Can. J. Chem. Downloaded from www.nrcresearchpress.com by 210.87.254.5 on 09/05/12
For personal use only.

Canadian Journal of Chemistry

Issued by THE NATIONAL RESEARCH COUNCIL OF CANADA

VOLUME 44 JANUARY 1, 1966 NUMBER 1

DELPHINIUM ALKALOIDS

THE STRUCTURES OF THE ALKALOIDS OF DELPHINIUM CARDINALE HOOK AND THE ALKALOID DELATINE

M. H. BENN

Department of Chemistry, University of Alberta, Calgary, Alberta

Received July 16, 1965

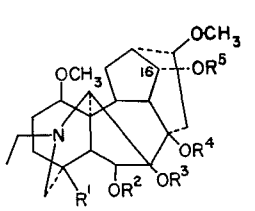
ABSTRACT

Browniine, dehydrobrowniine, lycoctonine, hetisine, and a dehydrohetisine were isolated from *Delphinium cardinale* Hook. Delatine, an alkaloid previously isolated from *D. elatum* L., was found to be hetisine. These are the first examples of the occurrence of the *Aconitum* alkaloid hetisine in *Delphinium* spp.

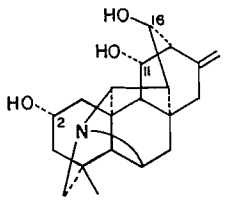
As part of a programme concerned with the chemotaxony of the genus *Delphinium*,[1] we have examined the alkaloids of *D. cardinale* Hook, a handsome, red-flowered species that sometimes exceeds 6 ft in height and is native to Southern and Baja California.

Extraction of the above-ground portion of the plant yielded an amorphous mixture of ester alkaloids which, on saponification, gave the parent alkaloids as a noncrystalline glass, together with benzoic and N-methylsuccinylanthranilic acids. Careful column chromatography of the mixed alkaloids on alumina initially yielded three crystalline alkaloids, one of which was recognized as lycoctonine. This alkaloid was first isolated as the (−)-N-(*o*-carboxyphenyl) methylsuccinimide ester,[2] methyllycaconitine, from *Aconitum lycoctonum*[3] (3, 4) and was subsequently found to be distributed quite widely in *Delphinium* spp. (2*a*). Lycoctonine has been shown to have the structure I (R^1 = OH, R^2 = CH_3, R^3 = R^4 = H, R^5 = CH_3) (6, 7). The other two crystalline alkaloids from the column chromatogram appeared to be unknown.

The first of these, m.p. 163–164°, was eluted from the column before lycoctonine and



I



II

[1]*Some 500 species of Delphinium that are almost exclusively native to the Northern Hemisphere and commonly blue flowered have been described (1). The genus has long been recognized by chemists as a rich source of alkaloids (2).*

[2]*The succinimide ring is easily opened by bases, hence the appearance of N-methylsuccinylanthranilic acid after saponification (4). We presume that lycoctonine is present in D. cardinale as methyllycaconitine.*

[3]*It has been suggested that this was actually A. vulparia Reichb. (5).*

had an infrared spectrum showing a strong resemblance to those of lycoctonine and the closely related alkaloid browniine[4] (I, $R^1 = OCH_3$, $R^2 = CH_3$, $R^3 = R^4 = R^5 = H$) (8), with, however, the additional feature of absorption in the carbonyl region at 1 750 cm^{-1}. Proton magnetic resonance spectroscopy (60 Mc/s) also revealed a striking similarity of the spectrum of the new alkaloid to those of lycoctonine and browniine, with signals caused by an ethyl group and four methoxyl groups as prominent features of the spectrum. However, in contrast to spectra of these two alkaloids, in which the methoxyl signals were completely resolved, in the spectrum of the new alkaloid two of the methoxyl signals overlapped to form a single, unresolved signal. The new alkaloid also showed low-intensity absorption in the ultraviolet at 288 mμ, while its optical rotatory dispersion curve exhibited a positive Cotton effect with extrema at 310 and 287 mμ.[5] All of these features seemed to be accommodated by dehydrobrowniine, in which the secondary hydroxyl at C-16 of browniine has been oxidized to give a cyclopentanone system. That this was, in fact, the correct structure of the alkaloid was readily shown by a sodium borohydride reduction, browniine being the only product formed. The stereospecific reduction of dehydroxobrowniine (to oxobrowniine) has already been described (8); in both cases shielding of one side of the carbonyl function results in exclusive formation of the 16α-alcohol.

The structure of the alkaloid of m.p. 163–164° was also established by a partial synthesis from browniine. Sodium dichromate in acetic acid[6] gave low yields of ketonic, basic material from which dehydrobrowniine was separated by chromatography and found to be identical with the naturally occurring alkaloid.

Thin-layer chromatography results had already suggested that browniine itself was probably present in the noncrystalline alkaloid fractions eluted before and together with dehydrobrowniine, and indeed browniine could be isolated as the crystalline perchlorate salt from these fractions, after all ketonic materials had been removed with Girard-T reagent.[7]

The second new crystalline alkaloid, m.p. 268–270°, eluted from the column after lycoctonine, had an infrared spectrum markedly different from that of lycoctonine (or browniine). In particular, the second new alkaloid exhibited absorption at 3 080, 1 650, and 900 cm^{-1} which suggested the presence of an exocylic methylene group, at 1 700 cm^{-1} which suggested a cyclohexanone, and at 1 050 cm^{-1} which suggested the presence of secondary hydroxyl functions. All these absorptions were absent in the spectra of lycoctonine and browniine, which in contrast had strong absorption bands at 2 820 and 1 085 cm^{-1}, caused by their methoxyl functions, which are not present in the spectrum of the unknown alkaloid. An analysis of the proton magnetic resonance spectrum of the unknown alkaloid confirmed that there were no methoxyl groups present, and also revealed the presence of one tertiary C-methyl group (and the probable absence of other simple alkyl groups) and two vinylic protons (as required for an exocyclic methylene function). The ultraviolet light absorption spectrum of the second new alkaloid showed low-intensity absorption at 290 mμ. The optical rotatory dispersion curve of the alkaloid dissolved in

[4]*This alkaloid was originally isolated from D. brownii Rydb. (synonym D. glaucum S. Wats.).*

[5]*Interestingly, in acid solution the optical rotatory dispersion curve shows a negative Cotton effect. A similar observation in the Lycopodium alkaloid series (9) has been interpreted as indicating that positively charged nitrogen has a large specific rotativity, like fluorine (10). We thank Dr. W. A. Ayer for drawing our attention to this observation (9).*

[6]*Oppenhauer oxidation failed to yield dehydrobrowniine, the starting material being recovered even under reasonably forcing conditions (cyclohexanone – aluminium t-butoxide in refluxing toluene for 8 h), presumably because of steric hindrance to the formation of the cyclic transition state required in this oxidation.*

[7]*Unless this was done, dehydrobrowniine perchlorate contaminated the product and could not be removed, even by repeated recrystallization.*

Can. J. Chem. Downloaded from www.nrcresearchpress.com by 210.87.254.5 on 09/05/12
For personal use only.

methanol showed only the vestige of an inflexion at 325 mμ; however, when dissolved in acetic acid or 1 *N* aqueous sulfuric acid the alkaloid showed a weak positive Cotton effect with extrema at 310 and 330 mμ. The molecular weight, determined by mass spectrometry, was 327 which, combined with the analytical results, gave a molecular formula for the alkaloid of $C_{20}H_{25}NO_3 \cdot \frac{1}{2}H_2O$.

In 1943, Goodson (11) reported the isolation of three alkaloids, methyllycaconitine, delpheline (I, R^1 = H, R^2 = OH, $R^3 + R^4 = CH_2$, $R^5 = CH_3$) (12), and delatine, from the seeds of *D. elatum*.[8] Delatine was much less heavily oxygenated than the other two alkaloids and was ascribed the molecular formula $C_{19}H_{25}NO_3 \cdot H_2O$ by Goodson, who also reported it to have m.p. 148° (hydrate), 261–264° (anhydrous), $[\alpha]_D^{23}$ +13.5° in dilute hydrochloric acid, and to contain neither methoxyl nor N-methyl groups. No further work on delatine appears to have been reported in the literature.

It appeared possible that our second alkaloid and delatine might be the same compound, and we obtained a sample of Goodson's delatine hydrochloride for comparative purposes. However, there was complete absence of carbonyl absorption in the infrared spectrum of delatine hydrochloride. There was, however, a striking similarity to the spectrum of hetisine hydrobromide, which we also had at hand.

Hetisine was first described in 1942, having been isolated from *Aconitum heterophyllum* Wall. by Jacobs and Craig (13), and its complete structure has very recently been established as that shown in II by X-ray crystallographic analysis of the hydrobromide (14). The physical constants reported by Jacobs and Craig for hetisine, m.p. 145° (effervescence), 253–256°, $[\alpha]_D^{25}$ +13.7° (ethanol), were suggestively similar to those of delatine, and indeed upon comparison of the alkaloids, as the free bases and hydrobromides, they were found to be identical. Thus delatine is in fact hetisine (II).

After this serendipitous outcome, we observed that there were certain general similarities in the infrared spectra of hetisine and our alkaloid. Acting on the premise that the second new alkaloid might be a dehydrohetisine, we therefore reduced it with sodium borohydride. The only product isolated was hetisine, which was characterized as the hydrobromide.

Our second alkaloid is therefore one of the three possible dehydrohetisines (III, IV, and V). High-resolution infrared spectroscopy[9] failed to reveal any shift (or splitting) of the carbonyl absorption band from the position expected for a simple cyclohexanone system, 1 707 cm^{-1}, i.e. there was no evidence for hydrogen bonding such as might have been expected had the keto function been at either C-11 (IV) or C-16 (V). There was also no sign of "abnormally" intense $n \rightarrow \pi^*$ ultraviolet light absorption at 290 mμ, such as would also have been anticipated had the keto function been in these positions, gamma to the exocylic methylene group.[10]

The remaining alternative of locating the keto function is at C-2, and this is not particularly attractive since one would have anticipated (octant rule) that this compound would have shown a large, negative Cotton effect in its optical rotatory dispersion spectrum. Furthermore, in this position, the stereospecific sodium borohydride reduction is much more unexpected than for the alternative positions (IV, V), where very pronounced shielding effects are apparent.[11] However, we tentatively advance the structure III for the alkaloid, m.p. 268–270°.

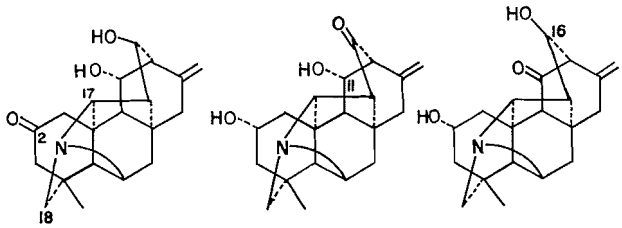
[8]*The seeds were those of a horticultural strain that was probably much crossed.*

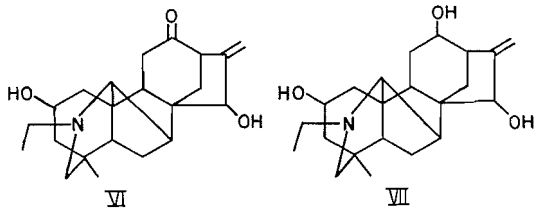
[9]*In very dilute solution in chloroform, with a Beckman IR-7 spectrometer having scale expansion.*

[10]*Molecular models of III and IV show that there should be perceptible overlap of the orbitals of the carbonyl and exocylic methylenic double bonds, the required conditions for enhanced $n \rightarrow \pi^*$ absorption (15), although the overlap is not as good as that in songorine (VI), which has λ_{max} 290 mμ, ε 500 (16).*

[11]*Possibly the β-oriented hydrogens at C-17 and C-18 do screen the "rear-side" of the keto function in III, but exclusive "front-side" attack and formation of the 2α-ol, by sodium borohydride, seems rather surprising.*

Can. J. Chem. Downloaded from www.nrcresearchpress.com by 210.87.254.5 on 09/05/12
For personal use only.





Finally, we reexamined the noncrystalline alkaloids eluted after dehydrohetisine and, from the infrared spectra of these, we were able to deduce that hetisine was present. Upon rechromatography of these fractions, hetisine was isolated and characterized as the hydrobromide.

The co-occurrence of the dehydroalkaloids and their parent alkaloids raises the question of whether the dehydro compounds are of genuine natural occurrence, or are artifacts produced by oxidation during the processing of the plant material and isolation of the alkaloids. From the evidence at our disposal,[12] however, we believe that the dehydroalkaloids which we isolated do actually coexist in the plant with the corresponding alkaloids.

It is interesting to see another diterpenoid alkaloid, hetisine, common to *Aconitum* and *Delphinium* species, reflecting the very close phylogenetic relationship of these two genera. Presumably the lycoctonine and hetisine skeletons are closely related biosynthetically, possibly arising from some common diterpenoid precursor, e.g. by some modification of the common biogenetic derivation suggested for the lycoctonine and atisine skeletons (2*b*, 17).

EXPERIMENTAL

Unless otherwise stated, all melting points are corrected, infrared spectra are of KBr disks and were made with a Perkin–Elmer 337 grating spectrometer, proton magnetic resonance spectra were measured at 60 Mc/s in deuterochloroform with tetramethylsilane as standard (τ = 10), optical rotatory dispersion measurements were made with a Durrum–Jasco spectrometer, and ultraviolet light absorptions are of solutions in 95% (v/v) ethanol. The alumina used for column chromatography was Woelm, neutral, grade 4. Thin-layer chromatography was performed on silica gel G with chloroform–methanol (4:1 v/v) as solvent and iodine vapor for location of the alkaloids.

Isolation of the Alkaloids

D. cardinale plants, collected in and just before blossoming, were cut up and preserved under isopropanol–methanol. After 7 days, the plants were repeatedly macerated with methanol, in a Waring Blendor, until the extracts were almost colorless. The dry plant residue amounted to 0.8 kg. Rapid concentration of the

[12]*On prolonged exposure to the atmosphere, in solution or as solids, browniine and hetisine were discolored. Infrared examination of the "aged" alkaloids revealed the formation of only traces of carbonyl-containing products from hetisine and not a trace of such material from browniine. There is a previous example of the co-occurrence of an aconite alkaloid and its dehydro derivative. Napelline (VII) and songorine (VI) have been isolated from Aconitum napellus (16).*

Can. J. Chem. Downloaded from www.nrcresearchpress.com by 210.87.254.5 on 09/05/12
For personal use only.

methanol extracts (cyclone evaporator) yielded a dark-green syrup which was partitioned between petroleum ether and 1 *N* aqueous sulfuric acid. The petroleum ether layer was re-extracted with dilute sulfuric acid (4 × 200 ml) and the combined aqueous extracts washed with petroleum ether (4 × 100 ml). The aqueous solution was made strongly alkaline with sodium hydroxide solution and then extracted with chloroform (7 × 200 ml). The combined, dried ($MgSO_4$) chloroform extracts were concentrated under reduced pressure (to about 200 ml) and then extracted with 1 *N* aqueous sulfuric acid (5 × 100 ml). The combined aqueous extracts were backwashed with chloroform (1 × 100 ml), make alkaline with sodium hydroxide solution, and extracted with chloroform (5 × 100 ml) as before. The combined, dried ($MgSO_4$) chloroform extracts were evaporated under reduced pressure to a residual oil which was dissolved in acetone, and the solution was then reevaporated under reduced pressure to yield the ester alkaloids as an amorphous off-white solid (3.5 g, 0.44%, based on dry plant residue).

Saponification of the Ester Alkaloids

The ester alkaloids (2.5 g) were dissolved in methanol (50 ml) containing sodium hydroxide (300 mg) and water (10 ml). The solution was refluxed for 90 min and then the bulk of the methanol was removed under reduced pressure. The residual solution was diluted with water (40 ml) and extracted with chloroform (4 × 30 ml). The combined, dried ($MgSO_4$) chloroform extracts were evaporated under reduced pressure to yield the alkaloids as an off-white glass (2.5 g).

The aqueous alkaline extracts were adjusted to pH 5 with dilute sulfuric acid and extracted with chloroform (4 × 25 ml). Evaporation of the dried ($MgSO_4$) extracts yielded a little off-white solid, which was recrystallized from water to give colorless laths, m.p. 120–121°, undepressed on admixture with authentic benzoic acid. The infrared spectrum of the recrystallized material was also superimposable on that of benzoic acid.

The aqueous extracts remaining from the chloroform extraction were brought to pH 1 with sulfuric acid and extracted continuously with ether for 48 h. Evaporation of the ether extract yielded an oil which crystallized from concentrated ether or acetone. Recrystallization of this acid from water gave colorless needles, m.p. 162–163°. Thin-layer chromatography showed that this acid was indistinguishable from synthetic (±)-N-methylsuccinylanthranilic acid,[13] and the infrared spectra of the synthetic and isolated acids, in chloroform solution, were identical. The literature m.p. for (−)-N-methylsuccinylanthranilic acid is 163–164° (18) and 155° (11).

Column Chromatography of the Mixed Alkaloids

The mixed, saponified alkaloids (2.5 g) were chromatographed on a column of alumina (2.0 cm × 40 cm). Fractions of 25 ml were collected and evaporated individually under reduced pressure, and the residues were examined by thin-layer chromatography. The fractions were then appropriately grouped. Details of the column chromatography are given in Table I.

Fractions 19–38 were crystallized from ether to give small colorless prisms of an alkaloid, m.p. 161–163° (128 mg, 5%).

Fractions 49–52 were crystallized from acetone – petroleum ether to give colorless needles of lycoctonine hydrate, m.p. 115–125° (open capillary) (104 mg, 4%). Lit. m.p. 120–139° (19). The infrared spectrum of the isolated alkaloid was identical with that of an authentic specimen of lycoctonine hydrate.

Fractions 67–69 were rechromatographed on alumina, neat chloroform being used as eluant and 10 ml fractions being collected. Fractions 5–10 from this separation yielded a white glass (229 mg) which was crystallized from acetone to give colorless needles of an alkaloid, m.p. 265–270° (104 mg, 4%).

Fractions 73–81 and 82–85 and the tail fractions from the rechromatographed fractions 67–69 had infrared spectra which indicated that they were almost pure hetisine. The tail fractions (105 mg) were converted into the hydrobromide salt, m.p. 260–266° (decomp.), undepressed on admixture with authentic hetisine hydrobromide. Lit. m.p. 266–269° (14*b*). The infrared spectrum of the hydrobromide was also identical with that of authentic material.

Alkaloid, m.p. 161–163°

$[\alpha]_D^{27}$ +19°; optical rotatory dispersion, Cotton effect, $[\phi]_{300}^{27}$ +1 380°, $[\phi]_{260}^{27}$ +650° (*c*, 0.2); optical rotatory dispersion in 1 *N* aqueous H_2SO_4, Cotton effect, $[\phi]_{310}^{30}$ −372°, $[\phi]_{287}^{30}$ +1 320° (*c*, 0.15). The ultraviolet absorption had a slight inflexion on the end absorption curve at 288 mμ, ε 30. The infrared spectrum had prominent absorption bands at 3 500, 3 400, 2 970, 2 910, 2 855, 2 830, 1 750, 1 470, 1 350, 1 290, 1 215, 1 100 (broad), 990, 940, 730, 650, 630, and 590 cm^{-1}. The proton magnetic resonance spectrum contained prominent signals at τ 8.9 (t) (3H) (CH_3 of N-ethyl group) and at τ 6.7 (s) (6H), 6.65 (s) (3H), 6.58 (s) (3H) (four OCH_3 groups).

Alkaloid, m.p. 265–270°

Anal. Found: C, 71.20; H, 7.70; N, 4.17; mol. wt. 327 (mass spectrometer). $C_{20}H_{25}NO_3 \cdot \frac{1}{2}H_2O$ requires C, 71.40; H, 7.79; N, 4.15.

$[\alpha]_D^{28}$ +18°; optical rotatory dispersion, plain curve, $[\phi]_{600}^{29}$ +60°, $[\phi]_{280}^{29}$ +420° (slight inflexion), $[\phi]_{340}^{29}$

[13]*This acid was obtained by saponification of the ester prepared by the reaction of (±)-methylsuccinic anhydride with ethyl anthranilate.*

Can. J. Chem. Downloaded from www.nrcresearchpress.com by 210.87.254.5 on 09/05/12
For personal use only.

TABLE I

Fraction Nos.	Eluant composition (v/v)	Wt. eluted (mg)	Appearance	Composition
1–6	Benzene	14	Pale brown wax	Essentially alkaloid free
7–18	5% ether–benzene	14	Pale yellow oil	At least two alkaloids, one (the slower moving) indistinguishable from browniine
19–38	5–50% ether–benzene	329	Pale yellow glass	Similar to fractions 7–18, but fastest moving alkaloid now predominant
39–48	50% ether–benzene and ether	95	Off-white glass	A third alkaloid now present, indistinguishable from lycoctonine
49–52	Ether	153	Colorless glass	The third alkaloid now predominant
53–66	Ether and chloroform	267	Off-white glass	As fractions 49–52
67–69	5% methanol–chloroform	777	Off-white glass	A mixture of several alkaloids
70–72	5 and 10% methanol–chloroform	409	Off-white glass	Similar to fractions 67–69
73–81	10% methanol–chloroform	117	Lemon-yellow glass	A mixture with a predominant (slow-running) alkaloid
81–85	25% methanol–chloroform	75	Brownish-yellow glass	Similar to fractions 73–81

+210° (*c*, 0.16); optical rotatory dispersion in 1 *N* aqueous H_2SO_4, Cotton effect, $[\phi]_{343}^{30}$ +175°, $[\phi]_{316}^{30}$ +92° (*c*, 0.16); ultraviolet absorption, λ_{max} 290 mμ, ε 40. The infrared spectrum had bands at 3 350, 3 080, 2 960, 2 940, 1 700, 1 650, 1 430, 1 285, 1 070, 1 050, 900, and 875 cm^{-1}. The proton magnetic resonance spectrum had signals at τ 5.1 (1H) and 5.3 (1H) (two vinylic protons) and 8.85 (s) (3H) (CH_3—C(—)—).

Isolation of Browniine from the "Front" Fractions of the Main Column Chromatogram

Fractions 4–14 (105 mg) were dissolved in ethanol (5 ml) containing acetic acid (0.5 ml), Girard-T reagent (100 mg) was added, and the reaction mixture was then refluxed for 8 h. After having been kept at room temperature overnight, the reaction mixture was concentrated under reduced pressure, the residue diluted with ice water (40 ml), and the solution made alkaline with ammonia and extracted with chloroform (4 × 10 ml). Removal of solvent, under reduced pressure, from the combined, dried ($MgSO_4$) chloroform extracts left an off-white glass (72 mg). This material showed no carbonyl absorption in the infrared spectrum (chloroform solution). Part of this material (38 mg) was chromatographed on alumina and the alkaloid (21 mg) that was eluted with 25% (v/v) ether–benzene was converted into the crystalline perchlorate salt, m.p. 208–210°, undepressed on admixture with authentic browniine perchlorate. Lit. m.p. 212° (8). The infrared spectrum was also identical with that of browniine perchlorate.

Sodium Borohydride Reduction of the Alkaloid, m.p. 161–163°

Sodium borohydride (50 mg) was added during the course of 1 h to a solution of the alkaloid (38 mg) in methanol (8 ml) containing water (1 ml). After 2 h at room temperature, two drops of concentrated hydrochloric acid was added to the solution to destroy any excess borohydride, the reaction mixture was evaporated to a small volume under reduced pressure and diluted with water (5 ml), and the solution was made alkaline with 6 *N* aqueous sodium hydroxide solution (5 ml) and extracted with chloroform (4 × 10 ml). The combined, dried ($MgSO_4$) chloroform extracts were evaporated under reduced pressure to a residual oil (44 mg), which was converted into the beautifully crystalline perchlorate salt, m.p. and mixed m.p. with browniine perchlorate 212–214°. The infrared spectrum of the perchlorate of the reduced alkaloid was also superimposable on that of authentic browniine perchlorate.

Preparation of Dehydrobrowniine

Browniine (from 363 mg of perchlorate salt) was dissolved in acetic acid (5 ml) and to this, at room temperature, was added 1.5 ml of a solution of sodium dichromate (0.60 g) in acetic acid (50 ml).

Can. J. Chem. Downloaded from www.nrcresearchpress.com by 210.87.254.5 on 09/05/12
For personal use only.

Further 1.5 ml volumes of the sodium dichromate solution were added to the reaction mixture after 30, 90, and 150 min. After 18 h at room temperature, the reaction mixture was diluted with ice water (30 ml), made alkaline with sodium hydroxide solution, and extracted with chloroform (4 × 20 ml). (Centrifugation was necessary at this stage.) The combined, dried ($MgSO_4$) chloroform extracts were evaporated under reduced pressure to yield a yellow glass (288 mg). This glass was redissolved in chloroform (15 ml) and extracted with 1 *N* aqueous sulfuric acid (2 × 15 ml). The combined aqueous extracts were backwashed with chloroform (1 × 10 ml) and the combined, dried ($MgSO_4$) chloroform extracts evaporated under reduced pressure to yield neutral material (85 mg). Basification of the aqueous extracts with sodium hydroxide solution followed by chloroform extraction (3 × 15 ml) gave, after solvent had been removed from the combined, dried ($MgSO_4$) chloroform extracts, the basic material (195 mg). The infrared spectrum of this material in chloroform solution suggested about 30% ketone content, and when it was chromatographed on alumina the fractions that were eluted with benzene and 5% (v/v) ether–benzene were crystallized from concentrated ether solution as colorless prisms, m.p. 161–163° (37 mg, 12%). The infrared spectrum was superimposable on that of the alkaloid of m.p. 161–163° isolated from *D. cardinale*.

Anal. Found: C, 64.64; H, 8.73; N, 3.03. $C_{25}H_{39}NO_7$ requires C, 64.49; H, 8.44; N, 3.01.

Sodium Borohydride Reduction of the Alkaloid, m.p. 261–265°

A solution of the alkaloid (10.8 mg) in 90% ethanol was reduced with a total of 30 mg of sodium borohydride and the product isolated as described before. The reduction product was converted into the hydrobromide, which formed thin, colorless needles, m.p. 265–270° (decomp.), undepressed on admixture with authentic hetisine hydrobromide. The infrared spectra of the hydrobromides of the reduction product and of hetisine were also identical.

Delatine

The free base was prepared from a sample of Goodson's hydrochloride salt and converted into the hydrobromide salt, m.p. 262–266° (decomp.), undepressed on admixture with authentic hetisine hydrobromide. The infrared spectrum was also superimposable on that of the authentic hetisine hydrobromide.

ACKNOWLEDGMENTS

For assistance with the collection of plant material, we thank Professor T. A. Geissman, Chemistry Department, U.C.L.A., Dr. Peter Raven, Botany Department, Stanford University, Dr. T. Mosquin, Research Branch, Canada Department of Agriculture, Ottawa, Dr. R. C. B. Hartland-Rowe, Biology Department, and Dr. T. S. Sorensen and Mr. D. Meakin, Chemistry Department, University of Alberta.

We are indebted to Drs. Adamson and Wilkinson of the Wellcome Foundation, Beckenham, Kent, England, who supplied the authentic sample of Dr. Goodson's delatine hydrochloride, and to Dr. E. O. Edwards of the National Research Council, Ottawa, for a gift of hetisine hydrobromide.

Dr. W. A. Ayer of the Chemistry Department, University of Alberta, Edmonton, kindly arranged for the measurement of mass spectra (one of which was provided by Dr. D. B. McLean of McMaster University) and some initial optical rotatory dispersion spectra, on which he made some extremely helpful comments.

Finally, we thank the National Research Council of Canada for a grant which made possible the collecting expedition and subsequent chemical investigations.

REFERENCES

1. Index Kewensis and Supplements. Clarendon Press, Oxford.
2. (*a*) H. G. Boit. Ergebnisse der Alkaloid-Chemie bis 1960. Akadamie Verlag, Berlin. 1961. (*b*) K. Wiesner and Z. Valenta. Fortschr. Chem. Org. Naturstoffe, **16**, 26 (1958). (*c*) E. S. Stern. *In* The alkaloids. Vol. 7. *Edited by* R. H. F. Manske. Academic Press, Inc., New York. 1960. p. 473.
3. F. Hubschmann. Schweiz. Wochschr. Pharm. **3**, 269 (1865). E. S. Stern. *In* The alkaloids. Vol. 4. *Edited by* R. H. F. Manske and H. L. Holmes. Academic Press, Inc., New York. 1954. p. 275.
4. R. C. Cookson, J. E. Page, and M. E. Trevett. J. Chem. Soc. 4028 (1954). A. D. Kuzovkov and A. V. Bocharnikova. Zh. Obshch. Khim. **28**, 556 (1958).
5. T. A. Henry. The plant alkaloids. 4th ed. J. & A. Churchill, Ltd., London. 1949. p. 692.
6. M. Przybylska and L. Marion. Can. J. Chem. **34**, 185 (1956).
7. O. E. Edwards, L. Marion, and D. K. R. Stewart. Can. J. Chem. **34**, 1315 (1956).
8. M. H. Benn, M. A. M. Cameron, and O. E. Edwards. Can. J. Chem. **41**, 477 (1963)
9. W. A. Ayer, J. A. Berezowsky, and D. A. Law. Can. J. Chem. **41**, 649 (1963).

Can. J. Chem. Downloaded from www.nrcresearchpress.com by 210.87.254.5 on 09/05/12
For personal use only.

10. W. MOFFIT, R. B. WOODWARD, A. MOSCOWITZ, W. KLYNE, and C. DJERASSI. J. Am. Chem. Soc. **83,** 4013 (1961).
11. J. GOODSON. J. Chem. Soc. 139 (1943).
12. R. C. COOKSON and M. E. TREVETT. J. Chem. Soc. 3121 (1956); 3864 (1956).
13. W. A. JACOBS and L. CRAIG. J. Biol. Chem. **143**, 605 (1942).
14. (*a*) M. PRZYBYLSKA. Can. J. Chem. **40**, 566 (1962). (*b*) M. PRZYBYLSKA. Acta Cryst. **16**, 871 (1963).
15. R. C. COOKSON and N. S. WARIYAR. J. Chem. Soc. 2302 (1956).
16. K. WIESNER, S. ITO, and Z. VALENTA. Experientia, **14**, 167 (1958). K. WIESNER, Z. VALENTA, J. F. KING, R. K. MAUGDAL, L. G. HUMBER, and S. ITO. Chem. Ind. London, 173 (1957). T. SUGASAWA. Unpublished. *Quoted by* S. W. Pelletier. Tetrahedron, **14**, 95 (1961).
17. Z. VALENTA and K. WIESNER. Chem. Ind. London, 354 (1956).
18. S. YUNUSOV and N. K. ABUBAKIROV. Zh. Obshch. Khim. **22**, 1461 (1952).
19. R. H. F. MANSKE and L. MARION. Can. J. Res. **248**, 1 (1946).

Can. J. Chem. Downloaded from www.nrcresearchpress.com by 210.87.254.5 on 09/05/12
For personal use only.

CHARGE-TRANSFER COMPLEXES OF BIPHENYLENE

P. H. EMSLIE, R. FOSTER, AND R. PICKLES
Chemistry Department, Queen's College, University of St. Andrews, Dundee, Scotland
Received June 24, 1965

ABSTRACT

An attempt has been made to redetermine the enthalpy and entropy of formation of the charge-transfer complex between tetracyanoethylene and biphenylene in dichloromethane solution from measurements of the equilibrium constant at different temperatures. The results obtained under conditions where biphenylene is in excess differ from those previously published in which tetracyanoethylene was in excess. It is argued that the optimum condition for determining equilibrium constants of a 1:1 complex is when the reactants are mixed in solution in this ratio. Determinations under this condition yield $\Delta H = -2.6$ kcal mole^{-1} and $\Delta S = -4.1$ e.u.

The energies of the intermolecular charge-transfer transitions of biphenylene with several different acceptors suggest that the ionization potential of biphenylene is ~7.4 eV.

The association constant of the charge-transfer complex between biphenylene, D, and tetracyanoethylene, A, in dichloromethane has recently been measured by Farnum *et al.* (1). This constant was evaluated by the Benesi–Hildebrand method (2) from measurements of the optical absorption caused by the characteristic charge-transfer transition. Because of the limited supply of biphenylene, measurements were made on a series of solutions in which [D] was constant and small compared with [A]. From such determinations an association constant K_c was determined where

$$K_c = [AD]/[A][D] \text{ l mole}^{-1}, \quad [1]$$

which was converted to a dimensionless association constant K_x:

$$K_x = [AD]/x_A[D], \quad [2]$$

where x_A = mole fraction of A; hence for dilute solutions

$$K_x = K_c\,(1000d/M), \quad [3]$$

where d = density of solvent and M = molecular weight of solvent. Farnum *et al.* (1) obtained a value of $K_x = 80$ at 22°, and a molar extinction coefficient $\epsilon = 500$. From measurements of a single solution at various temperatures, the temperature variation of K_x was calculated on the assumption that ϵ is temperature independent. From van't Hoff plots, $\Delta H = -2.8$ kcal mole^{-1} and $\Delta S = -1.0$ e.u., the pure complex being used as the standard state.

An attempt has been made to redetermine these constants by using the condition [D] $\gg$ [A], in which K_c and ϵ are evaluated by a variant (3) of the Benesi–Hildebrand relationship. It may be shown (3) that

$$d/[D] = -Kd + K[A]\epsilon, \quad [4]$$

where, for a series of solutions of constant [A] and varying [D], and [A] $\ll$ [D], d represents the optical density of a 1 cm path length at a wavelength λ caused by absorption by the complex alone, at which wavelength the extinction coefficient is ϵ. A plot of $d/[D]$ against d should be linear, with a gradient of $-K_c$.

Can. J. Chem. Downloaded from www.nrcresearchpress.com by 210.87.254.42 on 09/05/12
For personal use only.

RESULTS AND DISCUSSION

Thermodynamic Constants of the Tetracyanoethylene Complex

Plots of $d/[D]$ against d, measured at the wavelength of maximum absorption (λ_{max} = 680 mμ) and 22° under the conditions described in the previous section, gave nonlinear correlations; the results of one such determination are shown in Fig. 1. Estimates of $K_c \approx 1.1 \pm 0.5$ l mole^{-1} (hence $K_x = 17 \pm 8$) and $\epsilon \approx 2\,300 \pm 1\,000$ are very different from the values obtained by Farnum *et al.* In contrast the values of the product $K_x\epsilon$ at a given temperature are equal within the admittedly large error.

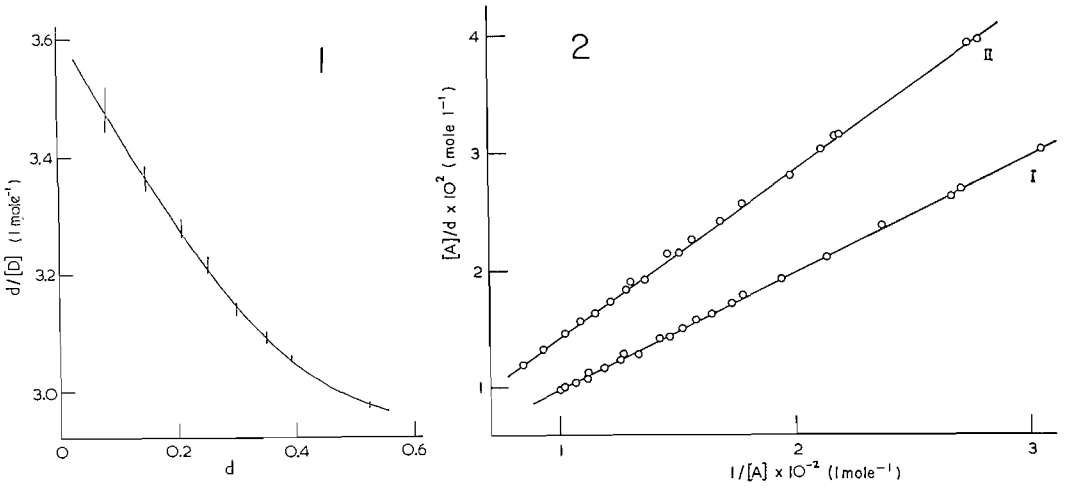


FIG. 1. Plot of $d/[D]$ against d for solutions of tetracyanoethylene, A, plus biphenylene, D, in dichloromethane, where [A] = 1.537 × 10^{-3} M, at 22.0°, with a 1 cm cuvette. The lengths of the lines marking the experimental points are measures of the error as reckoned in terms of the reproducibility of the measurements of d.

FIG. 2. Plots of $[A]/d$ against $[A]^{-1}$ for solutions of tetracyanoethylene, A, plus biphenylene, D, in dichloromethane, where [A] = [D], at 6.5° (I) and at 25.1° (II), with a 3 cm cuvette.

We consider (4) that these differences in K_x and ϵ and the nonlinearity of $d/[D]$ with d shown in the present determination are the results of the deviations from Beer's law shown by the optical absorption of the species AD. Both the method of evaluation used by Farnum *et al.* and that used by ourselves assume that Beer's law is strictly obeyed. The consequences of deviations have been discussed recently (4), where it was pointed out that the optimum condition needed to minimize such deviations is to use systems which involve a minimum *total* concentration of solute. To obtain maximum concentrations of complex under such conditions, [A] = [D] for a 1:1 complex. We have now used this condition to re-evaluate the association constant. It may be shown (5) that, when [A] = [D],

$$[5] \qquad \frac{[A]}{d} = \frac{1}{[A]K_c\epsilon} + \frac{2}{\epsilon}$$

for a 1 cm path length. For a 3 cm path length as used in the present determination,

$$[6] \qquad \frac{[A]}{d} = \frac{1}{[A]3K_c\epsilon} + \frac{2}{3\epsilon}.$$

Can. J. Chem. Downloaded from www.nrcresearchpress.com by 210.87.254.42 on 09/05/12
For personal use only.

Hence a plot of $[A]/d$ against $[A]^{-1}$ should be linear, and from this plot K_c and ϵ may be evaluated. Such plots are shown in Fig. 2. The values of K_c and ϵ calculated by this method are given in Table I, together with the calculated values of K_x, ΔH, and ΔS, based on the same standard states as the values quoted by Farnum *et al.*

TABLE I

Values of equilibrium constants (K_c, K_x), extinction coefficient (ϵ), enthalpy (ΔH), and entropy (ΔS) of formation of the complex biphenylene–tetracyanoethylene in dichloromethane

Temp. (°C)	K_c (l mole^{-1})	K_x	ϵ	ΔH (kcal mole^{-1})	ΔS (e.u.)
6.5	$0.95_4 \pm 0.008$	$14.9_8 \pm 0.1$	$3\,540 \pm 30$	-2.6_5	-4.1_0
25.1	$0.71_0 \pm 0.007$	$11.1_4 \pm 0.1$	$3\,290 \pm 30$		

Ionization Potential of Biphenylene from Charge-Transfer Spectra

Farnum *et al.* have compared the value of the frequency of the maximum of the charge-transfer band (ν_{max}) with ν_{max} for other tetracyanoethylene complexes. From the empirical relationship described by Merrifield and Phillips (6) the value of ν_{max} for the biphenylene complex would correspond to an ionization potential (I_p) of 6.4 eV. Merrifield and Phillips suggested that for tetracyanoethylene complexes a better linear correlation exists between the free energy of formation of the complex and the I_p. From such a relationship, Farnum *et al.* obtained a value of $I_p = 7.37$ eV for biphenylene.

Tetracyanoethylene complexes give a poorer correlation of ν_{max} with I_p of the donor than do complexes with many other acceptors. It has recently been suggested that this may be the result of multiple overlapping charge-transfer bands (7). From an analysis of such spectra it is suggested (7) that eq. [7] provides a better correlation of I_p and ν_{ct} for tetracyanoethylene complexes.

$$\nu_{ct} = 0.83 I_p - 4.42, \qquad [7]$$

where ν_{ct} is the frequency of the charge-transfer bands and is measured in electron volts. The position of λ_{max} for the biphenylene complex (680 mμ) corresponds to $I_p = 7.5$ eV by eq. [7].

Although Mulliken (8) and others have emphasized the lack of a theoretical basis for such linear correlations, consistent and reasonable results may be obtained from them (9). ν_{max} for complexes of biphenylene with several acceptors have now been compared with ν_{max} for complexes of these acceptors with a series of donors. Dichloromethane was used as the solvent in most cases; otherwise 1,2-dichloroethane or chloroform was used. Recently, it has been shown that ν_{max} is virtually independent of the solvent for these particular solvents (10). The donors have been selected from those for which the ionization potential has been determined experimentally by the photoionization method (11). Plots of ν_{max} against I_p of the donor molecules (Fig. 3) suggest that I_p for biphenylene is ~7.35–7.45 eV.

EXPERIMENTAL

Analytical

Solutions were made up and measured as described previously (3, 12) with an Optica CF4 spectrophotometer. The spectra of complexes referred to in Fig. 3 were recorded with an Optica CF4DR spectrophotometer. For weaker complexes, concentrated solutions of the mixture of components were measured in cells having a short path length.

The best straight lines and root-mean-square deviations for the data depicted in Fig. 2 were obtained by using a standard root-mean-square program on a Stantec Zebra computer.

Can. J. Chem. Downloaded from www.nrcresearchpress.com by 210.87.254.42 on 09/05/12
For personal use only.

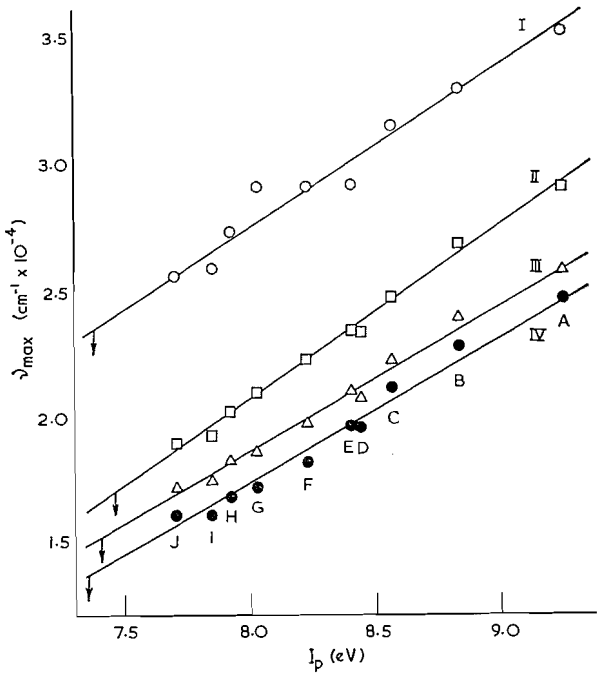


FIG. 3. Plots of the frequencies of the maxima (ν_{max}) of the charge-transfer bands for the complexes of the acceptors (I) 1,3,5-trinitrobenzene, (II) chloranil, (III) 2,3-dicyano-*p*-benzoquinone, (IV) 2,3-dichloro-5,6-dicyano-*p*-benzoquinone, with the donors (A) benzene, (B) toluene, (C) *o*- and *m*-xylene, (D) *p*-xylene, (E) mesitylene, (F) anisole, (G) durene, (H) pentamethylbenzene, (I) hexamethylbenzene, (J) aniline, (↓) biphenylene, against the ionization potentials (I_p) of the respective electron donors A–J.

Materials

Tetracyanoethylene was prepared and purified as described previously (13). Biphenylene was prepared by the method of Baker *et al.* (14) by the pyrolysis of diphenyleneiodonium iodide (15). It was recrystallized three times from methanol. Dichloromethane was distilled three times from phosphoric oxide and then from anhydrous potassium carbonate, and finally redistilled; b.p. 40° at 760 mm.

ACKNOWLEDGMENTS

The authors thank the Department of Scientific and Industrial Research for a grant (to P. H. E.), and the Royal Society for the provision of cells of variable path length (to R. F.).

REFERENCES

1. D. G. FARNUM, E. R. ATKINSON, and W. C. LOTHROP. J. Org. Chem. **26**, 3204 (1961).
2. H. A. BENESI and J. H. HILDEBRAND. J. Am. Chem. Soc. **71**, 2703 (1949).
3. R. FOSTER, D. LL. HAMMICK, and A. A. WARDLEY. J. Chem. Soc. 3817 (1953).
4. P. H. EMSLIE, R. FOSTER, C. A. FYFE, and I. HORMAN. Tetrahedron, **21**, 2843 (1965).
5. R. FOSTER. J. Chem. Soc. 5098 (1957).
6. R. E. MERRIFIELD and W. D. PHILLIPS. J. Am. Chem. Soc. **80**, 2778 (1958).
7. E. M. VOIGT and C. REID. J. Am. Chem. Soc. **86**, 3930 (1964).
8. C. REID and R. S. MULLIKEN. J. Am. Chem. Soc. **76**, 3869 (1954). R. S. MULLIKEN and W. B. PERSON. Ann. Rev. Phys. Chem. **13**, 107 (1962).
9. R. FOSTER. Nature, **183**, 1253 (1959).
10. P. H. EMSLIE and R. FOSTER. Rec. Trav. Chim. **84**, 255 (1965).
11. K. WATANABE, T. NAKAYAMA, and J. MOTTL. Final report on ionisation potentials of molecules by a photoionisation method. University of Hawaii, Honolulu. Department of Army contract No. DA-04-200-ORD 480 and 737. 1959. R. BRALSFORD, P. V. HARRIS, and W. C. PRICE. Proc. Roy. Soc. London, Ser. A, **258**, 459 (1960).
12. R. FOSTER. J. Chem. Soc. 1075 (1960).
13. P. H. EMSLIE and R. FOSTER. Tetrahedron, **21**, 2851 (1965).
14. W. BAKER, M. P. V. BOARLAND, and J. F. W. MCOMIE. J. Chem. Soc. 1476 (1954).
15. J. COLLETTE, D. MCGREER, R. CRAWFORD, F. CHUBB, and R. B. SANDIN. J. Am. Chem. Soc. **78**, 3819 (1956).

Can. J. Chem. Downloaded from www.nrcresearchpress.com by 210.87.254.42 on 09/05/12
For personal use only.

Can. J. Chem. Downloaded from www.nrcresearchpress.com by 210.87.254.42 on 09/05/12
For personal use only.

INVESTIGATION OF THE STRUCTURE OF 1,5-METHYLENE-QUINOLIZIDINIUM ION[1]

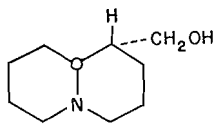
O. E. EDWARDS, GÁBOR FODOR,[2] AND LÉO MARION
Division of Pure Chemistry, National Research Council, Ottawa, Canada

Received November 3, 1964

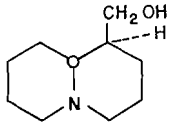
ABSTRACT

Galinovsky observed that O-tosyllupinine (II) readily isomerized to a quaternary tosylate. Without rigorous proof he assigned to this a monomeric azetidinium salt structure. A study of the infrared and nuclear magnetic resonance spectra and molecular weight of the compound confirms the 1,5-methylene-quinolizidinium salt structure III.

Galinovsky (1) demonstrated that the tosyl ester (II) of the alkaloid lupanine (I*a*) was isomerized on heating into a quaternary salt, in contrast to the thermal stability of the tosyl ester of epilupinine (I*b*). He interpreted this isomerization as an internal nucleophilic displacement to give the azetidinium salt (III*a*). The fact that the quaternary salt could be converted into lupinine by alkali confirmed that no skeletal rearrangement was involved in the thermal reaction.



Ia



Ib

The relative configurations of lupinine and its epimer have been demonstrated, by conformational analysis (2), infrared evidence for internal hydrogen bonding (3, 4), and dipole moment measurements (4), to be those illustrated in I*a* and I*b*, and the absolute configuration was proved by degradation of lupinine to (+)-4-methyl-nonane (5). Thus the stereochemistry of lupinine permits the formation of the internal salt III.

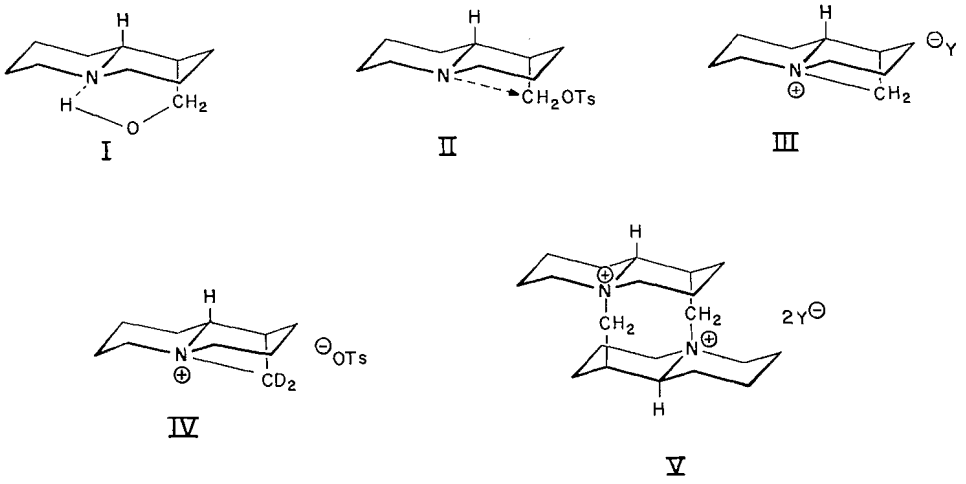
As pointed out recently by Leonard (6), however, Galinovsky produced no rigorous evidence for structure III, and a strain-free dimeric salt containing a diazaoctane system (V) would account equally well for his observations. Molecular models of the dimer V demonstrate the presence of bad hydrogen interactions and make this a priori unlikely. Nevertheless, a reexamination of the quaternary salt seemed desirable.

When completely dissociated, salt III should give an apparent molecular weight of 161.5, while IV should have one of 215.3. The salt was slightly associated in ethanol, but in methanol increasing dilution caused progressive dissociation. Extrapolation of the apparent molecular weight curve to infinite dilution in this solvent gave a value of 158.5 (Fig. 1), in excellent agreement with the requirement for III. Infrared spectral and nuclear magnetic resonance (n.m.r.) evidence supports this structure.

Infrared Evidence

Although the spectra of azetidinones have been investigated thoroughly because of interest in the penicillins, only limited data are available on the azetidines (7). Sheinker

[1]*Issued as N.R.C. No. 8672.*
[2]*Visiting scientist, National Research Council, Ottawa. Present address: Chemistry Department, Laval University, Quebec, Quebec.*



and Peresleni (8) studied the infrared and Raman spectra of cyclic imines to determine the influence of ring size on basicity. Later, Lippert and Prigge (9) assigned specific infrared and Raman absorption bands to symmetrical and antisymmetrical skeletal vibrations in the four-membered ring. A comparison is given in Table I between the infrared absorption frequencies for azetidine, piperidine, and (incomplete) 1-methyl-*trans*-quinolizidine (10) and the frequencies that we have observed for the quaternary bromide from lupinine (presumably *IIIb*) (Fig. 2).

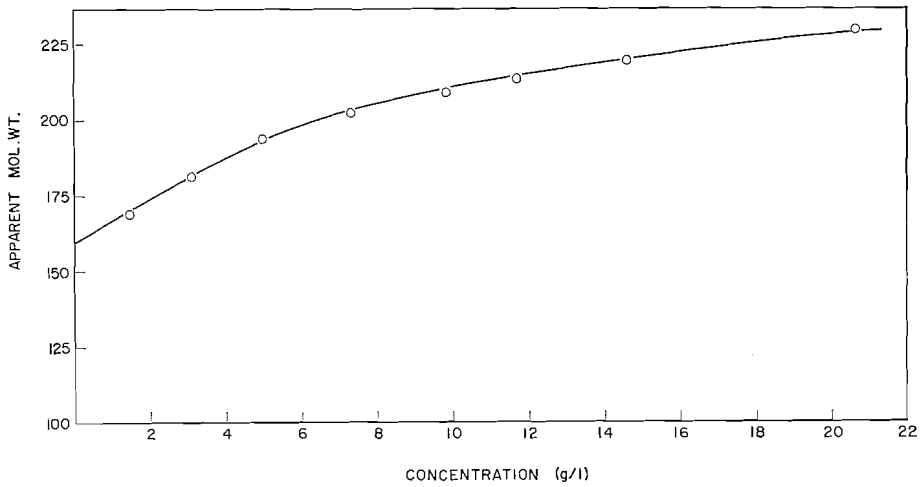


FIG. 1. Molecular weight determination.

The possible structures under consideration contain either (*a*) one four-membered and one six-membered ring, both strained, together with a less distorted six-membered ring, or (*b*) four six-membered rings and one eight-membered ring, all strainless. A significant absorption is found around 1 449–1 460 cm^{-1} in the spectrum of azetidine, which is ascribed by the Russian authors (8) to internal deformation vibrations of the methylene groups; comparable methylene groups in compounds having larger rings gave only

Can. J. Chem. Downloaded from www.nrcresearchpress.com by 210.87.254.42 on 09/05/12
For personal use only.

Can. J. Chem. Downloaded from www.nrcresearchpress.com by 210.87.254.42 on 09/05/12
For personal use only.

TABLE I

Infrared spectra

Azetidine (8)	3 266 s	2 990 s(i)	2 960 vs	2 857 vs		1 465 w 1 449 m	1 336 s 1 317 w	1 251 m 1 240 m	1 151 s	1 084 s	983 s 950 w	900 s 755 s	
N,N-(Dimethyl-d_6)-azetidinium iodide VIII	3 440 vs		2 965 s	2 250 s 2 065 m	1 635 vs	1 468 s 1 445 s 1 437 vs	1 350 m 1 318 w	1 270 s 1 240 s	1 182 s 1 162 vs	1 080 s 1 055 s	982 m 930 m	880 m 835 w 810 w	
1,5-Methylene-quinolizidinium bromide (III*b*)		3 020 s 2 990 s(i)	2 955 s 2 948 vs 2 915 vs 2 895 vs 2 885 vs	2 860 vs 2 855 vs(i) 2 820 s 2 778 s 2 735 s(i) 2 720 s 2 690 s 2 648 vs 2 625 vs 2 605 vs 2 575 vs 2 540 vs 2 510 vs		1 468 vs 1 458 m 1 445 vs 1 442 vs(i) 1 430 vs 1 423 vs 1 408 s	1 385 w 1 352 w 1 345 w 1 340 w 1 318 w 1 320 w 1 308 w	1 282 s 1 280 m(i) 1 265 m 1 237 w 1 210 w	1 152 w	1 085 w 1 095 w 1 075 m 1 068 w 1 052 w 1 028 m 1 020 s	998 m 980 w 964 s 954 w 940 m(i) 928 w 1 006	905 w(i) 902 w 890 w 855 m 845 (d) 820 w(d) 793 w 755 765 w(d) 904 866	700 m
Piperidine (9)	3 310		2 893	2 853 2 806 2 732		1 446	1 348	1 289 1 267	1 172 1 150	1 057 1 039			
trans-1-Methyl-quinolizidine (10)			2 945	2 865 2 805 2 755 2 680 2 610									

NOTE: Wave numbers (cm^{-1}) are given; i, inflection; d, double peak; s, strong; vs, very strong; m, medium; w, weak.

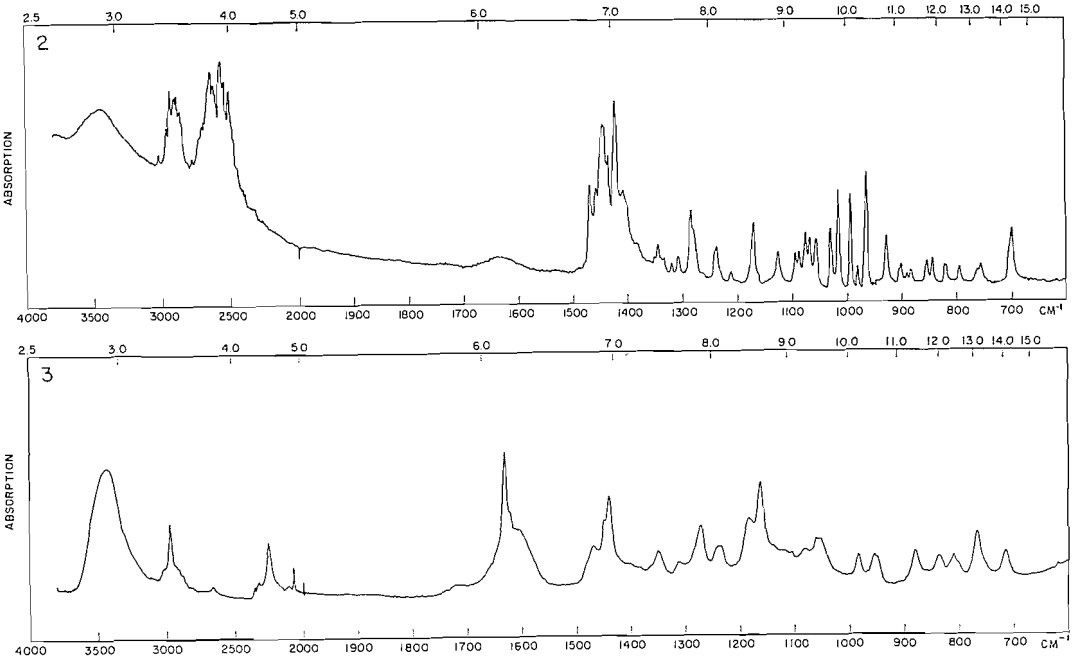
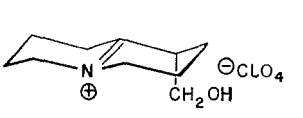


FIG. 2. Infrared spectrum of 1,5-methylene-quinolizidinium bromide.
FIG. 3. Infrared spectrum of N,N-(dimethyl-d_6)-azetidinium iodide.

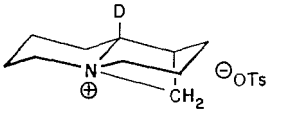
weak absorption in this region. The infrared spectrum of III*b* contains a very strong multiple peak between 1 425 and 1 468 cm^{-1}.

In their consideration of the effect of ring size on symmetrical and antisymmetrical skeletal vibrations Lippert and Prigge (9) ascribed to symmetrical skeletal vibrations a peak at 1 084 cm^{-1} in the spectrum of azetidine and one at 820 cm^{-1} in the spectrum of piperidine. The spectrum of III*b* shows a strong multiple peak between 1 050 and 1 090 cm^{-1} and a weak double peak at 820 cm^{-1}.

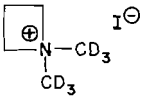
A maximum at 983 cm^{-1} in the spectrum of the imine having a four-membered ring and a maximum at 1 110 cm^{-1} in the imine having a six-membered ring were ascribed to antisymmetrical skeletal vibrations. The spectrum of III*b* shows a multiplet between 965 and 1 030 cm^{-1} and a single sharp peak at 1 125 cm^{-1}. These comparisons, together



VI



VII



VIII

Can. J. Chem. Downloaded from www.nrcresearchpress.com by 210.87.254.42 on 09/05/12
For personal use only.

with the general shape of the absorption curve, point to the close resemblance of III*b* to azetidine. It may be questioned whether it is justified to compare a quaternary azetidinium salt (with positively charged nitrogen) with a secondary amine of the same series. However, Sheinker and Peresleni (8) report only a slight change in spectra in going from the cyclic bases to their hydrochlorides. To meet this objection N,N-(dimethyl-d_6)-azetidinium iodide (VIII) was prepared and its infrared spectrum (see Table I and Fig. 3) compared with that of azetidine and with that of our quaternary bromide. The characteristic absorption near 1 465 and 1 084 cm^{-1} remained unaltered in the quaternary salt, and the medium peak attributable to antisymmetrical skeletal vibrations was only slightly displaced to 982 cm^{-1}, thus providing a close analogy to the spectrum of II*b*.

Nuclear Magnetic Resonance Spectra

The n.m.r. spectrum of Galinovsky's tosylate (III*a*) determined on a Varian A-60 instrument is reproduced in Fig. 4. The sharp signals at δ 7.20, 7.42, 7.68, and 7.80

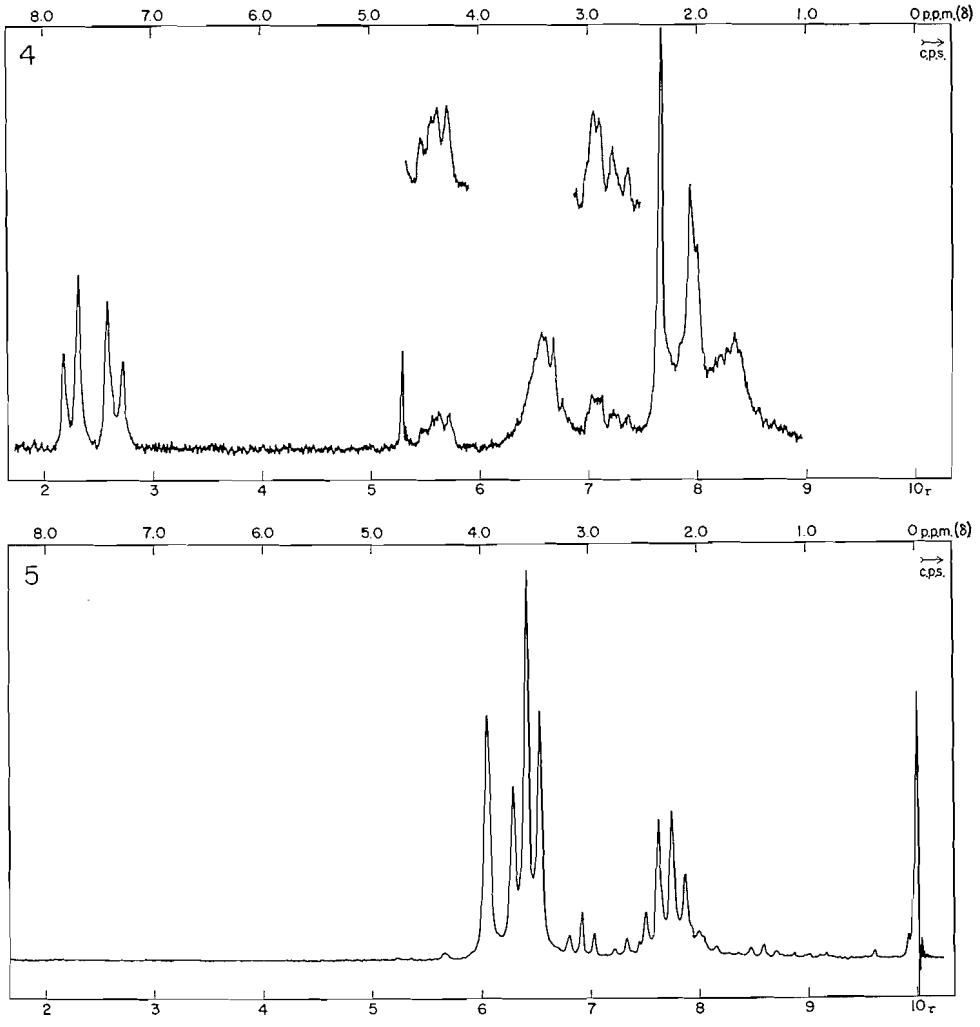


FIG. 4. Nuclear magnetic resonance spectrum of Galinovsky's tosylate.
FIG. 5. Nuclear magnetic resonance spectrum of azetidine.

Can. J. Chem. Downloaded from www.nrcresearchpress.com by 210.87.254.42 on 09/05/12
For personal use only.

correspond to four aromatic protons, and the methyl signal of the tosyl group is at δ 2.32. The remaining signals are rather complex and broadened. The quartet from 4.16 to 4.42 corresponds to one proton; the broad quartet at 3.20–3.32 corresponds to four protons, while the three peaks between δ 2.50 and 2.82 equal two protons. The higher field resonance corresponds to 11 protons.

In looking for n.m.r. criteria for the possible azetidinium ion structure of Galinovsky's salt, we noted that methylenes in four-membered rings are deshielded to an unusual extent. For example, cyclobutane methylenes resonate at δ 1.98 as contrasted with δ 0.22 for cyclopropane, 1.51 for cyclopentane, and 1.44 for cyclohexane; azetidine α-methylene protons resonate at δ 3.54 (cf. Fig. 5, also Table II), while those in ethyleneimine resonate

TABLE II

Nuclear magnetic resonance spectra

Compound	Solvent	Chemical shifts (p.p.m.)			
		α-Protons			$\beta(\gamma\delta)$-Protons
Azetidine*	Homogeneous	3.95 (N—H)			2.48
		3.70			2.38
		3.58			2.25
		3.45			2.13
Azetidine	D_2O	3.43			2.25
		3.29			2.12
		3.17			2.00, 1.89
N,N-(Dimethyl-d_6)-azetidinium iodide†	D_2O	4.38			2.69
		4.24			2.50
		4.10			2.42
					2.36
1,5-Methylene-quinolizidinium tosylate‡	D_2O	4.42	3.32	2.82	1.95
		4.32	3.27	2.77	1.91
		4.25	3.20	2.66	1.71
		4.16		2.50	1.66
					1.54
1,5-Methylene-quinolizidinium tosylate*	$CDCl_3$	4.61	3.79	3.18	2.06
		4.46	3.73	2.97	2.02
		4.35	3.64	2.81	1.80
					1.67
1,5-(Methylene-d_2)-quinolizidinium tosylate‡	D_2O		3.58	2.98	2.06
			3.48	2.91	2.03
			3.36	2.78	1.83
				2.67	1.68
N-Methyl-1-methyl-quinolizidinium iodide§			3.30		1.74
			3.16		
1-Methyl-*trans*-quinolizidine§			2.76		1.59
			2.55		

*Internal reference was tetramethylsilane.
†Internal reference was sodium *p*-toluenesulfonate.
‡The methyl signal of *p*-toluenesulfonate anion taken as 2.52 was used as internal reference.
§Moynehan *et al.* gave τ values in their paper (10).

at δ 1.36, in pyrrolidine at δ 2.75, and in piperidine at δ 2.71 (11, 13). The signals at δ 3.20 in the spectrum of III*b* thus are very suggestive of the presence of the four-membered ring. It was surprising, however, if this were so, that the charge on the nitrogen had not produced further deshielding in the quaternary salt. Moynehan *et al.* (10) observed a downfield shift of 0.4–0.6 p.p.m. of the α-methylenes on quaternization of 1-methylquinolizidine (Table II). Indeed, the α-methylenes of N,N-(dimethyl-d_6)-azetidinium iodide (VIII) gave rise to a triplet centered at δ 4.3 (Fig. 6). In the n.m.r. spectrum of

Can. J. Chem. Downloaded from www.nrcresearchpress.com by 210.87.254.42 on 09/05/12
For personal use only.

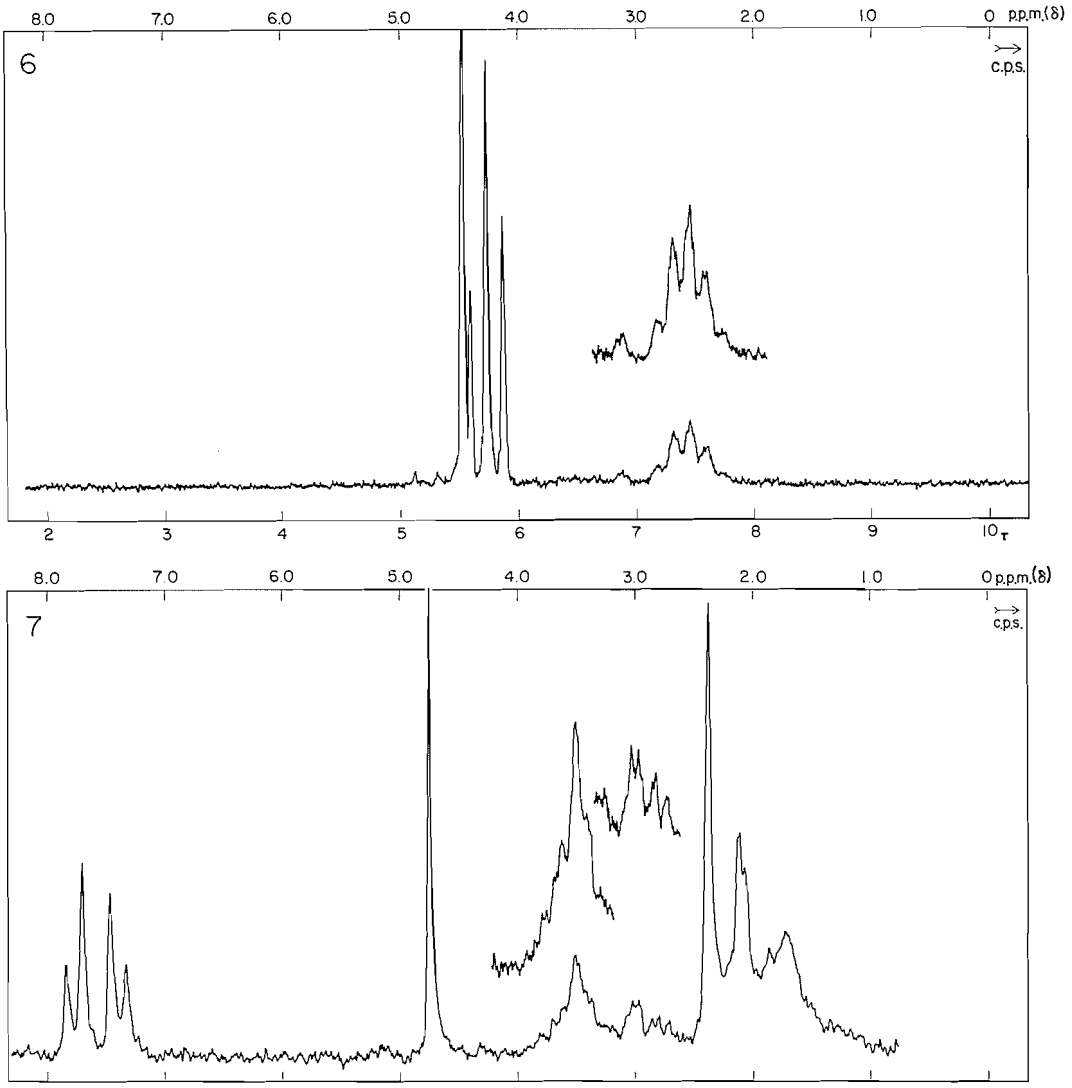


FIG. 6. Nuclear magnetic resonance spectrum of N,N-(dimethyl-d_6)-azitidinium iodide.
FIG. 7. Nuclear magnetic resonance spectrum of 1,5-(methylene-d_2)-quinolizidinium tosylate.

III*a* the one-hydrogen signal at δ 4.1–4.38 seemed likely to be caused by the tertiary 10-hydrogen, provided it were linked to the alleged azetidinium ring; the 10-hydrogen in the quinolizidinium ion itself has no signal at such a low field (10). To assign the low-field hydrogen signals of III*a* with confidence, recourse was had to deuteration. The tosylate of lupinine-11,11-d_2 was prepared and converted into the d_2-salt of Galinovsky (IV). Its n.m.r. spectrum now lacked the signal at δ 4.16–4.42, and integration showed that the signal of a second proton was missing in the region δ 3.2–3.32. Three protons still resonated in the region δ 2.5–3.3 (Fig. 7). We conclude that the azetidinium ion is present but is somewhat twisted, so that the magnetic environment of the two methylene hydrogens is different, only one experiencing the strong deshielding characteristic of an azetidinium salt. Furthermore, the 10-proton resonates at higher field than one of the

Can. J. Chem. Downloaded from www.nrcresearchpress.com by 210.87.254.42 on 09/05/12
For personal use only.

11-methylene protons. To allocate it precisely, an attempt was made to replace the 10-hydrogen by deuterium, i.e. by synthesizing VII. Mercuric acetate converted (−)-lupinine into 5(10)-dehydrolupininium acetate, which was converted directly into the crystalline perchlorate (VI). This analyzed correctly and had the characteristic immonium ion absorption at 1 680 cm^{-1} (12). However, it had no optical activity at the D-line, and hence may have been racemized despite the attempt to avoid basic conditions under which $\Delta^{1(10)}$-enamine might be formed. Catalytic deuteration or reduction with lithium aluminium deuteride converted this into a high-boiling base. In the latter case this was shown to analyze correctly for 10-monodeutero-lupinine, and hence was probably racemic 10-deutero-epilupinine. As a consequence, these attempts were abandoned.

In summary, the evidence from molecular weight determinations and infrared and n.m.r. spectroscopy is consistent with the azetidinium salt structure for Galinovsky's product. The high percentage of internal quaternization in a melt is remarkable, especially since a strained ring is being produced. A large factor must be the shielding of the unshared pair in the all-*trans* conformation by the axial tosyloxymethyl group (thereby preventing bimolecular reaction) coupled with an entropy effect favoring the internal quaternization.

The tosylate III*a* is relatively stable and could not be reductively cleaved by sodium borohydride.

An X-ray crystallographic examination of the tosylate of III has been initiated in these laboratories.[3]

EXPERIMENTAL

All melting points were determined on a Kofler stage and were not corrected.

O-Tosyl-lupinine (II)

Lupinine I*a* (19.98 g, 0.118 mole) was dissolved in dry acetone (300 ml), and *p*-toluenesulfonyl chloride (11.3 g, 0.059 mole) dissolved in acetone (210 ml) was added. The pale yellow solution was stirred magnetically for 15 h at 25°. The separated lupinine hydrochloride was removed by filtration; m.p. 212° (10), wt. 10.9 g (yield 90%). The acetone was removed from the filtrate at 25° under 15 mm pressure in a rotatory evaporator, and the brownish oily residue was dissolved in 300 ml of *n*-heptane and 30 ml of water. After the solution was shaken, the two layers were separated. The aqueous layer was adjusted with 0.5 *N* sodium hydroxide to pH 9 and extracted 5 times with methylene chloride (total 200 ml). The combined heptane and methylene chloride extracts were dried over drierite, filtered, and evaporated as above. It left the product II as an oily residue (18 g). A small quantity was converted into the picrate, m.p. 165°; Galinovsky (1) reported m.p. 145°.[4]

Anal. Calcd. for $C_{23}H_{28}O_{10}N_4S$: N, 10.14. Found: N, 10.02.

Rearrangement of II to IIIa

Lupinine tosyl ester (17.8 g) was heated in a 500 ml round-bottomed flask fitted on a rotatory evaporator, in a boiling water bath under 15 mm pressure for 4 h. After 1 h most of the oil had formed a solid film-like layer on the wall of the flask. At this point, dry ether (100 ml) was added, whereupon crystallization was initiated. After completion of the reaction the white precipitate was filtered off, washed with dry ether (20 ml), finely ground under ether in a mortar, and filtered again. After it was allowed to dry in a desiccator, the tosylate III*a* thus obtained (16.2 g; 84.6% yield based on the lupinine) melted at 128–130°. For analysis and spectroscopic measurements a sample was crystallized twice from dry ethanol–ether (1:4); m.p. 139°. Galinovsky (1) reported the same melting point, as determined in an evacuated capillary tube.

Anal. Calcd. for $C_{17}H_{25}NO_3S$: C, 63.10; H, 7.79; N, 4.02. Found: C, 63.26; H, 7.97; N, 4.15.

1,5-Methylene-quinolizidinium Bromide (IIIb)

Via the Picrate

The tosylate III*a* was converted into the picrate III*c*, m.p. 208°, as described by Galinovsky (1). The picrate (691 mg) was treated with 0.2 *N* hydrobromic acid, and the picric acid was removed by extracting 10 times with a total of 1 l ether. The extracted aqueous solution was evaporated to dryness in a rotatory evaporator under 15 mm pressure, the oily residue was dissolved in absolute ethanol, dry benzene was added, and the solution was evaporated, this process of solution and evaporation being repeated several times to

[3]*C. Saunderson, unpublished.*

[4]*He prepared his tosyl ester in pyridine (1), which gives a less pure product than the method we used, with lupinine both as substrate and as proton acceptor.*

Can. J. Chem. Downloaded from www.nrcresearchpress.com by 210.87.254.42 on 09/05/12
For personal use only.

drive off the water. Finally, the residue was crystallized from butanol–ether (1:2), wt. 50 mg, m.p. 167°, infrared spectrum shown in Fig. 2.

Because of some inorganic contamination the C and H values are usually low.

Via the Iodide

The tosylate III*a* (5.83 g, 0.01805 mole) was dissolved in dry ethanol (8 ml), and a solution of dry sodium iodide (2.70 g) dissolved in ethanol (5 ml) and dry acetone (20 ml) was added. The precipitated sodium tosylate was filtered off and washed with acetone, wt. 3.492 g (99.8%). The combined acetone–alcohol filtrate and washings were evaporated under reduced pressure in a rotatory evaporator, the residual crystalline iodide III*d* was dissolved in methylene chloride (25 ml), alcohol (1 ml) was added, the solution was filtered to remove the last traces of sodium tosylate, and the filtrate was evaporated to dryness. The residual iodide was dissolved in water (20 ml), silver bromide (5 g) added, and the mixture stirred for 14 h until no more iodide ion was present in a sample of liquid drawn from the mixture. After filtration the aqueous filtrate was evaporated to dryness and the residue crystallized from methylene chloride – *n*-hexane, wt. 0.100 g. The low yield is due to the tendency of the bromide to give a volatile product. This will be discussed in a forthcoming paper.

*Attempted Reductive Cleavage of the Tosylate III*a*

The tosylate (271.2 mg, 0.837 mmole) was dissolved in water (5 ml), sodium borohydride (380 mg, 10 mmoles) was added, and the solution was adjusted to pH 9 by the addition of a few drops of 0.2 *N* potassium hydroxide. After 3 days, seven extractions with a total of 500 ml of ether failed to remove any basic material. The aqueous solution was neutralized with 2 *N* hydrochloric acid and evaporated to dryness, and the residue was extracted with dry ethanol. Addition of dry ether to the ethanol extract caused the crystallization of the unchanged tosylate III*a*, m.p. 139°.

Azetidine

This was prepared by Kraut from tosylamide and 1-chloro-S-bromopropane according to Searles *et al.* (14), with subsequent cleavage of N-tosyl-azetidine with sodium and amyl alcohol (15).

The main problem consisted in the removal of the last traces of water from azetidine. Drying over barium oxide (16) alone proved unsufficient; so sodium–lead alloy was used thereafter, yielding a pure product after distillation, b.p. 72–73°, n.m.r. spectrum shown in Fig. 5.

N,N-(Dimethyl-d_6)-azetidinium Iodide (VIII)

Azetidine (0.5425 g) was dissolved in 10 ml of methanol; then 0.5167 g powdered sodium methoxide was added followed by 5 g deuteromethyl iodide, with cooling to maintain the temperature at 15°. Water (1 ml) was added and the solution was kept at 20° for 20 h, during which time the pH was kept near neutrality by addition of sodium methoxide. The filtered solution was evaporated in a vacuum, and the residue was extracted first with acetone to remove sodium iodide and then with absolute ethanol. The residue, after evaporation of the ethanol solution, crystallized on the addition of acetone. The needle-like crystals were collected by filtration, giving 0.502 g, m.p. 276°, n.m.r. spectrum shown in Fig. 6.

Anal. Calcd. for $C_5H_6D_6NI$: C, 27.4; H + D, 6.45; D, 6 atoms. Found: C, 27.13; H + D, 6.1; D, 5.6 atoms.

1,5-(Methylene-d_2)-quinolizidinium tosylate (IV)

Methyl lupininate (0.9272 g) dissolved in 5 ml dry ether was added over the course of 5 min to a stirred solution of lithium aluminium deuteride (0.5 g) in 25 ml anhydrous ether, while the solution was kept cool with ice. Stirring was continued for 30 min at 20°. After decomposition of excess lithium aluminium deuteride by 3 ml deuterium oxide (with cooling) the precipitate was removed by filtration and washed with a total of 30 ml ether. After removal of the ether the residual oil soon solidified to a white crystalline mass. The product was distilled under 0.001 mm pressure from an oil bath at 100–120° (yield: 577.5 mg (72.5%)), giving low-melting crystals of 1-hydroxymethyl-quinolizidine-d_3.

The compound has no signal for a hydroxyl at δ 5.2. It lacked the quartet at δ 3.6–3.8 present in lupinine, which corresponds obviously to the C—H protons in the CH_2OH group.

Lupinine-d_3 (5.775 mg) was dissolved in 5 ml dry acetone, tosyl chloride (322 mg) in dry acetone (5 ml) was added, and the solution was kept overnight at 20°. Lupinine-d_3-deuterochloride (129 mg; calcd. 300 mg), which separated, was filtered off.

Anal. Calcd. for $C_{10}M_{16}D_4ONCl$: D, 4.0 atoms. Found: D, 3.78 atoms.

The mother liquor was evaporated, and the residue was dissolved in 10 ml *n*-hexane and shaken with 2 ml 0.2 *N* NaOH. Then the alkaline layer was extracted several times with a total of 50 ml *n*-hexane. The combined hexane extracts were dried (K_2CO_3) and the solvent removed to give O-tosyl-lupinine-d_2 (506.7 mg; calcd. 554 mg). It was converted into the internal quaternary salt by heating for 3 h at 95° in a rotatory evaporator under a vacuum; yield, 330 mg, after washing with ether. When recrystallized from ethanol–ether (1:3), this gave 220 mg, m.p. 137–139°.

Anal. Calcd. for $C_{17}H_{23}D_2O_3NS$: D, 2 atoms. Found: D, 1.87 atoms.

Can. J. Chem. Downloaded from www.nrcresearchpress.com by 210.87.254.42 on 09/05/12
For personal use only.

Mercuric Acetate Oxidation of Lupinine to the 5(10)-Dehydrolupininium Salt

Mercuric acetate (75 mg) was dissolved in glacial acetic acid (30 ml) and to it was added a solution of lupinine (800 mg) in a minimum volume of glacial acetic acid. The reaction was heated under a reflux condenser for 2 h in an oil bath at 80°. The mercurous acetate formed (~85% of theory) was removed by filtration. The filtrate was diluted with water and the excess mercuric acetate precipitated by hydrogen sulfide. The mercurous sulfide was filtered off and the aqueous solution evaporated nearly to dryness. The residue was dissolved in water and evaporated once more to get rid of the acetic acid. It was then dissolved in methanol and the calculated amount of 1.63 *N* perchloric acid (2.8 ml) was added. The perchlorate VI crystallized as white leaflets. After one recrystallization from MeOH–H_2O it had m.p. 172–174°, $[\alpha]_D$ 0° ± 0.3° (*c*, 9.7 in dimethylformamide).

Anal. Calcd. for $C_{10}H_{18}O_5NCl$: C, 44.90; H, 6.72; N, 5.26. Found: C, 44.70; H, 6.25; N, 5.26.

Attempts to Deuterate 5(10)-Dehydrolupininium Perchlorate

Catalytic Deuteration of 5(10)-Dehydrolupininium Perchlorate VI

Crude 5(10)-dehydrolupininium perchlorate (231.9 mg) was reduced by deuterium gas over PtO_2 (30 mg) in glacial acetic acid (10 ml). Because of the presence of traces of sulfur in the substance the catalyst was being poisoned and had to be replaced at intervals. The deuteration was continued until the calculated amount of D_2 had been adsorbed. The resulting reduced material was recovered by removing the solvent, and the base was liberated. Its infrared and n.m.r. spectra showed that more than one atom had entered the molecule.

By Lithium Aluminium Deuteride

Lithium aluminium deuteride (200 mg) was dissolved in dry ether (20 ml), dehydrolupininium perchlorate (540 mg, 2 mmoles) was added with magnetic stirring, and the whole was refluxed for 3 h. The complex was decomposed by 2 ml of water, the ethereal layer was decanted and dried (K_2CO_3), and the solvent was distilled. A viscous oil (300 mg) remained in the flask, which could be driven over at 10^{-4} mm pressure from an oil bath at 190–200°. The nearly colorless oil gave analytical figures corresponding to lupinine-d_2.

Anal. Calcd. for $C_{10}H_{17}D_2ON$: C, 70.02; H, 11.19; N, 8.19. Found: C, 69.73; H, 10.72; N, 8.34.

ACKNOWLEDGMENTS

We thank Mr. H. Seguin, who carried out the molecular weight determinations as well as the microanalyses including deuterium determinations, Mr. R. Lauzon for measuring the infrared absorption spectra, and Mr. M. Lesage, who measured n.m.r. spectra and made the mercuric acetate oxidations of lupinine.

REFERENCES

1. H. Galinovsky and H. Nesvadba. Monatsh. Chem. **85**, 1300 (1954).
2. R. C. Cookson. Chem. Ind. London, 337 (1953).
3. A. F. Thomas, H. J. Vipond, and L. Marion. Can. J. Chem. **33**, 1290 (1955).
4. J. Ratusky, A. Reiser, and F. Sorm. Chem. Listy, **48**, 1795 (1954); Collection Czech. Chem. Commun. **20**, 798 (1955).
5. P. Karrer, F. Canal, K. Zohner, and R. Widner. Helv. Chim. Acta, **11**, 1062 (1928).
6. N. J. Leonard. *In* The alkaloids. Vol. 7. *Edited by* R. H. F. Manske. Academic Press, Inc., New York. 1961. pp. 253–317.
7. L. Fowden. Nature, **176**, 347 (1955).
8. I. N. Sheinker and H. M. Peresleni. Zh. Fiz. Khim. **32**, 2112 (1958).
9. E. Lippert and H. Prigge. Ber. Bunsenges. Physik. Chem. **67**, 554 (1963).
10. T. M. Moynehan, K. Schofield, R. A. Y. Jones, and A. R. Katritzky. J. Chem. Soc. 2637 (1962).
11. E. Lippert and H. Prigge. Ber. Bunsenges. Physik. Chem. **67**, 415 (1963).
12. N. J. Leonard, A. S. Hay, R. W. Fulmer, and W. Gash. J. Am. Chem. Soc. **77**, 439 (1955).
13. A. T. Bottini and J. D. Roberts. J. Am. Chem. Soc. **80**, 5203 (1958).
14. S. Searles, M. Tamres, F. Block, and L. A. Quarterman. J. Am. Chem. Soc. **78**, 4917 (1956).
15. W. R. Vaughan, R. S. Klonowsky, R. S. McElhinney, and B. M. Millward. J. Org. Chem. **26**, 138 (1961).
16. C. C. Howard and W. Marckwald. Ber. **32**, 2032 (1899).

Can. J. Chem. Downloaded from www.nrcresearchpress.com by 210.87.254.42 on 09/05/12
For personal use only.

Can. J. Chem. Downloaded from www.nrcresearchpress.com by 210.87.254.5 on 09/05/12
For personal use only.

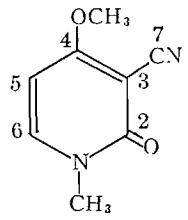
THE ROLE OF ASPARTIC ACID IN THE BIOSYNTHESIS OF RICININE[1]

S. R. JOHNS[2] AND LÉO MARION[3]
Division of Pure Chemistry, National Research Council, Ottawa, Canada
Received August 27, 1965

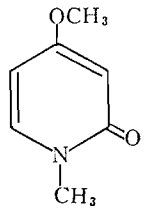
ABSTRACT

Ricinine, isolated from *Ricinus communis* L. fed aspartic acid-3-^{14}C and aspartic acid-4-^{14}C, was degraded, and in each case the activity of all the carbon atoms was determined. The results obtained indicate that aspartic acid is incorporated into ricinine via the Krebs tricarboxylic acid cycle rather than directly as aspartic acid. Experiments with aspartic acid-^{15}N support this suggestion; they indicate that the ring nitrogen from ricinine is not derived directly from the nitrogen of aspartic acid, since both it and the nitrile nitrogen contain essentially the same abundance of ^{15}N.

Previous studies (1, 2) on the biosynthesis of ricinine (I) in *Ricinus communis* L. indicate that succinic acid or a closely related four-carbon dicarboxylic acid found in the Krebs tricarboxylic acid cycle is the source of carbon atoms 2, 3, and 7. The distribution of labelling in ricinine produced in feeding experiments with acetate-2-^{14}C is essentially the



I



II

same as that when succinate-2,3-^{14}C is fed to the plant, since acetate is converted into succinate via the Krebs cycle.

Aspartic acid has been shown to be incorporated into ricinine (3), nicotine (4, 5), and nicotinic acid (6). The question remained unsolved concerning whether the aspartic acid was incorporated as such, or whether the amino group was lost and the resulting four-carbon dicarboxylic acid was the true precursor. Schiedt and Boeckh-Behrens (3) found that, in ricinine isolated after aspartic acid-3-^{14}C had been fed to the plant, 42% of the total activity was at C-3 while C-2 was not radioactive. This result would indicate either that the aspartic acid is incorporated as a unit with the amino group attached or that the amino group is lost and the resulting dicarboxylic acid is incorporated without passing through the Krebs cycle. The work of Gross *et al.* (6) involving the feeding of aspartic acid-1,4-^{14}C,^{15}N to *Mycobacterium tuberculosis* (Stam BCG) and subsequent isolation of nicotinic acid further supports the view that aspartic acid is incorporated as a unit. These authors found the incorporation of ^{14}C and ^{15}N to be essentially the same and assumed that this implied no breakdown of the amino acid.

In contrast to the above results, Griffith *et al.* (4) report that aspartic acid-3-^{14}C is not a

[1]*Issued as N.R.C. No. 8712.*
[2]*National Research Council of Canada Postdoctorate Fellow. Present address: Chemical Research Laboratories, Division of Organic Chemistry, C.S.I.R.O., Melbourne, Australia.*
[3]*Present address: Faculty of Pure and Applied Science, University of Ottawa, Ottawa, Canada.*

direct precursor of nicotine in *Nicotiana rustica*. Only approximately half of the ^{14}C activity of the pyridine ring is located at C-3. Similarly, Christman and Dawson (5) fed aspartic acid-^{15}N to excised tobacco (*Nicotiana tabacum* L.) roots in sterile culture and found that the nitrogen label was equilibrated during the culture period with the general nitrogen pool. The approximate mean excess of ^{15}N present in the tobacco roots and culture fluids was 2%; this was also the concentration in each ring of the nicotine produced.

The present work describes the results obtained in feeding aspartic acid-3-^{14}C, aspartic acid-4-^{14}C, and aspartic acid-^{15}N to *Ricinus communis* L. The ricinine isolated after the aspartic acid-3-^{14}C and aspartic acid-4-^{14}C feedings was diluted in each case with synthetic ricinine. The carbons were individually isolated as suitable derivatives and their activity determined. Carbon atoms 2, 3, and 7 were obtained by the method of Juby and Marion (2) respectively as benzoic acid and bromopicrin, and by difference between ricinine and 4-methoxy-N-methyl-2-pyridone (II), i.e. loss of the C-7 nitrile. Carbon atoms 4, 5, and 6 were isolated as described by Essery *et al.* (7) as benzoic acid, bromopicrin, and formaldehyde dimedone respectively. The methyl groups attached to oxygen and nitrogen were each isolated as tetramethylammonium iodide. All derivatives were converted by combustion into carbon dioxide which was precipitated as barium carbonate, and counted as thin layers on aluminium planchets.

The results obtained for aspartic acid-3-^{14}C and aspartic acid-4-^{14}C are shown in Table I.

TABLE I

Location of activity in ricinine

Incorporation of aspartic acid-3-^{14}C, 2.4%			Incorporation of aspartic acid-4-^{14}C, 0.66%		
Position	Activity (d.p.m./mg $BaCO_3$)	% of ricinine activity	Position	Activity (d.p.m./mg $BaCO_3$)	% of ricinine activity
OCH_3†	3.91	1.5	OCH_3‡	5.55	8.7
NCH_3†	3.33	1.3	NCH_3‡	4.75	7.5
C-2*	67.7	37.2			
C-3*	497	39	C-3‡	10.2	4.0
C-4†	0	0			
C-5†	8.0	0.8			
C-6	Not determined				
C-7*	150	18	C-7‡	7.75	78.2

*Activity of diluted ricinine used, 160 d.p.m./mg $BaCO_3$.
†Activity of diluted ricinine used, 127 d.p.m./mg $BaCO_3$.
‡Activity of diluted ricinine used, 32 d.p.m./mg $BaCO_3$.

These results indicate that aspartic acid-3-^{14}C is incorporated into ricinine to an extent comparable with the incorporation of labelled succinic acid (2). The distribution of activity among carbon atoms 2, 3, and 7 of ricinine in the ratio 2:2:1 is indicative of a precursor randomized in the Krebs tricarboxylic acid cycle. The percentage activities on carbons 2, 3, and 7 are similar to those observed when succinate-2,3-^{14}C and acetate-2-^{14}C are fed to the plant, and suggest that the amino group of aspartic acid is eliminated first, and that the resulting acid goes through the Krebs cycle before incorporation.

The results of feeding aspartic acid-4-^{14}C are in complete accord with such a mechanism, and the lower overall incorporation of the aspartic acid-4-^{14}C precursor further supports the breakdown to a symmetrical dicarboxylic acid similar to succinic acid. The labelling on the carboxylic acid group would then be distributed equally between carbon atom 7 of ricinine and the carbon atom of the acid lost by decarboxylation. An incorporation of approximately half that observed after aspartic acid-3-^{14}C had been fed to the plant would be expected in the aspartic acid-4-^{14}C experiment, but because of the possibility of a number of cycles through the Krebs cycle the figures are approximately in the ratio 1:3.

Can. J. Chem. Downloaded from www.nrcresearchpress.com by 210.87.254.5 on 09/05/12
For personal use only.

Can. J. Chem. Downloaded from www.nrcresearchpress.com by 210.87.254.5 on 09/05/12
For personal use only.

The ^{15}N content of the ricinine isolated from *Ricinus communis* L. after aspartic acid-^{15}N was fed was determined by mass spectrometric analysis. Nitrogen was isolated from ricinine and 4-methoxy-N-methyl-2-pyridone (II) by the method and apparatus of Rittenberg (8). The alkaloid was digested under Kjeldahl conditions for 18 h. The extended time of digestion was meant to remove all carbonaceous material and prevent carry through of any material with mass 28, 29, or 30. After the reaction mixture had been made basic, it was steam distilled into dilute hydrochloric acid. The ammonium chloride in the distillate was oxidized with sodium hypobromite and the resulting nitrogen analyzed in the mass spectrometer. Initially, contamination with oxygen gave inconsistent results. This oxygen could originate either from air contamination or from decomposition of the hypobromite solution. To prevent loss of oxygen from the hypobromite, the reagent was stabilized with 1% potassium iodide as suggested by Sims and Cocking (9). Further modification of the original Rittenberg procedure involved complete removal of solvent from the ammonium chloride solution, and repeated degassing of the hypobromite solution by freezing it and allowing it to warm to room temperature. Mass spectrometer analyses in which the 32 peak (O_2) content was greater than 2–3% of the 28 peak (N_2) were discarded as a result of the possibility of CO(28) contamination of the N_2 peak by reaction of the oxygen with the carbon filament in the mass spectrometer.

The results obtained from separate feeding experiments are given in Table II. The

TABLE II

^{15}N excess in nitrogen samples

	Feeding *i*	Feeding *ii*
Aspartic acid	71.9%	93%
Ricinine	0.50%	0.77%
4-Methoxy-N-methyl-2-pyridone	0.49%	0.82%

nitrogen isolated from ricinine originates from both the pyridine ring and the nitrile group. Removal of the nitrile group by hydrolysis and decarboxylation with 57% sulfuric acid (10) gave 4-methoxy-N-methyl-2-pyridone (II), from which the nitrogen was isolated and analyzed as before. This gives the value of the isotopic nitrogen content of the pyridone ring.

Again the results indicate that aspartic acid is not incorporated as such into the ricinine molecule. The ^{15}N abundance in both nitrogens of ricinine was the same, indicating that deamination of the aspartic acid has taken place and that the nitrogen was equilibrated with the nitrogen pool before incorporation into the alkaloid. If the pyridone nitrogen were derived from aspartic acid, it is unlikely that the incorporation into the ring would be the same as that into the nitrile group.

Our results are at variance with those reported by Schiedt and Boeckh-Behrens (3), but agree with those of Griffith *et al.* (4) and of Christman and Dawson (5). Although Mothes and his co-workers (6) claimed that aspartic acid was incorporated as such into nicotinic acid, they did their work with a microorganism, not a higher plant in which biosynthetic pathways are not necessarily the same. Hence, both in *Ricinus communis* and in the tobacco plant (4) aspartic acid is deaminated and goes through the Krebs cycle before incorporation.

With aspartate-4-^{14}C the label is found mostly in the nitrile group; this is in agreement with the observation of Waller and Henderson (11) after succinic acid-1,4-^{14}C had been fed to the plant.

Can. J. Chem. Downloaded from www.nrcresearchpress.com by 210.87.254.5 on 09/05/12
For personal use only.

EXPERIMENTAL

Melting points were determined on a Kofler hot stage and corrected. Radioactive samples were burned and counted as thin layers of barium carbonate on aluminium planchets in a Baird-Atomic Inc. end-window proportional counter using methane gas. Appropriate corrections were made for background count, counter efficiency, and sample self-absorption. Nitrogen mass spectrometric analyses were carried out on an analytical instrument.

Growth of Plants and Administration of Tracers

Seeds of *Ricinus communis* L. were planted just beneath the surface of moist vermiculite in wooden flats in a greenhouse kept at 20–25°. After approximately 14 days (depending upon the time of the year) when the plants were 15–20 cm high and the primary leaves were emerging, an aqueous solution of the precursor was introduced into the base of the stem of each plant by means of glass capillary tubes. The tubes were previously partly filled with the solution by capillary rise (2). The following precursors were administered by this method: (*a*) a solution of (±)-aspartic acid-3-^{14}C (1.79 mg, 1.77×10^8 d.p.m., California Corporation for Biochemical Research, Los Angeles) and (−)-aspartic acid-^{15}N (13.10 mg, 71.9% ^{15}N excess, Schwarz Bioresearch Inc., Orangeburg, New York) in 0.1 *N* aqueous sodium hydroxide (0.8 ml) to 31 plants; (*b*) a solution of (±)-aspartic acid-3-^{14}C (2.22×10^8 d.p.m., Merck, Sharpe and Dohme, Montreal) in 0.1 *N* aqueous sodium hydroxide (0.7 ml) to 26 plants; (*c*) a solution of (−)-aspartic acid-4-^{14}C (2.22×10^8 d.p.m., California Corporation for Biochemical Research, Los Angeles) and (−)-aspartic acid-^{15}N (10.31 mg, 71.9% ^{15}N excess) in 0.1 *N* aqueous sodium hydroxide (1.0 ml) to 35 plants; (*d*) a solution of (−)-aspartic acid-^{15}N (33.3 mg, 93% ^{15}N excess, Merck, Sharpe and Dohme, Montreal) in 0.5 *N* aqueous sodium hydroxide (0.5 ml) to 16 plants.

Isolation of Ricinine

Ricinine was isolated from the plant and purified as previously described (1, 2, 7).

In experiment 1, in which a mixture of (±)-aspartic acid-3-^{14}C and (−)-aspartic acid-^{15}N was fed, the ricinine isolated (147 mg, m.p. 202–203°) had an activity of 3.18×10^3 d.p.m./mg $BaCO_3$. This represents an incorporation of 2.4%.

After (±)-aspartic acid-3-^{14}C (experiment 2) had been fed to the plant the latter yielded ricinine (187 mg, m.p. 202°) with an activity of 3.08×10^3 d.p.m./mg $BaCO_3$. This represents an incorporation of 2.3%.

In experiment 3, in which a mixture of (−)-aspartic acid-4-^{14}C and (−)-aspartic acid-^{15}N was fed, the ricinine (201 mg, m.p. 202°) isolated from the plant had an activity of 9.02×10^2 d.p.m./mg $BaCO_3$, which shows an incorporation of 0.66%.

Degradation of Ricinine

Active ricinine was diluted with inactive synthetic ricinine prepared by the method of Schroeter *et al.* (12) as modified by Schiedt *et al.* (13). The procedures used for the isolation of the individual carbon atoms were essentially those previously reported (1, 2, 7). The N-methyl and methoxyl carbons were isolated as tetramethylammonium iodide by a modification of the Herzig–Meyer method. Carbon 2 was isolated as the carboxylic group of benzoic acid, and carbon 3 as bromopicrin (2). Also, carbon 4 was isolated as the carboxylic group of benzoic acid, and carbon 5 as bromopicrin by oxidation of 5-nitroricinine with calcium hypobromite (7). The activity of carbon 7 was determined by the difference between the activity of ricinine and that of 4-methoxy-N-methyl-2-pyridone (II), the product obtained by removal of the nitrile group. All isolated products were purified and burned to carbon dioxide, and the gas was converted into barium carbonate by absorption in a solution of barium hydroxide. The results are listed in Table I, in which the activity of a derivative of ricinine is given as disintegrations per minute per milligram of barium carbonate.

Samples for Mass Spectrometric Analysis

Nitrogen was determined from samples of aspartic acid, ricinine, and 4-methoxy-N-methyl-2-pyridone (II) by the modified method and apparatus described by Rittenberg (8, 9). To prevent contamination of the nitrogen samples by oxygen, the hypobromite solution used in the oxidation of the ammonium chloride was stabilized with 1% potassium iodide. Further precautions to prevent any contamination involved removal of the solvent from the ammonium chloride solution and prolonged degassing of the hypobromite solution by alternate freezing and warming at least three times. Mass spectrometric determinations in which the oxygen peak (32) was more than 3% of that of the nitrogen peak (28) were discarded. The results of the determinations of ^{15}N excess in the aspartic acid-^{15}N fed to the plant, of the isolated ricinine, and of the derived 4-methoxy-N-methyl-2-pyridone are recorded in Table II.

ACKNOWLEDGMENTS

The authors thank Mr. H. Séguin for carrying out the sample combustions, and Mr. R. Pilon for the mass spectrometric analyses. One of us (S. R. J.) acknowledges with thanks a travel grant from the Burroughs Wellcome Trust.

REFERENCES

1. P. F. JUBY and L. MARION. Biochem. Biophys. Res. Commun. **5**, 461 (1961).
2. P. F. JUBY and L. MARION. Can. J. Chem. **41**, 117 (1963).
3. U. SCHIEDT and G. BOECKH-BEHRENS. Z. Physiol. Chem. **330**, 58 (1962).
4. T. GRIFFITH, K. P. HELLMAN, and R. U. BYERRUM. Biochemistry, **1**, 336 (1962).
5. D. R. CHRISTMAN and R. F. DAWSON. Biochemistry, **2**, 182 (1963).
6. D. GROSS, H. R. SCHÜTTE, G. HUBNER, and K. MOTHES. Tetrahedron Letters, **9**, 541 (1963).
7. J. M. ESSERY, P. J. JUBY, L. MARION, and E. TRUMBULL. Can. J. Chem. **41**, 1142 (1963).
8. D. RITTENBERG. Preparation and measurement of isotopic tracers. J. W. Edwards, Ann Arbor, Michigan. 1946.
9. A. P. SIMS and E. C. COCKING. Nature, **181**, 474 (1958).
10. E. WINTERSTEINER, J. KELLER, and A. B. WEINHAGEN. Arch. Pharm. **255**, 513 (1917).
11. G. R. WALLER and L. M. HENDERSON. Biochem. Biophys. Res. Commun. **6**, 398 (1961).
12. A. SCHROETER, C. SEIDLER, M. SULZBACHER, and R. KANITZ. Ber. **65**, 432 (1932).
13. U. SCHIEDT, G. BOECKH-BEHRENS, and A. M. DELLUVA. Z. Physiol. Chem. **330**, 46 (1962).

Can. J. Chem. Downloaded from www.nrcresearchpress.com by 210.87.254.5 on 09/05/12
For personal use only.

Can. J. Chem. Downloaded from www.nrcresearchpress.com by 210.87.254.40 on 09/05/12
For personal use only.

ALKALOIDS OF THE SEEDS OF ASPIDOSPERMA FENDLERI WOODSON

R. H. BURNELL[1] AND J. D. MEDINA
Department of Chemistry, Instituto Venezolano de Investigaciones Cientificas, Caracas, Venezuela

AND

W. A. AYER
Department of Chemistry, University of Alberta, Edmonton, Alberta

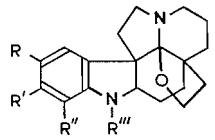
Received September 8, 1964

ABSTRACT

The structures of three new alkaloids from the seeds of *A. fendleri* have been elucidated and two of the bases have been converted into aspidolimidine. A fourth base has been shown to be present in small amounts but its nature remains unknown.

Extraction of the seeds of the Venezuelan tree *Aspidosperma fendleri* (1) has yielded four alkaloids, of which fendlerine, $C_{23}H_{30}N_2O_4$, is the most abundant; this alkaloid is also found in large quantities in the trunk and root bark. The structures of fendlerine and the minor base fendleridine have been discussed in preliminary reports (2, 3).

Fendleridine, $C_{19}H_{24}N_2O$, is the simplest of the bases present and, on the basis of its ultraviolet spectrum, belongs to the unsubstituted dihydroindole group of alkaloids. The infrared spectrum reveals peaks characterizing the dihydroindole imino group and the aromatic ring but gives no information concerning the nature of the oxygen atom, which is probably ethereal. The nuclear magnetic resonance spectrum confirms the presence of four aromatic protons (multiplet: 6.55 to 7.50 δ), but absorption typical of olefinic protons and of methyl groupings of any type is absent. A two-proton quartet (centered at 3.98 δ), which has also been observed in other dihydroindolic aspidosperma alkaloids, has been shown to be characteristic of the —O—CH_2— grouping as found in aspidoalbine (V) (4) and aspidolimidine (IV) (5). This region of the nuclear magnetic resonance spectrum of fendleridine is strikingly similar to that of O-methyl-N-despropionylaspidoalbine (6)



I R = R′ = R″ = R‴ = H
II R = H; R′ = OCH_3; R″ = OH; R‴ = $COCH_2CH_3$
III R = H; R′ = R″ = OH; R‴ = $COCH_3$
IV R = H; R′ = OCH_3; R″ = OH; R‴ = $COCH_3$
V R = R′ = OCH_3; R″ = OH; R‴ = $COCH_2CH_3$

(except for the methoxyl bands in the latter). A plausible structure for fendleridine is that shown by I; this is supported by the mass spectrometric fragmentation pattern (Fig. 1). Confirmation of the analytical figures was shown by the molecular ion peak at 296 *m/e*; the typical aspidospermine type M-28 peak (*a*) arising from the loss of ethylene is also present. Rupture of the C-10—C-11 bond (at *x* in *a*) gives rise to fragment *b*, which is responsible for the base peak at 138 *m/e*. This fragment has also been observed in the

[1]*Present address: Chemistry Department, Laval University, Quebec 10, Quebec.*

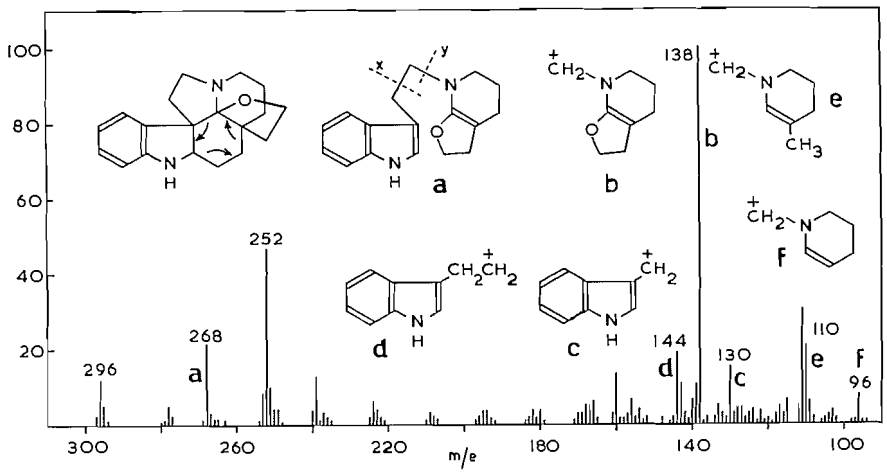


FIG. 1. Mass spectrum of fendleridine. Peaks with an intensity greater than 2% of the most intense peak are shown.

fragmentation of aspidoalbine (V) (4) and aspidolimidine (IV) (5). The indolic portion of the molecule gives rise to weaker peaks at 144 *m/e* (rupture at *y*) and 130 *m/e* (rupture at *x*). The other significant peaks in the mass spectrum arise from expulsion of the oxide bridge (intense peak at 252 *m/e*) and subsequent fragmentation as described above.

Fendlerine shows ultraviolet absorption attributable to a phenolic N-acyldihydroindole and, as expected, the spectrum changes in basic solution. The infrared spectrum confirms the presence of the N-acyl residue (1 635 cm^{-1}), which is presumably hydrogen bonded with the phenolic hydroxyl since virtually no absorption is observed in the hydroxyl-stretching region. From the nuclear magnetic resonance spectrum the N-acyl grouping was shown to be a propionyl residue (triplet and quartet centered at 1.24 δ and 2.53 δ respectively); this was confirmed by acidic hydrolysis of fendlerine and vapor phase chromatography of the volatile acid. Only propionic acid was detected. Other peaks in the nuclear magnetic resonance spectrum include a quartet from two aromatic protons (centered at 6.89 δ), one methoxyl residue (3.84 δ), and a one-proton peak at 12.42 δ attributable to the chelated phenolic hydroxyl. Since the nature of one of the oxygen functions remained obscure, the probability that fendlerine contained an ethereal moiety (other than the methoxyl) was a tempting assumption. This hypothesis was to some extent strengthened by the appearance of a peak in the hydroxyl region of the infrared spectrum of the product obtained by hydrogenating the base over platinum on charcoal. Under the conditions employed, most of the peaks in the mass spectrum of fendlerine were of low intensity, but the base peak was at 138 *m/e* (fragment *b*) as in the case of fendleridine (I). The analytical figures were confirmed by the molecular ion peak at 398 *m/e*; other peaks of importance were those associated with the loss of the N-propionyl residue. The most prominent indolic fragment (the dihydroxy derivative of *c*) gave rise to a peak at 161 *m/e*. Structure II was in all respects compatible with the spectral data on fendlerine; this was confirmed by the conversion of the latter into aspidolimidine (IV). Acid hydrolysis of fendlerine gave the des-N-propionyl derivative, which could not be crystallized but which was acetylated with acetyl chloride in pyridine. The product, a mixture of the N-acetyl and O,N-diacetyl derivatives, was hydrolyzed in methanolic sodium hydroxide under nitrogen to give the pure N-acetyl compound, which was in all respects identical with aspidolimidine

Can. J. Chem. Downloaded from www.nrcresearchpress.com by 210.87.254.40 on 09/05/12
For personal use only.

Can. J. Chem. Downloaded from www.nrcresearchpress.com by 210.87.254.40 on 09/05/12
For personal use only.

(IV). Since the number of bases with this same hexacyclic skeleton is increasing, it would seem logical to name them as derivatives of the simplest member. Preference is given to the name aspidoalbidine, which has already been used to describe this system (7). Thus fendlerine is N-propionyl-16-methoxy-17-hydroxyaspidoalbidine (II).

The small amount of the high-melting aspidofendlerine (m.p. 278° (decomp.)) was easily purified by fractional sublimation; analysis indicated the molecular formula $C_{21}H_{26}N_2O_4$. The ultraviolet spectrum is similar to that of fendlerine (II) and changes in basic ethanol and in the presence of buffered boric acid, thus suggesting a catechol residue (8). The infrared spectrum shows the presence of hydroxyl and N-acyl functions. Peaks in the nuclear magnetic resonance spectrum are interpreted as showing both bonded and unbonded phenolic hydroxyl groups (11.06 and 5.79 δ respectively), two adjacent aromatic protons (quartet centered at 6.84 δ), and a N-acetyl residue (2.30 δ). The mass spectrum gave peaks of extremely low intensity, with the exception of the base peak at 138 *m/e* (fragment *b* in Fig. 1), which confirmed the suspicion that this base was also of the fendleridine (I) skeletal type. On a small scale, aspidofendlerine, assumed to be N-acetyl-16,17-dihydroxyaspidoalbidine (III), was treated with diazomethane; aspidolimidine (IV) was isolated as the major product, thus confirming the structure.

The fourth base obtained from the extraction appears to be unrelated to the three already described. Absorption in the ultraviolet is similar to that of a dihydroindole, and the infrared spectrum suggests the presence of an ester residue. The mass spectrum is unlike that of a member of the hexacyclic aspidoalbidine series.

EXPERIMENTAL

Melting points are uncorrected. Unless otherwise stated ultraviolet spectra were measured in ethanol (ϵ values in parentheses) and infrared spectra in Nujol mulls. Nuclear magnetic resonance spectra were measured on 5–10% solutions in deuteriochloroform with a Varian Associates model HR-100 spectrometer. Tetramethylsilane protons were taken as 0 p.p.m. An AEI MS2-H mass spectrometer was used and the samples were introduced through a heated inlet system maintained at 200°.

Isolation of the Alkaloids

The dried seeds (480 g) of *A. fendleri* Woodson (1) were continuously extracted with methanol in a Soxhlet extractor. Concentration gave a brown tar which was dissolved in 2% hydrochloric acid; after filtration the non-basic material was removed by continuous extraction with chloroform. The aqueous solution was then basified with ammonia and the crude mixture of bases (14.8 g) was obtained by chloroform extraction. Shaking the chloroform containing the non-basic material with dilute hydrochloric acid, basification, and extraction yielded a further quantity of crude base (12.7 g; total = 27.5 g).

The crude base (27 g) was distributed between chloroform (stationary phase) and acetate buffer (pH 4.45) in a countercurrent distribution apparatus for a total of 20 transfers. The buffer entering the first tube of the apparatus was then replaced by acetate buffer of pH 4.0, and a further 20 transfers were completed. The mixture of stronger bases contained in the leading aqueous fractions (tubes 33 to 40; 917 mg) was chromatographed over type H alumina in benzene. The first eluate which contained alkaloid (benzene–chloroform, 3:1) gave white crystals of *fendleridine* (209 mg).

Fractions 15 to 32 yielded *aspidofendlerine* (135 mg), which was recrystallized from methanol.

Chromatography of fractions 1 to 12 over alumina in benzene gave the major base, *fendlerine* (12.6 g), as a thick, pale yellow oil which crystallized on contact with acetone.

Fractions 13 and 14 from the distribution contained, in addition to fendlerine, a small amount of another *base* which was purified by repeated preparative chromatography on Whatman 3MM paper. In this manner a total of 64 mg (m.p. 176–178°) was obtained but, apart from the ultraviolet spectrum (λ_{max} 240 (8 000) and 290 (3 100) mμ) and the infrared spectrum (no OH or NH bands, an ester carbonyl peak at 1 735 cm^{-1}), this base has resisted more positive characterization.

Fendleridine (Aspidoalbidine)

The base was recrystallized from acetone and then sublimed for analysis, m.p. 185–186°. Ultraviolet spectrum: λ_{max} 242 (7 300) and 293 (3 050) mμ. Infrared peaks at 3 300 (N—H) and 1 600 (aromatic) cm^{-1}.

Anal. Found: C, 77.3; H, 8.0; N, 9.4; O, 5.8. $C_{19}H_{24}N_2O$ requires C, 77.0; H, 8.2; N, 9.4; O, 5.4.

Fendlerine (N-Propionyl-16-methoxy-17-hydroxyaspidoalbidine)

After several recrystallizations from acetone the base melted at 179–181°. Ultraviolet spectrum: λ_{max} 225 (19 200) and 258 (3 560) mμ, $\lambda_{max}^{EtOH \cdot NaOH}$ 220 (17 200) and 300 (2 440) mμ. Infrared peaks at 1 635, 1 602, and 1 570 cm^{-1}.

Anal. Found: C, 69.1; H, 7.5; N, 7.2; O, 16.2; OMe, 7.7. $C_{23}H_{30}N_2O_4$ requires C, 69.3; H, 7.6; N, 7.0; O, 16.1; OMe (one), 7.8.

To confirm the presence of the N-propionyl group, the base (50 mg) was hydrolyzed in 20% sulfuric acid and a sample of the aqueous distillate was injected into a vapor phase chromatograph, yielding only propionic acid (by comparison with an authentic sample).

The *perchlorate*, m.p. 245–248°, was prepared by dissolving fendlerine in dilute aqueous perchloric acid and extracting with chloroform. The chloroform solution was dried over sodium sulfate and evaporated to give the crystalline salt, which was recrystallized from ethanol.

Anal. Found: N, 5.0; O, 26.6; Cl, 6.5. $C_{23}H_{30}N_2O_4 \cdot HClO_4 \cdot C_2H_5OH$ requires N, 5.1; O, 26.4; Cl, 6.5.

Aspidofendlerine (N-Acetyl-16,17-dihydroxyaspidoalbidine)

The small amount of base was sublimed twice and then recrystallized from ethanol, m.p. 278° (decomp.). Ultraviolet spectrum: λ_{max} 225 (11 500) and 259 (5 000) mμ, $\lambda_{max}^{buffered\ boric\ acid}$ 250 (broad plateau) and 290 (shoulder) mμ. Peaks in the infrared at 3 240 (OH), 1 635 (N-acyl), and 1 615 and 1 580 (aromatic) cm^{-1}.

Anal. Found: C, 67.9; H, 7.2; N, 7.5; O, 17.5. $C_{21}H_{26}N_2O_4$ requires C, 68.1; H, 7.1; N, 7.6; O, 17.3.

Aspidolimidine (from Fendlerine)

Fendlerine (330 mg) was hydrolyzed by refluxing it with 10% sulfuric acid for 4 h. The solution was cooled and, in an atmosphere of nitrogen, made basic with ammonia and then extracted with chloroform. The dried solution gave a glass (260 mg) which could not be induced to crystallize. The ultraviolet spectrum showed peaks at 215, 240 (shoulder), and 296 mμ; N-acyl absorption was absent in the infrared spectrum. The hydrolysis product (230 mg) was dissolved in pyridine (10 ml), acetyl chloride (0.5 ml) was added, and the mixture was shaken well for 10 min and then allowed to stand at room temperature for 2 h. After the mixture was poured into ice water and basified with ammonia, it was extracted with chloroform to give a brown foam (240 mg), which showed both N-acetyl and O-acetyl absorption in the infrared spectrum. Under nitrogen, the crude product was hydrolyzed with dilute methanolic sodium hydroxide (3 h) and then poured into water; a yellow foam was obtained by extraction with chloroform. Alumina chromatography of the latter gave the crystalline product (150 mg), which was recrystallized from ethanol and sublimed for analysis, m.p. 194–197°. The ultraviolet, infrared, and nuclear magnetic resonance spectra were identical with those of aspidolimidine, and a mixed melting point gave no depression.

Anal. Calcd. for $C_{22}H_{28}N_2O_4$: C, 68.7; H, 7.3; N, 7.3; O, 16.6. Found: C, 68.6; H, 7.3; N, 7.3; O, 16.6.

Aspidolimidine (from Aspidofendlerine)

Aspidofendlerine (35 mg) was dissolved in methanol and treated with ethereal diazomethane for 4 h. The volatile materials were removed at the pump and the residue triturated with acetone. An insoluble residue was shown to be unchanged aspidofendlerine (15 mg) and the soluble portion was repeatedly sublimed to give a crystalline product (17 mg), identical (melting point, mixed melting point, and infrared spectrum) with aspidolimidine.

ACKNOWLEDGMENTS

We thank Dr. B. Gilbert (Brazil) and Prof. C. Djerassi (Stanford University) for a sample of aspidolimidine.

REFERENCES

1. R. E. Woodson. Ann. Missouri Botan. Garden, **38**, 185 (1951).
2. R. H. Burnell, J. D. Medina, and W. A. Ayer. Chem. Ind. London, 33 (1964).
3. R. H. Burnell, J. D. Medina, and W. A. Ayer. Chem. Ind. London, 235 (1964).
4. C. Djerassi, L. D. Antonaccio, H. Budzikiewicz, J. M. Wilson, and B. Gilbert. Tetrahedron Letters, 1001 (1962).
5. B. Gilbert, J. A. Brissolese, J. M. Wilson, H. Budzikiewicz, L. J. Durham, and C. Djerassi. Chem. Ind. London, 1949 (1962).
6. J. N. Shoolery. Discussions Faraday Soc. **34**, 104 (1962).
7. K. S. Brown, H. Budzikiewicz, and C. Djerassi. Tetrahedron Letters, 1731 (1963).
8. S. McLean, K. Palmer, and L. Marion. Can. J. Chem. **38**, 1547 (1960).

Can. J. Chem. Downloaded from www.nrcresearchpress.com by 210.87.254.40 on 09/05/12
For personal use only.

THE SYNTHESIS OF D-*glycero*-L-*altro*-HEPTOSE, D-*glycero*-L-*allo*-HEPTOSE, AND *meso*-*glycero*-*altro*-HEPTITOL[1]

ROBERT YOUNG[2] AND G. A. ADAMS
Division of Biosciences, National Research Council, Ottawa, Canada
Received August 18, 1965

ABSTRACT

Condensation of D-talose with nitromethane in alkaline methanol gave the corresponding epimeric 1-deoxy-1-nitroheptitols which were converted into D-*glycero*-L-*altro*-heptose and D-*glycero*-L-*allo*-heptose (1.5:1) in 44% yield. Reduction of D-*glycero*-L-*altro*-heptose with sodium borohydride gave the hitherto unknown *meso*-*glycero*-*altro*-heptitol. The gas–liquid chromatography retention times of the 10 geometrically isomeric heptitol heptaacetates were determined. These data provide the necessary information for the key step in a procedure for the rapid identification of an unknown heptose.

Can. J. Chem. Downloaded from www.nrcresearchpress.com by 210.87.254.42 on 09/05/12
For personal use only.

Structural investigations of the polysaccharides from *Serratia marcescens* showed the presence of L-*glycero*-D-*manno*-heptose and D-*glycero*-D-*manno*-heptose (1), which were identified initially by gas–liquid chromatography of the derived heptitol acetates (2). It was apparent that this latter method of analysis provided a facile and reliable method for identifying heptoses in polysaccharides of unknown composition. If one disregards enantiomorphs, since they have identical chromatographic mobilities, there are 10 possible heptitols. One of these, *meso*-*glycero*-*altro*-heptitol, has not yet been prepared (3); consequently to complete the reference standards for the gas–liquid chromatography of the heptitol acetates its synthesis was undertaken. Heptitols can be prepared by the reduction of aldoheptoses or heptuloses. The former route was followed in the present study as it had the added advantage of involving the synthesis of two hitherto unknown heptoses, D-*glycero*-L-*altro*-heptose and D-*glycero*-L-*allo*-heptose.

Heptoses have been prepared successfully from the corresponding aldohexose by condensation of nitromethane with the aldehydic group of the glycose (4) and subsequent acid hydrolysis (5) of the derived 1-deoxy-1-nitroheptitols. Since the two essential requisites of this process, high solubility of the hexose and low solubility of the alcohol products in the reaction medium, were both met, this method was used in the present work.

D-Talose was prepared from D-galactose, via D-galactal, by described procedures (6, 7). Nitromethane was condensed with D-talose in alkaline methanol solution and the precipitated sodium salts of the 1-deoxy-1-nitroheptitols were recovered. Hydrolysis of the epimeric mixture with sulfuric acid yielded the expected mixture of D-*glycero*-L-*altro*-heptose and D-*glycero*-L-*allo*-heptose in 44% yield, together with unreacted starting material, D-talose. This mixture was fractionated successfully by cellulose column chromatography to give pure samples of each heptose. The ratio of D-*glycero*-L-*altro*-heptose to D-*glycero*-L-*allo*-heptose obtained was 1.5:1, as estimated by gas–liquid chromatography (2) of the mixture before chromatographic separation; this was confirmed by the yields from chromatographic fractionation. It was noteworthy that the chromatographic mobility of the heptoses was the same as that predicted by Davies in 1957 (8).

Although the heptoses themselves failed to crystallize, crystalline acetates were prepared. D-*glycero*-L-*altro*-Heptose, on reduction with borohydride, gave the expected

[1]*Issued as N.R.C. No. 8730.*
[2]*National Research Council Postdoctorate Fellow, 1963–1965.*

optically inactive *meso-glycero-altro*-heptitol. This alditol was characterized by the formation of a crystalline acetate. D-*glycero*-L-*allo*-Heptose, when reduced, gave the crystalline alcohol D-*glycero*-L-*allo*-heptitol. This heptitol is already known by its synonym D-*glycero*-D-*altro*-heptitol, which has been prepared (9) from D-*glycero*-D-*altro*-heptose.

Final proof for the structure of the synthetic heptoses was provided by selective periodate oxidation. This method (10) involves the oxidation of methyl heptopyranosides with 1 mole of periodate, which cleaves the exocyclic C_6—C_7 glycol system. Reduction of the aldehyde group at C_6 followed by hydrolysis of the methyl glycosides gave the expected hexose. D-*glycero*-L-*allo*-Heptose yielded mainly allose and the unreacted heptose. Arabinose and altrosan were obtained from D-*glycero*-L-*altro*-heptose. Altrosan and not altrose is to be expected, since hydrolysis of methyl altroside produces the anhydro derivative as the predominant product (11). Glycosidation of altrose results in almost equal amounts of furanosides and pyranosides (12) together with a small amount of altrosan. It can be assumed that D-*glycero*-L-*altro*-heptose behaves in a similar fashion, and so the production of arabinose can be explained by oxidation of the methyl furanoside at the exocyclic C_5—C_6 glycol system.

The 10 heptitol acetates were examined by gas–liquid chromatography on two different column packings, and the retention times are given in Table I.

TABLE I

Retention times of heptitol heptaacetates relative to that of hexa-*O*-acetyl-galactitol (T_g)

Heptitol acetate	Column packing material	
	i	*ii*
meso-glycero-allo-Heptitol	1.61	1.47
D-*glycero*-L-*allo*-Heptitol D-*glycero*-D-*altro*-Heptitol	1.80	1.67
D-*glycero*-D-*manno*-Heptitol D-*glycero*-D-*talo*-Heptitol	1.98	1.90
meso-glycero-altro-Heptitol	2.05	1.93
D-*glycero*-D-*gluco*-Heptitol L-*glycero*-D-*talo*-Heptitol	2.11	1.93
meso-glycero-gulo-Heptitol	2.25	2.25
D-*glycero*-D-*ido*-Heptitol D-*glycero*-L-*gulo*-Heptitol	2.28	2.31
D-*glycero*-L-*manno*-Heptitol L-*glycero*-L-*galacto*-Heptitol	2.32	2.28
D-*glycero*-L-*gluco*-Heptitol D-*glycero*-L-*galacto*-Heptitol	2.47	2.41
meso-glycero-ido-Heptitol	2.66	2.66

NOTE: The brace denotes two synonyms for the same compound.

A procedure can now be given for the consecutive steps involved in identifying a heptose. The presence of heptose in the intact polysaccharide can be detected with the sulfuric acid – cysteine reaction (13), which gives a characteristic absorption maximum at 505 mμ as a result of aldoheptose constituents. Detection of aldoheptoses on paper chromatograms with the *p*-anisidine hydrochloride spray reagent (14) reveals these compounds as brown-black spots, which are quite different in color from those given by any other class of sugar. Examination by gas–liquid chromatography (2) of the alditol acetates derived from the polysaccharide hydrolysate, using the standard relative retention times given in Table I, will identify the heptitol. A meso heptitol can arise from one

Can. J. Chem. Downloaded from www.nrcresearchpress.com by 210.87.254.42 on 09/05/12
For personal use only.

heptose precursor, and an optically active heptitol from one of two heptose precursors. Where one heptitol can be derived from two different heptoses, the latter are fortunately easily differentiated by the paper chromatographic mobilities (8) of the original aldoheptoses. Finally, after the heptose has been isolated the determination of the optical form can be made, and proof of structure can be obtained by means of selective periodate oxidation to the hexose with the same configuration as the upper six carbon atoms of the heptose (10).

EXPERIMENTAL

Paper chromatograms were run by the descending method on Whatman No. 1 filter paper with the following solvent systems (v/v): (*a*) ethyl acetate – pyridine – water (10:4:3), (*b*) butan-1-ol–ethanol–water (4:1:5), (*c*) butan-1-ol–pyridine–water (6:4:3), (*d*) ethyl acetate – acetic acid – formic acid – water (18:3:1:4). Sugars were detected on the chromatograms with the *p*-anisidine hydrochloride (14) or alkaline silver nitrate (15) spray reagents. The rates of movement of the sugars are quoted relative to that of D-glucose (R_g).

Gas–liquid partition chromatography (16) was carried out on a Pye argon chromatograph fitted with an ionization detector by using straight glass columns (120 × 0.5 cm inside diameter) with the following packings: (*i*) 10% (w/w) neopentyl glycol succinate on 80–100 mesh nonacid-washed Chromosorb W (temperature 210°); (*ii*) 1:1 (w/w) mixture of 15% w/w butanediol succinate polyester on 100–120 mesh Chromosorb W and 15% w/w Apiezon M grease on 100–120 mesh Chromosorb W (temperature 205°).

The retention times of the acetylated polyols are quoted relative to that of hexa-*O*-acetyl-galactitol (T_g).

Melting points were determined on a Fisher–Johns apparatus and are corrected.

Specific rotations are reported as equilibrium values.

Condensation of D-*Talose with Nitromethane*

A solution of sodium (1.8 g) in dry methanol (40 ml) at 0 °C was added to a vigorously stirred solution of α-D-talose (4.00 g) in dry methanol (50 ml) and nitromethane (50 ml). The solution was clear immediately after the addition, but 10 min later a precipitate began to appear. Stirring was continued for 8 h at room temperature, and the solution gradually turned yellow. The mixture was kept at 0 °C overnight, and the precipitated sodium salts of the 1-deoxy-1-nitroheptitols (5.22 g) were removed by filtration and washed with cold methanol and finally with ether. The solid material was dissolved in 0.5 *M* sodium hydroxide (50 ml) and the solution was added dropwise, with stirring, to 12 *N* sulfuric acid (61 ml), which was cooled externally with ice. Stirring was continued for 1 h, water (110 ml) was added, and the solution was adjusted to pH 3 by the addition of saturated aqueous barium hydroxide (ca. 1 400 ml). The removal of sulfate ions was completed with 12% aqueous barium acetate solution (55 ml). Barium salts were removed by centrifugation and the supernatant was evaporated to a smaller volume (ca. 300 ml). Deionization was effected by stirring the solution with Rexyn 101 (H^+) and Duolite A4 (OH^-) ion-exchange resins. Evaporation of the deionized solution to dryness gave a syrup (3.2 g), which was shown by paper chromatography to contain the two heptoses with some unreacted talose.

A small portion of the mixture was reduced with sodium borohydride and acetylated with acetic anhydride and sulfuric acid, and the resulting polyol acetates were examined by gas–liquid chromatography (2) on column *i*. Three peaks were obtained corresponding to D-talitol, D-*glycero*-D-*altro*-heptitol, and an unknown heptitol acetate. The ratio of D-*glycero*-D-*altro*-heptitol to the unknown heptitol was 1.0:1.50, as assessed by measurement of the peak areas.

The rest of the syrup was fractionated on a cellulose column (60 × 3 cm) with butan-1-ol (¼ saturated with water) as eluent, and the following fractions were collected.

Fraction 1, D-*Talose*

This fraction (872 mg) was shown by paper chromatography and by gas–liquid chromatography of the derived polyol acetate (hexa-*O*-acetyl-D-talitol, T_g 0.88 on column *i* (2)) to be homogeneous and to be chromatographically indistinguishable from D-talose, R_g 1.45 in solvent *a*. The syrup was dissolved in boiling methanol and, when it was cooled, crystals of α-D-talose were obtained, m.p. 134 °C, $[\alpha]_D$ +21° (equilibrium) (*c*, 3.0 in water).

Fraction 2, D-*Talose and* D-*glycero*-L-*altro-Heptose*

Paper chromatography of fraction 2 (347 mg) showed that it contained D-talose and D-*glycero*-L-*altro*-heptose. The ratio of hexose to heptose in the mixture was 3:4, as assessed by gas–liquid chromatography of the polyol acetates (2). Chromatographic fractionation on filter paper in solvent *a* gave a pure sample of each component. The syrup (192 mg) containing D-*glycero*-L-*altro*-heptose was added to fraction 3.

Fraction 3, D-*glycero*-L-*altro-Heptose*

This fraction (332 mg) was shown to be homogeneous by paper chromatography. It had R_g 1.09 in solvent *a*, 1.08 in solvent *b*, and 1.02 in solvent *c*. Attempts to crystallize the heptose were unsuccessful. The colorless

Can. J. Chem. Downloaded from www.nrcresearchpress.com by 210.87.254.42 on 09/05/12
For personal use only.

syrup had $[\alpha]_D$ −22° (*c*, 1.96 in water). Gas–liquid chromatography (2) of the derived heptitol heptaacetate indicated the presence of only one peak, T_g 2.05 on column *i*.

D-*glycero*-L-*altro*-Heptose (100 mg) was acetylated with acetic anhydride (10 ml) and sulfuric acid (0.1 ml), the solution being shaken at room temperature for 48 h. The mixture was poured onto ice, and extraction with chloroform yielded a syrup which gave crystals from methanol solution. Hexa-*O*-acetyl-D-*glycero*-L-*altro*-heptose was recrystallized from methanol, and the crystals were found to contain 2 moles of methanol of crystallization. The crystalline product had m.p. 221 °C and $[\alpha]_D$ +52° (*c*, 0.95 in chloroform).

Anal. Calcd. for $C_{21}H_{34}O_{15}$: C, 47.91; H, 6.47. Found: C, 47.92; H, 6.50.

The rest of the syrup yielded an isomeric crystalline product from ethyl ether – light petroleum (b.p. 30–60°) which, on recrystallization from the same solvent, gave hexa-*O*-acetyl-D-*glycero*-L-*altro*-heptose·$2CH_3OH$, m.p. 125 °C, $[\alpha]_D$ −25° (*c*, 1.01 in chloroform).

Anal. Calcd. for $C_{21}H_{34}O_{15}$: C, 47.91; H, 6.47. Found: C, 47.83; H, 6.46.

These two isomers could have different anomeric configurations or could have different ring sizes, and so no attempt is made to assign a definite structure to them.

D-*glycero*-L-*altro*-Heptose (100 mg) was dissolved in water (10 ml) and stirred with sodium borohydride (120 mg) for 2 h at room temperature. Amberlite IR 120 (H^+) ion-exchange resin was added to bring the pH of the solution to 5, and boric acid was removed by evaporation with methanol. The resulting *meso-glycero-altro*-heptitol failed to crystallize but the syrup had $[\alpha]_D$ 0° (*c*, 3.0 in water). A portion (70 mg) of the syrup was acetylated with acetic anhydride (20 ml) and concentrated sulfuric acid (0.15 ml), yielding crystalline hepta-*O*-acetyl-*meso-glycero-altro*-heptitol. The acetate, on recrystallization from ethyl ether – light petroleum (b.p. 30–60°), had m.p. 70 °C and $[\alpha]_D$ 0° (*c*, 3.0 in chloroform).

Anal. Calcd. for $C_{21}H_{30}O_{14}$: C, 49.80; H, 5.96. Found: C, 49.64; H, 5.68.

Fraction 4, D-*glycero*-L-*altro-Heptose and* D-*glycero*-L-*allo-Heptose*

Fraction 3 (329 mg) was shown by paper chromatography to contain the above two heptoses. Gas–liquid chromatography (2) indicated the relative proportions of D-*glycero*-L-*altro* heptose and D-*glycero*-L-*allo* heptose to be 3:1.

Fraction 5, D-*glycero*-L-*allo-Heptose*

Paper chromatography in several solvent systems showed that this fraction (448 mg) was homogeneous. It had R_g 0.77 in solvent *a*, 0.77 in solvent *c*, and 0.89 in solvent *d*. Attempts to obtain the sugar in a crystalline form were unsuccessful. D-*glycero*-L-*allo*-Heptose had $[\alpha]_D$ −10° (*c*, 1.90 in water). Gas–liquid chromatography of the derived polyol acetate on column *i* gave only one peak, T_g 1.80.

D-*glycero*-L-*allo*-Heptose was acetylated with a mixture of concentrated sulfuric acid, acetic anhydride, and acetic acid (17). Hexa-*O*-acetyl-D-*glycero*-L-*allo*-heptose was obtained in a crystalline form from ethyl ether – light petroleum and was recrystallized twice from the same solvent. The crystals had m.p. 142 °C and $[\alpha]_D$ +32° (*c*, 1.24 in chloroform).

Anal. Calcd. for $C_{19}H_{26}O_{13}$: C, 49.33; H, 5.66. Found: C, 49.41; H, 5.73.

Reduction of D-*glycero*-L-*allo*-heptose (100 mg) with sodium borohydride (120 mg) in a manner analogous to the reduction of the other heptose gave D-*glycero*-L-*allo*-heptitol, already known by its synonym D-*glycero*-D-*altro*-heptitol. Recrystallization from ethanol gave a crystalline product (m.p. 131 °C, undepressed on admixture with an authentic sample) having $[\alpha]_D$ −0.7° (*c*, 3.0 in water) and $[\alpha]_D$ +53° (*c*, 0.7 in 5% ammonium molybdate) (9).

Selective Periodate Oxidation of the Heptoses (10)

Samples of D-*glycero*-L-*allo*-heptose (26.4 mg) and D-*glycero*-L-*altro*-heptose (27.4 mg) were heated with 2% methanolic hydrogen chloride at 100 °C for 17 h. After neutralization with silver carbonate, the solutions were evaporated to dryness, yielding syrups (24.4 mg and 21.7 mg respectively). The latter were dissolved in water (2.0 ml), the calculated amount of an aqueous solution of 0.015 *M* sodium metaperiodate (7.2 ml and 6.4 ml respectively) was added slowly at 0 °C, and the mixtures subsequently were shaken at room temperature overnight. A solution of sodium borohydride (30 mg) in water (5.0 ml) was added slowly to each and the mixtures again left overnight. After work-up in the usual way, hydrolysis was effected with *N* hydrochloric acid at 100 °C for 2 h. The neutralized products were examined by paper chromatography and by gas–liquid chromatography of the derived polyol acetates (2).

D-*glycero*-L-*allo*-Heptose gave equal amounts of the unreacted heptose and allose (R_g 1.05 in solvent *c*) together with smaller amounts of nonreducing sugars (R_g 1.17 and 1.38 in solvent *c*).

D-*glycero*-L-*altro*-Heptose yielded equal amounts of a reducing and a nonreducing sugar. The former was identified as arabinose and the latter as altrosan (R_g 1.41 in solvent *c*).

ACKNOWLEDGMENTS

The authors thank Dr. N. K. Richtmyer for a sample of D-*glycero*-D-*ido*-heptose, and our colleague, Dr. M. B. Perry, for several samples of heptitol heptaacetates and also for many valuable discussions.

Can. J. Chem. Downloaded from www.nrcresearchpress.com by 210.87.254.42 on 09/05/12
For personal use only.

REFERENCES

1. R. YOUNG and G. A. ADAMS. Can. J. Chem. **43**, 2929 (1965).
2. S. W. GUNNER, J. K. N. JONES, and M. B. PERRY. Can. J. Chem. **39**, 1892 (1961).
3. J. M. WEBBER. Advan. Carbohydrate Chem. **17**, 15 (1962).
4. J. C. SOWDEN. Advan. Carbohydrate Chem. **6**, 291 (1951).
5. J. U. NEF. Ann. **280**, 263 (1894).
6. W. G. OVEREND, F. SHAFIZADEH, and M. STACEY. J. Chem. Soc. 671 (1950).
7. W. W. PIGMAN and H. S. ISBELL. J. Res. Natl. Bur. Std. **19**, 189 (1937).
8. D. A. L. DAVIES. Biochem. J. **67**, 253 (1957).
9. J. W. PRATT and N. K. RICHTMYER. J. Am. Chem. Soc. **77**, 6326 (1955).
10. N. J. ANTIA and M. B. PERRY. Can. J. Chem. **38**, 1917 (1960).
11. G. J. ROBERTSON and C. F. GRIFFITH. J. Chem. Soc. 1193 (1935).
12. T. YAMAKAWA, N. UETA, and I. ISHIZUKA. Japan. J. Exptl. Med. **34**, 231 (1964).
13. Z. DISCHE. Methods Biochem. Analy. **2**, 313 (1954).
14. L. HOUGH, J. K. N. JONES, and W. H. WADMAN. J. Chem. Soc. 1702 (1950).
15. W. E. TREVELYAN, D. P. PROCTER, and J. S. HARRISON. Nature, **166**, 444 (1950).
16. C. T. BISHOP. Advan. Carbohydrate Chem. **19**, 95 (1964).
17. R. M. HANN and C. S. HUDSON. J. Am. Chem. Soc. **56**, 2465 (1934).

Can. J. Chem. Downloaded from www.nrcresearchpress.com by 210.87.254.42 on 09/05/12
For personal use only.

Can. J. Chem. Downloaded from www.nrcresearchpress.com by 210.87.254.105 on 09/05/12
For personal use only.

NUCLEAR MAGNETIC RESONANCE STUDIES

VIII. DETERMINATION OF THE THERMODYNAMIC PARAMETERS GOVERNING ASSOCIATIONS OF SUBSTITUTED BENZALDEHYDES IN TOLUENE SOLUTION[1,2]

R. E. KLINCK[3] AND J. B. STOTHERS

Department of Chemistry, University of Western Ontario, London, Ontario

Received August 9, 1965

ABSTRACT

The temperature dependence of the proton chemical shifts of four substituted benzaldehydes in toluene solution has been measured. From these results, estimates have been made of the enthalpies and entropies of formation of the stereospecific solute–solvent complexes which were previously shown to exist in these systems. These calculations indicate that the ΔH and ΔS values are -0.9 ± 0.2 kcal/mole and -4.9 ± 1.3 e.u., respectively. No correlation with substitution is apparent; the results are compared with other available data.

INTRODUCTION

In an earlier paper, the pronounced effect of substituents on the solvent shift of formyl proton shieldings in benzaldehydes caused by aromatic solvents was described (1); subsequently, a more detailed examination of this phenomenon was reported (2). In the latter work, the solvent shift for each non-equivalent proton site in a series of *p*-substituted benzaldehydes, acetophenones, and toluenes was measured, and the results gave strong evidence for the existence of stereospecific solute–solvent interactions in a variety of aromatic solvents. At that time it was noted that measurements of the temperature dependence of these solvent shifts could, in principle, provide the necessary data with which to evaluate the thermodynamic parameters governing these associations. With this object in mind, we present the results of an investigation of the variation with temperature of the proton chemical shifts of four benzaldehydes in toluene solution.

For this study, *p*-substituted examples were chosen to permit a straightforward measurement of the chemical shifts of all solute protons without a detailed analysis. To compare the influence of an electron-withdrawing substituent with that of an electron donor, the *p*-nitro and *p*-N,N-dimethylamino derivatives were examined. Terephthalaldehyde was included to show the effects for a symmetrically substituted solute, and benzaldehyde itself was examined for comparison with the others, although only the temperature dependence of its formyl proton is readily determined. Toluene was selected as the solvent because of the relatively wide temperature range over which measurements are possible.

The existence of solute–solvent complex formation in a variety of systems involving aromatic solvents is well established and a number of discussions of the phenomenon have appeared (2–11). In general, these investigations have been carried out at a single temperature and, thus, the relative strengths of the complexes were not determined. Abraham (5), however, has examined the temperature variation of the solute proton shieldings of both chloroform and methyl iodide in toluene solutions, and the effect of temperature on pyrimidine–toluene solutions has been reported (10). The present results may be compared with the ΔH and ΔS values obtained for these cases.

[1]*For part VII in this series see D. J. Aberhart, Y. S. Chen, P. de Mayo, and J. B. Stothers, Tetrahedron, 21, 1417 (1965).*

[2]*Some of these results were presented at the 47th conference of the Chemical Institute of Canada, Kingston, Ontario, June 1964.*

[3]*Petroleum Research Fund Predoctorate Fellow, summer 1962, 1963, 1964; holder of a Dow Fellowship, 1963–1964. Present address: Department of Physics, Duke University, Durham, North Carolina, U.S.A.*

Can. J. Chem. Downloaded from www.nrcresearchpress.com by 210.87.254.105 on 09/05/12
For personal use only.

EXPERIMENTAL

The solutes used in this work are commercially available and were purified by recrystallization or distillation before their spectra were recorded. Toluene-d_8 (98 atom % D minimum) was obtained from Merck, Sharp and Dohme, Montreal. To approximate infinite dilution conditions, 5 mole % solutions of each solute were examined in the first instance. To permit observations over a larger temperature range, and to examine the effects of further dilution, the *p*-NO_2 and *p*-N,N-$(CH_3)_2$ derivatives were studied at concentrations down to 0.5 mole %.

All spectra were obtained with a Varian DP-60 instrument and peak positions were determined by interpolation between audio side bands of an internal tetramethylsilane reference signal placed on either side of the peak to be measured. The precision is estimated to be ±0.5 c/s. The variable temperature studies were performed with a Varian V-4340 probe accessory which has been modified to allow operation over a much wider range.

TREATMENT OF EXPERIMENTAL DATA

The formation of the postulated stereospecific solute–solvent complexes may be considered in terms of a dynamic equilibrium of the type

[1] $$\text{aldehyde (A)} + \text{solvent (S)} \rightleftharpoons \text{complex (C)},$$

if one assumes a 1:1 solute–solvent molecular ratio. Since the energies of the unassociated aldehyde and the complex may be expected to differ, the equilibrium will be temperature dependent. As the temperature is lowered it is expected that the relative amount of complex present will increase. It follows that the observed shielding of a given solute proton will be temperature dependent, because any specific chemical shift measurement will reflect the average magnetic environment of that proton. On the basis of the earlier studies (1, 2), the shielding of the solute protons, therefore, will be increased as the temperature decreases, and, in the limit of very low temperatures, the observed chemical shift should be characteristic of the complex itself. An estimate of the shielding for the solute protons in unassociated molecules can be obtained from measurements in an "inert" solvent. From these two limiting values, one can determine an equilibrium constant for any temperature according to the following method.

For eq. [1], let the original concentrations be represented by n_A^0 and n_S^0, the number of moles of aldehyde and solvent initially present. At equilibrium, the number of moles of the various species are n_A, n_S, and n_C and, if fraction p of the solute is complexed, $n_C = pn_A^0$. In terms of mole fractions the equilibrium constant, K, is given by

[2] $$K = X_C/(X_A \cdot X_S) = \exp(\Delta S/R) \exp(-\Delta H/RT),$$

where $X_C = pn_A^0/n_A^0 + n_S^0 - pn_A^0$, etc. ΔH and ΔS are the enthalpy and entropy of formation of the complex. Substitution of the appropriate expressions gives

[3] $$K = \frac{p}{(1-p)}\left[1 + \frac{X_A^0}{X_S^0 - pX_A^0}\right],$$

where X_A^0 and X_S^0 are the initial mole fractions of aldehyde and solvent, respectively. The fraction p can be obtained from the chemical shift measurements for a specific solute proton such that ν is an observed shift and is the weighted mean of the shifts for the unassociated solute, ν_A, and for the complex, ν_C. Thus

$$p = (\nu - \nu_A)/(\nu_C - \nu_A),$$

which for convenience may be reduced to $p = \nu/\nu_C$ by taking ν_A as the reference point (i.e. $\nu_A = 0$).

To obtain values of ν_A for the various solute protons it seemed most reasonable to use the data for dilute solutions in carbon tetrachloride. Since all of the solutes employed

Can. J. Chem. Downloaded from www.nrcresearchpress.com by 210.87.254.105 on 09/05/12
For personal use only.

are not sufficiently soluble to permit the determination of precise chemical shifts in this solvent, data for chloroform solutions were used for certain cases. For the latter, small corrections were made for the effects of hydrogen bonding between the solvent and the carbonyl group on the basis of our earlier results (1). All raw chemical shift measurements were made relative to that of internal tetramethylsilane and then converted, for purposes of calculation, to a scale having ν_A for a specific proton set as zero. Values for ν_C for the various solute protons were obtained by extrapolation to absolute zero of the curve defined by the chemical shift data over the experimentally accessible temperature range. From these figures, values for p are obtained from which, by using eq. [3], the equilibrium constants were calculated. From plots of $\log K$ vs. $1/T$, ΔH and ΔS are obtained in the usual fashion.

The principal feature of the approach employed in this study is the use of the chemical shift variation with temperature for more than one proton site in a given solute molecule. Previously, similar estimates have been made by an analogous analysis, but these have been confined to measurements of the shift variations of a single solute proton. The use of more than one set of experimental results for a given case should lead to a more reliable estimate of the ΔH and ΔS parameters as well as providing an internal check on the precision of the calculated results.

As a further test of the analysis, the calculated values of ΔH and ΔS may be used together with the value of ν_C to calculate the theoretical curve of chemical shift vs. temperature for a given solute proton.

RESULTS

To illustrate the approach employed in this study, the experimental results for p-nitrobenzaldehyde in toluene solution will be considered in detail. Four concentrations were examined for this particular case, namely, 10.0, 5.0, 2.5, and 1.0 mole %. The largest temperature range over which measurements were possible was the most dilute of these, and the analysis of these results is presented in the following paragraphs.

The variation with temperature of the chemical shifts of the formyl, ortho, and meta protons is illustrated by the points in Fig. 1 over the range -71.5 to $+100$ °C. Extrapolation of these curves to 0 °K gave the values 472 ± 20, 339 ± 20, and 377 ± 20 c/s (from tetramethylsilane) for these three non-equivalent proton sites, respectively. The corresponding values of ν_A for these protons were taken as 606.9, 481.9, and 499.9 c/s, respectively, from results for dilute carbon tetrachloride solutions. Thus, the ν_C values are found, by subtraction, to be 135 ± 20, 143 ± 20, and 123 ± 20 c/s for the formyl, ortho, and meta protons, respectively. By using eq. [3], the equilibrium constants were calculated for the various temperatures at which measurements were made. As an example of typical experimental results, the data for the meta protons of p-nitrobenzaldehyde are collected in Table I. Since the data for the other nuclei in this and the following examples are similar, only one case is presented in detail.[4] Plots of the results for $\log K$ vs. $1/T$ are illustrated in Fig. 2 for each of the three non-equivalent protons in p-nitrobenzaldehyde. Values for ΔH and ΔS obtained from the three lines in Fig. 2 are presented in Table II, together with the corresponding results for the other concentrations for which a reasonable interval could be examined. From the results for the 1 mole % solutions, the theoretical curves of temperature vs. chemical shift were calculated, and these are given in Fig. 1 as the solid lines.

[4]*The full experimental details for all other cases examined during the course of this investigation are available in ref. 12.*

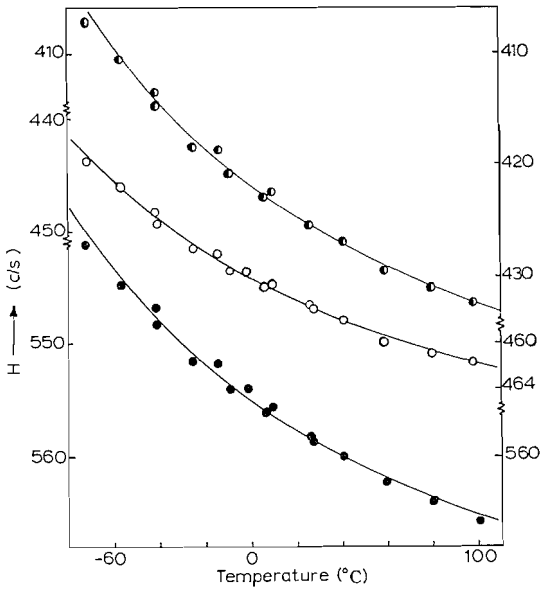


FIG. 1. Temperature dependence of the proton shieldings for 1 mole % solutions of *p*-nitrobenzaldehyde in toluene-d_8 (in cycles per second from tetramethylsilane at 60 Mc/s). Experimental points are shown for the formyl proton (●), ortho protons (◐), and meta protons (○); the full lines are the calculated temperature variations (see text).

TABLE I

Experimental data and results for meta protons in *p*-nitrobenzaldehyde (1 mole % in toluene-d_8)

Temp. (°C)	Chemical shift (c/s)		$1/T \times 10^{-3}$	K	$-\log K$
	Observed	ν			
98.0	461.7	38.2	2.695	0.458	0.3395
80.0	461.0	38.9	2.833	0.470	0.3278
59.2	459.9	40.0	3.010	0.490	0.3101
41.2	457.9	42.0	3.183	0.527	0.2781
27.7	457.0	42.9	3.326	0.544	0.2641
26.8	456.6	43.3	3.336	0.552	0.2578
10.2	454.8	45.1	3.531	0.589	0.2301
6.7	455.0	44.9	3.575	0.584	0.2333
−1.1	453.6	46.3	3.678	0.614	0.2119
−8.5	453.6	46.3	3.781	0.614	0.2119
−13.5	452.1	47.8	3.854	0.646	0.1896
−24.5	451.6	48.3	4.024	0.658	0.1820
−40.8	449.4	50.5	4.307	0.708	0.1498
−41.0	448.3	51.6	4.310	0.735	0.1336
−56.5	446.0	53.9	4.619	0.794	0.1003
−71.5	443.8	56.1	4.963	0.854	0.0687

Although, in principle, the temperature dependence of four different proton chemical shifts in *p*-N,N-dimethylaminobenzaldehyde could be analyzed by the method outlined above, the temperature variation of the shielding for only two of these, the *N*-methyl and meta protons, is very pronounced. A series of equilibrium constants at various temperatures were calculated from the data for these two sites. From the results for the 1 mole % solutions, the plots shown in Fig. 3 were constructed. The average shielding (see the next paragraph) of the ortho protons is virtually independent of temperature

Can. J. Chem. Downloaded from www.nrcresearchpress.com by 210.87.254.105 on 09/05/12
For personal use only.

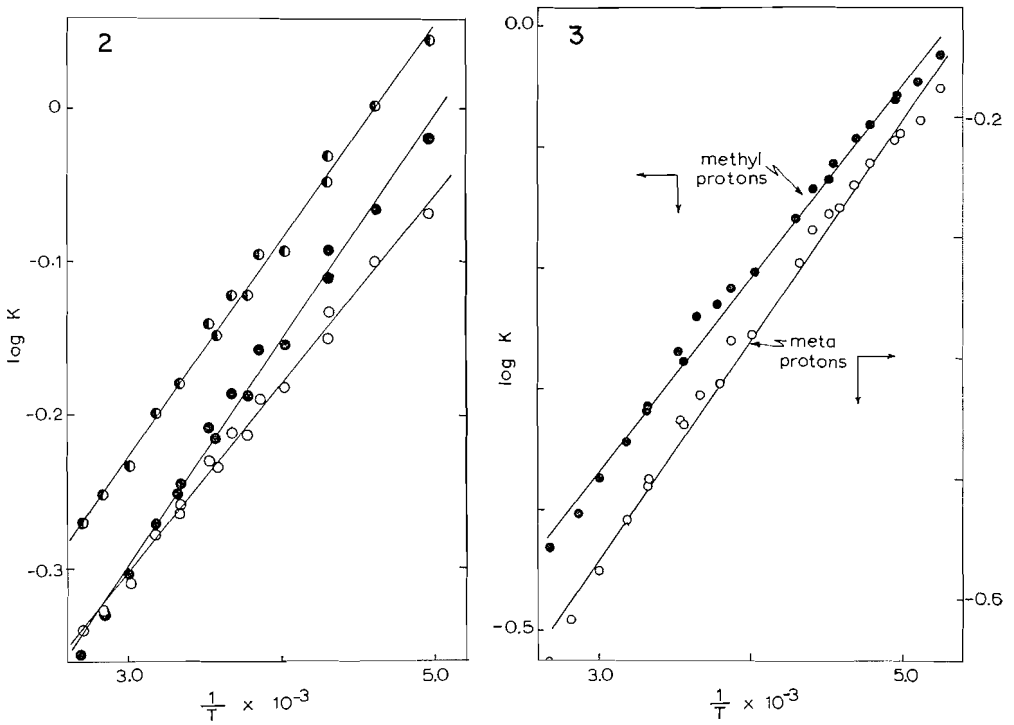


FIG. 2. Plots of log K vs. $1/T$ for the non-equivalent protons of p-nitrobenzaldehyde in toluene-d_8 (1 mole % solutions; ●, formyl proton; ◐, ortho protons; ○, meta protons).

FIG. 3. Plots of log K vs. $1/T$ for the methyl and meta protons of p-N,N-dimethylaminobenzaldehyde in toluene-d_8 (1 mole % solutions).

TABLE II

Thermodynamic parameters for complex formation of p-nitrobenzaldehyde in toluene-d_8

Solution concentration (mole %)	Temp. range (°K)	Non-equivalent proton sites					
		Formyl group		Ortho protons		Meta protons	
		$-\Delta H$ (kcal/mole)	$-\Delta S$ (e.u.)	$-\Delta H$ (kcal/mole)	$-\Delta S$ (e.u.)	$-\Delta H$ (kcal/mole)	$-\Delta S$ (e.u.)
1.0	202–373	0.68	3.4	0.65	3.0	0.56	3.1
2.5	252–375	0.75	3.9	0.69	3.5	0.61	3.6
5.0	250–372	0.80	4.3	0.73	3.7	0.60	4.0
Averaged values*		0.74±0.06	3.9±0.4	0.69±0.04	3.4±0.3	0.59±0.03	3.6±0.4

*These are the statistical averages with the standard deviation shown.

while that of the formyl proton changes by only 3 c/s over the interval −104 to +103 °C. Both of these observations are entirely consistent with our original ideas on the relative orientation of the solvent molecule in the complex (2). As in the previous case, several different concentrations were examined (10, 5.0, 2.5, 1.0, and 0.5 mole %), and the behavior was similar for all. The parameters obtained for each of these dilutions are collected in Table III and the temperature ranges are indicated.

At the lower temperatures (<−50 °C) the proton spectra for the p-N,N-$(CH_3)_2$ derivative become more complex because of the decreased rate of rotation of the formyl

Can. J. Chem. Downloaded from www.nrcresearchpress.com by 210.87.254.105 on 09/05/12
For personal use only.

TABLE III

Thermodynamic parameters for complex formation of *p*-N,N-dimethylaminobenzaldehyde in toluene-d_8

Solute concentration (mole %)	Temp. range (°K)	Non-equivalent sites: N-Methyl protons $-\Delta H$ (kcal/mole)	N-Methyl protons $-\Delta S$ (e.u.)	Meta protons $-\Delta H$ (kcal/mole)	Meta protons $-\Delta S$ (e.u.)
0.5	186–300	0.71	3.9	0.84	5.2
1.0	176–373	0.72	3.9	0.83	5.1
2.5	169–375	0.74	3.5	0.80	4.9
5.0	239–375	0.80	4.6	0.97	5.7
10.0	273–372	0.78	3.9	1.03	5.5
Averaged values*		0.75±0.04	3.9±0.2	0.89±0.09	5.3±0.3

*These are statistical averages with the standard deviation shown.

group about the bond connecting it to the aromatic ring. This feature has been noted before (13) but, for the present case in an aromatic solvent, the relative shift between the two non-equivalent ortho proton sites is substantially increased (in the limit of slow rotation) such that the spectral changes characteristic of a slow exchange process are apparent at a temperature higher than that observed in the published account (13), for which vinyl chloride and methylene chloride were employed as solvents. We have determined the potential barrier to rotation in this and several closely related systems (12, 14) by a detailed study of the spectra at low temperatures; a full account of this work will be published in the near future.

Chemical shift measurements were carried out for the formyl and aryl protons of terephthalaldehyde with 5 mole % solutions over the rather limited temperature range 26 to 98.5 °C. For benzaldehyde, measurements were confined to the temperature dependence (over the range −35 to +100 °C) of the formyl proton shielding, since chemical shift data for the aryl protons are not so readily obtained. For these two examples, the $\log K$ vs. $1/T$ plots are presented in Figs. 4 and 5, respectively.

A summary of the calculated results for the ΔH and ΔS parameters found for all of the solutes included in this study is presented in Table IV. For those cases in which several different concentrations were examined, the results were averaged statistically

TABLE IV

Thermodynamic parameters for complex formation of substituted benzaldehydes in toluene-d_8

Substituent	Solute concentration (mole %)	Temp. range (°K)	K (300°)	$-\Delta H^*$ (kcal/mole)	$-\Delta S^*$ (e.u.)
4-H	5.0	238–373	0.499	0.95±0.05	4.6±0.4
4-CHO	5.0	273–371	0.313	1.17±0.13	6.2±0.5
4-N,N-$(CH_3)_2$	0.5–10	168–378	0.449	0.78±0.05	4.6±0.7
4-NO_2	1.0–5.0	201–373	0.5941	0.67±0.08	3.6±0.4

*Averaged values for all experimental data with standard deviations given.

and the Chauvenet Principle (15) was employed to eliminate widely divergent values. The error limits given in the table are the standard deviations (σ). A reasonable estimate of the precision of the measurements may be set at about twice the standard deviation. It is important to note that the calculated ΔH for terephthalaldehyde is without doubt the least precise because of the relatively narrow temperature range examined.

Can. J. Chem. Downloaded from www.nrcresearchpress.com by 210.87.254.105 on 09/05/12
For personal use only.

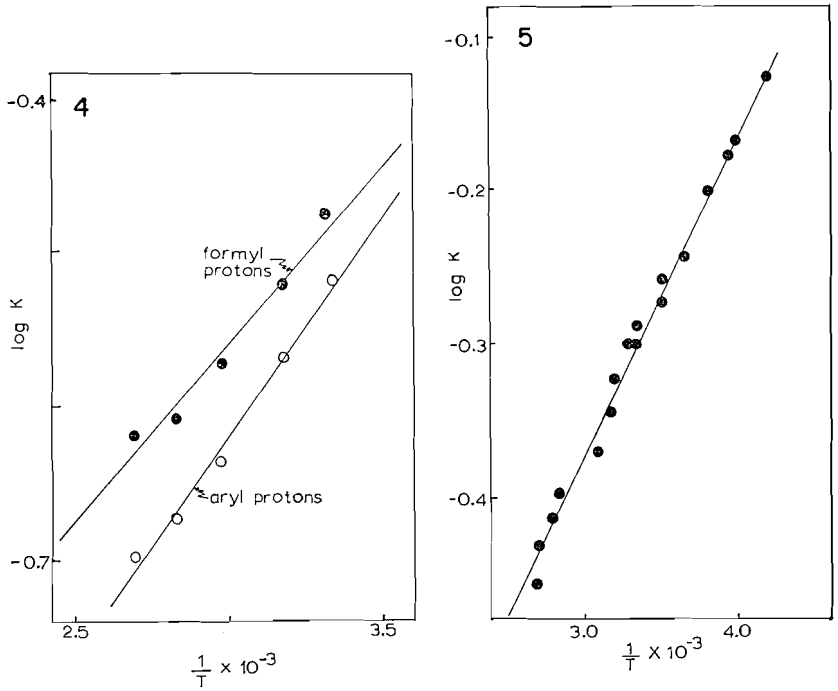


FIG. 4. Plots of log K vs. $1/T$ for the formyl and aryl protons of terephthalaldehyde in toluene-d_8 (5 mole %).
FIG. 5. Plot of log K vs. $1/T$ for the formyl proton of benzaldehyde in toluene-d_8 (5 mole %).

DISCUSSION

From the values given in Table IV it is clear that the solute–solvent associations are very weak interactions indeed. The calculated ΔH values of -0.9 ± 0.2 kcal/mole are significantly smaller than those obtained from analyses of the results for either chloroform or methyl iodide in toluene solutions (5), which have been reported as -1.6 and -1.3 kcal/mole, respectively, but only slightly less than that given for the pyrimidine–toluene association (10). It is interesting that the observed solvent shifts (2) in aromatic as opposed to nonpolar aliphatic solvents are so marked for such weak interactions. The present results emphasize the sensitivity with which nuclear magnetic resonance techniques can detect the presence of such interactions. Although the basic assumption underlying the considerations presented in this paper has been that the complex has a 1:1 solute–solvent ratio, it should be stressed that the methods employed do not permit a clear distinction between this, the simplest model, and other more complicated forms. In fact, the magnitudes of the observed ΔH parameters show that the complex is a very loose one, and any conclusions regarding a more precise description would be unwise and unwarranted.

Although the estimates of the proton shieldings for the complex itself are crude because of the long extrapolation, and consequently are subject to rather large error, trial calculations show that a 10–15% error in the ν_C values produces changes of less than 5% in the calculated ΔH values. Another source of error inherent in the method employed is the inaccuracy of the values chosen for ν_A, which may be in error by a few cycles per second. There is little doubt that the solvent shift caused by the aromatic solvent is

Can. J. Chem. Downloaded from www.nrcresearchpress.com by 210.87.254.105 on 09/05/12
For personal use only.

far greater than that arising from other mechanisms (2), and it seems reasonable to assume that the calculated ΔH values are within 0.2 kcal/mole of the correct magnitude.

A priori one may have expected the complex formed by *p*-N,N-dimethylaminobenzaldehyde to be more stable than the others, since the lone pair of electrons on nitrogen can interact directly with the carbonyl group by resonance and so give a more highly polarized solute molecule. It is clear, however, that no trends with substitution are revealed by the present results. There seems to be little doubt that specific solute–solvent associations do occur in these systems, and it is mildly surprising to find that the interactions are so weak. These results suggest that the problem of interpretation of solute proton shieldings in aromatic solvents should be approached cautiously, particularly in the case of large solute molecules for which a number of sites may be available for similar weak interactions. Potentially, the use of selective solvent shifts for unravelling subtle points of stereochemistry is most interesting but the way to a complete understanding of these may be difficult. In the meantime, careful studies using well-known model compounds offer a practical and valuable means of exploiting some of the more pronounced solvent shifts (9, 16).

ACKNOWLEDGMENTS

We thank the donors of the Petroleum Research Fund, administered by the American Chemical Society, for generous support of this research project through grant PRF No. 1165, A1. We also thank the Dow Chemical Co. for a fellowship granted to one of us (R. E. K.).

REFERENCES

1. R. E. Klinck and J. B. Stothers. Can. J. Chem. **40**, 1071 (1962).
2. R. E. Klinck and J. B. Stothers. Can. J. Chem. **40**, 2329 (1962).
3. J. V. Hatton and R. E. Richards. Mol. Phys. **3**, 253 (1960); **5**, 139 (1962); **5**, 153 (1962).
4. T. Schaeffer and W. G. Schneider. J. Chem. Phys. **32**, 1218 (1960).
5. R. J. Abraham. Mol. Phys. **4**, 369 (1961).
6. J. V. Hatton and W. G. Schneider. Can. J. Chem. **40**, 1285 (1962).
7. W. G. Schneider. J. Phys. Chem. **66**, 2653 (1962).
8. L. A. LaPlanche and M. T. Rogers. J. Am. Chem. Soc. **86**, 337 (1964).
9. N. S. Bhacca and D. H. Williams. Tetrahedron Letters, No. 42, 3127 (1964).
10. J. N. Murrell and V. M. S. Gill. Trans. Faraday Soc. **61**, 402 (1965).
11. M. T. Rogers and J. L. Burdett. Can. J. Chem. **43**, 1516 (1965).
12. R. E. Klinck. Ph.D. Thesis, University of Western Ontario, London, Ontario. 1965.
13. F. A. L. Anet and M. Ahmad. J. Am. Chem. Soc. **86**, 119 (1964).
14. R. E. Klinck, D. H. Marr, and J. B. Stothers. 47th Conf. Chem. Inst. Canada, Kingston, Ontario, June 1964.
15. J. F. Kenney and E. S. Keeping. Mathematics of statistics. Part 2. 2nd ed. D. Van Nostrand Co., Inc., New York. 1953.
16. D. H. Williams. Tetrahedron Letters, No. 27, 2305 (1965).

Can. J. Chem. Downloaded from www.nrcresearchpress.com by 210.87.254.105 on 09/05/12
For personal use only.

NUCLEAR MAGNETIC RESONANCE STUDIES

IX. THE CHEMICAL SHIFT OF THE FORMYL PROTON IN ALIPHATIC ALDEHYDES[1]

R. E. KLINCK[2] AND J. B. STOTHERS
Department of Chemistry, University of Western Ontario, London, Ontario
Received August 27, 1965

ABSTRACT

The effects of structure on the shielding of formyl protons of aliphatic aldehydes have been examined. The survey included examples of acyclic, alicyclic, and α,β-unsaturated aldehydes. The potential use of these results as an aid for structural elucidations is discussed, and the limitations are noted.

As part of a survey of the variation of the chemical shift of the formyl proton with structure in a variety of organic aldehydes (1), the nuclear magnetic resonance spectra of 36 aliphatic examples have been determined. These include aldehydes in which the formyl group is bonded to acyclic, alicyclic, and α,β-unsaturated carbon skeletons. Certain general trends which have potential application for structural elucidations are evident from these shielding results; these data constitute the subject of the present paper.

In an earlier paper (1), the major factors which could be expected to influence the shielding of formyl protons were considered in detail, and the present results are examined in light of these ideas. Briefly, these effects include (*a*) the deshielding influence of the carbonyl bond itself, (*b*) the shielding of the formyl proton by conjugative electron release to the carbonyl bond in suitable systems, and (*c*) the long-range effects attributable to neighboring anisotropic bonds. As before, it may be expected that only *b* and *c* will be variable throughout the series, since the orientation of the formyl proton with respect to the carbonyl bond is invariant. Support for these considerations has been provided by recent ^{13}C nuclear magnetic resonance studies (2–4), and some comparison of the ^{1}H and ^{13}C data is presented below.

For the purpose of intercomparing the results, all chemical shift values were determined in carbon tetrachloride solutions and, for most cases, concentrations of 20, 10, and 5% (w/v) were examined. In general, little effect of dilution was apparent over this range, since for most examples the total change is less than 0.01 p.p.m. The formyl proton chemical shifts for all compounds included in this study are listed in Table I for 5% solutions, and the shift observed upon dilution from 20% is indicated.

From the data for the first six entries in the table it can be seen that an increased chain length in the linear acyclic cases produces very small changes in the shielding of the formyl proton. A shift of 0.03 p.p.m. toward higher field is apparent upon substitution of an additional carbon to propionaldehyde but further extension of the chain is without effect. It is interesting that the ^{13}C shieldings of the carbonyl carbon nuclei of these simplest examples are also unaffected by chain extension (2), except for the significant change of ca. -2 p.p.m. from CH_3CHO to CH_3CH_2CHO. While this behavior is typical for methyl substitution in a variety of systems (5), the absence of a change in the formyl proton shielding for the same structural modification makes it difficult to

[1]*For part VIII in this series see R. E. Klinck and J. B. Stothers, Can. J. Chem., 44, 37 (1966).*
[2]*Petroleum Research Fund Predoctorate Fellow, summer 1962, 1963, 1964; holder of a Dow Fellowship, 1963–1964. Present address: Department of Physics, Duke University, Durham, North Carolina, U.S.A.*

TABLE I

Formyl proton shifts of some aliphatic aldehydes (5% solutions (w/v) in CCl_4)

Entry	Compound	Chemical shift (p.p.m.)*	J (c/s)	Entry	Compound	Chemical shift (p.p.m.)*	J (c/s)
I	Acetaldehyde	9.73 (+0.02)	2.8	XXII	2,4-Hexadienal	9.46 (−0.01)	7.7
II	Propionaldehyde	9.73 (+0.02)	1.3	XXIII†	Citral *a*	9.85 (0.00)	7.7
III	*n*-Butyraldehyde	9.70 (+0.01)	1.7		Citral *b*	9.80 (0.00)	7.8
IV	*n*-Valeraldehyde	9.69 (0.00)	1.4	XXIV	2-Methyl-2-butenal (tiglaldehyde)	9.32 (0.00)	—
V	Octanal	9.69 (0.00)	1.7	XXV	Cinnamaldehyde	9.64 (+0.01)	8.0
VI	Dodecanal	9.69 (0.00)	1.6	XXVI	*p*-N,N-Dimethylaminocinnamaldehyde	9.53 (−0.02)	7.6
VII	Citronellal	9.68 (0.00)	2.0	XXVII	α-Methylcinnamaldehyde	9.57 (+0.03)	—
VIII	Hydroxycitronellal	9.69 (0.00)	1.7	XXVIII	α-Amylcinnamaldehyde	9.47 (+0.01)	—
IX	Isobutyraldehyde	9.57 (0.00)	1.3	XXIX	Phenylpropynal	9.38 (+0.02)	—
X	2-Ethylbutanal	9.51 (−0.01)	2.3	XXX	1-Cyclopentene-1-carboxaldehyde	9.72 (0.00)	—
XI	2-Phenylpropanal	9.59 (−0.03)	1.2	XXXI	1-Cyclohexene-1-carboxaldehyde	9.33 (+0.01)	—
XII	Cyclopentanecarboxaldehyde	9.53 (−0.01)	2.0	XXXII	1-Cycloheptene-1-carboxaldehyde	9.26 (+0.01)	—
XIII	Cyclohexanecarboxaldehyde	9.53 (+0.01)	1.0	XXXIII	6-Methyl-1,3-cyclohexadiene-1-carboxaldehyde	9.42 (0.00)	—
XIV	Cycloheptanecarboxaldehyde	9.56 (+0.01)	0.9				—
XV	3-Cyclohexene-1-carboxaldehyde	9.62 (0.00)	0.8	XXXIV	2-Chloro-1-cyclopentene-1-carboxaldehyde	9.95 (−0.01)	
XVI	4-Cyano-2,2-dimethylbutanal	9.38 (−0.01)	—	XXXV	2-Chloro-1-cyclohexene-1-carboxaldehyde	10.11 (0.00)	—
XVII	2,2,4-Trimethyl-3-pentenal	9.32 (−0.01)	—	XXXVI	2-Chloro-1-cycloheptene-1-carboxaldehyde	10.03 (0.00)	—
XVIII	1-Methylcyclopentane-1-carboxaldehyde	9.38 (−0.01)	—	XXXVII	Furfural	9.67 (+0.03)	—
XIX	1-Methylcyclohexane-1-carboxaldehyde	9.34 (−0.01)	—				
XX	Acrolein	9.54 (+0.01)	—				
XXI	Crotonaldehyde	9.43 (0.00)	7.6				

*From internal tetramethysilane. The quantity in parentheses is the shift (in p.p.m.) observed upon dilution of 20% solutions.
†Reported values (10): citral *a*, 9.84 p.p.m. (J = 7.8 c/s); citral *b*, 9.80 p.p.m. (J = 8.4 c/s).

offer an explanation for both experimental observations. In fact, a satisfactory rationalization of the methyl substitution effect on ^{13}C shieldings has not yet appeared but the problems involved have been discussed (5). In any event it appears that a proton chemical shift of 9.71 ± 0.02 p.p.m. is characteristic of the structure RCH_2CHO, since chain branching at the β-C (i.e. C-3) has no effect on the formyl shieldings (entries VII and VIII in the table). The appearance of a triplet pattern for the formyl absorption proves, of course, the presence of a monosubstituted α-carbon. For the examples included in the table, the observed coupling constants are listed, but no discussion of these is given since a careful examination and detailed interpretation of these spin–spin coupling interactions have been presented recently by Karabatsos and Hsi (6).

The effect of alkyl substitution at the α-carbon in the aliphatic series is illustrated by the results for entries IX–XV. Clearly the trend is toward higher field upon replacement of an α-C—H bond by a C—C bond. Presumably the origin of this shift is the diamagnetic anisotropy of the additional α-C—C bond since, according to the currently accepted view, the formyl proton lies in the shielding region of this bond (7). These protons absorb in the range 9.54 ± 0.03 p.p.m., with the exception of Δ^3-cyclohexene-1-carboxaldehyde (XV), and the fact that the latter compound exhibits formyl absorption at slightly lower field can be attributed to a long-range deshielding influence of the olefinic bond. Another feature of these results is that there is no apparent effect of ring size for the compounds having five-, six-, and seven-membered rings. While each of these undoubtedly exists as a mixture of conformations, it is interesting that the time-average shielding is similar for each. It is well known that rather larger chemical shift differences are observed between the protons of axial and equatorial formyl groups on six-membered rings in a number of natural products (8), but preliminary results in these laboratories indicate that the differences probably arise from more remote structural features than the cyclohexyl ring. We are currently engaged in a more detailed study of this particular aspect.

The shielding results for entries XVI–XIX exhibit an additional shift to higher field as a result of the replacement of the remaining α-C—H bond by a C—C bond. Presumably the reason for this is the same as that noted for the immediately preceding examples. It is expected that the effect of the β–γ double bond in XVII will be negligible, in contrast to the result for XV mentioned above, since free rotation is possible for the acyclic example so that a rapid interconversion among a host of conformers effectively averages the long-range influence of the olefinic bond to zero. These results indicate that, for structures of the type R_3CCHO, the formyl proton absorption occurs in the range 9.36 ± 0.03 p.p.m.

The next group of aldehydes listed have the common feature of an α,β-unsaturated structure. In the earlier paper (1), the notion was advanced that conjugation of the carbonyl group leads to a decreased polarization of the formyl C—H bond and hence an up-field shift of the formyl proton absorption. A considerable body of ^{13}C data for carbonyl compounds (2–4) also supports the original hypothesis (1). The present results are in complete accord with this view. For example, acrolein exhibits formyl absorption at 0.2 p.p.m. higher field than propionaldehyde, and a further shift of 0.1 p.p.m. is found for crotonaldehyde, as would be expected for the additional electron release by the β-methyl group. Thus it appears that the conjugative shielding effect outweighs the deshielding influence of the olefinic bond (9) in the α,β-unsaturated cases. Since a planar conformation will be preferred in these systems, it is not unreasonable that the formyl proton for *trans*-2,4-hexadienal (XXII) appears at slightly lower field than that for crotonaldehyde (XXI) as a result of the deshielding effect of the second olefinic bond

through space. Similarly, a low-field shift can be seen for the second double bond in XXXIII relative to that in XXXI. A detailed study of the two isomeric forms of citral has recently appeared (10) and the data in the table are in reasonable agreement with those published. It is somewhat surprising that these formyl protons appear at such low field, 9.80 and 9.85 p.p.m. These results are atypical for the α,β-unsaturated cases considered here with one other exception, which is discussed later. Dilution of the citral samples over the concentration range 20–2.5% (w/v) gives no change in the position of the formyl signals, and so it would appear that a self-association of solute molecules is not responsible for the low-field position of these peaks.

As in the saturated cases, α-alkyl substitution leads to shielding of the formyl proton, as indicated by the shift for 2-methyl-2-butenal (tiglaldehyde) as well as for the α-methyl and α-amyl derivatives of cinnamaldehyde relative to that for crotonaldehyde and cinnamaldehyde, respectively.

In our earlier paper (1), it was argued that the appearance of the formyl proton absorption for cinnamaldehyde (XXV) at 9.64 p.p.m. is consistent with the view that the ring-current effect of the aromatic ring is substantially reduced from that operative in the case of benzaldehyde (9.96 p.p.m.) while the conjugative shielding should be similar for each. Since the absorption position of a given formyl proton appears to be determined by the relative influence of these two opposing factors, we conclude that the conjugative contribution tends to dominate in XXV. The fact that the aryl ring still tends to deshield in this system, albeit to a lesser extent, can be seen by a comparison of the results for acrolein and cinnamaldehyde. Other evidence to support the interpretation is given by the chemical shift of 9.36 p.p.m. for the formyl proton of phenylpropynal (XXIX), a value which is at 0.27 p.p.m. higher field than that for cinnamaldehyde. Since the spatial effect of a triple bond caused by its magnetic anisotropy is approximately opposite to that of a double bond (11), one would expect the formyl proton in a structure of the type —C≡C—CHO to be shielded relative to one of the type —CH=CH—CHO, other things remaining essentially constant. Thus, the formyl shieldings for the series benzaldehyde, cinnamaldehyde, acrolein, and phenylpropynal are entirely consistent with our original interpretations.

Another example for which a ring-current contribution could be expected to be appreciable is furfural (XXXVII). The question of a possible ring current arising from the furan ring has received attention recently by several authors using both theoretical and experimental approaches (12, 13), and there is little doubt of the existence of this effect. Controversy has arisen, however, over its magnitude relative to that of the benzene ring. Some workers (12) have concluded that the ring-current effect of furan is significantly less than that of benzene whereas others (13) believe that they are comparable in magnitude. The results of the present study point to the conclusion that the ring-current effect of the furan nucleus is real but smaller than the benzene effect, since the formyl proton of furfural absorbs at 9.67 p.p.m.

Formyl proton shieldings have been shown to respond to the influence of polar substituents in conjugated systems (1), and the result for *p*-N,N-dimethylaminocinnamaldehyde provides another example of this trend. The change of 0.08 p.p.m. to higher field upon substitution of this substituent on the cinnamaldehyde skeleton, however, is significantly smaller than the 0.31 p.p.m. change found earlier (1) for the corresponding substitution in the benzaldehyde series.

In contrast to the saturated cases, the results for the 1-cycloalkene-1-carboxaldehydes show a pronounced change in chemical shift with ring size. The formyl proton for the

cyclopentenyl derivative absorbs at much lower field than that in the cyclohexenyl and cycloheptenyl systems. In fact, the shift for cyclohexene-1-carboxaldehyde (XXI) agrees well with the value for *trans*-2-methyl-2-butenal (tiglaldehyde) (XXIV), indicating that there is no special effect from the ring. The origin of this remarkable deshielding found for the compound with a five-membered ring is not evident, but some additional observations are pertinent to the problem. Dilution of the sample produces no change in the observed shift; therefore the possibility of self-association can be ruled out. It is interesting that the ultraviolet absorption of cyclopentene-1-carboxaldehyde (XXX) is unlike that of many other disubstituted α,β-unsaturated aldehydes (14), several of which absorb near 228 mμ while XXX absorbs at 237 mμ. The intensities of the absorption for these cases, however, are similar (ϵ_{max} 11 000 – 12 000), indicating no appreciable conformational differences. Another possible explanation for the low shielding in XXX, which could be considered, is the existence of a ring current for the nearly planar cyclopentenyl ring. It is conceivable that this might account for the observations, but examination of the 2-chloro derivatives of the cycloalkenylaldehydes (XXXIV–XXXVI) shows that the formyl protons absorb over a much narrower range, 10.03 ± 0.08 p.p.m., which appears to rule out a significant ring-current contribution for the cyclopentenyl ring. If all other factors were approximately constant, one would expect formyl absorption for 2-chloro-1-cyclopentene-1-carboxaldehyde (XXXIV) to be near 10.5 p.p.m. rather than the observed 9.95 p.p.m. position. The observed shift for XXX at 9.72 p.p.m., therefore, would seem to indicate that another, as yet undefined, influence is operative for this structure. This behavior, however, appears to be characteristic of the 1-formyl-1-cyclopentenyl system, since two other examples having this basic structure have been found. These are helminthosporal (15) and lycoctamone (16), which absorb at 9.90 and 9.75 p.p.m., respectively, in $CDCl_3$ solution.

In summary, it can be said that variations of the formyl proton shieldings of aliphatic aldehydes are, for the most part, qualitatively interpretable in terms of conjugative interactions involving the carbonyl group and anisotropic effects of neighboring groups. For structural studies, indications of the nature of the environment of specific formyl protons may be obtained from their resonance positions and multiplicities, but the narrow range of shifts encountered in this study shows that such data must be employed with caution.

EXPERIMENTAL

All spectra were determined with a Varian DP-60 spectrometer and the peak positions were measured by using audio modulation in the usual way. All chemical shift results are the average of at least 10 separate measurements.

Most of the compounds used in this study are commercially available and were purified by distillation or recrystallization before use. A sample of 2,2,4-trimethyl-3-pentenal was kindly provided by Dr. R. H. Hasek, Tennessee Eastman Co. The preparations employed for the other aldehydes are described below.

Cycloalkanecarboxaldehydes

Cycloheptanecarboxaldehyde (XIV)

Cycloheptyl chloride (10 g), prepared as described by Goering and McCarron (17), in dry ether (10 ml) was added to magnesium turnings (1.9 g) in dry ether (100 ml) under nitrogen and refluxed gently for 12 h. The Grignard reagent formed was treated with 10 g N,N-dimethylformamide and worked up in the usual way to give XIV (5.0 g, 53%), b.p. 75° at 25 mm, n_D^{20} 1.4698. Its semicarbazone had m.p. 154–155°. The reported physical constants are: XIV, b.p. 74° at 25 mm, n_D^{21} 1.4720 (18); semicarbazone, m.p. 155–156° (19).

Cyclopentanecarboxaldehyde (XII)

In a similar manner, cyclopentyl chloride gave XII (28%), b.p. 138°, n_D^{20} 1.4452; semicarbazone, m.p. 123–124°. The reported values are: XII, b.p. 41–42° at 18 mm, n_D^{25} 1.4470; semicarbazone, m.p. 123–124° (20).

1-Methyl-1-cycloalkanecarboxaldehydes

1-Methyl-1-cyclohexanecarboxaldehyde (XIX)

Cycloheptanol (11 g) treated with formic acid (1.77 g) and concentrated H_2SO_4 (60 ml) as described by Koch and Haaf (21) yielded 1-methyl-1-cyclohexanecarboxylic acid. The crude acid was reduced with $LiAlH_4$ (4.0 g) in ether (200 ml) to give the corresponding carbinol (3.8 g, 31%). Oxidation of the carbinol after the method of Barton *et al.* (22) gave XIX (1 g, 27%), b.p. 161–163°, n_D^{20} 1.4492; semicarbazone, m.p. 155–156°. The reported constants are: XIX, b.p. 120° at 54 mm, n_D^{21} 1.4490; semicarbazone, m.p. 154–155° (23).

1-Methyl-1-cyclopentanecarboxaldehyde (XVIII)

In a similar manner, cyclohexanol gave 1-methyl-1-cyclopentanecarboxaldehyde (29%), b.p. 140–141°, n_D^{20} 1.4557; semicarbazone, m.p. 165–166°. The reported values are: XVIII, b.p. 31–33° at 10 mm, n_D^{25} 1.4560; semicarbazone, m.p. 166–168° (20).

1-Cycloalkene-1-carboxaldehydes

A slight modification of the general method of Braude and Evans (24) was employed for these preparations.

1-Cycloheptene-1-carboxaldehyde (XXXII)

Freshly distilled 1-chloro-1-cycloheptene (15 g), prepared as described previously (25), was added slowly to a stirred suspension of finely cut lithium (2 g) in dry pentane (150 ml) under nitrogen and the mixture gently heated under reflux for 12 h. After the mixture was cooled to the ambient temperature, N,N-dimethylformamide (10 g) in dry ether (30 ml) was added dropwise. The mixture was stirred for 2 h and worked up as usual to give XXXII (3.0 g, 20%), b.p. 80° at 10 mm, n_D^{20} 1.4982, λ_{max} (hexane) 228 mμ (ϵ 11 500); semicarbazone, m.p. 205–206°, λ_{max} (EtOH) 268 mμ (ϵ 27 000). The reported constants are: XXXII, b.p. 82–83° at 9 mm, n_D^{20} 1.4983, λ_{max} 228 mμ (ϵ 12 000); semicarbazone, m.p. 310–311°, λ_{max} 268 mμ (ϵ 27 000) (24).

1-Cyclohexene-1-carboxaldehyde (XXXI)

In a similar manner, 1-chloro-1-cyclohexene (14 g), as prepared previously (26), gave XXXI (3.0 g, 23%), b.p. 70° at 13 mm, n_D^{20} 1.4924, λ_{max} (hexane) 227 mμ (ϵ 11 000); semicarbazone, m.p. 216–217°, λ_{max} (EtOH) 266 mμ (ϵ 25 500). The reported values are: XXXI, b.p. 72° at 15 mm, n_D^{20} 1.4920, λ_{max} 227 mμ (ϵ 11 000); semicarbazone, m.p. 217–218°, λ_{max} (EtOH) 266 mμ (ϵ 26 000) (24).

1-Cyclopentene-1-carboxaldehyde (XXX)

Similarly, XXX was prepared from 1-chloro-1-cylcopentane (27) in very low yield (~1%) and had b.p. 40° at 10 mm and λ_{max} 237 mμ (ϵ 12 000), which can be compared with the literature values (28): b.p. 45° at 16 mm and λ_{max} 237 mμ (ϵ 12 000).

2-Chloro-1-cycloalkene-1-carboxaldehydes

2-Chloro-1-cycloheptene-1-carboxaldehyde (XXXVI)

Cycloheptanone (5.6 g) was treated with phosphoryl chloride (15.7 g) and N,N-dimethylformamide (9.5 g) as described by Ziegenbein and Lang (29) to give XXXVI in 57% yield. The material had b.p. 92° at 11 mm and n_D^{20} 1.5223, while the literature values (29) are b.p. 108–111° at 19 mm and n_D^{20} 1.5215.

2-Chloro-1-cyclohexene-1-carboxaldehyde (XXXV)

In an analogous manner, cyclohexanone gave XXXV in 68% yield, having b.p. 87° at 11 mm and n_D^{20} 1.5201. The reported constants are b.p. 88–90° at 11 mm and n_D^{20} 1.5198 (29).

2-Chloro-1-cyclopentene-1-carboxaldehyde (XXXIV)

Cyclopentanone was employed in a similar manner to yield XXXIV in poor yield (5%). This material exhibited the following constants: b.p. 80–81° at 22 mm, n_D^{20} 1.5150, which may be compared with the reported values (29): b.p. 42–44° at 1 mm, n_D^{20} 1.5145.

6-Methyl-1,3-cyclohexadiene-1-carboxaldehyde (XXXIII)

Following the method described by Wichterle and Hudlicky (30) for the preparation of 1-acetoxy-1,3-butadiene, the higher boiling fractions yielded XXXIII, b.p. 62° at 5 mm; semicarbazone, m.p. 201° (decomp.); phenylhydrazone, m.p. 84–85°. The literature values (30) are: XXXIII, b.p. 62.5° at 5 mm; semicarbazone, m.p. 200°; phenylhydrazone, m.p. 83–84°.

ACKNOWLEDGMENTS

We thank the donors of the Petroleum Research Fund, administered by the American Chemical Society, for generous support of this project, the National Research Council for support in the early stages of this work, and the Dow Chemical Co. for a fellowship granted to one of us (R. E. K.). We acknowledge the generosity of Dr. R. H. Hasek, Tennessee Eastman Co., for providing a sample of 2,2,4-trimethyl-3-pentenal, and thank Dr. G. J. Karabatsos for providing us with a preprint of his work before publication.

REFERENCES

1. R. E. KLINCK and J. B. STOTHERS. Can. J. Chem. **40**, 1071 (1962).
2. J. B. STOTHERS and P. C. LAUTERBUR. Can. J. Chem. **42**, 1563 (1964).
3. K. S. DHAMI and J. B. STOTHERS. Can. J. Chem. **43**, 479 (1965); **43**, 498 (1965); **43**, 510 (1965).
4. D. H. MARR and J. B. STOTHERS. Can. J. Chem. **43**, 596 (1965).
5. J. B. STOTHERS. Quart. Rev. London, **19**, 144 (1965).
6. G. J. KARABATSOS and N. HSI. J. Am. Chem. Soc. **87**, 2874 (1965).
7. D. W. DAVIES. Mol. Phys. **6**, 489 (1963).
8. T. J. KING and J. P. YARDLEY. J. Chem. Soc. 4308 (1961). E. WENKERT, P. W. JEFFS, and J. R. MAHAJAN. J. Am. Chem. Chem. Soc. **86**, 2218 (1964). W. R. CHAN, C. WILLIS, M. P. CAVA, and R. P. STEIN. Chem. Ind. London, 495 (1963).
9. K. TORI, Y. HATA, R. MUNEYUKI, Y. TAKANO, T. TSUJI, and H. TANIDA. Can. J. Chem. **42**, 926 (1964).
10. P. B. VENUTO and A. R. DAY. J. Org. Chem. **29**, 2735 (1964).
11. J. A. POPLE. J. Chem. Phys. **24**, 1111 (1956).
12. H. A. P. DE JONGH and H. WYNBERG. Tetrahedron, **21**, 515 (1965). J. A. ELVIDGE. Chem. Commun. 160 (1965). D. W. DAVIES. Chem. Commun. 258 (1965).
13. R. J. ABRAHAM, R. C. SHEPPARD, W. A. THOMAS, and S. TURNER. Chem. Commun. 43 (1965).
14. L. K. EVANS and A. E. GILLAM. J. Chem. Soc. 565 (1943).
15. P. DE MAYO, E. Y. SPENCER, and R. W. WHITE. Can. J. Chem. **39**, 1608 (1961).
16. O. E. EDWARDS, L. MARION, J. D. CONNOLLY, M. BENN, and Z. STOJANAC. I.U.P.A.C. Symp. Chem. Nat. Prod., Kyoto, Japan, April 12–18, 1964. Abstr. p. 114.
17. H. L. GOERING and F. H. MCCARRON. J. Am. Chem. Soc. **78**, 2270 (1956).
18. M. FINKELSTEIN. Chem. Ber. **90**, 2097 (1957).
19. A. C. COPE, N. A. NELSON, and D. S. SMITH. J. Am. Chem. Soc. **76**, 1100 (1954).
20. S. M. NAQVI, J. P. HORWITZ, and R. FILLER. J. Am. Chem. Soc. **79**, 6283 (1957).
21. H. KOCH and W. HAAF. Ann. **618**, 251 (1958).
22. D. H. R. BARTON, B. J. GARNER, and R. H. WIGHTMAN. J. Chem. Soc. 1855 (1964).
23. W. PARKER and R. A. RAPHAEL. J. Chem. Soc. 1723 (1955).
24. E. A. BRAUDE and E. A. EVANS. J. Chem. Soc. 3334 (1955).
25. E. A. BRAUDE, W. F. FORBES, and E. A. EVANS. J. Chem. Soc. 2202 (1953).
26. E. A. BRAUDE and J. A. COLES. J. Chem. Soc. 2014 (1950).
27. E. A. BRAUDE and W. F. FORBES. J. Chem. Soc. 1755 (1951).
28. I. HEILBRON, E. R. H. JONES, J. B. TOOGOOD, and B. C. L. WEEDON. J. Chem. Soc. 1827 (1949).
29. W. ZIEGENBEIN and W. LANG. Chem. Ber. **93**, 2743 (1960).
30. O. WICHTERLE and M. HUDLICKY. Collection Czech. Chem. Commun. **12**, 572 (1947).

Can. J. Chem. Downloaded from www.nrcresearchpress.com by 210.87.254.5 on 09/05/12
For personal use only.

POLYOXYPHENOLS OF WESTERN RED CEDAR (THUJA PLICATA DONN)

III. STRUCTURE OF PLICATIC ACID

J. A. F. GARDNER,[1] E. P. SWAN,[2] S. A. SUTHERLAND,[3] AND HAROLD MACLEAN[2]

Department of Forestry of Canada, Forest Products Laboratory, Vancouver, British Columbia

Received August 24, 1965

ABSTRACT

Periodate oxidation studies, nuclear magnetic resonance spectra of derivatives, and X-ray crystallographic data have shown that plicatic acid, the major component of the heartwood extractive of western red cedar (*Thuja plicata* Donn), is 2,3,6-trihydroxy-7-methoxy-2-hydroxymethyl-4-(3′,4′-dihydroxy-5′-methoxyphenyl)-tetralin-3-carboxylic acid. The asymmetric configuration by X-ray data is 2R,3S,4R or its enantiomer, by Cahn–Ingold nomenclature.

Analytical and degradation studies described in previous papers (1, 2) provided a partial structure for plicatic acid, the reactive strong acid polyoxyphenol present in the heartwood of western red cedar. Plicatic acid, now shown to be I, forms a γ-lactone, termed plicatin, which also occurs in the heartwood, although in smaller quantities. To assist in the location of the alcoholic hydroxyls, the oxidation with sodium periodate of various crystalline methyl ether derivatives of plicatic acid was examined. The results are summarized in Table I.

The usual arsenite (3) technique for determining the periodate consumption, which involves treatment of aliquots with sodium bicarbonate solution, could not be used. The raising of the pH by the bicarbonate induced rapid over-oxidation in the aliquot solution, with the formation of yellow and then blue dyes, which are presently under investigation. It was therefore necessary to use the Malaprade (3) technique.

TABLE I

Periodate oxidation (pH 4) of plicatic acid derivatives

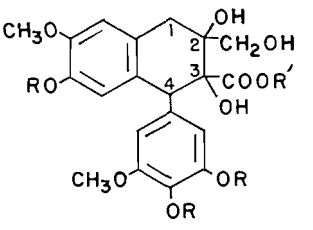
Derivative	Temperature (°C)	Time	Periodate consumed (moles)	Formaldehyde formed (moles)
Trimethyl ether, II	0	1 h	3.05	0.97
	0	6 h	3.30	0.97
Trimethyl ether methyl ester, III	20	1 h	2.30	0.98
	20	1½ h	2.52	—
	0	10 min	1.17	0.97
	0	1½ h	2.10	—
	0	4 h	2.40	0.97
Tetrol by $LiAlH_4$ reduction of III	20	15 min	2.90	—
	20	40 min	3.10	1.97
	20	1 h	3.15	—
	20	3½ h	3.30	1.98

[1]*Present address: Dean of Forestry, University of British Columbia, Vancouver 8, British Columbia.*

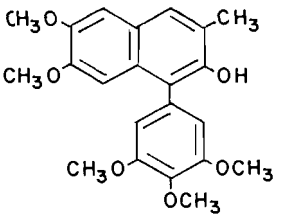
[2]*Research Scientist, Vancouver Forest Products Laboratory, Department of Forestry of Canada, 6620 N.W. Marine Drive, Vancouver 8, British Columbia.*

[3]*Assistant Professor, Department of Chemistry, University of British Columbia, Vancouver 8, British Columbia.*

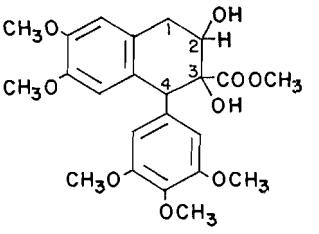
The trimethyl ether II consumed 3 moles of sodium periodate in 1 h and formed 1 mole of formaldehyde. For the methyl ester III, however, only 2 moles of periodate were consumed rapidly and additional oxidation was slow. This behavior was consistent with the acid being an α-hydroxy acid (3), as indicated by its strong acidity and color reactions (1, 2). Following the oxidation carefully at 0 °C showed that the 1 mole of formaldehyde formed was produced during consumption of the first mole of periodate. These results and lactone formation were consistent with structure I for plicatic acid and structure III for its tri-O-methyl ether methyl ester.



I R = R′ = H
II R = CH_3, R′ = H
III R = R′ = CH_3



IV



V

The trimethyl ether γ-lactone and the monoacetate of the ester were inert to the periodate in the cold. In carbohydrates, the presence of an additional ring as in the 1,6-anhydrofuranoses confers stability (4); esterification of the primary alcohol removed the first point of attack and lack of reaction with the tertiary hydroxyls on carbons 2 and 3 indicated a sterically hindered *trans* configuration.

In further confirmation of structure III, a tetrol was formed by lithium aluminium hydride reduction of its ester carbonyl function. As expected, this tetrol rapidly consumed 3 moles of periodate while 2 moles of formaldehyde were formed. Furthermore, repeated attempts to form a podophyllotoxone analogue by manganese dioxide oxidation of III failed, indicating the absence of a hydroxyl group in the 1 position (5).

Presence of the tetrahydronaphthalene ring was supported by the ready formation of a crystalline naphthalene derivative by heating the trimethyl ether lactone (1) to 340 °C. The product had an ultraviolet absorption spectrum characteristic of a substituted naphthalene and gave a positive phenol test with anhydrous ferric chloride in chloroform. On the basis of analysis, infrared and ultraviolet spectra, nuclear magnetic resonance spectra of the product and its acetate, and the successful, although difficult, coupling reaction with diazotized sulfanilic acid (color test) (6), this compound appeared to be the β-naphthol IV. This structure was indicated further by its inability to be methylated with either diazomethane or dimethyl sulfate. Also, nitric acid oxidation in a Carius tube failed to yield any benzoic acid derivatives.

To fix the position of the hydroxymethyl and carboxylic acid group on carbon atoms 2 and 3 of the tetrahydronaphthalene ring, the oxidation of methyl tri-O-methyl plicatate (III) with periodate was limited to 1 mole to produce the ketone at carbon 2. Catalytic hydrogenation then gave the diol V, in which a new proton on the saturated ring replaced the hydroxymethyl group. Nuclear magnetic resonance (n.m.r.) spectra of III and V show the spin–spin coupling of this new proton with the two protons of carbon 1, thereby positioning the original hydroxymethyl group at carbon 2 and giving plicatic acid the structure I.

Can. J. Chem. Downloaded from www.nrcresearchpress.com by 210.87.254.5 on 09/05/12
For personal use only.

The n.m.r. spectrum of III together with an integral curve summed for all proton species believed present was obtained, and agreed well with the proposed structure. Figure 1 (upper curve) shows the n.m.r. spectrum of III in deuteriochloroform containing deuterium oxide and trifluoroacetic acid to exchange the protons of the hydroxyl group.

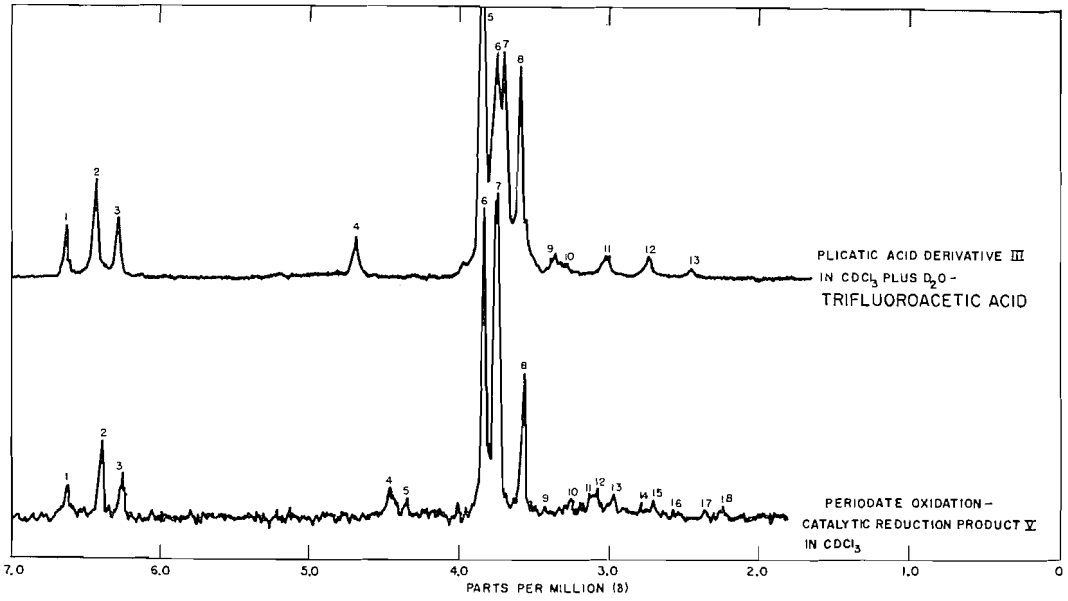


FIG. 1. Nuclear magnetic resonance spectrum at 60 Mc/s of methyl tri-O-methyl plicatate (III) and its periodate oxidation – catalytic reduction product (V).

Assignation of proton signals at the various numbered positions is given in Table II. Relatively few lignan n.m.r. spectra have been published but, of those available, the above assignations agree well with those of lyoniresinol and its derivatives (7).

Optimum reaction conditions for the periodate oxidation of III were studied by means of thin-layer chromatography. Preparative thick-layer chromatography was used to obtain a small yield of desired product with the correct infrared spectrum and analyses. This oxidation product, which was susceptible to further air oxidation, was readily reduced to the desired product (V), which was a mixture of two isomers. The major product was purified by preparative thick-layer chromatography to yield the desired product with an infrared spectrum very similar to that of III. The n.m.r. spectrum was taken as before but the solution was rather dilute, necessitating high amplification with consequent high noise level so that the integral curve was not obtained. After the n.m.r. spectrum was taken, the sample was reexamined by thin-layer chromatography to demonstrate that no changes had occurred.

The n.m.r. spectrum of the oxidation–reduction product V was similar to that from III and is shown in Fig. 1 (lower curve). The positions of the absorptions from the aromatic and methyl protons were unchanged. The signal from the C4 proton was unchanged but shifted by 0.22 δ, and was attributed to the removal of the hydroxymethyl group (by the periodate oxidation) which had given long-range shielding of this proton in III. The signal from the C1 proton was changed from the regular AB pattern to a poorly resolved complex pattern of the AB portion of an ABX spectrum. Similar poorly resolved spectra are found in the literature (9). The interpretation of the spectrum of V was facilitated by obtaining

Can. J. Chem. Downloaded from www.nrcresearchpress.com by 210.87.254.5 on 09/05/12
For personal use only.

TABLE II

Proton assignments of n.m.r. spectra (Fig. 1)

Compound	Peak No.	Position (δ)	Assignment
III	1	6.63	C8
	2	6.43	C2′ and C6′
	3	6.28	C5
	4	4.69	C4
	5, 6	3.85, 3.75	Methoxyl
	7	3.70	Hydroxymethylene
	8	3.60	Methyl ester
	9	3.37	Hydroxyl†
	10–13 incl.	2.63, 3.12*	C1 (J_{AB} −17 c.p.s.)
V	1	6.63	C8
	2	6.40	C2′ and C6′
	3	6.25	C5
	4	4.47	C4
	5	4.37	C2 or hydroxyl‡
	6, 7	3.85, 3.75	Methoxyl
	8	3.59	Methyl ester
	11	3.13	Hydroxyl
	Remainder	3.23–2.20	C1
Acetate of V	Not shown in Fig. 1	5.80, 5.65, 5.57	C3
		4.70	C4
		3.64–2.63	C1

*Peak positions and height calculated according to Jackman (8). Height agreed with theory.
†Poorly exchanged, probably the tertiary OH group α to the $COCCH_3$ (on C3).
‡See text for explanation.

and comparing it with the spectrum of the acetate of V, which showed that it was the monoacetate derivative. Acetylation of a secondary hydroxyl group shifts the attached proton downfield by about 1.0 δ (10). New signals appeared at 5.57, 5.65, and 5.80 δ for the C2 proton but it was not certain from what position they had shifted. By allowing for the difference in chemical shifts between V and its acetate, it was certain that the signals from C1 protons (peaks 9–18 except peak 11) were the same in both cases. Proton-exchange experiments, carried out by the addition of two drops of deuterium oxide to the n.m.r. tube, showed that the tertiary hydroxyl group α to the carbonyl was giving peak 11 and thus did not acetylate. The position of the remaining hydroxyl group was uncertain. Since peak 5 disappeared upon acetylation, it was either this hydroxyl group or the C2 proton; upon deuterium exchange it was uncertain whether the peak disappeared or not because of a low ratio of signal to noise.

The *p*-bromoanilide of tri-O-methylplicatic acid crystallizes in the orthorhombic system, space group $P2_12_12_1$, with unit cell dimensions $a = 21.08$, $b = 5.79$, $c = 23.08$ Å. There are four molecules of $C_{29}H_{32}O_9NBr$ in the cell. Three-dimensional X-ray data were collected on a Nonius equi-inclination Weissenberg camera, and intensities of the 1 778 observed reflections were estimated visually. The coordinates of the bromine atom were determined from a Patterson synthesis, and the calculated phase angles applied to a first three-dimensional Fourier synthesis. Bromine is not heavy enough to give optimum phase agreement, although it was possible to identify the basic ring skeleton. Addition of increasing numbers of light atoms to subsequent structure-factor calculations improved the phases until all atoms were clearly visible (Fig. 2). Refinement of the structure is continuing. Since X-ray data did not differentiate between this compound and its enantiomer, the asymmetric configuration is either 2R,3S,4R or 2S,3R,4S by Cahn–Ingold nomenclature (12), i.e. all carbons attached to the tetralin ring are *trans*.

Can. J. Chem. Downloaded from www.nrcresearchpress.com by 210.87.254.5 on 09/05/12
For personal use only.

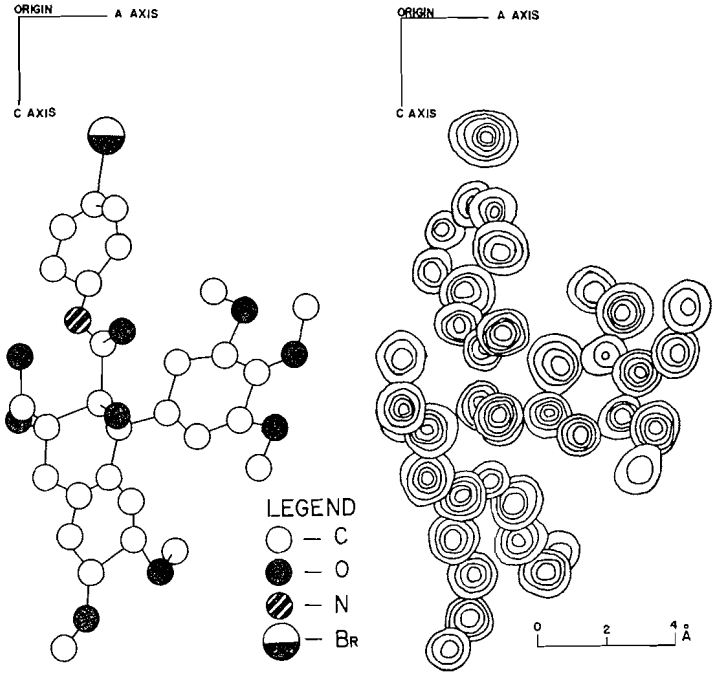


FIG. 2. X-ray crystallographic projection of *p*-bromoanilide of tri-O-methyl plicatic acid.

Plicatic acid is therefore 2,3,6-trihydroxy-7-methoxy-2-hydroxymethyl-4-(3′,4′-dihydroxy-5′-methoxyphenyl)-tetralin-3-carboxylic acid. The nomenclature of Freudenberg and Weinges (11) does not allow for the naming of a free acid lignan. The proposed name by this system is 3,4,8,4′,8′,9′-hexahydroxy-5,3′-dimethoxy-9-cyclolignanoic acid. This lignan is novel in that it is the first to be known to have a monomethylated pyrogallol ring. It is also the first lignan to have a free carboxylic acid group in the side chain.

EXPERIMENTAL

All melting points are uncorrected. The n.m.r. spectra were run in deuteriochloroform on a Varian A-60 machine of the Chemistry Department, University of British Columbia, with tetramethylsilane as an internal standard. X-ray crystallographic calculations were performed on an IBM 7040 computer with programmes written by Dr. J. Trotter of the University of British Columbia. Analyses were performed by Clark Microanalytical Laboratories, Urbana, Illinois. Thin-layer and preparative chromatography was carried out on silica gel G with dichloromethane – acetone – acetic acid (80:20:1 v/v/v) as the developing solvent; the detecting reagent used was a concentrated nitric acid – sulfuric acid (1:1 v/v) mixture. Infrared spectra were taken as KBr disks.

Periodate Oxidations; Methylated Plicatic Acid Derivatives

The following example illustrates the reaction techniques used to obtain the data shown in Table I. Tri-O-methyl plicatic acid (II; 0.121 g) was dissolved in ethanol (1.5 ml) and water (35 ml), cooled to 0 °C, and added to 0.1 *M* aqueous sodium metaperiodate (10 ml), also at 0 °C. The total volume was adjusted to 50 ml with cold water and the solution stored at 0 °C. Periodate consumption was determined on aliquots (5 ml) at ½, 1, and 6 h intervals by the Malaprade (3) technique. Formaldehyde yields were determined colorimetrically by the chromotropic acid method of Lambert and Neish (13).

Pyrolysis Product V of Tri-O-methyl Plicatic Acid

Tri-O-methyl plicatic acid (II; 1.03 g) was intimately mixed with small glass helices in a glass tube and heated in a current of nitrogen gas in a muffle furnace at 290 °C, the temperature being increased to 340 °C over a period of 1 h. The yellowish solid that condensed on the tube walls outside the furnace was crystallized from benzene to yield pale yellow crystals (0.466 g), m.p. 202–204 °C, which on repeated recrystallization melted at 210–211 °C. Ultraviolet spectrum in ethanol ($m\mu$ (log ϵ)): 236 (4.82), 282 (3.82), 293 (3.79) shoulder, 321 (3.56), and 334 (3.68); in 0.002 *M* sodium ethylate: 238 (4.61), 253 (4.54) shoulder.

Anal. Calcd. for $C_{22}H_{24}O_6$: C, 68.7; H, 6.29; OCH_3, 40.3. Found: C, 68.6; H, 5.93; OCH_3, 39.6.

Can. J. Chem. Downloaded from www.nrcresearchpress.com by 210.87.254.5 on 09/05/12
For personal use only.

Kuhn–Roth oxidation showed 0.97 mole C-methyl (14). This product, after acetylation (15) and recrystallization from methanol–water, melted at 152–153 °C. Infrared spectral comparison showed complete acetylation by the disappearance of the phenolic hydroxyl band. Nuclear magnetic resonance spectra of both the pyrolysis product and its acetate indicated both the number and species of protons expected.

Preparation of Methyl Tri-O-methyl Plicatate; Oxidation–Reduction Product V

Methyl tri-O-methyl plicatate (III; 100 mg) was dissolved in ethanol (25 ml) and cooled to 0 °C. Sodium metaperiodate (672 mg) in water (75 ml) containing three drops of 0.1 *N* hydrochloric acid was cooled and added. The mixture was kept for 1 h in the dark at the same temperature and then extracted with chloroform (3 × 25 ml); the combined extracts were dried over anhydrous sodium sulfate, filtered, and evaporated under reduced pressure. The keto-ester product was purified by preparative thin-layer chromatography (R_f 0.8) and recrystallized from ether to give slightly green crystals, m.p. 69–70 °C, yield 47 mg. It had the expected infrared spectrum, showing in comparison with that of III a very much decreased hydroxyl absorption at 3 450 cm^{-1} and the appearance of another carbonyl absorption at 1 750 cm^{-1} for the six membered ring ketone.

Anal. Calcd. for $C_{23}H_{26}O_9$: C, 61.90; H, 5.87; OCH_3, 41.70. Found: C, 60.85; H, 5.97; OCH_3, 39.01.

The keto-ester product (40 mg) was dissolved in ethanol (10 ml), and hydrogenated at room temperature and 3 atmospheres pressure in a Parr apparatus for 1 h with platinum catalyst. The catalyst was recovered on the filter, the ethanol evaporated under reduced pressure, and the product purified by thick-layer chromatography. The main product (21 mg) had R_f 0.25 (slightly more than that of III) and after recrystallization from ethanol–ether melted sharply at 165 °C. The infrared spectrum was as expected, with only carbonyl absorption from the ester group.

Anal. Calcd. for $C_{23}H_{28}O_9$: C, 61.62; H, 6.29; OCH_3, 41.51. Found: C, 60.87; H, 6.23; OCH_3, 39.58.

After the n.m.r. spectrum of this product was obtained the recovered material was crystallized from benzene. The crystals were treated with pyridine (1 ml) and acetic anhydride (1 ml) at 40 °C for 1 h. The reagents were evaporated under high vacuum and the n.m.r. spectrum of the product was obtained.

p-Bromoanilide of Tri-O-methyl Plicatic Acid

Tri-O-methyl plicatic acid (II; 1 g) was mixed with *p*-bromoaniline (2 g), refluxed for 2 h at 140 °C, cooled overnight, dissolved in $CHCl_3$ (50 ml), and filtered. The solution was extracted with 10% HCl (3 × 15 ml), washed once with water (10 ml), re-extracted with 10% NaOH (3 × 15 ml), dried, and evaporated. The product, recrystallized from ethanol, melted at 247–248 °C (yield 57%). Infrared spectrum: carbonyl shifted to 1 672 cm^{-1} with additional amide absorption (16) at 3 325, 1 535, and 1 308 cm^{-1} when compared with the spectrum of methyl tri-O-methyl plicatate (III).

Anal. Calcd. for $C_{29}H_{32}O_9BrN$: C, 56.3; H, 5.21; N, 2.26; Br, 12.93. Found: C, 55.74, 56.01; H, 4.75, 4.91; N, 2.20, 2.17; Br, 12.76, 13.00.

Reduction of Methyl Tri-O-methyl Plicatate

Methyl tri-O-methyl plicatate (III; 3.0 g) was reacted with lithium aluminium hydride (1.86 g) in accordance with the procedure of Schrecker and Hartwell (17) and yielded, on three recrystallizations from ethyl acetate – hexane (1:2), a tetrol derivative, 2,3-dihydroxy-6,7-dimethoxy-2,3-dihydroxymethyl-4-(3′,4′,5′-trimethoxyphenyl)-tetralin (1.58 g). After this product was dried in a vacuum at 100 °C for 2 h it showed a partial melting, without gasification, at 150–155 °C, followed by recrystallization on the melting point stage and remelting at 164–164.5 °C. Recrystallization from methanol–water (1:10) and similar drying yielded crystals melting at 125–126 °C. Infrared spectra of both crystal forms were identical, showing enhanced hydroxyl and no acid carbonyl band when compared with the spectrum of the starting material.

Anal. Calcd. for $C_{23}H_{30}O_9$: C, 61.3; H, 6.72; OCH_3, 34.4. Found: C, 60.83; H, 6.87; OCH_3, 33.9.

ACKNOWLEDGMENTS

We thank Dr. L. D. Hall of the Chemistry Department, University of British Columbia, for many helpful discussions on the interpretation of the n.m.r. spectra; Dr. J. B. Armstrong, Department of Biochemistry, University of Wisconsin, for work on the crystallographic data; and the National Research Council of Canada for financial support to S. A. S. for the crystallographic study.

REFERENCES

1. J. A. F. Gardner, G. M. Barton, and H. MacLean. Can. J. Chem. **37**, 1703 (1959).
2. J. A. F. Gardner, B. F. MacDonald, and H. MacLean. Can. J. Chem. **38**, 2387 (1960).
3. J. R. Dyer. Methods Biochem. Analy. **3**, 111 (1956).
4. R. J. Dimler, H. A. Davis, and G. E. Hilbert. J. Am. Chem. Soc. **68**, 1377 (1946).
5. W. J. Gensler, F. Johnson, and A. D. B. Sloan. J. Am. Chem. Soc. **82**, 6074 (1960).
6. L. F. Fieser and M. Fieser. *In* Advanced organic chemistry. Reinhold Publishing Corp., New York. p. 852.
7. Y. Kato. Chem. Pharm. Bull. Tokyo, **11**, 823 (1963).

Can. J. Chem. Downloaded from www.nrcresearchpress.com by 210.87.254.5 on 09/05/12
For personal use only.

8. L. M. JACKMAN. *In* Applications of nuclear magnetic resonance spectroscopy in organic chemistry. Pergamon Press, New York. 1959. p. 89.
9. Varian high resolution nuclear magnetic resonance spectra catalog. Vol. 2. Varian Associates, Palo Alto, California. 1963. Spectra Nos. 503, 517, 518.
10. L. M. JACKMAN. *In* Applications of nuclear magnetic resonance spectroscopy in organic chemistry. Pergamon Press, New York. 1959. p. 55.
11. K. FREUDENBERG and K. WEINGES. Tetrahedron, **15**, 115 (1961).
12. R. S. CAHN, C. K. INGOLD, and V. PRELOG. Experientia, **12**, 81 (1956).
13. M. LAMBERT and A. C. NEISH. Can. J. Res., B, **28**, 83 (1950).
14. W. F. BARTHEL and F. B. LAFORGE. Ind. Eng. Chem. Anal. Edition, **16**, 434 (1944).
15. J. S. FRITZ and G. H. SCHENK. Anal. Chem. **31**, 1808 (1959).
16. L. J. BELLAMY. *In* The infra-red spectra of complex molecules. 2nd ed. John Wiley & Sons, Inc., New York. 1958. p. 205.
17. A. W. SCHRECKER and J. L. HARTWELL. J. Am. Chem. Soc. **77**, 435 (1955).

Can. J. Chem. Downloaded from www.nrcresearchpress.com by 210.87.254.5 on 09/05/12
For personal use only.

Can. J. Chem. Downloaded from www.nrcresearchpress.com by 210.87.254.5 on 09/05/12
For personal use only.

1,2,3,4-TETRAPHENYLDIAZETIDINE

A REEXAMINATION[1]

J. G. SMITH
Exploratory Research Laboratory, Dow Chemical of Canada, Limited, Sarnia, Ontario

Received August 13, 1965

ABSTRACT

The reported synthesis of 1,2,3,4-tetraphenyldiazetidine by treating the sodium adduct of N-benzylidene aniline with benzaldehyde or benzoate ester is reexamined. It is shown that the original report is in error. The products from the reaction are the two diastereomeric N-benzoyl-N,N′,1,2-tetraphenylethylenediamines and *dd,ll*-N,N′,1,2-tetraphenylethylenediamine. When diethyl ether was used as a reaction medium, another product, N-benzoyl-N,N′-diphenylstilbene-α,α'-diamine, was formed. An explanation is offered for the formation of these compounds and for the differences in reaction products caused by the two reaction media employed, diethyl ether and tetrahydrofuran.

In 1928 it was reported (1) that the treatment of the sodium addition product (I) of N-benzylidine aniline with either ethyl benzoate or benzaldehyde produced 1,2,3,4-tetraphenyldiazetidine (II), as shown in eq. [1]. Because of the rarity of compounds such as (II)

[1] $C_6H_5—CH=N—C_6H_5 \xrightarrow[(C_2H_5)_2O]{Na}$ $C_6H_5—CH(Na)—CH(Na)—C_6H_5$ (I) $\xrightarrow[C_6H_5—CO_2—C_2H_5]{C_6H_5CHO\ or}$ $C_6H_5—CH—CH—C_6H_5$ (II)

and the possibility that such a reaction may be a synthetic route to them, the reaction was reexamined.

RESULTS

Tetrahydrofuran was initially used as the preparative solvent and reaction medium because of the greater solubility of the organometallic compound in it. The addition of sodium to N-benzylidene aniline proceeded rapidly and smoothly to give the expected 2:2 adduct (I) (2, 3).

The reaction of this adduct with either benzaldehyde or esters of benzoic acid proceeded in a manner quite unlike that previously described. While the same compound was isolated from the two reactions, the melting point was some 30° higher than that reported.

On the basis of its analysis and its infrared spectrum, which showed a NH band at 3 380 cm^{-1} and an amide carbonyl band at 1 625 cm^{-1}, the compound was identified as N-benzoyl-N,N′,1,2-tetraphenylethylenediamine. Synthesis of the monobenzamides from the known diastereomeric N,N′,1,2-tetraphenylethylenediamines established its identity as the monobenzamide of the *dd,ll* diamine.

In addition to this, a second amide was isolated in low yield, which, on the basis of its analysis, infrared spectrum (NH band at 3 360 cm^{-1}, amide carbonyl at 1 635 cm^{-1}), and

[1]*Contribution No. 136 from the Exploratory Research Laboratory.*

Can. J. Chem. Downloaded from www.nrcresearchpress.com by 210.87.254.5 on 09/05/12
For personal use only.

mixed melting point, was shown to be the N-benzoyl derivative of meso-N,N′,1,2-tetraphenylethylenediamine. The *dd,ll*-N,N′,1,2-tetraphenylethylenediamine was also detected in the products arising from the reaction with benzaldehyde.

Thinking that the course of the reaction may have been influenced by the choice of solvent, we repeated the experiments with diethyl ether, the solvent originally employed (1, 2). With methyl benzoate, no change in the course of the reaction was noticed. The products isolated were *dd,ll*-N,N′,1,2-tetraphenylethylenediamine and again the N-benzoyl derivatives of the *dd,ll* and meso diamines. There was, however, a change in the relative amounts of the two diastereomeric benzamides. With diethyl ether as solvent approximately equal quantities were formed, whereas with tetrahydrofuran the benzamide was largely derived from *dd,ll*-N,N′,1,2-tetraphenylethylenediamine.

Benzaldehyde generated a new compound which appeared as a yellow precipitate when the reaction mixture was hydrolyzed with water. This material decomposed at its melting point, was oxidized in boiling solvents, and lost its yellow color on treatment with acids. Its infrared spectrum showed a NH band at 3 340 cm^{-1} and an amide carbonyl band at 1 645 cm^{-1}. The chemical properties matched closely those described (4) for N-benzoyl-N,N′-diphenylstilbene-α,α'-diamine. Its identity was established by synthesis, by comparison of its infrared spectrum, and by the mixed melting point of its picrate.

Table I summarizes the reaction products and yields obtained.

TABLE I

Summary of reaction products and yields

			Products and yields			
Reagent	Solvent	Mole ratio*	*dd,ll*-TPED,† % yield	N-Benzoyl-TPED,† % yield	*dd,ll*/meso	Others, % yield
Methyl benzoate	Tetrahydrofuran	1	3	77	10	5‡
Methyl benzoate	Diethyl ether	1	30	62	0.35	
Benzaldehyde	Tetrahydrofuran	0.5	72	4	—	
Benzaldehyde	Tetrahydrofuran	1	28	63	20	
Benzaldehyde	Tetrahydrofuran	2	—	90	—	
Benzaldehyde	Diethyl ether	1	33	38	2.1	21§
Benzaldehyde	Diethyl ether	2	32	52	0.7	

*Moles of reagent/moles N-benzylidene aniline.
†N,N′,1,2-Tetraphenylethylenediamine.
‡N-Benzylidene aniline.
§N-Benzoyl-N,N′-diphenylstilbene-α,α'-diamine.

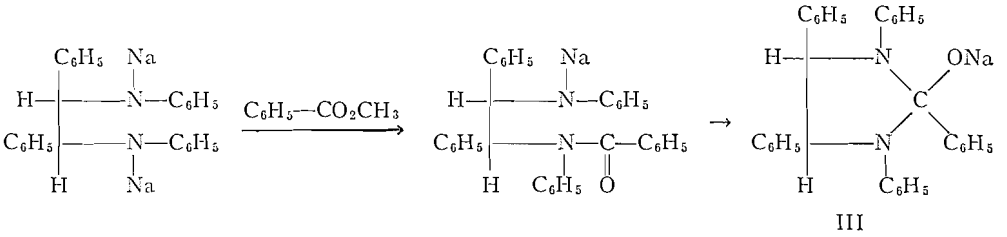
DISCUSSION

It must be concluded that 1,2,3,4-tetraphenyldiazetidine is not formed in any significant quantity in these reactions. The question remains concerning the identity of the compound isolated by Schlenk and Bergmann (1). Two pieces of evidence were offered for its identity, its analysis and its melting point, 153–154°, which differed markedly from that (136–139°) of the N,N′,1,2-tetraphenylethylenediamine obtained on hydrolysis of the organosodium compound.

At the time of the original work the fact was not appreciated that the hydrolysis product is actually a mixture of the meso and *dd,ll* diastereomers, whose individual melting points are 167° and 153° respectively (5). It seems likely that the reported compound was *dd,ll*-N,N′,1,2-tetraphenylethylenediamine, whose melting point and analysis agree with those reported. Its formation was probably due to premature hydrolysis of the reaction mixture.

Treatment of the sodium compound in ether with benzaldehyde results in the immediate formation of a yellow precipitate. Hydrolysis of the reaction mixture at this point produced only the diastereomeric mixture of the tetraphenylethylenediamines. It is only after the reaction mixture has been allowed to stand at room temperature for several hours before hydrolysis that appreciable quantities of benzoylated products are detected.

The formation of N-benzoylated derivatives with benzoate esters is to be expected. The interesting feature is the formation of only the monobenzamide. Possibly, after the formation of the monobenzamide, further reaction occurs intramolecularly to form (III),

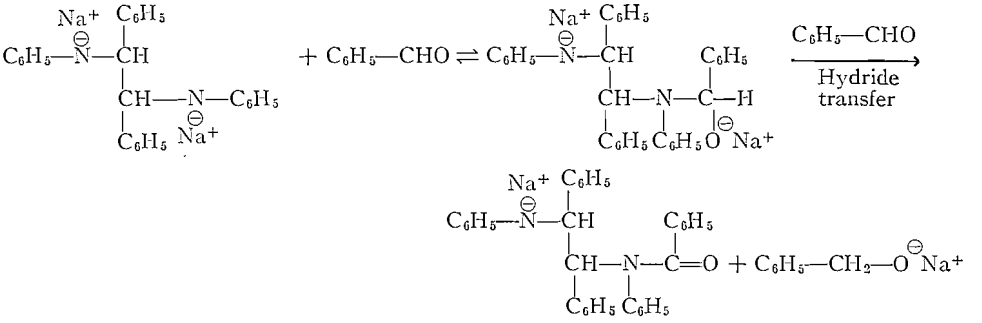
[2] 

III

as shown in eq. [2]. Hydrolysis of the reaction product results in the ring opening of (III), thereby forming the N-benzoyl derivative.

Differences in the ratio of the monobenzamides of meso- and *dd,ll*-N,N′,1,2-tetraphenylethylenediamine formed in tetrahydrofuran versus those formed in diethyl ether are due to the difference in the ratio of the diastereomeric N,N′-disodio-N,N′,1,2-tetraphenylethylenediamines formed in the two solvents. It has been established (*5b*) that the ratio of the diastereomeric diamines formed by reductive dimerization of N-benzylidene aniline in wet ether is approximately 1:1. By using this published melting point – composition phase diagram, the diamine mixture obtained on hydrolysis of the sodium compound formed in tetrahydrofuran contained approximately 10% of the meso diamine.

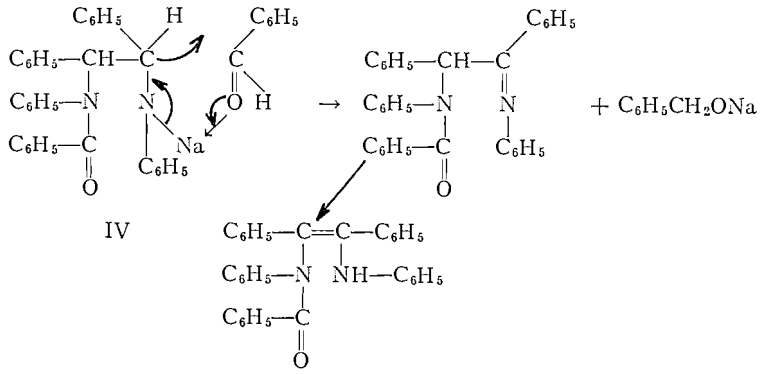
In the case of the reaction with benzaldehyde, the substituted benzamide can arise from two sources. The amine anion can take part in a Cannizarro reaction, as shown in eq. [3],

[3] 

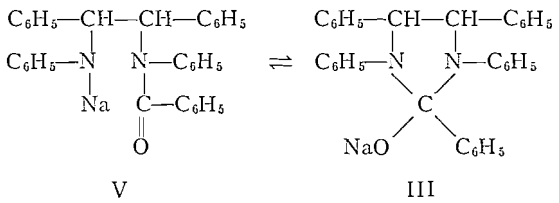
to produce the product and an alkoxide ion. This anion in turn can react with benzaldehyde in a Cannizarro reaction to produce benzyl benzoate, which acts as a second source of the benzamide.

Since the stilbene derivative arises in diethyl ether, it is a reasonable assumption that the meso-disodio compound, which is formed in large amounts in diethyl ether, is its source. Presumably it is formed by a hydride transfer within a cyclic complex (IV), as shown in eq. [4]. A similar hydride transfer has been noted in the reactions of lithium diethylamide with benzophenone (6).

Can. J. Chem. Downloaded from www.nrcresearchpress.com by 210.87.254.5 on 09/05/12
For personal use only.

[4] 

The ability of the meso-disodio derivative to engage in this reaction is probably connected with the position of the equilibrium between the "open" mono-N-benzoyl compound (V) and the cyclic isomer (III), as shown in eq. [5]. It will be noted that the *dd,ll*

[5] 

isomer of (V) produces the *trans* arrangement of the two phenyl groups in (III) whereas the diastereomeric *dl,ld* isomer of (V) produces the *cis* arrangement. It would be anticipated that, in the latter case, a higher concentration of the open structure (V) would exist in the equilibrium because of the greater steric interaction of the phenyl groups in the corresponding stereoisomer of (III).

An increase in the benzaldehyde concentration increases the rate of the Cannizarro reaction much faster than it increases the rate of the cyclic hydride transfer. The benzyl benzoate so formed reacts with the sodium compound, producing the monobenzamide before the internal hydride transfer can occur within the complex to produce the stilbene derivative.

EXPERIMENTAL

Melting points are uncorrected and were determined in an open capillary in a Gallenkamp melting point apparatus. Infrared spectra were taken on a Beckmann IR9 or a Perkin–Elmer 421G.

All operations involving the organometallic compound were performed under a positive head of purified nitrogen (7). N,N′,1,2-Tetraphenylethylenediamine (TPED) was prepared by an aluminium amalgam reduction of N-benzylidene aniline in wet ether (5*b*). The diastereomers were separated by means of their complexes with N,N-dimethylformamide (5*a*); *dd,ll*-TPED had m.p. 150–153°, meso-TPED m.p. 167–168°.

The tetrahydrofuran and diethyl ether used in the experiments were purified by refluxing them under nitrogen over sodium metal until the addition of benzophenone produced the permanent blue color of the ketyl. The solvent was then distilled onto lithium aluminium hydride and stored in this fashion. When needed, the solvent was refluxed over the lithium aluminium hydride for 2 to 4 h and then distilled into the reaction vessel, a modified Schlenk tube (8).

Preparation of the Organosodium Compound

The Schlenk tube containing the freshly distilled solvent was transferred to a dry box where the N-benzylidene aniline and sodium metal (freshly cut) were weighed and added. The tube was removed from the dry box and shaken in a horizontal shaker. The reaction began at once, accompanied by the formation of an orange or orange-red color. The completeness of reaction was determined by permitting weighed amounts

Can. J. Chem. Downloaded from www.nrcresearchpress.com by 210.87.254.5 on 09/05/12
For personal use only.

of the solution to flow into 50% aqueous ethanol. The solution was then titrated with standardized hydrochloric acid and phenolphthalein indicator. Under these conditions the TPED is not titrated. Table II demonstrates that the reaction is quite rapid.

Table III summarizes the properties of the mixed diastereomeric diamines isolated from the hydrolysis.

TABLE II

Reaction of N-benzylidene aniline with sodium

Duration of agitation, min	Equivalents NaOH per mole $C_6H_5CH{=}NC_6H_5$	
	Tetrahydrofuran*	Diethyl ether†
15	0.425	—
45	0.93	0.99
100	1.02	0.98
180	1.03	0.99
1 225	1.02	—

*N-Benzylidene aniline (0.01 mole) and tetrahydrofuran (35 g).
†N-Benzylidene aniline (0.01 mole) and diethyl ether (50 g).

TABLE III

N,N′,1,2-Tetraphenylethylenediamines formed on hydrolysis

Solvent	Melting point	% meso*	% meso†
Tetrahydrofuran	135–139	50	46
Diethyl ether	144.5–149	10	6.6

*From the melting point – composition data of Stuhmer and Messwarb (*5b*).
†Isolated through the complex with N,N-dimethylformamide (*5a*).

Preparation of Monobenzamide of Meso-N,N′,1,2-tetraphenylethylenediamine

Meso-N,N′,1,2-tetraphenylethylenediamine (1.09 g, 0.003 mole) was dissolved in 15 ml of benzene and 15 ml of pyridine. Benzoyl chloride (0.632 g, 0.0045 mole) was added and the solution refluxed for 18 h. To the cooled mixture, 15 ml of benzene and 15 ml of 10% aqueous potassium hydroxide was added. The aqueous phase was separated, and the organic phase was washed once with 10 ml of 10% potassium hydroxide and three times with 15 ml portions of water, and then dried over magnesium sulfate. Evaporation of the solution gave 1.332 g of solid, m.p. 170–182 °C. The material was dissolved in 30 ml of hot carbon tetrachloride, the solution was filtered hot, and when the solution was allowed to cool 1.133 g of a voluminous white precipitate separated, m.p. 188–192 °C. The infrared spectrum (Nujol mull) showed a NH band at 3 360 cm^{-1} and an amide carbonyl band at 1 635 cm^{-1}.

Anal. Calcd. for $C_{33}H_{28}N_2O$: C, 84.59; H, 6.02; N, 5.97. Found: C, 84.90; H, 5.92; N, 6.00.

Preparation of Monobenzamide of dd,ll-N,N′,1,2-Tetraphenylethylenediamine

dd,ll-N,N′,1,2-Tetraphenylethylenediamine (0.723 g, 0.002 mole) was dissolved in 25 ml of diethyl ether and 5 ml of benzene. Benzoyl chloride (0.912 g, 0.0021 mole) was added and the solution was allowed to stand at room temperature for 40 h. A white precipitate separated. The mixture was evaporated to dryness and the residue dissolved, with heating, in 15 ml of ethanol and 5 ml of water. Potassium hydroxide (0.40 g) dissolved in 10 ml of ethanol and 2 ml of water was added to the hot solution. The precipitate which formed was dissolved in 20 ml of benzene, and the organic phase was separated, washed twice with 10 ml of water, and dried over magnesium sulfate. Evaporation gave 0.882 g of a glassy residue. Treatment with 10 ml of diethyl ether effected crystallization. Filtration gave 0.349 g of derivative, m.p. 176.5–182 °C. Recrystallization from 5 ml of *n*-butanol gave 0.336 g, m.p. 180–183 °C. The infrared spectrum (Nujol mull) showed a NH band at 3 380 cm^{-1} and an amide carbonyl band at 1 625 cm^{-1}.

Anal. Calcd. for $C_{33}H_{28}N_2O$: C, 84.59; H, 6.02; N, 5.97. Found: C, 84.79; H, 5.97; N, 6.08.

Reaction in Tetrahydrofuran with Methyl Benzoate

The sodium adduct from 5.43 g (0.03 mole) of N-benzylidene aniline, 75.3 g of tetrahydrofuran, and 1.4 g (0.06 atom) of sodium was transferred to a 250 ml flask which was filled with dry nitrogen and which was equipped with a magnetic stirring bar. The solution was stirred, and 4.08 g (0.03 mole) of freshly distilled methyl benzoate dissolved in 15 ml of dry tetrahydrofuran was added all at once. A deep ruby-red color developed immediately. During the next 24 h, an orange-red precipitate formed and the color of the solution became orange. Water (25 ml) was then added and the precipitate dissolved.

Can. J. Chem. Downloaded from www.nrcresearchpress.com by 210.87.254.5 on 09/05/12
For personal use only.

Can. J. Chem. Downloaded from www.nrcresearchpress.com by 210.87.254.5 on 09/05/12
For personal use only.

The solution was transferred to a separatory funnel with 50 ml of benzene, and the aqueous phase was separated. The organic phase was washed three times with 25 ml portions of water, dried over magnesium sulfate, and evaporated, giving 6.84 g of residue. This was dissolved in 25 ml of hot benzene and treated with 40 ml of petroleum ether (b.p. 30–60°). A precipitate separated and (after 5 h) was filtered off, wt. 5.22 g, m.p. 163–175°. This material had an infrared spectrum identical with that of the N-benzoyl-*dd,ll*-TPED. However, the presence of a small amount of the diastereomer N-benzoyl-meso-TPED was demonstrated by allowing a solution of 0.6 g of the mixture in 50 ml of toluene–heptane (1:1) to evaporate to half volume spontaneously at room temperature over a period of 1 week. The crystals which separated consisted of small needles intermixed with relatively massive parallelopipeds. These were easily separated mechanically. The needles (0.05 g, m.p. 178–182°) had an infrared spectrum (Nujol mull) identical with that of the monobenzamide of the meso-TPED; the parallelopipeds (0.49 g, m.p. 165–182°) were similarly shown to be the monobenzamide of the *dd,ll* diamine.

The filtrate from the mixed monobenzamides was evaporated and the residual oil dissolved in 5 ml of methylene chloride and 25 ml of petroleum ether (b.p. 30–60 °C). The solution was chromatographed on 60 g of Woelm, grade I, basic alumina, elution being carried out with petroleum ether containing increasing amounts of methylene chloride. The first 350 ml of petroleum ether – 10% methylene chloride gave, on evaporation, 0.173 g of an amorphous solid. Crystallization from 5 ml absolute ethanol gave 0.018 g of N-benzylidene aniline, m.p. 50–54°.

The filtrate from this gave 0.086 g of the 2,4-dinitrophenylhydrazine derivative of benzaldehyde, m.p. 235–237 °C, on treatment with 2,4-dinitrophenylhydrazine reagent. An additional 0.104 g of this material was eluted with the next 200 ml of petroleum ether – 25% methylene chloride. After this, 300 ml of petroleum ether – 50% methylene chloride eluted 0.186 g of a solid which was recrystallized from 3 ml of ethanol. There was obtained 0.105 g of *dd,ll*-TPED, m.p. 148–150°, mixed melting point with an authentic sample 148–153°.

The next 275 ml of methylene chloride eluted 0.191 g of a solid which, on recrystallization from 3 ml of ethanol, gave 0.163 g of the monobenzamide of *dd,ll*-TPED, m.p. 170–176°, mixed melting point with an authentic sample 174–180°.

The yields obtained for the various compounds are: N-benzoyl-TPED (mixed isomers), 77%; *dd,ll*-TPED, 3%; N-benzylidene aniline, 5%.

Reaction in Tetrahydrofuran with Benzaldehyde (Mole Ratio 1:1)

The sodium adduct from 3.62 g (0.02 mole) of N-benzylidene aniline and 0.8 g (0.04 atom) of sodium in 62.2 g of tetrahydrofuran was transferred to a 125 ml flask which was filled with dry nitrogen and which was equipped with a magnetic stirring bar. The solution was stirred and 2.12 g (0.02 mole) of benzaldehyde was added all at once. A deep red color immediately developed. The solution was allowed to stand for 16 h, during which time a dark red precipitate formed.

Water (15 ml) was added with stirring. The color of the solution changed to orange and the precipitate dissolved. Diethyl ether (75 ml) was added, the aqueous phase was separated, and the ether layer was washed five times with 20 ml portions of water. After drying over magnesium sulfate, the solution was filtered and evaporated. The residue, a semicrystalline gummy solid, was dissolved in 20 ml of benzene and added to 50 ml of petroleum ether (b.p. 30–60°). The solid which separated was filtered off, washed with 1:1 benzene – petroleum ether, and dried; wt. 2.564 g, m.p. 174–180°. A comparison of the infrared spectrum with that of an authentic sample of N-benzoyl-*dd,ll*-TPED showed that the materials were identical.

The filtrate was evaporated, and the residue was dissolved in 20 ml of ether and 10 ml of benzene, and chromatographed on 60 g of Woelm, grade I, basic alumina. Elution with 50 ml of 1:1 petroleum ether – diethyl ether and then 100 ml of diethyl ether removed 1.02 g of *dd,ll*-N,N′,1,2-tetraphenylethylenediamine, m.p. 145–148°. Recrystallization from absolute ethanol raised the melting point to 150–153°; the mixed melting point with an authentic sample was 151–153°. The next 200 ml of ether containing 10% benzene eluted 0.161 g of N-benzoyl-meso-TPED, m.p. 180–186°, which after recrystallization from toluene melted at 186–192°; the mixed melting point with an authentic sample was 186–192°. The next 200 ml of ether containing 25% benzene, 150 ml of 1:1 ether–benzene, 200 ml of 1:1 ether–benzene containing 0.5% methanol, and 200 ml of 1:1 ether–benzene containing 2% methanol yielded a total of 0.25 g of N-benzoyl-*dd,ll*-TPED. The yields of these various compounds are: *dd,ll*-TPED, 28%; N-benzoyl-*dd,ll*-TPED, 60%; N-benzoyl meso-TPED, 3%.

Reaction in Tetrahydrofuran with Benzaldehyde (Mole Ratio 1:2)

This last experiment was repeated, except that only 1.06 g (0.01 mole) benzaldehyde was added. Evaporation of the solvent after washing gave a residue of 3.61 g. The infrared spectrum of this material showed only a weak band at 1 630 cm^{-1} characteristic of the amide carbonyl. The rest of the spectrum was identical with that of *dd,ll*-TPED.

Chromatography of the crude product as described above enabled 2.61 g (72% yield) of *dd,ll*-TPED, m.p. 141–153°, and 0.176 g (4% yield) of the monobenzamide, m.p. 173–184°, to be isolated.

Reaction in Tetrahydrofuran with Benzaldehyde (Mole Ratio 2:1)

The adduct prepared from 1.81 g (0.01 mole) of N-benzylidene aniline and 0.5 g (0.02 atom) of sodium in 43.6 g of tetrahydrofuran was transferred to a 125 ml flask which was filled with dry nitrogen. The solution

was stirred and 2.12 g (0.02 mole) of benzaldehyde was rapidly added. A red color developed at once and deepened when the solution was allowed to stand for 20 h. Addition of water (15 ml) caused the color to change to yellow. Diethyl ether (50 ml) was added, the aqueous layer was separated, and the organic layer was washed twice with 20 ml portions of water, twice with 20 ml portions of 10% sodium bisulfite solution, and twice with 20 ml portions of water. After drying over magnesium sulfate, the solution was filtered and evaporated, giving a yellow crystalline residue.

The material was dissolved in 10 ml of benzene and added to 30 ml of petroleum ether (b.p. 30–60°). A crystalline solid separated; wt. 2.113 g, m.p. 170–180°. The infrared spectrum showed that this material was N-benzoyl-*dd,ll*-TPED (90% yield). The filtrate was not examined further.

Reaction in Diethyl Ether with Methyl Benzoate

The sodium adduct from 3.26 g (0.02 mole) of N-benzylidene aniline, 0.9 g (0.04 atom) sodium, and 103 g of diethyl ether was transferred to a 250 ml flask which was filled with dry nitrogen. The solution was stirred with a magnetic stirrer and 2.72 g (0.02 mole) of methyl benzoate added all at once. An immediate orange color developed and, when the solution was allowed to stand overnight, a precipitate formed. On the addition of 25 ml of water the color changed to yellow and the precipitate dissolved. When the solution was allowed to stand, small needle-like crystals separated. After 24 h, the precipitate was filtered off, washed with ether, and dried. This solid amounted to 0.938 g, m.p. 190–193°, mixed melting point with an authentic sample of N-benzoyl-meso-TPED 189–193°.

The ether phase was separated from the filtrate, washed twice with 25 ml portions of water, dried over magnesium sulfate, and evaporated. The residue amounted to 2.985 g and melted at 122–152°. Its infrared spectrum (Nujol mull) revealed the presence of the two diastereomeric N-benzoyl-TPED's.

A sample of material (1.50 g) was dissolved in 50 ml of ether–benzene (3:1) and chromatographed on 60 g of Woelm, grade I, basic alumina. Elution with diethyl ether gave 0.341 g (100 ml) of *dd,ll*-TPED, m.p. 127–134°; recrystallization from absolute ethanol raised the melting point to 147–153°, no depression with an authentic sample. The next 50 ml gave 0.270 g of a mixture of *dd,ll*-TPED and N-benzoyl-meso-TPED. These were separated by treating the mixture with 20 ml diethyl ether, at which time the N-benzoyl compound crystallized, giving 0.032 g, m.p. 188–191°, no depression with an authentic sample. The filtrate was evaporated and the residue recrystallized from 4 ml of absolute ethanol, giving 0.130 g of *dd,ll*-TPED, m.p. 149–153°; the mixed melting point with an authentic sample was not depressed. The next 200 ml of ether eluted an additional 0.545 g of N-benzoyl-meso-TPED, m.p. 183–187°, identified by its infrared spectrum. The next 200 ml of ether–benzene (3:1) and 350 ml ether–benzene (1:1) eluted 0.369 g of N-benzoyl-*dd,ll*-TPED; its melting point after recrystallization from ethanol was 182–184°, not depressed by an authentic sample.

Correcting the isolated samples for the aliquot sample of crude material and dividing the one mixture in the ratio of the amounts isolated gives total yields of *dd,ll*-TPED of 1.12 g (30%), N-benzoyl-meso-TPED 2.14 g (46%), and N-benzoyl-*dd,ll*-TPED 0.735 g (16%).

Reaction in Diethyl Ether with Benzaldehyde (Mole Ratio 1:1)

The sodium adduct from 3.62 g (0.02 mole) of N-benzylidene aniline, 0.9 g (0.04 atom) of sodium, and 104 g of diethyl ether was transferred to a 250 ml flask. The solution was stirred with a magnetic stirrer and 2.12 g (0.02 mole) of benzaldehyde dissolved in 10 ml of ether was added all at once. An orange color immediately developed together with a dense yellow precipitate. The mixture was stirred for 6 h, during which time the color deepened to a dark red-brown and the precipitate partially dissolved, changing color to a dark red or brown. Water (25 ml) was added with stirring. The precipitate dissolved to give a clear yellow solution, and then after 5 min a yellow solid began separating. After standing overnight, the mixture was filtered, and the solid was washed with ether. After drying it amounted to 0.996 g, m.p. 212–214°.[2] Its infrared spectrum (Nujol mull) showed a NH band at 3 340 cm^{-1} and an amide carbonyl at 1 645 cm^{-1}. Comparison of the spectrum with that of an authentic sample (4) of N-benzoyl-N,N′-diphenylstilbene-α,α'-diamine showed that they were identical. The compound yielded a picrate, m.p. 274–277°, mixed melting point with the picrate of N-benzoyl-N,N′-diphenylstilbene-α,α'-diamine 273.5–278.5°.

The filtrate was chromatographed on 60 g of Woelm, grade I, basic alumina. Elution with 300 ml of petroleum ether – benzene (2:1) removed 1.207 g of *dd,ll*-TPED, m.p. 140–153°. The next 200 ml of 2:1:1 benzene – petroleum ether – methylene chloride removed 0.561 g of the N-benzoyl derivative of meso-TPED, m.p. 148–173°. The N-benzoyl derivative was dissolved in 1 ml of hot ethyl acetate, and 5 ml of ethanol was added. The material which crystallized had m.p. 180–197°, mixed melting point with an authentic sample 188–198°. The next 900 ml of petroleum ether – methylene chloride (1:1) and 400 ml of methylene chloride eluted 1.198 g of N-benzoyl-*dd,ll*-TPED, m.p. 173–180°; the mixed melting point with an authentic sample was undepressed. The combined yields of these materials are: *dd,ll*-N,N′,1,2-tetraphenylethylenediamine, 33%; N-benzoyl-N,N′-diphenylstilbene-α,α'-diamine, 21%; N-benzoyl-N,N′,1,2-tetraphenylethylenediamine (mixed isomers), 38%.

[2]*This material was degraded during the determination of the melting point. The reported value was obtained by inserting the sample in a melting point apparatus preheated to 205 °C.*

Can. J. Chem. Downloaded from www.nrcresearchpress.com by 210.87.254.5 on 09/05/12
For personal use only.

Reaction in Diethyl Ether with Benzaldehyde (Mole Ratio 1:2)

The sodium compound from 1.81 g (0.01 mole) of N-benzylidene aniline and 0.5 g (0.02 atom) of sodium in 61 g of diethyl ether was treated with 2.12 g (0.02 mole) of benzaldehyde. An immediate formation of a yellow precipitate occurred and the solution became orange. Over the next 12 h no change occurred in the appearance of the mixture. Water (13 ml) was added and the precipitate dissolved, accompanied by a color change from orange to yellow. A small amount of a granular white precipitate remained. This was filtered off (wt. 0.243 g, m.p. 188–290°), dissolved in benzene, filtered from the insoluble material, and evaporated to give 0.167 g of N-benzoyl-meso-TPED, m.p. 180–195°.

The ether filtrate was evaporated to 2.32 g of a gummy residue. This was dissolved in 20 ml of benzene and the solution was added to 50 ml of diethyl ether. The small amount of solid which separated was filtered off to give 0.058 g, m.p. 189–195°; the mixed melting point with an authentic N-benzoyl derivative of meso-TPED was not depressed.

An aliquot portion (1.35 g solids) of filtrate was then chromatographed on 65 g of Woelm, grade I, basic alumina, diethyl ether being used as the eluting agent. The first 150 ml of eluate removed 0.666 g of gum (A). The next 150 ml eluted 0.217 g of the N-benzoyl derivative of meso-TPED, m.p. 189–192°, undepressed by an authentic sample. The next 175 ml eluted 0.122 g of a mixture of the N-benzoyl derivatives of meso- and *dd,ll*-TPED. After this, 250 ml of 3:1 ether–benzene and 150 ml of 1:1 ether – methylene chloride eluted 0.240 g of the N-benzoyl derivative of *dd,ll*-TPED, m.p. 173–177°. When it was recrystallized from absolute ethanol it had m.p. 177–180°; the mixed melting point with an authentic sample was undepressed. No further material was eluted from the column.

The infrared spectrum of gum (A) showed a NH absorption band at 3 380 cm^{-1} and a carbonyl band at 1 725 cm^{-1} but no amide carbonyl band at 1 630 – 1 650 cm^{-1}. This material was treated with 10 ml of petroleum ether (b.p. 30–60°) and allowed to stand. A solid separated, 0.339 g, m.p. 139–141°. When this solid was recrystallized from cyclohexane it had m.p. 138–146°; the mixed melting point with authentic *dd,ll*-TPED was 144–150°. The petroleum ether filtrate, on evaporation, gave a mobile yellow oil whose infrared spectrum was identical with that of benzyl benzoate. The total yields, after they were corrected for the aliquot portion chromatographed, were: *dd,ll*-TPED (0.583 g), 32%; N-benzoyl-TPED (1.221 g), 52%. If the fraction of mixed diastereomers obtained during chromatography is arbitrarily assumed to be a 1:1 mixture of the two diastereomers, then the yield of N-benzoyl-meso-TPED is 30% and that of N-benzoyl-*dd,ll*-TPED is 22%.

ACKNOWLEDGMENTS

The author is indebted to Mr. I. J. Bastien (Dow Chemical of Canada, Limited) for the infrared spectra and Mr. L. E. Swim (The Dow Chemical Company, Midland, Michigan) for the microanalyses.

REFERENCES

1. W. SCHLENK and E. BERGMANN. Ann. **463**, 321 (1928).
2. W. SCHLENK, J. APPENRODT, A. MICHAEL, and A. THAL. Ber. **47**, 473 (1914).
3. M. SCHLOSSER. Angew. Chem. Intern. Ed. Engl. **3**, 368 (1964).
4. A. E. EVEREST and H. MCCOMBIE. J. Chem. Soc. **99**, 1752 (1911).
5. (*a*) R. JAUNIN. Helv. Chim. Acta, **39**, 111 (1956); **43**, 2029 (1960).
   (*b*) W. STUHMER and G. MESSWARB. Arch. Pharm. **286**, 221 (1953).
6. G. WITTIG and H.-D. FROMMELD. Ber. **97**, 1964 (1964).
7. L. F. FIESER. J. Am. Chem. Soc. **46**, 2639 (1924).
8. J. W. B. REESOR, J. G. SMITH, and G. F. WRIGHT. J. Org. Chem. **19**, 940 (1954).

Can. J. Chem. Downloaded from www.nrcresearchpress.com by 210.87.254.5 on 09/05/12
For personal use only.

Can. J. Chem. Downloaded from www.nrcresearchpress.com by 210.87.254.42 on 09/05/12
For personal use only.

ÉTUDE QUANTITATIVE DES RÉACTIONS D'OZONOLYSE

I. OZONATION DU TÉTRAPHÉNYLÉTHYLÈNE

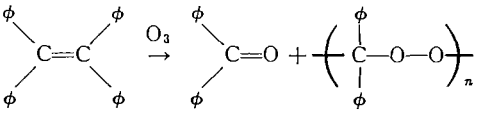
S. FLISZÁR, D. GRAVEL ET E. CAVALIERI
Département de Chimie, Université de Montréal, Montréal, Québec

Reçu le 23 août 1965

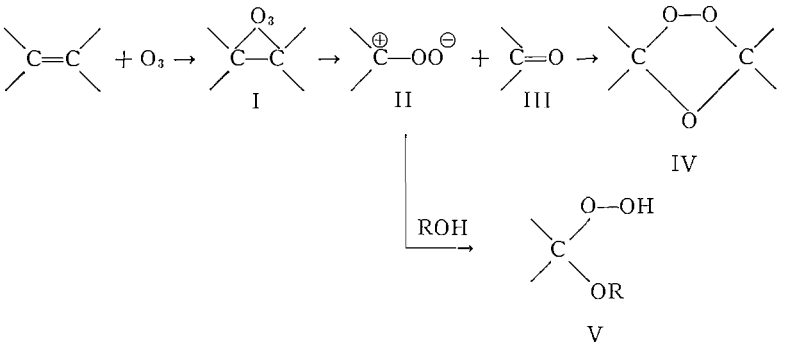
RÉSUMÉ

L'étude quantitative de l'ozonation du tétraphényléthylène en solution dans du CCl_4 montre que l'ozonolyse de 1 mole d'oléfine engendre 1 mole de benzophénone, 0.57 mole d'oxyde de carbonyle sous forme de peroxyde cyclique et 0.43 mole d'oxyde de carbonyle sous forme de polymère (supposé en chaîne ouverte); ce bilan est indépendant du débit d'ozone et de la température, dans l'intervalle compris entre 0 et 45 °C.

Contrairement à ce qui se passe avec de nombreuses oléfines, l'ozonation du tétraphényléthylène ne conduit pas à la formation d'un ozonide mais engendre de la benzophénone et des peroxydes polymères (1).



La théorie de Criegee (2) sur le mécanisme de formation des ozonides rend bien compte de cette réaction: l'attaque de l'ozone sur la double liaison engendre un ozonide primaire[1] (I) qui se scinde en un zwitterion (II) plus un composé carbonylé (III) (aldéhyde ou cétone).



En absence d'un réactif (alcool ou acide, par exemple) amenant la destruction du zwitterion (II) en engendrant un hydroperoxyde (V), le zwitterion réagit soit avec le composé carbonylé (III) pour former l'ozonide (IV), soit se polymérise en formant un peroxyde. Sauf dans des cas particuliers où la fonction carbonyle est activée (2, 4) (esters α-cétoniques, par exemple) ou se trouve sur la même molécule que la partie zwitterion (5), il n'y aura généralement pas de réaction entre II et III avec formation de l'ozonide (IV) si III est une cétone;[2] alors, dans un solvant inerte, il n'y aura production que de peroxydes à

[1] *Pour plus de détails au sujet de la structure de I, c.f. réf. 3.*
[2] *La formation d'ozonides par réaction de zwitterions aldéhydiques avec de l'acétone (ce dernier en grand excès) est décrite dans réf. 6.*

différents degrés de polymérisation, en plus de la cétone engendrée lors de la scission de l'ozonide primaire (I) très instable. Par contre, si III est un aldéhyde, il y aura presque toujours formation de l'ozonide; ce cas sera discuté lors d'un prochain travail.

Les difficultés qui se présentent lors de l'interprétation quantitative des résultats d'ozonations ont trait particulièrement à une connaissance insuffisante (*a*) du sens de rupture de l'ozonide primaire et (*b*) du comportement du zwitterion, en relation avec un mécanisme de cage plus ou moins prononcé. Ces difficultés se reflètent dans les travaux établissant des bilans de production d'ozonides "naturels" et "non naturels" engendrés lors de l'ozonation d'oléfines non symétriques (7).

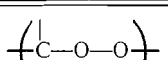
Le but de nos recherches est d'étudier plus en détail le comportement du zwitterion de Criegee. A cet égard l'ozonation du tétraphényléthylène offre l'exemple le plus simple, vu que cette oléfine n'engendre pas d'ozonide (1), du moins pas en quantité appréciable: le groupement carbonyle des cétones étant en général moins susceptible à une attaque nucléophile que celui des aldéhydes, et du fait de la grande facilité de formation de peroxydes à partir du zwitterion, la non-production d'ozonide est facilement expliquée.

Concernant la formation de peroxydes il importe de relever les faits expérimentaux suivants: (*i*) les solutions de tétraphényléthylène fraîchement ozonées libèrent rapidement de l'iode à partir d'une solution acétique de NaI (1*b*) et (*ii*) le peroxyde dimère (VI) isolé par Marvel et Nichols ne donne pas cette réaction; ceci suggère que nous aurons à tenir compte de deux types de peroxydes. Nous désignerons par peroxyde "actif" celui qui libère l'iode et par diperoxyde de benzophénone le produit connu (VI).

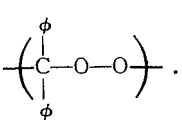
Des bilans[3] d'ozonation nous ont renseigné sur les quantités des différents produits engendrés par l'attaque de l'ozone sur le tétraphényléthylène. Les quantités d'oléfine consommée et de benzophénone formée ont été calculées d'après des mesures d'absorption infrarouge; le peroxyde "actif" a été déterminé par voie iodométrique (Tableau I); le diperoxyde de benzophénone a été calculé par différence et, dans d'autres expériences, mesuré par pesée.

TABLEAU I

Ozonation du tétraphényléthylène dans CCl_4 à 25°

[C=C]	Débit O_3	Durée	O_3 consommé	C=C consommée	>C=O formée	 formé
0.05	0.0178	15	0.19	0.21	0.20	0.09
	0.0205	60	0.71	0.75	0.72	0.32
	0.0325	20	0.46	0.45	0.46	0.18
	0.0310	30	0.58	0.69	0.64	0.29
	0.0365	40	0.90	0.90	0.91	0.42
	0.135	5	0.38	0.37	0.39	0.15
	0.140	10	0.66	0.67	0.66	0.33
0.085	0.152	5	0.43	0.42	0.43	0.18
	0.152	10	0.78	0.76	0.76	0.33

NOTONS: [C=C]: concentration (mole/l) de l'oléfine; débit: millimole/min; durée: min; O_3 et C=C consommés, C=O et (actif) formés: millimole. La quantité de diperoxyde de benzophénone se calcule en soustrayant le peroxyde "actif"de C=C consommée.

[3]*Dans ces bilans, les peroxydes seront comptés sous forme d'oxyde de carbonyle monomère*  .

Can. J. Chem. Downloaded from www.nrcresearchpress.com by 210.87.254.42 on 09/05/12
For personal use only.

Une constatation importante se dégage de ces résultats: la quantité de benzophénone formée est, aux erreurs expérimentales près, égale à la quantité d'oléfine consommée; nous nous en sommes encore assurés par des ozonations poussées jusqu'à consommation complète de l'oléfine et avons confirmé ainsi que 1 mole d'oléfine ozonée engendre seulement 1 mole de benzophénone. On en conclut que, dans nos conditions expérimentales, il n'y a pas de décomposition d'oxyde de carbonyle avec formation de benzophénone.

En vue d'établir en quelle mesure le bilan d'ozonation dépend des conditions expérimentales, nous avons procédé à une confrontation des proportions de benzophénone et de peroxyde "actif" formés. La Fig. 1 rend compte des résultats obtenus par l'ozonation de 20 ml de solution d'oléfine dans CCl_4 à 25 °C (±0.3°) par un courant de gaz O_2–O_3.

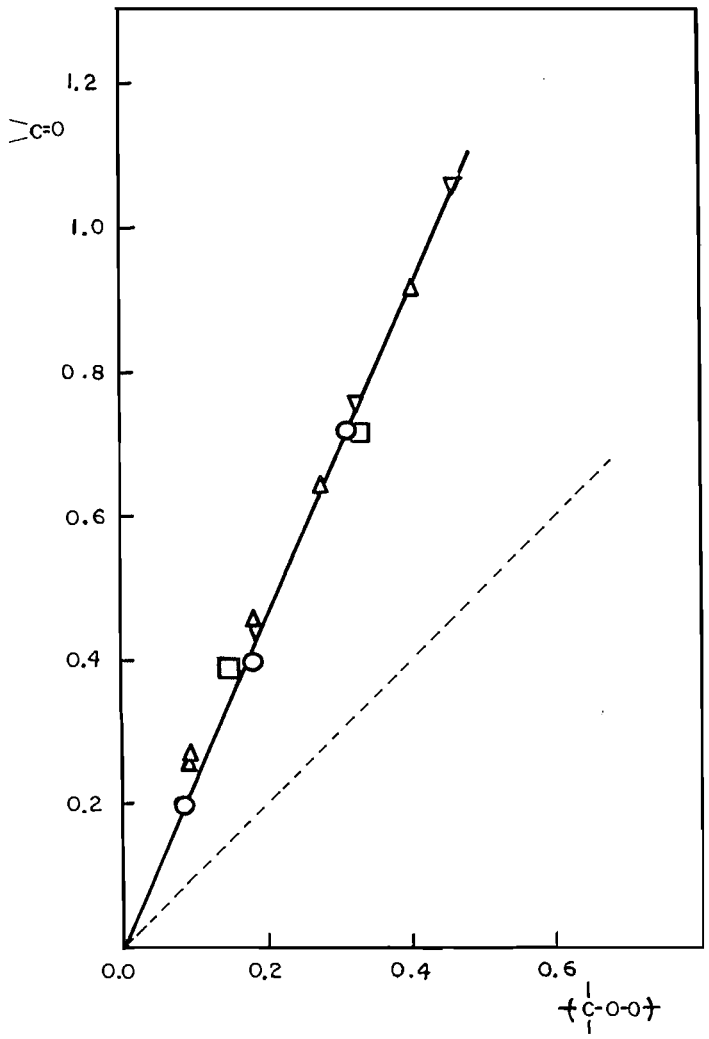


FIG. 1. Ozonation du tétraphényléthylène dans CCl_4 à 25 °C: millimoles de benzophénone et peroxyde "actif" produits. Concentration initiale de l'oléfine: 0.05 *M*; débit O_3: ○, 0.0175–0.0205 mmole/min; △, 0.0310–0.0370 mmole/min; □, 0.135–0.140 mmole/min; ▽, 0.152 mmole/min (concentration oléfine 0.085 *M*).

Can. J. Chem. Downloaded from www.nrcresearchpress.com by 210.87.254.42 on 09/05/12
For personal use only.

Des valeurs rapportées dans cette figure il se dégage que le rapport r = (benzophénone formée/peroxyde "actif" formé) est indépendant du débit en O_3 et de la concentration en oléfine de la solution; on calcule, d'après ces valeurs, $r = 2.30$. La Fig. 1 montre clairement la constance de r jusqu'à un degré avancé de la réaction (environ 95%). La ligne en pointillé se rapporte à une formation équimolaire de benzophénone et d'oxyde de carbonyle. Notons encore que la valeur de r est indépendante de la température dans le domaine de 0 à 45 °C, ce qui est attesté par les valeurs reproduites dans la Fig. 2, I.

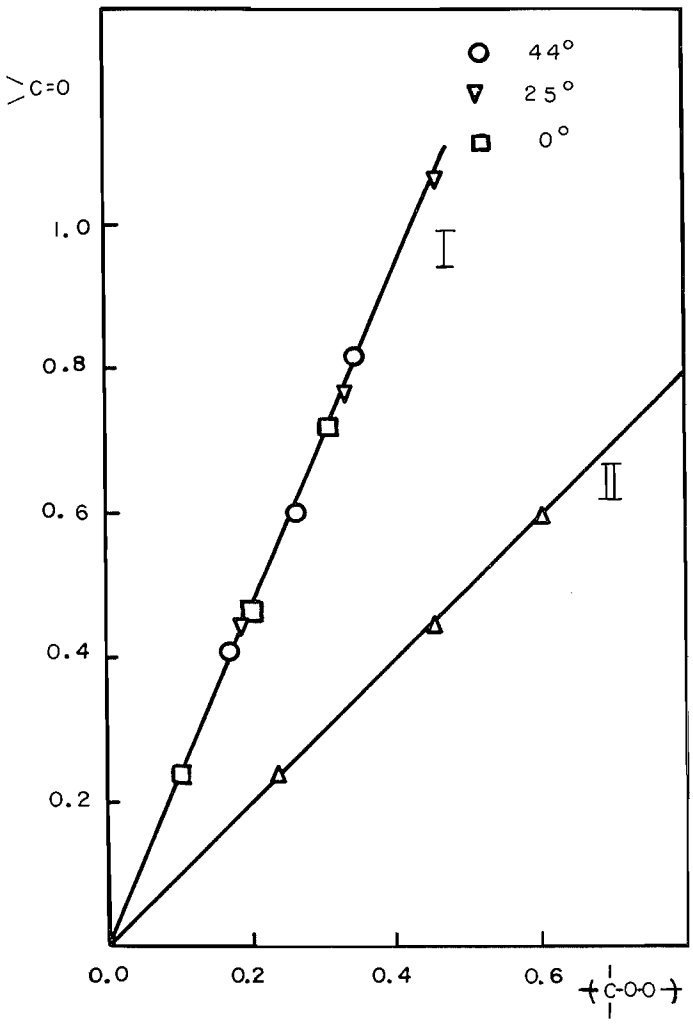


FIG. 2. I. Ozonation du tétraphényléthylène dans CCl_4 à différentes températures. LÉGENDE: ○ et ▽, concentration oléfine 0.085 M, débit O_3 0.128–0.153 mmole/min; □, concentration oléfine 0.05 M, débit O_3 0.068 mmole/min. II. Ozonation en présence de CH_3OH (0.3 M) dans CCl_4, à 0 °C.

La constatation que la benzophénone formée est 2.30 fois plus abondante que le peroxyde "actif" formé ne pouvant s'interpréter par une scission d'un oxyde de carbonyle qui engendrerait de la benzophénone, la somme[3] peroxyde "actif" plus diperoxyde de benzophénone doit être égale à la quantité de benzophénone formée, soit égale à la quantité

Can. J. Chem. Downloaded from www.nrcresearchpress.com by 210.87.254.42 on 09/05/12
For personal use only.

d'oléfine consommée. Nous nous sommes d'ailleurs assurés que l'ozonolyse de 1 mole d'oléfine conduit bien à la formation de 1 mole de zwitterion en effectuant des expériences d'ozonolyse en présence de CH_3OH (Tableau II) et montrant qu'il se forme autant d'hydroperoxyde (V) que de cétone.

TABLEAU II

Ozonation d'une solution 0.05 *M* de tétraphényléthylène dans CCl_4 at 0 °C, en présence de 0.3 *M* de CH_3OH

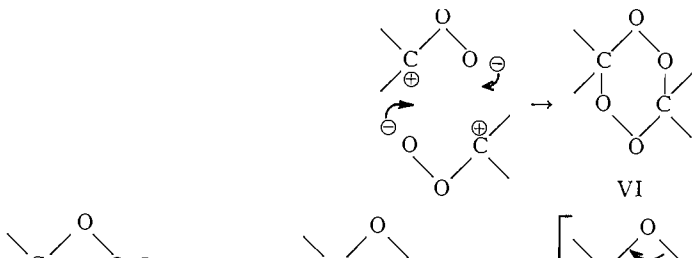
Débit O_3	Durée	O_3 consommé	$>C{=}O$ formée	$-\overset{|}{C}-O-OH$ formé
0.068	5	0.20	0.23	0.24
0.079	10	0.44	0.44	0.46
0.077	15	0.60	0.59	0.61

NOTONS: Débit O_3: millimole/min; durée: min; O_3 consommé, $>C{=}O$ et $-\overset{|}{C}-O-OH$ formés: millimole.

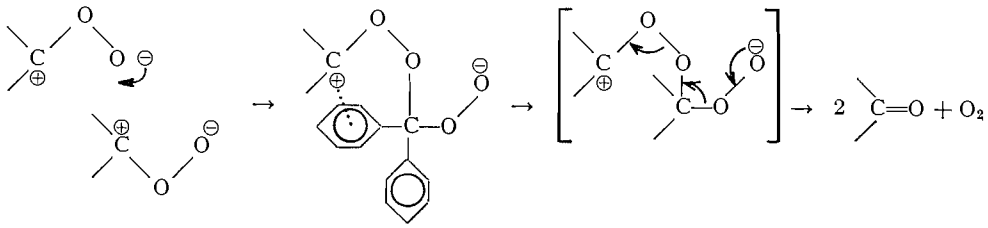
Ce fait est bien démontré par la Fig. 2, II, la ligne tracée étant celle calculée pour la formation équimolaire de II et de III.

Dès lors le bilan d'ozonation du tétraphényléthylène en solution dans le CCl_4 s'établit comme suit aux températures comprises entre 0 et 45 °C: 1.0 mole d'oléfine engendre 1.0 mole d'ozonide primaire (I) qui se scinde en 1.0 mole de benzophénone plus 1.0 mole de zwitterion. C'est le processus de Criegee confirmé par les expériences effectuées en présence de CH_3OH. Le zwitterion engendre ensuite un peroxyde stable (57%), principalement sous forme de dimère cyclique (VI) n'oxydant pas l'ion iodure en I_2, le restant du zwitterion (43%) engendrant un polymère capable d'oxyder l'ion iodure en I_2.

Il paraît raisonnable d'admettre pour le polymère "actif" la forme en chaîne ouverte (VII), représentée ici par son dimère, sans pour autant présumer de la possibilité de polymérisation à un plus haut degré. On note en effet la possibilité d'interaction de l'ion $C^{\oplus}$ provenant d'une molécule zwitterion avec le système d'électrons π des noyaux benzéniques, comme le montre le schéma (VII). Une telle interaction pourrait, en quelque sorte, être comparée aux liaisons H intramoléculaires comme elles s'établissent, par exemple, dans les alcools benzylique et phényléthylique (VIII); une interaction similaire



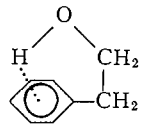
VI



VII

Can. J. Chem. Downloaded from www.nrcresearchpress.com by 210.87.254.42 on 09/05/12
For personal use only.

de carbocations avec des noyaux benzéniques a été décrite récemment par Cram et Goldstein (8). Cette stabilisation aurait pour effet d'empêcher la libre rotation autour de la liaison C—O avec cyclisation conséquente.



VIII

Pour confirmer que le produit libérant l'iode est composé uniquement de fragments d'oxyde de carbonyle nous avons dosé la benzophénone engendrée par la réaction du peroxyde "actif" avec I^-. Les solutions fraîchement ozonées ont été additionnées d'un peu de CH_3COOH; après mesure de l'intensité de la bande carbonyle de la cétone à 1 667 cm^{-1}, on ajoute un peu de NaI et procède (après $\frac{1}{2}$ h) à une nouvelle mesure de l'intensité de cette bande. Ces expériences montrent que par l'adjonction de I^- la quantité de benzophénone augmente de 1.43 fois par rapport à l'expérience faite en absence de I^-. Le fait qu'il se forme exactement 1 mole de benzophénone par mole d'oxygène actif titré iodométriquement confirme bien que le produit "actif" est uniquement constitué de fragments oxyde de carbonyle ce qui exclut la présence, du moins en quantité appréciable, d'ozonide.

Ainsi, par exemple, avons-nous obtenu les résultats suivants[3] (en millimoles) par l'ozonation à 25 °C de 70 ml d'une solution 0.085 *M* de tétraphényléthylène: O_3 consommé, 3.3; oléfine consommée, 3.3; benzophénone formée, 3.2; peroxyde "actif", 1.45; diperoxyde de benzophénone, 1.85 (dosé par voie spectrographique), 1.80 et 1.93 (par isolation et pesée). Bilan: obtenu 1.85 + 1.45 + 3.2 = 6.50 mmoles de produits, correspondant à 6.50/2 = 3.25 mmoles d'oléfine consommée. Après adjonction de 10% d'acide acétique glacial, la densité optique de la bande carbonyle, mesurée dans une cellule de 0.203 mm d'épaisseur, est de 0.137; la densité optique de cette bande mesurée dans les mêmes conditions, mais en présence de I^-, est de 0.197, soit 0.197/0.137 = 1.43 fois plus grande.

Pour terminer, nous avons encore étudié la stabilité du peroxyde "actif". En laissant reposer les solutions ozonées pendant 24 h à 25 °C on note une diminution d'environ 30% de la teneur en peroxyde "actif", sans pour autant déceler une augmentation de la quantité de benzophénone; par contre on note un accroissement de la teneur en diperoxyde de benzophénone, difficile à doser du fait que ce produit cristallise à partir du mélange réactionnel en raison de sa très faible solubilité. A l'ébullition, par contre, la diminution de la quantité de peroxyde "actif" est accompagnée d'une forte augmentation de la quantité de benzophénone. Ainsi, par exemple, la solution dont nous avons décrit ci-haut le bilan en détail donne, après 1 h de reflux (79–80 °C), 0.56 mmole de benzophénone, accompagnant une diminution de 0.60 mmole de peroxyde "actif".

PARTIE EXPÉRIMENTALE

Le débit d'ozone a été mesuré par le dosage de l'iode libéré par l'ozone dans une solution aqueuse de KI; la quantité d'ozone consommé par l'oléfine a été calculée par différence, en connaissant d'une part le débit d'O_3 et la durée d'ozonation et, d'autre part, en dosant l'iode libéré dans une solution de KI receuillant le gaz d'ozonation après son passage dans la solution d'oléfine. Les ozonations ont été effectuées en faisant barbotter le mélange gazeux O_2–O_3, avec un débit variant (selon les expériences) entre 4 et 7 l par heure, dans la solution d'oléfine dans du CCl_4 anhydre. Lors des expériences faites à 25° et à 45° la partie supérieure du récipient contenant la solution à ozoner, et notamment le tube d'évacuation du gaz d'ozonation, était refroidi afin de limiter les pertes de solvant. Chaque ozonation était suivie d'un balayage de la solution par de l'azote sec pendant 10 min.

Can. J. Chem. Downloaded from www.nrcresearchpress.com by 210.87.254.42 on 09/05/12
For personal use only.

La benzophénone et le tétraphényléthylène ont été dosés par voie spectrographique infrarouge d'après les densités optiques de la bande de vibration du groupement carbonyle à 1 667 cm^{-1} pour la benzophénone et la fine bande à 1 493 cm^{-1} du tétraphényléthylène. Le diperoxyde de benzophénone possédant également une bande faible à 1 493 cm^{-1}, nous en avons tenu compte lors de l'évaluation de la quantité d'oléfine consommée: pour ce faire nous avons établi un diagramme de calibration en admettant la validité de la loi de Lambert–Beer et en déterminant soigneusement les densités optiques (i) des solutions d'oléfine de départ et (ii) des mêmes solutions ozonées à 100%. Dès lors il est facile, à l'aide de tels diagrammes, de déterminer les concentrations d'olefine non consommée et, pour les réactions suffisamment avancées (ozonées à plus que 50%), d'estimer la quantité de diperoxyde de benzophénone formé. Ce dernier composé a également été isolé en suivant la méthode de Marvel et Nichols (1*a*) avec des rendements variant entre 52 et 59%, en bon accord avec le bilan proposé.[4] Le point de fusion, après recristallisation dans du benzène, était 205–206 °C.

Anal. Calc. pour $C_{26}H_{20}O_4$: C, 78.77; H, 5.09. Trouvé: C, 79.36; H, 5.03.

Quant aux corps peroxydiques libérant l'iode, nous avons recouru à leur dosage chimique selon Lohaus (9): une partie de la solution d'oléfine ozonée est ajoutée à une solution fraîchement préparée de NaI dans l'acide acétique glacial, en présence d'un peu de CO_2 solide; après un repos de 30 min à l'obscurité on titre l'iode libéré par une solution de thiosulfate de sodium. On opère parallèlement sur un témoin, constitué par un mélange de CCl_4, CH_3COOH et NaI, additionné de benzophénone et de tétraphényléthylène. Nous nous sommes d'ailleurs assurés que ces derniers corps n'influencent pas le dosage des peroxydes; on a vérifié d'autre part que les analyses effectuées après un repos du mélange réactionnel de 20, 30 et 40 min donnent les mêmes résultats, aux erreurs expérimentales près; après seulement 10 min de temps de réaction, les valeurs sont environ 5–10% trop faibles. Le dosage des hydroperoxydes engendrés lors des expériences faites en présence de méthanol a été effectué de manière identique.

REMERCIEMENTS

Nous sommes reconnaissants à M. le Professeur C. Sandorfy, Directeur du Laboratoire de Spectroscopie chimique, ainsi qu'à M. le Professeur J. C. Richer pour toutes les facilités qu'ils nous accordent dans nos recherches expérimentales. Nous remercions également M. G. Bélanger de son assistance technique précieuse et le Conseil National de Recherches du Canada pour une subvention qui a permise ces recherches.

BIBLIOGRAPHIE

1. (*a*) C. S. MARVEL et V. E. NICHOLS. J. Org. Chem. **6**, 296 (1941). (*b*) E. BRINER et S. FLISZÁR. Helv. Chim. Acta, **43**, 1113 (1960).
2. R. CRIEGEE. Record Chem. Progr. Kresge-Hooker Sci. Lib. **18**, 111 (1957).
3. P. S. BAILEY. Chem. Rev. **58**, 926 (1958).
4. R. CRIEGEE. Advan. Chem. Ser. **21**, 133 (1958). R. CRIEGEE, S. S. BATH et B. V. BORNHAUPT. Chem. Ber. **93**, 2891 (1960).
5. R. CRIEGEE et G. LOHAUS. Chem. Ber. **86**, 1 (1953).
6. R. W. MURRAY, P. R. STORY et L. D. LOAN. J. Am. Chem. Soc. **87**, 3025 (1965).
7. O. LORENZ et C. R. PARKS. J. Org. Chem. **30**, 1976 (1965). L. D. LOAN, R. W. MURRAY et P. R. STORY. J. Am. Chem. Soc. **87**, 737 (1965).
8. D. J. CRAM et M. GOLDSTEIN. J. Am. Chem. Soc. **85**, 1063 (1963).
9. G. LOHAUS. Ann. **583**, 4 (1953).

[4]*Marvel et Nichols trouvent (1a) des rendements de 53 et 57%.*

Can. J. Chem. Downloaded from www.nrcresearchpress.com by 210.87.254.42 on 09/05/12
For personal use only.

Can. J. Chem. Downloaded from www.nrcresearchpress.com by 210.87.254.40 on 09/05/12
For personal use only.

THE OCCURRENCE OF 2,3-DIBROMOBENZYL ALCOHOL 4,5-DISULFATE, DIPOTASSIUM SALT, IN POLYSIPHONIA LANOSA[1]

J. H. HODGKIN,[2] J. S. CRAIGIE, AND A. G. MCINNES
Atlantic Regional Laboratory, National Research Council, Halifax, Nova Scotia

Received August 9, 1965

ABSTRACT

A new brominated phenolic compound, isolated in 5% yield from the red alga *Polysiphonia lanosa*, has been characterized as 2,3-dibromobenzyl alcohol 4,5-disulfate, dipotassium salt. The structural determination, synthesis, and properties of this compound and its derivatives are described.

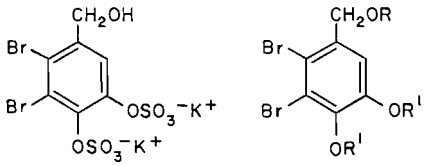
INTRODUCTION

Evidence for the presence of brominated phenolic compounds in the Rhodomelaceae family of algae has been based principally on the results of paper chromatographs, and characteristic color reactions with ferric chloride (1). However, 5-bromo-3,4-dihydroxybenzaldehyde has been shown to occur in *Polysiphonia morrowii* (2), and two other compounds (believed to be brominated sulfonated hydroxybenzoic acids) with the empirical formulae $C_7H_2O_9S_2Br_2K_2$ and $C_7H_3O_9S_2BrK_2$ have been isolated from *Polysiphonia lanosa* (3).

The purpose of this communication is to report the isolation of 2,3-dibromobenzyl alcohol 4,5-disulfate, dipotassium salt (I), in high yield from *Polysiphonia lanosa* (L.) Tandy.

RESULTS AND DISCUSSION

A colorless compound (I), with the molecular formula $C_7H_4O_9S_2Br_2K_2$, crystallized from solution when aqueous–alcoholic extracts of *P. lanosa* were concentrated. The infrared spectrum (Fig. 1) of this compound indicated the presence of a hydroxyl group (3 320 cm^{-1}, broad), a benzene ring (3 055, 1 603, 1 572, and 880 cm^{-1}), a benzylic methylene group (2 970, 2 910, and 1 455 cm^{-1}), and the anion of a sulfate ester (1 250 and 1 030 cm^{-1}). Mild acid hydrolysis of I gave 2 moles of sulfuric acid per mole of compound, and a crystalline phenol (II*a*), molecular formula $C_7H_6O_3Br_2$. Proton magnetic resonance (p.m.r.) studies showed that this phenol contained a single aromatic hydrogen (τ 2.83), a methylene group (τ 5.38) of a benzyl alcohol, and three hydroxyl protons (broad signal centered at about τ 6.9).



I

Compound II*a* formed a triacetate (II*b*), molecular formula $C_{13}H_{12}O_6Br_2$, on acetylation with acetic anhydride in pyridine. The p.m.r. spectrum established the presence of two non-equivalent aromatic acetoxyl groups (τ 7.70 and 7.77), an aliphatic acetoxyl group (τ 7.92), a methylene group (τ 4.85) of a benzyl acetate, and a single aromatic hydrogen

[1]*Issued as N.R.C. No. 8754.*
[2]*National Research Council of Canada Postdoctorate Fellow, 1963–1965.*

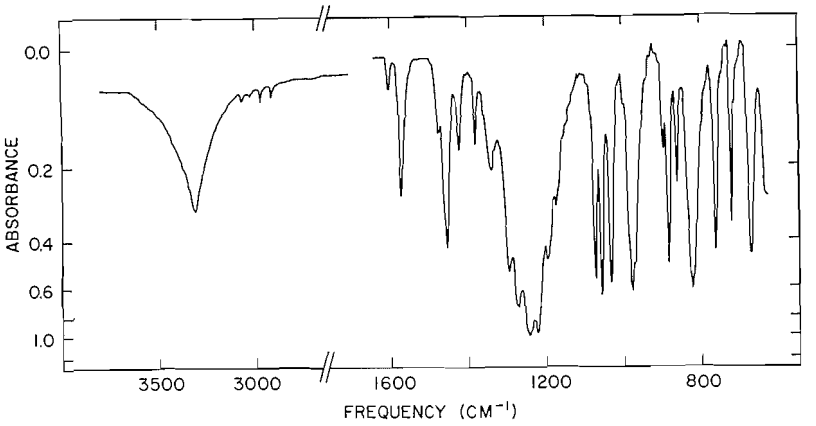


FIG. 1. The infrared spectrum of 2,3-dibromobenzyl alcohol 4,5-disulfate, dipotassium salt (KBr disk).

(τ 2.70). Moreover, "field sweep" double resonance experiments with a Varian V-6058 decoupler established that the aromatic hydrogen was coupled to the methylene group (4). Consequently, the phenol II*a* must contain two non-equivalent phenolic hydroxyl groups, a benzylic hydroxymethylene group, and a single aromatic proton.

Reduction of II*a* with Raney nickel in sodium hydroxide solution (5, p. 143) yielded a compound which was shown to be identical with an authentic sample of 3,4-dihydroxytoluene by p.m.r. and infrared examination. The phenolic hydroxyls in the parent compound must therefore occupy the 3- and 4-positions relative to the hydroxymethylene group, which was hydrogenolized to a methyl group (5, p. 127) during the reduction. The three structures for phenol II*a*, which are compatible with the above results, are 2,3-dibromo-4,5-dihydroxybenzyl alcohol (as shown), 2,5-dibromo-3,4-dihydroxybenzyl alcohol, and 2,6-dibromo-3,4-dihydroxybenzyl alcohol.

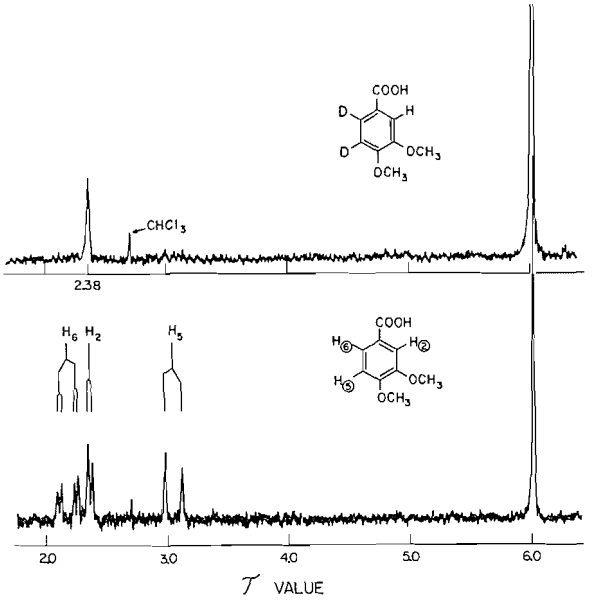


FIG. 2. The p.m.r. spectra of veratric acid and 5,6-dideuteroveratric acid in deuterochloroform with tetramethylsilane as an internal standard.

Can. J. Chem. Downloaded from www.nrcresearchpress.com by 210.87.254.40 on 09/05/12
For personal use only.

Can. J. Chem. Downloaded from www.nrcresearchpress.com by 210.87.254.40 on 09/05/12
For personal use only.

It was possible to determine the structure of the phenol by comparing the p.m.r. spectra of veratric acid with that of a dideuteroveratric acid (Fig. 2) prepared from II*a*. The isotopically labelled acid was obtained by methylation and oxidation of a deuterated 3,4-dihydroxytoluene that was produced from II*a* by reduction with Raney nickel (*vide supra*) in sodium deuteroxide solution. Proton magnetic resonance signals at average τ values of 2.38, 2.20, and 3.07 in the spectrum of veratric acid (Fig. 2) could be assigned to protons H_2, H_5, and H_6 on the basis of the ortho, meta, and para coupling constants ($J_{H_5H_6}$ = 8.2 c.p.s., $J_{H_2H_6}$ = 2.0 c.p.s., and $J_{H_2H_5} < 0.5$ c.p.s.). The presence of the single aromatic proton at τ 2.38 for the deuterated derivative (Fig. 2) is therefore proof that it is at the 2-position in the benzene ring, and establishes the structure of the compound as 5,6-dideuteroveratric acid. As the two deuterium atoms replaced the bromine atoms in II*a*, this compound must be 2,3-dibromo-4,5-dihydroxybenzyl alcohol. This structure is consistent with the fact that the two aromatic methoxyl and acetoxyl groups in II*c* and II*b* are in magnetically non-equivalent environments, as shown by p.m.r. (see Experimental section).

Final proof of the structure of II*a* was obtained when II*c* was shown to be identical with an authentic sample of 2,3-dibromo-4,5-dimethoxybenzyl alcohol that was synthesized from 5,6-dibromovanillin (6) by methylation and sodium borohydride reduction. Moreover, synthetic 5,6-dibromoveratraldehyde (7) and 5,6-dibromoveratric acid (8) were also shown to be identical with the products of the partial or complete oxidation of II*c*.

It is interesting to note that one of the phenolic hydroxyls in II*a* is much more acidic than the other because the reaction with 1 molecular equivalent of diazomethane produces a single monomethyl ether. This ether was not identical with synthetic 2,3-dibromo-4-hydroxy-5-methoxybenzyl alcohol, as shown by p.m.r., and consequently must be the other possible isomer, 2,3-dibromo-4-methoxy-5-hydroxybenzyl alcohol.

When compound II*a* was caused to react with sulfur trioxide – pyridine complex in aqueous potassium carbonate, it formed a disulfate dipotassium salt whose infrared spectrum was identical with that of the salt isolated from *P. lanosa*. Since aliphatic hydroxyl groups do not form sulfate esters under these conditions, the salt must be 2,3-dibromobenzyl alcohol 4,5-disulfate, dipotassium salt (I).

As far as the authors are aware, this is the first aromatic compound isolated from a natural source which contains bromine on contiguous carbon atoms. A knowledge of the mechanism of bromination of the aromatic ring by the organism would be of considerable interest to both the biochemist and the organic chemist. Studies have been initiated to investigate this matter.

EXPERIMENTAL

Melting points were carried out on a Kofler hot stage. Infrared spectra were determined on a Perkin–Elmer model 237 spectrometer as potassium bromide disks. Proton magnetic resonance spectra were obtained with a Varian A-60 spectrometer equipped with a V-6058 spin-decoupler accessory, and were determined as 5–15% solutions in deuterochloroform or deuterated acetone (where specifically indicated) with tetramethylsilane as an internal standard.

Isolation of the P. lanosa Salt (I)

Freshly harvested alga (17 kg) was blotted and then extracted for 3 h with boiling aqueous ethanol (40 l, 80%). The extract was filtered to remove debris, and the filtrate was concentrated under reduced pressure (to 4 l). The dark-brown crystals, which deposited as the filtrate cooled, were collected and washed with methanol until the wash solvent remained colorless. The yield of light-grey product was 77 g (4%, dry wt. basis). Similar extractions of material collected at different times of the year yielded between 1 and 5% of the crystalline product. The salt was purified by repeated recrystallization from water to yield fine colorless needles of I.

Anal. Calcd. for $C_7H_4O_9S_2Br_2K_2$: C, 15.74; H, 0.75; O, 26.96; S, 11.98; Br, 29.91. Found: C, 15.96; H, 0.85; O, 27.12; S, 11.76; Br, 29.77.

The determination of sulfate by gravimetric methods (9), after hydrolysis of I with dilute hydrochloric acid, indicated the presence of two sulfate groups per molecule.

Hydrolysis of the P. lanosa Salt (I)

The potassium salt (16 g) in dilute hydrochloric acid (500 ml, 0.1 *N*) was heated on a steam bath until the solution turned slightly milky (0.5 h). The reaction mixture was then cooled and continuously extracted with ether to yield phenol II*a* as a colorless solid (8 g). The product was crystallized from ethyl acetate to give fine needles, m.p. 123–125°; p.m.r. spectrum: 2.83 τ (1H, singlet), 5.38 τ (2H, singlet), $\approx$6.9 τ (3H, very broad singlet).

Anal. Calcd. for $C_7H_6O_3Br_2$: C, 28.22; H, 2.03; Br, 53.62. Found: C, 28.21; H, 2.27; Br, 53.67.

The phenol, on treatment with excess acetic anhydride in pyridine, formed a triacetate derivative (II*b*), which was crystallized from methanol as fine colorless prisms, m.p. 105–106°; p.m.r. spectrum: 7.70 and 7.77 τ (6H, two singlets), 7.92 τ (3H, singlet), 4.85 τ (2H, doublet, $J \simeq 0.4$ c.p.s.), 2.70 τ (1H, triplet, $J \simeq 0.4$ c.p.s.).

Anal. Calcd. for $C_{13}H_{12}O_6Br_2$: C, 36.83; H, 2.85; Br, 37.69. Found: C, 36.87; H, 3.12; Br, 37.18.

The phenol formed a dimethyl ether (II*c*) when it was allowed to stand for 16 h with excess diazomethane in ether. This derivative was crystallized from petroleum ether (b.p. 60–80°) as fine, colorless needles, m.p. 92°; p.m.r. spectrum (deuterated acetone): 6.21 and 6.11 τ (6H, two singlets), 5.38 τ (2H, singlet), 2.64 τ (1H, singlet).

Anal. Calcd. for $C_9H_{10}O_3Br_2$: C, 33.16; H, 3.10; Br, 49.02. Found: C, 33.28; H, 3.29; Br, 48.53.

The phenol II*a* also formed a monomethyl ether on treatment with approximately 1 mole of diazomethane, for 1 h. This was separated from the dimethyl ether and unchanged phenol by chromatography on alumina. The monomethyl ether, on crystallization from benzene, gave colorless needles, m.p. 160–162°; p.m.r. spectrum (deuterated acetone): 6.18 τ (3H, singlet), 5.41 τ (2H, broad singlet), 2.75 τ (1H, broad singlet).

*Reduction of Phenol II*a *with Raney Nickel*

(*i*) The phenol (0.81 g) was dissolved in 5% sodium hydroxide solution (100 ml) and Raney alloy (4 g) added in small portions, with shaking. The mixture was heated on a steam bath for 1 h, cooled, filtered, and then acidified with concentrated hydrochloric acid. The resulting solution was continuously extracted with ether to yield 3,4-dihydroxytoluene as a pale yellow oil (0.25 g), b.p. 65° at 0.3 mm. This was shown by p.m.r. and infrared spectra to be identical with an authentic sample synthesized from 3,4-dihydroxybenzaldehyde by reduction, first with sodium borohydride by the procedure of Vogel (10, p. 881) and then with Raney alloy (as above).

(*ii*) The phenol II*a* (0.97 g) was dissolved in sodium deuteroxide solution (5 g of sodium in 70 ml D_2O), Raney alloy (4 g) was added in small portions over 20 min, and the mixture was heated on a steam bath for 1 h (care being taken to exclude any water vapor). The solution was cooled, filtered, acidified with concentrated hydrochloric acid, and continuously extracted with ether to yield, on removal of the solvent, a light oil (0.32 g). This was immediately methylated with diazomethane in ether solution to yield a dideutero-3,4-dimethoxytoluene as a colorless oil (0.29 g). The dimethoxytoluene was then treated with potassium permanganate (0.5 g) in aqueous sodium carbonate solution (50 ml, 5%). The mixture was warmed on a steam bath for 1 h, cooled, and decolorized with acidic sodium metabisulfite solution. The solution was continuously extracted with ether and the solvent removed under vacuum. The resulting solid was purified by dissolving it in sodium bicarbonate, extracting the impurities with ether, and then reprecipitating the solid with acid and re-extracting it with ether. The material was recrystallized from water and sublimed under vacuum to give 2,3-dideuteroveratric acid (51 mg) as fine needles, m.p. 180°.

Preparation of 2,3-Dibromo-4,5-dimethoxybenzyl Alcohol

5,6-Dibromoveratraldehyde (0.46 g, prepared by the method of Raiford and Wittmer (7)) was dissolved in methanol (10 ml), and a solution of sodium borohydride (80 mg) in sodium hydroxide (7 ml, 0.1 *N*) was added, with stirring. The methanol was removed on a steam bath and the residue was diluted with water (20 ml) and extracted with ether. The ethereal solution was taken to dryness and the residue was crystallized from petroleum ether to give 2,3-dibromo-4,5-dimethoxybenzyl alcohol (II*c*) as fine needles, m.p. 91–92°. This was shown by p.m.r., infrared spectra, and mixed melting point to be identical with the dimethyl ether obtained from the natural phenol (II*a*). The oxidation products of the natural dimethyl ether (method of Vogel (10, p. 520)) were shown to be identical with synthetic 5,6-dibromoveratraldehyde (7) and 5,6-dibromoveratric acid (8) by p.m.r., infrared spectra, and mixed melting point. The melting point of our sample of synthetic 5,6-dibromoveratric acid was 194° (lit. m.p. 186–187° (8)).

*Sulfonation of Phenol II*a

The phenol (0.36 g) was dissolved in water (10 ml) containing potassium carbonate (0.5 g), and sulfur trioxide – pyridine complex (0.24 g) was added slowly, with stirring. The solution was then cooled to 5° for 24 h and the resulting crystals were collected and recrystallized from a small amount of water to give fine needles of 2,3-dibromobenzyl alcohol 4,5-disulfate, dipotassium salt (I) (0.33 g). This was shown by infrared spectra to be identical with the natural sulfate salt isolated from *Polysiphonia lanosa*.

Can. J. Chem. Downloaded from www.nrcresearchpress.com by 210.87.254.40 on 09/05/12
For personal use only.

ACKNOWLEDGMENT

We acknowledge the excellent technical assistance of Mrs. M. G. Flack.

REFERENCES

1. M. PEGUY. Intern. Seaweed Symp. 4th, Halifax, Nova Scotia. 1964. p. 366.
2. J. AUGIER and P. MASTAGLI. Compt. Rend. **229**, 775 (1949); **242**, 190 (1956).
3. T. SAITO and Y. ANDO. Nippon Kagaku Zasshi, **76**, 478 (1955).
4. H. ROTTENDORF and S. STERNHELL. Australian J. Chem. **17**, 1315 (1964).
5. V. I. KOMAREWSKY, C. H. RIESZ, and F. L. MORRITZ. *In* Technique of organic chemistry. Vol. II. 2nd ed. *Edited by* A. Weissberger. Interscience Publishers, Inc., New York. 1956.
6. L. C. RAIFORD and G. C. HILLMAN. J. Am. Chem. Soc. **49**, 1571 (1927).
7. L. C. RAIFORD and F. B. WITTMER. J. Org. Chem. **10**, 527 (1945).
8. L. C. RAIFORD and R. P. PERRY. J. Org. Chem. **7**, 354 (1942).
9. A. I. VOGEL. A textbook of quantitative inorganic analysis including elementary instrumental analysis. John Wiley & Sons, Inc., New York. 1961. p. 462.
10. A. I. VOGEL. A textbook of practical organic chemistry. Longmans, Green & Co., Ltd., London. 1962.

Can. J. Chem. Downloaded from www.nrcresearchpress.com by 210.87.254.40 on 09/05/12
For personal use only.

SELECTIVE NUCLEOPHILIC SUBSTITUTION AND PREFERENTIAL EPOXIDE FORMATION

A. J. DICK[1] AND J. K. N. JONES
Department of Chemistry, Queen's University, Kingston, Ontario
Received July 20, 1965

ABSTRACT

The tri-*O*-methanesulfonyl derivatives of methyl β-D-xylopyranoside, methyl β-L-arabinopyranoside, and methyl α-L-arabinopyranoside undergo selective substitution at C-4, when heated with sodium azide in *N*,*N*-dimethylformamide, to yield 4-azido derivatives with inversion of configuration at C-4. The resultant 4-azido-2,3-di-*O*-methanesulfonyl derivatives were converted, by reaction with sodium methoxide, into 2,3-anhydro compounds whose configurations were assigned by nuclear magnetic resonance analysis. The mechanism of epoxide formation is discussed.

INTRODUCTION

The many attempts to effect nucleophilic substitution of isolated sulfonate ester groups attached to furanoside and pyranoside rings have met with only limited success (1), although the replacement of 4-sulfonates of certain hexopyranosides has been achieved (2), as has also the replacement of the 3-toluene-*p*-sulfonyl-β-D-glucopyranose (3). The course of the reactions of tosyl derivatives of cyclitols with sodium benzoate in *N*,*N*-dimethylformamide has also been described (4). The present study is concerned with the competitive nucleophilic substitution of methyl 2,3,4-tri-*O*-methanesulfonyl-pentopyranosides with azide ion in *N*,*N*-dimethylformamide solution. This work was prompted by a related investigation of the reaction of methyl hexopyranoside tetrachlorosulfates with chloride ion (5), to which the results reported here are strictly analogous.

The 2,3,4-tri-*O*-methanesulfonyl derivatives of methyl α-D-xylopyranoside (I) (6), methyl β-D-xylopyranoside (II), methyl β-L-arabinopyranoside (III), and methyl α-L-arabinopyranoside (IV) were each caused to react with 1 mole of sodium azide in *N*,*N*-dimethylformamide at 130° to yield 4-azido-4-deoxy derivatives with inversion of configuration at C-4. Thus the 4-azido-4-deoxy-2,3-di-*O*-methanesulfonyl derivatives of methyl β-L-arabinopyranoside (V) (6), methyl α-L-arabinopyranoside (VI), methyl α-D-xylopyranoside (VII), and methyl β-D-xylopyranoside (VIII) were obtained from I, II, III, and IV, respectively. Of the four azido-di-*O*-methanesulfonyl derivatives described, only methyl 4-azido-4-deoxy-2,3-di-*O*-methanesulfonyl-β-D-xylopyranoside (VIII) could be substituted further in the presence of an excess of sodium azide; these results will be described in a later publication.

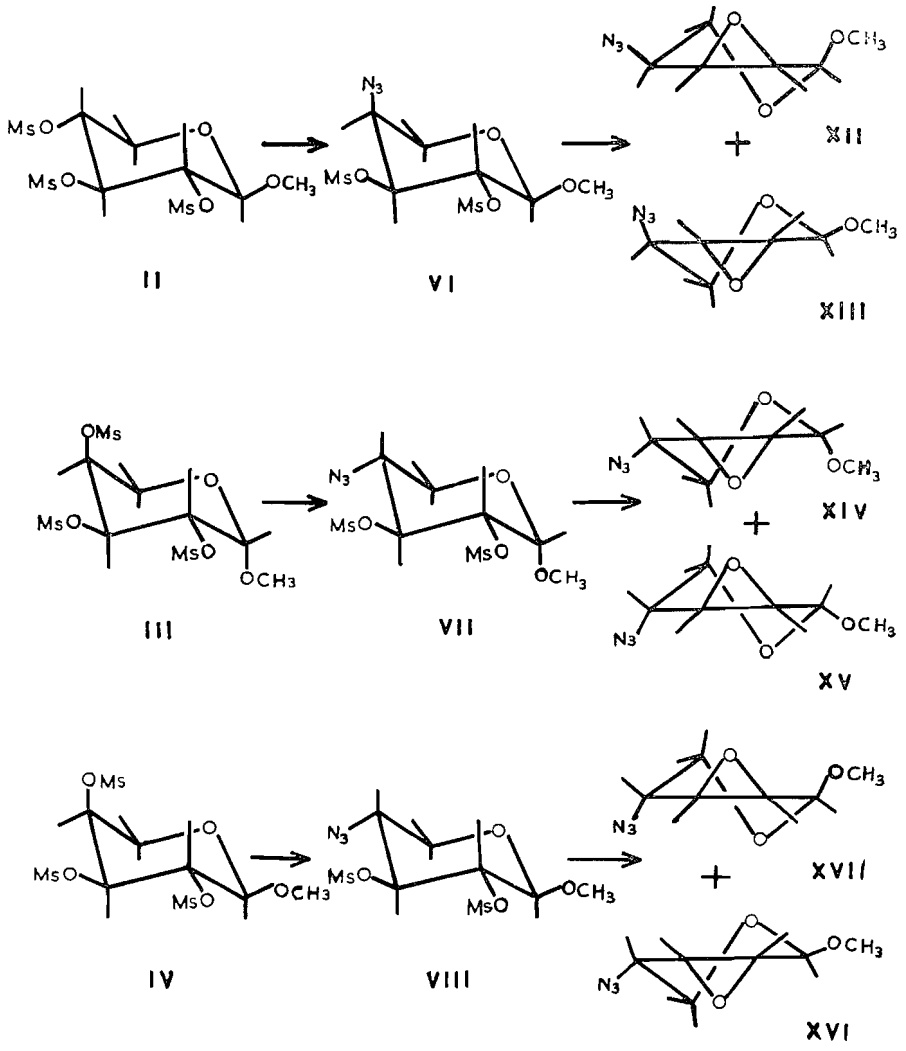
That V, VI, and VII were resistant to further substitution may be rationalized according to the arguments put forward by Jennings and Jones (5). The ester group on C-2 would be expected to be unreactive as compared with those on C-3 and C-4 because of their different electronic environments, that on C-2 being in the proximity of two β-oxygen atoms (ring oxygen and anomeric groups). Hindrance to attack at the rear side of the sulfonyloxy groups at C-3 of V and VII by the axial methyl glycosidic group would prevent further substitution in these compounds. To explain the unreactivity of the ester group at C-3 of VI it is necessary to invoke deactivation of the equatorial ester group by the vicinal axial substituent at C-4. Jennings and Jones referred to hindrance

[1]*Present address: University of Bristol, Bristol, England.*

Can. J. Chem. Downloaded from www.nrcresearchpress.com by 210.87.254.5 on 09/05/12
For personal use only.

of the attainment of the substitution transition state as a result of the eclipsing of the large substituents at C-3 and C-4 in the transition state. The ester group at C-3 of VIII, which is not subject to the types of interaction described above, would be expected to be replaced.

Reist *et al.* (7) observed a similar selective replacement reaction of methyl 2-*O*-acetyl-3,4-di-*O*-toluene-*p*-sulfonyl-β-L-arabinopyranoside with sodium azide in *N*,*N*-dimethylformamide, and thereby achieved the synthesis of 4-acetamido-4-deoxy-D-ribose. 4-Acetamido-4-deoxy-L-xylose has been synthesized from methyl tri-*O*-methanesulfonyl-α-D-xylopyranoside (I) (6).



It was shown that VI, VII, and VIII were 4-azido derivatives by conversion into 2,3-anhydro-4-azido-4-deoxy derivatives with sodium methoxide in methanol. It was also reported that V gave predominantly methyl 2,3-anhydro-4-azido-4-deoxy-β-L-ribopyranoside (IX) (6) on treatment with methanolic potassium hydroxide. The structural assignment of IX was made on the basis of its nuclear magnetic resonance (n.m.r.) spectrum

Can. J. Chem. Downloaded from www.nrcresearchpress.com by 210.87.254.5 on 09/05/12
For personal use only.

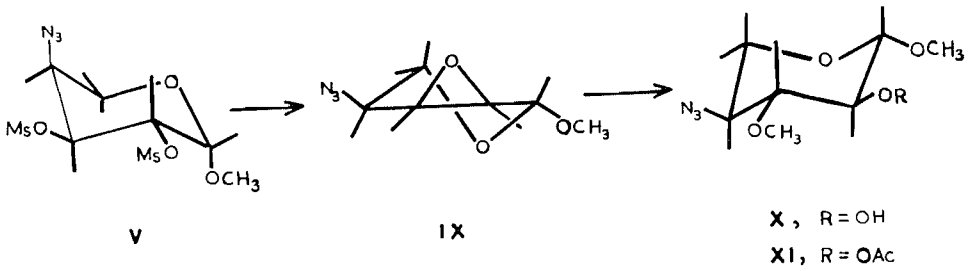
(Table I) and has since been confirmed by its further reaction with potassium hydroxide in methanol, but for a longer time. A crystalline mono-*O*-methyl derivative (X) was isolated from the reaction. Acetylation of this in pyridine yielded a syrupy acetate whose n.m.r. spectrum (Fig. 1) showed it to be methyl 2-*O*-acetyl-4-azido-4-deoxy-3-*O*-methyl-β-L-xylopyranoside (XI). The singlets caused by the methoxyl and *O*-acetyl hydrogens

TABLE I

Chemical shifts (τ values) and first-order coupling constants (c.p.s.)

Methyl 2,3-anhydro-4-azido-4-deoxy-pyranoside	H-1	H-2, H-3*
β-L-*ribo* (IX)	5.13 $J_{1,2} < 0.5$	
α-L-*ribo* (XII)	5.12 $J_{1,2} = 2.5$	
α-*lyxo* (XIII)	5.17 $J_{1,2} < 0.5$	6.77 $J_{2,3} = 4.0$
α-D-*ribo* (XIV)	5.23 $J_{1,2} = 2.5$	
α-D-*lyxo* (XV)	5.26 $J_{1,2} < 0.5$	6.82 $J_{2,3} = 3.5$
β-D-*ribo* (XVI)	5.20 $J_{1,2} < 0.5$	
β-D-*lyxo* (XVII)	5.12 $J_{1,2} = 3.0$	

*Center of the "AB" quartet.



are immediately assignable. The doublet at τ 5.75 ($J_{1,2}$ = 7.0 c.p.s.) was assigned to H-1, and since the triplet at τ 5.14 contained the same 7.0 c.p.s. spacing, it was therefore assigned to H-2. Because H-2 resonates at low field, the acetyl group must be on C-2. The relative intensities of the lines in the multiplets confirmed these assignments. The comparatively large couplings between H-1 and H-2 and between H-2 and H-3 indicated that these pairs of hydrogens are disposed *trans* diaxially, and since the configuration at C-1 is already known, the β-L-*xylo* configuration may be assigned to this compound. This 3-*O*-methyl-L-xylose derivative could only have been derived from a 2,3-anhydro-L-ribose precursor. The sequence of reactions (I → V → IX → X) leads to inversion of configuration, namely, at C-2, C-3, and C-4 (i.e. α-D-*xylo* to β-L-*xylo*).

The di-*O*-methanesulfonyl derivatives (VI, VII, and VIII), when treated with sodium methoxide, each gave a mixture of two 2,3-anhydro derivatives, namely, methyl 2,3-anhydro-4-azido-4-deoxy-α-L-ribopyranoside (XII) and methyl 2,3-anhydro-4-azido-4-deoxy-α-L-lyxopyranoside (XIII) from VI, methyl 2,3-anhydro-4-azido-4-deoxy-α-D-ribopyranoside (XIV) and methyl 2,3-anhydro-4-azido-4-deoxy-α-D-lyxopyranoside (XV) from VII, and methyl 2,3-anhydro-4-azido-4-deoxy-β-D-ribopyranoside (XVI) and methyl

Can. J. Chem. Downloaded from www.nrcresearchpress.com by 210.87.254.5 on 09/05/12
For personal use only.

Can. J. Chem. Downloaded from www.nrcresearchpress.com by 210.87.254.5 on 09/05/12
For personal use only.

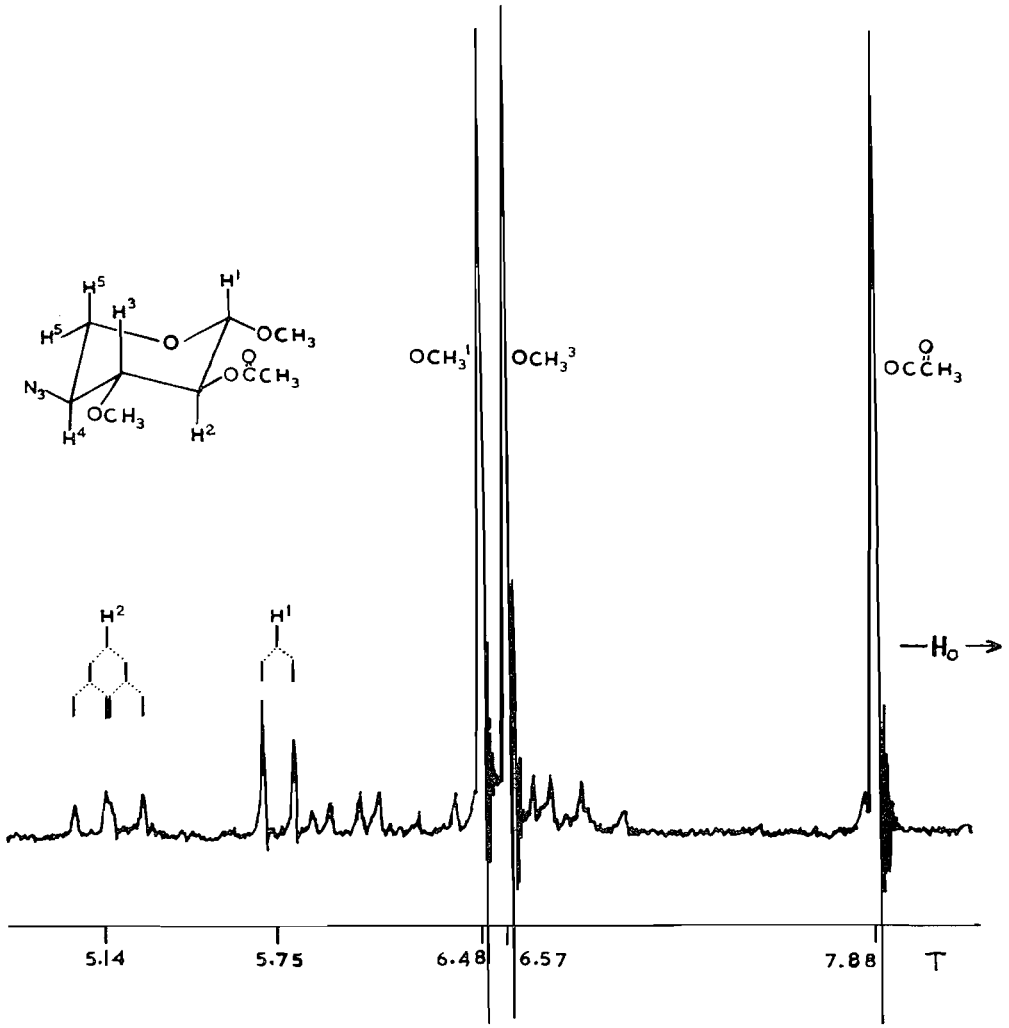


FIG. 1. Partial n.m.r. spectrum of methyl 2-*O*-acetyl-4-azido-4-deoxy-3-*O*-methyl-β-L-xylopyranoside.

2,3-anhydro-4-azido-4-deoxy-β-D-lyxopyranoside (XVII) from VIII. The anhydro-pyranosides from VI and VII were easily separated by column chromatography on silica gel, but it was necessary to separate those prepared from VIII by preparative thin-layer chromatography.

Structural assignments of the anhydro-pyranoside derivatives were made on the basis of partial analysis of their n.m.r. spectra. The chemical shifts and first-order coupling constants which were obtained for the ring protons of these compounds and which are collected in Table I are in sufficient agreement with those obtained by Buss *et al.* in their n.m.r. study of carbohydrate 2,3-epoxides (8) to assign the epoxide ring to the 2,3 position. For example, the spectrum of XIII (Fig. 2*b*) has a singlet (τ 5.17) assignable to H-1 and an "AB" quartet (centered at τ 6.77) assignable to H-2 and H-3. The very small couplings between H-1 and H-2 and between H-3 and H-4 indicate that these pairs of protons contain a *trans* relationship. In Fig. 2*a* is shown the spectrum of XII, which reveals a doublet at τ 5.12 ($J_{1,2} = 2.5$) assignable to H-1, thus indicating that H-1 and H-2 are *cis*.

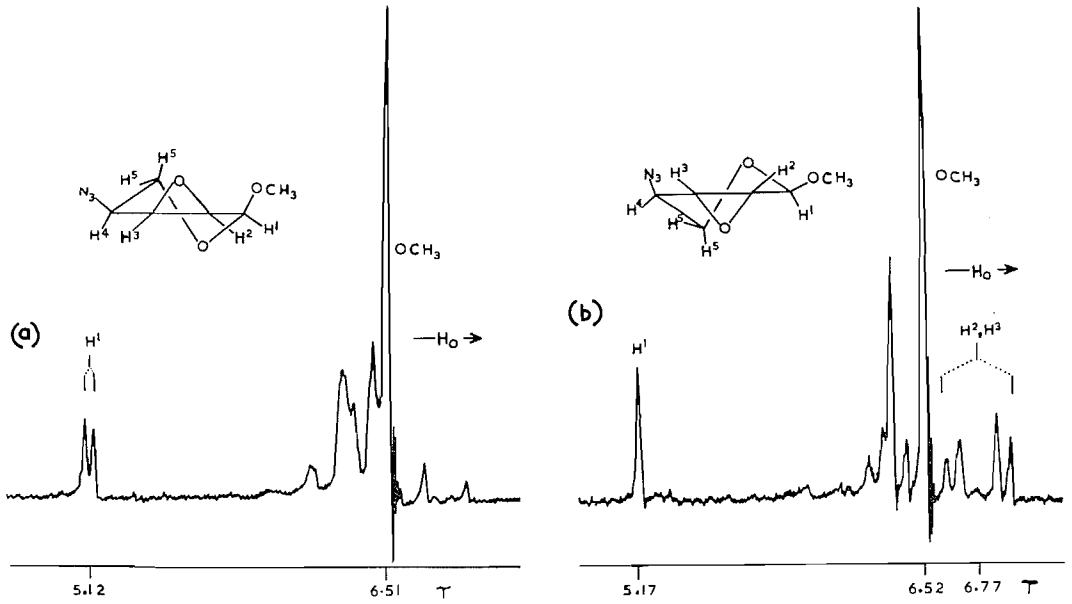


FIG. 2. Partial n.m.r. spectra of (*a*) methyl 2,3-anhydro-4-azido-4-deoxy-α-L-ribopyranoside and (*b*) methyl 2,3-anhydro-4-azido-4-deoxy-α-L-lyxopyranoside.

Also we noted in an earlier publication (6) the synthesis of methyl 4,6-diazido-4,6-dideoxy-2,3-di-*O*-methanesulfonyl-α-D-galactopyranoside (XXIII) from methyl 2,3,4,6-tetra-*O*-methanesulfonyl-α-D-glucopyranoside (XXII). The details of this preparation are now given. Proof of structure of XXIII was achieved by mesylating methyl 4,6-diazido-4,6-dideoxy-α-D-galactopyranoside (2), which gave a di-*O*-methanesulfonyl derivative identical in all respects with XXIII.

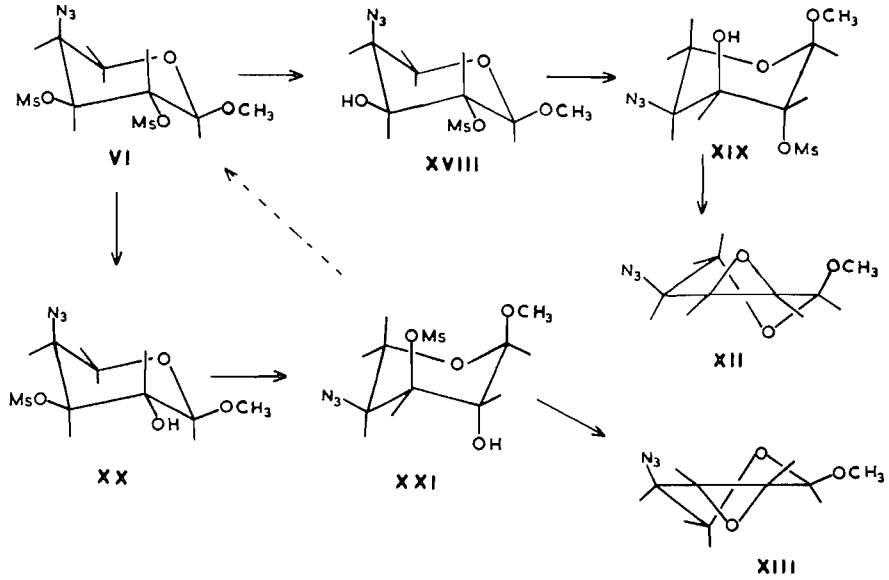
DISCUSSION

The mechanism of the sequence of reactions leading to epoxide formation is of interest in view of the relative yields of the two anhydro derivatives obtained. But the interpretation is complex. Angyal and Gilham, in their synthesis of anhydroinositols from vicinal *trans* di-*O*-tosylates (9), favored removal of one of the sulfonyl groups by *O*—*S* fission (S_N2_S type), a process that is facilitated by the inductive effect of the adjacent sulfonyloxy group, followed by participation of the free hydroxyl in the elimination of the neighboring sulfonyl group to give the epoxide. Although a preponderance of one anhydro-pyranoside over the other is obtained in most cases in the present study, it is difficult to imagine that one sulfonyloxy group is more accessible to hydrolysis than the other (e.g. C-2 of VII), because an equatorial substituent is equidistant from a vicinal equatorial or axial substituent. However, the inductive effect of the neighboring methoxyl and azido groups is probably a major influence. Moreover, the situation is complicated by the possibility of "transsulfonylation", since Cope and Shen (10) have obtained evidence that "transtosylation" is operating in the formation of 1,4:2,5:3,6-trianhydro-D-mannitol from the ditosylate of 1,4:3,6-dianhydro-D-glucitol. Our attempts to achieve transmesylation have, however, been unsuccessful. Methyl 4-azido-4-deoxy-β-L-xylopyranoside (6) and methyl 3,4-di-*O*-isopropylidene-2-*O*-methanesulfonyl-α-L-arabinopyranoside (11) were boiled under reflux in methanol solution containing sodium methoxide. Hydrolysis of the

Can. J. Chem. Downloaded from www.nrcresearchpress.com by 210.87.254.5 on 09/05/12
For personal use only.

2-*O*-methanesulfonyl group occurred, but the formation of an anhydro derivative or a mono-*O*-methyl compound derived from the epoxide was not observed. Similarly, reaction of methyl 4-azido-4-deoxy-β-L-arabinopyranoside (6) with methyl 4,6-diazido-4,6-dideoxy-2,3-di-*O*-methanesulfonyl-α-D-galactopyranoside failed to yield an anhydro derivative from the *arabino* compound.

Nevertheless, the relative yields of anhydro-pyranosides that were obtained may be explained on purely conformational grounds. Initial hydrolysis, by *O*—*S* cleavage of the sulfonyloxy group, at C-3 of VI would give XVIII, which would have to undergo a change in chair conformations for the participating substituents to be *trans*-diaxial in the



transition state in order to yield the epoxide XII, which was obtained as the major product. On the other hand, if the sulfonyloxy group at C-2 of VI were hydrolyzed first, the chair conformation (XXI) would be formed to give *trans* coplanarity of the participating groups and subsequently would give the epoxide XIII.

If the two transition states are considered as approximating to XIX and XXI, the formation of the latter would be the least favored on conformational grounds because of the passing interaction of the methanesulfonyloxy group on C-3 with the axial azido group on C-4 when XX changes to that conformation (e.g. XXI) where the substituents on C-2 and C-3 are diaxial. In the case of XVIII, the same passing interaction involves a less bulky hydroxyl group. Also, there would be a larger 1,3-diaxial interaction in XXI than in XIX. Thus, although XVIII and XX may be formed with similar ease, the former would be the more reactive and the anhydro-pyranoside (XII) derived from it would predominate. Furthermore, transmesylation of XXI by VI followed by S_N2_S cleavage at C-3 would yield XVIII and thus increase the final yield of XII.

Similar considerations of passing interactions that are incurred when there is a change in conformation, and of transtosylation are useful in explaining the virtually exclusive formation of the *allo*-epoxide from methyl 4,6-*O*-benzylidene-2,3-di-*O*-toluene-*p*-sulfonyl-α-D-glucopyranoside (12) and of the *talo*-epoxide from methyl 4,6-*O*-benzylidene-2,3-di-*O*-toluene-*p*-sulfonyl-β-D-galactopyranoside (13).

Can. J. Chem. Downloaded from www.nrcresearchpress.com by 210.87.254.5 on 09/05/12
For personal use only.

Can. J. Chem. Downloaded from www.nrcresearchpress.com by 210.87.254.5 on 09/05/12
For personal use only.

EXPERIMENTAL

Solutions were concentrated under reduced pressure below 50° with a rotating vacuum-type evaporator, except *N,N*-dimethylformamide solutions which were evaporated at 60°. Melting points were determined on a Reichert melting point apparatus and are uncorrected. Optical rotations were measured at 23 ± 3° with a Hilger standard polarimeter. All infrared spectra obtained for the compounds described were consistent with the assigned structures. Thin-layer chromatograms (silica gel G, Merck) were irrigated with 4% v/v methanol in benzene and the spots located by spraying the chromatograms with a 5% solution of sulfuric acid in ethanol and heating the plates at 120°. Epoxides were also detected with a sodium iodide and methyl red reagent (14). Nuclear magnetic resonance spectra were measured in $CDCl_3$ solution with a Varian A60 spectrometer.

*Methyl 2,3,4-Tri-O-methanesulfonyl-β-*D*-xylopyranoside (II) and Methyl 2,3,4-Tri-O-methanesulfonyl-β-*L*-arabinopyranoside (III)*

Methyl β-D-xylopyranoside and methyl β-L-arabinopyranoside were methanesulfonylated as usual with 3 moles of methanesulfonyl chloride in pyridine solution. The respective trimethanesulfonates were isolated by pouring the reaction mixtures into ice water and were recrystallized from methanol to give II (78% yield), m.p. 147.5–148.5°, $[\alpha]_D$ −33.6° (*c*, 1.4 in chloroform), and III (92% yield), m.p. 127.5–128°, $[\alpha]_D$ +143° (*c*, 4.6 in chloroform).

Anal. Calcd. for $C_9H_{18}O_{11}S_3$: C, 27.1; H, 4.5; S, 24.1. Found for II: C, 27.3; H, 4.5; S, 23.8. Found for III: C, 26.9; H, 4.2; S, 24.1.

*Methyl 2,3,4-Tri-O-methanesulfonyl-α-*L*-arabinopyranoside (IV)*

A crystalline mixture (20 g) containing ca. 70% methyl α-L-arabinopyranoside (15) plus 30% of the anomer (calculated from the specific rotation) was dissolved in pyridine (250 ml), and methanesulfonyl chloride (3.2 moles) was added slowly, the temperature of the reaction mixture being kept below 0°. After the reaction mixture had been kept at room temperature for 3 h, it was poured into ice water (500 ml). The crystalline precipitate was collected and recrystallized from methanol to give 19.3 g of a solid which melted at 177–181°. Two further recrystallizations from methanol gave the pure α-anomer (IV), which melted at 190.5–191.5° and had $[\alpha]_D$ +34.3° (*c*, 1.02 in chloroform).

Anal. Calcd. for $C_9H_{18}O_{11}S_3$: C, 27.1; H, 4.5; S, 24.1. Found: C, 26.7; H, 4.8; S, 24.4.

*Methyl 2,3,4,6-Tetra-O-methanesulfonyl-α-*D*-glucopyranoside (XXII)*

Methyl α-D-glucopyranoside was treated with methanesulfonyl chloride (4 moles) as described above to give XXII, which melted at 146.5–147.5° and had $[\alpha]_D$ +91° (*c*, 1.76 in chloroform).

Anal. Calcd. for $C_{11}H_{22}O_{14}S_4$: C, 26.1; H, 4.34; S, 25.3. Found: C, 25.7; H, 4.0; S, 24.9.

Reaction of the Tri-O-methanesulfonyl Derivatives with Sodium Azide

A 10% solution of the methanesulfonyl derivative in *N,N*-dimethylformamide containing sodium azide (ca. 1.2 moles) was heated at 130°. The disappearance of starting material was followed by thin-layer chromatography, and the reaction mixture was cooled 2 h after starting material was no longer evident. The solution was then filtered to remove precipitated sodium methanesulfonate and the filtrate evaporated to dryness. The residue was partitioned between water and chloroform, and the chloroform layer was washed several times with water, dried ($MgSO_4$), and concentrated to a syrup which crystallized when it was allowed to stand. Recrystallization from methanol or ethanol gave the corresponding azido-deoxy-di-*O*-methanesulfonyl derivative.

*Methyl 4-Azido-4-deoxy-2,3-di-O-methanesulfonyl-α-*L*-arabinopyranoside (VI)*

Reaction of methyl 2,3,4-tri-*O*-methanesulfonyl-β-D-xylopyranoside (II) as above required 24 h for complete disappearance of the starting material and gave VI, isolated in 40% yield, which melted at 124.5–125.5° and had $[\alpha]_D$ +1.3° (*c*, 3.76 in chloroform).

Anal. Calcd. for $C_8H_{15}N_3O_8S_2$: C, 27.8; H, 4.35; N, 12.2; S, 18.5. Found: C, 27.5; H, 4.3; N, 12.4; S, 18.7.

*Methyl 4-Azido-4-deoxy-2,3-di-O-methanesulfonyl-α-*D*-xylopyranoside (VII)*

The reaction of methyl 2,3,4-tri-*O*-methanesulfonyl-β-L-arabinopyranoside (III) was essentially complete in 12 h and gave 84% yield of VII, which melted at 117.5–118° and had $[\alpha]_D$ +121° (*c*, 2.94 in chloroform).

Anal. Calcd. for $C_8H_{15}N_3O_8S_2$: C, 27.8; H, 4.35; N, 12.2; S, 18.5. Found: C, 27.5; H, 4.4; N, 12.5; S, 18.6.

When VI and VII were treated with sodium azide as above, no further substitution products were observed on thin-layer chromatograms after 24 h reaction, and only starting material was recovered.

*Methyl 4-Azido-4-deoxy-2,3-di-O-methanesulfonyl-β-*D*-xylopyranoside (VIII)*

Methyl 2,3,4-tri-*O*-methanesulfonyl-α-L-arabinopyranoside (IV), when caused to react with sodium azide (1.2 moles) for 36 h as described above, gave VIII in 38% yield. In addition to the desired monoazido derivative, several other components were observed on thin-layer chromatograms. Starting material (12%) was recovered by fractional crystallization from methanol. VIII remained in the mother liquors and was purified by evaporation of the solvent and crystallization of the residue from ethanol; it had m.p. 140–141° and $[\alpha]_D$ +1.4° (*c*, 3.55 in chloroform).

Anal. Calcd. for $C_8H_{15}N_3O_8S_2$: C, 27.8; H, 4.35; N, 12.2; S, 18.5. Found: C, 27.6; H, 4.4; N, 11.9; S, 18.3.

Reaction of Methyl 2,3,4,6-Tetra-O-methanesulfonyl-α-D-glucopyranoside with Sodium Azide

The methanesulfonyl derivative (XXII) (20 g) was heated in *N,N*-dimethylformamide solution (300 ml) containing sodium azide (7.7 g) at 115° for 40 h. The reaction was worked up as above and gave methyl 4,6-diazido-4,6-dideoxy-2,3-di-*O*-methanesulfonyl-α-D-galactopyranoside (XXIII) (12.8 g; 81%), which melted at 144–144.5° and had $[\alpha]_D$ +92° (*c*, 1.06 in chloroform).

Anal. Calcd. for $C_9H_{16}O_8N_6S_2$: C, 27.0; H, 4.0; N, 21.0; S, 16.0. Found: C, 26.9; H, 4.0; N, 21.2; S, 15.6.

Reaction of Methyl 4,6-Diazido-4,6-dideoxy-α-D-galactopyranoside with Methanesulfonyl Chloride

Methyl 4,6-diazido-4,6-dideoxy-α-D-galactopyranoside (2) (0.10 g) was treated with methanesulfonyl chloride (0.2 ml) as usual, in pyridine solution. A crystalline product was obtained which, after recrystallization from methanol, melted at 144–144.5°. The melting point was undepressed on admixture with methyl 4,6-diazido-4,6-dideoxy-2,3-di-*O*-methanesulfonyl-α-D-galactopyranoside.

Reaction of Methyl 4-Azido-4-deoxy-2,3-di-O-methanesulfonyl-pentopyranosides with Sodium Methoxide

A 5% solution of the 4-azido-4-deoxy-2,3-di-*O*-methanesulfonyl derivative in methanol containing ca. 2 moles sodium methoxide was boiled under reflux. The reaction was continued until the starting material had disappeared, as shown by thin-layer chromatography. Methanol was removed and the residue was partitioned between chloroform and water. The chloroform layer was dried ($MgSO_4$) and concentrated to a syrup from which a little starting material was removed by crystallization from methanol. The oily residue remaining after evaporation of the methanol was fractionated by chromatography on a column of silica gel (Davison). Elution with 4:1 v/v petrol (b.p. 40–60°) – ether gave a good separation of the anhydro derivatives obtained from VI and VII.

Anhydro Derivatives from Methyl 4-Azido-4-deoxy-2,3-di-O-methanesulfonyl-α-L-arabinopyranoside (VI)

After VI (5.52 g) was allowed to react for 4 h as described above, starting material (2.14 g) was recovered together with an oily mixture (1.35 g). When this oil was fractionated on silica gel (70 g), with benzene – 0.2% methanol as eluent, methyl 2,3-anhydro-4-azido-4-deoxy-α-L-lyxopyranoside (XIII) (12.5%) was eluted first as an oil, which had $[\alpha]_D$ −104° (*c*, 0.77 in chloroform), followed by methyl 2,3-anhydro-4-azido-4-deoxy-α-L-ribopyranoside (XII) (40.5%), which had $[\alpha]_D$ −252° (*c*, 0.43 in chloroform).

Anal. Calcd. for $C_6H_9O_3N_3$: C, 42.1; H, 5.3; N, 24.6. Found for XII: C, 42.3; H, 5.3; N, 24.1. Found for XIII: C, 42.4; H, 5.5; N, 24.2.

Anhydro Derivatives from Methyl 4-Azido-4-deoxy-2,3-di-O-methanesulfonyl-α-D-xylopyranoside (VII)

Reaction of VII (27 g) for 4 h as described above yielded starting material (VII) (16 g), methyl 2,3-anhydro-4-azido-4-deoxy-α-D-lyxopyranoside (XV) (0.40 g) (as an oil which had $[\alpha]_D$ +105° (*c*, 1.08 in chloroform)), and methyl 2,3-anhydro-4-azido-4-deoxy-α-D-ribopyranoside (XIV) (7) (3.33 g) (which melted at 43–44°).

Anal. Calcd. for $C_6H_9O_3N_3$: C, 42.1; H, 5.3; N, 24.6. Found for XV: C, 42.1; H, 5.4; N, 24.5.

Anhydro Derivatives from Methyl 4-Azido-4-deoxy-2,3-di-O-methanesulfonyl-β-D-xylopyranoside (VIII)

Treatment of VIII (3.22 g) with methoxide for 6 h as described above yielded starting material (1.55 g) and an oily product (0.78 g). Chromatography of the latter on silica gel gave a mixture (0.36 g) of two anhydro derivatives which were separated on thin-layer chromatograms, with 0.2% methanol in benzene as solvent, to give methyl 2,3-anhydro-4-azido-4-deoxy-β-D-ribopyranoside (XVI), m.p. 64–64.5°, $[\alpha]_D$ 0° (*c*, 0.30 in chloroform), and methyl 2,3-anhydro-4-azido-4-deoxy-β-D-lyxopyranoside (XVII) as an oil, $[\alpha]_D$ ca. −54° (*c*, 0.39 in chloroform). The relative amounts of XVI and XVII, obtained by estimation of the anomeric hydrogen from an integrated n.m.r. spectrum of the mixture, were 9:16 respectively.

Anal. Calcd. for $C_6H_9O_3N_3$: C, 42.1; H, 5.3; N, 24.6. Found for XVI: C, 42.4; H, 5.4; N, 25.1. Found for XVII: C, 42.1; H, 5.3; N, 24.1.

Methyl 4-Azido-4-deoxy-3-O-methyl-β-L-xylopyranoside (X)

A mixture of methyl 4-azido-4-deoxy-2,3-di-*O*-methanesulfonyl-β-L-arabinopyranoside (V) (6) (5.0 g), methanol–water (2:1) (125 ml), and potassium hydroxide (5.0 g) was boiled under reflux for 3 h. The solution was concentrated to remove methanol and was then extracted with ether. The ethereal extract was washed several times with water, and the aqueous washings were deionized by passage through Amberlite IR-120 (H^+ form) and Duolite A-4 (OH^- form) ion-exchange resins. Concentration of the aqueous solution gave a syrup (3 g) which was fractionated on a column of silica gel by elution with benzene containing 10% methanol. The first fraction obtained was methyl 4-azido-4-deoxy-3-*O*-methyl-β-L-xylopyranoside (X) (1.3 g) which, after recrystallization from petrol (60–80°), melted at 111–111.5° and had $[\alpha]_D$ −21.2° (*c*, 2.45 in chloroform).

Anal. Calcd. for $C_7H_{13}O_4N_3$: C, 41.4; H, 6.4; N, 20.7. Found: C, 41.1; H, 6.2; N, 20.8.

Methyl 2-O-Acetyl-4-azido-4-deoxy-3-O-methyl-β-L-xylopyranoside (XI)

Methyl 4-azido-4-deoxy-3-*O*-methyl-β-L-xylopyranoside (X) (0.20 g) was acetylated with acetic anhydride in pyridine solution in the usual manner and gave XI (0.22 g) as a colorless syrup which had $[\alpha]_D$ +25.7° (*c*, 4.1 in chloroform).

Anal. Calcd. for $C_9H_{15}O_5N_3$: C, 44.1; H, 6.1; N, 17.1. Found: C, 44.0; H, 6.2; N, 17.2.

Can. J. Chem. Downloaded from www.nrcresearchpress.com by 210.87.254.5 on 09/05/12
For personal use only.

ACKNOWLEDGMENTS

We thank the National Research Council for a grant (N.R.C. T-19) and Queen's University for a McLaughlin Travelling Scholarship (to A. J. D.). We also thank Dr. L. Hough for many helpful suggestions and Dr. Bruce Coxon for assistance in the interpretation of the n.m.r. spectra.

REFERENCES

1. P. A. LEVENE and R. S. TIPSON. J. Biol. Chem. **105**, 419 (1934). R. S. TIPSON. Advan. Carbohydrate Chem. **8**, 107 (1953). N. K. MATHESON and S. J. ANGYAL. J. Chem. Soc. 1133 (1952). M. L. WOLFROM, J. BERNSMANN, and D. HORTON. J. Org. Chem. **27**, 4505 (1962). M. JACKSON and L. D. HAYWARD. Can. J. Chem. **37**, 1048 (1959). K. S. RYAN, H. ARZOUMANIAN, E. M. ACTON, and L. GOODMAN. J. Am. Chem. Soc. **86**, 2497 (1964); **86**, 2503 (1964). J. F. CODINGTON, R. FECHER, and J. J. FOX. J. Am. Chem. Soc. **82**, 2794 (1960).
2. B. HELFERICH and A. GNÜCHTEL. Ber. **71**, 712 (1938). E. J. REIST, D. E. GUEFFROY, and L. GOODMAN. J. Org. Chem. **24**, 1618 (1959). E. J. REIST, R. R. SPENCER, B. R. BAKER, and L. GOODMAN. Chem. Ind. London, 1794 (1962). J. HILL, L. HOUGH, and A. C. RICHARDSON. Proc. Chem. Soc. 346 (1963). E. J. REIST, D. E. GUEFFROY, and L. GOODMAN. J. Am. Chem. Soc. **85**, 3715 (1963).
3. N. A. HUGHES and P. R. H. SPEAKMAN. J. Chem. Soc. 2236 (1965).
4. S. J. ANGYAL and T. S. STEWART. Proc. Chem. Soc. 331 (1964).
5. H. J. JENNINGS and J. K. N. JONES. Can. J. Chem. **43**, 3018 (1965).
6. A. J. DICK and J. K. N. JONES. Can. J. Chem. **43**, 977 (1965).
7. E. J. REIST, D. E. GUEFFROY, and L. GOODMAN. J. Am. Chem. Soc. **87**, 677 (1965).
8. D. H. BUSS, L. HOUGH, L. D. HALL, and J. F. MANVILLE. Tetrahedron, **21**, 69 (1965).
9. S. J. ANGYAL and P. T. GILHAM. J. Chem. Soc. 3691 (1957).
10. A. C. COPE and T. Y. SHEN. J. Am. Chem. Soc. **78**, 5913 (1956).
11. H. B. WOOD, JR. and H. G. FLETCHER, JR. J. Am. Chem. Soc. **80**, 5242 (1958).
12. J. HONEYMAN and J. W. W. MORGAN. J. Chem. Soc. 3660 (1955).
13. E. SORKIN and T. REICHSTEIN. Helv. Chim. Acta. **28**, 1 (1945); **28**, 662 (1945).
14. J. G. BUCHANAN and J. C. P. SCHWARZ. J. Chem. Soc. 4770 (1962).
15. C. S. HUDSON. J. Am. Chem. Soc. **47**, 265 (1925).

Can. J. Chem. Downloaded from www.nrcresearchpress.com by 210.87.254.5 on 09/05/12
For personal use only.

STRUCTURES OF CHLOROBIUM CHLOROPHYLLS (660)[1]

A. S. HOLT, J. W. PURDIE,[2] AND J. W. F. WASLEY[3]
Division of Biosciences, National Research Council, Ottawa, Canada
Received June 2, 1965

ABSTRACT

The *Chlorobium* chlorophylls (660) consist of six different pigments, all of which are derivatives of δ-alkyl-2-desvinyl-2-α-hydroxyethylpyropheophorbide *a*. The six compounds differ in their substituents at C_4 (isobutyl, *n*-propyl, ethyl), C_5 (ethyl, methyl), and C_δ (ethyl, methyl).

INTRODUCTION

Initial studies (1–4) on the *Chlorobium* chlorophylls (660) established the presence of magnesium and a conjugated carbonyl group, and the absence of a methoxyl group. Removal of the magnesium by acid and hydrolysis of the product by hot, methanolic potassium hydroxide yielded crude "pheophorbide" and farnesol (5, 6). Oxidative degradation of the crude "pheophorbide" yielded *trans*-dihydrohematinic acid imide, methylethylmaleimide, and methyl-*n*-propylmaleimide. Crude "pheophorbide" was separated into six different fractions by column partition chromatography between ether and hydrochloric acid (6–8). These were designated 1 to 6 in the order of their decreasing acid numbers (order of elution). Their respective visible absorption spectra were not significantly different but resembled those of purpurins.

Fractions 1 and 2 yielded methylisobutylmaleimide; fractions 3 and 4, methyl-*n*-propylmaleimide; and fractions 5 and 6, methylethylmaleimide. All fractions possessed a hydroxyalkyl group (6, 7, 9) which could be oxidized to a conjugated carbonyl group (10) or dehydrated to an alkenyl group (11), the latter being converted into an alkyl group by catalytic hydrogenation to yield a "meso" derivative (12). The "meso" derivatives of fractions 3 and 4 yielded methylethylmaleimide in addition to methyl-*n*-propylmaleimide. This established the hydroxyalkyl group as an α-hydroxyethyl substituent. It was assumed to be at ring I by analogy with the *Chlorobium* chlorophylls (650).

The porphyrin that was obtained when fraction 5 was treated with hydriodic acid in acetic acid (65 °C) contained a conjugated carbonyl group, and an ethyl group in place of the hydroxyethyl group (7), and gave an "etio"-type visible absorption spectrum (13).

Oxidation of fraction 5 in alkaline dimethylformamide gave a diketone which was cleaved with hydrogen peroxide to yield a tricarboxylic acid. This, when decarboxylated at 185 °C in 1% HCl, gave a porphyrin with a "phyllo"-type absorption spectrum. It was concluded that the chlorophylls (660) possess a cyclopentanone ring, together with an alkyl substituent on a methine bridge carbon atom, and that it is this substituent which changes the effect of the cyclopentanone ring on the visible absorption spectrum of the porphyrin (13). The extra alkyl group was assigned to the δ methine bridge on the basis of nuclear magnetic resonance spectroscopy (7).

The purpose of the following work was to confirm the C_δ assignment and to identify the substituents at C_5 and C_δ in each fraction.

[1]*Issued as N.R.C. No. 8670.*
[2]*National Research Council Postdoctorate Fellow, 1961–1963. Present address: Defence Chemical, Biological and Radiation Laboratories, Defence Research Board, Ottawa.*
[3]*National Research Council Postdoctorate Fellow, 1962–1964. Present address: Department of Medicinal Chemistry, Geigy Chem. Corp., New York.*

Can. J. Chem. Downloaded from www.nrcresearchpress.com by 210.87.254.40 on 09/05/12
For personal use only.

Can. J. Chem. Downloaded from www.nrcresearchpress.com by 210.87.254.40 on 09/05/12
For personal use only.

DISCUSSION

Comparison of the proton magnetic resonance spectra of the methyl esters of mesopyropheophorbide *a*, δ-chloromesopyropheophobide *a*, and the "meso" derivative of fraction 5 indicates that the alkyl group is at C_δ. Mesopyropheophorbide *a* has signals at $\tau = 0.67$ and 0.90 which are assigned to the α and β methine bridge protons, and a signal at $\tau = 1.53$ which is assigned to the C_δ proton (14). δ-Chloromesopyropheophorbide *a* has only two bridge proton signals, at $\tau = 0.69$ and 0.76. Similarly, the "meso" derivative of fraction 5 has only two signals in this region, at $\tau = 0.48$ and 0.65. The absence of a signal at about $\tau = 1.5$ indicates that there is an alkyl substituent on C_δ. This is supported by the fact that the "meso" derivative of fraction 5 of chlorophylls (660) does not give a chloro derivative when treated by the methods used to prepare δ-chloromesopyropheophorbide *a* (7). The nuclear magnetic resonance spectra of fractions 3 and 4 give only two methine bridge proton signals: fraction 3, $\tau = 0.23$ and 0.65; fraction 4, $\tau = 0.28$ and 0.70.

Rapoport and co-workers (15, 16) have also investigated the main fraction of the *Chlorobium* chlorophylls (660), presumably that designated fraction 5 in our work (7). On the basis of nuclear magnetic resonance studies, they concluded that the structure proposed by Holt *et al.* (7) was probably correct, except that the alkyl group was suggested to be at either the α or the β methine bridge. This conclusion is invalidated by assignment of the signal $\tau = 0.67$ to a δ-proton, which differs to an inadmissible extent from the assignments of δ-proton signals of chlorophylls *a* and *b*: $\tau = 1.85$ and 1.86, respectively.

In our studies it was found that fraction 5 has methine bridge proton signals at $\tau = 0.28$ and 0.61. Similarly, fraction 6 has signals at $\tau = 0.30$ and 0.85; its "meso" derivative has signals at $\tau = 0.63$ and 0.75. Thus, conversion of the 2-α-hydroxyethyl group into an ethyl group affects mainly the lower field signals. In fractions 5 and 6, respectively, $\tau = 0.28$ and 0.30 are provisionally assigned to the C_α protons, and $\tau = 0.65$ and 0.85 to the C_β protons. Treatment of fraction 5 with warm CH_3COOD removes the peak at $\tau = 0.28$, as observed by Rapoport and co-workers. The C_α proton appears to exchange in this compound.

The arrangement of the peripheral substituents was assumed to be analogous to the (650) *Chlorobium* chlorophylls so that only the groups at C_4 and C_5 remained to be determined. The C_5 substituents could have been determined by converting the "meso" derivative of each fraction into the corresponding δ-phylloporphyrin and oxidizing this derivative with chromic acid. The δ-phylloporphyrins gave only low yields. Oxidation of the porphyrins also gave low yields of the imide from ring III. On the other hand, chromic acid oxidation of the phyllochlorin from chlorophyll *a* gave a very good yield of citraconimide. Conversion of the (660) pheophorbides into chlorins with ring V removed (and the hydroxyethyl group still present) gave good yields by the following method (Fig. 1).

The pheophorbide (I) was oxidized by oxygen in dimethylformamide to a diketone (II), which was further oxidized with hydrogen peroxide to the tricarboxylic acid (III) with carboxyl groups on C_6 and C_γ. Refluxing the tricarboxylic acid in 10% HCl for 1 h caused the absorption maximum to shift from 672 mμ to 653 mμ, indicating removal of the γ-carboxyl group (IV). Further refluxing in a mixture of pyridine and acetic acid yielded V with an absorption maximum at 640 mμ.

Treatment of V with 1% HCl in a sealed tube at 185 °C gave VI, the corresponding porphyrin. Analyses of the esters from fraction 5 showed the presence of two methoxyl groups in IV and one in V. The tricarboxylic acid corresponding to III from the "meso" derivative of fraction 5 was described previously (7). The visible absorption spectrum of VI, after purification, was identical with that of the δ-phylloporphyrin prepared from fraction 5.

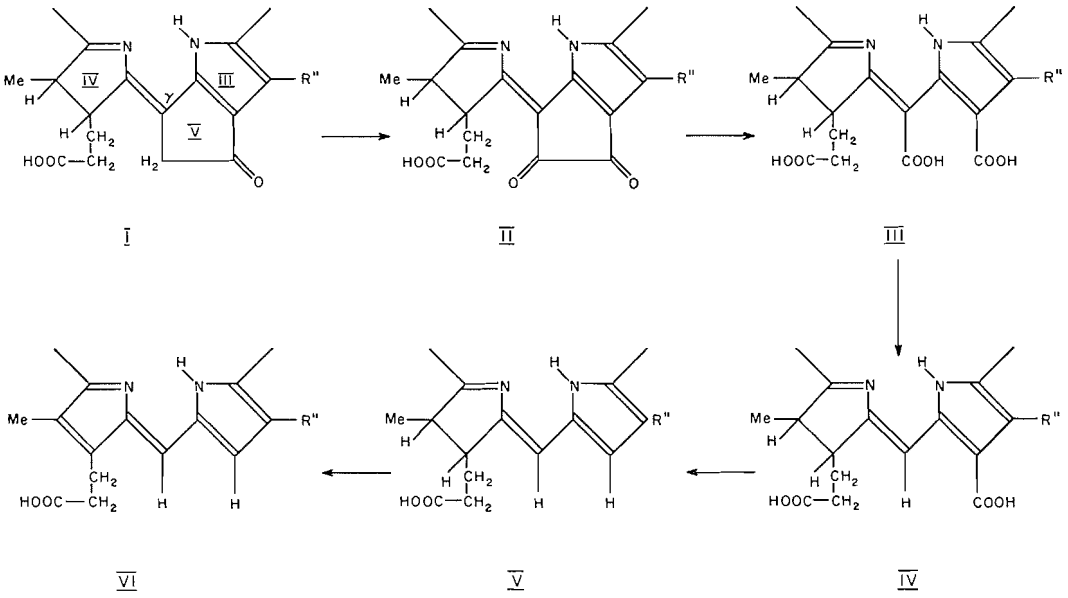


FIG. 1. Stepwise degradation of pheophorbides (660).

The chlorin derivatives (V) from fractions 1 to 6 (0.5–1 mg) were degraded with chromium trioxide in acetic acid by using a slight modification of the method described previously (9). The neutral imides produced were identified by comparison with synthetic imides by using gas–liquid partition chromatography on a column of polyphenyl ether, and the results were confirmed on a column of butanediol succinate. Fractions 1 to 5 all yielded ethylmaleimide, and fraction 6 citraconimide, from ring III, in addition to the expected imide from ring II, leaving only the δ-alkyl group undetermined.

TABLE I

Gas–liquid partition chromatography of the neutral imides from the oxidation of derivative V from fractions 1 to 6 (polyphenyl ether column; 175 °C; 100 ml argon per min)

Source of derivative V	Retention times relative to that of methylethylmaleimide
Mesopyropheophorbide *a*	0.535, 1.00
Fraction 1	0.53, 1.69
Fraction 2	0.81, 1.69
Fraction 3	0.81, 1.44
Fraction 4	0.81, 1.44
Fraction 5	0.81, 1.00
Fraction 6	0.53, 1.00
Synthetic imides	
Citraconimide	0.53
Ethylmaleimide	0.81
Methylethylmaleimide	1.00
Methyl-*n*-propylmaleimide	1.44
Methylisobutylmaleimide	1.69

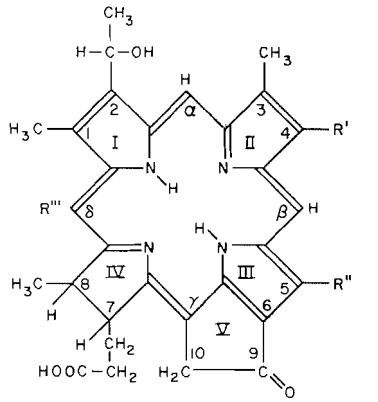
Fractions 3 to 6 were converted into "meso" derivatives and then into δ-phylloporphyrins. In addition to the δ-phylloporphyrin, a small amount of the corresponding pyrroporphyrin (δ-alkyl group removed) was obtained from each fraction. This result was not unexpected, because the conditions used for decarboxylation were similar to those used by Fischer (19). The pyrroporphyrins obtained from fractions 3 and 4 were purified and compared with

Can. J. Chem. Downloaded from www.nrcresearchpress.com by 210.87.254.40 on 09/05/12
For personal use only.

synthetic 1,3,8-trimethyl-2,5-diethyl-4-*n*-propylporphin-7-propionic acid (9, 17). The methyl esters of both pyrroporphyrins had m.p. 205–208 °C alone and 205–210 °C in admixture with the methyl ester of the synthetic compound (m.p. 207–211 °C). The pyrroporphyrin from fraction 4 was further shown to be identical with the synthetic compound by comparison of X-ray powder photographs. This confirmed that fractions 3 and 4 had identical peripheral substituents and that they therefore differed only at the δ-position.

MacDonald and co-workers (17, 18) prepared synthetic δ-phylloporphyrins and compared them with the phylloporphyrins from fractions 3, 4, 5, and 6. Fraction 5 phylloporphyrin was identical with synthetic 1,3,8,δ-tetramethyl-2,4,5-triethylporphin-7-propionic acid (17). Similarly, fraction 6 yielded δ-phylloporphyrin XV. This confirmed that, in fractions 5 and 6 at least, the order of the substituents in the *Chlorobium* chlorophylls (660) was the same as that found in the *Chlorobium* chlorophylls (650) (9), and that they possessed δ-methyl substituents.

Mass spectrometric molecular weight determinations were recently made of the methyl esters of fractions 2, 4, 5, and 6 (21). The values found for fractions 5 and 6 agree with those deduced from the degradative and analytical results. Those found for fractions 2 and 4 correspond to those of δ-methyl compounds. Consequently, previously proposed structures of fractions 1–4 (22) are here revised (Fig. 2).



Fraction	R′	R″	R‴
1	Isobutyl	Et	Et
2	Isobutyl	Et	Me
3	*n*-Propyl	Et	Et
4	*n*-Propyl	Et	Me
5	Et	Et	Me
6	Et	Me	Me

FIG. 2. Proposed structures of the pheophorbides from *Chlorobium* chlorophylls (660).

EXPERIMENTAL

Materials and Methods

Melting points (uncorrected) were measured on a Koffler hot stage. Imides were separated and identified as reported previously (4, 8). Nuclear magnetic resonance spectra were determined with a Varian V-4300 B spectrometer operating at 60 Mc/s. Visible absorption spectra were determined with a Cary model 14 spectrophotometer. Relative intensities of absorption bands are listed in parentheses.

Separation of Pheophorbides (660)

Initial separations by partition chromatography on a Celite column (8) were made with hydrochloric acid (8.5% w/w). Fractions 1 and 2 were purified with 11% hydrochloric acid; fractions 3 and 4, 9.5%; fraction 5, 8.0%; and fraction 6, 7.0%.

A large-scale preparation gave the following yields of pure pheophorbides from 13 g of *Chlorobium* chlorophyll (660): fraction 1, 25 mg; fraction 2, 30 mg; fraction 3, 84 mg; fraction 4, 715 mg; fraction 5, 3 150 mg; fraction 6, 462 mg. Thus fraction 5 accounted for 70% of the pure pheophorbides obtained.

Can. J. Chem. Downloaded from www.nrcresearchpress.com by 210.87.254.40 on 09/05/12
For personal use only.

Preparation of Tricarboxylic Acid Derivative (III); General Procedure

Fraction 5 (200 mg) was dissolved in dimethylformamide (100 ml), and oxygen was bubbled through for 5 min to saturate the solution. Aqueous potassium hydroxide (15%, w/v; 7 ml) was added and the mixture shaken for 3 min. Hydrogen peroxide (30%, 2 ml) was added and the mixture shaken for 30 s. It was then poured into a mixture of ether and water, and extracted into the ether layer by adding citric acid. The ethereal extract was washed well with water and the solvent was removed under reduced pressure. The residue was dissolved in a minimum of tetrahydrofuran and precipitated by addition to petroleum ether; yield 190 mg. Visible absorption spectrum (ether): λ_{max} 672 mμ (1.00); 620 mμ (0.12); 538 mμ (0.17); 507 mμ (0.24).

Preparation of Dicarboxylic Acid Derivative (IV); General Method

The tricarboxylic acid (III) from fraction 5 (200 mg) was dissolved in a minimum of acetic acid (80 ml), and hydrochloric acid (10%, 250 ml) was added. The mixture was refluxed for 1 h. The mixture was added to ether and neutralized. The ethereal extract was concentrated under reduced pressure, and the product (IV) was purified on a Celite column with 8% HCl; yield 140 mg. Visible absorption spectrum (ether): λ_{max} 653 mμ (1.00); 598 mμ (0.12); 540 mμ (0.17); 510 mμ (0.25).

A sample of IV was esterified (CH_2N_2), but the product failed to crystallize from ether.

Anal. Found: MeO, 10.15. $C_{34}H_{38}O_3N_4{\cdot}(OMe)_2$ requires MeO, 10.10.

Preparation of V; General Method

The dicarboxylic acid (IV) from fraction 5 (25 mg) was dissolved in a mixture of pyridine and glacial acetic acid (1:3, 80 ml) and refluxed for 8 h. The mixture was poured into ether and neutralized with sodium bicarbonate. The ethereal extract was washed well and the product (V) purified on a Celite column (hydrochloric acid, 8%); yield 5.8 mg. Visible absorption spectrum (ether): λ_{max} 640 mμ (1.00); 582 mμ (0.12); 527 mμ (0.15); 502 mμ (0.30).

Oxidative Degradation of Derivative V; General Procedure

The pigment (1.5 mg) was dissolved in glacial acetic acid (ca. 5 ml) and the solution cooled to 10 °C. Aqueous chromium trioxide (0.03 ml; 6.7%, w/v) was added to the cooled solution. Chromium trioxide (0.3 ml) was again added and the mixture was allowed to stand overnight. The isolation and the identification of the imides by gas–liquid partition chromatography has been described earlier (4, 8).

Preparation and Purification of "Meso" Derivatives; General Procedure

The "meso" derivatives of pheophorbides (660) were prepared by a method analogous to that used for the "meso" pheophorbides (650) (9).

The pheophorbide (50 mg) was dissolved in 100% phosphoric acid (20 ml) and maintained at 60 °C for 30 min, with vigorous stirring. The pigment was extracted with ether and chromatographed on a Celite column between ether and hydrochloric acid. The vinyl derivative separated as the lower band, leaving the unchanged material (which could again be treated with phosphoric acid to produce more of the vinyl derivative), and was hydrogenated (palladium black – H_2) in acetone; the "meso" derivative that was formed was purified by using hydrochloric acid that was 0.5% weaker than that required for the corresponding vinyl compound.

Preparation of δ-Phylloporphyrins; General Procedure

The "meso" compound was oxidized by oxygen to a tricarboxylic acid (Fig. 1). The product was dissolved in glacial acetic acid to which an equal volume of hydrochloric acid (1%) was added. The mixture was heated in a Teflon-lined brass bomb at 175° for 3½ h. After it had cooled, the solution was filtered to remove any decomposition products, and extracted with ether.

Hydrochloric acid (1%) extraction of the ether solution removed any δ-phylloporphyrin, and pyrroporphyrin that was formed as a by-product was obtained by a further extraction with hydrochloric acid (5%). The porphyrins obtained were then re-extracted with ether.

The δ-phylloporphyrins of fractions 3 to 6 of the pheophorbides (660) were prepared from the pure "meso" derivatives as outlined above, and were purified on acid-washed Celite with hydrochloric acid (1.5%). The pyrroporphyrins were purified (hydrochloric acid, 4.5%). Further purification was effected by crystallization from ether.

The purified free acids of the porphyrins were methylated with methanolic hydrogen chloride, and purified by chromatography on alumina (Shawinigan, reagent grade, deactivated with chloroform–methanol (95:5)) with chloroform as eluant.

The copper complexes of the phylloporphyrin methyl esters were also prepared, purified in the same way, and crystallized from chloroform–methanol.

Samples of the free acids, methyl esters, and copper complexes were all examined and compared with synthetic samples. The criteria used for identifying the natural samples with the synthetic materials were visible absorption spectra, melting and mixed melting points, and X-ray powder photographs.

Fraction 3.—δ-Phylloporphyrin (free acid), long needles from ether. δ-Phylloporphyrin methyl ester, needles from chloroform–methanol; m.p. 196–199°. Pyrroporphyrin methyl ester, needles from ether; m.p. 205–208°.

Can. J. Chem. Downloaded from www.nrcresearchpress.com by 210.87.254.40 on 09/05/12
For personal use only.

Fraction 4.—Pyrroporphyrin methyl ester, needles from ether; m.p. 205–208°. δ-Phylloporphyrin (free acid), long feathery needles from ether. δ-Phylloporphyrin methyl ester, small needles from chloroform–methanol; m.p. 195–197 °C (slight changes at 164 to 190 °C). δ-Phylloporphyrin methyl ester, copper complex, bright red prisms from chloroform–methanol; m.p. 174–179°.

Fraction 5.—δ-Phylloporphyrin (free acid), long needles from ether. δ-Phylloporphyrin methyl ester, from chloroform–methanol; m.p. 215–215.5°. δ-Phylloporphyrin methyl ester, copper complex from chloroform–methanol; m.p. 213.5–215°.

Fraction 6.—δ-Phylloporphyrin (free acid), long purple needles from ether. δ-Phylloporphyrin methyl ester, purple rods from chloroform–methanol; m.p. 209–213°. δ-Phylloporphyrin methyl ester, copper complex, small red purple needles from chloroform–methanol; m.p. 210–212.5°.

The δ-phylloporphyrins all possess almost identical visible absorption spectra; the pyrroporphyrins have spectra identical with that of pyrroporphyrin XV derived from chlorophyll *a*. Fraction 5 δ-phylloporphyrin: λ_{max} (ether): 629 mμ (0.10); 578 mμ (0.38); 535 mμ (0.39); 502 mμ (1.00). Bands II and III absorb almost equally, as compared with the same bands of γ-phylloporphyrin (II > III) (20).

ACKNOWLEDGMENTS

The authors thank Dr. S. F. MacDonald and Dr. H. J. Bernstein of the Division of Pure Chemistry for generous assistance. We are also grateful to Mr. R. G. Carriere for technical assistance.

REFERENCES

1. A. S. Holt and H. V. Morley. J. Am. Chem. Soc. **82**, 500 (1960).
2. A. S. Holt and H. V. Morley. *In* Comparative biochemistry of photoreactive systems. M. B. Allen (*Editor*). Academic Press, Inc., New York. 1960. p. 168.
3. H. V. Morley and A. S. Holt. Can. J. Chem. **39**, 755 (1961).
4. H. V. Morley, F. P. Cooper, and A. S. Holt. Chem. Ind. London, **32**, 1018 (1959).
5. H. Rapoport and H. F. Hamlow. Biochem. Biophys. Res. Commun. **6**, 134 (1961).
6. A. S. Holt, D. W. Hughes, H. J. Kende, and J. W. Purdie. Plant Cell Physiol. Tokyo, **4**, 49 (1963).
7. A. S. Holt, D. W. Hughes, H. J. Kende, and J. W. Purdie. J. Am. Chem. Soc. **84**, 2835 (1962).
8. D. W. Hughes and A. S. Holt. Can. J. Chem. **40**, 171 (1962).
9. J. W. Purdie and A. S. Holt. Can. J. Chem. In press.
10. H. Fisher, R. Lambrecht, and H. Mittenzwei. Z. Physiol. Chem. **253**, 32 (1938).
11. H. Fischer and J. Hasenkamp. Ann. **519**, 42 (1935).
12. H. Fischer and G. Spielberger. Ann. **515**, 130 (1935).
13. A. Stern and H. Wenderlein. Z. Physik. Chem. Leipzig, **176**, 81 (1936).
14. R. B. Woodward and V. Škavrić. J. Am. Chem. Soc. **83**, 4676 (1961).
15. J. W. Mathewson, W. R. Richards, and H. Rapoport. J. Am. Chem. Soc. **85**, 364 (1963).
16. J. W. Mathewson, W. R. Richards, and H. Rapoport. Biochem. Biophys. Res. Commun. **13**, 1 (1963).
17. J. L. Archibald, S. F. MacDonald, and K. B. Shaw. J. Am. Chem. Soc. **85**, 644 (1963).
18. J. L. Archibald, D. M. Walker, K. B. Shaw, A. Markovac, and S. F. MacDonald. Can. J. Chem. In press.
19. H. Fischer and H. Orth. Die chemie des pyrrols. Vol. II. Akademische Verlagsgesellschaft, Leipzig. 1937. Part 1. pp. 357–358.
20. A. Stern and H. Wenderlein. Z. Physik. Chem. Leipzig, **174**, 321 (1935).
21. A. H. Jackson, G. W. Kenner, and K. M. Smith. Personal communication.
22. A. S. Holt. *In* chemistry and biochemistry of plant pigments. T. W. Goodwin (*Editor*). Academic Bks., Ltd., London. 1965. pp. 3–28.

Can. J. Chem. Downloaded from www.nrcresearchpress.com by 210.87.254.40 on 09/05/12
For personal use only.

Can. J. Chem. Downloaded from www.nrcresearchpress.com by 210.87.254.6 on 09/05/12
For personal use only.

SYNTHESIS AND NUCLEAR MAGNETIC RESONANCE SPECTRUM OF 3′,4′,6′-TRI-O-ACETYL-2-(METHYLTHIO)-D-GLUCOPYRANO[2′,1′: 4,5]-2-THIAZOLINE

TEIICHIRO ITO
Research Laboratories, Meiji Seika Kaisha Ltd., Yokohama, Japan
Received June 15, 1965

ABSTRACT

1,3,4,6-Tetra-O-acetyl-2-deoxy-2-(dithiocarbomethoxy)-2-amino-β-D-glucopyranose, when it was treated with trifluoroacetic acid, gave 3′,4′,6′-tri-O-acetyl-2-(methylthio)-D-glucopyrano-[2′,1′:4,5]-2-thiazoline (III). Compound III showed a nuclear magnetic resonance spectrum capable of full interpretation. Long-range coupling between H_2 and H_4 was observed. The conformation of this compound in solution was discussed on the basis of the coupling constants for ring hydrogens.

Derivatives of amino sugars containing thiazoline rings have been prepared as intermediates for the synthesis of 2,3- and 3,2-thioamino sugars. In 1961, Goodman and Christensen (1) reported that a thiazoline ring was formed when a derivative of D-altropyranose 2-methanesulfonate with a dithiocarbomethoxyamino group at carbon 3 was heated in pyridine. Reckendorf and Bonner (2) synthesized a derivative of D-allopyrano-[3′,2′:5,4]-2-thiazoline by a similar reaction. The derivative of D-glucopyrano[2′,1′:4,5]-2-thiazoline, however, has not yet been described. As reported in a previous paper (3), N-benzyloxycarbonyl-tetra-O-acetyl-D-glucosamine, on treatment with trifluoroacetic acid, gave a glucose derivative containing an oxazolidone ring.

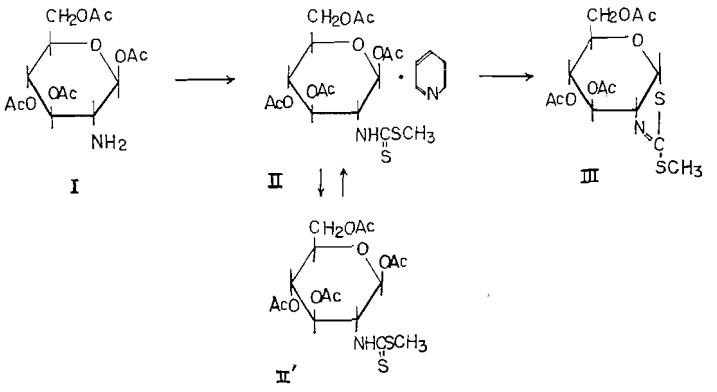
In this paper, application of the reaction using trifluoroacetic acid for the preparation of the derivative of D-glucopyrano-thiazoline, and the nuclear magnetic resonance (n.m.r) spectrum of this compound, will be described.

When 1,3,4,6-tetra-O-acetyl-2-deoxy-2-amino-β-D-glucopyranose (I) (4) was treated with carbon disulfide, triethylamine, and methyl iodide in pyridine, 1,3,4,6-tetra-O-acetyl-2-deoxy-2-(dithiocarbomethoxy)-2-amino-β-D-glucopyranose was isolated as needle crystals (II) which contained 1 mole of pyridine. The n.m.r. spectrum of compound II in $CDCl_3$ indicated the presence of a methylthio group (singlet, τ 7.40), O-acetyl groups (three peaks, τ 7.89, 7.91, and 7.96), and pyridine (multiplet, τ 1.3–1.5, 1.6–1.9, and 2.5–2.7).

The pyridine-free compound (II′) was obtained as an amorphous powder. In the n.m.r. spectrum (in $CDCl_3$), the peaks caused by ring hydrogens were identical in the spectra of compounds II and II′. The infrared spectrum (in Nujol) of compound II showed bands at 1 590, 1 578, and 1 564 cm^{-1}, while compound II′ showed bands at 1 545, 1 530, and 1 512 cm^{-1}.

When compound II was treated with trifluoroacetic acid at 70° for 12 min, the reaction product was obtained as a syrup which crystallized gradually when it was allowed to stand in a refrigerator. It showed m.p. 51–54°. Elemental analysis and infrared and n.m.r. spectra showed that the product was 3′,4′,6′-tri-O-acetyl-2-(methylthio)-D-glucopyrano-[2′,1′:4,5]-2-thiazoline (III).

The n.m.r. spectrum showed the presence of a methylthio group (τ 7.46) and O-acetyl groups (two peaks, τ 7.86 and 7.92; intensity 1:2). As shown in Fig. 1, the peaks caused by ring hydrogens gave such different chemical shifts that they were assigned readily from



their splittings. The observed first-order coupling constants (J) for ring hydrogens are shown in Table I. It is noteworthy that long-range coupling (J, 1 c.p.s.) between H_2 and H_4 is observed.

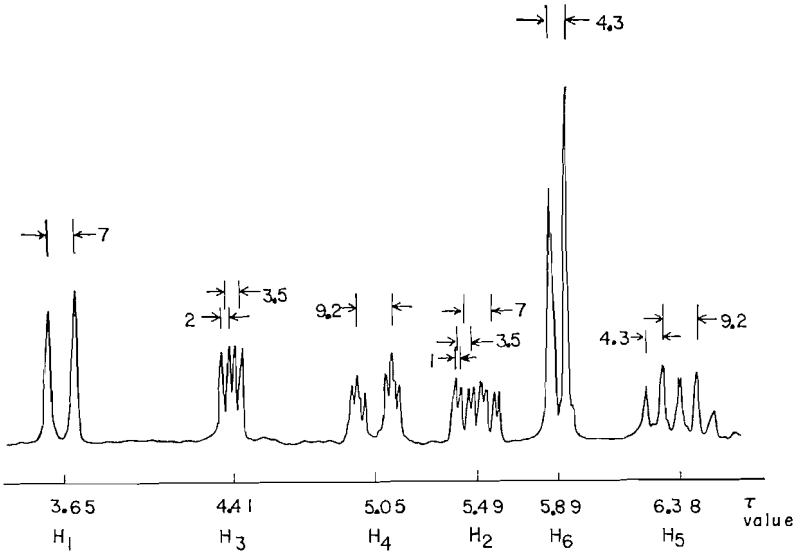


FIG. 1. The 60 Mc.p.s. n.m.r. spectrum of 3′,4′,6′-tri-O-acetyl-2-(methylthio)-D-glucopyrano[2′,1′:4,5]-2-thiazoline (III) in $CDCl_3$. The peaks caused by methylthio and O-acetyl groups are omitted.

Lemieux (5), Hall (6, 7), and their co-workers have observed the long-range interactions in numerous carbohydrates. It has been shown that the long-range couplings are highly stereoselective, occurring only between hydrogens possessing a critical relationship (6, 8).

Recently, a number of n.m.r. spectra of carbohydrates have been examined for information on their conformations through application of the relationships that appear to exist between the coupling constant and the dihedral angles defined by vicinal protons (7, 9–13). It has been recognized that the theoretical Karplus relation (9) has its own limitations (14).

However, it was thought to be of interest to show the dihedral angles of compound III, which were calculated from the Karplus equation (9). The calculated dihedral angles and the theoretical angles corresponding to the chair and skew-boat conformations are shown in Table I.

Can. J. Chem. Downloaded from www.nrcresearchpress.com by 210.87.254.6 on 09/05/12
For personal use only.

TABLE I

Coupling constants, calculated dihedral angles, and theoretical angles for chair and skew-boat conformations

	CH—CH					
	1,2	2,3	3,4	4,5	5,6	2,4
Coupling constant, J_{HH} (c.p.s.)	7	3.5	2.0	9.2	4.3	1.0
Dihedral angle calculated from Karplus equation*	22°	48° 129°	58° 119°	179°		
Theoretical angle						
Chair	60°	180°	180°	180°		
Skew-boat	30°	60°	90°	150°		

*$J = J_0 \cos^2 \phi - 0.28$ c.p.s., where $J_0 = 8.5$ for $0° \leqslant \phi \leqslant 90°$ and 9.5 for $90° \leqslant \phi \leqslant 180°$.

Since compound III contains a thiazoline ring fused to a pyranose ring, the dihedral angle for H_1–H_2 is expected to be less than 60°. The value of 22° calculated from the Karplus equation suggests that a partial flattening of the chair conformation occurs. The coupling constant of 9.2 c.p.s. for H_4 and H_5 suggests that the dihedral angle for H_4–H_5 is about 180° (15); thus this part of the pyranose ring remains virtually unaltered. The above data, including the small values for $J_{2,3}$ and $J_{3,4}$, indicate that the pyranose ring of compound III is somewhat distorted from the normal chair conformation.

Coxon and Hall (7) suggested a skew-boat conformation for 1,2-O-alkylidene-α-D-glucopyranoses. If we assume a skew-boat form for compound III, we find some differences between the calculated and theoretical angles for H_3–H_4 (Table I). Most likely, the observed spectra are time-averaged spectra of various half-chair and skew-boat conformations.

Recently, Williams and Bhacca (16) reported that, in the chair form of a cyclohexane ring, the variation of vicinal coupling constant with the orientation of an electronegative substituent such as —OH or —OAc is quite large. Therefore, to determine an exact conformation of the distorted pyranose ring, more experimental data must be available.

EXPERIMENTAL

Melting points are uncorrected. The n.m.r. spectra were measured with a Varian A-60 spectrometer, tetramethylsilane being used as internal reference.

1,3,4,6-Tetra-O-acetyl-2-deoxy-2-(dithiocarbomethoxy)-2-amino-β-D-glucopyranose

Crystals (II) Containing 1 Mole of Pyridine

To a chilled solution of 2.4 g of 1,3,4,6-tetra-O-acetyl-2-deoxy-2-amino-β-D-glucopyranose (I) in 8 ml of dry pyridine was added 1.5 ml of triethylamine and then 0.8 ml of carbon disulfide, with stirring. The temperature was maintained below 5°. The solution was stirred at the ice-bath temperature for 1.5 h, and then 0.8 ml of methyl iodide was added. After being stirred for an additional 30 min at 0°, the mixture was stored overnight at 5° and then poured into ice water. The separated crystalline precipitates were filtered off and washed with water; yield 3 g (72%). It was recrystallized from a mixture of ethyl acetate and hexane. The recrystallized compound has the following properties: m.p. 106–108°; $[\alpha]_D^{20}$ −44° (*c*, 0.5 in chloroform); $\lambda_{max}^{CH_3OH}$ 223 mμ (ε 4 100), 251 mμ (ε 13 100), 275 mμ (ε 5 100).

Anal. Calcd. for $C_{16}H_{23}NS_2O_9 \cdot C_5H_5N$: C, 48.82; H, 5.46; N, 5.42; S, 12.41. Found: C, 48.72; H, 5.37; N, 5.53; S, 12.57.

Pyridine-Free Compound (II′)

The above compound (II) (0.5 g) was dissolved in methylene dichloride, and washed with cold 1 *N* hydrochloric acid, cold sodium bicarbonate aqueous solution, and then cold water. The solvent layer was separated, dried, and evaporated to a white powder (300 mg).

Anal. Calcd. for $C_{16}H_{23}NS_2O_9$: C, 43.92; H, 5.29. Found: C, 43.91; H, 5.28.

Crystallization of compound II′ as such was unsuccessful; however, it was crystallized readily as crystals (II) by dissolving it in ethyl acetate and mixing the solution with hexane and a small amount of pyridine.

Can. J. Chem. Downloaded from www.nrcresearchpress.com by 210.87.254.6 on 09/05/12
For personal use only.

3′,4′,6′-Tri-O-acetyl-2-(methylthio)-D-glucopyrano[2′,1′:4,5]-2-thiazoline (III)

Compound II (700 mg) was dissolved in trifluoroacetic acid (5 ml) and the solution was refluxed for 12 min at 70°. It was evaporated *in vacuo*, and the resulting syrup was dissolved in chloroform and washed with cold sodium bicarbonate aqueous solution and then cold water. The chloroform solution was dried and evaporated to a syrup, which crystallized gradually when it was allowed to stand in a refrigerator. (The crystallization was very slow. It required about 1 week.) The crystalline product was recrystallized from a mixture of ether and petroleum ether; yield 320 mg (62%), m.p. 51–54°, $[\alpha]_D^{18}$ −70° (*c*, 0.3 in chloroform), $\lambda_{max}^{CH_3OH}$ 221 mμ (ε 9 600). The infrared spectrum (in Nujol) showed bands at 1 720 (O-acetyl), 1 570 (—N=C—), 1 220–1 200, 1 070, 1 030, 950, 880, 812, and 755 cm^{-1}.

Anal. Calcd. for $C_{14}H_{19}NS_2O_7$: C, 44.55; H, 5.07; N, 3.71; S, 16.99. Found: C, 44.88; H, 4.84; N, 3.92; S, 17.39.

ACKNOWLEDGMENTS

The author expresses his gratitude to Dr. T. Nishida, Kobayashi Institute of Physical Research, for the determination of the n.m.r. spectrum. The author is grateful to Dr. S. Inouye of this laboratory for his helpful suggestions regarding the interpretation of the n.m.r. spectrum.

REFERENCES

1. L. Goodman and J. E. Christensen. J. Am. Chem. Soc. **83**, 3823 (1961).
2. W. M. zu Reckendorf and W. A. Bonner. Proc. Chem. Soc. 429 (1961).
3. T. Ito. Chem. Pharm. Bull. Tokyo, **12**, 499 (1964).
4. M. Bergmann and L. Zervas. Ber. **64**, 975 (1931).
5. R. U. Lemieux and R. Nagarajan. Can. J. Chem. **42**, 1270 (1964). R. U. Lemieux, D. R. Lineback, W. L. Wolfrom, F. B. Moody, E. G. Wallace, and F. Komitsky, Jr. J. Org. Chem. **30**, 1092 (1965). R. U. Lemieux and J. Howard. Can. J. Chem. **41**, 393 (1963).
6. L. D. Hall and L. Hough. Proc. Chem. Soc. 382 (1962).
7. B. Coxon and L. D. Hall. Tetrahedron, **20**, 1685 (1964).
8. A. Rassat, C. W. Jefford, J. M. Lehn, and B. Waegell. Tetrahedron Letters, 233 (1964).
9. M. Karplus. J. Chem. Phys. **30**, 11 (1959).
10. R. U. Lemieux, J. D. Stevens, and R. R. Fraser. Can. J. Chem. **40**, 1955 (1962).
11. R. J. Abraham, L. D. Hall, L. Hough, and K. A. McLauchlan. J. Chem. Soc. 3699 (1962).
12. R. W. Lenz and J. P. Heeschen. J. Polymer Sci. **51**, 247 (1961).
13. L. D. Hall. Advan. Carbohydrate Chem. **19**, 51 (1964).
14. M. Karplus. J. Am. Chem. Soc. **85**, 2870 (1963).
15. R. U. Lemieux, R. K. Kullnig, H. J. Bernstein, and W. G. Schneider. J. Am. Chem. Soc. **80**, 6098 (1958).
16. D. H. Williams and N. S. Bhacca. J. Am. Chem. Soc. **86**, 2742 (1964).

Can. J. Chem. Downloaded from www.nrcresearchpress.com by 210.87.254.6 on 09/05/12
For personal use only.

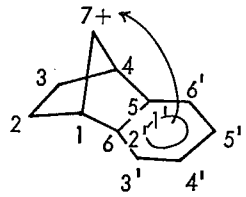
Can. J. Chem. Downloaded from www.nrcresearchpress.com by 210.87.254.40 on 09/05/12
For personal use only.

NOTES

POLAROGRAPHY OF 7-BENZONORBORNENONES[1]

HIROSHI TANIDA, HIROSHI MIYAZAKI, AND HIROYUKI ISHITOBI

Polarographic half-wave reduction potential distinguishes between aryl ketones and alkyl ketones. The reduction under neutral or acidic conditions is believed to involve a free radical process, followed by dimerization (pinacol formation) (1–3). As shown in previous papers (4), reactivity at the 7-position of benzonorbornenes demonstrated a typical homobenzylic conjugation; direct conjugate interaction was shown between the



C_7 carbonium ion formed in acetolysis of anti-7-benzonorbornenyl *p*-bromobenzenesulfonate and the aromatic ring. Interest in a radical reaction at this position led us to measure half-wave reduction potentials ($-E_{\frac{1}{2}}$) of benzonorbornen-7-one (I) and 4′-substituted derivatives (II–VI).

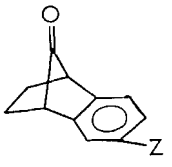
The Oppenauer oxidation of the 4′-substituted anti-7-benzonornenols (4) provided the materials used in this study. The $-E_{\frac{1}{2}}$'s measured under neutral conditions (see Experimental section), where a one-electron reduction process was observed for acetophenone, are summarized in Table I. For comparison, the results of benzonorbornen-2-one (VII), acetophenone, cyclohexanone, and cyclopentanone under the same conditions are also listed. The most significant result was that the $-E_{\frac{1}{2}}$ of the 7-ketones (I–VI) was almost the same as that of acetophenone; on the other hand, the 2-ketone (VII) did not yield a result similar to that of acetophenone, but instead resembled cyclohexanone and cyclo-

TABLE I

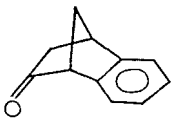
Half-wave potentials (saturated calomel electrode) and limiting currents of benzonorbornenones

Compound	$-E_{\frac{1}{2}}$, V	i_l, μA	Concentration × 10^3, moles/l
I	1.653	0.35	5.38
II	1.637	0.37	5.13
III	1.638	0.19	5.19
IV	1.614	0.32	5.07
V	1.623	0.43	4.97
VI	1.621	0.89	5.31
VII	No wave		
Acetophenone	1.616	9.43	5.93
Cyclohexanone	No wave		
Cyclopentanone	No wave		

[1]*Paper XI of a series on bicyclic systems; for paper X see H. Tanida and R. Muneyuki, J. Am. Chem. Soc., in press.*

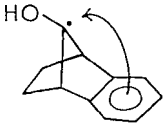


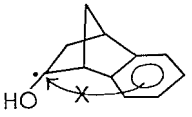
I, Z=H
II, Z=CH_3O
III, Z=CH_3
IV, Z=Cl
V, Z=Br
VI, Z=CN



VII

pentanone. Therefore, one might be able to argue that the 7-ketones behave as a kind of aryl ketone. However, the limiting current of 7-ketones was very small for reasons that cannot be explained at present. No significant substituent effect was observed.





Absence of anchimeric assistance in the homolytic reactions of 2-norbornyl and 2-norbornenyl systems has recently been demonstrated by several workers (5). In this connection, the indication of phenyl participation in the polarographic reduction reported here may be of interest in considering a radical reaction at the 7-position of the norbornenyl system.

EXPERIMENTAL

Melting points were taken by capillary and are corrected; boiling points are uncorrected.

Materials

4′-Methoxy-, 4′-methyl-, 4′-chloro-, and 4′-bromo-benzonorbornen-7-one (II, III, IV, and V) were prepared by the Oppenauer oxidation of the corresponding anti-alcohols (4) according to the procedure of Bartlett and Giddings (6) which was used for the preparation of I. The cyano compound (VI) was prepared by refluxing a solution of V and cuprous cyanide in dimethylformamide (7). Properties and analyses of the new 7-ketones prepared in this study are listed in Table II.

TABLE II

4′-Substituted benzonorbornen-7-ones (I)

4′-Substituent	Melting or boiling point (mm), °C	n_D (temp., °C)	Formula	% carbon		% hydrogen	
				Calcd.	Found	Calcd.	Found
CH_3O	140* (1)	1.5632 (25.7)	$C_{12}H_{12}O_2$	76.57	76.76	6.43	6.68
CH_3	101–102 (1)	1.5547 (23)	$C_{12}H_{12}O$	83.69	83.75	7.02	7.08
H	126 (16)	1.5597 (27.8)					
Cl	109 (2)	1.5748 (28.0)	$C_{11}H_9OCl$	68.58	68.47	4.71	4.97
Br	130* (1)	1.5953 (28.3)	$C_{11}H_9OBr$	55.72	56.00	3.83	3.89
CN	107–108	Crystal	$C_{12}H_9ON$	78.67	78.50	4.95	5.08

*Bath temperature.

Polarography

The half-wave reduction potentials were measured on a Yanagimoto pen-recording polarograph, model 102. The dropping mercury electrode that was used had the following characteristics in distilled water under an open circuit: $m = 0.865$ mg/s; $n = 70$ cm; $t = 4.33$ s. The supporting electrolytic solution was prepared by mixing 10 ml of 95% ethanol, 0.01% gelatin solution, and 1 *N* lithium chloride solution, adjusted to a total volume of 20 ml. Dissolved oxygen was removed from the solutions by bubbling nitrogen gas through them for 10 min. A saturated calomel electrode was used as an external reference electrode and the measurements were made in triplicate at 25 ± 0.1 °C.

Under acidic conditions (supporting electrolytic solution prepared by mixing 10 ml of 95% ethanol, 0.01% gelatin solution, and 10 ml of pH = 3.59 buffer), the wave of I became blurred. For acetophenone, $E_{\frac{1}{2}} = -1.273$ V and $i_d = 7.16$ μA (5.64×10^{-3} mole/l) were observed.

Can. J. Chem. Downloaded from www.nrcresearchpress.com by 210.87.254.40 on 09/05/12
For personal use only.

1. R. PASTERNAK. Helv. Chim. Acta, **31**, 753 (1948).
2. M. SUZUKI and P. J. ELVING. J. Phys. Chem. **65**, 391 (1961).
3. A. STREITWIESER, JR. Molecular orbital theory for organic chemists. John Wiley & Sons, Inc., New York. 1961. p. 183.
4. H. TANIDA, T. TSUJI, and H. ISHITOBI. J. Am. Chem. Soc. **86**, 4904 (1964). H. TANIDA. J. Am. Chem. Soc. **85**, 1703 (1963).
5. P. D. BARTLETT and R. E. PINCOCK. J. Am. Chem. Soc. **84**, 2445 (1962). M. M. MARTIN and D. C. DEJONGH. J. Am. Chem. Soc. **84**, 3526 (1962). H. HART and F. J. CHLOUPEK. J. Am. Chem. Soc. **85**, 1155 (1963). P. D. BARTLETT and J. M. MCBRIDE. J. Am. Chem. Soc. **87**, 1727 (1965).
6. P. D. BARTLETT and W. P. GIDDINGS. J. Am. Chem. Soc. **82**, 1240 (1960).
7. J. E. CALLEN, C. A. DORNFELD, and G. H. COLEMAN. Org. Syn. Collective Vol. **III**, 212 (1955). M. S. NEWMAN. Org. Syn. Collective Vol. **III**, 631 (1955).

RECEIVED AUGUST 4, 1965.
SHIONOGI RESEARCH LABORATORY,
SHIONOGI & CO., LTD.,
FUKUSHIMA-KU, OSAKA, JAPAN.

Can. J. Chem. Downloaded from www.nrcresearchpress.com by 210.87.254.40 on 09/05/12
For personal use only.

GAS CHROMATOGRAPHY OF ESTRONE AND RELATED COMPOUNDS

RAFAEL MONTALVO AND OWEN H. WHEELER

Gas chromatography at high temperatures has been used widely for the analysis of mixtures of steroids (1). The liquid phases most generally used are the nonpolar SE-30 silicone gum (2) and the polar QF-1 fluorinated alkyl silicone (3). However, only a few measurements have been reported on estrone, estradiol, and estrone methyl ether (4, 5).

This note reports a study of the retention times of estrone and a series of its derivatives, principally those substituted in ring A, on QF-1 and SE-30 columns (Table I), both as the free compounds and as their trimethylsilyl ethers (4).

The retention times (R_t) on the QF-1 column depend on the polarity of the compound, and methylation in position-3 reduced the R_t values. Similarly, estrolactone showed a greatly increased R_t value, whereas 17-deoxyestrone gave a low retention time.

Hydroxylation in position-2 of estradiol increased the R_t value to about twice that of estradiol, as did hydroxylation at position-16, although a 4-hydroxyl substituent caused an increase of only about 70%. The retention time for 2-acetoxy substitution was also greater than that for the 4-isomer. These differences are probably steric in origin, since a 2,3-disubstituted compound can be absorbed more easily in a direction along the length of the steroid molecule.

The trimethylsilyl ethers had lower values of R_t on the QF-1 column (Table I) than did the corresponding free compounds. Estradiol gave two peaks, one of the monoether and the second of the diether. However, the derivatives of 4-hydroxyestradiol and 4-hydroxyestrone showed only one peak.

The usefulness of the QF-1 column in separating estrone derivatives was shown by the fact that a commercial sample of estradiol monoacetate was readily analyzed as estradiol (33%), estradiol 3-acetate (25%), estradiol 17β-acetate (22%), and estradiol diacetate (20%). A sample of Werbin's dilactone (6) showed the following peaks (and relative areas): 6.3 (2%), 7.5 (2%), 9.0 (6%), and 9.4 min (90%). The compound may be a mixture of isomers, as originally suggested (6), although the peaks of low retention time are probably the result of decomposition.

1. R. PASTERNAK. Helv. Chim. Acta, **31**, 753 (1948).
2. M. SUZUKI and P. J. ELVING. J. Phys. Chem. **65**, 391 (1961).
3. A. STREITWIESER, JR. Molecular orbital theory for organic chemists. John Wiley & Sons, Inc., New York. 1961. p. 183.
4. H. TANIDA, T. TSUJI, and H. ISHITOBI. J. Am. Chem. Soc. **86**, 4904 (1964). H. TANIDA. J. Am. Chem. Soc. **85**, 1703 (1963).
5. P. D. BARTLETT and R. E. PINCOCK. J. Am. Chem. Soc. **84**, 2445 (1962). M. M. MARTIN and D. C. DEJONGH. J. Am. Chem. Soc. **84**, 3526 (1962). H. HART and F. J. CHLOUPEK. J. Am. Chem. Soc. **85**, 1155 (1963). P. D. BARTLETT and J. M. MCBRIDE. J. Am. Chem. Soc. **87**, 1727 (1965).
6. P. D. BARTLETT and W. P. GIDDINGS. J. Am. Chem. Soc. **82**, 1240 (1960).
7. J. E. CALLEN, C. A. DORNFELD, and G. H. COLEMAN. Org. Syn. Collective Vol. **III**, 212 (1955). M. S. NEWMAN. Org. Syn. Collective Vol. **III**, 631 (1955).

RECEIVED AUGUST 4, 1965.
SHIONOGI RESEARCH LABORATORY,
SHIONOGI & CO., LTD.,
FUKUSHIMA-KU, OSAKA, JAPAN.

Can. J. Chem. Downloaded from www.nrcresearchpress.com by 210.87.254.105 on 09/05/12
For personal use only.

GAS CHROMATOGRAPHY OF ESTRONE AND RELATED COMPOUNDS

RAFAEL MONTALVO AND OWEN H. WHEELER

Gas chromatography at high temperatures has been used widely for the analysis of mixtures of steroids (1). The liquid phases most generally used are the nonpolar SE-30 silicone gum (2) and the polar QF-1 fluorinated alkyl silicone (3). However, only a few measurements have been reported on estrone, estradiol, and estrone methyl ether (4, 5).

This note reports a study of the retention times of estrone and a series of its derivatives, principally those substituted in ring A, on QF-1 and SE-30 columns (Table I), both as the free compounds and as their trimethylsilyl ethers (4).

The retention times (R_t) on the QF-1 column depend on the polarity of the compound, and methylation in position-3 reduced the R_t values. Similarly, estrolactone showed a greatly increased R_t value, whereas 17-deoxyestrone gave a low retention time.

Hydroxylation in position-2 of estradiol increased the R_t value to about twice that of estradiol, as did hydroxylation at position-16, although a 4-hydroxyl substituent caused an increase of only about 70%. The retention time for 2-acetoxy substitution was also greater than that for the 4-isomer. These differences are probably steric in origin, since a 2,3-disubstituted compound can be absorbed more easily in a direction along the length of the steroid molecule.

The trimethylsilyl ethers had lower values of R_t on the QF-1 column (Table I) than did the corresponding free compounds. Estradiol gave two peaks, one of the monoether and the second of the diether. However, the derivatives of 4-hydroxyestradiol and 4-hydroxyestrone showed only one peak.

The usefulness of the QF-1 column in separating estrone derivatives was shown by the fact that a commercial sample of estradiol monoacetate was readily analyzed as estradiol (33%), estradiol 3-acetate (25%), estradiol 17β-acetate (22%), and estradiol diacetate (20%). A sample of Werbin's dilactone (6) showed the following peaks (and relative areas): 6.3 (2%), 7.5 (2%), 9.0 (6%), and 9.4 min (90%). The compound may be a mixture of isomers, as originally suggested (6), although the peaks of low retention time are probably the result of decomposition.

TABLE I

Compound	QF-1 column		SE-30 column	
	Relative R_t*	Relative R_t (TMSE)*,†	Relative R_t*	Relative R_t (TMSE)*,†
Cholestane	1.0	(1.0)	1.0	(1.0)
Estrone	2.5	1.6	0.45	0.51
Estrone acetate	3.9	—	0.54	—
Estradiol	1.8	0.89 (mono) 0.63 (di)	0.46	0.65 (di)
Estradiol 3-acetate	2.6	1.7	0.55	0.68
Estradiol 17β-acetate	2.8	—	0.55	—
Estradiol diacetate	3.9	—	0.68	—
Estradiol 3-methyl ether	1.3	0.89	0.42	0.54
Estradiol 17β-acetate 3-methyl ether	1.8	—	0.55	—
Estrone methyl ether	1.8	—	0.38	—
Estrolactone	6.8	1.8	1.1	—
Estrolactone acetate	—	—	1.3	—
17-Deoxyestrone	0.64	0.61	0.29	0.46
17-Deoxyestrone acetate	1.0	—	0.38	—
Estriol	3.5	1.5	1.2	1.5
Estriol triacetate	—	—	0.94	—
2-Hydroxyestradiol	3.5	0.95	1.1	—
4-Hydroxyestradiol	—	—	0.89	—
4-Hydroxyestrone	4.9	1.9	1.4	—
4-Hydroxyestrone 3-methyl ether	—	—	0.76	—
2-Hydroxyestrone 3-methyl ether	—	—	0.92	—
2-Hydroxyestrone dimethyl ether	2.7	—	0.50	—
2-Hydroxyestradiol 3-methyl ether	2.7	—	—	—
4-Hydroxyestradiol 3-methyl ether	2.3	—	—	—
2-Hydroxyestradiol 2,3-dimethyl ether	2.0	1.2	0.57	0.67
2-Hydroxyestrone diacetate	2.6	—	0.60	—
2-Hydroxyestradiol 3,17-dimethyl ether	—	—	0.57	0.67
2-Hydroxyestradiol 17β-acetate 2,3-dimethyl ether	2.8	—	0.72	—
2-Hydroxyestradiol 2-acetate 3-methyl ether	2.7	—	—	—
4-Hydroxyestradiol 4-acetate 3-methyl ether	2.0	—	—	—
2-Nitroestrone	—	—	0.68	—
4-Nitroestrone	—	—	0.61	—
2-Nitroestrone acetate	—	—	0.85	—
4-Nitroestrone acetate	—	—	0.72	—
2,2-Dihydroxyestran-1(10),4-diene-3,17-dione diacetate	—	—	1.2	—
4,4-Dihydroxyestra-1,5(10)-diene-3,17-dione diacetate	—	—	0.89	—
10-Hydroxyestra-1,4-diene-3,17-dione acetate	—	—	0.59	—
Testosterone	3.4	2.1	0.67	0.79
Testosterone acetate	4.7	—	0.85	—
19-Nortestosterone	3.4	2.1	0.67	0.78
Androstane-3,17-dione	2.6	—	0.54	—
Androsta-1,4-diene-3,17-dione	5.6	—	0.73	—

*At 255°; helium flow, 25 ml/min; 3% liquid phase on Chromosorb W in capillary column. R_t relative to cholestane = 1. R_t of cholestane = 4.2 min on QF-1 and 12.3 min on SE-30.
†TMSE = trimethylsilyl ethers, at 258°.

The data obtained with a column of silicon rubber (SE-30) showed much smaller differences in the retention times. This is consistent with the nonpolar nature of the liquid phase, and the retention times are usually lower than those obtained with a QF-1 column (5). Moreover, the order of retention times for different functional groups is different, that for QF-1 being deoxy < ether < alcohol < ketone < acetate, and that for SE-30 being deoxy < ether < ketone < alcohol < acetate. For the simple estrone derivatives, the small differences in R_t approximately follow the molecular weights (7). However, the

Can. J. Chem. Downloaded from www.nrcresearchpress.com by 210.87.254.105 on 09/05/12
For personal use only.

Can. J. Chem. Downloaded from www.nrcresearchpress.com by 210.87.254.105 on 09/05/12
For personal use only.

polyhydroxy compounds, such as 2-hydroxyestradiol, estriol, and estrolactone, had R_t values much larger than those expected for their molecular weights (see also 2- and 4-nitro derivatives); some form of specific interaction with the liquid phase must occur in these cases.

The relative R_t values of the trimethylsilyl ethers on the SE-30 column are only slightly higher than those of the free derivative. In general, the same reduction in retention time that was obtained with trimethylsilyl ethers on a QF-1 column can be achieved by using a SE-30 column for the free compounds. Moreover, there seems to be no advantage in running compounds on a SE-30 column as their trimethylsilyl ethers.

The steroid numbers (k_x) of Clayton (7) and the factor (ΔR_{mg}) of Knights and Thomas (8, 9) ($\Delta R_{mg} = \log k_x$) have been calculated (Table II). The values reflect the differences

TABLE II

Factors for estrone derivatives

Function	QF-1 column		SE-30 column	
	k_x*	ΔR_{mg}†	k_x*	ΔR_{mg}†
Acetylation at C-3	1.51	0.18	1.20	0.08
Acetylation at C-16	—	—	1.38	0.14
Acetylation at C-17	1.41	0.15	1.28	0.11
Methylation at C-3	0.73	−0.14	0.90	−0.05
Methoxylation at C-2	1.51	0.18	1.28	0.11
Carbonyl at C-17	3.85	0.59‡	1.53	0.18
Hydroxylation at C-17	2.81	0.45§	1.56	0.19
Hydroxylation at C-16	1.34	0.13	2.64	0.42
Hydroxylation at C-2	1.98	0.30	2.36	0.37
Hydroxylation at C-4	1.83	0.26	2.00	0.30
Nitration at C-2	—	—	1.56	0.19
Nitration at C-4	—	—	1.35	0.13
Trimethylsilyl ether at C-3	0.66‖	−0.18	1.15‖	0.06
Trimethylsilyl ether at C-17	0.64‖	−0.19	1.28‖	0.11

*Factor $k_x = R_t$ (derivative)/R_t (parent), at 255°.
†$\Delta R_{mg} = \log k_x$.
‡Reference 9 reports 0.65.
§Reference 9 reports 0.44, at 250°.
‖Corrected to 255°.

found in the retention times. Thus k_x is generally larger on the QF-1 column. However, compounds with two neighboring functional groups (k_x factor for acetylation at C-16α and hydroxylation at C-2 and C-4) showed larger values on the SE-30 column. These factors can be used to calculate the expected values of retention time of non-interacting functional groups (e.g. calculated R_t for estradiol diacetate, 16.2 min; experimental R_t, 16.4 min). However, the calculated values will be less accurate for the smaller k_x factors found with the SE-30 column (e.g. calculated R_t for estradiol 17β-acetate 3-methyl ether, 6.5 min; experimental R_t, 6.8 min).

EXPERIMENTAL

Apparatus

A Wilkens A-90 Aerograph was modified by incorporating small variable transformers, thermocouples, and a meter to control the temperature of the injector block. A hydrogen flame ionization detector was mounted in the column oven. The columns used were 3% QF-1 or 3% SE-30 on Chromosorb W, 60/80 mesh, 0.101 inch × 6 ft, prepared by Research Specialties. The gas flows were: helium and hydrogen, 25 ml/min; air, 250 ml/min. Samples of 1 μl of solution of the steroids of about 50 mg/ml were injected into the column. The detector response was linear for 20–75 μg of estrone, estradiol, and estradiol 3-methyl ether. The columns were saturated with 150 μg, and gave broad peaks. 2-Hydroxyestradiol and 4-hydroxyestradiol also gave broad peaks. The retention times were measured from the air peak. The QF-1 column had 500 and 1 020 theoretical plates for cholestane and estrone, respectively; the SE-30 column had 4 300 and 270 plates, respectively.

Steroids

Samples of analytical purity were used. Some were prepared as described elsewhere (10). 17-Desoxyestrone was prepared by Wolf–Kishner reduction of estrone (11). Estrolactone was synthesized by oxidizing estrone with hydrogen peroxide in aqueous sodium hydroxide (12). Nitration of estrone (13) yielded 2-nitro- and 4-nitro-estrone.

Trimethylsilyl Ethers

The steroid (30 mg) was dissolved in anhydrous tetrahydrofuran (0.2 ml), treated with trimethylchlorosilane (0.5 μl) and hexamethyldisilazane (2 ml), and left at room temperature overnight. The mixture was evaporated in a current of inert gas. The residue was extracted with tetrahydrofuran, the solution was centrifuged, and the upper layer was reevaporated. The residue that was left was dissolved in hexane, and this solution was used for chromatography.

ACKNOWLEDGMENTS

The authors are grateful to L. R. Axelrod (Southwest Foundation for Research and Education), J. Fishman (Sloan-Kettering Institute for Cancer Research), W. Klyne (Westfield College, London), and H. Werbin (University of California Medical School) for gifts of estrone derivatives, and Syntex, Souedad Anonima, for samples of estrone and estradiol.

The Puerto Rico Nuclear Center is operated by the University of Puerto Rico for the U.S. Atomic Energy Commission under contract No. AT(40-1)-1833.

1. E. C. Horning, W. J. A. VandenHeuvel, and B. G. Creech. Methods Biochem. Analy. **11**, 69 (1963).
2. W. J. A. VandenHeuvel, C. C. Sweely, and E. C. Horning. J. Am. Chem. Soc. **82**, 3481 (1960).
3. W. J. A. VandenHeuvel, E. O. A. Haahti, and E. C. Horning. J. Am. Chem. Soc. **83**, 1513 (1961).
4. T. Lukkainen, W. J. A. VandenHeuvel, E. O. Haahti, and E. C. Horning. Biochim. Biophys. Acta, **52**, 599 (1961).
5. T. Lukkainen, W. J. A. VandenHeuvel, and E. C. Horning. Biochim. Biophys. Acta, **62**, 153 (1962).
6. H. Werbin. Biochim. Biophys. Acta, **58**, 136 (1962).
7. B. C. Clayton. Biochemistry, **1**, 357 (1962).
8. B. A. Knights and G. H. Thomas. Nature, **194**, 833 (1962).
9. B. A. Knights and G. H. Thomas. Anal. Chem. **34**, 1046 (1962).
10. O. H. Wheeler and R. Montalvo. Radiation Res. In press.
11. C. Djerassi and G. H. Thomas. J. Am. Chem. Soc. **79**, 3835 (1957).
12. W. W. Westerfeld. J. Biol. Chem. **143**, 177 (1942).
13. H. Werbin and C. Holoway. J. Biol. Chem. **223**, 651 (1950).

Received July 22, 1965.
Puerto Rico Nuclear Center,
University of Puerto Rico,
Mayaguez, Puerto Rico.

ERRATUM: THE ALCOHOLYSIS OF TRIALKYLALKOXYSILANES PART II. THE PREPARATION AND CHEMISTRY OF METHYL 2,3,4-TRI-*O*-TRIMETHYLSILYL-α-D-GLUCOPYRANOSIDE

D. T. Hurst and A. G. McInnes

(Ref. Can. J. Chem. 43, 2004 (1965))

On page 2006, line 4, the molecular formula and analytical figures should read: Anal. Calcd. for $C_{23}H_{42}O_7Si_3$: C, 53.66; H, 8.22. Found: C, 53.52; H. 8.30.

Atlantic Regional Laboratory,
National Research Council,
Halifax, Nova Scotia.

Can. J. Chem. Downloaded from www.nrcresearchpress.com by 210.87.254.105 on 09/05/12
For personal use only.

Can. J. Chem. Downloaded from www.nrcresearchpress.com by 210.87.254.6 on 09/05/12
For personal use only.

Canadian Journal of Chemistry

Issued by THE NATIONAL RESEARCH COUNCIL OF CANADA

VOLUME 44 JANUARY 15, 1966 NUMBER 2

REACTIONS OF AMIDES AND RELATED COMPOUNDS

III. N.M.R. INVESTIGATION OF THE PROTONATION OF N,N-DIMETHYLNITROSOAMINE, N,N-DIETHYLNITROSOAMINE, AND N-NITROSOPIPERIDINE[1]

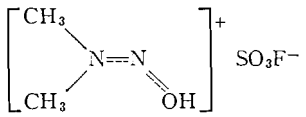
STEPHEN J. KUHN AND JOHN S. MCINTYRE

Dow Chemical of Canada, Limited, Exploratory Research Laboratory, Sarnia, Ontario

Received August 4, 1965

ABSTRACT

Protonation of N,N-dimethylnitrosoamine has been investigated by dissolving the nitrosoamine in different acids and recording the proton magnetic resonance spectra of these solutions. Concentrated sulfuric acid, sulfuric acid monohydrate, perchloric acid (72%), trifluoroacetic acid, and fluorosulfuric acid have been used in this study. Only in fluorosulfuric acid near 0 °C and lower was a new signal observed for the protonated nitrosoamine molecule. Integration of the peaks has shown that only one proton is captured by the nitrosoamine. The following structure is suggested for the protonated nitrosoamine.



The n.m.r. spectra of fluorosulfuric acid solutions of N,N-diethylnitrosoamine and N-nitrosopiperidine also show separate signals for the captured proton.

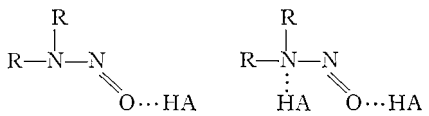
The n.m.r. spectrum of an equimolar solution of N,N-dimethylnitrosoamine, N,N-dimethylformamide, and trifluoroacetic acid in 2-nitropropane indicates that N,N-dimethylnitrosoamine is a weaker base.

INTRODUCTION

N,N-Dialkylnitrosamines with their four pairs of non-bonded electrons are potential Lewis bases. Recently Layne, Jaffe, and Zimmer (1, 2) have investigated the behavior of dialkylnitrosoamines and their interaction with acids in nonpolar and polar solvents by using ultraviolet spectroscopy. In a nonpolar solvent they found that two species are formed with trichloroacetic acid.

$$R_2N-NO\cdots HA \text{ and } HA\cdots R_2N-NO\cdots HA$$

The interaction is through hydrogen bonding and the structures suggested for the compounds are the following.

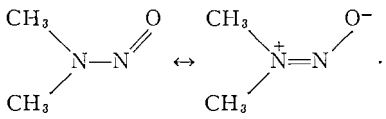


In aqueous sulfuric acid solution they observed a complicated series of changes rather than the expected simple change due to acid–base interaction. Assuming that some of the equilibria observed in more concentrated aqueous H_2SO_4 solution involved the formation of a

[1]*Contribution No. 135.*

conjugate acid, they attempted the isolation of these salts. By mixing pure dialkyl-N-nitrosoamines with concentrated sulfuric acid no precipitation of salts occurred. When the reaction was repeated with 70% aqueous perchloric acid, crystalline salts were obtained from di-*n*-heptyl-N-nitrosoamine and bis-(2-ethylhexyl)-N-nitrosoamine. The crystals slowly decompose above 30 °C and cannot be purified, but titration of the crude product suggested that their composition corresponded to a 1:1 molar adduct of the nitrosoamine and perchloric acid.

Looney, Phillips, and Reilly (3) have investigated the proton resonance spectra of nitrosoamines and have found that at room temperature the nuclear magnetic resonance (n.m.r.) spectrum of dimethylnitrosoamine consists of two sharp peaks of equal intensity which at higher temperature collapse into a singlet. The rotational barrier about the N—N bond in N,N-dimethylnitrosoamine is 23 kcal (considerably higher than in dimethylformamide ($\approx$ 7 kcal (4))), and probably arises largely from the partial double bond character of the N—N bond. Looney, Phillips, and Reilly conclude that the main contributors to the electronic structure of dimethylnitrosoamine are the two resonance forms:



The methyl protons occurring at higher fields are assigned as *cis* with respect to the oxygen and those at lower field as *trans* (5).

In the study reported here, the protonation of N,N-dimethylnitrosoamine was investigated in a number of protonating acids. N,N-diethylnitrosoamine and N-nitrosopiperidine were also examined in fluorosulfuric acid.

EXPERIMENTAL

All the nitrosoamines were obtained from Distillation Products and were used without further purification. Fluorosulfuric acid, obtained from Allied Chemical Corporation was distilled under vacuum before use; perchloric acid was obtained from Fisher Scientific Company.

Solutions of N-Nitroso Secondary Amines in Acids

(*a*) The acid solutions of N,N-dimethylnitrosoamine were prepared by adding the nitrosoamine to the well-stirred cold acid. For fluorosulfuric acid solutions of N,N-dimethylnitrosoamine, N,N-diethylnitrosoamine, and N-nitrosopiperidine, the acid was cooled to −30 °C and the nitrosoamine added slowly with stirring. All solutions were 7.5 wt. % nitrosoamine.

(*b*) Solutions for the concentration study were prepared by diluting a 22% fluorosulfuric acid solution with fluorosulfuric acid to 18, 10, 7 and 1%.

(*c*) Solutions for investigating the basicity of N,N-dimethylnitrosoamine relative to N,N-dimethylformamide were prepared by adding CF_3COOH (0.1 mole) to solutions of N,N-dimethylnitrosoamine (0.1 mole) or N,N-dimethylformamide (0.1 mole) or both (0.1 mole each) in 80 g of 2-nitropropane.

Nuclear Magnetic Resonance

The n.m.r. spectra of the solutions were recorded on a Varian A-60 spectrometer. A capillary of tetramethylsilane (TMS) in the sample was used as an external reference. Low temperatures were obtained by the Varian Variable Temperature Controller Model C-6040; the temperature was determined by separation of the methyl and hydroxyl protons in methanol prior to and after the recording of the spectra.

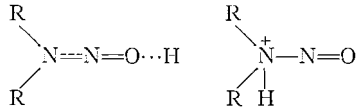
RESULTS AND CONCLUSIONS

Solution of N,N-Dimethylnitrosoamine in Acids

The n.m.r. spectra of N,N-dimethylnitrosoamine in concentrated sulfuric acid, sulfuric acid monohydrate, trifluoroacetic acid, and 70% perchloric acid show that there is a strong interaction between the nitrosoamine and the acids, indicated by the shifts of the

Can. J. Chem. Downloaded from www.nrcresearchpress.com by 210.87.254.6 on 09/05/12
For personal use only.

methyl proton signals. The results also indicate that the nitrosoamine retains its conjugated structure shown by the presence of two different methyl protons. This observation indicates that the protonation takes place on the oxygen atom of the nitroso group (I) and eliminates the possibility of the protonation on the nitrogen atom (II) of the dialkylamine group.



I II

No signal for the captured proton has been observed in any of these solutions. The relatively high freezing point of the acids prohibited using temperatures below −18°. The data obtained in these solutions is summarized in Table I.

TABLE I

N,N-Dimethylnitrosoamine in protonating acids*

Acid	Me position†	
	cis‡	*trans*‡
Neat	169	213
H_2SO_4	266	284
$H_2SO_4.H_2O$	256	276
CF_3COOH	215	239
$HClO_4$ (70%)	254	272

*These spectra were recorded at −18 °C, with the exception of H_2SO_4 which was determined at room temperature.
†Shifts are in c.p.s. relative to external tetramethylsilane.
‡*cis* or *trans* to the oxygen atom (5).

Solutions of N,N-Dimethylnitrosoamine, N,N-Diethylnitrosoamine, and N-Nitrosopiperidine in Fluorosulfuric Acid

Fluorosulfuric acid is a convenient acid for protonation studies. It is a strong protonating acid with a low freezing point and is a good solvent for nitrosoamines. A solution of N,N-dimethylnitrosoamine in fluorosulfuric acid was investigated between 45 °C and −19 °C (Table II).

TABLE II

N,N-Dimethylnitrosoamine in fluorosulfuric acid: temperature effect

Temp. (°C)	Me position*		Proton*
	cis†	*trans*†	
45	253	269	—
Room temperature	248	264	—
10	243	259	850 broad
−5	242	259	854
−19	241	258	854

*Shifts are in c.p.s. relative to external tetramethylsilane.
†*cis* or *trans* to the oxygen atom (5).

At 10° there is a broad band appearing below the fluorosulfuric acid proton. At lower temperatures this becomes a well-resolved singlet (see Fig. 1). Integration of the peaks showed that only one proton was present in the lower peak. We have assigned this peak to the proton captured by the nitrosoamine molecule.

Can. J. Chem. Downloaded from www.nrcresearchpress.com by 210.87.254.6 on 09/05/12
For personal use only.

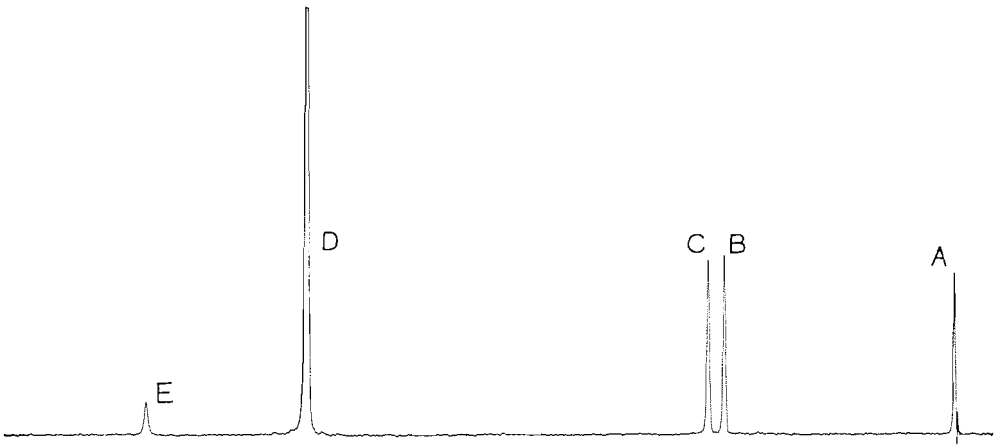


FIG. 1. N,N-Dimethylnitrosoamine in $HFSO_3$ at −19°. A, tetramethylsilane; B and C, methyls *cis* and *trans* with respect to the oxygen atom; D, $HFSO_3$; E, captured proton.

A solution of N,N-diethylnitrosoamine in fluorosulfuric acid at −5° showed a single peak at 837 c.p.s. The methyl peaks were centered at 100 and 106; the methylene at 269 and 276. The relative areas were 6 (combined methyl) and 4 (combined methylene). Also N-nitrosopiperidine in fluorosulfuric acid at −5° showed a singlet at 844 with area 1. The methylene peaks occurred at 134 (broad) and at 278 (multiplet) with relative areas of 6 and 4.

As expected the position of the single proton peak is concentration dependent whereas there is no appreciable change in the position of the methyl proton signals (Table III).

TABLE III

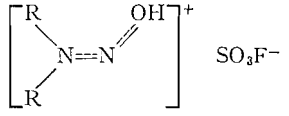
N,N-Dimethylnitrosoamine in fluorosulfuric acid at −17 °C: concentration effect

Concentration (% in $HFSO_3$)	Me position*		OH proton*
	cis†	*trans*†	
22	241	259	951
18	240	258	931
10	242	258	865
7	242	259	849
1	241	257	829

*Shifts are in c.p.s. relative to external tetramethylsilane.
†*cis* or *trans* to the oxygen atom (5).

In acid solution the N-nitrosoamine molecule with its four pairs of non-bonding electrons might be expected to interact with more than one molecule of acid. On the basis of the n.m.r. investigation of solutions of N,N-dialkylnitrosoamines in HSO_3F it seems clear that only one proton is captured by the nitrosoamine molecule. The spectra have also indicated that the site of protonation is on the oxygen atom of the molecule.

Formula III would be consistent with the n.m.r. results.



III

Can. J. Chem. Downloaded from www.nrcresearchpress.com by 210.87.254.6 on 09/05/12
For personal use only.

The delocalization of the positive charge shown in the above structure would likely prevent further protonation of the molecule. Similar structures have been suggested for the adducts of N-nitroso secondary amines with alkyl carbonium ions (7) and boron trifluoride (8). Gillespie and Birchall (6) have found a fast exchange between the acid protons and the captured proton in fluorosulfuric acid solution of amides; a signal corresponding to the hydroxyl proton in the adduct separates only at −80 °C. The present study shows that in fluorosulfuric acid solutions of N-nitroso secondary amines the acid-OH proton exchange is relatively slow and the n.m.r. signal corresponding to the OH proton in the adducts already appears at slightly below room temperature.

Competitive Protonation of N,N-Dimethylnitrosoamine and N,N-Dimethylformamide

A yellow solution of N,N-dimethylnitrosoamine in 2-nitropropane gives a colorless solution when protonated with an equimolar quantity of trifluoroacetic acid. When N,N-dimethylformamide is added to the colorless solution, the yellow color returns suggesting that N,N-dimethylformamide is the stronger base. The competition of N,N-dimethylnitrosoamine and N,N-dimethylformamide for acid protons was also investigated by measuring the relative downfield shifts of their methyl proton signals (Table IV). A comparison of these shifts again indicates that N,N-dimethylnitrosoamine is a weaker base than N,N-dimethylformamide.

TABLE IV

Competitive protonation of N,N-dimethylnitrosoamine and N,N-dimethylformamide at 30°

	D.M.F.*		D.M.N.A.†	
Solutions in 2-nitropropane	*cis*‡·§	*trans*‡·§	*cis*‡·‖	*trans*‡·‖
D.M.F.	102	94		
D.M.N.A.			88	42
D.M.F., D.M.N.A.	101	93	88	43
D.M.F., CF_3COOH	90	81		
D.M.N.A., CF_3COOH			72	35
D.M.F., D.M.N.A., CF_3COOH¶	91	83	81	41

*N,N-Dimethylformamide.
†N,N-Dimethylnitrosoamine.
‡Shifts in c.p.s. upfield from second peak in nitropropane septuplet.
§The methyl is *cis* or *trans* with respect to the aldehyde proton.
‖The methyl is *cis* or *trans* with respect to the oxygen atom.
¶Addition of D.M.F. to the solution of D.M.N.A. and CF_3COOH or addition of D.M.N.A. to the solution of D.M.F. and CF_3COOH gave identical shifts.

REFERENCES

1. W. S. LAYNE, H. H. JAFFE, and H. ZIMMER. J. Am. Chem. Soc. **85**, 435 (1963).
2. W. S. LAYNE, H. H. JAFFE, and H. ZIMMER. J. Am. Chem. Soc. **85**, 1816 (1963).
3. C. E. LOONEY, W. D. PHILLIPS, and E. L. REILLY. J. Am. Chem. Soc. **79**, 6136 (1957).
4. H. S. GUTOWSKY and C. H. HOLM. J. Chem. Phys. **25**, 1228 (1956).
5. G. J. KARABATSOS and R. A. TALLER. J. Am. Chem. Soc. **86**, 4373 (1964).
6. R. J. GILLESPIE and T. BIRCHALL. Can. J. Chem. **41**, 148 (1963).
7. S. HUNIG, L. GELDERN, and E. LUCKE. Angew. Chem. **75**, 476 (1963).
8. D. KLAMANN and W. KOSER. Angew. Chem. **75**, 1104 (1963).

Can. J. Chem. Downloaded from www.nrcresearchpress.com by 210.87.254.6 on 09/05/12
For personal use only.

ORGANOPHOSPHORUS–URANYL COMPLEXES STUDIED BY NUCLEAR MAGNETIC RESONANCE SPECTROSCOPY[1]

JANE L. BURDETT AND L. L. BURGER
Battelle Memorial Institute, Pacific Northwest Laboratory, Richland, Washington
Received July 27, 1965

ABSTRACT

The effect of extraction of uranyl nitrate on certain neutral organophosphorus compounds has been observed by nuclear magnetic resonance (n.m.r.) spectroscopy. Proton and phosphorus chemical shifts have been measured for the complexed and uncomplexed material. The effect of complexation on proton–proton and proton–phosphorus coupling constants has been noted.

INTRODUCTION

The metal-extracting ability of organophosphorus compounds has been investigated previously by many workers (1). Solvation complexes involving neutral organophosphorus compounds are formed with many salts, and of particular interest are the very strong complexes formed with uranyl nitrate and several other salts. These have the structure, $UO_2X_2(OP)_2$, where OP represents the phosphorus compound.

Numerous studies of the nuclear magnetic resonance of organophosphorus compounds have been published (2–8), but quantitative measurements of the effects of complex formation have not been reported. The present study has involved the effect of uranyl nitrate on the proton and phosphorus n.m.r. spectra of organophosphorus compounds. A series of compounds has been investigated, including phosphates, phosphonates, phosphinates, and phosphine oxides. Both the chemical shifts of ^1H and ^{31}P and the spin–spin coupling constants have been measured.

EXPERIMENTAL

Instrumental

Proton measurements have been made at 60.0 Mc on the Varian DP-60 and A-60 nuclear magnetic resonance spectrometers. Chemical shifts are reported within ±1 c.p.s. Phosphorus chemical shifts were measured at 24.3 Mc on the Varian DP-60 spectrometer and are reported within ±0.5 p.p.m. Proton–proton and proton–phosphorus coupling constants were measured on the Varian A-60 spectrometer and are reported to within ±0.1 c.p.s. All measurements have been made at room temperature (probe 33 ± 2 °C). Double resonance experiments have been performed using the Varian V-3521 integrator and inserting a 0.01 μF capacitor between the modulator output and the probe sweep coils, according to the technique developed by Johnson (9). Spectra were obtained using the first lower sideband.

Synthesis of Organophosphorus Compounds

Preparation of the compounds and their physical properties have been described elsewhere (10).

Preparation of Solutions

$UO(NO_3)_2.2H_2O$ was added to about 2 ml of the organophosphorus compound until the solution was saturated. The mixture was equilibrated with stirring for about 5 min and then was centrifuged. The supernatant was used to prepare carbon tetrachloride solutions of the complex. Concentrations of both complexed and uncomplexed material were 20% by volume.

RESULTS AND DISCUSSION

Chemical Shift Measurements

Proton chemical shifts are given in Table I for a series of organophosphorus compounds in c.p.s. from tetramethylsilane (TMS). Doubling of the β-alkoxy proton signal due to the

[1]*Work performed under contract AT(45-1)-1830 for the U.S. Atomic Energy Commission.*

Can. J. Chem. Downloaded from www.nrcresearchpress.com by 210.87.254.42 on 09/05/12
For personal use only.

presence of the phenyl ring in diisopropyl phenylphosphonate has been observed previously.

Representative proton spectra of the uncomplexed and complexed diethyl methylphosphonate are shown in Figs. 1*a* and 1*b*, respectively. Dissociation is negligible so that the spectrum does indeed represent that of the complex alone.

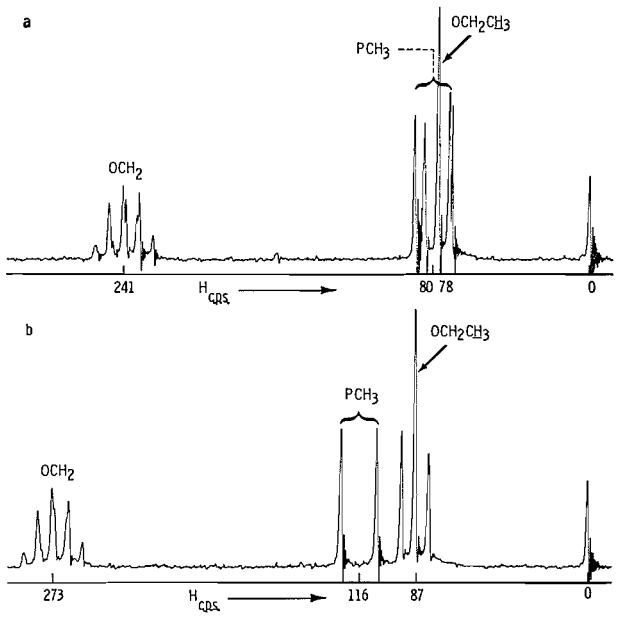


FIG. 1. (*a*) Proton magnetic resonance spectrum of diethyl methylphosphonate in carbon tetrachloride (20% v/v). (*b*) Proton magnetic resonance spectrum of diethyl methylphosphonate – uranyl nitrate complex in carbon tetrachloride (20% v/v).

The changes in chemical shift for protons in organophosphorus compounds on complexation with uranyl nitrate are seen in Table I. These changes are in the same order of magnitude as those observed in methylenediphosphonate complexes of uranyl nitrate (12). The greatest changes in chemical shift are observed for those protons closest to the phosphoryl group, i.e., the site of complexation. In every case the protons are effectively deshielded as a result of complexation. This is in agreement with the results of Ferraro for the α-protons of phosphoryl ligands in another uranyl complex, but not for the methyl protons which were more shielded in the complex (13). Presumably the structure of the complexed species is that of two bidentate nitrato and two phosphoryl groups as ligands in the plane perpendicular to the linear uranyl ion, similar to that for the trinitrato uranyl complex (14, 15). These paramagnetic shifts may be accounted for, at least in part, by the anisotropy of the uranyl group (12).

For the present series of compounds differences in chemical shifts *for protons* do not appear to be a sufficiently sensitive function of extracting ability. Apparently the major contribution to the chemical shift changes is the anisotropy of the uranyl group, and only a minor contribution is made by changes in the P—X bonds on complexation.

Phosphorus chemical shifts of carbon tetrachloride solutions are shown in Table II. As observed by earlier workers (3, 5), the substitution of stronger electron-donating groups on phosphorus results in less shielding of the quadruply-bound phosphorus nucleus. Recent

Can. J. Chem. Downloaded from www.nrcresearchpress.com by 210.87.254.42 on 09/05/12
For personal use only.

Can. J. Chem. Downloaded from www.nrcresearchpress.com by 210.87.254.42 on 09/05/12
For personal use only.

TABLE I

Proton chemical shifts for organophosphorus compounds and their uranyl complexes*

	Alkyl				Alkoxy					
	α-H		β-H		α-H		β-H		Other	
	σ	Δσ	σ	Δσ	σ	Δσ	σ	Δσ	σ	Δσ
$(CH_3CH_2O)_3PO$	—	—	—	—	+242	+30	+79	+9	—	—
$[CH_3(CH_2)_3O]_2PO(OCH_3)$	—	—	—	—	220†,234‡	28,36	§	§	—	—
$[CH_3(CH_2)_3O]_2PO(C_6H_{11})$	—	—	—	—	235	35	§	§	—	—
$(CH_3CH_2O)_2PO(H)$	—	—	—	—	245	30	80	10	401‖	+52
$(CH_3CH_2O)_2PO(CH_3)$	+81	+35	—	—	241	32	78	9	—	—
$(CH_3CH_2O)_2PO(CH_2CH_3)$	103	33	+69	+11	241	33	78	10	—	—
$[CH_3(CH_2)_3O]_2PO(CH_2Cl)$	209	36	—	—	245	30	§	—	§	—
$[(CH_3)_2CH—O]_2PO(C_6H_5)$	—	—	—	—	277	47	71,80¶	9,9¶	446**,465††	7**,27††
$[CH_3(CH_2)_2O]_2PO(C_6H_5)$	—	—	—	—	235	33	96	3	56‡‡,448**,465††	6**,27††
$(CH_3O)PO[(CH_2)_3CH_3]_2$	§	—	§	—	216	31	—	—	—	—

*Chemical shifts (σ) are in c.p.s. relative to TMS in 20% v/v carbon tetrachloride solutions. Changes in shifts on complexation (Δσ) are relative to the free ligand. Positive shifts indicate resonance at lower applied field relative to TMS.
†OCH_3.
‡OCH_2.
§Involved spectrum.
‖PH proton.
¶Two separate resonance peaks. Doubling is due to the presence of the benzene ring (11).
**3 Ring protons.
††2 Ring protons.
‡‡Methyl protons.

LCAO-MO calculations show that in quadruply connected phosphorus compounds the shielding of the phosphorus nucleus may be interpreted in terms of the polarity of the σ-bonds and the amount of π-character associated with the phosphorus (16, 17). An increase in ^{31}P shielding is accompanied by an increase in P=O bonding (16) or in π-electrons per phosphorus nucleus (17) in a series progressing from R_3PO to $(RO)_3PO$. The position of the phosphorus resonance of the dialkyl phenylphosphonates at higher applied fields than other phosphonates may also be explained in terms of an increase in the π-character of the P=O bond.

TABLE II

Phosphorus chemical shifts for organophosphorus compounds and their uranyl complexes*

Compound	Chemical shift (p.p.m.)		
	σ_{CCl_4}	$\sigma_{UO_2^{++},CCl_4}$	$\Delta\sigma$
$(CH_3CH_2O)_3PO$	−0.5	+0.2	+0.7
$[CH_3(CH_2)_3O]_2PO(OCH_3)$	+0.2	1.9	1.7
$(CH_3O)_2PO(H)$	9.8	17.3	7.5
$(CH_3CH_2O)_2PO(H)$	6.2	10.8	4.6
$[CH_3(CH_2)_3O]_2PO(H)$	6.7	12.5	5.8
$(CH_3CH_2O)_2PO(CH_3)$	29.4	37.6	8.2
$(CH_3CH_2O)_2PO(CH_2CH_3)$	32.2	39.0	6.8
$[CH_3(CH_2)_3O]_2PO[(CH_2)_3CH_3]$	31.1	37.9	6.8
$[(CH_3)_2CH—O]_2PO(C_6H_5)$	15.7	20.0	4.3
$[CH_3(CH_2)_2O]_2PO(C_6H_5)$	17.8	22.6	4.8
$(CH_3O)PO[(CH_2)_3CH_3]_2$	56.8	72.1	15.3
$[CH_3(CH_2)_7]_3PO$	42.0	74.1	32.1

*Chemical shifts are given in p.p.m. and are relative to external 85% phosphoric acid. Positive values represent chemical shifts at lower applied field than the reference.

Molecular orbital calculations have not been attempted for the unsymmetrically substituted phosphoryl compounds in the present study because of their inherent complexity. Use of the results of Wagner (16) and of Letcher and Van Wazer (17) has been restricted to a qualitative interpretation because of uncertainties in the ZPZ′ angles, and because of the uncertain relative effect of ligands of differing electronegativities on the π-bonding. Both the ^{31}P shifts and the π-character associated with the phosphorus nucleus may be estimated roughly for unsymmetrical compounds, assuming that each substituent makes an additive contribution. Results obtained from these calculations based on the above assumptions give either increasing π-character of the P=O bond or greater π-bonds per phosphorus in the order of increased phosphorus shielding.

Of primary importance in complexation is the unshared electron pair on the phosphoryl oxygen which is available for covalent bonding. Phosphine oxide, which forms the strongest complex, presumably has the most negative oxygen of the compounds studied (16, 18, 19). As a second order effect, complexation results in phosphorus chemical shifts downfield from those of the free ligand. This paramagnetic shift may be seen to increase with increasing extracting ability of the organophosphorus compound to a maximum in the phosphine oxide. Undoubtedly changes in the nature of the P=O bond with complexation are reflected in this shift. Also the phosphorus nucleus is in the paramagnetic region of the uranyl ion.

Infrared Measurements

Infrared P=O stretching frequencies for several complexed and uncomplexed organophosphorus compounds are given in Table III. The P=O stretching frequency gives a

Can. J. Chem. Downloaded from www.nrcresearchpress.com by 210.87.254.42 on 09/05/12
For personal use only.

linear correlation with extracting ability for these compounds (19). Thus a decrease in the stretching frequency is observed as extracting ability increases, i.e. phosphate < phosphonate < phosphinate < phosphine oxide. However, the change in stretching frequency on complexation, $\Delta_{P=O}$, does not correlate well with extracting ability (see Table III).

TABLE III

Infrared P=O stretching frequencies for organophosphorus compounds in carbon tetrachloride and complexed with UO_2^{++}*

Compound	P=O (cm^{-1})		$\Delta_{P=O}$ (cm^{-1})
	CCl_4	CCl_4,UO_2^{++}	
$(CH_3CH_2O)_3PO$	1 260	1 185	75
$[CH_3(CH_2)_3O]_2P(O)(OCH_3)$	1 274	1 190	84
$(CH_3CH_2O)_2PO(H)$	1 260	1 192	68
$(CH_3CH_2O)_2PO(CH_3)$	1 240	1 167	73
$(CH_3CH_2O)_2PO(CH_2CH_3)$	1 242	1 172	70
$[CH_2(CH_2)_3O]_2PO[(CH_2)_3CH_3]$	1 250	1 170	80
$[(CH_3)_2CH—O]_2PO(C_6H_5)$	1 253	1 185	68
$(CH_3O)PO[(CH_2)_3CH_3]_2$	1 230	1 140	90
$[CH_3(CH_2)_7]_3PO$	1 160	1 065	95

*Measurements have been made on a Perkin–Elmer Model 521 grating infrared spectrophotometer, using a CaF_2 cell. Concentrations were 10% in the solvent.

Spin–Spin Coupling Constants

Several proton–proton and proton–phosphorus coupling constants have been measured in the organophosphorus compounds (see Table IV). The very large J(P—H) coupling in the alkyl hydrogenphosphonates supports the structure in which hydrogen is directly attached to the phosphorus (2, 4, 5, 7). The alkoxy $^{31}P—^{1}H$ coupling forms an interesting series. Axtmann, Shuler, and Eberly (20) indicated an increase in J(P—O—C—H) coupling in trialkyl phosphates with increasing electron-withdrawing character of the alkyl group. In general the data in Table IV show that this picture may be extended to include phosphonates and phosphinates. Furthermore, comparison of J(P—O—C—H) in dimethyl methylphosphonate and diethyl methylphosphonate shows that the electron-withdrawing ability of an alkyl group affects the coupling in the alkoxy group of these compounds in the same manner.

Relative signs of coupling constants have been assigned in general from the literature (21–25). However, the relative sign of J(P—C—H) differs among several compounds (21, 23, 26–28). To determine its sign in the present organophosphorus compounds, proton double resonance experiments have been performed on diethyl ethylphosphonate and on the uranyl nitrate complex of this compound. In Fig. 2*a* is shown the normal proton spectrum for the diethyl ethylphosphonate – uranyl complex which has a doublet quartet (PCH_2) and a doublet triplet (PCH_2CH_3) whose lower triplet is masked by the ethoxy methyl protons. In Fig. 2*b* the upper triplet at 81 c.p.s. has been irradiated and, as a result, the lower quartet has collapsed, which indicates that J(P—C—H) and J(P—C—C—H) have unlike signs (29). Thus J(P—C—H) has a negative sign because J(P—C—C—H) has a positive sign (23). This negative sign for J(P—C—H) agrees with the conclusion of Duval and Koide (30, 31) that Hund coupling does make an important contribution to phosphorus–proton coupling.

The change in $^{31}P—^{1}H$ coupling constants on formation of uranyl complexes, although relatively small in most cases, is in the direction of increased coupling. In general the largest increase occurs for those protons closest to the phosphorus atom. Thus J(P—H) in

Can. J. Chem. Downloaded from www.nrcresearchpress.com by 210.87.254.42 on 09/05/12
For personal use only.

Can. J. Chem. Downloaded from www.nrcresearchpress.com by 210.87.254.42 on 09/05/12
For personal use only.

TABLE IV

Spin–spin coupling constants in organophosphorus compounds*

Compound	Coupling constant (c.p.s.)					
		Alkyl		Alkoxy		
	J_{HH}	$J_{\alpha H-P}$	$J_{\beta H-P}$	$J_{\alpha H-P}$	$J_{\beta H-P}$	Other
$(CH_3CH_2O)_3PO$	±7.3	—	—	±8.7	±0.9	—
$(CH_3O)PO[O(CH_2)_3CH_3]_2$	±6.6	—	—	±8.0† ±11.7‡	—	—
$(CH_3O)_2PO(H)$	—	—	—	±12.2	—	±696§
$(CH_3CH_2O)_2PO(H)$	±7.4	—	—	±9.9	—	±690§
$[CH_3(CH_2)_3O]_2PO(H)$	±6.5	—	—	±9.2	—	±690§
$(CH_3CH_2O)_2PO(CH_3)$	±7.3	∓18.1	—	±8.7	n.r.‖	—
$(CH_3CH_2O)_2PO(CH_2CH_3)$	±7.2¶	∓19.2**	±21.6**	±8.5	—	—
$[(CH_3)_2CH—O]_2PO(C_6H_5)$	±6.3	—	—	±8.1	—	—
$[CH_3(CH_2)_3O]_2PO(CH_2Cl)$	±6.6	∓11.2	—	±8.2	—	—
$(CH_3O)PO[(CH_2)_3CH_3]_2$	—	—	—	±10.9	—	—

*Solntions are 20% v/v in carbon tetrachloride.
†J_{POCH_2}.
‡J_{POCH_3}.
§J_{PH} for proton attached directly to a phosphorus atom.
‖n.r. = not resolved.
¶Alkoxy protons.
**Measurement is within ±0.4 c.p.s.

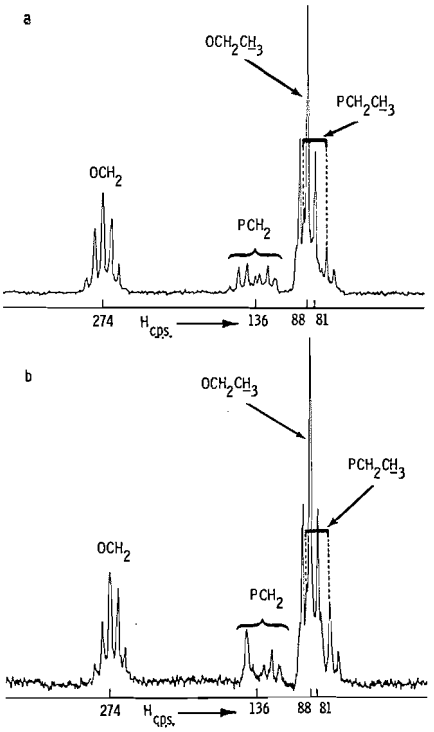


FIG. 2. (*a*) Proton magnetic resonance spectrum of diethyl ethylphosphonate – uranyl nitrate complex in carbon tetrachloride (20% v/v). (*b*) Proton double resonance spectrum of diethyl ethylphosphonate – uranyl nitrate complex in carbon tetrachloride (20% v/v).

the dialkyl hydrogenphosphonates increases by as much as 61 c.p.s. There appears to be no marked trend relating the change in coupling constant to complexing ability of the parent compound, although J(P—O—C—H) increases from 0.4 c.p.s. in $(RO)_3PO$ to 0.7 c.p.s. in $(RO)_2PO(R')$. No change in proton–proton coupling constants is observed with complexation. The observed increases in coupling constant with complexation are in part a consequence of changes in the hybridization of the P—X bond orbitals. The effective withdrawal of electrons from the P=O bond is presumably accompanied by an increase in the amount of s-character in the P—X bonds.

ACKNOWLEDGMENTS

We wish to acknowledge assistance from the following people: Mrs. Thelma W. Lawell for infrared measurements, Mr. Earl C. Martin for synthesis of compounds, Mr. Bernard L. Nist for use of the Varian A-60 spectrometer, Mr. Ross Pitcher for obtaining 100 Mc spectra, Dr. E. Duval for a preprint of long-range spin–spin interaction between nuclei and saturated compounds, Dr. J. R. Van Wazer for a preprint of the theoretical interpretation of phosphorus chemical shifts, and Dr. E. L. Wagner for stimulating discussions.

REFERENCES

1. L. L. BURGER. Nucl. Sci. Eng. **16**, 428 (1963).
2. N. MULLER, P. C. LAUTERBUR, and J. GOLDENSON. J. Am. Chem. Soc. **78**, 3557 (1956).
3. J. R. VAN WAZER, C. F. CALLIS, J. N. SHOOLERY, and R. C. JONES. J. Am. Chem. Soc. **78**, 5715 (1956).
4. C. F. CALLIS, J. R. VAN WAZER, J. N. SHOOLERY, and W. A. ANDERSON. J. Am. Chem. Soc. **79**, 2719 (1957).

Can. J. Chem. Downloaded from www.nrcresearchpress.com by 210.87.254.42 on 09/05/12
For personal use only.

5. H. FINEGOLD. Ann. N.Y. Acad. Sci. **70**, 875 (1958).
6. NUCLEAR MAGNETIC RESONANCE SPECTRAL DATA. Manufacturing Chemists Association Research Project, Agricultural and Mechanical College of Texas, College Station, Texas. 1962.
7. L. C. D. GROENWEGHE, L. MAIER, and K. MOEDRITZER. J. Phys. Chem. **66**, 901 (1962).
8. J. B. HENDRICKSON, M. L. MADDOX, J. J. SIMS, and H. D. KAESZ. Tetrahedron, **20**, 449 (1964).
9. L. F. JOHNSON. Private communication.
10. (*a*) L. L. BURGER and R. M. WAGNER. Chem. Eng. Data Ser. 3, 311 (1958). (*b*) L. L. BURGER and E. C. MARTIN. Presented at the 139th National Meeting of the American Chemical Society, St. Louis. March 1961.
11. T. H. SIDDALL III and C. A. PROHASKA. J. Am. Chem. Soc. **84**, 3467 (1962).
12. T. H. SIDDALL III and C. A. PROHASKA. Inorg. Chem. **4**, 783 (1965).
13. J. R. FERRARO. J. Inorg. Nucl. Chem. **26**, 225 (1964).
14. J. L. HOARD and J. D. STROUPE. Natl. Nucl. Energy Ser. Div. III, **2**, 15 (1949).
15. J. E. FLEMING and H. LYNTON. Chem. Ind. London, 1409 (1959).
16. E. L. WAGNER. J. Am. Chem. Soc. **85**, 161 (1963).
17. J. H. LETCHER and J. R. VAN WAZER. J. Chem. Phys. Submitted.
18. G. MAVEL. J. Chim. Phys. **61**, 1191 (1964).
19. L. L. BURGER. J. Phys. Chem. **62**, 590 (1958).
20. R. C. AXTMANN, W. E. SHULER, and J. H. EBERLY. J. Chem. Phys. **31**, 850 (1959).
21. G. M. WHITESIDES, J. L. BEAUCHAMP, and J. D. ROBERTS. J. Am. Chem. Soc. **85**, 2665 (1963).
22. M. KARPLUS. J. Chem. Phys. **30**, 11 (1959).
23. S. L. MANATT, G. L. JUVINALL, and D. D. ELLEMAN. J. Am. Chem. Soc. **85**, (1963).
24. G. J. BENE, E. DUVAL, A. FINAZ, G. HOCHSTRASSER, and S. KOIDE. Phys. Rev. Letters, **7**, 34 (1963).
25. G. J. BENE, E. DUVAL, A. FINAZ, and G. HOCHSTRASSER. Compt. Rend. **256**, 2365 (1963).
26. P. T. NARASIMHAN and M. T. ROGERS. J. Chem. Phys. **34**, 1049 (1961).
27. J. D. LANCASTER. Private communication.
28. W. A. ANDERSON, R. FREEMAN, and C. A. REILLY. J. Chem. Phys. **39**, 1518 (1963).
29. J. P. MAHER and D. F. EVANS. Proc. Chem. Soc. 208 (1961).
30. E. DUVAL and S. KOIDE. Phys. Rev. Letters, **8**, 314 (1964).
31. S. KOIDE and E. DUVAL. J. Chem. Phys. **41**, 315 (1964).

Can. J. Chem. Downloaded from www.nrcresearchpress.com by 210.87.254.42 on 09/05/12
For personal use only.

Can. J. Chem. Downloaded from www.nrcresearchpress.com by 210.87.254.6 on 09/05/12
For personal use only.

KINETIC STUDIES OF PROTON TRANSFER FROM PHENOLS TO TRINITROBENZYL ANION

J. A. Blake, M. J. B. Evans, and K. E. Russell
Department of Chemistry, Queen's University, Kingston, Ontario
Received August 18, 1965

ABSTRACT

The rates of reaction of various phenols with the 2,4,6-trinitrobenzyl anion in the solvent ethanol have been determined by a spectrophotometric method. The rate constants at −40 °C are related to the dissociation constants of the phenols in water at 25 °C and the value of α in the Brönsted relation is 0.84 ± 0.07; α drops to 0.44 ± 0.05 if the results for the substituted acetic acids (1) are included. The rate constants for the phenols are also correlated by the Hammett relationship, the ρ value at −40 °C being 1.82 ± 0.2. The activation energies range from 9.4 to 10.9 kcal/mole.

The rate of reaction of trinitrobenzyl anion with 3-methylphenol at −30 °C is reduced by a factor of 12 if the phenol is deuterated at the OH group and the solvent is deuteroethanol. The large isotope effect confirms that the rate-determining step involves proton transfer from the OH group of the phenol. Substitution of lithium or potassium cations for the sodium cation does not affect the rate constant at −10 °C.

In the reaction with 3-methylphenol, a measurable concentration of trinitrobenzyl anion remains at equilibrium and the equilibrium constant for the reaction is 1.3 ± 0.2 at 25 °C. The heat and entropy changes are approximately −6.5 kcal/mole and −21 e.u./mole respectively.

INTRODUCTION

The broad objective of this work is to determine the factors which influence the rates of proton transfer from weak acids to carbanion bases. Caldin and Long have shown (1) that the purple anion produced by the reaction of sodium ethoxide with 2,4,6-trinitrotoluene (TNT) is probably the 2,4,6-trinitrobenzyl ion (TNT^-) and that the rates of reaction of this anion with substituted acetic acids can be determined by conventional means at temperatures of the order of −70 °C. An extension of this work to phenols is desirable because it is possible to study by appropriate choice of substituted phenols the influence of inductive, resonance, and steric effects on the rate of proton transfer. In this paper the influence of inductive effects is examined by determining the rates of reaction of the TNT^- ion with meta-substituted phenols.

EXPERIMENTAL

Apparatus

The absorbance of the TNT^- ion was determined using a modified Fisher electrophotomer with a 650 mμ filter. The glass cells were similar in design to those used by Caldin and Trickett (2). The volumes of the main cell and side chamber were 60 ml and 10 ml respectively and the corresponding values for the smaller cell used in the isotope work were 10 ml and 2 ml respectively. Each glass cell was sealed into the thermostat by means of a silicone rubber gasket which was held in place by a ring of high density polythene. Condensation on the windows was prevented by a stream of nitrogen produced by evaporation of liquid nitrogen; the temperature of the nitrogen was controlled by passing it over a heater in a glass flask.

The cell was sealed into a small brass tank surrounded by styrofoam. One side of the tank was removable to facilitate exchange of cells and the seal was made by an indium gasket. The bath liquid, methanol, was cooled using a tube of dry ice and acetone and the rate of cooling was adjusted by varying the extent to which the tube was immersed in the methanol. The temperature was maintained to better than ±0.1 °C using a 20 W heater controlled by a Yellow Springs Instrument Company thermistor unit. The temperature of the bath was determined by means of a multi-junction copper–constantan thermocouple calibrated against a platinum resistance thermometer.

Equilibria between phenols and ethoxide ion in ethanol solution were studied using a Beckmann DU spectrophotometer, the quartz cells being maintained at −10 °C by passing cooled ethanol through the modified cell holder (3).

Can. J. Chem. Downloaded from www.nrcresearchpress.com by 210.87.254.6 on 09/05/12
For personal use only.

Procedure

A solution of approximately 0.008 *N* sodium ethoxide in absolute ethanol was prepared and standardized in an atmosphere of nitrogen against 0.1 *N* hydrochloric acid using a pH meter. Forty-four milliliters of this ethoxide solution was placed in the main chamber of the cell and 5 ml of a solution of phenol in ethanol in the side chamber. When temperature equilibrium was attained, the electrophotometer was adjusted for 100% transmission. One milliliter of a 0.003 *M* solution of TNT in an ethanol–toluene mixture was added to the ethoxide solution and the solution stirred until the absorbance reached a maximum. For reaction temperatures below −30 °C it was more convenient to mix the TNT and ethoxide solutions outside the cell and cool the mixture before placing it in the cell; at −60 °C it was necessary to wait about half an hour before equilibrium was reached.

The phenol solution was forced into the reaction cell using a rubber bulb attached to the side chamber and complete mixing effected by forcing some of the reaction mixture back and forth between the two chambers. Readings of absorbance could be obtained within 20 s of mixing, and half-lives were generally in the range 2–30 min. Rates of disappearance of TNT^- anion were determined for a range of phenol concentrations at appropriate temperatures in the −10 °C to −60 °C region; for any one phenol the temperature range was 20 to 30 °C. Density corrections were made using the data of Smyth and Stoops (4) for pure ethanol.

The reaction of the TNT^- anion with deuterated 3-methylphenol was studied with deuteroethanol as solvent. The 3-methylphenol was dissolved in 1 ml deuteroethanol to obtain the deuterated phenol and this solution was mixed with 7 ml TNT^- anion solution in the small cell.

Lithium and potassium ethoxide solutions (0.008 *M*) were prepared by dissolving the metals in absolute ethanol and were standardized against hydrochloric acid. The reactions of 3-methylphenol with TNT^- anion prepared using these ethoxides were studied at −30 °C, −20 °C, and −10 °C.

Equilibria between sodium ethoxide and phenol, 3-methylphenol, and 4-chlorophenol were investigated at −10 °C and 25 °C. Sodium ethoxide was added to the phenol solution in an atmosphere of nitrogen and the degree of conversion of phenol to phenoxide determined using absorbance measurements at 290 mμ (305 mμ for 4-chlorophenol). The initial concentration of phenol was close to 0.003 *M* and the cell thickness was 1 mm.

The equilibrium constant of the reaction between TNT^- and 3-methylphenol was obtained by measurement of the concentrations of TNT^- at equilibrium with various concentrations of 3-methylphenol. The solutions initially contained TNT and 0.008 *M* sodium ethoxide, and 3-methylphenol was added until its equilibrium concentration was in the range 0.02–0.07 *M*. Under these conditions the reaction of 3-methylphenol with ethoxide ion goes virtually to completion so that the equilibrium concentration of 3-methylphenoxide ion is close to 0.008 *M* in each experiment. The maximum concentration of TNT^- is 6×10^{-5} *M* and variations in its value do not significantly affect the concentrations of phenol and phenoxide. The equilibrium concentration of TNT^- was estimated from the absorbance of the solution. The extinction coefficient of TNT^- was determined from separate measurements of absorbances of solutions containing 0.008 *M* sodium ethoxide and various amounts of added TNT.

RESULTS AND DISCUSSION

Caldin and Long (1) have shown that the reaction of ethoxide ion with TNT probably proceeds according to the equation

$$[1] \qquad TNT + OEt^- \rightleftharpoons TNT^- + HOEt$$

and that the proton is transferred from the methyl group of the TNT to the ethoxide ion. Equilibrium is rapidly reached at room temperature and at the low ethoxide concentrations used in this work the side reaction to give a brown complex (1) proceeds to a negligible extent. On addition of phenol almost all the ethoxide is removed by reaction [2]

$$[2] \qquad XOH + OEt^- \rightleftharpoons HOEt + XO^-$$

and the excess phenol reacts with the TNT^- ion by reaction [3].

$$[3] \qquad TNT^- + XOH \rightleftharpoons TNT + XO^-$$

The rate of disappearance of the TNT^- ion is given by

$$[4] \qquad -\frac{d[TNT^-]}{dt} = (k_3[XOH] + k_{-1}[EtOH] + k_f)[TNT^-] - (k_1[OEt^-] + k_{-3}[XO^-])[TNT]$$

where k_1 and k_3 are rate constants for the forward reactions of [1] and [3], k_{-1} and k_{-3} are rate constants for the corresponding reverse reactions and k_f is included to take account

of a very slow fade of the purple anion in the absence of added phenol. The concentration of TNT is given by its initial concentration less the TNT^- concentration; solutions of TNT^- obey Beer's law at the concentrations used. Thus upon integration, eq. [5] is obtained

$$[5] \quad \ln (D - D_e) = -(k_3[XOH] + k_1[OEt^-] + k_{-1}[EtOH] + k_{-3}[XO^-] + k_f)t + b$$

where D, D_e are the absorbances of the reacting solution at time t and at equilibrium and b is a constant. Fig. 1 shows a typical plot of ln D vs. time, t, for the reaction of 3-acetylphenol with TNT^- at -40 °C; the absorbance at equilibrium, D_e, is too small to be measured with this phenol. The slopes, s, of such plots are used to evaluate k_3.

$$[6] \quad s = -(k_3[XOH] + k_1[OEt^-] + k_{-1}[EtOH] + k_{-3}[XO^-] + k_f)$$

At a given temperature with a given ethoxide concentration, the last four terms of eq. [6] are either constant or small compared with $k_3[XOH]$ provided that reaction [2] proceeds almost to completion. Thus a graph of s vs. [XOH] gives a straight line for each phenol at constant temperature and the rate constant k_3 is determined from the slope of the graph. The second and fourth terms of eq. [6] vary appreciably when low concentrations of 3-methylphenol are used at -10 °C but the error in k_3 from this cause is small.

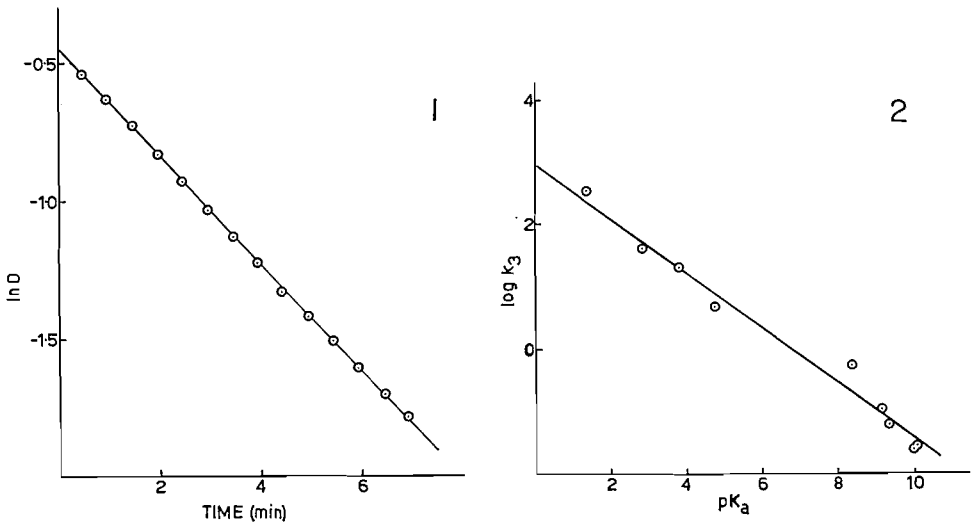


FIG. 1. Dependence of ln D on time for the reaction of TNT^- with 3-acetylphenol at -40 °C.
FIG. 2. Dependence of log k_3 (-40 °C) on pK_a in water.

The rate of reaction of TNT^- ion with deuterated 3-methylphenol in deuteroethanol is considerably less than that with 3-methylphenol in ethanol. The ratio of the rate constants k_3^H/k_3^D is 12 ± 2 at -30 °C. The rate constant may be affected by the change in solvent but the reduction in rate on deuteration is so great that it must be mainly due to a primary isotope effect. This confirms that the rate-determining step of the discharge of color of TNT^- ion by 3-methylphenol, and presumably other acids, is the proton transfer process of eq. [3]. The base strengths of the 3-methylphenoxide and TNT^- ions are not widely different and the transition state should be fairly symmetrical, so that a relatively large value of k_3^H/k_3^D is to be expected (5).

Can. J. Chem. Downloaded from www.nrcresearchpress.com by 210.87.254.6 on 09/05/12
For personal use only.

The kinetic results for phenol, 3-methyl-, 3-acetyl-, 3-cyano-, 3-nitro-, and 4-chlorophenol are summarized in Table I. The uncertainty in k_3 at -40 °C is estimated to be $\pm 8\%$, and the activation energies are probably correct to ± 0.8 kcal/mole; the resultant uncertainty in the values of log A at -40 °C is ± 0.9. The rate constants k_3 at -40 °C can be correlated by the Bronsted relation

$$[7] \qquad \log k_3 = \log G + \alpha \log K_a$$

where G and α are constants and K_a is the dissociation constant of the acid. Fig. 2 is a plot of log k_3 against pK_a in water at 25 °C for substituted phenols and acetic acids (1) showing that α is 0.44 ± 0.05 for acids whose pK_a values range from 1.4 to 10.1. This compares with a value of 0.54 observed by Bell and Higginson (6) in their study of the dehydration of acetaldehyde hydrate catalyzed by a wide variety of carboxylic acids and phenols. The rate constants of the meta-substituted phenols alone show a much more marked dependence on acid dissociation constant and the α value derived over the limited pK_a range 8.3–10.1 is 0.84 ± 0.07. The relatively high value of α may be due to solvation effects in the reactions of TNT^- with meta-substituted phenols. The rate constants for the more weakly acidic phenols are lower because of significantly lower A factors, rather than higher activation energies. This suggests that the formation of the activated complex in the reaction of TNT with phenol, for example, involves a larger increase in solvation than in the reaction with 3-nitrophenol.

TABLE I

Kinetic data for the reactions of phenols with TNT^- ion

Phenol	k_3 at -40 °C (l mole^{-1} s^{-1})	Activation energy (kcal/mole)	A factor (l mole^{-1} s^{-1})
Phenol	0.025	9.4	1.6×10^7
3-Methylphenol	0.029	9.8	4.4×10^7
3-Acetylphenol	0.108	10.1	3.2×10^8
3-Cyanophenol	0.30	10.9	4.9×10^9
3-Nitrophenol	0.55	10.9	9.1×10^9
4-Chlorophenol	0.066	10.0	1.6×10^8

The meta-substituted phenols were studied in an attempt to isolate inductive contributions of substituents to the reactivities of the phenols in this proton transfer reaction. The results are complicated by solvation effects but rate constants at -40 °C obey the Hammett relationship and a ρ value of 1.82 ± 0.2 is obtained. Only one para-substituted phenol, 4-chlorophenol, has been used as donor and the rate constant indicates that the resonance contribution to the reactivity of this phenol is small.

The effect on the rate of reaction of TNT^- with 3-methylphenol of varying the alkali metal cation from sodium to lithium or potassium was small. The rate constants with lithium, sodium, and potassium cations at -10 °C were 0.33, 0.33, and 0.32 l mole^{-1} s^{-1} respectively; although the rate constant for the reaction involving the lithium cation was somewhat greater than that for the reaction involving the potassium cation at -30 °C, the difference was not outside experimental error. Reactions of carbanions in solvents of fairly low dielectric constant, e.g. the addition of styrene to polystyrene anions in tetrahydrofuran (7), are frequently sensitive to the nature of the alkali metal counterion, and the lack of sensitivity in the reaction of TNT^- with 3-methylphenol in alcohol solution probably indicates that interaction between the TNT^- and the alkali metal cation is weak.

Can. J. Chem. Downloaded from www.nrcresearchpress.com by 210.87.254.6 on 09/05/12
For personal use only.

Can. J. Chem. Downloaded from www.nrcresearchpress.com by 210.87.254.6 on 09/05/12
For personal use only.

Equilibria in Proton-Transfer Reactions

Reaction [3] is reversible and the rate constant for the reverse reaction is dependent upon the base strength of the anion. Acetate ion (1) and 3-nitrophenoxide ion are relatively weak bases and reactions of TNT^- with their conjugate acids appear to proceed to completion. With 3-methylphenoxide ion, however, the rate of the reverse reaction is significant compared with that of the forward reaction. If the slow fade reaction which occurs even in the absence of added phenol is ignored, the equilibrium constant of reaction [3] can be derived from absorbance measurements at equilibrium of reaction mixtures containing 4 to 10×10^{-2} M excess 3-methylphenol. Equilibrium constants, K_3, at 25 °C and −10 °C are 1.3 ± 0.2 and 5.6 ± 1 respectively; the heat of reaction [3] is estimated to be −6.5 kcal/mole and the entropy change is approximately −21 entropy units (e.u.)/mole. K_3 can also be estimated from the equilibrium constants K_1 and K_2 of reactions [1] and [2], as $K_3 = K_2/K_1$. Interpolation of Caldin and Long's data (1) gives values of K_1 of 2 040 and 850 l/mole at 25° and −10 °C respectively; the concentration of ethanol is absorbed into the equilibrium constants K_1 and K_2. K_2, determined from absorbance measurements of mixtures of 3-methylphenol and ethoxide ion, was found to be 1 700 and 2 500 l/mole at 25 °C and −10 °C so that the derived K_3 values at these temperatures are 0.8 and 3.0. K_2 was determined for ionic concentrations an order of magnitude smaller than those used in the direct determination of K_3 and no account has been taken of activity coefficients in this work. In addition, it was observed that even with purified ethanol ethoxide ion at a concentration of 10^{-4} M was required to be added to the phenol solution before any appreciable conversion to phenoxide occurred. In these circumstances the agreement between the two sets of values of K_3 is satisfactory.

For the reaction of ethoxide ion with TNT the equilibrium constant at −10 °C is 850 l/mole and the heat and entropy of reaction are 3.6 kcal/mole and 27.2 e.u./mole (1) if the standard state of ethanol is taken as the pure liquid. The reaction of 3-methylphenoxide ion with TNT has an equilibrium constant at −10 °C of 0.18 and a heat and entropy of reaction of 6.5 kcal/mole and 21 e.u./mole. The lower equilibrium constant and higher heat of reaction reflect the weaker basicity of the 3-methylphenoxide ion as compared with ethoxide. In both reactions there appears to be considerable desolvation as the ethoxide or phenoxide ion in which the charge is relatively localized is converted to the TNT^- ion in which it is delocalized (1). The rate constant for the reaction of 3-methylphenoxide ion with TNT in ethanol solution can be estimated using the relationship $K_3 = k_3/k_{-3}$. At −10 °C k_{-3} is 0.06 ± 0.02 l $mole^{-1}$ s^{-1} and the activation energy is 16.3 ± 1.7 kcal/mole; the corresponding figures for the reaction of the more basic ethoxide ion with TNT are 3.8 l $mole^{-1}$ s^{-1} and 10.0 kcal/mole (1).

The equilibrium constant K_3 for the reaction of 3-methylphenol with TNT^- is relatively low and the dependence of the equilibrium concentration of TNT^- on phenol concentration is measurable. It was not possible to make comparable studies of the reaction of other phenols because the equilibrium concentration of TNT^- could not be determined with sufficient accuracy. K_3 for the reaction of phenol with TNT^- was estimated from the ratio K_2/K_1 to be 2.3 at 25 °C and the value for 4-chlorophenol is higher. These results suggest that equilibrium studies of reactions between TNT^- and dialkyl and trialkyl phenols would be fruitful, particularly at temperatures of the order of 25 °C. The occurrence of high equilibrium concentrations of ethoxide ion in reactions of TNT^- with such phenols will, however, complicate the interpretation of the kinetics of such reactions and it may be difficult to determine the exact magnitude of steric effects. Accurate quantitative studies of reactions with ortho-substituted phenols would be of considerable interest because the

proton transfer would be sterically hindered and might be susceptible to quantum mechanical tunnelling.

ACKNOWLEDGMENTS

The authors wish to thank Dr. E. F. Caldin for helpful discussions. They are grateful to the National Research Council for a grant and to Queen's University for a Milton Hersey fellowship (J.A.B.). The indium was a gift from Consolidated Mining and Smelting Co. Ltd.

REFERENCES

1. E. F. CALDIN and G. LONG. Proc. Roy. Soc. London, Ser. A, **226**, 263 (1955).
2. E. F. CALDIN and J. C. TRICKETT. Trans. Faraday Soc. **49**, 772 (1953).
3. D. POULI and W. MACF. SMITH. Can. J. Chem. **38**, 567 (1960).
4. C. P. SMYTH and W. N. STOOPS. J. Am. Chem. Soc. **51**, 3315 (1929).
5. R. P. BELL and J. E. CROOKS. Proc. Roy. Soc. London, Ser. A, **286**, 285 (1965).
6. R. P. BELL and W. C. E. HIGGINSON. Proc. Roy. Soc. London, Ser. A, **197**, 141 (1949).
7. D. N. BHATTACHARYYA, J. SMID, and M. SZWARC. J. Phys. Chem. **69**, 624 (1965).

Can. J. Chem. Downloaded from www.nrcresearchpress.com by 210.87.254.6 on 09/05/12
For personal use only.

Can. J. Chem. Downloaded from www.nrcresearchpress.com by 210.87.254.6 on 09/05/12
For personal use only.

SUR LES SPECTRES INFRAROUGES DES PHTALOCYANINES

H. F. SHURVELL[1] ET L. PINZUTI
Laboratoire de Physique P.C.B.1. et
Centre Technique de Spectrographie Infrarouge, Faculté des Sciences, Marseille, France

Reçu le 18 août 1965

RÉSUMÉ

Nous avons enrégistré les spectres infrarouges de la phtalocyanine sans métal, la phtalocyanine de cuivre (chlorée et non chlorée) et trois nouvaux derivés métalliques de la phtalocyanine: MoPc, Na_2Pc et AlOH—Pc (Pc = $C_{32}H_{16}N_8$). Nous proposons des interprétations pour la plupart des bandes des spectres infrarouges des phtalocyanines étudiées.

ABSTRACT

Infrared spectra of metal-free phthalocyanine, chlorinated and unchlorinated copper phthalocyanines, and three new metal derivatives of phthalocyanine: MoPc, Na_2Pc, and AlOH—Pc (Pc = $C_{32}H_{16}N_8$), have been recorded. Assignments have been suggested for many of the peaks in the infrared spectra of the phthalocyanines.

INTRODUCTION

Le spectre infrarouge de la phtalocyanine (H_2Pc*), Fig. 1*a*, a été étudié pour la première fois par Cannon et Sutherland (1). Par la suite, deux articles relatifs aux spectres infra-

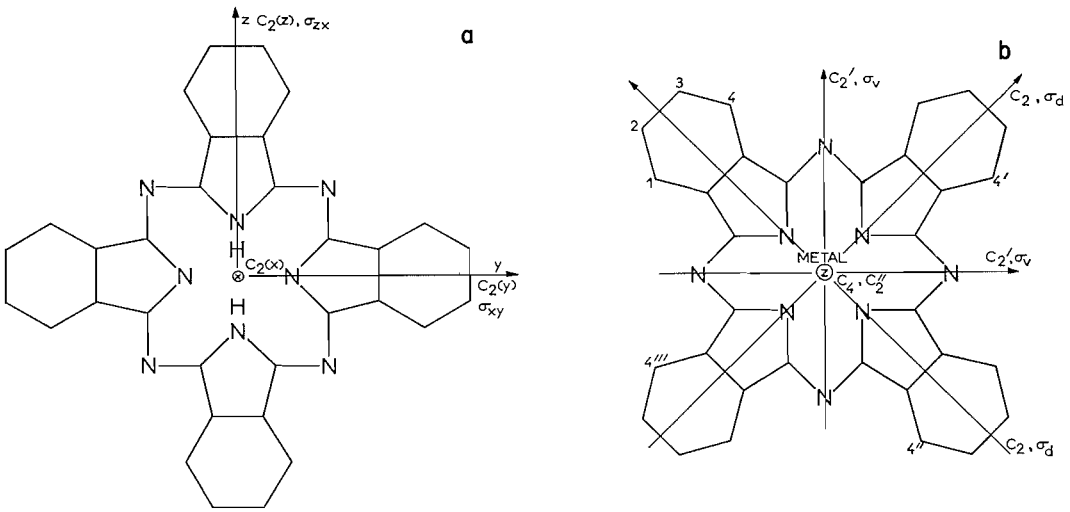


FIG. 1. Structure et symétrie des phtalocyanines: (*a*) H_2Pc (D_{2h}); (*b*) Metal–Pc (D_{4h}).

rouges des deux formes α et β de CuPc et d'autres phtalocyanines ont été publiés (2, 3). Terenin et Sidorov (4) ont étudié les effets produits par l'adsorption de vapeurs sur les spectres infrarouges de H_2Pc et de plusieurs dérivés métalliques, plus récemment Sidorov et Kotlyar (5) ont publié les spectres d'échantillons sublimés des deux variétés α et β

[1]*Adresse actuelle*: *Department of Chemistry, Queen's University, Kingston, Ontario.*
* *Le symbole Pc sera souvent utilisé ici pour représenter le noyau de la phthalocyanine*: $C_{32}H_{16}N_8$.

de H_2Pc (normale et partiellement *N*-deutériée) et des dérivés métalliques suivants: MgPc, ZnPc, CuPc, FePc, CoPc, NiPc et un dérivé de l'argent de composition non spécifiée. Ces auteurs ont trouvé plusieurs différences dans les spectres des formes α et β. Ils ont aussi donné quelques attributions. Très récemment les spectres infrarouges de plusieurs phtalocyanines de l'étain et du plomb ont été publiés (6).

Le présent article est une étude des spectres infrarouges de trois nouvelles phtalocyanines: MoPc, Na_2Pc et AlOH—Pc. Les spectres de toute une série de composés: H_2Pc, CuPc, 4,4′,4″,4‴-tétrachloro-CuPc et hexadécachloro-CuPc ont également été enregistrés. La comparaison de ces spectres entre eux et avec les spectres de molécules contenant des arrangements similaires d'atomes (benzènes ortho-disubstitués et pyrroles) peut permettre, avons nous pensé, de donner des attributions vibrationelles qualitatives.

Le Tableau I donne un résumé des changements attendus dans le spectre de H_2Pc quand les deux atomes d'hydrogène du groupement imine sont remplacés par un atome métallique puis quand, en plus, les hydrogènes des noyaux benzéniques sont substitués par des atomes de chlore.

TABLEAU I

Comportement prévu pour le spectre infrarouge de H_2Pc

Vibrations de H_2Pc	Changements du spectre attendus		
	Métal–Pc	Métal–Pc tétrachlorée	Métal–Pc hexadécachlorée
Vibrations des groupes N—H	Disparition	—	—
Vibrations des groupes C—H	Peu de changement	Quelques changements	Disparition
Vibrations des noyaux pyrroliques	Quelques changements dépendant du métal	Pas de changement	Pas de changement
Vibrations des noyaux benzéniques	Peu de changement	Peu de changement	Peu de changement

PARTIE EXPÉRIMENTALE

Les phtalocyanines étudiées ont été fournies par la S.A. Française des Matières Colorantes. L'échantillon d'hexadécachloro CuPc contient en réalité 15.5 atomes de chlore par molécule. Les fournisseurs ont signalé que les produits sont des produits techniques donc pas absolument purs.

Les spectres infrarouges (Figs. 2, 3 et 4) ont été obtenus avec un spectrophotomètre, Perkin-Elmer, modèle 125, à deux réseaux (300 et 60 traits/mm) et avant-prisme de KBr. L'étalonnage de l'instrument a été réalisé par l'enregistrement de spectres gazeux de: H_2O, NH_3 et CH_4, dont les fréquences sont connues avec une grande précision (7). Nous estimons que les fréquences figurant sur le Tableau IV ont une précision de ± 1.5 cm^{-1} dans la région de 3 000 cm^{-1} et une précision de ± 0.5 cm^{-1} dans les régions de plus grande longueur d'onde.

STRUCTURE ET SYMÉTRIE

Robertson (8) a étudié en détail le cristal et la structure moléculaire de H_2Pc (Fig. 1*a*). Plus tard Robertson et Woodward (9) ont publié la structure de NiPc (Fig. 1*b*). Ils ont montré que la structure du cycle de la phtalocyanine est peu perturbée par la substitution des deux hydrogènes iminiques par un atome métallique, à l'exception d'un glissement vers l'intérieur des quatre atomes d'azote pyrroliques (9).

Les symétries des phtalocyanines étudiées dans ce travail sont discutées dans les paragraphes qui suivent. Les nombres de vibrations normales de chaque type de symétrie appartenant aux différents groupes ponctuels sont donnés dans les Tableaux II (H_2Pc) et III (dérivés métalliques). Pour ces calculs nous avons utilisé les tableaux de Herzberg (10) et le choix des axes et plans de symétrie est conforme aux recommandations du "Joint Commission for Spectroscopy" (11).

Can. J. Chem. Downloaded from www.nrcresearchpress.com by 210.87.254.6 on 09/05/12
For personal use only.

Can. J. Chem. Downloaded from www.nrcresearchpress.com by 210.87.254.6 on 09/05/12
For personal use only.

TABLEAU II

Symétries possibles et dénombrements des vibrations de la H_2Pc

Groupe ponctuel	L'arrangement des atomes d'hydrogènes pyrroliques	Dénombrement des vibrations*	Vibrations actives en infrarouge	
			Total	N–H
D_{2h}	Atomes H dans le plan du cycle de la Pc (Fig. 1*a*)	$29A_g+13A_u+13B_{1g}+\underline{28B_{1u}}+14B_{2g}+\underline{28B_{2u}}+28B_{3g}+\underline{15B_{3u}}$	71	3
C_{2h}	Atomes H situés de part et d'autre du plan du cycle, dans un plan perpendiculaire au cycle, qui passe par deux atomes d'azote	$43A_g+41B_g+\underline{41A_u}+\underline{43B_u}$	84	3
C_i	Atomes H situés de part et d'autre du plan du cycle, mais sur aucun élément de symétrie.	$84A_g+\underline{84A_u}$	84	3

*Les types de symétrie soulignés sont actifs en infrarouge.

TABLEAU III

Dénombrement des vibrations des dérivés métaliques de la phtalocyanine

Molécule	Groupe ponctuel	Dénombrement des vibrations*	Vibrations actives en infrarouge
CuPc, MoPc, CuPc hexadécachlorée	D_{4h}	$14A_{1g}+6A_{1u}+13A_{2g}+\underline{8A_{2u}}+14B_{1g}+7B_{1u}+14B_{2g}+7B_{2u}+13E_g+\underline{28E_u}$	36
Pc (rien au centre)	D_{4h}	$14A_{1g}+6A_{1u}+13A_{2g}+\underline{7A_{2u}}+14B_{1g}+7B_{1u}+14B_{2g}+7B_{2u}+13E_g+\underline{27E_u}$	34
CuPc-4,4′,4″,4‴-tétrachlorée	C_{4h}	$27A_g+\underline{14A_u}+28B_g+14B_u+13E_g+\underline{28E_u}$	42
AlOH–Pc	C_{4v}	$\underline{24A_1}+19A_2+21B_1+21B_2+\underline{43E}$	67
Na_2Pc	C_{2h}	$43A_g+41B_g+\underline{41A_u}+\underline{43B_u}$	84

*Les types de symétrie soulignés sont actifs en infrarouge.

Can. J. Chem. Downloaded from www.nrcresearchpress.com by 210.87.254.6 on 09/05/12
For personal use only.

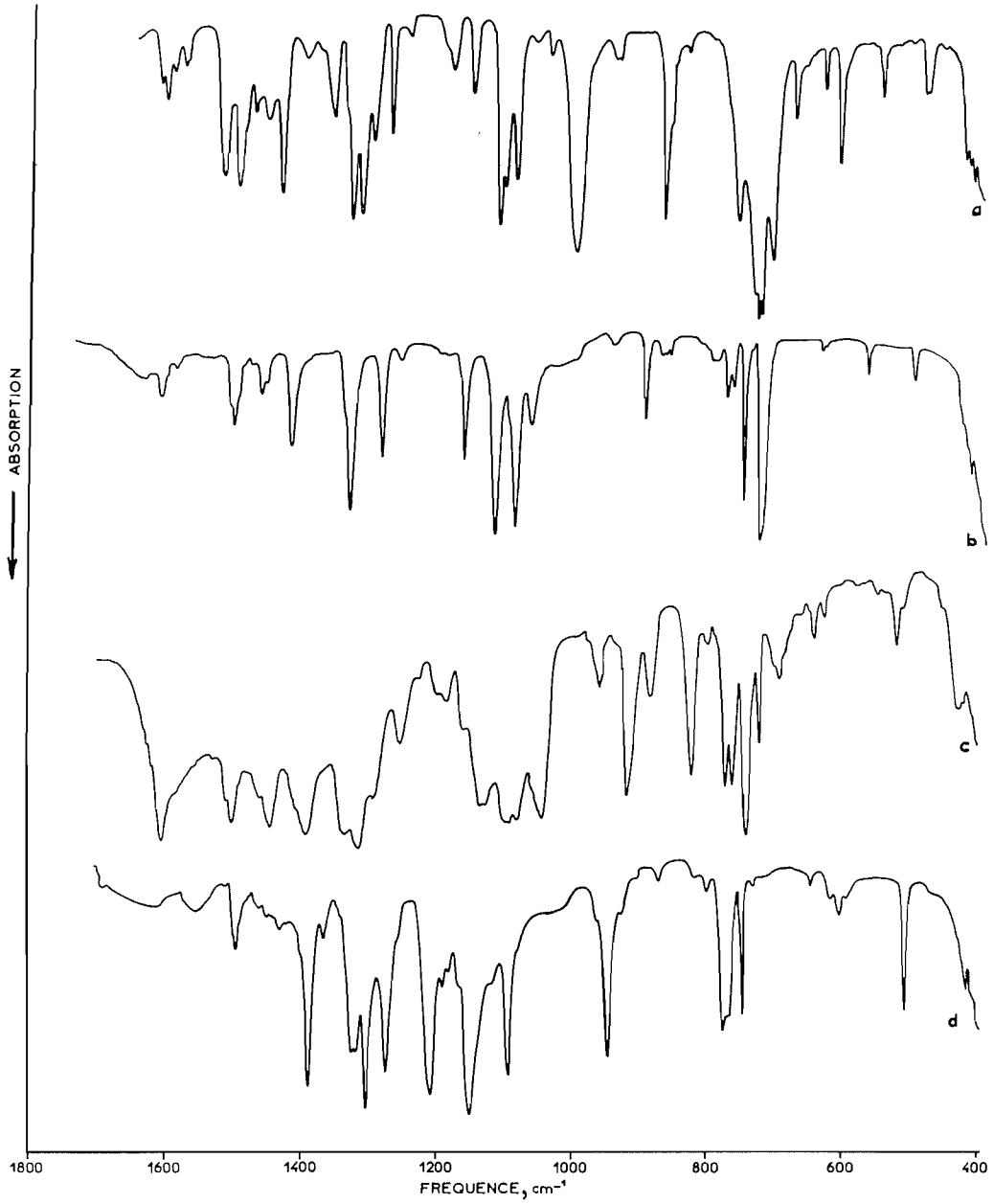


FIG. 2. Spectres infrarouges des phtalocyanines: (*a*) H_2Pc (0.5 mg); (*b*) CuPc (1 mg); (*c*) CuPc-4,4′,4″, 4‴-tétrachlorée (3 mg); (*d*) CuPc-hexadécachlorée (1 mg).

1. H_2Pc

La symétrie du noyau de phtalocyanine est sans doute voisine de D_{4h} (8) mais la présence de deux hydrogènes pyrroliques abaisse cette symétrie. Parmi les chercheurs précédents, plusieurs semblent avoir tacitement supposé que les hydrogènes pyrroliques sont dans le plan du noyau Pc sur un axe binaire (groupe ponctuel D_{2h}, Fig. 1*a*). Cependant, Linstead (12) et Lyons (13) ont indiqué que les hydrogènes pyrroliques pourraient être

Can. J. Chem. Downloaded from www.nrcresearchpress.com by 210.87.254.6 on 09/05/12
For personal use only.

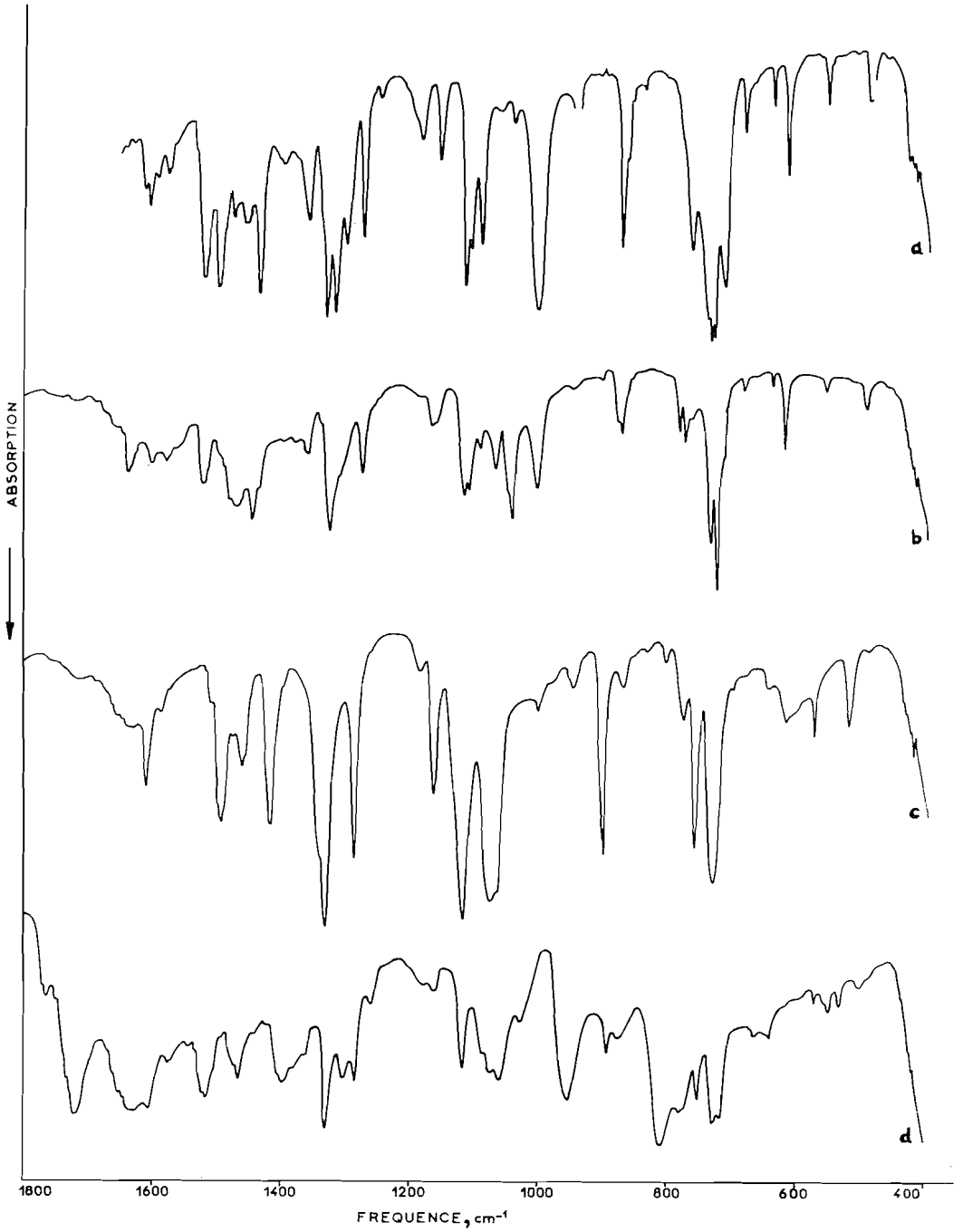


FIG. 3. Spectres infrarouges des phtalocyanines: (*a*) H_2Pc (0.5 mg); (*b*) Na_2Pc (1 mg); (*c*) AlOH—Pc (0.2 mg); (*d*) MoPc (1 mg).

extérieurs au plan du noyau Pc. De plus, en utilisant les valeurs fournies par Pauling (14) pour les longueurs des liaisons et des rayons de van der Waals, on s'aperçoit que les sphères de van de Waals des hydrogènes se recouvrent considérablement dans l'hypothèse d'une structure plane.

Si les atomes d'hydrogène en question sont situés de part et d'autre du noyau Pc dans un plan perpendiculaire au cycle et passant par les deux atomes d'azote pyrroliques, le groupe ponctuel est alors C_{2h}. Si les atomes d'hydrogène ne sont pas sur un tel plan, le groupe ponctuel est C_i; le seul élément de symétrie qui subsiste alors étant un centre de symétrie.

Le Tableau II dénombre les modes normaux de vibration de H_2Pc, actifs en infrarouge, (y compris les vibrations N—H), selon que le groupe est D_{2h}, C_{2h} ou C_i. On notera que, pour chacun de ces trois groupes, trois vibrations N—H, actives en infrarouge, sont prévues ce qui, malheureusement, ne permet pas de choisir entre les trois modèles à l'aide des spectres infrarouges.

2. CuPc, hexadécachloro-CuPc et MoPc

La symétrie de ces molécules est approximativement D_{4h}* (Fig. 1*b*). Le Tableau III donne l'analyse des vibrations normales, nous y avons inclus la molécule hypothétique Pc, sans rien au centre, pour montrer que les trois vibrations *N*-métal associées à l'atome central sont actives en infrarouge (un mode A_{2u} et un couple dégénéré E_u). La symétrie de MoPc est, elle aussi, probablement voisine de D_{4h}.

3. 4,4′,4″,4‴-Tétrachloro-CuPc

Quand on remplace par des atomes de chlore les hydrogènes en positions 4,4′,4″,4‴ (Fig. 1*b*) de CuPc, la symétrie est abaissée à C_{4h}.

4. AlOH—Pc

Nous suggérons, pour cette molécule, une symétrie C_{4v}, l'atome d'aluminium étant au centre du noyau Pc et le groupement O—H hors du plan du cycle.

5. Na_2Pc

Les atomes de sodium sont vraisemblablement situés de part et d'autre du noyau Pc de la même façon que dans le modèle C_{2h} de H_2Pc. Une similitude entre les spectres de Na_2Pc et H_2Pc impliquerait donc une similitude de structure entre ces deux molécules.

Formes α et β

Selon Kendall (3) les pigments commerciaux des phtalocyanines se présentent sous la forme β. Cependant, il y a dans la littérature une certaine confusion de notation entre les formes α et β. Si on compare entre les spectres infrarouges de CuPc produits par Kendall (3) et par Sidorov (5) on s'aperçoit que la form α de Kendall correspond à la forme β de Sidorov et vice versa.

Afin de savoir avec certitude quelle forme nous avons étudiée, nous avons enregistré les spectres des deux formes α et β de CuPc fournies par un autre producteur (Badische Anilin & Soda Fabrik A.G.). Ces spectres ont montré que notre échantillon était la variété β de Kendall (donc la forme α de Sidorov). En fait les spectres des deux variétés diffèrent peu et les attributions suggérées plus loin sont valables pour les deux variétés de H_2Pc et des dérivés métalliques.

La nature de la différence entre les formes α et β de H_2Pc et des dérivés métalliques n'est pas connue: seule la variété α a été étudiée aux rayons X (8, 9).† Kendall (3) a suggéré que la difference entre les spectres infrarouges, enregistrés pour les deux variétés α et β de CuPc, pourrait être due à un arrangement différent des molécules (régulier ou non), dans le cristal.

**Robertson et Woodward (9) trouvent, pour* NiPc, *de légères distorsions par rapport à une vraie symétrie D_{4h}.*
†Les composés étudiés par Robertson n'étaient pas des pigments commerciaux (forme β) mais des cristaux formés pas sublimation sous faible pression.

Can. J. Chem. Downloaded from www.nrcresearchpress.com by 210.87.254.6 on 09/05/12
For personal use only.

Can. J. Chem. Downloaded from www.nrcresearchpress.com by 210.87.254.6 on 09/05/12
For personal use only.

RÉSULTATS ET DISCUSSION

Les Figs. 2, 3 et 4 reproduisent les spectres. Le Tableau IV fournit les fréquences observées pour H_2Pc et les dérivés métalliques ainsi que les attributions que nous proposons.

Dans la discussion qui suit, nous avons parfois utilisé les abréviations suivantes; ν pour une vibration de valence, β pour une vibration C—H de déformation dans le plan, γ pour une vibration C—H de déformation hors du plan et ϕ pour une déformation du cycle benzénique exterieure du plan.

Allure générale des spectres

Le spectre dû au noyau Pc dans H_2Pc (en faisant abstraction des vibrations N—H) est assez voisin de celui de CuPc (comparer les Figs. 2*a* et 2*b*). Ceci indique que la symétrie du noyau de H_2Pc diffère peu de D_{4h}, puisque selon les Tableaux II et III, les règles de sélection permettent beaucoup plus de vibrations actives en infrarouge pour les groupes de plus basse symétrie. Ceci était d'alleurs prévisible puisque seuls les atomes d'hydrogène centraux ne respectent pas la symétrie D_{4h} et déterminent la symétrie exacte de la molécule.

L'éclatement des vibrations dégénérées E_u, ainsi que l'apparition de bandes supplémentaires interdits par les règles de sélection pour le groupe D_{4h}, permettent une évaluation de l'écart par rapport à cette symétrie D_{4h}. En fait, dans le spectre de H_2Pc plusieurs bandes d'absorption sont éclatées en doublets et on observe plusieurs maximums faibles qui ne se trouvent pas dans le spectre de CuPc.

Mises à part quelques différences d'intensité et de fréquences évidentes, le spectre de Na_2Pc ressemble beaucoup à celui de H_2Pc (voir Figs. 3 et 4).* La structure de Na_2Pc est donc vraisemblablement très voisine de celle de H_2Pc. Ceci confirme l'hypothèse d'une structure C_{2h} pour H_2Pc puisque les autres modèles sont moins raisonnables pour Na_2Pc. Malheureusement aucune étude de la structure de Na_2Pc n'a été publiée à ce jour.

Les fréquences du spectre de AlOH—Pc correspondent bien à celles de CuPc. Cependant, du fait de la différence de concentration, les intensités des bandes correspondantes sont entre 5 et 20 fois plus grandes dans le spectre de AlOH—Pc. Apparemment la présence du groupement O—H influe considérablement la variation de moment dipolaire mais n'affecte guère la symétrie du noyau Pc.

Le spectre de AlOH—Pc présente une bande floue vers 3 420 cm^{-1}, due sans doute à une vibration de valence ν O—H. La largeur et la position de cette bande, environ 200 cm^{-1} au dessous de la zone habituelle des vibrations ν O—H (15), indique une forte liaison hydrogène, qui est très probablement intermoléculaire.

En raison de l'excessive perte d'énergie infrarouge en traversant l'échantillon, le spectre de MoPc n'est pas aussi bien résolu que ceux des autres phtalocyanines. Il ressemble néanmoins grossièrement à celui de CuPc. Une forte bande, observée à 1 723 cm^{-1} ne se retrouve dans le spectre d'aucune des autres phtalocyanines étudiées. La seule interprétation que nous pouvons en donner est qu'elle est due à une impureté.

Attributions

On peut considérer que la molécule H_2Pc est construite à partir de quatre noyaux iso-indoles réunis par quatre atomes d'azote. Les noyaux iso-indoles eux mêmes sont composés d'un cycle benzénique et d'un cycle pyrrole. C'est pourquoi des travaux antérieurs sur les benzènes ortho-disubstitués et les pyrroles polysubstitués sont utiles pour attribuer les bandes observées dans le spectre de H_2Pc.

On peut supposer que les vibrations des cycles pyrroliques sont fortement couplées.

**Les bandes 3 290 cm^{-1} et 1 008 cm^{-1} dans le spectre de* Na_2Pc *sont dues à* H_2Pc *présent sous forme d'impureté.*

TABLEAU IV

Bandes d'absorption infrarouge des spectres des phtalocyanines (fréquences en cm^{-1})*

H_2Pc	CuPc	CuPc tétrachlorée	CuPc hexadéca-chlorée	Na_2Pc	MoPc	AlOHPc	Description
421f	420f	421f	421f	421f	422f	421f	ϕ C—C
—	—	429m	—	—	—	—	
490, 494 m	506f	520m	510F	498f	504tf	521m	Voir texte
558m	574f	—	—	561tf	573tf	576f	
620mF	—	627tf	620tf	624m	—	619f	
642m	641tf	640tf	649tf	642tf	642f	646tf	Voir texte
686m	—	692m	—	687tf	665f	—	ϕ C—C
716TF	—	—	—	—	—	—	Déf. N—H
731, 736 TF	730TF	724m	—	729, 739 TF	719, 730 F	730TF	γ C—H
—	—	742F	749F	—	—	—	
—	755F	764mF	—	—	754m	759F	
767F	771m	774mF	772ép	778f	—	778f	Voir texte
—	781m	—	779F	787f	782m	—	
—	—	800tf	804tf	—	810F	806tf	
—	—	824F	—	—	—	—	
841tf	—	—	—	—	—	—	
875F	871f	—	—	876m	877f	870f	γ C—H
—	—	884m	—	—	—	—	
—	900m	—	—	—	896f	903F	
—	—	920F	929ép	—	—	—	
943, 949 f	949tf	959m	949TF	952tf	957TF	949f	
1006TF	—	—	—	1008m†	—	—	Déf. N—H
1045f	—	1046FL	—	1046F	1031tf	—	β C—H
1068tf	1069m	—	—	1072m	1063, 1077 FL	1068ép	β C—H
—	—	1083FL	—	—	—	1079TF	
1095F	1091TF	1097FL	1097F	1096tf	1089ép	—	Voir texte
1111, 1120 TF	1121TF	—	—	1114, 1121 F	1120F	1120TF	β C—H
—	—	1134FL	—	—	—	—	
1160m	1168F	1161ép	1154TF	1167m	1164f	1165F	Voir texte
1189m	—	1187f	1194tf	1188tf	1181f	1187f	
—	—	—	1211TF	—	—	—	
1252tf	1260tf	1254m	—	1253tf	1263tf	—	
1277F	1288F	1293ép	1276F	1278m	1288m	1288F	ν C—C
1303m	—	1315TF	1306TF	1313ép	1306m	—	
1320, 1335 F	1334TF	1335ép	1320, 1327 F	1329F	1333F	1333TF	Voir texte
1362m	—	—	1365tf	1363f	1367ép	—	
1402f	—	—	—	1383tf	1383ép	—	
1438F	1421F	1391FL	1391TF	1438ép	1402Lm	1418F	ν C—C
1458, 1478 f	1457, 1465 f	1445F	—	1449F			
		1462ép		1473FL	1468m	1463F	
1501F	1505m	1502F	1497m	1485ép	—	1496F	ν C—C
1523F	1509ép	1511ép	—	1525m	1519m	—	
1580f	—	—	1553f	1580m	1578tf	1589tf	
1608, 1616 m	1611f	1606F	1610tf	1605Lm	1608m	1611m	ν C—C
—	—	—	—	1640m	1633Lm	—	
—	—	—	—	—	1723F	—	
2922tf	2922m	2920m	2925f	2922tf	2923tf	2926tf	
—	2954ép	2954ép	2954ép	2952tf	2962tf	—	
3030ép	3030tf	—	—	—	—	—	ν C—H
3050mF	3050f	—	—	3048m	—	3050m	ν C—H
3064ép	3059ép	3058tf	—	—	3060ép	—	ν C—H
3074ép	3082ép	—	—	3069ép	—	3082ép	ν C—H
—	—	—	—	—	3190Lm	—	
3290mF	—	—	—	3290tf†	—	—	ν N—H
—	—	—	—	—	—	3420FTL	ν O—H

*TF = très fort, F = fort, m = moyen, f = faible, tf = très faible, ép = épaulement et L = large.
†Ces deux bandes sont dues à la présence de H_2Pc sous forme d'impureté.

Can. J. Chem. Downloaded from www.nrcresearchpress.com by 210.87.254.6 on 09/05/12
For personal use only.

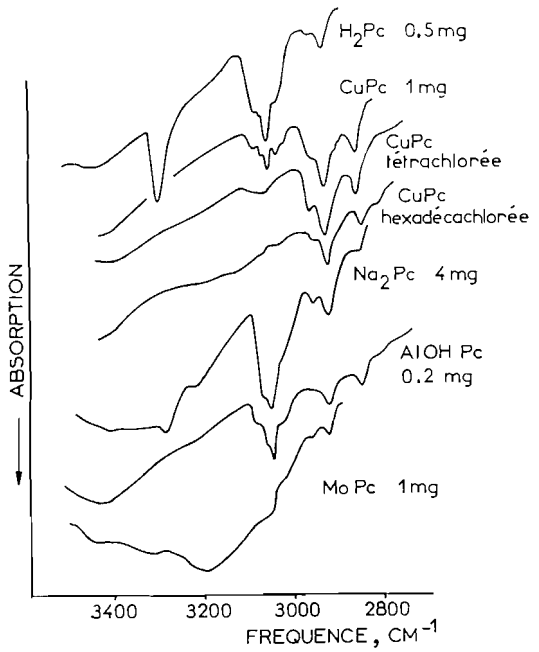


FIG. 4. Spectres infrarouges de quelques phtalocyanines entre 2 800 et 3 400 cm^{-1}.

D'autre part les vibrations du cycle benzénique seraient peu modifiées et les interactions entre les vibrations C—H des différents cycles benzéniques négligeables. Il nous est apparu que cette hypothèse est raisonnable, parce que les vibrations ν C—H ont été trouvées entre 3 000 et 3 100 cm^{-1}, les vibrations β C—H se trouvent entre 1 000 et 1 300 cm^{-1}, les vibrations γ C—H se trouvent entre 700 et 1 000 cm^{-1} et les vibrations ν C—C du cycle benzénique ont été trouvées entre 1 300 et 1 600 cm^{-1}. C'est à dire dans les régions ou on les observe pour un noyau benzénique substitué isolé.

Les spectres des molécules chlorées CuPc se sont révélés très utiles pour identifier les vibrations β C—H et γ C—H. Plusieurs vibrations propres au cycle benzénique ont été déterminées avec assez de certitude; mais il a été difficile d'identifier les vibrations provenant des liaisons C—N et du cycle pyrrolique.

(a) Vibrations N—H

Dans le spectre de H_2Pc, la bande forte à 3 290 cm^{-1} est sans doute une vibration de valence ν N—H. Cette vibration se manifeste vers 3 400 cm^{-1} dans les composés de l'indole (16) et dans la même région pour les pyrroles (17, 18). Cet abaissement de fréquence de l'ordre de 100 à 150 cm^{-1} par rapport aux indoles et aux pyrroles indique une forte liaison hydrogène dans H_2Pc. Mason (19) a trouvé un résultat analogue pour les porphines où les azotes et hydrogènes centraux sont arrangès de façon similaire. Cet auteur a également conclu que les liaisons hydrogènes étaient presque totalement intramoléculaire car les fréquences ν N—H étaient à peine changées quand on passe de l'état solide à la solution diluée dans CCl_4. Malheureusement aucun des solvants organiques connus ne dissout H_2Pc, ce qui nous a empêchés d'effectuer une expérience similaire.

On trouve les fréquences de déformation N—H à 716 et 1 006 cm^{-1}. Ces bandes étaient absentes des spectres de toutes les autres phtalocyanines étudiées (exception faite pour le spectre de Na_2Pc où on observe une bande à 1 008 cm^{-1}, mais cette bande est certainement due à H_2Pc présent sous forme d'impureté.

Can. J. Chem. Downloaded from www.nrcresearchpress.com by 210.87.254.6 on 09/05/12
For personal use only.

Can. J. Chem. Downloaded from www.nrcresearchpress.com by 210.87.254.6 on 09/05/12
For personal use only.

A la suite d'une étude sur des produits partiellement *N*-deutéries, Sidorov et Kotlyar (5) ont attribué deux bandes très faibles à 1 250 et 1 539 cm^{-1} à des vibrations de déformation N—H. Ces chercheurs ont suggéré qu'une bande à 753 cm^{-1} qui apparait seulement dans le spectre de la variété β est aussi liée aux fréquences de déformation des groupes imine. Mais d'autrepart, les recherches de Mason (19), montrent pour la porphine, que les déformations des groupes N—H ont lieu à 719 et 970 cm^{-1}; ceci vient donc à l'appui de notre attribution. Dans tous les cas, la théorie des groupes prévoit seulement deux fréquences de déformation N—H.

Il faut noter que la vibration N—H, 1 006 cm^{-1} de H_2Pc est inférieure de 140 cm^{-1} à la vibration correspondante du pyrrole (20). Ceci pourrait s'expliquer par l'existence d'une liaison hydrogène. Cependant, habituellement, les liaisons hydrogène augmentent plutôt la fréquence des vibrations de déformation (15). Pour la porphine, Mason (19) a expliqué cette anomalie en calculant le chevauchement des orbitales hybrides sp des quatre atomes d'azote pyrroliques avec les orbitales 1s d'un hydrogène. Ce calcul montre que la déformation de N—H dans le plan, devrait apparaître à une fréquence plus basse dans la porphine que dans le pyrrole. En fait ces calcules ne s'appliquent pas à H_2Pc puisque, pour les raisons indiquées plus haut, nous avons préféré adopter un modèle où l'arrangement des atomes d'hydrogène pyrroliques ne soit pas plan, avec une hybridation sp^3 des azotes iminiques. On peut alors imaginer une autre explication selon laquelle la vibration de déformation N—H serait couplée avec une vibration du cycle pyrrolique.

(b) Vibrations C—H

Pour les benzènes ortho-disubstitués on attend quatre vibrations de valence ν C—H entre 3 000 et 3 100 cm^{-1} (21, 22). Le spectre de la phtalocyanine H_2Pc présent quatre bandes d'absorption: 3 030, 3 050, 3 064 et 3 074 cm^{-1} qui correspondent pour CuPc aux fréquences: 3 030, 3 050, 3 059 et 3 082 cm^{-1}. Dans les spectres des autres phtalocyanines ces quatre pics ne sont pas résolus. Enfin, comme on pouvait le prévoir, la bande ν C—H est plus faible pour CuPc tétrachlorée et absente du spectre de CuPc hexadécachlorée.

D'après les spectres d'un certain nombre de benzènes ortho-disubstitués (21, 22, 23), on attend quatre vibrations β C—H dans les régions: 1 025 – 1 040 cm^{-1}, 1 070 – 1 130 cm^{-1}, 1 130 – 1 160 cm^{-1} et 1 250 – 1 290 cm^{-1}. Dans le spectre de H_2Pc on observe des bandes à 1 068 et 1 252 cm^{-1} ainsi qu'un doublet à 1 111, 1 120 cm^{-1} qui correspond aux sommets: 1 069, 1 121 et 1 260 cm^{-1} de CuPc. On observe des fréquences similaires pour les autres molécules métal–Pc sauf pour CuPc hexadécachlorée. Il est normal d'attribuer ces fréquences à des vibrations β C—H. Quant à la quatrième vibration β C—H de H_2Pc, elle est vraisemblablement mais avec moins de certitude située vers 1 045 cm^{-1}. Elle n'a pas été trouvée dans le spectre de CuPc mais ceci est peut être dû au fait que cette molécule a une plus haute symétrie. On observe une fréquence correspondante pour CuPc tétrachlorée mais cette absorption disparait de nouveau pour CuPc hexadécachlorée.

Le doublet 731, 736 cm^{-1} ainsi que la bande à 875 cm^{-1} du spectre de H_2Pc ont été attribués à des vibrations γ C—H. Pour CuPc il leur correspond les fréquences 730 et 871 cm^{-1}. Ces bandes sont absentes du spectre de CuPc hexadécachlorée.

Sidorov et Kotlyar (5) attribuent l'absorption à 716 cm^{-1} de H_2Pc à des déformations hors du plan des liaisons C—H des cycles benzéniques (γ C—H). Ils pensent que cette vibration donne lieu à une bande entre 719 et 739 cm^{-1} dans les spectres des phtalocyanines métalliques et n'existerait pas pour la CuPc chlorée. Ils affirment de plus que le doublet 731, 736 cm^{-1} du spectre de H_2Pc correspond aux bandes voisines de 755 cm^{-1} dans les spectres des phtalocyanines métalliques. Nous pensons qu'il parait beaucoup plus raisonnable de supposer que le doublet 731, 736 cm^{-1} correspond aux absorptions des métal–Pc

du massif ou de la bande situées entre 719 et 739 cm^{-1}. La bande à 716 cm^{-1} n'a d'équivalent ni dans les spectres des métal–Pc ni dans ceux des CuPc chlorées; cette bande serait donc due à une vibration du groupement N—H et on peut alors sûrement attribuer le doublet 731, 736 cm^{-1} à des vibrations γ C—H.

(c) Vibrations de l'ossature du cycle benzénique

Les trois modes ν C—C du benzène (1 594 cm^{-1} E_{2g}, 1 479 cm^{-1} E_{1u} et 1 309 cm^{-1} B_{2u}) (24) donnent, pour les benzènes ortho-disubstitués, cinq vibrations qui dépendent peu de la nature des substituants (21, 22, 23). La vibration dégénérée E_{2g} se sépare généralement en deux vibrations de fréquences voisines de 1 600 cm^{-1}. La vibration E_{1u} se sépare également, en donnant deux vibrations, plus espacées: entre 1 440 et 1 520 cm^{-1}; enfin le mode B_{2u} est généralement observé à une fréquence inférieure: entre 1 260 et 1 310 cm^{-1}. On observe dans les spectres de tous les composés étudiés des absorptions dans les régions 1 276 – 1 293 cm^{-1}, 1 391 – 1 438 cm^{-1}, 1 485 – 1 505 cm^{-1} et 1 605 – 1 616 cm^{-1}; nous suggérons d'admettre qu'elles proviennent de vibrations ν C—C du cycle benzénique.

On observe pour le benzène deux vibrations de déformation extérieures au plan du cycle ϕ C—C à 404 cm^{-1} (E_{2u}) et 707 cm^{-1} (B_{2g}) (24). La vibration 707 cm^{-1} ainsi qu'une des composantes du mode dégénéré 404 cm^{-1} sont assez peu sensibles aux substituants du cycle benzénique; on les trouve respectivement dans les régions 680–710 cm^{-1} et 400–450 cm^{-1} pour un grand nombre de benzènes mono- et disubstitués (21–23, 25). On observe dans les spectres de toutes les phtalocyanines étudiées, entre 420 et 421 cm^{-1}, une absorption qui correspond à la vibration 404 cm^{-1} du benzène. La bande 686 cm^{-1} du spectre de H_2Pc est peut être due à un autre mode ϕ C—C. On observe des absorptions correspondantes à 687 cm^{-1} pour Na_2Pc et 692 cm^{-1} pour CuPc-tétrachlorée, mais aucune bande analogue n'est observée dans les spectres de MoPc, CuPc et AlOH—Pc; encore une fois ceci est peut être dû à la plus grande symétrie de ces molécules.

(d) Autres bandes d'absorption caracteristiques

Plusieurs bandes apparaissant à des fréquences plus ou moins constantes dans les spectres de toutes les phtalocyanines étudiées n'ont pas été interprétées dans l'analyse précédente. Certains d'entre elles donnent lieu à des suites dans les spectres des divers composés étudiés (Tableau IV) on les observe dans le spectre de la H_2Pc à 642, 767, 1 095 et 1 160 cm^{-1}, et sous forme de doublets à 490, 494 cm^{-1} et 1 320, 1335 cm^{-1}. Nous pensons que ces absorptions sont dues à un couplage des vibrations de la partie centrale du cycle Pc considéré soit comme quatre cycles pyrroles reliés entre eux par quatre atomes d'azote soit comme un système continu de seize membres conjugués. Dans le premier cas, la bande 1 095 cm^{-1} pourrait être reliée à une vibration du cycle pyrrole trouvée à 1 144 cm^{-1} pour le pyrrole (20) et à 1 130 – 1 140 cm^{-1} pour les pyrroles substitués (17).

CONCLUSION

Il est évidemment hors de question d'interpréter complètement l'ensemble des fréquences de vibration d'une aussi grosse molécule que la phtalocyanine. Cependant, du fait du haut degré de symétrie de cette molécule particulière et des analogies de structure avec des molécules similaires dont les spectres sont assez bien connus, nous avons pu proposer des attributions pour de nombreuses bandes du spectre infrarouge.

Nos interprétations pour les vibrations N—H diffèrent de celles de Sidorov et Kotlyar (5) mais s'accordent avec celles de Mason pour les porphines (19). Les molécules CuPc chlorées se sont révélés utiles pour l'interprétation des vibrations C—H. Cependant, une étude des CuPc deutériées confirmerait mieux notre interprétation.

Can. J. Chem. Downloaded from www.nrcresearchpress.com by 210.87.254.6 on 09/05/12
For personal use only.

Nous avons publié les spectres de trois nouvelles phtalocyanines: MoPc, Na_2Pc et AlOH—Pc. Un travail ultèrieur sur AlOH—Pc devrait servir à rechercher le rôle joué par les liaisons hydrogènes dans la structure de cette molécule. Il existe peut être une liaison hydrogène OH . . . N intermoléculaire entre molécules adjacentes qui aurait pu être étudiée à partir des spectres de solutions (15) mais ceci présente des difficultés experimentales considérables dues à l'insolubilité des phtalocyanines. Le composé sodé Na_2Pc est également intéressant du point de vue structural puisque, comme nous l'avons suggéré, les atomes de sodium de Na_2Pc et d'hydrogène de H_2Pc pourraient être disposés de façon similaire. Une étude aux rayons X de la structure de Na_2Pc, permettant de localiser avec précision les positions des atomes de sodium, serait très utile.

REMERCIEMENTS

Nous voudrions exprimer notre gratitude à Messieurs les Professeurs J. Chouteau et P. Pesteil qui ont mis leurs laboratoires à notre disposition. Nous remercions aussi Monsieur le Professeur A. Julg pour de fructueuses discussions. Nous sommes également reconnaissants aux S. A. Française des Matières Colorantes et Badische Anilin Soda Fabrik A.G. qui nous ont fourni gracieusement les échantillons étudiés. Nous exprimons enfin notre reconnaissance au Gouvernement français et au C.N.R.S. qui nous ont apporté leur soutien financier.

BIBLIOGRAPHIE

1. G. G. Cannon et G. B. B. M. Sutherland. Spectrochim. Acta, **4**, 373 (1951).
2. A. A. Ebert, Jr. et H. B. Gottlieb. J. Am. Chem. Soc. **74**, 2806 (1952).
3. D. N. Kendall. Anal. Chem. **25**, 385 (1953).
4. A. N. Terenin et A. N. Sidorov. Spectrochim. Acta, **11** Suppl., 573 (1957). (Proc. Coll. Spect. Int. **VI**, Amsterdam, May 1956.)
5. A. N. Sidorov et I. P. Kotlyar. Optics and Spectroscopy, **11**, 92 (1961).
6. W. J. Kroenke et M. E. Kenney. Inorg. Chem. **3**, 696 (1964).
7. I.U.P.A.C. Tables of wavenumbers. Butterworths. 1961.
8. J. M. Robertson. J. Chem. Soc. 1195 (1936).
9. J. M. Robertson et I. Woodward. J. Chem. Soc. 219 (1937).
10. G. Herzberg. Infrared and Raman spectra. Van Nostrand. 1945.
11. Joint Commission for Spectroscopy. J. Chem. Phys. **23**, 1997 (1955).
12. C. E. Dent, R. P. Linstead et A. R. Lowe. J. Chem. Soc. 1037 (1934).
13. L. E. Lyons, J. R. Walsh et J. W. White. J. Chem. Soc. 167 (1960).
14. L. Pauling. The nature of the chemical bond. Cornell. 1960.
15. G. C. Pimentel et A. L. McLellan. The hydrogen bond. W. H. Freeman. 1960.
16. Y. Kanoaka *et coll.* Chem. Pharm. Bull. Japan, **8**, 294 (1960).
17. R. A. Jones. Australian J. Chem. **16**, 93 (1963).
18. U. Eisner et R. L. Erskine. J. Chem. Soc. 971 (1958).
19. S. F. Mason. J. Chem. Soc. 976 (1958).
20. R. C. Lord et F. A. Miller. J. Chem. Phys. **10**, 328 (1942).
21. J. H. S. Green, W. Kynaston et H. M. Paisley. J. Chem. Soc. 473 (1963).
22. J. R. Scherer et J. C. Evans. Spectrochim. Acta, **19**, 1739 (1963).
23. H. F. Shurvell, B. Dulaurens et P. Pesteil. A paraître.
24. S. Brodersen et A. Langseth. Mat. Fys. Skr. Dan. Vid. Selsk. **1**, 1 (1956).
25. D. H. Whiffen. J. Chem. Soc. 1350 (1956).

Can. J. Chem. Downloaded from www.nrcresearchpress.com by 210.87.254.6 on 09/05/12
For personal use only.

Can. J. Chem. Downloaded from www.nrcresearchpress.com by 210.87.254.6 on 09/05/12
For personal use only.

PREPARATION OF METAL NITRIDES BY THE EXPLODING WIRE TECHNIQUE[1]

MICHEAL J. JONCICH, JOE W. VAUGHN, AND BYRON F. KNUTSEN[2]
Michael Faraday Laboratories, Northern Illinois University, DeKalb, Illinois

Received July 6, 1965

ABSTRACT

An exploratory research program investigated the possibility of preparing metal nitrides by electrically exploding metal wires and foils in an atmsophere of (*a*) nitrogen, (*b*) ammonia, or (*c*) nitrogen and hydrogen. The explosions were carried out in an enclosed stainless steel pressure vessel. In a few cases, the wire was exploded while covered with liquid nitrogen in a stainless steel container maintained at liquid nitrogen temperatures.

The samples were analyzed using a modified Kjeldahl method for nitrogen. Greater yields of nitrides were obtained when a greater charge was given the oil-filled condensers used to supply the current, and when the pressure of gas surrounding the wire was increased. Yields as high as 50% were obtained in some cases. Clearly defined nitrides were obtained with magnesium, titanium, zirconium, tantalum, zinc, and aluminium. The metals iron, rhodium, platinum, copper, and cadmium did not appear to form stable nitrides under the experimental conditions.

A brief discussion of a mechanism by which a wire may explode is given.

INTRODUCTION

The exploding wire phenomenon (e.w.p.) is currently receiving considerable attention, particularly with regard to properties of the exploding wire, mechanism of the explosion process, and applications. The phenomenon was discovered in 1774 when Nairne (1) caused a wire to explode in his demonstration that the current in all parts of a series circuit is the same. Since shock waves may be produced during e.w.p. if the wire is confined, the exploding wire has been used recently to study shock waves in air and water. Chemical applications include the production of mirrors on the inside of vessels (2), the synthesis of inorganic compounds (3, 4), and the initiation of photochemical reactions (5, 6).

In 1964, Joncich and Reu (3) reported the preparation of sulfides, carbides, and iodides of aluminium and magnesium by electrically exploding a wire coated with the appropriate non-metal. Also, Mahieux (4) reported the formation of $PtXeF_6$ prepared by exploding platinum in an atmosphere of xenon and fluorine, although there appears to be some question as to the actual nature of the compound produced since no analysis for platinum was carried out. It was the purpose of this research to prepare various metallic nitrides by exploding the metal with an electrical discharge. The metal, in the form of wire or foil, was in an atmosphere containing nitrogen gas, ammonia, liquid nitrogen, or a mixture of hydrogen and nitrogen. There are several advantages in this method of chemical synthesis. (1) Preparation of very hygroscopic compounds can be accomplished since the system can be kept dry. (2) One of the reactants (nitrogen) can be removed easily from the products by evaporation. (3) Since considerable activation energy is available in e.w.p., it may be possible to synthesize new compounds, which under normal laboratory conditions cannot be prepared. (4) The equipment required is relatively simple.

[1]*Presented at the Symposium on High-Temperature Inorganic Chemistry, Ottawa, Canada, September 1964. This work is supported by the Petroleum Research Fund of the American Chemical Society.*
[2]*National Science Foundation research participant, 1964.*

Can. J. Chem. Downloaded from www.nrcresearchpress.com by 210.87.254.6 on 09/05/12
For personal use only.

In addition to these four advantages, there are two aspects of this technique which are unique to e.w.p. (1) The reaction is completed within microseconds. (2) The reaction is rapidly quenched. This is particularly true when the explosion is carried out under liquid nitrogen.

The discussion of the results of the experimental work will cover three aspects: (1) the mechanism by which wires explode when subjected to a large electrical discharge, (2) the equipment used in e.w.p. technique, and (3) the results of the preparation of a number of different nitrides.

Figure 1, which shows an ideal current–time oscilloscope tracing, will be referred to in the discussion of the different stages in the mechanism of the exploding wire. Of course, the actual tracing will depend on inductance of the circuit, pressure of gas surrounding the wire, size of the wire, switch characteristics, charging voltage, spacing of the electrodes, etc. A more detailed description of the mechanism can be found in articles by Chace (7) and others (8).

At time t_0 the circuit is closed and current commences to flow through the wire. The maximum initial current surge may be as great as 250 000 A depending on the system used. The time duration of the surge is less than 100 μs. If a heavy metallic bar were placed in the position of the wire, the discharge curve would then have the shape of a damped sine curve. As the current increases, the wire is heated very rapidly and is converted to a liquid at its normal melting point. The temperature of the molten wire increases towards its boiling point; however, since there is no interfacial surface between the molten wire and the walls of the container, the metal does not boil at its normal boiling point. Because of the large current flowing through the conductor, the wire is surrounded by a very strong magnetic field. The effect of this field is to increase the normal boiling temperature of the molten wire. The wire becomes superheated until it finally flash boils at time t_1. The boiling is accompanied by a loud noise and a flash of light. The wire in the vapor state continues to expand while the current drops to a relatively low value, but remains appreciable. The current drops because the wire, in the vapor state, has a very high resistance. It has been found that a current of 50 – 500 A flows through the vaporized wire during the "dark" or "dwell" period beginning at t_2. As the distance between the vaporized metal atoms continues to increase, ionization occurs, followed by a "restrike" or second surge of current at t_3. The duration of the "restrike" is a function of the velocity of the metallic vapors.

The duration of the "dwell" period depends on the pressure of the atmosphere surrounding the wire (9) as well as on many other factors. Pressures below 6 mm Hg may cause the "dwell" time to decrease or disappear. In this case it is likely that a great deal of the current is bypassing the wire and is arcing through the air gap. Since there is a plasma state associated with the wire during its transitions in the vapor state, it would seem advisable to have the current pass through the wire in one initial surge. Although the mechanism given above may not agree with all other mechanisms, many workers in the field consider it to be fairly accurate.

EXPERIMENTAL

The diagram of the electrical circuit used in the experimental work is given in Fig. 3. The energy source for the synthesis was provided by ten 31-μF capacitors (C) connected in parallel. The total energy stored on the capacitors was 12 000 J when the capacitors were charged to 9 000 V by the d.-c. power supply (P). Prior to the explosion, switch (S) was connected to resistor (R) to protect the power supply. Switch (S′) was an air gap switch designed in our laboratory and used to discharge the condensers through the wire (W).

It is important that the condensers, switch, and connecting leads have as low an inductance as possible. The lower the inductance of the system, the more rapidly the current will rise when the switch is closed.

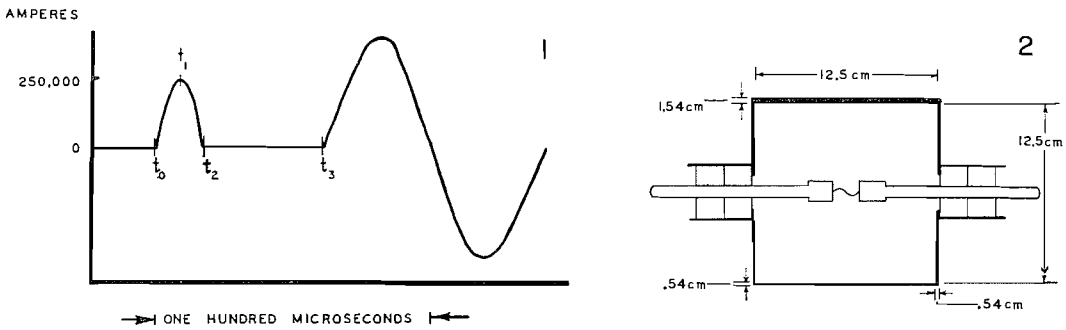


FIG. 1. An ideal current versus time oscilloscope tracing.
FIG. 2. Reaction vessel.

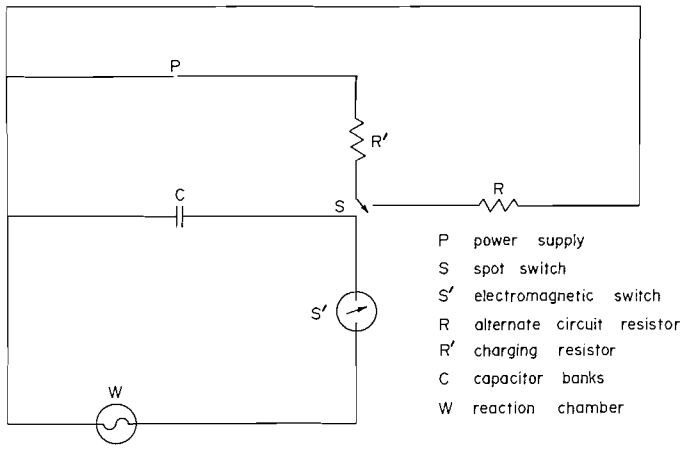


FIG. 3. Modified exploding wire circuit.

The investigations of Joncich and Reu (3) were performed in an evacuated glass reaction vessel, since the syntheses involved the reactions of two solids. The preparations of nitrides were carried out in a nitrogen atmosphere; a stainless steel cylindrical vessel was constructed to withstand the shock wave accompanying the explosion of the wire. Figure 2 is a side view of the 1 700 ml reaction chamber; a 500 ml reaction vessel was used in some experiments. In both cases, the top was removable and secured by heavy bolts with a Teflon gasket between the lid and the body of the vessel.

Various wire sizes were exploded and it was found that a wire weighing from 75–120 mg was the maximum weight that could be exploded without having large pieces of the unreacted wire in the collected sample. At a nitrogen pressure of 1 atm, the stoichiometric ratio of nitrogen to metal was approximately 1 000:1. After the explosion, it was necessary to wait 30 min before opening the chamber to prevent appreciable loss of the finely divided product.

The metals which were exploded in nitrogen were magnesium, iron, titanium, zirconium, tantalum, rhodium, platinum, copper, zinc, and aluminium. The products obtained for each element were grouped according to color and were analyzed for nitrogen by the Gunning modification of the Kjeldahl method. To test the analytical technique, it was found that 96% of the nitrogen in 20AlN·SiC* could be recovered by this method. Yields are reported as percentage nitride. Samples collected from wires exploded in gaseous ammonia were heated to 100 °C to drive off free ammonia prior to the determination of the nitrogen content.

RESULTS

Magnesium

Many samples of magnesium nitride (see Table I) were tan or white. These were predominately mixtures of the oxide and the metal and contained only a trace of nitrogen

**Available from Allis-Chalmers Co., Cerac Division, Milwaukee, Wisconsin.*

Can. J. Chem. Downloaded from www.nrcresearchpress.com by 210.87.254.6 on 09/05/12
For personal use only.

(0.2–0.5%). Magnesium exploded in an ammonia atmosphere under similar conditions gave a product with a nitride content of 6.4%. Increasing the charging voltages from 9 to 12 kV gave a product with a nitride content of 21.5%. Magnesium exploded in mixtures of hydrogen and nitrogen (1:1 molar ratio) showed a nitride content of 15.6%. Smaller wires were exploded in nitrogen; the product obtained had a nitride content of 6.23%. The use of smaller wires and a larger charge on the capacitors favors the production of the nitride. X-Ray powder photographs indicated the product contained Mg_3N_2 in all cases.

TABLE I

Results of explosions of wires in various atmospheres (condensers were charged to 9 kV)

Possible compound	Average weight of wire (mg)	Gas present	Total pressure of gas (mm Hg)	% yield of nitride	Total % metal in sample
Mg_3N_2*	170	N_2	736	Trace N	63
Mg_3N_2	176	$1N_2$ and $1H_2$	736	15.6	60
Mg_3N_2	80	N_2	736	6.23	ND‖
Mg_3N_2§	121	N_2	976	6.25	ND
Mg_3N_2§	115	$1N_2$ and 2He	976	3.0	ND
Mg_3N_2 or $Mg(NH_2)_2$*	172	NH_3	736	6.4†	ND
Mg_3N_2 or $Mg(NH_2)_2$‡	171	NH_3	736	21.5†	ND
Mg_3N_2	65	N_2	240	Red 3.05	44.9
				Yellow 3.05	46.8
TiN	84	$1N_2$ and $1H_2$	736	49.1	ND
TiN	81	$1NH_3$ and $2H_2$	736	52.5	ND
ZrN	158	N_2	736	24.8	75.5
ZrN	78	N_2	736	41.0	70.4
ZrN	79	N_2	976	47.4	70.8
TaN§	200	N_2	976	Gray 17.3	ND
Fe_2N	89	N_2	956	0	ND
Fe_2N	111	N_2	956	0	See Results
RhN§	98	N_2	976	0	ND
Pt_3N_4*	279	N_2	736	0	ND
Pt_3N_4	240	NH_3	736	0	97
Pt_3N_4	240	$1N_2$ and $1H_2$	736	0	96
Pt_3N_4	69	N_2	956	0	95
Pt_3N_4	73	N_2	736	0	96
Pt_3N_4§	90	N_2	956	0	ND
Cu_3N§	119	N_2	966	0	See Results
Zn_3N_2	119	N_2	966	0	ND
Zn_3N_2	118	N_2	966	0	ND
Al_3N_2	127	N_2	976	17.5	ND
Cd_3N_2	136	N_2	976	0	97.0

*The capacitors were charged to 8 kV instead of 9 kV.
†Based on the nitrogen content of Mg_3N_2.
‡The capacitors were charged to 12 kV.
§The nitrogen was passed over hot copper before filling the reaction vessel.
‖ND = no data collected.

Titanium

Titanium exploded in a 1:1 molar ratio of nitrogen to hydrogen gave a black product, corresponding to a 49.1% yield of nitride. Titanium was also exploded in a 1:2 mixture of ammonia and hydrogen; the yield of the nitride was 52.5%. Titanium nitride was prepared in 26.4% yield by exploding titanium under liquid nitrogen. The major product was TiN.

Zirconium

Rather large wires of zirconium (155 mg) were exploded in pure nitrogen at a pressure of 1 atm. This procedure gave the nitride in 24.8% yield. A smaller wire (78 mg) was exploded under the same conditions and the yield was increased to 41%. The yield of

Can. J. Chem. Downloaded from www.nrcresearchpress.com by 210.87.254.6 on 09/05/12
For personal use only.

the reaction was improved to 47.4% by increasing the pressure of the nitrogen to 976 mm Hg. X-Ray powder photographs confirmed the presence of ZrN in the samples.

Tantalum

Tantalum forms two nitrides, TaN, which is a metallic gray in color, and Ta_3N_5, which is red. Judging from the color of the samples, both forms were obtained. The red form was preferentially produced with small wires and large charge on the capacitors. However, the X-ray photographs of both forms were identical and showed the presence of TaN.

Iron

All explosions of iron except one gave a gray product which could be finely divided metal, Fe_2N, or the polymeric $(Fe_2N)_n$ which is also gray. However, the samples did not contain nitrogen and the X-ray data indicated the absence of any iron nitride.

Rhodium

Explosion of a rhodium wire in a nitrogen atmosphere produced a very dark green product, which did not contain nitrogen.

Platinum

Many attempts were made to prepare the unknown compound, platinum nitride. All attempts were unsuccessful. Nitrogen could not be detected in the samples, and chemical analysis as well as X-ray data indicated the product of the explosion was pure platinum.

Copper

Copper was exploded successfully but gave products which ranged in color from dark olive green to yellowish green and which contained a small amount of nitrogen. X-Ray data did not indicate the presence of Cu_3N in the sample. The product exhibited reactions characteristic of copper(I) compounds (10). However, chemical analysis indicated the presence of very small amounts of nitrogen, and X-ray diffraction patterns contained some lines characteristic of copper azide.

Zinc

A water soluble product was formed by the explosion of zinc in a nitrogen atmosphere. Kjeldahl analysis did not indicate the presence of nitrogen in the compound; however, it was later determined that the addition of concentrated sulfuric acid decomposes zinc nitride to the metal and free nitrogen. X-Ray data indicated the sample contained Zn_3N_2.

Aluminium

Aluminium foil exploded completely and gave the nitride in 17.5% yield. The color of the sample indicated the presence of the oxide. Since the nitrogen contained 0.3% impurity, which may have been oxygen, it was passed over hot copper before it was used in the exploding chamber. There is considerable evidence that when a metal is exploded in air, the oxide is formed in preference to the nitride (11). The presence of AlN in the sample was confirmed by X-ray data.

Cadmium

Cadmium exploded in a nitrogen atmosphere gave a product which had a nitrogen content of 0.39%. The cadmium content was 97.0%; the remainder was an acid insoluble residue. The nitride of cadmium may decompose into the metal and nitrogen upon the addition of acid; this possibility was previously pointed out in the case of zinc nitride.

It has been demonstrated that it is possible to prepare various nitrides using the techniques of e.w.p. Further work is needed to investigate the optimum conditions for

Can. J. Chem. Downloaded from www.nrcresearchpress.com by 210.87.254.6 on 09/05/12
For personal use only.

the preparation of the various nitrides. A conclusion from this exploratory work is that an increase in the voltage used to explode the wire and in the pressure surrounding the wire, accompanied by a decrease in the size of the wire, favors the formation of the nitride. In cases in which the nitride was not obtained, it is possible that the nitride will not form, or if formed, is unstable and rapidly decomposes to the metal and nitrogen. The results of these experiments are summarized in Table I.

ACKNOWLEDGMENT

The authors are grateful for helpful discussions concerning this work with Dr. Walter A. Yeranos. The aid received from Dr. Aubrey J. Serewicz on the X-ray diffraction studies is gratefully acknowledged.

REFERENCES

1. E. NAIRNE. Phil. Trans. Roy. Soc. London, **64**, 79 (1774).
2. M. FARADAY. Proc. Roy. Inst. G. Brit. **8**, 356 (1857).
3. M. J. JONCICH and D. REU. *In* Exploding wires. Vol. 3. *Edited by* W. G. Chace and H. K. Moore. Plennum Press, N. Y. 1964. p. 353.
4. M. F. MAHIEUX. Compt. Rend. **257**, 1083 (1963); **258**, 3497 (1964).
5. G. K. OSTER and R. A. MARCUS. J. Chem. Phys. **27**, 189 (1957).
6. R. A. MARCUS. *In* Exploding wires. Vol. 1. *Edited by* W. G. Chace and H. K. Moore. Plenum Press, New York. 1959. p. 307.
7. W. G. CHACE and H. K. MOORE (*Editors*). Exploding wires. Vols. I–3. Plenum Press, New York. 1959, 1962, 1964.
8. C. P. NASH and W. G. MCMILLAN. Phys. Fluids, **4**, 911 (1961).
9. G. S. ROSE. J. Appl. Phys. **33**, 1604 (1962).
10. R. T. SANDERSON. Chemical periodicity. Reinhold Publishing Co., New York. 1960. p. 206.
11. F. G. KARIORIS and B. R. FISH. J. Colloid Chem. **17**, 155 (1962).

Can. J. Chem. Downloaded from www.nrcresearchpress.com by 210.87.254.6 on 09/05/12
For personal use only.

Can. J. Chem. Downloaded from www.nrcresearchpress.com by 210.87.254.6 on 09/05/12
For personal use only.

EFFECT OF CO AND N_2 ON MERCURY-PHOTOSENSITIZED REACTIONS[1]

J. B. HOMER[2] AND F. P. LOSSING
Division of Pure Chemistry, National Research Council, Ottawa, Canada
Received August 25, 1965

ABSTRACT

The addition of CO is found to increase the rate of the mercury-photosensitized decomposition of certain compounds (ethylene, acetone, anisole) by a factor in excess of 2.5, but does not affect the rate with paraffin hydrocarbons. The addition of N_2, known to quench $Hg(^3P_1)$ to the metastable $Hg(^3P_0)$ state, does not produce an increase in rate. The results are discussed with reference to a possible HgCO* complex which contains most of the original excitation energy of $Hg(^3P_1)$ atom.

INTRODUCTION

This publication is concerned with some phenomena associated with the effect of foreign gases, particularly CO and N_2, on $Hg(^3P_1)$ photosensitized decomposition reactions at relatively low pressures. The effect was observed quite unexpectedly when the addition of moderate amounts of CO was found to give a twofold increase in the rate of decomposition of anisole by $Hg(^3P_1)$ atoms. Further investigation of this effect showed that addition of CO similarly increased the decomposition rates of ethylene and acetone, but left those of paraffin hydrocarbons unaffected. A possible explanation in terms of formation of metastable $Hg(^3P_0)$ atoms was quickly rejected when it was found that the addition of N_2, which also quenches $^3P_1$ atoms to the metastable $^3P_0$ state, gave no enhancement in the rates of decomposition. Further work on this unusual phenomenon was therefore felt to be justified.

A comprehensive review of the reactions of excited mercury atoms, summarizing the known cross sections and nature of such reactions has recently been published by Cvetanović (1), so that further background on such reactions need not be given here.

EXPERIMENTAL

The experimental arrangements were similar to those previously described (2, 3), but for the sake of clarity they are briefly described here. The reactor is shown in Fig. 1. A stream of helium at 12 mm pressure carried the reactant together with mercury vapor through a fused silica tube illuminated by an intense low pressure mercury lamp. The reactor, the lamp, and the supply of mercury to the stream were held at 55 °C by circulating water. The residence time in the illuminated zone was about 10^{-3} s. Directly after passing the illuminated zone the reaction stream passed over a small orifice through which a portion flowed directly into the ionization chamber of a mass spectrometer. The partial pressures of reactant and product gases in the reactor in the immediate neighborhood of the orifice can be measured with the mass spectrometer after appropriate calibrations. Changes in composition can be measured with 1–2% accuracy, at least for non-radical products. In the present experiments the extent of decomposition (in a constant residence time) was measured from the decrease in the parent peak of the compound brought about by turning on the mercury lamp. Isotopic corrections from interfering peaks were applied where necessary.

Some experiments were carried out using a static reactor. This consisted of a fused silica vessel 2 cm in diameter and 12 cm long containing a drop of mercury and irradiated by a U-shaped low pressure mercury lamp. The lamp and reactor were immersed in water at 25°. Illumination periods, controlled by a rotating electrical contact driven by a synchronous motor, varied from 0.6 s to 3 s. The reproducibility of measurement of C_2H_4 decomposed and C_2H_2 formed in identical repetitive runs was about 5%.

[1]*National Research Council Contribution No. 8711.*
[2]*National Research Council Postdoctorate Fellow, 1963–1965.*

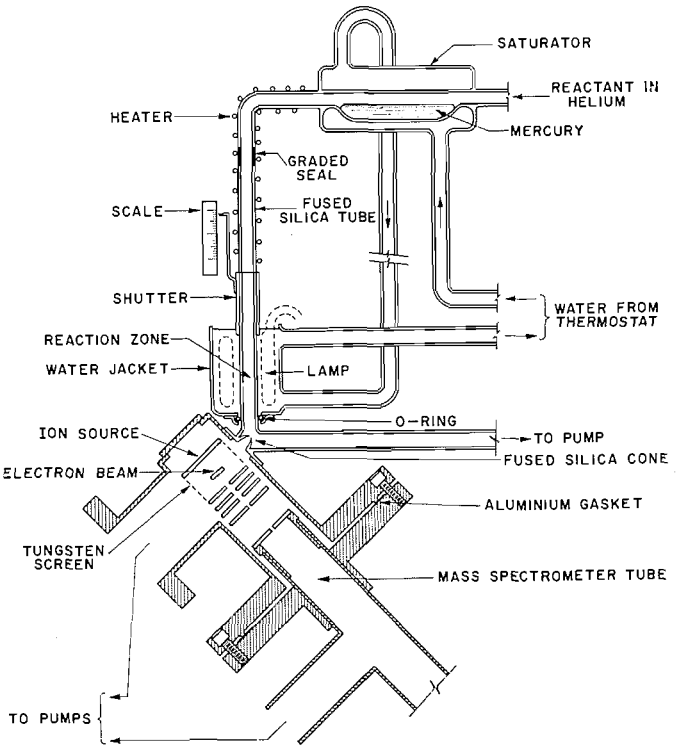


FIG. 1. Diagram of photochemical reactor.

RESULTS

Hg($^3P_1$) Photosensitized Decomposition of Ethylene

Although, as mentioned above, enhancement of the rate of photosensitized decomposition by CO was observed for several compounds, the effect was mainly studied with ethylene since this reaction is perhaps the most clearly understood, and the reaction products are mainly non-radical and therefore undergo a minimum of secondary reactions. The interaction of $Hg(^3P_1)$ atoms with ethylene leads to formation of an excited C_2H_4 which decomposes almost entirely through elimination of a H_2 molecule (4). A concurrent reaction giving $H + C_2H_3$ amounts to only 3–4% of the total reaction (2, 6) or lower (1, 5, 7). Moreover, the quantum yield of H_2 is close to unity at low pressures (8). Assuming the reaction sequence

[1] $$Hg + h\nu \rightarrow Hg(^3P_1)$$

[2] $$Hg(^3P_1) \rightarrow Hg(^1S_0) + h\nu$$

[3] $$Hg(^3P_1) + C_2H_4 \rightarrow Hg(^1S_0) + C_2H_2 + H_2$$

leads to a kinetic equation

$$-\frac{dt}{dP} = \frac{1}{I_a} + \frac{k_2}{I_a k_3[C_2H_4]}$$

where I_a is the rate of production of $Hg(^3P_1)$ by reaction [1], t = time, and P = partial pressure of ethylene. When the amount of decomposition is small

$$dt/dP = \Delta t/\Delta P$$

Can. J. Chem. Downloaded from www.nrcresearchpress.com by 210.87.254.6 on 09/05/12
For personal use only.

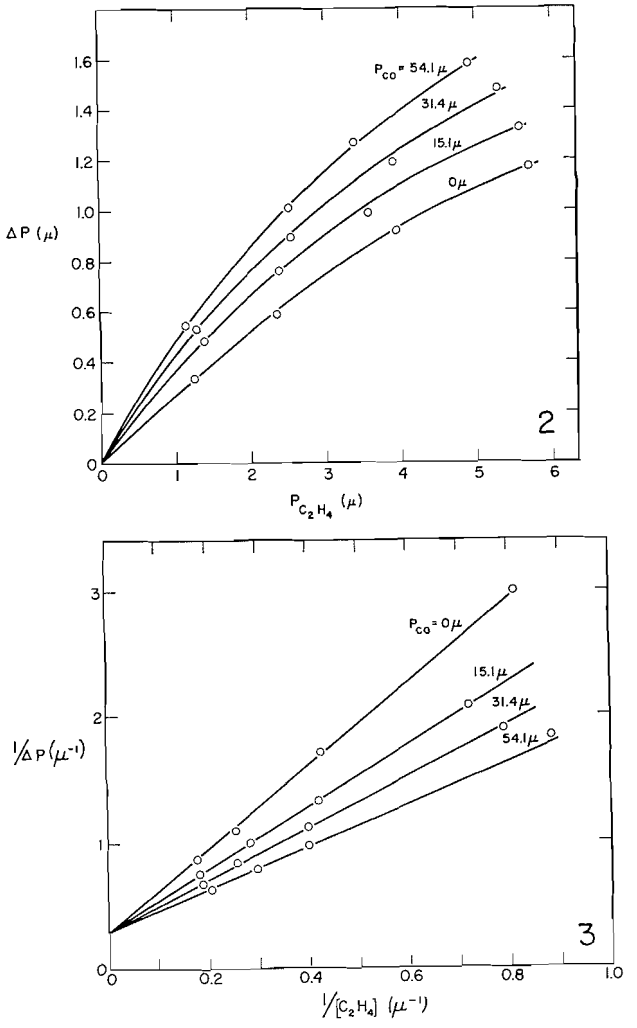


FIG. 2. Amount of ethylene decomposed as a function of its partial pressure.
FIG. 3. Reciprocal plot of data in Fig. 2.

where Δt is the residence time, and ΔP is the amount of ethylene decomposed. For the sake of simplicity, this is assumed to apply for decompositions of the order of 20%.

A plot of the amount of ethylene decomposed against the partial pressure of ethylene is shown in Fig. 2, and is transformed into a reciprocal plot in Fig. 3. When $P_{CO} = 0$, the intercept in Fig. 3 gives a value of $1/I_a\Delta t$; this and the slope of the line give k_2/k_3 to be 5.82×10^{-7} mole l^{-1}. The value of k_3 is known (1) to be 3.7×10^{11} l mole^{-1} s^{-1}, so that $k_2 = 2.15 \times 10^5$ s^{-1}. The effective lifetime of a quantum of 2 537 Å radiation in this system is therefore 4.65×10^{-6} s, which by comparison with the radiative lifetime of $Hg(^3P_1)$ of 1×10^{-7} s indicates the extent of radiative imprisonment in this reactor under the conditions employed.

Effect of Foreign Gas Addition

When CO was added to the reaction stream of ethylene and helium the amount of ethylene decomposed was greatly increased. The results obtained by varying the partial

Can. J. Chem. Downloaded from www.nrcresearchpress.com by 210.87.254.6 on 09/05/12
For personal use only.

pressure of both ethylene and CO are also shown in Fig. 2 and Fig. 3. The plots in Fig. 3 are a series of essentially straight lines fanning out from a common intercept on the $1/\Delta P$ axis. This shows, firstly, that the proportionality between $1/\Delta P$ and $1/[C_2H_4]$ is still retained in the presence of CO, and, secondly, that $I_a\Delta t$ is unchanged. Since the amounts of CO added were too small compared with the 12 mm of helium gas to affect the flow rate (and consequently Δt) significantly, the latter shows that no increase in the amount of chemically effective light occurred with the CO addition, either by pressure broadening or by absorption by CO itself.

At a partial pressure of ethylene of ~ 2 μ, the amount decomposed was about 20%. The change in this amount by the addition of CO, N_2, CO_2, and H_2O is recorded in Fig. 4 as a plot of Δ_2/Δ_1 against the partial pressures of the added gas. Here Δ_2 is the amount of decomposition in the presence, and Δ_1, in the absence, of the added gas. It can be seen that although CO greatly increases the extent of decomposition, N_2 shows practically no effect.

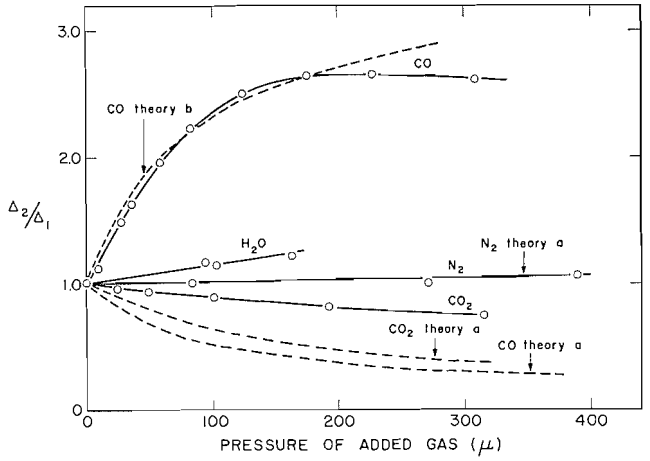


FIG. 4. Effect of added gas on the decomposition of ethylene. Δ_2 is the amount of decomposition in the presence, and Δ_1 in the absence, of the added gas.

From existing data it is possible to predict what effects the addition of CO and N_2 should have on the reaction of $Hg(^3P_1)$ with C_2H_4. CO and N_2 have no known electronic states low enough in energy to be excited by collision with $Hg(^3P_1)$ atoms. They can, however, absorb energy in internal and translational forms, thereby converting $Hg(^3P_1)$ to the metastable $^3P_0$ state or even to the $^1S_0$ ground state.

[4] $$Hg(^3P_1) + CO \text{ (or } N_2) \rightarrow Hg(^3P_0) + CO^* \text{ (or } N_2^*)$$

[5] $$\rightarrow Hg(^1S_0) + CO^{**} \text{ (or } N_2^{**})$$

Zemansky (9, 10) studied the quenching of the fluorescence of Hg 2 537 Å and found that CO was 20 times more efficient than N_2:

$$\text{i.e. } (k_4^{CO} + k_5^{CO})/(k_4^{N_2} + k_5^{N_2}) \approx 20.$$

This is a large difference for apparently similar molecules, and Zemansky proposed that $k_4^{CO} \gg k_4^{N_2}$ on the grounds that the energy discrepancy in reaction [4] was smaller for the formation of $Hg(^3P_0) + CO_{(v=1)}$ than for $Hg(^3P_0) + N_{2(v=1)}$. Scheer and Fine (11) showed this proposition to be false by measuring the amount of $Hg(^3P_0)$ atoms produced, concluding that, in fact, $k_4^{CO} = 1.35k_4^{N_2}$. In addition Callear and Norrish (12) have pointed

Can. J. Chem. Downloaded from www.nrcresearchpress.com by 210.87.254.6 on 09/05/12
For personal use only.

out that if N_2 is added to a Hg resonance lamp, the decreased quantum output can be returned almost to normal by heating, an act that could easily reverse reaction [4] but not [5]. They inferred that $k_5^{N_2}$ is negligibly small.

From the values determined by Mitchell and Zemansky (10) the rates at 55 °C are:

$$k_4^{CO} + k_5^{CO} = 5.84 \times 10^{10}\ \text{l mole}^{-1}\ \text{s}^{-1}$$
$$k_4^{N_2} + k_5^{N_2} = 0.275 \times 10^{10}\ \text{l mole}^{-1}\ \text{s}^{-1}.$$

From the above arguments the separated rate constants are:

$$k_4^{CO} = 0.37 \times 10^{10}\ \text{l mole}^{-1}\ \text{s}^{-1}$$
$$k_4^{N_2} = 0.275 \times 10^{10}\ \text{l mole}^{-1}\ \text{s}^{-1}$$
$$k_5^{CO} = 5.47 \times 10^{10}\ \text{l mole}^{-1}\ \text{s}^{-1}$$
$$k_5^{N_2} = 0.$$

Although metastable $Hg(^3P_0)$ atoms decompose ethylene by a much lower rate of 0.7×10^{10} l mole^{-1} s^{-1} (1) compared with 37×10^{10} l mole^{-1} s^{-1} for $Hg(^3P_1)$ atoms, they have a much longer radiative lifetime, $\sim 4 \times 10^{-4}$ s. The presence of $Hg(^3P_0)$ atoms in the present reaction system could therefore be significant. If the additional reaction steps are then written

[6] $$Hg(^3P_0) \rightarrow Hg(^1S_0) + h\nu$$

[7] $$Hg(^3P_0) + C_2H_4 \rightarrow Hg(^1S_0) + C_2H_4 + H_2$$

and a steady state treatment is applied to $Hg(^3P_1)$ and $Hg(^3P_0)$ in this system, the following equation can be deduced.

$$\frac{-\Delta_2}{\Delta t} = \frac{I_a[C_2H_4][k_3k_6 + k_3k_7[C_2H_4] + k_4k_7[CO]]}{[k_6 + k_7[C_2H_4]][k_2 + k_3[C_2H_4] + (k_4 + k_5)[CO]]}$$

In the absence of CO

$$\frac{-\Delta_1}{\Delta t} = \frac{I_a k_3[C_2H_4]}{k_2 + k_3[C_2H_4]}$$

so that

$$\frac{\Delta_2}{\Delta_1} = \frac{1 + k_4k_7[CO]/k_3(k_6 + k_7[C_2H_4])}{1 + (k_4 + k_5)[CO]/(k_2 + k_3[C_2H_4])}.$$

If the values of the rate constants already evaluated are inserted in this equation, the theoretical dependence of Δ_2/Δ_1 on the pressure of added gas can be calculated for CO and N_2. The result is shown superimposed on Fig. 4 as theory *a*. Theory and experiment are identical for N_2, the small enhancement caused by the longer life of $Hg(^3P_0)$ being counterbalanced by its slower rate of reaction with ethylene. Theory predicts, however, that CO would *decrease* the amount of decomposition because of rapid deactivation of $Hg(^3P_1)$ to the ground state, whereas the experimental result shows an opposite effect. Indeed if, hypothetically, k_4^{CO} were infinite and all other rates remained the same, the maximum enhancement possible would still be much lower than that observed, that is, Δ_2/Δ_1 for the C_2H_4 concentration corresponding to Fig. 4 would reach a limit of 1.49.

It is evident that the formation of $Hg(^3P_0)$ is not the major factor in the observed effect of CO addition.

Dependence on Light Intensity

Wire gauze screens of known optical transmission were inserted between the lamp and the reactor, and the amount of decomposition of ethylene was measured with and without

Can. J. Chem. Downloaded from www.nrcresearchpress.com by 210.87.254.6 on 09/05/12
For personal use only.

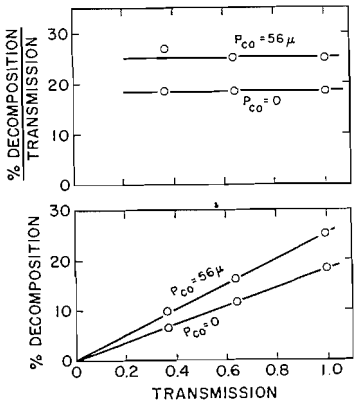


FIG. 5. Plot showing first-order dependence on light intensity with and without added CO.

the addition of 56 μ of CO to the stream. The results (Fig. 5) confirm that the dependence on light intensity was not greater than the first power. This immediately ruled out any stepwise excitation paths to excited species, for instance an electronically excited CO molecule.

A metal sleeve (shown in Fig. 1) was lowered in stages between the lamp and the reactor, thus varying the length of the illuminated zone. The amount of decomposition (Fig. 6) increased linearly with the length of the illuminated zone. No buildup of active species, as observed previously in the photosensitized decomposition of biacetyl (13), was therefore taking place along the reactor. This restricts all chemically active species to a lifetime much shorter than the time of transit along the reactor. The fact that both lines in Fig. 6 have the same extrapolated zero in terms of distance emphasizes this fact.

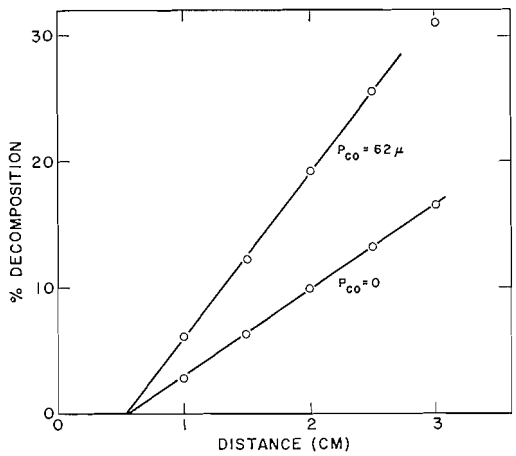


FIG. 6. Amount of decomposition as a function of the length of the illuminated zone.

Search for Abnormal Products

No products other than acetylene and hydrogen could be found at moderate pressures of ethylene ($\sim$ 20 μ) and high pressures of CO (200 μ). The additional decrease in ethylene caused by the addition of CO was as far as could be assessed ($\pm$2%) always equal to the increase in acetylene produced. A particularly close search was made for products such as

Can. J. Chem. Downloaded from www.nrcresearchpress.com by 210.87.254.6 on 09/05/12
For personal use only.

formaldehyde, acetaldehyde, or addition products of Hg and CO, but none was detected. A negative result was also obtained when N_2, CO_2, or H_2O were added.

In runs made in the static reactor system at higher pressures (see Experimental) no evidence for addition products of CO with ethylene could be found, in particular no acrolein, methyl ketene, or cyclopentanone. Butane, butene, and butadiene were produced in appreciable amounts, both in the presence and absence of CO. In order for CO to more than double the amount of decomposition of ethylene by the competition of reactions [6] and [7]

[6] $$C_2H_4^* + M \rightarrow C_2H_4 + M$$

[7] $$C_2H_4^* + CO \rightarrow \text{products}$$

the quantum yield for ethylene decomposition in the absence of CO would have to be <0.5. This seems unlikely in view of the probable inefficiency of 12 mm of helium as a medium for deactivation, and the observed high quantum yield for H_2 even at moderately high pressures (8).

Effect of CO on the Decomposition of Other Compounds

The extent of the photosensitized decomposition of *n*-butane, propane, and cyclopropane was unaffected by the addition of 100 μ of CO. Ethane showed a slight decrease and isobutane a slight increase, possibly larger than experimental error. Anisole and acetone, on the other hand, showed the same substantial increase as did ethylene. It would appear that the new active species formed by the CO addition has a preference for an attack on π-bonds.

Experiments with the Static Reactor System

It was thought that the enhancement of decomposition of ethylene in the presence of CO might result from some peculiarity of the fast-flow system or mercury lamp used in the mass-spectrometric experiments, or possibly from wall effects. It was found, however, that the enhancement effect of CO could be reproduced in the static reactor, in which the geometry and the lamp were quite different. For these experiments, a mixture of foreign gas and ethylene in the ratio of 10:1 was made up. Samples of this mixture at different pressures were irradiated in the reactor for times of 0.6 to 3 s, and analyzed for C_2H_4 and C_2H_2 with the mass spectrometer. The rates of decomposition were compared with those of pure ethylene under identical conditions. Variations in Δ_2/Δ_1 with total pressure are shown in Fig. 7 for the three foreign gases, CO, N_2, and He. At the lowest pressures, the effect of CO was to increase the rate of decomposition by a factor approaching that found in the flow reactor, while N_2 and He showed no effect. With increasing pressure, the special effect of CO vanished. This would be expected since the region of complete quenching is being approached, and the rate would be determined by the rate of absorption of quanta, i.e. by the useful output of the lamp, and the partial pressure of mercury in the reactor.

Consideration as to the Active Species Introduced by CO Addition

From the discussion above, it is apparent that the enhancement effect of CO cannot be attributed to the absorption of additional quanta. The explanation must therefore lie in the utilization of quanta which are, in the absence of CO, re-radiated from the reactor. This requires the introduction by CO of an active species with a large cross section toward ethylene. The high reactivity of the active species toward molecules decomposing by way of a triplet state (ethylene, acetone) compared with its inactivity toward paraffins would seem to define the species as being itself a triplet. The lowest triplet of CO, $A^3\pi$, lies over

Can. J. Chem. Downloaded from www.nrcresearchpress.com by 210.87.254.6 on 09/05/12
For personal use only.

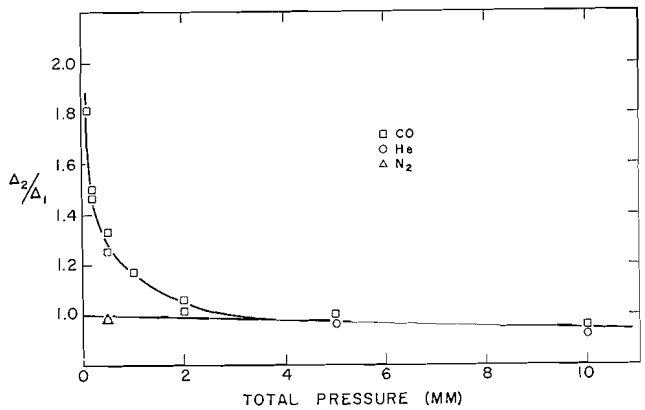


FIG. 7. Enhancement by CO of the rate of decomposition of ethylene in a static reactor system. Addition of He and N_2 has essentially no effect.

1 V above the $Hg(^3P_1)$ level, and could only be formed by stepwise excitation, or by collision with $Hg(^1P_1)$ atoms. Stepwise excitation has been ruled out on the grounds of first-order dependence on the light intensity. The formation of significant amounts of $Hg(^1P_1)$ atoms by 1 849 Å radiation present in the output of the lamp appears improbable, since this radiation would be greatly attenuated by the water surrounding the reactor. In any case the formation of $CO(A^3\pi)$ by $Hg(^1P_1)$ would be inefficient because of violation of the spin conservation rule.

The presence of vibrationally excited CO molecules, at levels up to $v = 8$ or higher, resulting from collision with Hg*, has been demonstrated by observation of the infrared emission (14). These observations suggested that a high vibrational state of CO was excited directly by collision with Hg* rather than by a stepwise excitation. Such vibrationally excited CO molecules could be the excited species responsible for the present observations, but this explanation runs into serious difficulties. Although the reaction $C_2H_4 \rightarrow C_2H_2 + H_2$ is only 41.7 kcal/mole endothermic, the photosensitized decomposition is extremely slow by $Cd(^3P_1)$ atoms (87.3 kcal/mole) and even, by $Zn(^3P_1)$ atoms (92.5 kcal/mole) (15). It seems reasonable, therefore, that vibrationally excited CO molecules with energies less than about 90 kcal/mole would be ineffective in exciting C_2H_4 to the required energy level, which is presumably a vibrationally excited triplet state. Even for CO molecules having vibrational energy in excess of this, the transfer in a single collision of such large amounts of vibrational energy to ethylene, as either vibrational or electronic excitation, seems most improbable.

It would appear that the proposal that $Hg(^3P_1)$ and CO form a complex with an appreciable lifetime, put forward by Scheer and Fine (11) to explain the large rate of reaction [5], might account for the presently observed effect. Such a complex has been further discussed by Polanyi (16) in relation to the vibrationally excited CO observed by Karl and Polanyi (14). If it is assumed that the HgCO* complex is a reasonably long-lived one, retaining essentially all the energy of $Hg(^3P_1)$ and decomposing to $Hg(^1S_0)$ and a vibrationally excited CO, reaction [5] can be replaced by

[8] $$Hg(^3P_1) + CO \rightarrow HgCO^*$$

[9] $$HgCO^* \rightarrow Hg(^1S_0) + CO^{**}$$

and a further reaction can be written:

[10] $$HgCO^* + C_2H_4 \rightarrow Hg(^1S_0) + CO + C_2H_2 + H_2.$$

Can. J. Chem. Downloaded from www.nrcresearchpress.com by 210.87.254.6 on 09/05/12
For personal use only.

Incorporation of these reactions into the previous scheme leads to the overall equation

$$\frac{\Delta_2}{\Delta_1} = \frac{1 + k_4k_7[CO]/k_3(k_6 + k_7[C_2H_4]) + k_8k_{10}[CO]/k_3(k_9 + k_{10}[C_2H_4])}{1 + (k_4 + k_8)[CO]/(k_2 + k_3[C_2H_4])}.$$

Now, if the rate formerly assigned to reaction [5] is assigned to reaction [8], values for the ratio k_{10}/k_9 can be evaluated from the experimental values of Δ_2/Δ_1. For the 80 μ CO point in Fig. 4, this leads to $k_{10}/k_9 = 1.10 \times 10^7$ l mole^{-1}.

The theoretical curve using this value is shown in Fig. 4 as theory *b*. While the fit to the Δ_2/Δ_1 vs. P_{CO} curve is fair, this theory leads to a slightly nonlinear plot between $1/\Delta_2$ and $1/[C_2H_4]$. The linearity can be improved on the assumption of other reactions leading to the loss of active species, e.g. the reverse of reaction [8] or an interaction between $Hg(^3P_0)$ and CO, but these considerations have to remain qualitative in the absence of the necesssary data. Moreover, it must be remembered that kinetic equations have been used which are ideally only applicable to small amounts of decomposition. It appears therefore that such a mechanism can approach correspondence with the experimental results. The assumption of a HgCO* complex remains the most plausible explanation of the observed effects.

Effect of CO_2 and H_2O Addition

CO_2 appears to quench $Hg(^3P_1)$ to the ground state only, no $Hg(^3P_0)$ atoms being formed (12). In the absence of other effects, the addition of CO_2 should reduce the amount of decomposition by competitive quenching. As seen in Fig. 4, a reduction was observed, but the reduction was smaller than predicted by the available quenching cross sections (1). It is not clear whether this should be regarded as evidence for a special effect of CO_2. The addition of H_2O slightly increased the amount of decomposition of ethylene (Fig. 4). It is known (12) that H_2O quenches $Hg(^3P_1)$ to $Hg(^3P_0)$ but the cross section for this reaction is not known. In this case also it is not clear whether a special effect of H_2O exists. Since these gases showed only minor effects compared with that found with CO, they were not investigated in detail.

CONCLUSION

The experimental results reported here concerning the interaction of $Hg(^3P_1)$ atoms and CO provide support for earlier evidence that this interaction involves the formation of a HgCO* complex of appreciable lifetime. Such a complex, if it had a cross section for reaction with ethylene the same as that for $Hg(^3P_1)$ atoms with ethylene, would need to have a lifetime of about 3×10^{-5} s (from the deduced value of k_{10}/k_9). A shorter lifetime would necessitate a corresponding increase in the reaction cross section. Such a large cross section is perhaps not incompatible with the known affinity of metallic carbonyls for π-bonds. Attempts to detect a HgCO* complex spectroscopically would appear to be worthwhile.

REFERENCES

1. R. J. CVETANOVIĆ. Progress in reaction kinetics. Vol. II. Pergamon Press, London. 1964. p. 41.
2. F. P. LOSSING, D. G. H. MARSDEN, and J. B. FARMER. Can. J. Chem. **34**, 701 (1956).
3. P. KEBARLE and F. P. LOSSING. Can. J. Chem. **37**, 389 (1959).
4. D. J. LEROY and E. W. R. STEACIE. J. Chem. Phys. **11**, 676 (1942).
5. R. J. CVETANOVIĆ and A. B. CALLEAR. J. Chem. Phys. **23**, 1182 (1955).
6. P. KEBARLE. J. Phys. Chem. **67**, 716 (1963).
7. J. R. MAJER, B. MILE, and J. C. ROBB. Trans. Faraday Soc. **57**, 1342, 1692 (1961).
8. KANG YANG. J. Am. Chem. Soc. **86**, 3941 (1964).
9. M. W. ZEMANSKY. Phys. Rev. **36**, 919 (1930).
10. A. C. G. MITCHELL and M. W. ZEMANSKY. Resonance radiation and excited atoms. Cambridge University Press, Cambridge. 1934.

Can. J. Chem. Downloaded from www.nrcresearchpress.com by 210.87.254.6 on 09/05/12
For personal use only.

11. M. D. SCHEER and J. FINE. J. Chem. Phys. **36**, 1264 (1962).
12. A. B. CALLEAR and R. G. W. NORRISH. Proc. Roy. Soc. London, Ser. A, **266**, 299 (1962).
13. A. G. HARRISON and F. P. LOSSING. Can. J. Chem. **37**, 1478 (1959).
14. G. KARL and J. C. POLANYI. J. Chem. Phys. **38**, 271 (1963).
15. E. W. R. STEACIE. Atomic and free radical reactions. Reinhold Publishing Corporation, New York. 1954.
16. J. C. POLANYI. Appl. Opt. Suppl. 2 of Chem. Lasers, 109 (1965).

Can. J. Chem. Downloaded from www.nrcresearchpress.com by 210.87.254.6 on 09/05/12
For personal use only.

Can. J. Chem. Downloaded from www.nrcresearchpress.com by 210.87.254.42 on 09/05/12
For personal use only.

PROTON MAGNETIC RESONANCE LINE WIDTH AS A FUNCTION OF POLYMER TACTICITY[1]

S. BROWNSTEIN AND D. M. WILES
Division of Applied Chemistry, National Research Council, Ottawa, Canada

Received August 6, 1965

ABSTRACT

The high resolution proton magnetic resonance spectra of five samples of poly(methyl methacrylate) in chloroform solution have been measured with 100 Mc/s equipment. The widths of the absorption lines arising from the protons of the α-methyl and the methoxyl groups have been compared. The widths are greater when the polymer is predominantly syndiotactic than when it is predominantly isotactic. It is concluded that isotactic samples have the more extended conformation in chloroform solution. An analogy with dilute solution viscosity measurements is outlined in support of this conclusion. Differences between the widths of the lines of the methylene protons in a completely isotactic poly(methyl methacrylate) sample are attributed to long range spin coupling.

INTRODUCTION

High resolution proton magnetic resonance measurements have been used with considerable success in recent years to determine differences in stereoregularity for a number of different polymers. The method is applicable, at least in principle, whenever the resonance absorption for a particular proton exhibits a chemical shift, determined by the magnetic environment of that proton, which is unique to a particular steric configuration.

Poly(methyl methacrylate) (PMMA) was the first polymer to which the technique was applied. It was shown (1) that the chemical shift of the α-methyl group protons was determined by the configuration of substituents about the pseudo-asymmetric α-carbon atom in each unit of the polymer chain. The measurement of PMMA tacticities, based on this principle, is now considered routine.

It is the purpose of this communication to describe differences in proton absorption line widths, for different PMMA samples, which can be correlated with differences in polymer tacticities. These data will be related qualitatively to chain flexibility and relative conformational geometry. It also appears to be possible with 100 Mc/s apparatus to detect differences in line widths which may be due to proton spin coupling over longer distances than have been considered heretofore for these materials.

EXPERIMENTAL

One fraction from each of five polymer samples was used in this work. The conditions under which these polymers were prepared can be summarized as follows.

A.—This sample was prepared in tetrahydrofuran solution at −78 °C with magnesium diethyl initiator; [MMA] = 1 M; [$Mg(Et)_2$] = 45 mM. After removal of the petroleum ether soluble material, this sample was used without further fractionation.

B.—This polymer was prepared in benzene solution at 60 °C with 2,2′-azo-bis-isobutyronitrile initiator.*

C.—Polymerization was carried out in toluene solution at −30 °C with *n*-butyllithium initiator; [MMA] = 0.25 M; [BuLi] = 3.85 mM.

D.—This sample was prepared in toluene solution at −30 °C with *n*-butyllithium initiator in the presence of added lithium methoxide; [MMA] = 0.125 M; [BuLi] = [LiOMe] = 7.6 mM.

E.—Polymerization was carried out in toluene solution at 0 °C with phenylmagnesium bromide initiator; [MMA] = 0.5 M; [ϕMgBr] = 36 mM.

The anionic polymerizations (A, C—E) were carried out in an all-glass vacuum apparatus which could be prewashed with butyllithium solution. The monomer and solvents were rigorously purified on a vacuum line.

[1]*Issued as N.R.C. No. 8705.*

**Prepared by Dr. J. M. G. Cowie of these laboratories.*

The butyllithium was obtained in hexane solution from the Foote Mineral Company and the Grignard reagent as a diethyl ether solution from Peninsular Chemical Research, Inc. Details of the manipulation of reagents and of the polymerization procedure were similar to those described elsewhere (2).

The polymers (except A) were separated into fractions by a precipitation technique which has been published previously (3). The molecular weights of the fractions were derived from their viscosities measured in chloroform solution at 25 °C with Cannon–Ubbelohde dilution viscometers. One fraction, having a molecular weight of the order of 1 to 2×10^4, was to be selected from each polymer sample. The viscosity – molecular weight relationship used (3) is not particularly accurate below 2×10^4 but would certainly be adequate for this purpose.

The proton magnetic resonance spectra of the five selected polymer fractions were measured in chloroform solution (12%, w/v) at 70 °C (thermostatted probe) with a Varian HR100 spectrometer which had been modified to operate by a "time division pulsing scheme" (4). The spectra were calibrated with sidebands produced by audio modulation. Line widths were measured in cycles/s at half height. The widths quoted for the peaks arising from protons in the polymer molecules have had the value of the line width of the solvent peak subtracted from them. This was done to compensate for any slight difference in spectrometer resolution when obtaining the various spectra.

RESULTS AND DISCUSSION

A summary of the data obtained from the proton resonance spectra is shown in Table I. The tacticities were obtained in the usual way by measuring the relative areas of the peaks due to absorption by the protons of the α-methyl group. The half-height widths of the peaks in the spectra of fractions A/2 and B/F7 which arise from α-methyl group protons in syndiotactic configurations are significantly larger than the corresponding widths of the isotactic peak for fractions C/I2, D/H2, and E/9A. Similarly the widths of the methoxyl peaks for the former fractions are greater than for the latter, more isotactic fractions. It seems most reasonable to attribute the difference in peak widths to differences in freedom of molecular motion within the samples. There being no significant differences in fraction molecular weight or in solution concentration the peak width change with changing tacticity must arise because of differences in polymer chain segment flexibility. It is logical to suggest, therefore, that at a given temperature in chloroform as solvent, more isolated segmental motion can occur in an isotactic PMMA molecule in concentrated solution than in a syndiotactic molecule.

There is evidence from viscosity measurements in theta solvents (5, 6) that the unperturbed chain dimension for isotactic PMMA is greater than for atactic PMMA* in dilute solutions. In nitromethane solution the order of decreasing PMMA chain dimension is isotactic > atactic > syndiotactic (6). In a good solvent such as chloroform, viscosity measurements with dilute solutions indicate that the dimensional differences are much less pronounced but nevertheless an isotactic chain appears to be more extended than a syndiotactic chain.

It is reasonable to suppose that the relative order of chain dimensions for the tactic forms of PMMA remains the same in the more concentrated solutions used for proton magnetic resonance measurements. Qualitative observations show that, for comparable polymer molecular weights, a chloroform solution of isotactic PMMA is more viscous than a solution of syndiotactic PMMA in the 10–15% concentration range. An analogy appears to exist, therefore, such that in concentrated solutions an isotactic PMMA chain is more extended than a syndiotactic chain, as is found to be the case in dilute solutions. It would be expected that in the more extended conformation greater localized segmental motion can occur. This concept provides some support for the explanation of the narrower peak widths reported in Table I for the isotactic fractions.

**Atactic or "conventional" PMMA has by no means a random arrangement of configurations. Ordinarily it is prepared above room temperature with a radical initiator and has an appreciable content of syndiotactic triads (cf. Table I, fraction B/F7).*

Can. J. Chem. Downloaded from www.nrcresearchpress.com by 210.87.254.42 on 09/05/12
For personal use only.

Can. J. Chem. Downloaded from www.nrcresearchpress.com by 210.87.254.42 on 09/05/12
For personal use only.

TABLE I

Effect of polymer tacticity on proton line widths

Sample/fraction	$\bar{M}_v \times 10^{-4}$	Triads (%)			Line widths (cycles/s)				
		Isotactic	Heterotactic	Syndiotactic	$\Delta CHCl_3$	W_s	W_I	W_{OCH_3}	W_{CH_2}
A/2	2.1	—	11	89	1.28	8.2		3.3	13.6
B/F7	2.2	5	30	65	1.24	7.3		3.7	
C/I2	1.2	68	22	10	1.23		4.9	1.4	
D/H2	2.0	79	14	7	1.72		5.3	1.9	
E/9A	1.0	100	—	—	1.26		5.0	2.0	4.0 and 6.4

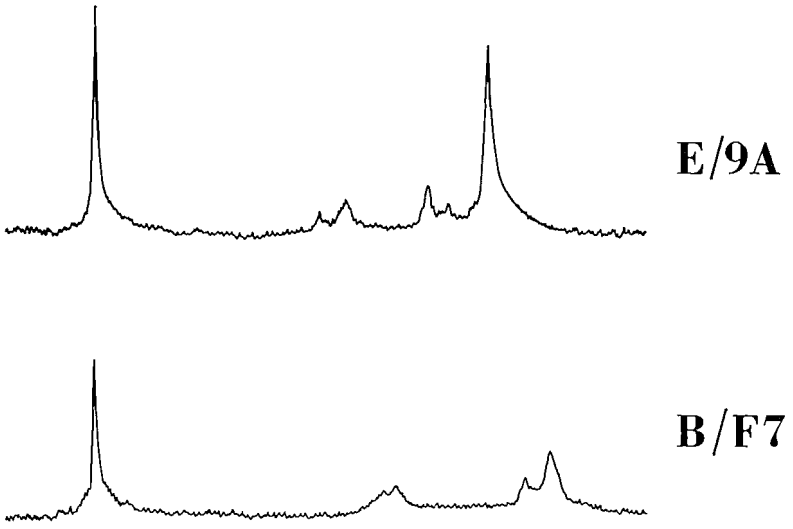


FIG. 1. The 100 Mc/s proton magnetic resonance spectra of two PMMA fractions with different tacticities.

In an isotactic sequence the methylene protons are magnetically non-equivalent. Therefore, a typical AB pattern of two non-equivalent, spin-coupled nuclei is obtained. Previously reported PMMA spectra were normally obtained at lower operating frequencies. Under these conditions the higher field peak of one of the methylene protons slightly overlapped the peak of the isotactic α-methyl group. By operation at 100 Mc/s it is possible to resolve clearly all the peaks from the isotactic methylene protons in fraction E/9A. Those at lower field are approximately 2.4 cycles/s wider than the ones at higher field (Table I). Since both methylene protons should experience the same freedom of motion the extra width for the low field protons may be attributed to a long range spin coupling to the protons of the α-methyl group.

It has generally been assumed, on the basis of spectra obtained at lower operating frequencies, that chemical shifts of methylene protons in syndiotactic and heterotactic sequences in the same polymer molecule are the same. From the proton resonance spectrum of fraction B/F7 it may be seen that separate peaks for each type are barely resolved. This slight difference in chemical shift may account for the unusually broad peak normally observed for the methylene group in largely syndiotactic and heterotactic samples. The spectra of polymer samples E/9A and B/F7 are shown in Fig. 1.

ACKNOWLEDGMENTS

The authors are grateful to Dr. S. Bywater and Dr. J. M. G. Cowie for helpful discussions, and to Mr. P. E. Black for technical assistance.

REFERENCES

1. F. A. BOVEY and G. V. D. TIERS. J. Polymer Sci. **44**, 173 (1960).
2. D. M. WILES and S. BYWATER. Polymer, **3**, 175 (1962).
3. B. J. COTTAM, D. M. WILES, and S. BYWATER. Can. J. Chem. **41**, 1905 (1963).
4. J. PAASIVIRTA and S. BROWNSTEIN. J. Am. Chem. Soc. **87**, 3593 (1965).
5. I. SAKURADA, A. NAKAJIMA, O. YOSHIZAKI, and K. NAKAMAE. Kolloid-Z. **186**, 41 (1962).
6. S. BYWATER, J. M. G. COWIE, and D. M. WILES. Paper presented at the 12th Canadian High Polymer Forum, Ste. Marguerite, P.Q. 1964.

Can. J. Chem. Downloaded from www.nrcresearchpress.com by 210.87.254.42 on 09/05/12
For personal use only.

Can. J. Chem. Downloaded from www.nrcresearchpress.com by 210.87.254.5 on 09/05/12
For personal use only.

STEREOCHEMISTRY AND SEVEN COORDINATION[1]

T. A. CLAXTON[2] AND G. C. BENSON
Division of Pure Chemistry, National Research Council, Ottawa, Canada

Received August 11, 1965

ABSTRACT

A method is described to calculate the equilibrium configuration of any number of identical particles restricted to a spherical surface and interacting with forces derivable from an interparticle potential of the form r^{-n}. It is shown that distributions of symmetry C_2 are expected for seven particles when n is small. In certain cases, the model can be used to explain the shape of molecules of the type MX_m. The importance of directed valence in these molecules is considered and the structure of IF_7 discussed.

INTRODUCTION

Gillespie (1) has proposed that the arrangement of the electron pairs in the valency shell of a central atom of a polyatomic molecule can be predicted by considering the equilibrium configuration of similar particles on the surface of a sphere with an appropriate law of force between the particles. For numbers from two to eight it has been shown by Shütte and van der Waerden (2) that the arrangements predicted by maximizing the least distance between any two particles agree with those given by Föppel (3) for an interparticle potential of r^{-1} (i.e. an inverse square law of force), except for the case of seven particles. It is concluded that for any number of particles from two to eight, except seven, the minimum energy arrangement is independent of the force law. For the case of seven electron pairs we reproduce in Fig. 1 the three possibilities (D_{5h}, C_{2v}, C_{3v}) suggested by Gillespie as the force law is varied.

The most probable arrangement, for an interparticle potential proportional to r^{-n}, with large n is the C_{3v} structure. For $n = 1$ the D_{5h} structure is energetically more favorable. Gillespie suggests that the C_{2v} structure is an equilibrium arrangement for $1 < n < \nu$, where ν is large. Britton (4) has shown that the energy of the C_{2v} configuration is indeed less than both the C_{3v} and D_{5h} structures in the region $n = 4$. Thus Gillespie's suggestion is supported but since the energies of all the structures considered in this region are nearly equal it implies that less important forces obeying a different analytical form may be dominant in determining the structure.

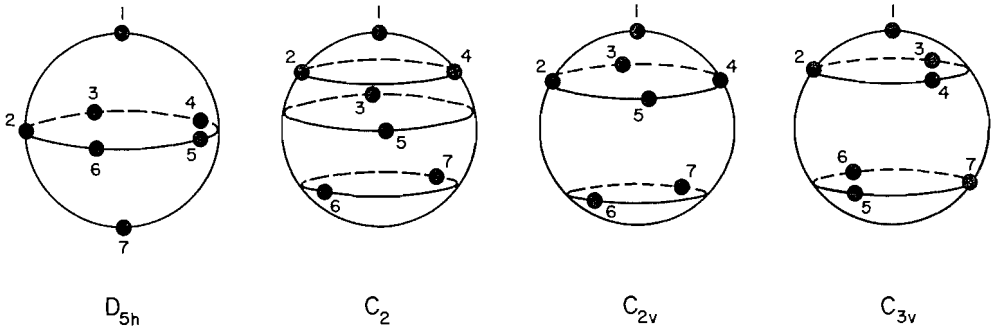


FIG. 1. Arrangements of seven particles on the surface of a sphere.

[1]*Issued as N.R.C. No. 8710.*
[2]*National Research Council of Canada Postdoctorate Fellow 1961–1963. Present address: Department of Chemistry, The University, Leicester, England.*

Since the three structures are not too different, it seems possible that the transition from one structure to another may occur through a complete spectrum of intermediate configurations. Indeed, it is reasonable to consider the C_{2v} structure as a perturbed form of either the C_{3v} or the D_{5h} structures. From Fig. 1 the similarity of the D_{5h} and C_{2v} structures can be appreciated by comparing the groups of particles 2;1,3,6,7;4,5 of D_{5h} with the groups 1;2,3,4,5;6,7 of C_{2v}. Also the groups 7;3,4,5,6;1,2 of C_{3v} are suitable for comparison with C_{2v}. The recent differences of opinion (5–8) concerning the structure of IF_7 may be attributed to this similarity especially since the molecule may be distorted (7). For this molecule, with identical ligands, it is somewhat surprising that the structure determined is not regular. As Gillespie and Nyholm (9) point out, the shapes predicted for molecules with electron pairs up to six are correct without exception. Any distortion incurred for systems with identical ligands is restricted to change in bond length along a unique axis (e.g. PCl_5). Such does not appear to be the case with IF_7. There does not seem to be any proof indicating that the D_{5h} structure is more stable than any other, except for $n = 1$. Britton has shown that both the C_{2v} and C_{3v} configurations have higher energies for $n < 4$, but did not prove that the D_{5h} structure has the lowest energy. From the comparison of the structures in Fig. 1 and the distorted form of IF_7, it would seem that intermediate structures of lower symmetry might be more favorable in the region of small n ($1 < n < 6$).

In order to investigate this possibility, a more general method than that of Britton is required. The latter restricts the number of degrees of freedom to those needed to specify configurations having a particular symmetry and then minimizes the energy. This approach is reasonable but becomes inadequate when the symmetry restrictions are removed.

A completely satisfactory solution of the problem calls for the determination of the configuration corresponding to an absolute minimum of the energy when the only condition imposed is that the particles must be located on a sphere. The method of calculation we have used falls somewhat short of the ideal goal since it provides a way only for finding relative minima of the energy and does not ensure the absolute stability of the configuration. However, it does offer a much more powerful approach than employed previously and merits brief description.

METHOD OF CALCULATION AND RESULTS

The location of each particle, of a set of m identical particles, is indicated by its Cartesian coordinates x_i, y_i, z_i (for the i-th particle). Restriction to a sphere of unit radius imposes the condition

$$x_i^2 + y_i^2 + z_i^2 = 1. \qquad [1]$$

The repulsive energy of interaction of the particles is assumed to be

$$E = \sum_{i=1}^{m-1} \sum_{j=i+1}^{m} r_{ij}^{-n} \qquad [2]$$

where r_{ij} is the distance between particles i and j and n is a constant (integer or non-integer).

Starting from any arbitrary configuration, an iterative procedure based on the method of steepest descent is used to displace the particles towards a minimum energy configuration. The latter is distinguished by the fact that the resultant tangential force on each particle is zero. This method of seeking a balance of forces, rather than attempting to minimize the energy directly, has the advantage of being more sensitive in situations where the energy surface is very flat near the minimum.

Can. J. Chem. Downloaded from www.nrcresearchpress.com by 210.87.254.5 on 09/05/12
For personal use only.

The x-component of the force on the i-th particle is

$$[3] \qquad F_{xi} = n \sum_{j=1}^{m}{}' (x_i - x_j)\ r_{ij}^{-(n+2)}$$

where the prime on the summation indicates the omission of the term for $j = i$. Defining the other components (F_{yi} and F_{zi}) by similar equations, the magnitude of the force on the i-th particle is given by

$$[4] \qquad F_i = (F_{xi}^2 + F_{yi}^2 + F_{zi}^2)^{1/2}.$$

At any stage in the iterative calculation, each particle is allowed to move in the direction of the resultant force acting on it. Generally this will take the particle off the sphere and the distance from the center must be renormalized. The new x-coordinate of particle i is then

$$[5] \qquad x_i(\text{new}) = (x_i + \gamma F_{xi})/[(x_i + \gamma F_{xi})^2 + (y_i + \gamma F_{yi})^2 + (z_i + \gamma F_{zi})^2]^{1/2}$$

and similar expressions can be written for the y- and z-coordinates. The quantity γ is a scale factor which determines the extent of the displacement. Assignment of an optimum value to γ is difficult; small values lead to excessive numbers of iterations while too large a γ causes instability of the calculation. Experience has shown that a reasonable compromise can be obtained by setting

$$[6] \qquad \gamma = K/F_{\max}$$

where K is a constant and $F_{\max}$ is the largest value of F_i ($i = 1$ to m). In our calculations a value of K equal to 0.1 or 0.2 generally was satisfactory.

In effect, eqs. [5] and [6] correspond to displacing the particle experiencing the largest force by a vector of magnitude K (the vector being in the direction of the force) and altering the positions of the other particles by proportionally smaller vectors. Each particle is then moved along its new radius vector until it is again on the unit sphere.

The resultant force on any particle in a distribution of a particular symmetry must obey the operations of the symmetry point group. Hence if we let each particle move from one distribution to another along the directions of force, the symmetry of the distribution will be maintained. This is important since it means the general method can be used to determine the equilibrium configuration of specified symmetries. But it can also be a disadvantage since an arbitrary initial configuration (ideally containing only the identity symmetry element) may accidentally pick up undesired elements of symmetry during the process of the calculation. The consequences are obvious but it is assumed that they can be avoided by taking more than one starting configuration.

TABLE I

Repulsive energies (in arbitrary units) at zero tangential force condition

n	$E(D_{3h})$	$E(C_2)$	$E(C_{2v})$	$E(C_{3v})$
2.0	10.2500	10.2502	10.2588	10.2601
2.5	8.7202	8.7202	8.7290	8.7305
3.0	7.4648	7.4641	7.4718	7.4734
3.5	6.4268	6.4248	6.4302	6.4318
3.84165	5.8196	5.8159	5.8196	5.8211
4.0	5.5625	5.5578	5.5606	5.5620
4.2	5.2576	5.2512	5.2532	5.2544
4.6	4.7075	4.6969	4.6973	4.6983
5.0	4.2269	4.2102	4.2102	4.2108
5.598	3.6159	3.5885	3.5885	3.5885

Can. J. Chem. Downloaded from www.nrcresearchpress.com by 210.87.254.5 on 09/05/12
For personal use only.

TABLE II

Spherical angular coordinates of particles in the C_2, C_{2v}, and C_{3v} configurations calculated for $n = 2$, 4, and 5.6

	C_2		C_{2v}		C_{3v}	
	ϕ	θ	ϕ	θ	ϕ	θ
$n=2$	.0	.0	.0	.0	.0	.0
	.0	72.4	.0	80.6	.0	73.5
	180.0	72.4	180.0	80.6	120.0	73.5
	−93.2	89.5	−97.9	80.6	−120.0	73.5
	86.8	89.5	82.1	80.6	60.0	129.1
	−11.7	144.0	−48.9	144.0	−60.0	129.1
	168.3	144.0	131.1	144.0	180.0	129.1
$n=4$	.0	.0	.0	.0	.0	.0
	.0	74.3	.0	79.9	.0	74.1
	180.0	74.3	180.0	79.9	120.0	74.1
	−96.3	86.8	−97.6	79.9	−120.0	74.1
	83.7	86.8	82.4	79.9	60.0	129.7
	−27.3	143.7	−48.8	143.7	−60.0	129.7
	152.7	143.7	131.2	143.7	180.0	129.7
$n=5.6$	.0	.0	.0	.0	.0	.0
	.0	79.2	.0	79.5	.0	74.5
	180.0	79.2	180.0	79.5	120.0	74.5
	−97.5	79.7	−97.5	79.5	−120.0	74.5
	82.5	79.7	82.5	79.5	60.0	130.1
	−48.0	143.4	−48.7	143.4	−60.0	130.1
	132.0	143.4	131.3	143.4	180.0	130.1

The treatment outlined above is well suited for calculation on a digital computer and, in our work, was programmed for an IBM 1620. A few initial calculations for the case of seven particles showed that distributions with lower energies than the configurations proposed by Gillespie did exist. We chose first to determine those values of n for which the configurations D_{5h} and C_{2v}, and C_{2v} and C_{3v} have identical energies. These situations occur for $n = 3.84165$ and 5.598 respectively. In the former case it is definite that a distribution of C_2 symmetry (see Fig. 1) has a lower energy. This finding prompted further calculations for other n, the results of which are summarized in Table I. These clearly indicate that the C_{2v} distribution never possesses the lowest energy uniquely. For the region $2 < n < 5.6$ a distribution with C_2 symmetry is favored. This configuration is illustrated in Table II where the polar coordinates (θ = colatitude, ϕ = azimuth) of the particles are given for calculations with $n = 2$, 4, and 5.6. For comparison, the corresponding C_{2v} and C_{3v} configurations are also listed.

DISCUSSION

The results show that for seven particles on a sphere the distribution of C_2 symmetry (1:2:2:2) is the most stable for $2 < n < 5.6$. On this basis, we expect seven-coordinated compounds to have similar structures with this symmetry. This conclusion is not strictly correct, since the distributions of particles are calculated using the condition that the tangential forces are zero. The perpendicular forces are not taken into account. For 2, 3, 4, and 6 particles on a sphere, the symmetry of the distributions require the perpendicular force to be the same for every particle. Such structures are found to be undistorted for molecules with the same number of equivalent ligands, unless the non-bonding electron distribution of the central atom is unsymmetrical, as it is in some transition metal ions. Five particles give a trigonal bipyramid. The two particles on the threefold symmetry axis belong to a different symmetry species from those on the twofold symmetry axes and

Can. J. Chem. Downloaded from www.nrcresearchpress.com by 210.87.254.5 on 09/05/12
For personal use only.

Can. J. Chem. Downloaded from www.nrcresearchpress.com by 210.87.254.5 on 09/05/12
For personal use only.

hence these two sets of particles may have different perpendicular forces. It is easily shown that the two particles on the threefold axis have a larger force for an interparticle potential r^{-1}. This explains the greater bond lengths along this axis for molecules such as PCl_5. Since for seven particles, we have suggested that the most probable symmetry is C_2, there are four different perpendicular forces possible, one for each of the groups 1:2:2:2 (corresponding to the particles 1;2,4;3,5;6,7 of the C_2 structure in Fig. 1). The restriction of the sphere is extremely important in this case. Possibly even for $n = 1$, the C_2 structure without the restraining influence of a sphere would be lower in energy than the D_{5h} structure, because of the higher number of degrees of freedom. Thus it is possible that the C_2 structure is the most favorable for a larger range of n than has already been suggested. Such an arrangement is shown later to be consistent with the structure of IF_7 (7). XeF_6 and $SbBr_6^{3-}$ can also be classified as having seven electron pairs in the valence shell. The structure of XeF_6 is unknown (10) but it behaves spectroscopically like a symmetrical molecule (11); $SbBr_6^{3-}$ is reported to be octahedral (12). Thus neither of these molecules appear to have the predicted distorted structure.* The basic arguments used by Gillespie and Nyholm (9), and later by Gillespie (1), require the use of directed valence orbitals which exist, in the same region of space as so-called lone pair orbitals, even when the orbital is not involved in bonding. This very useful picture has been extensively employed although (13) 'there is no causal relationship between the mathematical convenience of the orbital approximation and the occurrence of directed valences'. Evidence from theoretical studies of simple hydrides of elements in the first row of the periodic table is accumulating which indicates that it is very doubtful that a directed lone pair orbital occupies the same region of space as it would if it were a bonding orbital. Theoretical work, based on the Hellmann–Feynman theorem, has been interpreted as showing that (14) 'in hydride molecules which possess at least one lone pair of electrons the bond orbitals will be primarily of p character and the lone pair orbitals will contain close to the maximum amount of s character'. Possibly the importance of the concept of directed valence, especially regarding the spatial distribution of the lone pairs, has been overstressed (15). Gray and Pritchard (13) are of this opinion and suggest dividing compounds of the type MH_m into two classes: (*a*) where the nuclear repulsion term dominates, and (*b*) where the *net* electron attraction term is most important.

The ideas of Gillespie and Nyholm (9) and of Gray and Pritchard (13) lead to similar predictions for the shapes of molecules not containing lone pairs of electrons and in which the central atom is less than seven coordinated. Gillespie (1) showed that for these cases the molecular shape could be predicted by assuming the arrangement depended on an interparticle potential r^{-n}. Since the results were found to be independent of n, it can be concluded that either nuclear electrostatic repulsions or Pauli forces are the major factors in determining the shape. The presence of lone pairs in the valence shell will generally make the *net* electron attraction term dominant. Gray and Pritchard do not indicate the qualitative expectations in such cases but Nyholm and Gillespie have discussed them very convincingly. However, situations must arise where so many ligands are crowded around a central atom that the nuclear repulsion term is dominant whether or not the valence shell contains lone pairs. It seems reasonable to suggest that for molecules of the type MX_m, for $m \geqslant 6$, the shape may be determined solely by the repulsion between the ligands. As mentioned earlier, a symmetrical structure is reported for $SbBr_6^{3-}$. The

**Since the manuscript of this paper was submitted, preliminary results of an electron diffraction study of gaseous XeF_6 have been reported by Bartell, Gavin, and Thompson (J. Chem. Phys. 43, 2547 (1965)). These indicate a definite departure of the XeF_6 molecule from octahedral symmetry.*

valence shell of this molecule contains 14 electrons and if the structure is determined by nuclear repulsions, the bonding orbitals used are of secondary importance. However, for true octahedral symmetry the electron distribution must be compatible. It is sufficient to note that the 14 valence electrons can occupy the 4f shell to achieve spherical symmetry. This is more than enough to satisfy the minimum symmetry requirements.

In any set of molecules, say MX_m, for $m = 2, 4, 6$, only one of these, $m = 6$, can possibly have the nuclear repulsion term dominant. If the MX_4 structure were governed by this term it would be difficult to explain the stability of MX_6. In some molecules, for example SiF_4, it is unnecessary to know which term is more important since both arguments lead to the tetrahedral structure when no lone pairs are present. Since SiF_6^{2-} exists, the *net* electron attractive term is apparently dominant. This idea is supported by the failure of the nuclear spin–spin coupling constant in its reduced form (16) to give a linear dependence on the atomic number of the central atom in the series CF_4, SiF_4, GeF_4. The similarly reduced coupling constants for the series SiF_6^{2-}, PF_6^-, SF_6 vary linearly with atomic number (16, 17). It appears that the correlations obtained by Reeves (18) hold in every case where the nuclear repulsion term is expected to be dominant, and that the latter may be responsible for their existence.

Since IF_7 has no lone pairs in the valence shell, we cannot distinguish between Gillespie's model of seven particles on a sphere and that of Gray and Pritchard. However, there is no doubt that the structure is determined by the nuclear repulsion term. Let us assume that the valence electrons are distributed with an overall spherical symmetry. This allows us to consider the interaction of the central iodine atom with the fluorines to be a function of the radial distance only. Thus there is some justification for using a spherical surface for distribution of the particles. Possibly we should use an inverse square force law to describe the interaction but as already mentioned the C_2 distribution will probably be more stable than the D_{5h}, once we allow particles to move off the spherical surface. Although calculations have indicated that this is true it is not clear how to make an unequivocal comparison. For example, one basis for a fair comparison would be to insist that all the particles have in addition to a zero tangential force an identical perpendicular force. The difficulty with this approach is that an assumption has to be made about the nature of the central attractive force holding the molecule together. It is therefore clear that predictions of molecular structure derived from calculations for particles on a sphere are less reliable in the case of seven particles than when smaller numbers are considered.

As a check on these ideas we have taken the results for $n = 3$ to 5 and have calculated the perpendicular force on each particle in the C_2 configuration. It is found that particles 6 and 7 experience the largest forces and we would expect these to move out radially relative to the other particles. This is consistent with the observation of Burbank (7) that the fluorine atoms in these positions have the largest I—F bond distances in IF_7. However, Donohue (8) has recently questioned the conclusions of Burbank and suggests that 'it is not possible at the present time to demonstrate that the molecular symmetry is different from D_{5h}'. This uncertainty in the molecular structure does not affect our arguments, but emphasizes the similarity of the different symmetry types already discussed. It should be stressed that none of our results can be used to contribute to the present controversy (7, 8).

Although we cannot expect to calculate the structural details of any molecule (especially in cases of low symmetry) from the model of particles on a sphere, it appears that this approach does offer some help in understanding the factors governing molecular shape. The concept of the localized bond, which is very useful, especially for molecules without lone pair electrons, is unnecessarily rigid and does not explain the structure of IF_7 in the

Can. J. Chem. Downloaded from www.nrcresearchpress.com by 210.87.254.5 on 09/05/12
For personal use only.

natural way outlined above. It is appreciated that this model was proposed by Gillespie to represent the interaction of electron pairs in the valence shell, but we have chosen to identify the particles with atoms in those cases where the nuclear repulsion term is expected to be dominant. In this way the structure of $SbBr_6^{3-}$ can be discussed.*

ACKNOWLEDGMENT

We are indebted to Messrs. L. Marks and J. Taylor of the N.R.C. Computation Centre for suggesting the method of steepest descent used in this work and for programming assistance.

REFERENCES

1. R. J. GILLESPIE. Can. J. Chem. **38**, 818 (1960).
2. K. SHÜTTE and B. L. VAN DER WAERDEN. Math. Ann. **123**, 96 (1951).
3. L. FÖPPEL. J. Reine Angew. Math. **141**, 251 (1912).
4. D. BRITTON. Can. J. Chem. **41**, 1632 (1963).
5. J. DONOHUE. J. Chem. Phys. **30**, 1618 (1959).
6. R. D. BURBANK. J. Chem. Phys. **30**, 1619 (1959).
7. R. D. BURBANK. Acta Cryst. **15**, 1207 (1962); **16**, 700 (1963).
8. J. DONOHUE. Acta Cryst. **18**, 1018 (1965).
9. R. J. GILLESPIE and R. S. NYHOLM. Quart. Rev. **11**, 339 (1957).
10. J. G. MALM, H. SELIG, J. JORTNER, and S. A. RICE. Chem. Rev. **65**, 199 (1965).
11. E. E. WEAVER, B. WEINSTOCK, and C. P. KNOP. J. Am. Chem. Soc. **85**, 111 (1963).
12. TABLES OF INTERATOMIC DISTANCES AND CONFIGURATION IN MOLECULES AND IONS. Chem. Soc. London, Spec. Publ. **11** (1958).
13. B. F. GRAY and H. O. PRITCHARD. J. Chem. Phys. **25**, 779 (1956).
14. R. F. W. BADER and G. A. JONES. Can. J. Chem. **41**, 586 (1963).
15. T. A. CLAXTON. Chem. Ind. London, 1713 (1964).
16. P. T. INGLEFIELD and L. W. REEVES. J. Chem. Phys. **40**, 2425 (1964).
17. L. W. REEVES. J. Chem. Phys. **40**, 2423 (1964).
18. L. W. REEVES. J. Chem. Phys. **40**, 2128 (1964).

**A referee has kindly pointed out that Brown (Can. J. Chem. 42, 2758 (1964)) has shown that $TeBr_6^{2-}$, which is isoelectronic with $SbBr_6^{3-}$, is also octahedral. The fact that Brown has ascribed the symmetry of this ion to repulsions between the closed shells of the ligands rather than to nuclear repulsion is in our opinion merely a matter of emphasis. Thus considered along the lines outlined above, $TeBr_6^{2-}$ is clearly a case where the nuclear repulsion term dominates over the net electron attraction term. Brown attributes the repulsion specifically to the interactions between the closed shells of the bromines.*

Can. J. Chem. Downloaded from www.nrcresearchpress.com by 210.87.254.5 on 09/05/12
For personal use only.

THERMAL OXIDATION OF SARAN CARBON

PART I. STUDIES UNDER STATIC OXYGEN SYSTEM

R. G. BARRADAS, M. J. DIGNAM, AND D. D. CHADHA
Department of Chemistry, University of Toronto, Toronto, Ontario

Received April 26, 1965

ABSTRACT

Oxidation studies from 425 to 600 °C of porous carbons obtained from the pyrolytic decomposition of pure polyvinylidene chloride have been carried out in static oxygen systems. Measurements of weight change were made by means of a sensitive thermal microbalance. Empirical activation energies for the oxidation reaction were determined to be approximately 1 eV in magnitude, and comparison is made with previously published results for graphite. Carbon samples obtained from polymers compressed at different molding pressures showed somewhat different temperature and pressure rate dependence. An unusual pressure dependence was observed for the rate of reaction, and a tentative explanation is offered.

Can. J. Chem. Downloaded from www.nrcresearchpress.com by 210.87.254.5 on 09/05/12
For personal use only.

INTRODUCTION

Adsorption studies (1, 2, 3) and surface diffusion of gases (4, 5) on "Saran charcoal", a carbon obtained by the complete pyrolytic decomposition of pure polyvinylidene chloride, have been previously reported. Other adsorption studies on a similarly named Saran charcoal were published earlier on carbon prepared from a commerical copolymer of vinylidene chloride and vinyl chloride (6). An extensive investigation of the physicochemical properties of porous carbons is now being carried out in this laboratory, but the present paper is confined to reporting only the results of thermal oxidation studies of Saran charcoal under static conditions.

Saran carbon has been selected for this investigation because of its unique properties. It is a hard, strong, highly porous form of carbon with very regular surface and bulk properties (7, 8). In contrast, pyrolysis of many other polymers leads initially to tar formation and hence to carbon residues with non-uniform surfaces and irregular pore structures (3).

Interest in oxidation studies of this carbon stems in part from its possible development as a diffusion-type fuel cell electrode (9, 10) as well as in other electrode applications where oxidation of the carbon electrode can be of importance. Examples of the latter are electrochemical oxidations of organic compounds at carbon electrodes in strong oxygenated mineral acids where complex anodic chronopotentiometric behavior is observed (11) and the oxidative deterioration of carbon electrodes in the industrial manufacture of chlorine and chlorates (12).

EXPERIMENTAL

The apparatus, which is described in detail elsewhere (13), consists of an automatically recording Sartorius-Werke vacuum microbalance in conjunction with a vacuum furnace and associated vacuum equipment. The balance assembly has a load capacity in excess of 1 g and can detect weight changes as low as 3×10^{-7} g. The furnace temperature is maintained constant to ± 0.1 °C or better and uniform over 4 in. of the central portion to about ± 0.05 °C. The internal diameter of the furnace chamber is 4 cm, and the entire apparatus may be evacuated to pressures of about 3×10^{-6} Torr.

Saran carbon samples of approximately 0.5 g were prepared from pure polyvinylidene chloride powder, which was compressed into "flat" cylinders in a stainless steel die of 0.5 in. diameter by means of a Carver hydraulic press. Samples of the molded polymer were made by the application of 10 000 and 15 000 lb/in.^{2} pressures (referred to as type A and type B samples respectively in subsequent discussion). Before pyrolysis a small hole was drilled in each sample to facilitate its attachment (when fully carbonized) to the platinum

wire suspended from the microbalance beam. The complete pyrolytic decomposition of the polyvinylidene chloride samples and the subsequent determination of porosities by argon adsorption measurements were carried out according to previously described procedures (8). Oxygen was purified by liquefaction in a trap, using liquid nitrogen as refrigerant, followed by distillation; the middle fraction of the distillate was stored in a 2 l storage bulb for subsequent use.

The Saran carbon was introduced into the apparatus and manipulated until it hung centrally in the reaction chamber. After the sample was counterbalanced, the apparatus was evacuated, and the reaction chamber heated to 600 °C and kept at that temperature for 24 h to ensure that the carbon was outgassed. With this procedure, pressures of 5×10^{-5} Torr or better could be maintained at 600 °C. For an experimental run the temperature of the reaction chamber was set at the desired value, then oxygen was admitted to a known pressure. The initial oxygen pressure and subsequent total pressure were measured with an oil (dibutyl phthalate) manometer which could be read by a cathetometer to within ±0.015 Torr. The first measurement of weight changes, shown as positive increments in Figs. 1 and 2, were made not less than 30 s after the introduction of oxygen. The effect on the oxidation rate of varying the temperature and the oxygen pressure was followed in a systematic manner for the two sets of Saran carbons prepared by the different initial molding compression pressures.

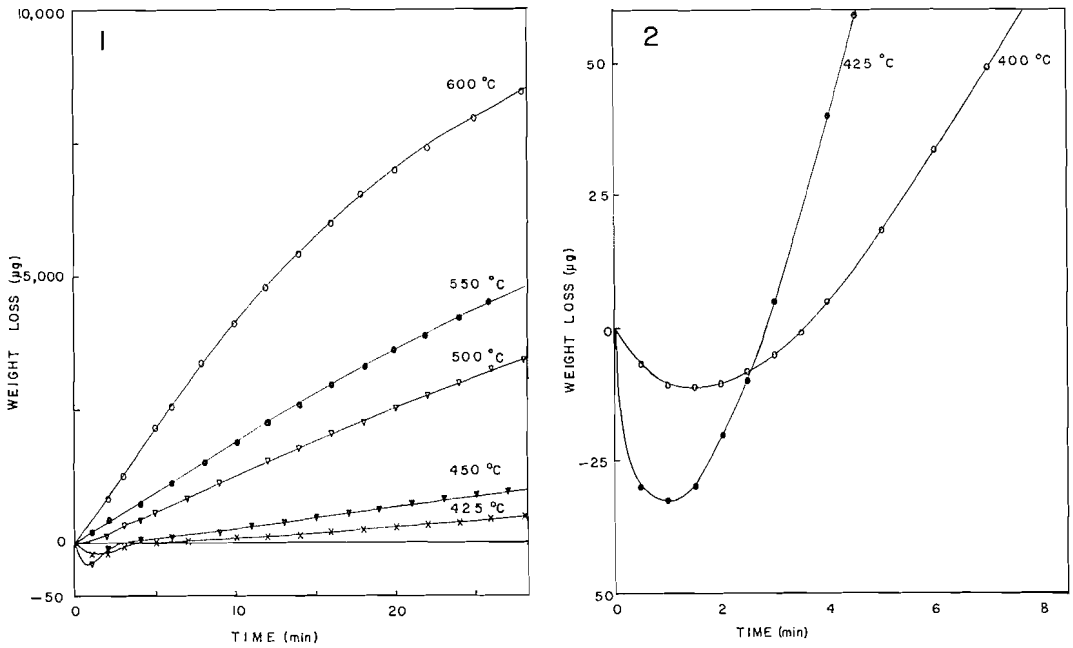


FIG. 1. Weight loss as a function of time for sample A for oxidation temperatures ranging from 425 to 600 °C and for an initial oxygen pressure of 4.5 Torr.

FIG. 2. Weight change as a function of time for sample A at 400 and 425 °C at an initial oxygen pressure of 19.7 Torr.

RESULTS

Outgassing at 400 °C for 24 h was inadequate to expel all sorbed species, and constancy in weight of the carbon could only be attained after heating the sample *in vacuo* at 600 °C for the same period of time.

The data for a sample of Saran carbon type A (pore volume 0.42 cm^3/g) are presented in Fig. 1. The weight scale in Fig. 1 has been expanded for positive weight changes to show the small initial weight increase which takes place at low temperatures (425–450 °C). A clearer illustration of this positive weight change is shown in Fig. 2. Although the detailed oxidation behavior at different pressures and for type B samples (pore volume 0.40 cm^3/g) is somewhat different, the qualitative features remain the same. The differences in their behavior can be inferred from Figs. 3 and 4. However, before pro-

Can. J. Chem. Downloaded from www.nrcresearchpress.com by 210.87.254.5 on 09/05/12
For personal use only.

ceeding to these data, it is worth noting that after a series of oxidation runs with a single sample, starting at 600 °C and finishing at 425 °C, a repeated run at 600 °C reproduces the results of the first run to within 10%. Although the rates of reaction at the respective temperatures are relatively constant, there appears to be no unequivocal evidence to suggest whether the internal pores have been significantly enlarged or not. Nevertheless, marked macroscopic changes in physical texture throughout the sample have been observed at the conclusion of a series of oxidation runs. The carbon then resembled "coke" in its ability to crumble easily on slight application of mechanical pressure, and inspection of the fragments showed that oxidation had taken place not only on the outer surface but also well within the interior of the sample.

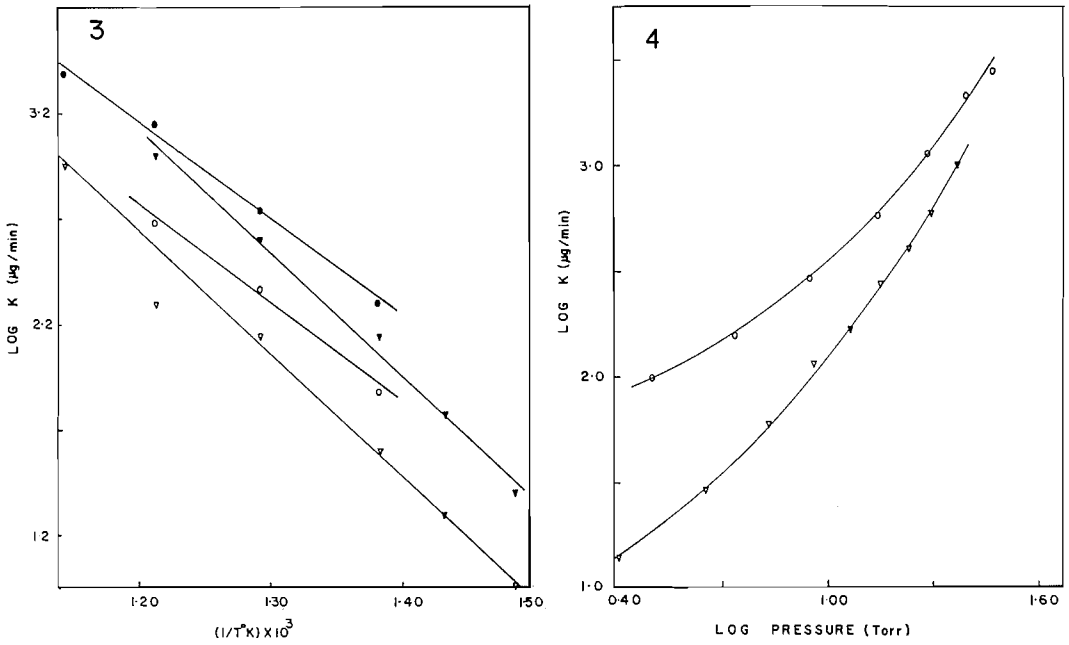


FIG. 3. Plot of logarithm of oxidation rate against reciprocal temperature in degrees absolute. Sample A: ○, 4.5 Torr (O_2); ●, 19.7 Torr (O_2). Sample B: ▽, 4.5 Torr (O_2); ▼, 19.5 Torr (O_2).
FIG. 4. Plot of logarithm of oxidation rate versus logarithm of initial oxygen pressure at 500 °C. ▽, Sample A. ○, Sample B.

The temperature dependence for oxidation of type A and type B Saran carbon is illustrated in Fig. 3 for two different initial oxygen pressures. The rates were calculated from the slopes of the initial linear regions of weight loss against time. The results for oxidation at 600 °C have been omitted from two of the curves of Fig. 1 as the pronounced curvature of the oxidation curves in conjunction with the rapid oxidation made the rate determination rather uncertain. In relation to the data shown in Fig. 1 we have calculated that the total amount of oxygen consumed at 425 °C is about 4% (on the basis that only CO is formed as the product) after 28 min of reaction. Higher oxygen consumption for the same period of reaction was obtained for each elevated temperature, and at 600 °C most of the oxygen appeared to have been consumed.

Figure 4 presents the pressure dependence of the rate for type A and type B samples at a temperature of 500 °C. Once again, the rates were determined from the linear region of the oxidation curves.

Can. J. Chem. Downloaded from www.nrcresearchpress.com by 210.87.254.5 on 09/05/12
For personal use only.

Can. J. Chem. Downloaded from www.nrcresearchpress.com by 210.87.254.5 on 09/05/12
For personal use only.

DISCUSSION

Dacey and Thomas (1) generally degassed their Saran carbons at 400 °C for several hours before carrying out adsorption studies. Our results indicate that this procedure is insufficient for the removal of more sorbed species. The decrease in oxidation rate with time at high temperatures (Fig. 1) undoubtedly arises from the consumption of oxygen and perhaps also from the formation of products* (presumably CO and (or) CO_2, cf. ref. 14 and the references contained therein).

The initial gain in weight at low temperatures (Figs. 1 and 2) is interesting as it can only result from chemisorption of oxygen or possibly from a pressure buildup within the porous carbon, which would be detectable if the diffusion constant for the reaction product(s) is sufficiently smaller than that for oxygen. In the present context, the diffusion constants are those for migration of the gases through the porous structure of the solid. It seems unlikely from the experimental conditions of our measurements that the initial gain in weight is caused by spurious effects resulting from "thermo-molecular flow" caused by thermal inhomogeneity or by various Knudsen Effects as reported by Poulis and Thomas (15). For the temperature and pressure ranges investigated in the present work, our calculations indicate that the mean free path of the oxygen molecules is well below the dimensions of the containing vessel (cf. ref. 15).

The relative constancy in the rates of reaction following a series of oxidation runs with a single carbon sample suggests that there may be a compensation between two operating parameters. If the surface area per unit volume of the carbon decreases (as porosity increases), this effect is balanced by a corresponding increase in the diffusion constants for the migration of the gases through the pores of the sample.

The linearity of the Arrhenius plots (Fig. 3) suggests a relatively simple interpretation of the temperature coefficient. Interpreting the slopes in terms of "activation energies" we obtain the values listed in Table I. These values are notably smaller than the 37

TABLE I

Energy of activation and oxygen pressure for type A and B samples

	Energy of activation (kcal/mole)	Oxygen pressure (Torr)
Saran carbon A	26.9	4.48±0.07
	26.9	19.74±0.06
Saran carbon B	21.5	4.54±0.17
	21.5	19.50±0.07

kcal/mole found by Gulbransen and Andrew (16) for the oxidation of artificial graphite in the same range of temperature and pressure. The activation energy for type A samples is significantly greater than that for type B samples, but this difference cannot be accounted for only on the basis of pore volume and density of the carbons. One cannot distinguish a carbon sample of pore volume 0.40 cm^3/g from another of 0.42 cm^3/g because the accuracy of measurement of porosities by argon adsorption is poorer than 0.02. Because of the difference in the initial molding compression pressures of the polymer, there is a good possibility that pore diameter and structure of the ultimate carbons may

**The apparatus is presently undergoing extensive modifications to allow oxidation studies to be carried out under dynamic flow conditions, thus enabling more precise control of the composition of the oxidizing environment. Modifications to permit monitoring of the product composition are also under way. The results of this complementary work under dynamic conditions will be communicated elsewhere later.*

be different. Saran carbon has been reported as being a system of uniform micropores, where the narrowest constrictions to flow are 10 to 15 Å wide (4). The observed differences in activation energy may arise as a result of different permeabilities of the samples to oxygen and (or) resultant products (cf. discussion which follows eq. [1] below).

A further interesting result concerns the unusual pressure dependence illustrated in Fig. 4. The slope of log (rate) versus log (oxygen pressure) is fairly close to 1 at low pressures, increasing to 2 or higher at high pressures. It might be supposed that the unusual pressure dependence could be explained simply by combining rate expressions for the interfacial reaction with conventional diffusion equations. This does not, however, appear to be the case. A detailed analysis of reaction kinetics in porous media will be presented by one of us (M. J. D.) in a subsequent publication. A brief summary of the pertinent results as they apply to the present static oxygen system will, however, be given below.

If the primary surface reaction rate is proportional to p^n where p is the oxygen pressure, and the diffusion constant for oxygen migration within the porous carbon is independent of the concentration of sorbed species, then the maximum possible pressure dependence for oxidation of the porous carbon will be given by p to the power of n or $(n + 1)/2$, whichever is greater. This postulate for the reaction of a gas in the pores of a solid is essentially the same as that derived by Wheeler from a somewhat different theoretical approach (17), and it has been applied by Blyholder and Eyring (18) to the interpretation of the kinetics of graphite oxidation. Furthermore, if diffusion plays a major role in the overall reaction kinetics, the empirical activation energy will be the mean of the activation energy for the primary reaction process and that for diffusion (*vide infra*).

In the present case it appears very unlikely that n is greater than 1. The data on graphite (16) would suggest a value between 0 and 1. It is extremely probable, therefore, that the observed pressure dependence arises as a result of an increase in the diffusion constant with increasing adsorbate concentration in the porous carbon. Although such a postulate appears somewhat contrary to expectation, a similar phenomenon has been observed by Dacey and Fendley (4) who measured the flow of non-reactive gases through Saran charcoal. They found that for certain samples the flow rate for a given pressure gradient increased linearly with increasing average pressure. The maximum dependence of the diffusion constant on pressure which may be inferred from their results is still insufficient to predict a p^2 dependence for $n \leqslant 1$. A more detailed examination of this problem will have to await the data obtained from the dynamic flow system.

It appears almost certain that diffusion of oxygen into the porous carbon plays a major role in the overall reaction kinetics. We may therefore write

$$[1] \qquad Q_{obs} = (Q_D + Q_R)/2$$

where Q_{obs}, Q_D, and Q_R are respectively the observed or empirical activation energy, the activation energy for diffusion, and that for the primary surface reaction (cf. ref. 18). Using the results in Table I, and noting that Q_R is probably not greater than the corresponding quantity for oxidation of graphite (37 kcal), we conclude that $Q_D \gtrsim 6$ kcal for type B samples, and $\gtrsim 14$ kcal for type A samples. The estimated value of Q_D for type B samples is in very good agreement with the activation energies of about 4 and 5 kcal/mole for diffusion of argon and methane as reported by Dacey and Fendley (4). This suggests that eq. [1] gives a good representation of the Q_D contribution, which arises from the permeability of the carbon to oxygen and (or) resultant gaseous products. The estimated value of Q_D for type A samples appears to be too large. One possible explanation for this

Can. J. Chem. Downloaded from www.nrcresearchpress.com by 210.87.254.5 on 09/05/12
For personal use only.

is that the permeability of type A samples is substantially greater than that of type B samples. If the type A permeability were sufficiently large, eq. [1] would not be valid in that Q_{obs} would be closer to Q_R than indicated by this equation. A further possibility is, of course, that Q_R differs for the two types of Saran carbons.

ACKNOWLEDGMENTS

We are indebted to the Defence Research Board and the University of Toronto for financial support of this work. One of us (M. J. D.) is grateful to the National Research Council for grants to construct the vacuum microbalance.

REFERENCES

1. J. R. DACEY and D. G. THOMAS. Trans. Faraday Soc. **50**, 740 (1954).
2. J. R. DACEY, J. C. CLUNIE, and D. G. THOMAS. Trans. Faraday Soc. **54**, 250 (1958).
3. J. J. KIPLING and R. B. WILSON. Trans. Faraday Soc. **56**, 557, 562 (1960).
4. J. R. DACEY and J. A. FENDLEY. *In* Structure and properties of porous materials. *Edited by* D. H. Everett and F. S. Stone. Butterworths, London. 1958. p. 142.
5. J. R. DACEY. Advan. Chem. Ser. **33**, 172 (1961).
6. R. V. CULVER and N. S. HEATH. Trans. Faraday Soc. **51**, 1569, 1575 (1955).
7. R. FRANKLIN. Proc. Roy. Soc. London, Ser. A, **209**, 196 (1951).
8. J. R. DACEY and R. G. BARRADAS. Can. J. Chem. **41**, 180 (1963).
9. G. YOUNG (*Editor*). Fuel cells. Vols. I and II. Reinhold, New York. 1960 and 1963.
10. J. WEISSBART. J. Chem. Educ. **38**, 267 (1961).
11. R. G. BARRADAS and M. E. BRERETON. Unpublished results.
12. J. S. SCONCE (*Editor*). Chlorine: its manufacture, properties and uses. Reinhold, New York. 1962.
13. M. J. DIGNAM and W. R. FAWCETT. J. Electrochem. Soc. In press. 1965.
14. P. L. WALKER, JR., F. RUSINKO, JR., and L. G. AUSTIN. Advances in catalysis. Vol. XI. Academic Press, New York. 1959. p. 133.
15. J. A. POULIS and J. M. THOMAS. J. Sci. Instr. **40**, 95 (1963).
16. E. A. GULBRANSEN and K. F. ANDREW. Ind. Eng. Chem. **44**, 1034 (1952).
17. A. WHEELER. Advances in catalysis. Vol. III. Academic Press, New York. 1951. p. 249.
18. G. BLYHOLDER and H. EYRING. J. Phys. Chem. **61**, 682 (1957); **63**, 1004 (1959).

Can. J. Chem. Downloaded from www.nrcresearchpress.com by 210.87.254.5 on 09/05/12
For personal use only.

Can. J. Chem. Downloaded from www.nrcresearchpress.com by 210.87.254.6 on 09/05/12
For personal use only.

SOME HYDROGEN ABSTRACTION REACTIONS OF PERFLUOROETHYL RADICALS

G. O. PRITCHARD,[1] J. R. DACEY, W. C. KENT, AND C. R. SIMONDS
Department of Chemistry, Royal Military College of Canada, Kingston, Ontario
Received August 19, 1965

ABSTRACT

With perfluoroazoethane as a photolytic source of C_2F_5 radicals, the hydrogen abstraction reactions of C_2F_5 with deuterium, ethane, cyclohexane, acetone, and trifluoroacetaldehyde have been studied, and the Arrhenius parameters derived. The H-atom abstraction reactions of the three perfluoroalkyl radicals, CF_3, C_2F_5, and C_3F_7, are discussed.

INTRODUCTION

Data on the H-atom abstraction reactions of perfluoroalkyl radicals (CF_3, C_2F_5, and C_3F_7) have recently been summarized (1, 2); they are quite limited, especially for C_2F_5 radicals, and the Arrhenius parameters obtained with a particular substrate RH show wide variations. The perfluoroketones have generally been used as a source of radicals, although some work has been done with the fluoroaldehydes, and hexafluoroazomethane has been used as a source of CF_3 radicals (3). Direct abstraction versus recombination data were not obtained in the last study because of the rapid addition of CF_3 radicals to —N=N—, which reduces their concentration so severely that the rate of formation of C_2F_6 cannot be accurately determined. However, perfluoroazo compounds can be photolyzed in the near ultraviolet, so that the range of compounds RH can be extended to aldehydes and ketones, without the latter being photolyzed. In contrast to hexafluoroazomethane, large yields of C_4F_{10} are obtained in the photolysis of perfluoroazoethane under comparable conditions (4), so that it has been used as the radical source in this work; and direct abstraction

[1] $$C_2F_5 + RH \rightarrow C_2F_5H + R$$

versus recombination

[2] $$2C_2F_5 \rightarrow C_4F_{10}$$

data have been obtained. Substrates RH were chosen so that comparison could be made with the available CF_3 and C_3F_7 radical data (see Table II).

EXPERIMENTAL

The beam from a high-pressure Hg arc was collimated and passed through a Corning 9863 blue-glass and $CuSO_4.5H_2O$ solution (100 g l^{-1}, 5 cm path). The cylindrical (5 cm diameter, 10 cm long) pyrex cell had a reaction volume of 192 cc, and it was fully illuminated. It was fitted with an outer jacket, and desired temperatures were obtained with refluxing liquids.

The perfluoroazoethane was prepared by the action of silver(I) fluoride on trifluoroacetonitrile (5); the contents of the bomb were bubbled through a KOH solution (twice) and then through a solution of Ag_2O suspended in water. The recovered gas was distilled on a Podbielniak column, the fraction between 18 and 21 °C being retained. After the gas was dried with P_2O_5, vapor density measurements gave a molecular weight (corrected) of 264 (calculated 266). Vapor phase chromatography indicated that the compound was >99.5% pure, although two trace impurities of greater volatility were detected. The more volatile of the two was found to be C_4F_{10} by vapor phase chromatographic characterization. Other possible impurities are C_2F_5Br and N-bromotetrafluoroethylidenimine, which are by-products of the preparation (5), although the purification technique was designed to remove them. Also, the mass spectrum of the perfluoroazoethane

[1]*Department of Chemistry, University of California, Santa Barbara, California.*

showed no conclusive evidence for Br^+, but spurious ion-peaks at *m/e* 30 and 46 were obtained. It is possible that these peaks are caused by NO_2 (b.p. 21°), which may be formed in some way in the preparation. The azo-compound was further purified by pumping at −110 to −115 °C, which completely removed the impurities from the chromatograms and the mass spectra. No variation in rate data was observed whether this final purification step was carried out or not.

The extinction coefficient (based on decadic logarithms) of perfluoroazoethane is 17.2 l mole^{-1} cm^{-1} at 3 840 Å (λ_{max}), and ϵ ranges from 12.4 to 15.6 l mole^{-1} cm^{-1} between 3 600 and 3 700 Å, showing the expected shift to the red when F atoms are substituted for H atoms (6). In azoethane, ϵ = 9.9 l mole^{-1} cm^{-1} at 3 550 Å (λ_{max}) (7).

At the completion of a run, N_2 could be collected at −190 °C and measured. Its purity was checked on the mass spectrometer. C_2F_5H was collected at −145 °C, and it was characterized and its purity established by vapor phase chromatography and mass spectrometry. A sample was then collected at −107 °C, and subjected to vapor phase chromatography on a 3% squalane on silica-gel column at 150 °C. The C_4F_{10} showed a retention time of 3½ min and the perfluoroazoethane 8½ min. The purity of the C_4F_{10} was checked on the mass spectrometer. When perfluoroazoethane, in which the final purification step had not been carried out, was used, the second impurity showed as a peak at 6½ min.[2] In runs above 220 °C, a small peak appeared at ~5 min, and tended to merge into the tail of the C_4F_{10} peak; the peak became slightly more pronounced at higher temperatures. It was observed when the azo-compound was photolyzed alone at these temperatures, but it was not formed in a dark reaction. Because of this peak, a slight correction (<3%) was made to the C_4F_{10} areas obtained above 220 °C. The retention time of the C_2F_5H, which sometimes contained a negligible quantity of C_4F_{10}, was 2½ min.

The compounds RH used were of spectroscopic or highest quality research grade. In the D_2 experiments, the D_2 was pumped off at −190°, together with the N_2. The D_2 used analyzed ~99% D_2, 1% HD, and < 0.3% H_2 on the mass spectrometer. The C_2F_5D produced in the reaction contained less than 2% C_2F_5H at the lowest temperature, as found by a comparison of *m/e* 51 and 52 (CF_2H^+ and CF_2D^+). In the ethane experiments, the excess ethane was pumped off the reaction mixture at −175°; attempts were made to identify $C_2F_5C_2H_5$ in the reaction products by vapor phase chromatography, but it was concluded that only trace amounts, if any, were formed.

Acetone and cyclohexane, and any other products formed in these systems, did not interfere with the analysis. In the experiments with CF_3CHO, after pumping off the N_2, a fraction was collected at −107° and subjected to vapor phase chromatography on the column at room temperature. Retention times were C_2F_5H 22 min, and C_4F_{10} 34 min. This procedure was adopted, since the excess CF_3CHO interfered with the Ward-still separation of C_2F_5H and C_4F_{10}.[3] Three small peaks at lower retention times were also observed, probably from CF_3H, C_2F_6, and C_3F_8 formed by the decomposition of the CF_3CO radical.

RESULTS AND DISCUSSION

The results for the five compounds studied are given in Table I. Pressures (measured at room temperature) of perfluoroazoethane used were: 1½–3 cm with D_2, ethane, and acetone; 3½–9 cm with cyclohexane; and 2–4½ cm with CF_3CHO. From the N_2 produced, it was calculated that about 10% of the perfluoroazoethane was photodecomposed in each experiment. The data give good Arrhenius plots, and $k_1/k_2^{1/2}$ in mole$^{-1/2}$ cc$^{1/2}$ s$^{-1/2}$ is: for D_2, $1.2 \times 10^6\ e^{-14100/RT}$; for ethane, $1.5 \times 10^5\ e^{-8700/RT}$; for cyclohexane, $1.5 \times 10^5\ e^{-6000/RT}$; for acetone, $5.1 \times 10^4\ e^{-8400/RT}$; and for CF_3CHO, $2.5 \times 10^5\ e^{-9700/RT}$. The value and limits of error for the D_2 activation energy are $E_1 - \frac{1}{2}E = 14.1 \pm 0.3$ kcal mole^{-1}. Including the low run at 232 °C, we obtain 13.8 ± 0.4 kcal mole^{-1}. The limits of error for the other activation energies are less than ±0.2 kcal mole^{-1}.

Table II shows all the available Arrhenius parameters on R_f(CF_3, C_2F_5, or C_3F_7) radical H-atom abstraction reactions.

[1] $$R_f + RH \rightarrow R_fH + R$$

[2] $$2R_f \rightarrow R_{f_2}$$

Two studies on the cross combination of perfluoroalkyl radicals, $CF_3 + C_3F_7$ (9), and $CF_3 + C_2F_5$ (10), yield ratios close to the collision theory value of 2, independent of the

[2]*This may suggest that the perfluoroazoethane exists to a small extent as two geometric isomers. An analysis of the infrared spectrum of hexafluoroazomethane has been presented (8), but it was not concluded whether the cis or the trans form predominated. It has been claimed that intensely yellow (cis) and colorless (trans) hexafluoroazomethane occur. (V. A. Ginsburg et al. Proc. Acad. Sci. USSR, Chem. Sect. Engl. Transl. 142, 34 (1962).*

[3]*The Ward-still separation used with the other compounds was as rapid, and the chromatograms were more accurate.*

Can. J. Chem. Downloaded from www.nrcresearchpress.com by 210.87.254.6 on 09/05/12
For personal use only.

temperature, showing that we may directly compare the values of $E_1 - \frac{1}{2}E_2$ in Table II, and the values of $A_1/A_2^{1/2}$ almost directly. The respective collision numbers at 400 °K for CF_3, C_2F_5, and C_3F_7 are 7.5×10^{13}, 1.1×10^{14}, and 1.3×10^{14} mole^{-1} cc s^{-1} ($\sigma_{CF_3} = 4.0$ Å, $\sigma_{C_2F_5} = 5.5$ Å, $\sigma_{C_3F_7} = 6.5$ Å). Very recent work (11) indicates that $E_2 = 0$ for CF_3 combination, so that we may equate $E_1 - \frac{1}{2}E_2$ with E_1 as an absolute value.

TABLE I

RH (moles × 10^5)	Time (s)	Temp. (°C)	Product (moles × 10^5) N_2	C_2F_5H	C_4F_{10}	$\frac{1}{2}[C_2F_5H] + [C_4F_{10}]$ / $[N_2]$
RH = deuterium						
77.6	2 500	153.5		0.197	2.60	
96.6	2 400	154.5		0.213	2.05	
77.8	2 300	159.5		0.428	1.87	
73.7	2 250	178.0		0.543	2.22	
76.3	1 700	190.5		0.618	1.73	
69.0	1 500	203.5		0.490	1.76	
53.0	1 200	221.0		0.799	1.21	
60.9	1 200	232.0		1.11	2.26	
45.3	1 200	234.5		1.17	1.75	
43.7	1 000	258.5		2.38	3.16	
RH = ethane						
29.0	2 500	84.0		0.304	1.47	
27.3	2 000	99.0		0.363	1.15	
19.3	2 500	110.5	2.83	0.573	2.04	0.83
18.6	2 000	139.0	2.44	0.803	1.14	0.63
24.3	1 500	153.7		1.16	0.891	
14.3	1 500	179.0		1.24	1.44	
13.8	1 400	193.0		1.29	0.605	
8.95	1 200	219.0		1.41	0.542	
23.3	1 000	226.0		2.74	0.539	
RH = cyclohexane						
7.38	2 000	28.0	2.83	0.656	1.49	0.64
9.07	1 500	27.0	3.10	0.751	1.49	0.60
17.0	1 500	42.0	3.34	1.50	1.11	0.56
14.8	1 500	57.8	2.66	1.73	0.663	0.57
12.2	1 500	82.0	3.18	2.48	0.410	0.52
5.94	1 500	100.0	3.71	2.37	0.715	0.51
9.25	1 500	112.0	3.82	2.75	0.468	0.48
10.5	1 000	112.0	3.52	2.71	0.455	0.51
5.55	1 200	132.0		3.14	0.396	
RH = acetone						
71.9	2 500	82.0	1.34	0.285	0.916	0.79
45.7	2 500	108.5	1.90	0.460	1.27	0.79
44.7	2 400	130.5	2.19	0.743	1.28	0.75
38.2	2 200	155.5	2.95	1.69	1.52	0.80
35.3	2 000	178.5	1.81	1.24	0.671	0.71
35.6	1 600	204.0	2.16	1.73	0.550	0.65
37.6	1 500	219.5	2.33	2.31	0.498	0.71
RH = CF_3CHO						
31.2	2 000	138.0	3.14	0.630	1.29	0.51
22.2	1 700	154.5	3.88	0.693	1.13	0.38
24.2	1 600	179.0	3.88	1.05	0.759	0.33
23.2	1 400	190.5	5.37	1.66	1.23	0.38
12.6	1 250	206.5	4.34	1.27	1.80	0.56
10.4	1 200	220.0	4.72	1.30	1.44	0.23

Limitations are put on the accuracy of the values of E_1 (and this applies to many radical abstraction studies) because additional R_fH (except in the aldehyde systems) may be formed by interaction of the R_f radical with the radical formed in reaction [1]

[3] $$R_f + R \rightarrow R_fH + R(-H)$$

Can. J. Chem. Downloaded from www.nrcresearchpress.com by 210.87.254.6 on 09/05/12
For personal use only.

Can. J. Chem. Downloaded from www.nrcresearchpress.com by 210.87.254.6 on 09/05/12
For personal use only.

TABLE II

RH	Activation energies $E_1 - \frac{1}{2}E_2$ (kcal mole^{-1})			Pre-exponential ratios $A_1/A_2^{1/2}$ (mole$^{-1/2}$ cc$^{1/2}$ s$^{-1/2}$ × 10^{-4})		
	CF_3	C_2F_5	C_3F_7	CF_3	C_2F_5	C_3F_7
Hydrogen	9.5, 8.6	11.9,* 12.4	12.3,* 12.1	14, (4–9)	53,* 158	44,* 72
Deuterium	10.2, 9.5	(12.6), 14.1	13.8,* 14.0, (12.9)	5.9, (3–6)	(28), 120	60,* 96, (49)
Methane	10.3, 10.4, 11.3	10.6	9.5	10, 9, 19	4.2	0.97
Ethane	7.5, (7.3)	8.7	9.2	0.99	15	17
Cyclohexane	5.0	6.0	5.2	5.7	15	1.2
Acetone	8.3, (7.8)	8.4	7.2	6.9	5.1	6.7
Aldehydes	8.2 (CF_3CHO)	9.7 (CF_3CHO)	4.0 (C_3F_7CHO)	9.0	25	0.19
	4.0 (CH_3CHO)	4.5 (C_2F_5CHO)		1.2	0.3	
Ketones	6.6 (CF_3COCH_3)	5.6 ($C_2F_5COC_2H_5$)	8.4 ($C_3F_7COC_2H_5$)	0.25	2.2	5.9

*[R_fH] and [R_fD] divided by 2, see text. Parenthetical values considered less reliable. Data mainly obtained from the compilations in refs. 1 and 2, and this work. Other data taken from G. O. Pritchard and G. H. Miller. J. Chem. Phys. 35, 1135 (1961); W. G. Alcock and E. Whittle. Trans. Faraday Soc. 61, 244 (1965); R. L. Thommarson and G. O. Pritchard. To be published; and refs. 11, 14, and 19.

which competes with

[4] $$R_f + R \rightarrow R_fR.$$

In the C_3F_7 + ethane system, allowance was made for this from a knowledge of the C_4H_{10} ($R + R \rightarrow R_2$) and the $C_3F_7C_2H_5$ formed (12), but the value of E_1 was not affected whether the correction was made or not, although the reason for this is not apparent (13). In many systems the necessary product analysis to assess the extent of reaction [3] has not been or is not easily performed, and if only a partial analysis is carried out the possible temperature dependence of k_3/k_4 must be considered (14). A more complete review (15) of the problem will be presented.

In this respect the perfluoroazo-compounds may be preferable sources to the perfluoroketones, since a large fraction of the R radicals can easily add to —N=N—, rather than enter into reactions [3] and [4]. In the experiments with ethane we were not able to obtain measurable quantities of $C_2F_5C_2H_5$. Since k_3/k_4 for C_2F_5 and C_2H_5 is less than 0.4, based on k_3/k_4 for $C_3F_7 + C_2H_5$ (12, 14), any C_2F_5H formed in reaction [3] was negligible. The mass balance, $(\frac{1}{2}[C_2F_5H] + [C_4F_{10}])/[N_2]$, indicates an increasing loss of C_2F_5 radicals with temperature, from increasing addition at —N=N—, and reactions [3] and [4]. No analysis was attempted for C_2F_5–cyclohexyl and C_2F_5–acetonyl, but in experiments with cyclohexane above 200 °C, when $[C_2F_5H]/[N_2]$ approaches 2, the perfluoroazoethane consumed indicated the addition of cyclohexyl to —N=N—.

In the hydrogen (H_2 and D_2) systems the fate of the atom liberated

$$R_f + D_2 \rightarrow R_fD + D$$

poses a problem, since it may combine with an R_f radical

[5] $$R_f + D + (M) \rightarrow R_fD + (M)$$

to produce additional R_fD (this reaction may or may not have a third-body restriction) as well as another atom.

[6] $$D + D + M \rightarrow D_2 + M$$

This competition has been treated by Kutschke (16), who concludes that if both modes of removal of hydrogen atoms occur over the temperature range, a varying correction to $[R_fD]$ is necessary. Although this consideration is important in perfluoroketone systems, when C_3F_7CHO was used as the radical source (2), the HD enrichment of the D_2 that occurred during reaction indicated that the major fate of the D atoms was

$$D + C_3F_7CHO \rightarrow HD + C_3F_7CO$$

and no correction to $[C_3F_7D]$ was required. Similarly, no correction to the $[C_2F_5D]$ produced in this work is necessary, if we assume that the major fate of the D atoms is addition to —N=N—. This is substantiated by the pre-exponential ratio obtained, 120×10^4 mole$^{-1/2}$ cc$^{1/2}$ s$^{-1/2}$, which compares favorably with the aldehyde values, 158×10^4 ($C_2F_5 + H_2$), 72×10^4 ($C_3F_7 + H_2$), and 96×10^4 ($C_3F_7 + D_2$), all in mole$^{-1/2}$ cc$^{1/2}$ s$^{-1/2}$. The lower (asterisk) values (Table II) were obtained in perfluoroketone systems where it was considered that reaction [5] was the predominant fate of the hydrogen atoms, and the rates of production of R_fH and R_fD were divided by 2. The data imply that atom recombination (reaction [6]) predominates in these systems, but Kutschke (16) has pointed out that there are too many uncertainties to fully justify this conclusion.

Although limits of error have not been quoted in Table II, it will be assumed for the remainder of the discussion that the values of E_1 given, as derived from the Arrhenius plots, are good to ±0.5 kcal mole^{-1}, although much of the experimental data certainly appears to be more precise than this. Despite the experimental uncertainties, the values of

Can. J. Chem. Downloaded from www.nrcresearchpress.com by 210.87.254.6 on 09/05/12
For personal use only.

E_1 for H_2 and D_2 with C_2F_5 and C_3F_7 show a pronounced increase over those with CF_3. Recent work (17) indicates that $D(CF_3—H)$ may exceed $D(C_2F_5—H)$, and $D(C_3F_7—H)$, which is identical with $D(C_2F_5—H)$ (1), by as much as 4–5 kcal mole^{-1}, so that the H_2 data could be explained in terms of the Evans–Polanyi relation, $E = \alpha\Delta H + c$, with $\alpha \simeq 0.6$.

Our previous conclusion, based on an assumed invariance for $D(R_f—H)$, that E_1 should remain constant for the three radicals for a particular substrate (1) is invalidated if one accepts the picture given for H_2 and D_2. Nevertheless, approximate constancy for E_1 is seen for methane, ethane, cyclohexane, and acetone in Table II. Any interpretation is further complicated by the greater than 10-fold variations in the $A_1/A_2^{1/2}$ ratios (acetone excepted), which in part is probably a result of internal compensation in the Arrhenius parameters. For instance, with the experimental value of $k_1/k_2^{1/2} = 24.7$ mole$^{-1/2}$ cc$^{1/2}$ s$^{-1/2}$ for CF_3 + ethane at 182 °C (18), if we assume $A_1/A_2^{1/2} = 10^5$ mole$^{-1/2}$ cc$^{1/2}$ s$^{-1/2}$ (rather than 10^4 as given in Table II), E_1 becomes 9.6 kcal mole^{-1}, which leads to a better correlation with the C_2F_5 and C_3F_7 + ethane data.

The variations in the Arrhenius parameters for the aldehydes are quite extreme. Based upon the value of $E_1 = 9.7$ kcal mole^{-1} that we have obtained for

$$C_2F_5 + CF_3CHO \rightarrow C_2F_5H + CF_3CO$$

it seems that the value of Dodd and Smith (19) of $E_1 = 8.2$ kcal mole^{-1} for

$$CF_3 + CF_3CHO \rightarrow CF_3H + CF_3CO$$

is experimentally justified, although it had previously seemed to be improbably high (20). Bromination studies (21) have demonstrated a marked deactivating effect for H abstraction when fluorine atoms are substituted for hydrogen atoms on the adjacent carbon atom. The values of E_1 for CF_3 + CF_3CHO and CH_3CHO are consistent with this.

The data on the ketones again suggest compensation in the Arrhenius parameters, although from steric considerations some attack at the primary rather than the secondary H-atoms could contribute to a real increase in E_1 for $C_3F_7 + C_2H_5COC_3F_7$.

Acetone shows very little variation for attack by the three radicals, which would lead one to conclude that the H_2 and D_2 data are best explained by compensation in the Arrhenius parameters, rather than by any real change in E_1. A complete interpretation must await further elucidation of all the factors involved, and at present it appears that it is only valid to compare the rate constant ratios, $k_1/k_2^{1/2}$, directly, and not the derived Arrhenius parameters.

ACKNOWLEDGMENTS

This work was generously supported by the Defence Research Board of Canada, under grant 9530/13. One of us (G.O.P.) thanks the National Science Foundation for assistance, and we also thank Dr. F. P. Lossing for mass-spectrometric analyses and for communication of unpublished data. We also thank Drs. J. G. Calvert and E. Whittle for private communications.

REFERENCES

1. G. O. Pritchard and R. L. Thommarson. J. Phys. Chem. **68**, 568 (1964).
2. G. O. Pritchard and J. K. Foote. J. Phys. Chem. **68**, 1016 (1964).
3. G. O. Pritchard, H. O. Pritchard, H. I. Schiff, and A. F. Trotman-Dickenson. Trans. Faraday Soc. **52**, 849 (1956).
4. J. A. Young and R. D. Dresdner. J. Org. Chem. **28**, 833 (1963). J. R. Dacey, R. F. Mann, and G. O. Pritchard. Can. J. Chem. **43**, 3215 (1965).
5. W. J. Chambers, C. W. Tullock, and D. D. Coffman. J. Am. Chem. Soc. **84**, 2337 (1962).
6. A. H. Dinwoodie and R. N. Haszeldine. J. Chem. Soc. 2266 (1965).
7. J. G. Calvert. Private communication.
8. W. O. Freitag. Ph.D. Thesis, University of Pennsylvania, Philadelphia, Pa. 1955.

Can. J. Chem. Downloaded from www.nrcresearchpress.com by 210.87.254.6 on 09/05/12
For personal use only.

9. G. O. PRITCHARD, G. H. MILLER, and J. R. DACEY. Can. J. Chem. **39**, 1968 (1961).
10. A. S. GORDON. Can. J. Chem. In press.
11. R. D. GILES and E. WHITTLE. Trans. Faraday Soc. **61**, 1425 (1965).
12. G. GIACOMETTI and E. W. R. STEACIE. Can. J. Chem. **36**, 1493 (1958).
13. G. O. PRITCHARD and G. H. MILLER. J. Phys. Chem. **63**, 2074 (1959).
14. G. O. PRITCHARD and R. L. THOMMARSON. J. Phys. Chem. **69**, 1001 (1965).
15. G. O. PRITCHARD and H. O. PRITCHARD. In preparation.
16. K. O. KUTSCHKE. Can. J. Chem. **42**, 1232 (1964).
17. A. M. TARR, J. W. COOMBER, and E. WHITTLE. Trans. Faraday Soc. **61**, 1182 (1965).
18. P. B. AYSCOUGH, J. C. POLANYI, and E. W. R. STEACIE. Can. J. Chem. **33**, 743 (1955).
19. R. E. DODD and J. W. SMITH. J. Chem. Soc. 1465 (1957).
20. G. O. PRITCHARD, G. H. MILLER, and J. K. FOOTE. Can. J. Chem. **40**, 1830 (1962).
21. E. WHITTLE. Private communication.

Can. J. Chem. Downloaded from www.nrcresearchpress.com by 210.87.254.6 on 09/05/12
For personal use only.

Can. J. Chem. Downloaded from www.nrcresearchpress.com by 210.87.254.5 on 09/05/12
For personal use only.

REACTIONS OF ORGANOTIN COMPOUNDS

VI. THE REACTIONS OF TIN HYDRIDES WITH PERFLUOROVINYL TIN COMPOUNDS

A. D. BEVERIDGE, H. C. CLARK,[1] AND J. T. KWON
Department of Chemistry, University of British Columbia, Vancouver, British Columbia

Received July 30, 1965

ABSTRACT

The reactions of methyltin hydrides with methylperfluorovinyltin compounds have been examined under heat or ultraviolet irradiation. In no case is there evidence of addition to the C=C bond. Instead, extensive reduction of the vinyl group occurs to give *cis*-1,2-difluorovinyltin derivatives as the principal products, with smaller amounts of the *trans*-1,2-difluorovinyltin isomers, 2,2′-difluorovinyltin compounds, and products containing one or more $-C_2H_2F$ groups. Trimethyl- or dimethyl-tin fluoride is formed quantitatively from the corresponding hydride. In the reaction of dimethyl bis(perfluorovinyl)tin with dimethyltin dihydride, vinyl-hydrogen exchange occurs at 60° in the dark to give dimethylperfluorovinyltin hydride, while under ultraviolet irradiation partially fluorinated vinyltin compounds are formed. On the other hand, no reaction takes place between dimethyl bis(perfluorovinyl)tin and 2 moles of trimethyltin hydride in the dark at 50°, but under ultraviolet irradiation at 25°, partial vinyl-hydrogen exchange occurs, accompanied by reduction, to yield both trimethyl and dimethyl partially fluorinated vinyltin compounds. The infrared and proton magnetic resonance spectra of the products are discussed.

INTRODUCTION

In earlier papers in this series (1–3), we examined the addition reactions of dimethyltin dihydride to a series of olefins, some partially fluorinated. It was concluded that such additions most probably occur by a free radical mechanism in which the formation of radicals from the tin dihydride may be the rate-determining step. A secondary and somewhat unexpected result from these studies centered about the apparent instability of groups such as $>Sn(C_2F_3H_2)_2$ or $>Sn(C_2F_3BrH)_2$. The latter should constitute part of the reaction product from dimethyltin dihydride and trifluorobromoethylene, but the reaction in fact proceeded chiefly according to the equation

$$(CH_3)_2SnH_2 + 2CF_2{=}CFBr \rightarrow (CH_3)_2SnBr_2 + 2CF_2{=}CFH.$$

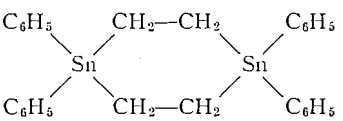
To gain further information about the reactivity of the C=C bond towards tin hydrides, and about the stability and decomposition of the fluoroalkyl group bonded to tin, we have now investigated the reactions of tin mono- and di-hydrides with some tin–perfluorovinyl compounds.

DISCUSSION

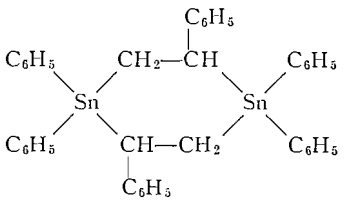
By analogy with the ready addition of tetrafluoroethylene to dimethyltin dihydride, one might anticipate a smooth reaction between trimethyltin hydride and trimethyl(perfluorovinyl)tin to give the product $(CH_3)_3SnCF_2CFHSn(CH_3)_3$. It is, however, well established (4) that such additions to the vinyl C=C bond do not occur readily for vinyltin compounds, although exceptions are observed. Thus diphenyltin dihydride and diphenyldivinyltin do not form the 1,4-distannacyclohexane compound (I), although a related product (II) has been obtained by reaction of diphenyltin dihydride with phenylacetylene (5). However, triphenyltin hydride and triphenylvinyltin, when heated under nitrogen at 70°, formed 1,2-bis(triphenyltin)ethane in 50% yield (6). It is noticeable that those

[1]*To whom correspondence concerning this paper should be sent. Present address: Department of Chemistry, University of Western Ontario, London, Ontario, Canada.*

cases in which addition to the vinyl C=C bond does occur are largely confined to triphenylvinyltin, and the suggestion has been made that this is a result of the activation



(I)



(II)

of the double bond by a conjugative $d\pi$–$p\pi$ mechanism (6). In one instance there is evidence of vinyl-hydrogen exchange. In the reaction of tri-*n*-butyltin hydride with triethylvinyltin at 90°, the products[2] were a mixture of tri-*n*-butyltin hydride and tri-*n*-butylvinyltin, triethyltin hydride, and 1,2-bis(tri-*n*-butyltin)ethane.

In general the perfluorovinyltin compounds are less stable thermally and kinetically than their vinyltin analogues, and their chemical behavior is often quite different. For example, the only reaction so far reported of a perfluorovinyltin compound with a tin hydride (7) appears to be a double decomposition reaction and not an addition.

$$(C_6H_5)_3SnCF{=}CF_2 + (C_6H_5)_3SnH \rightarrow CF_2{=}CFH + (C_6H_5)_3SnSn(C_6H_5)_3$$

This is in contrast to the addition to triphenylvinyltin described above. Clearly, the extension of our previous studies with fluoro-olefins to similar reactions of perfluorovinyltin compounds allows a number of possibilities.

Trimethyltin hydride and trimethylperfluorovinyltin do not react at 25° in the dark, and raising the temperature to 70° caused only 3% reaction. This is in contrast to the smooth reaction of the triphenyltin compounds described above, and perhaps emphasizes the importance of $d\pi$–$p\pi$ interactions in the latter case. Very ready reaction of the trimethyltin compounds, however, does occur under ultraviolet irradiation at 25°. Addition to the C=C bond does not take place, and in fact the vinyl group is reduced, accompanied by the quantitative formation of trimethyltin fluoride. The principal volatile product is trimethyl (*cis*-1,2-difluorovinyl)tin; smaller amounts of the *trans*-1,2-difluorovinyl compound, trimethyl (2,2′-difluorovinyl)tin, and a product of empirical composition $(CH_3)_3SnC_2H_2F$ are also formed. The principal reaction is therefore described by the equation

$$(CH_3)_3SnCF{=}CF_2 + (CH_3)_3SnH \rightarrow (CH_3)_3SnCF{=}CFH \text{ (}cis\text{ and }trans\text{ in ratio 3:1)} \; [+ (CH_3)_3SnCH{=}CF_2] + (CH_3)_3SnF.$$

To obtain a compound with a monofluorovinyl group, $-C_2H_2F$, however, a secondary reaction must be postulated. All the above products have been characterized by their infrared and proton magnetic resonance spectra (*vide infra*), and by hydrolysis with trifluoroacetic acid. Thus, for example, trimethyl (*cis*-1,2-difluorovinyl)tin quantitatively forms 1,2-difluoroethylene on treatment with trifluoroacetic acid.

$$(CH_3)_3SnCF{=}CFH\ (cis) + CF_3COOH \rightarrow CFH{=}CFH + (CH_3)_3SnOOCCF_3$$

It was found that under ultraviolet irradiation with a twofold excess of the hydride, the conversion of trimethylperfluorovinyltin to protonated vinyl derivatives was complete, and also that the yield of $(CH_3)_3SnC_2H_2F$ increased threefold. Although there were

[2]*D. Seyferth and M. A. Weiner, quoted in ref. 4, p. 226.*

Can. J. Chem. Downloaded from www.nrcresearchpress.com by 210.87.254.5 on 09/05/12
For personal use only.

indications of other secondary products, further reaction of the 1,2-difluorovinyl compounds gives principally $(CH_3)_3SnC_2H_2F$. This is confirmed by the fact that trimethyl (*cis*-1,2-difluorovinyl)tin could be further reduced, by ultraviolet irradiation with trimethyltin hydride, to form $(CH_3)_3SnC_2H_2F$. Interestingly, in this reaction some of the *cis*-1,2-difluorovinyl compound is converted to the *trans* isomer.

$$(CH_3)_3SnCF{=}CFH\ (cis) + (CH_3)_3SnH \rightarrow (CH_3)_3SnC_2H_2F\ [+ (CH_3)_3SnCF{=}CFH\ (trans)] + (CH_3)_3SnF$$

The configuration of the SnC_2H_2F group is uncertain, although the spectra of the products always gave the same coupling constants for the $-C_2H_2F$ group, clearly establishing that only the one isomer was always formed, although three are possible. The most reasonable assignments are in terms of the configuration shown in Table I, but this requires a fluorine–proton coupling constant for the *trans* —HC=CF— group of 100 c.p.s., at least twice as great as any known value (8). Other configurations cannot be correlated with the other observed coupling constants.

In the reaction of dimethyl bis(perfluorovinyl)tin with 2 moles of trimethyltin hydride, there exist such possibilities as reduction to form either protonated vinyl products such as $(CH_3)_2Sn(CF{=}CFH)_2$ bis-*cis*, or mixed products such as $(CH_3)_2Sn(CF{=}CF_2)(CF{=}CFH)$, or vinyl-hydrogen exchange to form trimethylperfluorovinyltin, or addition. Although no reaction was apparent even after 35 h at 50° in the dark, some vinyl-hydrogen exchange and reduction were observed after heating for 24 h at 60° in the dark, followed by exposure to daylight for 24 h. Under ultraviolet irradiation at 25°, complete reaction was achieved, and both vinyl-hydrogen exchange and reduction were observed. The principal products of the reaction were trimethyl *cis*-1,2-difluorovinyltin, trimethylperfluorovinyltin, trimethyl *trans*-1,2-difluorovinyltin, dimethyl bis(*cis*-1,2-difluorovinyltin), smaller amounts of trimethyl 2,2-difluorovinyltin, and dimethyl bis(2,2-difluorovinyltin), and still lesser amounts of the secondary products $(CH_3)_3SnC_2H_2F$ and $(CH_3)_2Sn(C_2H_2F)_2$.

Therefore, it is clear that the two initial competing reactions must be

$$[a] \qquad (CH_3)_2Sn(CF{=}CF_2)_2 + 2(CH_3)_3SnH \rightarrow 2(CH_3)_3SnCF{=}CF_2 + (CH_3)_2SnH_2$$

$$[b] \qquad (CH_3)_2Sn(CF{=}CF_2)_2 + 2(CH_3)_3SnH \rightarrow (CH_3)_2Sn(CF{=}CFH)_2\ (cis) + (\text{others})$$

with the exchange reaction dominant. Extensive reduction of the fluorinated vinyl species by trimethyltin hydride, and dimethyltin dihydride (from [*a*]), must then ensue. This was completely borne out by identification of a white solid produced in the reaction as a mixture of trimethyltin fluoride and dimethyltin difluoride, with the latter present in higher yield. There was no evidence for addition.

Finally, the reaction of dimethyltin dihydride with dimethyl bis(perfluorovinyl)tin was examined, and here markedly different results were obtained according to the conditions employed. At 60° in the dark, although products from the decomposition of the starting materials and from reduction were formed in small amounts, the only major product was dimethylperfluorovinyltin hydride, $(CH_3)_2SnH(CF{=}CF_2)$. This was identified unambiguously by its proton magnetic resonance and infrared spectra. Although one other example of vinyl-hydrogen exchange has been reported[2] in addition to that described in the preceding reaction, this appears to be the only compound so far known which contains simultaneously the Sn—C=C and Sn—H groups. This demonstrates in a unique way the lack of reactivity of the C=C bond in perfluorovinyltin compounds towards addition. The basic reaction under these conditions is therefore the following:

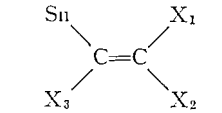
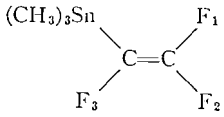
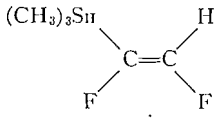
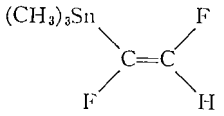
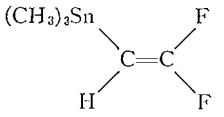
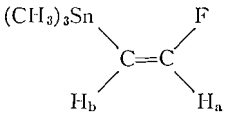
$$(CH_3)_2Sn(CF{=}CF_2)_2 + (CH_3)_2SnH_2 \rightarrow 2(CH_3)_2SnH(CF{=}CF_2).$$

Can. J. Chem. Downloaded from www.nrcresearchpress.com by 210.87.254.5 on 09/05/12
For personal use only.

Can. J. Chem. Downloaded from www.nrcresearchpress.com by 210.87.254.5 on 09/05/12
For personal use only.

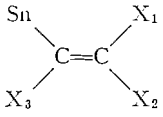
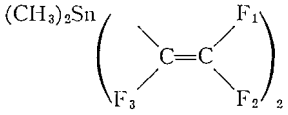
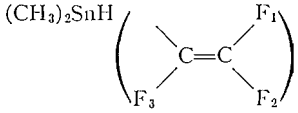
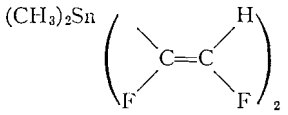
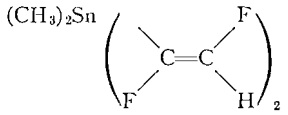
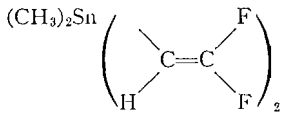
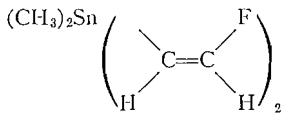
TABLE I

Nuclear magnetic resonance assignments for trimethyl and dimethyl perfluorovinyl and fluorovinyl species

	δ_{CH_3}*	$J_{^{119}Sn-CH_3}$*	$J_{^{117}Sn-CH_3}$	$J_{^{13}C-CH_3}$	$\delta_{vinyl\ H}$	J_{12}	J_{23}	J_{13}
	−0.33	60.5	58.0	131	—	—	—	—
 *cis*	−0.26	59.5	57.0	132	−5.93 quartet	77	—	25.5
 *trans*	−0.32	60	57.5	131	−7.60 quartet	78	15	—
	—	— (Not distinguished)	—	—	−3.92 quartet	—	9	46
	−0.20	58.0	55.5	129	−4.97 (H_a) quartet −6.91 (H_b) quartet	76	5.5	(100?)

Can. J. Chem. Downloaded from www.nrcresearchpress.com by 210.87.254.5 on 09/05/12
For personal use only.

TABLE I (*Concluded*)

	δ_{CH_3}*	$J_{^{119}Sn-CH_3}$*	$J_{^{117}Sn-CH_3}$	$J_{^{13}C-CH_3}$	$\delta_{vinyl\ H}$	J_{12}	J_{23}	J_{13}
	−0.58	61.6	58.6	131				
	−0.37 −0.41	64.4	61.3	2.2				
	−0.53	—	—	—	−5.93 quartet	75.5	—	25
	—	—	—	—	−7.53 quartet	76.5	15	
	—	—	—	—	−4.03 quartet	—	9	45
	−0.47	—	—	—	−5.13 quartet −7.04 quartet	72	5.5	(98?)

*All chemical shifts are given in p.p.m. with respect to internal tetramethylsilane, and coupling constants are in c.p.s.

However, when the two compounds were allowed to react under ultraviolet irradiation at 25°, the vinyl-hydrogen exchange was not observed; instead the formation of dimethyltin difluoride and partially fluorinated dimethylvinyltin compounds was noted.

TABLE II

Characteristic C=C stretching and C—F frequencies observed in trimethyl and dimethyltin perfluorovinyl and fluorovinyl species

	C=C region (±2 cm^{-1})	C—F region (±2 cm^{-1})*
Vapor phase		
$Me_3SnCF{=}CF_2$	1 712 s	1 278 sh, 1 268 s, 1 110 s, 998 s
$Me_3SnCF{=}CFH$ (*cis*)	1 649 s	1 106 s, 1 065 m, 1 045 m
$Me_3SnCF{=}CFH$ (*trans*)	1 637 s	~1 105 s,br
$Me_3SnCH{=}CF_2$	1 683 s	1 266 s, 1 103 s, 930 s
$Me_3SnC_2H_2F$	1 608 s	1 190 w,sh, 1 160 m,sh, 1 100 s, 973 s
$Me_2Sn(CF{=}CF_2)_2$	1 711 s,	1 271 s, 1 102 s, 1 002 s
$Me_2Sn(H)(CF{=}CF_2)$	1 718 s	1 285 s, 1 120 s, 1 010 s
$Me_2Sn(CF{=}CFH)_2$ bis-*cis*	1 647 s	1 102 s, 1 065 m, 1 039 m
$Me_2Sn(CF{=}CFH)_2$ bis-*trans*	—†	—†
$Me_2Sn(CH{=}CF_2)_2$	1 685 s	—†, —†, 928
$Me_2Sn(C_2H_2F)_2$	1 608 s	1 148 m,sh, 1 105 s, 973 s
Liquid film		
$Me_3SnCF{=}CF_2$	1 712 s	1 280 s, 1 265 s, 1 145 m,sh, 1 100 s, 997 s
$Me_3SnCF{=}CFH$ (*cis*)	1 643 s	1 086 s, 1 058 s, 1 038 s
$Me_3SnCF{=}CFH$ (*trans*)	1 635 s	~1 100 s
$Me_3SnCH{=}CF_2$	1 676 s	—†, —†, 925 s
$Me_3SnC_2H_2F$	1 604 s	—†, —†, 1 087 s, 966 s

*Some listed peaks in the 900 – 1 000 cm^{-1} region may be assigned C—H bending bands.
†Not distinguishable because other species present.

From the infrared and proton magnetic resonance spectra of the reduction products, mixed products of the type $(CH_3)_2Sn(CF{=}CF_2)(CF{=}CFH)$ were clearly not formed, as was also the case in the reaction with trimethyltin hydride. For example, only one C=C stretching vibration could be assigned to each component (Table II), confirming that only one type of vinyl group was present in each dimethyltin product. Dimethyl bis(*cis*-1,2-difluorovinyl)tin was again the major product, and minor products were $(CH_3)_2Sn(CF{=}CFH)_2$ *trans*, $(CH_3)_2Sn(CH{=}CF_2)_2$, and $(CH_3)_2Sn(C_2H_2F)_2$ formed in the ratio 2:1:4. Trimethylperfluorovinyltin and trimethyl *cis*-1,2-difluorovinyltin were also detected in small amounts, presumably formed by the formation of trimethyltin hydride from dimethyltin dihydride (1), followed by vinyl-hydrogen exchange and partial reduction. Other unidentified compounds were also formed in small amounts. When the ultraviolet irradiation was prolonged (6 h) decomposition was extensive, and from the color and air sensitivity of the resulting involatile solid, it appeared that polymeric forms of dimethyltin (9) were also formed. The complex variation of the course of this reaction with the experimental conditions is thus well illustrated.

Meaningful conclusions about the mechanism by which perfluorovinyl groups are converted to fluorovinyl groups, because of reaction with a tin hydride, are difficult to draw. Clearly, ultraviolet light greatly accelerates this process, although vinyl-hydrogen exchange may also occur under such conditions. One is tempted to suggest that free radical formation from the tin hydride is again the determining factor, but there is no obvious reason for the favored formation of the *cis*-1,2-difluorovinyltin compound, and equally acceptable alternatives based on a four-center mechanism, or on an addition followed immediately by trimethyl or dimethyltin fluoride elimination, can be suggested. It should also be noted that vinyl-hydrogen exchange could occur undetected in the reactions of trimethylperfluorovinyltin and trimethyltin hydride, and dimethyl bis(perfluorovinyl)tin and dimethyltin dihydride.

Can. J. Chem. Downloaded from www.nrcresearchpress.com by 210.87.254.5 on 09/05/12
For personal use only.

The characterization of the fluorovinyl products of these reactions is based to a considerable extent on their proton magnetic resonance spectra. These are not discussed in detail, since all the observed spectra could be readily interpreted in terms of the fluorine – vinyl proton couplings, by comparison with previously reported (8) and other (10) values. Sidebands arising from coupling of the methyl protons with ^{119}Sn, ^{117}Sn, and ^{13}C were observed in all spectra, but complete assignments could not be made in all cases because of overlapping with similar bands due to other components in inseparable mixtures. Coupling constants, together with other data, are presented in Table I, and may be compared with earlier data (11, 12).

Since the C=C frequencies in the infrared spectra of the vinyltin compounds also provide a useful means of characterization, the variations in these frequencies are listed in Table II.

EXPERIMENTAL

Standard high vacuum techniques were used for most reactions, except where stated. Reactions involving heat only were carried out in pyrex glass Carius tubes, whereas those involving ultraviolet irradiation were carried out in silica tubes. Infrared spectra were recorded on model 137 sodium chloride and potassium bromide, and model 21 double-beam, Perkin–Elmer spectrophotometers, while nuclear magnetic resonance spectra were obtained with Varian A 60 and H.R. 60 spectrometers. Gas chromatographic separations were carried out on a Beckman GC – 2A instrument with a dinonyl phthalate column at 147°, and helium carrier gas (10 p.s.i.g.).

Dimethyl bis(perfluorovinyl)tin and trimethyl(perfluorovinyl)tin were prepared essentially according to the method of Kaesz, Stafford, and Stone (13) in 52% and 50% yields respectively. Both were characterized by their infrared spectra, molecular weights, elemental analyses, and nuclear magnetic resonance spectra (see Tables I and II).

Trimethylperfluorovinyltin, which had previously been reported by Seyferth *et al.* (14) as having been obtained in 64% yield from the reaction between perfluorovinyllithium and trimethyltin bromide, was prepared by the reaction of trimethyltin bromide and perfluorovinylmagnesium bromide in anhydrous tetrahydrofuran. The product (b.p. 110.5°) was separated from the tetrahydrofuran (b.p. 66°) by distillation at 760 mm with a Vigreaux column. Final purification was achieved by vacuum fractionation and gas chromatography.

Dimethyltin dihydride and trimethyltin hydride were obtained by the procedure described by Finholt *et al.* (15), and characterized by the above methods.

Reactions of Trimethyltin Hydride with Trimethylperfluorovinyltin

(*a*) Trimethyltin hydride (0.944 g, 5.70 mmoles) and trimethylperfluorovinyltin (1.41 g, 5.73 mmoles) were condensed into an evacuated Carius tube and left for 250 h in the dark at 25°. Fractional condensation of the volatile products in the vacuum system gave trimethyltin hydride (0.933 g, 5.67 mmoles) and trimethylperfluorovinyltin (1.29 g, 5.27 mmoles). A small amount of involatile white solid remained in the tube.

(*b*) Trimethyltin hydride (0.738 g, 4.46 mmoles) and trimethylperfluorovinyltin (1.09 g, 4.46 mmoles) were sealed in a pyrex Carius tube, and kept at 50° in the dark for 66 h. Fractionation of the reaction mixture gave unreacted hydride (0.692 g, 4.20 mmoles) and a fraction composed almost entirely of unchanged trimethylperfluorovinyltin (1.05 g, 98% recovery). However, this contained a small amount of a new compound which gave characteristic infrared bands at 1 649 (C=C stretch), 1 106, 1 065, 1 045 cm^{-1} (C—F stretch). A new, minor peak was observed in a gas chromatographic analysis of the recovered perfluorovinyltin. The new component was identified as trimethyl (*cis*-1,2-difluorovinyl)tin (*vide infra*). A small amount of involatile white solid remained in the reaction tube.

(*c*) In a reaction similar to *b*, equimolar amounts of trimethyltin hydride and trimethylperfluorovinyltin were allowed to react at 70° in the dark for 18 h. Vacuum fractionation led to a 97% recovery of the reactents, although again the trimethylperfluorovinyltin was shown by gas chromatography to contain not more than approximately 1% of trimethyl (*cis*-1,2-difluorovinyl)tin.

(*d*) Trimethyltin hydride (1.65 g, 10.00 mmoles) and trimethylperfluorovinyltin (2.45 g, 10.00 mmoles) were allowed to react in a silica Carius tube at 25° under ultraviolet irradiation (100 watt Henovia lamp) for 18 h. After 3 h, a white solid was visible in the tube, and at the conclusion of the experiment, the inside walls were coated with this solid. When the tube was opened, No non-condensable gas was observed, and the volatile products were separated by trap-to-trap distillation into fractions which condensed at −23° (1.44 g), −36° (0.283 g), −46° (0.421 g), −78° (0.059 g), and −196° (0.009 g).

The involatile white solid remaining in the reaction tube was washed out with ether, and, by comparison of its infrared spectrum and X-ray powder photograph with those of an authentic sample, was identified as trimethyltin fluoride. Yield 1.84 g, 100% based on trimethyltin hydride.

Anal. Calcd. for C_3H_9FSn: C, 19.6; H, 4.9. Found: C, 19.9; H, 4.2.

Can. J. Chem. Downloaded from www.nrcresearchpress.com by 210.87.254.5 on 09/05/12
For personal use only.

Can. J. Chem. Downloaded from www.nrcresearchpress.com by 210.87.254.5 on 09/05/12
For personal use only.

The −23° to −78° fractions contained at least three components in addition to unreacted trimethylperfluorovinyltin, determined on the basis of additional bands in the C=C stretching vibration and C—F stretching vibration regions in their infrared spectra (vapor state). Repeated trap-to-trap distillation eventually gave a fraction at −23° which showed only one C=C stretching frequency. This was identified by elemental analysis, its proton magnetic resonance spectrum, and by quantitative hydrolysis with trifluoroacetic acid, as trimethyl (*cis*-1,2-difluorovinyl)tin, obtained in 49% yield.

Anal. Calcd. for $C_5H_{10}F_2Sn$: C, 26.5; H, 4.41. Found: C, 26.7, H, 4.21.

Trimethyl (*cis*-1,2-difluorovinyl)tin (0.222 g, 0.98 mmole) was allowed to react with trifluoroacetic acid (0.264 g, 2.6 mmoles) at room temperature. Vacuum fractionation gave unreacted trifluoroacetic acid (0.142 g; amount calculated for 100% reaction 0.152 g) and 1,2-difluoroethylene (0.0605 g, 0.95 mmole), identified by its infrared spectrum (16) and molecular weight (calcd. 64, obs. 64).

The proton magnetic resonance spectrum of trimethyl (*cis*-1,2-difluorovinyl)tin consists of a quartet centered at −5.93 p.p.m., with methyl resonance at −0.26 p.p.m., with respect to internal tetramethylsilane. The infrared spectrum of this compound (vapor phase) showed absorption at 3 002 (m), 2 925 (m) (CH stretch); 1 649 (vs) (—CF=CFH (*cis*) stretch); 1 295 (w), 1 198 (vw) (CH_3 symmetric deformation); 1 125 (w,sh), 1 113 (vs), 1 068 s, 1 045 s (C—F stretch); 800 (sh); 779 (s) (CH_3—Sn rock); 715 (m); 537 (vs), 516 (m) (Sn—C stretch). In the liquid phase, absorption was observed at 3 125 w, 3 000 m, 2 925 m, 2 894 w, (C—H stretch); 1 645 s (CF=CFH stretch); 1 296 w, 1 195 w; 1 086 s, 1 058 s, 1 038 s (C—F stretch); 795 vs,sh; 780 vs (CH_3—Sn rock); 723 w, 540, 518 (Sn—C stretch).

The remaining volatile material, after this separation of some pure trimethyl(*cis*-1,2-difluorovinyl)tin, could not be separated into other pure components by further vacuum fractionation, and was split into three fractions by passage over a dinonyl phthalate column.

The first fraction eluted, present in only a small amount, was hydrolyzed with trifluoroacetic acid to give 1,1-difluoroethylene, identified by its infrared spectrum, suggesting that the original compound could only have been trimethyl(2,2-difluorovinyl)tin. Its infrared spectrum showed absorption at 3 015 (w), 2 970 (w), (C—H stretch); 1 683 (vs) ($CH=CF_2$ stretch); 1 266 (s), (C—F stretch); 1 200 (w,sh); 1 103 (s), 930 (s) (C—F stretch); 778 (s) (CH_3—Sn rock); 724 (w).

The second and largest fraction to be eluted was recycled through the chromatograph three times to remove the last traces of $(CH_3)_3SnCH=CF_2$ and $(CH_3)_3SnCF=CFH$ (*cis*) The infrared spectrum (vapor) of the remaining material showed it to contain unreacted trimethylperfluorovinyltin together with at least two other components. Qualitative hydrolysis with trifluoroacetic acid gave a mixture of fluoro-olefins, whose infrared spectrum contained all the expected bands for $CF_2=CFH$, CFH=CFH (16), and $CFH=CH_2$ (17). The following conclusions were therefore drawn: (i) The formation of $CF_2=CFH$ on hydrolysis confirms the infrared observation that unreacted $(CH_3)_3SnCF=CF_2$ was present. (ii) the formation of CFH=CFH shows the presence of $(CH_3)_3SnCF=CFH$ in the original volatile mixture. Since the *cis* isomer was quantitatively removed as the third fraction to be eluted from the chromatogram, this species must be trimethyl (*trans*-1,2-difluorovinyl)tin. (iii) the formation of $CH_2=CFH$ indicates the presence of reduction product(s) of composition $(CH_3)_3SnCH=CFH$ (*cis* or *trans*) or $(CH_3)_3SnCF=CH_2$.

These conclusions were further supported by the proton magnetic resonance spectrum of this second chromatographic fraction. The spectrum showed six doublets and two CH_3 peaks, of which, from the integrals, the former could be grouped as one set of four doublets, and a separate set of two doublets. The set of four doublets was consistent with a reduced vinyl group containing two protons, and the other set of two doublets with a reduced vinyl group containing one proton. Of the CH_3 peaks, that at −0.20 p.p.m. (with respect to internal tetramethylsilane) must be associated with the set of four doublets since, from the integrals, the ratio of CH_3 protons to vinyl protons was 1:4.2. The ratio expected for $(CH_3)_3SnC_2H_2F$ was 1:4.5. The other CH_3 peak at $\delta = -0.33$ p.p.m. was clearly due to unreacted $(CH_3)_3SnCF=CF_2$, and also to CH_3 groups which associated with the pair of doublets. The latter were at −7.60 p.p.m. with coupling constants of 78 c.p.s. and 15 c.p.s. These values were consistent (9) with C=CFH and CH=CF— (*cis*) couplings respectively, which confirmed the existence of $(CH_3)_3SnCF=CFH$ (*trans*). Since the observed ratio, obtained from the integrals, of vinyl proton (CF=CFH):methyl proton was 1:20, in contrast to the ratio of 1:9 expected for $(CH_3)_3SnCF=CFH$ (*trans*), the ratio of the latter compound to $(CH_3)_3SnCF=CF_2$ must be approximately 9:11. The four doublets could be grouped in two sets having $\delta = -4.97$ and −6.91 p.p.m. respectively and coupling constants of 76 and 5.5 c.p.s., and 100 and 5.5 c.p.s. respectively. To explain the 5.5 c.p.s. value, the occurrence of CH=CH— (*cis*) must be advanced. The value of 76 c.p.s. could then arise from the coupling in —CH=CFH. However, 100 c.p.s. is at least twice as great as any known value for the coupling of —CH=CF— (*trans*). The assignment is therefore uncertain, and the compound is just referred to as $(CH_3)_3SnC_2H_2F$.

From the infrared spectrum of this three-component mixture, and the spectra of $(CH_3)_3SnCF=CF_2$ and $(CH_3)_3SnC_2H_2F$ (see later), the following bands were assigned to $(CH_3)_3SnCF=CFH$ (*trans*): 1 637 (CF=CFH *trans*, stretch), 1 105 (C—F stretch), and 812 cm^{-1}.

(*e*) Trimethyl(perfluorovinyl)tin (1.08 g, 4.40 mmoles) and trimethyltin hydride (0.725 g, 4.40 mmoles) were allowed to react under conditions identical to experiment *d* above. To determine the relative yield of each species, the proton magnetic resonance spectrum of the total volatile products was recorded. From the integrated spectrum, the values in Table III were obtained, from a total of 0.972 g volatile material, this

TABLE III

	Weight (g)	Mole % (based on $(CH_3)_3SnCF{=}CF_2$)
$(CH_3)_3SnCF{=}CF_2$ (recovered)	0.209	19
$(CH_3)_3SnCF{=}CFH$ (*cis*)	0.509	51
$(CH_3)_3SnCF{=}CFH$ (*trans*)	0.170	17
$(CH_3)_3SnCH{=}CF_2$	0.01	1
$(CH_3)_3SnC_2H_2F$	0.044	5

being 54% of the total weight of reactants. Note that the yield of the *cis* isomer agrees well with the value obtained in the previous experiment. Trimethyltin fluoride (0.762 g, 4.2 mmoles, 95.4% yield) was also isolated.

(*f*) Trimethyltin hydride (1.59 g, 9.66 mmoles) and trimethylperfluorovinyltin (1.15 g, 4.70 mmoles) were allowed to react in a silica Carius tube at 25° under ultraviolet irradiation for 18 h. The volatile products were then transferred to a nuclear magnetic resonance sample tube, leaving a trace of an unidentified involatile liquid together with an involatile solid. The latter was washed out with ether, dried, and identified as trimethyltin fluoride (1.66 g, 9.09 mmole, 94.3% yield).

The proton magnetic resonance spectrum showed the presence of $(CH_3)_3SnCF{=}CFH$ (*cis*), $(CH_3)_3SnCF{=}CFH$ (*trans*), $(CH_3)_3SnH$, and $(CH_3)_3SnC_2H_2F$, but not of $(CH_3)_3SnCF{=}CF_2$. Some additional peaks, not observed in previous experiments and which could not be satisfactorily assigned, were also seen. From the integrated spectrum, the percentage yields and calculated weights shown in Table IV were obtained.

TABLE IV

	% of volatiles	Weight (g)	Mole % (based $(CH_3)_3SnCF{=}CF_2$)
$(CH_3)_3SnCF{=}CFH$ (*cis*)	52	0.429	40.2
$(CH_3)_3SnCF{=}CFH$ (*trans*)	11	0.091	8.5
$(CH_3)_3SnCH{=}CF_2$	—	—	—
$(CH_3)_3SnC_2H_2F$	18	0.148	15.1
$(CH_3)_3SnH$	9	0.074	4.6 (of original hydride)
Others (unidentified)	10	0.082	~10

Reactions of Trimethyltin Hydride with Trimethyl(cis-1,2-difluorovinyl)tin

(*a*) The vinyltin compound (0.175 g, 0.773 mmole) and trimethyltin hydride (0.165 g, 1.00 mmole) were irradiated with ultraviolet light for 15 h at 25°. The volatile products were separated chromatographically to give unreacted trimethyl(*cis*-1,2-difluorovinyl)tin and slightly impure $(CH_3)_3SnC_2H_2F$. The infrared spectrum (vapor) showed absorption at 3 090 (w), 3 000 (m), 2 093 (m); 1 608 (s); 1 190 (w), 1 160 (m), 1 100 (s), 973 (s); 800 (m,sh); 775 (vs); 725 (m,w).

Anal. Calcd. for $C_5H_{11}FSn$: C, 28.6; H, 5.24. Found: C, 27.7; H, 5.03. Molecular weight calcd. 209; found 209, 212.

The fraction identified as $(CH_3)_3SnC_2H_2F$ (0.228 g, 0.109 mmole) gave immediate reaction with excess trifluoroacetic acid in a Carius tube at 25°. The resulting olefin was trapped at −196° and shown by its infrared spectrum to contain $CFH{=}CH_2$ and a little $CFH{=}CFH$ (0.0475 g, molecular weight 55.0; molecular weight calcd. for $CFH{=}CH_2$, 46; for $CFH{=}CFH$, 64). The impurity was thus $CFH{=}CFH$, from trimethyl(*trans*-1,2-difluorovinyl)tin.

(*b*) Trimethyl(*cis*-1,2-difluorovinyl)tin (1.25 g, 5.49 mmoles) and trimethyltin hydride (0.904 g, 5.49 mmoles) were allowed to react under the conditions of the last experiment. The volatile products (1.00 g) were then transferred to a nuclear magnetic resonance sample tube, and, from an analysis of the spectrum and from the values of the integrals, the proportions shown in Table V were calculated.

TABLE V

	% of volatiles	Weight (g)	Mole %
$(CH_3)_3Sn(CF{=}CFH)$ (*cis*)	50	0.5	40
$(CH_3)_3SnCF{=}CFH$ (*trans*)	10	0.1	8
$(CH_3)_3SnC_2H_2F$	30	0.3	24
Others (unassigned peaks)	10	0.1	—

Can. J. Chem. Downloaded from www.nrcresearchpress.com by 210.87.254.5 on 09/05/12
For personal use only.

Can. J. Chem. Downloaded from www.nrcresearchpress.com by 210.87.254.5 on 09/05/12
For personal use only.

Reactions of Dimethyl Bis(perfluorovinyl)tin with Trimethyltin Hydride

(*a*) Trimethyltin hydride (1.06 g, 6.44 mmoles) and dimethyl bis(perfluorovinyl)tin (1.00 g, 3.22 mmoles) were kept at 50° in the dark for 35 h. Approximately 94% of the hydride as well as 78% of the unchanged perfluorovinyl compound, was recovered. A trace of an involatile solid and a small amount of CF_2=CFH were also formed.

(*b*) Trimethyltin hydride (2.15 g, 13.0 mmoles) and dimethyl bis(perfluorovinyl)tin (2.04 g, 6.55 mmoles) were heated to 70° in a Carius tube for 17 h and then left in daylight for a further 24 h. Hydrogen (0.009 g) was observed on opening the tube, and a white solid (0.85 g), identified as mainly dimethyltin difluoride, but containing traces of metallic tin and other species, remained in the tube after removal of all volatile products. The latter were separated into a −23° fraction (1.34 g), a −45° fraction (0.18 g), a −78° fraction (1.43 g) shown to be unreacted trimethyltin hydride, and a −196° fraction (0.065 g) identified as CF_2=CFH. Gas chromatographic examination of the −23° and −45° fractions showed them to consist largely of unreacted dimethyl bis(perfluorovinyl)tin, along with trimethylperfluorovinyltin and trimethyl *cis*-1,2-difluorovinyltin, with lesser amounts of the *trans* isomer.

(*c*) Trimethyltin hydride (0.566 g, 3.44 mmoles) and dimethyl bis(perfluorovinyl)tin (0.536 g, 172 mmoles) were allowed to react at 25° under ultraviolet irradiation for 11 h. The resulting involatile white solid (0.635 g), washed out with ether, was refluxed with toluene to remove soluble impurities. It was identified by its X-ray powder photograph as largely dimethyltin difluoride, along with some trimethyltin fluoride. The volatile products (0.380 g) were separated chromatographically into several fractions, which from their nuclear magnetic resonance and infrared spectra were shown to be: 1. $(CH_3)_3SnCH$=CF_2 (minor); 2. $(CH_3)_3SnCF$=CF_2, $(CH_3)_3SnCF$=CFH (*trans*), $(CH_3)_3SnC_2H_2F$ (major); 3. $(CH_3)_2Sn(CH$=$CF_2)_2$ (minor); 4. $(CH_3)_2Sn(CF$=$CF_2)_2$ (minor); 5. $(CH_3)_2Sn(CF$=CFH$)_2$ (*cis*), $(CH_3)_3SnCF$=CFH (*cis*) (major); 6. Unidentified species (minor). A very negligible amount of unreacted hydride, and a little CF_2=CFH were also observed.

(*d*) Trimethyltin hydride (0.425 g, 2.58 mmoles) and dimethyl bis(perfluorovinyl)tin (0.40 g, 1.29 mmoles) were reacted as in *c*. The involatile white solid (0.42 g), which was isolated and purified as in *c*, consisted of a mixture of dimethyltin difluoride and trimethyltin fluoride, with the difluoride in excess. The volatile products (0.36 g) were transferred to a nuclear magnetic resonance sample tube, after removal of CF_2=CFH by vacuum fractionation. From analysis of the proton spectrum, and from the integrated spectrum, the proportions shown in Table VI were obtained.

TABLE VI

	% of volatiles	Weight (g)	Mole %*
$(CH_3)_3SnCF$=CFH (*cis*)	49	0.18	30
$(CH_3)_3SnCF$=CF_2	17	0.060	9.5
$(CH_3)_3SnCF$=CFH (*trans*)	14	0.050	8.6
$(CH_3)_2Sn(CF$=CFH$)_2$ (*cis*)	5.5	0.020	5.7
$(CH_3)_3SnC_2H_2F$	3.8	0.014	2.5
$(CH_3)_3SnCH$=CF_2	3.5	0.013	2.1
$(CH_3)_2Sn(C_2H_2F)_2$	1.1	0.0041	1.3
$(CH_3)_2Sn(CH$=$CF_2)_2$	1.1	0.0041	1.2
$(CH_3)_2Sn(CF$=$CF_2)_2$	0.9	0.0021	0.78
Others	4.5	0.017	—

*Taken with respect to trimethyltin hydride for the trimethyltin species, and with respect to dimethyl bis(perfluorovinyl)tin for the dimethyltin species.

Reactions of Dimethyltin Dihydride with Dimethyl Bis(perfluorovinyl)tin

In these reactions complete separation of the vinyl products from involatile residues was not always achieved, so that accurate yields cannot be given. According to the infrared spectra, however, recovery of unreacted hydride and of other hydride species was complete.

(*a*) Dimethyltin dihydride (1.247 g, 8.29 mmoles) and dimethyl bis(perfluorovinyl)tin (1.996 g, 5.67 mmoles) were heated to 60° in a sealed tube in the dark for 2 h. Removal of most of the volatile products left a white solid, and the following fractions were separated: (i) A −16° (0.042 g) fraction identified spectroscopically as unreacted perfluorovinyl compound. (ii) A −45° fraction (1.19 g) of which 87% was dimethyl (perfluorovinyl)tin hydride, $(CH_3)_2SnH(CF$=$CF_2)$. Molecular weight: calcd. 251; obs. 248. The infrared and proton resonance spectra support this characterization. The former shows absorption at 3 010 (m), 2 920 (m), (C—H stretch); 1 872 (s) (Sn—H stretch); 1 718 (s) (C=C stretch); 1 285 (s), 1 120 (s), 1 010 (s), (C—F stretch); 775 (s) (Sn—CH_3 rock); 725 (m), 576 (m), and 522 (s). The proton spectrum shows the Sn—H peak at −5.46 p.p.m. This is a broad, partially resolved multiplet, where for the proton attached to tin in $(CH_3)_2SnH(CF$=$CF_2)$, 56 components are expected. The methyl protons are seen as a doublet at −0.37 and −0.41 p.p.m. with the ^{119}Sn and ^{117}Sn sidebands at −0.93 and −0.89, and −0.90 and −0.86 p.p.m. respectively. The proton spectrum also showed that this −45° fraction contained approximately 7% of the $(CH_3)_2Sn(CF$=CFH$)_2$ bis-*cis* isomer, and 4% of the corresponding bis-*trans* isomer. (iii) A −64°

fraction (0.77 g, molecular weight 250) identified as pure $(CH_3)_2SnH(CF{=}CF_2)$. The total yield of $Me_2SnH(CF{=}CF_2)$ was thus 1.21 g, 4.82 mmoles. (iv) A −125° fraction (0.375 g, 2.50 mmoles) shown by its infrared spectrum and molecular weight (150) to be unreacted dimethyltin dihydride (95.4% of the excess). (v) A −196° fraction (0.02 g) identified spectroscopically as trifluoroethylene.

As further confirmation of the characterization of dimethyl(perfluorovinyl)tin hydride, a sample was reacted at 50° in the dark for 40 h with excess tetrafluoroethylene. Much of the product was separated as a fraction of molecular weight approximately 340 (calcd. for $(CH_3)_2Sn(CF{=}CF_2)(CF_2CF_2H)$, 330) and with an infrared spectrum which showed the presence of both $-CF{=}CF_2$ and $-C_2F_4H$ groups (1).

(*b*) Dimethyl bis(perfluorovinyl)tin (2.357 g, 6.73 mmoles) and dimethyltin dihydride (1.113 g, 7.38 mmoles) were exposed to ultraviolet irradiation for 1 h at 25–30°. When the tube was opened to the vacuum line, hydrogen (0.045 mmole) was evolved. The volatile products (0.900 g) were removed *in vacuo*, and a yellow solid was left in the tube. An infrared spectrum of the yellow solid showed the presence of $-CF{=}CF_2$, $-CF{=}CFH$, and $-C_2H_2F$ groups. When the solid was refluxed with toluene for 2 h, a white residue formed which was found by spectroscopy to contain no vinyl groups, and whose powder photograph was identical with that of an authentic sample of dimethyltin difluoride. The volatile products were transferred to a nuclear magnetic resonance sample tube, and from the proton spectrum, the integrated spectrum, and the known values of coupling constants, species containing $-CF{=}CFH$ (*cis*), $-CF{=}CFH$ (*trans*), and $-CH{=}CF_2$ groups were identified as well as dimethyltin dihydride and some unassigned peaks. It was concluded from the integral values that the volatile dimethyltin products were unreacted dimethyl bis(perfluorovinyl)tin (30%), $(CH_3)_2Sn(CF{=}CFH)_2$ (*cis*), $(CH_3)_2Sn(CF{=}CFH)_2$ (*trans*), $(CH_3)_2Sn(CH{=}CF_2)_2$, and $(CH_3)_2Sn(C_2H_2F)_2$, the last four in the approximate ratio 10:2:1:4, and an unidentified component. In addition, small amounts of trimethylperfluorovinyltin and trimethyl-1,2-difluorovinyltin were also detected. The latter presumably arose from decomposition of dimethyltin dihydride (1), followed by vinyl-hydrogen exchange, and partial reduction.

(*c*) Dimethyltin dihydride (0.82 g, 5.41 mmoles) and dimethyl bis(perfluorovinyl)tin (1.847 g, 5.26 mmoles) were irradiated at 25° for 6 h. When the tube was opened, hydrogen (1 mmole) was evolved, and only 14% of the total weight of reactants was recovered as volatile products, mainly as the unreacted perfluorovinyl compound. There remained a brightly colored, air-sensitive solid.

ACKNOWLEDGMENTS

The financial support of the National Research Council, Ottawa, is gratefully acknowledged.

REFERENCES

1. H. C. Clark, S. G. Furnival, and J. T. Kwon. Can. J. Chem. **41**, 2889 (1963).
2. C. Barnetson, H. C. Clark, and J. T. Kwon. Chem. Ind. London, 458 (1964).
3. H. C. Clark and J. T. Kwon. Can. J. Chem. **42**, 1288 (1964).
4. D. Seyferth. *In* Progress in inorganic chemistry. Vol. III. *Edited by* F. A. Cotton. Interscience Publishers, New York. 1962. pp. 129–280.
5. M. C. Henry and J. C. Noltes. J. Am. Chem. Soc. **82**, 561 (1960).
6. M. C. Henry and J. C. Noltes. J. Am. Chem. Soc. **82**, 558 (1960).
7. D. Seyferth, G. Raab, and K. A. Brändle. J. Org. Chem. **26**, 2934 (1961).
8. J. A. Pople, W. G. Schneider, and H. J. Bernstein. High resolution nuclear magnetic resonance. McGraw-Hill Book Co., New York. 1959.
9. T. L. Brown and G. L. Morgan. Inorg. Chem. **2**, 736 (1963).
10. H. C. Clark, W. S. Tsang, and J. H. Tsai. Chem. Comm. 171 (1965).
11. H. C. Clark, J. T. Kwon, L. W. Reeves, and E. J. Wells. Can. J. Chem. **41**, 3005 (1963).
12. H. C. Clark, J. T. Kwon, L. W. Reeves, and E. J. Wells. Inorg. Chem. **3**, 907 (1964).
13. H. D. Kaesz, S. L. Stafford, and F. G. A. Stone. J. Am. Chem. Soc. **82**, 6232 (1960).
14. D. Seyferth, D. E. Welch, and G. Raab. J. Am. Chem. Soc. **84**, 4266 (1962).
15. A. E. Finholt, A. C. Bond, Jr., K. E. Wilzbach, and H. I. Schlesinger. J. Am. Chem. Soc. **69**, 2692 (1947).
16. R. N. Haszeldine and B. R. Steele. J. Chem. Soc. 2800 (1957).
17. B. Bak and D. Christensen. Spectrochim. Acta, **12**, 355 (1958).

Can. J. Chem. Downloaded from www.nrcresearchpress.com by 210.87.254.5 on 09/05/12
For personal use only.

Can. J. Chem. Downloaded from www.nrcresearchpress.com by 210.87.254.40 on 09/05/12
For personal use only.

^{60}Co γ-RADIOLYSIS OF HYDROGEN HALIDES AT 77 °K[1]

R. C. RUMFELDT[2] AND D. A. ARMSTRONG
Department of Chemistry, University of Alberta, Calgary, Calgary, Alberta

Received August 31, 1965

ABSTRACT

Yields of hydrogen formed in the ^{60}Co γ-radiolyses of pure polycrystalline samples of HBr and HCl at 77 °K decrease with increasing dose in the range 0 to 1×10^{18} eV per g. The true initial yields are $G(H_2)_{\text{solid HCl at 77°K}} = 6.3 \pm 0.2$ and $G(H_2)_{\text{solid HBr at 77°K}} = 12.3 \pm 0.3$. Within experimental error these are the same as the respective liquid-phase yields at −79 °C. For doses in excess of 2×10^{18} eV per g the dose dependence is no longer significant and the yields tend toward plateau values of 3.2 ± 0.1 and 10.3 ± 0.1 for HCl and HBr respectively. The dose dependence of the hydrogen yields is attributed to the scavenging of a reactive intermediate by the halogen atoms and molecules which accumulate in the solid matrix as the dose increases.

In independent experiments with an apparatus of the Klein–Scheer type it was shown that hydrogen atoms react readily with films of HBr at 77 °K. There is, however, no evidence of a significant reaction with HCl at this temperature. The difference in behavior of the two hydrogen halides may be explained by their different activation energies for reaction with hydrogen atoms. The results of the γ-radiolyses are discussed in the light of these experiments and it is suggested that the dose dependence may be a result of the scavenging of an ionic intermediate rather than a thermal hydrogen atom.

INTRODUCTION

Earlier publications (1–3) from this laboratory have dealt largely with the γ-radiolysis of liquid and gaseous hydrogen halides. The present study was designed to investigate the radiolysis of solid polycrystalline HCl and HBr at 77 °K. Since it seemed that hydrogen atoms might be formed within the irradiated solids, an independent experimental technique was employed to investigate their reactivity toward HCl and HBr at this temperature.

EXPERIMENTAL

Materials

The hydrogen halides were purified and stored prior to irradiation as previously described (1, 3).

Apparatus

The apparatus and technique for the ^{60}Co γ-irradiations were essentially the same as in the earlier work. In this study the use of much larger samples (up to 5 g) of hydrogen halide and very careful experimental technique permitted the measurement of yields to within ±3% at doses as low as 2×10^{17} eV per g.

A number of experiments were performed in an apparatus of the type developed by Klein and Scheer (4) for studying hydrogen atom reactions at liquid nitrogen temperature. A uniform polycrystalline film of about 1 g of hydrogen halide was deposited on the inner wall of an evacuated 500 ml vessel immersed in a liquid nitrogen bath. Hydrogen atoms were produced by admitting a small pressure of hydrogen gas (50–100 μ of Hg) and dissociating the hydrogen molecules on an incandescent tungsten filament. At the pressures used most of these atoms diffuse to the walls of the vessel, where they may recombine or react with molecules in the hydrogen halide film to form hydrogen molecules, viz:

$$[1] \qquad H + HX \rightarrow H_2 + X.$$

Two different experimental arrangements were employed. In the first arrangement the apparatus consisted of a spherical bulb with the tungsten filament situated at its center. With this geometry the hydrogen halide film was exposed to the direct radiation from the incandescent filament as well as to the hydrogen atoms. In the second arrangement the filament was situated in a tube 2 cm in diameter attached to the cylindrical reaction vessel as shown in Fig. 1. The hydrogen atoms were carried into the vessel by convection and diffusion, and the film was shielded from the direct photon irradiation of the filament by an aluminium shield. In both arrangements the entire apparatus was immersed in liquid nitrogen.

[1]*Presented in part at the 150th meeting of the American Chemical Society, held September 1965 in Atlantic City.*
[2]*Present address: Department of Chemistry, University of Windsor, Windsor, Ontario.*

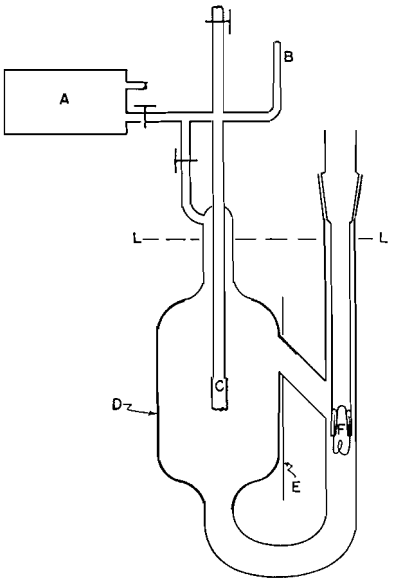


FIG. 1. Reaction vessel for the study of H-atom reactions with hydrogen halide films at 77 °K. (A) Equibar pressure meter coupled to recorder. (B) Palladium thimble for introducing pure gaseous hydrogen. (C) Sintered glass plug used to control deposition of the HX film on the surface of the reaction vessel. (D) Reaction vessel; double thickness indicates area in which the film is deposited. (E) Aluminium sheet to shield the film from direct visible radiation from F. (F) Tungsten filament and mercury pools for electrical contact. (L) Liquid nitrogen level.

The course of reaction [1] at 77 °K was followed by observing the pressure of hydrogen in the reaction vessel. In initial experiments this was done with a pirani gauge. In later work the pressure was monitored continuously with a Transonics type 120 equibar pressure meter coupled to a recorder.

RESULTS AND DISCUSSION

The hydrogen yields from pure polycrystalline hydrogen chloride are plotted against absorbed dose in Fig. 2. There is an obvious dependence on dose at doses less than 2×10^{18} eV per g. The true initial yield, obtained by extrapolation of the curve through the experimental points, is $G(H_2)^0_{\text{solid HCl at } 77°K} = 6.3 \pm 0.2$. Within experimental error this is the same as the liquid-phase yield of 6.5 ± 0.1 (1, 3). The hydrogen yields from pure polycrystalline HBr show a similar dependence on dose (see Fig. 2) and the experimental points also extrapolate to the liquid-phase yield (data have been included in Fig. 2 for comparison).

The liquid-phase yields in Fig. 2 show no evidence of a dose dependence. In control experiments no hydrogen was found: (*a*) in empty cells which had been subjected to the usual degassing procedure, sealed off under vacuum, and then subjected to irradiation at 77 °K, or (*b*) in cells filled with hydrogen halide and left unirradiated for periods equivalent to the duration of the average irradiation. From these observations and the fact that the G values were independent of sample size (and quantity of hydrogen determined), it may be concluded that the dose dependence is not an artifact of the experimental procedure or analytical technique.

The dose dependence of the hydrogen yields indicates that some product of the radiolysis accumulates in the solid hydrogen halides and scavenges reactive intermediates which under other circumstances react to form hydrogen molecules. It is apparent that the scavenger must consist of halogen atoms trapped in the HX matrix or halogen molecules

Can. J. Chem. Downloaded from www.nrcresearchpress.com by 210.87.254.40 on 09/05/12
For personal use only.

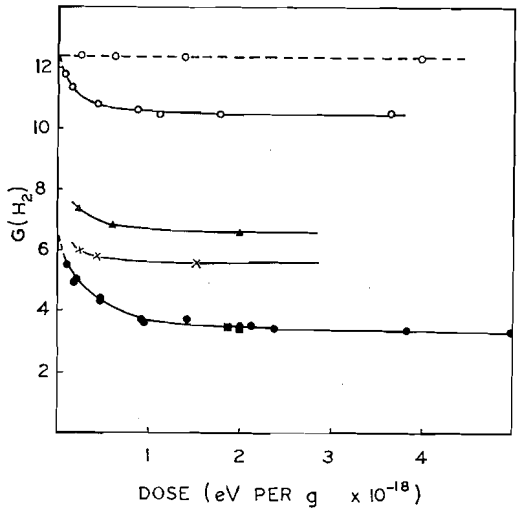


FIG. 2. Plots of $G(H_2)$ vs. dose for polycrystalline samples of hydrogen halides irradiated at 77 °K with ^{60}Co γ-rays. ○, Pure HBr; ●, pure HCl; ■, pure HCl, intermittent irradiations (see text); ×, 0.017 mole % HBr in HCl; ▲, 0.076 mole % HBr in HCl; the points on the broken line at the top represent corresponding yields in liquid HBr.

formed by atom recombination in the radiation tracks, or a combination of both. If a G value of 6.3 for the initial splitting of the H—Cl bond is assumed, it can be shown that approximately 2×10^{16} Cl atoms will have been formed per g of HCl when the hydrogen yield from the HCl has fallen halfway between 6.3 and the "plateau yield" (see below) of 3.3. This concentration corresponds to an average distance between Cl atoms of 300–400 Å. With the realization that these atoms would in fact be distributed in clusters and that some would probably have recombined, it is obvious that the species being scavenged must on the average traverse distances greater than 400 Å before reacting to form hydrogen molecules. Similar considerations apply in the case of HBr.

The value of $G(H_2)$ from solid HCl at a dose of 2 to 3 $\times$ 10^{18} eV per g is $3.3_6 \pm 0.1_0$, in good agreement with an earlier result (3). Beyond this dose range the dose dependence is very small for both hydrogen halides. Values of $G(H_2)$ in the dose range 2 to 3 $\times$ 10^{18} eV per g are therefore referred to as plateau yields.

Since the plateau yields in Fig. 2 are all much greater than zero it is clear that only a fraction of the total hydrogen formation from HCl and HBr is dependent on dose. In the case of HCl the remainder of the hydrogen may be attributed largely to a species, $H_{(s)}''$, the reactions of which are insensitive to the radical scavengers Cl and Cl_2 in the concentrations produced during the irradiations. Further evidence for such a reactive species comes from an earlier observation of the effect of chlorine added to the HCl prior to freezing and irradiation (3). A concentration of 2×10^{-4} mole of chlorine per g of HCl caused $G(H_2)$ to decrease from the plateau yield of 3.3 to 2.7. An increase of the chlorine concentration to 6×10^{-4} mole per g had no additional effect. The value of $G_{H(s)}''$ must therefore be 2.7. It is to be noted, also, that there is considerable evidence for corresponding species in both the liquid- and gas-phase radiolysis of HCl (1, 2, 3). The data for the gas-phase radiolysis of HBr (5) indicate that an analogous species is formed in this hydrogen halide, its yield ($G_H'' = 9$ to 10) being much greater than in HCl (cf. refs. 1, 5). The plateau yield of $G(H_2) = 10.3$ in solid HBr at 77 °K is in accord with these observations.

Can. J. Chem. Downloaded from www.nrcresearchpress.com by 210.87.254.40 on 09/05/12
For personal use only.

Can. J. Chem. Downloaded from www.nrcresearchpress.com by 210.87.254.40 on 09/05/12
For personal use only.

The reactive species responsible for the dose-dependent portion of the hydrogen yield from solid hydrogen halides (hereafter designated as $H_{(s)}'$) should be related to the species H′ observed in the liquids at −79 °C. The latter has the kinetic properties of a hydrogen atom (1) and is thought to be formed in the dissociative capture of electrons by suitable constellations of hydrogen halide molecules (1). This capture process must give rise to X—H—X⁻ as well as H. If capture occurred at 77 °K, $H_{(s)}'$ would have the kinetic properties of a thermal hydrogen atom (H) and two situations might arise. In the first, H atoms would be mobile and undergo reactions [1] and [2]

$$H + X + M \rightarrow HX + M \qquad [2]$$

in the solid hydrogen halides. In the case of HBr it can be shown on the basis of $A_1 \simeq A_2$, $E_2(H + Br) = 0$ kcal per mole, and $E_1(H + HBr) = 2$ kcals per mole activation energy (cf. ref. 1) that k_1/k_2 has a value of the order of 10^{-6} at 77 °K. Thus a relatively large concentration of Br atoms (10^{-5} per molecule of HBr or 10^{17} per g of HBr) would have to accumulate in the solid HBr before reaction [1] were suppressed. Depending on the yield of trapped bromine atoms (which has an upper limit of G(trapped Br) = 24) this would occur at an absorbed dose of 10^{18} to 10^{19} eV per g. Hence, although the approach to the plateau yield in Fig. 2 might have been expected at a somewhat higher dose than was observed, it is conceivable that this situation could be tenable in solid HBr. In contrast the corresponding value of k_1/k_2 for HCl at 77 °K based on $E_1(H + HCl) = 4.7$ kcals per mole (cf. ref. 1) would be about 10^{-13}. Thus as little as 10^{-12} Cl atoms per molecule of HCl (or 2×10^{10} per g of HCl) should serve to virtually suppress reaction [1] in HCl. If for example G(trapped Cl) $\geqslant 1$, it can be shown that this atom concentration would have been reached at a dose $\leqslant 2 \times 10^{12}$ eV per g. With allowance for an increase in $k_1(H + HCl)$ of up to 10^3 to take account of the enhanced contribution of quantum mechanical tunneling at 77 °K and other uncertainties in the calculation, the upper limit on this dose may be set at 2×10^{15} eV per g. This is some three orders of magnitude smaller than the dose at which the limiting plateau yield was attained in Fig. 2, and the discrepancy is sufficient to exclude the first situation in HCl.

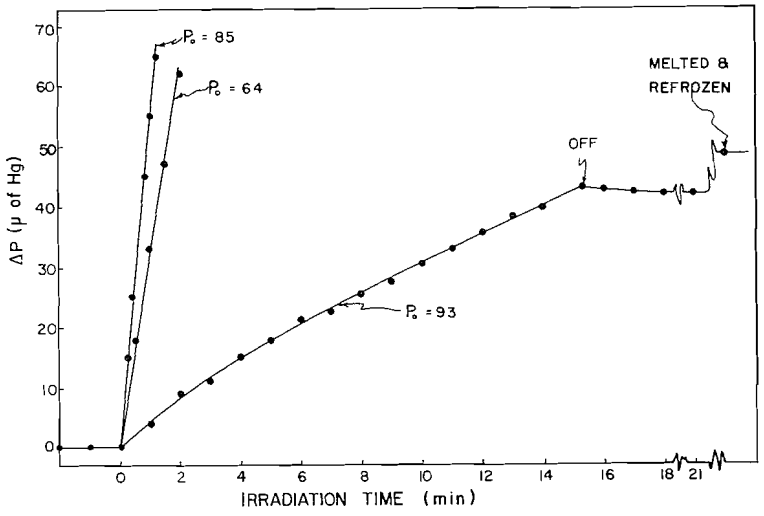


FIG. 3. Reaction time curves for H-atom reactions with HBr films at 77 °K. The tungsten filament was lighted at time zero. The curve for $P_0 = 93$ μ of Hg pressure was obtained with a film in the apparatus shown in Fig. 1. The apparatus used to obtain the other curves is described in the text.

Can. J. Chem. Downloaded from www.nrcresearchpress.com by 210.87.254.40 on 09/05/12
For personal use only.

In view of the foregoing considerations additional information about the reactivity of H atoms toward HCl and HBr at 77 °K was desirable. The application of the Klein–Scheer technique appeared to be the best method of obtaining this. Typical results are shown in Fig. 3, where the increase in the pressure of hydrogen in the reaction bulb has been plotted against the time elapsed after heating the tungsten filament. With an HBr film on the surface of the reaction bulb there was a pressure rise (see Fig. 3) with both of the experimental arrangements (described in Experimental). Although the reaction rate was much faster in the reaction vessel with the filament at its center, the second apparatus was considered more satisfactory for observing reaction [1] at 77 °K. In addition to eliminating the direct irradiation of the film, which might have caused a temperature rise of several degrees at the film surface, it ensured that all hydrogen atoms were brought to kinetic energies characteristic of 77 °K by collisional deactivation before they reached the film. The pressure increase observed in this vessel may therefore be regarded as a true indication of thermal hydrogen atom reactions with an HBr film at 77 °K. The slight decrease in the rate of the pressure rise as the reaction proceeded is to be expected, since the bromine atoms formed in reaction [1] will accumulate in the crystal lattice with the consequent occurrence of reaction [2]. The effect of this competition would have been alleviated to some extent by the increase in the rate of hydrogen atom formation, which would have accompanied the rise in the pressure of molecular hydrogen. Nevertheless the fact that the system did not rapidly approach a steady state indicates that the reaction does not proceed only at the crystal surfaces, and that the hydrogen atoms are able to penetrate to considerable depths. As a corollary, the observed pressure increase shows that hydrogen molecules are also mobile in the film, since the majority of them must escape very rapidly. However, a significant fraction of them appear to be formed too deep within the crystal to escape during the time of reaction. They are only observed on melting the film (see Fig. 3, the increase in pressure of hydrogen after melting and refreezing).

In the case of an HCl film in the first apparatus, which provides the optimum conditions for reaction [1], there was no increase in pressure over a prolonged period of exposure. Increasing the filament temperature and doubling the initial pressure also failed to initiate any reaction. It can be shown that $k_1(H + HCl)/k_2(H + Cl)$ would have to have approximately the same value as $k_1(H + HBr)/k_2(H + Br)$ to explain the dose dependence on the basis of hydrogen atom scavenging. Thus the above observations strongly support the arguments previously used against the occurrence of reaction [1] in solid HCl irradiated at 77 °K.

The second situation which must be considered is that H atoms would remain trapped in the hydrogen halide matrices at 77 °K and become mobile during the "warm-up" period before the bulkier halogen atoms could recombine. This situation is untenable in HBr in view of the foregoing observations. In addition it should be noted that Mitchell, Green, and Spinks (6) failed to find definite evidence for the presence of trapped H atoms in their electron spin resonance study of γ-irradiated HBr at 77 °K. For HCl the second situation would require that reaction [1] be in competition with [2] during the "warm-up" period at temperatures where the ratio k_1/k_2 was higher than 10^{-13}.* The dose dependence could be explained on this basis since, the larger the dose received prior to melting, the larger the concentration of chlorine atoms would be, and hence the greater the suppression of reaction [1]. In two experiments the HCl samples were successively irradiated to a dose of 0.24 $\times$

**In contrast to the value of 10^{-13} at 77 °K, $k_1(H + HCl)/k_2(H + Cl)$ would have a value of about 10^{-6} at the melting point of HCl (−114.3 °C). At this temperature $k_1(H + HCl)/k(H + Cl_2)$ would have a value of $\simeq 8 \times 10^{-4}$. Note that these and all similar calculations are based on the kinetic data given in ref. 1.*

10^{18} eV per g, melted to convert the accumulated chlorine atoms to molecules, refrozen, and reirradiated until a total final dose of about 1.9×10^{18} eV per g had been attained. If hydrogen formation took place on melting, one would expect the yields from these intermittent irradiations to be higher than those from a continuous irradiation to the same total dose. To be precise, they should have corresponded to the G value for a dose of 0.24×10^{18} eV per g. In fact the observed G values (see the squares in Fig. 3) corresponded to those for the total accumulated dose of 1.9×10^{18} eV/g. This indicates that the second situation is an extremely unlikely one in HCl. In this connection it is also to be noted that few crystalline solids are able to trap hydrogen atoms at 77 °K (cf. their behavior in ice (7)). Furthermore an electron spin resonance study of samples of HCl irradiated at 77 °K was carried out in this laboratory, and failed to reveal the presence of trapped hydrogen atoms (8).

The foregoing arguments show that reactions of thermal hydrogen atoms do not provide an acceptable explanation for the dose dependence of the hydrogen yields from solid HCl. Thus it appears that in crystalline HCl at 77 °K electrons may undergo processes other than the capture reaction referred to above. The low temperature phases, in which HCl and HBr exist at 77 °K, consist of orthorombic crystal lattices, and Hornig and his co-workers (9) have concluded that the hydrogen halide molecules are arranged in the form of zig-zag hydrogen-bonded chains. The component molecules are coupled in their infrared modes, and there is no evidence of rotation of the molecules in the spectroscopic sense of the term. In ordered crystalline solids of this type the rate of energy loss of sub-excitation electrons is much less than in liquids (10). Furthermore the regular lattice structure may provide preferred paths for electron and charge transfer. As a result, electrons are extremely mobile in such solids (11). Trapping and capture are most likely to occur at crystal defects present initially or created by radiation damage. Two alternative reactions of electrons are therefore probable: (*a*) reaction with H_2Cl^+ positive ions to form hydrogen molecules or atoms

[3]* $$H_2Cl^+ + e \rightarrow H_2 + Cl \text{ (or } H + Cl) + \text{energy}$$

and (*b*) reaction with the trapped Cl atoms which accumulate in the HCl matrix. Since these are probably formed in the reactions of $H_{(s)}''$ as well as in reaction [3], their concentrations should increase much more rapidly than that of H_2Cl^+, thus providing for eventual repression of reaction [3]. It should be noted that this electron-trapping mechanism is not subject to the objections encountered previously for hydrogen atom reactions in HCl. Furthermore electron trapping at crystal sites occupied by Cl_2 (or Br_2 in HBr) would probably also be a highly efficient process, since it should result in the formation of Cl_2^-, which is stable at 77 °K.† On this basis it is possible to explain the fact that the molecular chlorine which was formed on melting the samples in the intermittent experiments described above was essentially as effective in suppressing the hydrogen yield as the Cl atoms which it replaced. This would certainly not have been the case for hydrogen atom scavenging at 77 °K.

Although a hydrogen atom mechanism is not entirely excluded in the case of HBr, the electron-trapping mechanism could also explain the effects observed in that hydrogen halide.

**If* H *atoms were formed they should possess sufficient kinetic energy to undergo reaction [1] without further activation.*

†*The molecular halogen ions* Cl_2^- *and* Br_2^- *have been observed in the* γ*-radiolysis of sulfuric acid glasses containing* Cl^- *and* Br^- *at 77 °K (12), and in the corresponding crystalline alkali halides after* γ*-irradiation (13). Both* Br_2^- *and* Cl_2^- *exhibit strong absorption maxima in the region 3 300 to 3 900 Å (12, 13) and in the halide crystals there is evidence of an additional maximum at about 7 500 Å (13). It is to be noted that the formation of these ions could also explain the fact that both* HCl *and* HBr *exhibit a grey-green color after irradiation.*

Can. J. Chem. Downloaded from www.nrcresearchpress.com by 210.87.254.40 on 09/05/12
For personal use only.

Spectroscopic techniques (9) have confirmed that HCl and HBr form homogeneous solid solutions as would have been expected. Several experiments were performed with solid solutions prepared by rapidly freezing homogeneous liquid solutions of HBr in HCl. The hydrogen yields from these showed a much less marked dependence on dose than did those from pure HCl (see Fig. 2). $G(H_2)$ values for a dose of 2×10^{18} eV per g (i.e. plateau yields) are given in Table I as a function of HBr concentration.

TABLE I

Hydrogen yields from solid solutions of HBr in HCl at 77 °K

HBr (mole fraction)	$G(H_2)$	HBr (mole fraction)	$G(H_2)$
0.00_0	3.3_6	0.01_7	5.7_0
0.001_5	4.0_6	0.03_8	6.2_1
0.006_5	4.7_2	0.05_1	6.4_7
0.01_7	5.4_4		

It can be seen that the hydrogen yields from HCl are extremely sensitive to minute traces of HBr. For example, 0.001_5 mole % HBr enhanced $G(H_2)$ by 0.7 G units. This sensitivity confirms the fact that long range chemical or physical interactions precede the actual process of hydrogen formation. It is not clear at present whether these involve energy transfer along the chains of HCl molecules to isolated HBr molecules (cf. ref. 14) or the capture of positive charges or radicals (including e) at HBr sites on the crystal lattice. It is possible that all these processes occur.

REFERENCES

1. R. C. Rumfeldt and D. A. Armstrong. J. Phys. Chem. **68**, 761 (1964).
2. R. A. Lee, R. S. Davidow, and D. A. Armstrong. Can. J. Chem. **42**, 1906 (1964).
3. D. A. Armstrong. Can. J. Chem. **40**, 1385 (1962).
4. M. D. Scheer and R. Klein. J. Phys. Chem. **65**, 375 (1961).
5. R. A. Lee and D. A. Armstrong. Nature, **200**, 552 (1963).
6. F. W. Mitchell, B. C. Green, and J. W. T. Spinks. Can. J. Chem. **38**, 689 (1960).
7. L. H. Piette, R. C. Rempel, H. E. Weaver, and J. M. Flournoy. J. Chem. Phys. **30**, 1623 (1959). J. M. Flournoy, L. H. Baum, and S. Siegel. J. Chem. Phys. **36**, 2229 (1962).
8. D. A. Stiles. Private communication.
9. D. F. Hornig and W. E. Osberg. J. Chem. Phys. **23**, 662 (1955). D. F. Hornig and G. L. Hiebert. J. Chem. Phys. **27**, 752, 1216 (1957); **28**, 316 (1958).
10. H. Frohlich and R. L. Platzman. Phys. Rev. **92**, 1152 (1953).
11. E. J. Hart and R. L. Platzman. *In* Mechanisms in radiobiology. *Edited by* M. Errera and A. Forssberg. Academic Press, New York. 1961. p. 157.
12. D. M. Brown and F. S. Dainton. Private communication.
13. C. J. Delbecq, W. Hayes, and P. H. Yuster. Phys. Rev. **121**, 1043 (1961).
14. J. L. Magee. *In* Comparative effects of radiation. *Edited by* Milton Burton *et al.* John Wiley and Sons, New York. 1960. Chap. 7.

Can. J. Chem. Downloaded from www.nrcresearchpress.com by 210.87.254.40 on 09/05/12
For personal use only.

Can. J. Chem. Downloaded from www.nrcresearchpress.com by 210.87.254.5 on 09/05/12
For personal use only.

THERMODYNAMIC AND ELECTROCHEMICAL PROPERTIES OF ZIRCONIUM CHLORIDES IN ALKALI CHLORIDE MELTS

B. SWAROOP[1] AND S. N. FLENGAS
Department of Metallurgy and Materials Science, University of Toronto, Toronto, Ontario

Received June 4, 1965

ABSTRACT

The liquidus curves in the binary equilibrium phase diagrams of the systems, $ZrCl_2$–MCl, and $ZrCl_3$–MCl, where M is potassium or sodium, have been determined where possible. The electrochemical properties of the dilute solutions of zirconium di-, tri-, and tetra-chlorides, in the temperature range 670 °C to 750 °C, were investigated by reversible electromotive force measurements. From the results various equilibria between zirconium metal and the solutions of zirconium tri- and tetra-chlorides, respectively, were determined. Activity calculations indicate that zirconium tetrachloride is heavily complexed in these melts.

INTRODUCTION

Measurements of the "apparent standard potentials" of several metal – metal chloride systems in dilute solutions in fused alkali chlorides have been reported in previous investigations (1, 2, 3). Such measurements provide data on activities, help determine the equilibrium constants of chemical reactions in fused salts, and provide some of the necessary information for the recovery of metals by fused salt electrolysis. An equimolar melt of potassium and sodium chlorides was used as the solvent melt in all these studies, and a silver – silver chloride electrode developed earlier in this work (1) was the reference electrode.

In this investigation, the technique has been applied to the determination of the reversible potentials of the zirconium chlorides in the temperature range 670 °C to 750 °C. Three zirconium chlorides are known to exist at room temperature: zirconium dichloride, zirconium trichloride, and zirconium tetrachloride.

Pure solid zirconium trichloride disproportionates at high temperatures by the reaction:

[1] $$2ZrCl_{3(s)} = ZrCl_{2(s)} + ZrCl_{4\ vap.}$$

Turnbull and Watts (4) have shown that the reaction pressure of zirconium tetrachloride vapor in equilibrium with the two solid phases reaches 1 atm at about 450 °C. Solutions of zirconium trichloride in alkali chloride melts have also been considered to be thermally unstable and recent measurements of the zirconium potential have been conducted in melts containing zirconium tetrachloride (5, 6).

Preliminary experiments in this laboratory have indicated that at 700 °C zirconium metal is soluble in an equimolar melt of potassium and sodium chlorides containing either zirconium trichloride or zirconium tetrachloride. Solidified material from these solutions had a dark blue color, indicating the presence of reduced zirconium species.

In the experimental work reported herein, the thermal stabilities of zirconium dichloride and of zirconium trichloride in solution were investigated by cryoscopic measurements and by X-ray analysis.

The liquidus curves of the binary systems MCl–$ZrCl_2$ and MCl–$ZrCl_3$, where M is potassium or sodium, were determined. The potentials of a zirconium electrode immersed in a solution containing zirconium dichloride and the redox potentials of the systems $ZrCl_2|ZrCl_3$ and $ZrCl_3|ZrCl_4$ were also investigated. From the results, the equilibrium

[1]*Present address: Department of Metallurgy, Northwestern University, Evanston, Illinois, U.S.A.*

constants for the reactions between zirconium metal and zirconium tri- or tetra-chlorides in solution were obtained and the mechanism of the reversible deposition of zirconium metal by electrolysis from a melt containing zirconium tetrachloride is predicted.

EXPERIMENTAL

The preparations of anhydrous zirconium dichloride and of zirconium trichloride of purity better than 98% by weight have been described in previous publications (7, 8). Zirconium tetrachloride was used as the stable complex compound K_2ZrCl_6. The preparation of this compound has also been reported in a previous publication (9). Zirconium di- and tri-chlorides are hygroscopic and oxidize readily in air; the potassium hexachlorozirconate compound is only hygroscopic. Accordingly, handling of these materials was done in a dry box filled with purified argon.

The liquidus curves of the binary systems $MCl–ZrCl_2$ and $MCl–ZrCl_3$, where M is sodium or potassium, were established by freezing point measurements. The mixtures were contained in heart-shaped quartz ampoules, with a thermocouple well blown in the center, sealed under vacuum. The cooling curves were recorded on a 1 mV full-scale deflection recorder. The cooling rate was automatically regulated to between 0.75 to 1.5 deg per min. Undercooling was generally below 1.5 deg. Calibrated platinum – platinum – 13% rhodium thermocouples were used for these measurements and the reproducibility of the measured freezing points on the same sample was ±1 °C. Potentials were measured with the cell shown in Fig. 1.

The cell was constructed from quartz glass and was operated under an atmosphere of purified argon. The melt was contained in a platinum crucible connected to a platinum lead wire. The crucible itself represented

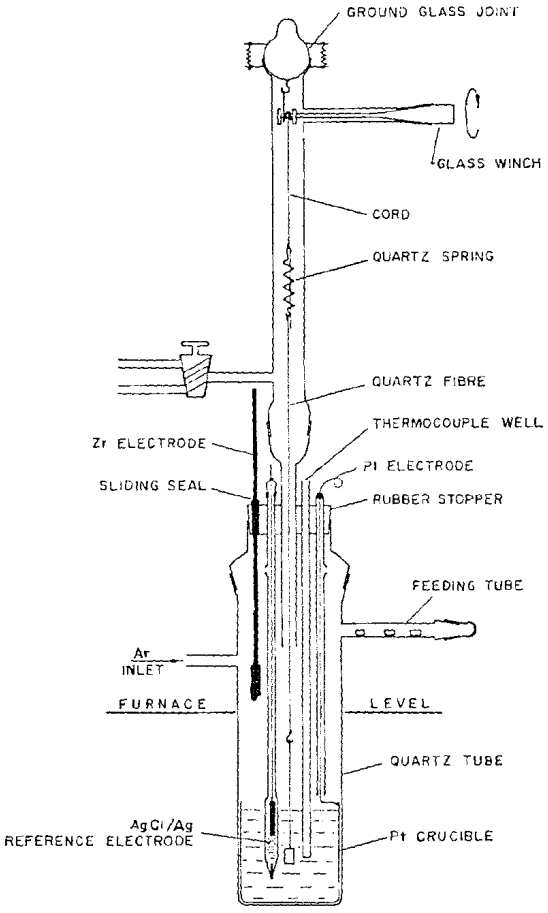


FIG. 1. Cell design.

Can. J. Chem. Downloaded from www.nrcresearchpress.com by 210.87.254.5 on 09/05/12
For personal use only.

the inert platinum electrode for the redox potential measurements of the systems $Zr^{2+}|Zr^{3+}$ and $Zr^{3+}|Zr^{4+}$. The potentials of the zirconium electrode were obtained with a solution containing zirconium dichloride. The electrode was of reactor-grade zirconium metal, containing less than 400 p.p.m. of metallic impurities. It could be lowered into the system using a sliding seal. The reference electrode in all these measurements was a silver – silver chloride electrode of a design given in a previous publication (1). The solutions in the two electrode compartments were separated by an asbestos fiber sealed at the tip of the reference electrode. Thermoelectric potentials caused by these electrodes were measured separately and the appropriate corrections were applied to the measured electrode potentials.

Solutions of zirconium dichloride were also prepared *in situ* by the direct reaction between zirconium metal and zirconium trichloride in solution:

$$[2] \qquad Zr_{(s)} + 2(ZrCl_3)_{solution} = 3(ZrCl_2)_{solution}.$$

For this purpose a quartz spring balance was incorporated in the cell. A zirconium rod, 1/2 in. long by 1/4 in. in diameter, was suspended from the lower end of the balance and dipped into a melt containing a known amount of zirconium trichloride. The loss of weight of zirconium in reaction [2] could then be followed by measuring the spring extension with a cathetometer. By this method 0.1 mg of reacted metal corresponding to the production of 0.53 mg of zirconium dichloride could be detected. A mixture of divalent and trivalent zirconium of any desired ratio could also be obtained by withdrawing the metal from the solution and thus interrupting the reaction at any given time prior to its completion. These solutions were then used for measurements of the redox potentials of the $Zr^{2+}|Zr^{3+}$ system.

Solutions of zirconium dichloride and mixtures containing known amounts of either zirconium di- and tri-chlorides, or zirconium tri- and tetra-chlorides were also prepared by adding weighed pellets of the pure anhydrous materials from the sidearm feeding tube shown in Fig. 1.

RESULTS AND DISCUSSION

(*a*) *Phase Diagram Determinations*

The liquidus curves for the binary systems KCl–$ZrCl_2$ and NaCl–$ZrCl_2$ were investigated and the results are given in Figs. 2 and 3.

The diagrams are of the simple eutectic type. The melting point of pure zirconium dichloride was found at 722 ± 1 °C. In the KCl–$ZrCl_2$ system, the eutectic is found at 698 ± 1 °C and 53.5 mole % zirconium dichloride. In the NaCl–$ZrCl_2$ system the eutectic lies at 695 ± 1 °C and at 69 mole % zirconium dichloride. X-ray patterns of material cooled from eutectic composition on the NaCl–$ZrCl_2$ system showed the same positions of the lines and the same order of relative intensities as found in pure zirconium dichloride (8) and sodium chloride, indicating that solid solubility is slight if it occurs.

X-ray patterns taken on KCl–$ZrCl_2$ samples cooled from a liquid of eutectic composition showed only a slight displacement in the position of the potassium chloride peaks, indicating the existence of solid solubility in this system. Disproportionation products such as zirconium metal, zirconium trichloride, or any of the hexachlorozirconate compounds could not be detected in these systems. Repeated freezing point determinations on the same sample were fully reproducible to within 1 °C, thus indicating the thermal stability of these solutions. The liquidus curve on the KCl-rich side of the system KCl–$ZrCl_3$ is shown in Fig. 4.

The melting point of pure zirconium trichloride could not be obtained because of disproportionation. The X-ray analysis of a solidified sample of zirconium trichloride included sharp lines for zirconium dichloride, a medium strong line for zirconium tetrachloride, and a weak line for zirconium trichloride. Similarly the $ZrCl_3$-rich solutions in this system indicated that disproportionation had taken place. On the potassium chloride side of the diagram, X-ray analysis on quenched samples obtained from a liquid solution containing 59.6 mole % zirconium trichloride showed very sharp lines for the trichloride. It appeared, however, that the lines were slightly displaced and their order of relative intensities had changed. The potassium chloride lines were also displaced, thus indicating solid solubility. The eutectic temperature was found at 581 ± 2 °C. The liquidus freezing

Can. J. Chem. Downloaded from www.nrcresearchpress.com by 210.87.254.5 on 09/05/12
For personal use only.

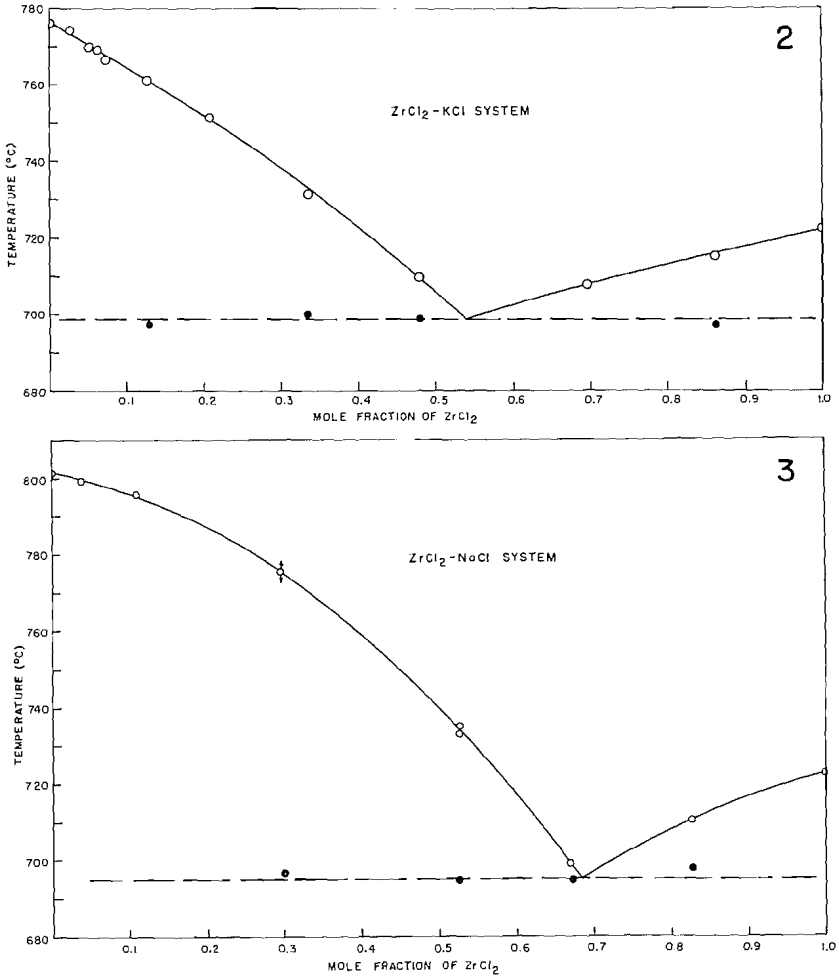


FIG. 2. Phase diagram of the $ZrCl_2$–KCl system.
FIG. 3. Phase diagram of the $ZrCl_2$–NaCl system.

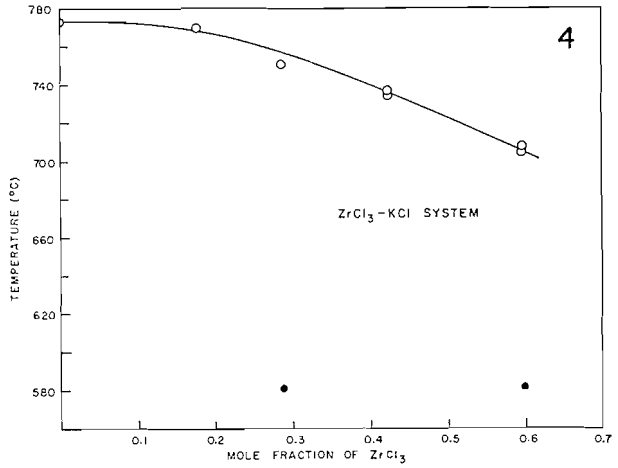
points were found to be lowered by 3 deg after the cooling curve had been repeated on the same sample.

Attempts to determine the phase diagram for the $ZrCl_3$–NaCl mixtures failed because of excessive disproportionation in this system.

In conclusion the phase diagram investigation indicates that zirconium dichloride is stable in its solutions with either potassium or sodium chlorides. On the other hand, zirconium trichloride is stable only in the presence of potassium chloride. It is probable that the formation of complex species with potassium chloride in the melt causes the shift of the equilibrium of disproportionation reaction [1] on the reactant side.

The stability of zirconium trichloride in the equimolar melt of potassium and sodium chlorides was also investigated by taking the X-ray diffraction patterns of a sample containing 15 mole % zirconium trichloride. The sample was raised to 750 °C, kept at that temperature for 24 h, and then quenched. The X-ray patterns showed clearly only the sharp lines for zirconium trichloride, along with those for potassium and sodium chlorides. The latter were slightly displaced because of the existence of solid solubility, as expected.

Can. J. Chem. Downloaded from www.nrcresearchpress.com by 210.87.254.5 on 09/05/12
For personal use only.



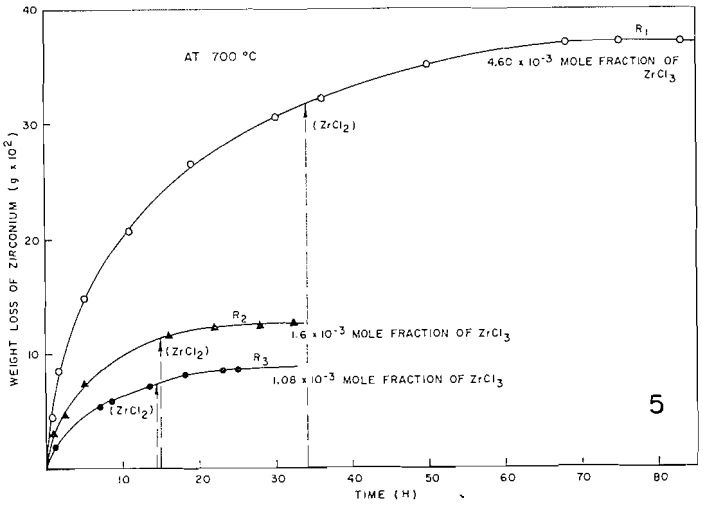


FIG. 4. Liquidus curve in the $ZrCl_3$-KCl system.
FIG. 5. Solubility of zirconium metal in zirconium trichloride in solution in the equimolar melt of potassium and sodium chlorides.

(b) Solubilities of Zirconium Metal in Zirconium Trichloride Solutions

The reaction between zirconium metal and zirconium trichloride in solution in the equimolar melt of potassium and sodium chlorides was investigated by the quartz spring balance apparatus. Typical solubility curves at 700 °C as a function of time are given in Fig. 5. The vertical dotted lines represent the weight loss of zirconium metal corresponding to the formation of zirconium dichloride from the initial amount of zirconium trichloride present in the melt. It was found that when all the trichloride had been reduced to the dichloride the zirconium rod continued to lose weight slowly. After periods of 96 h, amounts to the order of 5×10^{-5} to 10^{-4} mole fraction excess metal in solution were obtained. Zirconium metal did not dissolve in the equimolar melt of potassium and sodium chlorides. However, slow dissolution was evident when zirconium dichloride was added to this melt. The mechanism of metal dissolution in molten salts is not too well understood at present. Particularly in this case, the observed excess solubility cannot be associated with

Can. J. Chem. Downloaded from www.nrcresearchpress.com by 210.87.254.5 on 09/05/12
For personal use only.

the existence of a species of a lower valence than divalent zirconium. From the potential measurements, to be discussed subsequently, it appears that the valence and the activity of divalent zirconium in solution are not affected by the presence of excess metal.

From the curves in Fig. 5 it is evident that at 700 °C the relative rate of metal dissolution is rather slow, and increases with increasing concentration of zirconium trichloride in solution, as expected.

(*c*) *Electromotive Force Measurements*

The reversible potentials of the cell,

$$\begin{array}{c|c||c|c} \text{Zr} & \text{ZrCl}_2\,(X_2) & \text{AgCl}\,(X_1) & \text{Ag} \\ (-) & \text{KCl} + \text{NaCl}\ ((1/1)\ \text{mole}) & \text{KCl} + \text{NaCl}\ ((1/1)\ \text{mole}) & (+) \end{array} \qquad \text{(cell A)},$$

were measured, at various concentrations of zirconium dichloride, as a function of temperature. At each concentration level, the potentials reached their equilibrium values within 3 to 4 h and remained constant thereafter. The results of these measurements are given in Fig. 6. Each curve corresponds to a complete temperature cycle in the range 670 °C to 750 °C. The readings were fully reproducible. During a temperature cycle that lasted 24 to 48 h, the potential drift on returning to the original temperature was less than ±2 mV. At temperatures higher than 750 °C readings became unstable and were not taken.

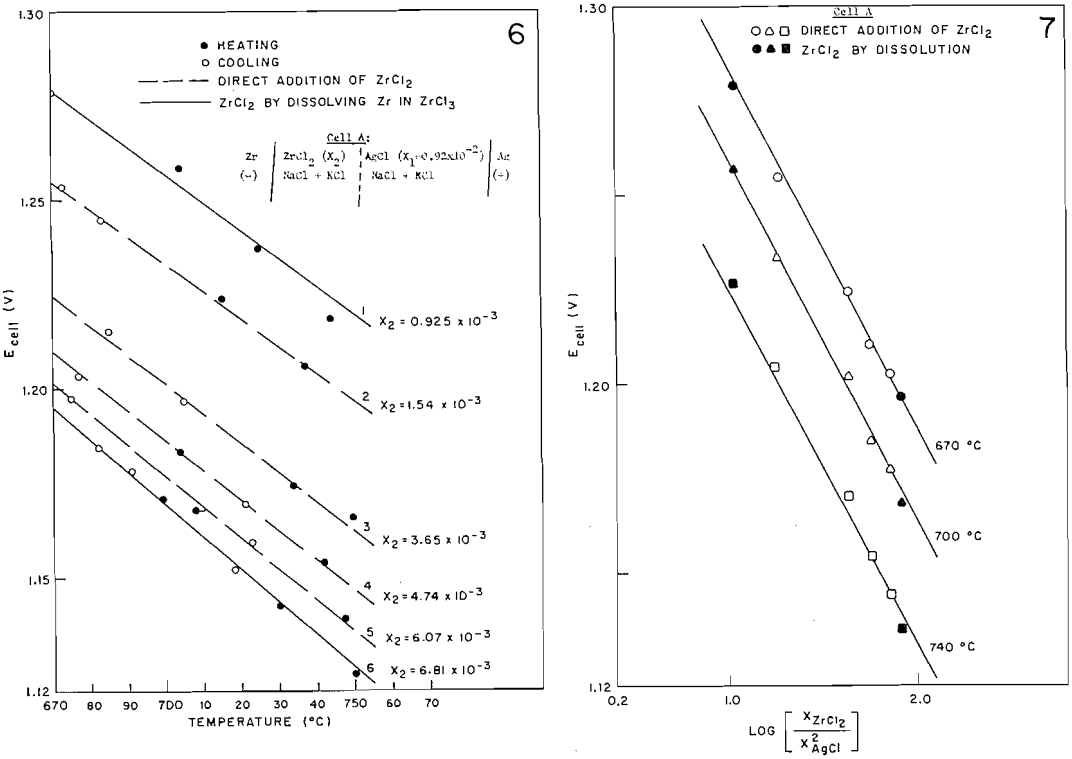


FIG. 6. Potentials of the $Zr|Zr^{2+}$ system as a function of temperature.
FIG. 7. Plot of the potentials of the $Zr|Zr^{2+}$ system against the logarithm of mole fractions.

Can. J. Chem. Downloaded from www.nrcresearchpress.com by 210.87.254.5 on 09/05/12
For personal use only.

In Fig. 6, the solid lines represent compositions of zirconium dichloride prepared by the dissolution method, and the dotted lines represent additions of pure zirconium dichloride. The reaction in cell A is given as

[3] $$Zr_{(s)} + 2(AgCl)_{solution} = (ZrCl_2)_{solution} + 2Ag_{(s)}$$

and the Nernst equation corresponding to this reaction is

[4] $$E_{cell} = (E_{ZrCl_2}{}^0 - E_{AgCl}{}^0) - \frac{RT}{2F} \ln \frac{\gamma_{ZrCl_2}}{\gamma_{AgCl}{}^2} - \frac{RT}{2F} \ln \frac{X_2}{X_1{}^2}$$

where, E_{cell} is the experimentally measured cell potential, and $E_{ZrCl_2}{}^0$ and $E_{AgCl}{}^0$ represent the formation potentials of the pure constituents. The formation potentials may be calculated from thermodynamic data available in the literature and will be referred to as "standard potentials" in all subsequent discussions. The X's and γ's are mole fractions and activity coefficients, respectively. The standard states of reference for the activity calculations are the pure compounds at the temperature of the experiment.

The plot of the cell potentials against log $(X_2/X_1{}^2)$ of eq. [4] is given in Fig. 7. Isotherms at the selected temperatures of 670 °C, 700 °C, and 740 °C are shown. The curves are linear indicating that the activity coefficients of zirconium dichloride and silver chloride are constant at constant temperature, and independent of concentration. Accordingly, the solutions obey Henry's law and the data may be used for the calculation of an "apparent standard cell potential", $E_{app}{}'^0$, given as

[5] $$E_{app}{}'^0 = E_{ZrCl_2}{}^0 - E_{AgCl}{}^0 - (RT/2F) \ln \gamma_2.$$

The activity coefficient for silver chloride has been neglected in eq. [5] since these solutions are known to be ideal (1).

The "apparent standard cell potential" defines the free energy of reaction [3] in hypothetical solutions of unit concentration, with reactants and products in their states at infinite dilution. The cell reactions for the two redox cells

Pt	$ZrCl_2$ (X_2)		AgCl (X_1)	Ag	
(−)	$ZrCl_3$ (X_3)	||	KCl + NaCl ((1/1) mole)	(+)	(cell B)
	KCl + NaCl ((1/1) mole)				

and

Pt	$ZrCl_3$ (X_3)		AgCl (X_1)	Ag	
(−)	$ZrCl_4$ (X_4)	||	KCl + NaCl ((1/1) mole)	(+)	(cell C)
	KCl + NaCl ((1/1) mole)				

are, respectively,

[5] $$(ZrCl_2)_{in\ solution} + (AgCl)_{in\ solution} = (ZrCl_3)_{in\ solution} + Ag_{solid}$$

and

[6] $$(ZrCl_3)_{in\ solution} + (AgCl)_{in\ solution} = (ZrCl_4)_{in\ solution} + Ag_{solid}$$

The appropriate forms of the corresponding Nernst equation are

[7] $$E_{cell} = [3E_{ZrCl_3}{}^0 - 2E_{ZrCl_2}{}^0 - E_{AgCl}{}^0 - (RT/F) \ln (\gamma_{ZrCl_3}/\gamma_{ZrCl_2})] - (RT/F) \ln (X_{ZrCl_3}/X_{ZrCl_2})$$

and

[8] $$E_{cell} = [4E_{ZrCl_4}{}^0 - 3E_{ZrCl_3}{}^0 - E_{AgCl}{}^0 - (RT/F) \ln (\gamma_{ZrCl_4}/\gamma_{ZrCl_3})] - (RT/F) \ln (X_{ZrCl_4}/X_{ZrCl_3})$$

Can. J. Chem. Downloaded from www.nrcresearchpress.com by 210.87.254.5 on 09/05/12
For personal use only.

where E^0's represent the standard potentials of the pure constituents, and γ's and X's are the corresponding activity coefficients and mole fractions. The quantities in brackets are the "apparent standard potentials" for the two redox systems.

The redox potentials of di- and tri-, and of tri- and tetra-valent zirconium were measured in the mole fraction range 10^{-3} to 10^{-4} and in the temperature range 670 °C to 750 °C. These potentials reached steady values in 3 to 6 h. Accordingly, at each concentration level, the potentials were measured as a function of time. When steady readings were obtained, the system was observed for at least another 3 h to ensure that true equilibrium had been reached. The equilibrium potentials as a function of temperature for these two systems are shown in Figs. 8 and 9. The results correspond to complete temperature

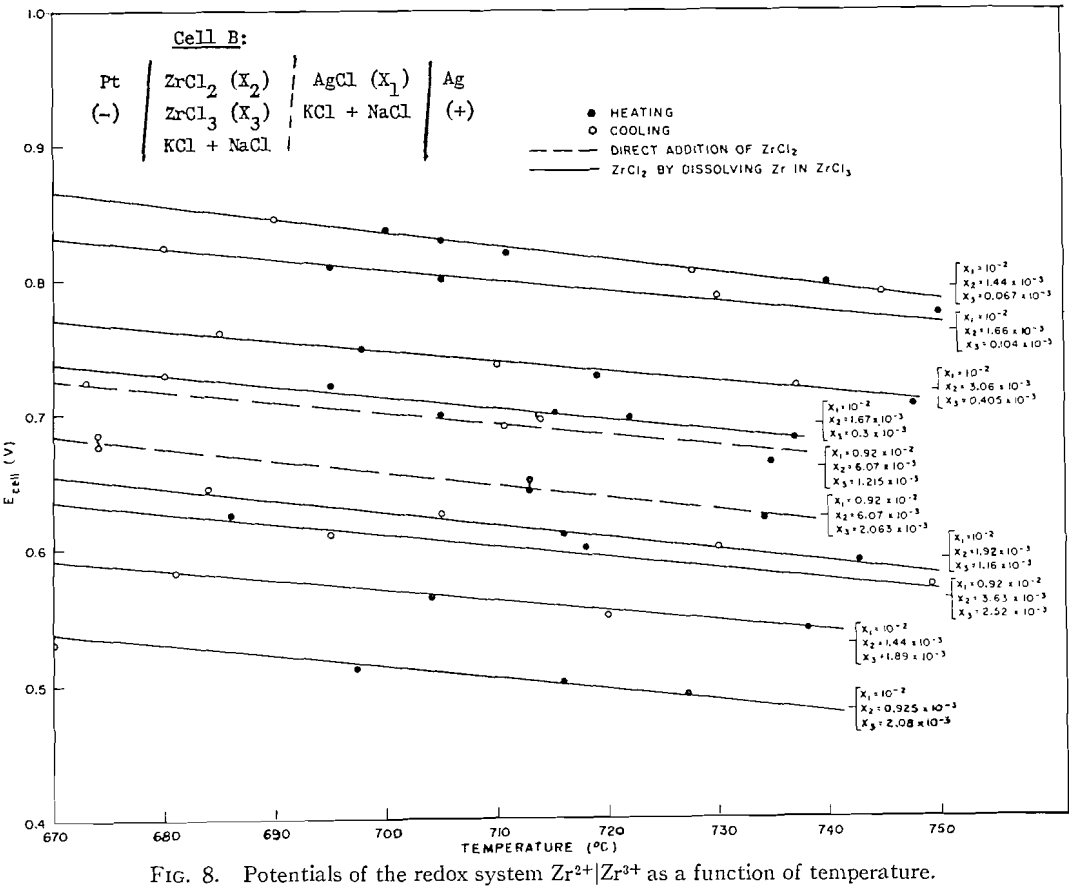


FIG. 8. Potentials of the redox system $Zr^{2+}|Zr^{3+}$ as a function of temperature.

cycles and were quite reproducible. Thus, during a temperature cycle, on cooling the potentials returned to the original values to within ±3 mV.

The corresponding Nernst isotherms for the two systems are given in Figs. 10 and 11. The curves are linear with a slope corresponding to a one-electron electrode process, as expected. The linearity of the curves also indicates that the solutions of trivalent and tetravalent zirconium follow Henry's law.

The "apparent standard" potentials of these three systems were calculated, at each concentration level, with eqs. [4], [7], and [8], and the arithmetic means of these values are given in Table I.

Can. J. Chem. Downloaded from www.nrcresearchpress.com by 210.87.254.5 on 09/05/12
For personal use only.

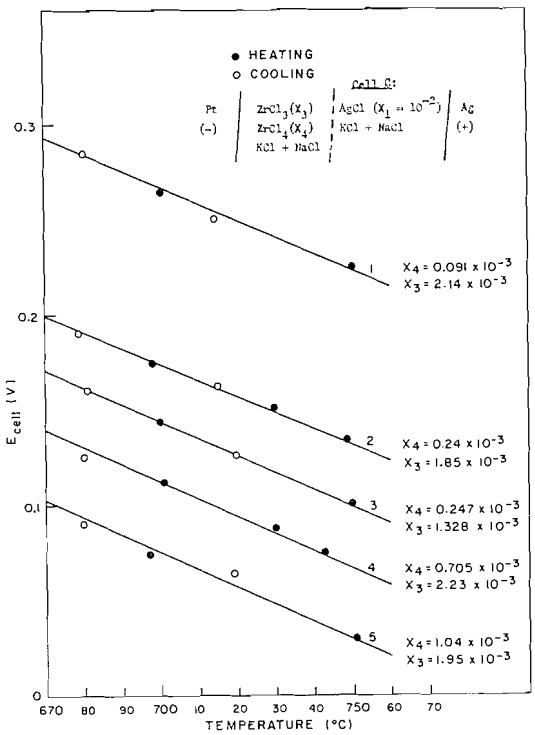


FIG. 9. Potentials of the redox system $Zr^{3+}|Zr^{4+}$ as a function of temperature.

TABLE I

Apparent standard electrode potentials with respect to the chlorine electrode* in 1/1 mole KCl + NaCl

Cell reaction†	$E_{app}'^{0}$(V) 670 °C	700 °C	740 °C
1. $Zr_{(s)} + Cl_{2(g)} = (ZrCl_2)$	−2.225±0.006	−2.200±0.008	−2.166±0.006
2. $(ZrCl_2) + \frac{1}{2}Cl_{2(g)} = (ZrCl_3)$	−1.837±0.015	−1.813±0.020	−1.784±0.018
3. $(ZrCl_3) + \frac{1}{2}Cl_{2(g)} = (ZrCl_4)$	−1.266±0.005	−1.240±0.010	−1.205±0.015
4. $Zr_{(s)} + \frac{3}{2}Cl_{2(g)} = (ZrCl_3)$	−2.096±0.009	−2.071±0.012	−2.039±0.010
5. $Zr_{(s)} + 2Cl_2 = (ZrCl_4)$	−1.888±0.008	−1.863±0.012	−1.830±0.011
6. $Ag_{(s)} + \frac{1}{2}Cl_{2(g,\,1\,atm)} = (AgCl)$[1]	−0.852±0.001	−0.845±0.001	−0.835±0.001
7. $Cl^-|Cl^0$	0.0	0.0	0.0

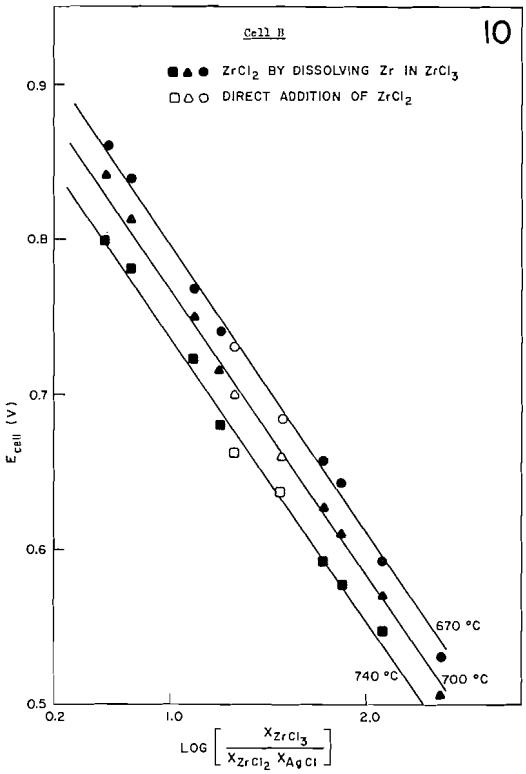
*Note that the sign of the experimentally obtained apparent standard potentials has been changed to conform with the recommendations of the Stockholm Convention of the International Union of Pure and Applied Chemistry as reported by Light and Bethune (10).

†Parentheses indicate components in solution.

The potentials in this table refer to the chlorine electrode as the zero potential reference. For the calculation, the known potentials of the silver – silver chloride electrode measured against a chlorine electrode (1) were added to the measured potentials. From these data the "apparent standard" potentials of the systems $Zr|Zr^{3+}$, and $Zr|Zr^{4+}$ were also calculated and are included in Table I.

"Apparent standard" potentials given in this table refer to the reactions between zirconium metal and chlorine gas at 1 atm to produce 1 gram mole of the corresponding chloride at a thermodynamic state having the properties of the solution at infinite dilution. From the data the mole fraction equilibrium constants for various reactions involving the zirconium chlorides were also calculated and are summarized in Table II.

Can. J. Chem. Downloaded from www.nrcresearchpress.com by 210.87.254.5 on 09/05/12
For personal use only.



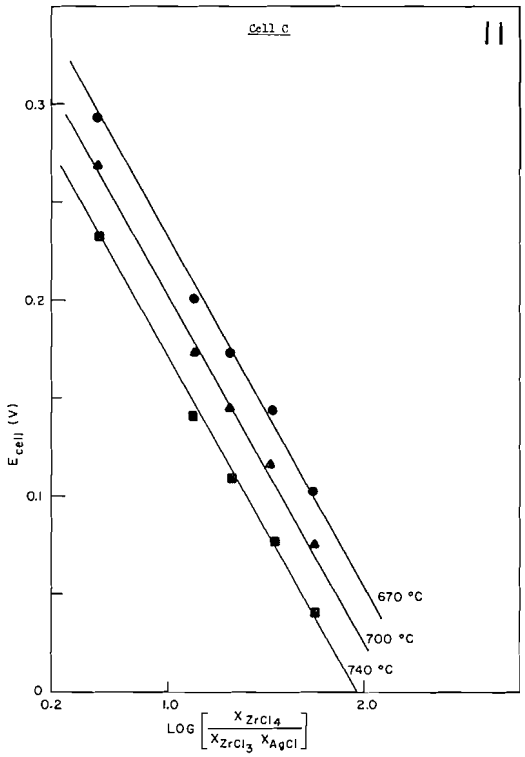


FIG. 10. Plot of the potentials of the redox system $Zr^{2+}|Zr^{3+}$ as a function of the logarithm of the mole fractions.

FIG. 11. Plot of the potentials of the $Zr^{3+}|Zr^{4+}$ redox system as a function of the logarithm of the mole fractions.

TABLE II

Reactions in 1/1 mole KCl + NaCl melt

Reaction*	Equilibrium constant K_X'		
	670 °C	700 °C	740 °C
1. $Zr_{(s)} + (ZrCl_4) = 2(ZrCl_2)$	1.75×10^{7}	8.77×10^{6}	5.14×10^{6}
2. $Zr_{(s)} + 3(ZrCl_4) = 4(ZrCl_3)$	2.56×10^{13}	8.90×10^{12}	3.33×10^{12}
3. $Zr_{(s)} + 2(ZrCl_3) = 3(ZrCl_2)$	1.45×10^{4}	9.42×10^{3}	6.4×10^{3}
4. $2(ZrCl_3) = (ZrCl_2) + (ZrCl_4)$	8.22×10^{-4}	1.10×10^{-3}	1.24×10^{-3}

*Parentheses indicate components in solution.

The high positive values of the equilibrium constants indicate that zirconium metal should reduce any tetra- or tri-valent zirconium present to the divalent species. The reduction in both cases should be almost quantitative. Thus the observed solubility of zirconium metal in a melt containing zirconium tetrachloride is supported by the thermodynamic calculations. It can also be predicted from these results that the potential of a zirconium electrode in a solution of zirconium tetrachloride cannot be interpreted in a simple manner. Measurements of this type represent nonequilibrium potentials which are not representative of the initial composition of the melt.

To provide further evidence on this matter, the potentials of a zirconium electrode immersed in a solution containing only zirconium tetrachloride were measured. The cell

Can. J. Chem. Downloaded from www.nrcresearchpress.com by 210.87.254.5 on 09/05/12
For personal use only.

was of the same design as before, including a zirconium and an inert platinum electrode. The potentials of these two electrodes were measured against the silver – silver chloride reference. Potential versus time curves were obtained and two such curves are plotted in Fig. 12. It is seen that the potential of the zirconium electrode appears to change rather

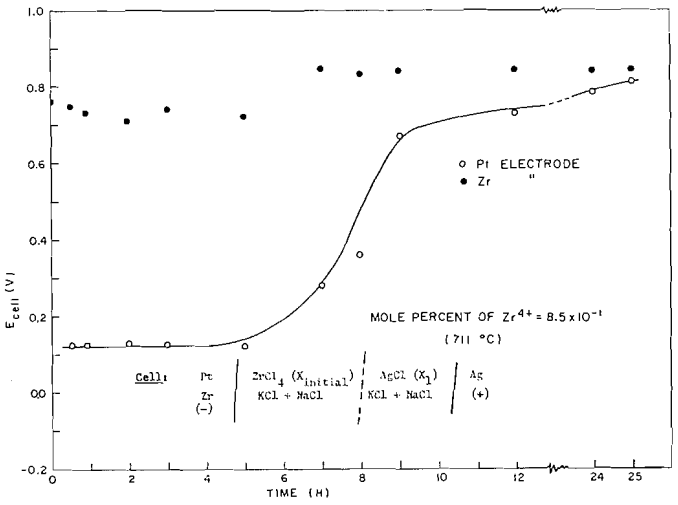


FIG. 12. Nonequilibrium potential measurements of zirconium and platinum electrodes immersed in a solution of zirconium tetrachloride.

slowly with time. However, the potential of the platinum electrode changes more rapidly. The shape of the potential versus time curve of the platinum electrode is characteristic of a redox titration. The behavior of such a reacting electrode may be predicted thermodynamically. For example, for the equilibrium between zirconium metal and zirconium tetrachloride, the final redox potential of the cell

Pt	$Zr^{4+} \rightleftharpoons Zr^{3+}$	Ag^+	Ag	(cell D)
(−)	(as $ZrCl_4$ and $ZrCl_3$)	(as AgCl)	(+)	

corresponds to an overall cell reaction which may be written as:

[9] $$(ZrCl_3) + (AgCl) = (ZrCl_4) + Ag_{(s)}$$

For this reaction $(ZrCl_3)$ and $(ZrCl_4)$ represent the equilibrium concentrations of tri- and tetra-valent zirconium in the presence of zirconium metal. Evidently, the concentration of tetravalent zirconium at equilibrium is entirely different from its initial concentration.

For reaction [9], the change in free energy is given as

[10] $$\Delta G_R = \bar{G}_{ZrCl_4} + G_{Ag_{(s)}}{}^0 - \bar{G}_{ZrCl_3} - \bar{G}_{AgCl} = -E_{cell}F$$

where $\bar{G}_{ZrCl_4}$ and $\bar{G}_{ZrCl_3}$ are the chemical potentials of these species at their equilibrium concentrations. These are determined by the reaction:

[11] $$Zr_{(s)} + 3(ZrCl_4) \rightleftharpoons 4(ZrCl_3).$$

At equilibrium $4\bar{G}_{ZrCl_3} - 3\bar{G}_{ZrCl_4} - G_{Zr}{}^0 = 0$ and

[12] $$\bar{G}_{ZrCl_4} - \bar{G}_{ZrCl_3} = (\bar{G}_{ZrCl_4} - G_{Zr}{}^0)/4.$$

Can. J. Chem. Downloaded from www.nrcresearchpress.com by 210.87.254.5 on 09/05/12
For personal use only.

Substituting this expression in eq. [10], we obtain the following relationship:

$$[13] \qquad 4\Delta G_R = \bar{G}_{ZrCl_4} - G_{Zr}{}^0 - 4\bar{G}_{AgCl} + 4G_{Ag}{}^0 = -4E_{cell}{}'F.$$

The chemical reaction corresponding to the free energy change above is

$$[14] \qquad Zr_{(s)} + 4(AgCl) = (ZrCl_4) + 4Ag_{(s)}$$

and may be realized in a galvanic cell containing a zirconium electrode immersed in a solution of zirconium tetrachloride at the previously established equilibrium concentration. It is evident that when the solution reaches its equilibrium composition, the platinum and the zirconium electrodes should indicate the same potential, i.e. $E = E'$. It may be shown in a similar manner that this potential is characteristic of *all* the possible redox combinations in the system and of *all* the various zirconium ions in solution.

The convergence of the two potential curves in Fig. 12 supports the theoretical interpretation. The initial differences in the two potentials are indicative of concentration changes occurring at the electrode solution interface as the result of the various competing reactions prior to equilibrium. The reliability of such measurements is therefore subject to the attainment of chemical equilibrium between all the possible species in the system. From the curves in Fig. 12, it is seen that the reduction processes at 711 °C are quite slow. During these measurements the potentials did not reach equilibrium even after a period of 25 h.

Potential measurements in the $Zr|Zr^{4+}$ system have been reported by Yang *et al.* (6). The measurements were obtained at 450 °C with solutions of zirconium tetrachloride in the eutectic melt of potassium and lithium chlorides. The reference electrode was a chlorine electrode (5). However, when these potentials are plotted against the concentration of zirconium tetrachloride on a logarithmic scale, a straight line is obtained with a slope indicating an electrode reaction corresponding only to 0.9 electron. In a later publication by Yang *et al.* (6), the measurements were repeated with a silver chloride reference electrode. Again the Nernst plot from these results gave a curve with a slope changing between one to three electrons. It appears that the system was reacting during the measurements. The "apparent standard" potentials could not be calculated from these results.

The potentials of the $Zr|Zr^{4+}$ system have also been measured recently by Smirnov *et al.* (11), with respect to a chlorine reference electrode. The measurements were taken in the solvent melt of potassium and sodium chlorides and in the temperature range 670 °C to 970 °C. The Nernst isotherms obtained from these measurements showed an appreciable curvature and were interpreted as implying the presence of divalent zirconium in the reaction:

$$[15] \qquad Zr_{(s)} + (Zr^{4+})_{solution} \rightleftharpoons 2(Zr^{2+})_{solution}.$$

From the mathematical analysis of the potential isotherms, the apparent standard potentials for the two systems $Zr|Zr^{2+}$ and $Zr|Zr^{4+}$ were calculated, and the results are in complete disagreement with the present values. Thus, at 700 °C, the apparent standard potentials for the two systems $Zr|Zr^{2+}$ and $Zr|Zr^{4+}$ are given as 1.927 V and 2.000 V, respectively. The corresponding values found in the present investigation are 2.200 V and 1.863 V. The equilibrium potential for a reacting electrode, representing reaction [15], is given by Smirnov as

$$[16] \qquad E_{cell} = (E_{app}{}'^0)_{ZrCl_2} - (RT/2F)\ln x[Zr]_t = (E_{app}{}'^0)_{ZrCl_4} - (RT/4F)\ln (1-x)[Zr]_t$$

Can. J. Chem. Downloaded from www.nrcresearchpress.com by 210.87.254.5 on 09/05/12
For personal use only.

Can. J. Chem. Downloaded from www.nrcresearchpress.com by 210.87.254.5 on 09/05/12
For personal use only.

where, $E_{app}{}'^{0}$'s are the apparent standard potentials for the two systems $ZrCl_2$ and $ZrCl_4$, x is the fraction of Zr^{2+} ions computed with respect to the total soluble zirconium content in the electrolyte, and $[Zr]_t$, is the ionic-fraction concentration of total zirconium, equal to $[Zr]_t = [Zr^{2+}] + [Zr^{4+}]$

The fraction x of divalent zirconium ions is then calculated from the *slope* of the isotherm representing the plot of E_{cell} vs. log $[Zr]_t$. It is readily seen that the fraction x changes continuously with the total zirconium content in the melt; the apparent standard potential $E_{app}{}^{0'}$ is the only true constant in the system at any given temperature. It is evident that from the slope of this curve only the ratio of the x's at two different compositions may be obtained. The authors do not indicate whether other limiting conditions were considered in order to solve eq. [16]. It appears, therefore, that the method used in calculating the potentials of the two systems by Smirnov *et al.* (11) is highly questionable.

In a later publication, Smirnov and co-workers (12) reported potential versus current curves obtained during the electrolysis of solutions of zirconium tetrachloride in the equimolar melt of potassium and sodium chlorides at 700 °C. Molybdenum cathodes were used in these experiments, and the polarization curves showed quite clearly three distinctive steps at about 1.1, 1.7, and 2.1 V. In spite of this observation, the results were interpreted as a two-step reduction during which tetravalent zirconium was first reduced to the divalent species at about 1.7 V. This was followed by the reduction of the divalent zirconium to metal at about 2.1 V. The latter value is in agreement with the reversible potential of divalent zirconium obtained in the present work (Table I). (The first step, at 1.1 V, was attributed to the deposition of molybdenum ions produced *in situ* in the melt by the direct reduction of zirconium tetrachloride by molybdenum metal.) However, from the results obtained in this investigation (Table I), it is indicated that the polarization plateaux at 1.1 and 1.7 V should correspond to the reactions $Zr^{4+} \rightarrow Zr^{3+}$ and $Zr^{3+} \rightarrow Zr^{2+}$, respectively. Furthermore, it appears that molybdenum ions deposited either at a much lower potential or at a potential similar to that required for the reduction of tetravalent zirconium.

From the magnitude of the equilibrium constants given in Table II, it may be predicted that zirconium trichloride in solution does not disproportionate to any significant extent. Furthermore, the reaction between zirconium di- and tetra-chloride to produce trivalent zirconium proceeds almost to completion. Therefore, these calculations substantiate the thermal stability of zirconium trichloride in these melts found by the X-ray investigation.

ACTIVITY CALCULATIONS

The "apparent potentials" given in Table I may be used for the calculation of the activity coefficients of the various zirconium species in solution. For the calculation, accurate data on the free energies of formation of the pure zirconium chlorides are required. Unfortunately, the data given by various authors are entirely contradictory. For example, the free energies of formation of zirconium trichloride given by Wicks and Block (13) and by Turnbull and Watts (4) differ by about 25 kcal. Similarly, the data available (4, 13) for the zirconium dichloride differ by about 9 kcal. The data for zirconium tetrachloride are slightly better. Free energies of formation of pure zirconium tetrachloride given by Kubaschewski and Evans (14) differ by about 5 kcal from those found in tabulations given by Wicks and Block (13), or Hamer *et al.* (15). The difference is due to the uncertainty in the heat of formation of solid zirconium tetrachloride at 298 °K.

Because of such discrepancies, the partial molar properties for zirconium di- and trichlorides were not calculated. For zirconium tetrachloride, the data given by Kubaschewski

and Evans (14) appear to be the most reliable as they are also substantiated by Turnbull and Watts (4). Accordingly, the approximate activity coefficients for zirconium tetrachloride were calculated from the equation

$$[17] \qquad E_{app}'^{0} = E_{ZrCl_4}{}^{0} - (RT/4F) \ln \gamma_{ZrCl_4}$$

where $E_{app}'^{0}$ is the "apparent standard" potential for zirconium tetrachloride obtained experimentally, and $E_{ZrCl_4}{}^{0}$ is the corresponding "standard" potential calculated from the available thermodynamic data (13). The Henrian activity coefficients of zirconium tetrachloride, γ_{ZrCl_4}, obtained from these calculations at the selected temperatures of 670 °C, 700 °C, and 740 °C are 4.67×10^{-3}, 6.08×10^{-3}, and 8.49×10^{-3}, respectively. The activity coefficients are of the order of 10^{-3} to 10^{-2} and increase with increasing temperature, as expected. These values should be compared to the activity coefficients for zirconium tetrachloride in alkali chloride melts obtained by direct vapor pressure measurements (16). For the KCl–$ZrCl_4$ system at 800 °C, the activity coefficient is about 0.5×10^{-4}, while for NaCl–$ZrCl_4$, the activity coefficient is only 0.4×10^{-3}. The values which are found from the potential measurements in the equimolar melt of potassium and sodium chlorides are higher and change from 5×10^{-3} at 670 °C to 8×10^{-3} at 740 °C. This difference of one to two orders of magnitude in the activity coefficients obtained by the two methods could be explained by an uncertainty in the free energy of formation of zirconium tetrachloride of about 4.5 kcal. Such a difference is well within the limits of accuracy of the thermodynamic data given in the literature.

An additional source of error could be the calculation of the apparent standard potential of zirconium tetrachloride from the combined results of the electromotive force measurements on three different cells. It should also be realized that the activity coefficients obtained in these two investigations represent measurements on three different systems; therefore, some difference due to the solvent effect should be expected. In any case, the pronounced negative deviations from ideality of zirconium tetrachloride indicate the formation of the complex $ZrCl_6^{2-}$ anions in the melt, as suggested previously (16).

CONCLUSIONS

The results of this investigation indicate that zirconium trichloride does not disproportionate in molten solutions containing an excess of potassium chloride. The mechanism of the electrolytic deposition of zirconium metal from a melt of potassium and sodium chlorides containing zirconium tetrachloride is predicted from the combined results of the potential measurements. The latter indicate a three-step reduction:

$$Zr^{4+} \rightarrow Zr^{3+} \rightarrow Zr^{2+} \rightarrow Zr^{0}.$$

The approximate deposition potentials are 1.2, 1.8, and 2.2 V, respectively. The final step corresponding to the deposition of zirconium metal occurs at about 2.2 V, well below the deposition potentials (~3.5 V) of the alkali metal cations in the solvent melt.

Furthermore, the solubility of zirconium metal in a melt containing zirconium tri- or tetra-chlorides indicates that the deposition process should be carried out preferably from a melt containing reduced zirconium species.

ACKNOWLEDGMENTS

The authors are indebted to the Defence Research Board of Canada for its financial assistance in support of this research.

Can. J. Chem. Downloaded from www.nrcresearchpress.com by 210.87.254.5 on 09/05/12
For personal use only.

REFERENCES

1. S. N. FLENGAS and T. R. INGRAHAM. J. Am. Electrochem. Soc. **106**, 714 (1959).
2. S. N. FLENGAS. Can. J. Chem. **41**, 773 (1963).
3. R. SRINIVASAN and S. N. FLENGAS. Can. J. Chem. **42**, 1315 (1964).
4. A. G. TURNBULL and J. A. WATTS. Australian J. Chem. **16**, 947 (1963).
5. L. YANG and R. G. HUDSON. Trans. AIME, **215**, 589 (1959).
6. L. YANG, R. G. HUDSON, and CHIEN-YEH CHIEN. Phys. Chem. of Process Met. Part II. Inst. Sci. Publ., New York. 1961. p. 925.
7. B. SWAROOP and S. N. FLENGAS. Can. J. Chem. **42**, 1495 (1964).
8. B. SWAROOP and S. N. FLENGAS. Can. J. Chem. **43**, 2115 (1965).
9. R. L. LISTER and S. N. FLENGAS. Can. J. Chem. **42**, 1102 (1964).
10. T. S. LIGHT and A. J. BETHUNE. J. Chem. Educ. **34**, 443 (1957).
11. M. V. SMIRNOV, V. E. KOMAROV, and A. N. BARABOSHKIN. Proc. All-Union Conf. on Phys. Chem. of Molten Salts and Slags, Moscow, Nov. 22–25, 1960. Eng. transl. by U.S. Atomic Energy Com. AEC-TR 5948. pp. 438–448.
12. M. V. SMIRNOV, A. N. BARABOSHKIN, and V. E. KOMAROV. Russian J. Phys. Chem. Engl. Transl. **37** (8), 901 (1963).
13. C. E. WICKS and F. E. BLOCK. Thermodynamic properties of elements. U.S. Bur. Mines Bull. **605**, 1963.
14. O. KUBASCHEWSKI and E. L. EVANS. Metallurgical thermochemistry. Pergamon Press, London. 1959.
15. W. J. HAMER, M. S. MALMBERG, and B. RUBIN. J. Electrochem. Soc. **103**, 8 (1956).
16. R. L. LISTER and S. N. FLENGAS. Can. J. Chem. **43**, 2947 (1965).

Can. J. Chem. Downloaded from www.nrcresearchpress.com by 210.87.254.5 on 09/05/12
For personal use only.

Can. J. Chem. Downloaded from www.nrcresearchpress.com by 210.87.254.105 on 09/05/12
For personal use only.

THEORIES OF INHIBITION BY NITRIC OXIDE

MARGARET H. BACK AND KEITH J. LAIDLER
Department of Chemistry, University of Ottawa, Ottawa, Canada
Received August 9, 1965

ABSTRACT

Theories of the inhibition by nitric oxide of pyrolysis and other reactions, proposed by Voevodsky, by Wojciechowski and Laidler, and by Norrish and Pratt, are critically discussed in this paper with reference to the experimental results. The Voevodsky scheme, involving the suppression by nitric oxide of a heteorgeneous initiation process, is shown to be inconsistent with the observed results for ethane pyrolysis. The Norrish–Pratt scheme, involving oxime formation and NO-induced oxime decomposition, is shown to be unsatisfactory in failing to predict nonintegral orders and in leading to activation energies that are much too high. It is concluded that it is necessary to postulate H abstraction by NO, as in the Wojciechowski–Laidler mechanisms.

INTRODUCTION

In recent years there has been considerable interest in the mechanisms of organic pyrolyses in the presence of inhibitors such as nitric oxide. It was originally thought that the sole effect of nitric oxide was to remove radicals from the system, but a number of studies of isotopic mixing have shown that free-radical chain processes are still important in the maximally inhibited reactions; this has been demonstrated for propane (1), ethane (2), butane (3), and dimethyl ether (4).

Three general schemes have recently been proposed to explain the kinetics of pyrolyses in the presence of nitric oxide. Voevodsky (5, 6) has suggested that initiation and termination both take place on the surface of the vessel, and that both irreversible and reversible surface initiation occurs, the former being suppressed by nitric oxide and other inhibitors. Wojciechowski and Laidler (7, 8) suggested that nitric oxide brings about an additional initiation reaction in which there is abstraction of a hydrogen atom.

$$M + NO \rightarrow R + HNO$$

Termination was suggested to occur by reaction between an organic radical R and either HNO or RNO. At higher NO concentrations termination becomes mainly RNO + RNO or HNO + HNO; under these circumstances the rate increases with NO concentration, as found experimentally.

Norrish and Pratt (9) have more recently put forward an alternative scheme which places emphasis on the reactions of oximes. They do not consider that nitric oxide abstracts hydrogen atoms; it adds on to radicals with the eventual formation of an oxime, e.g.

$$C_2H_5 + NO \rightarrow C_2H_5NO \rightarrow CH_3CH{=}NOH.$$

These oximes undergo decomposition in two ways, by reaction with an additional molecule of NO, and by direct unimolecular decomposition. Norrish and Pratt apply their scheme in a general way to the decomposition of *n*-pentane, and show that it can account qualitatively for the variation of rate with nitric oxide concentration. They also obtain quantitative agreement by making a plausible choice of rate constants.

The object of this paper is to discuss critically these schemes with reference to the experimental data. It will be seen that recent results on the ethane pyrolysis are at variance with Voevodsky's proposals. With the Norrish–Pratt scheme two serious difficulties arise. In the first place, the scheme is incapable of predicting fractional orders

for the maximally inhibited reactions; secondly, it does not account for the activation energies observed in the regions of maximal inhibition and accelerated reaction.

THE VOEVODSKY PROPOSAL

Several recent investigations, by Quinn (10), Gordon (11), and Back and Lin (12), have been concerned with the rate of production of methane in the ethane pyrolysis. The main initiation process is

$$C_2H_6 \rightarrow 2CH_3,$$

and the rate of production of methane, by the reaction

$$CH_3 + C_2H_6 \rightarrow CH_4 + C_2H_5$$

is therefore a measure of the rate of initiation. All three investigations have led to the conclusion that an increase in surface/volume ratio has a very small effect on the rate of initiation. For Voevodsky's suggestion to be applicable the heterogeneous initiation would have to be about 90% of the whole, since at maximal inhibition the rate is reduced to approximately one-tenth of the uninhibited value. The actual contribution of the surface initiation is very much less than this.

It might be argued that the surface brings about an alternative initiation process, namely

$$C_2H_6 \rightarrow C_2H_5 + H$$

and that it is this process that is suppressed by nitric oxide. This proposal also leads to difficulty, however. Back and Lin's results (12) show that the rate of production of butane by the reaction

$$2C_2H_5 \rightarrow C_4H_{10}$$

is not increased by packing the reaction vessel. If this is the main termination process the net rate of initiation must be unaffected by surface, since rates of initiation and termination must be equal. The possibility remains that there is an additional termination process

$$C_2H_5 + H \rightarrow C_2H_6$$

which occurs on the surface. This would require, however, that there would be an *equilibrium* concentration of C_2H_5; this being so, nitric oxide, by reducing the rate of formation of C_2H_5, could not affect the concentration of C_2H_5, since it would equally affect the rate of its removal. The results for ethane therefore cannot be reconciled with Voevodsky's proposal. His suggestions might, of course, be valid for other reactions.

THE WOJCIECHOWSKI–LAIDLER MECHANISMS

The Wojciechowski–Laidler proposals, which have been applied in detail to the decompositions of ethane (13), propane (14), butane (15), dimethyl ether (4), diethyl ether (16), acetaldehyde (17), and propionaldehyde (18) involve the following main features:

(i) Addition of nitric oxide leads to an *additional* initiation process, the abstraction of a hydrogen atom from the substrate molecule.

$$RH + NO \rightarrow R + HNO$$

(*ii*) There are formed species such as HNO and RNO, the latter becoming converted into the oxime which may break down further.

(*iii*) In the presence of nitric oxide there is an *additional* chain-ending step involving the reaction of a radical with HNO, RNO, or the oxime.

Can. J. Chem. Downloaded from www.nrcresearchpress.com by 210.87.254.105 on 09/05/12
For personal use only.

The most likely chain-ending step in the presence of nitric oxide is the one involving the predominant radical or radicals in the particular chain mechanism. Table I summarizes the situation with the various pyrolyses that have been investigated in detail. In each case the most probable chain-ending step leads to the correct order for the maximally inhibited reaction.

TABLE I

Wojciechowski-Laidler mechanisms for inhibition by nitric oxide. Initiation: RH + NO → R + HNO

Decomposition of:	Predominant radicals	Postulated chain-ending step	Overall order of maximally inhibited reaction	Ref.
C_2H_6	C_2H_5, H	$C_2H_5 + HNO \rightarrow C_2H_6 + NO$	1	13
C_3H_8	C_3H_7, H	$C_3H_7 + HNO \rightarrow C_3H_8 + NO$	1.5	14
C_4H_{10}	C_2H_5	$C_2H_5 + C_2H_4NOH \rightarrow C_4H_{10} + NO$	1.5	15
CH_3OCH_3	CH_3	$CH_3 + CH_2NOH \rightarrow C_2H_6 + NO$	1.5	4
$C_2H_5OC_2H_5$	C_2H_5	$C_2H_5 + C_2H_4NOH \rightarrow C_4H_{10} + NO$	1–1.5	16
CH_3CHO	CH_3	$CH_3 + CH_2NOH \rightarrow C_2H_6 + NO$	1.5	17
C_2H_5CHO	C_2H_5	$C_2H_5 + CH_3CH{=}NOH \rightarrow C_4H_{10} + NO$	1.5	18

Voevodsky (6) has recently objected to the Wojciechowski–Laidler scheme as applied to the ethane pyrolysis, mainly on the grounds that the chain length for the uninhibited reaction is "not large"; if the chain length in the uninhibited reaction were indeed short it would be impossible to explain inhibition on the basis of a mechanism which increases the rate of initiation. Voevodsky quotes the mass-spectrometric studies of Eltenton (19) as indicating short chains. The latest work (12), however, on the rate of methane production, leads to the result that the chain length is about 100. Wojciechowski and Laidler (13) concluded that the chain length is about 5 in the maximally inhibited reaction. A tenfold inhibition would therefore be produced if the addition of nitric oxide doubled the rate of initiation; there is therefore no difficulty along these lines.

Support for the suggestion that the main initiation reaction in the maximally inhibited reactions is the abstraction of a hydrogen atom by nitric oxide is provided by the behavior in the region in which the rate increases linearly with the nitric oxide concentration. Activation energies for the reaction in this region are given in the last column of Table II; the values for the paraffins are calculated from the rates measured by Blackmore and Hinshelwood (20), assuming a frequency factor of 10^{11} l mole^{-1} s^{-1}, while those for the ethers and acetaldehyde were measured directly by Laidler *et al.* (4, 17, 18). It is to be noted that the activation energies are consistent with the endothermicities of the postulated initiation reactions, listed in the next to last column of Table II.

TABLE II

Activation energies in the region of acceleration by nitric oxide

Decomposition of:	D(R—H) (kcal/mole)	Endothermicity of RH + NO → R + HNO	Activation energy of accelerated reaction (kcal/mole)
C_2H_6	98	50	52
C_3H_8	97	49	48
n-C_5H_{12}	95	47	52
iso-C_5H_{12}	94	46	45
neo-C_5H_{12}	96	48	48
CH_3OCH_3	92	44	43
$C_2H_5OC_2H_5$	93	45	45
CH_3CHO	85	37	39

Can. J. Chem. Downloaded from www.nrcresearchpress.com by 210.87.254.105 on 09/05/12
For personal use only.

Can. J. Chem. Downloaded from www.nrcresearchpress.com by 210.87.254.105 on 09/05/12
For personal use only.

THE NORRISH–PRATT PROPOSAL

The general scheme proposed by Norrish and Pratt (9) is

[1] $$M \rightarrow R_L + R_S$$

[2] $$R_S + M \rightarrow P_1 + R_L$$

[3] $$R_L \rightarrow P_2 + R_S$$

[4] $$R_L \rightarrow \text{products (chain ending)}$$

[5] $$R_L + NO \rightarrow R_LNO \rightarrow Ox$$

[6] $$Ox + NO \rightarrow R_S + \text{products}$$

[7] $$Ox \rightarrow \text{products}$$

where M is the substrate molecule, P_1 and P_2 are product molecules, Ox is an oxime, and R_L and R_S are large (μ) and small (β) radicals respectively. Reaction [4] is written as a first-order reaction for simplicity; this reaction is in any case unimportant in the presence of much nitric oxide.

Norrish and Pratt applied their scheme only to the *n*-pentane decomposition; we will now apply it to a number of other pyrolyses.

Pyrolysis of Ethane

A number of investigations (13, 21–25) have shown that small amounts of nitric oxide reduce the rate of the ethane pyrolysis to a limiting value; higher concentrations bring about an acceleration, the rate in this region being proportional to [NO] and to $[C_2H_6]$. In the maximally inhibited region the order with respect to ethane is unity at higher pressures and 3/2 at lower pressures. In the region of maximal inhibition the activation energy is 77.3 kcal per mole, whereas it is 52 kcal per mole in the region where the rate is proportional to [NO].

On the basis of the Norrish–Pratt proposals the mechanism would be*

[1] $$C_2H_6 \rightarrow 2CH_3$$

[2] $$CH_3 + C_2H_6 \rightarrow CH_4 + C_2H_5$$

[3] $$C_2H_5 \rightarrow C_2H_4 + H$$

[4] $$H + C_2H_6 \rightarrow H_2 + C_2H_5$$

[5] $$C_2H_5 + NO \rightarrow C_2H_5NO$$

[5′] $$C_2H_5NO \rightarrow CH_3CH{=}NOH$$

[6] $$CH_3CH{=}NOH + NO \rightarrow C_2H_4 + 2NO + H$$

[7] $$CH_3CH{=}NOH \rightarrow \text{products } (CH_3CN + H_2O?)$$

Application of the steady-state treatment to this scheme leads to

[*a*] $$[Ox] = \frac{k_1[C_2H_6]}{k_7}$$

[*b*] $$[C_2H_5] = \frac{k_1k_7 + k_1k_6[NO]}{k_5k_7[NO]}[C_2H_6]$$

[*c*] $$v = \frac{d[C_2H_4]}{dt} = k_3[C_2H_5] + k_6[Ox][NO]$$

**In the Norrish–Pratt scheme it is postulated that* NO *reacts with* $CH_3CH{=}NOH$ *to form* $CH_3 + HNO_2 +$ HCN, *in addition to reaction [6];* CH_3 *would produce* C_2H_5 *and then* H. *The essential feature of their scheme is the regeneration of* R_S *(in this case* H*) from the oxime. The* HNO_2 *is involved in the chain-branching processes at higher* NO *concentrations.*

$$[d] \qquad = \frac{k_1k_3}{k_5}\frac{[C_2H_6]}{[NO]} + \frac{k_1k_3k_6}{k_5k_7}[C_2H_6] + \frac{k_1k_6}{k_7}[C_2H_6][NO].$$

This equation is of the right form, in that it explains a reduction in rate at low NO concentrations, a flat region, and an acceleration at high NO concentrations.

A difficulty arises with this scheme when one considers the activation energies. The activation energy in the region of maximal inhibition would be

$$[e] \qquad E_{max} = E_1 + E_3 + E_6 - E_5 - E_7$$

and the experimental value is 77 kcal. E_1 is about 85 kcal and E_3 about 40 kcal. It follows that if the scheme is correct

$$[f] \qquad E_5 + E_7 - E_6 = 48 \text{ kcal.}$$

E_5 must be small, and it seems impossible that E_7 could be 48 kcal greater than E_6. In the region of acceleration by NO

$$[g] \qquad E_{ind} = E_1 + E_6 - E_7$$

or

$$[h] \qquad E_{max} - E_{ind} = E_3 - E_5.$$

Experimentally E_{max} is 77 kcal and E_{ind} is 52 kcal; therefore $E_3 - E_5 = 25$ kcal. Since E_3 is about 40 kcal, E_5 must be 15 kcal, which is unreasonably large.

The Wojciechowski–Laidler scheme, on the other hand, leads to a square-root relationship in the rate constants, and has no difficulty in explaining the experimental value of E_{max}, as explained in detail in the original paper (13). At high NO concentrations the Wojciechowski–Laidler mechanism predicts that the activation energy should be that of the initial abstraction reaction

$$C_2H_6 + NO \rightarrow C_2H_5 + HNO$$

This reaction is endothermic by about 50 kcal, so that an activation energy of 52 kcal is entirely reasonable.

The Norrish–Pratt scheme further predicts that the rate of the accelerated reaction will equal the rate of the maximally inhibited reaction when $[NO] = k_3/k_5$. With Bywater and Steacie's value (25) for $k_3 = 10^{13}\, e^{-39500/RT}\, s^{-1}$ and the value for k_5 of 3×10^{10} cc mole^{-1} s^{-1}, as suggested by Norrish and Pratt, $k_3/k_5 = 4.5$ mm at 900 °K and 1.0 mm at 850 °K. These estimates are upper limits since k_3 is probably no longer unimolecular in this region and k_5 is unlikely to be smaller. With ethane, however, these pressures of NO are barely sufficient to cause maximum inhibition, and much larger pressures are required to cause acceleration (20).

Furthermore, the accelerated reaction would be expected to occur at low pressures of NO when k_3, the rate constant for the decomposition of R_L, is small or when E_3 is large. In fact the opposite trend is observed. The accelerated reaction sets in earliest with acetaldehyde, for which R_L is one of the least stable radicals. Much larger pressures of NO are required to accelerate the reaction with hydrocarbons (26) and the greatest pressure of NO is required with ethane for which R_L is the most stable, i.e. E_3 is the argest.

Dimethyl Ether Pyrolysis

The effect of nitric oxide on the pyrolysis of dimethyl ether (4) is similar to that on ethane; there is again a flat region, followed by a region of acceleration. The order at

Can. J. Chem. Downloaded from www.nrcresearchpress.com by 210.87.254.105 on 09/05/12
For personal use only.

maximal inhibition is 3/2, and the activation energy is 64.6 kcal per mole. At higher concentrations of NO the rate is proportional to $[CH_3OCH_3]$ and to [NO], and the activation energy is 43.4 kcal per mole.

The Norrish–Pratt mechanism would be

[1] $$CH_3OCH_3 \rightarrow CH_3 + CH_3O$$

[2] $$CH_3 + CH_3OCH_3 \rightarrow CH_4 + CH_2OCH_3$$

[3] $$CH_2OCH_3 \rightarrow CH_2O + CH_3$$

[4] $$CH_3O \rightarrow CH_2O + H$$

[5] $$H + CH_3OCH_3 \rightarrow H_2 + CH_2OCH_3$$

[6] $$NO + CH_3OCH_2 \rightarrow CH_3OCH_2NO \rightarrow CH_3OCH{=}NOH$$

[7] $$CH_3OCH{=}NOH + NO \rightarrow 2NO + CH_2O + CH_3$$

[8] $$CH_3OCH{=}NOH \rightarrow \text{products } (CH_3OCN + H_2O?)$$

The steady-state equations lead to

[*i*] $$[Ox] = (2k_1/k_8)[CH_3OCH_3]$$

[*j*] $$[CH_3OCH_2] = \frac{2k_1[CH_3OCH_3]}{k_6[NO]} + \frac{2k_1k_7[CH_3OCH_3]}{k_6k_8}$$

[*k*] $$v = k_3[CH_3OCH_2] + k_7[Ox][NO]$$

[*l*] $$= \frac{2k_1k_3[CH_3OCH_3]}{k_6[NO]} + \frac{2k_1k_3k_7}{k_6k_8}[CH_3OCH_3] + \frac{2k_1k_7}{k_8}[CH_3OCH_3][NO].$$

Again the equation is of the right general form, leading first to inhibition and then to catalysis. The mechanism does not, however, account for the 3/2 order at maximal inhibition. It is to be noted that since in the Norrish–Pratt mechanisms the chain-ending steps are always first order, the steady-state equations are linear in free radical concentrations and cannot lead to nonintegral orders.

The experimental activation energies again present a difficulty for the mechanism. At maximal inhibition

[*m*] $$E_{max} = E_1 + E_3 + E_7 - E_6 - E_8 = 64.6 \text{ kcal (expt.)}.$$

$E_1 = 87$ kcal and $E_3 = 19$ kcal so that

[*n*] $$E_6 + E_8 - E_7 = 41 \text{ kcal}.$$

Such a high value seems impossible. At high NO concentrations

[*o*] $$E_{ind} = E_1 + E_7 - E_8 = 43 \text{ kcal (expt.)}.$$

With $E_1 = 87$ kcal

[*p*] $$E_8 - E_7 = 44 \text{ kcal}$$

which requires an impossibly high activation energy for the decomposition of the oxime.

Alternatively it might be suggested that since the CH_3 radicals are more plentiful than the CH_3OCH_2, the oxime will be formed from CH_3 by the reaction

[6′] $$CH_3 + NO \rightarrow CH_3NO \rightarrow CH_2{=}NOH$$

followed by

[7′] $$CH_2{=}NOH + NO \rightarrow 2NO + CH_3$$

[8′] $$CH_2{=}NOH \rightarrow \text{products } (HCN + H_2O?)$$

Can. J. Chem. Downloaded from www.nrcresearchpress.com by 210.87.254.105 on 09/05/12
For personal use only.

The result is now

$$[q] \qquad v = \frac{d[CH_2O]}{dt} = k_3[CH_2OCH_3]$$

$$[r] \qquad = \frac{2k_1k_2}{k_{6'}}\frac{[CH_3OCH_3]^2}{[NO]} + \frac{2k_1k_2k_{7'}}{k_{6'}k_{8'}}[CH_3OCH_3]^2 + k_1[CH_3OCH_3][NO].$$

This mechanism again fails to explain the 3/2 order at maximal inhibition, and is inconsistent with the experimental activation energies.

MODIFIED NORRISH–PRATT MECHANISMS

It is clear on the basis of the foregoing discussion that an important difficulty with the Norrish–Pratt mechanisms arises from their suggestion that the chain-ending steps are unimolecular, involving only the oxime molecule. As a result of this the steady-state equations are linear and not quadratic in radical concentrations, so that no explanation is provided for 3/2 kinetics, as found in the dimethyl ether pyrolysis. Furthermore, the rate expressions involve k_1 and not $k_1^{1/2}$, and therefore lead to much too high a value for the activation energy.

In view of this it is natural to modify the Norrish–Pratt proposals by replacing their unimolecular chain-ending step by a bimolecular one. For ethane pyrolysis, if we replace reaction [7] above by

$$[7'] \qquad Ox + C_2H_5 \rightarrow \text{products}$$

the result is

$$[l] \qquad v = \frac{d[C_2H_4]}{dt} = k_3\left(\frac{k_1k_6}{k_5k_{7'}}\right)^{1/2}[C_2H_6]^{1/2} + \left(\frac{k_1k_5k_6}{k_7}\right)^{1/2}[C_2H_6]^{1/2}[NO].$$

In the region of maximal inhibition the scheme therefore leads to an order slightly higher than 1/2 (since the order of reaction [3] is somewhat greater than unity); experimentally the order is somewhat larger than unity (~1.1). A further difficulty is that the scheme leads to a dependence on $[C_2H_6]^{1/2}$ at higher NO pressures, whereas the experimental dependence is on $[C_2H_6]$.

For the dimethyl ether pyrolysis, replacement of reaction [8] by

$$[8'] \qquad Ox + CH_3 \rightarrow \text{products}$$

leads to

$$[m] \qquad v = \frac{d[CH_4]}{dt} = k_2\left(\frac{k_1k_7}{k_6k_{8'}}\right)^{1/2}[CH_3OCH_3]^{3/2}$$

This mechanism correctly predicts the 3/2 order behavior, but fails to account for acceleration at high NO pressures.

CONCLUSION

The general conclusion of this analysis is that the H-abstraction reactions by NO must be important in the pyrolyses occurring in the presence of nitric oxide. The oxime decompositions may also be important, but do not have a very large effect on the overall kinetic behavior.

ADDENDUM: Gowenlock (27) has recently reviewed inhibition mechanisms, and has raised some objections to the Wojciechowski–Laidler proposals:

Can. J. Chem. Downloaded from www.nrcresearchpress.com by 210.87.254.105 on 09/05/12
For personal use only.

(*a*) *The Wojciechowski–Laidler mechanisms do not account for nitric oxide consumption, which has been shown to occur in some cases.* The main feature of the mechanisms is that in the region of maximal inhibition there is a chain reaction that is zero order in nitric oxide. It is possible to introduce reactions leading to removal of nitric oxide, but these do not modify the explanation of the kinetic behavior. Undoubtedly such reactions are important, particularly at high nitric oxide concentrations, and should certainly be considered in a more detailed treatment.

(*b*) *The Wojciechowski–Laidler mechanism for the ethane pyrolysis "implicitly excludes methyl radical participation and methane production from the inhibited decomposition, although these appear in the uninhibited decomposition".* This is not the case; the uninhibited initiation process ($C_2H_6 \rightarrow 2CH_3$) is unaffected by nitric oxide addition.

(*c*) *The proposed termination steps are improbable.* The chemical evidence, however, nearly all relates to much lower temperatures than used in the pyrolysis experiments. This criticism may have validity, but still remains to be substantiated.

(*d*) *The proposals have the weakness that they attempt to produce a general mechanism for inhibited decompositions.* In fact, the Wojciechowski–Laidler mechanisms are significantly different for the various pyrolyses. The mechanisms resemble one another only in postulating the *same types* of initiation and termination steps.

Undoubtedly the Wojciechowski–Laidler mechanisms will have to be modified, but the discussion of the present paper strongly suggests that H-atom abstraction by NO must be included as an important step in inhibited decompositions. Work is at present being carried out in these laboratories to establish the nature of the subsequent processes.

REFERENCES

1. V. A. Poltorak and V. V. Voevodsky. Dokl. Akad. Nauk SSSR, **91**, 584 (1953).
2. F. O. Rice and R. E. Varnerin. J. Am. Chem. Soc. **76**, 324 (1954).
3. A. Kuppermann and L. G. Larson. J. Chem. Phys. **33**, 1264 (1960).
4. D. J. McKenney, B. W. Wojciechowski, and K. J. Laidler. Can. J. Chem. **41**, 1993 (1963).
5. V. V. Voevodsky. Trans. Faraday Soc. **55**, 65 (1959).
6. V. V. Voevodsky. Kinetics Catalysis USSR Engl. Transl. **5**, 603 (1964).
7. B. W. Wojciechowski and K. J. Laidler. Can. J. Chem. **38**, 1027 (1960).
8. B. W. Wojciechowski and K. J. Laidler. Trans. Faraday Soc. **59**, 369 (1963).
9. R. G. W. Norrish and G. L. Pratt. Nature, **197**, 143 (1963).
10. C. P. Quinn, Proc. Royal Soc. London, Ser. A, **275**, 190 (1963).
11. A. S. Gordon. Chemical Institute of Canada Symposium on the Kinetics of Pyrolytic Reactions, University of Ottawa, September 1964.
12. M. C. Lin and M. H. Back. Can. J. Chem. In press. 1966.
13. K. J. Laidler and B. W. Wojciechowski. Proc. Roy. Soc. London, Ser. A, **260**, 103 (1961).
14. K. J. Laidler, N. H. Sagert, and B. W. Wojciechowski. Proc. Roy. Soc. London, Ser. A, **270**, 254 (1962).
15. N. H. Sagert and K. J. Laidler. Can. J. Chem. **41**, 848 (1963).
16. K. J. Laidler and D. J. McKenney. Proc. Roy. Soc. London, Ser. A, **278**, 517 (1964).
17. M. Eusuf and K. J. Laidler. Can. J. Chem. **42**, 1861 (1964).
18. K. J. Laidler and M. Eusuf. Can. J. Chem. **43**, 278 (1965).
19. G. Elteton. J. Chem. Phys. **15**, 455 (1947).
20. D. R. Blackmore and C. N. Hinshelwood. Proc. Roy. Soc. London, Ser. A, **268**, 36 (1962).
21. L. A. K. Staveley. Proc. Roy. Soc. London, Ser. A, **162**, 558 (1937).
22. J. E. Hobbs and C. N. Hinshelwood. Proc. Roy. Soc. London, Ser. A, **167**, 447 (1938).
23. E. W. R. Steacie and G. Shane. Can. J. Res. B, **18**, 351 (1940).
24. K. V. Ingold, F. J. Stubbs, and C. N. Hinshelwood. Proc. Roy. Soc. London, Ser. A, **208**, 285 (1951).
25. S. Bywater and E. W. R. Steacie. J. Chem. Phys. **19**, 326 (1951).
26. D. R. Blackmore and C. N. Hinshelwood. Proc. Roy. Soc. London, Ser. A, **268**, 21 (1962).
27. B. G. Gowenlock. The inhibition of gaseous force radical chain reactions. *In* Progress in reaction kinetics. Vol. 3. *Edited by* G. Porter. Pergamon Press, Oxford. 1965. p. 171.

Can. J. Chem. Downloaded from www.nrcresearchpress.com by 210.87.254.105 on 09/05/12
For personal use only.

Can. J. Chem. Downloaded from www.nrcresearchpress.com by 210.87.254.5 on 09/05/12
For personal use only.

A PERTURBATION CALCULATION OF THE EFFECT OF ELECTRIC INTERACTION ON PROTON MAGNETIC SHIELDING

T. YONEMOTO[1]

Department of Chemistry, University of Manitoba, Winnipeg, Manitoba

Received February 19, 1965

ABSTRACT

The effect of electric interaction of molecular systems on proton magnetic shielding is calculated by a perturbation method, and a general expression of this effect is obtained. It is shown that the effect consists of three parts. Two of them are dependent on the time average of the field at the proton, and correspond to the linear and the square terms of Buckingham's equation of the (external) electric field effect. The third part is proportional to the van der Waals interaction energy between the hydrogen and the interacting object. The magnitude of the former two terms is calculated for a polarized hydrogen atom and a hydrogen molecule. The van der Waals deshielding caused by halogen atoms is also estimated.

I. INTRODUCTION

The theoretical treatment of the electric field effect on proton magnetic shielding was first taken up by Marshall and Pople (1). They obtained the perturbed wave function of a hydrogen atom in a uniform external electric field, and from this wave function they calculated the change of the magnetic shielding constant. Because of the spherical symmetry of the hydrogen atom, the effect of the electric field depends on the square of the field strength. In molecules, the electron distribution around a proton is not spherically symmetric, so that the shielding will also be expected to depend linearly on the field. Buckingham (2) showed, by application of the equation of Marshall and Pople, that such a linear term could arise if the hydrogen atom were in two constant fields, one external and one molecular. His formula proved to be successful in the explanation of the solvent effect in a polar solute (3). Buckingham's equation has been used also for the interpretation of the proton chemical shift in other cases (4, 5).

Bloembergen (6) pointed out that a linear variation of the nuclear quadrupole interaction with applied field can be obtained from the second-order perturbation energy which is bilinear in the nuclear quadrupole interaction and in the field. The same approach was made by Musher (7) to calculate the linear effect on the proton magnetic shielding. He used an approximate third-order perturbation formula and variation function method, and found that the linear change is of the same order of magnitude as that given by Buckingham. However, the square term was discarded in Musher's calculation, as he was interested in only the linear effect.

The van der Waals (dispersion) interaction, also an electric interaction, contributes an important part to the solvent shift (3, 8). The effect of this interaction has been calculated for a two-hydrogen atom system (9). Recently Schaefer *et al.* (10) proposed that shielding of this type could also operate on an intramolecular basis. In terms of this concept, an interpretation of the anomalous low shift in some halogen compounds and mesitylene derivatives was given (10, 11), although no exact information on the magnitude of this effect was available. Thus it was hoped to derive it by a quantum mechanical treatment of a molecular system in general.

In this paper, a general formulation of the effect of electric interaction is carried out with certain approximations in the fourth-order perturbation calculation. The electric

[1]*N.R.C. Postdoctorate Fellow, 1962–1964. On leave of absence from the Electrotechnical Laboratory, Nagatacho, Chiyoda-ku, Tokyo, Japan.*

interaction of the molecular system is included as another perturbation term in the problem of finding the magnetic shielding (12). In the expression of the shielding change that results from this interaction, the first-order term with respect to the electric perturbation is found to correspond to the linear term of Buckingham's equation, and the second-order term to correspond to the square term of Buckingham's equation and the so-called van der Waals effect. The magnitude of these terms is estimated for some cases.

II. PROCEDURE OF CALCULATION AND APPROXIMATIONS

Interaction Energy

Consider the interaction of a group of charged particles (electrons and (or) nuclei) with a hydrogen atom in a molecule. This group will be called group A. It may be either a part of the molecule which contains the proton in question (intramolecular case), or a molecule, or a part of a molecule to which the proton does not belong (intermolecular case). We assume that group A is close enough to the proton to perturb the wave function of the shielding electron, but not so close that there is appreciable overlap between the density distribution of the shielding electron and that of the group-A electrons. Thus the exchange repulsion is excluded. The interaction energy can then be approximated by the dipole–dipole interaction term, when we are interested in the effect of neutral molecules or group of atoms and there is no quadrupole moment in it. The generalization of the theory by the inclusion of these terms can be applied in a straightforward way.

The magnetic shielding in a molecule in liquid is given by averaging over the situations where the magnetic field is parallel and perpendicular to the proton – group A direction denoted by a vector $\boldsymbol{R}$. In the intramolecular case, the direction of the H—X bond axis (X is the atom to which the hydrogen is bonded) is fixed with respect to $\boldsymbol{R}$. We take the z'-axis of the external (laboratory) coordinates (x', y', z') along the direction of the magnetic field, and the molecular coordinates (x, y, z) on the proton with the z-axis along and opposite to the H—X bond direction. Two typical cases will be investigated, i.e. $\boldsymbol{R} \parallel z$ and $\boldsymbol{R} \perp z$. The interaction energy is

$$[1] \qquad \begin{aligned} U &= (e/R^3)(xX + yY - 2zZ) \equiv U_{\parallel} \qquad (\boldsymbol{R} \parallel z) \\ &= (e/R^3)(xX - 2yY + zZ) \equiv U_{\perp} \qquad (\boldsymbol{R} \perp z) \end{aligned}$$

where

$$[1a] \qquad X = \sum_i q_i x_i \text{ etc.},$$

and x_i is the x-component of the i-th charge (q_i) of the group A referred to its electric center. The summation in [1*a*] extends over all the charges in the group. The interaction U is of the form of the van der Waals interaction Hamiltonian, but in case there is a permanent dipole moment in A, the interaction includes dipolar field interaction as well as the so-called van der Waals interaction. In this case, the expectation values $\langle X \rangle$, etc. are non-zero and are related to the steady dipolar field F of the group A at the proton, as

$$[2] \qquad F_x = (1/R^3)\langle X \rangle \text{ etc.}$$

Hamiltonian

The perturbation Hamiltonian is

$$[3] \qquad \mathscr{H}' = U + \mathscr{H}_{\mathrm{H}},$$

$$\begin{aligned} \mathscr{H}_{\mathrm{H}} &= -\frac{ie\hbar}{2mc}\left(H + \frac{2\mu}{r^3}\right)\frac{\partial}{\partial \phi} + \frac{e^2}{8mc^2}\left(H + \frac{2\mu}{r^3}\right)^2 (x'^2 + y'^2) \\ &= AH + B\mu + CH\mu + D(H^2, \mu^2) \end{aligned}$$

Can. J. Chem. Downloaded from www.nrcresearchpress.com by 210.87.254.5 on 09/05/12
For personal use only.

where H is the external magnetic field, μ is the nuclear magnetic moment of the proton, and ϕ is the azimuthal coordinate around the z'-axis. $\mathscr{H}_{\mathrm{H}}$ is the interaction of the magnetic field with the shielding electron, which can be written as a sum of linear and bilinear terms in H and μ. Other notations have the usual meanings. It should be mentioned here that the magnitude of the electric perturbation is of the order of one-tenth of the total electronic energy under conditions where the concept of the electric field effect is ordinarily applied. $\mathscr{H}_{\mathrm{H}}$ is many orders smaller than U, so that the first-order field effect on the magnetic shielding is obtained from the second- and the third-order perturbation energy, and the second-order field effect from the third- and the fourth-order perturbation calculation.

Perturbation Energy

The perturbation energy in the fourth-order approximation can be obtained by the ordinary procedure (13). As in most perturbation calculations, use is made of the mean excitation energy approximation. This approximation may be good when the discrete energy levels lie within a narrow range (14). The weight of the states in the continuum of energy levels is expected to be small. At any rate, the results should be valid as to the order of magnitude.

The explicit form of $\mathscr{H}'$ given in eqs. [3], [1], and [2] is brought into the energy expression, which is then expanded in terms of H and μ, and as in Ramsey's theory, terms proportional to $H\mu$ are picked out. The introduction of U in $\mathscr{H}'$ gives rise to more terms of different types other than those that appear in Ramsey's theory. However, from the fact that U is of the order of one-tenth of the excitation energy ΔE, it is easily shown that only terms proportional to $H\mu U/\Delta E$ and $H\mu U^2/\Delta E^2$ are significant. All the other terms are negligible or are independent of the nuclear transition energy. The sum of these $H\mu$-terms thus represents the interaction energy of the nuclear spin – electron system with the external magnetic field, i.e. the term additional to the nuclear Zeeman energy. The magnetic shielding of the proton is the coefficient of $H\mu$ in this additional energy, averaged over random orientation of the molecule.

Result

The calculation of the matrix elements that appear in the above-mentioned energy formula is made possible by the assumption of no overlap between the wave function of the hydrogen part and that of the group A. The operators X, X^2, etc. are thus replaced by their expectation values for the unperturbed state of the group A. Using [2] and

$$[4] \qquad \langle X^2\rangle = \langle \sum_i q_i x_i\rangle^2 + [\langle \sum_i q_i^2 x_i^2\rangle - \sum_i \langle q_i x_i\rangle^2]$$

$$\equiv R^6 F_x^2 + a_0^2 e^2 Q_x \text{ etc.}$$

which holds when the Hartree approximation is made for the wave function of the group A, we obtain

$$[5] \qquad \Delta\sigma = (e^2/3mc^2a_0)(A_1 + A_2 + B_1 + B_2 + C_1 + C_2),$$

where

$$A_1 = (a_0 e/\Delta E)a_1 F_z,$$

$$A_2 = (a_0^2 e^2/\Delta E^2)a_2 F_z,$$

$$B_1 = (a_0 e^2/\Delta E^2)[b_{11}(F_x^2 + F_y^2) + (b_{12} + b_{13})F_z^2],$$

$$B_2 = (a_0^2 e^4/\Delta E^2)[(b_{21} + b_{23})(F_x^2 + F_y^2) + (b_{22} + b_{24})F_z^2],$$

Can. J. Chem. Downloaded from www.nrcresearchpress.com by 210.87.254.5 on 09/05/12
For personal use only.

for both $\boldsymbol{R} \parallel z$ and $\boldsymbol{R} \perp z$, and

$$\left.\begin{aligned} C_1 &= (a_0^3e^4/R^6\Delta E^2)(b_{11}Q_x + b_{11}Q_y + 4b_{12}Q_z) \\ C_2 &= (a_0^4e^6/R^6\Delta E^3)(b_{21}Q_x + b_{21}Q_y + 4b_{22}Q_z) \end{aligned}\right\} \quad (\boldsymbol{R} \parallel z),$$

$$\left.\begin{aligned} C_1 &= (a_0^3e^4/R^6\Delta E^2)(b_{11}Q_x + 4b_{11}Q_y + b_{12}Q_z) \\ C_2 &= (a_0^4e^6/R^6\Delta E^3)(b_{21}Q_x + 4b_{21}Q_y + b_{22}Q_z) \end{aligned}\right\} \quad (\boldsymbol{R} \perp z).$$

The expressions for a_1, a_2, b_{11}, etc. are given in the Appendix. In the derivation of the above results, it was assumed that the wave function for the hydrogen part is axially symmetric about the z-axis. We shall later choose the form of the wave function for actual calculation of the matrix elements. However, this assumption was made beforehand, because it simplifies the result to a great extent.

In the above expressions, $A_1 + A_2$ and $B_1 + B_2$ are dependent respectively on the time average of the field and the square of its components at the proton. Thus we obtained incidentally the expression for intramolecular and (or) external field effect, by solving a van der Waals type perturbation problem. When the interacting group has no net dipole moment, terms A_1 to B_2 all vanish and the shielding change is of pure van der Waals effect, represented by $C_1 + C_2$.

III. TWO-HYDROGEN ATOM SYSTEM

The system of two slightly interacting hydrogen atoms, which is the simplest example of a perturbed hydrogen, has already been dealt with by a variational method (9). This problem is studied in this section, because the result of the present treatment can be compared with the former, and also because it affords an insight into more complex systems.

As the ground state wave function of a hydrogen atom is spherically symmetric, the effect is of the van der Waals type:

$$\Delta\sigma = \Delta\sigma_{HH} = -\frac{e^2}{3mc^2a_0}\left(9\frac{a_0^4e^4}{\Delta E^2} + 4\frac{a_0^3e^6}{\Delta E^3}\right)R^{-6}. \qquad [6]$$

For example, a hydrogen atom at 4 Bohr radius from another one is desheilded by 0.3 p.p.m. if the ionization energy of a hydrogen atom (2.2×10^{-11} erg) is adopted as ΔE. This result is three times larger than that found by the variational method (10^{-7} for $R = 4$ Bohr radius (9)). When the interatomic distance is 3 Å, $\Delta\sigma_{HH}$ is -0.025 p.p.m. Since only electric interaction is considered, no R^{-3} term appears in this treatment.

The van der Waals interaction energy between two hydrogen atoms, calculated by the second-order perturbation energy is (15)

$$\epsilon_{HH} = -6a_0^4e^4/R^6\Delta E.$$

Thus the shielding change in the two-hydrogen atom system is written as

$$\Delta\sigma_{HH} = \frac{e^2}{3mc^2a_0}\frac{\epsilon_{HH}}{\Delta E}\left(\frac{3}{2} + \frac{2}{3}\frac{e^2}{a_0\Delta E}\right). \qquad [7]$$

IV. VAN DER WAALS DESHIELDING BY A HALOGEN ATOM

The result of the calculations in the preceding section, that the field effect caused by the van der Waals interaction between two hydrogen atoms is proportional to the interaction energy, suggests that there will be a larger deshielding when a hydrogen interacts

Can. J. Chem. Downloaded from www.nrcresearchpress.com by 210.87.254.5 on 09/05/12
For personal use only.

with heavier atoms with which the van der Waals interaction is larger. This has been pointed out by Marshall and Pople (9) and by Musher (16). In proton resonance of organic molecules, there are many cases where a halogen atom is near a proton. These are the examples (intramolecular case) of the situation mentioned above.

A precise calculation of this effect is difficult because no accurate molecular wave function is available that describes the state of ionization, hybridization, or state of inner and lone pair electrons, etc. of a halogen in a bond. Thus we are obliged to estimate it from a calculation of the effect of a slightly interacting halogen atom on the shielding of a proton.

TABLE I

$\langle \sum_i x_i^2 \rangle / a_0^2$ values of halogen atoms and ions

Atoms or ions	F	F^-	Cl^-	Br	Br^-
$\langle \sum_i x_i^2 \rangle / a_0^2$	3.1	3.6	12.5	14	18

The spherical symmetry of these two atoms is the same as in the case of the two-hydrogen atom system, so that the result of the calculations in the preceding section can be applied to the present problem if Q for a hydrogen atom ($=1$) is replaced by that of the halogen value. The magnitude of Q ($=\langle \sum_i x_i^2 \rangle / a_0^2$ in this case) is calculated for some halogen atoms and ions by the use of the Hartree–Fock wave functions (17–20). The results are shown in Table I. These values are multiplied into [6] to obtain the deshielding by the van der Waals interaction of the halogens. The effect of a fluorine atom at 3 Å from a proton is not significant, but a chlorine atom at the same distance may deshield the proton by about 0.3 p.p.m.

V. POLARIZED HYDROGEN ATOM

The wave function for a hydrogen in a bond may in some cases be approximated by a function made up of the ground and the excited states. This approximation is not good at distances far from the proton, but in the region near the proton, where the main contribution to the shielding arises, the electron distribution will be expanded in terms of excited states wave functions. Thus

$$\psi_0 = C_0(1s) + C_1(2s) + C_2(2p) + \ldots .$$

The simplest form of this approximation is

[8] $$\psi_0 = (1 + C^2)^{-1/2}[(1s) + C(2p_{-z})]$$

where C is a small combination constant. By the directional character of the bond, the 2p-function is the hydrogen $2p_z$-orbital in the $-z$-direction, which is denoted as $2p_{-z}$. For simplicity, the 2s-function was omitted. This does not change the essential feature of the results.

The wave function [8] is actually that of a polarized hydrogen atom. Although this is a very crude model for a hydrogen in a molecule, it is worthwhile to examine the nature of the electric field effect on this model, because as long as we use a one-center wave function approximation, in which the calculation of the matrix elements is simple, the essential characteristics of any wave function of this type are contained in this form.

The result is

[9] $$\Delta\sigma = -6.3C \times 10^{-12}F_z - 0.68(1 + 5.9C^2) \times 10^{-18}F^2 - 1.25C^2 \times 10^{-18}F_z^2 + \Delta\sigma_W,$$

Can. J. Chem. Downloaded from www.nrcresearchpress.com by 210.87.254.5 on 09/05/12
For personal use only.

for $\Delta E = 2.2 \times 10^{-11}$ erg. It is shown that the linear dependence of the field effect is a result of the polarization of the shielding electron, or of the interaction of the field with the atomic dipole at the proton. The first and the second term of eq. [9] correspond to the two terms of Buckingham's equation, and the third term can be regarded as the correction to the first. The fourth term is the van der Waals contribution. When the interacting object has spherical symmetry, it can be written in a simple form. Using the mean excitation energy as mentioned above, but writing it as $e^2/2a_0$ rather than its magnitude, we get

$$\Delta\sigma_W = -(1\,204)(1 + 11.6C^2)Q(a_0/R)^6 \times 10^{-6} \quad [10]$$

for $\boldsymbol{R} \parallel z$. The coefficient to C^2 in [10] becomes 5.6 for $\boldsymbol{R} \perp z$ and 7.6 for the intermolecular case, if the mutual orientation of the two molecules is completely random. As in the two-hydrogen atom system, $\Delta\sigma_W$ is proportional to the corresponding interaction energy. For both $\boldsymbol{R} \parallel z$ and $\boldsymbol{R} \perp z$,

$$\Delta\sigma_W = 50(1 - 1.4C^2)(\epsilon/\Delta E) \times 10^{-6}. \quad [11]$$

It should be mentioned that, although eq. [9] was derived on the basis of the dipolar interaction between a hydrogen and a charge group, it holds also for a steady external field (in this case, of course, the van der Waals term does not appear). One can derive from [9] the equation of the external electric field effect on a hydrogen atom. However, this gives the average value over random direction of F, because eq. [5] is already in the averaged form. When F is an external field, the direction of it is fixed with respect to the magnetic field. The shielding in this case can be obtained from equations similar to [5] but for specific mutual direction of F and H, the average of which leads to [5]. The result is

$$\Delta\sigma = -(e^2/3mc^2a_0)[8.4(a_0^4/e^2)F^2] \qquad (F \parallel H), \quad [12]$$

$$= -(e^2/3mc^2a_0)[12.8(a_0^4/e^2)F^2] \qquad (F \perp H).$$

These equations are very close to the results of Marshall and Pople (1), in which the numerical coefficients in the square bracket are 439/40 and 193/15 for $F \parallel H$ and $F \perp H$, respectively.

VI. HYDROGEN MOLECULE

It is desirable to calculate the field effect with better wave functions than the polarized hydrogen atom model. A LCAO-molecular orbital is nearer reality. The use of this wave function, however, requires carrying out bi-central integrations, which is not always easy. It was found that the calculation for a hydrogen molecule is workable: the integrations were performed on the surface of an ellipsoid with the two nuclei as foci.

A simple form of the localized LCAO-MO

$$\psi_0 = (2 + 2S)^{-1/2}(\psi_1 + \psi_2) \quad [13]$$

was used, taking into account the approximate nature of the present treatment. ψ_1 and ψ_2 are the Slater type hydrogen atomic 1s orbitals (21) for the two nuclei, and S is the overlap integral between ψ_1 and ψ_2. Internuclear distance is 0.74 Å (22). As the procedure of the integration is tedious, only the result is given here. For $\Delta E = 2.2 \times 10^{-11}$ erg,

$$\Delta\sigma = -4.5 \times 10^{-12}F_z - 1.16 \times 10^{-18}F^2 + 1.02 \times 10^{-18}F_z^2 + \Delta\sigma_W \quad [14]$$

and when the charge distribution in the group A is isotropic,

$$\Delta\sigma_W = -(2\,369)Q(a_0/R)^6 \times 10^{-6}. \quad [15]$$

Can. J. Chem. Downloaded from www.nrcresearchpress.com by 210.87.254.5 on 09/05/12
For personal use only.

The van der Waals interaction energy can be calculated with the LCAO-MO given above. An equation of the form of [11] with a factor 37.5 in place of $50(1 - 1.4C^2)$ is valid in this case.

VII. SUMMARY OF THE RESULTS AND DISCUSSION

The results of the above calculation are summarized as follows:

(*a*) By the use of the fourth-order perturbation theory and mean excitation energy approximation, the general formula for the electric field effect on the proton magnetic shielding is obtained. This is

$$\Delta\sigma = \Delta\sigma(1) + \Delta\sigma(2) + \Delta\sigma_W \qquad \text{(eq. [5])}.$$

In this equation, $\Delta\sigma(1)$ is the part proportional to the steady field strength at the proton, $\Delta\sigma(2)$ is dependent on the square of the steady field and its z-component, and $\Delta\sigma_W$ is the van der Waals contribution.

(*b*) The field effect on a proton in a molecule, estimated with the polarized hydrogen atom model and a localized LCAO-MO for a hydrogen molecule, is given by eqs. [9] and [14], respectively. Although the magnitude of C is not certain, the linear term of [9] nearly coincides with that of Buckingham's equation when $C = 0.3$. The result for a hydrogen molecule is somewhat larger.

(*c*) Calculation of the van der Waals contribution $\Delta\sigma_W$ is in general difficult. However, it is possible to calculate it for a simple case of a two-hydrogen atom system (eq. [6]). It is also possible to estimate the effect of a heavy atom. This is $\Delta\sigma_{HH}$ (given by eq. [6] for the hydrogen – heavy atom distance R) times a factor such as given in Table I. In general, if the value of Q is obtained, $\Delta\sigma_W$ can be calculated by eq. [10] or [15]. The van der Waals contribution is shown to be proportional to the interaction energy. A heavy halogen near a halogen gives rise to a considerable amount of the van der Waals low shift.

There have been some experimental studies to determine the magnitude of the linear and the square terms of the field effect. The experimental values of the former for some molecules as obtained by different methods are in the range of $1.3\text{–}3.4 \times 10^{-12}\ F_z$ (23–25), and the square terms have been found to be $0.8\text{–}1.0\ (\pm 0.3) \times 10^{-18}\ F^2$, except for hydrogen chloride (26). In view of the approximations made, the agreement of the present results with the experimental findings is satisfactory both for the polarized hydrogen atom model with $C \simeq 0.3$ and for the LCAO-MO calculation for H_2. It should be noted also that $\Delta\sigma$ contains functions of the derivatives of the wave function, which may change greatly with the choice of the latter. Thus we encounter the same difficulty as that found in calculating the paramagnetic part of the magnetic shielding, if we attempt to obtain an exact value of the field effect. The exceptionally large effect found in HCl is either caused by the strong ionic character of the bond, namely, a very large atomic dipole at the hydrogen, or attributable to an interaction other than the dipole–dipole term that contributes much to the shielding change in this case.

The intermolecular field effect is the statistical average of $\Delta\sigma$ over the mutual orientations of the molecule. If it is completely random, one obtains the isotropic average, and the linear term vanishes in this case. The system of two hydrogen atoms, or solutions in which symmetric solute molecules are dispersed among symmetric solvent molecules, represents this case. In general, however, there exists the reaction field on which experiments to determine the linear field effect are based. In complex molecules, there will be specific interactions between different parts of the two (or more) molecules, which will result in non-isotropic orientation and different reaction fields on different parts of a molecule (27).

Can. J. Chem. Downloaded from www.nrcresearchpress.com by 210.87.254.5 on 09/05/12
For personal use only.

The constant C in the polarized hydrogen atom model has so far been assumed to be positive. This means that the electron cloud is shifted towards the atom to which the hydrogen is bonded, and this is a reasonable postulate. In the present treatment of the polarized hydrogen atom, C can be taken as the parameter which determines the atomic dipole moment $\mathbf{p}$ of the hydrogen. It is clear from the procedure of the present calculation that the linear term originates in the interaction of the form $-\mathbf{p}\cdot\mathbf{F}$, so that the direction of $\mathbf{p}$ with respect to the electric field determines the sign of the linear term. If $\mathbf{p}$ is in the direction H to X, the linear term reverses the sense. This is not found in proton resonance, but in fluorine resonance it has been found in the CHF_3 molecule, from a study of the medium effect (26).

A theoretical calculation of the electronic state in a HF molecule (28, 29) reveals that the atomic dipole on the fluorine is in the direction from the fluorine nucleus away from the bond, although the net dipole moment of the HF molecule is in the opposite direction. Presumably this holds also for a C—F bond, so that the direction of $\mathbf{p}$ on the fluorine atom with respect to the bond is the same as in the case of hydrogen in a C—H bond. On the other hand, the mean field remaining along the C—F bond is from F to C, because the bond moment of the C—F bond is C^+—F^- (26). The energy $-\mathbf{p}\cdot\mathbf{F}$ thus becomes opposite in sign, leading to the apparent positive effect (shielding rather than deshielding), when it is obtained from the medium effect. However, the coefficient of the linear term of the field effect equation for fluorine should have the same sign as in the proton. This may be verified by a study of an intramolecular field effect on the fluorine chemical shift.

ACKNOWLEDGMENTS

The author expresses his thanks to Professor T. Schaefer of the University of Manitoba for his interest in and valuable discussion on this work. He also thanks Dr. M. Shibuya of the Electrotechnical Laboratory (Tokyo) and the referees for their comments, and the National Research Council of Canada for a fellowship.

APPENDIX

$$a_1 = -8\langle r^{-1}\rangle\langle r\cos\theta\rangle + 4\langle\cos\theta\rangle$$

$$a_2 = -4\langle r^{-2}\cos\theta\rangle + 6\left\langle r^{-2}\cos\theta\frac{\partial^2}{\partial\theta^2}\right\rangle - 12\langle r\cos\theta\rangle\left\langle r^{-3}\frac{\partial^2}{\partial\theta^2}\right\rangle$$

$$b_{11} = -6\langle r^{-1}\rangle\langle r^2\sin^2\theta\rangle + 3\langle r\sin^2\theta\rangle$$

$$b_{12} = -12\langle r^{-1}\rangle\langle r^2\cos^2\theta\rangle + 6\langle r\cos^2\theta\rangle$$

$$b_{13} = \langle r\cos\theta\rangle[48\langle r^{-1}\rangle\langle r\cos\theta\rangle - 24\langle\cos\theta\rangle]$$

$$b_{21} = -5\langle r^{-1}\sin^2\theta\rangle + 6\langle r^{-1}\cos^2\theta\rangle + 6\left\langle r^{-1}\sin^2\theta\frac{\partial^2}{\partial\theta^2}\right\rangle - 8\langle r^2\sin^2\theta\rangle\left\langle r^{-3}\frac{\partial^2}{\partial\theta^2}\right\rangle$$

$$b_{22} = 6\langle r^{-1}\sin^2\theta\rangle - 16\langle r^{-1}\cos^2\theta\rangle + 12\left\langle r^{-1}\cos^2\theta\frac{\partial^2}{\partial\theta^2}\right\rangle - 16\langle r^2\cos^2\theta\rangle\left\langle r^{-3}\frac{\partial^2}{\partial\theta^2}\right\rangle$$

$$b_{23} = -32\langle r\cos\theta\rangle\langle r^{-2}\cos\theta\rangle$$

$$b_{24} = \langle r\cos\theta\rangle\left[32\langle r^{-2}\cos\theta\rangle - 48\left\langle r^{-2}\cos\theta\frac{\partial^2}{\partial\theta^2}\right\rangle + 80\langle r\cos\theta\rangle\left\langle r^{-3}\frac{\partial^2}{\partial\theta^2}\right\rangle\right]$$

In these equations, $\langle K\rangle$ represents $\pi\int\phi_0{}^*K\phi_0 r^2\sin\theta\,dr\,d\theta$ where ϕ_0 is the r–θ part of ψ_0. r, θ, and φ are the molecular polar coordinates on the proton.

Can. J. Chem. Downloaded from www.nrcresearchpress.com by 210.87.254.5 on 09/05/12
For personal use only.

REFERENCES

1. T. W. MARSHALL and J. A. POPLE. Mol. Phys. **1**, 199 (1958).
2. A. D. BUCKINGHAM. Can. J. Chem. **38**, 300 (1960).
3. A. D. BUCKINGHAM, T. SCHAEFER, and W. G. SCHNEIDER. J. Chem. Phys. **32**, 1227 (1960).
4. T. SCHAEFER and T. YONEMOTO. Can. J. Chem. **42**, 2318 (1964).
5. G. KOTOWYCZ, T. SCHAEFER, and E. BOCK. Can. J. Chem. **42**, 2541 (1964).
6. N. BLOEMBERGEN. J. Chem. Phys. **35**, 1131 (1961).
7. J. I. MUSHER. J. Chem. Phys. **37**, 34 (1962).
8. A. A. BOTHNER-BY. J. Mol. Spectry. **5**, 52 (1960).
9. T. W. MARSHALL and J. A. POPLE. Mol. Phys. **3**, 339 (1960).
10. T. SCHAEFER, W. F. REYNOLDS, and T. YONEMOTO. Can. J. Chem. **41**, 2969 (1963).
11. V. M. S. GIL and W. A. GIBBONS. Mol. Phys. **8**, 199 (1964).
12. N. F. RAMSEY. Phys. Rev. **78**, 669 (1950).
13. L. D. LANDAU and E. M. LIFSHITZ. Quantum mechanics. Pergamon, London. 1958. p. 136.
14. L. JANSEN and P. MAZUR. Physica, **21**, 193 (1955).
15. L. I. SCHIFF. Quantum mechanics. McGraw-Hill, Toronto. 1955. p. 180.
16. J. I. MUSHER. J. Chem. Phys. **41**, 2671 (1964).
17. E. CLEMENTI, C. C. J. ROOTHAAN, and M. YOSHIMINE. Phys. Rev. **127**, 1618 (1962).
18. E. CLEMENTI and A. D. MCLEAN. Phys. Rev. **133**, A419 (1964).
19. E. CLEMENTI and A. D. MCLEAN. Phys. Rev. **133**, A1274 (1964).
20. E. CLEMENTI. J. Chem. Phys. **41**, 303 (1964).
21. C. A. COULSON. Valence. Clarendon, Oxford. 1952. p. 40.
22. TABLES OF INTERATOMIC DISTANCES AND CONFIGURATION IN MOLECULES AND IONS. The Chemical Society, London. 1958.
23. W. T. RAYNES, A. D. BUCKINGHAM, and H. J. BERNSTEIN. J. Chem. Phys. **36**, 3481 (1962).
24. L. PETRAKIS and H. J. BERNSTEIN. J. Chem. Phys. **37**, 2731 (1962).
25. F. HRUSKA, E. BOCK, and T. SCHAEFER. Can. J. Chem. **41**, 3043 (1963).
26. L. PETRAKIS and H. J. BERNSTEIN. J. Chem. Phys. **38**, 1562 (1963).
27. P. LASZLO and J. I. MUSHER. J. Chem. Phys. **41**, 3906 (1964).
28. A. B. F. DUNCAN and J. A. POPLE. Trans. Faraday Soc. **49**, 217 (1953).
29. A. B. F. DUNCAN. J. Am. Chem. Soc. **77**, 2107 (1955).

Can. J. Chem. Downloaded from www.nrcresearchpress.com by 210.87.254.5 on 09/05/12
For personal use only.

KINETIC STUDIES OF CHLORO COMPLEXES OF RHODIUM AS HYDROGENATION CATALYSTS

B. R. JAMES AND G. L. REMPEL
Department of Chemistry, University of British Columbia, Vancouver, British Columbia
Received August 23, 1965

ABSTRACT

The anionic complexes $[RhCl_6]^{3-}$, $[Rh(H_2O)Cl_5]^{2-}$, and $[Rh(H_2O)_2Cl_4]^-$ activate molecular hydrogen for the reduction of ferric ion in aqueous acid solution; the catalytic activity increased with increasing number of chloride ligands present. Cationic and neutral chloroaquorhodium(III) complexes did not homogeneously catalyze the reduction of ferric ion, the complexes themselves being reduced to metallic rhodium, a powerful heterogeneous catalyst.

Chloro complexes of rhodium(III) and rhodium(I) were not effective catalysts in aqueous solution for the homogeneous hydrogenation of the olefinic bond in maleic acid. Anionic chlororhodate(III) complexes were reduced by hydrogen to the univalent state, this state being stabilized against further reduction to the metal by complexing with the maleic acid present. Preliminary studies indicate that in dimethylacetamide solution rhodium(III) trichloride is an effective homogeneous catalyst for the reduction of maleic acid to succinic acid by hydrogen, the reaction proceeding through a rhodium(I) – maleic acid complex.

INTRODUCTION

Previous workers (1) in this laboratory had found that rhodium(III) trichloride in aqueous 3 *M* HCl solution homogeneously activated molecular hydrogen for the reduction of a substrate such as ferric ion. It seemed likely that the species predominantly present was $[RhCl_6]^{3-}$, although there was no direct experimental evidence for this. More recently data have been published giving the absorption spectra and stability constants of the Rh(III)–chloride complexes (2). In the present investigations the kinetics of the $Rh(III)/H_2/Fe(III)$ system were studied in aqueous solution over a wide range of chloride concentration in an attempt to find correlation between catalytic activity and the nature of the Rh(III) chloride species present. This paper describes these studies.

The use of chloro complexes of rhodium as possible catalysts for the homogeneous hydrogenation of olefinic bonds is also considered in this paper. Most metal ions and complexes which activate molecular hydrogen homogeneously in solution and catalyze the reduction of inorganic substrates (3) are not effective catalysts for the hydrogenation of olefin bonds. Acid aqueous solutions containing chlororuthenate(II) complexes, however, did successfully hydrogenate, under homogeneous conditions, several olefinic compounds including maleic acid (4), and it seemed worthwhile to study the reactions of chloro complexes of rhodium under similar conditions. We have also started some studies on the $Rh(III)/H_2$/maleic acid system in dimethylacetamide solution. Recent publications have reported that certain rhodium(III) complexes can activate molecular hydrogen to give hydrogenation of olefinic bonds under homogeneous but nonaqueous conditions (5, 6). Hex-1-ene can be converted into *n*-hexane by ethanol—benzene solutions of tertiary phosphine and arsine complexes such as 1,2,3-tris-(triphenylphosphine)trichlororhodium (III) and by ethanolic solutions of rhodium(III) trichloride or 1,2,6-trichlorotripyridine rhodium(III). These reports are short communications and little detail is given. However, the reactions are probably complex, e.g. hex-1-ene is catalytically isomerized by ethanolic rhodium trichloride (7). It is also known that reaction with ethanol of the triphenylphosphine- and arsine-type complexes of the platinum transition metal ions can give

Can. J. Chem. Downloaded from www.nrcresearchpress.com by 210.87.254.105 on 09/05/12
For personal use only.

hydrido- and hydridocarbonyl-type complexes with the metal in a reduced valency state (8, 9) and so the hydrogenation systems described are likely to be complex kinetically. A very recent communication describes a more well-defined system in which a hydride intermediate has been detected during the catalyzed hydrogenation of olefins and acetylenes by the complex $(Ph_3P)_3Rh^{I}Cl$ in benzene solutions (10). In view of the recent activity in the field of catalysis by rhodium complexes we have included in this paper results of some preliminary studies carried out in dimethylacetamide solutions.

EXPERIMENTAL

The H_2 was obtained from Canadian Liquid Air Co. and was passed through a deoxo catalytic purifier to remove O_2 before use. $Fe(ClO_4)_3$ and $TiCl_3$ were reagent grade products obtained from Alpha Inorganics Inc. The titanium salt was dissolved in 3 *M* HCl to give a solution about 2 *M* in Ti(III); this was stored in a burette in the absence of air. Maleic acid was obtained as C.P. grade from Eastman Kodak and was recrystallized before use. A stock 9.0 *M* $HClO_4$ solution was obtained by dilution of reagent grade 60% $HClO_4$ solution obtained from Nichols Chemical Company. B.D.H. concentrated HCl was diluted to give stock HCl solutions which were standardized against alkali solutions prepared from B.D.H. standard NaOH ampuls.

Rhodium(III) trichloride was obtained as the trihydrate $RhCl_3.3H_2O$ from Platinum Chemicals; $Na_3RhCl_6.12H_2O$ was a product of K and K Laboratories. These solids were dissolved in HCl to give stock rhodium solutions. The method of Pantani (11) was used to estimate the concentration of Rh in these solutions, the Rh(III) being oxidized by hypochlorite at pH 11.2 to a violet color, probably Rh(VI), with a characteristic absorption at 530 mμ (ϵ = 1 270); the results indicated concentrations within 10% of those expected for solutions made by the weighing out of the salts as pure compounds. Because of the strict conditions of concentrations, pH, and time required for the full development of the violet color it seemed that the rhodium compounds were essentially pure and could be weighed out as such to give standard Rh(III) solutions. A 0.2 *M* solution of $Na_3RhCl_6.12H_2O$ in 6 *M* HCl exhibited absorption spectrum maxima at 411 mμ (ϵ = 85) and 518 mμ (ϵ = 100) corresponding closely to the reported spectrum of the $[RhCl_6]^{3-}$ species (2). The spectrum of a freshly prepared solution of $RhCl_3.3H_2O$ in 3 *M* HCl exhibited a single absorption peak at 505 mμ (ϵ = 80); it has been suggested (12, 13) that this solution contains polynuclear species and complexes with both chloride ions and water molecules coordinated, both cationic and anionic Rh(III) species being present. The absorption spectrum very slowly changes when the solution is left at room temperature for several weeks, a second peak developing in the region of 400 mμ. This spectrum change can be accomplished rapidly by heating the initial solution. The final constant spectrum showed maxima at 404 mμ (ϵ = 67) and 511 mμ (ϵ = 74) and comparison with the data of Wolsey and co-workers (2) suggests that the major species present is $[Rh(H_2O)Cl_5]^{2-}$ with small amounts of the 6:1 chloro complex. A solution of the $[Rh(H_2O)_6]^{3+}$ species was made by digestion of $RhCl_3.3H_2O$ in strong $HClO_4$, the chloride being distilled off as HCl. The spectrum of the final solution corresponded to that of the fully aquated species (2) and showed maxima at 310 mμ (ϵ = 57) and 396 mμ (ϵ = 53); this solution was diluted to give a standard solution 6.0 *M* in $HClO_4$ and was used to prepare other solutions containing Rh(III) chloro complexes by the method described by Wolsey (2). In these solutions the chloride concentration was varied from 0.01 *M* to 3.25 *M* by the addition of HCl solution, the total acid strength and ionic strength always being 6.0 *M*: the solutions were made up in pyrex tubes which were subsequently sealed and maintained at 120° for 2 weeks. This period of time was necessary for the attainment of equilibrium among the complex species.

Kinetic measurements were made by following the uptake of H_2 at constant pressure by the procedure described earlier by Halpern and co-workers (14, 15). Gas uptake is indicated by a difference in levels of a liquid of negligible vapor pressure (e.g. butyl phthalate) in a capillary manometer thermostated with a gas burette at 25°. H_2 is then added to the system through a needle valve, a constant pressure being maintained by the resulting rise of mercury in a calibrated tube of the burette. The height of the mercury column is followed with a travelling microscope.

Visible and ultraviolet absorption spectra were measured on a Cary 14 recording spectrophotometer with matched Beckman standard silica cells of 1 cm optical path length.

RESULTS

Hydrogen Solubility from Kinetic Measurements

The kinetics of the reduction by H_2 of ferric ion in the presence of rhodium(III) chloride were of the form

$$-d[H_2]/dt = k[H_2][Rh^{III}] = k'[Rh^{III}]$$

Can. J. Chem. Downloaded from www.nrcresearchpress.com by 210.87.254.105 on 09/05/12
For personal use only.

where $k' = k[H_2]$, as previously found by other workers (1). Since the concentrations of Rh^{III} and H_2 remain constant while the ferric species is being reduced, the kinetics are pseudo zero order. When all the Fe^{III} had been reduced to Fe^{II} reduction of Rh^{III} to metallic rhodium occurred, and was marked by an increase in the rate of H_2 uptake caused by autocatalysis by the metal. Figure 1 shows typical H_2 uptake plots at 80° for some of the experiments summarized in Table I; this shows results for the $RhCl_3/H_2/FeCl_3$ systems over a range of chloride concentration from 0.43 *M* to 5.57 *M* at a constant acidity. The chloride concentration was varied by the addition of HCl, the total acid strength and ionic strength in the series always being 5.57 *M*; the Rh^{III} and initial Fe^{III} concentrations were the same throughout. Values of k' were calculated from the slopes of the zero order H_2 uptake plots.

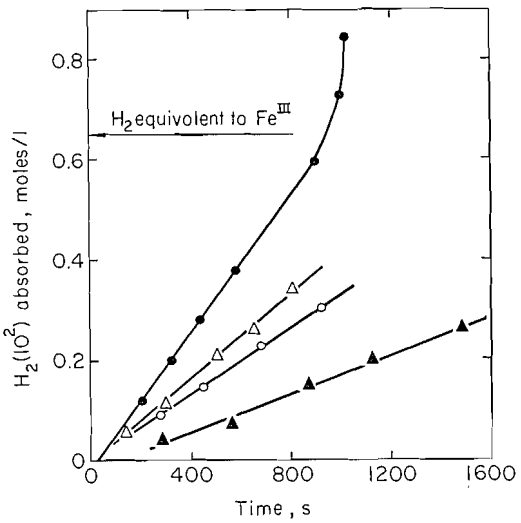


FIG. 1. Typical rate plots at 80°, 450 mm H_2, 0.011 *M* $RhCl_3$, 0.013 *M* $FeCl_3$; various media with $[HCl] + [HClO_4] = 5.57$ *M*: (●) 0.43 *M* HCl; (△) 3.00 *M* HCl; (○) 3.86 *M* HCl; (▲) 5.57 *M* HCl.

The spectra of the Rh^{III} solutions used in the two extreme concentrations (0.43 *M* and 5.57 *M* chloride) were measured near the end of the hydrogenation experiments and were found to be very similar, exhibiting peaks in the regions of 405 mμ ($\epsilon \sim 70$) and 510 mμ ($\epsilon \sim 80$), indicating that the chlororhodate(III) species present in the two solutions are essentially the same; comparison with the published data (2) shows that both solutions contain predominantly the $[Rh(H_2O)Cl_5]^{2-}$ species with smaller amounts (~20%) of the 6:1 chloro species. The available formation constant data (2) at 120° for the Rh(III)-chloride complexes indicate that the 5:1 chloro species would predominate in the 0.43 *M* $[Cl^-]$ conditions and the 6:1 species in the 5.57 *M* $[Cl^-]$ conditions. The hydrogenation experiments were carried out at 80° over a period of about 30 min; the slow equilibration of the species during this time must account for the perseverance of the 5:1 species at the higher $[Cl^-]$,

The relatively large variation in rate of H_2 uptake for this series of experiments is not then due to the presence of different chloro species but must be principally due to variation in the H_2 solubility in the different media. The concentration of H_2 in 5.57 *M* HCl was estimated as 5.3×10^{-4} mole atm^{-1} from the solubility data of Weibe and Gaddy (16), correcting for the effect of HCl (17); this gives a rate constant k of 0.60 l

Can. J. Chem. Downloaded from www.nrcresearchpress.com by 210.87.254.105 on 09/05/12
For personal use only.

TABLE I

Kinetic data at 80° for $RhCl_3/H_2/FeCl_3$ systems; $[Rh^{III}] = 0.011\ M$; $[Fe^{III}] = 0.013\ M$; $H_2 = 450$ mm; $Rh(H_2O)Cl_5^{2-}$ predominant species

Medium		Rate of H_2 uptake $\times 10^6$ (moles l^{-1} s^{-1})	$k' \times 10^4$ (s^{-1})	k (l $mole^{-1}$ s^{-1})	$[H_2] \times 10^4$ (moles l^{-1})
HCl (M)	$HClO_4$ (M)				
5.57	0.00	2.10	1.91	0.60	3.2
4.71	0.86	2.78	2.53	0.60	4.2
3.86	1.71	3.35	3.05	0.60	5.1
3.00	2.57	4.28	3.89	0.60	6.5
2.14	3.43	5.62	5.11	0.60	8.5
0.43	5.14	7.11	6.46	0.60	10.8

$mole^{-1}$ s^{-1} in this medium. The solubility of hydrogen in the varying media can then be calculated approximately, assuming a rate constant of 0.60 l $mole^{-1}$ s^{-1} throughout the series. These data are included in Table I. The variation of H_2 solubility with media is shown in Fig. 2. The solubility of noble gases such as Kr increases by a factor of about two on going from pure H_2O to 6 M $HClO_4$ (18) and this together with the known decrease in H_2 solubility with increasing HCl strength (17) suggests that the magnitude of the solubility variation shown in Fig. 2 is reasonable.

Catalytic Reduction of Ferric Ion by the Complexes $[Rh(H_2O)_{6-n}Cl_n]^{(n-3)-}$

Kinetic results at 80° for two experiments with solutions of Na_3RhCl_6 at high and low chloride concentration and for the series of experiments with the prepared $Rh(H_2O)_6^{3+}/HCl/HClO_4$ solutions are summarized in Table II. Absorption spectra were measured before and, when possible (with the anionic complexes), after the hydrogenation experiment; the spectra of the Rh^{III} species were unaffected by the catalytic reduction. The principal species present were again determined by comparison with the spectroscopic data of Wolsey and co-workers (2). In the 0.64 M HCl, 5.14 M $HClO_4$ medium, Na_3RhCl_6 dissociated principally into the 5:1 chloro species. The hydrogen solubilities were estimated from the data shown in Fig. 2.

TABLE II

Kinetic data at 80° for Rh(III)/H_2/Fe(III) systems. $[Fe^{III}] = 0.013\ M$; $H_2 = 450$ mm. The number given for the species present represents the number of coordinated chloride ions*

Predominant species present	Medium		Rate of H_2 uptake $\times 10^6$ (moles l^{-1} s^{-1})	$[H_2] \times 10^4$ (moles^{-1})	k (l $mole^{-1}$ s^{-1})
	HCl (M)	$HClO_4$ (M)			
5 (6)	0.64	5.14	6.10	10.8	0.40
6	5.79	0.00	3.19	3.2	0.71
0	0.00	6.00	Metal precipitates		
1	0.01	6.00	Metal precipitates		
2	0.02	5.98	Metal precipitates		
3	0.04	5.96	Metal precipitates		
4 (5)	0.08	5.92	2.06	12.0	0.20
5 (4)	0.20	5.80	3.18	12.0	0.31
6	3.50	2.50	3.10	6.5	0.55

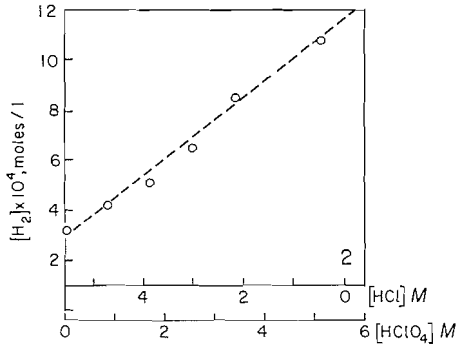
*Na_3RhCl_6 solution was used for the first two experiments listed, the $[Rh^{III}]$ being 0.014 M; the $[Rh^{III}]$ in the remaining systems was 0.0087 M.

Can. J. Chem. Downloaded from www.nrcresearchpress.com by 210.87.254.105 on 09/05/12
For personal use only.

The two experiments with the hexachloro salt indicate that the 6:1 chloro species is more active catalytically than the 5:1 species, the estimated rate constants being compatible with the data of Table I. The experiments with the complexes prepared from the $[Rh(H_2O)_6^{3+}]$ solution confirm this and demonstrate that the activities of the anionic complexes decrease in the order

$$[RhCl_6]^{3-} > [Rh(H_2O)Cl_5]^{2-} > [Rh(H_2O)_2Cl_4]^{-}$$

The rate constants determined in this series of experiments are about 25% lower than might be expected in comparison with those obtained with the $RhCl_3/HCl$ and Na_3RhCl_6/HCl systems. However, in consideration of the somewhat uncertain H_2 solubility corrections and the slight variations in ionic strength from one series of experiments to another, this is not too unreasonable. There is no doubt in the order of activity of the complexes.



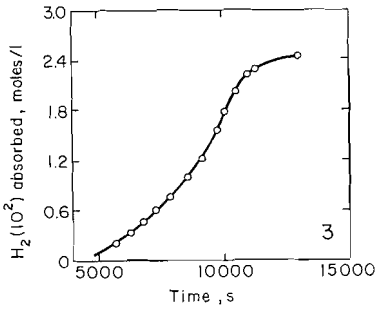


FIG. 2. Solubility of H_2 in $HCl/HClO_4$ media.
FIG. 3. Rate plot for cationic species $Rh(H_2O)_5Cl^{2+}$ at 80°, 450 mm H_2, 0.0087 *M* Rh^{III}, 0.025 *M* Fe^{III}, 6.0 *M* $HClO_4$, 0.01 *M* HCl.

Homogeneous hydrogenation of Fe^{III} was not observed when the $[Rh(H_2O)_6]^{3+}$, $[Rh(H_2O)_5Cl]^{2+}$, $[Rh(H_2O)_4Cl_2]^{+}$, and $Rh(H_2O)_3Cl_3$ complexes were initially present in solution. Figure 3 shows the H_2 uptake plot for a $[Rh(H_2O)_5Cl]^{2+}$ system. There was no gas uptake or change in species present (confirmed spectrophotometrically) for about 5 000 s; a slow autocatalytic uptake of H_2 was then observed, metallic rhodium being precipitated from solution. The uptake at the end point corresponded exactly to complete reduction of Fe^{III} to Fe^{II} and Rh^{III} to Rh^0. The other cationic and neutral Rh(III)–chloride complexes gave similar rate plots.

In the absence of Fe^{III} substrate, acid solutions containing $[Rh(H_2O)_{6-n}Cl_n]^{(n-3)-}$ species where $n = 0$ to 6 were all rapidly reduced by H_2 in an autocatalytic manner to the metal at temperatures above 40°, the final H_2 uptake corresponding to reduction of Rh^{III} to Rh^0.

Rh^{III}/H_2/Maleic Acid Systems

Excess maleic acid in 3 *M* HCl solution was added to the solution of $RhCl_3$ in 3 *M* HCl which contained principally the 5:1 chloro species and hydrogenation was attempted in the usual way at 80°. H_2 was taken up as shown in Fig. 4. The rate of uptake falls off with time and becomes very slow after about 16 000 s. At this stage the uptake corresponded to reduction of Rh(III) to Rh(I).

$$Rh^{III} + H_2 \xrightarrow{k} Rh^{I} + 2H^{+}$$

Can. J. Chem. Downloaded from www.nrcresearchpress.com by 210.87.254.105 on 09/05/12
For personal use only.

Spectrophotometric measurements showed that the Rh(III) chloro complexes did not complex with maleic acid. The Rh^{I} state must be stabilized by complexing with the maleic acid in a rapid step which prevents further reduction to the metal.

$$Rh^{I} + \text{maleic acid} \xrightarrow{\text{fast}} \text{complex.}$$

A rate law of the form

$$-d[H_2]/dt = -d[Rh^{III}]/dt = k[Rh^{III}][H_2]$$

indicates that at constant $[H_2]$ the reaction becomes one of pseudo first order. A good linear plot of $\log [Rh^{III}]$ versus time was obtained from the rate data, assuming the decrease in $[Rh^{III}]$ is proportional to the H_2 uptake (Fig. 4). From the slope of the rate plot the pseudo first order rate constant can be evaluated and, taking the solubility of H_2 as 6.1×10^{-4} mole atm^{-1} in this medium, the bimolecular rate constant k was calculated (Table III). The values obtained for two different initial Rh^{III} concentrations, 0.51 and 0.59 l $mole^{-1}$ s^{-1}, confirm that the reaction is first order in rhodium and agree with the values obtained for the catalytic reduction of Fe^{III} under similar conditions (1). This indicates that the rate-determining step is the same for both systems (see Discussion).

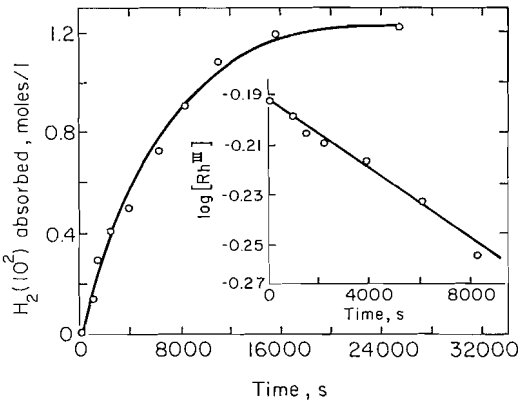


FIG. 4. Rate plot at 80°, 450 mm H_2, 0.011 M $RhCl_3$, 0.10 M maleic acid, 3 M HCl. Inset: plot of $\log [Rh^{III}]$ against time.

The original reddish Rh(III) solution gradually became light yellow during the course of the reaction; the spectrum of the final solution (Fig. 5) exhibited absorption maxima at 353 mμ ($\epsilon = 400$) and 425 mμ ($\epsilon = 180$). The same yellow species in solution was formed by reducing the Rh(III)/maleic acid/3 M HCl solution with Ti^{III} (in the absence of maleic acid, Ti^{III} rapidly reduced Rh^{III} to the metal). The solution certainly contains a complex of maleic acid with rhodium in a reduced valency state and the stoichiometry of the reaction with H_2 indicates a Rh^{I} complex.

Table III also summarizes results obtained for the maleic acid systems with the complexes prepared from the $Rh(H_2O)_6^{3+}/HCl/HClO_4$ solutions. With the cationic species $[Rh(H_2O)_6]^{3+}$ and $[Rh(H_2O)_4Cl_2]^{+}$ in solution a rapid uptake of H_2 was observed and reduction to Rh^{0} occurred with a resulting heterolytically catalyzed H_2 reduction of the maleic acid. With the solution containing predominantly the 5:1 chloro species reduction to the Rh^{I} – maleic acid complex again occurred, but there was also slight

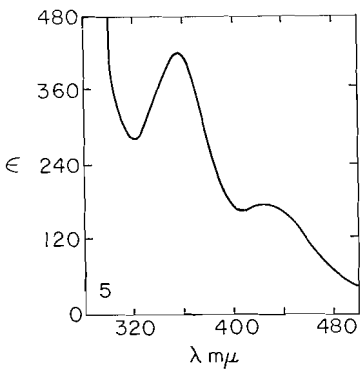
Can. J. Chem. Downloaded from www.nrcresearchpress.com by 210.87.254.105 on 09/05/12
For personal use only.

TABLE III

Kinetic data at 80° for the Rh(III)/H_2/maleic acid system; H_2 = 450 mm; maleic acid = 0.10 *M*

Major species	$[Rh^{III}]$ (*M*)	Medium HCl (*M*)	Medium $HClO_4$ (*M*)	$[H_2] \times 10^4$ (moles l^{-1})	*k* ($l\,mole^{-1}\,s^{-1}$)
5	0.011	3.00	0.00	3.6	0.51
5	0.015	3.00	0.00	3.6	0.59
0	0.007	0.00	3.00	Metal precipitates	
2	0.006	0.01	4.12	Metal precipitates	
5 (4)	0.006	0.14	4.00	Slight metal precipitates	
6	0.006	2.18	1.95	Slight metal precipitate?	

reduction to the metal; the resulting heterogeneous hydrogenation complicated the H_2 uptake plot. The $RhCl_6^{3-}$ solution was also reduced to the same yellow species but the H_2 uptake did not level off and continued at a very slow rate, suggesting some further reaction, possibly heterolytic, might be involved. Because of this irreproducibility of the aqueous Rh^{III}/H_2/maleic acid systems, which probably resulted from slight reduction of Rh^{III} to the metallic state, a detailed kinetic study was not carried out.



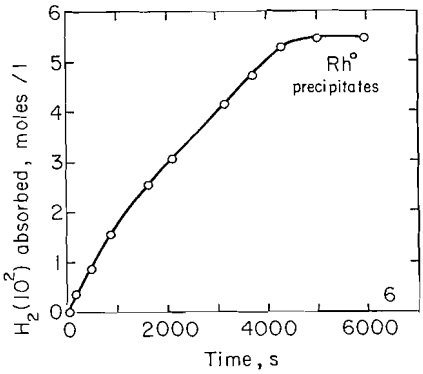


FIG. 5. Absorption spectrum of Rh^I – maleic acid complex in 3 *M* HCl.
FIG. 6. Rate plot at 80°, 730 mm H_2, 0.005 *M* $RhCl_3$, 0.05 *M* maleic acid in dimethylacetamide solution.

Preliminary experiments in dimethylacetamide solution have given reproducible results. The experiments consist of adding excess maleic acid to a neutral solution of $RhCl_3.3H_2O$ in dimethylacetamide; hydrogenation is carried out in the usual way. Figure 6 shows a typical H_2 uptake plot. In contrast to the aqueous system complete homogeneous hydrogenation of the maleic acid occurs, the total H_2 uptake being equivalent to the sum of that required for reduction of the olefinic bond and reduction of Rh^{III} to Rh^I. The initial more rapid rate of H_2 uptake, which is first order in both Rh^{III} and H_2, is concerned with the production of a Rh^I – maleic acid complex as in the aqueous system. The later linear uptake could be explained by the reactions

$$Rh^I - \text{maleic acid} + H_2 \xrightarrow{k} Rh^I + \text{succinic acid}$$

$$Rh^I + \text{maleic acid} \xrightarrow{\text{fast}} Rh^I - \text{maleic acid}.$$

At the end point in these systems metallic rhodium is precipitated. These systems are being more fully studied.

Can. J. Chem. Downloaded from www.nrcresearchpress.com by 210.87.254.105 on 09/05/12
For personal use only.

Can. J. Chem. Downloaded from www.nrcresearchpress.com by 210.87.254.105 on 09/05/12
For personal use only.

DISCUSSION

It has been found that in acid solution only anionic chlororhodate(III) complexes will activate molecular H_2 for the homogeneous reduction of ferric ion. The activity of the species increases with increasing number of chloride ligands attached to the metal ion, i.e.

$$[RhCl_6]^{3-} > [Rh(H_2O)Cl_5]^{2-} > [Rh(H_2O)_2Cl_4]^{-}$$

A common feature of the mechanisms of many homogeneously catalyzed hydrogenation reactions appears to be a rate-determining heterolytic splitting of H_2 by the catalytic species with the formation of a metal hydride complex which reduces the substrate in a subsequent fast step (1, 3). For the present reactions, for example,

[1] $$RhCl_6^{3-} + H_2 \underset{k_{-1}}{\overset{k_1}{\rightleftharpoons}} HRhCl_5^{3-} + Cl^-$$

[2] $$HRhCl_5^{3-} + 2FeCl_3 \xrightarrow[\text{fast}]{k_2} RhCl_6^{3-} + HCl + 2FeCl_2.$$

Harrod and Halpern (1) had carried out their studies with $RhCl_3$ in 3.0 M to 5.0 M HCl solutions; they had suggested that $[RhCl_6]^{3-}$ was likely to be the predominant species in solution, but the present results show that the 5:1 chloro species persists over this range of HCl concentration. The rate constants we obtained are in excellent agreement with those obtained earlier under comparable conditions (1).

Reaction [1] is essentially the replacement of chloride ion by hydride ion; easier removal of chloride ion would be expected with increasing negative charge in agreement with the observed activities of the complexes. This factor is also reflected in the stepwise formation constants of the complexes $K_1 > 10^3$, $K_2 > 10^3$, $K_3 \sim 10^3$, $K_4 \sim 250$, $K_5 \sim 25$, $K_6 \sim 0.56$ (2); increasing strength of the metal chloride bonding in the lower species makes removal of the chloride or its replacement by hydride increasingly difficult. A similar trend has been reported for the catalytic hydrogenation of dichromate by chloro complexes of Cu^{II} (19). The catalytic activity increases with increasing concentration of chloride ion in solution, levelling off to a maximum when the $CuCl_4^{2-}$ species is fully formed.

In the absence of ferric substrate cationic, neutral, and anionic rhodium(III)–chloride complexes are all rapidly reduced to the metal by H_2 at 80° in acid solution. The equilibrium represented by reaction [1] must still exist but the hydride complex is rapidly converted by some process to metallic rhodium, i.e.

[3] $$Rh^{III} + H_2 \underset{k_{-1}}{\overset{k_1}{\rightleftharpoons}} Rh^{III}H^- + H^+$$

[4] $$Rh^{III}H^- \xrightarrow{k_3} Rh^0$$

where k_3 is likely to be $> k_{-1}$. The experiments involving the maleic acid systems indicate that process [4] goes via the Rh^I state. The rate-determining step for the formation of the Rh^I – maleic acid complex is again governed by reaction [3] since the determined rate constant is the same as that determined for the H_2-catalyzed reduction of Fe^{III}. Production of Rh^I must proceed by the rapid step

[5] $$Rh^{III}H^- \rightarrow Rh^I + H^+.$$

Rhodium metal could then be produced by further reduction of Rh^{I} by H_2 or by a disproportionation reaction. (It is of course possible that the reduction of ferric species involves a Rh^{I} species rather than the postulated hydride $Rh^{III}H^{-}$; this will depend on the relative rates of the two fast steps shown in reactions [2] and [5].)

There is stabilization of the Rh^{I} state by complexing with maleic acid only when anionic chlororhodate(III) complexes are initially present; with the cationic complexes present metal was precipitated. More information is required about the nature of the Rh^{I} – maleic acid complex; the d acceptor orbitals of the chloride ion might be important for stabilizing the low valency state of the metal, the stabilization increasing with the number of chloride ligands present. A simple dimer olefin complex of Rh^{I}, μ-dichlorotetraethylenedirhodium(I) $(C_2H_4)_4Rh_2^{I}Cl_2$ has recently been isolated by Cramer (20) by reacting ethylene with an aqueous methanolic solution of $RhCl_3$.

The cationic and neutral chlororhodium(III) complexes do not act as hydrogenation catalysts for the homogeneous reduction of ferric ion; metallic rhodium was always precipitated from solution. From the reaction schemes listed above this suggests that for these systems k_3 is $> k_2$, i.e. the dissociation of the $Rh^{III}H^{-}$ species for the cationic and neutral species is more rapid than its reaction with Fe^{III}; for the anionic species k_2 must be $> k_3$. Cationic and neutral complexes of Rh^{III} are like their Co^{III} analogues, usually kinetically inert whereas the anionic complexes are generally labile (21).

Rhodium – chloride complexes, with rhodium in the tri- or uni-valent state, in aqueous acid solutions are not effective catalysts for the homogeneous hydrogenation of the olefinic bond in maleic acid. An olefin complex is formed with Rh^{I}, but this shows no reaction with H_2. This is in contrast somewhat with the corresponding ruthenium systems: Ru^{III} chloro complexes have been shown to be ineffective as catalysts for the homogeneous hydrogenation of olefinic bonds, but Ru^{II} complexes were active (4). A 1:1 complex of Ru^{II} with maleic acid is formed, but this reacted with H_2 to yield again succinic acid and free Ru^{II}.

The preliminary experiments in the dimethylacetamide solvent, however, indicate that the Rh^{I} – maleic acid complex does react at measurable rates with H_2 in neutral solutions to produce succinic acid in a homogeneous catalytic reaction. Wilkinson and co-workers (10) have reported that a solution of $(Ph_3P)_3Rh^{I}Cl$ in benzene takes up molecular H_2 to give an intermediate hydride stable enough for the Rh—H bond to be detected by nuclear magnetic resonance; this hydride rapidly reduces olefins such as hex-1-ene and acts as a catalytic intermediate in the homogeneous hydrogenation of the olefin. In our studies, solutions of $RhCl_3.3H_2O$ in dimethylacetamide take up molecular H_2 to give the Rh^{I} valence state which rapidly complexes with the olefin present; the Rh^{I}–olefin complex then reacts further with H_2 to give the catalytic reduction. The kinetics of this system will be reported in a later paper.

ACKNOWLEDGMENTS

Grateful acknowledgment is made to the National Research Council of Canada for support of this research.

REFERENCES

1. J. F. Harrod and J. Halpern. Can. J. Chem. **37**, 1933 (1959).
2. W. C. Wosley, C. A. Reynolds, and J. Kleinberg. Inorg. Chem. **2**, 463 (1963).
3. J. Halpern. Advan. Catalysis, **11**, 301 (1959).
4. J. Halpern, J. F. Harrod, and B. R. James. J. Am. Chem. Soc. **83**, 753 (1961).
5. R. D. Gillard, J. A. Osborn, P. B. Stockwell, and G. Wilkinson. Proc. Chem. Soc. 284 (1964).
6. J. A. Osborn, G. Wilkinson, and J. F. Young. Chem. Comm. 17 (1965).
7. A. J. Chalk and J. F. Harrod. J. Am. Chem. Soc. **86**, 1776 (1964).

Can. J. Chem. Downloaded from www.nrcresearchpress.com by 210.87.254.105 on 09/05/12
For personal use only.

8. L. VASKA. J. Am. Chem. Soc. **86**, 1943 (1964).
9. J. CHATT. J. Chem. Soc. 3466 (1964).
10. J. F. YOUNG, J. A. OSBORN, F. H. JARDINE, and F. WILKINSON. Chem. Comm. 131 (1965).
11. F. PANTANI. Talanta, **9**, 15 (1962).
12. J. S. FORRESTER and G. H. AYRES. J. Phys. Chem. **63**, 1979 (1959).
13. A. M. KRISTJANSON and M. LEDERER. J. Less-Common Metals, **1**, 245 (1959).
14. J. HALPERN, J. F. HARROD, and P. E. POTTER. Can. J. Chem. **37**, 1446 (1959).
15. A. J. CHALK and J. HALPERN. J. Am. Chem. Soc. **81**, 5846, 5854 (1959).
16. R. WEIBE and V. L. GADDY. J. Am. Chem. Soc. **56**, 76 (1934).
17. A. SEIDELL. Solubilities of inorganic and metal organic compounds. Vol. I. 3rd ed. D. Van Nostrand Co., Inc., New York. 1940. p. 557.
18. G. J. AKERLOF. J. Am. Chem. Soc. **57**, 1196 (1935).
19. E. PETERS and J. HALPERN. Can. J. Chem. **34**, 554 (1956).
20. R. D. CRAMER. Inorg. Chem. **1**, 722 (1962).
21. F. A. COTTON and G. WILKINSON. Advanced inorganic chemistry. Interscience, New York. 1962. p. 839.

Can. J. Chem. Downloaded from www.nrcresearchpress.com by 210.87.254.105 on 09/05/12
For personal use only.

Can. J. Chem. Downloaded from www.nrcresearchpress.com by 210.87.254.105 on 09/05/12
For personal use only.

NOTES

THE RADIOLYSIS OF TRIFLUOROETHANOL

J. C. RUSSELL[1] AND K. J. MCCALLUM

Information is being gathered on the radiolysis of related simple halogenated compounds. Woods and Spinks (1, 2) have studied the radiolysis of aqueous solutions of trichloroethanol, tribromoethanol, and dibromoethanol, as well as the trisubstituted acetaldehydes fluoral hydrate, chloral hydrate, and bromal hydrate. With the exception of fluoral hydrate, aqueous solutions of all the above compounds gave yields of the corresponding halogen acid in the range $G_{HX} = 25$–400. The size of the acid yields and the dose rate dependence that were found indicate that these compounds undergo chain reactions forming the halogen acids.

The radiation chemistry of ethanol, both pure and in aqueous solution, has been investigated in detail (3–5). No chain reaction was found and a detailed mechanism has been proposed by Adams and Sedgewick (4) and Myron and Freeman (5).

The present note reports an investigation of the ^{60}Co γ-radiolysis of trifluoroethanol, both as the pure alcohol and in aqueous solution. The halogen acid was formed in moderate yield; hydrogen and products similar to those found in ethanol radiolysis were also formed.

RESULTS

Most of the results are shown in Figs. 1 and 2 and Table I. All values except those for the vicinal glycol and gas analyses (for which duplicate determinations were made) represent at least four separate irradiations. Most values represent the average of eight or

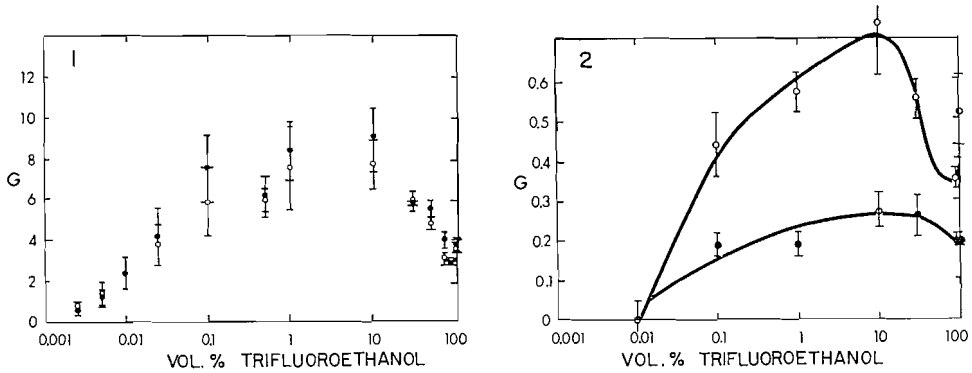


FIG. 1. The yield of acid and fluoride vs. concentration of trifluoroethanol. (●) Acid, (○) fluoride.
FIG. 2. The yield of carbonyl and formaldehyde vs. concentration of trifluoroethanol. (○) Total reactive carbonyl, (●) formaldehyde.

more separate irradiations. The vertical bars in Figs. 1 and 2 represent experimental standard deviations.

Trifluoroethanol samples containing 0.408% and 0.093% water by weight gave the same yield of acid and fluoride on irradiation.

[1]*Present Address*: *Department of Chemistry, University of Alberta, Edmonton, Alberta.*

TABLE I

Trifluoroethanol (moles/l)	Volume % trifluoroethanol	G					
		Vicinal glycol	H_2	CO_2	Organic acid	Unreactive carbonyl	Reactive carbonyl
11.4	99.6	0.10±0.02	3.2±0.2	<0.004	<0.05	0.4±0.2	0.52±0.1
1.14	10	0.27±0.02	2.4±0.2	0.016±0.002	0.5±0.2	0.9±0.4	0.75±0.1

Samples of pure irradiated trifluoroethanol were analyzed with a gas chromatograph equipped with a Carbowax column. Nine significant peaks were found, six of which could be considered to be large enough to indicate organic products of some importance. None of these compounds corresponded to known non-fluorinated aliphatic compounds. No identification could be made, since no authentic samples of the possible compounds were available.

The yields of acid and fluoride were measured for pure trifluoroethanol and 1.1 *M* trifluoroethanol in water at the dose rates 2×10^{18} eV/g h and 2×10^{17} eV/g h. The yields were found to be independent of the dose rate.

The yield of HF from aqueous solutions of trifluoroethanol is relatively small, being slightly larger than that found by Woods and Spinks (1) for fluoral hydrate ($G_{HF} = 7.1$). It is very much lower than the $G_{HCl} = 27$ found by Woods and Spinks for trichloroethanol and the $G_{HBr} = 89$ found for tribromoethanol. The yield of $G_{HF} = 7.9$ is, however, larger than the sum of the yields of free radicals and solvated electrons in γ-irradiated water (6). This might indicate that there is some contribution from a chain reaction, but that this is too small to give a detectable dose rate effect over the dose rate range studied.

Three distinct types of carbonyl compounds were found. These were formaldehyde, another reactive carbonyl which has not been identified, and an unreactive carbonyl (believed to be fluoral hydrate).

The radiolysis of pure trifluoroethanol gives products which are analogous to those found for ethanol. The yield of HF is small and there would appear to be little or no contribution from a chain reaction. The sum of the yields of HF and H_2 is only slightly larger than the radiolytic yield of H_2 from ethanol (5).

The radiolysis of trifluoroethanol is very similar to that of ethanol, but quite different from that of the related halogenated compounds. Trifluoroethanol is thus best regarded as a modified ethanol, rather than as an analogue of the other halogenated compounds.

EXPERIMENTAL

Materials

Trifluoroethanol, $CF_3—CH_2—OH$, was obtained from K and K Laboratories, Jamaica, N.Y. The trifluoroethanol was analyzed by gas chromatography. The total impurities were estimated to be less than 1%. The content of water was found by Karl Fisher titration (7) to be 0.408% by weight. This was not objectionable when making up aqueous solutions. A small quantity of trifluoroethanol was dried by fractional distillation through a 6 in. glass column, packed with glass helices. This material contained 0.093% water. Efforts to dry trifluoroethanol with silica gel and barium oxide were not successful. The dried trifluoroethanol gave the same yields of acid and fluoride on irradiation as trifluoroethanol containing 0.408% water. The undried material was used for subsequent irradiations of pure trifluoroethanol.

All water used in making up solutions which were irradiated was triply distilled. Ordinary distilled water was distilled from an alkaline permanganate solution and then redistilled from an acid solution of potassium dichromate.

All irradiations were performed in capped 10 mm × 75 mm polypropylene test tubes supplied by Nalgene Company Inc., Rochester, N. Y. The tubes were chosen on the basis of their inertness towards trifluoroethanol and the radiolysis products. One of the products, HF, attacks glass, giving low yields if glass vessels are used.

Experimental Methods

All samples were deoxygenated with a flow of dry oxygen-free nitrogen before irradiation. The irradiations were performed with a 50 curie ^{60}Co source. This gave a dose rate of 2×10^{18} eV/g h, and doses in the range

Can. J. Chem. Downloaded from www.nrcresearchpress.com by 210.87.254.105 on 09/05/12
For personal use only.

0.26–1.6 $\times$ 10^{20} eV/g were used. The dose rates were measured with a "Fricke" dosimeter (8) and a Farmer Baldwin X-ray dosimeter MkII made by the Baldwin Instrument Company, Dartford, Kent, England. For the "Fricke" dosimeter $G_{Fe^{3+}}$ was taken as 15.5 and $\epsilon_{Fe^{3+}}$ as 2 201 at 25 °C and 304 mμ (8). The dose rates as measured by the two methods agreed within the experimental error of 2%.

The acid yields were determined by visual microtitration with 0.1 *N* NaOH and chlorophenol red indicator. The fluoride yields were determined by reaction with thorium chloranilate to give a colored complex. The concentration of the complex was measured spectrophotometrically at 304 mμ wavelength. The procedure followed was adapted by Fisher Scientific Company (9) from that of Fine and Wynne (10). The yields of hydrogen and carbon dioxide were determined by a gas chromatographic technique on a silica gel column.

The analytical method used to determine the total carbonyl yield was that of Lappin and Clark (11). The unreactive carbonyl (possibly fluoral hydrate) was estimated by a modification of the total carbonyl analysis of Lappin and Clark. Under the conditions of analysis by this procedure fluoral hydrate does not react with the 2,4-dinitrophenylhydrazine reagent. It was found that if the heating time at 80 °C was extended from 5 min to 60 min, approximately 20% reaction could be achieved. In this way the yield of such unreactive carbonyl compounds was estimated by comparison with known amounts of fluoral hydrate dissolved in trifluoroethanol.

The analytical method of Tanenbaum and Bricker (12) was used to determine the formaldehyde yields. The "chromotropic acid" (4,5-dihydroxy-2,7-naphthalene disulfonic acid) method of Bricker and Johnson (13) for the determination of formaldehyde was investigated and found to be unsuitable in the system of trifluoroethanol and water used. The method gave higher values for the formaldehyde concentration in irradiated samples than the total carbonyl concentration. The presence of trifluoroethanol also caused large negative errors in the analysis.

The analytical method of Siggia (14) was used for the determination of the yields of vicinal glycol. The yields of organic acid were estimated by treating the samples with diazomethane after the trifluoroethanol and water had been evaporated. The resulting methyl glycollate was then detected and the amount present estimated by gas chromatography. Known amounts of glycollic acid in trifluoroethanol were used for reference.

ACKNOWLEDGMENT

This work was supported by the National Research Council.

1. R. J. Woods and J. W. T. Spinks. Can. J. Chem. **38**, 77 (1960).
2. R. J. Woods and J. W. T. Spinks. Can. J. Chem. **35**, 1475 (1957).
3. G. G. Jayson, G. Scholes, and J. Weiss. J. Chem. Soc. 1358 (1957).
4. G. E. Adams and R. D. Sedgewick. Trans. Faraday Soc. **60**, 865 (1964).
5. J. J. J. Myron and G. R. Freeman. Can. J. Chem. **43**, 381 (1965).
6. F. S. Dainton and D. B. Peterson. Proc. Roy. Soc. London, Ser. A, **267**, 443 (1962).
7. J. Mitchell and D. M. Smith. Aquametry. Interscience Publishers, New York. 1948.
8. J. Weiss, A. O. Allen, and H. A. Swarz. Proc. Intern. Conf. Peaceful Uses of At. Energy, Geneva 1955, **14**, 179 (1956).
9. Technical Data Sheet TD-138. Fisher Scientific Company, Limited.
10. L. Fine and E. A. Wynne. Microchem. J. **3**, 515 (1959).
11. G. R. Lappin and L. C. Clark. Anal. Chem. **23**, 541 (1951).
12. M. Tanenbaum and C. E. Bricker. Anal. Chem. **23**, 354 (1951).
13. C. E. Bricker and H. R. Johnson. Ind. Eng. Chem. Anal. Ed. **17**, 400 (1945).
14. S. Siggia. *In* Qualitative organic analysis via functional groups. 2nd ed. John Wiley and Sons, Inc., New York. 1954.

Received July 20, 1965.
Department of Chemistry and Chemical Engineering,
University of Saskatchewan,
Saskatoon, Saskatchewan.

COMMENT: DEFINITION OF A BIRADICAL

G. R. Freeman

It is evident from the literature of the past few years that there is disagreement or lack of clarity about the meaning of the term "biradical". The concept of a biradical is of sufficient importance in several types of reaction that it should be clarified, even if arbitrarily. The purpose of the present note is to suggest a better definition of the term

Can. J. Chem. Downloaded from www.nrcresearchpress.com by 210.87.254.105 on 09/05/12
For personal use only.

0.26–1.6 $\times$ 10^{20} eV/g were used. The dose rates were measured with a "Fricke" dosimeter (8) and a Farmer Baldwin X-ray dosimeter MkII made by the Baldwin Instrument Company, Dartford, Kent, England. For the "Fricke" dosimeter $G_{Fe^{3+}}$ was taken as 15.5 and $\epsilon_{Fe^{3+}}$ as 2 201 at 25 °C and 304 mμ (8). The dose rates as measured by the two methods agreed within the experimental error of 2%.

The acid yields were determined by visual microtitration with 0.1 *N* NaOH and chlorophenol red indicator. The fluoride yields were determined by reaction with thorium chloranilate to give a colored complex. The concentration of the complex was measured spectrophotometrically at 304 mμ wavelength. The procedure followed was adapted by Fisher Scientific Company (9) from that of Fine and Wynne (10). The yields of hydrogen and carbon dioxide were determined by a gas chromatographic technique on a silica gel column.

The analytical method used to determine the total carbonyl yield was that of Lappin and Clark (11). The unreactive carbonyl (possibly fluoral hydrate) was estimated by a modification of the total carbonyl analysis of Lappin and Clark. Under the conditions of analysis by this procedure fluoral hydrate does not react with the 2,4-dinitrophenylhydrazine reagent. It was found that if the heating time at 80 °C was extended from 5 min to 60 min, approximately 20% reaction could be achieved. In this way the yield of such unreactive carbonyl compounds was estimated by comparison with known amounts of fluoral hydrate dissolved in trifluoroethanol.

The analytical method of Tanenbaum and Bricker (12) was used to determine the formaldehyde yields. The "chromotropic acid" (4,5-dihydroxy-2,7-naphthalene disulfonic acid) method of Bricker and Johnson (13) for the determination of formaldehyde was investigated and found to be unsuitable in the system of trifluoroethanol and water used. The method gave higher values for the formaldehyde concentration in irradiated samples than the total carbonyl concentration. The presence of trifluoroethanol also caused large negative errors in the analysis.

The analytical method of Siggia (14) was used for the determination of the yields of vicinal glycol. The yields of organic acid were estimated by treating the samples with diazomethane after the trifluoroethanol and water had been evaporated. The resulting methyl glycollate was then detected and the amount present estimated by gas chromatography. Known amounts of glycollic acid in trifluoroethanol were used for reference.

ACKNOWLEDGMENT

This work was supported by the National Research Council.

1. R. J. Woods and J. W. T. Spinks. Can. J. Chem. **38**, 77 (1960).
2. R. J. Woods and J. W. T. Spinks. Can. J. Chem. **35**, 1475 (1957).
3. G. G. Jayson, G. Scholes, and J. Weiss. J. Chem. Soc. 1358 (1957).
4. G. E. Adams and R. D. Sedgewick. Trans. Faraday Soc. **60**, 865 (1964).
5. J. J. J. Myron and G. R. Freeman. Can. J. Chem. **43**, 381 (1965).
6. F. S. Dainton and D. B. Peterson. Proc. Roy. Soc. London, Ser. A, **267**, 443 (1962).
7. J. Mitchell and D. M. Smith. Aquametry. Interscience Publishers, New York. 1948.
8. J. Weiss, A. O. Allen, and H. A. Swarz. Proc. Intern. Conf. Peaceful Uses of At. Energy, Geneva 1955, **14**, 179 (1956).
9. Technical Data Sheet TD-138. Fisher Scientific Company, Limited.
10. L. Fine and E. A. Wynne. Microchem. J. **3**, 515 (1959).
11. G. R. Lappin and L. C. Clark. Anal. Chem. **23**, 541 (1951).
12. M. Tanenbaum and C. E. Bricker. Anal. Chem. **23**, 354 (1951).
13. C. E. Bricker and H. R. Johnson. Ind. Eng. Chem. Anal. Ed. **17**, 400 (1945).
14. S. Siggia. *In* Qualitative organic analysis via functional groups. 2nd ed. John Wiley and Sons, Inc., New York. 1954.

Received July 20, 1965.
Department of Chemistry and Chemical Engineering,
University of Saskatchewan,
Saskatoon, Saskatchewan.

COMMENT: DEFINITION OF A BIRADICAL

G. R. Freeman

It is evident from the literature of the past few years that there is disagreement or lack of clarity about the meaning of the term "biradical". The concept of a biradical is of sufficient importance in several types of reaction that it should be clarified, even if arbitrarily. The purpose of the present note is to suggest a better definition of the term

Can. J. Chem. Downloaded from www.nrcresearchpress.com by 210.87.254.105 on 09/05/12
For personal use only.

"biradical" and to discuss several aspects of biradicals, some of which are frequently ignored.

An often used definition of biradical is—a molecule with two unpaired electrons (1). This definition is inadequate because it restricts biradicals to triplet species and those that contain a pair of doublets. A better definition is—*a biradical is an atom or molecule that reacts as though it has two monoradical functions.** The latter definition includes electronically excited singlet species such as $O(^1D)$ atoms and singlet carbenes.

There is no difficulty with the concept of biradicals when speaking of their reacting in bimolecular reactions. However, part of the controversy over whether certain unimolecular isomerization and decomposition reactions occur via biradical intermediates or via concerted mechanisms seems to contain a lack of clarity about the concept of biradicals. For example, tests which are frequently applied to detect monoradicals, such as the addition of a scavenger, cannot easily be used to detect biradicals that can combine or disproportionate internally. Two radical groups in one molecule corresponds to a local monoradical concentration of the order of 10 M. If both the intra-biradical disproportionation and combination reactions are not sterically hindered, the concentration of even a very efficient scavenger would have to be $\gtrsim 10$ M to intercept the intra-biradical reactions. In reaction systems where radical scavengers, such as oxygen or olefins, have been used to detect monoradicals, the monoradical concentrations have usually been less than micromolar. Conveniently low scavenger concentrations have therefore been adequate to intercept inter-monoradical reactions. Similar reasoning shows that the lifetime of this type of biradical is many orders of magnitude shorter than that of monoradicals in most systems, so it would be extremely difficult to detect the biradicals by electron spin resonance spectroscopy. In spite of the difficulty of detection of this type of biradical, the concept is useful when one is trying to visualize the precise mechanism of certain isomerization and decomposition reactions. The controversy over whether these reactions occur via concerted or biradical mechanisms is not trivial. A concerted mechanism is one in which the transition state does not have free radical character.

At what point does a vibrationally excited ring (cyclic molecule) become a biradical? Consider the following sequence of events in a hydrocarbon molecule: (*a*) energy is absorbed by the molecule; (*b*) sufficient energy becomes localized in a C—C bond that it can break; (*c*) the groups involved in the bond in question move away from each other and as they become more and more separated in space, the correlation between the spins of the odd electrons in the free-radical ends decreases.

The probability of occurrence of a spin change during the collision of two doublet atoms is large when the change of internal energy is small compared with the energy of relative motion (2, 3). The energy of relative motion, E_{rm}, of the two ends of a biradical will be somewhere between the excess vibrational energy in the biradical (i.e. the amount of vibrational energy in excess of that required to break the bond in the molecule) and the thermal energy of the surrounding medium. Thus, if the ends of the breaking bond can become sufficiently separated that the difference in energy between the triplet and singlet states, $|E_t - E_s|$, is less than E_{rm}, then the species can be considered to be a biradical rather than an excited molecule.

The foregoing discussion is consistent with recent observations of Hammond (4).

The results of crude calculations indicate that a low-lying "pair of doublets" electronic state of the trimethylene biradical cannot exist in a vibrational ground state because the tetrahedral separation distance between the two end carbon atoms is too small (2.5 Å).

**This particular choice of words was partly suggested by one of the referees.*

Can. J. Chem. Downloaded from www.nrcresearchpress.com by 210.87.254.105 on 09/05/12
For personal use only.

It would very rapidly form cyclopropane (singlet). A vibrationally excited trimethylene biradical would also have a considerable amount of singlet or triplet character mixed with its "pair of doublets" character. This is in agreement with the product distributions obtained by Crawford *et al.* (5) from substituted trimethylene biradicals produced by the decomposition of pyrazolines.

NOTE ADDED IN PROOF: The 8.2 kcal/mole activation energy for ring closing of the trimethylene biradical calculated by Benson (6) is probably too high, for the following reasons.

(*a*) The primary C—H bond dissociation energies in propane are higher than those in ethane (7). The recalculated value of ΔH_f^0 ($\dot{C}H_2CH_2\dot{C}H_2$ at 25° and 1 atm) is 69 kcal/mole, as opposed to 67 kcal/mole used by Benson. Benson (6) removed a hydrogen atom from each end of a propane molecule and assumed that the two radical ends were independent of each other. The same procedure was used in the present calculation.

(*b*) The value 64.2 kcal/mole reported by Rabinovitch (8) and used by Benson (6) as the activation energy for opening the cyclopropane ring is too high by the amount of the activation energy for rotation of a CH_2 group in the biradical. The calculated activation energy for ring closure is also too high by this amount.

(*c*) All the hydrogens in cyclopropane are in the eclipsed conformation, so the biradical formed initially upon C—C cleavage might also be mainly in this conformation. Since the eclipsed conformation of ethane is 3 kcal/mole higher in potential energy than is the staggered conformation (10), the totally eclipsed conformation of the trimethylene biradical would have a ΔH_f^0 a bit less than 73 kcal/mole, calculated by the same method as before.

Thus the activation energy for ring closure in an eclipsed trimethylene biradical should be 2–3 kcal/mole.

A skew trimethylene biradical would tend to form "π-cyclopropane" (10), which is equivalent to an electronically excited state of cyclopropane.

1. L. N. FERGUSON. Electron structures of organic molecules. Prentice-Hall Inc., New York. 1952. p. 211.
2. A. DALGARNO. Proc. Roy. Soc. London, Ser. A, **262**, 132 (1961).
3. D. R. BATES. Atomic and molecular processes. Academic Press, New York. 1962. pp. 607–608.
4. J. R. FOX and G. S. HAMMOND. J. Am. Chem. Soc. **86**, 4031 (1964).
5. R. J. CRAWFORD, R. J. DUMMEL, and A. MISHRA. J. Am. Chem. Soc. **87**, 3023 (1965). A. MISHRA. Unpublished results.
6. S. W. BENSON. J. Chem. Phys. **34**, 521 (1961). W. B. DEMORE and S. W. BENSON. Advan. Photochem. **2**, 219, 256 (1964).
7. C. T. MORTIMER. Reaction heats and bond strengths. The Pergamon Press, Ltd., London. 1962. p. 127.
8. B. S. RABINOVITCH, E. W. SCHLAG, and K. B. WIBERG. J. Chem. Phys. **28**, 504 (1958).
9. M. HANACK. Conformation theory. Academic Press, Inc., New York. 1965. p. 29.
10. R. J. CRAWFORD and A. MISHRA. J. Am. Chem. Soc. **87**, 3768 (1965).

RECEIVED JUNE 17, 1965.
DEPARTMENT OF CHEMISTRY,
UNIVERSITY OF ALBERTA,
EDMONTON, ALBERTA.

Can. J. Chem. Downloaded from www.nrcresearchpress.com by 210.87.254.105 on 09/05/12
For personal use only.

Can. J. Chem. Downloaded from www.nrcresearchpress.com by 210.87.254.42 on 09/05/12
For personal use only.

Canadian Journal of Chemistry

Issued by THE NATIONAL RESEARCH COUNCIL OF CANADA

VOLUME 44 FEBRUARY 1, 1966 NUMBER 3

THE PROTON MAGNETIC RESONANCE SPECTRA AND TAUTOMERIC EQUILIBRIA OF ALDOSES IN DEUTERIUM OXIDE[1]

R. U. LEMIEUX AND J. D. STEVENS[2]

Department of Chemistry, University of Alberta, Edmonton, Alberta

Received April 6, 1965

ABSTRACT

The proton magnetic resonance spectra of D-xylose, D-lyxose, D-arabinose, D-ribose, D-glucose, D-mannose, and D-galactose were determined at 100 Mc.p.s. in deuterium oxide. The chemical shifts and structures of a number of ring protons in these compounds were determined either by spin-decoupling experiments or by synthesis of specifically deuterated compounds. The proton magnetic resonance parameters are shown to provide considerable information on the conformations and tautomeric equilibria for the sugars in aqueous solution. It is concluded that, for aldopyranoses in a chair conformation, the chemical shift of equatorial protons at a given position is virtually independent of configurational changes at other positions. However, an axial proton is shielded about 0.3 p.p.m. less by an axial hydroxyl group at a neighboring position than when the hydroxyl group is in an equatorial orientation. An axial hydroxyl group leads to deshielding of an opposing axial proton by about 0.35 p.p.m. By using the chemical shifts of the ring protons of β-D-xylopyranose and β-D-glucopyranose as reference point, the chemical shifts of protons in other pyranose structures could be anticipated to within a useful degree of accuracy.

Evidence was obtained that D-ribose and 2-deoxy-D-ribose exist in aqueous solution both in the pyranose and in the furanose forms. None of the other pentoses showed readily detectable amounts of the furanose forms at equilibrium. Although D-allose does not give readily detectable amounts of the furanose forms when at equilibrium in aqueous solutions, D-altrose does. D-Talose showed only two forms, one of which was the β-pyranose structure.

Lenz and Heeschen (1) examined the nuclear magnetic resonance (n.m.r.) spectra of D-glucose, D-mannose, 2-deoxy-D-glucose, and D-xylose with deuterium oxide as solvent. Only the signals of the anomeric protons were readily observed, and the spacings of these signals were used as coupling constants to estimate conformational features for these sugars in aqueous solution. The observed spacings were undoubtedly strongly influenced by virtual long-range coupling (2, 3) and, therefore, were not a direct measure of the coupling constants involved. Also, it is now evident (4, 5) that the relationship between the coupling constant and the dihedral angle defined by neighboring protons (the Karplus relationship) is subject to parameters other than the dihedral angle. Therefore, attempts to relate the spacings of the doublet signals for the anomeric protons of sugars to precise molecular geometry are without either a theoretical or an empirical basis. Although coupling constants between neighboring protons cannot be used to predict precise conformational features, their use in appropriate instances for establishing configurational features (6) remains unchallenged.

Use has also been made of chemical shifts for establishing the configurations of sugars

[1]*Presented in part at the 142nd meeting of the American Chemical Society, Atlantic City, New Jersey, September 9–14, 1962. Abstracts of papers, p. 18D.*

[2]*Corn Industries Research Foundation Postdoctorate Fellow, 1960–1962.*

Can. J. Chem. Downloaded from www.nrcresearchpress.com by 210.87.254.42 on 09/05/12
For personal use only.

and their derivatives. To our knowledge, there is no exception to the rule that an equatorial proton will produce its signal to lower field than a chemically similar but axial proton (7), when the compounds considered are epimeric and both in the same chair conformation, and when the protons considered are not at the α-position to a carbonyl group (8). However, as will be seen later, this rule may not apply, for example, to the anomeric forms of D-altropyranose in the C1-conformation.

It has long been recognized that important shielding effects can arise from positions other than the neighboring positions (3, 9, 10), so that any rationalization of chemical shift must take into consideration the total structure of the molecule. We have demonstrated (3) that the chemical shifts of the ring protons of acetylated sugars are strongly dependent on configurational changes at positions other than the neighboring positions. Also, it is clearly apparent that chemical shifts are subject to specific solvent effects which cannot, as yet, be predicted. Nevertheless, it proved possible to establish simple empirical rules for correlating chemical shift measured under standard conditions with the configurational and conformational properties of acetylated sugars (3), and the purpose of this communication is to report a similar success for free sugars dissolved in deuterium oxide. Furberg (11) has commented on the use of n.m.r. to establish points of configuration and on its application to reducing sugars dissolved in deuterium oxide. Both Lenz and Heeschen (1) and Hall (12) have commented on the diamagnetic anisotropy of the C—O bond and have rationalized the chemical shifts of axial anomeric protons in sugars (glucose and mannose) differing in the configuration of the 2-position. Lenz and Heeschen considered the chemical shifts of protons at positions other than the anomeric center, but had no experimental evidence to support the "intuitive" rationalizations. This effort was premature since, for example, it took no cognizance of the strong deshielding influence of an axial hydroxyl on an opposing axial proton (10). We have now determined the chemical shifts of a number of protons at positions other than the anomeric center for sugars in deuterium oxide by employing both double irradiation and specific deuteration techniques.

The procedure used in these investigations was to dissolve the sugar in deuterium oxide and to determine the n.m.r. spectrum on the Varian A60 spectrometer with tetramethylsilane as the external standard. Normally, the course of the mutarotation was readily followed in the spectrometer. The 100 Mc.p.s. spectra of the solutions at equilibrium were measured. The line positions were established relative to calibration side bands and placed on the scale in parts per million from tetramethylsilane using the positions for the anomeric protons found in the A60 spectra. The spin-decoupling experiments were obtained as described by Johnson (13) with the Varian H.R. 100 spectrometer (10).

A freshly prepared solution of α-D-xylopyranose in deuterium oxide showed a sharp, one-proton doublet at 5.26 p.p.m. The rest of the spectrum was a fairly narrow band in the region 3.5–3.9 p.p.m. When it was allowed to stand the solution mutarotated to equilibrium and at 35° showed signals (Fig. 1A) for anomeric protons at 5.26 and 4.65 p.p.m. with spacings of 3.1 and 7.4 c.p.s.; these signals were assigned to the α- and β-anomers, respectively. Integration of these signals showed that the mixture contained 67% of the β-anomer.

Spin decoupling at 1.63 p.p.m. to higher field from the signal for H_1^α collapsed the doublet; therefore, the chemical shift for H_2^α is at 3.63 p.p.m. The quartet at 4.00 p.p.m. with spacings of 4.3 and 10.4 c.p.s. was assigned to the 5-proton in an equatorial orientation, H_{5e}^β, in view of its intensity and structure. The intensity of the quartet was equal to that of the signal for H_1^β and, as the small coupling constant can only arise from H_4^β to H_{5e}^β coupling, this signal must belong to H_{5e}^β, since the signal for H_4^β should be more complex. The assignment of the H_{5e} signal was confirmed by examination of the spectrum of the

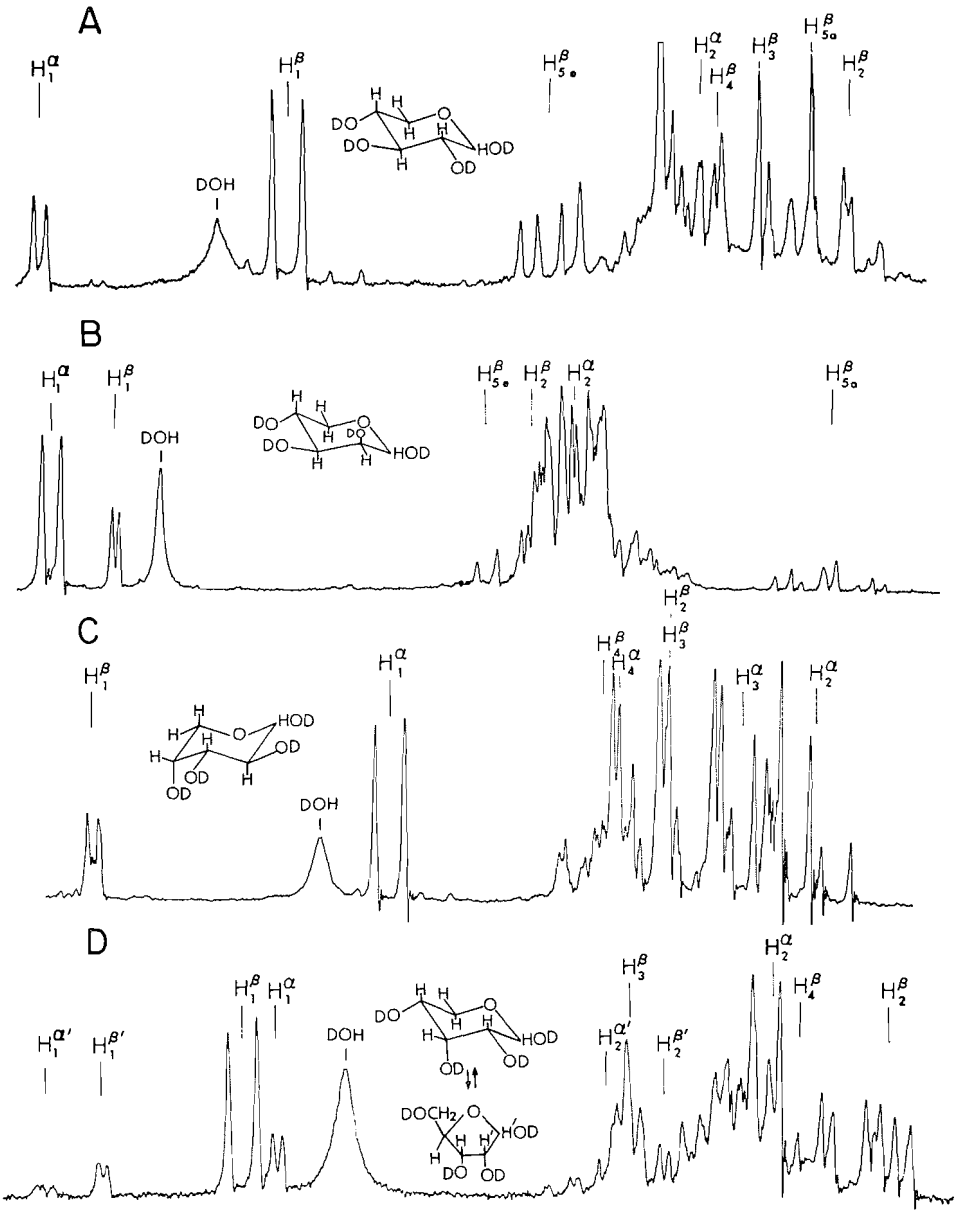


FIG. 1. Nuclear magnetic resonance spectra at 100 Mc.p.s. of aldopentoses at tautomeric equilibrium in deuterium oxide at 35°. LEGEND: A, D-xylose; B, D-lyxose; C, D-arabinose; D, D-ribose.

5-deuterio-D-xylose prepared by Lemieux and Howard (14). The quartet was now a doublet with an intensity corresponding to that expected from the composition of the compound. Irradiation at 42 c.p.s. to higher field than the signal for H^{β}_{5e} caused the quartet to collapse to a doublet with the larger spacing. Therefore, the signal for H^{β}_{4} is centered at about 3.58 p.p.m. The intensitites of the signals to higher field than 3.5 p.p.m. corresponded to three protons, based on the intensity of H^{β}_{1}. It was apparent, therefore, in view of the spectrum of the α-anomer, that H^{β}_{2}, H^{β}_{3}, and H^{β}_{5a} gave their signals in this region. Since irradiation

Can. J. Chem. Downloaded from www.nrcresearchpress.com by 210.87.254.42 on 09/05/12
For personal use only.

of H^{β}_{5e} caused extensive collapse of the signal at 3.36 p.p.m., it was most likely that the signal for H^{β}_{5a} was near this position. Irradiation of H^{β}_{1} caused the quartet with spacings of about 7.4 and 8.5 c.p.s. at 3.26 p.p.m. to collapse to a doublet. Therefore, the chemical shift of H^{β}_{2} is 3.26 p.p.m. and $J^{\beta}_{3,2} = 8.5$ c.p.s. The spectrum resulting from this double irradiation experiment showed clearly the triplets for H^{β}_{3} at 3.49 p.p.m. and for H^{β}_{5a} at 3.36 p.p.m. The spacings require $J^{\beta}_{3,4} = 8.5$ and $J^{\beta}_{4,5a} = 10$, and confirmed $J^{\beta}_{5a,5e} \simeq 10$ c.p.s.

The spacings observed in the spectrum for β-D-xylopyranose (see Table I) require that the compound exist in a near C1-chair conformation as anticipated from conformational analysis. All that can be said for the α-form is that the spacing from the H_1 signal agrees with that for a gauche interaction between H_1 and H_2. Also, as will be seen below, the chemical shift for H_2 is in the region expected for the compound in the chair conformation.

A freshly prepared solution of α-D-lyxopyranose showed a one-proton signal at 5.08 p.p.m. with a spacing of 4.2 c.p.s.; this signal was assigned to H^{α}_{1}. The rest of the spectrum was a rather narrow band in the region 3.7–4.1 p.p.m. On equilibration at 35°, a doublet appeared at 4.94 p.p.m. with a spacing of 1.5 c.p.s.; this signal was assigned to H^{β}_{1} (see Fig. 1B). An octet appeared that was centered at about 3.32 p.p.m. and had an intensity corresponding to that of the signal for H^{β}_{1}. This signal is provisionally assigned to H^{β}_{5a}. The signal collapsed to a much narrower complex multiplet on irradiation at 4.07 p.p.m. It seems most probable, in view of the chemical shift for H^{β}_{5e} of D-xylose, that the quartet centered at 4.09 p.p.m. is the signal for H^{β}_{5e}. The spacings suggest $J^{\beta}_{4,5e} \simeq 5$ c.p.s. and $J^{\beta}_{5a,5e} \simeq 10$ c.p.s. Irradiation at 3.90 p.p.m. collapsed the signal for H^{α}_{1} to a singlet, and it is concluded, therefore, that the chemical shift for $H^{\alpha}_{2} = 3.90$ p.p.m. Irradiation of H^{β}_{1} caused the quartet centered at 4.04 p.p.m. to collapse to a doublet. Therefore the chemical shift for $H^{\beta}_{2} = 4.04$ and $J^{\beta}_{2,3} \simeq 3$ c.p.s. Integration of the anomeric signals showed that the mixture contained 71% of the α-anomer at 35°.

A freshly prepared solution of β-D-arabinose in deuterium oxide gave a one-proton doublet signal at 5.34 p.p.m. with a spacing of 2.7 c.p.s.; this signal was assigned to H^{β}_{1}. The crystalline sugar is known by X-ray analysis (15) to have the pyranose ring in the 1C-conformation, wherein H_1 is in the equatorial orientation. On mutarotation, the solution produced a signal for H^{α}_{1} as a doublet with a spacing of 7.2 c.p.s. at 4.60 p.p.m. (see Fig. 1C). Although the DOH signal was reduced to an intensity of about that of H^{α}_{1} at equilibrium, no other signals for anomeric protons were observed. The shape of the signal for H^{β}_{1} showed the presence of second-order effects from virtual long-range coupling and, therefore, a small chemical shift for H^{β}_{2} and H^{β}_{3} (3). Irradiation at 3.93 p.p.m. collapsed the signal for H^{β}_{1}; therefore the signal for H^{β}_{2} is at this position. The signal for H^{α}_{1} is a sharp doublet and, therefore, H^{α}_{2} and H^{α}_{3} must be well shifted chemically. Double irradiation showed that H^{α}_{2} gave its signal at 3.58 p.p.m. The chemical shifts of the 3- and 4-protons in both the β- and α-forms were determined by examining the n.m.r. spectra of the 2,5,5-trideuterio derivatives. These compounds were prepared from D-glucurone as described in the Experimental section. The spectra measured at 60 Mc.p.s. are reproduced in Fig. 2B for both the freshly prepared solution of exchanged crystalline 2,5,5-trideuterio-β-D-arabinopyranose and the equilibrated solution. Figure 2A shows the corresponding spectra for ordinary D-arabinose. The two doublets for H^{β}_{3} and H^{β}_{4} seen on the spectrum of the freshly prepared solution of the deuterated compound must be at 3.93 and 4.07 p.p.m., respectively, in view of the strong second-order effects noted in the signal for H^{β}_{1} and the fact that the chemical shift for $H^{\beta}_{2} = 3.93$ p.p.m. The spacings of the signals require $J^{\beta}_{3,4} = 3.4$ c.p.s. Mutarotation caused the appearance of two new doublets at 3.75 and

Can. J. Chem. Downloaded from www.nrcresearchpress.com by 210.87.254.42 on 09/05/12
For personal use only.

Can. J. Chem. Downloaded from www.nrcresearchpress.com by 210.87.254.42 on 09/05/12
For personal use only.

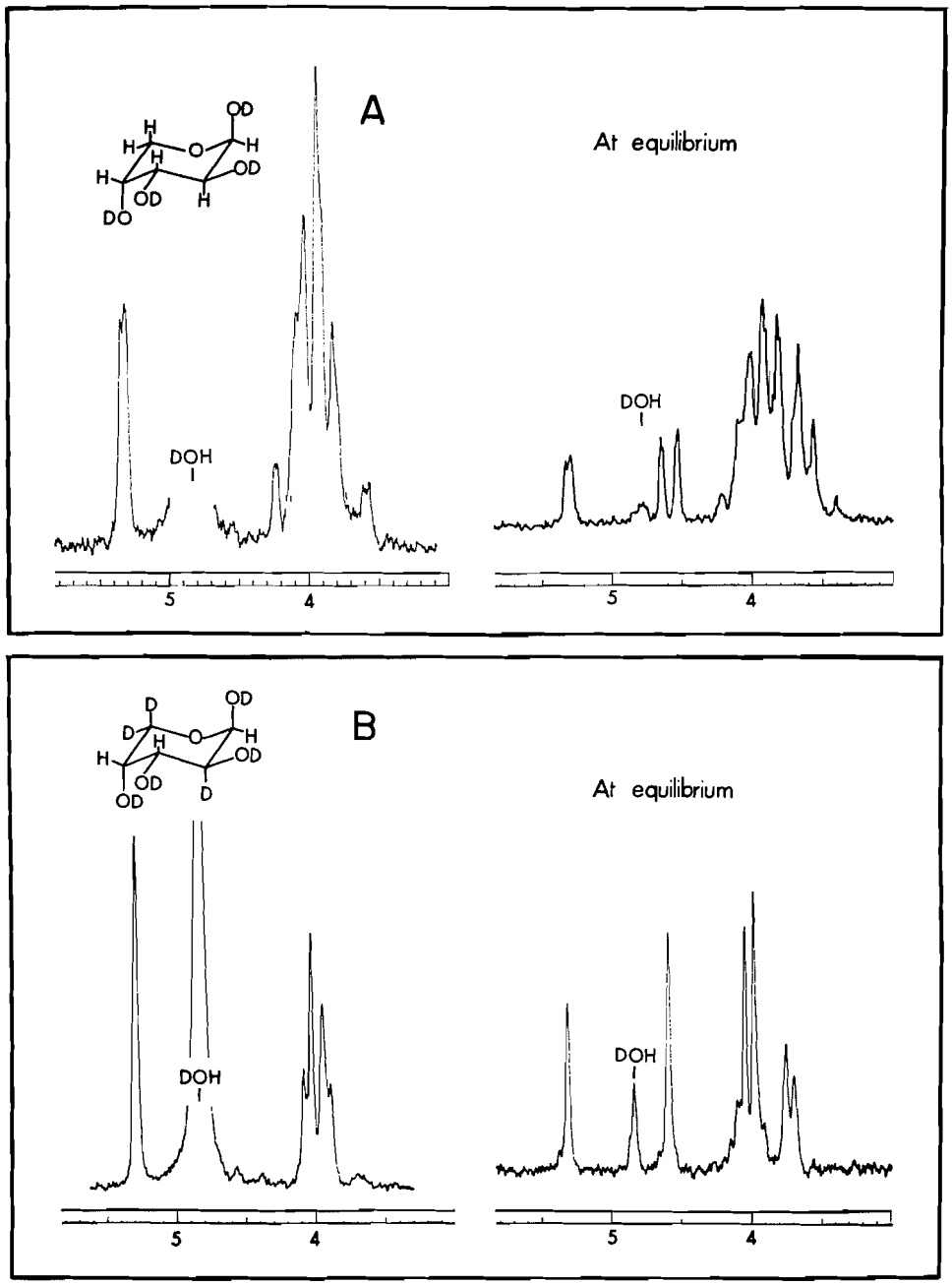


FIG. 2. Nuclear magnetic resonance spectra at 60 Mc.p.s. in deuterium oxide at 35°. LEGEND: A, β-D-arabinopyranose within a few minutes of dissolution and at tautomeric equilibrium; B, 2,5,5′-trideuterio-β-D-arabinopyranose within a few minutes of dissolution and at tautomeric equilibrium.

4.04 p.p.m. which are assigned to H_3^α and H_4^α, respectively. This assignment is based mainly on the rule that the anomerization from the β- to the α-form will lead to a greater shielding of the 3-proton. This effect is discussed in detail below. The spacings of the signals require $J_{3,4}^\alpha = 3.6$ c.p.s. The spectrum of this equilibrated solution substantiates the evidence discussed above that only the α- and β-forms of arabinopyranose are in appreciable concentration at 35°. Integration of the signals for the anomeric protons requires 63% of the α-anomer. The signal for H_2^α appears as a well-defined quartet at 3.58 p.p.m., from which it can be concluded that $J_{2,3}^\alpha = 9.9$ c.p.s. The coupling constants observed for $J_{1,2}$, $J_{2,3}$, and $J_{3,4}$ for the α-form are clearly in accord with the 1C-chair conformation for this compound in aqueous solution. It will be seen below that the observed chemical shifts also agree with this conclusion.

A freshly prepared solution of β-D-ribose in deuterium oxide showed rapid mutarotation, and it was not possible to obtain a spectrum of the crystalline material in a virtually unchanged condition. The mutarotation at 35° gave rise to a solution the n.m.r. spectrum (Fig. 1D) of which had four readily discernible signals of total intensity one at 5.42, 5.30, 4.99, and 4.91 p.p.m. The relative intensities were 6:18:56:20. When the sample was heated to 80°, the signal for DOH moved upfield from 4.75 p.p.m. to 4.3 p.p.m. No further signals for anomeric protons were observed and the integration showed that the total of the intensities for anomeric protons was one-fifth of those of the other protons in the molecule. It was therefore clearly apparent that only four of the tautomeric forms for D-ribose are at appreciable concentrations in water in the temperature range 35–80°. Only the position of the signal for the high-field doublet changed appreciably from 4.91 to 4.83 p.p.m. when the solution was heated to 80°. The relative intensities of the signals changed to 11:19:47:23.

The doublet at 4.99 p.p.m. with a spacing of 6.4 c.p.s. was evidently from H_1^β of the pyranose form. Irradiation at 3.60 p.p.m. caused collapse of the H_1^β signal and therefore corresponds to the chemical shift for H_2^β. Irradiation of H_2^β collapsed the signal for H_3^β at 4.13 p.p.m. This signal was also collapsed by irradiation at 3.79 p.p.m., the signal for H_4^β. It was apparent, therefore, that $J_{2,3}^\beta = 3.1$ c.p.s. and $J_{3,4}^\beta = 3$ c.p.s. The quartet signal for H_4^β suggests that $J_{4,5}^\beta \simeq 10$ c.p.s. The coupling interactions for the vicinal protons of β-D-ribopyranose leave no doubt that the compound has a C1-chair conformation. The axial 3-hydroxyl group probably has caused some distortion, which has decreased the dihedral angle defined by H_1 and H_2.

The n.m.r. spectrum of 5-*O*-methyl-D-ribose was determined to provide a basis for the assignment of the signals for the anomeric proton. Unfortunately, at the time the compound was available, it was not possible to apply heat to move the DOH sample upfield. Nevertheless, the DOH signal was reduced to a very low level, and only two signals for anomeric protons were observed at 5.40 and 5.51 p.p.m. with spacings of 1.5 and 3 c.p.s., respectively. The signals for the two protons at the 5-position in this compound occurred as a band centered at about 3.75 p.p.m. with an intensity double that of the total intensity of the two signals for anomeric protons. Also, a band centered at about 4.2 p.p.m. had an intensity of three, as expected for the total signals for H_2, H_3, and H_4 protons. Only two methoxy-group signals were observed at 60 Mc.p.s. It seems probable, therefore, that 5-*O*-methyl-D-ribose does not exist to any appreciable extent in more than two tautomeric forms (either the two furanose forms or a furanose form and the open-chain form). In view of the equilibrium between the methyl D-ribosides in 1% methanolic hydrogen chloride at 35° and the apparent absence of dimethyl acetal (16), it is most probable that the signals at 5.40 and 5.51 p.p.m. correspond to those of the anomeric protons for the anomeric D-ribofuranoses. The ratio of the intensities of these signals was 2.6:1,

Can. J. Chem. Downloaded from www.nrcresearchpress.com by 210.87.254.42 on 09/05/12
For personal use only.

Can. J. Chem. Downloaded from www.nrcresearchpress.com by 210.87.254.42 on 09/05/12
For personal use only.

respectively. The signals are assigned to the β- and α-furanose forms, respectively, since, in general, derivatives of β-ribofuranose have $J_{1,2}$ of about 1 c.p.s. as compared to 4–5 c.p.s. for the α-anomers. Also, it can be expected that the 1,2-*trans*-β configuration will provide the more stable anomer in aqueous solution. For these reasons, the signals at 5.30 and 5.42 p.p.m. in the spectrum of D-ribose are assigned to the anomeric protons of the β- and α-furanose forms, respectively. Bishop and Cooper (16) found that the methyl ribosides at equilibrium contained 5.2% α-furanoside, 17.4% β-furanoside, 11.6% α-pyranose, and 65.8% β-pyranosides. The close correspondence between these values and those now estimated for the mutarotation of ribose at 35°, namely, 6% α-furanose, 18% β-furanose, and 56% β-pyranose, supports the above assignments and suggests that the signal with a spacing of 2.1 c.p.s. at 4.91 p.p.m. arose from the α-D-pyranose form which was present to an extent of 20%. The observed coupling of H_1 with H_2 for the open-chain form would be expected to be the weighted average of the coupling constants for the staggered conformations and, on this basis, to have a value substantially greater than 3 c.p.s. On this basis, the signal at 4.91 p.p.m. cannot have arisen from the open-chain form. This argument can also be applied to the signals at 5.30 and 5.42 p.p.m. There seems to be no alternative, therefore, to the conclusion that the signal at 4.91 p.p.m. arose from the α-D-ribopyranose form. The rather well defined doublet for this signal would be in keeping with the expectation of a substantial chemical shift between H_2 and H_3. It is noteworthy that the signal assigned to the anomeric proton of the α-furanose (H_1^{α}, Fig. 1D) seems to be too complex and, therefore, part of this signal may have arisen from the 1-proton of the hydrated open-chain form. On the other hand, the complexity of the signal may be caused by either long-range coupling or virtual long-range coupling, or both. Certainly, the indications are that the open-chain form is present at much lower concentrations than the 8.5% suggested by the results of a polarographic investigation (17).

Inspection of the chemical shifts for the ring protons of the pentopyranoses shows that there exists a good correlation of the shifts with the configuration of the sugar. This correlation is most readily appreciated by using the chemical shifts for β-D-xylopyranose as reference point and adjusting these shifts according to the following empirical rules. (*i*) If the proton under consideration is in an equatorial orientation, add 0.60 p.p.m. (3, 10). (*ii*) If the proton under consideration is in an axial orientation, (*a*) add 0.30 p.p.m. for each neighboring axial hydroxyl group and (*b*) add 0.35 p.p.m. for each axial hydroxyl group which is in opposition to the axial proton.

The results of these calculations are presented in Table I for the protons of known chemical shift. It is seen that the agreement is reasonably good, if one considers the inaccuracies in determining the chemical shifts by spin decoupling (at least ±0.05 p.p.m.) and the fact that at least some of the rings must be distorted appreciably from the perfect chair form. Certainly, the agreement is sufficiently good to support the conformations assigned above and to indicate that the empirical rules deal with the main configurational effects on chemical shift in the n.m.r. spectra of the sugars. The main discrepancies are in the values for the chemical shifts of the anomeric protons for α-D-lyxopyranose, β-D-arabinopyranose, and α-D-ribopyranose, compounds which, in chair conformations, have two of the four hydroxyl groups in an axial orientation.

As was seen above, H_1 for α-D-ribopyranose gives its signal at 4.91 p.p.m., which is much to higher field than that, 5.25 p.p.m., expected for the compound in the C1-conformation. On the other hand, this chemical shift is in good agreement with that, 4.95 p.p.m., expected for the compound in the 1C-conformation. The chemical shift for H_2 agrees with that expected for the compound in either of the chair conformations. Thus, as

is also concluded by Rudrum and Shaw (18), the indications are that α-D-ribopyranose strongly prefers the 1C-conformation.

α-D-Lyxopyranose has an anomalously high value for $J_{1,2} = 4.2$ c.p.s. when compared to that, 1.7 c.p.s., for the configurationally related α-D-mannopyranose. Also, the chemical shifts for H_1 calculated for α-D-lyxopyranose in either the 1C- or C1-conformations are in poor agreement (see Table I) with the experimental value. However, the n.m.r. parameters are well rationalized by assuming that the compound exists in about equal amounts in the two chair conformations. Thus, by using the spacings for the signals of H_1 in β-D-ribopyranose and α-D-mannopyranose as those to be expected for α-D-lyxopyranose in the 1C- and C1-conformations, respectively, a value for $J_{1,2} = 0.5(6.4 + 1.7) = 4.1$ c.p.s. is obtained. The chemical shift for H_1 would be expected, on this basis, to be $0.5(5.25 + 4.99) = 5.12$ p.p.m., which agrees well with the experimental value of 5.08 p.p.m. Also, on this basis, the chemical shift for H_2 is expected to be 3.89 p.p.m., in good agreement with the observed value of 3.90 p.p.m. Thus, it can be concluded that crystalline α-lyxose is in the pyranose ring form and exists in both chair forms in about equal amounts when dissolved in water. This conclusion was also reached by Rudrum and Shaw (18).

The values for $J_{1,2}$ and $J_{3,4}$ determined for β-D-arabinopyranose do not distinguish between the 1C- and C1-conformations for this compound. It is seen in Table I that the observed chemical shifts for protons 1 to 4 are in as good agreement with those calculated on the basis of the 1C-conformation as with those calculated on the basis of the C1-conformation. In fact, the agreement, especially for H_3 and H_4, is not at all good. Furthermore, the signal for H_1 is at a rather anomalously low field and, therefore, the n.m.r. data would not have sufficed to establish the pyranose ring form. Since it is known (15) that the compound is in the pyranose form, perhaps the conformations are rather seriously distorted from the chair forms. A knowledge of $J_{2,3}$ would shed light on the problem of the chair–chair equilibrium for this compound, but this was not available since the 2- and 3-protons are not appreciably shifted chemically. This lack of chemical shift is to be expected for the compound in chair forms, since these protons are in very similar environments in both chair conformations. Rudrum and Shaw (18) assigned the 1C-conformation to the compound in aqueous solution, but this conclusion must obviously be held in reservation.

It is of interest to note that, as was to be expected, the configurational effects on chemical shift are much simpler for the free sugars than for their acetylated derivatives (3). A consideration of a molecular model of an acetoxy group in axial orientation on a six-membered ring and the anisotropy of the carbonyl group of the acetoxy group (9) makes evident the fact that the carbonyl group should strongly deshield the geminal proton but tend to shield equatorial protons at the neighboring and next to neighboring positions. Thus, whereas an axial hydroxyl group has no appreciable effect on the chemical shifts of these protons, an axial acetoxy group leads, in both cases (3), to a shielding of about 0.2 p.p.m. relative to that when the acetoxy group is in an equatorial orientation.

As seen in Table II, the chemical shifts for the 1- and 2-protons of β-D-glucopyranose are in close agreement with those found for β-D-xylopyranose. Therefore, the introduction of the hydroxymethyl group has little effect on these chemical shifts. By using the observed values for β-glucose as reference point and the foregoing empirical rules, the chemical shifts of protons in the other hexoses were calculated; the results are given in Table II. It is seen that the agreement is quite good and the trends excellent. That is, for example, the same chemical shift for the 2-hydrogens of the anomeric mannopyranoses was predicted. Also, although the absolute chemical shifts for the 2-hydrogens of the α- and

Can. J. Chem. Downloaded from www.nrcresearchpress.com by 210.87.254.42 on 09/05/12
For personal use only.

Can. J. Chem. Downloaded from www.nrcresearchpress.com by 210.87.254.42 on 09/05/12
For personal use only.

TABLE I

Nuclear magnetic resonance parameters for pentopyranoses in deuterium oxide

	Xylose		Lyxose		Arabinose		Ribose	
	α	β	α	β	β	α	α	β
Chemical shifts in p.p.m. from tetramethylsilane (external)*								
H_1	5.26	4.65	5.08	4.94	5.34	4.60	4.91	4.99
	[5.25]		[5.00],† [5.25]‡	[4.95]	[5.25],† [5.30]‡	[4.65]	[4.95],† [5.25]‡,	[5.00]
H_2	3.63	3.26	3.90	4.04	3.93	3.58	3.85	3.60
	[3.56]		[3.91],† [3.86]‡	[3.86]	[3.91],† [3.86]‡	[3.61]	[3.86]†, [3.86]‡	[3.56]
H_3	—	3.49	—	—	3.93	3.75	—	4.13
					[4.14],† [4.09]‡	[3.79]		[4.09]
H_4	—	3.58	—	—	4.07	4.04	—	3.79
					[4.18],† [4.23]‡	[4.18]		[3.88]
H_{5a}	—	3.36	—	3.32	—	—	—	—
				[3.36]				
H_{5e}	—	4.00	—	4.09	—	—	—	—
				[4.00]				
Observed spacings (approximate coupling constants) in c.p.s.								
H_1–H_2	3.1	7.4	4.2	1.5	2.7	7.2	2.1	6.4
H_2–H_3	—	~8.5	—	3	—	9.9	—	3.1
H_3–H_4	—	~8.5	—	—	3.4	3.6	—	~3
H_4–H_{5a}	—	~10	—	—	—	—	—	~10
H_3–H_{5e}	—	4.3	—	~5	—	—	—	—
H_{5a}–H_{5e}	—	10.4	—	~10	—	—	—	—

*The results in brackets refer to calculated chemical shifts obtained by using the empirical rules presented in the text.
†1C-conformation.
‡C1-conformation.

TABLE II

Nuclear magnetic resonance parameters for hexoses in deuterium oxide

	Glucose		Mannose		Allose*		Galactose†		Talose	
	α	β	α	β	α	β	α	β	α	β
Chemical shifts in p.p.m. from tetramethylsilane (external)										
H_1	5.32	4.74	5.25	4.97	—	5.00	5.34	4.68	5.37	4.88
	[5.34]	—	[5.34]	[5.04]		[5.09]	[5.34]	[4.74]	[5.34]	[5.04]
H_2	3.60	3.32	4.01	4.03	—	—	3.87	3.55	—	—
	[3.62]	—	[3.92]	[3.92]			[3.97]	[3.67]		
Observed spacings (approximate coupling constants) in c.p.s.										
$J_{1,2}$	3.5	7.5	1.7	1.0	—	8.2	2.8	7.1	<1	<1

*The chemical shift for H_3^β was 4.28 p.p.m. with $J^\beta_{2,3} \simeq J^\beta_{3,4} \simeq 2.5$ c.p.s.

†Spin-decoupling experiments showed H_3^β and H_5^β to differ little in chemical shift at about 24 c.p.s. to higher field (3.73 p.p.m.) than H_4^β which gave a rough doublet at 3.97 p.p.m. with $J_{3,4}$ about 3 c.p.s.

β-forms of galactopyranose were not estimated with precision, the difference in the chemical shifts was the same as that found by experiment. It is quite evident, therefore, that these simple rules should find widespread application for determination of structure. For example, if the chemical shifts of the 2-hydrogens of a pyranose structure, as determined by spin decoupling of the signals for the anomeric hydrogens, are nearly the same, then it can be concluded that the 2-hydroxyl group is in an axial orientation. It should prove possible to extend this method to rules for differentiating between pyranose and furanose structures, and this matter will be examined primarily in an attempt to establish the ring forms of the rare hexoses in aqueous solution. In the case of D-ribose, the chemical shifts of the 2-protons for the α- and β-furanose forms were 4.19 and 4.07 p.p.m., respectively. These chemical shifts are to substantially lower field than those for the α- and β-pyranose forms, 3.85 and 3.60 p.p.m., respectively. It is to be expected that the ring protons of furanose structures will, in general, have chemical shifts intermediate to chemically similar protons in an axial and equatorial orientation. Also, the long-range configurational effects on chemical shift should be diminished in furanose structures.

The spectra of allose, talose, and altrose were determined but not subjected, as yet, to extensive investigation. The spectrum for allose at equilibrium clearly required the compound to exist virtually entirely in the β-D-allopyranose form. It was apparent that some mutarotation occurred, since the signal for the anomeric proton diminished in intensity as compared with the signal for the 3-proton at 4.28 p.p.m. when the solution was allowed to come to equilibrium. However, the signal of no other anomeric proton was readily observable. It is therefore apparent that the anchoring effect of the hydroxymethyl group for the chair conformation destabilizes the α-pyranose form by forcing a strong interaction between the axial 1- and 3-hydroxyl groups. Also, it is apparent that the introduction of a hydroxymethyl group on C-5 of the ribose structure leads to substantial destabilization of the furanose rings relative to that of the β-pyranose ring. The intensities of the signals attributable to anomeric protons found in the spectrum of D-talose require the compound to exist almost entirely in two tautomeric forms. If talose assumed either one of the furanose forms, then the 1-hydrogen would be in very much the same environment as in the corresponding ribofuranose. For this reason, the signal at 4.88 p.p.m. appears to be at too high a field to be assigned to H_1 of a furanose form. Instead, this signal likely arises from the β-pyranose structure in a distorted-chair or twist-boat conformation. The form of talose which gives a signal for H_1 at 5.37 p.p.m. could be either α-pyranose or β-furanose

Can. J. Chem. Downloaded from www.nrcresearchpress.com by 210.87.254.42 on 09/05/12
For personal use only.

Can. J. Chem. Downloaded from www.nrcresearchpress.com by 210.87.254.42 on 09/05/12
For personal use only.

(19). The spectrum for D-altrose in deuterium oxide at 35° showed four signals attributable to anomeric protons with a total intensity of one proton. The chemical shifts were 5.00, 5.13, 5.26, and 5.32 p.p.m. with spacings of 4.0, 1.5, 2.0, and 4.5 c.p.s., respectively. The relative intensities were about 29:37:11:23. Obviously, therefore, altrose exists in aqueous solution to a large extent in the furanose forms. This is not surprising in view of the axial hydroxyl groups at the 2- and 3-positions of the pyranose forms (especially the axial group at the 3-position) and the favorable all-*trans* configuration of the furanose form (17). Although it is possible to speculate on the origin of the signals, this matter seems best to be reserved for a future publication when more detailed information will be available. It may be noted, however, that, according to the above rules for the correlation of chemical shift with the configuration of sugars, the chemical shift of H_1 (equatorial) for α-D-altropyranose in the C1-conformation is expected to be at 5.34 p.p.m. and that for the β-anomer (H_1 axial) in the same conformation to be at 5.39 p.p.m.

Experiments with 2-deoxy-D-ribose conducted with L. Anderson confirmed the X-ray evidence (20) for the β-pyranose form in the crystals, m.p. 77–84°, $[\alpha]_D^{22}$ −97° → −48° after 20 min (*c*, 2 in water). The mutarotation was readily followed in the n.m.r. spectrometer at 0° and found to lead to a mixture of four tautomers. The α- and β-pyranose forms were present in about equal amounts at equilibrium and comprised about 70% of the mixture at 60°. The quartet signal for the anomeric proton of the α-anomer was at 4.90 p.p.m. with spacings of 2.5 and 8.2 c.p.s., and requires the 1C-conformation for this compound. The anomeric proton of the β-form gave a triplet signal at 5.36 p.p.m. with a spacing of 3.5 c.p.s. Certainly, therefore, the compound must exist, at least to a substantial extent, in the C1-conformation which is present in the crystalline solid (20). The furanose forms gave signals for the anomeric protons of about equal intensity at 5.69 p.p.m. (triplet with spacing of 4.5 c.p.s.) and 5.63 p.p.m. (quartet with spacings of 2.1 and 5.5 c.p.s.), which for obvious reasons likely arose from the α- and β-forms, respectively.

Since this manuscript was first submitted for publication, a paper appeared on the same subject by Rudrum and Shaw (18). In general, the conclusions are the same as those we communicated in 1962 from spectra measured at 60 Mc.p.s. The generally larger "coupling constants" reported herein are no doubt caused by a greater absence of second-order effects resulting from reduced virtual long-range coupling. A comparison of the spacings in these two publications further emphasizes (3) the hazard of using spacings as coupling constants. In the absence of knowledge related to this effect, Rudrum and Shaw (18) assigned the 1C-conformation to β-D-arabinopyranose. This conclusion was based on the belief that an equatorial orientation was required to account for the chemical shift of H_1. The present data indicate that the agreement between the observed and expected values would be even better with the compound in the C1-conformation. Thus, as was found for the acetylated sugars (3), the simple rule that equatorial protons give their signals to lower field than chemically similar but axial protons can have exceptions depending on the chemical nature and orientation of nearby substituent atoms or groups.

Finally, it is of interest to compare the amounts of the anomeric forms found by integration of the signals for the anomeric protons with the values obtained by other methods. The results given in Table III show excellent agreement for xylose, glucose, mannose, and galactose. The values for lyxose and arabinose agree well with Angyal's calculated values (21) but definitely differ from those determined by rotation and bromine oxidation (22) to an extent greater than the experimental error (about ±2%). Perhaps these pentoses exist to a small extent in the furanose form. The signal for the anomeric proton of β-talose was directly under the DOH signal; therefore, the n.m.r. value is only a rough estimate.

TABLE III

Percentage proportions of the α-aldopyranose form at equilibrium

	Nuclear magnetic resonance at 35°	Rotation*	Bromine oxidation*	Calculated†
Xylose	33	34.8	32.1	36
Glucose	36	36.2	37.4	36
Lyxose	71	76	79.7	73
Mannose	67	68.8	68.9	68
Ribose	38‡	—	—	11
Allose	<10?	—	—	—
Arabinose	63	73.5	67.6	61
Galactose	27	29.6	31.4	36
Talose	66?	—	65.9	77.5

*Reference 22.
†Reference 21.
‡Of the pyranose forms.

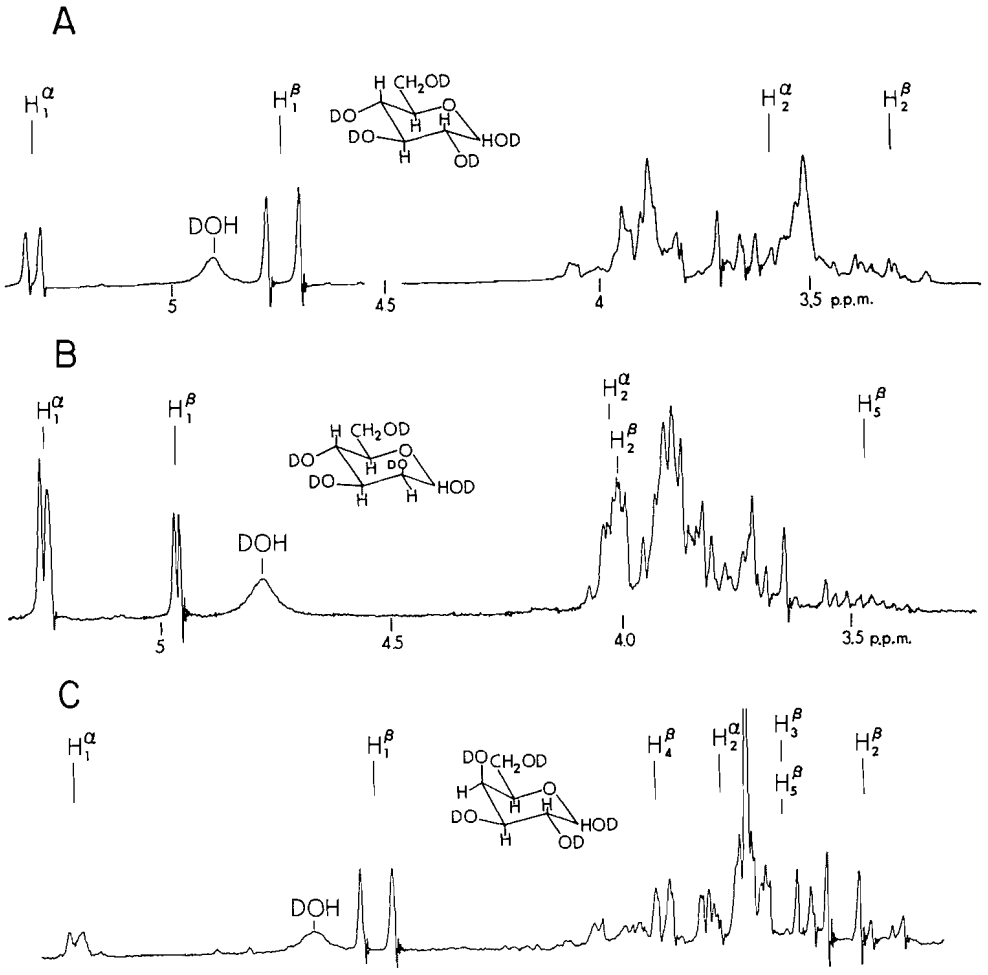


FIG. 3. Nuclear magnetic resonance spectra at 100 Mc.p.s. of aldohexoses at tautomeric equilibrium in deuterium oxide at 35°. LEGEND: A, D-glucose; B, D-mannose; C, D-galactose.

Can. J. Chem. Downloaded from www.nrcresearchpress.com by 210.87.254.42 on 09/05/12
For personal use only.

Can. J. Chem. Downloaded from www.nrcresearchpress.com by 210.87.254.42 on 09/05/12
For personal use only.

EXPERIMENTAL

The physical measurements were made as described previously (10).

6,6′-Dideuterio-1,2:5,6-di-O-isopropylidene-α-D-glucofuranose

1,2-*O*-Isopropylidene-α-D-glucofuranurono-6,3-lactone, m.p. 120–122°, was prepared from D-glucurone according to the directions described by Owens *et al.* (23). The compound, 32.5 g, was dissolved in 200 ml of tetrahydrofuran freshly distilled from lithium aluminium hydride, and the solution was added dropwise to a stirred solution of 5.06 g of lithium aluminium deuteride (Metal Hydrides Inc., 96.3%) in 600 ml of the tetrahydrofuran. The addition took 3.5 h and the reaction mixture was refluxed for a further 1 h. Water, 15 ml, was then carefully added and this was followed by the addition of 10 ml of 15% aqueous sodium hydroxide and 55 ml of water (24). The precipitated aluminium hydroxide was removed by filtration with Celite as a filter aid. The filtrate was deionized with Amberlite IR 120, H^+, and evaporated to dryness *in vacuo*. The residue was triturated with acetone and ethanol to provide 30.5 g of a product which was dissolved in 900 ml of dry acetone. The solution was cooled to 0° and 36 ml of concentrated sulfuric acid was added dropwise to the stirred solution. After the mixture had been kept at about 15° for 4.5 h, it was cooled to below 10° and neutralized with a solution of 54 g of sodium hydroxide in 60 ml of water. The precipitated salts were removed by filtration and the filtrate was evaporated under reduced pressure. A chloroform solution of the syrupy residue was extracted with water, and the material in the aqueous extract was dried and retreated with acetone and sulfuric acid as described above. The combined chloroform solutions were evaporated and the residue recrystallized from benzene – petroleum ether. The total yield was 16.7 g (41.4% based on the lithium aluminium deuteride) of 6,6′-dideuterio-1,2:5,6-di-*O*-isopropylidene-α-D-glucofuranose, m.p. 108–110°, in agreement with the melting point of the undeuterated compound prepared in a similar manner (25).

The compound, 1.0 g, was dissolved in 50 ml of 50% aqueous methanol, and 0.2 ml of concentrated sulfuric acid was added. The solution was heated at 100° for 3 h and then neutralized with barium hydroxide. Removal of solvent left a syrup which was acetylated with acetic anhydride and sodium acetate in the usual manner to provide 6,6′-dideuterio-β-D-glucopyranose pentaacetate, m.p. 132–133°, in 0.69 g yield. Treatment of a sample of this product with a 1:1 mixture of acetic acid – acetic anhydride containing sulfuric acid provided 6,6′-dideuterio-α-D-glucopyranose pentaacetate, m.p. 111.5–112.5°. The n.m.r. spectra of these two pentaacetates are reported in a separate communication (3).

2-O-Benzyl-D-arabinose

3-*O*-Benzyl-1,2:5,6-di-*O*-isopropylidene-α-D-glucofuranose (26), 201 g, was dissolved in a mixture of 400 ml of ethanol and 200 ml of *N* sulfuric acid. The solution was heated at 75° for 7.5 h, and then evaporated *in vacuo* to a light syrup which was dissolved in about 500 ml of water. This solution was heated at 90° for 1.5 h. The cooled solution was extracted twice with chloroform and then neutralized with barium hydroxide. Evaporation of the filtered solution and crystallization of the residue from acetone–benzene gave 128 g (95% yield) of 3-*O*-benzyl-D-glucopyranose (27), m.p. 134–136°.

The procedures (28) for the conversion of this compound into 2-*O*-benzyl-D-arabinose were modified (29) as follows. Sodium metaperiodate, 45 g, was dissolved by heating in 150 ml of water, and the rapidly cooled solution was added to 54 g of 3-*O*-benzyl-D-glucose in 150 ml of water. The resulting solution was cooled in ice water and then left at room temperature. The mass of crystals which formed in 15 min was collected and washed with cold water. The yield was 37 g of 2-*O*-benzyl-4-*O*-formyl-D-arabinose, m.p. 124–130°. Methanol, 500 ml, was added to the filtrate and the mixture was refrigerated for 2 h. The precipitated salts were removed by filtration and washed with methanol. The combined filtrates were evaporated to a syrup which was dissolved in 25 ml of water. On cooling, a further crop of the formyl ester, 11.3 g, was deposited. The total yield was 90% of material of sufficient purity for the next stage in the preparation.

The above compound was saponified in aqueous solution with sodium hydroxide. The solution was deionized with Amberlite IR 120, H^+, and then evaporated to a light syrup which deposited crystals after refrigeration for several days. These crystals, plus a second crop obtained from the mother liquors, were recrystallized from ethyl acetate. The yield was 83% of 2-*O*-benzyl-D-arabinose (28), m.p. 111–113°, $[\alpha]_D$ −73° after 0.5 h (*c*, 2.1 in water).

2-Deuterio-β-D-arabinose

2-*O*-Benzyl-D-arabinose, 12.0 g, was dissolved in 8 ml of deuterium oxide and the solvent was removed by freeze-drying. This procedure was repeated and the product was then dissolved in 30 ml of deuterium oxide which had been treated with 550 mg of sodium. After standing at room temperature for 7 days, the solution was neutralized with *O*-deuterated acetic acid and extracted three times with 300 ml volumes of ethyl acetate. The combined extracts were evaporated to dryness *in vacuo* and the residue was crystallized from ethyl acetate to give 3.4 g of 2-deuterio-2-*O*-benzyl-D-arabinose, m.p. 108–109.5°, $[\alpha]_D$ −71.5 (*c*, 1.7 in water).

The compound was dissolved in ethanol for hydrogenolysis at atmospheric pressure with 10% palladium-on-charcoal catalyst. The yield of 2-deuterio-β-D-arabinose isolated in the usual manner and crystallized from 80% aqueous methanol (30) was nearly quantitative.

2,5,5'-Trideuterio-β-D-arabinose

The compound was prepared from the above described 6,6'-dideuterio-1,2:5,6-di-*O*-isopropylidene-α-D-glucofuranose by the same procedures as described for the preparation of 2-deuterio-β-D-arabinose from 1,2:5,6-di-*O*-isopropylidene-α-D-glucofuranose. The overall yield of material melting at 151–153° was 8%.

ACKNOWLEDGMENTS

The authors thank the Corn Products Refining Company for a generous gift of D-glucurone. The n.m.r. spectra at 60 Mc.p.s. were determined by R. Swindlehurst and Mrs. G. Conway, and those at 100 Mc.p.s. by G. Bigam of this department. The research was supported in part by the National Research Council of Canada through grant T172 to R. U. Lemieux.

REFERENCES

1. R. W. LENZ and J. P. HEESCHEN. J. Polymer Sci. **51**, 247 (1961).
2. J. I. MUSHER and E. J. COREY. Tetrahedron, **18**, 791 (1962).
3. R. U. LEMIEUX and J. D. STEVENS. Can. J. Chem. **43**, 2509 (1965).
4. R. U. LEMIEUX, J. D. STEVENS, and R. R. FRASER. Can. J. Chem. **40**, 1955 (1962).
5. M. KARPLUS. J. Am. Chem. Soc. **85**, 2870 (1963).
6. R. U. LEMIEUX, R. K. KULLNIG, and R. Y. MOIR. J. Am. Chem. Soc. **80**, 2237 (1958).
7. R. U. LEMIEUX, R. K. KULLNIG, H. J. BERNSTEIN, and W. G. SCHNEIDER. J. Am. Chem. Soc. **80**, 6098 (1958).
8. A. NICHON, M. A. CASTLE, R. HARADA, C. E. BERKOFF, and R. O. WILLIAMS. J. Am. Chem. Soc. **85**, 2185 (1963).
9. L. M. JACKMAN. Applications of nuclear magnetic resonance spectroscopy in organic chemistry. Pergamon Press, New York. 1959.
10. R. U. LEMIEUX and J. W. LOWN. Can. J. Chem. **42**, 893 (1964).
11. S. FURBERG and B. PEDERSEN. Acta Chem. Scand. **17**, 1160 (1963).
12. L. D. HALL. Tetrahedron Letters, **23**, 1457 (1964).
13. L. F. JOHNSON. Varian Associates Technical Bull. No. 87-100-082. 1962.
14. R. U. LEMIEUX and J. HOWARD. Can. J. Chem. **41**, 308 (1963).
15. A. HORDVIK. Acta Chem. Scand. **15**, 16 (1961).
16. C. T. BISHOP and F. P. COOPER. Can. J. Chem. **41**, 2743 (1963).
17. S. M. CANTOR and Q. P. PENISTON. J. Am. Chem. Soc. **62**, 2113 (1940).
18. M. RUDRUM and D. F. SHAW. J. Chem. Soc. 52 (1965).
19. R. U. LEMIEUX. *In* Molecular rearrangements. Paul de Mayo (*Editor*). Interscience Publishers, Inc., New York. Part 2. pp. 713–715.
20. S. FURBERG. Acta Chem. Scand. **14**, 1357 (1960).
21. E. L. ELIEL, N. L. ALLINGER, S. J. ANGYAL, and G. A. MORRISON. Conformational analysis. John Wiley & Sons, Inc., New York. 1965. p. 408.
22. H. S. ISBELL. J. Res. Natl. Bur. Std. **66A**, 233 (1962).
23. L. N. OWENS, S. PEAT, and W. J. G. JONES. J. Chem. Soc. 339 (1941).
24. V. M. MIĆOVIĆ and M. LJ. MIHAILOVIĆ. J. Org. Chem. **18**, 1190 (1953).
25. O. TH. SCHMIDT. *In* Methods in carbohydrate chemistry. Vol. 2. R. L. Whistler and M. L. Wolfrom (*Editors*). Academic Press, Inc., New York. 1963. p. 321.
26. M. H. ADAMS, R. E. REEVES, and W. F. GOEBEL. J. Biol. Chem. **140**, 653 (1941).
27. K. FREUDENBERG, H. VON HOCHSTETTER, and H. ENGELS. Ber. **58**, 666 (1925).
28. J. C. P. SCHWARZ and M. MACDOUGALL. J. Chem. Soc. 3065 (1956).
29. R. K. NESS and H. G. FLETCHER, JR. J. Am. Chem. Soc. **74**, 5341 (1952).
30. R. C. HOCKETT and C. S. HUDSON. J. Am. Chem. Soc. **56**, 1632 (1934).

Can. J. Chem. Downloaded from www.nrcresearchpress.com by 210.87.254.42 on 09/05/12
For personal use only.

Can. J. Chem. Downloaded from www.nrcresearchpress.com by 210.87.254.42 on 09/05/12
For personal use only.

THE OXIDATION OF PHENOLS

I. THE OXIDATION OF 2,6-DI-*t*-BUTYL-4-METHYLPHENOL, 2,6-DI-*t*-BUTYLPHENOL, AND 2,6-DIMETHYLPHENOL WITH PEROXY RADICALS[1]

E. C. HORSWILL AND K. U. INGOLD
Division of Applied Chemistry, National Research Council, Ottawa, Canada

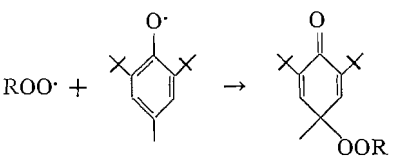
Received September 24, 1965

ABSTRACT

Previous work on the oxidation of alkyl phenols with peroxy radicals is summarized. The yields of the peroxy-cyclohexadienones formed from 2,6-di-*t*-butyl-4-methylphenol in the α,α'-azo-bis-isobutyronitrile-initiated oxidation of tetralin at 40 °C have been measured quantitatively. The results suggest that not all the oxidation chains are initiated by isobutyronitrile peroxy radicals.

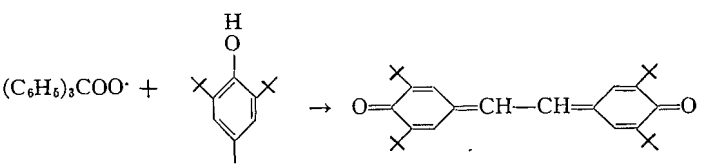
The products from the oxidation of 2,6-di-*t*-butylphenol and 2,6-dimethylphenol with *t*-butyl peroxy radicals are found to be mainly dialkyl-*p*-benzoquinones and tetraalkyl diphenoquinones.

Although the kinetics of the phenol – peroxy radical reaction[2] have been investigated intensively in recent years, comparatively little attention has been paid to the products of this reaction. About 10 years ago the products from 2,4,6-trialkyl phenols were examined by several groups of workers (1–6), but there has been very little activity in this field since that time. Peroxy radicals generated by the cobalt-catalyzed decomposition of hydroperoxides (1, 2) or by the thermal decomposition of compounds such as α,α'-azo-bis-isobutyronitrile (AIBN) in the presence of oxygen (2, 3) generally gave mainly 4-peroxy-cyclohexadienones (1–3), the yields of which depended upon the phenol, the peroxy radical, and the experimental conditions. Extremely high yields approaching 100% were obtained with 2,6-di-*t*-butyl-4-methylphenol (BMP) and *t*-butyl peroxy radicals. After the initial abstraction of the phenolic hydrogen (cf., however, ref. 7), the reaction can be represented, for example, as



I

Under certain conditions phenols containing a *p*-methyl group gave stilbenequinones (e.g. see ref. 2),



II

This product is formed from two phenoxy radicals by a very complicated sequence of reactions (8). The less highly oxidized dihydroxy bibenzyl dimers have been isolated after

[1]*Issued as N.R.C. No. 8757.*
[2]*That is, the kinetics for the inhibition of hydrocarbon autoxidation by phenols.*

the high-temperature air oxidation of hydrocarbons retarded with phenols containing a *p*-methyl group, e.g. 2,6-di-*t*-butyl-4-methylphenol (4, 5), 2-*t*-butyl-4,6-dimethylphenol (5), and 2,4,6-trimethylphenol (5). With a *n*-alkyl group in the para position trialkyl phenols generally give 4-hydroxyaryl ketones (6).

In contrast to the wealth of information on trialkyl phenols only two di- and one mono-alkyl phenol have been examined. When cumene was oxidized, Moore and Waters (5) identified traces of 2,2′-dihydroxy diphenyls from *p*-cresol and 2,4-dimethylphenol, while 2,6-dimethylphenol gave the tetramethyl 4,4′-dihydroxy diphenyl and 4,4′-diphenoquinone (see also ref. 9).

Our interest in this subject arose from our studies of the kinetics of the inhibition of hydrocarbon autoxidation by phenols (10). In particular, we felt that more information on the products from phenols other than trialkyl phenols would be a great help in further elucidating the overall mechanism of this reaction. The present paper describes the products formed by the *t*-butyl peroxy radical oxidation of two dialkyl phenols, 2,6-di-*t*-butyl- and 2,6-dimethyl-phenol. In addition, the development of a thin-layer chromatographic (t.l.c.) method for separating and tentatively identifying oxidation products prompted us to look for a compound having structure I under the conditions actually employed in kinetic studies of inhibition. That is, no compound of this structure in which R is derived from an oxidizing hydrocarbon RH has ever been identified. The actual formation of such a product is of importance in connection with the assumptions involved in determining rates of chain initiation by the induction-period method of Boozer *et al.* (3). That is, rates of chain initiation in hydrocarbon autoxidation are generally determined by measuring the induction period produced by small quantities of BMP (3, 10), it being assumed that each molecule of the phenol reacts with just *two* peroxy radicals (see, however, ref. 11). This plausible assumption is based on the identification of 2,6-di-*t*-butyl-4-methyl-4-peroxy-isobutyronitrile-2,5-cyclohexadiene-1-one (I, R = $(CH_3)_2(CN)C$, hereafter referred to as IBN-1) after the decomposition of AIBN in chlorobenzene containing BMP in the presence of oxygen (3).

A somewhat better justification for this assumption is provided by the present results on the products formed from BMP during the oxidation of tetralin at 40 °C under conditions fairly typical of those normally used in induction-period studies. The reaction mixture in these experiments consisted of 3 ml of tetralin and 10 ml of chlorobenzene with 2.7×10^{-4} mole/l BMP and 0.66 g (2.94×10^{-1} mole/l) AIBN. The oxygen absorption curve is shown in Fig. 1. The induction period is 2 760 s, giving an efficiency of chain initiation, e, equal to 0.64. (The rate constant, k_1, for AIBN decomposition at 40 °C was taken to be 5.2×10^{-7} s^{-1}.) The reaction was stopped at various times between 3 600 and 5 500 s, since all the BMP should by now be consumed as the oxidation rate is equal to its uninhibited value. Work-up of the reaction mixtures for t.l.c. analysis is described in the Experimental section. The t.l.c. plates showed three well-resolved spots travelling ahead of a long streak which started at the origin and is due to residual AIBN and tetralin hydroperoxide. The spot with the largest R_f is formed from AIBN and chlorobenzene rather than from BMP or tetralin. The second spot corresponded in position to the expected α-tetralyl peroxy derivative of BMP (hereafter referred to as TET-1). Positive identification was achieved by extracting this spot (from a large sample) with CCl_4 and comparing its infrared spectrum with that of an authentic sample prepared by the method of Bickel and Kooyman (2). The third spot, which was relatively weak, corresponded in position to IBN-1. There was no spot corresponding to the stilbenequinone nor to either its di- or tetra-hydro derivatives. The yield of TET-1 was estimated by running the reaction

Can. J. Chem. Downloaded from www.nrcresearchpress.com by 210.87.254.42 on 09/05/12
For personal use only.

mixture and several standard solutions on the same thin-layer sheet. The chromatogram was photographed and analyzed with a photodensitometer, as this proved to be more satisfactory than direct measurement on the chromatogram (see Experimental section). There was an excellent straight-line relation between the sample weight and the area under the densitometer curve in the range of concentrations from 5 to 40 g/l. From this calibration line the best estimate of the yield of TET-1 (based on the starting phenol) was 86 ± 10% (standard deviation) at 3 600 s and 84 ± 5% at 5 500 s. The IBN-1 spot was too faint for this method to be applied. Its yield was estimated to be 10 ± 3% by visual comparison with spots from solutions of known strength. The overall yield of compounds with structure I is, therefore, ~95 ± 10%. This provides a sound justification for the assumption that each molecule of BMP reacts with two peroxy radicals under normal kinetic conditions.

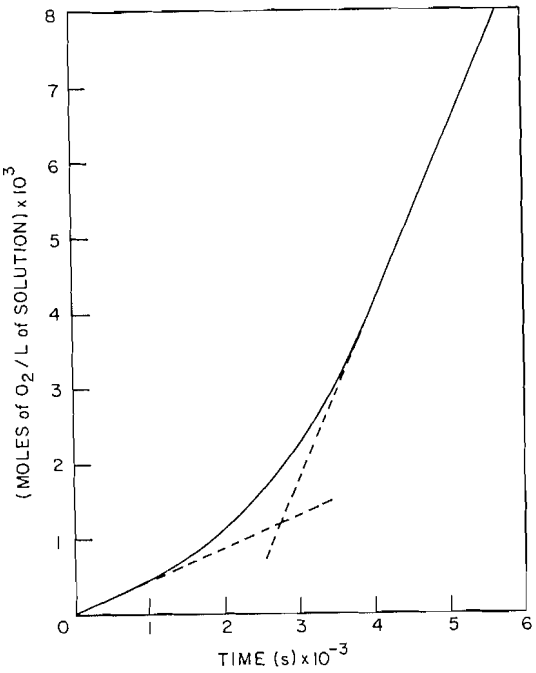


FIG. 1. Oxygen absorption by 3 ml tetralin in 10 ml chlorobenzene with 0.66 g AIBN and 2.7×10^{-4} mole/l BMP at 40 °C.

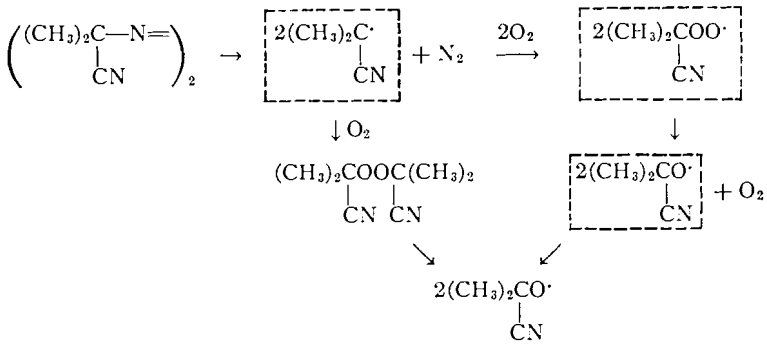
The relative yields of IBN-1 and TET-1 can roughly be predicted by comparing the rate of chain initiation ($2ek_1$[AIBN] = 2×10^{-7} mole/l s) with the amount of oxygen absorbed at the point where the rate reaches its uninhibited value (i.e. 3.10×10^{-3} mole/l at 3 600 s).[3] If the rate of isobutyronitrile peroxy radical production is equal to the rate of chain initiation, then $2 \times 10^{-7} \times 3\,600 = 7.2 \times 10^{-4}$ mole/l of these radicals was formed by the end of the induction period. Since 3.1×10^{-3} mole/l of α-tetralyl peroxy radicals was formed in this time, the expected yield of TET-1 is (3.1/3.1 + 0.72) × 100 = 81%, and of IBN-1 (0.72/3.82) × 100 = 19%. The fact that only about half the expected IBN-1 was formed indicates that fewer isobutyronitrile peroxy radicals

[3]*The measured change in gas volume amounts to* 3.25×10^{-3} *mole/l. This must be corrected for nitrogen evolution by the AIBN and oxygen absorption by the initiator radicals (10). This correction is* $-(2e - 1)k_1$[*AIBN*] $\times$ 3 600 $= -0.15 \times 10^{-3}$ *mole/l.*

Can. J. Chem. Downloaded from www.nrcresearchpress.com by 210.87.254.42 on 09/05/12
For personal use only.

Can. J. Chem. Downloaded from www.nrcresearchpress.com by 210.87.254.42 on 09/05/12
For personal use only.

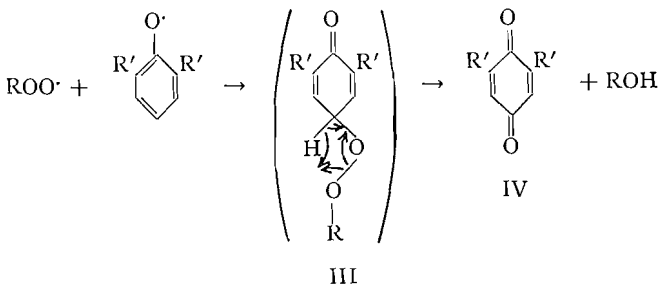
are involved in the main reaction sequence than is suggested by this simple calculation, since it seems unlikely that these radicals would add to the phenoxy radical any less readily than α-tetralyl peroxy radicals. A possible explanation for the low yield of IBN-1 is that two isobutyronitrile peroxy radicals can frequently be formed while they are still in the same solvent cage in which their precursors were produced. Mutual interaction would give two tertiary alkoxy radicals, which could both initiate oxidation but probably could not add to the phenoxy radical (cf. the reaction of *t*-butoxy radicals with this phenol (12)). An alternative possibility would be the formation of an unstable peroxide from a single molecule of oxygen and its subsequent decomposition to the same two alkoxy radicals. That is,



In this connection, the yield of IBN-1 in the absence of tetralin, but otherwise under the same experimental conditions, was only 62 ± 4% at 3 600 s and 71 ± 4% at 5 500 s, which also suggests that BMP is a relatively ineffective trap for the radicals formed from AIBN and oxygen.

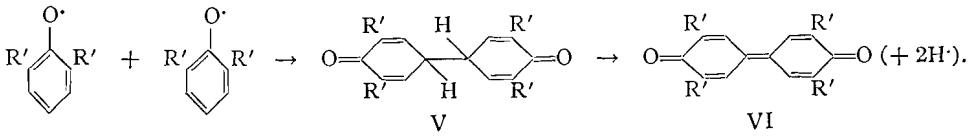
The 2,6-di-*t*-butylphenol and 2,6-dimethylphenol were oxidized by the method of Bickel and Kooyman (2). That is, 0.1 mole of *t*-butyl hydroperoxide in 50 ml of benzene containing 0.05 mole of the phenol was catalytically decomposed by the slow addition of powdered cobalt toluate, the temperature being kept below 30 °C. Unfortunately, this simple procedure does not give very reproducible product yields. However, this disadvantage is more than offset when unstable products are formed by the low temperature of the reaction. After all the hydroperoxide had been decomposed, the products were separated by column chromatography on silica gel, mixtures of hexane, benzene, and ethyl acetate being used as eluents. Every fraction was checked for purity by t.l.c. on silica before being worked up for the products.

The principal products from 2,6-di-*t*-butylphenol and 2,6-dimethylphenol result from two competing radical coupling reactions. That is, the initially formed phenoxy radical can react with either a peroxy radical



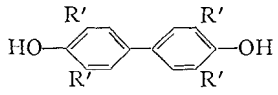
III

or a second phenoxy radical



V VI

The 2,6-dimethylphenol–hydroperoxide solution turns the deep red color characteristic of diphenoquinones (VI) almost immediately after the addition of the cobalt catalyst. In contrast, the 2,6-di-*t*-butylphenol–hydroperoxide solution turns only light yellow, which is characteristic of *p*-benzoquinones (IV), although gas chromatography shows that all the starting phenol has been consumed. This yellow color very gradually darkens and finally becomes a deep red after several hours. This suggests that the tetra-*t*-butyl VI is not formed by the direct oxidation of V under these conditions.[4] Instead, this keto compound must first rearrange to its enol tautomer, the bis-phenol V*a*.



V*a*

This rearrangement is catalyzed by the *t*-butanol formed in the oxidation (cf. refs. 13 and 14). The bis-phenol is then oxidized to VI by the peroxy radicals. The rearrangement of V to V*a* must be a much faster process for the methyl than for the *t*-butyl compound. It is therefore not surprising that, although tetra-*t*-butyl V was a minor product (~1%) from 2,6-di-*t*-butylphenol, none of the tetramethyl compound was isolated or identified from 2,6-dimethylphenol. Compound III was not identified in either case, but its similarity to I provides a logical path for the production of the *p*-benzoquinone IV.

The relative importance of IV and VI in the products depends on the nature of the alkyl group. The dimethylphenol yields approximately 12% IV[5] and up to 75% VI, whereas the dibutylphenol yields approximately 59% IV and 31% VI. The higher yield of IV in the latter case can probably be attributed to the greater stability of the 2,6-di-*t*-butyl phenoxy radical. Both phenols also gave some brown polymeric material and a few additional crystalline products that were not isolated in sufficient quantity for identification.

EXPERIMENTAL

2,6-Di-t-butyl-4-methylphenol

When the oxidation was stopped after the rate had reached its uninhibited value, the reaction mixture was placed overnight in a freezer at −30 °C to crystallize the unreacted AIBN. After filtration the tetralin and chlorobenzene were removed under high vacuum with gentle warming. The semisolid residue, which consisted mainly of unreacted AIBN and tetralin hydroperoxide, was extracted with 5–10 ml of cold *n*-hexane (in which both these compounds are very insoluble). The hexane was removed under vacuum, and the very small oily residue was dissolved in toluene and made up to 0.1 ml. Handling losses were probably not more than 2–3% unless some compound was strongly adsorbed on the surface of the AIBN crystals.

A 1 μl sample of the toluene solution was spotted on an Eastman Chromagram sheet (with fluorescent indicator) along with the same volumes of three known concentrations of TET-1 (e.g. 5, 10, and 20 g/l). After t.l.c. was carried out in trichloroethylene, a transverse strip of the TET-1 spots was excised and evaluated on a Spinco model R Analytrol. This instrument was modified by using the ultraviolet light source to excite the fluorescent strip and the visible-sensitive photocell as the detector. To reduce the visible light from

[4]*However, the tetra-t-butyl V does inhibit the α,α′-azo-bis-isobutyronitrile-initiated oxidation of cumene at 65 °C. This inhibition may be due to the promotion by the higher temperature of either an isomerization to V*a* or a direct reaction of V with peroxy radicals.*

[5]*All product yields are based on the percentage conversion of the starting phenol.*

Can. J. Chem. Downloaded from www.nrcresearchpress.com by 210.87.254.42 on 09/05/12
For personal use only.

the source a Corning 7-54 filter was used between the light and fluorescent strip. The sensitivity of this method was later increased by photographing the uncut fluorescent chromatogram under ultraviolet light. An enlarged positive transparency was then prepared, cut into strips lengthwise, and evaluated in the Analytrol in visible light, to which the machine is more sensitive.

The average of triplicate (three t.l.c.) determinations of the yield of TET-1, based on the starting phenol concentration, was 86 ± 10% after 3 600 s and 84 ± 5% after 5 500 s. In the absence of tetralin the yield of IBN-1 (t.l.c. in benzene) was 62 ± 4% after 3 600 s and 71 ± 4% after 5 500 s.

The IBN-1 and TET-1 were both prepared by the methods of Bickel and Kooyman (2). The purified materials melted at 92–93.5° (lit. m.p. 92.5° (2) and 91–92° (3)) and 105–106.5° (lit. m.p. 104°(2)) respectively.

2,6-Dimethylphenol

The precipitate of reacted cobalt and of most of the deep red compound VI was filtered and weighed. Benzene was removed from the filtrate under vacuum. The residue was eluted through a 4 ft silica column with mixtures of benzene and ethyl acetate; the fractions were automatically collected in the order IV, VI, and *p*-toluic acid from the cobalt catalyst. Compounds IV and VI were identified by comparison with authentic samples of these compounds by means of melting point, mixed melting point, and X-ray powder pattern. The yield of IV was confirmed by gas–liquid chromatography on a polyester succinate column at 185 °C.

2,6-Di-t-butyl-phenol

The cobalt precipitate was filtered off and the benzene removed under vacuum. The products were eluted in the order V, VI, IV, and *p*-toluic acid. The products were identified by comparison with authentic samples by means of melting point, mixed melting point, X-ray powder pattern, and infrared spectra. Authentic V was prepared by the oxidation of 2,6-di-*t*-butylphenol with silver oxide (14). The melting point is 152–156° (lit. m.p. 151–152° (13, 14)); at 156° there is a sudden dendritic growth of red crystals of VI which do not melt until 249°. In separate experiments, it was shown that, at its melting point, V decomposed to VI and 2,6-di-*t*-butylphenol. The infrared spectrum of V shows the doublet characteristic of *p*-quinolides at 1 637 and 1 661 cm^{-1}, and the nuclear magnetic resonance spectrum of V shows protons with chemical shifts (in parts per million to low field of tetramethylsilane) of 1.18 (*t*-butyl), 3.36 (4H), and 6.33 (3H and 5H).

REFERENCES

1. T. W. Campbell and G. M. Coppinger. J. Am. Chem. Soc. **74**, 1469 (1952).
2. A. F. Bickel and E. C. Kooyman. J. Chem. Soc. 3211 (1953).
3. C. E. Boozer, G. S. Hammond, C. E. Hamilton, and J. N. Sen. J. Am. Chem. Soc. **77**, 3233 (1955).
4. C. D. Cook. J. Org. Chem. **18**, 261 (1953).
5. R. F. Moore and W. A. Waters. J. Chem. Soc. 243 (1954).
6. M. E. Hey and W. A. Waters. J. Chem. Soc. 2753 (1955).
7. G. M. Coppinger. J. Am. Chem. Soc. **86**, 4385 (1964).
8. R. H. Bauer and G. M. Coppinger. Tetrahedron, **19**, 1201 (1963).
9. W. A. Waters and C. Wickham-Jones. J. Chem. Soc. 2420 (1952).
10. J. A. Howard and K. U. Ingold. Can. J. Chem. **40**, 1851 (1962); **41**, 1744 (1963); **41**, 2800 (1963); **42**, 1044 (1964); **42**, 2324 (1964).
11. C. E. Boozer, G. S. Hammond, C. E. Hamilton, and C. Peterson. J. Am. Chem. Soc. **77**, 3380 (1955).
12. K. U. Ingold. Can. J. Chem. **41**, 2807 (1963).
13. M. S. Kharasch and B. S. Joshi. J. Org. Chem. **22**, 1439 (1957).
14. H. S. Blanchard. J. Org. Chem. **25**, 264 (1960).

Can. J. Chem. Downloaded from www.nrcresearchpress.com by 210.87.254.42 on 09/05/12
For personal use only.

THE OXIDATION OF PHENOLS

II. THE OXIDATION OF 2,4-DI-*t*-BUTYLPHENOL WITH PEROXY RADICALS[1]

E. C. HORSWILL AND K. U. INGOLD
Division of Applied Chemistry, National Research Council, Ottawa, Canada

Received September 24, 1965

ABSTRACT

Ten products from the oxidation of 2,4-di-*t*-butylphenol with *t*-butyl peroxy radicals have been identified. They can be subdivided into three groups, depending on the type of radical–radical coupling reaction by which they are produced or in which their precursors are formed: (*i*) phenoxy–peroxy coupling, (*ii*) phenoxy–phenoxy coupling at the 6 positions, and (*iii*) phenoxy–phenoxy coupling through the oxygen atom of one radical and the 6 position of the second radical. Products resulting from still other phenoxy–phenoxy coupling reactions are undoubtedly formed in minor amounts.

Can. J. Chem. Downloaded from www.nrcresearchpress.com by 210.87.254.6 on 09/05/12
For personal use only.

The products from the oxidation of 2,4-di-*t*-butylphenol with *t*-butyl peroxy radicals have been studied as a part of our general investigation into the oxidation of phenols (1). This compound was chosen as a representative 2,4-dialkyl phenol which might be expected to give a simpler mixture of products than a phenol containing a methyl group, since products coupled through the methyl group (such as dihydroxy bibenzyls and stilbenequinones) would not be formed. In spite of this simplification no less than 10 products were identified, and the thin-layer chromatographic (t.l.c.) plates showed that many others were present. The products were separated by column chromatography on silica (1). Their relative yields depended not only on the exact conditions of the reaction but also on the speed with which they were separated. The latter variation is due to the fact that many of the initial products are unstable peroxides which decompose on exposure to light and heat and even to the mildly acidic silica column itself.

By analogy with 2,6-dialkyl phenols (1) we may expect to get products resulting from phenoxy–peroxy and phenoxy–phenoxy radical coupling reactions. However, in the present case, the existence of a hydrogen atom in the 6 position leads to products of increased complexity because of the rapid rearrangement of those intermediates with an *o*-quinolide structure. For convenience, the overall reaction is divided into three parts.

Firstly, combination of the initially formed phenoxy radical with a *t*-butyl peroxy radical.

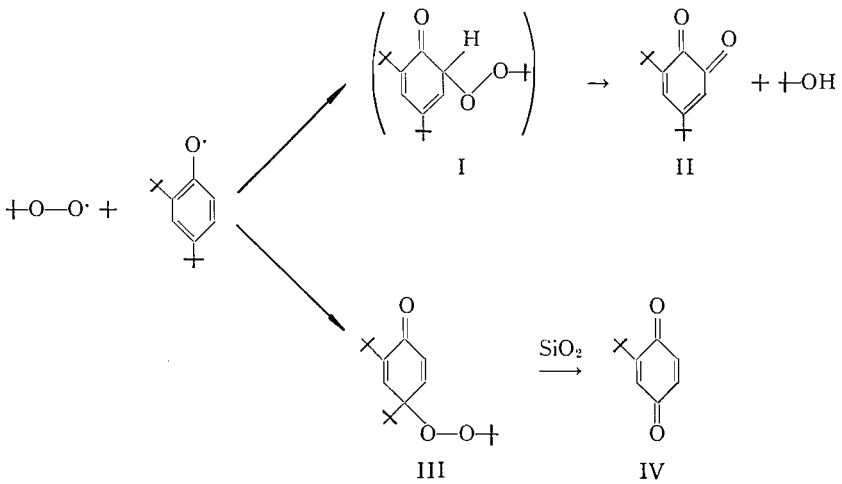
3,5-Di-*t*-butyl-*o*-benzoquinone (II) was one of the major products (~10%), but its probable precursor (I) was not identified. The conversion of I into II may occur either directly (cf. ref. 1) or after rearrangement to an *o*-peroxy phenol. The 4-peroxy-cyclohexadienone, III, found in 5–10% yield, is similar to the major products formed from 2,4,6-trialkyl phenols (1). Compound III decomposed slowly on the t.l.c. plates to give 2-*t*-butyl-*p*-benzoquinone (IV) and other unidentified products. No compound corresponding to the addition of the peroxy radical at the 2 position of the original phenol was identified, nor was its expected decomposition product, 4-*t*-butyl-*o*-benzoquinone, detected.

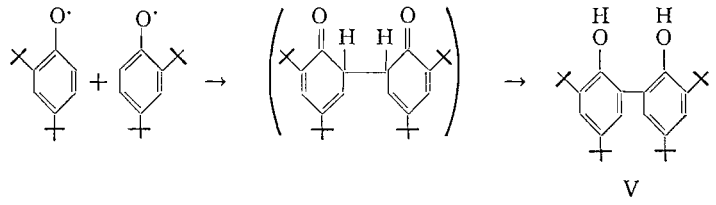
Secondly, combination of two phenoxy radicals through their carbon atoms in position 6.

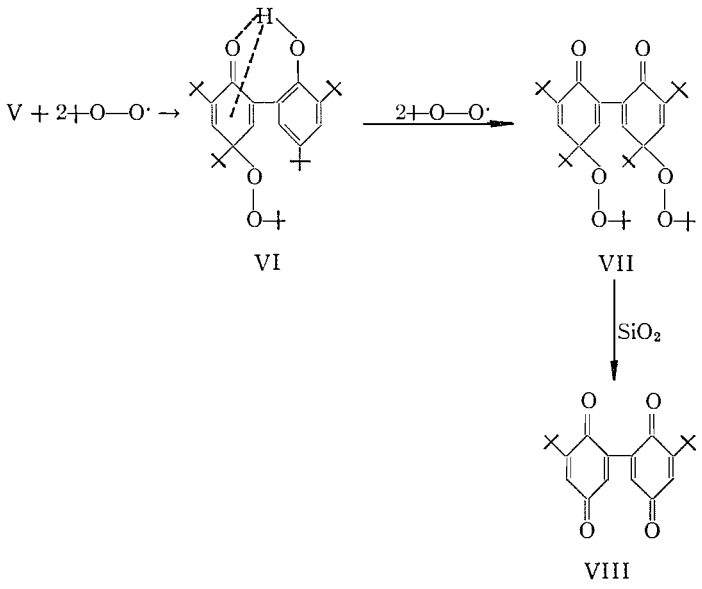
The biphenol V and its precursor were not identified among the products under the standard experimental conditions, that is, with a ratio of not less than 2 moles of hydroperoxide per mole of phenol. However, in a separate experiment with only 1 equivalent

[1]*Issued as N.R.C. No. 8758.*

Can. J. Chem. Downloaded from www.nrcresearchpress.com by 210.87.254.6 on 09/05/12
For personal use only.



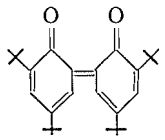




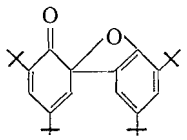
Can. J. Chem. Downloaded from www.nrcresearchpress.com by 210.87.254.6 on 09/05/12
For personal use only.

of hydroperoxide, compound V was isolated in 37% yield. The yield of VI varied from about 12% for a 2:1 hydroperoxide–phenol ratio to less than 1% for a 3:1 ratio, there being a corresponding increase in the yield of VII and, hence, VIII. These variations suggest that the phenolic hydrogen in VI is much less readily abstracted by peroxy radicals than is the first phenolic hydrogen in V or the hydrogen in the starting phenol. This conclusion is supported by the infrared spectrum of VI, which indicates that the hydroxyl group is not "free" but is involved in *two* intramolecular hydrogen bonds. That is, the spectra in the OH fundamental stretching region shows two bands, the frequencies of which correspond to the formation of hydrogen bonds with the cyclohexadienone ring and with the quinone oxygen (see Experimental section). A hydrogen-bonded OH group is much less readily attacked than a "free" OH group (2); therefore, VI is a relatively unreactive phenol. The maximum yield of VII (slightly less than 10%) was isolated from a reaction with a 3:1 hydroperoxide–phenol ratio. This compound decomposes rather readily on the silica column to give VIII. For instance, in the course of one experiment where a product initially containing ~10–12% VII remained on a column for several weeks, the separated products contained less than 1% VII but over 10% VIII. No attempt was made to identify or to isolate the corresponding decomposition product from VI, but it is undoubtedly present and responsible for one of the many unidentified spots on the t.l.c. analytical plates.

The basic carbon skeleton in VI and VII was confirmed by their preparation in high yield by the cobalt-catalyzed oxidation of V with 2 moles and 4 moles of *t*-butyl hydroperoxide, respectively. The biphenol itself was prepared by the oxidative coupling of 2,4-di-*t*-butylphenol in the presence of sodium hydroxide (3). The two tautomers, IX and X, resulting from the removal of only the two phenolic hydrogen atoms, were also prepared from V by its oxidation with silver oxide. Compound IX was not isolated from



IX

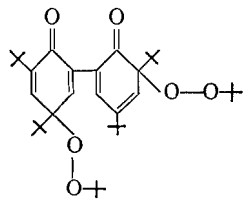


X

solution, but its presence was inferred by the rather stable, deep blue color of the products (cf. refs. 4 and 5). It rearranges to X slowly in ether or benzene but extremely rapidly in methanol or ethanol. The preparation of X by the oxidation of V with $K_3Fe(CN)_6$ and with 2,6-di-*t*-butyl-4-cyanophenoxy radicals has been described by Müller *et al.* (5). The absence of IX (by color) and X (by a spot test comparison on a t.l.c. plate) from the peroxy radical oxidation products of 2,4-di-*t*-butylphenol under the usual experimental conditions emphasizes the fundamental difference between oxidation with reagents that can add to the initial phenoxy radical and those which cannot.

Compound VIII was shown to be identical with the product obtained by the oxidation of 4,4′-dimethoxy-6,6′-di-*t*-butyl-*o*,*o*′-biphenol with chromium trioxide (6) and nitric acid (7). This dimethoxy biphenol was prepared by the oxidative coupling of 2-*t*-butyl-4-methoxyphenol with silver oxide.

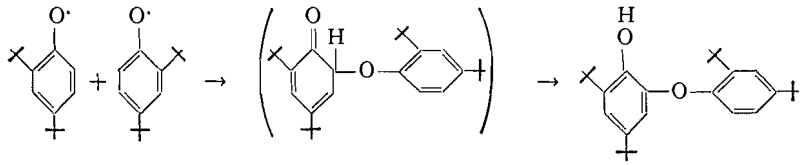
A product which appears to be isomeric with VII, except that the two rings are not equivalent, was also isolated in extremely small yield. Although it was not detected on the t.l.c. plates on which the raw product mixtures from the reaction of V with *t*-butyl peroxy radicals were run, its nuclear magnetic resonance spectrum suggests that it probably has



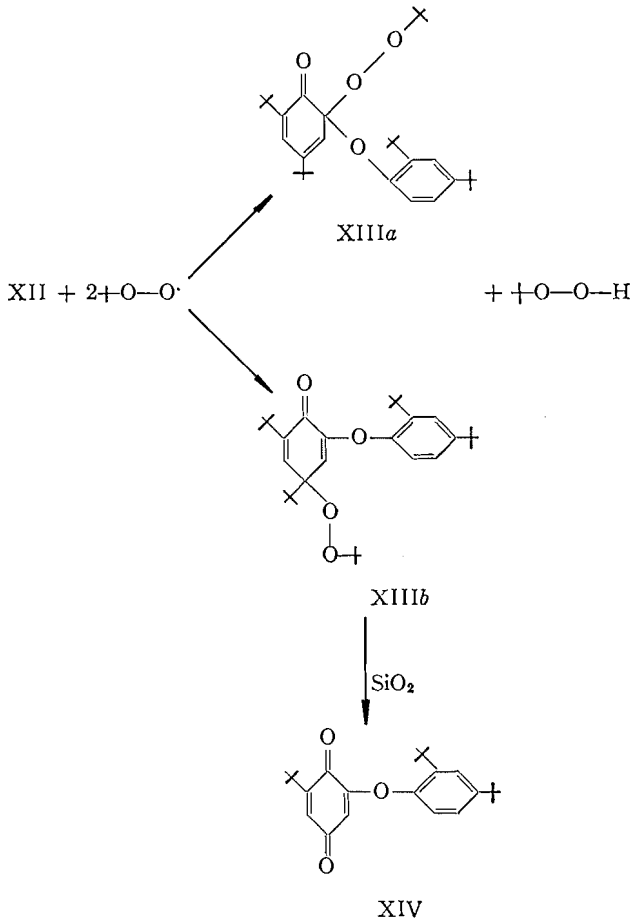
XI

structure XI. The apparent absence of XI from these t.l.c. plates could be due to its low yield in the reaction, since minor products are, in general, not readily detected by thin-layer chromatography of raw products because of the streaking of the major components when the sample is heavily spotted.

Thirdly, combination of two phenoxy radicals through the oxygen atom of one of them to give a 2-hydroxy diphenyl ether (XII).



XII



XIV

Can. J. Chem. Downloaded from www.nrcresearchpress.com by 210.87.254.6 on 09/05/12
For personal use only.

Can. J. Chem. Downloaded from www.nrcresearchpress.com by 210.87.254.6 on 09/05/12
For personal use only.

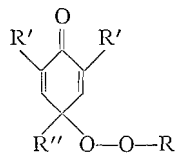
The phenol XII and its precursor were not identified, but its oxidation product XIII appears to be one of the major components in the reaction mixture (~20%). The yield of XIV was less than 5%. There is a slight doubt about whether the peroxy radical in XIII is in the *a* (ortho) or *b* (para) position, since this compound does not have a double band at around 1 667 cm^{-1} (6 μ) in its infrared spectrum. This doublet has generally been considered to be a characteristic feature in the spectra of *p*-quinolides (see below), so that its absence would seem to favor structure XIII*a*. However, most of the remaining evidence, including the nuclear magnetic resonance spectrum, certain other infrared bands, and the conversion of XIII into XIV thermally or on the silica column, favors structure XIII*b*. The detailed evidence relating to the structure of these and other products is given below. An attempt to synthesize XII by an Ullman condensation of 2,4-di-*t*-butyl-6-bromophenol or 2,4-di-*t*-butyl-6-bromoanisole with 2,4-di-*t*-butylphenol was unsuccessful, yielding V as the only crystalline product (cf. ref. 8).

The reaction schemes given above provide an obvious explanation for the occurrence of many spots on the t.l.c. plates which were not correlated with any particular compound. It is obvious, for example, that the peroxy radicals in VI and VII could also add to either ortho position or, alternatively, phenoxy radicals could add to V to give similar types of addition compounds. Even if we neglect all the products formed by the decomposition of the primary peroxides and all the products resulting from the combination of V and XII via their phenoxy radicals, we can calculate that over 40 primary products could be formed in the reaction. We have identified only seven of these (i.e. II, III, V, VI, VII, XIII, and, tentatively, XI), together with three secondary products (i.e. IV, VIII, and XIV).

Assignment of Structure

Structural assignments were based mainly on a comparison of the nuclear magnetic resonance, ultraviolet, and infrared spectra of the products with those of model compounds.

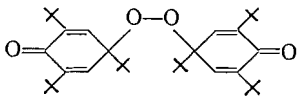
The nuclear magnetic resonance spectra of a number of model compounds were examined in carbon tetrachloride solution containing tetramethylsilane as an internal reference. A Varian Associates high-resolution spectrometer was used at an operating frequency of 100 Mc. The magnitudes of the chemical shifts for the *t*-butyl group (in parts per million to low field of tetramethylsilane) are as follows: (*a*) in six phenols the *t*-butyl group at the 2 or 2 and 6 positions was in the range 1.30–1.50, and at the 4 position was in the range 1.20–1.37; (*b*) in two *o*- and two *p*-quinones 1.20–1.30; (*c*) in *t*-butyl peroxide and hydroperoxide 1.18–1.24; (*d*) in 4-alkyl-4-peroxy-cyclohexadienones with the structure



XV

for R′ = *t*-butyl, 1.15–1.25, for R″ = CH_3 and R = $(CH_3)_2(CN)C$, α-tetralyl, and *t*-butyl, (1.16). The shift for the CH_3 group changes from 2.20 in the original phenol to 1.25–1.40 in these three dienones. For R′ = R″ = R = *t*-butyl, the assignments were 1.25, 0.95, and 1.22, respectively. These four compounds were all prepared by the method of Bickel and Kooyman (9).

We also attempted to prepare bis(1,3,5-tri-*t*-butyl-2,5-cyclohexadien-4-one) peroxide (XVI) by the oxidation of 2,4,6-tri-*t*-butylphenol with silver oxide in the presence of oxygen (10). Recrystallization of the raw product from methanol gave yellowish crystals,



XVI

m.p. 142–148° (lit. m.p. 148–149° (10, 11)). This melting point was not improved by a further recrystallization from ethanol. The nuclear magnetic resonance spectrum showed three peaks in the *t*-butyl region, the main one at 1.25 and two smaller bands at 0.85 and 0.79 present in a ratio of roughly 5:2:1, respectively. The ultraviolet spectrum had a maximum in the absorption at 317 mμ as well as the expected maxima at 385 and 238 mμ (see below). The band at 317 mμ suggested the presence of a compound with an *o*-quinolide structure (9). Thin-layer chromatography showed that three products were present. These correspond, in order of importance, to products coupled at the 4,4′; 4,2′; and 2,2′ positions (12). These products were not separated in bulk for complete characterization.

The data given above show that there is considerable overlap in the range of chemical shifts for *t*-butyl groups in different positions in these types of compounds. However, the results do suggest that a shift of 1.10 or less will generally be due to a *t*-butyl-peroxy-cyclohexadienone in which the *t*-butyl group and the peroxy group are both attached to the same carbon atom[2] (e.g. XV with R″ = *t*-butyl). The small shifts for CH_3 groups in this position also support this generalization.

In agreement with the results of Bickel and Kooyman (9), the ultraviolet spectra of all four model 4-peroxy-cyclohexadienones showed a distinctive, though rather weak ($\epsilon \sim 25$), absorption band at around 365 mμ and a much stronger absorption at ~235 mμ. In contrast, the oxidation products rarely showed a distinctive band at 365 mμ, although there was often a hump or shoulder on the side of a much stronger absorption. Several products also showed a maximum or a shoulder at ~280 mμ characteristic of an aromatic ring. None of the products had an absorption maximum at ~310 mμ which is probably characteristic of 2-peroxy-cyclohexadienones (9), although XI does have a band at 296 mμ which is fairly near this frequency.

The infrared spectra of many compounds with a *p*-quinolide structure show a characteristic double band at about 1 667 cm^{-1} (6.0 μ), generally with a separation of about 20 cm^{-1} between the bands. There are many examples of this feature in the literature both for 4-peroxy-cyclohexadienones (e.g. refs. 9, 14, 15) and, chiefly as a result of the extensive investigation into phenol oxidation by Müller, Ley, Rieker, and co-workers, for 4-oxy-cyclohexadienones (e.g. refs. 7, 13, 16, 17).[3] These workers also noted that bands at ~1 250 and ~1 000 cm^{-1} seemed to be characteristic of this structure (16). We have confirmed the presence of the 6 μ doublet in each of our four model 4-peroxy-cyclohexadienones, but the bands at ~1 250 and ~1 000 cm^{-1} were too variable in frequency and intensity to be very useful diagnostically. However, XV, with *t*-butyl groups at R, R′, and R″, had a strong absorption band at 975 cm^{-1} which was not present in the other

[2]*This rule is not always obeyed, as the nuclear magnetic resonance spectrum of the trimer of 2,5-di-t-butyl-4-methoxyphenol (13) has a t-butyl group with a shift of only 0.97. We are deeply indebted to Dr. Anton Rieker for a generous sample of this trimer.*

[3]*Only one exception to this general rule has so far been observed. That is, 2,6-di-t-butyl-4-triphenylmethyl-4-pentachlorophenoxy-2,5-cyclohexadien-1-one has only a single band at 1 680 cm^{-1}. However, it is possible that this compound was actually the o-quinol ether (17).*

Can. J. Chem. Downloaded from www.nrcresearchpress.com by 210.87.254.6 on 09/05/12
For personal use only.

three compounds with structure XV. A strong band at 977 cm^{-1} is also present in XVI, and we therefore attribute this band to the 4-*t*-butyl-4-(per)oxy-cyclohexadien-1-one structure.

Although the presence of only a single 6 μ band in XIII (at 1 655 cm^{-1}) argues against the *b* structure, the presence of a fairly strong band at 993 cm^{-1} favors this structure. Structure *b* is also supported by the small shift (1.05) for one of the five *t*-butyl bands in the nuclear magnetic resonance spectrum of XIII and by its ultraviolet spectrum (shoulders at 382 and 365 mμ and maxima at 289 and 242 mμ). These results suggest that the 6 μ doublet is not a required feature in the infrared spectra of *p*-quinolides.[4]

The structure of XI is very uncertain. The small chemical shifts (1.00 and 1.08) for two of the six *t*-butyl groups suggest that the peroxy radicals have added to carbon atoms with *t*-butyl substituents. This is also suggested by the strong band at 965 cm^{-1} in the infrared spectrum of XI. However, it is rather surprising that there is only one moderately strong band in the 6 μ region, the one at 1 700 cm^{-1}. The ultraviolet spectrum of XI is quite similar to the spectra of a number of *p*-quinol ethers derived from 2,4,6-tri-*t*-butylphenol (16). Structure XI is suggested here mainly because the carbon and hydrogen analyses and molecular weight data are virtually the same as those for compound VII, while the nuclear magnetic resonance spectrum shows that the *t*-butyl groups on the two rings are not equivalent.

EXPERIMENTAL

The cobalt-catalyzed decomposition of *t*-butyl hydroperoxide in the presence of phenols has been described previously (1). The products were eluted from a silica column with hexane, benzene, and ethyl acetate in the following order: V, VI, XIII, XI, XIV, VII, III, VIII, II. Unless otherwise stated the infrared spectra were measured in KBr pellets. The molecular weights were measured in benzene on a Mechrolab vapor pressure osmometer. All melting points were measured on a Kofler hot stage.

3,5-Di-t-butyl-o-benzoquinone (II)

Formed in about 10% yield based on the amount of 2,4-di-*t*-butylphenol reacted. Dark red needles from benzene, m.p. 116.5–117°. Identical (by mixed melting point and X-ray powder crystallography) with an authentic sample prepared by oxidizing 3,5-di-*t*-butylcatechol with Ag_2O.

2,4-Di-t-butyl-4-t-butylperoxy-2,5-cyclohexadien-1-one (III)

Formed in 5–10% yield. White needles from MeOH, m.p. 60.8–61.3°, decomposition with evolution of gas at 140°. This compound can be sublimed without decomposition under high vacuum. Infrared spectrum: bands at 1 672, 1 645, and 975 cm^{-1}. Ultraviolet spectrum: shoulder at 365 mμ, maximum at 230 mμ. Nuclear magnetic resonance spectrum: *t*-butyl groups at 0.97 (1) and 1.17 (2), several aromatic protons between 5.90 and 6.72. Gives IV on decomposition on the silica t.l.c. plates.

Anal. Calcd. for $C_{18}H_{30}O_3$: C, 73.43; H, 10.27; mol. wt. 294.4. Found: C, 73.37; H, 10.27; mol. wt. 293.

2-t-Butyl-p-benzoquinone (IV)

An authentic sample was prepared by oxidizing 2-*t*-butyl hydroquinone with Ag_2O. Yellow needles from hexane, m.p. 58.5–59°.

4,4',6,6'-Tetra-t-butyl-o,o'-biphenol (V)

Synthesized by the air oxidation of the sodium salt of 2,4-di-*t*-butylphenol (3). White needles from MeOH, m.p. 200–201°.

This compound was also prepared by the cobalt toluate catalyzed decomposition of 0.09 g of *t*-butyl hydroperoxide in 0.4 ml benzene containing 0.2 g 2,4-di-*t*-butylphenol. Recrystallization from methanol yielded 74 mg (37%) V, m.p. 199–200.5°.

2,4-Di-t-butyl-4-t-butylperoxy-6,6'-(2,4-di-t-butylphenol)-2,5-cyclohexadien-1-one (VI)

The yield depends on the initial hydroperoxide–phenol ratio (see text). Yellow needles from MeOH, m.p. 136–139° (decomp.). These yellow crystals turn green in a few minutes on exposure to light. Infrared spectrum: bands at 1 657, 1 630, and 980 cm^{-1}. There is also a strong hydrogen-bonded OH band at about

[4]*The absence of the doublet is not simply due to the presence of an aryloxy group in the ortho position, since the 2,5-di-t-butyl-4-methoxyphenol trimer has the usual type of spectrum with bands at 1 663 and 1 677 cm⁻¹.*

Can. J. Chem. Downloaded from www.nrcresearchpress.com by 210.87.254.6 on 09/05/12
For personal use only.

3 230 cm^{-1} and a much weaker hydrogen-bonded band at about 3 500 cm^{-1}. In CCl_4 the bands are at 3 495,[5] 3 224, 1 658, 1 635, and 970 cm^{-1}. The ratio of the intensities of the two OH bands in CCl_4 is unaffected by a change in the concentration of VI from 0.005 to 0.025 *M*. Both bands therefore involve intramolecular hydrogen bonds. Ultraviolet spectrum: shoulder at ~365 mμ, maximum at 270 and 230 mμ. Nuclear magnetic resonance spectrum: *t*-butyl groups at 1.07 (1), 1.29 (3), and 1.39 (1), other protons at 6.82–8.09. This compound is identical in all respects with the product obtained by catalytically decomposing 0.1 g *t*-butyl hydroperoxide in 1 ml benzene containing 0.2 g V.

Anal. Calcd. for $C_{32}H_{50}O_4$: C, 77.06; H, 10.10; mol. wt. 498.7. Found: C, 77.07; H, 10.18; mol. wt. 500.

6,6′-Bis-2,4-di-t-butyl-4-t-butylperoxy-2,5-cyclohexadien-1-one (VII)

The yield depends on the initial hydroperoxide–phenol ratio. White needles from MeOH, m.p. 144–147° (decomp.). Infrared spectrum: bands at 1 662, 1 650, and 981 cm^{-1}. Ultraviolet spectrum: band maxima at 365 and 236 mμ. Nuclear magnetic resonance spectrum: *t*-butyl groups at 1.05 (1), 1.19 (1), and 1.23 (1), the only other protons are at 6.73. To judge by its X-ray powder pattern, this compound appears to exist in two polymorphic forms, depending on whether it is recrystallized from MeOH or benzene. It is identical with the product obtained in over 60% yield by causing V to react with an excess of *t*-butyl peroxy radicals.

Anal. Calcd. for $C_{36}H_{58}O_6$: C, 73.68; H, 9.96; mol. wt. 586.9. Found: C, 73.41; H, 9.84; mol. wt. 586.

6,6′-Bis-2-t-butyl-p-benzoquinone (VIII)

Formed from VII on the silica column (see text). Orange-yellow needles from carbon tetrachloride – hexane, m.p. 161–162°. Infrared spectrum: single band at 1 658 cm^{-1}. Ultraviolet spectrum: band maxima at 430 and 254 mμ. Nuclear magnetic resonance: *t*-butyl at 1.30, other protons at 6.50 and 6.58. This product is identical in all respects with that obtained by the chromic acid oxidation in acetone (6) of 6,6′-di-*t*-butyl-4,4′-dimethoxy-*o,o′*-biphenol. This dimethoxy biphenol was prepared by the oxidative coupling of 2-*t*-butyl-4-methoxyphenol with silver oxide in ether. The resultant deep purple solution was reduced with sodium iodide in acetic acid. Recrystallization from benzene gave white needles, m.p. 232° (lit. m.p. 228° (4)). To a solution of 0.1 g of this biphenol in 5 ml acetone was quickly added 1.0 ml chromic acid prepared according to Bowden *et al.* (6). The addition of excess water after 1 min precipitated fine yellow needles, which were extracted with ether, washed with 1% sodium bicarbonate solution, and dried over magnesium sulfate. Filtration and evaporation gave 70 mg of yellow crystals, m.p. 149–160°, which did not contain any of the starting material. Recrystallization fron carbon tetrachloride – hexane gave 42 mg of orange needles of VIII, m.p. 161–162 °C. Compound VIII was also prepared from the dimethoxy biphenol by oxidation with nitric acid (cf. ref. 7). A sample was purified by vacuum sublimation for analysis.

Anal. Calcd. for $C_{20}H_{22}O_4$: C, 73.60; H, 6.79; mol. wt. 326.4. Found: C, 73.26; H, 7.08; mol. wt. 324.

2,2′,4,4′-Tetra-t-butyl-o,o′-diphenoquinone (IX)

The deep purple color of an *o,o′*-diphenoquinone (4, 5) is produced in a very short time when 0.5 g V (or 2,4-di-*t*-butylphenol) are mixed, with shaking, with 0.3 g Ag_2O in 20 ml absolute ether containing 1 g of anhydrous Na_2SO_4. The color is fairly stable in ether or benzene but is rapidly destroyed by adding methanol or ethanol. This purple color is only transiently observed when 2,4-di-*t*-butylphenol is oxidized with $K_3Fe(CN)_6$ by the method of Müller *et al.* (5). We did not attempt to isolate IX.

The Spirocyclic Quinolide Ether (X)

The deep purple solution of IX was filtered, a few drops of MeOH was added to effect the interconversion of IX into X, and the solvents were removed under vacuum. Recrystallization from MeOH gave yellow crystals, m.p. 154.0–155.5° (lit. m.p. 152–154° (5)). Infrared spectrum: relatively weak bands at 1 656, 1 638, and 1 607 cm^{-1}. Ultraviolet spectrum: shoulder at 310 mμ, maximum at 275 mμ, and the absorption increases from 260 to 220 mμ without any maximum. Nuclear magnetic resonance spectrum: four *t*-butyl groups of equal intensity at 1.19, 1.25, 1.34, and 1.46, other protons at 5.39–7.03. These data support structure X, which was originally proposed by Müller *et al.* (5).

2,4-Di-t-butyl-4-t-butylperoxy-6-(3,5-di-t-butyl-3-t-butylperoxy-4,6-cyclohexadien-2-one)-2,5-cyclohexadienone (XI)

A very minor product. White crystals from MeOH, m.p. 123.0–123.5°. Infrared spectrum: bands at 1 700 and 965 cm^{-1}. Ultraviolet spectrum: an increase in absorption from 400 to 350 mμ; the absorption then remains constant to 325 mμ, after which it rises to a maximum at 296 mμ. This is followed by a strong increase in the absorption with shoulders at ~240 and ~220 mμ. Nuclear magnetic resonance spectrum: six *t*-butyl groups at 1.00, 1.08, 1.18, 1.20, 1.24, and 1.32, other protons at 5.64 and 7.25.

Anal. Calcd. for $C_{36}H_{58}O_6$: C, 73.68; H, 9.96; mol. wt. 586.9. Found: C, 73.50; H, 9.27; mol. wt. 587.

[5]*This frequency is too low to represent a "free" phenolic hydroxyl group in* CCl_4 *(18), which suggests that it is bonded to the π electrons of the cyclohexadienone ring (see ref. 19). The* OH *stretching fundamental in V is also at about this frequency (i.e. 3 527 cm⁻¹). This suggests that each of the* OH *groups in V is hydrogen bonded to the π electrons of the opposite aromatic ring. The main* OH *band in VI at 3 224 cm⁻¹ must correspond to a hydrogen bond with the quinonoid oxygen.*

Can. J. Chem. Downloaded from www.nrcresearchpress.com by 210.87.254.6 on 09/05/12
For personal use only.

2,4-Di-t-butyl-4-t-butylperoxy-6-(2,4-di-t-butylphenoxy)-2,5-cyclohexadien-1-one (XIIIb)

One of the most important products of the reaction (~20%). White needles from MeOH, m.p. 161–164° (decomp.). Infrared spectrum: bands at 1 665 and 993 cm^{-1}. Ultraviolet spectrum: maxima at 289 and 242 mμ, shoulders at 382 and 365 mμ. Nuclear magnetic resonance spectrum: five *t*-butyl groups at 1.05, 1.10, 1.28, 1.36, and 1.46, other protons at 6.58, 7.18, and 7.98.

Anal. Calcd. for $C_{32}H_{50}O_4$: C, 77.06; H, 10.10; mol. wt. 498.7. Found: C, 77.01; H, 10.05; mol. wt. 501.

2-t-Butyl-6-(2,4-di-t-butylphenoxy)-p-benzoquinone (XIV)

A very minor product produced by the decomposition of XIII on the silica column. It is also formed by the thermal decomposition of XIII. Yellow needles (which can be sublimed under vacuum) from MeOH, m.p. 181–183°. Infrared spectrum:[6] bands at 1 679 and 1 669 cm^{-1}. There are also strong bands at 1 584 and 1 145 cm^{-1}. The last band may be connected specifically with the 2,6-disubstituted-*p*-benzoquinone structure, since VIII and 2,6-di-*t*-butyl- and 2,6-dimethyl-*p*-benzoquinone have strong bands at 1 161, 1 160, and 1 185 cm^{-1}, respectively. Ultraviolet spectrum: maxima at 380, 287, and 240 mμ, and shoulders at 262 and 247 mμ. Nuclear magnetic resonance spectrum: three *t*-butyl groups at 1.38, 1.42, and 1.54.

Anal. Calcd. for $C_{24}H_{32}O_3$: C, 78.91; H, 8.48; mol. wt. 380.5. Found: C, 78.77; H, 8.22; mol. wt. 370.

ACKNOWLEDGMENTS

The authors thank Mr. D. A. Lindsay for his help with the t.l.c. and column chromatographic separation of the products. Our thanks are also due to Dr. S. K. Brownstein for the nuclear magnetic resonance spectra, to Mr. R. Ironside for the infrared spectra, to Mr. G. R. Duval for the ultraviolet spectra, to Dr. L. D. Calvert for numerous X-ray powder photographs, and to Mr. A. E. Castagne and Mr. J. R. H. Seguin for the carbon and hydrogen analyses. We are also grateful to Dr. I. E. Puddington for his continued interest in, and encouragement of, this work.

REFERENCES

1. E. C. HORSWILL and K. U. INGOLD. Can. J. Chem. This issue.
2. J. A. HOWARD and K. U. INGOLD. Can. J. Chem. **42**, 1044 (1964).
3. J. H. FOOKES, E. L. PELTON, and M. W. LONG, JR. U.S. Patent No. 2,885,444 (May 1959).
4. J. BALTES and F. Volbert. Fette Seifen Anstrichmittel, **57**, 660 (1955).
5. E. MÜLLER, R. MAYER, B. NARR, A. RIEKER, and K. SCHEFFLER. Ann. **645**, 25 (1961).
6. K. BOWDEN, I. M. HEILBRON, E. R. H. JONES, and B. C. L. WEEDON. J. Chem. Soc. 39 (1946).
7. E. MÜLLER and K. LEY. Chem. Ber **88**, 601 (1955).
8. R. G. R. BACON, S. C. RENNISON, and O. J. STEWART. Proc. Chem. Soc. 409 (1964).
9. A. F. BICKEL and E. C. KOOYMAN. J. Chem. Soc. 3211 (1953).
10. H. S. BLANCHARD. J. Org. Chem. **25**, 264 (1960).
11. C. D. COOK and R. C. WOODWORTH. J. Am. Chem. Soc. **75**, 6242 (1953).
12. G. M. COPPINGER. Private communication.
13. E. MÜLLER, H. KAUFMANN, and A. RIEKER. Ann. **671**, 61 (1964).
14. T. W. CAMPBELL and G. M. COPPINGER. J. Am. Chem. Soc. **74**, 1469 (1952).
15. G. M. COPPINGER. J. Am. Chem. Soc. **79**, 2758 (1957).
16. E. MÜLLER, K. LEY, and G. SCHELTE. Chem. Ber. **90**, 2660 (1957).
17. E. MÜLLER, A. RIEKER, and A. SCHICK. Ann. **673**, 40 (1964).
18. K. U. INGOLD. Can. J. Chem. **38**, 1092 (1960).
19. A. W. BAKER and A. T. SHULGIN. J. Am. Chem. Soc. **80**, 5358 (1959).

[6]*The spectrum is not similar to that of 2,5-di-t-butyl-6-(2,5-di-t-butyl-4-methoxyphenoxy)-p-benzoquinone (13). We are indebted to Dr. Rieker for a copy of the infrared spectrum of this compound.*

Can. J. Chem. Downloaded from www.nrcresearchpress.com by 210.87.254.6 on 09/05/12
For personal use only.

Can. J. Chem. Downloaded from www.nrcresearchpress.com by 210.87.254.40 on 09/05/12
For personal use only.

STEREOCHEMICAL STUDIES

V. REARRANGEMENTS ACCOMPANYING ATTEMPTS TO EPIMERIZE 4-OXA-3-OXO-5α-CHOLESTANE AND 4-OXA-3-OXO-5β-CHOLESTANE BY BREWSTER AND KUCERA'S METHOD

W. H. LUNN[1] AND J. T. EDWARD
Department of Chemistry, McGill University, Montreal, Quebec

AND

SEYMOUR MEYERSON
Research and Development Department, American Oil Company, Whiting, Indiana

Received August 5, 1965

ABSTRACT

Epimerization of 4-oxa-3-oxo-5α-cholestane by Brewster and Kucera's method gave only a 23% yield of the 5β-lactone; several other compounds were formed, apparently via skeletal rearrangement during hydrolysis of the tosylate. The attempted epimerization of 4-oxa-3-oxo-5β-cholestane gave mainly unsaturated acids, but no 5α-lactone (a small amount of skeletal rearrangement also occurred). Both epimers undergo rearrangement to γ-lactones when treated with trifluoroacetic acid.

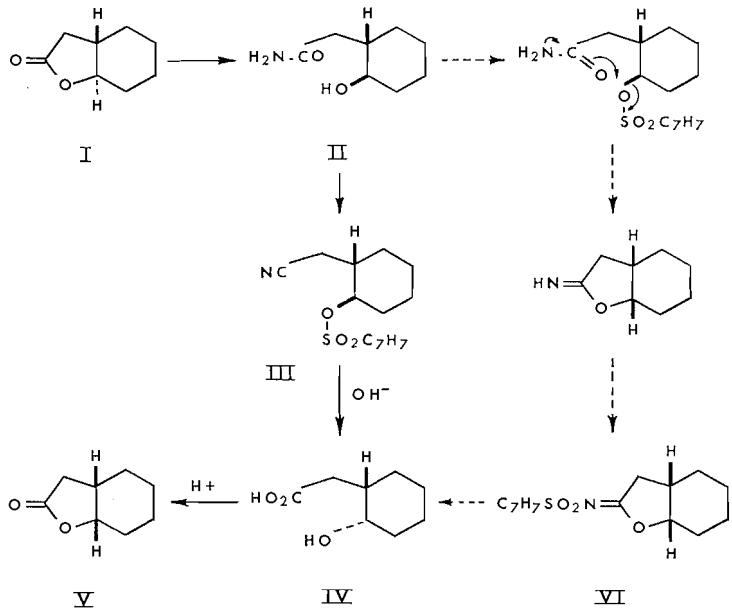
Mass spectra, used in conjunction with infrared and nuclear magnetic resonance spectra and other data to make structural assignments, were found to be highly sensitive to certain structural features. In particular, they can usually distinguish sharply between molecules that contain a pendant ring structure and those that do not.

Brewster and Kucera (1) epimerized the *trans*-fused lactone I, as shown in Reaction Scheme 1, by converting it with ammonia into the hydroxyamide II, transforming II with *p*-toluenesulfonyl (tosyl) chloride in pyridine into a compound having the molecular formula $C_{15}H_{19}NO_3S$, hydrolyzing this compound with aqueous sodium hydroxide to the hydroxyacid IV, and cyclizing IV with acid to the *cis*-fused lactone V. In accord with our own experience in applying this procedure to other lactones, as well as other evidence (2) that hydroxyamides react with tosyl chloride in pyridine to form nitriles, the intermediate $C_{15}H_{19}NO_3S$ is formulated here as the cyanotosylate III rather than VI, which was postulated (1) to arise via the steps shown by broken arrows. The cyanotosylate structure is supported by a nitrile band at 2 249 cm^{-1} in the infrared spectrum (3, p. 263).

In an attempt to obtain large quantities of the *cis* lactone X, which was required in another connection, we have applied Brewster and Kucera's epimerization procedure to the readily available *trans* lactone, 4-oxa-3-oxo-5α-cholestane VII (4, 5), as shown in Reaction Scheme 2. However, alkaline hydrolysis of the cyanotosylate IX gave a complex mixture from which the *cis* lactone X was obtained in only 23% yield. By contrast, Brewster and Kucera obtained relatively pure lactone V from the cyanotosylate III in 75% yield. It accordingly became of interest to identify other products of the hydrolysis of IX, in an attempt to discover the cause of the divergent behavior of the cyanotosylates III and IX. We also applied Brewster and Kucera's procedure to the isomeric *cis* lactone X (Reaction Scheme 3). The use of isomeric lactones in this procedure permitted us to discern the effect of differing stereochemistry in the hydrolysis of the cyanotosylates IX and XXV (Reaction Scheme 3).

Fractionation of the mixtures obtained by hydrolysis of the cyanotosylates proved to be a formidable task. In addition to adsorption chromatography, a technique that we term "split crystallization" proved to be highly useful. This consists of watching under a magnifying glass the shape of the crystals being formed, and filtering the mixture as

[1]*Holder of National Research Council Studentships, 1959–1961.*



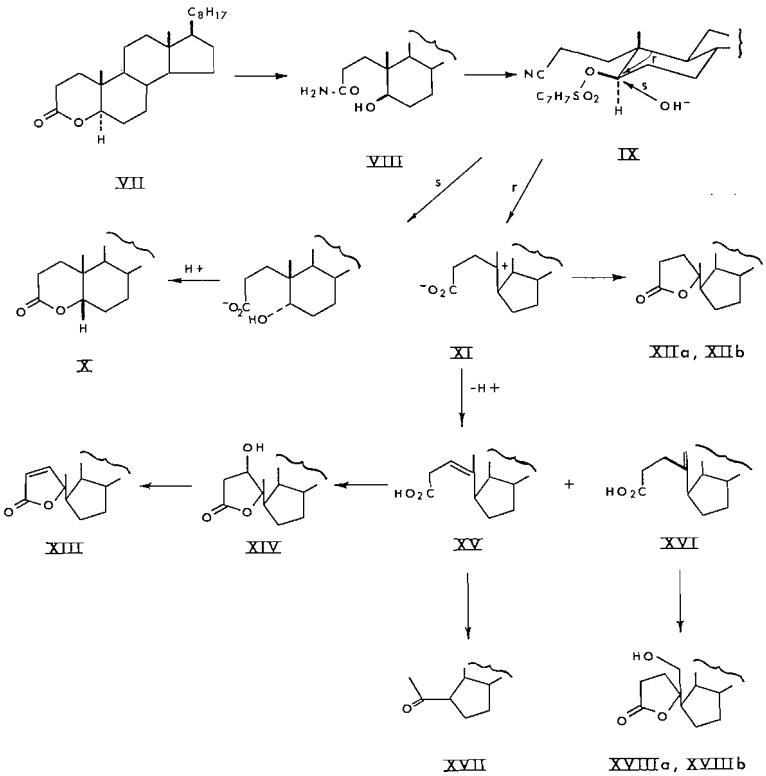
REACTION SCHEME 1.

soon as a second crystalline form appears, thereby indicating a second compound. Concentration of the filtrate often leads to preferential crystallization of the second compound, the mixture being filtered as soon as crystals of the first compound become visible. Further concentration of the filtrate leads to crystallization of one or the other of the two compounds; the various crops are combined on the basis of crystalline shape and recrystallized to complete purification. In many instances this technique proved to be more successful than chromatography. Thus reduction of 5-oxo-3,5-seco-A-norcholestan-3-oic acid with sodium borohydride gave a mixture from which the lactones VII and X were obtained in yields of 37% and 4.5% by crystallization and chromatography; split crystallization from ethanol raised the yields to 64% of VII (needles) and 17.5% of X (plates).

Products from Applying the Epimerization Procedure to 4-Oxa-3-Oxo-5α-cholestane

Fractionation of the mixture obtained from the hydrolysis of the cyanotosylate IX yielded, besides the δ-lactone X, two crystalline isomeric γ-lactones XII*a* and XII*b*, an oily mixture of unsaturated acids, and several intractable oily fractions. From the unsaturated acid fraction, the acid XVI was obtained in a crystalline form; evidence for the presence of the isomeric acid XV comes from the products XIII, XIV, and XVII obtained by various chemical treatments of the fraction, as described below. The structures postulated for the different products, shown in Reaction Scheme 2, rest mainly on spectral evidence which is described below and which in aggregate seems reasonably convincing. These structures indicate that hydrolysis of the cyanotosylate IX (reaction *s*) is accompanied by a competing solvolysis (reaction *r*) in which Wagner–Meerwein shift of the antiparallel 9–10 bond synchronous with the loss of tosylate ion gives the carbonium ion XI. Rearrangements of this stereoelectronic character are common in ring A of triterpenes, and lead to its contraction to a five-membered ring (6). In these cases, as well as in that now under consideration, the rearrangement is made possible by *gem*-dialkyl substitution of the carbon atom next to the developing carbonium ion, because the alkyl shift then gives a relatively stable tertiary carbonium ion. The cyanotosylate

Can. J. Chem. Downloaded from www.nrcresearchpress.com by 210.87.254.40 on 09/05/12
For personal use only.

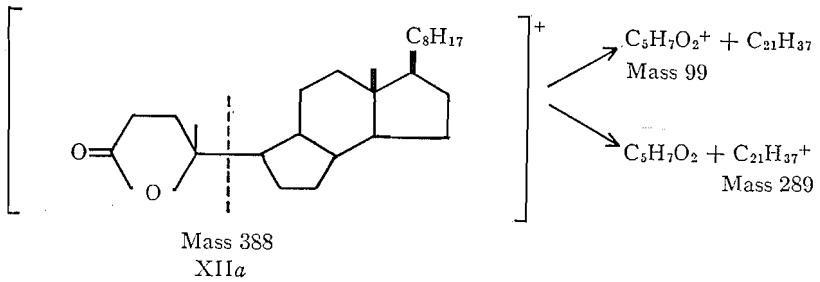


REACTION SCHEME 2.

III will have less tendency to undergo rearrangement, because this would provide a secondary carbonium ion. Hence, it would be expected to give a better yield of epimerized lactone.

γ-Lactones XIIa and XIIb

A crystalline product $C_{26}H_{44}O_2$, obtained in about 7% yield, appeared to be compound XII*a* for the following reasons. The infrared spectrum (ν_{max} 1 769 cm^{-1}; cf. ref. 3, p. 179) indicates a γ-lactone and, in contrast to X, the compound is extremely resistant to ring opening by hydroxide ion or ammonia, as would be expected for a *gem*-disubstituted γ-lactone (7). The pendant lactone structure is indicated by the mass spectrum of the compound, which shows the most intense peaks at masses 99, 287, and 289 (Table I). Those at masses 99 and 289 correspond to the complementary products from the expected bond cleavage in the parent ion of XII*a*:



Mass 388
XII*a*

Can. J. Chem. Downloaded from www.nrcresearchpress.com by 210.87.254.40 on 09/05/12
For personal use only.

Fission of the single bond joining the pendant lactone to the rest of the molecule should be a highly preferred process, both because the bond is β to an oxygen atom (8), and because it joins two branched carbon atoms (8*d*, 9). When the lactone group is not joined by a single bond to the rest of the molecule, as in the isomeric spiro-γ-lactone XXVI*a*, the genesis of which is discussed later (Reaction Scheme 3), the intense peaks at masses 99, 287, and 289 are missing (Table I).

TABLE I

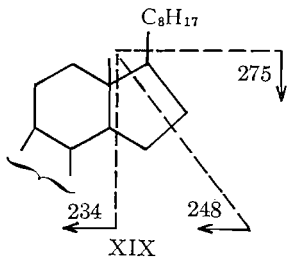
Partial mass spectra of lactones XII*a* and XXVI*a*

	Relative intensity*		
Mass	XII*a*	XXVI*a*	Loss†
388	26.0	100.0	(Parent ion)
373	7.3	13.2	CH_3
370	6.9	7.4	H_2O
331	0.4	9.2	C_3H_5O
289	34.0	0.8	$C_5H_7O_2$
287	64.6	1.3	$C_5H_9O_2$
275	15.0	25.6	C_8H_{17}
248	6.2	18.6	$C_8H_{17}CHCH_2$
234	9.8	42.0	$C_8H_{17}CHCH_2CH_2$
99	100.0	3.1	$C_{21}H_{37}$

*The scale of relative intensities was defined by assigning a value of 100.0 to the most intense peak of mass greater than 90 in each spectrum; this is also the strongest peak in the entire spectrum of XII*a*, XXVI*a*, XVIII*b*, and XIV, except for a peak of mass 43.

†Probable composition of neutral particle(s) lost from parent ion.

The other peaks in the mass spectrum are also consistent with the structure XII*a*. That at mass 287 corresponds to the loss of the pendant lactone group plus two hydrogen atoms. The mechanism of this reaction is not known; no evidence is available to pinpoint the source of the two extra atoms. Precedents for such double-hydrogen migration are known, although the most familiar ones, those of alkyl esters of oxygen acids (8*c*, 10), are not directly analogous to the present case. Peaks at masses 275, 248, and 234 correspond to characteristic cleavages of the cholestane skeleton leading to loss of C_8H_{17}, $C_8H_{17}CHCH_2$, and $C_8H_{17}CHCH_2CH_2$ from ring D (11):



XIX

Loss of C_3H_5O, as evidenced by the peak at mass 331 in the spectrum of XII*a*, occurs also in γ-valerolactone (12). The low intensity at mass 331 in the spectrum of XII*a* contrasts with that in the spectrum of XXVI*a*, and suggests that this reaction is too slow to compete effectively with other, more favored reactions in the former compound.

The nuclear magnetic resonance (n.m.r.) spectrum of $C_{26}H_{44}O_2$ confirms the structure of the lactone moiety of XII*a*. At high field it shows, as do all the other reaction products mentioned below, the spectrum characteristic of cholestane derivatives (13). The protons associated with the lactone moiety appear at lower field as multiplets centered at 7.45

Can. J. Chem. Downloaded from www.nrcresearchpress.com by 210.87.254.40 on 09/05/12
For personal use only.

and 8.00 τ, corresponding to the α- and β-protons, respectively; the areas under the peaks indicate two α- and two β-protons. For comparison, γ-butyrolactone shows peaks at 7.69 and 7.92 τ for α- and β-protons (14). The absence of any peaks below 7 τ is significant, because a proton at the γ-position of the lactone would give a signal at about 5.5 τ (15, spectrum No. 63). Evidently, the γ-position is disubstituted. One of the substituents must be a methyl group, because a sharp, unsplit peak (area: three protons) appears at 8.61 τ; the γ-methyl groups of 3,3,4,4-tetramethylbutyrolactone give a signal at 8.67 τ (15, spectrum No. 214). This is well below the field at which the signals from the methyl groups of cholestane are observed (13).

Concentration of the mother liquors from the crystallization of the lactone XII*a* yielded very small quantities of another compound $C_{26}H_{44}O_2$, having the probable structure XII*b* and differing from XII*a* only in the configuration at C-10. The infrared spectrum of this product above 1 400 cm^{-1} is superimposable on that of XII*a* (Fig. 1), and the n.m.r. spectrum is similar, with a sharp peak at 8.65 τ.

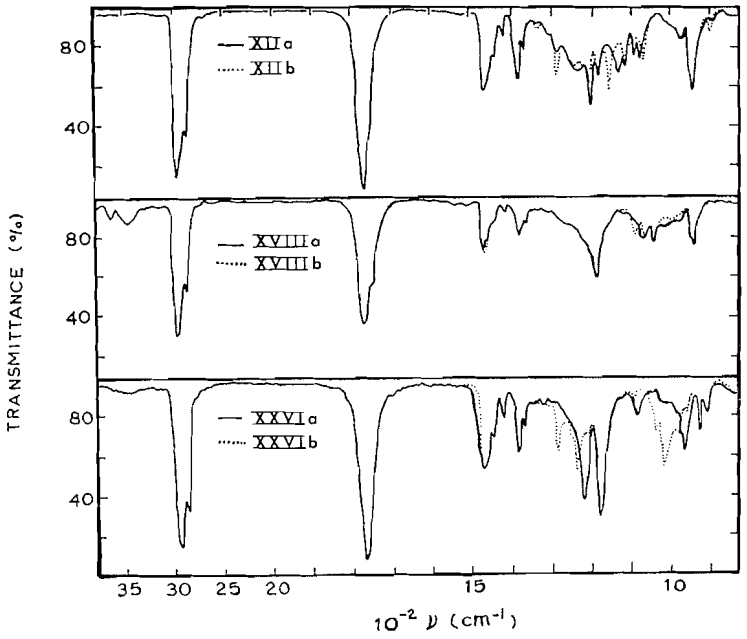


FIG. 1. Infrared spectra of some lactones (presumed to be epimeric).

Unsaturated Acids XV and XVI and Products Derived from Them

The crude mixture from the hydrolysis of IX contained acids (ν_{max} 1 710 cm^{-1}) (3, p. 162). A small quantity of crystalline acid $C_{26}H_{44}O_2$, for which the structure XVI is suggested, was obtained after considerable manipulation. The terminal olefinic methylene of this structure was indicated by infrared peaks at 3 078, 1 638, and 885 cm^{-1} (3, p. 34), and its presence in the unsaturated acid fraction was confirmed by oxidizing a portion of the fraction with osmium tetroxide and sodium metaperiodate in aqueous dioxane (16) and identifying formaldehyde among the oxidation products.

Because no other unsaturated acid could be isolated in a crystalline state from this fraction, a portion of the fraction was oxidized with osmium tetroxide in the hope of obtaining more crystalline products. Chromatography of this reaction mixture on alumina

Can. J. Chem. Downloaded from www.nrcresearchpress.com by 210.87.254.40 on 09/05/12
For personal use only.

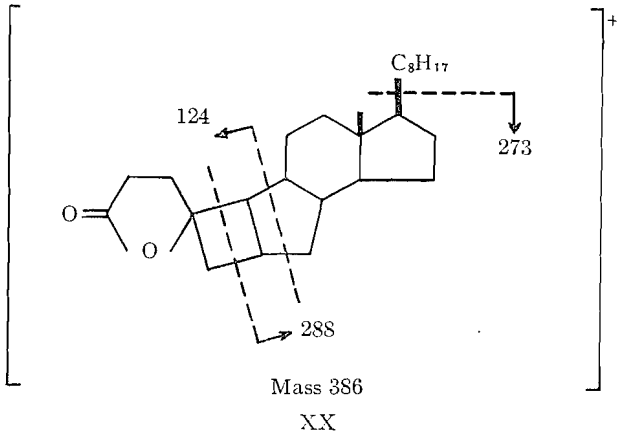
gave two hydroxylactones having the properties to be expected of the isomeric compounds XVIII*a* and XVIII*b*, produced by the two possible approaches of the oxidizing agent to the double bond of XVI. The infrared spectra of the two compounds are closely similar (Fig. 1) and show asymmetric peaks at 1 771 cm^{-1} (cf. ref. 17). The mass spectra (Table II) are also remarkably similar. In a manner characteristic of primary alcohols, which lose H_2O readily (18), the compounds give essentially no parent peaks, but show prominent

TABLE II

Partial mass spectra of hydroxylactones XVIII*a* and XVIII*b*

	Relative intensity		
Mass	XVIII*a*	XVIII*b*	Loss
404	0	0.02	(Parent ion)
386	59.5	59.4	H_2O
371	18.0	12.0	H_2O and CH_3
358	5.1	5.1	H_2O, and CO or CH_2CH_2
288	5.5	8.7	H_2O and $C_5H_6O_2$
273	31.2	31.4	H_2O and C_8H_{17}
124	100.0	100.0	H_2O and $C_{19}H_{34}$

peaks at the parent mass less 18. In *n*-hexanol, 91% of the hydrogen lost with hydroxyl as water comes from C-4, and considerable evidence indicates that 1,4-elimination is general in primary alcohols (19). In the present case, such elimination might plausibly give rise to the ion XX which can, by further fragmentation as shown, account for the peaks of masses 124, 273, and 288.



XX

As would be expected for the formulae XVIII*a* and XVIII*b*, the n.m.r. spectra of the lactones lack the peak at about 8.6 τ caused by a γ-methyl group on the lactone ring; instead, low-field peaks appear at 6.33 τ for XVIII*a* and at 6.34 τ (two protons) for XVIII*b*. These values are slightly lower than the usual value of 6.44 τ for the methylene protons of $—CH_2OH$ (20), but are reasonable when the deshielding effect that is to be expected from the lactone ring is taken into account.

A third compound obtained from the osmium tetroxide oxidation of the unsaturated acid fraction is most plausibly formulated as the hydroxylactone XIV. The infrared spectrum shows hydroxyl (3 620, 3 459 (broad) cm^{-1}) (3, p. 96) and carbonyl (1 776 cm^{-1}, with an inflection at 1 758 cm^{-1}) (3, p. 179) peaks. The mass spectrum (Table III) shows

Can. J. Chem. Downloaded from www.nrcresearchpress.com by 210.87.254.40 on 09/05/12
For personal use only.

TABLE III

Partial mass spectrum of hydroxylactone XIV

Mass	Relative intensity	Loss
404	0.5	(Parent ion)
386	52.8	H_2O
371	5.0	H_2O and CH_3
360	3.4	CO_2 or, more likely, CH_2CHOH
289	100.0	$C_5H_7O_3$
288	43.7	$C_5H_8O_3$
232	17.6	H_2O and $C_8H_{17}CHCH_2CH_2$
175	24.4	$C_5H_8O_3$ and C_8H_{17}
149	73.5	$C_5H_7O_3$ and $C_8H_{17}CHCH_2$
135	62.4	$C_5H_7O_3$ and $C_8H_{17}CHCH_2CH_2$
134	43.9	$C_5H_8O_3$ and $C_8H_{17}CHCH_2CH_2$

a small peak for the parent ion and a strong peak at mass 386 for the parent ion less H_2O, as expected for a secondary alcohol (18). The most intense peak, at mass 289, corresponds to cleavage of the pendant hydroxylactone group ($C_5H_7O_3$) from the parent ion; the peak at mass 288 arises presumably by the same cleavage accompanied by migration of a hydrogen atom. The peak at mass 360 probably arises by loss of CH_2CHOH from the lactone ring. Other prominent peaks can be accounted for by further characteristic cleavages at ring D (as shown in XIX) of the ions of masses 288, 289, and 386.

In agreement with the structure XIV, the n.m.r. spectrum of this compound shows a sharp unsplit peak at 8.72 τ caused by a γ-methyl group on the lactone ring (cf. structure XII*a* above). A weaker, more diffuse band centered at 5.29 τ (one proton) may be attributed to the single β-hydrogen of the lactone (20). Again, the n.m.r. spectrum indicates that the lactone contains no γ-hydrogen.

A fourth compound isolated after the oxidation of fraction A may be the α,β-unsaturated γ-lactone XIII, produced by dehydration of XIV or of a more reactive isomer. Such dehydration should take place easily (21). The infrared (ν_{max} 1 758 cm^{-1}) (17) and ultraviolet (λ_{max} 206 mμ, ϵ_{max} ~11 000, in ethanol) (22) spectra indicate an α,β-unsaturated γ-lactone, and the most abundant ion in the mass spectrum (Table IV), which occurs at mass 97, almost certainly consists of the γ-methyl-α,β-unsaturated lactone moiety ($C_5H_5O_2$). Loss of this group as a radical from the parent ion accounts for the complementary ion of mass 289; other prominent peaks can be accounted for by further breakdown of this ion at ring D.

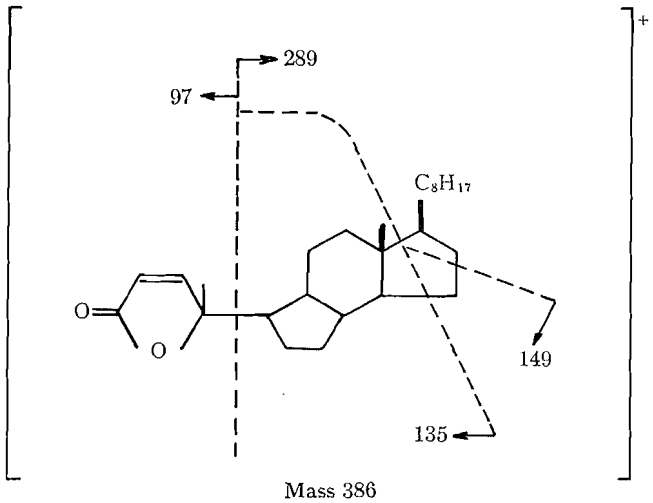
TABLE IV

Partial mass spectrum of unsaturated lactone XIII

Mass	Relative intensity	Loss
386	60	(Parent ion)
371	58	CH_3
289	87	$C_5H_5O_2$
149	85	$C_5H_5O_2$ and $C_8H_{17}CHCH_2$
135	62	$C_5H_5O_2$ and $C_8H_{17}CHCH_2CH_2$
97	100*	$C_{21}H_{37}$

*To facilitate handling the very small quantity of lactone available, it was introduced into the spectrometer in hexane solution. The peak at mass 97 was the strongest peak in the spectrum free of interference from hexane.

Can. J. Chem. Downloaded from www.nrcresearchpress.com by 210.87.254.40 on 09/05/12
For personal use only.



Mass 386
XIII

The oxidation products XIII and XIV point to the presence of XV in the unsaturated acid fraction. Further evidence for this acid was obtained by oxidizing another portion of the fraction with the Lemieux–Rudloff reagent (23). The mixture of carbonyl compounds thus formed gave two 2,4-dinitrophenylhydrazones whose analyses and ultraviolet (24) and n.m.r. spectra (25) were consonant with their being isomeric derivatives (possibly geometrical isomers) of the methyl ketone XVII.

Products from Applying the Epimerization Procedure to 4-Oxa-3-oxo-5β-cholestane

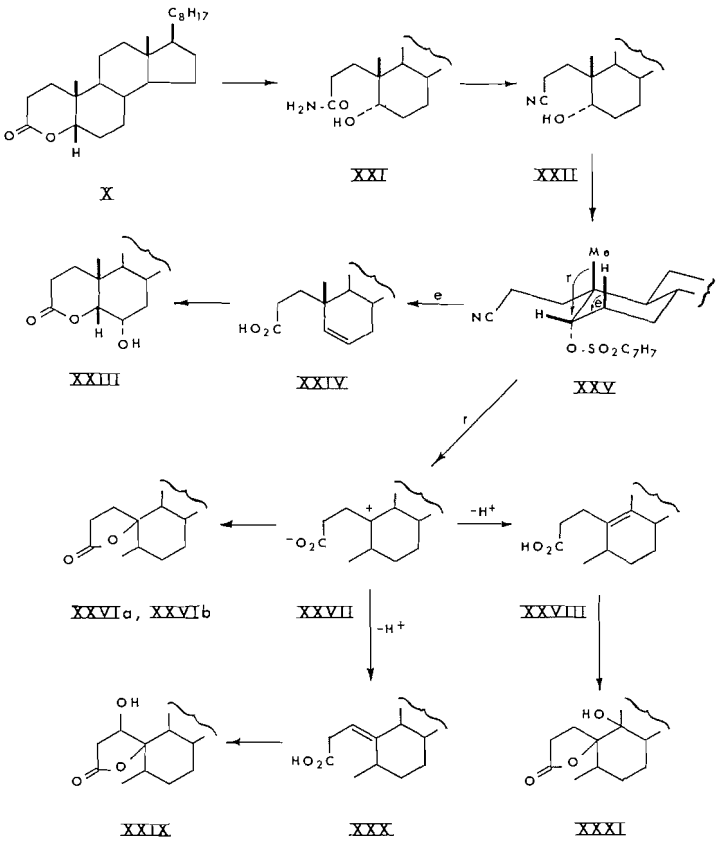
The results of applying the epimerization procedure to 4-oxa-3-oxo-5β-cholestane X are shown in Reaction Scheme 3. The hydroxyamide XXI (5) reacted with *p*-toluenesulfonyl chloride in pyridine to give the hydroxynitrile XXII. Under the same conditions, the equatorial hydroxyl group of VIII is tosylated, but evidently the axial hydroxyl of XXI is less reactive. However, at a higher temperature we were able to tosylate this hydroxyl group and obtain the cyanotosylate XXV.

Alkaline hydrolysis of this compound under the conditions specified by Brewster and Kucera gave a gum, which was separated into an unsaturated acid fraction and minute quantities of two crystalline compounds G and H, probably the isomers XXVI*a* and XXVI*b*. The unsaturated acids could not be obtained in a crystalline form, but appeared to consist chiefly of XXIV, with small amounts of XXVIII and XXX, as evidenced by the crystalline compounds XXIII, XXIX, and XXXI (the latter two formulations very tentative) obtained by oxidation of the mixture. The δ-lactone VII, which has a prominent peak at 1 740 cm^{-1} (5), could not be detected in the reaction mixture. A hydroxide ion approaching the top face of the cyanotosylate XXV is apparently prevented by the angular methyl group from attacking at C-5 and displacing the tosylate ion (as in reaction *s*, Reaction Scheme 2), and instead attacks the axial hydrogen at C-6 to give the elimination reaction *e*. The competing solvolysis to give the rearranged carbonium ion XXVII (reaction *r*), from which XXVI*a*, XXVI*b*, XXVIII, and XXX could arise, would be governed by the same stereoelectronic factors that govern the rearrangement IX → XI.

γ-Lactones XXVIa and XXVIb

The two crystalline products G and H were obtained in only minute amounts, but

Can. J. Chem. Downloaded from www.nrcresearchpress.com by 210.87.254.40 on 09/05/12
For personal use only.



REACTION SCHEME 3.

fortunately product H, $C_{26}H_{44}O_2$, was readily available by the acid-catalyzed rearrangement of X as described later. It appears to be a γ-lactone (ν_{max} 1 769 cm^{-1}), and has a n.m.r. spectrum similar in many respects to that of XII*a*. Thus, it shows multiplets at 7.43 τ (two protons) and 8.06 τ (two protons), which can be assigned to the α- and β-protons of a γ-lactone. These multiplets are symmetrical about their common center, the fine detail resembling that of A_2B_2 systems (e.g. β-propiolactone (26)) having J_{AB} and J_{AB}' equal. The absence of a proton from the γ-position is clear, because this would give an unsymmetrical A_2B_2C spectrum; confirmation comes from the absence of a peak at about 5.5 τ. The γ-position, hence, must be disubstituted and, because neither substituent is methyl (no sharp peak at about 8.6 τ), the spiro formulation XXVI*a* is suggested.

This spiro formulation is supported by the mass spectrum (Table I), which gives no evidence for a pendant lactone ring. The parent ion makes up a far larger part of the total ion yield than does that of XII*a*, and relatively strong peaks correspond to cleavages in ring D (cf. structure XIX) and loss of C_3H_5O (12); these processes are overshadowed in XII*a* by rupture of the pendant bond.

The structure XXVI*b*, epimeric at the spiro position, is tentatively suggested for product G on the basis of the very close similarity of its infrared spectrum to that of product H (Fig. 1). It was obtained in too small an amount (4 mg) for more extensive investigation.

Can. J. Chem. Downloaded from www.nrcresearchpress.com by 210.87.254.40 on 09/05/12
For personal use only.

Unsaturated Acids XXIII, XXVIII, and XXX and Products Derived from Them

The unsaturated acids that were the chief products from the solvolysis of the tosylate XXV could not be obtained in a crystalline form. Consequently, the fraction containing them was oxidized with osmium tetroxide. The major product from this reaction was a hydroxy-δ-lactone (ν_{max} 3 596, 1 742 cm^{-1}), for which the structure XXIII was suggested by the close similarity of the infrared spectrum below 1 060 cm^{-1} to that of the lactone X. The mass spectrum of the hydroxylactone (Table V) shows a weak peak for the parent

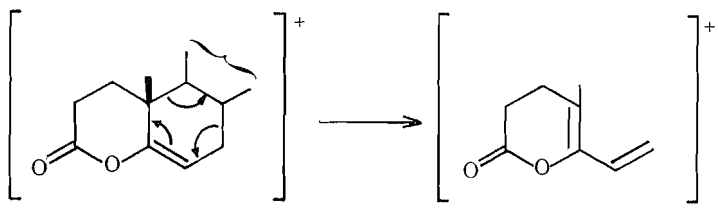
TABLE V

Partial mass spectrum of hydroxylactone XXIII

Mass	Relative intensity	Loss
404	0.8	(Parent ion)
389	0.6	CH_3
386	15.7	H_2O
371	100.0*	H_2O and CH_3
331	1.5	$C_3H_5O_2$
315	2.5	
291	0.4	C_8H_{17}
273	3.1	H_2O and C_8H_{17}
264	0.1	$C_8H_{17}CHCH_2$
248	1.2	
247	4.5	
246	1.4	
138	94.2	H_2O and $C_{18}H_{32}$

*Strongest peak in the entire spectrum.

ion and a strong one corresponding to loss of H_2O, as expected for a secondary alcohol. The intense peak at mass 138 suggests a reverse Diels–Alder reaction (27) via an intermediate that arises by primary loss of H_2O, either by 1,2-elimination or by 1,4-elimination followed by isomerization (19*a*). Other features of the mass spectrum seem to be consistent with the structure XXIII.



Mass 138

Osmium tetroxide would be expected to attack the unsaturated acid XXIV on the α-face (28, p. 14). An α-configuration for a 6-hydroxyl group of the hydroxylactone is indicated by its molecular rotation (−35°), as compared with that of the parent lactone X (+72°); the shift caused by introducing the hydroxyl group (−107°) is close to that expected for a 6α-hydroxyl group in the coprostane series (−100°) (28, p. 179).

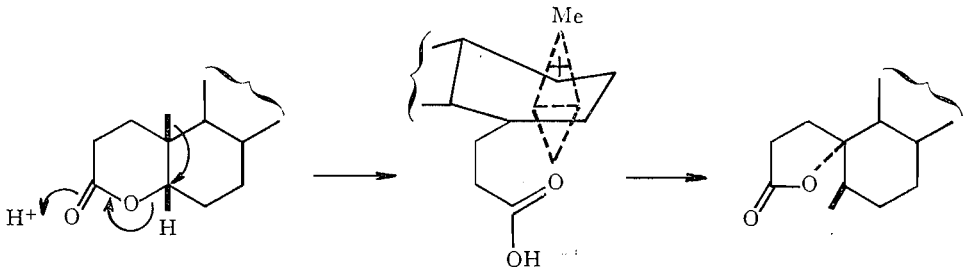
Besides the hydroxy-δ-lactone XXIII, minute amounts of hydroxy-γ-lactones are formed by oxidation of the unsaturated acid fraction. Tentative structures XXIX and XXXI may be assigned to these compounds on the basis of their infrared spectra (ν_{max} 3 617, 3 440, 1 772 cm^{-1}; and 3 580, 1 772 cm^{-1}, respectively) and their possible genesis as shown in Reaction Scheme 3. The spectrum of the second lactone showed no bonded

Can. J. Chem. Downloaded from www.nrcresearchpress.com by 210.87.254.40 on 09/05/12
For personal use only.

hydroxyl peak, unlike the spectra of all of the other hydroxylactones encountered in this study. This indicates a highly hindered hydroxyl group, as in XXXI.

Rearrangement of 4-Oxa-3-oxo-5α-cholestane and 4-Oxa-3-oxo-5β-cholestane in Acid

The low yields of the lactones G and H from alkaline hydrolysis of XXV because of the competing elimination reaction led us to attempt to prepare the compounds by treatment of the lactone X with acid. With hot formic (4 days) or trifluoroacetic acid (10 h), lactone H was obtained in 60–70% yield, together with starting material and small amounts of uncrystallizable products, which were indicated by their infrared spectra to be unsaturated acids. Selective formation of the single epimer H suggests that, in this reaction, the carbonium ion is the bridged ion XXXII, and that the stereochemistry of lactone H is as shown in XXVI*a*.



X XXXII XXVI*a*

The *trans*-δ-lactone VII was more stable in acid. After it had been heated under reflux for 13 days in trifluoroacetic acid, it was converted into a complex mixture, from which two uncrystallizable gums (each showing a single strong infrared absorption band in the carbonyl region) were separated by protracted chromatography. The first gum had an infrared spectrum very similar to those of XII*a* and XII*b*, and may possibly be a mixture of these lactones and of others epimeric at C-5. The second gum was yellow, and had an ultraviolet absorption suggesting an unsaturated ketone (28, p. 19); such compounds have been reported from the treatment of δ-lactones with acid (29 and references therein).

EXPERIMENTAL

All melting points are corrected. Unless otherwise stated, optical rotations were measured in chloroform solution, infrared spectra in carbon tetrachloride, and nuclear magnetic resonance spectra in chloroform or deuteriochloroform. Mass spectra were measured with 70 V electrons on a modified (30) Consolidated model 21-103*c* instrument, with the sample-introduction system heated to 250°. Woelm alumina was used for chromatography. Proportions indicated for solvent mixtures are by volume.

trans-1-Cyanomethyl-2-tosyloxycyclohexane (III)

This compound, m.p. 84.6–85.6°, was prepared according to the method described by Brewster and Kucera (1).

Anal. Calcd. for $C_{15}H_{19}NO_3S$: C, 61.40; H, 6.53; N, 4.77; S, 10.93. Found: C, 61.62; H, 6.45; N, 4.97; S, 11.04.

4-Oxa-3-oxo-5α-cholestane (VII) and 4-Oxa-3-oxo-5β-cholestane (X)

5-Oxo-3,5-seco-A-norcholestan-3-oic acid (40 g) (31) was reduced with sodium borohydride (5). The reaction products were split crystallized from 95% ethanol, successive crops being obtained by concentration of the solution until finally only an oil was obtained. The various crops were combined according to crystal shape and recrystallized three times to give pure 5α-lactone (VII) (24.5 g; 64% yield) and 5β-lactone (X) (6.73 g; 17.5%).

5β-Tosyloxy-3,5-seco-A-norcholestan-3-nitrile (IX)

4-Oxa-3-oxo-5α-cholestane (12.5 g) was converted into the corresponding hydroxyamide VIII (5). The crude dried product was dissolved together with vacuum-dried, recrystallized *p*-toluenesulfonyl chloride

Can. J. Chem. Downloaded from www.nrcresearchpress.com by 210.87.254.40 on 09/05/12
For personal use only.

(60 g) in dry pyridine (900 ml), and left in a stoppered flask for 24 h at room temperature. Slow addition of water, with stirring, and cooling gave a crystalline precipitate which was collected by filtration, washed with water until it was pyridine-free, dried under vacuum, and recrystallized from 95% ethanol to give white needles of cyanotosylate IX (13.65 g), m.p. 165.2–166°. Concentration of the mother liquors provided a second crop which, after being recrystallized twice (0.64 g), melted at 165–166°. Further concentration of the resultant mother liquors yielded the lactone VII (0.45 g; 4%), m.p. 114–115.2°. The total yield of the cyanotosylate IX amounted to 82%.

Recrystallization of the cyanotosylate, $[\alpha]_D^{26}$ +1° (*c*, 2.98), m.p. 165.2–166°, did not raise its melting point. Infrared: ν_{max} 2 250 (w) cm^{-1}.

Anal. Calcd. for $C_{33}H_{51}NO_3S$: C, 73.13; H, 9.51; N, 2.58; S, 5.92. Found: C, 73.08; H, 9.48; N, 2.62; S, 5.79.

In a previous pilot experiment the cyanotosylate was crystallized in the form of plates, m.p. 156.7–157.1°, whose infrared spectrum was identical with that of the material melting at 165.2–166°.

5α-Hydroxy-3,5-seco-A-norcholestan-3-nitrile (XXII)

Similar treatment of crude 5α-hydroxy-3,5-seco-A-norcholestan-3-amide (XXI) (5), prepared from 4-oxa-3-oxo-5β-cholestane (X) (11.54 g), with *p*-toluenesulfonyl chloride (58 g) in dry pyridine (950 ml) for 24 h gave a solid which was recrystallized three times from aqueous ethanol. Colorless plates of 5α-hydroxy-3,5-seco-A-norcholestan-3-nitrile (XXII) (7.83 g) were obtained; m.p. 153–153.7°; $[\alpha]_D^{26}$ +45° (*c*, 2.02); ν_{max} 3 665, 2 254 cm^{-1}.

Anal. Calcd. for $C_{26}H_{45}NO$: C, 80.56; H, 11.70; N, 3.61. Found: C, 80.30; H, 11.67; N, 3.82.

Concentration of the mother liquors gave a solid which, after three recrystallizations from aqueous ethanol, produced a second crop (0.44 g), m.p. 152.8–153.7°, thereby raising the yield to 72%. The final residue, after five recrystallizations from aqueous ethanol, gave 4-oxa-3-oxo-5β-cholestane (X) (0.24 g), m.p. 107.2–108°, equivalent to 2.1% of the starting material.

5α-Tosyloxy-3,5-seco-A-norcholestan-3-nitrile (XXV)

A solution of the 2-cyano-5α-hydroxy compound (XXII) (8.23 g) and vacuum-dried, recrystallized *p*-toluenesulfonyl chloride (47 g) in dry pyridine (470 ml) was kept at 67–71°. Infrared examination of the solid that was precipitated by dilution of small samples with water at 6 h intervals showed that the concentration of the tosyloxy compound reached a maximum in 96–102 h. After 102 h a large volume of water was slowly added to the reaction mixture, with stirring, the temperature being maintained below 5° by external cooling. The mixture was extracted with ether, and the ether extract was washed thoroughly with water and with saturated sodium chloride solution and then dried over magnesium sulfate. Evaporation of the extract to dryness at reduced pressure yielded a semicrystalline mass (9.48 g), which was chromatographed on alumina (285 g, 10% water). Evaporation of the fractions eluted with hexane gave an oil (3.92 g), which was proved by its infrared spectrum (ν_{max} 3 010 (w sh), 2 254 (w), and 1 650 (w) cm^{-1}) to be an unsaturated nitrile. Benzene–ether (9:1) then eluted a gum (4.55 g), which was crystallized three times from methanol–ether to give crystals of 5α-tosyloxy-3,5-seco-A-norcholestane-3-nitrile (XXV) (1.67 g), m.p. 91.3–92.8°, $[\alpha]_D^{29}$ +44° (*c*, 3.06), ν_{max} 2 247 cm^{-1}.

Anal. Calcd. for $C_{33}H_{51}NO_3S$: C, 73.13; H, 9.51; N, 2.58; S, 5.92. Found: C, 73.02; H, 9.58; N, 2.64; S, 5.80.

Concentration of the mother liquors at reduced pressure gave a solid which, after four crystallizations from methanol–ether, yielded a second crop (0.95 g), m.p. 92–92.6°.

The benzene–ether (8:1) eluates (0.96 g), after two recrystallizations from aqueous ethanol, gave starting material (0.75 g), m.p. 153–153.7°. A further crop (0.1 g), m.p. 152.8–153.6°, was obtained when the mother liquors were concentrated and the solid that was obtained was recrystallized three times from aqueous ethanol. The yield of cyanotosylate XXV was 22.5%, and the recovery of starting material was 10%.

Hydrolysis of 5β-Tosyloxy-3,5-seco-A-norcholestan-3-nitrile (IX)

The tosyloxy compound (14.2 g) was heated under reflux in a solution of sodium hydroxide (225 g) in 83% aqueous ethanol (2.8l) for 9 h. The tosylate had completely dissolved after 1 h. The bulk of the ethanol was removed at reduced pressure, and the mixture was acidified with cooling and extracted with ether. The ether extract was washed with water until the washings were neutral to litmus, washed with saturated sodium chloride solution, dried over magnesium sulfate, and evaporated to dryness at reduced pressure. The infrared spectrum of the resultant oil showed peaks at 1 770 (s), 1 735 (s), and 1 710 (s) cm^{-1}. The presence of a broad, rather weak band from 3 660 to 2 500 cm^{-1} indicated that the 1 710 cm^{-1} absorption could be attributed to carboxylic acids (3, p. 162); however, attempts to remove these acids from the ether solution by extraction with aqueous sodium hydroxide failed.

The hydrolysis products were dissolved in anhydrous ether (50 ml) and treated with an ether solution (50 ml) of diazomethane which had been obtained by the action of 50% potassium hydroxide (30 ml) on N-nitroso-N-methyl-N′-nitroguanidine (8 g). After 2 h, the excess diazomethane was destroyed with 0.1 *N* hydrochloric acid, and the ether solution was washed with water until it was acid free and then with saturated sodium chloride solution, dried over magnesium sulfate, and evaporated at reduced pressure. The infrared spectrum of the oil (10.14 g) thus obtained showed maxima at 1 700 (s) and 1 737 (m) cm^{-1}, the 1 710 and 3 660 – 2 500 cm^{-1} bands having disappeared.

Can. J. Chem. Downloaded from www.nrcresearchpress.com by 210.87.254.40 on 09/05/12
For personal use only.

Can. J. Chem. Downloaded from www.nrcresearchpress.com by 210.87.254.40 on 09/05/12
For personal use only.

The oil was chromatographed on alumina (315 g; 6% water) and the following fractions, clearly defined by their infrared spectra, were collected: A, an oil (3.75 g; 37% of material placed on column), eluted with hexane and hexane–benzene (9:1); B, an oil (0.38 g; 3.8%), eluted with hexane–benzene (7:1, 6:1, and 5:1); C, crystals (0.93 g; 9.2%), eluted with benzene; D, an oil (0.80 g; 7.9%), eluted with benzene–ether (4:1); E, crystals (3.04 g; 30%), eluted with ether – water – acetic acid (94:1:5). The total recovery amounted to 89%, a further 3% of mixed fractions being discarded.

Fraction A

The infrared spectrum (peaks at 3 080, 1 735, 1 655 – 1 635, and 890 cm^{-1}) showed that this fraction was probably a mixture of the methyl esters of unsaturated acids. Portions were treated as described below, yields being calculated on the assumption that fraction A has the approximate composition $C_{26}H_{44}O_2$.

Acid XVI

A part (200 mg) of the oil was heated under reflux for 2 h in a 1 *N* solution of sodium hydroxide in ethanol–water (9:1) (7 ml). The reaction mixture was then cooled, acidified with 1 *N* hydrochloric acid, diluted with water, and extracted with ether. The ether extract was washed with water until the washings were neutral, washed with aqueous saturated sodium chloride, dried over magnesium sulfate, and evaporated to dryness at reduced pressure. A solution of the resultant oil (192 mg) in 95% ethanol was made just alkaline to phenolphthalein by the addition of 0.01 *N* sodium hydroxide, and a hot solution of S-benzylisothiuronium chloride (0.8 g) in 95% ethanol (4 ml) was added. After 10 min, the organic salts were precipitated with water and collected by filtration as a whitish powder, m.p. 127.5–130°. Eight recrystallizations from aqueous ethanol raised the melting point to 144.8–145.3°. The purified salt was dissolved in 95% ethanol (5 ml), and the resultant solution was acidified with 1 *N* hydrochloric acid and then diluted with water. The oily solid that was precipitated was recrystallized three times from aqueous ethanol to give white crystals of XVI (10 mg; 5% yield), m.p. 90.5–92.3°. Infrared: ν_{max} 3 660 – 2 500 (m w), 3 078 (m sh), 2 870 (s sh), 1 745 (w), 1 710 (s), 1 638 (w), and 885 (m) cm^{-1}.

Anal. Calcd. for $C_{26}H_{44}O_2$: C, 80.35; H, 11.41. Found: C, 80.45; H, 11.28.

Oxidative Production of Formaldehyde

A solution of fraction A (0.5 g) and osmium tetroxide (50 mg) in dioxane (24 ml, freshly distilled from lithium aluminium hydride) and water (5 ml) was stirred for 30 min at room temperature. Finely ground sodium metaperiodate (0.8 g) was then slowly added over a period of 15 min and the tan-colored slurry agitated for a further 3 h. The mixture was steam-distilled until the distillate gave a negative reaction with Brady's reagent. The addition of a 6% solution (10 ml) of dimedone in 50% ethanol to the steam distillate (150 ml) resulted in the separation of white crystals after about 20 min, though the whole mixture darkened with time. After the mixture was allowed to stand overnight in the refrigerator, it was filtered. The grey crystalline solid was dissolved in boiling 95% ethanol and filtered through carbon, which was washed with more boiling 95% ethanol. The clear colorless filtrate and washings were concentrated to a small volume (10 ml) and diluted with water (30 ml). On refrigeration the solution deposited white crystals of the dimedone derivative of formaldehyde (73.8 mg), m.p. 190.5–191°.

Oxidation of Fraction A with Osmium Tetroxide

A solution of fraction A (1 g) in dry ether (50 ml) and dry pyridine (1.2 ml) was treated with osmium tetroxide (0.8 g) and left at room temperature in the dark for 10 days. Removal of the ether and pyridine at reduced pressure gave a brown oil, which was added to a solution of sodium sulfite (5 g) in 57% aqueous ethanol (65 ml). The solution was heated under reflux for 2 h, then sodium hydroxide (1 g) was added, and heating under reflux was continued for 1 h. The hot solution was filtered and the insoluble residue washed thoroughly with hot 95% ethanol. The bulk of the ethanol was removed from the filtrate and washings by distillation at reduced pressure. The concentrated solution was acidified with 5 *N* hydrochloric acid and extracted with ether. The ether extract was washed with water until it was free from acid, then washed with saturated sodium chloride solution, and dried over magnesium sulfate. Evaporation of the solution to dryness left an oil (844 mg). This oil was chromatographed on alumina (36 g, 10% water) and the following fractions were collected.

(*i*) Elution with hexane–benzene (2:1) gave crystals which, after two recrystallizations from aqueous methanol, yielded fine needles of XIII (6 mg), m.p. 119–120.2°, $[\alpha]_D^{29}$ +20° (*c*, 0.15), $\lambda_{max}^{CHCl_3}$ 206 mμ (ϵ ~11 000), ν_{max} 1 758 (s) cm^{-1}.

Anal. Calcd. for $C_{26}H_{42}O_2$: C, 80.76; H, 10.95. Found: C, 80.61; H, 11.14.

Recrystallization of the solid that was obtained by evaporating the mother liquors yielded a second crop (7 mg), m.p. 118.7–119.8°.

(*ii*) Elution with benzene–ether (9:1 and early 8:1 fractions) provided crystals (289 mg), which, on one split crystallization from petroleum ether (b.p. 60°), gave fine needles. These were recrystallized from hexane to produce XVIII*a* (13 mg); m.p. 172–173°; $[\alpha]_D^{29}$ −11° (*c*, 0.61); $\nu_{max}^{CHCl_3}$ 3 617 (w), 3 424 (w b), 1 771 (s), 1 753 (s i) cm^{-1}; $\nu_{max}^{CHCl_3}$ 3 570 (w), 3 350 (w b), 1 756 (s) cm^{-1}.

Anal. Calcd. for $C_{26}H_{44}O_3$: C, 77.18; H, 10.96. Found: C, 76.62; H, 10.87.

Concentration of the mother liquors from split crystallization gave a solid. After three recrystallizations from hexane this was obtained in long plates of XVIII*b* (60 mg); m.p. 159.2–161°; $[\alpha]_D^{26}$ +28° (*c*, 3.20); ν_{max} 3 617 (w), 3 424 (w b), 1 771 (s), 1 753 (s i) cm^{-1}; $\nu_{max}^{CHCl_3}$ 3 591 (w), 3 380 (w b), 1 755 (s) cm^{-1}.

Can. J. Chem. Downloaded from www.nrcresearchpress.com by 210.87.254.40 on 09/05/12
For personal use only.

Anal. Calcd. for $C_{26}H_{44}O_3$: C, 77.18; H, 10.96. Found: C, 77.03; H, 10.61.

The mother liquors from XVIII*b* gave more solid on concentration. On recrystallization from petroleum ether (b.p. 60°) this gave a crop of needles which was recrystallized twice from hexane to give a second crop of XVIII*a* (7 mg), m.p. 171.8–173°.

(*iii*) Elution with benzene–ether (8:1, 7:1, and 6:1) gave crystals (132 mg). These were recrystallized four times from aqueous methanol to give flat rhombs of XIV (36 mg); m.p. 189.4–190.2°; $[\alpha]_D^{26}$ +31° (*c*, 1.96); ν_{max} 3 620 (w), 3 459 (w b), 1 776 (s), 1 758 (s i) cm^{-1}.

Anal. Calcd. for $C_{26}H_{44}O_3$: C, 77.18; H, 10.96. Found: C, 76.97; H, 10.64.

Concentration of the mother liquors and recrystallization from aqueous methanol of the solid thus obtained yielded a second crop (24 mg) of the same product, m.p. 188.2–189.9°.

The yields of pure XIII, XVIII*a*, XVIII*b*, and XIV were 0.6, 1.9, 5.7, and 5.7%, respectively. However, the weights of the crude fractions from the chromatogram before the wasteful crystallizations indicate that the yield of XVIII*a* and XVIII*b* together was about 28%, and that that of XIV was 10%.

(*iv*) Elution with ether – water – acetic acid (94:1:5) gave an oil (270 mg), which could not be crystallized. The infrared spectrum showed bands attributable to a hydroxy-δ-lactone.

Oxidation of Fraction A with the Lemieux–Rudloff Reagent (23)

Potassium carbonate (0.25 g) in water (14 ml) was added, with vigorous stirring, to a solution of another portion (1.2 g) of fraction A in *t*-butanol (62 ml), followed by a portion (28 ml) of a solution prepared from sodium metaperiodate (4.1 g) and water (55 ml), and then 1% aqueous potassium permanganate solution (0.7 ml). The rest of the periodate was added over the next 30 min, permanganate solution (0.8 ml) being added when necessary to maintain the permanganate color throughout the next 3 h. Stirring was continued overnight, after which time the excess oxidant was destroyed with sodium bisulfite and the *t*-butanol removed by distillation at reduced pressure. The resultant mixture was extracted with ether. The ether layer was washed with water and then with saturated sodium chloride solution, dried over magnesium sulfate, filtered, and treated with an ether solution of diazomethane that was prepared from N-nitroso-N-methyl-N′-nitroguanidine (1.4 g). The excess diazomethane was destroyed with 0.1 *N* hydrochloric acid, and the solution was washed with water and then with saturated sodium chloride solution, dried over magnesium sulfate, and evaporated to dryness. The resultant oil (1.11 g) was chromatographed over alumina (34 g, 10% water). The initial hexane fractions gave a light oil (344 mg), the infrared spectrum of which indicated that it consisted primarily of ketonic material. It was dissolved in boiling ethanol (8 ml) and mixed with a hot solution of 2,4-dinitrophenylhydrazine (0.8 g) in sulfuric acid (2 ml) and 70% ethanol (20 ml). Yellow crystals were obtained which, on a single split crystallization and three recrystallizations from 95% ethanol containing a little ethyl acetate, produced small yellow needles of the 2,4-dinitrophenylhydrazone of XVII (224 mg); m.p. 142–142.5°; $[\alpha]_D^{26}$ +32° (*c*, 2.20); $\lambda_{max}^{CHCl_3}$ 367 mμ (ε 22 000); ν_{max} 3 312 (w), 3 095 (w), 1 618 (s) cm^{-1}; n.m.r. unsplit peak at 7.95 τ (methyl adjacent to C=N; cf. ref. 25).

Anal. Calcd. for $C_{29}H_{44}N_4O_4$: C, 67.92; H, 8.65; N, 10.92. Found: C, 67.75, 67.92; H, 8.86, 8.95; N, 10.94, 10.88.

Concentration of the filtrate from the split crystallization gave a solid which, after one recrystallization from 95% ethanol – ethyl acetate (4:1), was obtained as orange-yellow crystals, m.p. 118–120.4°. Two subsequent recrystallizations from hexane gave orange plates of an isomeric 2,4-dinitrophenylhydrazone of XVII (25 mg); m.p. 125.7–126.8°; $[\alpha]_D^{29}$ +18° (*c*, 1.60); $\lambda_{max}^{CHCl_3}$ 367 mμ (ε 22 500); ν_{max} 3 304 (w), 3 084 (w), 1 618 (s) cm^{-1}; n.m.r. peaks at 7.93 and 8.01 τ.

Anal. Calcd. for $C_{29}H_{44}N_4O_4$: C, 67.92; H, 8.65; N, 10.92. Found: C, 67.53; H, 8.99; N, 11.07.

Concentration of the mother liquors and two recrystallizations from hexane of the solid residue thus obtained gave a second crop (13 mg), m.p. 124.2–125.9°.

The residue that was obtained by allowing the mother liquors from all the recrystallizations of the two isomeric 2,4-dinitrophenylhydrazones to evaporate to dryness at room temperature was recrystallized three times from 95% ethanol to give pale yellow needles of a third 2,4-dinitrophenylhydrazone (23 mg); m.p. 125.6–126.7°; $[\alpha]_D^{31}$ −19° (*c*, 0.87); $\lambda_{max}^{CHCl_3}$ 367 mμ (ε 23 000); ν_{max} 3 313 (w), 3 087 (w), 1 618 (s) cm^{-1}.

Anal. Calcd. for $C_{31}H_{48}N_4O_4$: C, 68.85; H, 8.95; N, 10.36. Found: C, 68.76; H, 8.53; N, 10.52.

Fraction B

This material exhibited a maximum at 1 735 (s) cm^{-1} and no peaks in the 1 700 – 1 600 cm^{-1} region; it was not attacked by osmium tetroxide or the Lemieux–Rudloff reagent, and so lacked an olefinic double bond. It (350 mg) was saponified for 2 h with a solution (under reflux) of 0.5 *N* sodium hydroxide in 90% aqueous ethanol (12 ml). After the usual extraction procedure, the resultant oil was chromatographed on Davison silica gel (11.5 g). The material (157 mg) from the benzene–ether (9:1) fractions was collected and rechromatographed on Davison silica gel (140 g), giving a series of fractions from benzene–ether (92:8 to 8:1) which could not be crystallized. These gave identical infrared spectra (ν_{max} 3 500 (w), 3 500 (w), 3 500 – 2 300 (w m), 1 746 (m sh), 1 705 (s) cm^{-1}); spectra and analysis suggested that these fractions consisted of impure ethoxyacids derived from XI by reaction with ethanol.

Anal. Calcd. for $C_{28}H_{50}O_3$: C, 77.36; H, 11.60. Found: C, 76.83; H, 11.36.

Fraction C

This crystalline fraction, on two recrystallizations from aqueous ethanol, gave colorless needles of XII*a* (474 mg), m.p. 114.5–115.5°, $[\alpha]_D^{29}$ +14° (*c*, 2.72).

Anal. Calcd. for $C_{26}H_{44}O_2$: C, 80.35; H, 11.41. Found: C, 80.34; H, 11.34.

Concentration of the mother liquors gave a solid which, after three recrystallizations from aqueous ethanol, produced a second crop (88 mg), m.p. 112.5–113.8°.

Fraction D

This oily fraction (ν_{max} 3 630 (m), 3 405 (w b), 1 724 (s), 1 709 (m i), 1 656 (m) cm^{-1}) could not be crystallized; treatment with sodium hydroxide in aqueous ethanol or with acetic anhydride in pyridine gave gummy products.

Fraction E

Three recrystallizations of this solid fraction from aqueous ethanol gave 4-oxa-3-oxo-5β-cholestane (X) (1.07 g), m.p. 107.2–108°, identified by mixed melting point and infrared spectrum. The residue (1.97 g) from the mother liquors was chromatographed on alumina (60 g, 10% water). The fractions eluted with hexane–benzene (6:1 to 1:6) yielded crystalline material (284 mg) which, after two recrystallizations from aqueous methanol, gave colorless needles (127 mg), which were identified by infrared spectrum, melting point, and mixed melting point as XII*a* (described above). Concentration of the mother liquors gave, after one split crystallization and five recrystallizations from the same solvent, long colorless plates of XII*b* (20 mg), m.p. 88.6–90.2°, $[\alpha]_D^{29}$ +1° (*c*, 2.40), ν_{max} 1 768 (s) cm^{-1}.

Anal. Calcd. for $C_{26}H_{44}O_2$: C, 80.35; H, 11.41. Found: C, 80.44; H, 11.44.

A second crop (32 mg), m.p. 88.5–90.2°, was obtained by further concentration of the mother liquors and five subsequent recrystallizations.

The fractions (1.53 g) eluted with ether – water – acetic acid (94:1:5) gave, on two recrystallizations from aqueous ethanol, a further crop of X (1.23 g), m.p. 107–107.8°.

Hydrolysis of 5α-Tosyloxy-3,5-seco-A-norcholestan-3-nitrile (XXV)

A solution of the cyanotosylate (2.4 g) and sodium hydroxide (37.5 g) in 83% aqueous ethanol (465 ml) was heated under reflux for 7 h (the tosylate had dissolved completely within 10 min). Removal of the bulk of the ethanol at reduced pressure and the usual ether-extraction procedure gave a gum (1.75 g), the infrared spectrum of which showed a large peak at 1 705 cm^{-1} (acid) and a small inflection at 1 770 cm^{-1} (γ-lactone). Relative values of the optical densities of these peaks, that of the C—H stretching peak at 2 939 cm^{-1} being taken as unity, were 1.02 and 0.04, respectively, minor corrections being made for band overlapping. Treatment of an ether solution of the gum with an ether solution of diazomethane (derived from N-nitroso-N-methyl-N′-nitroguanidine (1.4 g)) and the usual work-up produced an oil (1.75 g), which was chromatographed on alumina (53 g, 6% water).

Elution with hexane gave a series of fractions having almost identical infrared spectra, with bands at 3 010 (w sh), 1 736 (s), and 1 650 cm^{-1} characteristic of unsaturated esters. The fractions were combined as fraction F (1.46 g) and oxidized as described below.

Benzene–ether (9:1) eluted an oil (35 mg) which, after three crystallizations from aqueous methanol, gave long needles of compound G (probably XXVI*b*) (4 mg), m.p. 97.5–99.5°, ν_{max} 1 770 (s).

The next eluate with benzene–ether (9:1) gave a gum (29 mg) which, after three crystallizations from aqueous methanol, yielded needles of a γ-lactone (12 mg) (compound H), m.p. 153.1–153.8°. This product was proved, by mixed melting point and infrared spectrum, to be identical with the compound obtained by the acid-catalyzed rearrangement of 4-oxa-3-oxo-5β-cholestane (X), described below, and was assigned the structure XXVI*a*.

Elution with ether – water – acetic acid (96:1:3) removed some ill-defined oils from the column; in no fraction was there any evidence, from the infrared spectrum, of 4-oxa-3-oxo-5α-cholestane. Total recovery from the column amounted to 102%.

Oxidation of Fraction F with Osmium Tetroxide

Fraction F was heated under reflux in 1 *N* sodium hydroxide in 90% aqueous ethanol for 2 h, and the solution was worked up by the usual acidification, ether-extraction, and drying procedures. Part (525 mg) of the uncrystallizable acidic material thus obtained was left in the dark at room temperature for 10 days in a solution of osmium tetroxide (0.8 g) in anhydrous ether (40 ml) containing dry pyridine (1.6 ml). Removal of the ether and pyridine at reduced pressure then gave a brown oil, which was treated for 1½ h with sodium sulfite (6 g) in boiling 57% aqueous ethanol (60 ml). The hot solution was filtered, the insoluble residue washed thoroughly with hot 95% ethanol, and the bulk of the ethanol removed at reduced pressure. The solution was acidified and extracted with ether. The extract was dried and evaporated, yielding a gum (489 mg), which was chromatographed on alumina (15 g, 12.5% water).

Hexane–benzene (1:1) eluted crystalline material (16 mg), m.p. 199–202°, which, after two recrystallizations from hexane, was obtained as fine needles (XXXI?) (8 mg); m.p. 202–203°; $[\alpha]_D^{31}$ −23° (*c*, 0.44); ν_{max} 3 580 (m), 1 772 (s) cm^{-1}.

Anal. Calcd. for $C_{26}H_{44}O_3$: C, 77.18; H, 10.96. Found: C, 77.12; H, 11.18.

Elution with benzene gave crystalline material (9 mg), m.p. 218–220°, which yielded, after two recrystallizations from hexane, heavy needles (XXIX?) (3 mg); m.p. 223–225°; ν_{max} 3 617 (w), 3 440 (w b), 1 772 (s) cm^{-1}.

The bulk of the material (385 mg) was recovered as a semicrystalline gum from the ether – water – acetic

Can. J. Chem. Downloaded from www.nrcresearchpress.com by 210.87.254.40 on 09/05/12
For personal use only.

acid (96.5:0.5:3 to 93:2:5) eluates. It was rechromatographed on Davison silica gel (19 g), from which was eluted, by ether–methanol (9:1), crystalline material (283 mg). Three recrystallizations from hexane gave plates of XXIII (118 mg), m.p. 123.8–124.5°, $[\alpha]_D^{29}$ −9° (*c*, 3.07).

Anal. Calcd. for $C_{26}H_{44}O_3$: C, 77.18; H, 10.96. Found: C, 77.47; H, 11.22.

Concentration of the mother liquors gave a solid which, after two recrystallizations from hexane, yielded a second crop (41 mg), m.p. 122.7–124°.

The amounts of XXIX, XXXI, and XXIII that were obtained correspond to respective yields for XXX, XXVIII, and XXIV of 0.5%, 1.2%, and 24.3% from the solvolysis of the cyanotosylate XXV. However, the high retention of XXIII on the columns suggests that this estimate is far too low for XXIV; an estimate based on the recovery of crude XXIII from the first column would be 59%.

Treatment of 4-Oxa-3-oxo-5α-cholestane (VII) with Trifluoroacetic Acid

A solution of the lactone (6.2 g) in trifluoroacetic acid (65 ml) was heated under reflux with the exclusion of moisture. Small samples were taken each day, and after removal of the trifluoroacetic acid at reduced pressure, their infrared spectra were measured. The peak at 1 740 – 1 737 cm^{-1}, attributable in part to the starting material, approached a minimum after 13 days, and other peaks appeared at 1 770, 1 706, and 1 649 cm^{-1}. At this time the bulk of the trifluoroacetic acid was removed by distillation, and the residue was diluted with water and extracted with ether. The ether solution, after washing and drying, was evaporated to give a heavy dark brown oil (5.9 g), which was chromatographed on Davison silica gel (230 g).

Hexane eluted a colorless oil (311 mg), the infrared spectrum of which showed C—H bands (2 910 (s), 2 850 (s sh), 1 463 (m), 1 380 (m), 1 368 (m sh) cm^{-1}) and no C=O band. Hexane–benzene (7:1) next eluted a light yellow oil (330 mg) having an additional peak at 3 022 (s sh) cm^{-1}. Benzene–ether (99:1 to 6:1) eluted the bulk of the material as a brown oil (fraction I) (3.94 g) with bands at 1 771 (m), 1 739 (m), 1 708 (m), and 1 649 (s) cm^{-1}. Benzene–ether (4:1), followed by pure ether, eluted an oil (fraction J) (0.82 g) which absorbed strongly at 1 649 cm^{-1}, with only smaller peaks in the 1 800 – 1 700 cm^{-1} region.

Rechromatography of fraction I on Davison silica gel (158 g) yielded, from the eluates with benzene–ether (98:2), a yellow oil (2.05 g) showing bands at 1 771 (s) and 1 708 (m) cm^{-1}. This oil was rechromatographed on alumina (72 g, 6% water). Elution with hexane–benzene (4:1) followed by benzene gave an oil (0.66 g) which showed a strong band at 1 771 cm^{-1} and a small band at 1 670 cm^{-1}. Further rechromatography on Florisil gave, on elution with benzene–ether (9:1 to 8:1), an almost colorless oil (0.55 g) showing only the 1 771 cm^{-1} peak between 1 800 and 1 600 cm^{-1}. However, rechromatography of this material on alumina (27.5 g, 10% water) again yielded an uncrystallizable oil (0.43 g), although the infrared spectrum was essentially changed.

Fraction J from the initial chromatogram was rechromatographed on Davison silica gel (35 g). The eluates with benzene–ether (92:8 to 6:1) yielded an oil (462 mg), which was further chromatographed on alumina (14 g, 12.5% water). From this, hexane to hexane–benzene (1:1) eluted a yellow oil (147 mg), the infrared spectrum of which was almost devoid of any absorption between 1 800 and 1 600 cm^{-1}, except for a strong band at 1 649 cm^{-1}. Ultraviolet: λ_{max} 323 mμ (ε 9 900) in 80% aqueous ethanol; in a 0.5 *N* solution of sodium hydroxide in 80% aqueous ethanol, after the solution had been allowed to stand overnight, λ_{max} 300 mμ (ε 7 500).

Treatment of 4-Oxa-3-oxo-5β-cholestane (X) with Formic Acid

A solution of the lactone (1 g) in formic acid (17 ml) was heated under reflux with the exclusion of moisture for 4 days. Removal of the bulk of the formic acid by distillation at reduced pressure and the usual ether extraction gave a white crystalline material which, after two recrystallizations from methanol, was obtained as long needles of compound H (320 mg), m.p. 153.2–153.8°, $[\alpha]_D^{29}$ +8° (*c*, 4.16 in chloroform).

Anal. Calcd. for $C_{26}H_{44}O_2$: C, 80.35; H, 11.41. Found: C, 80.05; H, 11.32.

The solid from the concentration of the mother liquors, on three recrystallizations from methanol, gave a second crop (60 mg), m.p. 152.7–153.7°. The residue from the evaporation of the mother liquors was dissolved in ether (20 ml) and treated with an ethereal solution of diazomethane derived from nitrosodimethylurea (1 g), and the product was chromatographed on Woelm alumina (18 g, 6% water).

Hexane–benzene (7:1 to 2:1) eluted a semicrystalline material (231 mg), which was recrystallized three times from methanol to give a further crop of compound H as needles (189 mg), m.p. 152.8–153.6°. Ether – water – acetic acid (95:2:3) eluted an oil which solidified. This, after two crystallizations from aqueous ethanol, gave starting material (8.3 mg), m.p. 106.8–107.8°. The total yield of rearranged product was 61%, and the recovery of starting material was 0.8%.

Treatment of 4-Oxa-3-oxo-5β-cholestane (X) with Trifluoroacetic Acid

A solution of the lactone (1.95 g) in trifluoroacetic acid (14 ml) was heated under reflux and anhydrous conditions for 10 h. Removal of the trifluoroacetic acid at reduced pressure, followed by the usual ether-extraction procedure, gave oily crystals (1.89 g). Three recrystallizations from methanol produced needles (510 mg), which were proved by mixed melting point and infrared spectrum to be identical with the product from formic acid treatment. The residue from the evaporation of the methanolic mother liquors was dried and chromatographed on alumina (40 g, 6% water), as described above, to give more crystals of compound H (529 mg), m.p. 153.2–153.8°, and starting material (182 mg), m.p. 106.7–107.8°. The total yield of compound H was 71%, and the recovery of starting material was 9%.

Can. J. Chem. Downloaded from www.nrcresearchpress.com by 210.87.254.40 on 09/05/12
For personal use only.

ACKNOWLEDGMENTS

We are grateful to Dr. E. H. Charlesworth and Dr. H. J. Campbell for a sample of the lactone of *trans*-2′-hydroxycyclohexylacetic acid, to Dr. A. Taurins for nuclear magnetic resonance measurements and for help with infrared measurements, to the referees for helpful suggestions, and to the National Research Council for financial support of the work performed at McGill University.

REFERENCES

1. J. H. Brewster and C. K. Kucera. J. Am. Chem. Soc. **77**, 4564 (1955).
2. C. R. Stephens, E. J. Bianco, and F. J. Pilgrim. J. Am. Chem. Soc. **77**, 1701 (1955).
3. L. J. Bellamy. The infrared spectra of complex molecules. John Wiley & Sons, Inc., New York. 1956.
4. R. B. Turner. J. Am. Chem. Soc. **72**, 579 (1950).
5. J. T. Edward and P. F. Morand. Can. J. Chem. **38**, 1325 (1960).
6. C. K. Ingold. Structure and mechanism in organic chemistry. Bell & Sons, Ltd., London. 1953. pp. 321 and 500. D. H. R. Barton. J. Chem. Soc. 1027 (1953). J. F. King and P. de Mayo. Molecular rearrangements. *Edited by* P. de Mayo. Interscience Publishers, Inc., New York. 1964. Part II. p. 827.
7. E. L. Eliel. Stereochemistry of carbon compounds. McGraw-Hill Book Co., Inc., New York. 1962. p. 197.
8. (*a*) F. W. McLafferty. Anal. Chem. **29**, 1782 (1957).
   (*b*) R. A. Friedel, J. L. Shultz, and A. G. Sharkey. Anal. Chem. **28**, 926 (1956).
   (*c*) A. G. Sharkey, J. L. Shultz, and R. A. Friedel. Anal. Chem. **31**, 87 (1959).
   (*d*) D. C. DeJongh and K. Biemann. J. Am. Chem. Soc. **86**, 67 (1964).
   (*e*) W. H. McFadden, E. A. Day, and M. J. Diamond. Anal. Chem. **37**, 89 (1965).
9. M. J. O'Neal and T. P. Wier. Anal. Chem. **23**, 830 (1951).
10. F. W. McLafferty. Anal. Chem. **31**, 82 (1959).
11. R. Ryhage and E. Stenhagen. J. Lipid Res. **1**, 361 (1960). H. Budzikiewicz and C. Djerassi. J. Am. Chem. Soc. **84**, 1430 (1962).
12. L. Friedman and F. A. Long. J. Am. Chem. Soc. **75**, 2832 (1953).
13. J. N. Shoolery and M. T. Rogers. J. Am. Chem. Soc. **80**, 5121 (1958). G. Slomp and F. A. MacKellar. J. Am. Chem. Soc. **84**, 204 (1962).
14. G. V. D. Tiers. Characteristic nuclear magnetic resonance 'shielding values' for hydrogen in organic structures. Minnesota Mining and Manufacturing Co., St. Paul, Minnesota. 1958. pp. 18 and 20.
15. High resolution nuclear magnetic resonance. Varian Associates, Palo Alto. 1962.
16. R. Pappo, D. S. Jones, R. U. Lemieux, and W. S. Johnson. J. Org. Chem. **21**, 478 (1956).
17. R. N. Jones and B. S. Gallagher. J. Am. Chem. Soc. **81**, 5242 (1959).
18. F. W. McLafferty. 8th Annual Meeting of the American Society for Testing and Materials, Committee E-14, on Mass Spectrometry, Atlantic City, New Jersey, 1960. F. W. McLafferty. *In* Determination of organic structures by physical methods. Vol. 2. F. C. Nachod and W. D. Phillips (*Editors*). Academic Press, Inc., New York. 1962. p. 93. F. W. McLafferty. *In* Mass spectrometry of organic ions. F. W. McLafferty (*Editor*). Academic Press, Inc., New York. 1963. p. 309.
19. (*a*) S. Meyerson and L. C. Leitch. J. Am. Chem. Soc. **86**, 2555 (1964).
   (*b*) W. Benz and K. Biemann. J. Am. Chem. Soc. **86**, 2375 (1964).
20. L. M. Jackmann. Applications of nuclear magnetic resonance spectroscopy in organic chemistry. The Pergamon Press, Ltd., London. 1959. p. 55.
21. E. S. Gould. Mechanism and structure in organic chemistry. Holt-Dryden, New York. 1959. p. 183.
22. W. G. Dauben and P. D. Hance. J. Am. Chem. Soc. **75**, 3352 (1953). A. T. Nielsen. J. Org. Chem. **22**, 1539 (1957). W. G. Dauben, D. A. Lightner, and W. K. Hayes. J. Org. Chem. **27**, 1897 (1962).
23. R. U. Lemieux and E. von Rudloff. Can. J. Chem. **33**, 1701 (1955); **33**, 1710 (1955). E. von Rudloff. Can. J. Chem. **33**, 1714 (1955); **34**, 1413 (1956).
24. G. D. Johnson. J. Am. Chem. Soc. **75**, 2720 (1953). L. A. Jones, J. C. Holmes, and R. B. Seligman. Anal. Chem. **28**, 191 (1956). J. P. Phillips. J. Org. Chem. **27**, 1443 (1962).
25. D. Y. Curtin, J. A. Gourse, W. H. Richardson, and K. L. Rinehart. J. Org. Chem. **24**, 93 (1959).
26. J. A. Pople, W. G. Schneider, and H. J. Bernstein. High-resolution nuclear magnetic resonance. McGraw-Hill Book Co., Inc., New York. 1959. p. 145.
27. S. Meyerson, J. D. McCollum, and P. N. Rylander. J. Am. Chem. Soc. **83**, 1401 (1961). K. Biemann. Angew. Chem. Intern. Ed. Engl. **1**, 98 (1962). H. Audier, M. Fétizon, and W. Vetter. Bull. Soc. Chim. France, 1971 (1963).
28. L. F. Fieser and M. Fieser. Steroids. Reinhold Publishing Corp., New York. 1959.
29. H. O. House and M. Schellenbaum. J. Org. Chem. **28**, 34 (1963).
30. H. M. Grubb, C. H. Ehrhardt, R. W. Vander Haar, and W. H. Moeller. 7th Annual Meeting of the American Society for Testing and Materials, Committee E-14, on Mass Spectrometry, Los Angeles, California, May, 1959.
31. J. T. Edward, D. Holder, W. H. Lunn, and I. Puskas. Can. J. Chem. **39**, 599 (1961).

Can. J. Chem. Downloaded from www.nrcresearchpress.com by 210.87.254.40 on 09/05/12
For personal use only.

Can. J. Chem. Downloaded from www.nrcresearchpress.com by 210.87.254.42 on 09/05/12
For personal use only.

SULFONATE ESTERS OF α-CHLOROALDOXIMES, ALDOXIMES, AND AMIDOXIMES VIA "SULFENE" ADDITION

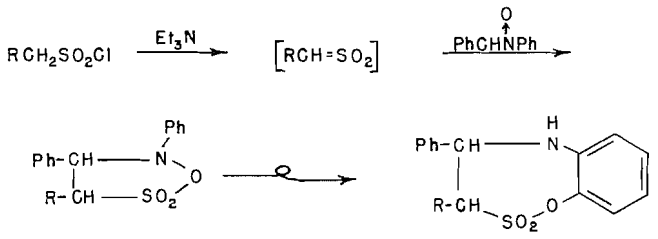
W. E. Truce and A. R. Naik
Department of Chemistry, Purdue University, Lafayette, Indiana

Received September 7, 1965

ABSTRACT

Reaction of aromatic nitrile oxides with methanesulfonyl and benzylsulfonyl chlorides in the presence of triethylamine yielded sulfonate esters of α-chloroaldoximes ($R-\overset{Cl}{\overset{|}{C}}=NO_3SCH_2R'$). Under the same reaction conditions, aldoximes yielded sulfonate esters, which decomposed to nitriles, and amidoximes yielded amidoxime O-sulfonates, which were also prepared by the action of ammonium hydroxide on $R-\overset{Cl}{\overset{|}{C}}=NO_3SCH_2Ph$. Chemical as well as nuclear magnetic resonance spectroscopic evidence confirms the formula $R-\overset{NH_2}{\overset{|}{C}}=NOH$ for amidoximes.

Inasmuch as cycloadditions of "sulfenes" to certain nucleophilic olefinic compounds to give products with four-membered rings have been realized (1), it became of interest to determine whether "sulfenes" would also cyclize with 1,3-dipolar systems. In fact, Truce *et al.* (2) have found that methanesulfonyl chloride reacts with C,N-diphenylnitrone in the presence of triethylamine to give a seven-ring aza-sultone, presumably via the sequence of steps shown in Reaction Scheme 1.



Reaction Scheme 1.

The present report concerns the behavior of another 1,3-dipolar system, nitrile N-oxides (3, 4), under "sulfene"-producing conditions. When an ethereal solution of benzonitrile oxide containing triethylamine was treated with benzylsulfonyl chloride, a crystalline product was obtained. Analysis of that product suggested the empirical formula $C_{14}H_{12}NO_3Cl$, indicating the presence of 1 mole of hydrogen chloride over that expected of a cycloadduct. The infrared spectrum showed bands at 1 180 cm^{-1} and 1 380 cm^{-1} ($\rangle SO_2$). The nuclear magnetic resonance spectrum showed a singlet at 4.7 p.p.m. (relative area 1) and aromatic protons at 7.4–8.2 p.p.m. (relative area 5). The singlet is nearly in the same position as the singlet for the benzylic protons (4.78 p.p.m.) in benzylsulfonic anhydride (5). From these limited data the product was assigned the structure α-chlorobenzaldoxime benzylsulfonate.

$$Ph-C\equiv N\rightarrow O + PhCH_2SO_2Cl \xrightarrow[Et_2O]{Et_3N} Ph-\overset{Cl}{\overset{|}{C}}=NO_3SCH_2Ph$$

Similar compounds were obtained by like reactions of benzylsulfonyl chloride (Et_3N) and methanesulfonyl chloride (Et_3N) with *p*-chlorobenzonitrile N-oxide and *m*-nitrobenzonitrile N-oxide. However, the structurally hindered 2,4,6-trimethylbenzonitrile N-oxide yielded only 2,4,6-trimethylphenylisocyanate.

Nitrile oxides are prepared by dehydrohalogenation of α-chloroaldoximes ($R-\overset{Cl}{\overset{|}{C}}=NOH$, hydroxamic acid chlorides) with triethylamine (3). However, the reverse can be effected, i.e. nitrile oxides add hydrogen chloride (6) and thiols (7). This suggests the occurrence of the following equilibrium under the above reaction conditions.

$$R-\overset{Cl}{\overset{|}{C}}=NOH + Et_3N \rightleftharpoons R-C\equiv N\rightarrow O + Et_3NHCl$$

Thus, there may be present a small but significant amount of α-chloroaldoxime in the medium, and this α-chloroaldoxime may be adding to "sulfene" to give the ester, with the equilibrium shifting to the left as the reaction proceeds.

$$R-CH_2SO_2Cl \xrightarrow{Et_3N} [R-CH=SO_2] \xrightarrow{R'-\overset{Cl}{\overset{|}{C}}=NOH} RCH_2SO_3N=\overset{Cl}{\overset{|}{C}}-R'$$

I–VI

I	R = C_6H_5, R′ = C_6H_5	(m.p. 105–107°)
II	R = C_6H_5, R′ = *p*-ClC_6H_4	(m.p. 102–103°)
III	R = C_6H_5, R′ = *m*-$NO_2C_6H_4$	(m.p. 144–146°)
IV	R = H, R′ = C_6H_5	(m.p. 110–111°)
V	R = H, R′ = *p*-ClC_6H_4	(m.p. 80°)
VI	R = H, R′ = *m*-$NO_2C_6H_4$	(m.p. 98–100°)

In fact, benzylsulfonyl chloride reacts with nitrile oxides in ether in the presence of triethylammonium chloride to give the corresponding esters. But, it adds to neither benzonitrile oxide nor *p*-chlorobenzonitrile oxide in the absence of triethylammonium chloride (the highly reactive *m*-nitrobenzonitrile oxide did give a small quantity of ester under the latter conditions). The maximum yield of ester was obtained when triethylamine was added to a mixture of α-chloroaldoxime and sulfonyl chloride in benzene or ether (Table I) at room temperature or ice-bath temperature.

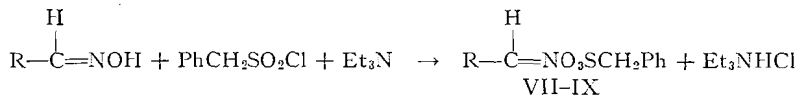
TABLE I

Yield of $R-\overset{Cl}{\overset{|}{C}}=NO_3SCH_2Ph$ in the reaction of $R-C\equiv N\rightarrow O$ with $PhCH_2SO_2Cl$

	R = C_6H_5 (I)	R = *p*-ClC_6H_4 (II)	R = *m*-$O_2NC_6H_4$ (III)
Ether + Et_3N	36%	37%	63%
Benzene + Et_3N	50%	43.6%	76%
Chloroform + Et_3N	24%	33.4%	
Ether	0%	0%	24%
Ether + $Et_3N\cdot HCl$	22%	39%	
Addition of Et_3N to a mixture of $RC(Cl)=NOH$ and $PhCH_2SO_2Cl$	57%	75%	81%

Can. J. Chem. Downloaded from www.nrcresearchpress.com by 210.87.254.42 on 09/05/12
For personal use only.

Also, *syn*-benzaldoxime, *syn*-*p*-chlorobenzaldoxime, and *anti*-*m*-nitrobenzaldoxime gave the corresponding sulfonic acid esters when treated under phenylsulfene-generating conditions.



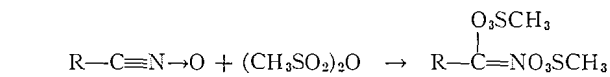
VII–IX

VII R = C_6H_5 (m.p. 77–79°)
VIII R = *p*-ClC_6H_4 (m.p. 103°)
IX R = *m*-$O_2NC_6H_4$ (m.p. 90–92°)

Under identical reaction conditions benzaldoxime did not react with *p*-toluenesulfonyl chloride.

Not many sulfonate esters of aldoximes are known (8, 9), because they are very unstable. *syn*-Aldoxime sulfonates decompose to nitriles spontaneously or when they are passed through an alumina column (8*a*). Such facile dehydrosulfonation was substantiated in this work and provided a simple and clean method for the overall dehydration of aldoximes to nitriles. The strained mesitaldoxime ester was too unstable to isolate, and decomposed to nitrile immediately.

It has been observed that methanesulfonic and benzylsulfonic anhydrides do generate "sulfenes" on reaction with triethylamine (5). Therefore, it was hoped that methanesulfonic anhydride might react with nitrile oxides as follows.



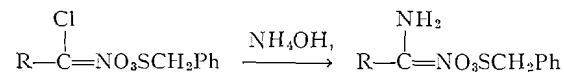
However, treatment of *p*-chlorobenzonitrile oxide and *m*-nitrobenzonitrile oxide with methanesulfonic anhydride in ether or chloroform in the presence of triethylamine yielded only starting nitrile oxide or its dimer.

In conclusion, the above facts do not clearly preclude a reaction sequence involving initial addition of "sulfene" to the nitrile oxide ($R'C\overset{+}{N}O_3\overset{-}{S}CHR$) followed by addition of hydrogen chloride, as against initial addition of hydrogen chloride to the nitrile oxide followed by addition of "sulfene".

Attempts were made, without success, to replace the "carbonyl" hydrogen of benzaldoxime benzylsulfonate and *p*-chlorobenzaldoxime benzylsulfonate with chlorine.

The esters I and II, on treatment with alcoholic KOH, gave benzonitrile and *p*-chlorobenzonitrile and, under more vigorous conditions, benzamide and *p*-chlorobenzamide, respectively. The ester III, on reaction with triethylamine, gave only *m*-nitrobenzonitrile. Presumably these reactions involve initial attack by the base on chlorine, with expulsion of the sulfonate anion to give the nitrile, which may be hydrolyzed further to the amide.

A cursory look at the structures of the esters indicates that there is a reactive chlorine atom, which should be replaced easily. The esters did not react with gaseous ammonia at room temperature. However, reaction with ammonium hydroxide in acetone at room temperature or higher yielded the corresponding amidoxime esters.



X–XII

X R = C_6H_5 (m.p. 102° (decomp.))
XI R = *p*-ClC_6H_4 (m.p. 89–90° (decomp.))
XII R = *m*-$NO_2C_6H_4$ (m.p. 127° (decomp.))

Can. J. Chem. Downloaded from www.nrcresearchpress.com by 210.87.254.42 on 09/05/12
For personal use only.

The amidoxime esters were also prepared by the reaction of amidoximes with benzylsulfonyl chloride in the presence of triethylamine. The required amidoximes were prepared by the reaction of nitriles with hydroxylamine or by the action of gaseous ammonia on α-chloroaldoximes.

$$R{-}C{\equiv}N + NH_2OH \rightarrow R{-}\overset{\overset{NH_2}{|}}{C}{=}NOH$$

$$R{-}\overset{\overset{Cl}{|}}{C}{=}NOH + NH_3 \rightarrow R{-}\overset{\overset{NH_2}{|}}{C}{=}NOH$$

$$R{-}\overset{\overset{NH_2}{|}}{C}{=}NOH + [PhCH{=}SO_2] \rightarrow R{-}\overset{\overset{NH_2}{|}}{C}{-}NO_3SCH_2Ph$$

Amidoximes theoretically could exist in two tautomeric forms *a* and *b*.

$$R{-}\overset{\overset{NH_2}{|}}{C}{=}NOH \qquad (a)$$

$$R{-}\overset{\overset{NH}{\|}}{C}{-}NHOH \qquad (b)$$

Although structure *a* has been accepted as the correct structure of amidoximes, this preference was based on infrared spectroscopy (10 and references therein). However, more definitive support for structure *a* was provided by nuclear magnetic resonance spectroscopy (10, 11). Our synthesis of these compounds not only provides a proof for the structures of the sulfonate esters of α-chloroaldoximes but also provides chemical evidence for the structure of amidoximes.

Infrared spectra of the amidoximes that were studied showed asymmetric and symmetric NH_2 stretching modes as two weak but sharp bands at 3 400 – 3 500 and 3 300 – 3 400 cm^{-1} and a broad band at 3 200 cm^{-1} caused by an associated OH function (11). On esterification only the band caused by OH disappeared. The amidoximes as well as their sulfonate esters exhibited strong bands at 1 630 – 1 675 cm^{-1} caused by C=N (11).

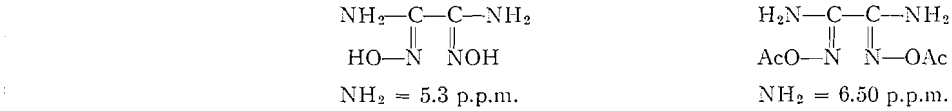
TABLE II

Chemical shifts (δ) in dimethyl sulfoxide

	Assignments:			
	OH	C_6H_5	NH_2	CH_2
$Ph{-}\overset{\overset{NH_2}{|}}{C}{=}NOH$	9.64	7.2–7.8	5.74	
$Ph{-}\overset{\overset{NH_2}{|}}{C}{=}NO_3SCH_2Ph$		7.0–8.0		4.74
p-$ClPh{-}\overset{\overset{NH_2}{|}}{C}{=}NOH$	9.64	7.2–7.8	5.8	
p-$ClPh{-}\overset{\overset{NH_2}{|}}{C}{=}NO_3SCH_2Ph$		7.0–8.0		4.8
m-$NO_2Ph{-}\overset{\overset{NH_2}{|}}{C}{=}NOH$	9.96	7.4–8.6	6.1	
m-$NO_2Ph{-}\overset{\overset{NH_2}{|}}{C}{=}NO_3SCH_2Ph$		6.8–8.6		4.8

Can. J. Chem. Downloaded from www.nrcresearchpress.com by 210.87.254.42 on 09/05/12
For personal use only.

The nuclear magnetic resonance spectra of the amidoximes and amidoxime sulfonates have been studied (Table II). The singlets at 9.6–10.0 p.p.m. are caused by N—OH (10, 11). The aromatic proton bands appear as a complex at 7.00 to 8.6 p.p.m., depending on the substitution on the aromatic ring. The NH_2 band appears as a singlet at 5.7 to 6.1 p.p.m. in amidoximes, a little higher than the literature values (10, 11). In the amidoxime sulfonate esters the singlet caused by OH disappears, and the singlet caused by NH_2 now shifts to the aromatic region and is not readily distinguished from the aromatic protons. However, the integration values support this conclusion. In the ester there is another band caused by benzylic protons at 4.78–4.80 p.p.m. as expected. The type of band shift observed for NH_2 has been reported (10) for oxamidoxime and its diacetate.



Variations in the chemical shifts observed and reported in the literature may be due to different solvents employed, e.g. it was observed that singlets caused by N—OH and NH_2 of benzamidoxime appear at 9.64 p.p.m. and 5.74 p.p.m. in dimethyl sulfoxide, but in deuterated chloroform they appear at 9.57 p.p.m. and 4.9 p.p.m., respectively.

EXPERIMENTAL*

Materials

The oximes were prepared according to the standard procedure. The α-chloroaldoximes were prepared by the action of chlorine on oximes in chloroform (12) or in 8 *N* HCl (4, 13) at ice-bath temperature. The solution first turns deep blue and finally slight orange. α-Chlorobenzaldoxime, m.p. 45–47° (lit. (4) m.p. 45°), is unstable and appears to be hydrolyzed to aldehyde when it is allowed to stand. *p*-Chloro(α-chloro)-benzaldoxime, m.p. 88–89° (lit. (4) m.p. 82–86°); *m*-nitro(α-chloro)benzaldoxime, m.p. 96–98° (lit. (4) m.p. 96°). Nitrile N-oxides were prepared *in situ* in most cases by the action of triethylamine on α-chloro-aldoximes in ether. However, *p*-chlorobenzonitrile oxide, m.p. 68–70° (lit. (14) m.p. 82–83°), was isolated for characterization. Triethylamine (Matheson, Coleman and Bell) was dried over KOH. Mallinckrodt anhydrous diethyl ether was used as obtained. Benzene was Baker spectrophotometric grade.

α-Chlorobenzaldoxime Benzylsulfonate (I)

To a continuously stirred solution of 1.55 g (0.01 mole) of α-chlorobenzaldoxime in about 100 ml of ether, maintained in an ice bath, was rapidly added 2 g (0.02 mole) of triethylamine. After 5 min, 2 g (slightly over 0.01 mole) of benzylsulfonyl chloride dissolved in about 15 ml of ether was added, dropwise, during a period of ½ h. After the solution was stirred for an additional hour, it was filtered and evaporated to dryness, and the residue was dissolved in benzene. Dilution with hexane and cooling yielded 0.5 g of 3,4-diphenylfuroxan, which, on further crystallization, had m.p. 112–114° (lit. (14) m.p. 114°). The mother liquor was evaporated to dryness and the residue was crystallized from alcohol to yield 1.1 g (36%) of the benzylsulfonate of α-chlorobenzaldoxime (I), m.p. 103–105° (raised to 105–107° after several crystallizations).

Anal. Calcd. for $C_{14}H_{12}ClNO_3S$: C, 54.28; H, 3.88; Cl, 11.45; N, 4.51; S, 10.32; mol. wt. 309.5. Found: C, 54.21; H, 4.13; Cl, 11.18; N, 4.71; S, 10.63; mol. wt. 313.

Infrared spectrum: 1 180 cm^{-1} (vs), 1 380 cm^{-1} (vs). Nuclear magnetic resonance spectrum: multiplets at 7.4–8.2 p.p.m. (relative area 5), singlet at 4.7 p.p.m. (relative area 1).

p-Chloro(α-chloro)benzaldoxime Benzylsulfonate (II)

To an ethereal solution containing 1 g of *p*-chlorobenzonitrile oxide and 1 g of triethylamine was added an ether solution of 1.5 g of benzylsulfonyl chloride as above. The residue remaining after the ether had been evaporated was dissolved in benzene, and the solution was filtered, diluted with hexane, and cooled. The precipitate was filtered off to give 0.6 g (37%) of the ester, m.p. 92–97°; after crystallization from benzene–hexane, m.p. 102–103°.

Anal. Calcd. for $C_{14}H_{11}Cl_2NO_3S$: C, 48.84; H, 3.20; Cl, 20.64; S, 9.30; mol. wt. 344. Found: C, 49.15; H, 3.56; Cl, 20.33; S, 9.71; mol. wt. 341.

The infrared spectrum was practically identical with that of I.

**All melting points are uncorrected. Microanalyses were performed by Dr. C. S. Yey and staff of the Microanalytical Laboratory, Purdue University. Nuclear magnetic resonance spectra were recorded on a Varian A-60 high-resolution spectrometer.*

Can. J. Chem. Downloaded from www.nrcresearchpress.com by 210.87.254.42 on 09/05/12
For personal use only.

Mesitonitrile N-Oxide

An aqueous basic solution of 12.7 g of the sodium salt of mesitaldoxime was added, while it was being filtered, to a stirred solution of sodium hypobromite (at 0 to 10°) prepared by adding 7 ml of bromine to 100 ml of 20% aqueous NaOH at 0 to 10°. The precipitate was filtered off, and the residue was washed with water and crystallized from hexane (first crop, m.p. 107–110°, yield 9.2 g; second crop, m.p. 104–106°, yield 2.1 g (lit. (6) m.p. 114°)).

Reaction of Mesitonitrile N-Oxide with Benzylsulfonyl Chloride in the Presence of Triethylamine

To an ether solution of 1.6 g (0.01 mole) of mesitonitrile oxide (m.p. 107–110°, lit. m.p. 114°) and 1 g of triethylamine was added an ethereal solution of 2 g of benzylsulfonyl chloride, as above. Evaporation of ether left a liquid residue, which was crystallized from hexane to give 1.1 g of 2,4,6-trimethylphenylisocyanate, m.p. 44–46°.

Anal. Calcd. for $C_{10}H_{11}NO$: C, 74.53; H, 6.83; N, 8.70. Found: C, 74.64; H, 6.93; N, 8.55.

In the infrared spectrum there was a very strong band at 2 260 cm^{-1}. In the literature (15) the isocyanate has been reported as a liquid. The urea derivative was prepared by treating the isocyanate with aniline, and had m.p. 240–242° (lit. (6) m.p. 245°).

m-Nitro(α-chloro)benzaldoxime Benzylsulfonate (III)

To an ice-cooled ethereal solution of 2 g (0.01 mole) of *m*-nitro(α-chloro)benzaldoxime was slowly added 1 g of triethylamine. After 5 min, 2 g of benzylsulfonyl chloride was added followed by the addition, over a ½ h period, of 1 g of triethylamine dissolved in ether. The residue obtained when the reaction mixture was filtered contained jelly-like material besides triethylammonium chloride. The residue was extracted with boiling benzene and the benzene solution evaporated to yield 1.65 g of the ester, m.p. 132–138°. The original ether mother liquor was evaporated to yield 550 mg of the ester, m.p. 135–140°; total yield 2.2 g (63%). After the product was crystallized from ether, it had m.p. 145–146°.

Anal. Calcd. for $C_{14}H_{11}ClN_2O_5S$: C, 47.46; H, 3.10; Cl, 10.00; N, 7.91; S, 9.00. Found: C, 47.73; H, 3.29; Cl, 10.28; N, 7.93; S, 8.72.

Although it is reported in the literature (14) that *m*-nitrobenzonitrile oxide is fairly stable, we could not isolate it in a pure form. On concentration it invariably turned to jelly-like material, possibly a dimer or trimer of the nitrile oxide. Therefore, the required nitrile oxide was always prepared *in situ* in dilute solution.

Reaction of Nitrile N-Oxides with Benzylsulfonyl Chloride in the Presence of Triethylamine in Benzene

The reactions in benzene were carried out the same as those in ether at a temperature of 10 to 15°. The yields of esters were: I, 50%; II, 43.6%; III, 76%.

Reaction of Nitrile N-Oxides with Benzylsulfonyl Chloride in the Presence of Triethylamine in Chloroform

The reactions in chloroform were carried out the same as those in ether at room temperature. The products could not be purified by crystallization and therefore were separated on acid-washed alumina columns. From the columns a 33.4% yield of compound II and a 24% yield of compound I were isolated.

Reaction of Nitrile N-Oxides and Benzylsulfonyl Chloride in Ether

Reaction of *p*-chlorobenzonitrile N-oxide with benzylsulfonyl chloride in ether yielded a white solid (after the solution had been stirred for 2 h at ice-bath temperature and the ether evaporated), which, when it was crystallized from benzene–hexane, yielded 1.55 g (75%) of benzylsulfonyl chloride and 0.9 g of crude nitrile oxide dimer.

Benzonitrile oxide which had similarly been treated with benzylsulfonyl chloride in ether yielded a white solid, which on work-up offered 1.9 g (95%) of benzylsulfonyl chloride.

After *m*-nitrobenzonitrile N-oxide had been treated with benzylsulfonyl chloride in ether as above, a small quantity (24%) of ester III (m.p. 140–143°) separated from the ether solution on concentration and cooling.

Reaction of Nitrile N-Oxides with Benzylsulfonyl Chloride in Ether in the Presence of 1 Equivalent of Triethylammonium Chloride

Without filtering off the triethylammonium chloride from the reaction of the α-chloroaldoxime and triethylamine (1 mole each) in ether, we treated the reaction mixture with 1 equivalent of benzylsulfonyl chloride, stirred it for 2 h at ice-bath temperature, and worked it up as before. When the ether was evaporated off, a liquid residue remained, in contrast to the preceding experiments. *p*-Chlorobenzonitrile oxide yielded 39% of ester II, and benzonitrile oxide yielded 22% of ester I.

Addition of 1 Equivalent of Triethylamine to a Mixture of 1 Mole of α-Chloroaldoxime and 1 Mole of Benzylsulfonyl Chloride

To an ether solution of a mixture of α-chloroaldoxime and benzylsulfonyl chloride (1 equivalent each) was added an ether solution of 1 equivalent of triethylamine at ice-bath temperature as before to yield: I, 57%; II, 75%; III, 81%.

α-Chlorobenzaldoxime Methanesulfonate (IV)

To an ether solution of 1.6 g of α-chlorobenzaldoxime was added 2 g of triethylamine at once at ice-bath

Can. J. Chem. Downloaded from www.nrcresearchpress.com by 210.87.254.42 on 09/05/12
For personal use only.

temperature followed by the addition of an ethereal solution of 1.2 g of methanesulfonyl chloride as before. From the residue, obtained after the ether had been evaporated, was isolated 0.8 g (33%) of ester IV (m.p. 106–109°), which, on further crystallization from benzene–hexane, had m.p. 110–111°.

Anal. Calcd. for $C_8H_8ClNO_3S$: C, 41.20; H, 3.43; Cl, 15.23; N, 6.01; S, 13.73. Found: C, 41.53; H, 3.46; Cl, 15.33; N, 5.94; S, 13.59.

p-Chloro(α-chloro)benzaldoxime Methanesulfonate (V)

Prepared as above, m.p. 80°.

Anal. Calcd. for $C_8H_7Cl_2NO_3S$: C, 35.82; H, 2.61; Cl, 26.50; N, 5.22; S, 11.94. Found: C, 35.76; H, 2.72; Cl, 26.35; N, 5.25; S, 12.21.

m-Nitro(α-chloro)benzaldoxime Methanesulfonate (VI)

Prepared as above with benzene as solvent (10 to 15° bath temperature); 1.4 g (50%) of crude ester VI was obtained (m.p. 91–95°), which, on further crystallization from benzene, had m.p. 98–100°.

Anal. Calcd. for $C_8H_7ClN_2O_5S$: C, 34.40; H, 2.51; Cl, 12.70; N, 10.03; S, 11.50. Found: C, 34.67; H, 2.51; Cl, 22.82; N, 9.96; S, 11.26.

syn-Benzaldoxime Benzylsulfonate (VII)

By using the method described for I, compound VII was prepared. The crude product, when it was dissolved in benzene and diluted with hexane, had m.p. 67–73°, and on further crystallization had m.p. 77–79°. The ester is unstable and decomposes to nitrile at room temperature in a couple of days. The infrared spectrum showed typical $\diagup\!\!\diagdown SO_2$ stretching bands at 1 175 cm^{-1} and 1 370 cm^{-1}.

The α-hydrogen of the aldoxime in the ester was not successfully replaced by chlorine as follows. (*a*) Dry chlorine was passed through a solution of 0.5 g of the ester at ice temperature for 20 min. When the solvent was evaporated, unchanged ester was recovered. (*b*) The same reaction was conducted at room temperature without success. (*c*) The ester was suspended in 8 *N* HCl and chlorine was passed through at room temperature, but only the unchanged ester was recovered.

syn-p-Chlorobenzaldoxime Benzylsulfonate (VIII)

The ester was prepared as above, m.p. 103°. The ester could not be chlorinated further.

Anal. Calcd. for $C_{14}H_{12}ClNO_3S$: C, 54.20; H, 3.87; N, 4.51; Cl, 11.42; S, 10.32; mol. wt. 310. Found: C, 54.29; H, 4.01; N, 4.42; Cl, 11.49; S, 10.19; mol. wt. 311.

The ester, when it was passed through an alumina column, decomposed to nitrile, m.p. 92° (lit. (16) m.p. 93–94°).

anti-m-Nitrobenzaldoxime Benzylsulfonate (IX)

The ester was prepared as above. The yield was quantitative (m.p. 90–92°).

Anal. Calcd. for $C_{14}H_{12}N_2O_5S$: C, 52.50; H, 3.75; N, 8.75; S, 10.00. Found: C, 52.48; H, 3.79; N, 8.55; S, 10.19.

Attempted Preparation of syn-2,4,6-Trimethylbenzaldoxime Benzylsulfonate

The same method was employed as described above, 3.26 g of oxime being used. The ester was a white solid at ice temperature. When it was dissolved in benzene at room temperature it decomposed spontaneously. Next day the solution was chromatographed on acid-washed alumina and the following compounds were isolated: 2,4,6-trimethylbenzonitrile (2 g), m.p. 49–51° (lit. m.p. 54°); *syn*-2,4,6-trimethylbenzaldoxime (100 mg), m.p. 125°; 2,4,6-trimethylformanilide (100 mg), m.p. 177–178° (lit. (17) m.p. 177°).

Hydrolysis of I and II

The esters (500 mg each) were hydrolyzed with 1 g of KOH dissolved in 50 ml of ethanol at room temperature (1 h) or at reflux temperature (½ h). The solution was diluted with water and the ethanol was removed under vacuum. The remaining solution was extracted with chloroform, dried over sodium sulfate, and evaporated to dryness. II at reflux temperature yielded 110 mg of *p*-chlorobenzamide, m.p. 172–174°, which, on further crystallization, had m.p. 176–177°; mixed melting point with an authentic sample, 175–176°. The same ester, on hydrolysis at room temperature, yielded a few milligrams of amide and 110 mg of crude *p*-chlorobenzonitrile, m.p. 80–87°. Hydrolysis of I at reflux temperature yielded 30 mg of benzamide, m.p. 125–126°, and at room temperature about 100 mg of crude benzonitrile.

Reaction of III with Triethylamine in Benzene

To a solution of 1.6 g of ester III in 50 ml of dry benzene was added 10 ml of triethylamine, and the solution was heated under reflux for 1 h. The solution was concentrated and added to an acid-washed alumina column prepared in hexane. Elution with benzene gave 340 mg of *m*-nitrobenzonitrile, m.p. 115–116° (lit. (18) m.p. 117–118°).

Reaction of m-Nitrobenzonitrile N-Oxide with Methanesulfonic Anhydride in Ether in the Presence of Triethylamine

To an ether (50 ml) solution of 1.75 g of methanesulfonic anhydride was added at ice-bath temperature

Can. J. Chem. Downloaded from www.nrcresearchpress.com by 210.87.254.42 on 09/05/12
For personal use only.

an ether solution of 1.65 g of *m*-nitrobenzonitrile oxide. To the stirred solution was added, dropwise, an ether solution of 1 g of triethylamine (20 min). The solution was evaporated and the residue was treated with benzene, from which 0.4 g of the dimer of *m*-nitrobenzonitrile oxide was isolated. The residue was an orange liquid, which could not be identified further. However, the liquid did not show any characteristic $\rangle SO_2$ stretching bands in the infrared spectrum.

Reaction of p-Chlorobenzonitrile N-Oxide with Methanesulfonic Anhydride in the Presence of Triethylamine

The reaction was conducted as above, 1.9 g of *p*-chloro(α-chloro)benzaldoxime being used. The residue (after the ether had been evaporated) was treated with water and filtered to yield only *p*-chlorobenzonitrile oxide, as determined from its infrared spectrum (band at 2 300 cm^{-1} (vs)). The product was dissolved in benzene and worked up the next day to yield 1.1 g of the dimer of the nitrile oxide (m.p. 139–142°).

In a similar reaction in chloroform at room temperature 0.9 g of the dimer of the nitrile oxide (m.p. 139–142°) was obtained; the remaining residue was also a solid which showed a weak band at 2 300 cm^{-1} in its infrared spectrum caused by nitrile oxide but no bands caused by $\rangle SO_2$ stretching.

m-Nitrobenzamidoxime

Gaseous ammonia was passed through a benzene (50 ml) solution of 2.5 g of *m*-nitro(α-chloro)benzaldoxime for 15 min. The benzene solution was evaporated to dryness, and the residue was treated with water to remove ammonium chloride and crystallized from aqueous ethanol. The first crop was orange, m.p. 164–167°. The infrared spectrum showed two sharp bands at 3 500 – 3 400 cm^{-1} (vw) and 3 400 – 3 300 cm^{-1} (vw), a broad band at 3 200 cm^{-1}, and a sharp peak at 1 675 cm^{-1}. The second crop was greyish white, m.p. 167–170°, and there was a depression in the mixed melting point of the two. The first crop, on further crystallization, had m.p. 169–170°, yield 0.9 g (lit. (19) m.p. 174°).

When a similar experiment was done in ethanol at room temperature, a large amount of solid precipitated from the ethanol solution, m.p. 179–181°, which was not the dimer of the nitrile oxide. The yield of *m*-nitrobenzamidoxime was about the same as above. When ammonia was passed through the alcoholic solution at *ice-bath* temperature, the yield of *m*-nitrobenzamidoxime was doubled.

m-Nitrobenzamidoxime was also prepared by the reaction of *m*-nitrobenzonitrile and hydroxylamine, and the product was crystallized from water.

Nuclear magnetic resonance spectrum: singlet at 9.96 p.p.m. (relative area 1), multiplets at 7.4–8.6 p.p.m. (relative area 4), singlet at 6.1 p.p.m. (relative area 2).

p-Chlorobenzamidoxime

Gaseous ammonia was passed through an ethanol solution of 1 g of *p*-chloro(α-chloro)benzaldoxime at ice-bath temperature for 5 min. The solution was diluted with water and filtered. The clear solution was concentrated and cooled to give 740 mg of *p*-chlorobenzamidoxime, m.p. 127–130°. On further crystallization from water it melted at 132–133° (lit. (20) m.p. 134°). The infrared spectrum showed two sharp bands at 3 400 – 3 500 cm^{-1} (vw) and 3 300 – 3 400 cm^{-1} (vw), a broad band at 3 200 cm^{-1}, and a strong band at 1 650 cm^{-1}. Nuclear magnetic resonance spectrum: singlet at 9.64 p.p.m. (relative area 1), multiplets at 7.2–7.8 p.p.m. (relative area 4), singlet at 5.8 p.p.m. (relative area 2).

p-Chlorobenzamidoxime was also prepared by heating under reflux overnight a clear aqueous alcoholic solution of *p*-chlorobenzonitrile and hydroxylamine.

Benzamidoxime

A clear aqueous alcoholic solution of 0.1 mole of hydroxylamine and 0.1 mole of benzonitrile was gently heated under reflux overnight, concentrated, and cooled. The oil which separated out was poured on a porous plate, where it solidified. The solid was dissolved in benzene and crystallized, m.p. 76–78° (lit. (21) m.p. 78°). Infrared spectrum: two sharp bands at 3 400 – 3 500 cm^{-1} (vw) and 3 300 – 3 400 cm^{-1} (vw), a broad band at 3 200 cm^{-1}, and a band at 1 640 cm^{-1} (vs). Nuclear magnetic resonance spectrum: singlet at 9.64 p.p.m. (relative area 1), multiplets at 7.2 to 7.8 p.p.m. (relative area 5), singlet at 5.74 p.p.m. (relative area 2).

m-Nitrobenzamidoxime O-Benzylsulfonate (XII)

To an acetone (30 ml) solution of 1.75 g (0.005 mole) of the ester III was added 5 ml of ammonium hydroxide, and the mixture was stirred for ½ h at room temperature. Most of the acetone was removed under vacuum and diluted with water. A brown oil separated which soon solidified. The solid was dissolved in chloroform and diluted with hexane to give 1.1 g of crude XII (m.p. 117–120°). The mother liquor, on further concentration, gave a second fraction (m.p. 135–141°) which was mainly III. The first fraction, on further crystallization from benzene, had m.p. 127° (decomp.).

Anal. Calcd. for $C_{14}H_{13}N_3O_5S$: C, 50.15; H, 3.91; N, 12.53; S, 9.55. Found: C, 50.40; H, 3.95; N, 12.36; S, 9.72.

Infrared spectrum: two sharp bands at 3 400 – 3 500 cm^{-1} (vw) and 3 300 – 3 600 cm^{-1} (vw), a band at 1 640 cm^{-1} (s). Nuclear magnetic resonance spectrum: multiplets at 6.8–8.6 p.p.m. (relative area 11), singlet at 4.8 p.p.m. (relative area 2).

Can. J. Chem. Downloaded from www.nrcresearchpress.com by 210.87.254.42 on 09/05/12
For personal use only.

When ammonia was passed through the solution of the ester III in benzene at room temperature, only the starting material was recovered quantitatively.

m-Nitrobenzamidoxime O-benzylsulfonate was also prepared by the reaction of *m*-nitrobenzamidoxime with benzylsulfonyl chloride in the presence of triethylamine in tetrahydrofuran at ice-bath temperature. The solution was evaporated to dryness under reduced pressure and water was added to remove *m*-nitrobenzamidoxime. The ester was crystallized from benzene. The yield was quantitative, m.p. 126–127° (decomp.). The mixed melting point with the above ester was 125–126° (decomp.) and the infrared spectra of the two were identical.

p-Chlorobenzamidoxime O-Benzylsulfonate (XI)

The reaction was done as above with 1 g of II, except that the solution was gently heated under reflux for ½ h. The crude product (510 mg) was crystallized from benzene–hexane, m.p. 89–90° (decomp.).

Infrared spectrum: two sharp bands at 3 400 – 3 500 cm^{-1} and 3 300 – 3 400 cm^{-1}, a band at 1 640 cm^{-1}.

Compound XI was also prepared from *p*-chlorobenzamidoxime in ether as above. The white residue obtained after the ether had been evaporated was shaken with water to remove unreacted *p*-chlorobenzamidoxime, and the residue (90%) was crystallized. The first fraction (1 g) was pure XI, m.p. 87–89° (decomp.). The infrared spectrum was identical with that of the above material and there was no depression in the mixed melting point. The second fraction melted at 87–89°, but left a residue. The third fraction, m.p. 139–140°, had an infrared spectrum which indicated that it was a quaternary ammonium salt; also present were characteristic $\rangle SO_2$ stretching vibrations, indicating that the ester might be unstable and might decompose in the process of purification.

Anal. Calcd. for $C_{14}H_{13}ClN_2O_3S$ (m.p. 87–89°): C, 51.45; H, 4.01; Cl, 10.8; N, 8.6; S, 10.00. Found: C, 51.61; H, 3.97; Cl, 10.97; N, 8.40; S, 9.60.

Benzamidoxime O-Benzylsulfonate (X)

The reaction was done as above with 1 g of ester I, except that the reaction mixture was kept (well corked) for 2½ h at room temperature; 440 mg of crude X was obtained, m.p. 94° (decomp.). The compound is slightly soluble in benzene and ether. On crystallization from ether it had m.p. 98° (decomp.).

Infrared spectrum: two sharp bands at 3 400 – 3 500 cm^{-1} and 3 300 – 3 400 cm^{-1}, a strong band at 1 629 cm^{-1}.

Compound X was also prepared from benzamidoxime in ether as above. When the crude product was crystallized from ether, the ester had m.p. 102° (decomp.). The infrared spectrum was identical with that of the above material and a mixed melting point of the two was 98° (decomp.).

Anal. Calcd. for $C_{14}H_{14}N_2O_3S$: C, 57.93; H, 4.82; N, 9.6; S, 11.03. Found: C, 57.82; H, 5.00; N, 9.39; S, 10.84.

ACKNOWLEDGMENT

This investigation was supported by Public Health Service grant No. CA-04536-06 from the National Cancer Institute.

REFERENCES

1. G. STORK and I. J. BOROWITZ. J. Am. Chem. Soc. **84**, 313 (1962). G. OPITZ and H. ADOLPH. Angew. Chem. **74**, 77 (1962). W. E. TRUCE *et al.* J. Am. Chem. Soc. **84**, 3030 (1962).
2. W. E. TRUCE, J. R. NORELL, R. W. CAMPBELL, D. G. BRADY, and J. W. FIELDHOUSE. Chem. Ind. London, 1870 (1965).
3. R. HUISGEN. Angew. Chem. Intern. Ed. Engl. **2**, 573 (1963).
4. R. H. WILEY and B. J. WAKEFIELD. J. Org. Chem. **25**, 546 (1960).
5. W. E. TRUCE and A. R. NAIK. Unpublished observations.
6. CH. GRUNDMANN and J. M. DEAN. Angew. Chem. Intern. Ed. Engl. **3**, 585 (1964).
7. M. H. BENN. Can. J. Chem. **42**, 2393 (1964).
8. (*a*) A. R. NAIK. Ph.D. Thesis, University of California, San Francisco, California. 1963. (*b*) M. O. FORSTER and H. H. JUDD. J. Chem. Soc. **97**, 263 (1910).
9. R. J. CRAWFORD and C. WOO. Can. J. Chem. **43**, 1534 (1965).
10. H. E. UNGNADE, L. W. KISSINGER, A. NARATH, and D. C. BARHAM. J. Org. Chem. **28**, 134 (1963).
11. C. L. BELL, C. N. V. NAMBURY, and L. BAUER. J. Org. Chem. **29**, 2873 (1964).
12. H. RHEINBOLDT. Ann. **451**, 161 (1927).
13. O. PILOTY and H. STEINBOCK. Ber. **35**, 3112 (1902).
14. A. QUILICO. The chemistry of heterocyclic compounds. Vol. 17. Interscience Publishers, Inc., New York. 1962. p. 21. Table II.
15. J. EISENBERG. Ber. **15**, 1017 (1882).
16. F. BEILSTEIN and A. KUHLBERG. Ann. **146**, 336 (1868).
17. A. HANTZSCH and A. LUCAS. Ber. **28**, 749 (1895).
18. I. RAMSEN, R. N. HARTMAN, and A. M. MAKENFUSS. Am. Chem. J. **18**, 169 (1896).
19. M. SCHOPFF. Ber. **18**, 1063 (1885). A. WERNER. Ber. **27**, 2848 (1894).
20. C. H. ANDREWES, H. KING, and J. WALKER. Proc. Roy. Soc. London, Ser. B, **133**, 20 (1946).
21. F. TIEMANN and P. KRUGER. Ber. **17**, 1685 (1884).

Can. J. Chem. Downloaded from www.nrcresearchpress.com by 210.87.254.42 on 09/05/12
For personal use only.

Can. J. Chem. Downloaded from www.nrcresearchpress.com by 210.87.254.6 on 09/05/12
For personal use only.

THE PREPARATION OF 5-ALKYLTHIO, BRANCHED TRYPTAMINES

J. KENNETH HORNER, J. I. DEGRAW, AND W. A. SKINNER

Department of Pharmaceutical Chemistry, Life Sciences Research, Stanford Research Institute, Menlo Park, California

Received August 9, 1965

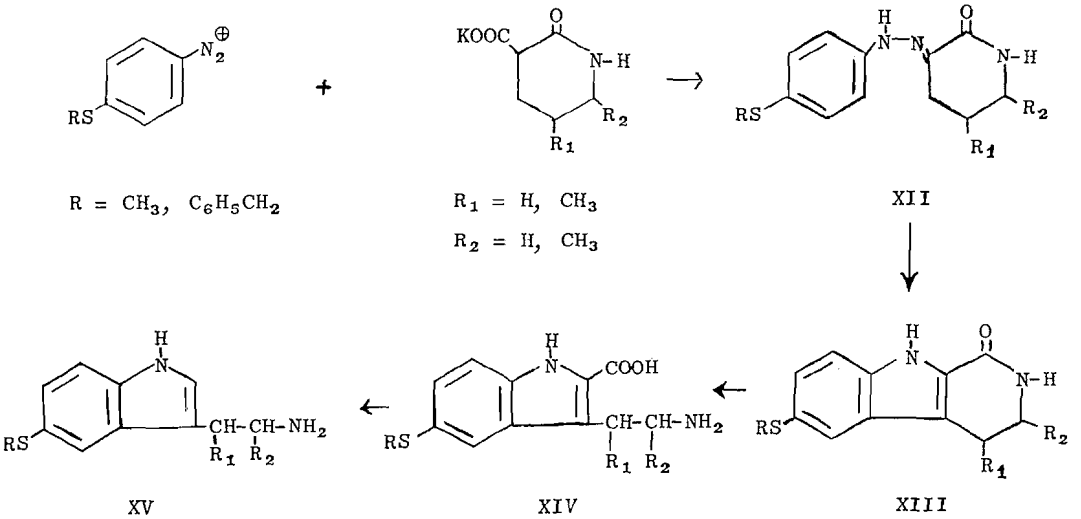
ABSTRACT

The Japp–Klingemann reaction has been employed to prepare six new tryptamines. Data on the intermediate phenylhydrazones, β-carbolines, and tryptamine carboxylic acids are presented. Syntheses of 5-methyl-, 6-methyl-, 5,5-dimethyl-, and 5,6-dimethyl-2-oxopiperidine-3-carboxylates are described.

Analogues of tryptamine have aroused considerable interest because of the implication of serotonin in the etiology of certain psychotic disorders. In a recent paper (1) we described the synthesis of the thiol analogue of serotonin. As an extension of this work we have now prepared some 5-alkylthio, branched-chain tryptamines.

The preparation of the various 5-alkylthiotryptamines was based on the piperidone procedure first introduced by Abramovitch and Shapiro (2). This route obviates the use of difficultly obtained indoles as starting materials and has been employed by several authors (1–5) for the synthesis of nuclear-substituted tryptamines. It was recently extended by Russian workers to include α-methyltryptamines (6, 7) and α,β-dimethyltryptamines (8). Abramovitch and Muchowski (9) further expanded the method to prepare β-methyltryptamines. An attempt by us to apply the method for the synthesis of 5-methylthio-β,β-dimethyltryptamine was unsuccessful when we were unable to hydrolyze the intermediate oxo-β-carboline (XIII-G; Table II). The general synthetic route is outlined in Reaction Scheme 1.

Utilizing the versatile Japp–Klingemann reaction, we prepared substituted 2,3-piperidione-3-(4′-alkylthio)phenylhydrazones (XII) from the various methyl-substituted



REACTION SCHEME 1.

Can. J. Chem. Downloaded from www.nrcresearchpress.com by 210.87.254.6 on 09/05/12
For personal use only.

3-carbethoxy-2-piperidones. The phenylhydrazones XII were cyclized in acid to the substituted 6-alkylthio-1,2,3,4-tetrahydro-1-oxo-β-carbolines (XIII). All β-carbolines underwent alkaline hydrolysis to the corresponding 3-aminoalkyl-5-alkylthio-2-indole carboxylic acid (XIV), except 4,4-dimethyl-6-methylthio-1,2,3,4-tetrahydro-1-oxo-β-carboline (XIII-G). With this compound, only starting material was isolated under a variety of alkaline hydrolytic conditions.

Infrared, ultraviolet, and nuclear magnetic resonance spectra were obtained for 6-methylthio-1,2,3,4-tetrahydro-1-oxo-β-carboline and for the 3-methyl-, 4-methyl-, and 4,4-dimethyl-6-methylthio-1,2,3,4-tetrahydro-1-oxo-β-carbolines. In each case the spectra were inspected in an effort to find some difference in the 4,4-dimethyl compound which would account for its stability to basic hydrolysis. Enolization of the amide moiety of the lactam would confer alkaline stability upon the molecule, but infrared data failed to show any indication of C=N absorption in the critical 5.75–6.05 μ region in any of the β-carbolines. Ultraviolet spectra were unchanged when run in neutral and alkaline media, again indicating a lack of enolization. Nuclear magnetic resonance data on the four compounds, obtained on a 100 Mc instrument, showed the expected peaks and frequency shifts, except for those protons in the 5-positions. The 5-proton was found at 7.56 p.p.m. in both the non-methylated β-carboline and the 3-methyl β-carboline spectra. The 4-methyl spectrum showed a shift downfield of 0.11 p.p.m., and the 4,4-dimethyl a downfield shift of 0.22 p.p.m., for the 5-proton.

Menon and Simonson (10) reported that 4,4-dimethyl-2-piperidone was not hydrolyzed in base, while Kuhn and Jerchel (11) reported that 6-methyl-2-piperidone was opened under the same conditions. This retardation of ring-opening reactions by geminal substitution is well known, and Bordwell and co-workers (12) have theorized that the stabilizing effect is due to decreased ability of the departing atoms to move away from each other in the transition state. In our case nuclear magnetic resonance data have indicated interaction between the *gem*-dimethyls and the 5-proton. Molecular models suggest that there would also be rotational restriction between the *gem*-dimethyls and the carboxylate ion in the lyate species. These conditions would promote rapid reclosure to the lactam ring.

The 5-alkylthio, branched tryptamines (XV) were obtained in good yield by facile decarboxylation of the carboxylic acids (XIV) in a mixture of aqueous hydrochloric and acetic acids. Physical and analytical data for the compounds obtained by the above sequence are listed in Tables I–IV.

Except for ethyl 2-oxo-5,5-dimethylpiperidine-3-carboxylate (XI), the carbethoxypiperidones used in this work were prepared by modified versions of previously described procedures. These modifications along with references to the original methods are described in the Experimental section. The synthesis of ethyl 2-oxo-5,5-dimethylpiperidine-3-carboxylate (XI) was achieved by a three-step procedure starting with diethyl methylene malonate (13). The vinyl ester was allowed to react with 1-piperidino-2-methylpropene (14) to yield the formyl diester IX. The oxime X was prepared as described previously and hydrogenated over Raney nickel to yield piperidone XI, as shown in Reaction Scheme 2.

EXPERIMENTAL

Ethyl 2-Oxo-6-methylpiperidine-3-carboxylate (III)

A mixture of 1.2 g of ethyl 2-carbethoxy-4-acetylbutyrate (I) (15), 1.2 g of hydroxylamine hydrochloride, 6 ml of pyridine, and 6 ml of ethyl alcohol was refluxed for 3 h. The colorless solution was evaporated to dryness *in vacuo* and the residual syrup was partitioned between 15 ml of ether and 15 ml of water. The aqueous portion was extracted with another 15 ml of ether and the combined ether extracts were washed with 10 ml of water. The ether was dried and evaporated *in vacuo* to leave 0.98 g of syrup; λ_{max}^{film} 2.9–3.0 μ

Can. J. Chem. Downloaded from www.nrcresearchpress.com by 210.87.254.6 on 09/05/12
For personal use only.

TABLE I

2,3-Piperidione-*p*-alkylthiophenylhydrazones (XII)

XII	R	R_1	R_2	Yield (%)	Melting point* (°C)	Calcd. C	Calcd. H	Calcd. N	Found C	Found H	Found N
A	CH_3	H	CH_3	76	215	59.3	6.51	16.0	59.1	6.58	16.0
B	$C_6H_5CH_2$	H	CH_3	27	225–227	67.2	6.24	12.4	67.0	6.18	12.3
C	CH_3	CH_3	H	47	222	59.3	6.51	16.0	59.2	6.57	15.8
D	$C_6H_5CH_2$	CH_3	H	58	215	67.2	6.24	12.4	67.1	6.23	12.4
E	CH_3	CH_3	CH_3	58	213	60.6	6.91	15.2	60.6	6.93	15.0
F	$C_6H_5CH_2$	CH_3	CH_3	92	215–217	68.0	6.56	11.9	67.8	6.58	12.1
G	CH_3	Di-CH_3	H	90	232	60.6	6.91	15.2	60.2	6.91	15.2

*All melting points are uncorrected and were taken on a Fisher–Johns melting block.

TABLE II

6-Alkylthio-1,2,3,4-tetrahydro-1-oxo-β-carbolines (XIII)

XIII	R	R_1	R_2	Method*	Yield (%)	Melting point (°C)	Calcd. C	Calcd. H	Calcd. N	Found C	Found H	Found N
A	CH_3	H	CH_3	B	47	214	63.4	5.73	11.4	63.1	5.77	11.3
B	$C_6H_5CH_2$	H	CH_3	B	90	†	70.8	5.63	8.69	70.9	5.60	8.65
C	CH_3	CH_3	H	A	58	158	63.4	5.73	11.4	63.3	5.85	11.5
D	$C_6H_5CH_2$	CH_3	H	A	42	180	70.8	5.63	8.69	70.5	5.76	8.61
E	CH_3	CH_3	CH_3	A	‡	—	Noncrystalline					
F	$C_6H_5CH_2$	CH_3	CH_3	A	96	73–75	69.8§	7.12	7.08	69.7	7.13	7.25
G	CH_3	Di-CH_3	H	A	50	213	64.6	6.20	10.8	64.8	6.00	10.8

*Method A, hydrogen chloride and acetic acid; method B, 88–90% formic acid.
†Obtained as a noncrystalline glass by evaporative distillation, 210° at 0.3 mm.
‡Noncrystalline material was isolated and used in the next reaction without purification.
§Calculated as the isopropyl alcohol solvate.

Can. J. Chem. Downloaded from www.nrcresearchpress.com by 210.87.254.6 on 09/05/12
For personal use only.

TABLE III

5-Alkylthiotryptamine-2-carboxylic acids (XIV)

XIV	R	R_1	R_2	Yield (%)	Melting point (°C)	Calcd. C	Calcd. H	Calcd. N	Found C	Found H	Found N
A	CH_3	H	CH_3	55	253 (decomp.)	59.2	5.65	10.6	59.2	5.70	10.8
B	$C_6H_5CH_2$	H	CH_3	50	—	Noncrystalline					
C	CH_3	CH_3	H	63	217–219	57.1*	6.28	10.2	56.9	5.92	9.98
D	$C_6H_5CH_2$	CH_3	H	95	207	65.4*	6.05	8.05	65.7	6.04	8.22
E	CH_3	CH_3	CH_3	42†	223–225	60.4	6.52	10.1	60.0	6.69	10.4
F	$C_6H_5CH_2$	CH_3	CH_3	94	200–202	67.8	6.26	7.91	67.4	6.43	7.97

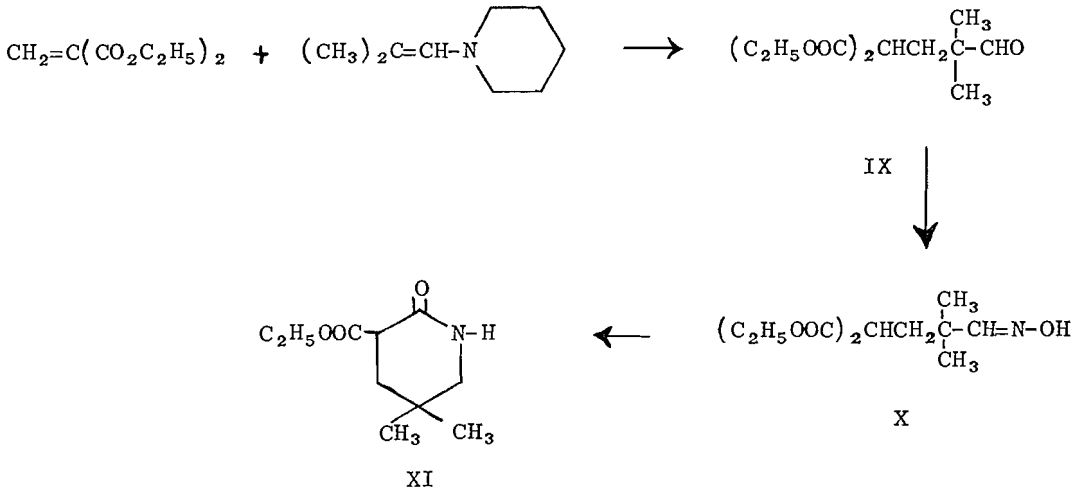
*Calculated as the hemihydrate.
†This yield includes the preparation of the noncrystalline β-carboline (XIII-E).

TABLE IV

5-Alkylthio, methyl-substituted tryptamines (XV)

XV	R	R_1	R_2	Yield* (%)		Melting or boiling point (°C)	Calcd. C	Calcd. H	Calcd. N	Found C	Found H	Found N
A	CH_3	H	CH_3	75	Free base	108	65.4	7.32	12.7	64.9	7.22	12.5
B	$C_6H_5CH_2$	H	CH_3	46	Picrate†	200	54.9	4.41	13.3	54.9	4.57	13.2
C	CH_3	CH_3	H	79	HCl	212–215	56.1	6.67	10.9	56.0	6.65	11.1
D	$C_6H_5CH_2$	CH_3	H	69	HCl	210	64.9	6.36	8.42	64.7	6.23	8.15
E	CH_3	CH_3	CH_3	68	Picrate	202–205	49.2	4.57	15.1	49.4	4.67	15.1
F	$C_6H_5CH_2$	CH_3	CH_3	72	Free base	170 at 0.3	73.5	7.14	9.03	73.8	7.20	8.99

*Yields calculated for free bases.
†XV-B hydrochloride, m.p. 219°.



REACTION SCHEME 2.

(NH, OH), 5.7–5.8 μ (ester C=O), 6.0 μ (C=N). The material was not purified further and was used directly in the next reaction.

A mixture of 185.7 g of ethyl 2-carbethoxy-4-acetylbutyrate ketoxime (II), 6 teaspoonfuls of W-2 Raney nickel, and 150 ml of ethyl alcohol was shaken under 3 atmospheres of hydrogen at 80°. The absorption of gas was complete after 98 h. The catalyst was removed by filtration and the filtrate was evaporated *in vacuo* to leave 117 g (84%) of off-white crystals. A portion was recrystallized from cyclohexane to yield an analytical sample, m.p. 71–73° (lit. m.p. 73° (7)). A more direct method (16) for the preparation of III has recently appeared.

Ethyl 2-Carbethoxy-4-acetylvalerate (IV)

To a solution of 0.2 g of sodium in 135 ml (0.84 mole) of diethyl malonate was added 18.0 g (0.21 mole) of methyl isopropenyl ketone over 15 min. The temperature rose to 45° and was maintained there by an external cold water bath. The mixture was stirred for 20 min, neutralized with acetic acid, and distilled *in vacuo* through a short Vigreux column. Excess diethyl malonate (95 g) was collected at 60–100° and 1.2 mm, and 39.7 g (76%) of product was collected at 122–132° and 1.2 mm. Redistillation of the latter fraction gave 32.2 g (62%), b.p. 116–122° at 1.0 mm.

In larger runs, the methyl isopropenyl ketone was distilled from a 50% monomer solution (K & K Chemical Co.) directly into the sodiomalonate solution. Yields of 70–75% were obtained by this procedure.

The analytical sample boiled at 124–125° and 1.7 mm.

Anal. Calcd. for $C_{12}H_{20}O_5$: C, 59.0; H, 8.25. Found: C, 59.1; H, 8.24.

Ethyl 2-Oxo-5,6-dimethylpiperidine-3-carboxylate (VI)

Ethyl 2-carbethoxy-4-acetylvalerate ketoxime (V) was prepared from the keto ester IV by the same procedure used to prepare oxime II.

A mixture of 126.8 g of oxime V, 2.5 teaspoonfuls of W-2 Raney nickel, and 150 ml of ethyl alcohol was shaken with hydrogen at 4 atmospheres and 100° for 66 h, thereby consuming 91% of the theoretical amount of gas. The catalyst was removed, and the solvent was evaporated to leave 96.3 g (99%) of the piperidone VI; λ_{max}^{film} 3.10 μ (NH), 5.75 μ (ester C=O), 5.99 μ (lactam C=O), *no* 10.69 μ band as seen in oxime V. The analytical sample was prepared by dissolving the oil in benzene and filtering the solution to separate a small amount of free acid. The benzene was concentrated and the residue was heated at 100° under reduced pressure. The residual oil did not crystallize. Reference 8 listed m.p. 67–68°.

Anal. Calcd. for $C_{10}H_{17}NO_3$: C, 60.3; H, 8.60; N, 7.03. Found: C, 60.0; H, 8.53; N, 7.10.

Ethyl 2-Oxo-5-methylpiperidine-3-carboxylate (VIII)

This compound was prepared essentially by the method of Abramovitch and Muchowski (9). The procedure involved the Michael addition of diethyl malonate and methacrylonitrile. The resulting ethyl 2-carbethoxy-4-cyanovalerate (VII) was hydrogenated to yield the piperidone VIII. We were able to effect this reduction over platinum oxide at low pressure, while the above authors utilized Raney nickel at high pressure.

Ethyl 2-Carbethoxy-4-formylisovalerate (IX)

To 88.0 g (0.63 mole) of 1-piperidino-2-methylpropene (14) was rapidly added 110.0 g (0.63 mole) of

Can. J. Chem. Downloaded from www.nrcresearchpress.com by 210.87.254.6 on 09/05/12
For personal use only.

diethyl methylene malonate (13). The resulting warm solution was cooled to room temperature and allowed to stand for 1 h. Ice water (100 ml) was added, and the mixture was adjusted to pH 3–4 with 6 *N* hydrochloric acid and stirred for 15 min. The acidic mixture was extracted with two 250 ml portions of ether. The ether was washed twice with 250 ml portions of water, and then with 100 ml of saturated sodium bicarbonate. The ethereal solution was dried and evaporated *in vacuo* to leave 110 g of a colorless syrup, which was distilled at 114–120° and 1.3 mm to give 71.5 g (46%). An analytical sample had b.p. 95–96° at 1.0 mm; λ_{max}^{film} 3.60 μ, 3.70 μ (aldehyde, C—H), 5.7–5.8 μ (ester, aldehyde C=O).

Anal. Calcd. for $C_{12}H_{20}O_5$: C, 59.0; H, 8.25. Found: C, 58.8; H, 8.39.

Ethyl 2-Oxo-5,5-dimethylpiperidine-3-carboxylate (XI)

Ethyl 2-carboxy-4-formylisovalerate aldoxime (X) was prepared from the formyl ester IX by the same procedure used to prepare the oxime II.

A mixture of 59.0 g of the oxime X, 5 teaspoonfuls of W-2 Raney nickel, and 150 ml of ethyl alcohol was shaken for 48 h under 3 atmospheres of hydrogen at 60°. The catalyst was removed and the solvent evaporated to leave 46.7 g (98%) of a syrup which crystallized after 2 weeks. A portion was triturated with cyclohexane to yield white crystals, m.p. 44–47°.

Anal. Calcd. for $C_{10}H_{17}NO_3$: C, 60.3; H, 8.60; N, 7.03. Found: C, 60.0; H, 8.55; N, 7.00.

2,3-Piperidione-p-alkylthiophenylhydrazones (XII)

All phenylhydrazones (XII-A–XII-G) listed in Table I were prepared by the same general procedure, which is described here for the preparation of 6-methyl-2,3-piperidione-3-(4′-methylthio)phenylhydrazone (XII-A).

Ethyl 2-oxo-6-methylpiperidine-3-carboxylate (III) (9.7 g, 0.05 mole) was dissolved in 25 ml of warm ethyl alcohol, cooled to 0°, and diluted with a solution of 3.5 g (0.05 mole) of potassium hydroxide in 75 ml of water. This clear solution was chilled overnight and diluted with 200 g of a mixture of cracked ice and water. The cold solution was stirred while a suspension of 4-methylthiobenzene diazonium chloride was added in one portion followed by the immediate addition of 6 g of sodium acetate. The diazonium salt was prepared from 0.05 mole of 4-methylthioaniline in 30 ml of 4 *N* hydrochloric acid and 0.05 mole of sodium nitrite. In the formation of this diazonium salt it was necessary to stir the reactants for 1–2 h at 0° to ensure complete reaction. The mixture was stirred at 0° for 6 h, and the tan solid was collected by filtration and washed well with water. The crude material was washed with ether, and then with cold ethyl alcohol, and was sufficiently pure for further reactions.

An analytical sample, m.p. 215°, was prepared by recrystallizations from 2-methoxyethanol and then from dilute ethyl alcohol.

All crystalline phenylhydrazones XII had infrared absorption spectra with these approximate values; λ_{max}^{Nujol} 3.10 μ, 3.15 μ (NH), 6.00 μ (amide C=O), 6.23 μ (aryl), 6.44 μ (amide II). The three benzyl-substituted hydrazones (XII-B, XII-D, and XII-F) showed 1,4-disubstituted benzene absorption near 12.1 μ.

5-Alkylthio-1,2,3,4-tetrahydro-1-oxo-β-carbolines (XIII)

The phenylhydrazones XII were cyclized to the β-carbolines (XIII-A–XIII-G) listed in Table II by a general method with either hydrogen chloride and glacial acetic acid or 88–90% formic acid. The preparation of 3-methyl-6-methylthio-1,2,3,4-tetrahydro-1-oxo-β-carboline (XIII-A) is described below. The acetic acid modification follows.

A solution of 9.5 g (0.035 mole) of 6-methyl-2,3-piperidione-3-(4′-methylthio)phenylhydrazone (XII-A) in 80 ml of 88–90% formic acid was refluxed for 1 h, cooled to 25°, and concentrated *in vacuo*. The residue was washed with ice and water, then separated, and triturated with ethyl alcohol to give a tan solid. This solid was collected and used in the next reaction without further purification. An analytical sample, m.p. 214°, was prepared by recrystallizations from butyl chloride – ethyl alcohol mixtures and finally from isopropyl alcohol.

In the preparation of the six β-carbolines XIII-C–XIII-G the phenyl hydrazones XII-C–XII-G were dissolved in glacial acetic acid either at 25° or by slight warming, and then hydrogen chloride was passed into the solutions for 15 min. To obtain maximum yields and to avoid decomposition, the resulting suspensions were heated for varying periods of time and at different temperatures: C, 15 min on a steam bath; D, 15 min at reflux; E, 10 min on a steam bath and 40 min at reflux; F, 1 min at reflux and 40 min at 25°; G, 15 min at reflux. These acetic acid solutions were then cooled, concentrated to approximately one-third volume under reduced pressure, and diluted with ice water. The aqueous portion was decanted and the gums were crystallized from hot isopropyl alcohol.

The β-carbolines XIII showed comparable infrared absorption spectra; λ_{max}^{Nujol} 2.90 μ, 3.07 μ (NH), 5.97 μ (amide C=O). Ultraviolet spectra: λ_{max}^{EtOH} XIII-A, 231 mμ (ϵ = 14 000); XIII-C, 248 mμ (ϵ = 16 000); XIII-G, 233 mμ (ϵ = 16 000). Nuclear magnetic resonance spectra were run in deuterated chloroform. Locations of the peaks for the 5-proton were: XIII-A, 7.56 p.p.m.; XIII-C, 7.67 p.p.m.; XIII-G, 7.78 p.p.m.

5-Alkylthiotryptamine-2-carboxylic Acids (XIV)

The tryptamine carboxylic acids XIV-A–XIV-F listed in Table III were prepared by the following

Can. J. Chem. Downloaded from www.nrcresearchpress.com by 210.87.254.6 on 09/05/12
For personal use only.

general procedure, which is described for the preparation of 3-(2′-aminopropyl)-5-methylthio-2-indole carboxylic acid (XIV-A). One β-carboline XIII-G did not yield an amino acid under these alkaline hydrolytic conditions.

A solution of 3.8 g (15 mmoles) of 3-methyl-6-methylthio-1,2,3,4-tetrahydro-1-oxo-β-carboline (XIII-A) in 75 ml of ethyl alcohol was mixed with a solution of 12 g (0.18 mole) of potassium hydroxide in 20 ml of water and heated under reflux for 12 h. The solution was cooled, concentrated to half volume *in vacuo*, and diluted with water. The alkaline aqueous solution was passed through filter aid and charcoal, and then adjusted to pH 5 with acetic acid. The resulting solid was isolated by filtration and was of sufficient purity for use in further reactions. An analytical sample, m.p. 253° (decomp.), was prepared by recrystallizations from dilute ethyl alcohol.

The solid tryptamine carboxylic acids XIV showed similar infrared absorption spectra; λ_{max}^{Nujol} 2.94 μ (NH), 3.10 μ (NH, OH), 5.90 μ (acid C=O), 6.20 μ (aryl).

5-Alkylthio, Branched Tryptamines (XV)

The acidic decarboxylations of the tryptamine carboxylic acids XIV-A–XIV-F to the corresponding tryptamines XV-A–XV-F were run as described below in the preparation of 3-(2′-aminopropyl)-5-methylthioindole (XV-A). The substituted tryptamines are listed in Table IV.

A solution of 2.0 g (7.6 mmoles) of 3-(2′-aminopropyl)-5-methylthio-2-indole carboxylic acid (XIV-A) in 30 ml of acetic acid and 40 ml of 2 *N* hydrochloric acid was heated under reflux for 15 h. The clear solution was concentrated to near dryness and diluted with water. The acidic solution was passed through filter aid and charcoal, and adjusted to pH 10. The separated oil was extracted with ether; the ethereal solution was dried and concentrated to yield the free crystalline tryptamine XIV-A. Recrystallization from dilute ethyl alcohol gave an analytical sample, m.p. 108°.

The remaining tryptamines XV-B–XV-F were oils. For analytical purposes they were either converted into the picrate salts and recrystallized from 2-methoxyethanol–water (XV-B, XV-E), or converted into the hydrochloride salts in 6 *N* hydrochloric acid and recrystallized from dilute hydrochloric acid (XV-C, XV-D). One tryptamine (XV-F) was evaporatively distilled in a short-path tube for analysis.

All of the tryptamines that were prepared showed closely related infrared absorption spectra; λ_{max}^{Nujol} 3.00 μ (indole NH), 6.20 μ, 6.25 μ (NH_2, aryl). The benzyl derivatives had monosubstituted benzene absorption at 12.9 μ and 14.2 μ.

REFERENCES

1. J. K. Horner and W. A. Skinner. Can. J. Chem. **42**, 2904 (1964).
2. R. A. Abramovitch and D. Shapiro. J. Chem. Soc. 4589 (1956).
3. E. Adlerova *et al.* Collection Czech. Chem. Commun. **25**, 784 (1960).
4. A. Allais. Fr. Patent No. 1,186,258 (August 19, 1959); Chem. Abstr. **55**, 23562 (1961).
5. M. von Strandtmann, M. P. Cohen, and J. Shavel, Jr. J. Med. Chem. **6**, 719 (1963).
6. A. G. Terzyan, R. R. Safrazbekyan, R. S. Sukasyan, and G. T. Tatevosyan. Izv. Akad. Nauk Arm. SSR Khim. Nauki, **14**, 261 (1961); Chem. Abstr. **57**, 8531 (1962); Experientia, **17**, 493 (1961).
7. N. N. Suvorov, M. N. Preobrazhenskaya, and N. V. Uvarova. Zh. Obshch. Khim. **32**, 1567 (1962); Chem. Abstr. **58**, 4499 (1963); Zh. Obshch. Khim. **33**, 3738 (1963); Chem. Abstr. **60**, 7975 (1964).
8. A. V. Mkhitaryan, A. A. Kogodovskaya, A. G. Terzyan, and G. T. Tatevosyan. Izv. Akad. Nauk Arm. SSR Khim. Nauki, **15**, 379 (1962); Chem. Abstr. **59**, 2753 (1963).
9. R. A. Abramovitch and J. M. Muchowski. Can. J. Chem. **38**, 554 (1960).
10. K. N. Menon and J. L. Simonson. J. Chem. Soc. 304 (1929).
11. R. Kuhn and D. Jerchel. Chem. Ber. **76**, 413 (1943).
12. F. G. Bordwell, C. E. Osborne, and R. D. Chapman. J. Am. Chem. Soc. **81**, 2698 (1959).
13. A. Sakurai, H. Midoridawa, and S. Aoyama. J. Sci. Res. Inst. Tokyo, **52**, 112 (1958).
14. E. Benzing. Angew. Chem. **71**, 521 (1959).
15. F. Korte and H. Machleidt. Chem. Ber. **90**, 2143 (1957). N. C. Ross and R. Levine. J. Org. Chem. **29**, 2346 (1964).
16. J. Shavel, Jr., M. von Strandtmann, and M. P. Cohen. U.S. Patent No. 3,182,071 (May 4, 1965).

Can. J. Chem. Downloaded from www.nrcresearchpress.com by 210.87.254.6 on 09/05/12
For personal use only.

A GENERAL METHOD FOR SELECTIVE N-METHYLATION OF SUBSTITUTED TRYPTAMINES[1]

J. KENNETH HORNER AND W. A. SKINNER

Department of Pharmaceutical Chemistry, Life Sciences Research, Stanford Research Institute, Menlo Park, California

Received August 16, 1965

ABSTRACT

A general method for selective N-methylation of substituted tryptamines is described. The method involves the lithium aluminium hydride reduction of an intermediate carbamate. Eleven new tryptamines and 11 new carbamoyltryptamines are described.

Can. J. Chem. Downloaded from www.nrcresearchpress.com by 210.87.254.105 on 09/05/12
For personal use only.

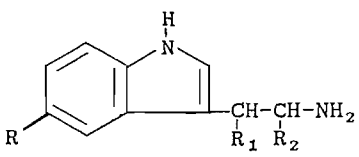
While preparing structural analogues of serotonin and bufotenin in this laboratory, we needed N-monosubstituted tryptamines (III) and N,N-disubstituted tryptamines (V). Until recently the method of choice for preparing N-substituted tryptamines was N-tosylation followed by N-alkylation with an alkyl halide and then reductive cleavage of the protective tosyl group with sodium in ammonia (1). This scheme, however, cannot be used if N,N-disubstitution is desired or if other functional groups sensitive to reductive cleavage are present on the molecule. In our laboratory 5-benzylthiotryptamine (I, R = $C_6H_5CH_2S$, $R_1 = R_2 = H$) was prepared and reduced to 5-mercaptotryptamine with sodium in ammonia (2); therefore, a different method of preparing 5-benzylthio-N-alkyltryptamines had to be found which would not cleave or reduce the labile benzylthio group.

While aryl tosylamides are sufficiently reactive to allow cleavage by hydrolysis with mineral acids (3), alkyl tosylates either are unaffected or polymerize. N,N-Dimethyl-5-aminoindole has been prepared by demethylation of the quaternary ammonium salt with sodium propoxide (4). In our laboratory the quaternary ammonium salt of N,N-dimethyltryptamine could not be demethylated by this procedure; the reaction only yielded material containing no amine function. A general method of converting β-phenethylamine into N,N-dimethylphenethylamine (5) by the Eschweiler–Clarke reaction yielded polymeric material when applied to tryptamines. Preparation of N-formyltryptamine followed by reduction with lithium aluminium hydride produced no identifiable product. N-Methyl-N-tosyltryptamine was not cleaved by boiling concentrated hydrochloric acid, nor was it reduced with lithium aluminium hydride.

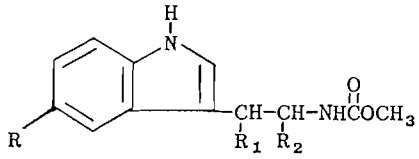
The method which yielded N-methyltryptamines (III) and N,N-dimethyltryptamines (V), and which we report here, involved preparation of the appropriate carbamates (6) (II and IV) with methyl chloroformate followed by reduction with lithium aluminium hydride. Physical properties and elemental analyses of the substituted tryptamines prepared by this procedure are summarized in Table I.

To explore the applicability of the method, commercial-grade tryptamine hydrochloride was used as a model compound. The reaction of tryptamine and methyl chloroformate yielded the only crystalline carbamate in the series of tryptamines, methyl 2-(3′-indolylethyl)-carbamate (II, $R = R_1 = R_2 = H$), which was recrystallized from ethyl alcohol – water to give the analytical sample melting at 79°. This sample gave a good elemental analysis and was insoluble in dilute acid; its infrared spectrum showed amide carbonyl

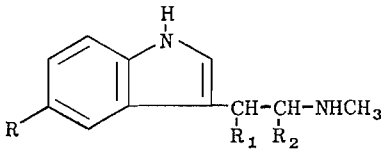
[1]*This work was supported by the U.S. Army Chemical Research and Development Laboratories, Edgewood Arsenal, Maryland.*



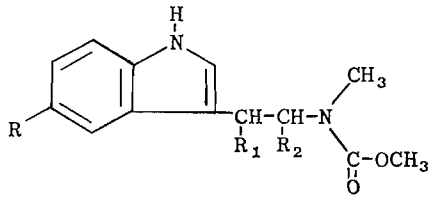
I



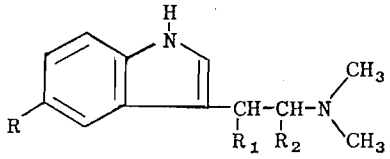
II



III



IV



V

absorption at 5.9 μ. All other carbamates that were synthesized were oils which decomposed upon attempted distillation. Their infrared absorption spectra and solubility behavior corresponded favorably with the characterized carbamate of tryptamine, and in all cases they were reduced without further purification.

The attempted preparation of the quaternary ammonium derivative of 5-methylthio-3-(2′-dimethylaminopropyl)indole (IX) by reaction with methyl iodide yielded a crystalline compound XVII having the stoichiometry $C_{16}H_{28}I_2N_2SO$. This elemental analysis was not consistent with that of a monomethiodide; however, the analysis agreed quite well with that of a dimethiodide monohydrate of IX. In the proof of the suspected sulfonium–ammonium structure, ultraviolet and infrared spectral data were inconclusive. The nuclear magnetic resonance spectrum of the starting amine IX in carbon tetrachloride (with tetramethylsilane as an internal standard) revealed that the singlet absorption of the methylthio proton occurs at 2.41 p.p.m. (three protons) and that the singlet of the dimethylamino proton occurs at 2.30 p.p.m. (six protons).

The nuclear magnetic resonance spectrum of the uncharacterized product XVII in deuterated dimethyl sulfoxide (with tetramethylsilane as an external standard) showed six protons at 3.45 p.p.m. and nine protons at 3.57 p.p.m. Tiers (7) locates the methyl proton peaks of the tetramethylammonium ion at 3.33 p.p.m. and the methylene proton peaks of the tetraethylammonium ion at 3.40 p.p.m. Comparison of the nuclear magnetic resonance spectra of ethyl octadecyl sulfide and ethyl methyloctadecyl sulfonium iodide[2] in deuterated chloroform (with tetramethylsilane as an internal standard) showed that the

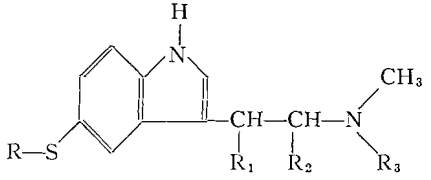
[2]*Eastman Organic Chemicals, Rochester, New York, Nos. 9434 and 9435.*

Can. J. Chem. Downloaded from www.nrcresearchpress.com by 210.87.254.105 on 09/05/12
For personal use only.

Can. J. Chem. Downloaded from www.nrcresearchpress.com by 210.87.254.105 on 09/05/12
For personal use only.

TABLE I

Yields, physical constants, and analytical results



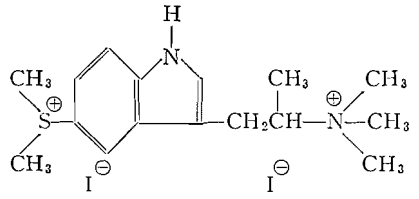
Compound	R	R_1	R_2	R_3	Yield* (%)		Melting or boiling point‡	Calcd. C	Calcd. H	Calcd. N	Found C	Found H	Found N
VI	CH_3	H	H	H	45	Picrate†	213° (decomp.)	48.1	4.26	15.6	48.3	4.45	15.6
VII	CH_3	H	H	CH_3	44	Free base	105–107°	66.6	7.74	12.0	66.4	7.75	11.8
VIII	CH_3	H	CH_3	H	78	Free base	180° at 0.4	66.6	7.74	12.0	66.5	7.92	12.0
IX	CH_3	H	CH_3	CH_3	81	Free base	200° at 0.5	67.7	8.12	11.3	67.4	8.27	11.3
X	CH_3	CH_3	H	H	84	Free base	160° at 0.3	66.6	7.74	12.0	66.8	7.74	12.0
XI	CH_3	CH_3	H	CH_3	72	Free base	102°	67.7	8.12	11.3	67.7	7.98	11.4
XII	CH_3	CH_3	CH_3	H	76	Bicarbonate†	210°	58.1	7.15	9.03	58.4	7.26	9.30
XIII	CH_3	CH_3	CH_3	CH_3	91	Free base	180° at 0.3	68.7	8.45	10.7	68.8	8.48	10.6
XIV	$C_6H_5CH_2$	H	H	H	84	HCl†	184–187°	64.9	6.36	8.42	65.1	6.40	8.42
XV	$C_6H_5CH_2$	H	CH_3	H	80	Free base	200° at 0.2	73.5	7.14	9.03	73.5	7.22	8.90
XVI	$C_6H_5CH_2$	H	CH_3	CH_3	80	Picrate†	90, 125°§	56.4	4.92	12.7	56.5	5.09	12.5

*Yields are of free bases and include preparation of the carbamate and reduction to the alkylamine.
†Analyzed as the salt.
‡All melting points are uncorrected and were taken on a Fisher–Johns melting block. Boiling points by evaporative distillation also are uncorrected.
§Compound XVI melted at 90°, and solidified and remelted at 125°.

multiplet of the sulfide methylene proton was centered at 2.5 p.p.m. (four protons). The complex absorptions of the sulfonium methylene proton were centered at 3.8 p.p.m. (four protons), and the signals of the sulfonium methyl proton were centered at 3.3 p.p.m. (three protons). These nuclear magnetic resonance spectral data, as summarized in Table II, in conjunction with the elemental analysis indicated that XVII was the monohydrate of 5-methylthio-3-(2′-dimethylaminopropyl)indole dimethiodide and that it had the ammonium–sulfonium structure.

TABLE II

Position of methyl and methylene protons in the nuclear magnetic resonance (all values are in parts per million)



XVII

Compound	N	N⊕	S	S⊕
IX	2.30 (CH_3)		2.41 (CH_3)	
XVII		3.57 (CH_3)		3.45 (CH_3)
Me_2N	2.25 (CH_3)			
$Me_4N⊕$		3.33 (CH_3)		
$Et_4N⊕$		3.40 (CH_2)		
EtS			2.5 (CH_2)	
Et S⊕ Me				3.3 (CH_3)

GENERAL EXPERIMENTAL

Methyl N-(5-Benzylthio-3-indolylpropyl-2′)-carbamate (II, R = $C_6H_5CH_2S$, R_1 = H, R_2 = CH_3)

All of the intermediate carbamoyltryptamines (II) and N-methylcarbamoyltryptamines (IV) were prepared by the following general procedure.

To a solution of 5.0 g (15.0 mmoles) of 3-(2′-aminopropyl)-5-benzylthioindole (8) in 150 ml of chloroform was added a solution of 0.1 mole of sodium hydroxide in 150 ml of water. The mixture was cooled in an ice bath and stirred while 30.0 mmoles of methyl chloroformate was added. The mixture was stirred, while cold, for 1 h, then acidified with 6 *N* hydrochloric acid, and stirred at 25° for 0.5 h. The layers were separated and the aqueous portion was extracted with chloroform. The organic portions were combined, washed with water, dried, and concentrated *in vacuo* to yield 4.4 g of the oily carbamate. The oil was insoluble in dilute hydrochloric acid and the infrared spectrum did not contraindicate the desired structure.

5-Benzylthio-3-(2′-methylaminopropyl)indole (XV)

All the N-methyltryptamines (III) and N,N-dimethyltryptamines (V) listed in Table I were prepared by the following general procedure.

To a stirred suspension of 3.8 g (0.1 mole) of lithium aluminium hydride in 100 ml of tetrahydrofuran was added a solution of 4.4 g (12.4 mmoles) of methyl N-(5-benzylthio-3-indolylpropyl-2′)-carbamate in 100 ml of tetrahydrofuran. The mixture was refluxed for 24 h and then cooled, and the excess reagent was decomposed either by careful addition of a few milliliters of a saturated ammonium chloride solution or by careful addition of a small amount of ethyl alcohol followed by water. The hydrolyzed mixture was concentrated *in vacuo* and extracted either with butyl alcohol – water (in the case of the aqueous ammonium chloride neutralization) or with ether–water (in the case of the ethyl alcohol – water neutralization). The butyl alcohol or ether portion was separated, washed with water, dried, and concentrated. The residual oil was dissolved in dilute hydrochloric acid; the solution was filtered, if necessary, and was then made basic with dilute sodium hydroxide. The free base was extracted with ether, dried, and concentrated under reduced

Can. J. Chem. Downloaded from www.nrcresearchpress.com by 210.87.254.105 on 09/05/12
For personal use only.

pressure to give 4.3 g of free amine XV (80% yield). For analytical purposes a small amount was evaporatively distilled in a short-path tube at 200° and 0.2 mm.

Tryptamines VII and XI were solids and were recrystallized from dilute ethyl alcohol and butyl chloride. All other alkylated tryptamines in this series were oils. Some were converted into picrates and recrystallized from alcohol–water. One tryptamine (XIV) was converted into the hydrochloride by rubbing the free amine in 6 *N* hydrochloric acid; the hydrochloride was recrystallized from 2 *N* hydrochloric acid. One substituted free amine (XII) quickly formed a bicarbonate salt when left in the air for a short period of time. This salt was water soluble and high melting, and showed the characteristic NH_2^+ stretching vibration absorptions at 3.70 μ in the infrared. The salt was recrystallized from ethyl alcohol for analytical purposes.

5-Methylthio-3-(2′-dimethylaminopropyl)indole Dimethiodide (XVII)

The reaction of 5-methylthio-3-(2′-dimethylaminopropyl)indole (IX) with an excess of methyl iodide in acetone gave a solid which was purified by recrystallizations from ethyl alcohol. Elemental analysis of the water-soluble analytical sample, m.p. 130° (decomp.), was inconsistent with a monomethiodide structure but did correspond to the dimethiodide monohydrate of the starting amine IX.

Anal. Calcd. for mono CH_3I: C, 46.2; H, 5.94; N, 7.18. Found for XVII: C, 35.0; H, 4.90; N, 5.17. Calcd. for $(CH_3I)_2 \cdot H_2O$: C, 34.9; H, 5.13; N, 5.09.

That XVII was the dimethiodide monohydrate in the sulfonium–ammonium form was proved by nuclear magnetic resonance.

REFERENCES

1. S. WILKINSON. J. Chem. Soc. 2079 (1958).
2. J. K. HORNER and W. A. SKINNER. Can. J. Chem. **42**, 2904 (1964).
3. W. A. SKINNER, H. F. GRAM, and B. R. BAKER. J. Org. Chem. **25**, 780 (1960).
4. E. SHAW. J. Am. Chem. Soc. **76**, 1384 (1954).
5. R. N. ICKE and B. B. WISEGARVER with G. A. ALLES. *In* Organic syntheses. Collective Vol. III. John Wiley & Sons, Inc., New York. 1955. p. 723.
6. J. B. HENDRICKSON, R. GOSCHKE, and R. REES. Tetrahedron, **20**, 576 (1964).
7. G. D. TIERS. Tables of τ-values for a variety of organic compounds. Minnesota Mining and Manufacturing Co., St. Paul, Minnesota. 1960.
8. J. K. HORNER, J. I. DEGRAW, and W. A. SKINNER. Can. J. Chem. This issue.

Can. J. Chem. Downloaded from www.nrcresearchpress.com by 210.87.254.105 on 09/05/12
For personal use only.

THE NUCLEAR MAGNETIC RESONANCE SPECTRUM OF VINYLENE CARBONATE

K. A. McLauchlan[1]
Basic Physics Division, National Physical Laboratory, Teddington, Middlesex, England

AND

T. Schaefer
Department of Chemistry, University of Manitoba, Winnipeg, Manitoba

Received August 16, 1965

ABSTRACT

The H and ^{13}C spectra of vinylene carbonate have been studied by double-resonance techniques. It was found that $J(^{13}C—H) = \pm 220.15 \pm 0.15$ c/s, $J(^{13}C—C—H) = \pm 17.47 \pm 0.12$ c/s, and $J(H—C—C'—H') = \pm 1.47 \pm 0.03$ c/s. A long-range coupling of 9.26 ± 0.10 c/s was observed between the carbon nucleus of the carbonate group and the vinyl protons. The magnitudes and signs of the geminal $^{13}C—C—H$ couplings are discussed in terms of the molecular orbital theory of Pople and Bothner-By.

INTRODUCTION

Early studies (1) of enriched samples of ethane, ethylene, and acetylene showed that the magnitude of the geminal couplings between ^{13}C and H nuclei varied considerably. Spectral analysis showed that the coupling in acetylene was of the same sign as the directly bonded $^{13}C—H$ coupling, and was therefore positive, while those in ethane and ethylene were negative. Freeman (2), using double-resonance techniques, discovered that the corresponding geminal coupling in *sym*-tetrabromoethane was positive and that couplings of both signs occurred in acrylonitrile (3). Studies of propene (4) and acetaldehyde (5) also demonstrated couplings of both signs, as did an investigation of vinyl bromide (6). The work reported here was initiated to discover the sign of the large geminal coupling constant observed in vinylene carbonate (structural formula given in Table I, No. 4).

EXPERIMENTAL

The sample of vinylene carbonate was obtained from the Koch-Light laboratories. Homonuclear double-resonance experiments were performed at "tickling" radio-frequency field strengths (7) in the frequency–sweep mode of a Varian H.A.100 spectrometer. Heteronuclear "tickling" experiments were carried out on a modified field–frequency stabilized V4300B spectrometer operating at 56.4 Mc/s in the proton region and with its transmitter coil double-tuned to the H and ^{13}C resonant frequencies. The ^{13}C irradiating field was derived from a Rohde and Schwarz frequency synthesizer.

RESULTS

The proton spectrum of vinylene carbonate showed three sets of satellite transitions caused by molecules containing ^{13}C nuclei. Two of these originated in the normal geminal and directly bonded coupling between ^{13}C and H nuclei of the ethylenic group. The third set, a doublet showing no H—H coupling, was derived from a long-range coupling between the carbon nucleus of the carbonyl group and the protons. This coupling, a *trans* one through oxygen and carbon, had a magnitude of 9.26 ± 0.10 c/s. Its sign could not be determined but its existence was confirmed by "tickling" experiments in the ^{13}C region.

A schematic representation of the spectrum caused by molecules containing a ^{13}C nucleus in one of the ethylenic positions is given in Fig. 1, the central proton peak caused

[1]*Present address: Physical Chemistry Laboratory, South Parks Road, Oxford, England.*

Can. J. Chem. Downloaded from www.nrcresearchpress.com by 210.87.254.42 on 09/05/12
For personal use only.

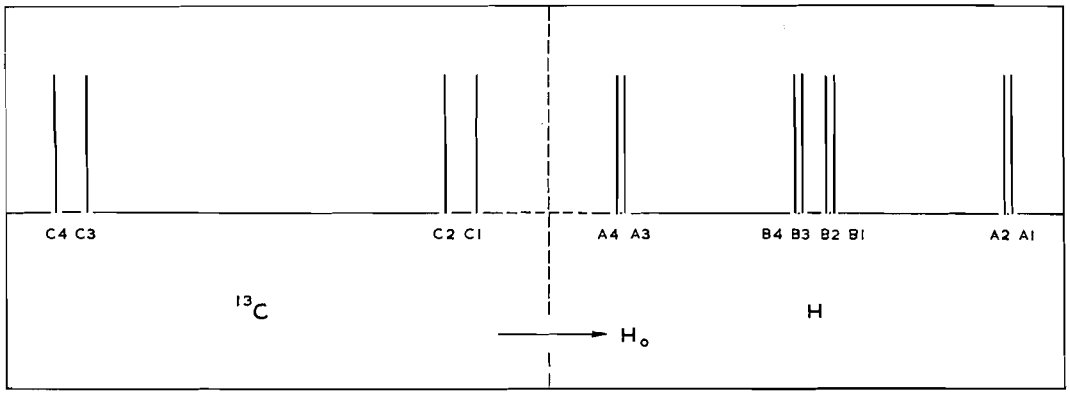
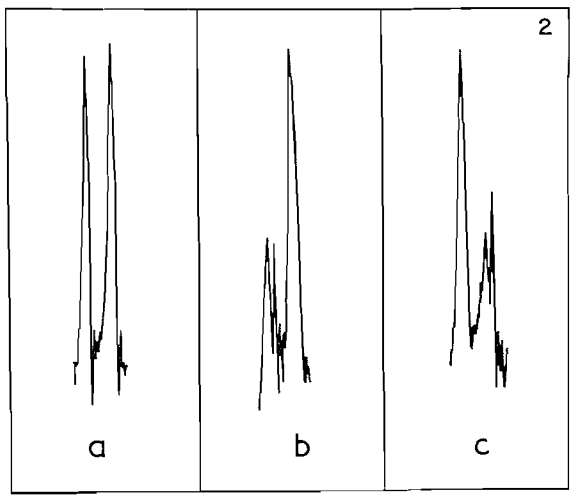


FIG. 1. A schematic diagram of the coupled spin system of molecules containing one ^{13}C nucleus in the vinyl group. Resonances caused by one of the carbons being ^{12}C are omitted for clarity. The numbering is in the order of increasing absolute frequency.

by the presence of a ^{12}C nucleus in the second ethylenic position being omitted to focus attention on the coupled spin system. Direct measurement of the proton spectrum gave the magnitudes of $J(^{13}C—H)$, $J(^{13}C—C—H)$, and $J(H—C—C'—H')$ quoted below, together with the standard deviations of the measurements. The relative signs of these coupling constants were obtained by "tickling" experiments. Figure 2 shows the results of one such experiment where the low-field satellite peaks A3 and A4 are shown while the proton transition B4 is irradiated (Fig. 2*b*) and while B3 is irradiated (Fig. 2*c*). Figure 3 shows the results of a further experiment performed with "tickling" in the ^{13}C region. Figure 3*a* shows the high-field doublet A1 and A2 while Fig. 3*b* shows the effect on this



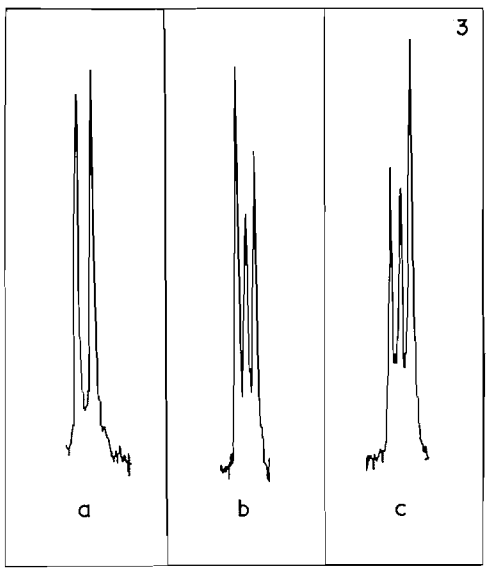


FIG. 2. (*a*) The low-field proton doublet A3 and A4, with (*b*) irradiation of the proton line B4 and (*c*) irradiation of B3.

FIG. 3. (*a*) The high-field proton doublet A1 and A2, with (*b*) irradiation of the ^{13}C transition C1 and (*c*) irradiation of the ^{13}C transition C2.

Can. J. Chem. Downloaded from www.nrcresearchpress.com by 210.87.254.42 on 09/05/12
For personal use only.

doublet of irradiating ^{13}C transition C1 and Fig. 3*c* shows the effect of irradiating C2. The observations are consistent only when all the couplings have like sign (2). The magnitudes and signs of the coupling constants are thus: $J(H—C—C'—H') = \pm 1.47 \pm 0.03$ c/s, $J(^{13}C—H) = \pm 220.15 \pm 0.15$ c/s, and $J(^{13}C—C—H) = \pm 17.47 \pm 0.12$ c/s.

A chemical shift of 23.07 p.p.m. was observed between the ethylenic and carbonyl ^{13}C resonances, the carbonyl ^{13}C nucleus being observed at the higher frequency, i.e. at low field. This result is consistent with other observations (8).

DISCUSSION

Proton–Proton Coupling

The coupling $J(H—C—C'—H')$ between the olefinic protons in cyclic compounds depends on ring size (9–12). Theory (13) agrees that it is inversely dependent on angles θ and θ' ($\theta = \angle HCC'$, $\theta' = \angle CC'H'$) of the HCC'H' fragment. $J(H—C—C'—H') = 5.3 \pm 0.1$ c/s in cyclopentene (11, 12). Replacement of the hydrogen atoms in ethylene by more electronegative atoms induces a rehybridization of the carbon atoms in the HCC'H' fragment (13) and decreases $J(H—C—C'—H')$. The observed decrease (14) in $J(H—C—C'—H')$ in substituted ethylenes is $11.7(1 - 0.34\Delta E)$, where $\Delta E = E_X - E_H$ (X = substituent). Replacement of two hydrogen atoms by carbon atoms would therefore result in $J(H—C—C'—H') = 8.5$ c/s, leaving 3.2 c/s as the decrease caused by ring closure, i.e. caused by increases in θ and θ'. Finally, if one writes $J(H—C—C'—H') = 5.3(1 - 2 \times 0.34\Delta E)$, where $\Delta E = E_0 - E_C = 1$, there results $J(H—C—C'—H') = 1.6$ c/s as the predicted value for vinylene carbonate, in satisfactory agreement with the experimental value of $+1.5$ c/s.

Geminal Carbon–Proton Coupling

General

In their theory of nuclear spin coupling between geminal hydrogens, Pople and Bothner-By (15) have indicated that the positive trend in $J(H—C—H)$ in going from ethane to ethylene arises because, with rising s character of the carbon atom, the lowest energy transition between a bonding antisymmetrical orbital and an antibonding symmetrical orbital is favored (the methylene group is described in terms of four molecular orbitals delocalized over both C—H bonds). Furthermore, inductive withdrawal of electrons from these orbitals is predicted to lead to a positive change in $J(H—C—H)$, while hyperconjugative withdrawal is predicted to lead to a negative change. The opposite predictions apply to a donation of electrons. These predictions are in qualitative agreement with experiment (15).

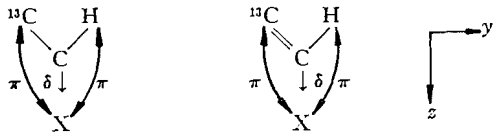
The positive trend of $J(H—C—H)$ with rising s character is also observed for $J(^{13}C—C—H)$ in ethane, ethylene, and acetylene (1). Now, it often happens that a linear relationship exists between s character in the bonding carbon orbital and $J(^{13}C—H)$ (16–19). On the assumption (16) that both $J(^{13}C—H)$ and $J(^{13}C—C—H)$ tend to reflect the s character in the carbon bonding orbitals, an increase is expected in both as the s character of the carbon atom in the C—H or C—C bonds increases. It is also normally accepted that the s character depends on inductive withdrawal or donation of electrons by the substituent (19). If it is now further assumed that hyperconjugative withdrawal or donation by the substituent does not affect $J(^{13}C—H)$ and that the theory of Pople and Bothner-By can be qualitatively extended to $^{13}C—C—H$ systems, then there exists a basis

$$\begin{array}{c} | \\ X \end{array}$$

for the semiquantitative discussion of the sign and magnitude of $J(^{13}C—C—H)$.

Can. J. Chem. Downloaded from www.nrcresearchpress.com by 210.87.254.42 on 09/05/12
For personal use only.

Assume that in structures I and II the approach of Pople and Bothner-By (15) can be



I II

qualitatively utilized. The electronegative substituent X withdraws δ electrons (straight arrow in I and II) from the C—C and C—H bonds, thus leading to a positive increase in $J(^{13}C—C—H)$. At the same time, by the theory of Juan and Gutowsky (19), the s character of the carbon-bonding orbital in C—H increases, leading to an increase in $J(^{13}C—H)$. If the substituent X is also able to donate or withdraw electrons in a hyperconjugative way (curved arrows in I and II), this will further increase or decrease, respectively, the value of $J(^{13}C—C—H)$ without affecting $J(^{13}C—H)$ very much.[2] Hence, a plot of $J(^{13}C—C—H)$ versus $J(^{13}C—H)$ should reflect hyperconjugative effects on $J(^{13}C—C—H)$ in a semi-quantitative way.

Application to Experimental Data

In Fig. 4 are plotted $J(^{13}C—C—H)$ values versus $J(^{13}C—H)$ values for the molecules listed in Table I. The solid circles represent ethane, ethylene, and acetylene. The points for vinylene carbonate, vinyl bromide, and *sym*-tetrabromoethane are represented by open circles. A smooth line is drawn through these six points. Deviations from this line are now discussed for individual compounds.

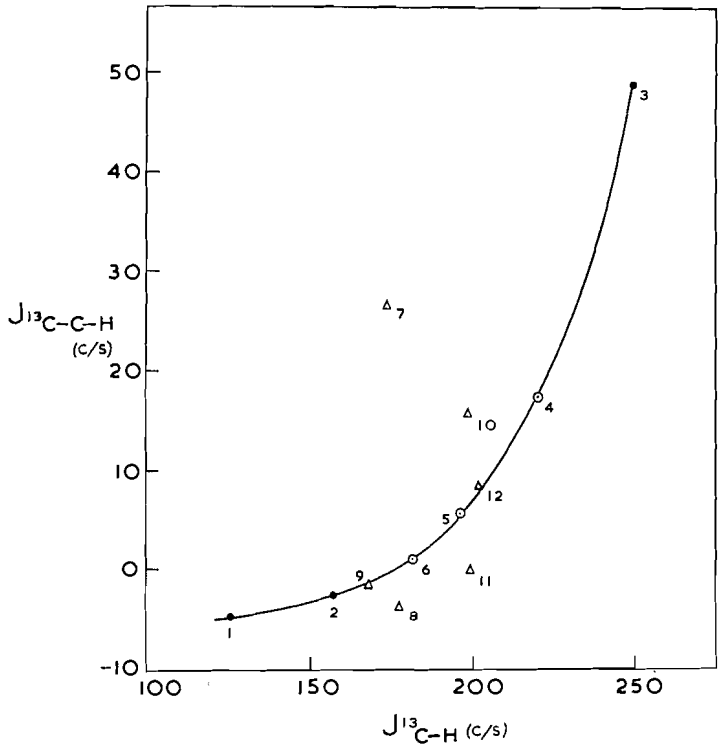


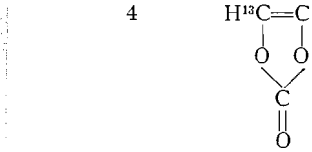
FIG. 4. $J(^{13}C—C—H)$ is plotted versus $J(^{13}C—H)$. The numbering corresponds to that in Table I. A smooth line is drawn through points 1 to 6.

[2]*There is some evidence that there are small contributions to* $J(^{13}C—H)$ *by* π *electrons (20).*

Can. J. Chem. Downloaded from www.nrcresearchpress.com by 210.87.254.42 on 09/05/12
For personal use only.

TABLE I

Carbon–proton coupling constants (in cycles per second) in some simple compounds

No.	Compound	$J(^{13}C—C—H)$*	$J(^{13}C—H)$†	Reference
1	$H_3{}^{13}C—CH_3$	−4.5±0.3	124.9±0.3	1
2	$H_2{}^{13}C=CH_2$	−2.4±0.2	156.4±0.3	1
3	$H{}^{13}C\equiv CH$	+49.15±0.3	249.0±0.3	1
4		+17.5±0.1	220.15±0.15	This paper‡
5	$H_2{}^{13}C=CHBr$	+5.8±0.5	196.1±0.2	6
6	$^{13}CHBr_2CHBr_2$	+1.1±0.1	181.0±1.5	2
7	$^{13}CH_3CHO$	+26.6	172.0	4
8	$H_2{}^{13}C=CHC\equiv N$	−3.67	176.74	3
9	*cis*-$(C_2H_5OOC)CH=CH(COOC_2H_5)$	±1.5±0.3	167.6±0.3	26
10	*cis*-$HCl{}^{13}C=CHCl$	±15.7±0.3	198.3±0.3	26
11	*trans*-$HCl{}^{13}C=CHCl$	0±0.3	199.1±0.3	26
12	$Cl_2{}^{13}C=CHCl$	±8.4	201.2‡±1	27

*Sign relative to $J(^{13}C—H)$.

†Note that the value given refers to the carbon to which the substituent is attached, e.g. in acrylonitrile (point 8) $J_\alpha(^{13}C—H)$ = 176.7 c/s.

‡Reference 28 gives $J(^{13}C—H)$ = 220.1 and 201.2 c/s for vinylene carbonate and trichloroethylene, respectively.

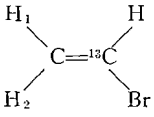
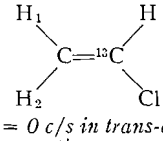
Acetaldehyde (point 7).—The greatest deviation of any is found for this compound in Fig. 4. Inductive electron withdrawal by the oxygen from the C—C and C—H bonds leads to an increase in both $J(^{13}C—H)$ and $J(^{13}C—C—H)$. However, hyperconjugative back donation of electrons (from the oxygen p_y orbital) is expected to increase $J(^{13}C—C—H)$ further. The effects reinforce one another to give $J(^{13}C—C—H)$ = +26.6 c/s. A similar explanation holds for the very large positive value of $J(H—C—H)$ in formaldehyde (15).

Vinyl cyanide (point 8).—Here the cyano group, being more electronegative than hydrogen, increases $J(^{13}C—H)$[3] to 176.7 c/s; however, it can also withdraw electrons from the $^{13}C{=}C—H$ fragment by hyperconjugation, and this is expected to lead to a negative change in $J(^{13}C—C—H)$. From Fig. 4 it appears that the hyperconjugative effect outweighs the inductive effect, and the net result is a negative deviation from the line. A similar shift in $J(H—C—H)$ is noted for the cyanomethanes (15).

In diethyl maleate (point 9) hyperconjugative withdrawal by the carbonyl group is hindered by the geometry of the system (combined steric hindrance and rotation), and no deviation is present *if* it is assumed that $J(^{13}C—C—H)$ is *negative*.

The chloroethylenes (points 10, 11, and 12).—If $J(^{13}C—C—H)$ for trichloroethylene (point 12) is assumed to be positive, it falls very near the line in Fig. 4. However, both 1,2-dichloroethylenes (points 11 and 12) deviate strongly, and the deviations, probably of opposite sign,[4] cannot be explained in terms of the concepts presented above. In this

[3] *$J(^{13}C—H)$ involves the substituted carbon whereas $J(^{13}C—C—H)$ involves the unsubstituted carbon; see structures I and II.*

[4] *In the molecule*  *, $J(^{13}C—C—H_1)$ = +7.5 c/s while $J(^{13}C—C—H_2)$ = −8.5 c/s (21). If a similar situation holds in*  *, then $J(^{13}C—C—H)$ in cis-dichloroethylene is positive. Furthermore, the values $J(^{13}C—C—H)$ = 0 c/s in trans-dichloroethylene and $J(^{13}C—C—H)$ = +8.4 c/s (assumed positive) are consistent with this assumption.*

Can. J. Chem. Downloaded from www.nrcresearchpress.com by 210.87.254.42 on 09/05/12
For personal use only.

connection it may be noted that the hybridization parameters calculated from $J(^{13}C—H)$ values in the methyl halides (18, 19) are among the most "unacceptable" (22). Doubt has recently been expressed (23, 24) about the validity of the rehybridization theory for $J(^{13}C—H)$. In any case, the deviations noted here may well indicate the presence of an important factor which has been neglected in this discussion. Further determinations of both the size and sign of $J(^{13}C—C—H)$ in model compounds are needed.

The Coupling $J(^{13}C—O—C—H)$

The only other values in the literature are ± 3.1 and ± 4.0 c/s and are for compounds (alkylesters) where ^{13}C is sp^2 hybridized (25). The higher value in vinylene carbonate may partly be the result of the second oxygen atom bonded to $^{13}C{=}O$, since it is known (23) that $J(^{13}C—C—C—H)$ increases slightly as the electronegativity of the substituent on ^{13}C increases. However, there appear to be a number of other factors involved in determining $J(^{13}C—C—C—H)$, in addition to the s character of the ^{13}C atomic orbital (23). The largest value found to date for $J(^{13}C—C—C—H)$ is ± 6.4 c/s in trimethylacetylbromide (23).

ACKNOWLEDGMENTS

The work reported here forms part of the research programme of the National Physical Laboratory and is published by permission of the Director. T. Schaefer thanks the laboratory for facilities as a Guest Worker and the National Research Council of Canada for financial assistance. The technical assistance of Miss J. Harris is gratefully acknowledged.

REFERENCES

1. R. M. Lynden-Bell and N. Sheppard. Proc. Roy. Soc. London, Ser. A, **269**, 385 (1962).
2. R. Freeman and W. A. Anderson. J. Chem. Phys. **39**, 806 (1963).
3. R. Freeman. J. Chem. Phys. **40**, 3571 (1964).
4. H. Dreeskamp, E. Sackmann, and F. Stegmeier. Z. Elektrochem. **67**, 860 (1963).
5. H. Dreeskamp and E. Sackmann. Proceedings of the meeting of the Società Italiana per il Progresso delle Scienze, Sardinia, Italy, 1964. To be published.
6. R. M. Lynden-Bell. Mol. Phys. **6**, 537 (1963).
7. R. Freeman and W. A. Anderson. J. Chem. Phys. **37**, 2053 (1962).
8. J. B. Stothers. Quart. Rev. London, **19**, 126 (1965).
9. J. A. Pople, W. G. Schneider, and H. J. Bernstein. High resolution nuclear magnetic resonance. McGraw-Hill Book Co., Inc., New York. 1959. p. 195.
10. O. L. Chapman. J. Am. Chem. Soc. **85**, 2014 (1963).
11. G. V. Smith and H. Kriloff. J. Am. Chem. Soc. **85**, 2016 (1963).
12. P. Laszlo and P. von R. Schleyer. J. Am. Chem. Soc. **85**, 2018 (1963).
13. M. Karplus. J. Am. Chem. Soc. **85**, 2870 (1963).
14. C. N. Banwell and N. Sheppard. Discussions Faraday Soc. **34**, 115 (1962).
15. J. A. Pople and A. A. Bothner-By. J. Chem. Phys. **42**, 1339 (1965).
16. J. Ranft. Ann. Physik, **10**, 399 (1963).
17. J. N. Shoolery. J. Chem. Phys. **31**, 1427 (1959).
18. N. Muller and D. E. Pritchard. J. Chem. Phys. **31**, 768 (1959); **31**, 1471 (1959).
19. C. Juan and H. S. Gutowsky. J. Chem. Phys. **37**, 2198 (1962).
20. H. S. Gutowsky and C. S. Juan. Discussions Faraday Soc. **34**, 52 (1962).
21. R. M. Lynden-Bell. Mol. Phys. **6**, 537 (1963).
22. N. Muller. J. Chem. Phys. **42**, 4309 (1965).
23. G. J. Karabatsos and C. E. Orzech. J. Am. Chem. Soc. **87**, 560 (1965).
24. W. J. Considine. J. Chem. Phys. **42**, 1130 (1965).
25. G. J. Karabatsos, J. D. Graham, and F. M. Vane. J. Am. Chem. Soc. **84**, 37 (1962).
26. N. Muller. J. Chem. Phys. **37**, 2729 (1962).
27. H. Dreeskamp and E. Sackmann. Z. Physik. Chem. Frankfurt, **34**, 273 (1962).
28. J. H. Goldstein and G. S. Reddy. J. Chem. Phys. **36**, 2644 (1962).

Can. J. Chem. Downloaded from www.nrcresearchpress.com by 210.87.254.42 on 09/05/12
For personal use only.

Can. J. Chem. Downloaded from www.nrcresearchpress.com by 210.87.254.40 on 09/05/12
For personal use only.

CHOLLA GUM

I. STRUCTURE OF THE DEGRADED CHOLLA GUM

V. M. PARIKH[1] AND J. K. N. JONES
Department of Chemistry, Queen's University, Kingston, Ontario

Received September 16, 1965

ABSTRACT

Purified cholla gum (*Opuntia fulgida*) contains L-arabinose (51.6%), D-galactose (31.7%), D-xylose (15.0%), L-rhamnose (2–3%), and D-galacturonic acid (11.2%). Partial hydrolysis of the gum by cold acid produced a polymer which contained only D-galactose and D-galacturonic acid in the proportion 9:2. Methylation and hydrolysis of the degraded gum produced 2,3,4,6-tetra-*O*-methyl-D-galactose (2 moles), 2,3,4-tri-*O*-methyl-D-galactose (1 mole), 2,4,6-tri-*O*-methyl-D-galactose (2 moles), 2,4-di-*O*-methyl-D-galactose (4 moles), and 2,3,4-tri-*O*-methyl-D-galacturonic acid (2 moles). Smith-type degradation of the degraded gum produced D-galactose (6 moles), glycolaldehyde (? moles), glycerol (2.5 moles), and glyceronic acid (2.5 moles).

Hydrolysis of the undegraded gum produced an aldobiouronic acid, which was proved to be 3-*O*-(β-D-galactopyranosyl uronic acid)-D-galactose by its reduction, methylation, and the identification of the methylated sugars obtained by the hydrolysis of the octamethyl galactobioside.

Based on these results, a possible structure for the average chain length of the degraded gum has been proposed.

The sample of the cholla gum (*Opuntia fulgida*) that was investigated was obtained through the kindness of Dr. B. A. Erukoff and Dr. K. Folkers of the New York Botanical Garden. The gum was earlier investigated by Anderson *et al.* (1) and by Sands and Klass (2), who reported D-galactose, D-galacturonic acid, L-rhamnose, and L-arabinose as constituent units. They also isolated an aldobiouronic acid and identified it as *O*-(D-galactopyranosyl uronic acid)-L-rhamnose. In a later investigation Brown *et al.* (3) detected significant quantities of D-xylose residues in it, but reported that their sample of gum contained only trace quantities of L-rhamnose. They also carried out the methylation of the gum and were able to isolate, from the hydrolysate of the methylated gum, the following sugars: (*i*) 2,3,5-tri-*O*-methyl-L-arabinose, (*ii*) 2,3,4-tri-*O*-methyl-D-xylose, (*iii*) 2,3-di-*O*-methyl-L-arabinose, (*iv*) 2,4-di-*O*-methyl-D-galactose, (*v*) L-arabinose (unsubstituted), and (*vi*) 2-*O*-methyl-D-galacturonic acid. In the present investigations a beginning has been made on a study of the detailed molecular architecture of the repeating unit of the gum.

Partial hydrolysis of the gum with 3% sulfuric acid on a boiling water bath produced an aldobiouronic acid, viz. 3-*O*-(β-D-galactopyranosyl uronic acid)-D-galactose, which, after formation of its ester glycoside, was reduced with lithium aluminium hydride to a neutral galactobioside and then completely methylated; the product was hydrolyzed to produce 2,3,4,6-tetra-*O*-methyl-D-galactose and 2,4,6-tri-*O*-methyl-D-galactose. The two methylated sugars were identified by conversion into their respective *N*-phenylglycosylamines. Partial hydrolysis of the gum with cold 6 *N* sulfuric acid for 21 days, on the other hand, produced a degraded gum, containing D-galactose and D-galacturonic acid only, together with a series of neutral oligosaccharides and monosaccharides. The pure degraded gum was obtained, as a barium salt, by removal of the mono- and oligo-saccharides by dialysis and the repeated precipitation of the undialyzable material from ethanol. A detailed report on the isolation and identification of the oligosaccharides

[1]*Present address: Department of Chemistry, Notre Dame University, Nelson, British Columbia.*

thus obtained will be published in a subsequent paper. However, it may be mentioned here that two of the major components were 6-*O*-β-D-galactopyranosyl-D-galactose and 3-*O*-β-D-galactopyranosyl-D-galactose. (The barium salt of the degraded gum was obtained as a white powder, and had $[\alpha]_D^{23}$ +46.5° (*c*, 1.5 in water).) The equivalent weight of the degraded gum acid was found to be 920, this amounting to a uronic acid anhydride content of 19.1%. On hydrolysis it gave mainly D-galactose and D-galacturonic acid in the approximate ratio of 9:2, together with trace quantities of L-arabinose (ca. 1%) and L-rhamnose (ca. 2–5%).

Polymers containing a high percentage of uronic acid residues are frequently very difficult to methylate by Haworth's method (4, 5). The degraded gum was, however, very rapidly methylated by the procedure described by Srivastava and co-workers (6). Methylation was completed by two treatments with Purdie's (7) reagents. Methanolysis and hydrolysis of the methylated degraded gum produced a mixture of partially methylated sugars, which were separated and identified as (i) 2,3,4,6-tetra-*O*-methyl-D-galactose (2 moles), (ii) 2,3,4-tri-*O*-methyl-D-galactose (1 mole), (iii) 2,4,6-tri-*O*-methyl-D-galactose (2 moles), (iv) 2,4-di-*O*-methyl-D-galactose (4 moles), 2,3,4-tri-*O*-methyl-D-galacturonic acid (2 moles), and trace quantities of a di-*O*-methyl (?) derivative of L-rhamnose. The average chain length of the degraded gum, which contains two D-galacturonic acid residues, was calculated to be 11 anhydrohexose units or a multiple of this. Isolation of 2 moles of tetra-*O*-methyl-D-galactose and 2 molecules of tri-*O*-methyl-D-galacturonic acid suggested that, out of a total of 11 hexopyranose residues constituting the average chain length of the degraded gum, 4 formed nonreducing terminal residues and that therefore the degraded gum must also be a highly branched molecule.

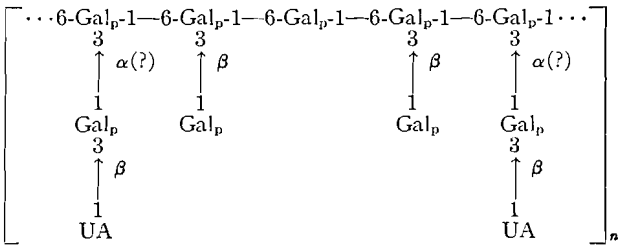
When subjected to periodic acid oxidation, the degraded gum consumed 0.93 mole of the oxidant and liberated 0.47 mole of formic acid per mole of anhydrohexose unit. As the average chain length of the degraded gum is believed to be composed of 11 anhydrohexopyranose units, the above results can be interpreted as the consumption of 10.2 moles of the oxidant and the liberation of 5.2 moles of formic acid per average repeating unit of the degraded polymer. During the methylation studies, 4 moles of 2,4-di-*O*-methyl-D-galactose and 2 moles of 2,4,6-tri-*O*-methyl-D-galactose residues were obtained. Thus, 6 moles of a total of 11 moles of the average repeating unit were not expected to consume any oxidant. The remaining five hexopyranose residues, resulting in the production of 2,3,4,6-tetra-*O*-methyl-D-galactose (2 moles), 2,3,4-tri-*O*-methyl-D-galactose (1 mole), and 2,3,4-tri-*O*-methyl-D-galacturonic acid (2 moles), were expected to consume 2 moles of the oxidant and to produce 1 mole of formic acid per hexose unit, thus accounting for a total consumption of 10 moles of the oxidant and production of 5 moles of formic acid per average repeating unit in the polymer.

The degraded gum was subjected to a Smith-type degradation (8, 9), whereby the polymer was oxidized by periodic acid and the polyaldehyde thus obtained was reduced to a polyol by sodium borohydride. The hydrolysate of the polyol, on chromatographic examination, was found to contain four components, viz. D-galactose (approximately 55–60%), glycolaldehyde (ca. 15–25%), and glycerol and glyceronic acid (almost equal proportions). (All estimations were visual.) D-Galacturonic acid was not detected in the mixture; similarly, L-arabinose and L-rhamnose, which formed trace quantities in the degraded polymer, were also absent from the hydrolysate. It is possible to compare these results with those expected from the methylation experiments. On the basis of the preceding methylation data 6 moles of galactose would be expected to be resistant to periodate oxidation and should be recovered after a Smith-type degradation. The

Can. J. Chem. Downloaded from www.nrcresearchpress.com by 210.87.254.40 on 09/05/12
For personal use only.

remaining 3 moles of D-galactose were each expected to produce 1 mole of glycerol and 1 mole of glycolaldehyde (Formula 2). The two D-galacturonic acid residues, which produced 2,3,4-tri-*O*-methyl-D-galacturonic acid on methylation, were each expected to give rise to 1 mole of glyceronic acid and 1 mole of glycolaldehyde. Thus, the hydrolysate was expected to contain a total of 6 moles (57.8%) of D-galactose, 5 moles (16.1%) of glycolaldehyde, 3 moles (14.7%) of glycerol, and 2 moles (11.4%) of glyceronic acid.

On the basis of these results, the degraded polymer is believed to be composed predominantly of $1 \rightarrow 6$ and $1 \rightarrow 3$ linked galactose residues. It is not possible, as yet, to assign a unique structure to this polymer, but a simple structure which can accommodate all the above facts can be written as shown in Formula 1.



FORMULA 1. A probable structure of the degraded cholla gum. A comparison of experimental results with those calculated on the basis of the proposed structure as given above. LEGEND: Gal$_p$, D-galactopyranose; UA, D-galacturonic acid.

The unexpectedly high positive rotation ($[\alpha]_D$ +46.5°) of the degraded polymer (the original gum had $[\alpha]_D$ −86.2°) could be attributed to the presence of some α-linkages in the polymer, although all the neutral oligosaccharides, as well as the aldobiouronic acid, isolated from the gum were found to be β-linked. If the two aldobiouronic acid residues are assumed to be α-linked (shown with a question mark in Formula 1) to the 3 position of the galactose residues in the main chain (the linkage between D-galacturonic acid and D-galactose being much more stable in comparison with the rest of the linkage in the polymer), isolation of the $1 \rightarrow 3$ α-linked disaccharide may not be possible. Furthermore, if Hudson's rules (10) of isorotation are used to calculate the approximate optical rotation of the degraded gum, the value obtained ($[\alpha]_D$ +30.4°) on the assumption of the presence of two α-linkages is closer to the experimental value ($[\alpha]_D$ +46.5°) than that calculated on the assumption that all the linkages are of the β-type ($[\alpha]_D$ −1.7). Therefore, in Formula 2, these two linkages are shown as α-linkages, and Smith-type degradation results of the degraded gum are explained.

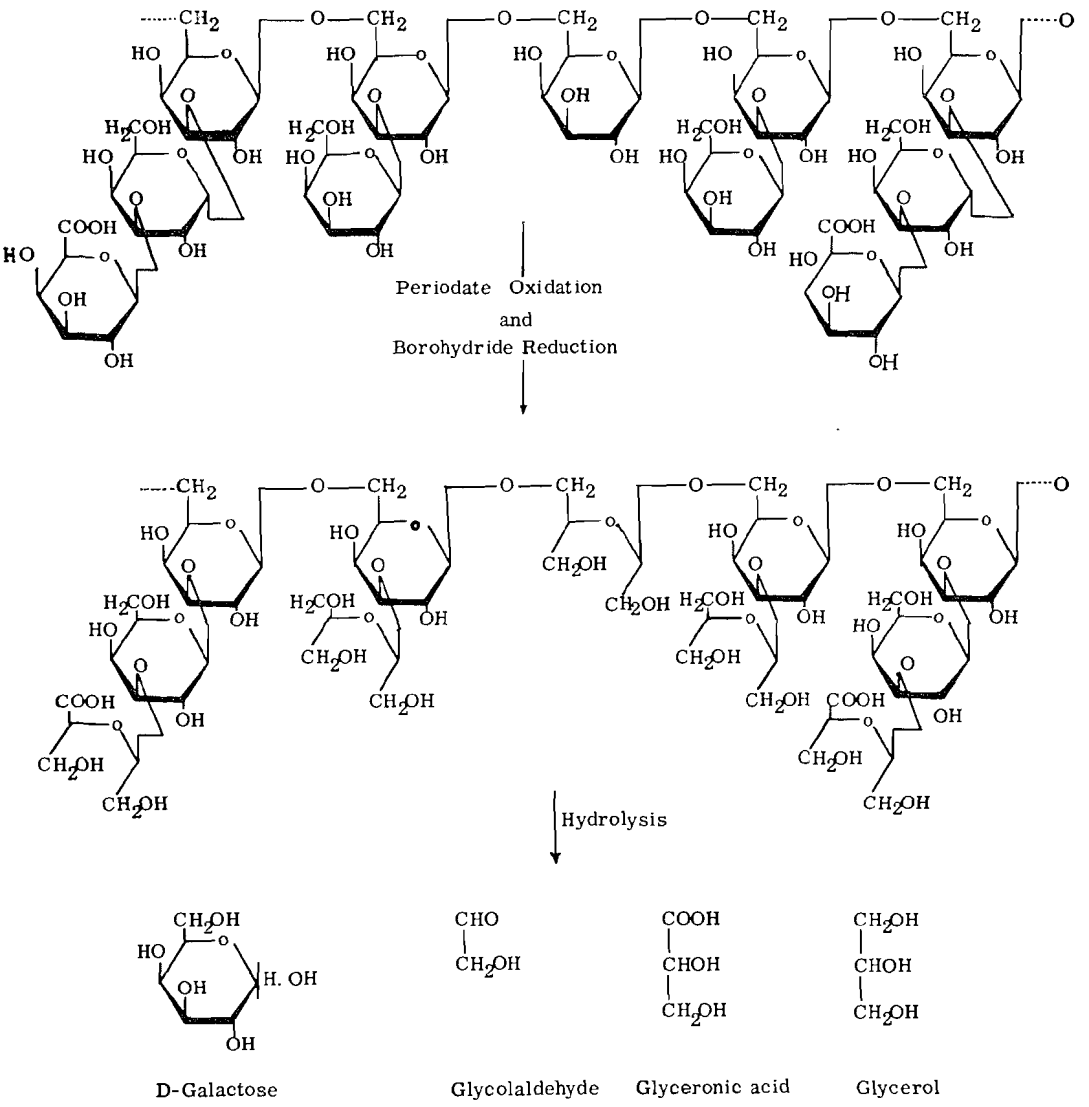
EXPERIMENTAL

Methods

Unless otherwise stated, all specific rotations are equilibrium values recorded at 23 ± 3°, and all solutions were concentrated under reduced pressure at 40–45°. All infrared spectra were made in chloroform solutions (6%) on a Perkin–Elmer model 21 infrared spectrophotometer. Whatman No. 1 papers were used for partition chromatography with the following solvent systems (by volume): (*a*) butan-1-ol–ethanol–water (3:1:1); (*b*) butan-1-ol–ethanol–water (5:1:4), top layer cleared by the addition of a minimum of ethanol; (*c*) ethyl acetate – acetic acid – formic acid – water (18:3:1:4); (*d*) butan-1-ol–pyridine–water–benzene (5:3:3:1); (*e*) ethyl acetate – pyridine – water (10:4:3); (*f*) butan-1-ol–ethanol–water (1:1:1); (*g*) benzene–ethanol–water (169:47:15). The spray reagents that were used were alkaline silver nitrate (11) and *p*-anisidine hydrochloride (12).

Whatman 3 MM paper and columns packed with Whatman cellulose powder by the wet method were used for the separation of sugar mixtures. All melting points are uncorrected.

Can. J. Chem. Downloaded from www.nrcresearchpress.com by 210.87.254.40 on 09/05/12
For personal use only.



FORMULA 2. Proposed structure of degraded cholla gum, and its Smith-type degradation.

Isolation and Purification of the Gum

The crude gum (120 g), which was dark brown and had a characteristic odor, was purified by dissolving the powdered material in warm, dilute sodium hydroxide (0.1 *N*), during which process some ammonia was evolved. The dark brown solution, after filtration, was cooled and then added slowly to ice-cold ethanol containing 1% hydrogen chloride. The precipitated product was washed twice by decantation, filtered off, dissolved in cold water, and reprecipitated by adding the solution to ice-cold ethanol containing 1% hydrogen chloride. The process was repeated three more times, after which the pale cream colored powder was separated by filtration, washed with acetone and ether, and dried *in vacuo* over silica gel for several days (yield, 58 g). The pure gum had: moisture, 4.8%; ash, 0.7%; $[\alpha]_D$ −86.2° (*c*, 1.8 in water); equivalent weight, 1 734 (acidimetry); uronic acid anhydride, 10.15% (acidimetry); L-arabinose, 51.6%; D-galactose, 31.7%; D-xylose, 15.0%; L-rhamnose, 2–3%; nitrogen, nil; methoxyl, nil. The uronic acid was identified as D-galacturonic acid (see below).

Examination of a sample of a gum by free-boundary electrophoresis in a Tiselius apparatus, with 0.05 *M* sodium borate buffer at 11 mA and 175 V, indicated that the polysaccharide was either homogeneous or inseparable under these conditions.

Can. J. Chem. Downloaded from www.nrcresearchpress.com by 210.87.254.40 on 09/05/12
For personal use only.

Can. J. Chem. Downloaded from www.nrcresearchpress.com by 210.87.254.40 on 09/05/12
For personal use only.

Isolation and Characterization of the Aldobiouronic Acid

The gum (15 g) was suspended in dilute sulfuric acid (3%, 400 ml), and the suspension was shaken vigorously overnight and then heated on a boiling water bath for 10 h. After neutralization ($BaCO_3$) and filtration, concentration of the hydrolysate gave a light brown, viscous syrup, which was poured slowly into ethanol (90%, 300 ml) to precipitate the barium salts of the uronic acid as a gummy mass. The precipitate was extracted several times with boiling ethanol (90%) until a dry, pale brown powder, free from monosaccharides, was obtained; yield, 1.85 g; $[\alpha]_D^{22}$ +56.2 (*c*, 1.0 in water); Ba, 14.9%. It was obviously a mixture, in the main, of the barium salts of the aldobiouronic (Ba, 16.1%) and aldotriouronic (Ba, 11.68%) acids. Chromatographic examination of the powder in solvent *c* gave one major spot (probably of the aldobiouronic acid) with a considerable trailing throughout the entire length of the chromatogram.

Complete hydrolysis of a portion of the above mixture and chromatographic examination, in solvent *c*, of the hydrolysate revealed the presence of D-galacturonic acid and D-galactose only in the hydrolysate, along with trace quantities of L-rhamnose. Unsuccessful attempts were made to convert the aldotriouronic acid into aldobiouronic acid by mild hydrolysis with 0.1 *N* sulfuric acid. The aldobiouronic acid was therefore purified by converting its barium salt into the free acid, by passage of the mixture through IR-120 ion-exchange resin, and by separation by partition chromatography of the mixture of acids on a cellulose column (80 × 4 cm), butan-1-ol fully saturated with water being used as the solvent phase. The aldotriouronic acid appeared to be adsorbed irreversibly on the column and could not be recovered even after the column had been eluted with distilled water.

The pure acid (equiv. wt. 340) was converted into its methyl ester methyl glycoside, which was reduced with lithium aluminium hydride to a neutral bioside, a small portion of which, on hydrolysis with 2 *N* sulfuric acid, gave only galactose. The methyl bioside was fully methylated by Haworth's procedure followed by Purdie's method to give a colorless syrup; OMe, 53.7%; η_D^{22} 1.4672; $[\alpha]_D$ +2.6° (*c*, 0.85 in water). This, on hydrolysis, gave a mixture of two methylated sugars (R_g 0.89 and 0.67 in solvent *b*), which were separated on Whatman 3 MM filter sheets and identified as 2,3,4,6-tetra-*O*-methyl-D-galactose (m.p. 74°; $[\alpha]_D$ +144 → +119° (in water) (13, 14)) and 2,4,6-tri-*O*-methyl-D-galactose (m.p. 98–104°; $[\alpha]_D$ +120 → +91 (in water) (15)). Both sugars were converted into their respective *N*-phenylglycosylamines. Found: *N*-phenyl-2,3,4,6-tetra-*O*-methyl-D-galactosylamine, m.p. and mixed m.p. 195–196° (16); *N*-phenyl-2,4,6-tri-*O*-methyl-D-galactosylamine, m.p. and mixed m.p. 178–180°, $[\alpha]_D$ −90 → 37° (24 h) (*c*, 0.8 in acetone) (17).

Hydrolysis of the Gum and Isolation of the Degraded Gum

The gum (100 g), once precipitated from its aqueous solution with ethanol, was suspended in dilute sulfuric acid (6 *N*, 1 200 ml); this suspension was left on a rotary shaker at room temperature (20–23°) for a period of 23 days. The dark brown solution was then filtered to remove some light, gelatinous residue (ca. 3–4 g), the filtrate was neutralized with barium carbonate, and the solution was again filtered. The filtrate was concentrated to a suitable volume (ca. 600 ml) and dialyzed against distilled water (3 × 4 l). The dialysate, on concentration, gave a mixture of mono- and oligo-saccharides (58 g); the undialyzed material, after further dialysis against running water and precipitation with ethanol, gave the barium salt of the degraded gum. The product was dissolved in cold water and reprecipitated with ethanol, the process being repeated four times until a chromatographically homogeneous, oligosaccharide-free white powder was obtained; yield, 26.4 g; $[\alpha]_D$ +46.5° (*c*, 1.5 in water); Ba, 7.13% (equivalent to an equiv. wt. 899). A portion of the barium salt was converted into the acidic degraded gum by passing its aqueous solution through a column of IR-120 ion-exchange resin, and the equivalent weight of the acid so obtained was determined by titration against standard alkali and found to be 920, equivalent to a D-galacturonic acid anhydride content of 19.1%.

Hydrolysis of the degraded gum by 2 *N* sulfuric acid and chromatographic examination of the hydrolysate revealed only two major spots, corresponding to D-galactose and D-galacturonic acid in an approximate ratio of 9:2. Trace quantities of L-rhamnose (ca. 2–3%) and L-arabinose (ca. 1% or less) were also present.

Methylation of the Degraded Gum (6)

Methylation of the degraded gum was carried out with ease by Srivastava's method (6), in which the dry polymer (3.5 g) was dispersed in warm, dry dimethyl sulfoxide, the suspension was cooled to 20°, and barium oxide (15 g) and methyl iodide (60 ml) were added to it. The mixture was stirred mechanically for 48 h at 30°, during which time it turned dark brown (as a result of the liberated iodine). The inorganic salts were then precipitated by addition of a large amount of chloroform, and the solution was centrifuged. The reddish brown colored organic phase was then washed with a small quantity (2 × 30 ml) of an aqueous solution of sodium thiosulfate (15%), followed by distilled water (25 ml). It was dried (Na_2SO_4) and concentrated to a brown mobile liquid (5–6 ml) containing dimethyl sulfoxide, which could not be removed by evaporation without some decomposition of the polysaccharide.

The mobile solution of partially methylated degraded gum in dimethyl sulfoxide was treated twice with Purdie's reagents (CH_3I and Ag_2O) (7), and the light yellow, syrupy product was examined by infrared spectrometry. It showed no absorption in the hydroxyl region (3 400 – 3 600 cm^{-1}) and in the region between 800 and 900 cm^{-1} which usually indicates the absence of α-linkages in the polymer.

Anal. Found: OMe, 41.6.

Methanolysis and Identification of Methylated Sugars of the Methylated Degraded Gum

A solution of the methylated degraded gum (0.95 g) in methanolic hydrogen chloride (7%, 50 ml) was heated to 100° in sealed tubes for 6 h. The solution was then diluted with 0.5 *N* hydrochloric acid (50 ml) and the mixture heated (4 h) on a boiling water bath to hydrolyze the glycosides. The cooled solution was then neutralized (silver carbonate) and filtered, and hydrogen sulfide was bubbled through the filtrate, which was again filtered. The filtrate, on evaporation under reduced pressure, gave a brown syrup (0.72 g). Chromatographic examination of the syrup in solvents *a*, *b*, *c*, *d*, and *f* showed it to be a mixture of at least five components, which were separated chromatographically on Whatman 3 MM filter sheets with solvent *b* as eluant. Table I shows the different fractions that were isolated from the mixture.

TABLE I

Components isolated from the hydrolysate of the methyl ether of degraded cholla gum

Fraction No.	Methylated sugar	Yield (approximate mole ratio)	R_g in solvent *b*	Color to *p*-anisidine
1	2,3,4,6-Tetra-*O*-methyl-D-galactose	114 mg (2 moles)	0.89	Reddish brown
2	2,3,4-Tri-*O*-methyl-D-galactose	60 mg (1 mole)	0.65	Yellowish brown
3	2,4,6-Tri-*O*-methyl-D-galactose	103 mg (2 moles)	0.67	Reddish brown
4	2,4-Di-*O*-methyl-D-galactose	189 mg (4 moles)	0.40	Yellow
5	2,3,4-Tri-*O*-methyl-D-galacturonic acid	102 mg (2 moles)	—	Pink
6	Not identified, probably a dimethyl-L-rhamnose	Trace	0.99	Yellow

Fraction 1, 2,3,4,6-Tetra-O-methyl-D-galactose

The syrup was crystallized from methanol–acetone; the crystals had m.p. 74°; $[\alpha]_D$ +142 → 118° (in water). It was chromatographically homogeneous, had R_g 0.89, and gave a reddish brown spot on chromatograms sprayed with *p*-anisidine hydrochloride. It was converted into *N*-phenyl-2,3,4,6-tetra-*O*-methyl-D-galactosylamine; m.p. and mixed m.p. 195–196°; $[\alpha]_D$ −82° (*c*, 1.2 in acetone) (18).

Fraction 2, 2,3,4-Tri-O-methyl-D-galactose

Fraction 2 (60 mg), on chromatographic examination, was found to contain ca. 10–15% of fraction 3. Similarly, chromatographic examination of fraction 3 revealed the presence of ca. 5% of fraction 2. The two fractions were therefore mixed together and purified by chromatographic separation on Whatman 3 MM paper with solvent *d*.

Fraction 2 so obtained (42 mg) was chromatographically pure and had $[\alpha]_D$ +138° (*c*, 0.4 in water). When its solution in ethanol (5 ml) was heated under reflux with redistilled aniline (22 mg) for 8 h, the *N*-phenyl-2,3,4-tri-*O*-methyl-D-galactosylamine was formed, which crystallized out, when the solution was kept for several days, in the form of large brown plates; these were washed with ice-cold ethanol – diethyl ether (9:1 v/v) and had m.p. 163–167°; $[\alpha]_D$ −58 → 46° (6 days) (*c*, 0.4 in methanol) (19).

Fraction 3, 2,4,6-Tri-O-methyl-D-galactose

The pure syrup (79 mg) obtained after the second chromatographic separation moved parallel, on chromatograms, to the 2,4,6-tri-*O*-methyl-D-galactose which had been obtained earlier from the aldobiouronic acid, and crystallized when seeded with it. When it was recrystallized from ethanol–acetone it gave fine needles, m.p. and mixed m.p. 103–104°; $[\alpha]_D$ +121 → 92° (*c*, 0.6 in water). Its *N*-phenyl glycosylamine had m.p. and mixed m.p. 178–180° (undepressed on admixture with an authentic specimen); $[\alpha]_D$ −90 → +37° (24 h) (*c*, 0.6 in acetone) (17).

Fraction 4, 2,4-Di-O-methyl-D-galactose

This component (189 mg) crystallized readily, and on recrystallization from benzene–ethanol–water had m.p. 103°; $[\alpha]_D$ +123 → +86° (*c*, 0.98 in water). Smith (19) gives m.p. 103°; $[\alpha]_D$ 122 → +86° (in water). It was further characterized as 2,4-di-*O*-methyl-D-galactose through its crystalline *N*-phenyl glycosylamine which, on recrystallization from benzene–methanol (1:2), had m.p. and mixed m.p. with authentic *N*-phenyl-2,4-di-*O*-methyl-D-galactosylamine 216–217°; $[\alpha]_D$ −182° (*c*, 1.2 in pyridine) (20).

Fraction 5, 2,3,4-Tri-O-methyl-D-galacturonic Acid

This component (102 mg) crystallized spontaneously, and on recrystallization from methanol–water (9:1 v/v) had m.p. 100°; $[\alpha]_D^{23}$ +128 → +106° (*c*, 0.88 in water).

Anal. Calcd. for $C_9H_{16}O_7 \cdot H_2O$: equiv. wt. 259. Found: equiv. wt. 254 (21).

The acidic sugar was oxidized by bromine water and converted into its dimethyl ester by boiling the product (8 h) with methanolic hydrogen chloride (1%, 25 ml). The resultant pale yellow syrup crystallized on trituration with a small amount of diethyl ether. Recrystallization from petrol – diethyl ether (1:1) gave the crystalline dimethyl ester of 2,3,4-tri-*O*-methyl-D-galactosaccharic acid, m.p. 101°; $[\alpha]_D$ +31° (*c*, 0.34 in water) (21).

Can. J. Chem. Downloaded from www.nrcresearchpress.com by 210.87.254.40 on 09/05/12
For personal use only.

Periodate Oxidation of the Degraded Gum

The ash-free degraded gum (60 mg dry wt) was dispersed in water (75 ml) and oxidized by shaking the suspension with 0.03 *M* periodic acid solution (25 ml) in the dark at 25°. The amount of periodic acid consumed and the formic acid liberated (after correction for the titratable acidity of the gum and of periodic acid) during the progress of the reaction were estimated in the usual way (22) at regular time intervals. The molar periodate consumption and formic acid liberation per mole of anhydrohexose unit were as shown in Table II.

TABLE II

Periodate oxidation of the degraded cholla gum (moles of periodate consumed and formic acid liberated per mole of anhydrosugar $C_6H_{10}O_5$)

Time (h)	1	4	8	12	24	28	32	48	72
Periodate	0.39	0.59	0.72	0.80	0.95	0.99	1.00	1.05	1.10
Formic acid	0.12	0.24	0.37	0.40	0.48	0.49	0.50	0.52	0.54

Extrapolation of the flat portions of the curves to zero time gave 0.93 mole of periodic acid consumed and 0.47 mole of formic acid liberated per $C_6H_{10}O_5$ unit.

Smith-Type Degradation of the Degraded Gum (8, 9)

The degraded gum (250 mg) was odixized by periodic acid for 24 h under conditions identical with those described above, after which excess oxidant was destroyed by ethylene glycol (25 ml) and the mixture was dialyzed against running distilled water. The undialyzed polyaldehyde solution was concentrated and the polyaldehyde was reduced by addition of aqueous sodium borohydride solution (1%, 25 ml) to the polyalcohol, which was obtained as a white powder (201 mg) on concentration of the solution. Hydrolysis of the polyol with 1 *N* sulfuric acid on a boiling water bath and concentration of the neutralized hydrolysate gave a syrup which, on chromatographic examination in various solvents, showed the presence of D-galactose (ca. 55–60%), glycolaldehyde (ca. 15–25%), and glycerol and glyceronic acid (almost equal proportions). (All estimations were visual.)

ACKNOWLEDGMENTS

The authors thank Drs. B. A. Erukoff and K. Folkers for the gift of cholla gum. They also thank the National Research Council for a grant (N.R.C. T-19) and Queen's University for financial assistance.

REFERENCES

1. E. Anderson, L. Sands, and N. Sturgis. Am. J. Pharm. **97**, 589 (1925).
2. L. Sands and R. Klass. J. Am. Chem. Soc. **51**, 3441 (1929).
3. F. Brown, E. L. Hirst, and J. K. N. Jones. J. Chem. Soc. 1761 (1949).
4. R. Montgomery and F. Smith. Methods Biochem. Analy. **3**, 153 (1954).
5. W. N. Haworth. J. Chem. Soc. **107**, 8T (1915).
6. H. C. Srivastava, S. N. Harshe, and P. P. Sing. Tetrahedron Letters, 1869 (1963).
7. T. Purdie. J. Chem. Soc. **83**, 1021 (1903).
8. M. Abdel-Akher, J. K. Hamilton, R. Montgomery, and F. Smith. J. Am. Chem. Soc. **74**, 4970 (1952).
9. I. J. Goldstein, G. W. Hay, B. A. Lewis, and F. Smith. Am. Chem. Soc. Abstr. Papers, **135**, 3D (1959).
10. C. S. Hudson. J. Am. Chem. Soc. **31**, 66 (1909).
11. W. E. Trevelyan, D. P. Procter, and J. S. Harrison. Nature, **166**, 444 (1950).
12. L. Hough, J. K. N. Jones, and W. H. Wadman. J. Chem. Soc. 1702 (1950).
13. W. N. Haworth and G. C. Leitch. J. Chem. Soc. **113**, 188 (1918).
14. E. L. Hirst, J. K. N. Jones, and W. O. Walder. J. Chem. Soc. 1443 (1947).
15. E. G. V. Percival and J. C. Somerville. J. Chem. Soc. 1615 (1937).
16. E. G. V. Percival and T. G. H. Thompson. J. Chem. Soc. 750 (1962).
17. E. L. Hirst and J. K. N. Jones. J. Chem. Soc. 1482 (1939).
18. E. V. White and P. S. Rao. J. Am. Chem. Soc. **75**, 2617 (1953).
19. F. Smith. J. Chem. Soc. 1724 (1939).
20. D. J. Bell and E. Baldwin. J. Chem. Soc. 125 (1941).
21. P. Andrews, D. H. Ball, and J. K. N. Jones. J. Chem. Soc. 4090 (1953).
22. G. Neumüller and E. Vasseur. Arkiv Kemi, **5**, 235 (1953).

Can. J. Chem. Downloaded from www.nrcresearchpress.com by 210.87.254.40 on 09/05/12
For personal use only.

Can. J. Chem. Downloaded from www.nrcresearchpress.com by 210.87.254.105 on 09/05/12
For personal use only.

PROTONATED CARBONYL GROUPS

VIII. ALKYLURACIL SALTS

DENYS COOK

Department of National Health and Welfare, Food and Drug Directorate, Ottawa, Canada

Received July 29, 1965

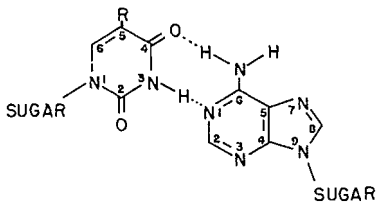
ABSTRACT

With 1,3-dimethyluracil and 1,3,6-trimethyluracil as models for nucleic acid bases, it was found by infrared spectroscopic methods that the site of protonation is a carbonyl group. Analysis of other evidence makes it likely that it is the carbonyl group in position 4. In 1,3,6-trimethyluracil salts, activation of the 5 position under acid conditions permits ready hydrogen–deuterium exchange.

Some anomalous 2 base – 1 acid salts with complex acids are considered in the light of base pairing errors in nucleic acids.

INTRODUCTION

Uracil and thymine (5-methyluracil) are two of the pyrimidine bases found in the nucleic acids. Thymine (I) is thought to be paired with adenine in deoxyribonucleic acid (DNA) (1), and uracil (II) with adenine in ribonucleic acid (2).



I R = CH_3 THYMINE...

II R = H URACIL...

These pyrimidines are weak bases, and are capable of forming salts although no pK values seem to have been published. It is of interest to find the site of protonation in simple dioxypyrimidines of this type, and methods previously found to be satisfactory have presently been employed (3). To simplify the interpretation of the spectra of the salts the 1,3-dialkyl derivatives have been used. The N-monoalkyl derivatives will be considered later.

RESULTS

Tables I and II show the absorption bands in the salts of 1,3-dimethyluracil and 1,3,6-trimethyluracil; Table III shows the bands caused by the protonated group.

DISCUSSION

There are four basic atoms in the N-alkyluracils, and the molecule resulting from protonation of each site in turn is depicted in structures III–VI. The salt spectra show a broad strong band in the 2 000 – 2 500 cm^{-1} region which is attributed to the protonated group, but neither its position nor its structure helps in the determination of the protonation site, and any of structures III–VI could equally well give rise to such a band. The deuteration shifts and isotopic ratios are normal.

TABLE I

Absorption bands in the spectra of 1,3-dimethyluracil salts

	HCl	HBr	DBr	HI	DI	$HSbCl_6$
ν_{CH}	3 098 w	3 092 m	3 090 w			
		3 080 m,sh		3 071 m	3 072 m	3 080 m
ν_{CH}	3 053 w	3 052 w	3 055 w	3 048 m	3 056 m	
	3 022 vw	3 024 w	3 023 w			
ν_{CH_3}	2 960 vw	2 955 w				
ν_{CH_3}		2 922 w				
ν_{OH}		2 300 m,sh				
		2 168 s,sh	1 720?	2 585 s	1 990 m	2 600 m
		2 120 s,sh		2 538 s		
		2 075 s,sh		2 495 s		
		2 032 m		2 440 s	1 854 m	
		1 981 m		2 398 s		
		1 905 w		2 360 s		
		1 730 m,sh	1 734 m,sh	1 725 s,sh	1 730 s,sh	
		1 719 vs,sh			1 720 s,sh	
ν_{CO}	1 710 vs	1 712 vs	1 714 vs	1 715 vs	1 716 vs	1 682 s
	1 695 m,sh	1 695 m,sh				
	1 664 m	1 674 m	1 680 m,sh	1 680 m,sh	1 680 m,sh	
	1 650 m	1 622 vs,sh	1 622 s,sh			
	1 642 m					
ν_{8a}	1 618 m	1 612 vs	1 617 vs	1 616 s	1 615 vs	1 632 s
				1 570 s,sh		1 612 s,sh
ν_{8b}	1 590 m	1 568 vs	1 568 s	1 566 s	1 568 vs	1 580 s
ν_{19a}	1 550 m,sh	1 552 m,sh	1 558 s,sh	1 555 m,sh	1 554 m,sh	1 555 m,sh
ν_{CO}	1 502 m,sh	1 512 s	1 515 s	1 524 m	1 509 s	1 510 m
		1 500 m,sh	1 505 s,sh	1 500 m,sh	1 502 s,sh	
ν_{19b}	1 456 m	1 461 m	1 464 w	1 450 m	1 454 w	
		1 450 m,sh	1 452 w			
	1 432 m	1 428 m,sh	1 420 w,sh			
	1 423 m	1 423 m	1 424 m	1 425 m	1 424 m	1 424 s
		1 387 s,sh	1 395 m	1 388 s,sh	1 390 s	
ν_{14}	1 375 m,sh	1 380 s	1 379 s	1 380 vs	1 379 vs	1 392 s
	1 338 s	1 335 m	1 333 m	1 338 m	1 334 m	1 328 m
δ_{OH}	1 352 m?	1 290 m	973 m	1 276 m	948 m	1 355 m
	1 275 m					
	1 260 m	1 260 m	1 258 m	1 249 m	1 256 m	1 267 m
	1 219 m	1 220 m	1 219 m	1 215 m	1 215 m	1 217 m
	1 172 m	1 160 m	1 165 m	1 160 m	1 160 m	1 173 w
	1 145 s	1 145 m	1 153 m	1 141 m	1 140 m	1 148 m
	1 128 m,sh		1 142 m			
ν_{12}	1 066 m	1 065 w	1 065 m	1 065 w	1 070 m	1 072 w
				1 010 w	1 010 m	
ν_1	1 014 m	1 018 m	1 018 m	996 m	996 m	1 020 m
	990 w,sh	980 vw				
γ_{OH}	958 m	872 m		760 m,sh		830 m,b
	941 m	941 w	942 w	940 m	936 m	938 w
	838 m	828 w	836 w			830 m,b
γ_{CH}	817 m	813 m	815 m	817 s	814 s	808 m
	791 m	790 m	787 m	790 m	780 m	795 m
δ_{CC}	769 vs	765 s	766 s	748 s	748 s	762 s
	761 m,sh					
	700 w	700 w		700 w	700 m	704 m

A consideration of the bands in the 1 700 cm^{-1} region leads to rejection of structures III and IV. N-Aroyltrialkylammonium ions (VII*a*) (4), N-acyltrialkylammonium halides (VII*b*) (5), and 2,2-dimethylquinuclid-6-one salts (VIII) (6), all possessing a quaternary nitrogen atom adjacent to a carbonyl group, have carbonyl stretching frequencies in the 1 780 – 1 810 cm^{-1} region. Even when the quaternary nitrogen atom has a trigonal sp^2 configuration, as in N-aroylpyridinium (IX*a*) (7) and N-acylpyridinium (IX*b*) (5) salts, the carbonyl stretching frequencies are in the region of 1 785 and 1 800 cm^{-1} respectively.

Can. J. Chem. Downloaded from www.nrcresearchpress.com by 210.87.254.105 on 09/05/12
For personal use only.

TABLE II

Absorption bands in the spectra of 1,3,6-trimethyluracil salts

	HCl	HBr	DBr	H_2SnCl_6	H_2SnBr_6
ν_{CH}	3 081 w	3 076 m	3 070 m	3 082 m	3 081 m
	2 995 vw			3 012 m	3 012 m
ν_{CH_3}	2 953 w	2 945 w	2 948 w		
ν_{CH_3}	2 918 vw	2 910 w	2 912 w		
ν_{OH}	1 788 m,sh	2 250 m,b	1 790 m,b	3 048 m,b	3 062 m,b
	1 730 s,sh				
	1 715 vs,sh		1 715 vs,sh		1 728 s
ν_{CO}	1 705 vs	1 712 vs	1 708 vs	1 730 vs	1 712 vs
	1 698 s,sh	1 696 s,sh	1 697 s,sh	1 700 m,sh	
	1 692 s,sh				
	1 680 m,sh	1 664 m,sh	1 665 m,sh		
		1 632 m,sh	1 625 s,sh		
	1 628 s,sh	1 625 m,sh	1 620 s,sh		
ν_{8a}	1 600 s	1 615 vs	1 611 vs	1 607 vs	1 602 vs
ν_{8b}	1 572 s	1 583 s	1 568 s	1 588 vs	1 583 vs
		1 572 s,sh			
	1 552 m,sh	1 552 m,sh	1 554 m,sh		1 550 w,sh
ν_{CO}	1 500 s	1 508 s	1 504 s	1 512 m	1 508 m
		1 502 s,sh			
	1 485 s,sh	1 485 m,sh	1 485 m,sh		
		1 454 m,sh	1 454 w,sh	1 452 m,sh	1 450 m,sh
		1 443 m,sh	1 440 m,sh		
	1 428 s	1 430 m	1 436 s	1 438 s	1 435 s
					1 402 m,sh
	1 402 m	1 408 m	1 406 m	1 398 m	1 393 m
					1 385 m,sh
ν_{14}	1 373 s	1 379 m	1 376 m	1 370 m	1 366 m
	1 370 s,sh				
	1 320 m	1 310 m	1 191 m	1 338 m	1 332 w
				1 290 w	1 285 w
		1 262 m,sh	1 262 m,sh		
δ_{OH}	1 258 m	1 250 m	999 m	1 231 m	1 223 m
	1 222 m,sh	1 235 m,sh	1 225 m		1 200 m,sh
	1 185 m,sh	1 180 w	1 180 w,sh	1 178 m	1 170 m
	1 128 w	1 128 w	1 128 w	1 120 m	1 116 m
	1 058 m	1 058 m	1 058 m	1 050 w	1 045 w,sh
	1 042 m	1 041 m	1 041 m	1 034 m	1 030 m,sh
					1 025 m
	992 m	992 m	993 m,sh	986 m	982 m
γ_{OH}	954 m	809 m			
	898 w	896 w,sh	888 w	890 w	886 w
	852 w	855 m,sh	855 w,sh		
	826 m	821 w	817 w		
	786 m,sh	786 w	788 vw		
	767 vs	765 vs	765 vs	756 vs	750 vs
	712 m	710 m	708 w	710 m	704 m
					696 m?
			644 w		659 m

This shows that delocalization of the positive charge around the carbon atoms in the pyridinium ring is present but small.

Since the highest frequency band in the carbonyl stretching region is near 1 715 cm^{-1}, no similarity in structure between uracil salts and VII, VIII, or IX can be assumed.

A further argument can be advanced to rule out structures III and IV. In tertiary (sp^3) amine salts the NH deformation mode has been found near 1 402 cm^{-1}, and this value has been suggested as a diagnostically useful group frequency (3). No band near 1 402 cm^{-1} showing a deuteration shift has been found in the uracil salts.

Oxygen protonation is thus proposed in uracil salts, and the chief source of confirmation comes from the in-plane hydrogen-bending mode. This has been found hitherto (3) to

Can. J. Chem. Downloaded from www.nrcresearchpress.com by 210.87.254.105 on 09/05/12
For personal use only.

TABLE III

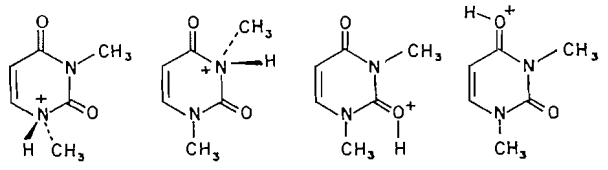
OH bands in the spectra of 1,3-dimethyluracil and 1,3,6-trimethyluracil salts

	1,3-Dimethyluracil				1,3,6-Trimethyluracil			
	HCl	HBr	HI	$HSbCl_6$	HCl	HBr	H_2SnCl_6	H_2SnBr_6
ν_{OH}		2 168	2 585 2 440	2 600	1 788	2 250	3 048	3 062
ν_{OD}		1 720	1 990 1 854			1 790		
ν_{OH}/ν_{OD}		1.26	1.30 1.30					
δ_{OH}	1 352	1 290	1 276	1 355	1 258	1 250	1 231	1 223
δ_{OD}		973	948			999		
δ_{OH}/δ_{OD}		1.32	1.34			1.25		
γ_{OH}	958	872	760	808	954	869	?	?

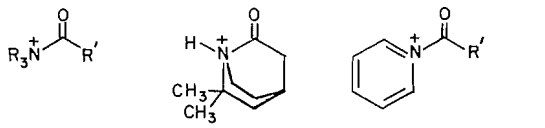
give an absorption band in protonated carbonyl groups near 1 257 cm^{-1}. There is indeed a band in all the uracil salts in the appropriate region (see Table III) which moves, on deuteration, to near 980 cm^{-1}, thereby giving normal isotopic ratios. In addition, this band is the only one (with the exception of the ~750 cm^{-1} band caused by the out-of-plane hydrogen-deformation γ_{OH}) which shifts on deuteration, thus unambiguously identifying it as δ_{OH}.

The other characteristic of protonated carbonyl groups is a lowered carbonyl frequency. These have previously been located near 1 500 cm^{-1}, except for that at ~1 400 cm^{-1} in the vibrationally coupled amides, with some reservations about the preciseness of the description as a result of possible mixing of the ring modes with carbonyl stretching modes.

Protonated uracils have a pattern of bands which is quite similar in each salt but which is very different from that of the free base. In the latter there are two bands, at ~1 700 and ~1 650 cm^{-1}, which are probably associated with carbonyl stretching vibrations (8–10). The ~1 650 cm^{-1} band is often overlapped by ring modes, so that it is quite broad. In the salts this region becomes nicely resolved into bands near 1 715, 1 615, 1 575, and 1 510 cm^{-1}. The highest and lowest bands are assigned to carbonyl group vibrations,



III IV V VI



VII
a, R′= ARYL
b, R′= ALKYL

VIII

IX
a, R′= ARYL
b, R′= ALKYL

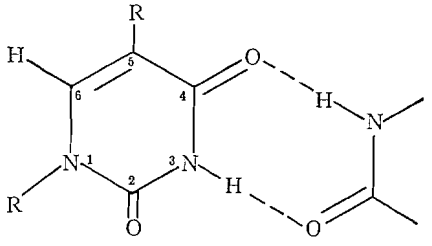
Can. J. Chem. Downloaded from www.nrcresearchpress.com by 210.87.254.105 on 09/05/12
For personal use only.

the lowest being caused by the protonated group. The middle two bands would then be assigned to ring modes ν_{8a} and ν_{8b}.* The 1 510 cm^{-1} band is in a position quite close to that seen in many protonated C=O bonds in heterocyclic ring systems, and the fact that it shows little movement in the deuterated salt has been taken as a sign that little or no mixing of C=O stretching vibrations and OH in-plane bending occurs. In peri-methoxyanthraquinone salts changes of ~20 cm^{-1} occur on deuteration, and other factors, too, have indicated coupling (11). On the other hand, α-pyridones (12) have shown changes in ν_{CO} and δ_{OH} similar to those observed in uracil salts. This is not too surprising in view of the similarity of the lactam grouping in each compound.

The question now arises as to which of the two carbonyl groups in the uracils is protonated. Nothing is known of the relative basicity of the two carbonyl groups in terms of pK values. Pullman and Pullman (13) have calculated bond orders and charge distribution in the uracil nucleotide, and give 0.770 and 1.501 for C_4O and 0.802 and 1.471 for C_2O respectively. Attempts to regard each C=O group as a prototype of a simpler system, e.g. C_2O as a part of $R_2N—CO—NR_2$ and C_4O as a part of an α-pyridone system, seem unsatisfactory. Since there is some structural evidence from crystallographic studies that C_4O is more basic than C_2O, this evidence will be examined; then an a posteriori justification of the spectra will be attempted.

TABLE IV

Systems exhibiting the $N_3H\cdots C_4O$ hydrogen bonds



	R_1	R_5
1-Methyluracil (14)	CH_3	H
1-Methylthymine (15)	CH_3	CH_3
Adenine–thymine pair in DNA (1)	Deoxyribose	CH_3
Adenine–uracil pair in RNA (2)	Ribose	H
1-Methylthymine–9-methyladenine complex (22)	CH_3	CH_3
1-Methyluracil–9-ethyladenine complex (31)	CH_3	H
Uracil (32)*	H	H
5′-Bromo-5′-deoxythymidine (33)†	Deoxyribose	CH_3

*N_1H also forms a hydrogen bond to C_4O, but there are no hydrogen bonds to C_2O.
†In the monoclinic form (A) N_3H and C_4O form hydrogen bonds to the appropriate part of the CH_2OH group in the sugar.

The crystal structures of 1-methyluracil (14) and 1-methylthymine (15) show that two molecules form a hydrogen-bonded dimer related by a center of symmetry (see partial structure in Table IV). The hydrogen bonds are formed between N_3H and C_4O. NR_1 cannot, and C_2O does not, form a hydrogen bond. These hydrogen-bonded dimers are arranged in a plane, and all other contacts in this plane, except for the hydrogen bonds, are weak van der Waals forces. Forces between planes are probably limited to van der Waals interactions, though there may be some weak dipole–dipole forces between

See ref. 12 for nomenclature.

Can. J. Chem. Downloaded from www.nrcresearchpress.com by 210.87.254.105 on 09/05/12
For personal use only.

Can. J. Chem. Downloaded from www.nrcresearchpress.com by 210.87.254.105 on 09/05/12
For personal use only.

the polar parts of molecules in different layers. If one now considers the 1-methylthymine molecule, a rotation of 180° about the 3,6 axis would give a configuration which has merely exchanged the N_1CH_3 group for the C_5CH_3 group, and transposed the carbonyl groups. The spatial requirements of N_1CH_3 and C_5CH_3 are so similar that their interchange should have an imperceptible effect on the crystal lattice. The effect of charge distribution, particularly the π-electron distribution, is more subtle (15). From this point of view the effect of interchanging N_1CH_3 and C_5R might make more difference to the interlayer forces and might modify arrangements in a direction perpendicular to the plane of the dimer. It is considered, therefore, that C_4O is more basic than C_2O, since the $N_3H\cdots OC_4$ hydrogen bonds are maintained in the structures in Table IV, even though reversal of the hydrogen bonds to $N_3H\cdots OC_2$ would give rise to no additional instability. The acidity of N_3H does not enter into the discussion, as it is common to both arrangements.

What has been said of 1-methylthymine applies to the same extent to 1-methyluracil. R_5 in this case is hydrogen, so that interchange of N_1CH_3 and C_5H will make a larger difference. Since the interdimer and interlayer forces are van der Waals forces of low directional specificity, slight rearrangement to accommodate an altered methyl group would make small differences.

Additional information can be derived from carbonyl group bond lengths in certain molecules. Although the C_4O distances are larger than the C_2O distances in 1-methylthymine and 1-methyluracil, this may be due in part to the hydrogen bond. In 1,3,7,9-tetramethyluric acid (16), in which no hydrogen bonds are possible, C_6O, which is the carbonyl group equivalent to C_4O in the pyrimidines, is 0.03 Å longer than C_2O (same numbering in both bases). The same situation occurs in caffeine (0.07 Å) (17) and in theophylline hydrate (0.03 Å) (18), though in the latter the N_7H bond may interfere. The longer carbonyl groups are associated with more $C^+—O^-$ character and greater donor activity.

This evidence makes it seem likely that C_4O is the more basic site, and that the structure of the cation would therefore be that shown by VI. In the hydrohalides a hydrogen bond in $C{=}O^+—H\cdots X^-$ would be preferred, and not $C{=}O^+—H\cdots O{=}C$, since ν_{OH} does vary with X^-. But in the $HSbCl_6$ salt the low value of ν_{OH} might be taken as evidence for the latter type of hydrogen bond, especially as the protonated carbonyl group stretching frequency is shifted from 1 720 to 1 682 cm^{-1}.

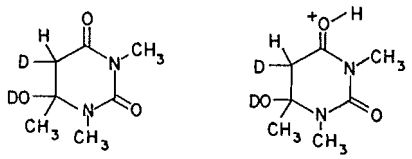
The vibrational behavior of VI can now be interpreted in terms of the assignments of the 1 510 cm^{-1} band to C_4O stretching and the 1 715 cm^{-1} band to C_2O stretching. The two intermediate bands at 1 615 and 1 575 cm^{-1} are then assigned to ν_{8a} and ν_{8b}, and the 1 550 and 1 460 cm^{-1} bands to ν_{19a} and ν_{19b}. The N-methyl and C-methyl group asymmetric deformation vibrations would give rise to the absorption band near 1 423 cm^{-1}, whereas the symmetric deformation band would be obscured by the strong 1 380 cm^{-1} band, which seems to be too strong to assign to $\delta_{CH_3}{}^s$. The 1 380 cm^{-1} band would be assigned to ν_{14}; its intensity in heterocyclic compounds is much greater than in homocyclic compounds (12).

The exchange experiments with D_2O provided some interesting information on the reactivity at the 5 position. 1,3,6-Trimethyluracil·HCl, on treatment with excess D_2O and evacuation, did not give the deuterated salt. Instead the free base was recovered, but it was found to have exchanged the hydrogen at position 5 for deuterium. It was thus possible to relate bands at 3 088, 1 226, 1 040, and 845 cm^{-1} to the C_5H bond. Corresponding bands in the C_5D compound were at 2 302 (1.34), 1 070 (1.14), 778 (1.33), and 632? (1.33) cm^{-1}. Since only three absorption bands should occur (ν_{CH}, δ_{CH}, and

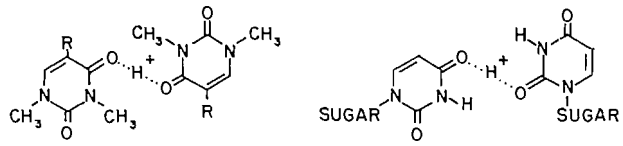
γ_{CH}), it is likely that some mixing of δ_{CH} with a ring mode occurs. The nuclear magnetic resonance spectrum of the deuterated material lacked the resonance at 338 c.p.s.

Two interesting points are raised with respect to this observation. One is concerned with the mechanism of exchange, whether by electrophilic substitution at position 5 or by covalent hydration across the 5:6 bond followed by dehydration to give the 5-d_1 derivative. The second one, which is independent of the mechanism, has to do with the protonation state during the reaction, for it will be recalled that no exchange took place with only D_2O (see Experimental section) or D_2O at pD > 7.

In view of the known ability of 1,3-dimethyluracil to add H_2O across the 5:6 double bond to give the 6-hydroxy derivative (19, 20), an intermediate of this nature (X) might be considered in the carbon deuteration of 1,3,6-trimethyluracil. The hydrogen atom at position 5 would be expected to be quite acidic and, upon isotopic exchange and subsequent D_2O elimination, would be replaced by deuterium. This acidity may only be generated in the protonated base XI. It is difficult to justify the exchange process without the acidic H_5 atom, since D_2O addition and elimination would be expected to follow the same stereochemical pathway. Some idea of the configuration of XI would be of value in these arguments, but unfortunately this is not known.



X XI



XII XIII

2 Base – 1 Acid Salts

The infrared spectra of the 2:1 salts show the usual broad strong band centered near 900 cm^{-1} with several deep transmission windows (21). The band near 1 700 cm^{-1} is thought to be caused by the carbonyl stretching vibration of position 2, though again there is no conclusive evidence about which carbonyl group is concerned in the hydrogen bond. A possible structure XII is indicated.*

The relevance of such structures to errors in base sequence in polynucleotides is determined by the geometry of the base pair. The distance between the 1′ carbon atoms of the deoxyribose sugar molecule attached to the base pairs was 11.1 Å in the Watson–Crick model (1) (see Table V). Calculations suggest that the corresponding distance in the 2:1 salts shown in XII may be close to 12.3 Å. This figure is large, but not unreasonably so. Just as Hoogsteen (22) has shown that a slightly distorted double-helix DNA model

**The structure of some of these 2:1 salts, their dimensions, and the question of the centrosymmetric hydrogen bond are being investigated by Dr. J. C. Speakman at the University of Glasgow, Scotland.*

Can. J. Chem. Downloaded from www.nrcresearchpress.com by 210.87.254.105 on 09/05/12
For personal use only.

TABLE V

C_1'—C_1' distances

Structure	C_1'—C_1' (Å)
Polyadenylic acid (27)	10.5
9-Ethyladenine–1-methyluracil complex (31)	7.5
9-Ethylguanine–1-methylcytosine complex (34)	10.55
9-Methyladenine–1-methylthymine complex (22)	8.65
Watson–Crick model	11.1

can be built incorporating the anomalous hydrogen-bonded system in the 1-methylthymine–9-methyladenine complex, in which the distance between the methyl carbon atoms is 8.645 Å, then it is likely that a model having a larger distance could be built involving similar distortions but in the opposite sense.

However, XII is not the only model that can be considered. As has been shown above, although the C_4O carbonyl group is probably more basic than the C_2O carbonyl group, the difference is slight, and other factors may override this. Thus in the non-centrosymmetric structure XIII, where the short hydrogen bond between C_4O and C_2O is energetically very similar to that in XII, the C—C distance is 9.8 Å. Other similar structures are listed in Table VI. This distance is much closer to the one probably existing in the nucleic

TABLE VI

C—C distances in model base pairs

		d_{CC}	Structures*	Symmetry elements
N_1O_4	N_1O_4§	12.3	3*,†	i, i*,†
N_1O_4	N_1O_4	10.0‡	2*	σ, σ*
N_3O_4	N_3O_4	8.0	1	i
N_3O_2	N_3O_2	8.0	1	i
N_1O_4	N_1O_2	10.1	2†	
N_1O_4	N_3O_2	9.4	2†	
N_3O_2	N_1O_2	8.0	1	
N_3O_4	N_1O_2	8.0	1	
N_3O_4	N_3O_2	8.0	1	

*Another structure of similar symmetry derived by rotation of both molecules around N_1C_4 axis.
†Another structure derived by rotation of *one* molecule around N_1C_4 axis.
‡Some angular distortions are necessary here, and possibly some tilted planes, to prevent N_3H interactions.
§The N subscript indicates the point of attachment of the methyl, and the O subscript indicates the oxygen atom involved in hydrogen bonding.
NOTE: i = center of symmetry; σ = mirror plane.

acids. The symmetry of the hydrogen-bonded partners in the 2:1 salts was formerly thought always to involve a center of symmetry (23, 24), but recently an exception was noted. The mesitaldehyde – perchloric acid 2:1 complex (25) was found to have a plane of symmetry through the carbonyl oxygen atoms and the shared proton perpendicular to the molecular plane. This precedent makes more plausible some of the structures in Table VI which do not have a center of symmetry. Another possibility for the introduction of errors in base sequence would arise if a uracil–sugar bond was formed at N_3 of the pyrimidine molecule. Many other additional structural arrangements could then be made for the incorporation of such nucleosides into a nucleic acid by proton sharing. Some of these are also shown in Table VI.

The number of structural types known to form 2:1 salts is quite large, but they have one thing in common. The basic atoms forming the bond are usually of low pK_a; for example, amides, α-pyrones, α-pyridones, γ-pyridones, aromatic aldehydes, and heterocy-

Can. J. Chem. Downloaded from www.nrcresearchpress.com by 210.87.254.105 on 09/05/12
For personal use only.

clic amine oxides have pK_a values less than about 3.3. Most compounds of higher basicity form conventional salts. It is significant that, of the nucleic acid bases, uracil and thymine probably have the lowest pK_a values: cytosine, 4.6; adenine, 4.25; guanine, 3.0; uracil, no listed value, but probably slightly higher than that of 2-thiouracil, −4.16 (26).

Finally, the source of the proton accommodated between the bases is not hard to find. The secondary phosphate linking two sugar molecules has one OH group remaining which could, under the appropriate circumstances, yield the proton to be shared by the bases. There are precedents for this behavior: in polyadenylic acid (27) the proton is transferred from the POH group to the N_1 position on the base; and in polycytidylic acid (28) a form is known to exist at pH 5.5 in which the cytosine NH_2 groups form hydrogen bonds to the carbonyl groups, and the protonated N_3 atom forms a hydrogen bond to the unprotonated N_3 atom in the second molecule. It is very unlikely that this bond could be a symmetrical one because of the large distance involved.

EXPERIMENTAL

Materials

1,3-Dimethyluracil and 6-methyluracil were obtained from the Aldrich Chemical Company. 6-Methyluracil was dimethylated according to the method published by Davidson and Baudisch (29).

1,3-Dimethyluracil Salts

HCl Salt

The base, dissolved in a small amount of $CHCl_3$ and then excess CCl_4, was treated with anhydrous HCl to give a white hygroscopic solid, m.p. 105–106°.

Anal. Calcd. for $C_6H_8N_2O_2 \cdot HCl$: HCl, 19.2. Found: HCl, 18.7.

HBr Salt

The same treatment gave a white hygroscopic solid, m.p. 179–180°.

Anal. Calcd. for $C_6H_8N_2O_2 \cdot HBr$: HBr, 36.6. Found: HBr, 36.7.

HI Salt

Equimolar portions of aqueous (50%) HI and the base gave long needles after 24 h, m.p. 163–165 (decomp.).

Anal. Calcd. for $C_6H_8N_2O_2 \cdot HI$: C, 26.88; H, 3.38; N, 10.45. Found: C, 26.75; H, 4.03; N, 10.48.

When $CHCl_3$ solutions were used the 2:1 salt $(C_6H_8N_2O_2)_2 \cdot HI$ was found.

$HAsF_6$ Salt

Aqueous (~60%) $HAsF_6$ (4.0 g) and 2.01 g base gave long needles about 0.5 h after mixing, m.p. 172–174.

Anal. Calcd. for $(C_6H_8N_2O_2)_2 \cdot HAsF_6$: C, 30.65; H, 3.64; N, 11.92. Found: C, 30.65; H, 3.45; N, 11.46.

Infrared (Nujol and fluorolube): 3 095 m, 3 068 m, 1 710 s, 1 642 s, 1 580 s, 1 430 m,b, 1 380 m, 1 337 s, 1 258 m, 1 225 m, 1 148 m, 1 062 m, 1 050 m,sh, 960 m,b, 925 m,b, 822 m, 806 s, 788 s, 770 s, 700 vs (AsF_6^-).

The two following salts are similar.

HPF_6 Salt

Aqueous (~60%) HPF_6 (2.30 g) and 2.86 g base gave a solid immediately after mixing, m.p. 129–133.

Anal. Calcd. for $(C_6H_8N_2O_2)_2 \cdot HPF_6$: C, 33.81; H, 4.02; N, 13.15. Found: C, 33.37; H, 4.06; N, 13.44.

$HSbF_6$ Salt

Aqueous (~60%) $HSbF_6$ (3.61 g) and 2.77 g base developed crystals after mixing, m.p. 155 (decomp.).

Anal. Calcd. for $(C_6H_8N_2O_2)_2 \cdot HSbF_6$: C, 27.87; H, 3.31; N, 10.84. Found: C, 28.06; H, 3.20; N, 10.53.

HBF_4 Salt

Attempts to prepare this salt have been described previously (30); only the BF_3 complex resulted.

1,3,6-Trimethyluracil Salts

HCl Salt

Same as above, m.p. 127–129.

Anal. Calcd. for $C_7H_{10}N_2O_2 \cdot HCl$: HCl, 18.6. Found: HCl, 18.2.

HBr Salt

As above, m.p. 194–195.

Anal. Calcd. for $C_7H_{10}N_2O_2 \cdot HBr$: HBr, 34.0. Found: HBr, 34.0.

HI Salt

Equivalents of the aqueous acid and base yielded a hydrate. Attempts to remove water required conditions so vigorous that some decomposition into 2:1 salts occurred.

Can. J. Chem. Downloaded from www.nrcresearchpress.com by 210.87.254.105 on 09/05/12
For personal use only.

H_2SnCl_6 Salt

The salt precipitated as a white solid when a $CHCl_3$ solution of the base was saturated with HCl and then treated with $SnCl_4$, m.p. 131–133°. Analytical figures for this and the following salt were difficult to obtain because of their hygroscopic nature; argentimetric titrations were usually low.

H_2SnBr_6 Salt

Same method as with HBr and $SnBr_4$, m.p. 138–139°.

$HSbCl_6$ Salt

A $CHCl_3$ solution of the base gave a pale yellow solid on treatment with dry HCl and $SbCl_5$, which was recrystallized from ethanol, m.p. 227–228°.

Anal. Calcd. for $(C_7H_{10}N_2O_2)_2 \cdot HSbCl_6$: C, 26.11; H, 3.29; N, 8.70. Found: C, 26.37; H, 3.28; N, 8.11.

Infrared (Nujol and fluorolube): 1 695 s,sh, 1 685 s, 1 632 s, 1 555 m,sh, 1 503 m, 1 426 m, 1 412 m, 1 378 m, 1 266 m, 1 215 m, 1 182 m, 1 125 m, 1 068 m, 1 046 m, 1 000 m, 895 m, 810 s, 805 s,sh, 794 s,vb, 759 vs, 688 s, 642 m.

Deuterated salts were prepared by exchange with D_2O. 1,3,6-Trimethyuracil·HCl gave 5-deuterio-1,3,6-trimethyluracil under these conditions, but neither the free base in D_2O nor a NaOD–D_2O solution of the base exchanged in this manner.

Spectra

The conditions under which the spectra were recorded have been described before (12).

ACKNOWLEDGMENTS

Most of the work reported here was done in the Exploratory Research Laboratory, Dow Chemical of Canada, Limited, Sarnia, Ontario; the assistance of Mrs. R. H. Veach in preparing many of the compounds and recording their spectra, and of Dr. J. S. McIntyre in recording the nuclear magnetic resonance spectra is gratefully acknowledged. The microanalytical data were obtained through the courtesy of Mr. L. E. Swim and his associates (The Dow Chemical Company, Midland, Michigan, U.S.A.).

REFERENCES

1. J. D. Watson and F. H. C. Crick. Nature, **171**, 737 (1953); **171**, 964 (1953).
2. A. Rich and D. R. Davies. J. Am. Chem. Soc. **78**, 3548 (1956).
3. D. Cook. Can. J. Chem. **42**, 2292 (1964).
4. R. Gompper and P. Altreuther. Z. Anal. Chem. **170**, 205 (1959).
5. D. Cook. Can. J. Chem. **40**, 2362 (1962).
6. H. Pracejus. Chem. Ber. **92**, 988 (1959).
7. D. Cook. Unpublished results.
8. H. M. Randall, R. G. Fowler, N. Fuson, and J. R. Dangl. Infrared determination of organic structures. D. Van Nostrand Co., Inc., New York. 1949.
9. L. N. Short and H. W. Thompson. J. Chem. Soc. 168 (1952).
10. C. L. Angell. J. Chem. Soc. 504 (1961).
11. D. Cook. Spectrochim. Acta. In press.
12. D. Cook. Can. J. Chem. **43**, 749 (1965).
13. A. Pullman and B. Pullman. J. Chim. Phys. **58**, 904 (1961).
14. D. W. Green, F. S. Mathews, and A. Rich. Acta Cryst. **16**, 907 (1963).
15. K. Hoogsteen. Acta Cryst. **16**, 28 (1963).
16. D. J. Sutor. Acta Cryst. **16**, 97 (1963).
17. D. J. Sutor. Acta Cryst. **11**, 453 (1958).
18. D. J. Sutor. Acta Cryst. **11**, 83 (1958).
19. A. M. Moore and C. H. Thompson. Science, **122**, 594 (1955).
20. A. M. Moore and C. H. Thompson. Can. J. Chem. **35**, 163 (1957).
21. D. Cook. Chem. Ind. London, 607 (1963).
22. K. Hoogsteen. Acta Cryst. **16**, 907 (1963).
23. W. Takei. Ph.D. Thesis, California Institute of Technology, Pasadena, California. 1957.
24. H. H. Mills and J. C. Speakman. Proc. Chem. Soc. 216 (1963).
25. C. D. Fisher, L. H. Jensen, and W. M. Schubert. J. Am. Chem. Soc. **87**, 33 (1965).
26. B. Stanovnik and M. Tišler. Arzneimittel-Forsch. **14**, 1004 (1964).
27. A. Rich, D. R. Davies, F. H. C. Crick, and J. D. Watson. J. Mol. Biol. **3**, 71 (1961).
28. R. Langridge and A. Rich. Nature, **198**, 725 (1963).
29. D. Davidson and O. Baudisch. J. Am. Chem. Soc. **48**, 2379 (1926).
30. D. Cook. Chem. Ind. London, 1259 (1964).
31. F. S. Mathews and A. Rich. J. Mol. Biol. **8**, 89 (1964).
32. G. S. Parry. Acta Cryst. **7**, 313 (1954).
33. M. Huber. Acta Cryst. **10**, 129 (1957).
34. E. J. O'Brien. J. Mol. Biol. **7**, 107 (1963).

Can. J. Chem. Downloaded from www.nrcresearchpress.com by 210.87.254.105 on 09/05/12
For personal use only.

Can. J. Chem. Downloaded from www.nrcresearchpress.com by 210.87.254.5 on 09/05/12
For personal use only.

THE SYNTHESIS OF PORPHYRINS DERIVED FROM CHLOROBIUM CHLOROPHYLLS[1,2]

J. L. ARCHIBALD,[3,4] D. M. WALKER,[3,5] K. B. SHAW,[3,6] A. MARKOVAC,[3] AND S. F. MACDONALD

Division of Pure Chemistry, National Research Council, Ottawa, Canada

Received September 23, 1965

ABSTRACT

The proofs of the structures proposed for the *Chlorobium* pheophorbides 650, fractions 1–5, and for the *Chlorobium* pheophorbides 660, fractions 5 and 6, are completed and the degradational evidence, where parallel, confirmed through the synthesis of derived porphyrins.

The photosynthetic bacteria *Chlorobium thiosulfatophilum*, strain L and strain VN, contain *Chlorobium* chlorophyll 650 and *Chlorobium* chlorophyll 660 respectively, the numbers indicating the wavelength of their absorption maxima in the red. These are magnesium complexes of farnesyl (not phytyl) esters of the *Chlorobium* pheophorbides 650 and 660. Like ordinary chlorophyll, both these chlorophylls are mixtures, for their pheophorbides can be resolved into several components, which are termed fractions: *Chlorobium* pheophorbide 650, fractions 1–6, and *Chlorobium* pheophorbide 660, fractions 1–6.

These fractions (pheophorbides) are more closely related to the pyrropheophorbide *a* than to the pheophorbide *a* from chlorophyll *a*, for they lack the 10-carbomethoxy group of the latter. All were shown to be homologues of 2-(α-hydroxyethyl)-2-desvinyl-pyrropheophorbide *a* (I, R^1 = Et, R^2 = Me, R^3 = H) (Reaction Scheme 1) and were formulated (2, 3) as shown in Table I, wherein the structures of the related porphyrins as well as some chlorophyll *a* derivatives are also indicated. It will be noted that some trivial names such as pyrroporphyrin (strictly pyrroporphyrin 15), phylloporphyrin, and desoxo-phylloerythrin are used in two senses. Without qualification, they refer to the prototypes derived from chlorophyll *a*; otherwise, they refer to the homologues of these, derived from the *Chlorobium* chlorophylls.

The analytical and degradational evidence (2, 3) did not completely prove these structures for, in the absence of special features, it could only reveal the pairs of substituents on positions 1–8 but not their order. In both the 650 and 660 series other structures in which the substituents on any of the pyrrole rings 1, 2, or 4 were reversed in order (e.g. 7-methyl-8-propionic acid) were equally compatible with it. The indicated structures were preferred, because they were more obviously related to pheophorbide *a*.

In the 650 series, there was no direct evidence concerning the nature of R^2 in fractions 3, 5, and 6, for citraconimide had not been detected among their oxidation products.

In the 660 series, improved analytical methods revealed the natures of R^2 in all fractions. However, in the absence of adequate models, the nuclear magnetic resonance evidence which placed the R^3 groups on the δ-positions was not conclusive (3, 4). Further, as

[1]*Issued as N.R.C. No. 8760.*

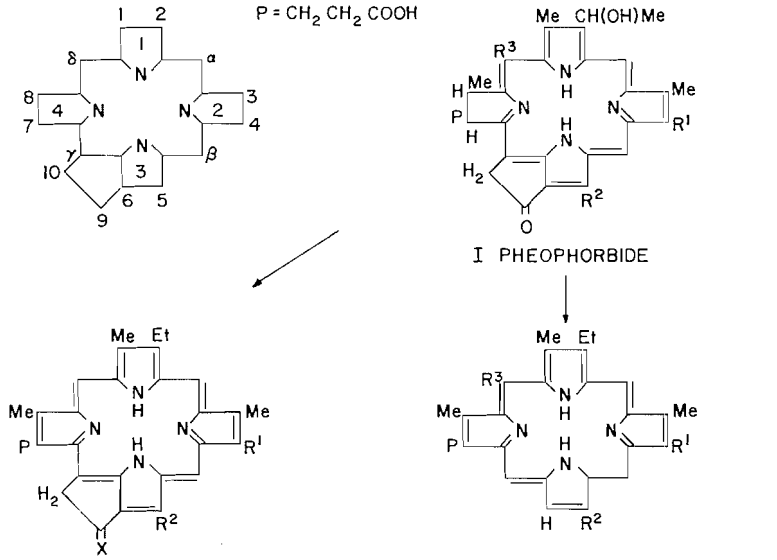
[2]*Part of this work has been reported briefly (1), and the results have been summarized in connection with the analytical work (2, 3).*

[3]*National Research Council Postdoctorate Fellow.*

[4]*Present address: Wyeth Laboratories Incorporated, Philadelphia, Pennsylvania.*

[5]*Present address: Imperial Chemical Industries Ltd., Petrochemical and Polymer Laboratory, Runcorn, Cheshire, England.*

[6]*Present address: Defence Research Board, Shirley's Bay, Ottawa, Canada.*



REACTION SCHEME 1. *Chlorobium* pheophorbides and derived porphyrins.

TABLE I
Pheophorbides and derived porphyrins

	Structure (Reaction Scheme 1)	R^1	R^2	R^3
Derivatives of pheophorbide *a* (from chlorophyll *a*)				
Pyrropheophorbide *a*	I ($CH{=}CH_2$ for CH(OH)Me)	Et	Me	H
Mesopyrropheophorbide *a*	I (Et for CH(OH)Me)	Et	Me	H
Phylloerythrin	II*a*	Et	Me	H
Desoxo-phylloerythrin	II*b*	Et	Me	H
Pyrroporphyrin 15	III*a*	Et	Me	H
γ-Phylloporphyrin 15	III*a* (Me for H on γ)	Et	Me	H
Chlorobium pheophorbide 650				
Fraction 1	I	CH_2CHMe_2	Et	H
Pyrroporphyrin from fraction 1	III*a*	CH_2CHMe_2	Et	H
Fraction 2	I	$CH_2CH_2CH_3$	Et	H
Pyrroporphyrin from fraction 2	III*a*	$CH_2CH_2CH_3$	Et	H
Fraction 3	I	CH_2CHMe_2	Me	H
Pyrroporphyrin from fraction 3	III*a*	CH_2CHMe_2	Me	H
Fraction 4	I	Et	Et	H
Pyrroporphyrin from fraction 4	III*a*	Et	Et	H
Fraction 5	I	$CH_2CH_2CH_3$	Me	H
Desoxo-phylloerythrin from fraction 5	II*b*	$CH_2CH_2CH_3$	Me	H
Fraction 6	I	Et	Me	H
Chlorobium pheophorbide 660				
Fraction 1	I	CH_2CHMe_2	Et	Et
Fraction 2	I	CH_2CHMe_2	Et	Me
Fraction 3	I	$CH_2CH_2CH_3$	Et	Et
Fraction 4	I	$CH_2CH_2CH_3$	Et	Me
Pyrroporphyrin from fractions 3 and 4	III*a* (cf. 650, fraction 2)	$CH_2CH_2CH_3$	Et	H
Fraction 5	I	Et	Et	Me
δ-Phylloporphyrin from fraction 5	III*b*	Et	Et	Me
Fraction 6	I	Et	Me	Me
δ-Phylloporphyrin from fraction 6	III*b*	Et	Me	Me

Can. J. Chem. Downloaded from www.nrcresearchpress.com by 210.87.254.5 on 09/05/12
For personal use only.

definite evidence about the nature of the R^3 groups was lacking, the 660 fractions were formulated by assuming the R^3 groups to be the simplest possible: R^3 = Me in all fractions except either 1 and 3 or 2 and 4, wherein R^3 = Et. The molecular weights of fractions 2, 4, 5, and 6, determined since the synthetic work was completed, are consistent only with the former alternative.

In the case of *Chlorobium* pheophorbide 650, fraction 6, the structure was subsequently confirmed and the assumptions validated by converting it into pyrropheophorbide *a* (3), wherein the order of the substituents and the 5-methyl group was known through Fischer's syntheses of related porphyrins. In the present work, the synthesis of the degradation products listed in Table I provides similar confirmation of the structures of the remaining *Chlorobium* pheophorbides 650, fractions 1–5, and of the *Chlorobium* pheophorbides 660, fractions 5, 6, and (in part) 3 and 4. This also supports the assumptions upon which these and the remaining structures were based. All the identities were established through the melting points, the mixed melting points, and the X-ray powder photographs of both the methyl esters and their copper complexes.

In the 650 series, the pyrroporphyrins from fractions 1–4 and the desoxo-phylloerythrin from fraction 5 were identified with synthetic specimens.

In the 660 series, not enough of fractions 1 and 2 were obtained for the degradations to be attempted. The two phylloporphyrins III*b* (R^1 = $CH_2CH_2CH_3$, R^2 = Et, R^3 = Me) and III*b* (R^1 = $CH_2CH_2CH_3$, R^2 = R^3 = Et) were synthesized for comparison with those from fractions 3 and 4, without prejudice about which should correspond to which. It was initially concluded from the X-ray powder photographs of the esters that the synthetic δ-methyl- and δ-ethyl-porphyrins might correspond with those from fractions 3 and 4 respectively, but the limited amounts of material were used before either of these identities had been established. Further, in view of the polymorphism of the specimens, none of the possible identities can be excluded on this evidence. Other difficulties here were the low yields in the syntheses, the relatively high solubilities, and the relative difficulty with which fractions 3 and 4 are separated. As these two synthetic δ-phylloporphyrins were neither well characterized (see Experimental) nor identified with material of natural origin, they are omitted from Table I. However, both fractions 3 and 4 were also degraded to one pyrroporphyrin which was shown (3) to be identical with the synthetic pyrroporphyrin corresponding to the 650 pheophorbide, fraction 2. This confirmed the structures of fractions 3 and 4 except for the nature and position of R^3. The δ-phylloporphyrins from fractions 5 and 6 were identified with synthetic specimens. That corresponding to fraction 6 (δ-phylloporphyrin 15) had been synthesized by Fischer (5), but none of his specimen remained. When his synthesis was repeated in a considerably modified form, we found that the melting point of its methyl ester – copper complex had been reported incorrectly.

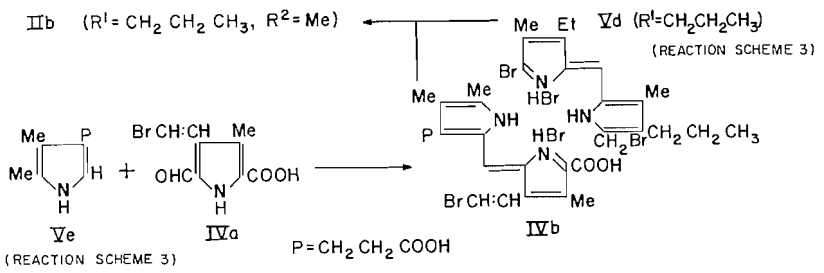
Porphyrins of the 650 Series

The obvious attack was to synthesize pyrroporphyrins for comparison with those obtained by degradation. This degradation seemed to be impracticable for, in contrast to that of pheophorbide *a*, the isocyclic ring of pyrropheophorbide *a* is not easily oxidized by Fischer's methods. In the first instance (fraction 5), this difficulty was avoided by comparing a synthetic desoxo-phylloerythrin with analytical ones. This confirmed the isocyclic ring, but the synthesis of desoxo-phylloerythrins is more laborious than that of pyrroporphyrins and is probably unsuited to 5-ethyl derivatives, for which the pyrrole intermediate providing ring 3 is reportedly unstable (6). Later, methods were found by which

Can. J. Chem. Downloaded from www.nrcresearchpress.com by 210.87.254.5 on 09/05/12
For personal use only.

the pheophorbides 650 were degraded to pyrroporphyrins, or the pheophorbides 660 to δ-phylloporphyrins and pyrroporphyrins (3). It was then possible to compare synthetic and analytical pyrroporphyrins, as was done with fractions 1–4.

The synthetic work was done concurrently with the analytical, before the potential of the developing analytical methods was known. A structure tentatively suggested for fraction 2 required it to be degraded to 2- or 4-*n*-propyl-2- or -4-desethyl-desoxophylloerythrin. Because the required pyrromethenes were known, the second of these was synthesized (Reaction Scheme 2) by the method which Fischer had used for desoxophylloerythrin itself (7, 8). All the intermediates were obtained by the reported methods or by modifications thereof (see Experimental).



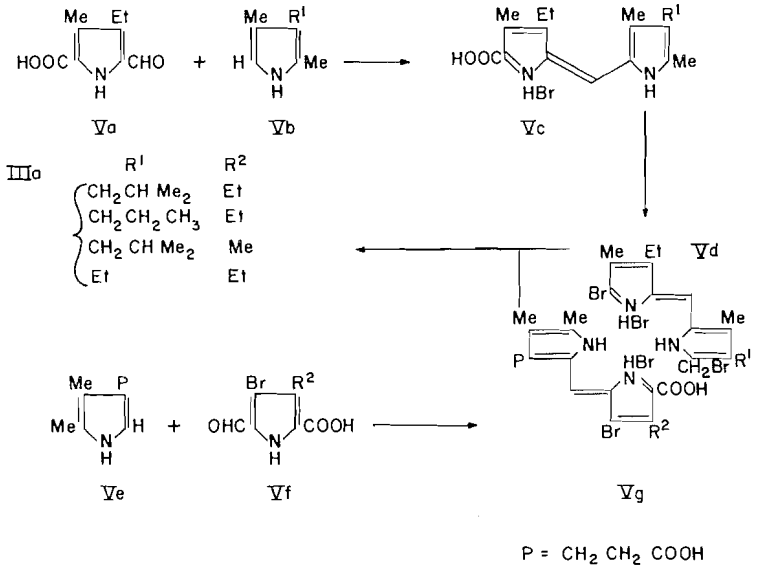
REACTION SCHEME 2. The synthesis of 4-*n*-propyl-4-desethyl-desoxo-phylloerythrin (II*b*, $R^1 = CH_2CH_2CH_3$, R^2 = Me).

The synthetic 4-*n*-propyl-4-desethyl-desoxo-phylloerythrin (II*b*, $R^1 = CH_2CH_2CH_3$, R^2 = Me) differed from that obtained when fraction 2 was degraded. Later analytical work showed that, in both fractions 2 and 5, R^1 was indeed *n*-propyl and was on ring 2 rather than on ring 1. However, it also showed that R^2 was ethyl in fraction 2, and thus was probably methyl in fraction 5. Fraction 5 was then degraded to a desoxo-phylloerythrin which was shown to be identical with the synthetic one.

Some work on the above degradations should be mentioned. In model experiments, the degradation of pyrropheophorbide *a* with hydrogen iodide in acetic acid to phylloerythrin, and of the latter to desoxo-phylloerythrin by the Wolf–Kishner method (9), was repeated. This gave an initially low melting desoxo-phylloerythrin ester (m.p. ca. 255°) which required extensive purification. The same method was used to degrade fraction 2. Further model experiments showed that the Wolf–Kishner reduction of mesopyrropheophorbide *a* gave a mixture of desoxo-phylloerythrin and desoxo-mesopyrropheophorbide *a* (10), and the latter gave more desoxo-phylloerythrin when heated with dilute acid. Here a high-melting product (ester m.p. 262–264°) resulted directly, so this method was used to degrade fraction 5.

The four pyrroporphyrins were synthesized by the scheme used by Fischer for one synthesis of pyrroporphyrin 15 (11) (Reaction Scheme 3). Unlike two possible alternatives, it utilized some pyrromethenes which could also be used in the synthesis of δ-phylloporphyrins (see below); also, one methene (V*d*, $R^1 = CH_2CH_2CH_3$) had already been prepared. Further, and unlike the fourth alternative, this scheme used the more easily available pyrroles, derivatives of 2,4- rather than 2,3-dimethyl-pyrrole, to construct rings 2 and 3 on which R^1 and R^2 varied. All the pyrroles and pyrromethenes in Reaction Scheme 3 were obtained essentially by the reported methods, or by standard ones (see Experimental). However, there had been no satisfactory preparation of V*b* (R^1 = isobutyl), and the following are new: V*c* (R^1 = isobutyl), V*d* (R^1 = isobutyl), V*f* (R^2 = Et), and V*g* (R^2 = Et).

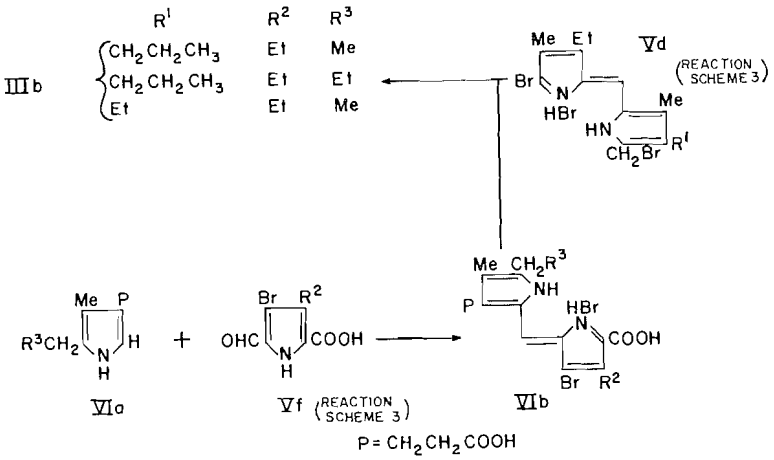
Can. J. Chem. Downloaded from www.nrcresearchpress.com by 210.87.254.5 on 09/05/12
For personal use only.



REACTION SCHEME 3. The synthesis of the pyrroporphyrins (V*d* (R^1 = Et)) is obtained directly by brominating 2,4-dimethyl-3-ethyl-pyrrole.

Porphyrins of the 660 Series

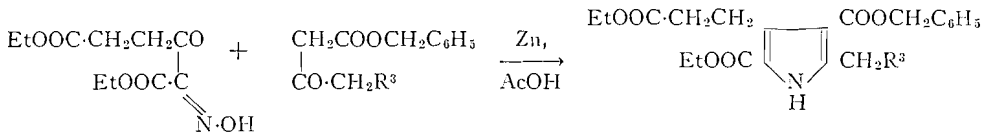
The syntheses of the δ-phylloporphyrins was undertaken by the method indicated in Reaction Scheme 4, for reasons mentioned in connection with the analogous synthesis of pyrroporphyrins. The 5-ethyl-5-desmethyl-δ-phylloporphyrin corresponding to fraction 5 was thus obtained. The δ-phylloporphyrins presumably corresponding to fractions 3 and 4, III*a* (R^1 = $CH_2CH_2CH_3$, R^2 = Et, R^3 = Me) and III*a* (R^1 = $CH_2CH_2CH_3$, R^2 = R^3 = Et), were also obtained, but, as mentioned above, were inadequately characterized. The data here (see Experimental) gave some misleading indications of identities, whereas the usual problem has been that of polymorphism obscuring identities (cf. 650, fraction 4, and 660, fraction 6); in both cases the criteria are near the limits of their usefulness. By using V*d* (R^1 = Et) and VI*b* (R^2 = R^3 = Me), this method failed to give δ-phylloporphyrin itself (III*a*, R^1 = Et, R^2 = R^3 = Me), which corresponds to fraction 6; the spectrum of the product suggested that it was the corresponding pyrroporphyrin.



REACTION SCHEME 4. The synthesis of homologues of δ-phylloporphyrin.

Can. J. Chem. Downloaded from www.nrcresearchpress.com by 210.87.254.5 on 09/05/12
For personal use only.

The syntheses of the pyrroles VI*a* (R^3 = Me and R^3 = Et) were analogous to a synthesis of VI*a* (R^3 = H) (12):



followed by $COOCH_2C_6H_5 \rightarrow COOH \rightarrow H \rightarrow CHO \rightarrow CH_3$, and then hydrolysis and decarboxylation. Here, as in analogous cases, the acids produced by hydrogenating the benzyl esters are most smoothly decarboxylated by heating the crude acids containing Raney nickel, a small amount first being decarboxylated to wet the walls of the flask with the product. We have since found that homologues such as the above are more readily obtained through the reaction of α-bromomethyl-pyrroles with Grignard reagents (13).

The benzyl propionyl acetate and benzyl *n*-butyryl acetate required in the above pyrrole syntheses were obtained, as was benzyl acetoacetate (14), by heating the ethyl esters with benzyl alcohol. The ethyl esters were obtained by boiling ethyl propionyl malonate and ethyl *n*-butyryl malonate with water (cf. refs. 15, 16). This may be the most generally useful method for preparing ethyl acyl acetates. The yields by a standardized procedure are competitive, consistent, and insensitive to the size of the run. Acyl malonic esters (17, 18) have also been split less reliably (19) by heating them with sulfonic acids (18), less conveniently by cold concentrated sulfuric acid (16) (see also Experimental), in low yield by steam distillation (20), and (together with undesirable by-products) by heating them with acid and a catalyst (21). When the product is not readily separated from the by-product (diethyl malonate) by distillation, it can be purified as its bisulfite complex or, if it does not form one, as its magnesium derivative (cf. ref. 22). Related methods employing ethyl acyl acetoacetates as intermediates give ethyl acetoacetate as the by-product, the separation of which, other than by distillation, requires more specialized methods. Although ethyl propionyl acetate is conveniently obtained from ethyl cyanoacetate and ethyl magnesium iodide, this method is less general and requires 2 moles of the Grignard reagent.

As δ-phylloporphyrin (III*a*, R^1 = Et, R^2 = R^3 = Me) was not obtained as above, we repeated Fischer's synthesis (5) (Reaction Scheme 5). Accordingly, the pyrroles VII*e* and VII*f*, obtained by more recent methods (see Experimental), were converted into VII*g* and hence into VII*h*. The preparation of VII*d* was modified, VII*b* being used instead of 3-methyl-4-ethyl-pyrrole, for it is doubtful that the latter always condenses under the methyl group (23). The two known pyrroles VII*a* and VII*b* were obtained by a method which was particularly convenient, because both were required: VIII*a* was converted through VIII*b*, IX*a*, and IX*b* into IX*c* and IX*d*; the latter gave VII*a* and VII*b* respectively. In effect, this sequence converts a pyrrole into its isomer with the β-substituents reversed, or into higher homologues thereof. Another alternative though unsatisfactory synthesis of VII*a* was found in the modified Knorr synthesis (cf. ref. 24) of its α-carbethoxy derivative from isonitroso-acetoacetic ester and 4-methyl-3,5-heptanedione.

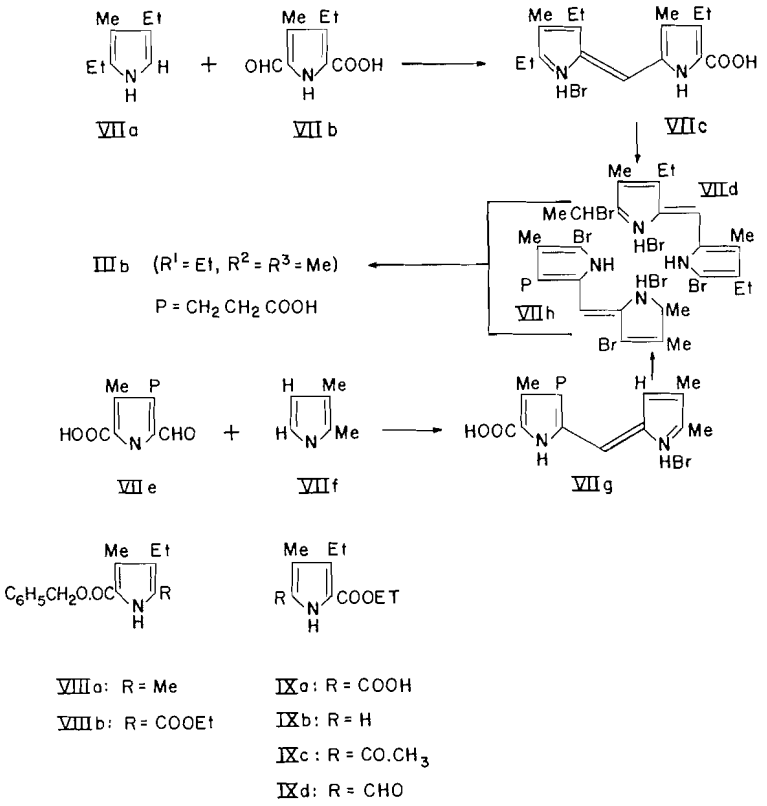
EXPERIMENTAL

Pyrroles

*2-Formyl-3-(ω-bromovinyl)-4-methyl-5-carboxy-pyrrole (IV*a*) (25)*

The reported yield and melting point of the intermediate, 2,4-dimethyl-3-(ω-bromovinyl)-5-carbethoxy-pyrrole, were only realized when the crude product (from ether) was recrystallized by extraction (thimble) successively with benzene (5 parts), with hexane (10 parts), and then with benzene.

Can. J. Chem. Downloaded from www.nrcresearchpress.com by 210.87.254.5 on 09/05/12
For personal use only.



REACTION SCHEME 5. The synthesis of δ-phylloporphyrin 15.

Only when the corresponding ester was hydrolyzed by heating it for 2 h under reflux (mantle) was the expected yield obtained.

2-Formyl-3-ethyl-4-methyl-5-carboxy-pyrrole (Va) (26)

2,4-Dimethyl-3-ethyl-5-carbethoxy-pyrrole (27) was oxidized in varying yield to the 2-aldehyde (28) (purified to m.p. ⩾ 90° from aqueous ethanol by high vacuum distillation or by extraction with pentane), and the latter was hydrolyzed (26), the product (m.p. ⩾ 200°) being precipitated by acetic acid. A specimen, m.p. 210° (lit. (26) m.p. 199°), was analyzed.

Anal. Calcd. for $C_9H_{13}O_3N$: C, 59.00; H, 7.15; N, 7.65. Found: C, 59.13; H, 6.88; N, 7.55.

2,4-Dimethyl-3-n-propyl-pyrrole (Vb, $R^1 = CH_2CH_2CH_3$) (29, p. 60)

The method developed for the 3-ethyl homologue (30) gave a 65% yield from 2,4-dimethyl-3-propionyl-5-carbethoxy-pyrrole (29, p. 200).

2,4-Dimethyl-3-isobutyl-5-carbethoxy-pyrrole

The corresponding 3-isobutyryl-pyrrole (31) (colorless prisms, 55%, m.p. 111–113° (lit. (31) m.p. 108°)) was isolated by extraction with ether, distillation (bath temperature 160° at 0.1 mm), and crystallization from aqueous ethanol. This was hydrogenated for 6 h in 2.5 parts of ethanol over Raney nickel (1 900 p.s.i., 160°), more nickel added, and the hydrogenation repeated. The product was filtered off and dissolved in ether. Ether was removed from the filtered solution and the residue crystallized from aqueous ethanol as colorless needles (52%), m.p. 116–117°.

Anal. Calcd. for $C_{13}H_{21}NO_2$: C, 69.92; H, 9.48; N, 6.27. Found: C, 70.03; H, 9.34; N, 6.31.

2,4-Dimethyl-3-isobutyl-pyrrole (Vb, $R^1 = CH_2CHMe_2$) (31)

The above 5-carbethoxy derivative (5 g) was heated under reflux for 3 h with 3 g of sodium hydroxide, 10 ml of water, and enough ethanol to maintain solution. It was taken to dryness *in vacuo*, the residue extracted with 150 ml of water, and the insoluble ester recycled. Acidifying the aqueous extracts with 10% hydrochloric acid to pH 6 precipitated the α-carboxy-pyrrole (92%), which decomposed at 92°. This was distilled *in vacuo* at 110° to give the product (87%) as a colorless oil.

Anal. Calcd. for $C_{10}H_{17}N$: C, 79.40; H, 11.34; N, 9.27. Found: C, 79.74; H, 11.12; N, 8.98.

The one-step method from 2,4-dimethyl-3-isobutyryl-5-carbethoxy-pyrrole was unsatisfactory by either the original (31) or the modified (30) Wolf–Kishner procedures.

Can. J. Chem. Downloaded from www.nrcresearchpress.com by 210.87.254.5 on 09/05/12
For personal use only.

2,3-Dimethyl-pyrrole-4-propionic Acid (Hemopyrrole-carboxylic Acid, Ve)

This (12) was always recrystallized just before use as yellow needles, m.p. 132–133°, by extraction with 50 parts of hexane (thimble) over 12 h while protected from light.

2-Formyl-3-bromo-4-methyl-5-carboxy-pyrrole (Vf, R^2 = Me)

2,4-Dimethyl-3-bromo-5-carbethoxy-pyrrole (29, p. 92) was chlorinated in chloroform (not ether (cf. ref. 11)), the chloroform removed at 20°, and the residue converted into the 2-aldehyde which was obtained as colorless needles (65–80%). This was hydrolyzed (11) under nitrogen and the product recrystallized as microneedles (60%) from aqueous acetone.

Ethyl Propionyl Acetate (with D. K. Dougall)[7]

Ethyl propionyl malonate was prepared (18) on a 5 *M* scale in a 5 l flask, the ether layer containing the crude product being further washed with dilute $NaHCO_3$ and then water before stripping. The combined undistilled residues from two such runs were gently boiled under a 12 inch Vigreux column with 2 l of water for 9 h, with vigorous stirring (cf. ref. 16). The combined ester layers in the flask and distillate were extracted with 10 × 350 ml of aqueous $NaHSO_3$ (4 lb). The extract was washed with pentane, and then stirred in an ice bath while the solution was being neutralized at 25° with 35% NaOH, ice being added as necessary. The mixture was extracted with benzene; the extract was washed with aqueous $NaHCO_3$ and then with water, dried (Na_2SO_4), and filtered; the benzene was removed. Distillation gave 543 g (38% overall), b.p. 89.5–91° at 20 mm, n_D^{25} 1.4213, copper complex m.p. 142–143° (lit. (32) m.p. 144–145°). Gas–liquid chromatography showed about 4% of a second component.

Anal. Calcd. for $C_7H_{12}O_3$: C, 58.31; H, 8.39. Found: C, 59.61; H, 8.41.

In preliminary experiments on a 1.25 *M* scale, the above method and the sulfuric acid method (cf. ref. 16) both gave 28% yields. When the purification with bisulfite was omitted, a 51% yield was reported by the above method (33). Using gas–liquid chromatography, we found a commercial specimen to be 50% pure.

Benzyl Propionyl Acetate

Ethyl propionyl acetate (432 g) and benzyl alcohol (324 g) were heated with a few boiling stones in a 1 l flask in a mantle under a 12 inch Vigreux column until thermometers in the liquid and at the top of the column registered 176° and 91° respectively. The rest was distilled to 83° (0.05 mm). The distillate was recycled by heating to 183° and then distilling to 83° (0.05 mm), this second distillate being recycled again. The three residues were combined and distilled to give the product (575 g, 93%), b.p. 80–85° or higher at 0.5 mm depending on the rate of distillation, n_D^{25} 1.5050.

Anal. Calcd. for $C_{12}H_{14}O_3$: C, 69.88; H, 6.84. Found: C, 69.23; H, 6.42.

2-Methyl-3-carbobenzoxy-4-ethyl-5-carbethoxy-pyrrole

This was prepared by the Knorr synthesis according to our usual procedure (compare the corresponding 4-(2′-carbethoxyethyl)-pyrrole (23)), ethyl propionyl acetate (see above) being nitrosated with amyl nitrite and the product being condensed with benzyl acetoacetate. The crude pyrrole was washed with 50% ethanol and crystallized from ethanol, m.p. 126–127° (51%). For analysis it was recrystallized to m.p. 127–129°.

Anal. Calcd. for $C_{18}H_{21}O_4N$: C, 68.55; H, 6.71. Found: C, 68.10; H, 6.67.

2-Methyl-3-bromo-4-ethyl-5-carbethoxy-pyrrole (29, p. 93)

The corresponding 3-carbobenzoxy-pyrrole (above) was reduced in 3 parts of ethanol over Raney nickel (1 000 p.s.i., 100°) to the 3-carboxylic acid (29, p. 257) (90%). This was decarboxylated at 260° and the resulting 3-free pyrrole (29, p. 240) was distilled at 15 mm and then twice crystallized from aqueous ethanol (69%). A solution of this (19 g) in 60 ml of carbon tetrachloride was stirred and protected from moisture while 5.8 ml of bromine was dropped in. Stirring was continued for ½ h, and the solution was concentrated *in vacuo* to one-half volume and then refrigerated overnight. The crystals were washed with ether and recrystallized from aqueous ethanol as needles (63%), m.p. 127–129° (lit. (29, p. 93) m.p. 124°).

2-Formyl-3-bromo-4-ethyl-5-carbethoxy-pyrrole (34)

Sulfuryl chloride (10.3 ml) was added over 20 min to a stirred solution of the corresponding 2-methyl pyrrole (above, 16.3 g) in 250 ml of chloroform (ethanol free). Next day the solvent was removed *in vacuo*. The residue was twice crystallized from 70% ethanol at 0° to give nearly colorless needles (68%), m.p. 96–97° (lit. (34) m.p. 93–95°).

Anal. Calcd. for $C_{10}H_{12}NO_3Br$: C, 43.81; H, 4.41; N, 5.11; Br, 29.16. Found: C, 43.99; H, 4.28; N, 5.06; Br, 28.69.

2-Formyl-3-bromo-4-ethyl-5-carboxy-pyrrole (Vf, R^2 = Et)

The corresponding ester (above, 11.74 g) was heated in the steam bath under nitrogen for 3 h with 36 ml of 5% NaOH. The cooled solution was diluted to 300 ml, filtered, acidified with HCl, and refrigerated. The nearly colorless precipitate (96%) was recrystallized from acetone as needles which decomposed above 230°.

Anal. Calcd. for $C_8H_8O_3NBr$: C, 39.05; H, 3.29; N, 5.69; Br, 32.48. Found: C, 39.07; H, 3.40; N, 5.71; Br, 32.11.

2-Ethyl-3-carbobenzoxy-5-carbethoxy-pyrrole-4-propionic Acid Ethyl Ester

This was prepared from ethyl β-keto-adipate (16), amyl nitrite, and benzyl propionyl acetate (above) on a

[7]*National Research Council Postdoctorate Fellow, 1956–1957.*

Can. J. Chem. Downloaded from www.nrcresearchpress.com by 210.87.254.5 on 09/05/12
For personal use only.

1.5 *M* scale exactly as was its 2-methyl homologue (23). It formed colorless prisms (58%) when it was crystallized from ethanol, m.p. 92–93°.

Anal. Calcd. for $C_{22}H_{27}O_6N$: C, 65.82; H, 6.78; N, 3.49. Found: C, 66.03; H, 6.91; N, 3.10.

2-Ethyl-3-carboxy-4-(2-carbethoxyethyl)-5-carbethoxy-pyrrole

The corresponding 3-carbobenzoxy-pyrrole (above) was hydrogenated in ethanol over Raney nickel for 6 h at 125° and 1 500 p.s.i. Ethanol was removed and the residue extracted with ice-cold 0.1 *N* sodium carbonate, from which the product was precipitated with acetic acid. When it was crystallized from 50% ethanol it formed colorless prisms, m.p. 186–188.5°.

Anal. Calcd. for $C_{15}H_{21}O_6N$: C, 57.86; H, 6.80; N, 4.50. Found: C, 57.81; H, 6.91; N, 4.84.

2-Ethyl-5-carbethoxy-pyrrole-4-propionic Acid Ethyl Ester

The corresponding 3-carbobenzoxy-pyrrole (above, 50 g) was hydrogenated as above and the crude acid was slowly distilled at 15 mm from a 250 ml flask heated in a mantle with the neck wrapped in heating tape. The distillate was redistilled from a Vigreux flask to give an oil (78%), b.p. 150° at 0.5 mm, solidifying to colorless prisms, m.p. 40–41°, unstable to air and light.

Anal. Calcd. for $C_{14}H_{21}O_4N$: C, 62.90; H, 7.92; N, 5.24. Found: C, 63.17; H, 7.89; N, 5.13.

2-Ethyl-3-formyl-5-carbethoxy-pyrrole-4-propionic Acid Ethyl Ester

The corresponding 3-free pyrrole (above, 17.5 g) was stirred with dimethylformamide (35 ml, distilled over P_2O_5), while 8.8 ml of phosphorus oxychloride was dropped in. The mixture was heated on the steam bath for 40 min, cooled, and poured into 300 ml of water containing 52 g of sodium acetate. The oily layer solidified when the solution was allowed to cool. It was recrystallized by extraction with 1 600 ml of hexane (thimble) to give colorless needles (79%), m.p. 85–86°.

Anal. Calcd. for $C_{15}H_{21}O_5N$: C, 61.00; H, 7.17; N, 4.74. Found: C, 60.79; H, 6.80; N, 5.08.

2-Ethyl-3-methyl-5-carbethoxy-pyrrole-4-propionic Acid Ethyl Ester

The corresponding 3-formyl pyrrole (above) was reduced in ethanol over Raney nickel at 180° and 1 300 p.s.i. for 4 h. After the catalyst had been separated and the ethanol removed, the residue was crystallized from aqueous ethanol to give colorless needles (82%), m.p. 80.5–81.5°. For analysis, it was recrystallized to m.p. 81–82°.

Anal. Calcd. for $C_{15}H_{23}O_4N$: C, 64.03; H, 8.29; N, 4.98. Found: C, 64.21; H, 8.19; N, 5.18.

2-Ethyl-3-methyl-pyrrole-4-propionic Acid (VIa, R^3 = Me)

The corresponding 5-carbethoxy ester (above, 21.4 g) was heated under reflux for 3 h on the steam bath with 100 ml of water, 30 ml of ethanol, and 22 g of sodium hydroxide. Ethanol was boiled off, more water added, and the solution saturated with sulfur dioxide under a layer of ether and extracted twice with ether. The ether layer was washed with water and dried (Na_2SO_4), and the ether was removed. The residual solid was heated on the steam bath for 5 min with 15 ml of water. The whole was quickly dried (oil pump) and the residue crystallized from 1 200 ml of hexane. The colorless needles (86%) that were initially formed rapidly turned pink, m.p. 85–88°, sensitive to air and light.

Anal. Calcd. for $C_{10}H_{15}O_2N$: C, 66.27; H, 8.34; N, 7.73. Found: C, 66.08; H, 7.95; N, 7.91.

Ethyl n-Butyryl Acetate

Crude ethyl *n*-butyryl malonate was prepared in two 4.1 *M* runs in the same manner as ethyl propionyl malonate was (above), and boiled with water in the same way for 6.5 h. Combining the ester layers in the flask and distillate gave 1 270 ml of crude product. Magnesia mixture (850 ml) (from 330 g of $MgCl_2 \cdot 6H_2O$, 420 g of NH_4Cl, 1 500 ml of water, and 450 ml of ammonium hydroxide), 800 ml of water, and 400 ml of ice were stirred vigorously at 10°, 110 ml of the crude ester was added, and stirring was continued for 20 min. The filtered precipitate was twice slurried (Waring Blendor) and filtered with 60 ml of magnesia mixture which had been diluted with 500 ml of ice water, and then dried to 0.02 mm. The magnesium complex from 310 ml of crude ester (194 g, m.p. 152.5–154° (lit. (22) m.p. 156–157°)) was shaken with 600 ml of ether, 110 ml of hydrochloric acid, and 800 ml of ice water. The ether layer was washed with 10% HCl and both acid layers washed in turn with ether. The combined ether layers were washed with water, aqueous disodium phosphate, and water, and then dried (Na_2SO_4) and the ether removed. The residue was distilled at 14 mm to give 14 g, b.p. 86–91°, $n_D^{16.5}$ 1.4265; 122 g, b.p. 91–92.5°, $n_D^{16.5}$ 1.4275; and 18 g, b.p. 92.5–93°, $n_D^{16.5}$ 1.4275; total 49% overall.

All three fractions were suitable for conversion into the benzyl ester (see below). The middle fraction (copper complex m.p. 126–126.5° (lit. (35) m.p. 125–126°)) appeared on gas chromatography to be homogeneous and indistinguishable from the product which was obtained from ethyl *n*-butyryl acetoacetate (29, p. 405), but both gave a carbon analysis which was 2.5% high.

Benzyl n-Butyryl Acetate

As in the preparation of benzyl propionyl acetate (above), 116.3 g of the above ethyl *n*-butyryl acetate and 93 ml of benzyl alcohol were heated to 195° and distilled to 95° (0.01 mm) through three cycles. Distillation of the combined residues gave 145 g (89%), b.p. (0.02 mm) 89–93° or higher depending on the rate of distillation, n_D^{15} 1.5040.

Anal. Calcd. for $C_{13}H_{16}O_3$: C, 70.89; H, 7.32. Found: C, 71.05; H, 7.41.

Can. J. Chem. Downloaded from www.nrcresearchpress.com by 210.87.254.5 on 09/05/12
For personal use only.

2-n-Propyl-3-carbobenzoxy-5-carbethoxy-pyrrole-4-propionic Acid Ethyl Ester

This was obtained from ethyl β-keto-adipate (16), amyl nitrite, and the above benzyl *n*-butyryl acetate in the same manner as its 2-methyl homologue was (23), except that more acetic acid was used to maintain solution and prevent foaming. It formed colorless prisms (42%) when it was crystallized from aqueous ethanol, m.p. 84.5–85.5°.

Anal. Calcd. for $C_{23}H_{29}O_6N$: C, 66.49; H, 7.04; N, 3.37. Found: C, 66.36; H, 6.96; N, 3.31.

2-n-Propyl-3-methyl-5-carbethoxy-pyrrole-4-propionic Acid Ethyl Ester

The corresponding 3-carbobenzoxy derivative (above), in the same manner as its 2-ethyl homologue above, was converted successively into the 3-carboxy pyrrole (colorless plates from ethanol, m.p. 178–180°, or changing at 160° to needles, m.p. 184–185°), the 3-free pyrrole (prisms from pentane at −10°, m.p. 35.5–36.5°), the 3-formyl pyrrole (needles from hexane, m.p. 87.5–88.5°), and the 3-methyl pyrrole (ca. 20% overall). The latter formed colorless needles when it was crystallized from aqueous ethanol, m.p. 77–79°.

Anal. Calcd. for $C_{16}H_{25}O_4N$: C, 65.06; H, 8.53; N, 4.74. Found: C, 65.33; H, 8.50; N, 4.78.

2-n-Propyl-3-methyl-pyrrole-4-propionic Acid (VIa, R^3 = Et)

This was obtained, in the same manner as its 2-ethyl homologue (above), from the corresponding 5-carbethoxy ester (above). It separated from hexane when the solution was allowed to stand under nitrogen, finally at 10°, as long colorless needles (68%), m.p. 80.5–81.5°.

Anal. Calcd. for $C_{11}H_{17}O_2N$: C, 67.66; H, 8.78; N, 7.17. Found: C, 67.43; H, 8.58; N, 7.42.

4-Methyl-3,5-diethyl-2-carbethoxy-pyrrole

Ethyl acetoacetate (48 g) in 200 ml of acetic acid was nitrosated at 8° with 28 g of sodium nitrite in 50 ml of water, and excess nitrite was destroyed the next day with ammonium sulfamate. This solution, zinc dust (150 g), and 4-methyl-3,5-heptanedione (36) (51 g) were added in 5 portions over 10 min to a stirred solution of ammonium acetate (40 g) in acetic acid (100 ml) maintained at 60–70°. More zinc dust was added at this temperature over 1 h. The mixture was then kept for 1 h at 105° and then decanted into ice water. The product was separated from 2,4-dimethyl-3,5-dicarbethoxy-pyrrole by extraction with pentane, distillation to 90° (1×10^{-4} mm), and crystallization from pentane at −20°. It formed large colorless prisms (7 g, 9%), m.p. 62–63°.

Anal. Calcd. for $C_{12}H_{19}NO_2$: C, 68.86; H, 9.15. Found: C, 68.77; H, 9.07.

References to this in the literature (5; 29, p. 57) refer to 4-formyl-3,5-diethyl-2-carbethoxy-pyrrole.

3-Methyl-2,4-diethyl-pyrrole (VIIa)

(*a*) 4-Methyl-3-ethyl-2-carbethoxy-5-acetyl-pyrrole (IX*c*, see below, 13 g) was heated for 16 h at 160° in an autoclave with 12 ml of hydrazine and 7 g of sodium dissolved in 220 ml of absolute ethanol. Ethanol was then distilled off through a column and 30 ml of water added to the residue, which was then extracted with ether. The extract was dried (potassium carbonate) and the ether distilled off through a column. A drop of hydrazine was added to the residue, which was distilled through a small column (95–98°, 12 mm) to give 7.5 g (94%) of a pale oil, picrate m.p. 110° (lit. (5) m.p. 110°). It is stable in an evacuated sealed tube protected from light.

Anal. Calcd. for $C_9H_{14}N$: C, 78.77; H, 11.02; N, 10.21. Found: C, 78.47; H, 10.76; N, 10.15.

(*b*) 4-Methyl-2,4-diethyl-2-carbethoxy-pyrrole (see above, 1 part) was heated for 5 h at 170° in a Teflon-lined metal tube with 8 parts of ethanolic potassium hydroxide (10% w/v). Ether was then added and the product (82%) isolated as above, picrate m.p. and mixed m.p. with the above picrate 109–110°.

Anal. Found: C, 78.64; H, 11.22; N, 10.01.

4-Methyl-3-ethyl-2-carboxy-pyrrole-5-aldehyde (VIIb)

The corresponding ester (IX*d*, see below, 9.5 g) was boiled for 5 min with 20 ml of 10% sodium hydroxide. The clear solution was cooled, filtered with Darco, and acidified with hydrochloric acid. The crystalline precipitate was separated and recrystallized from 60% ethanol, m.p. 176° (7.5 g, 91%). For analysis it was recrystallized three times from 70% ethanol as long needles, m.p. 180–181° (lit. (37) m.p. 174°).

Anal. Calcd. for $C_9H_{11}O_3N$: C, 59.66; H, 6.12; N, 7.73. Found: C, 59.38; H, 5.98; N, 7.67.

2-Formyl-4-methyl-5-carboxy-pyrrole-3-propionic Acid Diethyl Ester

(*a*) A solution of 10.7 g of 2,4-dimethyl-5-carboxy-pyrrole-3-propionic acid diethyl ester (24) in 50 ml of chloroform (dried over calcium chloride) was stirred in an ice bath and protected from moisture while 7.2 ml of sulfuryl chloride was added over 1 h. Next day the chloroform was removed *in vacuo* and the residue was boiled for 5 min with 15 g of sodium acetate in 100 ml of water. The insoluble oil was washed by decantation and dissolved in ether. The washed (aqueous sodium carbonate and then water) and dried ether solution was evaporated and the residue distilled in high vacuum. The product (8 g, 71%) solidified when the solution was allowed to cool, m.p. 62–67°. For analysis it was recrystallized from pentane as pale yellow prismatic needles, m.p. 64.5–65.5° (lit. (38) m.p. 62–66°).

Anal. Calcd. for $C_{14}H_{19}NO_5$: C, 59.77; H, 6.81. Found: C, 59.95; H, 6.84.

(*b*) The corresponding half ester (free propionic acid (39)) was esterified at 20° in ethanolic hydrogen chloride and crystallized from pentane to give prismatic needles, m.p. and mixed m.p. with the above diethyl ester 64.5–65.5°.

Can. J. Chem. Downloaded from www.nrcresearchpress.com by 210.87.254.5 on 09/05/12
For personal use only.

2-Formyl-4-methyl-5-carboxy-pyrrole-3-propionic Acid (VIIe)

Either the above diethyl ester or the monoethyl ester (39) was hydrolyzed in ethanolic potassium hydroxide, crystallized from formic acid as colorless needles (39), and dried (63°, 1×10^{-4} mm).

Anal. Calcd. for $C_{10}H_{11}NO_5 \cdot HCOOH$: C, 48.71; H, 4.83; N, 5.16; equiv. wt. 90.4. Found in the product from the diethyl ester: C, 48.45; H, 4.73; N, 5.16; equiv. wt. 80.6. Found in the product from the monoethyl ester: equiv. wt. 79.4.

After recrystallization from water, the former melted at 220–235° (decomp.) (lit. (38) m.p. 232–234° (decomp.)) with intervening phase changes.

2,3-Dimethyl-pyrrole (VIIf)

2-Methyl-3-carbethoxy-pyrrole (40) was reduced by lithium aluminium hydride (41).

4-Methyl-3-ethyl-5-carbobenzoxy-pyrrole-2-carboxylic Acid (cf. VIIIb)

Sulfuryl chloride (6.6 g) was dropped into a stirred solution of 2,4-dimethyl-3-ethyl-5-carbobenzoxy-pyrrole (42) (VIII*a*, 3.6 g) in 50 ml of absolute ether at 10–15°. Next day the ether was removed *in vacuo*, hot aqueous sodium acetate (7 g in 30 ml) added to the residue, and the mixture boiled for 5 min. After the solution was allowed to cool, the insoluble material was dissolved in 10% sodium hydroxide, and the solution was washed with ether and then acidified with hydrochloric acid. The precipitate was separated, washed with water, and crystallized from ethanol (thimble) to give 2.5 g (62%), m.p. 166°. For analysis it was recrystallized from ethanol as colorless prisms, m.p. 175°.

Anal. Calcd. for $C_{16}H_{17}O_4N$: C, 66.88; H, 5.96; N, 4.88. Found: C, 67.02; H, 5.95; N, 5.02.

4-Methyl-3-ethyl-2-carbethoxy-5-carbobenzoxy-pyrrole (VIIIb)

As in the preparation of the corresponding carboxylic acid (above), 26.7 g of 2,4-dimethyl-3-ethyl-5-carbobenzoxy-pyrrole in 250 ml of ether was treated with 40.8 g of sulfuryl chloride. Ethanol (150 ml) was added to the residue that was left after the ether had been evaporated. Water (200 ml) was added to the clear solution, and the mixture extracted with ether. The extract was washed with 5% sodium hydroxide, with saturated sodium bisulfite, and with water, and then dried (sodium sulfate) and the ether evaporated. Crystallizing the residue from *n*-hexane gave 28 g (92%), m.p. 51°. For analysis it was recrystallized from *n*-hexane as colorless needles, m.p. 53°.

Anal. Calcd. for $C_{18}H_{21}O_4N_2$: C, 68.55; H, 6.71; N, 4.44. Found: C, 68.39; H, 6.66; N, 4.65.

4-Methyl-3-ethyl-2-carbethoxy-pyrrole-5-carboxylic Acid (IXa)

The corresponding benzyl ester (VIII*b*, see above, 15.75 g) in 250 ml of ethanol was hydrogenated at atmospheric pressure over 500 mg of palladium black (uptake 1 100 ml, calcd. 1 180 ml). The mixture was heated to dissolve the precipitate, filtered, and cooled. The colorless product (10.2 g, 91%) separated, m.p. 230°. For analysis it was recrystallized from ethanol as colorless elongated prisms, m.p. 233° (lit. (37) m.p. 218°).

Anal. Calcd. for $C_{11}H_{15}O_4N$: C, 58.65; H, 6.71; N, 6.22. Found: C, 58.74; H, 6.68; N, 6.43.

4-Methyl-3-ethyl-2-carbethoxy-pyrrole (IXb)

The corresponding acid (IX*a*, see above) was decarboxylated (37) to give the distilled product (53%), m.p. 69–70°. For analysis it was recrystallized from *n*-hexane as colorless plates, m.p. 75° (lit. (37) m.p. 76°).

Anal. Calcd. for $C_{10}H_{15}NO_2$: C, 66.27; H, 8.34; N, 7.73. Found: C, 66.09; H, 8.25; N, 7.90.

4-Methyl-3-ethyl-2-carbethoxy-5-acetyl-pyrrole (IXc)

Anhydrous aluminium chloride (21 g) was added, in portions, to a cooled and stirred solution of the corresponding α-free pyrrole (see above, 14 g) in 150 ml of carbon disulfide and 10 ml of acetyl chloride. The mixture was heated under reflux for 15 min, cooled, and poured into ice water. The product was extracted with ether; the extract was washed with 5% sodium hydroxide and then with water, and dried (sodium sulfate); the solvents were removed *in vacuo*. The residue was crystallized from *n*-hexane (thimble) to give 13 g (75%) of colorless needles, m.p. 107°.

Anal. Calcd. for $C_{12}H_{17}NO_3$: C, 64.55; H, 7.68; N, 6.27. Found: C, 64.30; H, 7.51; N, 6.04.

4-Methyl-3-ethyl-2-carbethoxy-pyrrole-5-aldehyde (IXd)

The corresponding α-free pyrrole (IX*b*, see above, 10 g) was converted into the aldimine hydrochloride (37). When this was dissolved in 50 ml of ice water (much less than suggested (37), the aldehyde being appreciably soluble), the aldehyde crystallized (9.5 g, 82%), m.p. 55°. For analysis it was crystallized from 60% ethanol, m.p. 65–66° (lit. (37) m.p. 68°).

Anal. Calcd. for $C_{11}H_{15}O_3N$: C, 63.14; H, 7.23; N, 6.69. Found: C, 63.33; H, 7.39; N, 6.88.

Pyrromethenes

4,4',5'-Trimethyl-3-(ω-bromovinyl)-5-carboxy-pyrromethene-3'-propionic Acid Hydrobromide (IVb) (8)

After washing with ethyl acetate until the washings were very pale, and then with ether, the product (57%) decomposed at about 105°.

5-Bromo-4,3'-dimethyl-5'-bromomethyl-3,4'-diethyl-pyrromethene Hydrobromide (Vd, R^1 = Et) (43)

The reported yield of a stable product was only obtained when *freshly* distilled cryptopyrrole was brominated; the resulting mixture of pyrromethenes was washed with a little acetic acid and then thoroughly with

Can. J. Chem. Downloaded from www.nrcresearchpress.com by 210.87.254.5 on 09/05/12
For personal use only.

much petrol ether (30–60°), and dried over KOH at 0.02 mm; then the methenes were separated. More of the desired product was obtained by boiling "methene II" with 15 parts of acetic acid for 5 min.

5-Carboxy-4,3',5'-trimethyl-3-ethyl-4'-n-propyl-pyrromethene Hydrobromide (Vc, $R^1 = CH_2CH_2CH_3$) (44)

2-Formyl-3-ethyl-4-methyl-5-carboxy-pyrrole (1.25 g) was finely ground in an agate mortar and then mixed with 0.95 g of freshly distilled 2,4-dimethyl-3-*n*-propyl-pyrrole in a 10 ml beaker which was cooled in ice. Acetic acid (0.7 ml) was added, with stirring, followed by 0.7 ml of hydrobromic acid (48%). The syrup was stirred and rubbed (5 to 15 min) until the whole solidified to orange prisms (ca. 70%). These were filtered on sintered glass and washed with ether until the washings were light yellow.

5-Bromo-4,3'-dimethyl-5'-bromomethyl-3-ethyl-4'-n-propyl-pyrromethene Hydrobromide (Vd, $R^1 = CH_2CH_2CH_3$) (44)

The intermediate 5-carboxy-pyrromethene (above) (1 g) was powdered and stirred with 0.5 ml of acetic acid, the solution being cooled with ice, while bromine (1 g) in 1 ml acetic acid was added dropwise. After the reaction had subsided, the mixture was heated for 40 min in the steam bath. Next day the product was filtered off, and washed with a little acetic acid and then with ether until the washings were colorless. It formed purple prisms (50–60%) which decomposed above 190°. For analysis it was recrystallized as violet rods from acetic acid.

Anal. Calcd. for $C_{17}H_{23}N_2Br_3$: Br, 48.44. Found: Br, 46.89.

5-Carboxy-4,3',5'-trimethyl-3-ethyl-4'-isobutyl-pyrromethene Hydrobromide (Vc, $R^1 = CH_2CHMe_2$)

This was obtained from 1.165 g of freshly redistilled 2,4-dimethyl-3-isobutyl-pyrrole, 1.42 g of 2-formyl-3-ethyl-4-methyl-5-carboxy-pyrrole, 0.8 ml of acetic acid, and 0.8 ml of 48% hydrobromic acid exactly as was the 4'-*n*-propyl homologue (above). It formed yellow crystals (66%).

Anal. Calcd. for $C_{19}H_{27}O_2N_2Br$: C, 57.70; H, 6.89; N, 7.09. Found: C, 57.34; H, 6.88; N, 7.16.

5-Bromo-4,3'-dimethyl-5'-bromomethyl-3-ethyl-4'-isobutyl-pyrromethene Hydrobromide (Vd, $R^1 = CH_2CHMe_2$)

This was obtained from the above 5-carboxy-pyrromethene (2.52 g), just as was the 4'-*n*-propyl homologue (above), by using 1.3 ml of acetic acid and then 1.05 ml of bromine in 2.6 ml of acetic acid, except that heat was applied for 1.5 h. It formed red crystals (69%).

Anal. Calcd. for $C_{18}H_{25}N_2Br_3$: C, 42.25; H, 4.95; N, 5.50. Found: C, 42.38; H, 4.89; N, 5.37.

3-Bromo-4,4',5'-trimethyl-5-carboxy-pyrromethene-3'-propionic Acid Hydrobromide (Vg, $R^2 = Me$) (11)

Hemopyrrole-carboxylic acid (1.67 g) and 2.32 g of 2-formyl-3-bromo-4-methyl-5-carboxy-pyrrole were ground together in an agate mortar, transferred to a 10 ml beaker, and stirred without cooling with 1 ml of acetic acid and then 2 ml of 48% hydrobromic acid. The orange product (96%) which rapidly separated was filtered off, washed with 150 ml dry ether, and dried.

3-Bromo-4',5'-dimethyl-4-ethyl-5-carboxy-pyrromethene-3'-propionic Acid Hydrobromide (Vg, $R^2 = Et$)

This was obtained, exactly as was its 4-methyl-5'-ethyl isomer (above), from hemopyrrole-carboxylic acid (1.42 g), 2-formyl-3-bromo-4-ethyl-5-carboxy-pyrrole (2.09 g), 0.25 ml of acetic acid, and 2 ml of 48% hydrobromic acid. It formed orange prisms (70%) which decomposed above 200° without melting.

Anal. Calcd. for $C_{17}H_{20}O_4N_2Br_2$: C, 42.87; H, 4.25; N, 5.89; Br, 33.56. Found: C, 42.79; H, 4.25; N, 5.82; Br, 33.38.

3-Bromo-4,4'-dimethyl-5'-ethyl-5-carboxy-pyrromethene-3'-propionic Acid Hydrobromide (VIb, $R^2 = R^3 = Me$)

2-Ethyl-3-methyl-pyrrole-4-propionic acid (0.91 g) and 2-formyl-3-bromo-4-methyl-5-carboxy-pyrrole (1.16 g) were ground in an agate mortar. Acetic acid (0.25 ml) was added and rubbing continued. In this case the intermediate may crystallize. Hydrobromic acid (1 ml of 48%) was added slowly, and rubbing gave a syrup from which the product crystallized, on further vigorous rubbing, as orange prisms (99%). These were filtered off on sintered glass, thoroughly washed with much dry ether, and dried *in vacuo* over sodium hydroxide.

Anal. Calcd. for $C_{17}H_{20}O_4N_2Br_2$: C, 42.87; H, 4.25; N, 5.89; Br, 33.56. Found: C, 42.73; H, 4.03; N, 5.51; Br, 33.41.

3-Bromo-4'-methyl-4,5'-diethyl-5-carboxy-pyrromethene-3'-propionic Acid Hydrobromide (VIb, $R^2 = Et$, $R^3 = Me$)

This was obtained, exactly as was its 4-methyl-5'-ethyl homologue (above), from 2-ethyl-3-methyl-pyrrole-4-propionic acid (1.45 g), 2-formyl-3-bromo-4-ethyl-5-carboxy-pyrrole (1.97 g), 0.25 ml of acetic acid, and 2 ml of 48% hydrobromic acid, with rubbing for about 15 min to induce crystallization. The product (75%) formed orange prisms which decomposed at about 200°. It decomposed when its recrystallization was attempted.

Anal. Calcd. for $C_{18}H_{22}O_4N_2Br_2$: C, 44.11; H, 4.53; N, 5.72; Br, 32.60. Found: C, 44.16; H, 4.86; N, 5.89; Br, 32.97.

3-Bromo-4'-methyl-4-ethyl-5'-n-propyl-5-carboxy-pyrromethene-3'-propionic Acid Hydrobromide (VIb, $R^2 = R^3 = Et$)

This was obtained, exactly as was its 4-methyl-5'-ethyl homologue (above), from 2-*n*-propyl-3-methyl-pyrrole-4-propionic acid (0.9 g), 2-formyl-3-bromo-4-ethyl-5-carboxy-pyrrole (1.2 g), 0.85 ml of acetic acid,

Can. J. Chem. Downloaded from www.nrcresearchpress.com by 210.87.254.5 on 09/05/12
For personal use only.

and 1.5 ml of 48% hydrobromic acid, with rubbing for 0.5 h; then seed was obtained by rubbing a portion on a glass plate. The product (80%) formed orange prisms.

Anal. Calcd. for $C_{19}H_{24}O_4N_2Br_2$: C, 45.25; H, 4.79; N, 5.56. Found: C, 44.98; H, 4.55; N, 5.61.

5-Carboxy-3,4'-dimethyl-4,3',5'-triethyl-pyrromethene Hydrobromide (VIIc)

This was obtained, exactly as were its analogues above, from 1 g of 4-methyl-3-ethyl-2-carboxy-pyrrole-5-aldehyde, 0.75 g of 3-methyl-2,4-diethyl-pyrrole, 0.7 ml of acetic acid, and 0.7 ml of 48% hydrobromic acid in a cooled 10 ml beaker, the product being washed with 10% methanol in ether and then with ether. A sample of the red crystals (1.2 g, 57%) was recrystallized from methanol–ether as orange-red needles, m.p. 120–124° (decomp.).

5-Bromo-3,4'-dimethyl-4,3'-diethyl-5'-bromoethyl-pyrromethene Hydrobromide (VIId) (5)

The corresponding 5-carboxy-pyrromethene above (VII*c*, 1.2 g) was suspended in 2 ml of acetic acid, 0.4 ml of bromine added, and the mixture heated for 5 min in the steam bath. The red crystalline product (1.4 g, 89%) was filtered off from the cooled mixture and washed with ether. A sample for analysis was dissolved in acetone, heated for 10 min, filtered off the next day, and crystallized twice from acetic acid to give red prisms which decomposed above 280°.

Anal. Calcd. for $C_{17}H_{23}N_2Br_3$: C, 41.19; H, 4.68; N, 5.66; Br, 48.46. Found: C, 41.05; H, 4.16; N, 5.50; Br, 48.29.

5,3'-Dibromo-4,4',5'-trimethyl-pyrromethene-3-propionic Acid Hydrobromide (VIIh)

This was obtained from 2,3-dimethyl-pyrrole (VII*f*, see above) and 2-formyl-4-methyl-5-carboxy-pyrrole-3-propionic acid (VII*e*, see above) over the 5-carboxy-pyrromethene VII*g*, as reported (5); it decomposed above 220°.

Anal. Calcd. for $C_{15}H_{17}O_2N_2Br_3$: C, 36.23; H, 3.42; N, 5.63; Br, 48.24. Found: C, 36.57; H, 3.50; N, 5.37; Br, 48.04.

Porphyrins (Ordered as the Corresponding "650" Fractions 1–5 and then "660" Fractions 3–6)

4-Isobutyl-5-ethyl-4-desethyl-5-desmethyl-pyrroporphyrin 15 Methyl Ester (1,3,8-Trimethyl-2,5-diethyl-4-isobutyl-porphin-7-propionic Acid Methyl Ester (IIIa, $R^1 = CH_2CHMe_2$, $R^2 = Et$))

5-Bromo-4,3'-dimethyl-5'-bromomethyl-3-ethyl-4'-isobutyl-pyrromethene hydrobromide (V*d*, $R^1 = CH_2CHMe_2$, 2.1 g), 3-bromo-4',5'-dimethyl-4-ethyl-5-carboxy-pyrromethene-3'-propionic acid hydrobromide (V*g*, $R^2 = Et$, 2.93 g), and 5 g of methylsuccinic acid were ground together, dried at 20° in high vacuum, and then heated, with stirring, in a test tube at 160° and then (10 min after melting) at 180° for 2 min. The partially cooled melt was poured into 1.5 l of warm water. The pH was brought to 5 with disodium phosphate, and the mixture was heated for 1 h on the steam bath and then allowed to cool overnight. The solid was filtered off, well washed with water, dried, powdered, and extracted with 3 l of ether for 3 days (thimble). The ether was repeatedly extracted with 100 ml portions of 0.5% hydrochloric acid until neither colored impurities were extracted nor precipitates formed. The acid porphyrins were precipitated as their sodium salts by shaking the ether with 10% sodium hydroxide (4 × 25 ml). These were filtered off, dissolved in concentrated hydrochloric acid, and brought into 1.5 l of ether with sodium acetate. The pyrroporphyrin was extracted from the washed ether solution with 4% hydrochloric acid, leaving bromoporphyrins in the ether. The pyrroporphyrin was returned to fresh ether by using sodium acetate. Its ether solution was washed, dried, concentrated, and chromatographed on a column of 6% hydrochloric acid on Celite 545, development being carried out with equilibrated ether (45). The large lower band was cut out, leaving three small red, yellow, and brown ones. The pigment in it was eluted with 2% hydrochloric acid in acetone and brought into ether by using water. When this ether solution was washed, dried, and concentrated, most of the product (13 mg) crystallized; visible spectrum in ether (relative density in parentheses): maxima at 622 (0.46), 595 (0.09), 568 (0.48), 526 (0.70), 497 (1.00), and 493 (0.98) mμ, with shoulders at 613, 573, and 471 mμ.

The crystalline acid was left overnight in 5% hydrogen chloride in methanol, and the product brought from this into chloroform by using water. The washed and dried (sodium sulfate) chloroform solution was filtered through a column of alumina (grade V, made up with the 5% methanol in chloroform that was also used for the elution), and concentrated. The chloroform was removed by boiling it off while methanol was being added. Part of the product (4 mg, m.p. 223–226°) crystallized. The rest (5.6 mg, m.p. 222.5–225.5°) was obtained by evaporating the mother liquors and crystallizing the residue from ether (final volume 2 ml) at 0°. The whole was recrystallized slowly from ether to give 5 mg of needles; visible spectrum in ether (relative density in parentheses): maxima at 622 (0.47), 596 (0.09), 568 (0.49), 526 (0.72), 496 (1.00), and 493 (1.00) mμ, with shoulders at 613, 573, and 470 mμ.

Anal. Calcd. for $C_{35}H_{42}O_2N_4$: C, 76.33; H, 7.63. Found: C, 75.95; H, 7.43.

It melted at 225.5–227.5°. The mixed melting point with the "pyrroporphyrin" ester from *Chlorobium* pheophorbide 650, fraction 1 (m.p. 229.5–231° (2)), was 226–230° with softening from 224°; the X-ray powder photographs of these two specimens were identical.

Copper Complex of the Methyl Ester

About 0.2 mg of the ester in 0.5 ml of chloroform was boiled in a 3 × $\frac{3}{8}$ inch test tube; copper acetate (0.5 mg), in methanol (0.5 ml) containing a trace of acetic acid, was added. Half the solvent was boiled off (a glass boiling stick made from melting point tubing being used), and replaced by methanol; this was

Can. J. Chem. Downloaded from www.nrcresearchpress.com by 210.87.254.5 on 09/05/12
For personal use only.

repeated three times as the product crystallized out. After a final concentration to ca. ¼ ml, the product was separated and washed with methanol (centrifuge). It formed a felt of hair-like crystals, m.p. 229–231.5°, mixed m.p. with the "pyrroporphyrin" ester copper complex from *Chlorobium* pheophorbide 650, fraction 1 (m.p. 230–232.5° (2)), 229–232.5°; the X-ray powder photographs of these two specimens were identical.

4-n-Propyl-5-ethyl-4-desethyl-5-desmethyl-pyrroporphyrin 15 Methyl Ester (1,3,8-Trimethyl-2,5-diethyl-4-n-propyl-porphin-7-propionic Acid Methyl Ester (IIIa, $R^1 = CH_2CH_2CH_3$, $R^2 = Et$))

5-Bromo-4,3′-dimethyl-5′-bromomethyl-3-ethyl-4′-*n*-propyl-pyrromethene hydrobromide (V*d*, $R^1 = CH_2CH_2CH_3$, 2.62 g), 3-bromo-4′,5′-dimethyl-4-ethyl-5-carboxy-pyrromethene-3′-propionic acid hydrobromide (Vg, $R^2 = Et$, 2.5 g), and 5 g of methylsuccinic acid were heated together and the melt worked up exactly as in the synthesis of the 4-isobutyl homologue above. The Celite column was eluted for 4 h to separate the single slow-moving porphyrin band from dark material at the top. The intermediate free acid (40 mg) crystallized when its ether solution (3 ml) was allowed to stand; visible spectrum in ether (relative densities in parentheses): maxima at 622 (0.47), 597 (0.09), 567 (0.47), 525 (0.71), 497 (1.00), and 493 (0.99) mμ, with shoulders at 613, 573, and 471 mμ.

The methyl ester (30 mg) was prepared exactly as was the 4-isobutyl homologue above. It crystallized from methanol displacing chloroform, as long glistening needles; visible spectrum in ether (relative density in parentheses): maxima at 622 (0.48), 595 (0.09), 568 (0.47), 525 (0.71), 497 (1.00), and 493 (1.00) mμ, with shoulders at 613, 573, and 470 mμ.

Anal. Calcd. for $C_{34}H_{40}O_2N_4$: C, 76.09; H, 7.51. Found: C, 75.93; H, 7.59.

It had m.p. 210–213°. The mixed melting point with the "pyrroporphyrin" ester from *Chlorobium* pheophorbide 650, fraction 2 (m.p. 207–210° (2)), was 207–211°. The X-ray powder photographs of these synthetic and analytical specimens were identical.

The copper complex of the ester formed needles, m.p. 211–213°, mixed m.p. with the "pyrroporphyrin" ester – copper complex from *Chlorobium* pheophorbide 650, fraction 2 (m.p. 208.5–211.5° (2)), 209–213°; the X-ray powder photographs of these two specimens were identical.

The synthetic porphyrin has also been identified (3) with the pyrroporphyrins from *Chlorobium* pheophorbide 660, fractions 3 and 4.

The Desoxo-phylloerythrin Methyl Ester from Chlorobium Pheophorbide 650 Fraction 2 (4-n-Propyl-5-ethyl-4-desethyl-5-desmethyl-desoxo-phylloerythrin Methyl Ester (IIb, $R^1 = CH_2CH_2CH_3$, $R^2 = Et$))

The corresponding phylloerythrin methyl ester (cf. II*a*) (38 mg, m.p. 249–251° from chloroform–methanol after chromatography on sucrose; this had been obtained from *Chlorobium* pheophorbide 650, fraction 2, with hydrogen iodide in acetic acid (46)) was reduced by the Wolf–Kishner method as in the reduction of phylloerythrin itself (9). The crude product was extracted with ether, purified on a column of Celite – 3.5% hydrochloric acid, esterified, and crystallized as usual. It formed needles (15 mg), m.p. 221–222°, unchanged after hydrolysis, refractionation, and reesterification; visible spectrum in tetrahydrofuran–ether (relative density in parentheses): maxima at 620 (0.52), 594 (0.08), 566 (0.38), 531 (0.22), and 498 (1.0) mμ, with shoulders at 613 and 572 mμ.

Anal. Calcd. for $C_{36}H_{42}O_2N_4$: C, 76.83; H, 7.52; N, 9.96. Found: C, 76.41; H, 7.85; N, 10.14.

The copper complex formed needles, m.p. 233–235°.

This was compared with the synthetic desoxo-phylloerythrin (see below) corresponding to fraction 5.

4-Isobutyl-4-desethyl-pyrroporphyrin 15 Methyl Ester (1,3,5,8-Tetramethyl-2-ethyl-4-isobutyl-porphin-7-propionic Acid Methyl Ester (IIIa, $R^1 = CH_2CHMe_2$, $R^2 = Me$))

5-Bromo-4,3′-dimethyl-5′-bromomethyl-3-ethyl-4′-isobutyl-pyrromethene hydrobromide (V*d*, $R^1 = CH_2CHMe_2$, 2 g), 3-bromo-4,4′,5′-trimethyl-5-carboxy-pyrromethene-3′-propionic acid hydrobromide (Vg, $R^2 = Me$, 2 g), and 5 g of methylsuccinic acid were heated together and the melt worked up exactly as in the synthesis of the 5-ethyl homologue above. On the Celite column, the pyrroporphyrin was in a dense bluish red band which was easily separated from two slower and weaker ones. The free acid did not crystallize from ether (3 ml), so the ether was evaporated and the residue esterified and crystallized from methanol displacing chloroform, as was its 5-ethyl homologue. The methyl ester formed prisms (2 mg); visible spectrum in ether (relative density in parentheses): maxima at 623 (0.47), 596 (0.09), 568 (0.47), 525 (0.71), 497 (1.00), and 493 (1.00) mμ, with shoulders at 614, 573, and 470 mμ. It melted at 224–226° after changing to needles at 220–221.5°. The mixed melting point with the "pyrroporphyrin" ester from *Chlorobium* pheophorbide 650, fraction 3, of m.p. 220–222° which has been analyzed (2) was 220–222.5°; the X-ray powder photographs of these two specimens were identical.

The copper complexes of these two esters, synthetic and of natural origin (2), both formed sheaves of needles, m.p. and mixed m.p. 222–223.5°; their X-ray powder photographs were identical.

The mixed melting point with synthetic 1,3,8-trimethyl-2,5-diethyl-4-isobutyl-porphin-7-propionic acid methyl ester (m.p. 225.5–227.5°) was 217 to ca. 223°.

5-Ethyl-5-desmethyl-pyrroporphyrin 15 Methyl Ester (1,3,8-Trimethyl-2,4,5-triethyl-porphin-7-propionic Acid Methyl Ester (IIIa, $R^1 = R^2 = Et$))

5-Bromo-4,3′-dimethyl-5′-bromomethyl-3,4′-diethyl-pyrromethene hydrobromide (V*d*, $R^1 = Et$, 1.5 g) and 3-bromo-4′,5′-dimethyl-4-ethyl-5-carboxy-pyrromethene-3′-propionic acid hydrobromide (Vg, $R^2 = Et$, 1 g) were heated with 5 g of methylsuccinic acid, etc., as usual to yield the washed ether extract of the melt. Part of the product was extracted from the ether with 2% hydrochloric acid and worked up as under *a*; the

Can. J. Chem. Downloaded from www.nrcresearchpress.com by 210.87.254.5 on 09/05/12
For personal use only.

balance was precipitated as the sodium salt and worked up as under *b*; etioporphyrin I (145 mg) remained in the ether.

(*a*) The pigment was returned to ether, and the product was separated from a faster band on Celite – 5% hydrochloric acid (5 × 12 cm), then esterified, and crystallized from methanol displacing chloroform. The product formed purple prisms (20 mg), m.p. 185–205°; visible spectrum in chloroform (relative intensities in parentheses): maxima at 619 (0.336), 566 (0.466), 534 (0.685), and 498 (1.00) mμ, with shoulders at 591 and 532 mμ and inflexions at 573, 526, 501, and 572 mμ. This ester (2 mg) was chromatographed three times in 4% chloroform – petrol (30–60°) on icing sugar (m.p. then 186–190°) and then in ether on successively Celite – 6.5% hydrochloric acid and then Celite – 7% hydrochloric acid (m.p. then 188–191°, remelt 208–210°). The balance was recrystallized for analysis, prisms m.p. 187–210°, remelt 205–210°.

Anal. Calcd. for $C_{33}H_{38}O_2N_4$: C, 75.83; H, 7.33; N, 10.72. Found: C, 75.91; H, 7.48; N, 10.61.

(*b*) The sodium salts were dissolved in hydrochloric acid. The pigment was brought from this into ether, extracted with 4% hydrochloric acid (the bromo-pyrroporphyrin being left in the ether), returned to ether, and re-precipitated as the sodium salt; these steps were repeated. The residue left when the final ether solution had been evaporated was esterified and crystallized from methanol displacing chloroform to give prisms (19 mg), m.p. 187–189°, resolidifying to needles, m.p. 205–211°. The mixed melting point with the analytical pyrroporphyrin from *Chlorobium* pheophorbide 650, fraction 4 (see below), was 210–216.5°, remelt 212–217°; the X-ray powder photographs of these analytical and synthetic materials differed only in that the former had a few extra lines.

The high-melting form of the synthetic porphyrin ester was obtained by heating it, in a tube sealed off at 1×10^{-4} mm, from 180 to 205° over 3 h and then 1 h at 205°; m.p. 213–216.5°, mixed m.p. with the pyrroporphyrin ester from fraction 4 (as originally crystallized, see below) 212.5–217°. After both specimens had been heated *in vacuo* to 205°, their X-ray powder photographs were consistent, with each being a mixture of two forms, with one predominant form in common.

The synthetic and analytical (from fraction 4) esters were recrystallized again in the same way as prisms, and now gave identical X-ray powder photographs (synthetic, m.p. 189–193°; analytical, m.p. 191–194°). These changed to, or when they were cooled resolidified to, needles (synthetic, m.p. 207–214°; analytical, m.p. 211–214°) or sheets (synthetic, m.p. 213–216°; analytical, m.p. 213–216.5°). The analytical specimen sometimes resolidified, when it was cooled, to crystals of uncertain form which changed to the above needles at 185–190°; here a fourth form sometimes appeared as prismatic needles, m.p. 215.5–216.5°. The mixed melting point of the synthetic and analytical prisms was 189–193°, resolidifying to needles, m.p. 206–214.5°.

The synthetic specimen – copper complex formed fine red needles, m.p. 220–226°, mixed m.p. with the analytical complex (m.p. 220–226°) 219–227°. The X-ray powder photographs of these two specimens were identical.

The mixed melting point with the copper complex of synthetic 1,3,5,8-tetramethyl-2-ethyl-4-isobutylporphin-7-propionic acid methyl ester (m.p. 222–223.5°) was 201 to ca. 213°.

The "Pyrroporphyrin" Methyl Ester from Chlorobium Pheophorbide 650 Fraction 4 (1,3,8-Trimethyl-2,4-5-triethyl-porphin-7-propionic Acid Methyl Ester (IIIa, $R^1 = R^2 = Et$))

The "pyrroporphyrin" free acid (2) in ether was chromatographed on Celite – 4.8% hydrochloric acid (2 × 10 cm). The single broad red band was eluted with ether. The pigment was esterified, its chloroform solution filtered through alumina, and the product crystallized from chloroform–methanol as purple prisms (4.6 mg), m.p. 214.5–216.5°, with some signs of a solid phase change at 180°; visible spectrum in chloroform (relative intensities in parentheses): maxima at 618 (0.335), 566 (0.461), 534 (0.672), and 497 (1.00) mμ, with shoulders at 592 and 532 mμ and inflexions at 573, 525, 500, and 472 mμ.

The copper complex formed fine red needles, m.p. 220–226°.

4-n-Propyl-4-desethyl-desoxo-phylloerythrin Methyl Ester (IIb, $R^1 = CH_2CH_2CH_3$, $R^2 = Me$)

Essentially as in the analogous synthesis of desoxo-phylloerythrin itself (7), 18 g of 5-bromo-4,3′-dimethyl-5′-bromomethyl-3-ethyl-4′-*n*-propyl-pyrromethene hydrobromide (Vd, $R^1 = CH_2CH_2CH_3$) and 18 g of 4,4′,5′-trimethyl-3-(ω-bromovinyl)-5-carboxy-pyrromethene-3′-propionic acid hydrobromide (IVb) were heated in succinic acid at 190–220°. The 18 melts, freed of succinic acid with hot water at pH 4 (disodium phosphate), were powdered, dried, and extracted for 3 days with 1 l of chloroform (thimble). The extract was poured into 20 volumes of ether, and the acidic porphyrins (1.66 g) were precipitated by shaking the filtered solution with 2% sodium hydroxide. A portion (0.5 g) was dissolved in acetic acid – hydrochloric acid and the pigments were brought into 3.5 l of ether by using sodium acetate. The washed and clarified ether solution was concentrated to 800 ml, shaken with 1% hydrochloric acid, and applied to a column of Celite 545 (9.5 × 42 cm, made up with 3.5% hydrochloric acid). Elution with ether separated the main band from much slower and much faster ones. It was extruded and eluted with 50% acetone, from which the pigment was brought into ether. The washed ether solution was evaporated and the residue esterified, crystallized, and recrystallized in the usual way. The product (48 mg, 0.8%) formed plates (occasionally needles), m.p. 235–237.5° after sintering and apparently a solid phase change from 234°; visible spectrum in tetrahydrofuran–ether (relative density in parentheses): maxima at 621 (0.54), 595 (0.07), 567 (0.37), 531 (0.22), and 498 (1.0) mμ, with shoulders at 613 and 573 mμ.

Anal. Calcd. for $C_{35}H_{40}O_2N_4$: C, 76.61; H, 7.35; N, 10.21. Found: C, 77.02; H, 7.15; N, 10.55.

Its mixed melting points with the desoxo-phylloerythrin esters from *Chlorobium* pheophorbide 650,

Can. J. Chem. Downloaded from www.nrcresearchpress.com by 210.87.254.5 on 09/05/12
For personal use only.

fractions 2 (see above) and 5 (see below), were respectively 213–216° and 235–237.5°. Its X-ray powder photograph was identical with that of the latter desoxo-phylloerythrin ester from fraction 5, and these two specimens had identical visible spectra in chloroform: λ_{max} (relative density in parentheses) 619 (0.41), 567 (0.40), 536.7 (0.24), 502 (1.0) mμ.

Its copper complex formed needles, m.p. 245–247.5°.

Anal. Calcd. for $C_{35}H_{38}O_2N_4Cu$: C, 68.89; H, 6.28; CuO, 13.04. Found: C, 68.56; H, 6.34; CuO, 12.39.

Its mixed melting points with the copper complexes of the desoxo-phylloerythrin esters from *Chlorobium* pheophorbide 650, fractions 2 and 5, were respectively 220–228° and 245.5–247°. Its X-ray powder photograph was identical with that of the latter complex from fraction 5.

1,3,5,7-Tetramethyl-2,6-diethyl-4,8-di-n-propyl-porphin

The chloroform–ether solution, from which the above synthetic desoxo-phylloerythrin had been precipitated as its sodium salt, was evaporated. An aliquot was dissolved in chloroform and passed through an alumina column (alkaline, grade II, made up with 5% methanol in chloroform). The eluate was concentrated and the pigment passed through a similar column. It was crystallized from chloroform–methanol as long prisms (17%) which decomposed at about 310°.

Anal. Calcd. for $C_{34}H_{42}N_4$: C, 80.59; H, 8.36; N, 11.06. Found: C, 80.72; H, 8.55; N, 11.54.

The Desoxo-phylloerythrin Methyl Ester from Chlorobium Pheophorbide 650 Fraction 5 (4-n-Propyl-4-desethyl-desoxo-phylloerythrin Methyl Ester (IIb, $R^1 = CH_2CH_2CH_3$, $R^2 = Me$))

The mesopyropheophorbide (2) (24 mg from *Chlorobium* pheophorbide 650, fraction 5), 0.4 g of sodium in 6 ml of absolute ethanol, and 0.3 ml of 95% hydrazine were frozen in a bomb tube, which was then sealed after it had been evacuated to 0.1 mm. The tube was warmed, shaken, and heated for 5 h at 170° in a rocking oven. The pigment was brought into ether by using acetic acid and the desoxo-phylloerythrin extracted with 2% hydrochloric acid. Evaporating the ether layer left the corresponding meso-desoxo-pyrropheophorbide, which was heated with 4 ml of acetic acid and 2 ml of 3% hydrochloric acid in a sealed tube, which had been deaerated as above, for 5 h at 180°. The resulting pigment was brought into ether and more of the product extracted with 2% hydrochloric acid. The pigment in the hydrochloric acid extracts was brought into ether with sodium acetate, and purified on a column of Celite – 5% hydrochloric acid, the single band being eluted with acetone after extrusion and the pigment being returned to ether. When the washed ether solution was concentrated, the product separated as needles of the free acid (7.7 mg). This was esterified and crystallized to give the product as plates, m.p. 235–237° after sintering and an apparent solid phase change at 234–235°.

The copper complex formed needles, m.p. 246–247°.

4-n-Propyl-5-ethyl-4-desethyl-5-desmethyl-δ-phylloporphyrin Methyl Ester (1,3,8,δ-Tetramethyl-2,5-diethyl-4-n-propyl-porphin-7-propionic Acid Methyl Ester (IIIb, $R^1 = CH_2CH_2CH_3$, $R^2 = Et$, $R^3 = Me$))

5-Bromo-4,3′-dimethyl-5′-bromomethyl-3-ethyl-4′-*n*-propyl-pyrromethene hydrobromide (V*d*, $R^1 = CH_2CH_2CH_3$, 2.75 g), 3-bromo-4′-methyl-4,5′-diethyl-5-carboxy-pyrromethene-3′-propionic acid hydrobromide (VI*b*, $R^2 = Et$, $R^3 = Me$, 2.6 g), and 5 g of methylsuccinic acid were heated together and stirred at 160–170° for 15 min and then at 180° for 5 min. The crude product was isolated and extracted with ether as in the case of the 4-isobutyl-5-ethyl-pyrroporphyrin (above). The ether was washed with 0.1% hydrochloric acid, and the acidic porphyrins were then separated as their sodium salts by shaking the ether with 10% sodium hydroxide. They were returned to fresh ether, extracted with 4% hydrochloric acid, again brought into ether, and passed through a column of Celite – 2% hydrochloric acid. Elution for 5 h removed a little porphyrin, leaving a blue band and, near the top, a black one. The blue band was separated, and the pigment was eluted with 2% hydrochloric acid in acetone and then transferred to ether. The residue that was left when the ether was evaporated was esterified and brought into chloroform. The solution was passed through a column of alumina, filtered, and then concentrated to 2 ml while methanol was being added to displace the chloroform.

The product (5 mg) separated overnight; visible spectrum in ether: λ_{max} (relative density in parentheses): 629 (0.10), 576 (0.35), 534 (0.35), and 501 (1.00) mμ. Recrystallization from methanol gave prisms melting from 173° to 190°, with partial solidification at 180° followed by intervening remelting at 183–187°. Recrystallization from ether then gave needles, m.p. 191–194°, with the suggestion of a phase change at 190°.

X-ray powder photographs showed that the forms from methanol and from ether were different. The photograph of the latter was almost identical with that of the δ-phylloporphyrin ester (3), m.p. 196–199°, from *Chlorobium* pheophorbide 660, fraction 3, there being small differences in the intensities of a few lines. The photographs of the synthetic ester had nothing in common with those of the δ-phylloporphyrin ester from fraction 4.

1,3,8-Trimethyl-2-5,δ-triethyl-4-n-propyl-porphin-7-propionic Acid Methyl Ester (IIIb, $R^1 = CH_2CH_2CH_3$, $R^2 = R^3 = Et$)

5-Bromo-4,3′-dimethyl-5′-bromomethyl-3-ethyl-4′-*n*-propyl-pyrromethene hydrobromide (V*d*, $R^1 = CH_2CH_2CH_3$, 1.88 g) and 3-bromo-4′-methyl-4-ethyl-5-*n*-propyl-5-carboxy-pyrromethene-3′-propionic acid hydrobromide (VI*b*, $R^2 = R^3 = Et$, 2.3 g) were fused with methylsuccinic acid, and the product was isolated exactly as was the δ-methyl analogue above; a single blue band appeared on the Celite column. The product (3 mg) formed poorly defined prisms, m.p. 140–156°; visible spectrum in ether (relative density in parentheses): λ_{max} 628 (0.10), 574 (0.34), 534 (0.32), and 502 (1.0) mμ.

Can. J. Chem. Downloaded from www.nrcresearchpress.com by 210.87.254.5 on 09/05/12
For personal use only.

It was recrystallized from methanol as prisms, m.p. 151–170°, with intervening darkening at 120° and partial phase changes to glistening prisms at 130–131°, to small needles from 151°, and to long needles at 164°.

The analytical δ-phylloporphyrin from *Chlorobium* pheophorbide 660, fraction 4 (3), had m.p. 195–197°, with the suggestion of phase changes at 164–190°. X-ray powder photographs showed that it existed in two (or more) forms, neither of which was identical with that of the synthetic material. The analytical and synthetic copper complexes, m.p. 174–179° and 172–180° respectively, mixed m.p. 172–180°, did not give identical X-ray powder photographs.

5-Ethyl-5-desmethyl-δ-phylloporphyrin 15 Methyl Ester (1,3,8,δ-Tetramethyl-2,4,5-triethyl-porphin-7-propionic Acid Methyl Ester (IIIb, $R^1 = R^2 = Et$, $R^3 = Me$))

Methylsuccinic acid (6.6 g), 3-bromo-4′-methyl-4,5′-diethyl-5-carboxy-pyrromethene-3′-propionic acid hydrobromide (VI*b*, $R^2 = Et$, $R^3 = Me$, 1 g), and 5-bromo-4,3′-dimethyl-5′-bromomethyl-3,4′-diethyl-pyrromethene hydrobromide (V*d*, $R^1 = Et$, 5.6 g) were ground together and heated in six portions at 160° for 20 min. The melt was freed of methylsuccinic acid, dried, powdered as usual, and then heated under reflux for 2 h in 200 ml of 5% methanolic hydrogen chloride. The pigment in the filtered solution was then brought into chloroform. The chloroform solution was filtered through deactivated alumina, washed with 45% aqueous resorcinol (10 × 50 ml subsequently backwashed), washed with water, dried, and again filtered through alumina; then the solvent was evaporated. The residue was stirred for 2 h with 500 ml of ether, and undissolved etioporphyrin separated. The pigments in the ether were chromatographed twice on Celite – 2% hydrochloric acid and once on Celite – 1.8% hydrochloric acid, in each case the blue band of the product being eluted with ether. The pigment in the final eluate was extracted with 2% hydrochloric acid and returned to ether. The solution was concentrated to 5 ml and left at 10° overnight. The product separated as needles, m.p. 209–211°, raised to 210–211.5° and then 214–215.5° (7.4 mg) when recrystallized from chloroform–methanol and then from ether; visible spectrum in ether (relative density in parentheses): maxima at 629.5 (0.11), 577 (0.39), 534 (0.40), and 502 (1.00) mμ.

Anal. Calcd. for $C_{34}H_{40}O_2N_4$: C, 76.09; H, 7.51; N, 10.44. Found: C, 76.27; H, 7.21; N, 10.61.

The mixed melting point with the phylloporphyrin ester from *Chlorobium* pheophorbide 660, fraction 5 (see below), was 214–215°, and the X-ray powder photographs of the two specimens were identical. The mixed melting point of the synthetic ester with synthetic δ-phylloporphyrin 15 methyl ester (m.p. 212–213.5°) (see below) was 202 to ca. 208°.

The copper complex formed needles, m.p. 212.5–215°, mixed m.p. with the copper complex of the above analytical phylloporphyrin 213–215°. The X-ray powder photographs of these two specimens were identical. The mixed melting point of the copper complex of the analytical phylloporphyrin with that of synthetic δ-phylloporphyrin 15 methyl ester (m.p. 206–209.5°) was 199 to ca. 206°.

The "Phylloporphyrin" Methyl Ester from Chlorobium Pheophorbide 660 Fraction 5 (1,3,8,δ-Tetramethyl-2,4,5-triethyl-porphin-7-propionic Acid Methyl Ester)

The analytical "phylloporphyrin" (free acid) (3) was left overnight in 5% methanolic hydrogen chloride, the ester brought into ether, and the solution chromatographed on Celite – 2% hydrochloric acid (2 × 12 cm). Two narrow brown bands followed a blue one. The pigment in the latter was eluted and its ether solution concentrated to 0.5 ml. The product (1.3 mg) separated as needles, m.p. 215–215.5°; visible spectrum in ether (relative density in parentheses): maxima at 629 (0.10), 578 (0.38), 535 (0.39), and 502 (1.00) mμ.

The copper complex formed needles, m.p. 213.5–215.5°.

δ-Phylloporphyrin 15 Methyl Ester (1,3,5,8,δ-Pentamethyl-2,4-diethyl-porphin-7-propionic Acid Methyl Ester (IIIb, $R^1 = Et$, $R^2 = R^3 = Me$)) (5)

5-Bromo-3,4′-dimethyl-4,3′-diethyl-5′-bromoethyl-pyrromethene hydrobromide (VII*d*, 4 g), 5,3′-dibromo-4,4′,5′-trimethyl-pyrromethene-3′-propionic acid hydrobromide (VII*h*, 4.01 g), and 16 g of methylsuccinic acid were heated together in portions, and the crystalline δ-phylloporphyrin free acid (40 mg) was isolated exactly as reported (5). This was dissolved in concentrated hydrochloric acid, brought into ether by using sodium tartrate, and chromatographed as usual on Celite – 2% hydrochloric acid. The pigment in the single red slow-moving band was eluted with acetone – 2% hydrochloric acid, and brought into ether; then the ether was evaporated. The residue was esterified and crystallized as usual from methanol displacing chloroform to give red needles (35 mg) of the ester, m.p. 210–212° (lit. (5) m.p. 214°), 212–213.5° after one or more recrystallizations from methanol displacing chloroform.

Anal. Calcd. for $C_{33}H_{38}O_2N_4$: C, 75.83; H, 7.33; N, 10.72. Found: C, 75.59; H, 7.54; N, 10.54.

X-ray powder photographs showed that it crystallized in either of two forms or in mixtures of the two. The usual pure form was obtained from both boiling and cold (20°) solutions; the other form was obtained pure only once, from a boiling solution. When the usual form was heated, a solid phase change at about 200° was sometimes apparent.

The phylloporphyrin ester from *Chlorobium* pheophorbide 660, fraction 6 (3) (m.p. 211–214°, mixed m.p. with the above 211–213°), separated sometimes as a mixture of these two forms and sometimes in a form giving an X-ray powder photograph identical with that of the usual form of the synthetic ester. The visible spectra of the two specimens in chloroform were identical; λ_{max} (relative density in parentheses): 628 (0.08), 576 (0.42), 539.5 (0.39), and 505 (1.0) mμ.

Can. J. Chem. Downloaded from www.nrcresearchpress.com by 210.87.254.5 on 09/05/12
For personal use only.

The copper complexes of these esters, synthetic and of natural origin, formed needles, m.p. 206–209.5° and 205.5–208° after sintering from 205.5 and 205° respectively (lit. (5) m.p. 189°), mixed m.p. 206–209.5° after sintering from 205.5°. The X-ray powder photographs of these two specimens were identical.

It has been reported (5) that the spectrum of the synthetic δ-phylloporphyrin 15 is identical with that of γ-phylloporphyrin 15, in which the intensity of band 2 is significantly greater than that of band 3. Elsewhere (47) these two bands in the spectrum of δ-phylloporphyrin 15 are reported to be nearly equal in intensity, as they are in the spectra of all the synthetic and degradational δ-phylloporphyrins mentioned above.

δ-Phylloporphyrin 15 (Free Acid)

Some of the synthetic ester was hydrolyzed at 20° overnight in acetic acid – hydrochloric acid (1:1) (alkaline hydrolysis apparently resulted in decomposition). The acid was brought into ether, precipitated by 5% sodium hydroxide as the sodium salt, and returned to ether with acid. Concentrating the ether gave the product as needles. The X-ray powder photographs of this and of the phylloporphyrin free acid (3) derived from the above *Chlorobium* pheophorbide 660, fraction 6, were identical.

ACKNOWLEDGMENTS

The authors thank Dr. A. S. Holt and his colleagues for their generous cooperation, and Dr. Maria Przybylska for the interpretation of the X-ray powder photographs.

REFERENCES

1. J. L. Archibald, S. F. MacDonald, and K. B. Shaw. J. Am. Chem. Soc. **85**, 644 (1963).
2. J. W. Purdie and A. S. Holt. Can. J. Chem. In press.
3. A. S. Holt, J. W. Purdie, and J. W. F. Wasley. Can. J. Chem. In press.
4. J. W. Mathewson, W. R. Richards, and H. Rapoport. J. Am. Chem. Soc. **85**, 346 (1963).
5. H. Fischer, W. Siedel, and L. LeThierry d'Ennequin. Ann. **500**, 137 (1933).
6. H. Fischer and E. Strobel. Ann. **531**, 251 (1937). E. Strobel. Dissertation, Technische Hochschule, Munich, Germany. 1936.
7. H. Fischer and J. Riedmair. Ann. **490**, 91 (1931).
8. H. Fischer and J. Riedmair. Ann. **499**, 288 (1932).
9. H. Fischer, O. Moldenhauer, and O. Süs. Ann. **585**, 1 (1931).
10. H. Fischer and H. Gibian. Ann. **550**, 208 (1942); **552**, 153 (1942).
11. H. Fischer, H. Berg, and A. Schormüller. Ann. **480**, 109 (1930).
12. F. Morsingh and S. F. MacDonald. J. Am. Chem. Soc. **82**, 4377 (1960).
13. S. F. MacDonald and A. Markovac. Can. J. Chem. In press.
14. R. F. Bacon. Am. Chem. J. **33**, 79 (1905).
15. B. R. Baker, R. E. Schaub, and J. H. Williams. J. Org. Chem. **17**, 116 (1952).
16. S. F. MacDonald and R. J. Stedman. Can. J. Chem. **33**, 458 (1955).
17. H. Lund. Ber. **67**, 935 (1934).
18. B. Riegel and W. M. Lilienfeld. J. Am. Chem. Soc. **67**, 1273 (1945).
19. F. Bohlmann, H. J. Mannhardt, and H. G. Viehe. Chem. Ber. **88**, 364 (1955).
20. D. S. Breslow, E. Baumgarten, and C. R. Hauser. J. Am. Chem. Soc. **66**, 1286 (1944).
21. A. Brandstrom. Acta Chem. Scand. **5**, 1413 (1951).
22. E. E. Blaise. Compt. Rend. **132**, 978 (1901).
23. S. F. MacDonald. J. Chem. Soc. 4176 (1952).
24. E. Bulloch, A. W. Johnson, E. Markham, and K. B. Shaw. J. Chem. Soc. 1430 (1958).
25. H. Fischer and O. Süs. Ann. **484**, 118 (1930).
26. H. Fischer, E. Sturm, and H. Friedrich. Ann. **461**, 244 (1928).
27. F. K. Signaigo and H. Adkins. J. Am. Chem. Soc. **58**, 709 (1936).
28. W. Siedel and F. Winkler. Ann. **554**, 162 (1943).
29. H. Fischer and H. Orth. Chemie des pyrrols. Vol. I. Akademische Verlagsgesellschaft, Leipzig. 1934.
30. A. Treibs and R. Schmidt. Ann. **577**, 111 (1952).
31. H. Fischer and M. Bertl. Z. Physiol. Chem. **229**, 52 (1934).
32. G. Dupont. Compt. Rend. **148**, 1522 (1909).
33. J. Ellis, A. H. Jackson, A. C. Jain, and G. W. Kenner. J. Chem. Soc. 1935 (1964).
34. R. A. Nicholaus and R. Nicholetti. Ann. Chem. **47**, 167 (1957).
35. A. Wahl. Compt. Rend. **152**, 95 (1911).
36. H. Musso and K. Figge. Ann. **668**, 1 (1963).
37. W. Siedel. Z. Physiol. Chem. **231**, 167 (1935).
38. G. M. Badger, R. L. N. Harris, and R. A. Jones. Australian J. Chem. **17**, 987 (1964).
39. H. Fischer and H. Andersag. Ann. **458**, 117 (1927).
40. A. Treibs and W. Ott. Ann. **615**, 156 (1958).
41. R. L. Hinman and S. Theodoropulos. J. Org. Chem. **28**, 3052 (1963).
42. A. Hayes, G. W. Kenner, and N. R. Williams. J. Chem. Soc. 3779 (1958).
43. H. Fischer and H. Orth. Chemie des pyrrols. Vol. II. Akademische Verlagsgesellschaft, Leipzig. 1937. Part I. p. 106.
44. H. Fischer and A. Rothhaas. Ann. **484**, 102 (1930).
45. D. W. Hughes and A. S. Holt. Can. J. Chem. **40**, 171 (1962).
46. A. S. Holt and D. W. Hughes. J. Am. Chem. Soc. **83**, 499 (1961).
47. F. Pruckner. Z. Physik. Chem. **190A**, 101 (1942).

Can. J. Chem. Downloaded from www.nrcresearchpress.com by 210.87.254.5 on 09/05/12
For personal use only.

Can. J. Chem. Downloaded from www.nrcresearchpress.com by 210.87.254.105 on 09/05/12
For personal use only.

KINETIC SULFUR ISOTOPE EFFECTS IN AROMATIC BROMODESULFONATION[1]

B. T. BALIGA[2] AND A. N. BOURNS
Department of Chemistry, McMaster University, Hamilton, Ontario

Received October 7, 1965

ABSTRACT

Both bromodeprotonation and bromodesulfonation occur during aqueous bromination of sodium *p*-methoxybenzenesulfonate, A, and potassium 1-methylnaphthalene-4-sulfonate, B. Whereas for A the bromodeprotonation increases appreciably in amount as the bromide ion concentration is raised, this reaction takes place to a relatively small extent for the less reactive B. A reinvestigation of the kinetics of bromination and a determination of sulfate yields for both of these compounds over a range of bromide ion concentration of 0 to 0.5 *M* have been made to evaluate the individual rates of these two competing reactions. The kinetic data for the bromodesulfonation of A favor a two-step mechanism with Br_2 as the brominating species, but are not considered to eliminate completely a one- or two-step process involving Br^+ (or H_2OBr^+). For B, the kinetics allow either a one- or two-step mechanism with molecular bromine as the brominating agent.

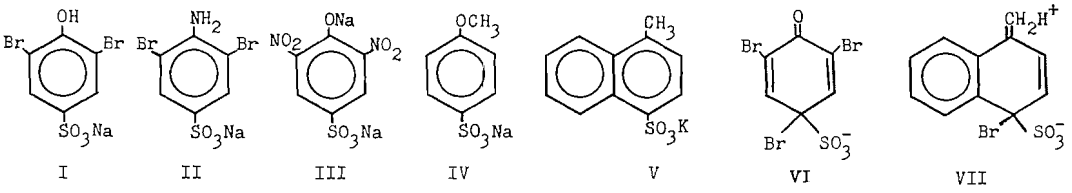
Kinetic sulfur isotope effects (k^{32}/k^{34}) have been measured for the bromodesulfonation of A at different bromide ion concentrations. The observed effects are: at $[Br^-] = 0$, 0.3%; at $[Br^-] = 0.03$ *M*, 1.3%; at $[Br^-] = 0.5$ *M*, 1.7%. These results confirm the two-step mechanism favored by kinetics and allow the rejection of the alternate mechanism with Br^+ (or H_2OBr^+) as the brominating species. A similar study of B gave the following results: at $[Br^-] = 0$, 0.2%; at $[Br^-] = 0.25$ *M*, 0.3%; at $[Br^-] = 0.5$ *M*, 0.4%; at $[Br^-] = 2.0$ *M*, 0.8%. These results establish the two-step mechanism for this compound and completely eliminate the alternate one-step process.

INTRODUCTION

The direct replacement by bromine of the sulfonate group in aromatic sulfonates in aqueous medium, known as bromodesulfonation, is a reaction generally shown by aromatic

$$Ar—SO_3^- + Br_2 \rightarrow Ar—Br + SO_3 + Br^-$$

sulfonates in which the sulfonate group is activated by powerful electron-releasing groups situated in a position ortho or para to the sulfonate group in the aromatic nucleus. Cannell (1, 2) in 1957 reported for sulfonates I to V a rather thorough investigation of the kinetics of bromodesulfonation in aqueous solution. For the highly reactive I, both kinetic and spectral studies provided evidence for the existence of a relatively long-lived quinoid-type intermediate VI, whose decomposition is the rate-determining step in bromodesulfonation.



I II III IV V VI VII

For the less highly activated sulfonates II, III, and IV, whose bromodesulfonation rates are suppressed by bromide ion, over and above that which can be attributed to tribromide ion formation

[1]*Issued as N.R.C. No. 8789.*

[2]*To whom all correspondence should be made. Present address: Division of Applied Chemistry, National Research Council, Ottawa, Canada.*

$$Br_2 + Br^- \overset{K}{\rightleftarrows} Br_3^-,$$

he proposed the following mechanism (mechanism A), in which $Ar\overset{+}{\underset{SO_3^-}{\overset{Br}{}}}$ is a metastable intermediate.

$$Ar{-}SO_3^- + Br_2 \underset{k_2}{\overset{k_1}{\rightleftarrows}} Ar\overset{+}{\underset{SO_3^-}{\overset{Br}{}}} + Br^-$$

$$Ar\overset{+}{\underset{SO_3^-}{\overset{Br}{}}} \xrightarrow{k_3} Ar{-}Br + SO_3$$

The rate expression for this mechanism has the form

$$[1] \qquad k_{obs} = \frac{k_1 k_3}{k_2[Br^-] + k_3} \cdot \frac{1}{1 + K[Br^-]},$$

where k_{obs} is the observed rate constant and K is the equilibrium constant for the tribromide ion formation.

For the least activated sulfonate, V, he found no sufficient depression in rate by added bromide ion beyond that which could be accounted for by the equilibrium between Br_2 and Br_3^-. The author drew no conclusion from this about the mechanism, and simply stated that "the kinetics require only a transition state and it is not necessary to propose a reaction intermediate". It is important, however, to note that his kinetic data for V can be accounted for either by mechanism A with $k_3 \gg k_2[Br^-]$ or by a one-step process. The latter possibility exists because the quinoid configuration VII, stabilized only by hyperconjugation, would be expected to possess a higher energy than in the case of the more highly activated systems I to IV and might, therefore, not correspond to a potential energy minimum along the reaction coordinate curve. Kinetic sulfur isotope effect measurements might be expected to shed some light on this question of mechanism for the bromodesulfonation of V. If the reaction takes place according to mechanism A with $k_3 \gg k_2[Br^-]$, then from eq. [1] may be obtained

$$[2] \qquad \left[\frac{k^{32}}{k^{34}}\right]_{obs} = \frac{k_1^{32}}{k_1^{34}}.$$

In this case, the formation of the intermediate (VII) being rate determining, the isotope effect should be zero or very close to it (at the most a few tenths of a percent). On the other hand, if the reaction takes place in a single step, then of course the C—S bond is being ruptured in the process and a sulfur isotope effect should result. It is true that the magnitude of this effect would be determined by the extent of bond rupture in the transition state and, conceivably, this could be such as to give rise to only a very small effect. If this result were observed, then no distinction could be drawn between the two mechanisms, although one would have gained a valuable insight into the extent to which bond rupture has proceeded in the highest energy state along the reaction coordinate. On the other hand, if a normal sulfur isotope effect, e.g. of the order of 1 to 2%, were to be found for this system, this result would clearly eliminate mechanism A and provide strong evidence in support of the one-step process.

To use kinetic sulfur isotope effects as a criterion to distinguish between these possibilities, it was felt necessary *first* to test this tool by applying it to the bromodesulfonation of a

Can. J. Chem. Downloaded from www.nrcresearchpress.com by 210.87.254.105 on 09/05/12
For personal use only.

compound which appeared on the basis of Cannell's kinetic results to proceed through mechanism A. Of the three compounds, II, III, and IV, whose bromination rates are suppressed by bromide ion beyond that attributable to Br_3^- formation, sodium *p*-methoxybenzenesulfonate (IV) seemed to be the most suitable for this test for the following reasons. Firstly, its reaction rate in the absence of bromide ion is sufficiently low to permit the use of reactant concentrations convenient for the isotope effect experiments and, furthermore, the bromide ion developed during the course of the reaction does not significantly affect the constancy of the rate constant, at least during the extent of reaction chosen for this study. Secondly, the ratio k_2/k_3 is of reasonable magnitude, namely 22 (as found by Cannell), to achieve the required condition $k_2[Br^-] \gg k_3$ at an attainable concentration of bromide ion. From the kinetic eq. [1] derived for mechanism A, which involves Br_2 as the brominating species, the ratio of the rate constants for the light and heavy sulfur isotopes, k^{32}/k^{34}, is given by eq. [3].

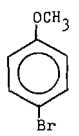
$$[3] \qquad \left[\frac{k^{32}}{k^{34}}\right]_{obs} = \frac{k_1^{32}}{k_1^{34}} \cdot \frac{k_3^{32}}{k_3^{34}} \cdot \frac{k_2^{34}[Br^-] + k_3^{34}}{k_2^{32}[Br^-] + k_3^{32}}$$

At zero or very low bromide ion concentration ($k_2[Br^-] \ll k_3$) this can be reduced to the form shown in eq. [2]. The observed isotope effect is, therefore, a measure of the relative rates with which the two isotopic species form a quinoid intermediate. Since this step does not involve the rupture of a C—S bond, the isotope effect can be expected to be small or zero ($k_1^{32}/k_1^{34} \simeq 1$). At a bromide ion concentration sufficiently high that $k_2[Br^-] \gg k_3$,

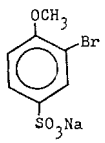
$$[4] \qquad \left[\frac{k^{32}}{k^{34}}\right]_{obs} = \frac{k_1^{32}}{k_1^{34}} \cdot \frac{k_2^{34}}{k_2^{32}} \cdot \frac{k_3^{32}}{k_3^{34}} = \frac{K^{32}}{K^{34}} \cdot \frac{k_3^{32}}{k_3^{34}},$$

in which K^{32}/K^{34} is the equilibrium isotope effect for the formation of the quinoid intermediate. Equation [4] now includes a rate constant ratio, k_3^{32}/k_3^{34}, for the step in which a C—S bond is being ruptured, and the isotope effect (a primary one) should be of normal magnitude (1 to 2%). Thus, it can be seen that for reaction by mechanism A the isotope effect should vary from zero to normal magnitude as the concentration of bromide ion changes. In other words, the isotope effect should be dependent on the concentration of bromide ion.

Initially, we assumed that Cannell's kinetic data on sodium *p*-methoxybenzenesulfonate were reliable and hence provided sound evidence for mechanism A. However, preliminary quantitative experiments, which involved the determination of sulfate yield (as related to the amount of bromine consumed) in the partial bromodesulfonation, disclosed the surprising fact that this yield is considerably less than that expected on the basis of the quantity of bromine consumed. This suggested that the bromination of sodium *p*-methoxybenzenesulfonate results in two competing reactions, bromodesulfonation and bromodeprotonation, the latter being the ordinary halogenation of the benzene ring in a position ortho to the methoxy group. This was further confirmed by product analysis: by isolating separately from the reaction mixture compounds VIII and IX, these being, respectively,



VIII



IX

Can. J. Chem. Downloaded from www.nrcresearchpress.com by 210.87.254.105 on 09/05/12
For personal use only.

the bromodesulfonated and bromodeprotonated products. Furthermore, it was established that these two competing reactions are of the same kinetic order, namely, first order with respect to sulfonate and first order with respect to bromine. The individual rate constants can therefore be evaluated from a knowledge of the rate constant for total bromination and the yield of sulfate. When the new kinetic data for the bromodesulfonation of compound IV were analyzed, it was found that, although the results favor mechanism A, a one- or two-step mechanism with Br^+ (or H_2OBr^+) as the brominating species cannot be eliminated completely. It now became apparent that the isotope effect study on compound IV was desirable to confirm the mechanism of bromodesulfonation, and was not, as originally intended, simply a test of reaction mechanism criterion.

When our attention was turned to compound V, again it was found that bromination results in two competing reactions, bromodesulfonation and bromodeprotonation. Also, there were strong indications that Cannell's salt was far from being of sufficient purity for reliable kinetic measurements. Consequently, with this compound also, the isotope effect investigation was preceded by a careful kinetic study involving the determination of total bromination rates and sulfate yields at different bromide ion concentrations. These results revealed that the product $k_{obs}(1 + K[Br^-])$, contrary to Cannell's findings, decreases somewhat as the bromide ion concentration increases, although not to an extent that cannot reasonably be attributed to a salt effect. Nevertheless, this result suggested the desirability of studying the kinetic isotope effect, not just at one bromide ion concentration, as had been originally planned, but at different concentrations, with the view to obtaining strong supporting evidence for mechanism A.

EXPERIMENTAL

Reagents

Anisole (Eastman Kodak, white label) was dried and fractionally distilled. α-Methylnaphthalene (99%) was obtained from L. Light and Co., England. Chlorosulfonic acid (British Drug Houses, laboratory reagent grade) was twice distilled before use. Carbon tetrachloride (Mallinckrodt, analytical reagent) was dried and fractionally distilled. All inorganic chemicals were analytical reagent grade.

Preparation of Sodium p-Methoxybenzenesulfonate

Anisole was sulfonated at −20 °C with chlorosulfonic acid by using carbon tetrachloride as solvent (3). The sulfonic acid that was formed was converted into its sodium salt, which was crystallized twice from water and twice from aqueous ethanol.

Cannell's kinetic experiment on the rate of bromination (expt. 26, p. 2935 of ref. 2) was repeated on this sulfonate. A steady rate constant, 0.0253 l mole^{-1} s^{-1}, compared with Cannell's value, 0.0254 l mole^{-1} s^{-1}, was obtained. The purity of the sulfonate was further established by estimating the yield of sulfate, gravimetrically, on complete bromodesulfonation. In several experiments, yields in the range 99.6–99.9% were obtained, in remarkable agreement with the theoretical yield of 100%.

Preparation of Potassium 1-Methylnaphthalene-4-sulfonate

For this preparation, direct sulfonation of α-methylnaphthalene by means of chlorosulfonic acid as used by Cannell (2) was first tried. The sulfonate that was obtained showed, however, after several recrystallizations unsteady rate constants when the rate of bromination was measured, and hence was impure. It was necessary, therefore, to employ a different method for purifying this sulfonate. Of the two purification methods tried for this purpose, only one proved to be successful.

The unsuccessful method was to convert the sulfonate into the *p*-toluidine salt, repeatedly recrystallize the *p*-toluidine salt to constant melting point, and then convert it back into the sulfonate. Although this method yielded a *p*-toluidine derivative of m.p. 234.8–235.8 °C, much higher than that reported by Cannell (227–229 °C), the material, after its conversion into the sulfonate, still showed unsteady rate constants.

In the second method the sulfonate was converted into the sulfonyl chloride by reaction with PCl_5, and the sulfonyl chloride that was formed was recrystallized repeatedly to constant melting point (melts very sharply at 81 °C; lit. (4) m.p. 81 °C) from benzene – petroleum ether (m.p. of anilide derivative, 157.5–158 °C; lit. (4) m.p. 158 °C). The sulfonyl chloride was then converted back into the sulfonate by refluxing with alcoholic KOH. The separated sulfonate was recrystallized twice from aqueous ethanol.

The question of the purity of this material and of the material prepared initially by the method used by Cannell is worth discussing. A number of kinetic experiments were first performed on material prepared

Can. J. Chem. Downloaded from www.nrcresearchpress.com by 210.87.254.105 on 09/05/12
For personal use only.

and purified by Cannell's method, the conditions used being identical with those of expts. 29 and 30 reported in his paper (p. 2935, ref. 2). It was found that, although the rate constants obtained from initial rates agreed fairly closely with Cannell's values, there was a serious fall off in the values of the rate constants as the reaction progressed. Nor could satisfactory results be obtained with material "purified" through the *p*-toluidine salt. On the other hand, the product obtained from the sulfonyl chloride purification procedure gave perfectly steady rate constants throughout the course of a kinetic run. It is of interest to note that the rate constant obtained for this material under the conditions of Cannell's expt. 29 was 0.0511 l mole^{-1} s^{-1}, which is to be compared with Cannell's reported value of 0.0985 l mole^{-1} s^{-1}. Since there seems to be little doubt that the salt used in the present study was of considerably higher purity than that used by Cannell, it is our view that no reliance can be placed on his rate constant for this compound.

Despite this elaborate purification procedure, the purity of the salt used in our work left something to be desired. The yields of sulfate obtained by "complete" bromodesulfonation in the presence of excess bromine at room temperature ranged from 92.6 to 93.1% of the theoretical amount, suggesting that the salt contained approximately 7% impurity. Since the same reactions carried out in a sealed tube at 210 °C for 8 days yielded sulfate in yields of 99.4–99.9%, it would appear that the impurity is an unreactive isomer, probably potassium 1-methylnaphthalene-5-sulfonate. Its presence, although introducing some error in the rate studies, should have no effect on the kinetic isotope effect results.

Product Analysis in the Bromination of Sodium p-Methoxybenzenesulfonate

Two separate aqueous solutions of 400 ml each, one containing the sulfonate (0.064 mole) and the other bromine (0.064 mole) and sodium bromide (0.4 mole), were cooled to 0 °C and then thoroughly mixed. The resulting solution was maintained at this temperature for about 3 h to permit the bromination to proceed to completion. At the end of the reaction, the bromodesulfonated product, *p*-bromoanisole, was extracted with carbon tetrachloride. After the latter had been distilled off, crude *p*-bromoanisole (2.45 g; 0.013 mole) was obtained in a yield corresponding to about 20% of the initial sulfonate. The product was identified by converting it into a derivative, *p*-methoxybenzoic acid (m.p. 183.5–184 °C), which gave no depression in melting point on admixture with an authentic sample of this acid (m.p. 183.5–184 °C).

After *p*-bromoanisole had been removed, the clear aqueous solution containing sodium 3-bromo-4-methoxybenzenesulfonate (the bromodeprotonated product) was first neutralized with solid sodium carbonate to a pH of 7. The solution was concentrated to about 125 ml by heating it at its boiling point and, when still hot, was saturated with sodium chloride before being allowed to cool. The separated solid weighed 15.1 g (0.051 mole), which corresponded in yield to about 80% of the initial sulfonate on the assumption that only one nuclear position is substituted by bromine. After recrystallization twice from water, it was converted into the sulfonamide via sulfonyl chloride. The melting point of the sulfonamide (139.5–140 °C) agreed with the literature value (139–140 °C (5)) for 3-bromo-4-methoxybenzenesulfonamide. The identity of the compound was further established by its infrared spectrum and by the lack of any melting point depression on admixture with an authentic sample of the sulfonamide prepared from *o*-bromoanisole.

Kinetics of Bromination

The rate of bromination was measured by following the rate of disappearance of bromine iodometrically. The technique was essentially the same as that adopted by Cannell (2). The aliquots (10 ml) of the reacting solution, withdrawn from time to time by means of a fast-delivery pipette (calibrated before use), were quenched in 10 ml of a 2% aqueous potassium iodide solution. The concentrations of sulfonate and bromine were varied but were kept, essentially, in the molar ratio of 4:1 to reduce the possibility of any dibromination. The reactions were carried out at constant acidity and ionic strength, which were adjusted by means of perchloric acid and sodium perchlorate, respectively. The rate constant for total bromination, k_{obs}, was evaluated by a least-square plot of $\log_{10}(A_0 - B_0 + B)/B$ versus t. (For definition of symbols, see ref. 2.) For the equilibrium

$$Br_2 + Br^- \underset{}{\overset{K}{\rightleftharpoons}} Br_3^-$$

the constant K at 0 °C, equal to 21.09 (l mole^{-1}), has been used in the present work. This value was obtained by extrapolating the values recently determined by Schaife and Tyrrel (6) at 5, 25, and 35 °C.

Resolution of Rate Constant for Total Bromination (k_{obs}) into Bromodesulfonation (k_{obs}^S) and Bromodeprotonation (k_{obs}^H) Rate Constants

In Cannell's study and also in the present work, the observed second-order rate constants, k_{obs}, were independent of the molar ratio of sulfonate to bromine. In addition, it was found in the present work that, at a given Br^- concentration, the ratio of the yield of sulfate to the total amount of bromine consumed was the same irrespective of the ratio of the two reactants or the extent of reaction. This established that the two competing reactions, bromodesulfonation and bromodeprotonation, are of the same kinetic order, namely, first order with respect to sulfonate and first order with respect to bromine. The resolution of k_{obs} into individual rate constants for bromodesulfonation, k_{obs}^S, and bromodeprotonation, k_{obs}^H, can therefore be achieved from a knowledge of the yield of sulfate and the amount of bromine consumed.

For determining the yield of sulfate, extensive preliminary experiments were done to establish that the

Can. J. Chem. Downloaded from www.nrcresearchpress.com by 210.87.254.105 on 09/05/12
For personal use only.

sulfate formed in the reaction could be recovered quantitatively and estimated gravimetrically as barium sulfate with a good degree of precision and without significant interference by foreign ions. For the sulfate yield results to be kinetically meaningful it was essential that only one molecule of bromine be consumed per molecule of sulfonate, or, in other words, that there be no dibromination. To avoid any possibility of the latter the molar ratio of sulfonate to bromine was always kept at 4:1 and the reaction was allowed to proceed only until about 12% of the sulfonate was consumed. The acidity and ionic strengths were the same as in kinetic experiments. However, to obtain sufficient barium sulfate (~70 mg) for gravimetric estimation and for conversion into sulfur dioxide for isotopic analysis, the concentrations of sulfonate and bromine were changed with changing Br^- concentration, since the extent of bromodesulfonation is strongly dependent upon the concentration of this ion.

In these partial brominations, since one knows the total amount of bromine consumed (as found by the difference between the initial concentration and the concentration when the reaction was stopped) and the correspondinging yield of sulfate formed (as found gravimetrically), the percentage of bromodesulfonation (as related to the total amount of bromine consumed), x, is given by (moles of sulfate formed/moles of bromine consumed) $\times$ 100, and $(100 - x)$ gives the percentage of bromodeprotonation.

Complete Bromodesulfonations

At room temperature, these were performed as follows. To a known amount of sulfonate solution, bromine solution was added, the concentration of bromine being kept at least 10 times greater than that of sulfonate. The system was allowed to stand for many days, during which period the bromodesulfonation would go to completion. At the end of this period, the excess bromine was first removed and the organic product was extracted with carbon tetrachloride. The organic extract was washed several times with water and the washings combined with the aqueous solution. From the resulting solution the sulfate was obtained gravimetrically as barium sulfate. The complete bromodesulfonation results served as a criterion of purity for the sulfonate; also, the barium sulfate samples obtained in these reactions were needed for determining the sulfur isotopic ratio in the reactant.

To carry out the complete bromodesulfonation of potassium 1-methylnaphthalene-4-sulfonate under drastic conditions, a known amount of sulfonate solution and excess bromine were put into a pyrex tube, which was then sealed. After this tube had been kept at 210 °C in a furnace for 8 days the products were isolated as described before.

Evaluation of Kinetic Sulfur Isotope Effect

The barium sulfate samples obtained in the partial and complete bromodesulfonations were converted into sulfur dioxide for mass spectrometric analysis.

The conversion of the sulfur of barium sulfate into sulfur dioxide involved the following steps. The barium sulfate samples were first reduced to hydrogen sulfide by using a mixture of hydrochloric, hypophosphorus, and hydriodic acids; the hydrogen sulfide was then precipitated as cadmium sulfide. The latter was converted into silver sulfide, which was then burned to sulfur dioxide by a high-vacuum technique (7). These procedures have been tested with standard barium sulfate samples and have been found to involve no significant isotopic fractionation.

The relative abundances of the sulfur isotopes were measured on a 6 inch, 90°, simultaneous collection mass spectrometer similar to that described by Wanless and Thode (8). This was a high-precision instrument capable of measuring changes in isotopic ratios with a precision of $\pm 0.02\%$. The $^{32}S/^{34}S$ ratios were obtained from the mass 64/mass 66 ion-current ratios after a suitable correction had been applied for the contribution to mass 66 of the molecular species $^{32}S^{16}O^{18}O$ (9).

The kinetic isotope effect was calculated by the expression shown in eq. [5], which had been derived by Stevens and Attree (10) for a reaction in which there is no complication of competing processes.

$$\frac{k^{32}}{k^{34}} = \frac{\ln\ (1 - f)}{\ln\ (1 - rf)} \qquad [5]$$

In this equation $r = (^{32}S/^{34}S)$ reactant/$(^{32}S/^{34}S)$ product) and f is the mole fraction of the reactant which has undergone reaction. Because of the competing bromodeprotonation, an estimate of f is given by $f'(1 - p)/(1 - f'p)$, where $f' = x/a$, the mole fraction of reactant which has undergone bromination, and p is the fraction of the total reaction which is the bromodeprotonation process.

RESULTS

Bromodesulfonation of Sodium p-Methoxybenzenesulfonate

The results of a series of kinetic experiments and sulfate yield determinations for the bromination of sodium *p*-methoxybenzenesulfonate, carried out at Br^- concentrations ranging from 0 to 0.5 M under conditions of constant ionic strength and acidity, are given in Table I. It can be seen from this table that the amount of bromodeprotonation increases as the Br^- concentration is increased. A plot of $\{k_{obs}(1 + K[Br^-])\}^{-1}$ versus $[Br^-]$ over a

Can. J. Chem. Downloaded from www.nrcresearchpress.com by 210.87.254.105 on 09/05/12
For personal use only.

TABLE I

Kinetic data for the bromination of sodium *p*-methoxybenzenesulfonate at 0 °C (ionic strength = 0.50 *M*; rate constants expressed in liter/mole second)

$[Br^-]$ (mole/l)	Sulfate yield (%)	k_{obs}	k_{obs}^H	k_{obs}^S	$k_{obs}^S(1 + K[Br^-])$
0.0000	88.2	0.538±0.0041*	0.0630	0.475	0.475
0.0300	65.9	0.177±0.0012	0.0600	0.117	0.191
0.0700	53.0	0.0800±0.0006	0.0380	0.0420	0.104
0.100	47.4	0.0549±0.0005	0.0289	0.0260	0.0808
0.200	36.0	0.0219±0.0002	0.0140	0.00790	0.0412
0.300	29.2	0.0132±0.0001	0.00935	0.00385	0.0282
0.400	24.1	0.00910±0.00008	0.00691	0.00219	0.0207
0.500	20.8	0.00674±0.00004	0.00534	0.00140	0.0162

*Precision limits are calculated from the standard deviation of the slope of the least-square plot of $\log_{10}(A_0 - B_0 + B)/B$ versus t.

range of Br^- concentration from 0 to 0.5 *M* is shown in Fig. 1 (points drawn by open squares), where it can be seen that the points at the higher Br^- concentrations deviate considerably from a straight line. On the other hand, a plot of $\{k_{obs}^S(1 + K[Br^-])\}^{-1}$ versus $[Br^-]$ (Fig. 1, points shown by open circles) shows excellent linearity over the range of Br^- concentrations used.[3] If one interprets this linear relationship in terms of

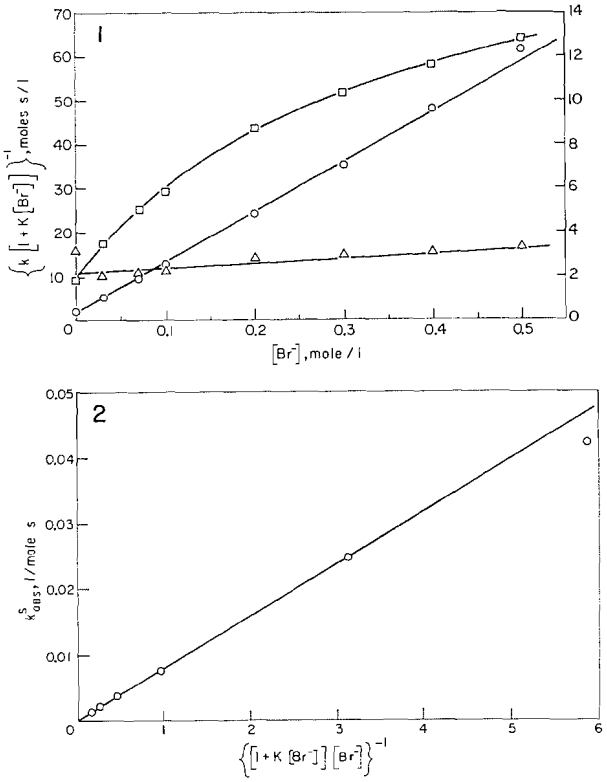


FIG. 1. Plot of rate constants (corrected for Br_3^- effect) for the total bromination, bromodesulfonation, and bromodeprotonation of sodium *p*-methoxybenzenesulfonate versus $[Br^-]$. LEGEND: □, $k = k_{obs}$ (right-hand ordinate); ○, $k = k_{obs}^S$ (left-hand ordinate); △, $k = k_{obs}^H$ (left-hand ordinate).

FIG. 2. Plot of rate constants, k_{obs}^S, for the bromodesulfonation of sodium *p*-methoxybenzenesulfonate versus $\{(1 + K[Br^-])[Br^-]\}^{-1}$.

[3]*The small deviation in the point at* $[Br^-] = 0.5$ *M can be attributed to experimental error in the determination of the very low yield of sulfate at this high* Br^- *concentration.*

Can. J. Chem. Downloaded from www.nrcresearchpress.com by 210.87.254.105 on 09/05/12
For personal use only.

Can. J. Chem. Downloaded from www.nrcresearchpress.com by 210.87.254.105 on 09/05/12
For personal use only.

TABLE II

Kinetic sulfur isotope effects for the bromodesulfonation of sodium *p*-methoxybenzenesulfonate at 0 °C

Expt. No.	Reaction	f'*	f†	$^{32}S/^{34}S$	$(^{32}S/^{34}S)$ partial)/ $(^{32}S/^{34}S)$ complete)	k^{32}/k^{34}	k_3^{32}/k_3^{34}
ES-SI-1	Complete			22.152			
ES-SI-2				22.139			
ES-SI-3				22.200			
ES-SI-5				22.129			
ES-SI-6				22.124			
				Mean 22.149±0.027‡			
ES-SII-1	Partial	0.125	0.112	22.245	1.0043	1.0045	
ES-SII-3	at $[Br^-]$ =	0.116	0.104	22.196	1.0021	1.0023	
ES-SII-4	0.0000 *M*	0.144	0.129	22.182	1.0015	1.0017	
ES-SII-5		0.148	0.133	22.232	1.0037	1.0041	
ES-SII-6		0.150	0.135	22.225	1.0034	1.0037	
						Mean 1.0032±0.0012‡	
ES-SIII-2	Partial	0.129	0.0889	22.391	1.0109	1.0113	
ES-SIII-3	at $[Br^-]$ =	0.131	0.0904	22.431	1.0127	1.0133	
ES-SIII-4	0.0300 *M*	0.160	0.112	22.435	1.0129	1.0136	
						Mean 1.0127±0.0009‡	1.0143
ES-SIV-1	Partial	0.144	0.0338	22.521	1.0168	1.0171	
ES-SIV-2	at $[Br^-]$ =	0.146	0.0345	22.489	1.0154	1.0160	
ES-SIV-3	0.500 *M*	0.146	0.0345	22.543	1.0178	1.0181	
ES-SIV-4		0.137	0.0319	22.532	1.0173	1.0178	
						Mean 1.0173±0.0008‡	1.0145

*f' is the mole fraction of the reactant which has undergone bromination.
†f is the corrected mole fraction of the reactant which has undergone bromodesulfonation.
‡The limit shown is the standard deviation.

Can. J. Chem. Downloaded from www.nrcresearchpress.com by 210.87.254.105 on 09/05/12
For personal use only.

mechanism A, the slope of the straight line is k_2/k_1k_3 and its intercept at $[Br^-] = 0$ is $1/k_1$. From these two quantities the ratio k_2/k_3 may be calculated and is found to have the value 66. This is to be compared with the value 22 obtained by Cannell from a plot of $\{k_{obs}(1 + K[Br^-])\}^{-1}$ versus $[Br^-]$ in the range of $[Br^-]$ from 0 to 0.15 M, on the assumption that bromodesulfonation is the only reaction. The remaining plot in Fig. 1 (points shown by open triangles) refers to the bromodeprotonation of sodium *p*-methoxybenzenesulfonate and will be discussed in a subsequent paper.

A plot of $k_{obs}{}^S$ versus $\{(1 + K[Br^-])[Br^-]\}^{-1}$, which will be discussed later, for the bromodesulfonation of sodium *p*-methoxybenzenesulfonate is shown in Fig. 2.

The sulfur isotopic ratios ($^{32}S/^{34}S$) of the reactant and of the product produced in various partial reactions are given in Table II. Each of the $^{32}S/^{34}S$ ratios reported in this table is for barium sulfate produced in a separate bromodesulfonation experiment, either complete or partial. The ratios for the product of the complete reactions are averaged and the mean combined with the individual isotopic ratios obtained for the product of the partial reactions to give (($^{32}S/^{34}S$) partial)/(($^{32}S/^{34}S$) complete) values recorded in the same table. These quotients are then substituted into eq. [5], along with the corresponding f values, for the calculation of the kinetic isotope effect, k^{32}/k^{34}, which is recorded in the same table.

Bromodesulfonation of Potassium 1-Methylnaphthalene-4-sulfonate

The kinetic results for the bromination of potassium 1-methylnaphthalene-4-sulfonate are given in Table III, where it can be seen that the competing bromodeprotonation

TABLE III

Kinetic data on the bromodesulfonation of potassium 1-methylnaphthalene-4-sulfonate at 0 °C (rate constants expressed in liter/mole second)

Ionic strength (M)	$[Br^-]$ (moles/l)	Sulfate yield (%)	k_{obs}	$k_{obs}{}^S$	$k_{obs}{}^S(1 + K[Br^-])$
0.50	0.0000	89.7	0.103±0.0008*	0.0924	0.0924
	0.100	88.5	0.0304±0.00022	0.0269	0.0836
	0.250	80.1	0.0143±0.00007	0.0115	0.0721
	0.400	76.8	0.00887±0.00004	0.00681	0.0643
	0.500	75.5	0.00709±0.00003	0.00535	0.0618
2.00†	0.0000	88.8	0.321±0.0032	0.321	
	2.00	59.6	0.00267±0.000024	0.00159	

*Precision limits are calculated from the standard deviation of the slope of the least-square plot of $\log_{10}(A_0 - B_0 + B)/B$ versus t.
†Kinetics investigated for the isotope effect study at high ionic strength.

reaction occurs only to a small extent. The product $k_{obs}{}^S(1 + K[Br^-])$ is not strictly a constant but shows a small decrease; a plot of $\{k_{obs}{}^S(1 + K[Br^-])\}^{-1}$ versus $[Br^-]$ is shown in Fig. 3.

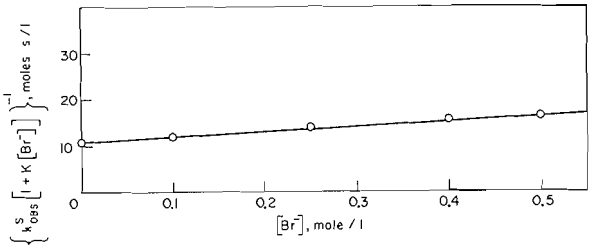


FIG. 3. Plot of rate constants (corrected for Br_3^- effect) for the bromodesulfonation of potassium 1-methylnaphthalene-4-sulfonate versus $[Br^-]$.

In Table IV are given the sulfur isotope abundances of barium sulfate produced in two kinds of "complete" bromodesulfonation reactions, one carried out at room temperature

TABLE IV

Mass spectrometric results for the product of the complete bromodesulfonation of potassium 1-methylnaphthalene-4-sulfonate

Expt. No.	Reaction conditions	$^{32}S/^{34}S$ (individual values)	Mean*
E'S-SI-3	Room temperature	22.236	
E'S-SI-4		22.216	
E'S-SI-5		22.213	
E'S-SI-8		22.188	
E'S-SI-9		22.202	
			22.211±0.019
E'S-SI-1	Sealed tube, 210 °C	22.200	
E'S-SI-2		22.193	
E'S-SI-6		22.219	
E'S-SI-7		22.213	
			22.206±0.012
		Overall mean	22.209±0.014

*The limits shown are standard deviations.

and giving a 93% yield of barium sulfate and the other performed under drastic conditions in a sealed tube and producing close to the theoretical yield of product. It can be seen from this table that the sulfur isotopic ratios of the barium sulfate produced in the two kinds of "complete" bromodesulfonation are identical (well within experimental error). This shows that the 7% impurity, which it will be recalled is considered to be an unreactive isomer of potassium 1-methylnaphthalene-4-sulfonate, has the same sulfur isotopic abundance as the compound in question.

In Table V are given the sulfur isotopic ratios for the barium sulfate produced in partial reactions carried out in a range of Br^- concentration from 0 to 2 M and at two different ionic strengths. Each of these ratios was divided by the overall mean value obtained for the products of the complete reaction (see Table IV), and the resulting quotients were separately used for the calculation of the isotope effect k^{32}/k^{34} given in the last column of this table.

DISCUSSION

Bromodesulfonation of Sodium p-Methoxybenzenesulfonate

A depression in rate with increasing Br^- concentration, over and above that which can be attributed to Br_3^- formation, found by Cannell for the bromodesulfonation of compounds II and III, and also found from our new kinetic data for the bromodesulfonation of compound IV, can be accommodated fully as well by *another* mechanism (mechanism B) not considered by Cannell. This mechanism is analogous to that proposed (11) for the iodination of phenols and aromatic amines, and involves Br^+ (or H_2OBr^+) as the brominating species.

$$Br_2 + H_2O \overset{K'}{\rightleftharpoons} H_2OBr^+ + Br^-$$

$$Ar{-}SO_3^- + H_2OBr^+ \underset{k_2'}{\overset{k_1'}{\rightleftharpoons}} Ar\begin{matrix}\diagup^{+}Br\\ \diagdown SO_3^-\end{matrix} + H_2O$$

$$Ar\begin{matrix}\diagup^{+}Br\\ \diagdown SO_3^-\end{matrix} \xrightarrow{k_3'} Ar{-}Br + SO_3$$

Can. J. Chem. Downloaded from www.nrcresearchpress.com by 210.87.254.105 on 09/05/12
For personal use only.

Can. J. Chem. Downloaded from www.nrcresearchpress.com by 210.87.254.105 on 09/05/12
For personal use only.

TABLE V

Kinetic sulfur isotope effects for the bromodesulfonation of potassium 1-methylnaphthalene-4-sulfonate at 0 °C

Expt. No.	[Br^-] (moles/l)	Ionic strength (moles/l)	f'*	f†	$^{32}S/^{34}S$	(($^{32}S/^{34}S$) partial)/(($^{32}S/^{34}S$) complete)‡	k^{32}/k^{34}§
E'S-SII-1	0.0000	0.50	0.0954	0.0864	22.235	1.0012	1.0013
E'S-SII-2	0.0000	0.50	0.0988	0.0895	22.244	1.0016	1.0015
							Mean 1.0014
E'S-SII'-1	0.0000	2.00	0.201	0.184	22.227	1.0008	1.0011
E'S-SII'-2	0.0000	2.00	0.200	0.183	22.262	1.0024	1.0025
E'S-SII'-3	0.0000	2.00	0.184	0.168	22.258	1.0022	1.0026
E'S-SII'-4	0.0000	2.00	0.184	0.169	22.274	1.0029	1.0032
							Mean 1.0023±0.0008
E'S-SIV-1	0.250	0.50	0.112	0.0917	22.259	1.0022	1.0026
E'S-SIV-2	0.250	0.50	0.111	0.0908	22.272	1.0028	1.0032
							Mean 1.0029
E'S-SIII-1	0.500	0.50	0.111	0.0862	22.292	1.0038	1.0043
E'S-SIII-2	0.500	0.50	0.105	0.0811	22.262	1.0024	1.0030
E'S-SIII-3	0.500	0.50	0.201	0.159	22.269	1.0027	1.0028
E'S-SIII-4	0.500	0.50	0.201	0.159	22.306	1.0044	1.0046
							Mean 1.0037±0.0008
E'S-SV-4	2.00	2.00	0.0542	0.0332	22.350	1.0064	1.0069
E'S-SV-5	2.00	2.00	0.0544	0.0333	22.399	1.0085	1.0088
E'S-SV-2	2.00	2.00	0.112	0.0771	22.383	1.0078	1.0081
E'S-SV-3	2.00	2.00	0.114	0.0786	22.366	1.0071	1.0075
E'S-SV-1	2.00	2.00	0.236	0.169	22.346	1.0062	1.0066
E'S-SV-1(D)	2.00	2.00	0.236	0.169	22.365	1.0070	1.0079
							Mean 1.0076±0.0007

*f' is the mole fraction of the reactant which has undergone bromination.
†f is the corrected mole fraction of the reactant which has undergone bromodesulfonation.
‡($^{32}S/^{34}S$) complete = 22.209 (see Table IV).
§The limits shown are standard deviations.

The rate equation for this mechanism has the form

$$[6] \qquad k_{obs} = \frac{K'k_1'k_3'}{(k_2' + k_3')(1 + K[Br^-])[Br^-]}.$$

If, instead of the two-step process involving the quinoid intermediate, the brominating species Br^+ (or H_2OBr^+) were to form the product directly in a single step having a rate constant k_4, an equation similar to eq. [6], namely,

$$[7] \qquad k_{obs} = \frac{K'k_4}{(1 + K[Br^-])[Br^-]},$$

would be followed. In either case a plot of k_{obs} versus $\{(1 + K[Br^-])[Br^-]\}^{-1}$ would be expected to be a straight line with a zero intercept. However, examination of eq. [1] shows that, under the circumstance $k_2[Br^-] \gg k_3$, mechanism A, like mechanism B, will also lead to a straight-line plot of k_{obs} versus $\{(1 + K[Br^-])[Br^-]\}^{-1}$. Now when the rate data for compounds II and III were analyzed by Cannell in terms of mechanism A, he obtained a k_2/k_3 ratio such that $k_2[Br^-]$ is large relative to k_3, even at quite low Br^- concentrations. It is therefore not surprising for us to find that Cannell's data for these two compounds give a good linear plot of k_{obs} versus $\{(1 + K[Br^-])[Br^-]\}^{-1}$, and hence do not distinguish between the two mechanisms.

It is tempting, therefore, to see whether our kinetic data for the bromodesulfonation of compound IV would distinguish between the two mechanisms. Inspection of eqs. [6] and [7] shows that mechanism B also predicts a straight-line plot of $\{k_{obs}^S(1 + K[Br^-])\}^{-1}$ versus $[Br^-]$, but, unlike mechanism A, requires a zero intercept.[4] The fact that a small but experimentally real intercept has been observed in the latter plot for the bromodesulfonation of sodium *p*-methoxybenzenesulfonate (Fig. 1) might argue against mechanism B for this compound. It is our opinion, however, that one would not be justified in completely eliminating mechanism B simply on the basis of this very small intercept. The usual way to see whether mechanism B is operative is to test the linearity of k_{obs}^S versus $\{(1 + K[Br^-])[Br^-]\}^{-1}$, as required by the relationships of eqs. [6] and [7]; such a plot for the bromodesulfonation of sodium *p*-methoxybenzenesulfonate is shown in Fig. 2. It can be seen from this figure that, over the range of Br^- concentrations of 0.5 to 0.1 M, the points perfectly fit a straight line. At Br^- concentrations of 0.03 and 0.07 M, deviations from linearity were observed, the deviation being quite considerable for the point corresponding to $[Br^-] = 0.03$ M (it was not convenient to include this point in the plot). These deviations from linearity appear exactly where one would expect them for a reaction by mechanism A with a k_2/k_3 ratio of 66. When $[Br^-]$ is above 0.1 M, $k_2[Br^-]$ is sufficiently large relative to k_3 to cause the kinetic points to fit a straight line within the limits of experimental error. Below 0.1 M, however, the product $k_2[Br^-]$ starts to assume a value comparable with that for k_3 and deviations from linearity become apparent. The kinetic results therefore clearly favor mechanism A over mechanism B, but outright rejection of mechanism B on the basis of the kinetic data alone was not considered justifiable. Strong supporting evidence, however, is desirable, and this has been sought through a kinetic sulfur isotope effect study of the reaction.

An inspection of mechanism B reveals that the sulfur isotope effect should be inde-

[4] *A more vigorously derived kinetic expression for mechanism B, which takes into account the very small amount of titratable bromine which is in the form* H_2OBr^+, *actually does require an intercept for this plot. It can be shown, however, that this intercept is equal to the product of the slope and K', the equilibrium constant for* H_2OBr^+ *formation. Since the slope is ~120 and K' has a value of* 10^{-20} *(12), the intercept required by mechanism B is obviously quite insignificant.*

Can. J. Chem. Downloaded from www.nrcresearchpress.com by 210.87.254.105 on 09/05/12
For personal use only.

pendent of the Br^- concentration, since Br^- is formed in a pre-equilibrium step which has nothing to do with the substitution step. For a two-step process in mechanism B,

$$[8] \qquad \left[\frac{k^{32}}{k^{34}}\right]_{obs} = \frac{k_1'^{32}}{k_1'^{34}} \cdot \frac{k_3'^{32}}{k_3'^{34}} \cdot \frac{k_2'^{34} + k_3'^{34}}{k_2'^{32} + k_3'^{32}},$$

and the observed isotope effect will depend on the relative magnitudes of k_3' and k_2'. If $k_3' \gg k_2'$, the effect will be zero (or close to it); if $k_3' \ll k_2'$, the effect will be a normal one. Also, for a one-step process in mechanism B, an isotope effect of appreciable magnitude can be expected since C—S bond rupture is involved in the rate-determining step. On the other hand, for mechanism A, as discussed earlier, the isotope effect can be expected to vary from zero to normal magnitude as the Br^- concentration is increased.

Kinetic sulfur isotope effects have been determined for the bromodesulfonation of sodium *p*-methoxybenzenesulfonate at three different initial Br^- concentrations: 0, 0.03, and 0.5 *M*. In a reaction with no added Br^-, the concentration of this ion will have reached 5×10^{-4} *M* during the 12% reaction (with respect to sulfonate) used in the isotope effect experiments. This means that, if mechanism A is operative, the ratio of the rate of reversion of the intermediate to its rate of conversion into product, $k_2[Br^-]/k_3$, will on the average be only $66 \times 0.00025 = 0.0165$. For all practical purposes then, one can consider that the intermediate proceeds only to product; that is, the formation of the intermediate is rate determining. At $[Br^-] = 0.03$ *M*, rate reverse/rate forward $= 66 \times 0.03 = \sim 2$; that is, of every three intermediates formed, two revert to reactant and one proceeds to product. Finally, at $[Br^-] = 0.5$ *M*, rate reverse/rate forward $= 66 \times 0.5 = 33$; under these conditions the intermediate should be essentially in equilibrium with reactants and a normal isotope effect can be expected.

Inspection of Table II reveals that the kinetic isotope effect does indeed increase with an increase in the concentration of bromide ion. These results completely eliminate mechanism B and provide strong supporting evidence for mechanism A in the bromodesulfonation of sodium *p*-methoxybenzenesulfonate. Thus, at very low Br^- concentrations, the rate-determining step is the formation of the quinoid intermediate in which the C—S bond is still intact. The isotope effect, which is a measure of the rate ratio k_1^{32}/k_1^{34}, is 1.0032. At $[Br^-] = 0.5$ *M*, the rupture of the C—S bond is fully rate determining and a normal isotope effect of 1.0173 is observed. At an intermediate Br^- concentration of 0.03 *M* the rupture of the C—S bond is partially rate determining and the isotope effect is 1.0127.

The magnitude of the isotope effect for the step involving C—S bond rupture, namely k_3^{32}/k_3^{34}, can be evaluated from eq. [3] and the observed isotope effect at the different Br^- concentrations, providing an assumption is made concerning the value of k_2^{32}/k_2^{34}. Since the quinoid intermediate is a high-energy species, it seems reasonable to assume that the transition state for the first step more closely resembles this intermediate than it does the reactant. If this is so, the ratio k_2^{32}/k_2^{34} should be considerably closer to unity than is the ratio k_1^{32}/k_1^{34}, for which the value 1.0032 has been observed. It would seem reasonable, therefore, to assume $k_2^{32} = k_2^{34}$; that is, there is no significant isotope effect for the reverse reaction within the limits of our measurements. With this assumption then, it follows from eq. [3] that

$$[9] \qquad \left[\frac{k^{32}}{k^{34}}\right]_{obs} = \frac{k_1^{32}}{k_1^{34}} \cdot \frac{\frac{k_3^{32}}{k_3^{34}} \cdot \frac{k_2^{32}}{k_3^{32}} \cdot [Br^-] + 1}{\frac{k_2^{32}}{k_3^{32}} \cdot [Br^-] + 1}.$$

Can. J. Chem. Downloaded from www.nrcresearchpress.com by 210.87.254.105 on 09/05/12
For personal use only.

In eq. [9], $k_1^{32}/k_1^{34} = 1.0032$, the isotope effect measured at $[Br^-] = 0$, and $k_2^{32}/k_3^{32} = 66$, a value obtained from the slope and intercept of the plot of $\{k_{obs}{}^S(1 + K[Br^-])\}^{-1}$ versus $[Br^-]$ in Fig. 1. Equation [9] reduces to

$$[10] \qquad \left[\frac{k^{32}}{k^{34}}\right]_{obs} = 1.0032\,\frac{(k_3^{32}/k_3^{34})\cdot 66\cdot[Br^-] + 1}{66\cdot[Br^-] + 1}.$$

In this equation if one substitutes the measured isotope effect $(k^{32}/k^{34})_{obs}$ at a given Br^- concentration, the desired ratio, k_3^{32}/k_3^{34}, can be calculated; the latter values at the two different Br^- concentrations are given in Table II. It is significant to note that exactly the same value, within experimental error, is obtained for the k_3^{32}/k_3^{34} ratio at the two different Br^- concentrations, 0.03 and 0.5 *M*. This internal self-consistency of the results, when interpreted in terms of mechanism A, lends further support to this mechanism for the reaction. Furthermore, the value 1.014 for k_3^{32}/k_3^{34} corresponds closely to the theoretical value, 1.016, for a transition state in which there is complete C—S bond rupture.

The evidence obtained in the present work for the operation of mechanism A for the bromodesulfonation of compound IV strongly suggests that this mechanism is being followed also in the same reaction of the more reactive compounds II and III.

There is a small, but certainly real, isotope effect, $k_1^{32}/k_1^{34} = 1.0032$, in the formation of the quinoid intermediate. Since the C—S bond remains intact in this process, one might have expected this effect to be zero. It might therefore be argued that this small effect arises from a slight reversion of the intermediate as a consequence of the bromide ion developed during the course of the reaction. We now intend to show by the method of successive approximations that this is not a primary effect, but rather quite definitely a secondary one.

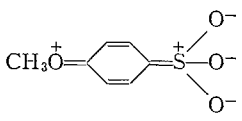
(*a*) If one assumes $k_1^{32}/k_1^{34} = 1$ (as one would have expected), eq. [10] is used to calculate k_3^{32}/k_3^{34} from the experimental data: $[Br^-] = 0.5$ *M*, $(k^{32}/k^{34})_{obs} = 1.0173$. The value of k_3^{32}/k_3^{34} turns out to be 1.0178.

(*b*) This value of k_3^{32}/k_3^{34} is substituted into eq. [10] to calculate k_1^{32}/k_1^{34} from the experimental data: $[Br^-] = 0.00025$ *M* (average concentration of Br^- developed during the course of the reaction in the partial run in which there is no added Br^-), $(k^{32}/k^{34})_{obs} = 1.0032$. The value of k_1^{32}/k_1^{34} so obtained, which should be somewhat better than the initially assumed value of unity, is 1.0030.

(*c*) Now, by using $k_1^{32}/k_1^{34} = 1.0030$, procedure *a* is repeated and a value of 1.0147 is obtained for k_3^{32}/k_3^{34}.

(*d*) Procedure *b* is again repeated with $k_3^{32}/k_3^{34} = 1.0147$. The value of k_1^{32}/k_1^{34} so obtained is 1.0030, identical with the result from operation *b*.

The fact that through a series of these operations k_1^{32}/k_1^{34} finally assumes a constant value of 1.0030, which is not significantly different from the observed effect, 1.0032, at a bromide ion concentration of 0, clearly shows that this effect is a secondary one associated with the step for the formation of the intermediate. This secondary isotope effect is probably caused by the fact that the sulfonate group in the initial state is capable of conjugated interaction with the benzene ring and that this interaction is destroyed in the formation of the intermediate, thus resulting in some C—S bond weakening.



Can. J. Chem. Downloaded from www.nrcresearchpress.com by 210.87.254.105 on 09/05/12
For personal use only.

Evidence in support of such conjugative interaction of the sulfonate group with the aromatic ring has been obtained in studies on the acid strength of naphthylammonium ions (13), $^{-}O_3SC_{10}H_6\overset{+}{N}H_3$, and of substituted benzenesulfonic acids (14). It is to be noted that the very small secondary isotope effects associated with the elements of higher atomic number usually are not detectable. To our knowledge, the only other example reported to date is a secondary ^{14}C effect in the formation of the 2,4-dinitrophenylhydrazone of acetophenone-β-^{14}C (15).

Bromodesulfonation of Potassium 1-Methylnaphthalene-4-sulfonate

Preliminary kinetic studies on the bromination of potassium 1-methylnaphthalene-4-sulfonate revealed that this compound, like compound IV, undergoes competing bromodesulfonation and bromodeprotonation reactions. Again, the latter reaction had been overlooked by Cannell in his kinetic study of the bromination of this compound. Furthermore, there was reason to believe that the salt used by Cannell was quite impure. For these reasons, a careful reinvestigation of the bromination kinetics, including the determination of sulfate yields, was made over a range of bromide ion concentrations from 0 to 0.5 M, and the results are given in Table III. It can be seen from this table that the product $k_{obs}^{S}(1 + K[Br^-])$ is not strictly a constant but shows a decrease of about 33% over this range of Br^- concentration. Similar small decreases in $k_{obs}(1 + K[Br^-])$ have been observed before in certain bromodeprotonation processes (16, 17) and have been attributed to a salt effect resulting from the replacement by sodium bromide of some inert salt used to maintain a constant ionic strength at the different Br^- concentrations. Clearly, this very small depression in rate by Br^- eliminates any form of mechanism with Br^+ (or H_2OBr^+) as the brominating species (see eqs. [6] and [7]), but it is fully consistent with either the one- or two-step mechanism with Br_2 as the brominating agent.

If potassium 1-methylnaphthalene-4-sulfonate does undergo bromodesulfonation by the one-step mechanism, then the small decrease in rate observed must be due entirely to the salt effect. On the other hand, if the reaction is proceeding in two steps through a quinoid intermediate, then the decrease in rate would be due, in part or entirely, to the return of this intermediate to reactant as the Br^- concentration is increased. The fact that a plot of $\{k_{obs}^{S}(1 + K[Br^-])\}^{-1}$ versus $[Br^-]$ (Fig. 3) is linear lends support to the two-step mechanism, although the possibility that a salt effect could take a similar form is not excluded. If one interprets this linearity solely in terms of a return of an intermediate to reactant, the slope and intercept of the line in Fig. 3 give a value of 1.1 for k_2/k_3, the ratio of the rate constants for reverse and forward reactions involving this intermediate.

A kinetic sulfur isotope effect study of this reaction was initiated in an attempt to distinguish between the two possibilities. Initial isotope effect experiments were carried out under the same conditions as those used in the sodium p-methoxybenzenesulfonate study. Inspection of Table V reveals that, over the range of Br^- concentration 0 to 0.5 M, the isotope effects are small and show a variation which is barely beyond experimental error. There is, however, a strong suggestion of a small increase in the isotope effect with increasing Br^- concentration, but the change is too small to be meaningful as a mechanistic criterion. These results obviously made it necessary to go to a higher bromide ion concentration. Since, in doing so, the ionic strength of the medium would also change, it was necessary first to demonstrate that a change in ionic strength alone does not significantly influence the magnitude of the isotope effect. That this is indeed the case can be seen from Table V by comparing the results obtained at the two ionic strengths in the absence of

Can. J. Chem. Downloaded from www.nrcresearchpress.com by 210.87.254.105 on 09/05/12
For personal use only.

added bromide ion. The difference in the mean k^{32}/k^{34} ratios does not exceed the experimental error.

After this crucial point had been established, a series of isotope effect measurements were made at $[Br^-] = 2\ M$. The mean value so obtained, 1.0076[5] ± 0.0007, is significantly different from the value, 1.0023 ± 0.0008, found at $[Br^-] = 0$ and the same ionic strength. This result amply confirms the trend suggested by the earlier experiments and, in our opinion, clearly establishes the two-step mechanism for the bromodesulfonation of potassium 1-methylnaphthalene-4-sulfonate.

It is of interest to see if the number 1.1 obtained from the plot in Fig. 3 is the true value for the ratio k_2/k_3. For this value of k_2/k_3, at $[Br^-] = 0.5\ M$ one intermediate returns to reactant to two going forward, and the isotope effect should have increased considerably over the value obtained at $[Br^-] = 0$. At $[Br^-] = 2\ M$, the observed isotope effect should have reached nearly a normal value. Clearly, therefore, much of the slope in Fig. 3 is due to the salt effect. It is possible to estimate the true value of the k_2/k_3 ratio from eq. [9]. In this equation $k_1^{32}/k_1^{34} = 1.0023$, while the ratio k_3^{32}/k_3^{34} can, to a first approximation, be considered to be the same as that found for compound IV, namely 1.0144. These ratios, when combined in eq. [9] with the observed isotope effect at $[Br^-] = 2\ M$, gave a value of 0.29 for the k_2/k_3 ratio. That some reliance can be placed on the k_2/k_3 ratio calculated in this way, and on the assumption that $k_3^{32}/k_3^{34} \approx 1.014$, is shown by the agreement between the isotope effects obtained experimentally at the other Br^- concentrations, 0.25 and 0.5 M, and the values calculated by substitution of the values for k_2/k_3, k_1^{32}/k_1^{34}, and k_3^{32}/k_3^{34} in eq. [9]. At $[Br^-] = 0.25\ M$, the experimentally observed isotope effect is 1.0029, and the calculated value is 1.0032; at $[Br^-] = 0.5\ M$, the corresponding values are 1.0037 and 1.0041. It can be inferred, therefore, that nearly 75% of the depression in the quantity $k_{obs}{}^{S}(1 + K[Br^-])$ by bromide ion results from the salt effect.

ACKNOWLEDGMENT

We are grateful to Mr. Jan Monster for the mass spectrometric analysis.

REFERENCES

1. L. G. CANNELL. J. Am. Chem. Soc. **79**, 2927 (1957).
2. L. G. CANNELL. J. Am. Chem. Soc. **79**, 2932 (1957).
3. R. E. STEIGER. Helv. Chim. Acta, **13**, 173 (1930).
4. K. ELBS and B. CHRIST. J. Prakt. Chem. **106**, 17 (1923).
5. E. H. HUNTRESS and F. H. CARTEN. J. Am. Chem. Soc. **62**, 603 (1940).
6. D. B. SCHAIFE and H. J. V. TYRREL. J. Chem. Soc. 386 (1958).
7. H. G. THODE, J. MONSTER, and H. B. DUNFORD. Bull. Am. Assoc. Petrol. Geologists, **42**, 2619 (1958).
8. R. K. WANLESS and H. G. THODE. J. Sci. Instr. **30**, 395 (1953).
9. H. G. THODE, J. MACNAMARA, and W. H. FLEMING. Geochim. Cosmochim. Acta, **3**, 235 (1953).
10. W. H. STEVENS and R. W. ATTREE. Can. J. Res., B, **27**, 807 (1949).
11. B. S. PAINTER and F. G. SOPER. J. Chem. Soc. 342 (1947).
12. M. C. SNEED, J. L. MAYNARD, and R. C. BRASTED. Comprehensive inorganic chemistry. D. Van Nostrand Co., Inc., New York. 1954. p. 180.
13. A. BRYSON. Trans. Faraday Soc. **47**, 528 (1951).
14. H. ZOLLINGER, W. BUCHLER, and C. WITTWER. Helv. Chim. Acta, **36**, 1711 (1953).
15. V. F. RAAEN, A. K. TSIOMIS, and C. J. COLLINS. J. Am. Chem. Soc. **82**, 5502 (1960).
16. E. GROVENSTEIN and U. V. HENDERSON. J. Am. Chem. Soc. **78**, 569 (1956).
17. R. P. BELL and D. J. RAWLINSON. J. Chem. Soc. 63 (1961).

[5]*It is of interest to note that the same isotope effect, within the precision of measurement, is obtained at* $[Br^-] = 2\ M$ *at widely varying extents of reaction. This establishes that the impurity present in the salt causes no complication in the isotope effect experiments.*

Can. J. Chem. Downloaded from www.nrcresearchpress.com by 210.87.254.105 on 09/05/12
For personal use only.

Can. J. Chem. Downloaded from www.nrcresearchpress.com by 210.87.254.40 on 09/05/12
For personal use only.

KINETIC HYDROGEN ISOTOPE EFFECTS IN AROMATIC BROMODEPROTONATION[1]

B. T. BALIGA[2] AND A. N. BOURNS
Department of Chemistry, McMaster University, Hamilton, Ontario

Received October 7, 1965

ABSTRACT

The bromodeprotonation of sodium *p*-methoxybenzenesulfonate is an ordinary halogenation reaction in which a hydrogen ortho to the methoxy group is replaced by bromine. The kinetic data for this reaction do not distinguish between a one- and a two-step mechanism with Br_2 as the brominating species. The two-step mechanism was confirmed by the observation of a variation in the kinetic hydrogen isotope effect, k^H/k^D, with changing bromide ion concentration. The observed isotope effects are 1.01, 1.07, 1.18, and 1.31 at bromide ion concentrations 0, 0.5, 1, and 2 *M*, respectively.

The isotope effect study strongly establishes that in this reaction the small depression in rate produced by bromide ion, beyond that due to Br_3^- formation, arises mainly from a salt effect, and only a small amount of this depression is caused by return of the intermediate to reactants.

INTRODUCTION

The displacement of a proton from an aromatic nucleus by a halogen is an important reaction in electrophilic aromatic substitution. In recent years there has been a great deal of interest in the mechanism of halodeprotonations, and a large number of studies have been directed to the problem of establishing the identity of the halogenating species and also to the question of elucidating the detailed pathway of the substitution process itself. Whereas ordinary kinetic studies (1) have frequently provided valuable information on the nature of the halogenating species, they have been of limited value in shedding light on the detailed mechanism of the substitution process itself. Since 1950 a number of kinetic hydrogen isotope effect studies have been made to provide a solution to this latter problem (2). A graded series of isotope effects have been observed with, as yet, no reported effects in chlorination, with effects ranging from zero to an appreciable magnitude in bromination, and with relatively large effects in almost all cases of iodination.

Although a knowledge simply of the magnitude of the isotope effect under a given set of conditions for a reaction provides valuable information about the extent of C—H bond rupture in the highest energy state, it can by no means distinguish between a one-step process (mechanism I)

$$ArH + X_2 \rightleftharpoons \text{transition state} \rightarrow ArX + X^- + H^+$$

and a two-step process (mechanism II)

$$ArH + X_2 \underset{k_2}{\overset{k_1}{\rightleftharpoons}} Ar\overset{+}{\underset{X}{\overset{H}{<}}} + X^-$$

$$Ar\overset{+}{\underset{X}{\overset{H}{<}}} \xrightarrow{k_3} ArX + H^+.$$

One way in which kinetic isotope effects may provide unambiguous support for the two-step mechanism is by the demonstration of a variation in the magnitude of this effect with a change in the concentration of halide ion, X^-. Changes in the concentration of X^- would

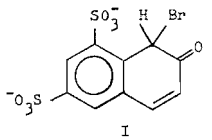
[1]*Issued as N.R.C. No. 8790.*
[2]*To whom all correspondence should be made. Present address: Division of Applied Chemistry, National Research Council, Ottawa, Canada.*

Can. J. Chem. Downloaded from www.nrcresearchpress.com by 210.87.254.40 on 09/05/12
For personal use only.

be expected to influence the relative rates of return of an intermediate to reactant and of decomposition to product, and hence would affect the extent to which the latter step (in which there is C—H bond rupture) contributes to the overall reaction rate.

Several attempts to achieve a variation in the magnitude of the hydrogen isotope effect by varying the concentration of halide ion have not been decisive. Grimison and Ridd (3) observed in the iodination of glyoxaline by molecular iodine a normal isotope effect ($k^H/k^D = 4.4$) that was unaffected by changes in halide ion concentration, while a similar result has been observed by Berliner (4) in the iodination of anisole with ICl ($k^H/k^D = 3.8$). These results can be interpreted by either a one- or a two-step mechanism with I^+ (or H_2OI^+) as the iodinating species, or by mechanism II in which I_2 or ICl acts as the electrophile. The latter possibility exists because, even at the lowest halide ion concentration used, the rate of reversal of the intermediate could still be faster than the proton loss ($k_2[I^-] \gg k_3$), and hence C—H bond rupture could still be fully rate determining. Finally, Berliner and Schueller (5) have observed in the bromination of diphenyl a small isotope effect ($k^H/k^D = 1.15$) invariant with Br^- concentration, a result which can be interpreted by either mechanism II, with the formation of the intermediate being rate determining (in this case the 15% isotope effect is a secondary one), or by mechanism I through a transition state in which the C—H bond is only slightly weakened.

To date, the positive application of the isotope effect criterion has been reported in only a few cases: (*i*) a variation in hydrogen isotope effect ($k^H/k^D = 6.55$–3.62) with a change in the concentration of base in the coupling reaction of *p*-chlorodiazobenzene with 2-naphthol-6,8-disulfonic acid (6); (*ii*) a variation in carbon isotope effect ($k^{12}/k^{13} = 1.002$–1.045) with changing concentration of Br^- in the bromodecarboxylation of 3,5-dibromo-4-hydroxybenzoic acid (7); (*iii*) a variation in sulfur isotope effect (8) with a change in the concentration of Br^- in the bromodesulfonation of sodium *p*-methoxybenzenesulfonate ($k^{32}/k^{34} = 1.003$–1.017) and potassium 1-methylnaphthalene-4-sulfonate ($k^{32}/k^{34} = 1.002$–1.008); and (*iv*) a variation in hydrogen isotope effect in the iodination of *p*-nitrophenol (9) ($k^H/k^D = 2.3$–5.4) and of aniline (10) ($k^H/k^D = 2.4$–3.6) with a change in the concentration of iodide ion. These results provide unambiguous evidence in support of the two-step mechanism and also establish that the halogenating species that is involved is molecular halogen. Also, Zollinger *et al.* (11–13) have recently demonstrated very strongly by kinetic and nuclear magnetic resonance study the existence of a fairly long-lived intermediate I in the direct bromination of the disodium salt of 2-naphthol-6,8-disulfonic acid. This



I

intermediate is formed rapidly from reactants, builds up to measurable proportions, and then decomposes by a slow unimolecular step which is base catalyzed. In accordance with this mechanism the hydrogen isotope effect ($k^H/k^D = 1.48$–2.34) increased with the ratio of the concentration of reactants.

The kinetic data on the bromodeprotonation of sodium *p*-methoxybenzenesulfonate (temperature 0 °C; ionic strength 0.50 *M*) are given in Table I, where it can be seen that the product $k_{obs}{}^H(1 + K[Br^-])$ is not strictly a constant but diminishes by a considerable amount (~37%) over a range of Br^- concentration of 0 to 0.5 *M*. A similar decrease in rate has been observed in the bromination of substituted anisoles (14) and of 2,6-dibromo-

TABLE I

$[Br^-]$ (mole/l)	k_{obs}^H (l mole^{-1} s^{-1})	$k_{obs}^H(1 + K[Br^-])$ (l mole^{-1} s^{-1})
0.0000	0.0630	0.0630
0.0300	0.0600	0.0980
0.0700	0.0380	0.0940
0.100	0.0289	0.0898
0.200	0.0140	0.0731
0.300	0.00935	0.0685
0.400	0.00691	0.0652
0.500	0.00534	0.0616

phenol (15). Although this small decrease in rate eliminates any form of mechanism involving Br^+ (or H_2OBr^+) as the brominating species (see eqs. [6] and [7] of ref. 8), it can be accommodated readily by either mechanism I or mechanism II with Br_2 as the brominating agent.

The question which now arises is whether the *decrease* in $k_{obs}^H(1 + K[Br^-])$ is purely a salt effect resulting from the replacement of sodium perchlorate by sodium bromide as the Br^- concentration is increased (at constant ionic strength), or whether it is due, at least in part, to the return of a reaction intermediate to reactant. The fact that a plot of $\{k_{obs}^H(1 + K[Br^-])\}^{-1}$ versus $[Br^-]$ is linear (see Fig. 1[3] of ref. 8) is certainly in accordance with mechanism II, in which the depression of rate with increasing Br^- concentration results from the return of the intermediate. The answer to this question may be provided through a study of the kinetic hydrogen isotope effect at different Br^- concentrations. If the depression in rate is due entirely to a salt effect, the isotope effect should not vary with Br^- concentration. This result cannot distinguish between mechanism I and mechanism II, in which the rate of decomposition of the intermediate is fast relative to its return to reactant at all experimentally realizable bromide ion concentrations, i.e. $k_2[Br^-] \ll k_3$. If, however, any significant part of the depression in $k_{obs}^H(1 + K[Br^-])$ is due to the return of an intermediate to reactant (mechanism II), then this should manifest itself in an increase in k^H/k^D with increasing concentration of Br^-. This observation would provide the strongest possible evidence for the two-step mechanism. In view of this, the kinetic hydrogen isotope effect (k^H/k^D) as a function of Br^- concentration was measured for the bromodeprotonation of sodium *p*-methoxybenzenesulfonate.

EXPERIMENTAL

Reagents

Deuterium oxide that was claimed to be 99.4% pure came from Oak Ridge National Laboratory, Tennessee. Deuteriosulfuric acid was prepared by distilling sulfur trioxide into deuterium oxide and later adjusting the freezing point to 14.21 °C (the freezing point of pure deuteriosulfuric acid) with deuterium oxide. Acetic anhydride (Fisher certified reagent grade) was fractionally distilled through a long column, and the middle fraction, boiling at 139.5–140.5 °C, was collected. This procedure was carried out to ensure that the substance was free of moisture and acetic acid. All other chemicals that were used were the same as before (8).

Sodium p-Methoxybenzenesulfonate-O,O′-d_2

Several attempts were made to prepare this compound by direct exchange between sodium *p*-methoxybenzenesulfonate and deuteriosulfuric acid. The results were unsuccessful and it was concluded that the sulfonic acid group has a pronounced deactivating effect in the exchange of hydrogen atoms on the benzene ring. A similar conclusion was reached by Ingold *et al.* (16) after their unsuccessful attempts to deuterate benzenesulfonic acid by direct exchange with deuteriosulfuric acid. An alternative method is to prepare

[3]*The deviation from linearity of the point at* $[Br^-] = 0$ *in this plot is undoubtedly due to the large experimental error in the value used for the percentage of bromodeprotonation. At* $[Br^-] = 0$, *the sulfate yield is* $88 \pm 1\%$; *hence, bromodeprotonation is* $12 \pm 1\%$.

Can. J. Chem. Downloaded from www.nrcresearchpress.com by 210.87.254.40 on 09/05/12
For personal use only.

Can. J. Chem. Downloaded from www.nrcresearchpress.com by 210.87.254.40 on 09/05/12
For personal use only.

2,4,6-trideuterioanisole first and then sulfonate it under conditions such that there would be no exchange in the ortho positions. 2,4,6-Trideuterioanisole can be prepared in two ways: either by methylation of 2,4,6-trideuteriophenol or by the deuteration of anisole itself. For economic and practical reasons, the method adopted by Brown *et al.* (17), involving direct exchange between anisole and deuterioacetic acid (CH_3COOD) with sulfuric acid as catalyst, was found to be most suitable. This method has a distinct advantage over the direct exchange of anisole with deuteriosulfuric acid, in the following respects: the deuterium source (D_2O) needed for the operations is much less; the yield of deuterioanisole is greater; and the exchange is exclusively in the 2,4,6-positions of anisole, as desired.

The deuterioacetic acid that was required was prepared by treating acetic anhydride (3.45 moles) with deuterium oxide (3.45 moles). The mixture was heated under reflux for 10 h, every precaution being taken to exclude moisture. To the resulting deuterioacetic acid was added deuteriosulfuric acid (4 ml) as catalyst.

Anisole (25 g; 0.23 mole) was treated with deuterioacetic acid (2.76 moles) in a 500 ml round-bottomed flask whose upper neck was constricted for vacuum sealing. The system was frozen by means of liquid nitrogen and the flask was evacuated. With the stopcock closed, the contents were allowed to thaw and were then frozen again by liquid nitrogen. The system was again evacuated and the flask was sealed off. The flask, enclosed in a copper wire net, was immersed in an oil bath at 90 ± 0.1 °C for 48 h. At the end of this period the flask was removed and well cooled. It was then opened and its contents were carefully poured onto chipped ice. In the meantime, 320 ml of 9 *M* sodium hydroxide solution was cooled in ice. The solution in chipped ice was then slowly poured into the alkali solution with constant stirring, the system being kept well cooled. When the entire solution was added the final pH was about 8.

The separated anisole was extracted with ether in many portions, and the combined extracts were repeatedly washed with water until the washings were neutral to litmus. The ether extract was then dried thoroughly with anhydrous sodium sulfate and the ether was finally removed by vacuum distillation. The recovered anisole was further subjected to two similar exchanges, 2.07 moles of deuterioacetic acid being used each time. The alkali used for neutralization after these exchanges was 9 *M* sodium hydroxide (240 ml). In each of the three exchanges there was approximately 25–30% loss of anisole, the major loss being almost certainly due to its destruction on prolonged heating with the acid. The anisole that was finally obtained was distilled over metallic sodium, and the distillate boiling at 153–153.5 °C was collected. The final yield was 9 g, which is about 36% of the starting material.

A nuclear magnetic resonance spectrum of the deuterioanisole in carbon tetrachloride (the solution was ~25% by weight) is shown in Fig. 1, and that of ordinary anisole obtained under similar conditions in Fig. 2.

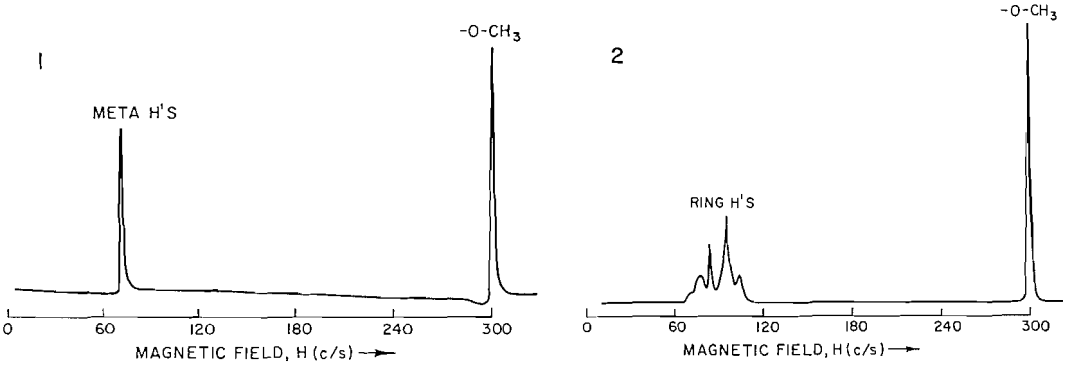


FIG. 1. Proton nuclear magnetic resonance spectrum of 2,4,6-trideuterioanisole at 60 Mc/s in carbon tetrachloride.

FIG. 2. Proton nuclear magnetic resonance spectrum of anisole at 60 Mc/s in carbon tetrachloride.

It can be seen that the multiple spectrum of the five hydrogens of the benzene ring in ordinary anisole is completely replaced by a single sharp peak (of 3,5-meta protons) in the deuterioanisole. The latter peak has two-thirds the area of that of the methyl protons, showing that the anisole is essentially completely deuterated in the 2,4,6-positions.

2,4,6-Trideuterioanisole (9 g; 0.083 mole) was sulfonated with chlorosulfonic acid (9.3 g; 0.08 mole) in 30 ml of carbon tetrachloride as solvent by the procedure described previously (8). The sulfonic acid was filtered and freed from any unreacted anisole by washing it with carbon tetrachloride. The solid acid was then carefully added to an ice-cold saturated solution of sodium carbonate, with constant stirring, such that when all the sulfonic acid was added the pH of the solution was about 7 to 8. The solution was then vacuum distilled at 50 °C to remove water. The dry solid that was left behind was then extracted with 80% ethanol in three portions of 100 ml, 50 ml, and 50 ml. The combined ethanol extracts were vacuum distilled, and the solid that was obtained was found to be almost free from inorganic impurities. It was then subsequently recrystallized twice from aqueous ethanol, and dried thoroughly at 110 °C before use.

Figure 3 shows the nuclear magnetic resonance spectrum of the deuterated sulfonate in deuterium oxide (the solution was 5% by weight), and Fig. 4 the spectrum of the unlabelled sulfonate obtained under similar

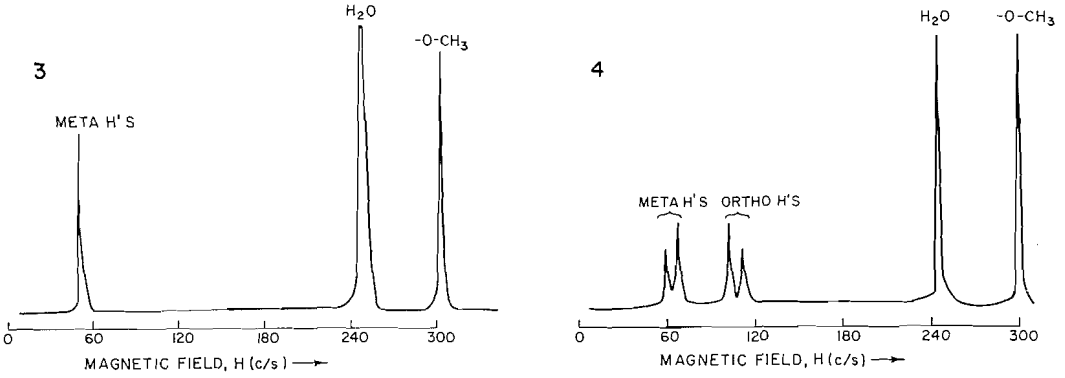


FIG. 3. Proton nuclear magnetic resonance spectrum of sodium *p*-methoxybenzenesulfonate-*O,O'*-d_2 at 60 Mc/s in D_2O.
FIG. 4. Proton nuclear magnetic resonance spectrum of sodium *p*-methoxybenzenesulfonate at 60 Mc/s in D_2O.

conditions. The spectrum of the unlabelled sulfonate consists of two doublets of the ortho and meta protons of the benzene ring. In the deuterated sulfonate the ortho doublet has completely disappeared and the meta doublet has coalesced into a single sharp peak. The latter peak has two-thirds the area of that of the methyl protons, showing that the sulfonate is essentially completely deuterated in the 2,6-positions.

Kinetics of Bromination

The experimental techniques used to measure the rates of bromination for the labelled and unlabelled sulfonates were the same as described previously (8). For the evaluation of bromodedeuteration rates in the bromination of the labelled sulfonate, the latter, being short in quantity, was not used for estimating the yield of sulfate. However, the desired ratio, k^H/k^D, can be obtained as follows. If $(k_{obs})_H$ and $(k_{obs})_D$ are the rate constants for the total bromination of unlabelled and labelled sulfonates, respectively, then

$$[1] \qquad \frac{(k_{obs})_H}{(k_{obs})_D} = \frac{k^S + k^H}{k^S + k^D} = \frac{k^S/k^H + 1}{k^S/k^H + k^D/k^H}$$

or

$$[2] \qquad \frac{k^H}{k^D} = \frac{\dfrac{(k_{obs})_H}{(k_{obs})_D}}{k^S/k^H\left[1 - \dfrac{(k_{obs})_H}{(k_{obs})_D}\right] + 1},$$

where k^S, k^H, and k^D are the rate constants for bromodesulfonation, bromodeprotonation, and bromodedeuteration, respectively. In deriving this equation the assumption is made that the rate constant, k^S, for bromodesulfonation is unaffected by deuterium substitution. Since k^S/k^H is known from the sulfate yield data for the unlabelled compound, the isotope effect can readily be evaluated.

RESULTS AND DISCUSSION

The kinetic isotope effects, k^H/k^D, for the bromodeprotonation of sodium *p*-methoxybenzenesulfonate over a range of Br^- concentration of 0 to 2 *M* are given in Table II, where it can be seen that there is a definite increase in the isotope effect with increasing Br^- concentration. Mechanism II is thus established. Now, if the depression in $k_{obs}{}^H(1 + K[Br^-])$ were due entirely to a return of the intermediate to reactant, then the slope of the linear plot of $\{k_{obs}{}^H(1 + K[Br^-])\}^{-1}$ versus $[Br^-]$ (this plot is shown in our preceding paper; see Fig. 1 of ref. 8) for the bromodeprotonation of sodium *p*-methoxybenzenesulfonate is k_2/k_1k_3 and the intercept is $1/k_1$. From these a value of 1.2 is calculated for the ratio k_2/k_3. That this value is much too high is evident from the small value of the

Can. J. Chem. Downloaded from www.nrcresearchpress.com by 210.87.254.40 on 09/05/12
For personal use only.

Can. J. Chem. Downloaded from www.nrcresearchpress.com by 210.87.254.40 on 09/05/12
For personal use only.

TABLE II

Kinetic hydrogen isotope effects for the bromodeprotonation reaction of sodium *p*-methoxybenzenesulfonate at 0 °C
(rate constants expressed in liters/mole second)

Ionic strength (M)	[Br^-] (moles/l)	$(k_{obs})_H$* $\times 10^3$	$(k_{obs})_D$* $\times 10^3$	$(k^S/k^H)_H$†	k^H/k^D Found	k^H/k^D Calcd.
0.50	0.0000	538±4	536±4	7.47	1.01±0.02‡	1.00
	0.100	54.9±0.5	54.4±0.2	0.901	1.02±0.02	1.02
	0.500	6.76±0.035	6.42±0.02	0.263	1.07±0.01	1.08
1.00	0.500	9.44±0.03	8.94±0.04	0.241	1.07±0.01	1.08
	1.000	4.24±0.026	3.67±0.018	0.119	1.18±0.02	1.16
2.00	2.00	3.04±0.012	2.34±0.012	0.0417§	1.31±0.02	1.31

*Precision limits are calculated from the standard deviation of slope of the least-square plot of $\log_{10}(A_0 - B_0 + B)/B$ versus t.
†$(k^S/k)_H$ = percentage of bromodesulfonation/percentage of bromodeprotonation for the undeuterated sulfonate.
‡Estimated maximum overall error based on variation in the $(k^S/k^H)_H$ and rate constant values.
§The sulfate yield at [Br^-] = 2 M was estimated to be 4%. An accurate experimental determination was not possible at this concentration of salt.

isotope effect (see Table II) and its relative insensitivity to changes in the concentration of bromide ion. Thus, if this ratio were correct, then at $[Br^-] = 2\ M$, for every seven molecules of the intermediate formed, five would return to reactant and only two would proceed to product. This is approaching an equilibrium condition between reactant and intermediate and would be expected to give rise to an isotope effect, k^H/k^D, of several fold.

An estimate of the true k_2/k_3 ratio, and with it the quantity k_3^H/k_3^D, the isotope effect for the C—H bond rupture step, can be obtained by a trial and error substitution into eq. [3][4] to give the best fit to the experimental values of k^H/k^D at the different concentrations of Br^-.

$$[3] \qquad \frac{k^H}{k^D} = \frac{k_1^H}{k_1^D} \cdot \frac{\frac{k_3^H}{k_3^D} \cdot \frac{k_2^H}{k_3^H} \cdot [Br^-] + 1}{\frac{k_2^H}{k_3^H} \cdot [Br^-] + 1}$$

In deriving this equation the reasonable assumption is made that the isotope effect for the return of the intermediate to reactants, k_2^H/k_2^D, is unity. The isotope effect at $[Br^-] = 0$, k_1^H/k_1^D, is, as seen from Table II, also unity. This procedure leads to $k_2/k_3 = 0.027$ and $k_3^H/k_3^D = 7.0$. The fit to the experimental data obtained by substitution of these values into eq. [3] can be seen by comparing the last two columns in Table II.[5]

The value obtained for k_2/k_3 (0.027) from isotope effect results is to be compared with the value (1.2) obtained on the assumption that the depression in $k_{obs}^H(1 + K[Br^-])$ with $[Br^-]$ (Fig. 1 of ref. 8) is due entirely to an increasing return of the intermediate to reactants as the Br^- concentration is increased. Clearly, therefore, almost all this depression in rate is the result of the salt effect. Indeed, it was fortunate that there was sufficient return of the intermediate to give a fruitful result in the application of the isotope effect test for the two-step mechanism. To our knowledge, the present work constitutes the first reported study of *variation* in kinetic hydrogen isotope effect during bromodeprotonation by variation of bromide ion concentration.

It is of interest to note that the isotope effect for the second step, k_3^H/k_3^D, is 7.0, which is about the value to be expected for C—H bond rupture in a reaction at 0 °C. Finally, it is most important to note that the ratio k_1^H/k_1^D, which is the ratio of the rates of formation of the intermediate from the two isotopic sulfonates, is unity within a precision of about ±0.02. The absence of a significant secondary isotope effect in this reaction is to be compared with other results, shown in Table III, where secondary effects of appreciable magnitude have been observed.

TABLE III

Reaction	Isotope effect	Reference
Bromination of benzene	$k^H/k^D = 0.97$	18
Bromination of diphenyl	$k^H/k^D = 1.15$	5
Nitration of benzene	$k^H/k^D = 0.893$	19
Nitration of toluene	$k^H/k^D = 0.855$	19
Nitration of fluorobenzene	$k^H/k^D = 0.820$	20
Chlorination of benzene	$k^H/k^D = 0.870$	21
Azo-coupling of 1,3,5-trimethoxybenzene with *p*-chlorodiazonium ion	$k^H/k^T = 0.885$	22

[4]*The corresponding equation for the sulfur isotope effect is given in our preceding paper (see eq. [9] of ref. 8).*

[5]*It is recognized that the k_2/k_3 ratio will not be entirely independent of ionic strength. The fact, however, that the isotope effect at two ionic strengths for $[Br^-] = 0.5\ M$ is the same within the limits of measurement indicates that the k_2/k_3 ratio is rather insensitive to changes in ionic strength.*

Can. J. Chem. Downloaded from www.nrcresearchpress.com by 210.87.254.40 on 09/05/12
For personal use only.

It is suggested that the similar rate of formation of the intermediate in the bromodeprotonation of undeuterated and deuterated sodium *p*-methoxybenzenesulfonate is a consequence of a fortuitous cancellation in the transition state of the effect of hyperconjugation and of the rehybridization of the carbon orbitals from sp^2 to sp^3 (2, 23).

ACKNOWLEDGMENTS

We thank Dr. R. J. Gillespie for recording the nuclear magnetic resonance spectra. The financial assistance of Dow Chemical of Canada is gratefully acknowledged.

REFERENCES

1. P. B. D. De La Mare and J. H. Ridd. Aromatic substitution. Butterworth Scientific Publications, London. 1959.
2. E. Berliner. *In* Progress in physical organic chemistry. Vol. 2. Interscience Publishers, Inc., New York. 1964. p. 253.
3. A. Grimison and J. H. Ridd. J. Chem. Soc. 3019 (1959).
4. E. Berliner. J. Am. Chem. Soc. **82**, 5435 (1960).
5. E. Berliner and K. E. Schueller. Chem. Ind. London, 1444 (1960).
6. H. Zollinger. Helv. Chim. Acta, **38**, 1597 (1955); **38**, 1617 (1955).
7. E. Grovenstein and G. A. Ropp. J. Am. Chem. Soc. **78**, 2560 (1956).
8. B. T. Baliga and A. N. Bourns. Can. J. Chem. This issue.
9. E. Grovenstein and N. S. Aprahamian. J. Am. Chem. Soc. **84**, 212 (1962).
10. F. M. Vainshtein, E. A. Shilov, and E. T. Tomilenko. Kinetika i Kataliz, **4**, 357 (1963).
11. M. Christen and H. Zollinger. Helv. Chim. Acta, **45**, 2057 (1962).
12. M. Christen and H. Zollinger. Helv. Chim. Acta, **45**, 2066 (1962).
13. M. Christen, W. Koch, W. Simon, and H. Zollinger. Helv. Chim. Acta, **45**, 2077 (1962).
14. R. P. Bell and D. J. Rawlinson. J. Chem. Soc. 63 (1961).
15. E. Grovenstein and U. V. Henderson. J. Am. Chem. Soc. **78**, 569 (1956).
16. C. K. Ingold, G. G. Raisin, and C. L. Wilson. J. Chem. Soc. 1637 (1936).
17. W. G. Brown, K. E. Wilzbach, and W. H. Urry. Can. J. Res., B, **27**, 398 (1949).
18. P. B. D. De La Mare, T. M. Dunn, and J. T. Harvey. J. Chem. Soc. 923 (1957).
19. G. A. Olah, S. J. Kuhn, and S. H. Flood. J. Am. Chem. Soc. **83**, 4571 (1961).
20. G. A. Olah, S. J. Kuhn, and S. H. Flood. J. Am. Chem. Soc. **83**, 4581 (1961).
21. G. A. Olah, S. J. Kuhn, and B. A. Hardie. J. Am. Chem. Soc. **86**, 1055 (1964).
22. E. Helgstrand and B. Lamm. Arkiv Kemi, **20**, 193 (1962).
23. E. A. Halevi. *In* Progress in physical organic chemistry. Vol. 1. Interscience Publishers, Inc., New York. 1963. p. 109.

Can. J. Chem. Downloaded from www.nrcresearchpress.com by 210.87.254.40 on 09/05/12
For personal use only.

Can. J. Chem. Downloaded from www.nrcresearchpress.com by 210.87.254.40 on 09/05/12
For personal use only.

THE SYNTHESIS OF 5-DIMETHYLAMINOINDOLE AND DERIVATIVES[1]

JOSEPH I. DEGRAW
Life Sciences Research, Stanford Research Institute, Menlo Park, California

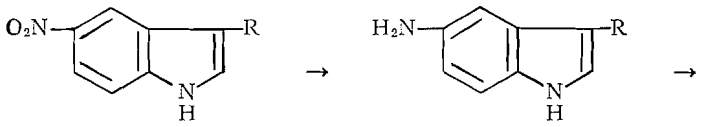
Received August 17, 1965

ABSTRACT

The preparation of 5-dimethylaminoindole is described. This compound underwent the usual reactions typical of 3-unsubstituted indoles, and various 3-substituted derivatives were prepared. Syntheses for 5-dimethylaminotryptophan, 5-dimethylaminotryptamine, 5-dimethylamino-N,N-dimethyltryptamine, and 5-dimethylamino-α-methyltryptamine are reported.

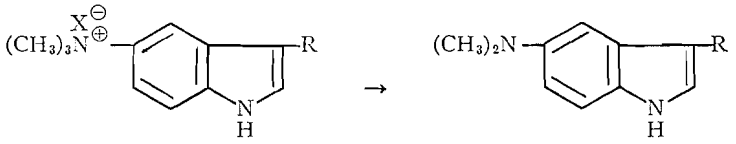
The preparation of some 2-methyl-5-dimethylaminoindoles bearing a substituent at the 3-position was reported by Shaw (1) in 1954. This appears to be the only work done in this area, and the simplest member of this class of indoles, 5-dimethylaminoindole (IV*a*), has not been described. A synthesis of IV*a* starting from 5-nitroindole (I*a*) has been achieved by employing Shaw's general method. Several reactions pertinent to 3-unsubstituted indoles could be carried out on this compound, and various substituents were introduced at the 3-position.

The preparation of 5-aminoindole (II*a*) from 5-nitroindole (I*a*) has previously been accomplished by catalytic hydrogenation (2), but the extreme sensitivity of II*a* to air oxidation presents a problem in the work-up and purification. A more convenient reduction of I*a* was achieved with hydrazine and palladium in boiling ethanol to give a high yield of II*a*, which, when used immediately, required no further purification. The aminoindole (II*a*) was then treated with excess dimethyl sulfate, and the quaternized base was isolated as its picrate salt (III*a*). Stirring the picrate with Dowex 2 (chloride) resin readily converted it into the chloride (III*b*). Treatment of III*b* with sodium propoxide in boiling *n*-propanol effected demethylation to yield 5-dimethylaminoindole (IV*a*) in an overall yield of 53% from 5-nitroindole (I*a*).



I*a*, R = H
I*b*, R = CH_2CN

II*a*, R = H
II*b*, R = CH_2CN



III*a*, R = H, X = picrate
III*b*, R = H, X = Cl
III*c*, R = CH_2CN, X = picrate
III*d*, R = CH_2CN, X = Cl

IV*a*, R = H
IV*b*, R = CH_2CN

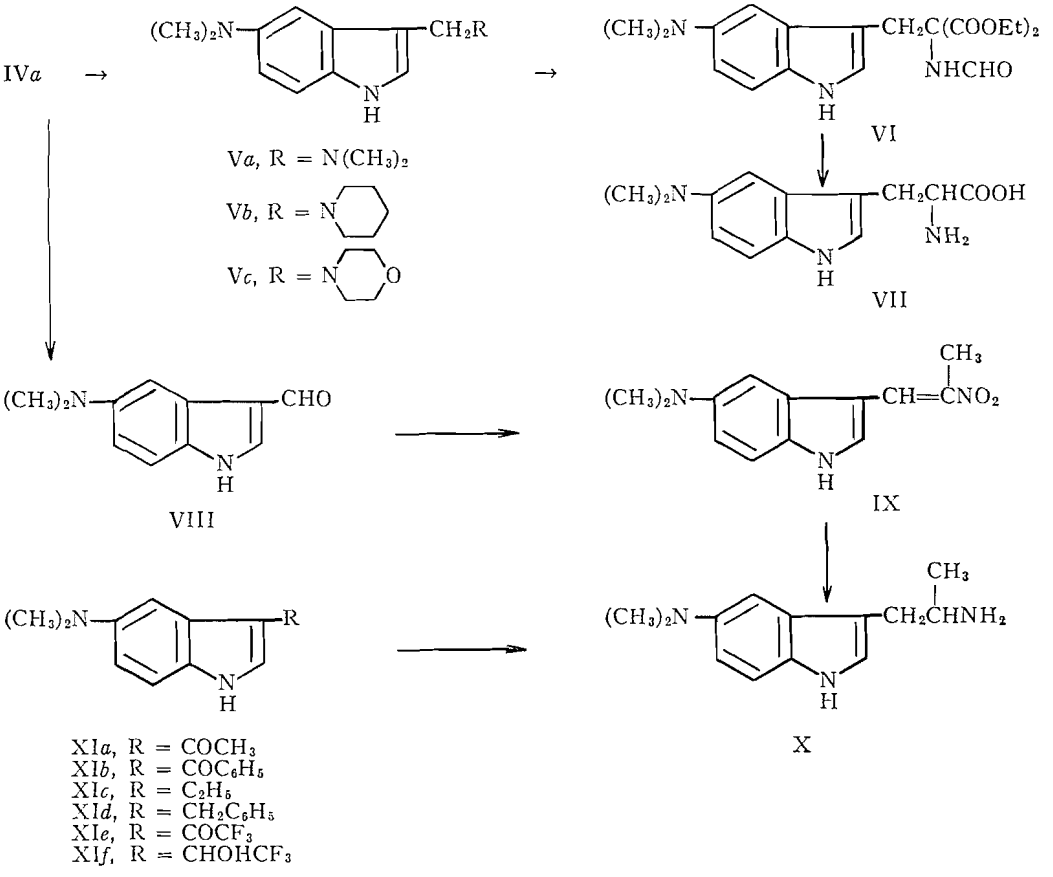
[1]*This work was supported by the United States Army Chemical Research and Development Laboratories, Edgewood Arsenal, Maryland.*

Can. J. Chem. Downloaded from www.nrcresearchpress.com by 210.87.254.40 on 09/05/12
For personal use only.

When IV*a* was treated with aqueous formaldehyde and secondary amines under the usual Mannich conditions, the 3-dialkylaminomethyl compounds (V*a*–V*c*) were obtained. Reaction of the gramine V*a* with diethyl formamidomalonate followed by acid hydrolysis and decarboxylation of the resulting amido diester (VI) gave 5-dimethylaminotryptophan (VII) as the hydrochloride salt. The biological properties of VII may be of interest; however, the related 5-aminotryptophan (3) did not seem to possess significant physiological activity (4).

Formylation of IV*a* with the phosphoryl chloride – dimethylformamide reagent according to the general procedure of Smith (5) gave the aldehyde (VIII) in a 51% yield. The aldehyde could not be condensed with nitromethane either by catalysis with ammonium acetate (6) or by water separation methods. However, VIII reacted quite readily with nitroethane and ammonium acetate to yield the nitrone (IX). Reduction of IX with lithium aluminium hydride produced 5-dimethylamino-α-methyltryptamine (X), which was isolated as its bis picrate salt.

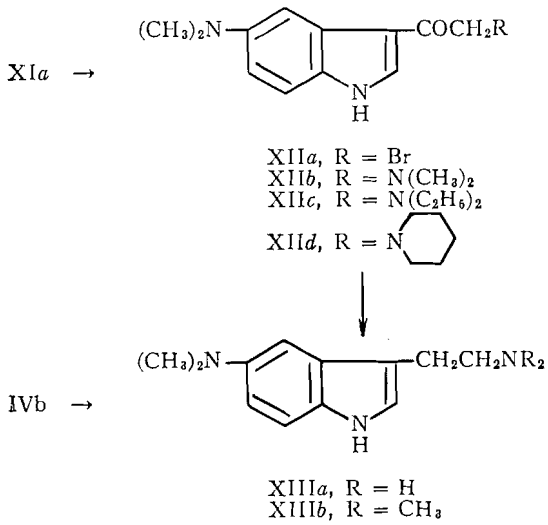
If IV*a* was allowed to react with acetyl chloride or benzoyl chloride in the presence of stannic chloride (7, 8), the 3-position was readily acylated to yield the methyl ketone (XI*a*) or the phenyl ketone (XI*b*). Reduction of the ketones with lithium aluminium hydride proceeded very smoothly, and 5-dimethylamino-3-ethylindole (XI*c*) and 5-dimethylamino-3-benzylindole (XI*d*) were obtained. When 5-dimethylaminoindole was stirred with trifluoroacetic anhydride for a few hours, the 3-trifluoromethylketone (XI*e*) was obtained. This ketone was reduced to the corresponding alcohol (XI*f*) with sodium borohydride.



XI*a*, R = $COCH_3$
XI*b*, R = COC_6H_5
XI*c*, R = C_2H_5
XI*d*, R = $CH_2C_6H_5$
XI*e*, R = $COCF_3$
XI*f*, R = $CHOHCF_3$

The methyl ketone was treated with bromine in warm methanol (9) to give the bromoketone (XII*a*) in a poor yield. Displacement of the bromine atom with secondary amines in hot isopropanol generated the 5-dimethylamino-α-alkylaminomethylketones (XII*b*–XII*d*). The α-dimethylamino ketone (XII*b*) was reduced with lithium aluminium hydride to yield 5-dimethylamino-N,N-dimethyltryptamine (XIII*b*), characterized as its picrate salt.

A better method for the synthesis of 5-dimethylaminotryptamines was to hydrogenate 5-dimethylamino-3-indoleacetonitrile (IV*b*) in the presence of an excess of an appropriate amine. 5-Dimethylaminotryptamine (XIII*a*) and its N,N-dimethyl derivative (XIII*b*) were readily prepared in this manner. The nitrile (IV*b*) was prepared from 5-nitro-3-indoleacetonitrile (2*a*, 10) (I*b*) by the sequence I*b* → IV*b*.



EXPERIMENTAL

5-Aminoindole (IIa)

To a mixture of 25.0 g of 5-nitroindole (I), 1.2 g of 10% palladium on carbon, and 200 ml of absolute ethanol was slowly added 25 ml of 98–100% hydrazine. After the resulting exothermic reaction had subsided, the mixture was boiled under reflux for 2 h. The catalyst was removed by filtration and the filtrate was evaporated to leave a yellow solid residue. The crystals were shaken with 200 ml of water and collected, and the cake was dried *in vacuo* to leave 16.5 g (81%) of 5-aminoindole. In this work the aqueous wash was decanted and the damp residue used immediately in the next step to minimize exposure to the air. Recrystallization of a portion from benzene gave a sample, m.p. 131–134° (lit. (2*a*) m.p. 132–133°).

5-Indolyltrimethylammonium Picrate (IIIa)

To a mixture of 2 g (15.5 mmoles) of 5-aminoindole in 32 ml of water containing 5.7 g (68 mmoles) of sodium bicarbonate was added 6.20 ml (65.5 mmoles) of dimethyl sulfate over 12 min with stirring. The resulting dark solution was stirred another 10 min, warmed to 65°, and poured into a warm solution of 3.60 g (15.7 mmoles) of picric acid in 240 ml of water. The yellow, crystalline precipitate was allowed to stand for 2 h. It was collected, washed thoroughly with water and ether, and dried to leave 5.2 g (85%) of the picrate. Recrystallization from 75% ethanol yielded 4.3 g (70%), m.p. 171–173°. An analytical sample, m.p. 172–174°, was obtained by recrystallization from absolute ethanol.

Anal. Calcd. for $C_{17}H_{17}N_5O_7$: C, 50.6; H, 4.25; N, 17.4. Found: C, 50.8; H, 4.58; N, 17.8.

5-Indolyltrimethylammonium Chloride (IIIb)

A mixture of 300 g of Dowex 2 (chloride) resin, 46.0 g of the picrate (III*a*), and 1 200 ml of 83% methanol was stirred for 17 h at room temperature. The resin was removed by filtration and washed with 100 ml of methanol. The filtrate was evaporated *in vacuo* to leave a dark sirup, which was dissolved in 120 ml of hot isopropanol and diluted with 800 ml of acetone. The dark gum that precipitated was removed by decantation and the supernatant was diluted with another 700 ml of acetone. The solution was chilled for 3 days to yield

Can. J. Chem. Downloaded from www.nrcresearchpress.com by 210.87.254.40 on 09/05/12
For personal use only.

beige crystals, which were collected, washed with acetone, and dried to leave 13.5 g (57%) of product, m.p. 200–201°. An analytical sample, previously obtained in the same manner from another run, had m.p. 188–191°.

Anal. Calcd. for $C_{11}H_{15}ClN_2$: C, 62.7; H, 7.17; N, 13.3. Found: C, 62.8; H, 7.35; N, 13.0.

5-Dimethylaminoindole (IVa)

To a solution of 1.54 g (0.067 g-atom) of sodium in 270 ml of *n*-propanol was added 13.0 g (62 mmoles) of 5-indolyltrimethylammonium chloride, and the mixture was stirred at reflux for 17 h. It was evaporated to dryness *in vacuo* and the residue partitioned between 100 ml of water and 100 ml of ether. The aqueous portion was extracted with another 50 ml of ether, followed by washing of the combined ether extracts with 50 ml of water. The ether solution was dried over magnesium sulfate and evaported *in vacuo* to leave 8.2 g of a dark sirup. The sirup was distilled at reduced pressure; a total of 7.5 g (76%) of IV*a* as a clear liquid was collected at b.p. 135–140° and 0.25 mm. The liquid solidified to form white crystals, m.p. 45–47°. A sample that was sublimed for analysis had m.p. 49–50°; λ_{max}^{EtOH} 238 mμ (ε 22 900).

Anal. Calcd. for $C_{10}H_{12}N_2$: C, 75.0; H, 7.56; N, 17.5. Found: C, 75.1; H, 7.47; N, 17.4.

An optimum yield of 53% from 5-nitroindole was realized by using the crude intermediates (no purification whatever) directly in the following steps. The final distillation of IV*a* was sufficient for its purification.

3-Cyanomethylindole-5-trimethylammonium Picrate (IIIc)

To a mixture of 1.17 g (5.8 mmoles) of 5-nitro-3-indoleacetonitrile (10), 50 mg of 5% palladium on carbon, and 10 ml of absolute ethanol was added 0.90 ml (28 mmoles) of 100% hydrazine. When the resulting reaction had subsided, the mixture was boiled under reflux for 1.5 h. The catalyst was removed by filtration and the solvent was evaporated *in vacuo* to leave an amber sirup, whose infrared spectrum was in agreement with that of the aminonitrile (II*b*). The crude material was mixed with 2 ml of ethanol, 12 ml of water, and 2.20 g (26 mmoles) of sodium bicarbonate. Then, with stirring, was added 2.40 ml (25 mmoles) of dimethyl sulfate over 5 min. The mixture was stirred for 15 min and the resulting solution was heated at 65° for 5 min. A warm solution of 1.5 g of picric acid in 90 ml of water was added to give a yellow, crystalline precipitate. The picrate was collected, thoroughly washed with water, and dried to leave 1.90 g (73%), m.p. 181–206°. The crude picrate was stirred with 30 ml of hot methanol and chilled for 2 days to yield 1.60 g, m.p. 212–224°. An analytical sample, m.p. 221–224°, was obtained by recrystallization from methanol.

Anal. Calcd. for $C_{19}H_{18}N_6O_7$: C, 51.6; H, 4.10; N, 19.0. Found: C, 51.8; H, 3.97; N, 19.0.

3-Cyanomethylindole-5-trimethylammonium Chloride (IIId)

A mixture of 1.60 g of the picrate (III*c*), 10 g of Dowex 2 (chloride) resin, and 50 ml of 90% methanol was stirred for 3 h. The resin was removed by filtration and washed with a little methanol, and the filtrate was evaporated *in vacuo* to leave 0.90 g (90%) of III*d* as dark crystals. A recrystallization from 10 ml of ethanol yielded 0.68 g of tan crystals, m.p. 221–223°. Another recrystallization from ethanol yielded an analytical sample of off-white crystals, m.p. 220–221°.

Anal. Calcd. for $C_{13}H_{16}ClN_3$: C, 62.5; H, 6.45; N, 16.8. Found: C, 62.1; H, 6.32; N, 17.0.

5-Dimethylamino-3-indoleacetonitrile (IVb)

To a solution of 62 mg (2.7 mg-atoms) of sodium in 12 ml of *n*-propanol was added 600 mg (2.4 mmoles) of the methochloride (III*d*), and the mixture was boiled under reflux for 16 h. The solvent was removed *in vacuo* and the dark residue was partitioned between 20 ml of water and 20 ml of ether. The dark aqueous portion was extracted with another 20 ml of ether and the combined ether extracts were washed with 10 ml of water. The ether was dried over magnesium sulfate and evaporated to leave 340 mg of tan crystals, which were recrystallized from benzene (4 ml) to give 210 mg, m.p. 121–122°; λ_{max}^{Nujol} 3.20 μ (NH), 4.48 μ (C≡N).

Anal. Calcd. for $C_{12}H_{13}N_3$: C, 72.3; H, 6.57; N, 21.1. Found: C, 72.5; H, 6.49; N, 21.1.

3-Dimethylaminomethyl-5-dimethylaminoindole (Va)

A solution of 0.50 g (3.1 mmoles) of 5-dimethylaminoindole, 0.60 ml (3.3 mmoles) of 25% aqueous dimethylamine, 0.28 ml (3.5 mmoles) of 37% formaldehyde, and 2 ml of acetic acid was heated at 50° for 2 h. The solution was chilled and adjusted to pH 10–11 with 10% sodium hydroxide to give a white precipitate, which was collected, washed with water, and dried to leave 0.37 g. Recrystallization from 4 ml of cyclohexane yielded 0.20 g (29%) of V*a* as white crystals, m.p. 110–111°.

Anal. Calcd. for $C_{13}H_{19}N_3$: C, 71.9; H, 8.83; N, 19.4. Found: C, 72.0; H, 8.68; N, 19.2.

The bis methiodide, m.p. 220–225° (decomp.), was prepared in an 80% yield by treatment of V*a* with an excess of methyl iodide in alcohol.

Anal. Calcd. for $C_{15}H_{25}N_3I_2$: I, 50.6. Found: I, 50.0.

3-Piperidinomethyl-5-dimethylaminoindole (Vb)

This compound, m.p. 112–115°, was prepared in a 59% yield by a procedure analogous to that used for V*a*.

Anal. Calcd. for $C_{16}H_{23}N_3$: C, 74.7; H, 9.01; N, 16.3. Found: C, 75.0; H, 8.84; N, 16.1.

Can. J. Chem. Downloaded from www.nrcresearchpress.com by 210.87.254.40 on 09/05/12
For personal use only.

3-Morpholinomethyl-5-dimethylaminoindole (Vc)

This compound, m.p. 82–85°, was prepared in a 15% yield by a procedure analogous to that used for V*a*.

Anal. Calcd. for $C_{15}H_{21}N_3O$: C, 69.5; H, 8.16; N, 16.2. Found: C, 69.7; H, 8.21; N, 16.1.

Diethyl 5-Dimethylamino-3-indolylmethylformamidomalonate (VI)

A mixture of 500 mg (2.3 mmoles) of 5-dimethylaminogramine, 470 mg (2.3 mmoles) of diethyl formamidomalonate, 60 mg (1.5 mmoles) of powdered sodium hydroxide, and 20 ml of toluene was stirred under reflux for 15 h in a nitrogen atmosphere. It was cooled to 70–80° and filtered, followed by evaporation of the filtrate *in vacuo* to a volume of 10 ml. The solution was chilled for 1 h, and the resulting white crystals were collected, washed with 3 ml of toluene, and dried to leave 580 mg of the amido diester (VI), m.p. 171–176°. Recrystallization from 10 ml of ethanol gave 420 mg (49%) of white crystals, m.p. 177–179°; λ_{max}^{Nujol} 3.05 μ, 3.15 μ (NH); 5.72 μ (ester C=O); 5.99 μ (amide C=O).

Anal. Calcd. for $C_{19}H_{25}N_3O_5$: C, 60.8; H, 6.72; N, 11.2. Found: C, 60.8; H, 6.91; N, 11.1.

5-Dimethylamino-dl-tryptophan (VII)

A solution of 350 mg of the formamidomalonate (VI) in 8 ml of 3 *N* hydrochloric acid was boiled under reflux for 1.5 h. The solution was evaporated to dryness *in vacuo* to give a sirup that was crystallized when mixed with 10 ml of acetone. The crystals were collected, washed with acetone, and dried to leave 160 mg (54%) of the amino acid hydrochloride, m.p. 208–212°; λ_{max}^{pH13} 232 mμ (ϵ 26 100). A thin-layer chromatoplate (cellulose, 1.5 *N* ammonia) showed a single ultraviolet-absorbing spot, R_f 0.8.

Anal. Calcd. for $C_{13}H_{17}N_3O_2 \cdot 2HCl \cdot H_2O$: C, 46.2; H, 6.27; N, 12.4; Cl, 21.0. Found: C, 46.2; H, 6.00; N, 11.9; Cl, 19.6.

The material was quite hygroscopic. A portion was dissolved in hot isopropanol and precipitated out with acetone to yield white crystals, m.p. 220–222°. A chromatoplate (cellulose, *n*-butanol – acetic acid – water (4:1:5)) showed a single spot, R_f 0.5, as detected by iodine vapor.

Anal. Calcd. for $C_{13}H_{17}N_3O_2 \cdot 1.5HCl \cdot H_2O$: C, 48.9; H, 6.32; N, 13.1; Cl, 16.7. Found: C, 49.0; H, 6.53; N, 12.9; Cl, 16.7.

3-Formyl-5-dimethylaminoindole (VIII)

To 1.0 ml of dimethylformamide at 5° was added 0.3 ml (3.4 mmoles) of phosphoryl chloride, the temperature being kept at 10–15°. A solution of 0.50 g (3.1 mmoles) of 5-dimethylaminoindole in 0.60 ml of dimethylformamide was added over 5 min, the temperature being maintained at 20–25°. The mixture was kept for 2 h at room temperature and diluted with 15 ml of ice water, with stirring, to give a yellow solution. The pH was adjusted to 10–11 with 10% sodium hydroxide to give a yellow, crystalline precipitate. The mixture was warmed on the steam bath for about 5 min, with the addition of small amounts of alkali to maintain the pH at 10–11. The precipitate was stirred for 20 min and was filtered. The yellow cake was thoroughly washed with water and dried to give 0.49 g of the aldehyde, m.p. 195–198°. A recrystallization from 12 ml of ethanol yielded 0.3 g (51%) of yellow crystals, m.p. 214.5–217.0°; λ_{max}^{Nujol} 3.15 μ (NH), 6.10 μ (aldehyde C=O); λ_{max}^{EtOH} 240 mμ (ϵ 19 300), 282 mμ (ϵ 11 500).

Anal. Calcd. for $C_{11}H_{12}N_2O$: C, 70.2; H, 6.43; N, 14.9. Found: C, 70.1; H, 6.47; N, 15.1.

1-(5-Dimethylamino-3-indolyl)-2-nitro-1-propene (IX)

A solution of 300 mg of 5-dimethylamino-3-formylindole and 120 mg of ammonium acetate in 5 ml of nitroethane was heated on the steam bath for 1.5 h in an open flask. The dark red solution was evaporated *in vacuo* and the residual sirup was stirred with 10 ml of water, thereby causing crystallization. The red-black crystals were collected, washed with water and ether, and dried to leave 290 mg of product. A recrystallization from 5 ml of ethanol yielded 145 mg, m.p. 168–170°; λ_{max}^{Nujol} 3.1 μ (NH), 6.18 μ (C=C), 7.9 μ (NO_2); λ_{max}^{EtOH} 238 mμ (ϵ 25 400), 415 mμ (ϵ 13 300).

Anal. Calcd. for $C_{13}H_{15}N_3O_2$: C, 63.7; H, 6.16; N, 17.1. Found: C, 63.9; H, 6.44; N, 17.2.

5-Dimethylamino-α-methyltryptamine Picrate (X)

The nitrone (IX) (1.23 g) was reduced with 1.9 g of lithium aluminium hydride in 30 ml of tetrahydrofuran by boiling the solution under reflux for 15 h. The excess hydride was cautiously decomposed at 0–5° by the addition of ethanol, followed by water. The solvent was removed *in vacuo* and the residue was suspended in 100 ml of ether. Water was added until the solid material became pasty, but mobile. The mixture was shaken thoroughly and the ether layer was decanted. Another 20 ml ether extraction was similarly conducted. The ether extract was dried over magnesium sulfate and evaporated *in vacuo* to leave 0.92 g of an amber sirup. The infrared spectrum showed loss of the nitro band at 7.9 μ. The sirup was dissolved in 10 ml of ethanol and added to 2.7 g of picric acid in 150 ml of warm water. The yellow, crystalline picrate was collected and recrystallized from 15 ml of acetone–ethanol (3:2) to give 1.1 g, m.p. 203–206°. A 200 mg portion was further recrystallized from 3 ml of acetone to yield 121 mg, m.p. 215.5–216.5°.

Anal. Calcd. for $C_{25}H_{25}N_9O_{14}$: C, 44.9; H, 3.73; N, 18.7. Found: C, 44.7; H, 3.82; N, 19.1.

3-Acetyl-5-dimethylaminoindole (XIa)

To an ice-cold, stirred solution of 0.50 g (3.1 mmoles) of 5-dimethylaminoindole (IV*a*) in 8 ml of benzene

Can. J. Chem. Downloaded from www.nrcresearchpress.com by 210.87.254.40 on 09/05/12
For personal use only.

was slowly added 0.32 ml (4.5 mmoles) of acetyl chloride. Then 0.93 ml (8.0 mmoles) of anhydrous stannic chloride in 2 ml of benzene was added over 10 min to precipitate an orange complex. The mixture was stirred for 1.75 h at room temperature and then poured into 25 ml of ice water. The benzene layer was removed and the aqueous portion was made strongly alkaline with 10% sodium hydroxide. The mixture was extracted with three 15 ml portions of ethyl acetate, which were combined, washed with 10 ml of water, and dried over magnesium sulfate. The solvent was evaporated to leave 0.53 g of a pale yellow, crystalline residue. The residue was treated with 15 ml of ether and the solid collected to give 0.37 g (59%) of XI*a* as yellow crystals, m.p. 223–231°. A recrystallization from ethyl acetate yielded an analytical sample, m.p. 227–230°; λ_{max}^{EtOH} 240 mμ (ϵ 20 900), 282 mμ (ϵ 9 900).

Anal. Calcd. for $C_{12}H_{14}N_2O$: C, 71.3; H, 6.98; N, 13.8. Found: C, 70.9; H, 6.87; N, 14.1.

3-Benzoyl-5-dimethylaminoindole (XIb)

To a well-stirred, ice-cold solution of 1.00 g (6.2 mmoles) of 5-dimethylaminoindole in 15 ml of benzene was slowly added 1.04 ml (9.0 mmoles) of benzoyl chloride. Then, at 0–5°, 1.86 ml (16 mmoles) of stannic chloride in 6 ml of benzene was added over 10 min. Stirring was continued for 1.5 h at room temperature and the mixture was poured into 100 ml of ice water. After the mixture was warmed on the steam bath to obtain complete solution, 10% sodium hydroxide was added until a pH of about 12 was reached. The resulting yellow precipitate was extracted with three 25 ml portions of *n*-butanol, dried over magnesium sulfate, and evaporated to dryness *in vacuo*. The residue was recrystallized from 25 ml of ethanol to yield 1.10 g (67%) of XI*b*, m.p. 213–214°.

Anal. Calcd. for $C_{17}H_{16}N_2O$: C, 77.3; H, 6.10; N, 10.6. Found: C, 76.9; H, 6.38; N, 10.4.

3-Ethyl-5-dimethylaminoindole Picrate (XIc)

5-Dimethylamino-3-acetylindole (XI*a*, 1.27 g) was reduced with 0.50 g of lithium aluminium hydride in 20 ml of tetrahydrofuran by boiling the mixture under reflux for 2.5 h. The excess hydride was destroyed with a little ethanol and water. The solvent was evaporated, the residue was diluted with 25 ml of ether, and enough water was added to create a pasty aqueous phase. The mixture was shaken and the ether decanted. Another extraction with 25 ml of ether was performed, and the ether was dried over magnesium sulfate and evaporated to leave 1.04 g of sirup. The sirup, in 10 ml of ethanol, was added to 1.6 g of picric acid in 120 ml of hot water to yield 2.1 g of the yellow, crystalline picrate. A recrystallization from 200 ml of 90% ethanol gave 1.15 g of yellow crystals, m.p. 197–198°. An analytical sample, m.p. 200–202°, was obtained by a similar recrystallization of material from another run.

Anal. Calcd. for $C_{18}H_{19}N_5O_7$: C, 51.8; H, 4.59; N, 16.8. Found: C, 52.1; H, 4.83; N, 17.0.

3-Benzyl-5-dimethylaminoindole (XId)

The phenyl ketone (XI*b*, 3.30 g) was reduced with lithium aluminium hydride (1.00 g) as described above to yield 3.05 g (99%) of XI*d* as the crystalline free base. A recrystallization from 40 ml of cyclohexane, with carbon treatment, yielded 1.60 g (52%) of white crystals, m.p. 63–64°.

Anal. Calcd. for $C_{17}H_{18}N_2$: C, 81.6; H, 7.25; N, 11.2. Found: C, 81.2; H, 7.19; N, 11.2.

3-Trifluoroacetyl-5-dimethylaminoindole (XIe)

A suspension of 0.5 g of 5-dimethylaminoindole in 5 ml of trifluoroacetic anhydride was stirred at room temperature for 5 h. The mixture was evaporated *in vacuo* and the residue was stirred with 20 ml of a saturated sodium bicarbonate solution for 1 h. The yellow crystals were collected, washed with water, and dried to leave 0.73 g of the trifluoroketone. Recrystallization from 8 ml of ethyl acetate gave 0.35 g of orange crystals, m.p. 234–238°, and a second crop of 0.14 g; λ_{max}^{Nujol} 3.1 μ (NH), 6.1 μ (C=O), 8.5 μ, 8.8 μ (CF_3); λ_{max}^{EtOH} 240 mμ (ϵ 18 200), 300 mμ (ϵ 10 000).

Anal. Calcd. for $C_{12}H_{11}F_3N_2O$: C, 56.4; H, 4.33; N, 10.9. Found: C, 56.4; H, 4.25; N, 11.3.

2,2,2-Trifluoro-1-(5-dimethylamino-3-indolyl)ethanol (XIf)

To a stirred suspension of 0.42 g of 5-dimethylamino-3-trifluoroacetylindole (XI*e*) in 6 ml of ethanol was slowly added 0.40 g of sodium borohydride. The mixture was stirred for 40 min and evaporated to dryness *in vacuo*. The residue was stirred with 25 ml of water for 30 min and filtered. The cake was washed with water and dried to leave 0.43 g (100%) of the product (XI*f*), m.p. 189–191°; λ_{max}^{Nujol} 3.05 μ (OH, NH), 8.65 μ, 8.95 μ (CF_3), *no* ketone at 6.1 μ. An analytical sample that was obtained by recrystallization from benzene of material from another run had m.p. 187–190°.

Anal. Calcd. for $C_{12}H_{13}F_3N_2O$: C, 55.8; H, 5.08; N, 10.9. Found: C, 55.9; H, 5.18; N, 10.8.

3-Bromcacetyl-5-dimethylamincindole (XIIa)

To an ice-cold, stirred suspension of 10.0 g of 5-dimethylamino-3-acetylindole in 200 ml of methanol was slowly added 3.5 ml of bromine in 50 ml of methanol over 15 min. The resulting dark solution was boiled under reflux for 2 h and evaporated to dryness *in vacuo*. The residue was dissolved in 300 ml of water and the solution was taken to pH 7–8 with saturated sodium bicarbonate. The brown precipitate was collected, washed with water, and dried to leave 11.3 g. It was extracted with four 100 ml portions of boiling ethyl acetate, and the solution was chilled for 15 h to yield 1.9 g of product that was suitable for further use.

Can. J. Chem. Downloaded from www.nrcresearchpress.com by 210.87.254.40 on 09/05/12
For personal use only.

The infrared spectrum was similar to that of the starting methyl ketone except for a probable C—Br band at 15.0 μ.

3-Dimethylaminoacetyl-5-dimethylaminoindole (XIIb)

A mixture of 1.4 g of the bromoketone (XII*a*), 1.5 ml of anhydrous dimethylamine, and 30 ml of isopropanol was boiled under reflux for 1.5 h. The solvent was evaporated and the residue dissolved in 20 ml of water. The pH was adjusted to 7–8 and a small amount of brown precipitate was removed. The solution was taken to pH 11–12 to precipitate the crystalline product, which was collected, washed with water, and dried to leave 0.97 g, m.p. 196–220°. A recrystallization from isopropanol gave 0.66 g (54%), m.p. 208–213°. An analytical sample, similarly prepared, had m.p. 217–220°.

Anal. Calcd. for $C_{14}H_{19}N_3O$: C, 68.5; H, 7.81; N, 17.1. Found: C, 68.4; H, 7.89; N, 17.0.

3-Diethylaminoacetyl-5-dimethylaminoindole (XIIc)

The bromoketone (280 mg) was allowed to react with diethylamine (1.0 ml) in the same manner as above, to yield 100 mg of XII*c* as white crystals, m.p. 167.5–170°, after recrystallization from ethyl acetate.

Anal. Calcd. for $C_{16}H_{23}N_3O$: C, 70.3; H, 8.48; N, 15.4. Found: C, 69.7; H, 8.26; N, 15.2.

3-Piperidinoacetyl-5-dimethylaminoindole (XIId)

The bromoketone (200 mg) was allowed to react with piperidine (0.4 ml) in the same manner as above, to yield 125 mg of XII*d* as white crystals, m.p. 203–206°, after recrystallization from isopropanol.

Anal. Calcd. for $C_{17}H_{23}N_3O$: C, 71.5; H, 8.12; N, 14.7. Found: C, 70.9; H, 7.93; N, 14.6.

3-(2-Dimethylaminoethyl)-5-dimethylaminoindole Dipicrate (XIIIb)

Method A

The α-dimethylaminoketone (XII*b*, 200 mg) was reduced with lithium aluminium hydride (150 mg) in hot tetrahydrofuran. The excess hydride was destroyed with alcohol and water, and the solvent removed *in vacuo*. The residue was partitioned between water and ether, and the ether was dried over magnesium sulfate. Evaporation of the ether left 120 mg of partially crystalline residue. The bis picrate, m.p. 190–194°, was prepared from aqueous–alcoholic picric acid and recrystallized from 50% 2-methoxyethanol. A second recrystallization from acetone gave yellow crystals, m.p. 193.5–196°.

Anal. Calcd. for $C_{26}H_{27}N_9O_{14}$: C, 45.3; H, 3.95; N, 18.3. Found: C, 45.3; H, 4.10; N, 18.7.

Method B

A mixture of 420 mg of 5-dimethylamino-3-indoleacetonitrile (IV*b*), ½ teaspoonful of W-2 Raney nickel, 15 ml of methanol, and 5 ml of anhydrous dimethylamine was shaken under 3 atmospheres of hydrogen for 18 h. The catalyst was removed and the solvent was evaporated *in vacuo* to leave 426 mg of an amber sirup, whose infrared spectrum was nearly similar to that of the material prepared by method A. The bis picrate (1.13 g) was prepared as above and treated with 25 ml of warm acetone to yield 0.63 g, m.p. 190–193°, and a second crop of 0.16 g, m.p. 189–193°.

5-Dimethylaminotryptamine Dipicrate (XIIIa)

The nitrile (IV*b*, 420 mg) was hydrogenated in the presence of Raney nickel and 25 ml of methanolic ammonia as described above. The bis picrate was similarly prepared to yield 1.06 g (76%) of yellow crystals, m.p. 210–215°. A treatment with hot acetone (12 ml) gave 0.88 g, m.p. 214–217°.

Anal. Calcd. for $C_{24}H_{23}N_9O_{14}$: C, 43.6; H, 3.51; N, 19.1. Found: C, 43.9; H, 3.58; N, 19.1.

REFERENCES

1. E. SHAW. J. Am. Chem. Soc. **76**, 1384 (1954).
2. (*a*) G. CAVALLINI and F. RAVENNA. Farmaco Pavia Ed. Sci. **13**, 105 (1958). (*b*) J. HARLEY-MASON and A. H. JACKSON. J. Chem. Soc. 1158 (1954).
3. F. RAVENNA. Experientia, **14**, 273 (1958). J. DEGRAW and L. GOODMAN. J. Org. Chem. **27**, 1395 (1962).
4. S. GARRATINI. Private communication.
5. G. F. SMITH. J. Chem. Soc. 3842 (1954).
6. E. H. YOUNG. J. Chem. Soc. 3493 (1958).
7. J. DEGRAW and L. GOODMAN. J. Med. Chem. **7**, 213 (1964).
8. J. DEGRAW, J. KENNEDY, and W. SKINNER. In press.
9. K. BODENDORF and A. WALK. Arch. Pharm. **294**, 484 (1961).
10. J. DEGRAW and L. GOODMAN. J. Org. Chem. **27**, 1728 (1962).

Can. J. Chem. Downloaded from www.nrcresearchpress.com by 210.87.254.40 on 09/05/12
For personal use only.

Can. J. Chem. Downloaded from www.nrcresearchpress.com by 210.87.254.42 on 09/05/12
For personal use only.

THE CHEMISTRY OF EPISULFIDES

I. THE REACTIVITIES OF PROPYLENE SULFIDE AND PROPYLENE OXIDE TOWARDS ANILINE

NEIL S. ISAACS
Department of Chemistry, University of Victoria, Victoria, British Columbia

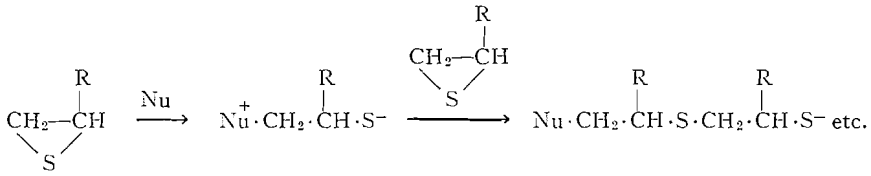
Received September 7, 1965

ABSTRACT

The rates of reaction of propylene sulfide and propylene oxide with aniline have been measured at three temperatures between 30° and 50°. The episulfide is found to be the less reactive and has the higher activation energy. The results are interpreted as indicating a considerable degree of ring opening in the transition state, with the strain energy of the ring providing a considerable portion of the activation energy.

Although the ring-opening reactions of 1,2-epoxides have been examined thoroughly and well documented (1, 2) with regard to both the products formed and rate measurements, their sulfur analogues have received scant attention. No kinetic or mechanistic investigations have yet been reported, despite the fact that such work might be expected to yield information concerning the importance of such factors as ring strain and electronic effects in both heterocyclic systems. It was for these reasons that we undertook initially a comparison of the reactivities of a typical episulfide, propylene sulfide, with its analogue, propylene oxide.

Ring opening of episulfides, unlike epoxides, is frequently complicated by polymerization (3, 4), since the initial thiolate ion is strongly nucleophilic.



Thus, hydroxide and alkoxide ions, carbanions, and primary and secondary aliphatic amines give rise to polymers which may account for anything from 10 to 90% of the products. These reactions are clearly unsuited to kinetic studies, and our attention was turned to weaker bases. Aniline was found to react smoothly, albeit slowly, with propylene sulfide in ethanol to give the β-anilinothiol in quantitative yield. The analogous product was obtained from the reaction of aniline with propylene oxide. Other reagents which were found to give no polymer were acetic acid and acetyl chloride. Results with these acidic reagents will be published elsewhere.

Products of the Reactions

Propylene Sulfide and Aniline

An unsymmetrically substituted episulfide was chosen to compare the reactivities at either carbon atom of the ring. Thus the products might be either I or II (Z = S), or a mixture of the two. It is necessary to establish that the directions of ring opening of the episulfide and epoxide are similar. The failure to meet this criterion might indicate mechanistic differences between the reactions and thus render comparisons dubious. Propylene oxide in basic solution is usually attacked at the primary carbon atom (1), but



there is at least one reference in the literature (5) to attack by a base on the secondary carbon atom in propylene sulfide. Since chemical tests cannot distinguish between a primary and a secondary thiol, attempts were made to determine the identity of the product by spectroscopic means. Attempted nuclear magnetic resonance measurements in a variety of solvents revealed that the thiol proton resonated very close to the complex methylene absorption and that the splitting pattern could not be differentiated unambiguously even after deuteration. The best structural evidence was given by the mass spectrum (Fig. 1), which confirmed the molecular weight of 167 and indicated an entirely reasonable

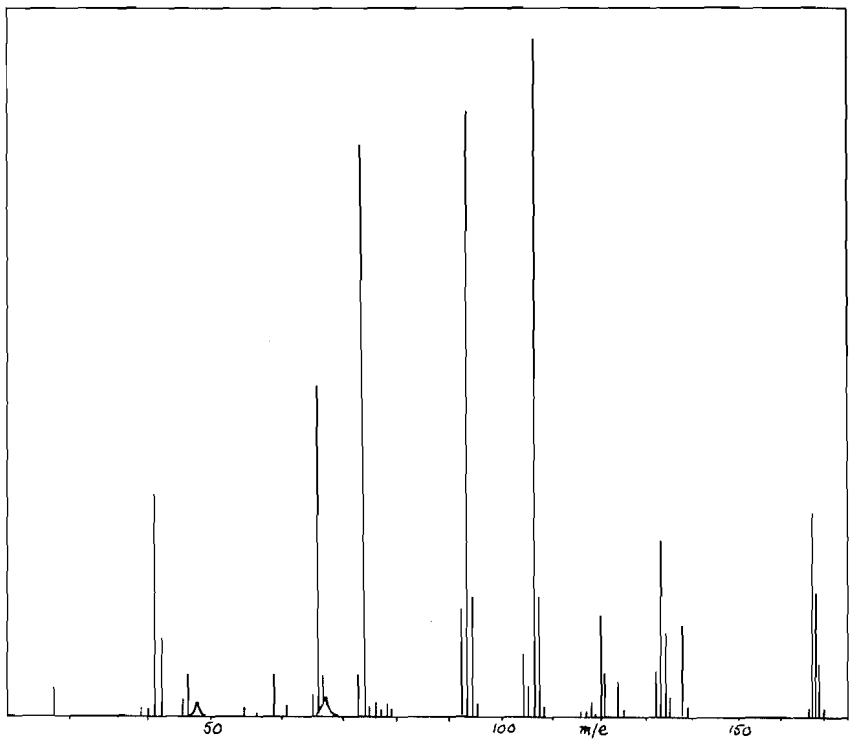
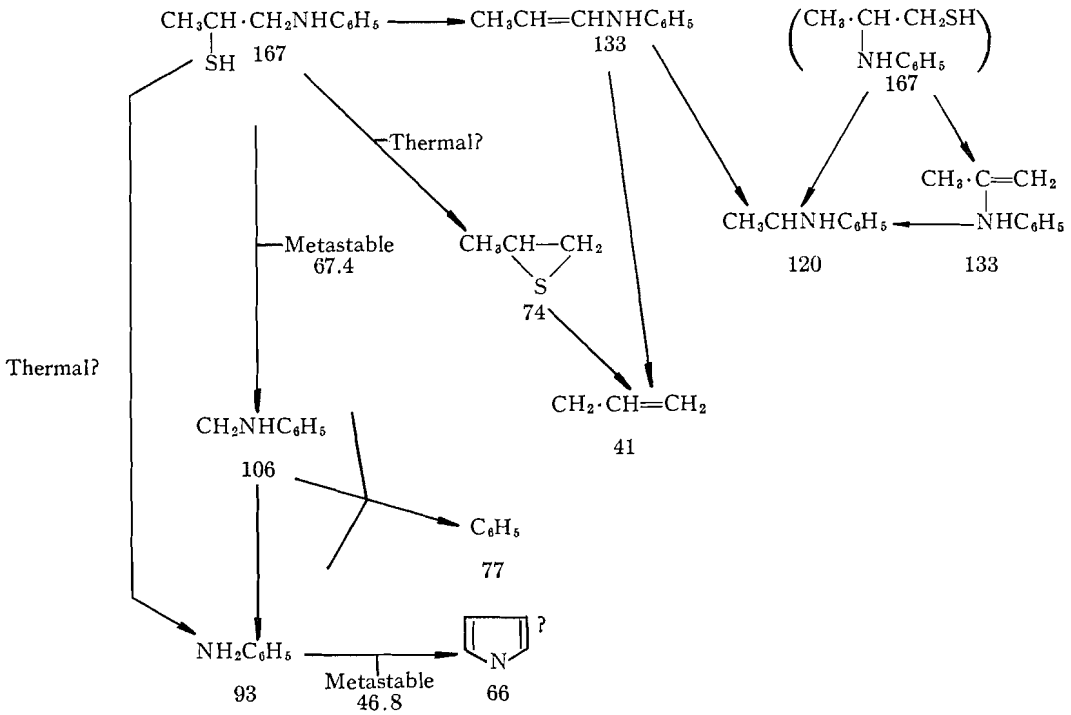


FIG. 1. Mass spectrum (20 V) of the propylene sulfide – aniline product.

degradation based on the secondary thiol (I, Z = S) (Reaction Scheme 1). In particular, the base peak at $m/e = 106$ corresponds to a loss of C_2H_5S, which readily results from the fission of the bond between the original ring carbon atoms of I (with the nitrogen-containing fragment retaining the charge) but which cannot be obtained from structure II (Z = S) without a minimum of two prior rearrangements. The much weaker peak at $m/e = 120$, corresponding to a loss of CH_3S from the molecular ion, could be due to a certain amount of the primary thiol, but could also be explained by successive losses of H_2S (giving rise to the peak at $m/e = 133$) and CH from I. Furthermore, the origin of the base peak by direct fission of the parent molecular ion is confirmed by the presence of a

Can. J. Chem. Downloaded from www.nrcresearchpress.com by 210.87.254.42 on 09/05/12
For personal use only.

strong metastable peak at $106^2/167 = 67.3$; no such transition is observed for $120^2/167 = 86.2$.



REACTION SCHEME 1.

Propylene Oxide and Aniline

Considerable evidence has been accumulated which points to the invariably greater susceptibility to attack by amines of the primary carbon of a monosubstituted ethylene oxide (1). The product of the reaction between aniline and propylene oxide has been studied by Petrov (10) and assigned the structure I (Z = O) on the grounds that it cyclized under the action of benzaldehyde to the known 2,3-diphenyl-5-methyloxazolidine. Confirmation of this is provided by the mass spectrum (Fig. 2, Reaction Scheme 2), which is analogous to that of the propylene sulfide product. From the molecular ion at $m/e = 151$ is derived the same base peak at $m/e = 106$ corresponding to a loss of $CH_3CH{\cdot}OH$, the direct transition being established by a metastable peak at $106^2/151 = 74.3$. Again, a weak peak at $m/e = 120$ may be explained as derived from II (Z = O) by scission of CH_2OH or by successive losses of water (leading to $m/e = 133$) and CH from I (Z = O). Precedents for this type of fission with rearrangement are known (6). The reason for the appearance of a peak of mass 79 (pyridine?) although the aniline moiety in the previous spectrum produced a fragment at mass 66 (pyrrole?) is not understood, but this result may indicate a slight change in the conditions under which the spectra were run. Accordingly, we regard the products derived from both propylene sulfide and propylene oxide as being entirely analogous and resulting from attack of the aniline on the primary carbon in either case, with the possibility of the presence of a small amount of the product of secondary attack.

Can. J. Chem. Downloaded from www.nrcresearchpress.com by 210.87.254.42 on 09/05/12
For personal use only.

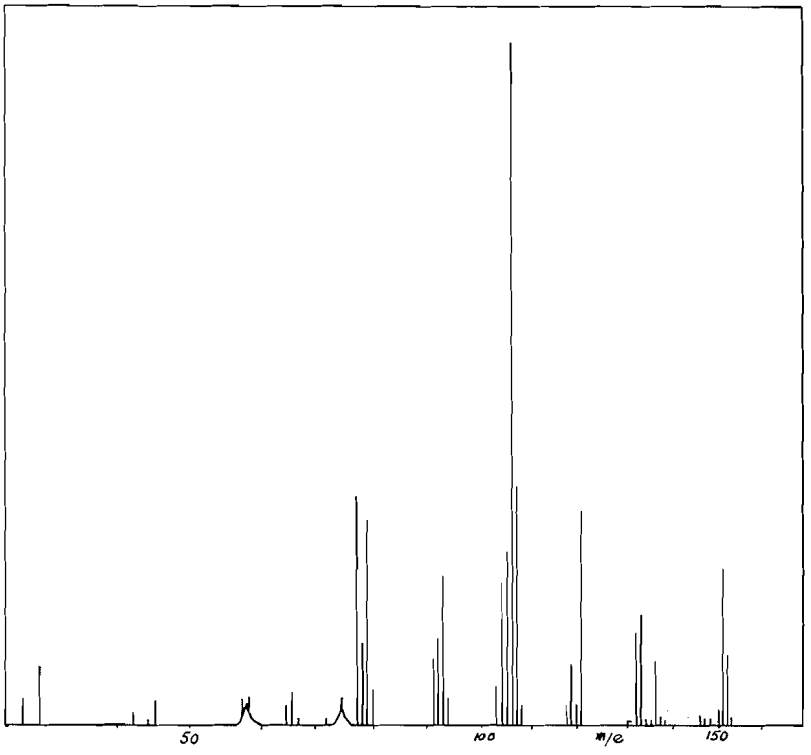
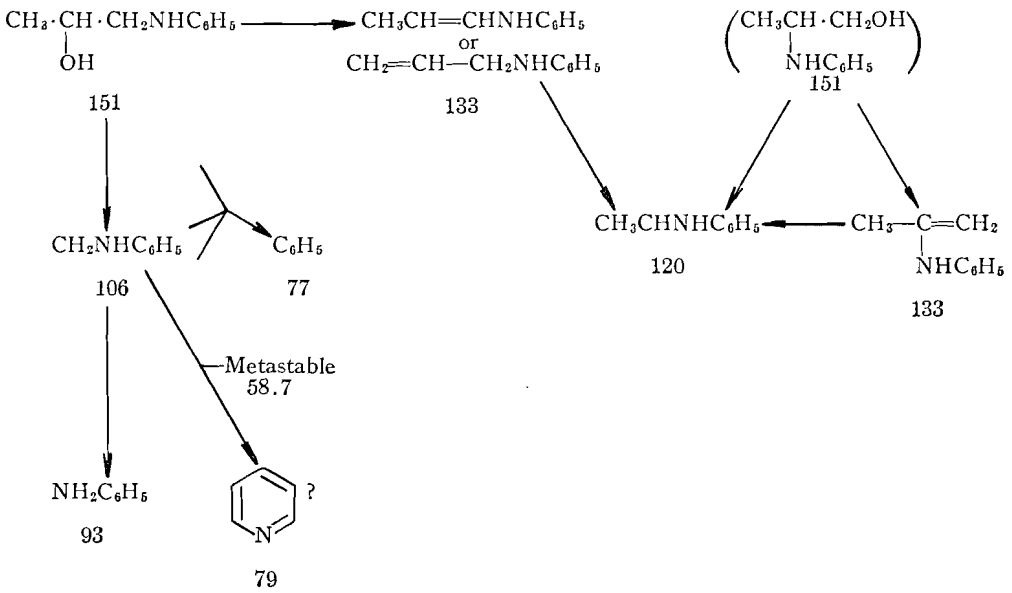


FIG. 2. Mass spectrum (20 V) of the propylene oxide – aniline product.



REACTION SCHEME 2.

Can. J. Chem. Downloaded from www.nrcresearchpress.com by 210.87.254.42 on 09/05/12
For personal use only.

Kinetic Methods

Sufficient pure aniline and either propylene sulfide or propylene oxide were weighed out, separately dissolved in 99.8% ethanol, and brought to the required temperature. The solutions were mixed at $t = 0$ and the mixture was quickly made up to a calibrated volume with ethanol. The initial concentrations were approximately 0.1 M in episulfide or epoxide and 0.15 M in aniline.

Aliquots of 1.0 ml volume were withdrawn at appropriate intervals and analyzed spectrophotometrically. Each aliquot was placed in a 50 ml graduated flask with a little 98% ethanol. The following reagents were added successively over a period of 3–4 min, to convert the aniline into phenylazo-β-naphthol: 2 ml 5% sodium nitrite solution, 5 ml 1.0 N hydrochloric acid, 5 ml 5% β-naphthol solution in ethanol, and 5 moles 2.0 N sodium hydroxide. The flask was then filled to the mark with ethanol. After dilution of 1.0 ml of the resulting deep red solution to 50 ml with ethanol containing 2 ml 2 N sodium hydroxide, the absorbance at 510 mμ was recorded spectrophotometrically with a 10 mm path length. The analytical method was calibrated against standard solutions of aniline in ethanol and with solutions of pure phenylazo-β-naphthol in ethanol, and was shown to be reproducible and accurate to 1.5%. The presence of the reaction product in the analytical solution contributed negligibly to the production of the color, and the very slight brown color inevitably accompanying the β-naphthol was compensated for by subtracting a blank determination carried out with each run. Duplicate kinetic runs were carried out in baths thermostatted to ±0.1° or better and at three or four different temperatures.

Kinetic Results

Good second-order rate plots were obtained as far as the reactions were followed, which, except for the slowest, was to 75% completion. Bimolecular rate constants are shown in Table I and activation parameters in Table II and Fig. 3. The reproducibility of the rate constants, measured as the ratio of the mean deviation of values obtained from individual points on the rate plot to the mean value obtained from the slope, was of the order of 2–3%.

TABLE I

Specific rate constants for reactions with aniline

Propylene sulfide		Propylene oxide	
T (°C)	10^5k (l mole^{-1} s^{-1})	T (°C)	10^5k (l mole^{-1} s^{-1})
49.60	1.59	50.90	3.65
	1.52		3.55
41.05	0.815	39.08	2.30
	0.852		2.20
39.75	0.722		
30.60	0.330	30.50	1.72
	0.334		1.59

TABLE II

Activation parameters for reactions with aniline

	E_A ($\Delta H^{\neq}$) (kcal mole^{-1})	log A	$\Delta S^{\neq}$ (e.u.)
Propylene sulfide	14.64	5.10	−35.2
Propylene oxide	7.10	0.35	−56.8

Can. J. Chem. Downloaded from www.nrcresearchpress.com by 210.87.254.42 on 09/05/12
For personal use only.

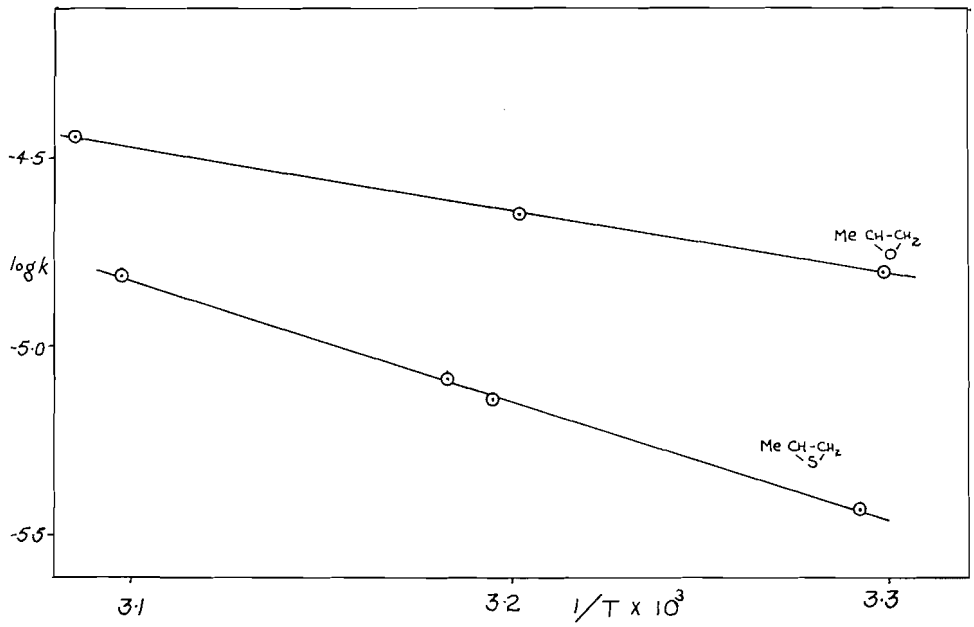


FIG. 3.

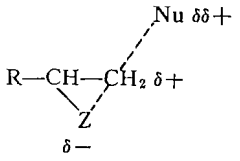
DISCUSSION

The results demonstrate the notably lower reactivity of the episulfide to nucleophilic attack as compared with the epoxide. The difference, a factor of from two to six over the temperature range studied, is remarkably small if one considers the profound structural change involved. However, the reaction rates of epoxides have been noted previously (7, 8) as being influenced very little by the electronic effects of substituents on the ring. The low value for the activation energy for propylene oxide is also striking and indicates convergence of the rates at around 85°. Parker and Isaacs (1) have discussed the ring-opening reactions of epoxides in terms of a gradation of mechanisms ranging from a 'S_N1-like' transition state (III), in which much polar character (though no free carbonium ion) is present, to a 'S_N2-like' transition state (IV), in which bond making and fission are smoothly concerted (though the incoming and leaving groups are not collinear with the carbon atom). The episulfides may similarly be considered.

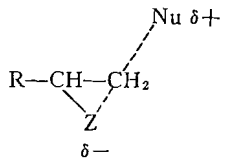
The attack of aniline should take place more readily on a primary carbon atom than on a secondary carbon atom for steric reasons, and would be expected to attack propylene oxide more readily than propylene sulfide by virtue of the greater polarization of the C—O bond as compared with that of the C—S bond. The latter, however, is probably the more easily broken (the energies for homolysis are of the order of 75 and 55 kcal $mole^{-1}$, respectively (9)). The balance of these effects will determine the reactivities of the compounds and the detailed reaction paths which they follow, each tending towards a minimum of activation energy. Thus we might expect to find in the transition state for propylene sulfide a smaller degree of bond making between aniline and carbon and a greater degree of bond breaking between carbon and the heteroatom than in the case of propylene oxide. In other words, the transition state for episulfide should be a looser structure than that for epoxide, though both are more akin to IV than to III. The greater radius of the sulfur

Can. J. Chem. Downloaded from www.nrcresearchpress.com by 210.87.254.42 on 09/05/12
For personal use only.

atom than of the oxygen atom would also contribute towards a lesser degree of solvation around the developing anionic site in the episulfide. That this is so is demonstrated by the less negative entropy of activation shown by propylene sulfide. Solvation effects are undoubtedly most important. Reactions between amines and epoxides may become very sluggish or immeasurably slow in nonpolar aprotic media (13).



III (Z = S, O)



IV (Z = S, O)

When the values obtained for the enthalpies of activation are discussed, a further factor must be considered, namely, the release of the potential energy of bond-angle deformations in the three-membered rings. This strain energy will tend to reinforce the activation process as the reaction proceeds, and to reduce the energy which has to be drawn from kinetic sources to reach the transition state. The ring-strain energies of ethylene oxide and ethylene sulfide have been estimated (11) by hydrogenation methods as 14 and 9 kcal mole^{-1}, respectively; these values should not be substantially different for propylene oxide and propylene sulfide. The difference between them, namely, 5 kcal mole^{-1}, should be the difference between the activation energies for the two reactions, other effects being equal. The difference found, 7.5 kcal mole^{-1}, is in the predicted direction and is larger by 2.5 kcal than the value suggested by ring-strain considerations alone. This may be accounted for by the factors discussed above, of which, in both reactions, bond formation is more pronounced than bond breaking in the transition state, and this to a greater extent with propylene oxide than with propylene sulfide.

EXPERIMENTAL

Mass spectra were recorded on a Hitachi Perkin–Elmer mass spectrometer with a 20 V electron beam and sample pressures of 1–2 × 10^{-7} Torr.

Visible spectrophotometry was carried out in a Beckman DB machine.

Propylene sulfide was prepared from propylene oxide in 40–60% yield by the method of Bordwell and Anderson (12) and was purified by careful fractionation through a fractionating column having 20 theoretical plates, the middle fraction being collected, b.p. 73.5 °C.

Propylene oxide, Eastman reagent grade, was purified by fractional distillation, b.p. 35 °C.

Aniline was purified by regeneration from the recrystallized hydrochloride followed by distillation through a short Vigreux column, the middle fraction being collected, b.p. 185°. This was stored under nitrogen and in the absence of light, under which conditions it remained colorless.

The Reaction between Propylene Sulfide and Aniline

Propylene sulfide was dissolved in four times its weight of 98% ethanol, and a 1.5-fold *M* excess of aniline added. The mixture was allowed to stand in a water bath at 50° for 3 days, after which the solvent and unreacted episulfide were removed at the pump; then the residue was distilled at 1 mm pressure, 1-anilinopropan-2-thiol being collected (after the excess aniline had passed over) as a colorless, unpleasant-smelling liquid, b.p. 86° at 1 mm, n_D^{25} 1.5829.

Anal. Found: C, 64.69; H, 7.68; mol. wt. (by mass spectrum) 167. $C_9H_{13}NS$ requires C, 64.70; H, 7.78; mol. wt. 167.

A negligible quantity of involatile material remained in the distillation flask. 1-Anilinopropan-2-ol was prepared according to Petrov (10). When the reaction between propylene oxide and aniline was allowed to go to completion, an undistillable material was isolated after the 1-anilinopropan-2-ol had been removed, presumably N,N-bis(2-hydroxypropyl) aniline, amounting to some 10% of the products. The formation of this compound was negligible at 50–70% reaction when an excess of aniline was used.

Can. J. Chem. Downloaded from www.nrcresearchpress.com by 210.87.254.42 on 09/05/12
For personal use only.

ACKNOWLEDGMENTS

Thanks are extended to the National Research Council for financial support of this work, and to Dr. J. Holmes, University of Ottawa, for determining the mass spectra.

REFERENCES

1. R. E. PARKER and N. S. ISAACS. Chem. Rev. 737 (1959).
2. R. ROSOWSKY. *In* Heterocyclic compounds with three- and four-membered rings. Vol. 1. A. Weissberger (*Editor*). Interscience Publishers, Inc., New York. 1964.
3. C. S. MARVEL and E. D. WEIL. J. Am. Chem. Soc. **76**, 61 (1945).
4. G. I. BRAZ. J. Gen. Chem. USSR Engl. Transl. **21**, 757 (1951).
5. B. HANSEN. Acta Chem. Scand. **13**, 151 (1959).
6. F. MCLAFFERTY. Mass spectral correlations. American Chemical Society, Washington, D.C. 1963.
7. N. B. CHAPMAN, N. S. ISAACS, and R. E. PARKER. J. Chem. Soc. 1925 (1959).
8. R. LAIRD and R. E. PARKER. J. Chem. Soc. 6065 (1963).
9. K. S. PITZER. J. Am. Chem. Soc. **70**, 2140 (1948).
10. K. D. PETROV. Sb. Statei Obshch. Khim. Akad. Nauk SSSR, **1**, 374 (1953).
11. R. A. NELSON and R. S. JESSUP. J. Res. Natl. Bur. Std. **48**, 206 (1952).
12. F. G. BORDWELL and H. M. ANDERSON. J. Am. Chem. Soc. **84**, 4961 (1953).
13. N. S. ISAACS. Unpublished work.

Can. J. Chem. Downloaded from www.nrcresearchpress.com by 210.87.254.42 on 09/05/12
For personal use only.

ÉTUDES SUR LES PHÉNYL-5 CYCLOHEXANEDIOLS-1,3 ISOMÈRES

JEAN-CLAUDE RICHER ET NGUYEN-THI-THANH-HOA[1]
Département de Chimie, Université de Montréal, Montréal, Québec

Reçu le 23 août 1965

RÉSUMÉ

Les trois phényl-5 cyclohexanediols-1,3 isomères ont été préparés et caractérisés. Les configurations de ces produits ont été attribuées grâce à leurs spectres infra-rouges et de résonance magnétique nucléaire. Les vitesses d'oxydation chromique de ces diols ont aussi été déterminées; il a été observé une fois de plus que ces vitesses relatives sont dans l'ordre prévu par l'encombrement stérique auquel est soumis chacun des groupes hydroxyles.

INTRODUCTION

Dans un travail précédent (1), les configurations des diméthyl-5,5 cyclohexanediols-1,3 (I et II) ont été assignées grâce à leurs vitesses relatives d'oxydation chromique. Cette preuve de configuration a récemment été attaquée par Finegold et Kwart (2), qui l'ont qualifiée de douteuse. Depuis, cette méthode a été confirmée pour la détermination des configurations de monoalcools (3, 4) alors que Durocher (5) et Durocher et Favre (6) l'ont appliquée avec succès dans le cas de diols bicycliques. Nous voulons rapporter dans le présent travail quelques observations ayant trait aux phényl-5 cyclohexanediols-1,3 (III–V); à cause de la présence du groupe phényle (7), nous considérons ces diols comme conformationnellement fixés.

RÉSULTATS

Les diols recherchés ont tous été obtenus à partir de la phényl-5 cyclohexanedione-1,3 (VI), préparée d'après les indications de Vorländer (8). D'une part, l'hydrogénation catalytique de cette cétone en présence de nickel de Raney, à pression atmosphérique et à la température de la pièce (9), conduit au phényl-5 cyclohexanediol-1,3 *cis* (diaxial III), p.f. 135–136°, dont le spectre infra-rouge en solution diluée montre une bande caractéristique due aux ponts hydrogènes intramoléculaires (10); les autres caractéristiques du composé sont résumées dans le Tableau I. D'autre part, la réduction de la dicétone VI par le sodium et l'éthanol d'après les indications de Crossley et Renouf (11) fournit en prépondérance le phényl-5 cyclohexanediol-1,3 *cis* (diéquatorial IV), p.f. 160–161°; une faible quantité du phényl-5 cyclohexanediol-1,3 *trans* (V), p.f. 132.5–133.5° (abaissé par mélange avec le *cis* diaxial), est formée aux côtés du diol IV. Les propriétés caractéristiques de ces produits sont résumées au Tableau I.

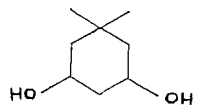
Afin de prouver d'une façon non-ambigüe la configuration du diol *trans* V, la synthèse proposée par Tamm (12) et Mühle et Tamm (13) et représentée dans le Schéma Réactionnel 1 a été réalisée en suivant fidèlement la procédure expérimentale décrite par Durocher et Favre (6). Cette synthèse conduit à un diol, p.f. 132.5–133.5, qui est en tous points identique au phényl-5 cyclohexanediol-1,3 *trans* (V) décrit plus haut et que Crossley et Renouf (11) appelaient "*cis* modification".

DISCUSSION

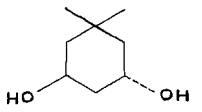
Les configurations proposées pour les diols sont cohérentes avec leurs modes de formation. En effet il est maintenant bien établi, d'une part, que la réduction des dicétones

[1]*Extrait du mémoire présenté par Mlle. Nguyen-Thi en vue de l'obtention du grade de Maître ès Sciences, Faculté des Sciences, Université de Montréal, mars 1965.*

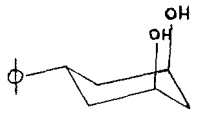
Can. J. Chem. Downloaded from www.nrcresearchpress.com by 210.87.254.6 on 09/05/12
For personal use only.



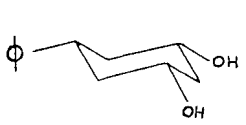
I



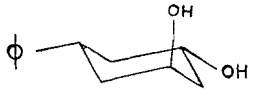
II



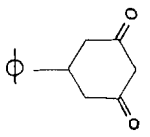
III



IV



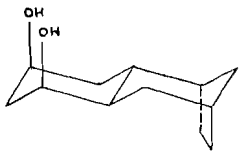
V



VI



VII



VIII

par le sodium et l'alcool conduit principalement aux glycols diéquatoriaux (1, 5, 6, 9, 14, 15); d'autre part, la synthèse du produit *trans* V d'après la méthode de Tamm (12, 13) reprise par Durocher et Favre (6) et Durocher (5) est non-ambigüe. Quant à l'hydrogénation catalytique des dicétones maintenues dans une conformation rigide comme dans

TABLEAU I

	cis diaxial III	*cis* diéquatorial IV	*trans* V
Point de fusion (°C)	135–136	160–161 (litt. (11) 160)	132.5–133.5 (litt. (11) 134)
Spectres infra-rouges (cm^{-1})			
OH	3 621.7 3 548.0	3 623.2	3 627.2
Phényle	1 595	1 600	1 600
C—O	970	1 010	1 035 980
Déplacements chimiques (p.p.m.) des hydrogènes carbinoliques	4.25	3.75	4.33 3.66
Vitesses d'oxydation chromiques ($10^5 k_2$ en l $mole^{-1}$ s^{-1})	145	30.5	99.3

le cas présent, les résultats obtenus jusqu'à maintenant (5, 6, 9) indiquent que les diols diaxiaux sont formés en prépondérance. De plus le pont hydrogène intramoléculaire observé dans le spectre infra-rouge du produit III ne peut être expliqué que par une configuration diaxiale des deux groupes hydroxyles (10). Le fait que le spectre de résonance magnétique nucléaire du produit V, p.f. 132.5–133.5°, montre deux bandes, à 3.66 et 4.33 p.p.m., dues à des hydrogènes carbinoliques indique que ce composé est non symétrique et supporte la configuration *trans* attribuée à ce produit.

Can. J. Chem. Downloaded from www.nrcresearchpress.com by 210.87.254.6 on 09/05/12
For personal use only.

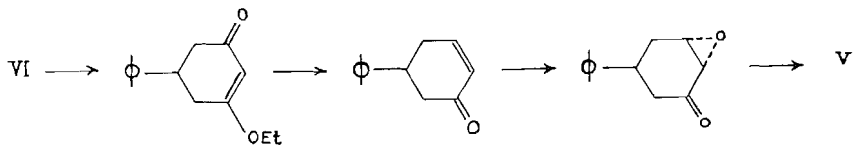


SCHÉMA RÉACTIONNEL 1.

Les vitesses relatives d'oxydation chromique (1:3.24:4.75) sont dans l'ordre prévu grâce à l'empêchement stérique auquel sont soumis les groupes hydroxyles (diéquatoriaux, axial–équatorial, diaxiaux), et confirment les configurations attribuées. Les résultats obtenus dans le présent travail montrent une fois de plus l'utilité des oxydations chromiques pour la détermination des configurations relatives des alcools et des diols secondaires cycliques; il semble donc que les objections soulevées par Finegold et Kwart (2) au sujet de cette méthode ne sont pas justifiées.

L'ordre de grandeur de la différence entre la fréquence d'absorption de l'hydroxyle libre et celle de l'hydroxyle lié intramoléculairement dans le spectre infra-rouge du diol diaxial III, $\Delta\nu$ de 73.7 cm^{-1}, est le même que celui observé par Kuhn (10) pour le cyclohexanediol-1,3, $\Delta\nu$ de 75 cm^{-1}, et par Durocher (5) pour les diols VII, $\Delta\nu$ de 79.5 cm^{-1}, et VIII, $\Delta\nu$ de 76.6 cm^{-1}. On peut donc admettre qu'une valeur de $\Delta\nu$ d'environ 75 cm^{-1} correspond à la valeur que l'on devrait observer pour un pont hydrogène intramoléculaire dans les cyclohexanediols-1,3 diaxiaux "standards". Il a déjà été noté (5, 6, 13) que des déviations majeurs de cette valeur indiquent une déformation de la molécule.

PARTIE EXPÉRIMENTALE

Les points de fusion ont été déterminés à l'aide d'un appareil "hot stage apparatus" de la Compagnie Reichert (Autriche). Les spectres infra-rouge de routine ont été déterminés à l'aide d'un spectrophotomètre Beckman, modèle IR-8, à double faisceaux. La position précise des bandes OH a été mesurée à l'aide d'un appareil, modèle 112, de la compagnie Perkin–Elmer avec optique de fluorure de lithium et calibré immédiatement avant et après les spectres grâce aux données de l'I.U.P.A.C. pour la vapeur d'eau; ces mesures, précises à ± 0.5 cm^{-1}, ont été effectuées dans une cellule de 30.9 mm et sur des solutions de produits dans CCl_4. Les spectres de résonance magnétique nucléaire ont été pris avec un appareil, modèle A 60, de la Compagnie Varian pour des solutions dans l'acétone deutériée et utilisant le tétraméthylsilane comme référence interne; les déplacements chimiques (δ) sont exprimés en parties par million (p.p.m.). Des analyses élémentaires satisfaisantes ont été obtenues pour les produits nouveaux par Claude Daesslé, Organic Microanalysis, Montréal. Les vitesses d'oxydation chromique ont été mesurées d'après la méthode décrite récemment (4); les conditions expérimentales sont: température de 25 °C, acide acétique aqueux à 90%.

REMERCIEMENTS

Les auteurs remercient le Conseil National de Recherches du Canada pour l'aide financière accordée sous forme d'octroi de recherches (A 1295); le Bureau de l'Aide Extérieure du Canada (Plan Colombo) pour l'aide financière accordée sous forme de bourses d'études; la Compagnie Bristol Laboratories pour l'aide financière apportée sous forme d'octroi de recherches; le Dr. Aldée Cabana, Université de Sherbrooke, pour la détermination des spectres infra-rouges des diols; et le Dr. Claude Gilardeau pour la mesure des vitesses d'oxydation chromique.

BIBLIOGRAPHIE

1. H. FAVRE et J. C. RICHER. Can. J. Chem. **37**, 411 (1959).
2. H. FINEGOLD et H. KWART. J. Org. Chem. **27**, 2361 (1962).
3. J. C. RICHER, L. A. PILATO et E. L. ELIEL. Chem. Ind. London, 610 (1962).
4. J. C. RICHER et C. GILARDEAU. Can. J. Chem. **43**, 538 (1965).
5. J. G. DUROCHER. Ph.D. Thèse, Université de Montréal, Montréal, Québec. 1965.
6. J. G. DUROCHER et H. FAVRE. Can. J. Chem. **42**, 260 (1964).

Can. J. Chem. Downloaded from www.nrcresearchpress.com by 210.87.254.6 on 09/05/12
For personal use only.

7. E. W. GARBISCH, JR. et D. B. PATTERSON. J. Am. Chem. Soc. **85**, 3228 (1963).
8. D. VORLÄNDER. Ber. **27**, 2054 (1894).
9. H. FAVRE et J. C. RICHER. Can. J. Chem. **37**, 417 (1959).
10. L. P. KUHN. J. Am. Chem. Soc. **74**, 2492 (1952).
11. A. W. CROSSLEY et N. RENOUF. J. Chem. Soc. 602 (1915).
12. C. TAMM. Helv. Chim. Acta, **43**, 1700 (1960).
13. H. MÜHLE et C. TAMM. Helv. Chim. Acta, **46**, 268 (1963).
14. A. W. ALLAN, R. P. A. SNEEDEN et J. COLVIN. J. Chem. Soc. 557 (1958).
15. V. P. HIRSJARVI. Ann. Acad. Sci. Fennicae, Ser. A II, **23**, 108 (1946).

Can. J. Chem. Downloaded from www.nrcresearchpress.com by 210.87.254.6 on 09/05/12
For personal use only.

Can. J. Chem. Downloaded from www.nrcresearchpress.com by 210.87.254.5 on 09/05/12
For personal use only.

NOTES

RADIATION-INDUCED BROMINATION OF 2,3-DIMETHYLBUTANE

OWEN H. WHEELER AND HILDA BATLLE DE PABON

Although the vapor-phase photochemical bromination (at 100°) of 2,3-dimethylbutane leads to a variety of products (1), the photochemical bromination of the liquid hydrocarbon at room temperature is reported (2, 3) to give largely 2,3-dibromo-2,3-dimethylbutane. The γ-induced (cobalt-60) bromination has now been studied and compared with photochemical bromination.

EXPERIMENTAL

γ-Induced Bromination

2,3-Dimethylbutane (10 ml) (Aldrich Chemical Co., 99% pure by gas chromatography) distilled from sodium was placed in a glass vessel from which the air had been displaced by helium, and bromine (0.5 ml) that had been distilled from phosphorus pentoxide was added. The vessel was fitted with a stopper and tube to allow the escape of hydrogen bromide, and irradiated in the gamma pool (4) for 16 h to a total corrected absorbed dose of 1.72 Mrads. After irradiation the dissolved hydrogen bromide was removed by passing nitrogen through the solution. The hydrolyzable organic bromide was determined by adding an aliquot (4.0 ml) of the irradiated solution to 50% aqueous ethanol (100 ml) at room temperature, and by titrating portions at intervals with 0.01 *N* sodium hydroxide. A total of 4.20 meq of bromide was liberated after 100 h (see Fig. 1*a*). The total organic bromide was determined by heating under reflux another aliquot (4.0 ml) with a solution of sodium in ethylene diglycol (0.25 *N*) for 15 h. Titration with hydrochloric acid showed the liberation of 5.41 meq of bromide.

The irradiation was repeated with the hydrocarbon (50 ml) and bromine (2.5 ml) to a corrected absorbed dose of 2.54 Mrads during 22 h. Solid (1.0 g), m.p. 150–160°, was precipitated in the vessel. The supernatant solution was distilled in a spinning-band column, giving a distillate of 2,3-dimethylbutane (infrared) and a solid residue (5.2 g), m.p. 155–160°. The solid fractions were purified by sublimation to give 2,3-dibromo-2,3-dimethylbutane, m.p. 159–160° (decomp.) (lit. (5) m.p. 160–164°). The nuclear magnetic resonance spectrum in deuteriochloroform showed a single sharp peak at δ 2.03, against tetramethylsilane as an internal standard. The dibromide was soluble in 2,3-dimethylbutane (0.15 g/ml at 26°).

The initial radiolytic yield (G-value = 2 760 $\pm$ 130) was determined by irradiating samples of a solution of bromine (5%) in 2,3-dimethylbutane for periods of 5–80 min in a helium atmosphere. This value remained constant for absorbed doses of 25 000 – 150 000 rads and bromine concentrations of 0.9–2.0 meq/ml. The unreacted bromine was determined by adding potassium iodide (1 g) in water (5 ml) and titrating the solution with 0.1 *N* sodium thiosulfate. The absorbed dose from the source was determined by the Fricke dosimeter with the same cells as used in the irradiations, a correction being made for the relative electron densities of the Fricke solution and the solution of 2,3-dimethylbutane.

2,3-Dimethylbutane was not detectably affected (boiling point and gas chromatography) on irradiation to 2.5 Mrads in an inert atmosphere.

Photochemical Bromination

Distilled 2,3-dimethylbutane (50 g) was contained in a flask immersed in a water bath maintained at 30° and illuminated by a 500 W tungsten lamp, placed 4 inches below the flask. Distilled bromine (8 g) was led in with a current of helium below the surface of the hydrocarbon, with mechanical stirring. After addition of the bromine the gas flow was maintained to remove the hydrogen bromide. A solid (16.4 g), m.p. 150–160°, was deposited in the flask.

A portion (25 ml) of the solution was solvolyzed in 50% aqueous ethanol (250 ml) at room temperature, and aliquots (10 ml) were titrated with 0.1 *N* sodium hydroxide (see Fig. 1*b*).

Another portion (10 ml) was hydrolyzed by heating it under reflux for 6 h with a 0.25 *N* solution of sodium in diethylene glycol (50 ml), and aliquots (10 ml) were titrated with 0.013 *N* hydrochloric acid, thereby showing 1.57 meq of bromine/ml.

A solution of bromine (0.1 *N*) in the hydrocarbon, maintained in the dark, showed no detectable decrease in concentration in 6 h and a decrease of 0.2% in 24 h.

DISCUSSION

In their study of the photochemical bromination of 2,3-dimethylbutane, Russell and Brown (3) determined the total organic bromide by hydrolyzing the solution with base, and the tertiary bromide by solvolyzing an aliquot in aqueous ethanol. They noticed that the liberation of bromide ion during the solvolysis increased with time, and they assumed that the true value of the amount of tertiary bromide could be obtained by extrapolation to zero time. The solution obtained in this work on the γ-induced bromination of 2,3-dimethylbutane showed a steady increase for periods up to more than 1 day (Fig. 1*a*).

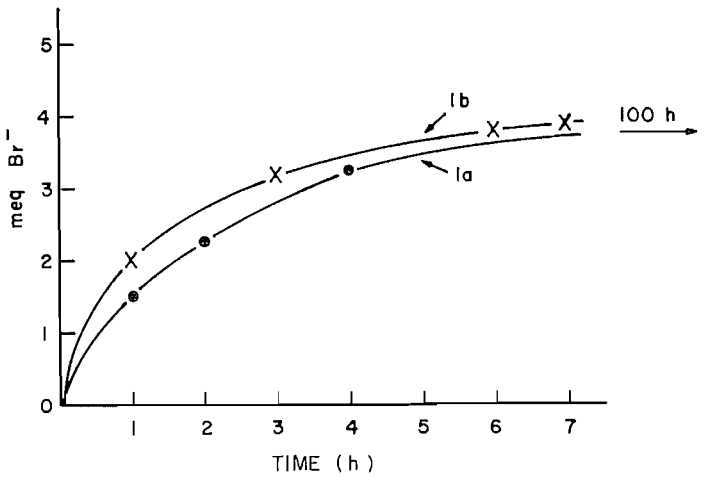


FIG. 1. Solvolysis of bromide solutions.

Distillation of the brominated solution left solid 2,3-dibromo-2,3-dimethylbutane (identified by its melting point and nuclear magnetic resonance spectrum) as the only product. No fraction corresponding to a liquid monobromide was detected. 2,3-Dibromo-2,3-dimethylbutane itself showed the same abnormal behavior on solvolysis, and the bromide analyses of the irradiated solution can be accounted for on the basis of the solubility of the solid dibromide in 2,3-dimethylbutane. The reported rate constant of solvolysis of this dibromide (6), based on only three experimental points, must be treated with reservation.

The photochemical (visible) bromination of 2,3-dimethylbutane also produced exclusively 2,3-dibromo-2,3-dimethylbutane, and the solution of the brominated hydrocarbon showed the same behavior on solvolysis (Fig. 1*b*).

The high G-value (2 760 $\pm$ 130) (molecules reacted per 100 eV) indicates that the reaction proceeds by an initial chain mechanism. (Russell and Brown (3) have suggested that the dibromide is formed from the monobromide in a rapid ionic mechanism.) The chlorination of hydrocarbons gives higher G-values (7). However, the γ-induced and photochemical chlorinations of benzene (8), toluene (9, 10), and *n*-butyric acid (8) give the same products. The photochemical and radiation-induced halogenations of organic compounds seem to produce the same products and probably proceed by similar mechanisms.

ACKNOWLEDGMENTS

The nuclear magnetic resonance spectrum was determined by Dr. L. M. Mateos at the Instituto de Quimica, Universidad Nacional Autonoma de Mexico. The Puerto Rico

Can. J. Chem. Downloaded from www.nrcresearchpress.com by 210.87.254.5 on 09/05/12
For personal use only.

Nuclear Center is operated by the University of Puerto Rico for the U.S. Atomic Energy Commission (contract No. AT(40-1)-1833).

1. M. S. KHARASCH, Y. C. LIU, and W. NUDENBURG. J. Org. Chem. **20**, 680 (1955).
2. A. V. GROSSE and V. N. IPATIEFF. J. Org. Chem. **8**, 438 (1943).
3. G. A. RUSSELL and H. C. BROWN. J. Am. Chem. Soc. **77**, 4025 (1955).
4. O. H. WHEELER and R. MONTALVO. Radiation Res. In press.
5. R. G. KELSO, K. W. GREENLEE, J. M. DERFER, and C. E. BOARD. J. Am. Chem. Soc. **74**, 287 (1952).
6. P. PETRENKO-KRISTSCHENKO. Ber. **61**, 845 (1928).
7. A. J. SWALLOW. Radiation chemistry of organic compounds. Pergamon Press, New York. 1960.
8. I. ROSEN. Large radiation sources in industry. Vol. II. International Atomic Energy Agency, Vienna. 1960. p. 97.
9. R. A. COX and A. J. SWALLOW. Chem. Ind. London, 1277 (1956).
10. R. A. COX and A. J. SWALLOW. J. Chem. Soc. 3727 (1958).

RECEIVED JULY 22, 1965.
PUERTO RICO NUCLEAR CENTER,
MAYAGUEZ, PUERTO RICO.

Can. J. Chem. Downloaded from www.nrcresearchpress.com by 210.87.254.5 on 09/05/12
For personal use only.

ORGANIC SULFUR MECHANISMS
III. A BRIEF INVESTIGATION INTO THE REACTION OF BENZONITRILE OXIDE WITH SULFENES[1]

J. F. KING AND T. DURST

As part of our scrutiny of the chemistry of sulfenes (1, 2 and references therein), we were led to consider whether these species were capable of 1,3-dipolar cycloaddition reactions. 1,2-Cycloadditions leading to products with four-membered rings appear to be well established (3–6); however, although certain reactions of sulfenes may be rationalized in terms of 1,3-dipolar additions, no such processes have actually been authenticated.[2] As the question seemed to have bearing on our study of the mechanism of the coupling of phenylsulfene to form *trans*-stilbene and *cis*-diphenylethylene sulfone (8–10), we sought some information on the point.

We chose to look at the reaction of sulfenes with a nitrile oxide, chiefly because such a species would appear to be able to react both as a dipolar reagent and as a dipolarophile,[3] and would therefore be potentially capable of detecting either type of reactivity in sulfenes. Of the various known nitrile oxides, benzonitrile oxide is comparatively readily accessible. Thus, when an ethereal solution of α-chlorobenzaldoxime (benzoyl chloride oxime) is treated with triethylamine, triethylammonium chloride forms a precipitate immediately, and the nitrile oxide remains in solution along with any excess triethylamine. Since triethylamine is known (1, 2) to react with phenylmethanesulfonyl chloride to give phenylsulfene, the nitrile oxide – triethylamine solution was added directly to a solution of the sulfonyl chloride, in the expectation of observing the reaction of the sulfene and the nitrile oxide. The crystalline product which was obtained (and which could also be

[1]*An independent and more extensive study, leading to the same conclusion about the structure of the new class of compounds, has been carried out by Professor W. E. Truce and Dr. A. R. Naik of Purdue University, and is described elsewhere in this issue.*

[2]*A 1,3-dipolar addition to a sulfene has been suggested by Strating (7) as a mechanism for the formation of oxythioacyl halides. The available evidence, however, permits other interpretations.*

[3]*Huisgen, however, questions the idea that benzonitrile oxide is functioning as a dipolarophile in the formation of diphenylfuroxan (11), the reaction which is probably the best-known example of the alleged dipolarophile activity of nitrile oxides.*

Nuclear Center is operated by the University of Puerto Rico for the U.S. Atomic Energy Commission (contract No. AT(40-1)-1833).

1. M. S. KHARASCH, Y. C. LIU, and W. NUDENBURG. J. Org. Chem. **20**, 680 (1955).
2. A. V. GROSSE and V. N. IPATIEFF. J. Org. Chem. **8**, 438 (1943).
3. G. A. RUSSELL and H. C. BROWN. J. Am. Chem. Soc. **77**, 4025 (1955).
4. O. H. WHEELER and R. MONTALVO. Radiation Res. In press.
5. R. G. KELSO, K. W. GREENLEE, J. M. DERFER, and C. E. BOARD. J. Am. Chem. Soc. **74**, 287 (1952).
6. P. PETRENKO-KRISTSCHENKO. Ber. **61**, 845 (1928).
7. A. J. SWALLOW. Radiation chemistry of organic compounds. Pergamon Press, New York. 1960.
8. I. ROSEN. Large radiation sources in industry. Vol. II. International Atomic Energy Agency, Vienna. 1960. p. 97.
9. R. A. COX and A. J. SWALLOW. Chem. Ind. London, 1277 (1956).
10. R. A. COX and A. J. SWALLOW. J. Chem. Soc. 3727 (1958).

RECEIVED JULY 22, 1965.
PUERTO RICO NUCLEAR CENTER,
MAYAGUEZ, PUERTO RICO.

ORGANIC SULFUR MECHANISMS
III. A BRIEF INVESTIGATION INTO THE REACTION OF BENZONITRILE OXIDE WITH SULFENES[1]

J. F. KING AND T. DURST

As part of our scrutiny of the chemistry of sulfenes (1, 2 and references therein), we were led to consider whether these species were capable of 1,3-dipolar cycloaddition reactions. 1,2-Cycloadditions leading to products with four-membered rings appear to be well established (3–6); however, although certain reactions of sulfenes may be rationalized in terms of 1,3-dipolar additions, no such processes have actually been authenticated.[2] As the question seemed to have bearing on our study of the mechanism of the coupling of phenylsulfene to form *trans*-stilbene and *cis*-diphenylethylene sulfone (8–10), we sought some information on the point.

We chose to look at the reaction of sulfenes with a nitrile oxide, chiefly because such a species would appear to be able to react both as a dipolar reagent and as a dipolarophile,[3] and would therefore be potentially capable of detecting either type of reactivity in sulfenes. Of the various known nitrile oxides, benzonitrile oxide is comparatively readily accessible. Thus, when an ethereal solution of α-chlorobenzaldoxime (benzoyl chloride oxime) is treated with triethylamine, triethylammonium chloride forms a precipitate immediately, and the nitrile oxide remains in solution along with any excess triethylamine. Since triethylamine is known (1, 2) to react with phenylmethanesulfonyl chloride to give phenylsulfene, the nitrile oxide – triethylamine solution was added directly to a solution of the sulfonyl chloride, in the expectation of observing the reaction of the sulfene and the nitrile oxide. The crystalline product which was obtained (and which could also be

[1]*An independent and more extensive study, leading to the same conclusion about the structure of the new class of compounds, has been carried out by Professor W. E. Truce and Dr. A. R. Naik of Purdue University, and is described elsewhere in this issue.*

[2]*A 1,3-dipolar addition to a sulfene has been suggested by Strating (7) as a mechanism for the formation of oxythioacyl halides. The available evidence, however, permits other interpretations.*

[3]*Huisgen, however, questions the idea that benzonitrile oxide is functioning as a dipolarophile in the formation of diphenylfuroxan (11), the reaction which is probably the best-known example of the alleged dipolarophile activity of nitrile oxides.*

Can. J. Chem. Downloaded from www.nrcresearchpress.com by 210.87.254.40 on 09/05/12
For personal use only.

prepared simply by mixing the three reagents and allowing the mixture to stand for 5 min) was not, however, any normal product of a dipolar cycloaddition.

Analysis indicated the empirical formula $C_{14}H_{12}NSO_3Cl$, implying a formal derivation from 1 molecule each of phenylsulfene, benzonitrile oxide, and hydrogen chloride. The nuclear magnetic resonance spectrum showed only a singlet at 4.67 p.p.m. (relative area 1) and aromatic protons from 7.4 to 8.1 p.p.m. (relative area 5). The chemical shift of the nonaromatic proton(s) is well within the range (4.1 to 5.0 p.p.m.) which we (10) have found for the benzylic hydrogens in about a dozen structurally varied compounds containing the $PhCH_2SO_2$ group; the value observed for these protons in benzophenone oxime phenylmethanesulfonate (4.68 p.p.m.) is effectively identical with that found for the compound from the nitrile oxide reaction. The compound shows absorption in the ultraviolet region (λ_{max} 252 mμ, ϵ 10 000) very similar to that of acetophenone oxime and the benzaldoximes (12), which have maxima near 250 mμ with extinction coefficients slightly over 10 000. Three very strong bands are found in the infrared spectrum at 1 386, 1 178, and 816 cm^{-1}. The positions of the two higher frequency bands are in good agreement with those expected for a sulfonic ester, but are distinctly higher than the corresponding bands in sulfones or sulfonamides (13). A strong band around 800 cm^{-1} has been noticed by Freeman and Hambly (14) in the spectra of a number of sulfonic esters, and has been tentatively assigned to the S—OR stretching mode.

The most straightforward assembling of these data leads to structure I*a* for the compound, i.e. the material is simply the phenylmethanesulfonyl ester of α-chlorobenzaldoxime.

$$PhC{\equiv}\overset{+}{N}{-}\overset{-}{O} + RCH_2SO_2Cl \xrightarrow{Et_3N} Ph{-}\overset{Cl}{\overset{|}{C}}{=}N{-}OSO_2CH_2R$$

I*a* R = Ph
I*b* R = H

A structure in which the $PhCH_2SO_2$ group and the chlorine are interchanged is not excluded, but would require a more complex mode of formation, and would therefore seem less likely in the absence of any evidence favoring it.

Though no attempt has been made to explore the full scope of the reaction, its generality is suggested by the fact that a very similar compound is formed when methanesulfonyl chloride replaces phenylmethanesulfonyl chloride in the reaction. By analogy, structure I*b* is assigned to the material.

There appear to be two simple routes by which these materials might be formed from a sulfene in the reactions: (*i*) attack of the sulfene on α-chlorobenzaldoxime, which may be present or re-formed (in small quantity) in the medium, or (*ii*) reaction of the sulfene with the nitrile oxide to form a cationic intermediate ($PhC{\equiv}\overset{+}{N}{-}OSO_2CH_2Ph$) which subsequently picks up a chloride anion. The apparent completeness of the conversion of α-chlorobenzaldoxime into benzonitrile oxide with base suggests that route *ii* is perhaps more probable than route *i*, but clearly distinguishing evidence is lacking.

To the original aim of this study, these observations contribute only the conclusion that benzonitrile oxide and sulfenes do not yield the products of a dipolar addition under the conditions tried. Whether these species would undergo dipolar addition in the absence of triethylammonium chloride remains uncertain, though it seems likely that the reaction would not be extremely rapid; at present, however, it is not particularly easy to obtain direct evidence on the point. The products of these reactions represent an appar-

Can. J. Chem. Downloaded from www.nrcresearchpress.com by 210.87.254.40 on 09/05/12
For personal use only.

ently hitherto unknown type of oxime (or hydroxamic acid) derivative. Their significance in the chemistry of sulfenes remains unestablished, but they promise interesting chemistry in their own right.

EXPERIMENTAL

Melting points were determined on a Kofler block and are uncorrected. Infrared spectra were obtained with Beckman IR-5 or IR-7 spectrophotometers equipped with sodium chloride optics, or a Beckman IR-5A instrument equipped with cesium bromide optics. The silica gel referred to is British Drug Houses "suitable for chromatography" grade.

Reaction of Benzonitrile Oxide, Phenylmethanesulfonyl Chloride, and Triethylamine

α-Chlorobenzaldoxime (15) (1.8 g, 12 mmoles) and phenylmethanesulfonyl chloride (Eastman Kodak white label, sold under the alternative name α-toluenesulfonyl chloride) (3.0 g, 16 mmoles) were dissolved in methylene chloride (30 ml) and treated quickly with excess triethylamine. The solution was allowed to stand at room temperature for 5 min, then poured into water, and extracted with ether. The material remaining after evaporation of the ether was chromatographed on silica gel. Elution with benzene gave a material (2.24 g, 7.3 mmoles, 60%) which was crystallized from methylene chloride – pentane as heavy colorless crystals, m.p. 104–105°.

Anal. Calcd. for $C_{14}H_{12}NSO_3Cl$: C, 54.29; H, 3.88; N, 4.52; S, 10.35; Cl, 11.42. Found: C, 54.22; H, 4.07; N, 4.57; S, 10.54; Cl, 11.59.

The ultraviolet spectrum showed a single maximum at 252 mμ (ε 10 000). Infrared spectrum (0.4 *M* in CH_2Cl_2; IR-7 above 800 cm^{-1}, IR-5A below 800 cm^{-1}): 3 070 (w), 1 593 (m), 1 566 (m), 1 496 (m), 1 457 (w), 1 448 (m), 1 386 (vs), 1 206 (s), 1 178 (vs), 1 143 (w), 1 075 (w), 1 030 (w), 1 001 (w), 978 (m), 899 (s), 874 (s), 816 (vs), 637 (m), 622 (w), 603 (m), 585 (w), 543 (s), 492 (m). The nuclear magnetic resonance spectrum showed complex absorption in the region 7.4 to 8.1 p.p.m. and a singlet at 4.67 p.p.m. (relative areas 5:1).

In a separate experiment α-chlorobenzaldoxime was treated with excess triethylamine in ether solution. The triethylammonium chloride was filtered off and the filtrate added to an ethereal solution of phenylmethanesulfonyl chloride; work-up as above gave the same product.

Reaction of Benzonitrile Oxide, Methanesulfonyl Chloride, and Triethylamine

α-Chlorobenzaldoxime (450 mg, 2.9 mmoles) was dissolved in anhydrous ether (20 ml) and treated with triethylamine (1 ml, 7.2 mmoles). The triethylammonium chloride which precipitated was filtered off. Methanesulfonyl chloride (350 mg, 3.1 mmoles) in ether (5 ml) was added to the filtrate and the solution was allowed to stand at room temperature for a day. The mixture was then poured into water and extracted with ether. Chromatography of the ether extract on silica gel gave, on elution with 1:1 low-boiling petroleum ether – benzene, a white solid (255 mg, 1.1 mmoles, 37%) which, after recrystallization from methylene chloride – pentane, melted at 110–112°.

Anal. Calcd. for $C_8H_8NSO_3Cl$: C, 41.11; H, 3.45; N, 6.03; S, 13.72; Cl, 15.15. Found: C, 41.05; H, 3.54; N, 6.10; S, 13.69; Cl, 15.06.

The nuclear magnetic resonance spectrum showed complex absorption from 8.0 to 7.3 p.p.m. and a singlet at 3.25 p.p.m. (relative areas 5:3). The principal bands in the infrared spectrum ($CHCl_3$, IR-5) between 1 700 and 800 cm^{-1} are: 1 385 (s), 1 265 (s), 1 188 (s), 969 (m), 897 (s), 819 (s).

ACKNOWLEDGMENTS

This work was supported through a grant-in-aid and a scholarship by the National Research Council of Canada, and via a grant-in-aid by the Petroleum Research Fund administered by the American Chemical Society.

1. J. F. King and T. Durst. J. Am. Chem. Soc. In press.
2. J. F. King and T. Durst. J. Am. Chem. Soc. **86**, 287 (1964).
3. R. Fusco, S. Rossi, and S. Maiorana. Chim. Ind. Milan, **44**, 873 (1962).
4. I. J. Borowitz. J. Am. Chem. Soc. **86**, 1146 (1964). G. Stork and I. J. Borowitz. J. Am. Chem. Soc. **84**, 313 (1962).
5. G. Opitz and H. Adolph. Angew. Chem. **74**, 77 (1962).
6. G. Opitz and K. Fischer. Z. Naturforsch. **18b**, 775 (1963).
7. J. Strating. Rec. Trav. Chim. **83**, 94 (1964).
8. E. Wedekind and D. Schenk. Ber. **44**, 198 (1911).
9. J. F. King and T. Durst. J. Am. Chem. Soc. **85**, 2676 (1963).
10. J. F. King and T. Durst. Unpublished observations.
11. R. Huisgen. Angew. Chem. **75**, 604 (1963).

Can. J. Chem. Downloaded from www.nrcresearchpress.com by 210.87.254.40 on 09/05/12
For personal use only.

12. R. F. REKKER and J. U. VEENLAND. Rec. Trav. Chim. **78**, 739 (1959).
13. L. J. BELLAMY. *In* Organic sulfur compounds. Vol. 1. *Edited by* N. Kharasch. Pergamon Press, New York. 1961. Chap. 6. p. 47.
14. D. E. FREEMAN and A. N. HAMBLY. Australian J. Chem. **10**, 239 (1957).
15. H. HENECKA and P. KURTZ. *In* Methoden der Organischen Chemie (Houben-Weyl). Vol. 8. 4th ed. Georg Thieme Verlag, Stuttgart. 1952. p. 691.

RECEIVED JULY 22, 1965.
DEPARTMENT OF CHEMISTRY,
UNIVERSITY OF WESTERN ONTARIO,
LONDON, ONTARIO.

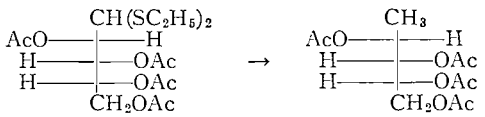
Can. J. Chem. Downloaded from www.nrcresearchpress.com by 210.87.254.40 on 09/05/12
For personal use only.

THE SEPARATION OF ALDOPENTOSE AND ALDOHEXOSE DIETHYL DITHIOACETAL DERIVATIVES BY GAS–LIQUID PARTITION CHROMATOGRAPHY

D. T. WILLIAMS AND J. K. N. JONES

INTRODUCTION

Numerous workers have separated and identified the aldopentoses and aldohexoses by gas–liquid partition chromatography (g.l.p.c.) of certain of their derivatives. The derivatives normally used have been the fully acetylated methyl glycosides, aldose acetates, and alditol acetates (1–5). More recently trimethylsilyl derivatives have been employed instead of the acetylated derivatives (6–8). Except for the alditol acetates, the presence of anomeric isomers invariably causes problems in interpretation when a mixture of sugars is being analyzed. The use of alditol derivatives avoids this confusion but, since the same alditol can arise from two different aldoses, an unambiguous assignment of the parent aldose cannot always be made. Bentley *et al.* (8) investigated the g.l.p.c. of the trimethylsilyl derivatives of aldose oximes, acetals, and thioacetals, but they reported unsatisfactory separations of these compounds. During our work on the oxidation of aldose thioacetals by *A. suboxydans* we have found that fully acetylated aldose diethyl dithioacetals can be separated satisfactorily by g.l.p.c. (Table I). The advantage of thioacetal derivatives is that each aldose gives a single product which has only one peak on g.l.p.c. but which still retains the complete individuality of the parent aldose. A second set of derivatives with these advantages is the fully acetylated 1-deoxyalditols (Table II), which can easily be obtained by boiling the corresponding thioacetal derivatives, shown below, under reflux with freshly prepared Raney nickel. From the relative



retention times of these pairs of derivatives an unambiguous assignment of the parent aldose dithioacetal acetate can be made.

It should be emphasized, however, that this technique is not suitable for the quantitative analysis of sugar mixtures because of the variation in yields of diethyl dithioacetal derivatives and because of the formation of other faster moving products formed during the desulfurization step. De-*O*-acetylation, which might conceivably occur because of the

12. R. F. REKKER and J. U. VEENLAND. Rec. Trav. Chim. **78**, 739 (1959).
13. L. J. BELLAMY. *In* Organic sulfur compounds. Vol. 1. *Edited by* N. Kharasch. Pergamon Press, New York. 1961. Chap. 6. p. 47.
14. D. E. FREEMAN and A. N. HAMBLY. Australian J. Chem. **10**, 239 (1957).
15. H. HENECKA and P. KURTZ. *In* Methoden der Organischen Chemie (Houben-Weyl). Vol. 8. 4th ed. Georg Thieme Verlag, Stuttgart. 1952. p. 691.

RECEIVED JULY 22, 1965.
DEPARTMENT OF CHEMISTRY,
UNIVERSITY OF WESTERN ONTARIO,
LONDON, ONTARIO.

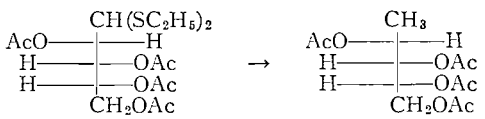
Can. J. Chem. Downloaded from www.nrcresearchpress.com by 210.87.254.6 on 09/05/12
For personal use only.

THE SEPARATION OF ALDOPENTOSE AND ALDOHEXOSE DIETHYL DITHIOACETAL DERIVATIVES BY GAS–LIQUID PARTITION CHROMATOGRAPHY

D. T. WILLIAMS AND J. K. N. JONES

INTRODUCTION

Numerous workers have separated and identified the aldopentoses and aldohexoses by gas–liquid partition chromatography (g.l.p.c.) of certain of their derivatives. The derivatives normally used have been the fully acetylated methyl glycosides, aldose acetates, and alditol acetates (1–5). More recently trimethylsilyl derivatives have been employed instead of the acetylated derivatives (6–8). Except for the alditol acetates, the presence of anomeric isomers invariably causes problems in interpretation when a mixture of sugars is being analyzed. The use of alditol derivatives avoids this confusion but, since the same alditol can arise from two different aldoses, an unambiguous assignment of the parent aldose cannot always be made. Bentley *et al.* (8) investigated the g.l.p.c. of the trimethylsilyl derivatives of aldose oximes, acetals, and thioacetals, but they reported unsatisfactory separations of these compounds. During our work on the oxidation of aldose thioacetals by *A. suboxydans* we have found that fully acetylated aldose diethyl dithioacetals can be separated satisfactorily by g.l.p.c. (Table I). The advantage of thioacetal derivatives is that each aldose gives a single product which has only one peak on g.l.p.c. but which still retains the complete individuality of the parent aldose. A second set of derivatives with these advantages is the fully acetylated 1-deoxyalditols (Table II), which can easily be obtained by boiling the corresponding thioacetal derivatives, shown below, under reflux with freshly prepared Raney nickel. From the relative



retention times of these pairs of derivatives an unambiguous assignment of the parent aldose dithioacetal acetate can be made.

It should be emphasized, however, that this technique is not suitable for the quantitative analysis of sugar mixtures because of the variation in yields of diethyl dithioacetal derivatives and because of the formation of other faster moving products formed during the desulfurization step. De-*O*-acetylation, which might conceivably occur because of the

possible presence of base in the Raney nickel catalyst, was not observed. However, any ambiguity which might be caused as a result of this possibility may be obviated if the mixture is reacetylated after reduction and before analysis.

DISCUSSION AND RESULTS

The best separations were generally obtained with LAC-4R-886 polyester grease on Chromosorb W, although in the case of the aldopentose diethyl dithioacetal tetraacetates 20% Apiezon M grease on Chromosorb W was found to be the most suitable column packing. With this second packing (column III) the aldopentose diethyl dithioacetal tetraacetates were easily identified both as individual standards and when run as mixtures. However, with a column packing of 5% LAC polyester grease (column I), a mixture of D-lyxose and D-arabinose diethyl dithioacetal tetraacetates gave only one peak, with a retention time intermediate between that of the two individual standards. Furthermore, the order of elution of the aldopentose thioacetals varied with the nature of the liquid phase (Table I); therefore, no attempt was made to correlate the structures of the thioacetals with their relative retention times.

TABLE I

Retention times of acetylated diethyl dithioacetals (in min and relative to that of D-ribose diethyl dithioacetal tetraacetate) (flow rate, 92 ml argon/min; temperature, 198°)

Diethyl dithioacetal acetates of:	Column packing: I		III	
	Min	Relative	Min	Relative
D-Ribose	12.2	1.00	26.7	1.00
D-Arabinose	13.5	1.11	29.0	1.08
D-Lyxose	14.0	1.15	30.4	1.14
D-Xylose	14.8	1.21	27.8	1.04
D-Allose	28.3	2.32		
D-Mannose	33.0	2.70		
D-Altrose	33.5	2.75		
D-Talose	33.7	2.76		
D-Glucose	35.3	2.89		
D-Galactose	40.0	3.28		
L-Gulose	40.8	3.34		
L-Idose	44.5	3.65		

The separation of the aldohexose dithioacetal pentaacetates was not as simple, since D-altrose and D-talose diethyl dithioacetal pentaacetates and D-galactose and L-gulose diethyl dithioacetal pentaacetates were not distinguishable from each other (Table I). However, examination of the acetylated 1-deoxyalditols (Table II) by g.l.p.c. on a column of 15% LAC polyester grease (column II) showed that all of these compounds were separable, except for 1-deoxy-D-glucitol and 1-deoxy-L-gulitol pentaacetates. A combination of the results from Tables I and II, therefore, gives an unambiguous identification of each aldose.

EXPERIMENTAL

Preparation of Aldose Diethyl Dithioacetals

The aldose (1 g) was dissolved in concentrated hydrochloric acid (1 ml), cooled to 0°, and then shaken with ethanethiol (1 ml) for 20–30 min. The reaction mixture was then poured into excess alkaline solution and the aqueous solution continuously extracted with chloroform for 3–4 h. The chloroform extract was

Can. J. Chem. Downloaded from www.nrcresearchpress.com by 210.87.254.6 on 09/05/12
For personal use only.

TABLE II

Retention times of acetylated 1-deoxyalditols (in min and relative to that of 1-deoxy-D-ribitol tetraacetate) (flow rate, 75 ml argon/min; temperature, 198°)

1-Deoxyalditol acetates of:	Column packing II	
	Min	Relative
D-Ribitol	5.9	1.00
D-Arabinitol	6.3	1.07
D-Lyxitol	6.75	1.14
D-Xylitol	8.7	1.47
D-Allitol	16.3	2.77
D-Mannitol	17.6	2.99
D-Altritol	18.1	3.07
D-Talitol	18.5	3.14
D-Galactitol	20.2	3.42
D-Glucitol	23.6	4.00
L-Gulitol	23.7	4.02
L-Iditol	28.7	4.88

dried (Na_2SO_4), filtered, and concentrated to a syrup which usually crystallized in seconds. Recrystallization from ethanol yielded the aldose diethyl dithioacetal.

The following thioacetals were prepared in this manner: D-arabinose, D-ribose, D-xylose, D-lyxose, D-glucose, D-galactose, D-mannose, D-altrose, D-talose, and D-allose.

Mixtures of D-mannose and L-gulose diethyl dithioacetals and D-glucose and L-idose diethyl dithioacetals were prepared by reduction, with $NaBH_4$, of D-*lyxo*-hexo-5-ulose-1,1-diethyl dithioacetal and D-*xylo*-hexo-5-ulose-1,1-diethyl dithioacetal respectively (9).

Aldose Diethyl Dithioacetal Pentaacetates

The aldose diethyl dithioacetal (0.5 g) was dissolved in dry pyridine (3 ml), and acetic anhydride (4 ml) was added. After the reaction mixture was allowed to stand at room temperature for 18 h, it was worked up in the usual manner to give the aldose diethyl dithioacetal acetates.

1-Deoxyalditol Pentaacetates

The aldose diethyl dithioacetal pentaacetate was boiled under reflux in ethanol for 16 h with approximately four times its weight of freshly prepared Raney nickel (10). The Raney nickel was filtered off and washed well with methanol. The filtrate and washings were then concentrated to a syrup, which consisted mainly of the 1-deoxyalditol acetate. Some other degradation products were also present, but these ran at a much faster rate on g.l.p.c. and did not interfere in any way. 1-Deoxy-D-galactitol and 1-deoxy-1-mannitol were also prepared by sodium borohydride reduction of L-fucose and L-rhamnose respectively. Acetylation with acetic anhydride and pyridine then gave the corresponding acetates.

Gas–Liquid Partition Chromatographic Separations

The recorded separations were made on a Pye argon chromatograph which was fitted with an ionization detector (80 μcuries radium D) and which employed straight glass columns (117 × 0.5 cm inside diameter) packed with the appropriate support and enclosed at each end by small glass wool plugs. The samples (5–20 μl) in dry chloroform were placed on top of the column by a micropipette, and development was carried out with dry argon as the carrier gas.

Column packing I consisted of 5% LAC-4R-886 polyester grease (Chromatographic Specialities, Brockville) on nonacid-washed Chromosorb W, 80–100 mesh. *Column packing II* consisted of 15% LAC-4R-886 polyester grease on nonacid-washed Chromosorb W, 80–100 mesh. *Column packing III* consisted of 20% Apiezon M grease (Fisher Scientific Co.) on nonacid-washed Chromosorb W, 100–120 mesh.

The dried column packings were run into the glass columns under gravity, with gentle tapping to ensure even packing.

ACKNOWLEDGMENTS

We thank the National Research Council for financial assistance (N.R.C. T-19) and for the award of a scholarship to one of us (D. T. W.). We also thank Dr. M. B. Perry and Mr. B. T. Lawton for generous gifts of D-talose and D-allose respectively.

Can. J. Chem. Downloaded from www.nrcresearchpress.com by 210.87.254.6 on 09/05/12
For personal use only.

1. S. W. GUNNER, J. K. N. JONES, and M. B. PERRY. Chem. Ind. London, 255 (1961).
2. A. W. KIRCHER. Tappi, **45**, 143 (1962).
3. R. J. FERRIER. Chem. Ind. London, 831 (1961).
4. S. W. GUNNER, J. K. N. JONES, and M. B. PERRY. Can. J. Chem. **39**, 1892 (1961).
5. C. T. BISHOP and F. P. COOPER. Can. J. Chem. **38**, 388 (1960).
6. R. J. FERRIER. Tetrahedron, **18**, 1149 (1962).
7. E. J. HEDGLEY and W. G. OVEREND. Chem. Ind. London, 378 (1960).
8. R. BENTLEY, M. MAKITA, C. C. SWEELEY, and W. W. WELLS. J. Am. Chem. Soc. **85**, 2497 (1963).
9. D. T. WILLIAMS and J. K. N. JONES. Can. J. Chem. **43**, 955 (1965).
10. A. I. VOGEL. Textbook of practical organic chemistry. Longmans, Green and Co., Inc., New York. 1951.

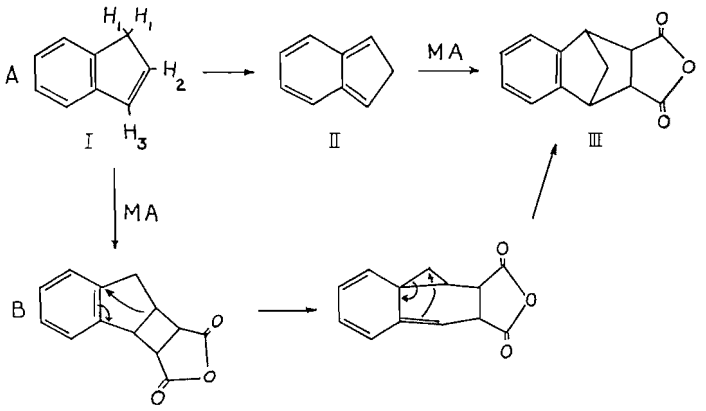
RECEIVED SEPTEMBER 24, 1965.
DEPARTMENT OF CHEMISTRY,
QUEEN'S UNIVERSITY,
KINGSTON, ONTARIO.

Can. J. Chem. Downloaded from www.nrcresearchpress.com by 210.87.254.6 on 09/05/12
For personal use only.

CONCERNING THE REACTION BETWEEN MALEIC ANHYDRIDE AND INDENE

NEIL S. ISAACS

The singular 1,3-addition of maleic anhydride (MA) to indene (1, 2) involving a concomitant hydrogen shift has recently been the subject of a study by Berson and co-workers (3, 4), who have distinguished between a mechanism proposed originally by Alder, in which prior isomerization to isoindene (II) occurs (Reaction Scheme 1A), and one that was postulated by themselves from analogy with a rearrangement in the bicyclo-(3,2,0)-heptene series and which involved 1,2-addition and rearrangement (Reaction Scheme 1B).



REACTION SCHEME 1.

In Reaction Scheme 1A, C-2 of the indene molecule becomes the methylene bridge of the adduct (III), whereas in Reaction Scheme 1B the latter is formed from C-1 with skeletal rearrangement but no hydrogen transfer. When he worked with partially deuterated indene (mostly on C-1 and C-3), Berson concluded that Reaction Scheme 1B

1. S. W. GUNNER, J. K. N. JONES, and M. B. PERRY. Chem. Ind. London, 255 (1961).
2. A. W. KIRCHER. Tappi, **45**, 143 (1962).
3. R. J. FERRIER. Chem. Ind. London, 831 (1961).
4. S. W. GUNNER, J. K. N. JONES, and M. B. PERRY. Can. J. Chem. **39**, 1892 (1961).
5. C. T. BISHOP and F. P. COOPER. Can. J. Chem. **38**, 388 (1960).
6. R. J. FERRIER. Tetrahedron, **18**, 1149 (1962).
7. E. J. HEDGLEY and W. G. OVEREND. Chem. Ind. London, 378 (1960).
8. R. BENTLEY, M. MAKITA, C. C. SWEELEY, and W. W. WELLS. J. Am. Chem. Soc. **85**, 2497 (1963).
9. D. T. WILLIAMS and J. K. N. JONES. Can. J. Chem. **43**, 955 (1965).
10. A. I. VOGEL. Textbook of practical organic chemistry. Longmans, Green and Co., Inc., New York. 1951.

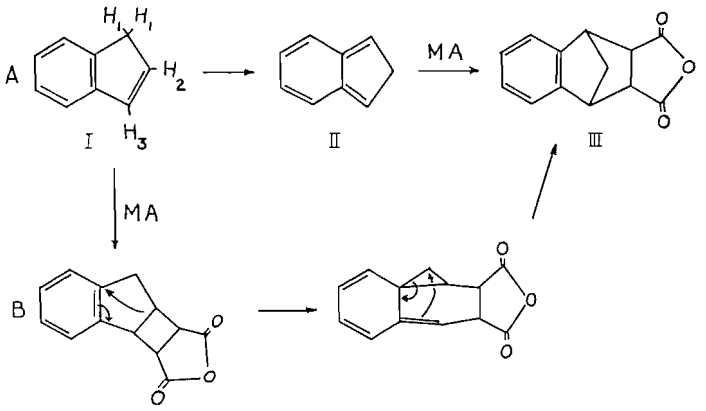
RECEIVED SEPTEMBER 24, 1965.
DEPARTMENT OF CHEMISTRY,
QUEEN'S UNIVERSITY,
KINGSTON, ONTARIO.

Can. J. Chem. Downloaded from www.nrcresearchpress.com by 210.87.254.42 on 09/05/12
For personal use only.

CONCERNING THE REACTION BETWEEN MALEIC ANHYDRIDE AND INDENE

NEIL S. ISAACS

The singular 1,3-addition of maleic anhydride (MA) to indene (1, 2) involving a concomitant hydrogen shift has recently been the subject of a study by Berson and co-workers (3, 4), who have distinguished between a mechanism proposed originally by Alder, in which prior isomerization to isoindene (II) occurs (Reaction Scheme 1A), and one that was postulated by themselves from analogy with a rearrangement in the bicyclo-(3,2,0)-heptene series and which involved 1,2-addition and rearrangement (Reaction Scheme 1B).



REACTION SCHEME 1.

In Reaction Scheme 1A, C-2 of the indene molecule becomes the methylene bridge of the adduct (III), whereas in Reaction Scheme 1B the latter is formed from C-1 with skeletal rearrangement but no hydrogen transfer. When he worked with partially deuterated indene (mostly on C-1 and C-3), Berson concluded that Reaction Scheme 1B

is untenable; we have confirmed this in work with indene-2-*d*, the adduct of which essentially retains all the deuterium on the methylene bridge.

In addition we have found that the rate, measured by the disappearance of indene, appears to depend upon the concentration of maleic anhydride (Fig. 1).

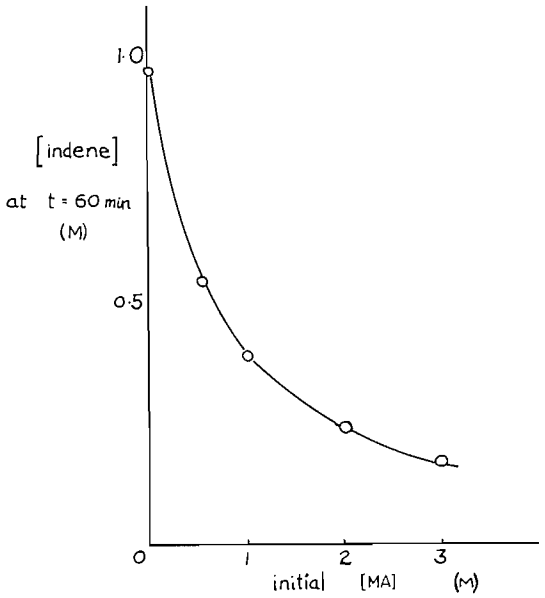
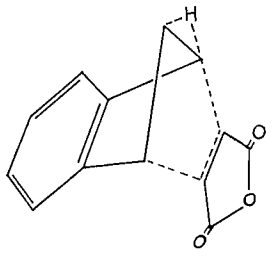


FIG. 1.

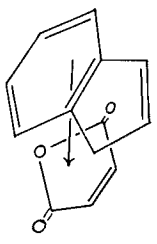
According to Reaction Scheme 1A, the slow step of the reaction is the isomerization of indene, which should be independent of maleic anhydride concentration. If a molecule of maleic anhydride is implicated in the rate-determining step, three possibilities may be considered. Firstly, the isomerization of indene to isoindene may be appreciably reversible, i.e. $k_{-1} \approx k_2$, although Roth's (5) recent study of the thermal isomerization of indene

$$\text{I} \underset{k_{-1}}{\overset{k_1}{\rightleftharpoons}} \text{II} \underset{k_2}{\overset{\text{MA}}{\rightleftharpoons}} \text{III}$$

does not support this. Secondly, a hitherto unconsidered mechanism, albeit one without exact precedent in Diels–Alder type additions, would involve a bimolecular reaction leading directly to 1,3-addition in concert with the hydrogen shift. This could occur through operation of the 'maximum overlapping' principle, thereby leading to the *endo* adduct via an essentially planar transition state (IV). A third way in which the maleic



IV



V

Can. J. Chem. Downloaded from www.nrcresearchpress.com by 210.87.254.42 on 09/05/12
For personal use only.

anhydride concentration might affect the rate is by charge-transfer complexing (6, 7), thereby leading to a lowering of the activation energy for the isomerization to isoindene and to stabilization of the isoindene intermediate. The maleic anhydride is then, incidentally, in a very favorable environment (V) to react with the diene. Isomerization induced by maleic anhydride before addition has been suggested to account for adducts formed with non-conjugated dienes such as limonene (8), although such reactions may involve hydrogen transfer to maleic anhydride (9). That charge transfer occurs between indene and maleic anhydride is evident from the yellow color (λ_{max} = 630 mμ) produced on admixture of the two compounds (cf. indene (λ_{max} = 245 mμ) and maleic anhydride (end absorption <240 mμ)).

The latter mechanism, perhaps, seems to be the most attractive at present, but further work with substituted indenes might permit a distinction to be made.

EXPERIMENTAL

Nuclear magnetic resonance and infrared spectra were recorded on Varian A60 and Beckman IR-4 spectrometers respectively. Integration measurements are the average of two or three recordings and are consistent to approximately 0.05 proton unit.

Preparation of Indene-2-d

Indan-2-ol-2-d

To indan-2-one (3.28 g, 24.3 mmoles), prepared by the method of Pfeiffer and Hesse (10) in dry ether (25 ml), was added a slurry of lithium aluminium deuteride (0.34 g, 8.1 mmoles). The mixture was stirred for 2 h and boiled under reflux for 1 h, after which water was added, the ethereal solution separated and dried with $MgSO_4$, and the solvent removed to give indan-2-ol-2-*d*.

Without further purification the deuterated indanol was added to acetic anhydride (5.01 ml) and the mixture warmed on a steam bath for 20 min. The acetic anhydride and acetic acid were removed by distillation, and indan-2-yl acetate-2-*d* was distilled at 75° and 3 mm; yield, 4.15 g (95%). Both the alcohol and the ester showed an absorption peak at 2 150 cm^{-1}.

Indene-2-d

The indanyl acetate-2-*d*, dissolved in an equal volume of benzene, was dropped, in a slow nitrogen stream, through a 6 inch tube that was packed with silica chips and which was surrounded by a furnace to maintain the center of the tube at 490 ± 10°. The rate of addition was adjusted to 4–6 drops per min, and the emerging vapors were condensed, washed with sodium bicarbonate solution, and dried with $MgSO_4$. Distillation yielded indene-2-*d*; b.p. 63° at 12 mm; yield, 1.52 g (55%). The deuterium content was estimated as better than 0.95 atom of deuterium per molecule by its proton resonance, in which the peak at 3.6 μ in the indene spectrum is assigned to H-2 and that at 3.3 μ to H-3.

Reaction between Indene-2-d and Maleic Anhydride

Indene-2-*d* (1.0 g), freshly sublimed maleic anhydride (0.6 g), and hydroquinone (2 mg) were dissolved in benzene (1 ml) and sealed under vacuum into a length of 3 mm bore glass tubing. The tube was heated at 210° for 2.5 h. When the solution was allowed to cool, the product crystallized. Recrystallization from ethyl acetate yielded the adduct III, m.p. 188° (lit. m.p. 187–188 (1)).

The nuclear magnetic resonance spectrum of this product in $CDCl_3$ (internal tetramethylsilane) showed 1.1 protons on the methylene bridge at approximately 8 μ, indicating that this is derived from C-2 of indene. The slight loss of deuterium is due to 'scrambling' of hydrogen around the five-membered ring, as studied by Roth (5); this was examined by us in a separate experiment in which partially deuterated indene-1,1,3-*d* was heated under the same conditions but in the absence of maleic anhydride. The results are summarized in Table I.

TABLE I

Thermal stability of indene-2-*d* (protons per molecule)

	Before heating	After heating
Aromatic	4.0	4.0
C-1	0.28	0.37
C-2	0.99	0.78
C-3	0.14	0.15

Can. J. Chem. Downloaded from www.nrcresearchpress.com by 210.87.254.42 on 09/05/12
For personal use only.

Kinetic Experiments

Indene was purified by repeated fractional distillation of reagent-grade indene (Eastman), and maleic anhydride by sublimation *in vacuo*.

Samples (1.00 ml) of a benzene solution of indene (1.0 *M*) containing a trace of hydroquinone and maleic anhydride in concentrations up to 3 *M* were heated for 1 h in sealed tubes at 184°. The samples were cooled, separately diluted to 10 ml with acetone, and analyzed for indene by gas chromatography with a silicone column at 180° and helium as the carrier gas. The results are shown in Fig. 1.

ACKNOWLEDGMENTS

We express our thanks to Professor R. C. Cookson, who suggested the problem and, together with Dr. L. D. Hall, made the nuclear magnetic resonance measurements; and to the Department of Scientific and Industrial Research for a fellowship, during which much of this work was carried on.

1. K. Alder, F. Pascher, and M. Vogt. Chem. Ber. **75**, 1501 (1942).
2. K. Alder and M. Fremery. Tetrahedron, **14**, 190 (1961).
3. J. A. Berson and J. W. Patton. J. Am. Chem. Soc. **84**, 3406 (1962).
4. J. A. Berson and G. B. Aspelin. Tetrahedron, **20**, 2697 (1964).
5. W. R. Roth. Tetrahedron Letters, **17**, 1009 (1964).
6. R. S. Mullikan. J. Am. Chem. Soc. **74**, 811 1952).
7. M. J. S. Dewar and A. R. Lepley. J. Am. Chem. Soc. **83**, 4560 (1961).
8. K. Hultzsch. Ber. **72**B, 1173 (1939).
9. A. Nickon. J. Am. Chem. Soc. **77**, 1190 (1955).
10. P. Pfeiffer and T. Hesse. J. Prakt. Chem. **158**, 315 (1941).

Received March 8, 1965.
Department of Chemistry,
University of Victoria,
Victoria, British Columbia.

Can. J. Chem. Downloaded from www.nrcresearchpress.com by 210.87.254.42 on 09/05/12
For personal use only.

Can. J. Chem. Downloaded from www.nrcresearchpress.com by 210.87.254.6 on 09/05/12
For personal use only.

Canadian Journal of Chemistry

Issued by THE NATIONAL RESEARCH COUNCIL OF CANADA

VOLUME 44 FEBRUARY 15, 1966 NUMBER 4

SELENIUM ISOTOPE EFFECTS IN THE REDUCTION OF SODIUM SELENITE AND OF SODIUM SELENATE

C. E. REES[1] AND H. G. THODE

Chemistry Department, McMaster University, Hamilton, Ontario

Received August 17, 1965

ABSTRACT

Selenium isotope effects in the reduction of sodium selenite and of sodium selenate have been studied. Rate constant ratios for the ^{76}Se and ^{82}Se species have been determined for the reactions $Se^{iv} \rightarrow Se^{0}$ (1.017), $Se^{vi} \rightarrow Se^{iv}$ (1.018), and $Se^{0} \rightarrow Se^{iv}$ (1.010) at room temperature. Theoretical predictions of the first two ratios, from the use of models in which the rate-controlling steps are assumed to be Se—O bond cleavages in SeO_3^{2-} and SeO_4^{2-}, respectively, lead to predictions in good agreement with experiment.

INTRODUCTION

Krouse and Thode (1) have shown that the isotopes of selenium are fractionated in nature and that, in general, the observed fractionations are similar to but smaller than those observed for sulfur. This paper presents the results of experiments on the fractionation of selenium isotopes during chemical reactions involving the reduction of selenite and selenate to selenium. Such a study is of interest in the interpretation of naturally observed fractionations, and provides results that may be compared with theoretical calculations based on statistical–mechanical methods.

Rate constants for isotopic reactions involving ^{76}Se and ^{82}Se have been compared by measuring the differences in the ^{82}Se:^{76}Se ratios between reactants and reaction products for fractional reductions. Changes in isotope abundance ratios are measured as

$$\delta \text{ (p.p.t.)} = \frac{(^{82}Se/^{76}Se)_x - (^{82}Se/^{76}Se)_{\text{standard}}}{(^{82}Se/^{76}Se)_{\text{standard}}} \times 1000,$$

where p.p.t = parts per thousand. This quantity may be related to ratios of rate constants and is also experimentally measurable with a double collection mass spectrometer. The spectrometer used in this work has previously been described (1).

THEORETICAL

For the competing isotopic reactions

$$A_1 + B + \text{----} \xrightarrow{k_1} P_1 + \text{----}$$
$$A_2 + B + \text{----} \xrightarrow{k_2} P_2 + \text{----}$$

[1]*Present Address: Department of Chemistry, University of California at San Diego, La Jolla, California, U.S.A.*

the isotope effect observed after partial reaction may be related to the ratio of rate constants. For small ($\sim 5\%$) fractions of reaction, the isotope effect, if we compare reaction products with the starting material, is given by:

$$-\delta = k_1/k_2 - 1.$$

More generally, if D is the depletion of the heavy isotope, defined as $[A_2]/[A_{20}]$, the fraction of the heavy isotope which has not yet reacted, and if δ is defined as the isotope effect for products compared with the starting material and δ' as that for substrate compared with starting material, then:

[1] $$-\delta = \frac{D - D^{k_1/k_2}}{1 - D^{k_1/k_2}}$$

[2] $$\delta' = \frac{D}{D^{k_1/k_2}} - 1.$$

The theory of isotope fractionation during chemical reactions is considered in terms of the theory of absolute rates and was first formulated by Bigeleisen (2). For the competing reactions above the ratio of rate constants is given by:

$$k_1/k_2 = ((Q_2/Q_1)/(Q_2^{\ddagger}/Q_1^{\ddagger}))(\upsilon_{1i}^{\ddagger}/\upsilon_{2i}^{\ddagger}).$$

This expression omits the transmission coefficient and Wigner tunnelling correction of absolute rate theory, the assumption being that for heavy elements these terms will remain invariant under isotopic substitution. The terms Q_2/Q_1 and $Q_2^{\ddagger}/Q_1^{\ddagger}$ are ratios of partition functions for the reactants and activated complexes respectively and each may be evaluated as

$$\prod_i^N \frac{u_{2_i}}{u_{1_i}} \frac{e^{-u_{2i}/2}}{e^{-u_{1i}/2}} \frac{1 - e^{-u_{1i}}}{1 - e^{-u_{2i}}},$$

where $u_i = h\upsilon_i/kT$ and υ_i is the i^{th} fundamental vibrational frequency of the molecule. If n is the number of atoms in the molecule, then for the reactants, N is $(3n - 6)$, and for the activated complexes it is $(3n - 7)$, since in an activated complex one of the vibrational degrees of freedom is non-genuine, corresponding to the cleavage of a bond, and is equivalent to a translation along the reaction coordinate.

According to Slater (3), the term $\upsilon_{1L}^{\ddagger}/\upsilon_{2L}^{\ddagger}$, the ratio of the two frequencies which become imaginary in the activated complex, may be evaluated in terms of the reduced masses of the activated complexes as they traverse the critical region of the reaction coordinate, so that:

$$\upsilon_{1L}^{\ddagger}/\upsilon_{2L}^{\ddagger} = (\mu_2^{\ddagger}/\mu_1^{\ddagger})^{1/2}.$$

The theoretical prediction of a ratio of rate constants requires precise knowledge of the form of the activated complex. Such information is not available and it is necessary to consider models in which the nature of the activated complex is assumed to be known. The merits of such models are gauged by their appropriateness to the physical conditions and the degree of agreement between predictions based on them and the observed isotope effects.

Three cases, which give for a particular form of model an estimate of k_1/k_2 and the extreme upper and lower values of k_1/k_2 which may arise from this model, will be considered.

I. The case where the activated complex is identical to the starting material, with the

Can. J. Chem. Downloaded from www.nrcresearchpress.com by 210.87.254.6 on 09/05/12
For personal use only.

exception that the frequency associated with the breaking bond is missing. Then

$$(Q_2/Q_1)/(Q_2^{\pm}/Q_1^{\pm}) = Q(\upsilon_{2L})/Q(\upsilon_{1L})$$

where this ratio is the same as the partition function ratio for diatomic isotopic molecules with frequencies υ_{2L} and υ_{1L}. The mass ratio is evaluated by considering the effective mass to be the reduced mass of the activated complex across the bond which breaks. Either mass or atom fragments may be used in this evaluation.

II. The case where the partition function ratio term is very close to unity. This gives a lower limit, and is also the high temperature limit of the ratio of rate constants. Then

$$k_1/k_2 = (\mu_2^{\pm}/\mu_1^{\pm})^{1/2}.$$

III. The case where the activated complex has some structure which is, strictly speaking, unknown, but for which the value of the partition function ratio lies between that for the starting material (with the omission of a frequency term) and unity. The extreme value of unity may be approached if in the transition state there is complexing of the reacting molecule with other material, so that a complicated structure is formed in which not many of the vibrational frequencies are sensitive to isotopic substitution. Then

$$k_1/k_2 = (Q_2/Q_1) \cdot (\mu_2^{\pm}/\mu_1^{\pm})^{1/2}.$$

This approach gives an upper limit for the value of k_1/k_2.

Calculations

To predict the isotope effects in the reductions of selenite and selenate, it is necessary to determine the fundamental vibrational frequencies of the species $^{76}SeO_3^{2-}$, $^{82}SeO_3^{2-}$, $^{76}SeO_4^{2-}$, and $^{82}SeO_4^{2-}$.

The fundamental frequencies for SeO_3^{2-} in Table I are the means of the values reported by Rocchiccioli (4) and Walrafen (5). These have been taken to be the frequencies appropriate to the most abundant species $^{80}SeO_3^{2-}$. The selenite ion has a pyramidal XY_3 structure and a force constant analysis must take into account the apex angle of the pyramid. Wells and Bailey (6) determined the structure of the SeO_3 groups in crystals of selenious acid and their mean apex angle of 100.6° has been used.

TABLE I

Vibrational frequency assignments

Molecule	υ_1	υ_2	υ_3	υ_4
$^{80}SeO_3^{2-}$	805 (1)*	433 (1)	735 (2)	376 (2)
$^{76}SeO_3^{2-}$	808 (1)	435 (1)	739 (2)	377 (2)
$^{82}SeO_3^{2-}$	804 (1)	431 (1)	733 (2)	376 (2)
$^{80}SeO_4^{2-}$	835 (1)	341 (2)	875 (3)	421 (3)
$^{76}SeO_4^{2-}$	835 (1)	341 (2)	882 (3)	423 (3)
$^{82}SeO_4^{2-}$	835 (1)	341 (2)	872 (3)	420 (3)

*Frequencies quoted in cm^{-1}; figures in parentheses indicate degeneracy.

The force constant analysis has been carried out by the *F–G* matrix method, the *F* and *G* matrix elements used being those given by Nakamoto (7). The following set of force constants was determined:

$$Fr = 4.497 \times 10^5 \text{ dyn cm}^{-1}$$
$$F\alpha = 0.629 \times 10^5 \text{ dyn cm}^{-1}$$
$$Frr = 0.420 \times 10^5 \text{ dyn cm}^{-1}$$
$$F\alpha\alpha = 0.092 \times 10^5 \text{ dyn cm}^{-1}.$$

Can. J. Chem. Downloaded from www.nrcresearchpress.com by 210.87.254.6 on 09/05/12
For personal use only.

These have been used to determine the frequencies for $^{76}SeO_3^{2-}$ and $^{82}SeO_3^{2-}$ quoted in Table I.

The fundamental frequencies for $^{80}SeO_4^{2-}$ listed in Table I are the means of values reported by Heath and Linnett (8), Pistorius (9), and Walrafen (10). SeO_4^{2-} has T_d symmetry. The force constants were calculated by the *F–G* matrix method, the matrix elements used being those given by Pistorius (9).

From the method of Pistorius, *Frr* is assumed to be 0.347, and, using the frequency data for $^{80}SeO_4^{2-}$, the following set of force constants was determined:

$$\begin{aligned} Fr &= 5.529 \times 10^5 \text{ dyn cm}^{-1} \\ Fr\alpha - Fr\alpha' &= -0.195 \times 10^5 \text{ dyn cm}^{-1} \\ F\alpha - F\alpha\alpha' &= 0.660 \times 10^5 \text{ dyn cm}^{-1} \\ F\alpha\alpha - F\alpha\alpha' &= 0.148 \times 10^5 \text{ dyn cm}^{-1}. \end{aligned}$$

These have been used to determine the frequencies for $^{76}SeO_4^{2-}$ and $^{82}SeO_4^{2-}$ listed in Table I.

Table II shows calculated ratios of partition functions for the molecules SeO_3^{2-} and

TABLE II

Partition function ratios for selenite and selenate

T, °C	$Q(^{82}SeO_3^{2-})/Q(^{76}SeO_3^{2-})$	$Q(^{82}SeO_4^{2-})/Q(^{76}SeO_4^{2-})$
0	1.029 (1.008)*	1.054 (1.015)
25	1.025 (1.007)	1.047 (1.013)
50	1.021 (1.006)	1.041 (1.012)

*The figures in parentheses represent the contributions of individual frequencies, as discussed in the text.

SeO_4^{2-}. Also shown are the contributions to these ratios of (i) for SeO_3^{2-}, one component of the doubly degenerate *E*-type asymmetric stretching vibration ν_3 and of (ii) for SeO_4^{2-}, one component of the triply degenerate F_2-type vibration ν_3.

EXPERIMENTAL

The mass spectrometer and the method for preparing SeF_6 samples for isotopic analysis of selenium have been described by Krouse and Thode (1).

The Reduction of Sodium Selenite

Reductions were performed with ascorbic acid ($C_6H_8O_6$), which gives quantitative reductions quickly at room temperature over a wide range of pH's. For fractional reductions, the percentage reaction can be easily and predictably controlled by the quantity of $C_6H_8O_6$ used. The stoichiometry of the reaction is:

$$SeO_3^{2-} + 2H^+ = H_2SeO_3$$
$$H_2SeO_3 + 2C_6H_8O_6 = Se^0 + 2C_6H_8O_6 + 3H_2O.$$

Two sets of reductions were performed; one, at 24 °C, varying the % reduction, and the other, a set of 20% reductions at 3 °C and 40 °C. In all reductions the procedure was to add the quantity of $C_6H_8O_6$ required to give the correct percentage reduction to a solution of Na_2SeO_3, the solution then being maintained at the required temperature until the precipitated selenium could be filtered and weighed.

The Reduction of Sodium Selenate

It has been reported (11, 12) that selenate is reduced to selenite in strong HCl solutions. However, from the oxidation potentials compiled by Latimer (13), the reaction may be written:

$$SeO_4^{2-} + 4H^+ + 2Cl^- = H_2SeO_3 + H_2O + Cl_2 - 0.21.$$

Thus, in 1 *M* solutions, the components on the left are favored. It has been suggested (14) that in fact the reduction of Se^{vi} to Se^{iv} proceeds as:

$$SeO_4^{2-} + 8Cl^- + 8H^+ \rightarrow SeCl_6^{2-} + Cl_2 + 4H_2O.$$

Can. J. Chem. Downloaded from www.nrcresearchpress.com by 210.87.254.6 on 09/05/12
For personal use only.

If Se^{iv} formed by the above reaction is reduced to Se^0 by the action of $C_6H_8O_6$, then there is the possibility of the reaction

$$2Se^{vi} + Se^0 \rightarrow 3Se^{iv}$$

or, from Latimer:

$$2SeO_4^{2-} + Se^0 + H_2O + 4H^+ = 3H_2SeO_3 + 0.41.$$

In practice this reaction only occurs if the Se^0 is present in the red active form.

Three experiments were performed, at 22 °C in each case, with HCl to reduce Se^{vi} to Se^{iv} and $C_6H_8O_6$ to reduce Se^{iv} to Se^0. In each of these 10 ml of 0.5 *M* Na_2SeO_4 together with 50 ml H_2O and 120 ml concentrated HCl was used.

1. $C_6H_8O_6$ (881 mg, 2.5 meq) was added to the solution. After the formation of red Se^0, 300 ml H_2O was added to quench the oxidation of Se^0.
2. The solution was allowed to stand overnight before the addition of 2.5 meq $C_6H_8O_6$. Red Se^0 was formed, some of which was lost by the oxidation reaction described above.
3. $C_6H_8O_6$ (2.5 meq) was added to the solution. Red Se^0 was formed and after 1 h had virtually disappeared by re-oxidation. A further 2.5 meq $C_6H_8O_6$ was added, more red Se^0 being formed. In each of these experiments, the red Se^0 was allowed to nucleate and was recovered by filtration for weighing and isotopic analysis.

RESULTS AND DISCUSSION

The Reduction of Sodium Selenite

Table III shows the results of the reduction experiments. Column 4 shows the isotope effects, comparing product selenium with the starting material, and column 5 gives the ratio of rate constants for the reactions:

$$^{76}Se^{iv} \xrightarrow{k_1} Se^0$$
$$^{82}Se^{iv} \xrightarrow{k_2} Se^0.$$

The ratios of rate constants are derived from the experimental isotope effects by eq. [1]. The isotope effects involved are appreciable, indicating that a bond involving selenium is broken in the rate-determining step for the reduction. The value for k_1/k_2 at 3 °C is in good agreement with the experimental value reported by Krouse and Thode (1).

TABLE III

Selenium isotope effects in the reduction of sodium selenite

Experiment	T, °C	% reduction	δ, p.p.t.*	k_1/k_2
1	24±1	10	−18.4±1	1.020±0.001
2	24±1	20	−16.9±1	1.019±0.001
3	3±1	20	−14.6±1	1.017±0.001
4	40±1	20	−14.2±0.7	1.016±0.0007

$$*\delta(\text{p.p.t.}) = \frac{(^{82}Se/^{76}Se)_x - (^{82}Se/^{76}Se)_{standard}}{(^{82}Se/^{76}Se)_{standard}} \times 1000.$$

Theoretical predictions of k_1/k_2 may be made from the three arguments discussed above and by supposing the rate-controlling step in the reduction to be the cleavage of an Se—O bond.

In case I (see theoretical section), the activated complex is the same as the starting material with the exception that one vibrational mode has taken on a non-genuine character. This mode is most probably one component of the doubly degenerate *E*-type asymmetric stretching vibration ν_3 ($\sim$730 cm^{-1}). The ratio of partition function terms will be (from Table II): 1.008, 1.007, and 1.006 at 0, 25, and 50 °C, respectively.

The mass term may be evaluated from either atomic masses or mass fragments for the reduced mass of the species O_2Se---O, yielding the values 1.006 and 1.004, respectively. The values for k_1/k_2 are shown in columns 4 and 5 of Table IV.

Can. J. Chem. Downloaded from www.nrcresearchpress.com by 210.87.254.6 on 09/05/12
For personal use only.

TABLE IV

Summary of calculated ratios of rate constants for the reduction of Se^{iv}

T of model, °C	k_1/k_2					
	II (low)		I (intermediate)		III (high)	
	Mass	Atom	Mass	Atom	Mass	Atom
0	1.004	1.006	1.012	1.014	1.033	1.035
25	1.004	1.006	1.011	1.013	1.029	1.031
50	1.004	1.006	1.010	1.012	1.025	1.027

In case II, the lower limit for k_1/k_2 is simply the mass term, 1.006 or 1.004 for atom or mass fragments. These values are shown in columns 2 and 3 of Table IV.

For case III, the upper limit for k_1/k_2 is given by

$$k_1/k_2 = Q(^{82}SeO_3^{2-})/Q(^{76}SeO_3^{2-}) \cdot (\mu_2^{\ddagger}/\mu_1^{\ddagger})^{1/2}$$

for which the values of k_1/k_2 are shown in columns 6 and 7 of Table IV. All three arguments predict a regular decrease in the value of k_1/k_2 with increase of temperature. Thus, while argument I yields predicted values of the right magnitude, the experimental temperature dependence is difficult to account for on the basis of this simple model. It is not possible to give any preference to either the atom or mass fragment estimates of the mass terms.

TABLE V

Experimentally observed isotope effects in the reduction of Se^{iv}

Experiment	Se recovery		δ, p.p.t.
	mg	%	
1	122	32.5	-14.0 ± 1.0
2	72	18.0	-10.4 ± 1.0
3	233	59.2	-8.3 ± 1.0

$$\delta(\text{p.p.t.}) = \frac{(^{82}Se/^{76}Se)_x - (^{82}Se/^{76}Se)_{standard}}{(^{82}Se/^{76}Se)_{standard}} \times 1000.$$

It is possible that at low temperatures some factor such as solvent effects is causing the value of k_1/k_2 to be depressed, but, because of the errors involved in the experimental results, it is not possible to rule out the possibility that this temperature dependence is spurious.

The Reduction of Sodium Selenate

Table V shows the yields of selenium from the experiments described above, together with the isotope effects in product selenium, measured relative to the starting material.

Three reactions are involved in the above experiments, viz

[3] $Se^{vi} \rightarrow Se^{iv}$

[4] $Se^{iv} \rightarrow Se^{0}$

[5] $Se^{0} \rightarrow Se^{iv}$

and from the experimental results it is possible to estimate k_{76}/k_{82} for each of them. Let us consider the experiments in turn.

Can. J. Chem. Downloaded from www.nrcresearchpress.com by 210.87.254.6 on 09/05/12
For personal use only.

Experiment 1

With 5 meq Se^{vi} in HCl solution, 2.5 meq $C_6H_8O_6$ was added, and, after the formation of Se^0, the acidity of the solution was reduced to prevent re-oxidation. The reaction may be written as:

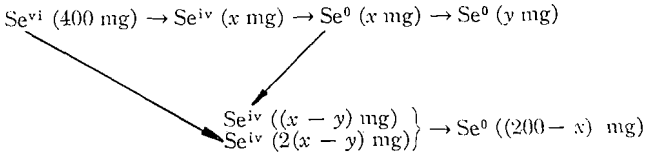
$$Se^{vi} \xrightarrow{32.5\%} Se^{iv} \xrightarrow{100\%} Se^0.$$

There is no isotope effect in the second step. The observed isotope effect is −14 p.p.t. for a 33% reduction, which from eq. [1] gives a value of 1.018 for k_1/k_2 in the reduction of Se^{vi} to Se^{iv}.

Experiment 2

Se^{vi} (5 meq) in HCl solution was allowed to stand for 24 h before 2.5 meq $C_6H_8O_6$ was added. No attempt was made to prevent oxidation of Se^0 and 72 mg of Se^0 was recovered.

The proposed reaction scheme is shown below.



Here, x mg Se^{vi} is reduced to Se^{iv} and 100% of the Se^{iv} is reduced to Se^0. Of the x mg Se^0, y mg remains unoxidized while $(x - y)$ mg is oxidized to Se^{iv}. In this oxidation, twice this quantity, the total remaining, of Se^{vi} is reduced to Se^{iv}. So $3(x - y)$ mg Se^{iv} are produced. There was sufficient $C_6H_8O_6$ added to reduce 200 mg Se^{iv} and x mg was reduced, so that a further $(200 - x)$ mg are reduced to Se^0 giving a total of $(200 - x) + y$ mg (72 mg experimentally).

From the above considerations:

$$(200 - x) + y = 72$$
$$2(x - y) = 400 - x.$$

So that:

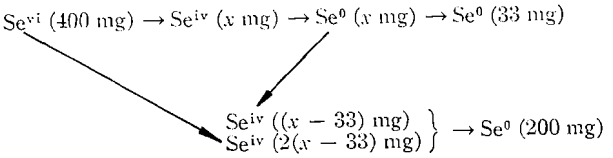
$$x = 144 \text{ mg}; \; y = 16 \text{ mg}.$$

If, in the oxidation of Se^0, one assumes the substrate to be at $+\Delta$ p.p.t. with respect to the original Se^0, so that the 128 mg Se^{iv} formed from the Se^0 is at $-(16/128)\Delta$ p.p.t., and, if k_1/k_2 for reactions [3] and [4] is taken as 1.018 and 1.015, respectively, then, with the observed Δ value of the final product Se^0 (−10.4 p.p.t.), it is possible to work through the reactions, using eqs. [1] and [2] to derive $\Delta = 17$ p.p.t. and k_1/k_2 for reaction [5] = 1.007.

Experiment 3

With 400 mg Se^{vi} in HCl solution, 2.5 meq $C_6H_8O_6$ was added, and red Se^0 formed, some of which was re-oxidized. A further addition of 2.5 meq $C_6H_8O_6$ was made, more red Se^0 being formed to give a total yield of 233 mg.

The proposed reaction scheme is shown below.



Can. J. Chem. Downloaded from www.nrcresearchpress.com by 210.87.254.6 on 09/05/12
For personal use only.

Here x mg Se^{VI} was reduced to Se^{IV} and to Se^0. Oxidation of Se^0 to Se^{IV} was accompanied by the reduction of all the remaining Se^{VI} to Se^{IV}. When the second addition of $C_6H_8O_6$ was made, only Se^{IV} and Se^0 remained, and this $C_6H_8O_6$ was sufficient to reduce 200 mg Se^{IV} to Se^0, there being no further oxidation.

This being the case, the amount of Se^0 not oxidized by the presence of Se^{VI} must have been 33 mg. From these considerations

$$2(x - 33) + x = 400$$

so that:

$$x = 155 \text{ mg.}$$

Using k_1/k_2 values for the reactions [3], [4], and [5] of 1.018, 1.015, and 1.007, respectively, and working through the various reactions, using eqs. [1] and [2], leads to a predicted value of -6.9 p.p.t. for the recovered Se^0, compared with the experimental value of -8.3 p.p.t.

Reinterpretation of the results of experiments 2 and 3 with adjustment of the value of k_1/k_2 for reaction [4] leads to an optimum set of values in which k_1/k_2 for reactions [3], [4], [5] is 1.018, 1.017, and 1.010, respectively, these values giving a δ-value of -9.1 p.p.t. for the recovered Se^0 in experiment 3, compared with the experimental value of -8.3 p.p.t.

Theoretical predictions of k_1/k_2 for reaction [3], the reduction of Se^{VI} to Se^{IV}, may be made from the three arguments discussed above and by supposing the rate-controlling step in the reduction to be the cleavage of a Se—O bond.

TABLE VI

Summary of the calculated ratios of rate constants for the reduction of Se^{VI} to Se^{IV} at 25 °C

	k_1/k_2 for model:		
	II (low)	I (intermediate)	III (high)
Mass fragments	1.002	1.015	1.049
Atom fragments	1.006	1.019	1.053

In case I (see theoretical section), the activated complex is the same as the starting material with the exception that one vibrational mode has taken on a non-genuine character. This mode is most probably one component of the triply degenerate F_2-type vibration $\nu_3(\sim 880 \text{ cm}^{-1})$. The partition function term will be (from Table II) 1.013 at 25 °C. The mass term may be evaluated from either atomic masses or mass fragments for the reduced mass of species O_3Se---O, yielding the values 1.006 and 1.002, respectively. The values for k_1/k_2 are shown in column 2 of Table VI.

In case II, the lower limit for k_1/k_2 is simply the mass term, 1.006 or 1.002 for atom or mass fragments. These values are shown in column 1 of Table VI.

In case III, the upper limit for k_1/k_2 is given by

$$k_1/k_2 = Q(^{82}SeO_4^{2-})/Q(^{76}SeO_4^{2-}) \cdot (\mu_2^{\ddagger}/\mu_1^{\ddagger})^{1/2}$$

for which the values of k_1/k_2 are shown in column 3 of Table VI.

Comparison of the figures in Table VI with the experimental results shows that the intermediate case, argument I, gives good agreement with experiment, but that it is not possible to give preference to either the atom or mass fragment estimates of the mass term.

Can. J. Chem. Downloaded from www.nrcresearchpress.com by 210.87.254.6 on 09/05/12
For personal use only.

The theoretical prediction of k_1/k_2 for reaction [5], the oxidation of Se^0 to Se^{IV}, requires that the partition function ratio for the reactant material, elemental selenium, be known. The elemental selenium will most likely be in the form of open-ended selenium chains, and partition function ratio data for these are not available. All that may be said concerning such a prediction is: If the activated complex is simply selenium or a diatomic molecule containing selenium, so that Q_2/Q_1 is unity and the mass term is either unity or greater than unity, then the predicted ratio k_1/k_2 will be greater than unity, as is observed experimentally.

CONCLUSIONS

The experiments on the reduction of sodium selenite show that the rate constant for the ^{76}Se species is about 1.017 times that for the ^{82}Se species. Theoretical prediction of this ratio, from a simple model where the rate-determining step is the breaking of a Se—O bond in SeO_3^{2-}, leads to good agreement with experiment for the magnitude of the isotope effect. It is not possible to explain the temperature dependence of k_1/k_2 on the basis of this model.

From the experiments on the reduction of sodium selenate, estimates can be made of the ratios k_{76}/k_{82} for the reduction of Se^{VI} to Se^{IV} and the oxidation of Se^0 to Se^{IV}, values of 1.018 and 1.010 being determined. Theoretical prediction of the former ratio, assuming the rate-determining step to be the cleavage of a Se—O bond in SeO_4^{2-}, gives good agreement with experiment.

ACKNOWLEDGMENTS

The authors wish to express their thanks to the National Research Council of Canada whose financial assistance made possible the above study.

REFERENCES

1. R. H. KROUSE and H. G. THODE. Can. J. Chem. **40**, 367 (1962).
2. J. BIGELEISEN. J. Chem. Phys. **17**, 675 (1949).
3. N. B. SLATER. The theory of unimolecular reactions. Cornell, Ithaca, N.Y. 1959.
4. C. ROCCHICCIOLI. Compt. Rend. **247**, 1108 (1958); Ann. Chim. Paris, **5**, 999 (1960).
5. G. E. WALRAFEN. J. Chem. Phys. **36**, 90 (1962).
6. A. F. WELLS and M. BAILEY. J. Chem. Soc. 1282 (1949).
7. K. NAKAMOTO. Infrared spectra of inorganic and co-ordination compounds. Wiley, New York. 1963.
8. D. F. HEATH and J. W. LINNETT. Trans. Faraday Soc. **44**, 873 (1948).
9. C. W. F. T. PISTORIUS. J. Chem. Phys. **27**, 965 (1957).
10. G. E. WALRAFEN. J. Chem. Phys. **39**, 1479 (1963).
11. E. B. BENGER. J. Am. Chem. Soc. **39**, 2171 (1917).
12. W. M. HILDEBRAND and G. E. F. LUNDELL. Applied inorganic analysis. Wiley, New York. 1929.
13. W. M. LATIMER. The oxidation states of the elements and their potentials. Prentice-Hall, New York. 1952.
14. R. H. TOMLINSON. Private communication.

Can. J. Chem. Downloaded from www.nrcresearchpress.com by 210.87.254.6 on 09/05/12
For personal use only.

SECOND VIRIAL COEFFICIENTS AND INTERMOLECULAR FORCES FOR THE AMMONIA–ACETYLENE SYSTEM

H. Y. Cheh, J. P. O'Connell, and J. M. Prausnitz
Department of Chemical Engineering, University of California, Berkeley, California

Received September 8, 1965

ABSTRACT

Volumetric data for gaseous ammonia–acetylene mixtures have been analyzed to obtain second virial coefficients as a function of temperature and composition. From the pure-component virial coefficients of ammonia and acetylene, Kihara-potential parameters were obtained and these were used to calculate the physical contributions to the second cross virial coefficients, B_{12}. The difference between the experimental B_{12} and that calculated from the physical contribution is attributed to chemical interaction, or complex formation, between the two molecules. Chemical equilibrium constants have been calculated, and ΔH^0 and ΔS^0 for complex formation were found to be $-(2\,210)$ cal/mole and -16.6 cal/mole °K respectively. These results indicate very weak hydrogen bond formation between the nitrogen atom in the ammonia and the hydrogen atom in acetylene.

1. INTRODUCTION

The study of chemical association and solvation in the gaseous phase by analysis of second virial coefficient data has been well established by various workers, notably by Lambert (1). Recent volumetric data for the ammonia–acetylene system reported by Khodeeva (2) have provided us with an opportunity to study the intermolecular forces between these two molecules.

2. CALCULATION OF SECOND VIRIAL COEFFICIENTS

2.1. Ammonia

Very precise measurements for the volumetric properties of ammonia have been reported by Meyers and Jessup (3), Beattie and Lawrence (4), and Kasarnowsky (5). Data covering the temperature range 298.2 to 598.2 °K and the pressure range 1 to 250 atm were used in the evaluation of the second virial coefficients of ammonia. The data reduction method used was similar to that of David and Hamann (6). The results are summarized in Table I and in Fig. 1.

TABLE I
Second virial coefficients of ammonia

Temp., °K	B_{11}, cc/mole
323.2	−202
348.2	−165
373.2	−137
398.2	−116
423.2	−99

2.2. Acetylene

Volumetric data of acetylene at various temperatures and pressures were measured by Hölemann and Hasselmann (7), by Teranishi (8), and also by Schäfer (9). The substantial disagreement between their results has been discussed by Weber (10). We also found the data to be inadequate for evaluating the second virial coefficients. Therefore second virial coefficients were calculated with the equation of Pitzer and Curl (11) based on a three-parameter theorem of corresponding states. Pitzer and Curl's equation utilizes the critical

Can. J. Chem. Downloaded from www.nrcresearchpress.com by 210.87.254.6 on 09/05/12
For personal use only.

pressure, the critical temperature, and an acentric factor which is determined from the experimental vapor pressure curve. These properties of acetylene and the calculated second virial coefficients are given in Table II and in Fig. 1. We estimate the uncertainty in the second virial coefficients to be about ±5 cc/mole at the lower temperatures and ±2 cc/mole at higher temperatures.

TABLE II

Second virial coefficients, critical properties, and acentric factor of acetylene. Critical temperature: 309.5 °K; critical pressure: 61.6 atm; acentric factor: 0.1985

Temp., °K	B_{22}, cc/mole
323.2	−131
348.2	−109
373.2	−91
398.2	−77
423.2	−64

2.3. Ammonia–Acetylene

Recently, Khodeeva (2) published measurements for the volumetric properties of the ammonia–acetylene system over the range 323.2 to 423.2 °K and 10 to 90 atm. Second virial coefficients for the mixture were calculated by the same method as that used for ammonia. The results are shown in Fig. 2.

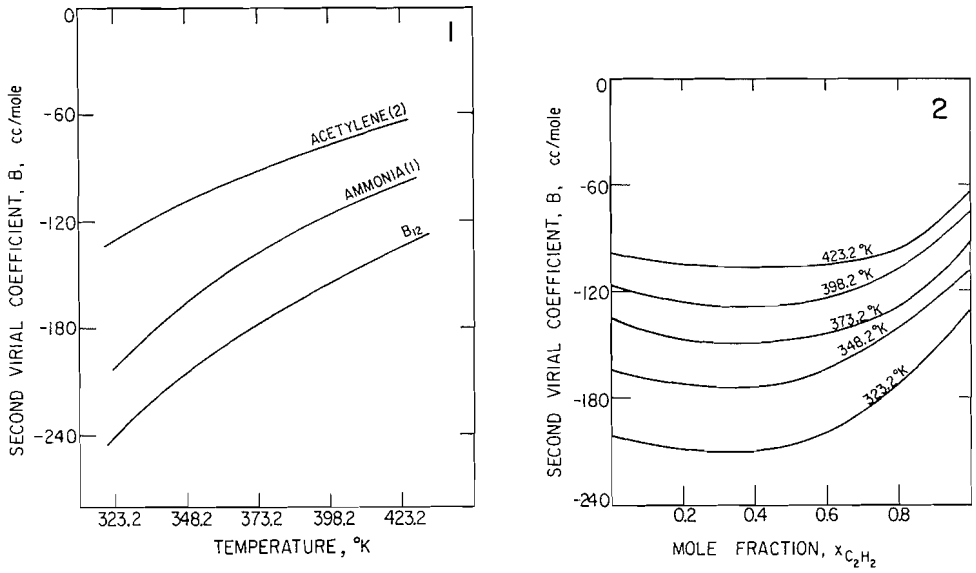


FIG. 1. Second virial coefficients for ammonia, acetylene, and ammonia–acetylene.
FIG. 2. Second virial coefficients for the ammonia–acetylene system.

The second virial coefficient B of a binary system is related to the second virial coefficients of the pure components and to the second cross virial coefficient B_{12} by

$$B = x_1^2 B_{11} + 2x_1 x_2 B_{12} + x_2^2 B_{22} \quad [1]$$

where x is the mole fraction and where the subscripts 1 and 2 stand for components 1 (ammonia) and 2 (acetylene).

Can. J. Chem. Downloaded from www.nrcresearchpress.com by 210.87.254.6 on 09/05/12
For personal use only.

From the experimental second virial coefficients for the pure gases and for the mixture, values of B_{12} were calculated and are given in Fig. 1 and in Table III.

TABLE III

Second cross virial coefficients for the ammonia–acetylene system

Temp., °K	B_{12}, cc/mole
323.2	−240
348.2	−204
373.2	−177
398.2	−155
423.2	−134

3. PHYSICAL INTERACTIONS AND SECOND VIRIAL COEFFICIENTS

3.1. Various Physical Interactions

Physical interactions among molecules possessing dipole and quadrupole moments include in the general case interactions resulting from dispersion, dipole–dipole, dipole–induced dipole, dipole–quadrupole, quadrupole–quadrupole, and off-center dipole forces. For the dispersion and dipole–dipole interactions tables of reduced second virial coefficients for the spherical-core potential have been calculated by O'Connell and Prausnitz (12). For other interactions, the following equations may be applied*

$$[2]\quad B_{\text{ind}} = -\frac{2}{3}\pi N\delta^3 \frac{\alpha\mu^2}{8\delta^6 U_0 y^2}\left[H_6(y) + \frac{\mu^4 y^4}{40\delta^6 U_0^2} H_{12}(y) + \frac{29\mu^8 y^8}{(134\,400)\delta^{12} U_0^4} H_{18}(y) + \dots\right]$$

$$[3]\quad B_{\text{dip–quad}} = -\frac{2}{3}\pi N\delta^3 \frac{\mu^2\theta^2}{64\delta^8 U_0^2}\left[H_8(y) - \frac{\mu^2 y^2}{5\delta^3 U_0} H_{11}(y) - \frac{6\theta^2 y^2}{35\delta^5 U_0} H_{13}(y) + \dots\right]$$

$$[4]\quad B_{\text{quad–quad}} = -\frac{2}{3}\pi N\delta^3 \frac{7\theta^4}{320\delta^{10} U_0^5}\left[H_{10}(y) - \frac{18\theta^2 y^2}{343\delta^5 U_0} H_{15}(y) + \dots\right]$$

$$[5]\quad B_{\text{off-center dip}} = -\frac{2}{3}\pi N\delta^3 \frac{\gamma^{*2}\mu^2}{2\delta^3 U_0}\left[H_8(y) - \frac{\mu^2 y^2 H_{11}(y)}{5\delta^3 U_0} + \dots\right]$$

where

$$y^2 = 4U_0/kT, \quad \gamma^* = 2a/\delta, \quad a^* = 2a/(\delta - 2a),$$

$$H_n(y) = y^{(4.5-(n/6))} \sum_{m=0}^{\infty} \Gamma\left(\frac{6m + n - 3}{12}\right)\frac{y^m}{m!},$$

U_0 = minimum potential energy,
a = radius of the spherical core of the molecule,
δ = distance between molecular centers when the potential energy is zero,
α = polarizability,
μ = dipole moment, and
θ = quadrupole moment.

In general, dispersion and dipole–dipole contributions are by far the most significant. However, the others are not negligible.

**To correct misprints in ref. 12, the exponent of δ in the factor outside the bracket should be changed from 3 to 6 in eq. [14] and from 5 to 8 in eq. [15].*

Can. J. Chem. Downloaded from www.nrcresearchpress.com by 210.87.254.6 on 09/05/12
For personal use only.

3.2. Evaluation of Intermolecular Parameters

3.2.a. Ammonia

Ammonia is a tetrahedral molecule with a dipole moment of 1.47 D (debye) (13) and a quadrupole moment of 1.0×10^{-26} electrostatic unit cm^2 (e.s.u. cm^2) (14). Hence all the additional interactions described by eqs. [2] to [5] are significant. The best Kihara parameters were obtained by a fit of the second virial coefficients by a nonlinear, least squares technique on an IBM 7094 computer to all the interaction equations simultaneously. The best values for the parameters and the root mean square (r.m.s.) deviation for the second virial coefficients from 298.2 to 598.2 °K are

$$U_0/k = 145\ ^\circ\text{K},\ \delta = 2.63\ \text{Å},\ 2a = 0.125\ \text{Å},\ \text{and r.m.s. deviation} = 1.36\ \text{cc/mole}.$$

3.2.b. Acetylene

Acetylene is a linear molecule with no dipole moment but a quadrupole moment of 3.0×10^{-26} e.s.u. cm^2 (14). Here only the dispersion and quadrupole–quadrupole interactions are important. The second virial coefficients were fitted to obtain a set of Kihara-potential parameters. These parameters were then used to calculate $B_{\text{quad–quad}}$ by eq. [4]. The difference between the overall second virial coefficients and $B_{\text{quad–quad}}$ thus obtained was then used to provide a new estimate of B_{disp} in order to obtain a better set of potential parameters. These parameters in turn gave a better approximation for $B_{\text{quad–quad}}$. This iterative process was continued until there was no change in the parameters by two successive approximations. The best values for the parameters and the r.m.s. deviation for the second virial coefficients from 273.2 to 533.2 °K are

$$U_0/k = 412\ ^\circ\text{K},\ \delta = 4.11\ \text{Å},\ 2a = 1.54\ \text{Å},\ \text{and r.m.s. deviation} = 0.10\ \text{cc/mole}.$$

3.3. Calculation of Second Cross Virial Coefficients $B_{12\ phys}$ resulting from Physical Interactions

The commonly recommended semiempirical mixing rules were used to obtain the Kihara-potential parameters for the mixtures:

[6] $$U_{0_{12}}/k = (U_{0_1}U_{0_2})^{1/2}/k = 245.2\ ^\circ\text{K}$$

[7] $$\delta_{12} = \tfrac{1}{2}(\delta_1 + \delta_2) = 3.367\ \text{Å}$$

[8] $$a_{12} = \tfrac{1}{2}(a_1 + a_2) = 0.416\ \text{Å}.$$

To calculate $B_{12\ \text{phys}}$, the parameters of eqs. [2] to [4] are as follows:

$$\mu = \mu_1,\ \alpha = \alpha_2,\ \theta = \theta_2$$

[9] (or $\theta = \sqrt{(\theta_1\theta_2)}$ for the quadrupole–quadrupole interaction).

The various contributions to $B_{12\ \text{phys}}$ were then found from the function $H_n(y)$ tabulated by Buckingham and Pople (15). The results are summarized in Table IV and Fig. 3.

TABLE IV

Various physical B_{12} for the ammonia–acetylene system

Temp., °K	B_{12} disp, cc/mole	B_{12} ind, cc/mole	B_{12} dip–quad, cc/mole	B_{12} quad–quad, cc/mole	B_{12} phys, cc/mole
323.2	−32.0	−11.7	−1.8	−1.3	−46.8
348.2	−25.0	−10.2	−2.3	−1.1	−38.6
373.2	−19.8	−9.0	−2.6	−1.0	−32.4
398.2	−15.4	−8.1	−2.7	−0.8	−27.0
423.2	−11.6	−7.3	−2.7	−0.7	−22.3

Can. J. Chem. Downloaded from www.nrcresearchpress.com by 210.87.254.6 on 09/05/12
For personal use only.

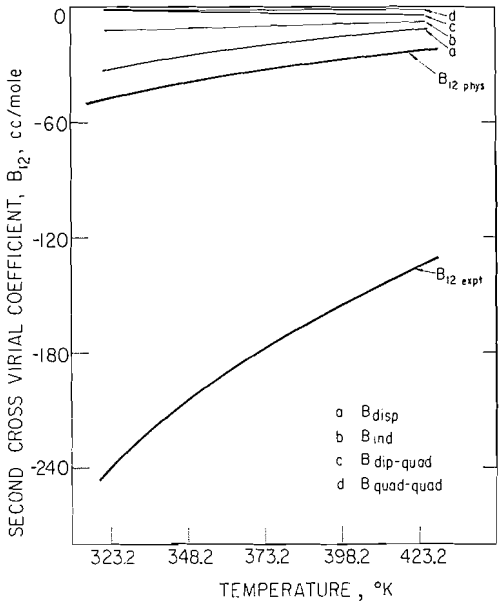


FIG. 3. Physical contributions to the cross coefficient B_{12}.

4. CHEMICAL SOLVATION BETWEEN AMMONIA AND ACETYLENE

Figure 3 clearly shows that the virial coefficients resulting from physical interactions between ammonia and acetylene account for only about 20% of the experimental B_{12}. This discrepancy is due to the chemical association between ammonia and acetylene which probably is a result of hydrogen bonding.

We postulate the following chemical equilibrium:

[10] $$C_2H_2 + NH_3 \rightleftharpoons C_2H_2{-}NH_3.$$

The stoichiometric coefficients are unity in eq. [10] since second virial coefficients represent only two-body interactions. Lambert *et al.* (16) derived the relationship between second virial coefficients and equilibrium constants for a bimolecular reaction provided that the degree of complex formation was small. This method has been applied to various mixtures by Lambert and associates (16, 17) and also by Prausnitz and Carter (18).

For the bimolecular chemical equilibrium,

[11] $$A + B \rightleftharpoons AB$$

the equilibrium constant K_p is defined as

[12] $$K_p = p_{AB}/p_A p_B$$

where p_{AB}, p_A, and p_B are the partial pressures of AB, A, and B respectively.

Lambert *et al.* (16) showed that

[13] $$-RTK_p = B_{12\ chem} = B_{12\ expt} - B_{12\ phys}.$$

The term $B_{12\ phys}$ can be considered to be a result of dispersion and electrostatic forces in instantaneous molecular collisions whereas the term $B_{12\ chem}$ results from the formation of weak chemical bonds. This division is necessarily somewhat arbitrary. The thermodynamic equilibrium constant K is defined by

[14] $$-RT \ln K = \Delta G^0$$

Can. J. Chem. Downloaded from www.nrcresearchpress.com by 210.87.254.6 on 09/05/12
For personal use only.

where ΔG^0 is the standard Gibbs free energy change, and where

[15] $$K = K_p K_\varphi$$

and

[16] $$K_\varphi = \varphi_{AB}/\varphi_A\varphi_B \ (\varphi = \text{fugacity coefficient}).$$

To obtain K from K_p data, it is necessary to extrapolate K_p to its value at zero pressure where $K_\varphi = 1$. Equation [13] then gives the relationship between $B_{12\ \text{chem}}$ and K. Since $B_{12\ \text{expt}}$ and $B_{12\ \text{phys}}$ were both evaluated by extrapolation to zero pressure, the above conditions are automatically satisfied.

The enthalpy and entropy of complex formation are given by the slope and intercept of a plot of ln K versus the reciprocal of the absolute temperature:

[17] $$-\ln K = (\Delta H^0/RT) - (\Delta S^0/R).$$

Table V shows our result for K at various temperatures. The heat and entropy are

$$\Delta H^0 = -(2\,210) \text{ cal/mole} \pm 300 \text{ cal/mole and}$$
$$\Delta S^0 = -16.6 \text{ cal/mole °K} \pm 0.9 \text{ cal/mole °K}.$$

The uncertainties in the enthalpy and entropy of reaction are due mainly to experimental error.

TABLE V

$B_{12\ \text{chem}}$ and equilibrium constants

Temp., °K	$B_{12\ \text{chem}}$, cc/mole	K_p, atm^{-1}
323.2	−193	0.00729
348.2	−165	0.00579
373.2	−145	0.00473
398.2	−128	0.00392
423.2	−112	0.00322

The enthalpy of complex formation is roughly one-half that for typical hydrogen bond formation (19). The enthalpies of the pure components in the ideal gas state at 373.2 °K calculated on the basis of structural parameters (20) are

$$H_{NH_3}{}^0 = 3\,060 \text{ cal/mole and } H_{C_2H_2}{}^0 = 3\,230 \text{ cal/mole}.$$

The enthalpy of the complex is then estimated from the heat of complex formation to be 4 080 cal/mole. If one follows Rowlinson's (21) suggestion and assumes that the complex behaves as an ideal diatomic gas (no vibration of the newly formed bond), the enthalpy would be $(7/2)RT$ which is only 2 600 cal/mole. The extra enthalpy of 1 480 cal/mole for the complex may be accounted for by consideration of the vibrational degrees of freedom. For instance, the introduction of two normal modes of very low vibrational frequencies produces an enthalpy of this magnitude.

Similarly, the entropies of ammonia and acetylene as ideal gases, calculated at 373.2 °K and 1 atm, are

[18]
$$\begin{cases} S^0 = S_{trans}{}^0 + S_{rot}{}^0 + S_{vib}{}^0 \\ S_{NH_3}{}^0 = (38.55 + 9.14 + 0.30) \text{ cal/mole °K} = 47.99 \text{ cal/mole °K} \\ S_{C_2H_2}{}^0 = (36.83 + 11.31 + 2.34) \text{ cal/mole °K} = 50.48 \text{ cal/mole °K} \end{cases}$$

Hence the entropy of the complex is 81.9 cal/mole °K.

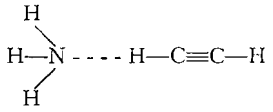
Can. J. Chem. Downloaded from www.nrcresearchpress.com by 210.87.254.6 on 09/05/12
For personal use only.

Shepp and Bauer (22) considered the change in entropy in gaseous, bimolecular association as being the sum of two terms

$$\Delta S^0 = \Delta S^0_{\text{trans+rot}} + \Delta S_{\text{vlb}}{}^0 \quad [19]$$

where $\Delta S^0_{\text{trans+rot}}$ is the change for rigid-body molecules and $\Delta S_{\text{vlb}}{}^0$ includes the difference in the entropy contributions from the nonrigid degrees of freedom, vibration and restricted rotation. They found that $\Delta S_{\text{vlb}}{}^0$ is always positive for the association process. The magnitude of $\Delta S_{\text{vlb}}{}^0$ is determined primarily by the strength of the new bond. For a weak bond, the frequencies are low and $\Delta S_{\text{vlb}}{}^0$ is large.

If one again considers the ammonia–acetylene complex as a diatomic gas held loosely by a hydrogen bond:



the translational and rotational entropy can be written as

$$S_{\text{trans}}{}^0 = R\left[\ln \frac{[2\pi(m_{NH_3} + m_{C_2H_2})kT]^{3/2}}{h^3}\frac{kT}{p}\right] + \frac{5}{2}R \quad [20]$$

$$S_{\text{rot}}{}^0 = R\left[\ln\left(\frac{8\pi^2 IkT}{\sigma h^2}\right) + 1\right] \quad [21]$$

where m_{NH_3} and $m_{C_2H_2}$ are the mass of the ammonia and acetylene molecules respectively, I is the moment of inertia of the complex, and σ is the symmetry factor of the complex. At 373.2 °K and 1 atm, $S_{\text{trans}}{}^0$ for the complex is 38.3 cal/mole °K. $S_{\text{rot}}{}^0$ depends on the N - - - H bond length and has values varying from 14.0 to 14.9 cal/mole °K if the distance between the two "big atoms" varies from 2 Å to 3.5 Å. Thus $S_{\text{rot}}{}^0$ is not very sensitive to the bond length. If we take $S_{\text{rot}}{}^0$ to be 14.5 cal/mole °K, $S^0_{\text{trans+rot}}$ is 52.8 cal/mole °K. Under these conditions $\Delta S_{\text{vlb}}{}^0$ is given as

$$\begin{aligned}\Delta S_{\text{vlb}}{}^0 &= \Delta S_{\text{total}}{}^0 - \Delta S^0_{\text{trans+rot}} \\ &= -16.6 - (52.8 - 48.1 - 47.7) \text{ cal/mole °K} \\ &= +26.4 \text{ cal/mole °K.}\end{aligned}$$

The magnitude of our value indicates that the N - - - H bond is a very weak one; this is in agreement with the conclusion reached from the enthalpy calculations. The $\Delta S_{\text{vlb}}{}^0$ value appears rather high when compared to most of the cases reported by Shepp and Bauer (22), and also by Slutsky and Bauer (23). But the equilibrium constants for the ammonia–acetylene system are also much lower and therefore a much weaker bond should be expected.

5. CONCLUSION

Evidence for chemical solvation between ammonia and acetylene in the gaseous phase has been obtained by analysis of the second virial coefficients for the ammonia–acetylene system. The chemical interaction contributes approximately 80% of the second cross virial coefficients. A molecular analysis of the heat and entropy changes resulting from chemical forces suggests that there is weak hydrogen bonding between ammonia and acetylene.

The authors are grateful to the Computer Center, University of California, Berkeley, for the use of their facilities.

Can. J. Chem. Downloaded from www.nrcresearchpress.com by 210.87.254.6 on 09/05/12
For personal use only.

REFERENCES

1. J. D. LAMBERT. Discussions Faraday Soc. **15**, 226 (1953).
2. C. M. KHODEEVA. Zh. Fiz. Khim. **38**, 1276 (1964).
3. C. H. MEYERS and R. S. JESSUP. Refrig. Eng. **11**, 345 (1925).
4. J. A. BEATTIE and C. K. LAWRENCE. J. Am. Chem. Soc. **52**, 6 (1930).
5. J. S. KASARNOWSKY. Acta Physiochim. URSS, **12**, 513 (1940).
6. H. G. DAVID and S. D. HAMANN. Proc. Conf. Thermodyn. Transport Properties Fluids, London, 1957. 1958. p. 74.
7. P. HÖLEMANN and R. HASSELMANN. Forschungsber. Wirtsch. Verkehrsministeriums Nordrhein-Westfalen, **78** (1954).
8. H. TERANISHI. Rev. Phys. Chem. Japan, **25**, 25 (1955).
9. K. SCHÄFER. Z. Physik. Chem. Frankfurt, **B36**, 85 (1937).
10. J. H. WEBER. A.I.Ch.E. J. **5**, 17 (1959).
11. K. S. PITZER and R. F. CURL. J. Am. Chem. Soc. **79**, 2369 (1957).
12. J. P. O'CONNELL and J. M. PRAUSNITZ. *In* Advances in thermophysical properties at extreme temperatures and pressures. *Edited by* S. Gratch. American Society Mechanical Engineers, New York. 1965. p.19.
13. A. L. MCCLELLAN. Tables of experimental dipole moments. Freeman, San Francisco. 1963.
14. A. D. BUCKINGHAM. Quart. Rev. London, **13**, 183 (1959).
15. A. D. BUCKINGHAM and J. A. POPLE. Trans. Faraday Soc. **51**, 1173 (1955).
16. J. D. LAMBERT, G. A. H. ROBERTS, J. S. ROWLINSON, and V. J. WILKINSON. Proc. Roy. Soc. London, Ser. A, **196**, 113 (1949).
17. J. D. LAMBERT, J. S. CLARKE, J. F. DUKE, C. L. HICKS, S. D. LAWRENCE, D. M. MORRIS, and M. G. T. SHONE. Proc. Roy. Soc. London, Ser. A, **249**, 414 (1959).
18. J. M. PRAUSNITZ and W. B. CARTER. A.I.Ch.E. J. **6**, 611 (1960).
19. G. C. PIMENTEL and A. L. MCCLELLAN. The hydrogen bond. Freeman, San Francisco. 1960.
20. E. A. MOELWYN-HUGHES. Physical chemistry. 2nd ed. Macmillan, New York. 1961.
21. J. S. ROWLINSON. Trans. Faraday Soc. **45**, 974 (1949).
22. A. SHEPP and S. H. BAUER. J. Am. Chem. Soc. **76**, 265 (1954).
23. L. SLUTSKY and S. H. BAUER. J. Am. Chem. Soc. **76**, 270 (1954).

Can. J. Chem. Downloaded from www.nrcresearchpress.com by 210.87.254.6 on 09/05/12
For personal use only.

Can. J. Chem. Downloaded from www.nrcresearchpress.com by 210.87.254.6 on 09/05/12
For personal use only.

ION PAIR EFFECTS IN THE REACTION BETWEEN POTASSIUM FERROCYANIDE AND POTASSIUM PERSULFATE

R. W. CHLEBEK AND M. W. LISTER
Department of Chemistry, University of Toronto, Toronto, Ontario

Received August 3, 1965

ABSTRACT

The rate of the reaction between potassium ferrocyanide and potassium persulfate has been measured over a range of conditions. The rate is dependent on the potassium ion concentration, and it is shown that this is explained if it is assumed that $KFe(CN)_6^{3-}$ and $KS_2O_8^-$ are the reacting species. The equilibrium constants governing the formation of these ion pairs were measured with a cation-sensitive glass electrode. Similar constants for the products $KFe(CN_6)^{2-}$ and KSO_4^-, and also for KNO_3, were measured. From these equilibrium constants, the true rate constants of the reaction can be obtained, and it is shown that these vary with ionic strength in the manner predicted by Brönsted's equation.

The reaction

$$2K_4Fe(CN)_6 + K_2S_2O_8 \rightarrow 2K_3Fe(CN)_6 + 2K_2SO_4$$

in aqueous solution was examined some time ago by Holluta and Herman (1). They found it to be a second-order reaction, but with rate constants that increased strikingly with the concentration of potassium ions. This might be attributed to an increase in ionic strength, and Brönsted's treatment (2) of the effect of ionic strength on reaction rate would, of course, predict such an increase, since the reacting ions are of the same sign. However, Holluta and Herman's results seem to correlate the rate constants with the potassium ion concentration rather than with the ionic strength; this is the sort of correlation that has been emphasized by Olson and Simonson (3) for other reactions. A possible explanation is that ion pairs such as $KFe(CN)_6^{3-}$ are the real reacting species, and this sort of explanation has been suggested in other cases (4). The object of the present work was, firstly, to investigate the extent of ion pair formation for the reagents and products in this reaction. This was done by measurements with a cation-sensitive glass electrode. Secondly, this information was used to find the nature of the actual reacting species, and hence the true rate constants of the reaction. Finally, the dependence of these rate constants on ionic strength was examined and compared with the predictions of Brönsted's equation.

EXPERIMENTAL

Chemicals

Potassium chloride.—Mallinckrodt analytical reagent was dried at 110 °C and stock solutions were made up by weight.

Tetramethylammonium chloride.—The salt, stated to be more than 99% pure, supplied by Matheson, Coleman and Bell Co. was used. Stock solutions were standardized by silver nitrate titration.

Tetramethylammonium hydroxide.—The 10% solution supplied by Eastman Organic Chemicals was diluted and standardized with potassium hydrogen phthalate.

Potassium nitrate.—The British Drug Houses AnalaR reagent was used after drying at 110 °C.

Potassium sulfate.—The Merck analytical reagent was used after grinding and drying at 110 °C.

Potassium persulfate.—The Fisher certified reagent was used. After drying, the salt was analyzed by adding excess ferrous ammonium sulfate to a solution of the salt, and titrating the excess with ceric ammonium sulfate. The salt was 100% pure within the error of the titration. Solutions were always used the same day that they were made up.

Potassium ferricyanide.—The Baker and Adamson reagent salt was used. Solutions were made up by weight, and standardized with iodometric titration.

Potassium ferrocyanide.—The Fisher certified reagent was used. The purity was checked by titration with ceric ammonium sulfate and found to be 100% within the experimental error. Solutions were always used the same day that they were made up.

RESULTS

Equilibrium Measurements

The concentrations of potassium ions in various solutions were measured with a Beckmann 39137 cation electrode. A saturated calomel electrode with a frit junction was used as a reference electrode, and the voltages were read on a Beckmann 101900 research pH meter. The voltages could be read to 0.05 mV. The apparatus was first calibrated by solutions of potassium chloride, containing 0.001 M tetramethylammonium hydroxide and adjusted to a fixed ionic strength by tetramethylammonium chloride. The tetramethylammonium hydroxide was added to keep the hydrogen ion concentration low, since the glass electrode is sensitive to hydrogen ions. Calibrations were made at different temperatures, which were controlled to within ±0.1 °C by a water thermostat.

It was expected that the variation of the measured voltage with concentration would follow the Nernst equation, in effect

$$dE/d \log [K^+] = 0.1984T,$$

where E is the voltage in mV and T is the absolute temperature. In fact, slightly different values for the slope of E against log [K^+] were obtained, and instead of 0.1984 the following values were found.

t (°C)	20	25	30	40	Mean
Slope	0.1923	0.1937	0.1912	0.1919	0.1923

These are for a range of [K^+] from 0.1 to 0.01 M, and are all at an ionic strength of 0.1. This deviation cannot be caused by formation of ion pairs of KCl, since this would have increased the slope; potassium chloride was chosen as the calibrating compound since earlier work (e.g. ref. 4, p. 169) had shown that ion pair formation was very slight. Probably the electrode responds slightly to tetramethylammonium ions. In practice, for the determination of equilibrium constants, the electrode was placed alternately in a calibrating solution of potassium chloride and in the salt solution whose equilibrium constant was being measured. Both solutions contained 0.001 M tetramethylammonium hydroxide and tetramethylammonium chloride to bring them to the same ionic strength (usually 0.1). It was assumed that the experimental values for $dE/d \log [K^+]$ held for this comparison.

Results for the various compounds investigated are given in Table I. The constants so obtained can be claimed to be only moderately accurate, as an error of 0.1 mV in δE (the difference between the voltage observed with the salt solution and with the calibrating solution) would cause a considerable change in K. For instance, for the second solution of potassium nitrate, a change of 0.1 mV in δE would increase K from 0.382 to 0.438. Table II summarizes the thermodynamic data calculated from the data in Table I. The equilibrium constants were measured at an ionic strength of 0.1. These can be converted to zero ionic strength, if single ion activity coefficients are assumed to be of the usual form,

$$[1] \qquad -\log f = Az^2\left(\frac{\sqrt{\mu}}{1 + Ba\sqrt{\mu}} - C\mu\right).$$

Can. J. Chem. Downloaded from www.nrcresearchpress.com by 210.87.254.6 on 09/05/12
For personal use only.

Kielland (5) has found that values of $a = 4$ Å for the $S_2O_8^{2-}$ ion and $a = 5$ Å for the $Fe(CN)_6^{4-}$ ion fit the activity coefficient data for salts of these ions. For potassium ions $a = 3$ Å is a commonly used value. The results in Table II were calculated using these values, 3.5 Å for sulfate and nitrate ions, and values for the ion pairs equal to that for the anion they contain. The values for K^0 in Table II may be compared with results in the literature obtained by other methods of measurement, mostly by conductivity. These are: KNO_3, 0.72 to 0.78 at 18 °C (6, 7) and 0.55 (7) to 0.63 at 25 °C (8); K_2SO_4, 6.6 at 18 °C and 9.1 at 25 °C (9); $K_3Fe(CN)_6$, 20 at 18 °C and 25 at 25 °C (10, 11); $K_4Fe(CN)_6$, 200 at 25 °C (12, 13). Considering the different methods of measurement, and the adjustment to zero ionic strength, these values are in reasonable agreement with the present ones.

Two other comments may be made on Table II. Firstly, ΔH^0 plotted against ΔS^0 gives an approximately straight line with slope about 220 °K. Secondly, ΔS^0 becomes larger as the charge on the ion increases. This would be expected if it arises from polarization of the

TABLE I

Equilibrium measurements

Salt	t (°C)	Total salt concn. (M)	Calibrating [KCl]	δE (mV)	Calcd. [K^+]	Equilibrium Constant (M^{-1})
KNO_3	24.65	0.08000	0.07537	0.675	0.07744	0.43
	24.65	0.07931	0.07751	−0.15	0.07704	0.38
	24.65	0.08923	0.08650	−0.125	0.08607	0.43
	24.65	0.09914	0.09549	−0.15	0.09492	0.47
	39.3	0.09949	0.09669	0.10	0.09632	0.34
	39.3	0.8954	0.08725	0.14	0.08678	0.37
	39.3	0.07950	0.07778	−0.055	0.07794	0.27
	39.3	0.06964	0.06826	0.035	0.06817	0.32
K_2SO_4	24.65	0.03200	0.06085	−0.675	0.05922	2.9
	24.65	0.03400	0.06440	−0.475	0.06318	2.6
	24.65	0.03600	0.06805	−0.625	0.06636	2.8
	24.65	0.03800	0.07170	−0.35	0.07070	2.3
	39.3	0.03600	0.06421	0.47	0.06538	3.4_5
	39.3	0.03494	0.06261	0.32	0.06338	3.6
	39.3	0.03401	0.06094	0.70	0.06260	3.0
	39.3	0.03700	0.06584	0.65	0.06750	3.2
$K_2S_2O_8$	24.65	0.03200	0.05915	−0.225	0.05862	3.4_5
	24.65	0.03400	0.06260	−0.075	0.06241	3.1_5
	24.65	0.03600	0.06605	−0.075	0.06585	3.1
	24.65	0.03800	0.06945	−0.225	0.06882	3.4
	39.3	0.03800	0.06864	−0.13	0.06830	3.7
	39.3	0.03700	0.06697	−0.12	0.06666	3.7
	39.3	0.03600	0.06530	−0.02	0.06525	3.5_5
	39.3	0.03500	0.06363	0.0	0.06363	3.5
$K_4Fe(CN)_6$	24.65	0.01600	0.04383	0.125	0.04405	7.4
	24.65	0.01700	0.04640	0.3	0.04696	6.6
	24.65	0.01806	0.04895	0.25	0.04944	7.2
	24.65	0.01900	0.05150	0.3	0.05213	6.6
	39.3	0.01900	0.05146	−0.01	0.05144	8.0
	39.3	0.01800	0.04894	−0.15	0.04866	8.7
	39.3	0.01700	0.04639	0.13	0.04662	7.4
	39.3	0.01600	0.04385	−0.13	0.04363	8.6
$K_4Fe(CN)_6$	24.65	0.00800	0.02850	−0.3	0.02816	32.8
	24.65	0.00900	0.03216	−0.25	0.03184	27.0
	24.65	0.01000	0.03461	0.15	0.03482	30.9
	24.65	0.01100	0.03868	−0.6	0.03776	34.7
	39.3	0.01000	0.03381	0.39	0.03432	38.3
	39.3	0.00950	0.03223	0.08	0.03233	45.8
	39.3	0.00900	0.03064	0.31	0.03101	40.1
	39.3	0.00850	0.02905	0.42	0.02952	37.8

Can. J. Chem. Downloaded from www.nrcresearchpress.com by 210.87.254.6 on 09/05/12
For personal use only.

TABLE II

Thermodynamic data calculated from the data in Table I (ΔF^0 and ΔH^0 are in kcal/g mole, ΔS^0 in cal/deg g mole, K and K^0 in g mole/l)

Salt	t (°C)	K ($\mu = 0.1$)	K^0	ΔF^0	ΔH^0	ΔS^0
KNO_3	24.65 39.3	0.42_5 0.32_5	0.69 0.53_6	0.22	−3.22	−11.5
K_2SO_4	24.65 39.3	2.67 3.31	6.90 8.83	−1.14	3.11	14.3
$K_2S_2O_8$	24.65 39.3	3.28 3.62	8.23 9.36	−1.25	1.62	9.6
$K_3Fe(CN)_6$	24.65 39.3	6.97 8.19	25.1 30.7	−1.91	2.57	15.0
$K_4Fe(CN)_6$	24.65 39.3	31.3 40.5	170 231	−3.04	3.86	23.2

solvent (the "Born charging effect") which has been applied by Laidler in treating the entropy of hydrated monatomic ions (14). His equation for these ions was (S^0 in cal/deg mole)

$$S^0 = \tfrac{3}{2}R \ln M + 10.2 - 11.6z^2/r,$$

where M is the atomic weight, z the charge, and r the radius of the ion. The last term is the one arising from polarization and, though many other effects must be involved in determining the entropy of these ions, it is worth noting that qualitatively the order for ΔS^0 is that predicted from considerations of polarization.

Kinetic Measurements

The reaction between potassium ferrocyanide and potassium persulfate was followed by taking samples from the reacting mixture and measuring the optical absorbance at 420 mμ with a Beckmann DU spectrophotometer. At this wavelength, the extinction coefficient is 1 025 cm^{-1} (g mole/l)$^{-1}$ for potassium ferricyanide, ~0.85 for potassium ferrocyanide, and negligibly small for all other substances present. Previous work (15) on the spontaneous decomposition of potassium persulfate showed that, under the conditions used, less than 1% of its total disappearance was due to spontaneous decomposition. This observation was confirmed in the present work by iodometric titration of the reaction mixtures at the beginning and end of a run. The titre, which measures both ferricyanide and persulfate, did not decrease detectably during the reaction.

The reaction is first order in both reagents. Rate constants, calculated on this assumption, did not drift during the runs, which were frequently continued until the reaction was 80% complete. Table III gives such constants defined by

$$-\frac{d[K_2S_2O_8]}{dt} = -\frac{1}{2}\frac{d[K_4Fe(CN)_6]}{dt} = k_{app}[K_4Fe(CN)_6].[K_2S_2O_8].$$

No assumption is made at present about whether free ions or ion pairs are the actual reacting species; hence these are apparent rate constants (indicated by k_{app} throughout). Table III gives the initial reagent concentrations and also the concentration of potassium nitrate, which was added to control the ionic strength. In addition, all reaction mixtures were 0.001 M in potassium hydroxide to prevent formation of hydrolyzed species, particularly $HFe(CN)_6^{3-}$.

Can. J. Chem. Downloaded from www.nrcresearchpress.com by 210.87.254.6 on 09/05/12
For personal use only.

TABLE III

Apparent rate constant, k_{app}, (g mole/l)$^{-1}$ min^{-1} (all mixtures contained 0.001 *M* KOH)

Run No.	*t* (°C)	Initial $[K_4Fe(CN)_6]$	Initial $[K_2S_2O_8]$	$[KNO_3]$	k_{app}
1	25.0	6.25×10^{-3}	3.125×10^{-3}	27.12×10^{-3}	0.879
2		6.25	6.25	17.75	0.814
3		1.248	2.50	79.0	1.48
4		9.00	3.00	0.0	0.56
5		9.00	3.00	0.0	0.56
6		1.00	2.00	83.0	1.52
7		3.50	4.00	52.0	1.18
8		1.00	2.00	90.5	1.62
9		1.00	2.00	95.85	1.70
10		1.00	0.90	148.0	2.44
11		1.00	0.90	137.0	2.26
12		1.00	0.90	121.0	2.06
13		1.00	0.80	41.8	1.01
14		1.00	1.00	25.35	0.794
15		1.00	15.00	0.0	0.523
16		1.00	6.00	20.59	0.587
17		1.00	6.00	9.82	0.402
18		1.00	6.00	0.0	0.239
19	40.0	1.00×10^{-3}	2.00×10^{-3}	32.59×10^{-3}	1.85
20		1.00	2.00	39.0	2.14
21		1.00	2.00	49.35	2.69
22		1.00	2.00	59.8	3.17
23		1.00	4.00	16.00	1.28
24		1.00	4.00	6.00	0.786
25		1.00	1.20	72.2	3.68
26		1.00	1.20	82.5	4.14
27		1.00	0.90	96.0	4.68
28		1.00	0.90	106.0	5.07
29		1.00	0.60	117.0	5.52
30		1.00	0.60	127.0	6.01
31		1.00	0.573	138.0	6.40
32		1.00	0.573	150.0	6.81
33		9.00	3.00	0.0	1.50
34		6.25	3.125	27.1	2.42
35		1.00	2.00	83.0	4.18

DISCUSSION

The results in Table III show the dependence on potassium ion concentration previously noted by Holluta and Herman (1). This is not simply a matter of ionic strength. For instance, runs 1, 3, and 4 all have an apparent ionic strength of almost exactly 0.10; but in run 4 k_{app} is 0.56 with total $[K^+] = 0.043$, in run 1 k_{app} is 0.88 with total $[K^+] = 0.058$, and in run 3 k_{app} is 1.48 with total $[K^+] = 0.089$ *M*. Runs 33, 34, and 35 form a similar series. The most plausible theory of this behavior is to suppose that one or both of the reacting species are ion pairs. The various possible combinations were examined, and the choice made on the basis of whether (i) the rate constants fell on a smooth curve when plotted against ionic strength, and (ii) whether the effect of ionic strength followed the predictions of Brönsted's theory. The details of these calculations were as follows.

Calculation of Ionic Strength

This was calculated for each run, with allowance for the effect of ion pairing. As it inevitably changes a little during each run, the calculation was made for a time halfway through each run. The procedure consisted of first calculating the ionic strength as if no ion pairing has occurred. Activity coefficients for this ionic strength were then calculated for all the species present, using the extended Debye–Hückel equation (i.e. eq. [1] above).

Can. J. Chem. Downloaded from www.nrcresearchpress.com by 210.87.254.6 on 09/05/12
For personal use only.

From these, and from values of the equilibrium constants at 0.1 ionic strength, the equilibrium constants at the first approximation to the ionic strength of the run were calculated. From these constants, the concentrations of all the species present were calculated, and hence a second approximation to the ionic strength was obtained. This cycle was repeated, giving new constants, hence new concentrations, and a new value for the ionic strength, until repetition gave no appreciable change in ionic strength. These values were then used in connection with the calculations on rate constants described below.

Calculation of Rate Constants

It was first assumed that some particular pair of ions were the main reacting species, and the appropriate rate constants were designated as follows.

Reacting Species	Constant
$Fe(CN)_6^{4-} + S_2O_8^{2-}$	k_1
$KFe(CN)_6^{3-} + S_2O_8^{2-}$	k_2
$Fe(CN)_6^{4-} + KS_2O_8^{-}$	k_3
$KFe(CN)_6^{3-} + KS_2O_8^{-}$	k_4

If the equilibrium constants are

$$K_1 = \frac{[KFe(CN)_6^{3-}]}{[K^+][Fe(CN)_6^{4-}]}$$

and

$$K_2 = \frac{[KS_2O_8^{-}]}{[K^+][S_2O_8^{2-}]},$$

then

$$k_1 = k_{app}(1 + K_1x)(1 + K_2x)$$

where x is the free potassium ion concentration, which was obtained during the calculation of ionic strength. It varied little during a run, and was assumed constant. Hence k_1 can be calculated from this equation. Similarly,

$$k_2 = k_{app}(1 + K_1x)(1 + K_2x)/K_1x$$
$$k_3 = k_{app}(1 + K_1x)(1 + K_2x)/K_2x$$
$$k_4 = k_{app}(1 + K_1x)(1 + K_2x)/K_1K_2x^2.$$

Each of these equations assumes that only one mechanism for the reaction is important. Rate constants k_1, k_2, k_3, and k_4 were calculated, and their variation with ionic strength was investigated. Brönsted's equation is

$$\log k = \log k^0 + 2Az_a.z_bF(\mu),$$

where k is the rate constant at some ionic strength μ, k^0 is the constant at zero ionic strength, A is the Debye–Hückel constant, z_a and z_b are the charges on the reacting species, and $F(\mu)$ is the function of the ionic strength in the Debye–Hückel equation (eq. [1] above). The constants in the Debye–Hückel equation are assumed to be the same both for the reacting species and for the activated complex, an assumption which can be avoided at the cost of making the equation somewhat more complicated.

Accordingly $\log k_1$, $\log k_2$, etc. were plotted against $F(\mu)$, taking a with an average value of 4.5 Å. The results are shown in Figs. 1 and 2, for 25 and 40 °C respectively. Two

Can. J. Chem. Downloaded from www.nrcresearchpress.com by 210.87.254.6 on 09/05/12
For personal use only.

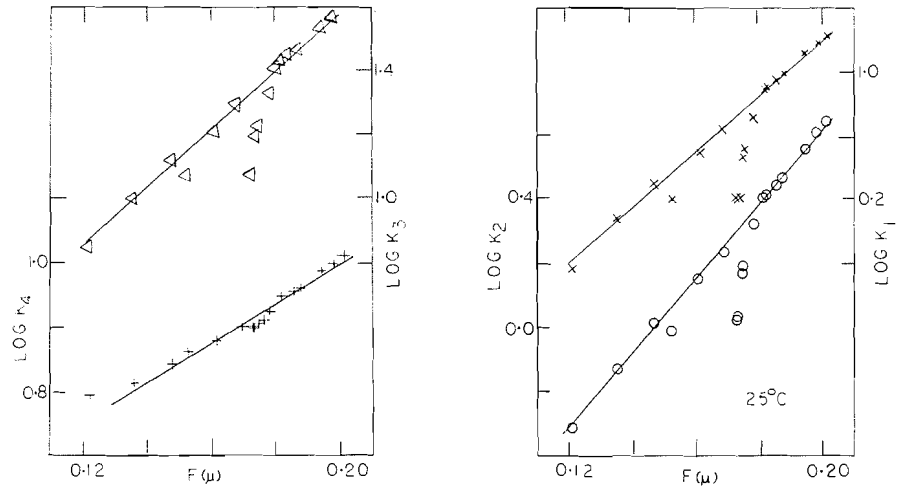


FIG. 1. Logarithms of various rate constants at 25 °C plotted against the Debye–Hückel function of the ionic strength: ×, log K_1; ○, log K_2; △, log K_3; +, log K_4.

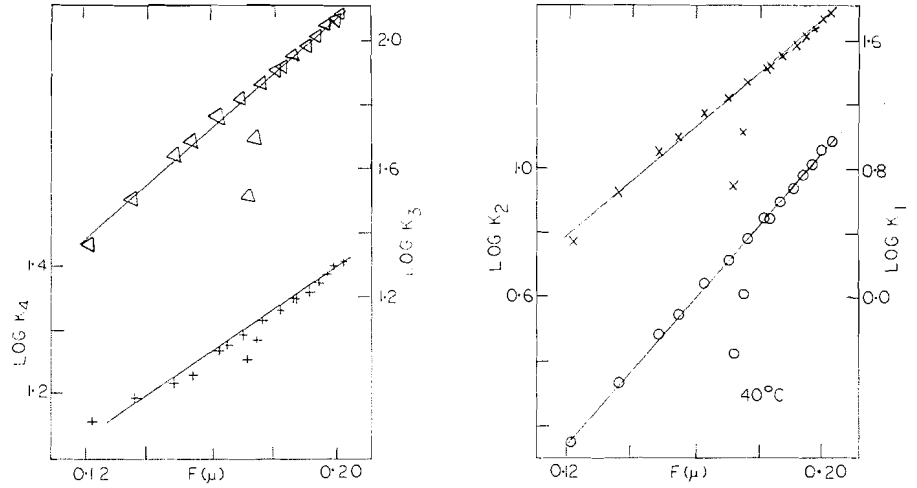


FIG. 2. Logarithms of various rate constants at 40 °C plotted against the Debye–Hückel function of the ionic strength: ×, log K_1; ○, log K_2; △, log K_3; +, log K_4.

things are apparent from these diagrams. (i) The runs with amounts of $K_4Fe(CN)_6$ other than the usual amount of 10^{-3} M fall off the general line (runs 1, 2, 4, 5, 7, 33, 34) but do so to a much smaller extent for log k_4. This is evidence that the reacting species are $KFe(CN)_6^{3-}$ and $KS_2O_8^-$. (ii) Lines can be drawn for all types of k through the points for runs in which the initial ferrocyanide concentration was 0.001 M. The slopes of these lines can be compared with the predictions of the Brönsted equation. This is perhaps most easily seen by comparing the values of $z_a z_b$ calculated from the slope with the actual values. This is done in Table IV, and it is seen that the values only agree for k_4. This also supports the view that the reacting species are $KFe(CN)_6^{3-}$ and $KS_2O_8^-$. To some extent this agreement is fortuitous since it depends on the exact values of the parameters chosen for the Debye–Hückel equations. Fairly large alterations of these parameters could

Can. J. Chem. Downloaded from www.nrcresearchpress.com by 210.87.254.6 on 09/05/12
For personal use only.

change the slope by about 20%, but could not possibly give agreement for any other reacting species in Table IV.

TABLE IV

Comparison of experimental values of $z_a z_b$ with values calculated from the slope of the lines in Figs. 1–2

Reacting species	Rate constant	t (°C)	$z_a z_b$	$z_a z_b$ calcd. from slope
$Fe(CN)_6^{4-} + S_2O_8^{2-}$	k_1	25	8	17.3
		40	8	16.8
$KFe(CN)_6^{3-} + S_2O_8^{2-}$	k_2	25	6	11.9
		40	6	11.1
$Fe(CN)_6^{4-} + KS_2O_8^{-}$	k_3	25	4	9.2
		40	4	8.5
$KFe(CN)_6^{3-} + KS_2O_8^{-}$	k_4	25	3	3.11
		40	3	2.94

These calculations assume only one mechanism is operative. At very low $[K^+]$, others must doubtless become important, but there is no sign of this under the conditions used above. It may be noted that if Holluta and Herman's (1) data are compared with ours, the rate constants appear to be considerably larger. The chief difference in their conditions was that they added no potassium hydroxide. Presumably $HFe(CN)_6^{3-}$, or even $KHFe(CN)_6^{2-}$, is contributing to the reaction.

The lines through the plots of log k_4 against $F(\mu)$, k_4 in units of (g mole/l)$^{-1}$ min^{-1}, give for 25 °C

$$\log k_4 = 0.376 + 3.17F(\mu),$$

and for 40 °C

$$\log k_4 = 0.693 + 3.33F(\mu).$$

This makes the activation energy at zero ionic strength, $\Delta H^{\ddagger}$, equal to 9.0 kcal/g mole. If, as usual, we write

$$k_4 = \frac{kT}{h} e^{\Delta S^{\ddagger}/R} . e^{-\Delta H^{\ddagger}/RT},$$

the entropy of activations, $\Delta S^{\ddagger}$, is found to be −34.7 cal/deg mole. This is rather strongly negative, but Laidler (16) deduces that for ionic reactions like the present one a value of $-10 z_a z_b$ might be expected. This would lead one to expect a value of −30 cal/deg mole in the present reaction, so the observed value is quite plausible. Similar calculations for $\Delta S^{\ddagger}$ at zero ionic strength give: for K_1, $\Delta S^{\ddagger} = 4.7$ cal/deg mole with $z_a z_b = 8$; for K_2, $\Delta S^{\ddagger} = 6.9$ cal/deg mole with $z_a z_b = 6$; and for K_3, $\Delta S^{\ddagger} = -7.8$ cal/deg mole with $z_a z_b = 4$. These results help to confirm the mechanism for the reaction suggested above. The conclusion is not altered if the calculations are made for $F(\mu) = 0.20$.

REFERENCES

1. J. Holluta and W. Herman. Z. Physik. Chem. Leipzig, **A166**, 453 (1933).
2. J. N. Brönsted. Z. Physik. Chem. Leipzig, **102**, 169 (1922); **115**, 337 (1925). S. W. Benson. The foundations of chemical kinetics. McGraw-Hill Book Co., Inc., New York. 1960. p. 525.
3. A. R. Olson and T. R. Simonson. J. Chem. Phys. **17**, 1167 (1949).
4. C. W. Davies. Ion association. Butterworths, London. 1962. p. 139.
5. J. Kielland. J. Am. Chem. Soc. **59**, 1675 (1937).

Can. J. Chem. Downloaded from www.nrcresearchpress.com by 210.87.254.6 on 09/05/12
For personal use only.

6. C. W. DAVIES. Trans. Faraday Soc. **23**, 351 (1927).
7. W. H. BANKS, E. C. RIGHELLATO, and C. W. DAVIES. Trans. Faraday Soc. **27**, 621 (1931).
8. T. SHEDLOVSKY. J. Am. Chem. Soc. **54**, 1411 (1932).
9. I. L. JENKINS and C. B. MONK. J. Am. Chem. Soc. **72**, 2695 (1950).
10. C. B. MONK. J. Chem. Soc. 423 (1949).
11. J. C. JAMES and C. B. MONK. Trans. Faraday Soc. **46**, 1041 (1950).
12. J. C. JAMES. Trans. Faraday Soc. **45**, 855 (1949).
13. S. R. COHEN and R. A. PLANE. J. Phys. Chem. **61**, 1096 (1959).
14. K. J. LAIDLER. Can. J. Chem. **34**, 1107 (1956).
15. E. HAKOILA. Ann. Univ. Turku. Ser. A, **66** (1963).
16. K. J. LAIDLER. Reaction kinetics. Vol. II. Pergamon Press, London. 1963. p. 12.

Can. J. Chem. Downloaded from www.nrcresearchpress.com by 210.87.254.6 on 09/05/12
For personal use only.

Can. J. Chem. Downloaded from www.nrcresearchpress.com by 210.87.254.6 on 09/05/12
For personal use only.

VISIBLE AND ULTRAVIOLET ABSORPTION SPECTRA OF RHODIUM(III) IN FUSED ALKALI CHLORIDES AND NITRATES

FREDRICK B. OGILVIE[1] AND OWEN G. HOLMES[2]
University of Saskatchewan, Regina, Saskatchewan

Received October 5, 1965

ABSTRACT

The spectrum of $RhCl_3$ in fused LiCl–KCl at 440 °C is sufficiently different from that of $RhCl_6^{3-}$ to suggest the existence of some other species such as dimeric or polymeric bridge-complexes, or, less likely, tetrahedral $RhCl_4^-$. The spectra of $RhCl_3$ and $K_3Rh(NO_2)_6$ in fused $NaNO_3$–KNO_3 at 300 °C indicate the occurrence of nitro coordination in both systems, probably completely in the latter case, but in competition with chloro coordination in the former. Addition of KCl to a solution of $RhCl_3$ in $NaNO_3$–KNO_3 causes spectral changes which suggest that $RhCl_6^{3-}$ is the principal rhodium species present.

INTRODUCTION

The rather complicated chemistry of rhodium(III) in aqueous solutions has recently been the subject of extensive and careful study. On the basis of crystal field theory, Jorgensen (1) was able to interpret the spectra, as measured by himself and by earlier workers, of a variety of rhodium complexes. Kristjanson and Lederer (2) applied chromatographic methods to the separation of the species present in hydrochloric acid solutions of rhodium(III). By ion-exchange techniques, Wolsey, Reynolds, and Kleinberg (3) isolated and characterized a number of chloro–aquo complexes from the rhodium(III)–chloride system in acid solution. Schmidtke (4) has reported the spectra and their theoretical interpretation for a number of species of the type RhA_6.

In this work, rhodium(III) has been dissolved in fused eutectic mixtures of $NaNO_3$ and KNO_3 and of LiCl and KCl, and in NaNO–KNO_3 with added Cl^- and NO_2^-. The visible and ultraviolet spectra of these solutions have been measured and have been compared to aqueous spectra in attempts to determine the rhodium-containing species present.

EXPERIMENTAL

Anhydrous $RhCl_3$ from Alfa Inorganics, Inc., $RhCl_3 . xH_2O$ from Fisher Scientific Co. Ltd., and $K_3Rh(NO_2)_6$ from Engelhard Industries, Inc., were the sources of rhodium for these experiments.

Rhodium was determined by the procedure given by Brito (5). In this method rhodium(III) is reduced by magnesium metal and then the resulting Rh is dried in a stream of H_2 and weighed as the metal.

A stock of $NaNO_3$–KNO_3 eutectic, 45.5 mole % $NaNO_3$, was prepared by fusing the ingredients. The mixture was then cooled, crushed, and stored over silica gel.

Hygroscopic LiCl–KCl, 41.2 mole % KCl, was prepared by a modification of the method of Boston and Smith (6). The mixture of salts for a given experiment was heated under a stream of dry HCl gas to remove traces of water and then under N_2 to remove residual HCl. The molten eutectic was transferred directly to an evacuated optical cell which was then sealed.

Spectral measurements on the fused salt solutions were made with a Beckman DU spectrophotometer, modified by interposing a small furnace assembly between the light source and the monochromator. For spectral study, specimens and blanks were placed in a furnace which was equipped with a light transmission path and a positioning device for 1 cm glass or quartz optical cells.

In each experiment, a sample of the corresponding solvent was used as a blank. Strong ultraviolet absorption by nitrate ion limited measurements to energies of less than 30 000 cm^{-1}.

Combined uncertainties in the determination of rhodium, spectrophotometer response, positioning reproducibility in the light path, and density of the $NaNO_3$–KNO_3 solvent lead to estimated uncertainties of less than 5% in the values for molar absorptivity.

[1]*Present address: Iowa State University, Ames, Iowa.*
[2]*Present address: Lethbridge College, Lethbridge, Alberta.*

Spectra for the $NaNO_3$–KNO_3 solutions were measured at 300 ± 5 °C and for the LiCl–KCl solutions at 440 ± 5 °C.

RESULTS

(a) $RhCl_3$ in LiCl–KCl

At 440 °C anhydrous $RhCl_3$ readily dissolved in fused LiCl–KCl to yield a rose-colored solution whose spectrum is shown in Fig. 1. Also in Fig. 1 is the spectrum obtained for a solution of $RhCl_3 . xH_2O$ refluxed for 4 h in 6 *M* HCl.

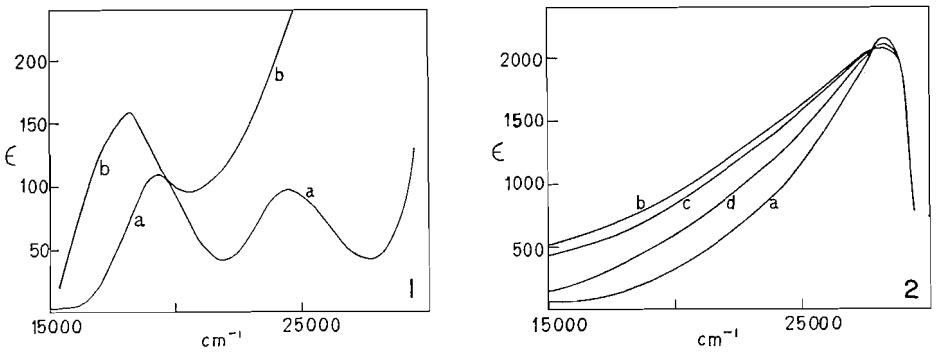


FIG. 1. Absorption spectra of $RhCl_3$: (*a*) 5.5 × 10^{-3} *M* $RhCl_3$ in 6 *M* HCl; (*b*) 1.4 × 10^{-3} *M* $RhCl_3$ in LiCl–KCl.

FIG. 2. Absorption spectra in $NaNO_3$–KNO_3: (*a*) 2 × 10^{-4} *M* $K_3Rh(NO_2)_6$; (*b*) $RhCl_3$, approximately 5 × 10^{-4} *M*; (*c*) $RhCl_3$, mole ratio Rh^{3+}:NO_2^- = 1:3; (*d*) $RhCl_3$, mole ratio Rh^{3+}:NO_2^- = 1:50.

(b) $RhCl_3$ and $K_3Rh(NO_2)_6$ in $NaNO_3$–KNO_3

At 300 °C anhydrous $RhCl_3$ dissolved in $NaNO_3$–KNO_3 over a period of several hours to produce a yellow solution whose spectrum is shown in Fig. 2. Maintenance of the solution at this temperature for 48 h led eventually to the deposition of a black precipitate. An increase in temperature to 350 °C accelerated this deposition, whereas addition of Na_2O_2 to the yellow solution caused immediate precipitation. After isolation and fusion with potassium pyrosulfate, analysis of the black residue showed 80.6% Rh; the theoretical value for Rh_2O_3 is 81.1% Rh.

Addition of $NaNO_2$ to the $NaNO_3$–KNO_3 solvent markedly increased the rate of solution of $RhCl_3$, but did not appreciably alter the rate of formation of the black precipitate. The variation of the spectrum of $RhCl_3$ in $NaNO_3$–KNO_3 with concentration of $NaNO_2$ is illustrated in Fig. 2. Also shown is the spectrum of the yellow solution formed by dissolution of $K_3Rh(NO_2)_6$ in $NaNO_3$–KNO_3.

Fig. 3 shows the spectrum, which varies as the solution ages, of aqueous $K_3Rh(NO_2)_6$.

(c) $RhCl_3$ in $NaNO_3$–KNO_3 with Added KCl

The dependence of the spectrum of $RhCl_3$ in fused $NaNO_3$–KNO_3 upon the concentration of added KCl is shown in Fig. 4. A change in color from yellow to rose accompanied the change in spectrum.

DISCUSSION

There is general agreement that the principal rhodium species in an aged solution of $RhCl_3$ in strong HCl is hexachlororhodate(III) ion. Kristjanson and Lederer (2) have estimated that in 6 *M* HCl, 95 ± 5% of the rhodium is in that form. Wolsey *et al.* (3) have found that even at 2 *M* HCl an equilibrium mixture of chloro-aquo complexes consists largely of $RhCl_6^{3-}$. Fig. 1*a* is therefore presented as that of $RhCl_6^{3-}$, there being

Can. J. Chem. Downloaded from www.nrcresearchpress.com by 210.87.254.6 on 09/05/12
For personal use only.

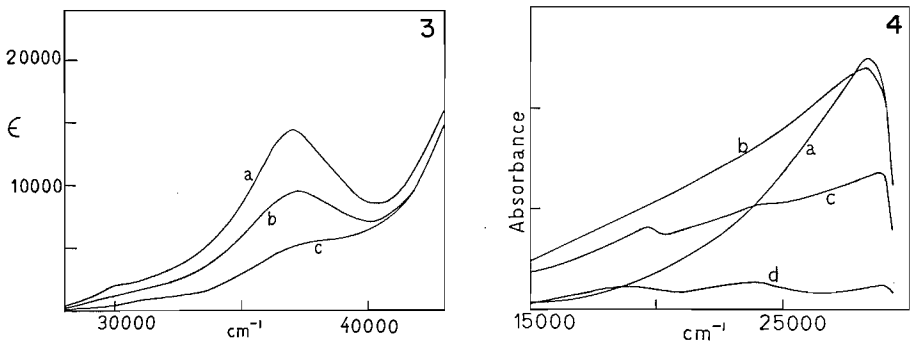


FIG. 3. Absorption spectra of 6×10^{-5} *M* $K_3Rh(NO_2)_6$ in water: (*a*) freshly prepared solution; (*b*) after 24 h at room temperature; (*c*) after 120 h at room temperature.

FIG. 4. Absorption spectra of rhodium(III) in $NaNO_3$–KNO_3: (*a*) 2×10^{-4} *M* $K_3Rh(NO_2)_6$; (*b*) $RhCl_3$, approximately 10^{-3} *M*; (*c*) $RhCl_3$, mole ratio $RhCl_3$:KCl = 1:260; (*d*) $RhCl_3$, mole ratio $RhCl_3$:KCl = 1:600.

two bands with maxima at 19 300 cm^{-1} (ϵ = 109) and 24 400 cm^{-1} (ϵ = 98). Also strong charge transfer absorption is observed at higher energies, beginning around 29 000 cm^{-1}. This spectrum is in good agreement with those reported by several authors, including Wolsey *et al.* (3) who obtained bands at 19 300 cm^{-1} (ϵ = 111.5) and 24 000 cm^{-1} (ϵ = 93.8).

A number of authors, see for example Jorgensen (1), have attributed the bands of $RhCl_6^{3-}$ to transitions from the ground state $^1\Gamma_1$ of the configuration γ_5^6 to states $^1\Gamma_4$ and $^1\Gamma_5$ of the configuration $\gamma_5^5\gamma_3$. Jorgensen also presented evidence for the weaker transitions to states $^3\Gamma_4$ and $^3\Gamma_5$ of the latter configuration.

In fused LiCl–KCl at 440 °C a single peak is observed at 18 200 cm^{-1} (ϵ = 160), along with intense absorption beginning at about 26 000 cm^{-1}. If this spectrum is due to $RhCl_6^{3-}$ in the melt, as might be expected, the lower energy band is shifted 1 100 cm^{-1} to lower energy relative to the aqueous system, with the higher energy band shifted to higher energy where it is obscured by the charge transfer absorption.

It may be that the species in the melt is other than $RhCl_6^{3-}$. Gruen and McBeth (7) have reviewed the coordination chemistry of the 3d transition metal ions in fused salts, pointing out several instances of tetrahedral chloro-complexes at the elevated temperatures. However, they generalized that tripositive 3d ions tend to six- rather than four-coordinate chloro-complexes, a tendency that one would expect to be more pronounced for the larger 4d ion Rh^{3+}.

A more likely possibility is that dimeric or polymeric chloro-bridged complexes exist in the melt. Kristjanson and Lederer (2) proposed that when a solution of $RhCl_6^{3-}$ in HCl was evaporated, and the residue redissolved in HCl, highly charged chloro-bridged ions were obtained, since they found some of the rhodium to be more strongly bound to ion-exchange columns than $RhCl_6^{3-}$. This solution displayed a spectrum with a band maximum at 18 900 cm^{-1} and strong absorption beyond 25 000 cm^{-1}. Upon aging, the solution reverted to the equilibrium with a high proportion of $RhCl_6^{3-}$.

In the range accessible with $NaNO_3$–KNO_3 as solvent, the spectrum of $RhCl_3$ is characterized by one rather strong band with a maximum at 28 200 cm^{-1} and ϵ = 2 100, the band being asymmetric with a long tail of absorption on the low energy side. The addition of NO_2^- to the melt reduces the low energy absorption until the spectrum approaches that of $K_3Rh(NO_2)_6$ in $NaNO_3$–KNO_3.

Can. J. Chem. Downloaded from www.nrcresearchpress.com by 210.87.254.6 on 09/05/12
For personal use only.

These results point to nitro-coordination in all of the nitrate solutions studied. The slow rate of solution of $RhCl_3$ in $NaNO_3$–KNO_3 correlates with the slow production of traces of NO_2^- which occurs in that system. The effect of added NO_2^- suggests a gradual shift from chloro- to nitro-coordination. The stability of the spectrum of $K_3Rh(NO_2)_6$ suggests preservation of $Rh(NO_2)_6^{3-}$ in the melt. Since the least absorption in the low energy range is observed for the chloride-free solution of $K_3Rh(NO_2)_6$, that absorption may be caused by the presence of mixed chloro–nitro-complexes in all of the other solutions.

Aqueous $Rh(NO_2)_6^{3-}$, which can be followed well into the ultraviolet, gives a spectrum with a band at 37 000 cm^{-1} (ϵ = 14 400), a shoulder at 30 000 cm^{-1} (ϵ = 2 000), and strong absorption beyond 45 000 cm^{-1}. Schmidtke (4) reported a more complete spectrum with bands at 37 000 cm^{-1} (ϵ = 16 500) and 50 000 cm^{-1} (ϵ = 54 000), both of which he attributed to the nitrite ion, and a ligand-field absorption (shoulder) at 29 800 cm^{-1} (ϵ = 2 380). The spectrum (and pH) of freshly prepared aqueous $Rh(NO_2)_6^{3-}$ changed markedly with time because of hydrolysis. The shoulder at around 30 000 cm^{-1} roughly corresponds to the well-defined band at 28 200 cm^{-1} for the $NaNO_3$–KNO_3 solutions.

A progressive increase in chloride concentration in $NaNO_3$–KNO_3 solution of $RhCl_3$ transforms the spectrum. At high chloride concentration the strong band attributed to $Rh(NO_2)_6^{3-}$ has become a small residual peak, while two new bands have resolved at 18 800 cm^{-1} and 24 000 cm^{-1}. The correspondence between these values and those for $RhCl_6^{3-}$ indicates the presence of $RhCl_6^{3-}$ in the chloride-containing melt. This in turn weighs against the existence of $RhCl_6^{3-}$ as the principal species in LiCl–KCl, one of the possibilities considered earlier in this discussion.

ACKNOWLEDGMENTS

The financial assistance of the National Research Council is gratefully acknowledged.

REFERENCES

1. C. K. JORGENSEN. Acta Chem. Scand. **10**, 500 (1956).
2. A. M. KRISTJANSON and M. LEDERER. J. Less-Common Metals, **1**, 245 (1959).
3. W. C. WOLSEY, C. A. REYNOLDS, and J. KLEINBERG. Inorg. Chem. **2**, 463 (1963).
4. H. SCHMIDTKE. Z. Physik. Chem. Neue Folge Frankfurt, **40**, 96 (1964).
5. F. BRITO. U.S. Dept. Comm. Office Tech. Serv. AD **267**, 432 (1961).
6. C. R. BOSTON and G. P. SMITH. J. Phys. Chem. **62**, 409 (1958).
7. D. M. GRUEN and R. L. MCBETH. Pure Appl. Chem. **6**, 23 (1963).

Can. J. Chem. Downloaded from www.nrcresearchpress.com by 210.87.254.6 on 09/05/12
For personal use only.

Can. J. Chem. Downloaded from www.nrcresearchpress.com by 210.87.254.42 on 09/05/12
For personal use only.

THE THERMODYNAMIC PROPERTIES OF HYDROGEN SELENIDE

J. R. RAWLING AND J. M. TOGURI
Chemistry Department, Noranda Research Centre, Pointe Claire, Quebec

Received August 31, 1965

ABSTRACT

Hydrogen selenide may be generated by the reaction of hydrogen gas with liquid selenium according to the reaction

$$H_{2(g)} + Se_{(l)} \rightleftharpoons H_2Se_{(g)}$$

where $$K = P_{H_2Se}/P_{H_2}a_{Se}.$$

The equilibrium constant K of this reaction was measured by passing hydrogen over liquid selenium at controlled rates of flow over the temperature range 525–625 °C. The equilibrium ratio of hydrogen to hydrogen selenide was determined by gas analysis. Over the temperature range 525–625 °C, the equilibrium constant can be expressed by the equation

$$\log K = 13.07 + 2.97 \times 10^{-4}T - 3.69 \log T - 2\,209T^{-1} - 4.81 \times 10^{3}T^{-2}.$$

This expression leads to $\Delta H_{298}^\circ = 9\,174 \pm 107$ cal mole^{-1}, $\Delta F_{298}^\circ = 5\,132$ cal mole^{-1}, and $\Delta S_{298}^\circ = 13.56$ e.u. (entropy units) for the respective heat, free energy, and entropy of formation of hydrogen selenide from hydrogen and crystalline selenium.

INTRODUCTION

One of the methods for the determination of the chemical potential of selenium in metal selenide systems is by equilibrating the metal in question with a mixture of hydrogen selenide and hydrogen according to the equilibrium,

[1] $$H_2Se_{(g)} + Me = MeSe + H_{2(g)}.$$

To carry out such a study the thermochemistry of hydrogen selenide must be well established. However, investigations (1, 2) on the equilibrium among hydrogen, selenium, and hydrogen selenide according to eq. [2]

[2] $$H_{2(g)} + Se_{(l)} = H_2Se_{(g)}$$

do not agree with the published thermochemical data (3, 4, 5). Furthermore, the only investigation of the reaction between hydrogen and selenium at temperatures above 500 °C (1) indicates a maximum in the equilibrium constant at 575 °C which cannot be explained by any known structural transformation. Consequently, the object of this investigation was to establish reliable values of the equilibrium constant of reaction [2] before a systematic study of the selenium potential in various alloy systems was undertaken.

EXPERIMENTAL

The well-known transpiration method was adopted to measure the equilibrium between liquid selenium, hydrogen, and hydrogen selenide. The procedure involved the bubbling of hydrogen or mixtures of hydrogen and hydrogen selenide through liquid selenium at constant velocity and temperature. The gas mixture leaving the furnace was then analyzed for hydrogen and hydrogen selenide. The important requirement in this method is to ensure the saturation of the equilibrating gases.

The apparatus is shown in Fig. 1. It consisted of a gas purification system, two equilibrating furnaces, and a gas-scrubbing system.

Hydrogen was passed through a Deoxo purifier to remove residual oxygen and then through an Anhydrone column to remove moisture. Argon utilized for flushing the system passed through an Anhydrone drying column and then through a furnace containing titanium turnings at 850 °C to remove oxygen and hydrogen. The required gases were then admitted to the furnace through calibrated flowmeters.

The selenium was contained in a Vycor crucible placed in a Kanthal resistance furnace. With this furnace a uniform temperature zone was readily obtained to within ±1.5 °C along the middle 8 cm of the furnace

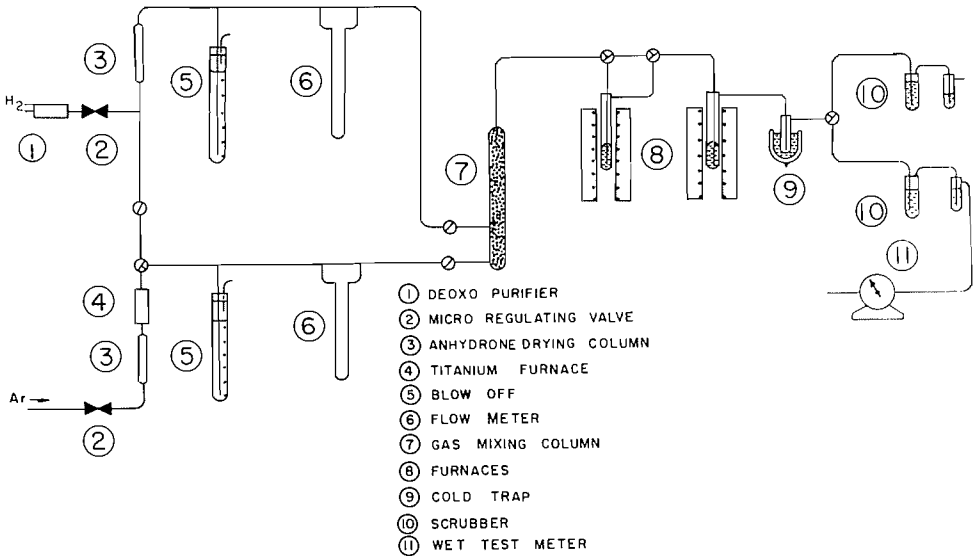


FIG. 1. Diagram of apparatus.

for temperatures of 400–700 °C. The furnace temperature was measured with a calibrated chromel–alumel thermocouple placed directly below the base of the crucible situated in the constant temperature zone.

A Vycor gas inlet tube penetrated to within 2 mm of the bottom of the crucible so that gas entering the crucible bubbled through a column of liquid selenium approximately 3.5 cm deep. Two such furnaces were used when a mixture of hydrogen and hydrogen selenide was required, the first furnace acting as a hydrogen selenide generator which supplied a gas mixture of known composition to the second.

The gases leaving the furnace passed through a cold trap which condensed any selenium vapor present. The cold trap was maintained at approximately −20 °C with an ice – ammonium chloride mixture. On leaving the cold trap the gas mixture passed through a solution containing 50 g/l (grams per liter) of reagent grade sodium hydroxide and 7 g/l of reagent grade potassium bromate. Hydrogen selenide was decomposed in this solution according to the reaction

$$[3] \qquad H_2Se + 2NaOH + 3(O) = Na_2SeO_3 + 2H_2O.$$

The effectiveness of this decomposition was ensured by passing the scrubbed gas through a solution containing 10 g.p.l. of copper sulfate. If decomposition was incomplete a black precipitate of copper selenide was formed. Finally the gas was passed through a wet-test meter to determine the volume of the residual hydrogen. The second scrubber system shown in Fig. 1 was employed as a bypass.

The experimental procedure adopted was to place 40 g of selenium in each furnace. As the furnaces were brought to the required temperature, argon was admitted to the system at a flow rate of approximately 100 ml/min. This gas was replaced with hydrogen when the required temperature was obtained. The hydrogen flow was continued until the solution in the bypass scrubber had turned to a deep brownish red indicating the deposition of selenium. The gas stream was then switched through the main scrubber and the flow rate adjusted to the desired value.

After the required amount of hydrogen, approximately 1 to 3 l, had passed through the apparatus the flow was stopped and the flask containing the scrubber solution removed. A flask of fresh scrubber solution was then put into place and the system purged with hydrogen for a few minutes using the bypass scrubber. The gas stream was then switched through the fresh scrubber and wet-test meter and the procedure repeated at a different flow rate. Approximately eight such experiments were carried out with a charge of 40 g of selenium.

The scrubber solutions obtained from each run were acidified with 80% excess of concentrated hydrochloric acid. The solutions were then heated to 80 °C and the selenium reduced to the elemental form with sulfur dioxide. The selenium thus precipitated was filtered, dried, and weighed.

The molar flow rates of hydrogen and hydrogen selenide leaving the furnace were calculated from the volume of hydrogen passing through the wet-test meter in a given time and from the weight of selenium absorbed in the scrubber system during the same period.

Can. J. Chem. Downloaded from www.nrcresearchpress.com by 210.87.254.42 on 09/05/12
For personal use only.

RESULTS AND DISCUSSION

The equilibrium constant for reaction [2] is given by

$$K = P_{H_2Se}/P_{H_2}, \quad [4]$$

since pure liquid selenium is present at unit activity.

In the present experiments

$$P_{H_2} = (n_{H_2}/V)RT = (m_{H_2}/M_{H_2})(RT/V) \quad [5]$$

and

$$P_{H_2Se} = (n_{H_2Se}/V)RT = (m_{H_2Se}/M_{H_2Se})(RT/V) \quad [6]$$

thus

$$K = P_{H_2Se}/P_{H_2} = n_{H_2Se}/n_{H_2} = (m_{H_2Se}/m_{H_2})(M_{H_2}/M_{H_2Se}), \quad [7]$$

where the symbols used have their usual meanings. Consequently, the results lead to a direct measurement of K. However, experiments of this kind are liable to two sources of error because of kinetic factors. Firstly, if the gas is passed through the crucible too rapidly, it will not have time to reach equilibrium with the liquid phase. Secondly, since the molecular weights of the two gaseous components are very different, a strong thermal diffusive effect is to be expected, causing the H_2Se molecules to migrate preferentially to the cold part of the system, and this effect is likely to become pronounced at slow gas flow rates. For true equilibrium conditions the ratio P_{H_2Se}/P_{H_2} will be independent of gas flow rate; therefore experiments were carried out over a range of flow rates in order to establish this condition.

If the ratio of P_{H_2Se}/P_{H_2} in equilibrium with selenium is independent of flow rate, the ratio of the molar flow rates of hydrogen and hydrogen selenide is also independent of flow rate. Under these conditions a plot of molar flow rate of hydrogen selenide n_{H_2Se} against molar flow rate of hydrogen n_{H_2} should yield a straight line passing through the origin. Any errors resulting from nonequilibrium or diffusion effects will cause deviations from this linear relationship. The equilibrium ratio P_{H_2Se}/P_{H_2} is given by the slope of this line since rearrangement of eq. [7] and division by time, t, leads to

$$n_{H_2Se}/t = K(n_{H_2}/t) + f(F) \quad [8]$$

where $f(F)$ represents any deviation from equilibrium conditions, such deviations being some function of the gas flow rate F. If equilibrium is achieved $f(F) \rightarrow 0$.

Fig. 2 shows a typical plot of the molar flow rate of hydrogen selenide against the molar flow rate of hydrogen at 600 °C. The flow rate of hydrogen was varied from 40 to 120 ml/min. Over this region the ratio of the mass flow of hydrogen selenide and hydrogen was found to be independent of the flow rate.

Measurements of the equilibrium constant were carried out over the temperature range 525 to 625 °C. Equilibrium was approached either by the decomposition of H_2Se or by its formation by controlling the H_2Se/H_2 input ratio to the second equilibration furnace. The results are shown in Fig. 3 and tabulated in Table I. The direction of the approach to equilibrium is indicated for each point shown on the figure. At temperatures below 525 °C the reaction proceeded too slowly for the attainment of equilibrium.

Can. J. Chem. Downloaded from www.nrcresearchpress.com by 210.87.254.42 on 09/05/12
For personal use only.

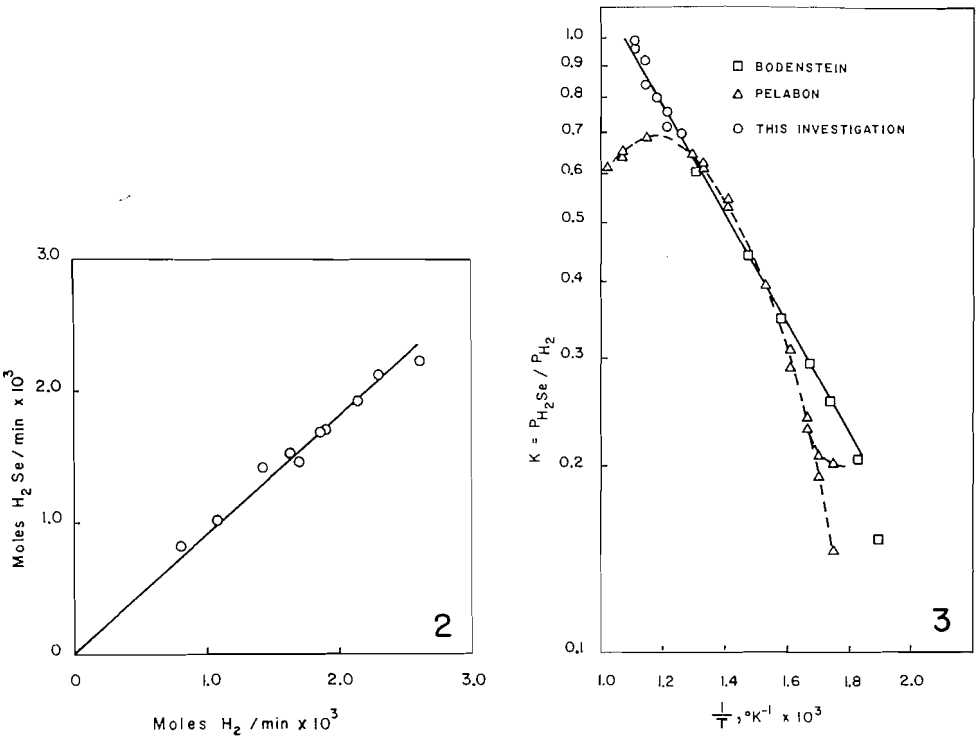


FIG. 2. Relation between molar flow rates of hydrogen selenide and hydrogen leaving the furnace at 600 °C.

FIG. 3. The effect of temperature on the equilibrium constant K for the reaction $H_{2(g)} + Se_{(l)} = H_2Se_{(g)}$.

Pelabon (1) has studied the same reaction over the temperature range 250 to 705 °C, whereas Bodenstein (2) measured this equilibrium over the temperature range 254 to 493 °C. Their results are also summarized in Fig. 3 together with the results of the present study. At temperatures below 300 °C, their results are in poor agreement possibly because of kinetic effects. Above 500 °C, Pelabon's results indicate that K passes through a maximum value of approximately 0.7 at 575 °C. Since there is no known structural

TABLE I

Equilibrium constant for the reaction $H_{2(g)} + Se_{(l)} = H_2Se_{(g)}$ $(K = P_{H_2Se}/P_{H_2})$

Temp. (°C)	Ratio H_2Se/H_2 entering furnace	Equilibrium constant K
525	0.70	0.70
550	0.62	0.72
		0.76
575	0.70	0.80
600	Pure H_2	0.84
	1.04	0.91
625	Pure H_2	0.99
	1.04	0.97

Can. J. Chem. Downloaded from www.nrcresearchpress.com by 210.87.254.42 on 09/05/12
For personal use only.

transformation in the system at this temperature, this phenomenon cannot be interpreted as one involving a state of equilibrium. On the other hand our results approximately fall on the extension of a straight line drawn through Bodenstein's data.

A Σ plot has been carried out with the specific heat data of Kelley (6) to permit the calculation of a free energy equation for reaction [2]. From a least square analysis of the Σ function, the following relationships were obtained.

$$\Delta F_T^0 = 10\,107 - 59.80T + 16.88T \log T - 1.36 \times 10^{-3}T^2 + 0.22 \times 10^5 T^{-1}$$
$$\Delta H_T^0 = 10\,107 - 7.33T + 1.36 \times 10^{-3}T^2 + 0.43 \times 10^5 T^{-1}$$
$$\log K = 13.07 + 2.97 \times 10^{-4}T - 3.69 \log T - 2\,209T^{-1} - 4.81 \times 10^3 T^{-2}.$$

For the reaction

[9] $$H_{2(g)} + Se_{(s)} = H_2Se_{(g)}$$

and with Kelley's (6) recommended value of the heat of fusion of selenium of 1 300 cal mole^{-1} at 490 °K, the following thermodynamic relationships were obtained.

$$\Delta F_T^0 = 9\,964 - 30.05T + 5.14T \log T + 3.04 \times 10^{-3}T^2 + 0.22 \times 10^5 T^{-1}$$
$$\Delta H_T^0 = 9\,964 - 2.23T - 3.04 \times 10^{-3}T^2 + 0.43 \times 10^5 T^{-1}$$
$$\log K = 6.57 - 6.64 \times 10^{-4}T - 1.12 \log T - 2\,178T^{-1} - 4.81 \times 10^3 T^{-2}.$$

This leads to $\Delta H_{298}^0 = +9\,174 \pm 107$ cal mole^{-1}, $\Delta F_{298}^0 = 5\,132$ cal mole^{-1}, and $\Delta S_{298}^0 = 13.56 \pm 0.36$ e.u. for the formation of hydrogen selenide from hydrogen and crystalline selenium. Values of the heat of formation summarized by Lumbroso (3) vary from 16.02 to 20.5 kcal mole^{-1} at 298 °K. More recently a value of 18.16 kcal mole^{-1} was obtained by Kapustinskii and Kankovskii (5) from measurements of the heat of combustion of H_2Se, whereas Gunn (7) estimates a value of 8 kcal mole^{-1} from the heat of explosion of H_2Te–H_2Se gas mixtures. This latter value is in close agreement with the value of 9 174 cal mole^{-1} obtained in this study.

The entropy change for the formation of hydrogen selenide from hydrogen and crystalline selenium at 298 °K of 13.56 ± 0.36 e.u. is in reasonable agreement with the calculated value of 10.95 e.u. from the tabulated data of Kelley (8), particularly if one takes into account the uncertainty of the existing literature data which is accumulated in the type of calculation given above.

CONCLUSIONS

The equilibrium constant for the reaction $H_{2(g)} + Se_{(l)} = H_2Se_{(g)}$ has been determined over the temperature range 525 to 625 °C and can be expressed by the relationship

$$\log K = 13.07 + 2.97 \times 10^{-4}T - 3.69 \log T - 2\,209T^{-1} - 4.81 \times 10^3 T^{-2}.$$

This equation leads to $\Delta H_{298}^0 = 9\,174 \pm 0.1$ cal mole^{-1}, $\Delta F_{298}^0 = 5\,132$ cal mole^{-1}, and $\Delta S_{298}^0 = 13.56$ e.u. for the respective heat, free energy, and entropy of formation of hydrogen selenide from hydrogen and crystalline selenium.

No anomaly in the equilibrium constant was observed as reported by Pelabon (1).

ACKNOWLEDGMENTS

The authors wish to express their thanks to Miss E. Schaffer for her assistance in carrying out the experiments and to Drs. P. H. Jennings and W. C. Cooper for their helpful discussion. They are grateful to Canadian Copper Refiners Ltd. for providing the financial support for this work.

Can. J. Chem. Downloaded from www.nrcresearchpress.com by 210.87.254.42 on 09/05/12
For personal use only.

REFERENCES

1. H. PELABON. *Quoted by* J. W. Mellor. Treatise on inorganic and theoretical chemistry. Vol. 10. Longmans, London. 1947. p. 758.
2. M. BODENSTEIN. Z. Physik. Chem. Leipzig, **29**, 429 (1899).
3. H. LUMBROSO. Nouveau traité de chimie minérale. Vol. 13. *Edited by* P. Pascal. Masson, Paris. 1961. p. 1775.
4. F. D. ROSSINI *et al.* Natl. Bur. Std. U.S. Circ. 500. 1952.
5. A. F. KAPUSTINSKII and R. T. KANKOVSKII. Zh. Fiz. Khim. **33**, 722 (1959).
6. K. K. KELLEY. U.S. Bur. Mines Bull. 584 (1960).
7. S. R. GUNN. J. Phys. Chem. **68**, 949 (1964).
8. K. K. KELLEY. U.S. Bur. Mines Bull. 592 (1961).

Can. J. Chem. Downloaded from www.nrcresearchpress.com by 210.87.254.42 on 09/05/12
For personal use only.

Can. J. Chem. Downloaded from www.nrcresearchpress.com by 210.87.254.6 on 09/05/12
For personal use only.

THE Hg $6(^3P_1)$ PHOTOSENSITIZATION OF SPIROPENTANE

G. R. De Maré, L. G. Walker, O. P. Strausz, and H. E. Gunning
Department of Chemistry, University of Alberta, Edmonton, Alberta

Received October 13, 1965

ABSTRACT

The triplet mercury photosensitization of spiropentane affords ethylene, allene, and methylenecyclobutane as major reaction products. This indicates an olefinic-type interaction with the quaternary C—C σ-bond of spiropentane, the cleavage of which results in a triplet state diradical. The initially formed diradical may undergo isomerization through ring cleavage or deactivation by collision. The open chain diradical then either decomposes unimolecularly into $C_2H_4 + C_3H_4$ or on collisional relaxation isomerizes to methylenecyclobutane.

The paraffinic-type interaction between Hg* and spiropentane which would lead to C—H bond scission appears to have minor significance.

INTRODUCTION

Our interest in the mercury photosensitization of spiropentane arose from our current investigations on the analogous reactions of cyclopropane. This topic has recently been reviewed (1); therefore only a very brief outline will be given here.

Cyclopropane, in most of its reactions, exhibits an intermediate behavior between olefins and paraffins. In its interaction with Hg* atoms the final reaction products can equally well be accounted for by an olefinic- or paraffinic-type reaction (2, 3). The olefinic interaction would imply quenching into the C—C σ-bond with the formation of a vibrationally excited triplet trimethylene which then may partly decompose into allyl + H. Alternately paraffinic interaction through C—H bond cleavage could lead to the formation of vibrationally excited cyclopropyl radicals which may subsequently isomerize to allyl either unimolecularly or on combination with other radicals.

This study was undertaken in the hope that with a more complex cyclopropane derivative such as spiropentane some of the complications mentioned above could be circumvented and a clear distinction made between the two possibilities.

EXPERIMENTAL

The reaction system and the method used to determine the fractional absorption of the resonance radiation have been described in a previous paper (4).

The light intensity, measured by propane actinometry at 730 Torr propane pressure, was 1.42×10^{15} quanta/s.

Spiropentane was prepared by the method of Applequist *et al.* (5) and purified extensively. A neat sample gave a single resonance on an A60 nuclear magnetic resonance instrument at maximum intensity, verifying the excellent purity. Nitric oxide (Matheson C.P.) was purified as previously described. Propylene (Phillips research grade) and propylene-1,1-d_2 (Merck) were degassed at −196° and distilled from −130°.

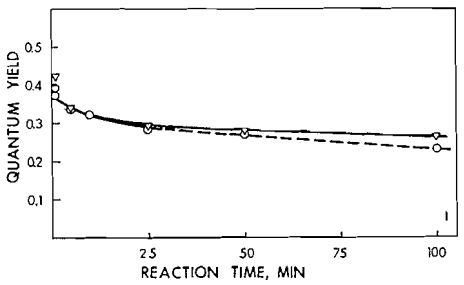
Ethylene and allene were identified by their mass spectra and relative gas chromatographic retention times. They were determined quantitatively on a 16 ft column of 30% tricresyl phosphate on 30/60 mesh firebrick at 75°. Methylenecyclobutane was identified by its relative gas chromatographic retention time and mass and nuclear magnetic resonance spectra and was determined quantitatively on a dimethylsulfolane column.

RESULTS AND DISCUSSION

The major products of the reaction were ethylene, allene, and methylenecyclobutane. Minor products were hydrogen ($\Phi \simeq 0.04$ at 50 Torr), two isomers of the substrate, and at longer exposure times, a product of mass 70, and a C_{10} compound.

The yields of ethylene and allene were examined as a function of exposure time at a substrate pressure of 53.0 ± 1.5 Torr (see Fig. 1) and as a function of substrate pressure

(see Fig. 2). The yield of methylenecyclobutane as a function of substrate pressure was measured in separate experiments and is also shown in Fig. 2, along with the sum of the yield of ethylene and methylenecyclobutane.



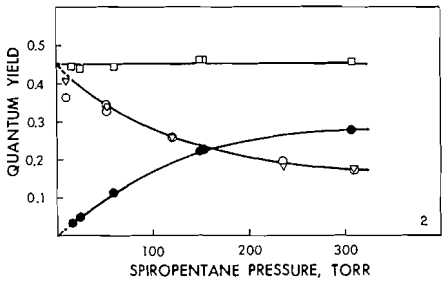


FIG. 1. Quantum yield of ethylene ▽ and allene ○ as a function of reaction time.
FIG. 2. Dependence of the product yields on spiropentane pressure: ethylene ▽, allene ○, methylenecyclobutane ●, and (ethylene + methylenecyclobutane) □.

The effect of added olefin and nitric oxide on the reaction was checked and it was found that besides their function as an inert gas they have no effect on the major reaction products.

The following mechanism is proposed to explain the results.

[1] $$Hg\ 6(^3P_1) + \text{spiropentane} \xrightarrow{\alpha} Hg\ 6(^1S_0) + \text{allene}$$

[2] $$\xrightarrow{\beta} Hg\ 6(^1S_0) + \text{methylenecyclobutyl radical} + H$$

[3] $$\text{methylenecyclobutyl radical} \rightarrow \text{vinylcyclopropyl radical}$$

[4] $$\text{vinylcyclopropyl radical} \rightarrow C_2H_4 + C_3H_4$$

[5] $$\text{vinylcyclopropyl radical} \xrightarrow{M} \text{methylenecyclobutane}$$

[6] $$\text{methylenecyclobutyl radical} \xrightarrow{M} \text{methylenecyclobutane}$$

[7] $$H + \text{methylenecyclobutane} \rightarrow \text{methylenecyclobutyl radical} + H_2$$

[8] $$2\ \text{methylenecyclobutyl radical} \rightarrow \text{dimer}$$

Steady-state treatment gives the following relation for the ratio of product yields:

[I] $$R(\text{methylenecyclobutane})/R(\text{ethylene}) = (k_5/k_4)[M].$$

A plot of the left-hand side of [I] vs. substrate pressure is shown in Fig. 3. A satisfactory straight line is obtained. From the slope then $k_5/k_4 = 5.5_5 \times 10^{-3}$ mm Hg^{-1}. If k_5 is set

Can. J. Chem. Downloaded from www.nrcresearchpress.com by 210.87.254.6 on 09/05/12
For personal use only.

equal to 1×10^{-10} cc/molecule s (ca. the collision frequency) then $k_4 = 5.8 \times 10^8$ s^{-1} and τ_4, the lifetime of the 1,4-diradical, 2-methylenebutane in this system, is equal to 1.7×10^{-9} s. Also

$$[II] \qquad 1/\Phi(C_2H_4) = 1/\Phi(C_3H_4) = (k_4 + k_5[M])(k_3 + k_6[M])/\Phi(1)k_3k_4$$

where $\Phi(1)$ is the quantum yield of step [1]. Equation [II] reduces to

$$1/\Phi(C_2H_4) = 1/\Phi(C_3H_4) = 1/\Phi(1)$$

at zero pressure. Plots of $1/\Phi(C_2H_4)$ and $1/\Phi(C_3H_4)$ vs. substrate pressure are shown in Fig. 4. Both lines extrapolate to 2.28 at zero pressure giving $\Phi(1) = 0.44$, which agrees well with the experimental value of 0.45 obtained from the sum of molecular split and methylenecyclobutane formation (cf. Fig. 2), and which is unaffected by pressure over the range studied. The actual value of $\Phi(1)$, owing to its exposure time dependence (cf. Fig. 1), is somewhat uncertain and is probably about 10–15% higher than given above, that is, ca. 0.50.

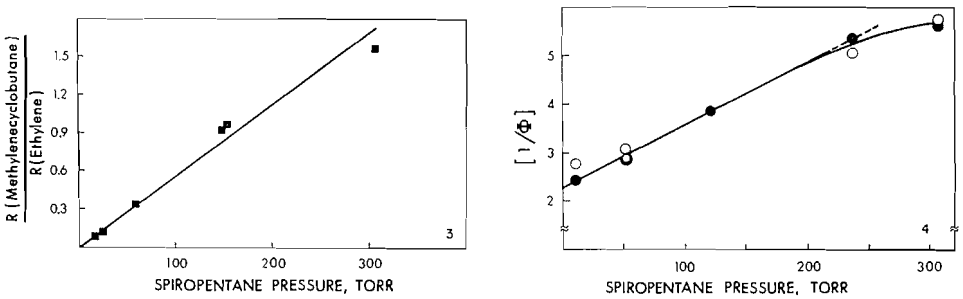


FIG. 3. Plot of R(methylenecyclobutane)/R(ethylene) vs. spiropentane pressure.
FIG. 4. Plot of $1/\Phi(C_2H_4)$ ● and $1/\Phi(C_3H_4)$ ○ vs. spiropentane pressure.

If now it is assumed that $k_5 = k_6 = 10^{-10}$ cc/molecule then from [II] a value of ca. 10^{-10} s is obtained for the lifetime of the  diradical, and therefore collisional stabilization should not be important for this species over the pressure range studied.

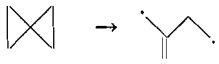
The quantum yield of step [2] is ca. 0.04 as determined from the yield of the H_2 product. Step [7] is probably more rapid with spiropentane than with cyclopropane but self-scavenging of H atoms by C_2H_4 and C_3H_4 still may be significant. In the cyclopropane reaction the main mode of H-atom disappearance is self-scavenging followed by polymerization, and H_2 actually is a very minor product (2, 3). The estimation of $\Phi(2)$ from the H_2 yield alone in the present system is quite uncertain since self-scavenging may also lead to polymer formation. However, in contrast to the cyclopropane case polymer formation could not be observed in the spiropentane system, consequently polymerization via self-scavenging cannot be important.

The two unidentified isomers of spiropentane formed in very small yields (Φ(combined) < 0.05) could have been either vinylcyclopropane, cyclopentene, or a pentadiene. Both of the major reactions, the molecular decomposition into ethylene and allene, [4], and the isomerization to methylenecyclobutane, [5], require no hydrogen migration in contrast to other possible but apparently less probable reactions.

The thermal reaction of spiropentane in the temperature interval of 360 and 410 °C has also been reported (6) to yield the same kind of products, $C_2H_4 + C_3H_4$ and methylenecyclobutane, as the photosensitization. The isomerization is truly unimolecular with an

Can. J. Chem. Downloaded from www.nrcresearchpress.com by 210.87.254.6 on 09/05/12
For personal use only.

activation energy of 57.6 kcal/mole and a pre-exponential factor of $10^{15.86}$. This large value of the pre-exponential factor indicates a very loose transition state in comparison with the highly strained spiropentane structure (strain energy = 63 kcal/mole (7)). The decomposition reaction has been found to be slower than the isomerization and to have a higher activation energy. Whether the thermolysis proceeds via the same reaction paths, that is, triplet potential surfaces, as the mercury sensitization cannot be decided, but the salient features of the reaction are in accord with such a mechanism (7, 8). If this is the case, the activation energy of the isomerization, 57.6 kcal/mole, may be assigned to the formation of 1,4-diradical, 2-methylenebutane



and for this reason the 1,4-diradical, 2-methylenebutane, formed in [3] should have ca. 55 kcal/mole excess vibrational energy.*

Finally it may be concluded that at least ca. 55% of the primary quenching act with spiropentane leads to an olefinic-type energy transfer by the promotion of a $\sigma \rightarrow \sigma^*$ transition in the ring C—C bond which results in a triplet state diradical formation. This unique reactivity of the cyclopropyl ring indicates that, unlike the higher cyclic alkane and non-cyclic alkanes, the cyclopropanes have C—C sigma electrons which are more readily available to electrophilic reagents than the C—H electrons. This behavior is in line with the well-established olefinic character of cyclopropanes (12).

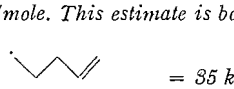
ACKNOWLEDGMENT

The authors gratefully acknowledge financial assistance from the National Research Council of Canada.

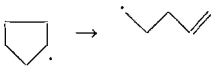
REFERENCES

1. R. J. Cvetanović. Progr. Reaction Kinetics, **2**, 39 (1964).
2. R. A. Holroyd and G. W. Klein. J. Phys. Chem. **69**, 2129 (1965).
3. P. Kozak, G. N. C. Woodall, A. G. Sherwood, O. P. Strausz, and H. E. Gunning. To be published.
4. G. R. De Maré, O. P. Strausz, and H. E. Gunning. Can. J. Chem. **43**, 1329 (1965).
5. D. E. Applequist, G. F. Fanta, and B. W. Henrikson. J. Org. Chem. **23**, 1715 (1958).
6. M. C. Flowers and H. M. Frey. J. Chem. Soc. 5550 (1961).
7. J. D. Cox. Tetrahedron, **19**, 1175 (1963).
8. P. Nangia and S. W. Benson. J. Am. Chem. Soc. **84**, 3411 (1962).
9. H. E. Gunning and R. L. Stock. Can. J. Chem. **42**, 357 (1964).
10. A. S. Gordon, S. R. Smith, and C. M. Drew. J. Chem. Phys. **36**, 824 (1962).
11. P. J. Kozak. Ph.D. Thesis, University of Alberta, Edmonton, Alberta. 1964.
12. M. Yu Lukina. Russ. Chem. Rev. English Transl. **31**, 419 (1962).

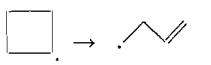
It would also follow that the bond dissociation energy D(C—CH_2) in spiropentane should be less than 57 kcal/mole, with an amount corresponding to the activation energy of the isomerization reaction



which may have a value of about 5–10 kcal/mole. This estimate is based on the following reported values for E_a,



= 35 kcal/mole (9),



= 18 kcal/mole (10),

and also on the observation that cyclopropyl radicals are quite stable at room temperature and readily undergo H-atom abstraction reactions (11).

Can. J. Chem. Downloaded from www.nrcresearchpress.com by 210.87.254.6 on 09/05/12
For personal use only.

Can. J. Chem. Downloaded from www.nrcresearchpress.com by 210.87.254.40 on 09/05/12
For personal use only.

THE RANGES OF INTERACTIONS IN THE RADIOLYSIS OF SOLID HYDROCARBON MIXTURES[1]

P. J. DYNE AND J. DENHARTOG
Research Chemistry Branch, Chalk River Nuclear Laboratories, Chalk River, Ontario

Received September 22, 1965

ABSTRACT

We describe a novel technique for measuring the ranges of interaction in the radiolysis of hydrocarbon mixtures, e.g. the distance between donor and acceptor molecules in an energy transfer process. Thin layers, 20 to 1 000 Å thick, of solid *c*-C_6D_{12} sandwiched between other materials which activate or deactivate the hydrocarbon, are irradiated. The yields of D_2 and HD are measured as a function of the layer thickness. These yields change rapidly when the layer thickness is comparable with the range of the interaction.

We find: (*a*) the activation of *c*-C_6D_{12} by *n*-C_6H_{14} has a very short range consistent with an ion–molecule reaction between nearest neighbor molecules; (*b*) the deactivation by CCl_4 or benzene has a longer range (180 Å or more) consistent with the average separation of positive ions and electrons in an irradiated hydrocarbon; (*c*) the intermediates in the bimolecular reaction giving HD in layers of C_6D_{12} and C_6H_{12} have a short range (< 100 Å) and cannot be thermal hydrogen atoms.

1. INTRODUCTION

It is now generally believed that charge separation plays an important role in the radiolysis of hydrocarbons. After ionization, electrons move a large distance away from the positive ions so that the time for recombination is long enough for both electrons and positive ions to react with other molecules. We (1), in common with many others (e.g. refs. 2–4), have argued that the inhibiting effects on the radiolysis of hydrocarbons of some additives (e.g. CCl_4) are due to electron capture; other effects of activation and deactivation in mixtures of hydrocarbons are due to charge exchange between a positive ion and a molecule of another hydrocarbon.

In this paper we describe experiments on the radiolysis of hydrocarbon mixtures in which the ranges of the interactions are measured. These may, in some cases, be the average distance between positive ions and electrons when electron capture occurs or, in others, it may be the distance between a positive ion and a molecule when charge transfer takes place.

We irradiate mixtures in which the components are separated into layers. Layers of a hydrocarbon are sandwiched between layers of another material which either activates or deactivates the decomposition of the hydrocarbon. If the layer of hydrocarbon has a thickness T and the range of the interaction with the adjacent layers is R then, when $T \gg R$, the decomposition of the hydrocarbon layer will be unaffected by its environment. If, however, $T \ll R$ the sample will approach the behavior of a homogeneous mixture; activation or deactivation of the hydrocarbon will be observed. Samples with layer thicknesses in the range 20 to 1 000 Å have been prepared. The anticipated changes in yield with thickness were observed and these are used to estimate the ranges of the interaction involved.

We shall interpret these ranges in terms of a mechanism recently suggested by us for the radiolysis of aliphatic hydrocarbons (1). The initial radiation act produces ions and excited molecules. (For this example, we choose deuterated cyclohexane, C_6D_{12}, since it was used in all the experiments described in this paper.)

[1]*Issued as AECL No. 2260.*

[1] $$C_6D_{12} \xrightarrow[[1b]]{[1a]} \begin{cases} C_6D_{12}^+ + e \\ C_6D_{12}^* \end{cases}$$

In the pure hydrocarbon, electron capture by the positive ion also produces the excited species $C_6D_{12}^*$.

[2] $$C_6D_{12}^+ + e \rightarrow C_6D_{12}^*$$

$C_6D_{12}^*$ can then decompose by two routes: forming D_2 by molecular detachment

[3] $$C_6D_{12}^* \begin{cases} \nearrow D_2 + \cdots \\ \searrow X_D + \cdots \end{cases}$$

or producing X_D which subsequently reacts in a bimolecular process as described in Section 4. If C_6D_{12} is present in a mixture with a hydrocarbon with a higher ionization potential (e.g. C_6H_{14}), charge exchange can occur.

[4] $$C_6D_{12} + C_6H_{14}^+ \rightarrow C_6D_{12}^+ + C_6H_{14}$$

Electron capture by the $C_6D_{12}^+$ ion gives an increased yield of C_6D_{12} and hence of D_2 and HD. An electron scavenger such as CCl_4 captures electrons,

[5] $$CCl_4 + e \rightarrow CCl_4^-,$$

and leads, on the reaction of CCl_4^- with $C_6H_{12}^+$, to decompositions other than reactions [2] and [3].

2. EXPERIMENTAL TECHNIQUES

A prerequisite of these 'layer' experiments is an analytical technique which can measure, with high precision, products formed from the layer whose thickness is being varied. Isotopic labelling of the thin layers provides an ideal method. In all these experiments deuterocyclohexane is the component in these layers which are sandwiched between very much thicker layers of a material whose interaction with C_6D_{12} is being studied. We call these the thin or indicator layer, and the thick or blanket layer respectively. For accuracy in analysis the sample must be about 1 g in weight and contain $\sim 1\%$ of C_6D_{12}. For a reasonably sized condensing surface (30 cm²), samples with layer thicknesses in the range of interest, 50–500 Å, must be made up of several hundred layers of deuterated hydrocarbons and blanket material. Automated sample preparation is essential.

The final form of the irradiation cell is shown in Fig. 1. Vapors are condensed onto a copper disc 5.5 cm in diameter which forms the bottom of a liquid nitrogen reservoir. The inner glass tube ensures that vapors condense wholly on the flat portion of the disc. The serrated metal baffle just above the valve disperses the stream of vapor so that it is evenly deposited. During deposition of a sample the cell is continuously evacuated through a lead of 1/4 in. copper tubing. When deposition is complete this tube is crimped and cut with a Kane cold-welding tool to make a vacuum tight seal. The cell is connected to the deposition apparatus (or, after irradiation, to a gas analysis line) through a Hoke metal bellows valve and an Edwards vacuum union. This valve is closed while the cell is being irradiated.

The deposition apparatus for metering out vapors is shown schematically in Fig. 2. Blanket material from ballast volume (1) and deuterated cyclohexane from ballast volume (2) are admitted alternately to the cell through ~ 2 ml metering volumes between valves V_1 and V_2 and between V_3 and V_4. These valves are magnetically operated (Edwards type D-11207).

The valves were opened and closed in a sequence which was actuated by a stepping switch. A microswitch provided the impulses which advanced the stepping switch and this microswitch was, in turn, closed and opened by studs on the circumference of a slowly rotating wheel. The spacing of the studs and the speed of rotation of the wheel controlled the time for each step and the time for a complete cycle.

We were particularly concerned about the possibility of inadvertent mixing of the two components during deposition, and so made liberal allowances for the time taken to complete deposition. Half a minute was allowed for deposition with either V_2 and V_3 open. A further half minute was taken with V_2 or V_3 closed before the next layer was deposited. The time for a complete cycle, deposition of a pair of layers, was 2 min. When our techniques were developed we chose to make samples with 310 layers of each component. The total amount of C_6D_{12} in the sample is, therefore, proportional to the thickness of the layers.

With this arrangement of valves most of the layer is deposited in perhaps a tenth of a second or less. We were concerned that, for the thick layers, this deposition rate could be so high that the latent heat of condensation could produce transient local melting and hence some mixing of the layers. To minimize this,

Can. J. Chem. Downloaded from www.nrcresearchpress.com by 210.87.254.40 on 09/05/12
For personal use only.

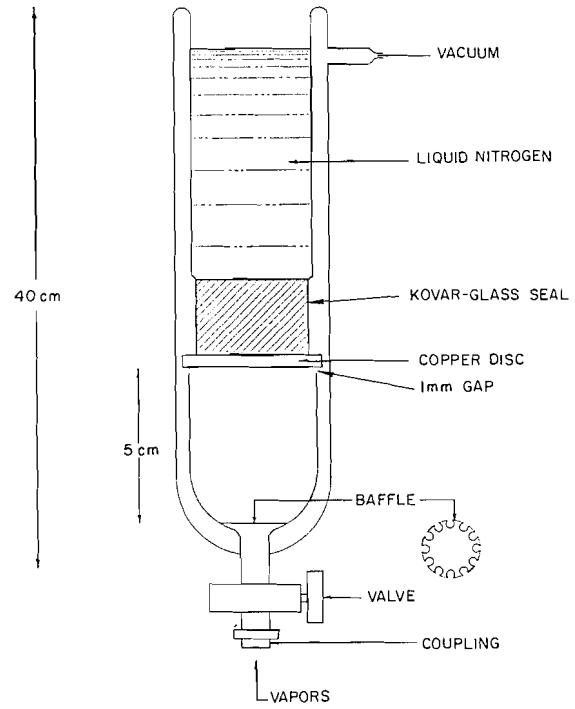


FIG. 1. Cell used for preparing and irradiating multilayered samples.

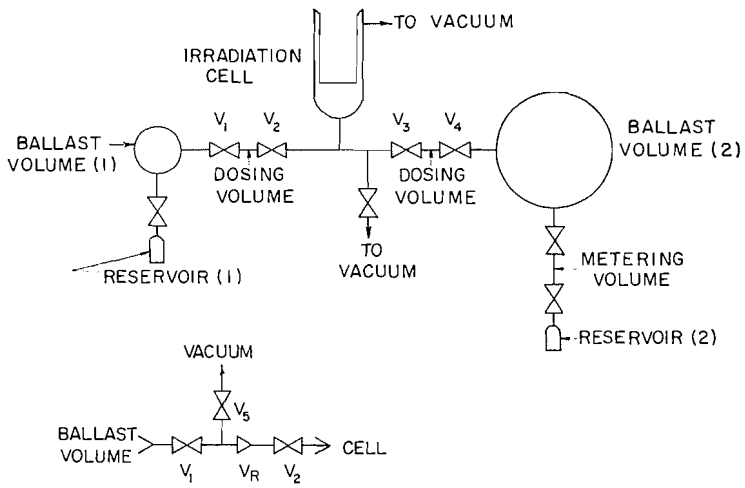


FIG. 2. Vacuum line for deposition of multilayered samples.

another arrangement, shown in the insert, was used for metering the blanket material. Vapor from the reservoir was bled continuously through a needle valve V_R whose setting was chosen so that the correct amount of vapor passed through it in 30 s. The cycle of operation was arranged so that deposition occurred with V_1 and V_2 open and V_5 closed. At the end of the deposition V_1 and V_2 were closed and the dead space between V_1 and V_R evacuated through V_5. The deposition rate with this arrangement is $\sim 10^{-7}$ mole/cm^2 s. This is two orders of magnitude slower than the rates used for trapping free radicals from gases which have been passed through an electric discharge (5). If local melting occurred in these experiments, free radicals could diffuse and recombine. As can be seen (Figs. 5 and 6), this modification produced no change in the experimental results. We are confident that the layers are truly segregated.

Can. J. Chem. Downloaded from www.nrcresearchpress.com by 210.87.254.40 on 09/05/12
For personal use only.

The amounts deposited in one layer of each component were set by the pressure in the ballast volumes. For the blanket layer, which is normally deposited in a constant thickness, whatever the thickness of the thin layer might be, this pressure was set by the vapor pressure of the liquid at the temperature of the thermostat bath in which the liquid reservoir (1) was placed. For the thin layers the pressure in the ballast volume was varied by adding aliquots from the intermediate metering volume. This metering volume was 50 ml and was filled at the vapor pressure of liquid C_6D_{12}. The ballast volume was ~ 20 l.

Separate vacuum systems, not shown in the figure, were used for evacuating both ballast volumes and the irradiation cell before sample preparation was started. The organic liquids were degassed by conventional freeze–thaw techniques.

After the sample was prepared it was irradiated with Co-60 gamma rays at liquid nitrogen temperature to doses of 1.4×10^{19} eV/ml C_6H_{12} at dose rates of 7.7×10^{17} eV/ml C_6H_{12} per minute. These doses are high because the sample is necessarily small. Because of the geometry of the cell, dosimetry was done by irradiating a thin layer of *n*-hexane on a disc and taking $G(H_2) = 4.3$ (as determined in this laboratory) for this solid material.

After irradiation the sample was melted and the radiolytic gas pumped to a conventional gas analysis line. After the volume of gas was measured, the isotopic composition was determined by mass spectrometry. For samples with blanket materials such as CCl_4 which have zero hydrogen yield, a quantity of H_2 was added to the gas extracted from the sample so that the radiolytic gas could be more conveniently handled. The amount of D_2 was obtained from the mass spectrometric analysis. The liquid mixture of blanket and indicator material in the irradiation cell was weighed and analyzed either by gas chromatography or by mass spectrometry to determine the weight of C_6D_{12} in the sample. From this and the number of layers the layer thickness was calculated. The thickness derived in this way was generally within 10% of that predicted from the pressures and volumes in the deposition apparatus.

3. THE VALIDITY AND PRECISION OF THE TECHNIQUE

As will be seen, we claim to be able to make reproducible layers of hydrocarbons as thin as 20 Å, which is of the order of four molecular layers. In this section we outline the reasons for our confidence in the technique.

The deposition of the thin C_6D_{12} layer could be imperfect in two different ways. There could be considerable mixing in the interfacial regions which would lead to the observation of excitation transfer at erroneously large distances. The observed range would then be a maximum value. Alternatively, the layers could be unevenly deposited. If this occurred to any significant extent it would be observed visually as the layers built up. All our samples have a uniform appearance. When very thin they are transparent and show interference colors; as they grow thicker they become uniformly translucent to opaque.

We regard adventitious mixing as the most likely source of error. If it occurred to a constant extent then we would observe the same long range for all systems. However, this is not the case; the observed ranges vary over a factor of about five. One can then argue that mixing, if it occurs, can only be significant for the system with the smallest range (30 Å) and must be relatively insignificant for all systems giving ranges greater than 30 Å.

The most convincing argument for the validity of these experiments is their reproducibility. In Fig. 4 we present the results we obtained for C_6D_{12} layers sandwiched between layers of $C_6H_{14} + 4\%$ C_6H_6. In this figure, and in all subsequent figures, yields per 100 eV absorbed in the C_6D_{12} are plotted against the thickness of the C_6D_{12} layer. By convention we plot the yields obtained in homogeneous mixtures at $T = 0$.

The cluster of experimental points in the thickness range 90–130 Å should be noted. These results also show the variation of the HD and D_2 yields which is observed when the thick layer consists of an undeuterated hydrocarbon. In thick C_6D_{12} layers D_2 is produced both by molecular detachment,

$$C_6D_{12} \xrightarrow{\sim\sim\sim} C_6D_{10} + D_2,$$

and by a second order process which we can write

$$C_6D_{12} \xrightarrow{\sim\sim\sim} X_D + \cdots$$
$$X_D + C_6D_{12} \rightarrow D_2 + \cdots.$$

Can. J. Chem. Downloaded from www.nrcresearchpress.com by 210.87.254.40 on 09/05/12
For personal use only.

As the C_6D_{12} layer decreases in thickness an increasing fraction of the intermediate X_D may escape from the layer and react to give HD.

$$X_D + RH \rightarrow HD + \cdots$$

In the homogeneous sample the D_2 yields have fallen to a finite value, the yield of the molecular detachment process in that solid matrix; at the same time the HD yield increases.

4. THE RELATIONS BETWEEN LAYER THICKNESS, RANGE, AND YIELD

First we shall discuss the case where the interaction between the two layers is due to a mobile intermediate with a range or diffusion length large compared to molecular dimensions. The matter in the layers can be regarded as continuous. This mobile species could be an electron, a hydrogen atom, a photon, or an exciton. Let the number of the intermediates formed during radiolysis be N per unit volume of material randomly distributed in the indicator layer and let the number which escape from a unit area of the indicator material into the blanket be N_e. We can then define an arbitrary average escape distance, t, to be such that

$$N_e = Nt. \tag{6}$$

Suppose the indicator layer has a thickness $T \gg t$. If it is remembered that the indicator layer has two sides, then the fraction of intermediates which escape is $2t/T$ and the fraction which is trapped in the layer is $1 - (2t/T)$. Intermediates which escape from the thin layer give product yields characteristic of a homogeneous mixture; intermediates which are trapped in the layer give yields characteristic of the segregated mixture. At a thickness T_h (= half-value thickness), when the yield from the layer is midway between the two extremes of homogeneous and segregated samples, we have

$$2t/T_h = 1 - (2t/T_h) \text{ or}$$

$$t = T_h/4. \tag{7}$$

We now have to find the relation between the escape distance t, which is measured experimentally through eq. [7], and the range of the mobile intermediate. Let the mobile intermediate have a range R and let us consider those which are formed at a distance D below the surface (Fig. 3) of the indicator layer. The fraction of these intermediates which escape through the surface is equal to the area of the cap divided by the total surface area of the sphere. That is, the fraction escaping equals

$$2\pi R(R - D)/4\pi R^2 = \tfrac{1}{2}(1 - (D/R)). \tag{8}$$

If N intermediates are formed per unit volume then dN_e, the fraction which escapes from an increment dD, is

$$dN_e = (N/2)(1 - D/R)\, dD \tag{9}$$

whence

$$N_e = \frac{N}{2}\int_0^R \left(1 - \frac{D}{R}\right) dD = \frac{NR}{4}.$$

It follows, therefore, from eqs. [6], [7], and [9] that $t = R/4$ and

$$R = T_h. \tag{10}$$

It is, however, unlikely that the mobile species would have a unique range. It is almost certain to have some dispersion so that values of R obtained from eq. [10] represent some averaged value of the range.

Can. J. Chem. Downloaded from www.nrcresearchpress.com by 210.87.254.40 on 09/05/12
For personal use only.

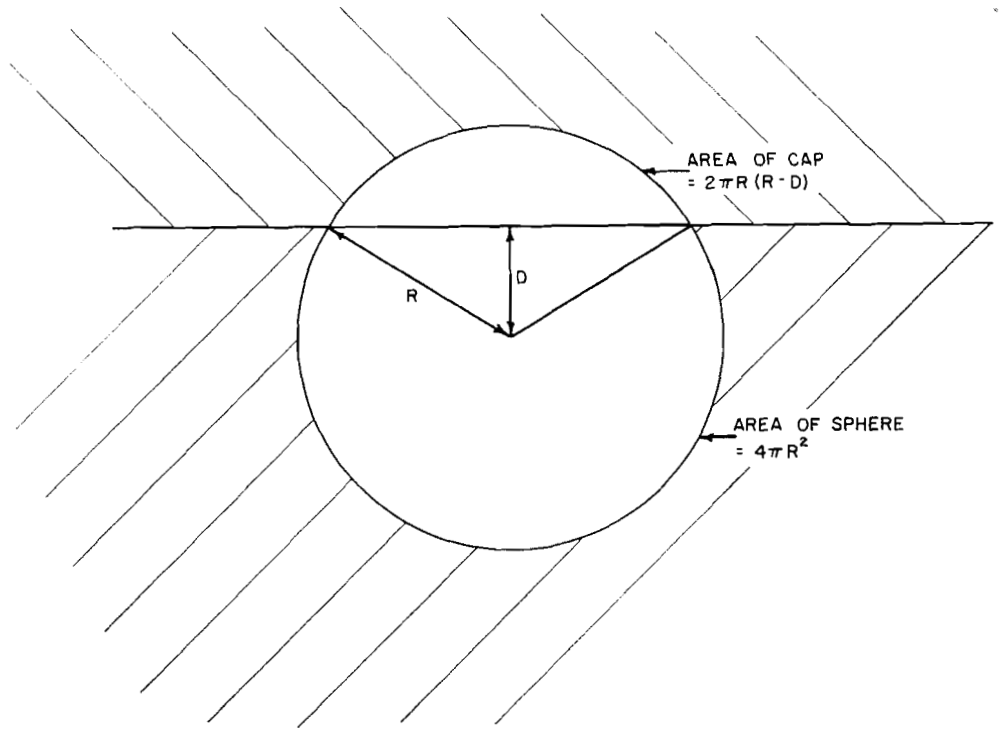


FIG. 3. Geometry of the escape of a particle from a layer.

The probability of an escape from a layer has been treated in detail by Case, de Hoffman, and Placzek (6) for a mobile species which is attenuated exponentially. Values of the escape probability are tabulated as a function of the ratio of the layer thickness to the mean free path λ of the diffusing species. The mean free path λ is the distance in which the species is attenuated by 1/e. For an escape probability of 0.5, equivalent to our condition defining T_h, $\lambda = 1.56T_h$. Values of R obtained from eq. [10] would, therefore, be approximately two thirds of the mean free path.

The tabulation in this reference also allows one to plot the shape of the yield curve as a function of the layer thickness. This plot appears in Fig. 6 which shows our results for the D_2 yield from layers of C_6D_{12} sandwiched between CCl_4 layers. Since the curve is fitted to the data at three points (T = 0, 180 Å, and "∞"), this is not a particularly sensitive test although the agreement is satisfactory. However, for most of our purposes, eq. [10] is an adequate approximation. We will use the symbol $\bar{R}$ to remind us that this range is probably arbitrarily averaged.

The above analysis is incorrect if the range is very short and comparable with molecular dimensions. Suppose that activation or deactivation is restricted to molecules in the surface layers; only molecules in contact with the molecules in the blanket layer interact. Half the layer, the two molecular layers in contact with the blanket material, interact, and the other half of the layer, consisting of the remaining two molecular layers in the middle, are unaffected. Hence T_h = 4 molecular diameters.

Our main interest is in distinguishing between mechanisms of excitation transfer through measurements of $\bar{R}$. We can first distinguish between interactions occurring

Can. J. Chem. Downloaded from www.nrcresearchpress.com by 210.87.254.40 on 09/05/12
For personal use only.

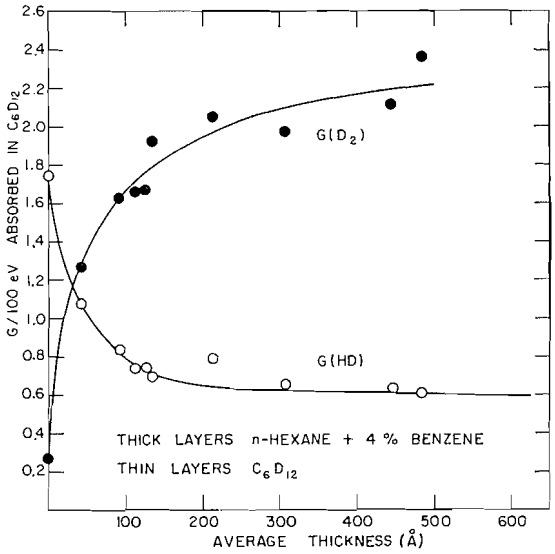


FIG. 4. Yields from the $(C_6D_{12})/(C_6H_{14} + 4\%\ C_6H_6)$ system.

between molecules in contact and interactions in which the diffusing species moves, on the average, several molecular diameters before reacting. For the hydrocarbon systems studied here, nearest neighbor interactions are indicated when $\bar{R} \leq 40$ Å, corresponding to molecular diameters of ≤ 10 Å. Interactions involving diffusing species are indicated by significantly larger values of $\bar{R}$ of 100 Å or more. Intermediate values of $\bar{R}$ = 40–80 Å are difficult to interpret. Suppose that the intermediate is a hot hydrogen atom which reacts efficiently within two molecular diameters. The apparent range will be larger than the 40 Å figure for nearest neighbor interactions and could be, say, 60 Å (as given by eq. [10]). The true range of the hot hydrogen atom is, however, shorter than this since the situation resembles nearest neighbor interactions more closely than it does the diffusion of a reactive intermediate through a continuum.

Values of $\bar{R}$ may be determined from measurements of HD or D_2 and we shall call these $\bar{R}_{HD}$ and $\bar{R}_{D_2}$ respectively. We shall refer to the system of a thin layer of material "X" placed between thick materials of "Y" as the (X)/(Y) system. Samples of thin layers of C_6D_{12} sandwiched between CCl_4 are described by $(C_6D_{12})/(CCl_4)$.

The scatter of the experimental points in these and other experiments suggests that the yield at the half-value is known to about ± 0.1 G units. The effect of this uncertainty on the value of $\bar{R}$ depends, of course, on the slope of the curve of yield vs. layer thickness. An accuracy of ± 10 Å in $\bar{R}$ is consistent with most of our data. These limits are perhaps somewhat reduced if $\bar{R}$ is small and the yield is changing rapidly with layer thickness.

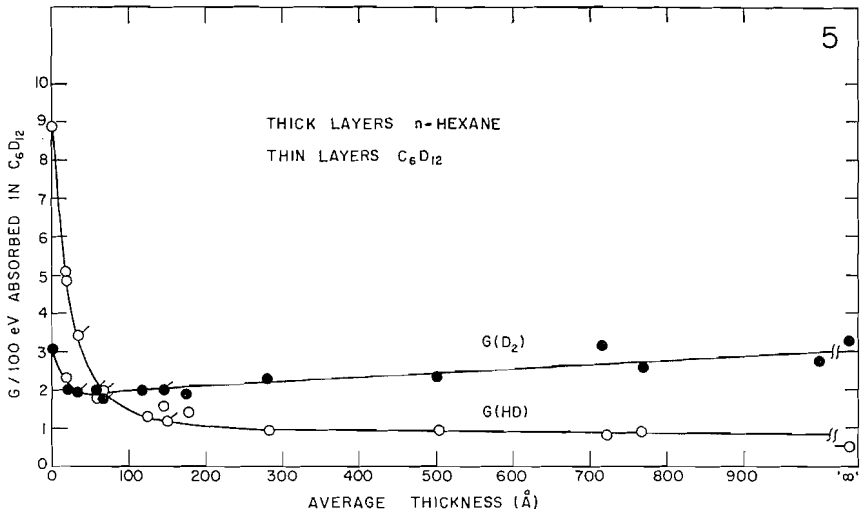
5. THE PRODUCTION OF H_2 AT 77 °K

It is essential for these layer experiments that the reaction chosen for study shall occur at a low temperature, when the layered structure is intact, and not after melting, when the layered structure has been destroyed.

For hydrocarbon samples about one quarter of all the radiolytic hydrogen can be pumped away from the sample before it is melted. If the sample contains a small amount of deuterocyclohexane distributed homogeneously, then the initial fraction contains both

Can. J. Chem. Downloaded from www.nrcresearchpress.com by 210.87.254.40 on 09/05/12
For personal use only.

HD and D_2 in percentage amounts comparable to that of the second fraction obtained on melting the sample.* Both molecular detachment processes giving D_2 and bimolecular processes giving HD are, therefore, taking place at 77 °K. The addition of benzene to these homogeneous mixtures again shows no large discrimination in D_2 and HD production between the two fractions.



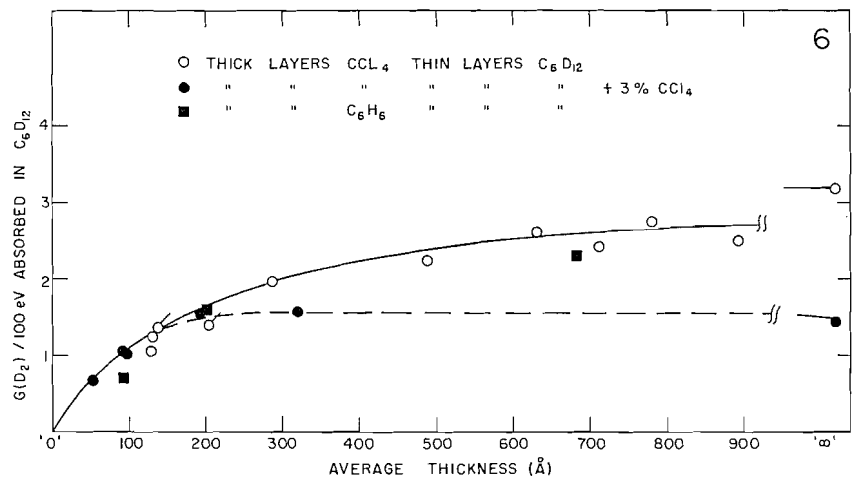


FIG. 5. Yields from the $(C_6D_{12})/(C_6H_{14})$ system. The flagged points were obtained from the slower deposition rates.

FIG. 6. Yields from the $(C_6D_{12})/(CCl_4)$, $(C_6D_{12})/(C_6H_6)$, and $(C_6D_{12} + 3\%\ CCl_4)/(CCl_4)$ systems. The full curve is calculated from the table of ref. 5 fitted to $\bar{R}_{D_2} = 180$ Å. The flagged points were obtained from the slower deposition rates.

In layered samples a similar behavior is observed in that about one fifth of the gas escapes before melting. However, the first fraction contains a much higher percentage of HD and D_2 than the second. For layers ~ 100 Å thick more than 70% of all the HD and D_2 appears in the first fraction. There is thus no question that all the HD and D_2 may be

*For example: In a matrix containing 5.72 mole % C_6D_{12} in n-C_6H_{14} the first fraction (17% of the total) contained 12.1% HD and 5.9% D_2, the second fraction contained 9.9% HD and 4.0% D_2.

Can. J. Chem. Downloaded from www.nrcresearchpress.com by 210.87.254.40 on 09/05/12
For personal use only.

formed at liquid nitrogen temperature. We attribute the fractionation to physical processes which permit the preferential escape of D_2 and HD from the thin layers. These multilayered samples cannot be ideally uniform and there are likely to be channels and interstices in the vicinity of the layer boundaries.

Further relevant observations were made on the isotopic composition of hydrogen evolved from samples having only one layer of C_6D_{12}. The isotopic composition of the first fraction was independent of the position of the C_6D_{12} layer: whether on top of the light hydrocarbon and thus exposed to the vacuum in the irradiation cell, or underneath a thickness of ~ 1 mm of light hydrocarbon. This supports the suggestion that part of the radiolytic hydrogen can escape from a bulk sample of hydrocarbon.

6. EXPERIMENTAL RESULTS

(a) Thick Layers of n-Hexane

In this system (Fig. 5) there is a strong activation of the C_6D_{12} at very small thicknesses, which is shown most clearly by the increase in the HD yield. The D_2 yield also shows this effect in a somewhat disguised form. From 1 000 Å to 60 Å the D_2 yield decreases because of the effect outlined in Section 4, that of X_D reacting with C_6H_{14} instead of C_6D_{12}. Below 60 Å this process is swamped by the short range processes activating C_6D_{12}. The magnitude of the activation is shown by the D_2 yield, which, in homogeneous mixtures of C_6D_{12} with C_6H_{14} is 3.2 as compared with a value of 0.5 found in homogeneous C_6D_{12}–C_6H_{12} mixtures. (Both values obtained in our laboratory.) The value of $\bar{R}_{D_2}$ is somewhat indeterminate. For the HD yield $\bar{R}_{HD} = 25$ Å. This indicates that the interaction occurs between molecules in contact.

(b) Thick Layers of Carbon Tetrachloride and Benzene

Results for samples with either CCl_4 or C_6H_6 are shown in Fig. 6. The range of the deactivation is identical for both materials. The two flagged points for CCl_4 were obtained in experiments in which the CCl_4 layer was deposited slowly through a small leak and not in one puff. As mentioned in Section 2 this is a reduction of two orders of magnitude in the deposition rate and the yields are unchanged. The long range implied by the results here is, therefore, real and is not due to mixing of the layers during deposition.

For both the $(C_6D_{12})/(CCl_4)$ and $(C_6D_{12})/(C_6H_6)$ systems we find $\bar{R}_{D_2} = 180$ Å.

It is well known that the homogeneous addition of carbon tetrachloride (or other additives) to a hydrocarbon reduces the yield in two stages (1, 7); a rapid reduction at low CCl_4 concentrations which terminates at concentrations of about 3% CCl_4, leaving a "residual yield" which is much more weakly reduced by further additions of CCl_4. We accordingly studied the $(C_6D_{12} + 3\%\ CCl_4)/(CCl_4)$ system in which $G(D_2) = 1.5$ in the infinitely thick layers; the yield curve is approximately horizontal until it intersects the curve for the $(C_6D_{12})/(CCl_4)$ system and is then coincident with that curve (Fig. 6). The range of this interaction is, therefore, 60 Å—considerably less than for the $(C_6D_{12})/(CCl_4)$ system. The value of $\bar{R}_{D_2}$ for the $(C_6D_{12})/(CCl_4)$ system is, therefore, the weighted sum of two ranges, 60 Å for the residual part of the yield and a much larger range ~ 340 Å for the part of the yield inhibited by 3% CCl_4 (assuming that the average is obtained by weighting the ranges according to the inhibited and residual yields respectively).

(c) Systems with C_6H_{12} in the Thick Layer

The study of the $(C_6D_{12})/(C_6H_{12})$ system would be expected to give information on the mobility of the species X_H and X_D, the intermediates in the bimolecular reaction giving

Can. J. Chem. Downloaded from www.nrcresearchpress.com by 210.87.254.40 on 09/05/12
For personal use only.

hydrogen. As we have already noted $G(D_2)$ will diminish when the C_6D_{12} layer is thin enough for a significant fraction of the X_D formed in the layer to escape and react in the C_6H_{12} layer to give HD. The yield of HD will, further, be increased to a similar extent by the diffusion of X_H from the C_6H_{12} layer into the C_6D_{12} layer. This yield depends on the total surface of C_6D_{12} exposed to the light hydrocarbon. Under our experimental conditions, where the amount of C_6D_{12} is kept constant, the number of layers and hence the surface area is inversely proportional to the layer thickness. If there were no isotope effects ($G(X_H) = G(X_D)$) and the diffusion lengths and reactivity of X_H and X_D were identical, then a reduction in $G(D_2)$ by a certain amount, as the layer thickness decreased, would be matched by an increase in $G(HD)$ of twice that amount. We would also observe $\bar{R}_{D_2} = \bar{R}_{HD}$. Isotope effects might alter the ratio of these changes in $G(D_2)$ and $G(HD)$ from the simple value of 1:2, but $G(HD)$ should always increase in the thinner layers to a greater extent than $G(D_2)$ decreases.

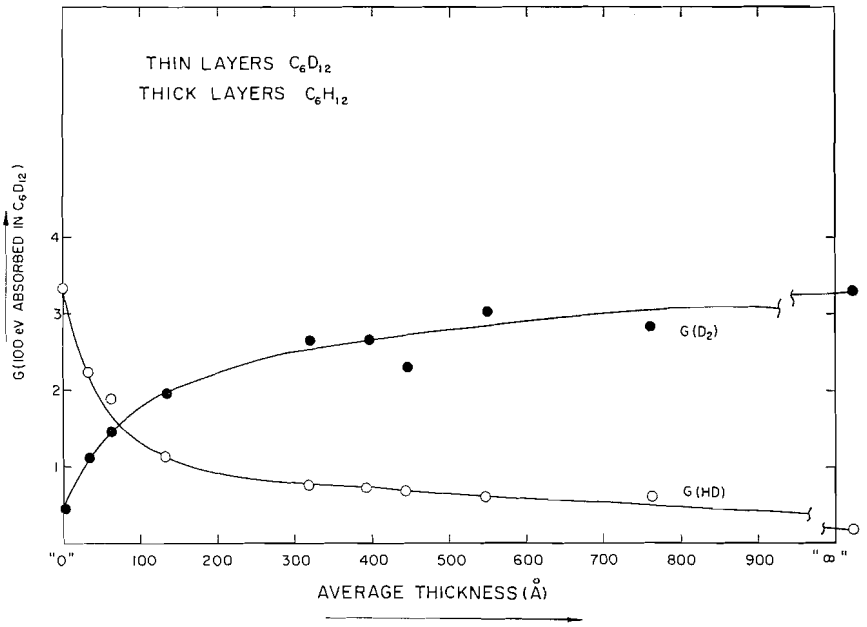
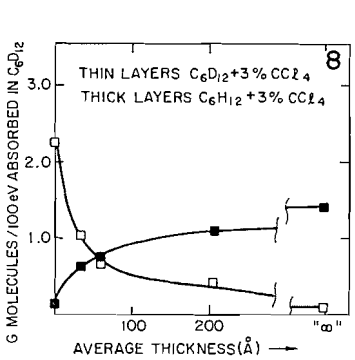


FIG. 7. Yields from the $(C_6D_{12})/(C_6H_{12})$ system.

Experimentally the $(C_6D_{12})/(C_6H_{12})$ system does not follow these predictions. We find $\bar{R}_{D_2} = 110$ Å and $\bar{R}_{HD} = 60$ Å and $G(HD)$ in the homogeneous sample is, at most, equal to $G(D_2)$ in the segregated mixture (Fig. 7). We conclude that there is a process in which C_6H_{12} quenches the decomposition of C_6D_{12} with a range of the order of 100 Å.

Three other systems with C_6H_{12} in the thick layer have been studied: $(C_6D_{12} + 3\%\ CCl_4)/(C_6H_{12} + 3\%\ CCl_4)$, $(C_6D_{12} + 3\%\ CCl_4)/(C_6H_{12})$, and $(C_6D_{12})/(C_6H_{12} + 3\%\ CCl_4)$. For brevity we will refer to the composite layers as $(C_6H_{12} + CCl_4)$ and $(C_6D_{12} + CCl_4)$. These systems were chosen because, on the interpretation we have proposed, electron scavenging is nearly complete at this concentration of CCl_4. The hydrogen from the solid CCl_4 solutions at these concentrations is, we suggest, formed through the decomposition of excited molecules which do not have ionic precursors. The results are shown in Figs. 8, 9, and 10 and in Table I.

Can. J. Chem. Downloaded from www.nrcresearchpress.com by 210.87.254.40 on 09/05/12
For personal use only.



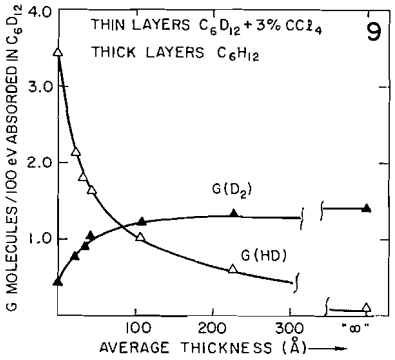


FIG. 8. Yields from the $(C_6D_{12} + 3\%\ CCl_4)/(C_6H_{12} + 3\%\ CCl_4)$ system. (■) $G(D_2)$, (□) G(HD).
FIG. 9. Yields from the $(C_6D_{12} + 3\%\ CCl_4)/(C_6H_{12})$ system.

All the systems with C_6H_{12} in the thick layer show values of $\bar{R}_{HD}$ of 40–60 Å so that interactions do not extend much further than nearest neighbors. It follows that X_H and X_D could be molecular species immobilized in the surface of the layers or mobile species which reacted inside one or, at the most, two molecular diameters.

TABLE I
Observed interaction ranges

Indicator layer	Blanket layer	Fig.	$\bar{R}_{HD}$ (Å)	$\bar{R}_{D_2}$ (Å)
C_6D_{12}	n-C_6H_{14}	5	25	See text
C_6D_{12}	CCl_4	6	—	180
C_6D_{12}	C_6H_6	6	—	180
$C_6D_{12} + 3\%\ CCl_4$	CCl_4	6	—	60
C_6D_{12}	C_6H_{12}	7	60	110
$C_6D_{12} + 3\%\ CCl_4$	$C_6H_{12} + 3\%\ CCl_4$	8	40	60
$C_6D_{12} + 3\%\ CCl_4$	C_6H_{12}	9	40	40
C_6D_{12}	$C_6H_{12} + 3\%\ CCl_4$	10	40	200

By contrast, values of $\bar{R}_{D_2}$ vary from 40 to 200 Å and here we must be observing, in addition, one or more processes inhibiting the decomposition of C_6D_{12} itself (to give D_2 by either a unimolecular or bimolecular route) which are independent of the reactions of X_H or X_D. These have already been noted in the $(C_6D_{12})/(C_6H_{12})$ system.

Systems in which the C_6D_{12} layer contains CCl_4, $(C_6D_{12} + CCl_4)/(C_6H_{12} + CCl_4)$ and $(C_6D_{12} + CCl_4)/(C_6H_{12})$, show a much closer agreement between $\bar{R}_{HD}$ and $\bar{R}_{D_2}$ than is seen in the $(C_6D_{12})/(C_6H_{12})$ system. Further, in both these systems the increase in G(HD), as the layers are made thinner, is approximately twice the decrease in $G(D_2)$. (See Figs. 8 and 9.) These systems approximately follow the predictions for the simple case, outlined above. It appears that addition of CCl_4 to the C_6D_{12} layer has removed or masked the other processes inhibiting the decomposition of C_6D_{12} which we noted in the $(C_6D_{12})/(C_6H_{12})$ system.

The $(C_6D_{12})/(C_6H_{12} + CCl_4)$ system has a large value of $\bar{R}_{D_2}$, 200 Å, which is essentially that observed in the $(C_6D_{12})/(CCl_4)$ system, 180 Å (Fig. 10). This low concentration of CCl_4 in the blanket is, therefore, apparently equivalent to a blanket layer consisting wholly of CCl_4.

Can. J. Chem. Downloaded from www.nrcresearchpress.com by 210.87.254.40 on 09/05/12
For personal use only.

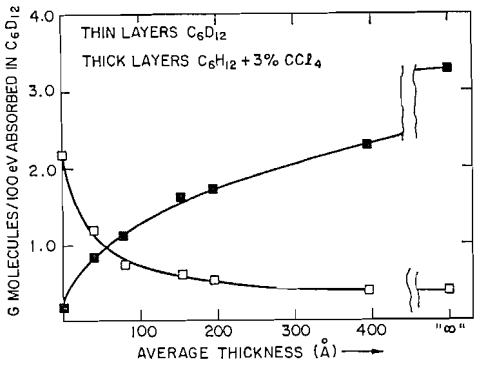


FIG. 10. Yields from the $(C_6D_{12})/(C_6H_{12} + 3\%\ CCl_4)$ system. (■) $G(D_2)$, (□) $G(HD)$.

7. DISCUSSION

This study is exploratory and we shall, accordingly, take a cautious view of the significance of the data. We regard differences in values of $\bar{R}$ to be significant if they amount to a factor of two; smaller differences will not be discussed in detail as they may or may not be significant.

We have distinguished four processes, in order of increasing range:

1. Activation of C_6D_{12} by n-C_6H_{14}, $\bar{R} \simeq 25$ Å.
2. Reactions of the intermediates X_H and X_D to give HD, $\bar{R} \simeq 40$–60 Å.
3. A deactivation of C_6D_{12} by C_6H_{12}, $\bar{R} \simeq 110$ Å.
4. A deactivation of C_6D_{12} by CCl_4 and C_6H_6, $\bar{R} \simeq 180$–200 Å. If the thin layer contains 3% CCl_4 then the range is shorter, $\bar{R} \simeq 60$ Å.

(a) Activation by n-C_6H_{14}

The value of $\bar{R}_{HD}$ observed in this system, 25 Å, is clearly in the region where the layer is ~ 4 molecular diameters thick. The charge transfer step which we suggest is responsible for the activation

$$C_6H_{14}^+ + C_6D_{12} \rightarrow C_6H_{14} + C_6D_{12}^+$$

can, we conclude, only occur between nearest neighbors.

Referring to the results discussed earlier for the $(C_6D_{12})/(C_6H_{14} + 4\%\ C_6H_6)$ system, we see that the addition of benzene at this low concentration has entirely destroyed the activation process: the sum of $G(D_2) + G(HD)$ in fact shows a net decrease from the thick to the thin layers. According to our proposed mechanism, benzene acts as an electron scavenger

$$C_6H_6 + e \rightarrow C_6H_6^-$$

and reaction of the $C_6H_6^-$ ion with $C_6D_{12}^+$ (or $C_6H_{14}^+$) does not result in decomposition of the positive ions to give hydrogen. In this system this neutralization cannot occur until the sample is melted and the molecules are mobile.

The charge exchange step will occur whether or not benzene is present. Its effect will, however, not be observed if the range of electrons is sufficiently large, since these will then pass into the benzene-containing layer. By hypothesis neutralization of positive ions by negative ions does not yield HD or D_2.

(b) Inhibition by Carbon Tetrachloride and Other Electron Scavengers

According to the arguments of ref. 1, the inhibited part of the yield, which is sharply

Can. J. Chem. Downloaded from www.nrcresearchpress.com by 210.87.254.40 on 09/05/12
For personal use only.

reduced by small additions of electron scavengers such as CCl_4, is identified as the yield of ions (reaction [1*a*]) and the residual yield is the yield of excited molecules [1*b*]. We have inferred that $\bar{R}_{D_2}$ for the $(C_6D_{12})/(CCl_4)$ system, 180 Å, is an average of two components: one with $\bar{R}_{D_2} \simeq 340$ Å which is equivalent to the interaction at low CCl_4 concentrations and the other with $\bar{R}_{D_2} \simeq 60$ Å for the interaction at high concentrations ($> 3\%$). We would accordingly identify the range of 340 Å as the average separation of positive ions and electrons in a matrix of solid C_6D_{12}. Recent studies with organic glasses have shown that G(ions) and $G(e^-)$ are ~ 3 (8) and that these electrons may travel considerable distances in the glass (100 to 1 000 Å) before being recaptured by the positive ion (9). A value for the average positive ion electron separation of 340 Å is, however, admittedly large, and greater than that suggested for liquid hydrocarbons (4).

The large value of $\bar{R}_{D_2}$ in the $(C_6D_{12})/(C_6H_{12} + CCl_4)$ system is relevant to this conclusion. This is also a composite range. On our mechanism the interaction consists of two parts: (i) electron capture in the thick layer inhibiting decomposition of the C_6D_{12} and (ii) escape of the intermediate X_D from the C_6D_{12} layer to give HD instead of D_2 when $t \sim 40$ Å (as will be discussed shortly). Accordingly, the range of the electrons alone must be significantly greater than 200 Å and this would be consistent with the 340 Å value deduced above for electron-positive ion separation.

The interaction in the $(C_6D_{12} + 3\%\ CCl_4)/(CCl_4)$ system for which $\bar{R}_{D_2} \sim 60$ Å could represent the short range part of the spectrum of positive ion electron separation or some other process entirely. If it did represent an interaction with electrons then it would follow that all the hydrogen formed in solid cyclohexane was formed through ionic precursors and none through molecules, a conclusion which would be in conflict with our interpretation of the "residual" yield.

In our opinion the balance of evidence favors the identification of the residual yield with the decomposition of excited molecules which do not have ionic precursors. The interaction of CCl_4 with this excited molecule would then be an energy transfer process. Such a process has also been suggested by Freeman (10) for the interaction in the benzene–cyclohexane system in the concentration range 3–100% C_6H_6. His rate constants for the reaction are small and would be consistent with the short range interactions we observe.

(c) Reactions of the Intermediates X_H and X_D

The small values of $\bar{R}_{HD}$, essentially the interaction distance of the species X_H and X_D, show that they are not thermal hydrogen or deuterium atoms. Firstly, the activation energy for H-atom abstraction by H atoms is sufficiently large (~ 7 kcal) (11) that this reaction could not occur at 77 °K. We have, however, found that the bimolecular process giving HD does occur at low temperatures. Further, Klein and Scheer (12) found that H atoms could diffuse rapidly at 77 °K without reaction through a layer of aliphatic hydrocarbons $\sim 10^4$ Å thick. This would mean that if thermal H atoms were reactive intermediates, $\bar{R}_{HD}$ would be of this order. This would also be true if the H atoms diffused through the sample at 77 °K but only reacted as the sample warmed up, or if they reacted by bimolecular combination. The difference of more than three orders of magnitude between $\bar{R}_{HD}$ values expected for thermal H atoms and those found experimentally is conclusive.

It is possible that X_H and X_D are hot hydrogen and deuterium atoms. Hot hydrogen atoms have often been postulated as reactive intermediates in the radiolysis of hydrocarbons and recent chemical evidence for them has been given by Toma and Hamill (2).

Can. J. Chem. Downloaded from www.nrcresearchpress.com by 210.87.254.40 on 09/05/12
For personal use only.

We might anticipate that hot hydrogen atoms, if formed, would initially have energies in the range of 1–10 eV. Our results would require then that the major fraction of these atoms would react before moderation in a distance of 40–60 Å. The efficiency of abstraction at one collision must be less than unity but greater than one hundredth.

Abstraction reactions of hot hydrogen and deuterium atoms have been studied by Martin and Willard (13). Photolysis of DBr and HBr produces D and H atoms with energies of about 3 eV. Abstraction from H_2, D_2, CH_4, and CD_4 was studied. The activation energy for abstraction from H_2 and D_2 is 7.5 ±1 kcal (close to that for the higher hydrocarbons we are studying). For D atoms reacting with H_2, Martin and Willard found that 62% reacted while hot and the remainder were moderated. Probabilities of reaction per collision as high as 0.35 were observed. It appears, therefore, that the high total reaction probability required in our systems is reasonable, as is a range corresponding to several molecular diameters. However, as we have already pointed out, the 40–60 Å ranges are in the intermediate region where we cannot properly describe the layers as continuous.

Thermodynamically possible ion–molecule reactions can be written for the production of HD and D_2 in mixtures of light and heavy hydrocarbons (14, 15). As we have argued, these should have small values of $\bar{R}_{HD}$, ~25 Å, as observed in the $(C_6D_{12})/(C_6H_{14})$ system. The somewhat larger values of $\bar{R}_{HD}$ (40–60 Å) observed in systems with C_6H_{12} in the thick layer may be significant evidence against such mechanisms.

(d) Excitation Transfer between C_6H_{12} and C_6D_{12}

Studies of the radiolysis of liquid mixtures of light hydrocarbons and their deuterated counterparts suggest that excitation transfer between the light and heavy molecules may be taking place; the light hydrocarbons being activated and the heavy counterpart being deactivated.

In dilute solutions of C_6D_{12} in C_6H_{12} the yields of D_2 and HD are low and much less than the yields of H_2 and HD from dilute solution of C_6H_{12} in C_6D_{12} (16). These yields are, indeed, so high that C_6H_{12} molecules must be activated by C_6D_{12}. Conversely, then, C_6D_{12} molecules are deactivated by C_6H_{12}. Similar observations have been made for mixtures of C_2D_6 and C_2H_6 (17). H_2 and HD yields in solutions of C_2H_6 in C_2D_6 are so large that activation of C_2H_6 must be occurring. The deactivation of C_6D_{12} by C_6H_{12} shown by the value of $\bar{R}_{D_2}$ in the $(C_6D_{12})/(C_6H_{12})$ system is further evidence for such an interaction.

8. CONCLUSIONS

Our principal conclusions are:

1. The intermediates in the bimolecular reaction which gives HD in mixtures of isotopic hydrocarbons have a short range. They cannot be thermal hydrogen atoms. Plausible arguments for their identification as hot hydrogen atoms can be advanced.

2. No energy transfer processes with extremely long ranges (i.e. ~1 000 Å) have been found. Activation in mixtures of hydrocarbons (e.g. cyclohexane and *n*-hexane) has a very short range corresponding to nearest neighbor interactions, consistent with our identification of these processes as charge transfer.

3. Deactivation by carbon tetrachloride has a long range (200–500 Å) which can be interpreted as the distance separating positive ions and electrons in the ionization process in solids.

4. There is evidence for an energy transfer process between deuterated and undeuterated hydrocarbons.

Can. J. Chem. Downloaded from www.nrcresearchpress.com by 210.87.254.40 on 09/05/12
For personal use only.

REFERENCES

1. P. J. DYNE. Can. J. Chem. **43**, 1080 (1965).
2. S. Z. TOMA and W. H. HAMILL. J. Am. Chem. Soc. **86**, 1478 (1964).
3. T. F. WILLIAMS. J. Am. Chem. Soc. **86**, 3954 (1964).
4. G. R. FREEMAN. J. Chem. Phys. **43**, 93 (1965).
5. B. A. THRUSH. *In* Formation and trapping of free radicals. *Edited by* A. M. Bass and H. P. Broida. Academic Press, New York. 1960.
6. K. M. CASE, F. DE HOFFMAN, and G. PLACZEK. Introduction to the theory of neutron diffusion. Los Alamos Scientific Laboratory. U.S. Govt. Printing Office. 1953. pp. 17–25.
7. P. J. DYNE, D. R. SMITH, and J. A. STONE. Ann. Rev. Phys. Chem. **14**, 313 (1963).
8. M. R. RONAYNE, J. P. GUARINO, and W. H. HAMILL. J. Am. Chem. Soc. **84**, 4230 (1962).
9. P. J. DYNE and O. A. MILLER. Can. J. Chem. **43**, 2696 (1965).
10. G. R. FREEMAN. J. Chem. Phys. **33**, 71 (1960).
11. H. A. KAZMI and D. J. LEROY. Can. J. Chem. **42**, 1145 (1964).
12. R. KLEIN and M. D. SCHEER. J. Phys. Chem. **62**, 1011 (1958).
13. R. M. MARTIN and J. E. WILLARD. J. Chem. Phys. **40**, 3007 (1964).
14. T. F. WILLIAMS. Trans. Faraday Soc. **57**, 755 (1961).
15. P. J. DYNE and J. DENHARTOG. Can. J. Chem. **40**, 1616 (1962).
16. P. J. DYNE and W. M. JENKINSON. Can. J. Chem. **40**, 1746 (1962).
17. J. A. STONE. Private communication.

Can. J. Chem. Downloaded from www.nrcresearchpress.com by 210.87.254.40 on 09/05/12
For personal use only.

Can. J. Chem. Downloaded from www.nrcresearchpress.com by 210.87.254.5 on 09/05/12
For personal use only.

DIFFUSION IN MULTICOMPONENT AQUEOUS SYSTEMS

J. E. LANE[1] AND J. S. KIRKALDY
Department of Metallurgy and Metallurgical Engineering, McMaster University, Hamilton, Ontario
Received July 20, 1965

ABSTRACT

A vacancy model, originally developed for the description of diffusion in substitutional alloys, is modified for application to aqueous solutions, including those containing ionic species. The results obtained with this model are similar to those of two recently published methods for estimating L-coefficients in dilute multicomponent liquid systems.

Agreement with experimental L-coefficients at relatively high concentrations can be improved for this model by assuming that the jump probability of a diffusing species is inversely proportional to the relative viscosity of the mixture. Good agreement is then found for some systems up to combined solute concentrations of 3 M.

INTRODUCTION

In two recent papers (1, 2), hereinafter referred to as I and II respectively, we have investigated the macroscopic implications of two simple microscopic models of diffusion in multicomponent systems. In I we showed that the form of the concentration dependence of the L-coefficients describing diffusion in multicomponent alloy systems was similar for both an exchange and a vacancy mechanism. In II we adapted the exchange mechanism to describe diffusion in a quasi-crystalline model of a liquid. The calculations based on this approach gave good quantitative agreement with experimental L-coefficients in several dilute ternary liquid systems and gave qualitative agreement in more concentrated solutions. We show in this communication that the vacancy mechanism of diffusion given in I, when suitably modified, gives just as good a description of diffusion in multicomponent liquid systems as the exchange mechanism.

MODEL

As in II, we postulate a quasi-crystalline liquid, with each diffusing entity occupying a lattice site; in addition we postulate that a very small fraction of the sites are vacant. Diffusion occurs by interchange of a diffusing unit (atom, ion, or molecule) with an adjacent vacant site. The lattice sites are all assumed to be equivalent, and hence the partial molar volumes are the same for each diffusing species, and the volume- and number-fixed frames of reference are coincident.

The flux of the i'th component in the lattice-fixed (or Kirkendall) frame of reference of the model was given in I for the vacancy mechanism as,

$$[1] \qquad (J_i)_K = -\frac{\lambda^2}{RT}\hat{C}_i P_i \frac{\partial \mu_i}{\partial x},$$

where λ is the lattice spacing in the direction of the chemical potential gradient, $\hat{C}_i$ is the concentration of the i'th component per unit volume of lattice as determined by averaging normal to the chemical potential gradient, and P_i is the jump probability of the i'th species at the concentration under consideration.

SOLUTIONS CONTAINING NO WEAK ELECTROLYTES

We consider a solution containing solvent, designated as component 0, nonelectrolyte components 1 and 2, and neutral salt components 3 and 4, composed of ions 3^1, 4^1, and 5^1,

[1]*Now at the C.S.I.R.O., Division of Physical Chemistry, Box 4331, G.P.O., Melbourne, Australia.*

the ions of type 5^1 being common to both salts. The ionic fluxes are given by [1] but are also subject to the condition of electrical neutrality, which in this particular case is,

$$[2] \qquad \sum_{k^i=3^i}^{5^i} Z_{k^i}(J_{k^i}) = 0,$$

where Z_{k^i} is the charge on the k^i'th species. In II, a method was given in detail for obtaining salt fluxes from the expressions for the ionic fluxes together with the condition of electrical neutrality. Use of this method and eq. [1] and [2] gives the salt fluxes as,

$$[3] \qquad (J_k)_{\substack{K \\ k,\,l=3,4}} = -\frac{\lambda^2}{RT}\alpha_{kk}\frac{\partial \mu_k}{\partial x} - \frac{\lambda^2}{RT}\alpha_{kl}\frac{\partial \mu_l}{\partial x},$$

where,

$$[4] \qquad \alpha_{kl} = (Z_{5^i})^{-2}\left\{\delta_{kl}\hat{C}_{k^i}P_{k^i} - \prod_{m^i=k,\,l} Z_{m^i}\hat{C}_{m^i}P_{m^i} \Big/ \sum_{m^i=3^i}^{5^i}(Z_{m^i})^2\hat{C}_{m^i}P_{m^i}\right\},$$

and δ_{kl} is the Kröneker delta. The chemical potential gradients in [3] are those of the neutral salts.

A completely general description of diffusion in the lattice-referred coordinate system is given by,

$$[5] \qquad (J_i)_K = -\sum_{j=0}^{4}(L_{ij}')_K\frac{\partial \mu_i}{\partial x},$$

where the $(L_{ij}')_K$ are not unique. For this particular model the $(L_{ij}')_K$ may be summarized as,

$$[6] \qquad (L_{ij}')_K = \frac{\lambda^2}{RT}\delta_{ij}\hat{C}_iP_i,$$

where $\qquad i = 0, 1, 2;\ j = 0, 1, 2, 3, 4 \quad \text{or} \quad i = 0, 1, 2, 3, 4;\ j = 0, 1, 2.$

$$(L_{ij}')_K = \frac{\lambda^2}{RT}\alpha_{ij}, \qquad i, j = 3, 4.$$

THE SYSTEM H_2O–Na_2SO_4–H_2SO_4

This sytem was discussed in detail in II. We designate the water as component 0, the neutral salts as components 1 and 2, and the ionic species Na^+, H^+, SO_4^{2-}, $NaSO_4^-$, HSO_4^- as $1^1, \ldots, 5^1$ respectively. The fluxes of the ions are given by eq. [1], written in terms of the relevant ionic quantities. By a procedure similar to that given in II, the salt fluxes may be written in the form of eq. [5] where the $(L_{ij}')_K$ are given by,

$$[7] \qquad (L_{i0}')_K = (L_{0i})_K = \frac{\lambda^2}{RT}\delta_{0i}\hat{C}_0P_0, \qquad i = 0, 1, 2,$$

$$(L_{kl}')_K = \frac{\lambda^2}{RT}\beta_{kl}, \qquad k, l = 1, 2$$

where

$$\beta_{kl} = \tfrac{1}{4}\left\{(\hat{C}_{k^i}P_{k^i} + \hat{C}_{(k+3)^i}P_{(k+3)^i}) - \prod_{m^i=k^i,\,l^i}(\hat{C}_{m^i}P_{m^i} - \hat{C}_{(m+3)^i}P_{(m+3)^i}) \Big/ \sum_{m=1^i}^{5^i}(Z_{m^i})^2\hat{C}_{m^i}P_{m^i}\right\}.$$

Can. J. Chem. Downloaded from www.nrcresearchpress.com by 210.87.254.5 on 09/05/12
For personal use only.

Can. J. Chem. Downloaded from www.nrcresearchpress.com by 210.87.254.5 on 09/05/12
For personal use only.

TRANSFORMATION TO THE VOLUME-FIXED FRAME OF REFERENCE

Comparison of the model with experimental systems can be most conveniently made if the L-coefficients are in their unique form pertaining to diffusion in the volume-fixed frame of reference, i.e.

$$[8] \qquad (J_i)_V = -\sum_{i,j\neq 0} (L_{ij})_V \left(\frac{\partial \mu_j}{\partial x} - \frac{\bar{V}_j}{\bar{V}_0}\frac{\partial \mu_0}{\partial x}\right).$$

The $(L_{ij})_V$ are unique and can be obtained from the $(L_{ij}')_K$ of eq. [5] by first transforming the fluxes to the volume-fixed frame of reference of the model, and then using the Gibbs–Duhem equation to replace the dependent forces $\partial\mu_i/\partial x$ by the independent forces

$$\left(\frac{\partial \mu_j}{\partial x} - \frac{\bar{V}_j}{\bar{V}_0}\frac{\partial \mu_0}{\partial x}\right).$$

This procedure was given in detail in I, and for this model,

$$[9] \qquad (L_{ij})_V = (L_{ij}')_K - N_i \sum_{k=0}^{4} \gamma_k (L_{kj}')_K - N_j \sum_{l=0}^{4} \gamma_l (L_{il}')_K + N_i N_j \sum_{k=0}^{4}\sum_{l=0}^{4} \gamma_k \gamma_l (L_{kl}')_K,$$

where γ_i is unity for the solvent and nonelectrolyte solutes, and is given in general by the sum of the moduli of the charges on the constituent ions for each electrolyte solute. The mole fractions N_k are given by (neglecting the vacancy concentration),

$$N_k = \hat{C}_k \Big/ \sum_{l=0}^{4} \hat{C}_l,$$

where for electrolytes the $\bar{C}_i$'s are the concentrations of the neutral salts.

EVALUATION OF THE JUMP PROBABILITIES AT INFINITE DILUTION

The jump probability of the solvent at infinite dilution P_0^0 is given by eq. [56] of I as,

$$[10] \qquad P_0^0 = (D_0^{*,0}) C_0^0 / \hat{C}_0^0 (\lambda^0)^2,$$

the superscript ^{0} indicating the value of a quantity at infinite dilution; $(D_0^{*,0})_V$ is the mutual diffusion coefficient on the molar concentration gradient scale of isotopically labelled solvent molecules in otherwise pure solvent, and C_i is the molar concentration. Equation [10] is approximate because it assumes that solvent molecules with different isotopic composition have the same transport properties. The solvent is water in every system discussed here and we take the value of $(D_0^{*,0})$ at 25 °C to be 2.27×10^{-8} cm^2/s. This value was obtained by Longsworth (3) for mixtures of D_2O–H_2O with a Gouy diffusiometer, and it is in good agreement with the value 2.29×10^{-8} obtained by Andreev (4) with a diaphragm-cell method.

The jump probability of the nonelectrolyte solute components are given by eq. [60] of I as,

$$[11] \qquad P_i^0 = (D_i^0)_V C_0^0 / \hat{C}_0^0 (\lambda^0)^2.$$

The ionic jump probabilities in aqueous solutions are obtained by an analysis similar to that given in II for obtaining the values of the frequency of the ion–water exchange, i.e.

$$[12] \qquad P_{k^i}^0 = (\lambda_{k^i}^0)_{\text{cond}}\, C_0^0 / |Z_{k^i}| F^2 \hat{C}_0^0 (\lambda^0)^2,$$

where $(\lambda_{k^i}^0)_{\text{cond}}$ is the limiting ionic conductance of the k^ith ion, and F is the Faraday.

Can. J. Chem. Downloaded from www.nrcresearchpress.com by 210.87.254.5 on 09/05/12
For personal use only.

CALCULATION OF THE $(L_{ii})_V$

In all calculations use is made of the following relations, $\hat{C}_i/\hat{C}_0^0 = C_i/C_0^0$, the value of C_0^0 at 25 °C for water being 55.344 (5), and

$$(\lambda/\lambda^0)^2 = \left\{C_0^0 \Big/ \left(\sum_{i=0}^{2} C_i + \sum_{k^i=3^i}^{5^i} C_{k^i} \right)\right\}^{2/3},$$

except in the H_2O–Na_2SO_4–H_2SO_4 system, where it is given by,

$$(\lambda/\lambda^0)^2 = \left\{C_0^0 \Big/ \left(C_0 + \sum_{k^i=1^i}^{3^i} C_{k^i} + \sum_{k^i=4^i}^{5^i} 2C_{k^i} \right)\right\}^{2/3},$$

obtained by neglecting the vacancy concentration. Here it has been assumed that the ion–pairs $NaSO_4^-$ and HSO_4^- each occupy two lattice sites (the same assumption was made in II).

Two different approximations are made for the P_i at finite concentrations,

[13] $$P_i \approx P_i^0,$$

and

[14] $$P_i \approx P_i^0/\eta_r,$$

where η_r is the relative viscosity.

Ezrokhi (6) has proposed the following empirical relationship for estimating the relative viscosity of mixtures,

[15] $$\log \eta_r(\text{mixture}) = \sum_i \log \eta_r(C_i)$$

where $\eta_r(C_i)$ is the relative viscosity of a binary solution containing the i'th solute at the same molar concentration as it is in the mixture. By eq. [15], Ezrokhi found very good agreement with experimental measurements for the system H_2O–NaCl–KCl.

TABLE I

Comparison of models with experimental L-coefficients for the system H_2O–NaCl–KCl at 25 °C

C_0	54.69	54.29	54.43	54.02	51.14
C_3	0.2500	0.2500	0.5000	0.5000	1.500
C_4	0.2500	0.5000	0.2500	0.5000	1.500
η_r	1.020	1.019	1.043	1.032	1.156
$(L_{33})_V \times RT \times 10^8$					
Calcd. [13]	0.271	0.292	0.494	0.538	1.57
Calcd. II	0.270	0.289	0.492	0.533	1.51
Calcd. Wendt (7)	0.273			0.541	1.54
Calcd. [14]	0.266	0.287	0.474	0.522	1.36
Expt.	0.260	0.277	0.470	0.510	1.27
$(L_{34})_V \times RT \times 10^8$					
Calcd. [13]	−0.090	−0.119	−0.124	−0.182	−0.580
Calcd. II	−0.088	−0.113	−0.120	−0.173	−0.492
Calcd. Wendt (7)	−0.092			−0.189	−0.643
Calcd. [14]	−0.089	−0.117	−0.119	−0.177	−0.501
Expt.	−0.077	−0.102	−0.108	−0.163	−0.477
$(L_{44})_V \times RT \times 10^8$					
Calcd. [13]	0.356	0.629	0.395	0.703	2.02
Calcd. II	0.355	0.629	0.393	0.701	1.99
Calcd. Wendt (7)	0.355			0.701	1.96
Calcd. [14]	0.349	0.617	0.381	0.681	1.75
Expt.	0.345	0.619	0.378	0.691	1.73

NOTE: 0 = H_2O; 3 = NaCl; 4 = KCl. All conductance data from ref. 10. Relative viscosities from ref. 6. Experimental L-coefficients from refs. 8 and 9.

TABLE II

Comparison of models with experimental L-coefficients for the system H_2O–glycine–KCl at 25 °C

C_0	54.55	54.35	53.95	53.94	53.74	53.33
C_1	0.2500	0.2500	0.2500	0.5000	0.5000	0.5000
C_3	0.1250	0.2500	0.5000	0.1250	0.2500	0.5000
η_r	1.036	1.035	1.033	1.077	1.076	1.074
$(L_{11})_V \times RT \times 10^8$						
Calcd. [13]	0.266	0.266	0.266	0.535	0.536	0.534
Calcd. II	0.263	0.264	0.267	0.517	0.519	0.519
Calcd. [14]	0.257	0.257	0.258	0.497	0.498	0.497
Expt.	0.259	0.259	0.258	0.502	0.501	0.498
$(L_{13})_V \times RT \times 10^8$						
Calcd. [13]	0.000	−0.001	−0.004	0.000	−0.001	−0.004
Calcd. II	−0.001	−0.003	−0.006	−0.003	−0.006	−0.011
Calcd. [14]	0.000	−0.001	−0.004	0.000	−0.001	−0.004
Expt.	0.000	0.000	0.000	0.001	−0.001	−0.002
$(L_{33})_V \times RT \times 10^8$						
Calcd. [13]	0.126	0.248	0.491	0.125	0.250	0.493
Calcd. II	0.123	0.246	0.491	0.123	0.244	0.485
Calcd. [14]	0.121	0.239	0.474	0.116	0.232	0.458
Expt.	0.122	0.245	0.486	0.118	0.238	0.467

NOTE: 0 = H_2O; 1 = glycine; 3 = KCl. $D_1^0 \times 10^5 = 1.061$, ref. 11. Conductance data from Robinson and Stokes (10). Relative viscosities estimated by eq. [15] and the binary data of refs. 11 and 12. Experimental L-coefficients from ref. 5.

In Table I are the calculated values of the L-coefficients of the system H_2O–NaCl–KCl at 25 °C using both approximations [13] and [14] with eq. [9], [6], [10], and [12]. The values calculated by the method given in II, and by Wendt (7), are also included, together with the experimental values of Dunlop and Gosting (8) and Dunlop (9). The ionic conductances at infinite dilution were obtained from Robinson and Stokes (10), and the relative viscosities from Ezrokhi (6).

The L-coefficients for the system H_2O–glycine–KCl at 25 °C are given in Table II. The diffusion coefficient of glycine at infinite dilution and 25 °C was obtained from Ellerton *et al.* (11). The relative viscosities were estimated with eq. [15], the experimental data for aqueous glycine solutions (11), and the data of Kaminsky (12). The experimental L-coefficients are those of Woolf *et al.* (5).

The calculations for the system H_2O–Na_2SO_4–H_2SO_4, using approximations [13] and [14] with eq. [9], [7], [10], and [12], are summarized in Table III. The ratios of H^+/HSO_4^- concentrations were calculated by a method given by Baes (13), and with the assumption that the $NaSO_4^-$ concentration was zero, except for the last column of Table III. The relative viscosities were calculated from [15] and the data of Kaminsky (14). The limiting ionic conductance of HSO_4^- at 25 °C is that of Kerker (15) and for the other ionic species those of Robinson and Stokes (10). The experimental L-coefficients are from Wendt (16).

In Table IV, calculations of the L-coefficients are given for the systems H_2O–raffinose–urea, H_2O–raffinose–KCl, H_2O–LiCl–NaCl, and H_2O–LiCl–KCl. These calculations were made by using approximation [14] with eq. [9], [6], [10], [11], and [12], estimating the relative viscosities by means of eq. [15], and using the binary solution data of Dunlop (17), Gosting and Akeley (18), Kaminsky (19, 14, 12) and the limiting ionic conductances given by Robinson and Stokes (10). The calculations of Miller (20) for the same systems are also given. Miller used ternary diffusion data and estimates of the thermodynamic quantities $\partial\mu_i/\partial C_j$ to obtain values of the L-coefficients.

DISCUSSION

The calculations presented here for the exchange and vacancy models of diffusion in multicomponent systems generate very similar macroscopic descriptions. This result is

Can. J. Chem. Downloaded from www.nrcresearchpress.com by 210.87.254.5 on 09/05/12
For personal use only.

TABLE III

Comparison of models with experimental L-coefficients for the system H_2O–Na_2SO_4–H_2SO_4 at 25 °C

C_0	53.47	52.58	52.29	51.24	51.24
C_1	0.5000	1.0000	0.5000	1.0000	1.0000
C_2	0.5000	0.5000	1.0000	1.0000	1.0000
C_1^i	1.00	2.00	1.00	2.00	1.80
C_2^i	0.45	0.38	1.07	0.90	0.90
C_3^i	0.45	0.88	0.57	0.90	0.70
C_4^i	0.00	0.00	0.00	0.00	0.20
C_5^i	0.55	0.62	0.93	1.10	1.10
η_r	1.40	1.62	1.60	1.86	1.86
$(L_{11})_V \times RT \times 10^8$					
Calcd. [13]	0.280	0.507	0.304	0.562	
Calcd. II	0.263	0.444	0.284	0.503	
Calcd. Wendt (7)	0.286			0.561	
Calcd. [14]	0.200	0.313	0.190	0.302	0.318
Expt.	0.231	0.381	0.226	0.371	0.371
$(L_{12})_V \times RT \times 10^8$					
Calcd. [13]	−0.155	−0.173	−0.244	−0.331	
Calcd. II	−0.155	−0.195	−0.201	−0.301	
Calcd. Wendt (7)	−0.133			−0.313	
Calcd. [14]	−0.111	−0.107	−0.153	−0.178	−0.158
Expt.	−0.072	−0.084	−0.091	−0.146	−0.146
$(L_{22})_V \times RT \times 10^8$					
Calcd. [13]	0.836	0.868	1.41	1.59	
Calcd. II	0.785	0.831	1.31	1.47	
Calcd. Wendt (7)	0.903			1.73	
Calcd. [14]	0.597	0.536	0.881	0.855	0.843
Expt.	0.515	0.444	0.802	0.725	0.725

NOTE: 0 = H_2O; 1 = Na_2SO_4; 2 = H_2SO_4. λHSO_{4cond}^{-0} from ref. 15, remaining conductance data from ref. 10. Ionic concentrations estimated by method of Baes (13). Relative viscosities estimated by [15] and the binary data of ref. 14. Experimental L-coefficients from ref. 16.

TABLE IV

Comparison of L-coefficients calculated by means of approximation [14] with those calculated by Miller (20) with experimental ternary diffusion data and estimated thermodynamic data

C_0	53.9	54.9	54.2	54.8	54.8
C_i	0.015	0.015	0.015	0.25	0.25
C_j	0.50	0.10	0.50	0.20	0.20
Component i	Raffinose	Raffinose	Raffinose	LiCl	LiCl
Component j	Urea	KCl	KCl	NaCl	KCl
η_r	1.041	1.021	1.018	1.056	1.036
$(L_{ii})_V \times RT \times 10^8$					
Calcd. [14]	0.0063	0.0064	0.0065	0.199	0.207
Miller (20)	0.0062	0.0063	0.0063	0.189	0.200
$(L_{ij})_V \times RT \times 10^8$					
Calcd. [14]	−0.001	0.000	−0.004	−0.046	−0.063
Miller (20)	−0.001	0.000	−0.002	−0.041	−0.060
$(L_{jj})_V \times RT \times 10^8$					
Calcd. [14]	0.651	0.098	0.487	0.205	0.281
Miller (20)	0.657	0.099	0.495	0.206	0.283

NOTE: $D_{raff}^0 \times 10^8 = 0.4359$, ref. 17. $D_{uren}^0 \times 10^8 = 1.381$, ref. 18. Ionic conductance data from ref. 10. Relative viscosities estimated by eq. [15] and binary solution data of refs. 12, 14, 17, 18, and 19.

somewhat analogous to that obtained for substitutional solids in I. Indeed, for infinitely dilute solutions this description may be obtained from purely macroscopic assumptions as shown by Wendt (7). His method for estimating L-coefficients is based on the assumption that the off-diagonal ionic L-coefficients in the solvent-fixed frame of reference are zero and that the mobilities of ionic species in the same frame have the same values as they do at infinite dilution. It is relevant to add that although Wendt proposed his method for electrolyte components only, it can also be used for nonelectrolyte solutes. Since in the limit of infinite dilution the solvent-fixed, volume-fixed, and lattice-fixed frames coincide,

Can. J. Chem. Downloaded from www.nrcresearchpress.com by 210.87.254.5 on 09/05/12
For personal use only.

the values of L-coefficients obtained by the various methods tend to coincide so that there is no macroscopic basis on which to choose between them. However, for a kinetic interpretation of the coefficients and extension of the theory to higher concentrations our formulation appears to be mandatory.

In the system H_2O–NaCl–KCl where relative viscosity data is available, and H_2O–glycine–KCl where the relative viscosities can be computed without introducing large errors, the approximation for the P_i from eq. [14] gives better estimates of the L-coefficients than any of the methods based on approximations similar to eq. [13]. For these two systems, the difference between estimated and experimental L-coefficients is within three times the experimental error at all concentrations. The agreement between the estimated values for the system in Table IV and the values given by Miller (20) is also good.

For the system H_2O–Na_2SO_4–H_2SO_4 where the electrolytes are incompletely ionized, approximation [14] still gives better agreement with experiment than approximation [13], but not as good as it does in the other systems considered. There are several reasons for this. The relative viscosities are likely to be in error by as much as 20%, since the relative viscosities of the binary solutions were calculated by methods that are only accurate for concentrations less than a few tenths molar. The estimates of the ratio of the concentrations H^+/HSO_4^-, by the method of Baes (13), is not expected to be accurate at the concentrations used here, and the approximation that the concentration of $NaSO_4^-$ is zero is known to be incorrect (21). There is no value of the limiting ionic conductance of $NaSO_4^-$ available, but on the assumption that it is the same as that of HSO_4^-, values of the L-coefficients at a concentration of 1 M for Na_2SO_4 and H_2SO_4 have been calculated from approximation [14] and the assumption that 10% of the sodium is transported as $NaSO_4^-$. These values are given in the last column of Table III, and are in better agreement with the experimental L-coefficients, the difference being about three times the experimental error.

The introduction of the relative viscosity into the calculations will also improve the accuracy of the other two methods of estimating the L-coefficients. However, there is at present no rigid theoretical justification for this procedure. Indeed, there appears to be no simple connection between viscous flow and the exchange mechanism of diffusion. The use of the relative viscosity with Wendt's (7) method is equivalent to the use of Stoke's law for particles of similar size to the solvent. Glasstone, Laidler, and Eyring (22) have described in detail a vacancy mechanism of viscous flow which also has a term corresponding to the jump probability of a diffusing unit with an adjacent hole. The jump probability in their model varies with viscosity as,

$$P_i = P_i^0(\lambda^0)^3/\eta_r(\lambda)^3,$$

which differs from [14] by the term $(\lambda^0/\lambda)^3$. Inclusion of this term in the calculation of the L-coefficients would lead to poorer agreement with experimental values in every system discussed here.

It is expected that the approximation [14] will fail in high polymer solutions. Stokes and Weeks (23) have reported that values of the limiting equivalent conductances of ions in aqueous solutions of the synthetic sucrose polymer Ficall are of similar magnitude to those in sucrose solutions of similar weight percent solute concentration, although the sucrose solutions are very much less viscous than the Ficall solutions. Osborne and Porter (24) also record that a diffusion-controlled quenching reaction has a rate constant in a high viscosity aqueous gelatin solution not significantly different from the value in pure water.

Can. J. Chem. Downloaded from www.nrcresearchpress.com by 210.87.254.5 on 09/05/12
For personal use only.

Estimates of the L-coefficients based on the approximation [14] would seem on the evidence available to be reliable for aqueous solutions of nonelectrolytes (except high polymers) and strong electrolytes of combined solute concentrations of a few molar. By inversion of the analysis of Dunlop and Gosting (8) and Woolf *et al.* (5) and with either experimental or estimated multicomponent thermodynamic data, it then becomes possible to compute the multicomponent diffusion coefficients. Wendt (7) has shown that this procedure yields reliable diffusion coefficients in very dilute solutions using his method of estimating the L-coefficients. Introduction of relative viscosities into the calculations will lead to correspondingly good agreement at higher concentrations, and the estimated diffusion coefficients should be sufficiently accurate for a number of applied problems requiring this information.

It is pertinent to discuss the information, in addition to relative viscosities, necessary for calculating the L-coefficients at finite concentrations. The exchange model requires a knowledge of the quantities C_0^0, C_0, ... , C_{n-1}, $(D_1^0)_V$, ... , $(D_{n-1}^0)_V$ (or limiting ionic conductances of ionic species), and some method of estimating the rate of exchange of the solutes. This latter information can only be obtained experimentally by recourse to multicomponent diffusion data, although, as shown in II, it may be estimated with sufficient accuracy for dilute solutions. The vacancy model requires knowledge of the quantities C_0^0, C_0, ... , C_{n-1}, $(D_0^{*,0})_V$, ... , $(D_{n-1}^0)_V$ (or limiting ionic conductances for ionic species) all of which can be obtained experimentally without the need of multicomponent diffusion data. The method given by Wendt requires less information than the vacancy model, since it does not require C_0^0, C_0, and $(D_0^{*,0})_V$ to estimate the L-coefficients in the solvent-fixed frame of reference. However, an exact transformation to the volume-fixed frame of reference requires a knowledge of the solute partial molar volumes which brings the two methods into equivalence, except for the term $(D_0^{*,0})_V$.

At the concentrations of ternary systems for which precise experimental data are thus far available, it is not possible to use the experimental values of the L-coefficients and their concentration dependence to decide which of the two atomic mechanisms we have investigated gives the better macroscopic description of diffusion in multicomponent liquid systems, although the differences should tend to be significant at the highest concentration of the system H_2O–Na_2SO_4–H_2SO_4. Indeed, it may not be possible to identify the mechanism by a purely macroscopic measurement. It would, nonetheless, be useful to have precise measurements of diffusion coefficients, chemical potential derivatives with concentration, and relative viscosities of ternary solutions in which the solute concentrations approach those of the solvent. In particular, information on ternary systems not containing electrolytes would be most helpful, since the presence of ionic species complicates the analysis of any model. This is particularly evident in the case of a ternary solution containing two electrolytes with a common ion. The relatively large off-diagonal L-coefficients observed in these systems are predominantly the result of the formal coupling of the chemical potentials of the two salts rather than a real coupling of the fluxes.

Since the evidence for a vacancy mechanism of diffusion in substitutional alloys is much better than for aqueous solutions, we believe that the macroscopic implication of the model should at least be as good a description of alloys as it is of aqueous solutions. In particular, the vacancy mechanism was shown in I to be equivalent to the phenomenological description,

$$[16] \qquad (J_i)_K = -(L_{ij}')_K \frac{\partial \mu_j}{\partial x},$$

$$(L_{ij}')_K = 0 \text{ for all } i \neq j.$$

Can. J. Chem. Downloaded from www.nrcresearchpress.com by 210.87.254.5 on 09/05/12
For personal use only.

This scheme consisting of a diagonal matrix of phenomenological coefficients is particularly useful in obtaining solutions of the integral equations of multicomponent diffusion (25) when the lattice- (Kirkendall) and volume-fixed frames of reference coincide. The scheme [16] has already been verified experimentally for interstitial components of ternary alloys (26, 27).

ACKNOWLEDGMENTS

This work was supported by the National Research Council. We wish to thank Professor R. P. Wendt of the Louisiana State University for making a preprint of his recent paper available to us.

REFERENCES

1. J. E. LANE and J. S. KIRKALDY. Can. J. Phys. **42**, 1643 (1964).
2. J. E. LANE and J. S. KIRKALDY. Can. J. Chem. **43**, 1812 (1965).
3. L. G. LONGSWORTH. J. Phys. Chem. **64**, 1914 (1960).
4. G. A. ANDREEV. Russ. J. Phys. Chem. English Transl. **37**, 186 (1963).
5. L. A. WOOLF, D. G. MILLER, and L. J. GOSTING. J. Am. Chem. Soc. **84**, 317 (1962).
6. L. L. EZROKHI. Zhr. Prikl. Khim. **26**, 802 (1953).
7. R. P. WENDT. J. Phys. Chem. **69**, 1227 (1965).
8. P. J. DUNLOP and L. J. GOSTING. J. Phys. Chem. **63**, 86 (1959).
9. P. J. DUNLOP. J. Phys. Chem. **63**, 612 (1959).
10. R. A. ROBINSON and R. H. STOKES. Electrolyte solutions. 2nd ed. Butterworths, London. 1959. p. 463.
11. H. D. ELLERTON, G. REINFELDS, D. E. MULCAHY, and P. J. DUNLOP. J. Phys. Chem. **68**, 403 (1964).
12. M. KAMINSKY. Z. Physik. Chem. Frankfurt, **12**, 206 (1957).
13. C. F. BAES. J. Am. Chem. Soc. **79**, 5611 (1957).
14. M. KAMINSKY. Discussions Faraday Soc. **24**, 171 (1957).
15. M. KERKER. J. Am. Chem. Soc. **79**, 3664 (1957).
16. R. P. WENDT. J. Phys. Chem. **66**, 1279 (1962).
17. P. J. DUNLOP. J. Phys. Chem. **60**, 1464 (1956).
18. L. J. GOSTING and D. F. AKELEY. J. Am. Chem. Soc. **74**, 2058 (1952).
19. M. KAMINSKY. Z. Physik. Chem. Frankfurt, **8**, 171 (1956).
20. D. G. MILLER. J. Phys. Chem. **63**, 570 (1959).
21. C. W. DAVIES, H. W. JONES, and C. B. MONK. Trans. Faraday Soc. **48**, 921 (1952).
22. S. GLASSTONE, K. J. LAIDLER, and H. EYRING. The theory of rate processes. McGraw-Hill, New York. 1941. Chap. 9.
23. R. H. STOKES and I. A. WEEKS. Australian J. Chem. **17**, 304 (1964).
24. A. D. OSBORNE and G. D. PORTER. Proc. Roy. Soc. London, Ser. A, **284**, 9 (1965).
25. J. S. KIRKALDY, J. E. LANE, and G. R. MASON. Can. J. Phys. **41**, 2174 (1963).
26. J. S. KIRKALDY and G. R. PURDY. Can. J. Phys. **40**, 208 (1962).
27. L. C. BROWN and J. S. KIRKALDY. Trans. AIME, **230**, 223 (1964).

Can. J. Chem. Downloaded from www.nrcresearchpress.com by 210.87.254.5 on 09/05/12
For personal use only.

THE SOLVENT ISOTOPE EFFECT AND THE PARTIAL MOLAR VOLUME OF IONS[1]

R. E. ROBERTSON, S. E. SUGAMORI, R. TSE,[2] AND C.-Y. WU[3]
Division of Pure Chemistry, National Research Council, Ottawa, Canada

Received September 1, 1965

ABSTRACT

The partial molar volume of ions in water furnishes an indication, if not precise information, about the nature of ionic solvation (1–5). Accordingly, it was hoped that differences in this term and particularly the effect of temperatures on the differences in the apparent partial molar volume for a series of ions in light and heavy water would provide a basis for decisions on the nature of solvation of the benzenesulfonic ion. This ion is of considerable interest in the study of solvolysis, but very little is known about the characteristics of solvation.

The present work was initiated as a consequence of a difference in the interpretation of the source of the kinetic solvent isotope effects observed in the solvolysis of halides and sulfonates in light and heavy water. Swain and co-workers (6–8) attached particular emphasis to differences arising from differential solvation of the quasi-ionic transition state, a viewpoint initially shared by ourselves. Subsequently, however, Laughton and Robertson (9), while admitting of the possibility of differences contributing to the kinetic solvent isotope effect k_{D_2O}/k_{H_2O} in the transition state, attributed the major determinant of this ratio to differences in what they referred to as "the stability of the initial state solvation shell" in the respective media. In previous papers evidence supporting this view have been presented (10, 11).

The data presented here marks an attempt to determine the isotope differences in the partial molar volume of two salts of known and different solvation characteristics as a basis of establishing, in a semi-quantitative way, the characteristics of the benzenesulfonic ion. Our choice was governed by the knowledge that the kinetic solvent isotope effect showed that the solvolysis of halides gave about the same values of the k_{D_2O}/k_{H_2O} ratio (0.7–0.8) while the value for the sulfonates was about 0.9; that the fluoride ion is regarded as a "structure builder" and the iodide as a net "structure breaker". The position of the sulfonic ion in this respect was unknown.

EXPERIMENTAL DETAIL

Distilled water passed through an ion exchange column with suitable precautions was the source of H_2O. The D_2O (99.97%) was obtained from Merck, Sharp and Dohme, Montreal, and was redistilled in a scaled down model of the water distillation system of Stuart and Wormwell (12). The efficiency of both systems was controlled by conductivity measurements. Sodium and potassium benzenesulfonate and potassium methanesulfonate were recrystallized at least twice from methanol and then dried under vacuum. Sodium methanesulfonate and butanesulfonate were first dissolved in water and then methanol was added to the saturated solution to initiate crystallization. Sodium methanesulfonate, which was prepared from practical grade methanesulfonic acid, was recrystallized four times by this method. Sodium fluoride and iodide were reagent grade salts and were dried at 110 °C before use. Solutions were made up by weight. All weighings were on a Mettler Semi-Micro Gramatic balance, in a balance room regulated to 22 °C and 55% humidity.

The pycnometer was of the modified Sprengel type described by Robertson (13) and was held in a special rack in a water bath controlled to $\leqslant 0.003$ °C, as determined by a platinum resistance thermometer. A series of pycnometers were used since it was necessary to leave each in the bath at least 20 min to achieve temperature equilibrium before reading the meniscus level, and another 20 min in the balance room after washing with pure acetone and wiping before taking readings.

[1] *Issued as N.R.C. No. 8781.*
[2] *Summer Research Assistant, 1957.*
[3] *National Research Council Postdoctorate Fellow, 1963–1965.*

Can. J. Chem. Downloaded from www.nrcresearchpress.com by 210.87.254.42 on 09/05/12
For personal use only.

While our method of determining densities does not appear to be capable of the same accuracy as the hydrostatic balance method (14) or some variant of the dilution method (15–17), the accuracy was about the same as that reported by Jones and Christian using a similar pycnometer (18). At the time the work was initiated, our main concern was with the solvent isotope effect on the partial molar volume and the simpler method seemed desirable. We now hold the view that the simplicity was apparent rather than real.

RESULTS AND DISCUSSION

The apparent partial molar volume for a solute can be determined from the expression

$$[1] \qquad \phi = M_2/d_0 - \frac{1\,000\,(d - d_0)}{d_0\,c},$$

where d and d_0 are densities of solution and solvent at a given temperature, M_2 is the molecular weight of the solute, and c is the concentration in moles/l. The partial molar volume at infinite dilution, $\bar{V}_0$, is obtained by a suitable extrapolation procedure. For ionic solutes, extrapolation usually (19–21) takes the form

$$[2] \qquad \phi = \phi_0 + sc^{1/2}.$$

In the original proposal (19), the coefficient s was empirical and varied with the electrolyte. Redlich has summarized the arguments and evidence in favor of a limiting equation of similar form based on the Debye–Hückel theory where s will have a common value for all electrolytes. As he rightly points out, a failure of the limiting law implies a failure of the Debye–Hückel theory.

However, the validity of eq. [2] has been criticized by several authors. Geffcken and collaborators found that in the range of low concentrations the curve $\phi_t = f(c^{1/2})$ was not linear, but S-shaped (15). Rutskov (22) proposed a modified equation to be used in regions of low concentrations. Stewart (23) further demonstrated that the linear correlation of $\bar{V}_0$ with $c^{1/2}$ is not satisfied by a major part of the data available for strong electrolytes, but the errors in much of the earlier data may exclude this data as valid for use as evidence (21). Bodanszky and Kauzmann (24) observed that the volume change accompanying the ionization of water using a dilatometer is quite different from the value calculated from existing partial molal volume data. It was demonstrated that $d\phi/dc^{1/2}$ was not linearly related to $c^{1/2}$.

A typical set of data for sodium iodide is given in Table I and the corresponding plots of ϕ versus m and $c^{1/2}$ are shown in Fig. 1. Similar sets of data and plots were obtained for each of the salts on which this report is based. It will be noted that the extrapolated value $\bar{V}_0$ for sodium iodide (35.19 ml) is about the same for each plot. The value reported by Owen and Brinkley (25) was 35.10, while that by McInnes and Dayhoff (26) was 35.37 ml as a consequence of much longer extrapolations. Using the Redlich equation we calculated a value of 35.19 ml from their data.

In their recent review of progress in this field during the past 25 years, Redlich and Meyer strongly support the limiting law previously advanced discounting the validity of alternate equations of a similar form on the basis of insufficient accuracy. Current work by Hepler and co-workers (17) shows that data for NaOH and $(CH_3)_4NCl$ approaches the limiting law at low concentrations and, as would be expected, deviates at higher concentrations. While the accuracy of our data is not such as would permit us to contribute to this aspect of the problem, we were unavoidably drawn into it because of our empirical observation that the apparent molar volume of the salts studied by us in the concentration range 0.1–0.01 M showed an unambiguous and consistent linear correlation with concentration rather than some fractional power of c, and d_0 was indistinguishable from d_0^0,

Can. J. Chem. Downloaded from www.nrcresearchpress.com by 210.87.254.42 on 09/05/12
For personal use only.

TABLE I

Apparent molar volume of NaI in H_2O at 25 °C,

$$\phi = \frac{M}{d_0} - \frac{1\,000\,(d-d_0)}{d_0 c}, \quad \frac{M}{d_0} = \frac{149.92}{0.9970471} = 150.364$$

m	c	$\sqrt{c}$	d_0	d_0c	$d - d_0$	$\frac{1\,000\,(d-d_0)}{d_0c}$	ϕ
0.06	0.060235	0.245	1.0039166	0.060057	0.0068695	114.383	35.981
0.05	0.050139	0.224	1.0027717	0.049991	0.0057246	114.514	35.850
0.04	0.040065	0.200	1.0016268	0.039947	0.0045797	114.645	35.719
0.03	0.030015	0.173	1.0004819	0.029926	0.0034348	114.776	35.588
0.02	0.019987	0.141	0.9993369	0.019928	0.0022898	114.905	35.459
0.015	0.014982	0.123	0.9987645	0.014937	0.0017174	114.975	35.389
0.010	0.009982	0.100	0.9981920	0.009952	0.0011449	115.037	35.327
0.008	0.007984	0.089	0.9979630	0.007960	0.0009159	115.061	35.303
0.007	0.006985	0.084	0.9978586	0.006964	0.0008015	115.087	35.277

the density of pure water, within our experimental limits. Correlation with $c^{1/2}$ gave a curved plot which extrapolated to approximately the same $\bar{V}_0$. If we accept the empirical correlation supported by Table II, then

[3] $$d = d_0 + \alpha m$$

and the volume is given by

$$V = \frac{1\,000 + mM}{d_0 + \alpha m},$$

where m is molarity and α an empirical constant.

The apparent molar volume is

$$\phi_2 = \frac{V}{M} - \frac{M}{d_0 + \alpha M} - \frac{(1\,000 + mM)^{\alpha}}{(d_0 + \alpha m)^2}$$

and the partial molar volume of the solute is

[4] $$\bar{V}_0 = \frac{M}{d_0} - \frac{1\,000\,\alpha}{d_0^2}$$

or

$$\bar{V}_0 = \frac{M}{d_0} - \frac{1\,000\,(d-d_0)}{m d_0^2}$$

or

[5] $$\bar{V}_0 = \frac{M}{d_0} - \frac{1\,000\,(d-d_0)}{d_0 c}\left(1 + \frac{\alpha m}{d_0}\right).$$

Since in this investigation $\alpha m/d_0$ is always much smaller than unity, eq. [5] becomes almost identical with eq. [1]; hence we are justified in using eq. [4] to calculate the respective apparent partial molar volumes* presented in Tables II and III. Thus we were able

Because we have used this empirical extrapolation, the apparent partial molar volumes so obtained need not coincide with the limiting values obtained by application of the Redlich–Rosenfeld equation. Were V_0 a fundamental quantity, such as melting point or absolute temperature, this might be disturbing. But when one reflects that even the V_0 based on a Redlich–Rosenfeld extrapolation is a pretty hazy quantity until we have a far better understanding of water and of aqueous solutions of ions, we do not see that the substitution of an extrapolation based on Debye–Hückel considerations offers any particular theoretical advantage and certainly entails practicar disadvantages. Had we chosen to give our values for 0.001 M, or a similar arbitrary concentration, our conclusions would have remained unchanged.

Can. J. Chem. Downloaded from www.nrcresearchpress.com by 210.87.254.42 on 09/05/12
For personal use only.

TABLE II

Ionic partial molar volumes of sulfonates in water using values for $\bar{V}_{ion}$ of $Na^+ = -1.5$ and $K^+ = 8.7$ (26)

Sulfonate	$\bar{V}_0$	Anion	$\bar{V}_0$ for anion
$Na\phi SO_3$	107.73	ϕSO_3^-	109.23
$K\phi SO_3$	117.88		109.18
$NaC_4H_9SO_3$	102.71	$C_4HgSO_3^-$	104.21
$NaCH_3SO_3$	54.95	$CH_3SO_3^-$	56.45
KCH_3SO_3	65.20		56.50

TABLE III

Density equation and partial molar volume in light and heavy water for temperatures between 5 and 25 °C

Salt	Solvent	T (°C)	d	$\bar{V}_0$
NaF	H_2O	25	$0.997073+0.04305\,m$	−1.19
		20	$0.998245+0.044429\,m$	−2.22
		10	$0.999721+0.045587\,m$	−4.34
		5	$0.999988+0.046802\,m$	−5.080
NaF	D_2O	25	$1.10430+0.0501832\,m$	−3.12
		20	$1.105365+0.050950\,m$	−3.71
		15	$1.106012+0.052108\,m$	−4.62
		10	$1.106028+0.052697\,m$	−5.11
		5	$1.105656+0.053989\,m$	−6.19
NaI	H_2O	25	$0.997047+0.11449\,m$	35.19
		20	$0.998239+0.116144\,m$	32.65
		15	$0.999170+0.117196\,m$	33.63
		5	$0.999968+0.119551\,m$	30.37
NaI	D_2O	25	$1.104530+0.124305\,m$	33.84
		20	$1.105414+0.124588\,m$	33.42
		15	$1.105883+0.127167\,m$	31.59
		10	$1.105976+0.128370\,m$	30.61
		5	$1.105603+0.130283\,m$	29.02
$Na\Phi SO_3$	H_2O	25	$0.997140+0.0725785\,m$	107.73
		15	$0.999182+0.0770944\,m$	103.09
		11	$0.999703+0.0782699\,m$	101.89
		8	$0.999825+0.0795332\,m$	100.63
$Na\Phi SO_3$	D_2O	25	$1.104106+0.0748492\,m$	101.77
		15	$1.105316+0.0770444\,m$	99.37
		11	$1.105449+0.0792319\,m$	98.13
		8	$1.105349+0.0801768\,m$	97.37

to obtain apparent partial molar volumes from our density data without facing the problem of whether ϕ should be plotted against $c^{1/2}$, c, or some other function of c. The apparent partial molar volumes in the tables are computed from density data using a least squares program with an IBM computer. Our density data show differences of not more than $1 \times 10^{-5} - 2 \times 10^{-5}$ from the computed lines.

Had our experimental techniques been suited to the exploration of densities at low concentrations with high precision, questions relating to the general problem of partial molal volumes in light and heavy water might have been explored. For the purpose of determining the isotope effect on the partial molar volume, the method of extrapolation was not important; hence the simpler form was adopted without prejudice.

The results of our investigation of the apparent partial molar volume for sodium benzenesulfonate, butanesulfonate, and methanesulfonate and for potassium benzenesulfonate and methanesulfonate at 25 °C are given in Table II. In Table III the density

Can. J. Chem. Downloaded from www.nrcresearchpress.com by 210.87.254.42 on 09/05/12
For personal use only.

equations and apparent partial molar volumes of NaF, NaI, and $NaC_6H_5SO_3$ in light and heavy water are given for temperatures between 5 and 25 °C.

We have been unable to find a value for the partial molar volume of sodium fluoride. Geffcken (27) gives a value of $\bar{V}_0 = 6.6$ ml for KF but this value was determined on the basis of an extrapolation from rather concentrated solutions (1.79–10.722 moles/l).

If we accept the value of $\bar{V}_0$ of -1.5 and 8.7 ml for Na^+ and K^+ respectively (25), the value of $\bar{V}_0$ for F^- from our work would be -0.31 ml compared to the value -2.1 ml derived from the data of Geffcken. This new value would remove the anomaly noted by Mukerjee (28) for the F^-.

The value of $\bar{V}_0$ for sodium iodide is in good agreement with earlier work (26), considering the difference in concentration range studied and method of extrapolation. Hence we accept the values of $\bar{V}_0$ for the sulfonic salts as being precise to 0.1–0.2 ml. There does not appear to have been a previous determination.

The value of $\bar{V}_0$ for the sulfonic ions will have two components characterized by quite different solute–solvent interaction. That surrounding the hydrocarbon will tend to enhance water–water interaction (29) while that about the SO_3^- group will be dominated by ion–water interaction. The presence of the charged group in close proximity to the neutral group will have some effect on the solvation of the latter (30) as will be apparent in the following. If the partial molal volume of methane is taken as 38.2 ml, ref. 31, and that of butane as 83.3 (allowing 15.8 ml. for CH_2, ref. 31, and 83.2 ml. for benzene, ref. 31,) the corresponding values for SO_3^- are 18.5 ml, 19.4 ml, and 26.4 ml respectively.

These results, while of certain intrinsic interest, were incidental to the basic problem of the relative isotope effect arising from the solvation of the fully charged ions and, more particularly, how these differences change with temperature. The necessary data are given in Table III but the significance of these data is more apparent in the plot of apparent partial molar volumes against temperature, Figs. 2–4.

For each of the three salts, the plot for the partial molar volume in D_2O lies below that in H_2O. This is consistent with the accepted hypothesis that the ion breaks down water structure in varying degrees and hence favors a more close-packed structure. D_2O has more structure than H_2O and since the relative molar volumes of the two solvents differ by only 0.1 ml/mole near 5 °C decreasing to 0.04 ml/mole near 60° (32), the overall effect on the more structured D_2O is greater than on H_2O. As the temperature increases it is apparent that the relative effect of the ions on the structure of H_2O relative to D_2O increases in the case of NaF and Na benzenesulfonate but decreases slightly, if at all, for the NaI. This qualitative observation suggests that the fluoride and the sulfonate have a similar overall effect on contiguous water structure which differs from the corresponding effect of sodium iodide. These are tentative conclusions and will require more precise data in order to be established conclusively.

There have been numerous attempts to correlate the radius and charge of ions with the corresponding thermodynamic properties of aqueous solutions. For our purpose, it is sufficient to assume the qualitative description of a primary solvation layer tightly oriented by ion–dipole interaction surrounded by layers of water, in which ion–dipole interaction competes progressively less successfully with water–water interaction and both with the kinetic energy of the individual water molecules. When allowance is made for varying charge density, size and shape of the ions, and the unique properties of water, the diversity of phenomena associated with ionic solvation can be easily compassed, and for the same reasons less easily defined.

Can. J. Chem. Downloaded from www.nrcresearchpress.com by 210.87.254.42 on 09/05/12
For personal use only.

Can. J. Chem. Downloaded from www.nrcresearchpress.com by 210.87.254.42 on 09/05/12
For personal use only.

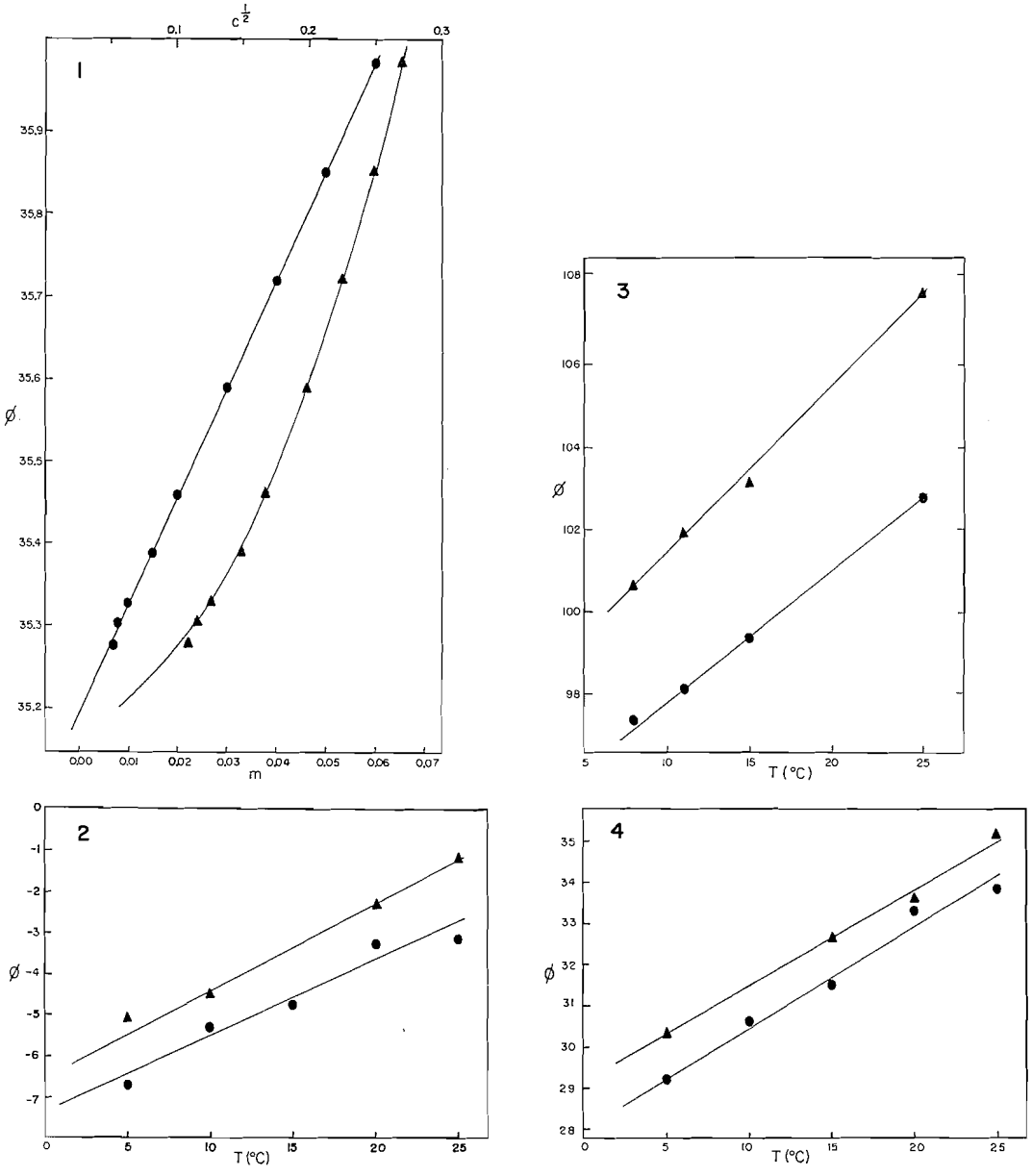


FIG. 1. Apparent partial molar volume of NaI at 25 °C: ▲, versus $c^{1/2}$ (top abscissa scale); ●, versus m (bottom abscissa scale).
FIG. 2. Temperature dependence of apparent partial molar volume of NaF: ▲, in H_2O; ●, in D_2O.
FIG. 3. Temperature dependence of apparent partial molar volume of Na benzenesulfonate: ▲, in H_2O; ●, in D_2O.
FIG. 4. Temperature dependence of apparent partial molar volume of NaI: ▲, in H_2O; ●, in D_2O.

In the lower temperature range where water is most ice-like, $\bar{V}_0$ for many salts first increases with temperature, then decreases (33). Our work is confined to the lower range (5–25 °C), and all $\bar{V}_0$ show an increase with temperature in both H_2O and D_2O. Approximate values of the temperature coefficient of $\bar{V}_0$ in ml/deg are given in Table IV. The

TABLE IV

Approximate values of $d\bar{V}_0/dT$, in the temperature range 5–25 °C, obtained from a least mean square calculation of slopes for Figs. 2–4

	NaF	NaI	Na benzenesulfonate
H_2O	0.198±0.008	0.236±0.013	0.417±0.022
D_2O	0.151±0.009	0.249±0.024	0.259±0.009

value of $d\bar{V}_0/dT$ for sodium iodide is the same as that reported by Eucken (34). One explanation for the increase would be that as the temperature increases there is a decrease in the structure of the water; hence the decrease due to the presence of the ion is reduced and the apparent partial molar volume increases accordingly. This behavior would tend to make the coefficient a function of the size, and there is a slight suggestion of such a trend. But this behavior must be but one of the factors involved, for it would lead to the prediction that $\bar{V}_0^{H_2O} - \bar{V}_0^{D_2O}$ would decrease. Such a trend may occur with NaI only, the tentative value of $d\bar{V}_0/dT$ in that case being greater in D_2O than in H_2O (Table IV). The combination of opposing factors has led some authors to divide ions according to their secondary solvation characteristics in groups designated as "structure breakers" and "structure builders". Whatever detailed significance these terms may have, qualitatively we may conclude that the benzenesulfonic ion appears to be similar to the fluoride, and hence would be considered a strong structure builder.

A question arises as to whether this effect may be attributed to the SO_3^- group or to the phenyl group. If we may judge from the relative constancy with T of the apparent partial molar volume of the methyl halides in water (35), the former must be responsible. This conclusion is consistent with the hypothesis that the solution of the neutral solute in water takes place without evidence of the breaking of water–water bonds (36). The above results provide further evidence that the kinetic solvent isotope effect for the hydrolysis of halides and sulfonates is not the same as that which characterizes the solvation of the product ions. The values of k_{D_2O}/k_{H_2O} for the hydrolysis of fluoride and iodide are very similar, while the value for the sulfonates is about half as large. Here by contrast we find that the fluoride and benzenesulfonate are grouped and the isotope effect for the latter is the largest of the three ions investigated (Na being common throughout). From this observation we may conclude that the factors which determine the kinetic solvent isotope effect are not the same as those determining the solvent isotope effect associated with the solvation of the ions. Davies and Benson (37) reached a similar conclusion from their study of the solvent isotope effect on the enthalpy of solvation of sodium benzenesulfonate in D_2O and H_2O.

REFERENCES

1. F. T. Gucker. Chem. Rev. **13**, 111 (1933).
2. K. Fajans and O. Johnson. J. Am. Chem. Soc. **64**, 668 (1942).
3. A. M. Couture and K. J. Laidler. Can. J. Chem. **34**, 1209 (1956).
4. L. G. Hepler. J. Phys. Chem. **61**, 1426 (1957).
5. R. E. Gibson and O. H. Loeffler. J. Am. Chem. Soc. **63**, 443 (1941).
6. C. G. Swain, R. Cardinaud, and A. D. Ketley. J. Am. Chem. Soc. **77**, 934 (1955).
7. C. G. Swain and R. F. W. Bader. Tetrahedron, **10**, 182 (1960).
8. C. G. Swain and E. R. Thornton. J. Am. Chem. Soc. **84**, 822 (1962).
9. P. M. Laughton and R. E. Robertson. Can. J. Chem. **34**, 1714 (1956).
10. R. E. Robertson and P. M. Laughton. Can. J. Chem. **43**, 154 (1965).
11. R. E. Robertson. Can. J. Chem. **42**, 1707 (1964).
12. J. M. Stuart and F. Wormwell. J. Chem. Soc. 85 (1930).
13. G. R. Robertson. Ind. Eng. Chem. Anal. Ed. **11**, 464 (1939).
14. O. Redlich and J. Bigeleisen. J. Am. Chem. Soc. **64**, 758 (1942).

Can. J. Chem. Downloaded from www.nrcresearchpress.com by 210.87.254.42 on 09/05/12
For personal use only.

15. W. GEFFCKEN, A. KRUIS, and L. SOLANA. Z. Physik. Chem., B, **35**, 317 (1937).
15. H. E. WIRTH, R. E. LINDSTROM, and J. N. JOHNSON. J. Phys. Chem. **67**, 2339 (1963).
17. L. G. HEPLER, J. M. STROKES, and R. H. STOKES. Trans. Faraday Soc. **61**, 20 (1965).
18. G. JONES and S. M. CHRISTIAN. J. Am. Chem. Soc. **59**, 484 (1937).
19. D. O. MASSON. Phil. Mag. **8** (7), 218 (1929).
20. O. REDLICH. J. Phys. Chem. **44**, 619 (1940).
21. O. REDLICH and D. M. MEYER. Chem. Rev. **64**, 221 (1964).
22. A. P. RUTSKOV. Zh. Fiz. Khim. **29**, 463 (1955).
23. G. W. STEWART. J. Chem. Phys. **7**, 381 (1939); **7**, 869 (1939).
24. A. BODANSZKY and W. KAUZMANN. J. Phys. Chem. **66**, 177 (1962).
25. B. B. OWEN and S. R. BRINKLEY. Chem. Rev. **29**, 461 (1941).
26. D. A. MACINNES and M. D. DAYHOFF. J. Am. Chem. Soc. **74**, 1017 (1952).
27. W. GEFFCKEN. Z. Physik. Chem. A, **155**, 1 (1931).
28. P. MUKERJEE. J. Phys. Chem. **65**, 740 (1961).
29. H. S. FRANK and M. W. EVANS. J. Phys. Chem. **13**, 507 (1945).
30. E. D. GODDARD, C. A. J. HOEVE, and G. C. BENSON. J. Phys. Chem. **61**, 593 (1957).
31. W. L. MASTERTON. J. Chem. Phys. **22**, 1830 (1954).
32. K. WIRTZ. Angew. Chem. A, **59**, 138 (1947).
33. M. EIGEN and E. WICKE. Z. Elektrochem. **55**, 334 (1951).
34. A. EUCKEN. Z. Elektrochem. **51**, 6 (1948).
35. H. G. HOLLAND and E. A. MOELWYN-HUGHES. Trans. Faraday Soc. **52**, 297 (1956).
36. D. D. ELEY. Trans. Faraday Soc. **35**, 1281 (1939).
37. D. DAVIES and G. C. BENSON. Can. J. Chem. **43**, 3100 (1965).

Can. J. Chem. Downloaded from www.nrcresearchpress.com by 210.87.254.42 on 09/05/12
For personal use only.

KINETICS AND MECHANISM OF COMPLEX FORMATION BETWEEN ETHYLENE AND RUTHENIUM(II) CHLORIDE IN AQUEOUS SOLUTION[1]

JACK HALPERN
Department of Chemistry, University of Chicago, Chicago, Illinois

AND

BRIAN R. JAMES
Department of Chemistry, University of British Columbia, Vancouver, British Columbia

Received October 8, 1965

ABSTRACT

The formation of a 1:1 π-complex between ethylene and ruthenium(II) in aqueous hydrochloric acid solution is described. The kinetics of the reaction were examined over a range of temperatures and of concentrations of ruthenium(II), ethylene, hydrogen ion, and chloride ion. The results suggest that complex formation proceeds through a stepwise (S_N1) mechanism in which the initial step involves the dissociation of a chlororuthenate(II) complex.

INTRODUCTION

In the course of an investigation of the homogeneous catalytic activation of molecular hydrogen in solution by metal complexes, it was found that chloro complexes of ruthenium(II) were effective catalysts for the hydrogenation of certain olefinic compounds (1). Maleic and fumaric acids were hydrogenated to succinic acid through mechanisms involving 1:1 ruthenium(II)–olefin complexes as catalytic intermediates. Although ethylene itself could not be hydrogenated with this catalyst, aqueous solutions of ruthenium(II) chloride were found to take up ethylene, the extent of the uptake and the accompanying spectral changes being in accord with the formation of a relatively stable 1:1 ruthenium(II)–ethylene complex.

This paper describes a kinetic study of this reaction, apparently the first such study of the formation of a stable metal olefin complex by direct reaction between the metal ion and olefin, uncomplicated by subsequent rearrangement or decomposition of the complex. The fact that the chloro complexes of ruthenium(II) in aqueous solution are not completely characterized imposed certain limitations on the interpretation of the results, but certain features of the mechanism could nevertheless be elucidated.

EXPERIMENTAL

The ruthenium chloride solutions were prepared by dissolving Johnson, Matthey Specpure ammonium aquochlororuthenite[2] in 3 *M* HCl. The spectrum of the resulting solution corresponded to that previously reported for ruthenium(IV) (3, 5). The solution was standardized by reduction with hydrogen to ruthenium(III), using the method of Harrod, Ciccone, and Halpern (2). Ruthenium(II) was generated by the reduction of ruthenium(IV) with an excess of titanium(III) chloride. The spectrum of the blue ruthenium(II) solution agreed with that reported by Jorgensen (6) and by Rechnitz (7).

Ethylene was Matheson Company C.P. grade. Titanium(III) chloride solutions were prepared under a nitrogen atmosphere by dissolving 98.6% $TiCl_3$ (from Stauffer Chemical Co.) in 3 *M* HCl and was stored under nitrogen. The titanium(III) was standardized by titration with ferric ammonium sulfate (8*a*) and by spectrophotometry (9), the two methods yielding consistent results. The chloride ion concentration was determined by the nitrobenzene modification of the Volhard method (8*b*).

Kinetic measurements were made by following the uptake of ethylene at constant pressure using the apparatus and procedure described earlier (10).

[1]*Work performed at the University of British Columbia and supported through grants from the National Research Council of Canada and the Petroleum Research Fund, administered by the American Chemical Society.*

[2]*Although designated* $(NH_4)_2Ru(H_2O)Cl_5$, *this compound is probably* $(NH_4)_2Ru(OH)Cl_5$. *Other workers (2–4) have also reported that commercial "ruthenium(III)" salts consist largely of ruthenium(IV).*

Can. J. Chem. Downloaded from www.nrcresearchpress.com by 210.87.254.40 on 09/05/12
For personal use only.

Can. J. Chem. Downloaded from www.nrcresearchpress.com by 210.87.254.40 on 09/05/12
For personal use only.

RESULTS

Stoichiometry

Blue solutions of ruthenium(II) chloride containing 3 *M* HCl were found to absorb ethylene at conveniently measurable rates in the temperature range 50–65°, the total ethylene uptake corresponding approximately to the number of moles of ruthenium(II) initially present (Fig. 1). The uptake of ethylene was accompanied by disappearance of the blue color of the solution, associated with the absorption band having a maximum at 680 mμ and attributed to $RuCl_4^{2-}$ (6). The final solution was faintly yellow, and its absorption spectrum exhibited a broad shoulder in the region of 360–380 mμ ($\epsilon \sim 200$), on the long wavelength tail of the ultraviolet absorption band.

This complex formation was not readily reversible, the yellow solutions apparently being stable on heating in vacuo. On contact with air the solutions were rapidly oxidized to give the well known spectrum of ruthenium(III) chloride (6). Maleic acid readily displaced the ethylene from the ruthenium(II)–ethylene complex suggesting that the latter is less stable than the ruthenium(II) – maleic acid complex whose formation constant has been determined (1) spectrophotometrically to be $5 \times 10^3\ M^{-1}$ (3 *M* HCl, 20°).

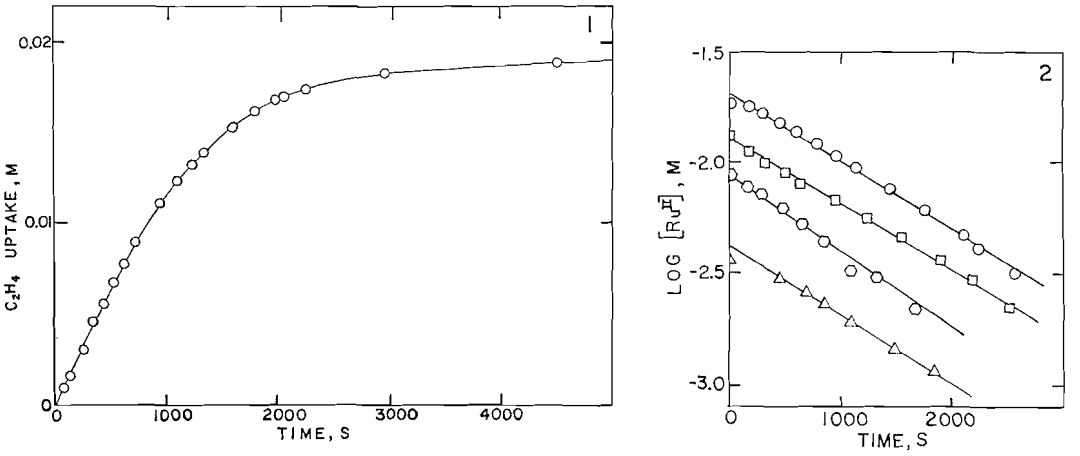


FIG. 1. Uptake of ethylene by a 2.0×10^{-2} *M* Ru^{II} solution at 60° (3.1 *M* HCl; 1.85×10^{-3} *M* C_2H_4).
FIG. 2. First-order rate plots for the uptake of ethylene by solutions of different initial Ru^{II} concentrations (55°; 3.1 *M* HCl; 2.15×10^{-3} *M* C_2H_4).

Kinetics

At constant ethylene and HCl concentrations the uptake of ethylene was found to follow pseudo-first order kinetics, the rate being proportional to the residual concentration of uncomplexed ruthenium(II) (designated as $[Ru^{II}]$), i.e.

$$[1] \qquad -d[Ru^{II}]/dt = k'[Ru^{II}]$$

where the relation

$$[2] \qquad [Ru^{II}] + [Ru^{II}(C_2H_4)] = [Ru^{II}]_{Initial}$$

was used to compute $[Ru^{II}]$ from the observed uptake of ethylene; k' was evaluated from the slopes of first-order plots such as those shown in Fig. 2 (which were generally linear over at least 75% of the reaction) and found to be independent of the initial Ru^{II} concentration when the latter was varied from 3.5×10^{-3} to 1.84×10^{-2} *M*.

Table I summarizes the results of several series of experiments at temperatures ranging from 50° to 65°, in which the ethylene partial pressure was varied to determine the order of the reaction in ethylene. The concentrations of ethylene given in Table I were computed by extrapolating available data (11) for the solubility of ethylene in pure water over the temperature range 0° to 40°, no correction being made for the effect of the ruthenium chloride and hydrochloric acid. The kinetic dependence on the ethylene concentration, revealed by the data in Table I, is complex, corresponding to an apparent order in ethylene of <1; this apparent order decreases with increasing ethylene concentration, the rate tending to approach a limiting value.

TABLE I

Summary of kinetic data (3.1 *M* HCl; 0.1 *M* $TiCl_3$)

Temp., °C	$[Ru^{II}]_{initial} \times 10^2$, *M*	C_2H_4, mm	$[C_2H_4] \times 10^3$, *M*	$k' \times 10^4$, s^{-1}
55	0.35	652	2.15	7.44
	0.875	652	2.15	8.27
	1.32	666	2.19	7.35
	1.84	651	2.15	7.48
50	1.05	670	2.44	4.79
		520	1.89	3.70
		376	1.37	3.03
		204	0.74	1.91
55	1.05	652	2.15	7.85
		494	1.62	7.07
		393	1.29	5.74
		258	0.85	4.29
		142	0.47	2.59
60	1.05	629	1.85	13.9
		436	1.28	11.1
		396	1.17	10.3
		264	0.78	7.67
		148	0.44	4.18
65	1.05	603	1.63	20.9
		403	1.09	16.2
		249	0.67	10.8
		119	0.32	5.63

TABLE II

Kinetic data at 55° (1.05×10^{-2} *M* Ru^{II}; 0.1 *M* $TiCl_3$; 2.2×10^{-3} *M* C_2H_4)

[HCl], *M*	$[Cl^-]_{total}$, *M*	$k' \times 10^4$, s^{-1}	[HCl], *M*	$[Cl^-]_{total}$, *M*	$k' \times 10^4$, s^{-1}
3.10	3.4	7.41	2.48	3.6	9.76
	3.4	8.03	2.15	3.5	9.93
	4.0	7.02	1.60	3.4	10.9
	4.4	6.40	1.60	3.4	11.5
	4.4	5.63	1.07	3.3	14.8
	4.9	4.67	0.53	3.2	16.0
	5.4	4.05			
	5.8	3.30			
	6.4	2.76			

Table II summarizes the results of experiments at 55°, made to determine the dependence of the rate on the concentrations of H^+ and Cl^-. The concentration of H^+ was varied from 0.5 to 3.1 *M* while the Cl^- concentration (and ionic strength) was kept constant at 3.4 *M* with LiCl. The Cl^- concentration was varied from 3.1 to 6.4 *M* by addition of LiCl

Can. J. Chem. Downloaded from www.nrcresearchpress.com by 210.87.254.40 on 09/05/12
For personal use only.

to solutions containing 3.1 *M* HCl. Unfortunately, no suitable inert anion could be found which could be substituted for Cl^- in order to keep the ionic strength constant in these experiments; ClO_4^- which is commonly used for this purpose is rapidly reduced by Ru(II). The results in Table II reveal a marked inverse dependence of the rate on the concentrations of both H^+ and Cl^-.

In all these experiments the Ti(III) added initially to reduce the Ru(IV) to Ru(II) was in at least tenfold excess over the initial Ru(IV) concentration. Providing this excess was maintained or exceeded, the rate was found to be unaffected by the Ti(III) concentration. The Cl^- concentrations listed in Tables I and II include the contribution from the added titanium(III) chloride.

In the absence of ruthenium(II), solutions containing ruthenium(III) or ruthenium(IV) exhibited no reactivity toward ethylene under the conditions of these experiments.

DISCUSSION

The inverse kinetic dependence of the reaction on the Cl^- concentration along with the observation that the rate tends to approach a limiting value with increasing ethylene concentration, suggest that formation of the $Ru^{II}(C_2H_4)$ complex proceeds through a two-step dissociation (S_N1) mechanism of the type,

$$Ru^{II}Cl_n \underset{k_{-1}}{\overset{k_1}{\rightleftarrows}} Ru^{II}Cl_{n-1} + Cl^- \qquad [3]$$

$$Ru^{II}Cl_{n-1} + C_2H_4 \overset{k_2}{\rightarrow} Ru^{II}Cl_{n-1}(C_2H_4). \qquad [4]$$

Assuming the steady state approximation for the intermediate $Ru^{II}Cl_{n-1}$ this mechanism yields the rate-law,

$$\frac{-d[Ru^{II}]}{dt} = \frac{k_1k_2[Ru^{II}Cl_n][C_2H_4]}{k_{-1}[Cl^-]+k_2[C_2H_4]}. \qquad [5]$$

At constant $[Cl^-]$ and $[C_2H_4]$, and assuming $[Ru^{II}] \simeq [Ru^{II}Cl_n]$,

$$k' = k_1k_2[C_2H_4]/(k_{-1}[Cl^-] + k_2[C_2H_4]), \qquad [6]$$

whence

$$\frac{1}{k'} = \frac{1}{k_1} + \frac{k_{-1}[Cl^-]}{k_1k_2[C_2H_4]}. \qquad [7]$$

The linear plots of $1/k'$ versus $1/[C_2H_4]$ at constant $[Cl^-]$, shown in Fig. 3, are in accord with this relation and yield the values of k_1 and $(k_{-1}[Cl^-]/k_2)$ listed in Table III. The values of k_1 are fitted by the Arrhenius relation,

$$k_1 = 2.5 \times 10^{12} \exp(-22\,800/RT) \quad s^{-1} \qquad [8]$$

corresponding to $\Delta S_1^{\ddagger} = -4$ e.u.

While the inverse dependence of k' on the Cl^- concentration, revealed by the data in Table II, is qualitatively in accord with the proposed mechanism, these data do not permit the Cl^- dependence predicted by eq. [7] to be tested quantitatively. The circumstances which preclude this are:

(*a*) the very significant variations in ionic strength, and possibly in the solubility of ethylene, which accompany the variations of the Cl^- concentration due to failure to find a suitably inert anion to substitute for Cl^-, and

(*b*) the effect of varying the Cl^- concentration on the distribution of ruthenium(II)–chloro complexes. Spectral evidence (12), including the observation that the absorbance

Can. J. Chem. Downloaded from www.nrcresearchpress.com by 210.87.254.40 on 09/05/12
For personal use only.

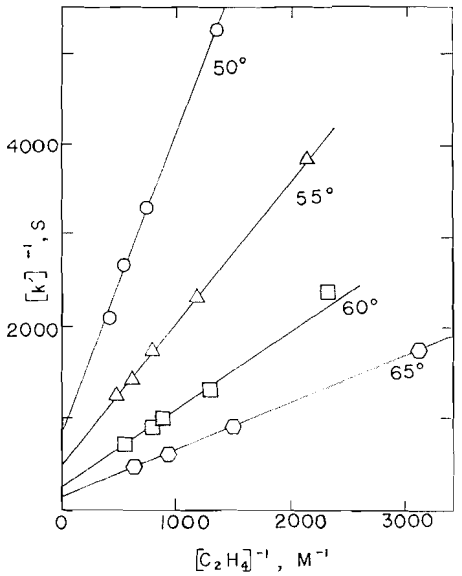


FIG. 3. Dependence of rate on the ethylene concentration plotted in accord with eq. [7] (3.1 *M* HCl).

TABLE III

Effect of temperature on rate constants at 3.1 *M* HCl

Temp., °C	$k_1 \times 10^3$, s^{-1}	$(k_{-1}[Cl^-]/k_2) \times 10^3$, *M*
50	1.2	4.0
55	1.9	2.9
60	3.4	2.8
65	5.7	2.9

at 680 mμ due to the blue complex (believed to be $RuCl_4^{2-}$) decreases as the Cl^- concentration is increased from 3 to 6 *M* indicates that the Cl^- variation examined in the kinetic experiments does affect the distribution of ruthenium(II)–chloro complexes in solution. Unfortunately, the equilibria involved have not thus far been elucidated.

The kinetic expressions deduced from the proposed mechanism also fail to account for the observed inverse dependence of k' on the H^+ concentration (Table III). This may reflect hydrolytic equilibria involving chlororuthenate(II) complexes whose reactivity is enhanced through hydrolysis. Some indication of such hydrolytic processes is also provided by recent observations (13) that at lower acidities (0.03 to 0.3 *M* H^+) chlororuthenate (II) complexes are readily oxidized by water to ruthenium (III), whereas this was not observed at the higher acidities (>0.5 *M* H^+) employed in the present investigation.

Because of these complications, the observed rate constant k', and the derived rate constant k_1, must be considered as composite constants which may reflect contributions from more than one ruthenium(II) complex.

The conclusions of the present investigation are consistent with, and derive some support from, those of a recent investigation (12, 14) of the reaction between ruthenium(II) and formic acid in aqueous hydrochloric acid, to yield a ruthenium(II)–carbonyl complex, in accord with

[9] $$Ru^{II} + HCOOH \rightarrow Ru^{II}(CO) + H_2O.$$

Can. J. Chem. Downloaded from www.nrcresearchpress.com by 210.87.254.40 on 09/05/12
For personal use only.

The rate law for this reaction was found to be analogous to that described above for the reaction between ruthenium(II) and ethylene, suggesting that the two reactions proceed through related mechanisms involving a common step, presumably the dissociative step represented by eq. [3].

REFERENCES

1. J. HALPERN, J. F. HARROD, and B. R. JAMES. J. Am. Chem. Soc. **83**, 753 (1961).
2. J. F. HARROD, S. CICCONE, and J. HALPERN. Can. J. Chem. **39**, 1372 (1961).
3. F. PANTANI. J. Less-Common Metals, **4**, 116 (1962).
4. D. SAWYER, R. GEORGE, and J. BAGGER. J. Am. Chem. Soc. **81**, 5893 (1959).
5. P. WEHNER and J. C. HINDMAN. J. Phys. Chem. **56**, 10 (1052).
6. C. K. JORGENSEN. Acta Chem. Scand. **10**, 518 (1956).
7. G. A. RECHNITZ. Inorg. Chem. **1**, 953 (1962).
8. A. I. VOGEL. A textbook of quantitative inorganic analysis. 3rd ed. John Wiley and Sons, Inc., New York. 1961. (*a*) p. 330. (*b*) p. 266.
9. H. HARTMANN and H. SCHLAFER. Z. Physik. Chem. **197**, 116 (1951).
10. A. J. CHALK and J. HALPERN. J. Am. Chem. Soc. **81**, 5846 (1959).
11. A. SEIDELL. Solubilities of organic compounds. Vol. 2. 3rd ed. D. Van Nostrand Co., Inc., New York. 1961. p. 94.
12. J. HALPERN and A. L. W. KEMP. To be published.
13. G. A. RECHNITZ and H. A. CATHERINO. Inorg. Chem. **4**, 112 (1965).
14. A. L. W. KEMP. Ph.D. Dissertation, The University of Chicago, 1964.

Can. J. Chem. Downloaded from www.nrcresearchpress.com by 210.87.254.40 on 09/05/12
For personal use only.

Can. J. Chem. Downloaded from www.nrcresearchpress.com by 210.87.254.40 on 09/05/12
For personal use only.

THE CLEAVAGE OF PHOSPHORUS TO NITROGEN BONDS WITH HYDROGEN FLUORIDE[1]

R. GREENHALGH AND J. R. BLANCHFIELD
Defence Chemical Biological and Radiation Laboratories, Ottawa, Canada
Received October 13, 1965

ABSTRACT

Dialkyl phosphoramidates and alkyl P–alkylphosphonamidates react with hydrogen fluoride breaking the P—N bond to yield the corresponding fluoridates. This cleavage occurred when the nitrogen was unsubstituted, but the yield of product was increased by methyl substitution on the nitrogen. The reaction with diphenyl N,N-dimethylphosphoramidate was not restricted to the P—N bond, since cleavage of the CO—P bonds took place giving, as the ultimate product, hexafluorophosphoric acid. The results obtained indicate that hydrogen fluoride is the most efficient of the hydrogen halides in cleaving P—N bonds.

The introduction of a fluorine atom into an organophosphorus molecule to form a P—F bond can be accomplished by a variety of fluorinating agents. Treatment of diisopropyl phosphorochloridate with sodium fluoride or ammonium fluoride in anhydrous solvents readily converts it into the phosphorofluoridate (1). Similarly, methylphosphonic difluoride can be prepared by bubbling 2 equivalents of hydrogen fluoride into the corresponding dichloride (2). In this latter reaction attempts to isolate the intermediate, methylphosphonic chlorofluoride, were unsuccessful, indicating that the intermediate is more reactive towards hydrogen fluoride than the dichloride (3). In these laboratories it has been found that isopropyl methylphosphonofluoridate can be prepared by the action of hydrogen fluoride on isopropyl N,N,P-trimethylphosphonamidate in anhydrous conditions. This result, however, appears to be at variance with the results reported for phosphoramidates (4), where hydrogen fluoride was the exception among the hydrogen halides in not cleaving the P—N bond. Consequently, it was decided to investigate further the reaction between hydrogen fluoride and phosphoramidates and two limited series of compounds were studied. The first involved varying the substitution on the nitrogen, and consisted of diisopropyl phosphoramidate and its monomethyl and dimethyl derivatives, whereas the second series, where the substitution on the phosphorus was changed, consisted of the dimethyl derivatives of diisopropyl phosphoramidate, diphenyl phosphoramidate, and isopropyl methylphosphonamidate.

The experiments were performed in carbon tetrachloride solution at room temperature. In both series of phosphoramidates it was found that the P—N bond was readily cleaved by hydrogen fluoride. The yields of diisopropyl phosphorofluoridate from diisopropyl phosphoramidate and the mono- and di-methyl derivatives did not vary in any set pattern, but there was sufficient difference in the yields from the substituted amides (79% and 84%) and the unsubstituted amide (61%) to allow speculation on the factors controlling the reaction. The nature of the P—N bond has been discussed by Clark (5). It was suggested that the bond order is enhanced by overlap of the p-orbital of the lone pair of electrons on the nitrogen atom with the d-orbitals of the phosphorus atom resulting in a reduction of the positive charge on the phosphorus and lower susceptibility to nucleophilic attack. Phosphoramidates are, in fact, stable in basic solution, although primary phosphoramidates are known to form salts by abstraction of a proton from the nitrogen (6).

[1]*Issued as DCBRL Report No. 479.*

However, the cleavage of phosphorus to nitrogen bonds under acidic conditions involves prior protonation of the nitrogen atom (5) and $p\pi$–$d\pi$ overlap becomes less important. The greater ease of reaction of the N-substituted derivatives may, therefore, lie in a higher basicity of the nitrogen atoms resulting from the inductive and hyperconjugative effects of the methyl groups, and we propose that the observed results are better explained by increased formation of protonated intermediate than by decrease in bond strength as suggested by Skrowaczewska and Mastalerz (4).

It is also of interest that hydrogen fluoride cleaves primary, secondary, and tertiary phosphoramidates, whereas the other hydrogen halides apparently cleave only the tertiary derivatives (4). This greater reactivity towards the P—N bond may be attributed to the anhydrous nature of the reaction, since it is well known that pure hydrogen fluoride is one of the most acidic media known (*7a*). It is possible, however, that it might also be related to the strength of the phosphorus–halogen bond that is formed in the various reactions. Of these, the P—F bond is by far the strongest (8).

In the other series, the reaction of diphenyl N,N-dimethylphosphoramidate was of special interest because of the reactions which occurred subsequent to P—N bond cleavage. A proton magnetic resonance spectrum of the crude product indicated that the P—N bond had cleaved, since the N-methyl protons appeared as a singlet, whereas if the nitrogen had still been attached to the phosphorus, a doublet would have resulted. However, the only product that was easily isolated was phenol. A fluorine nuclear magnetic resonance (n.m.r.) spectrum was more revealing, showing the presence of two compounds having P—F bonds. The major product showed a doublet, $J = 960$ c.p.s., and the minor product exhibited another doublet, $J = 715$ c.p.s. The coupling constant of 715 c.p.s. is very unusual and is indicative of hexafluorophosphoric acid (9). Although it proved to be impossible to isolate the major product of this reaction, the minor product could be isolated by extending the reaction time and changing the working-up procedure; and it was shown to be, in fact, hexafluorophosphoric acid.

The facts that the major earlier product showed a doublet in the fluorine n.m.r. spectrum and a triplet in the phosphorus n.m.r. spectrum and that the yield of phenol was insufficient for the cleavage of both the phenyl ester bonds led to the postulation that this product was phenyl phosphorodifluoridate. The cleavage of the CO—P bond by hydrogen fluoride was unexpected, since there had been no evidence of the production of isopropanol from the amides of diisopropyl phosphoric acid or any report of the formation of phenol in the conversion of diphenyl N,N-dimethylphosphoramidate to diphenyl phosphorochloridate with hydrogen chloride (10). It is, however, reminiscent of the reaction of hydrogen fluoride with methylphosphonyldichloride (3). Since the P—N bond is cleaved so readily in the case of the other phosphoramidates, it is assumed that this is the bond which breaks first in diphenyl N,N-dimethylphosphoramidate followed by production of 1 molecule of phenol to give the postulated intermediate, phenyl phosphorodifluoridate. The mechanism by which this compound is converted to hexafluorophosphoric acid is unknown, since no other compounds were isolated from the reaction. However, many phosphorus compounds, including phosphorus oxyfluoride, are known to react with hydrogen fluoride to give this acid (*7b*) and it seems probable that this is an intermediate in the formation of hexafluorophosphoric acid from diphenyl N,N-dimethylphosphoramidate.

Summarizing, phosphoramidates and phosphonamidates were found to react with hydrogen fluoride under anhydrous conditions to form fluoridates. The yield of the product appeared to increase with increasing methyl substitution on the nitrogen, a fact attributed to ease of formation of the protonated intermediate. The ability of hydrogen fluoride to

Can. J. Chem. Downloaded from www.nrcresearchpress.com by 210.87.254.40 on 09/05/12
For personal use only.

cleave N-substituted and unsubstituted amidates is in contrast to that of the other hydrogen halides which cleave only the N,N-disubstituted derivatives (4).

EXPERIMENTAL

The infrared spectra were recorded on a Perkin-Elmer 221-G spectrophotometer and the n.m.r. spectra on a Varian V4300C spectrometer operating at 60 mc/s for protons, 24.288 mc/s for ^{31}P and at 56.445 mc/s for ^{19}F. Extreme care was necessary in handling the cleavage products because of their high toxicities.

The amidates were prepared by the action of the appropriate amine on the phosphorochloridate or phosphonochloridate by the methods of McCombie *et al.* (11), and Coe *et al.* (12) respectively. They were characterized by their infrared and proton magnetic resonance spectra and by their melting or boiling points: diisopropyl phosphoramidate, m.p. 55–56° (lit. (13) 56–57°); diisopropyl N-methylphosphoramidate, b.p. 76° at 0.05 mm (lit. (14) 84° at 0.4 mm); diisopropyl N,N-dimethylphosphoramidate, b.p. 61° at 1 mm (lit. (14) 68° at 2 mm); diphenyl N,N-dimethylphosphoramidate, m.p. 30–31° (lit. (15) 30–32°); isopropyl trimethylphosphonamidate, b.p. 75° at 6 mm (lit. (12) 43° at 0.04 mm).

Cleavage of Diisopropyl N-Methylphosphoramidate with Hydrogen Fluoride

Diisopropyl N-methylphosphoramidate (2 g) was dissolved in carbon tetrachloride (10 ml) in a Teflon bottle which was kept at room temperature by cooling in a water bath. The bottle was connected via a trap to a cylinder of anhydrous hydrogen fluoride by a small bore Teflon tube (i.d. 1 mm) and a similar tube was used to lead off the effluent gas. After the system was swept with dry nitrogen gas, a brisk stream of hydrogen fluoride was passed through the solution and within a few minutes an oil separated. The flow of hydrogen fluoride was continued for a total of 17 min. No attempt was made to meter the hydrogen fluoride, whose solubility in carbon tetrachloride is 0.94% at 23°. After the flow of hydrogen fluoride was stopped, the system was again swept with dry nitrogen and then neutralized by adding a solution of triethylamine (2 ml) in chloroform (35 ml). The solution was then washed with 5% sodium bicarbonate solution, dried, and distilled, giving diisopropyl phosphorofluoridate, b.p. 57° at 3 mm (lit. (1) 73° at 16 mm), 1.58 g (yield 84%). The product was identified by means of its infrared and n.m.r. spectra which were identical with those of an authentic sample. Infrared (film): 1 298 cm^{-1}, P=O; 1 180, 1 140, and 1 105 cm^{-1}, $(CH_3)_2CHOP$; 1 013 cm^{-1}, P—OC; and 860 cm^{-1}, P—F. The proton magnetic resonance spectrum in carbon tetrachloride solution showed a doublet centered at $\tau = 8.63$ (isopropyl CH_3) and an octet centered at $\tau = 5.30$ (isopropyl CH) with $J_{P-CH} = J_{CH-CH_3} = 6.2$ c.p.s.

Cleavage of Diisopropyl N,N-Dimethylphosphoramidate with Hydrogen Fluoride

Similar treatment of diisopropyl N,N-dimethylphosphoramidate (2 g) with hydrogen fluoride yielded diisopropyl phosphorofluoridate, 1.38 g (79% yield), which was again identified by its infrared and n.m.r. spectra.

Cleavage of Diisopropyl Phosphoramidate with Hydrogen Fluoride

Prior to reaction, diisopropyl phosphoramidate (2 g) was dissolved in carbon tetrachloride which was then distilled off to remove any traces of water from the starting material. The product isolated after treatment with hydrogen fluoride was identified by spectral methods as diisopropyl phosphorofluoridate, 1.25 g (61% yield).

Cleavage of Isopropyl Trimethylphosphonamidate with Hydrogen Fluoride

Isopropyl trimethylphosphonamidate (2 g) on treatment with hydrogen fluoride as above yielded isopropyl methylphosphonofluoridate, b.p. 46° at 10 mm (lit. (16) 46° at 8 mm), 1.37 g (81% yield). The product was identified by comparison of its infrared and n.m.r. spectra with those of an authentic sample. Infrared (film): 1 315 cm^{-1}, P—CH_3; 1 277 cm^{-1}, P=O; 1 180, 1 142, and 1 105 cm^{-1}, $(CH_3)_2CHOP$; 1 015 cm^{-1}, P—OC; and 838 cm^{-1}, P—F. The proton magnetic resonance spectrum in carbon tetrachloride solution showed a doublet at $\tau = 8.63$ (isopropyl CH_3) with $J_{CH_3-CH} = 6.15$ c.p.s. and a double doublet centered at $\tau = 8.45$ (CH_3P) with $J_{CH_3-F} = 5.5$ c.p.s. and $J_{CH_3-P} = 18.7$ c.p.s.

Reaction of Diphenyl N,N-Dimethylphosphoramidate with Hydrogen Fluoride

With the apparatus described above, hydrogen fluoride was bubbled through a solution of diphenyl N,N-dimethylphosphoramidate (9.8 g) in carbon tetrachloride (25 ml) for 2.5 h and the solution swept with dry nitrogen for a further 1.5 h. Potassium hydroxide solution (2 *N*) (100 ml) was then added and the aqueous layer separated and concentrated to 10 ml. The crystals which precipitated on cooling were recrystallized from water and dried over phoshorus pentoxide to give potassium hexafluorophosphate, 3.67 g (56% yield). The phosphorus and fluoride n.m.r. spectra and an X-ray powder pattern were identical with those obtained from an authentic sample prepared by the method of Woysie (17). The phosphorus n.m.r. spectrum in D_2O solution showed a septet centered at 145.4 p.p.m. upfield from 85% phosphoric acid with $J_{P-F} = 711$ c.p.s., and the fluorine spectrum exhibited a doublet centered at 6.9 p.p.m. downfield from trifluoracetic acid. The X-ray diffraction pattern with a cobalt source, = 1.78890 Å, gave the following lines: 4.5 (s), 3.87 (vs), 2.75 (s), 2.34 (m), 2.24 (m), 1.94 (w), 1.74 (m), 1.59 (m), 1.38 (w), 1.30 (m), 1.23 (w), 1.17 (w), 1.08 (w), and 1.04 (vw).

Can. J. Chem. Downloaded from www.nrcresearchpress.com by 210.87.254.40 on 09/05/12
For personal use only.

The aqueous solution remaining after removal of the crystals was saturated with carbon dioxide when an oil separated which was removed by extraction with ether. The ether layer was dried and distilled to give phenol, b.p. 181°, 3.62 g (yield 55%), which later crystallized and had an infrared spectrum identical with that of an authentic sample.

ACKNOWLEDGMENTS

The authors wish to thank Miss P. A. Lutley for determining the n.m.r. spectra, Miss J. A. Rodgers for the infrared spectra, and Mr. L. G. Wilson for the X-ray powder pattern. We are also grateful to Dr. R. M. Heggie and Dr. M. A. Weinberger for helpful discussions.

REFERENCES

1. B. C. Saunders and G. J. Stacey. J. Chem. Soc. 695 (1948).
2. T. D. Dawson and K. C. Kennard. J. Org. Chem. **22**, 1671 (1957).
3. F. W. Hoffmann and A. M. Reeves. J. Org. Chem. **26**, 3040 (1961).
4. Z. Skrowaczewska and P. Mastalerz. Roczniki Chem. **29**, 415 (1955).
5. V. M. Clark. Proc. Chem. Soc. 129 (1964).
6. A. N. Pudovik and G. P. Krupnov. J. Gen. Chem. USSR Eng. Transl. **33**, 1612 (1963).
7. (*a*) J. H. Simons. *In* Fluorine chemistry. *Edited by* J. H. Simons. Academic Press, New York. 1950. Chap. 6.
   (*b*) W. Lange. *In* Fluorine chemistry. *Edited by* J. H. Simons. Academic Press, New York. 1950. Chap. 3.
8. S. B. Hartley, W. S. Holmes, J. K. Jaques, M. F. Mole, and J. C. McCoubrey. Quart. Rev. London, **17**, 216 (1963).
9. H. S. Gutowsky, D. W. McCall, and C. P. Slichter. J. Chem. Phys. **21**, 279 (1953).
10. Z. Skrowaczewska and P. Mastalerz. Roczniki Chem. **27**, 443 (1953).
11. H. McCombie, B. C. Saunders, and G. J. Stacey. J. Chem. Soc. 380 (1945).
12. D. G. Coe, B. J. Perry, and E. S. Sherwood. J. Org. Chem. **24**, 1018 (1959).
13. F. R. Atherton, H. T. Openshaw, and A. R. Todd. J. Chem. Soc. 660 (1945).
14. J. W. Maarsen, M. C. Smit, and J. Matze. Rec. Trav. Chim. **76**, 713 (1957).
15. A. Kovache, H. Jean, and G. Garnier. Chim. Ind. Paris, **64**, 287 (1950).
16. P. J. R. Bryant, A. H. Ford-Moore, B. J. Perry, A. W. H. Wardrop, and T. F. Watkins. J. Chem. Soc. 1553 (1960).
17. M. M. Woysie. *In* Inorganic synthesis. Vol. 3. *Edited by* L. F. Audrieth. McGraw-Hill, New York. 1950. p. 111.

Can. J. Chem. Downloaded from www.nrcresearchpress.com by 210.87.254.40 on 09/05/12
For personal use only.

THE THERMAL DECOMPOSITION OF ETHANE

PART I. INITIATION AND TERMINATION STEPS

M. C. LIN AND M. H. BACK
Chemistry Department, University of Ottawa, Ottawa, Canada

Received August 27, 1965

ABSTRACT

The rates of production of methane and butane in the pyrolysis of ethane have been measured over the temperature range 550–620 °C and at pressures of 40–600 mm. At high pressure the rates of formation of both products were first order in ethane, but below 200 mm the first-order rate coefficients decreased. The ratio of methane to butane was consistent with the interpretation that methane is a measure of the initiation reaction and that the combination and disproportionation of ethyl radicals is the main termination step. The order of the decomposition of the ethyl radical with respect to ethane varied between 0.38 and 0.59. The results are discussed in terms of the mechanism of the overall process.

INTRODUCTION

The initiation and termination steps in the chain decomposition of ethane have been the subject of much controversy. There is general agreement that the rate is first order with respect to ethane and that hydrogen atoms and ethyl radicals are the chain carriers. The mechanisms proposed generally include the following reactions.

[1] $$C_2H_6 \rightarrow 2CH_3$$

[2] $$CH_3 + C_2H_6 \rightarrow CH_4 + C_2H_5$$

[3] $$C_2H_5 \rightarrow C_2H_4 + H$$

[4] $$H + C_2H_6 \rightarrow H_2 + C_2H_5$$

[5*a*] $$C_2H_5 + C_2H_5 \rightarrow C_4H_{10}$$

[5*b*] $$\rightarrow C_2H_4 + C_2H_6$$

[6] $$H + C_2H_5 \rightarrow C_2H_6$$

[7] $$CH_3 + C_2H_5 \rightarrow C_3H_8$$

Rice and Herzfeld (1) pointed out that termination by reaction [6] would lead to first-order kinetics, as observed. Küchler and Theile (2), however, showed that the rate was increased on addition of inert gases and suggested that the initiation step was a second-order process and that termination occurred by the combination of ethyl radicals. This mechanism also gave first-order kinetics. In an experimental and theoretical examination of the problem, Laidler and Wojciechowski (3) concluded that the Küchler–Theile mechanism was more consistent with the evidence then available. For example, the concentration of ethyl radicals was shown to be much greater than that of hydrogen atoms (4) so that termination by combination of ethyl radicals should predominate. Also, the Küchler–Theile mechanism predicted an activation energy for the decomposition close to that observed, and a change in the order of the decomposition to 3/2 in the regions of temperature and pressure in which this change was found.

More recently, however, several investigations of the initial rate of formation of methane (5–8) have shown that this reaction is first order with respect to ethane, indicating that the initiation step is a first-order process. This fact has been reconciled with the other evidence in various ways. Davis and Williamson (6), whose experiments were done in a flow system at high temperatures (676–775 °C), found that the rate of formation

Can. J. Chem. Downloaded from www.nrcresearchpress.com by 210.87.254.5 on 09/05/12
For personal use only.

of methane was slightly pressure-dependent. They favored the combination of ethyl radicals as the chain-ending step and suggested that the pressure sensitivity of both the initiation step and the decomposition of the ethyl radical combined to give first-order kinetics, which were, at any rate, only roughly obeyed under their conditions. Quinn (7) made this suggestion more specific by proposing that when the overall rate and the rate of production of methane were exactly first order, the rate constant for decomposition of the ethyl radical should be proportional to the square root of the pressure. Evidence from a previous study of the pyrolysis of *n*-butane (9) supported this view. Gordon (8) found a considerable surface dependence of the rate and suggested that one of the termination reactions was heterogeneous. This probably involved hydrogen atoms, because of their high diffusion coefficient.

The present experiments were undertaken to measure the rate of production of butane and, by a comparison with the rate of production of methane, to establish whether this is the main termination product.

EXPERIMENTAL

Apparatus

The decomposition was studied in a conventional static system. The reaction vessel was a quartz sphere of 511.5 cc with S/V ratio of 0.6 cm^{-1} enclosed in an electrically heated steel cylinder about 2 cm thick. The temperature of the vessel was controlled with a Thermoelectric thermoregulator. When evacuated the temperature could be maintained within 0.2° but because of fluctuations in temperature on admission of reactant, especially at high pressures, the temperature during an experiment was precise only to 0.5°. A reaction vessel packed with silica tubes was used to increase the S/V ratio to 9.4 cm^{-1}, an increase of 15 times that of the unpacked vessel. Both vessels were treated with hot nitric acid followed by several washings with distilled water. Gases to be mixed prior to decomposition were condensed into a large flask on an inner-sealed cold finger. When the finger was warmed rapidly the gases were mixed by convection.

Reagents

Phillips Research Grade ethane was distilled from trap-to-trap several times and finally degassed at −160 °C.

Procedure and Analysis

Before each experiment the system was evacuated to a pressure lower than 10^{-4} mm. At the end of an experiment the products and reactant were removed through a series of traps, which were, in order, a spiral trap, a Le Roy still, a conventional trap, and a final spiral trap, followed by a Toepler pump and gas burette. A mercury diffusion pump between the last two traps aided collection of the non-condensable gases. Initially all traps were cooled with liquid nitrogen. When most of the non-condensable gases had been collected in the gas burette, the first spiral trap was warmed to room temperature and the Le Roy still was warmed to −162 °C. Final traces of occluded non-condensable gases were then collected while most of the ethane distilled into the conventional trap. Butane remained in the Le Roy still and was analyzed by gas chromatography on a 12 ft column of hexanedione on Firebrick maintained at 0 °C. Careful checks of the distillation showed that losses of butane were never more than 10% and could be reliably corrected for. In experiments with carbon dioxide, an additional trap filled with ascarite removed the carbon dioxide before condensation in the Le Roy still.

The mixture of methane and hydrogen collected in the gas burette was analyzed by combustion of hydrogen in a copper oxide furnace maintained at 280 °C. Attempts to separate ethylene from the non-condensable gases by using a trap packed with copper filings maintained at −196 °C resulted in loss of methane, and the packing was finally abandoned. Instead, traces of ethylene were collected in the Toepler pump with the hydrogen and methane, but the gases were admitted to the combustion furnace through a liquid nitrogen trap. The concentration of ethylene in the furnace was then negligible. When combustion of hydrogen was complete the gases were expanded into the large bulb of the Toepler pump, isolated from the combustion furnace, and measured in the gas burette. An amount of ethylene equivalent to the saturated vapor pressure at −196 °C in the Toepler bulb was thus collected in the gas burette, and correction for this amount was made to the final measurement of methane. This correction was not more than 10% of the amount of methane. The yield of hydrogen was obtained by subtracting the yield of methane from the total non-condensable gases.

RESULTS

The yields of hydrogen, methane, and butane were measured as a function of reaction time over the temperature range 550–620 °C and the pressure range 40–600 mm. The

Can. J. Chem. Downloaded from www.nrcresearchpress.com by 210.87.254.5 on 09/05/12
For personal use only.

measurements of hydrogen and methane were extended to the range 640–726 °C over a lower pressure range. Initial rates of hydrogen production were obtained by extrapolation of plots of the rate against time. From 400 to 150 mm the order of hydrogen production was 1.0. At higher pressures a slight decrease in order was observed, while at lower pressures the order increased. This continuous change in order of the hydrogen production is shown in Fig. 1, in which the complete temperature range is represented. The first-order rate constant could be represented by the following expression.

$$\log k\ (s^{-1}) = (16.22 \pm 0.11) - \frac{77\,600 \pm 600}{2.303RT}$$

Typical plots of methane yield as a function of time are shown in Fig. 2. The rate of production of methane was constant only in the initial stages of the decomposition and increased at all temperatures as secondary reactions became important. The initial rate was not obtained directly from plots such as Fig. 2, but from an extrapolation to

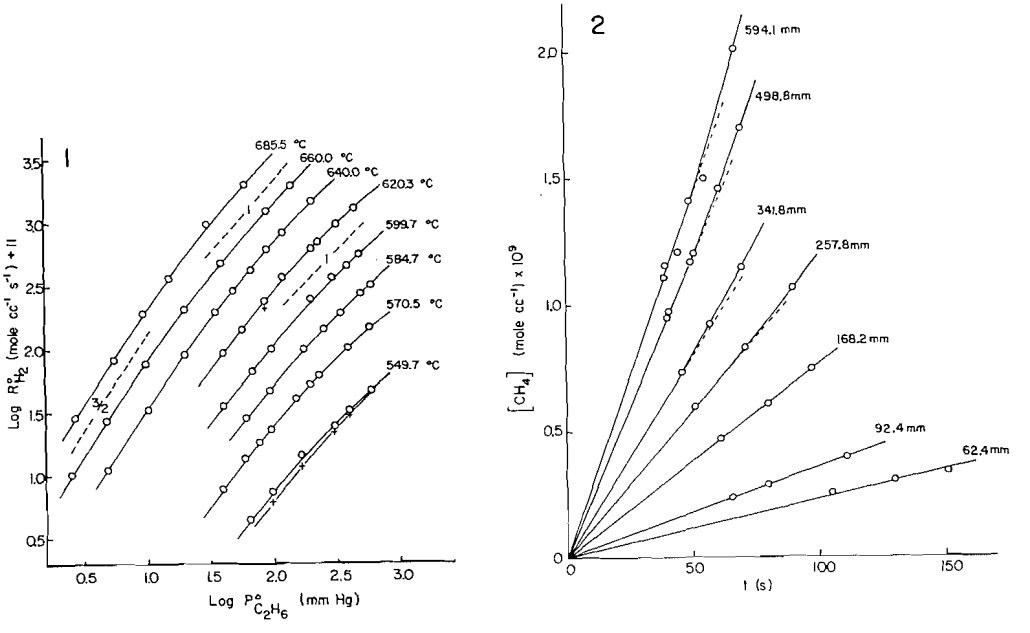


FIG. 1. Log rate of hydrogen production against log ethane pressure: O, for unpacked vessel; +, for packed vessel.
FIG. 2. Yield of methane as a function of time at 584.7 °C.

zero time of the rate as a function of time. This procedure, which is described in Part III (23), was particularly important at high temperatures where secondary reactions occur at very low conversions. The order of the rate of production of methane with respect to ethane was 1.0 above ~200 mm and is illustrated in Fig. 3. The falloff in the first-order rate coefficient is discussed in detail in Part II (23). First-order rate constants were calculated from the equation

$$k_1 = \frac{\frac{1}{2}R^0_{CH_4}}{[C_2H_6]}$$

Can. J. Chem. Downloaded from www.nrcresearchpress.com by 210.87.254.5 on 09/05/12
For personal use only.

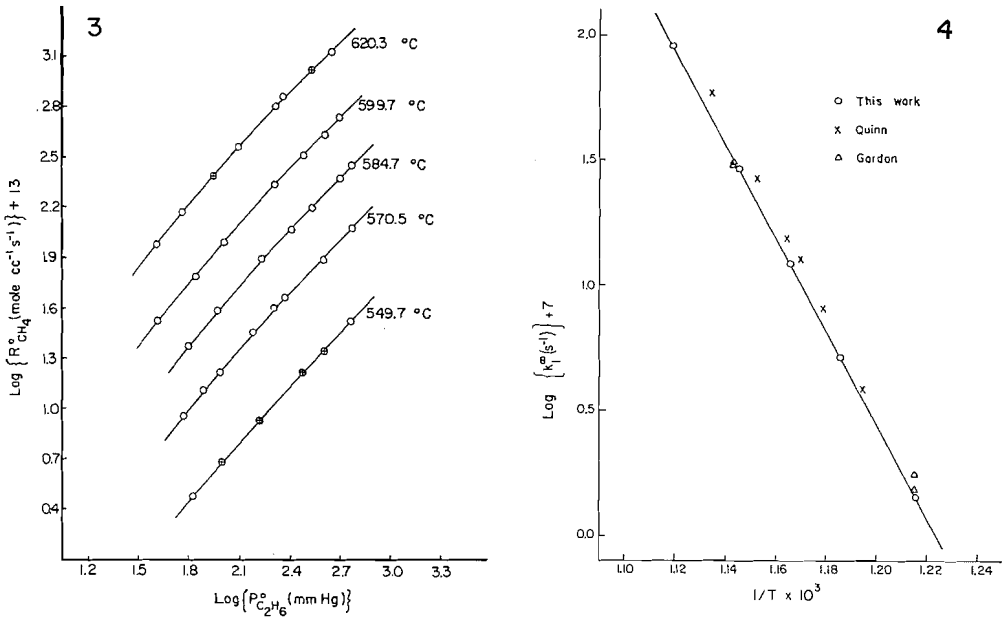


FIG. 3. Log rate of methane production against log ethane pressure: ○, for unpacked vessel; +, for packed vessel.

FIG. 4. Arrhenius plot of first-order rate constant, k_1^{∞}, for rate of methane production: ×, ref. 8; △, ref. 9; ○, present results.

and are listed in Table I. The Arrhenius plot of the first-order constants is shown in Fig. 4 together with the measurements of Quinn (7) and Gordon (8). The following relation was found.

$$\log k_1\ (s^{-1}) = (16.00 \pm 0.066) - \frac{86\,000 \pm 370}{2.303RT}$$

At low temperatures the kinetics of butane production followed a similar pattern to that of methane production, the rate increasing from the initial value at about the same conversion. At 585 °C and above the rate decreased as the reaction time increased. Typical plots of yield as a function of time are shown in Fig. 5. Again, initial yields were obtained by extrapolation of rate vs. time curves. The order of butane production was 1.0 at high pressures but increased as the pressure was lowered. The double logarithmic plot is shown in Fig. 6. The Arrhenius plot of the first-order rate constants gave an activation energy of 89.8 kcal/mole.

The ratio $\frac{1}{2}R^0_{CH_4}/R^0_{C_4H_{10}}$ varied from 1.3 to 1.8 and is included in Table I. If methane is a measure of the initiation step and butane of the termination step and if the ratio of disproportionation to combination for ethyl radicals is 0.15 (10), then the ratio $\frac{1}{2}R^0_{CH_4}/R^0_{C_4H_{10}}$ is 1.15.

If hydrogen is formed only by reactions [3] and [4] and butane only by combination of ethyl radicals then

$$\frac{R^0_{H_2}}{(R^0_{C_4H_{10}})^{1/2}} = \frac{k_3}{k_{5a}^{1/2}}.$$

A plot of log $\{R^0_{H_2}/(R^0_{C_4H_{10}})^{\frac{1}{2}}\}$ against log $[C_2H_6]$ is shown in Fig. 7. If it is assumed that k_{5a} is independent of pressure, the slopes of these curves give the order of reaction

Can. J. Chem. Downloaded from www.nrcresearchpress.com by 210.87.254.5 on 09/05/12
For personal use only.

TABLE I

First-order rate coefficients for rate of methane production in units of s^{-1}

T (°C)	$P^0_{C_2H_6}$ (mm Hg)	$\frac{R^0_{CH_4}}{2[C_2H_6]_0}$	$\frac{R^0_{CH_4}}{2R^0_{C_4H_{10}}}$
549.7	592.8	1.43	1.35
	401.5	1.44	1.59
	299.7	1.41	1.53
	164.7	1.34	1.57
	97.4	1.28	1.72
	67.3	1.15	1.55
570.5	590.5	5.48	1.67
	400.0	5.19	1.55
	236.0	5.12	1.73
	199.7	5.13	1.61
	153.4	4.92	1.62
	96.0	4.63	1.80
	78.3	4.50	1.68
	59.4	3.96	1.63
	40.1	—	—
584.7	594.1	12.7	1.44
	498.8	12.7	1.44
	341.8	12.5	1.46
	257.5	12.3	1.46
	168.2	12.5	1.51
	92.4	11.4	1.48
	62.4	10.4	1.63
599.7	500.6	29.5	1.40
	402.1	29.3	1.40
	298.9	29.6	1.49
	203.1	29.1	1.59
	99.9	26.7	1.69
	68.4	24.6	1.76
	41.0	22.4	2.15
620.3	448.3	88.8	1.18
	335.6	89.7	1.23
	236.1	89.9	1.27
	209.8	84.3	1.20
	124.5	83.9	1.47
	87.6	78.2	1.43
	57.9	73.1	1.63
	40.7	66.5	1.76

[3] with respect to ethane. This varied from 0.38 at low temperatures and high pressures to 0.59 at high temperatures and low pressures. The activation energy for the decomposition of the ethyl radical, if the combination of ethyl radicals involves no activation energy, is 32.7 ± 1.5 kcal/mole. No trend was observed with pressure.

Rates of hydrogen, methane, and butane production were measured at 585 °C in the presence of various pressures of carbon dioxide. On addition of 100 mm of carbon dioxide to 100 mm of ethane, the rates of methane and butane production were unchanged but the rate of hydrogen production increased by about 20%.

Rates of formation of products measured using the packed reaction vessel are compared with those from the unpacked vessel in Figs. 1, 3, 6, and 7. The rate of methane production was unaffected by the increase in S/V ratio, but the yields of both butane and hydrogen decreased. The effect was greatest at the lower temperatures and pressures, as would be expected for a surface reaction. The order of both butane and hydrogen production increased slightly.

Can. J. Chem. Downloaded from www.nrcresearchpress.com by 210.87.254.5 on 09/05/12
For personal use only.

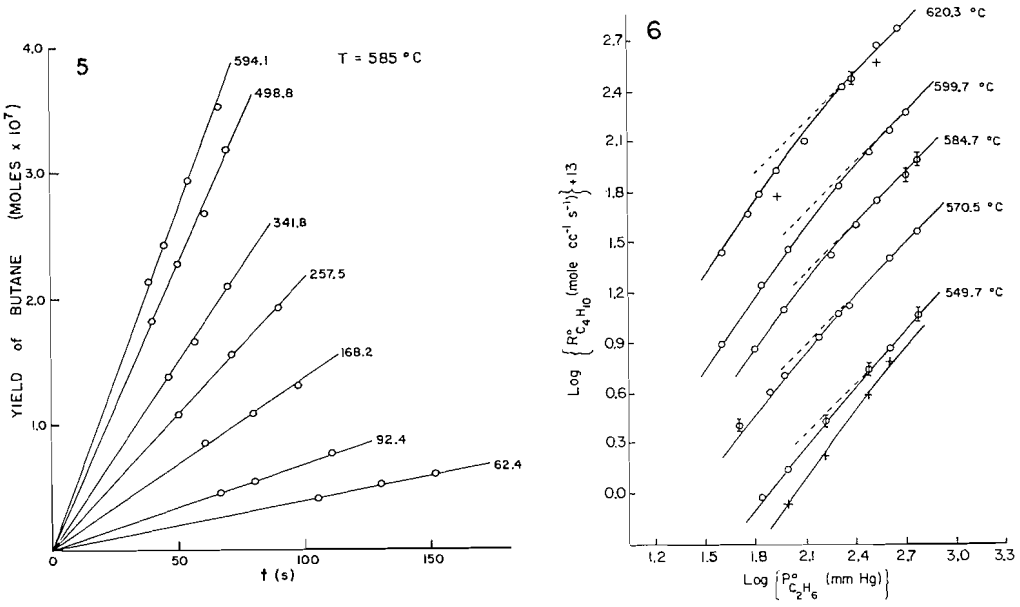


FIG. 5. Yield of butane as a function of time at 585 °C.
FIG. 6. Log rate of butane production against log ethane pressure: O, for unpacked vessel; +, for packed vessel.

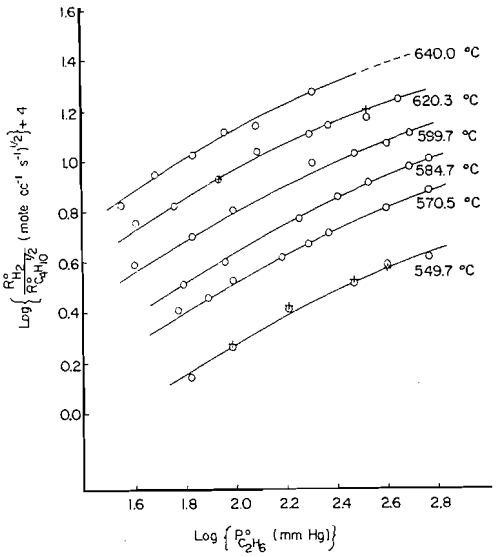


FIG. 7. Plot showing order with respect to ethane of the decomposition of the ethyl radical: O, unpacked vessel; +, packed vessel.

DISCUSSION

The present results largely confirm the mechanism of the decomposition proposed by Davis and Williamson (6) and by Quinn (7). In particular, the measurement of the production of butane supports the combination of ethyl radicals as the main termination step.

Can. J. Chem. Downloaded from www.nrcresearchpress.com by 210.87.254.5 on 09/05/12
For personal use only.

We have assumed that the initial decomposition of the ethane molecule occurs by the rupture of the C—C bond to give two methyl radicals. An alternative mode of initiation to give methane and a methylene radical has been suggested (11)

[1a] $$C_2H_6 \rightarrow CH_4 + CH_2$$

but from the present results this appears less likely than reaction [1]. In the subsequent reaction of the methylene radical with ethane, the excited molecule of propane formed would either be stabilized or dissociate into radical fragments, probably $CH_3 + C_2H_5$. By comparison with the reaction of methylene radicals with methane (12), it may be deduced that stabilization would be dependent on pressure in the range of the present experiments. If some of the "hot" propane formed is stabilized, then methane is formed without the production of an ethyl radical and hence without the formation of butane. This would give a high ratio of methane to butane, as actually found, but would show a marked increase with increasing pressure, whereas the observed ratio decreased as the pressure increased. It is very unlikely that formation of propane by reaction of methylene with ethane would be independent of pressure in the range covered by the present experiments. Reaction [1a] must therefore be at most only a minor mode of dissociation of the ethane molecule.

The rate of production of methane is a measure of the rate of reaction [1] only if all methyl radicals react with ethane and none are lost by termination. The most likely termination step involving methyl radicals is reaction [7] and the relative rates of reaction [2] and [7] may be calculated from the following equation.

$$\frac{\text{Rate [7]}}{\text{Rate [2]}} = \frac{k_7(R^0_{C_4H_{10}})^{1/2}}{k_{5a}^{1/2}k_2[C_2H_6]}$$

Inserting the values $k_2 = 10^{11.20}\,e^{-10400/RT}$ (13), $k_{5a} = 2.0 \times 10^{13}$ (14), and $k_7 = 4 \times 10^{13}$ in the units cc mole^{-1} s^{-1}, we obtain for 100 mm ethane $R_7/R_2 = 5.0 \times 10^{-3}$ at 550 °C and 2.8×10^{-2} at 620 °C. The temperature coefficient of k_5 has been ignored in these and later calculations because of the uncertainty involved in the long extrapolation. These ratios are therefore upper limits since an activation energy of 2 kcal/mole causes an increase in k_5 of almost a factor of 10 at 550 °C. In the present experiments it is thus unlikely that methyl radicals are involved in termination, and the first-order production of methane shows that the dissociation of ethane into two methyl radicals is a first-order process above about 200 mm in the temperature range 550–620 °C.

In Fig. 4 the Arrhenius plot of k_1 is compared with two recent measurements in the same temperature range. The absolute values for k_1 agree very well at temperatures in the neighborhood of 570 °C, but some divergence at the higher and lower ranges caused a considerable deviation in the activation energies. We feel that the method of extrapolation which was used in the present experiments at each pressure and temperature to obtain the initial rate of methane production gives rate constants more reliable than those obtained by Quinn, and that his activation energy is consequently too high.

The errors quoted in the present results are the probable errors obtained by a least-squares analysis of the data. The systematic errors are undoubtedly much larger, but because of the difficulty in estimating these quantitatively we have not attempted to state the total error limits. Recent measurements of the Arrhenius parameters of k_1 are summarized in Table II.

Can. J. Chem. Downloaded from www.nrcresearchpress.com by 210.87.254.5 on 09/05/12
For personal use only.

TABLE II

Arrhenius parameters of k_1

Reference	Temp. range (°C)	log A (s^{-1})	E (kcal/mole)
(5)	766–836	14.85–15.7	85–89
(6)	675–770	16.29	86.0
(7)	564–608	17.45±0.82	91.7
(8)	475–600	14.5	81.0
Present results	550–620	16.00±0.066	86.0

For a reaction which involves the rupture of one bond and for which the reverse combination of radicals has no activation energy, the activation energy may be related to the bond dissociation energy in the following general way (15).

$$D \leqslant E \leqslant D + RT$$

From the present results and from the values (16) for ΔH_f at 0 °K given in the first column below, one may calculate the values given in the second column.

$\Delta H_f(C_2H_6) = -16.517$ kcal/mole
$\Delta H_f(CH_4) = -15.987$ kcal/mole
$\Delta H_f(H) = 51.620$ kcal/mole

$D(CH_3—CH_3) = 85.0 \pm 0.5$ kcal/mole
$\Delta H_f(CH_3) = 34.2$ kcal/mole
$D(CH_3—H) = 102$ kcal/mole

The observed order with respect to total pressure of the decomposition of the ethyl radical confirms previous suggestions (6, 7) that in this range of temperature and pressure the ethyl radical is roughly halfway into its second-order region. The activation energy for decomposition is in agreement with that found by Purnell and Quinn (9) if an activation energy of 10.4 kcal/mole (17) is taken for the abstraction of hydrogen from butane by the ethyl radical, instead of 15.2 kcal/mole as used by these authors. As expected, the activation energy of 32.7 ± 1.5 kcal/mole is lower than the activation energy of 39.5 kcal/mole (18) for the first-order decomposition. The relation of this decrease to the number of effective oscillators in the ethyl radical is discussed in Part II (23).

In agreement with previous results (7, 8), the rate of methane production was unchanged by increasing the S/V ratio by a factor of about 15. It seems well substantiated that the initiation reaction is the homogeneous dissociation of ethane. The decrease in the rate of hydrogen production, however, would suggest an increased rate constant for the termination process in the packed vessel. This would lower the radical concentration, thus decreasing the overall rate, while the rate of removal of radicals would still equal the rate of initiation. Since butane production was not enhanced, but was in fact decreased, this heterogeneous termination does not yield butane and thus probably does not involve an adsorbed ethyl radical. The adsorbed species must therefore be a hydrogen atom which may become attached to the surface by reaction with an ethyl radical as well as by direct adsorption.

[8] $$H + S \rightleftarrows H—S$$

[9] $$C_2H_5 + S \rightarrow C_2H_4 + H—S$$

Termination may then take place as follows.

[10] $$H + H—S \rightarrow H_2 + S$$

[11] $$C_2H_5 + H—S \rightarrow C_2H_6 + S$$

The surface reaction becomes more predominant at low pressures and its rate is thus probably dependent in some way on the homogeneous concentration of hydrogen atoms.

Can. J. Chem. Downloaded from www.nrcresearchpress.com by 210.87.254.5 on 09/05/12
For personal use only.

Although in the present experiments the concentration of hydrogen atoms is always lower than that of ethyl radicals, the rate of reaction [8] may be faster than that of [9] if an appreciable activation energy is required for the latter. This is quite reasonable in view of the strength of the bond broken. Termination may occur by either reaction [10] or [11], since the rate constant of reaction [10] may be much larger than that of reaction [11] and may outweigh the difference in concentration of H atoms and ethyl radicals. Our results therefore favor the occurrence of reaction [8] followed by reactions [10] or [11].

The magnitude of the effect of the surface on the rate was smaller than that observed by Gordon (8). The heterogeneous reaction may be very sensitive to the nature of the surface, which in turn may be a function of the treatment of the vessel prior to the experiments or even of the purity of the quartz of which the vessel is made. For these reasons it may be difficult to obtain quantitative agreement for the surface reaction from one laboratory to another.

The fact that in both vessels the ratio of methane to butane is higher than that expected on the basis of reactions [1] to [5] suggests that a second termination reaction, which does not produce butane, makes a minor contribution. The most probable reaction is reaction [6], but this interpretation is unlikely for two reasons. Calculation of the relative concentrations of hydrogen atoms and ethyl radicals indicates that the concentration of the former is too low to make a significant contribution to the termination, unless the rate constant for reaction [6] is much greater than for reaction [5]. The ratio of hydrogen atoms to ethyl radicals is given by $k_3/k_4[C_2H_6]$, and values for k_3 may be taken from Fig. 7 with $k_{5a} = 2.0 \times 10^{13}$ cc mole^{-1} s^{-1} (14). Using Berlie and Le Roy's measurement of $k_4 = 10^{12.53} e^{-6800/RT}$ cc mole^{-1} s^{-1} (19) at 100 mm ethane $k_3/k_4[C_2H_6] = 7.0 \times 10^{-3}$ at 550 °C and 3.0×10^{-2} at 620 °C. With a recent measurement of $k_4 = 10^{14.12} e^{-9700/RT}$ cc mole^{-1} s^{-1} (20) these ratios are slightly lower. To account for the ratios of methane/butane of 1.7, however, the percentage termination by a reaction other than [5] may be shown to be 33% and for a ratio of 1.4, 20%. Furthermore, even if the calculated values were in error to the extent that at 550 °C reaction [6] could account for about 25% of the termination, the relative temperature coefficients of k_3 and k_4 are such that at 620 °C hydrogen atoms should be the predominant radical and termination should be largely by [6]. The trend, however, in the ratio of methane/butane is in the reverse direction and at 620 °C and high pressures the ratio is exactly as predicted.

Another possible explanation may be that the ratio of disproportionation/combination of 0.15 for ethyl radicals, measured in a temperature region lower than the present experiments, is not the correct ratio under the conditions of these experiments. It seems unlikely, however, that the activation energy difference between the combination and disproportionation reactions would be more than 1 kcal/mole. This was the upper limit suggested by Ivin and Steacie (21). This difference raises the ratio k_{5b}/k_{5a} to 0.27 at 550 °C, which is not sufficient to account for the ratios in Table I.

It seems probable that a heterogeneous termination may contribute to a sufficient extent in the unpacked vessel to account for the ratios of methane/butane. This would necessitate a non-linear extrapolation of the rate of butane production as a function of S/V ratio, the rate rising steeply towards zero S/V ratio to give the required rate of butane production. Such a curve was found by Voevodsky (22) in a study of the decomposition of propane in vessels packed with various amounts of tubing. The heterogeneous reaction would be consistent with the trend of less participation at high temperatures

Can. J. Chem. Downloaded from www.nrcresearchpress.com by 210.87.254.5 on 09/05/12
For personal use only.

and high pressures. It is worth noting that this discrepancy between the rates of production of methane and butane affects neither the calculation of k_3 nor the conclusions regarding the order of reaction [3] with respect to ethane, provided only that the yield of butane gives a measure of the concentration of ethyl radicals and that production of hydrogen from possible termination steps is negligible compared to that from reaction [4].

ACKNOWLEDGMENTS

The authors wish to thank Professor K. J. Laidler for many helpful discussions.

The authors also thank the National Research Council for a grant in support of this work and the Ontario Research Foundation for a fellowship awarded to M. C. Lin.

REFERENCES

1. F. O. Rice and K. F. Herzfeld. J. Am. Chem. Soc. **56**, 284 (1934).
2. L. Küchler and H. Theile. Z. Physik. Chem. B, **42**, 359 (1939).
3. K. J. Laidler and B. W. Wojciechowski. Proc. Roy. Soc. London, Ser. A, **260**, 91 (1961).
4. E. W. R. Steacie. Atomic and free radical reactions. Reinhold Publishing Corp., New York. 1954.
5. C. H. Leigh, M. Szwarc, and J. Bigeleisen. J. Am. Chem. Soc. **77**, 2193 (1955).
6. H. G. Davis and K. D. Williamson. Fifth World Petroleum Congress, 1959. Section IV, p. 37.
7. C. P. Quinn. Proc. Roy. Soc. London, Ser. A, **275**, 190 (1963).
8. A. S. Gordon. C.I.C. Symposium on the Kinetics of Pyrolytic Reactions, Ottawa, September 1964.
9. J. H. Purnell and C. P. Quinn. Proc. Roy. Soc. London, Ser. A, **270**, 267 (1962).
10. A. F. Trotman-Dickenson and J. A. Kerr. Progress in reaction kinetics. Vol. I. Pergamon Press, Ltd., London. 1961.
11. C. J. Danby, B. C. Spall, F. J. Stubbs, and C. N. Hinshelwood. Proc. Roy. Soc. London, Ser. A, **218**, 450 (1953).
12. J. A. Bell and G. B. Kistiakowsky. J. Am. Chem. Soc. **84**, 3417 (1962).
13. A. F. Trotman-Dickenson and E. W. R. Steacie. J. Chem. Phys. **19**, 329 (1951).
14. A. Shepp and K. O. Kutschke. J. Chem. Phys. **26**, 1020 (1957).
15. M. Szwarc. Chem. Rev. **47**, 75 (1950).
16. Selected values of physical and thermodynamic properties of hydrocarbons. American Petroleum Institute of Research Project, Carnegie Press. 1953.
17. P. J. Boddy and E. W. R. Steacie. Can. J. Chem. **38**, 1576 (1960).
18. S. Bywater and E. W. R. Steacie. J. Chem. Phys. **19**, 326 (1951).
19. M. R. Berlie and D. J. Le Roy. Discussions Faraday Soc. **14**, 50 (1953).
20. R. R. Baldwin and A. Melvin. J. Chem. Soc. 1785 (1964).
21. K. J. Ivin and E. W. R. Steacie. Proc. Roy. Soc. London, Ser. A, **208**, 25 (1951).
22. V. V. Voevodsky. Trans. Faraday Soc. **55**, 65 (1959).
23. M. C. Lin and M. H. Back. The thermal decomposition of ethane. Parts II and III. To be published.

Can. J. Chem. Downloaded from www.nrcresearchpress.com by 210.87.254.5 on 09/05/12
For personal use only.

Can. J. Chem. Downloaded from www.nrcresearchpress.com by 210.87.254.40 on 09/05/12
For personal use only.

THE CHEMISTRY OF IRIDIUM IN BASIC AQUEOUS SOLUTION

A POLAROGRAPHIC STUDY

GARY VAN LOON AND JOHN A. PAGE

Department of Chemistry, University of Toronto, Toronto, Ontario

Received August 19, 1965

ABSTRACT

The polarographic behavior of iridium(IV) has been studied in basic solutions at 25 °C at an ionic strength maintained with sodium chloride at 0.50 *M*. Between pH 11.3 and 13.0, a reversible, diffusion-controlled, one Faraday per mole reduction wave was obtained. The $E_{1/2}$ was −0.60 V versus a saturated calomel reference electrode at pH 12.0; a shift of −57 mV per pH unit indicated that one hydrogen ion is involved in the reduction. With basic solutions of iridium(III), the corresponding oxidation wave was obtained, but the metal was easily air oxidized. The basic iridium(IV) species gave an absorption peak at 313 mμ. The rate of formation of the basic iridium(III) complex from an acid iridium(III) solution was found to be more rapid than that of the basic iridium(IV) complex from an acid iridium(IV) solution. The reaction of iridium(IV) with ethylenediaminetetracetate was also studied.

INTRODUCTION

There has been some work on the direct polarography of iridium in aqueous solutions, but the only positive results have been obtained with hydrochloric acid solutions (1, 2). Willis (3) was unable to obtain polarographic waves with either iridium(III) or iridium(IV) in the presence of bromide, cyanide, ethylenediamine, pyridine, and thiocyanate electrolytes. Repin (4) was unable to obtain polarographic waves with iridium(III) in chloride, phosphate, tartrate, and tetraethylammonium iodide electrolytes. With solutions of $IrCl_3$ buffered at pH 5 with acetate, Simpson, Evans, and Saroff (5) did obtain a reduction wave with a relatively small diffusion current; this might well be due to the presence of some iridium(IV) in the solution. A precipitate gradually appeared when the solution was left standing. Ezerskaya and Filimonova (6) could not obtain a wave with iridium(III) or indium(IV) in a solution containing ethylenediaminetetracetate at pH 5 to 6. West, Dean, and Breda (7) observed a reduction wave with $E_{1/2}$ of −1.4 V with iridium(IV) in a 0.5 *M* Na_2F_2 electrolyte of pH 5, but the limiting current plateau was very poorly defined.

With a 0.2 *M* HCl electrolyte, Page (1) found that the reduction $Ir^{IV} \rightarrow Ir^{III}$ took place at the dropping mercury electrode (d.m.e.). The $E_{1/2}$ was more positive than the oxidation potential of the mercury, but the limiting current plateau was well defined. Pshenitysn, Ezerskaya, and Ratinova (2) found an $E_{1/2}$ of +0.73 V for this reduction with a rotating platinum microelectrode in an acid 0.1 *M* NaCl electrolyte. They also found that iridium(III) produced an anodic wave with a slightly more positive $E_{1/2}$ under the same conditions, indicating that the $Ir^{IV} + e \rightleftarrows Ir^{III}$ reaction was somewhat irreversible.

This work is a study of the polarographic behavior of iridium in basic solutions. It augments the previous spectrophotometric investigations of iridium by MacNevin and Kriege (8) and Desideri and Pantani (9).

EXPERIMENTAL

All potentials reported, *V*, are in volts relative to the saturated calomel reference electrode.

Polarograms were recorded on a Leeds and Northrup type E electrochemograph with the damping set in the No. 1 position. The cell was of the conventional H-type with a saturated calomel reference electrode, and all polarography was carried out at 25.0 °C. The polarographic currents reported have been corrected for the residual current found on blank polarography. The mercury electrode had a flow rate of 1.850 mg s^{-1} at an effective height, *h*, of 82.7 cm of mercury. Polarographic currents were measured in acid solution at −0.20 V,

at a drop time of 4.21 s and corresponding capillary constant of 1.916 $mg^{2/3}\ s^{-1/2}$. In basic solutions, the polarographic currents were measured at −0.90 V, corresponding to a drop time of 4.20 s and capillary constant of 1.915 $mg^{2/3}\ s^{-1/2}$.

The controlled potential coulometric titrations were carried out with the apparatus and cells previously described (1). A Beckman model G pH meter with a 40495 blue-glass electrode and a saturated calomel reference electrode was used for pH measurements. Corrections were made for the sodium ion present in the solutions. The meter was standardized against a borax solution prepared according to the directions of the National Bureau of Standards from their sample 187a (pH = 9.18 at 25.0 °C). Spectra in the visible and ultraviolet region were recorded with a Bausch and Lomb Spectronic 505 with matched quartz cells of 1 and 10 cm path length. For measurements at a single wavelength (313 mμ) a Beckman DU spectrophotometer was used.

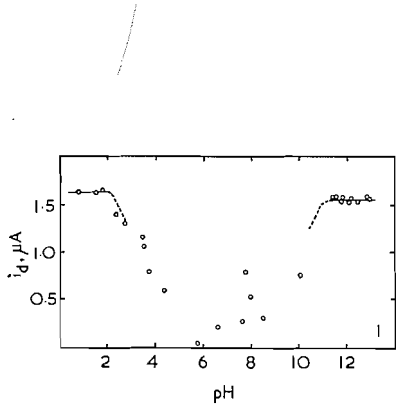
Deaeration of solutions for polarography and coulometry was done with prepurified nitrogen (less than 20 p.p.m. oxygen), but in critical cases the nitrogen was further purified by passage over copper turnings at 500 °C.

All chemicals used were reagent grade. The standard iridium solution was prepared from hydrated sodium hexachloroiridate ($Na_2IrCl_6.6H_2O$) obtained from Englehard Industries Limited (lot A-32). Preliminary experiments showed that the salt contained approximately 5% lead. This was originally detected by a polarographic wave with $E_{1/2}$ of −0.43 V in 0.2 *M* HCl solution and confirmed by spectrographic analysis.

The standard iridium solution was prepared as follows. The salt (4.34 g) was dissolved in 600 ml of aqueous solution containing 4 ml of concentrated hydrochloric acid. The pH of the resulting solution was 1.0. The solution was then passed through a column of Dowex 50W-X8 cation exchange resin according to the procedure prescribed by Marks and Beamish (10) for the separation of base metals from rhodium and iridium. Polarography of the resulting solution showed that the lead had been completely removed. The solution was then diluted to 2 000 ml with water and 13 ml of concentrated hydrochloric acid. This working solution was thus 0.1 *M* in hydrochloric acid. It was standardized according to the method of Page (1) by controlled potential coulometry. The concentration was found to be 0.446 ± 0.006 mg Ir/ml from five such determinations on 5 or 10 mg samples. Chlorination of samples of the solution before electrolysis (1) resulted in the same value, showing that there was no significant amount of iridium(III) in the solution.

RESULTS AND DISCUSSION

The polarographic behavior of iridium(IV) was investigated over a range of pH. Solutions were prepared by dilution of the standard iridium(IV) solution, with the final ionic strength controlled at 0.50 *M* with sodium chloride. The appropriate volume of a standard sodium chloride solution was added before the adjustment of pH by the addition of a sodium hydroxide solution. The final chloride concentration was thus a constant 0.50 *M* up to pH 12, but was lower at the higher pH's where the concentration of free hydroxide was appreciable. The solutions were diluted to final volume, and stabilized at 100 °C for 15 to 30 min before polarography at 25 °C.



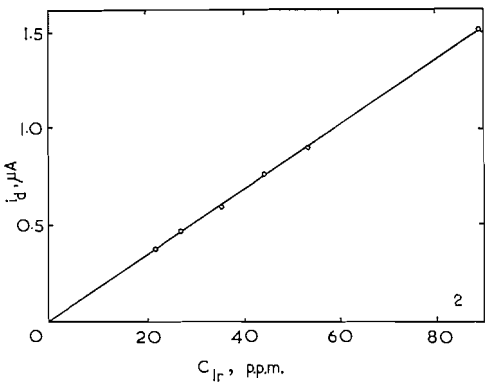


FIG. 1. Diffusion current as a function of pH in stabilized iridium(IV) solutions. μ = 0.50, C_{Ir} = 0.464 m*M*.

FIG. 2. Diffusion current as a function of concentration in stabilized iridium(IV) solutions. μ = 0.50, pH = 11.5 to 12.3.

Can. J. Chem. Downloaded from www.nrcresearchpress.com by 210.87.254.40 on 09/05/12
For personal use only.

Can. J. Chem. Downloaded from www.nrcresearchpress.com by 210.87.254.40 on 09/05/12
For personal use only.

The diffusion current, i_d, was a function of pH (Fig. 1). From pH 0 to 2, the previously reported reduction wave with $E_{1/2}$ more positive than the oxidation potential of the mercury was obtained. Above pH 2, the diffusion current of this wave decreased, the wave disappearing completely at pH 6. Above pH 6, a second reduction wave developed, with a diffusion current that was independent of pH above pH 11.3. In the pH range 2 to 11.3, a precipitate was frequently observed in the stabilized solutions, indicating that hydrolysis to an insoluble neutral species had occurred, at least in part. Above pH 11.3, the stabilized solutions were clear.

A linear calibration curve, i_d versus concentration of iridium(IV), was obtained for solutions stabilized in the pH range 11.5 to 12.3 (Fig. 2). A diffusion control of the reduction process was indicated by a proportionality between i_d and the square root of the height of the mercury column of the dropping electrode. The value of $i_d/Ch^{1/2}$ was 1.85 and 1.88 μA mM^{-1} cm$^{-1/2}$ at h 64.8 and 82.7 cm respectively.

The reduction appeared to be a reversible one-electron process. Plots of $E_{d.m.e.}$ versus log $(i/(i_d - i))$ were linear with slopes of 58, 63, 66, 60, and 64 mV at pH's of 11.9, 12.2, 12.4, 12.8, and 13.0 respectively. The half-wave potential was a function of pH, shifting by 57 mV per pH unit in the pH range 11.3 to 13.0; the reduction was more difficult in more basic solutions (Fig. 3).

Since the shift in $E_{1/2}$ is very close to 59 mV per pH unit, it would appear that one hydrogen ion is involved in the one-electron reduction of the iridium(IV). If the iridium (IV) species in the basic solution is $Ir(OH)_6^{2-}$, then the reduction corresponds to:

$$Ir(OH)_6^{2-} + H_2O + e^- \rightarrow Ir(OH)_5(H_2O)^{2-} + OH^-.$$

The one-electron reduction was confirmed by controlled potential electrolyses at a mercury cathode at −0.80 V. The iridium(IV) solutions were prepared and stabilized as in the polarographic experiments, with the final pH in the range 11.5 to 12.5. The reductions proceeded smoothly to low background currents, but the calculated number of electrons was variable, close to but always greater than one (Table I). During the electrolyses, a white precipitate, presumably of iridium(III), formed. This precipitate partially dissolved when the solution was allowed to stand in air subsequent to electrolysis. Coulometry of

TABLE I

Ir taken (mg)	Coulombs*	Faradays/mole
4.46	0.295	1.31
	0.249	1.11
	0.244	1.09
	0.245	1.10
	0.231	1.03
	0.233	1.04
	0.245	1.09
	0.250†	1.12
	0.252†	1.13
3.55	0.185†	1.04
	0.183†	1.03
5.20‡	0.308	1.18
5.45	0.285†	1.04
	0.287†	1.05

*Corrected for background current.
†Solutions are 0.001 M in ethylenediaminetetracetate.
‡Solution standardized gravimetrically with 2-mercaptobenzothiazole by Dr. K. S. Chung.

these air-oxidized solutions always gave low results of about 60 to 80% of the initial value, as would be expected if some iridium was present as a nonreactive precipitate.

Polarography was also carried out on iridium(III) solutions prepared by controlled potential electrolysis. Solutions of iridium(IV) in a 0.2 *M* HCl electrolyte were reduced at a mercury cathode at 0 V. When these solutions were made basic with sodium hydroxide in the pH range 11.5 to 12.5, in the absence of oxygen, an anodic wave was obtained on polarography. Subsequent partial air oxidation gave a composite anodic–cathodic wave, while complete air oxidation gave the cathodic wave characteristic of iridium(IV). The $E_{1/2}$'s of the anodic, composite, and cathodic waves were identical, confirming the reversible nature of the polarographic wave.

Although the polarography of iridium in basic solution has not been reported, the spectral characteristics have been investigated. Desideri and Pantani (9) noted an absorption peak at 313 mμ (molar absorptivity, ϵ = 2 880, our value) starting with acid solutions of iridium(IV) or even iridium(III) in the presence of dissolved air. They showed that the iridium(IV) was present in the basic solutions as an $Ir(OH)_6^{2-}$ species. MacNevin and Kriege (8) also produced an absorption peak with iridium(IV) in a basic ethylenediaminetetracetate (EDTA) electrolyte. They postulated that an iridium(IV)–EDTA complex was formed, but since the peak had the same characteristics as that produced in basic solution in the absence of EDTA it may be assumed that the absorbing species is not an EDTA complex.

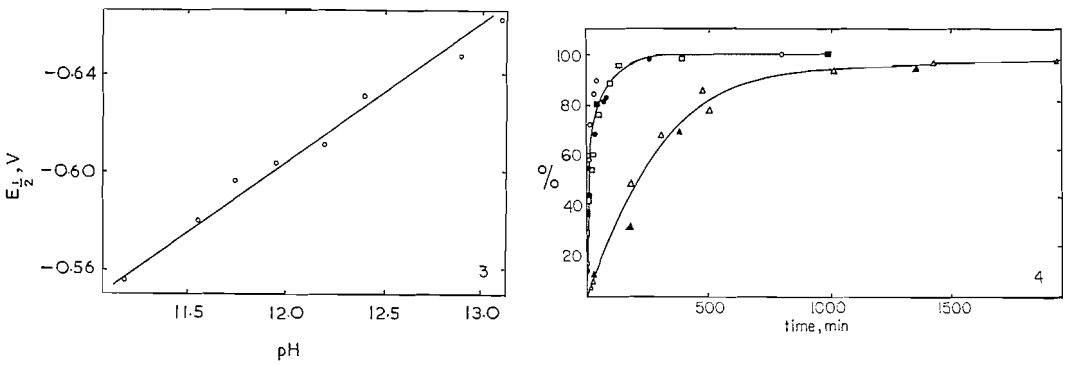


FIG. 3. $E_{1/2}$ as a function of pH in stabilized iridium(IV) solutions. μ = 0.50, C_{Ir} = 0.464 m*M*.
FIG. 4. Development of the polarographic wave in the absence of oxygen: wave height (% of final) as a function of time. μ = 0.50, C_{Ir} = 0.2 m*M*, pH = 11.5 to 12.5. (□, ■) Ir^{III} (anodic wave), (○, ●) Ir^{IV} + ethylenediaminetetracetate (anodic wave), (△, ▲) Ir^{IV} (cathodic wave).

In both of these investigations, chloride ion was present in the basic solutions and may be involved in the absorbing species; however, we have prepared a basic iridium complex with the same absorption characteristics in the absence of chloride ion. Aliquots of the stock iridium(IV) solution were fumed twice with perchloric acid to remove chloride, diluted, and electrolyzed at a mercury cathode at 0 V to give iridium(III). The iridium was then precipitated from the solution with sodium hydroxide and the precipitate was filtered off, washed, and then fused with solid sodium hydroxide in a nickel crucible. The melt when dissolved in water gave the same polarographic and absorption characteristics as previously noted with iridium(IV) in basic solution.

The rate of formation of the active polarographic and absorbing species in the aqueous solutions has been followed at room temperature (Fig. 4).

Can. J. Chem. Downloaded from www.nrcresearchpress.com by 210.87.254.40 on 09/05/12
For personal use only.

With the standard iridium(IV) solution as the starting solution, there was a rapid (< 5 min) disappearance of the iridium(IV) chloride spectrum when the solution was made basic. This was followed by a slow development of the new polarographic reduction wave; there was a matching development in absorbance at 313 mμ indicating that the same species is active in both polarography and absorption in the basic solution. On the other hand, with an air-free iridium(III) solution, prepared by controlled potential electrolysis as before, as the starting solution, there was a more rapid growth of the polarographic oxidation wave when the solution was made basic. There was no change in absorbance at 313 mμ. If air was admitted after complete development of the anodic wave, there was a rapid (< 1 min) oxidation of the iridium(III) with a complete development of both the cathodic wave and the absorbance at 313 mμ. These final characteristics could be obtained directly with the solutions of iridium(IV) or iridium(III) in the presence of dissolved air by 15 to 30 min stabilization at 100 °C.

The reactions involved in the presence of EDTA were also studied. On addition of the sodium salt of EDTA to an acid iridium(IV) solution, the characteristic red-brown color changed to pale green over a period of several hours at room temperature. The transformation could be accelerated by heating to 100 °C. The final spectrum closely matched that of iridium(III) prepared by controlled potential electrolysis. The acidic solution gave no characteristic polarographic wave, but the red-brown color of iridium(IV) could be restored by chlorine oxidation.

If an acid 0.2 mM iridium(IV) solution was made 0.001 M in dissolved EDTA, stabilized at 100 °C, and then made air free and basic, a polarographic oxidation wave developed at a rate close to that found when the iridium(III) solution was made basic (Fig. 4). This suggests that there is first a reduction of the iridium(IV) by the EDTA and a subsequent formation of the polarographically active species. The EDTA does not influence the rate of formation of the active species from the iridium(III). The final iridium(III) species was readily air oxidized to give a polarographic reduction wave.

At a given pH, the polarographic wave in a basic solution with added EDTA had the same $E_{1/2}$ as in similar solutions without EDTA.

A second reduction wave appeared in the basic EDTA solutions. It had an $E_{1/2}$ of −1.35 V, corresponding to that of glyoxylate in basic solution. Enns (11) has already found that EDTA can be oxidized by riboflavin in acid solution, and has identified glyoxylic acid as an oxidation product of the EDTA. This second wave does not occur with the EDTA if iridium(III) is used as a starting material in place of iridium(IV).

If air is admitted to the basic solution of iridium(III) and EDTA, there is rapid and complete oxidation of the iridium. Controlled potential coulometry on such solutions gave results consistent with a one-electron reduction process (Table I).

CONCLUSIONS

The polarography of the iridium(IV) in basic solution is suitable for quantitative work and the reversible nature of the one Faraday per mole reduction is in contrast to the irreversible nature of the polarography in other electrolytes. The polarography of iridium (III) was also quantitative, but not of practical use in analysis because of the easy air oxidation of iridium(III) in basic solution.

The controlled potential coulometry consistently gave high results, despite the fact that the reductions proceeded rapidly to a small final background current. The iridium(III) species formed on controlled potential reduction in the basic solution was insoluble, in contrast to that formed on making an acid iridium(III) species basic.

Can. J. Chem. Downloaded from www.nrcresearchpress.com by 210.87.254.40 on 09/05/12
For personal use only.

The polarographic behavior in basic solution matches the spectrophotometric behavior previously reported, although it appears that in the procedure of MacNevin and Kriege (8) the EDTA does not form a complex with iridium. The EDTA does act as a reducing agent for iridium(IV) in acid solution, but not in basic solution.

The formation of the basic iridium(IV) species from an initially acid solution of $IrCl_6^{2-}$ was found to be slow. It is known that $IrCl_6^{2-}$ is kinetically fairly inert (12), and the formation of the basic iridium(IV) species is evidently a two-step process, for while there is a rapid disappearance of the $IrCl_6^{2-}$ spectrum, there is only a slow growth of the polarographically reducible species. The formation of the basic iridium(III) species from an initially acid solution (prepared either by controlled potential or EDTA reduction) is more rapid. This is in agreement with the observations that anionic iridium(III) complexes are labile (12).

ACKNOWLEDGMENTS

The authors are indebted to the National Research Council of Canada for a grant in aid of this research and for scholarship aid (G.V.L.). They are also indebted to the University of Toronto and the Ontario Research Foundation for financial assistance. Thanks are also due to Dr. K. S. Chung for samples of standardized iridium solution.

REFERENCES

1. J. A. PAGE. Talanta, **2**, 365 (1962).
2. N. K. PSHENITSYN, N. A. EZERSKAYA, and V. D. RATNIKOVA. Russ. J. Inorg. Chem. English Transl. **8**, 1791 (1958).
3. J. B. WILLIS. J. Am. Chem. Soc. **67**, 547 (1945).
4. S. A. REPIN. J. Appl. Chem. USSR English Transl. **20**, 55 (1947); Chem. Abstr. **41**, 5813*e* (1947).
5. R. B. SIMPSON, R. L. EVANS, and H. A. SAROFF. J. Am. Chem. Soc. **77**, 1438 (1955).
6. N. A. EZERSKAYA and V. N. FILIMONOVA. J. Anal. Chem. USSR English Transl. **17**, 946 (1962).
7. P. W. WEST, J. DEAN, and E. J. BREDA. Collection Czech. Chem. Commun. **13**, 1 (1948).
8. W. M. MACNEVIN and O. H. KRIEGE. Anal. Chem. **28**, 16 (1956).
9. P. G. DESIDERI and F. PANTANI. Ric. Sci. Rend. **1**, 265 (1961).
10. A. G. MARKS and F. E. BEAMISH. Anal. Chem. **30**, 1464 (1958).
11. K. ENNS. Ph.D. Thesis, University of Toronto, Toronto, Ontario. 1963.
12. F. A. COTTON and G. WILKINSON. Advanced inorganic chemistry. Interscience Publishers, New York. 1962. pp. 841–842.

Can. J. Chem. Downloaded from www.nrcresearchpress.com by 210.87.254.40 on 09/05/12
For personal use only.

Can. J. Chem. Downloaded from www.nrcresearchpress.com by 210.87.254.105 on 09/05/12
For personal use only.

A SOLVENT-EXTRACTION STUDY OF THE THERMODYNAMICS OF ANILINE AND ITS NITRATE

A. ABOUL-SEOUD AND M. DOHEIM

Chemical Engineering Department, Faculty of Engineering, University of Alexandria, Egypt, U.A.R.

Received September 21, 1965

ABSTRACT

The distribution coefficients of aniline between *n*-heptane and aqueous sodium nitrate solutions were measured at different temperatures. The activity coefficients of aniline in aqueous sodium nitrate solutions were determined. The effect of sodium nitrate on the dissociation of the anilinium ion was studied at different temperatures by a modified distribution method. Attention was directed to the choice of the extracting solvent and of the analytical method. The effect of the presence of undissociated anilinium ions on the distribution coefficients was taken into consideration.

K_0, K_b, ΔH, ΔF, and ΔS for the dissociation of the anilinium ion were evaluated.

INTRODUCTION

During a study of the effect of electrolytes on the rate of diazotization of aniline, it was found necessary to study the dissociation of the anilinium ion in the presence of sodium nitrate solutions of different ionic strengths, and to evaluate thermodynamic quantities such as the activity coefficient of aniline in aqueous sodium nitrate solutions, and the basic dissociation constant of aniline, at different temperatures. These results (1) are to be combined with the results of equilibrium (2) and kinetic measurements involving aniline.

The values were determined by a modified distribution method (3, 5, 7), in which attention was directed to the choice of the extracting solvent and of the analytical method.

EXPERIMENTAL

The distribution method (3, 5, 7) seems to be the most suitable for this and similar studies.

n-Heptane was used as extracting solvent. It is not too volatile, and it does not react with any of the substances involved in this study. Unlike benzene, it is very slightly soluble in water (5.2 mg/100 ml H_2O at 15.5° C (4)), so that there is no need for solubility corrections (5); also, it does not lead to distribution coefficients which are inconveniently high (3, 5).

The aniline in the heptane phase was determined by ultraviolet spectroscopy with a Unicam SP. 500 spectrophotometer. Absorption curves for solutions of aniline in heptane, of different concentrations, showed that 287 mμ is the wavelength of maximum absorption. Consequently, all spectrophotometric measurements of the concentration of aniline in heptane were carried out at this wavelength. The accuracy of this analytical method is estimated to be $\pm 0.01\%$.

Materials

Aniline.—Extra pure quality was used. This was distilled with zinc dust and then redistilled before use; b.p. 184 °C.

Sodium nitrate.—An A.R. product was used.

n-Heptane.—A pure quality was used. This was further purified by distillation; b.p. 98 °C.

Aniline nitrate solution.—Standard solutions of purified aniline in boiled-out distilled water, and of nitric acid prepared from an A.R. product, were mixed together, just before use, in such volumes as to give aniline nitrate solution of the desired concentration.

Procedure

Distribution coefficient measurements.—Twenty milliliters of an aqueous solution, containing a known amount of aniline and the calculated amount of sodium nitrate, were equilibrated at the desired temperature with 20 ml of *n*-heptane. The two phases were then separated by removal of the aqueous layer by suction.

Dissociation constant measurements.—These measurements were carried out in the same way, substituting aniline by aniline nitrate.

All measurements were carried out in duplicate, or in triplicate when necessary.

RESULTS, CALCULATIONS, AND CONCLUSIONS

The Distribution of Aniline between n-Heptane and Aqueous Sodium Nitrate Solutions

In the range of concentrations investigated, the distribution of aniline between *n*-heptane and water was found to be independent of the total concentration of aniline, indicating that no association or compound formation took place in either phase (6). This was determined from the linearity of the plot of the concentration of aniline in heptane (c_H) against its concentration in the aqueous phase (c_A), in distribution experiments at 5, 15, 25, and 35 °C. The results are given in Table I.

TABLE I

The equilibrium concentrations of aniline in the heptane phase (c_H) and in the aqueous phase (c_A), at different temperatures

Temp. (°C)	c_H or c_A	Concentration of aniline (mg/l)			
5	c_H	5.88	15.37	29.50	36.65
5	c_A	12.74	31.19	63.62	75.09
15	c_H	6.65	16.60	32.65	39.65
15	c_A	11.97	29.96	60.47	72.09
25	c_H	7.75	19.15	38.35	46.55
25	c_A	10.87	27.41	54.77	65.19
35	c_H	8.65	21.20	43.85	52.75
35	c_A	9.97	25.36	49.27	58.99

The distribution of aniline between *n*-heptane and aqueous sodium nitrate solutions was studied at 5, 15, 25, and 35 °C. The results are given in Table II.

The values of the distribution coefficients in terms of molalities (m_H/m_A) were calculated, and plotted against the sum of the molalities of the amine and of sodium nitrate in the aqueous phase. The curves thus obtained were extrapolated to zero molality. From the values of m_H/m_A and the corresponding values at zero molality, the values of the activity coefficients of aniline (f_{An}) in aqueous sodium nitrate solutions were determined (7).

The plot of log f_{An} against the sum of the molalities of aniline and of sodium nitrate, in the aqueous phase, was found to be linear up to a salt molality of 2. This is in concordance

TABLE II

The distribution coefficients of aniline between *n*-heptane and aqueous sodium nitrate solutions

Temp. (°C)	$NaNO_3$ (mole/l)	$NaNO_3$ (m)	Aniline in heptane (mg/l)	Mean m_H/m_A	f_{An}	k_m
	0.0	0.000	29.5	0.68	1.00	
	0.5	0.510	30.9	0.72	1.10	
5±0.05	1.0	1.040	33.5	0.80	1.19	0.07
	2.0	2.136	37.5	0.93	1.37	
	4.0	4.625	47.3	1.31	1.92	
	0.0	0.000	32.6	0.79	1.00	
	0.5	0.510	35.2	0.88	1.11	
15±0.05	1.0	1.040	39.0	1.02	1.29	0.08
	2.0	2.136	42.3	1.15	1.46	
	4.0	4.625	51.3	1.56	1.96	
	0.0	0.000	38.3	1.03	1.00	
	0.5	0.510	42.2	1.20	1.16	
25±0.05	1.0	1.040	45.3	1.34	1.30	0.095
	2.0	2.136	49.7	1.58	1.53	
	4.0	4.625	60.4	2.34	2.27	
	0.0	0.000	43.8	1.30	1.00	
	0.5	0.510	47.6	1.50	1.15	
35±0.05	1.0	1.040	50.8	1.70	1.30	0.114
	2.0	2.136	55.1	1.99	1.53	
	4.0	4.625	63.2	2.69	2.01	

Can. J. Chem. Downloaded from www.nrcresearchpress.com by 210.87.254.105 on 09/05/12
For personal use only.

with the relationship reported by Harned and Owen (8, p. 398) and the findings of Randall and Failey (9). This plot may be represented by the equation

$$[1] \qquad \log f_{An} = k_m(m_{An} + m_{NaNO_3})$$

where k_m is the salting coefficient (8, p. 398), and m is the molality.

The values of the salting coefficient were found to be 0.07, 0.08, 0.095, and 0.114 at 5, 15, 25, and 35 °C respectively. The value of k_m at 25 °C may be compared with 0.074 for ethyl acetate (10), and with 0.019 for phenyl thiourea (11), at the same temperature.

The fact that k_m is dependent on the nature of the nonelectrolyte is in accord with earlier findings (12).

The plot of $1/f_{An}$ against the molality (8, pp. 58, 403, 404) of sodium nitrate was found to be linear up to a molality of 1. The linearity of this plot indicates that the results conform in a general way to the Debye theory of salt effects (8, pp. 58, 403, 404; 13).

The Dissociation of the Anilinium Ion

The results of the study of the effect of ionic strength and temperature on the dissociation of the anilinium ion are given in Table III, where K_m is the dissociation constant in terms of molalities,

$$[2] \qquad K_m = m_{H^+}m_{Aniline}/m_{Anilinium^+}.$$

In the calculation of K_m, the effect of the presence of undissociated anilinium ions on the distribution coefficients was taken into consideration. Thus, the values of m_H/m_A, corresponding to the values of $m_{NaNO_3} + m_{AnHNO_3}$, in the curves obtained by plotting m_H/m_A against the sum of the molalities of sodium nitrate and of aniline in the aqueous phase, were used for calculating the molality of free aniline in the aqueous phase, in dissociation measurements.

TABLE III

The effect of sodium nitrate on the dissociation of anilinium nitrate

Temp. (°C)	$NaNO_3$ (mole/l)	$NaNO_3$ (m)	m_H/m_A	$m_{An} \times 10^4$	$K_m \times 10^5$ (±0.3%)
	0.0	0.000	0.80	3.0	1.76
	0.5	0.508	0.89	5.5	5.59
15±0.05	1.0	1.034	0.98	10.4	20.98
	2.0	2.135	1.17	15.6	52.43
	4.0	4.635	1.59	39.1	667.50
	0.0	0.000	1.03	3.4	2.43
	0.5	0.508	1.18	5.8	7.10
25±0.05	1.0	1.034	1.33	9.4	19.77
	2.0	2.135	1.63	12.5	38.81
	4.0	4.635	2.34	28.7	405.81
	0.0	0.000	1.32	3.8	3.32
	0.5	0.508	1.48	6.0	8.47
35±0.05	1.0	1.034	1.64	8.6	18.39
	2.0	2.135	1.97	11.5	36.73
	4.0	4.635	2.37	25.1	331.94

The thermodynamic dissociation constant (K_0) was obtained for each temperature by plotting pK_m against the sum of the molalities of anilinium and sodium salts, and extrapolating to zero molality.

$$[3] \qquad K_0 = (f_{An}f_{H^+}/f_{AnH^+})\ (m_{An}m_{H^+}/m_{AnH^+}) = (f_{An}f_{H^+}/f_{AnH^+})K_m,$$

where f_{An}, f_{H^+}, and f_{AnH^+} are the activity coefficients of, and m_{An}, m_{H^+}, and m_{AnH^+} are the molalities of, aniline, hydrogen, and anilinium ions, respectively, in the aqueous phase.

Can. J. Chem. Downloaded from www.nrcresearchpress.com by 210.87.254.105 on 09/05/12
For personal use only.

With zero molality as the standard state, therefore, and when by definition $f = 1$, it follows from eq. [3] that at zero molality $K_m = K_0$.

It may be seen from eq. [3] that the value of K_0 is independent of the sodium nitrate concentration. The increase in K_m with sodium nitrate concentration may be attributed to the influence of sodium nitrate on the activity coefficients of aniline, hydrogen, and anilinium ions. From Table II, however, it is seen that the influence on the activity coefficients of aniline is not large. The relatively large increase in K_m with salt concentration is due, therefore, to either a relatively large increase of f_{AnH^+} or decrease of f_{H^+} with sodium nitrate concentration or both. Similar effects of electrolytes on f_{H^+} have already been reported (14). This problem is the subject of further investigation in this laboratory.

Evaluation of K_b, ΔH, ΔF, and ΔS

The plot of log K_0 against $1/T$ was found to be a straight line. From the slope of this line the heat of dissociation of the anilinium ion (ΔH), was calculated to be 5.78 ± 0.02 kcal.

In Table IV, the values of the thermodynamic dissociation constant (K_0), the ionic product of water (K_w), the basic dissociation constant (15) of the anilinium ion (K_b), the heat of dissociation (ΔH), the free energy change (16) (ΔF), and the entropy change (16) (ΔS) are given.

TABLE IV

Evaluation of K_b for aniline and ΔH, ΔF, and ΔS for the dissociation of the anilinium ion, at different temperatures

Temp. (°C)	$K_0 \times 10^5$	$K_w^* \times 10^{14}$	$K_b \times 10^9$	ΔH (kcal)	ΔF (kcal)	ΔS (e.u.)
15	1.76	0.450	0.253	5.78±0.02	6.26±0.02	−1.7±0.01
25	2.43	1.008	0.414	5.78±0.02	6.29±0.02	−1.7±0.01
35	3.32	2.089	0.629	5.78±0.02	6.31±0.02	−1.7±0.01

*From ref. 8, p. 485.

The fact that ΔH is independent of temperature over the range 15–35 °C indicates that in this range the difference of the partial molar heat capacity in the dissociation of the anilinium ion (ΔC_p) equals zero.

The values in Table IV may be compared with Pedersen's (17) values of $\Delta H = 7100$ cal, $\Delta F = 6265$ cal, and $\Delta S = +3.4$ e.u., at 25 °C, and with Everett and Wynne-Jones' (18) values of $\Delta C_p = 0.0$, $\Delta H = 7105$, $\Delta F = 6265$, and $\Delta S = +2.8$, at 25 °C.

REFERENCES

1. H. SCHMID and CH. ESSLER. Monatsh. Chem. **91**, 496 (1960). H. SCHMID. Chemiker Ztg. **86**, 812 (1962).
2. T. A. TURNEY. J. Chem. Soc. 4263 (1960). C. A. BUNTON and G. STEDMAN. J. Chem. Soc. 2440 (1958).
3. R. C. FARMER and F. J. WARTH. J. Chem. Soc. 1726 (1904).
4. HANDBOOK OF PHYSICS AND CHEMISTRY. 39th ed. Chemical Rubber Publishing Co., Cleveland, Ohio. 1957. p. 969.
5. G. WILLIAMS and F. G. SOPER. J. Chem. Soc. 2469 (1930).
6. R. E. TREYBAL. Liquid extraction. McGraw-Hill, New York. 1951. p. 24. W. NERNST. Z. Physik. Chem. **8**, 110 (1891).
7. A. ABOUL-SEOUD and A. EL-HADY. Rec. Trav. Chim. **81**, 958 (1962).
8. H. S. HARNED and B. B. OWEN. The physical chemistry of electrolytic solutions. Reinhold, New York. 1950. p. 398.
9. M. RANDALL and C. F. FAILEY. Chem. Rev. **4**, 271, 285, 291 (1927).
10. S. GLASSTONE and A. POUND. J. Chem. Soc. 2660 (1925). S. GLASSTONE, D. W. DIMOND, and E. C. JONES. J. Chem. Soc. 2935 (1926).

Can. J. Chem. Downloaded from www.nrcresearchpress.com by 210.87.254.105 on 09/05/12
For personal use only.

11. W. BLITZ. Z. Physik. Chem. **43**, 41 (1903). V. ROTHMUND. Z. Physik. Chem. **33**, 401 (1900).
12. H. S. HARNED AND B. B. OWEN. The physical chemistry of electrolytic solutions. Reinhold, New York. 1950. p. 403. P. GROSS and K. SCHWARZ. Österr. Akad. Wiss. Math. Naturw. Kl. Sitzber. Abt. I, **139**, 179 (1930). P. GROSS and M. ISER. Österr. Akad. Wiss. Math. Naturw. Kl. Sitzber. Abt. I, **139**, 221 (1930).
13. P. DEBYE. Z. Physik. Chem. **130**, 56 (1927).
14. H. M. DAWSON. Trans. Faraday Soc. **24**, 640 (1928).
15. W. J. MOORE. Physical chemistry. Longmans, London. 1956. pp. 471–473.
16. J. A. V. BUTLER. Chemical thermodynamics. Macmillan, London. 1951. p .459.
17. K. J. PEDERSEN. Kgl. Danske Videnskab. Selskab. Mat.-Fys. Medd. **14**, 28 (1937).
18. D. H. EVERETT and W. F. K. WYNNE-JONES. Trans. Faraday Soc. **35**, 1380 (1939).

Can. J. Chem. Downloaded from www.nrcresearchpress.com by 210.87.254.105 on 09/05/12
For personal use only.

Can. J. Chem. Downloaded from www.nrcresearchpress.com by 210.87.254.105 on 09/05/12
For personal use only.

NOTES

PARAMAGNETIC CENTERS IN IRRADIATED POTASSIUM SULFATE[1]

V. V. GROMOV[2] AND J. R. MORTON

Recent investigations (1, 2) into the radiolysis of polycrystalline sulfates prompted this examination of the electron spin resonance (e.s.r.) spectra of irradiated potassium sulfate single crystals. By irradiating the samples and studying their spectra at 77 °K and at 300 °K different stages in the radiation damage process were revealed.

The e.s.r. spectra of single crystals of K_2SO_4 irradiated and examined at 77 °K demonstrated the presence of a single paramagnetic species, A, characterized by a highly anisotropic g-tensor. By monitoring the spectrum during warm-up of the sample it could be seen that over 90% of A decomposed to form a second species, B, although the amount of A surviving at 300 °K was sufficient to permit the determination of its g-tensor at this temperature. The radical B was characterized by an almost isotropic g-tensor. The principal values of the g-tensors of the two radicals are given in Table I. Examination of a very large, heavily irradiated crystal revealed ^{33}S hyperfine structure in the spectrum of radical B, the interaction being 275, 270, and 315 Mc/s with H_0 along the a, b, and c crystallographic axes respectively. No ^{33}S hyperfine structure was detected in the spectrum of radical A. However, since a very much smaller crystal had to be used for experiments at 77 °K, the anticipated signal/noise ratio was less than 5:1, and so the absence of ^{33}S signals was not proved unequivocally.

The maximum-slope line widths of the spectra of both radicals were approximately 5 G, and were independent of temperature. The major contributions to the line widths are therefore presumed to be crystal imperfections and unresolved ^{39}K hyperfine structure.

The identification of the two radicals trapped in irradiated K_2SO_4 depended on a comparison of their spectral parameters with those of already well-substantiated species, and it was concluded that A and B were SO_4^- and SO_3^- respectively.

TABLE I

The principal values of the g-tensors of radicals detected in irradiated K_2SO_4 crystals

Radical	Principal g-factors
A (SO_4^-)	2.0486, 2.0082, 2.0037
B (SO_3^-)	2.0033, 2.0033, 2.0023

The g-tensor of radical A has three different principal values (Table I) indicating C_{2v} or lower symmetry. Axially symmetric radicals such as SO_3^- (3), O_2^- (4), or O^- (5) are therefore excluded; even apart from symmetry considerations, their principal g-factors are not similar to those of radical A. The radical SO_2^-, although possessing C_{2v} symmetry, has a maximum g-factor of 2.01 (6) and cannot therefore be identified with radical A. The radical SO_4^- has been observed (7) in both γ-irradiated and ultraviolet-photolyzed alkali–metal persulfates, where it is formed as a result of S–S bond scission. In potassium

[1]*N.R.C. No. 8807.*

[2]*Visiting scientist. Present address: Institute of Physical Chemistry, Soviet Academy of Sciences, Moscow.*

persulfate, for example, SO_4^- has principal g-factors 2.0327, 2.0084, 2.0035; these values are sufficiently similar to those presently reported to suggest the identification of radical A in K_2SO_4 as SO_4^-. The lack of ^{33}S hyperfine interaction for SO_4^-, although not unequivocally established in the present case, is consistent with this identification. Molecular orbital calculations on the perchlorate ion (8), which is isoelectronic with the sulfate ion, suggest that in SO_4^- the unpaired electron would occupy the $1t_1$ orbital, composed entirely of oxygen 2p orbitals. It has also been suggested (7) that as a result of either Jahn–Teller or crystal-field distortion T_d symmetry is lost, the $1t_1$ orbital giving rise to b_1, b_2, and a_2 orbitals under C_{2v} symmetry. With the unpaired electron entering the a_2 orbital, spin–orbit interaction between the ground $^2A_2$ state and a low-lying $^2B_2$ state would account for one principal g-factor being considerably greater than the free spin value 2.0023. None of the principal g-factors would be expected to be lower than 2.0023, however, since recent calculations (9) indicate that no unoccupied orbital is less than 10 eV above the $1t_1$ orbital of SO_4^-.

The radical SO_3^- has been detected as a result of γ-irradiation in several compounds containing the —SO_3 function (3). It is characterized by an almost isotropic g-factor of 2.0036 ± 0.0007 and by a hyperfine interaction in the range 300–400 Mc/s involving the ^{33}S nucleus (spin 3/2) of the 0.74% $^{33}SO_3^-$ radicals present in natural abundance. The unpaired electron occupies an a_1 orbital (symmetry C_{3v}) possessing considerable sulfur 3s character. There can be little doubt that radical B in irradiated K_2SO_4 is SO_3^-. Alternatives such as SO_2^- or SO^-, being π-electron radicals, would not be expected to exhibit a large ^{33}S interaction. In SO_2^-, for example, the isotropic ^{33}S hyperfine interaction is only 41 Mc/s (6).

EXPERIMENTAL

Crystals of K_2SO_4 were grown by slow evaporation of aqueous solution. The unit cell is orthorhombic, having dimensions $a = 5.731$, $b = 10.008$, $c = 7.424$ Å, and contains four molecules of K_2SO_4 (10). The crystal habit was inferred goniometrically and confirmed by X-ray diffraction photographs, being prismatic along [100] and developing {021}. The crystals were irradiated with a Philips X-ray tube type 25623-62, and examined after irradiation with a Varian V-4502 spectrometer previously described (11). To determine the g-tensors of the radicals the K_2SO_4 crystals were mounted on a two-circle goniometer (12) and rotated about each of the orthorhombic axes in turn, spectra being taken every 10°. From these data the principal values of the g-tensors were determined in the usual way (13).

ACKNOWLEDGMENT

The authors are grateful to Dr. L. D. Calvert for determining the unit-cell dimensions and directions of the crystals.

1. V. I. Spitsyn, V. V. Gromov, and L. G. Karaseva. Dokl. Akad. Nauk SSSR, **159**, 178 (1964).
2. V. V. Gromov and J. W. T. Spinks. To be published.
3. G. W. Chantry, A. Horsfield, J. R. Morton, J. R. Rowlands, and D. H. Whiffen. Mol. Phys. **5**, 233 (1962).
4. W. Kanzig. Phys. Chem. Solids, **23**, 479 (1962).
5. W. Sander. Z. Physik, **169**, 353 (1962).
6. P. W. Atkins, A. Horsfield, and M. C. R. Symons. J. Chem. Soc. 5220 (1964).
7. P. W. Atkins, J. A. Brivati, A. Horsfield, M. C. R. Symons, and P. A. Trevalion. Proc. Int. Symp. on Free Radicals, 6th, Cambridge, 1963.
8. M. Wolfsberg and L. Helmholz. J. Chem. Phys. **20**, 837 (1952).
9. D. M. Bishop, M. Randič, and J. R. Morton. To be published.
10. R. W. G. Wyckoff. The structure of crystals. 2nd. ed. Chem. Cat. Co. Inc., New York. 1931. p. 291.
11. J. R. Morton. Can. J. Chem. **43**, 1948 (1965).
12. G. Roberts and W. Derbyshire. J. Sci. Instr. **38**, 511 (1961).
13. J. E. Geusic and L. C. Brown. Phys. Rev. **112**, 64 (1958).

Received October 14, 1965.
Division of Applied Chemistry,
National Research Council,
Ottawa, Canada.

Can. J. Chem. Downloaded from www.nrcresearchpress.com by 210.87.254.105 on 09/05/12
For personal use only.

PHOTOLYSIS OF MIXES OF PERFLUOROACETONE AND PERFLUORODIETHYL KETONE REACTIONS OF CF_3 AND C_2F_5 RADICALS

ALVIN S. GORDON

It has been reported that alkyl radicals easily displace a perfluoroalkyl radical from a perfluoroketone (1–3). In the work reported here, the evidence indicates that a perfluoroalkyl radical does not displace a perfluoroalkyl radical from a perfluoroketone even at 300 °C.

The combination reactions of perfluoroethyl and perfluoromethyl radicals result in a ratio for the rate of formation of the various radical–radical addition products,

$$[1] \qquad \frac{k_{CF_3,C_2F_5}}{k_{CF_3,CF_3}^{1/2}\, k_{C_2F_5,C_2F_5}^{1/2}} = \frac{R_{C_3F_8}}{R_{C_2F_6}^{1/2}\, R_{C_4F_{10}}^{1/2}} = 2.08 \pm 0.04 .$$

This ratio is independent of temperature. The k's are the rate constants for the subscripted radical–radical combinations, and the R's are the rate of formation of the subscripted compound. The results are in good agreement with the previously published value of 1.77 ± 0.10 for perfluoromethyl and perfluoro n-propyl radical combinations (4).

It has been shown previously that F atoms are not abstracted by disproportionation of perfluoro radicals or by abstraction from perfluoroketones at temperatures as high as 200° (4, 5). The present work adds further evidence and extends the temperature to 300°, since no CF_4 is found in the products.

Two mixes of perfluoroacetone and perfluorodiethyl ketone were employed, 1:1 and 3:1. As may be noted in Table I, the composition had no effect on the ratio in eq. [1], consonant with a radical–radical combination mechanism. The reactants were photolyzed in a quartz cell with the radiation from a medium pressure mercury lamp; products were analyzed by gas chromatography, with a 1% squalane on pelletex column, temperature programmed from −196 °C to 100 °C. All the peaks were trapped and identified by mass spectrometry. The peak areas were converted to micromoles by instrument calibration factors obtained with pure materials.

TABLE I

Combination of ratios of CF_3 and C_2F_5 radicals from photolysis of perfluoroacetone and perfluoropentanone-3

Temp. (°C)	Pressure of mix (cm)	$\frac{C_3F_8}{(C_2F_6)^{1/2}(C_4F_{10})^{1/2}}$
Perfluoropentanone-3/perfluoroacetone = 1		
151.0	8.1	2.1
150.5	3.7	2.1
201.0	10.1	2.0
201.0	10.1	2.1
251.0	10.0	2.1
300.0	10.0	2.1
Perfluoropentanone-3/perfluoroacetone = 3		
100.0	10.0	2.0
151.0	10.0	2.1

Since the possibility existed that perfluoromethylethyl ketone would appear on the chromatogram at the same place as perfluorobutane, the products of the reaction at the highest temperature were resolved by a silene column which retains ketones. The mass spectral pattern of the perfluorobutane from the silene column proved to be identical

Can. J. Chem. Downloaded from www.nrcresearchpress.com by 210.87.254.40 on 09/05/12
For personal use only.

with that from the pelletex column, showing that no perfluoromethylethyl ketone was produced, and that the displacement reactions

[2] $$\dot{C}F_3 + C_2F_5COC_2F_5 \rightarrow CF_3COC_2F_5 + \dot{C}_2F_5$$

and

[3] $$\dot{C}_2F_5 + CF_3COCF_3 \rightarrow CF_3COC_2F_5 + \dot{C}F_3$$

do not occur. Since the heat of reaction in reactions [2] and [3] is about zero, the high activation barrier against the reaction probably results from the electropositive character of both the carbon atom of the attacking radical and that of the attacked carbon atom of the carbonyl group, because of the influence of the F and O atoms. By a similar argument, Gordon (6) has proposed that the electropositive $\dot{C}F_3$ radicals attack the electronegative oxygen atom rather than the carbon atom of the carbonyl group in perfluoroacetone; the present work substantiates the hypothesis.

In combination reactions of unlike radicals, ratio [1] would be temperature independent even if the same barrier existed for the three reactions. A small barrier for such reactions (not over 1.5 kcal/mole) has been suggested for such combinations (7, 8) but very recent work on cross combination of CH_3 and CF_3 (9, 10) indicates no temperature dependence. The results indicate that CF_3 combination has no barrier, since CH_3 combination has no activation barrier.

The results in Table I show that the cross combination ratio for CF_3 and C_2F_5 is very close to 2. The ratio is calculated to be 2.0 on the basis of collisions of CF_3 and C_2F_5 assuming equal diameters, and 2.3 assuming the diameter of C_2F_5 is twice that of CF_3. A realistic choice would be between these extreme values. Since the calculations show that the relative diameters will have little effect on the calculated ratio, any large deviations from a value of 2 must be due to the reaction probabilities. A comparison of the values of ratio [1] obtained in this work with the analogous value from the work of Pritchard, Miller, and Dacey (4) on perfluoromethyl and perfluoro *n*-propyl combination reactions suggests that the probability of reaction on collision is equal for all these radicals. There is an indication that the analogous alkyl radicals also have equal probability for reaction, although the data have considerable error (11). The alkyl radical data also are not corrected for disproportionation reactions; for methyl, ethyl, and *n*-propyl radicals, the correction is quite small (12).

I wish to thank G. O. Pritchard for fruitful discussions.

1. G. O. Pritchard and E. W. R. Steacie. Can. J. Chem. **35**, 1216 (1957).
2. S. J. W. Price and K. O. Kutschke. Can. J. Chem. **38**, 2128 (1960).
3. W. G. Alcock and E. Whittle. Trans. Faraday Soc. **61**, 244 (1965).
4. G. O. Pritchard, G. H. Miller, and J. R. Dacey. Can. J. Chem. **39**, 1968 (1961).
5. G. H. Miller, G. O. Pritchard, and E. W. R. Steacie. Z. Physik. Chem. Frankfurt, **16**, 262 (1958).
6. A. S. Gordon. J. Chem. Phys. **36**, 1330 (1962).
7. P. B. Ayscough. J. Chem. Phys. **24**, 944 (1956).
8. G. O. Pritchard and J. R. Dacey. Can. J. Chem. **38**, 182 (1960).
9. G. O. Pritchard and J. T. Bryant. J. Phys. Chem. **69**, 1085 (1965).
10. R. D. Giles and E. Whittle. Trans. Faraday Soc. **61**, 1425 (1965).
11. J. A. Kerr and A. F. Trotman-Dickinson. Chem. Ind. London, 125 (1959).
12. Carl A. Heller. Private communication.

Received May 25, 1965.
Chemistry Division,
U.S. NOTS,
China Lake, California.

Can. J. Chem. Downloaded from www.nrcresearchpress.com by 210.87.254.40 on 09/05/12
For personal use only.

Can. J. Chem. Downloaded from www.nrcresearchpress.com by 210.87.254.40 on 09/05/12
For personal use only.

BENZOPHENONE-SENSITIZED PHOTOLYSIS OF CYCLOPENTENE. PREPARATION OF *meso*- AND DL-3,3′-BICYCLOPENTENYL

K. S. SIDHU, O. P. STRAUSZ, AND H. E. GUNNING

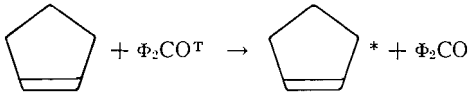
Triplet state energy transfer from benzophenone to simple monoolefins is an inefficient process (1) because the triplet state energy of simple monoolefins lies above the triplet level of benzophenone. No such restriction exists, however, on the photoreduction of benzophenone. Cyclohexene, for example, while being a poor quencher, readily brings about the photoreduction of benzophenone (2). The reactivity of the lowest-lying (n, π^*) state of benzophenone in its photoreduction reactions has been shown to be very selective and sensitive toward electron availability (3). The reactivity, in general, parallels that of *t*-butyl hypochlorite, which reacts with the allylic hydrogen in cyclohexene and cyclopentene 25 and 30 times faster, respectively, than with the hydrogen of the corresponding cycloalkanes (4).

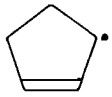
In this note we describe an example of the use of this selective reactivity of triplet state benzophenone for preparative purposes. When we photolyzed solutions of benzophenone in cyclopentene we found 3,3′-bicyclopentenyl ($C_{10}H_{14}$) as the only hydrocarbon product, formed in good yields. The results of some representative runs in which quantum yield values for benzophenone disappearance and benzopinacol and 3,3′-bicyclopentenyl formation were measured are summarized in Table I.

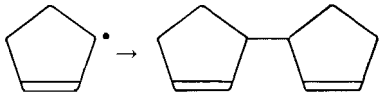
The results can be accounted for by the following scheme,

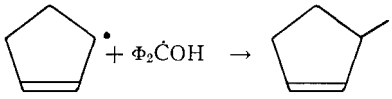
[1] $\Phi_2CO + h\nu \rightarrow \Phi_2CO^S$

[2] $\Phi_2CO^S \rightarrow \Phi_2CO^T$

[3]  $+ \Phi_2CO$

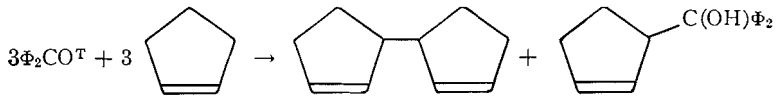
[3a]  $+ \Phi_2\dot{C}OH$

[4]  (isomers I and II)

[5]  $+ \Phi_2\dot{C}OH \rightarrow$ $C(OH)\Phi_2$ (III)

[6] $2\Phi_2\dot{C}OH \rightarrow (\Phi_2C(OH))_2$ (IV)

where Φ_2CO^S and Φ_2CO^T are excited singlet and triplet states of benzophenone. C_5H_8* is electronically or vibrationally excited cyclopentene. The overall reaction is



$3\Phi_2CO^T + 3$ → I and II + III + $(\Phi_2C(OH))_2$ IV

III has not been definitely identified; however, the petroleum ether soluble fraction of the solid products shows an infrared spectrum which is compatible with this structure. Moreover, similar cross-recombination has been observed in the benzophenone-photosensitized oxidation of toluene and cumene (5). Within the uncertainty in benzopinacol determinations, the results of Table I are in agreement with the above mechanism.

TABLE I

Quantum yield determination results*

Einsteins absorbed $\times 10^3$	Quantum yields (moles einstein^{-1})		
	$-\Phi_2CO$	$C_{10}H_{14}$	$(\Phi_2C(OH))_2$
2.88	0.48	0.15	0.14
4.20	0.49	0.14	0.10
6.02	0.47	0.13	0.12
Average	0.48	0.14	0.12

*With 0.1 *M* solutions of benzophenone in cyclopentene (cf. Experimental).

TABLE II

Values of τ for the different protons of the two 3,3′-bicyclopentenyl isomers

Protons	τ	
	Isomer I	Isomer II
Olefinic	4.38*	4.35*
Tertiary	7.35	7.39
$>CH_2$ (α to π bond)	7.73	7.70
$>CH_2$ (β to π bond)	(i) 8.04	8.06
	(ii) 8.48	8.48

*The corresponding internal olefinic protons absorb near $\tau = 4.38$ in 3- and 4-vinylcyclopentene.

From the quantum yield data the ratio of rate constants of deactivation to abstraction, k_3/k_{3a}, is equal to 1.1.*

No dicyclopentadiene, cyclopentyl cyclopentene, or polymer formation was observed. Therefore, thermalized cyclopentenyl radicals do not disproportionate or add to cyclopentene. It may be noted that no cyclopentadiene was observed in the mercury-photosensitized decomposition of cyclopentene (6). Cyclohexene does not give any oxetane in a similar reaction (2) and a specific search for oxetane in the present case failed to reveal its presence. Since no $C_{10}H_{14}$ product other than 3,3′-bicyclopentenyl was detected, the attack of benzophenone is exclusively on the allylic hydrogen.

On the gas chromatographic column the $C_{10}H_{14}$ product resolved into two fractions with relative retention times of 46 (I) and 53 (II) with respect to cyclopentene. (Column: 19 ft 30% β,β'-oxidipropionitrile on fire brick, at 63 °C, with He-carrier flow 110 ml/min.) Authentic samples (cf. Experimental) gave retention times identical with them. The two peaks were symmetrical and equal in area. They were separately collected and analyzed.

**This figure should be viewed from the standpoint that energy transfer reactions may proceed with near-collision efficiency, whereas abstraction reactions have low frequency factors and considerable activation energies.*

Can. J. Chem. Downloaded from www.nrcresearchpress.com by 210.87.254.40 on 09/05/12
For personal use only.

Their infrared and mass spectra were identical with each other and with those obtained on synthetic samples. Their nuclear magnetic resonance (n.m.r.) spectra were also identical with the n.m.r. spectra of synthetic materials, but a small difference appeared between I and II. The values of the complex multiplet resonances for the two isomers are listed in Table II. The important difference is in the fine splitting of olefinic protons (shown in Fig. 1). Among the various optical isomers of 3,3′-bicyclopentenyl which have not yet been reported in the literature, the meso structure, in equilibrium position, has the two double bonds closer than the optically active forms. The meso isomer may therefore be expected to show the observed greater splitting (cf. Fig. 1(*a*).) due to proximity effects. This view is supported by the n.m.r. spectrum of 3-cyclopentenylcyclopentane. The two olefinic protons of this molecule appear at a τ value of 4.38 and have almost identical structure to the olefinic protons of II. Thus I and II are most likely the meso- and DL-stereoisomers of 3,3′-bicyclopentenyl, respectively.

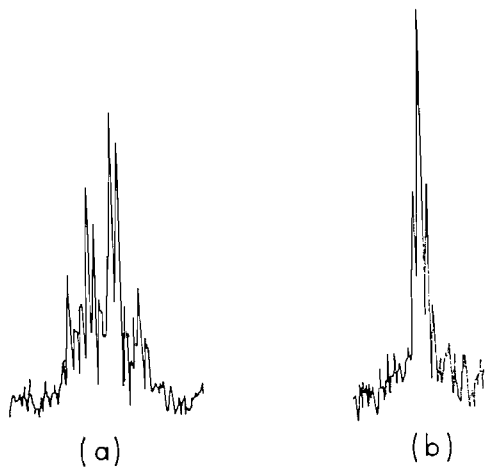


FIG. 1. Nuclear magnetic resonance spectra of the olefinic protons of (*a*) *meso*- and (*b*) DL-3,3′-bicyclopentenyl. HR-100.

Finally a series of experiments for the determination of the effect of conversion of the reaction on the 3,3′-bicyclopentene yield were carried out. Solutions (2.1 *M*) of benzophenone in cyclopentene were irradiated in pyrex vessels with unfiltered radiation from a Hanovia medium-pressure mercury lamp for various durations. The reaction mixtures were separated by distillation (unreacted cyclopentene b.p. 42° at 710 mm, and 3,3′-bicyclopentenyl b.p. 70° at 18 mm). No complications due to secondary reactions were observed up to 12% conversion and the yield for $C_{10}H_{14}$ was 85% based on the benzophenone consumption and the suggested mechanism.

In summary, the photochemical route described in this note offers a convenient single step synthesis from simple starting materials for the preparation of 3,3′-bicyclopentyls. Furthermore, these results confirm the observations of Walling and Thaler (4) on the reactivity of allylic hydrogen in cyclopentene.

EXPERIMENTAL

Solutions (0.1 *M*) of benzophenone (Fisher reagent grade) in freshly distilled cyclopentene (Phillips research grade) were degassed by repeated freezing and thawing. The irradiations were carried out in a cylindrical pyrex cell with a high pressure mercury lamp. The filter system consisted of $CuSO_4.5H_2O$ solution (400 g/l) and a Corning filter 7-51(5970). The passing band observed on a Cary spectrophotometer

Can. J. Chem. Downloaded from www.nrcresearchpress.com by 210.87.254.40 on 09/05/12
For personal use only.

had a maximum at 3 725 Å and was 500 Å wide at half-height. A solution of 0.1186 *M* uranyl oxalate and 0.1210 *M* oxalic acid was used as the actinometer, and a CBS Laboratories type CL-1010 phototube was used to monitor the light intensities.

After irradiation, samples of the reaction mixture were injected into a gas–liquid chromatograph (g.l.c.) column with a microliter syringe and $C_{10}H_{14}$ determined. Benzophenone disappearance was measured by the standard spectrophotometric technique (7). The absorbencies were measured on a Cary spectrophotometer model 14M. For benzopinacol determination an aliquot of the reaction mixture was placed in a tube and the volatile part slowly pumped off. The residue was mixed with petroleum ether (b.p. 60–70°) and allowed to stand overnight. The residual crystalline solid was filtered, dried, and weighed. It was identified by its decomposition point (184°) and infrared spectrum.

Two methods were used to prepare the authentic samples of 3,3′-bicyclopentenyl. (*a*) A good yield for 3,3′-bicyclohexenyl has been reported in the reaction of *t*-butoxy radicals with cyclohexene. Accordingly, a mixture of di-*t*-butyl peroxide and cyclopentene in molar ratio 1:6 was degassed and sealed in a Carius tube and heated to 130° for 40 h. The reaction mixture was then distilled to give the desired fraction (b.p. 70° ± 2° at 18 mm). The yield was poor. (*b*) 3-Chlorocyclopentene was prepared by passing dry HCl through cyclopentadiene. The final product was obtained via Grignard reaction.

The infrared and n.m.r. spectra were obtained in CCl_4 solvent. Tetramethylsilane was the internal standard in the n.m.r. analyses.

1. G. S. Hammond and P. A. Leermakers. J. Phys. Chem. **66**, 1148 (1962).
2. D. R. Arnold, R. L. Hinman, and A. H. Glick. Tetrahedron Letters, **22**, 1425 (1964).
3. C. Walling and M. J. Gibian. J. Am. Chem. Soc. **87**, 3361 (1965).
4. C. Walling and W. Thaler. J. Am. Chem. Soc. **83**, 3877 (1961).
5. G. S. Hammond, W. P. Baker, and W. M. Moore. J. Am. Chem. Soc. **83**, 2795 (1961).
6. W. A. Gibbons, W. F. Allen, and H. E. Gunning. Can. J. Chem. **40**, 568 (1962).
7. W. M. Moore, G. S. Hammond, and R. P. Foss. J. Am. Chem. Soc. **83**, 2789 (1961).

Received October 14, 1965.
Department of Chemistry,
University of Alberta,
Edmonton, Alberta.

REACTIONS OF HYDRAZINE WITH ALKOXIDES

M. S. Bains

It has been reported (1, 2) that coordination complexes of titanium and zirconium alkoxides with hydrazine undergo further chemical reactions when they stand in solution and under vacuum with or without being heated. The reactions of boron and aluminium halides with hydrazine are noteworthy (3). Some of the results of further work on similar reactions of hydrazine with boron alkoxides and boric acid are briefly reported here.

Boron ethoxide and boron isopropoxide do not react with simple amines to give addition complexes of the type $B(OR)_3NR'_3$ where R′ = H or alkyl. In attempts to isolate complexes of boron alkoxides, compounds of hydrazine with boron methoxide and boron mixed methoxide were obtained (4) either when the base reacted with pure boron methoxide, or when boron ethoxide or boron isopropoxide was mixed with it in a large excess of methanol. In addition to these adducts the products $[B(OMe)_{2.5}]_2N_2H_3$, $[B(OPr^i)_{0.75}(OMe)_2]N_2H_{3.75}$, and $[B(OMe)_{2.3}]N_2H_{3.3}$ were isolated from the reaction of boron ethoxide or boron isopropoxide with the base in the presence of excess methanol (5). It appeared that stable adducts are obtained after the ethoxide and isopropoxide groups are replaced by methoxide groups, and subsequently elimination reactions that give these products take place. However, it has now been observed that when pure boron ethoxide or pure boron isopropoxide is mixed with anhydrous hydrazine no simple addition complex can be isolated; replacement of alkoxide groups by hydrazido groups has been observed. The analytical results of a few typical experiments are shown in Table I.

Can. J. Chem. Downloaded from www.nrcresearchpress.com by 210.87.254.40 on 09/05/12
For personal use only.

had a maximum at 3 725 Å and was 500 Å wide at half-height. A solution of 0.1186 *M* uranyl oxalate and 0.1210 *M* oxalic acid was used as the actinometer, and a CBS Laboratories type CL-1010 phototube was used to monitor the light intensities.

After irradiation, samples of the reaction mixture were injected into a gas–liquid chromatograph (g.l.c.) column with a microliter syringe and $C_{10}H_{14}$ determined. Benzophenone disappearance was measured by the standard spectrophotometric technique (7). The absorbencies were measured on a Cary spectrophotometer model 14M. For benzopinacol determination an aliquot of the reaction mixture was placed in a tube and the volatile part slowly pumped off. The residue was mixed with petroleum ether (b.p. 60–70°) and allowed to stand overnight. The residual crystalline solid was filtered, dried, and weighed. It was identified by its decomposition point (184°) and infrared spectrum.

Two methods were used to prepare the authentic samples of 3,3′-bicyclopentenyl. (*a*) A good yield for 3,3′-bicyclohexenyl has been reported in the reaction of *t*-butoxy radicals with cyclohexene. Accordingly, a mixture of di-*t*-butyl peroxide and cyclopentene in molar ratio 1:6 was degassed and sealed in a Carius tube and heated to 130° for 40 h. The reaction mixture was then distilled to give the desired fraction (b.p. 70° ± 2° at 18 mm). The yield was poor. (*b*) 3-Chlorocyclopentene was prepared by passing dry HCl through cyclopentadiene. The final product was obtained via Grignard reaction.

The infrared and n.m.r. spectra were obtained in CCl_4 solvent. Tetramethylsilane was the internal standard in the n.m.r. analyses.

1. G. S. Hammond and P. A. Leermakers. J. Phys. Chem. **66**, 1148 (1962).
2. D. R. Arnold, R. L. Hinman, and A. H. Glick. Tetrahedron Letters, **22**, 1425 (1964).
3. C. Walling and M. J. Gibian. J. Am. Chem. Soc. **87**, 3361 (1965).
4. C. Walling and W. Thaler. J. Am. Chem. Soc. **83**, 3877 (1961).
5. G. S. Hammond, W. P. Baker, and W. M. Moore. J. Am. Chem. Soc. **83**, 2795 (1961).
6. W. A. Gibbons, W. F. Allen, and H. E. Gunning. Can. J. Chem. **40**, 568 (1962).
7. W. M. Moore, G. S. Hammond, and R. P. Foss. J. Am. Chem. Soc. **83**, 2789 (1961).

Received October 14, 1965.
Department of Chemistry,
University of Alberta,
Edmonton, Alberta.

REACTIONS OF HYDRAZINE WITH ALKOXIDES

M. S. Bains

It has been reported (1, 2) that coordination complexes of titanium and zirconium alkoxides with hydrazine undergo further chemical reactions when they stand in solution and under vacuum with or without being heated. The reactions of boron and aluminium halides with hydrazine are noteworthy (3). Some of the results of further work on similar reactions of hydrazine with boron alkoxides and boric acid are briefly reported here.

Boron ethoxide and boron isopropoxide do not react with simple amines to give addition complexes of the type $B(OR)_3NR'_3$ where R′ = H or alkyl. In attempts to isolate complexes of boron alkoxides, compounds of hydrazine with boron methoxide and boron mixed methoxide were obtained (4) either when the base reacted with pure boron methoxide, or when boron ethoxide or boron isopropoxide was mixed with it in a large excess of methanol. In addition to these adducts the products $[B(OMe)_{2.5}]_2N_2H_3$, $[B(OPr^i)_{0.75}(OMe)_2]N_2H_{3.75}$, and $[B(OMe)_{2.3}]N_2H_{3.3}$ were isolated from the reaction of boron ethoxide or boron isopropoxide with the base in the presence of excess methanol (5). It appeared that stable adducts are obtained after the ethoxide and isopropoxide groups are replaced by methoxide groups, and subsequently elimination reactions that give these products take place. However, it has now been observed that when pure boron ethoxide or pure boron isopropoxide is mixed with anhydrous hydrazine no simple addition complex can be isolated; replacement of alkoxide groups by hydrazido groups has been observed. The analytical results of a few typical experiments are shown in Table I.

Can. J. Chem. Downloaded from www.nrcresearchpress.com by 210.87.254.105 on 09/05/12
For personal use only.

Can. J. Chem. Downloaded from www.nrcresearchpress.com by 210.87.254.105 on 09/05/12
For personal use only.

TABLE I

Reactions of boron alkoxides and of boric acid with hydrazine

Expt. No.	Reactants: Boron ethoxide, g	Reactants: Boron isopropoxide, g	Reactants: Boric acid, g	Reactants: Hydrazine, g	Product: Boron Found	Product: Boron Calcd.	Product: Hydrazine Found	Product: Hydrazine Calcd.	Empirical formula
1	3.9			2.0	8.39	8.19	24.05	24.24	$B(OEt)_2N_2H_3$
2	3.3			1.4	8.36	8.19	24.07	24.24	$B(OEt)_2N_2H_3$
3	2.1			2.1	9.68	9.54	28.40	28.17	$B(OEt)_{1.6}N_2H_{2.6}$
4		3.3		2.6	8.60	8.32	24.29	24.61	$B(OPr^i)_{1.5}N_2H_{2.5}$
5		5.9		1.7	10.90	10.82	32.26	32.00	$B(OPr^i)N_2H_2$
6		2.8		1.3	10.70	10.82	32.44	32.00	$B(OPr^i)N_2H_2$
7			10.0	6.0	14.51	14.48	40.00	40.10	$B(OH)_2N_2H_3$
8			4.0	2.5	26.20	26.19	38.10	38.19	$B_2(OH)_2N_2$
9			1.1	1.2	19.05	19.10	55.25	55.50	$B(OH)N_2H_2$

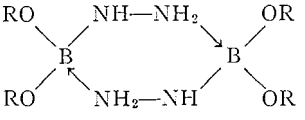
One alkoxide group of boron ethoxide and two alkoxide groups of boron isopropoxide are replaced at room temperature under vacuum (1 mm Hg). It is also significant that the product $B(OEt)_2N_2H_3$ on azeotropic distillation with benzene lost a molecule of hydrazine giving a product $[B(OEt)_2]_2N_2H_2$. This may also signify that the product $B(OEt)_2N_2H_3$ contains a hydrazine of solvolysis according to the formula $[B(OEt)_2]_2N_2H_2.N_2H_4$. Further heating of the product $[B(OEt)_2]_2N_2H_2$ to 200 °C and under vacuum of 0.2 mm Hg resulted in the elimination of a molecule of alcohol per boron atom, the final product having the composition $(BOEt)_2N_2$ with possible B=N double bonds.

Hydrazine also reacts with boric acid, with the elimination of water and the introduction of B—N bonds. The products obtained are given in Table I.

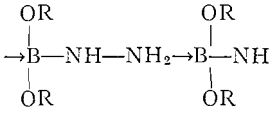
A brief comment on these results may be appropriate. It is well established that the B—N bond is fairly stable and is formed at the expense of B—H, B—X (X = halogen), B—C, and B—O bonds (6). In this context the compounds reported above are quite likely to be formed. These products are not soluble in inert organic solvents, therefore their molecular weights could not be determined; this may mean that the products are polymeric.

The following tentative structures proposed for the products of different general composition as given in the following four categories would emphasize the significance of these results.

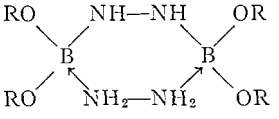
(i) For $B(OR)_2N_2H_3$



(I)

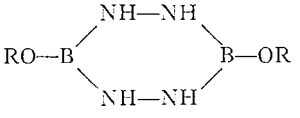


(II)

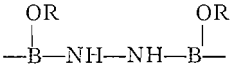


(III)

(ii) For $B(OR)N_2H_2$

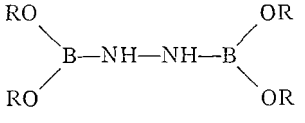


(IV)



(V)

(iii) For $B_2(OR)_4N_2H_2$



(VI)

Can. J. Chem. Downloaded from www.nrcresearchpress.com by 210.87.254.105 on 09/05/12
For personal use only.

(iv) For $B_2(OR)_2N_2$



(VII) (VIII)

All these types of products where R may be alkyl or H have been isolated. Due to boron acceptor and nitrogen donor atoms these products may be further polymerized. The formula VIII may, however, not be feasible on grounds of hybridization.

An ethereal solution of anhydrous hydrazine and titanium isopropoxide takes on a violet coloration, the color deepening with time. The reaction

$$4Ti(OPr^i)_4 + N_2H_4 \rightarrow 4Ti(OPr^i)_3 + 4Pr^iOH + N_2$$

accounts for the development of color and may be the result of a trace of titanium(III). However, a mixture of titanium isopropoxide and hydrazine in benzene or toluene turned deep violet when heated under reflux. When the volatile constituents were distilled off under high vacuum a brownish solid was obtained. The titanium content of such products in four experiments was 33–35%, conforming to the formula $(Pr^iO)TiN_2H$. Furthermore, when hydrazine and titanium isopropoxide were heated together and the temperature raised gradually in the absence of any solvent, an explosive reaction took place at about 130 °C bath temperature.

TABLE II

Reaction of zirconium isopropoxide isopropylate with hydrazine

Expt. No.	Volume of ether, ml	Reactants: Zirconium isopropoxide isopropylate, g	Reactants: Hydrazine, g	Product: Zirconium Found	Product: Zirconium Calcd.	Product: Empirical formula
1	150	4.0	1.0	52.5	50.9	$Zr(OPr^i)N_2H$
2	100	7.1	1.0	39.0	38.9	$Zr(OPr^i)_2N_2H_2$

These experiments pointed to the introduction of metal–nitrogen bonds. The following experiment is very instructive in this connection.

Tetrakis(diethylamide)titanium (2 g) was treated with an almost stoichiometric amount of anhydrous hydrazine in ether solution. After the reaction mixture had stood for some time, high vacuum was applied to remove ether and any other volatile materials. After this distillation of ether, when the flask and its contents were still cold, a violent explosion took place. The probable reaction appears to be the following

$$Ti(NEt_2)_4 + N_2H_4 \rightarrow TiN_2 + 4Et_2NH \text{ (explodes)}.$$

For zirconium isopropoxide isopropylate ($Zr(OPr^i)_4Pr^iOH$) and excess hydrazine the results are given in Table II. In the second experiment, since the volume of the solution was less and the concentration of isopropoxide was relatively high, the equilibrium of

Can. J. Chem. Downloaded from www.nrcresearchpress.com by 210.87.254.105 on 09/05/12
For personal use only.

the reaction, which is reversible, moved toward the left, and therefore a small number of isopropoxide groups were replaced.

$$Zr(OPr^i)_4Pr^iOH + N_2H_4 \rightleftharpoons Zr(Pr^iO)_{4-n}N_2H_{4-n} + (n+1)Pr^iOH$$

These reactions with titanium and zirconium isopropoxide are remarkable, since amines do not generally displace alkoxide groups whereas alcohols very readily displace amines from dialkylamino derivatives (7). The reactions present an analogy with those between metal chloride and ammonia and metal chloride and hydrazine (8, 9) and they suggest that alkoxide groups are replaced by hydrazine to give products of the general composition $M(OR)_{4-n}N_2H_{4-n}$. Further work to elucidate these reactions and the structure of the products is in progress.

It should be noted that experiments with transition metal alkoxides may result in explosions and therefore caution is necessary. The work with boron compounds is safe, however, and explosions were neither expected nor observed.

ACKNOWLEDGMENT

The author wishes to thank Prof. D. C. Bradley for his encouragement and his interest in this work.

1. M. S. Bains and D. C. Bradley. Can. J. Chem. **40**, 1350 (1962).
2. M. S. Bains. Ph.D. Thesis, University of London, London, England. 1959.
3. W. G. Paterson and M. Onyszchuk. Can. J. Chem. **41**, 1872 (1963).
4. M. S. Bains and L. Jain. Res. Bull. Panjab Univ. **16**, 45 (1965).
5. M. S. Bains and C. L. Jain. Unpublished work.
6. W. Gerrard. Organic chemistry of boron. Academic Press, London. 1961.
7. D. C. Bradley and I. M. Thomas. J. Chem. Soc. 3857 (1960).
8. (*a*) G. W. A. Fowles and F. H. Pollard. J. Chem. Soc. 2588, 4128 (1953).
   (*b*) G. W. A. Fowles and D. Nicholls. J. Chem. Soc. 990 (1959).
9. (*a*) O. Schmitz-Dumont, P. Simons, and G. Broja. Z. Anorg. Allgem. Chem. **258**, 307 (1949).
   (*b*) O. Schmitz-Dumont and F. Raabe. Z. Anorg. Allgem. Chem. **277**, 297 (1954).

Received June 29, 1965.
Department of Chemistry,
Panjab University,
Chandigarh-3, India.

Can. J. Chem. Downloaded from www.nrcresearchpress.com by 210.87.254.105 on 09/05/12
For personal use only.

Can. J. Chem. Downloaded from www.nrcresearchpress.com by 210.87.254.5 on 09/05/12
For personal use only.

Canadian Journal of Chemistry

Issued by THE NATIONAL RESEARCH COUNCIL OF CANADA

VOLUME 44 MARCH 1, 1966 NUMBER 5

HYDROXYL PROTON MAGNETIC RESONANCE IN RELATION TO RING SIZE, SUBSTITUENT GROUPS, AND MUTAROTATION OF CARBOHYDRATES[1]

A. S. PERLIN

National Research Council of Canada, Prairie Regional Laboratory, Saskatoon, Saskatchewan

Received July 13, 1965

ABSTRACT

Some magnetic resonance properties of hydroxyl protons are described for a variety of sugars and derivatives in dimethyl sulfoxide. Spectral information of this kind is shown to be useful, particularly for differentiating between certain types of interconvertible molecular species. For example, a reducing sugar may be characterized as pyranose or furanose depending upon whether it exhibits a resonance signal that can be ascribed to OH-4 or OH-5, respectively. According to the data obtained, α-D-glucose, α-D-xylose, β-D-arabinose, α-D-lyxose, and α- and β-D-ribose are pyranoses when freshly dissolved, whereas the 2,3-carbonate of D-mannose or D-lyxose is in a furanose form. Selective deuteration and spin decoupling were of primary importance in making some of the spectral assignments.

Although arabinose, ribose, and galactose exist partly as furanoses in mutarotated aqueous solutions, their tendency to adopt the structure of the five-membered ring is much greater in dimethyl sulfoxide. Such variability may be due to an interplay of effects; for example, the furanose forms are relatively stable, but this property is masked in water by preferential solvent stabilization of the pyranose structures.

Depending on the number and kinds of hydroxyl proton signals detected, it is possible to distinguish between cyclic and acyclic forms of certain sugar derivatives, as illustrated with hydrazones and with dialdehydes obtained by oxidative glycol scission. Hydroxyl proton magnetic resonance data are of value also for characterizing partially acetylated sugars.

INTRODUCTION

Hydroxyl protons of alcohols dissolved in dimethyl sulfoxide give magnetic resonance signals that, in contrast to their properties in the more common nuclear magnetic resonance (n.m.r.) solvents, are generally well resolved and permit the detection of spin–spin splitting (1).[2] The anomeric hydroxyl groups of sugars are characterized by resonance at lower field than the other hydroxyl groups (1, 2), and their signals should be of value in assigning configuration and in determining the composition of anomeric mixtures of reducing sugars (2).

The current study utilizes the magnetic resonance characteristics of hydroxyl protons mainly to derive some information about compounds capable of adopting more than one type of structure. Thus attention is centered on reducing sugars that may exist in both pyranose and furanose forms, and on certain carbohydrate derivatives that can be described by cyclic or acyclic formulae. A related application is the use of hydroxyl proton magnetic resonance spectroscopy in the structural elucidation of partially acetylated sugars, compounds that may suffer acyl migration when examined by chemical methods.

[1]*Issued as N.R.C. No. 8791.*

[2]*See, however, a recent communication by J. G. Trayham and G. A. Knesel, J. Am. Chem. Soc. 87, 4220 (1965), and also the Experimental section.*

In addition, some comments are made on the equilibration of reducing sugars in dimethyl sulfoxide as compared with their well-known mutarotation characteristics in water.

Ring Size of Reducing Sugars

It is not always easy to determine the ring size of reducing sugars and derivatives. X-ray crystallography has firmly established that several sugars are pyranoid in the crystalline state (see ref. 3), and there is a great deal of evidence showing that pyranose forms also predominate when these sugars are dissolved (4–6). A particularly facile demonstration of the pyranose structure of α-D-glucose in dimethyl sulfoxide solution is provided by hydroxyl proton resonance data (Fig. 1).[3]

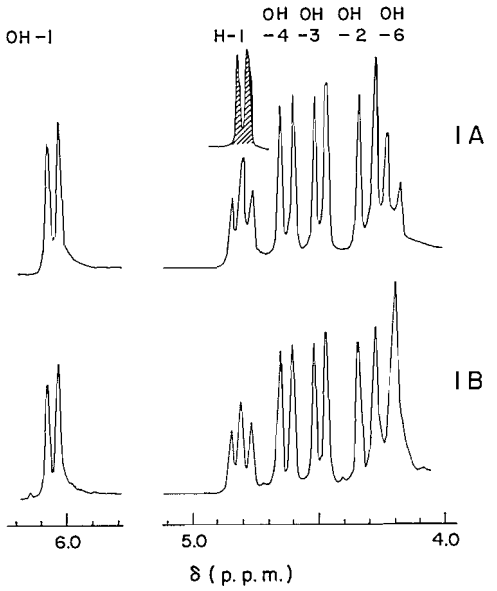


FIG. 1. Partial n.m.r. spectra at 100 Mc.p.s. of (A) α-D-glucose and (B) α-D-glucose-5,6,6′-d_3 in dimethyl sulfoxide solution, showing hydroxyl proton signals (OH) and the anomeric proton signal (H-1). The inset doublet in A represents the only signal (H-1) detected after the addition of deuterium oxide to the solution.

In the region of the spectrum shown, five of the six signals are attributable to hydroxyl protons since they no longer appear after deuterium oxide is introduced. The remaining signal, initially a triplet, collapses to a doublet (inset). Since it is the most strongly deshielded of the protons bonded to carbon, and also since it is coupled with the hydroxyl proton giving a doublet at lowest field, i.e. OH-1 (1, 2), it can be ascribed to H-1 (7). The other three doublets (Fig. 1A) are signals of secondary hydroxyl protons, i.e. OH-2, OH-3, and either OH-4 (pyranose ring) or OH-5 (furanose ring). By using a sample deuterated at position 5, a clear choice between the latter two alternatives is possible. Thus, if one of these three doublets is caused by OH-5 rather than by OH-4, it should be replaced in the spectrum of the deuterated sample by a strongly modified signal, most likely a broad singlet.[4] α-D-Glucose-5,6,6′-d_3 (8) was utilized for this purpose, and as seen in Fig. 1B, the

[3]*The spectrum (Fig. 1A) is the same irrespective of whether the solution is prepared from the crystalline sugar directly or from a syrup obtained by concentrating a fresh aqueous solution of the sugar.*

[4]*This effect was cross-checked by comparing the spectrum of 1,2-O-isopropylidene-α-D-glucofuranose in dimethyl sulfoxide with that of the compound deuterated at position 5 (8); the latter gave a singlet in place of one of the doublets exhibited by the undeuterated compound.*

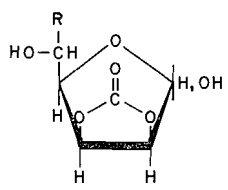
Can. J. Chem. Downloaded from www.nrcresearchpress.com by 210.87.254.5 on 09/05/12
For personal use only.

signals for its secondary hydroxyl groups are the same as those shown in Fig. 1A. This shows that the 5 position must be engaged in forming the pyranose ring. In addition, the presence of a broad singlet at 4.20 p.p.m.[5] in Fig. 1B establishes that the high-field triplet in Fig. 1A is caused by the hydroxyl proton of the primary carbinol group.[6]

Assignments in Fig. 1A for signals of the 2, 3, and 4 hydroxyl groups are based on double-resonance experiments (11, 12), frequency-swept spin decoupling being employed and dimethyl sulfoxide-d_6 being used as the solvent. Signals for the protons bonded to carbons 2, 3, and 4 (not shown in Fig. 1), which are not well shifted from each other, were also first located with the aid of the spin-decoupling technique. Each of these protons was then irradiated in turn at the appropriate resonance frequency, causing one or another of the hydroxyl proton doublets to become wholly, or largely, spin decoupled.

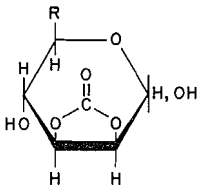
α-D-Xylose exhibits four well-resolved hydroxyl proton doublets that correspond closely both in chemical shift and spacings to hydroxyl protons 1 to 4 of α-D-glucose. Aside from the apparent similarity in molecular architecture between the pentose and hexose, this evidence that the compound has four secondary hydroxyl groups (1) shows clearly that α-D-xylose is a pyranose sugar in dimethyl sulfoxide solution. In this respect, the spectra of α-D-lyxose and β-D-arabinose are also in accord with a pyranose structure for each of these pentoses when first dissolved in dimethyl sulfoxide (however, see below).

An additional problem involving ring size, for which hydroxyl proton magnetic resonance data have proven useful, concerns the preferred size of the sugar ring in some fused-ring derivatives. In an earlier study (13) it was noted that, although D-mannose 2,3-carbonate (I) and related compounds behave chemically as furanose sugars (and certain n.m.r. data support this assignment), the observed coupling between H-3 and H-4 (ca. 3.2 c.p.s.) appears to favor a pyranose (IB) rather than a furanose (IA) structure, if the Karplus curve (7, 14, 15) is closely applicable for compounds of this type. However, the furanose structure has now been confirmed by taking into account hydroxyl proton resonance data.



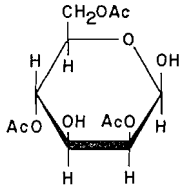
IA (R=CH_2OH)

IIA (R=H)

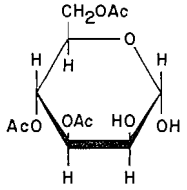


IB (R=CH_2OH)

IIB (R=H)



III



IV

The spectrum of I in dimethyl sulfoxide is very similar to that already presented (13) for the compound in deuterium oxide, aside mainly from the added presence of hydroxyl proton signals (two doublets and a triplet). Of particular note is the absence of detectable coupling between H-4 and a hydroxyl group, since H-4 gives virtually the same quartet signal with either solvent, and since this signal is unaffected when deuterium oxide is

[5]*See Experimental section for the basis of the chemical shift values.*

[6]*For a relatively large and diverse group of known compounds examined during this study, the signal ascribable to the proton of a primary hydroxyl group has almost invariably appeared as a triplet. However, n.m.r. spectroscopy has amply confirmed (see ref. 9) that the methylene protons of such groups in sugar molecules usually are magnetically non-equivalent. Since the hydroxyl proton thus constitutes the X part of an ABX system (10), there is the likelihood that a quartet or higher multiplet will be encountered in some instances. Although the presence of a hydroxyl proton triplet or higher multiplet in a spectrum is itself indicative of a primary carbinol group, detection of coupling between that proton and the α-methylene protons is a more rigorous criterion (see below).*

Can. J. Chem. Downloaded from www.nrcresearchpress.com by 210.87.254.5 on 09/05/12
For personal use only.

added to the dimethyl sulfoxide solution. Although this clearly indicates that there cannot be a free hydroxyl group at position 4 of I, it is not equally evident that H-5 *is* coupled with a hydroxyl group, because its signal is obscured by those of the 6 protons. However, such coupling was readily demonstrable with the 6-*O*-trityl derivative of I (13) by using the double-resonance technique. In the spectrum of this derivative (Fig. 2) the appearance

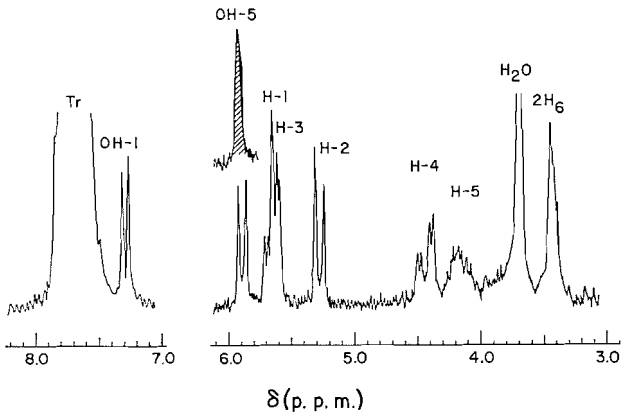


FIG. 2. The n.m.r. spectrum at 100 Mc.p.s. of 6-*O*-trityl-D-mannose 2,3-carbonate in dimethyl sulfoxide-d_6, with tetramethylsilane, contained in a coaxial capillary, as reference. The assignments are based on those reported in ref. 13. The inset signal illustrates the effect on the hydroxyl proton doublet at 5.9 p.p.m. of spin decoupling by irradiation at the resonance frequency of H-5 (Tr = protons of trityl group).

of the H-4 and most other signals is essentially the same as that in the spectrum of I itself, but the H-5 signal is well isolated. By irradiating at the resonance frequency of this proton the doublet at 5.9 p.p.m. is spin decoupled, appearing as a broad singlet (inset). These overall data obviously are not consistent with the pyranose structure (IB), and permit the conclusion that the bicyclic sugar derivative is furanose (IA).

Hydroxyl proton resonance data also help to demonstrate that a related compound, D-lyxose 2,3-carbonate (II) (16), contains a furanose ring. The spectrum of II closely resembles that of I (both in deuterium oxide and dimethyl sulfoxide), again giving an apparent value for $J_{3,4}$ of 3.3 c.p.s. As seen from Fig. 3B and its deuterium-exchanged counterpart (Fig. 3A) the pentose carbonate gives rise to a triplet caused by a hydroxy proton (at 4.9 p.p.m. in Fig. 3B). Furthermore, the C-5 methylene protons show coupling with a hydroxyl group (Fig. 3B) that is removed on addition of deuterium oxide (Fig. 3A). Therefore, the primary carbinol group in II must be free and the sugar can accordingly be ascribed a furanose structure (IIA).

Spectra of Partially Acetylated Derivatives

Hydroxyl protons resonate in dimethyl sulfoxide at lower field than do most protons that are bonded to carbon atoms of sugar molecules. With derivatives containing strongly deshielding substituent groups (e.g. acetyl), both OH and CH signals are found in the same region of the spectrum, but they then can readily be differentiated by "cancelling out" through the addition of deuterium oxide (1). For example, in the spectra of 1,2,3,4- and 1,3,4,6-tetra-*O*-acetyl-α-D-glucose and 1,2,3,6-tetra-*O*-acetyl-β-D-glucose, OH and CH signals are found in close proximity, but, on addition of deuterium oxide, a doublet is removed from each of the latter two spectra and a triplet from that of the 1,2,3,4 derivative. This clearly confirms the presence of a free primary carbinol group in the one instance

Can. J. Chem. Downloaded from www.nrcresearchpress.com by 210.87.254.5 on 09/05/12
For personal use only.

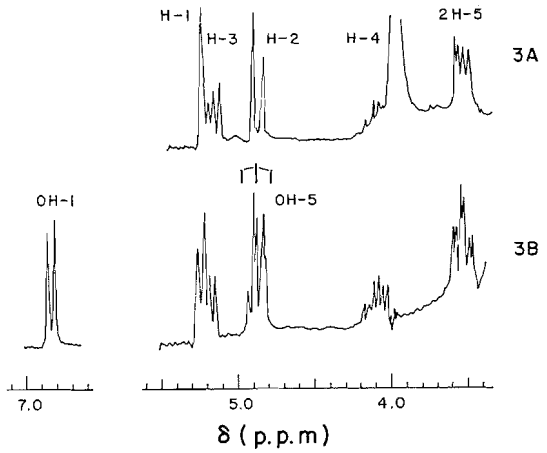


FIG. 3. The n.m.r. spectra at 100 Mc.p.s. of D-lyxose 2,3-carbonate in dimethyl sulfoxide (B) before and (A) after the addition of deuterium oxide to the solution (OH = hydroxyl proton).

and, at least, that the unacetylated hydroxyl group in each of the other two tetraacetates is secondary.[7]

An examination of two tri-*O*-acetyl-D-mannoses illustrates how OH and CH data can supplement each other in defining structure. Earlier, these triacetates were assigned the β-2,4,6 (III) and α-3,4,6 (IV) structures, respectively, mainly on the basis of chemical properties (17). The spectrum of III (Fig. 4B and, after addition of deuterium oxide,

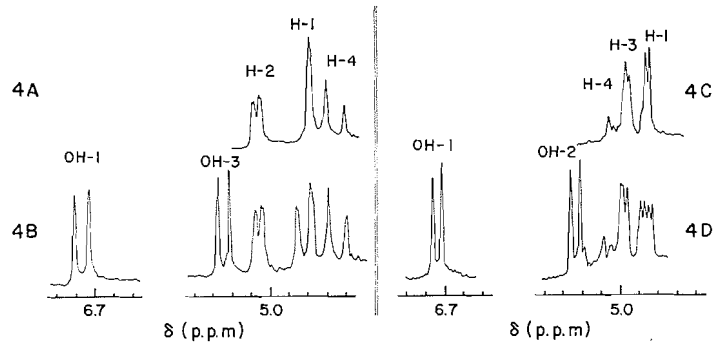


FIG. 4. Partial n.m.r. spectra at 100 Mc.p.s. of 2,4,6-tri-*O*-acetyl-β-D-mannose in dimethyl sulfoxide (B) before and (A) after the addition of deuterium oxide to the solution, and of 3,4,6-tri-*O*-acetyl-α-D-mannose in dimethyl sulfoxide (D) before and (C) after the addition of deuterium oxide (OH = hydroxyl proton).

Fig. 4A) shows the presence of two hydroxyl proton doublets. That at lower field is ascribed to OH-1 because of its location; also, it has the same spacing (7.4 c.p.s.) as the signal at 4.78 p.p.m. (Fig. 4A; 4.82 p.p.m. in Fig. 4B), which, because of its location at relatively low field for a proton bonded to carbon, undoubtedly is that of H-1. Since the anomeric position is free and the primary carbinol group is substituted (only OH doublets are detected), the two CH signals remaining unchanged in going from Fig. 4B to Fig. 4A must be those of protons alpha to secondary acetoxyl groups. The proton exhibiting a

[7]*Such information is rendered particularly accessible by the fact that dimethyl sulfoxide is a very good solvent for compounds of this type.*

Can. J. Chem. Downloaded from www.nrcresearchpress.com by 210.87.254.5 on 09/05/12
For personal use only.

quartet at 5.05 p.p.m. shows weak coupling with H-1 and hence is H-2, but since it is not coupled with the doublet at 4.65 p.p.m., the latter can only be on the nonadjacent carbon atom-4 (if one assumes a pyranose ring). This confirms that III is a 2,4,6-triacetate.

Similarly, the spectrum of IV shows that OH-1 in this compound is unsubstituted and that the other free hydroxyl group is secondary. The doublet at 4.99 p.p.m. (spacing of 2.2 c.p.s.) and the broad multiplet that overlaps it must be caused by protons alpha to acetoxyl groups. Since neither is coupled with H-1 (spacing of 1.5 c.p.s.), these signals can be ascribed to H-3 and H-4. A choice between these two follows from the fact that the observed spacing (2.2 c.p.s.) for the doublet is close to that expected for H-3, but far too small for H-4 in the D-*manno* series (7). Hence, these data confirm that IV is the 3,4,6-triacetate. An additional point to be noted in Fig. 4 is that OH-1 splittings are 7.5 and 4.5 c.p.s. for III and IV, respectively. These values are close to those for β-D-mannose (7.9 c.p.s.) and α-D-mannose (4.3 c.p.s.), respectively, in agreement with assignments made on the basis of rotational data (17). In these instances, the corresponding values for H-1 splitting (7) are all much smaller (1.0–1.5 c.p.s.) and hence less satisfactory for configurational assignments. Relative chemical shifts for the OH-1 signals are less reliable for the purpose because of differences in the proximity of each anomeric center to the acetoxyl groups.

Cyclic vs. Acyclic Forms

Hydroxyl proton magnetic resonance spectra may be of value in differentiating between cyclic and acyclic forms of compounds. Hydrazones, for example, may be depicted in either of these forms (18, 19) and, although they may be distinguished chemically (18, 19), the number of hydroxyl proton signals displayed should provide a simple, independent diagnosis. Several hydrazones examined during the current study were found to exist in dimethyl sulfoxide as acyclic compounds. Thus, D-erythrose-2,5-dichlorophenylhydrazone shows two doublets (OH-2 and OH-3) and a triplet (OH-4), and D-fucose-*p*-toluenesulfonylhydrazone shows four doublets (OH-2 to OH-5). The hydroxyl proton signals given by D-mannose-phenylhydrazone are too closely grouped to distinguish individually, but the total integral of these signals (relative to that of the phenyl protons) corresponds to the presence of five free hydroxyl groups. As pointed out in a recent study of acetylated hydrazones (20), the acyclic form of these compounds is characterized by a low-field signal caused by the C-1 formyl proton which, however, is sometimes obscured by resonance signals for the aromatic protons. An additional type of signal clearly observable in the above-mentioned spectra of the unsubstituted hydrazones is that of the NH groups, which was found in the region of 8.5–9.5 p.p.m. Accordingly, these signals no longer were produced after the addition of deuterium oxide.[8]

Dialdehydes formed by oxidative glycol scission of cyclic carbohydrate derivatives are easily hydrated and tend to exist predominantly in forms such as hemialdals, hydrates, or internal hemiacetals (21, 22). The dialdehyde V, produced by cleaving the 2,3-diol group of 4,6-*O*-benzylidene methyl α-D-glucopyranoside and its stereoisomers (21, 23, 24), forms a crystalline dihydrate. Although the latter may be depicted as in VI, its chemical properties are best accounted for by a hemialdal (VII) monohydrate structure (21, 23). The n.m.r. spectrum of the compound in dimethyl sulfoxide (Fig. 5A) clearly favors the latter formulation, since it contains two hydroxyl proton doublets (at 6.74 and 6.80 p.p.m., respectively), whereas the *gem*-diol groups of VI require the presence of four hydroxyl proton doublets.

[8]*However, the* NH *group of* D-*erythrose-2,5-dichlorophenylhydrazone was found to exchange with the deuterium much more slowly than the* NH *group of the other hydrazones.*

Can. J. Chem. Downloaded from www.nrcresearchpress.com by 210.87.254.5 on 09/05/12
For personal use only.

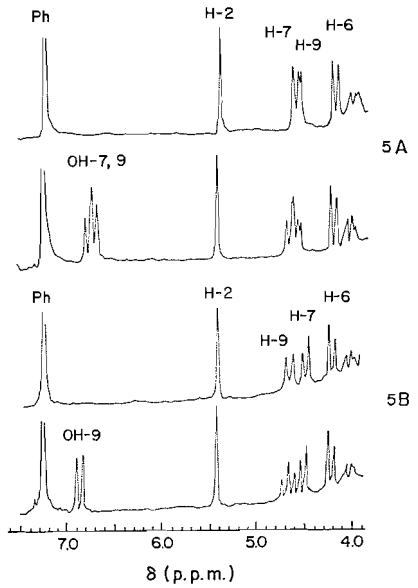
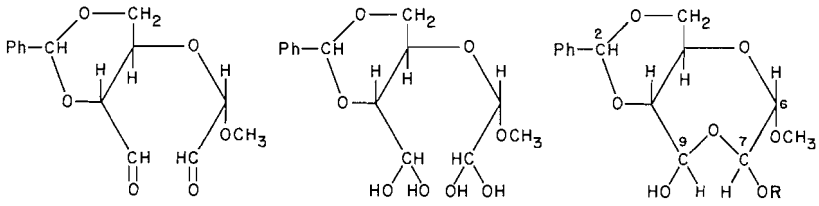


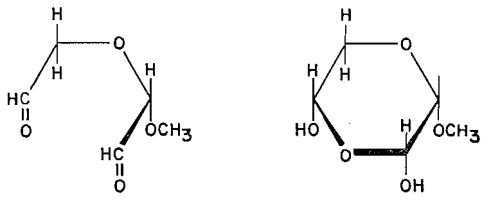
FIG. 5. Partial n.m.r. spectra at 100 Mc.p.s of (A) hemialdal VII and (B) hemialdal ethanolate VIII in dimethyl sulfoxide. The upper portions of A and B show the signals displayed after the addition of deuterium oxide to the two solutions (OH = hydroxyl proton; Ph and H-2 represent the aryl and alkyl protons, respectively, of the benzylidene grouping).

By treating the hemialdal VII with various alcohols crystalline alcoholates are produced (23). These may be depicted as in VIII or, alternatively, by an isomer in which the OR group is at position 9 (22). In accord with this type of structure, the methyl or ethyl derivative, examined in the present study, shows only one hydroxyl doublet (Fig. 5B). By deuterium exchange, the proton alpha to this hydroxyl group (H-9) is accounted for and a doublet at 4.54 p.p.m., not present in Fig. 5A, can be attributed to the proton alpha to the OR group of VIII. This latter proton shows coupling with a proton giving the doublet at 4.25 p.p.m., which is undoubtedly H-6. Hence the dialdehyde methanolate and ethanolate



V VI VII (R = H)

VIII (R = CH_3, etc.)



IX X

Can. J. Chem. Downloaded from www.nrcresearchpress.com by 210.87.254.5 on 09/05/12
For personal use only.

may, in fact, be represented by VIII, in which the alkoxyl group is at position 7 and the free hydroxyl group at C-9. However, at least one other isomer of each alcoholate is formed in minor proportion, as shown by an examination of the total solvolysis products.

Among other dialdehydes examined are those (IX) derived by oxidative scission of the 2,3,4-triol grouping in methyl pentopyranosides (22, 25). These also are thought to exist as hemialdals (e.g. X) when hydrated, with those derived from a pair of anomers constituting mirror-image forms (22). However, based on the properties of *p*-nitrobenzoate derivatives of the hemialdals, it has been suggested recently that the mirror-image relationship is no longer a tenable concept (26). The current spectral data are nevertheless entirely compatible with the earlier view. Thus the two products obtained by treating methyl α- and β-D-xylopyranosides with 2 molar equivalents of periodic acid (25) give n.m.r. spectra that are indistinguishable. When the freshly prepared, syrupy products are dissolved in dimethyl sulfoxide, signals attributable to hydroxyl protons are detected (Fig. 6A), but they are not well resolved and are broadly dispersed, showing that a mixture

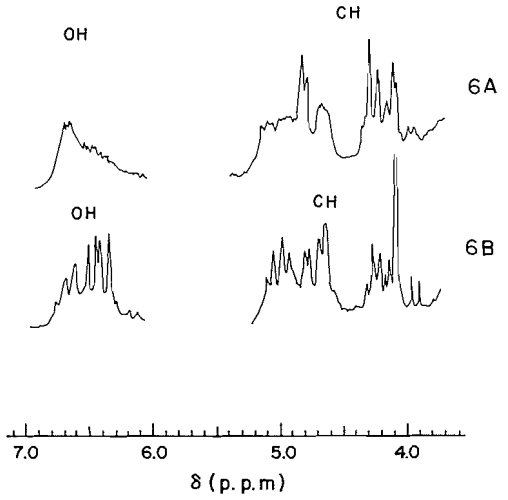


FIG. 6. Partial n.m.r. spectra at 100 Mc.p.s. of the syrupy product obtained by concentrating an aqueous solution of dialdehyde IX prepared from either methyl α- or β-D-xylopyranoside (A) after a few minutes in dimethyl sulfoxide and (B) after 4 days in dimethyl sulfoxide (OH = hydroxyl protons; CH = protons bonded to carbon).

of forms is present. Signals for other protons also display a highly complex pattern. The resolution is considerably improved when the solutions are stored in dimethyl sulfoxide (Fig. 6B) and when, as shown by the changes in the relative intensity of the signals, the composition of the mixture changes markedly. Although the observed changes and the multiplicity of signals make analysis of these spectra difficult, they nevertheless provide a large number of points of reference for comparing the products obtained from the two anomers. On this basis, the oxidation products cannot be differentiated and hence must be regarded as enantiomeric, with each being composed of the same mixture of stereoisomers. To these observations may be added the fact that, when the anomeric D-xylosides are treated in deuterium oxide with 2 molar equivalents of sodium metaperiodate, the spectra of their oxidation products are found to be highly complex but, again, indistinguishable.

Anomeric Composition and Mutarotation

The slow mutarotation of reducing sugars in dimethyl sulfoxide facilitates estimation of mixtures of anomers (2). By the same token, the spectrum of a reducing sugar in this

Can. J. Chem. Downloaded from www.nrcresearchpress.com by 210.87.254.5 on 09/05/12
For personal use only.

Can. J. Chem. Downloaded from www.nrcresearchpress.com by 210.87.254.5 on 09/05/12
For personal use only.

solvent provides a good criterion of the sample's anomeric purity. In this respect, several crystalline compounds examined during the current study were found to consist of mixtures. Usually one component greatly predominated, but in some instances a substantial proportion of each anomer was detected. For example, 3,4-*O*-isopropylidene-2-*O*-methyl-D-arabinose (27), recently described in an analytically pure, crystalline form (28), shows no detectable mutarotation in water, methanol, or chloroform. According to the spectrum of the compound in dimethyl sulfoxide this anomalous behavior can now be attributed to co-crystallization of both anomers; thus, their ratio in the freshly prepared solution was about the same as that after the sugar had first been dissolved in water. Similarly, samples of D-glucose that had been crystallized from a mixture of methanol and isopropanol were found to contain both anomers, with the β-anomer generally predominant.

Some characteristics of the equilibration of reducing sugars in dimethyl sulfoxide deserve comment. Of particular note is the fact that solutions of D-galactose, D-arabinose, and D-ribose show at least three different hydroxyl proton signals that may be attributed to anomeric protons, whereas D-glucose or D-mannose shows, at most, two such low-field signals. These observations are perhaps not surprising in view of the complex way in which the former sugars mutarotate in water (6), behavior that has been ascribed to the existence of furanose forms together with the anomeric pyranoses in the solutions.

When β-D-arabinose is dissolved in dimethyl sulfoxide each of the hydroxyl groups displays a doublet, consistent with a pyranose structure, as noted above. The anomeric hydroxyl proton resonates at 5.88 p.p.m., but in 24 h a relatively strong overlapping signal is found at 5.94 p.p.m. and a more minor OH-1 resonance at 6.23 p.p.m. In 4 days (Fig. 7A) the latter signal (ascribed to the α-pyranose form) is only slightly more prominent, although it is the major OH-1 signal when the sugar has mutarotated in water (Fig. 7B). The other new signal (ascribed to a furanose form) becomes a main component of the spectrum (Fig. 7A), but represents a trace constituent of the material transferred

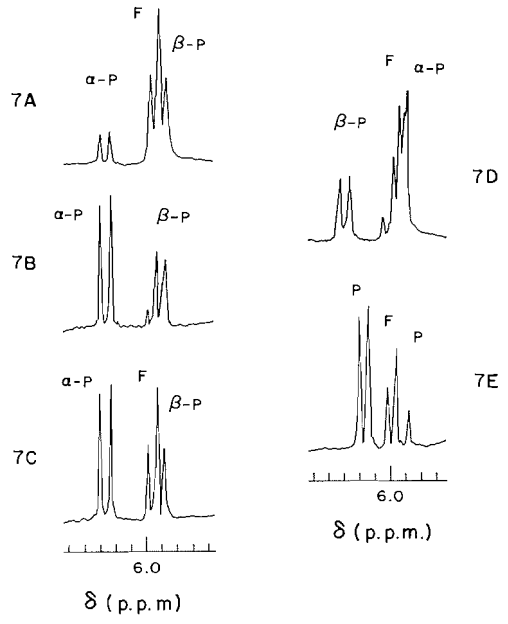


FIG. 7. Partial n.m.r. spectra at 100 Mc.p.s. of (A) D-arabinose, after 4 days in dimethyl sulfoxide; (B) D-arabinose, fresh solution in dimethyl sulfoxide of syrup obtained by concentrating a mutarotated aqueous solution of the sugar; (C) sample B, 2 days later; (D) D-galactose, after 4 days in dimethyl sulfoxide; and (E) D-ribose, after 4 days in dimethyl sulfoxide.

from the aqueous solution (Fig. 7B), although when the latter sample is stored in dimethyl sulfoxide this signal again becomes very prominent (Fig. 7C). The assignments that are made are supported by an examination of the signals for other hydroxyl protons (not shown) which were displayed by solutions of D-arabinose and D-arabinose-5,5′-d_2 and which had the compositions represented by Figs. 7B and 7C. With the undeuterated sample, a signal at 4.52 p.p.m. becomes more complex and intense as the proportion of the presumed furanose form increases. In the spectrum of the deuterated sugar, however, a sharp singlet develops in this region. This shows that the primary carbinol group is liberated as the OH-1 signal at 5.94 p.p.m. becomes more prominent, and hence that the latter is caused by D-arabinofuranose.

Spectral changes closely similar to those for D-arabinose are found with D-galactose (e.g. Fig. 7D; also, the spectrum of the mixture obtained after mutarotation in water strongly resembles that shown in Fig. 7B, except that the pyranose anomeric designations are reversed). Different samples of D-ribose were found to be initially mixtures of two anomers. Although a number of the hydroxyl proton signals overlap in the spectrum of these mixtures, there was no evidence of the presence of a primary carbinol multiplet; therefore, both anomers that were detected are presumed to be pyranoses. Hence, a third OH-1 signal that slowly becomes evident (shown in Fig. 7E) is probably that of D-ribofuranose and, in accord with this likelihood, its appearance is accompanied by that of a triplet at 4.36 p.p.m.

In general, pyranose forms of reducing sugars greatly predominate over furanose forms in aqueous solution. One factor that may contribute substantially to this difference is the relatively satisfactory way in which a pyranose chair can fit into the tridymite structure of water, particularly when the hydroxyl groups are equatorially oriented (30). In addition, if two sugars such as D-glucose and D-galactose are compared, the former is regarded as the *more* stable in a pyranose conformation but the less stable in a furanose conformation (see ref. 29 for a recent discussion of these factors). Therefore, of these two sugars, D-galactose (and similarly D-arabinose) is more likely to exist in a furanose form than is D-glucose. According to the present findings, furanose forms are particularly prominent in dimethyl sulfoxide for those sugars showing complex mutarotation in water. Although dimethyl sulfoxide also is strongly hydrogen bonding, its chain-like structure (31, 32) appears unlikely to favor the stabilization of one form of a sugar over another. Hence, if a particular sugar is "inherently" relatively stable in a furanose form, this fact should become more evident with dimethyl sulfoxide as the solvent than with water.

Other observations appear to be consistent with the possibility of an interplay of effects of this kind. Thus, although hemialdal X appears to prefer one particular conformation in dimethyl sulfoxide, the spectrum of the compound when first transferred from water (Fig. 6A) shows that other forms are dominant initially. Effects such as these suggest that dimethyl sulfoxide, or other solvents, might provide some specific advantage as a medium for comparing the conformational stability of interconvertible forms, by minimizing orienting effects caused by the structure of water itself.

EXPERIMENTAL

Proton magnetic resonance data were recorded with a Varian-100 high-resolution spectrometer. Unless otherwise specified, dimethyl sulfoxide, dried by storage over anhydrous calcium sulfate or by distillation, was used as the solvent. The signal for the methyl protons of the solvent served as a reference signal for the internally stabilized lock system of the spectrometer. For a solution of dimethyl sulfoxide and tetramethylsilane in carbon tetrachloride this signal is 249 c.p.s. downfield from that of the tetramethylsilane protons. Accordingly, all reported chemical shift values are 2.5 p.p.m. (250 c.p.s.) larger than the values actually recorded.

Can. J. Chem. Downloaded from www.nrcresearchpress.com by 210.87.254.5 on 09/05/12
For personal use only.

The concentration of solute was generally 25–50 mg/ml of solvent.

On a few occasions, resonance signals expected for hydroxyl protons were not detected, or the signals were poorly resolved. These effects could usually be attributed to the presence of traces of acid in the sample, particularly with syrupy compounds. In such instances, the dimethyl sulfoxide solution was diluted with water and then treated with a slight excess of ammonia, after which the water and excess of base were removed *in vacuo* at 40 °C.

Materials

Most of the compounds examined in the current study were prepared in this laboratory during the course of other studies, e.g. α-D-glucose-5,6,6′-d_3 (8), D-mannose 2,3-carbonate (13), D-lyxose 2,3-carbonate (16), 2,4,6-tri-*O*-acetyl-β-D-mannose and 3,4,6-tri-*O*-acetyl-α-D-mannose (17), D-erythrose 2,5-dichlorophenylhydrazone (33), and dialdehyde V (22).

Dialdehydes of type X were prepared by oxidizing methyl α- and β-D-xylopyranosides with periodic acid according to ref. 23, except that formic and iodic acids and the excess of the oxidant were removed by use of Dowex-1 (bicarbonate form).

1,2-O-Isopropylidene-β-D-arabinofuranose-5,5′-d_2

1,2-*O*-Isopropylidene-β-D-arabinofuranuronic acid methyl ester (34) (0.15 g) was reduced (35) by slow addition to a solution of sodium borodeuteride (Merck, Sharp and Dohme) (0.10 g) in ice water (3 ml). After 5 h the reaction mixture was treated with Amberlite IR-120 (H^+) and Dowex-1 (bicarbonate form), and concentrated; then residual boric acid was removed as the volatile methyl ester. The product solidified (yield, 0.10 g) and was recrystallized from ethyl acetate – hexane, m.p. 113–116 °C, $[\alpha]_D$ +26° (*c*, 0.9 in water).

Anal. Calcd. for $C_8H_{12}D_2O_5$: C, 50.0. Found: C, 49.8.

In accord with the assigned structure, the n.m.r. spectrum of the compound in deuterium oxide showed the presence of the isopropylidene group (singlets at 1.80 and 1.97 p.p.m.), and signals attributable to protons 1 to 4 at 6.44, 5.10, 4.64, and 4.52 p.p.m. (relative to tetramethylsilane as an external coaxial reference).

D-*Arabinose-5,5′-d_2*

The *O*-isopropylidene derivative (40 mg) was hydrolyzed with 0.1 *N* sulfuric acid (5 ml) on the steam bath for 3 h; the solution was neutralized with Dowex-1 (bicarbonate form), and concentrated to dryness. The n.m.r. spectrum of the syrupy product, freshly dissolved in dimethyl sulfoxide, was virtually indistinguishable from that of the syrup obtained by concentrating a mutarotated aqueous solution of D-arabinose.

ACKNOWLEDGMENTS

The author expresses his gratitude to M. Mazurek, who recorded the n.m.r. spectra, and to Drs. J. C. MacDonald and A. P. Tulloch, who drew the author's attention to the publications listed herein as refs. 1 and 2.

REFERENCES

1. O. L. Chapman and R. W. King. J. Am. Chem. Soc. **86**, 1256 (1964).
2. B. Casu, M. Reggiani, G. G. Gallo, and A. Vigevani. Tetrahedron Letters, **39–40**, 2839 (1964); **27**, 2253 (1965).
3. G. A. Jeffrey and R. D. Rosenstein. Advan. Carbohydrate Chem. **19**, 7 (1964).
4. C. S. Hudson and E. Yanovsky. J. Am. Chem. Soc. **39**, 1013 (1917).
5. P. A. Levene. J. Biol. Chem. **59**, 129 (1924).
6. H. S. Isbell and W. W. Pigman. J. Res. Natl. Bur. Std. **18**, 141 (1937).
7. R. U. Lemieux, R. K. Kullnig, H. J. Bernstein, and W. G. Schneider. J. Am. Chem. Soc. **80**, 6098 (1958).
8. W. Mackie and A. S. Perlin. Can. J. Chem. **43**, 2921 (1965).
9. L. D. Hall. Advan. Carbohydrate Chem. **19**, 51 (1964).
10. J. A. Pople, W. G. Schneider, and H. J. Bernstein. High resolution nuclear magnetic resonance. McGraw-Hill Book Co., Inc., New York. 1959.
11. F. Bloch. Phys. Rev. **94**, 496 (1954).
12. W. A. Anderson. Phys. Rev. **98**, 1279 (1956).
13. A. S. Perlin. Can. J. Chem. **42**, 1365 (1964).
14. M. Karplus. J. Chem. Phys. **30**, 11 (1959).
15. F. A. L. Anet. Can. J. Chem. **39**, 789 (1961).
16. P. A. J. Gorin. Unpublished preparation.
17. A. S. Perlin. Can. J. Chem. **41**, 555 (1963).
18. E. G. V. Percival. Advan. Carbohydrate Chem. **3**, 23 (1948).
19. L. Mester. Advan. Carbohydrate Chem. **13**, 105 (1958).
20. M. L. Wolfrom, G. Fraenkel, D. R. Lineback, and K. Komitsky, Jr. J. Org. Chem. **29**, 457 (1964).
21. I. J. Goldstein, B. A. Lewis, and F. Smith. J. Am. Chem. Soc. **80**, 939 (1958).
22. R. D. Guthrie. Advan. Carbohydrate Chem. **16**, 105 (1961).

Can. J. Chem. Downloaded from www.nrcresearchpress.com by 210.87.254.5 on 09/05/12
For personal use only.

23. R. D. GUTHRIE and J. HONEYMAN. J. Chem. Soc. 2441 (1959).
24. H. R. GOLDSCHMID and A. S. PERLIN. Can. J. Chem. **38**, 2280 (1960).
25. E. L. JACKSON and C. S. HUDSON. J. Am. Chem. Soc. **59**, 994 (1937).
26. G. J. F. CHITTENDEN and R. D. GUTHRIE. J. Chem. Soc. 2271 (1965).
27. G. R. BARKER and D. C. C. SMITH. Chem. Ind. London, 1035 (1952).
28. W. MACKIE and A. S. PERLIN. Can. J. Chem. **43**, 2645 (1965).
29. R. U. LEMIEUX. *In* Molecular rearrangements. *Edited by* P. de Mayo. Interscience Publishers, Inc., New York. 1964. Part 2. p. 709.
30. M. A. KABAYAMA and D. PATTERSON. Can. J. Chem. **36**, 563 (1958).
31. H. L. SCHLAFER and W. SCHAFFERNICHT. Angew. Chem. **72**, 618 (1960).
32. A. J. PARKER. Quart. Rev. London, **16**, 163 (1962).
33. A. S. PERLIN and C. BRICE. Can. J. Chem. **33**, 1216 (1955).
34. P. A. J. GORIN and A. S. PERLIN. Can. J. Chem. **34**, 693 (1956).
35. M. L. WOLFROM and K. ANNO. J. Am. Chem. Soc. **74**, 5583 (1952).

Can. J. Chem. Downloaded from www.nrcresearchpress.com by 210.87.254.5 on 09/05/12
For personal use only.

Can. J. Chem. Downloaded from www.nrcresearchpress.com by 210.87.254.40 on 09/05/12
For personal use only.

ELECTRON SPIN RESONANCE STUDIES OF PHOTOLYTICALLY GENERATED AROMATIC KETYLS

RAYMOND WILSON[1]
Department of Chemistry, University of Saskatchewan, Saskatoon, Saskatchewan
Received August 31, 1965

ABSTRACT

Electron spin resonance observations on the photolytically generated ketyls of benzaldehyde, acetophenone, and benzophenone in protic solvents are reported. Proton coupling constants differ considerably from those reported by other workers for the same ketyls generated by other methods in aprotic solvents.

Molecular orbital calculations of unpaired electron spin densities, in which the effective electronegativities of the oxygen atoms on the ketyls are assumed to be increased by hydrogen bonding in protic solvents, are reported. The calculated changes in spin densities agree qualitatively with the semi-empirical changes calculated by the McConnell relationship.

Observations on the dynamics of solvation of the benzaldehyde ketyl in a mixture of a protic and an aprotic solvent are reported and discussed.

INTRODUCTION

Previous publications (1, 2) have reported electron spin resonance (e.s.r.) studies on the ketyls of benzophenone and fluorenone and on many nitrobenzene radical anions generated by the photolysis of alkaline aqueous ethanolic or methanolic solutions. The mechanism by which these radical anions are formed is suggested by the flash photolysis work of Porter and Wilkinson on benzophenone (3). Benzophenone is excited by ultraviolet radiation (3 300 Å) to the singlet state, which then undergoes a radiationless transition to the triplet state.

[1] $$(C_6H_5)_2CO \xrightarrow{h\nu} (C_6H_5)_2\overset{*}{C}O \text{ (singlet)}$$

[2] $$(C_6H_5)_2\overset{*}{C}O \text{ (singlet)} \rightarrow (C_6H_5)_2\overset{*}{C}O \text{ (triplet)}$$

Benzophenone in the triplet state quite readily abstracts hydrogen atoms from suitable solvents to give the ketyl radical.

[3] $$(C_6H_5)_2\overset{*}{C}O \text{ (triplet)} + RH \rightarrow (C_6H_5)_2\dot{C}OH + \dot{R}$$

A lifetime of 10^{-3} s for this ketyl radical in liquid paraffin (viscosity 30 cP) at room temperatures has been reported (3). In alkaline solutions formation of the familiar blue ketyl radical anion (hereafter referred to as ketyl), which has a lifetime of several seconds, is favored.

[4] $$(C_6H_5)_2\dot{C}OH + OH^- \rightarrow (C_6H_5)_2\dot{C}O^- + H_2O$$

A similar mechanism seems to be followed in the photolytic generation of the nitrobenzene radical anions in alkaline protic solvents (2). This mechanism is also indicated by the detection, by e.s.r. spectroscopy, of the $C_6H_5 \cdot NO_2H$ radical formed by photolyzing a neutral solution of nitrobenzene in tetrahydrofuran (4).

The present report extends previous e.s.r. studies on the photolytically generated ketyls of benzophenone and fluorenone (1) to the far less stable benzaldehyde and

[1]*Postdoctorate Fellow, 1962–1963. Present address: National Physical Laboratory, Teddington, Middlesex, England.*

acetophenone ketyls, which appear to be formed by a similar mechanism. Benzophenone ketyl is included for comparison purposes. Observations on the effects of solvation on the unpaired electron distributions are reported and compared with theoretically estimated values.

EXPERIMENTAL

Reagents

"Eastman grade" benzaldehyde and acetophenone were used without further purification. Freshly prepared absolute ethanolic or acetone-free methanolic solutions, 10^{-2} M in the carbonyl compound and 10^{-1} M in sodium ethoxide or sodium methoxide, respectively, were used.

"Eastman grade" acetonitrile – methanol solutions, 10^{-2} M in the carbonyl compound and 10^{-1} M in sodium methoxide, were freshly prepared for the mixed-solvent experiments.

Ultraviolet Radiation

A 125 W Hanovia quartz alpine sun burner, type S-100, was enclosed in an aluminium tube designed to direct the radiation onto the sample solution within the Varian electron paramagnetic resonance spectrometer multipurpose cavity. The ultraviolet lamp was cooled by a jet of dry air and the aluminium tube was cooled by a water jacket. A water filter, 4 mm wide, between quartz plates was incorporated into the tube to eliminate direct heating of the sample by infrared radiation.

Electron Spin Resonance Observations

The Varian Associates V 4500 electron paramagnetic resonance spectrometer was used. Continuous irradiation of the sample while spectra were being recorded was made possible by utilizing the Varian multipurpose cavity. Reduction of the cavity quality factor by lossy solvents was largely eliminated by the use of Varian flat quartz, aqueous solution sample cells.

The Varian 6 inch magnet system with a pole gap of $2\frac{1}{2}$ inches was used, and the magnetic field was modulated at 100 kc/s.[2]

Spectra were recorded as first derivatives under "standard sweep" conditions, and line spacings were determined by comparison with the known spacings for the nitrobenzene radical anion (2) and the benzophenone ketyl (1). Absolute values of the hyperfine coupling constants are estimated to be better than 2%, while the relative values are better than 1%.

RESULTS

Spectra were observed a few seconds after the ultraviolet irradiations had been begun; maximum intensities were reached after about 20 s. The short inhibition period was probably caused by oxygen or other scavengers that were present as small impurities and which were reacting with the radicals formed initially. Spectra recorded during continuous photolysis of alkaline solutions of benzaldehyde and acetophenone in methanol and ethanol at room temperature (25 °C) are given in Figs. 1–4.

Continuous photolysis caused the spectra to decay almost completely within half an hour. In Figs. 1–4, the asymmetry of line intensity about the center of the spectra is largely caused by this decay.

Accurate line-width measurements were not made. It was necessary to modulate the magnetic field at about 50 mG to obtain a tolerable ratio of signal to noise. The minimum line width that was observed, with low microwave power to avoid saturation and the non-ideal modulation amplitude, was never less than 120 mG.

Careful inspection of the spectra indicated that they could be accounted for by the coupling constants shown in Table I. The calculated "stick" spectra in Figs. 1–4 correspond to these coupling constants. Agreement between experimental and calculated spectra is seen to be good. Assignment of coupling constants to specific protons is not possible from the aforementioned experimental data alone. However, from considerations of molecular orbital calculations described in a later section, the assignations given in Table I are suggested. The absence of a twofold rotation axis through the 1 and 4 positions of the benzaldehyde and acetophenone ketyls should be noted.

[2]*The 100 kc/s oscillator and detector were constructed in the chemistry department by Mr. J. A. Williams.*

Can. J. Chem. Downloaded from www.nrcresearchpress.com by 210.87.254.40 on 09/05/12
For personal use only.

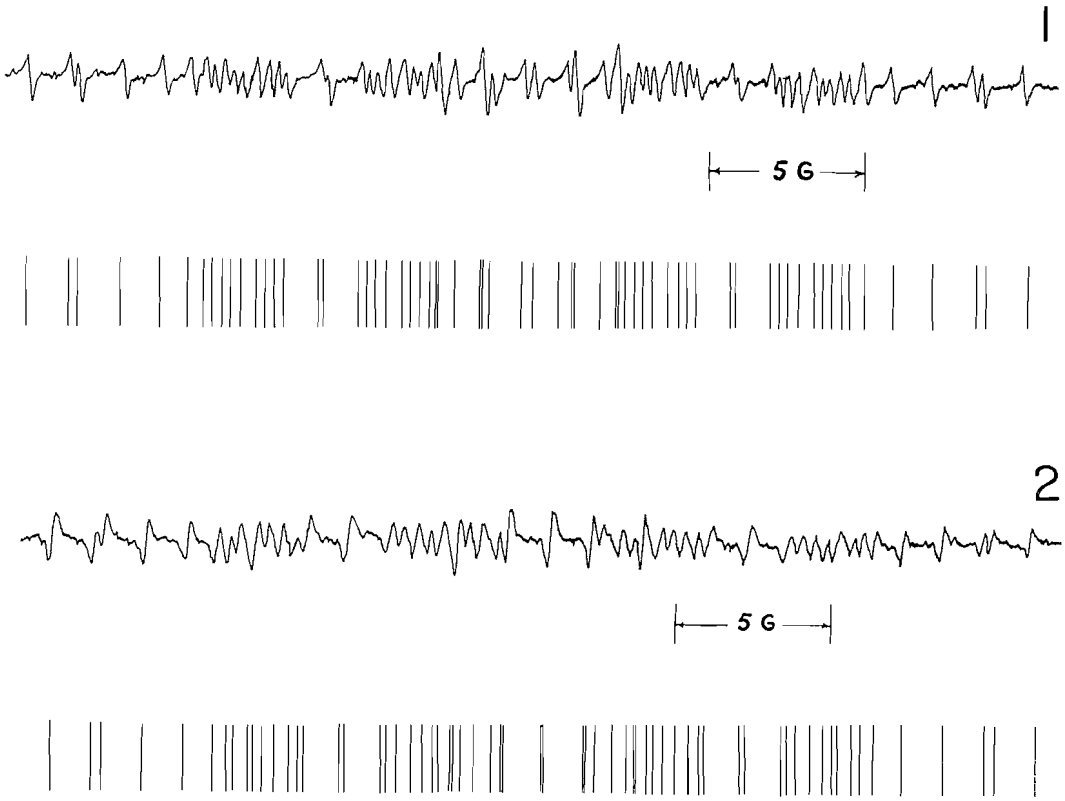


FIG. 1. The observed first-derivative e.s.r. spectrum and the calculated "stick" spectrum of benzaldehyde ketyl in methanol at 25 °C.
FIG. 2. The observed first-derivative e.s.r. spectrum and the calculated "stick" spectrum of benzaldehyde ketyl in ethanol at 25 °C.

The spectra of the benzaldehyde ketyl are slightly but distinctly different in the solvents methanol and ethanol. This is also the case for the acetophenone ketyl. The slight differences in the spectra are paralleled by slight changes in the coupling constants; the changes in the proton coupling constant of the CHO group and the coupling constant of the CH_3 group are the most marked. No differences in the spectrum of the benzophenone ketyl in the solvents methanol and ethanol were detected.

The spectrum resulting from the photolysis of an alkaline solution of benzaldehyde in a mixture of methanol and ethanol is a hybrid and not a superposition of the spectra in the two separate solvents.

The effect of solvent on the benzaldehyde ketyl was investigated further by photolyzing alkaline solutions of benzaldehyde in mixtures of methanol and the aprotic solvent acetonitrile. Increasing the fraction of acetonitrile caused changes of increasing magnitude in all the proton coupling constants, particularly in that of the CHO group, a_7. The experimentally determined points for a_7 versus the fractional volume of methanol in the mixed methanol–acetonitrile solvent are given in Fig. 5. The curve is drawn according to an equation discussed later. Increasing the fraction of acetonitrile caused an apparent decrease in the stability of the ketyl. This resulted in deterioration of the spectra, and it was not possible to obtain a spectrum for 100% acetonitrile.

Can. J. Chem. Downloaded from www.nrcresearchpress.com by 210.87.254.40 on 09/05/12
For personal use only.

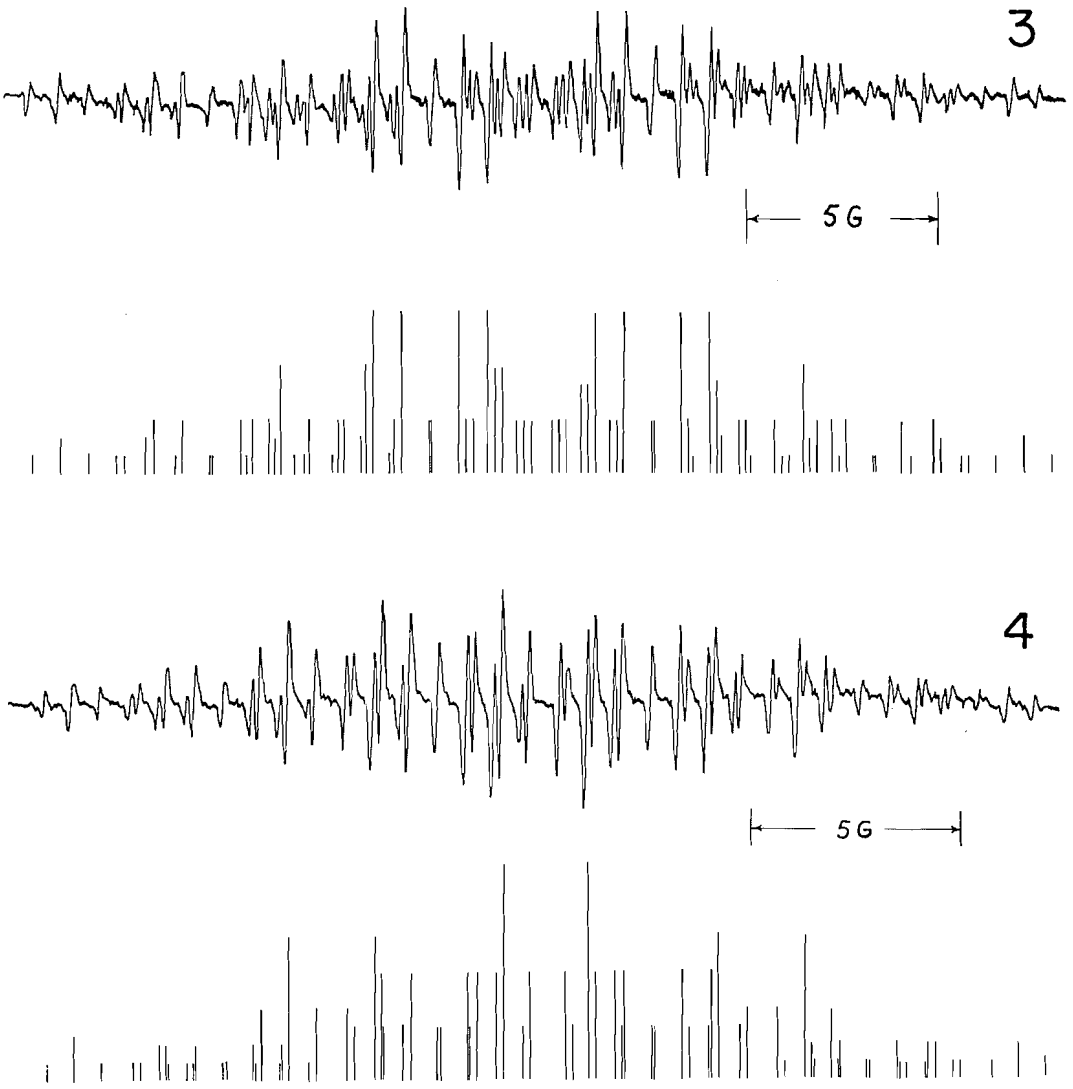


FIG. 3. The observed first-derivative e.s.r. spectrum and the calculated "stick" spectrum of acetophenone ketyl in methanol at 25 °C.

FIG. 4. The observed first-derivative e.s.r. spectrum and the calculated "stick" spectrum of acetophenone ketyl in ethanol at 25 °C.

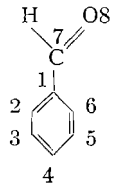
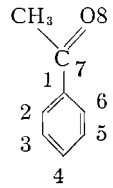
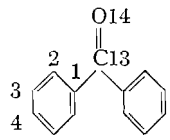
MOLECULAR ORBITAL CALCULATIONS

The McLachlan modification of the Huckel theory (5), with a value of 1.2 for λ, was used to calculate unpaired electron spin densities. It was assumed that in the solvents used the ketyls were solvated. In particular, the oxygen atoms of the carbonyl groups are most likely to be hydrogen bonded to methanol or ethanol. The proximity of hydrogen atoms to the carbonyl group increases the effective electronegativity of the oxygen atom. This effect can be introduced into molecular orbital calculations by decreasing the value of the oxygen atom Coulomb integral, α_O (6). α_O is given by the familiar relationship $\alpha_O = \alpha + \delta_O\beta$, where α and β are the Coulomb and resonance integrals, respectively, for the benzene molecule. δ_O is a molecular orbital parameter; since β is negative, increasing

Can. J. Chem. Downloaded from www.nrcresearchpress.com by 210.87.254.40 on 09/05/12
For personal use only.

TABLE I

Proton isotropic coupling constants at 25 °C (in Gauss)

Ketyl of:	Solvent	a_2	a_3	a_4	a_5	a_6	a_7	a_{Mo}
Benzaldehyde								
	MeOH	5.14	1.62	6.24	1.36	4.26	13.00	—
	EtOH	5.14	1.67	6.29	1.31	4.23	12.70	—
Acetophenone								
	MeOH	4.78	1.45	6.24	1.45	4.45	—	11.37
	EtOH	4.79	1.45	6.22	1.41	4.42	—	11.00
Benzophenone								
	MeOH and EtOH	2.80	1.03	3.46	1.03	2.80	—	—

δ_O decreases α_O. The resonance integral for the carbonyl group is given by $\beta_{CO} = \gamma_{CO}\beta$. A constant value of 1.6 was used for γ_{CO} irrespective of solvent. Similarly, a value of 0.9 was used for γ_{C-CO}, which gives the resonance integral for the bond between the carbonyl group and the aromatic ring. This is quite reasonable if one considers that the C—CO bond is not typically aromatic and that there is a possibility of oscillation of the aromatic ring about this bond.

Asymmetry was introduced into the calculations on the benzaldehyde and acetophenone ketyls by utilizing the suggestion of Rieger and Fraenkel (7) that the Coulomb integrals of the carbon atoms at the 6 position, that is, the carbon atoms near the oxygen atoms,

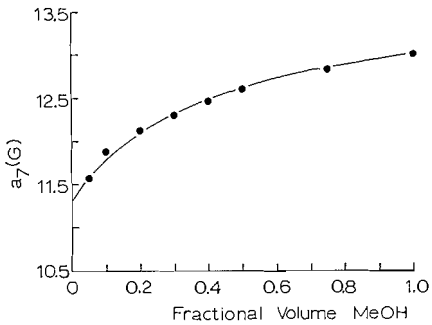


FIG. 5. a_7 versus fractional volume of methanol for the benzaldehyde ketyl in a methanol–acetonitrile mixture.

Can. J. Chem. Downloaded from www.nrcresearchpress.com by 210.87.254.40 on 09/05/12
For personal use only.

are slightly more positive than those for typically aromatic carbon atoms. This reflects a slight decrease in the electronegativity of these carbon atoms because of the proximity of the oxygen atoms. For the benzaldehyde ketyl, a value of -0.1 was used for δ_6, whereas for the acetophenone ketyl, which the e.s.r. spectra indicate is more symmetrical, a value of -0.05 was used. For the completely symmetrical benzophenone ketyl, the value of δ for all the ortho carbon atoms was set equal to 0.

For calculations on the acetophenone ketyl which involves the methyl group, the grouping C—C′—H_3 was considered and the values used for the molecular orbital parameters are $\delta_{H_3} = -0.5$, $\delta_{C'} = -0.1$, $\gamma_{C'-H_3} = 2.5$, and $\gamma_{C-C'} = 0.9$ (8).

In Table II, unpaired spin densities calculated by using various values of δ_O are compared with the semi-empirical values for the ketyls in various solvents. The semi-empirical values for protons attached to the aromatic system were calculated by the McConnell relationship $a_i = Q_H|\rho_i|$, where ρ_i is the unpaired electron spin density at the aromatic carbon atom i adjacent to the proton under consideration. For methyl groups, the relation $a_{Me} = Q_{Me}|\rho|$ was used, where ρ is the spin density on the aromatic carbon atom adjacent to the methyl group. Values of 23.7 G and 27.2 G were used for the constants Q_H and Q_{Me}, since these values have been used extensively with considerable success by Fraenkel and co-workers (6, 7, 9). Semi-empirical values of unpaired spin densities for the electrochemically generated ketyls in N,N-dimethylformamide from publications by Fraenkel and co-workers (7, 9) have been included in Table II for comparison purposes.

Values of unpaired spin density calculated from molecular orbital theory with $\delta_O = 2.9$ and 2.2 are given in columns 1 and 2, and should be compared with the experimental values for the ketyls in the solvents methanol and ethanol. Similarly, the values in column 3 calculated with $\delta_O = 1.5$ should be compared with the experimental values for the solvent N,N-dimethylformamide. A considerable dependence of the unpaired spin density at the carbonyl group carbon atom on the electronegativity of the oxygen atom is expected and in fact observed. Greater effort was therefore made to fit the molecular orbital data with the semi-empirical data at the 7 positions of the benzaldehyde and acetophenone ketyls. The better quantitative agreement at these positions in Table II is therefore not surprising. Quantitative agreement elsewhere is not good but not unreasonable when the limitations of molecular orbital theory are considered. Qualitative trends are indicated quite clearly. For example, increasing the electronegativity of the oxygen atom, that is, increasing δ_O, increases the positive spin density at the ortho positions, and the increase at the carbonyl group carbon atom is particularly marked; the spin densities at the meta positions become more negative and the spin densities at the para positions decrease. All these changes of spin density are paralleled qualitatively in every case by changes with solvent of the semi-empirical spin densities.

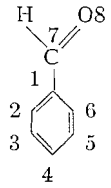
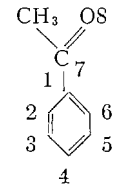
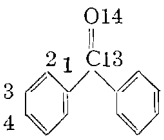
DISCUSSION

From the assignation of the proton coupling constants in Table I, it is apparent that the benzaldehyde and acetophenone ketyls do not have a twofold center of symmetry through the 1 and 4 positions as might be expected. It seems that these are examples of hindered rotation of the carbonyl groups about the C—CO bond. The phenomenon was first observed with e.s.r. spectroscopy by Maki and Geske for the *p*-nitrobenzaldehyde radical anion (10) and has since been noted on several other occasions (7, 11), including the electrochemically generated benzaldehyde and acetophenone radical anions in aprotic solvents (9).

Can. J. Chem. Downloaded from www.nrcresearchpress.com by 210.87.254.40 on 09/05/12
For personal use only.

TABLE II

Unpaired electron spin densities

Ketyl of:		Calculated* I†	Calculated* II‡	Calculated* III§	Experimental‖ MeOH	Experimental‖ EtOH	Experimental‖ N,N-Dimethyl-formamide¶
Benzaldehyde	1	0.004		0.098	—	—	—
	2	0.167		0.166	0.217	0.217	0.198
	3	−0.064		−0.052	0.068	0.070	0.055
	4	0.194		0.247	0.263	0.265	0.273
	5	−0.047		−0.038	0.057	0.055	0.032
	6	0.139		0.128	0.180	0.178	0.143
	7	0.537		0.314	0.549	0.536	0.359
	8	0.066		0.130	—	—	—
Acetophenone	1	0.012	0.045	0.096	—	—	—
	2	0.155	0.156	0.151	0.202	0.202	0.179
	3	−0.054	−0.051	−0.047	0.061	0.061	0.045
	4	0.188	0.209	0.235	0.263	0.262	0.278
	5	−0.048	−0.044	−0.035	0.061	0.061	0.037
	6	0.143	0.142	0.133	0.188	0.186	0.157
	7	0.501	0.418	0.303	0.418	0.404	0.248
	8	0.067	0.091	0.134	—	—	—
Benzophenone	1	−0.016		0.027	—		—
	2	0.111		0.098	0.118		0.106
	3	−0.039		−0.032	0.043		0.035
	4	0.123		0.133	0.146		0.148
	13	0.429		0.270	—		—
	14	0.070		0.145	—		—

*See text for molecular orbital parameters.
†$\delta_O = 2.9$.
‡$\delta_O = 2.2$.
§$\delta_O = 1.5$. Values for acetophenone and benzophenone ketyls are taken from refs. 9 and 7, respectively.
‖Spin densities are calculated from the isotropic coupling constants by using $a_i = 23.7|\rho_i|$ and $a_{Me} = 27.2|\rho_7|$.
¶Spin densities from refs. 7 and 9 are reduced to three figures after the decimal point.

The slight differences in the ortho protons and also in the meta protons arise because rotation is slow compared with the hyperfine frequency difference. In the case of benzaldehyde ketyl in methanol, the CHO group is rotating about the C—CO bond with a frequency $\omega < \gamma|a_2 - a_6| \sim 1.55 \times 10^7$ s^{-1}, where γ is the magnetogyric ratio of the electron.

The acetophenone ketyl also exhibits the hindered rotation phenomenon. In this case, the difference between the ortho coupling constants is less and the undoubted slight difference in the meta protons was not resolved. The expected difference in the meta protons is about 100 mG, which could well have been masked by the line width. Inspection of the three outermost lines in Figs. 3 and 4 does, in fact, show that the observed intensity ratio is less than 1:2:1, which is the ratio expected for two exactly equivalent meta protons.

The benzophenone ketyl appears to have four exactly equivalent meta protons. Apparently, steric hindrance between the ortho protons forces the rings out of a common plane, and it is possible that relatively free, out-of-phase rotation of the phenyl groups about the C—CO bonds occurs.

Can. J. Chem. Downloaded from www.nrcresearchpress.com by 210.87.254.40 on 09/05/12
For personal use only.

Can. J. Chem. Downloaded from www.nrcresearchpress.com by 210.87.254.40 on 09/05/12
For personal use only.

The coupling constants reported in Table I for ketyls in protic solvents differ considerably from those reported previously for the same ketyls in aprotic solvents such as acetonitrile, dimethylformamide, and 1,2-dimethoxyethane (1, 7, 9, 12). Similar results have been noted for the nitrobenzene radical anion (2, 13) and the semiquinones (6).

Solvation of ketyls via hydrogen bonding to the carbonyl group oxygen atom is certain to occur, and the resultant effect on the unpaired electron spin distributions is quite marked. In the molecular orbital calculations described previously, the effect of hydrogen bonding on the electronegativity of the oxygen atom was considered; it was noted that the calculated changes in unpaired spin density correspond qualitatively with the semi-empirical changes calculated from the isotropic coupling constants. A possible point of significance is the observation that the semi-empirical spin densities, particularly at the 7 position, of the benzaldehyde ketyl in protic solvents agree best with the theoretical values calculated by using a value of 2.9 for δ_O. The acetophenone ketyl data indicate that a value of 2.2 for δ_O gives a better fit. The difference in the values of δ_O reflects a greater electronegativity of the benzaldehyde ketyl oxygen atom, which could be interpreted as resulting from greater solvation. The lesser degree of solvation of the acetophenone ketyl could result from possible steric hindrance by the bulky CH_3 group. Another point is the observation of slightly greater unpaired spin densities at the 7 positions for both benzaldehyde and acetophenone ketyls in methanol than in ethanol. This indicates the slightly greater solvation powers of the smaller methanol molecule, compared with ethanol.

It is difficult to decide what the nature of the solvated ketyl is. The formation of several different species with any one solvent is possible. Each species could give rise to a different e.s.r. spectrum provided the exchange frequency of solvent molecules between the various species is low compared with the hyperfine frequency differences in their e.s.r. spectra. The observation of a single spectrum for each ketyl in the various solvents indicates that either there is a single species, solvated or unsolvated, or the exchange between the various species is fast.

The observation of a single spectrum for the benzaldehyde ketyl in mixed solvents indicates that exchange is fast. Gendell *et al.* (6) have derived a simple expression for the expected value of a coupling constant, a, resulting from the fast exchange of solvent molecules X and Y between singly solvated species RX and RY. In the case of a mixture of acetonitrile, X, and methanol, Y, the expression becomes

$$[5] \qquad a = \frac{a_{RX} - x(a_{RX} + 1.30Ka_{RY})}{1 - x(1 - 1.30K)}.$$

a_{RX} and a_{RY} are the coupling constants for RX and RY respectively. x is the fractional volume of methanol, and the factor of 1.30 arises because of differences in the molecular weights and densities of methanol and acetonitrile. K is the equilibrium constant for the exchange of solvent molecules.

$$[6] \qquad RX + Y \overset{K}{\rightleftharpoons} RY + X$$

In Fig. 5, eq. [5] for a_7 of the benzaldehyde ketyl is plotted for the acetonitrile–methanol mixture, with $K = 2.65$, $a_{RX} = 11.3$ G, and $a_{RY} = 13.01$ G. The agreement with the observed results is better than could be expected when one considers the gross assumptions that were made. Multi-solvation is quite possible and it cannot be assumed that the nature of methanol, which is normally highly associated, remains constant throughout the mixture range.

The value of the equilibrium constant indicates that solvation by methanol is favored over possible solvation by acetonitrile. The e.s.r. spectra also indicate that the benzaldehyde ketyl in acetronitrile is less stable than that in methanol, which implies that solvation by methanol imparts a greater degree of protection to the ketyl. That is, decay of the ketyl by mechanisms such as disproportionation and association or reaction with other molecules is inhibited to a greater extent.

The predicted value of 11.3 G for a_7 in acetonitrile does not compare too well with the value of 8.507 G reported by Steinberger and Fraenkel (9) in the similar solvent, dimethylformamide. This difference could arise from the greater influence of the sodium cation on the unpaired electron distribution compared with the influence of the bulky tetra-*n*-propylammonium cation used by Steinberger and Fraenkel. Cationic field effects have been observed to cause a blue shift of absorption maxima in the ultraviolet spectra of various metal benzophenone ketyls (14 and references therein).[3] Cationic field effects are more likely in acetonitrile than in the strongly solvating protic solvents, which protect the ketyl to a greater extent. They are even more likely in such nonpolar solvents as 1,2-dimethoxyethane. In this case, association between the ketyl and cations such as Na^+ and K^+ occurs (12), thereby resulting in hyperfine interaction with the metal. Hirota (12) has noted that the effect on the unpaired electron distribution in the benzophenone ketyl increases with an increasing ratio of charge to cationic radius. The effect at the 13 position was followed by observing the hyperfine interaction with ^{13}C substituted at that position. The influence at other positions in the aromatic system was observed to be much less and almost negligible at the para positions. One can assume, therefore, that these positions are relatively far from the cation. The observations by Hirota parallel results in this work; protic solvents effect the positions nearest the carbonyl group quite markedly and effect the para positions to a very small degree.

ACKNOWLEDGMENTS

The support of the National Research Council of Canada, and the very capable assistance of Mr. J. A. Williams with the instrumentation are gratefully acknowledged. The University of California at Los Angeles is thanked for the use of their computing facilities.

REFERENCES

1. P. B. Ayscough and R. Wilson. J. Chem. Soc. 5412 (1963).
2. P. B. Ayscough, F. P. Sargent, and R. Wilson. J. Chem. Soc. 5418 (1963).
3. G. Porter and F. Wilkinson. Trans. Faraday Soc. **57**, 1686 (1961).
4. R. L. Ward. J. Chem. Phys. **38**, 2588 (1963).
5. A. D. McLachlan. Mol. Phys. **3**, 233 (1960).
6. J. Gendell, J. H. Freed, and G. K. Fraenkel. J. Chem. Phys. **37**, 2832 (1962).
7. P. H. Rieger and G. K. Fraenkel. J. Chem. Phys. **37**, 2811 (1962).
8. C. A. Coulson. Valence. Oxford University Press, London. 1952. V. W. Crawford. J. Chem. Soc. 2052 (1953). P. H. Rieger and G. K. Fraenkel. J. Chem. Phys. **39**, 609 (1963).
9. N. Steinberger and G. K. Fraenkel. J. Chem. Phys. **40**, 723 (1964).
10. A. H. Maki and D. H. Geske. J. Am. Chem. Soc. **83**, 1852 (1961).
11. E. W. Stone and A. H. Maki. J. Chem. Phys. **38**, 1999 (1963).
12. P. B. Ayscough and R. Wilson. Proc. Chem. Soc. 229 (1962). N. Hirota. J. Chem. Phys. **37**, 1884 (1962).
13. L. H. Piette, P. Ludwig, and R. N. Adams. J. Am. Chem. Soc. **84**, 4212 (1962).
14. D. C. Powell and E. Warhurst. Trans. Faraday Soc. **58**, 953 (1962).

[3]*The referee is thanked for bringing these papers to the author's attention.*

Can. J. Chem. Downloaded from www.nrcresearchpress.com by 210.87.254.40 on 09/05/12
For personal use only.

Can. J. Chem. Downloaded from www.nrcresearchpress.com by 210.87.254.105 on 09/05/12
For personal use only.

THE ALKALOIDS OF FUMARIACEOUS PLANTS

LV. THE STRUCTURE OF CULARIDINE

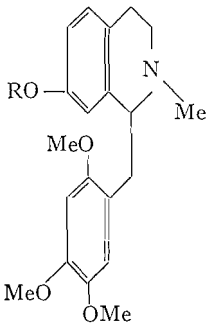
RICHARD H. F. MANSKE
Research Laboratories, Dominion Rubber Co., Ltd., Guelph, Ontario

Received November 19, 1965

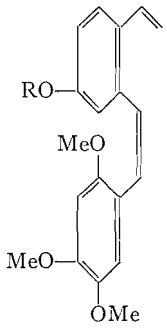
ABSTRACT

Cularidine, which on O-methylation yields cularine, has one phenolic hydroxyl group. It was O-ethylated with diazoethane, and the resultant O-ethylcularidine was degraded to asaronic and 4-ethoxyphthalic acids via sodium – liquid ammonia fission, O-methylation, double Hofmann degradation, and oxidation. These fragments prove the structure of cularidine to be that shown by III.

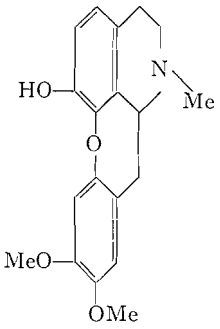
The alkaloid cularidine has been isolated from *Dicentra cucullaria* (L.) Bernh. (1) and from *Corydalis claviculata* (L.) DC. (2). It is monophenolic and upon methylation with diazomethane is converted into cularine; therefore, it can have only one of three possible structures. It is evident that the procedure used in determining the structure of cularine (3), when applied to cularidine O-ethyl ether, will give an unambiguous answer. The experimental difficulties, however, are twofold: difficult O-methylation and poor yields on oxidation; hence pilot experiments with cularine were carried out first.



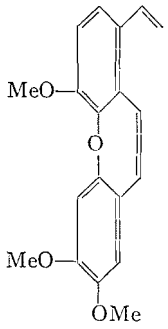
I



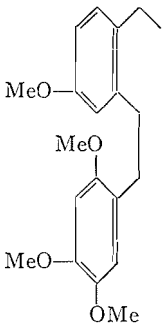
II



III



IV



V

The scission of the diphenyl ether bridge with sodium in liquid ammonia is almost quantitative, but the methylation of the resultant phenolic base offered considerable difficulty until the method of Rodionow (4) was used; then moderate yields of the tetramethoxybenzylisoquinoline (I, R = Me) were obtained. The exhaustive methylation of this base also proceeded in moderate yields to give II (R = Me). However, the oxidation of the latter, although it gave the phthalic acid derivative in acceptable yields, gave asaronic (2,4,5-trimethoxybenzoic) acid in very poor yields, presumably because it is attacked rather easily by the oxidizing agent (permanganate). Nevertheless, a very small amount of asaronic acid was obtained not only from the cularine degradation but also from cularidine O-ethyl ether. This observation alone indicates that III is the structure of cularidine; however, it was also possible to isolate 4-ethoxyphthalic acid in better yield from the degradation products, and this fact alone is also sufficient to establish the suggested structure. The ethoxyphthalic anhydride showed the characteristic anhydride infrared peaks at 1 773 and 1 840 cm^{-1} and was characterized as its N-methylimide. A nuclear

magnetic resonance spectrum of the latter clearly showed the signals associated with the O-ethyl group (a quartet at τ 5.92 (2H, J = 7.0 c.p.s.) and a triplet at τ 8.53 (3H, J = 7.0 c.p.s.)) as well as the singlet of the methyl protons (at τ 6.85 shifted to lower field because of the deshielding of the two electronegative carbonyl groups).

An attempt to obtain recognizable degradative fragments from cularine by another route failed at the penultimate stage. When the doubly unsaturated product (IV) of the second stage of the Hofmann degradation was treated with sodium in liquid ammonia, the product was not the phenolic vinylstilbene but a phenolic ethyldibenzyl which, on O-methylation, generated the fully saturated ethyltetramethoxydiphenylethane V, the nuclear magnetic resonance spectrum of which was entirely consistent with this structure.

The help of Dr. Kju Hi Shin in interpreting the nuclear magnetic resonance spectra is gratefully acknowledged.

EXPERIMENTAL

2-Methyl-7,2',4',5'-tetramethoxy-1-benzyltetrahydroisoquinoline (I, R = Me)

The phenolic base obtained by the sodium – liquid ammonia fission of cularine (4 g) was added to phenyltrimethylammonium hydroxide (prepared from 8 g of the corresponding *p*-toluenesulfonate), and the mixture was heated at 110–120° for 1 h. Steam was passed into the reaction mixture to remove the dimethylaniline and then the solution was extracted with ether. The washed ether solution was dried over solid potassium hydroxide and the solvent largely removed. The base (2.5 g) crystallized shortly, and when it was recrystallized from dry ether – hexane it was obtained as stout colorless prisms melting sharply at 98°.*

Anal. Calcd. for $C_{21}H_{27}O_4N$: four OMe, 34.76. Found: OMe, 34.54, 34.38.

Degradation of Cularidine

A solution of cularidine (1.5 g) in ethanol was treated with an ethereal solution of diazoethane, and after 24 h the excess reagent was removed. The base, in ether solution, was washed with water and dried over potassium hydroxide. It was then added to ca. 50 cc liquid ammonia and treated with a dilute solution of sodium in the same solvent until the blue color was permanent for 1 min. After evaporation of the ammonia, the residue was extracted with ether and the residue from the ether extract was heated with an excess of phenytrimethylammonium hydroxide. The non-phenolic base was isolated as described above and converted into the nitrogen-free compound (II, R = Et) by a double Hofmann degradation (3). The resultant product weighed 0.24 g and consisted of a colorless resin. It was dissolved in acetone and treated with a saturated aqueous solution of potassium permanganate until the color was permanent for 30 min. The acetone was boiled off, a little calcium chloride added, and the hot mixture filtered through a layer of Filtercel. The acidified filtrate was exhausted with ether and the residue from the extract sublimed from a distillation tube. There was a small amount of sublimate at 110° and 0.2 mm which melted at 130–141° either alone or in admixture with asaronic acid. This quantity was insufficient for further characterization. A second distillate was obtained at ca. 150° and 0.2 mm; this, when resublimed, melted at 65–70° either alone or in admixture with 4-ethoxyphthalic anhydride. It was treated in methanol with methylamine, the mixture evaporated, and the residue sublimed (140° at 0.2 mm). The crystalline sublimate, when recrystallized from ether–hexane, melted at 108° either alone or in admixture with an authentic specimen of N-methyl 4-ethoxyphthalimide.

4-Ethoxyphthalic Anhydride

This compound has been described by Fritsch (5), but for the present it was prepared by ethylating 4-hydroxyphthalic acid (6) with ethyl sulfate and alkali. From 12 g of diethyl 4-aminophthalate via the hydroxy acid was obtained 5.5 g of twice-sublimed 4-ethoxyphthalic anhydride which, when recrystallized from dry ether, melted at 76°. The *methylimide*, which had been prepared from the anhydride, sublimed *in vacuo*, and recrystallized from dry ether, melted at 109°. The *ethylimide*, similarly prepared and purified, melted at 102°.

Anal. Calcd. for $C_{12}H_{13}O_3N$: C, 65.74; H, 5.98. Found: C, 65.39, 65.34; H, 5.66, 6.13.

O-Ethylcularidine

Though the free base could not be obtained in crystalline form, it gave an acid oxalate (m.p. 218°) which was only sparingly soluble in cold methanol. The *picrate*, crystallized from acetone–methanol, melted at 210°. The hydrochloride was obtained as colorless needles melting at 172° when recrystallized twice from hot acetone, in which it is moderately soluble. It appears to be a monohydrate.

Anal. Calcd. for $C_{21}H_{25}O_4N \cdot HCl \cdot H_2O$: C, 61.54; H, 6.84. Found: C, 61.34, 61.99; H, 7.28, 7.27.

When this hydrochloride was recrystallized from methanol a solvated form melting at 195° was obtained. The *methiodide* of the O-ethyl ether melted at 236° and the *methine methiodide* prepared therefrom consisted of fine needles, which were sparingly soluble in methanol and which melted at 205° without darkening.

**All melting points are corrected.*

Can. J. Chem. Downloaded from www.nrcresearchpress.com by 210.87.254.105 on 09/05/12
For personal use only.

2-Ethyl-5,2',4',5'-tetramethoxy-1,2-diphenylethane (V)

A solution of compound IV (3) in tetrahydrofuran was added to liquid ammonia in which a small piece of sodium had been dissolved. The blue color was discharged at once. Sodium in small pieces was added until the blue color of the solution remained for 5 min. The ammonia was then evaporated in a current of air, and the residue was treated with an excess of sodium bicarbonate and extracted with ether. The phenolic residue from the washed and dried ether solution did not crystallize. It was methylated with an excess of dimethyl sulfate and caustic soda; the non-phenolic product thus obtained was dried in ether solution with potassium hydroxide. Partial evaporation of the ether and the addition of hexane to the concentrate gave a nearly quantitative yield of the saturated compound (V), m.p. 93°. It was stable to permanganate in acetone solution.

Anal. Calcd. for $C_{20}H_{26}O_4$: C, 72.70; H, 7.93. Found: C, 72.61, 72.44; H, 7.82, 7.83.

REFERENCES

1. R. H. F. MANSKE. Can. J. Res., B, **16**, 81 (1938).
2. R. H. F. MANSKE. Can. J. Chem. **43**, 989 (1965).
3. R. H. F. MANSKE. J. Am. Chem. Soc. **72**, 55 (1950).
4. W. RODIONOW. Bull. Soc. Chim. France, **39**(4), 305 (1926).
5. P. FRITSCH. Ann. 24 (1895).
6. A. BAEYOR. Ber. **10**, 1079 (1877).

Can. J. Chem. Downloaded from www.nrcresearchpress.com by 210.87.254.105 on 09/05/12
For personal use only.

Can. J. Chem. Downloaded from www.nrcresearchpress.com by 210.87.254.5 on 09/05/12
For personal use only.

THE CHEMISTRY OF THE AMINOCHROMES

IX. THE REACTIONS OF GLUTATHIONE WITH SOME HALOGENATED AMINOCHROMES[1,2]

G. L. MATTOK AND R. A. HEACOCK[3]

Psychiatric Research Unit, University Hospital, Saskatoon, Saskatchewan

Received June 28, 1965

ABSTRACT

7-Iodoadrenochrome reacts with glutathione to give 5,6-dihydroxy-7-iodo-1-methylindole, 5,6-dihydroxy-1-methylindole, 7-*S*-glutathionyl-5,6-dihydroxy-1-methylindole, and a trace of a product that is probably 4-*S*-glutathionyl-5,6-dihydroxy-7-iodo-1-methylindole. It reacts with the monosodium salt of glutathione to give mainly 5,6-dihydroxy-7-iodo-1-methylindole and 4-*S*-glutathionyl-5,6-dihydroxy-7-iodo-1-methylindole, with smaller quantities of 7-*S*-glutathionyl-5,6-dihydroxy-1-methylindole and 5,6-dihydroxy-1-methylindole. 7-Bromoadrenochrome reacts with glutathione (free acid or monosodium salt) to give mainly 7-bromo-5,6-dihydroxy-1-methylindole and a second product, which is probably 7-bromo-4-*S*-glutathionyl-5,6-dihydroxy-1-methylindole. The main products that are obtained in reactions of this type result from either direct reduction of the aminochrome or 1,4-addition of the thiol to either of the α,β-unsaturated C_5-carbonyl systems in the aminochrome molecule.

INTRODUCTION

It has been shown that the main products of the reaction between adrenochrome and glutathione (GSH)[4] result from the 1,4-addition of the thiol to the C_5-unsaturated carbonyl systems in the aminochrome molecule that involve the C_6—C_7 and C_4—C_9 double bonds. These products are probably 7-*S*-glutathionyl-5,6-dihydroxy-1-methylindole (I) and 9-*S*-glutathionyl-2,3,6,9-tetrahydro-3,5-dihydroxy-6-oxo-1-methylindole respectively (1). It was observed that small quantities of DHMI[5] (II) were formed at the same time (1). A preliminary study by paper chromatography of the products of the reaction between GSH and 7-iodoadrenochrome (III) showed that, in addition to 7-iodo-DHMI (IV), two substances with R_f values[6] of 0.44 and 0.67 were formed (2). In some earlier publications it was reported that the iodine atom occupied the 2-position in iodoaminochromes (cf. ref. 3). It has recently been shown, however, that the halogen atom in halogenated aminochromes and derived products is invariably in the 7-position (4).

This paper reports the results of an extensive examination by spectroscopy and paper chromatography of the products obtained from a number of 7-iodo- and 7-bromoaminochromes when they react with GSH or GSH(Na).

EXPERIMENTAL

Materials

7-Iodoadrenochrome (5), 1-ethyl-7-iodonoradrenochrome (6), 7-iodo-1-isopropylnoradrenochrome (6), 7-iodoadrenochrome methyl ether (6), 5,6-dihydroxy-1-methylindole (7), and 5,6-dihydroxy-7-iodo-1-methylindole (2) were prepared by methods described in the literature (cf. ref. 4). GSH, GSH(Na), and GSSG were obtained from Nutritional Biochemicals Corporation.

[1]*This investigation was supported by grants from the Department of National Health and Welfare (Ottawa) and the Government of Saskatchewan (Department of Public Health).*

[2]*For part VIII in this series, see R. A. Heacock and O. Hutzinger, Can. J. Chem., 43, 2535 (1965).*

[3]*Present address: Atlantic Regional Laboratory, National Research Council, 1411 Oxford Street, Halifax, Nova Scotia.*

[4]*GSH, GSH(Na), and GSSG are used respectively as abbreviations for glutathione (free acid), glutathione (monosodium salt), and oxidized glutathione.*

[5]*DHMI is used as an abbreviation for 5,6-dihydroxy-1-methylindole and the 5,6-dihydroxy-1-methylindole nucleus in its derivatives.*

[6]*All the R_f values reported in this paper were obtained by descending development on Whatman No. 1 paper, with 2% acetic acid in water as the developing solvent.*

Reaction Mixtures

The reaction mixtures were prepared by suspending the 7-iodo- or 7-bromo-aminochrome (10 mg) in a solution of GSH or GSH(Na) (25 mg) in water (1 ml). When the violet color of the solutions had totally disappeared, which usually occurred within several minutes of their preparation, the reaction mixtures were filtered, and samples (30 μl) of the clear filtrates were used directly for chromatographic or spectroscopic investigation.

To investigate the possibility of reactions between 7-iodo- or 7-bromo-adrenochrome and GSSG, an aqueous suspension (1 ml) of the halogenated aminochrome (10 mg) was treated with an excess of GSSG, and the reaction mixture was examined by paper chromatography.

An aqueous suspension of 7-iodo-DHMI (10 mg/ml) was treated with excess GSH and the reaction mixture allowed to stand at room temperature for 2 h. It was then extracted with ether, and the dried (Na_2SO_4) ether extract was examined by paper chromatography.

Paper Chromatography

Descending chromatography was carried out on Whatman No. 1 paper, with acetic acid (2%) in water as the running solvent. In all cases the solvent was allowed to descend ca. 15 inches, which required 2.5–3 h. After they were dried in air at room temperature, the developed chromatograms were examined for fluorescence in ultraviolet light and were then sprayed with one of the following chromogenic reagents:[7] Ehrlich's reagent, cinnamaldehyde, *p*-dimethylaminocinnamaldehyde, diazotized *p*-nitroaniline, Gibb's reagent, or ninhydrin.

In some cases the aqueous solution of the aminochrome reaction products was extracted with peroxide-free ether (4 × 1.0 ml). Samples of both the dried (Na_2SO_4) ether extracts and the aqueous mother liquors (ca. 120–150 μl and 50 μl respectively) were examined chromatographically on paper in the manner described above.

Relatively pure solutions of the individual products were obtained by chromatography on Whatman No. 3MM paper (23 cm × 57 cm) by a procedure previously described (1).

Spectroscopy

Spectra were obtained from suitably diluted solutions of the reaction mixtures or ether extracts, and were recorded on a Beckman DK-2 or a Unicam SP.800 recording spectrophotometer.

RESULTS

The results of a survey by paper chromatography of the products obtained by the action of GSH on five different 7-iodo- and 7-bromo-aminochromes, and of GSH(Na) on 7-iodo- and 7-bromo-adrenochrome are given in Table I. Paper chromatograms of 7-iodoadrenochrome–GSH reaction mixtures usually showed three main spots with R_f values of ca. 0.18, 0.44, and 0.65 after they were sprayed with any one of most of the chromogenic reagents that react positively with indoles and phenols. The developed chromatograms often exhibited a weak pink spot in the 0.8–0.9 R_f zone before spray was applied. As the paper dried, this area slowly developed a yellow-green fluorescence, typical of a 5,6-dihydroxyindoxyl derivative. This suggests that the pink spot was due to free aminochrome (cf. ref. 9) that was produced during the chromatographic procedure from decomposition of one of the materials originally present in the reaction mixture. When the 7-iodoadrenochrome–GSH reaction mixture was exhaustively extracted with peroxide-free ether, and both the ether extracts and aqueous mother liquors were examined separately by paper chromatography, it was observed that one product (R_f 0.18) was totally extracted by the ether and the other (R_f 0.62) was not. At first it appeared that the substance that produced the spot with R_f ca. 0.44 was only partially extracted by the ether. Careful examination of the color reactions and ultraviolet absorption spectra of the products with R_f values of ca. 0.44 on chromatograms of the ether extracts and the mother liquors that had been run individually, however, showed that they were different (see Table I). The product that is not extractable with ether (R_f 0.45) shows color reactions that would be expected of an indole, a catechol, or an α-amino acid (see Table I), and it gives a positive reaction with the ceric sulfate – sodium arsenite reagent (cf. ref. 10), which suggests that it still contains iodine.

[7]*The chromogenic reagents were prepared by common methods described in the literature (cf. ref. 8).*

Can. J. Chem. Downloaded from www.nrcresearchpress.com by 210.87.254.5 on 09/05/12
For personal use only.

Can. J. Chem. Downloaded from www.nrcresearchpress.com by 210.87.254.5 on 09/05/12
For personal use only.

In the reaction of 7-iodoadrenochrome with GSH(Na), much more of the substance with a R_f of 0.18 (probably 7-iodo-DHMI (IV)) was formed, and only traces of DHMI (II) could be detected in ether extracts of these reaction mixtures. The major product of this reaction was the one that could not be extracted with ether (R_f 0.45), but traces of the product with R_f 0.63 were also present. 7-Iodoadrenochrome–GSH(Na) reaction mixtures were extracted with ether; the mother liquors were kept overnight at room temperature and then examined by paper chromatography. This showed that very little of the product (R_f ca. 0.45) that was not extractable with ether was present, but that a new product with R_f ca. 0.60 was formed. It did not contain iodine and it showed color reactions similar to those of 7-*S*-glutathionyl-5,6-dihydroxy-1-methylindole (I).

Paper chromatograms of the mixtures obtained from the reaction of 7-bromoadrenochrome with either GSH or GSH(Na) were essentially similar in appearance (see Table I). The overall chromatographic picture in both was more comparable to that obtained in the reaction of 7-iodoadrenochrome with GSH(Na) than with GSH. The main products that were observed had R_f values of ca. 0.22 and 0.48. The former is most probably 7-bromo-DHMI and the latter, which is not extractable with ether, appears to be analogous to the substance (R_f ca. 0.45) not extractable with ether that is one of the major products of the 7-iodoadrenochrome–GSH(Na) reaction.

Paper chromatographic examination of the products obtained from 1-ethyl-7-iodonoradrenochrome, 7-iodo-1-isopropylnoradrenochrome, and 7-iodoadrenochrome methyl ether by the action of GSH in aqueous solution showed that they were basically similar to those obtained from 7-iodoadrenochrome under similar conditions (see Table I). Reaction mixtures of 7-iodoadrenochrome methyl ether and GSH gave a chromatographic pattern that was virtually identical with that obtained from a reaction mixture of 7-iodoadrenochrome and GSH, which indicates that the alkoxy group in the 3-position of the aminochrome ring system has no significant effect on the course of the reaction with GSH (cf. ref. 1).

No reaction that could be detected by paper chromatography occurred in aqueous solution between GSSG and either 7-bromoadrenochrome or 7-iodoadrenochrome, which suggested that the thiol group of GSH (or of GSH(Na)) must have been involved in all the reactions described above. Consequently, none of these reaction products were formed by the interaction of the 7-halogeno substituent of the aminochrome molecule and the primary amino group of the amino acid. Aqueous solutions of 7-bromo-DHMI and of 7-iodo-DHMI were treated individually with GSH, GSH(Na), and GSSG in turn. Paper chromatographic examination of the ether extracts of these reaction mixtures, after they had stood at room temperature for several hours, showed the presence of DHMI, which indicated that dehalogenation of the 7-halogeno-DHMI derivatives had occurred.

The products obtained from 7-iodoadrenochrome by the action of GSH or GSH(Na) in aqueous solution exhibited absorption maxima at 306 mμ and 385 mμ, whereas reaction mixtures obtained from 7-bromoadrenochrome exhibited them at 305 mμ and 380 mμ. The longer wavelength peak was about three times relatively more intense in both cases when the reaction was carried out with GSH(Na) than with GSH. It was not possible in either case, however, to obtain solutions of the substances that absorb in the 380–385 mμ region, by elution of any part of the developed chromatograms.

When freshly prepared reaction mixtures, which are yellow, were diluted with water they became red-pink in color. After they had stood at room temperature for ca. 2 h, however, they showed no significant absorption at 380 mμ and the intensity of the peak at ca. 300 mμ was increased, but the solutions did not become pink after dilution. These

Can. J. Chem. Downloaded from www.nrcresearchpress.com by 210.87.254.5 on 09/05/12
For personal use only.

TABLE I

Paper chromatography* and ultraviolet absorption characteristics of the products obtained from reactions of glutathione (free acid or monosodium salt) with some 7-iodoaminochromes and with 7-bromoadrenochrome

Reaction mixture	R_f values and intensities† of main spots‡	λ_{max} (mμ)	Colors with chromogenic reagents§					
			Ehr.	Cinn.	DMAC	DPNA	Gib.	Nin.
7-Iodoadrenochrome–GSH	0.18 (w)‖	282; 303	BV	RP → VBr	BG → B	GyM → Br	GyBr → Br	—
	0.44 (m)¶	300	BV	OrBr → VBr	BG → B	M → VBr	Br	—
	0.45 (w)	311	V → BV	P → Gy	BGy → GyV	GyP	Br	Gy
	0.65 (s)	303	V → BV	RP → GyV	BG → GyV	M → VBr	PBr → Br	BGy
	0.84 (w)**							
7-Iodoadrenochrome–GSH(Na)	0.18 (s)‖	282; 303	BV	RP → VBr	BG → B	GyM → Br	GyBr → Br	—
	0.42 (w)¶	300	BV	OrBr → VBr	BG → B	M → VBr	Br	—
	0.45 (s)	311	V → BV	P → Gy	BGy → Gy	GyP	Br	Gy
	0.63 (w)	303	V → BV	RP → GyV	BG → GyV	M → VBr	PBr → Br	BGy
	0.85 (w)**							
1-Ethyl-7-iodonoradreno-chrome–GSH	0.25 (w)		BV	RP → VBr	BG → B	GyM → Br	GyV → Br	—
	0.50 (m)		PV → BV	P → GyV	BGy → GyV	GyP	Br	Gy
	0.52 (m)		BV	OrBr → VBr	BG → B	M → VBr	Br	—
	0.68 (s)		V → BV	RP → GyV	BG → GyV	M → VBr	PBr → Br	BGy
	0.85 (w)**							
7-Iodo-1-isopropylnoradreno-chrome–GSH	0.28 (m)		BV	RP → GyP	BG → BV	GyM → Br	GyV → Br	—
	0.50 (m)		PV → BV	P → Gy	BGy → GyV	GyP	Br	Gy
	0.58 (m)		BV → V	OrBr → VBr	BG → BGy	RBr → Br	Br	—
	0.69 (s)		V → BV	RP → GyV	BGy → Gy	M → VBr	PBr → Br	BGy
	0.84 (w)**							

Can. J. Chem. Downloaded from www.nrcresearchpress.com by 210.87.254.5 on 09/05/12
For personal use only.

TABLE I (*Concluded*)

Reaction mixture	R_f values and intensities† of main spots‡	λ_{max} (mμ)	Colors with chromogenic reagents§					
			Ehr.	Cinn.	DMAC	DPNA	Gib.	Nin.
7-Iodoadrenochrome methyl ether – GSH	0.19 (w)‖		BV	RP → VBr	BG → B	GyM → Br	GyBr → Br	—
	0.42 (w)¶		BV	OrBr → VBr	BG → B	M → VBr	Br	—
	0.44 (w)		V → BV	P → Gy	BGy → GyV	GyP	Br	Gy
	0.65 (s)		V → BV	RP → GyV	BG → GyV	M → VBr	PBr → Br	BGy
	0.80 (w)**							
7-Bromoadrenochrome–GSH	0.22 (m)††	280; 301	BV	RP → VBr	BG → BGy	GyM → VBr	GyBr → Br	—
	0.42 (w)¶	300	BV	OrBr → VBr	BG → B	M → VBr	Br	—
	0.49 (s)	310	V → BV	P → GyV	BG → GyV	GyBr → Gy	Br	BGy
	0.60 (w)		V	GyP → GyV	GyV	P → GyV	—	BGy
	0.84 (w)**							
7-Bromoadrenochrome-GSH(Na)	0.22 (s)††	280; 301	BV	RP → VBr	BG → BGy	GyM → VBr	GyBr → Br	—
	0.42 (w)¶	300	BV	OrBr → VBr	BG → B	M → VBr	Br	—
	0.47 (s)	310	V → BV	P → GyV	BG → GyV	GyBr → Gy	Br	BGy
	0.84 (w)**							

*Descending development on Whatman No. 1 paper with 2% acetic acid in water.
†s = strong, m = medium, w = weak.
‡All the R_f values reported are the average of at least six determinations. Spots caused by unchanged glutathione and oxidized glutathione, which have R_f values of ca. 0.90 and ca. 0.95 in this system, were invariably present on the developed chromatograms; therefore for the sake of brevity they are not shown in the table.
§REAGENTS: Ehr. = Ehrlich's reagent, Cinn. = cinnamaldehyde, DMAC = *p*-dimethylaminocinnamaldehyde, DPNA = diazotized *p*-nitroaniline, Gib. = Gibb's reagent (*N*,2,6-trichloro-*p*-quinoneimine), Nin. = ninhydrin. COLORS: B = blue, BV = blue-violet, BG = blue-green, BGy = blue-grey, V = violet, VBr = violet-brown, GyV = grey-violet, PV = pink-violet, M = magenta, GyM = grey-magenta, P = pink, RP = red-pink, GyP = grey-pink, PBr = pink-brown, Br = brown, RBr = red-brown, OrBr = orange-brown, Gy = grey, GyBr = grey-brown.
‖5,6-Dihydroxy-7-iodo-1-methylindole.
¶5,6-Dihydroxy-1-methylindole.
**This spot was invariably weak and its color reactions were difficult to describe accurately because, in part, of the contamination of this region with excess glutathione.
††7-Bromo-5,6-dihydroxy-1-methylindole.

facts indicate that the product (λ_{max} 380 mμ) is relatively unstable and readily decomposes in aqueous solution to give a compound characterized by λ_{max} 300 mμ, and also that the unstable compound is necessary for the regeneration of an aminochrome-type structure.

DISCUSSION

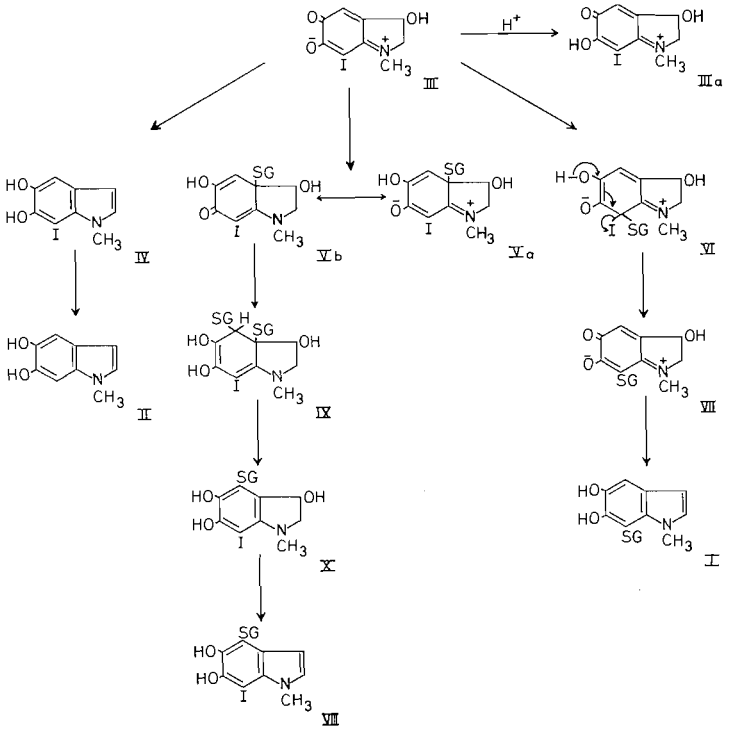
Two of the three main products of the reaction between 7-iodoadrenochrome (III) and GSH or GSH(Na) are extractable with ether, and from the nature of their paper chromatographic and spectroscopic properties (see Table I) they appear to be 7-iodo-DHMI (IV) and DHMI (II). 7-Iodo-DHMI (IV) is a relatively minor product in reactions involving GSH, but much larger amounts of it are formed when GSH(Na) is the reactant. When 7-iodoadrenochrome (III) and GSH react, the main product that is not extractable with ether has a R_f of 0.63. Because of this value, its color reactions, and its absorption maximum it appears to be identical with the main product of the adrenochrome–GSH reaction with the same R_f value, which was previously provisionally identified (1) as 7-*S*-glutathionyl-DHMI (I). The product with a λ_{max} of ca. 380 mμ, that is initially present in the 7-iodoadrenochrome–GSH reaction mixtures, is probably analogous to the substance (R_f ca. 0.80, λ_{max} ca. 350 mμ) in the adrenochrome–GSH reaction mixtures that was tentatively identified as 9-*S*-glutathionyl-2,3,6,9-tetrahydro-3,5-dihydroxy-6-oxo-1-methylindole (1). In the present case the product would be 9-*S*-glutathionyl-2,3,6,9-tetrahydro-3,5-dihydroxy-7-iodo-6-oxo-1-methylindole (V). The shift of the observed λ_{max} towards longer wavelengths in the spectra of compounds of this type is compatible with iodine substitution in the 7-position of the molecule (cf. ref. 11).

It has been suggested that little of the DHMI that is formed during the course of the adrenochrome–GSH reaction results from the direct reduction of adrenochrome by the thiol (1). The presence of a halogen substituent in the aminochrome nucleus, however, may raise its oxidation potential sufficiently to permit direct reduction by GSH (cf. ref. 12). In this case the initial product would be the corresponding true leuco compound 3,5,6-trihydroxy-7-iodo-1-methylindoline, which would readily give 7-iodo-DHMI (IV) by loss of water from the 2- and 3-positions of the indoline ring system (cf. ref. 11).

The formation of 7-*S*-glutathionyl-DHMI (I) could occur as the result of a 1,4-addition–elimination process. 1,4-Addition of GSH to the α,β-unsaturated C_5-carbonyl system in 7-iodoadrenochrome (III), involving the C_6—C_7 double bond, would give an intermediate compound (VI), which could readily give 7-*S*-glutathionyladrenochrome (VII) by the elimination of hydrogen iodide. Reduction of 7-*S*-glutathionyladrenochrome (VII) would initially give 7-*S*-glutathionylleucoadrenochrome, which would be expected rapidly to undergo intramolecular dehydration (cf. ref. 11) with the formation of 7-*S*-glutathionyl-DHMI (I).

The unstable product showing absorption at ca. 380 mμ (probably 9-*S*-glutathionyl-7-iodo-2,3,6,9-tetrahydro-3,5-dihydroxy-6-oxo-1-methylindole (V*a*)) presumably results from the 1,4-addition of GSH to the α,β-unsaturated C_5-carbonyl system in 7-iodoadrenochrome (III), involving the C_4—C_9 double bond (cf. ref. 1). The formation of the product V*a* probably represents the first stage in the formation of the product (R_f 0.45) that is not extractable with ether. The color reactions and the ultraviolet absorption maximum (see Table I) of this latter substance indicate that it retains the indole nucleus and contains an *o*-diphenol system, an α-amino acid residue, and an iodine atom, which suggests that it is an iodinated DHMI derivative containing a GSH residue. If it is assumed that the iodine atom is retained in the 7-position, the *S*-glutathionyl residue would be in the 4-position of the indole ring system. The final product would therefore

Can. J. Chem. Downloaded from www.nrcresearchpress.com by 210.87.254.5 on 09/05/12
For personal use only.



REACTION SCHEME 1.

appear to be 4-*S*-glutathionyl-5,6-dihydroxy-7-iodo-1-methylindole (VIII). 7-Iodo substitution in compounds of this type usually results in a lowering of the R_f value in 2% acetic acid and in an increase in the wavelength of the main ultraviolet absorption maximum (e.g. DHMI: λ_{max} 300 mμ, R_f 0.44; 7-iodo-DHMI: λ_{max} 303 mμ and 313 mμ (shoulder), R_f 0.18). Deiodination of VIII occurs readily in aqueous solution at room temperature with the formation of a product, presumably 4-*S*-glutathionyl-DHMI, which has chromatographic properties similar to those of 7-*S*-glutathionyl-DHMI (I).

It has already been pointed out that relatively more deiodinated products are formed in cases when 7-iodoadrenochrome (III) reacts with GSH rather than with GSH(Na). A satisfactory explanation of this is not available at the moment. The course of the reaction may be influenced, however, by the degree of zwitterionic character of the structure of 7-iodoadrenochrome,[8] which would determine the extent of conjugation in the C_5—C_7 α,β-unsaturated C_5-carbonyl system. The formation of the intermediate VI would require a considerable degree of conjugation in this system, which would result from a high degree of dipolarity in the aminochrome molecule. Under the strongly acid conditions of the GSH reaction (pH ca. 3.5), the C_6—C_7 double bond in the zwitterionic form of the 7-iodoaminochrome molecule would be stabilized by the protonation of the polarized C_6-carbonyl group (cf. III*a*), and the addition mechanism III $\rightarrow$ VI (i.e. the route leading to the formation of I) will be favored. The addition product V is probably a resonance hybrid (V*a* $\leftrightarrow$ V*b*). A second molecule of GSH could be added to V*b* by a 1,4-addition to the α,β-unsaturated C_6-carbonyl system, involving the C_4—C_5 double bond, to give the intermediate IX. The elimination of a molecule of GSH (involving the angular GSH

[8]*The properties of the aminochromes are generally better explained by a zwitterionic structure than by a true m-amino-o-quinone structure (cf. ref. 13).*

Can. J. Chem. Downloaded from www.nrcresearchpress.com by 210.87.254.5 on 09/05/12
For personal use only.

residue) from IX by a β-elimination mechanism would lead to the formation of the 3,5,6-trihydroxyindoline derivative (X), which would readily give 4-*S*-glutathionyl-5,6-dihydroxy-7-iodo-1-methylindole (VIII) by an internal dehydration mechanism (cf. ref. 11).

There are two different α,β-unsaturated C_5-carbonyl systems in an aminochrome molecule that will accept a thiol by a 1,4-addition mechanism (cf. ref. 1). The degree of conjugation in one of these systems, i.e. that involving the C_4—C_9 double bond, will not be affected materially by the degree of zwitterionic character of the aminochrome molecule. The degree of conjugation in the system involving the C_6—C_7 double bond, however, will be influenced strongly by the degree of dipolarity of the molecule. A high degree of conjugation in the latter system will depend on a large contribution from the zwitterionic form of the molecule. Consequently, addition to the C_5—C_7 α,β-unsaturated carbonyl system will be favored by the relatively acid conditions of the GSH reaction. Under the less acid conditions of the GSH(Na) reaction, however, this route (i.e. III $\rightarrow$ VI) will not be as dominant, which will allow the III $\rightarrow$ V reaction to occur to a relatively greater extent. The addition of a second molecule of GSH to the unsaturated C_6-carbonyl system in V, involving the C_4—C_5 double bond, would be facilitated by a large contribution of the nonpolar form (V*b*) to the overall molecular structure of V, which would be favored by the less acid conditions of the GSH(Na) reaction.

The reactions of 7-bromoadrenochrome with GSH or GSH(Na) are comparable to that of 7-iodoadrenochrome with GSH(Na). Two of the main products obtained from 7-bromoadrenochrome appear to be 7-bromo-DHMI (R_f 0.22, λ_{max} 280 and 301 mμ) and a product that is probably 7-bromo-4-*S*-glutathionyl-DHMI (R_f 0.48, λ_{max} 310 mμ). A third unstable product (λ_{max} ca. 380 mμ), which cannot be detected by paper chromatography, is initially present in these reaction mixtures. It is presumably analogous to the product derived from 7-iodoadrenochrome with a λ_{max} in the same region, and consequently is 7-bromo-*S*-glutathionyl-2,3,6,9-tetrahydro-3,5-dihydroxy-6-oxo-1-methylindole. As with the 7-iodo compound, there was evidence that more dehalogenation occurred when the reaction was carried out with GSH than with GSH(Na). There was also spectroscopic evidence that there was greater formation (by about a factor of three) of the product with a maximum absorption band at ca. 380 mμ when GSH(Na) was used. The overall amount of dehalogenation observed with both GSH and GSH(Na) was much less in reactions with 7-bromoadrenochrome than in those with the corresponding iodo compound. This phenomenon parallels the order of displacement rates of halides from substituted quinones by sulfite, i.e. I $\gg$ Br $>$ Cl (14). The formation of the products that were obtained in the reaction of 7-bromoadrenochrome with GSH or GSH(Na) may be explained satisfactorily by mechanisms similar to those proposed for the corresponding reactions with 7-iodoadrenochrome.

ACKNOWLEDGMENT

The assistance of Mrs. B. D. Scott with some of the paper chromatographic work is gratefully acknowledged.

REFERENCES

1. G. L. Mattok and R. A. Heacock. Can. J. Chem. **43**, 119 (1965).
2. R. A. Heacock and B. D. Scott. Can. J. Chem. **38**, 508 (1960).
3. R. A. Heacock. Chem. Rev. **59**, 181 (1959).
4. R. A. Heacock, O. Hutzinger, B. D. Scott, J. W. Daly, and B. Witkop. J. Am. Chem. Soc. **85**, 1825 (1963).
5. H. Sobotka and J. Austin. J. Am. Chem. Soc. **73**, 3077 (1951).
6. R. A. Heacock and B. D. Scott. Can. J. Chem. **38**, 516 (1960).

Can. J. Chem. Downloaded from www.nrcresearchpress.com by 210.87.254.5 on 09/05/12
For personal use only.

7. G. L. MATTOK and R. A. HEACOCK. Can. J. Chem. **42**, 484 (1964).
8. R. A. HEACOCK, M. E. MAHON, and B. D. SCOTT. Can. J. Chem. **39**, 231 (1961).
9. R. A. HEACOCK, C. NERENBERG, and A. N. PAYZA. Can. J. Chem. **36**, 853 (1958).
10. C. H. BOWDEN, N. F. MACLAGAN, and J. H. WILKINSON. Biochem. J. **59**, 93 (1955).
11. R. A. HEACOCK. Advan. Heterocyclic Chem. In press.
12. L. F. FIESER and M. FIESER. Advanced organic chemistry. Reinhold Publishing Corp., New York. 1961. p. 849.
13. J. HARLEY-MASON. Experientia, **4**, 307 (1948).
14. C. A. BISHOP, R. F. PORTER, and L. K. J. TONG. J. Am. Chem. Soc. **85**, 3991 (1963).

Can. J. Chem. Downloaded from www.nrcresearchpress.com by 210.87.254.5 on 09/05/12
For personal use only.

Can. J. Chem. Downloaded from www.nrcresearchpress.com by 210.87.254.42 on 09/05/12
For personal use only.

THE REACTION OF CHLORAL WITH HALOBENZENES AND WITH 2,4-DICHLOROPHENOL

SYNTHESIS OF HALOGENATED ETHYLBENZENES AND OF α-METHOXYPHENYLACETIC ACIDS

WILKINS REEVE, JOHN P. MUTCHLER, AND CHARLES L. LIOTTA[1]
Chemistry Department, University of Maryland, College Park, Maryland
Received June 24, 1965

ABSTRACT

The Friedel–Crafts reaction of chloral with aromatic compounds to form aryltrichloromethylcarbinols is reviewed. The molar ratio of aluminium chloride to chloral is critical and varies from 0.15 to 2.0 depending on the solvent, steric considerations, and the reactivity of the aromatic ring. The reaction has been used to prepare several new compounds with carbon disulfide or excess aromatic compound as the solvent. From 2,4-dichlorophenol, an *o*-hydroxy-α-trichloromethylbenzyl alcohol is obtained. Both the phenolic and side-chain hydroxy groups of this alcohol are methylated with equal ease by dimethyl sulfate.

It has now been found that changing the solvent from carbon disulfide to methylene chloride results in the hydroxy group of the initial carbinol also being replaced by chlorine. This role of the solvent in controlling the course of the reaction has not been observed previously.

The trichloromethylcarbinols are converted into α-methoxy acids by treatment with methanolic potassium hydroxide. Sodium in liquid ammonia removes the α-methoxy group, as well as the halogens, from 3,5-dichloro-α,2-dimethoxyphenylacetic acid.

Aryltrichloromethylcarbinols may be prepared by a Friedel–Crafts reaction between chloral and aromatic compounds such as benzene, toluene, *p*-xylene, and anisole (1); bromobenzene and chlorobenzene (2); and *o*-dichlorobenzene (3). Naphthalene has been reported to condense in the β-position (4). Other methods of preparing trichloromethylcarbinols have been reviewed (5). Aluminium chloride differs from other acid catalysts in that the reaction can easily be stopped at the carbinol stage. In contrast, the sulfuric acid catalyzed reaction of benzene (6) or chlorobenzene with chloral gives rise exclusively to diaryltrichloroethanes, as in the well-known synthesis of dichlorodiphenyltrichloroethane (DDT).

A general procedure for preparing the aryltrichloromethylcarbinols (Table I) involves mixing 1 equivalent of anhydrous chloral with an excess of the hydrocarbon (which serves as both reactant and solvent) and slowly adding at 0 to 30° sufficient solid aluminium chloride to cause the reaction to occur. The amount of aluminium chloride to be used per mole of chloral is a critical factor, since the use of more than the optimum amount results in the successive formation of diaryltrichloroethanes, diaryldichloroethylenes, tri- and tetra-arylethyl chlorides, and tetraarylethylenes. With large amounts of aluminium chloride, all of the first-formed carbinol is converted into these products. The importance of the amount of aluminium chloride in determining the nature of the reaction products has not been recognized adequately in reviews of the older literature (7).

It is apparent that, for the preparation of the carbinols, the optimum molar ratio of aluminium chloride to chloral is approximately 0.2 when aromatic hydrocarbons are employed as both the reactant and the solvent, and that increased amounts of aluminium chloride are required with the introduction of two chloro groups into the aromatic ring. With carbon disulfide as the solvent, a complex between the aryltrichloromethylcarbinol and the aluminium chloride precipitates. Consequently, an equal molar amount of

[1]*Celanese Fellow, 1962–1963.*

TABLE I

Preparation of aryltrichloromethylcarbinols

Aromatic compound	Moles reactant/mole chloral: Aromatic compound	$AlCl_3$	Solvent	Yield of Ar—CHOH—CCl_3, %
Benzene	Excess‖	0.22	Benzene	80*
Toluene	Excess‖	0.22	Toluene	Good*
Naphthalene	0.5	0.15	$C_6H_5NO_2$	61†
Anisole	Excess‖	0.20	Anisole	39‡
2,4-Dichloroanisole	1.0	2.0	CS_2	0
2,4-Dichlorophenol	0.9	2.1	CS_2	60
Fluorobenzene	1.0	1.0	CS_2	62
Chlorobenzene	Excess‖	0.2	C_6H_5Cl	50§
Chlorobenzene	1.0	1.0	CS_2	50
o-Dichlorobenzene	Excess‖	0.9	$C_6H_4Cl_2$	76
Bromobenzene	Excess‖	0.2	C_6H_5Br	55§
Bromobenzene	1.0	1.0	CS_2	49
Iodobenzene	1.0	1.0	CS_2	30

*Reference 1.
†Unpublished work.
‡33% of 1,1,1-trichloro-2,2-bis(*p*-methoxyphenyl)ethane was also obtained.
§Reference 2 reports 42 to 45% yield.
‖When used in excess, 7 to 10 moles is employed.

aluminium chloride was always used with this solvent. With 2,4-dichloroanisole, the reaction could not be induced to occur even under relatively severe conditions at 46°. That this unreactivity was primarily a steric effect caused by the bulky methoxy group was shown by the successful reaction of 2,4-dichlorophenol with chloral.

Methylene Chloride Solvent

With methylene chloride as the solvent (Table II), the reaction products were found to be α-trichloromethylbenzyl chlorides, the carbinol hydroxy group being replaced by chlorine. This was surprising, since the hydroxy group in the aryltrichloromethylcarbinols neither reacts with concentrated hydrochloric acid nor gives a test with the Lucas reagent.

TABLE II

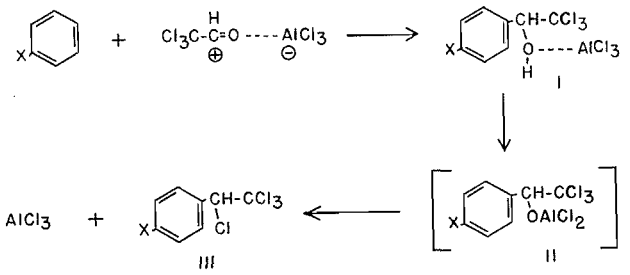
Reaction of chloral with aromatic compounds, methylene chloride being used as solvent*

Aromatic compound	Yield of Ar—CHCl—CCl_3, %
Acetanilide	29†
Fluorobenzene	68
Chlorobenzene	78
Bromobenzene	79
Iodobenzene	66

*0.3 mole of aromatic compound and 0.3 mole anhydrous chloral in 150 ml of methylene chloride were treated at 0° with 0.3 mole aluminium chloride over a 1 h period and allowed to warm to room temperature over a 5 h period.
†Twice the usual amount of aluminium chloride and chloral was used.

The above results strongly suggest that the reactions are proceeding by the mechanism shown in Reaction Scheme 1. The mechanism of formation of complex I closely corresponds to the usually accepted mechanism for the Friedel–Crafts acylation reaction (8). With carbon disulfide as the solvent, the reaction stops at this stage because the complex is insoluble. Further reaction would be difficult in a rigid crystal structure and in the absence of a solvent shell. With methylene chloride as the solvent, the reaction mixture remains

Can. J. Chem. Downloaded from www.nrcresearchpress.com by 210.87.254.42 on 09/05/12
For personal use only.



REACTION SCHEME 1.

homogeneous, and the elimination of hydrogen chloride leads to intermediate II. The conversion of this into tetrachloroethylbenzene (III) is analogous to the conversion of alcohols into alkyl chlorides with retention of configuration by reaction with boron trichloride; the latter reaction is believed to occur by a S_Ni mechanism involving a quasi four atom ring transition state (9). That the reaction in methylene chloride solvent does go through the carbinol complex stage (I) was shown by the fact that phenyltrichloromethylcarbinol reacted with an equal molar amount of aluminium chloride in methylene chloride at 0° to form α-trichloromethylbenzyl chloride in 66% yield.

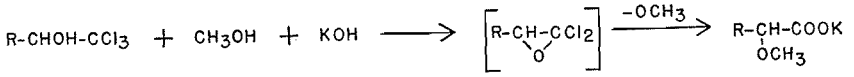
The condensation reaction between benzene itself and chloral to form the tetrachloroethylbenzene fails under the standard conditions employed; only a tar was obtained.

Infrared Data

The spectra of 20 secondary trichloromethylcarbinols prepared in these laboratories have been determined. In addition to the expected absorption bands caused by the hydroxy and aryl groups, two characteristic bands (835 to 815 and 780 to 760 cm^{-1}) are almost always strong. These are associated with the $Cl_3C—CHR—O—$ group.

Reactions of the Carbinols

The most important reaction of the carbinols is their conversion into α-substituted acids, where the nature of the substituent depends on the nucleophile used. Two examples follow in which the aryltrichloromethylcarbinols are converted into α-methoxy acids by treatment with methanolic potassium hydroxide. This conversion is presumed to occur by the mechanism postulated for the reaction of aromatic aldehydes with chloroform, methanol, and base (10) (Reaction Scheme 2).

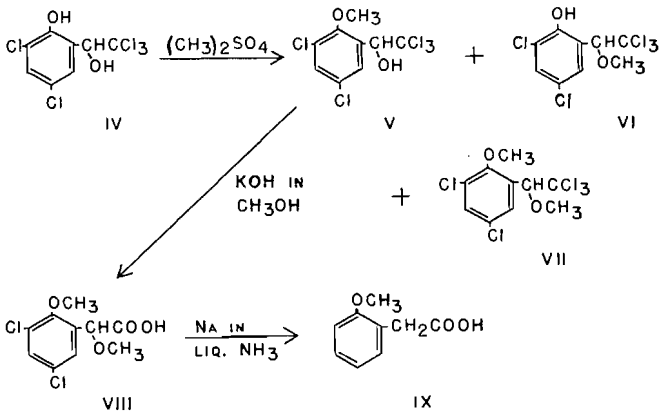


REACTION SCHEME 2.

3,5-Dichloro-2-hydroxyphenyltrichloromethylcarbinol (IV) was converted into the methoxy carbinol V and then into the dichlorodimethoxy acid VIII. The methylation step was interesting, since the carbinol hydroxy group was almost as reactive as the phenolic hydroxy group and since a mixture composed of more or less equal amounts of the methoxy compounds V, VI, and VII was obtained. The use of excess dimethyl sulfate and base gave only the neutral dimethoxy compound VII. The reaction of the mixture of methoxy compounds with potassium hydroxide in methanol at 65° converted methoxy compound V into the methoxy acid VIII, which could be separated from the other components (Reaction Scheme 3). The dimethoxy compound VII was inert. The position of the side

Can. J. Chem. Downloaded from www.nrcresearchpress.com by 210.87.254.42 on 09/05/12
For personal use only.

chain in the methoxy acid VIII was established by treatment of it with sodium in liquid ammonia. The two chlorines were removed as expected, and most unexpectedly, the side-chain methoxy group was also removed, with the formation of the known 2-methoxyphenylacetic acid.



REACTION SCHEME 3.

3,4-Dichlorophenyltrichloromethylcarbinol was likewise converted by treatment with methanolic potassium hydroxide into the known 3,4-dichloro-α-methoxyphenylacetic acid in 53% of the theoretical yield. The orientation of the chlorine atoms was established by this transformation, and also by preparing the carbinol independently from 3,4-dichlorophenylmagnesium bromide and chloral, and by comparing the crystalline acetate esters.

Physiological Activity in Plants

3,4-Dichloro-α-methoxyphenylacetic acid has been tested as a plant growth regulator on a wide variety of plants. It is qualitatively similar in physiological effects to 2,4-dichlorophenoxyacetic acid but is less active (11). The 3,5-dichloro-α,2-dimethoxyphenylacetic acid was most unusual for a member of this series of compounds, as it exhibited no physiological activity when tested on bean plants.

EXPERIMENTAL

All melting and boiling points are corrected. Analyses were performed by Mrs. Christine Neilson and Dr. Franz Kasler. The infrared spectra were determined on a Beckman IR-5 spectrophotometer, with the liquid, melt, or mull being measured as a film between sodium chloride plates. Mulls were prepared with polychlorotrifluoroethylene[2] for the region 5 000 to 1 310 cm^{-1}, and with Nujol for 1 310 to 650 cm^{-1}.

General Procedure for Preparation of α-Trichloromethylbenzyl Alcohols

3,4-Dichloro-α-trichloromethylbenzyl Alcohol

In a 5 l three-necked flask equipped with a Hershberg stirrer, thermometer, and dropping funnel was placed 2 100 ml of *o*-dichlorobenzene. A solution was prepared consisting of 456 g (3.1 moles) of freshly distilled anhydrous chloral dissolved in 296 ml of *o*-dichlorobenzene. This amounted to 600 ml and was subsequently added to the reaction mixture in 10 equal portions. The *o*-dichlorobenzene in the 5 l flask was cooled to 5° and 60 ml of the chloral solution was added. The first of 10 portions of powdered anhydrous aluminium chloride (40 g each, 0.3 mole) was added, and then 60 ml of the chloral solution was dripped in over a 7 min period. The alternate additions of chloral and aluminium chloride were continued until all had been added. The temperature was kept at 5 to 7° during the first 20% of the reaction. The ice bath was then removed, and during the subsequent additions the temperature slowly rose to, and was maintained at, 20°. After the additions were complete, the dark red reaction mixture was stirred for an additional 10 min at 20°. The reaction mixture was stirred, cooled in an ice bath, and decomposed by the slow addition of 800 ml of 6 *N*

[2]*Series 11–14 light oil from Halocarbon Products Corp., Hackensack, New Jersey.*

Can. J. Chem. Downloaded from www.nrcresearchpress.com by 210.87.254.42 on 09/05/12
For personal use only.

ice-cold hydrochloric acid followed by 400 ml of water. The temperature was not allowed to exceed 35°. The organic layer was washed with water, and stirred for 0.5 h each time with two portions of 1 500 ml of 5% sodium carbonate solution to remove chloral polymers. The excess *o*-dichlorobenzene was removed by distillation under water pump pressure and the residual 3,4-dichloro-α-trichloromethylbenzyl alcohol was distilled at 160–165° and 3 mm, in agreement with the literature value (3). The yield was 699 g or 76% of theory.

An alternative preparation of 3,4-dichloro-α-trichloromethylbenzyl alcohol was from 3,4-dichlorophenylmagnesium bromide and chloral. The Grignard reagent was prepared by converting acetanilide successively into *p*-bromoacetanilide, 4-bromo-2-chloroacetanilide, 4-bromo-2-chloroaniline, and 3,4-dichlorobromobenzene, and by allowing 108 g (0.80 mole) of the latter to react with 32 g (0.85 mole) of magnesium suspended in 350 ml of ether. Chloral (125 g, 0.85 mole) reacted with the Grignard reagent to form 75 g (32% of theory) of 3,4-dichloro-α-trichloromethylbenzyl alcohol, b.p. 160° at 3 mm.

The 3,4-dichloro-α-trichloromethylbenzyl alcohol from each of the above preparations was purified by conversion into the crystalline acetate, m.p. 83–84° (3), according to Howard's procedure (12). The acetate ester was hydrolyzed by refluxing overnight a solution of 26 g (0.07 mole) of it dissolved in 60 ml of ethanol containing 8 ml (0.1 mole) of concentrated hydrochloric acid and 5 ml of water. The 3,4-dichloro-α-trichloromethylbenzyl alcohol (16 g, 75% of theory) distilled as a clear liquid, b.p. 160° at 3 mm. The infrared spectrum showed absorption bands at 3 530, 3 080, 2 930, 1 590, 1 560, 1 460, 1 365, 1 290, 1 260, 1 190, 1 133, 1 075, 1 030, 1 005, 905, 890, 830, 800, 705, and 692 cm^{-1}.

General Procedure for Preparation of α-Trichloromethylbenzyl Chlorides

1-Chloro-4-(1,2,2,2-tetrachloroethyl)benzene

Chlorobenzene (34 g, 0.3 mole) and chloral (44 g, 0.3 mole) were dissolved in 150 ml of methylene chloride. The stirred solution was cooled to 0° and 40 g (0.3 mole) of anhydrous aluminium chloride was added over a period of 1 h. The reaction mixture was then allowed to warm up to room temperature over about a 5 h period, and was decomposed by adding it to a hydrochloric acid – ice mixture. The methylene chloride solution was washed twice with sodium bicarbonate solution, and with water. On distillation, 65 g (78% yield) of 1-chloro-4-(1,2,2,2-tetrachloroethyl)benzene was obtained, b.p. 158–160° at 15 mm. The infrared spectrum showed absorption bands at 3 040, 2 960, 1 500, 1 455, 1 345, 1 270, 1 230, 1 190, 1 085, 1 035, 1 015, 1 005, 925, 870, 820, 790–778, 760, 740–730, and 697 cm^{-1}.

Anal. Calcd. for $C_8H_5Cl_5$: C, 34.48; H, 1.81; Cl, 63.69. Found: C, 34.75; H, 2.07; Cl, 63.80.

This compound has previously been prepared by the action of phosphorus pentachloride (13) or thionyl chloride (14) on *p*-chlorophenyltrichloromethylcarbinol.

Results similar to those obtained with chlorobenzene were obtained with the compounds listed in Table II. The experimental conditions were identical with those given above, except for acetanilide. The results are summarized in Table III.

TABLE III

Product	Boiling point, °C (mm)	Melting point, °C	Analyses			
			Carbon		Hydrogen	
			Calcd.	Found	Calcd.	Found
p-$FC_6H_4CHCl—CCl_3$	145–148 (15)		37.08	36.88	1.93	1.97
p-$BrC_6H_4CHCl—CCl_3$	198–200 (30)		29.76	30.04	1.56	1.33
p-$IC_6H_4CHCl—CCl_3$	173 (10)	57	25.98	26.25	1.37	1.65
p-$AcNHC_6H_4CHCl—CCl_3$		205–206	39.86	40.02	3.02	3.30

With acetanilide, 20 g (0.15 mole) was allowed to react with the 0.3 *M* amounts of chloral and aluminium chloride as in the above procedure, except that the reaction temperature was 4 to 13°. Most of the product was isolated by filtration from the methylene chloride – water mixture after decomposition with the acid. Additional amounts were obtained by evaporating the methylene chloride and adding petroleum ether to a toluene extract of the tarry material. There was obtained a total of 13 g of *4'-(1,2,2,2-tetrachloroethyl)acetanilide*, which was recrystallized from methanol containing a small amount of water. The material has previously been prepared from acetanilide, chloral, and sulfuric acid (15).

1,2-Dichloro-4-(1,2,2,2-tetrachloroethyl)benzene (15 g, 80% of theory; b.p. 140° at 2.5 mm) was prepared by the general procedure of Haller *et al.* (13) from a solution of 17 g (0.06 mole) of 3,4-dichloro-α-trichloromethylbenzyl alcohol in 20 ml of dry benzene and 25 g (0.12 mole) of phosphorus pentachloride. Its infrared spectrum showed absorption bands at 1 475, 1 400, 1 230, 1 195, 1 140, 1 040, 1 015, 920, 885, 835, 825, 805, 760, 705, and 685 cm^{-1}.

Anal. Calcd. for $C_8H_4Cl_6$: C, 30.71; H, 1.29. Found: C, 31.00; H, 1.58.

α,β,β,3,4-Pentachlorostyrene

To 6.5 g (0.02 mole) of 1,2-dichloro-4-(1,2,2,2-tetrachloroethyl)benzene dissolved in 50 ml of 95% ethanol was added a solution of 1.1 g (0.02 mole) of potassium hydroxide dissolved in 15 ml of ethanol. A white

Can. J. Chem. Downloaded from www.nrcresearchpress.com by 210.87.254.42 on 09/05/12
For personal use only.

precipitate formed immediately. The reaction mixture was boiled for 1 min and filtered while hot. White crystals (5.1 g, 93% of theory) of the pentachlorostyrene separated out when the filtrate was cooled. After recrystallization from 95% ethanol, the α,β,β,3,4-pentachlorostyrene melted at 48–49°. The infrared spectrum of the melt showed absorption bands at 1 910, 1 770, 1 595, 1 550, 1 470, 1 380, 1 270, 1 225, 1 138, 1 062, 1 035, 998, 992, 952, 908, 880, 812, 802, 723, 717, 695, and 673 cm^{-1}.

Anal. Calcd. for $C_8H_3Cl_5$: C, 34.76; H, 1.09; Cl, 64.14. Found: C, 35.01; H, 1.35; Cl, 63.90.

p-Bromo-α,β,β-trichlorostyrene was likewise prepared in 76% yield from 1-bromo-4-(1,2,2,2-tetrachloroethyl)benzene by treatment with a sevenfold excess of methanolic potassium hydroxide; m.p. 36° from methanol. The infrared spectrum of the mull showed absorption bands of 1 585, 1 490, 1 395, 1 075, 1 015, 980, 880, 830, and 780 cm^{-1}.

Anal. Calcd. for $C_8H_4BrCl_3$: C, 33.55; H, 1.41. Found: C, 33.63; H, 1.70.

3,5-Dichloro-2-hydroxy-α-trichloromethylbenzyl Alcohol (IV)

In a 2 l three-necked flask was placed 250 g (1.53 moles) of 2,4-dichlorophenol dissolved in 650 ml of carbon disulfide. The mixture was cooled to 4° and 240 g (1.63 moles) of freshly distilled anhydrous chloral was added. Powdered anhydrous aluminium chloride (454 g, 3.35 moles) was spooned into the efficiently stirred reaction mixture over a 50 min period. The flask was cooled by an ice bath during the addition. The temperature rose to 15° during the addition of the first few portions of aluminium chloride and then fell slowly. Between additions, the reaction mixture was protected from atmospheric moisture by a calcium chloride drying tube.

After the last of the aluminium chloride had been added, the reaction mixture was warmed to 30° and stirred for another 20 min. It was then cooled to 0° and decomposed by the dropwise addition of 400 ml of cold 6 *N* hydrochloric acid. The temperature was maintained below 20° to prevent the reaction from becoming violent. The solid 3,5-dichloro-2-hydroxy-α-trichloromethylbenzyl alcohol was filtered, washed with dilute hydrochloric acid and with water, and recrystallized from a water–methanol solution. The white crystals (270 g, 60% of theory) melted at 128–129°. The analytical sample was recrystallized from cyclohexane. The infrared spectrum of a Nujol mull showed absorption bands at 3 450, 3 120, 2 950, 1 750, 1 590, 1 470, 1 430, 1 370, 1 330, 1 295, 1 250, 1 215, 1 170, 1 095, 1 070, 1 010, 918, 873, 853, 827, 808, 732, and 675 cm^{-1}.

Anal. Calcd. for $C_8H_5O_2Cl_5$: C, 30.95; H, 1.62; Cl, 57.12. Found: C, 31.02; H, 1.50; Cl, 57.30.

Methylation of 3,5-Dichloro-2-hydroxy-α-trichloromethylbenzyl Alcohol

A well-stirred mixture of 3,5-dichloro-2-hydroxy-α-trichloromethylbenzyl alcohol (IV) (130 g, 0.42 mole) and 170 ml of water was cooled to 0°, and 106 g (0.84 mole) of freshly distilled dimethyl sulfate was added. A solution of 16.8 g (0.42 mole) of sodium hydroxide in 150 ml of water was then dripped in over a 1 h period. After the solution was allowed to stand overnight, the organic layer was extracted with chloroform, washed with an ice-cold 10% sodium hydroxide solution to remove the phenolic components, and then washed with water. On distillation, there was obtained 80 g of a pale yellow oil, b.p. 140° at 3 mm, which was a mixture of approximately equal parts of 3,5-dichloro-2-methoxy-α-trichloromethylbenzyl alcohol (V) and 3,5-dichloro-2-methoxy-α-trichloromethylbenzyl methyl ether (VII), with some of the 3,5-dichloro-2-hydroxy-α-trichloromethylbenzyl methyl ether (VI) still present. The isolation of compound VI is described under the preparation of 3,5-dichloro-α,2-dimethoxyphenylacetic acid.

When the methylation was carried out with 54 g of the starting 3,5-dichloro-2-hydroxy-α-trichloromethylbenzyl alcohol (IV) under the same conditions, except with twice the relative amount of sodium hydroxide and four times as much water, 28 g of crude *3,5-dichloro-2-methoxy-α-trichloromethylbenzyl methyl ether (VII)* separated from the alkaline reaction mixture. On recrystallization from 95% ethanol, 24 g (37% yield) of white crystals, m.p. 79–80°, was obtained. The infrared spectrum of a Nujol mull showed absorption bands at 1 620, 1 425, 1 330, 1 250, 1 230, 1 200, 1 165, 1 120, 1 032, 995, 922, 878, 868, 847, 808, 775, and 724 cm^{-1}.

Anal. Calcd. for $C_{10}H_9O_2Cl_5$: C, 35.46; H, 2.68; OCH_3, 18.34. Found: C, 35.75; H, 3.05; OCH_3, 18.60.

3,5-Dichloro-α,2-dimethoxyphenylacetic Acid (VIII)

Sixty grams of the above mixture of compounds V, VI, and VII from the methylation step was dissolved in 200 ml of methanol, the solution heated to reflux, and a solution of 71 g (0.92 mole) of potassium hydroxide in 170 ml of methanol added. The reaction mixture was stirred and refluxed for 1 h. After the mixture had cooled to room temperature, the potassium chloride was filtered off and washed with small portions of methanol. An equal volume of water was added to the combined filtrates, and the mixture was extracted with chloroform to remove the neutral materials. The aqueous layer was acidified with dilute hydrochloric acid and extracted with chloroform. The chloroform was evaporated and the residual crude acid fraction dissolved in 20 ml of hot carbon tetrachloride. When the solution had cooled in an ice bath, 4 g of white crystalline *3,5-dichloro-2-hydroxy-α-trichloromethylbenzyl methyl ether* (VI) separated and was filtered off. It melted at 150–151°. The infrared spectrum of a mull showed absorption bands at 3 380, 1 595, 1 465, 1 415, 1 325, 1 255, 1 190, 1 150, 1 100, 1 040, 990, 920, 900, 870, 813–795, 750, 730, and 665 cm^{-1}.

Anal. Calcd. for $C_9H_7O_2Cl_5$: C, 33.31; H, 2.17; Cl, 54.63; OCH_3, 9.57. Found: C, 33.38; H, 2.43; Cl, 54.90; OCH_3, 9.55.

The carbon tetrachloride mother liquor was evaporated and 20 ml of water added to the crude residual acid. The mixture was neutralized with 10% sodium hydroxide solution to the phenolphthalein end point, and the solution was evaporated to dryness. The crystals were stirred with acetone, filtered to remove the organic

Can. J. Chem. Downloaded from www.nrcresearchpress.com by 210.87.254.42 on 09/05/12
For personal use only.

impurities, and washed with small portions of acetone until they were white. The resulting 20 g (35% of theory, based on methylated carbinol mixture) of sodium 3,5-dichloro-α,2-dimethoxyphenylacetate was recrystallized from 95% ethanol, and converted into the free acid by acidifying an aqueous solution of the salt. 3,5-Dichloro-α,2-dimethoxyphenylacetic acid (VIII) separated as an oil which solidified after it was stirred for a few minutes. The yield was 14.6 g. It was recrystallized twice from cyclohexane, and then melted at 80–82°. The infrared spectrum of a mull showed absorption bands at 2 940, 1 730, 1 475, 1 420, 1 335, 1 310, 1 250, 1 210, 1 190, 1 110, 1 100, 995, 920, 865, 850, 770, 715, and 670 cm^{-1}.

Anal. Calcd. for $C_{10}H_{10}Cl_2O_4$: C, 45.31; H, 3.80; Cl, 26.75; OCH_3, 23.41. Found: C, 45.40; H, 4.07; Cl, 27.04; OCH_3, 23.72.

Treatment of Acid VIII with Sodium in Liquid Ammonia

In a 400 ml beaker was placed 50 ml of liquid ammonia. Sodium (1 g) and 3,5-dichloro-α,2-dimethoxyphenylacetic acid (0.72 g) were added in small portions with intermittent stirring. The liquid ammonia was allowed to evaporate, and 10 ml of water was added to the residue. The solution was filtered, and the filtrate was acidified with 1 *N* hydrochloric acid and extracted with chloroform. On evaporation of the chloroform, a brown oil remained which solidified when it was allowed to stand. It was recrystallized twice from cyclohexane, and the 0.4 g of *o-methoxyphenylacetic acid* melted at 119–122°, in agreement with the literature value (16). It was identified by analysis and by comparison with an authentic sample prepared from α,2-dimethoxyphenylacetic acid (10) by a similar treatment with sodium in liquid ammonia.

3,4-Dichloro-α-methoxyphenylacetic Acid

In a 5 l three-necked flask equipped with a thermometer, stirrer, and dropping funnel were placed 441 g (1.5 moles) of distilled 3,4-dichloro-α-trichloromethylbenzyl alcohol, as obtained from the Friedel–Crafts reaction without subsequent purification, and 440 ml of methanol. The temperature was brought to 50° by means of a warm water bath, and a solution of 420 g (7.5 moles) of technical flake potassium hydroxide dissolved in 1 680 ml of methanol was added dropwise over a 45 min period. Hot water and ice were available for changing the water bath temperature quickly to maintain the reaction temperature at 50 ± 1°. (The yield drops drastically if the reaction is run at 35 or 65°.) The reaction mixture was stirred for an additional 2 h at 50–55°, after which time heat evolution had stopped; it was allowed to stand overnight.

The precipitated potassium chloride was filtered off and washed with 250 ml of 4:1 methanol–water. An equal volume of water was added to the combined filtrates, and the pH of the alkaline mixture brought to approximately 8 with 6 *N* hydrochloric acid. The solution was poured off from an insoluble neutral oil (about 40 g), and treated with activated carbon to yield a clear, yellow filtrate. It was acidified to a pH of 3.3 with 6 *N* hydrochloric acid, and 400 g of sodium chloride was added. The pH determinations were made with a pH meter on small samples diluted with four volumes of water. After the solution was stirred at room temperature for 2 h, the major crop of the crude sodium acid salt was filtered off. An additional small amount (20 g) was obtained by readjusting the pH to 3.3, seeding the solution, and maintaining the temperature near 0° for several days with occasional stirring. The precipitates were combined, and the impurities were removed by stirring with 300 ml of acetone for 10 min, filtering, and repeating the treatment with 500 ml of water at 0°. After another such washing cycle, the air-dried precipitate of *sodium hydrogen di(3,4-dichloro-α-methoxyphenylacetate)* weighed 195 g (53% of theory). It was converted into the free acid by dissolving it in dilute base and pouring a filtered solution of this into a 100% excess of 6 *N* hydrochloric acid. The acid separated as an oil. It was washed once with water by decantation. It solidified on seeding and stirring and was recrystallized from cyclohexane. The free acid melted at 88–89.5°, in agreement with the literature value (17).

ACKNOWLEDGMENTS

The financial support provided by the Celanese Corporation to C. L. L. is deeply appreciated. The examination of the various compounds for their plant growth regulating properties was carried out by L. L. Danielson or J. W. Mitchell and their co-workers at the U.S. Department of Agriculture Plant Industry Station, Beltsville, Maryland.

REFERENCES

1. A. Dinesmann. Compt. Rend. **141**, 201 (1905).
2. V. Ettel and J. Weichet. Collection Czech. Chem. Commun. **15**, 520 (1950).
3. R. Riemschneider. Monatsh. **82**, 600 (1951).
4. G. Cauquil and J. Boyer-Houard. Bull. Soc. Chim. France, 1391 (1955). R. Quelet, C. Borgel, and R. Durand. Compt. Rend. **240**, 1900 (1955). C. Broquet-Borgel. Ann. Chim. Paris, **3**, 204 (1958).
5. J. H. T. Ledrut and G. Combes. Ind. Chim. Belge, **27**, 635 (1962).
6. A. Bayer. Ber. **5**, 1098 (1872).
7. J. E. Hofmann and A. Schriesheim. Friedel-Crafts and related reactions. Vol. 2. G. A. Olah (*Editor*). Interscience Publishers, Inc., New York. 1964. Part 1. p. 616 is an example.
8. F. R. Jensen and G. Goldman. Friedel-Crafts and related reactions. Vol. 3. G. A. Olah (*Editor*). Interscience Publishers, Inc., New York. 1964. Part 2. p. 1004.

Can. J. Chem. Downloaded from www.nrcresearchpress.com by 210.87.254.42 on 09/05/12
For personal use only.

9. W. GERRARD and M. F. LAPPERT. J. Chem. Soc. 1020 (1951).
10. W. REEVE and C. W. WOODS. J. Am. Chem. Soc. **82**, 4062 (1960).
11. J. W. MITCHELL, B. C. SMALE, and W. H. PRESTON. J. Agr. Food Chem. **7**, 841 (1959). W. A. GENTNER, L. L. DANIELSON, and W. C. SHAW. An evaluation of several chemicals for their herbicidal properties—1959 field results. U.S. Department of Agriculture, Plant Industry Station, Beltsville, Maryland. 1960. Table 25.
12. J. W. HOWARD. J. Am. Chem. Soc. **52**, 5059 (1930).
13. H. L. HALLER *et al.* J. Am. Chem. Soc. **67**, 1601 (1945).
14. T. C. CHEN and W. T. SUMERFORD. J. Am. Chem. Soc. **72**, 5124 (1950).
15. A. YA. BERLIN, M. N. SHCHUKINA, and E. D. SAZONAVA. Zh. Obshch. Khim. **19**, 677 (1949); Chem. Abstr. **44**, 3448 (1950).
16. R. PSCHORR, O. WOLFES, and W. BUCKOW. Ber. **33**, 166 (1900).
17. W. REEVE and P. E. PICKERT. J. Am. Chem. Soc. **79**, 1932 (1957).

Can. J. Chem. Downloaded from www.nrcresearchpress.com by 210.87.254.42 on 09/05/12
For personal use only.

Can. J. Chem. Downloaded from www.nrcresearchpress.com by 210.87.254.42 on 09/05/12
For personal use only.

THE CORRELATION OF CHASMANINE WITH BROWNIINE[1]

O. E. EDWARDS, L. FONZES,[2] AND LÉO MARION[3]
Division of Pure Chemistry, National Research Council, Ottawa, Canada

Received October 15, 1965

ABSTRACT

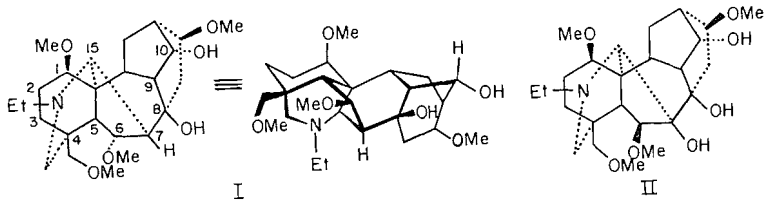
By means of oxidative and reductive fission, respectively, of the 7,15-bridge, the alkaloids browniine and chasmanine were converted into 7,15-seco-7,10-diketones. After epimerization of its C-6 methoxyl the diketone derived from chasmanine was identical with that obtained from browniine. This correlation confirms the structure previously tentatively assigned to chasmanine, and establishes its stereochemistry since browniine and lycoctonine have been interrelated.

RÉSUMÉ

Au moyen de la fission oxidative et réductive respectivement du pont en 7,15, la browniine et la chasmanine ont été converties en 7,15-seco-7,10 dicétones. Après épimérisation de son groupement méthoxyl en C-6, la dicétone dérivée de la chasmanine est identique à la dicétone obtenue à partir de la browniine. Cette conversion confirme la structure déjà attribuée à la chasmanine, et établie sa stéréochimie puisque la corrélation de la browniine et de la lycoctonine a été préalablement accomplie.

The alkaloid chasmanine, whose empirical formula can be expanded to $C_{19}H_{22}(N{\cdot}C_2H_5)(OH)_2(OCH_3)_4$, was recently discovered among the strong bases of *Aconitum chasmanthum* Stapf (1). Several of its reactions paralleled those of pseudaconitine and bikhaconitine, and on this basis it was tentatively assigned structure I, which accommodated all its reactions (2). No evidence, however, was available concerning the methoxyl assigned to C-1, except by analogy. A notable feature of the postulated structure is the absence of a tertiary hydroxyl on C-11. Neoline (3) is the only other known aconitine-type[4] diterpenoid alkaloid lacking this hydroxyl.

Neoline has not been related to an alkaloid of known structure, and attempts to relate chasmanine to bikhaconine were unsuccessful (2). We now report the conversion of browniine (II), whose structure is known with certainty (4), and chasmanine (I) into a common derivative, thus confirming the structure and proving the stereochemistry of the latter. In this correlation use was made of two unusual reactions of the lycoctonine-type and aconitine-type alkaloids which lead to 7,15-seco derivatives.



I II

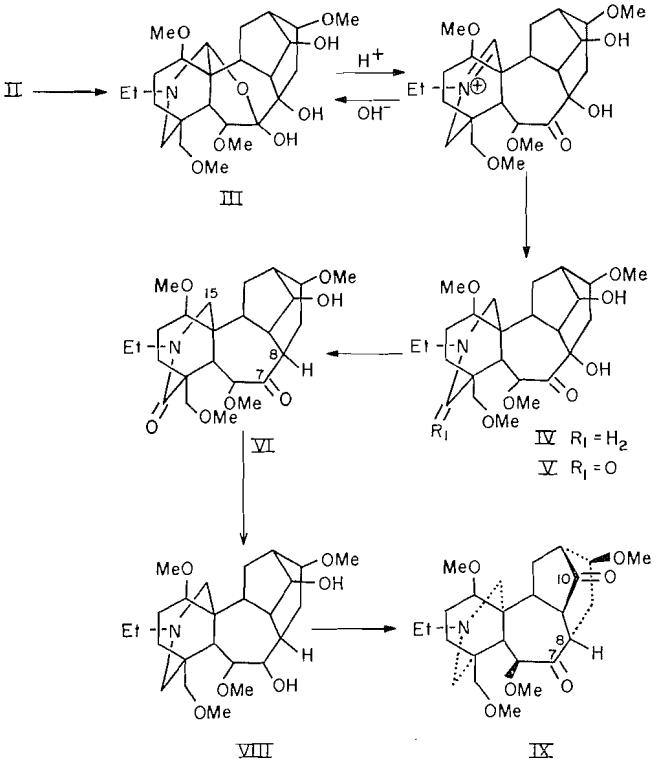
The alkaloid browniine, which is closely related to lycoctonine, differs from chasmanine in that it contains a 7-hydroxyl, and its 6-methoxyl is β-oriented; in contrast, this methoxyl in chasmanine is α-oriented. The 6-α-methoxyl of chasmanine is crowded by the substituents on C-4; hence we considered it probable that, if a 7,15-seco-7-ketone could be

[1]*Issued as N.R.C. No. 8796.*
[2]*National Research Council of Canada Postdoctorate Fellow (1964–1965).*
[3]*Present address: Faculty of Pure and Applied Science, University of Ottawa, Ottawa.*
[4]*We use the term aconitine-type to denote alkaloids with the lycoctonine skeleton but with hydrogen on C-7. Lycoctonine-type alkaloids are those with a hydroxyl on this carbon.*

prepared, this could be epimerized to the 6-β-methoxyl analogue. Correlation could then be made with a 7,15-seco-7-ketone derived from browniine.

When lycoctonine was oxidized with lead tetraacetate (5) it gave rise to a compound originally thought to be a simple carbinolamine, and therefore named hydroxylcoctonine. This compound, which was later shown to contain a carbinolamine masked as a hemiketal (6, 7), produced a ketone (isolycoctonine) when hydrogenated catalytically (7). It was anticipated that browniine would behave in a manner parallel to that of lycoctonine when treated with lead tetraacetate. Indeed, a nearly quantitative yield of hydroxybrowniine[5] (III), m.p. 115–118°, was obtained. The infrared spectrum of this base contained no carbonyl absorption whereas that of its perchlorate showed a strong band at 1 706 cm^{-1}. Hydrogenation of hydroxybrowniine perchlorate produced isobrowniine (IV), which in the infrared showed a carbonyl band at 1 710 cm^{-1}.

Oxidation of IV in acetone with potassium permanganate during 3 min (8) gave a fair yield of oxoisobrowniine (V), which in the infrared showed absorption at 1 710 cm^{-1} (CO) and 1 635 cm^{-1} (lactam CO). That the N-ethyl group was still present was shown by a triplet centered at δ 1.1 in the nuclear magnetic resonance (n.m.r.) spectrum. After one chromatographic purification on a column, the lactam V produced a single spot in thin-layer chromatography, but could not be induced to crystallize.



The reduction of V with a mixture of acetic anhydride, acetic acid, and zinc (9) gave in rather poor yield a mixture of two products, VI (R_f 0.56) and VII (R_f 0.35), accompanied by a small quantity of unchanged starting material. The compound VI, m.p. 152–159°, was identified as the expected 8-deoxyoxoisobrowniine, $C_{25}H_{39}O_7N$, showing in the infrared

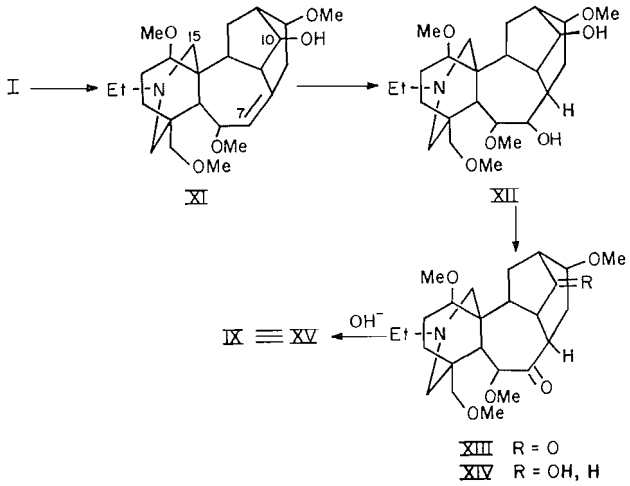
[5]*The trivial names used for the analogues in the lycoctonine series have been adopted for the browniine derivatives.*

Can. J. Chem. Downloaded from www.nrcresearchpress.com by 210.87.254.42 on 09/05/12
For personal use only.

absorption bands at 1 697 cm^{-1} (CO) and 1 635 cm^{-1} (lactam CO). Compound VII, m.p. 161–166°, gave analytical figures corresponding to the empirical formula $C_{25}H_{41}O_7N$. Its infrared spectrum contained no ketonic carbonyl absorption, but contained a lactam carbonyl band (1 635 cm^{-1}). That it was 8-deoxy-7-dihydrooxoisobrowniine, the product of the reduction of the ketone carbonyl of 8-deoxyoxoisobrowniine (VI), was proven by its formation from the latter via borohydride reduction.

The total reduction of compounds VI and VII with lithium aluminium hydride gave rise in each case to 8-deoxy-7-dihydroisobrowniine (VIII) which, on oxidation, produced the corresponding diketone, i.e. 10-dehydro-8-deoxyisobrowniine (IX), m.p. 156–158°. The infrared spectrum of IX contained absorption bands at 1 762 cm^{-1} (cyclopentanone) and 1 702 cm^{-1} (six-membered or larger cyclic ketone).

Starting with chasmanine (cf. ref. 2) we obtained the same derivative by a different route (9). Diacetylchasmanine (X), when treated with lithium tri-*t*-butoxyaluminohydride at 140° in diglyme,[6] produced the 7,15-seco olefin XI, m.p. 104–105°, showing in the n.m.r. a badly resolved doublet centered at δ 5.6 (vinyl proton), a triplet centered at δ 0.99 caused by the N-ethyl group (shielded by the double bond), and singlets at δ 3.40 (3H) and δ 3.38 (9H) indicative of four methoxyl groups. Hydration of XI with diborane by Brown's method (10) produced a 7,15-seco-7-hydroxy base XII, $C_{25}H_{43}O_6N$, m.p. 179–181°.



Oxidation of XII with chromic oxide in acetone gave a mixture of two ketones, XIII and XIV, which were separated by column chromatography. The ketone XIII was the expected 7,10-diketone, $C_{25}H_{39}O_6N$ (R_f 0.76). It had infrared absorption at 1 750 cm^{-1} (cyclopentanone) and 1 710 cm^{-1} (carbonyl in a six-membered or larger ring). The ketone XIV was a monoketone with the carbonyl function in a six-membered or larger ring (ν_{max} 1 710 cm^{-1}).

The diketone XIII, when refluxed in a 50:50 ethanol–water solution containing 15% of potassium hydroxide, was epimerized slowly at position 6. The yield of the epimer, however, was low, with degradation products predominating. The epimeric diketone XV thus obtained was in every respect identical with the diketone IX derived from browniine.

This interrelation confirms the structure originally assigned to chasmanine (2) and establishes that, except at C-6, it has the same relative and absolute configuration as

[6]*Trivial name of diethyleneglycol dimethyl ether.*

Can. J. Chem. Downloaded from www.nrcresearchpress.com by 210.87.254.42 on 09/05/12
For personal use only.

browniine. It also dispels any slight doubt that the C-6 methoxyl group of browniine has the β-configuration (4). The oxidation studies of Achmatowicz *et al.* (8) were also consistent with this assignment, since browniine gave predominantly the lactam.

It now seems possible to test the structure and configuration proposed for neoline (3) by interrelation with chasmanine through appropriate methyl ethers.

EXPERIMENTAL

For thin-layer chromatography, use was made of glass plates covered with a thickness of 250 μ of Merck's silica gel G which had been reactivated 15 min before utilization by drying in an oven at 120°. The developing solvents consisted of 90:10 dichloromethane–methanol (solvent I), 96:4 dichloromethane–methanol (solvent II), and 99:1 dichloromethane–methanol (solvent III). This last solvent was used in a jar saturated with ammonia vapors. The spots were located by means of modified Dragendorff's reagent, or iodine vapor. Melting points were taken on a Kofler stage and not corrected. Unless otherwise mentioned, the infrared spectra were measured in KBr pellets on a Perkin–Elmer infracord spectrometer, and the n.m.r. spectra were measured in deuteriochloroform solution containing tetramethylsilane as an internal reference, on a Varian A-60 instrument.

Hydroxybrowniine (III)

Browniine perchlorate (580 mg) was dissolved in water and the base liberated by the addition of sodium carbonate. The solution was extracted with dichloromethane, the extract dried over sodium sulfate, and the solvent evaporated under reduced pressure. To the residual base dissolved in glacial acetic acid (10 ml) was added a solution of lead tetraacetate (520 mg) in glacial acetic acid (20 ml). The mixture was allowed to stand at room temperature for 1 h, after which the reaction was stopped by the addition of two drops of glycerol. A concentrated aqueous solution of sodium sulfate was added, and the precipitated lead sulfate was filtered and washed with water. The combined filtrate and washings were evaporated under reduced pressure, the residue was dissolved in water, and the solution was made basic with sodium carbonate and extracted with dichloromethane. The extract was dried over sodium sulfate and the solvent evaporated under reduced pressure. Hydroxybrowniine was left as a colorless oil (485 mg, yield 97%). Thin-layer chromatography showed the presence of very little unchanged browniine. The product was dissolved in benzene and chromatographed on a column of neutral alumina, grade III (20 g). It was eluted with first benzene, then benzene–ether, and finally ether–methanol. The pure hydroxybrowniine was crystallized with difficulty from ether, m.p. 115–118; R_f 0.51 (solvent II). Its n.m.r. spectrum contained a triplet centered at δ 1.08 indicative of a N-ethyl group and singlets at δ 3.30, 3.38, 3.42, and 3.61 caused by four methoxyl groups. The infrared spectrum of the base contained no carbonyl absorption, but that of its amorphous perchlorate showed a carbonyl band at 1 706 cm^{-1}.

Anal. Calcd. for $C_{25}H_{41}O_8N$: C, 62.09; H, 8.55. Found: C, 62.09; H, 8.41.

Isobrowniine (IV)

To platinic oxide (120 mg) suspended in glacial acetic acid (10 ml) and previously hydrogenated was added a solution of hydroxybrowniine (485 mg) in glacial acetic acid (10 ml), and the mixture was shaken at room temperature in an atmosphere of hydrogen. After 10 min the theoretical quantity of hydrogen had been absorbed and the reaction was stopped. The platinum was filtered off and washed with methanol. The combined filtrate and washings were evaporated under reduced pressure and the residue was dissolved in water. After alkalization with sodium carbonate, the solution was extracted with dichloromethane, and the extract was dried with sodium sulfate and evaporated under reduced pressure. Isobrowniine (460 mg) was left as a colorless froth (yield 98%). In thin-layer chromatography a single spot appeared (R_f 0.64, solvent II), but even after chromatography on alumina, the product could not be induced to crystallize. Its infrared spectrum in dichloromethane solution contained a carbonyl absorption band (1 708 cm^{-1}). The n.m.r. spectrum showed a triplet centered at δ 0.95 (N-ethyl) and singlets at δ 3.30, 3.32, 3.35, and 3.40 (four methoxyl groups).

Oxoisobrowniine (V)

A solution of isobrowniine (700 mg) in 80:20 acetone–water (200 ml) was added all at once to a solution of potassium permanganate (500 mg) in 60:40 acetone–water (200 ml). After the solution had been stirred at room temperature for 3 min, the excess permanganate was destroyed by the addition of sodium bisulfite. The mixture was filtered through Celite and the filtrate evaporated to remove the acetone and part of the water. The residual solution, after addition of sulfuric acid (10 ml, 2 *N*), was extracted with dichloromethane. The extract was dried over sodium sulfite and evaporated to dryness under reduced pressure. Oxoisobrowniine was left as a colorless froth (390 mg), which was dissolved in benzene, chromatographed on alumina, and eluted with benzene and benzene–dichloromethane. The colorless oil thus obtained could not be induced to crystallize (R_f 0.93, solvent II). In the infrared taken in dichloromethane solution it showed absorption at 1 710 cm^{-1} (CO) and 1 635 cm^{-1} (lactam CO). Its n.m.r. spectrum contained a triplet centered at δ 1.1 (N-ethyl) and singlets at δ 3.38 (6H), 3.42 (3H), and 3.48 (3H) caused by four methoxyl groups.

Can. J. Chem. Downloaded from www.nrcresearchpress.com by 210.87.254.42 on 09/05/12
For personal use only.

Can. J. Chem. Downloaded from www.nrcresearchpress.com by 210.87.254.42 on 09/05/12
For personal use only.

8-Deoxyoxoisobrowniine (VI) and 8-Deoxy-7-dihydrooxoisobrowniine (VII)

Oxoisobrowniine (200 mg) was dissolved in acetic anhydride (10 ml) and acetic acid (10 ml). To the refluxing solution, during 1 h, was added zinc powder (14 g) in small portions. Boiling was continued for 30 min after the addition of the zinc, and the cooled mixture was filtered. The filtered zinc was washed thoroughly with benzene. The combined filtrate and washings were evaporated to dryness at 50° under reduced pressure. The white residue that was left was dissolved in water and the solution extracted with dichloromethane. The extract was washed with water, dried over potassium carbonate, and evaporated under reduced pressure. The residue (210 mg) was hydrolyzed by refluxing it for 1 h with 60:40 methanol–water (60 ml) containing 3% potassium hydroxide. The reaction mixture was concentrated at 40° under reduced pressure until the methanol had been removed, and the cooled solution was extracted with dichloromethane. The extract was dried over sodium sulfate and the solvent evaporated under reduced pressure. It left a residual, slightly yellowish oil (175 mg). Thin-layer chromatography revealed that this oil consisted of two products, VI (R_f 0.56) and VII (R_f 0.35), together with a small quantity of unreacted material. The crude product was dissolved in benzene and chromatographed on neutral alumina, grade III (7 g). It was eluted with benzene, dichloromethane, and methanol and the eluant was collected in 25 ml fractions. Elution with benzene gave fraction 1 (20 mg mixture) and fraction 2 (pure VI). Benzene–CH_2Cl_2 (90:10) gave fractions 3–6 (16 mg V and VI). Benzene–CH_2Cl_2 (50:50) gave fractions 7–8 (15 mg V and VI). Together, benzene–CH_2Cl_2 (20:80) and pure dichloromethane gave fractions 9–12 (10 mg V). With CH_2Cl_2 containing 1% methanol, fraction 13 gave 40 mg V and VII and fractions 14–16 gave pure VII (37 mg).

8-Deoxyoxoisobrowniine (VI) (R_f 0.56, solvent II) was crystallized from benzene–hexane, m.p. 152–154°; ν_{max} 1 697 cm^{-1} (CO) and 1 635 cm^{-1} (lactam CO).

Anal. Calcd. for $C_{25}H_{39}O_7N$: C, 64.49; H, 8.44; N, 3.01. Found: C, 64.48; H, 8.55; N, 3.20.

8-Deoxy-7-dihydrooxoisobrowniine (VII) (R_f 0.35, solvent II) was crystallized from benzene–hexane, m.p. 161–166°; ν_{max} 1 635 cm^{-1} (lactam CO).

Anal. Calcd. for $C_{25}H_{41}O_7N$: C, 64.21; H, 8.84. Found: C, 64.39; H, 8.35.

8-Deoxy-7-dihydroisobrowniine (VIII)

To a crude mixture of VI and VII dissolved in dioxane (30 ml) was added lithium aluminium hydride (350 mg) dissolved in ether. The mixture was heated until the ether had evaporated, and then refluxed for 45 min. The excess reagent was destroyed by the cautious addition of methanol. Celite was added to facilitate filtration, followed by water. The mixture was filtered through a Celite bed, the filter cake was washed with methanol, and the combined filtrate and washings were evaporated under reduced pressure. The residue was dissolved in dichloromethane, and the solution was dried over sodium sulfate and evaporated *in vacuo* to leave a colorless froth (360 mg) of crude product containing a quantity of starting material. It was dissolved in hexane and chromatographed on a column of neutral alumina, grade III. The eluate was collected in 20 ml fractions. Twelve fractions were obtained by elution with (*a*) 50:50 benzene–hexane, (*b*) 80:20 benzene–hexane, (*c*) benzene, (*d*) 90:10 benzene–CH_2Cl_2, and (*e*) 80:20 benzene–CH_2Cl_2, which yielded 70 mg of 8-deoxy-7-dihydroisobrowniine (VIII). Further elution yielded 260 mg of a mixture of VIII and starting material. The compound VIII was amorphous and colorless, and could not be induced to crystallize (R_f 0.8, solvent I). Its infrared spectrum contained no carbonyl, but did contain OH absorption bands (3 500, 3 600 cm^{-1}). The n.m.r. spectrum showed a triplet centered at δ 1.04 (N-ethyl) and singlets at δ 3.8 (3H) and 3.30 (9H) caused by four methoxyl groups.

Anal. Calcd. for $C_{25}H_{43}O_6N$: C, 66.19; H, 9.56. Found: C, 66.01; H, 9.59.

10-Dehydro-8-deoxyisobrowniine (IX)

To a solution of the compound VIII (70 mg) in acetone (5 ml) cooled in ice was added an ice-cold solution of chromic oxide (140 mg) in acetone, and the reaction mixture was allowed to stand at room temperature for 15 h. The acetone was evaporated under reduced pressure and the residue dissolved in 2 *N* sulfuric acid (10 ml). Sodium sulfite was added until the green color persisted, and the solution was neutralized with sodium carbonate and extracted with dichloromethane. The extract, after it had been dried over sodium sulfate and evaporated under reduced pressure, left a residual yellowish oil (70 mg). Thin-layer chromatography showed this oil to be a mixture of a small quantity of a weakly polar substance, some unreacted VIII, and several strongly polar products. The crude product was dissolved in hexane and chromatographed on neutral alumina, grade III (3 g). The eluate was collected in 15 ml fractions. Four fractions were obtained by elution with 50:50 hexane–benzene and 20:80 hexane–benzene. Further elution with benzene gave two fractions yielding 12 mg of the desired 10-dehydro-8-deoxyisobrowniine, which was crystallized from ether and recrystallized from ether–hexane, m.p. 156–158°; R_f 0.8 (solvent II); ν_{max} 1 762 cm^{-1} (five-membered cyclic ketone) and 1 702 cm^{-1} (CO in six-membered or larger ring), measured in a KBr pellet on a Perkin–Elmer double-beam, model 21B spectrometer; $[\alpha]_D^{25}$ +12.5° (*c*, 0.48 in absolute ethanol).

Anal. Calcd. for $C_{25}H_{39}O_6N$: C, 66.79; H, 8.75. Found: C, 66.49; H, 8.80.

Reductive Cleavage of Chasmanine (7,15-Seco Olefin XI)

Lithium aluminium hydride (2.5 g) dissolved in ether was added dropwise to anhydrous *t*-butanol (20 ml) maintained at the reflux temperature of ether. After completion of the reaction the precipitated lithium tri-*t*-butoxyaluminohydride was filtered off, washed rapidly and thoroughly with anhydrous ether, and dried

in vacuo. It was dissolved in diglyme (20 ml) which had been previously heated to 100°, and rapidly added to a solution of diacetylchasmanine (X) (3 g) in diglyme (20 ml) previously heated to 140°. The temperature was maintained at 140° for 15 min and the mixture cooled. The excess reagent was destroyed by the cautious addition of methanol. Celite was added to facilitate filtration, followed by water, and the mixture was filtered through Celite. The filter cake was washed thoroughly with methanol, and the combined filtrate and washings were evaporated under the reduced pressure first of a water pump and subsequently of an oil pump. The residue was dissolved in water and the solution extracted with dichloromethane. The extract was washed with several portions of 2 *N* sulfuric acid, and the combined acid washings were made basic with sodium carbonate and extracted with dichloromethane. This last extract was dried over sodium sulfate and evaporated to dryness under reduced pressure. It left the product as a crystalline residue (2 g) which, after crystallization from ether, melted at 104–105°; R_f 0.85 (solvent III); ν_{max} 3 520 cm^{-1} (OH). Its n.m.r. spectrum showed a badly resolved doublet at δ 5.60 indicative of a single olefinic proton, and singlets at δ 3.40 (3H) and 3.38 (9H) caused by four methoxyl groups.

Anal. Calcd. for $C_{25}H_{41}O_5N$: C, 68.93; H, 9.49. Found: C, 69.38; H, 9.45.

7,15-Seco-7-hydroxy Base XII

The seco olefin XI (800 mg) dissolved in tetrahydrofuran (20 ml) was cooled in ice, and to this solution was added a 1 *M* solution (20 ml) of diborane in tetrahydrofuran. After the mixture had been allowed to stand at room temperature for 3 h, 5% aqueous sodium hydroxide (10 ml) was slowly added, followed by 30% hydrogen peroxide. The mixture was then kept on the steam bath for 5 min, and allowed to stand at room temperature until the evolution of gas had ceased. It was then extracted with dichloromethane, and the extract was dried over sodium sulfate and evaporated under reduced pressure. The residual product XII was crystallized twice from ether, m.p. 179–181°; R_f 0.69 (solvent III); ν_{max} 3 450 cm^{-1}. Its n.m.r. spectrum contained a triplet centered at δ 1.00 (N-ethyl) and singlets at δ 3.38 (3H), 3.35 (3H), and 3.33 (6H) caused by four methoxyl groups.

Anal. Calcd. for $C_{25}H_{43}O_6N$: C, 66.19; H, 9.56. Found: C, 66.22; H, 9.73.

The 7,10-Diketone XIII and the 7-Ketone XIV

When compound XII (600 mg) was oxidized exactly as described for the oxidation of 8-deoxy-7-dihydroisobrowniine (VIII), the yield of crude product was 460 mg. In thin-layer chromatography the product showed two main spots. It was dissolved in hexane and chromatographed on a column of neutral alumina, grade III (15 g). The eluant was collected in 25 ml fractions. Elution with 50:50 hexane–benzene, with the 20:80 mixture, with benzene, and with 90:10 benzene–CH_2Cl_2 gave in fractions 3–13 the pure diketone XIII (135 mg). Continued elution with 90:10 benzene–CH_2Cl_2 and the 80:20 mixture gave in fractions 14–16 a mixture of XIII and XIV. Elution with 50:50 and 20:80 benzene–CH_2Cl_2 and with CH_2Cl_2 gave in fractions 17–24 pure compound XIV (61 mg).

Compound XIII was a colorless froth; R_f 0.76 (solvent III); ν_{max} 1 760 cm^{-1} (five-membered cyclic ketone) and 1 700 cm^{-1} (CO in six-membered or larger ring). Its n.m.r. spectrum contained a triplet centered at δ 1.07 (N-ethyl) and singlets at δ 3.37 (3H) and 3.50 (9H) indicative of four methoxyl groups.

Anal. Calcd. for $C_{25}H_{39}O_6N$: C, 66.79; H, 8.75. Found: C, 66.68; H, 8.81.

Compound XIV was crystallized from ether, m.p. 142–146°; R_f 0.59 (solvent III); ν_{max} 1 696 cm^{-1} (CO in six-membered or larger ring).

Anal. Calcd. for $C_{25}H_{41}O_6N$: C, 66.49; H, 9.15. Found: C, 67.08; H, 9.51.

Epimerization of the 7,10-Diketone XIII

Compound XIII (135 mg), dissolved in 50:50 ethanol–water containing potassium hydroxide (6 g), was refluxed and the course of the reaction followed by thin-layer chromatography. After 4 h, XIII had almost entirely disappeared, and a spot with a R_f value identical with that of 10-dehydro-8-deoxyisobrowniine (IX) was observed together with numerous spots of very polar substances. The reaction was then stopped, the ethanol evaporated under reduced pressure, and the remaining aqueous solution extracted with dichloromethane. The extract was washed with water, dried over sodium sulfate, and evaporated to dryness under reduced pressure. The residue (80 mg) was dissolved in hexane and chromatographed on a column of neutral alumina, grade III (4 g). Elution of the column with 20:80 hexane–benzene yielded the epimerized product XV (15 mg), which was crystallized first from ether and then from ether–hexane, m.p. 158–160°; R_f 0.8 (solvent II); $[\alpha]_D^{25}$ +12.3° (*c*, 0.57 in absolute ethanol). A mixture with compound IX derived from brownine melted at 156–159°; ν_{max} 1 762 cm^{-1} (CO in five-membered ring) and 1 702 cm^{-1} (CO in six-membered or larger ring). The infrared spectrum was taken in a KBr pellet on a Perkin–Elmer double-beam, model 21B spectrometer and was identical with that of compound IX. The X-ray powder pattern was exactly superimposable on that of 10-dehydro-8-deoxyisobrowniine (IX).

ACKNOWLEDGMENTS

We acknowledge our indebtedness to Mr. K. L. Handa, Jammu, India, who kindly provided a quantity of *A. chasmanthum*. Thanks are due to Mr. A. Knoll, who isolated the

Can. J. Chem. Downloaded from www.nrcresearchpress.com by 210.87.254.42 on 09/05/12
For personal use only.

alkaloid from the plant, to Mr. H. Séguin for the microanalyses, to Mr. M. Lesage for taking the n.m.r. spectra, and to Mr. R. Lauzon for the infrared spectra of the final products, measured on the double-beam instrument.

REFERENCES

1. O. Achmatowicz, Jr. and L. Marion. Can. J. Chem. **42**, 154 (1964).
2. O. Achmatowicz, Jr., Y. Tsuda, L. Marion, T. Okamoto, M. Natsume, H. H. Chang, and K. Kajima. Can. J. Chem. **43**, 825 (1965).
3. K. Wiesner, H. W. Brewer, D. L. Simmons, D. R. Babin, F. Bickelhaupt, J. Kallos, and T. Bogri. Tetrahedron Letters, **3**, 17 (1960).
4. M. H. Benn, M. A. M. Cameron, and O. E. Edwards. Can. J. Chem. **41**, 477 (1963).
5. R. C. Cookson and M. E. Trevett. Chem. Ind. London, 276 (1956).
6. Z. Valenta. Chem. Ind. London, 633 (1959).
7. O. E. Edwards, M. Los, and L. Marion. Can. J. Chem. **37**, 1996 (1959).
8. O. Achmatowicz, Jr., Y. Tsuda, and L. Marion. Can. J. Chem. **43**, 2336 (1965).
9. O. E. Edwards. Chem. Commun. London, 318 (1965).
10. H. C. Brown. Hydroboration. W. A. Benjamin, Inc., New York. 1962.

Can. J. Chem. Downloaded from www.nrcresearchpress.com by 210.87.254.42 on 09/05/12
For personal use only.

Can. J. Chem. Downloaded from www.nrcresearchpress.com by 210.87.254.6 on 09/05/12
For personal use only.

REDUCTIVE CLEAVAGE WITH METAL IN LIQUID AMMONIA

I. THE SELECTIVE CLEAVAGE OF THE BENZYLTHIO C—S BOND VERSUS THE BENZYLIDENEDIOXY C—O BOND IN METHYL *S*-BENZYL-4,6-*O*-BENZYLIDENE-2-THIO-α-D-ALTROPYRANOSIDES; THE INFLUENCE OF THE COSOLVENT 1,2-DIMETHOXYETHANE ON THE COURSE OF THE REACTION

U. G. NAYAK[1] AND R. K. BROWN
Department of Chemistry, University of Alberta, Edmonton, Alberta

Received July 28, 1965

ABSTRACT

The improved solubility of methyl *S*-benzyl-4,6-*O*-benzylidene-2-thio-α-D-altropyranoside (I) in liquid ammonia diluted with 1,2-dimethoxyethane has permitted the selective cleavage by metallic sodium or lithium of the C—S bond to give methyl 4,6-*O*-benzylidene-2-thio-α-D-altropyranoside in 70–75% yield. On the other hand, the slight solubility of I in liquid ammonia alone results only in the completely hydrogenolyzed material, methyl 2-thio-α-D-altropyranoside, along with unchanged I.

Generally, in liquid ammonia alone, reductive cleavage is rapid (15–20 min) and the benzylidene and benzyl groups are converted largely into toluene accompanied by a small amount of bibenzyl. In liquid ammonia – 1,2-dimethoxyethane mixtures the reaction is much slower ($\geqslant$ 1.5 h); under these conditions the benzylidene and benzyl groups are converted to a larger extent into bibenzyl, the rest becoming toluene.

The two strong infrared absorption bands (in Nujol) in the region of 766 to 778 cm^{-1} and 706 to 718 cm^{-1} have been assigned to the phenyl moiety of the benzylidene group, and the one strong band in the region of 702 cm^{-1} to the phenyl moiety of the *S*-benzyl group.

INTRODUCTION

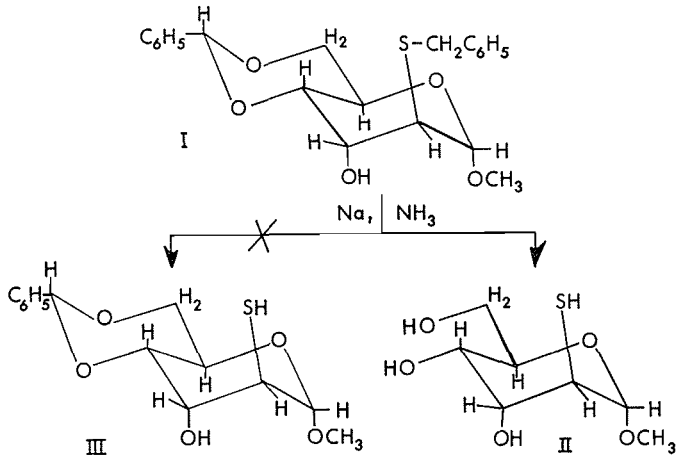
Birch (1, 2) has pointed out that a carbonyl group can be converted into a non-reducible species by acetal or ketal formation, but only if the resulting alkoxy group involved is neither benzylic nor allylic. Groups such as benzyl, benzyloxycarbonyl, and *p*-toluenesulfonyl, which are used to protect amino, hydroxy, or mercapto functions, are readily removed by the reducing action of sodium and liquid ammonia. Several articles have appeared (3–6) which illustrate the use of this technique in the synthesis of carbohydrate derivatives.

A report from this laboratory (3) has described the preparation of some monomercaptomonosaccharides by reductive cleavage of *S*-benzyl-4,6-*O*-benzylidene-2- (or -3-) thioglycopyranosides with sodium and liquid ammonia. At that time some attempts were made, by use of a limited proportion of sodium, to effect a selective cleavage of the *S*-benzyl group with retention of the protecting 4,6-*O*-benzylidene moiety (III, Reaction Scheme 1). However, the only isolable compounds were the unchanged methyl *S*-benzyl-4,6-*O*-benzylidene-2- (or -3-) thioglycoside (I) and the glycoside minus both protecting groups (II, Reaction Scheme 1).

To our knowledge few accounts exist wherein attempts at such selective metal–ammonia hydrogenolysis have been reported. In this connection it is noteworthy that a large excess of Raney nickel removes both the benzylidene and the methylthio groups from methyl 4,6-*O*-benzylidene-*S*-methyl-3-thio-α-D-altropyranoside (7) whereas, with only a fourfold excess of the metal, reductive desulfurization takes place unaccompanied by extensive removal of the benzylidene group (8).

Pinder and Smith (9) found no selective cleavage in the sodium – liquid ammonia reduction of 2-methyl-2-phenyl-1,3-oxathiolane or of 2-methyl-2-phenyl-1,3-dioxolane.

[1] *University of Alberta Postdoctorate Fellow.*



REACTION SCHEME 1.

It has been shown, however, that dialkyl thioethers are readily cleaved by sodium in liquid ammonia whereas the analogous oxygen ethers are practically unaffected (10). Thus one would expect, in a competitive reaction, that a benzylthio group should be hydrogenolyzed in preference to a benzyloxy group. This paper describes the results of attempts at selective cleavage of the benzylthio linkage with sodium and liquid ammonia in the presence of the benzylidene dioxy moiety, examples from the field of carbohydrate chemistry being used as substrates.

RESULTS AND DISCUSSION

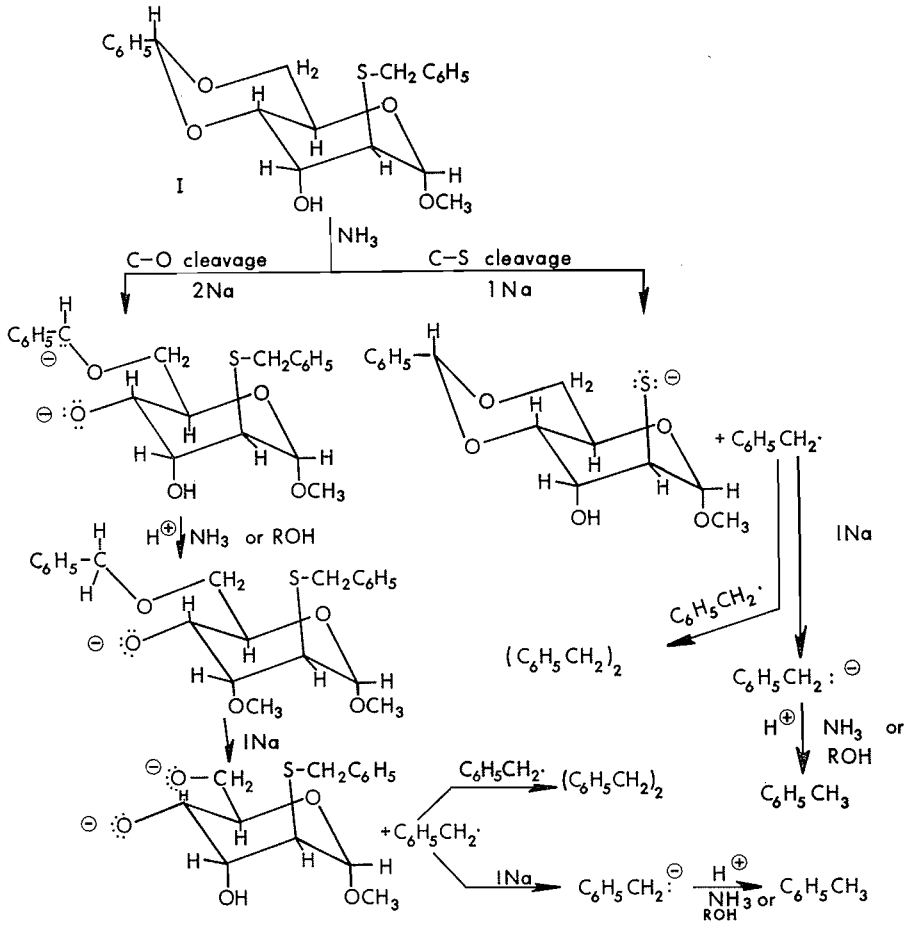
Amount of Sodium Required for Cleavage of the C—S and C—O Bonds

Experiments were designed to measure the proportion of sodium required to cleave the C—S and C—O bonds in a molecule such as methyl *S*-benzyl-4,6-*O*-benzylidene-2-thio-α-D-altropyranoside (I). This information was deemed to be necessary in approaching the problem of selective bond cleavage.

The theoretically required amounts of metal are illustrated in Reaction Scheme 2. It is seen that C—S cleavage requires 2 g-atoms of sodium if toluene alone is produced but just 1 g-atom of sodium if bibenzyl is formed exclusively. Whether bibenzyl is made by free-radical coupling as shown in Reaction Scheme 2 or by an anionic process as suggested by Birch (1) is not yet clear, but by either process 1 g-atom of sodium is required for C—S cleavage of 1 mole of compound I to produce the half mole of bibenzyl. For C—O cleavage, 2 g-atoms of sodium are expected to cleave one leg of the acetal (either at C_4—O or C_6—O) to form the *O*-benzyl group, after proton abstraction from the solvent or any alcoholic group present. This is followed by consumption of either 1 or 2 g-atoms of sodium to produce bibenzyl or toluene respectively. Thus, 3 or 4 g-atoms of sodium are required per mole of I depending upon the fate of the benzylidene group (as bibenzyl or toluene).

These predictions were substantiated by the results of experiments which measured the proportion of sodium metal required for the reductive cleavage of methyl 4,6-*O*-benzylidene-α-D-glucopyranoside (IV), methyl *S*-benzyl-4,6-O-ethylidene-3-thio-α-D-altropyranoside (V*a*), and methyl *S*-benzyl-4,6-*O*-ethylidene-2-*O*-methyl-3-thio-α-D-altropyranoside (V*b*) (Table I, experiments 1–5). The ethylidene group in compounds V*a* and

Can. J. Chem. Downloaded from www.nrcresearchpress.com by 210.87.254.6 on 09/05/12
For personal use only.



REACTION SCHEME 2.

V*b* is unaffected by the metal, and hence permitted estimation of the sodium consumption in the cleavage of the benzyl group from sulfur. In liquid ammonia, the 4,6-*O*-benzylidene group required 4 equivalents of sodium[2] for cleavage, yielding essentially toluene along with a minor amount (3%) of bibenzyl (expt. 1). But in the mixed solvent NH_3–1,2-dimethoxyethane somewhat less than 4 equivalents of sodium were consumed and a larger amount of bibenzyl was formed (16%, expt. 2). Accordingly, as expected, methyl *S*-benzyl-4,6-*O*-benzylidene-2-thio-α-D-altropyranoside (I) in liquid ammonia required 6 equivalents of sodium for complete reduction to methyl 2-thio-α-D-altropyranoside (II) (Table I, expt. 6).

Selective Cleavage of the C—S Rather Than the C—O Bond

When 2 equivalents of sodium was added to 1 equivalent of methyl *S*-benzyl-4,6-*O*-benzylidene-2-thio-α-D-altropyranoside (I) in liquid ammonia, only methyl 2-thio-α-D-altropyranoside (II), bibenzyl, and much unchanged I were obtained. This lack of selective reduction was due to the sparing solubility of I in liquid ammonia.[3] When 1,2-dimethoxy-

[2]*The hydroxyl groups in IV and Va consumed no metal under our conditions.*
[3]*A separate test showed that the bulk of a 100 mg quantity of I failed to dissolve in 500 ml of liquid ammonia*

Can. J. Chem. Downloaded from www.nrcresearchpress.com by 210.87.254.6 on 09/05/12
For personal use only.

Can. J. Chem. Downloaded from www.nrcresearchpress.com by 210.87.254.6 on 09/05/12
For personal use only.

TABLE I

Metal consumption and products obtained in the reductive cleavage of C—O and C—S bonds by sodium in liquid ammonia

Expt. No.	Compound (1 mole)	Solvent	Amount of Na consumed (g-atoms)	Products (%)*				
				Reduced substrate	Starting compound	Bibenzyl	Toluene	Unknown
1	IV	NH_3	4	VI (79)	0	3	69	
2	IV	NH_3–DME (3:2)	~4	VI (?)	0	16	?	
3	V*a*	NH_3	~2	VII*a* (95)	0	~10	⩾58	
4	V*b*	NH_3	~2	VII*b* (98)	0	8	?	
5	V*a*	NH_3–DME (1:1)	~1	VII*a* (66)	33	32	?	
6	I	NH_3	~6	II (87–94)	0	9	⩾56	
7	I	NH_3–DME (6:5)	1.5	III (71)	21	48	?	~7

*The question mark indicates that the percentage yield was not measured but that the compound was found to be present in the product.

NOTE: I, methyl *S*-benzyl-4,6-*O*-benzylidene-2-thio-α-D-altropyranoside; II, methyl 2-thio-α-D-altropyranoside; III, methyl 4,6-*O*-benzylidene-2-thio-α-D-altropyranoside; IV, methyl 4,6-*O*-benzylidene-α-D-glucopyranoside; V*a*, methyl *S*-beuzyl-4,6-*O*-ethylidene-3-thio-α-D-altropyranoside; V*b*, methyl *S*-benzyl-4,6-*O*-ethylidene-2-*O*-methyl-3-thio-α-D-altropyranoside; VI, methyl α-D-glucopyranoside; VII*a*, methyl 4,6-*O*-ethylidene-3-thio-α-D-altropyranoside; VII*b*, methyl 4,6-*O*-ethylidene-2-*O*-methyl-3-thio-α-D-altropyranoside; DME, 1,2-dimethoxyethane.

Can. J. Chem. Downloaded from www.nrcresearchpress.com by 210.87.254.6 on 09/05/12
For personal use only.

ethane was added as a cosolvent, to improve the solubility of I in liquid ammonia (4, 11, 13), selective reductive cleavage of the C—S bond did occur (Table I, expt. 7). Optimum results were obtained when the ratio of 1,2-dimethoxyethane to NH_3 was 4 or 5 to 6 (by volume).

Several interesting features became evident when 1,2-dimethoxyethane was used as cosolvent. (*i*) For the quantities of reagents taken (see Table II), the time required for consumption of sodium increased from 15 to 20 min when only ammonia was used, to $1\frac{1}{2}$–$3\frac{1}{2}$ h in the mixed solvent. A larger ratio of 1,2-dimethoxyethane to NH_3 increased the time to several hours. (*ii*) The proportion of bibenzyl increased markedly (>50% of theory) over that (~9%) obtained in just liquid ammonia. The yield of toluene dropped sharply as a consequence. (*iii*) The proportion of sodium metal required for C—S cleavage decreased also. This is in keeping with the requirement of 1 g-atom of metal when bibenzyl is the product of C—S cleavage, and 2 g-atoms when only toluene is obtained (see Reaction Scheme 2). The influence of solvent composition and amount of metal on the proportion of products obtained is shown in Table II. It is noteworthy that the use of lithium instead of sodium, under otherwise identical conditions, gave a larger yield (76%) of the selectively cleaved product III. Table III shows the effects, on the reduction of V*a*, of solvent composition and proportion of metal to substrate, with particular attention to bibenzyl (and therefore toluene) production.

Assignment of Absorption Bands for the Benzylthio and Benzylidene Dioxy Groups

The selective removal of the benzyl group from I has permitted the assignment of infrared absorption bands caused by the two monosubstituted phenyl groups. Strong absorption for monosubstituted phenyl in compound I in Nujol is found at 770 cm^{-1}, 710 cm^{-1}, and 702 cm^{-1}. For methyl 4,6-*O*-benzylidene-2-thio-α-D-altropyranoside (III), absorption (in Nujol) occurred at 766 cm^{-1} and 706 cm^{-1} caused by the benzylidene moiety. The completely reduced substance, methyl 2-thio-α-D-altropyranoside (II), showed none of these three absorption bands. Accordingly, for these altrosides, the 4,6-*O*-benzylidene group absorbs in the region of 766–770 cm^{-1} and 706–710 cm^{-1} (Δcm^{-1} = ~60) whereas the 2-benzylthio group absorbs at 702 cm^{-1}. In agreement with this, methyl 4,6-*O*-benzylidene-2-*O*-methyl-α-D-altropyranoside (14) shows absorption bands at 778 cm^{-1} and 718 cm^{-1} (Δcm^{-1} = 60), methyl 4,6-*O*-benzylidene-2,3-di-*O*-methyl-α-D-altropyranoside (14) exhibits strong absorption at both 766 cm^{-1} and 706 cm^{-1} (Δcm^{-1} = 60), and methyl 4,6-*O*-benzylidene-2-deoxy-α-D-allopyranoside absorbs at 778 cm^{-1} and 718 cm^{-1} (Δcm^{-1} = 60) (Fig. 1).

EXPERIMENTAL

Melting points are uncorrected. Infrared spectra were taken with a Perkin–Elmer model 421 instrument. Nuclear magnetic resonance spectra were obtained with a Varian Associates A-60 instrument. Gas–liquid chromatography was accomplished with a Burrell K-2 Kromo-Tog by using a 2.5 m column packed with 25% silicone rubber on Gas Chrom P (60–80 mesh) and a helium flow rate of 100 ml/min.

Syntheses of Compounds

Methyl 4,6-O-Ethylidene-2-O-(p-toluenesulfonyl)-α-D-glucopyranoside

The published procedure (12, 15) was employed, but with the following modifications which improved the isolation and more than tripled the yield. (*a*) The methyl 4,6-*O*-ethylidene-α-D-glucopyranoside (12) was treated with a 15% rather than 48% excess of *p*-toluenesulfonyl chloride. (*b*) The chloroform extract of the reaction mixture was first washed with ice-cold 6 *N* HCl to remove pyridine, and then washed with bicarbonate solution and water. (*c*) The oil left upon removal of the chloroform from the decolorized solution was dissolved in ether. When this was left in a refrigerator overnight a solid was obtained. A hot absolute ethanol solution of this solid, when cooled, gave 11.7% of pure methyl 4,6-*O*-ethylidene-2,3-di-*O*-(*p*-toluenesulfonyl)-α-D-glucopyranoside, m.p. 156° (lit. m.p. 156–157° (12), 154–155° (16)). (*d*) The brownish solid left after removal of solvent from the above alcoholic filtrate, when dissolved in chloroform and diluted with petroleum

Can. J. Chem. Downloaded from www.nrcresearchpress.com by 210.87.254.6 on 09/05/12
For personal use only.

TABLE II

Influence of solvent composition and amount of metal on the proportion of products in the ammonia–1,2-dimethoxyethane–sodium reduction of I

Solvent composition (ml)		I		Sodium consumed		Time	Yield of	Yield of bibenzyl	Recovered	Yield of
NH_3	1,2-Dimethoxyethane	g	Mole	g	Mole	(h)	III (%)	(%)	I (%)	II (%)
600	0	19.4	0.05	6.7	0.29	$\frac{1}{4}$	—	—	—	94
150	0	3.88	0.01	1.34	0.058	$\frac{1}{4}$	—	99	—	87
400	250	9.7	0.025	1.15	0.05	$2\frac{1}{2}$	48	35	21.7	19
400	250	9.7	0.025	1.725	0.075	$3\frac{1}{2}$	36	35	23.7	41
350	200	7.76	0.02	0.69	0.03	$1\frac{1}{2}$	56.6	45	27	13
300	250		0.02		0.03	$2\frac{1}{2}$	70.5	48	21	0.409 of impure viscous oil
300	250		0.02		0.03*	$1\frac{1}{2}$	75.7	60	16.1	0.429 of impure viscous oil
300	450		0.025		0.05	7	28	—	—	—
200	300		0.025		0.05	5	30.6	—	—	—

*Lithium.

NOTE: I, methyl *S*-benzyl-4,6-*O*-benzylidene-2-thio-α-D-altropyranoside; II, methyl 2-thio-α-D-altropyranoside; III, methyl 4,6-*O*-benzylidene-2-thio-α-D-altropyranoside.

Can. J. Chem. Downloaded from www.nrcresearchpress.com by 210.87.254.6 on 09/05/12
For personal use only.

TABLE III

Influence of solvent composition and amount of metal on the proportion of products in the ammonia–1,2-dimethoxyethane–sodium reduction of V*a* to VII*a* (amount of V*a* used in all cases = 3.26 g (0.01 mole))

Solvent composition (ml)		Sodium consumed		Time required for Na consumption (min)	Yield of VII*a* (%)*	Recovered V*a* (%)*	Yield of bibenzyl (mg)	Theoretical amount of Na required for reduction		
NH_3	1,2-Dimethoxyethane	mg	Mole					For the amount of bibenzyl produced‡ (mg)	For the amount of toluene produced§ (mg)	Total (mg)
200	0	230	0.01	5	51	49	Negligible		~230	~230
150	0	440	0.019	15	100	Nil	80	20	420	440
150	100	230	0.01	45	72.4	27.6	400	102	131	233
150	100	310	0.135	150	84.3	13.9	300	76	236	312
250	250	230	0.01	40	67.3	32.7	300	76	158	234
250	300	230	0.01	45	67.5	32.5	350	88	133	221
250	200	310	0.019	150	86.1	13.9	400	102	205	307
150	125	92	0.0133†	120	85.5	14.5	394	30	59	89

*Yield is based on the total amount of V*a* used.
†Lithium.
‡Calculated on the basis that 1 g-atom equivalent of sodium is required by 1 mole of V*a* if only bibenzyl is produced.
§Calculated on the assumption that the metal not used to produce bibenzyl was used to form toluene, thus requiring 2 equivalents of sodium for 1 mole of V*a*. The toluene was not actually isolated or estimated quantitatively.
NOTE: V*a*, methyl *S*-benzyl-4,6-*O*-ethylidene-3-thio-α-D-altropyranoside; VII*a*, methyl 4,6-*O*-ethylidene-3-thio-α-D-altropyranoside.

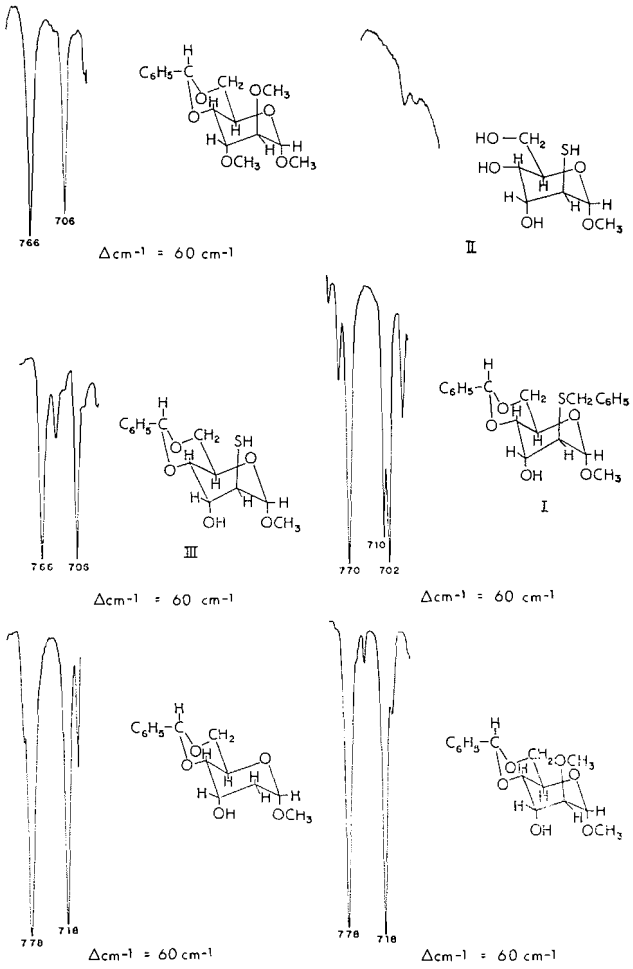


FIG. 1. Infrared absorption in Nujol of a number of altropyranosides in the region of 700 to 780 cm^{-1}.

ether (60–80°) to faint turbidity, gave 42.3% of methyl 4,6-*O*-ethylidene-2-*O*-(*p*-toluenesulfonyl)-α-D-glucopyranoside, m.p. 151° (lit. m.p. 150–151° (12)). (*e*) The mother liquors from the precipitated mono- and di-*p*-toluenesulfonyl compounds, freed from solvent and the residue acetylated (12), gave 11% of methyl 3-*O*-acetyl-4,6-*O*-ethylidene-2-*O*-(*p*-toluenesulfonyl)-α-D-glucopyranoside as long needles, m.p. 171° (lit. m.p. 169–171° (12)).

Methyl 2,3-Anhydro-4,6-O-ethylidene-α-D-mannopyranoside

The following modifications of the published procedure (12) greatly simplified the preparation of pure product. Methyl 4,6-*O*-ethylidene-2-*O*-(*p*-toluenesulfonyl)-α-D-glucopyranoside (or its acetate) was treated with a 25% rather than 100% excess of sodium methoxide in refluxing methanol for 4 h. The cooled mixture (needles separated) was poured into ice water. The water mixture was extracted with chloroform and the extract dried (Na_2SO_4) and freed from solvent. The residual solid was crystallized from methanol to give needles (84%) melting at 100° (lit. m.p. 100–100.5° (12)).

Methyl S-Benzyl-4,6-O-ethylidene-3-thio-α-D-altropyranoside (Va)

Published directions (12) were followed for most of this preparation. However, the isolation and crystallization procedures were modified advantageously. The precipitate obtained when the reaction mixture was poured into ice water was washed with water and petroleum ether as described (12), dissolved in diethyl ether, and dried (Na_2SO_4). The filtered ethereal solution was diluted with an equal volume of petroleum ether (60–80°) and the resulting solution gently refluxed on a water bath. When much of the ether had been

Can. J. Chem. Downloaded from www.nrcresearchpress.com by 210.87.254.6 on 09/05/12
For personal use only.

removed and the boiling point of the solvent had reached 50°, the flask and contents were allowed to cool to room temperature, whereupon V*a* separated as long colorless needles, yield 93%, m.p. 133° (lit. m.p. 132–133° (12)).

*Methyl S-Benzyl-4,6-O-ethylidene-2-O-methyl-3-thio-α-*D*-altropyranoside (Vb)*

To a solution of 16.3 g (0.05 mole) of V*a* in 90 ml of methyl iodide was added 24 g of silver oxide. The mixture, first stirred for 1.5 h at room temperature and then for 1.5 h at reflux, was filtered (cold) and the silver salts were washed with 50 ml of dry ether. The combined methyl iodide and ether solutions were freed from solvent under vacuum. The viscous oily residue showed no absorption for OH in the infrared spectrum. Chromatography on neutral alumina, activity grade I (Alupharm Chemicals, New Orleans, Louisiana), gave, by benzene elution, 11.1 g (65.3%) of an oil which solidified when cooled. Crystallization from cold hexane gave a compound melting at 84–85°; $[\alpha]_D^{24}$ −91° (*c*, 0.5 in chloroform). The infrared spectrum in Nujol showed bands at 710 cm^{-1} (phenyl) but none for OH.

Anal. Calcd. for $C_{17}H_{24}O_5S$: C, 59.97; H, 7.11; S, 9.42. Found: C, 59.84; H, 6.88; S, 9.68.

Ether elution of the column gave 2.5 g (25%) of a compound melting at 98–99° (from methanol). The infrared spectrum in Nujol was identical with that of authentic methyl 2,3-anhydro-4,6-*O*-ethylidene-α-D-mannopyranoside (ref. 12; see also above). No absorption for OH was evident. A mixed melting point was undepressed.

*Methyl S-Benzyl-4,6-O-benzylidene-2-thio-α-*D*-altropyranoside (I)*

This compound was prepared by an improved variation of the literature directions (3). Commercial sodium methoxide (Fisher Scientific Co.) (21.9 g, 0.115 mole) was dissolved in 200 ml of pure, dry methanol. A continuous current of nitrogen was passed through the apparatus, and benzyl mercaptan (67.9 g, 0.58 mole) was then added. When the solution had been stirred for 15 min, 26.4 g (0.1 mole) of methyl 2,3-anhydro-4,6-*O*-benzylidene-α-D-allopyranoside (14, 17) was added and the solution refluxed for 24 h (N_2). When cooled and poured with stirring into 1 l of ice water, the solution gave a precipitate of I. The solid was separated by filtration and dissolved in chloroform; this was combined with chloroform extracts (2 × 250 ml) of the filtrate. After the organic solution had been washed with water, it was dried (Na_2SO_4), separated from the drying agent, and freed from solvent under vacuum in a rotary evaporator. The semisolid residue was triturated with 500 ml of petroleum ether (60–80°), whereupon solidification occurred, yield (crude) 39 g (~100%). Recrystallization from 250 ml of absolute ethanol gave needles (35 g, 90%) melting at 136–137°; $[\alpha]_D^{25}$ +94.7° (*c*, 1 in chloroform) (lit. m.p. 136–137°; $[\alpha]_D^{24}$ +90.6° (*c*, 1.668 in chloroform) (3)). The infrared spectrum in Nujol showed absorption at 3 505 cm^{-1} (OH), 770 cm^{-1} and 710 cm^{-1} (phenyl of the benzylidene group), and 702 cm^{-1} (phenyl of the benzyl group).

Sodium – Liquid Ammonia Reduction

*Methyl 4,6-O-Ethylidene-2-O-methyl-3-thio-α-*D*-altropyranoside (VIIb) from Methyl S-Benzyl-4,6-O-ethylidene-2-O-methyl-3-thio-α-*D*-altropyranoside (Vb) (a Typical Procedure for Estimation of the Consumption of Sodium by Reaction in Liquid Ammonia)*

A dry, 500 ml, three-necked, round-bottomed flask (A) was fitted with a gas inlet tube (C), mercury seal stirrer, and dry ice condenser (B) whose outlet accommodated a tube containing sodium hydroxide pellets as protection against moisture from the atmosphere. The apparatus (A and B) was gently heated with a free flame for 5 min while a current of dry nitrogen was passed through via C to drive out surface moisture. When the system had been cooled (under a constant flow of dry nitrogen) gaseous ammonia from a cylinder of commercial anhydrous liquid ammonia was collected (150 ml) in a dry ice – acetone cooled receiver (D) fitted with a dry ice – acetone condenser (E) whose outlet was protected by a sodium hydroxide pellet tube. Metallic sodium was added to the liquid in D to destroy moisture, and then the ammonia was distilled, by using a cold water bath gradually warmed to 50°, into the dried vessel (A) previously cooled in a dry ice – acetone bath. A few milligrams of metallic sodium were added at intervals to A until the blue color persisted (for about 1 h). To this flask was then added 3.4 g (0.01 mole) of V*b*. A clear solution was obtained. Freshly cut sodium (0.46 g) was weighed in dry toluene, and from this four small pieces of about 100 mg each were added to the reaction mixture in A, one at a time only when the blue color caused by each preceding piece of metal had disappeared. Then the size of each subsequent piece of metal was reduced to ~10 mg and these were added until the blue color persisted for at least 15 min. In all, 440 mg was necessary, over a total reaction time of about 20 min.

The reaction mixture was then decomposed with excess ammonium chloride (5 g) and the ammonia allowed to evaporate in a current of nitrogen. The residue was dissolved in chloroform, and filtered free of solid; then the solvent was removed under vacuum. The remaining solid, when crystallized from cold ether, gave 2.35 g (98%) of VII*b*, m.p. 103–104°, $[\alpha]_D^{24}$ +113.7° (*c*, 1 in chloroform). Absorption in the infrared (Nujol) occurred at 2 600 cm^{-1} (SH) but none between 700 and 800 cm^{-1} for phenyl.

Anal. Calcd. for $C_{10}H_{18}O_5S$: C, 47.98; H, 7.25; S, 12.81. Found: C, 48.13; H, 6.96; S, 12.72.

The residual ethereal filtrate was evaporated and the residue triturated with 20 ml of petroleum ether (60–80°) to dissolve bibenzyl. The petroleum ether extract was freed from solvent to give 80 mg (8.3%) of bibenzyl, m.p. 51° (mixed melting point undepressed).

Can. J. Chem. Downloaded from www.nrcresearchpress.com by 210.87.254.6 on 09/05/12
For personal use only.

Methyl 4,6-O-Ethylidene-3-thio-α-D-altropyranoside (VIIa) from Methyl S-Benzyl-4,6-O-ethylidene-3-thio-α-D-altropyranoside (Va)

Method A: with sodium and liquid ammonia.—The reduction of this compound was carried out by using the apparatus and typical procedure described above. The 3.26 g (0.01 mole) of V*a* required 440 mg (0.02 mole) of sodium over a 15 to 20 min period. The reaction mixture was worked up accordingly to the preceding description to give a solid, after removal of the chloroform solvent, which, when dissolved in ether and diluted with petroleum ether (60–80°) to slight turbidity, gave 2.26 g (95.5%) of VII*a* as needles melting at 106–107°; $[\alpha]_D^{24}$ −123° (*c*, 1 in chloroform).

Anal. Calcd. for $C_9H_{16}O_5S$: C, 45.75; H, 6.83; S, 13.57. Found: C, 45.83; H, 6.91; S, 13.72.

Infrared absorption occurred at 3 465 cm^{-1} (OH) and 2 600 cm^{-1} (SH). There was no absorption for phenyl.

The residual ethereal filtrate, worked up as before, gave 80 mg of bibenzyl.

Method B: with sodium and liquid ammonia and modification to isolate the product toluene.—The preparation of the system and the reduction of the thioether V*a* (3.26 g, 0.01 mole) were carried out exactly as in the typical procedure above, except that the sodium was weighed and cut up in Skellysolve B. The work-up differed as follows. After the decomposition of the reaction mixture with ammonium chloride, the condenser (B) was filled with an ice–salt freezing mixture to retain the toluene but permit vaporization of the ammonia. The stream of nitrogen that was passed through the solution was discontinued, since it might promote loss of toluene by entrainment. The ammonia was allowed to volatilize and escape through B, without the use of a warmed water bath, by allowing the apparatus to remain overnight exposed to room temperature conditions. The residue in A was stirred with dry ether (200 ml) for half an hour and the solution then filtered. Careful fractionation removed the ether (which showed no peak for toluene by gas–liquid chromatography) until the residue was concentrated to about 15 ml. To this residue was added 0.499 g of ethylbenzene as internal standard; the resulting solution was analyzed by gas–liquid chromatography. An authentic mixture of known amounts of toluene and ethylbenzene was used for comparison. A total of 540 mg (58%) of toluene was thus determined. Removal of the ethylbenzene, toluene, and ether by distillation *in vacuo* gave a residue which was washed with water to eliminate the water-soluble VII*a*. The solid remaining (100 mg, 11%) was bibenzyl, m.p. 51°.

Method C: with sodium and liquid ammonia diluted with 1,2-dimethoxyethane.—A quantity of dry ammonia (250 ml) was put into a 1 l, three-necked, round-bottomed flask according to the typical procedure above. To this was added, via a dried dropping funnel, 100 ml of dry 1,2-dimethoxyethane (distilled from potassium metal) followed by a solution of 3.26 g (0.01 mole) of V*a* in 100 ml of dry 1,2-dimethoxyethane. An additional 50 ml of 1,2-dimethoxyethane was used to rinse the funnel, thus giving a 1:1 mixture (by volume) of ammonia and 1,2-dimethoxyethane in the reaction flask. To this solution was added freshly cut sodium (230 mg, 0.01 mole) in four pieces, one at a time, according to the typical procedure. The time required for this sodium to react was 45 min. The mixture was then decomposed with ammonium chloride as usual and the ammonia allowed to escape overnight, without the use of a warmed water bath, by using a constant current of dry nitrogen gas. About 150 ml of chloroform was then added and the mixture stirred for 1 h. This process eliminated the rest of the ammonia (pH paper test). The material was filtered, and chloroform (100 ml) was used to rinse the flask and to wash the collected solid. Removal of the chloroform and 1,2-dimethoxyethane on a rotary evaporator under vacuum left a semisolid. Trituration with water dissolved the mercaptan, and unreacted V*a* and bibenzyl remained as a solid. The mixture was filtered, and the aqueous filtrate concentrated *in vacuo* until the residue solidified. The crude yield was 1.59 g (67.3%). Crystallization from a mixture of ether and petroleum ether (60–80°) gave 1.55 g (66%) of material melting at 106–107°. The infrared spectrum and mixed melting point showed this to be identical with VII*a*.

Anal. Calcd. for $C_9H_{16}O_5S$: C, 45.75; H, 6.83; S, 13.57. Found: C, 46.00; H, 6.87; S, 13.66.

The mixture of unreacted material and bibenzyl left after removal of the aqueous solution was heated in 50 ml of refluxing petroleum ether (60–80°). The cooled mixture was filtered, leaving 1.07 g (32.6%) of solid melting at 132–133° and identical (infrared, mixed melting point) with starting material (V*a*). The petroleum ether filtrate was freed from solvent, leaving 300 mg (32%) of solid bibenzyl melting at 51°.

When the solvent was composed of 250 ml of ammonia and 200 ml of 1,2-dimethoxyethane, and 3.26 (0.01 mole) of V*a* and 0.31 g (0.0134 mole) of sodium were used, an 86% yield of VII*a*, 0.451 g (14%) of unchanged V*a*, and 400 mg (42%) of bibenzyl were obtained.

Table III illustrates the influence of solvent composition and amount of metal on the proportion of products in the ammonia–1,2-dimethoxyethane–sodium reduction of V*a* to VII*a*.

Methyl 4,6-O-Benzylidene-2-thio-α-D-altropyranoside (III) from Methyl S-Benzyl-4,6-O-benzylidene-2-thio-α-D-altropyranoside (I)

Method A: with sodium and liquid ammonia.—Details of the procedure followed those in method A for the reduction of the 3-benzylthioaltroside V*a* described above. The 19.4 g (0.05 mole) of I in 600 ml of ammonia consumed a total of 6.7 g (0.29 mole) of sodium in 200 mg pieces over a period of 15 min. The solution, after decomposition with excess ammonium chloride, was extracted with hot chloroform (4 × 250 ml). The solid left after removal of the chloroform from these extracts was triturated with 100 ml of petroleum ether (60–80°) to remove any bibenzyl, and the residue was dissolved in 50 ml of hot ethanol. When cooled overnight in a refrigerator, the solution yielded II as long colorless needles (8.4 g). A second crop (1.37 g) was

Can. J. Chem. Downloaded from www.nrcresearchpress.com by 210.87.254.6 on 09/05/12
For personal use only.

obtained upon concentration of the mother liquor. The total yield was 9.87 g (94%) of material melting at 146–147° (lit. m.p. 145–146° (3), 145–148° (4)). The infrared spectrum in Nujol showed absorption at 3 415 cm^{-1} (OH) and 2 570 cm^{-1} (SH) but no phenyl absorption.

Method B: with sodium and liquid ammonia and modifications to isolate toluene and bibenzyl.—The procedure used in method B for the reduction of the 3-benzylthioaltroside V*a* was followed here. A total of 1.34 g (0.058 mole) of sodium was required by 3.88 g (0.01 mole) of compound I in 150 ml of ammonia. After decomposition of the reaction mixture with ammonium chloride, 250 ml of dry ether was added to the flask and the ammonia allowed to evaporate through the condenser B cooled by a salt–ice freezing mixture. The residual ethereal mixture was filtered and the solid residue extracted with 200 ml of hot chloroform. Removal of the chloroform from this extract and crystallization of the resulting material from ethanol gave II as colorless needles (1.822 g, 87%), m.p. 146–147°. The ethereal extract was reduced in volume and ethylbenzene added as internal standard according to the details of method B for compound V*a*; 1.02 g (~56%) of toluene and 0.163 g (~9%) of solid bibenzyl, m.p. 51–52°, were obtained.

Method C: with sodium and liquid ammonia diluted with 1,2-dimethoxyethane.—The apparatus and the procedure used for the preparation of the ammonia–1,2-dimethoxyethane solution and subsequent reduction were the same as those in method C described for the reduction of V*a*.

To a mixture of 300 ml of ammonia and 250 ml of 1,2-dimethoxyethane containing 7.76 g (0.02 mole) of I was added 0.69 g (0.03 mole) of sodium cut into seven pieces, each piece being added in accordance with previous directions. The time required for total addition was 2.5 h. The decomposition and solvent elimination also followed cited directions. The solid that was obtained was dissolved in 50 ml of hot ethanol (rather than being triturated with water), and the solution was cooled to room temperature to give 2.3 g of the selectively reduced compound III as needles, m.p. 167–169°. The ethanol was removed from the filtrate with a rotary evaporator under vacuum, and the residue was dissolved in benzene and subjected to chromatography on 100 g of neutral alumina, activity grade II (Alupharm Chemicals, New Orleans, Louisiana). Initial benzene elution gave bibenzyl and unreacted I. With continued elution by benzene the mercaptan III began to appear, as shown by infrared absorption at 2 500 cm^{-1}, whereupon ether replaced benzene as the eluant to hasten the exit of the rest of component III still on the column (1.9 g). The total yield of III was 4.2 g (70.5%). Crystallization of the combined material from ethanol raised the melting point slightly to 168–169°; $[\alpha]_D^{24}$ +80.5° (*c*, 1 in chloroform).

Anal. Calcd. for $C_{14}H_{18}O_5S$: C, 56.37; H, 6.08; S, 10.74. Found: C, 56.23; H, 6.04; S, 10.76.

The infrared spectrum in Nujol showed absorption at 3 483 cm^{-1} (OH), 2 540 cm^{-1} (SH), and 766 cm^{-1} and 706 cm^{-1} (monosubstituted phenyl for the benzylidene group), but none at 702 cm^{-1} (monosubstituted phenyl for benzyl group). The integrated nuclear magnetic resonance spectrum in $CDCl_3$, with tetramethylsilane as reference, agreed with the structure assigned. Signals appeared at τ = 2.35 to 2.75 (multiplet for five phenyl protons), τ = 6.58 (singlet for three methyl protons), and τ = 7.95 and 8.15 (J = 10 c.p.s.) (doublet for SH proton).

The combined benzene eluates, freed from solvent, gave a solid which was heated with 50 ml of refluxing petroleum ether (60–80°). Separation by filtration left 1.61 g (21%) of unreacted I (undepressed melting point and identical infrared spectrum). From the petroleum ether filtrate was obtained, upon solvent removal, 0.87 g (48%) of bibenzyl, m.p. 51°.

Final methanol elution of the column above gave 0.47 g of unidentified oil which showed absorption for SH (2 540 cm^{-1}).

Table II illustrates the effect on product yield of different proportions of mixed solvent and starting materials with compound I as the reducible substance.

Selective Reduction of I with Lithium in Liquid Ammonia – 1,2-Dimethoxyethane

A solution of compound I in ammonia–1,2-dimethoxyethane, with the same quantities of materials as in the preceding experiment for method C, was treated with 0.208 g (0.03 mole) of lithium according to the detailed directions in method C. The solid obtained upon decomposition of the reaction mixture and removal of the 1,2-dimethoxyethane and chloroform used for extraction was heated with benzene to permit separation of the lithium chloride by filtration. The benzene was removed from the filtrate and the solid residue was dissolved in 100 ml of hot ethanol. When cooled, the solution deposited 2.7 g of III as needles, m.p. 168–169°. Chromatography of the residue as described above (method C) gave a further 1.81 g of III. The total yield of the mercaptan was 4.51 g (75.7%). Unreduced starting material amounted to 1.248 g (16%), and bibenzyl to 1.09 g (59%). Here again the same unidentified oil (420 mg) was obtained via the final methanol elution.

Reduction of Methyl 4,6-O-Benzylidene-α-D-glucopyranoside (IV)

Method A: with sodium in liquid ammonia.—Details of the procedure were the same as those in method B for the reduction of I to obtain the products II, toluene, and bibenzyl. Methyl 4,6-*O*-benzylidene-α-D-glucopyranoside (11) (5.64 g, 0.02 mole) in 300 ml of ammonia required 1.785 g (0.0776 mole) of sodium over a period of about 15 min. The ethereal extract obtained after removal of the solid by filtration gave, by gas–liquid chromatographic analysis, 1.14 g (62%) of toluene and 0.053 g (~3%) of bibenzyl.

Methanol extraction of the solid obtained after separation of the ether filtrate gave 3.08 g (79%) of methyl α-D-glucopyranoside melting at 164–165° (lit. m.p. 165° (11)).

Method B: with sodium and liquid ammonia containing 1,2-dimethoxyethane.—Details for this experiment

Can. J. Chem. Downloaded from www.nrcresearchpress.com by 210.87.254.6 on 09/05/12
For personal use only.

followed those in method C for the reduction of I to obtain III. A solution of 5.64 g (0.02 mole) of IV in 300 ml of ammonia diluted with 200 ml of 1,2-dimethoxyethane consumed 1.770 g (0.0756 mole) of sodium over a period of 4 h. After evaporation of the ammonia, however, the residue was extracted with ether to remove bibenzyl.[4] This amounted to 0.30 g (16%). The glycoside that was produced was not isolated in this case and was believed to be only methyl α-D-glucopyranoside. We were concerned in this experiment only with the amount of bibenzyl formed in an ammonia–1,2-dimethoxyethane mixture compared with the amount produced in ammonia alone under otherwise identical conditions.

ACKNOWLEDGMENTS

The financial assistance given by the National Research Council of Canada for part of this work is greatly appreciated. Infrared and nuclear magnetic resonance spectra were made by Mrs. G. Conway of the Department of Chemistry, University of Alberta, Edmonton, Alberta. Elemental analyses were performed by Dr. C. Daessle, Organic Microanalyses, 5757 Decelles Avenue, Montreal, Quebec, and by Dr. F. Pascher, Mikroanalytisches Laboratorium, Buschstrasse, Bonn, Germany.

REFERENCES

1. A. J. BIRCH. Quart. Rev. London, **4**, 69 (1950).
2. A. J. BIRCH and H. SMITH. Quart. Rev. London, **12**, 17 (1958).
3. N. C. JAMIESON and R. K. BROWN. Can. J. Chem. **39**, 1765 (1961).
4. J. E. CHRISTENSEN and L. GOODMAN. J. Am. Chem. Soc. **82**, 3827 (1961).
5. G. CASINI and L. GOODMAN. J. Am. Chem. Soc. **86**, 1427 (1964).
6. E. J. REIST, V. J. BARTUSKA, and L. GOODMAN. J. Org. Chem. **29**, 3725 (1964).
7. H. R. BOLLIGER and D. A. PRINS. Helv. Chim. Acta, **29**, 1061 (1946).
8. A. C. MAEHLY and T. REICHSTEIN. Helv. Chim. Acta, **30**, 496 (1947).
9. A. R. PINDER and H. SMITH. J. Chem. Soc. 113 (1954).
10. F. E. WILLIAMS and E. GEBAUER-FÜLNEGG. J. Am. Chem. Soc. **53**, 352 (1931).
11. N. K. RICHTMEYER. Methods Carbohydrate Chem. 1, 107 (1962).
12. L. GOODMAN and J. E. CHRISTENSEN. J. Org. Chem. **28**, 158 (1963).
13. N. D. SCOTT, T. F. WALKER, and V. L. HANSLEY. J. Am. Chem. Soc. **58**, 2442 (1936).
14. G. T. ROBERTSON and C. F. GRIFFITH. J. Chem. Soc. 1199 (1935).
15. H. R. BOLLIGER and D. A. PRINS. Helv. Chim. Acta, **28**, 465 (1945).
16. E. G. ANSELL and J. HONEYMAN. J. Chem. Soc. 2778 (1952).
17. N. K. RICHTMEYER and C. S. HUDSON. J. Am. Chem. Soc. **63**, 1727 (1941).

[4]*No attempt was made to isolate or to estimate toluene on the assumption that it must have been present as part of the product. Its amount was assumed to be equal to that portion of the benzylidene group which did not form bibenzyl. The latter compound was readily obtained almost quantitatively.*

Can. J. Chem. Downloaded from www.nrcresearchpress.com by 210.87.254.6 on 09/05/12
For personal use only.

Can. J. Chem. Downloaded from www.nrcresearchpress.com by 210.87.254.6 on 09/05/12
For personal use only.

REACTION OF THIOLS WITH EPOXIDES OF CONJUGATED 1,4-DIKETONES

H. S. WILGUS III, E. FRAUENGLASS, P. P. CHIESA, G. H. NAWN,[1] F. J. EVANS, AND J. W. GATES, JR.

Research Laboratories, Eastman Kodak Company, Rochester, New York

Received July 6, 1965

ABSTRACT

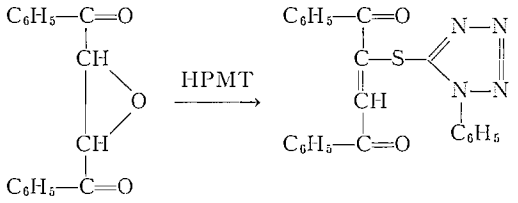
The reaction of thiols with 2,3-epoxides of bicyclo, conjugated 1,4-diketones was found to proceed readily to give the dehydrated thio-substituted enediones or their enolized isomers, depending upon the reaction conditions and the bicyclic bridging of the starting materials. In no case was a mixture of these isomers observed. Enediones generally resulted from these reactions with and without triethylamine catalysis, whereas the use of an equimolar amount of triethylamine generally gave hydroquinones. The ease of rearrangement of enedione to hydroquinone followed the order: 2,3-dimethylbutadiene adduct ≫ reduced cyclopentadiene adduct > cyclopentadiene adduct = 1,3-cyclohexadiene adduct.

Recent reviews on epoxides (1) reveal only one reference to the attack of a sulfhydryl group on an epoxide conjugated to a carbonyl group. In this case (2) hydrogen sulfide in the presence of barium hydroxide reacted with ethyl β,β-dimethylglycidate to give a small amount of ethyl 3-hydroxy-2-mercapto-3-methylbutyrate. The reactions of thiols with 2,3-epoxides of conjugated carbonyl or conjugated 1,4-dicarbonyl compounds have not been reported before. Alder *et al.* (3) have reported the preparation of several epoxides of cyclopentadiene–quinone adducts. The reactions of thiols with these and similar epoxides are reported in this paper.

The thiols that were studied were 1-phenyl-5-mercaptotetrazole (HPMT), 2-mercaptobenzthiazole (HMBT), *p*-toluenethiol (HPTT), 2-quinolinethiol (HQT), methanethiol (HMT), and ethanethiol (HET). Triethylamine (TEA) was often employed, either in catalytic or equimolar amounts. Trimethylamine or sodium salts of some mercaptans were also used.

In all but one case, the diketoepoxides were part of a cyclic system. The exception, *trans*-dibenzoylethylene epoxide (I), reacted with HPMT to produce 1,4-diphenyl-2-(1′-phenyl-5′-tetrazolylthio)-2-buten-1,4-dione (II), as shown in eq. [1]. The structure of II was assigned on the basis of a combustion analysis and an infrared spectrum which shows a conjugated carbonyl doublet at 1 630 and 1 650 cm^{-1}.

[1]



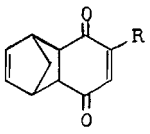
I II

The new diene adducts and epoxides used in this study are described in Tables I and II. Tables III and IV list the products obtained when these epoxides were treated with the various mercaptans. Two possible products of these reactions are the enedione III and the hydroquinone IV (eq. [2]). These structures were assigned on the basis of combustion

[1]*Present address: Polaroid Corporation, Cambridge 39, Massachusetts.*

TABLE I

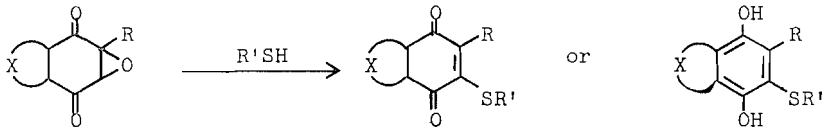
Adducts*



R	Yield, %	Melting point, °C, and crystallization solvent
4′-$C_6H_4CH_3$	76	128–129, methanol
$CH(CH_3)_2$	84	49–51, petroleum ether
$C(CH_3)_3$	82	81–82, ethanol
4′-$SC_6H_4CH_3$†	86	144–154, ethanol

*General procedure of Porter *et al.* (5).
†See Experimental section.

analyses and infrared spectra. In several cases, the products were known compounds synthesized in an unambiguous manner. The infrared spectra show conjugated carbonyl bands at 1 650 cm^{-1} for III and O—H bands at 3 325 cm^{-1} for IV.

[2] 

III IV

Inspection of Tables III and IV reveals that when no catalyst was used the product was the enedione III. Only one exception was noted: the 2,3-dimethylbutadiene–quinone adduct epoxide (XVII), which gave a substituted hydroquinone. This result is not surprising in view of the ease of rearrangement of the dimethylbutadiene–quinone adducts to the aromatic system (4). Since the enedione from XVII is a known compound, it was prepared by a different synthetic route (5).

The use of a catalytic amount of triethylamine generally gave enediones III. When an equimolar amount of triethylamine was used, the products were naphthohydroquinones. The enediones XXXIV and XXXV are not exceptions to this reaction, since they cannot rearrange to hydroquinones. The use of the sodium salt of the thiol also led to the naphthohydroquinone, as shown by XXIII.

In a previous paper (6) it is shown that the diene–quinone adducts have the *endo-cis* configuration and that the epoxide ring has the *exo* configuration. To determine whether the isolated double bond at the 6,8-position, because of its possible close proximity, had any effect on the reactivity of the epoxide and on the reaction mechanism, several examples of saturated epoxides were prepared. It is clear from the reactions of these epoxides (XLI–L) that the isolated double bond does not affect the reaction course. To verify this type of structure, XLVI was also prepared from the known quinone LIV (7), as shown in eq. [3]. The reduction of the isolated double bond appears to have decreased the strain on the bicyclic ring system, for the enedione XLV readily rearranged after the addition of a trace of mineral acid or after a long reflux period; the corresponding unsaturated enediones of XIX, XXVII, and XXXI required a base for rearrangement (4, 5).

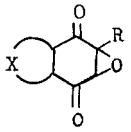
A phenyl or *p*-tolyl substituent did not exhibit any appreciable steric hindrance, as was shown by the reactions of epoxides V, VI, and XIV. When the substituent was isopropyl

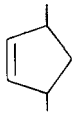
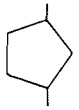
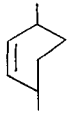
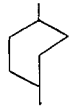
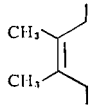
Can. J. Chem. Downloaded from www.nrcresearchpress.com by 210.87.254.6 on 09/05/12
For personal use only.

Can. J. Chem. Downloaded from www.nrcresearchpress.com by 210.87.254.6 on 09/05/12
For personal use only.

TABLE II

Epoxides prepared by the procedure of Alder *et al.* (3)



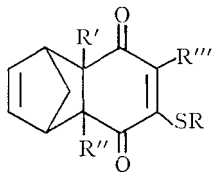
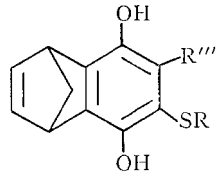
Compound No.	Starting material	X	R	Reaction conditions	Yield, %	Melting point, °C
V	See ref. 5		C_6H_5	60 min, room temp.	90	143–144
VI	See Table I		4′-$C_5H_4CH_3$	60 min, room temp.	88	134–136
VII	See Table I		$CH(CH_3)_2$	30 min, room temp.	90	119–120
VIII	See Table I		$C(CH_3)_3$	60 min, room temp.	84	144–146
IX	See ref. 2		H	*	83	111.5–113.5
X	See ref. 2		CH_3	*	82	132–134
XI	V		C_6H_5	*	62	127–130
XII	See ref. 3		H	10 min, 5 °C	80	137–138
XIII	See ref. 5		CH_3	30 min, 5 °C	80	116–117
XIV	See ref. 5		C_6H_5	30 min, room temp.	84	142.5–143
XV	XII		H	*	51	119–122
XVI	XIII		CH_3	*	75	130–132
XVII	See ref. 10		H	10 min, 5 °C	30	77–79

*Obtained by hydrogenation of the parent epoxides with Raney nickel – ethyl acetate at room temperature and 40 p.s.i.

Can. J. Chem. Downloaded from www.nrcresearchpress.com by 210.87.254.6 on 09/05/12
For personal use only.

TABLE III

Reaction products

Compound No.	R′	R″	R‴	Thiol reagent*	Yield, % 	Yield, % 	Melting point, °C
XIX	H	H	H	HPMT – cat. TEA†	70	—	133–134
XX	H	H	H	HMBT‡	27	—	141–142
XXI	H	H	H	HQT§	33	—	126–128
XXII	H	H	H	TEAPMT	—	94	179–181.5
XXIII	H	H	H	HMBT – cat. TEA‖	—	78	240–241
	H	H	H	NaMBT¶	—	77	
XXIV	H	H	H	TEAPTT§	—	89‡‡	144–145
XXV	H	H	H	TEAMT**	—	87‡‡	135–137
XXVI	H	H	H	TEAET**	—	30‡‡	95–96
XXVII	H	H	CH_3	HPMT – cat. TEA§	43	—	140–141
XXVIII	H	H	CH_3	TEAPMT	—	41	182–183
XXIX	H	H	CH_3	TEAMBT	—	90	213–214
XXX	H	H	CH_3	TEAPTT§	—	80‡‡	118–119
XXXI	H	H	C_6H_5	TEAPMT	—	50	125–134 (decomp.)
XXXII	H	H	C_6H_5	TEAPTT**	—	76	151–153 (decomp.)
XXXIII	H	H	4′-$C_6H_4CH_3$	HPMT – cat. TEA††	48	—	178–180 (decomp.)
XXXIV	CH_3	H	CH_3	TEAPMT	22	—	129–130
XXXV	H	CH_3	CH_3	TEAPMT	16	—	119–122 (decomp.)

*General procedure: Equimolar amounts of the reactants were refluxed for ¼ to 48 h in ethanol. A solid was obtained when the solution was allowed to cool or when the solvent was concentrated, and recrystallization was effected from ethanol or dilute acetic acid.

†Reaction time, 2 weeks at room temperature.

‡Reaction time, 3 weeks at room temperature.

§Refluxed for 1 h.

‖Refluxed for 48 h.

¶Reaction time, 18 h at room temperature in 50% ethanol.

**Refluxed for ½ h.

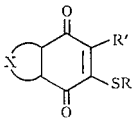
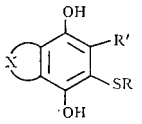
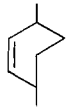
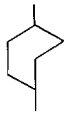
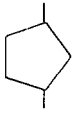
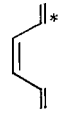
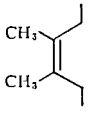
††Refluxed for 1½ h.

‡‡Isolated as the diacetate by acetylation of the solvent-stripped reaction mixture, with acetic anhydride and a catalytic amount of pyridine.

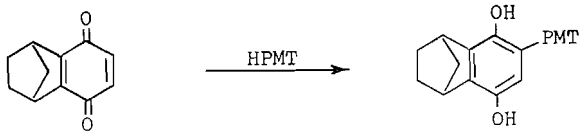
Can. J. Chem. Downloaded from www.nrcresearchpress.com by 210.87.254.6 on 09/05/12
For personal use only.

TABLE IV

Reaction products

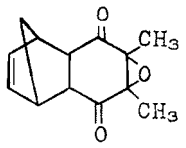
Compound No.	X	R′	Thiol reagent†	Yield, % 	Yield, % 	Melting point, °C
XXXVI		H	HPMT – cat. TEA	—	70	204–205 (decomp.)
XXXVII		H	HMBT – cat. TEA‡	—	25	217–218 (decomp.)
XXXVIII		CH_3	HPMT – cat. TEA§	60	—	145–146
XXXIX		CH_3	TEAPMT	—	40	185–186
XL		C_6H_5	TEAPMT	—	58	211–213 (decomp.)
XLI		H	HPMT – cat. TEA	44	—	135–136
XLII		H	TEAPMT	—	52	201–202 (decomp.)
XLIII		CH_3	HPMT – cat. TEA	77	—	121–122
XLIV		CH_3	TEAPMT	—	79	195–196 (decomp.)
XLV		H	HPMT‖	62	—	132–133
XLVI		H	HPMT¶	—	52	179–181
XLVII		CH_3	HPMT – cat. TEA‖	54	—	150–152
XLVIII		CH_3	TEAPMT	—	85	120–122
XLVIX		C_6H_5	HPMT – cat. TEA‖	100	—	Oil
L		C_6H_5	TEAPMT‖	—	70	132–134
LI		H	HPMT	78	—	144–145
LII		H	HMBT	64	—	171–173 (decomp.)
LIII		H	HPMT¶	—	65	185–186

*Epoxide was obtained by the procedure of Wertz *et al.* (11).
†General procedure is that of Table III.
‡Refluxed for 1½ h in benzene.
§Refluxed for 2 h.
‖Refluxed for 1 h.
¶Refluxed for 4 h in benzene.

[3] 

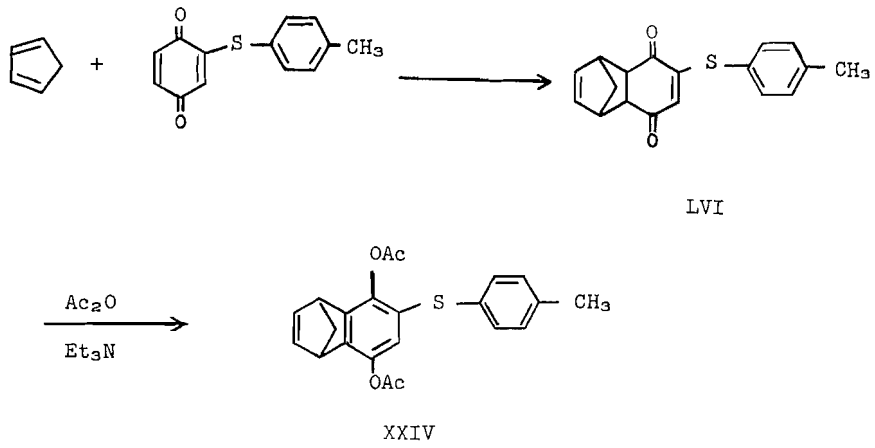
LIV XLVI

(VII) or *t*-butyl (VIII), no reaction was observed, even with the sodium mercaptides. In addition, the epoxides of the three isomeric dimethyl quinone – cyclopentadiene adducts were prepared (3). The 2,3-dimethyl epoxide LV did not react. This result is consistent with a S_N2 reaction mechanism.



LV

When nonheterocyclic mercaptans were used in this study, the enedione form could not be isolated and the hydroquinone derivatives were usually not stable; the presence of the latter was indicated by infrared spectra. These reaction products were usually isolated as their stable diacetates. The structure of one of these diacetates (XXIV) was confirmed by an alternate synthesis, as shown in eq. [4]. The conversion of LVI into XXIV was effected by a method of rearrangement used by Meinwald and Wiley (8).

[4] 

LVI

XXIV

EXPERIMENTAL

Unless otherwise specified, all chemicals were Eastman Kodak Company materials. The elemental analyses of all the new compounds reported in this paper were within the accepted tolerances.

1,4-Diphenyl-2-(1'-phenyl-5'-tetrazolylthio)-2-buten-1,4-dione (II)

Chalcone epoxide (9) was allowed to react at room temperature for 2 weeks with an alcoholic solution containing an equimolar amount of HPMT. The solvent was removed and the product was recrystallized from benzene–alcohol to give a 65% yield, m.p. 158–159° (decomp.).

1,4-Diacetoxy-5,8-dihydro-5,8-methano-2-(4'-toluenethio)-1,4-naphthohydroquinone (XXIV)

To a mixture of 1.4 g of 5,8-methano-4*a*,5,8,8*a*-tetrahydro-2-(4'-toluenethio)-1,4-naphthoquinone (LVI) in 25 ml of acetic anhydride was added 0.6 g of triethylamine. Tetrahydrofuran (1 ml) was then added to produce a clear solution. This solution was allowed to stand at room temperature for 3 days and was then

Can. J. Chem. Downloaded from www.nrcresearchpress.com by 210.87.254.6 on 09/05/12
For personal use only.

poured into 300 ml of cold water. Through continued stirring and trituration, the gummy material which separated solidified to give a red-brown solid. This material was collected and recrystallized from alcohol to give 1.4 g (73.7%) of an off-white powder, m.p. 145–147°. This material was identical in all respects with the sample of XXIV prepared as given in Table III.

5,8-Methano-1-(1'-phenyl-5'-tetrazolylthio)-5,6,7,8-tetrahydro-1,4-naphthohydroquinone (XLV)

To 5.0 g of 5,6,7,8-tetrahydro-5,8-methano-1,4-naphthoquinone (5) (LIV) was added 50 ml ethanol, followed by 5.1 g of HPMT. After the mixture had been refluxed for 3 h, the solvent was removed on a rotary evaporator and the residue was dissolved in chloroform. After 2 days, white crystals (2.83 g) were collected, m.p. 174–175° (decomp.). An additional 7.20 g of less-pure product was obtained. An infrared spectrum of this compound was identical with that of the sample prepared by another route, as shown in Table IV.

4'-Toluenethio-p-benzoquinone

To a chilled solution of 18.6 g of *p*-benzoquinone in 100 ml of methanol was added, with stirring, 10.7 g of *p*-toluenethiol in 50 ml of methanol during 30 min. Stirring was continued for 1 h while the reaction mixture warmed to room temperature. At the end of this time, the suspension was poured into 200 ml of ice water and the rust-colored precipitate was collected. The crude product, 19 g, m.p. 100–107°, was crystallized from ethanol to give 16 g of product, m.p. 108–110°.

REFERENCES

1. R. E. Parker and N. S. Isaacs. Chem. Rev. **59**, 737 (1959). S. Winstein and R. B. Henderson. Heterocyclic Compds. 1, 1 (1950).
2. V. F. Martynov and N. A. Razepina. Zh. Obshch. Khim. **22**, 1577 (1952); Chem. Abstr. **47**, 8016 (1953).
3. K. Alder, F. H. Flock, and H. Beumling. Chem. Ber. **93**, 1896 (1960).
4. O. Diels and K. Alder. Ber. **62**, 2337 (1929). L. W. Butz and A. W. Rytina. Org. Reactions, **5**, 136 (1949).
5. R. F. Porter, W. W. Rees, E. Frauenglass, H. S. Wilgus III, G. H. Nawn, P. P. Chiesa, and J. W. Gates, Jr. J. Org. Chem. **29**, 588 (1964).
6. D. F. O'Brien and J. W. Gates, Jr. J. Org. Chem. In press.
7. T. Pasternak and R. Castro. Helv. Chim. Acta, **31**, 536 (1948).
8. J. Meinwald and G. A. Wiley. J. Am. Chem. Soc. **80**, 3667 (1958).
9. R. E. Lutz and F. W. Wilder. J. Am. Chem. Soc. **56**, 1987 (1934).
10. I. G. Farbenindustrie A.G. Fr. Patent No. 677,296 (June 25, 1929); Chem. Abstr. **24**, 3118 (1930).
11. E. Wertz, H. Schobbert, and H. Seibert. Ber. **68**, 1163 (1935).

Can. J. Chem. Downloaded from www.nrcresearchpress.com by 210.87.254.6 on 09/05/12
For personal use only.

Can. J. Chem. Downloaded from www.nrcresearchpress.com by 210.87.254.6 on 09/05/12
For personal use only.

LYCOPODIUM ALKALOIDS

XVII. MASS SPECTRA OF ANNOTINE AND SOME ANNOTINE DERIVATIVES

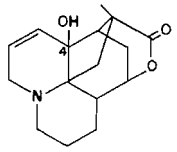
D. B. MacLean and M. Curcumelli-Rodostamo
Department of Chemistry, McMaster University, Hamilton, Ontario

Received October 13, 1965

ABSTRACT

The mass spectra of annotine and some of its derivatives are recorded and discussed. Fragmentation mechanisms are proposed to account for the formation of the major peaks in the spectra. The composition of the ions has been verified by measurement of the high-resolution spectra of four of the five compounds. The results lend support to the structure previously proposed for this alkaloid.

In a recent publication (1) it was proposed that annotine (2–5) has structure I. This proposal was based upon a number of degradation experiments, upon the examination of annotine and some of its derivatives by infrared and nuclear magnetic resonance spectroscopy, and upon biogenetic considerations. In this communication we report on the mass spectrometric examination of annotine and some of its derivatives.



I

The mass spectra of a representative group of *Lycopodium* alkaloids were reported several years ago (6); they showed that the loss of the bridge carbon atoms was characteristic of all alkaloids examined. Since then mass spectrometric studies have been used as an aid in the elucidation of the structure of several new alkaloids of this family, and in all cases this behavior has again been observed. Among other alkaloids, lycodoline (6, 7), des-N-methyl-hydroxy-α-obscurine (8), and lycofawcine (9), which carry a hydroxyl group at C_4 in the hydrojulolidine system, as has been proposed for annotine, were investigated. In the spectra of the first two of these compounds a large M-17 peak was observed as a result of loss of a hydroxyl radical. The M-17 ion so formed then underwent further fragmentation with loss of the bridge carbon atoms. Lycofawcine and its derivatives do not exhibit a prominent M-17 peak, but the C_4 hydroxyl is eliminated along with the bridge carbon atoms. One might expect that, if annotine has structure I, its fragmentation would follow a pattern similar to that of other alkaloids bearing a C_4—OH group. This expectation was borne out, as the results reported below indicate.

The major peaks in the mass spectrum of annotine, shown in Fig. 1*a*, may be explained by invoking two fragmentation processes. In one process the first step involves loss of the hydroxyl group, giving rise to an ion of mass 258. A metastable peak at *m/e* 242.0 is in accord with this change; the value of m^* calculated for the transformation $275 \rightarrow 258$ is 242.0. The peaks observed at *m/e* 172 and 144 may be considered to arise from the ion of mass 258 as shown in Scheme 1*a*. A metastable peak associated with the change $258 \rightarrow 172$ is observed at *m/e* 115.0 (m^* calcd. = 114.7). The last step, *m/e* $172 \rightarrow 144$, is analogous to the *m/e* $174 \rightarrow 146$ transformation encountered in the fragmentation of dihydrolycopodine and other *Lycopodium* alkaloids (6).

Can. J. Chem. Downloaded from www.nrcresearchpress.com by 210.87.254.6 on 09/05/12
For personal use only.

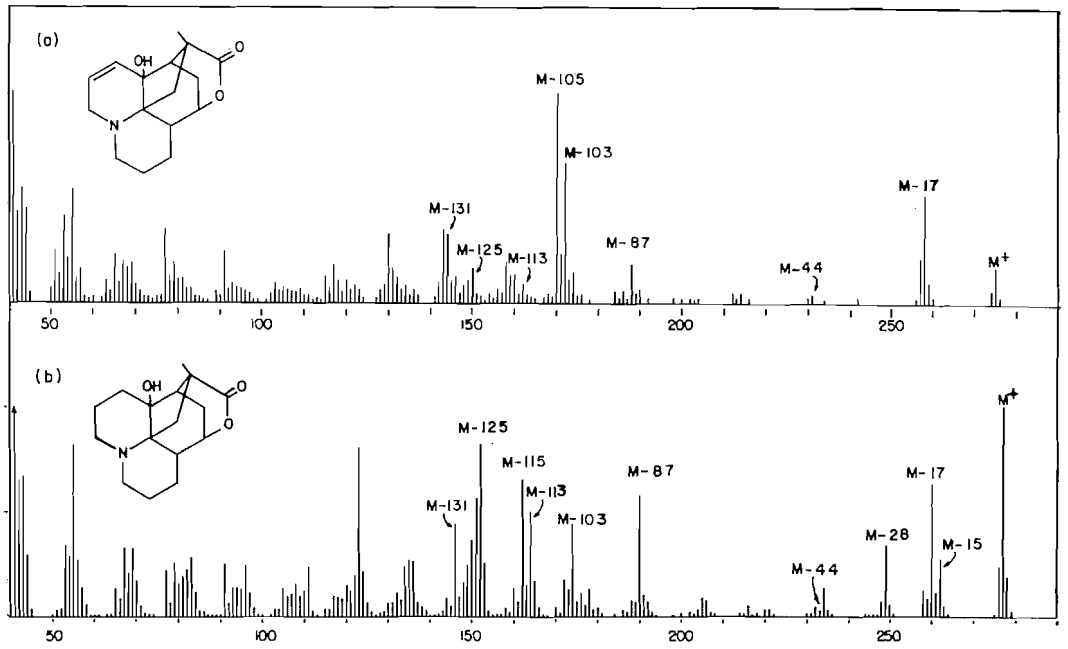


FIG. 1. Mass spectra of (*a*) annotine and (*b*) dihydroannotine.

The peaks at *m/e* 274, 188, 170, and 162 may be accounted for in a second fragmentation sequence as outlined in Scheme 1*b*. A metastable peak associated with the change 274 → 188 is observed at *m/e* 129.5 (*m** calcd. = 129.0).

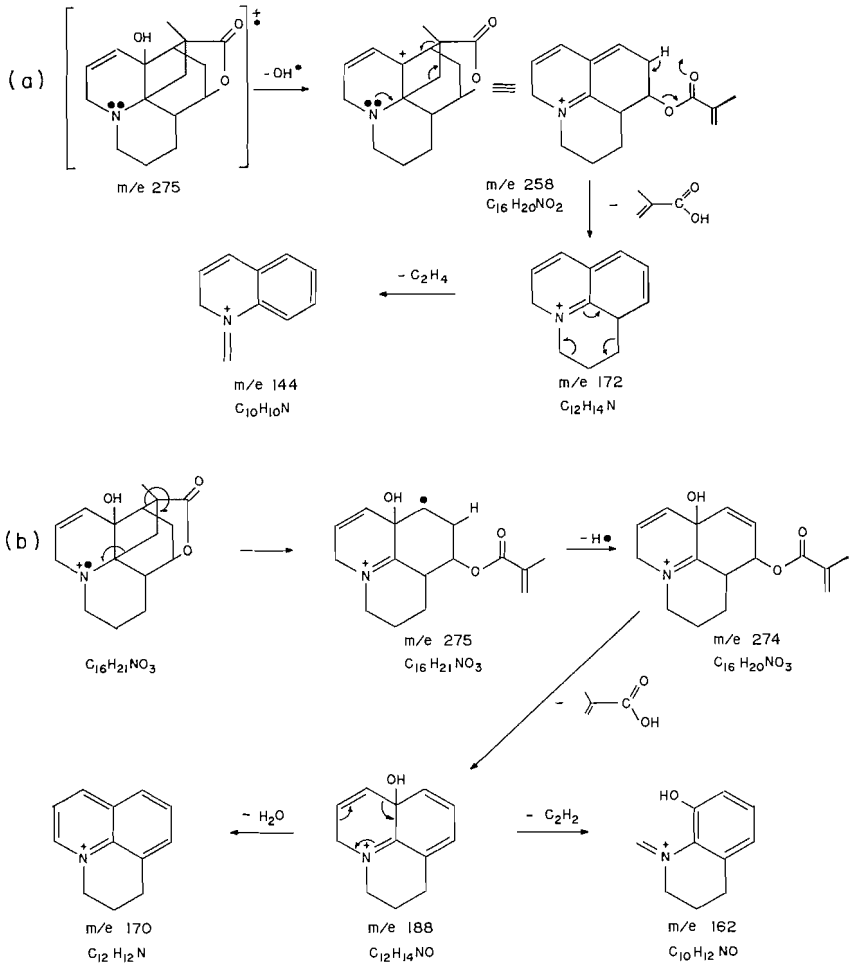
Other peaks in the spectrum of low intensity which merit consideration are those appearing at *m/e* 260 and *m/e* 231 corresponding, respectively, to loss of a methyl group and of carbon dioxide. The presence of the latter peak corroborates the proposal of a lactone function in annotine.

The results of an analysis of the high-resolution spectrum of annotine are recorded in Table I. In every case the composition of the ions is in accord with the mechanism proposed from a study of the low-resolution spectrum. In some cases, however, doublets

TABLE I

Accurate mass measurement of annotine

Measured mass	Error (obs. − calcd.) in milli mass units	Elemental composition	Mass difference from molecular ion
276.1550	−0.5	$C_{15}H_{21}{}^{13}C_1NO_3$	M+1
275.1521	−0.1	$C_{16}H_{21}NO_3$	M
274.1449	0.6	$C_{16}H_{20}NO_3$	M-1
260.1294	0.7	$C_{15}H_{18}NO_3$	M-15
258.1504	1.0	$C_{16}H_{20}NO_2$	M-17
231.1636	1.3	$C_{15}H_{21}NO$	M-44
188.1461	2.2	$C_{13}H_{18}N$	M-87
188.1111	3.6	$C_{12}H_{14}NO$	M-87
172.1149	2.2	$C_{12}H_{14}N$	M-103
172.0796	3.4	$C_{11}H_{10}NO$	M-103
170.1004	3.4	$C_{12}H_{12}N$	M-105
162.1282	−0.1	$C_{11}H_{16}N$	M-113
162.0917	−0.2	$C_{10}H_{12}NO$	M-113
144.0787	−2.6	$C_{10}H_{10}N$	M-131



SCHEME 1.

are observed, e.g. at *m/e* 188, 172, and 162, but in each case the major component of the doublet corresponds in composition to the ion proposed in the fragmentation mechanism. In particular it should be noted that the ion of *m/e* 231 corresponds in composition to loss of CO_2 from the molecular ion.

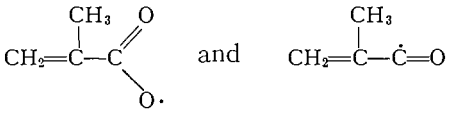
The mass spectrum of dihydroannotine is more complex than that of annotine, but closer examination reveals that both compounds undergo common fragmentation processes upon electron impact. This is shown in Fig. 1*b*, where the peaks are designated by their mass difference from the molecular ion. The fragmentation process discussed in Scheme 1*a* explains the presence of peaks at *m/e* 260, 174, and 146, each appearing 2 mass units above the corresponding peaks in annotine. Metastable peaks are observed at *m/e* 244.5, 116.8, and 123.0 corresponding, respectively, to the transformations 277 $\rightarrow$ 260 (m^* calcd. = 244.0), 260 $\rightarrow$ 174 (m^* calcd. = 116.4), and 174 $\rightarrow$ 146 (m^* calcd. = 122.5).

Scheme 1*b*, when applied to dihydroannotine, gives rise to ions of mass 276, 190, 172, and 162. A metastable peak is present at *m/e* 131.4 (m^* calcd. 276 $\rightarrow$ 190 = 130.8) in accord with the loss of methacrylic acid from the ion of *m/e* 276.

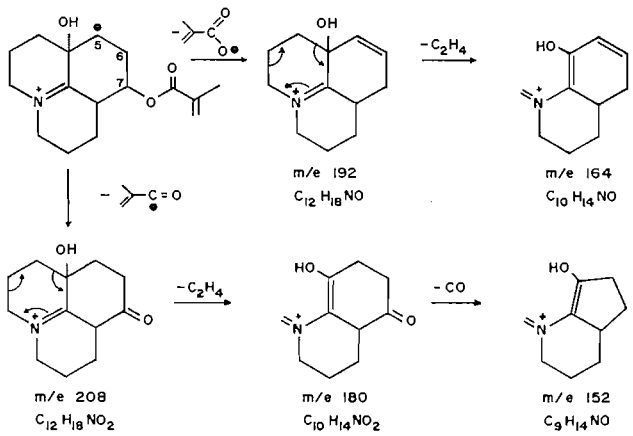
Can. J. Chem. Downloaded from www.nrcresearchpress.com by 210.87.254.6 on 09/05/12
For personal use only.

Can. J. Chem. Downloaded from www.nrcresearchpress.com by 210.87.254.6 on 09/05/12
For personal use only.

There are differences, however, as well as similarities, in the mass spectra of the two compounds. These differences, to a large extent, reflect the diminished tendency of the molecular ion of dihydroannotine to lose the hydroxyl radical, caused by the fact that such a process does not lead to a resonance-stabilized carbonium ion, as in the case of annotine. The relative difficulty with which the hydroxyl radical is lost from the molecular ion is demonstrated by the intense peak corresponding to the latter. As the molecular ion of dihydroannotine is not consumed to a large extent in the 277 → 260 transformation, other processes, which are insignificant in the fragmentation of annotine, here gain considerable importance. Thus a relatively intense peak is present at *m/e* 262 presumably caused by the loss of a methyl group; it provides evidence, independent from that available earlier, of the presence of this group in the alkaloid. Other peaks prominent in the spectrum of dihydroannotine appear at *m/e* 164, 152, 150, and 123. A possible route to the formation of the first two is outlined in Scheme 2. The peak at *m/e* 150 may be considered to be formed in part by loss of hydrogen from the ion of *m/e* 152. In this mechanism expulsion of the radicals



must be accompanied by hydrogen migration. In the first case hydrogen migration is postulated to occur from C_6 to C_7 and in the second from C_7 to C_5. The formation of a cyclopropane ring between C_5 and C_7 could account equally well for the ion of *m/e* 192. The presence of the strong peak at *m/e* 123 is not easily interpreted on the basis of the low-resolution spectrum alone.



SCHEME 2.

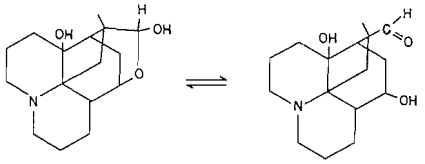
Examination of the high-resolution spectrum of dihydroannotine was carried out, and the results are shown in Table II. The composition of the ions discussed previously has been verified and additional information obtained. Thus the peak at *m/e* 249, formed by the loss of 28 mass units, is a doublet caused by loss of C_2H_4 and of CO from the molecular ion. The peak at *m/e* 123 is actually a quartet and thus not as important in the overall fragmentation as the examination of the low-resolution spectrum alone infers. The peaks at 190, 174, and 162 are O—CH_4 doublets, just as the corresponding ions at *m/e* 188, 172, and 162 are in the case of annotine. Similarly, O—CH_4 doublets are noted for the peaks at *m/e* 164 and 150.

TABLE II

Accurate mass measurement of dihydroannotine

Measured mass	Error (obs. − calcd.) in milli mass units	Elemental composition	Mass difference from molecular ion
278.1712	0.0	$C_{15}{}^{13}C_1H_{23}NO_3$	M+1
277.1659	−1.9	$C_{16}H_{23}NO_3$	M
276.1576	−2.4	$C_{16}H_{22}NO_3$	M-1
262.1415	−2.9	$C_{15}H_{20}NO_3$	M-15
260.1640	−1.0	$C_{16}H_{22}NO_2$	M-17
249.1702	−2.7	$C_{15}H_{23}NO_2$	M-28
249.1341	−2.4	$C_{14}H_{19}NO_3$	M-28
190.1582	−1.4	$C_{13}H_{20}N$	M-87
190.1218	−1.4	$C_{12}H_{16}NO$	M-87
174.1279	−0.4	$C_{12}H_{16}N$	M-103
174.0925	0.6	$C_{11}H_{12}NO$	M-103
172.1141	1.4	$C_{12}H_{14}N$	M-105
164.1060	−1.5	$C_{10}H_{14}NO$	M-113
164.0689	−2.3	$C_9H_{10}NO_2$	M-113
162.1262	−2.1	$C_{11}H_{16}N$	M-115
162.0898	−2.1	$C_{10}H_{12}NO$	M-115
152.1056	−1.9	$C_9H_{14}NO$	M-125
150.1244	−3.9	$C_{10}H_{16}N$	M-127
150.0898	−2.1	$C_9H_{12}NO$	M-127
146.0956	−1.4	$C_{10}H_{12}N$	M-131
123.1052	0.4	$C_8H_{13}N$	—
123.0799	−1.1	$C_8H_{11}O$	—
123.0663	−2.1	C_7H_9NO	—
123.0415	−3.1	$C_7H_7O_2$	—

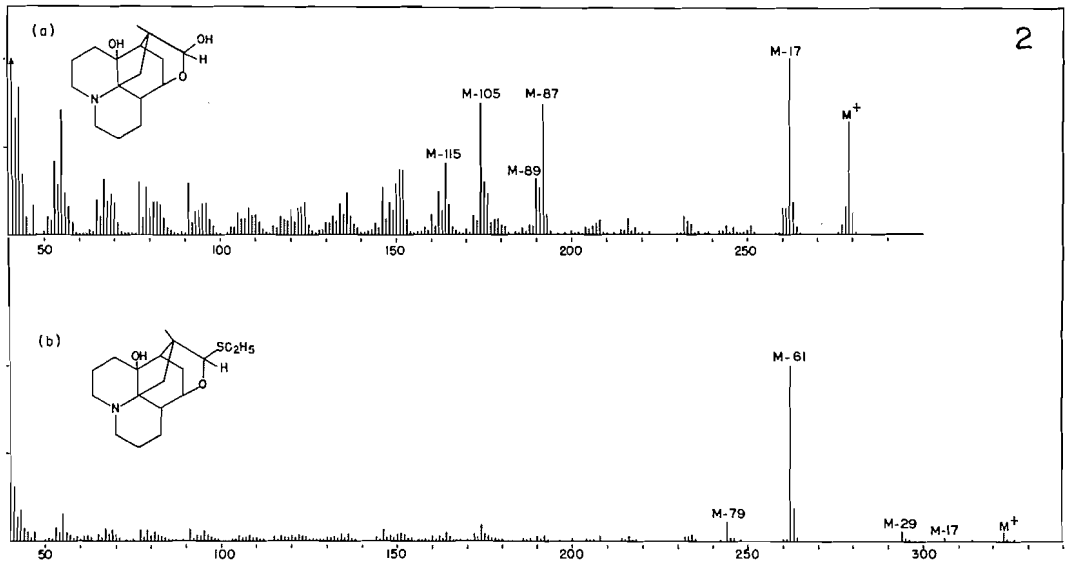
The infrared spectrum of dihydroannotinol (1) shows that the compound in the solid state as well as in solution exists in a hemiacetal form. In the ion source of the mass spectrometer, however, dihydroannotinol is present in the gaseous phase, and may exist in both the hemiacetal and the hydroxy aldehyde forms as shown below. We make use of both isomers in the proposed fragmentation mechanisms.



A study of the mass spectrum of dihydroannotinol (Fig. 2*a*) reveals, as expected, an analogy with the patterns present in the spectra of annotine and dihydroannotine. Here also, we find the two main fragmentation mechanisms advanced previously. The process initiated by the M → M-17 transformation is formulated in Scheme 3*a* for the hydroxy aldehyde form. This mechanism is supported by the presence of metastable peaks at *m/e* 246.5 (*m** calcd. 279 → 262 = 246.0) and 159.0 (*m** calcd. 192 → 174 = 157.7). A metastable peak present at *m/e* 141.0 could be caused by either one of the following transformations: 262 → 192 (*m** calcd. = 140.7) and 192 → 164 (*m** calcd. = 140.1).

The ions of mass 278, 191, 190, 172, and 162 may be accounted for by the fragmentation scheme shown in Scheme 3*b*. The ion–radical of mass 279 may lose methacrylaldehyde and water to form the species of mass 191, or it may be converted into the ion of mass 278 by loss of a hydrogen radical. As shown, both processes may lead to the formation of the ion of mass 190. In Table III are recorded the results of the analysis of the high-resolution spectrum of dihydroannotinol. The composition of the ions postulated according to the proposed fragmentation mechanism have been verified. Some ions appear as

Can. J. Chem. Downloaded from www.nrcresearchpress.com by 210.87.254.6 on 09/05/12
For personal use only.



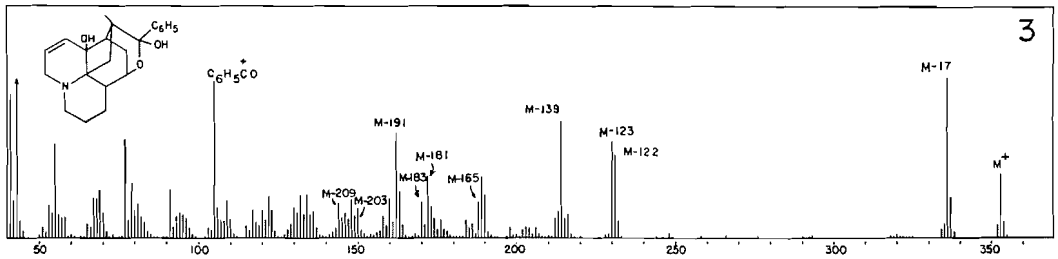


FIG. 2. Mass spectra of (*a*) dihydroannotinol and (*b*) its thioethyl analogue.
FIG. 3. Mass spectrum of phenylannotine.

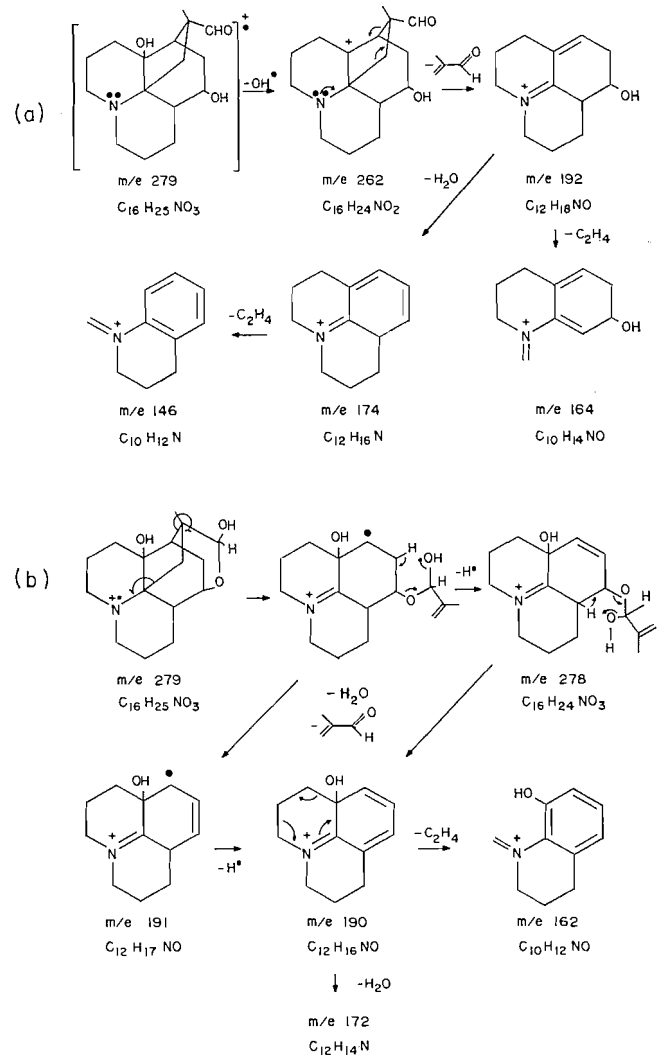
doublets as in the case of annotine and dihydroannotine. The ions of mass 150 and 152 may arise in a manner similar to that postulated for dihydroannotine.

TABLE III

Accurate mass measurement of dihydroannotinol

Measured mass	Error (obs. − calcd.) in milli mass units	Elemental composition	Mass difference from molecular ion
280.1863	−0.5	$C_{15}H_{25}{}^{13}C_1NO_3$	M+1
279.1821	−1.4	$C_{16}H_{25}NO_3$	M
278.1735	−2.2	$C_{16}H_{24}NO_3$	M-1
262.1782	−2.5	$C_{16}H_{24}NO_2$	M-17
192.1383	−0.6	$C_{12}H_{18}NO$	M-87
192.1057	3.3	$C_{11}H_{14}NO_2$	M-87
191.1297	−1.4	$C_{12}H_{17}NO$	M-88
190.1589	−0.6	$C_{13}H_{20}N$	M-89
190.1225	−0.7	$C_{12}H_{16}NO$	M-89
174.1259	−2.4	$C_{12}H_{16}N$	M-105
172.1101	−2.6	$C_{12}H_{14}N$	M-107
164.1403	−3.6	$C_{11}H_{18}N$	M-115
164.1042	−3.3	$C_{10}H_{14}NO$	M-115
162.1240	−4.3	$C_{11}H_{16}N$	M-117
162.0892	−2.7	$C_{10}H_{12}NO$	M-117
152.1061	−1.4	$C_9H_{14}NO$	M-127
150.1257	−2.6	$C_{10}H_{16}N$	M-129
150.0906	−1.3	$C_9H_{12}NO$	M-129
146.0952	−1.8	$C_{10}H_{12}N$	M-133

Can. J. Chem. Downloaded from www.nrcresearchpress.com by 210.87.254.6 on 09/05/12
For personal use only.

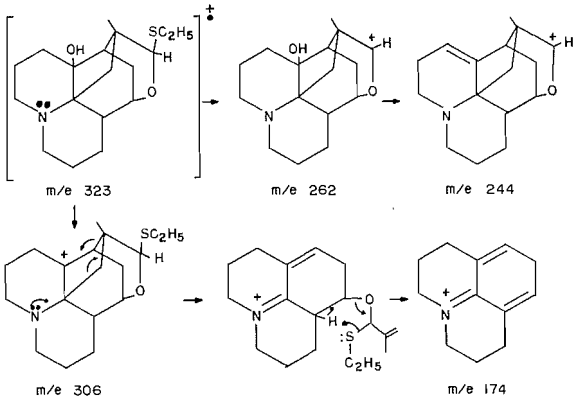


SCHEME 3.

Cleavage of the C—S bond is the dominant feature in the fragmentation of the thioethyl analogue of dihydroannotinol (1) (Fig. 2*b*). The peak at *m/e* 262 is by far the most intense in the spectrum. The peak at *m/e* 244 results from loss of water from the ion of mass 262. Metastable peaks are observed at *m/e* 213.0 (m^* calcd. $323 \rightarrow 262 = 212.5$) and 228.0 ($m^*$ calcd. $262 \rightarrow 244 = 227.2$) in accord with these changes. The peak at *m/e* 294 can be considered to arise by loss of the ethyl group from the molecular ion. Other peaks of low intensity are found at *m/e* 306 and 174; they probably arise by the already familiar process involving loss of the hydroxyl radical followed by expulsion of the bridge. These processes are illustrated in Scheme 4. A metastable peak is observed at 290.5 corresponding to the process $323 \rightarrow 306$ (m^* calcd. = 289.9).

A fourth derivative of annotine, whose spectrum (Fig. 3) is of considerable interest, is phenylannotine, to which we have assigned the structure shown. Instead of a lactone ring it contains a hemiketal function. In the solid state and in solution phenylannotine shows no carbonyl absorption. In the ion source of the mass spectrometer, however, it

Can. J. Chem. Downloaded from www.nrcresearchpress.com by 210.87.254.6 on 09/05/12
For personal use only.



SCHEME 4.

may well exist in the open-chain form as we have proposed for dihydroannitonol, and undergo fragmentation as such. Thus the ions of *m/e* 336, 190, 172, 162, and 144, shown in Scheme 5*a*, are postulated to arise from the open-chain form. The peaks at 352, 189, 188, 170, and 162 may form via Scheme 5*b* from the hemiketal form. The remaining peaks of high intensity which merit consideration are at *m/e* 105, which corresponds to the benzoyl cation, and at *m/e* 231, 230, and 214. The latter three peaks can best be accommodated if one invokes a fragmentation mechanism of the type shown in Scheme 5*c*.

Here again we have corroborated the composition of the ions by examination of the high-resolution spectrum. The data are shown in Table IV and include those ions discussed previously. It is observed that the peaks at *m/e* 188 and 162 are doublets of the

TABLE IV

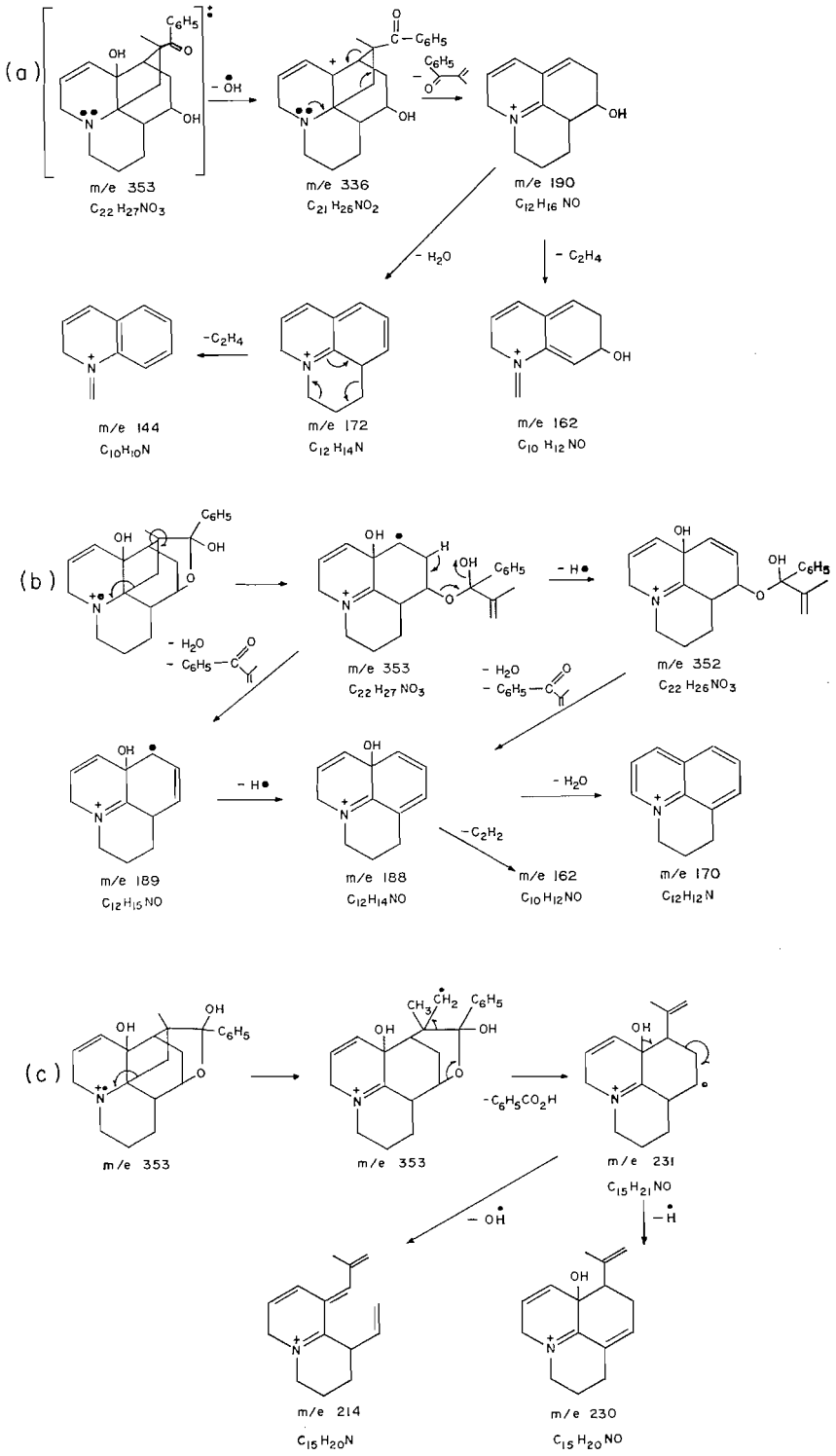
Accurate mass measurement of phenylannotine

Measured mass	Error (obs. − calcd.) in milli mass units	Elemental composition	Mass difference from molecular ion
354.2036	1.1	$C_{21}H_{27}{}^{13}C_1NO_3$	M+1
353.1973	−1.8	$C_{22}H_{27}NO_3$	M
352.1916	0.3	$C_{22}H_{26}NO_3$	M-1
336.1960	−0.4	$C_{22}H_{26}NO_2$	M-17
231.1596	−2.7	$C_{15}H_{21}NO$	M-122
230.1539	−0.6	$C_{15}H_{20}NO$	M-123
214.1598	0.2	$C_{15}H_{20}N$	M-139
190.1208	−2.4	$C_{12}H_{16}NO$	M-163
189.1135	−1.9	$C_{12}H_{15}NO$	M-164
188.1424	−1.5	$C_{13}H_{18}N$	M-165
188.1068	−0.7	$C_{12}H_{14}NO$	M-165
172.1113	−1.4	$C_{12}H_{14}N$	M-181
170.0966	−0.4	$C_{12}H_{12}N$	M-183
162.1257	−2.6	$C_{11}H_{16}N$	M-191
162.0895	−2.4	$C_{10}H_{12}NO$	M-191
144.0826	1.3	$C_{10}H_{10}N$	M-209

same composition as those in annotine. The loss of benzoic acid from phenylannotine is equivalent to loss of CO_2 in annotine, showing that the molecules fragment in an analogous manner in each system. Modification of the structure, however, as in phenylannotine, makes the formation of the ion of *m/e* 231 a much more favorable mode of fragmentation. The oxygen-free ions at *m/e* 188 and 162 in phenylannotine and in

Can. J. Chem. Downloaded from www.nrcresearchpress.com by 210.87.254.6 on 09/05/12
For personal use only.

Can. J. Chem. Downloaded from www.nrcresearchpress.com by 210.87.254.6 on 09/05/12
For personal use only.



SCHEME 5.

annotine may owe their origin to further fragmentation of the ions at *m/e* 231, 230, and 214. The oxygen-free ions at *m/e* 190 and 164 in dihydroannotine and dihydroannotinol may form in an analogous manner.

These results lend strong support to the proposal of structure I for annotine, since they provide evidence for the presence of a bridged hydrojulolidine skeleton in the alkaloid. Annotine and its derivatives lose the bridge carbon atoms in one of their major pathways of fragmentation and undergo further fragmentation to ions, appearing at *m/e* 170, 172, and 174, containing a $C_{12}N$ unit but differing in their hydrogen content. This behavior is analogous to that of other *Lycopodium* alkaloids having a bridged hydrojulolidine system (6).

EXPERIMENTAL

Apparatus, Methods, and Materials

The low-resolution spectra were recorded on a CEC21-103C mass spectrometer at an ionizing potential of 70 eV and an ionizing current of 50 μA. Samples were injected directly into the ion source by using a vacuum lock system. Peaks with an intensity $\geqslant 2\%$ of the most intense peak have been plotted. The high-resolution spectra were recorded on a CEC21-110 mass spectrometer. Spectra were measured by the method described by Biemann *et al.* (10).

The compounds used in this investigation were prepared according to methods described in a previous paper in this series (1).

ACKNOWLEDGMENTS

The authors are greatly indebted to Professor K. Biemann, Massachusetts Institute of Technology, in whose laboratory all spectra were recorded. Financial assistance from the National Research Council of Canada is gratefully acknowledged.

REFERENCES

1. W. A. Szarek, K. A. H. Adams, M. Curcumelli-Rodostamo, and D. B. MacLean. Can. J. Chem. **42**, 2584 (1964).
2. R. H. F. Manske and L. Marion. Can. J. Res., B, **21**, 92 (1943).
3. A. Bertho and A. Stoll. Chem. Ber. **85**, 663 (1952).
4. O. Achmatowicz and W. Rodewald. Roczniki Chem. **32**, 485 (1958).
5. G. S. Perry and D. B. MacLean. Can. J. Chem. **34**, 1189 (1956).
6. D. B. MacLean. Can. J. Chem. **41**, 2654 (1963).
7. W. A. Ayer and G. G. Iverach. Can. J. Chem. **42**, 2514 (1964).
8. S. N. Alam, K. A. H. Adams, and D. B. MacLean. Can. J. Chem. **42**, 2456 (1964).
9. W. A. Ayer, W. R. Bowman, P. Kebarle, and R. H. Burnell. Can. J. Chem. **43**, 328 (1965).
10. K. Biemann, P. Bommer, A. L. Burlingame, and W. J. McMurray. J. Am. Chem. Soc. **86**, 4624 (1964).

Can. J. Chem. Downloaded from www.nrcresearchpress.com by 210.87.254.6 on 09/05/12
For personal use only.

Can. J. Chem. Downloaded from www.nrcresearchpress.com by 210.87.254.6 on 09/05/12
For personal use only.

THE REACTION OF CARYOPHYLLENE AND DIAZOACETIC ESTER; SOME OBSERVATIONS ON CYCLOPROPANES

E. W. WARNHOFF AND V. DAVE
Department of Chemistry, University of Western Ontario, London, Ontario
Received October 20, 1965

ABSTRACT

The crystalline acid obtained in 1928 from saponification of the caryophyllene – diazoacetic ester reaction product has been found to be a 1:1 mixture of the stereoisomers V and VII. Compound III is an exception to the observation that cyclopropane CH bonds absorb in the 1.55–1.70 μ near-infrared region.

Addition of diazoacetic ester to caryophyllene (I) at 170° in the presence of copper has been reported (1) to yield a 1:1 reaction product whose saponification liberated an acid, $C_{17}H_{26}O_2$, m.p. 165°, $[\alpha]_{5460}$ −40°. The stated failure of this acid to decolorize bromine or to react rapidly with permanganate indicated the absence of double bonds, and, consequently, the presence of *four* rings. This remarkable result was in contrast to the reaction of isocaryophyllene with diazoacetic ester, which produced a normal cyclopropanecarboxylic ester with one double bond remaining (2). If the acid from caryophyllene were indeed saturated, it would require an unusual structure and genesis, and therefore merited reinvestigation.

Repetition of the reaction of diazoacetic ester with caryophyllene followed by saponification of the product gave in 17% yield an acid of constant m.p. 166.5–168°, $[\alpha]_{5460}$ −39.5°, presumably the compound described earlier (1). However, the acid rapidly decolorized both bromine in chloroform and aqueous permanganate solutions.* The presence of an unsymmetrically disubstituted double bond was demonstrated by infrared peaks at 1 650 and 896 cm^{-1} and by absorption (two protons) at δ 4.80–5.13 p.p.m. in the nuclear magnetic resonance (n.m.r.) spectrum (Fig. 1). Being unsaturated, the acid was most likely the normal cyclopropanecarboxylic acid II*a* from the reaction of the more nucleophilic and strained trisubstituted double bond.

In spite of the apparent purity of the acid, two features of the n.m.r. spectrum were not compatible with the acid being a single compound. Instead of the vinyl proton pattern being a pair of broad singlets, it had the appearance (Fig. 1) of two pairs of overlapping singlets, and the methyl group absorption at δ 1.1 p.p.m. was a closely spaced pair of peaks rather than a singlet. Such a spectrum could, however, be displayed by an approximately equimolar mixture of two stereoisomers of II*a*. Although the acid could not be separated into components by thin-layer chromatography or by attempted fractional crystallization from several solvents, its methyl ester was partially resolved into two peaks of about equal area on gas–liquid chromatography. Since saponification of this methyl ester mixture regenerated the original acid, the latter must consist of two isomers; this mixture of stereoisomers was used for the determination of structure and stereochemistry.

On catalytic reduction (Pd/C) the acid absorbed 1.01 mole equivalents of hydrogen. The resulting dihydroacid III (73% yield), which is also an approximately equimolar mixture of stereoisomers notwithstanding its narrow melting range, no longer had C=C

**Eventually, after the present work was completed, it became possible (through the kindness of Dr. D. T. Gibson) to compare the acid with that prepared earlier (1). The two were identical and both gave positive tests with bromine and permanganate solutions (see Experimental).*

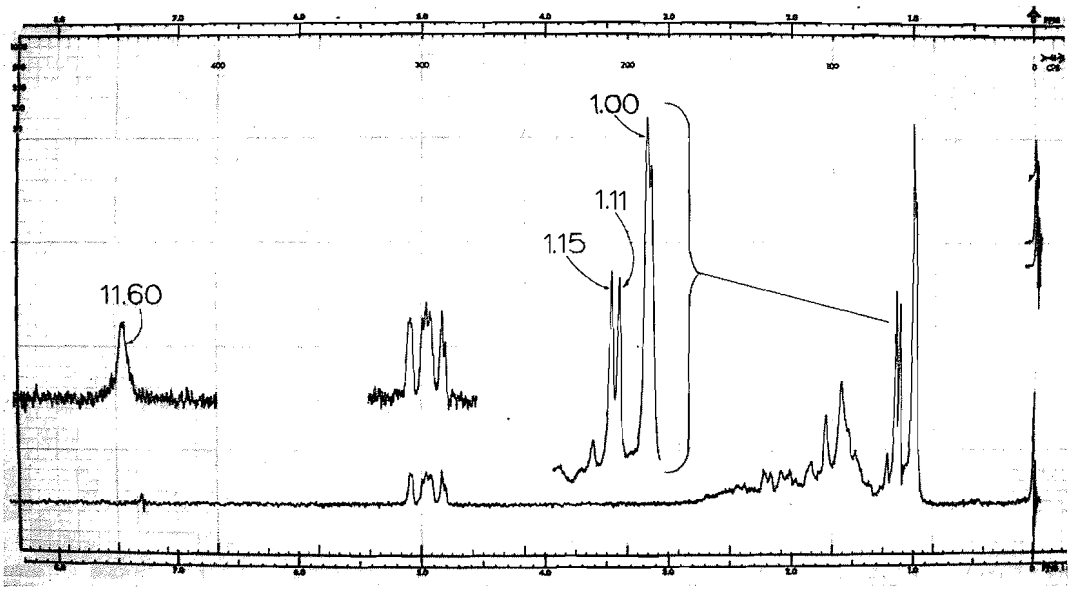
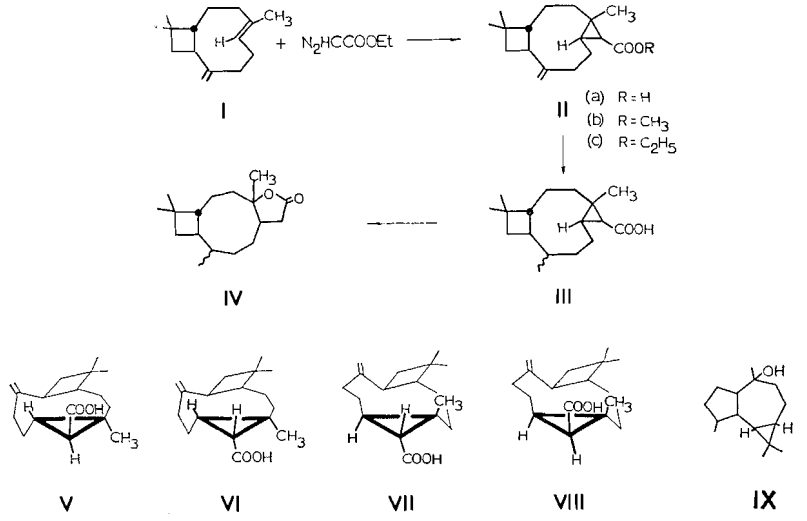


FIG. 1. The n.m.r. spectrum of the crystalline acid from the reaction of caryophyllene and diazoacetic acid.

double bond infrared absorption or vinyl hydrogen n.m.r. absorption, and did not react with bromine in carbon tetrachloride or with permanganate in aqueous acetone. The n.m.r. spectrum of III contained two overlapping doublets at δ 0.82 p.p.m. ($J \sim 6$ c.p.s.) and δ 0.87 p.p.m. ($J \sim 6$ c.p.s.) from the CH_3—CH groups generated, as well as two peaks at δ 1.15 and 1.27 p.p.m. from the quaternary cyclopropane methyl groups of the two stereoisomers.

Physical evidence for the presence of a cyclopropane ring conjugated with the carboxyl group includes the position of the carbonyl infrared peak in the series of compounds (1 700 cm^{-1} in acid II*a*, 1 690 cm^{-1} in dihydroacid III, 1 726 cm^{-1} in ethyl ester II*c*, and



Can. J. Chem. Downloaded from www.nrcresearchpress.com by 210.87.254.6 on 09/05/12
For personal use only.

1 715 cm^{-1} in methyl ester II*b*), and the ultraviolet end absorption (ϵ_{220} 290, ϵ_{210} 544) of dihydroacid III. On the other hand, while it is not unusual for cyclopropane C—H bonds to absorb at lower field than δ = 0–1 p.p.m. in n.m.r. spectra (3), dihydroacid III did not have any peak in the 1.55–1.70 μ near-infrared region (Fig. 2) attributable to the first overtone of the cyclopropane C—H stretching vibration. Although this spectral correlation has been found to be valid for all cyclopropanes containing at least one methylene group (4), it has been noted that cyclopropanes containing methine groups but no methylene group may not exhibit a recognizable near-infrared absorption peak (4*d*, 4*e*). In agreement, we find that ledol (IX) has no peak between 1.55 and 1.70 μ. Therefore, the interpretation of the absence of peaks in the 1.6 μ spectral region as being indicative of the absence of cyclopropane hydrogen bonds must be treated with reserve.

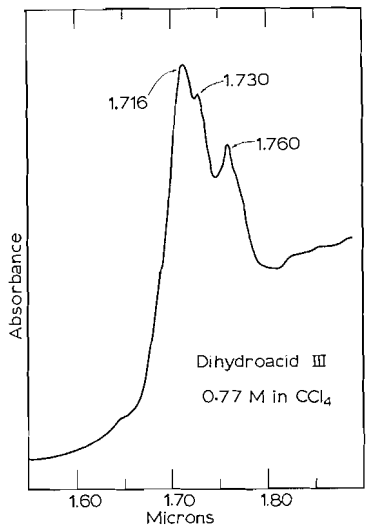


FIG. 2. The near-infrared spectrum of dihydroacid III.

Chemical evidence for the cyclopropane ring was provided by ring opening at room temperature with hydrobromic acid to produce from dihydroacid III the expected (5, 6) saturated γ-lactone IV, $\nu_{C=O}^{CHCl_3}$ 1 760 cm^{-1}. The attachment of the lactone oxygen atom to the carbon atom bearing the methyl group is supported by the singlet (3H) at δ 1.24 p.p.m. in the n.m.r. spectrum. Although both the acid II*a* and the dihydroacid III are known to be mixtures of stereoisomers, the lactone is probably a single pure compound, since the unsaturated acids in equilibrium with the lactone permit the epimerization of both asymmetric centers of the lactone ring, and since on gas–liquid chromatography the lactone gave a single peak.

Assignment of stereochemistry to the two isomers comprising the acid may be made on the following basis. Since the excess caryophyllene recovered from the reaction with diazoacetic ester is identical with the starting material, no isomerization of the *trans* double bond has occurred, and therefore the *trans* arrangement of groups is probably retained in the cyclopropane acid. There is ample precedent for preservation of double bond configuration in the reaction of *cis*- and *trans*-2-butene (7), *cis*- and *trans*-4-octene (8), *cis*-5-decene (9), and *cis*- and *trans*-stilbene (8) with diazoacetic ester under similar conditions. The possible isomers are then limited to two pairs of cyclopropanecarboxylic

Can. J. Chem. Downloaded from www.nrcresearchpress.com by 210.87.254.6 on 09/05/12
For personal use only.

acids (V and VI, VII and VIII) formed by addition to the two non-equivalent faces of the *trans* double bond. By analogy with known substituted cyclopropanes, such as the 2-methylcyclopropanecarboxylic acids (10) and the 2-phenylcyclopropanecarboxylic acids (11), each of the acids VI and VIII with the carboxyl and methyl groups *cis* will be appreciably less stable than its epimeric acid V or VII with the *trans* arrangement of these substituents. Of the six possible pairings of the four stereoisomers, V + VI and VII + VIII should be largely epimerizable at the α-position of the acid or its derivative to one of the original components; V + VIII, VI + VII, and VI + VIII should be epimerizable to a mixture containing one or two components not present in the starting material; only V + VII might remain almost unchanged.

When the methyl ester of the acid isomers was refluxed with sodium methoxide in methanol-O-d_1, the recovered ester contained deuterium, thus proving that the α-proton of the ester had been removed, but the composition of the ester was the same as that of the starting material (within experimental error). Therefore, both methyl esters must possess the more stable configuration at the α-carbon atom, and the acid II*a* is most likely a mixture of the *trans* stereoisomers V and VII. Both of these isomers are present in the original diazoacetic ester reaction product, along with two or three other isomers, and were not formed during saponification of the ethyl ester, because hydrolysis of the ethyl ester II*c* with sodium deuteriooxide in dioxane gave acid II*a* containing no deuterium bound to carbon. With no removal of the α-proton occurring during saponification, the stereochemistry of the acid isomers must be the same as that present in the original esters. It is satisfying that these two stereoisomers, which together constituted more than half of the acid mixture, are those expected on the basis of the empirical rule that reaction of diazoacetic esters with double bonds usually occurs to give, as the major cyclopropane product, that isomer in which the carboalkoxy group is subject to the fewest repulsive non-bonded interactions. This generalization is based, *inter alia*, on the examples of *cis*-stilbene (8), *cis*-2-butene (7), *cis*-4-octene (8), cyclohexene (12), styrene (11, 13), 1,3-cyclohexadiene (14), cyclopentadiene (15), and phenanthrene (16). *cis*-5-Decene (9) would appear to be an exception in which the products are formed in nearly equal amounts (57% *cis*, 43% *trans*).

EXPERIMENTAL

General

Melting points were determined on a Reichert microscope hot stage and are corrected.

Optical rotations were measured on a Rudolph model 80 polarimeter with a 1 dm tube, in 95% ethanol solutions unless otherwise specified.

Infrared spectra were carried out on a Beckman IR-5 or IR-7 spectrometer, near-infrared spectra on a Beckman model DK-1 spectrometer with carbon tetrachloride solutions, ultraviolet spectra on a Bausch and Lomb Spectronic 505 spectrometer, and nuclear magnetic resonance spectra on a Varian A-60 spectrometer with deuteriochloroform solutions.

Thin-layer chromatography was performed with Camag Kieselgel DF-5 silica gel. R_f values quoted were taken from one plate developed in petroleum ether – acetic acid (92:8) on which all compounds were present. For detection, plates were sprayed with concentrated sulfuric acid – concentrated nitric acid (1:1) and heated.

Analyses were carried out by Dr. A. Bernhardt and associates, Mülheim, Germany. Combustion deuterium analyses by the falling-drop method were by Josef Nemeth, Urbana, Illinois.

Petroleum ether refers to the fraction boiling at 35–60°.

Methanol-O-d_1 was prepared by deuterium oxide hydrolysis of methyl orthoformate according to a procedure for the preparation of ethanol-O-d_1 (17). The product was estimated to be 98% methanol-O-d_1 from its n.m.r. spectrum.

Caryophyllene was obtained by fractional distillation of saponified clove bud terpenes and had b.p. 120° at 10 mm, $[\alpha]_{21}^{D}$ −9.38° (neat).

Reaction of Caryophyllene and Diazoacetic Ester

To a mixture of 30 g of *trans*-caryophyllene ($[\alpha]_{D}^{21}$ −9.38° (neat)) and 1 g of copper powder (British Drug

Can. J. Chem. Downloaded from www.nrcresearchpress.com by 210.87.254.6 on 09/05/12
For personal use only.

Houses, precipitated) heated to 165–170° was added dropwise a solution of 5.00 g of ethyl diazoacetate (18) in 5.0 g of *trans*-caryophyllene at such a rate that vigorous nitrogen evolution and a temperature around 170° were maintained. When the addition was complete after 20 min, the mixture was maintained at 165–170° for 30 min more. The copper was removed by filtration and the filtrate fractionally distilled through a 1 m Nester and Faust spinning spiral column. There was collected 23 g (66% recovery) of *trans*-caryophyllene, $[\alpha]_D^{21}$ −9.4° (neat), b.p. 121–123° at 10.5 mm. The ethyl ester II*c* distilled at 135–160° and 2 mm; 7.5 g (59% yield based on the diazoester); $[\alpha]_D$ −12.7° (*c*, 2.74); $\nu_{max,\,IR\text{-}7}^{CCl_4}$ 1 726 (C=O), 1 637 (C=C), and 892 cm^{-1} (C=CH$_2$); $\epsilon_{215}^{95\%\ EtOH}$ 3 490.

Anal. Calcd. for $C_{19}H_{30}O_2$ (290.43): C, 78.57; H, 10.41. Found: C, 76.75; H, 9.89.

Gas–liquid chromatography of this product on a 3 m column of 4% SE-30 supported on 100–120 mesh Gas Chrom P at 198° in an all-glass apparatus gave two major peaks of retention times 5.0 and 5.8 min and an overlapping minor peak of retention time 6.4 min.

Unsaturated Acid (IIa)

(*a*) A solution of 5.00 g of the ethyl ester from the previous experiment in 30 ml of 5% ethanolic potassium hydroxide was refluxed for 3 h. The reaction mixture was diluted with water and washed with ether. Acidification of the aqueous layer and extraction with ether yielded 3.90 g of slightly yellow, oily crystals. Several recrystallizations from methanol and ethanol gave 0.80 g (17%) of colorless needles, m.p. 166.5–168°, $[\alpha]_{5460}^{23.5}$ −39.5° (*c*, 1.39), $[\alpha]_D^{23}$ −32.6° (*c*, 2.10), R_f 0.63 (lit. (1): m.p. 165°, $[\alpha]_{5460}$ −40° (alcohol)); $\epsilon_{210}^{95\%\ EtOH}$ 3 524; $\nu_{max,\,IR\text{-}5}^{CHCl_3}$ 1 700 (C=O), 1 650 (C=C), and 896 cm^{-1} (C=CH$_2$). Nuclear magnetic resonance spectrum: δ 0.99 and 1.00 p.p.m. (2s, 6H, *gem*-dimethyl), 1.11 and 1.15 p.p.m. (2s, 3H, CH$_3$—▽), 4.80–5.13 p.p.m. (m, 2H, C=CH$_2$), and 11.60 p.p.m. (s, 1H, COOH).

Anal. Calcd. for $C_{17}H_{26}O_2$ (262.38): C, 77.82; H, 9.99. Found: C, 77.87; H, 9.87; neutral equiv. 260.

Dropwise addition of 5% bromine in carbon tetrachloride solution to the acid dissolved in chloroform gave immediate decolorization. When 2% aqueous potassium permanganate solution was added to the acid dissolved in acetone, the purple color changed within 20 s, but there was no observable change in an acetone blank.

A sample of the acid prepared by Gibson (1) from supa oil caryophyllene and found by him to be identical with the acid from clove bud caryophyllene was compared with the above acid. The melting points (165.5–167°) and infrared and n.m.r. spectra were identical. There was no depression in the melting point of a mixture of the two acids.

(*b*) To a solution of 0.40 g of sodium in a mixture of 4 ml of deuterium oxide (>99%) and 7 ml of dioxane was added 0.47 g of the distilled mixture of ethyl esters from the caryophyllene – diazoacetic ester reaction. The reaction mixture was refluxed for 7 days, diluted with water, and extracted with ether. Acidification of the aqueous layer precipitated 0.45 g (106%) of crystalline acid which, after recrystallization from methanol, had m.p. 164–165.5° (35 mg). The infrared spectrum and R_f were identical with those of II*a*.

Anal. Calcd. for $C_{17}H_{25}DO_2$: D, 3.85 atom % excess. Found: D, 0.00 atom % excess.

Dihydro Acid III

(*a*) A mixture of 40 mg of 5% palladium on carbon catalyst (MCB) and 4 ml of absolute ethanol was equilibrated with hydrogen. Addition of 16.5 mg (0.063 mmole) of unsaturated acid II*a* resulted in the uptake of 1.73 ml (1.01 mole equivalents) of hydrogen at 27° and 738 mm.

(*b*) A mixture of 225 mg of 5% palladium on carbon catalyst and 100 ml of absolute ethanol was equilibrated with hydrogen. Then 1.90 g of the unsaturated acid II*a* was added and the reaction mixture shaken until hydrogen uptake ceased. The solution was evaporated to dryness after the catalyst had been removed by filtration, and the residue was recrystallized twice from methanol to yield 1.40 g (73%) of colorless needles of dihydroacid III, m.p. 152–154°, $[\alpha]_D^{23}$ +23.9° (*c*, 2.06), R_f 0.66, $\epsilon_{210}^{95\%\ EtOH}$ 544, $\nu_{max,\,IR\text{-}7}^{CCl_4}$ 1 690 cm^{-1} (C=O). Nuclear magnetic resonance spectrum: δ 0.82 and 0.87 p.p.m. (2d, $J \sim 6$ c.p.s., 3H, CH$_3$—CH), 0.96 p.p.m. (s, 6H, two unsplit methyls), 1.15 and 1.27 p.p.m. (2s, 3H, CH$_3$—▽), and 11.33 p.p.m. (s, 1H, COOH).

Anal. Calcd. for $C_{17}H_{28}O_2$ (264.39): C, 77.22; H, 10.67. Found: C, 77.23; H, 10.36.

Methyl Ester IIb

To a solution of 350 mg of acid II, m.p. 166.5–168°, in 5 ml of ether was added an ethereal solution of diazomethane at room temperature with stirring. Excess diazomethane was destroyed with a few drops of acetic acid. The ethereal solution was washed with 10% aqueous bicarbonate, water, and saturated sodium chloride solution, and then dried over magnesium sulfate. Evaporation of the ether left 320 mg (89%) of pale yellow oil which was distilled in a tube at 150° and 0.1 mm; $[\alpha]_D^{25}$ −32.8 ± 1.5° (*c*, 1.89); R_f 0.82; $\nu_{max,\,IR\text{-}5}^{CHCl_3}$ 1 715 (C=O), 1 635 (C=C), and 892 cm^{-1} (C=CH$_2$). Nuclear magnetic resonance spectrum: δ 0.98 and 1.00 p.p.m. (2s, 6H, *gem*-dimethyl), 1.09 and 1.12 p.p.m. (2s, 3H, CH$_3$—▽), 3.64 p.p.m. (s, 3H, OMe), and 4.75–5.02 p.p.m. (m, 2H, C=CH$_2$).

Anal. Calcd. for $C_{18}H_{28}O_2$ (276.40): C, 78.21; H, 10.21. Found: C, 77.71; H, 10.03.

Gas–liquid chromatography on a 2 m column of 1% SE-30 supported on 100–120 mesh Gas Chrom P at 147° in an all-glass apparatus gave two partially resolved peaks of approximately equal area and with retention times 9.09 and 9.47 min.

Can. J. Chem. Downloaded from www.nrcresearchpress.com by 210.87.254.6 on 09/05/12
For personal use only.

A solution of 320 mg of the methyl ester in 5 ml of 5% ethanolic potassium hydroxide was refluxed for 6 h. The reaction mixture was diluted with water and washed with ether. Acidification of the aqueous layer and extraction with ether gave 296 mg of crystalline acid. One recrystallization from methanol yielded 282 mg (93% recovery) of colorless needles of II*a*, m.p. 166–168°, $[\alpha]_D^{24.5}$ −32.9° (*c*, 2.08), R_f 0.63.

Dihydrolactone IV

Hydrogen bromide gas was slowly passed for 2 h into a solution of 1.40 g of dihydroacid III, m.p. 149–153°, in 20 ml of glacial acetic acid. After the reaction mixture had been kept at room temperature for 34 h more, the acetic acid was evaporated at reduced pressure. The residual brown oil was dissolved in ether and the acids removed by extraction with 10% sodium carbonate solution. Removal of ether from the dried solution left 1.08 g (77%) of yellowish-brown oily crystals. Sublimation at 100–110° and 0.1 mm followed by recrystallization from methanol, ethanol, and finally ethyl acetate gave colorless prisms, m.p. 143.5–145°, $[\alpha]_D^{22.5}$ −19.9° (*c*, 1.75), R_f 0.36, $\epsilon_{215}^{95\%\ EtOH}$ 49, $\nu_{max,\ IR\text{-}5}^{CHCl_3}$ 1 760 cm^{-1} (γ-lactone C=O). Nuclear magnetic resonance spectrum: δ 0.89 p.p.m. (d, $J \sim 7$, 3H, CH_3—CH), 0.97 and 1.00 p.p.m. (2s, 6H, *gem*-dimethyl), and 1.24 p.p.m. (s, 3H, CH_3—C—O).

Anal. Calcd. for $C_{17}H_{28}O_2$ (264.39): C, 77.22; H, 10.67. Found: C, 76.79; H, 10.65.

Gas–liquid chromatography on a 2 m column of 2% SE-33 supported on 80–100 mesh Gas Chrom A at 200° in an all-glass apparatus gave a single symmetrical peak of retention time 0.91 min.

Attempts to open the cyclopropane ring of III by treatment in chloroform solution with anhydrous hydrogen chloride at room temperature and at reflux were unsuccessful; starting material was recovered.

Attempted Epimerization

(*a*) *Deuterium exchange.*—To a solution of 0.5 g of sodium metal dissolved in 10 ml of dry methanol-O-d_1 was added 1.10 g of methyl ester II*b* prepared from pure acid II*a*. The reaction mixture was protected from moisture, refluxed for 24 h, cooled, and diluted with ether. The ethereal solution was washed with 10% aqueous sodium carbonate, water, and saturated aqueous sodium chloride, and then dried over magnesium sulfate. Evaporation of the ether left 0.95 g (86% recovery) of liquid which was distilled at 140–150° and 2 mm, $[\alpha]_D^{23}$ −29.7° ± 1.5° (*c*, 1.93).

Anal. Calcd. for $C_{18}H_{27}DO_2$: D, 3.57 atom % excess. Found: D, 2.63 atom % excess.

The n.m.r. spectrum of the product could not be distinguished in appearance from that of the starting material. Gas–liquid chromatography on a 2 m column of 2% SE-33 supported on 80–100 mesh Gas Chrom A at 140° in an all-glass apparatus gave two partially resolved peaks of retention times 3.50 and 3.68 min, unchanged on 1:1 admixture with untreated methyl ester.

(*b*) To a solution of 1 g of sodium in 20 ml of dry methanol was added 1.20 g of not quite pure methyl ester II*b*, $[\alpha]_D^{26.5}$ −25.0° ± 1° (*c*, 2.29). The solution was refluxed for 2 h, cooled, diluted with water, acidified, and extracted with ether. The organic layer was washed with aqueous sodium bicarbonate, dried, and concentrated to remove the ether. There remained 0.890 g of light tan oil which was distilled at 115° and 0.1 mm, $[\alpha]_D^{24}$ −27.2° ± 2° (*c*, 1.87).

The n.m.r. spectrum of the product could not be distinguished in appearance from that of the starting material. The gas–liquid chromatogram was identical with that of pure methyl ester II*b*, except for the presence of a minor impurity which was also present in the starting material used for this experiment.

ACKNOWLEDGMENTS

We thank Dr. D. T. Gibson for supplying an authentic sample of acid II*a*, and the National Research Council for financial support. The gas–liquid chromatograms were kindly run by Mrs. P. F. Highet, National Institutes of Health, Bethesda, Maryland.

REFERENCES

1. D. T. Gibson. J. Chem. Soc. 750 (1928). J. Simonsen and D. H. R. Barton. The terpenes. Vol. III. Cambridge University Press, London. 1952. p. 71.
2. E. Deussen and P. Hacker. J. Prakt. Chem., Ser. 2, **117**, 282 (1927).
3. W. G. Dauben and R. L. Cargill. Tetrahedron, **15**, 197 (1961). H. Weitkamp, U. Hasserodt, and F. Korte. Chem. Ber. **95**, 2280 (1962).
4. (*a*) W. H. Washburn and M. J. Mahoney. J. Am. Chem. Soc. **80**, 504 (1958). (*b*) P. G. Gassman. Chem. Ind. London, 740 (1962). (*c*) P. G. Gassman and W. M. Hooker. J. Am. Chem. Soc. **87**, 1079 (1965). (*d*) H. Weitkamp and F. Korte. Tetrahedron, **20**, 2125 (1965). (*e*) L. Skattebøl. Personal communication.
5. E. P. Kohler and J. B. Conant. J. Am. Chem. Soc. **39**, 1404 (1917).
6. J. Meinwald, A. Lewis, and P. G. Gassman. J. Am. Chem. Soc. **84**, 979 (1962). R. R. Sauers and P. E. Sonnet. Tetrahedron, **20**, 1032 (1964).
7. W. von E. Doering and T. Mole. Tetrahedron, **10**, 65 (1960).
8. I. A. D'Yakonov, M. I. Komendantov, F. Gui-Siya, and G. L. Korichev. J. Gen. Chem. USSR Engl. Transl. **32**, 917 (1962).

Can. J. Chem. Downloaded from www.nrcresearchpress.com by 210.87.254.6 on 09/05/12
For personal use only.

9. I. A. D'YAKONOV and R. R. KOSTIKOV. J. Gen. Chem. USSR Engl. Transl. **34**, 1385 (1964).
10. D. E. APPLEQUIST and A. H. PETERSON. J. Am. Chem. Soc. **82**, 2372 (1960).
11. H. L. DE WAAL and G. W. PEROLD. Chem. Ber. **85**, 574 (1952).
12. P. S. SKELL and R. M. ETTER. Proc. Chem. Soc. 443 (1961).
13. A. BURGER and W. L. YOST. J. Am. Chem. Soc. **70**, 2198 (1948).
14. J. A. BERSON and E. S. HAND. J. Am. Chem. Soc. **86**, 1978 (1964).
15. P. BESINET, R. FRAISSE, R. JACQUIER, and P. VIALLEFONT. Bull. Soc. Chim. France, 1377 (1960). B. FOHLISCH. Chem. Ber. **97**, 88 (1964).
16. G. E. HALL and J. P. WARD. Tetrahedron Letters, **8**, 437 (1965).
17. V. J. SHINER and M. L. SMITH. J. Am. Chem. Soc. **83**, 598 (1961).
18. E. B. WOMACK and A. B. NELSON. Org. Syn. **24**, 56 (1944).

Can. J. Chem. Downloaded from www.nrcresearchpress.com by 210.87.254.6 on 09/05/12
For personal use only.

Can. J. Chem. Downloaded from www.nrcresearchpress.com by 210.87.254.40 on 09/05/12
For personal use only.

UTILIZATION OF SULFUR

SYNTHESIS OF SYMMETRICAL THIIRANES FROM KETOHYDRAZONES

N. LATIF, I. FATHY, N. MISHRIKY, AND B. HAGGAG
National Research Center, Cairo, United Arab Republic

Received July 13, 1965

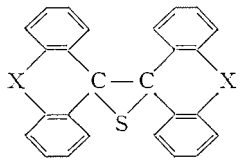
ABSTRACT

Dispiro(xanthene-9,2′-thiirane-3′,9″-xanthene), dispiro(thioxanthene-9,2′-thiirane-3′,9″-thioxanthene), epithiobidiphenyleneethane, epithiotetraphenylethane, epithiotetra-*p*-anisylethane, and epithiotetra-*p*-tolylethane are directly synthesized by the base-catalyzed interaction of the corresponding ketohydrazones, elemental sulfur, and yellow mercuric oxide. The reaction mechanism is discussed. Epithiotetra-*p*-tolylethane is also obtained by the uncatalyzed reaction of sulfur with the corresponding diazoalkane.

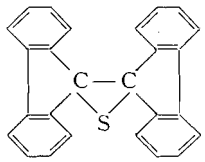
The successful use of thiiranes in industry and biology stimulated various authors to investigate the chemistry of this group of compounds in more detail. Thiiranes are usually prepared by the action of diazoalkanes on thioketones (1). Recently, it has been reported that diazoalkanes react with sulfur to give the corresponding thiiranes (2); however, the instability and the inaccessibility of some of the diazo compounds limited the usefulness of this method.

In the present study, the synthesis of symmetrical thiiranes is brought about directly from the readily available and stable ketohydrazones, thus obviating the necessary preparation of the diazoalkanes and thioketones (3). Thus, dispiro(xanthene-9,2′-thiirane-3′,9″-xanthene) (I*a*), dispiro(thioxanthene-9,2′-thiirane-3′,9″-thioxanthene) (I*b*), epithiobidiphenyleneethane (II), epithiotetraphenylethane (III*a*), epithiotetra-*p*-anisylethane (III*b*), and epithiotetra-*p*-tolylethane (III*c*) are produced when the corresponding ketohydrazones are allowed to react with elemental sulfur and yellow mercuric oxide in boiling ether or benzene, and in the presence of ethanolic potassium hydroxide. The corresponding ketazines are also produced in this reaction. In the absence of mercuric oxide and (or) alkali, the episulfides are not obtained. The dimethoxybenzophenone azine, which is produced in the experiment with *p*,*p*′-dimethoxybenzophenone hydrazone, is found to be yellow and melts at 184°, whereas Staudinger and Kupfer (4) reported that the azine is violet and melts at 124°. The structure of the product obtained in the present investigation is supported by analytical data and is rigorously confirmed by the fact that it is synthesized by three established procedures: (*a*) by oxidizing the hydrazone with mercuric oxide in benzene, (*b*) by heating *p*,*p*′-dimethoxydiphenyldiazomethane above its melting point, and (*c*) by fusing the ketone with the hydrazone at 160–170°. It is known that *p*-substituted benzophenone azines are generally high-melting yellow products. The sulfides I*a*, I*b*, II, III*a*, III*b*, and III*c* have been obtained previously by other methods (2, 5). III*c* is now also obtained by the uncatalyzed reaction of sulfur with di-*p*-tolyldiazomethane. The thiiranes are desulfurized by copper bronze or Raney nickel to give the corresponding ethylenes; however, the use of Raney nickel usually gives better yields of the pure ethylenes.

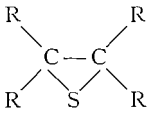
It is believed that the direct production of thiiranes from ketohydrazones may proceed through the intermediate formation of the corresponding diazoalkane VII. The latter gives the corresponding thioketone through its nucleophilic attack on sulfur and the simultaneous splitting off of nitrogen. The thioketone reacts further with another molecule



Ia, X = O Ib, X = S



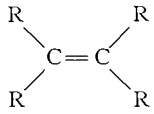
II



IIIa, R = 

IIIb, R = CH_3O 

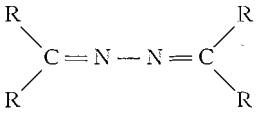
IIIc, R = CH_3 



IVa, R = 

IVb, R = CH_3O 

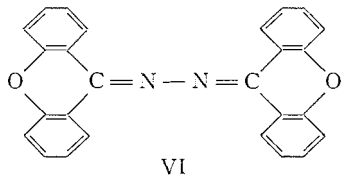
IVc, R = CH_3 



Va, R = 

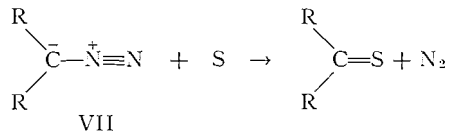
Vb, R = CH_3O 

Vc, R = CH_3 

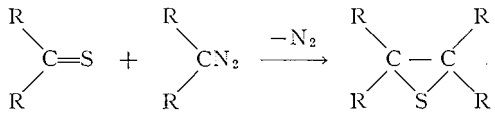


VI

of the diazo compound to give the cyclic sulfide (cf. Reaction Scheme 1). It has been pointed out (6) that the S—S bonds in sulfur and organic polysulfides are readily broken by nucleophilic reagents. The production of the corresponding diazo compound as an intermediate is evidenced by the fact that its characteristic color is developed during the reaction, and in some experiments it has been isolated from the reaction mixture.



VII



REACTION SCHEME 1.

The alternative mechanism which might suggest itself is that the diazoalkane first splits off nitrogen to give a carbene which then coordinates with sulfur to give the thioketone (2). Production of the carbene as an intermediate is usually accompanied by the formation of the corresponding ethylene as a by-product; however, the ethylenes are not produced in this reaction, except in the case of fluorenone hydrazone, where it is presumably formed through the decomposition of the first-formed sulfide. It is found that II decomposes easily during crystallization from benzene. A polar, rather than a free-radical,

Can. J. Chem. Downloaded from www.nrcresearchpress.com by 210.87.254.40 on 09/05/12
For personal use only.

mechanism is also strongly supported by the fact that the reaction is remarkably retarded by benzoyl peroxide, which is a free-radical initiator, and that it is uncatalyzed by sunlight. Addition of an aqueous dimethylamine solution instead of alkali also catalyzes the reaction, but a lower yield is obtained. The presence of heteroatoms having mobile unshared electron pairs, or electron-releasing substituents, which increase the nucleophilic character (basicity) of the diazoalkane carbanion VII, enhances the reaction. Thus, better yields of the sulfides are obtained with xanthone or thioxanthone rather than with fluorenone hydrazone. With substituted benzophenone hydrazones, the best yield is obtained in the case of the dimethoxy derivative.

EXPERIMENTAL

Melting points were not corrected. Microanalyses were performed by A. Bernhardt, Germany, and the Microanalyses Unit, National Research Center, Cairo.

Preparation of Dispiro(xanthene-9,2′-thiirane-3′,9″-xanthene) (Ia)

Freshly prepared ethanolic potassium hydroxide solution (0.5 ml) was added to a suspension of xanthone hydrazone (2 g), yellow mercuric oxide (4 g), and powdered sulfur (0.5 g) in dry ether (30 ml). The mixture was boiled under reflux for 6 h, the green ethereal solution was filtered while hot, the black residue was extracted with boiling acetone, and the acetone extract was concentrated and left to cool. The solid that was obtained (0.52 g) was recrystallized from acetone to give dispiro(xanthene-9,2′-thiirane-3′,9″-xanthene), m.p. 206–207 °C (undepressed when admixed with an authentic sample (2)).

The residue that was left after the acetone extraction was extracted with boiling xylene, the extract was concentrated and left to cool, and the separated crystals were shown to be xanthone azine (VI) (m.p. and mixed m.p. 285°).

When the reaction was repeated with a 20–25% aqueous dimethylamine solution instead of potassium hydroxide, I*a* was produced.

Preparation of Dispiro(thioxanthene-9,2′-thiirane-3′,9″-thioxanthene) (Ib)

Thioxanthone hydrazone was allowed to react with sulfur and mercuric oxide as above. The product that was obtained (0.48 g) was shown to be dispiro(thioxanthene-9,2′-thiirane-3′,9″-thioxanthene) (its infrared spectrum is identical with that of an authentic sample (2)).

Preparation of Epithiobidiphenyleneethane (II)

Fluorenone hydrazone (2 g), yellow mercuric oxide (4 g), and sulfur (0.5 g) were allowed to react in boiling dry benzene (20 ml) for 6 h. The red-brown reaction mixture was filtered while hot and evaporated to dryness, and a few milliliters of acetone was added to the residue. The separated solid (0.17 g) was shown to be epithiobidiphenyleneethane, m.p. 162–163° (undepressed when admixed with an authentic sample (2)). The filtrate was concentrated and cooled, and the separated solid (0.34 g) was shown to be bidiphenyleneethylene (melting point and mixed melting point). The mother liquor was evaporated to dryness, a few milliliters of ether was added to the oily residue, and the solution was cooled. The solid that separated (0.7 g) was shown to be 9-diazofluorene (melting point and mixed melting point).

When the reaction was carried out in dry ether instead of benzene, a small amount of II only was obtained.

Preparation of Epithiotetraphenylethane (IIIa)

The reaction was carried out as above. The violet benzene solution was filtered while hot, concentrated, and left to cool. The separated solid (0.35 g) was shown to be epithiotetraphenylethane (2) (m.p. and mixed m.p. 178°). The mother liquor was evaporated to dryness, a few milliliters of methanol was added, and the solid that was obtained was shown to be diphenyl ketazine (V*a*).

When the reaction was carried out with a dimethylamine solution instead of potassium hydroxide, III*a* was obtained.

When III*a* was heated under reflux with Raney nickel in ethanol, tetraphenylethylene (IV*a*), m.p. 222–224° (undepressed when admixed with an authentic sample), was obtained.

Preparation of p,p′-Dimethoxybenzophenone Azine (Vb)

Method A

p,p′-Dimethoxybenzophenone hydrazone (1 g) and yellow mercuric oxide (2 g) in dry benzene (15 ml) were heated under reflux for 6 h. The violet reaction mixture was filtered while hot, concentrated, and left to cool. The separated solid was crystallized from acetone to give the azine as yellow crystals, m.p. 182–184 °C.

Anal. Calcd. for $C_{30}H_{28}N_2O_4$: C, 74.98; H, 5.87; N, 5.83. Found: C, 74.64; H, 6.10; N, 5.02.

Method B

p,p′-Dimethoxydiphenyldiazomethane (0.2 g) was heated at 150 °C (bath temperature) for 1 h and left to cool. The yellow solid that was obtained was extracted with boiling acetone, and was proved to be the azine (melting point and mixed melting point).

Can. J. Chem. Downloaded from www.nrcresearchpress.com by 210.87.254.40 on 09/05/12
For personal use only.

Method C

A mixture of *p,p'*-dimethoxybenzophenone (0.5 g) and the corresponding hydrazone (0.5 g) was heated at 160–170 °C for 3 h. The reaction mixture was left to cool, and the yellow product that was formed was crystallized from acetone and shown to be the azine (melting point and mixed melting point).

Preparation of Epithiotetra-p-anisylethane (IIIb)

A mixture of *p,p'*-dimethoxydiphenyldiazomethane (1 g) and sulfur (0.25 g) in dry ether (25 ml) was heated under reflux for 3 h. The reaction mixture was filtered off, and the residue was extracted with boiling ether. The ether extract was concentrated and cooled, and the separated solid (0.45 g) was crystallized from benzene to give epithiotetra-*p*-anisylethane as colorless crystals, m.p. 220–222°.

Anal. Calcd. for $C_{30}H_{28}O_4S$: C, 74.38; H, 5.78; S, 6.61. Found: C, 74.57; H, 5.91; S, 6.45.

This compound, when heated under reflux with Raney nickel in ethanol, gave tetra-*p*-anisylethylene (IV*b*), m.p. 186–188°.

Anal. Calcd. for $C_{30}H_{28}O_4$: C, 79.62; H, 6.24. Found: C, 80.13; H, 6.14.

Reaction of p,p'-Dimethoxybenzophenone Hydrazone with Sulfur

The hydrazone, sulfur, and mercuric oxide were allowed to react together in dry benzene as usual. The reaction mixture was filtered off, the residue was extracted with boiling benzene, and the benzene solution was concentrated and cooled. The separated solid was extracted with boiling acetone, and the acetone extract was cooled to give *p,p'*-dimethoxybenzophenone azine (melting point and mixed melting point). The acetone-insoluble fraction was crystallized from benzene to give III*b* (0.67 g).

Preparation of Epithiotetra-p-tolylethane (IIIc)

The reaction between di-*p*-tolyldiazomethane (2 g) and sulfur (0.5 g) was carried out as in the case of the dimethoxy analogue. The product (0.37 g) was crystallized from acetone to give epithiotetra-*p*-tolylethane, m.p. 195–196° (5).

Anal. Calcd. for $C_{30}H_{28}S$: C, 85.71; H, 6.66; S, 7.61. Found: C, 85.35; H, 6.81; S, 7.68.

This compound, when heated under reflux with Raney nickel in alcohol, yielded the ethylene (IV*c*) (7), m.p. 150 °C.

Anal. Calcd. for $C_{30}H_{28}$: C, 92.74; H, 7.26. Found: C, 93.10; H, 7.25.

Reaction of p,p'-Dimethylbenzophenone Hydrazone with Sulfur

The reaction was carried out as in the case of the dimethoxy analogue to give III*c*, m.p. 195–196° (0.37 g), and *p,p'*-dimethylbenzophenone azine (V*c*), m.p. 197–198° (Staudinger and Goldstein (8) gave m.p. 190–191°).

Anal. Calcd. for $C_{30}H_{28}N_2$: C, 86.50; H, 6.78; N, 6.73. Found: C, 86.93; H, 6.94; N, 6.96.

REFERENCES

1. B. EISTERT. *In* Newer methods of preparative organic chemistry. Interscience Publishers, Inc., New York. 1948. p. 513.
2. N. LATIF and I. FATHY. J. Org. Chem. **27**, 1633 (1962); Ann. Rept. Progr. Chem. Chem. Soc. London, **59**, 321 (1962).
3. N. LATIF, I. FATHY, and B. HAGGAG. Tetrahedron Letters, **17**, 1155 (1965).
4. H. STAUDINGER and O. KUPFER. Ber. **44**, 2209 (1911).
5. A. SCHÖNBERG and M. BARAKAT. J. Chem. Soc. 1074 (1939).
6. E. BERTOZZI, F. DAVIS, and E. FETTES. J. Polymer Sci. **19**, 17 (1956). P. BARTLETT and G. MEGUERIAN. J. Am. Chem. Soc. **78**, 3710 (1956). L. BATEMAN *et al.* J. Chem. Soc. 2838 (1958); 2866 (1958). J. ROSS. J. Chem. Soc. 2863 (1958).
7. H. GILMAN and F. FLICK. Rec. Trav. Chim. **48**, 461 (1929); Chem. Abstr. **23**, 2950 (1929).
8. H. STAUDINGER and J. GOLDSTEIN. Ber. **49**, 1925 (1916).

Can. J. Chem. Downloaded from www.nrcresearchpress.com by 210.87.254.40 on 09/05/12
For personal use only.

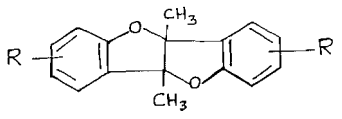
Can. J. Chem. Downloaded from www.nrcresearchpress.com by 210.87.254.6 on 09/05/12
For personal use only.

ON THE CONDENSATION OF *p*-CRESOL WITH GLYOXAL

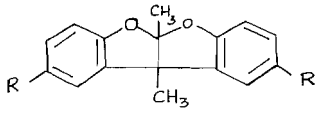
B. S. THYAGARAJAN, K. K. BALASUBRAMANIAN, AND R. BHIMA RAO

Two different methods of synthesis for the formation of coumarano(3,2-*b*)coumarans have long been known in the literature (1–3). One of these is the condensation of phenols with 1,2-dicarbonyl compounds in the presence of sulfuric acid, and the other is the acid-catalyzed cyclodehydration of 2,3-bis-(*o*-hydroxyaryl)-2,3-bis-hydroxybutanes. In both instances, the assumption has tacitly been made that the ultimate products have the benzofuro(3,2-*b*)benzofuran structure (I).

In the course of an attempt to provide synthetic evidence for the products of the acid-catalyzed rearrangement of 1,4-bis-aryloxybut-2-ynes (4), we have recently pointed out the erroneous nature of this assignment and have presented a more rational, alternate representation for two such products (II).

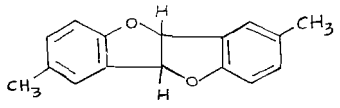


I

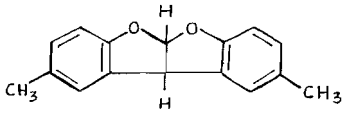


IIa, R = H

IIb, R = CH_3



III



IV

Although the condensation of *p*-cresol with glyoxal is not germane to our main efforts in the rearrangements of the 1,4-bis-aryloxybut-2-ynes, we have reinvestigated the former reaction to verify the validity of a similar structural assignment (III) (5).

The earlier structural formulation III rested on the evidence that the same product was obtainable by way of the acid-catalyzed dehydration of 1,2-bis-(2-hydroxy-5-methylphenyl)-ethane-1,2-diol (6). Repetition of the published procedure (5) yielded a compound in complete agreement with the earlier description. However, a nuclear magnetic resonance spectrum of the compound (taken in $CDCl_3$ with tetramethylsilane as an internal reference) (Fig. 1) revealed the following characteristics: a singlet at 2.25 p.p.m. caused by the aromatic methyl group integrating for six protons; a signal at 4.8 p.p.m. integrating for one proton; a signal at 4.9 p.p.m. integrating for one proton; and a multiplet centered at 6.95 p.p.m. integrating for six protons.

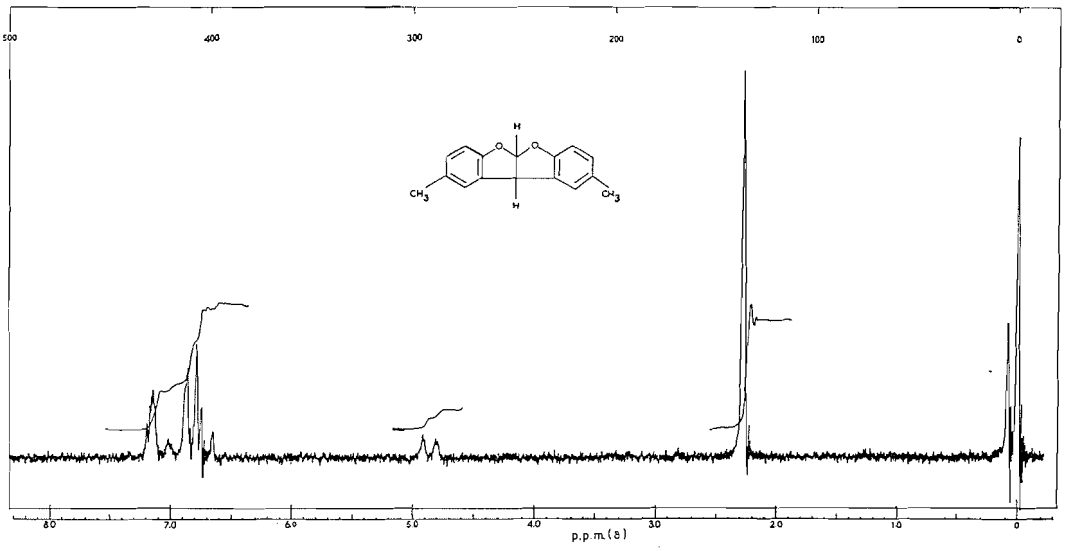


FIG. 1.

The benzofuro(3,2-*b*)benzofuran structure III would be expected to show only a singlet for the benzylic protons, in view of their location on identical environments. On the other hand, the benzofuro(2,3-*b*)benzofuran structure IV would exhibit split absorptions for the bridgehead protons because of the fact that one of them is now benzylic whereas the other is not. The observed nuclear magnetic resonance spectrum leaves no doubt that the product is a benzofuro(2,3-*b*)benzofuran (IV).

Thus, in all the three cyclodehydrations of symmetrical (*o*-hydroxyaryl) glycols as well as the 1,2-dicarbonyl condensations, the products are not the reported coumarano(3,2-*b*)-coumarans but the coumarano(2,3-*b*)coumarans.

ACKNOWLEDGMENTS

Our grateful thanks are due to Riker Laboratories Inc., Northridge, California, U.S.A., for the nuclear magnetic resonance spectrum. We thank the Government of India for a fellowship to R. B. R., and the Council for Scientific and Industrial Research, New Delhi, for a fellowship to K. K. B.

1. W. BAKER and J. C. MCGOWAN. J. Chem. Soc. 559 (1937).
2. G. J. GIE. Chem. Abstr. **41**, 1661 (1947).
3. K. SISIDO, H. NOZAKI, and T. IWAKO. J. Am. Chem. Soc. **71**, 2037 (1949).
4. B. S. THYAGARAJAN, K. K. BALASUBRAMANIAN, and R. BHIMA RAO. Tetrahedron, **21**, 2289 (1965).
5. A. ROSENTHAL and A. ZAIONCHKOVSKY. Can. J. Chem. **38**, 2277 (1960).
6. O. ANSELMINO. Ber. **41**, 621 (1908).

RECIEVED AUGUST 17, 1965.
DEPARTMENT OF ORGANIC CHEMISTRY,
UNIVERSITY OF MADRAS,
MADRAS, INDIA.

Can. J. Chem. Downloaded from www.nrcresearchpress.com by 210.87.254.6 on 09/05/12
For personal use only.

THE PREPARATION AND CHARACTERIZATION OF *cis*- AND *trans*-2-HYDRO-3-CHLORO-HEXAFLUORO-2-BUTENE

DONALD J. BURTON, RICHARD L. JOHNSON, AND RICHARD T. BOGAN

Although the preparation of the 2-hydro-3-chlorohexafluoro-2-butenes has been reported several times in the literature (1–4), no separation or identification of the individual isomers has been reported. In some recent work on the selective reduction of vinylic halogen in polyfluorinated olefins (5), we have carried out the reduction of a mixture of *cis*- and *trans*-2,3-dichlorohexafluoro-2-butene. Gas chromatographic analysis indicated two product peaks (presumed to be the *cis*- and *trans*-2-hydro-3-chlorohexafluoro-2-butenes). Since very few geometrical isomers of highly fluorinated olefins have been reported, and since these isomers are of potential interest in mechanistic studies of polyfluorinated olefins, we undertook the separation and identification of each geometrical isomer.

The isomer mixture was prepared by the monoreduction of the 2,3-dichlorohexafluoro-2-butene mixture with sodium borohydride in diglyme. Each isomer was separated and purified by vapor phase chromatography. Vapor density molecular weight determinations and infrared analysis demonstrated that the two compounds were indeed the isomeric 2-hydro-3-chlorohexafluoro-2-butenes. Assignment of the geometrical configuration of each isomer was made on the basis of the analysis of the ^{19}F nuclear magnetic resonance spectra of the pure isomers. The physical properties and the spectral data for each isomer are tabulated in Tables I and II, respectively.

TABLE I

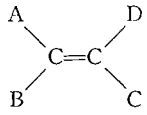
Physical properties of *cis*- and *trans*-$CF_3CH{=}CClCF_3$

	Boiling point (°C)*	n_D^{20}	Molecular weight†	—C=C—‡
cis-Isomer	41–42	1.3078	195	6.02 μ
trans-Isomer	34.5–35.5	1.3014	195	5.98 μ

*Microboiling point measured at 743 mm.
§Average of two determinations, calcd. mol. wt. 198.
‡Spectra were calibrated versus polystyrene film. Values are consistent with the presence of the —CH=CCl— grouping.

TABLE II

Spectral data for *cis*- and *trans*-$CF_3CH{=}CClCF_3$



	A	B	C	D	J_{AD}*	J_{AC}	J_{AB}	J_{BC}
cis-Isomer	CF_3	H	Cl	CF_3	10.8	—	8.0	—
trans-Isomer	CF_3	H	CF_3	Cl	—	1.0	5.4	1.2

*Spectra were measured at 56.4 Mc.p.s. with CCl_3F as an internal standard; J values are in cycles per second.

Can. J. Chem. Downloaded from www.nrcresearchpress.com by 210.87.254.105 on 09/05/12
For personal use only.

The ^{19}F nuclear magnetic resonance spectrum of the *trans*-2-hydro-3-chlorohexafluoro-2-butene consisted of two sets of lines: a line at $\phi^* = +61.2$ which was broken down into two quartets caused by coupling of the CF_3 group (A) with the hydrogen and with the *trans*-CF_3 group (C), and another line at $\phi^* = +70.8$ which consisted of two condensed quartets caused by coupling of the CF_3 group (C) with the *trans*-CF_3 (A) and with the hydrogen.

The spectrum of the *cis*-isomer consisted of two sets of lines: a line at $\phi^* = +57.7$ consisting of a complex pattern (octet) caused by splitting of the CF_3 group (A) by the hydrogen and the other CF_3 group (D), and a second line at $\phi^* = +65.0$ consisting of a quartet caused by splitting of the CF_3 group (D) by the other CF_3 group (A).

The assignment of the *trans*- or *cis*-structure was made on the basis of the magnitude of the coupling constants. The coupling constant between two CF_3 groups (*trans* across the double bond) has been reported to be 1.3–1.5 c.p.s. (6–8). The coupling constant between two CF_3 groups (*cis* across the double bond) has been reported to be 11–13 c.p.s. (6–8). The values of $J(CF_3, CF_3)$ of 1.0 c.p.s. and 10.8 c.p.s. are consistent with these previous assignments.

EXPERIMENTAL

$CF_3CCl{=}CClCF_3 + NaBH_4$

In a four-necked flask were placed 25 ml of dry diglyme (distilled from lithium aluminium hydride) and 23.3 g (100 mmoles) of 2,3-dichlorohexafluoro-2-butene (mixture of the *cis*- and *trans*-isomers). The mixture was cooled to 0 °C, and 99.0 ml of 1.01 *M* sodium borohydride (100 mmoles) in diglyme was added dropwise, the temperature being kept below 5 °C. During the addition of the borohydride solution, 29 mmoles (corrected to s.t.p.) of hydrogen was evolved. After the addition of the borohydride solution was completed, the reaction mixture was stirred at 0 °C for an additional 0.5 h and then cautiously hydrolyzed with water. On hydrolysis, 162 mmoles (corrected to s.t.p.) of hydrogen was evolved. After complete hydrolysis, the reaction mixture was poured into 50 ml of ice water and the organic layer separated.

The pure *cis*- and *trans*-isomers of 2-hydro-3-chlorohexafluoro-2-butene were separated and purified by preparative vapor phase chromatography on a F&M model 720 gas chromatograph having a 10 ft by 0.5 inch (outside diameter) copper column packed with 20% w/w dinonylphthalate supported on 100–120 mesh Gas Chrom P maintained at 40 °C, with the vaporizer at 200 °C and a helium flow rate of 300 ml/min. The retention times were 5.05 min and 9.05 min for the *trans*- and the *cis*-isomers, respectively.

ACKNOWLEDGMENTS

This work was supported in part by a grant from the U.S. Public Health Service (GM 11809-02), for which grateful acknowledgment is made. We are indebted to Mr. Robert S. Sudol and Dr. Paul R. Resnick of the DuPont Company for measuring the ^{19}F nuclear magnetic resonance spectra and for assistance in their interpretation.

1. A. L. Henne, J. B. Hinkamp, and W. J. Zimmerschied. J. Am. Chem. Soc. **67**, 1906 (1945).
2. A. L. Henne and W. G. Finnegan. J. Am. Chem. Soc. **71**, 298 (1949).
3. R. N. Hazeldine. J. Chem. Soc. 2504 (1952).
4. J. A. Sedlak. Ph.D. Thesis, Ohio State University, Columbus, Ohio. 1960.
5. D. J. Burton and R. L. Johnson. J. Am. Chem. Soc. **86**, 5361 (1964).
6. G. V. D. Tiers. J. Chem. Phys. **35**, 2263 (1961).
7. S. Andreades. J. Am. Chem. Soc. **84**, 864 (1962).
8. G. V. D. Tiers. J. Phys. Chem. **66**, 1192 (1962).

Received September 8, 1965.
Department of Chemistry,
University of Iowa,
Iowa City, Iowa.

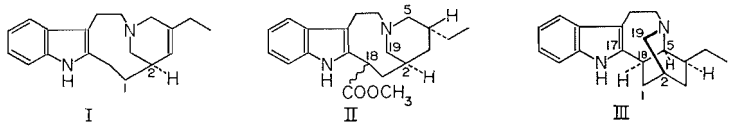
Can. J. Chem. Downloaded from www.nrcresearchpress.com by 210.87.254.105 on 09/05/12
For personal use only.

THE ABSOLUTE CONFIGURATION OF THE IBOGA ALKALOIDS

JAMES P. KUTNEY, RICHARD T. BROWN, AND EDWARD PIERS

Can. J. Chem. Downloaded from www.nrcresearchpress.com by 210.87.254.5 on 09/05/12
For personal use only.

The Iboga alkaloids have received considerable attention during recent years; in particular, several groups of workers, including our own, have been interested in the total synthesis of the Iboga skeleton. Indeed we were able to provide a synthetic entry into this series by means of a transannular cyclization process (1), and recently two publications (2, 3) have revealed totally synthetic pathways to the Iboga series. Although the basic structure of this group, initially proposed by the Ciba workers (4), was subsequently confirmed by the X-ray analysis of ibogaine hydrobromide (5), in which the relative configuration was also determined, the absolute configuration of this series was, until recently, an open question. The crucial evidence which allowed a solution to this problem came from our work on cleavamine, in which the structure and absolute configuration were determined by the X-ray method to be as depicted in I (6). A subsequent detailed paper illustrating the three-dimensional structure of cleavamine methiodide has also appeared (7). The isolation of cleavamine from an acid cleavage reaction on catharanthine and the subsequent demonstration that carbomethoxydihydrocleavamine (II) can be cyclized in a stereospecific manner to the alkaloids coronaridine and dihydrocatharanthine (1) provided indisputable evidence for the stereochemical relationship between cleavamine and the Iboga alkaloids. In our most recent paper (8) we discussed our results along with those previously published by other workers, and indicated that structure III represents the absolute configuration of ibogamine, one of the members of the Iboga family. Our purpose in publishing the present note is to emphasize that through a careless error on our part we have drawn the *incorrect* absolute configuration in structure III. We illustrate below that the *correct* absolute configuration for the Iboga family is in fact *antipodal* to the one presented in III.



I II III

Since our previous paper (8) has already mentioned all the relevant work in this area, we merely wish to emphasize presently the crucial arguments which invalidate the stereoformula III and which point out that it is in fact impossible to derive III from cleavamine (I) and (or) from carbomethoxydihydrocleavamine (II).

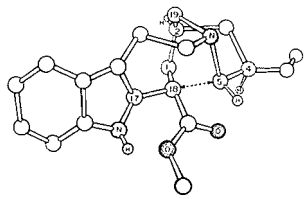
Carbomethoxydihydrocleavamine (II) has the same absolute configuration at C_2 (Iboga alkaloid numbering) as cleavamine (I). Since II, via its iminium salt involving the $C_5{=}\overset{+}{N}$ group, has been cyclized to the Iboga alkaloid system as already mentioned above (1), the absolute configuration at C_2 in the rigid Iboga skeleton must remain the same. It may be argued that an alteration in configuration at C_2 could have taken place in the iminium salt derivative *before* the cyclization process. This argument is made invalid for two reasons. First of all, both cleavamine and carbomethoxydihydrocleavamine are derived from a ring-opening reaction on catharanthine (9, 10). When this result is

taken in conjunction with the above cyclization result, it becomes obvious that either *no* epimerization or *two* epimerizations at C_2 must occur to allow regeneration of the catharanthine system in the cyclization process. Secondly, we have excluded the possibility of epimerization at C_2 in a related series of investigations. We have shown that an iminium salt intermediate with the $C_{19}{=}\overset{+}{N}\!\!\diagup\!\!\diagdown$ group, which is the only intermediate in which epimerization at C_2 could occur, cyclizes to an Aspidosperma skeleton; an X-ray analysis of this product establishes that the absolute configuration at this asymmetric center remains *unchanged* (11).

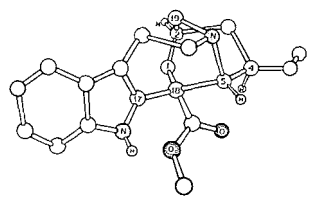
With the above evidence on hand one immediately notes that, although there are numerous conformations which structures I and II with nonrigid nine-membered rings can attain, there is in fact only *one* conformation of II which allows C_{18} and C_5 to come into reasonable proximity for bond formation. This particular conformation is reproduced in II*a*. It becomes immediately obvious that in II*a* the C_2—C_{19}—N bridge is now α-oriented and that the eventual ring closure between these two centers results in formation of the rigid Iboga system shown in IV, which now represents the complete structure for coronaridine. The absolute configuration in IV is antipodal to that shown above in III. On this basis the complete structure and absolute configuration of ibogamine are now correctly represented by V.

We wish to indicate that the alternate conformation for II, in which the C_2—C_{19}—N bridge is β-oriented, places C_{18} and C_5 far apart and clearly provides an impossible situation for bond formation between these two centers. However, even if such a cyclization were possible, it would in fact provide the Iboga alkaloid with the *wrong* relative configuration, the latter being already available from the X-ray determination of ibogaine hydrobromide (5) as mentioned above.

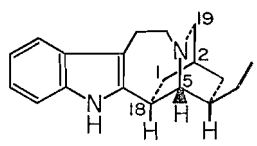
The absolute configuration of the Iboga family as illustrated above for ibogamine is *opposite* to that originally suggested in the publication from the Ciba group (4). More recently Buchi has also postulated the *opposite* absolute configuration for voacangine based on an incorrect interpretation of our X-ray work on cleavamine (12). For this reason the absolute configuration for the voacangine unit in the dimeric alkaloid voacamine (12) must be altered. Similarly, the absolute configuration of the velbanamine unit in the oncolytic Vinca alkaloids vinblastine and vincristine is now established, since velbanamine can readily be converted into cleavamine. The absolute configuration is antipodal to the stereochemistry presented in a recent communication (10).[1]



II a



IV



V

[1]*After our paper had been submitted for publication, a communication on the X-ray analysis of leurocristine methiodide appeared (13) wherein the absolute configuration for the cleavamine-like unit was shown to be in complete agreement with our previous work. We also acknowledge some recent correspondence with Professor G. Buchi on this point.*

Can. J. Chem. Downloaded from www.nrcresearchpress.com by 210.87.254.5 on 09/05/12
For personal use only.

1. J. P. KUTNEY, R. T. BROWN, and E. PIERS. J. Am. Chem. Soc. **86**, 2287 (1964).
2. G. BUCHI, D. L. COFFEN, K. KOCSIS, P. E. SONNET, and F. E. ZIEGLER. J. Am. Chem. Soc. **87**, 2073 (1965).
3. J. W. HUFFMAN, C. B. S. RAO, and T. KAMIYA. J. Am. Chem. Soc. **87**, 2288 (1965).
4. M. F. BARTLETT, D. F. DICKEL, and W. I. TAYLOR. J. Am. Chem. Soc. **80**, 126 (1958).
5. G. ARAI, J. COPPOLA, and G. A. JEFFERY. Acta Cryst. **13**, 553 (1960).
6. J. P. KUTNEY, J. TROTTER, T. TABATA, A. KERIGAN, and N. CAMERMAN. Chem. Ind. London, 648 (1963).
7. N. CAMERMAN and J. TROTTER. Acta Cryst. **17**, 384 (1964).
8. J. P. KUTNEY, R. T. BROWN, and E. PIERS. Can. J. Chem. **43**, 1545 (1965).
9. N. NEUSS, M. GORMAN, H. E. BOAZ, and N. J. CONE. J. Am. Chem. Soc. **84**, 1509 (1962). M. GORMAN, N. NEUSS, and N. J. CONE. J. Am. Chem. Soc. **87**, 93 (1965).
10. N. NEUSS, M. GORMAN, W. HARGROVE, N. J. CONE, K. BIEMANN, G. BUCHI, and R. E. MANNING. J. Am. Chem. Soc. **86**, 1440 (1964).
11. A. CAMERMAN, N. CAMERMAN, J. P. KUTNEY, E. PIERS, and J. TROTTER. Tetrahedron Letters, 637 (1965).
12. G. BUCHI. Pure Appl. Chem. **9**, 21 (1964). G. BUCHI, R. E. MANNING, and S. A. MONTI. J. Am. Chem. Soc. **86**, 4631 (1964).
13. J. W. MONCRIEF and W. N. LIPSCOMB. J. Am. Chem. Soc. **87**, 4963 (1965).

RECEIVED OCTOBER 29, 1965.
DEPARTMENT OF CHEMISTRY,
UNIVERSITY OF BRITISH COLUMBIA,
VANCOUVER, BRITISH COLUMBIA.

ERRATUM: SYNTHESIS OF 4-ACETAMIDO-4-DEOXY-SUGARS

A. J. DICK AND J. K. N. JONES

(Ref. Can. J. Chem. 43, 977 (1965))

On page 977, structure IV should have the "ribo" and not the "lyxo" configuration.
On page 978, paragraph 4, line 5, the symbol XII should be replaced by IV.
In the footnote on page 978, XII should read IV.

DEPARTMENT OF CHEMISTRY,
QUEEN'S UNIVERSITY,
KINGSTON, ONTARIO.

Can. J. Chem. Downloaded from www.nrcresearchpress.com by 210.87.254.5 on 09/05/12
For personal use only.

Can. J. Chem. Downloaded from www.nrcresearchpress.com by 210.87.254.105 on 09/05/12
For personal use only.

Canadian Journal of Chemistry

Issued by THE NATIONAL RESEARCH COUNCIL OF CANADA

VOLUME 44 MARCH 15, 1966 NUMBER 6

ANODIC OXIDE FILMS ON INDIUM ANTIMONIDE[1]

A. C. HARKNESS
British Columbia Research Council, Vancouver, British Columbia

AND

L. YOUNG
Department of Electrical Engineering, University of British Columbia, Vancouver, British Columbia

Received September 7, 1965

ABSTRACT

The kinetics of formation of anodic oxide films on different crystal faces of single crystal indium antimonide have been investigated by measurements of charge passed, capacitance, and optical properties. Below a transition or breakdown region of voltage no difference in kinetics was found. Above this voltage a marked difference appeared. The transition voltage was found to depend on both the crystal face and the current density at which the film was formed.

INTRODUCTION

Most observations on the growth of high resistance anodic oxide films can be explained in terms of the ionic conduction properties of the oxide film itself (1): that is, the movement of ions through the oxide under the influence of the applied field controls the growth process. The movement of ions across the metal–oxide interface is not an important factor in determining the overall rate.

Dewald (2) anodized different crystal faces of indium antimonide and reported that there were marked differences in the kinetics of film formation on different faces. He reported that the ionic current density and field were not related by the simple equation $i = A \exp BE$ (where i is the current density, E is the field, and A and B are constants); rather there were two such equations, one describing the behavior at low formation rates and the other at high formation rates. At the low rates (0.1 V/s) the field on the (332) face was about 15% lower than the field on the ($\bar{3}32$) face. At higher rates (10 V/s) the fields converged and both faces exhibited the same kinetics.

Venables and Broudy (3) anodized (111) and ($\bar{1}\bar{1}\bar{1}$) faces of indium antimonide at a current density of 2×10^{-4} A/cm^2 which corresponds to Dewald's low rate. Like Dewald they used 0.1 M KOH as the electrolyte. The formation rates on the two surfaces were the same until the voltage had increased to 11 V. At this point the rate of voltage increase on the (111) face decreased sharply, but the film thickness as indicated by the interference colors increased at a greater rate. The ($\bar{1}\bar{1}\bar{1}$) face showed the same behavior at 13 V.

Lavine, Rosenberg, and Gatos (4) have also reported that the rate of anodic oxidation of indium antimonide is faster on (111) surfaces than on ($\bar{1}\bar{1}\bar{1}$) surfaces.

Indium antimonide crystallizes in the zinc blende structure which lacks a center of symmetry and has crystallographic polarity along the ⟨111⟩ axis. The structure may be

[1]*Paper presented at the 48th Chemical Institute of Canada Conference, Montreal, 31 May 1965.*

visualized as composed of tetrahedra of indium atoms interlocked with tetrahedra of antimony atoms in such a manner that each indium atom is at the center of a tetrahedron of antimony atoms and vice versa. If the bonding is considered to be only between nearest neighbors, then each atom is held by four bonds to the other species in the interior of the crystal. In the ⟨111⟩ direction layers of atoms of the same species are alternately singly and triply bound to parallel layers of atoms of the other species. Since surfaces arise by severing single bonds, opposite {111} surfaces are composed of different atom species triply bound to the lattice. Gatos (5) has given a detailed discussion of the bonding and reactivity of group III–IV compounds.

The assignment of the {111} surfaces is quite arbitrary. Dewald defined (111) as that surface showing the faster rate of film formation and others have adopted the same convention. It has since been determined that the (111) face terminates with indium atoms (6).

It would be expected that the free energy of formation of extremely thin oxide films would be different on different crystal faces. However, if the films are thick enough so that surface perturbations become negligible, then the properties of the film and the rate of growth should be independent of crystal face and oxide thickness at constant current density and temperature.

This paper describes experiments on oxide films formed on opposite {111} faces of single crystal indium antimonide. It was hoped that some insight into the previously reported anomalous behavior might be obtained.

EXPERIMENTAL

The indium antimonide was Cominco Grade 35S, a high mobility *n*-type single crystal grown in the ⟨111⟩ direction. Slices were cut parallel to {111} faces with a tungsten wire saw. Specimens were normally prepared by abrasion on metallurgical papers down to 4/0. Those which survived this treatment then had wires soldered to them. Picien wax was applied to stop off one side and the edges. The specimens were chemically polished in a solution containing concentrated nitric acid, concentrated hydrofluoric acid, and glacial acetic acid in the ratio 5:3:3 by volume. The (111) face polishes to a bright finish while the $(\overline{1}\overline{1}\overline{1})$ face is lightly etched and gives a matte finish.

All film forming was done in an electrolyte of 0.1 *M* borax (pH = 9.2) at 25.0°. This electrolyte was chosen to minimize the possible solution of antimony oxide. The cathode was platinized platinum and voltages were measured with respect to the cathode with the solution saturated with hydrogen. The cell was shielded from direct light to avoid the photoeffects reported by Venables and Broudy (3, 7).

Nearly all formation experiments were conducted with a constant current generator with a control apparatus designed and built by Mr. R. Cuthbert in the laboratories of the British Columbia Research Council. This device displays the time required to form through selected voltage intervals and terminates the current on arrival at a preset voltage. During anodization the solution was not stirred, since this resulted in bubbles on the anode. The currents employed were normally too low to cause appreciable heating of the anode.

Specimen areas were determined by photographing the specimen on squared paper and comparing the area covered by the specimen to the area of a square by planimeter measurement or by weighing. An alternative, simpler procedure was to make Xerox copies of the specimens backed by squared paper. No allowance was made for surface roughness.

The series equivalent capacity and resistance of the films were measured with a conventional bridge.

The wavelengths of minimum reflectivity of the interference colors were measured with a Cary Model 14 recording spectrophotometer. Specimens were mounted in a holder so that light was incident at an angle of 11°. A polished (111) surface was used as reference.

The specimens used for ellipsometer determinations were mechanically polished. After abrading on metallurgical papers they were rubbed on a soft cloth soaked with a slurry of fine alumina. This treatment produces bright mirror finishes on both (111) and $(\overline{1}\overline{1}\overline{1})$ faces. Measurements were made with a Gaertner L119 ellipsometer with monochromatic light of 5 461 Å. The method of measurement was the same as that used for oxide films on tantalum (8).

RESULTS AND DISCUSSION

Typical formation curves are illustrated in Fig. 1. Both crystal faces exhibited similar behavior. There is a nearly linear rise in voltage followed by a period where the rate of

Can. J. Chem. Downloaded from www.nrcresearchpress.com by 210.87.254.105 on 09/05/12
For personal use only.

rise decreases. During anodization quite bright interference colors are developed through the sequence light gold, deep gold, bronze, pink, purple, blue, green, grey. Second order colors are not well defined and the films break down and evolve gas.

On both surfaces the transition voltage, defined as the voltage where linear growth ceases, increases with increasing current density. Furthermore, the final voltage reached before complete failure is higher with higher current densities.

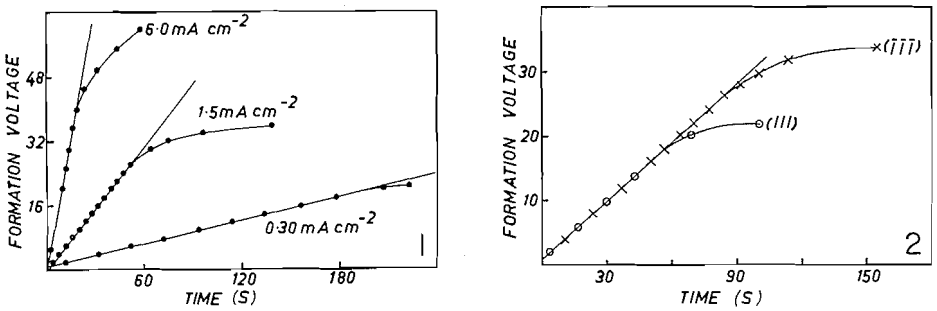


FIG. 1. Formation curves for $(\bar{1}\bar{1}\bar{1})$ surface of InSb. Various current densities.
FIG. 2. Formation curves for (111) and $(\bar{1}\bar{1}\bar{1})$ surfaces of InSb. Current density 1.00 mA/cm².

In agreement with Venables and Broudy (3), it was found that the transition voltage was higher for films formed on $(\bar{1}\bar{1}\bar{1})$ surfaces than for those formed on (111) surfaces. Figure 2 shows formation curves for specimens of each surface formed at the same current density. Until the transition voltage for the (111) surface is reached the rates of formation are identical. This behavior was encountered through the range of current densities used. In Fig. 3, transition voltages are plotted against the logarithms of the formation rates for the linear region. The curve for $(\bar{1}\bar{1}\bar{1})$ specimens lies above that for the (111) specimens.

The colors of the films indicate that past the transition voltage their thickness increases rapidly. Thus, for a given current density, the (111) surface will show a faster rate of film growth over a certain voltage range. This of course assumes that no significant change in the optical properties of the film occurs at the transition voltage. The wavelength of minimum reflectivity is a measure of film thickness. A plot of this parameter against formation voltage for {111} specimens formed at similar current densities is given in Fig. 4.

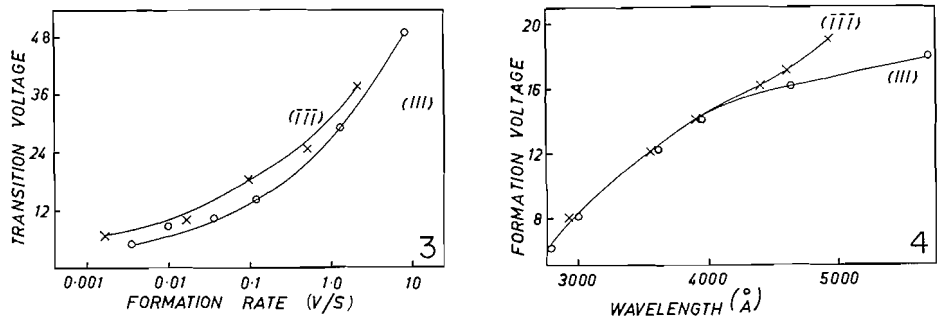


FIG. 3. Variation of transition voltage with formation rate for (111) and $(\bar{1}\bar{1}\bar{1})$ surfaces of InSb.
FIG. 4. Wavelength of minimum reflectivity vs. formation voltage for films formed on (111) and $(\bar{1}\bar{1}\bar{1})$ surfaces of InSb. Current density 0.3 mA/cm².

Can. J. Chem. Downloaded from www.nrcresearchpress.com by 210.87.254.105 on 09/05/12
For personal use only.

To detect differences in the kinetics of film formation, quite accurate estimates of fields are necessary. Measurements of capacity have proved to be particularly effective (1). If the current efficiency is high, measurement of the charge, Q, passed to form through a voltage interval, ΔV, may be combined with a measurement of the increase in reciprocal capacity, $\Delta(1/C)$, to give an estimate of the field which is independent of the specimen area. The quantity $\Delta V/(Q\Delta(1/C))^{1/2}$ is an estimate of the field strength.

Figure 5 shows the field estimate, $\Delta V/(Q\Delta(1/C))^{1/2}$, as a function of the logarithm of the formation rate (below the transition voltage). The scatter is about $\pm 5\%$. This is an order of magnitude worse than can be obtained with tantalum. The results, however, tend to confirm that there is no difference between the {111} faces.

The reflection of polarized light from a surface results in changes in the amplitude and phase of both the p- and s-components. The appropriate equation which relates the ratio of the reflection coefficients to these changes is $R_p/R_s = \tan \psi e^{i\Delta}$. Here, ψ is the relative amplitude change and Δ the relative phase change. These quantities are the experimental parameters. The character of the reflected light is dependent on the wavelength and angle of incidence of the incident light, the optical constants of the substrate (metal), and on the optical constants and thickness of the surface film (oxide).

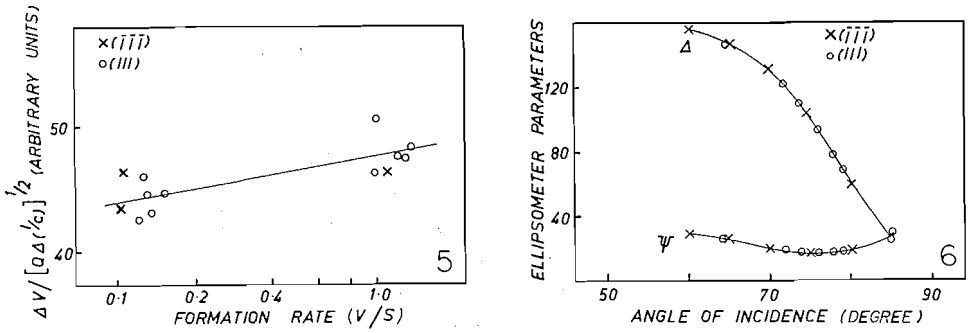


FIG. 5. Field estimates from charge and capacity data vs. formation rate for films formed on (111) and $(\bar{1}\bar{1}\bar{1})$ surfaces of InSb below the transition voltage.
FIG. 6. Variation of ellipsometer parameters ψ and Δ with angle of incidence for unanodized (111) and $(\bar{1}\bar{1}\bar{1})$ surfaces of InSb.

In principle, the method allows the determination of the optical constants of the film and its thickness provided the optical constants of the bare metal are known. In practice, ultrahigh vacuum techniques would be required to obtain film-free metal in order to measure its optical constants by ellipsometry. For some metals, e.g. tantalum, the optical constants may be obtained by other methods (9). Kumagai and Young (8) have shown that curve-fitting methods (with an IBM 1620 computer) may be used with ellipsometer data to obtain good values of the optical constants of both metal and oxide film. Their procedure was followed in this study.

A plot of the ellipsometer parameters, ψ and Δ, as a function of angle of incidence of 5 461 Å light for unanodized {111} surfaces of indium antimonide is given in Fig. 6. The surfaces had been mechanically polished with alumina. It is seen that there is no apparent difference between the two surfaces.

From data on unanodized metal preliminary estimates of the optical constants of the metal were found to be $n = 3.5$ and $k = 2.1$ for the (111) surface. The corresponding estimates for the $(\bar{1}\bar{1}\bar{1})$ surface were 3.6 and 2.1. These should of course be equal. We are using the convention that the complex index of refraction is written $\bar{n} = n - ik$.

Can. J. Chem. Downloaded from www.nrcresearchpress.com by 210.87.254.105 on 09/05/12
For personal use only.

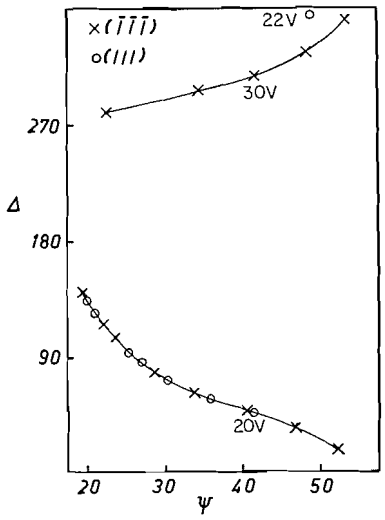


FIG. 7. Ellipsometer curve for films formed on (111) and ($\bar{1}\bar{1}\bar{1}$) surfaces of InSb. Current density 1.00 mA/cm².

Figure 7 shows Δ vs. ψ plots for films formed on (111) and ($\bar{1}\bar{1}\bar{1}$) surfaces at 1.00 mA/cm². For these specimens the film was formed to a preset voltage and the specimen removed from the cell, rinsed, and dried. After the ellipsometer measurements were made, the film was removed by dissolving in hydrofluoric acid. A new film was formed to a different voltage and the procedure repeated. The formation data for these films are those displayed in Fig. 2.

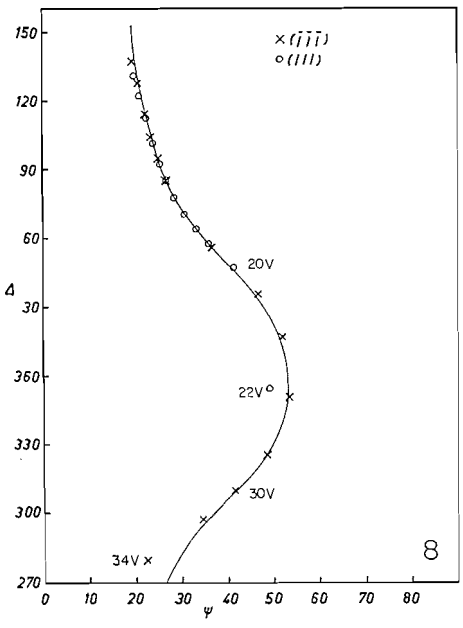
The significance of Fig. 7 is that, up to the transition voltage of the (111) specimen (18 V), there is complete coincidence of the ellipsometer curves. This indicates that the oxide films formed on both surfaces have identical properties. This, combined with the identical rates of voltage rise, is strong evidence for the same kinetics of formation on both (111) and ($\bar{1}\bar{1}\bar{1}$) surfaces of indium antimonide.

The experimental Δ vs. ψ plot of Fig. 7 was fitted by trial and error curves calculated for various values of the optical constants n_2 and k_2 for the metal and n_1 for the oxide. The oxide was assumed to be non-absorbing, i.e. $k_1 = 0$. Figure 8 shows the calculated curve giving the best fit of the experimental points. The values used in calculating this curve were (for oxide) $n_1 = 2.15$ and (for metal) $n_2 = 4.6$ and $k_2 = 1.6$. Kurdiani (10) reports $n_2 = 4.6$ and $k_2 = 0.5$.

A plot was constructed of Δ and film thickness from the calculated curve. From this plot, thicknesses corresponding to experimental values of Δ for particular formation voltages were read off. This allowed the construction of formation voltage – film thickness plots as shown in Fig. 9. The slopes of these plots yield values of the field across the oxide of 4.6×10^6 V/cm for the (111) surface and 4.3×10^6 V/cm for the ($\bar{1}\bar{1}\bar{1}$) surface (for current density 1 mA/cm²). The difference should be considered as due to experimental variation rather than real field differences.

The evidence indicates that below a transition voltage there is no difference in the formation behavior of anodic films formed on (111) and ($\bar{1}\bar{1}\bar{1}$) surfaces of indium antimonide. Above the transition voltage the ellipsometer data deviate from the calculated curve. This suggests that there has been a change in the optical properties of the films.

Can. J. Chem. Downloaded from www.nrcresearchpress.com by 210.87.254.105 on 09/05/12
For personal use only.



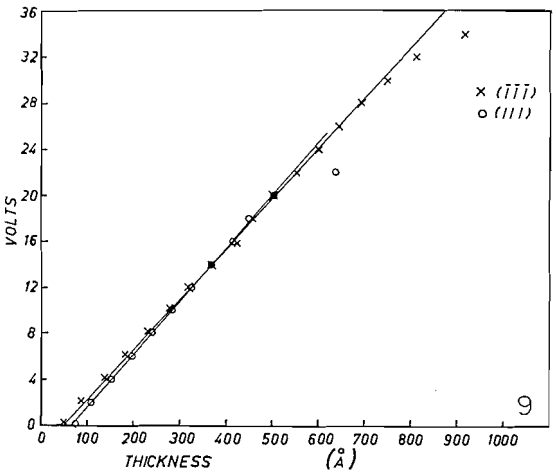


FIG. 8. Calculated ellipsometer curve with (for oxide) $n_1 = 2.15$ and (for metal) $n_2 = 4.6$, $k_2 = 1.6$. Compared with data from Fig. 7.

FIG. 9. Thickness, from ellipsometer data, of films formed on (111) and $(\overline{111})$ surfaces of InSb vs. formation voltage.

The nature of the change at the transition voltage and its dependence on crystal face remain obscure.

ACKNOWLEDGMENT

This work was supported by a grant from the Sprague Electric Company, North Adams, Massachusetts.

REFERENCES

1. L. YOUNG. Anodic oxide films. Academic Press, London and New York. 1961.
2. J. F. DEWALD. J. Electrochem. Soc. **104**, 244 (1957).
3. J. D. VENABLES and R. M. BROUDY. J. Electrochem. Soc. **107**, 296 (1960).
4. M. C. LAVINE, A. J. ROSENBERG, and H. C. GATOS. J. Appl. Phys. **29**, 1131 (1958).
5. H. C. GATOS. Science, **137**, 311 (1962).
6. H. C. GATOS and . C. LAVINE. J. Electrochem. Soc. **107**, 427 (1960).
7. J. D. VENABLES Md R. M. BROUDY. J. Appl. Phys. **30**, 1110 (1959).
8. S. KUMAGAI andan YOUNG. J. Electrochem. Soc. **111**, 1411 (1964).
9. L. MASING, J. E. L. ORME, and L. YOUNG. J. Electrochem. Soc. **108**, 428 (1991).
10. N. I. KURDIANI. Soviet Phys.–Solid State English Transl. **5**, 1310 (1964).

Can. J. Chem. Downloaded from www.nrcresearchpress.com by 210.87.254.105 on 09/05/12
For personal use only.

Can. J. Chem. Downloaded from www.nrcresearchpress.com by 210.87.254.5 on 09/05/12
For personal use only.

ÉTUDE DE LA FORMATION DES COMPLEXES DU PROTACTINIUM AVEC LES ACIDES DI- ET POLY-CARBOXYLIQUES PAR LA MÉTHODE D'ÉCHANGE D'IONS

IOAN GALATEANU

Institut de Physique Atomique Bucarest, Roumanie[1]

Reçu le 28 juin 1965

RÉSUMÉ

On a étudié la formation de complexes du protactinium avec les acides malique, tartrique, trioxyglutarique, oxalique, aconitique, citrique et éthylènediaminetétraacétique, à l'aide de la méthode d'échange d'ions. On en a calculé les constantes d'instabilité. L'ordre de stabilité croissante de ces complexes est le suivant: aconitique, malique, tartrique, oxalique, trioxyglutarique, citrique, éthylènediaminetétraacétique.

ABSTRACT

The formation of the protactinium complexes with malic, tartaric, trioxyglutaric, oxalic, aconitic, citric, and ethylenediaminetetraacetic acids has been studied by the ion-exchange method, and the instability constants have been calculated. The stability of the complexes increases in the following order: aconitic, malic, tartaric, oxalic, trioxyglutaric, citric, ethylenediaminetetraacetic acid.

Dans les travaux scientifiques concernant la chimie du protactinium on trouve des opinions différentes sur la forme du protactinium dans les solutions acides. D'après Elson (1) dans les solutions faiblement acides, le protactinium se trouve sous la forme de complexes hydrolysés: $Pa(OH)_{4.5}^{0.5+}$, $PaO(OH)_{2.5}^{0.5+}$, etc., mais dans les solutions fortement acides, il peut se présenter sous forme ionique Pa^{5+}. Goble, Golden et Maddock (2) ont montré l'existence des complexes du protactinium respectivement $PaOCl_6^{2-}$ et $PaO_2(NO_3)_4^{3-}$ dans les solutions de HCl et HNO_3. En outre, Kraus et Moore (3) pensent qu'il existe un complexe $H_nPaX_5Cl_{n+1}^{1-}$ dans la solution HCl 8 *M*. Starik *et al.* (4) ont étudié le comportement du protactinium dans l'acide nitrique (1–12 *M*) à l'aide de la méthode d'échange d'ions et démontré l'existence des complexes: $Pa(OH)_4^{1+}$, $Pa(OH)_3^{2+}$, $[Pa(OH)_3(NO_3)]^{1+}$, $[Pa(OH)_3(NO_3)_2]^0$, $[Pa(OH)(NO_3)_5]^{1-}$, $[Pa(OH)(NO_3)_7]^{3-}$, etc.

Dans nos travaux antérieurs nous avons étudié le processus de la formation des complexes du protactinium avec les acides lactique (5), α-hydroxy-iso-butyrique et mandélique (6) par la méthode d'échange d'ions. Les résultats obtenus nous montrent que le protactinium, dans les solutions de ces acides (pH = 0.5–1), se trouve sous la forme des complexes du type: $[PaO(OH)_yR_j]^{(5-2-y-j)+}$ où R est le coordinat respectif, mais dans les solutions des mêmes acides à pH plus élevés (pH = 2) prédomine la forme de complexes: $[Pa(OH)_yR_j]^{(5-y-j)+}$ où $y = 1,2,3 \ldots$ et $j = 1$.

Nous avons calculé les valeurs des constantes d'instabilité des complexes du protactinium avec plusieurs acides organiques, à l'aide des méthodes de Froneus (7–10) et de Paramonova (11–15) et nous avons publié ces résultats dans une brève note (16).

Dans la présente communication nous avons décrit le processus de la formation des complexes du protactinium avec les acides malique, tartrique, trioxyglutarique, oxalique, citrique, aconitique et éthylènediaminetétraacétique.

PARTIE EXPÉRIMENTALE

Les solutions de ces acides, préparées avant chaque série d'expériences, avaient des concentrations dans les limites 8×10^{-5} à 7×10^{-1} *M*, et une force ionique $\mu = 0.25$.

[1]*Adresse actuelle: Agence Internationale de l'Énergie Atomique, Vienne I, Kaerntnerring 11, Autriche.*

Tous les réactifs étaient de haute pureté. Le protactinium-233 que nous avons utilisé comme indicateur dans toutes les expériences a été obtenu par la réaction nucléaire:

$$^{232}\mathrm{Th} + \mathrm{n} \rightarrow {}^{233}\mathrm{Th} \xrightarrow{\beta^-} {}^{233}\mathrm{Pa} \xrightarrow{\beta^-} {}^{233}\mathrm{U}.$$

On a effectué la séparation du protactinium-233 à l'aide d'échangeurs d'ions par adsorption (sur anionite Dowex-1, Cl^-) de solutions HCl 10 *M*, puis par élution avec une solution HCl 4 *M* (17). Après séparation, les solutions chlorhydriques du protactinium-233 ont été évaporées à sec et finalement le protactinium a été mis en solution 2 *M* d'acide perchlorique et conservé dans des bouteilles de Teflon. Toutes les expériences, pour la détermination des constantes d'instabilité, ont toujours été effectuées avec des solutions fraîches de protactinium. En ce cas on peut éviter la formation des radiopseudocolloïdes. Des parts aliquotes de solution du protactinium ont été ajoutées aux solutions de chacun des acides, puis mises en contact avec les quantités calculées de cationite (Dowex-50, 400 mesh) et d'anionite (Amberlite IRA-400, 100 mesh). Pour chaque échantillon placé dans un cylindre de Teflon la durée du contact a été de 3 h pour le cationite et 5 h dans le cas de l'anionite, avec agitation dans un thermostat maintenu à la température constante (25 °C). Ensuite on a pris des parts aliquotes de chaque solution et on a mesuré l'activité résiduelle, en déterminant le coefficient de distribution du protactinium-233, à l'aide de la formule:

$$\zeta = I_0 - I/I \cdot v/m \quad \mathrm{l/g}$$

où I_0 est l'activité initiale, I est l'activité après la formation des complexes, v est le volume de la part aliquote et m est la quantité de résine en grammes.

RÉSULTATS

Pour déterminer les constantes d'instabilité, d'après la méthode de Paramonova, il a fallu calculer tout d'abord le rapport $\gamma_+ = G/G^0 . C^0/C$ (l'adsorption relative). Dans cette formule G représente la quantité de protactinium adsorbée sur cationite, en présence du complexant; G^0 est la quantité de protactinium adsorbée sur cationite mais en absence du complexant. La fraction C^0/C en ce cas joue le rôle du facteur de correction où C représente la concentration totale du protactinium en solution (%) en présence du complexant et C^0 est la concentration totale du protactinium (%) dans la solution, en absence du complexant (Tableaux I à III).

TABLEAU I

Détermination des constantes d'instabilité des malates et tartrates du protactinium (μ = 0.25)

C_{H_2A} (mole/l)	pH	ζ (l/g$\times 10^3$)	γ_+	γ_2	K_1 $\times 10^{-3}$	K_2 $\times 10^{-5}$	K_1'* $\times 10^{-3}$	K_2'* $\times 10^{-5}$
Acide malique								
0.01	0.65	97.0	0.97	—	0.6	—	1.2	—
0.05	0.80	105.0	0.98	—	9.8	—	1.2	—
0.10	0.80	98.5	0.95	—	7.6	—	1.2	—
0.20	0.83	60.0	0.77	0.02	2.6	—	1.2	—
0.30	0.83	50.0	0.71	0.07	2.9	—	1.2	—
0.40	0.85	40.0	0.65	0.08	2.9	—	1.2	—
0.50	0.85	27.5	0.49	0.26	1.9	1.5	1.2	—
0.60	0.85	22.1	0.42	0.31	1.7	2.5	1.2	—
0.65	0.85	22.1	0.44	0.26	2.1	0.8	1.2	—
				Moyenne	3.8	1.6	1.2	—
Acide tartrique								
0.01	0.80	110.0	0.99	—	—	—	7.7	—
0.05	0.80	105.0	0.95	—	10.4	—	7.7	—
0.10	0.80	91.5	0.88	—	8.0	—	7.7	—
0.20	0.75	47.7	0.59	0.24	3.2	1.2	7.7	—
0.30	0.75	26.5	0.38	0.51	2.0	0.6	7.7	3.9
0.40	0.80	25.0	0.34	0.55	2.2	1.1	7.7	—
0.50	0.80	19.2	0.28	0.62	2.1	1.3	7.7	9.0
0.60	0.80	15.0	0.23	0.69	1.9	1.4	7.7	4.9
0.65	0.75	11.2	0.18	0.78	7.0	1.2	7.7	1.6
				Moyenne	4.6	1.1	7.7	4.8

*Dans les Tableaux I, II, III et VI les constantes K_1 et K_2 sont calculées par la méthode de Paramonova. Les constantes K_1', K_2' et K_3' sont calculées par la méthode de Froneus.

Can. J. Chem. Downloaded from www.nrcresearchpress.com by 210.87.254.5 on 09/05/12
For personal use only.

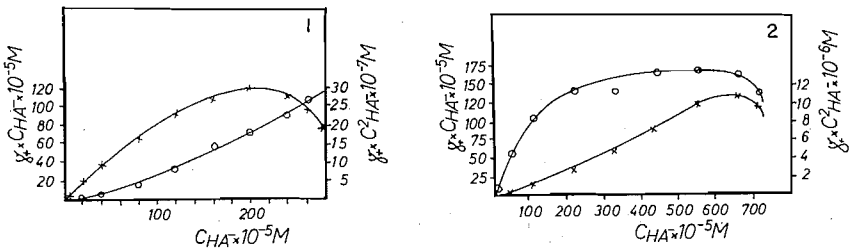


FIG. 1. Formation des complexes du protactinium avec l'acide malique. ×, Pa:HMal$^-$ = 1:1; ○, Pa:HMal$^-$ = 1:2.
FIG. 2. Formation des complexes du protactinium avec l'acide tartrique. ○, Pa:HTart$^-$ = 1:1; ×, Pa:HTart$^-$ = 1:2.

En utilisant le système de coordonées $\gamma_+ . C_{HA^-}$ vs. C_{HA^-} (où C_{HA^-} représente la concentration du coordinat moles/l), nous avons obtenu des courbes (Figs. 1 à 6) qui nous montrent le domaine d'existence du premier complexe, en fonction de la concentration du coordinat. La présence des maximums sur ces courbes indiquent, qualitativement, la formation des complexes du protactinium qui ont le rapport Pa:HA$^-$ = 1:1. A l'aide du système de coordonées log $\gamma_+/1 - \gamma_+$ vs. log C_{HA^-} nous avons aussi déterminé quantitativement le rapport Pa:HA$^-$ pour tous les complexes du protactinium avec les acides mentionnés plus haut. Par exemple pour les acides malique, tartrique et trioxyglutarique de tels graphiques sont montrés dans les Figs. 7 à 9. La pente des droites dans ce système de coordonnées exprime le nombre de molécules du coordinat dans le complexe.

TABLEAU II

Détermination des constantes d'instabilité des trioxyglutarates et oxalates du protactinium (μ = 0.25)

C_{H_2A} (mole/l)	pH	ζ (l/g×10^3)	γ_+	γ_2	K_1 ×10^{-3}	K_2 ×10^{-4}	K_1' ×10^{-3}	K_2'	K_3' ×10^{-7}
Acide trioxyglutarique									
0.0005	1.1	2010.0	0.73	—	—	—	—	—	—
0.0010	1.2	255.0	0.92	—	0.96	—	—	—	—
0.0050	1.2	159.0	0.73	—	1.10	—	—	—	—
0.0100	1.0	130.0	0.77	—	2.70	—	—	—	—
0.0500	1.0	4.3	0.06	—	—	—	1.10	—	—
0.1000	1.0	2.3	0.03	—	—	—	1.10	—	—
0.2000	1.0	4.5	0.05	—	—	—	1.10	—	—
0.3000	0.95	3.9	0.04	—	—	—	1.10	—	—
0.4000	1.0	0	—	—	—	—	1.10	—	—
0.5000	1.0	0	—	—	—	—	1.10	1.3×10^{-8}	—
0.6000	0.95	8.6	0.1	—	—	—	1.10	1.3×10^{-8}	—
0.7000	1.10	4.5	0.07	—	—	—	—	1.3×10^{-8}	—
				Moyenne	1.6	—	1.10	1.3×10^{-8}	—
Acide oxalique									
0.0001	0.65	38.0	0.90	—	0.45	—	—	—	—
0.0005	0.65	75.0	—	—	—	—	—	—	—
0.0010	0.80	37.9	0.92	—	5.00	—	—	—	—
0.0100	0.80	32.5	0.76	—	1.50	—	2.8	—	—
0.0500	0.80	5.5	0.18	0.01	5.50	1.10	2.8	—	—
0.1000	0.80	0.6	0.02	0.27	1.00	1.80	2.80	—	—
0.2000	0.75	0.40	0.01	0.01	1.42	—	2.8	2.0×10^{-6}	9.0
0.3000	0.75	0.08	—	0.02	—	0.35	2.8	0.5×10^{-6}	9.0
0.4000	0.75	0.02	—	—	—	—	—	—	9.0
0.5000	0.75	0	—	—	—	—	—	—	—
0.6000	0.75	0.80	0.03	—	—	—	—	—	—
0.7000	0.75	0.15	—	—	—	—	—	—	—
				Moyenne	2.51	1.12	2.8	1.25×10^{-6}	9.0

Can. J. Chem. Downloaded from www.nrcresearchpress.com by 210.87.254.5 on 09/05/12
For personal use only.

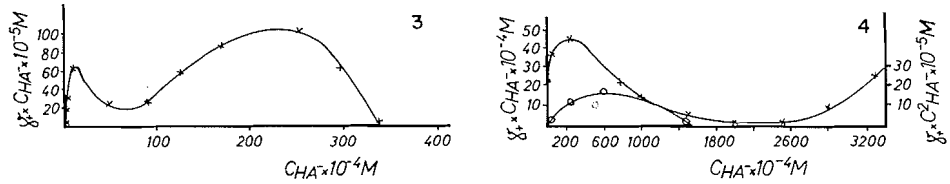


FIG. 3. Formation des complexes du protactinium avec l'acide trioxyglutarique.
FIG. 4. Formation des complexes du protactinium avec l'acide oxalique. ×, Pa:HOxal$^-$ = 1:1; ○, Pa:HOxal$^-$ = 1:2.

Pour le second complexe (Pa:HA$^-$ = 1:2) le domaine d'existence a été déterminé à l'aide des graphiques de coordonées $\gamma_+ . C^2_{HA^-}$ vs. C_{HA^-}. Le nombre des molécules du coordinat a été calculé à l'aide de graphiques de coordonées $\log \gamma_+/1 - \gamma_+ - \gamma_2$ vs. $\log C_{HA^-}$, où γ_2 est la fraction de ce complexe (Tableaux I à III).

TABLEAU III

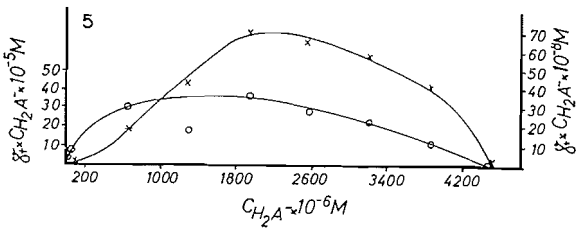
Détermination des constantes d'instabilité des citrates et aconitates du protactinium (μ = 0.25)

C_{H_3A} (mole/l)	pH	ζ (l/g)	γ_+	γ_2	K_1	K_2 ×10^{-6}	K_1'	K_2' ×10^{-6}	K_3' ×10^{-9}
Acide citrique									
0.0005	0.65	117.0	0.98	—	2.1×10^{-4}	—	2.2×10^{-4}	—	—
0.0010	0.65	79.0	0.81	—	—	—	2.2×10^{-4}	—	—
0.0100	0.95	93.5	0.92	—	7.4×10^{-4}	—	2.2×10^{-4}	—	—
0.0500	0.95	157.0	—	—	—	—	2.2×10^{-4}	—	—
0.1000	0.95	30.6	0.45	0.06	5.2×10^{-4}	—	2.2×10^{-4}	—	—
0.2000	0.95	7.0	0.15	0.45	1.9×10^{-4}	0.72	2.2×10^{-4}	3.1	—
0.3000	0.85	10.7	0.19	—	4.5×10^{-4}	—	2.2×10^{-4}	—	—
0.4000	0.85	5.4	0.10	0.26	2.8×10^{-4}	2.50	—	8.0	—
0.5000	0.85	7.9	0.14	—	5.2×10^{-4}	—	—	—	1.6
0.6000	0.85	1.6	0.03	0.70	1.1×10^{-4}	0.60	—	1.8	1.6
0.7000	0.85	0	—	—	—	—	—	—	—
				Moyenne	3.7×10^{-4}	1.2	2.2×10^{-4}	4.4	1.6
Acide aconitique									
0.001	0.75	114.0	0.50	—	—	—	—	—	—
0.005	0.80	285.0	0.74	—	—	—	—	—	—
0.010	0.80	145.0	0.64	—	—	—	—	—	—
0.050	0.75	132.0	0.60	—	—	—	—	—	—
0.100	0.80	138.0	0.56	—	1.5×10^{-3}	—	—	—	—
0.200	0.80	130.5	0.51	—	2.5×10^{-3}	—	—	—	—
0.300	0.80	120.0	0.49	—	3.5×10^{-3}	—	6.6×10^{-2}	—	—
0.400	0.80	143.5	0.46	—	4.1×10^{-3}	—	6.6×10^{-3}	—	—
0.500	0.80	92.5	0.34	—	3.1×10^{-3}	—	6.6×10^{-3}	—	—
0.600	0.80	114.5	0.47	—	6.4×10^{-3}	—	6.6×10^{-3}	—	—
0.700	0.75	135.0	0.46	—	7.2×10^{-3}	—	6.6×10^{-3}	—	—
				Moyenne	4.1×10^{-3}	—	6.6×10^{-3}	—	—

Les constantes d'instabilité ont été calculées en conditions d'équilibre de l'échange ionique, à l'aide des formules adéquates des méthodes de Froneus (7–10) et de Paramonova (11–15) (Tableaux I à III et VI).

Afin de vérifier la présence des complexes avec des charges négatives on a étudié l'adsorption sur l'anionite (Tableau IV). De la même manière on a constaté que le protactinium forme des complexes anioniques avec les acides mentionnés plus haut aussi à concentrations plus petites de l'acide.

Can. J. Chem. Downloaded from www.nrcresearchpress.com by 210.87.254.5 on 09/05/12
For personal use only.



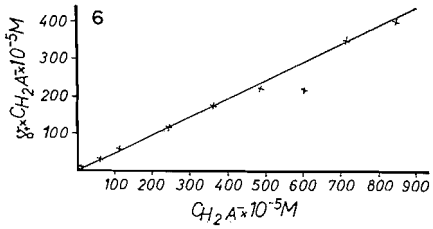


FIG. 5. Formation des complexes du protactinium avec l'acide citrique. ○, $Pa:H_2Cit^- = 1:1$; ×, $Pa:H_2Cit^- = 1:2$.

FIG. 6. Formation des complexes du protactinium avec l'acide aconitique.

TABLEAU IV

L'adsorption des complexes du protactinium sur l'anionite Amberlite IRA-400 ($\mu = 0.25$)

C_{H_2A} (mole/l)	pH	ζ (l/g×10³)	C_{H_2A} (mole/l)	pH	ζ (l/g×10³)
Malique*			Citrique		
0.01	0.65	3.05	0.0005	0.65	0.40
0.05	0.80	10.00	0.0010	0.65	7.00
0.10	0.80	5.25	0.0100	0.95	0
0.20	0.83	8.65	0.0500	0.95	0
0.30	0.83	5.80	0.1000	0.95	0
0.40	0.85	5.15	0.2000	0.85	0
0.50	0.85	3.90	0.3000	0.85	0
0.60	0.85	3.35	0.400	0.85	0
0.65	0.87	0.75	0.500	0.85	0
Tartrique*			0.600	0.85	3.25
0.01	0.80	15.3	0.700	0.85	4.5
0.05	0.80	49.5	Aconitique		
0.10	0.80	0	0.001	0.75	0
0.20	0.75	0	0.005	0.80	0
0.30	0.75	0	0.010	0.80	0
0.40	0.80	0	0.050	0.75	0
0.50	0.80	5.6	0.100	0.80	1.9
0.60	0.80	4.0	0.200	0.80	11.5
0.65	0.80	6.8	0.300	0.80	9.5
Trioxyglutarique			0.400	0.80	9.0
0.0005	1.1	0	0.500	0.80	10.2
0.0010	1.2	7.35	0.600	0.75	9.70
0.0050	1.2	5.35	0.700	0.75	15.5
0.0100	1.0	2.60	EDTA		
0.0500	1.0	2.75	0.00008	2.4	48.2
0.1000	1.0	2.00	0.00080	2.6	3.2
0.2000	1.0	0	0.00400	2.4	0
0.3000	0.95	0	0.00800	2.4	0
0.4000	1.0	0	0.01280	2.4	0
0.5000	1.0	0	0.02560	2.7	0
0.6000	0.95	0			
0.7000	1.1	0			
Oxalique					
0.0001	0.65	4.15			
0.0005	0.65	0.45			
0.0010	0.65	0.25			
0.0100	0.80	30.50			
0.0500	0.80	6.00			
0.1000	0.80	3.50			
0.2000	0.80	0			
0.3000	0.75	0			
0.4000	0.75	0			
0.5000	0.75	0			
0.6000	0.75	0.69			
0.7000	0.75	0.51			

*Dans ces cas on a utilisé l'anionite Dowex-1×16.

Can. J. Chem. Downloaded from www.nrcresearchpress.com by 210.87.254.5 on 09/05/12
For personal use only.

Pour déterminer la charge des complexes nous avons employé la méthode de Trofimov et de Stepanova (18) qui permet de calculer la charge moyenne effective (Tableau V). On a observé que la charge des complexes est fonction de la concentration du coordinat et du pH des solutions.

TABLEAU V

Détermination de la charge moyenne effective des complexes du protactinium ($\mu = 0.25$)

C_{H_2A} (mole/l)	pH	$\bar{z}$	C_{H_2A} (mole/l)	pH	$\bar{z}$
Malique			Citrique		
0.10	1.0	4.5+	0.010	0.8	5.0+
0.30	1.0	4.5+	0.010	1.5	2.0+
0.50	1.0	4.5+	0.010	1.7	*
Tartrique			0.010	2.0	*
0.10	1.0	3.5+	0.010	2.8	*
0.30	1.0	3.0+	0.010	0.95	6.0+
0.50	1.0	1.5+	0.010	1.35	6.0+
Trioxyglutarique			0.010	1.75	5.5+
0.29	1.1	7.0+	0.010	2.35	5.5+
0.29	2.0	4.0+	0.010	3.00	6.0+
0.0005	1.1	5.0+	0.0005	0.65	7.5+
0.0010	1.2	5.0+	0.0010	0.65	8.5+
0.0050	1.2	5.5+	0.0100	0.95	6.5+
0.0500	1.0	10.0+	0.0500	0.95	2.0+
0.1000	1.0	8.0+	0.1000	0.95	4.0+
0.01	1.1	4.0+	Aconitique		
0.01	1.4	4.0+	0.001	0.75	7.5+
0.01	1.5	1.5+	0.005	0.80	4.5+
0.01	1.8	1.0+	0.010	0.80	6.5+
Oxalique			0.050	0.75	7.5+
0.0001	0.65	10.0+	0.100	0.80	7.5+
0.0005	0.65	7.0+	0.200	0.80	7.0+
0.0010	0.65	6.0+			
0.0100	0.80	5.0+			

*En ce cas il n'y a pas d'adsorption sur cationite.

DISCUSSIONS

Selon les valeurs du coefficient de distribution ζ (Tableaux I à III) l'adsorption du protactinium sur le cationite de solutions d'acides mentionnés plus haut, est fonction de la concentration du coordinat et du pH. Les courbes des Figs. 1 à 6 montrent que le protactinium avec les acides hydroxy forme des complexes qui ont des rapports $Pa:HA^-$ différents. Par exemple les acides malique et tartrique dans l'intervalle de concentration $10^{-2} - 6.5 \times 10^{-1}$ M forment des complexes ayant le même rapport $Pa:HA^-$ et les constantes d'instabilité respectivement $K_1 = 3.8 \times 10^{-3}$ et $K_1 = 4.6 \times 10^{-3}$ (Tableau I). Par contre les acides trioxyglutarique, oxalique et citrique forment des complexes avec le protactinium qui se comportent de façon différente (Figs. 3 à 5). L'augmentation de la concentration de l'acide trioxyglutarique conduit à la diminution brusque des valeurs du coefficient de distribution sur cationite. Le phénomène est dû à la formation de complexes qui contiennent un nombre différent de molécules d'acide, ayant, comme il a été trouvé, plusieurs charges positives. En même temps la diminution brusque du coefficient de distribution est fortement influencée également par la formation des complexes dimérisés. La dimérisation des complexes du protactinium avec l'acide trioxyglutarique (dans certaines conditions de pH et de concentration du coordinat) est indiquée également par le nombre de molécules du coordinat dans ces complexes et par leur charge moyenne effective (Tableau V et Fig. 9).

Les résultats que nous avons obtenus dans l'étude de la complexation du protactinium

Can. J. Chem. Downloaded from www.nrcresearchpress.com by 210.87.254.5 on 09/05/12
For personal use only.

avec les acides lactique (5), α-hydroxy-iso-butyrique et mandélique (6), montrent que la dimérisation de ces complexes est possible aussi à une concentration constante du protactinium mais en variant le pH et la concentration du coordinat. En ce cas nous pensons qu'une telle dimérisation est due à la formation des liaisons hydrogène intermoléculaires. Analogiquement, pour les acides malique, tartrique, trioxyglutarique et citrique la dimérisation des complexes du protactinium, dans ces conditions de pH et concentration mentionneés plus haut, est due à la formation des liaisons hydrogène intermoléculaires.

TABLEAU VI

Détermination des constantes d'instabilité des complexes du protactinium avec l'EDTA

C_{H_4Y} (mole/l)	$C_{H_3Y^-}$ (mole/l)	pH	ζ (l/g×10³) Sur cationite	Sur anionite	K_1	K_2
8×10^{-5}	8×10^{-7}	2.4	25.3	48.2		
8×10^{-4}	8×10^{-6}	2.6	5.2	3.2		
4×10^{-3}	4×10^{-5}	2.4	4.8	0	6.5×10^{-9}	1.1×10^{-12}
8×10^{-3}	8×10^{-5}	2.4	4.3	0		
12×10^{-3}	12×10^{-5}	2.4	1.3	0		
25×10^{-3}	25×10^{-5}	2.7	1.4	0		

La variation du pH et de la concentration du coordinat conduit également à une variation des valeurs de la charge moyenne effective (Tableau V). L'augmentation du pH renforce le processus d'hydrolyse du protactinium (19, 20) qui favorise la formation des liaisons hydrogène entre les groupes OH du protactinium hydrolysé et le coordinat.

En ce qui concerne la complexation du protactinium avec l'acide oxalique, d'après l'allure de la courbe (Fig. 4) et les valeurs des constantes d'instabilité des oxalates (Tableau II), on a observé une ressemblance avec celles de l'acide trioxyglutarique. Cela conduit à penser que l'acide oxalique se comporte comme un acide hydroxy.

L'augmentation de la concentration des acides citrique, aconitique et éthylènediaminetétracétique conduit à la diminution brusque des valeurs du coefficient de distribution (Tableaux III, IV et VI). Le pH a aussi une influence semblable.

En déterminant le domaine d'existence des complexes du protactinium avec les acides citrique et aconitique, dans l'intervalle de concentrations de 10^{-4} à 10^{-1} M et de pH = 0.65–0.95 (Figs. 5 et 6) on a trouvé que l'acide citrique forme des complexes ayant le rapport $Pa:H_2Cit^- = 1:1$ et 1:2, tandis que l'acide aconitique forme des complexes avec le rapport

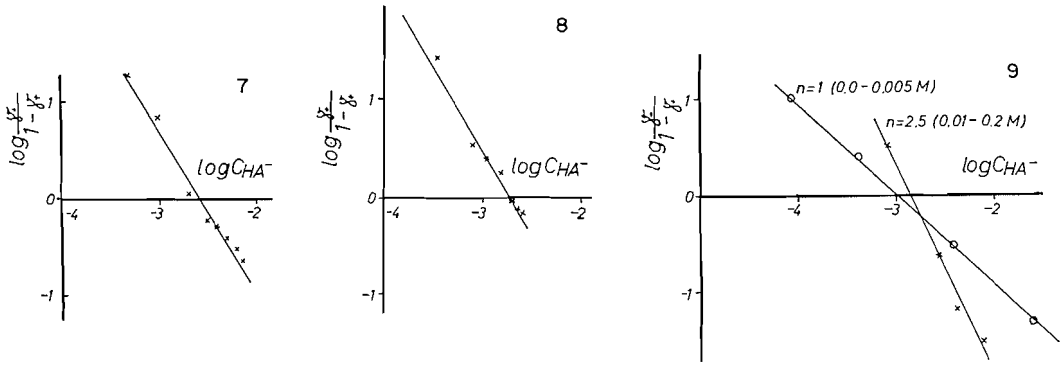


FIG. 7. Détermination du nombre des molécules du coordinat dans les malates de protactinium: $n = 1$.
FIG. 8. Détermination du nombre des molécules du coordinat dans les tartrates de protactinium: $n = 1$.
FIG. 9. Détermination du nombre des molécules du coordinat dans les trioxyglutarates de protactinium: $n_1 = 1$; $n_2 = 2.5$.

Can. J. Chem. Downloaded from www.nrcresearchpress.com by 210.87.254.5 on 09/05/12
For personal use only.

Can. J. Chem. Downloaded from www.nrcresearchpress.com by 210.87.254.5 on 09/05/12
For personal use only.

TABLEAU VII

Formes possibles des complexes du protactinium avec quelques acides di-carboxyliques, en solution

Acide	Intervalle de concentrations (mole/l)	Valeurs expérimentales			Formes proposées des complexes	
		n_1	n_2	$\bar{z}$	Milieu fortement acide	Milieu faiblement acide
Malique	$10^{-2}-6.5\times10^{-1}$	—	2	4.5+	$[Pa_2O(OH)_{1.5}(HMal)_2]^{4.5+}$	$[Pa_2(OH)_{3.5}(HMal)_2]^{4.5+}$
Tartrique	$10^{-2}-6.5\times10^{-1}$	1	2	3.5+	$[Pa_2O(OH)_{3.5}(HTart)]^{3.5+}$	$[Pa_2(OH)_{5.5}(HTart)]^{3.5+}$
				1.5+	$[Pa_2O(OH)_{4.5}(HTart)_2]^{1.5+}$	$[Pa_2(OH)_{6.5}(HTart)_2]^{1.5+}$
Trioxyglutarique	$5\times10^{-4}-7\times10^{-1}$	1	2.5	4+	$[Pa_2O(OH)_3(HTogl)]^{4+}$	$[Pa_2(OH)_5(HTogl)]^{4+}$
Oxalique	$10^{-4}-7\times10^{-1}$	1	2	4+	$[Pa_2O(OH)_3(HOxal)]^{4+}$	$[Pa_2(OH)_5(HOxal)]^{4+}$
					$[Pa_2O(OH)_2(HOxal)_2]^{4+}$	$[Pa_2(OH)_4(HOxal)_2]^{4+}$

$Pa:H_2Acon^-$ = 1:0.5. L'augmentation de la concentration du coordinat dans les limites ci-dessus citées, conduit dans le cas des citrates, à une diminution de la charge des complexes de $\bar{z} = 8.5+$ à $\bar{z} = 2+$. Pour l'acide aconitique, dans ces conditions, $\bar{z}$ reste presque constant.

En comparant les constantes d'instabilité des citrates et des aconitates de protactinium, on a observé que l'acide aconitique forme des complexes plus instables que les citrates. La diminution de la stabilité des aconitates par rapport aux citrates de protactinium peut être expliquée par le fait que, dans ce cas il n'y a pas comme avec les acides citrique et oxalique, de formation de cycles penta (qui sont plus stables) par l'intermédiaire des groupes hydroxy de l'acide.

En se basant sur les valeurs des coefficients $\bar{z}$ (la charge moyenne effective) et $\bar{n}$ (le nombre des molécules du coordinat dans le complexe respectif) expérimentalement trouvées, nous sommes arrivés à la conclusion que la forme des complexes du protactinium avec les acides hydroxy mentionnés plus haut, dépend du milieu (fortement ou faiblement acide). Les formes les plus adéquates des quelques complexes sont montrées dans le Tableau VII.

Le comportement de l'acide éthylènediaminetétracétique (EDTA) (sel disodique), lors de la formation de complexes, est complètement différent de celui des acides mono-, di- et tri-carboxyliques, que nous avons étudiés. La diminution rapide des valeurs du coefficient de distribution en fonction de la concentration du coordinat nous indique la grande tendance de cet acide à former avec le protactinium des complexes ayant des charges négatives. Par exemple à la concentration très faible du coordinat de 8×10^{-7} M et à pH = 2.4, la formation de complexes est encore appréciable. Dans ces conditions, on trouve environ 50% de l'activité totale du protactinium en solution sur l'anionite et seulement 20% sur le cationite. Ce résultat montre que le protactinium, en dehors des complexes ayant des charges négatives et positives, forme aussi des complexes neutres.

Le rapport $Pa:H_3Y^-$ déterminé à l'aide des graphiques et à la concentration en coordinat de 8×10^{-7} M (pH = 2.4–2.7) a pour valeur 1:1. L'augmentation de la concentration du coordinat conduit aussi à la formation de complexes de type $Pa:H_3Y^-$ = 1:2 et $Pa:H_2Y^{2-}$ = 1:1.

En réalité, le processus de la formation des complexes chelatés du protactinium avec l'EDTA est plus compliqué qu'il n'a été décrit dans cette communication.

BIBLIOGRAPHIE

1. R. E. Elson. The actinide elements. *Edited by* G. T. Seaborg and J. J. Katz. New York. 1954. Chap. 5.
2. A. Goble, J. Golden et A. C. Maddock. Can. J. Chem. **34**, 284 (1956).
3. K. A. Kraus et G. E. Moore. J. Am. Chem. Soc. **72**, 4293 (1950).
4. J. E. Starik, L. D. Sheidina et L. I. Il'menkova. Radiokhimiya, **1**, 168 (1959); **1**, 391 (1959).
5. I. Galateanu et A. V. Lapitzkii. Radiokhimiya, **4**, 421 (1962).
6. A. V. Lapitzkii et I. Galateanu. Radiokhimiya, **5**, 330 (1963).
7. S. Froneus. Acta Chem. Scand. **4**, 72 (1950).
8. S. Froneus. Acta Chem. Scand. **5**, 139 (1951).
9. S. Froneus. Acta Chem. Scand. **6**, 1200 (1952).
10. S. Froneus. Svensk Kem. Tidskr. **64**, 317 (1952).
11. V. I. Paramonova. Zh. Neorgan. Khim. **3**, 523 (1957).
12. V. I. Paramonova et A. S. Voevodskii. Zh. Neorgan. Khim. **1**, 1905 (1956).
13. V. I. Paramonova, A. I. Mosevič et A. I. Subotina. Zh. Neorgan. Khim. **1**, 88 (1958).
14. V. I. Paramonova. Zh. Neorgan. Khim. **1**, 212 (1958).
15. V. I. Paramonova, A. S. Kreičuk et B. A. Shishlyakov. Radiokhimiya, **1**, 650 (1959).
16. I. Galateanu et A. V. Lapitzkii. Dokl. Acad. Nauk SSSR, **147**, 372 (1962).
17. K. A. Kraus, G. E. Moore et F. Nelson. J. Am. Chem. Soc. **78**, 2692 (1956); **72**, 4283 (1950); **77**, 1383 (1955); **73**, 2900 (1951).
18. A. V. Trofimov et L. N. Stepanova. Radiokhimiya, **2**, 73 (1960).
19. R. Guillaumont, R. Muxart, R. Bouissières et M. Haissinsky. J. Chim. Phys. **57**, 1019 (1960).
20. D. Brown, T. Sato, A. J. Smith et R. G. Wilkins. J. Inorg. Nucl. Chem. **23**, 91 (1961).

Can. J. Chem. Downloaded from www.nrcresearchpress.com by 210.87.254.5 on 09/05/12
For personal use only.

Can. J. Chem. Downloaded from www.nrcresearchpress.com by 210.87.254.40 on 09/05/12
For personal use only.

THE SYSTEM: ALUMINIUM–INDIUM–SILVER

PART I. THE BINARY AND TERNARY MISCIBILITY GAPS

A. N. CAMPBELL AND R. WAGEMANN

Department of Chemistry, University of Manitoba, Winnipeg, Manitoba

Received November 4, 1965

ABSTRACT

The miscibility gap in the binary system: Al–In has been investigated and the critical temperature and composition estimated as 945 °C and 68.8% In, 31.2% Al (by weight).

The liquid–liquid partial miscibility region of the ternary system has also been determined. The lowest temperature at which two liquids can exist in equilibrium before a third (solid) phase appears was found to be approximately 590°. At this temperature, the ternary gap extends to 30.5% Ag, 34.7% Al, and 34.8 In. Isotherms of the ternary gap are given for 50° intervals between 650° and 900°. A true ternary critical point does not exist, i.e. the binary critical temperature is lowered continuously by addition of silver.

INTRODUCTION

In the course of a lengthy investigation of the complicated system named in the title, we have become convinced that the accepted equilibrium diagram for the component binary system: silver–indium, is seriously in error and, indeed, a preliminary experimental investigation has shown that this is so. Since this will delay the completion of the work for some time, we thought it advisable at this stage to give a report on the interesting two-liquid relations.

Valentiner and Puzicha (1) stated that the two metals, indium and aluminium, are largely immiscible in both solid and liquid states. These authors, as well as Raub and Engel (2) give rather inaccurate limits for the liquid gap at the monotectic temperature, which they report as 634°. The latest, most extensive, work is that of Campbell, Buchanan, Kuzmak, and Tuxworth (3), who used a quenching technique and investigated the course of the indium-rich curve between the monotectic and eutectic temperatures. They reported the limits of the gap as 17.5 and 97.2 wt. % indium, at 638.6°: the eutectic contained less than 0.05% aluminium. Campbell and co-workers determined the compositions of conjugate layers up to 800°. In the present work, by raising the temperature to 950°, we have succeeded in closing the gap, and we have deduced the binary critical temperature and composition with reasonable certainty. The addition of silver to the binary system: In–Al increases the mutal solubility and we have completed the determination of the two-liquid surface.

EXPERIMENTAL

Purity of Metals

Silver (Johnson, Matthey) 99.995% Ag.

Indium (Consolidated Mining and Smelting Company of Canada) 99.99% In.

Aluminium (Department of Mines and Technical Surveys, Mines Branch, Ottawa) 99.994% Al, 0.0019% Fe, 0.0018% Si, 0.0018% Cu.

Miscibility Gap (in Binary and Ternary System)

Previous work by Campbell, Buchanan, Kuzmak, and Tuxworth (3) had indicated that the miscibility gap in the system: Al–In might close somewhere between 800° and 900°. In the present investigation the two liquid layers were brought to equilibrium in a furnace at constant temperature and the liquid layers were sampled directly. An investigation of analytical methods, including the flame spectrometer, led us to the conclusion that no really accurate method exists for the chemical determination of indium in the presence of aluminium. The method of analysis adopted was therefore to analyze directly for silver by the Volhard method and, for ternary alloys, determine the composition from density measurements. From calibration graphs of experimentally observed density versus aluminium–indium content for various fixed silver contents, the aluminium–indium ratio could be established as soon as the silver content was known. The relatively large differences in density of the three metals made this method fairly accurate.

A chromel–alumel thermocouple was calibrated in the usual way from the freezing points of pure metals. A Brown recorder permitted an accuracy of reading of 1°; including other sources of error, we estimate the final error of our temperatures to be ±2°. The molten alloys were kept in an argon atmosphere in the Vycor cell shown in Fig. 1.

The cell was evacuated after loading, filled with argon, and connected to a mercury valve to allow for expansion after heating. For isothermal work, a separate chromel–alumel thermocouple, placed in the furnace immediately above the crucible (Fig. 1) was connected to a Wheelco thermostatic control. The furnace temperature was constant to ±1°.

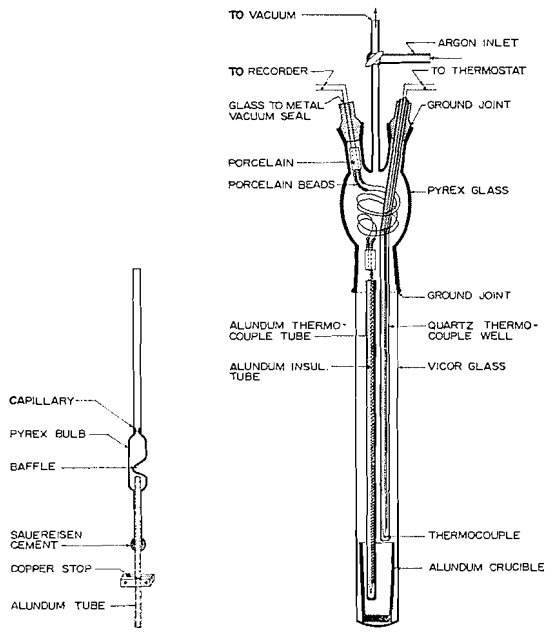


FIG. 1. The alloy pipette and the isothermal and thermal analysis cell.

Preparation of Alloys

Alundum crucibles of 25 ml capacity were used for melting the alloys. For thermal analysis alloys of different composition were obtained from an original alloy by adding increments of one component along a line of constant ratio of concentration of the other two components. Alloys were given a preliminary melting in an induction furnace at 1 000°. In the isothermal work the alloys were equilibrated at the desired temperature, for 14 h. Samples of alloys were withdrawn from the top and bottom layers with the pipette shown in Fig. 1. The depth to which the pipette was lowered was controlled by the copper stop. Immediately after a sample was withdrawn, the pipette was removed from the cell and immersed in cold water, the whole operation requiring less than 30 s. The cracked glass was then removed and the whole sample cut into small pieces for density determination and chemical analysis.

Density Determination

Densities were determined in a 25 ml Weld pycnometer, using redistilled *n*-butyl ether as the inert liquid: some of the alloys react with water. Sixty determinations of density were made in duplicate, for calibration purposes. The results are expressed graphically in Fig. 2. The temperature of all determinations was 25.00 ± 0.02°. We estimate our results to be accurate to 0.002 g/cc corresponding to an error in composition of about ±0.8% In for low concentrations of indium or ±0.02% In for high concentrations of indium. Each curve of Fig. 2 represents a 10% increase in indium content, while the abscissa represents the percentage of silver. It will be observed that the curves have steep slopes indicating that density is very sensitive to composition. To use this set of curves for the analysis of a ternary alloy, determination of the silver content and of the density provides sufficient data (with suitable interpolation) for the determination of indium.

RESULTS

Some 60 isothermal experiments were carried out and the data are available in the thesis of the junior author (R. Wagemann, ref. 4). Figure 3 gives the limits of the ternary isothermal liquid gap at 650°, 700°, 750°, 800°, and 900°.

Can. J. Chem. Downloaded from www.nrcresearchpress.com by 210.87.254.40 on 09/05/12
For personal use only.

The 650° isotherm is separately reproduced in Fig. 4 in order that the slopes of tie lines joining congruent solutions may be evident. The binary liquid gap of the system: aluminium–indium is reproduced in Fig. 5.

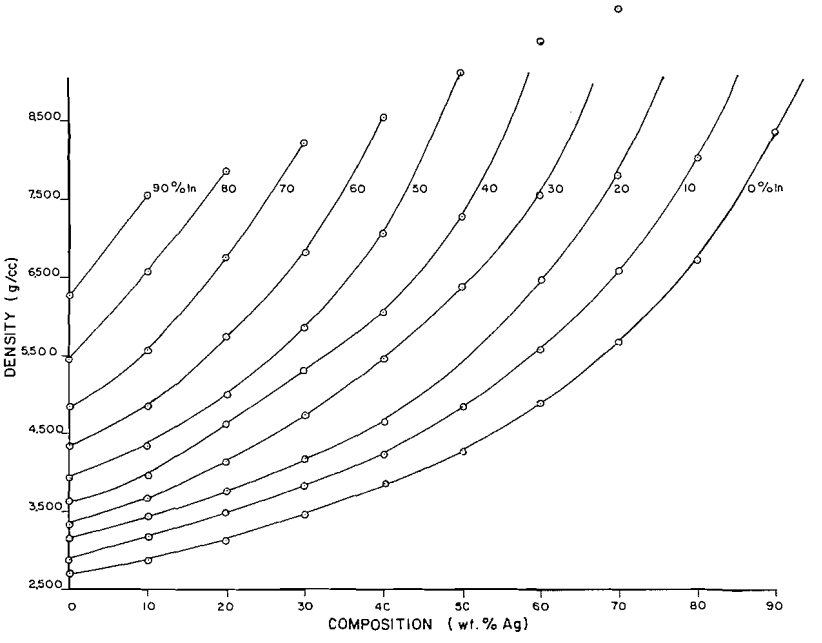


FIG. 2. Density vs. composition for the binary system: Ag–In.

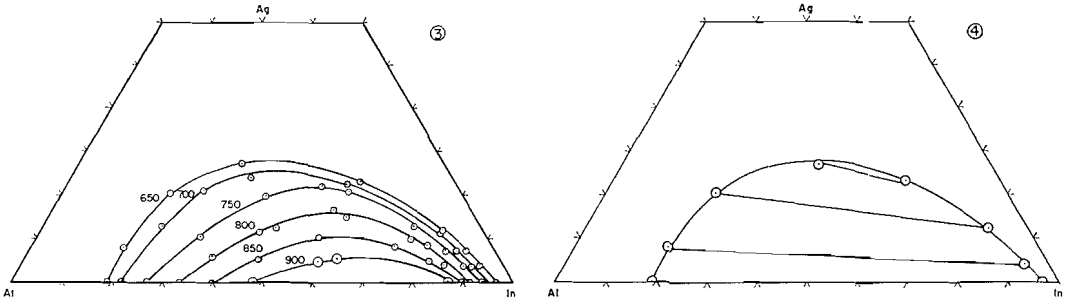


FIG. 3. Isotherms through liquid–liquid immiscibility space at 650, 700, 750, 800, 850, and 900 °C.
FIG. 4. The isotherm at 650 °C for the system: Al–In–Ag showing direction of the tie lines.

The Binary Miscibility Gap

For the binary system: indium–aluminium, an approximate critical temperature of 945° was obtained by the extrapolation of our experimental measurements, which extended to 900° (Fig. 5). The law of the rectilinear diameter is followed rather closely and the extrapolation of this straight line to the critical temperature gave the critical composition as 68.8% In. An alloy of composition 70% In was found to be completely homogeneous at 950°, in the sense that the density was the same throughout.

The Ternary Miscibility Gap

Isotherms through the ternary liquid–liquid space (ternary gap) at 650°, 700°, 750°, 800°, 850°, and 900° are shown in polytherma projection in Fig. 3. A true ternary critical

Can. J. Chem. Downloaded from www.nrcresearchpress.com by 210.87.254.40 on 09/05/12
For personal use only.

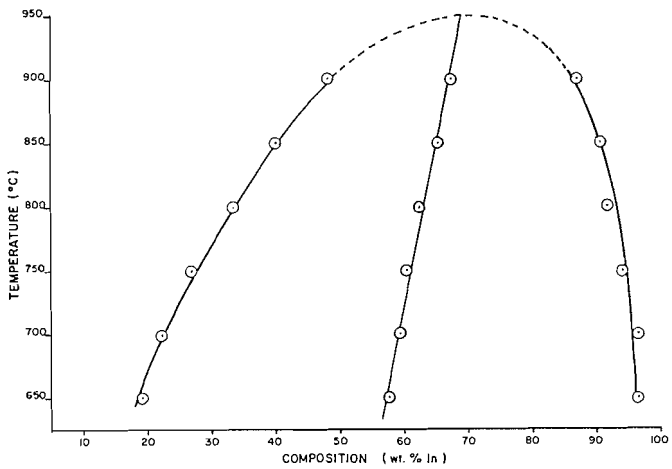


FIG. 5. Liquid–liquid immiscibility in the binary system: Al–In.

temperature does not exist in this system; in other words, the addition of silver to the binary critical mixture of the system: Al–In progressively lowers the temperature of complete miscibility. The lowest temperature at which two liquid layers can coexist, in absence of solid phase, is 590°. The critical composition at 650° is approximately 26 wt. % Ag, 47% In, 27% Al. At 590°, the content of silver has risen to 30%. Attempts by thermal analysis to detect the boundaries of the three-phase region ($L_1 + L_2 + S$), which lies below the ternary miscibility gap, failed, no doubt on account of the smallness of the heat effect.

ACKNOWLEDGMENT

We are indebted to the Consolidated Mining and Smelting Company of Canada, in this as in all our other investigations of indium alloys, for the presentation of a constant supply of pure indium.

REFERENCES

1. S. VALENTINER and I. PUZICHA. Metallforsch. **2**, 127 (1947).
2. E. RAUB and M. ENGEL. Metallforsch. **1**, 148 (1946).
3. A. N. CAMPBELL, L. B. BUCHANAN, J. M. KUZMAK, and R. H. TUXWORTH. J. Am. Chem. Soc. **74**, 1962 (1952).
4. R. WAGEMANN. M.Sc. Thesis, University of Manitoba, 1964.

Can. J. Chem. Downloaded from www.nrcresearchpress.com by 210.87.254.40 on 09/05/12
For personal use only.

Can. J. Chem. Downloaded from www.nrcresearchpress.com by 210.87.254.5 on 09/05/12
For personal use only.

THE TRANSMISSION OF POLAR EFFECTS

PART III.[1] THE KINETICS OF THE ACID-CATALYZED ESTERIFICATION OF 3-SUBSTITUTED ACRYLIC ACIDS AND THE ALKALINE HYDROLYSIS OF THE METHYL ESTERS

KEITH BOWDEN[2]

Department of Pure and Applied Chemistry, Royal College of Advanced Technology, Salford, Lancashire, England

Received September 21, 1965

ABSTRACT

The rate coefficients for the acid-catalyzed esterification in methanol at 35.0° of fourteen 3-substituted acrylic acids have been determined. Rate coefficients have also been determined for the alkaline hydrolysis in 70% v/v dioxan–water at 18.8° of 13 methyl esters and the carbonyl-stretching frequencies of the esters have been examined. The effect of *trans*-substitution is assessed by use of the Hammett equation. In the alkaline hydrolysis, the transmission of polar effects is approximately 1.9 that of the meta- and para-substituted benzoates. An analysis of the steric effects in the *cis*-isomers in both reactions shows that the steric effects of the halogeno-substituents in the two reactions differ and an explanation is offered. The application of the Taft–Ingold equation to ortho-substituted benzoates is criticized. The carbonyl-stretching frequencies of the *cis*-halogeno-esters exhibit a shift of $+8$ cm^{-1} compared with the *trans*-isomers; this shift is attributed to an electrostatic effect.

INTRODUCTION

Previous studies, in this series, have been made on the reactivity of 3-substituted acrylic acids (1). The results indicated that there was a similar polar effect from the *cis*- or *trans*-position and that the transmission was about twice that for a similarly substituted *p*-benzoic acid. It was felt that this information equipped us to test thoroughly the Taft separation of polar and steric effects in ester hydrolysis (2), using the 3-substituted acrylic system. Taft's separation of these effects in arylaliphatic and aliphatic systems has received support (3, 4), whereas the related treatment of the ortho-benzoic systems has recently been criticized (5). The latter workers suggest that the separation does not give a true estimate of the polar effect of the ortho-substituent and that the steric effects in alkaline and acidic hydrolysis and esterification are not the same.

In this study, the reactivity of both *cis*- and *trans*-3-substituted acrylic esters and acids have been measured in their alkaline hydrolysis and acid-catalyzed esterification reaction. These results, together with the carbonyl-stretching frequencies of the esters, are reported here.

EXPERIMENTAL

Materials

Methyl acrylate was obtained commercially and was redistilled immediately before use. The preparation and purity of the acids have been described previously (1). The preparation of the other esters was made more difficult because the olefinic bond in a number of the halogeno-substituted acrylic acids is reactive towards diazomethane, which is usually the best methylating agent (cf. ref. 6). Therefore, the methyl esters were prepared by esterification of the acids by methanolic hydrogen chloride. The less stable *cis*-esters could be isomerized by prolonged heating in acid solution. Because of this, these esters were prepared by treatment of the corresponding acids with dry methanolic hydrogen chloride for from 3 to 6 h at 50°. After isolation, the methyl esters were distilled under reduced pressure. Details of the physical properties and, where relevant, the elemental analyses are given in Table I. No evidence of isomer or other impurities was found by gas–liquid chromatography, by nuclear magnetic resonance spectroscopy, or from their saponification equivalents.

Methanol was purified by Lund and Bjerrum's method (9) and had b.p. 64° at 754 mm, d_4^{20} 0.7922 (lit. (10) 64.5°, 0.7914). The water content was found to be less than 0.08% w/w by Karl Fischer titration.

[1]*Part II; see Can. J. Chem. 43, 3354 (1965).*

[2]*Present address: Department of Chemistry, The University of Essex, Colchester, Essex, England.*

TABLE I

Physical properties of esters

Methyl ester	b.p. or m.p. (°C)	Literature b.p. (°C)	Reference
Acrylate	81–82 at 755 mm	85	7
trans-Crotonate	119–120 at 755 mm	121	7
cis-Crotonate	73–74 at 110 mm	102–104 at 754 mm	8
trans-3-Chloroacrylate	124 at 755 mm	*a*	—
cis-3-Chloroacrylate	44–45 at 45 mm	*b*	—
trans-3-Bromoacrylate	148 at 755 mm	*c*	—
cis-3-Bromoacrylate	38–39 at 12 mm	*d*	—
trans-3-Iodoacrylate	41–42	*e*	—
cis-3-Iodoacrylate	62–63 at 12 mm	*f*	—
trans-3-Methoxyacrylate	155–156 at 755 mm	*g*	—
trans-3-Chlorocrotonate	59–60 at 12 mm	64–67 at 14 mm	7
cis-3-Chlorocrotonate	42–43 at 12 mm	42–43 at 13 mm	7
3,3-Dimethylacrylate	135–136 at 755 mm	135–138	7

(*a*) Anal. Calcd. for $C_4H_5O_2Cl$: C, 39.86; H, 4.18; Cl, 29.42. Found C, 39.80; H, 4.12; Cl, 29.32.
(*b*) Anal. Calcd. for $C_4H_5O_2Cl$: C, 39.86; H, 4.18; Cl, 29.42. Found C, 39.79; H, 4.08; Cl, 29.49.
(*c*) Anal. Calcd. for $C_4H_5O_2Br$: C, 29.12; H, 3.05; Br, 48.43. Found C, 29.06; H, 3.16; Br, 48.49.
(*d*) Anal. Calcd. for $C_4H_5O_2Br$: C, 29.12; H, 3.05; Br, 48.43. Found C, 29.15; H, 3.10; Br, 48.28.
(*e*) Needles from water.
Anal. Calcd. for $C_4H_5O_2I$: C, 22.67; H, 2.38; I, 59.87. Found C, 22.71; H, 2.29; I, 59.81.
(*f*) Anal. Calcd. for $C_4H_5O_2I$: C, 22.67; H, 2.38; I, 59.87. Found C, 22.60; H, 2.31; I, 59.75.
(*g*) Anal. Calcd. for $C_6H_8O_3$: C, 51.71; H, 6.95. Found C, 51.85; H, 7.07.

Dioxan was purified by the method of Cavell, Chapman, and Johnson (11) and had b.p 101.5° at 754 mm (lit. (10) 101.3° at 760 mm). Anhydrous toluene-*p*-sulfonic acid (microanalytical reagent grade, Hopkins and Williams Limited) was dried in a vacuum desiccator and had m.p. 105–106° (lit. (10) 106–107°).

Measurements

Acid-Catalyzed Esterification

The method used was similar to that of Smith and Reichardt (12). The acid catalyst used in these studies was, however, toluene-*p*-sulfonic acid. The Goldschmidt eq. [i] (see ref. 12)

$$[i] \qquad k = \frac{(a + r)\ \ln\ [a/(a - x)] - x}{rt[\text{catalyst}]}$$

was used to calculate the rate coefficient k (l mole^{-1} min^{-1}), where a is the initial concentration of the carboxylic acid (approximately 0.05 M) and $(a - x)$ is the concentration at time t. The catalyst concentration was approximately 0.05 or 0.1 M. The constant r was found to be 0.28 at 35.0° which is in agreement with the interpolated value (i.e. 0.28) from earlier work (12). The reaction times were short and no isomerization was detected for less stable *cis*-isomers. There was no trend to faster rates with time, and nuclear magnetic resonance measurements on test samples indicated no detectable (i.e. less than 1%) conversion.

Alkaline Ester Hydrolysis

Rate coefficients were measured as described previously (3). Equal concentrations of ester and alkali (approximately 0.025 or 0.05 M) were used and the reaction studied by the "H" bulb method. The choice of solvent as 70% v/v dioxan–water was dictated by the lack of solubility of the least soluble ester in highly aqueous solution and the occurrence of nucleophilic substitution of the halogen in alkaline methanol–water. The latter reaction appeared to be due to methoxide ion completely. This ion is in equilibrium with the hydroxide ion in these solutions (3, 5). Saponification equivalents indicated no significant (i.e. $< 1\%$) substitution at 18.8° in aqueous dioxan. The solutions were prepared in a manner similar to that previously described (3, 5). The rate coefficient k (l mole^{-1} min^{-1}) was calculated from the second-order expression [ii] when the reactants are present in equal initial concentrations,

$$[ii] \qquad k = x/at(a - x),$$

where a is the initial concentration of the reactants and $(a - x)$ is their concentration at time t.

Since there were no available data for the hydrolysis of methyl benzoates in this medium, rate coefficients were also measured for a series of these esters.

Infrared Spectra

The carbonyl-stretching vibrations of the methyl esters were examined with a Perkin–Elmer Model 221 infrared recording spectrophotometer equipped with sodium chloride prism and cells. The bands were scanned

Can. J. Chem. Downloaded from www.nrcresearchpress.com by 210.87.254.5 on 09/05/12
For personal use only.

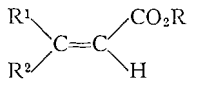
at 6 cm^{-1} min^{-1} (1 μ in 50 cm of the chart) and a 1 mm cell was used. The solutions were approximately 0.02 *M* in carbon tetrachloride (Hopkin and Williams, Ltd., "Spectrosol" grade) solution. The calibration was checked with a solution of acetone in carbon tetrachloride (band at 1 719 cm^{-1}) and at least two independent measurements were made on each ester. The values of ν_{max} (wave number at the absorption maximum) were measured.

RESULTS AND DISCUSSION

The results are summarized in Tables II and III.

TABLE II

Acid-catalyzed esterification of the acids, alkaline hydrolysis, and carbonyl-stretching vibration frequencies of the methyl esters



R^1	R^2	Acid-catalyzed esterification in methanol at 35.0° (10^2k)	Alkaline hydrolysis in 70% v/v dioxan–water at 18.8° ($10k$)	Carbonyl-stretching frequencies in carbon tetrachloride ν_{max} (cm^{-1})
H	H	20.0*	41.1†	1 735
H	Me	9.07*	4.20†	1 730‡
Me	H	3.87	2.36†	1 728
H	Cl	5.13	149	1 733
Cl	H	3.40	36.5	1 742.5
H	Br	5.99	209	1 733
Br	H	3.82	23.1	1 740.5
H	I	4.10	159	1 733
I	H	1.62	15.0	1 739.5
Cl	Me	2.82	7.60	1 740.5
Me	Cl	1.40	11.3	1 728.5
Me	Me	1.83*	0.148	1 728
H	OMe	4.70	2.24	1 713
H	NO_2	2.62	—	—

NOTE: Values of k (1 $mole^{-1}$ min^{-1}) are accurate to ±2.5% or better. The accuracy of the wave number (*relative* to the standard) is considered to be ±1 cm^{-1}.

*Sudborough and Davies (13) found, at 15° with an earlier, inexact rate equation and hydrogen chloride as the catalyst, the ratio of rate coefficients to be 1.00 (acrylic):0.408 (*trans*-crotonic):0.0737 (3,3-dimethylacrylic).

†For the alkaline hydrolysis in water, the ratio of the rate coefficients has been found to be 1.00 (acrylate):0.167 (*trans*-crotonate): 0.100 (*cis*-crotonate) (14, 15).

‡Barrow (16) found ν_{max} as 1 729 cm^{-1}.

TABLE III

Alkaline hydrolysis of substituted methyl benzoates in 70% v/v dioxan–water at 18.8°

Substituent	10^2k*	Substituent	10^2k*
p-MeO	5.62	*p*-Cl	63.2
p-Me	7.03	*p*-Br	69.0
m-Me	12.2	*m*-Cl	80.0
H	17.4		

*Values of k (1 $mole^{-1}$ min^{-1}) are accurate to ±2% or better.

The Effect of Substitution on the Alkaline Hydrolysis Reaction

The effect of the substituents is shown in Table II. The effect of the *trans*-substituents is linearly related to their effect on the ionization reaction (1), as shown in Fig. 1. However, the unsubstituted ester deviates and has an apparently enhanced rate (this is discussed later). It is omitted from the following correlations. Like the ionization reaction, the effect of the *trans*-substituents on the alkaline hydrolysis is well correlated by the Hammett eq. [iii],

[iii] $$\log (k/k_0) = \rho\sigma,$$

Can. J. Chem. Downloaded from www.nrcresearchpress.com by 210.87.254.5 on 09/05/12
For personal use only.

using either para-σ-values (see ref. 1) or σ^n-values (17). The correlations are shown in Table IV, together with the related benzoate series. The value found for the alkaline ester hydrolysis of the *trans*-isomers, 3.739 or 4.431, is about twice the value, 2.048 or 2.331, found for meta- and para-substituted methyl benzoates under the same conditions. Thus, the reaction constant ratio ϕ is 1.87, in 70% dioxan–water, which agrees well with the ratio of 1.71 and 2.19 found for two other carboxylic acid reactions, in ethanol and water respectively, in our previous studies (1). The dielectric constants of the media are 20.0, 24.3, and 78.5 respectively.

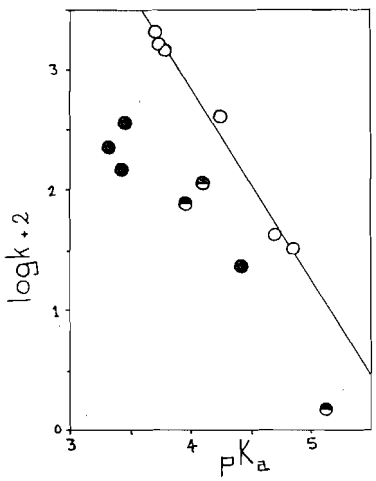


FIG. 1. Relation between the rates of alkaline hydrolysis of the esters and the aqueous pK_a values of the acids (○, *trans*; ●, *cis*; ◓, di-3-substituted).

The reactivity of the *cis*-isomers obviously shows the rate retardation due to a steric influence from the proximate substituents (see Fig. 1). In our previous studies, we found the normal polar effect was almost the same from the *cis*- and *trans*-position. A very reasonable assumption is that this is also true for these ester reactions. The rate decrease of the *cis*- compared with the *trans*-isomers will then be a measure of the "steric" effect of the proximate *cis*-substituent. These values of log (k_c/k_t) are shown in Table V.

TABLE IV

Hammett equation analysis*

Reaction	ρ	Log k_0	n	r
1. Alkaline hydrolysis of methyl esters in 70% dioxan–water at 18.8°				
trans-3-Substituted acrylates	3.739†	0.316	5	0.995
	4.431‡	0.032	5	0.986
Meta- and para-substituted benzoates	2.048†	−0.744	7	0.986
	2.331‡	−0.829	7	0.978
2. Acid-catalyzed esterification in methanol at 35.0°				
trans-3-Substituted acrylics	−0.360†	−1.244	6	0.750
	−0.437‡	−1.211	6	0.811
Meta- and para-substituted benzoics	−0.226†	−1.856	6	0.585
	−0.291‡	−1.836	6	0.682

*n is the number of substituents; r is the correlation coefficient.
†Using σ.
‡Using σ^n.

Can. J. Chem. Downloaded from www.nrcresearchpress.com by 210.87.254.5 on 09/05/12
For personal use only.

TABLE V
Steric effect of *cis*-substituent

Substituent	Log (k_c/k_t)	
	Acid-catalyzed esterification	Alkaline hydrolysis
H	0.0	0.0
Me	−0.37	−0.25
Cl	−0.18	−0.61
Br	−0.20	−0.96
I	−0.40	−1.03

The Effect of Substitution on the Acid-Catalyzed Esterification

The effect of substituents is shown in Table II. These bear a relationship to the ionization of the acids which is similar to that previously seen for the alkaline reaction. An important exception is the marked deviation of the unsubstituted acid, which is excluded from the correlation. This is discussed later. The Hammett reaction constant ρ, for the *trans*-substituents, is −0.360 or −0.437 (see Table IV). The correlation is rather poor. The reaction constant for the *same* para-substituted benzoic acids is −0.226 or −0.291 and the correlation is also poor.[3] The increased transmission of polar effects from the *trans*-position compared with the *para*-substituted benzoic acid is shown and ϕ is given as 1.55. Nevertheless, we can make the same assumption of the equality of the polar effect from the *cis*- and *trans*-position as was made for the alkaline hydrolysis. The "steric" effect of the *cis*-substituent can then be measured by log (k_c/k_t) and these values are shown in Table IV. Our implicit assumption here, as before, that the *trans*-isomers have a negligible steric effect seems very reasonable in view of the occurrence of the polar linear free energy relations and the substituent's "distant" position. The apparently greatly enhanced rate of the unsubstituted acid, however, is difficult to explain.

A consideration of the disubstituted compounds' reactivity confirms our previous indications. Thus, the decreased rate of the 3,3-dimethylacrylic acid in the esterification reaction is only sufficient (log (k_{Me_2}/k_{t-Me}) = −0.69) to account for a very small, favorable polar contribution overcome by a steric effect greater than that present in the *cis*-methyl isomer (log (k_{c-Me}/k_{t-Me}) = −0.37). This increase in steric effect would arise from the increase in internal interactions caused on forming the transition state (3, 21). This rate is impossible to account for by the rate relative to the unsubstituted compound, e.g. log (k_{t-Me}/k_H) = −0.34, log (k_{c-Me}/k_H) = −0.71, and log (k_{Me_2}/k_H) = −1.04, because steric effects are *not* additive, buttressing causing increasing steric effect with increasing substitution (2, 3, 21). The pattern of reactivity of the chloro-crotonic acids verify this. The relative rate (log ($k_{c-Me,t-Cl}/k_{c-Cl,t-Me}$) = −0.30) is identified with the difference in steric effect of the *cis*-substituents (see Table V). The rate coefficient for the unsubstituted acid appears to be enhanced by a factor of $\Delta \log k$ equal to approximately 0.40. An analysis of the rates of the disubstituted esters in the alkaline hydrolysis reaction also indicates that the enhancement of the rate of the unsubstituted ester is a real effect. In this $\Delta \log k$ equals approximately 0.30.

The cause of this effect appears to be obscure. Since it occurs only on the substitution of

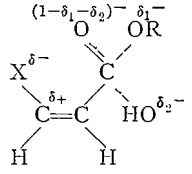
[3]*These esterification studies (18) have been correlated by Jaffé using all substituents (19) (ρ = −0.229, r = 0.457, and n = 16) and by Wepster and co-workers (17) using only selected substituents with negligible resonance interactions (ρ = −0.521, r = 0.979, and n = 8). A consideration of the pattern of reactivities of the para-substituents seems to indicate a substituent polar effect* without *its resonance contribution.*

Can. J. Chem. Downloaded from www.nrcresearchpress.com by 210.87.254.5 on 09/05/12
For personal use only.

the first substituent, a displacement resulting from a resonance effect, such as hyperconjugation (4), appears unlikely and it also appears unlikely to be a ponderal effect (20). However, it was not observed in our earlier study (1) on these systems.

Steric Effects

It is immediately obvious from a consideration of Table V that the "steric" effect of the dipolar halogeno-substituents is very much greater in the alkaline ester hydrolysis than in the acid-catalyzed esterification, whereas it is quite comparable for the alkyl group. The steric effect of the proximate substituents in ester reactions is normally ascribed to the "bulk" effect of the substituent causing crowding in the tetrahedral transition state. These interactions have been used very satisfactorily to account for the steric effects in aliphatic systems (21). The steric effects observed in the acid-catalyzed esterification reaction and, for alkyl substituents, in the alkaline ester hydrolysis appear to be of this kind. The steric factors in Table V, column 1, are more absolute measures of the steric effect than the E_s values of Taft (2) (see below). Their order of size is very reasonable (see ref. 2). The extra-"steric" effect observed in the alkaline hydrolysis has been qualitatively discussed as a steric effect on polar-facilitated solvation (5). Although this is a possibility, a simpler explanation can be offered. It is suggested that this effect is due to an electrostatic repulsion between the negative charge (δ^-) on the halogeno-substituent and the negative charge on the reaction site, as below (I). This effect is similar to one recently postulated to explain certain proximity interactions in nucleophilic substitution reactions (S_N2) (22, 23). The present results clearly demonstrate that steric effects for the *cis*-halogeno-substituents are very different from those in the acid-catalyzed reaction.



I

The Taft Separation of Polar and Steric Effects

Taft (2, 24) proposed the following Taft–Ingold eq. [iv] to separate the polar and steric effects in the hydrolysis of esters,

$$[\text{iv}] \qquad (\rho_B - \rho_A)\sigma^* = \log (k/k_0)_B - \log (k/k_0)_A,$$

where σ^* is the polar substituent constant and the subscripts B, A, and 0 refer to the acidic and basic hydrolysis and the unsubstituted compound respectively. The steric substituent constant E_s is defined by eq. [v].

$$[\text{v}] \qquad \log (k/k_0)_A = E_s$$

Ideally the acid and alkaline ester reactions should be otherwise identical, i.e. same alkyl ester, solvent, and temperature. Suitable data is very limited and difficult to obtain. Taft had previously found linear correlations between ester reactions of the same type (25), the slope being always close to unity, and was able to calculate averaged values. An important modification was to employ the acid-catalyzed esterification reaction to replace or reinforce the less available or accessible acid-catalyzed ester hydrolysis data. This appears a reasonable approximation since the reactant and transition states correspond. The reference ester, in the aromatic series, was usually the ortho-methyl benzoate; but alternatively the

Can. J. Chem. Downloaded from www.nrcresearchpress.com by 210.87.254.5 on 09/05/12
For personal use only.

ortho-fluoro or unsubstituted benzoate was used (2, 24). The assumptions are that there are independent contributions from polar, resonance, and steric effects; steric and resonance effects are the same in corresponding acidic and alkaline reactions, and the polar effects are much greater in the alkaline than in the acidic reaction. Taft assumed that $\rho_B - \rho_A$ equalled 2.48. Implicit in this separation is the identity of the steric effects in the alkaline and acid ester reactions. The increased interactions inhibiting the formation of the tetrahedral transition state will only be the same if the transition states for the acidic and alkaline ester reactions can be equated. This in fact appears to be a reasonable assumption (2, 3, and 5).

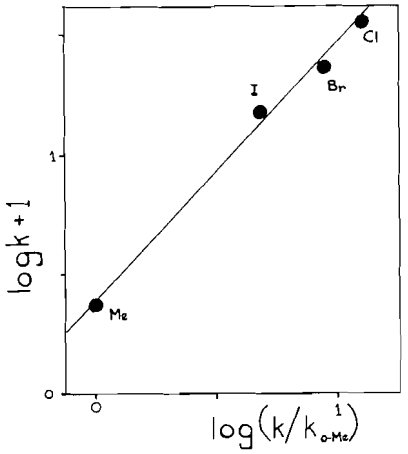


FIG. 2. Relation between the rates of alkaline hydrolysis of the *cis*-esters and Taft's averaged values of log (k/k_{o-Me}) for the alkaline hydrolysis of ortho-substituted benzoates (25).

We may now consider the evidence of our model system. The relative rates of the alkaline hydrolysis of the *cis*-isomers are linearly related (slope almost unity) to the corresponding rates of alkaline hydrolysis of methyl ortho-substituted benzoates (25) (see Fig. 2). Likewise the acid-catalyzed esterification rates of reaction are similarly related to the data available for the corresponding ortho-substituted benzoic acids (18). The unsubstituted compound must be excluded. This has been previously discussed. This is an extension of the relation found by Taft (25). It is thus extremely likely that our previous considerations of the steric effects of *cis*-substituents are directly applicable to ortho-substituted benzoates. The conclusions which have previously been reached for the former system are applicable to the latter system.

Thus, the Taft separation of the polar and steric effects involved in the reactions of ortho-substituted benzoates fails on the following counts: (1) the "steric" effects in the acid and alkaline reactions are quite different for a number of strongly dipolar substituents;[4] (2) the factor of $\rho_B - \rho_A$ cannot, in any case, be simply obtained from studies on the meta- and para-substituted benzoic system. The more efficient transmission from the ortho-position would probably require a factor of about 4.10 for the reactions used in this study.

The latter comment derives from our previous studies (1) in identifying the transmission of polar effects from the ortho-benzoic with the *cis*- and thus the *trans*-acrylic system. The

[4]*The ortho-fluoro-substituent (log $(k/k_0) = 0.70$), in alkaline hydrolysis of ethyl benzoates (see ref. 26), appears to have a polar effect alone and have no steric effect. It is presumably due to its small size that it exerts neither of the "steric" effects observed for the other halogens.*

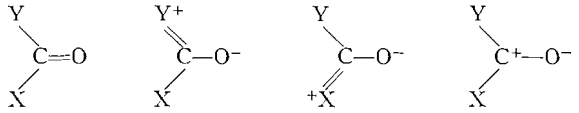
Can. J. Chem. Downloaded from www.nrcresearchpress.com by 210.87.254.5 on 09/05/12
For personal use only.

transmission from the ortho-position for alkaline hydrolysis would then be 1.9 times that from the para-position. Indirect reasoning by earlier workers (5) gave rise to a similar conclusion, i.e. polar effect of ortho-halogeno-substituents being about three times that of a similar para-substituent.

This criticism is not meant to apply to the separation of polar and steric effects in the aliphatic and arylaliphatic system (2–4). However, it seems possible that the alkyl esters with strongly dipolar substituents may exhibit the extra-"steric" effect found in this study for basic hydrolysis, e.g. see ref. 27.

The Carbonyl-Stretching Vibration

Thompson and co-workers (28) have represented the carbonyl-stretching vibration as being primarily determined by the relative contributions of the canonical structures II–V. As the frequency of the vibration indicates the energy needed to produce a dipolar state, a



II III IV V

reduction in the contribution of structures III, IV, and V will increase the frequency. The smaller steric requirement of the carbonyl oxygen compared to the methoxyl group will cause the proximity of the *cis*-substituent to the carbonyl oxygen when the molecule is coplanar. The direct "bulk" steric effect of these *cis*-substituents appears to be quite small in these esters.

The results in Table II indicate that the strongly dipolar halogeno-substituents result in an increase in the carbonyl-stretching frequency of approximately 8 cm^{-1} when the substituent is *cis*- rather than *trans*-orientated. The methyl substituent has a small effect in the *opposite* direction of 2 cm^{-1}. The effect in the *cis*-halogeno-esters appears to be the same as that previously suggested for related systems (29, 30). The effect of the proximate charge interaction will be to decrease the contribution of the canonical structure V and increase the frequency. This will be especially effective in the solvent used, carbon tetrachloride, which has a low dielectric constant. This effect in a physical property appears to be related to that postulated in the alkaline ester reaction.

REFERENCES

1. K. Bowden. Can. J. Chem. **43**, 3354 (1965).
2. R. W. Taft. *In* Steric effects in organic chemistry. *Edited by* M. S. Newman. John Wiley and Sons, Inc., New York. 1956. Chap. 13.
3. K. Bowden, N. B. Chapman, and J. Shorter. J. Chem. Soc. 5239 (1963).
4. (*a*) C. K. Hancock, E. A. Meyers, and B. J. Yager. J. Am. Chem. Soc. **83**, 4211 (1961).
(*b*) C. K. Hancock and C. P. Falls. J. Am. Chem. Soc. **83**, 4214 (1961).
(*c*) C. K. Hancock, B. J. Yager, C. P. Falls, and J. O. Schreck. J. Am. Chem. Soc. **85**, 1297 (1963).
5. N. B. Chapman, J. Shorter, and J. H. P. Utley. J. Chem. Soc. 1291 (1963).
6. L. N. Owen and H. M. Babatunde Somade. J. Chem. Soc. 1030 (1947).
7. I. Heilbron and H. M. Bunbury. Dictionary of organic compounds. 3rd ed. Eyre and Spottiswoode, London. 1953.
8. J. L. H. Allan, E. R. H. Jones, and M. C. Whiting. J. Chem. Soc. 1862 (1955).
9. H. Lund and J. Bjerrum. Ber. **64**, 210 (1931).
10. A. Weissberger. Techniques of organic chemistry. Vol. VII. 2nd ed. Interscience Publishers, Inc., New York. 1955.
11. E. A. S. Cavell, N. B. Chapman, and M. D. Johnson. J. Chem. Soc. 1413 (1960).
12. H. A. Smith and C. H. Reichardt. J. Am. Chem. Soc. **63**, 605 (1941).
13. J. J. Sudborough and M. J. P. Davies. J. Chem. Soc. 975 (1909).
14. L. Pekkarinen. Ann. Acad. Sci. Fennicae, Ser. A, II, **62**, 77 (1954).
15. A. Skrabal and W. Stockmair. Monatsh. **63**, 244 (1933).

Can. J. Chem. Downloaded from www.nrcresearchpress.com by 210.87.254.5 on 09/05/12
For personal use only.

16. G. M. BARROW. J. Chem. Phys. **21**, 2008 (1953).
17. H. VAN BEKKUM, P. E. VERKADE, and B. M. WEPSTER. Rec. Trav. Chim. **78**, 815 (1959).
18. (*a*) R. J. HARTMAN and A. B. GASSMAN. J. Am. Chem. Soc. **62**, 1559 (1940).
(*b*) R. J. HARTMAN and A. M. BORDERS. J. Am. Chem. Soc. **59**, 2107 (1937).
19. H. H. JAFFÉ. Chem. Rev. **53**, 191 (1953).
20. M. WOLFSBERG. Tetrahedron Letters, No. 46, 3405 (1964).
21. F. BECKER. Z. Naturforsch. **16b**, 236 (1961).
22. H. D. HOLTZ and L. M. STOCK. J. Am. Chem. Soc. **87**, 2404 (1965).
23. A. J. SISTI and W. MEMEGER. J. Org. Chem. **30**, 2102 (1965).
24. R. W. TAFT. J. Am. Chem. Soc. **74**, 3120 (1952).
25. R. W. TAFT. J. Am. Chem. Soc. **74**, 2729 (1952).
26. J. G. WATKINSON, W. WATSON, and B. L. YATES. J. Chem. Soc. 5437 (1963).
27. I. V. TALVIK and V. A. PALM. Sposobnost Organ. Soedin. Tartusk. Gos. Univ. Reaktsionnaya, **1**, 108 (1964); *see* Chem. Abs. **61**, 11865*b* (1964).
28. E. J. HARTWELL, R. E. RICHARDS, and H. W. THOMPSON. J. Chem. Soc. 1436 (1948).
29. L. J. BELLAMY and R. L. WILLIAMS. J. Chem. Soc. 4294 (1957).
30. R. N. JONES, D. A. RAMSAY, F. HERLING, and K. DOBRINER. J. Am. Chem. Soc. **74**, 2828 (1952).

Can. J. Chem. Downloaded from www.nrcresearchpress.com by 210.87.254.5 on 09/05/12
For personal use only.

Can. J. Chem. Downloaded from www.nrcresearchpress.com by 210.87.254.6 on 09/05/12
For personal use only.

HOMOGENEOUS CATALYSIS OF D_2–H_2O EXCHANGE BY RUTHENIUM(III) CHLORIDE: EVIDENCE FOR THE HETEROLYTIC SPLITTING OF HYDROGEN[1]

JACK HALPERN
Department of Chemistry, University of Chicago, Chicago, Illinois
AND
BRIAN R. JAMES
Department of Chemistry, University of British Columbia, Vancouver, British Columbia

Received October 29, 1965

ABSTRACT

The prediction, based on earlier studies of the ruthenium(III) chloride catalyzed oxidation of H_2 by iron(III), that in the absence of iron(III) or other oxidants ruthenium(III) chloride should catalyze homogeneously the isotopic exchange between D_2 and H_2O has been confirmed. A kinetic study was made of this exchange reaction in which the dependence of the exchange rate and of the exchange product distribution (HD:H_2 ratio) on the concentrations of ruthenium(III), hydrogen ion, and chloride ion were determined. The results, and in particular the observation that the HD:H_2 ratio of the exchange product increases with the concentrations of H^+ and Cl^-, support the view that the ruthenium(III)-catalyzed oxidation of D_2 by iron(III) and the D_2–H_2O exchange reaction proceed through related mechanisms involving a common rate-determining step in which D_2 is split heterolytically and a deuteridoruthenium(III) complex is formed.

INTRODUCTION

The ruthenium(III) chloride catalyzed oxidation of H_2 by Fe^{III} and Ru^{IV} in aqueous solution, reported by Harrod, Ciccone, and Halpern (1), was interpreted in terms of the mechanism

$$[1] \qquad Ru^{III} + H_2 \overset{k_1}{\rightarrow} Ru^{III}H^- + H^+$$

$$[2] \qquad Ru^{III}H^- + 2Fe^{III} \rightarrow Ru^{III} + 2Fe^{II} + H^+$$

in which the first step, involving the heterolytic splitting of H_2, is rate-determining. In line with this, the kinetics of the oxidation of H_2 were found to be $-d[H_2]/dt = k_1[H_2][Ru^{III}]$. Under the conditions of these measurements (80°, ~1 atm H_2, 3–6 *M* HCl) it was found that there was no appreciable uptake of H_2 by a solution of ruthenium(III) chloride (i.e., no reduction of Ru^{III}) in the absence of an oxidizing agent such as Fe^{III}, which implies that under these conditions reaction [1] must be proceeding reversibly. This should be reflected in isotopic exchange (i.e., formation of HD and (or) H_2) if D_2 is used in place of H_2, a result which has been confirmed by Schindewolf (2). In this paper we describe a more detailed study of this exchange reaction, with particular emphasis on measurement of the HD:H_2 ratio of the exchange product, the results of which provide additional support for the proposed heterolytic splitting mechanism.

EXPERIMENTAL

The preparation and characterization of the aqueous solutions of ruthenium(III) chloride have been described previously (1).

The D_2–H_2O exchange was measured as follows. A bulb of approximately 15 ml volume containing 1–3 ml of an aqueous solution of ruthenium(III) chloride, and immersed in a 80.0° oil bath, was filled to atmospheric pressure with D_2 (obtained from Stuart Oxygen Co.). The bulb was shaken for a given time, and the gas was then sampled and its isotopic composition determined mass spectrometrically using a Consolidated 21-611 mass spectrometer. The H^+ and Cl^- concentrations of the solution were adjusted with HCl and LiCl.

[1]*Work performed at the University of British Columbia and supported through grants from the National Research Council of Canada and the Petroleum Research Fund, administered by the American Chemical Society.*

Can. J. Chem. Downloaded from www.nrcresearchpress.com by 210.87.254.6 on 09/05/12
For personal use only.

RESULTS

Kinetic plots depicting the ruthenium(III) chloride catalyzed D_2–H_2O exchange are shown in Fig. 1. The rate plots for the formation of both HD and H_2 are seen to be approximately linear over a range corresponding to exchange of some 30% of the D_2 initially present. The overall exchange rate of D_2 in this experiment, $-d[D_2]/dt = d[HD]/dt + d[H_2]/dt = 9.5 \times 10^{-6}$ mole/l s, was about 25% lower than the corresponding rate of oxidation of D_2 by Fe^{III} (1.3×10^{-5} mole/l s) under the same conditions.[2] As will be shown below, this discrepancy is attributable to neglect of multiple exchange processes in computing the exchange rate.

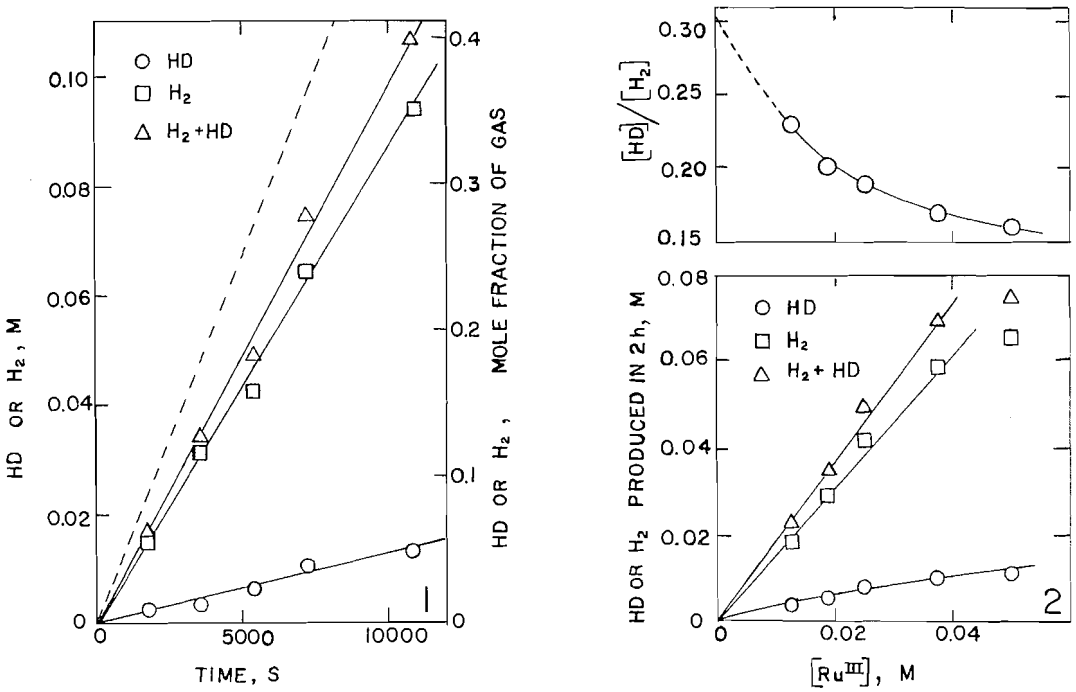


FIG. 1. Rate plots for the exchange of 13 ml D_2 gas (450 mm) with 1 ml H_2O containing 0.05 *M* Ru^{III} and 3.0 *M* HCl at 80°. The broken line corresponds to the rate of oxidation of D_2 by Fe^{III} under the same conditions.

FIG. 2. Dependence of the rate of exchange and the exchange product distribution on the Ru^{III} concentration (13 ml D_2 gas (450 mm) exchanged with 1 ml Ru^{III} solution containing 3 *M* HCl at 80°).

In subsequent experiments the total extent of exchange at the end of a given reaction period (generally 1 h) was used as a measure of the exchange rate. In no case did the extent of exchange (i.e., HD + H_2 produced) during this period exceed 30% of the initial D_2. In view of the linearity of the rate plots over this range (Fig. 1) this method of estimating the exchange rate appears justified.

The dependence of the exchange rate (measured in 3 *M* HCl) on the Ru^{III} concentration is depicted in Fig. 2. The total exchange rate is seen to be approximately first order in Ru^{III}, while the [HD]/[H_2] ratio of the exchange product increases with decreasing [Ru^{III}]. This presumably reflects the contribution to the H_2 yield from a multiple exchange

[2]*The corresponding rate of oxidation of* H_2 *was found to be* 1.46×10^{-5} *mole/l s. The kinetic isotope effect,* $k_1(H_2)/k_1(D_2)$ *is thus* ~*1.12.*

process whereby a dissolved HD molecule, produced by the primary exchange reaction between D_2 and H_2O, undergoes a second exchange reaction with H_2O to produce H_2 before escaping from the solution into the gas phase. The probability of occurrence of such multiple exchanges should decrease with decreasing exchange rate, i.e., with decreasing $[Ru^{III}]$, which would account for the observed inverse dependence of the $[HD]/[H_2]$ ratio on $[Ru^{III}]$. Extrapolation to $[Ru^{III}] = 0$, where such multiple exchange is negligible, gives $[HD]/[H_2] \simeq 0.3$. This value presumably corresponds to the primary product distribution, so that both HD and H_2 are primary products of the exchange reaction.

When corrected for this multiple exchange contribution the total D_2–H_2O exchange rate in Fig. 1 ($\sim 1.3 \times 10^{-5}$ mole/l s) approaches the corresponding rate of oxidation of D_2 by Fe^{III}.

A series of experiments was made to determine the effects of varying the H^+ and Cl^- concentrations on the exchange rate and product distribution. At each of three constant total Cl^- concentrations (3.0, 5.0, and 7.0 *M*) the H^+ concentration was varied by varying the proportions of HCl and LiCl in the solution. In each experiment the isotopic composition of the gas was determined after 1 h. The results are summarized in Table I.

TABLE I

Dependence of exchange rate and product distribution on concentrations of H^+ and Cl^- (based on exchange experiments at 80° between 13.0 ml D_2 (at 450 mm) and 3.0 ml 0.017 *M* Ru^{III})

Total Cl^-, *M*	HCl, *M*	LiCl, *M*	Exchange product after 1 h, (moles/l of solution) $\times 10^5$		
			H_2	HD	HD+H_2
3.0	1.0	2.0	9.3	1.0	10.3
	2.0	1.0	8.5	1.1	9.6
	3.0	0	13.0	2.0	15.0
5.0	1.0	4.0	10.2	2.0	12.2
	2.0	3.0	11.1	2.7	13.8
	3.0	2.0	11.9	3.2	15.1
	4.0	1.0	12.4	3.9	16.3
	5.0	0	12.0	4.2	16.2
7.0	1.0	6.0	6.6	2.1	8.7
	2.0	5.0	7.4	2.5	9.9
	3.0	4.0	8.2	3.5	11.7
	4.0	3.0	7.7	3.6	11.3
	5.0	2.0	7.1	4.1	11.2
	6.0	1.0	8.0	5.1	13.1
	7.0	0	7.9	5.5	13.4

The slight increase in the exchange rate with increasing H^+ concentration is consistent with the trend noted earlier (1) for the Ru^{III}-catalyzed oxidation of H_2 by Fe^{III}. No appreciable trend is apparent in the dependence of the exchange rate at constant $[H^+]$ on the Cl^- concentration. The distribution of the exchange products, however, exhibits a marked dependence, depicted in Fig. 3, on the concentrations of both H^+ and Cl^-. The $[HD]/[H_2]$ ratio is approximately proportional[3] to $[Cl^-]$ at constant $[H^+]$, and also increases linearly with $[H^+]$ at constant $[Cl^-]$.

Addition of Fe^{III} to solutions containing Ru^{III} inhibited the exchange between D_2 and H_2O completely until the Ru^{III}-catalyzed reduction of Fe^{III} to Fe^{II} was complete.

[3]*This observation should be interpreted with caution in view of the variation in ionic strength which accompanies variation of the* Cl^- *concentration.*

Can. J. Chem. Downloaded from www.nrcresearchpress.com by 210.87.254.6 on 09/05/12
For personal use only.

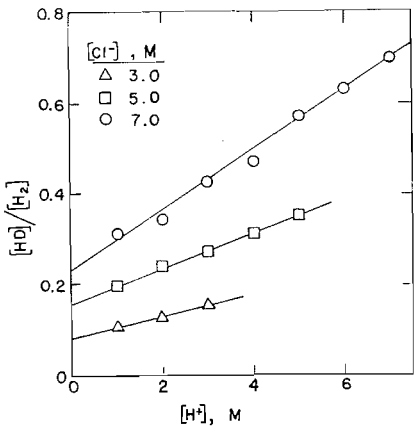


FIG. 3. Dependence of the exchange product distribution on the concentrations of H^+ and Cl^- (based on data in Table I).

DISCUSSION

The similarity of the kinetics of the Ru^{III}-catalyzed D_2–H_2O exchange and oxidation of D_2 by Fe^{III} reinforces the view already advanced that the two reactions proceed through related mechanisms involving a common rate-determining step. The mechanism proposed earlier (eq. [1] and [2]) for the oxidation of $H_2(D_2)$ by Fe^{III} can be extended to accommodate both reactions according to the following scheme (where $Ru^{III}Cl^-$ denotes one of the catalytically active chlororuthenate(III) complexes which are believed (1) to include $RuCl_6^{3-}$, $Ru(H_2O)Cl_5^{2-}$, and $Ru(H_2O)_2Cl_4^-$).

[3] $$Ru^{III}Cl^- + D_2 \xrightarrow{k_1} Ru^{III}D^- + D^+ + Cl^-$$

[4a] $$Ru^{III}D^- \xrightarrow[H^+ + Cl^-]{k_{-1}} Ru^{III}Cl^- + HD$$

[4b] $$Ru^{III}D^- \xrightarrow[+ H_2O]{k_2} Ru^{III}H^- + HDO$$

[5] $$Ru^{III}H^- \xrightarrow[H^+ + Cl^-]{k_{-1}} Ru^{III}Cl^- + H_2$$

[6] $$Ru^{III}D^- + 2Fe^{III} + Cl^- \rightarrow Ru^{III}Cl^- + 2Fe^{II} + D^+$$

This mechanism incorporates the following assumptions and conclusions:

(*a*) The rate-determining step [3] involves the heterolytic splitting of D_2 with formation of a deuteridoruthenium(III) complex. The D^- which is transferred to Ru^{III} displaces a Cl^- from the coordination shell. This implies that D^- occupies one of the normal ligand positions in the coordination shell of the ruthenium ion, in line with what is known about other hydrido complexes of transition metals (3).

(*b*) Isotopic exchange between D_2 and H_2O occurs through the reversal of step [3] (i.e., through steps [4*a*] and [5]). The D^+ which is released in step [3] undergoes complete exchange (conversion to H^+) with H_2O, whereas the $Ru^{III}D^-$ complex exchanges more slowly with H_2O, by what is assumed to be a pH-independent mechanism. According to

Can. J. Chem. Downloaded from www.nrcresearchpress.com by 210.87.254.6 on 09/05/12
For personal use only.

this, the total exchange rate $(-d[D_2]/dt)$ is determined by step [3], whereas the distribution of primary exchange products is determined by competition between steps [4*a*] and [4*b*]. This predicts that

$$[7] \qquad \frac{[HD]}{[H_2]} = \frac{k_{-1}[H^+][Cl^-]}{k_2}.$$

Interference from the multiple exchange process referred to earlier makes it difficult to determine the primary $[HD]/[H_2]$ ratio of the exchange product in order to test this prediction rigorously. Nevertheless, it is evident that eq. [7] is at least qualitatively in accord with the observed increase of the $[HD]/[H_2]$ ratios (which are not corrected for multiple exchange) with increasing H^+ and Cl^- concentrations (Fig. 3). The finite intercepts obtained on extrapolating to $[H^+] = 0$ the linear plots of $[HD]/[H_2]$ versus $[H^+]$ (Fig. 3) are, however, not predicted by eq. [7] and may reflect contributions to exchange at low H^+ concentrations from an H^+-independent back reaction (in addition to [4*a*]), e.g.,

$$[8] \qquad Ru^{III}D^- + H_2O + Cl^- \rightarrow Ru^{III}Cl^- + HD + OH^-.$$

(*c*) Oxidation of the intermediate, $Ru^{III}D^-$, by Fe^{III} (reaction [6]) is rapid and competes effectively with the back reactions [4*a*] and [5]. Thus, Fe^{III} inhibits the D_2–H_2O exchange reaction while undergoing reduction to Fe^{II} at the same rate as the Ru^{III}-catalyzed D_2–H_2O exchange in the absence of Fe^{III}.

Despite the difficulties involved in subjecting eq. [7] to a completely satisfactory quantitative test, it appears that, qualitatively at least, the observed dependence of the $[HD]/[H_2]$ ratio on the H^+ and Cl^- concentrations provides strong evidence for a mechanism involving heterolytic splitting of D_2 and the displacement of a Cl^- ligand. In favorable cases, this approach to the study of isotopic exchange patterns can provide evidence of a heterolytic splitting mechanism and can identify the displaced ligand, even without an explicit knowledge of the nature of the catalytic species or of the kinetics. It is of interest that an early suggestion by Rittenberg and Krasna (4) that the hydrogen-activating enzyme, hydrogenase, splits H_2 heterolytically was based on an essentially similar observation, namely that the initial product of the hydrogenase-catalyzed H_2–D_2O exchange is predominantly HD rather than D_2.

REFERENCES

1. J. F. Harrod, S. Ciccone, and J. Halpern. Can. J. Chem. **39**, 1372 (1961).
2. V. Schindewolf. Ber. Bunsenges. Physik. Chem. **67**, 219 (1963).
3. J. Chatt. Proc. Chem. Soc. 318 (1962). P. L. Orioli and L. Vaska. Proc. Chem. Soc. 333 (1962). S. J. LaPlaca and J. Ibers. J. Am. Chem. Soc. **85**, 3501 (1963).
4. D. Rittenberg and A. Krasna. Disc. Faraday Soc. **20**, 185 (1955).

Can. J. Chem. Downloaded from www.nrcresearchpress.com by 210.87.254.6 on 09/05/12
For personal use only.

EFFECT OF α-METHYLATION ON THE PARAMETERS CHARACTERIZING HYDROLYSIS IN WATER FOR A SERIES OF HALIDES AND SULFONATES[1]

R. L. HEPPOLETTE[2] AND R. E. ROBERTSON
Division of Pure Chemistry, National Research Council, Ottawa, Canada
Received October 15, 1965

ABSTRACT

The aim of this work was to explore the effect of α-methylation on the reactivity and detailed mechanism of hydrolysis. Accordingly, rate data and derived parameters are given for the hydrolysis of a series of halides and sulfonates in water. From the differences in kinetic parameters, an attempt is made to infer further information relating structure and mechanism.

This paper summarizes the results of a study of the effect of α-methylation on the solvolytic displacement of halides and sulfonates in water, thus extending our earlier study on the corresponding methyl compounds (1).

As a medium for solvolysis, water is known to have excellent ionizing properties and to be a fair nucleophile. Its position in these respects, relative to other solvents, is well known (2) and is not altered by our rate studies.

Relative rates, however, provide little evidence on which to base conclusions concerning the detailed mechanism, particularly with respect to solvent reorganization. This point has been repeatedly illustrated in the studies of Tommila (3) and of Winstein and Fainberg (4) and may be attributed to the compensating effect of solvent reorganization on $\Delta H^{\ddagger}$ and $\Delta S^{\ddagger}$. Hence it was from the latter terms and particularly from the values of $\Delta C_p^{\ddagger}$ that more detailed information about the reactions was expected. Even though the relation between changes in these parameters and mechanism is not as yet defined, these values should provide both an indication and a guide to the development of an acceptable hypothesis.

The basic aim here was to explore the pattern of values for a series of compounds rather than to investigate the temperature dependence of the rates for a few substrates with highest precision. To achieve this aim certain approximations were accepted, but there is no evidence that these approximations introduce significant differences in the derived parameters (see Experimental section).

EXPERIMENTAL

Halides

The halides were reagent grade samples, purified by distillation to give physical constants in agreement with the literature and passed through alumina for adsorption. These purified samples were protected from light and refrigerated during the kinetic study. The final criteria for kinetic purity was adherence to first order linearity. Because of the low solubility, particularly for the chlorides and iodides, the experimental difficulties here were much greater than for the corresponding sulfonates or even the methyl halides (1) and the experimental errors were correspondingly increased.

Sulfonates

Ethyl *p*-toluenesulfonate was obtained from distillation products and recrystallized several times from the melt; m.p. 32.1 °C. Isopropyl *p*-toluenesulfonate, methanesulfonate, and ethyl methanesulfonate were

[1]*Issued as N.R.C. No. 8831.*
[2]*N.R.C. Fellow 1956-1958.*

Can. J. Chem. Downloaded from www.nrcresearchpress.com by 210.87.254.105 on 09/05/12
For personal use only.

synthesized by the method of Morgan and Cretcher (5). All gave satisfactory neutral equivalents. Isopropyl *p*-Me: m.p. 19.8 °C, n_D^{25} 1.5002; ethyl mesylate: n_D^{25} 1.4151, d_4^{21} 1.20492; isopropyl mesylate: n_D^{25} 1.4167, d_4^{25} 1.01521.

Water

Distilled water was passed through an ion exchange column and sufficient backing electrolyte of the common anion added to give a concentration 0.001–0.003 *M*. The solution was evacuated and the halide introduced under vacuum. The sulfonates were added to the water prior to evacuation.

Rate Determinations

Rates were determined by the conductance method described previously (6). Details of temperature control, determination of time, and calculations were identical with the earlier work, save where noted specifically. The rate data reported in this paper were determined at a time when techniques and equipment were evolving. Temperature control was usually ±0.001–0.002 °C though in longer runs ($t_{1/2} > 6$ h) somewhat larger variation may have occurred. Some temperature variation may have arisen in the faster runs which would now be avoided (7). Errors in time may have also been present in the latter, but these should not have been large and should have been random. Temperature determination was by a platinum thermometer and temperature-controlled Mueller bridge.

The approximation (8)

$$\log (1/R_2 - 1/R_1) = k_1 t + c$$

was justified by the low concentrations used, and the small range of concentration involved (0.002–0.005 *M*). This approximation may have introduced a small error in $\Delta C_p^{\neq}$, but this would tend to be the same for all halides and unimportant in comparisons. Empirical calibrations of *R* vs. concentration (9) by dilution techniques do not alter the rates significantly.

RESULTS

Since it was our intention to relate changes in the derived parameters $\Delta H^{\neq}$, $\Delta S^{\neq}$, and $\Delta C_p^{\neq}$ to changes in mechanism and in solvent reorganization, there seemed little to be gained in a detailed study of the rates of hydrolysis of the ethyl halides; all evidence suggested these results would be similar to those for the corresponding methyl halides (1). Accordingly, rate determinations on the former, save for ethyl bromide, were made over a limited range only (Table I). With these exceptions, rate determinations covered the range 40–60 °C.

TABLE I

Kinetic data for the hydrolysis of a series of ethyl halides in water

Halide	*T* (°K)	*k* ($s^{-1} \times 10^5$)	*n*
Chloride	373.151	11.69±0.01*	5
	363.168	4.824±0.007	5
	353.170	1.841±0.002	4
Iodide	373.147	99.34±0.17	3
	363.160	40.61±0.01	4
	353.157	15.53±0.01	3

*Average deviation of *n* repetitive runs.

The temperature dependence of the rate could be fitted within experimental error to the usual three-constant equation

$$\log_{10} k = A/T + B \log T + C.$$

The corresponding constants determined from a least mean square fit for *n* individual rates together with standard deviations are given in Table II.[3]

If the above rate data are treated in terms of transition state hypotheses, and as a first approximation we assume that $d\Delta C_p^{\neq}/dT = 0$ within our experimental error, the

[3]*The complete rate data have been placed in The Depository of Unpublished Data, National Science Library, National Research Council, Ottawa, Canada, and photocopies may be obtained upon request to the Depository.*

Can. J. Chem. Downloaded from www.nrcresearchpress.com by 210.87.254.105 on 09/05/12
For personal use only.

TABLE II

Empirical constants for the temperature–rate relation
$\log_{10} k_1 = A/T + B \log T + C$

Compound	A	B	C	Δ^*	$n_{T_2}^{T_1}$
Ethyl bromide	−8 812.887	−23.832	82.1140	0.0009	$33_{57.5}^{95}$
Ethyl tosylate	−7 447.254	−18.930	66.6540	0.0024	35_{75}^{9}
Isopropyl benzenesulfonate	−7 206.575	−17.7736	64.9694	0.0016	45_{35}^{2}
Isopropyl toluenesulfonate	−7 580.71	−20.3306	72.3457	0.0022	41_{40}^{2}
Isopropyl methanesulfonate	−7 127.675	−16.695	61.5095	0.0006	52_{32}^{55}
Isopropyl chloride	−8 154.513	−18.259	65.8562	0.0013	45_{100}^{55}
Isopropyl bromide	−9 489.457	−28.677	97.3690	0.0017	45_{75}^{29}
Isopropyl iodide	−9 636.662	−27.875	95.7418	0.0022	48_{75}^{25}

*In Table II $\Delta = (\Sigma(\log k_{calc} - \log k_{obs})^2/(n-1))^{1/2}$ where Δ was calculated by computer using 18-digit accuracy. The 12-digit output was arbitrarily rounded to be consistent with experimental error. The quantity $n_{T_2}^{T_1}$ = number of individual rates used in the least mean square calculation, where T_1 and T_2 are temperature limits of experimental range.

corresponding pseudo-thermodynamic constants $\Delta H^{\ddagger}$, $\Delta S^{\ddagger}$, and $\Delta C_p^{\ddagger}$ may be derived according to the relations:

$$A = -\Delta H_0^{\ddagger}/2.303R$$

$$B = \Delta C_p^{\ddagger}/R + 1$$

$$C = (\Delta S_0^{\ddagger} - \Delta C_p^{\ddagger})/2.3026R + \log k/h$$

$$\Delta H_T^{\ddagger} = \Delta H_0^{\ddagger} + \Delta C_p^{\ddagger} T$$

$$\Delta S_T^{\ddagger} = \Delta S_0^{\ddagger} + 2.3026 \Delta C_p^{\ddagger} \log T.$$

These constants together with those for the methyl compounds from an earlier study are given in Table III.

TABLE III

Derived parameters for hydrolysis at 50 °C

Solute	k_1 ($s^{-1} \times 10^5$)	$\Delta H^{\ddagger}$ (cal/mole)	$\Delta S^{\ddagger}$ (cal/mole deg)	$\Delta C_p^{\ddagger}$ (cal/mole deg)	Ref.
Ethyl bromide	1.09_1	24 380	−6.0	−49	This work
Ethyl tosylate	12.67	21 280	−10.7	−40	This work
2-Propyl benzene sulfonate		20 920	−2.8	−37	This work
2-Propyl tosylate		20 990	−3.5	−42	This work
2-Propyl mesylate	89.11	21 239	−4.3	−35	This work
2-Propyl chloride	0.634	24 940	−5.3	−38	This work
2-Propyl bromide	11.01	24 360	−1.4	−59	This work
2-Propyl iodide	9.35	25 550	1.93	−57	This work
Methyl tosylate	13.80	20 770	−12.1	−33	(8)
Methyl benzene sulfonate	19.65	20 570	−12.1	−36	(10)
Methyl mesylate	8.40	20 440	−14.1	−37	(11)
Methyl chloride	0.076	25 250	−8.6	−50	(1)
Methyl bromide	1.11	24 140	−6.7	−46	(1)
Methyl iodide	0.26	25 950	−3.9	−56	(1)

DISCUSSION

Until recently, the question of whether the isopropyl halides and sulfonates hydrolyzed in water by an S_N1 or S_N2 mechanism was uncertain, a position dignified by the label, "borderline case". This uncertainty was supported by the "normal" α-deuterium isotope effect found for the hydrolysis of secondary halides in water, compared to the inverse effect found for primary compounds (12). It is known now that this isotopic difference

Can. J. Chem. Downloaded from www.nrcresearchpress.com by 210.87.254.105 on 09/05/12
For personal use only.

does not provide a test for detecting nucleophilic interaction (13–15). Similarly the k_{OH^-}/k_{H_2O} ratio is inconclusive as a test for mechanism where the nucleophilic assistance required is small.

Positive evidence of an important difference in solvent reorganization is apparent in the systematic difference in $\Delta C_p^{\ddagger}$ for reactions involving primary and secondary centers compared to those involving displacement from a tertiary carbon (7, 16).

Moreover, recent studies of temperature dependence of the β-deuterium isotope effect in displacement from secondary and from tertiary carbon centers (17) and theoretical calculations of Wolfsberg and Stern (18) may be taken as empirical evidence of differences related to mechanism and hence for the conclusion that solvolytic displacement from primary and secondary carbon centers in water normally involve some degree of nucleophilic interaction while corresponding displacement from a tertiary does not. In the latter case the question of "limiting mechanism" is unimportant.

The probability of attaining the degree of nucleophilic overlap required as a prerequisite for the activation of primary and secondary compounds may be an important factor in evaluating $\Delta S^{\ddagger}$ in particular, and our lack of an a priori method for estimating these differences imposes limitations on the present utility of this parameter.

Effect of α-Methylation on Reactivity

Relative rates provide a direct guide to the effect of structure on reactivity, a matter of practical importance to the synthetic chemist but of less obvious utility in revealing mechanistic details. In Table IV a systematic difference is apparent in the ratio $k_{i\text{-Pr}}/k_{Et}$ between the sulfonates and the halides. This difference can readily be accounted for in terms of the relative requirements of nucleophilic overlap in the two series and the opposing effect of enhanced steric opposition of the α-methyl in those examples where nucleophilic interaction is presumed to be greater.

TABLE IV

A comparison of relative rates of hydrolysis in water at 50 °C

Displaced anion	k_{Me}/k_{Et}	$k_{i\text{-Pr}}/k_{Et}$
Benzenesulfonate	1.03	63.2
Tosylate	1.08	57.8
Methanesulfonate	1.18	50.9
Chloride	1.15	9.5
Bromide	0.99	9.9
Iodide	0.51	17.4

Effect of α-Methylation on $\Delta C_p^{\ddagger}$

While solvent reorganization contributes to changes in $\Delta H^{\ddagger}$ and $\Delta S^{\ddagger}$, it is recognized that $\Delta C_p^{\ddagger}$ should be a much better indicator of solvent changes associated with the activation process. The particular utility of the latter parameters in this respect has been presented elsewhere and stems from the nature of aqueous solutions of weakly polar solutes (19–22). In water, such a solute may be regarded as surrounded by a dynamic hydrogen-bonded solvation shell. Insofar as the process of hydrolysis is concerned, the significant characteristics of this shell are (i) halide–water interaction is much smaller than water–water interaction, and (ii) the structure of the solvent shell appears to be more stable than the structure of bulk solvent. This may be attributed to a loss of librational freedom due to the presence of the solute: (iii) the stability of this solvent

Can. J. Chem. Downloaded from www.nrcresearchpress.com by 210.87.254.105 on 09/05/12
For personal use only.

shell decreases with increasing temperature, and (iv) charge development on the anion, as a consequence of nucleophilic interaction and favorable collisions, will lead to a breakdown of this solvation shell in the immediate neighborhood of the anion.

Since the work required to break down the initial state solvation shell alters with temperature, $\Delta H^{\ddagger}$, which includes this factor, will show a corresponding negative temperature coefficient due to this cause whatever other temperature dependent factors may be involved. For example, the contribution of varying degrees of nucleophilic interaction on $\Delta C_p^{\ddagger}$ is by no means clear but appears to be small. As a working hypothesis (21) we assume that the transition state is reached when, by a suitable combination of activating forces,

[1] anion–water interaction = water–water interaction.

According to this hypothesis, charge development will be the same for S_N2 mechanism whether displacement is from a primary or secondary halide. Accordingly, the contribution to $\Delta C_p^{\ddagger}$ from the breakdown of water structure about the halide will tend to be the same whether displacement is from a primary or secondary carbon. Thus in Table III there is no large unidirectional shift in $\Delta C_p^{\ddagger}$ with α-methylation. Closer inspection of a series of $\Delta C_p^{\ddagger}$ values suggests, however, that the values for S_N2 displacement from a secondary carbon are somewhat more negative than from the corresponding primary center. Such a difference might very well be related to specific initial state differences and seems more prominent for the halides than for the sulfonates. In this connection, the value of $\Delta C_p^{\ddagger}$ for the hydrolysis of isopropyl chloride (−38 cal/deg) would appear to be atypical. Similar positive shifts have been noted where a sparingly soluble reactant has been studied (23).

Effect of α-Methylation on $\Delta H^{\ddagger}$ and $\Delta S^{\ddagger}$

In an earlier paper (24) a correlation between $\Delta S^{\ddagger}$ and ΔS_{sol} (where ΔS_{sol} is the entropy change for the solvation of the corresponding product halide ion) prompted the conclusion that the quasi-anion was 80–98% solvated at the transition state in the case of the solvolysis of methyl and isopropyl halides in water. By using this approximation, the earlier calculations of the energy of activation, E_A, for the S_N1 solvolytic reactions by Evans (25) and by Franklin (26) were extended to cover the corresponding S_N2 hydrolysis of the above halides in water, and satisfactory agreement was obtained between the observed and calculated activation energies. As we have noted elsewhere (21), such agreement is not conclusive since the calculation involves essentially the difference of large numbers and there must always be some degree of reaction where the difference $(E_A)_{calc}$ will correspond to the observed activation parameter. It is equally clear that this type of calculation is not consistent with the qualitative hypothesis advanced above to define the condition for the transition state, eq. [1].

A comparison of the difference in $\Delta H^{\ddagger}$ resulting from α-methylation (Tables IV and V) shows that these are small compared with the total values (Table III) and compared with the differences in bond strengths and corresponding values for gas phase ionization. (Table 21 of ref. 27). It is possible that such nice cancellation of large differences occurs, but it seems equally feasible that we have in E_A (or $\Delta H^{\ddagger}$) a summation of smaller terms which do not change much with α-methylation. For such a structural change it is reasonable to expect a compensation between enhanced steric hindrance and the reduced requirement for nucleophilic overlap. If these opposing effects are approximately the same, the apparent lack of system in $(\Delta H_{Me}^{\ddagger} - \Delta H_{Et}^{\ddagger})$ and $(\Delta H_{i\text{-}Pr}^{\ddagger} - \Delta H_{Et}^{\ddagger})$ with different displaced groups is not surprising.

Can. J. Chem. Downloaded from www.nrcresearchpress.com by 210.87.254.105 on 09/05/12
For personal use only.

TABLE V

Comparison of enthalpy changes with α-methylation at 50 °C

Displaced group	$\Delta H_{Me}^{\neq} - \Delta H_{Et}^{\neq}$ (cal/mole)	$\Delta H_{i\text{-}Pr}^{\neq} - \Delta H_{Et}^{\neq}$ (cal/mole)
Benzenesulfonate	−600	−250
Tosylate	−520	−290
Mesylate	−680	120
Chloride	−290	−560
Bromide	−40	20
Iodide	350	−60

TABLE VI

A comparison of entropy differences resulting from α-methylation

Leaving group	$\Delta S_{Me}^{\neq} - \Delta S_{Et}^{\neq}$ (e.u.)	$\Delta S_{i\text{-}Pr}^{\neq} - \Delta S_{Et}^{\neq}$ (e.u.)
Benzenesulfonate	−1.3	6.4
Tosylate	−1.5	7.4
Mesylate	−1.8	8.3
Chloride	−0.2	3.4
Bromide	−0.7	4.6
Iodide	−0.3	5.5

By contrast, a regularity is apparent in $\delta_R\Delta S^{\neq}$ (Table VI) with different leaving groups and this difference ($\Delta S_{i\text{-}Pr}^{\neq} - \Delta S_{Et}^{\neq}$) would appear to be the main determinant of rate differences. For the halides, there is a fair correlation between $\delta_R\Delta S^{\neq}$ and the polarizability, α, (Fig. 1), an observation probably related to the correlation noted by Edwards (28) and Bunnett (29). The value for the sulfonates was not included because of uncertainty as to an acceptable approximation (29). Since the differences in $\Delta H^{\neq}$ among the sulfonates are about the same as for the halides (Table V), we would expect the sulfonates to occupy the same position relative to the halides in the upper curve where the entropy difference is plotted against polarizability as in the lower plot where the ordinate represents the difference in free energy. In the latter, the relative order of the sulfonates can be understood in terms of relative dispersal of charge on the sulfonic oxygens. Thus the methanesulfonate will be most effective in terms of eq. 1 because of the small polarizability of the methyl group compared to that of phenyl.

This is borne out both by the differences apparent in relative hydrogen bonding ability through this series (30), and the small but significant differences in the kinetic solvent isotope effect for the methanesulfonates and benzenesulfonates (31). In the benzenesulfonic series, while the phenyl group will tend to increase the polarizability, it will do so by dispersing the charge; hence the corresponding $\Delta S^{\neq}$ will be less than for the mesylate, and also less for the benzenesulfonate than for the tosylate, where the *p*-Me group will tend to reduce charge dispersal due to the phenyl group.

Apparently[4] the difference, $\delta_R\Delta S^{\neq}$, is not necessarily related to the degree of overlap required since we find approximately the same value for $\Delta S_{i\text{-}Pr}^{\neq} - \Delta S_{Et}^{\neq}$ for the solvolysis of the benzenesulfonates in water ($\delta_R\Delta S^{\neq}$ = 6.4 cal/mole deg), in methanol ($\delta_R\Delta S^{\neq}$ = 6.8 cal/mole deg), and in ethanol ($\delta_R\Delta S^{\neq}$ = 6.3 cal/mole deg). The corresponding relative rates are 62, 5, and 3.3 (32). The difference in the rate ratio is most easily accounted for

[4]*The assumption is made that a greater degree of nucleophilic interaction would be required where the solvent had poorer ionizing properties.*

Can. J. Chem. Downloaded from www.nrcresearchpress.com by 210.87.254.105 on 09/05/12
For personal use only.

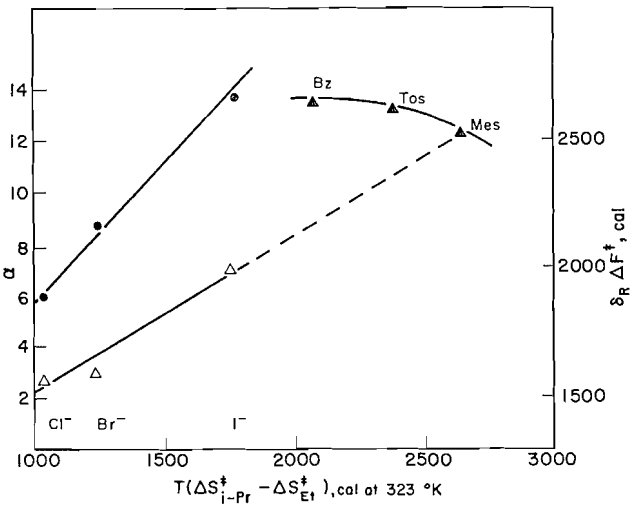


FIG. 1. Effect of α-methylation on the entropy of activation compared to the polarizability, α, and to the free energy difference, $\delta_R \Delta F^{\ddagger}$.

in terms of the effect of increased steric hindrance arising from a corresponding increased requirement for nucleophilic overlap.

The lack of any apparent systematic change in $\Delta H^{\ddagger}$ or $\Delta C_p^{\ddagger}$ with α-methylation stands in contrast to the effect of this change on the entropy, hence the familiar "compensatory effect" is absent (33–35), and this would seem to dispose of solvent reorganization as a root cause in this instance. This may be taken as a further support for our argument that the subtraction of $\Delta S_{Et}^{\ddagger}$ removes solvation differences associated with the anionic moiety in the activation process. Those uncertainties associated with $\Delta S^{\ddagger}$ in the transition state theory are also minimized.

Polarizability has been recognized to be an important factor in determining the rate of nucleophilic displacement (36–38), and is an essential feature of several empirical correlations relating structure and reactivity. Logically, this interaction would seem to require changes in $\Delta H^{\ddagger}$ or possibly in both $\Delta H^{\ddagger}$ and $\Delta S^{\ddagger}$. Clearly, such is not the case here, though the reason remains obscure.

ACKNOWLEDGMENTS

We wish to acknowledge the numerous discussions which we have had with Prof. J. M. W. Scott of Memorial University and the technical assistance of Mr. S. Sugamori.

REFERENCES

1. R. L. HEPPOLETTE and R. E. ROBERTSON. Proc. Roy. Soc. London, Ser. A, **252**, 273 (1959).
2. E. GRUNWALD and S. WINSTEIN. J. Am. Chem. Soc. **70**, 3731 (1948).
3. E. TOMMILA, E. PAAKKALA, U. K. VIRTANEN, A. ERVA, and S. VARITA. Ann. Acad. Sci. Fennicae, Ser. A II, **91**, (1959).
4. A. H. FAINBERG and S. WINSTEIN. J. Am. Chem. Soc. **79**, 1597 (1957) and others in same series.
5. M. S. MORGAN and L. H. CRETCHER. J. Am. Chem. Soc. **70**, 375 (1948).
6. R. L. HEPPOLETTE and R. E. ROBERTSON. J. Am. Chem. Soc. **83**, 1834 (1961).
7. E. A. MOELWYN-HUGHES, R. E. ROBERTSON, and S. SUGAMORI. J. Chem. Soc. 1965 (1965).
8. R. E. ROBERTSON. Can. J. Chem. **33**, 1536 (1955).
9. S. MARTIN, R. E. ROBERTSON, and G. C. BENSON. J. Sci. Instr. **41**, 237 (1964).
10. R. E. ROBERTSON. Can. J. Chem. **35**, 623 (1957).
11. P. W. C. BARNARD and R. E. ROBERTSON. **39**, 881 (1961).
12. J. A. LLEWELLYN, R. E. ROBERTSON, and J. M. W. SCOTT. Can. J. Chem. **38**, 222 (1960).

Can. J. Chem. Downloaded from www.nrcresearchpress.com by 210.87.254.105 on 09/05/12
For personal use only.

13. K. T. LEFFEK. Can. J. Chem. **42**, 851 (1964).
14. S. SELTZER. Private communication.
15. R. E. ROBERTSON and C. Y. WU. Chem. Ind. London, 1803 (1964).
16. K. T. LEFFEK, R. E. ROBERTSON, and S. SUGAMORI. J. Am. Chem. Soc. **87**, 2097 (1965).
17. L. HAKKA, A. QUEEN, and R. E. ROBERTSON. J. Am. Chem. Soc. **87**, 161 (1965).
18. M. WOLFSBERG and M. J. STERN. Pure Appl. Chem. **8**, 325 (1964).
19. H. S. FRANK and M. EVANS. J. Chem. Phys. **13**, 507 (1945).
20. D. N. GLEW. J. Phys. Chem. **66**, 605 (1962).
21. R. E. ROBERTSON. Can. J. Chem. **42**, 1707 (1964).
22. R. E. ROBERTSON and P. M. LAUGHTON. Can. J. Chem. **43**, 154 (1965).
23. G. HAMILTON and R. E. ROBERTSON. Can. J. Chem. **37**, 966 (1959).
24. R. E. ROBERTSON, R. L. HEPPOLETTE, and J. M. W. SCOTT. Can. J. Chem. **37**, 803 (1959).
25. A. G. EVANS. The reactions of organic halides in solution. Manchester University Press, Manchester, England. 1946.
26. J. L. FRANKLIN. Trans. Faraday Soc. **48**, 443 (1952).
27. A. STREITWIESER, JR. Chem. Rev. **56**, 571 (1956).
28. J. O. EDWARDS. J. Am. Chem. Soc. **78**, 1819 (1956).
29. J. F. BUNNETT. J. Am. Chem. Soc. **79**, 5969 (1957).
30. V. B. KARTHA, R. N. JONES, and R. E. ROBERTSON. Proc. Indian Acad. Sci. Sect. A, **58**, 216 (1963).
31. P. M. LAUGHTON and R. E. ROBERTSON. Can. J. Chem. **35**, 1319 (1957).
32. R. E. ROBERTSON. Can. J. Chem. **31**, 989 (1953).
33. K. J. LAIDLER. Trans. Faraday Soc. **55**, 1725 (1959).
34. L. L. SCHALEGER and F. A. LONG. Advances in physical organic chemistry. Vol. 1. Academic Press, Inc., New York. 1963. p. 21.
35. J. E. LEFFLER and E. GRUNWALD. Rates and equilibria of organic reactions. J. Wiley and Sons, Inc., New York. 1963. Ch. 9.
36. E. D. HUGHES. Trans. Faraday Soc. **34**, 195 (1938).
37. C. G. SWAIN and J. M. W. SCOTT. J. Am. Chem. Soc. **75**, 141 (1953).
38. J. O. EDWARDS. J. Am. Chem. Soc. **76**, 1540 (1954).

Can. J. Chem. Downloaded from www.nrcresearchpress.com by 210.87.254.105 on 09/05/12
For personal use only.

Can. J. Chem. Downloaded from www.nrcresearchpress.com by 210.87.254.40 on 09/05/12
For personal use only.

THE HYDROLYSIS OF SUBSTITUTED METHYL BENZENESULFONATES IN WATER[1]

R. E. ROBERTSON, A. STEIN,[2] AND S. E. SUGAMORI
Division of Pure Chemistry, National Research Council, Ottawa, Canada

Received October 29, 1965

ABSTRACT

Rate data and derived parameters for the hydrolysis of a series of para-substituted methyl benzenesulfonates are given. The introduction of such substituents has negligible effect on $\Delta C_p^{\neq}$, and the difference in rate is largely reflected in $\delta_X \Delta S^{\neq}$.

In this paper we report rate data for the hydrolysis of a series of substituted methyl benzenesulfonates in water. These, together with similar data already presented (1, 2), reveal certain trends in $\Delta H^{\neq}$, $\Delta S^{\neq}$, and $\Delta C_p^{\neq}$ which we hope will be of assistance in developing an understanding of the detailed mechanism of ionogenic reactions in water. The esters were the same as used in a previous investigation (3) redistilled or recrystallized where needed to give acceptable physical constants.

RESULTS AND DISCUSSION

Rates of hydrolysis for a series of temperatures[3] were determined by a conductance method as described in earlier papers (4). Here, as in previous papers, we take advantage of the convenience of using the approximation $\log (1/R_i' - 1/R_i) = \log (c_i' - c_i)$ where R and c are the measured resistance of the solution and the concentration of the product acid at times t and $t - \gamma$ respectively as required by the relation (5)

$$[1] \qquad kt_i - \log_e (c_{2_i} - c_{1_i}) = \log_e (c_\infty - c_0)(1 - e^{-kt}).$$

Where the concentrations of solute were low, a normal consequence of studying halides in water, and where γ was in the range of one or two half-lives, there was no indication of rate dependence on the individual cell constants. Hence, the error introduced through a neglect of the Onsager term was not larger than the random variation due to other causes. We have recently shown that, in the case of *t*-butyl chlriode, this approximation makes a negligible change in the derived parameters and a change in k_i in the order of 0.1%.

For each compound, the temperature dependence of the rate of hydrolysis has been shown to fit the empirical three-constant equation $\log_{10} k = A/T + B \log_{10} T + C$ within experimental error. The corresponding least mean square constants are given in Table I along with the temperature range over which the rates were determined, the number of determinations, and the unbiased standard deviation

$$\sigma = \left(\frac{\sum (\log k_{calc} - \log k_{obs})^2}{n - 1} \right)^{1/2}.$$

In Table I, $n_{T_2}^{T_1}$ refers to the number of individual rates used in the least mean square calculation, where T_1 and T_2 are the upper and lower temperatures defining the experimental range.

[1]*Issued as N.R.C. No. 8822.*
[2]*N.R.C. Summer Worker, 1960. Present address: Department of Chemistry, Memorial University, St. John's, Newfoundland.*
[3]*Individual rates have been placed in The Depository of Unpublished Data, National Science Library, National Research Council, Ottawa, Canada, and photocopies may be obtained upon request to the Depository.*

TABLE I

Empirical constants for the equation: $\log_{10} k = A/T + B \log_{10} T + C$

Compound	$-A$	$-B$	C	$n_{T_2}^{T_1}$	σ	Ref.
Me MeS	7133.19	17.985	63.132	37_0^{60}	0.0018	10*
Me *p*-MeO	7307.599	18.428	64.884	36_5^{70}	0.0021	
Me *p*-Me	6867.299	15.589	56.5090	45_0^{80}	0.0018	1*
Me *p*-H	7048.300	17.1925	61.2481	37_0^{65}	0.0018	
Me *p*-Br	6996.022	16.813	60.3558	40_5^{65}	0.0037	
Me *p*-NO_2	5816.123	8.726	36.895	37_5^{55}	0.0021	
Me *m*-NO_2	6727.626	14.861	55.059	33_5^{55}	0.003	

*Recalculated.

While it is true that the k_{OH^-}/k_{H_2O} ratio is smaller for the methyl benzenesulfonate than for the halides (6), there is no evidence that excludes the requirement for some degree of nucleophilic interaction in order to achieve the transition state. Whether the degree of nucleophilic interaction alters with para substitution was not explored, but it is worth noting that the relative effect of para substitution shows no unusual increase for attack by EtO^- in ethanol compared to solvolysis in ethanol. The secondary α-deuterium isotope effect for the hydrolysis of Me *p*-NO_2 ester is essentially the same ($k_H/k_D = 0.95$) as that reported for the *p*-Me ester (7). The value of the rate at 40.008 °C for the protonated ester was $3.49_3 \pm 0.007 \times 10^{-4}$ on four determinations, (3.498×10^{-4} calculated, see Table I) and for the deuterated compound $3.67_2 \pm 0.002 \times 10^{-4}$ on three determinations. The inferential value of this ratio as a test for differences in the degree of nucleophilic interaction is seriously weakened by the findings of Leffek (8) and of Wu and Robertson (9) in another system, but it is obvious that if para substitution causes a difference in respect to required overlap, it is not large. The change in the relative effect of para substitution on the rate of solvolysis in various solvents is probably a better indicator, but other factors (e.g. initial state differences) could account for the modest differences apparent in Table II.

In keeping with previous work, we accept the transition state hypotheses with the usual approximation of $d\Delta C_p^{\ddagger}/dT = 0$ and by analogy with true equilibria interpret the constants of the temperature–rate equation as follows.

$$A = -\Delta H_0^{\ddagger}/2.3026R \quad [2]$$

$$B = (\Delta C_p^{\ddagger}/R) + 1 \quad [3]$$

$$C = (\Delta S_0^{\ddagger} + \Delta C_p^{\ddagger})/2.3026R + \log_{10} k/h \quad [4]$$

The corresponding derived parameters are given in Table III.[4] We are well aware that it has been frequently argued that $\Delta F^{\ddagger}$ gives the truest reflection of the effect of a substituent on E_0, or on the potential energy (10), but it is just because substitution alters the rate of reaction through other factors than bond strength, that added useful information may be derived from a comparison of the derived constants $\Delta H^{\ddagger}$, $\Delta S^{\ddagger}$, and $\Delta C_p^{\ddagger}$.

If the transition state is reached when

anion–water interaction = water–water interaction,

[4]*The errors in these terms have not been specified. We are particularly grateful that Dr. D. N. Glew has recently provided an estimate for the case of isopropyl bromide where $\sigma = 0.0017$ from our calculation. The quantity $\delta\Delta H^{\ddagger}$ was shown to have a value of ~30 cal at 25 °C, 8.3 at 50 °C, and 32.5 at 75 °C. The corresponding error in $\Delta C_p^{\ddagger}$ was about 1.0 cal/mole deg over the entire range.*

Can. J. Chem. Downloaded from www.nrcresearchpress.com by 210.87.254.40 on 09/05/12
For personal use only.

TABLE II

Relative rates of solvolysis of substituted methyl benzenesulfonates

Para substituent	Water	MeOH	EtOH
MeO	0.5	—	0.45
Me	0.7	0.65	0.64
H	1	1	1
Br	1.67	2.20	2.2
NO_2	5.9	8.6	9.3

then the observed activation parameters are not reduced to "reasonable levels" (11–13) by solvation of the developing anions, but rather the contribution from this source is just about to begin. This hypothesis which was introduced to account for our solvolytic results for the halides (13) would be expected to hold for the hydrolysis of sulfonates as well. The $\Delta H^{\ddagger}$, $\Delta S^{\ddagger}$, and $\Delta C_p^{\ddagger}$ (Table III) then relate to those processes leading up to the critical conditions given above. The most important factors in the activation process will still be related to (*a*) repulsion energy, (*b*) bond strength/bond stretching, (*c*) reorganization of the solvent. Here, the question is how para substitution will be expected to alter these contributors.

TABLE III

Thermodynamic parameters for the hydrolysis of a series of methyl para-substituted benzenesulfonates in water at 50 °C

Compound	k_1 (s × 10^5)	$\Delta H^{\ddagger}$ (cal/mole)	$\Delta S^{\ddagger}$ (cal/mole deg)	$\Delta C_p^{\ddagger}$ (cal/mole deg)
Me Mes	8.40	20 450	−14.1	−38
Me *p*-MeO	10.71	20 960	−12.0	−39
Me *p*-Me	13.78	20 770	−12.1	−33
Me *p*-H	19.66	20 570	−12.0	−36
Me *p*-Br	54.50	20 570	−11.0	−35
Me *p*-NO_2	100.0	20 370	−9.3	−19
Me *m*-NO_2	89.13	20 600	−9.0	−32

If we take methyl methanesulfonate as an arbitrary reference, then the change to the benzenesulfonate series will probably (*a*) lower the repulsion, (*b*) lower the bond energy, (*c*) disperse the charge.

While the effect of para substitution on the rate is relatively small, it is the modification of electron density under nucleophilic attack which appears to be effective in determining differences in $\Delta F^{\ddagger}$, i.e. a combination of inductive ability and polarizability (14–16), which, it will be noted, appears to influence $\Delta S^{\ddagger}$ more than $\Delta H^{\ddagger}$, the latter save in one example being higher than for the reference compound.

The $\Delta C_p^{\ddagger}$ values for the series, in common with the sulfonates previously studied (2, 10), give values which are some 10–15 cal less negative than the corresponding term where a halide ion is the displaced group. All evidence available suggests that this difference arises from a difference in the degree of interaction between the sulfonic oxygens and the initial state solvation shell. The similarity of the $\Delta C_p^{\ddagger}$ values throughout the series suggests that solvent reorganization is about the same whatever the substituent—with the exception of the *p*-NO_2 derivative.

In spite of the difference in the size of the anion, the similarity in the value of $\Delta C_p^{\ddagger}$ throughout the series (with one exception) may be taken as an indication of uniform

Can. J. Chem. Downloaded from www.nrcresearchpress.com by 210.87.254.40 on 09/05/12
For personal use only.

solvent reorganization in the activation process. In the exceptional case (p-NO_2) there is the added possibility of hydrogen bonding to the oxygens of the NO_2 group which might, in principle, introduce an unusual factor. Against this may be cited the unexceptional value of $\Delta C_p^{\neq}$ for the m-NO_2 homologue; hence we attribute the low value of $\Delta C_p^{\neq}$ for the p-NO_2 compound to some feature associated with low solubility rather than interaction with the initial state solvent shell. Kartha (17) found that the effect of para substitution on hydrogen bonding as shown by Δ cm^{-1} vs. the displacement of the maximum of the OH band of the hydrogen-bonded complex from that of the free p-Cl phenol was in the order:

$$p\text{-}NO_2\ (83.5) < p\text{-Br}\ (97.6) < p\text{-H}\ (111.1);$$

$$p\text{-Me}\ (116.4) < \text{Mesylate}\ (117.9) < p\text{-MeO}\ (121.4).$$

These differences follow the trend to be expected from normal electronic effects of the respective substituents on the unshared electrons of the sulfonic oxygens. Since interaction of this kind in the initial state will tend to make $\Delta C_p^{\neq}$ less negative (this is the same argument used to account for the difference between the halides and the sulfonates) we may assume that initial state differences as a consequence of para substitution or transition state differences due to solvent exclusion are unimportant throughout this series.

REFERENCES

1. R. E. Robertson. Can. J. Chem. **33**, 1536 (1955).
2. R. E. Robertson. Can. J. Chem. **35**, 613 (1957).
3. R. E. Robertson. Can. J. Chem. **31**, 589 (1953).
4. R. L. Heppolette and R. E. Robertson. J. Am. Chem. Soc. **83**, 1834 (1961).
5. E. A. Guggenheim. Phil. Mag. Ser. 7, **2**, 538 (1926).
6. S. Hartman and R. E. Robertson. Can. J. Chem. **38**, 2033 (1960).
7. J. A. Llewellyn, R. E. Robertson, and J. M. W. Scott. Can. J. Chem. **38**, 222 (1959).
8. K. T. Leffek. Can. J. Chem. **42**, 851 (1964).
9. C. Y. Wu and R. E. Robertson. Chem. Ind. London, 1803 (1964).
10. P. W. C. Barnard and R. E. Robertson. Can. J. Chem. **39**, 881 (1961).
11. A. Streitwieser, Jr. Chem. Rev. **56**, 615 (1956).
12. R. E. Robertson, R. L. Heppolette, and J. M. W. Scott. Can. J. Chem. **37**, 803 (1959).
13. R. E. Robertson. Can. J. Chem. **42**, 1707 (1964).
14. J. F. Bunnett and J. Y. Bassett, Jr. J. Am. Chem. Soc. **81**, 2104 (1959).
15. R. F. Hudson. Chimica Milan, **16**, 173 (1962).
16. J. O. Edwards and R. G. Pearson. J. Am. Chem. Soc. **84**, 16 (1962).
17. V. B. Kartha, R. Norman Jones, and R. E. Robertson. Proc. Indian Acad. Sci. Sect. A, **58**, 216 (1963).

Can. J. Chem. Downloaded from www.nrcresearchpress.com by 210.87.254.40 on 09/05/12
For personal use only.

ISOTOPE EFFECTS IN MIXTURES OF LIQUID H_2O AND T_2O

MARK SALOMON
School of Chemistry, Rutgers, The State University, New Brunswick, New Jersey
Received August 31, 1965

ABSTRACT

Calculations are presented for the equilibrium tritium isotope effect involving water, hydronium ion, and hydroxide ion. The results are used to predict the kinetic isotope effect in the transfer of protons to a mercury cathode.

INTRODUCTION

The use of tritium for studying the kinetics of proton transfer reactions has some major advantages over the deuterium isotope. This is particularly true for reactions which proceed by small amounts of proton tunneling. The use of deuterium to evaluate proton tunneling contributions may not, in this case, be critical enough unless the kinetics are studied down to very low temperatures. In aqueous solutions one is severely limited to a relatively small temperature range. Hence criteria more diagnostic than the H/D isotope effect is sought. By employing the tritium isotope, which gives larger isotope effects, the experimental confirmation of proton tunneling may indeed be more significant. It is of interest, therefore, to calculate the solvent isotope effects for equilibria involving mixtures of H_2O and T_2O and to apply these calculations to a kinetic mechanism involving a proton transfer.

CALCULATION OF EQUILIBRIUM CONSTANTS

The calculations presented below were performed by the method of Bader (1, 2). This method was used recently by Thornton (3) to calculate the equilibrium properties for water containing the ^{16}O–^{18}O isotopes. This method, applied to hydrogen and tritium, has enabled the following equilibrium constants (for aqueous systems at 25 °C) to be calculated.

$H_2O + H_2TO^+ = HTO + H_3O^+$	$K_1 = 1.051$
$H_2O + T_3O^+ = HTO + HT_2O^+$	$K_2 = 9.474$
$H_2O + T_3O^+ = T_2O + H_2TO^+$	$K_3 = 7.459$
$2T_3O^+ + 3H_2O = 3T_2O + 2H_3O^+$	$L_T = 15.36$
$H_2O + T_2O = 2HTO$	$K_4 = 4.00$

These equilibrium constants were caclulated by first evaluating the partition function ratios, q_T/q_H, for the various isotopic species involved. The rotational partition function is calculated by Bader's method (1, 2) of treating the librations of the solvated H and T species as harmonic oscillators. The librational and vibrational frequencies for H_2O and OH^- were taken from Bader's work (1) and the corresponding frequencies for T_2O were calculated from Herzberg's equations (4). The force constants for H_2O given by Herzberg (4) were used in this calculation. The force constants and vibrational frequencies for H_3O^+ were obtained from Wolfsberg (5). The force constants for H_3O^+ are: $k_s = 4.915$, $k_\phi = 0.5$, $k_w = 0.06$, and $k_{int} = -0.4896$ mdyn Å^{-1}. The subscripts s, ϕ, w, and int refer, respectively, to the O—H stretch, the H—O—H bend, the O—H wag, and the OH . . . . OH interaction. The corresponding vibrational frequencies for T_3O^+ were calculated from Herzberg's equations (6).

Can. J. Chem. Downloaded from www.nrcresearchpress.com by 210.87.254.6 on 09/05/12
For personal use only.

The librational frequency shifts for T_2O and T_3O^+ were calculated from the inverse square roots of the average moments of inertia (cf. Bader, ref. 1). The moments of inertia were calculated from the formulae given by Moelwyn-Hughes (7). The bond length and valency angle for H_2O were taken, respectively, as 0.96 Å and 105° (7). The bond length and valency angle for pyramidal H_3O^+ were taken, respectively, as 1.05 Å (8) and 107° (3). The bond length for OH^- is not required. The vibrational and librational frequencies for the various H and T species in aqueous solution at 25 °C are given in Table I.

TABLE I

Frequency assignments for liquid waters at 25 °C

Molecule	Frequency (cm^{-1}) H species	Frequency (cm^{-1}) T species	Mode	Degeneracy
H_2O	3 400	2 003	ν_1	1
	1 645	988	ν_2	1
	3 440	2 183	ν_3	1
	667	408	ν_{lib}	3
H_3O^+	2 600	1 680	ν_1	1
	1 086	738	ν_2	1
	3 171	1 993	ν_3	2
	1 729	1 058	ν_4	2
	643	385	ν_{lib}	3
OH^-	3 615	2 206	ν_1	1
	477	291	ν_{lib}	2

Using the frequencies in Table I, the following partition function ratios were calculated.

$$\frac{q_{T_2O}}{q_{H_2O}} = 4.034 \times 10^4; \qquad \frac{q_{T_3O^+}}{q_{H_3O^+}} = 2.068 \times 10^6; \qquad \frac{q_{OT^-}}{q_{OH^-}} = 286.5$$

By applying the rule of the geometric mean (cf. ref. 2) the following partition function ratios were calculated.

$$\frac{q_{HTO}}{q_{H_2O}} = 402 \qquad \frac{q_{T_2O}}{q_{HTO}} = 100.5$$

$$\frac{q_{H_2TO^+}}{q_{H_3O^+}} = 382.2 \qquad \frac{q_{T_3O^+}}{q_{H_2TO^+}} = 5\,410$$

$$\frac{q_{HT_2O^+}}{q_{H_2TO^+}} = 127.4 \qquad \frac{q_{T_3O^+}}{q_{HT_2O^+}} = 42.47$$

The equilibrium constants, K_1 to K_4 and L_T, were calculated using these partition function ratios.

DISCUSSION

In this section, the above results are applied to the kinetics of electrochemical proton transfer with the primary object of trying to correlate the available experimental data with either a non-tunneling or a tunneling mechanism. Most of the experimental data for proton transfer to a mercury cathode involves the use of the deuterium isotope (9–13). In all cases the H/D isotope effect was observed to be quite small and potential dependent. Low temperature studies for transfer from alcoholic solutions to mercury cathodes indicates that proton tunneling plays a very negligible role in the overall rate of proton transfer (13). Similar conclusions have been reached for the aqueous system where one is considerably limited by the temperature range over which the kinetic isotope effect

Can. J. Chem. Downloaded from www.nrcresearchpress.com by 210.87.254.6 on 09/05/12
For personal use only.

can be studied (13–15). These conclusions are based upon the experimental findings that in both aqueous and non-aqueous systems (i) the activation energies for H and D transfer are temperature independent and (ii) the ratio of "true" frequencies factors, A_H/A_D, is equal to 1.2. If tunneling were a significant pathway in this reaction then, according to Bell (16), $A_H/A_D \leqslant 0.5$ is an excellent criteria.

The isotopic quantity most often studied in electrochemical kinetics is the separation factor S. In terms of a rate-determining proton transfer from an acid species to a mercury cathode, the tritium separation factor is defined (cf. 15, 17) as

$$S_T = \frac{C_T[H_3O^+]}{C_H[H_2TO^+]} \frac{q_{H_2TO^+}}{q_{H_3O^+}} \frac{q_H^{\ddagger}}{q_T^{\ddagger}},$$

where C_T/C_H is the atomic ratio of tritium to hydrogen in solution and ‡ refers to the activated complex. This relation is valid for the case where the only significant source of tritium is the species H_2TO^+. This condition is easily met by making C_T/C_H very small; e.g. when 10^{-5} mole of T_2O is placed in 1 l of normal acid solution, the concentration ratio $[H_3O^+]/[H_2TO^+] = 2.958 \times 10^6$ as calculated from the equilibrium relations for K_1 and K_4. The species HT_2O^+ is present in a concentration of the order of 10^{-11} M so that it need not be considered as a source of tritium. Inserting these quantities into the above equation with the value for $q_{H_2TO^+}/q_{H_3O^+}$ calculated above, one now has

$$S_T = 204.3 \frac{q_H^{\ddagger}}{q_T^{\ddagger}}. \qquad [1]$$

The partition function ratio for the activated complex, $q_H^{\ddagger}/q_T^{\ddagger}$, can be evaluated by empirical or semiempirical methods and different answers will result depending upon the method used. Hence Bockris *et al.* (17) assumed the rate-determining step to be

$$Hg + H_3O^+ + e \rightarrow HgH + H_2O, \qquad [2]$$

and from thermodynamic cycles an Eyring–Polanyi semiempirical potential energy surface was constructed. The use of the semiempirical method has been questioned even for *qualitative* analysis (18, 19). Also if one considers the mechanism to be that as written above, then one could not in fact use the semiempirical method because it uses a single eigenfunction to represent the state of the electron throughout the course of reaction (20). Hence the use of a single potential energy surface to represent mechanism [2] is a violation of the so-called adiabatic principle (20). The results of this calculation (17) gives an activation of around 2–6 kcal mole^{-1} which becomes *negative* when zero point energies are included. Also, the symmetric stretching frequency of Hg—H—OH_2 was calculated to be 3 000 cm^{-1} and this was attributed to the results obtained from the potential energy surface in which it was found that the O—H bond in the activated complex was *not* stretched from its equilibrium position in H_3O^+. This high frequency gave very small isotope effects which could be increased somewhat by assuming the bending frequencies to approach zero. Even with the assumption that the bending frequencies approach zero, the predicted isotope effect was still too small and a tunneling factor was required to increase it. In a more recent paper, Bockris and Matthews (21) have offered a model of charge transfer which involves stretching of the O—H bond and is therefore contrary to the model used in the quantitative calculations (17).

Conway *et al.* (14, 15, 22) have proposed a different model for slow proton discharge. According to this model the slow step corresponds to the reaction

$$Hg + H_3O^+ \rightleftharpoons X^{\ddagger} \rightarrow HgH^+ + H_2O, \qquad [3]$$

Can. J. Chem. Downloaded from www.nrcresearchpress.com by 210.87.254.6 on 09/05/12
For personal use only.

Can. J. Chem. Downloaded from www.nrcresearchpress.com by 210.87.254.6 on 09/05/12
For personal use only.

and electron transfer proceeds either by tunneling to the fully charged activated state, $X^{\pm}$, or by tunneling to the final state, HgH^{+}. This model of the activated complex was proposed in order to explain the observed results that (i) proton tunneling plays an insignificant role in the overall mechanism [2] for proton discharge and (ii) the potential dependence of S_D could be explained in terms of a non-tunneling mechanism if a fully charged activated complex could be justified.

The reasons leading to conclusion (i) has been discussed above and in more detail elsewhere (12–15, 22). The concept of a charged activated complex results from the successful application (15, 22) of Bader's model of proton transfer (23, 24) to the present electrochemical case. In this model, $q_H^{\pm}/q_D^{\pm}$ is evaluated by using a three center model. The activated complex is formed by electrons from mercury ($6s^2$) and oxygen ($2p^2$) and can be considered to form σ-bonding and σ-antibonding orbitals. According to Bader (23, 24), the antibonding effects will give rise to higher bending force constants when electrons are supplied to either end of the linear M . . . H . . . O complex and therefore result in smaller isotope effects. Since electron supply to the electrode surface is a variable in electrochemical kinetics, one would expect the bending frequency to be a function of electrode potential such that the kinetic isotope effect will decrease as the potential is made more cathodic. Calculation of bending frequencies from first principles then becomes exceedingly difficult and we have therefore chosen this frequency by comparing the activated complex with similar stable structures in which ν_ϕ is known, e.g. as in FHF^- (14, 15, 22). The variation of ν_ϕ has been used to explain the dependence of the H/D isotope effect on electron-donating substituents (23) and has been treated theoretically by the same author (24). We have found (14, 15) that bending frequencies of $\nu_{\phi,H} = 1\,000$ to $1\,200\ cm^{-1}$ could explain the observed decrease in the deuterium separation factor, S_D, from 3.7 at -0.9 V to 2.5 at -1.4 V (the potentials are referred to the reversible hydrogen electrode (12)). The vibrational frequency for the symmetrical stretching mode was calculated from Johnston's empirical method of bond orders (19). This method has been shown to predict activation energies to within ± 2 kcal $mole^{-1}$ for hydrogen transfer reactions and is therefore considered to be superior to the semiempirical method. The symmetrical stretching mode for the electrochemical proton transfer was found (22) to have a frequency $\nu_{s,H} = 1\,503\ cm^{-1}$. This is rather high for this type of vibration (e.g. in FHF^- $\nu_{s,H} = 600\ cm^{-1}$) and is attributed to the calculated result that the $(Hg—H—OH_2)^+$ complex is asymmetric (22).

Bockris *et al.* (17) and Christov (25) agree that, while tunneling is not a significant pathway in proton discharge at Hg cathodes in alcoholic solutions, in aqueous solutions up to 80% of the total rate of discharge is due to proton tunneling. The tritium isotope effect studied experimentally and theoretically has been offered as more dramatic proof for large amounts of proton tunneling in the aqueous system (17). It was found that the experimental S_T values decreased from ~ 9 at -0.9 V to ~ 4 at -1.4 V; also theoretical calculations based on a tunneling mechanism were presented which gave a satisfactory fit to the experimental data.

Values of S_T can be calculated from eq. [1] by evaluating $q_H^{\pm}/q_T^{\pm}$ as follows: first, the activated complex is assumed to be immobile (22); second, we can use the frequencies found for the $(Hg—H—OH_2)^+$ activated complex to calculate the corresponding frequencies for the $(Hg—T—OH_2)^+$ complex. It is found that $\nu_{s,T} = 870\ cm^{-1}$ for the stretch and $\nu_{\phi,T} = 584\ cm^{-1}$ at -0.9 V and $\nu_{\phi,T} = 696\ cm^{-1}$ at -1.4 V for the variable bending frequency. These last two bending frequencies were calculated from the H isotope frequencies which were used to fit the observed S_D versus potential relationship

(15). Hence the values of S_T calculated from eq. [1] are 5.3 and 2.9 for potentials of -0.9 and -1.4 V, respectively. Providing the mechanism proposed by Conway *et al.* (14, 15, 22) is correct, then the values of S_T predicted here should be fairly reliable and the problem is to explain the difference between these results and the experimental values of Bockris *et al.* (17).

There appears to be a serious anomaly in the experimental values in that the temperature coefficient of S_T, i.e. dS_T/dT, is positive; i.e. the isotope effect was observed to *increase* as the temperature was increased. The results for the H/D isotope effect all show a negative value for dS_D/dT when discharge is kinetically rate-determining. One cannot theoretically predict this effect based on a kinetic mechanism when k_H/k_D (the ratio of rate constants) is greater than unity, which it is (10, 13). Yet Bockris *et al.* do in fact predict this phenomena and this becomes even more difficult to comprehend if, as claimed, 80% of the rate proceeds by a tunneling mechanism. The experimental results indicating a positive dS_T/dT value could possibly be explained by slow diffusion of H_2TO^+ since it is present in micromolar quantities in the bulk. Such a process was suggested by Rome and Hiskey (11) to explain their one point where $(dS_D/dT)_i$ was positive. This occurred at the highest current density (i.e. the highest rate of reaction) in isotopically mixed solutions dilute in its D content. In no other case did Rome and Hiskey (11) or Walton and Wolfenden (9) observe this anomolous value for $(dS_D/dT)_i$.* It is quite possible therefore that the experimental S_T values are too high because of a further isotopic separation by slow diffusion. Hence the values of S_T predicted here would be expected to be lower than the experimental values, and the conclusion that proton tunneling is a significant pathway (based on the observed S_T values and the theoretical calculations including tunneling corrections) is not well founded. The values calculated here on the basis of a non-tunneling mechanism indicate low values of S_T and this is, partially at least, borne out by a low experimental value. It might be mentioned that the maximum isotope effect which would occur if there were no difference in zero point energies of the H and T activated complexes is 204 as obtained from eq. [1]. Hence the maximum theoretical S_T value is at least 20 times greater than the experimental value and this in itself is suggestive of a non-tunneling mechanism. Conclusive evidence in support of a non-tunneling mechanism should, however, involve values for the activation energies over a wide temperature range and the frequency factor ratio A_H/A_T. Although this information is not yet available, the present results are considered to be sufficient evidence in favor of the non-tunneling mechanism since they were derived by a simple extension of our previous H/D results as discussed above.

REFERENCES

1. C. G. Swain and R. F. W. Bader. Tetrahedron, **10**, 182 (1960).
2. C. G. Swain, R. F. W. Bader, and E. R. Thornton. Tetrahedron, **10**, 200 (1960).
3. E. R. Thornton. J. Am. Chem. Soc. **84**, 2474 (1962).
4. G. Herzberg. Infrared and Raman spectra. D. Van Nostrand Co., Inc., New York. 1945. p. 187.
5. M. Wolfsberg. Private communication. 1962. G. C. Walrafen. J. Chem. Phys. **36**, 1035 (1962).
6. G. Herzberg. Infrared and Raman spectra. D. Van Nostrand Co., Inc., New York. p. 188.
7. E. A. Moelwyn-Hughes. Physical chemistry. The Pergamon Press, Ltd., London. 1961. pp. 455, 502.
8. B. E. Conway. Modern aspects of electrochemistry. Vol. 3. *Edited by* Bockris and Conway. Butterworths, London. 1965. Chap. 2.
9. H. F. Walton and J. H. Wolfenden. Trans. Faraday Soc. **34**, 436 (1938).
10. B. Post and C. F. Hiskey. J. Am. Chem. Soc. **72**, 4203 (1950); **73**, 161 (1951).
11. M. Rome and C. F. Hiskey. J. Am. Chem. Soc. **76**, 5207 (1954).
12. M. Salomon and B. E. Conway. J. Phys. Chem. **68**, 2009 (1964).
13. B. E. Conway and M. Salomon. J. Chem. Phys. **41**, 3169 (1964).
14. B. E. Conway and M. Salomon. Ber. Bunsenges. Physik. Chem. **68**, 331 (1964).
15. M. Salomon and B. E. Conway. Disc. Faraday Soc. **39**, In press. 1965.

**At constant overpotential, $(dS_D/dT)_\eta$ was always observed to be negative, as it must be.*

Can. J. Chem. Downloaded from www.nrcresearchpress.com by 210.87.254.6 on 09/05/12
For personal use only.

16. R. P. BELL. The proton in chemistry. Cornell Univ. Press, Ithaca, N.Y. 1959.
17. J. O'M. BOCKRIS and S. SRINIVASAN. J. Electrochem. Soc. **111**, 844 (1964). J. O'M. BOCKRIS, S. SRINIVASAN, and D. B. MATTHEWS. Disc. Faraday Soc. **39**, In press. 1965.
18. J. H. DAVY, C. R. GUERRA, H. S. JOHNSTON, C. F. WEAVER, and C. E. YOUNG. J. Chem. Phys. **41**, 1517 (1964).
19. H. S. JOHNSTON and C. PARR. J. Am. Chem. Soc. **85**, 2544 (1963).
20. S. GLASSTONE, K. J. LAIDLER, and H. EYRING. Theory of rate processes. McGraw-Hill Book Co., Inc., New York and London. 1941.
21. J. O'M. BOCKRIS and D. B. MATTHEWS. J. Electroanal. Chem. **9**, 325 (1965).
22. M. SALOMON, C. G. ENKE, and B. E. CONWAY. J. Chem. Phys. **43**, 3989 (1965).
23. C. G. SWAIN, R. A. WILES, and R. F. W. BADER. J. Am. Chem. Soc. **83**, 1945 (1961).
24. R. F. W. BADER. Can. J. Chem. **42**, 1822 (1964).
25. ST. V. CHRISTOV. Disc. Faraday Soc. **39**, In press. 1965.

Can. J. Chem. Downloaded from www.nrcresearchpress.com by 210.87.254.6 on 09/05/12
For personal use only.

THE ANIONIC POLYMERIZATION OF ALLYL ACRYLATE AND OF ALLYL METHACRYLATE[1,2]

S. Bywater, P. E. Black, and D. M. Wiles
Division of Applied Chemistry, National Research Council, Ottawa, Canada

Received October 29, 1965

ABSTRACT

The low temperature polymerization of allyl acrylate in toluene solution has been investigated with *n*-butyllithium and 1,1-diphenyl-*n*-hexyllithium initiators. The latter was also used in a study of the polymerization of allyl methacrylate under the same conditions. The reactions between initiator and monomer were rapid in all cases. More than half of the initiator molecules reacted with monomer acrylic double bonds to start polymer chains, only a few of which grew to a high molecular weight, highly isotactic product. Most of the chains remained as a low molecular weight, precipitant-soluble product. The remaining initiator molecules reacted with the carbonyl groups of the monomers to produce species which could be detected as allyl alcohol, after termination of the reaction with acetic acid. The allyl double bonds were not involved in reactions during polymerization but were presumably responsible for the cross-linking which occurred when the polymers were exposed to air.

INTRODUCTION

Several of the many complex aspects of the anionic polymerization of methyl methacrylate in toluene solution have been shown to be due to the presence of the two unsaturated bonds in this monomer (1, 2). Both the acrylic double bond and the carbonyl group are susceptible to reaction with organometallic compounds (3). The reaction with the carbonyl group leads to kinetic complications (4, 5) and unusual polymer molecular weight distributions (6) when the initiator is *n*-butyllithium (BuLi). Some simplification of the kinetics is obtained by the use of a relatively less reactive initiator, 1,1-diphenyl-*n*-hexyllithium (DPHL), in toluene solution (2). Nevertheless, there is still evidence of reaction between DPHL and methyl methacrylate carbonyl groups at −78 °C.

A recent publication by Donati and Farina (7) deals with the organometallic-initiated polymerization of allyl acrylate (AA) in toluene solution. It is implied that BuLi reacts only with the acrylic double bond of the monomer. If this were so, allyl acrylate would then be preferable to methyl methacrylate for kinetic studies; the results could be more amenable to interpretation and explanation.

This paper is a report in some detail of the polymerization of AA in toluene solution at low temperatures with BuLi and DPHL initiators. The DPHL-initiated polymerization of allyl methacrylate (AMA) under the same conditions is also described. Polymer structures have been investigated in some cases by infrared, X-ray diffraction, and proton magnetic resonance techniques. The electronic spectra of living poly(allyl methacrylate) (PAMA) initiated by DPHL have been measured in toluene and tetrahydrofuran (THF) solutions.

EXPERIMENTAL

The sources of the initiators, BuLi and DPHL, and the handling and measurement of them has been described elsewhere (2). The monomers were obtained from the Borden Chemical Company and were purified as follows. After fractional distillation in a dry nitrogen environment at reduced pressure, the monomers were degassed on a vacuum line, stirred over calcium hydride, stirred in contact with a sodium mirror at −30 °C for 30 min, stirred on fresh calcium hydride again, and finally stored in a connected bulb at 0 °C in the dark. The desired quantity was distilled into a calibrated tube and then distilled into and sealed in a pre-weighed break-seal container. A final weighing determined the amount of monomer.

[1]*Issued as N.R.C. No. 8825.*
[2]*Paper presented in part at the Thirteenth Canadian High Polymer Forum, Ottawa, Ontario, September 22–24, 1965.*

Can. J. Chem. Downloaded from www.nrcresearchpress.com by 210.87.254.6 on 09/05/12
For personal use only.

An all-glass polymerization apparatus (4) was used for the kinetic experiments. The toluene solvent, purified as before (4), and all the glass surfaces with which the toluene solutions of initiator came in contact were pre-washed with BuLi. Details of the polymerization procedure have been published previously (2, 4). After polymerization occurred for various times to different degrees of conversion, acetic acid was added to terminate reaction. Triplicate 10 μl samples of each reaction mixture were analyzed for allyl alcohol by gas chromatography with a 2 m column of diglycerol on chromosorb W. The reaction mixture was then poured into a 10-fold excess of petroleum ether (boiling range 30–90 °C). The product was separated into precipitant-soluble and precipitant-insoluble portions. The latter portion from AA polymerizations was washed repeatedly with warm distilled water to remove lithium salts; the petroleum ether insoluble product from AMA polymerizations cross-linked too rapidly in air for the washing to be effective. All products were weighed after final drying in a vacuum desiccator under pumping at room temperature. The product yields were corrected to take into account the weight of diphenylhexyl end groups.

Number-average molecular weights of some of the soluble products were measured with a Mechrolab vapor-pressure osmometer. Viscosity-average molecular weights of a few samples of precipitant-insoluble polymers were determined from the relationship (8) which is quoted for poly(butyl acrylate) in acetone solution at 25 °C. The details of the proton magnetic resonance measurements are described elsewhere (9). Optical densities of some of the polymerizing allyl methacrylate systems were measured in the wavelength range 250–500 mμ with a Bausch and Lomb 505 recording spectrophotometer. The apparatus and techniques were similar to those described previously (10). The polymerization vessel and the quartz cell fastened to it were maintained at the desired temperature in the cell compartment by immersion in cold, absolute ethanol in a large quartz dewar vessel with optical windows.

RESULTS

The same general features found in the organometallic-initiated polymerization of methyl methacrylate have been observed in the polymerizations reported here. There is an initial rapid (< 2 min) consumption of monomer and initiator to form low molecular weight, precipitant-soluble polymer, followed by a slower process which produces high polymer. Much of the initiator is consumed in the first process. Most of the monomer, however, is incorporated in the molecules of high polymer which necessarily have a molecular weight higher than predicted from the [monomer]/[initiator] ratio used. Evidently there is attack of organometallics on the carbonyl groups in the system because lithium alkoxides, which appear in the terminated reaction mixtures as allyl alcohol, are formed.

Allyl Acrylate

The kinetic data for allyl acrylate polymerizations are shown in Fig. 1 as first order plots of monomer consumption. With a constant number of growing chains such plots would be linear. The rapid decrease in slope indicates that the number of active polymer chains decreased with time, with both initiators. This correlates with the visual observation that the yellow color, previously ascribed to the presence of the methacrylate – lithium ion pair (10), faded steadily during polymerization. The decrease in number of active centers proceeds to such an extent at higher [monomer]/[initiator] ratios that complete conversion to polymer could not be obtained in any reasonable time.

When BuLi initiator was used, about 10% of the monomer was converted to precipitant-soluble product ($\bar{M}_n \approx 900$) early in the reaction and there was a gradual increase in weight, as polymerization proceeded, to about $1\frac{1}{2}$ times the initial quantity. With DPHL initiator the weight of soluble product ($\bar{M}_n \approx 600$) was in general much higher initially but remained constant throughout a polymerization. When the initial concentrations of BuLi or DPHL were increased the weight of soluble product was higher, but there was no simple relationship between [initiator] or [monomer]/[initiator] and the weight of soluble product.

Allyl alcohol was detected in terminated reaction mixtures when either initiator was used. With BuLi, about 25% of the initiator was recovered as this product within the first 2 min of reaction. The amount subsequently increased rapidly until at long reaction

Can. J. Chem. Downloaded from www.nrcresearchpress.com by 210.87.254.6 on 09/05/12
For personal use only.

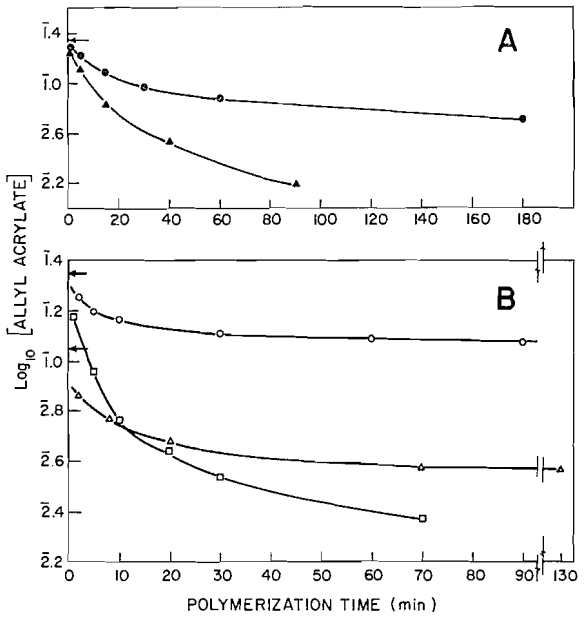


FIG. 1. Allyl acrylate polymerization in toluene at −78 °C. The symbol ← denotes initial monomer concentration. A: [AA] = 0.223 M; (●) [BuLi] = 4.0 mM; (▲) [BuLi] = 8.0 mM. B: (○) [DPHL] = 2.9 mM, [AA] = 0.223 M; (△) [DPHL] = 2.9 mM, [AA] = 0.112 M; (□) [DPHL] = 7.2 mM, [AA] = 0.223 M.

times virtually all the initiator was recovered in this form. The results for DPHL are shown in Fig. 2. About 35% of the initiator is rapidly converted to alkoxides at 2.9 mM initiator; at 7.6 mM an even larger fraction appears rapidly as lithium alkoxide. In all cases subsequent production increases steadily but monomer consumption does not.

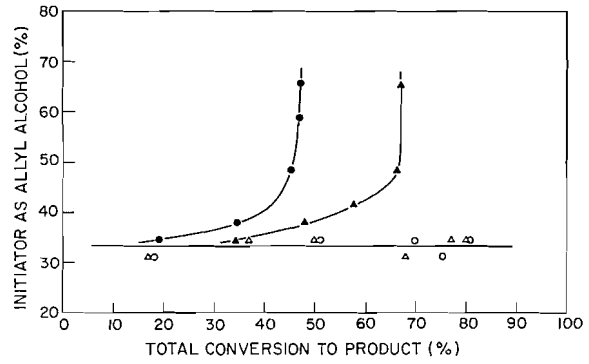


FIG. 2. Allyl alcohol in terminated reaction mixtures. Polymerization temperature = −78 °C. [DPHL] = 2.9 mM. (●) [AA] = 0.223 M; (▲) [AA] = 0.112 M; (○) [AMA] = 0.223 M; (△) [AMA] = 0.112 M.

Infrared analysis of typical poly(allyl acrylate) (PAA) showed that there was no detectable acrylic unsaturation but a great deal of carbonyl and allylic unsaturation. An oriented fibre of one PAA sample gave an X-ray diffraction pattern typical of a highly crystalline material probably having an isotactic polymer backbone (7).

Can. J. Chem. Downloaded from www.nrcresearchpress.com by 210.87.254.6 on 09/05/12
For personal use only.

Allyl Methacrylate

From Fig. 3 it can be concluded that the DPHL-initiated polymerization of AMA is less complicated than the polymerizations of AA described above. The consumption of monomer is first order, both internally and externally, at −78 °C and has been shown to be internally first order at −30 °C. This correlates with the visual observation that with this monomer the yellow color present in polymerizing systems faded little or not at all before termination.

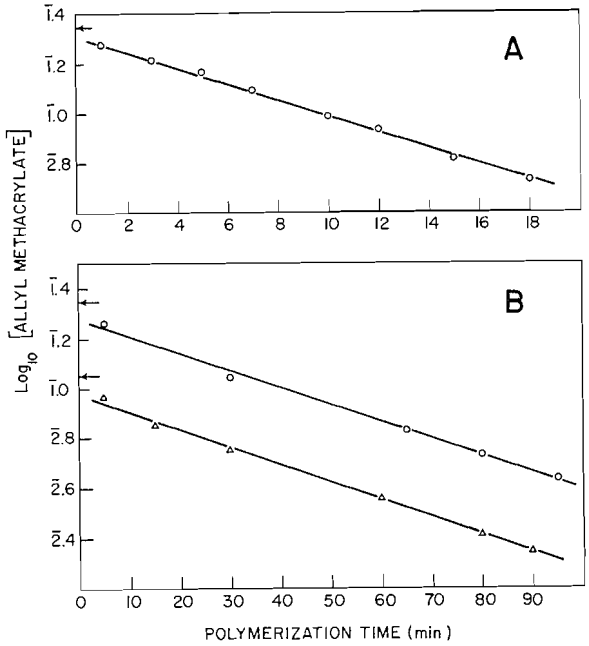


FIG. 3. Allyl methacrylate polymerization in toluene solution. The symbol ← denotes initial monomer concentration. [DPHL] = 2.9 mM. A: polymerization temperature = −30 °C; [AMA] = 0.223 M. B: polymerization temperature = −78 °C; (○) [AMA] = 0.223 M; (△) [AMA] = 0.112 M.

The absorption spectra for living PAMA anion – lithium cation systems in toluene and in THF are shown in Fig. 4. The curves represent the difference, in each of the two solvents, between the absorption at complete conversion and the absorption following termination with absolute ethanol. The spectra are very similar to those observed with the poly(methyl methacrylate) anion (10), as would be expected.

The conversion of monomer to polymer during polymerization in either solvent was accompanied by a decrease in optical density in the region 390–500 mμ and by an increase below 390 mμ. The gross optical density around 300 mμ actually increased by about 30% during polymerization, but this seemed to be largely due to an increase in background absorption in this wavelength region, since the absorption in the killed systems was greater than that of the reactants. The changes in optical density continued while polymer chains were growing and then stopped when monomer had been used up. Since there was no change, in particular no decrease thereafter in the region of absorption of the living polymer – lithium ion pair, it is reasonable to conclude that there was a constant number of living PAMA chains over the period of the experiments reported here. This conclusion is in agreement with the kinetic data shown in Fig. 3.

Can. J. Chem. Downloaded from www.nrcresearchpress.com by 210.87.254.6 on 09/05/12
For personal use only.

The weight of soluble product remains reasonably constant throughout the course of any given polymerization. The weight changes from one system to another, that is, varies with changing monomer concentration in a non-systematic way. The number-average molecular weight was found to be 450 for one system and was assumed to be similar in the other two.

The concentration of allyl alcohol (Fig. 2) was the same (about 33% of the initial [DPHL]) in each terminated reaction mixture for both systems at −78 °C. The value was a bit higher (39%) and also independent of polymerization time in the experiments at −30 °C.

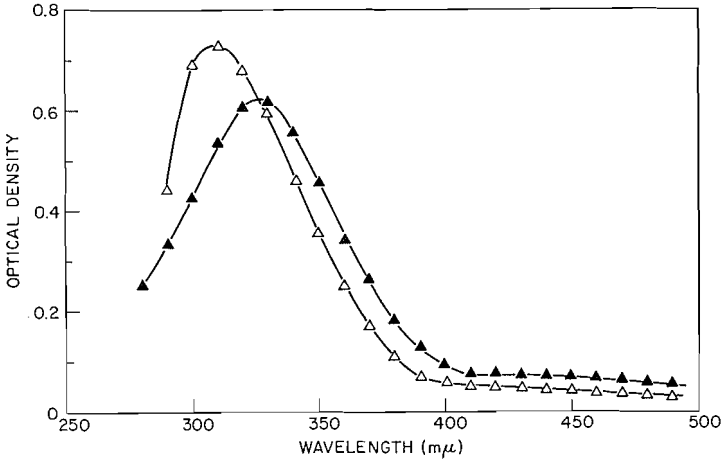


FIG. 4. Electronic absorption spectra of PAMA anions at −30 °C. 1.0 cm cell; [DPHL] = 0.725 mM, [AMA] = 0.112 M. (△) Toluene solvent; (▲) THF solvent.

The PAMA samples cross-linked very rapidly on exposure to air. Perhaps partly because of this it was not possible to crystallize these polymers. The proton magnetic resonance spectrum of samples prepared and recovered in vacuum showed that polymerization had occurred through the acrylic double bond and that polymers prepared in toluene solvent were highly isotactic. The tacticity changed to stereoblock, then to syndiotactic (9) as the polymerization solvent was altered to partly and then entirely tetrahydrofuran. There is much the same effect of reaction medium upon PAMA tacticity as was found (11) for fluorenyllithium-initiated poly(methyl methacrylate).

DISCUSSION

The kinetics of the organolithium-initiated polymerization of AA or of AMA are influenced by the fact that, for each of these monomers, two of the three unsaturated bonds are susceptible to reaction with initiator. There is apparently no appreciable reaction with the allylic double bonds of the monomers. Comparison with the anionic polymerization of methyl methacrylate indicates that the monomer acrylic double bonds are involved in polymer formation and the monomer carbonyl bonds cause complicating side reactions.

A diagram showing the two possible reactions of an organolithium compound with either AA or AMA is given in Fig. 5. Whereas reactions [1] and [2] are believed to be quite rapid it is not known to what extent reaction [3] occurs, before the polymerization is terminated. It is assumed that lithium allyl oxide present in a polymerizing system will be converted

Can. J. Chem. Downloaded from www.nrcresearchpress.com by 210.87.254.6 on 09/05/12
For personal use only.

quantitatively to allyl alcohol by reaction with acetic acid terminating agent. In the discussion to follow, reference to allyl alcohol should be regarded as synonymous with reference to its precursor(s) in an unterminated system in which, of course, there is no allyl alcohol as such.

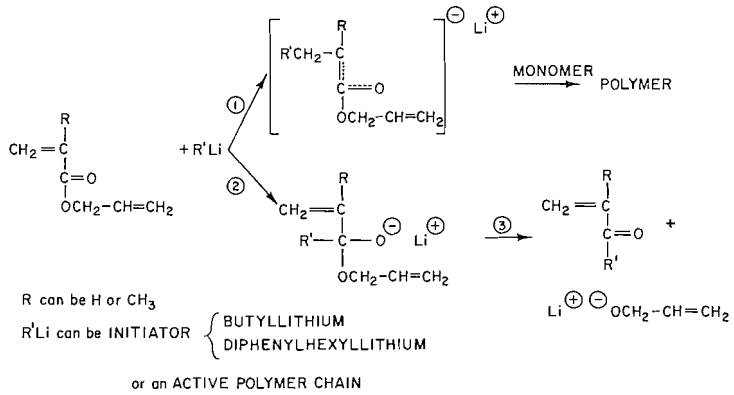


FIG. 5. The reactions of organolithium compounds with either AA or AMA.

Lithium allyl oxide or its precursor must be formed during the early stages of polymerization since allyl alcohol is invariably found in reaction mixtures terminated after short polymerization times. This amount of allyl alcohol probably reflects the extent of reaction between initiator and monomer carbonyl groups. Subsequently any reaction between growing polymer chains and monomer carbonyl groups would only give rise to a small increase, linear with conversion, in allyl alcohol concentration. This presumably occurs in the polymerizations of AA where the kinetic data and yellow color observations indicate a decreasing number of growing chains. It does not seem to occur in the DPHL-initiated polymerizations of AMA at −78° and −30 °C.

The percentage of added initiator which appears as allyl alcohol increases faster than conversion in AA polymerizations (Fig. 2). The increase in concentration of allyl alcohol precursor during chain growth is, in fact, far greater than the maximum concentration of polymer chains growing to high molecular weight. In addition, the concentration of allyl alcohol in reaction mixtures terminated at longer times continues to increase with increasing time before termination, even after polymerization has virtually ceased. There must, therefore, be a third source of allyl alcohol. Figure 6 shows a possible source which is connected with the formation of precipitant-soluble product. The idea of a short-chain, cyclic structure for this product, originally proposed by Glusker *et al.* (11), has since been used to explain some features of the polymerization of methyl methacrylate by DPHL (2). In the latter investigation the evidence indicates that the formation of soluble product is not concomitant with or followed immediately by the formation of lithium alkoxide. The sequence in the AA polymerizations seems to be a rapid formation of polymerization-inactive cyclic complex followed by a much slower irreversible cyclization with the eventual formation of lithium allyl oxide (cf. ref. 2). Although precipitant-soluble product is produced in the polymerizations of AMA also, there is no change in allyl alcohol concentration from low to higher percentage conversions to polymer. Presumably there is no reaction in these systems between growing polymer chains and monomer carbonyl groups nor is there any complete sequence of reactions like the one shown in Fig. 6 to produce allyl alcohol. The substitution of a methyl group (AMA) for the hydrogen

Can. J. Chem. Downloaded from www.nrcresearchpress.com by 210.87.254.6 on 09/05/12
For personal use only.

atom (AA) in the α-position to the acrylic double bond at which polymerization occurs may have the effect of preventing the inactive cyclic complex from undergoing true cyclization, just as it seems to prevent the reaction of a growing polymer chain with a monomer carbonyl group.

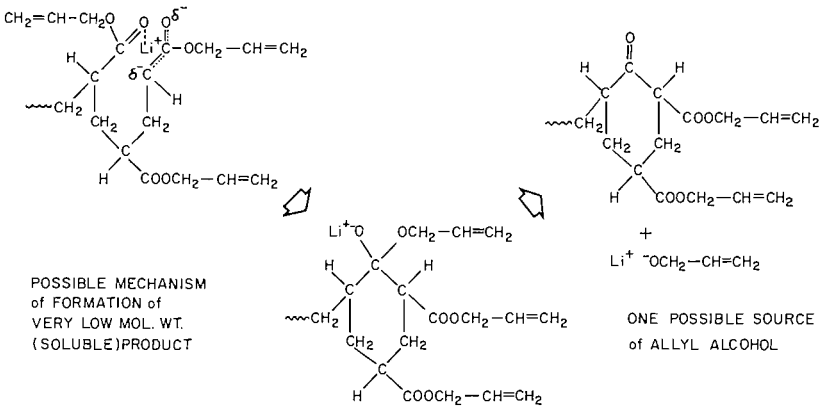


FIG. 6. A possible mechanism of lithium allyl oxide formation during AA chain propagation.

Other differences between AA and AMA (and their polymers) may also be the result of replacing an α-hydrogen with an α-methyl group. PAA has been found to cross-link slowly over a period of days at room temperature on exposure to air. PAMA on the other hand cross-links very rapidly under the same conditions. The polymerization of both monomers was attempted in tetrahydrofuran solution with DPHL initiator at −78 °C. In both cases a large proportion of the initiator led to the formation of precipitant-soluble product, a strong yellow color persisted until terminating agent was added, and allyl alcohol was present in the terminated reaction mixture. However, only with AMA monomer was a high molecular weight, precipitant-insoluble polymer formed.

The differences in crystallizability between highly isotactic PAA and PAMA presumably also arises because of the α-methyl group in each unit of the latter. It is relatively simple to induce sufficient ordering in the PAA such that a crystalline X-ray diffraction pattern is obtained. The same treatment of PAMA samples which have as high as 90% isotacticity does not provide sufficient ordering. There may be some connection between this situation and the observation (12) that butyllithium-initiated poly(methyl methacrylate), which may be highly isotactic if prepared in toluene solution at low temperatures, can not be crystallized by ordinary methods.

It can be assumed that the molar extinction coefficient which has been calculated (10) for poly(methyl methacrylate)-lithium in THF applies to the PAMA–lithium systems as well. This assumption would lead to the conclusion that approximately 1/3 of the DPHL initiator gives rise to growing PAMA chains, but this must be regarded as a rather unreliable estimate. A more accurate estimation of the number of growing chains in the polymerization systems being considered here would involve a calculation of the number of short chains in the precipitant-soluble products. Ordinarily the $\bar{M}_n$ of the material could be used for this purpose (cf. ref. 2), but in this work the values obtained were unacceptable. If both the weight and $\bar{M}_n$ values obtained were taken literally, the soluble material would account for more chains than there were initiator molecules added. The $\bar{M}_n$ values are believed to be too low because the soluble products (tacky, semisolids)

Can. J. Chem. Downloaded from www.nrcresearchpress.com by 210.87.254.6 on 09/05/12
For personal use only.

could not be pumped to constant weight at an elevated temperature as was normally done (4). Such a procedure would have led to a cross-linked material insoluble in benzene, the solvent for $\bar{M}_n$ measurements. The weights of the soluble products are believed to be too high owing to the presence of lithium salts and perhaps a component such as allyl alcohol which was not completely removed by pumping overnight at room temperature. For these reasons the concentrations of growing polymer chains could not be estimated from the soluble-product data, and a complete kinetic investigation was not attempted.

REFERENCES

1. S. BYWATER. Adv. Polymer Sci. **4**, 66 (1965).
2. D. M. WILES and S. BYWATER. Trans. Faraday Soc. **61**, 150 (1965).
3. D. M. WILES and S. BYWATER. Chem. Ind. London, 1209 (1963).
4. D. M. WILES and S. BYWATER. Polymer, **3**, 175 (1962).
5. D. M. WILES and S. BYWATER. J. Phys. Chem. **68**, 1983 (1964).
6. B. J. COTTAM, D. M. WILES, and S. BYWATER. Can. J. Chem. **41**, 1905 (1963).
7. M. DONATI and M. FARINA. Makromol. Chem. **60**, 233 (1963).
8. G. MEYERHOFF. Adv. Polymer Sci. **3**, 59 (1961).
9. D. M. WILES and S. BROWNSTEIN. J. Polymer Sci. Pt. B, **3**, 951 (1965).
10. D. M. WILES and S. BYWATER. J. Polymer Sci. Pt. B, **2**, 1175 (1964).
11. D. L. GLUSKER, I. LYSLOFF, and E. STILES. J. Polymer Sci. **49**, 315 (1961).
12. S. BYWATER and D. M. WILES. Unpublished data.

Can. J. Chem. Downloaded from www.nrcresearchpress.com by 210.87.254.6 on 09/05/12
For personal use only.

THE PHOTOCHEMICAL DECOMPOSITION OF SODIUM AZIDE

P. W. M. JACOBS[1] AND A. R. TARIQ KUREISHY[2]
Department of Chemistry, Imperial College, London, S.W. 7, England
Received November 1, 1965

ABSTRACT

When sodium azide is irradiated with ultraviolet light the rate of photolysis at first decreases and then becomes constant. Two reaction mechanisms are involved: the first occurs only in salt which has not previously been irradiated, whereas the second requires the presence of metallic sodium. These two reactions are interpreted as the formation and linear growth of nuclei in the dislocation network of the salt and an equation developed from this model gives good agreement with the experimental results. Incorporation of Fe^{3+} ions in NaN_3 leads to a greater number of nucleus-forming sites.

Can. J. Chem. Downloaded from www.nrcresearchpress.com by 210.87.254.105 on 09/05/12
For personal use only.

When crystals of the inorganic azides are irradiated with light of wavelength corresponding to a characteristic absorption band of the solid, photochemical decomposition takes place according to the equation

$$2MN_3 + h\nu \rightarrow 2M + 3N_2.$$

The kinetics of the reactions may thus be followed by measuring the pressure of nitrogen evolved as a function of time. A preliminary study of photolysis of sodium azide (1) has shown that the reaction possesses unique features. The characteristic behavior of barium (2), strontium (1), and potassium (1) azides is that the rate of photolysis at first decreases with the time of exposure to ultraviolet light and then subsequently increases again, finally attaining a constant rate. The initial deceleratory process is absent in a second irradiation of the sample. The secondary acceleratory process may be prevented (1, 2) by inserting a water filter between the low-pressure mercury lamp and the reaction vessel, thus showing that the reaction is initiated by light of wavelength $< 2\,000$ Å. The absorption spectra (3) of sodium and potassium azides are, however, very similar and so it does not seem likely that the explanation for the lack of the acceleratory process in sodium azide lies in the energy band structure of the salt.

Because of this apparently anomalous behavior of sodium azide we have investigated its photolysis in greater detail. The analysis of these results has important implications in discussions of the mechanism of the photolytic decomposition of azides generally.

EXPERIMENTAL

The experimental technique has been described in a previous paper (2). Since it has been shown (1) that 'static' and 'dynamic' runs yield essentially the same results, only the 'static' method was used, the kinetics of the reaction being followed by measuring the change in the pressure of nitrogen in a constant volume system with a Pirani gauge. The initial pressure in the system was $< 10^{-6}$ Torr and the outgassing rate about 10^{-5} Torr/h. Details of the method of preparation of the four sodium azide samples used have been given in a paper on their thermal decomposition (4). Preserving the same labels (4), these were:

II: Commercial grade sodium azide (from Hopkin and Williams) twice recrystallized from aqueous solution.

III: Commercial grade sodium azide twice recrystallized from a solution acidified with hydrazoic acid.

V*a*, V*b*: Commercial grade sodium azide recrystallized from solutions containing respectively, 0.06 mole % and 1 mole % ferric chloride.

[1]*Present address: Department of Chemistry, University of Western Ontario, London, Ontario.*
[2]*Present address: Department of Chemistry, University of Karachi, Karachi, Pakistan.*

Can. J. Chem. Downloaded from www.nrcresearchpress.com by 210.87.254.105 on 09/05/12
For personal use only.

RESULTS

Effect of Impurities

Plots of the rate of photochemical decomposition of 200 mg samples of sodium azide II, III, V*a*, and V*b* against the total number of nitrogen molecules evolved are shown in Fig. 1. The runs were carried out at room temperature (24 °C) and the light intensity was 1.2×10^{15} quanta $cm^{-2}\,s^{-1}$, calculated on the basis of a 2 537 Å monochromatic source. For II, III, and V*a* the usual (1) deceleratory process is evident, the photolysis rate finally attaining a constant value. For the sodium azide more highly doped with Fe^{3+}, however, the rate at first increases, then becomes constant, and finally decreases slowly (not shown in the figure) in a manner similar to the other preparations. There is evidence for an initial acceleratory process in V*a* also, but this is not so well marked.

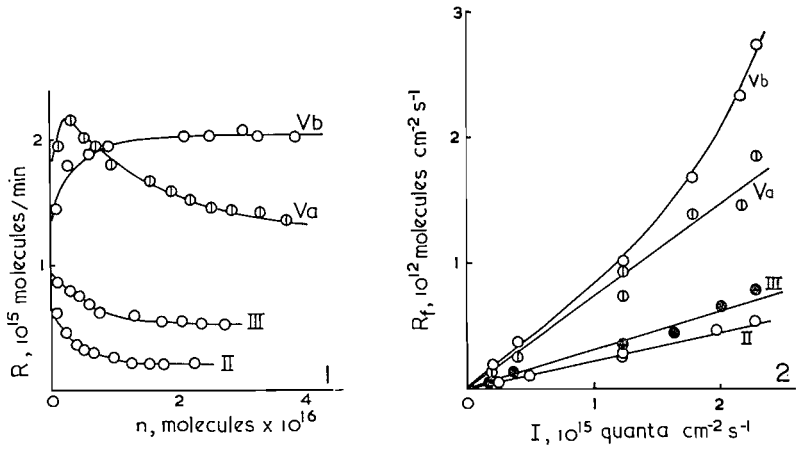


FIG. 1. Rate of photolysis R of 200 mg samples of sodium azide at room temperature and constant intensity as a function of n, the total number of nitrogen molecules evolved in the reaction. The methods used for the preparation of the azide samples are given in the text.
FIG. 2. Variation of the final constant rate of photolysis, R_f, with intensity of radiation.

The intensity dependence of the constant rate, R_f, is shown in Fig. 2. For II, III, and V*a* the plots of R_f against intensity are linear, but again V*b* behaved differently. By measuring the constant rate R_f at ice temperature also, the thermal activation energy E for the photolytic reaction was evaluated. The results were:

Sodium azide	II	III	V*a*	V*b*
E, kcal $mole^{-1}$	4.1	1.1	1.2	0

Kinetics

Plots of log $(R - R_f)$ against t are shown in Fig. 3, where R denotes the rate at time t and R_f is the final constant rate. Within the limits of experimental error, the points for preparations II and III scatter about the same line but those for the Fe^{3+}-doped sample V*a* lie on a different line of lower slope.

Quantitatively reproducible results were obtained when 400 mg samples of III were decomposed at room temperature. (The significance of the mass used is that it must be sufficient for the azide to cover the bottom of the silica reaction cell.) Plots of R against t for two different runs at the same temperature and intensity are shown in Fig. 4*a*. A series of runs at different intensities showed that both the initial and final rates, R_0 and

R_f, are proportional to the first power of the intensity (Fig. 5). The quantum yields for R_0 and R_f calculated from the slopes of these lines are 1.5×10^{-3} and 0.5×10^{-3} molecules of nitrogen per incident quantum, respectively.

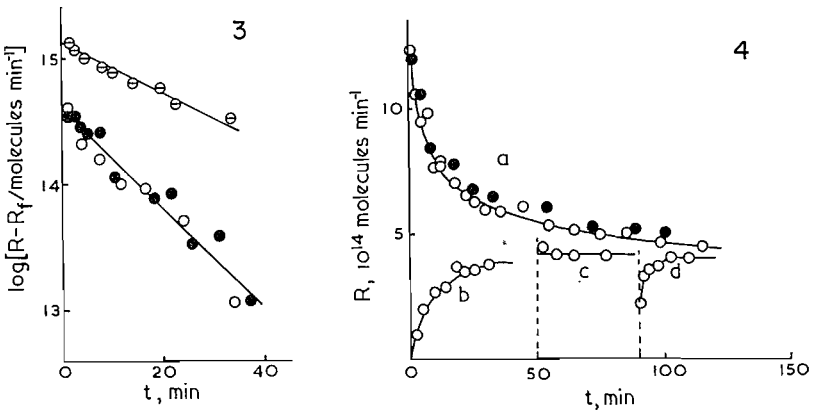


FIG. 3. Plots of log $(R - R_f)$ against time. (○) NaN_3 II; (●)III; (⊖) V*a*.
FIG. 4. Rate of photolysis of 400 mg samples of NaN_3 III at room temperature and constant intensity: (*a*) first run, showing reproducibility of the kinetics; (*b*) after 17 h exposure to gaseous products from first run; (*c*) after 2 h pumping in the dark; (*d*) after 1 h exposure to nitrogen.

Effect of Nitrogen

A sample of sodium azide was photolyzed until the rate of decomposition became constant (Fig. 4*a*). The decomposed sample was then left in contact with nitrogen for about 17 h in the dark. The variation of the rate of photolysis with time on resuming irradiation of the sample is shown in Fig. 4*b*. The rate starts at zero and rises to a constant value which is slightly lower than the previous constant rate. The lamp was then switched off and the sample left open to the pumps for 2 h. On re-irradiation photolysis commences at a rate which is slightly higher than the previous value (Fig. 4*c*) and it remains constant at this value. Fig. 4*d* shows that if the sample is left in contact with nitrogen for only 1 h the initial rate of photolysis is lower than the previous constant rate, but not zero, and that it rises more rapidly to the constant value.

DISCUSSION

Mechanisms

Previously (1, 2) we have associated distinct reaction mechanisms with the deceleratory and acceleratory reactions found in potassium, barium, and strontium azides. The primary deceleratory reaction occurs only in azides which have not been irradiated previously, whereas the acceleratory reaction is dependent on the presence of metal produced by the primary reaction. Since sodium azide does not show the acceleratory reaction, the question arises as to whether there are one or two mechanisms for the decomposition of the sodium salt. The results for successive irradiations of the same specimen (Fig. 4) show clearly that there are in fact two mechanisms and that the second of these, which is responsible for the constant-rate process, requires the presence of sodium metal. As in other azides the deceleratory reaction occurs only in the first run on a new sample. Successive runs either show a constant rate (Fig. 4*c*) or an accelerating reaction leading to a constant rate (Fig. 4*b*, *d*), depending on whether or not the sample has been exposed to nitrogen between irradiations. When the photolyzed azide is exposed

Can. J. Chem. Downloaded from www.nrcresearchpress.com by 210.87.254.105 on 09/05/12
For personal use only.

to nitrogen the gas evidently diffuses into the partly decomposed crystal and reacts with the metallic product. The extent of reaction is not determined by these experiments but it probably amounts only to chemisorption or surface nitridation, since macroscopic nitride formation requires much higher temperatures (4). This surface reaction is sufficient to prevent the catalysis of the photolysis by sodium metal until the metal has been reformed.

Absorption spectra (3) show that the primary process (1) is the production of excited azide ions N_3^{-*}. If these are adjacent to special sites S they may become trapped yielding the temporary species N_3eS, the electron e being shared between the trap S and the positive hole, N_3. Formation of a second excited azide ion then leads to decomposition, the whole process being represented by the equations

$$[1] \qquad N_3^- \overset{h\nu}{\rightleftarrows} N_3^{-*}$$

$$[2] \qquad N_3^{-*} + S \rightleftarrows N_3eS$$

$$[3] \qquad N_3^{-*} + N_3eS \rightarrow 3N_2 + \ominus e \ominus + S^-.$$

A combination of absorption spectra and electron spin resonance measurements (5) has shown that the F_2^+ center is the major product at low temperatures although F centers are also formed. At room temperature the F_2^+ center is unstable and forms a Na atom and two anion vacancies.

$$[4] \qquad Na^+ + \ominus e \ominus \rightarrow Na + 2\ominus$$

Whether or not the site S can hold an extra electron permanently depends on its nature. An impurity ion (e.g. Fe^{3+}) could be reduced but other sites (dislocation jogs) may prefer to shed it to form a second Na atom.

$$[5] \qquad S^- + Na^+ \rightarrow Na + S'$$

Nevertheless the site S′ will not be the same as before the reaction (S), since it is now associated with two sodium atoms and two anion vacancies. Repetition of this process r times leads to the *formation* of a stable nucleus of sodium. It is unknown as yet what value should be given to r; provisionally we assume that r is unity, that is, a single cycle of reactions [1] to [5] prevents the further functioning of the site S. The rate of nucleus formation is clearly a deceleratory process, since potential nucleus-forming sites S are being steadily consumed during the reaction.

The subsequent constant-rate reaction in the photolysis of sodium azide is due to the growth of these nuclei. After ultraviolet irradiation of sodium azide at room temperature, a broad absorption band (6) peaking at 3.60 eV is formed. This band is associated with the photoemission of electrons from sodium specks, which are probably filamentary in shape, the result of linear growth of the nuclei produced by the first process. Suppose a nucleus contains initially n atoms (where $n \sim 2r$). Then electrons may tunnel from excited azide ions to be trapped by nuclei which have become ionized by the light.

$$[6] \qquad Na_n \overset{h\nu}{\rightleftarrows} Na_n^+ + e$$

$$[7] \qquad N_3^{-*} + Na_n^+ \rightarrow Na_n + N_3.$$

Either by a repetition of [6] and [7], or by the reaction of an excited azide ion and a positive hole,

$$[8] \qquad N_3^{-*} + N_3 \rightarrow 3N_2 + 2\ominus + e,$$

there are formed three molecules of nitrogen, two electrons, and two anion vacancies.

Can. J. Chem. Downloaded from www.nrcresearchpress.com by 210.87.254.105 on 09/05/12
For personal use only.

The electrons produced in reactions [6] and [8] are trapped by anion vacancy pairs forming (transient) F_2^+ centers which then react with Na^+ (eq. [4]) to form Na atoms, the net result being:

[9] $$Na_n + 2e + 2Na^+ \rightarrow Na_{n+2}.$$

Repetition of the cycle leads to *growth* of the nucleus.

Kinetics

A steady state analysis is only possible when all the original centers (S) have been converted to growth nuclei. Once this has happened there are a constant number (n_0) of nuclei, equal to the number of original sites S, and the rate of photolysis is given by

[10] $$d(N_2)/dt = p_6 n_0 I = k_2 n_0,$$

if reaction [7] is preferred to reaction [−6]. p_6 is the rate constant for the forward step in [6] and k_2 is a new constant equal to $p_6 I$. Equation [10] predicts a linear dependence of the final constant rate, R_f, on intensity, as found experimentally (Figs. 2, 5). The converse assumption, reaction [−6] more important than reaction [7], does not lead to a rate linearly dependent on intensity (7).

To analyze the initial process, let r_j denote the rate of the elementary step j; then the rates of the forward and reverse steps of reactions [1]–[3] can be placed in order intuitively as $r_1 > r_{-1} \gg r_2 \gg r_{-2}, r_3$, if we accord a long lifetime to the excited state N_3eS. If this is correct, it follows that the rate of consumption of sites is

[11] $$-dn/dt = (p_3 p_1 I/p_{-1})[N_3^-]n_S = k_1 n_S,$$

where p is the rate constant for the jth step and k_1 is a constant at constant I because the consumption of N_3^- available is negligibly small. Equation [11] predicts that the initial rate $R_0(n_s = n_0)$ is proportional to I (Fig. 5) and that there will be a unimolecular decay in the number of sites at which this reaction can occur.

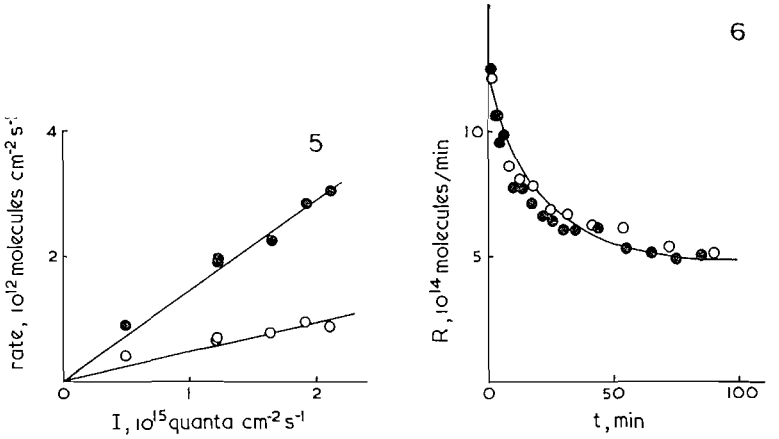


FIG. 5. Intensity dependence of the initial (●) and final (○) rates of photolysis of sodium azide.
FIG. 6. Rate of photolysis of NaN_3 as a function of time, showing the fit of eq. [15].

The kinetics of the photolysis of sodium azide may now be analyzed in terms of the nucleation and growth processes. There are n_0 potential nucleus-forming sites which are being transformed into growth nuclei at a rate given by the unimolecular decay law, the rate constant for this process being k_1. Since nuclei are postulated to grow linearly at a constant rate, a nucleus formed at time y will have attained a size $k_2(t - y)$ at time t.

Can. J. Chem. Downloaded from www.nrcresearchpress.com by 210.87.254.105 on 09/05/12
For personal use only.

There will be $n_0k_1 \exp(-k_1y)$ such nuclei. If n denotes the total number of nitrogen molecules produced by reaction in time t and n_1, n_2 are the numbers of molecules produced by the nucleation and growth mechanisms respectively, then

$$[12] \qquad n = n_1 + n_2 = 3n_0(1 - e^{-k_1 t}) + \int_0^t n_0k_1 e^{-k_1 y} k_2(t - y)\, dy.$$

On integration

$$[13] \qquad n = 3n_0(1 - e^{-k_1 t}) + (n_0k_2/k_1)(e^{-k_1 t} + k_1t - 1)$$

and therefore

$$[14] \qquad R = dn/dt = 3n_0k_1 e^{-k_1 t} + n_0k_2(1 - e^{-k_1 t}).$$

When $t = 0$, $R_0 = 3n_0k_1$ and when $t \rightarrow \infty$, $R_f = k_2n_0$. Substituting these values in eq. [14] and rearranging gives

$$[15] \qquad R - R_f = (R_0 - R_f) e^{-k_1 t}.$$

Equation [15] predicts that log $(R - R_f)$ should be a linear function of the time t. The photolysis data are in reasonable accord with this prediction (Fig. 3). From the slopes of such plots, and the values of the initial and final rates, the three constants k_1, k_2, and n_0 may be evaluated.

Figure 3 shows that the nucleation constant k_1 is the same for NaN_3 precipitated from alkaline and acid solutions and that the difference in rates is due primarily to a difference in n_0. Thus OH^- appears to poison some of the potential nucleus-forming sites. For the Fe^{3+}-doped sample, n_0 is higher still (some 4 times larger than for NaN_3 III) but k_1 has half its value for the undoped azides. Thus in NaN_3 containing Fe^{3+}, it is more difficult to nucleate the sites, but the larger number of them means that the overall reaction rate is higher.

TABLE I

Values of the nucleation rate constant k_1, growth rate constant k_2, and number of sites n_0 for 400 mg samples of NaN_3 III

Intensity, 10^{14} quanta cm^{-2} s^{-1}	$k_1 \times 10^4$, s^{-1}	$k_2 \times 10^4$, s^{-1}	$n_0 \times 10^{-16}$
5.0	5.5	7.0	0.6
12.3	7.7	8.3	1.0
12.3	7.7	7.9	0.9
16.6	10.9	11.3	0.8
19.2	10.4	10.3	1.1
22.1	11.6	10.0	1.0

Values of the constants for 400 mg samples of NaN_3 III decomposed at different intensities are given in Table I. The values are significant more for their order of magnitude than for the actual values quoted; nevertheless it may be seen that n_0 is independent of intensity whereas k_1, k_2 increase with increasing intensity (eqs. [10], [11]). The order of magnitude n_0 is $1\text{–}2 \times 10^{18}$ per mole or 1 in 4×10^5. This is a reasonable result for the number of nucleus-forming sites, but unfortunately does not identify them unequivocally. Nevertheless, we favor a model in which nucleation occurs at sites along dislocations whereupon the nuclei grow one-dimensionally, in both directions, along the dislocations. It would be hard to justify one-dimensional growth (an essential feature of the model) ssociated with point defects, for example. There are 6.7×10^{14} ion pairs per cm^2 in

Can. J. Chem. Downloaded from www.nrcresearchpress.com by 210.87.254.105 on 09/05/12
For personal use only.

NaN_3 so that, if the nucleation sites are points on dislocations, this would imply a dislocation density of $10^9/cm^2$. Dislocation counts of $10^5/cm^2$ have been recorded (8) for well-annealed ionic crystals, whereas a density of 10^{12} dislocations $/cm^2$ can occur in cold-worked metals (9). The calculated value, though high, would thus not appear unreasonable for NaN_3 precipitated as a mass of fine crystals. The dislocation model is the basis for eq. [14] and to show how well this equation is capable of representing the data we have calculated R from the values of the constants in Table I. This line is shown, together with data points for two runs, in Fig. 6. The dislocation model is also applicable to the thermal decomposition (4) of NaN_3, though at elevated temperatures the nuclei spread very rapidly along the dislocations and then grow two-dimensionally into the regions of good crystal surrounding the dislocations.

The effect of doping with Fe^{3+} can also be understood in terms of our model. The experimental results show that (i) n_0 increases, (ii) k_1 is reduced, and (iii) there is an initial acceleratory process (Fig. 1). An increase in n_0 is to be expected if Fe^{3+} ions incorporated along the dislocations act as nucleation sites. A change in k_1 the nucleation rate constant is to be expected with change in site, but one cannot say a priori whether nucleation will be easier or more difficult at the Fe^{3+} sites. However, p_1, p_{-1} should not be affected since they involve only the transition probabilities between ground and excited states of the azide ion. A decrease in k_1 thus means a decrease in p_3. This may indicate that the Fe^{3+} ions are complexed.

Equation [11] only applies once the traps are filled and for undoped azide this process (eq. [2]) takes place too rapidly to be distinguished. For the Fe^{3+} -doped samples, however, the initial process is visible because it takes longer to fill the greater number of traps. Thus additionally p_2 might be smaller at Fe^{3+} sites.

ACKNOWLEDGMENT

This research was supported financially by the U.S. Department of the Army, through its European Research Office.

REFERENCES

1. P. W. M. JACOBS, J. G. SHEPPARD, and F. C. TOMPKINS. Reactivity of Solids Fifth International Symposium, Munich 1964. Elsevier, Amsterdam. 1965. p. 509.
2. P. W. M. JACOBS, F. C. TOMPKINS, and V. PAI VERNEKER. J. Phys. Chem. **66**, 1113 (1962).
3. S. K. DEB. J. Chem. Phys. **35**, 2122 (1961).
4. P. W. M. JACOBS and A. R. T. KUREISHY. J. Chem. Soc. 4718 (1964).
5. G. J. KING, B. S. MILLER, F. F. CARLSON, and R. C. MCMILLAN. J. Chem. Phys. **35**, 1442 (1961).
6. B. S. MILLER. J. Chem. Phys. **33**, 889 (1960).
7. P. W. M. JACOBS, F. C. TOMPKINS, and D. A. YOUNG. Discussions Faraday Soc. **28**, 234 (1959).
8. L. W. BARR, I. M. HOODLESS, J. A. MORRISON, and R. RUDHAM. Trans. Faraday Soc. **56**, 697 (1960).
9. C. KITTEL. Introduction to solid state physics. 2nd ed. Wiley, New York. 1957. p. 556.

Can. J. Chem. Downloaded from www.nrcresearchpress.com by 210.87.254.105 on 09/05/12
For personal use only.

ELECTROLYTIC FORMATION OF LIVING POLYMERS FROM STYRENE

B. L. FUNT, D. RICHARDSON, AND S. N. BHADANI
Department of Chemistry, University of Manitoba, Winnipeg, Canada
Received November 16, 1965

ABSTRACT

Electrolysis of solutions of styrene in tetrahydrofuran produced living polymers and the typical colors of the living anions were observed. $NaAl(C_2H_5)_4$ and $NaB(C_6H_5)_4$ were each found suitable as conducting electrolytes.

When naphthalene was added to the solution in the absence of monomer the green sodium naphthalene complex was produced by electrolysis. Upon the addition of styrene monomer the orange living polystyryl anions were formed immediately. These changes were followed spectrophotometrically.

At the anode a terminating species was formed in a corresponding ratio to the living ions generated at the cathode. A mixing of the anode and cathode solutions resulted in a destruction of the living species and decolorization of the solution. The substances responsible were believed to be $Al(C_2H_5)_3$ and $B(C_6H_5)_3$ for the corresponding salts.

Possible mechanisms for the electro-polymerization reaction are proposed and discussed.

It is now generally recognized that the passage of an electrolytic current through a suitable solution of monomer can produce species which will initiate polymerization (1–4). Although the majority of investigations have been confined to free radical polymerizations (1, 2, 5–9), a significant number of reports of anionic polymerization initiated electrolytically have appeared. Most of these studies were performed in polar organic solvents, such as dimethyl formamide (3, 4, 10), which react readily with polymeric anions. The characteristic colors of the 'living' carbanions were never, therefore, observed in such systems, nor did polymerization continue after the cessation of current passage.

The first report of the production of 'living' polymers by an electrolytic method must be attributed to Yamazaki, Nakahama, and Kambara (11), who used tetrahydrofuran as solvent, and lithium aluminium hydride or sodium aluminium tetraethyl as electrolyte, for the polymerization of α-methylstyrene. Passage of an electric current through the solution did not immediately yield polymer, but rather a deep-red solution of the 'living' anion in the cathode compartment of a divided cell. Cooling the cell to -80 °C resulted in almost quantitative yields of high molecular weight polymer ($\sim 10^4$). From a comparison of the calculated with experimental molecular weight the authors concluded that the polymerization propagation mechanism was identical with the living polymerizations described by Szwarc (12). Further, the reduction potentials indicated that the initiation step proceeded by a direct electron addition to the double bond of α-methylstyrene.

In this paper we report investigations of the polymerization of styrene by a living anionic mechanism. It was expected that the charge transferred at the electrode could be correlated with the number of living anions produced in the solution. In the ideal case each electron transferred at the cathode would result in the formation of a living end, the concentration of which can be readily determined by absorption spectrophotometry. This living anion concentration, in turn, determines the kinetics of the reaction and the molecular weight of the product. Thus the estimation and control of the population of living ends could be expected to yield a new insight into the kinetics of the reaction and a refined control over the progress of the polymerization.

Inasmuch as this represents the first full reort of a living anionic polymerization with electrolytic control, a relatively complete description of the experimental technique is included.

Can. J. Chem. Downloaded from www.nrcresearchpress.com by 210.87.254.6 on 09/05/12
For personal use only.

Can. J. Chem. Downloaded from www.nrcresearchpress.com by 210.87.254.6 on 09/05/12
For personal use only.

EXPERIMENTAL

The complete absence of both oxygen and water is desirable in polymerizations of this type, and in endeavoring to achieve this, all materials were handled in vacuum or under an atmosphere of purified nitrogen.

The nitrogen was purified by passing it through a liquid nitrogen trap, columns of potassium hydroxide, heated copper turnings, a further liquid nitrogen trap, a silica gel column, a magnesium perchlorate column, and glass wool to remove dust.

The solvent tetrahydrofuran (THF) was refluxed over calcium hydride for over 24 h and distilled into a flask containing lumps of sodium. To this was added 10–20 mg of recrystallized naphthalene, and the flask was fitted to the reflux condenser of the vacuum system. With the pressure release open, refluxing was continued until formation of sodium naphthalene complex, characterized by the appearance of a dark green color. Following this the THF solution of sodium naphthalene was thoroughly degassed by alternate freezing and thawing, with pumping to the main vacuum line at 10^{-6} mm Hg. The THF solvent was then distilled under vacuum to a storage bulb coated with a fresh sodium film. When required it was distilled into an evacuated graduated tube.

The styrene, supplied by Matheson, Coleman and Bell, was first carefully fractionated under reduced nitrogen pressure. Finely ground calcium hydride was added and the mixture was stirred magnetically for about 16 h, all the while being attached to the vacuum line. The mixture was degassed by occasionally flashing to the backing pump. Further to this it was flash-distilled past a sodium-coated bulb to a flask containing calcium hydride. On warming, the styrene was quickly distilled into a vessel provided with several break-seals, degassed several times, and sealed from the line. The container was stored at −20 °C in the dark and, when required, styrene was transferred under vacuum via a break-seal to a graduated tube.

Whenever possible, glassware was thoroughly flamed under vacuum before use.

Electrolytes

$NaAl(Et)_4$

The $NaAl(Et)_4$ was prepared according to the following reaction (13).

$$3Na + 4Al(Et)_3 \rightarrow 3Na[Al(Et)_4] + Al\downarrow$$

The apparatus used is shown in Fig. 1. An excess of freshly cut sodium was placed in a 500 ml flask which was then attached by a Teflon joint, A, to the $Al(Et)_3$ container, I. Benzene was pumped off the sodium and the tube to the container was evacuated via B, which was connected to a backing pump. When sufficient alkyl had been added E was closed. From time to time the flask was opened to the pump momentarily at B. Eventually the sodium became coated with aluminium and the reaction almost ceased. To reactivate it the temperature of the flask was raised to >100 °C and further reaction took place in a homogeneous molten phase. At the completion of the reaction the flask and contents were allowed to cool, removed at A with C and D closed, and transferred to the dry-box; the $NaAl(Et)_4$ product was removed by crystallization from freshly distilled benzene. After further recrystallizations the product was pumped on the vacuum line for several hours, yielding white crystals. The storing and all subsequent handling of the electrolyte was performed under a nitrogen atmosphere in the dry-box.

$Na(C_6H_5)_4B$

This was acquired from Fisher (99.7%) and used without further purification as all attempts to recrystallize it from aqueous acetone failed (14).

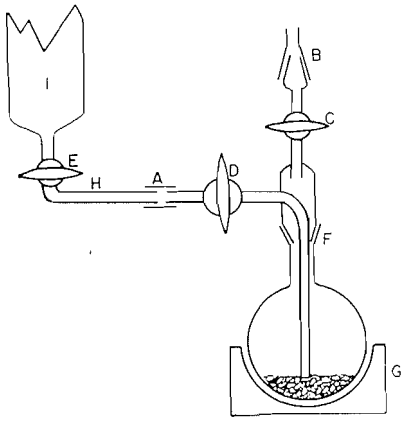


FIG. 1. Apparatus for preparation of $NaAl(Et)_4$: A, Teflon connector; B and F, B-24 joints C and; D Teflon-plug stopcocks; E, metal tap; G, heating mantle; H, copper tubing; I, $Al(Et)_3$ cylinder.

Experimental Procedure

All the early investigations were performed in the cell shown in Fig. 2, hereafter referred to as the single cell, since there is no separation of anode and cathode compartments.

With reference to the figure, A is a glass-enclosed magnetic stirring bar, BB are 1 × 1 in. platinum electrodes, D is a 1.0 cm quartz optical cell joined to the reaction vessel by a Pyrex-to-quartz graded seal, CC are tungsten electrode leads which make a vacuum tight seal with glass and appear to be inert to the reaction components, and E is a glass constriction. The reaction vessel itself is of Pyrex glass. In later experiments it was found necessary to use a divided cell of the type shown in Fig. 3.

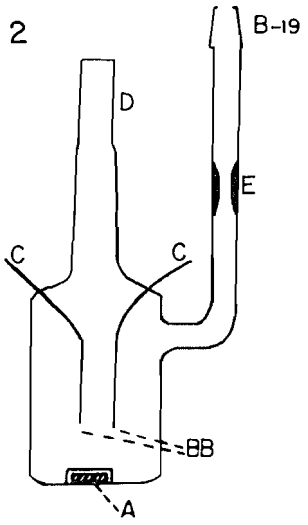


FIG. 2. Single cell.

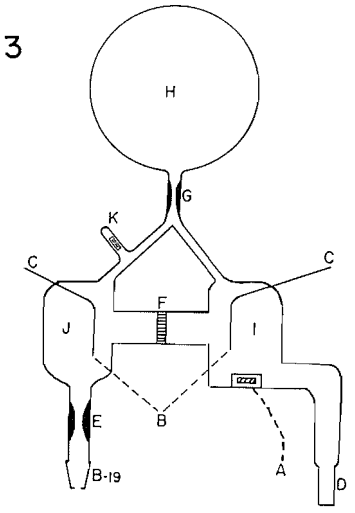


FIG. 3. Divided cell.

This figure bears the same notation as for Fig. 2 with the additions: F is a coarse porosity sintered glass disc, G is a further constriction, H is a 100 ml flask, I is the cathode compartment, J is the anode compartment, and K allows for a break-seal attachment. In addition, provision was made for the insertion of a 9 mm quartz spacer into the optical cell.

The experimental procedure involved charging the vessel with a weighed quantity of electrolyte through the B-19 joint, in the dry box under completely anhydrous conditions. Transfer of the vessel to the vacuum line in the absence of air was facilitated with a joint–stopcock–socket arrangement. The vessel was subsequently pumped on the vacuum line for several hours until the pressure, as recorded on the McLeod gauge, was 10^{-5}–10^{-6} mm Hg. Measured quantities of THF solvent and styrene monomer were distilled in from graduated tubes on other parts of the line and the vessel was sealed off at E. The contents of the flask H or the single cell were thoroughly mixed at room temperature. Inversion of the divided cell filled the anode and cathode compartments, J and I, with solution above the level of the electrodes, and the flask H was sealed and removed. The tube between the two compartments was intended to equalize the vapor pressures. The total volume of the single cell was approximately 50 ml and that of the double cell 100 ml.

After equilibration of the cell to room temperature a current was supplied from a constant direct current supply (0–16 mA at 0–600 V), stirring being maintained by the magnetic stirring bar, A. The progress of the electrolysis was followed optically on a Beckmann DB spectrophotometer, coupled with a pen recorder. The increase in optical density in the 340 mμ region of the spectrum caused by the CH_2—$CH(PH)^-$ Na^+ ion-pair in THF solvent was measured. Any attempt to measure the decrease in concentration of styrene from the characteristic absorption maxima in the 291 mμ region of its spectrum was prevented by a broad background absorption in this region. This may be seen from Fig. 4, which shows the absorption curves of a 0.012 *M* solution of $NaAl(Et)_4$ in THF before and after electrolysis.

RESULTS AND DISCUSSION

Preliminary investigations of the formation of living polystyryl anions were conducted in the cell shown in Fig. 2 with $NaAl(Et)_4$ as electrolyte. The characteristic orange color of the ion was formed at the cathode surface, but the solution became quickly decolorized with stirring. Only at very high viscosities, where diffusion was obviously a limiting factor,

Can. J. Chem. Downloaded from www.nrcresearchpress.com by 210.87.254.6 on 09/05/12
For personal use only.

was there any prolonged persistence of the characteristic color. Nevertheless in all these single cell experiments polystyrene was formed at high electrical efficiencies.

To investigate the nature of the polymerization process in greater detail, the divided cell shown in Fig. 3 was constructed. The cathode and anode compartments of this cell were separated by a sintered glass disc. Under these conditions a colored solution was formed in the cathode compartment and the color persisted for long periods of time after the current was switched off. Obviously living polystyryl anions were formed and were not being terminated. In the same cell the anode compartment was colorless and no polymer was recovered from this region. The nature of the species responsible for the destruction of the living ions is still indeterminate. Experiments have shown, however, that the color can be discharged by mixing the anolyte into the cathode compartment or by pouring the living ions into the anolyte solution. As expected the color was also discharged by exposing the solution to the atmosphere. The fact that color persists longer in the solutions which are more viscous and which have been subjected to greater electrolysis suggests that there is no buildup of any quenching impurity and that it is likely that the living ions and the killing species are formed in a 1:1 ratio in the electrolysis.

The divided and single cell experiments were repeated with $Na(C_6H_5)_4B$ with exactly the same results as for $NaAl(Et)_4$. The color formation and destruction follow the same pattern for the two different electrolytes.

Attempts to measure the optical spectrum of the polymer solution in the divided cell were aborted by the difficulties encountered in rendering the solution homogeneous. The polymerization tends to be heterogeneous in nature and the polymer formed at the cathode surface dissolves slowly in the solution.

In addition to direct formation of living polystyryl anions subsidiary experiments were performed in which naphthalene was added to the electrolyte solution. After a period of electrolysis the green color typical of sodium naphthalene was obtained. Its spectrum was considered to be identical with that of the complex formed by conventional methods (15). On the addition of styrene to this solution, the green color changed very rapidly to orange and then quickly decolorized. No polymer was extracted from the mixture. In the presence of styrene, it is of interest to note that on prolonged electrolysis the sodium naphthalene spectrum was again eventually obtained, but no polymer was isolated.

These experiments could suggest that the styrene added was impure and that the impurities prevented the formation of the living polystyryl anions. To check this possibility the styrene was added to conventionally prepared sodium naphthalene and there was an immediate and lasting formation of the characteristic color of the anion. Thus, again, the existence of a species which interfered with the polymerization was confirmed, even though this did not apparently interfere with the formation of sodium naphthalene itself.

When these experiments were repeated using a divided cell, the sodium naphthalene complex was formed in the cathode compartment. Its optical absorption spectrum is shown in Fig. 5, and is considered to be identical with the one obtained by Szwarc (15) using a conventional technique. Addition of styrene to the cathode compartment caused a rapid and lasting conversion to the living polystyryl anions, with their characteristic color (Fig. 6).

A further experiment was performed with $(Bu)_4NBr$ as electrolyte in the presence of naphthalene and, though a green color formed slowly, its absorption spectrum could in no way be reconciled with that in which an alkali metal acted as counterion.

Our information is not sufficiently complete to enable us to formulate a detailed reaction mechanism to explain the polymerization process. However, enough is known to delineate the more likely possibilities.

Can. J. Chem. Downloaded from www.nrcresearchpress.com by 210.87.254.6 on 09/05/12
For personal use only.

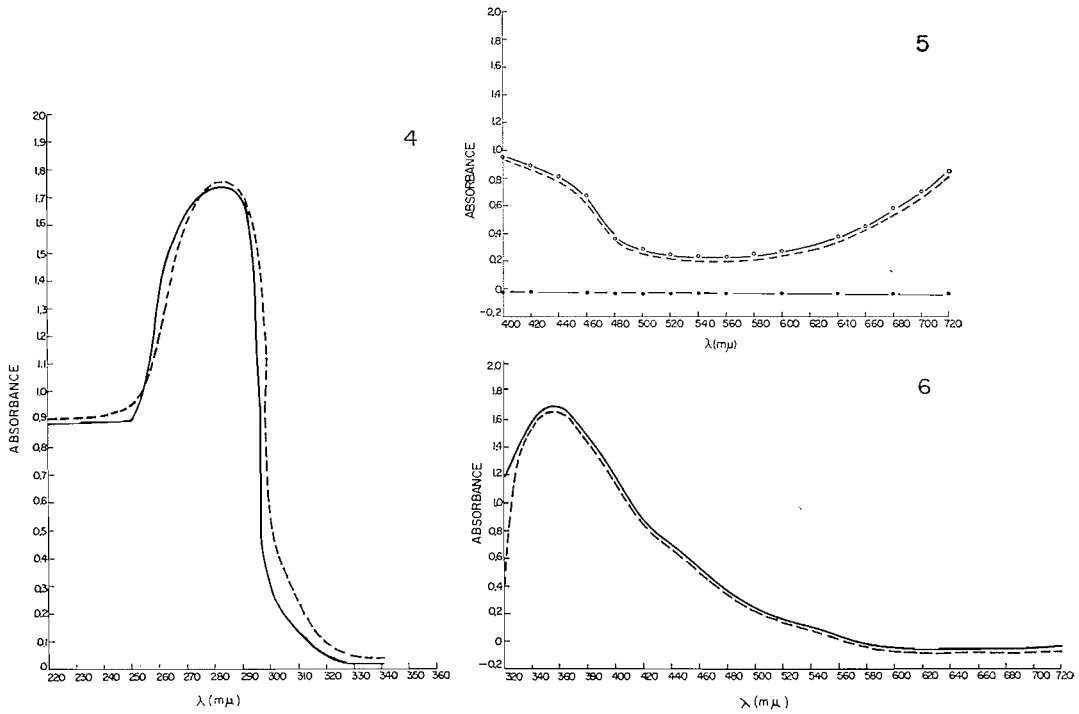


FIG. 4. Absorption spectrum of 0.012 *M* $NaAl(Et)_4$ solution in THF before electrolysis (solid curve) and after electrolysis at 1.3 mA for 18 min (broken curve).

FIG. 5. Absorption spectrum of solutions of naphthalene and $Na(C_6H_5)_4B$ in THF versus a THF reference: ○, after electrolysis for 14 min at 5.9 mA; ●, before electrolysis. The broken curve represents the differential spectrum.

FIG. 6. Spectrum of living polystyryl anions obtained on the addition of styrene to the cathode solution shown in Fig. 5. The solid curve represents the absorption spectrum, and the broken curve the differential spectrum relative to that of the solution before electrolysis.

If initiation proceeds at the cathode by the transfer of an electron from an electron donor, whether this be the electrode or sodium metal, then the end result for styrene is the same, namely the formation of a primary radical ion $\dot{M}^-$.

Following this step there are two possibilities of further reaction (16).

[i] $$C_6H_5CH{=}CH_2^- + C_6H_5CH{=}CH_2 \rightarrow \cdot CH(C_6H_5){-}CH_2{-}CH_2{-}CH(C_6H_5)^-$$

Thus a dimer is formed upon addition of one monomer molecule. This dimer possesses one "true" radical end and one "true" carbanion end and may grow in further polymerization by mechanisms involving both centers.

[ii] $$2CH(C_6H_5){=}CH_2^- \rightarrow {}^-CH(C_6H_5){-}CH_2{-}CH_2{-}CH(C_6H_5)^-$$

Monomeric radical ions $\dot{M}^-$ may also dimerize and form dimeric dicarbanions which may continue their growth by an anionic mechanism only.

Any initiation process which gives rise to a relatively high concentration of radical ions, e.g. homogeneous initiation by sodium naphthalene, favors mechanism [ii], the formation of dicarbanions. On the other hand, slow heterogeneous initiation by metallic mirrors, particularly if carried out at high monomer concentrations, favors mechanism [i], with the formation of dimeric radical ions.

At the anode the following process has been postulated by Ziegler (13, p. 251).

$$Al(Et)_4^- - e \rightarrow Al(Et)_4 \rightarrow Al(Et)_3 + \cdot Et$$

Can. J. Chem. Downloaded from www.nrcresearchpress.com by 210.87.254.6 on 09/05/12
For personal use only.

Disproportionation of ethyl radicals to form ethane and ethylene would be expected, but no gas evolution whatsoever is observed in these polymerizations, though this may reflect the solubility of the gases in the solution. It seems likely that the $Al(Et)_3$ or, in the case of $Na(C_6H_5)_4B$, the $B(C_6H_5)_3$ formed represent suitable terminators for the anionic polymerization of styrene.

We are not yet able to distinguish between the two initiation processes, but favor mechanism [ii]. The fact that polymer is formed in good yield and at high electrical efficiency in the single cell might be explained by radical growth of the radical anion formed by mechanism [i], the anion end having been terminated by anode products. This is unlikely, as previous work has shown that both current efficiencies and rates of polymer formation are low in radical polymerization (1, 2). On the other hand, a dianion propagation mechanism could only be possible if the individual polymer chain grew to its final length before termination. Although the living ions may have a short existence, new species are continually being formed at the electrode and a high current efficiency may still be consistent with the mechanism. It is, however, possible that both mechanisms contribute to the overall polymerization process.

In conclusion the experimental findings demonstrate that polystyryl anions are produced via electron transfer processes at the cathode, and their concentration can be controlled by the impressed current. The influence of added naphthalene on the course of the reaction is not clear, but the electrolytic formation of sodium naphthalene complex has been established in this work. Further work on the quantitative aspects of the kinetics of the polymerization is in progress.

ACKNOWLEDGMENTS

The authors thank the National Research Council for a grant and for the provision of a post-doctoral fellowship (D. R.). The financial assistance of the Camille and Henry Dreyfus Foundation is gratefully acknowledged.

REFERENCES

1. J. W. Breitenbach and C. H. Srna. Pure Appl. Chem. **4**, 245 (1962).
2. B. L. Funt and F. D. Williams. J. Polymer Sci. A, **2**, 865 (1964).
3. B. L. Funt and S. W. Laurent. Can. J. Chem. **42**, 2728 (1964).
4. B. L. Funt and S. N. Bhadani. Can. J. Chem. **42**, 2733 (1964).
5. B. L. Funt and K. C. Yu. J. Polymer Sci. **62**, 359 (1962).
6. E. Dineen, T. C. Schwan, and C. L. Wilson. J. Electrochem. Soc. **96**, 226 (1949).
7. W. B. Smith and H. Georg Gilde. J. Am. Chem. Soc. **31**, 5325 (1959).
8. N. S. Tsvetkov. Vysokomolekul. Soyedin. **3**, 549 (1961); Polymer Sci. USSR, **3**, 570 (1962).
9. I. V. Shelepin and A. I. Fedorova. Zh. Fiz. Khim. **38**, 2676 (1964).
10. B. L. Funt and S. N. Bhadani. J. Polymer Sci. In press. 1966.
11. N. Yamazaki, S. Nakahama, and S. Kambara. J. Polymer Sci. Pt. B, **3**, 57 (1965).
12. M. Szwarc, M. Levy, and R. Milkovitch. J. Am. Chem. Soc. **78**, 2656 (1956).
13. K. Ziegler. *In* Organo-metallic chemistry. *Edited by* H. Zeiss. Reinhold Publishing Corp., New York. 1960. Chap. 5. p. 205.
14. D. N. Bhattacharyya, C. L. Lee, J. Smid, and M. Szwarc. J. Phys. Chem. **69**, 608 (1965).
15. J. Jagur-Grodzinski, M. Feld, S. L. Yang, and M. Szwarc. J. Phys. Chem. **69**, 628 (1965).
16. M. Levy and M. Szwarc. J. Am. Chem. Soc. **82**, 521 (1960).

Can. J. Chem. Downloaded from www.nrcresearchpress.com by 210.87.254.6 on 09/05/12
For personal use only.

THE INFRARED SPECTRA OF SOME MIXED ALKYLARYLARSONIUM SALTS

W. R. CULLEN
Chemistry Department, University of British Columbia, Vancouver 8, British Columbia

G. B. DEACON
William Ramsay and Ralph Forster Laboratories, University College London, England

AND

J. H. S. GREEN
Chemical Standards Division, National Physical Laboratory, Teddington, Middlesex, England

Received October 5, 1965

ABSTRACT

The infrared spectra (4 000 to 200 cm^{-1}) of some trimethylphenyl-, dimethyldiphenyl-, methyltriphenyl-, triethylphenyl-, and diethyldiphenyl-arsonium salts have been recorded. Vibrational assignments have been made for the quaternary 'onium cations and have been compared with those for related compounds including one alkylarylgermane.

The vibrational spectra of some simple alkylarsonium cations have been recorded and assigned previously (1). The present paper reports an extension of the work to some salts of mixed alkylarylarsonium cations, for which infrared spectral data have been obtained over the range 4 000 to 200 cm^{-1}. Assignments have been made by reference to those for the alkylarsonium compounds (1) and to those made by one of us (2) for dimethylphenylarsine, methyldiphenylarsine, and triphenylarsine. They are consistent with partial assignments previously reported for the methyltriphenylarsonium cation and triphenylarsine (3).

RESULTS AND ASSIGNMENTS

Trimethylphenylarsonium Salts

The infrared spectra of three trimethylphenylarsonium salts are given in Table I together with the assignments. All the bands are attributable to the 'onium cations and show only small variations with the nature of the anion. The assignments are considered first in terms of the alkyl groups and skeleton, and then in terms of the phenyl group and the phenyl–arsenic modes.

The skeleton of the cation has C_{3v} symmetry and the $(CH_3)_3As$ group therefore has infrared active modes as follows: CH_3 asym. stretch $(a_1 + 2e)$; CH_3 sym. stretch $(a_1 + e)$; CH_3 asym. deformations $(a_1 + 2e)$; CH_3 sym. deformations $(a_1 + e)$; CH_3 rock $(a_1 + 2e)$; CH_3—As stretch $(a_1 + e)$; CH_3—As—CH_3 deformations $(a_1 + e)$, and CH_3 torsion (e). While the effect of the phenyl group might be to lift the degeneracies of the e class modes, the spectra do not reveal this for the internal methyl modes. From the results (1) for the tetramethylarsonium ion, the assignments of Table I follow readily. For $(CH_3)_4As^+$, the methyl rocking modes are evidently coincident at about 924 cm^{-1}, whereas in the trimethylphenylarsonium salts they are clearly resolved into at least three bands. Likewise, the CH_3—As—CH_3 deformation modes, not detectable above 200 cm^{-1} in the infrared spectrum of the tetramethylarsonium ion (1), are both seen in $(CH_3)_3(C_6H_5)As^+$, where they are assigned by comparison with trimethylarsine (4). No assignment is made here for the CH_3 torsion.

Can. J. Chem. Downloaded from www.nrcresearchpress.com by 210.87.254.5 on 09/05/12
For personal use only.

TABLE I

Vibrational frequencies (cm^{-1}) and assignments for trimethylphenylarsonium salts

Me_3PhAsI	$Me_3PhAsHgI_3$	$[Me_3PhAs]_2HgI_4$	Assignments
		3 062 w	
3 054 w	3 057 w	3 053 w	ν(CH) of phenyl ($a_1 + b_2$)
		3 021 w	
2 982 m	3 000 m	3 000 m	CH_3 asym. stretch ($a_1 + 2e$)
2 912 m	2 916 m	2 922 m	CH_3 sym. stretch ($a_1 + e$)
1 590 vw	1 584 vw	1 584 vw	ν(CC) ($a_1 + b_2$)
1 487 m	1 486 m	1 488 m	ν(CC) (a_1)
1 465 vw	1 464 vw	1 465 vw	304 + 1 160 = 1 464 (B_2)
1 439 s	1 439 m	1 440 m	ν(CC) (b_2)
1 423 m	1 408 m,br	1 417 m	CH_3 asym. def. ($a_1 + 2e$)
1 402 m		1 406 m,br	
1 336 m	1 336 m	1 336 m	ν(CC) (b_2)
1 308 m	1 309 w	1 310 w	395 + 905 = 1 300 (B_2)
1 289 vw	1 293 vw	1 288 vw	β(CH) (b_2)
1 261 m	1 268 m	1 268 w	CH_3 sym. def. ($a_1 + e$)
1 186 w	1 186 w	1 188 w	β(CH) (a_1)
1 158 m	1 160 w	1 162 w	β(CH) (b_2)
1 090 m	1 090 m	1 093 m	'X-sens.' q (a_1)
1 067 w	1 069 w	1 068 w	β(CH) (b_2)
1 027 w	1 026 w	1 024 w	β(CH) (a_1)
1 000 w	1 002 w	1 003 sh	Ring breathing (a_1)
		1 000 w	
—	—	974 w	γ(CH) ($a_2 + b_1$)
943 vs,br	924 s,br	929 vs	CH_3 rock ($a_1 + 2e$)
919 sh	863 sh	858 s,br	
870 s	853 m	847 s	
840 m	843 m		
746 vs	743 m	746 vs	γ(CH) (b_1)
	740 vs		
690 vs	690 vs	690 vs	ϕ(CC) (b_1)
649 s	646 m	655 m	ν(CH_3—As) asym. (e)
		648	
618 vw	616 vw	616 vw	α(CCC) (b_2)
595 m	600 w	601 m	ν(CH_3—As) sym. (a_1)
459 m	463 m	463 s	'X-sens.' y (b_1)
395 vw	—	—	ϕ(CC) (a_2)
302 s	304 s	303 s	'X-sens.' t (a_1)
275 m	277 m	278 m	'X-sens.' u (b_2)
236 m	234 m	238 m	CH_3—As—CH_3 asym. def. (e)
218 m,br	226 m,br	220 m,br	CH_3—As—CH_3 sym. def. (a_1)
	220		

INTENSITIES: s, strong; m, medium; w, weak; v, very; br, broad.

The phenyl vibrations fall into two groups: firstly those whose positions change little with mass and nature of the substituent, and secondly the 'X-sensitive' modes. (We use the notation of Whiffen (5) for the symmetry and form of the phenyl modes, but with the recommended (6) orientation of axes for C_{2v} symmetry.) The assignments follow from those for dimethylphenylarsine (2) and only a few points require comment. The region 1 250 to 1 340 cm^{-1} is rather confused in several phenyl derivatives, and in the present compounds the methyl symmetric deformations also occur here. These are taken as coincident at 1 268 cm^{-1}. There remain three bands to be allocated to two fundamentals, both in the b_2 class, and the choice made (cf. refs. 2 and 5) leaves the band at 1 310 cm^{-1}, which can be satisfactorily explained as either of two possible transitions to a b_2 level: 275 + 1 027 = 1 302 and 395 + 905 = 1 300. Three out-of-plane C—H deformations, γ(CH), are to be expected near 990(b_1), 960(a_2), and 905(b_1) cm^{-1}, but only what is probably the first of these is observed, in one salt only. The others are probably obscured by the CH_3 rocking absorptions. A fourth γ(CH) mode is expected around 840 cm^{-1}, but in all the spectra this absorption is too intense to be due to this fundamental alone and is

Can. J. Chem. Downloaded from www.nrcresearchpress.com by 210.87.254.5 on 09/05/12
For personal use only.

considered to derive from the third CH_3 rocking mode. The a_1 'X-sensitive' modes q and t are shifted by some 10 cm^{-1} to higher wavenumbers relative to their positions in dimethylphenylarsine (2) and a third such mode (r) is believed to have shifted to at least the same extent and become obscured by the strong band at 690 cm^{-1} (see Discussion). Thus all the fundamentals expected in the recorded region are accounted for; there remains the lowest b_1 mode, the 'X-sensitive' mode x, which is probably below 200 cm^{-1}.

Dimethyldiphenylarsonium Triiodomercurate(II)

The infrared spectrum of this salt is given in Table II together with the assignment and that (7) of dimethyldiphenylgermane, which is based on the available infrared and Raman spectra (8). The skeleton of the cation has C_{2v} symmetry and the $(CH_3)_2As$ group will therefore have infrared active modes as follows: CH_3 asym. stretch ($a_1 + b_1 + b_2$); CH_3

TABLE II

Vibrational frequencies (cm^{-1}) and assignments for dimethyldiphenylarsonium triiodomercurate(II) and dimethyldiphenylgermane

$Me_2Ph_2AsHgI_3$	Me_2Ph_2Ge		
Infrared	Infrared	Raman*	Assignments
	3 075 s		
3 054 w	3 040 s	3 075(0)	ν(CH) of phenyl ($a_1 + b_2$)
	3 017 m		
	2 998 m		
3 010 m	2 980 m	2 979(1b)	CH_3 asym. stretch ($a_1 + b_1 + b_2$)
2 920 m	2 909 m	2 910(3b)	CH_3 sym. stretch ($a_1 + b_2$)
		1 583(8)	
1 580 w	1 589 w	1 572(1)	ν(CC) ($a_1 + b_2$)
1 487 m	1 486 m		ν(CC) (a_1)
1 443 s	1 430 s		ν(CC) (b_2)
1 412 m	1 410 w	1 389(0)	CH_3 asym. def. ($a_1 + b_1 + b_2$)
1 407 sh	1 376 w		
1 336 m	1 333 w		ν(CC) (b_2)
1 301 w	1 302 w		277 + 1 017 = 1 294 (B_2)
1 285 m	1 261 w	1 243(1)	CH_3 sym. def. ($a_1 + b_2$)
1 268 m	1 242 m		
1 180 m	1 183 w	1 187(1)	β(CH) (a_1)
1 160 m	1 154 w	1 154(2)	β(CH) (b_2)
1 091			
1 087 m	1 098 w	1 088(2)	'X-sens.' q (a_1)
1 061 w	1 063 w		β(CH) (b_2)
1 017 w	1 026 w	1 029(4sp)	β(CH) (a_1)
1 000 m	998 w	999(10)	Ring breathing (a_1)
		942(3sp)	669 + 290 = 959 (A_1)
971 w	—		γ(CH) ($a_2 + b_1$)
	908 w		γ(CH) (b_1)
926 m	849 m		
893 s	826 s		CH_3 rock ($a_1 + b_1 + b_2$)
840 m	808 s		
741 vs	732 s		γ(CH) (b_1)
690 vs	703 s		ϕ(CC) (b_1)
680 sh	677 w	669(4)	'X-sens.' r (a_1)
645 m			ν(CH_3—As) asym. (b_2)
		616(3sp)	α(CCC) (b_2)
610 m			ν(CH_3—As) sym. (a_1)
	608 m	601(4sp)	ν(CH_3—Ge) asym. (b_2)
	587 m	580(8)	ν(CH_3—Ge) sym. (a_1)
463 m	467 m		'X-sens.' y (b_1)
329 s		290(3)	'X-sens.' t (a_1)
304 m			
277 m		233(3)	'X-sens.' u (b_2)
222 m			CH_3—As—CH_3 def. (a_1)
		206(2)	'X-sens.' x (b_1)
		180(3)	+ CH_3—Ge—CH_3 def. (a_1)

*Raman intensities: ref. 8.

Can. J. Chem. Downloaded from www.nrcresearchpress.com by 210.87.254.5 on 09/05/12
For personal use only.

sym. stretch ($a_1 + b_2$); CH_3 asym. deformations ($a_1 + b_1 + b_2$); CH_3 sym. deformations ($a_1 + b_2$); CH_3 rock ($a_1 + b_1 + b_2$); CH_3—As stretch ($a_1 + b_2$); CH_3—As—CH_3 deformation (a_1); and CH_3 torsion (b_1). Assignments for all of these fundamentals can be made, but for the internal modes the components are not all resolvable. (Examined as a disc in potassium chloride, the spectrum of the compound showed additional splitting of several bands, but the mean positions agreed well with the listed (mull) values.)

On the basis of C_{2v} symmetry for the skeleton of the cation, the phenyl '*X*-sensitive' modes *q*, *r*, and *t* are expected to show splitting into a_1 and b_2 components, as observed in methyldiphenylarsine (2). While the doublet attributed to mode *q* may be due to a crystal field effect, that of mode *t* is to be compared with the 298/310 cm^{-1} doublet in the arsine. In $(CH_3)_2(C_6H_5)_2As^+$, *r* is again obscured by the very strong band at 690 cm^{-1}, though it may contribute to the shoulder at 680 cm^{-1}. The strength of the 840 cm^{-1} band is considered too great to be solely due to the γ(CH) (a_2) mode expected here and is believed to derive from the third methyl rocking vibration.

Methyltriphenylarsonium Compounds

The infrared spectra and assignments for the iodide and the tetraiodomercurate are given in Table III. The former, examined both as mulls and discs, shows very considerable splitting of the bands which suggests a different site symmetry for the cation in this salt from that in the tetraiodomercurate. Assignments of the modes of the single methyl group and of the CH_3—As stretching frequency are straightforward. The C_{3v} symmetry of the skeleton of the cation may result in splitting of the phenyl–arsenic modes into a_1 and *e* components, but this is observed only for the lowest mode (*t*) involving stretching of the C_6H_5—As bond.

Ethylphenylarsonium Compounds

The infrared spectra of triethylphenylarsonium and diethyldiphenylarsonium triiodomercurates are listed in Table IV, together with assignments made, so far as the ethyl group is concerned, with reference to these for $(C_2H_5)_4As^+$ and $(C_2H_5)_3(CH_3)As^+$ (1). Some overlapping of the ethyl frequencies with those of the phenyl group is found, but all the expected fundamentals can be assigned if the band intensities are considered. Thus, the band at 1 000 cm^{-1} is much stronger than in the corresponding methylphenylarsonium compounds owing to a coincidence of the C—C stretching of the ethyl group with the relatively weakly absorbing a_1 phenyl ring mode. Again, the shifted position of the methyl rocking modes compared with the methylphenyl compounds reveals the three γ(CH) modes near 973, 923, and 846 cm^{-1}, and the weakness of the last confirms that in the methyl compounds the intensity of the 840 cm^{-1} band derives from a methyl rocking mode. The strong γ(CH) band near 740 cm^{-1} has, in the ethyl compounds, shoulders attributable to the adjacent strong methylene rocking mode, observed at 738 cm^{-1} in the triethylmethylarsonium ion (1). Additional bands, observed at 345 and 324 cm^{-1} in the triethylphenylarsonium compound compared with $(CH_3)_3(C_6H_5)As^+$, are clearly due to the C—C—As deformation. Similarly, bands of the diethyl compound at 357 and 338 cm^{-1} are due to C—C—As deformation, whereas the band at 328 cm^{-1} may either be due to this mode, or to the second of the two possible components of vibration *t*. However, *q* is not split, whereas in $(CH_3)_2(C_6H_5)_2As^+$ both *q* and *t* show splitting.

DISCUSSION

The results of the present work enable a number of comparisons to be made among the frequencies of certain vibrations in these and related compounds. The relevant values are assembled in Table V, and the alkyl groups and skeleton are considered first.

Can. J. Chem. Downloaded from www.nrcresearchpress.com by 210.87.254.5 on 09/05/12
For personal use only.

TABLE III

Vibrational frequencies (cm^{-1}) and assignments for methyltriphenylarsonium salts

$MePh_3AsI$	$[MePh_3As]_2HgI_4$	Assignments
3 077 m 3 045 m 3 029 m	3 080 sh 3 060 m 3 041 m 3 022 m	ν(CH) of phenyl ($a_1 + b_2$)
3 012 m	3 000 m	CH_3 asym. stretch
2 965 m 2 890 m	2 919 m	CH_3 sym. stretch
1 581 w	1 577 w	ν(CC) ($a_1 + b_2$)
1 489 1 487 m	1 485 m	ν(CC) (a_1)
1 449 sh 1 445 sh 1 441 m	1 442 s	ν(CC) (b_2)
1 414 1 407 m	1 410 m,br	CH_3 asym. def.
1 346 1 340 m	1 339 m	ν(CC) (b_2)
1 323 1 311 m	1 313 m	Combination
1 289 w 1 278 w	1 280 w,br	β(CH) (b_2) + CH_3 sym. def.
1 194 w 1 190 sh 1 184 m	1 185 m	β(CH) (a_1)
1 164 sh 1 159 m	1 162 m	β(CH) (b_2)
1 100 w 1 085 s	1 085 s	'*X*-sens.' *q* (a_1)
1 071 m	1 069 m	β(CH) (b_2)
1 021 m	1 022 m	β(CH) (a_1)
998 s	1 000 s	Ring breathing (a_1)
986 w	983 w	γ(CH) (b_1)
975 w		γ(CH) (a_2)
941 w		
928 w	926 w	γ(CH) (b_1)
912 901 890 s	892 vs 884 sh	CH_3 rock
856 849 w	852 w	γ(CH) (a_2)
753 746 742 vs	746 vs	γ(CH) (b_1)
691 vs	690 vs	ϕ(CC) (b_1)
682 sh	683 sh	'*X*-sens.' *r* (a_1)
628 sh 626 m	625 m	ν(CH_3—As)
615 w	620 vw	α(CCC) (b_2)
479 468 463 452 s	474 s	'*X*-sens.' *y* (b_1)
	391 w	ϕ(CC) (a_2)
348 sh 340 s 300 m	342 s 302 m	'*X*-sens.' *t* (a_1)
—	241 w	'*X*-sens.' *u* (b_2)

It was shown previously (1) that the carbon–arsenic stretching frequencies are shifted to higher wavenumbers from $(CH_3)_3As$ to $(CH_3)_4As^+$. For purposes of comparison it is convenient to use the average value of the ν(C—As) frequencies weighted according to the degeneracies. For $(CH_3)_3As$ (4) and $(CH_3)_4As^+$ (1), this is 580 and 635 cm^{-1}, respectively. Replacement of successive methyl groups in $(CH_3)_4As^+$ by phenyl groups causes the value

Can. J. Chem. Downloaded from www.nrcresearchpress.com by 210.87.254.5 on 09/05/12
For personal use only.

TABLE IV

Vibrational frequencies (cm^{-1}) and assignments for ethylphenylarsonium salts

$Et_3PhAsHgI_3$	$Et_2Ph_2AsHgI_3$	Assignments
	3 054 w	
3 054 w	3 018 w	ν(CH) of phenyl ($a_1 + b_2$)
2 982 m	2 964 m	ν(CH) asym. of CH_2
2 956 m	2 947 m	ν(CH) asym. of CH_3
2 921 m	2 912 m	ν(CH) sym. of CH_2
2 880 m	2 881 w	ν(CH) sym. of CH_3
1 580 vw	1 581 vw	ν(CC) ($a_1 + b_2$)
1 486 m	1 487 m	ν(CC) (a_1)
—	1 454 m	CH_3 asym. def.
1 443 s	1 433 s	ν(CC) (b_2)
1 412 m	1 412 m	CH_2 def.
1 383 m	1 383 m	CH_3 sym. def.
1 336 m	1 336 m	ν(CC) (b_2)
1 310 w	1 310 w	Combination
1 282 vw	1 281 vw	β(CH) (b_2)
1 247 m,br	1 250 sh 1 236 m,br	CH_2 wag
1 186 vw	1 187 w	β(CH) (a_1)
	1 173 w	β(CH) (b_2)
1 160 m	1 162 vw	CH_2 twist (?)
1 084 s	1 084 s	'X-sens.' q (a_1)
1 067 m	1 067 w	β(CH) (b_2)
1 044 s	1 048 s	CH_3 rock
1 023 m	1 023 m	β(CH) (a_1)
999 s	1 000 s	Ring breathing (a_1) + ν(CC) of C_2H_5
972 m	973 w	γ(CH) (b_1)
922 vw	925 vw	γ(CH) (b_1)
847 w	853 845 w	γ(CH) (a_2)
743 vs 734 s 728 sh	747 sh 743 sh 738 vs	γ(CH) (b_1) + CH_2 rock
690 s	690 s	ϕ(CC) (b_1)
685 sh	—	'X-sens.' r (a_1)
—	618 w	α(CCC) (b_2)
614 m 606 m	608 w 595 m	ν(C_2H_5—As) asym.
564 m	578 w	ν(C_2H_5—As) sym.
470 s	465 s	'X-sens.' y (b_1)
345 m 324 m	357 m 338 sh	C—C—As def.
297 m	328 m 304 m	'X-sens.' t (a_1)
222 m	220 m	CH_2—As—CH_2 def.

to drop only to 632, 627, and 625 cm^{-1}, and implies very little change in the strength of the methyl–arsenic bond. Conversion of $(CH_3)_2(C_6H_5)As$ and $(CH_3)(C_6H_5)_2As$ to $(CH_3)_3(C_6H_5)As^+$ and $(CH_3)_2(C_6H_5)_2As^+$, respectively, increases the methyl–arsenic stretching frequency by at least 53 cm^{-1}. The changes in the methyl rocking frequencies follow the same trend, as do the much smaller changes in the methyl symmetric deformations. In the alkyl compounds (1) the increase in the ν(C—As) frequency on 'onium ion formation was found to be accompanied by a small but significant increase in the carbon–hydrogen stretching frequencies. The same effect is observed here in the mixed methylphenyl compounds, so that evidently 'onium ion formation again results in both stronger C—As and C—H bonding. Comparison of the frequencies of the dimethyldiphenylarsonium cation with those of the isoelectronic germane (Table II) shows that methyl–metal

Can. J. Chem. Downloaded from www.nrcresearchpress.com by 210.87.254.5 on 09/05/12
For personal use only.

TABLE V

Comparison of some fundamental frequencies (cm^{-1}) of some alkylarylarsines and alkylarylarsonium compounds

Fundamental	Me_2PhAs*	Me_3PhAs^+†	$MePh_2As$*	$Me_2Ph_2As^+$†	Ph_3As*	$MePh_3As^+$‡
ν(Me—As) (average)§	575	632	574	627	—	625
Me rock	889 847	924 853 843	837	926 893 843	—	892
Me sym. def.	1 258 1 242	1 268	1 247	1 268	—	1 280
Me stretch	2 980 2 915	3 000 2 916	2 993 2 912	3 010 2 920	—	3 000 2 919
'X-sens.' q	1 079	1 090	1 081	1 091 1 087	1 074	1 085
'X-sens.' r	671 667	[690]§	672 668	[690]§ 680	667	683
'X-sens.' t	295	304	310 298	329 304	310	342 302

*Reference 2.
†HgI_3 salt.
‡HgI_4 salt.
§See text.

stretching, methyl rocking, methyl symmetric deformation, and carbon–hydrogen (of methyl) stretching frequencies are all higher in the cation than in the germane, as was found (1) for the corresponding tetramethyl compounds.

Stretching of the phenyl–arsenic bond makes contributions to all the a_1 'X-sensitive modes q, r, and t. Accordingly the shift of these vibrations to higher wavenumbers on 'onium ion formation is in accord with stronger phenyl–arsenic bonding in the cations than in the corresponding tertiary arsines. Both r and t are at higher frequencies in $(CH_3)_2(C_6H_5)_2As^+$ than in $(CH_3)_2(C_6H_5)_2Ge$. The findings and conclusions for the alkylarsonium salts (1) can therefore be extended to the mixed alkylaryl compounds, and the behavior of the phenyl–arsenic bond on 'onium ion formation parallels that of the methyl–arsenic bond.

Finally, it is to be noted that all the present compounds show strong absorption near 1 440 cm^{-1}, assigned to a b_2 ν(CC) mode. Similar intense absorption is generally found in the spectra of other phenyl–metal compounds (9 and references therein; 10 and references therein) and is not specific for a particular phenyl–metal link.

EXPERIMENTAL

The preparation of the majority of the compounds has been reported (11, 12).

Trimethylphenylarsonium iodide was obtained from the reaction of dimethylphenylarsine with methyl iodide and had m.p. 257° (lit. (13) m.p. 250°).

Anal. Calcd. for $C_9H_{14}AsI$: C, 33.4; H, 4.3. Found: C, 33.6; H, 4.6.

Bis(trimethylphenylarsonium) tetraiodomercurate (II) was obtained from the above iodide and mercuric iodide (14) and had m.p. 194–195° (lit. (14) m.p. 192°).

Anal. Calcd. for $C_{18}H_{28}As_2HgI_4$: C, 19.6; H, 2.5; Hg, 18.2. Found: C, 19.85; H, 2.6; Hg, 17.5.

Microanalyses were by Dr. A. Bernhardt.

Infrared spectra of the compounds as Nujol and hexachlorobutadiene mulls were obtained as described previously (1).

ACKNOWLEDGMENT

One of us (G. B. D.) thanks Imperial Chemical Industries Limited for a Fellowship.

Can. J. Chem. Downloaded from www.nrcresearchpress.com by 210.87.254.5 on 09/05/12
For personal use only.

Can. J. Chem. Downloaded from www.nrcresearchpress.com by 210.87.254.5 on 09/05/12
For personal use only.

REFERENCES

1. W. R. CULLEN, G. B. DEACON, and J. H. S. GREEN. Can. J. Chem. **43**, 3193 (1965).
2. J. H. S. GREEN, W. KYNASTON, and G. A. RODLEY. In preparation. G. A. RODLEY. Ph.D. Thesis, University College, London. 1963.
3. G. B. DEACON and R. A. JONES. Australian J. Chem. **16**, 499 (1963). D. H. BROWN, A. MOHAMMED, and D. W. A. SHARP. Spectrochim. Acta, **21**, 659 (1965).
4. H. SIEBERT. Z. Anorg. Allgem. Chem. **273**, 161 (1953). E. J. ROSENBAUM, D. J. RUBIN, and C. R. SANDBERG. J. Chem. Phys. **8**, 366 (1940).
5. D. H. WHIFFEN. J. Chem. Soc. 1350 (1956).
6. J. Chem. Phys. **23**, 1997 (1955).
7. J. H. S. GREEN. In course of publication.
8. L. A. LEITES, YU. P. EGOROV, J. YA, ZUEVA, and V. A. PONOMARENKO. Izv. Akad. Nauk SSSR Otd. Khim. Nauk, 2132 (1961).
9. G. B. DEACON, R. A. JONES, and P. E. ROGASCH. Australian J. Chem. **16**, 360 (1963).
10. L. C. THOMAS and R. A. CHITTENDEN. Spectrochim. Acta, **21**, 1905 (1965).
11. M. M. BAIG and W. R. CULLEN. Can. J. Chem. **39**, 420 (1961).
12. M. M. BAIG, W. R. CULLEN, and D. S. DAWSON. Can. J. Chem. **40**, 46 (1962).
13. A. E. GODDARD. *In* Textbook of inorganic chemistry, Vol. XI. *Edited by* J. Newton Friend. Griffen, London. 1930. Pt. 2. p. 91.
14. R. C. CASS, G. E. COATES, and R. G. HAYTER. J. Chem. Soc. 4007 (1955).

Can. J. Chem. Downloaded from www.nrcresearchpress.com by 210.87.254.40 on 09/05/12
For personal use only.

PREPARATION AND CHARACTERIZATION OF SULFONATED POLYSTYRENE LATEXES

F. S. CHAN AND D. A. I. GORING

Physical Chemistry Division, Pulp and Paper Research Institute of Canada, and Department of Chemistry, McGill University, Montreal, Quebec

Received October 26, 1965

ABSTRACT

The purpose of the work was the preparation of aqueous suspensions of model spherical particles stabilized by ionizable groups covalently bound to the surface. Starting material was a 80/20 styrene/divinylbenzene latex. The latex had an average particle diameter of 500 Å as determined in the electron microscope. The copolymer was sulfonated in dichloroethane with a 3/1 SO_3/triethylphosphate complex in a concurrent-flow fast-reaction apparatus and was purified by dialysis and ion exchange.

Three main fractions with neutralization equivalents, N_e of 0.9, 1.8, and 2.7 meq g^{-1} were prepared. Elemental analysis revealed that the varying N_e in these fractions resulted from the absorption of Ca^{2+} and Mg^{2+} ions which were tightly bound to the inner-lying sulfonic groups of the particles. Treatment with strong acid followed by ion exchange eliminated the bivalent ions and increased N_e, but the titration pattern was markedly changed after such treatment. Sulfonation caused both the partial specific volume and the refractive index increment to decrease. Electron micrographs showed that the latex particles were only slightly polydisperse and that there was little change in size and shape after sulfonation. Light-scattering measurements established the absence of aggregates in the sulfonated latex. Particle sizes, determined from the intrinsic viscosities, indicated some swelling of the particles in 1 *M* aqueous NaCl. The extent to which the sulfonated latex satisfies the criteria required of a model colloid to be used for a study of electroviscous behavior is discussed.

INTRODUCTION

The electroviscous behavior of polyelectrolytes is of fundamental importance in processes involving the interaction of colloidal materials and water. For experimental study, it would be useful to have a system of charged particles in which parameters such as size, shape, and potential are accurately known for all conditions of concentration and ionic strength of the aqueous medium. Results obtained would permit easier and more precise interpretation. The purpose of the present work is to prepare and characterize such a colloidal polyelectrolyte. Subsequent reports will deal with the investigation of the primary and secondary electroviscous effects by using this model system.

Certain desired features for the model particles are listed below.

Criterion No. I. Spheres of uniform size.
II. Macromolecular dimensions (200 – 2 000 Å in diameter).
III. Density near to that of water.
IV. Permanently stabilized in aqueous solutions by having strongly ionizable groups attached by covalent bonds to their surface.
V. Constant in size and shape over a wide range of ionic strengths.

The criterion of spherical shape is adopted because hydrodynamic theories are most complete for spheres. In addition, spherical particles are conveniently prepared. Despite their wide use, inorganic sols (1) usually violate criterion I by their irregular shape and polydispersity. Criterion II is necessary because of the much diminished electroviscous effect of the double layer with larger particles. Goldfarb *et al.* (2) recently prepared surface-charged spheres by emulsifying a mixture of molten paraffin and a long-chain surface-active compound. When the mixture was poured into cold water and fractionated by sieving and sedimentation, surface-charged paraffin particles with diameters of 3 and 10 μ were obtained. This particle size is much larger than the present requirement. Our attempts to use such paraffin sols have been unsuccessful because of a low yield in the

size range specified above. Schenkel and Kitchener (3) have described a "model suspension" consisting of spherical particles of cross-linked polystyrene which were sulfonated near the surface by a complex of SO_3/dioxane dissolved in dry dibutyl phthalate. However, the large particle size (10 μ) and the instability of the suspension would make this system unsuitable for the study of electroviscous effects.

The criterion of approximately aqueous density is needed to avoid settling due to the effect of gravity. In this respect, heavy metal sols (4), though spherical and monodispersed, may be unsatisfactory. Criterion IV establishes the condition that the number of charges attached to the particle is always well defined. A strongly ionizable group is preferred because weak acids are susceptible to hydrolysis and conversion of the salt into the corresponding undissociated acids (5, 6). Charged particles for hydrodynamic studies have been prepared by absorption of surface-active agents on latexes (7, 8) or emulsions (9, 10). But the tendency of the soap or stabilizer to desorb at low ionic strength (11) reduces the number of charges on the particle and renders the suspension unstable.

Exact knowledge of the size and shape of the particle is of primary importance in the interpretation of electroviscous effects. Hence the requirement of constant dimensions is listed as criterion V. A considerable variety of theory and experiment can be found in the literature dealing with the solution properties of polyelectrolytes. Such macromolecules are capable of large molecular expansion, and their configuration in solution may lie anywhere between that of a Gaussian coil and a rigid rod (12). The exact assignment of size and shape to the polyion is difficult. Therefore, linear polyelectrolytes cannot be regarded as being suitable models for a study of the primary and secondary electroviscous effects. The use of detergent micelles is also unsatisfactory because of the fluid interior and the possible decrease in size at low ionic strengths (13).

In the present investigation, the approach of Schenkel and Kitchener (3) was followed for the preparation of sulfonated latex particles of about 500 Å in diameter. The use of synthetic latexes has the advantage of yielding spheres of narrow particle-size distribution. The particle would be permanently stabilized by the sulfonic groups and, if heavily cross-linked, would retain its size and shape under all conditions of ionic strength. Also, the density of the dispersed phase would be similar to that of water. The drawback of this method appears to be the problem of avoiding coagulation and of limiting sulfonation to the surface of the particle. An attempt has been made to overcome these difficulties by use of a simple concurrent-flow fast-reaction apparatus, which allows reduction of the reaction time to less than 10^{-1} s. Also, sulfonation was carried out in an organic medium by the method of Turbak (14) to avoid coagulation of the latex by sulfone formation. This method is described in the first part of the paper. The second part of the paper deals with the characterization of the sulfonated latex particles with respect to their size, their shape, and the number of charges introduced. The methods used include potentiometric titration, elemental analysis, light scattering, electron microscopy, and viscometry. Finally certain anomalous properties of the sulfonated latex particles are described and the extent to which they satisfy the listed requirements is discussed.

PREPARATION

Starting Material

The starting material was a highly cross-linked styrene/divinylbenzene (80/20) latex kindly made for us by the Polymer Corporation, Sarnia, Canada,* with the characteristics given in Table I. The three lots

We are especially indebted to Drs. L. Brietman and W. G. Forbes for the gift of the samples without which the investigation would have been much more difficult. The electron micrographs and particle-size determinations described later in the paper were also made for us by Polymer Corporation.

Can. J. Chem. Downloaded from www.nrcresearchpress.com by 210.87.254.40 on 09/05/12
For personal use only.

shown in Table I were thoroughly mixed in equal proportions and filtered through Whatman papers to remove the aggregated particles. The filtrate was freeze-dried and stored over magnesium perchlorate before sulfonation.

TABLE I

Characteristics of the styrene/divinylbenzene latexes

Code No.	% conversion	% stripped solids	Particle size (Å)
LB/7-1	74.5	27.8	486
LB/7-2	72.1	27.3	468
LB/7-3	73.1	29.9	495

Sulfonating Agent

Initial attempts were made to sulfonate the latex particles by use of concentrated sulfuric acid and chlorosulfonic acid. These reagents produced dark-brown agglomerates because of charring and the probable formation of sulfones which gave rise to cross-linking between particles. These difficuties were obviated by using the SO_3/phosphate complex system discovered by Turbak (14).

Reaction Apparatus

A fast reaction apparatus was constructed and used in the sulfonation of the latex particles. A schematic diagram of the apparatus is shown in Fig. 1. The reactants are mixed in a flat cylindrical chamber machined on the surface of a stainless-steel plate and covered with a Teflon block. The mixing chamber (diameter = 0.5 cm, thickness = 0.1 cm) is fed by four jets which deliver reactants tangentially thus imparting a rotary motion to the fluid in the chamber and down the reaction tube (length = 14 cm, inside diameter = 0.2 cm). The reaction is stopped by flow into a bath of vigorosly stirred quenching solution. The driving force is supplied by a cylinder of compressed nitrogen fitted with a precision automatic regulator to give a constant pressure of 5 p.s.i. Under such conditions, the total resident time of the reaction mixture in the mixing chamber and the reaction tube was approximately 10^{-1} s.

The reagent was prepared by adding freshly distilled liquid SO_3 (Sulfan B) dropwise to an agitated solution of triethyl phosphate in dichloroethane at room temperature. Before use, the dichloroethane was distilled over P_2O_5. The molar ratio of SO_3/phosphate was 3/1, and the percentage of the complex in dichloroethane was 2–4%. All glassware was thoroughly dried and the complex reagent was used within a few hours after

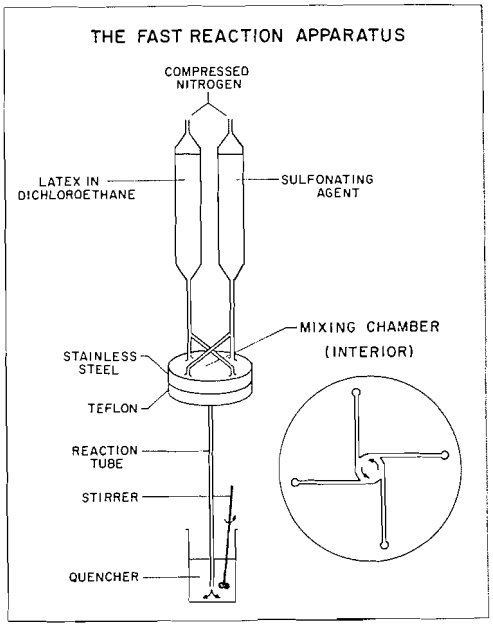


FIG. 1. Schematic diagram of the fast-reaction apparatus.

Can. J. Chem. Downloaded from www.nrcresearchpress.com by 210.87.254.40 on 09/05/12
For personal use only.

preparation to prevent deterioration due to the absorption of moisture from the atmosphere. Just before reaction, distilled dichloroethane was added to the freeze-dried latex particles to make up a solution of 0.5% by weight. Ultrasonic waves from an M.S.E. 60 W disintegrator operated at 20 kilocycles/s were passed through the solution for about 2 min to obtain a homogeneous dispersion. Electron micrographs of the ultrasonically treated latex showed that the particles were not damaged by this treatment.

Several types of quencher were tried. Some stopped the reaction by decomposition of the complex (water), others by formation of sulfonates (methanol, thiopene) or of non-reactive complexes (triethyl phosphate). The difference in their effectiveness seemed to be small. For all subsequent sulfonations, an aqueous solution containing enough NaOH for the neutralization of the reaction mixture was used as the quencher. The conversion of the sulfonic groups to the sodium form stopped the reaction and the resulting neutrality of the solution facilitated the purification process.

Purification

After the reaction was quenched, the sulfonated latex particles were found in the upper aqueous phase. The lower dichloroethane layer was removed in a separating funnel. Any remaining dichloroethane was evaporated off at 45 °C in a rotary evaporator. The aqueous suspension was then dialyzed in cellophane bags to remove excess inorganic ions and traces of low molecular weight impurities. To conserve distilled water, tap water was used in the initial stage of the dialysis. Finally, the solution was dialyzed for 4–6 d with 12 changes of distilled water, and then neutralized to pH 8 with carbonate-free sodium hydroxide. The product was a milky-white stable suspension of sulfonated latex particles which, when oven-dried at 110 °C, formed a feathery, translucent film. Freeze-drying produced white, fluffy, very fine powders. Both types of solid product could be redispersed instantaneously on addition of water to form a homogeneous, stable suspension having the same appearance as the sulfonated latex before drying.

Main Fractions

Considerable trial and error were applied to the fast-reaction method. Changes in the concentrations of the reactants and the flow rate were studied in an attempt to control the neutralization equivalent, N_e, of the sulfonated product. But in spite of great care in the preparation of the reagents, N_e varied unpredictably from batch to batch. It was then decided that the reaction was particularly sensitive to some unknown variable. Accordingly, 40 batches of the sulfonated latex particles were prepared. Each batch weighed about 2 g. The neutralization equivalent was determined (see "Characterization") for each batch, and was found to vary from 0.5 to 3.0 meq/g of solid. Based on their N_e values, the small batches were combined into three main fractions of about 25 g each, designated F1, F2, and F3. The maximum variation of N_e in each main fraction was ± 0.25 meq g^{-1}. An additional fraction, F4, was also prepared by simple mixing of the reagents without using the fast-reaction apparatus. In this case, the reaction time was increased to 2 h and the sulfonated latex had a slightly yellowish color. The main fractions were stored in aqueous suspensions in polyethylene bottles at -10 °C to avoid the growth of bacteria.

CHARACTERIZATION

Potentiometric Titration and Elemental Analysis

The sulfonated latex particles (hereafter designated as s.l.p.) were converted to the hydrogen form by a number of passes through a mixed-bed ion-exchange column (Rexyn 1-300, H–OH). The solution was titrated with carbonate-free 0.01 N NaOH by means of a Beckman model G pH meter with glass and calomel electrodes under an atmosphere of nitrogen, and pH readings were taken 2 min after each addition of titrant. Curve A in Fig. 2 is an example of the titration curves obtained. The shape of the curve is similar to that observed in the titration of strong mineral acids with NaOH. The neutralization equivalent was calculated from the amount of NaOH added at the equivalent point (pH = 8), and the weight of the solid was determined by evaporation of the solution to constant weight. Three or four determinations were made for each fraction and the mean values (average deviation from the mean = ± 0.05 meq g^{-1}) are given in the second column of Table II.

The sulfur contents determined in a Leco apparatus are given in the third column of Table II. Fraction F4 contains the highest percentage of sulfur, but the sulfur content is roughly the same for the other fractions which were sulfonated in the fast-reaction apparatus. All the sulfur contents are higher than the potentiometrically determined values of N_e. To check the efficiency of the ion-exchange column in converting the sodium sulfonate groups to the acidic form before titration, the sodium content of each fraction

Can. J. Chem. Downloaded from www.nrcresearchpress.com by 210.87.254.40 on 09/05/12
For personal use only.

TABLE II
Analytical results (meq/g solid)

Fraction	N_e	Sulfur	Na (in neutralized latex)	Ca	Mg
Non-sulfonated	—	0	0.1	0.01	—
F1	0.9	2.6	0.9	2.2	0.6
F2	1.8	3.0	2.0	1.4	0.4
F3	2.7	2.8	2.7	0.8	0.3
F4	2.0	4.0	2.1	1.7	0.5

after passage through the column was determined in a Beckman DU flame spectrophotometer at $\lambda = 589$ mμ. No trace of sodium was detected in any of the fractions. Using the same method the sodium content of the neutralized s.l.p. was determined. As shown in the fourth column of Table II there is good agreement between the sodium content and N_e for all fractions.

The question then arises why the sulfur content should be higher than the neutralization equivalent of the sulfonic groups. Examination of the emission spectrum of the s.l.p. in the acid form revealed the presence of calcium ($\lambda = 554$ and 622 mμ) and magnesium ($\lambda = 370$ mμ); approximate amounts are given in the last two columns of Table II. The calcium and magnesium contents decreased from F1 to F3 in contrast with the trend of increasing N_e values.

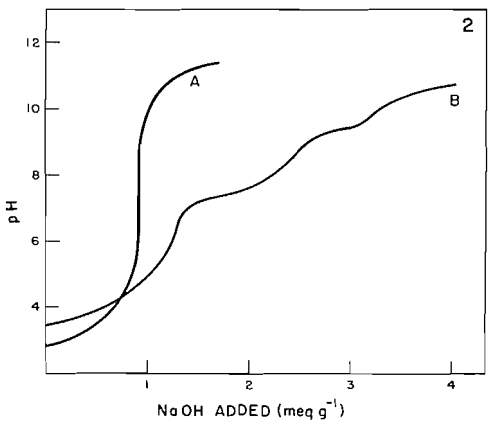
Absorption of Bivalent Ions

The latex did not contain calcium or magnesium before sulfonation (Table II). The source of these bivalent ions was traced back to the tap water which was used in the initial stage of dialysis to remove the excess inorganic ions in the reaction mixture. The fact that the bivalent ions were not removed by later dialysis against distilled water and passage through the ion-exchange column was unexpected. To confirm this point, solutions of a fraction which contained no bivalent ion were dialyzed against $1.4 \times 10^{-4} M$ $Ca(NO_3)_2$ for different intervals of time. Values of N_e for the dialyzed s.l.p. were determined as previously after several passages through an ion-exchange column. The amount of Ca^{2+} ion immobilized in the s.l.p. was likewise determined by flame photometry. As shown in Fig. 3, the neutralization equivalent decreases to 0.4 meq g^{-1} after prolonged treatment with dilute calcium nitrate. In the opposite sense, the amount of bound calcium increases until it reaches a value about the same as N_e before dialysis. These results leave little doubt that the absorption of various amounts of bivalent ions led to the different values of N_e shown in Table II.

Attempts to remove the absorbed bivalent ions were first made by repeated passage through ion-exchange columns. Between each passage, the solution was shaken for at least 24 h in the hope that the absorbed ions would diffuse out by osmotic forces. But the method failed either to increase the neutralization equivalent or to reduce the calcium content of the s.l.p. Similarly, repeated electrodialysis against distilled water (15) did not remove the bound Ca^{2+} ions. These experiments illustrated how strongly the bivalent ions were held by the s.l.p.

When the s.l.p. was treated with an excess of 0.5 M HCl which was subsequently removed by ion exchange, the emission spectrum of the acid-treated s.l.p. showed almost complete absence of calcium and magnesium. Titration curves of the s.l.p. after acid treatment were flatter and exhibited more than one inflection point. An example is

Can. J. Chem. Downloaded from www.nrcresearchpress.com by 210.87.254.40 on 09/05/12
For personal use only.



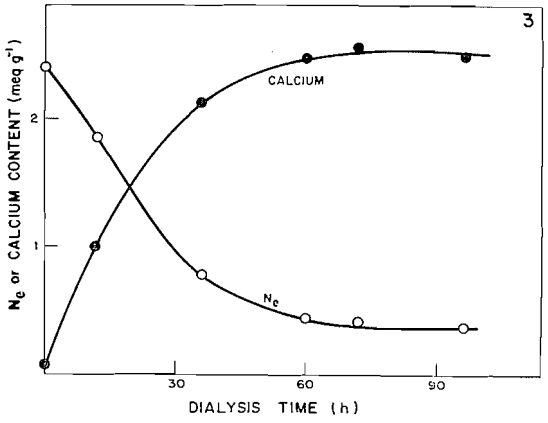


FIG. 2. Potentiometric titration curves: A, fraction F1; B, fraction F1 after acid treatment.
FIG. 3. Variation of N_e and calcium content of the s.l.p. with time of dialysis against aqueous calcium nitrate solution.

curve B in Fig. 2. If the equivalent point is taken at pH = 8, the exchange capacity increased to a value corresponding to the sulfur content of the s.l.p. When the acid-treated s.l.p. was dialyzed against dilute $Ca(NO_3)_2$, the titration curve approached the shape of curve A in Fig. 2.

The shape of the titration curve for the acid-treated material is similar to that obtained in titrating a mixture of weak and strong acids. In the present instance, however, the phenomenon is probably related to the structural properties of the s.l.p. rather than to the titration behavior of the $—SO_3^-$ functional group. Steric hindrance offered by the compact polymer network to the exchange of Na^+ ions with the protons of the inner layers of sulfonate groups seems a reasonable postulate. A similar type of titration curve has been observed for some compact globular proteins (16, 17).

Partial Specific Volume

The partial specific volume, $\bar{v}$, was determined with 5 ml Lipkin pycnometers (18) by the method of Svedberg and Pedersen (19). Measurements were made at 25 °C in distilled water with concentrations varying from 1% to 5% of solid. Values of $\bar{v}$ were constant over this range of concentrations. Partial specific volumes are listed in Table III. Pugh and Heller (20) have reported 0.9461 $cm^3\ g^{-1}$ for the specific volume of polystyrene latex particles which agrees well with $\bar{v}$ for the non-sulfonated latex in Table III. It can be seen, however, that $\bar{v}$ decreased markedly after sulfonation. This is caused by the acquisition of the relatively heavy cation and sulfonate groups by the particle. Butler *et al.* (21) have reported 0.697 ± 0.013 ml g^{-1} for the partial specific volume of sodium styrene sulfonate, which is comparable with the $\bar{v}$ values for F1 → F3 in Table III.

Refractive Index Increment

Refractive index differences were measured with a Brice–Phoenix differential refractometer (22, 23) at λ = 5 461 Å and 25 °C. The increments, dn/dc, obtained are given in Table III. The value for the non-sulfonated latex agrees well with 0.257 ± 0.005 ml g^{-1} found by Dandliker (24) for polystyrene latex particles at λ = 4 358 Å. Orofino and Flory (25) have reported an increment of 0.197 ml g^{-1} for polystyrene–*p*-sulfonic acid, which is in reasonable accord with dn/dc for the s.l.p. Thus, like the partial specific volume, the refractive index increment also decreased after sulfonation.

Can. J. Chem. Downloaded from www.nrcresearchpress.com by 210.87.254.40 on 09/05/12
For personal use only.

TABLE III

Partial specific volumes, refractive index increments, light scattering dissymmetries, and molecular weights of the neutralized latex

Fraction	$\bar{v}$ (ml g^{-1})	dn/dc (ml g^{-1})	$[z]_{c=0}$	$\bar{M}_w \times 10^6$ By light scattering	$\bar{M}_w \times 10^6$ Calculated
Non-sulfonated	0.9467	0.256	1.16	35	—
F1	0.7023	0.212	1.39	52	48
F2	0.6925	0.207	1.45	53	50
F3	0.6947	0.205	1.41	49	49
F4	0.5920	0.195	1.50	73	59

Light Scattering

Light scattering measurements were made at a wavelength of 5 461 Å with a Brice–Phoenix (26) photometer by methods described in several previous publications (22, 23, 27). The solvent was 0.05 M NaCl for F1 and F2 and 0.1 M NaCl for F3 and F4. Distilled water was used for the non-sulfonated latex since addition of a slight amount of salt caused rapid coagulation. All the solutions were filtered through 0.2 μ Millipore filters. Concentrations were between 0.005 and 0.05 g dl^{-1} and were determined by evaporation of aliquots and volumetric dilution with the solvent. Scattered intensities were measured at 0°, 45°, 90°, and 135° to the direction of the incident beam. The data were plotted by the usual methods. The weight-average molecular weight $\bar{M}_w$ was computed from an extrapolation of the turbidity function to zero concentration and was corrected for dissymmetry by means of the factors available in the literature (28). Values of the dissymmetry at zero concentration, $Z_{c=0}$, and of $\bar{M}_w$ are given in Table III. Also listed in Table III are molecular weights for the s.l.p. derived by adding to the weight of the original latex particle the sulfonate and cation content shown in Table II. The agreement for F1, F2, and F3 is excellent indicating that no aggregation occurred on sulfonation. The discrepancy in the case of F4 will be discussed later.

Electron Microscopy

Electron micrographs of the latex particles before and after sulfonation are shown in Figs. 4 and 5. The number-average diameter, D_n, weight-average diameter, D_w, and z-average diameter, D_z, of the particles together with the polydispersities, P, for different fractions are given in Table IV. Measurements were made of the diameters of 1 000 particles in each fraction, and average dimensions were calculated from the relation

$$[1a] \qquad D_n = \frac{\sum n_i D_i}{\sum n_i}$$

$$[1b] \qquad D_w = \frac{\sum n_i D_i^4}{\sum n_i D_i^3}$$

$$[1c] \qquad D_z = \frac{\sum n_i D_i^5}{\sum n_i D_i^4}$$

$$[1d] \qquad P = \frac{D_w}{D_n}$$

where n_i is the number of particles having diameter equal to D_i. The results demonstrate that the latex particles are fairly monodisperse spheres whose size and shape does not

Can. J. Chem. Downloaded from www.nrcresearchpress.com by 210.87.254.40 on 09/05/12
For personal use only.

seem to have altered by sulfonation. The lower particle size and higher polydispersity for F4 is probably due to slight fragmentation as a result of a longer sulfonation time.

TABLE IV

Particle dimensions from electron microscopy and viscosity

Fraction	D_n (Å)	D_w (Å)	D_z (Å)	P	$[\eta]_{1M}$ (dl g^{-1})	$D_{[\eta]}$ (Å)
Non-sulfonated	480	580	600	1.20	0.040	560
F1	510	590	610	1.16	0.068	760
F2	500	580	600	1.16	0.080	810
F3	490	600	620	1.21	0.074	770
F4	420	560	590	1.32	0.072	880

Viscometry

The intrinsic viscosity, $[\eta]$, was measured in Ubbelohde-type viscometers (29) at 25 ± 0.002 °C. To eliminate the electroviscous effect, measurements were made in 1 M NaCl solution for the sulfonated fractions. The diameter, $D_{[\eta]}$, of the equivalent Einstein sphere was computed from

$$[2] \qquad D_{[\eta]} = 2\left(\frac{30\bar{M}_w[\eta]_{1M}}{\pi N}\right)^{1/3}.$$

Values of $[\eta]_{1M}$ and $D_{[\eta]}$ are given in Table IV.

DISCUSSION

Let us review the degree to which the s.l.p. fractions meet the listed criteria. The electron micrographs shown in Figs. 4 and 5 indicate that the latex particles are spherical and that sulfonation has produced no visible change in their shape and general appearance. With the exception of F4, the average polydispersity is 1.18 (Table IV), which is sufficiently low for the latex particles to be considered monodisperse. Figures 4 and 5 show some agglomeration of the particles. The agreement of $\bar{M}_w$ from light scattering with the $\bar{M}_w$ computed by adding the sulfonate and cation weight to the particle (Table III) for fractions F1, F2, and F3 suggests that the aggregation is an artifact produced by the drying process in the preparation of specimens for electron microscopy. The absence of aggregates in polystyrene latexes has previously been reported by Dandliker (24) and more recently by Kratohvil and Smart (30). Thus the first two criteria are satisfactorily met by fractions F1, F2, and F3.

Fraction F4 is an exception to the above consistent picture. This fraction was in contact with the sulfonating agent for a longer period of time than F1, F2, and F3. The smaller particle size and higher polydispersity by electron microscopy (Table IV) is an indication of chemically-induced fragmentation of the latex and leaching out of degraded products. Furthermore, $\bar{M}_w$ (from light scattering) for F4 is 25% higher than $\bar{M}_w$ (calculated) (Table III), which suggests that the longer reaction time caused aggregation by interparticle cross-linking. Hence, in this respect, the fast-reaction technique yielded a sulfonated latex which was superior to the product obtained by conventional mixing of the reactants.

From Table III, the density of the s.l.p. is about 1.4 g ml^{-1}. This is slightly lower than that of polysaccharides or proteins (~1.5 g ml^{-1}) and considerably less than for many inorganic sols such as AgI (5.67 g ml^{-1}), with which many interesting hydrodynamic studies have been made (31, 32). Thus the s.l.p. can be regarded as having approximately the density of water in accordance with criterion III.

Can. J. Chem. Downloaded from www.nrcresearchpress.com by 210.87.254.40 on 09/05/12
For personal use only.



FIG. 4. Electron micrograph of the latex particles before sulfonation.
FIG. 5. Electron micrograph of the latex particles after sulfonation: fraction F1.

Can. J. Chem. Downloaded from www.nrcresearchpress.com by 210.87.254.40 on 09/05/12
For personal use only.

$[\eta]$ value of 1.4×10^3 dl g^{-1} in 0.5 M NaCl, from which $D_{[\eta]}$ would be 2×10^4 Å. This is approximately 30 times greater than the diameter of the corresponding dry sphere. In contrast, $D_{[\eta]}$ exceeds D_z for the s.l.p. by a factor of only 1.3. Hence, it is likely that the imbibed water stretched the highly cross-linked network to the fullest extent at 1 M and that further swelling at lower ionic strength was eliminated by the large contractile energy of the network. A test of the correctness of the above speculation will be described in a later report dealing with the primary electroviscous effect.

Concluding Remarks

These experiments have indicated the feasibility of preparing permanently stabilized suspensions of charged spheres by direct sulfonation of a cross-linked styrene/divinylbenzene latex in the macromolecular range of particle size. The inactivation of some of the $—SO_3^-$ groups in the interior of the particles by the absorption and immobilization of bivalent ions was unexpected, but it opened up the possibility of producing particles of low surface charge for hydrodynamic studies. Undoubtedly, a superior method would be to limit sulfonation to the surface as originally planned, perhaps by repeated sulfonation at very fast flow rates or by a rapid reaction in a non-swelling or gaseous medium.

In the succeeding investigation of electroviscous effects, it was decided to use materials already prepared rather than to embark on the uncertainties of a new preparation technique. Among the fractions in Table II, F1 contained the lowest number of ionizable groups and was closest to the requirements of our model polyelectrolyte. Therefore, it was chosen for subsequent use.

In addition to the primary interest of measuring the various electroviscous effects of charged spheres, the sulfonated latex particles may be used for other definitive investigations of colloidal behavior. Examples are the influence of charge on the concentration dependence of the sedimentation coefficient, or the effect of the double layer in light scattering. For such purposes, it would be useful to prepare fractions covering a range of particle size. Lastly, the possibility of using the sulfonated latex particles in the physiological characterization of diffusion paths in living organisms should be mentioned. Here the permanent absorption of bivalent ion might be an asset, since radioactive ions could be chosen and thus permit use of the extremely sensitive tracer technique in following the movement of the particle in vivo.

REFERENCES

1. WEISER, H. B. Inorganic colloid chemistry. Vol. I, The colloidal elements (1933); Vol. II, The hydrous oxides and hydroxides (1935); Vol. III, The colloidal salts (1938). John Wiley and Sons, Inc., New York.
2. J. GOLDFARB, G. A. JOHNSON, A. LAGOS, and L. SEPULVEDA. J. Colloid Sci. **17**, 690 (1962).
3. J. H. SCHENKEL and J. A. KITCHENER. Trans. Faraday Soc. **56**, 161 (1960).
4. B. V. ENÜSTÜN and J. TURKEVICH. J. Am. Chem. Soc. **85**, 3317 (1963).
5. B. E. CONWAY and J. A. V. BUTLER. Nature, **172**, 153 (1953).
6. B. E. CONWAY. J. Polymer Sci. **18**, 257 (1955).
7. C. L. SIEGLAFF and J. MAZUR. J. Colloid Sci. **15**, 437 (1960).
8. J. G. BRODNYAN and E. L. KELLEY. J. Colloid Sci. **20**, 7 (1965).
9. M. VAN DER WAARDEN. J. Colloid Sci. **9**, 215 (1954).
10. W. ALBERS and J. TH. G. OVERBEEK. J. Colloid Sci. **14**, 501 (1959).
11. C. L. SIEGLAFF and J. MAZUR. J. Colloid Sci. **17**, 66 (1962).
12. C. TANFORD. Physical chemistry of macromolecules. John Wiley and Sons Inc., New York. 1961.
13. K. J. MYSELS and L. H. PRINCEN. J. Phys. Chem. **63**, 1696 (1959).
14. A. F. TURBAK. J. Ind. Eng. Chem. **1**, 275 (1962).
15. W. Q. YEAN and D. A. I. GORING. Tappi, **47**, 16 (1964).
16. C. TANFORD and J. C. HAUENSTEIN. J. Am. Chem. Soc. **78**, 5287 (1956).
17. C. TANFORD, S. A. SWANSON, and W. S. SHORE. J. Am. Chem. Soc. **77**, 6414 (1955).
18. M. R. LIPKIN, J. A. DAVISON, W. T. HARVEY, and S. S. KURTZ, JR. Ind. Eng. Chem. **16**, 55 (1944).
19. T. SVEDBERG and K. O. PEDERSEN. The ultracentrifuge. Oxford University Press, London, New York, Toronto. 1940.

Can. J. Chem. Downloaded from www.nrcresearchpress.com by 210.87.254.40 on 09/05/12
For personal use only.

20. T. L. PUGH and W. HELLER. J. Colloid Sci. **12**, 173, 294 (1957).
21. J. A. V. BUTLER, A. B. ROBINS, and K. V. SHOOTER. Proc. Roy. Soc. London, Ser. A, **241**, 299 (1957).
22. D. A. I. GORING, M. SENEZ, B. MELANSEN, and M. M. HUQUE. J. Colloid Sci. **12**, 412 (1957).
23. M. M. HUQUE, J. JAWORZYN, and D. A. I. GORING. J. Polymer Sci. **39**, 9 (1959).
24. W. B. DANDLIKER. J. Am. Chem. Soc. **72**, 5110 (1950).
25. J. A. OROFINO and P. J. FLORY. J. Phys. Chem. **63**, 283 (1959).
26. B. A. BRICE, M. HALWER, and R. SPEISER. J. Opt. Soc. Am. **40**, 768 (1950).
27. D. A. I. GORING and T. E. TIMELL. J. Phys. Chem. **64**, 1426 (1960).
28. P. DOTY and R. F. STEINER. J. Chem. Phys. **18**, 1211 (1950).
29. A. W. CRAIG and D. A. HENDERSON. J. Polymer Sci. **19**, 215 (1956).
30. J. P. KRATOHVIL and C. SMART. J. Colloid Sci. **20**, 875 (1965).
31. R. H. OTTEWILL and R. F. WOODBRIDGE. J. Colloid Sci. **16**, 581 (1961); **19**, 606 (1964).
32. G. J. HARMSEN, J. VAN SCHOOTEN, and J. TH. G. OVERBEEK. J. Colloid Sci. **8**, 64, 72 (1953).
33. R. KUNIN and R. E. BARRY. Ind. Eng. Chem. **41**, 1269 (1949).
34. H. HEYMANN and I. J. O'DONNELL. J. Colloid Sci. **4**, 395 (1949).
35. R. M. FUOSS. J. Polymer Sci. **12**, 185 (1954).
36. I. KAGAWA and K. KATSUURA. J. Polymer Sci. **17**, 365 (1955).
37. F. T. WALL. J. Phys. Chem. **61**, 1344 (1957).
38. F. HARRIS and S. A. RICE. J. Phys. Chem. **58**, 725, 733 (1954).
39. U. P. STRAUSS and P. D. ROSS. J. Am. Chem. Soc. **81**, 5295, 5299 (1959).
40. H. INAGAKI, S. HOTTA, and M. HIRAMI. Makromol. Chem. **23**, 1 (1957).
41. G. DEŽELIĆ and J. P. KRATOHVIL. J. Colloid Sci. **16**, 561 (1961).
42. M. KATO, T. NAKAGAWA, and H. AKAMATU. Bull. Chem. Soc. Japan, **33**, 322 (1960).

Can. J. Chem. Downloaded from www.nrcresearchpress.com by 210.87.254.40 on 09/05/12
For personal use only.

THE RADIOLYSIS OF ALKALINE AQUEOUS SOLUTIONS CONTAINING HYDROGEN AND OXYGEN[1]

W. A. ARMSTRONG

Defence Chemical Biological and Radiation Laboratories, Department of National Defence, Ottawa, Canada

Received October 13, 1965

ABSTRACT

The initial yields of H_2O_2 in aerated water, $G(H_2O_2)^{O_2}$, and in water containing H_2 and O_2, $G(H_2O_2)^{H_2,O_2}$, have been measured for alkaline solutions irradiated with ^{60}Co γ-rays. $G(H_2O_2)^{O_2}$ decreases with increasing pH from a value of 1.22 in neutral solution to 0.63 in solutions of pH 13.92 and the relationship

$$G(H_2O_2)^{O_2} = G_{H_2O_2} - \tfrac{1}{2}G_{OH} + \tfrac{1}{2}G_{red}$$

is valid over the pH range 7 to 14.

$G(H_2O_2)^{H_2,O_2}$ decreases from 3.30 in neutral solution to a minimum of 2.00 at pH 11.35 and then increases to 2.65 at pH 13.92. The equation

$$G(H_2O_2)^{H_2,O_2} = G_{H_2O_2} + \tfrac{1}{2}G_{OH} + \tfrac{1}{2}G_{red},$$

which is applicable for neutral solutions, is not valid for basic solutions.

A reaction mechanism in accordance with the observed results and the literature values of the rate constants of likely radical reactions has been developed. It is assumed that in the alkaline solutions investigated OH radicals react with OH^- ions to form O^- radicals which react preferentially with O_2 to form O_3^- radicals which then react either with H_2 or H_2O_2. The increase in $G(H_2O_2)^{H_2,O_2}$ at pH > 12 is attributed to a difference in the rate of reaction of O_3^- with H_2O_2 and HO_2^-, $k(O_3^- + H_2O_2)/k(O_3^- + HO_2^-) = 2.45$.

INTRODUCTION

Studies of the hydrogen–oxygen–water system have produced valuable information about the yields of the primary products of the radiolysis of neutral water (1–3). Therefore, it was decided to attempt similar studies in the higher pH range where reported primary yields are not in agreement (3).

EXPERIMENTAL

Solutions were prepared with specially purified water (4) and reagent grade KOH and $Ba(OH)_2$. Solutions of pH 12 or greater were made 5×10^{-3} *M* in $Ba(OH)_2$ to remove carbonate ions while those of lower pH were prepared with either KOH or $Ba(OH)_2$. Certified 99.93% H_2 and O_2 gases, after being monitored with flowrators, were passed through activated charcoal, mixed, bubbled through a gas washer containing water at the same pH as the solution to be irradiated, and passed through a trap cooled with a dry ice – acetone mixture. The gas mixture was then bubbled for 30 min through the desired solution which was in a quartz flask equipped with a sidearm vent. After bubbling, the solution was poured through the sidearm to fill clean quartz tubes (4) which had been swept out with the gas mixture. Clamped wet ball-and-socket joints were used throughout the apparatus.

Samples were irradiated with ^{60}Co γ-radiation at a dose of 200 rads/min to doses of 2 000 to 8 000 rads. The dosimetry has been described elsewhere (4).

Initial dissolved H_2 and O_2 concentrations were calculated from the partial pressure of each gas at the measured barometric pressure and solution temperature (5).

Hydrogen peroxide was determined by the Ghormley method (4, 6). To verify the accuracy of the method with solutions of pH > 12, H_2O_2 solutions of known concentration were brought to the desired pH and analyzed. No effect due to high pH could be detected with H_2O_2 solutions which had been neutralized with potassium acid phthalate immediately before analysis.

RESULTS AND DISCUSSION

Typical $[H_2O_2]$ vs. dose plots are given for aerated water in Fig. 1 and for solutions of H_2 and O_2 in Fig. 2. The yield of H_2O_2 increases linearly with dose up to about 6 000 rads. The small intercept on the H_2O_2 axis in some of the plots is probably due to impurities.

[1]*Issued as DCBRL Report No. 482.*

Can. J. Chem. Downloaded from www.nrcresearchpress.com by 210.87.254.5 on 09/05/12
For personal use only.

The effects of increasing pH on the initial yield of H_2O_2 in irradiated aerated water, $G(H_2O_2)^{O_2}$, and solutions of H_2 and O_2, $G(H_2O_2)^{H_2,O_2}$, are listed in Table I. These G-values were determined from the slopes of $[H_2O_2]$ vs. dose plots. The yield of H_2O_2 in aerated solutions decreases as the pH increases from neutrality to $\sim$ pH 11, remains constant from pH 11 to 13, and then drops sharply at pH $>$ 13. With solutions containing both H_2 and O_2, the yield of H_2O_2 decreases rapidly as the pH increases from neutrality to $\sim$ pH 11, then increases rapidly at pH $>$ 12. It should be noted that $G(H_2O_2)^{H_2,O_2}$ is dependent on the ratio $[H_2]/[O_2]$ only for solutions of pH 10.62 and 11.35.

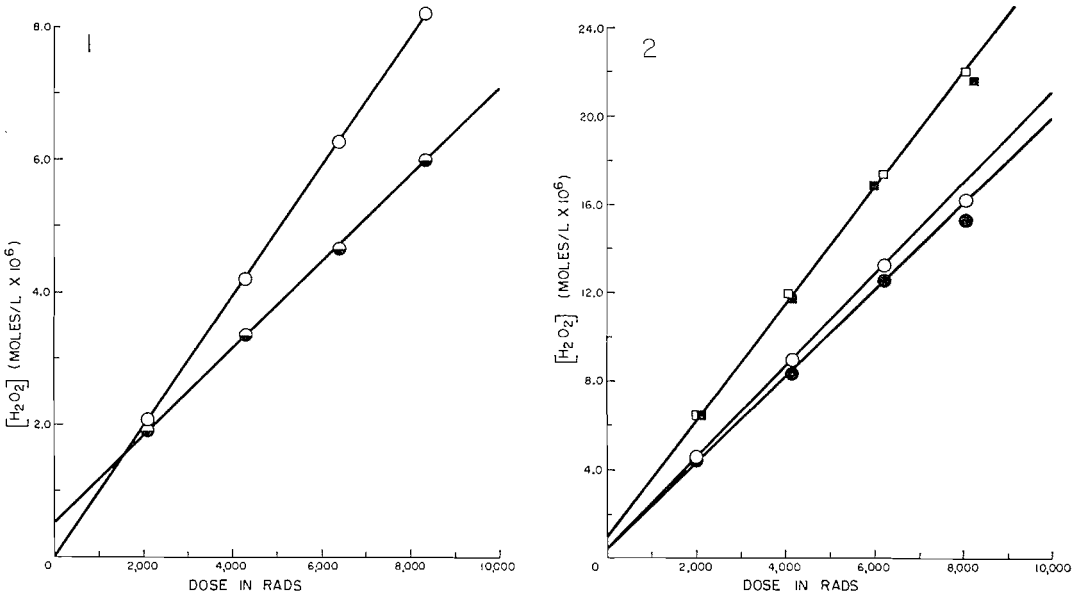


FIG. 1. H_2O_2 yields in aerated water: (○) 5×10^{-4} M KOH, pH 10.62; (◒) 0.5 M KOH – 5×10^{-3} M $Ba(OH)_2$, pH 13.55.

FIG. 2. H_2O_2 yields in water containing H_2 and O_2: (○) 5×10^{-4} M KOH, pH 10.62; (□) 0.1 M KOH – 5×10^{-3} M $Ba(OH)_2$, pH 12.85. (Open symbols $[H_2]/[O_2] = 1.20$, closed symbols $[H_2]/[O_2] = 0.60$.)

Allen (3) has shown that the yield of oxidizing radicals, G_{OH}, may be determined by comparing the initial yields of hydrogen peroxide in neutral water containing both dissolved oxygen and hydrogen and in water containing only oxygen (aerated water).

[A] $$G(H_2O_2)^{H_2,O_2} = G_{H_2O_2} + \tfrac{1}{2}G_{OH} + \tfrac{1}{2}G_{red}$$

[B] $$G(H_2O_2)^{O_2} = G_{H_2O_2} - \tfrac{1}{2}G_{OH} + \tfrac{1}{2}G_{red}$$

[C] $$G_{OH} = G(H_2O_2)^{H_2,O_2} - G(H_2O_2)^{O_2}$$
$$= 2.2 \text{ for neutral water.}$$

Where $G_{H_2O_2}$ is the "molecular" yield of H_2O_2, and G_{red} is the sum of the yield of hydrated electrons, $G_{e_{aq}^-}$, and the yield of H atoms, G_H.

During the course of the present investigation, Hayon (7) published the results of his studies on the radiolysis of alkaline aqueous solutions of nitrate + formate ions, ferricyanide + formate + O_2, and ferricyanide + ethanol + O_2 in the pH range 6 to 14. From these data he determined the yields of radicals and molecular products for the radiolysis of water at many pH values. We have used some of these values and expressions

Can. J. Chem. Downloaded from www.nrcresearchpress.com by 210.87.254.5 on 09/05/12
For personal use only.

TABLE I

The effect of pH on the initial yields of H_2O_2 in irradiated aerated water and aqueous solutions of H_2 and O_2

pH	$G(H_2O_2)^{O_2}$ Meas.	$G(H_2O_2)^{O_2}$ Calcd.*	$[H_2]$ (moles/l $\times 10^4$)	$[O_2]$ (moles/l $\times 10^4$)	$G(H_2O_2)^{H_2,O_2}$ Meas.	$G(H_2O_2)^{H_2,O_2}$ Calcd.†	$\Delta G(H_2O_2)$ Meas.	$\Delta G(H_2O_2)$ Calcd.	
Neutral	1.22	1.01	4.99	4.16	3.30	3.26	2.08	2.25	
Neutral			3.72	6.20	3.30				
9.25	1.06		4.99	4.16	2.81		1.75	1.81	
9.25			3.72	6.20	2.81		1.75	1.72	
10.10	1.00		4.99	4.16	2.29		1.29	1.22	
10.10			3.72	6.20	2.29		1.29	1.19	
10.62	0.95	0.98	5.02	4.18	2.01	3.25	1.06	1.03	
10.62			3.75	6.22	1.89		0.94	0.98	
11.35	0.92		5.02	4.18	2.00		1.08	0.98	
11.35			3.75	6.22	1.87		0.95	0.94	
12.10	0.88	0.90	4.86	4.01	2.10	3.30	1.22	0.99	1.50
12.10			3.62	5.98	2.10		1.22	0.96	1.49
12.85	0.87		4.86	4.01	2.54	3.52	1.67	1.68	
12.85			3.62	5.98	2.54		1.67	1.66	
13.25	0.74	0.73	4.63	3.78	2.74		2.00	1.79	
13.25			3.45	5.63	2.74		2.00	1.77	
13.55	0.63	0.60	4.29	3.39	2.71	3.68	2.08	1.89	
13.55			3.20	5.06	2.71		2.08	1.87	
13.92	0.63		3.67	2.79	2.65		2.02	2.01	
13.92			2.74	4.17	2.65		2.02	2.01	

*$G(H_2O_2)^{O_2} = G_{H_2O_2} + \frac{1}{2}G_{red} - \frac{1}{2}G_{OH}$, calculated with Hayon's values (7) for $G_{H_2O_2}$, G_{red}, and G_{OH}.
†$G(H_2O_2)^{H_2,O_2} = G_{H_2O_2} + \frac{1}{2}G_{red} + \frac{1}{2}G_{OH}$, calculated with Hayon's values (7) for $G_{H_2O_2}$, G_{red}, and G_{OH}.

[B] and [A] to determine the calculated values of $G(H_2O_2)^{O_2}$ and $G(H_2O_2)^{H_2,O_2}$ listed in Table I. The measured and calculated values of $G(H_2O_2)^{O_2}$ are in good agreement, whereas those of $G(H_2O_2)^{H_2,O_2}$ are not in agreement. These results infer that each of the oxidizing radicals present in irradiated alkaline aerated water reacts in such a way as to ultimately destroy $\frac{1}{2}$ molecule of H_2O_2, whereas in solutions of H_2 and O_2 the fraction of the oxidizing radicals which reacts with H_2 to ultimately form $\frac{1}{2}$ molecule of H_2O_2 decreases from unity at neutral pH to a minimum at about pH 12 then increases at pH > 12 but does not return to unity. This abrupt change at pH $\sim$ 12 may be related to a difference in the reactivity of the dissociated and undissociated forms of H_2O_2 since the pK value for the dissociation of H_2O_2 is 11.75 (8).

A reaction mechanism in accordance with these observed results may be developed from a consideration of the following reactions and their respective rate constants.

$$H_2O \longrightarrow\!\!\!\!\!\sim\!\!\!\!\!\sim\!\!\!\!\!\sim

[12] $O_3^- + H_2O_2 \rightarrow O_2^- + O_2 + H_2O$

[12a] $O_3^- + HO_2^- \rightarrow O_2^- + O_2 + OH^-$

[13] $O_3^- + H_2 \rightarrow O_2 + OH^- + H$ or $O_2^- + H_2O$

[14] $O_2^- + O_2^- + 2H_2O \rightarrow H_2O_2 + 2OH^-$ $\quad k_{14} = 1.7 \times 10^7$ (14)

Many of the above reactions are accepted in the mechanism for the radiolysis of neutral water. However, reactions [4] and [8] to [13] can occur only in basic solutions. Reaction [4] has been demonstrated by Matheson and Rabani (12), and Adams, Boag, and Michael (15) have presented evidence for [8]. The rate constant for reaction [10] has been determined from the optical absorption of the O_3^- (13) species but very little is known about its reactivity. The only demonstrated reaction is the oxidation of ferrocyanide (15).

In aerated solutions for initial yields, reactions [1] and [3] will predominate over [2] and [5] and each reducing radical will result in the formation of $\frac{1}{2}$ molecule of H_2O_2 either via [1] and [14], [3] and [14], or [4], [1], and [14]. Reactions [6], [9], and [13] will be negligible and each oxidizing radical will result in the destruction of $\frac{1}{2}$ molecule of H_2O_2 either directly by [7] or through [8] followed by either [11] or [10] and [12]. Hence

$$G(H_2O_2)^{O_2} = G_{H_2O_2} + \tfrac{1}{2}G_{red} - \tfrac{1}{2}G_{OH}.$$

In solutions containing both H_2 and O_2, each reducing radical will again react to ultimately form $\frac{1}{2}$ molecule of H_2O_2. For initial yields, reactions [7] and [11] will be negligible and H_2 and OH^- will compete for OH radicals in reactions [6] and [8]. There will also be a competition between H_2 and O_2 for O^- radicals in reactions [9] and [10] and between H_2O_2 and H_2 for O_3^- radicals in [12] and [13]. Assuming this reaction scheme

$$G(H_2O_2)^{H_2,O_2} = G_{H_2O_2} + \tfrac{1}{2}G_{red} + \tfrac{1}{2}G_{OH} - \frac{G_{OH}}{(1 + (k_6[H_2]/k_8[OH^-]))(1 + (k_9[H_2]/k_{10}[O_2]))(1 + (k_{13}[H_2]/k_{12}[H_2O_2]))}$$

$$[D] \quad \Delta G(H_2O_2) = G(H_2O_2)^{H_2,O_2} - G(H_2O_2)^{O_2} = G_{OH}\left(1 - \frac{G_{OH}}{(1 + (k_6[H_2]/k_8[OH^-]))(1 + (k_9[H_2]/k_{10}[O_2]))(1 + (k_{13}[H_2]/k_{12}[H_2O_2]))}\right).$$

At neutral pH, $k_6[H_2]/k_8[OH^-]$ is very large and the expression reduces to $\Delta G(H_2O_2) = G_{OH}$.

At pH > 12, $k_6[H_2]/k_8[OH^-]$ is negligibly small and as the pK value for the dissociation of H_2O_2 is 11.75 (8), reaction [12a] replaces [12]. Substitution in [D] of the appropriate values from Table I for solutions of pH 12.85 along with the literature values for the rate constants k_9 and k_{10} and Hayon's value (7) of $G_{OH} = 2.72$ at pH 12.90 gives $k_{13}[H_2]/k_{12a}[H_2O_2] = 1.52$. A similar calculation with literature values for k_6, k_8, k_9, and k_{10}, experimental results at pH 10.60, and Hayon's $G_{OH} = 2.27$ at this pH gives $k_{13}[H_2]/k_{12}[H_2O_2] = 0.62$. Thus $k_{12}/k_{12a} = 2.45$.

During an investigation of transient species in irradiated alkaline oxygenated solutions, Dorfman (14) observed a dependence on pH of the half-life of the transient absorption at 430 mμ due to O_3^-. The half-life increased from 0.4 ms at pH 11 to 2 ms at pH 13. On the assumption that the O_3^- disappeared by reaction with hydrogen peroxide, this observation supports our contention that the rate of reaction of O_3^- with H_2O_2 is greater than that with HO_2^- ($k_{12} > k_{12a}$).

Can. J. Chem. Downloaded from www.nrcresearchpress.com by 210.87.254.5 on 09/05/12
For personal use only.

In the final column of Table I, the values of $\Delta G(H_2O_2)$ calculated with expression [D] using the G_{OH} figures of Hayon and $k_{13}[H_2]/k_{12}[H_2O_2] = 0.62$ for solutions of pH < 12 and $k_{13}[H_2]/k_{12a}[H_2O_2] = 1.52$ for solutions of pH > 12 are compared with the measured values. Differences between the two throughout the entire alkaline pH range are never greater than 10% except at pH 12.10 where the experimental value lies between the two calculated values of 0.99, assuming $k_{13}[H_2]/k_{12}[H_2O_2] = 0.62$, and 1.50, assuming $k_{13}[H_2]/k_{12a}[H_2O_2] = 1.52$. Since the experimental error in measuring $G(H_2O_2)^{H_2,O_2}$ or $G(H_2O_2)^{O_2}$ at a given pH is about $\pm 5\%$, the proposed mechanism fits the data reasonably well.

One reaction that might be questioned is

$$O_3^- + H_2 \rightarrow O_2 + OH^- + H.$$

If this does not occur, only O^- can react with H_2 at pH > 12 and the high yield of $G(H_2O_2)^{H_2,O_2}$ will require k_9/k_{10} to be approximately 2 instead of the value 0.0308 derived from rate constants appearing in the literature. Also $G(H_2O_2)^{H_2,O_2}$ will be more dependent on $[H_2]/[O_2]$ than is indicated by the experimental results. In most alkaline systems the formation of O_3^- can be suppressed by employing a solute concentration much greater than the oxygen concentration. The low solubility of hydrogen prevented this in the present investigation.

The observed effects of increasing pH on $G(H_2O_2)^{H_2,O_2}$ may also be explained by postulating the presence in irradiated H_2O of an additional oxidizing species, X, different from OH. This proposed radical, first suggested by Allen (3), would have to react much less readily with H_2 than with H_2O_2. If such a species were present, reaction [13] could be replaced by

$$X + H_2 \rightarrow H + HX$$

and all O_3^- radicals could be assumed to react with H_2O_2 or its precursors. The increase in $G(H_2O_2)^{H_2,O_2}$ at pH > 12 might then be explained by assuming $k_{X+H_2O_2} > k_{X+HO_2^-}$.

Since there is no direct evidence for the presence of radical X in irradiated water, we prefer to base the mechanism on reactions of known species.

ACKNOWLEDGMENT

The author wishes to thank Mr. W. G. Humphreys for valuable technical assistance and Drs. P. J. Dyne and A. W. Boyd for helpful discussions.

REFERENCES

1. C. J. HOCHANADEL. J. Phys. Chem. **56**, 587 (1952).
2. A. O. ALLEN and R. A. HOLROYD. J. Am. Chem. Soc. **77**, 5852 (1955).
3. A. O. ALLEN. Radiation Res. Suppl. **4**, 54 (1964).
4. W. A. ARMSTRONG and W. G. HUMPHRIES. Can. J. Chem. **43**, 2576 (1965).
5. C. J. HOCHANADEL. Radiation Res. **17**, 286 (1962).
6. C. J. HOCHANADEL. J. Phys. Chem. **56**, 587 (1952).
7. E. HAYON. Trans. Faraday Soc. **61**, 734 (1965).
8. M. EVANS and N. URI. Trans. Faraday Soc. **45**, 244 (1949).
9. M. S. MATHESON. Radiation Res. Suppl. **4**, 1 (1964).
10. H. A. SCHWARZ. J. Phys. Chem. **62**, 255 (1962).
11. J. K. THOMAS. Trans. Faraday Soc. **61**, 702 (1965).
12. M. S. MATHESON and J. RABANI. J. Phys. Chem. **69**, 1324 (1965).
13. G. E. ADAMS, J. W. BOAG, and B. D. MICHAEL. Nature, **205**, 898 (1965).
14. G. CZAPSKI and L. M. DORFMAN. J. Phys. Chem. **68**, 1169 (1964).
15. G. E. ADAMS, J. W. BOAG, and B. D. MICHAEL. Trans. Faraday Soc. **61**, 492 (1965).

Can. J. Chem. Downloaded from www.nrcresearchpress.com by 210.87.254.5 on 09/05/12
For personal use only.

Can. J. Chem. Downloaded from www.nrcresearchpress.com by 210.87.254.5 on 09/05/12
For personal use only.

INFRARED SPECTRA OF GeH_2Br_2 AND GeD_2Br_2

ALEXANDER L. BEACH AND JAMES E. GRIFFITHS

Earlier studies of the infrared spectra of GeH_2F_2, GeH_2Cl_2, and GeH_2Br_2 (1, 2) satisfactorily located all of the fundamental frequencies except $\nu_4(a_1)$, the symmetric GeX_2 bending mode. With the availability of samples of GeH_2Br_2 and GeD_2Br_2, synthesized for another purpose, it was convenient to observe their infrared spectra as a check on previous work and to locate ν_4 with certainty. In $(CH_3)_2GeBr_2$ and $(CD_3)_2GeBr_2$ the fundamentals analogous to ν_4 occur at 99 and 98 cm^{-1} respectively (3).

Dibromogermane-d_2 was prepared by the reaction of GeD_4 with bromine in a glass vacuum system (4). Increased yields of the dibromide at the expense of the monobromide were obtained by the addition of larger quantities of bromine to the reaction tube than is usual when high yields of GeD_3Br are desired. Purification of the dibromide was effected by fractional vaporization and condensation in the usual way (4). The corresponding hydrogen compound was made similarly. Spectra of GeD_2Br_2 and GeH_2Br_2 were recorded with Beckman IR-11 and IR-12 spectrophotometers (33 to 4 000 cm^{-1}) and liquid and gas phase samples were confined in cells fitted with KBr or high density polyethylene windows.

The instrument was calibrated to ± 0.2 cm^{-1} throughout with the spectra of HCl, DCl, HBr, DBr, CH_4, NH_3, CO_2, CO, and H_2O. Frequencies reported are as accurate as this except when bands are naturally broad and the determination of the band center becomes less definite. In such cases the band centers are probably accurate to ± 1 cm^{-1}.

TABLE I

Fundamental frequencies (cm^{-1}) of GeH_2Br_2 and GeD_2Br_2

No.	Species	Description	GeH_2Br_2	GeD_2Br_2
1	a_1	$GeH_2(D_2)$ stretch	2 121.5	1 521.9
2	a_1	$GeH_2(D_2)$ bend	847.8	607.1
3	a_1	$GeBr_2$ stretch	298.3	297.2
4	a_1	$GeBr_2$ bend	104*	104*
5	a_2	Torsion	—	—
6	b_1	$GeH_2(D_2)$ stretch	2 138.3	1 543.0
7	b_1	$GeH_2(D_2)$ rock	491.8	362.6
8	b_2	$GeH_2(D_2)$ wag	756.8	543.1
9	b_2	$GeBr_2$ stretch	324.3	320.0

*Liquid state values.

Arguments favoring particular assignments in terms of a C_{2v} structure have been given previously (1, 2) and need not be repeated here. The results are summarized in Table I where frequency shifts clearly identify fundamentals associated with hydrogen or deuterium motions and the absence of significant changes in frequency confirm assignments of the $GeBr_2$ modes. The value for ν_4 is for the liquid. Product rule ratios, based upon reasonable structural parameters r(Ge—H) = 1.52 Å, r(Ge—Br) = 2.30 Å and

tetrahedral angles (5, and references therein), for $a_1 = 0.51$ (calcd. 0.50), $b_1 = 0.52$ (calcd. 0.51), and $b_2 = 0.71$ (calcd. 0.71) species agree satisfactorily with the calculated values.

In one sample sufficient $GeDBr_3$ was present to allow the measurement of the two Ge—Br_3 stretching fundamentals. These occur at $\nu_2(a_1) = 292.6$ and $\nu_5(e) = 316.4$ cm^{-1}.

1. T. N. Srivastava, J. E. Griffiths, and M. Onyszchuk. Can. J. Chem. **41**, 2101 (1963).
2. E. A. V. Ebsworth and A. G. Robiette. Spectrochim. Acta, **20**, 1639 (1964).
3. J. E. Griffiths. Unpublished results.
4. T. N. Srivastava, J. E. Griffiths, and M. Onyszchuk. Can. J. Chem. **40**, 739 (1962).
5. J. E. Griffiths, T. N. Srivastava, and M. Onyszchuk. Can. J. Chem. **40**, 579 (1962).

Received September 13, 1965.
Bell Telephone Laboratories, Incorporated,
Murray Hill, New Jersey.

Can. J. Chem. Downloaded from www.nrcresearchpress.com by 210.87.254.5 on 09/05/12
For personal use only.

DIMETHYLBERYLLIUM BIS(TRIMETHYLAMINE) AND DIMETHYLBERYLLIUM TETRAMETHYL-*o*-PHENYLENEDIAMINE

N. A. Bell and G. E. Coates

The ready formation of complexes in which one molecule of dimethylberyllium is coordinated to two molecules of pyridine or one of tetramethylethylenediamine (1), and the recent description (2) of the addition of a second molecule of trimethylamine at low temperature to the diethylberyllium–trimethylamine complex ($Et_2Be.NMe_3$) (3), prompted us to reexamine the reported nonexistence of dimethylberyllium bis(trimethylamine) (4).

Addition of successive quantities of trimethylamine to the solid 1:1 complex, $Me_2Be.NMe_3$, at 0° resulted in very slow reactions and the attainment of equilibrium required many hours. When an excess of trimethylamine was condensed on the 1:1 complex, and the excess removed in successive amounts, then equilibration occurred in 15–20 min. At 0° the pressure of amine fell until the composition of the condensed crystalline phase corresponded to a Be:N ratio of 1:2.03. Further removal of amine resulted in a steady amine pressure of 22.7 mm until the Be:N ratio became nearly 1:1. There was no evidence for a complex of composition $(Me_2Be)_2(NMe_3)_3$ described earlier (4). The results now reported are entirely consistent with the presence of two solid complexes, $Me_2Be.NMe_3$ and $Me_2Be(NMe_3)_2$. By repeating the above procedure at −9° and −4.5°, the dissociation pressure of the bis(trimethylamine) adduct was measured as 9.7 and 16.0 mm respectively. Dimethylberyllium bis(trimethylamine) melts sharply at 20° under 1 atm pressure of trimethylamine.

We also find that dimethylberyllium forms a complex, sufficiently stable to be purified by vacuum sublimation, with the chelating aromatic amine N,N,N′,N′-tetramethyl-*o*-phenylenediamine.

EXPERIMENTAL

Dimethylberyllium mono(trimethylamine) was prepared as described earlier (4), and after a tensimetric experiment the amount of beryllium complex was determined by hydrolysis and gas-volumetric measurement of methane by vacuum-line methods.

tetrahedral angles (5, and references therein), for $a_1 = 0.51$ (calcd. 0.50), $b_1 = 0.52$ (calcd. 0.51), and $b_2 = 0.71$ (calcd. 0.71) species agree satisfactorily with the calculated values.

In one sample sufficient $GeDBr_3$ was present to allow the measurement of the two Ge—Br_3 stretching fundamentals. These occur at $\nu_2(a_1) = 292.6$ and $\nu_5(e) = 316.4$ cm^{-1}.

1. T. N. Srivastava, J. E. Griffiths, and M. Onyszchuk. Can. J. Chem. **41**, 2101 (1963).
2. E. A. V. Ebsworth and A. G. Robiette. Spectrochim. Acta, **20**, 1639 (1964).
3. J. E. Griffiths. Unpublished results.
4. T. N. Srivastava, J. E. Griffiths, and M. Onyszchuk. Can. J. Chem. **40**, 739 (1962).
5. J. E. Griffiths, T. N. Srivastava, and M. Onyszchuk. Can. J. Chem. **40**, 579 (1962).

Received September 13, 1965.
Bell Telephone Laboratories, Incorporated,
Murray Hill, New Jersey.

Can. J. Chem. Downloaded from www.nrcresearchpress.com by 210.87.254.105 on 09/05/12
For personal use only.

DIMETHYLBERYLLIUM BIS(TRIMETHYLAMINE) AND DIMETHYLBERYLLIUM TETRAMETHYL-*o*-PHENYLENEDIAMINE

N. A. Bell and G. E. Coates

The ready formation of complexes in which one molecule of dimethylberyllium is coordinated to two molecules of pyridine or one of tetramethylethylenediamine (1), and the recent description (2) of the addition of a second molecule of trimethylamine at low temperature to the diethylberyllium–trimethylamine complex ($Et_2Be.NMe_3$) (3), prompted us to reexamine the reported nonexistence of dimethylberyllium bis(trimethylamine) (4).

Addition of successive quantities of trimethylamine to the solid 1:1 complex, $Me_2Be.NMe_3$, at 0° resulted in very slow reactions and the attainment of equilibrium required many hours. When an excess of trimethylamine was condensed on the 1:1 complex, and the excess removed in successive amounts, then equilibration occurred in 15–20 min. At 0° the pressure of amine fell until the composition of the condensed crystalline phase corresponded to a Be:N ratio of 1:2.03. Further removal of amine resulted in a steady amine pressure of 22.7 mm until the Be:N ratio became nearly 1:1. There was no evidence for a complex of composition $(Me_2Be)_2(NMe_3)_3$ described earlier (4). The results now reported are entirely consistent with the presence of two solid complexes, $Me_2Be.NMe_3$ and $Me_2Be(NMe_3)_2$. By repeating the above procedure at −9° and −4.5°, the dissociation pressure of the bis(trimethylamine) adduct was measured as 9.7 and 16.0 mm respectively. Dimethylberyllium bis(trimethylamine) melts sharply at 20° under 1 atm pressure of trimethylamine.

We also find that dimethylberyllium forms a complex, sufficiently stable to be purified by vacuum sublimation, with the chelating aromatic amine N,N,N′,N′-tetramethyl-*o*-phenylenediamine.

EXPERIMENTAL

Dimethylberyllium mono(trimethylamine) was prepared as described earlier (4), and after a tensimetric experiment the amount of beryllium complex was determined by hydrolysis and gas-volumetric measurement of methane by vacuum-line methods.

The Dimethylberyllium N,N,N',N'-Tetramethyl-o-phenylenediamine Complex

The diamine (2.0 g, 0.012 mole) was added to 10 cc of a 0.929 *M* solution of dimethylberyllium (0.0093 mole) in diethyl ether, resulting in a perceptibly exothermic reaction. Solvent was removed by evaporation and colorless crystals appeared when the solution had become concentrated. The complex was separated by removal of all the solvent under reduced pressure, and was purified by sublimation at 80–90° and 10^{-2} mm (m.p. 103–104° in a sealed tube). Hydrolysis of a sample followed by measurement of evolved methane and determination of beryllium gave results in agreement with the formula $C_{12}H_{22}BeN_2$.

Anal. Calcd.: Be, 4.42; hydrolyzable methyl, 14.8. Found: Be, 4.52, 4.29; hydrolyzable methyl, 14.6.

The molecular weight, determined cryoscopically in 0.42, 0.65, and 0.92 wt. % benzene solution, was 206, 211, and 215 respectively, corresponding to degrees of association of 1.01, 1.03, and 1.05.

ACKNOWLEDGMENT

The authors wish to thank Mr. T. Caygill for experimental assistance. This work was supported by the Science Research Council.

1. G. E. Coates and S. I. E. Green. J. Chem. Soc. 3340 (1962).
2. F. M. Peters. J. Organometal. Chem. Amsterdam, **3**, 334 (1965).
3. N. A. Bell and G. E. Coates. J. Chem. Soc. 692 (1965).
4. G. E. Coates and N. D. Huck. J. Chem. Soc. 4501 (1952).

Received October 18, 1965.
Chemistry Department,
University of Durham,
Durham, England.

THE REACTION OF HEXAFLUOROACETONE WITH SILANOLS

A. F. Janzen and C. J. Willis

We have recently shown (1) that hexafluoroacetone will react readily with a variety of compounds containing Si—H bonds, the products being hexafluoroisopropoxysilanes containing the grouping Si—O—$CH(CF_3)_2$. These reactions proceed under radical conditions, and also, in the case of trimethylsilane, ionic conditions. It has also been reported (2) that similar addition of hexafluoroacetone occurs across Ge—H and Sn—H bonds.

We now find that a ready reaction occurs between hexafluoroacetone and silanols, e.g. with trimethylsilanol at 20°:

$$(CH_3)_3SiOH + (CF_3)_2CO \rightarrow (CH_3)_3SiOC(CF_3)_2OH.$$

The product, 2-trimethylsiloxy-hexafluoroisopropanol, is readily purified by distillation (b.p. 106° at 740 mm) and may be kept in a sealed tube at 20° with no sign of decomposition. This behavior may be contrasted with that of the corresponding products from the reaction of hexafluoroacetone with other hydroxylic compounds. With water, the adduct is the "hydrate", i.e. hexafluoropropane-2,2-diol (3). This is a hygroscopic solid, m.p. 44°, which even at 20° shows a slight equilibrium dissociation to give hexafluoroacetone. With alcohols, hexafluoroacetone reacts reversibly to give unstable hemiketals (4), which are difficult to purify and readily dissociate:

$$(CF_3)_2CO + ROH \rightleftharpoons (CF_3)_2C\begin{matrix}\diagup OH \\ \diagdown OR\end{matrix}$$

where R = CH_3 or C_2H_5.

Can. J. Chem. Downloaded from www.nrcresearchpress.com by 210.87.254.105 on 09/05/12
For personal use only.

The Dimethylberyllium N,N,N',N'-Tetramethyl-o-phenylenediamine Complex

The diamine (2.0 g, 0.012 mole) was added to 10 cc of a 0.929 *M* solution of dimethylberyllium (0.0093 mole) in diethyl ether, resulting in a perceptibly exothermic reaction. Solvent was removed by evaporation and colorless crystals appeared when the solution had become concentrated. The complex was separated by removal of all the solvent under reduced pressure, and was purified by sublimation at 80–90° and 10^{-2} mm (m.p. 103–104° in a sealed tube). Hydrolysis of a sample followed by measurement of evolved methane and determination of beryllium gave results in agreement with the formula $C_{12}H_{22}BeN_2$.

Anal. Calcd.: Be, 4.42; hydrolyzable methyl, 14.8. Found: Be, 4.52, 4.29; hydrolyzable methyl, 14.6.

The molecular weight, determined cryoscopically in 0.42, 0.65, and 0.92 wt. % benzene solution, was 206, 211, and 215 respectively, corresponding to degrees of association of 1.01, 1.03, and 1.05.

ACKNOWLEDGMENT

The authors wish to thank Mr. T. Caygill for experimental assistance. This work was supported by the Science Research Council.

1. G. E. Coates and S. I. E. Green. J. Chem. Soc. 3340 (1962).
2. F. M. Peters. J. Organometal. Chem. Amsterdam, **3**, 334 (1965).
3. N. A. Bell and G. E. Coates. J. Chem. Soc. 692 (1965).
4. G. E. Coates and N. D. Huck. J. Chem. Soc. 4501 (1952).

Received October 18, 1965.
Chemistry Department,
University of Durham,
Durham, England.

THE REACTION OF HEXAFLUOROACETONE WITH SILANOLS

A. F. Janzen and C. J. Willis

We have recently shown (1) that hexafluoroacetone will react readily with a variety of compounds containing Si—H bonds, the products being hexafluoroisopropoxysilanes containing the grouping Si—O—$CH(CF_3)_2$. These reactions proceed under radical conditions, and also, in the case of trimethylsilane, ionic conditions. It has also been reported (2) that similar addition of hexafluoroacetone occurs across Ge—H and Sn—H bonds.

We now find that a ready reaction occurs between hexafluoroacetone and silanols, e.g. with trimethylsilanol at 20°:

$$(CH_3)_3SiOH + (CF_3)_2CO \rightarrow (CH_3)_3SiOC(CF_3)_2OH.$$

The product, 2-trimethylsiloxy-hexafluoroisopropanol, is readily purified by distillation (b.p. 106° at 740 mm) and may be kept in a sealed tube at 20° with no sign of decomposition. This behavior may be contrasted with that of the corresponding products from the reaction of hexafluoroacetone with other hydroxylic compounds. With water, the adduct is the "hydrate", i.e. hexafluoropropane-2,2-diol (3). This is a hygroscopic solid, m.p. 44°, which even at 20° shows a slight equilibrium dissociation to give hexafluoroacetone. With alcohols, hexafluoroacetone reacts reversibly to give unstable hemiketals (4), which are difficult to purify and readily dissociate:

$$(CF_3)_2CO + ROH \rightleftharpoons (CF_3)_2C\begin{matrix}\diagup OH \\ \diagdown OR\end{matrix}$$

where R = CH_3 or C_2H_5.

Can. J. Chem. Downloaded from www.nrcresearchpress.com by 210.87.254.105 on 09/05/12
For personal use only.

The trimethylsilanol adduct, by contrast, shows no sign of dissociation, and infrared spectroscopic examination (vapor phase at 20°) shows no hexafluoroacetone to be present. Since p_π–d_π back bonding from oxygen to silicon is a well-recognized factor in the stabilization of siloxy compounds (5), it may be suggested that such an effect enhances the stability of the trimethylsilanol adduct over similar carbon compounds.

It was of interest to extend this reaction to silanediols, since a similar addition of two molecules of hexafluoroacetone should produce a bifunctional adduct, $R_2Si[OC(CF_3)_2OH]_2$, which might condense to give linear or cyclic compounds with the interesting chain structure $[—SiR_2—O—C(CF_3)_2—O—]_n$, given similar stability by p_π–d_π bonding.

Such systems appear to have received little study in the organosilicon field. Henglein and co-workers (6) have prepared compounds of structure $C_2H_5OSi(CH_3)_2[OCH_2OSi(CH_3)_2]_nOC_2H_5$, where n = 1–5, and report that they show fair stability to water and alkali. In later papers (7), they describe the preparation of compounds containing the grouping Si—O—CH(CCl_3)—O—Si and claim that the —CCl_3 group exerts a stabilizing influence on the Si—O—C bond.

We now find that hexafluoroacetone will react readily with diphenylsilanediol in a donor solvent, such as ether or glyme, at 20°. The molar combining ratio is slightly above the 2:1 ratio which would be in accordance with the formation of the product $(C_6H_5)_2Si[OC(CF_3)_2OH]_2$. Removal of the solvent cannot be completed, however, without the decomposition of the product to evolve hexafluoroacetone and deposit of a mixture of the cyclic compounds $[(C_6H_5)_2SiO]_3$ and $[(C_6H_5)_2SiO]_4$.

It is apparent, then, that, in spite of the added stability expected from the π-bonding described above, the system Si—O—$C(CF_3)_2$—O—Si is unstable with respect to hexafluoroacetone and the silyl oxide. Consistent with this, we have failed to prepare, by several routes, the compound $(CH_3)_3SiOC(CF_3)_2OSi(CH_3)_3$, the inevitable products being hexafluoroacetone and hexamethyldisiloxane. This instability may be ascribed to the formation of an intermediate involving coordination from an oxygen atom to a more distant, rather than adjacent, silicon atom, i.e.

$$\begin{array}{c}(CF_3)_2C—O\\ \quad\quad|\quad\quad|\\ —R_2Si—O\quad SiR_2—\end{array} \rightarrow \begin{array}{c}(CF_3)_2C—O\\ \quad\quad|\quad\quad|\\ —R_2Si—O\rightarrow SiR_2—\end{array} \rightarrow \begin{array}{c}(CF_3)_2C{=}O\\ \\ —R_2Si—O—SiR_2—\end{array}$$

EXPERIMENTAL

General techniques have been described previously (1).

Reaction of Hexafluoroacetone with Trimethylsilanol

Hexafluoroacetone (6.86 g, 41.3 mmole) was condensed onto trimethylsilanol (1.90 g, 21.1 mmole, prepared by the method of Sommer *et al.* (8)) in an evacuated reaction tube (100 ml). On sealing the tube and warming to 20° immediate reaction was apparent. Fractionation after 5 h at 20° gave unreacted hexafluoroacetone (3.69 g, 22.2 mmole) and 2-trimethylsiloxy-hexafluoroisopropanol (3.6 g, 14.1 mmole, b.p. 105–106° at 740 mm).

Anal. Calcd. for $C_6H_{10}F_6O_2Si$: C, 28.1; H, 3.93; F, 44.5. Found: C, 27.5; H, 4.4; F, 44.3.

Infrared spectroscopic examination (gas phase) showed absorptions at 3 600 cm^{-1} (O—H), 2 960 cm^{-1} (C—H), and strong absorption centered on 1 250 cm^{-1} (C—F). The proton nuclear magnetic resonance spectrum showed a broad singlet at 3.59 p.p.m. and a sharp singlet at 0.18 p.p.m. (at 60 Mc/s to low field of tetramethylsilane). The former is assigned to the hydroxylic proton, the broadening being due to coupling with the fluorine atoms to give an unresolved septet, and the latter peak is assigned to the methyl protons. Integrated peak areas support these assignments.

The compound showed no sign of change after it was stored in a sealed tube for 3 months.

Reaction of Hexafluoroacetone with Diphenylsilanediol

No reaction was found when the two substances were kept together at 20° for 24 h.

When hexafluoroacetone (1.45 g, 8.75 mmole) was condensed onto diphenysilanediol (0.32 g, 1.5 mmole) in glyme (3.3 g) in a reaction tube (100 ml), a reaction was apparent on warming to 20°. After it was kept at

Can. J. Chem. Downloaded from www.nrcresearchpress.com by 210.87.254.105 on 09/05/12
For personal use only.

20° for 20 h, excess hexafluoroacetone and the bulk of the glyme were removed, leaving a viscous liquid. The amount of hexafluoroacetone recovered (0.86 g, 5.15 mmole) showed that the molar reacting ratio, $(CF_3)_2CO$ to $(C_6H_5)_2Si(OH)_2$, was 2.3:1.

Infrared spectroscopic examination of the viscous liquid showed that it still contained glyme, with O—H and C—F absorptions also present. The remaining solvent was not removable under vacuum at 20°. On heating to 80°, rapid evolution of hexafluoroacetone occurred and a white residue remained. After recrystallization from acetone, the residue had m.p. 160° and an infrared spectrum consistent with a mixture of $[(C_6H_5)_2SiO]_3$ and $[(C_6H_5)_2SiO]_4$. It has been reported (9) that these two compounds give a eutectic with m.p. 164–165°.

When ether was used as a solvent instead of glyme, the reaction followed a similar course, with the viscous liquid decomposing to give hexafluoroacetone even at 20°.

ACKNOWLEDGMENTS

This work was supported in part by the Defence Research Board of Canada, grant number 7583-05. We also gratefully acknowledge award of an Ontario Graduate Fellowship (to A. F. J.).

1. A. F. JANZEN and C. J. WILLIS. Can. J. Chem. **43**, 3063 (1965).
2. W. R. CULLEN and G. E. STYAN. Inorg. Chem. **4**, 1437 (1965).
3. W. J. MIDDLETON and R. V. LINDSEY. J. Am. Chem. Soc. **86**, 4948 (1964).
4. I. L. KNUNYANTS, CH'EN CH'ING-YUN, and N. P. GAMBARYAN. Izv. Akad. Nauk SSSR Otd. Khim. Nauk, 686 (1960).
5. C. EABORN. Organosilicon compounds. Butterworths, London. 1960. p. 91.
6. F. A. HENGLEIN and P. SCHMULDER. Makromol. Chem. **13**, 53 (1954).
7. F. A. HENGLEIN and H. NIEBERGALL. Chemiker Ztg. **80**, 611 (1956). F. A. HENGLEIN and H. GRÄSER. Makromol. Chem. **26**, 236 (1958).
8. L. H. SOMMER, E. W. PIETRUSZA, and F. C. WHITMORE. J. Am. Chem. Soc. **68**, 2282 (1946).
9. J. F. HYDE *et al.* J. Am. Chem. Soc. **69**, 488 (1947).

RECEIVED NOVEMBER 29, 1965.
DEPARTMENT OF CHEMISTRY,
UNIVERSITY OF WESTERN ONTARIO,
LONDON, ONTARIO.

LA SOLUBILITÉ DANS LES MÉLANGES ÉTHER ÉTHYLIQUE – ACIDES INORGANIQUES DE CERTAINS SELS DE FER, COBALT ET MANGANÈSE

R. A. A. MUZZARELLI

INTRODUCTION

Les connaissances actuelles sur la solubilité des sels inorganiques dans l'éther éthylique sont très limitées. Il est pourtant bien connu que certains composés inorganiques y sont solubles, en particulier $LiAlH_4$, et y sont légèrement dissociés, bien que les sels minéraux soient beaucoup moins dissociés que les organo-magnésiens, par exemple.

Le chlorure ferrique dans ses différents états d'hydratation est très soluble dans l'éther éthylique et il a été étudié (1). Encore quelques chlorures comme $TiCl_4$, $SnCl_4$ et $SiCl_4$ ont été l'objet d'études (2) et aussi on a noté que dans l'éther éthylique peuvent exister des complexes tels que $HFeCl_4$, $HSbCl_6$, H_2SnCl_6, qui sont des acides forts.

Mais les sels les plus intéressants du point de vue de la technologie moderne, capables de se dissoudre dans l'éther, sont les nitrates de thorium et d'uranyle. Ces nitrates représentent les sels qu'on obtient quand on veut mettre en solution le thorium ou l'uranium métalliques: les deux passent en solution facilement par réaction avec HNO_3 sous reflux.

Can. J. Chem. Downloaded from www.nrcresearchpress.com by 210.87.254.105 on 09/05/12
For personal use only.

20° for 20 h, excess hexafluoroacetone and the bulk of the glyme were removed, leaving a viscous liquid. The amount of hexafluoroacetone recovered (0.86 g, 5.15 mmole) showed that the molar reacting ratio, $(CF_3)_2CO$ to $(C_6H_5)_2Si(OH)_2$, was 2.3:1.

Infrared spectroscopic examination of the viscous liquid showed that it still contained glyme, with O—H and C—F absorptions also present. The remaining solvent was not removable under vacuum at 20°. On heating to 80°, rapid evolution of hexafluoroacetone occurred and a white residue remained. After recrystallization from acetone, the residue had m.p. 160° and an infrared spectrum consistent with a mixture of $[(C_6H_5)_2SiO]_3$ and $[(C_6H_5)_2SiO]_4$. It has been reported (9) that these two compounds give a eutectic with m.p. 164–165°.

When ether was used as a solvent instead of glyme, the reaction followed a similar course, with the viscous liquid decomposing to give hexafluoroacetone even at 20°.

ACKNOWLEDGMENTS

This work was supported in part by the Defence Research Board of Canada, grant number 7583-05. We also gratefully acknowledge award of an Ontario Graduate Fellowship (to A. F. J.).

1. A. F. JANZEN and C. J. WILLIS. Can. J. Chem. **43**, 3063 (1965).
2. W. R. CULLEN and G. E. STYAN. Inorg. Chem. **4**, 1437 (1965).
3. W. J. MIDDLETON and R. V. LINDSEY. J. Am. Chem. Soc. **86**, 4948 (1964).
4. I. L. KNUNYANTS, CH'EN CH'ING-YUN, and N. P. GAMBARYAN. Izv. Akad. Nauk SSSR Otd. Khim. Nauk, 686 (1960).
5. C. EABORN. Organosilicon compounds. Butterworths, London. 1960. p. 91.
6. F. A. HENGLEIN and P. SCHMULDER. Makromol. Chem. **13**, 53 (1954).
7. F. A. HENGLEIN and H. NIEBERGALL. Chemiker Ztg. **80**, 611 (1956). F. A. HENGLEIN and H. GRÄSER. Makromol. Chem. **26**, 236 (1958).
8. L. H. SOMMER, E. W. PIETRUSZA, and F. C. WHITMORE. J. Am. Chem. Soc. **68**, 2282 (1946).
9. J. F. HYDE *et al.* J. Am. Chem. Soc. **69**, 488 (1947).

RECEIVED NOVEMBER 29, 1965.
DEPARTMENT OF CHEMISTRY,
UNIVERSITY OF WESTERN ONTARIO,
LONDON, ONTARIO.

LA SOLUBILITÉ DANS LES MÉLANGES ÉTHER ÉTHYLIQUE – ACIDES INORGANIQUES DE CERTAINS SELS DE FER, COBALT ET MANGANÈSE

R. A. A. MUZZARELLI

INTRODUCTION

Les connaissances actuelles sur la solubilité des sels inorganiques dans l'éther éthylique sont très limitées. Il est pourtant bien connu que certains composés inorganiques y sont solubles, en particulier $LiAlH_4$, et y sont légèrement dissociés, bien que les sels minéraux soient beaucoup moins dissociés que les organo-magnésiens, par exemple.

Le chlorure ferrique dans ses différents états d'hydratation est très soluble dans l'éther éthylique et il a été étudié (1). Encore quelques chlorures comme $TiCl_4$, $SnCl_4$ et $SiCl_4$ ont été l'objet d'études (2) et aussi on a noté que dans l'éther éthylique peuvent exister des complexes tels que $HFeCl_4$, $HSbCl_6$, H_2SnCl_6, qui sont des acides forts.

Mais les sels les plus intéressants du point de vue de la technologie moderne, capables de se dissoudre dans l'éther, sont les nitrates de thorium et d'uranyle. Ces nitrates représentent les sels qu'on obtient quand on veut mettre en solution le thorium ou l'uranium métalliques: les deux passent en solution facilement par réaction avec HNO_3 sous reflux.

Can. J. Chem. Downloaded from www.nrcresearchpress.com by 210.87.254.40 on 09/05/12
For personal use only.

Il faut rappeler que l'éther éthylique a été un des cinq solvants considérés pour le projet d'extraction "Butex", et qu'il a été écarté car il ne donnait pas une satisfaisante séparation de l'uranium de ses impuretés (3). Or, il semble que cette même propriété de l'éther, de pouvoir dissoudre les sels de nombreux métaux, peut être mise à profit. Par exemple, une solution de 50 g de nitrate d'uranyle dans 95 cc d'éther éthylique a été soumise à chromatographie sur colonne de cellulose (4, 5), et il a été possible de séparer l'uranium des traces des lanthanides et de 15 autres métaux, tous retenus sur la cellulose.

Ces solutions de nitrate d'uranyle dans l'éther sont convenables pour la chromatographie sur cellulose, car la poudre de cellulose ne se gonfle pas en contact avec l'éther, à différence de ce qu'elle fait avec les solutions aqueuses; il est aussi très facile de récupérer le sel d'uranium. Le fait que le nitrate d'uranyle, à différence des autres nitrates, ne soit pas retenu sur la cellulose est expliqué par l'hypothèse que il est capable de se complexer à $UO_2(NO_3)_4^{2-}$ (6).

Les études citées offrent les perspectives suivantes:

(*a*) Les métaux contenus dans l'uranium comme impuretés doivent posséder eux aussi une bien que limitée solubilité dans l'éther. Il serait intéressant d'établir quelles sont ces limites de solubilité, soit pour prévoir s'il est possible de purifier par la méthode chromatographique un échantillon d'uranium à haute téneur d'impuretés, soit pour expliquer pourquoi les différents métaux forment dans la colonne des bandes à niveaux différents (5).

(*b*) Les connaissances en fait de solubilité pourraient orienter pour le choix des conditions favorables à la séparation des traces métalliques d'entre elles-mêmes par chromatographie de précipitation sur couche mince ou sur papier.

Les sels considérés dans cette étude ont été choisis à titre d'exemple. On a tenu compte de l'intérêt qu'on a, à l'heure actuelle, à purifier des mélanges de fluorures (7, 8), spécialement provenant des réacteurs nucléaires à sels fondus. La possibilité de mettre en solution les fluorures dans l'éther serait mise à profit dans les projets de chromatographie.

PARTIE EXPÉRIMENTALE

Ont été utilisés les solvants et les produits de degré analytique.

Solvants.—Les solvants étaient: acide nitrique fumant 98% (Canlab); fluorure d'hydrogène gazeux 100% (Matheson) et éther éthylique anhydre (Fisher).

Sels.—Les sels étaient: nitrate cobalteux hexahydrate; chlorure cobalteux hexahydrate; fluorure cobalteux anhydre; nitrate ferrique ennéahydrate; chlorure ferrique hexahydrate; fluorure ferrique anhydre; chlorure manganeux tetrahydrate et fluorure manganeux anhydre.

Solutions de ^{60}Co, ^{59}Fe et ^{54}Mn

Le cobalt-60, et le fer-59, ont été fournis par Atomic Energy of Canada Ltd., sous forme de fils métalliques, et chacun a été mis en solution dans la quantité indispensable de HNO_3 5 *N*, et porté à volume avec HNO_3 concentré.

Le manganèse-54 a été fourni par l'Oak Ridge National Laboratory, sous forme de solution de $MnCl_2$ en HCl 5 *N*. Cette solution a été diluée 1:10 avec HNO_3 concentré.

Préparation des solutions

Le fluorure d'hydrogène gazeux a été condensé, et mesuré avec des pipettes en polypropylène. Généralement la quantité prévue de fluorure d'hydrogène ou d'acide nitrique a été diluée à 50 cc avec l'éther éthylique, et un poids de sel, variant entre 1 g et 0.5 g, a été ajouté. Quelques microlitres de solution de métal radioactif ont été introduits dans la solution. Les solutions ont été tenues en agitation pendant 18 h, en thermostat à 29 °C. La phase solide a été toujours présente.

Vingt centimètres cubes de solution, après centrifugation, ont été prélevés et leur activité gamma a été enregistrée immédiatement. Les récipients en polypropylène ont été largement employés à toutes les étapes.

Mesures de radioactivité

Les bouteilles en polypropylène contenant la solution à mesurer ont été déposées sur un cristal de NaI, couplé électroniquement au spectromètre de rayonnements gamma à 128 canaux.

Les hauteurs des pics de 1.173 MeV, 0.835 MeV et 1.097 MeV respectivement pour ^{60}Co, ^{54}Mn et ^{59}Fe ont été mesurées et comparées avec celles des solutions étalons. Le rapport entre la quantité du sel utilisé et la

Can. J. Chem. Downloaded from www.nrcresearchpress.com by 210.87.254.40 on 09/05/12
For personal use only.

radioactivité qui la représente est le même pour la quantité inconnue de sel en solution et la radioactivité mesurée.

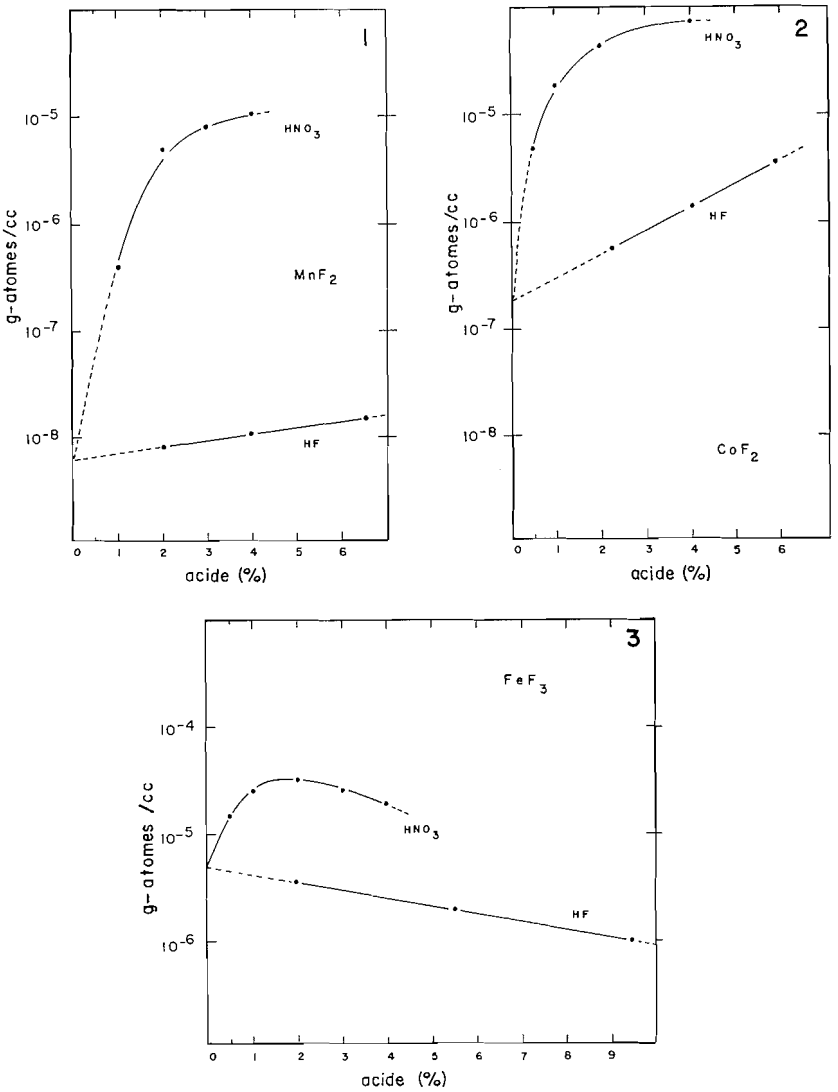
Evidemment, pour que le composé radioactif ajouté représentât tout le sel, ou en d'autres mots, pour que le sel utilisé fût homogènement radioactif, il a été nécessaire de permettre que les échanges isotopiques prissent place.

La précision des mesures, incluant toutes les erreurs expérimentales (principalement dues à la volatilité de l'éther), est environ de ±8%.

DISCUSSION DES RÉSULTATS

Solubilités dans l'éther éthylique

La mesure de la solubilité en éther éthylique saturé de sel a été obtenue pour chaque sel par extrapolation des deux courbes correspondantes aux solubilités dans les deux mélanges éther–HNO_3 et éther–HF (Figs. 1 à 7).



FIGS. 1–3. Les solubilités des fluorures de manganèse, de cobalt et de fer dans l'éther éthylique pur, l'éther–HNO_3 et l'éther–HF, à 29 °C. (Logarithme de g-atomes de métal, par cc.)

Can. J. Chem. Downloaded from www.nrcresearchpress.com by 210.87.254.40 on 09/05/12
For personal use only.

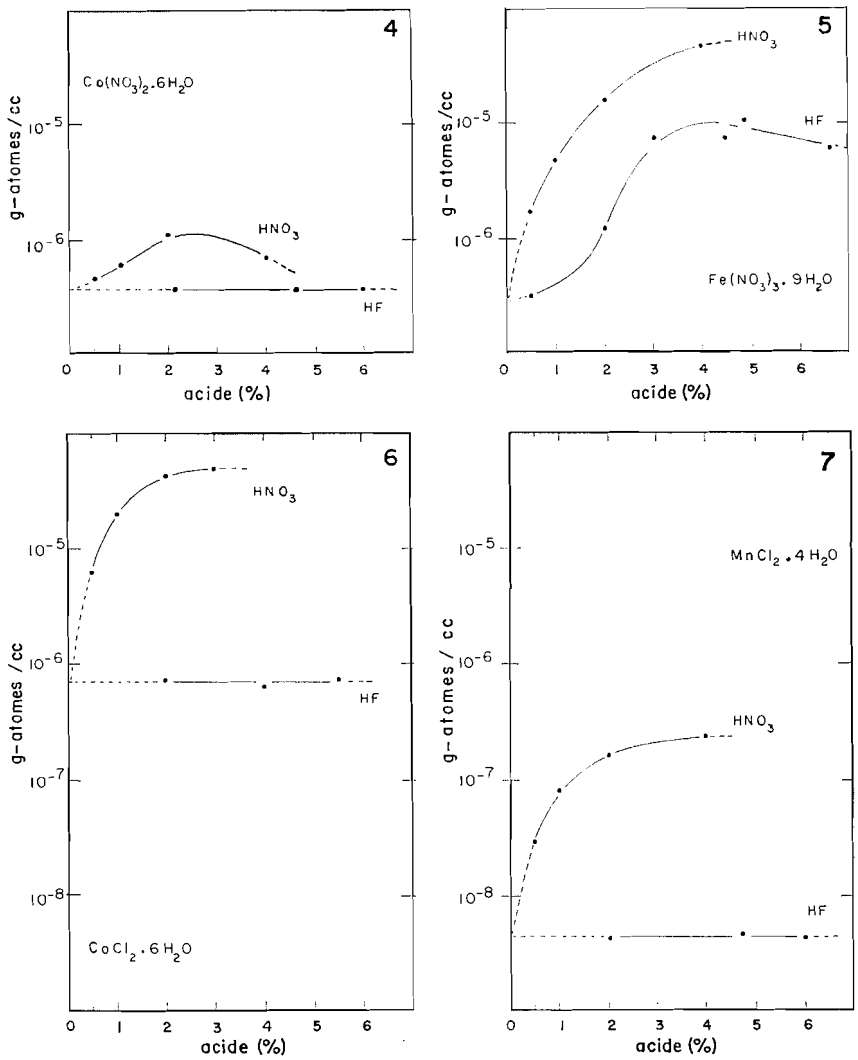
Can. J. Chem. Downloaded from www.nrcresearchpress.com by 210.87.254.40 on 09/05/12
For personal use only.

Puisque cette technique radiosotopique comporte l'introduction d'une quantité de sel radioactif dissous en HNO_3, il est clair que la mesure dans l'éther pur est impossible; l'extrapolation des deux courbes, d'ailleurs, donne une mesure assez précise et indique l'accord des résultats obtenus par deux voies différentes. L'extrapolation est aussi légitime, car la plupart des courbes sont des droites ou des branches de paraboles.

Les Figs. 1 et 7 montrent que les halogénures de manganèse sont moins solubles dans l'éther pur, que ceux des autres métaux. En général, on peut voir que les sels étudiés sont solubles dans l'éther, à un niveau suffisant pour permettre l'analyse et la chromatographie des traces des métaux en solution dans l'éther.

Solubilités dans les mélanges éther–HNO_3 et éther–HF

Les courbes qui illustrent les concentrations de métal dans la solution éther–HF, au varier du pourcent de HF, sont essentiellement des droites, avec l'exception remarquable



FIGS. 4–7. Les solubilités des nitrates et des chlorures de manganèse, de cobalt et de fer dans l'éther éthylique pur, l'éther–HNO_3 et l'éther–HF, à 29 °C. (Logarithme de g-atomes de métal, par cc.)

de la courbe du $Fe(NO_3)_3.9H_2O$ qui présente un point d'inflection. Il n'est pas possible de donner une explication de ce phénomène, mais les fluorures complexes qui se forment en solution aqueuse (9) se forment aussi dans l'éther (Figs. 1-3); et dans le cas illustré en Fig. 5, il se forme probablement un complexe particulièrement soluble.

Les courbes relatives aux mélanges éther–HNO_3 indiquent que les sels étudiés y sont beaucoup plus solubles que dans le mélange éther–HF, spécialement dans le cas du MnF_2 (Fig. 1). Généralement, à l'augmenter du pourcent de HNO_3, ces courbes montrent une nette et progressive augmentation de la concentration du métal.

Le mélange éther–HNO_3 est de mineure importance pour des teneurs en HNO_3 supérieures à 4%, étant donné qu'il devient un mélange explosif, du fait que des peroxides se forment. Mais aux faibles teneurs en HNO_3, ce mélange est de grand intérêt. D'autre part, en chromatographie sur cellulose, l'effet de l'acide nitrique sur la retention du cobalt de la part de plusieures celluloses a été trouvé négligeable (10).

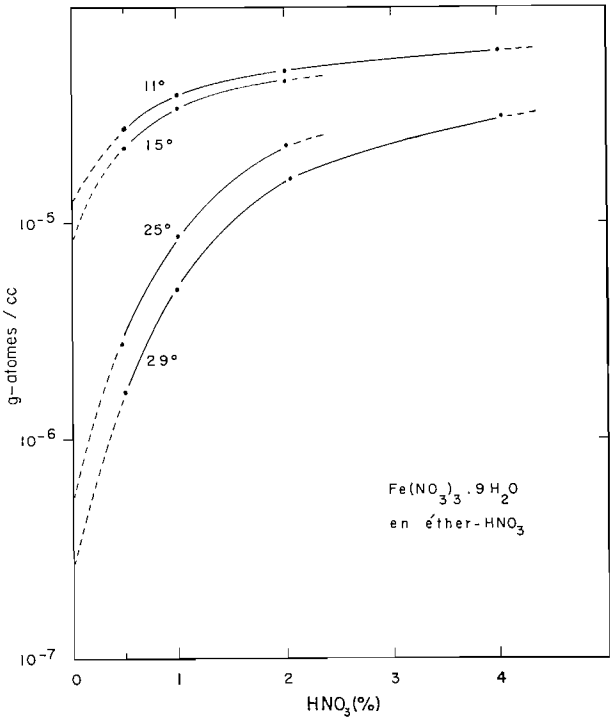


FIG. 8. La solubilité du nitrate ferrique ennéahydrate en éther éthylique pur et en éther–HNO_3, en fonction de la température. (Logarithme de g-atomes de métal, par cc.)

Variation de la solubilité en fonction de la température

La température a certainement un effet important sur la solubilité des sels dans l'éther.

Le nitrate ferrique ennéahydrate a été étudié en éther–HNO_3, et les résultats sont illustrés en Fig. 8.

CONCLUSIONS

Sur la base de ces résultats, il a été possible de séparer par chromatographie descendante les traces de chlorures de cobalt et manganèse d'avec microgrammes de chlorure ferrique (11).

Can. J. Chem. Downloaded from www.nrcresearchpress.com by 210.87.254.40 on 09/05/12
For personal use only.

En outre, si un échantillon d'uranium doit être analysé pour déterminer les traces de fer, de manganèse et de cobalt, et s'il est dissous en HNO_3, le nitrate d'uranyle cristallisé peut être facilement dissous dans l'éther–HNO_3, 2%. Compte tenu des résultats de cette étude, on pourra être sûrs que les traces des trois métaux passeront complètement en solution dans l'éther, pour une successive séparation chromatographique.

REMERCIEMENT

L'auteur remercie le Conseil National des Recherches du Canada pour la subvention accordée.

1. P. A. McCusker et S. M. S. Kennard. J. Am. Chem. Soc. **81**, 2976 (1959).
2. E. Wertyporoch et B. Altmann. Z. Physik. Chem. **1**, 168 (1934).
3. J. F. Flagg. Chemical processing of reactor fuels. Academic Press, New York. 1961.
4. Ch. A. Berthelot, S. Herrmann, K. F. Lauer et R. A. A. Muzzarelli. Communità Europea Energia Atomica, EUR 587, e (1964).
5. R. A. A. Muzzarelli et L. C. Bate. Talanta, **12** (9), 823 (1965).
6. C. Feldman et. J. Y. Ellenburg. Anal. Chem. **30**, 418 (1958).
7. E. A. Huff. Anal. Chem. **36**, 1921 (1964).
8. J. P. Faris. Anal. Chem. **32**, 521 (1960).
9. G. Goldstein. Anal. Chem. **36**, 243 (1964).
10. R. A. A. Muzzarelli. Talanta. Sous presse.
11. R. A. A. Muzzarelli. Microchem. J. Sous presse.

Reçu le 23 septembre 1965.
Faculté des Sciences,
Université de Sherbrooke,
Sherbrooke, Québec.

Can. J. Chem. Downloaded from www.nrcresearchpress.com by 210.87.254.40 on 09/05/12
For personal use only.

THE NUMERICAL ANALYSIS OF ELECTRON SPIN RESONANCE SPECTRA WITH HYPERFINE STRUCTURE[1]

R. Newton, K. F. Schulz, and R. M. Elofson

Numerical techniques have been devised that provide for the complete analysis of an electron spin resonance spectrum with any amount of hyperfine structure, provided the source material contains not more than two radicals.[2] These techniques depend primarily on the condition that each separate splitting constant has a symmetric effect on the spectrum, and their successful application depends equally on the accuracy with which this symmetry is recorded.

In the simplest case, a recorded spectrum of a single radical may be defined mathematically as $S(x)$, x being the magnetic intensity measured relative to the center of the spectrum. If the spectrum is known to have a splitting constant of value s and a corresponding spin of one half, then the definition of this splitting constant requires that the spectrum $S'(x)$, which is defined as the spectrum $S(x)$ with s removed, be related to $S(x)$ by:

$$[1] \qquad S(x) = S'(x + s) + S'(x - s).$$

[1]*Contribution No. 319, Research Council of Alberta, Edmonton, Alberta.*
[2]*A detailed account has been placed in the Depository of Unpublished Data. Photocopies may be obtained upon request to Depository of Unpublished Data, National Science Library, National Research Council, Ottawa, Canada.*

En outre, si un échantillon d'uranium doit être analysé pour déterminer les traces de fer, de manganèse et de cobalt, et s'il est dissous en HNO_3, le nitrate d'uranyle cristallisé peut être facilement dissous dans l'éther–HNO_3, 2%. Compte tenu des résultats de cette étude, on pourra être sûrs que les traces des trois métaux passeront complètement en solution dans l'éther, pour une successive séparation chromatographique.

REMERCIEMENT

L'auteur remercie le Conseil National des Recherches du Canada pour la subvention accordée.

1. P. A. McCusker et S. M. S. Kennard. J. Am. Chem. Soc. **81**, 2976 (1959).
2. E. Wertyporoch et B. Altmann. Z. Physik. Chem. **1**, 168 (1934).
3. J. F. Flagg. Chemical processing of reactor fuels. Academic Press, New York. 1961.
4. Ch. A. Berthelot, S. Herrmann, K. F. Lauer et R. A. A. Muzzarelli. Communità Europea Energia Atomica, EUR 587, e (1964).
5. R. A. A. Muzzarelli et L. C. Bate. Talanta, **12** (9), 823 (1965).
6. C. Feldman et. J. Y. Ellenburg. Anal. Chem. **30**, 418 (1958).
7. E. A. Huff. Anal. Chem. **36**, 1921 (1964).
8. J. P. Faris. Anal. Chem. **32**, 521 (1960).
9. G. Goldstein. Anal. Chem. **36**, 243 (1964).
10. R. A. A. Muzzarelli. Talanta. Sous presse.
11. R. A. A. Muzzarelli. Microchem. J. Sous presse.

Reçu le 23 septembre 1965.
Faculté des Sciences,
Université de Sherbrooke,
Sherbrooke, Québec.

Can. J. Chem. Downloaded from www.nrcresearchpress.com by 210.87.254.42 on 09/05/12
For personal use only.

THE NUMERICAL ANALYSIS OF ELECTRON SPIN RESONANCE SPECTRA WITH HYPERFINE STRUCTURE[1]

R. Newton, K. F. Schulz, and R. M. Elofson

Numerical techniques have been devised that provide for the complete analysis of an electron spin resonance spectrum with any amount of hyperfine structure, provided the source material contains not more than two radicals.[2] These techniques depend primarily on the condition that each separate splitting constant has a symmetric effect on the spectrum, and their successful application depends equally on the accuracy with which this symmetry is recorded.

In the simplest case, a recorded spectrum of a single radical may be defined mathematically as $S(x)$, x being the magnetic intensity measured relative to the center of the spectrum. If the spectrum is known to have a splitting constant of value s and a corresponding spin of one half, then the definition of this splitting constant requires that the spectrum $S'(x)$, which is defined as the spectrum $S(x)$ with s removed, be related to $S(x)$ by:

$$[1] \qquad S(x) = S'(x + s) + S'(x - s).$$

[1]*Contribution No. 319, Research Council of Alberta, Edmonton, Alberta.*
[2]*A detailed account has been placed in the Depository of Unpublished Data. Photocopies may be obtained upon request to Depository of Unpublished Data, National Science Library, National Research Council, Ottawa, Canada.*

By replacing x in this equation with $x + 2s$, $x + 4s$, etc. the following series of equations result:

$$[2] \qquad \begin{aligned} S(x + 2s) &= S'(x + 3s) + S'(x + s) \\ S(x + 4s) &= S'(x + 5s) + S'(x + 3s) \\ &\text{etc.} \end{aligned}$$

By alternately adding and subtracting these equations, all the terms on the right hand side disappear in the limit, except for the first.

$$[3] \qquad \text{i.e. } S(x) - S(x + 2s) + S(x + 4s) - \text{etc.} = S'(x - s)$$

By putting $x = s$ on the left of eq. [3] a function $F(s)$ is defined which is a valid function of s, regardless of whether s is an actual splitting constant of $S(x)$ or not.

$$[4] \qquad F(s) = S(s) - S(3s) + S(5s) - \text{etc.}$$

However, if s does take the value of one of the splitting constants then

$$[5] \qquad F(s) = S'(0) = 0$$

since $x = 0$ is the center of a validly defined spectrum $S'(x)$. This eq. [5] represents a necessary condition for a value of s to be valid as a splitting constant of $S(x)$.

The basic approach used above has been elaborated for all the conditions which might be encountered in an electron spin resonance spectrum. In addition, a suitable curve-fitting technique has been detailed that allows an analysis of the line shape function and a more accurate determination of the splitting constants, when they are known approximately.

These techniques have been applied to a series of methyl-anthrasemiquinone spectra (1) and the results are discussed relative to the analysis.

1. R. M. Elofson, B. E. Galbraith, K. F. Schultz, and R. Newton. Can. J. Chem. **43**, 1553 (1965).

Received December 14, 1965.
Research Council of Alberta,
Edmonton, Alberta.

THE ISOTROPIC ELECTRON PARAMAGNETIC RESONANCE SPECTRUM OF THE 1-HYDROXY-2,2,2-TRIFLUOROETHYL RADICAL[1]

P. Smith, J. T. Pearson,[2] and R. V. Tsina

Electron paramagnetic resonance (e.p.r.) spectral data for simple fluorinated alkyl radicals in solution are scarce, the only report on this topic having come to our attention after this present investigation had been completed (1). Consequently, this present investigation set out to obtain a well-resolved e.p.r. spectrum for the 1-hydroxy-2,2,2-trifluoroethyl radical, $CF_3\dot{C}HOH$, in aqueous solution by use of a recently developed flow technique (2, 3). In this technique hydroxyl radicals are generated within the cavity

[1]*This investigation was supported by United States Public Health Service grant GM 07653, Division of General Medical Sciences.*
[2]*Postdoctoral Research Associate, 1962–1964. Present address: Department of Chemistry, College of Technology, Huddersfield, England.*

Can. J. Chem. Downloaded from www.nrcresearchpress.com by 210.87.254.42 on 09/05/12
For personal use only.

By replacing x in this equation with $x + 2s$, $x + 4s$, etc. the following series of equations result:

$$[2] \qquad \begin{aligned} S(x + 2s) &= S'(x + 3s) + S'(x + s) \\ S(x + 4s) &= S'(x + 5s) + S'(x + 3s) \\ &\text{etc.} \end{aligned}$$

By alternately adding and subtracting these equations, all the terms on the right hand side disappear in the limit, except for the first.

$$[3] \qquad \text{i.e. } S(x) - S(x + 2s) + S(x + 4s) - \text{etc.} = S'(x - s)$$

By putting $x = s$ on the left of eq. [3] a function $F(s)$ is defined which is a valid function of s, regardless of whether s is an actual splitting constant of $S(x)$ or not.

$$[4] \qquad F(s) = S(s) - S(3s) + S(5s) - \text{etc.}$$

However, if s does take the value of one of the splitting constants then

$$[5] \qquad F(s) = S'(0) = 0$$

since $x = 0$ is the center of a validly defined spectrum $S'(x)$. This eq. [5] represents a necessary condition for a value of s to be valid as a splitting constant of $S(x)$.

The basic approach used above has been elaborated for all the conditions which might be encountered in an electron spin resonance spectrum. In addition, a suitable curve-fitting technique has been detailed that allows an analysis of the line shape function and a more accurate determination of the splitting constants, when they are known approximately.

These techniques have been applied to a series of methyl-anthrasemiquinone spectra (1) and the results are discussed relative to the analysis.

1. R. M. Elofson, B. E. Galbraith, K. F. Schultz, and R. Newton. Can. J. Chem. **43**, 1553 (1965).

Received December 14, 1965.
Research Council of Alberta,
Edmonton, Alberta.

THE ISOTROPIC ELECTRON PARAMAGNETIC RESONANCE SPECTRUM OF THE 1-HYDROXY-2,2,2-TRIFLUOROETHYL RADICAL[1]

P. Smith, J. T. Pearson,[2] and R. V. Tsina

Electron paramagnetic resonance (e.p.r.) spectral data for simple fluorinated alkyl radicals in solution are scarce, the only report on this topic having come to our attention after this present investigation had been completed (1). Consequently, this present investigation set out to obtain a well-resolved e.p.r. spectrum for the 1-hydroxy-2,2,2-trifluoroethyl radical, $CF_3\dot{C}HOH$, in aqueous solution by use of a recently developed flow technique (2, 3). In this technique hydroxyl radicals are generated within the cavity

[1]*This investigation was supported by United States Public Health Service grant GM 07653, Division of General Medical Sciences.*
[2]*Postdoctoral Research Associate, 1962–1964. Present address: Department of Chemistry, College of Technology, Huddersfield, England.*

Can. J. Chem. Downloaded from www.nrcresearchpress.com by 210.87.254.5 on 09/05/12
For personal use only.

of an e.p.r. spectrometer by the reduction of hydrogen peroxide with titanous ions in acidified aqueous solution. When an organic substrate is included in the reactant streams, it is attacked by the hydroxyl radicals to give products which can be detected by e.p.r. spectroscopy. 2,2,2-Trifluoroethanol, CF_3CH_2OH, was employed as the substrate and yielded a well-resolved e.p.r. spectral absorption of the form expected for the $CF_3\dot{C}HOH$ radical, i.e. a doublet of quartets resulting from coupling with the single CH proton and three equivalent CF_3–fluorine nuclei, respectively. In addition, each line of the quartets was split further into a narrow doublet. This narrow splitting is attributed to hyperfine interaction with the OH proton, a form of interaction which has been reported before for only a few organic radicals (4, 5). This spectrum is compared with that of the $CH_3\dot{C}HOH$ radical formed from ethanol under similar reaction conditions.

EXPERIMENTAL

The technique was essentially as before (2). The reactant streams were of line-distilled water 0.1 *M* in sulfuric acid (Baker and Adamson, chemically pure) and, respectively, 0.04 and 0.01 *M* in hydrogen peroxide (Becco, 98% w/w) and titanous chloride (Fisher, 20% w/w solution). The total flow rate was 5 ml s^{-1}, this being divided equally between the two streams. The reaction temperature was 27 ± 1 °C. Fresh samples of 2,2,2-trifluoroethanol (Halocarbon Products Co.) and ethanol (U.S. Industrial Chemical Co.) were used as substrates without further purification, since no impurities, except water, were detected by vapor-phase chromatography. The substrate was included in both reactant streams at the same concentration. When 2,2,2-trifluoroethanol was employed this concentration was 1 *M*, the value necessary for complete quenching of the absorption attributed to the hydroxyl radical. In the case of ethanol, a concentration of 0.1 *M* was easily enough for the signal of the hydroxyl radical to be suppressed. However, the concentration was varied over the range 0.1–1 *M*, no change being noticed in the results that were obtained. As before (2), spectra were recorded in the first-derivative form and all hyperfine coupling constants were measured against peroxylamine disulfonate as reference standard.

RESULTS AND DISCUSSION

A typical spectrum for 2,2,2-trifluoroethanol as substrate is shown in Fig. 1. The spectral structure is composed of 16 narrow lines, and is ascribed to the $CF_3\dot{C}HOH$ radical formed

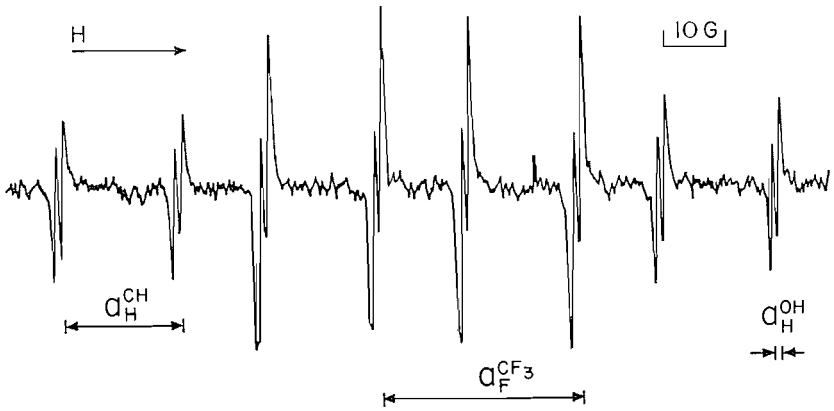


FIG. 1. First-derivative e.p.r. spectrum for the reaction of hydroxyl radicals with 2,2,2-trifluoroethanol (chart speed, 1 in. min^{-1}; time of scan, 10 min).

by the abstraction of a secondary hydrogen atom. These lines display the expected doublet (1:1) of quartets (1:3:3:1) arising from coupling with one CH proton and three CF_3–fluorine nuclei, respectively. However, each quartet is split further into a closely spaced doublet (1:1) which is attributed to coupling with the OH proton. This coupling

Can. J. Chem. Downloaded from www.nrcresearchpress.com by 210.87.254.5 on 09/05/12
For personal use only.

is reasonably interpreted by a resonance-stabilization mechanism similar to that proposed (3) to operate in the $\cdot CH_2OH$ radical, as shown in eq. [1].

[1] $$CF_3\dot{C}H\ddot{O}H \leftrightarrow CF_3\ddot{\dot{C}}H\dot{\ddot{O}}H$$

Support for this view is provided by the fact that a coupling with the OH proton of a similar size has been noticed for $\cdot CH_2OH$ (6–8) and for a number of related radicals where resonance stabilization of the above sort might be expected, e.g. $\cdot CH(COOH)OH$ (6, 9) and $\cdot CH(CN)OH$ (10). In the case of $CH_3\dot{C}HOH$, coupling with the OH proton has not definitely been reported so far (3, 8). This is perhaps not surprising in view of the probable electron-releasing character (11) of the CH_3 group with respect to radical stabilization by the resonance mechanism. Neverthless, for comparison purposes, ethanol was examined as substrate over a range of concentration, particular attention being directed to the detection of the possible presence of coupling with the OH proton in the $CH_3\dot{C}HOH$ radical. The spectral absorption that was produced was essentially as previously observed (3, 8), a doublet (1:1) of quartets (1:3:3:1) with no resolved doublet splitting arising from the OH proton. Table I summarizes all the spectral results that were obtained.

TABLE I

Hyperfine coupling constants for radicals formed by hydroxyl radical attack on 2,2,2-trifluoroethanol and ethanol*

Radical	Isotropic hyperfine coupling constants, G			
	a_H^{CH}	$a_H^{CH_3}$	$a_F^{CF_3}$	a_H^{OH}
$CF_3\dot{C}HOH$	18.1±0.4	—	31.8±0.6	1.17±0.28
$CH_3\dot{C}HOH$†	15.0±0.2	22.5±0.3	—	—‡

*Each coupling constant given is the arithmetical mean of all measurements of that coupling constant taken from several field scans. The cited precision index is the maximum absolute deviation from the arithmetic mean.

†In addition, there was a weak background absorption. Subsequent work has shown (8, 10) that this weak absorption can be made of comparable intensity to the signal from $CH_3\dot{C}HOH$ by decreasing the initial value of the ratio $[TiCl_3]/[H_2O_2]$ in the mixed streams while keeping the other reaction conditions unchanged; consequently, it is possible to identify this absorption as a triplet (1:2:1) of triplets (1:2:1) consistent with the radical $\cdot CH_2CH_2OH$.

‡Less than 0.3–0.4 G, the estimated resolution limit of the instrument.

The temperature dependence of the spectral data obtained with 2,2,2-trifluoroethanol was not investigated. The results from such a study might have some bearing on the possible contribution of hydrogen bonding between the OH proton and the CF_3 group similar to that now established to occur (12–16) in 2,2,2-trifluoroethanol itself. However, the occurrence of this kind of intramolecular hydrogen bonding in the $CF_3\dot{C}HOH$ radical would appear to be sterically less favored than in the CF_3CH_2OH molecule. This is because of the trigonal bond hybridization at the unsaturated carbon atom in the former compared with the tetrahedral bond hybridization at the 1-carbon atom in the latter.

Of particular concern is the result for the CF_3–fluorine coupling constant, $a_F^{CF_3}$, for which no directly comparable data appear to have been published before. Perhaps the most nearly comparable investigation reported so far is the single-crystal study of the radical $^-O_2C—CF_2—\dot{C}F—CO_2^-$ trapped in irradiated sodium perfluorosuccinate (17). For this radical the two CF_2–fluorine nuclei gave roughly equivalent coupling tensors, the isotropic components being equal to 34.6 and 40.3 G. These data are not greatly different from the value of 31.8 G for $a_F^{CF_3}$ in $CF_3\dot{C}HOH$ reported in Table I. Another pertinent investigation concerns perfluoroalkyl polymeric radicals of functional structure

Can. J. Chem. Downloaded from www.nrcresearchpress.com by 210.87.254.5 on 09/05/12
For personal use only.

$-CF_2-\dot{C}F-CF_2-$ trapped in irradiated, randomly oriented polytetrafluoroethylene (18).[3] For these radicals the observed value of $a_F^{CF_2}$ was 33 G (18), in reasonable agreement with the result of this present research. This agreement provides support for the claim by Rexroad and Gordy (18) that the CF_2–fluorine coupling for perfluoroalkyl polymeric radicals of the type they investigated appears to be predominantly isotropic in character. However, it should be emphasized that anisotropy is generally difficult to evaluate in randomly oriented samples such as those studied by Rexroad and Gordy. The fact that $a_F^{CF_3}$ ($CF_3\dot{C}HOH$) is so much larger than $a_H^{CH_3}$ ($CH_3\dot{C}HOH$) appears to be consistent with the powerful inductive effect ($-I$) of the CF_3 group relative to the $+I$ effect of the CH_3 group (11). Furthermore, it is in general agreement with the possibility of differences in the spin-delocalization mechanism operating in fluorocarbon radicals compared with that in hydrocarbon radicals (17, 20–22); for example, in the $CF_3\dot{C}HOH$ radical there is the likelihood of fluorine (2s) orbital mixing with the unsaturated-carbon (2p) orbital, whereas in the $CH_3\dot{C}HOH$ radical methyl-proton coupling is thought to arise via a hyperconjugative mechanism involving hydrogen (1s) orbitals and the unsaturated-carbon (2p) orbital.

That a a_H^{CH} is larger for $CF_3\dot{C}HOH$ than for $CH_3\dot{C}HOH$ is worth noting and may be another consequence of the factors discussed above in relation to the difference between $a_F^{CF_3}$ ($CF_3\dot{C}HOH$) and $a_H^{CH_3}$ ($CH_3\dot{C}HOH$). It might be mentioned that a part of the difference is presumably accountable on the basis of the expected (23) difference in excess charge density on the unsaturated carbon atom in the two radicals that were compared. Detailed consideration of these possibilities is hampered by the scarcity of e.p.r. data on comparable systems. Recently, Fischer (24) has developed a first-order treatment of substituent effects on the size of α-proton coupling constants in substituted simple alkyl radicals. For a similar reason, this approach is not readily extended to the $CF_3\dot{C}HOH$ radical at present. Moreover, it is likely that Fischer's approach would not be directly applicable here, inasmuch as both the CF_3 and OH groups are strongly inductive (11). Clearly, it would be interesting to have experimental data for other fluorinated aliphatic radicals.

The minimum concentrations of substrate needed to quench the signal of the hydroxyl radical under otherwise essentially identical reaction conditions are 1 and <0.1 M for 2,2,2-trifluoroethanol and ethanol, respectively. These results are somewhat preliminary, for the effect of changes in reaction conditions was not studied (8, 10). Nevertheless, the following qualitative comment may be made. The apparent difference in reactivity toward hydrogen atom abstraction at the 1 position is in line with the greater electron-withdrawing power of the CF_3 group compared with that of the CH_3 group (11) and the expected electrophilicity of hydroxyl radicals in reactions of this sort (6, 8, 10).

NOTE ADDED IN PROOF: After this present work was submitted for publication a pertinent paper (25) became available. This claims that the OH-proton splitting in the e.p.r. spectrum of the $\cdot CH_2OH$ radical under conditions similar to those employed in this present work is pH dependent as a consequence of OH-proton exchange. Similar spectral results for the $\cdot CH_2OH$ radical have recently been observed (10) in these laboratories as part of an already started investigation (8) which includes simple unsubstituted aliphatic alcohols; it might be noted that quantitative study of this phenomenon is complicated by the possibility of spectral-line broadening brought about by the presence of titanous ion.

[3]*It is relevant to add that results of size similar to those of Rexroad and Gordy (18) have been reported for irradiated samples of randomly oriented (19) and oriented (20) polytetrafluoroethylene.*

Can. J. Chem. Downloaded from www.nrcresearchpress.com by 210.87.254.5 on 09/05/12
For personal use only.

Consequently, the present work is being extended to cover a wider range of reaction conditions. It is hoped to report the resultant findings together with those arising from a current investigation of other fluorinated aliphatic substrates.

1. R. W. FESSENDEN and R. H. SCHULER. 150th Meeting of the American Chemical Society, Atlantic City, New Jersey, September 13–17, 1965. Abstr. p. 39V.
2. J. T. PEARSON, P. SMITH, and T. C. SMITH. Can. J. Chem. **42**, 2022 (1964).
3. W. T. DIXON and R. O. C. NORMAN. J. Chem. Soc. 3119 (1963).
4. G. P. RABOLD, K. H. BAR-ELI, and K. WEISS. Chem. Commun. 38 (1965).
5. G. P. RABOLD, K. H. BAR-ELI, E. REID, and K. WEISS. J. Chem. Phys. **42**, 2438 (1965).
6. W. T. DIXON, R. O. C. NORMAN, and A. L. BULEY. J. Chem. Soc. 3625 (1964).
7. L. H. PIETTE, G. BULOW, and K. LOEFFLER. Unpublished work.
8. P. SMITH, J. T. PEARSON, P. B. WOOD, and T. C. SMITH. J. Chem. Phys. **43**, 1535 (1965).
9. D. E. HENN and D. H. WHIFFEN. Mol. Phys. **8**, 407 (1964). G. C. MOULTON and H. T. CRENSHAW. Radiation Res. **25**, 139 (1965.)
10. J. C. BAILEY, J. T. PEARSON, P. SMITH, T. C. SMITH, R. V. TSINA, and P. B. WOOD. Unpublished work.
11. J. HINE. Physical organic chemistry. McGraw-Hill Book Co., Inc., New York. 1962. Chap. 4.
12. R. N. HASZELDINE. J. Chem. Soc. 1757 (1953).
13. L. M. MUKHERJEE and E. GRUNWALD. J. Phys. Chem. **62**, 1311 (1958).
14. C. G. CANNON and B. C. STACE. Spectrochim. Acta, **13**, 253 (1958).
15. M. OKI and H. IWAMURA. Bull. Chem. Soc. Japan, **35**, 1744 (1962).
16. P. J. KRUEGER and H. D. METTEE. Can. J. Chem. **42**, 340 (1964).
17. M. T. ROGERS and D. H. WHIFFEN. J. Chem. Phys. **40**, 2662 (1964).
18. H. N. REXROAD and W. GORDY. J. Chem. Phys. **30**, 399 (1959).
19. YA. S. LEBEDEV, YU. D. TSVETKOV, and V. V. VOEVODSKII. Opt. i Spektroskopiya, **8**, 811 (1960).
20. D. W. OVENALL. J. Chem. Phys. **38**, 2448 (1963).
21. D. R. EATON, A. D. JOSEY, W. D. PHILLIPS, and R. E. BENSON. Mol. Phys. **5**, 407 (1962).
22. D. J. E. INGRAM. Free radicals as studied by electron spin resonance. Butterworth Scientific Publications, London. 1958. Chap. 4.
23. J. P. COLPA and J. R. BOLTON. Mol. Phys. **6**, 273 (1963).
24. H. FISCHER. Z. Naturforsch. **20a**, 428 (1965).
25. H. FISCHER. Mol. Phys. **9**, 149 (1965).

RECEIVED AUGUST 23, 1965.
DEPARTMENT OF CHEMISTRY,
DUKE UNIVERSITY,
DURHAM, NORTH CAROLINA.

Can. J. Chem. Downloaded from www.nrcresearchpress.com by 210.87.254.5 on 09/05/12
For personal use only.

Can. J. Chem. Downloaded from www.nrcresearchpress.com by 210.87.254.40 on 09/05/12
For personal use only.

Canadian Journal of Chemistry

Issued by THE NATIONAL RESEARCH COUNCIL OF CANADA

VOLUME 44 APRIL 1, 1966 NUMBER 7

ORGANIC AND BIOLOGICAL SPECTROCHEMICAL STUDIES

XXII. THE INFRARED, ULTRAVIOLET, AND NUCLEAR MAGNETIC RESONANCE SPECTRA OF SOME SUBSTITUTED 2-INDANONES AND REFERENCE COMPOUNDS[1,2]

EMIL J. MORICONI AND JOHN P. ST. GEORGE[3]
Department of Chemistry, Fordham University, New York, New York

AND

W. F. FORBES
Department of Chemistry, University of Waterloo, Waterloo, Ontario

Received September 20, 1965

ABSTRACT

Infrared, ultraviolet, and nuclear magnetic resonance spectra of the following compounds are reported: 2-indanone (I), *trans*- and *cis*-hexahydro-2-indanone (V and XI), 1-chloro-2-indanone-1,3,3-d_3 (III), 1-bromo-2-indanone-1,3,3-d_3 (IV), 1-chloro-*trans*-hexahydro-2-indanone (VII), 1-bromo-*trans*-hexahydro-2-indanone (VIII), some deuterated forms of these compounds, 2-chlorocyclohexanone-2,6,6-d_3, and 2-bromocyclohexanone-2,6,6-d_3.

2-Indanone and *trans*-hexahydro-2-indanone each display two peaks in the carbonyl infrared region with intensity ratios of approximately 40:1. The origin of these doublets is discussed.

Nuclear magnetic resonance spectra were determined to indicate the presence or absence of ring mobility, and spin–spin coupling data were used to support some of the conclusions deduced from the infrared data for some of the compounds.

INTRODUCTION

It has previously been reported (see ref. 1 and references cited there) that film, solution, and KBr pellet infrared spectra of the 2-indanone ring system consistently gave a carbonyl doublet, whereas only one carbonyl frequency is reported for the 1-halo-2-indanones (2). To determine the origin of this doublet, we have re-investigated these spectra and prepared some appropriate α-substituted indanones. In addition, the ultraviolet and nuclear magnetic resonance (n.m.r.) spectra of these compounds are reported.

EXPERIMENTAL

Most of the infrared spectra were determined in replicate on a Perkin–Elmer model 21 spectrophotometer calibrated against atmospheric water vapor peaks at 1 784.95, 1 772.6, 1 768.17, and 1 756.82 cm^{-1} (25°), with a calcium fluoride prism at a computed spectral slit width (S') of 1.75 cm^{-1} in the carbonyl band region (3). The precision of the carbonyl band positions is estimated to range between 0.5 and 0.1 cm^{-1} depending on the symmetry of the peaks that are measured. The frequency accuracy of the ν^{I} values is believed to be better than ± 1 cm^{-1}, but the lower frequency ν^{II} peaks may be accurate to only ± 2 cm^{-1}

[1] *For part XXI in this series see A. Balasubramanian et al., Can. J. Chem., 43, 2603 (1965). Earlier papers in this series appeared under the general title "Light Absorption Studies".*

[2] *Contribution No. 739 from the Department of Chemistry, Fordham University.*

[3] *National Science Foundation Predoctorate Fellow, 1959–1962. Present address: Chemistry Department, Woodstock College, Woodstock, Maryland, U.S.A.*

Can. J. Chem. Downloaded from www.nrcresearchpress.com by 210.87.254.40 on 09/05/12
For personal use only.

because of overlapping with the stronger, higher frequency peaks. The integrated absorption intensities (mole^{-1} l cm^{-2} $\times$ 10^{-4}) were calculated from the equation (4)

$$A = \frac{2.303}{2cl} \pi \log_{10} (T_0/T)_{max} \times \Delta\nu_{\frac{1}{2}}^{a}.$$

The accuracy of the A values is estimated to be $\pm 5\%$. Solute concentrations were about 0.015 ± 0.002 mole/l. Base lines were determined by Wright's method (5). The cell thickness (0.548 mm) was determined from interference fringes. A Perkin–Elmer heated cell assembly (sodium chloride windows; Bodenseewerk, Germany) was used to obtain spectra of liquids at elevated temperatures.

Ultraviolet absorption spectra were determined by standard methods in 1 cm cells with a Cary model 15 spectrophotometer. The accuracy of the λ_{max} values is estimated to be ± 1 mμ, and the precision of the molar absorptivities $\pm 5\%$ or better. Most molar absorptivity values were reproducible to within $\pm 2\%$.

Nuclear magnetic resonance spectra were obtained in carbon tetrachloride solutions on a Varian A 60 model with tetramethylsilane as an internal standard. A microcell (Varian) was used for compounds which were available only in small amounts.

All solvents that were used were commercially available, spectroanalyzed solvents, redistilled when necessary. Chloroform was freed from its preservative by shaking it with concentrated sulfuric acid. After separation and filtration through soda lime and anhydrous sodium sulfate, the chloroform was distilled; a center fraction was used.

Some of the compounds were prepared and purified by standard methods, as described in the literature, or were commercially available. The remaining compounds were prepared as follows (melting and boiling points are corrected; elemental analyses by Schwarzkopf Microanalytical Laboratory, 56-19 37th Avenue, Woodside 77, New York; deuterium analyses by Mr. J. Nemeth, Department of Chemistry, University of Illinois, Urbana, Illinois).

2-Indanone-1,1,3,3-d_4 (II) was prepared by refluxing 2-indanone (I; 6.6 g) eight times for 4 h with 10 ml portions of D_2O (99.5%, Isomet Corp.). No basic catalyst was used since its presence was found to accelerate self-condensation. The product was purified by steam distillation (with D_2O), chromatographed from a 10 cm column of silica (Mallinckrodt, 100 mesh) with redistilled pentane (Eastman) containing 5% reagent grade anhydrous ether (Fisher), and finally crystallized from pentane to yield *2-indanone-1,1,3,3-d_4* (II; 2.2 g), m.p. 57.0–57.5 °C.

Anal. Calcd. for $C_9D_4H_4O$: D, 50.00 atom % excess D. Found: D, 49.05 atom %.

trans-Hexahydro-2-indanone-1,1,3,3-d_4 (VI) was prepared by refluxing *trans*-hexahydro-2-indanone (V; prepared by Hückel's method (6)) four times for 4 h with 10 ml portions of D_2O, each containing 15 mg of sodium carbonate. After extraction with peroxide-free anhydrous ether, the product was dried (Na_2SO_4), evaporated in vacuum to 2 ml, and chromatographed on a 19 mm (inside diameter) column of specially prepared silicic acid. (Mallinckrodt 100 mesh silicic acid (300 g) was washed five times with distilled water (3 l), the water being decanted after ca. 5 min settling. After filtration, this silicic acid was further washed with 95% ethanol and absolute ethanol and then heated for 2 days at 120 °C. To this was then added 3% D_2O, and the mixture was shaken for 24 h.) Elution with pentane containing 3% anhydrous ether and solvent removal gave *trans-hexahydro-2-indanone-1,1,3,3-d_4*, n_D^{25} 1.4741. The infrared spectrum showed complete α-deuteration in a freshly prepared sample (see Discussion).

1-Chloro-*trans*-hexahydro-2-indanone (VII) was prepared by direct chlorination at 0 °C of *trans*-hexahydro-2-indanone (V; 500 mg) in the presence of a small amount of water (3 ml) until a slight excess of the theoretical amount of chlorine that was necessary (257 mg) had been added. After extraction with peroxide-free ether, the products were dried (Na_2SO_4), reduced in volume, and chromatographed as previously described, but protected from light and heat as much as possible. Re-chromatography gave *1-chloro-trans-hexahydro-2-indanone* (VII; 25 mg), n_D^{25} 1.4998.

Anal. Calcd. for $C_9H_{13}OCl$: C, 62.6; H, 7.6; Cl, 20.5. Found: C, 62.6; H, 7.45; Cl, 20.7.

1-Bromo-*trans*-hexahydro-2-indanone (VIII) was prepared by direct bromination (bromine; 578 mg dissolved in methylene chloride; 10 ml) of *trans*-hexahydro-2-indanone (V; 500 mg) dissolved in methylene chloride (15 ml). Sunlight was usually necessary to initiate and to accelerate the reaction, and sometimes more concentrated solutions had to be used. After solvent removal under vacuum, the products were worked up as described for the chloro compound, but in addition all processes were carried out in an atmosphere of nitrogen. *1-Bromo-trans-hexahydro-2-indanone* (VIII) thus obtained had $n_D^{25.2}$ 1.5289.

Anal. Calcd. for $C_9H_{13}OBr$: C, 49.8; H, 6.0. Found: C, 49.0; H, 5.8.

1-Chloro-*trans*-hexahydro-2-indanone-1,3,3-d_3 (IX) was prepared by direct chlorination of *trans*-hexahydro-2-indanone-1,1,3,3-d_4 (VI; 447.5 mg) as described for the preparation of 1-chloro-*trans*-hexahydro-2-indanone (VII), except that D_2O was used instead of H_2O in all instances. *1-Chloro-trans-hexahydro-2-indanone-1,3,3-d_3* (IX; 35 mg) thus obtained had $n_D^{24.4}$ 1.5002.

Anal. Calcd. for $C_9H_{10}D_3OCl$: C, 61.5; H (+ D), 7.65; Cl, 20.2; D, 23.1 atom % excess D. Found: C, 61.7; H (+ D), 7.9; Cl, 20.1; D, 18.5 atom %.

1-Bromo-*trans*-hexahydro-2-indanone-1,3,3-d_3 (X) was prepared by bromination of *trans*-hexahydro-2-indanone-1,1,3,3-d_4 (VI; 391.8 mg) as described for the preparation of 1-bromo-*trans*-hexahydro-2-indanone

(VIII), except that D_2O was used instead of H_2O in all instances and that fluorotrichloromethane (Freon 11) was used as the solvent. *1-Bromo-trans-hexahydro-2-indanone-1,3,3-d_3* (X) was obtained in poor yield (9 mg) and, not consistently so, as a light yellow-brown liquid.

Anal. Calcd. for $C_9H_{10}D_3OBr$: C, 49.1; H (+ D), 6.1. Found: C, 47.5; H (+ D), 5.9.

Irradiation with a mercury lamp resulted almost exclusively in the dibromo compound.

1-Chloro-*cis*-hexahydro-2-indanone (XII) was prepared from *cis*-hexahydro-2-indanone (XI; prepared as described in ref. 6) as in the preparation of the corresponding *trans* isomer. It showed n_D^{25} 1.5068, but the elemental analysis indicated that, even after three chromatographs, the product still contained some dichloro impurity.

Anal. Calcd. for $C_9H_{13}OCl$: C, 62.6; H, 7.6; Cl, 20.5. Found: C, 61.5; H, 7.3; Cl, 23.2.

1-Bromo-cis-hexahydro-2-indanone (XIII) was prepared in the same way as the *trans* isomer (VIII) and had n_D^{24} 1.5283. The elemental analysis indicated the presence of some dibromo compound as an impurity.

Anal. Calcd. for $C_9H_{13}OBr$: C, 49.8; H, 6.0; Br, 36.8. Found: C, 49.3; H, 5.8; Br, 38.2.

2-Chlorocyclohexane-2,6,6-d_3 was prepared from cyclohexanone-2,2,6,6-d_4 (489.4 mg) by chlorination (343.5 mg chlorine) as in the preparation of 1-chloro-*trans*-hexahydro-2-indanone-1,3,3-d_3 (IX). *2-Chlorocyclohexanone-2,6,6-d_3* (123.2 mg) thus obtained had $n_D^{23.5}$ 1.4827.

Anal. Calcd. for $C_6H_6D_3OCl$: C, 53.1; H (+ D), 6.9; Cl, 26.1; D, 33.3 atom % excess D. Found: C, 53.3; H (+ D), 7.1; Cl, 26.1; D, 31.5 atom %.

2-Bromocyclohexanone-2,6,6-d_3 was prepared from cyclohexanone-2,2,6,6-d_4 (748 mg) by sunlight-catalyzed bromination (1.17 g bromine) as in the preparation of 1-bromo-*trans*-hexahydro-2-indanone (VIII). Purification and redistillation yielded *2-bromocyclohexanone-2,6,6-d_3* (149.7 mg), $n_D^{22.5}$ 1.5107.

Anal. Calcd. for $C_6H_6D_3OBr$: C, 40.0; H (+ D), 5.2; Br, 44.4; D, 33.3 atom % excess D. Found: C, 40.2; H (+ D), 5.3; Br, 44.1; D, 29.6 atom %.

1-Chloro-2-indanone-1,3,3-d_3 (III) was prepared from 2-indanone-1,1,3,3-d_4 (II; 509.9 mg) by chlorination (150 mg chlorine) as in the preparation of 1-chloro-*trans*-hexahydro-2-indanone-1,3,3-d_3 (IX). After crystallization from pentane, *1-chloro-2-indanone-1,3,3-d_3* (III; 174.1 mg) had m.p. 71–71.5° (Brutcher *et al.* (7) report m.p. 71–71.5° for the non-deuterated analogue).

Anal. Calcd. for $C_9H_4D_3OCl$: C, 63.7; H (+ D), 4.36; Cl, 20.9; D, 42.9 atom % excess D. Found: C, 63.9; H (+ D), 4.5; Cl, 21.1; D, 42.9 atom %.

1-Bromo-2-indanone-1,3,3-d_3 (IV) was prepared by direct bromination (bromine; 471.8 mg dissolved in methylene chloride; 10 ml) of 2-indanone-1,1,3,3-d_4 (II; 401.9 mg) dissolved in methylene chloride (10 ml). After solvent removal under vacuum, the products were worked up as for compound II. *1-Bromo-2-indanone-1,3,3-d_3* (IV; 424.7 mg) was crystallized from 5% ether in pentane and had m.p. 90–91° (Brutcher *et al.* (7) report m.p. 91° for the non-deuterated analogue).

Anal. Calcd. for $C_9H_4D_3OBr$: C, 50.5; H (+ D), 3.45; Br, 37.3; D, 42.9 atom % excess D. Found: C, 50.2; H (+ D), 3.3; Br, 37.2; D, 41.0 atom %.

DISCUSSION

Infrared Spectra

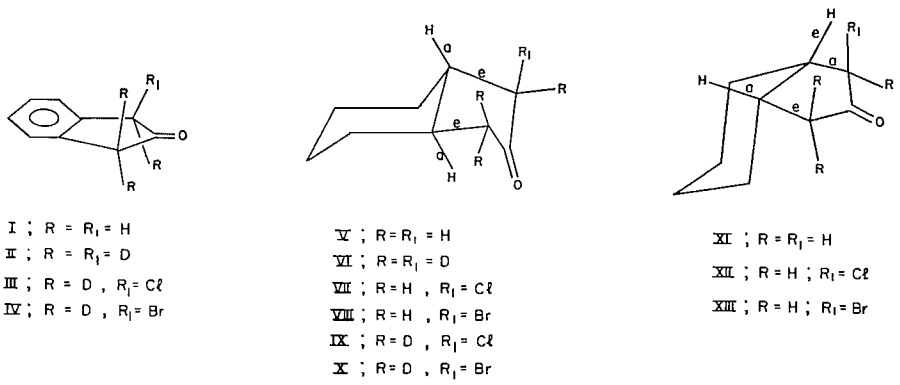
The relevant spectral data are listed in Table I. 2-Indanone-1,1,3,3-d_4 (II) and 2-indanone (I) are presumably planar or near-planar molecules (see also discussion of n.m.r. spectra). The frequency displacements of the main carbonyl bands in carbon tetrachloride solution observed on halogen substitution for compounds III and IV relative to these bands in compound II (20 and 9.9 cm^{-1}; see Table I) are similar to the displacements observed on halogen substitution of the non-deuterated analogues (19 and 13 cm^{-1}; see Table II) and in other related molecules (7). The halogen-substituted indanones III and IV may be slightly non-planar (see discussion of n.m.r. spectra), but there is no reason to suppose that the planarity of the indanone system is appreciably disturbed.

A small spectral displacement is observed between the main carbonyl bands of compounds I and II (0.5 cm^{-1}), if the bands are measured under identical conditions; similar small displacements may occur between compounds III and IV and their respective non-deuterated analogues. Inspection of the actual traces (Fig. 1) also shows that for 2-indanone (I) and compound V subsidiary bands occur at 1 728.8 cm^{-1} and 1 706.1 cm^{-1}, respectively, which are less intense and displaced in the deuterated compounds II and VI.

A number of possible explanations can account for the appearance of two carbonyl bands. Before these are discussed, however, a number of possibilities may be ruled out.

First, the absence of any concentration dependence within the concentration range 0.25

Can. J. Chem. Downloaded from www.nrcresearchpress.com by 210.87.254.40 on 09/05/12
For personal use only.



to 0.025 mole/l for compounds I and V (see Table I) eliminated intermolecular association complexes. The absence of such interactions is also indicated by the absence of a subsidiary band in the *cis* isomer (XI).

Next, enolization is unlikely as an explanation since no OH absorption could be detected in the infrared spectra, even at elevated temperatures. Figure 2 shows the overtone bands at 2.859 μ (3 498 cm^{-1}) and 2.878 μ (3 475 cm^{-1}) for compounds I and V, respectively, which are identified as such since these bands also occur in the deuterated analogues at 2.863 μ (3 493 cm^{-1}) for compound II and at 2.885 μ (3 466 cm^{-1}) for compound VI (see Fig. 2). Moreover, the n.m.r. spectra of compounds I, V, and XI show no hydroxyl protons (see Figs. 4*d*, 4*i*, and 4*l*).

Conformational isomerism also seems unlikely, since in such an equilibrium, when the

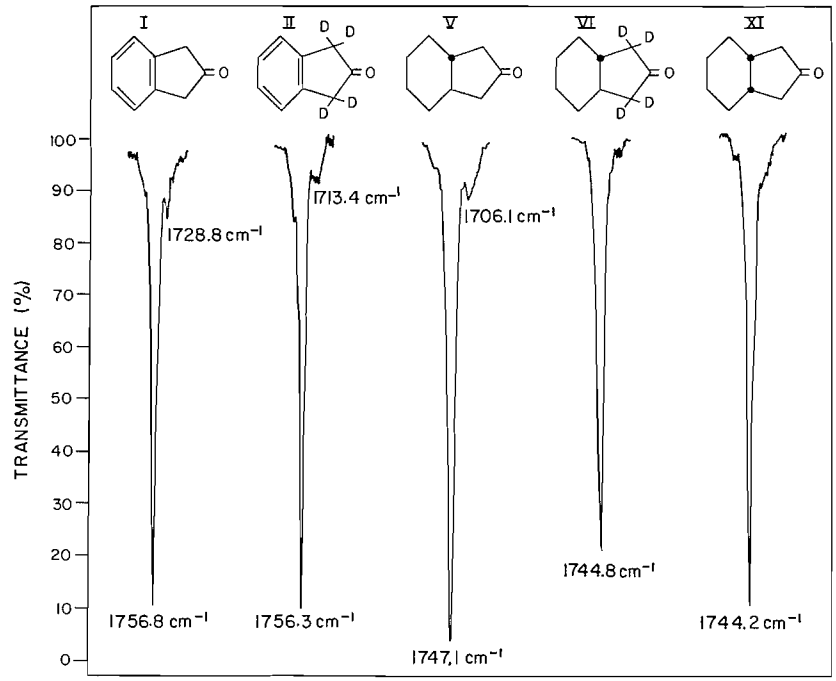


FIG. 1. Carbonyl bands in carbon tetrachloride solutions of 2-indanone (I), 2-indanone-1,1,3,3-d_4 (II), *trans*-hexahydro-2-indanone (V), *trans*-hexahydro-2-indanone-1,1,3,3-d_4 (VI), and *cis*-hexahydro-2-indanone (XI).

Can. J. Chem. Downloaded from www.nrcresearchpress.com by 210.87.254.40 on 09/05/12
For personal use only.

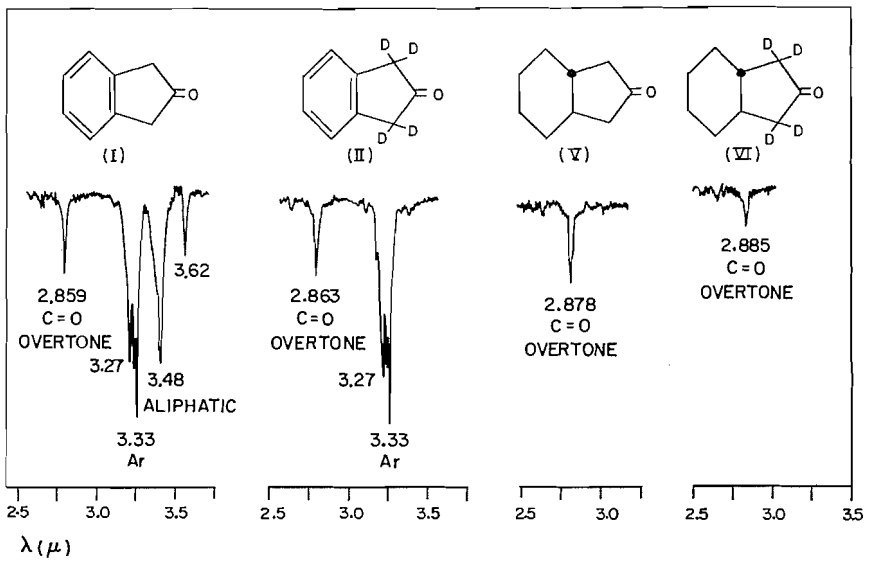


FIG. 2. Infrared spectra of compounds I, II, V, and VI (carbon tetrachloride solution) in the 2.5–3.5 μ region.

temperature is raised, the less-favored isomer would be expected to equilibrate with the more stable form. Figure 3 shows no such equilibrium for compounds I and V.

"Hot bands" also probably do not account for the subsidiary bands in compounds I and V, because such an explanation cannot readily account either for the changes observed in the deuterated analogues or for the observed spectral changes when the solvent is altered (see Table I). Moreover, hot transitions would be expected to be temperature dependent, and no such dependence is observed (see Fig. 3).

Finally, the presence of impurities, particularly water vapor, was looked for as a possible explanation of the subsidiary band, but careful repurification did not affect the observed spectra.

On the other hand, weak Fermi coupling is a possible explanation for the subsidiary bands observed in compounds I and V; such weak coupling between overtones and (or) combination bands on the one hand, and the strong carbonyl fundamental band on the other hand, may account partly for the small displacements observed in the main carbonyl bands of compounds II, III, IV, and VI and their non-deuterated analogues. The hypothesis of Fermi coupling similarly may also account, at least partly, for the decreased intensity of the subsidiary band in compound II and in compounds where the α-hydrogen atoms have been replaced by deuterium (see Fig. 1). If this explanation is correct, Fermi coupling seems to be more effective in compound V than in 2-indanone (I). This can be rationalized on the basis that the cyclopentanone ring in *trans*-hexahydro-2-indanone (V), unlike this ring in 2-indanone (I), is not planar (see discussion of n.m.r. spectra and refs. 7 and 8 and references cited there); possibly the molecule is then in a more favorable conformation for Fermi coupling to occur. No pronounced doublet formation could be detected in the *cis* isomer (see Fig. 1), which, however, may exist in a different conformation.

Moreover, some of the solvent changes (see Table I) are similar to those occurring in cyclopentanone (9) and ethylene carbonate (10), where Fermi resonance has been suggested as an explanation of the observed doublet.

However, there are difficulties with this explanation, based on Fermi coupling. First, the

Can. J. Chem. Downloaded from www.nrcresearchpress.com by 210.87.254.40 on 09/05/12
For personal use only.

Can. J. Chem. Downloaded from www.nrcresearchpress.com by 210.87.254.40 on 09/05/12
For personal use only.

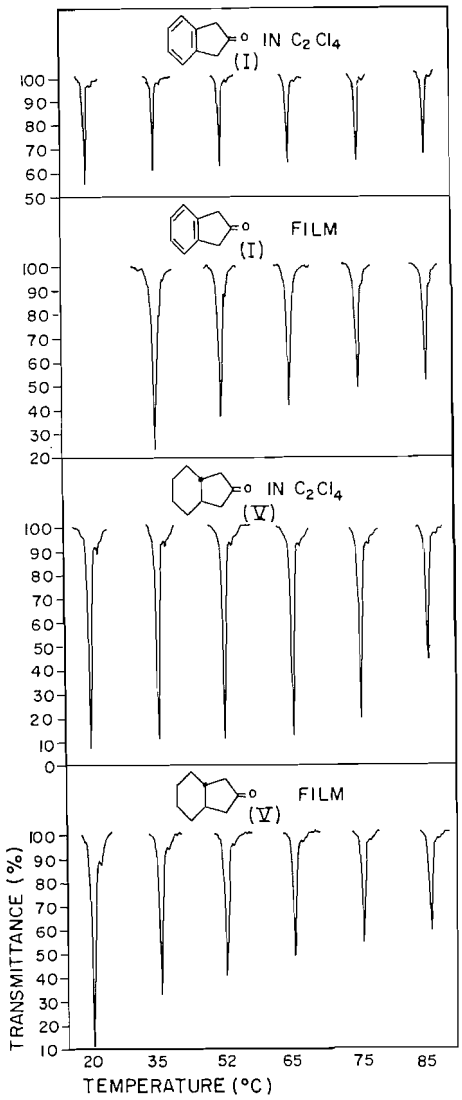


FIG. 3. Effect of temperature on the C=O stretching absorption in film and *sym*-tetrachloroethylene solutions of 2-indanone (I) and *trans*-hexahydro-2-indanone (V).

main carbonyl bands in compounds I and V are only weakly sensitive to isotopic substitution; hence, it is unlikely that one of the excitations corresponds to a combination band or overtone involving predominantly α-hydrogen motions. Also, there are no plausible bands in the infrared spectrum, overtones or combination bands of which could readily account for the Fermi coupling.

Next, it may be noted that the observed weak band could represent a weak fundamental vibration of the complex molecule. Such a vibration may be forbidden in a molecule in which the local symmetry (carbonyl and α-carbonyl region) is relatively high, as in the *cis* isomer (IX), where no subsidiary band is observed. If this is so, the various changes of position and intensity with substitution may predominantly reflect mass changes.

TABLE I

Main infrared carbonyl bands of some indanones

Compound	Solvent	ν_{max}^{I} (cm^{-1})	$\Delta\nu^{I}$ (cm^{-1})	A	ν_{max}^{II} (cm^{-1})
I*	CCl_4	1 756.8	8.7	1.98	1 728.8
	$CHCl_3$	1 751.8	12.3	2.69	1 731.6
	CH_2Cl_2	1 752.6	9.6	2.59	1 729.9
	CH_3CN	1 753.2	8.5	2.53	1 731.4
II	CCl_4	1 756.3	8.2	2.58	1 713.4
III	CCl_4	1 776.3			
IV	CCl_4	1 766.2			
V*	CCl_4	1 747.1	10.3	2.52	1 706.1
	$CHCl_3$	1 736.6	16.1	3.49	1 706.0
	CH_2Cl_2	1 738.9	13.4	2.45	1 701.1
	CH_3CN	1 740.4	12.7	3.43	1 704.0
VI	CCl_4	1 744.8	10.8	2.58	
VII	CCl_4	1 760.5			
VIII	CCl_4	1 763.0			
IX	CCl_4	1 759.1			
X	CCl_4	1 753.6			
XI	CCl_4	1 744.2	8.7	2.44	
Cyclopentanone (9)	CCl_4	1 747			1 731
	$CHCl_3$	1 743			1 728
	CH_2Cl_2	1 744			1 729
	CH_3CN	1 745			1 732
Ethylene carbonate (10)	CCl_4	1 819			1 773
	$CHCl_3$	1 811			1 780
	CH_2Cl_2	1 812			1 778
	CH_3CN	1 808			1 778

*These bands were found to be concentration independent (by using different path lengths) within the concentration range 0.25 to 0.025 mole/l.

Also, it is possible that the weak transition corresponds to a combination band which for symmetry reasons, or because of the absence of anharmonic mixing with the carbonyl fundamental vibration, is behaving independently with respect to substitution. That is, no Fermi coupling need be involved for at least some of the molecules studied.

Further, it is possible that in the aromatic systems the symmetry tends to inhibit Fermi coupling but that in some of the *trans*-hexahydro molecules it allows more Fermi coupling. Then, if the local symmetry (carbonyl and α-carbonyl region) is greater in the *cis* molecule, as seems likely, this could account for the absence of the subsidiary band in the *cis* molecules. In any case, Fermi coupling applies only to the interaction between a fundamental vibration and an overtone or combination tone, and carbonyl stretching modes not only involve stretching of the C=O bond but also motions of the adjacent C—C and C—H bonds and bond angles. Hence, it is probable that changing the adjacent masses changes significantly the form of the mode and thus its frequency. Any Fermi coupling may therefore only be a secondary interaction superimposed on this more fundamental effect. For example, the displacement in the carbonyl band for compound VIII on deuteration (-9.4 cm^{-1}; see Table I) may be caused by the non-equivalence of the α-positions on bromo substitution. Whatever their precise origin, these perturbations are unfortunate, since therefore the displacements observed on 1-chloro or 1-bromo substitution, *in the*

Can. J. Chem. Downloaded from www.nrcresearchpress.com by 210.87.254.40 on 09/05/12
For personal use only.

absence of the above-mentioned effects, cannot readily be determined. It is these displacements which are used to provide information concerning the conformation of the halogen-substituted compound. The uncorrected displacements obtained for these and some reference compounds on chloro and bromo substitution are listed in Table II.

TABLE II

Displacements (in CCl_4 solution) observed on substituting a chlorine or bromine atom in the position adjoining the carbonyl group

Reference compound	ν_{max} (cm^{-1})	ν_{max} (cm^{-1}) 1-Chloro derivative	ν_{max} (cm^{-1}) 1-Bromo derivative	Displacement (cm^{-1}) observed on substitution with: Cl	Br
2-Indanone* (I)	1 753	1 772	1 766	19	13
2-Indanone-1,1,3,3-d_4 (II)	1 756.3	1 776.3	1 766.2	20	9.9
Cyclohexanone†	1 712	1 740	1 730	28	18
Cyclohexanone-2,2,4,4-d_4	1 715.6	1 726.3	1 718.5	10.7	2.9
trans-Hexahydro-2-indanone (V)	1 747.1	1 760.5	1 763	13.4	15.9
trans-Hexahydro-2-indanone-1,1,3,3-d_4 (VI)	1 744.8	1 759.1	1 753.6	14.3	8.8
cis-Hexahydro-2-indanone (XI)	1 744.2	1 760.3	1 753.3	16.1	9.1

*Data from ref. 2.
†Data from ref. 11.

Ultraviolet Spectra

The data (Table III) show that, in some of the compounds investigated, slight spectral variations are observed in the $n \rightarrow \pi^*$ carbonyl band transitions on deuteration of the neighboring carbon atom. This is not inconsistent with the infrared data, which have indicated that the carbonyl stretching mode in the ground state is affected by α-substitution; hence the excited-state carbonyl stretching mode may also be affected by such substitution. However, the ultraviolet data must be interpreted cautiously since most of the compounds studied exhibit, like cyclopentanone, a number of peaks in the region studied; hence the location of the maximal absorption cannot readily be determined. Only the main maxima are recorded in Table III. For compounds I to IV, the low-intensity $n \rightarrow \pi^*$ electronic transition could not be measured, because of the large benzenoid absorption.

TABLE III

Main ultraviolet maxima ($n \rightarrow \pi^*$ transitions) of *trans*-hexahydro-2-indanone and of appropriate reference compounds in cyclohexane solution

Compound	λ_{max}	ϵ_{max}
trans-Hexahydro-2-indanone (V)	301	30
trans-Hexahydro-2-indanone-1,1,3,3-d_4 (VI)	301	30
1-Chloro-*trans*-hexahydro-2-indanone (VII)	322	50
1-Chloro-*trans*-hexahydro-2-indanone-1,3,3-d_3 (IX)	317	50
1-Bromo-*trans*-hexahydro-2-indanone (VIII)	321	70
1-Bromo-*trans*-hexahydro-2-indanone-1,3,3-d_3 (X)	318	115*
Cyclohexanone	293	15
Cyclohexanone-2,2,6,6-d_4	291	15
2-Chlorocyclohexanone	304	35
2-Chlorocyclohexanone-2,6,6-d_3	303	35
2-Bromocyclohexanone	312	100
2-Bromocyclohexanone-2,6,6-d_3	312	100

*Shoulder superimposed on another peak.

Nuclear Magnetic Resonance Spectra

The n.m.r. spectrum of cyclohexanone exhibits two peaks, one caused by four α-carbonyl hydrogens and the other by the six remaining hydrogens (12). Cyclohexanone-2,2,6,6-d_4, on the other hand, exhibits only one peak with no spin–spin splitting (see

Can. J. Chem. Downloaded from www.nrcresearchpress.com by 210.87.254.40 on 09/05/12
For personal use only.

Can. J. Chem. Downloaded from www.nrcresearchpress.com by 210.87.254.40 on 09/05/12
For personal use only.

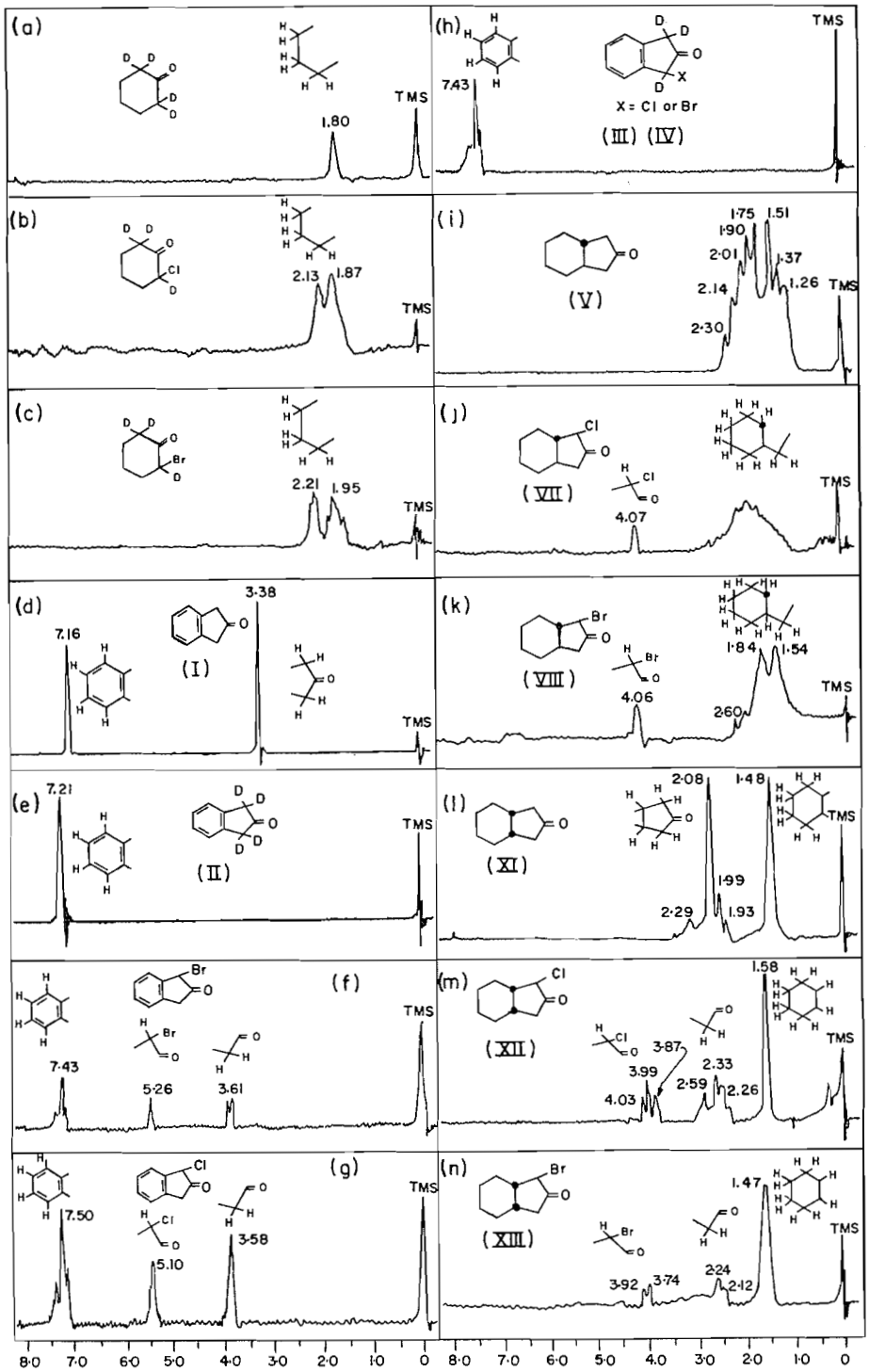


FIG. 4. Nuclear magnetic resonance spectra in carbon tetrachloride solution of (*a*) cyclohexanone-2,2,6,6-d_4, (*b*) 2-chlorocyclohexanone-2,6,6-d_3, (*c*) 2-bromocyclohexanone-2,6,6-d_3, (*d*) I, (*e*) II, (*f*) 1-bromo-2-indanone, (*g*) 1-chloro-2-indanone, (*h*) III and IV, (*i*) V, (*j*) VII, (*k*) VIII, (*l*) XI, (*m*) XII, and (*n*) XIII (TMS = tetramethylsilane).

Fig. 4*a*). This shows that the ring is mobile. Likewise, the n.m.r. spectrum of 2-chlorocyclohexanone (12) gives no indication of ring rigidity. The n.m.r. spectra of the chlorinated and brominated trideuterio analogues (see Figs. 4*b* and 4*c*) show two distinct peaks, one caused by the two hydrogens vicinal to the halogen and the other by the remaining four hydrogens on the ring. All these data confirm the mobility of the cyclohexanone ring.

The n.m.r. spectrum of compound I does not show any splitting (Fig. 4*d*), and that of its deuterated analogue (II; see Fig. 4*e*) shows only one sharp peak. 1-Bromo-2-indanone (see Fig. 4*f*) and 1-chloro-2-indanone (see Fig. 4*g*) yield three peaks in the ratio 4:2:1. Both spectra show a small amount of fine structure in the peak caused by the aromatic hydrogen atom; similar effects are observed in the deuterated analogues (III and IV; see Fig. 4*h*). This splitting is ascribed to the inductive effect of the halogen atom. The spectrum of 1-bromo-2-indanone shows a doublet for the geminal hydrogens (see Fig. 4*f*), thus suggesting that these hydrogens are not identical, one being slightly axial and the other slightly equatorial, presumably because of the steric effect of the larger bromine atom and its more axial character.

The spectra of *trans*-hexahydro-2-indanone (V) and its halogenated analogues (VII and VIII) suggest a rigid system with considerable spin coupling (see Figs. 4*i*, 4*j*, and 4*k*). The spectrum of the corresponding hydrocarbon also indicates a rigid system (13). Moreover, 1-chloro-*trans*-hexahydro-2-indanone (VII) gives a single peak (see Fig. 4*j*) at 4.07 p.p.m. with a band width of about 8 c.p.s. This relatively large band width suggests a limited amount of splitting between the angular hydrogen and the hydrogen geminal to the chlorine atom. Such a splitting is consistent if the angle between the two hydrogen atoms is about 85° (see Karplus' corrected equation (14)), but splitting probably also occurs across the carbonyl group with the methylene protons. 1-Bromo-*trans*-hexahydro-2-indanone (VIII) shows a similar peak with a band width of about 16 c.p.s. (Fig. 4*k*); this splitting is consistent with an angle, as defined above, of about 40°. The chloro and bromo derivatives (IX and X) of the appropriate deuterated compound (VI), as anticipated, give n.m.r. spectra identical with that of the parent compound (VI). The spectrum of *cis*-hexahydro-2-indanone (XI; see Fig. 4*l*) indicates a mobile molecule, as do the spectra of the corresponding halogen derivatives (XII and XIII; see Figs. 4*m* and 4*n*). *cis*-Hydrindane has been shown to have a low energy barrier to rotation (13).

1-Chloro-*cis*-hexahydro-2-indanone (XII) exhibits four peaks for the hydrogen geminal to chlorine (see Fig. 4*m*), which can be explained by assuming two non-equivalent α-positions, located in a molecule which itself can assume two conformational isomers. 1-Bromo-*cis*-hexahydro-2-indanone shows two peaks, with a possibility of further unresolved spin–spin splitting for the hydrogen geminal to bromine. This can be explained by assuming that, for this compound in both isomers, the conformation containing the bromine atom in the axial position is preferred.

ACKNOWLEDGMENTS

E. J. M. thanks the Directorate of Chemical Sciences, Air Force Office of Scientific Research, for their support of this research under grants AF-AFOSR 62-18 and 488-64, and acknowledges the assistance of National Science Foundation grant GP-1482 to the Department of Chemistry, Fordham University, towards the purchase of a nuclear magnetic resonance spectrometer.

The financial assistance from the National Research Council of Canada (to W. F. F.) is also gratefully acknowledged.

Can. J. Chem. Downloaded from www.nrcresearchpress.com by 210.87.254.40 on 09/05/12
For personal use only.

REFERENCES

1. A. T. BLOMQUIST and E. J. MORICONI. J. Org. Chem. **26**, 3761 (1961).
2. F. V. BRUTCHER, JR., T. ROBERTS, S. J. BARR, and N. PEARSON. J. Am. Chem. Soc. **81**, 4915 (1959).
3. R. N. JONES and C. SANDORFY. *In* Techniques of organic chemistry. Vol. IX. *Edited by* W. West. Interscience Publishers, Inc., New York. 1956. p. 274.
4. D. A. RAMSAY. J. Am. Chem. Soc. **74**, 72 (1952).
5. N. WRIGHT. Ind. Eng. Chem. Anal. Ed. **13**, 1 (1941).
6. W. HÜCKEL and H. FRIEDRICH. Ann. **451**, 132 (1926). A. KANDIAH. J. Chem. Soc. 922 (1931).
7. F. V. BRUTCHER, JR., T. ROBERTS, S. J. BARR, and N. PEARSON. J. Am. Chem. Soc. **81**, 4915 (1959).
8. W. KLYNE. Bull. Soc. Chim. France, 1396 (1960).
9. G. ALLEN, P. S. ELLINGTON, and G. D. MEAKINS. J. Chem. Soc. 1909 (1960).
10. L. J. BELLANY and R. L. WILLIAMS. Trans. Faraday Soc. **55**, 14 (1959).
11. E. J. COREY. J. Am. Chem. Soc. **75**, 2301 (1953).
12. W. D. KUMLER, J. N. SHOOLERY, and F. V. BRUTCHER, JR. J. Am. Chem. Soc. **80**, 2533 (1958).
13. N. B. MONIZ and J. A. DIXON. J. Am. Chem. Soc. **83**, 1671 (1961).
14. N. S. BHACCA and D. H. WILLIAMS. Applications of nuclear magnetic resonance spectroscopy in organic chemistry. Holden-Day, Inc., San Francisco. 1964. p. 49.

Can. J. Chem. Downloaded from www.nrcresearchpress.com by 210.87.254.40 on 09/05/12
For personal use only.

HYDROGEN EXCHANGE IN *s*-TRINITROBENZENE

E. BUNCEL AND E. A. SYMONS
Department of Chemistry, Queen's University, Kingston, Ontario
Received November 15, 1965

ABSTRACT

Hydrogen exchange in *s*-trinitrobenzene has been observed in the medium 90% dimethylformamide – 10% deuterium oxide containing sodium deuteriooxide (0.01 *M*). The proton transfer process between *s*-trinitrobenzene and base is therefore established. The factors which may contribute to the importance of the proton transfer process relative to the formation of Meisenheimer-type complexes are considered.

Can. J. Chem. Downloaded from www.nrcresearchpress.com by 210.87.254.42 on 09/05/12
For personal use only.

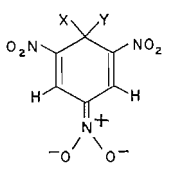
A particularly challenging problem is presented by the nature of the colored solutions formed in the interaction of aromatic polynitro compounds with bases. The following types of interaction have been proposed: attachment of the base to aromatic carbon with formation of an adduct having a pentadienyl structure (e.g. I) (1–7); formation of charge transfer complexes caused by partial overlap of electronic charge to the nitro compound (8–12); formation of anions such as II resulting from abstraction of nuclear hydrogen from the nitro compound (13–15).[1]

The pentadienyl anion structure (I, X = OR, Y = OR′) has now been well established through studies of visible (2), infrared (5), and most particularly nuclear magnetic resonance (17) spectroscopy; its role as the intermediate in nucleophilic aromatic substitution processes is understood (18). Theoretical aspects of the charge transfer process have been discussed (19 and references therein). In contrast, there is considerable uncertainty about the circumstances under which proton transfer processes are possible and about the role of the resulting anions in the overall scheme.

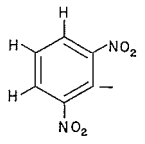
The formation of II, at least in a small concentration, from *m*-dinitrobenzene was demonstrated (15) by the observation of hydrogen exchange with a medium of dimethylformamide – deuterium oxide containing sodium deuteriooxide (0.005 *M*). It was suggested (15) that this anion may be responsible for the deep color of the solution, but this was not supported by other work (20). Even more uncertain was the situation with regards to the formation of the anion from *s*-trinitrobenzene. Thus Kharasch *et al.* (21) reported that treatment of *s*-trinitrobenzene with 0.02 *M* sodium hydroxide in ethanol – deuterium oxide resulted in the dilution of the deuterium of the medium, equivalent to the exchange of over 2 g-atoms of hydrogen from the trinitrobenzene. However, Ketelaar *et al.* (22) detected no deuterium enrichment in the *s*-trinitrobenzene recovered from 8 *M* sodium hydroxide in D_2O, and Miller and Wynne-Jones (8) observed no exchange after treatment with pyridine–D_2O. Recently an alternative explanation has been offered (6) to account for the observations of Kharasch *et al.*

Opinions based on measurements of conductivity and cryoscopy are likewise not unanimous. From both types of measurement Baliah and Ramakrishnan (14) concluded that in ethanolamine solutions *s*-trinitrobenzene does ionize by a proton transfer mechanism. A similar explanation was given by Lewis and Seaborg (13) for the conductivity of *s*-trinitrobenzene in pyridine. On the other hand, from conductivity and spectroscopic data Briegleb *et al.* (23) concluded that the ionic species formed from *s*-trinitrobenzene and piperidine in acetonitrile solution was the Meisenheimer-type adduct III.

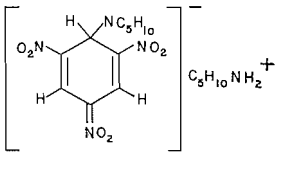
[1] *Under certain conditions the formation of radical anions has also been reported (16).*



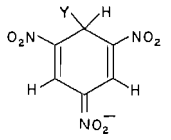
I



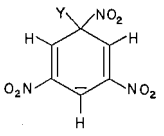
II



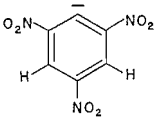
III



IV



V



VI

In view of this apparently conflicting evidence and in light of our previous findings (24) of an aromatic hydrogen exchange under mild conditions (CH_3ONa–CH_3OD), it was decided to re-investigate hydrogen exchange in the polynitrobenzenes.

RESULTS AND DISCUSSION

In the present study the exchange of hydrogen was investigated by two methods: measurement of the dilution of the deuterium of the medium during reaction by hydrogen by means of infrared spectroscopy, and estimation of the deuterium content in the recovered *s*-trinitrobenzene by spectral means and by analysis. We now report that *s*-trinitrobenzene does in fact undergo extensive hydrogen exchange in a medium of dimethylformamide–D_2O containing NaOD.[2]

The addition of NaOD in D_2O to a solution of *s*-trinitrobenzene in dimethylformamide gave a solution (0.01 *M* NaOD in 90% dimethylformamide – 10% D_2O) which was ruby red in color. The entry of hydrogen into the medium was first followed at room temperature; during 24 h there was only a small development of OH (measured at 3 450 cm^{-1}), indicating that exchange had occurred to about 15%. The temperature was then raised to 100 °C; in 30 min the OH peak increased to about 95% of its theoretical value. There was no significant increase in the OH peak during the next hour. The reaction was then stopped and the trinitrobenzene recovered. It was identified by its melting point, elemental analysis, and ultraviolet and visible spectra. In the infrared spectrum a band at 2 310 cm^{-1} showed the presence of C—D. The nuclear magnetic resonance spectrum showed a barely detectable signal corresponding in position to the hydrogens of *s*-trinitrobenzene. Deuterium analysis corresponded to 93.8% deuteration (the theoretical value for complete equilibration, if one ignored any possible isotope effects, was 96.9% deuteration). Hence it can be concluded that practically complete exchange of hydrogen in the *s*-trinitrobenzene had occurred.

s-Trinitrobenzene can be considered to be in equilibrium with anions IV, V, and VI as a result of the interaction with base Y^- (charge transfer complexes being disregarded). Of the two pentadienyl-type anions the Meisenheimer-type anion IV will be present in far greater concentration, even though V must be the reactive intermediate (6) in the formation 1-Y-3,5-dinitrobenzene, which is the main product of substitution (6). However,

[2]*Hydrogen exchange in s-trinitrobenzene has also been observed recently by Crampton and Gold: cited in ref. 25 as "unpublished observations" and in a personal communication from Professor Gold.*

Can. J. Chem. Downloaded from www.nrcresearchpress.com by 210.87.254.42 on 09/05/12
For personal use only.

Can. J. Chem. Downloaded from www.nrcresearchpress.com by 210.87.254.42 on 09/05/12
For personal use only.

only anion VI, formed by proton abstraction, leads to hydrogen exchange. In terms of the terminology recently advanced by Parker (26) and by Bunnett (27), the nucleophile Y^- takes part in competing processes resulting from its "carbon basicity" (equilibrium formation of IV and V) and its "hydrogen basicity" (equilibrium formation of VI). Any factor which will displace the balance between these equilibria will have an effect on the relative importance of hydrogen exchange in the overall scheme. An important example of such a factor is solvation of the nucleophile Y^-.[3] Parker (26) has shown that the nucleophilic reactivity, in rate processes, and the basicity, in equilibria, towards carbon of a number of nucleophiles are greatly enhanced by a change from a hydroxylic medium to a dipolar aprotic one (e.g. dimethylformamide), and that even relative orders of efficacy of the nucleophiles may be reversed in the two types of media. Cram *et al.* (32) observed that the nucleophilic reactivity of alkoxide ion in proton abstraction from carbon increased by as much as 10^9 when the solvent was changed from alcohol to dimethyl sulfoxide. Similarly it has recently been shown that deuteriooxide ion can bring about hydrogen exchange of dimethyl sulfoxide in its aqueous solutions (33). The observation of hydrogen exchange with *s*-trinitrobenzene in 90% dimethylformamide – 10% D_2O medium containing NaOD is in accord with the above discussion. It is hoped that a combination of rate and equilibrium studies will allow a dissection of the various possible processes.

The apparently conflicting evidence in the literature on the importance of the proton transfer process is, at least in part, explainable. The reaction medium and temperature were sufficiently diverse in the various studies to allow a shift in emphasis in the equilibria referred to above, in favor of or against the proton transfer process. The respective conclusions are thus not necessarily incompatible with one another. A systematic study is called for.

EXPERIMENTAL

Materials

s-Trinitrobenzene (Eastman) was recrystallized from ethanol, m.p. 122.0–122.5°.[4] Dimethylformamide was dried over molecular sieves and distilled under reduced pressure. NaOD solution was prepared by dissolving freshly cut sodium in 99.5% D_2O (Diaprep Inc.), and was standardized by titration with acid.

Methods

The infrared method for OH analysis in the aqueous dimethylformamide solutions was based on the measurement of absorbance at 3 450 – 3 500 cm^{-1} caused by OH stretching. Spectra were taken on a Perkin–Elmer model 21 instrument, usually over the region 3 700 – 2 300 cm^{-1}, cells with calcium fluoride or "irtran" (Connecticut Instrument Co.) windows, and a hypodermic syringe (for transfer of the solutions) being used. A calibration curve was first prepared with solutions of known H_2O and D_2O content; these solutions always contained 90% of dimethylformamide by volume. The calibration curve (absorbance versus hydrogen concentration) was almost linear up to a concentration of 1.0 g-atom hydrogen/l. The reproducibility of a measurement of hydrogen concentration was between 2 and 5%.

Hydrogen Exchange

In one experiment a solution was prepared containing 1.065 g *s*-trinitrobenzene in 50 ml of 0.01 *M* NaOD in 10% D_2O – 90% dimethylformamide. The red solution was sampled for OH analysis, first at room temperature (26°) and then while immersed in a constant temperature bath at 100°. To stop the reaction, the solution was added to dilute sulfuric acid (1 ml of 1 *N*) on ice; the red color was immediately discharged. The precipitated solid was recrystallized twice from ethanol to give pale yellow crystals (0.608 g), m.p. 122°, mixed m.p. with *s*-trinitrobenzene (after evaporation to dryness of a mixture of the two materials) 122°. This recrystallized material was used in the identification tests described below. An additional 0.132 g material (m.p. 119–121°) was recovered by ether extraction of the acidified reaction mixture.

Comparison of the infrared spectra in chloroform solution of the trinitrobenzene used in the exchange reaction (A) and of the recovered material (B) showed the following characteristics. Both A and B had bands at 924, 1 345, 1 545, and 1 620 cm^{-1}. B had new bands at 2 315 (C—D stretching), 1 385, and 1 400 cm^{-1} (doublet). Bands present in A but absent in B were those at 3 080 (C—H stretching) and 1 076 cm^{-1} (C—H in-plane vibration (15)).

[3]*Other factors which influence nucleophilicity and basicity have been considered by several authors (27–31).*
[4]*All melting points are uncorrected.*

The ultraviolet and visible spectra of A and B were identical, both qualitatively and quantitatively: in 96% ethanol, $\lambda_{max} = 225$ mμ, log $\epsilon_{225} = 4.41$ (lit. (34) values for *s*-trinitrobenzene in 96% ethanol are $\lambda_{max} = 225$ mμ, log $\epsilon_{225} = 4.41$).

The nuclear magnetic resonance spectrum (in deuteriochloroform with tetramethylsilane as external standard) of A showed a sharp singlet at $\tau = 0.59$. The spectrum of B had only a barely detectable signal at $\tau = 0.59$.

Carbon, hydrogen, and nitrogen analytical data for A and B were obtained consecutively.

Anal. Calcd. for A: C, 33.80; H, 1.42; N, 19.71. Found for A: C, 33.73, 33.82; H, 1.47, 1.50; N, 19.72. Found for B: C, 33.52, 33.27; H, 1.74, 1.60; N, 19.36.

Deuteration of A will cause the carbon and nitrogen analytical data to decrease slightly and the hydrogen value to increase slightly, in the region of the observed results for B.

Deuterium analysis was done by combustion and analysis by the falling-drop method (performed by J. Nemeth, Urbana, Illinois) of the water that was formed. To optimize the sensitivity of the analytical method, the sample submitted for analysis was a 50:50 mixture of A and B; this mixture had a deuterium content of 46.9%. The deuterium content of B was hence 93.8%.

ACKNOWLEDGMENTS

The authors thank the donors of the Petroleum Research Fund administered by the American Chemical Society for a grant (PRF 1841-A4) in support of this work. Discussions with Dr. A. R. Norris are also acknowledged.

REFERENCES

1. J. Meisenheimer. Ann. **323**, 205 (1902).
2. R. Foster and D. Ll. Hammick. J. Chem. Soc. 2153 (1954). R. Foster and R. K. Mackie. J. Chem. Soc. 3796 (1963).
3. J. B. Ainscough and E. F. Caldin. J. Chem. Soc. 2528 (1956).
4. R. C. Farmer. J. Chem. Soc. 3425 (1959).
5. L. K. Dyall. J. Chem. Soc. 5160 (1960).
6. V. Gold and C. H. Rochester. J. Chem. Soc. 1687 (1964); 1692 (1964).
7. T. Abe. Bull. Chem. Soc. Japan, **37**, 508 (1964).
8. R. E. Miller and W. F. K. Wynne-Jones. J. Chem. Soc. 2375 (1959); 4886 (1961).
9. G. Briegleb and H. Delle. Z. Elektrochem. **64**, 347 (1960).
10. P. H. Elmslie and R. Foster. Tetrahedron, **20**, 1489 (1964).
11. R. J. Pollitt and B. C. Saunders. J. Chem. Soc. 1132 (1964).
12. S. Iwata, H. Tsubomura, and S. Nagakura. Bull. Chem. Soc. Japan, **37**, 1506 (1964).
13. G. N. Lewis and G. T. Seaborg. J. Am. Chem. Soc. **62**, 2122 (1940).
14. V. Baliah and V. Ramakrishnan. Rec. Trav. Chim. **78**, 783 (1959); **79**, 1150 (1960).
15. R. J. Pollitt and B. C. Saunders. Proc. Chem. Soc. 176 (1962).
16. G. A. Russell, and E. G. Janzen. J. Am. Chem. Soc. **84**, 4153 (1962). G. A. Russell, E. G. Janzen, and E. T. Strom. J. Am. Chem. Soc. **86**, 1807 (1964).
17. M. R. Crampton and V. Gold. J. Chem. Soc. 4293 (1964).
18. J. F. Bunnett and R. E. Zahler. Chem. Rev. **49**, 273 (1951). J. Miller. Rev. Pure Appl. Chem. **1**, 171 (1951). J. F. Bunnett. Quart. Rev. London, **12**, 1 (1958). S. D. Ross. Progr. Phys. Org. Chem. **1**, 31 (1963).
19. G. Briegleb. Angew. Chem. Intern. Ed. Engl. **3**, 617 (1964).
20. R. Foster and R. K. Mackie. Tetrahedron, **19**, 691 (1963).
21. M. S. Kharasch, W. G. Brown, and J. McNab. J. Org. Chem. **2**, 36 (1937).
22. J. A. A. Ketelaar, A. Bier, and H. T. Vlaar. Rec. Trav. Chim. **73**, 37 (1954).
23. G. Briegleb, W. Liptay, and M. Canter. Z. Physik. Chem. Frankfurt, **26**, 55 (1960).
24. E. F. Ullman and E. Buncel. J. Am. Chem. Soc. **85**, 2106 (1963).
25. M. R. Crampton and V. Gold. Chem. Commun. 256 (1965).
26. A. J. Parker. Proc. Chem. Soc. 371 (1961); Quart. Rev. London, **16**, 163 (1962); Australian J. Chem. **16**, 585 (1963).
27. J. F. Bunnett. Ann. Rev. Phys. Chem. **14**, 271 (1963).
28. R. F. Hudson. Chimia Aarau, **16**, 173 (1962).
29. J. O. Edwards and R. G. Pearson. J. Am. Chem. Soc. **84**, 16 (1962). R. G. Pearson. J. Am. Chem. Soc. **85**, 3533 (1963).
30. W. P. Jencks. Progr. Phys. Org. Chem. **2**, 63 (1964).
31. J. Hine and R. D. Weimar, Jr. J. Am. Chem. Soc. **87**, 3387 (1965).
32. D. J. Cram, B. Rickborn, C. A. Kingsbury, and P. Haberfield. J. Am. Chem. Soc. **83**, 3678 (1961).
33. E. Buncel, E. A. Symons, and A. W. Zabel. Chem. Commun. 173 (1965).
34. P. Fielding and R. J. W. Le Fèvre. J. Chem. Soc. 2812 (1950).

Can. J. Chem. Downloaded from www.nrcresearchpress.com by 210.87.254.42 on 09/05/12
For personal use only.

Can. J. Chem. Downloaded from www.nrcresearchpress.com by 210.87.254.105 on 09/05/12
For personal use only.

CYCLOHEXANE COMPOUNDS

VI. NUCLEAR MAGNETIC RESONANCE SPECTRA OF SOME DERIVATIVES OF THE STEREOISOMERIC 3-BROMO-1,2-CYCLOHEXANEDIOLS AND THE 2-BROMO-1,3-CYCLOHEXANEDIOLS[1]

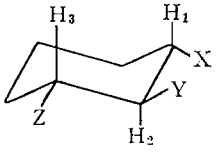
R. A. B. BANNARD
Defence Chemical, Biological and Radiation Laboratories, Ottawa, Canada

Received October 1, 1965

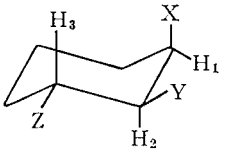
ABSTRACT

First-order analysis of the 60 Mc.p.s. proton magnetic resonance spectra of 1α-methoxy-2β-acetoxy-3α-bromocyclohexane, 1α-methoxy-2α-acetoxy-3β-bromocyclohexane, 1α-methoxy-2β-bromo-3α-acetoxycyclohexane, 1α-methoxy-2α-bromo-3β-acetoxycyclohexane, and the corresponding diol diacetates confirmed the stereochemical interrelationships of substituents which were assigned previously on chemical grounds, and demonstrated that the compounds exist in chair conformations. The chemical shifts of the methoxy methyl and acetoxy methyl protons did not provide reliable criteria for the assignment of conformations to these substituents in this series. The coupling constants of the methine protons followed, in general, the pattern predicted by the Karplus equation, and the smaller $J_{2,3}$ values observed in the *cis,trans* compounds relative to those in the *trans,trans* compounds are interpreted mainly on the basis of conformational equilibration, upon which is superimposed a small dihedral angular distortion or a remote substituent orientational effect.

Analysis of the multiplet patterns and chemical shifts of the methine protons in the nuclear magnetic resonance spectra of the stereoisomeric 1-methoxy-2-acetoxy-3-acetylaminocyclohexanes I*a* and II*a*, their ethoxy analogues (I*c* and II*c*), and certain of their derivatives (I*b*–I*e* and II*b*–II*e*) (1) permitted unambiguous assignment of both gross structure and conformation to these compounds. This work also indicated that the chemical



I



II

I*a*	X = OCH_3,	Y = OAc,	Z = NHAc	II*a*
I*b*	X = OCH_3,	Y = OAc,	Z = NAc_2	II*b*
I*c*	X = OC_2H_5,	Y = OAc,	Z = NHAc	II*c*
I*d*	X = OC_2H_5,	Y = OAc,	Z = NAc_2	II*d*
I*e*	X = OAc,	Y = OAc,	Z = NHAc	II*e*
I*f*	X = OAc,	Y = NHAc,	Z = OAc	II*f*
I*g*	X = OCH_3,	Y = OH,	Z = Br	II*g*
I*h*	X = OCH_3,	Y = Br,	Z = OH	II*h*
I*j*	X = OCH_3,	Y = OAc,	Z = Br	II*j*
I*k*	X = OAc,	Y = OAc,	Z = Br	II*k*
I*l*	X = OCH_3,	Y = Br,	Z = OAc	II*l*
I*m*	X = OAc,	Y = Br,	Z = OAc	II*m*

shifts of axially (6.59–6.62 τ) and equatorially (6.63–6.66 τ) oriented methoxy methyl protons are not sufficiently well separated to serve as criteria for the assignment of conformations to these substituents in these particular compounds (however, cf. ref. 3), whereas the chemical shifts of equatorially oriented acetoxy (7.90–7.99 τ) and acetamido (8.00–8.09 τ) methyl proton resonances appeared of possible utility in this series as well as

[1]*Issued as D.C.B.R.L. Report No. 483.*

Can. J. Chem. Downloaded from www.nrcresearchpress.com by 210.87.254.105 on 09/05/12
For personal use only.

in acetylated pyranose carbohydrates (4–8). In view of the potential usefulness of such correlations for conformational assignment in alicyclic molecules which contain these substituents in environments in which analysis of the methine proton resonances is complicated or prevented by the presence of numerous adjacent protons, it was considered desirable to extend the study to other cyclohexane derivatives of known structure. In this connection the nuclear magnetic resonance spectra of the stereoisomeric 1-methoxy-2(3)-hydroxy-3(2)-bromocyclohexanes (I*g*, I*h*, and II*g*, II*h*) (9, 10), their acetyl derivatives (I*j*, I*l*, and II*j*, II*l*), and the diacetates of the corresponding bromodiols (I*k*, I*m*, and II*k*, II*m*) were measured.

The spectra of the bromohydrins (I*g*, I*h*, and II*g*, II*h*) did not prove to be amenable to analysis because of overlap in the multiplet patterns of the methine protons. This situation was not improved when the compounds were acidified with trifluoroacetic acid to eliminate coupling between the hydroxylic proton and that attached to C_2. The only readily assignable resonances in these spectra were those caused by the methoxy methyl protons, which are given in Table I. On the other hand, in the spectra of the methoxybromoacetates (I*j*, I*l*, and II*j*, II*l*) and bromodiol diacetates (I*k*, I*m*, and II*k*, II*m*), the methine proton resonances were, in general, sufficiently chemically shifted from one another and from those of the methylene protons (7.4–9.2 τ) to permit first-order analysis of the spectra in the same manner as described previously (1). The chemical shifts and coupling constants thus obtained are shown in Tables I and II, respectively. That the measured splittings correspond closely to the true coupling constants was confirmed by measuring the spectra of compounds I*k*, I*l*, and I*m* (which had the largest J/δ ratios) at 100 Mc.p.s. (11, p. 139). The coupling constants thus found agreed within 0.2 c.p.s. with those recorded in Table II.

The magnitudes of the coupling constants ($J_{1,2}$ and $J_{2,3}$) together with the multiplet patterns (triplet or quartet) and signal widths of the H_2 resonances (8, 12) confirmed that the structures of the methoxybromoacetates and bromodiol diacetates, which were assigned previously (9, 10) on chemical grounds, are indeed correct and that the conformations of the substituents are mainly as shown in formulae I and II.

It is evident from Table I that the chemical shifts of the acetoxy and methoxy methyl protons do not provide reliable criteria for the assignment of conformation to these substituents in 1,2,3-trisubstituted cyclohexanes, because of overlap in the ranges of values observed for these groups in the axial (acetoxy, 7.88–7.94 τ; methoxy, 6.61–6.65 τ) and equatorial (acetoxy, 7.87–8.04 τ; methoxy, 6.55–6.66 τ) orientations.

In the 3-bromo series (I*j*, I*k*, and II*j*, II*k*), equatorial H_1 is shifted downfield 0.5–0.6 p.p.m. from axial H_1. The change in orientation of H_1 from axial to equatorial also causes a paramagnetic shift of 0.4–0.5 p.p.m. in the resonance of axial H_3, whereas axial H_2 is either unaffected or slightly shielded (0.1 p.p.m.). The 1-alkoxy-2-acetoxy-3-acetylaminocyclohexanes (I*a* and II*a*) exhibit parallel but slightly smaller shifts in the resonances of the methine protons, and it thus appears likely that the downfield shift in axial H_3 which accompanies the change in orientation of H_1 from axial to equatorial in these derivatives may owe its origin principally to the interaction of the axial anisotropic methoxyl or acetoxyl group at C_1 with axial H_3. A similar effect has recently been observed in acetylated methyl glycopyranosides of some aminohexoses (13). In the 2-bromo series (I*l*, I*m*, and II*l*, II*m*), equatorial H_1 is deshielded with respect to axial H_1 to a smaller extent (0.1–0.3 p.p.m.) than in the 3-bromo series, and the concomitant downfield shift in axial H_3 is likewise reduced. However, the shift in the resonance of axial H_2 which accompanies the change in orientation of H_1 from axial to equatorial is opposite in direction to and larger in magnitude than that observed in the 3-bromo series. Thus the chemical shifts of methine protons in these compounds depend upon the nature and orientation of adjacent and

Can. J. Chem. Downloaded from www.nrcresearchpress.com by 210.87.254.105 on 09/05/12
For personal use only.

TABLE I

Chemical shifts (τ values)

Compound	OMe (1)	OEt (1)	OAc (1)	OAc (2)	OAc (3)	NAc (2)	NAc (3)	NAc_2 (3)	H_1	H_2	H_3
I*a**	6.62			7.93			8.09		6.79	5.30	6.05
II*a**	6.63			7.90			8.08		6.39	5.29	5.61
I*b**	6.65			7.99				7.69	—	4.40	6.22
II*b**	6.66			7.99				7.66	6.22	4.51	5.81
I*c**		6.37, 8.84		7.92			8.08		6.64	5.26	5.99
II*c**		6.41, 8.81		7.90			8.07		6.25	5.23	5.65
I*d**		8.88		8.01				7.68	6.44	4.53	6.44
II*d**		6.43, 8.84		7.97				7.64	6.10	4.55	5.76
I*e**			7.98	7.95			8.07		5.14	5.14	5.98
II*e**			7.90	7.97			8.04		4.60	5.18	5.67
I*f*†			7.98		7.98	8.10			5.30	5.85	5.30
II*f*†			7.93		7.95	8.04			4.80	5.85	4.80
I*g*	6.55										
II*g*	6.62										
I*h*	6.61										
II*h*	6.61										
I*j*	6.66			7.88					6.82	4.98	6.17
II*j*	6.65			7.87					6.30	4.97	5.65
I*k*			7.99	7.92					5.25	4.86	6.12
II*k*			7.94	7.92					4.65	4.98	5.77
I*l*	6.54				8.04				6.78	6.22	5.08
II*l*	6.61				7.93				6.47	5.78	4.78
I*m*			7.90		7.92				5.03	6.14	5.03
II*m*			7.92		7.88				4.9	5.78	4.9

*Data from Anet *et al.* (1) or Bannard (2).
†Data from Suami and Ogawa (21).

Can. J. Chem. Downloaded from www.nrcresearchpress.com by 210.87.254.105 on 09/05/12
For personal use only.

TABLE II

Coupling constants

Compound	$-\Delta F^0$ (kcal/mole)	K	% e,a,a or a,a,a	Predicted $J_{2,3}$	Observed $J_{1,2}$	Observed $J_{2,3}$	Observed $J_{1,6a}$	Observed $J_{1,6e}$	Observed $J_{3,4a}$	Observed $J_{3,4e}$
I*a*					9.1	9.1				
II*a**					2.3	10.4				
I*b**					9.2	9.2				
II*b**					2.8	10.6				
I*c**					8.8	8.8				
II*c**					2.5	10.5				
I*d**					8.9	8.9				
II*d**					3.0	10.7				
I*e**					—	—				
II*e**					2.8	10.7				
I*f*†					10.5	10.5				
II*f*†					3.0	9.0				
I*j*	1.9§	25.2	4	10.0‡	10.1	10.3	9.0	4.6	10.8	4.8
II*j*	0.5	2.3	30	8.1	2.8	8.9	2.9	2.9	8.8	4.8
I*k*	1.9	25.2	4	10.0	9.7	9.7	9.7	4.9	10.6	4.7
II*k*	0.5	2.3	30	8.1	3.0	9.4	2.9	2.9	9.2	4.7
I*l*	1.9	25.2	4	10.0	9.8	9.9	10.8	5.0	10.0	4.9
II*l*	0.5	2.3	30	8.1	3.0	7.3	3.0	3.0	7.1	3.7
I*m*	1.9	25.2	4	10.0	10.1	10.1	9.6	4.6	9.6	4.6
II*m*	0.5	2.3	30	8.1	3.0‖	7.9‖	—	—	—	—

*Data from Anet *et al.* (1) or Bannard (2).
†Data from Suami and Ogawa (21).
‡On the basis of conformational equilibration, if one assumes $J_{180°} = 10.3$ c.p.s.
§See ref. 18.
‖The overlap of H_1 and H_3 in this compound renders the first-order analysis less accurate than in the other compounds, but no significant broadening of the H_2 multiplet was observed.

Can. J. Chem. Downloaded from www.nrcresearchpress.com by 210.87.254.105 on 09/05/12
For personal use only.

remote substituents as well as upon the conformation of the proton and the substituent attached to the same carbon atom. The anisotropic effects of all possible conformations of the substituents cannot be estimated; it is therefore not surprising that it is not possible to define narrow chemical shift ranges which are highly characteristic of the orientation of the methine proton concerned and of the functional group which is bonded to the same carbon atom.

The magnitudes of the coupling constants ($J_{1,2}$ and $J_{2,3}$) shown in Table II fall within the general ranges of values observed for $J_{a,e}$ (2–7 c.p.s.) and $J_{a,a}$ (5–13.4 c.p.s.) in six membered ring compounds in the chair form (14 and references therein). The dihedral angles between protons on adjacent carbon atoms for the chair, boat, and skew-boat forms of *trans,trans*- and *cis,trans*-1,2,3-trisubstituted cyclohexanes were obtained from measurements on Drieding models. Coupling constants corresponding to these angles were calculated by using the original Karplus parameters (15), and also by using a modification in which the entire curve was displaced upward by 1.1 c.p.s. (see below) at $J_{0°}$ and $J_{180°}$. Comparison of the observed couplings with the calculated values made it quite clear that the former are best rationalized on the grounds that the compounds are in the chair form principally in the conformations indicated in structures I and II.

Because of the rather wide range of $J_{a,a}$ values (7.3–10.3 c.p.s.) in the 1-methoxy-2(3)-acetoxy-3(2)-bromocyclohexanes as opposed to the narrow range for $J_{e,a}$ (2.8–3.0 c.p.s.), it was not clear how the Karplus parameters (15) should be modified, if at all, for the calculation of possible angular deformations in this series. However, a small upward displacement of the entire curve (cf. ref. 16) appeared to offer a reasonable approach. Compound I*j* has the largest $J_{2,3}$, and if it is assumed that $J_{180°} = 10.3$ c.p.s., displacement of the Karplus curve by an amount sufficient to give this magnitude of coupling constant at 180° (1.1 c.p.s.) would make $J_{60°} = 2.9$ c.p.s., which is in good agreement with the observed small couplings.

The observed variations in $J_{2,3}$ could owe their origin to the existence of an equilibrium between chair conformers, to distortion of dihedral angles between axially oriented protons, to electronegativity effects of substituents (17), or to differences in the orientation of remote functional groups (1; 11, p. 49). The earlier studies on the 1-alkoxy-2-acetoxy-3-acetylaminocyclohexanes (1, 2) made it seem unlikely that conformational equilibration is a major factor contributing toward the variations in $J_{a,a}$ in that series, but the same situation does not apply to the 1-methoxy-2(3)-bromo-3(2)-acetoxycyclohexanes. An exact determination of the extent of conformational equilibration in these compounds would be a major research project and is beyond the scope of this study. However, the equilibrium constants can roughly be estimated by making use of the conformational free-energy differences for the methoxyl group, acetoxyl group, and bromine (18). The values obtained, together with their predicted effects on $J_{2,3}$, are given in Table II, from which it is clearly apparent that all the experimentally observed values for $J_{2,3}$ in the *trans,trans*-bromocyclohexanediol derivatives (I*j*–I*m*) agree with the calculated couplings within experimental error (±0.3 c.p.s.). In the *cis,trans* analogues (II*j*–II*m*), however, there remains a significant difference between the observed and calculated couplings (except for II*m*), and it must be concluded that conformational equilibration is not the only one of the above-mentioned factors responsible for the changes in $J_{2,3}$. Since the same three (or two) substituents are always involved, electronegativity effects can probably be discounted. The residual discrepancies could be caused by small dihedral angular distortions of the protons caused by crowding of the *cis*-oriented substituents at C_1 and (or) by the change in orientation of the substituent at C_1 relative to those at C_2 and C_3. Evidence supporting the viewpoint that sizes of coupling constants can significantly be affected by changes in the

orientation of remote substituents has recently been presented (14, 19). The constancy of the small couplings in relation to the variability of the large couplings (Table II) would seem to be inconsistent with an interpretation based solely upon the dihedral angular distortion factor. However, there is insufficient evidence at present to differentiate between which of these factors is mainly responsible for the discrepancies observed.

The large 2,3 couplings in the acetylamino analogues (I*a*–I*f* and II*a*–II*f*) which were referred to earlier (1) present a picture quite different from those of the bromocyclohexanediol derivatives (I*j*–I*m* and II*j*–II*m*). The changes in the sizes of the coupling constants are in different directions in the two series as the orientation of the substituent at C_1 is changed in relation to those at C_2 and C_3 (Table II). Conformational equilibration and dihedral angular distortion were discounted as possible causes for the changes observed in the acetylamino series, and it was suggested that a remote substituent orientational effect is implicated (1) since electronegativity effects can also probably be discounted for isomeric pairs. The large divergences in $J_{2,3}$ for analogues of similar gross stereochemistry in the two series, e.g. I*a* and I*j*, II*a* and II*j*, undoubtedly owe their origin to a complex interplay of the four factors mentioned earlier, the complete analysis of which is beyond the scope of this work. It is sufficient to say that, although the relative electronegativities of substituents would be anticipated to play an important role in interpreting the observed divergences, the application of simple electronegativity considerations similar to those used by Williamson (17) in the more rigid hexachlorobicyclo[2.2.1]heptenes does not provide even an approximate rationalization.

EXPERIMENTAL

The proton magnetic resonance spectra were measured on a Varian V-4300C spectrometer operating at 60 Mc.p.s., a Varian V-3521 integrator being used for base-line stabilization. All solutions were 25% w/v in chloroform and were calibrated with reference to internal tetramethylsilane by the usual side-band technique. The preparation of all the compounds used herein was described previously (1, 2, 9, 10, 20, 21).

ACKNOWLEDGMENTS

The author is indebted to Dr. M. A. Weinberger and Miss P. Lutley for recording all the 60 Mc.p.s. spectra; to Dr. S. Brownstein for recording the 100 Mc.p.s. spectra of compounds I*j*, I*k*, and I*l*; and to Dr. R. R. Fraser for several helpful discussions.

REFERENCES

1. F. A. L. Anet, R. A. B. Bannard, and L. D. Hall. Can. J. Chem. **41**, 2331 (1963).
2. R. A. B. Bannard. Can. J. Chem. **42**, 744 (1964).
3. S. A. Barker, J. Hamer, M. C. Keith, and L. F. Thomas. J. Chem. Soc. 1538 (1963).
4. A. C. Richardson and K. A. McLaughlan. J. Chem. Soc. 2499 (1962).
5. L. D. Hall, L. Hough, K. A. McLaughlan, and K. Pachler. Chem. Ind. London, 1465 (1962).
6. L. Hough and S. H. Shute. Chem. Ind. London, 1827 (1962).
7. L. D. Hall. Advan. Carbohydrate Chem. **19**, 51 (1964).
8. R. U. Lemieux, R. K. Kullnig, H. J. Bernstein, and W. G. Schneider. J. Am. Chem. Soc. **80**, 6098 (1958).
9. R. A. B. Bannard and L. R. Hawkins. Can. J. Chem. **39**, 1530 (1961).
10. R. A. B. Bannard, A. A. Casselman, and L. R. Hawkins. Can. J. Chem. **43**, 2398 (1965).
11. N. S. Bhacca and D. H. Williams. Applications of nuclear magnetic resonance spectroscopy in organic chemistry. Holden-Day, Inc., San Francisco. 1964. p. 183.
12. R. U. Lemieux, R. K. Kullnig, and R. Y. Moir. J. Am. Chem. Soc. **80**, 2237 (1958).
13. H. Agahigian, G. D. Vickers, M. H. von Saltza, J. Reid, A. I. Cohen, and H. Gauthier. J. Org. Chem. **30**, 1085 (1965).
14. A. C. Huitric, J. B. Carr, W. F. Trager, and B. J. Nist. Tetrahedron, **19**, 2145 (1963).
15. M. Karplus. J. Chem. Phys. **30**, 11 (1959).
16. R. U. Lemieux, J. D. Stevens, and R. R. Fraser. Can. J. Chem. **40**, 1955 (1962).
17. K. L. Williamson. J. Am. Chem. Soc. **85**, 516 (1963).
18. E. L. Eliel, N. L. Allinger, S. J. Angyal, and G. A. Morrison. Conformational analysis. John Wiley & Sons, Inc., New York. 1965. p. 44.
19. D. H. Williams and N. S. Bhacca. J. Am. Chem. Soc. **86**, 2742 (1964).
20. R. A. B. Bannard and L. R. Hawkins. Can. J. Chem. **36**, 1241 (1958).
21. T. Suami and S. Ogawa. Bull. Chem. Soc. Japan, **37**, 194 (1964).

Can. J. Chem. Downloaded from www.nrcresearchpress.com by 210.87.254.105 on 09/05/12
For personal use only.

MASS SPECTRA OF OXYGENATED QUINOLINES

D. M. CLUGSTON AND D. B. MACLEAN
Department of Chemistry, McMaster University, Hamilton, Ontario
Received November 18, 1965

ABSTRACT

The mass spectra of the monohydroxyquinolines, the monomethoxyquinolines, N-methyl-2-quinolone, and N-methyl-4-quinolone have been recorded. The isomeric hydroxy compounds vary somewhat in the stability of the molecular ion, but all show the same fragmentation mechanism. Two general fragmentation patterns are discernible in the spectrum of each of the monomethoxyquinolines, but there is considerable variation among the isomers in the extent to which the two patterns occur. In addition, 8-methoxyquinoline undergoes a peculiar fragmentation wherein all three methyl hydrogens are lost. The 3-methoxy compound is unusual in that loss of 43 mass units from the molecular ion occurs in one step. Deuterium- and ^{13}C-labelling experiments have proved to be useful in interpreting the fragmentation pathways. The spectra of the two N-methylquinolones prove that O to N methyl rearrangement does not occur to any significant extent upon electron impact.

In a recent paper we reported on the behavior of some furoquinoline alkaloids upon electron impact (1). Except for quinoline (2) and some alkylquinolines (2, 3), no other systematic study of fragmentation in a quinoline system has been reported. It seemed appropriate, therefore, to examine the mass spectra of some simple oxygenated quinolines without the complicating effect of the furan ring present in the furoquinoline alkaloids. In this investigation, therefore, we report on the fragmentation of the seven monomethoxyquinolines, the seven monohydroxyquinolines, and the two isomeric N-methylquinolones.

Although the spectra of substituted quinolines have not been discussed, the spectra of other substituted aromatic systems have been examined in detail. The spectra of some methoxy derivatives of benzene (2, p. 174ff; 4) and naphthalene (5) have been reported, as have the spectra of phenols (6). In these compounds as well as in aromatic systems containing other substituents (2, p. 186ff; 4; 7), marked differences in the fragmentation of isomers have been noted. The mass spectra of several nitrogen-containing heterocyclic aromatic systems have been examined, and in many of them the loss of hydrogen cyanide has been found to be a major fragmentation pathway (2, p. 251ff). In 2- and 4-pyridone the spectra exhibit intense peaks for the loss of carbon monoxide (8). One might expect, therefore, that the quinoline derivatives discussed below would undergo fragmentation by pathways similar to those cited above. Our results show that this is so and that the expected differences among the various isomers are found.

The spectra of the monomethoxyquinolines are recorded in Fig. 1. It will be noted that there is considerable variation among the isomers, but that they can be divided into two main groups. The first group is made up of the 2- and 8-isomers while the second group comprises the rest. The major peaks found in each spectrum can be accounted for by two fragmentation schemes, both of which involve the methoxyl group in the initial fragmentation. Scheme 1 depicts the mechanism proposed for the formation of the ions appearing at M-1 (*m/e* 158), M-29 (*m/e* 130), M-30 (*m/e* 129), M-57 (*m/e* 102), and M-83 (*m/e* 76), and Scheme 2 outlines the mechanism by which the ions appearing at M-15 (*m/e* 144), M-43 (*m/e* 116), M-70 (*m/e* 89), and M-96 (*m/e* 63) are believed to arise. Both schemes are shown for 7-methoxyquinoline since the spectrum of this compound contains all the pertinent peaks, as well as metastable peaks supporting all the proposed fragmentations. Table I lists the metastable peaks which are observed for the various transformations for each of the seven isomers.

Can. J. Chem. Downloaded from www.nrcresearchpress.com by 210.87.254.5 on 09/05/12
For personal use only.

Can. J. Chem. Downloaded from www.nrcresearchpress.com by 210.87.254.5 on 09/05/12
For personal use only.

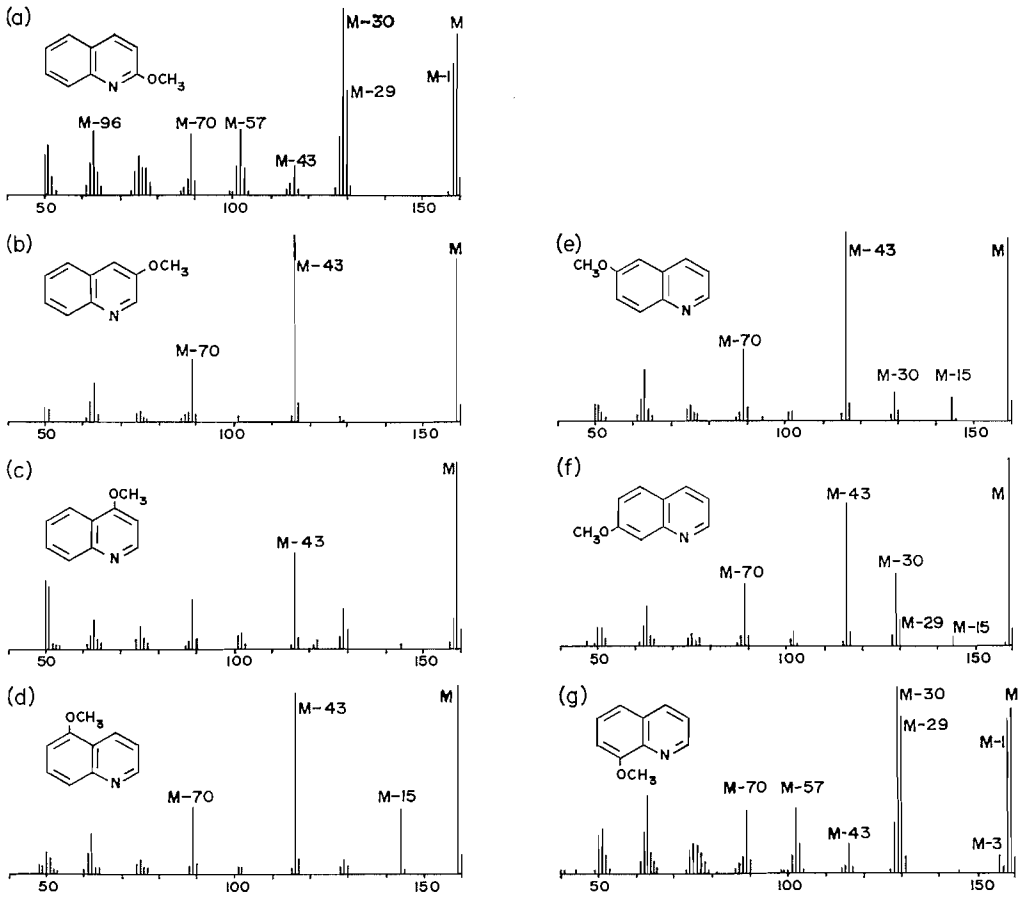


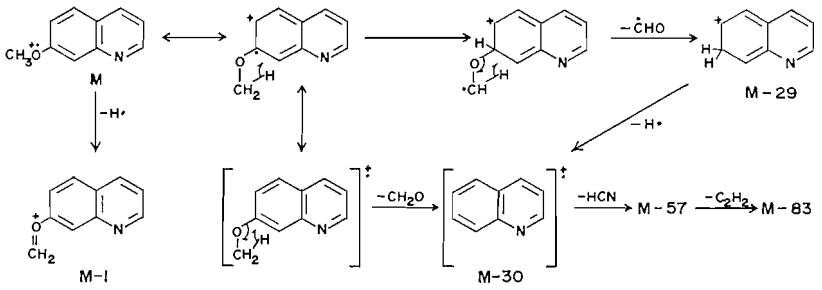
FIG. 1. Mass spectra of (*a*) 2-methoxyquinoline, (*b*) 3-methoxyquinoline, (*c*) 4-methoxyquinoline, (*d*) 5-methoxyquinoline, (*e*) 6-methoxyquinoline, (*f*) 7-methoxyquinoline, and (*g*) 8-methoxyquinoline.

TABLE I

Metastable peaks in the spectra of the methoxyquinolines

Transformation	Calcd.	Observed in the spectra of:
M → M-1 159 → 158	157.0	2-, 4-, 5-, 7-, 8-
M → M-15 159 → 144	130.4	3-, 5-, 7-
M → M-29 159 → 130	106.3	2-, 4-, 7-, 8-
M → M-30 159 → 129	104.7	4-, 5-, 6-, 7-
M-15 → M-43 144 → 116	93.4	4-, 5-, 6-, 7-
M-30 → M-57 129 → 102	80.7	2-, 4-, 7-, 8-
M-43 → M-70 116 → 89	68.3	2-, 3-, 4-, 5-, 6-, 7-, 8-
M-70 → M-96 89 → 63	44.6	2-, 3-, 4-, 5-, 6-, 7-, 8-

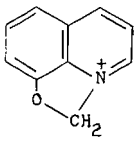
The spectra of 2- and 8-methoxyquinoline are similar in that the major fragment ions in each case are those which arise by the transformations depicted in Scheme 1. Both show intense peaks for the molecular ion, as expected for aromatic compounds, and at M-1,



SCHEME 1.

M-29, and M-30. That the methoxyl group is involved in the formation of all the major fragment ions is verified by examination of the mass spectra of the OCD_3 analogues of 2- and 8-methoxyquinoline. The spectra of the deuterated compounds are recorded in Figs. 2*a* and 2*c*. It is seen that the M-1, M-29, and M-30 peaks of the undeuterated compounds are found at M-2, M-30, and M-32, respectively, in the spectra of the deuterated compounds. Therefore, the M-1 peak arises by loss of one of the methyl hydrogens, and the M-29 and M-30 fragments arise by loss of CHO· and CH_2O, respectively, from the methoxyl group. The mechanism shown in Scheme 1 for loss of CHO· and CH_2O is that originally proposed by Barnes and Occolowitz (4) for the fragmentation of 1,3-dimethoxybenzene.

In a previous paper on the mass spectra of furoquinoline alkaloids (1) we noted that the furoquinolines containing an 8-methoxy substituent in the quinoline ring gave rise to an intense peak at M-1 in their mass spectra. We suggested that a hydrogen was lost from the methoxyl group and that the positive charge on the methyl carbon was stabilized by the unshared pair of electrons on the nearby nitrogen atom as shown below. A similar structure for the ion derived by loss of a hydrogen atom from the methyl group of the molecular ion of 2-methoxyquinoline may be written. The fact that, of all the methoxyquinolines examined, only the 2- and 8-isomers exhibit an intense M-1 peak in their spectra indicates that stabilization by neighboring nitrogen may indeed be involved.



We also suggested in our paper on the furoquinoline alkaloids that those alkaloids containing an 8-methoxyl substituent might undergo methyl migration from oxygen to nitrogen followed by elimination of CO or CHO·. The lack of any significant M-28 peak in the mass spectrum of 8-methoxyquinoline casts doubt on such a rearrangement, and the deuterium-labelling experiments discussed above all but eliminate such a possibility. An examination of the spectrum of 8-methoxyquinoline labelled in the methoxyl carbon with ^{13}C disproves completely any possibility of methyl migration before fragmentation. The spectrum of the ^{13}C-labelled compound is shown in Fig. 2*d*. It is evident that the peaks at *m/e* 129 (M-CH_2O) and *m/e* 130 (M-CHO·) are not shifted in the labelled compound, occurring in the same position as in the unlabelled analogue. The methoxyl carbon atom, therefore, is lost when these fragment ions are formed.

Can. J. Chem. Downloaded from www.nrcresearchpress.com by 210.87.254.5 on 09/05/12
For personal use only.

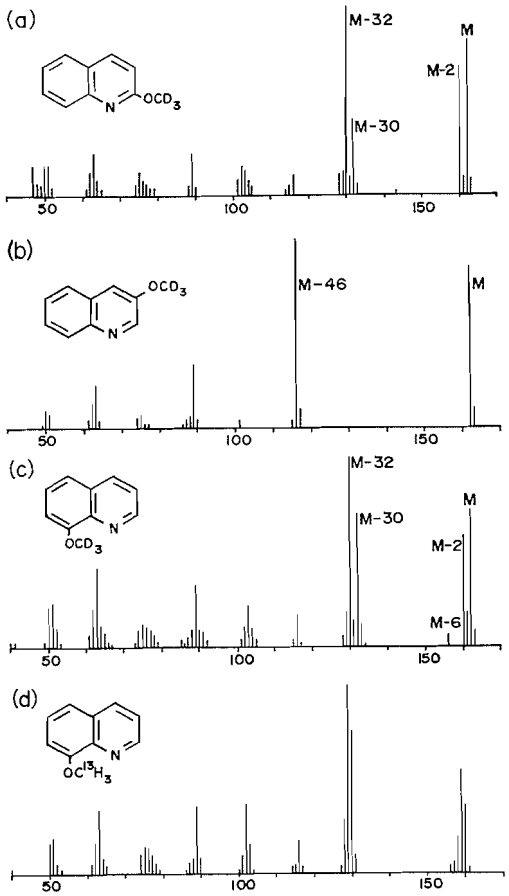


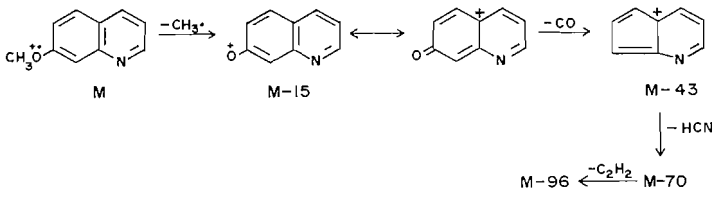
FIG. 2. Mass spectra of (*a*) 2-methoxy-d_3-quinoline, (*b*) 3-methoxy-d_3-quinoline, (*c*) 8-methoxy-d_3-quinoline, and (*d*) 8-methoxy-^{13}C-quinoline.

The presence of a peak at M-3 in the mass spectrum of 8-methoxyquinoline enables one to differentiate it from all the other methoxyquinolines examined. The fact that a similar fragmentation giving rise to a M-6 peak occurs in the deuterium-labelled analogue (Fig. 2*c*) indicates that all three methyl hydrogens, and only the methyl hydrogens, are lost to form the M-3 fragment ion from 8-methoxyquinoline. The M-3 ion apparently arises by loss of H_2 from the M-1 ion (m^* calcd. for $158 \rightarrow 156 = 154.0$; m^* obs. = 154.3), or in the case of the deuterated compound the M-6 ion arises by loss of D_2 from the M-2 ion (m^* calcd. for $160 \rightarrow 156 = 152.1$; m^* obs. = 152.5). A M-3 peak is apparently characteristic of quinolines carrying an 8-methoxyl substituent, although it is usually of much lower intensity than in the case of 8-methoxyquinoline itself. Thus, we have observed a M-3 peak in the mass spectra of 8-methoxyquinaldine and of three furoquinoline alkaloids containing an 8-methoxy substituent, skimmianine, maculosidine, and flindersiamine (1). In every case we have also observed a metastable peak corresponding to loss of H_2 from the M-1 fragment ion.

Both 2- and 8-methoxyquinoline exhibit peaks at *m/e* 116 (M-43) in their mass spectra, but of low intensity. This fragment is apparently formed in each case by the mechanism

Can. J. Chem. Downloaded from www.nrcresearchpress.com by 210.87.254.5 on 09/05/12
For personal use only.

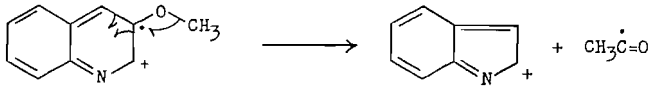
outlined in Scheme 2, even though the intensity of the M-15 peaks is too low to plot. The possibility that the ion of M-43 may arise by a concerted loss of 43 mass units cannot be excluded (see below).



SCHEME 2.

The most intense fragment ion peak in the mass spectra of 3-, 4-, 5-, 6-, and 7-methoxyquinolines is found at *m/e* 116 (M-43). A peak is also observed at *m/e* 144 (M-15) in every case except that of the 3-methoxy compound. Thus, the fragmentation pattern outlined in Scheme 2 would appear to be dominant in the cases of the 4-, 5-, 6-, and 7-methoxy compounds. Fragmentation according to Scheme 1 is discernible in all the isomers, but it is only in the 7-methoxy compound that it is apparent to any appreciable degree. Metastable peaks in the spectra of the 4-, 5-, 6-, and 7-isomers corroborate the major fragmentation processes (Table 1) as proposed in Schemes 1 and 2.

Apparently 3-methoxyquinoline is unique in that the loss of 43 mass units occurs in a concerted fashion. The peak at M-15 is of very low intensity whereas that at M-43 is the base peak of the spectrum. A metastable peak at *m/e* 85.0 corresponds to the transformation M → M-43 (*m** calcd. for 159 → 116 = 84.6). A possible mechanism for such a fragmentation is shown below. Confirmation of the fact that the methoxyl methyl group is

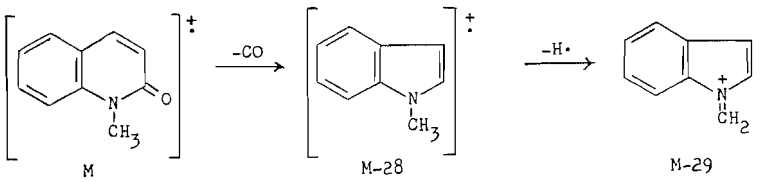


lost in this fragmentation is obtained by an examination of the spectrum of the deuterium-labelled analogue (Fig. 2*b*). The base peak is again at *m/e* 116, corresponding to the loss of 46 mass units from the molecular ion, and a metastable peak at *m/e* 83.4 corresponds to the fragmentation 162 → 116 (*m** calcd. = 83.1). To our knowledge, this is the first report of the loss of 43 mass units in a concerted step involving a methoxyl substituent.

We considered it possible that the 2- and 4-methoxyquinolines might undergo electron impact induced rearrangement of the methyl group from oxygen to nitrogen with subsequent fragmentation of the N-methylquinolone that was formed. It is known that such a rearrangement is induced thermally (9, 10). Accordingly, we prepared and recorded the mass spectra of N-methyl-2-quinolone and N-methyl-4-quinolone. The spectra, shown in Fig. 3, are distinctly different from the isomeric O-methyl compounds in that they contain only very small M-1 peaks and in that the major fragment in each case is formed by the loss of 28 mass units (CO) from the molecular ion. Metastable peaks in both spectra indicate that the fragmentation occurs in the sequence M → M-28 → M-29, as shown below for N-methyl-2-quinolone.

In the mass spectra of all of the monohydroxyquinolines the peak corresponding to the molecular ion (*m/e* 145) is the strongest in the spectrum. The spectra of the hydroxyquinolines may be divided, however, into two distinct groups on the basis of the intensities

Can. J. Chem. Downloaded from www.nrcresearchpress.com by 210.87.254.5 on 09/05/12
For personal use only.



of the peaks of the fragment ions. The two groups are represented in Fig. 4 by the spectra of 2- and 3-hydroxyquinoline. The first group, composed of the 2-, 4-, and 8-hydroxy compounds, exhibits relatively strong peaks for the fragment ions corresponding to the loss of 28 mass units (CO) followed by the loss of 27 mass units (HCN) and then 1 mass unit (H·) from the molecular ion. The second group, composed of the 3-, 5-, 6-, and 7-hydroxy compounds, exhibits the same fragment peaks, but at greatly reduced intensities. Facile loss of CO from the molecular ions of 2- and 4-hydroxyquinolines may

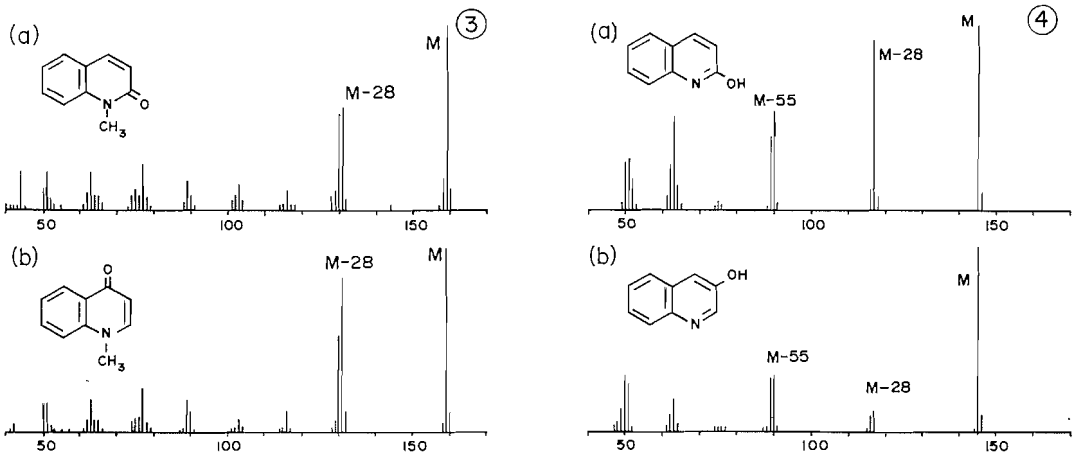


FIG. 3. Mass spectra of (*a*) N-methyl-2-quinolone and (*b*) N-methyl-4-quinolone.
FIG. 4. Mass spectra of (*a*) 2-hydroxyquinoline and (*b*) 3-hydroxyquinoline.

be explained on the basis of participation of the tautomeric quinolone structures shown below. In the case of 8-hydroxyquinoline, however, no such structure is permitted, and it is more difficult to rationalize the loss of carbon monoxide. It may be that the nearby nitrogen accepts the hydrogen of the 8-hydroxyl function, thereby allowing for the facile loss of CO.



EXPERIMENTAL

Apparatus, Methods, and Materials

Mass spectra were determined on a Hitachi Perkin–Elmer RMU-6A mass spectrometer at an ionizing potential of 80 eV and an ionizing current of 50 μA. Samples were introduced through an all-glass inlet system maintained at 200°. Spectra are plotted in terms of relative abundance, with the most intense peak (base peak) being taken as 100%. Only peaks equal to or greater than 2% of the base peak are recorded.

Can. J. Chem. Downloaded from www.nrcresearchpress.com by 210.87.254.5 on 09/05/12
For personal use only.

All samples were purified by vapor phase chromatography on a 6 ft column of 3% SE-30 silicone gum rubber on Chromosorb P. The column temperature was maintained at 150° or 200° depending on the volatility of the material. 6-Methoxyquinoline and 2-, 4-, and 8-hydroxyquinoline were obtained commercially; CD_3OH (99 atom % D), CD_3I (99 atom % D), and $^{13}CH_3I$ (53 atom % ^{13}C) were obtained from Merck, Sharp and Dohme of Canada Ltd.

2-Methoxyquinoline and 4-Methoxyquinoline

The hydroxyquinoline was converted into the chloroquinoline by treatment with phosphorus oxychloride (11). The chloro compound was heated under reflux with an excess of sodium methoxide in methanol for 3 h (11). The methanol was removed, water added, and the mixture extracted with chloroform. The chloroform extract was dried and evaporated to dryness, and the residue was purified by vapor phase chromatography.

2-Methoxyquinoline-d_3 and 4-Methoxyquinoline-d_3

The procedure used was identical with that above, except that sodium methoxide-d_3 and CD_3OH were used.

3-Hydroxyquinoline and 3-Methoxyquinoline

The diazonium chloride obtained from 3-aminoquinoline by the method of Abramovitch (12) was slowly added to boiling water. The resulting solution was cooled, excess $NaHCO_3$ added, and the hydroxyquinoline filtered off. The product was recrystallized from ethanol–water. Conversion into 3-methoxyquinoline was accomplished with diazomethane in ether.

5-Hydroxyquinoline

5-Nitroquinoline was converted into 5-hydroxyquinoline by the method of Kochanska and Brobanski (13).

5-Methoxyquinoline

5-Methoxyquinoline was prepared by the method of Bradford *et al.* (14).

6-Hydroxyquinoline

6-Methoxyquinoline was heated under reflux with 47% HI for 5 h. The acidic solution was neutralized and the 6-hydroxyquinoline recovered by extraction with chloroform. A sample for mass spectrometry was purified by vapor phase chromatography.

7-Methoxyquinoline

m-Anisidine (6 g), nitrobenzene (6 g), glycerol (45 g), and powdered $FeSO_4$ (4 g) were mixed together and stirred, and concentrated H_2SO_4 (35 g) was added slowly. The mixture was brought to a boil, allowed to stand for 0.5 h, and then heated under reflux for 4 h. Nitrobenzene was removed by steam distillation and primary amine destroyed by adding excess $NaNO_2$ and boiling the reaction mixture. The resulting solution was made basic with KOH and steam-distilled until the distillate was clear. The distillate was extracted with chloroform, and the oil (7 g) obtained from the $CHCl_3$ extract was distilled at 12 mm. A fraction collected up to 140° was discarded and a second fraction collected from 140–145° was further purified by vapor phase chromatography.

7-Hydroxyquinoline

This compound was prepared in the same manner as 6-hydroxyquinoline.

8-Methoxyquinoline

8-Hydroxyquinoline was treated with excess methyl iodide in the presence of sodium hydroxide in a solution of methanol–water. The solution was heated in a sealed tube at 100° for 0.5 h. The reaction mixture was poured into H_2O and extracted with chloroform. The dried chloroform solution was evaporated to dryness and the residue purified by vapor phase chromatography.

8-Methoxyquinoline-d_3

The procedure used was that described above, except that CD_3I was used instead of CH_3I.

8-Methoxyquinoline-^{13}C

The procedure used was that described for 8-methoxyquinoline, except that $^{13}CH_3I$ was used instead of CH_3I.

N-Methyl-2-quinolone and N-Methyl-4-quinolone

The hydroxyquinoline, aqueous sodium hydroxide, methyl iodide, and sufficient methanol to give a homogeneous solution were heated under reflux for 2 h (15, 16). The N-methylquinolones were isolated and purified by conventional procedures.

ACKNOWLEDGMENTS

We thank Dr. A. Corsini of this university for a sample of 8-methoxyquinaldine and Mr. John Wells of these laboratories for technical assistance in the preparation of the

Can. J. Chem. Downloaded from www.nrcresearchpress.com by 210.87.254.5 on 09/05/12
For personal use only.

methoxyquinolines. This work was supported through grants from the Dominion Rubber Co. Ltd. and the National Research Council of Canada.

REFERENCES

1. D. M. CLUGSTON and D. B. MACLEAN. Can. J. Chem. **43**, 2516 (1965).
2. H. BUDZIKIEWICZ, C. DJERASSI, and D. H. WILLIAMS. Interpretation of mass spectra of organic compounds. Holden-Day, Inc., San Francisco. 1964. p. 257.
3. W. A. AYER, T. E. HABGOOD, V. DEULOFEU, and H. R. JULIANI. Tetrahedron, **21**, 2169 (1965).
4. C. S. BARNES and J. L. OCCOLOWITZ. Australian J. Chem. **16**, 219 (1963).
5. K. BIEMANN. Mass spectrometry: organic chemical applications. McGraw-Hill Book Co., Inc., New York. 1962. p. 140.
6. T. ACZEL and H. E. LUMPKIN. Anal. Chem. **32**, 1819 (1960).
7. S. MEYERSON, H. DREWS, and E. K. FIELDS. Anal. Chem. **36**, 1294 (1964).
8. G. SPITELLER and M. SPITELLER-FRIEDMANN. Monatsh. **93**, 1395 (1963).
9. H. MEYER. Monatsh. **27**, 255 (1906).
10. H. MEYER and R. BEER. Monatsh. **34**, 1173 (1913).
11. A. ALBERT and J. N. PHILLIPS. J. Chem. Soc. 1294 (1956).
12. R. A. ABRAMOVITCH. J. Chem. Soc. 3839 (1954).
13. L. KOCHANSKA and B. BROBANSKI. Ber. **69**, 1807 (1936).
14. L. BRADFORD, T. J. ELLIOTT, and F. M. ROWE. J. Chem. Soc. 437 (1947).
15. P. FRIEDLÄNDER and F. MÜLLER. Ber. **20**, 2009 (1887).
16. E. SPÄTH and A. KOLBE. Monatsh. **43**, 469 (1922).

Can. J. Chem. Downloaded from www.nrcresearchpress.com by 210.87.254.5 on 09/05/12
For personal use only.

Can. J. Chem. Downloaded from www.nrcresearchpress.com by 210.87.254.5 on 09/05/12
For personal use only.

MASS SPECTRA AND REACTION MECHANISM STUDIES

THE FAVORSKY–MARKER REARRANGEMENT OF 17α-BROMOPREGNENOLONES IN DEUTERATED METHANOL[1]

R. DEGHENGHI, G. SCHILLING, AND G. PAPINEAU-COUTURE
Ayerst Research Laboratories, Montreal, Quebec
Received October 13, 1965

ABSTRACT

An examination of the mass spectra of the products isolated from a Favorsky rearrangement of 17α-bromopregnenolone acetate (Marker's conditions) in deuterated solvents offers a clue to the reaction mechanism. The stereochemical implications and the mass fragmentation pattern of the products examined are discussed.

The reaction of α-halo ketones in alkaline media, known as the Favorsky rearrangement, has received considerable attention recently (1–7, 29, 30). The proposed mechanisms have been numerous, and it is now obvious that, more than questioning their multiplicity, one has to limit their validity to the appropriate substrate and conditions of the reaction under study.

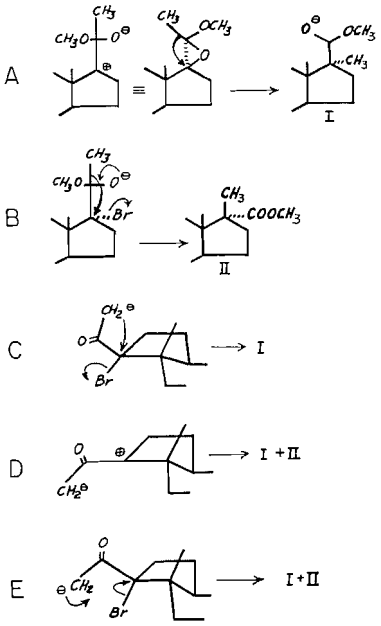
In 1942, Marker (8) reported the alkaline rearrangement of 17-bromo-20-ketopregnanes in aqueous methanolic potassium bicarbonate. The methyl ester of a 17-methyletianic acid was the principal product of the reaction. The stereochemistry of this type of compounds was later established by Plattner and co-workers (9), on the basis of the biological activities of the derived epimeric 17-methylprogesterones, and, more rigorously, by Wendler (10), who also established the configuration of the starting 17-bromo-20-ketones.

The mechanism of the Favorsky–Marker rearrangement of this type of compounds is particularly interesting in that a substantial stereospecificity with *retention of configuration* is achieved. Our careful study of the products of the alkaline rearrangement of 17α-bromopregnenolone (*vide infra*) shows that, of the two epimeric esters (or acids) formed, the 17α-methyl epimer (retention) is present to the extent of 85–90%. Both the (Tchoubar) (12) semibenzilic mechanism (11) (B) and the (Loftfield) synchronous (12) cyclopropanone intermediate (C) therefore have to be excluded for the formation of the major product, thereby leaving the original (Favorsky) epoxyether mechanism (13) (A), the zwitterionic non-synchronous (Aston–Dewar) cyclopropanone formation (14) (D), and the bromine transfer (31) from C-17 to C-21 proposed by Wendler (10) (E).[2]

The epoxyether mechanism, which was favored in the quasi-Favorsky rearrangement (15), found early supporters (16, 17) in the open-chain or monocyclic series. It is analogous to the quantitative formation of epoxynitrile from the reaction of 17-bromo-20-ketopregnanes and KCN in aqueous alcohol (18), and is the most plausible mechanism for the formation of D-homo ketolic steroids when 17-bromo-20-ketopregnanes react with aqueous NaOH in acetone (19). However, the failure of epoxyethers in general to yield Favorsky-type products (1) does not favor, although it does not rigorously exclude, this mechanism.

[1]*Presented in part at the meetings of the "Association Canadienne Française pour l'Avancement des Sciences", Ottawa, November 1961, and Quebec, November 1963, and at the 47th Canadian Chemical Conference, Kingston, Ontario, June 1964.*

[2]*We thank a referee for pointing out an earlier reference to this mechanism (31).*



The Aston–Dewar and Wendler non-synchronous mechanisms both postulate a cyclopropane intermediate preceded by a zwitterionic "no-bond" species (D), or by a bromoenolate resulting from an allylic shift of the bromine from C-17 to C-21 (3).

Evidence for a delocalized intermediate in monocyclic systems has recently (3) been claimed, and the allylic shift of Wendler is analogous to the "internal return" of Winstein (20) (shift from a tertiary to a primary allylic halide).

In a recent review (21) Engel, because of discrepancies in the epimer ratio after the rearrangement of 21- versus 17-halogenated 20-ketopregnanes, did not favor Wendler's suggestion.[3] Wendler's bromoenolate is also rather improbable because of the absence of solvolysis products derived from it (*vide infra*).

The influence of the solvent on the stereochemical outcome of the Favorsky rearrangement has been analyzed thoroughly by House (22, 29) and by Tchoubar (5). Their modified versions of the detailed Loftfield mechanism overcome the stereochemical objections to that mechanism.

A reexamination of the Favorsky–Marker rearrangement in methanolic aqueous potassium bicarbonate solution of pure[4] 17α-bromopregnenolone acetate (I) followed by reacetylation revealed the presence of five products: two epimeric esters II and III, two epimeric acids IV and V, and 17α-methoxypregnenolone acetate (VI).

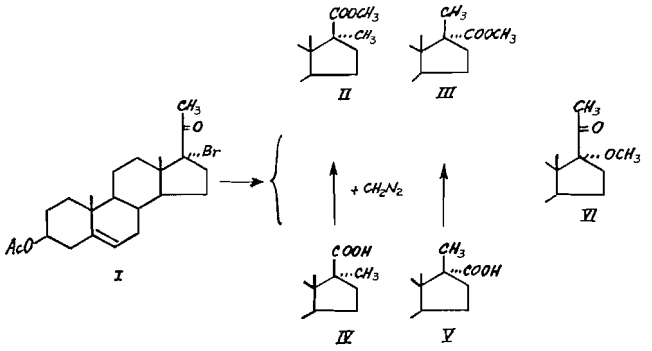
The acid fraction (IV + V) amounted to 4% of the total, and the neutral fraction had the following composition (by vapor phase chromatography): II, 90%; III, 5%; VI, <1% of the total. When the same reaction was run in the presence of K_2CO_3 instead of $KHCO_3$,[5] a slight change in the ratio of the epimers was observed, namely, II, 80%;

[3]*On closer analysis, this argument alone fails to be convincing if one considers that the rearrangement of a 21-halo-20-ketopregnane involves the abstraction of a 17-proton, and that Wendler's enolate derived from a 17-halo-20-ketone owes its negative charge to an allylic displacement through possibly a four-membered intermediate. The different origin of the two species, particularly in a polar solvent like methanol, may well account for differences in the reaction products.*

[4]*Recrystallized from methanol to a constant melting point and rotation, and to absolute homogeneity as judged by thin-layer chromatography and nuclear magnetic resonance spectra.*

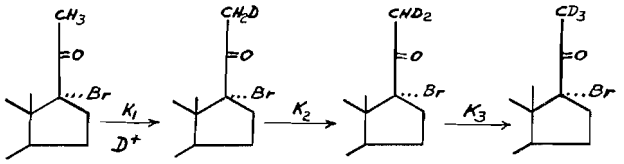
[5]*To avoid proton species in the deurated experiment (vide infra).*

Can. J. Chem. Downloaded from www.nrcresearchpress.com by 210.87.254.5 on 09/05/12
For personal use only.

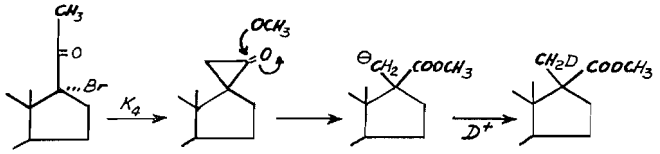


III, 12%; VI, 2%; IV, 5.5%; V, 0.5%. The reaction was then run in the presence of K_2CO_3 and deuterated solvents (CH_3OD, D_2O), and the products isolated as usual. The infrared spectra of the products revealed incorporation of deuterium, which conceivably could have been introduced by one or both of the following routes:

A. Before Favorsky rearrangement, by enolization and exchange with the medium.



B. By opening of a cyclopropane intermediate.



An examination of the products for the D_1, D_2, or D_3 species as well as for the non-deuterated material suggested itself for the following reasons: (*a*) The presence of any non-deuterated material should favor the epoxyether mechanism or (for the epimers III and V) the semibenzilic mechanism, indicating also that the exchange rates K_1, K_2, and K_3 are negligible. (*b*) The presence of polydeuterated (D_2, D_3) species is of course inconclusive, since the incorporation of deuterium could have occurred before any rearrangement (K_1, K_2, and K_3 not negligible). (*c*) The presence of only the monodeuterated species in both epimers, although not rigorously excluding the non-cyclopropanonic mechanisms, strongly favors a cyclopropanone fission (route *B*), indicating also that exchange before rearrangement is negligible.

An examination of the nuclear magnetic resonance spectra of the products was not revealing, since the band attributed to the 17-methyl group, reduced to approximately two-thirds of the original intensity, could have been attributed to the presence of some non-deuterated species together with a multideuterated (CHD_2 or CD_3) group, to the presence of a pure monodeuterated (CHD_2 or CD_3) group, or to the presence of a pure monodeuterated (CH_2D) substituent.[6]

[6]*We thank Dr. G. Just, Montreal, for suggesting this point to us.*

Can. J. Chem. Downloaded from www.nrcresearchpress.com by 210.87.254.5 on 09/05/12
For personal use only.

An examination of the mass spectra of the epimeric pairs (Figs. 1–4) provided the unequivocal answer: both deuterated epimers contain essentially one deuterium atom, and non-deuterated or polydeuterated species are absent.

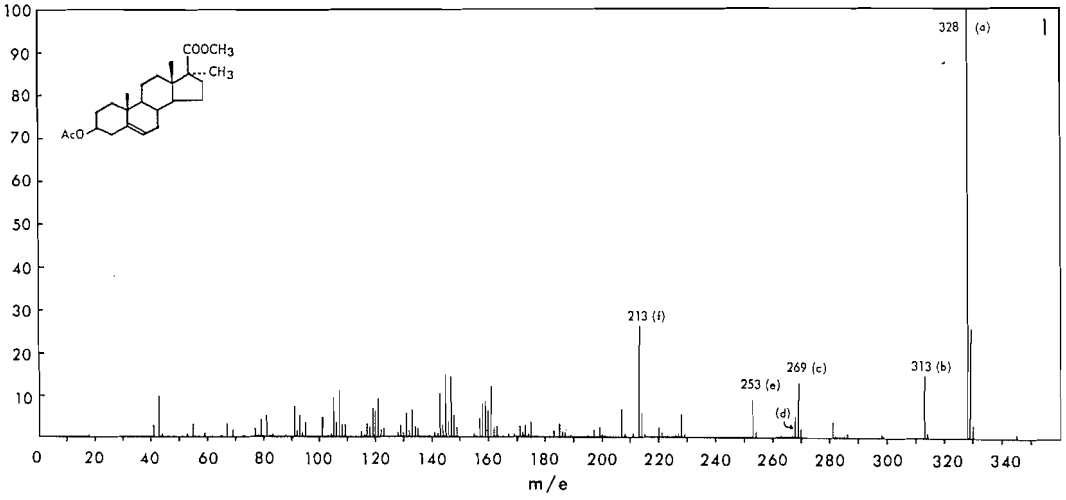


FIG. 1.

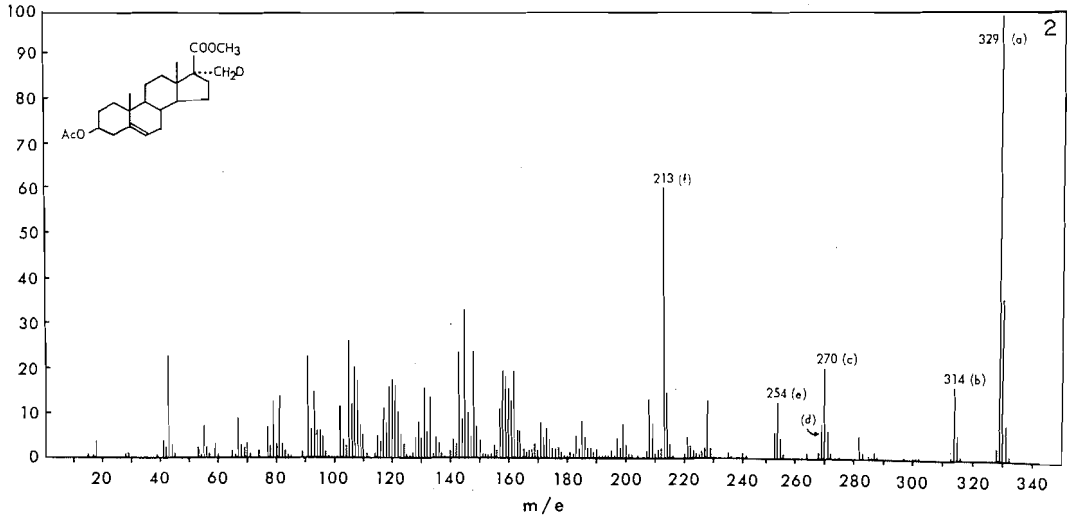


FIG. 2.

It seems reasonable to conclude, therefore, that *the deuterium is incorporated during an intermediate cyclopropanone fission and that the rate of deuterium exchange before rearrangement is negligible.* This finding militates strongly against the epoxyether or the semibenzilic rearrangements, the products of which would have contained all possible combinations of non- and poly-deuterated species.

The interesting solvolysis by-product, 17α-methoxypregnenolone acetate (23) (VI), was unequivocally characterized by comparison with an authentic sample prepared by methylation of 17α-hydroxypregnenolone acetate.

Can. J. Chem. Downloaded from www.nrcresearchpress.com by 210.87.254.5 on 09/05/12
For personal use only.

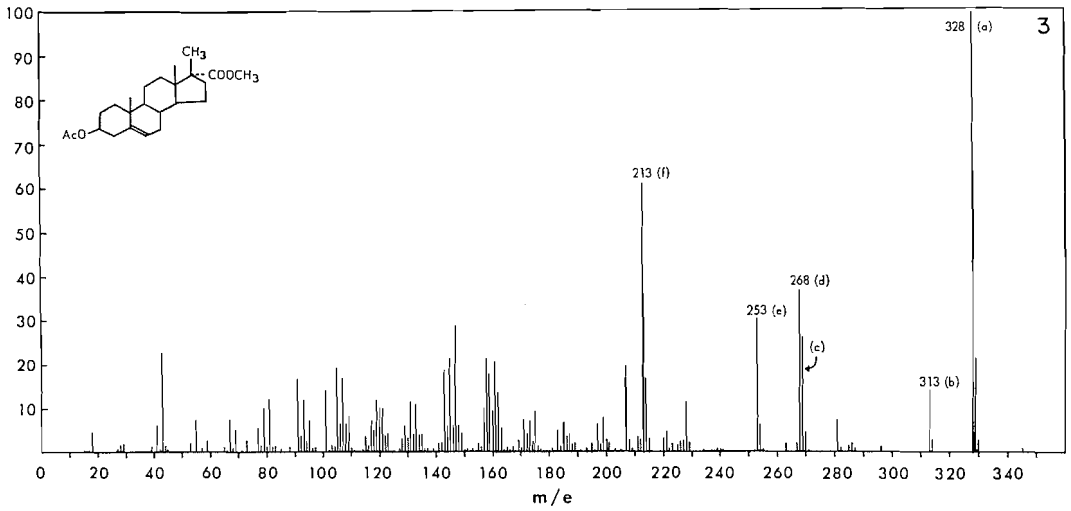


FIG. 3.

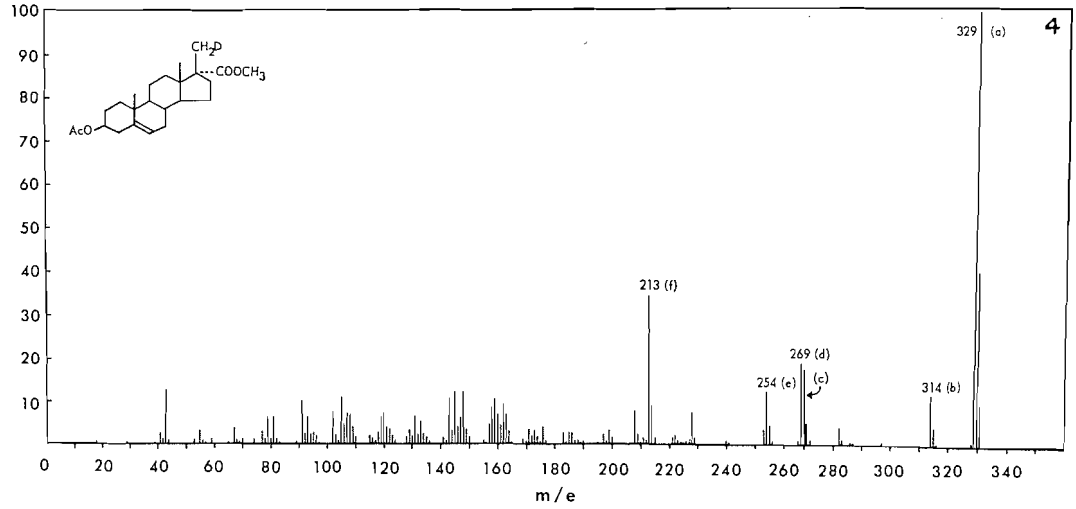


FIG. 4.

DISCUSSION

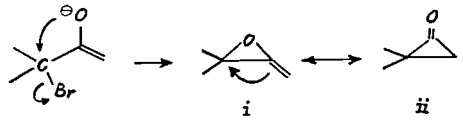
The Favorsky–Marker rearrangement of 17-bromo-20-ketopregnanes results in products with predominant retention of configuration. Careful analysis of the reaction mixture revealed the presence of only one solvolysis product, a 17α-methoxy-20-ketopregnane derivative. The incorporation of deuterium was homogeneous in both epimeric Favorsky products and D_1 was by far the predominant, if not the only, species.

These experimental facts can best be accommodated by a mechanism involving a common intermediate with a lifetime sufficient to give the solvolysis product VI before collapsing to the cyclic structures responsible for the epimeric esters II and III. The fact that no appreciable incorporation of deuterium occurs before rearrangement, as evidenced by the absence of D_2 or D_3 species, seems to indicate that the cyclopropanone formation goes faster than the ketonization of the enolate.

Can. J. Chem. Downloaded from www.nrcresearchpress.com by 210.87.254.5 on 09/05/12
For personal use only.

Can. J. Chem. Downloaded from www.nrcresearchpress.com by 210.87.254.5 on 09/05/12
For personal use only.

We can speculate about a stepwise mechanism for the Favorsky–Marker rearrangement for 17α-bromo-20-ketopregnanes as follows: step 1, enolate ion formation favored by the polarity of the solvent medium; step 2, oxygen–bromine dipole repulsion, bringing the oxygen to the beta side of the molecule; and step 3, loss of the halide to provide a delocalized intermediate which then collapses stereospecifically to a cyclopropanone (carbonyl on the beta side) or, alternatively, loss of halide assisted by a S_N2-type displacement to give structure *i*, which is a valency tautomer (30) of structure *ii* with the predominant stereochemistry.



Step 1 would be peculiar to Marker's conditions (methanol – aqueous alkali) whereas step 2 would be favored particularly by the stereochemistry of the steroidal side chain (24). A clockwise rotation of about 90° along the $C_{20} \rightarrow C_{17}$ axis of the solvated enolate is required to alleviate dipole interaction, thereby bringing the negatively charged oxygen to the beta side.

Unassisted loss of bromine or concerted bromine displacement (step 3) by the negative oxygen should then provide a "no-bond" zwitterion or the valency tautomer *i*, respectively, *with the oxygen always on the beta side* of the molecule. Both species can react with the solvent to provide the solvolysis product 17α-methoxypregnenolone, or collapse to the sterically predominant cyclopropane structure *ii*.

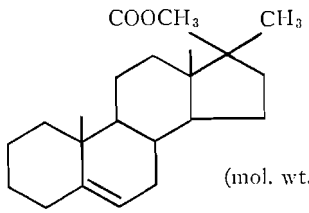
We believe that the 18-methyl and the 12-methylene groups responsible for the preferred rotational configuration (24) of the halogenated side chain are indirectly governing the stereochemistry of the Favorsky–Marker rearrangement, more than affecting the chemistry of the transition state.[7]

Mass Spectra of the Favorsky Products

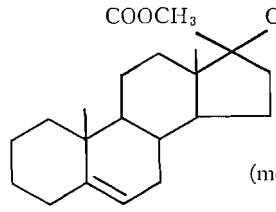
Significant peaks in the deuterated and non-deuterated pair of epimers are tabulated in Table I.

TABLE I

Mass spectra of the Favorsky products



(mol. wt. 388)



(mol. wt. 389)

Peak	*m/e*		*m/e*	
a	328	M′ (M-60)	329	M′ (M-60)
b	313	M′-15	314	M′-15
c	269	M′-59	270	M′-59
d	268	M′-60	269	M′-60
e	253	M′-75	254	M′-75
f	213	M′-115	213	M′-116

[7]*The noted (21) influence of a carbonyl group in position 11, in view of Woodward's analysis of the geometry of cyclic ketones (25), can hardly be explained only by a minimal steric distortion of the 18-methyl group. It is known that a bulky 12α-acetoxy group does not interfere with the steric retention of the Favorsky–Marker rearrangement (21). An influence of the 11-carbonyl on the reactivity of a 17,20-epoxynitrile system has been noted (18), but could not be accounted for on steric grounds. See also ref. 26 for other influences of the 11-keto group on reactions involving the side chain.*

The molecular ion is not present in the spectra. The base peaks (100%) are attributable to M-60 (loss of acetic acid) (27) (peaks *a*). Peaks *b* (M′-15) are attributable to a further loss of CH_3 from the ester group, peaks *c* (M′-59) to loss of the carbomethoxy group ($COOCH_3$), peaks *d* (M′-60) to loss of $COOCH_3$ + H, peaks *e* (M′-75) to loss of $COOCH_3$ + CH_4, and peaks *f* (M′-113 and M′-114) to loss of ring D ($C_6H_{11}O_2$ and $C_6H_{10}DO_2$).

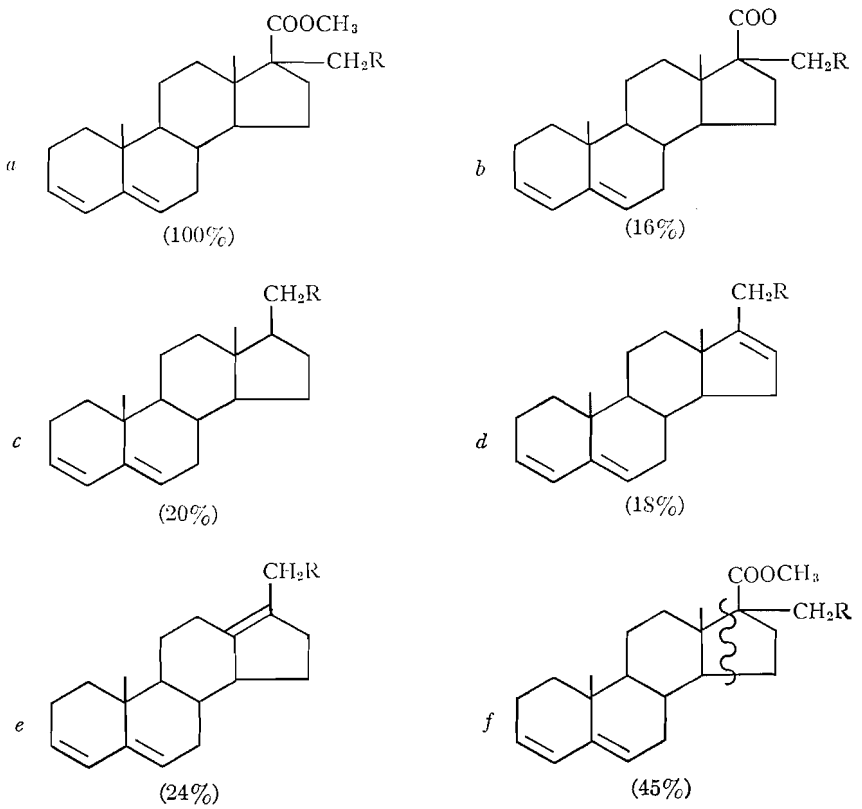
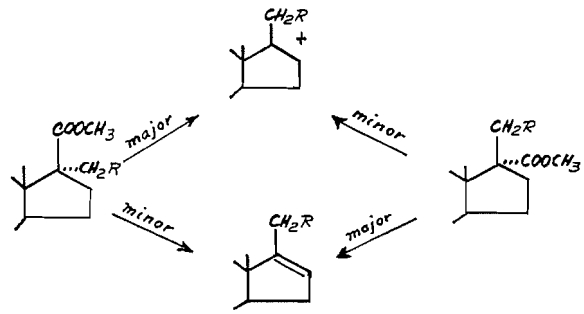


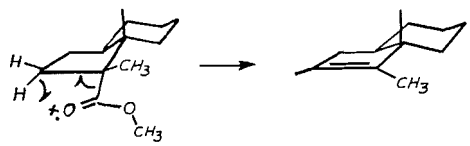
FIG. 5. The probable structure of fragments (R = H, D). The percentages in parentheses indicate the relative percentage intensity of the peaks.

The fragmentation pattern of the epimeric pairs (A and B) was remarkably similar, the only difference being in the relative intensity of peaks *c* and *d* (see spectra). These peaks (*m/e* 269 and 268 when R = H, *m/e* 270 and 269 when R = D) correspond to loss of a carbomethoxy ($COOCH_3$) and of a carbomethoxy plus hydrogen group.



Can. J. Chem. Downloaded from www.nrcresearchpress.com by 210.87.254.5 on 09/05/12
For personal use only.

This fact can be accounted for by invoking a cyclic mechanism for the elimination of a carbomethoxy plus hydrogen group favored by coplanarity of the two leaving groups. The more freely rotating 17α-carbomethoxy group can better satisfy a coplanar accommodation of the carboxyl with a 16-hydrogen, thus facilitating the concerted expulsion.



EXPERIMENTAL

Melting points are corrected. Rotations were determined at 10% concentration.

Favorsky–Marker Rearrangement in Deuterated Solvents

A quantity of 17-bromo-pregn-5-en-3β-ol-20-one 3-acetate (28) (5.0 g), which was purified by repeated crystallization from methylene dichloride – methanol to m.p. 149° and which was chromatographically homogeneous, was suspended in 20 ml CH_3OD and 5 ml D_2O (both >99.5% pure). To this was added 5 g of K_2CO_3, and the mixture was stirred and refluxed during 4 h with the exclusion of moisture. The cooled and clear solution was extracted twice with ether, and the organic phase was washed with water to neutrality, dried over $MgSO_4$, and evaporated to give 3.563 g of a neutral residue, which was dissolved in 25 ml dry pyridine and acetylated with 5 ml acetic anhydride for 1 h at 90°. The usual work-up gave a neutral crystalline *residue (A)* (4.149 g). The alkaline aqueous layer from the Favorsky rearrangement was acidified with 100 ml 1 *N* H_2SO_4 and extracted 4 times with CH_2Cl_2. The organic phase was washed once with water, dried over $MgSO_4$, and evaporated to give 0.467 g of acidic *residue (B)*.

The neutral residue A was resolved on thin-layer chromatography (system: 10% diisopropyl ether in CCl_4) into three spots, corresponding to the 17-isomeric etienic esters II and III and the solvolyis product 17α-methoxy-pregn-5-en-20-one-3β-ol acetate (VI). Gas–liquid chromatographic analysis (6 ft column, 2.2 mm inside diameter, packed with 5% DC 710-phenylmethylpolysiloxane on Gas Chrom P silanized (80–100 mesh), temperature 270 °C, helium 40 p.s.i.) revealed 86.5% of isomer II (17α-deuteriomethyl-17β-carbomethoxyandrost-5-en-3β-ol acetate), 11.3% of isomer III (17β-deuteriomethyl-17α-carbomethoxy-androst-5-en-3β-ol acetate), and 2.2% of 17α-methoxypregnenolone acetate (VI) (*vide infra*). This mixture was recrystallized twice from methanol to give 1.506 g of crystals, m.p. 163–166°, consisting of essentially pure isomer II. Further recrystallization from methanol yielded the analytically pure product, m.p. 166–169°, $[\alpha]_D^{23}$ −61.5° ($CHCl_3$). The infrared spectrum contained a weak deuterium band at 2 190 cm^{-1}, and the fingerprint region was different from that of the corresponding non-deuterated compound (9). The nuclear magnetic resonance spectrum showed a decreased intensity of the peak at 8.81 τ (17-methyl) to about two-thirds of the intensity of the peak in the non-deuterated product. The mass spectrum is shown in Fig. 2.

Anal. Calcd. for $C_{24}H_{35}O_6D$: C, 74.00; H, 9.57. Found: C, 73.75; H, 9.34.

The mother liquors of the first crystallization were recrystallized to give a crystalline (m.p. 135–140°) mixture (0.678 g) of II (90%) and III (10%); the filtrate (0.892 g), which was shown by gas–liquid chromatographic analysis to contain 67.5% of the isomer III, was separated on preparative thin-layer chromatography (system: 10% diisopropyl ether in CCl_4) to give pure isomer III, 0.150 g, m.p. 153.5° from *n*-heptane, $[\alpha]_D^{23}$ −70.6° ($CHCl_3$). The nuclear magnetic resonance spectrum showed that the 17-methyl peak at 8.85 τ had decreased to about two-thirds of the intensity of the peak in the non-deuterated product (9). The mass spectrum is shown in Fig. 4.

Anal. Calcd. for $C_{24}H_{35}O_4D$: C, 74.00; H, 9.57. Found: C, 74.08; H, 9.55.

The acidic residue B (0.467 g) was methylated with excess diazomethane in ether at room temperature and acetylated as described above to give a mixture consisting of 17α-deuteriomethyl-17β-carbomethoxy-androst-5-en-3β-ol acetate (II, 92%), the 17β-deuteriomethyl isomer (III, 6.9%), and 17α-methoxypregnenolone acetate (VI, 1.1%), as shown by gas–liquid chromatography. The solvolysis product VI (17α-methoxy-pregn-5-en-20-one-3β-ol acetate) was isolated by preparative thin-layer chromatography and recrystallized from *n*-heptane to m.p. 179–181 °C; $[\alpha]_D^{23}$ −10.4° ($CHCl_3$). The nuclear magnetic resonance spectrum showed a methoxy peak at 3.12 p.p.m., and the product was identical with authentic 17α-methoxypregnenolone acetate prepared according to the procedure of Hoffmann (23).

Anal. Calcd. for $C_{24}H_{36}O_4$: C, 74.19; H, 9.34. Found: C, 73.94; H, 9.15.

REFERENCES

1. A. S. KENDE. Org. Reactions, **11**, 261 (1960).
2. M. MAYER. Compt. Rend. **253**, 488 (1961).
3. A. FORT. J. Am. Chem. Soc. **84**, 2620 (1962).
4. H. O. HOUSE and H. W. THOMPSON. J. Org. Chem. **28**, 164 (1963).

Can. J. Chem. Downloaded from www.nrcresearchpress.com by 210.87.254.5 on 09/05/12
For personal use only.

5. A. GAUDEMER, J. PARELLO, A. SKROBEK, and B. TCHOUBAR. Bull. Soc. Chim. France, 2405 (1963).
6. S. A. ACHMAD and G. W. K. CAVILL. Australian J. Chem. **16**, 858 (1963).
7. J. M. SONIA and J. SALAUN. Tetrahedron Letters, 1175 (1963).
8. R. E. MARKER and R. B. WAGNER. J. Am. Chem. Soc. **64**, 216 (1942).
9. H. L. HEUSSER, CH. R. ENGEL, and PL. A. PLATTNER. Helv. Chim. Acta, **33**, 2237 (1950).
10. N. L. WENDLER, R. P. GRABER, and G. G. HAZEN. Tetrahedron, **3**, 144 (1958).
11. B. TCHOUBAR and O. SACKUR. Compt. Rend. **208**, 1020 (1939).
12. R. B. LOFTFIELD. J. Am. Chem. Soc. **72**, 632 (1950); **73**, 4707 (1951).
13. A. FAVORSKY. J. Prakt. Chem. **88**[2], 641 (1913).
14. J. G. BURR and M. J. S. DEWAR. J. Chem. Soc. 1201 (1954).
15. C. L. STEVENS and E. FARKAS. J. Am. Chem. Soc. **74**, 5352 (1952).
16. J. G. ASTON and R. B. GREENBERG. J. Am. Chem. Soc. **62**, 2590 (1940).
17. R. B. WAGNER and J. A. MOORE. J. Am. Chem. Soc. **72**, 2884 (1950).
18. R. DEGHENGHI and R. GAUDRY. Can. J. Chem. **39**, 1553 (1961).
19. R. DEGHENGHI. U.S. Patent No. 3,041,358 (June 26, 1962).
20. W. G. YOUNG, S. WINSTEIN, and H. L. GOERING. J. Am. Chem. Soc. **73**, 1958 (1951).
21. CH. R. ENGEL, S. K. ROY, J. BILODEAU, and P. LACHANCE. XIX I.U.P.A.C. Congr. London, July 1963. Abstr. Congr. Lectures, p. 53. CH. R. ENGEL, G. JUST, and R. BUTTERY. Can. J. Chem. **39**, 1805 (1961).
22. H. O. HOUSE and W. F. GILMORE. J. Am. Chem. Soc. **83**, 3980 (1961).
23. E. R. GLAZIER. J. Org. Chem. **27**, 4397 (1962). F. J. HOFFMANN. U.S. Patent No. 3,098,860 (July 23, 1963).
24. C. DJERASSI. Optical rotary dispersion. McGraw-Hill Book Co., Inc., New York. 1960. p. 128.
25. R. B. WOODWARD. *In* Mechanism of action of steroid hormones. C. A. Villee and L. L. Engel (*Editors*). Pergamon Press, New York. 1961. pp. 197–198.
26. R. GARDI and R. VITALI. Gazz. Chim. Ital. **93**, 1520 (1963).
27. R. RYHAGE and E. STENHAGEN. J. Lipid Res. **1**, 361 (1960).
28. P. L. JULIAN and W. J. KARPEL. J. Am. Chem. Soc. **72**, 362 (1950).
29. H. O. HOUSE and G. A. FRANK. J. Org. Chem. **30**, 2948 (1965).
30. R. C. COOKSON and M. J. NYE. J. Chem. Soc. 2009 (1965).
31. W. D. MCPHEE and E. KLINGSBERG. J. Am. Chem. Soc. **66**, 1132 (1944).

Can. J. Chem. Downloaded from www.nrcresearchpress.com by 210.87.254.5 on 09/05/12
For personal use only.

SYNTHESIS OF POSSIBLE ACTINOMYCIN D PRECURSORS[1]

JOHN P. MARSH, JR. AND LEON GOODMAN
Life Sciences Research, Stanford Research Institute, Menlo Park, California
Received November 1, 1965

ABSTRACT

The preparation of a number of polypeptides whose sequences are found in the actinomycin D molecule is described. The 4-methyl-3-hydroxyanthranoyl derivatives of these peptides were also prepared as possible substrates for an enzyme that forms the phenoxazinone system of the antibiotic.

Can. J. Chem. Downloaded from www.nrcresearchpress.com by 210.87.254.42 on 09/05/12
For personal use only.

An enzyme that has been named phenoxazinone synthetase (1) catalyzes the oxidative condensation of 2 moles of 4-methyl-3-hydroxyanthranilic acid to 1 mole of actinocin, the chromophoric unit of the actinomycins;[2] this enzyme is believed to play an important role in actinomycin biosynthesis. In order to try to elucidate the steps in the biosynthesis of this family of antibiotics, a group of polypeptides whose sequences appear in actinomycin D has been attached to the 4-methyl-3-hydroxyanthranoyl unit for study as possible substrates for the oxidative enzyme;[3] the preparation of these compounds is the subject of this manuscript.

Because we were interested in obtaining both the free polypeptides and the anthranoyl peptides, a stepwise addition of a N-carbobenzyloxyamino acid to a *t*-butyl aminoester was generally employed to give a blocked peptide that could serve as a common intermediate. Catalytic hydrogenation of the blocked peptide prepared in this way yielded an aminoester suitable for coupling with 3-(benzyloxy)-2-nitro-*p*-toluic acid (XXVIII) (3) to prepare the anthranoyl peptides, whereas a two-step process of hydrogenation and cleavage of the tertiary ester with trifluoroacetic acid yielded the free peptide, usually as a trifluoroacetic acid salt.

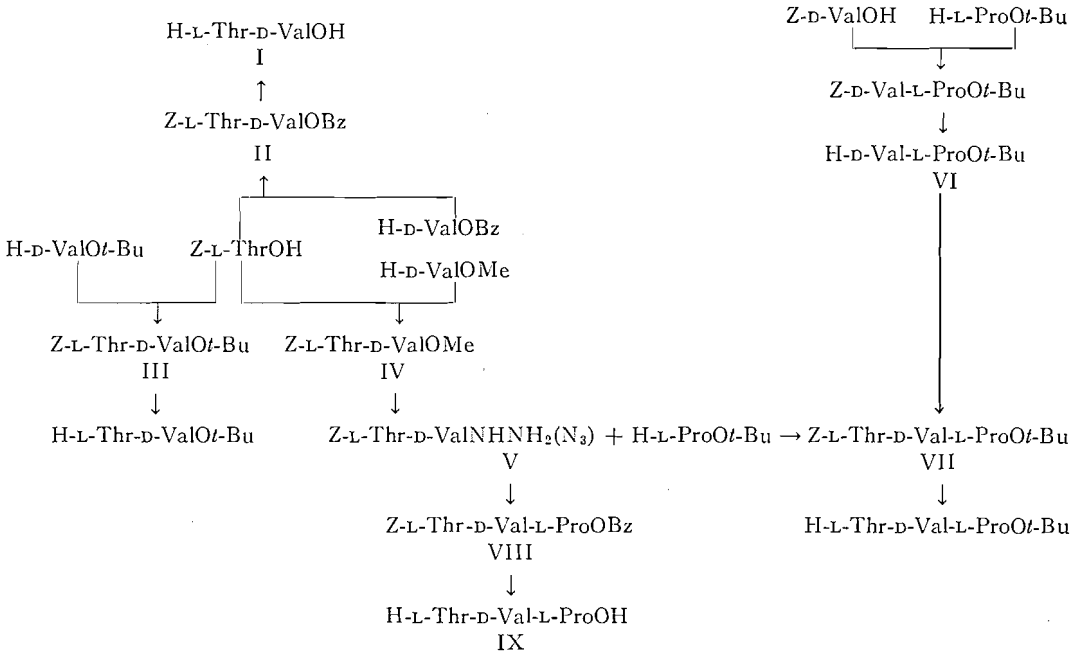
The phosphoryl chloride coupling method (4, p. 1006), because of its convenience, was used mostly in preparing the peptides (see Reaction Schemes 1 and 2). The blocked tripeptide (VII) was also prepared by the azide method (4, p. 1949), which is known to proceed without racemization, and by the carbodiimide technique (4, p. 1016); the products from the three preparations had identical optical rotations. The blocked pentapeptide (XXIV) was more conveniently prepared by coupling of the azide derived from V with the tripeptide ester (XXI); the alternative preparation of XXIV by the stepwise route using phosphoryl chloride couplings, however, gave an essentially identical product.

Hydrogenolysis of the blocked dipeptide (XI) proceeded normally, but the product, L-ProSarO*t*-Bu, cyclized to the diketopiperazine (XXVII) very readily at room temperature; special reaction conditions were required to obtain useful yields of the blocked tripeptide (XII). Ordinarily the *t*-butyl esters of dipeptides are quite stable to diketopiperazine cyclization and are thus advantageous in synthetic work. For example, Anderson (5) noted that *t*-butyl glycylphenylalaninate showed no evidence of diketopiperazine when held at room temperature for 23 days. The present work shows that, at least in

[1]*This work was carried out under the auspices of the Cancer Chemotherapy National Service Center, National Cancer Institute, National Institutes of Health, U.S. Public Health Service, contract No. PH 43-64-500. The opinions expressed are those of the authors and not necessarily those of the Cancer Chemotherapy National Service Center.*

[2]*For pertinent reviews see ref. 2.*

[3]*The enzymatic studies will be reported separately by Dr. Katz and his co-workers.*



REACTION SCHEME 1.

certain cases, *t*-butyl esters of dipeptides are not stable to intramolecular cyclization. The ease of cyclization of L-ProSarO*t*-Bu may be attributable to the presence of the proline moiety; recently, the enhanced tendency of proline dipeptides to undergo intramolecular cyclization has been noted in some mass spectral work (6). However, in our own work SarSarO*t*-Bu also cyclizes readily, and the presence of the sarcosine moiety in the dipeptide ester derived from XI may be the dominant factor.

The nuclear magnetic resonance (n.m.r.) spectra of all the peptides containing sarcosine and N-methyl-L-valine showed the double resonances for the N-methyl protons that result from amide *cis–trans* isomerism.

To prepare the anthranoyl peptides (XXXI) the respective *t*-butyl peptide esters were coupled with the acid (XXVIII) (3) by the phosphoryl chloride method (4, p. 1006) to form XXIX (Reaction Scheme 3). Reaction of XXIX with trifluoroacetic acid cleaved both the ester group and the aromatic O-benzyl group (7) to give XXX. Catalytic hydrogenation of XXX yielded the anthranoyl peptides that were stable in the form of their hydrochlorides (XXXI).

EXPERIMENTAL[4]

t-Butyl N-(Carbobenzoxy)-L-threonyl-D-valyl-L-prolinate (VII)

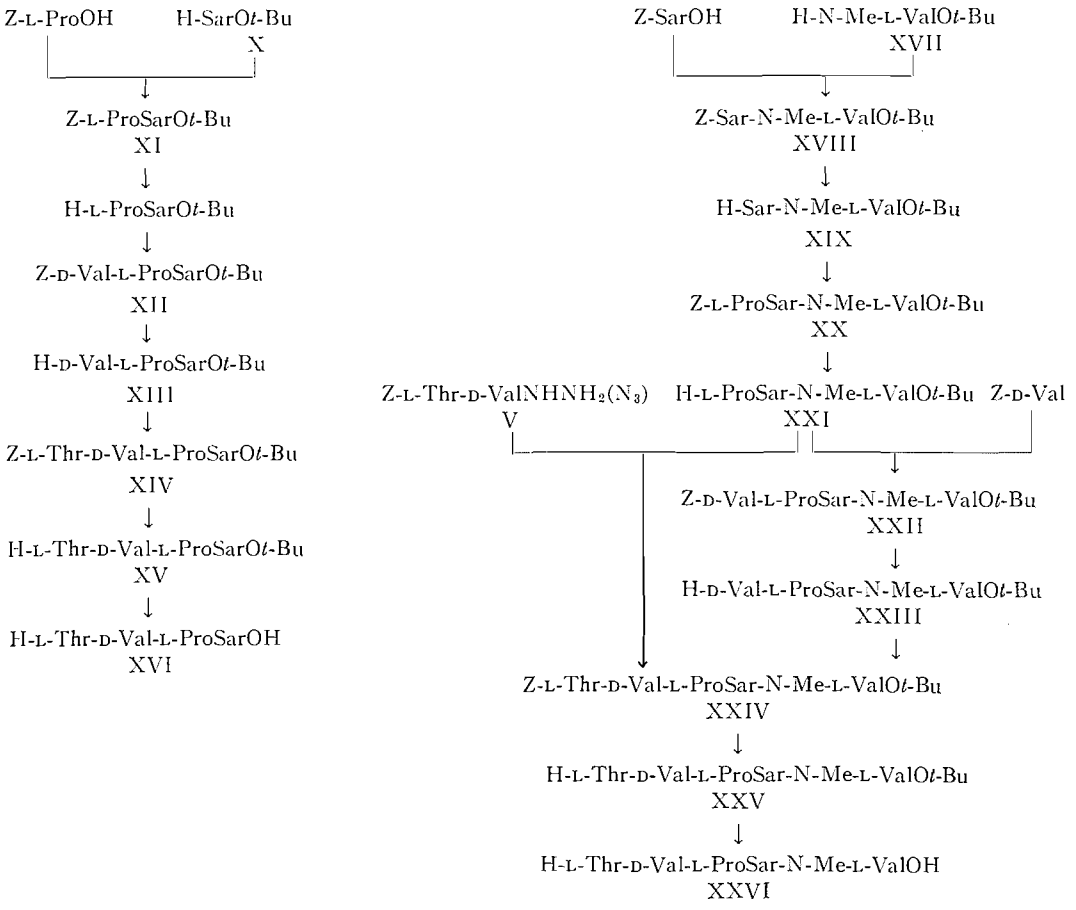
Phosphoryl Chloride Method

A solution of 1.319 g (4.76 mmoles) of *t*-butyl D-valyl-L-prolinate (VI) and 1.206 g (4.76 mmoles) of N-(carbobenzoxy)-L-threonine in 32 ml of dry, freshly distilled tetrahydrofuran was prepared and cooled

[4]*Boiling points and melting points are uncorrected; the latter were obtained with the Thomas–Hoover apparatus. Paper chromatography was run by the descending technique on Whatman No. 1 paper with the solvent system n-butanol – acetic acid – water (5:2:3); ninhydrin was used for detection. Magnesium sulfate was used to dry organic solutions unless otherwise noted. The n.m.r. spectra were run in deuteriochloroform on the Varian A-60 spectrometer with tetramethylsilane as the internal standard unless otherwise noted. Thin-layer chromatography was carried out on Brinkman silica gel HF, 0.25 mm thick. Detection was accomplished by ultraviolet and by 20% H_2SO_4 (v/v) spray. Silicic acid used for chromatography was a reagent grade, 90–200 mesh material. Optical rotations were run in chloroform at the D line unless otherwise noted. Gas chromatography was run in a 5 ft × $\frac{3}{8}$ inch phenyldiethanolamine succinate column, helium being used as a carrier gas.*

Can. J. Chem. Downloaded from www.nrcresearchpress.com by 210.87.254.42 on 09/05/12
For personal use only.

Can. J. Chem. Downloaded from www.nrcresearchpress.com by 210.87.254.42 on 09/05/12
For personal use only.



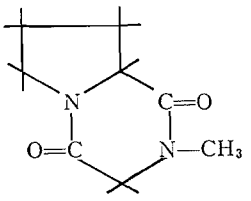
REACTION SCHEME 2.

to −15 to −20°. Phosphoryl chloride (0.436 ml (4.76 mmoles)) was added rapidly followed immediately by 1.32 ml (9.52 mmoles) of triethylamine. The mixture was stirred for 1 h at −15 to −20°, water (20 ml) was added, and then the tetrahydrofuran was evaporated *in vacuo* at room temperature. Water (20 ml) was added to the residue and the mixture was extracted with 25 ml of dichloromethane. The organic solution was washed with two 20 ml portions of water, two 20 ml portions of saturated aqueous sodium bicarbonate solution, and finally 20 ml of water; then the solution was dried and evaporated *in vacuo* to give 1.808 g (75%) of an oil that showed a major single spot on thin-layer chromatography (t.l.c.), with a trace spot at the origin. The oil was chromatographed on 60 g of silicic acid, and VII was obtained, by elution with ethyl acetate – chloroform (1:9), as an oil with $[\alpha]^{23}$ −33.3 ± 1.0° (*c*, 1.89).

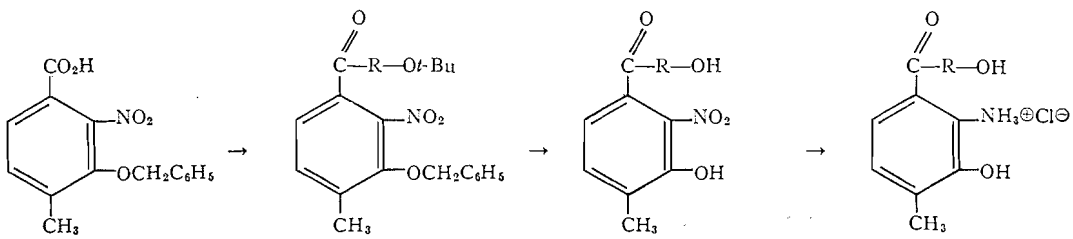
Anal. Calcd. for $C_{26}H_{39}N_3O_7$: N, 8.31. Found: N, 7.99.

Carbodiimide Method

A mixture of 1.455 g (5.25 mmoles) of VI, 1.364 g (5.38 mmoles) of N-(carbobenzoxy)-L-threonine, and 1.11 g (5.38 mmoles) of dicyclohexylcarbodiimide in 25 ml of dichloromethane was prepared, stirred for 18 h at room temperature, and then cooled to 0°. Glacial acetic acid (1 ml) was added, the mixture was filtered, and the filtrate was washed successively with 10 ml portions of water, 2 *N* hydrochloric acid, water, saturated



XXVII



XXVIII XXIX XXX XXXI

a series, R = L-Thr-D-Val
b series, R = L-Thr-D-Val-L-Pro
c series, R = L-Thr-D-Val-L-ProSar
d series, R = L-Thr-D-Val-L-ProSar-N-Me-L-Val

REACTION SCHEME 3.

aqueous sodium bicarbonate, and water; then the filtrate was dried and evaporated. The residue, which contained some solid, was dissolved in 25 ml of cyclohexane, filtered through Celite, and evaporated *in vacuo* to give 2.26 g of an oil that showed several spots on t.l.c. The oil was chromatographed on 76 g of silicic acid to yield, by elution with chloroform and ethyl acetate – chloroform (1:9), 1.819 g (67%) of an oil that showed a single spot on t.l.c. and had $[\alpha]^{25}$ $-33.1 \pm 0.9°$ (*c*, 1.91).

Azide Method

To a stirred solution at 0° of 4.20 g (11.5 mmoles) of N-(carbobenzoxy)-L-threonyl-D-valyl hydrazide (V) in a mixture of 42 ml of glacial acetic acid and 28 ml of 2 *N* hydrochloric acid was added 0.79 g (11.5 mmoles) of sodium nitrite dissolved in 4 ml of cold water. The mixture was diluted with 3 volumes of ice water and was extracted with 40 ml of cold ethyl acetate. The organic layer was washed with two 20 ml portions of ice water and two 20 ml portions of cold saturated aqueous sodium bicarbonate, dried over sodium sulfate, and decanted into a solution of 2.07 g (12.1 mmoles) of *t*-butyl L-prolinate in 10 ml of cold ethyl acetate. All operations were carried out rapidly in a cold room maintained at 4°. The mixture was stirred at 4° for 48 h; washed successively with 25 ml portions of water, saturated aqueous sodium bicarbonate, water, 2 *N* hydrochloric acid, and water; dried; and evaporated *in vacuo* to leave 4.44 g of a glass. This residue showed several spots on t.l.c. A portion of it, 3.218 g, was chromatographed on 76 g of silicic acid and the material that was eluted with ethyl acetate – chloroform (1:9) (1.971 g (45% from V)) had $[\alpha]^{23}$ $-33.1 \pm 1.0°$ (*c*, 1.94) and showed a single spot on t.l.c.

Anal. Calcd. for $C_{26}H_{39}N_3O_7$: C, 61.8; H, 7.77; N, 8.31. Found: C, 61.0; H, 7.51; N, 7.94.

Benzyl N-(carbobenzoxy)-L-threonyl-D-valinate (II) was prepared by the carbodiimide route to give an 80% yield of II, m.p. 90.1–90.6° (from methanol–water), that had $[\alpha]^{24}$ $-19.3 \pm 0.4°$ (*c*, 4.63).

Anal. Calcd. for $C_{24}H_{30}N_2O_6$: C, 65.2; H, 6.83; N, 6.33. Found: C, 65.1; H, 6.81; N, 6.53.

L-*Threonyl-D-valine (I)* was prepared by catalytic hydrogenolysis of II in 80% aqueous acetic acid over 5% palladium on carbon to give a 56% yield of I, m.p. 238.2–239.5° (from water–ethanol), that had $[\alpha]^{22}$ $+47.1 \pm 1.0°$ (*c*, 2.20 in water). On paper chromatography the compound showed a single spot with R_f 0.62.

Anal. Calcd. for $C_9H_{18}N_2O_4$: C, 49.5; H, 8.31; N, 12.8. Found: C, 49.6; H, 8.19; N, 12.6.

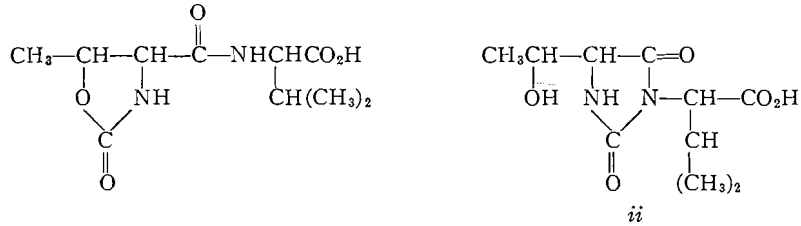
Methyl N-(carbobenzoxy)-L-threonyl-D-valinate (IV) was prepared by the carbodiimide route to give a 45% yield of IV, m.p. 121–122.5° (from benzene – petroleum ether (30–60°)), that had $[\alpha]^{22}$ $-33.7 \pm 0.5°$ (*c*, 4.97).

Anal. Calcd. for $C_{18}H_{26}N_2O_6$: C, 59.0; H, 7.16; N, 7.84. Found: C, 59.3; H, 7.23; N, 7.84.

N-(Carbobenzoxy)-L-threonyl-D-valine hydrazide (V) was prepared conventionally in 60% yield from IV[5] and had m.p. 244.8–246.5° (decomp.) (from absolute ethanol).

Anal. Calcd. for $C_{17}H_{26}N_4O_5$: C, 55.7; H, 7.16; N, 15.3. Found: C, 55.2; H, 7.22; N, 15.0.

[5]*An attempt to saponify IV with dilute base in aqueous dioxane gave a low yield of a solid, m.p. 225–228° (decomp.), whose elemental analysis and spectral data are compatible with the cyclic urethan i. As a referee has pointed out, these data do not eliminate the isomeric hydantoin ii as a possible structure.*



ii

Can. J. Chem. Downloaded from www.nrcresearchpress.com by 210.87.254.42 on 09/05/12
For personal use only.

*t-Butyl N-(carbobenzoxy)-*L*-threonyl-*D*-valinate (III)* was prepared by the carbodiimide method to give a 68% yield of solid, m.p. 112.8–115.0° (from cyclohexane–hexane), that had $[\alpha]^{24}$ −27.1 ± 0.5° (*c*, 5.07).

Anal. Calcd. for $C_{21}H_{32}N_2O_6$: C, 61.8; H, 7.90; N, 6.86. Found: C, 61.8; H, 7.87; N, 6.95.

t-Butyl D*-valyl-*L*-prolinate (VI)* was prepared by catalytic hydrogenation over 5% palladium on carbon in 95% ethanol of crude *t*-butyl N-(carbobenzoxy)-D-valyl-L-prolinate that had been prepared as an oil in 77% yield by the phosphoryl chloride method. The dipeptide ester (VI) was an oil with $[\alpha]^{23}$ −107 ± 2° (*c*, 1.56).

Anal. Calcd. for $C_{13}H_{26}N_2O_3$: C, 60.7; H, 9.79; N, 10.9. Found: C, 60.1; H, 9.67; N, 10.6.

*Benzyl N-(carbobenzoxy)-*L*-threonyl-*D*-valyl-*L*-prolinate (VIII)* was prepared from V in 68% yield by the azide method to give an oil that was purified by silicic acid chromatography and which had $[\alpha]^{23}$ −37.4 ± 1.7° (*c*, 1.12).

Anal. Calcd. for $C_{29}H_{37}N_3O_7$: C, 64.5; H, 6.91; N, 7.79. Found: C, 63.4; H, 7.00; N, 7.60.

L*-Threonyl-*D*-valyl-*L*-proline (IX)* was prepared by catalytic hydrogenolysis of VIII in 80% aqueous acetic acid over 5% palladium on charcoal. The tripeptide (IX) had m.p. 180.0–181.5° (decomp.) (from water–ethanol) and $[\alpha]^{25}$ −2.8 ± 0.7° (*c*, 1.48 in water). On paper chromatography the compound showed a single spot with R_f 0.64.

Anal. Calcd. for $C_{14}H_{25}N_3O_5 \cdot 0.8H_2O$: C, 51.0; H, 8.13; N, 12.7. Found: C, 50.9; H, 8.01; N, 13.0.

t-Butyl sarcosinate (X) was prepared by catalytic hydrogenolysis of crude *t*-butyl N-(carbobenzoxy)-sarcosinate (prepared from N-(carbobenzoxy)-sarcosine by Anderson's (5) procedure) in 95% ethanol over 5% palladium on carbon. The hydrogenolysis product was purified by distillation to give material that had b.p. 76.5–78° at 40 mm and which showed a single peak on vapor phase chromatography with a retention time of 1.80 min, a column temperature of 130° and a flow rate of 51 ml/min being used. The analytical sample had n_D^{23} 1.4148.

Anal. Calcd. for $C_7H_{15}NO_2$: C, 57.9; H, 10.4; N, 9.65. Found: C, 57.7; H, 10.4; N, 9.42.

*t-Butyl N-(carbobenzoxy)-*L*-prolylsarcosinate (XI)* was prepared in 85% yield by the phosphoryl chloride procedure to give the blocked dipeptide as an oil that showed a trace impurity on t.l.c. and had $[\alpha]^{22.5}$ −52.1 ± 0.9° (*c*, 2.85 in ethanol).

Anal. Calcd. for $C_{20}H_{28}N_2O_6$: C, 63.8; H, 7.49; N, 7.44. Found: C, 63.8; H, 7.47; N, 7.39.

2,5-Dioxo-1-methyl-3,4-trimethylenepiperazine (XXVII)

The blocked dipeptide (XI, 2.92 g) was dissolved in 30 ml of 95% ethanol and was hydrogenated conventionally with 5% palladium on carbon. After evaporation there was an oil (1.80 g) whose n.m.r. spectrum indicated loss of the *t*-butyl group by the reduced integrated intensity of the *t*-butyl protons relative to the rest of the molecule. Distillation (short path) of the material gave 0.68 g (bath temperature 125° at 0.008 mm) of a semisolid which was crystallized from ethyl acetate – cyclohexane to give the hygroscopic product, m.p. 46.2–47.5°, $[\alpha]^{22}$ −131.8 ± 2.9° (*c*, 0.613 in ethanol).

Anal. Calcd. for $C_8H_{12}N_2O_2$: C, 57.1; H, 7.20; N, 16.7. Found: C, 56.7; H, 7.20; N, 16.3.

*t-Butyl N-(carbobenzoxy)-*D*-valyl-*L*-prolylsarcosinate (XII)* was prepared in 71% yield by the phosphoryl chloride method from *t*-butyl L-prolylsarcosinate to give XII as an oil that showed two trace contaminants on t.l.c. The *t*-butyl dipeptide used in the condensation was prepared from XI by hydrogenation at 0°, rapid removal of the solvent at −10 to 0° in a high vacuum, and immediate use of the crude product in the coupling.

Anal. Calcd. for $C_{25}H_{37}N_3O_6$: C, 63.1; H, 7.84; N, 8.83. Found: C, 63.0; H, 7.91; N, 8.81.

t-Butyl D*-valyl-*L*-prolylsarcosinate (XIII)* was obtained in 93% yield as a solid with no definite melting point, by conventional hydrogenolysis in 95% ethanol. It had $[\alpha]^{23}$ −103 ± 1.3° (*c*, 1.55 in ethanol).

Anal. Calcd. for $C_{17}H_{31}N_3O_4$: C, 59.8; H, 9.16; N, 12.3. Found: C, 59.3; H, 9.11; N, 12.3.

*t-Butyl N-(carbobenzoxy)-*L*-threonyl-*D*-valyl-*L*-prolylsarcosinate (XIV)* was prepared in 67% yield by the phosphoryl chloride method to give the blocked tetrapeptide as a foam that showed a single spot on t.l.c. and had $[\alpha]^{23}$ −37.8 ± 1.4° (*c*, 0.923 in ethanol).

Anal. Calcd. for $C_{29}H_{44}N_4O_8$: C, 60.4; H, 7.69; N, 9.72. Found: C, 59.9; H, 7.80; N, 9.79.

t-Butyl L*-threonyl-*D*-valyl-*L*-prolylsarcosinate (XV)* was obtained in 92% yield as a white solid with no definite melting point, by conventional catalytic hydrogenolysis of XIV. It had $[\alpha]^{23}$ −28.1 ± 5.0° (*c*, 0.354 in ethanol).

Anal. Calcd. for $C_{21}H_{38}N_4O_6 \cdot H_2O$: C, 54.8; H, 8.75; N, 12.2. Found: C, 54.5; H, 8.40; N, 11.8.

L*-Threonyl-*D*-valyl-*L*-prolylsarcosine (XVI) Trifluoroacetate*

The tetrapeptide ester (XV, 0.700 g) was dissolved in 15 ml of trifluoroacetic acid, and the solution was allowed to stand at room temperature for 45 min and then was evaporated *in vacuo*. The residue was treated with 20 ml of benzene, the mixture evaporated *in vacuo*, and the treatment repeated. The residue was then dissolved in 10 ml of absolute ethanol, the solution filtered, and the filtrate treated with excess dry ether to precipitate the peptide salt. After a second ethanol–ether precipitation the product was isolated by centrifugation to yield 0.415 g (55%) of the salt, m.p. 147–160° (decomp.), $[\alpha]^{23}$ +9.1 ± 1.5° (*c*, 0.667 in ethanol). On paper chromatography the compound showed a single spot with R_f 0.67.

Anal. Calcd. for $C_{17}H_{30}N_4O_6 \cdot CF_3CO_2H$: C, 45.6; H, 6.25; F, 11.4; N, 11.2. Found: C, 45.6; H, 6.65; F, 11.7; N, 11.7.

Amino acid analysis of the tetrapeptide showed a molar ratio for Thr:Val:Pro:Sar of 1.06:1.04:1.01:0.77.

Can. J. Chem. Downloaded from www.nrcresearchpress.com by 210.87.254.42 on 09/05/12
For personal use only.

*t-Butyl N-Methyl-*L*-valinate (XVII)*

Liquid isobutylene (25 ml) was added to a solution of 2.9 g of N-methyl-L-valine (8) in 25 ml of dry dioxane containing 2.4 ml of concentrated sulfuric acid. The mixture, in a heavy-walled, tightly stoppered bottle, was stirred vigorously for 18 h at room temperature; then the excess isobutylene was vented and the residue was poured into an ice-cold mixture of 100 ml of water and 200 ml of ether. The water layer was separated, adjusted to pH 10 with 1 *N* sodium hydroxide, and extracted with three 25 ml portions of ether. The ether extract was dried and the ether removed by distillation through a short Vigreux column. Finally some dioxane was removed by application of an aspirator vacuum at room temperature. The residual liquid (3.0 g) was distilled through a spinning-band column to give 1.87 g (77%) of distillate collected in two fractions, b.p. 64–76° at 16 mm and 70–73° at 12 mm. The second fraction was used for analysis and had $[\alpha]^{20}$ +4.7 ± 0.9° (*c*, 0.95). Vapor phase chromatography showed a single peak with a retention time of 1.55 min, a column temperature of 139° and a flow rate of 143 ml/min being used.

Anal. Calcd. for $C_{10}H_{21}NO_2$: C, 64.1; H, 11.3; N, 7.48. Found: C, 63.8; H, 11.5; N, 7.36.

On a larger scale the removal of the dioxane was troublesome and caused difficulty in the isolation of XVII. The conversion of N-benzyl-N-methyl-L-valine (8) into the *t*-butyl ester, isolated as a crystalline hydrochloride, was simpler, but no practical system for debenzylation of the ester could be found.

*t-Butyl N-(carbobenzoxy)sarcosyl-N-methyl-*L*-valinate (XVIII)* was prepared in 71% yield by the phosphoryl chloride method to give the product as an oil that showed several trace spots on t.l.c. and had $[\alpha]^{23}$ −78.0 ± 0.9° (*c*, 1.08 in ethanol). The integration of the n.m.r. spectrum of the product showed the proper ratios for structure XVIII.

Anal. Calcd. for $C_{21}H_{32}N_2O_5$: C, 64.3; H, 8.22; N, 7.14. Found: C, 63.9; H, 7.95; N, 7.41.

*t-Butyl sarcosyl-N-methyl-*L*-valinate (XIX)* was prepared by conventional hydrogenolysis of XVIII to give a 65% yield of an oil that had $[\alpha]^{22}$ −68.1 ± 3.2° (*c*, 1.71 in ethanol) and which showed no signs of cyclization at room temperature.

Anal. Calcd. for $C_{13}H_{26}N_2O_3$: C, 60.4; H, 10.1; N, 10.9. Found: C, 60.4; H, 10.2; N, 11.0.

*t-Butyl N-(carbobenzoxy)-*L*-prolylsarcosyl-N-methyl-*L*-valinate (XX)* was prepared by the phosphoryl chloride method to give a 75% yield of an oil that was purified by silicic acid chromatography. The fraction eluted with chloroform represented a 44% yield and had $[\alpha]^{21}$ −102.8 ± 2.0° (*c*, 0.864 in ethanol).

Anal. Calcd. for $C_{26}H_{39}N_3O_6$: C, 63.8; H, 8.03; N, 8.58. Found: C, 63.7; H, 8.05; N, 8.79.

t-Butyl L*-prolylsarcosyl-N-methyl-*L*-valinate (XXI)* was prepared conventionally from XX to give 95% of an oil that had $[\alpha]^{23}$ −141.2 ± 0.6° (*c*, 0.91 in ethanol).

Anal. Calcd. for $C_{18}H_{33}N_3O_4$: C, 60.8; H, 9.36; N, 11.8. Found: C, 60.7; H, 9.21; N, 11.9.

*t-Butyl N-(carbobenzoxy)-*D*-valyl-*L*-prolylsarcosyl-N-methyl-*L*-valinate (XXII)* was prepared by the phosphoryl chloride procedure to give, after silicic acid chromatography, a 63% yield of an oil that had $[\alpha]^{21}$ −75.3 ± 2.0° (*c*, 1.00 in ethanol).

Anal. Calcd. for $C_{31}H_{48}N_4O_7$: C, 63.2; H, 8.22; N, 9.53. Found: C, 63.0; H, 8.71; N, 9.43.

t-Butyl D*-valyl-*L*-prolylsarcosyl-N-methyl-*L*-valinate (XXIII)* was prepared from XXII to give a 97% yield of a gum that had $[\alpha]^{25}$ −125.2 ± 2.4° (*c*, 1.15 in methanol).

Anal. Calcd. for $C_{23}H_{42}N_4O_5$: C, 60.8; H, 9.31; N, 12.3. Found: C, 60.9; H, 9.09; N, 12.4.

*t-Butyl N-(carbobenzoxy)-*L*-threonyl-*D*-valyl-*L*-prolylsarcosyl-N-methyl-*L*-valinate (XXIV)* was prepared both by the phosphoryl chloride procedure from XXIII and by the azide coupling of XXI and the azide derived from V. The phosphoryl chloride procedure provided, after chromatography on activated Florosil, 57% of a gum that gave a single spot on t.l.c. and had $[\alpha]^{21}$ −78.3 ± 1.0° (*c*, 0.548 in ethanol).

Anal. Calcd. for $C_{35}H_{55}N_5O_9$: C, 60.9; H, 8.04; N, 10.2. Found: C, 60.5; H, 8.16; N, 9.78.

The product from the azide coupling reaction was obtained in 60% yield after chromatography on Florosil and showed t.l.c. behavior identical with that of the phosphoryl chloride product; it had $[\alpha]^{21}$ −74.4 ± 1.7° (*c*, 1.10 in ethanol).

t-Butyl L*-threonyl-*D*-valyl-*L*-prolylsarcosyl-N-methyl-*L*-valinate (XXV)* was prepared from XXIV to give 92% of a foam that had $[\alpha]^{21}$ −75.4 ± 1.8° (*c*, 0.966 in ethanol).

Anal. Calcd. for $C_{27}H_{49}N_5O_7$: C, 58.4; H, 8.89; N, 12.6. Found: C, 57.8; H, 8.72; N, 12.3.

L*-Threonyl-*D*-valyl-*L*-prolylsarcosyl-N-methyl-*L*-valine (XXVI) trifluoroacetate* was prepared from XXV by the procedure described for XVI to give an 81% yield of a white foam that had $[\alpha]^{22}$ −42.4 ± 1.6° (*c*, 1.05 in ethanol). On paper chromatography the compound showed a single spot with R_f 0.69.

Anal. Calcd. for $C_{23}H_{41}N_5O_7 \cdot CF_3CO_2H$: C, 48.9; H, 6.90; F, 9.29; N, 11.4. Found: C, 48.7; H, 7.05; F, 9.66; N, 11.9.

*t-Butyl N-[3-(benzyloxy)-2-nitro-p-toluoyl]-*L*-threonyl-*D*-valinate (XXIXa)* was prepared by the phosphoryl chloride coupling of XXVIII and *t*-butyl L-threonyl-D-valinate to give a 60% yield of a crystalline solid having an undefined melting point after crystallization from cyclohexane.

Anal. Calcd. for $C_{28}H_{37}N_3O_8$: C, 61.9; H, 6.86; N, 7.73. Found: C, 61.8; H, 6.75; N, 7.53.

*N-(2-Nitro-3,4-cresotoyl)-*L*-threonyl-*D*-valine (XXXa)*

A solution of 3.578 g of XXIX*a* in 25 ml of trifluoroacetic acid was allowed to stand at room temperature for 1.5 h, and then was evaporated *in vacuo*. The residue was freed of acid by the successive addition and

Can. J. Chem. Downloaded from www.nrcresearchpress.com by 210.87.254.42 on 09/05/12
For personal use only.

evaporation of three 25 ml portions of benzene. The residue was partitioned between 25 ml each of chloroform and saturated aqueous sodium bicarbonate. The aqueous extract was acidified to pH 1 with 3 *N* hydrochloric acid and was extracted with 25 ml of chloroform. The organic extract was dried and evaporated *in vacuo* to leave 2.59 g of a yellow solid. Recrystallization from benzene yielded three crops of crystalline solid, 1.63 g (62%). A sample that was recrystallized for analysis had m.p. 101.2–104.0°.

Anal. Calcd. for $C_{17}H_{23}N_3O_8$: C, 51.4; H, 5.83; N, 10.6. Found: C, 51.6; H, 6.31; N, 10.3.

N-(2-Amino-3,4-cresotoyl)-L-*threonyl*-D-*valine Hydrochloride (XXXIa)*

A stirred mixture of 1.467 g of XXX*a*, 25 ml of absolute ethanol that contained 5 drops of glacial acetic acid, and 350 mg of 5% palladium on carbon was maintained under a hydrogen atmosphere for 18 h, during which time 343 ml (corrected for catalyst absorption) of hydrogen was absorbed. The mixture was filtered through Celite and the filtrate was treated with 10 ml of hydrogen chloride saturated ether. Dry hydrogen chloride was bubbled through the chilled solution for about 15 min, and then the solution was evaporated *in vacuo*. The residue was dissolved in the minimum amount of absolute ethanol, and the product was precipitated with excess dry ether. The precipitate (1.135 g (76%)) was collected by centrifugation to give a solid that showed no definite melting behavior and had $[\alpha]^{23}$ +13.8 ± 0.4° (*c*, 3.82 in 1 *N* hydrochloric acid), λ_{max}^{pH1} 221 mμ (ε 27 400) and 285 mμ (ε 6 450).

Anal. Calcd. for $C_{17}H_{26}ClN_3O_6$: C, 50.6; H, 6.49; Cl, 8.78; N, 10.4. Found: C, 50.8; H, 6.65; Cl, 8.66; N, 10.4.

t-Butyl N-[3-(benzyloxy)-2-nitro-p-toluoyl]-L-*threonyl*-D-*valyl*-L-*prolinate (XXIXb)* was a foam that was chromatographed on silicic acid to give a low yield of an amorphous material that gave a single spot on t.l.c. and whose n.m.r. spectrum was in good agreement with that of the postulated structure.

N-(2-Nitro-3,4-cresotoyl)-L-*threonyl*-D-*valyl*-L-*proline (XXXb)* was prepared from crude XXIX*b* with trifluoroacetic acid to give a 61% yield of solid after crystallization from ethyl acetate – cyclohexane. The material did not have a definite melting point; it had $[\alpha]^{26}$ −19.6 ± 0.8° (*c*, 1.87 in ethanol).

Anal. Calcd. for $C_{22}H_{30}N_4O_9$: C, 53.4; H, 6.14; N, 11.33. Found: C, 53.5; H, 6.73; N, 11.2.

Crystallization of the compound from carbon tetrachloride gave a solvate.

Anal. Calcd. for $C_{22}H_{30}N_4O_9 \cdot 0.4CCl_4$: C, 48.4; H, 5.44; Cl, 10.2; N, 10.1. Found: C, 48.6; H, 5.77; Cl, 9.90; N, 10.2.

N-(2-Amino-3,4-cresotoyl)-L-*threonyl*-D-*valyl*-L-*proline hydrochloride (XXXIb)* was an amorphous powder that was prepared in 66% yield from XXX*b* and which had $[\alpha]^{23}$ −16.9 ± 0.6° (*c*, 2.28 in 1 *N* hydrochloric acid).

Anal. Calcd. for $C_{22}H_{33}ClN_4O_7$: C, 52.8; H, 6.64; Cl, 7.08; N, 11.2. Found: C, 52.6; H, 6.77; Cl, 6.68; N, 10.6.

t-Butyl N-[3-(benzyloxy)-2-nitro-p-toluoyl]-L-*threonyl*-D-*valyl*-L-*prolylsarcosinate (XXIXc)* was obtained as a chromatographically homogeneous foam in 35% yield after chromatography on Florosil. It had $[\alpha]^{23}$ −20.9 ± 1.2° (*c*, 0.94 in ethanol).

Anal. Calcd. for $C_{36}H_{49}N_5O_{10}$: C, 60.8; H, 6.94; N, 9.84. Found: C, 60.9; H, 6.90; N, 9.17.

N-(2-Nitro-3,4-cresotoyl)-L-*threonyl*-D-*valyl*-L-*prolylsarcosine (XXXc)* was obtained from XXIX*c* as an amorphous solid after the usual trifluoroacetic acid treatment and a final precipitation from ethyl acetate with hexane. The material gave poor analytical results.

N-(2-Amino-3,4-cresotoyl)-L-*threonyl*-D-*valyl*-L-*prolylsarcosine hydrochloride (XXXIc)* was obtained as an ethanol solvate from hydrogenation of XXX*c*. It had $[\alpha]^{24}$ −30.3 ± 1.2° (*c*, 0.99 in 1 *N* hydrochloric acid) and λ_{max}^{pH1} 216 mμ (ε 31 200), 222 mμ (shoulder, ε 28 900), and 330 mμ (ε 2 205).

Anal. Calcd. for $C_{25}H_{38}ClN_5O_8 \cdot C_2H_5OH$: C, 52.4; H, 7.17; Cl, 5.74; N, 11.3. Found: C, 52.1; H, 6.85; Cl, 5.71; N, 11.3.

The presence of ethanol was confirmed by mass spectrometry.

t-Butyl N-[3-(benzyloxy)-2-nitro-p-toluoyl]-L-*threonyl*-D-*valyl*-L-*prolylsarcosyl-N-methyl*-L-*valinate (XXIXd)* was obtained in 58% yield as a chromatographically homogeneous foam after chromatography on activated Florosil.

Anal. Calcd. for $C_{42}H_{60}N_6O_{11}$: C, 61.1; H, 7.33; N, 10.2. Found: C, 61.0; H, 7.65; N, 9.45.

N-(2-Nitro-3,4-cresotoyl)-L-*threonyl*-D-*valyl*-L-*prolylsarcosyl-N-methyl*-L-*valine (XXXd)* was obtained in 85% yield from XXIX*d* as a yellow powder that showed a single spot on t.l.c.

Anal. Calcd. for $C_{31}H_{46}N_6O_{11}$: C, 54.9; H, 6.84; N, 12.4. Found: C, 55.3; H, 7.00; N, 12.3.

N-(2-Amino-3,4-cresotoyl)-L-*threonyl*-D-*valyl*-L-*prolylsarcosyl-N-methyl*-L-*valine hydrochloride (XXXId)* was obtained conventionally in 76% yield as an amorphous powder that had $[\alpha]^{22}$ −84.0 ± 2.1° (*c*, 0.61 in ethanol).

Anal. Calcd. for $C_{31}H_{49}ClN_6O_9$: C, 54.3; H, 7.21; Cl, 5.17; N, 12.3. Found: C, 54.1; H, 7.31; Cl, 4.86; N, 12.0.

ACKNOWLEDGMENTS

The authors thank Dr. Peter Lim and his staff for the infrared, ultraviolet, and n.m.r. spectra, the optical rotations, and the paper chromatography. They also are indebted to Mr. O. P. Crews and his group for the preparation of certain intermediates.

Can. J. Chem. Downloaded from www.nrcresearchpress.com by 210.87.254.42 on 09/05/12
For personal use only.

REFERENCES

1. E. KATZ. Unpublished work.
2. H. BROCKMANN. Angew. Chem. **72**, 939 (1960); Fortschr. Chem. Org. Naturstoffe, **18**, 1 (1960).
3. B. WEINSTEIN, O. P. CREWS, M. A. LEAFFER, B. R. BAKER, and L. GOODMAN. J. Org. Chem. **27**, 1389 (1962).
4. J. P. GREENSTEIN and M. WINITZ. Chemistry of the amino acids. Vol. 2. John Wiley & Sons, Inc., New York. 1961.
5. G. W. ANDERSON and F. M. CALLAHAN. J. Am Chem. Soc. **82**, 3359 (1960).
6. H. J. SVEC and G. A. JUNK. J. Am. Chem. Soc. **86**, 2278 (1964).
7. J. P. MARSH, JR. and L. GOODMAN. J. Org. Chem. **30**, 2491 (1965).
8. P. QUITT, J. HELLERBACH, and K. VOGLER. Helv. Chim. Acta, **66**, 327 (1963)

Can. J. Chem. Downloaded from www.nrcresearchpress.com by 210.87.254.42 on 09/05/12
For personal use only.

Can. J. Chem. Downloaded from www.nrcresearchpress.com by 210.87.254.5 on 09/05/12
For personal use only.

STEROIDS AND RELATED NATURAL PRODUCTS

XXVIII. STEREOCHEMISTRY OF 3-HYDROXY-4-OXA-5α-CHOLESTANE AND RELATED HEMIACETALS[1,2]

GEORGE R. PETTIT,[3] JOHN C. KNIGHT,[4] AND WILLIAM J. EVERS

Department of Chemistry, University of Maine, Orono, Maine, and Department of Chemistry, Arizona State University, Tempe, Arizona

Received November 23, 1965

ABSTRACT

Several new 3-hydroxy-4-oxa type steroidal hemiacetals (V and VII) have been prepared by diborane reduction of the corresponding δ-lactones. A detailed proton magnetic resonance study of the hemiacetal (IX*a*) derived from 3-oxo-4-oxa-5α-cholestane (VIII) indicated that diborane reduction led in each case to an epimeric mixture. Treating hemiacetal IX*a* with methanol – hydrochloric acid gave a mixture of acetals IX*b* and IX*c*. Pure specimens of the epimeric acetals were obtained by preparative thin-layer chromatography, and configurational assignments based on proton magnetic resonance studies were provided for each isomer. Allowing lactone VIII (in tetrahydrofuran solution) to react with 1 equivalent of diborane during 4 min resulted in approximately 80% conversion into hemiacetal IX*a*, and provided an illustration of the potential utility of the reduction reaction.

After the discovery (2) that certain steroidal lactones could conveniently be reduced to cyclic hemiacetals with diborane, the reduction reaction was applied (2, 3) to four A-ring steroidal lactones.[5] The first hemiacetal prepared in our laboratory by the diborane route was 3ξ-hydroxy-4-oxa-5α-cholestane (IX*a*), and the isomer (m.p. 197–199°) that was characterized was assumed (2*b*) to represent the 3β-equatorial epimer. Concurrently, Edward and his colleagues (4*c*) performed the same experiment by a lithium aluminium hydride procedure and isolated one isomer (m.p. 188–190°) that was assigned, on the basis of molecular rotation studies, the 3α-axial configuration. Although fractional recrystallization of the hemiacetal failed to reveal the presence of the 3β-isomer, a solution of the hemiacetal in tetrahydrofuran–water was found (4*c*) to represent 45% equatorial isomer and 55% axial epimer. Later, when we began a general study of the lactone → hemiacetal reduction reaction with diborane, the stereochemistry of A-ring steroidal hemiacetals became of increasing importance. Accordingly, a detailed examination of hemiacetal IX*a* was undertaken by proton magnetic resonance (p.m.r.) spectroscopy, and the study was expanded to include related hemiacetals representing the androstane (V) and pregnane (VII*a*) ring systems.

Synthesis of the required hemiacetals was conveniently achieved as follows. First, dehydroepiandrosterone (I) was converted into 3-oxo-androst-4-ene (II) essentially as previously reported (6) and the ketone was oxidized to lactone III*a* with peroxydisulfuric acid (2*b*, 3*a*). For chemical and subsequent biological comparative purposes, lactone III*a* was reduced by boron trifluoride – sodium borohydride to tetrahydropyran III*b* and by lithium aluminium hydride to diol IV. Then lactone III*a* in tetrahydrofuran was readily reduced to hemiacetal V by externally generated (sodium borohydride – boron trifluoride)

[1] *For part XXVII of this series, see ref. 1.*

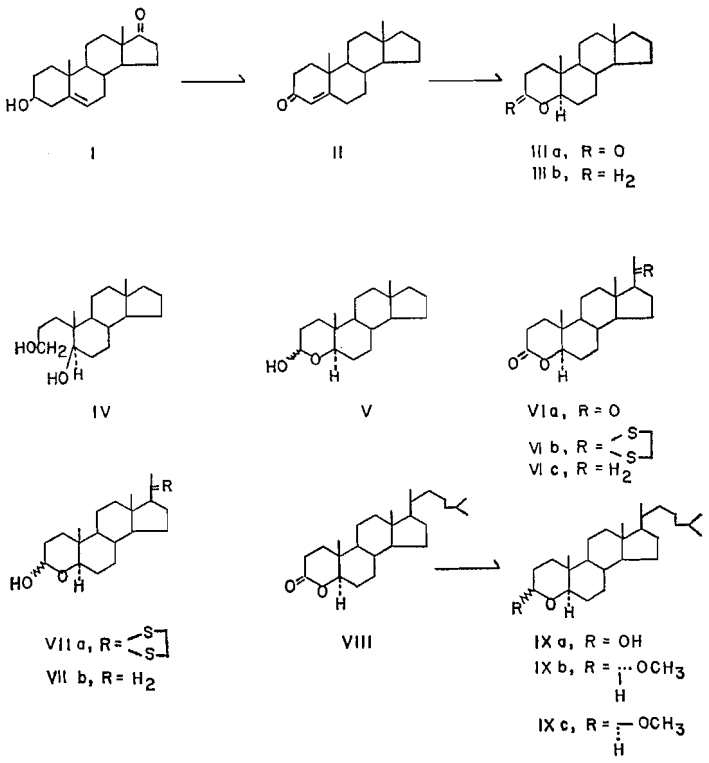
[2] *Based on part of the Ph.D. dissertation submitted by W. J. Evers to the Graduate School, University of Maine, Orono, Maine, December 1964.*

[3] *Correspondence should be addressed to this author at the Department of Chemistry, Arizona State University, Tempe, Arizona.*

[4] *Smith, Kline, and French Postdoctorate Fellow, 1962.*

[5] *Meanwhile, a variety of other steroidal hemiacetals have been prepared from the corresponding lactone by specialized lithium aluminium hydride or sodium borohydride techniques (4). In the same period, several novel approaches to steroidal hemiacetals and (or) acetal derivatives were also reported (5).*

diborane. Next, progesterone was converted (2*b*) into lactone VI*a*. Treating the 20-ketone (VI*a*) with boron trifluoride – ethanedithiol yielded thioketal VI*b*. Raney nickel desulfurization (7) of ethylenethioketal VI*b* gave the required lactone (VI*c*). Diborane (externally generated) reduction of lactones VI*b* and VI*c* provided the corresponding hemiacetal derivatives (VII*a* and VII*b*). At this point, the reduction reaction appeared to be of a general nature, and the necessary experimental conditions were more carefully defined, lactone VIII being used as a model substrate. Eventually, a 4 min reaction period at room temperature and with equivalent quantities of standard diborane in tetrahydrofuran[6] was found to convert lactone VIII in good yield (approximately 80%) into hemiacetal IX*a*. The remaining product, as evidenced by thin-layer chromatography, was the corresponding diol resulting from further reduction. In general, a 30 min reaction period was found to be satisfactory.



A chromatographically pure specimen of hemiacetal IX*a*, m.p. 185–190°, in deuteriochloroform was found by p.m.r. spectral comparison (Fig. 1) with specimens of 3β-hydroxy-5α-cholestane (8) and 3α-hydroxy-5α-cholestane (9) to represent a mixture of 3β- and 3α-epimers in approximately equal amounts. In the 5α-steroid series an axial C-3 proton generally exhibits a broad response upfield from the more well defined signal usually exhibited by an equatorial C-3 proton (10). The p.m.r. spectra of the 3-hydroxy-5α-cholestanes (Fig. 1) were in agreement with these observations. The 3β-hydroxy epimer of hemiacetal IX*a* displayed a broad 3α-proton signal at 4.58 δ and a broad 5α-proton signal centered at 3.07 δ. Corresponding signals at 5.08 (3β-proton) and 3.6–3.8 (5α-proton) δ of the composite spectrum were attributed to the 3α-hydroxy isomer (IX*a*).

[6]*Recently 1M borane in tetrahydrofuran has become commercially available (metal hydride division of Ventron Corporation) and is now being routinely employed (e.g. for preparation of hemiacetals) in our laboratory.*

Can. J. Chem. Downloaded from www.nrcresearchpress.com by 210.87.254.5 on 09/05/12
For personal use only.

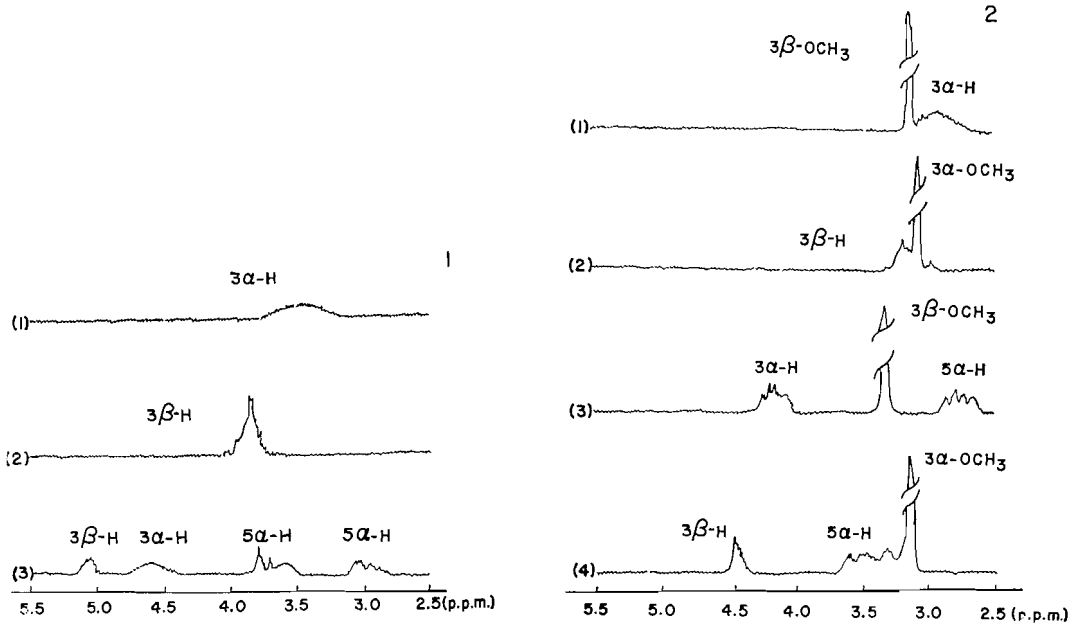


FIG. 1. The p.m.r. spectra of 3β-hydroxy-5α-cholestane (1), 3α-hydroxy-5α-cholestane (2), and the epimeric 3α- and 3β-hydroxy-4-oxa-5α-cholestanes (3) in deuteriochloroform. Resonance frequencies are recorded downfield from tetramethylsilane at 0.0 δ.

FIG. 2. The p.m.r. spectra of 3β-methoxy-5α-cholestane (1), 3α-methoxy-5α-cholestane (2), 3β-methoxy-4-oxa-5α-cholestane (3), and 3α-methoxy-4-oxa-5α-cholestane (4) in benzene recorded as noted in Fig. 1.

Analogous p.m.r. evidence was compiled and used to assign configurations to the epimeric methylacetals (IX*b* and IX*c*) derived from hemiacetal IX*a*.[7] Preparative thin-layer chromatography was used to separate the epimeric mixture of methylacetals obtained by treating hemiacetal IX*a* with methanol containing a drop of hydrochloric acid. By this method, pure specimens of the axial (IX*b*, m.p. 101–102°) and equatorial (IX*c*, m.p. 79–80°) epimers were obtained. A comparison (Fig. 2) of the p.m.r. spectra of both epimers in benzene solution with the p.m.r. spectra of 3α-methoxy- (13) and 3β-methoxy-5α-cholestane confirmed the structures previously assigned by Edward and collaborators.[7,8] Interestingly, the 5α-proton of the axial hydroxyl (IX*a*) and methoxy (IX*b*) isomers gave a p.m.r. signal displaced downfield by 0.6–0.7 δ from that of the C-3 equatorial isomers.[9]

A survey of hemiacetals V and VII indicated that each represented (in deuteriochloroform solution) a nearly equal mixture of epimers. Thus, the anomeric effect in 3-hydroxy-4-oxa steroids, in solution, is as important as conformational factors, and in the case of 3-methoxy-4-oxa-5α-steroids becomes of major importance. These conclusions reached on the basis of p.m.r. data support and confirm the earlier conclusions of Edward and his colleagues (4*c*, 11) regarding the stereochemistry of 3-hydroxy-4-oxa-5α-cholestane (IX*a*).

[7]*The isomeric acetals corresponding to structures IXb and IXc were prepared (2b, 4c, 11) in conjunction with earlier studies of hemiacetal IXa. The isomer, m.p. 98–99.5°, obtained from hemiacetal IXa and methanol – hydrogen chloride was shown (4c), on the basis of careful mutarotation determinations, to represent a 3α-methoxy configuration. Similarly, the β-anomer (m.p. 74–76°) obtained (11) by acid-catalyzed isomerization of the 3α-methoxy epimer was assigned structure IXc. Before these reports Fieser and his colleagues isolated a sample of the acetal melting at 89–92° (12).*

[8]*Edward and Puskas (11) also noted that acid-catalyzed isomerization of the 3-methoxy anomers favored formation of the 3α-methoxy isomer in the approximate ratio 7:3. A p.m.r. spectrum of the crude methylation product in benzene solution, prepared as described in the Experimental section, clearly verified the 3α-methoxy epimer as the major product.*

[9]*An example of 1,3-diaxial deshielding in the reverse direction, that is, of a C-3 proton by a bromine substituent at C-5, has been recorded (14).*

Can. J. Chem. Downloaded from www.nrcresearchpress.com by 210.87.254.5 on 09/05/12
For personal use only.

Can. J. Chem. Downloaded from www.nrcresearchpress.com by 210.87.254.5 on 09/05/12
For personal use only.

EXPERIMENTAL

The diethyl ether, diglyme (diethylene glycol dimethyl ether), and tetrahydrofuran were redistilled from sodium or lithium aluminium hydride and stored over sodium wire. Final purification of diglyme by distillation from lithium aluminium hydride in one case (observed by Dr. A. K. Das Gupta) resulted in an explosion. The same observation has recently been reported by Watson (15). In view of these experiences, distillation of diglyme from lithium aluminium hydride is not now recommended. All other solvents and boron trifluoride etherate were also redistilled. The sodium borohydride was used as supplied by Metal Hydrides, Inc. Each reduction reaction was conducted in a nitrogen atmosphere. Solvent extracts of aqueous solutions were dried over magnesium sulfate. Activated alumina refers to Merck "suitable for chromatography". Thin-layer chromatography plates were prepared with silica gel G (E. Merck, AG, Darmstadt) and developed with concentrated sulfuric acid.

A Kofler melting point apparatus was employed for melting point determinations (corrected). Optical rotation (chloroform solution) and elemental composition values were determined, respectively, in the laboratories of Dr. P. Demoen, Janssen Pharmaceutica, Beerse, Belgium, and Dr. A. Bernhardt, Mülheim, Germany. The infrared (potassium bromide) and p.m.r. spectra were recorded by Dr. R. A. Hill (University of Maine).

3-Oxo-4-oxa-5α-androstane (IIIa)

After chromatography on activated alumina in 1:1 petroleum ether – benzene, 3-oxo-androst-4-ene (II) (10 g (6)) was obtained as colorless needles, m.p. 106–108°. Oxidation to lactone III*a* was accomplished as previously described for 19-nortestosterone acetate (3*a*) with a reagent prepared from sulfuric acid (28 g), potassium persulfate (26 g), and glacial acetic acid (500 ml). The crude lactone (III*a*) was crystallized from petroleum ether – acetone as tacky yellow prisms (4.4 g). A solution of the product in 1:1 petroleum ether – benzene was percolated through a column of neutral alumina (Merck, Darmstadt) and, after removal of solvent, the filtrate residue was crystallized from petroleum ether – acetone as colorless needles (1.9 g), m.p. 115–116°. Repeated recrystallization from the same solvent mixture did not alter the melting point, and an analytical specimen exhibited $[\alpha]_D^{22}$ +77.3° (*c*, 1.25) and ν_{max} 1 735 cm^{-1}.

Anal. Calcd. for $C_{18}H_{28}O_2$: C, 78.21; H, 10.21. Found: C, 78.61; H, 10.27.

3,5β-Dihydroxy-3,5-seco-A-nor-5α-androstane (IV)

A solution of lactone III*a* (0.5 g) in tetrahydrofuran (20 ml) was reduced with lithium aluminium hydride (0.5 g in 30 ml of tetrahydrofuran) by the technique employed with 3-oxo-17β-hydroxy-4-oxa-5α-androstane (see ref. 3*a*). The diol (IV) was recrystallized from chloroform–methanol as needles weighing 0.45 g and melting at 189–190°. Several recrystallizations from the same solvent mixture provided an analytical sample (unchanged melting point); $[\alpha]_D^{22}$ 0.0° (*c*, 1.31);[10] ν_{max} 3 300, 1 085, 1 065, 1 040, and 1 025 cm^{-1}.

Anal. Calcd. for $C_{18}H_{32}O_2$: C, 77.09; H, 11.50; active H, 0.72. Found: C, 76.99; H, 11.26; active H, 0.62.

3ξ-Hydroxy-4-oxa-5α-androstane (V)

A solution of lactone III*a* (0.60 g) in tetrahydrofuran (20 ml) was treated with diborane generated from sodium borohydride (0.7 g) and boron trifluoride etherate (2.0 g) in diglyme (35 ml) as noted in earlier experiments (2, 3*a*). A solution of the solid product in 3:1 benzene–chloroform was chromatographed on neutral alumina. Elution with 60 ml of the same solvent mixture led to the recovery of lactone III*a* (0.05 g). Continued elution provided the epimeric hemiacetals (V). Three recrystallizations from chloroform – petroleum ether gave needles (0.40 g) melting at 188–192° (sintering from 178°). A thin-layer chromatogram of the hemiacetal mixture on Kieselguhr G (with chloroform or 19:1 chloroform–methanol as mobile phase) indicated that the analytical specimen represented only hemiacetal V: the epimeric mixture displayed $[\alpha]_D^{22}$ +56.4° (*c*, 1.17); ν_{max} 3 300, 1 115, 1 082, 1 042, and 1 030 cm^{-1}; p.m.r. (deuteriochloroform solution) response at 0.7, 0.95, 1–2 (broad), 3.1, 3.2, 4.75 (broad), and 5.2 δ.

Anal. Calcd. for $C_{18}H_{30}O_2$: C, 77.65; H, 10.86; active H, 0.36. Found: C, 77.92, 77.81; H, 11.01, 10.89; active H, 0.40.

Further elution of the column with 1:1 chloroform–methanol gave 0.10 g, m.p. 189–190°, of diol IV.[11]

4-Oxa-5α-androstane (IIIb)

Reduction of lactone III*a* (1.0 g) to tetrahydropyran III*b* was accomplished with the sodium borohydride (0.3 g) – boron trifluoride etherate (15 g) reagent in diglyme (30 ml) as previously described (1). A solution of the crude product in petroleum ether was passed through a column of activated alumina. After removal of the solvent *in vacuo* the residue was recrystallized from methanol–water; yield 0.45 g. Four recrystallizations from the same solvent yielded a pure specimen as colorless needles; m.p. 56–57°; $[\alpha]_D^{20}$ +34.7° (*c*, 1.86); ν_{max} 1 085, 1 105 cm^{-1}.

Anal. Calcd. for $C_{18}H_{30}O$: C, 82.38; H, 11.52. Found: C, 82.35, 82.34; H, 11.77, 11.46.

[10] *Methanol as solvent.*

[11] *By mixture melting point determination and infrared spectral comparison, the substance was found to be identical with an authentic sample.*

3-Oxo-4-oxa-5α-pregnane 20-Ethylenethioketal (VIb)

A solution of 3,20-dioxo-4-oxa-5α-pregnane (1.0 g, VI*a* (2*b*)) in boron trifluoride etherate (11 g) – ethanedithiol (3.0 g) was prepared at room temperature. Within a few minutes, the thioketal crystallized from solution as colorless needles. After a total of 1.5 h the mixture was cooled and diluted with methanol; the thioketal (VI*b*) was collected, washed with methanol, and recrystallized from acetone to yield 0.81 g melting at 237–239°; $[\alpha]_D^{23}$ +68.8° (*c*, 1.25); ν_{max} 1 740 cm^{-1}.

Anal. Calcd. for $C_{22}H_{34}O_2S_2$: C, 66.96; H, 8.69; S, 16.26. Found: C, 66.70; H, 8.58; S, 16.54.

3ξ-Hydroxy-4-oxa-5α-pregnane 20-Ethylenethioketal (VIIa)

Conversion of lactone VI*b* (0.45 g) in tetrahydrofuran (20 ml) into the epimeric mixture of hemiacetals corresponding to structure VII*a* was accomplished with diborane generated from sodium borohydride (0.5 g) and boron trifluoride etherate (2.9 g) in diglyme (18 ml) as described for hemiacetal V. The epimeric hemiacetals were recrystallized from chloroform – petroleum ether as colorless needles (0.32 g) melting at 187–188°; $[\alpha]_D^{21}$ 0.0°; ν_{max} 3 350 cm^{-1}.

Anal. Calcd. for $C_{22}H_{36}O_2S_2$: C, 66.60; H, 9.15; S, 16.17. Found: C, 66.28, 66.07; H, 8.89, 9.07; S, 16.36, 16.55.

3-Oxo-4-oxa-5α-pregnane (VIc)

Raney nickel (30 ml, W-4 (7)) was added to a solution of thioketal VI*b* (2.0 g) in ethanol (150 ml), and the mixture was heated at reflux for 4 h. After the solution was filtered, the nickel residue was washed with warm ethanol and the combined filtrate was concentrated to a colorless solid. Recrystallization from ethanol – petroleum ether gave 0.49 g of needles melting at 186–187°. Placing the nickel residues in a Soxlet apparatus and extracting with ethanol gave 0.16 g, and final dissolution of the nickel by-products in hydrochloric acid gave another 0.22 g of crude product. An analytical sample that was recrystallized from methanol – petroleum ether melted at 188–190°; $[\alpha]_D^{23}$ +107.4° (*c*, 0.619); ν_{max} 1 740 cm^{-1}.

Anal. Calcd. for $C_{20}H_{32}O_2$: C, 78.89; H, 10.59. Found: C, 78.38; H, 10.33.

3ξ-Hydroxy-4-oxa-5α-pregnane (VIIb)

Lactone VI*c* (0.3 g) in tetrahydrofuran (20 ml) was reduced to a mixture of epimeric hemiacetals (VII*b*, 0.2 g) by (see V) diborane prepared from sodium borohydride (0.4 g) and boron trifluoride etherate (2.2 g). Recrystallization from chloroform – petroleum ether yielded colorless crystals melting at 161–163°; $[\alpha]_D^{23}$ 69.3° (*c*, 1.0); ν_{max} 3 350 cm^{-1}.

Anal. Calcd. for $C_{20}H_{34}O_2$ (306): C, 78.38; H, 11.18; O, 10.44; active H, 0.33. Found: C, 78.33, 77.93; H, 11.19, 11.11; O, 10.79; active H, 0.25; mol. wt. (Rast) 271.

3ξ-Hydroxy-4-oxa-5α-cholestane (IXa)

In a typical experiment, 0.38 *M* borane in tetrahydrofuran (30 ml (16)) was added at room temperature to 3-oxo-4-oxa-5α-cholestane (5.1 g, VIII). Before dilution with water (10 ml) and extraction with diethyl ether (60 ml), the solution was allowed to stand for 0.5 h. The combined ethereal extracts were washed with water and dried (potassium carbonate). Removal of solvent *in vacuo* gave a solid residue (5.0 g). A solution of the crude product in tetrahydrofuran–benzene (1:3) was chromatographed on silica gel (250 g). Elution with the same solvent mixture led to 4.2 g of hemiacetal IX*a*, m.p. 183–190°. Recrystallization from either methylene chloride – acetone or tetrahydrofuran–ligroin (b.p. 90–120°) gave a specimen (IX*a*) melting at 185–190°. In both cases, thin-layer chromatograms (7:3 benzene – diethyl ether being used as the mobile phase) and mixture thin-layer chromatograms with an authentic sample (2*b*) indicated the presence of only hemiacetal IX*a* (see Fig. 1). Melting points of 188–190° (4*c*) and 197–199° (2*b*), representing different proportions of the epimeric hemiacetals, have been reported.

When the preceding experiment was repeated with 0.5 g of lactone VIII (and with appropriately adjusted amounts of the other reagents) for a total reaction time of 4 min, essentially the same result was obtained. A thin-layer chromatogram of the crude product suggested the presence of approximately 80% hemiacetal IX*a* accompanied by 3,5β-dihydroxy-3,5-seco-A-nor-5α-cholestane (2*b*). However, conducting the same reaction with one-half the previous quantity of diborane and a 30 min reaction period yielded a mixture (as evidenced by a thin-layer chromatogram) composed of approximately equal amounts of lactone VIII, hemiacetal IX*a*, and the diol resulting from complete reduction.

3α-Methoxy- and 3β-Methoxy-4-oxa-5α-cholestane (IXb and IXc)

A solution composed of the epimeric hemiacetals (0.40 g, IX*a*) prepared above, tetrahydrofuran (7 ml), methanol (15 ml), and 1 drop of concentrated hydrochloric acid was prepared by warming the mixture for approximately 3 min. Next, the solution was cooled and concentrated (*in vacuo*) to a crystalline residue. Six 0.06 g portions of the crude product were applied to each of six preparative silica gel G (1 mm layer) thin-layer chromatography plates. Each plate was developed 3 times with 9:1 hexane – diethyl ether, and the bands were identified by holding the plate in iodine vapor for a few seconds. Two very close bands were observed at approximately the middle of the plate, and each was carefully collected. Elution of the less-polar component with diethyl ether gave 0.19 g of acetal IX*b*, which was rechromatographed on four preparative thin-layer plates. By this means, a 0.16 g sample of 3α-methoxy-4-oxa-5α-cholestane (IX*b*) melting at 98–101.5° was obtained. Recrystallization from acetone raised the melting point to 101–102.5° (melting points of 98–99.5° and 106–107° have been reported (2*b*, 4*c*)).

Can. J. Chem. Downloaded from www.nrcresearchpress.com by 210.87.254.5 on 09/05/12
For personal use only.

The more polar acetal was eluted from the silica gel in the same manner, and rechromatographed (twice) on two preparative silica gel thin-layer plates to yield 0.06 g of 3β-methoxy-4-oxa-5α-cholestane (IX*c*) melting at 77–80°. Two recrystallizations from acetone and one from methanol–acetone raised the melting point to 79–80° (ref. 11 reports m.p. 78°).

The configuration assigned to each hemiacetal was supported by a p.m.r. study (see Fig. 2).

ACKNOWLEDGMENTS

This investigation was supported in part by Public Health Service research grants Nos. CA-04074-04 to CA-04074-07 and CA-08705-01 from the National Cancer Institute. We are also grateful for financial support provided to W. J. E. (1960–1963) in the form of a NDEA Predoctorate Fellowship, and to Dr. George Slump, The Upjohn Co., for determining the p.m.r. response of hemiacetal V.

REFERENCES

1. G. R. PETTIT, H. KLINGER, N. O. JORGENSEN, and J. OCCOLOWITZ. Phytochemistry. In press.
2. (*a*) G. R. PETTIT, T. R. KASTURI, B. GREEN, and J. C. KNIGHT. J. Org. Chem. **26**, 4773 (1961). (*b*) G. R. PETTIT and T. R. KASTURI. J. Org. Chem. **26**, 4553 (1961).
3. (*a*) G. R. PETTIT, A. K. DAS GUPTA, and U. R. GHATAK. Steroids, **1**, 137 (1963). (*b*) R. PAPPO. U. S. Patent No. 3,101,350 (August 20, 1963); Chem. Abstr. **60**, 596 (1964).
4. (*a*) W. S. JOHNSON, J. C. COLLINS, JR., R. PAPPO, M. B. RUBIN, P. J. KROPP, W. F. JOHNS, J. E. PIKE, and W. BARTMANN. J. Am. Chem. Soc. **85**, 1409 (1963). (*b*) K. HEUSLER and A. WETTSTEIN. Helv. Chim. Acta, **45**, 347 (1962). (*c*) J. T. EDWARD, P. F. MORAND, and I. PUSKAS. Can. J. Chem. **39**, 2069 (1961). (*d*) N. W. ATWATER. J. Am. Chem. Soc. **83**, 3071 (1961).
5. G. NOMINE, R. BUCOURT, and A. PIERDET. Fr. Patent No. 1,366,725 (July 17, 1964); Chem. Abstr. **61**, 14751 (1964). D. BERTIN and J. PERRONNET. Bull. Soc. Chim. France, 564 (1964). W. F. JOHNS. U.S. Patent No. 3,137,690 (June 16, 1964); Chem. Abstr. **61**, 4428 (1964). J. E. PIKE, M. A. REBENSTORF, G. SLOMP, and F. A. MACKELLAR. J. Org. Chem. **28**, 2499 (1963). K. HEUSLER, J. KALVODA, P. WIELAND, G. ANNER, and A. WETTSTEIN. Helv. Chim. Acta, **45**, 2575 (1962).
7. C. W. SHOPPEE and G. KRUEGER. J. Chem. Soc. 3641 (1961).
8. G. R. PETTIT and E. VAN TAMELEN. Org. Reactions, **12**, 356 (1962).
9. G. R. PETTIT and D. M. PIATAK. J. Org. Chem. **27**, 2127 (1962). M. NEEMAN and W. S. JOHNSON. Org. Syn. **41**, 9 (1961).
9. A. WINDAUS and C. UIBRIG. Ber. **47**, 2384 (1914). A. FURST and P. A. PLATTNER. Helv. Chim. Acta, **32**, 275 (1949).
10. D. A. SWANN and J. H. TURNBULL. Tetrahedron, **20**, 1265 (1964). R. E. COUNSELL. Tetrahedron, **15**, 202 (1961). L. F. FIESER and T. GOTO. J. Am. Chem. Soc. **82**, 1693 (1960). J. N. SHOOLERY and M. T. ROGERS. J. Am. Chem. Soc. **80**, 5121 (1958).
11. J. T. EDWARD and I. PUSKAS. Can. J. Chem. **40**, 711 (1962).
12. L. F. FIESER, T. GOTO, and B. K. BHATTACHARYYA. J. Am. Chem. Soc. **82**, 1700 (1960).
13. M. NEEMAN, M. J. CASERIO, J. D. ROBERTS, and W. S. JOHNSON. Tetrahedron, **6**, 36 (1959).
14. A. VAN DER GEN. Ph.D. Dissertation, University of Amsterdam, Amsterdam, Netherlands. 1964.
15. H. R. WATSON. Chem. Ind. London, 665 (1964).
16. G. ZWEIFEL and H. C. BROWN. Org. Reactions, **13**, 1 (1963).

Can. J. Chem. Downloaded from www.nrcresearchpress.com by 210.87.254.5 on 09/05/12
For personal use only.

ANTINEOPLASTIC AGENTS

XVII. N-(2-BROMOETHYL)-N-(2-CHLOROETHYL)AMINES[1,2]

GEORGE R. PETTIT[3] AND MAURICE R. CHAMBERLAND

Department of Chemistry, University of Maine, Orono, Maine, and Department of Chemistry, Arizona State University, Tempe, Arizona

Received December 7, 1965

ABSTRACT

A convenient synthesis (I*a* → IV*a*) starting with N-bis(2-chloroethyl)amine has been devised for obtaining N-(2-bromoethyl)-N-(2-chloroethyl)amine. Several N-alkyl (IV*b* and VIII) and N-benzyl (VII) derivatives of the unsymmetrically halogenated amine (IV*a*) were prepared for cancer chemotherapeutic evaluation.

The majority of characterized N-bis(2-haloethyl)amines are those bearing symmetrically substituted chlorine atoms (1). With the exception of derivatives of N-(2-chloroethyl)-N-(2-fluoroethyl)amine (see e.g. ref. 2), only a few examples of unsymmetrically halogenated nitrogen mustards have been described. Of the five remaining analogous possibilities, only derivatives of N-(2-chloroethyl)-N-(2-iodoethyl)amine appear to have been reported (3). For example, Ross has isolated N-(2′-chloroethyl)-N-(2′-iodoethyl)-4-methoxybenzylamine among products obtained by treating the corresponding dichloro derivative with sodium iodide in aqueous acetone (3*a*). Continued interest in utilizing (for the design of nitrogen mustards with more desirable antineoplastic properties) differences in chemical reactivity based on variance of halogen substituents in N-bis(2-haloethyl)amines led us to evaluate N-(2-bromoethyl)-N-(2-chloroethyl)amines. Interesting biological properties discovered recently in the case of several bromine-containing amines (5), combined with the results of our prior study of N-bis(2-bromoethyl)amines (6), suggested that amine IV*a* and several selected derivatives should receive biological evaluation.

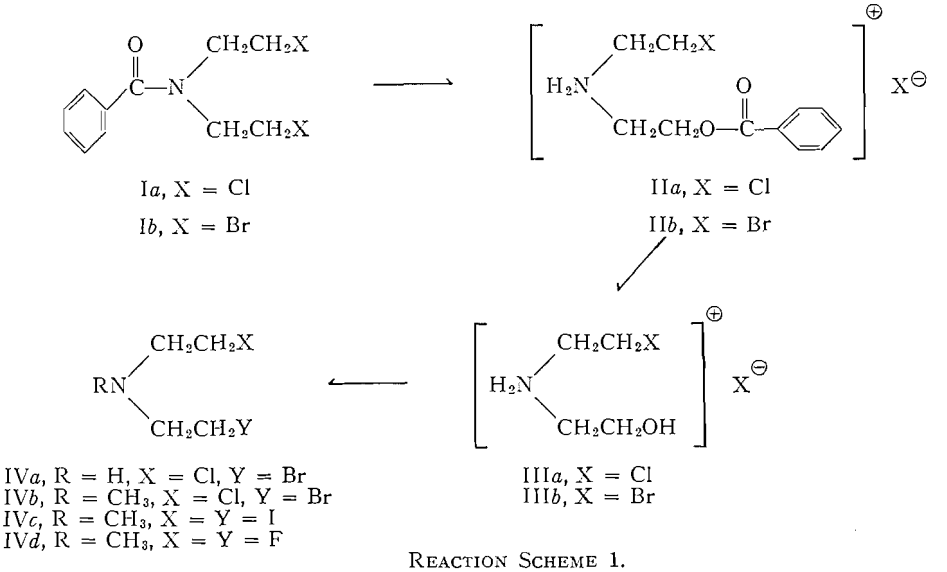
Although a number of synthetic methods were initially considered, the general route illustrated in Reaction Scheme 1 appeared to be the most promising from a practical standpoint, and emphasis was placed on this approach. Also, a useful procedure for obtaining amine III would provide, in principle, a method for obtaining the remaining unknown unsymmetrically halogenated nitrogen mustards. A sequence based on N-bis(2-chloroethyl)amine was first investigated. Preparation of amide I*a* and subsequent rearrangement in ethanol to ester II*a* was effected by a routine method previously developed in our laboratory (7). Ester II*a* was subjected to acid hydrolysis and 2-(2′-chloroethylamino)ethyl alcohol hydrochloride (III*a*) was isolated in essentially quantitative yield. Of several procedures explored for the bromination of alcohol III*a*, one based on phosphorus tribromide (providing 78% conversion into amine IV*a* hydrobromide) was found to be most satisfactory whereas another employing thionyl bromide (75% conversion of amine IV*a* hydrobromide) was considered to be less useful. An alternate reaction sequence starting with N-bis(2-bromoethyl)amine was also studied. Here amide I*b* was prepared and converted into ester II*b* as described earlier (6), and the ester was hydrolyzed with hydrobromic acid to yield alcohol III*b*. Although chlorination of alcohol III*b* with thionyl chloride readily gave amine IV*a* hydrochloride in good yield (98%), the overall method

[1] *For part XVI in this series, see G. R. Pettit and L. Garson, Can. J. Chem., 43, 2640 (1965).*

[2] *This investigation was aided by grants Nos. T-79E and T-79F from the American Cancer Society.*

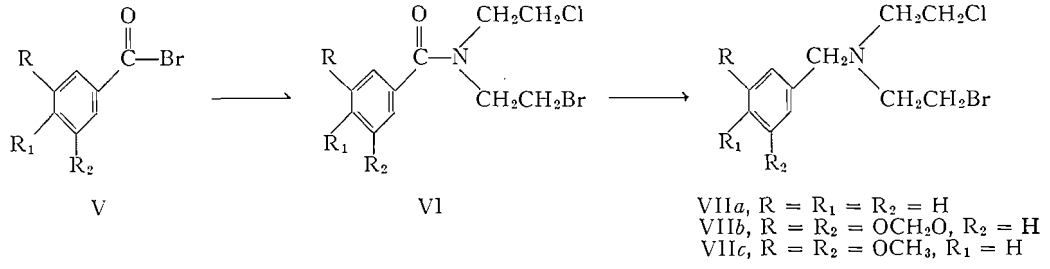
[3] *Present address: Department of Chemistry, Arizona State University, Tempe, Arizona.*

Can. J. Chem. Downloaded from www.nrcresearchpress.com by 210.87.254.40 on 09/05/12
For personal use only.



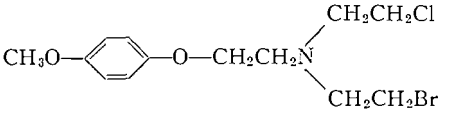
REACTION SCHEME 1.

was less suitable, as N-bis(2-chloroethyl)amine is a more readily available starting material. To compare the antineoplastic activity of N-methylamine IV*b* with that of N-methyl-N-bis(2-chloroethyl)amine, nitrogen mustard IV*a* hydrobromide was methylated by a formaldehyde – formic acid technique (8). Methylation of N-bis(2-fluoroethyl)-amine and N-bis(2-iodoethyl)amine was performed for the same reason.



REACTION SCHEME 2.

For biological studies four derivatives (VII*a*–VII*c*, VIII) of N-(2-bromoethyl)-N-(2-chloroethyl)amine were selected for preparation. Two of these substances, amines VII*b* and VII*c*, were chosen because of promising antitumor activity evidenced by the corresponding dichloro derivatives (7*a*). Synthesis of benzylamines VII*a*–VII*c* and aliphatic amine VIII proceeded as shown in Reaction Scheme 2.[4] The acyl bromide was



VIII

[4]*Previously (7a) a novel halogen exchange reaction provided the key step in a route believed to yield amine VIIb hydrochloride. However, the synthesis of amine VIIa described in the present contribution provides a more uniformly reliable synthetic approach to substances of this type.*

Can. J. Chem. Downloaded from www.nrcresearchpress.com by 210.87.254.40 on 09/05/12
For personal use only.

prepared with oxalyl bromide[5] or phosphorus tribromide. Reaction between the acyl bromide and 2 equivalents of amine IV*a* (in benzene solution) yielded the corresponding amide (VI), which was easily reduced with lithium aluminium hydride. In each case, the amine derivative was characterized as the hydrobromide salt. Structural assignments were confirmed by the results of infrared and proton magnetic resonance (p.m.r.) (e.g. see ref. 4*b*) spectral studies. Presently available results of biological studies[6] allow comparison of the effects of amine VII*a* and its dichloro (7*a*) and dibromo (6) analogues against Walker 256 (subcutaneous) in randomly bred albino rats. The N-(2-bromoethyl)-N-(2-chloroethyl)-amine VII*c* hydrobromide at a dose of 12.5 mg/kg caused 92% inhibition of tumor growth whereas the N-bis(2-chloroethyl)amine (at 4.8 mg/kg) and N-bis(2-bromoethyl)amine (at 12.5 mg/kg) counterparts showed, respectively, complete and 95% inhibition. The dose (in saline solution given intraperitoneally) regimen was begun on the first day of tumor transport and continued for 5 days. Tumor growth was measured on the 10th day.

EXPERIMENTAL

The p.m.r. spectra were obtained in deuterium oxide solution and are reported relative to the peak response of HDO as internal reference. The p.m.r. equipment and general experimental techinques used below are described in introductions to the Experimental sections of refs. 4*b* and 6. All analytical samples were colorless, and infrared spectra were recorded in potassium bromide.

2-(2′-Chloroethylamino)ethyl Benzoate Hydrochloride (IIa)

First, preparation of N-bis(2-chloroethyl)benzamide (I*a*) was achieved by condensing (cf. ref. 7*a*) N-bis(2-chloroethyl)amine (from 100 g of the hydrochloride derivative) with benzoyl chloride (40 g) in benzene (250 ml) solution. After N-bis(2-chloroethyl)amine hydrochloride was collected, the filtrate was concentrated *in vacuo* to a pale yellow oil. A solution of the crude amide in 95% ethanol (300 ml) was heated at reflux for 2 h. Evaporation (*in vacuo*) of solvent yielded ester II*a* as pale yellow crystals weighing 58.6 g (79%). Recrystallization from acetone gave colorless needles melting at 134–135° (ref. 9 reports m.p. 135°).

N-(2-Bromoethyl)-N-(2-chloroethyl)amine (IVa) Hydrobromide

Method A

A solution of 2-(2′-chloroethylamino)ethyl benzoate hydrochloride (II*a*, 50.0 g) in 10% hydrochloric acid (200 ml) was heated at reflux for 3 h. After cooling, the solution was filtered to remove benzoic acid (22.6 g, corresponding to a 98% recovery) and washed with chloroform (2 × 100 ml). The hydrochloric acid solution was concen trated *in vacuo* to a clear viscous oil, which was further dried azeotropically with benzene. The oily sample of *2-(2′-chloroethylamino)ethyl alcohol hydrochloride (IIIa)* was obtained in a quantitative yield and resisted a number of attempts at crystallization. However, the viscous oil proved to be satisfactory for conversion into amine IV*a*.

A sample (18 g) of hydrochloride III*a* was slowly added with rapid stirring to warm (steam bath) phosphorus tribromide (43 ml). Heating at steam bath temperature and stirring were continued for an additional hour while a deep straw colored solid separated. The mixture was washed with benzene (3 × 100 ml); the residual solid was dissolved in water (150 ml), neutralized (with cooling) with 6 *N* sodium hydroxide (60 ml), and extracted with benzene (500 ml). The dry benzene solution was treated with anhydrous hydrogen bromide and diluted with diethyl ether to yield 23.4 g (78%) of colorless crystals melting at 190–194°. Two recrystallizations from methanol – diethyl ether gave needles[7] melting at 198–200°; ν_{max} 2 900, 2 750, 2 400, 1 580, 1 450, 1 430, 1 395, and 1 280 cm^{-1}.

Anal. Calcd. for $C_4H_{10}Br_2ClN$: C, 17.96; H, 3.77; Br, 59.77; Cl, 13.26; N, 5.27. Found: C, 17.85; H, 3.77; Br, 59.96; Cl, 13.14; N, 5.11.

The procedure described directly above for obtaining amine IV*a* hydrobromide gave consistently good results and was used routinely.

Method B

A sample (25 g) of hydrochloride III*a* was suspended in dry benzene (100 ml) and treated with thionyl bromide (63.0 g, freshly prepared as described in ref. 10 during a 45 h reaction period) in benzene (50 ml). The mixture was stirred at reflux for 1 h and at room temperature for an additional hour. During the reaction

[5]*A cursory examination of the reaction between benzoyl chloride and amine IVa indicated that concomitant halogen exchange as previously observed in the case of N-bis(2-bromoethyl)amine (7a) might generally preclude use of the acyl chloride approach.*

[6]*We are indebted to the Cancer Chemotherapy National Service Center, National Institutes of Health, U.S. Public Health Service, for this valuable information.*

[7]*Consult ref. 4b for the p.m.r. spectrum of this substance.*

Can. J. Chem. Downloaded from www.nrcresearchpress.com by 210.87.254.40 on 09/05/12
For personal use only.

period, a color change from golden yellow to reddish brown was noted, and a more dense and darker oily phase appeared. The upper layer was decanted and the residue was diluted with methanol. The methanol solution in turn was diluted with diethyl ether. Cooling the solution led to amine IV*a* hydrobromide as colorless needles weighing 30.9 g (75%), m.p. 197–199°.

N-(2-Bromoethyl)-N-(2-chloroethyl)amine (IVa) Hydrochloride

Method A

A 1.0 g specimen of amine IV*a* hydrobromide (prepared by method B in the preceding experiment) was neutralized with 3 *N* sodium hydroxide. The base was extracted with benzene and the dry organic phase was treated with ethereal hydrogen chloride. The resulting hydrochloride derivative was recrystallized (3 times) from methanol – diethyl ether to yield an analytical sample melting at 195–197°.

Anal. Calcd. for $C_4H_{10}BrCl_2N$: C, 21.55; H, 4.52; Br, 35.85; Cl, 31.80; N, 6.28. Found: C, 21.48; H, 4.34; Br, 36.21; Cl, 32.01; N, 6.01.

Method B

A mixture of 2-(2′-bromoethylamino)ethyl benzoate (II*b*, 23 g, prepared as described in ref. 6) and 10% hydrobromic acid (150 ml) was heated at reflux for 3 h. After cooling, filtration, and washing with chloroform, the hydrobromic acid solution was concentrated *in vacuo* to a pale yellow oil (15.8 g, nearly quantitative conversion into amine III*b*). The oil was suspended in chloroform (130 ml) and treated (dropwise) with thionyl chloride (25 ml) in chloroform (30 ml). The mixture was heated at reflux for 0.5 h. Cooling the solution led to separation of amine IV*a* hydrochloride as yellow crystals, yield 16.9 g (98%), m.p. 185–189°. Three recrystallizations from ethanol – diethyl ether gave pure colorless needles melting at 195–197°. An infrared spectral comparison of the product and that obtained by method A confirmed the mutual identity of both hydrochloride salts.

Anal. Found: C, 21.26; H, 4.40; Br, 36.70; Cl, 31.80; N, 6.30.

N-Methyl-N-(2-bromoethyl)-N-(2-chloroethyl)amine (IVb) Hydrobromide

A mixture of amine IV*a* hydrobromide (3.0 g), 37% formalin (2.5 ml), and 98% formic acid (2 ml) was heated on a steam bath for 2 h. The solution was concentrated (*in vacuo*) to dryness and the residue dissolved in water (20 ml). The solution was neutralized with 6 *N* sodium hydroxide (20 ml) and the aqueous mixture extracted with benzene. Treating the benzene solution with ethereal hydrogen bromide yielded 2.8 g (87%) of amine IV*b* hydrobromide as colorless crystals, m.p. 114–115°. Two recrystallizations from methanol – diethyl ether yielded an analytical sample as needles melting at 122–125°; ν_{max} 2 900, 2 650, 2 575, 2 500, 2 350, 1 470, 1 375, 1 320, 1 285, 1 290, 950, and 760 (broad) cm^{-1}; p.m.r. responses at 3.15 (three methyl protons) and 3.7–4.3 (complex, eight methylene protons, principal signal at 3.91) δ.

Anal. Calcd. for $C_5H_{12}Br_2ClN$: C, 21.34; H, 4.30; Br, 56.79; Cl, 12.60; N, 4.98. Found: C, 21.36; H, 4.60; Br, 56.73; Cl, 12.65; N, 4.85.

N-Methyl-N-bis(2-iodoethyl)amine (IVc) Hydroiodide

Amine IV*c* hydroiodide was prepared from N-bis(2-iodoethyl)amine hydroiodide (4.5 g (6)), 37% formalin (3 ml), and 98% formic acid (2.0 g) as described in the preceding experiment (see IV*b*). The product weighed 4.1 g (88%) and melted at 165–167°. Three recrystallizations from methanol gave an analytical specimen as needles; m.p. 173–175° (11); ν_{max} 2 900, 2 700, 1 460, 1 450, 1 425, 1 365, 1 210, 1 190, 1 060, 1 010, 965, and 930 cm^{-1}.

Anal. Calcd. for $C_5H_{12}I_3N$: C, 12.86; H, 2.59; I, 81.56; N, 3.00. Found: C, 12.74; H, 2.74; I, 81.66; N, 3.13.

N-Methyl-N-bis(2-fluoroethyl)amine (IVd) Hydrobromide

The procedure used for converting N-bis(2-fluoroethyl)amine hydrobromide (2.3 g (4*a*)) into amine IV*d* hydrobromide (m.p. 96–98°, 1.4 g, 57% yield) with 37% formalin (2 ml) and 98% formic acid (1.0 g) was that illustrated in the case of amine IV*b* hydrobromide. Recrystallization (twice) from methanol – diethyl ether gave an analytical sample as needles melting at 102–104°; ν_{max} 2 900, 2 700, 2 650 (doublet with shoulder at 2 500), 1 460, 1 450, 1 435, 1 420, 1 240, 1 195, 1 170, 1 110, 1 090, 1 070, 1 045, 1 035, 1 010, 970, 900, 880, and 860 cm^{-1}.

Anal. Calcd. for $C_4H_{10}BrF_2N$: C, 29.43; H, 5.93; Br, 39.16; N, 6.86. Found: C, 29.64; H, 6.00; Br, 39.15; N, 6.68.

Childs (12) has summarized a route to amine IV*d*, and more recently Nemets and Epshtein (13) reported conversion of bromofluoroethane (with methylamine) into amine IV*d* hydrochloride.

N-(2-Bromoethyl)-N-(2-chloroethyl)benzylamine (VIIa) Hydrobromide

In a typical experiment, amine IV*a* hydrobromide (10.0 g) was dissolved in water (50 ml) – ice (20 g) and treated with 6 *N* sodium hydroxide (20 ml). The mixture was extracted with benzene, and the dry (magnesium sulfate) extract was treated (dropwise during 10 min) with benzoyl bromide (3.5 g, prepared from benzoic acid and phosphorus tribromide). Before the solution was cooled, stirring was continued at room temperature for 2 h. The solution was filtered to remove amine IV*a* hydrobromide (4.5 g, 89% recovery) and the filtrate was slowly added with stirring during 0.5 h to a mixture of lithium aluminium hydride (0.76 g)

Can. J. Chem. Downloaded from www.nrcresearchpress.com by 210.87.254.40 on 09/05/12
For personal use only.

and dry diethyl ether (100 ml). After a total reaction period at room temperature of 1 h, water (approximately 4 ml) was cautiously added to the mixture. The general procedure employed at this point has been described in a prior contribution (6). Next, the solution was filtered, dried, and treated with anhydrous hydrogen bromide. Further dilution with diethyl ether led to the separation of amine VII*a* hydrobromide as colorless crystals, yield 4.3 g (63%), m.p. 165–170°. Two recrystallizations from methanol – diethyl ether gave a pure sample as needles; m.p. 176–179°; ν_{max} 2 900, 2 650, 2 550, 2 350, 1 490, 1 450, 1 430, 1 375, 1 245, 1 210, 1 010, 960, 930, 765, 750, and 700 cm^{-1}; p.m.r. responses at 3.8–4.2 (complex, eight methylene protons, principal signal at 3.92), 4.70 (two benzyl protons), and 7.72 (five aromatic protons) δ.

Anal. Calcd. for $C_{11}H_{16}Br_2ClN$: C, 36.95; H, 4.51; Br, 44.70; Cl, 9.92; N, 3.92. Found: C, 36.85; H, 4.46; Br, 44.97; Cl, 9.76; N, 3.92.

N-(2′-Bromoethyl)-N-(2′-chloroethyl)-3,4-methylenedioxybenzylamine (VIIb) Hydrobromide

The acid bromide prepared from piperonylic acid (2.5 g) and oxalyl bromide (6 g) was allowed to react with the base corresponding to amine IV*a* hydrobromide (10.7 g) as described in the preceding experiment (see VII*a*). The crude amide was reduced by the lithium aluminium hydride (0.6 g) procedure (compare VII*a*), and the resulting amine hydrobromide weighed 5.3 g (88%), m.p. 159–163°. After two recrystallizations from methanol – diethyl ether the analytical sample (needles) melted at 164–165°; ν_{max} 2 900, 2 625, 2 500, 2 350, 1 500, 1 490, 1 445, 1 385, 1 260, 1 245, 1 105, 1 045, 950, 930, 880, 820, 810, 780, and 765 cm^{-1}; p.m.r. responses at 3.4–4.2 (complex, eight methylene protons, principal signal at 3.78), 4.50 (two benzyl protons), 6.08 (two methylenedioxy protons), and 7.08 (three aromatic protons) δ.

Anal. Calcd. for $C_{12}H_{16}Br_2ClNO_2$: C, 35.89; H, 4.02; Br, 39.80; Cl, 8.83; N, 3.49. Found: C, 35.76; H, 4.08; Br, 40.04; Cl, 8.75; N, 3.41.

N-(2′-Bromoethyl)-N-(2′-chloroethyl)-3,5-dimethoxybenzylamine (VIIc) Hydrobromide

A sample of 3,5-dimethoxybenzoyl bromide (3.7 g, prepared as noted in ref. 6) was allowed to react with the amine corresponding to 10.7 g of nitrogen mustard IV*a* hydrobromide. The resulting amide was reduced with lithium aluminium hydride (0.57 g). The hydrobromide derivative of the product weighed 4.8 g (80%) and melted at 160–163°. The general experimental technique and method used for purifying the product was that illustrated in the case of amine VII*a*. The analytical specimen was obtained as needles; m.p. 165–167°; ν_{max} 2 850, 2 800, 2 600, 2 575, 1 595, 1 480, 1 460, 1 430, 1 360, 1 305, 1 215, 1 170, 1 160, 1 070, 1 060, and 845 cm^{-1}; p.m.r. responses at 3.4–4.2 (complex, eight methylene protons and six methoxy protons, principal signals at 3.80–3.90), 4.50 (two benzyl protons), and 6.80 (three aromatic protons) δ.

Anal. Calcd. for $C_{13}H_{20}Br_2ClNO_2$: C, 37.39; H, 4.83; Br, 38.28; Cl, 8.49; N, 3.35. Found: C, 37.41; H, 5.10; Br, 38.60; Cl, 8.35; N, 3.47.

N-(2′-Bromoethyl)-N-(2′-chloroethyl)-4-methoxyphenoxyethylamine (VIII) Hydrobromide

Oxalyl bromide (9 g) containing 4-methoxyphenoxyacetic acid (3.6 g) was heated at reflux for 2 h. After removal (*in vacuo*) of excess oxalyl bromide the acyl bromide was obtained as a light brown oil. Without further purification the acyl bromide was treated with the free amine corresponding to 11.8 g of amine IV*a* hydrobromide. Subsequent reduction and purification of the product was accomplished as described for the isolation of amine VII*a* hydrobromide. The hydrobromide derivative of amine VIII was obtained in 63% yield (5.3 g). A pure specimen melted at 143–145°; ν_{max} 2 900, 2 650, 2 550, 2 350, 1 510, 1 485, 1 465, 1 440, 1 230, 1 020, 830, and 735 cm^{-1}; p.m.r. responses at 3.7–4.2 (complex, ten methylene and three methoxy protons, principal signals at 3.75 and 3.82), 4.22–4.50 (two methylene protons), and 6.90 (four aromatic protons) δ.

Anal. Calcd. for $C_{13}H_{20}Br_2ClNO_2$: C, 37.39; H, 4.83; Br, 38.28; Cl, 8.49; N, 3.35. Found: C, 37.09; H, 4.90; Br, 38.40; Cl, 8.35; N, 3.23.

REFERENCES

1. R. P. Bratzel, R. B. Ross, R. H. Goodridge, W. T. Huntress, M. T. Falather, and D. E. Johnson. Cancer Chemotherapy Rept. **26**, 1 (1963).
2. Z. B. Papanastassiou and R. J. Bruni. J. Org. Chem. **29**, 2870 (1964).
3. (*a*) W. C. J. Ross. J. Chem. Soc. 2589 (1949).
   (*b*) O. M. Friedman and A. M. Seligman. J. Am. Chem. Soc. **76**, 658 (1954).
   (*c*) A. M. Rutenburg, L. Persky, O. M. Friedman, and A. M. Seligman. J. Pharmacol. Exptl. Therap. **111**, 483 (1954); Chem. Abstr. **48**, 13960 (1954).
4. (*a*) G. R. Pettit and R. L. Smith. Can. J. Chem. **42**, 572 (1964).
   (*b*) G. R. Pettit, J. A. Settepani, and R. A. Hill. Can. J. Chem. **43**, 1792 (1965).
5. P. Hebborn and D. J. Triggle. J. Med. Chem. **8**, 541 (1965). J. D. P. Graham and K. Clarke. Brit. J. Pharmacol. **23**, 285 (1964). S. Sass, C. E. Williamson, S. P. Kramer, L. E. Goodman, A. Ulfohn, A. M. Seligman, and B. Witten. J. Med. Chem. **8**, 14 (1965). M. H. Benn, A. M. Creighton, B. J. Johnson, L. N. Owen, and G. R. White. J. Chem. Soc. 3395 (1964).
6. G. R. Pettit, M. R. Chamberland, D. S. Blonda, and M. A. Vickers. Can. J. Chem. **42**, 1699 (1964).
7. (*a*) G. R. Pettit, D. S. Blonda, and E. C. Harrington. Can. J. Chem. **41**, 2962 (1963).
   (*b*) G. R. Pettit, D. S. Blonda, and R. A. Upham. Can. J. Chem. **43**, 1798 (1965).

Can. J. Chem. Downloaded from www.nrcresearchpress.com by 210.87.254.40 on 09/05/12
For personal use only.

8. G. R. PETTIT and J. A. SETTEPANI. J. Org. Chem. **27**, 1714 (1962).
9. D. H. PEACOCK and U. G. DUTTA. J. Chem. Soc. 1303 (1934).
10. R. C. ELDERFIELD, W. J. GENSLER, F. BRODY, J. D. HEAD, S. C. DICKERMAN, L. WIEDERHOLD III, C. B. KREMER, H. A. HAGEMAN, F. J. KREYSA, J. M. GRIFFING, S. M. KUPCHAN, B. NEWMAN, and J. T. MAYNARD. J. Am. Chem. Soc. **68**, 1579 (1946).
11. A. M. SELIGMAN, O. M. FRIEDMAN, and A. M. RUTENBURG. Cancer, **3**, 342 (1950); Chem. Abstr. **44**, 5019 (1950).
12. A. F. CHILDS, L. J. GOLDSWORTHY, G. F. HARDING, F. E. KING, A. W. NINEHAM, W. L. NORRIS, S. G. P. PLANT, B. SELTON, and A. L. L. TOMPSETT. J. Chem. Soc. 2174 (1948).
13. V. G. NEMETS and G. L. EPSHTEIN. Izv. Vysshikh Uchebn. Zavedenii Khim. i Khim. Tekhnol. **5**, 101 (1962); Chem. Abstr. **58**, 3297 (1962).

Can. J. Chem. Downloaded from www.nrcresearchpress.com by 210.87.254.40 on 09/05/12
For personal use only.

THE REACTION OF PHENYLMETHANESULFONYL CHLORIDE WITH TERTIARY AMINES: FORMATION OF GEOMETRICAL ISOMERS ABOUT A CARBON–SULFUR DOUBLE BOND[1]

J. F. KING and T. DURST
Department of Chemistry, University of Western Ontario, London, Ontario
Received November 23, 1965

ABSTRACT

In methylene chloride or ether solution, phenylmethanesulfonyl chloride reacts with triethylamine to give a mixture consisting primarily of *trans*-stilbene and *cis*-diphenylethylene sulfone. In cyclohexane the same reagents yield principally a material which is shown to be a roughly 2:1 mixture of *cis*- and *trans*-oxythiobenzoyl chlorides (I and II, respectively). The latter compounds represent the first examples of geometrical isomerism about a double bond in which one of the atoms of the double bond is outside the first short period of the Periodic Table.

In 1911 Wedekind and Schenk (1) reported that the action of tertiary amines on phenylmethanesulfonyl chloride yielded *trans*-stilbene, and suggested that a species $RR'C{=}SO_2$, for which they coined the name "sulfene", was an intermediate in the reaction. The next 50 years yielded little that contributed directly to anything that could be regarded as a satisfactory description of the mechanism of the reaction in modern terms, although some, rather sporadic, reports on related aspects of the chemistry of sulfenes have appeared (for recent reviews of the latter see refs. 2–4). A few years ago we began a reexamination of the Wedekind reaction, starting with a simple repetition of the early work. We have confirmed Wedekind's report as far as it went, but in addition have encountered other aspects of the reaction which we have found to be of considerable interest. The most notable of these is the isolation of compounds which we will show in this account are the first examples of geometrical isomerism about a carbon–sulfur double bond, indeed about any double bond in which one of the atoms is of a higher atomic number than nitrogen.

In this paper the various products of the reaction of phenylmethanesulfonyl chloride with triethylamine are discussed and their structures (where previously unknown) proved, primarily with the aid of analytical and physical measurements. In a forthcoming paper corroborative evidence derived from *chemical* studies will be presented for the structures of the *cis*- and *trans*-oxythiobenzoyl chlorides. Two preliminary communications describing some of the work in these papers have already appeared (5, 6).

RESULTS AND DISCUSSION

The Reaction in Methylene Chloride and Ether

When the reaction of phenylmethanesulfonyl chloride and triethylamine was carried out in either ether or methylene chloride solution, sulfur dioxide was produced together with *trans*-stilbene and a material which was found to be *cis*-diphenylethylene sulfone, along with a small amount of the mixed *cis*- and *trans*-oxythiobenzoyl chlorides. (The isolation and proof of structure of the latter materials are discussed in a later section, those of the ethylene sulfone in the next paragraph.) The yields varied somewhat with the amount of care taken, but when the reactions were carried out at $-60°$ with appropriate precautions to exclude moisture, the yield of the isolated, crystalline *trans*-stilbene was 48%, that of the sulfone 28%.

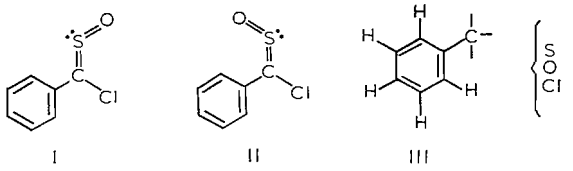
[1]*Part 4 in the series Organic Sulfur Mechanisms.*

Can. J. Chem. Downloaded from www.nrcresearchpress.com by 210.87.254.5 on 09/05/12
For personal use only.

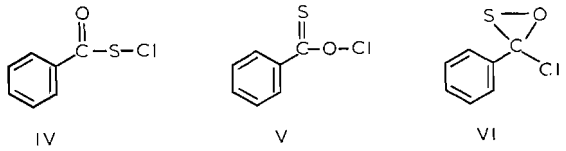
cis-Diphenylethylene sulfone was obtained directly by crystallization from the crude reaction mixture as a white solid melting with decomposition at 83–85°. Its structure is implied by (*i*) analysis, which indicates the formula $C_{14}H_{12}SO_2$, (*ii*) its infrared spectrum, which shows strong bands at 1 333 and 1 140 cm^{-1} characteristic of the sulfonyl group, and (*iii*) the nuclear magnetic resonance (n.m.r.) spectrum, which shows only two peaks, a singlet at 4.89 p.p.m. and a slightly broadened band at 7.3 p.p.m. (relative areas 1:5). Heating the compound to its melting point, or refluxing in a low-boiling solvent such as carbon disulfide or methylene chloride, causes loss of sulfur dioxide with concomitant production of *cis*-stilbene. The infrared spectrum of the stilbene thus produced showed it to be almost entirely free of the *trans* isomer. The fact that this reaction is highly stereospecific and is induced under such mild conditions may be reasonably accounted for only on the basis of a cyclic, concerted reaction in which the stereochemical relationship of the substituents is unchanged; in other words, it is highly probable that the phenyl groups are also *cis* in the starting material. Confirmation of this view appeared shortly after these experiments were completed, in the form of a communication by Neureiter and Bordwell (7), who showed that ethylene sulfones lose sulfur dioxide with preservation of the orientation of the substituents.

The Reaction in Cyclohexane and Benzene Solutions

In remarkable contrast to what occurs in either methylene chloride or ether, the reaction of phenylmethanesulfonyl chloride and triethylamine in cyclohexane yields a product which contains only a small amount of *trans*-stilbene, and which consists primarily of triethylammonium phenylmethanesulfonate (as well as triethylammonium chloride) and a reddish-brown oily product. This latter material, which was dubbed "red oil", was found to be a mixture of the geometrical isomers *cis*- and *trans*-oxythiobenzoyl chloride (I and II, respectively). These compounds were most conveniently isolated by silica gel chroma-



I II III



IV V VI

tography of the cyclohexane-soluble portion of the reaction mixture. The *trans* isomer (II), which was eluted first, crystallized from cold pentane to give slightly pink needles melting at 5°. Further elution of the chromatographic column yielded the *cis* isomer (I) as yellowish plates, m.p. 38–39°, in about double the quantity of the *trans* compound (II). The *cis* isomer was also obtained by a short-path distillation of the crude cyclohexane-soluble product, followed by recrystallization. Both compounds can be kept without significant decomposition for a few weeks in a refrigerator at −5°, but at room temperature, especially in the light or in a humid atmosphere, they are much more rapidly decomposed.

Can. J. Chem. Downloaded from www.nrcresearchpress.com by 210.87.254.5 on 09/05/12
For personal use only.

When the reaction of phenylmethanesulfonyl chloride and triethylamine was carried out in benzene solution, a mixture of all of the above products was obtained, viz. *trans*-stilbene, *cis*-diphenylethylene sulfone, *cis*- and *trans*-oxythiobenzoyl chloride, triethylammonium chloride, and triethylammonium phenylmethanesulfonate. These results correspond to the observations of Wedekind and Schenk (1), who, under similar conditions, isolated *trans*-stilbene and triethylammonium chloride, and described the residue as a "rötlich gefärbte Masse", clearly essentially the same material as our "red oil".

Preliminary experiments (8) indicate that phenylmethanesulfonyl bromide also yields, on reaction with triethylamine, a mixture containing the oxythiobenzoyl halides. When phenylmethanesulfonyl fluoride, however, was treated with triethylamine under similar conditions, the sulfonyl fluoride was recovered unchanged. More vigorous conditions gave reaction but no isolated product.

Proof of Structure of the Oxythiobenzoyl Chlorides

Because there is no adequately established precedent for structures I and II, it was felt that more than usual care ought to be exercised in assigning the structures of the compounds isolated from the "red oil". To this end both physical and chemical evidence was adduced, though this account deals primarily with the former. Table I summarizes a

TABLE I

Physical properties of *cis*- and *trans*-oxythiobenzoyl chlorides

	trans isomer (m.p. 5°)	*cis* isomer (m.p. 38–39°)
Molecular weight		
Cryoscopic (calcd. 172.6)	170, 167	178, 170
Mass spectrometric	172 (+ 174)	172 (+ 174)
Refractive index, n_D^{20}	1.657	1.605
Density, d_4^{20}	1.285	1.205
Molar refractivity, R_D	49.3	49.1
^1H n.m.r.	δ ~8.3 and ~7.5 p.p.m. (multiplets, ratio 2:3)	δ ~7.5 p.p.m. (multiplet)
^{13}C n.m.r. (relative to CS_2, $\delta_c = 0$)	$\delta_c = 12$ (singlet) and ~67 p.p.m. (complex absorption)	$\delta_c = 12$ (singlet) and ~65 p.p.m. (complex absorption)
Dipole moment, μ	2.6_3 D	3.9_7 D

number of physical data, and Figs. 1 and 2 show, respectively, the infrared and ultraviolet spectra of the compounds. Elemental analyses (see Experimental) taken together with the molecular weight (as determined by mass spectrometry and from the freezing point depression of cyclohexane solutions) establish the molecular formula as C_7H_5ClOS. The five hydrogen atoms in each compound are shown to be attached to an aromatic nucleus, from (*a*) the absorption around 7.5 to 8.5 p.p.m. (only) in the proton n.m.r. spectra (Table I), and (*b*) the observation of bands at 685 ± 3 and 755 ± 3 cm^{-1} in the infrared spectra. (The latter infrared band, which is not visible in the spectra of the CCl_4 solutions shown in Fig. 1, was obtained from solutions in CS_2.) This then leads to the partial structure III. Further confirmation of III is given by the hydrolytic reactions of these compounds (8, 9), which gave in each case a mixture of benzoic acid and dibenzoyl disulfide (Ph—CO—S—S—CO—Ph). It can readily be shown that the only full structures, in addition to I and II, which can be derived by completing III without involving electron-deficient species or placing a formal positive charge on either carbon or chlorine are formulae IV, V, and VI.

Can. J. Chem. Downloaded from www.nrcresearchpress.com by 210.87.254.5 on 09/05/12
For personal use only.

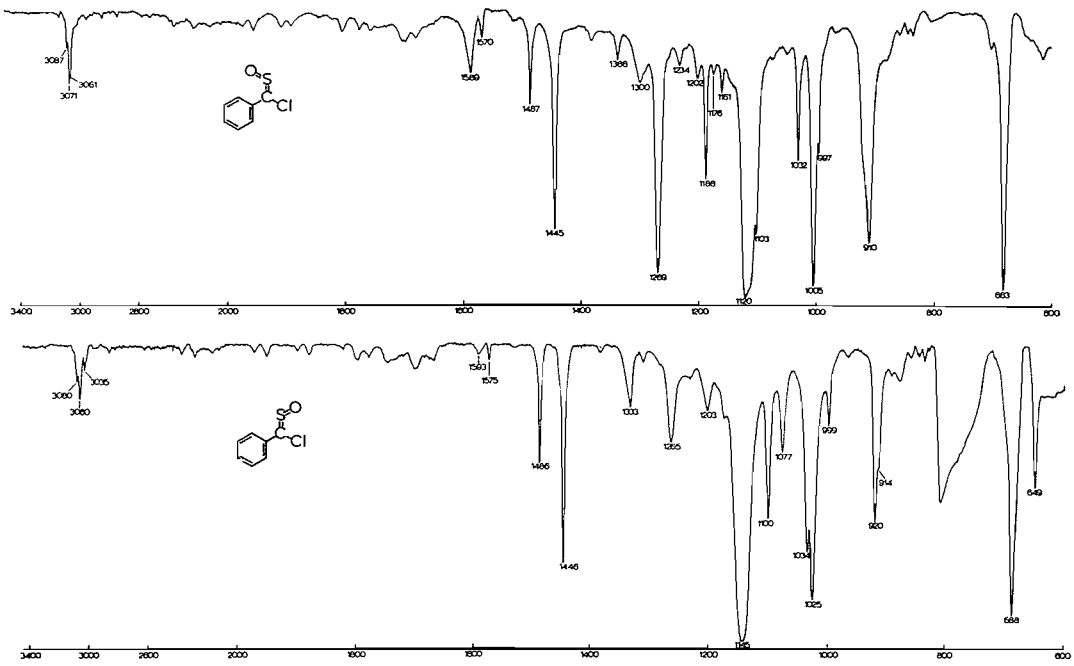


FIG. 1. Infrared spectra of *trans*- and *cis*-oxythiobenzoyl chlorides (0.6 *M* in CCl_4, 0.1 mm path length).

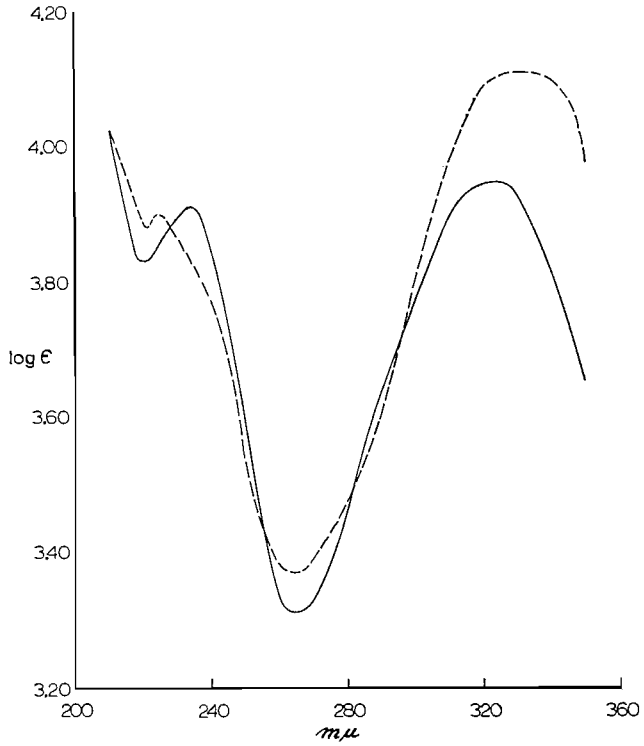


FIG. 2. Ultraviolet spectra of *cis*-oxythiobenzoyl chloride (solid line, $\lambda\lambda_{max}$ 229 mμ (ε 8 000) and 323 mμ (ε 9 000)) and *trans*-oxythiobenzoyl chloride (broken line, $\lambda\lambda_{max}$ 226 mμ (ε 8 000) and 328 mμ (ε 14 000)).

Can. J. Chem. Downloaded from www.nrcresearchpress.com by 210.87.254.5 on 09/05/12
For personal use only.

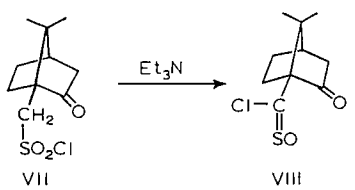
Can. J. Chem. Downloaded from www.nrcresearchpress.com by 210.87.254.5 on 09/05/12
For personal use only.

Examination of the properties of the two materials reveals a number of similarities which strongly suggest that the compounds are stereoisomers rather than merely structural isomers. The ultraviolet and ^{13}C n.m.r. spectra and the molecular refractivities are very similar. In the infrared spectrum of the lower melting isomer the strongest bands are at 1 120, 1 005, and 910 cm^{-1} (in addition to those at 758 and 683 cm^{-1}), and these have intense counterparts in the spectrum of the other isomer at 1 145, 1 025, and 920 cm^{-1}. If one of the isomers had either structure IV, V, or VI, then this would mean that two compounds with quite different functional groups would coincidentally show very similar physical properties. Structures I and II, on the other hand, account very well for the observed similarities.

There are, in addition, specific reasons for excluding structures IV, V, and VI, for each of these is incompatible with at least one physical property of the compounds. Structure IV would require absorption in the infrared spectrum appropriate to a carbonyl group. It is clear from Fig. 1 that there is no such band in either spectrum. On the other hand, structure V would be expected to absorb at longer wavelengths in the ultraviolet-visible region than is observed for either compound. For example, allylic thionbenzoates (e.g. Ph—CS—O—CH_2CH=CH_2) show a band at 420 mμ with an extinction coefficient of 97. Neither of the compounds under discussion shows any absorption maximum in the visible region of the spectrum; the extinction coefficient at 420 mμ is less than 4 for both materials. On the other hand, the spectrum of N-sulfinylaniline (PhN=SO), with bands at 231 mμ (ϵ 6 000) and 314 mμ (ϵ 10 000) (10), is strikingly similar to those of the "red oil" components (Fig. 2), in excellent agreement with the oxythiobenzoyl chloride structures, I and II. Finally, structure VI would be expected to display only the ultraviolet spectrum of a monosubstituted benzene ring superimposed on absorption caused by the individual sulfur and chlorine atoms. Such a structure does not adequately account for the maxima found around 325 mμ. The ^{13}C n.m.r. spectra also clearly rule out structure VI. In addition to the complex bands around 60–70 p.p.m. from carbon disulfide, both compounds show a singlet at 12 p.p.m. corresponding to one carbon atom. This signal is in the region characteristic of carbons constituting double bonds (particularly carbon–oxygen and carbon–sulfur double bonds), but is well below the range appropriate to singly bonded carbon atoms (11–13).

Having thus limited the possible structures of the two compounds to formulae I and II, we proceeded to decide which material corresponded to which structure. If one assumes that the C—Cl and S—O bonds are polarized so that the more electronegative elements Cl and O are partially negatively charged, the *cis* isomer (I) must have the higher dipole moment. On this basis, the *cis* structure (I) is assigned to the higher melting isomer (which also has the higher dipole moment (see Table I)); the lower melting isomer therefore has the *trans* structure (II).

The proposal of an oxythioacyl halide structure (such as I or II) is in itself not new, since it had been made in 1923 by Wedekind and co-workers (14) for the product (VIII)



VII VIII

of a very similar reaction of camphor-10-sulfonyl chloride (VII). What are new in the present study, however, are the isolation of both geometrical isomers and the presentation

of convincing evidence for the oxythioacyl halide structures. Wedekind's work, though admirable when judged with regard to the tools available at that time, gives little basis for excluding structures analogous to IV and V and none at all for the structure analogous to VI. As we have already mentioned in one of the preliminary communications (5), we have prepared Wedekind's "chlorsulfoxyd-campher" and have found its n.m.r. and infrared spectra to be in good agreement with his structure (VIII).

The Stoichiometry and Mechanism of the Reactions

Since the structures of the products have just been derived, it is appropriate to consider, briefly at least, the nature of the actual processes leading to these products. The overall transformation for the principal reaction in methylene chloride solution may be summarized by eq. [1].

[1] $$2PhCH_2SO_2Cl + 2Et_3N \rightarrow \left\{ \begin{array}{c} \begin{array}{cc} H & Ph \\ & C{=}C \\ Ph & H \end{array} \\ \text{or} \\ \begin{array}{ccc} H & SO_2 & H \\ & C{-}C & \\ Ph & & H \end{array} \end{array} \right\} + 2Et_3NH^+Cl^-$$

With the reaction in cyclohexane solution, certain factors make the picture a little more complicated. The major products are low-melting, highly soluble compounds which tend to decompose during isolation, thereby making quantitative recovery difficult. In addition, the reaction does not proceed entirely with formation of the oxythiobenzoyl chlorides, but also with production of a small amount of stilbene (presumably via eq. [1]) together with what appears to be a polymeric material, perhaps a "polysulfene", $(PhCHSO_2)_n$. The yields of the various products, however, are consistent with the major reaction being as shown in eq. [2] accompanied by a polymer-forming process and a limited amount of reaction via eq. [1].

[2] $$2PhCH_2SO_2Cl + 2Et_3N \rightarrow \underset{\displaystyle Cl}{\overset{\displaystyle |}{PhC{=}SO}} + Et_3NH^+Cl^- + Et_3NH^+PhCH_2SO_3^-$$

The above equations merely summarize the stoichiometry of the reactions and indicate neither how these products are actually formed nor how a change in solvent effects such a remarkable change in the course of the reaction. In a preliminary communication (5), we tentatively put forward a scheme in which the first step was the formation of phenylsulfene, as initially proposed by Wedekind. More recent work on the interaction of the same reagents in alcohols and amines (15–17) has demonstrated that sulfenes are intermediates in these reactions. The latter experiments, and others as well, have generally lent support to our tentative description,[2] though one modification seems necessary. In the original proposal we postulated the formation of the ethylene sulfone by the reaction of phenylsulfene with phenylcarbene, the latter being formed from another molecule

[2]*The mechanistic scheme in the communication contains an unfortunate mistake stemming from inadequate checking of the manuscript: the intermediate in the proposed conversion of α-chlorophenylmethanesulfinate anion (structure X in the scheme) into oxythiobenzoyl chloride should be* $\underset{\displaystyle Cl}{\overset{\displaystyle |}{PhCHSOZ}}$, *where* Z = Cl *or* SO_3CH_2Ph.

Can. J. Chem. Downloaded from www.nrcresearchpress.com by 210.87.254.5 on 09/05/12
For personal use only.

of phenylsulfene by loss of sulfur dioxide. However, it no longer seems likely that the formation of stilbene and the ethylene sulfone takes place via a carbene, since attempts both by us (8) and others (3, 18, 19) to trap such a species have been fruitless. We have carried out further studies designed to test aspects of our mechanistic proposal, but prefer to leave further discussion of the nature of these reactions to a forthcoming paper describing these experiments.

Geometrical Isomerism about Double Bonds with Sulfur Atoms

As was pointed out earlier, the isolation and characterization of the *cis*- and *trans*-oxythiobenzoyl halides represents the first demonstration of *cis–trans* isomerism about a double bond in which one of the atoms of the double bond is a second (or higher) period element. Previous examples of geometrical isomerism had been restricted to double bonds made up of first-period elements exclusively—notably carbon and nitrogen, though a case of geometrical isomerism involving boron has been suggested (20). To be sure, occasions in which a second-period element might show such geometrical isomerism are severely limited. If one confines the discussion to known functional groups, such isomerism would appear to be restricted to the carbon–sulfur double bond (as in the oxythioacyl compounds in the present study) and the analogous nitrogen–sulfur double bond (as in N-sulfinylamines, R—N=SO). The latter class of compounds has been known for 75 years, though no *cis–trans* isomers have been isolated or even been proved to exist. They have, however, been postulated to account for certain kinetic data (21). In addition, a study of the infrared spectra of some N-sulfinylamines (22) notes the possibility of *cis–trans* isomerism in these compounds, as does also a lecture (23) mentioning an investigation of the microwave spectrum of thionylimide (HN=SO). By analogy with the results of the present study it would seem probable that N-sulfinylamines should be capable of existing as *cis–trans* isomers, perhaps even with a sufficiently high energy barrier to their interconversion to enable their separation and characterization in the traditional manner.

The discovery of geometrical isomerism about a carbon–sulfur double bond is noteworthy both as a stereochemical curiosity and also, rather more significantly, because it provides evidence about the location of the atoms in a C=SO system. This fact, in turn, should be of value in testing any theoretical description of such bonds, or indeed of any double bonds between a first-row element and one from the second period of the Periodic Table.

EXPERIMENTAL

Infrared spectra were obtained on Beckman IR-5 or IR-7 spectrophotometers equipped with sodium chloride optics; if not otherwise specified, all values quoted for infrared frequencies were obtained on the IR-7 instrument. Ultraviolet spectra were determined on a Beckman DK-1 instrument with 1 cm quartz cells. Proton n.m.r. spectra were measured on Varian A-60 or DP-60 instruments with tetramethylsilane as internal standard. The ^{13}C n.m.r. spectra were obtained on the DP-60 instrument at 15.1 mc/s by the rapid-passage dispersion mode technique (11, 12). Refractive indices were measured with a thermostatically controlled Bausch and Lomb refractometer. Melting points were determined on a Kofler hot stage and are uncorrected. Density determinations were carried out with a Fisher–Davidson gravitometer.

Petroleum ether refers to the fraction of boiling range 35–60°. The silica gel used was British Drug Houses "suitable for chromatography" grade. Eastman Kodak "white label" grade phenylmethanesulfonyl chloride (α-toluenesulfonyl chloride) and triethylamine were used without further purification, except when otherwise specified.

Reaction of Phenylmethanesulfonyl Chloride and Triethylamine in Cyclohexane

Phenylmethanesulfonyl chloride (1.91 g, 10.0 mmoles) was dissolved in cyclohexane (150 ml) freshly distilled from calcium hydride. Addition of triethylamine (1.6 ml, 11.4 mmoles) in one portion gave an immediate white precipitate and a yellow color which slowly turned to red. The reaction was allowed to stand at room temperature for 3 h. The cyclohexane solution was decanted off and the solvent evaporated under reduced pressure. The yield of the reddish oil was 462 mg; its infrared spectrum showed it to be almost

Can. J. Chem. Downloaded from www.nrcresearchpress.com by 210.87.254.5 on 09/05/12
For personal use only.

Can. J. Chem. Downloaded from www.nrcresearchpress.com by 210.87.254.5 on 09/05/12
For personal use only.

entirely a mixture of *cis*- and *trans*-oxythiobenzoyl chlorides. (The isolation of the *cis*- and *trans*-oxythiobenzoyl chlorides from the "red oil" is described below.) The cyclohexane-insoluble material was dissolved in water (100 ml) and extracted with ether. Evaporation of the ether left a yellow oil (189 mg) whose infrared spectrum showed that it consisted of the isomeric oxythiobenzoyl chlorides together with a small amount of what appeared to be dibenzoyl disulfide. The total material extracted by the organic solvents is therefore 651 mg, which (if pure) would correspond to 3.8 mmoles of the oxythiobenzoyl chlorides (or, on the basis of eq. [2], a 76% yield of the crude oxythiobenzoyl chloride mixture).

A 25 ml aliquot of the aqueous layer (one-quarter of the total) was made basic by addition of 10% KOH solution. The liberated triethylamine was extracted with ether and the solution added to a solution of picric acid in ether. The resultant precipitate of triethylammonium picrate was filtered off, dried, and weighed; yield 753 mg (2.3 mmoles), m.p. 167–169°.

Glacial acetic acid (1 ml) was added to a second portion (33 ml) of the original aqueous phase. Aliquots of 15, 10, and 8 ml gave, respectively, titers of 8.84, 5.94, and 4.80 ml with 0.1 *N* $AgNO_3$, corresponding in turn to a total chloride ion content in the original cyclohexane-insoluble portion of the reaction mixture of 5.8, 5.9, and 6.0 mmoles.

Finally, a third portion of the aqueous solution (40 ml) was made basic and extracted with ether. The aqueous layer was evaporated to dryness and the residue treated with phosphorus pentachloride (1 g) in the usual manner (17). The reaction mixture was poured into water and extracted with ether. Evaporation of the ether gave an oil (235 mg, 1.2 mmoles) which was recrystallized from chloroform – petroleum ether, m.p. 90–92°, mixed m.p. with an authentic sample of phenylmethanesulfonyl chloride 90–92°.

In a separate experiment, the original aqueous phase was acidified after the ether extraction. Subsequent continuous extraction with ether for several hours followed by evaporation of the ether yielded a gummy material equal in weight to approximately 10% of the original sulfonyl chloride. The material resisted all attempts at crystallization and appeared to be polymeric. The infrared spectrum showed only a few very broad bands.

Isolation of the cis- and trans-Oxythiobenzoyl Chlorides

Crude "red oil" (285 mg) was placed on a column of silica gel (11 g). Elution with petroleum ether gave *trans*-stilbene (10 mg), identified by comparison of its infrared spectrum with that of an authentic sample. Elution with 3:1 petroleum ether – benzene yielded *trans*-oxythiobenzoyl chloride (60 mg). The *trans*-oxythiobenzoyl chloride was further purified by recrystallization from pentane at dry ice – acetone temperatures to give slightly pink needles, m.p. 5°.

Anal. Calcd. for C_7H_5SOCl: C, 48.70; H, 2.92; S, 18.54; Cl, 20.55. Found: C, 48.88; H, 3.07; S, 18.85; Cl, 20.44.

Finally, on elution with benzene, *cis*-oxythiobenzoyl chloride (150 mg) was obtained. Three recrystallizations from ether – petroleum ether and one from pentane gave slightly yellowish plates, m.p. 38–39°.

Anal. Calcd. for C_7H_5SOCl: C, 48.70; H, 2.92; S, 18.54; Cl, 20.55. Found: C, 48.59; H, 3.02; S, 18.67; Cl, 20.81.

Other physical properties are given in Table I. The infrared and ultraviolet spectra of the isomers are reproduced in Figs. 1 and 2. The quantities of the high-melting (*cis*) and low-melting (*trans*) isomers obtained directly from the chromatogram correspond to, respectively, 0.06 and 0.14 mmole from 1.0 mmole of phenylmethanesulfonyl chloride.

The dipole moments were determined in benzene solution with a Dipolmeter DM 01 instrument. The values were calculated according to the method of Guggenheim (24) from data obtained from solutions at four different concentrations. To ensure that the low-melting (*trans*) isomer was chemically unchanged, the infrared spectrum was determined after the measurements were completed, and was found to be unaltered.

The cryoscopic molecular weight determinations were carried out in cyclohexane solution. The cyclohexane (Fisher spectranalyzed) was purified by stirring it overnight with concentrated H_2SO_4, then for 5 h with 10% H_2SO_4 and $KMnO_4$, followed by drying with Na_2SO_4 and distillation from CaH_2. With the low-melting (*trans*) isomer, 156.6 mg in 29.78 g of cyclohexane lowered the freezing point by 0.644°, corresponding to a molecular weight of 170 (calcd. mol. wt. 172.6). In a repeat run 128.5 mg in 30.30 g gave a depression of 0.509°; mol. wt. 167. With the high-melting (*cis*) isomer, 151.8 mg in 32.50 g of cyclohexane lowered the freezing point by 0.553°; mol. wt. 170. In a repeat determination 223.9 mg in 33.48 g gave a lowering of 0.752°; mol. wt. 178.

Reaction of Phenylmethanesulfonyl Chloride with 2,4,6-Trimethylpyridine in Cyclohexane

Phenylmethanesulfonyl chloride (450 mg) was dissolved in cyclohexane (50 ml) and added over a period of 15 min to a solution of 2,4,6-trimethylpyridine (collidine) in cyclohexane (10 ml). The ultraviolet spectrum of a sample removed immediately after the addition of the sulfonyl chloride showed no 325 mμ peak. The reaction was allowed to stand for 12 h at 50°; the 325 mμ band was then found to be present in the ultraviolet spectrum. Work-up of the reaction mixture yielded a product whose infrared spectrum was virtually identical with that of the crude "red oil".

Reaction of Phenylmethanesulfonyl Chloride with Triethylamine in Methylene Chloride

Phenylmethanesulfonyl chloride (1.65 g) was dissolved in methylene chloride (30 ml) and the solution cooled to −60°. Triethylamine (2 ml) was added slowly during 2 min. The reaction was worked up by

washing the solution with water, drying it, and evaporating the methylene chloride under reduced pressure without heating. The crude yield of solid material was 826 mg. Recrystallization from methylene chloride – pentane yielded *cis*-1,2-diphenylethylene sulfone (259 mg, 27%), m.p. 83–85° (with bubbling).

Anal. Calcd. for $C_{14}H_{12}O_2S$: C, 68.84; H, 4.95; S, 13.10. Found: C, 68.81; H, 5.24; S, 13.28.

Infrared absorption ($CHCl_3$, IR-5) at 1 333 and 1 140 cm^{-1}; n.m.r. absorption ($CDCl_3$) at 4.89 (singlet) and 7.2 p.p.m. (complex phenyl hydrogen absorption), relative areas 1:5. The mother liquor was chromatographed on silica gel. Elution with petroleum ether gave *trans*-stilbene (419 mg, 48%), m.p. 124–126°, mixed m.p. with an authentic sample of *trans*-stilbene 124–126°.

Conversion of cis-1,2-Diphenylethylene Sulfone into Stilbene(s)

cis-1,2-Diphenylethylene sulfone (21.6 mg) was heated in an oil bath at 90° for 15 min. Bubbling was observed as the sulfone melted. The yield of *cis*-stilbene was 16.1 mg (100%). It was identified by comparison of its infrared spectrum with that of an authentic sample, and by conversion into *dl*-stilbene dibromide (in 73% yield) by treatment with bromine in carbon tetrachloride; m.p. of the dibromide 110–113°, mixed m.p. with an authentic sample 110–113°. The sulfone could also be decomposed by refluxing in carbon disulfide or methylene chloride for 1 h. The product was mainly *cis*-stilbene. Chromatography of *cis*-diphenylethylene sulfone on silica gel yielded a mixture containing mostly *cis*-stilbene plus a little *trans*-stilbene. Decomposition by refluxing in methylene chloride and triethylamine, or by dissolving in aniline for 4 h, yielded almost pure *cis*-stilbene, as determined by comparison of its infrared spectrum with that of an authentic sample.

Reaction of Phenylmethanesulfonyl Chloride with Triethylamine in Ether

Phenylmethanesulfonyl chloride (1.20 g) was dissolved in anhydrous ether (35 ml). The solution was cooled to −60° and triethylamine (2.0 ml) was added over a period of about 2 min. On addition of triethylamine a white precipitate was obtained immediately. The solution was allowed to stand at −60° for 10 min and then allowed to warm up to room temperature. The reaction mixture was washed with water, the ether layer was dried, and the solvent was evaporated to yield a white solid (570 mg). Chromatography on grade III neutral alumina (17 g) yielded, on elution with 1:1 benzene – petroleum ether, *trans*-stilbene (349 mg, 62%); its infrared spectrum was identical with that of an authentic specimen. A similar yield of *trans*-stilbene was obtained when the reaction was carried out at room temperature.

Reaction of Phenylmethanesulfonyl Chloride with Triethylamine in Benzene

Triethylamine (500 mg) was added in one portion under a nitrogen atmosphere to a solution of phenylmethanesulfonyl chloride (950 mg) in dry benzene (20 ml). On addition of the triethylamine the solution turned reddish orange, but this color soon faded to yellow. The reaction mixture was allowed to stand at room temperature for 10 min; then it was poured into water and extracted with ether. The ether layer was dried and the solvent evaporated to yield a reddish oil (247 mg) whose infrared spectrum showed the presence of *trans*-stilbene and *cis*- and *trans*-oxythiobenzoyl chlorides. Chromatography on grade III neutral alumina yielded, on elution with petroleum ether, *trans*-stilbene (141 mg, 31%), m.p. 125–126°, mixed m.p. with an authentic sample 125–126°. The infrared spectrum of the sample was identical with that of an authentic specimen of *trans*-stilbene.

Reaction of Phenylmethanesulfonyl Fluoride with Triethylamine

Phenylmethanesulfonyl fluoride was dissolved in ether containing a threefold quantity (on a molar basis) of triethylamine. The reaction was allowed to stand for 2 months, during which time a small amount of white material precipitated. The reaction was worked up by pouring the mixture into water and extracting it with ether. The ether-soluble material was identified as phenylmethanesulfonyl fluoride by comparison of its infrared spectrum with that of the starting material. When phenylmethanesulfonyl fluoride was refluxed with excess triethylamine for 1 h, a product was formed which appeared, from thin-layer chromatography, to consist of at least five products, and was not studied further.

ACKNOWLEDGMENTS

This work was supported by the National Research Council of Canada via scholarships and grants-in-aid. We thank Dr. W. A. Ayer (University of Alberta, Edmonton) for the mass spectra; Dr. J. B. Stothers, Dr. K. S. Dhami, and Dr. R. E. Klinck for the n.m.r. spectra and for help in their interpretation; and Dr. R. K. Chan for aid and advice in determining dipole moments.

REFERENCES

1. E. WEDEKIND and D. SCHENK. Ber. 44, 198 (1911).
2. J. F. KING, P. DE MAYO, E. MORKVED, A. B. M. A. SATTAR, and A. STOESSL. Can. J. Chem. **41**, 100 (1963).
3. W. E. TRUCE and J. R. NORELL. J. Am. Chem. Soc. **85**, 3231 (1963).
4. I. J. BOROWITZ. J. Am. Chem. Soc. **86**, 1146 (1964).
5. J. F. KING and T. DURST. Tetrahedron Letters, 585 (1963).

Can. J. Chem. Downloaded from www.nrcresearchpress.com by 210.87.254.5 on 09/05/12
For personal use only.

6. J. F. KING and T. DURST. J. Am. Chem. Soc. **85**, 2676 (1963).
7. N. P. NEUREITER and F. G. BORDWELL. J. Am. Chem. Soc. **85**, 1209 (1963).
8. T. DURST. Ph.D. Thesis, University of Western Ontario, London, Ontario. 1964.
9. J. F. KING and T. DURST. Unpublished observations.
10. W. T. SMITH, JR., D. TRIMNELL, and L. D. GRINNINGER. J. Org. Chem. **24**, 664 (1959).
11. P. C. LAUTERBUR. Ann. N.Y. Acad. Sci. **70**, 841 (1958).
12. P. C. LAUTERBUR. *In* Determination of organic structures by physical methods. Vol. 2. *Edited by* F. C. Nachod and W. D. Phillips. Academic Press, Inc., New York. 1962. Chap. 7.
13. J. B. STOTHERS. Quart. Rev. London, **19**, 144 (1965).
14. E. WEDEKIND, D. SCHENK, and R. STÜSSER. Ber. **56**, 633 (1923).
15. J. F. KING and T. DURST. J. Am. Chem. Soc. **86**, 287 (1964).
16. W. E. TRUCE, R. W. CAMPBELL, and J. R. NORELL. J. Am. Chem. Soc. **86**, 288 (1964).
17. J. F. KING and T. DURST. J. Am. Chem. Soc. **87**, 5684 (1965).
18. U. SCHÖLLKOPF. *Cited in* G. OPITZ, H. SCHEMPP, and H. ADOLPH. Ann. Chem. **684**, 92 (1965).
19. H. KLOOSTERZIEL. Unpublished observations. *Cited in* Chem. Weekblad, **59**, 77 (1963).
20. M. F. LAPPERT and M. K. MAJUMDAR. Proc. Chem. Soc. 88 (1963).
21. L. JANNELLI and L. SENATORE. Ann. Chim. Rome, **53**, 1356 (1963).
22. W. K. GLASS and A. D. E. PULLIN. Trans. Faraday Soc. **57**, 546 (1961).
23. E. B. WILSON, JR. Pure Appl. Chem. **7**, 23 (1963).
24. E. A. GUGGENHEIM. Trans. Faraday Soc. **47**, 573 (1951).

Can. J. Chem. Downloaded from www.nrcresearchpress.com by 210.87.254.5 on 09/05/12
For personal use only.

Can. J. Chem. Downloaded from www.nrcresearchpress.com by 210.87.254.5 on 09/05/12
For personal use only.

THE REACTION OF SOME COMPOUNDS CONTAINING THIOAMIDE GROUPS WITH 2,4,6-TRICHLORO-1,3,5-TRIAZINE

A. Pollak, B. Stanovnik, and M. Tišler
Department of Chemistry, University of Ljubljana, Ljubljana, Yugoslavia

Received November 23, 1965

ABSTRACT

The reaction between some compounds containing thioamide groups and cyanuric chloride was investigated. Evidence is presented that the reaction proceeds on the thioamide sulfur and not on the nitrogen as postulated earlier. The reaction with thiourea was used for the preparation of trithiocyanuric acid, as well as for the preparation of 3-chloro-6(1*H*)-pyridazinethione or 3-mercapto-6(1*H*)-pyridazinethione, and presents a new and convenient method for the synthesis of these compounds.

In connection with our investigations of the reactivity of heterocyclic compounds containing thioamide groups as a part of the ring system (1–4), it seemed of interest to investigate the reaction between compounds with thioamide groups and compounds with reactive halogens, particularly cyanuric chloride. An examination of the literature (5) revealed that the reaction of cyanuric chloride (2,4,6-trichloro-1,3,5-triazine) with different thiosemicarbazones was interpreted as proceeding on the N_2-nitrogen of the thiosemicarbazones. N-(4,6-Dichloro-1,3,5-triazinyl-2)-thioureas are also known, but they were prepared in a different manner (6).

A substantial amount of work on alkylations and acylations of different compounds with thioamide groups has been reported (7). Several recent publications have enlarged the earlier reports on the alkylation or acylation of thioureas (8), thioamides (9), thiosemicarbazides and thiosemicarbazones (10, 11), and heterocyclic compounds containing thioamide groups as a part of the ring system (12–15). In all cases the reaction proceeds with the attack on the thioamide sulfur, except in the reaction between 2-thiobenzothiazoline and diethylaminomethylchloride, in which case a N-substituted product was isolated; this is explained by the predisposition of these compounds to undergo unimolecular substitution (12).

Compounds containing thioamide groups were formerly postulated as reacting in their normal form (I) or in their tautomeric iminothiol form (II). This must certainly not be a

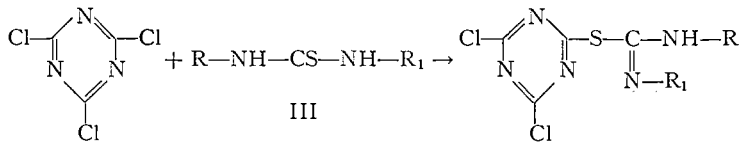


I II

condition, as in recent years the dipolar character of the thioamide group has been established (1, 2, 16–22). Thioamides are protonated on the sulfur atom and not on the nitrogen (23, 24), and the evidence, obtained from measurements of bond distances (25), provides additional support for the dipolar character. Furthermore, alkylations of ambident anions have been discussed (26) and evidence has been presented that the reaction course depends on the character of the transition state.

Finally, one must take into account the possibility of the migration of the initially bound alkyl group. So far, only the spontaneous O → S alkyl migration is known in the case of solid thioisobiuret hydrohalides at room temperature (27), and it seems very unlikely that, under the relatively mild reaction conditions used, a migration from the sulfur of the initially bound triazine would occur to give a N-substituted derivative.

Thus, the reaction between cyanuric chloride and compounds with thioamide groups (III) should proceed preferentially in the direction of the formation of isothiuronium salts or their derivatives; the present findings give a satisfactory basis for such an interpretation of the reaction course.



III IV

Regardless of which compound containing a thioamide group was employed for the reaction with cyanuric chloride, all reaction products gave a negative iodine–azide reaction (28), characteristic of the presence of a mercapto or thiocarbonyl group. This test was positive with all starting compounds containing thioamide groups. An assignment of the thiocarbonyl stretching frequency, which was used for the indication that such a reaction does proceed as N-substitution (5), seems to be very delicate, as this frequency is dependent on the structural environment and falls within a wide range, 1 400 – 1 000 cm^{-1} (29, 30).

Further evidence for the alkylation site could be obtained from the hydrolysis of the alkylation products that were obtained, as this is one of the possible methods of introducing a thiol (thione) group in many heterocyclic systems. The method involving the action of aqueous alkali on isothiuronium salts has superseded most of the others used for the laboratory-scale syntheses (31).

Thiourea, which appears to have the required combination of a considerable nucleophilic power and a weak basic strength ($pK_a = -1.19$) (32), reacted readily with cyanuric chloride or with 3,6-dichloropyridazine; the initially formed isothiuronium salts were then hydrolyzed to the corresponding trithiocyanuric acid (2,4,6-trimercapto-1,3,5-triazine), 3-chloro-6(1*H*)-pyridazinethione, or 3-mercapto-6(1*H*)-pyridazinethione. It is well known that the reactivity of the 1,3,5-triazine system is very great and exceeds the reactivity of different 3-substituted pyridazines (33). This was also observed in the case of the above reaction where, regardless of the amount of the thiourea used in the reaction, the trithiocyanuric acid was always obtained, in a smaller yield of course.

Some evidence of the reaction course may also be obtained from the ultraviolet spectra. Only a few publications have dealt with the ultraviolet spectra of 1,3,5-triazines; a useful compilation of some spectral data was presented by Koopman (34). He reported that 2,4-dichloro-6-amino- or substituted amino-1,3,5-triazines possess two absorption bands, one in the 2 250 – 2 440 Å region (high intensity) and the other in the 2 600 – 2 800 Å region (low intensity), whereas the 2,4-dichloro-6-alkylthio- or arylthio-1,3,5-triazines exhibit only one absorption band, that in the 2 600 – 2 670 Å region (high intensity). The ultraviolet spectra of some of our products all show a high-intensity band in the 2 960 – 3 180 Å region; these findings present additional evidence for the proposed S-alkylated products.

EXPERIMENTAL

Melting points were determined on a Kofler heating microscope. Ultraviolet spectra were measured on a Beckman model DU spectrophotometer.

S-(4,6-Dichloro-1,3,5-triazinyl-2)-acetone Thiosemicarbazone (IV, R = H, R_1 = N=C(CH_3)$_2$)

A solution of acetone thiosemicarbazone (2.6 g, 0.02 mole) (35) in acetone (100 ml) was added slowly to a stirred solution of cyanuric chloride (3.7 g, 0.02 mole) in acetone (300 ml). The reaction mixture was stirred at room temperature for 20 min and a saturated aqueous solution of sodium bicarbonate added until the

Can. J. Chem. Downloaded from www.nrcresearchpress.com by 210.87.254.5 on 09/05/12
For personal use only.

pH reached 7. The solvent was evaporated *in vacuo*, the residue treated with cold water (50 ml), and the precipitate collected by filtration and dried. The product was crystallized from a mixture of cyclohexane and ethyl acetate, yield 56%, m.p. >340 °C. The compound gave a negative iodine–azide reaction. Ultraviolet spectrum (in methanol): λ_{max} 3 020 Å, ϵ = 12 850.

Anal. Calcd. for $C_7H_8Cl_2N_6S$: C, 30.11; H, 2.89; N, 30.11; S, 11.48. Found: C, 29.92; H, 3.15; N, 30.32; S, 11.73.

In the same way as described above the following compounds were prepared, and in all cases the iodine–azide reaction was negative.

S-(4,6-Dichloro-1,3,5-triazinyl-2)-acetone 4'-phenylthiosemicarbazone (IV, R = C_6H_5, R_1 = N=CH$(CH_3)_2$) was obtained from acetone 4-phenylthiosemicarbazone (36). The product was crystallized from benzene, yield 47%, m.p. 193 °C. Ultraviolet spectrum (in dioxane): λ_{max} 2 540 and 3 180 Å, ϵ = 10 520 and 23 050.

Anal. Calcd. for $C_{13}H_{12}Cl_2N_6S$: C, 43.94; H, 3.38; N, 23.66; S, 9.02. Found: C, 44.14; H, 3.67; N, 23.55; S, 9.48.

S-(4,6-Dichloro-1,3,5-triazinyl-2)-phenylthiourea (IV, R = C_6H_5, R_1 = H) was obtained from phenylthiourea. The crude product was dissolved in ethyl acetate and poured into water. The precipitate was separated by filtration, washed with water, and air-dried, yield 12%, m.p. 198 °C.

Anal. Calcd. for $C_{10}H_7Cl_2N_5S$: C, 40.01; H, 2.35; N, 23.33; S, 10.67. Found: C, 40.18; H, 2.56; N, 23.64; S, 10.45.

S-(4,6-Dichloro-1,3,5-triazinyl-2)-1'-phenyl-3'-methylthiourea (IV, R = C_6H_5, R_1 = CH_3) was obtained from 1-phenyl-3-methylthiourea (37). The product was purified from ethanol, yield 10%, m.p. 136 °C.

Anal. Calcd. for $C_{11}H_9Cl_2N_5S$: C, 42.04; H, 2.89; N, 22.29. Found: C, 42.30; H, 3.02; N, 22.46.

S-(4,6-Dichloro-1,3,5-triazinyl-2)-n-heptanal thiosemicarbazone (IV, R = H, R_1 = N=CH$(CH_2)_5CH_3$) was prepared according to the procedure of Gingras *et al.* (5), m.p. 179 °C. Ultraviolet spectrum (in methanol): λ_{max} 2 960 Å, ϵ = 19 310.

S-(6-Chloropyridazinyl-3)-acetone Thiosemicarbazone

To a solution of acetone thiosemicarbazone (1.3 g, 0.01 mole) (35) in acetone (50 ml) was added 3,6-dichloropyridazine (1.5 g, 0.01 mole), and the mixture was left overnight at room temperature. The precipitated product was collected and dissolved in water (30 ml), and a saturated solution of sodium bicarbonate added until the pH reached 7. The precipitate was separated by filtration, dried, and crystallized from ethanol with the addition of some N,N-dimethylformamide, yield 18%, m.p. 121 °C.

Anal. Calcd. for $C_8H_{10}ClN_5S$: C, 39.42; H, 4.11; N, 28.75. Found: C, 39.56; H, 3.84; N, 28.98.

S-(6-Chloropyridazinyl-3)-benzaldehyde Thiosemicarbazone

The same reaction as above was applied, and the starting compound was benzaldehyde thiosemicarbazone (35, 37). After neutralization with sodium bicarbonate solution, the solvent was evaporated *in vacuo* and a red oil separated. This oil was separated from the residual liquid and, after it was allowed to stand overnight, crystals separated. The product was washed with ether and crystallized from ethanol with the addition of some N,N-dimethylformamide, yield 29%, m.p. 159 °C. Ultraviolet spectrum (in dioxane): λ_{max} 3 020 Å, ϵ = 20 450.

Anal. Calcd. for $C_{12}H_{11}ClN_5S$: C, 49.23; H, 3.76; N 23.93. Found: C, 49.46; H, 3.79; N, 23.88.

Trithiocyanuric Acid

To a solution of thiourea (6.8 g, 0.09 mole) in acetone (130 ml) was added cyanuric chloride (5.55 g, 0.03 mole), and the mixture was heated under reflux for 2 h on a water bath. The precipitated isothiuronium compound was filtered off and transferred to a solution of sodium hydroxide (6 g in 50 ml of water). The resulting solution was filtered, acidified with concentrated hydrochloric acid until the pH reached 1, filtered, and dried. The product was purified by dissolution in a 5% aqueous solution of sodium bicarbonate (30 ml) and subsequent acidification with concentrated hydrochloric acid to a pH of 1. The product was collected by filtration and dried *in vacuo*, yield 86%, m.p. >300 °C (38, 39).

Anal. Calcd. for $C_3H_3N_3S_3$: S, 54.18. Found: S, 54.01.

The above reaction was also conducted with a different mole ratio of the starting compounds (2:1 and 1:1), but in both cases only trithiocyanuric acid was obtained; however, the yields were correspondingly lower.

3-Chloro-6(1H)-pyridazinethione

To a solution of thiourea (1.52 g, 0.02 mole) in acetone (50 ml) was added 3,6-dichloropyridazine (3.0 g, 0.02 mole), and the reaction mixture was heated under reflux on a water bath for 2 h. The cooled reaction mixture was separated by filtration and the isolated isothiuronium compound was dissolved in an aqueous solution of sodium hydroxide (1 g in 20 ml of water). The solution was acidified with concentrated hydrochloric acid to a pH of 1, and the precipitate was separated and dried. It was purified by dissolution in 5% sodium bicarbonate solution (30 ml), filtration, and acidification with concentrated hydrochloric acid to a pH of 1, yield 80%, m.p. 150 °C (lit. (40) m.p. 130–140 °C). The mixed melting point with an authentic specimen was not depressed.

3-Mercapto-6(1H)-pyridazinethione

By the above procedure, but with double the amount of thiourea, the compound was obtained in 74% yield, m.p. 246 °C (1) (lit. (40) m.p. 230–240 °C). The mixed melting point with an authentic specimen was undepressed.

Can. J. Chem. Downloaded from www.nrcresearchpress.com by 210.87.254.5 on 09/05/12
For personal use only.

REFERENCES

1. B. STANOVNIK and M. TIŠLER. Croat. Chem. Acta, **36**, 81 (1964).
2. B. STANOVNIK and M. TIŠLER. Croat. Chem. Acta, **37**, 17 (1965).
3. A. POLLAK and M. TIŠLER. Tetrahedron, **21**, 1323 (1965).
4. A. POLLAK and M. TIŠLER. Monatsh. Chem. **96**, 642 (1965).
5. B. A. GINGRAS, T. SUPRUNCHUK, and C. H. BAYLEY. Can. J. Chem. **41**, 3050 (1963).
6. Y. KODAMA and S. HINOHARA. Yuki Gosei Kagaku Kyokai Shi, **22**, 669 (1964).
7. H. WEYL. Methoden der organischen Chemie. Vol. IX. G. Thieme Verlag, Stuttgart. 1955. pp. 898, 900.
8. D. C. SCHROEDER. Chem. Rev. **55**, 181 (1955).
9. R. N. HURD and G. DE LA MATER. Chem. Rev. **61**, 45 (1961).
10. J. GOERDELER, J. OHM, and O. TEGTMEYER. Chem. Ber. **89**, 1534 (1956).
11. H. BEYER and G. WOLTER. Chem. Ber. **89**, 1652 (1956).
12. K. N. AYAD, E. B. MCCALL, A. J. NEALE, and L. M. JACKMAN. J. Chem. Soc. 2070 (1962).
13. L. KATZ and M. S. COHEN. J. Org. Chem. **19**, 767 (1954).
14. T. V. L. ULBRICHT and C. C. PRICE. J. Org. Chem. **21**, 567 (1956).
15. R. SCHÖNBECK. Monatsh. Chem. **90**, 284 (1959).
16. A. LÜTTRINGHAUS. Arzneimittel-Forsch. **3**, 333 (1953).
17. M. J. JANSSEN. Rec. Trav. Chim. **79**, 1066 (1960).
18. R. MECKE, R. MECKE, and A. LÜTTRINGHAUS. Chem. Ber. **90**, 975 (1957).
19. J. T. EDWARD and H. STOLLAR. Can. J. Chem. **41**, 721 (1963).
20. B. STANOVNIK and M. TIŠLER. Arzneimittel-Forsch. **14**, 1004 (1964).
21. B. STANOVNIK and M. TIŠLER. Anal. Biochem. **9**, 68 (1964).
22. B. STANOVNIK and M. TIŠLER. Anal. Biochem. **9**, 411 (1964).
23. A. R. KATRITZKY and R. A. Y. JONES. Chem. Ind. London, 722 (1961).
24. W. KUTZELNIGG and R. MECKE. Spectrochim. Acta, **17**, 530 (1961).
25. M. R. TRUTER. J. Chem. Soc. 997 (1960).
26. N. KORNBLUM, R. A. SMILEY, R. K. BLACKWOOD, and D. C. IFFLAND. J. Am. Chem. Soc. **77**, 6269 (1955).
27. F. KURZER and S. A. TAYLOR. J. Chem. Soc. 470 (1960).
28. F. FEIGL. Spot tests. Vol. 2. Elsevier Pub. Co., Inc., Amsterdam. 1954. p. 164.
29. J. I. JONES, W. KYNASTON, and J. L. HALES. J. Chem. Soc. 614 (1957).
30. N. KHARASCH. Organic sulfur compounds. Vol. I. Pergamon Press, New York. 1961. p. 47.
31. E. E. REID. Organic chemistry of bivalent sulfur. Vol. I. Chemical Pub. Co., Inc., New York. 1958. p. 32.
32. M. J. JANSSEN. Rec. Trav. Chim. **81**, 650 (1962).
33. A. R. KATRITZKY. *In* Advances in heterocyclic chemistry. Vol. 4. Academic Press, Inc., New York. 1965. p. 266.
34. H. KOOPMAN. Rec. Trav. Chim. **80**, 158 (1961).
35. M. FREUND and A. SCHANDER. Ber. **35**, 2602 (1902).
36. H. W. STEPHEN and F. J. WILSON. J. Chem. Soc. 2531 (1926).
37. M. L. WILLARD and M. Z. JONES. J. Am. Chem. Soc. **62**, 2876 (1940).
38. A. HOFFMANN. Ber. **18**, 2196 (1885).
39. P. KLASON. J. Prakt. Chem. **33**, 121 (1886).
40. J. DRUEY, K. MEIER, and K. EICHENBERGER. Helv. Chim. Acta, **37**, 121 (1954).

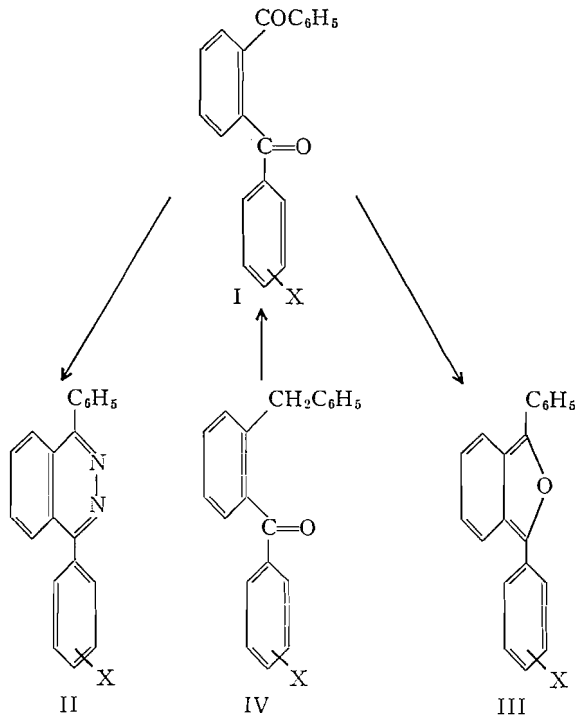
Can. J. Chem. Downloaded from www.nrcresearchpress.com by 210.87.254.5 on 09/05/12
For personal use only.

Can. J. Chem. Downloaded from www.nrcresearchpress.com by 210.87.254.105 on 09/05/12
For personal use only.

1,4-DIARYLPHTHALAZINES AND 1,3-DIARYLISOBENZOFURANS

WALTER W. ZAJAC, JR. AND DONALD E. PICHLER[1]

In connection with our studies on polynuclear aromatic compounds it became necessary to synthesize a series of unsymmetrically substituted 1,4-diarylphthalazines and 1,3-diarylisobenzofurans. Unsymmetrically substituted 2-benzoylbenzophenones (I) were the starting compounds for both the phthalazines and the isobenzofurans.



The most general route for the synthesis of the diketones (I) is via the oxidation of the substituted 2-benzylbenzophenones (IV) (1–4). During this investigation the chromium trioxide – acetic acid system (3) was used to effect the oxidation of the substituted 2-benzylbenzophenones (IV; X = 4′-CH_3, 4′-Cl, or 4′-Br) (see Table I). The remaining diketones (I; X = 2′-Cl, 2′-Br, 3′-CF_3, and 4′-F) used in this work had been prepared previously (3–5).

The diketones (I) were smoothly condensed with 85% hydrazine hydrate in acetic acid to the corresponding 1,4-diarylphthalazines (II) (see Table II).

The method of Cava *et al.* (6) employing potassium borohydride for the conversion of 1,2-diaroylbenzenes (I) into 1,3-diarylisobenzofurans (III) was used in this work and

[1]*Abstracted in part from the thesis of Donald Pichler presented to Villanova University, Villanova, Pennsylvania, in partial fulfillment of the requirements for the M.S. degree (1964).*

Can. J. Chem. Downloaded from www.nrcresearchpress.com by 210.87.254.105 on 09/05/12
For personal use only.

TABLE I

1,2-Diaroylbenzenes (I)

X	Yield (%)	Melting point (°C)	Formula	Analysis (%) Calcd. C	Calcd. H	Calcd. Halogen	Found C	Found H	Found Halogen	λ_{max} (mμ)	$\lambda_{C=O}$ (μ)
4′-Cl	94	136–137	$C_{20}H_{13}ClO_2$	74.89	4.09	11.05	75.01	4.25	11.04	257	6.03
4′-Br	98	146–147	$C_{20}H_{13}BrO_2$	65.77	3.59	21.88	65.69	3.46	21.75	257	6.03
4′-CH_3	86	144–145*	$C_{21}H_{16}O_2$	83.98	5.37		84.19	5.32		258	6.03

*Guyot and Vallette (10) report m.p. 139°.

TABLE II

1,4-Diarylphthalazines (II)

X	Yield (%)	Melting point (°C)	Formula	Analysis (%) Calcd. C	Calcd. H	Calcd. Halogen	Calcd. N	Found C	Found H	Found Halogen	Found N	λ_{max} (mμ)
2′-Cl	95	139	$C_{20}H_{13}ClN_2$	75.83	4.14	11.19	8.84	75.78	4.10	10.78	9.46	230, 295
4′-Cl	95	185–187	$C_{20}H_{13}ClN_2$	75.83	4.14	11.19	8.84	75.75	4.25	11.27	8.76	226, 298
2′-Br	67	134–135	$C_{20}H_{13}BrN_2$	66.50	3.63	22.12	7.75	66.57	3.90	22.12	7.67	224, 294
4′-Br	88	192–193	$C_{20}H_{13}BrN_2$	66.50	3.63	22.12	7.75	66.55	3.57	22.24	7.58	234, 298
3′-CF_3	89	193–194	$C_{21}H_{13}F_3N_2$	71.99	3.74	16.27	8.00	71.70	3.95	15.55	8.45	225, 296
4′-F	84	191–192	$C_{20}H_{13}FN_2$	79.98	4.36	6.33	9.33	80.05	4.39		9.65	244, 297
4′-CH_3	95	171–172*	$C_{21}H_{16}N_2$	85.11	5.44		9.45	84.69	5.60		9.92	224, 300

*Guyot and Vallette (10) report m.p. 117°.

Can. J. Chem. Downloaded from www.nrcresearchpress.com by 210.87.254.105 on 09/05/12
For personal use only.

TABLE III

1,3-Diarylisobenzofurans (III)

X	Yield (%)	Melting point (°C)	Formula	Analysis (%) Calcd. C	Calcd. H	Calcd. Halogen	Found C	Found H	Found Halogen	λ_{max} (mμ)
2′-Cl	49	70–71	$C_{20}H_{13}ClO$	78.82	4.30	11.63	79.01	4.15	11.95	266, 413
4′-Cl	51	101–102	$C_{20}H_{13}ClO$	78.82	4.30	11.63	78.52	4.14	11.81	265, 415
2′-Br	51	59–60	$C_{20}H_{13}BrO$	68.79	3.75	22.88	69.10	3.86	23.07	266, 415
4′-Br	48	120–121	$C_{20}H_{13}BrO$	68.79	3.75	22.88	69.11	3.79	22.99	267, 416
3′-CF_3	37	103–104	$C_{21}H_{13}F_3O$	74.55	3.87	16.85	74.30	3.80	16.05	267, 410
4′-F	71	82–83	$C_{20}H_{13}FO$	83.32	4.54	6.59	83.07	4.92	7.12	260, 398
4′-CH_3	75	84–85*	$C_{21}H_{16}O$	88.70	5.67		88.89	5.48		268, 410

*Guyot and Vallette (10) report m.p. 83°.

was also found to be superior to the older methods employing zinc and acetic acid (7) or zinc and alcoholic sodium hydroxide (8). The new isobenzofurans that were prepared are listed in Table III.

EXPERIMENTAL

Melting points were determined on a Thomas–Hoover melting point apparatus and are uncorrected. Microanalyses were carried out by Alfred Bernhardt, Mülheim, Germany. Infrared spectra were obtained on a Perkin–Elmer infracord, 0.25% in KBr. Ultraviolet and visible spectra were obtained on a Perkin–Elmer model 202 spectrophotometer, 1 cm cells, 95% ethanol as solvent.

The 2-benzoylbenzophenones (I) were prepared by the method of Vingiello *et al.* (3). The 1,4-diarylphthalazines (II) were prepared by the method of Blicke and Swisher (9). The 1,3-diarylisobenzofurans (III) were prepared by the method of Cava *et al.* (6).

1. C. K. Bradsher and F. A. Vingiello. J. Am. Chem. Soc. **71**, 1434 (1949).
2. C. K. Bradsher and F. A. Vingiello. J. Org. Chem. **13**, 786 (1948).
3. F. A. Vingiello, M. O. L. Spangler, and J. E. Bondurant. J. Org. Chem. **25**, 2091 (1960).
4. F. A. Vingiello, J. G. Van Oot, and H. H. Hannabass. J. Am. Chem. Soc. **74**, 4548 (1952).
5. F. A. Vingiello and J. G. Van Oot. J. Am. Chem. Soc. **73**, 5070 (1951).
6. M. P. Cava, M. J. Mitchell, and A. A. Deana. J. Org. Chem. **25**, 1481 (1960).
7. D. Boyd and D. Ladhams. J. Chem. Soc. 2089 (1928).
8. R. Adams and M. Gold. J. Am. Chem. Soc. **62**, 56 (1940).
9. F. F. Blicke and R. D. Swisher. J. Am. Chem. Soc. **56**, 923 (1934).
10. A. Guyot and F. Vallette. Ann. Chim. Phys. **23**[8], 363 (1911).

Received November 25, 1965.
Department of Chemistry,
Villanova University,
Villanova, Pennsylvania.

Can. J. Chem. Downloaded from www.nrcresearchpress.com by 210.87.254.105 on 09/05/12
For personal use only.

THE OXIDATION OF 1,2;5,6-DI-*O*-ISOPROPYLIDENE-D-GLUCOSE BY DIMETHYL SULFOXIDE – ACETIC ANHYDRIDE

W. Sowa and G. H. S. Thomas

A simple method of selective oxidation with a readily available reagent would be of great value in the field of carbohydrate chemistry. Recently Albright and Goldman reported a general method for the oxidation of alcohols to their corresponding carbonyl derivatives with dimethyl sulfoxide (DMSO) and certain acid anhydrides (1). The procedure, especially useful for the oxidation of sterically hindered hydroxyl groups, was recommended for compounds such as indole alkaloids which are sensitive to nonselective oxidizing agents. The present communication reports the use of DMSO – acetic anhydride for the oxidation of 1,2;5,6-di-*O*-isopropylidene-α-D-glucofuranose (I). Although it is possible to convert this compound into 1,2;5,6-di-*O*-isopropylidene-α-D-*ribo*-hexofuranos-3-ulose (II) in 80% yield with ruthenium tetroxide (2), oxidation with more common reagents is difficult (3, 4). By careful control of the conditions, Theander (4) oxidized I with chromium trioxide – pyridine complex in acetic acid and obtained the 3-keto derivative (II) in 6% yield. Theander also found that sodium borohydride reduced II stereospecifically and practically quantitatively to 1,2;5,6-di-*O*-isopropylidene-α-D-allofuranose (III), which crystallized with ease. This provided a convenient route to the rare monosaccharide D-allose, as well as evidence for the presence of II.

In the present work, the oxidation of I by DMSO – acetic anhydride was found to be virtually complete after 24 h at room temperature. After removal of the solvents by distillation, the oxidized residue was dissolved in aqueous ethanol and reduced with sodium

was also found to be superior to the older methods employing zinc and acetic acid (7) or zinc and alcoholic sodium hydroxide (8). The new isobenzofurans that were prepared are listed in Table III.

EXPERIMENTAL

Melting points were determined on a Thomas–Hoover melting point apparatus and are uncorrected. Microanalyses were carried out by Alfred Bernhardt, Mülheim, Germany. Infrared spectra were obtained on a Perkin–Elmer infracord, 0.25% in KBr. Ultraviolet and visible spectra were obtained on a Perkin–Elmer model 202 spectrophotometer, 1 cm cells, 95% ethanol as solvent.

The 2-benzoylbenzophenones (I) were prepared by the method of Vingiello *et al.* (3). The 1,4-diarylphthalazines (II) were prepared by the method of Blicke and Swisher (9). The 1,3-diarylisobenzofurans (III) were prepared by the method of Cava *et al.* (6).

1. C. K. Bradsher and F. A. Vingiello. J. Am. Chem. Soc. **71**, 1434 (1949).
2. C. K. Bradsher and F. A. Vingiello. J. Org. Chem. **13**, 786 (1948).
3. F. A. Vingiello, M. O. L. Spangler, and J. E. Bondurant. J. Org. Chem. **25**, 2091 (1960).
4. F. A. Vingiello, J. G. Van Oot, and H. H. Hannabass. J. Am. Chem. Soc. **74**, 4548 (1952).
5. F. A. Vingiello and J. G. Van Oot. J. Am. Chem. Soc. **73**, 5070 (1951).
6. M. P. Cava, M. J. Mitchell, and A. A. Deana. J. Org. Chem. **25**, 1481 (1960).
7. D. Boyd and D. Ladhams. J. Chem. Soc. 2089 (1928).
8. R. Adams and M. Gold. J. Am. Chem. Soc. **62**, 56 (1940).
9. F. F. Blicke and R. D. Swisher. J. Am. Chem. Soc. **56**, 923 (1934).
10. A. Guyot and F. Vallette. Ann. Chim. Phys. **23**[8], 363 (1911).

Received November 25, 1965.
Department of Chemistry,
Villanova University,
Villanova, Pennsylvania.

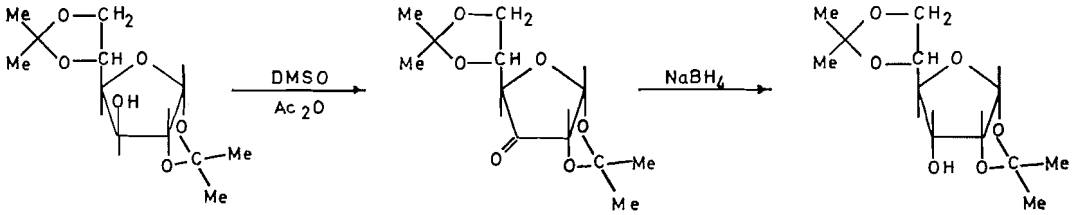
Can. J. Chem. Downloaded from www.nrcresearchpress.com by 210.87.254.42 on 09/05/12
For personal use only.

THE OXIDATION OF 1,2;5,6-DI-*O*-ISOPROPYLIDENE-D-GLUCOSE BY DIMETHYL SULFOXIDE – ACETIC ANHYDRIDE

W. Sowa and G. H. S. Thomas

A simple method of selective oxidation with a readily available reagent would be of great value in the field of carbohydrate chemistry. Recently Albright and Goldman reported a general method for the oxidation of alcohols to their corresponding carbonyl derivatives with dimethyl sulfoxide (DMSO) and certain acid anhydrides (1). The procedure, especially useful for the oxidation of sterically hindered hydroxyl groups, was recommended for compounds such as indole alkaloids which are sensitive to nonselective oxidizing agents. The present communication reports the use of DMSO – acetic anhydride for the oxidation of 1,2;5,6-di-*O*-isopropylidene-α-D-glucofuranose (I). Although it is possible to convert this compound into 1,2;5,6-di-*O*-isopropylidene-α-D-*ribo*-hexofuranos-3-ulose (II) in 80% yield with ruthenium tetroxide (2), oxidation with more common reagents is difficult (3, 4). By careful control of the conditions, Theander (4) oxidized I with chromium trioxide – pyridine complex in acetic acid and obtained the 3-keto derivative (II) in 6% yield. Theander also found that sodium borohydride reduced II stereospecifically and practically quantitatively to 1,2;5,6-di-*O*-isopropylidene-α-D-allofuranose (III), which crystallized with ease. This provided a convenient route to the rare monosaccharide D-allose, as well as evidence for the presence of II.

In the present work, the oxidation of I by DMSO – acetic anhydride was found to be virtually complete after 24 h at room temperature. After removal of the solvents by distillation, the oxidized residue was dissolved in aqueous ethanol and reduced with sodium



I II III

borohydride. Extraction of the product with ethyl acetate was followed by chromatography on a column of silicic acid. The D-allose derivative (III) was obtained in 62% yield based on I. The major by-product after oxidation was an unidentified reducing compound with a high R_F* value. A minor by-product was an ester, probably the 3-*O*-acetyl derivative of I.

The good yield of II indicates the usefulness of DMSO – acetic anhydride for the oxidation of hydroxyl groups of carbohydrates which are difficult to oxidize by other means. After the completion of this work, similar results were published by Onodera *et al.* (5), who obtained II in 65% yield by oxidation of I with DMSO containing phosphorus pentoxide.

EXPERIMENTAL

Thin-layer chromatography was carried out on layers (250 μ thick) of silica gel G on glass plates in (*a*) ethyl acetate – light petroleum, b.p. 30–60° (3:1 v/v), or (*b*) benzene–methanol (95:5 v/v). Compounds on the plates were detected by the following spray reagents: (*i*) sulfuric acid (30% v/v), followed by heating in an oven at 100–110°; (*ii*) saturated silver nitrate solution (1 ml) in aqueous acetone (100 ml), followed by a solution of sodium hydroxide (2 g) in aqueous ethanol (100 ml) (6); and (*iii*) ester spray reagent for thin-layer chromatography based on ferric hydroxamate reaction, according to Tate and Bishop (7). Preparative chromatography was carried out on a column of silicic acid (4 × 33 cm) with solvent *a*. Aliquots (15 ml) were collected at 30 min intervals. Evaporations were done under diminished pressure below 40 °C.

1,2;5,6-Di-*O*-isopropylidene-α-D-glucofuranose (I, 2.60 g) was dissolved in a mixture of DMSO (30 ml) and acetic anhydride (20 ml). Thin-layer chromatography of the solution during the course of the reaction showed that only a faint trace of I remained after 24 h at room temperature. The mixture was distilled at 0.05–0.1 mm, bath temperature 35–40°, to yield a syrupy residue (2.96 g) which consisted mainly of 1,2;5,6-di-*O*-isopropylidene-α-D-*ribo*-hexofuranos-3-ulose (II). It had R_I* 1.14 in solvent *a* and R_I 1.33 in solvent *b*; the reported value is R_I 1.04 in ethyl acetate – light petroleum, b.p. 40–60° (3:1 v/v) (3). The major by-product, also a reducing compound (spray *ii*), had R_I 1.34 in solvent *a*. In addition, there was a trace of an ester (spray *iii*) with R_I 1.25 in solvent *a*. A solution of the syrupy mixture in aqueous ethanol (100 ml, 70% v/v) was cooled and treated with sodium borohydride (2.6 g) for 30 min. The reaction mixture was poured into water (150 ml) and extracted with ethyl acetate (8 × 100 ml). Separation of the aqueous and organic layers was promoted by the addition of a small amount of sodium chloride. The combined extracts were dried over anhydrous sodium sulfate and concentrated to a syrup (2.81 g). This was redissolved in ethyl acetate and fractionated by column chromatography. First to be eluted was the reduced by-product (0.70 g), R_I 1.33 in solvent *a*. A mixture (0.05 g) of the reduced by-product and ester then followed. The starting material (I, 0.03 g) was next obtained and was well separated from the product, 1,2;5,6-di-*O*-isopropylidene-α-D-allose (III, 1.60 g, 62% yield based on I), R_I 0.85 in solvent *a* and R_I 1.00 in solvent *b*. I and III crystallized spontaneously when the eluting solvent was evaporated. After recrystallization of crude III (m.p. 72–75°) from benzene – light petroleum (b.p. 30–60°), it had m.p. 77–78° and $[\alpha]_D^{22}$ +36° (*c*, 0.5 in water). The reported values are m.p. 76–77° and $[\alpha]_D^{22}$ +37.7° (*c*, 0.5 in water) (4).

ACKNOWLEDGMENTS

The authors are grateful to Mrs. Claire Isaac for technical assistance. This research was made possible by a grant received by the Ontario Research Foundation from the Province of Ontario through the Department of Economics and Development.

R_F and R_I are the rates of movement of the sugars relative to that of the solvent front and of 1,2;5,6-di-O-isopropylidene-α-D-glucofuranose (I), respectively.

Can. J. Chem. Downloaded from www.nrcresearchpress.com by 210.87.254.42 on 09/05/12
For personal use only.

1. J. D. ALBRIGHT and L. GOLDMAN. J. Am. Chem. Soc. **87**, 4214 (1965).
2. P. J. BEYNON, P. M. COLLINS, and W. G. OVEREND. Proc. Chem. Soc. 342 (1964).
3. O. THEANDER. Acta Chem. Scand. **17**, 1751 (1963).
4. O. THEANDER. Acta Chem. Scand. **18**, 2209 (1964).
5. K. ONODERA, S. HIRANO, and N. KASHIMURA. J. Am. Chem. Soc. **87**, 4651 (1965).
6. W. E. TREVELYAN, D. P. Procter, and J. S. HARRISON. Nature, **166**, 444 (1950).
7. M. E. TATE and C. T. BISHOP. Can. J. Chem. **40**, 1043 (1962).

RECEIVED NOVEMBER 22, 1965.
DEPARTMENT OF ORGANIC CHEMISTRY,
ONTARIO RESEARCH FOUNDATION,
TORONTO, ONTARIO.

Can. J. Chem. Downloaded from www.nrcresearchpress.com by 210.87.254.42 on 09/05/12
For personal use only.

REACTION OF AROYL HALIDES WITH AROMATIC ALDEHYDES AND ACETOPHENONES

ROBERT FILLER AND FREDRIC N. MILLER

Adams and Vollweiler (1) reported in 1918 that aromatic acid chlorides and bromides react slowly at room temperature with aromatic aldehydes to form addition compounds, which were shown to be α'-halo esters (eq. [1]). The structures of the products were

[1] $$\underset{X = Cl, Br}{ArC(=O)-X} + O{=}CHAr' \rightarrow ArC(=O)-O-\underset{X}{CHAr'}$$

established by elemental analyses and by conversion of the halo ester into a diester on reaction with silver benzoate. The addition reaction has attracted little attention since that time, although recently it has been used as a method for obtaining an authentic sample of a diester (2).

In the discussion which follows, we provide infrared spectral evidence for the ester structure, as well as other observations concerning the reaction.

Infrared spectral analysis of the products reveals intense ester carbonyl absorption in the 1 755 – 1 735 cm^{-1} region, the position depending on the nature of the Ar group. The presence of the α'-halo group causes a substantial shift to higher frequencies (Table I).

TABLE I

Esters prepared from aroyl halides and aromatic aldehydes

Reactants	Product	$\nu_{C=O}$ (cm^{-1})*
$C_6H_5COBr + C_6H_5CHO$	$C_6H_5CO_2CHBrC_6H_5$	1 735
$C_6H_5COBr + p\text{-}ClC_6H_4CHO$	$C_6H_5CO_2CHBrC_6H_4Cl\text{-}p$	1 740
$p\text{-}NO_2C_6H_4COCl + C_6H_5CHO$	$p\text{-}NO_2C_6H_4CO_2CHClC_6H_5$	1 745
$C_6F_5COCl + C_6H_5CHO$	$C_6F_5CO_2CHClC_6H_5$	1 755
$C_6F_5COCl + C_6F_5CHO$	No reaction after 3 months, $p\text{-}NO_2C_6H_4CO_2CH_2C_6H_5$†	1 722

*All infrared spectra were measured in $CHCl_3$ except $C_6F_5CO_2CHClC_6H_5$, which was measured in CCl_4.
†Reference compound, prepared from the acid chloride and benzyl alcohol.

Adams and Vollweiler (1) reported that these compounds reacted with water according to eq. [2]. Ammonia and ethanol similarly gave the corresponding amide and ester.

[2] $$ArCO_2CHXAr' + H_2O \rightarrow ArCO_2H + HX + Ar'CHO$$

We found that, immediately after isolation, most of the products exhibited some absorption near 1 695 cm^{-1} caused by the presence of carboxylic acid. There was also some

1. J. D. ALBRIGHT and L. GOLDMAN. J. Am. Chem. Soc. **87**, 4214 (1965).
2. P. J. BEYNON, P. M. COLLINS, and W. G. OVEREND. Proc. Chem. Soc. 342 (1964).
3. O. THEANDER. Acta Chem. Scand. **17**, 1751 (1963).
4. O. THEANDER. Acta Chem. Scand. **18**, 2209 (1964).
5. K. ONODERA, S. HIRANO, and N. KASHIMURA. J. Am. Chem. Soc. **87**, 4651 (1965).
6. W. E. TREVELYAN, D. P. Procter, and J. S. HARRISON. Nature, **166**, 444 (1950).
7. M. E. TATE and C. T. BISHOP. Can. J. Chem. **40**, 1043 (1962).

RECEIVED NOVEMBER 22, 1965.
DEPARTMENT OF ORGANIC CHEMISTRY,
ONTARIO RESEARCH FOUNDATION,
TORONTO, ONTARIO.

Can. J. Chem. Downloaded from www.nrcresearchpress.com by 210.87.254.5 on 09/05/12
For personal use only.

REACTION OF AROYL HALIDES WITH AROMATIC ALDEHYDES AND ACETOPHENONES

ROBERT FILLER AND FREDRIC N. MILLER

Adams and Vollweiler (1) reported in 1918 that aromatic acid chlorides and bromides react slowly at room temperature with aromatic aldehydes to form addition compounds, which were shown to be α'-halo esters (eq. [1]). The structures of the products were

[1] $$\underset{X = Cl, Br}{\overset{\overset{O}{\|}}{ArC}—X} + O{=}CHAr' \rightarrow \overset{\overset{O}{\|}}{ArC}—O—\underset{X}{\overset{|}{C}}HAr'$$

established by elemental analyses and by conversion of the halo ester into a diester on reaction with silver benzoate. The addition reaction has attracted little attention since that time, although recently it has been used as a method for obtaining an authentic sample of a diester (2).

In the discussion which follows, we provide infrared spectral evidence for the ester structure, as well as other observations concerning the reaction.

Infrared spectral analysis of the products reveals intense ester carbonyl absorption in the 1 755 – 1 735 cm^{-1} region, the position depending on the nature of the Ar group. The presence of the α'-halo group causes a substantial shift to higher frequencies (Table I).

TABLE I

Esters prepared from aroyl halides and aromatic aldehydes

Reactants	Product	$\nu_{C=O}$ (cm^{-1})*
$C_6H_5COBr + C_6H_5CHO$	$C_6H_5CO_2CHBrC_6H_5$	1 735
$C_6H_5COBr + p\text{-}ClC_6H_4CHO$	$C_6H_5CO_2CHBrC_6H_4Cl\text{-}p$	1 740
$p\text{-}NO_2C_6H_4COCl + C_6H_5CHO$	$p\text{-}NO_2C_6H_4CO_2CHClC_6H_5$	1 745
$C_6F_5COCl + C_6H_5CHO$	$C_6F_5CO_2CHClC_6H_5$	1 755
$C_6F_5COCl + C_6F_5CHO$	No reaction after 3 months, $p\text{-}NO_2C_6H_4CO_2CH_2C_6H_5$†	1 722

*All infrared spectra were measured in $CHCl_3$ except $C_6F_5CO_2CHClC_6H_5$, which was measured in CCl_4.
†Reference compound, prepared from the acid chloride and benzyl alcohol.

Adams and Vollweiler (1) reported that these compounds reacted with water according to eq. [2]. Ammonia and ethanol similarly gave the corresponding amide and ester.

[2] $$ArCO_2CHXAr' + H_2O \rightarrow ArCO_2H + HX + Ar'CHO$$

We found that, immediately after isolation, most of the products exhibited some absorption near 1 695 cm^{-1} caused by the presence of carboxylic acid. There was also some

evidence of the aldehyde. The presence of these hydrolysis products is probably the result of exposure to atmospheric moisture as suggested previously (1). Indeed, on continued exposure, a progressive increase in the intensity of the acid carbonyl band is observed, accompanied by a corresponding diminution in the ester carbonyl frequency. This sensitivity to moisture made it difficult to obtain reliable analytical data for new compounds, except in the cases of a pentafluorophenyl ester (*vide infra*), and two esters derived from substituted acetophenones.

In confirmation of the earlier studies, we observed that esters in which Ar′ = C_6H_5 and Ar contains an electron-withdrawing group, e.g. *p*-$NO_2C_6H_4$ or C_6F_5, form much more slowly and are more stable to hydrolysis, thus indicating that attack of water on the carbonyl carbon is not involved in the rate-determining step. An example of a fairly stable ester is $C_6F_5CO_2CHClC_6H_5$, whose spectrum is shown in Fig. 1.

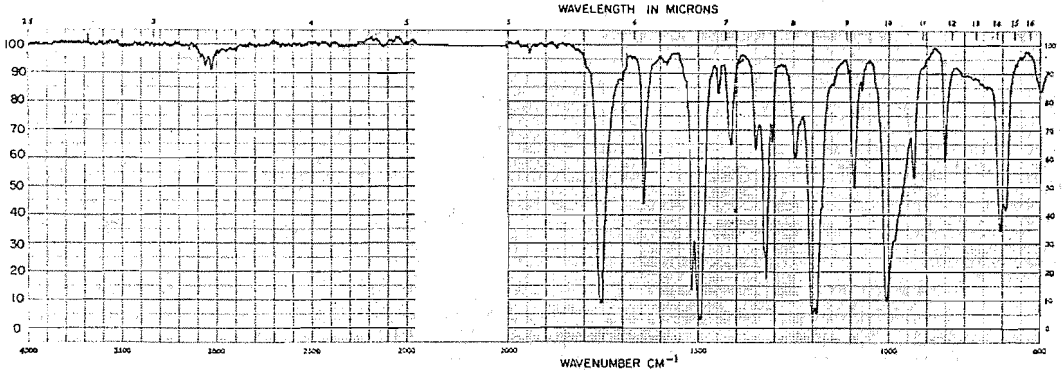


FIG. 1. The infrared spectrum of $C_6F_5CO_2CHClC_6H_5$ (in CCl_4 solvent) prepared from C_6F_5COCl and C_6H_5CHO.

p-Bromoacetophenone and *p*-nitroacetophenone also react slowly (8 days) with *p*-nitrobenzoyl chloride, and the infrared spectra of the products indicate the presence of esters of the type $ArCO_2CCl(CH_3)Ar'$. When the esters are heated, they revert to starting materials. Acetophenone and *p*-methylacetophenone failed to react with *p*-nitrobenzoyl chloride after 4 days.

From Adams' data and our own observation on the attempted reaction of pentafluorobenzaldehyde with pentafluorobenzoyl chloride, it appears that electron-withdrawing groups on the aromatic nucleus of the aldehyde slow down or inhibit the reaction. Although we have insufficient information to support a specific mechanism for the formation of the ester, it is apparent that increased nucleophilic character of the aldehyde oxygen (for attack on the carbonyl carbon of the acid halide) enhances the rate of reaction. Moreover, the observation that acid bromides react much faster than acid chlorides is consonant with the evidence that bromide is the better leaving group. At this stage, both stepwise mechanisms and a four-center transition state are possible.

EXPERIMENTAL

Infrared spectra were obtained on a Beckman IR-8 grating spectrophotometer.

Benzoyl Bromide and Benzaldehyde

Equimolar amounts of the two compounds were mixed in a flask and stoppered tightly. Solidification occurred after 2 days to give a product which fumed in air and decomposed readily. It was not possible to purify this material, in agreement with previous observations (1). The infrared spectrum in $CHCl_3$ showed two peaks in the carbonyl region at 1 695 cm^{-1} (with a shoulder at 1 705 cm^{-1}) and at 1 735 cm^{-1}.

Can. J. Chem. Downloaded from www.nrcresearchpress.com by 210.87.254.5 on 09/05/12
For personal use only.

Benzoyl Bromide and p-Chlorobenzaldehyde

Solidification took place 3 h after equimolar amounts of the two liquids were mixed. The grey-white solid decomposed rapidly with fuming in the air. Again it was not possible to purify the product, and the infrared spectrum showed that it underwent rapid decomposition in solution.

The spectrum in $CHCl_3$ was very similar to that of the product obtained in the previous reaction, with a strong band at 1 740 cm^{-1} attributed to the addition product, another strong band at 1 695 cm^{-1}, and a shoulder at 1 705 cm^{-1}. Also present was a broad band centered at 3 000 cm^{-1} and attributed to the bonded OH of the carboxylic acid.

A spectrum of the solution taken 1 h after the first showed the same features, although the band at 1 740 cm^{-1} had diminished in intensity and the others increased in intensity. The sample was then stored for 20 h and another spectrum taken at that time. This spectrum showed even greater changes, although the 1 740 cm^{-1} band was still fairly intense.

p-Nitrobenzoyl Chloride and Benzaldehyde

An equimolar amount of *p*-nitrobenzoyl chloride was dissolved in benzaldehyde, and the tightly stoppered flask kept at room temperature. Solidification occurred after 5 days, and the solid was recrystallized from Skellysolve B to give white crystals, m.p. 119–120° (lit. (1) m.p. 118–118.5°). The compound appears to be stable in the air, and a sample stored in a bottle for 3 months melted at 119–120°.

The spectrum in $CHCl_3$ showed a band in the carbonyl region at 1 745 cm^{-1} (strong) with shoulders at 1 740 cm^{-1} and 1 735 cm^{-1}. These bands are all assigned to the addition compound.

Pentafluorobenzoyl Chloride and Benzaldehyde

Equimolar amounts of the two compounds were mixed in a tightly stoppered flask and kept at room temperature. After 1 week the solution had turned yellow but no solid had formed. After an additional 2 weeks the mixture had solidified. Crystallization from petroleum ether gave white crystals (later turning pink), m.p. 93–94°. The infrared spectrum in CCl_4 showed strong absorption at 1 755 cm^{-1}, the only absorption in the carbonyl region.

Anal. Calcd. for $C_{14}H_6ClF_5O_2$: F, 28.3. Found: F, 29.5.

Pentafluorobenzoyl Chloride and Pentafluorobenzaldehyde

Equimolar amounts of the two compounds were mixed in a tightly stoppered flask and kept at room temperature. The solution turned light brown after 4 days and progressively darkened for 3 months, but no solid precipitated. After 3 months a small amount of pentane was added and an oil separated, but no product could be isolated.

p-Nitrobenzoyl Chloride and p-Bromoacetophenone

The reaction was conducted by dissolving equimolar amounts of the two compounds (0.1 mole each) in a minimum amount of anhydrous ether and keeping the tightly stoppered flask at room temperature for 8 days. On addition of *n*-pentane, a solid was obtained which was crystallized from Skellysolve B to give white needles, m.p. 49–52°.

Anal. Calcd. for $C_{15}H_{11}NO_4BrCl$: C, 46.84; H, 2.88. Found: C, 46.56; H, 2.96.

The spectrum of a CCl_4 solution showed four peaks in the carbonyl region. When the solution was allowed to stand in the spectrometer, the ester reverted to starting materials; the spectrum showed a strong band at 1 785 cm^{-1} caused by *p*-nitrobenzoyl chloride, a very strong band at 1 760 cm^{-1} and a medium band at 1 725 cm^{-1} caused by the addition compound, and a very strong band at 1 690 cm^{-1} caused by *p*-bromoacetophenone.

p-Nitrobenzoyl Chloride and p-Nitroacetophenone

The reaction was carried out in the same manner as above, and the product was isolated after 8 days as brownish-white needles, m.p. 62–64°. The infrared spectrum showed a strong band at 1 785 cm^{-1} caused by *p*-nitrobenzoyl chloride, a very strong band at 1 760 cm^{-1} and a medium band at 1 728 cm^{-1} caused by the addition compound, and a very strong band at 1 695 cm^{-1} caused by *p*-nitroacetophenone.

Anal. Calcd. for $C_{15}H_{11}N_2O_6Cl$: C, 51.37; H, 3.16. Found: C, 52.44; H, 3.50.

p-Nitrobenzoyl Chloride and Acetophenone (p-Methylacetophenone)

p-Nitrobenzoyl chloride (0.1 mole) was dissolved in 0.1 mole of acetophenone with the aid of a small amount of anhydrous ether. The tightly stoppered flask was kept at room temperature for 4 days and enough *n*-pentane was added to precipitate a solid. This solid was crystallized from Skellysolve B to give an off-white compound, m.p. 73–75°, shown by mixed melting point to be unreacted *p*-nitrobenzoyl chloride. *p*-Methylacetophenone behaved similarly.

1. R. Adams and E. H. Vollweiler. J. Am. Chem. Soc. **40**, 1732 (1918).
2. J. K. Stille and D. D. Whitehurst. J. Am. Chem. Soc. **86**, 4871 (1964).

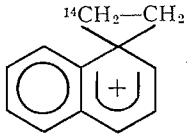
Received August 9, 1965.
Department of Chemistry,
Illinois Institute of Technology,
Chicago, Illinois.

Can. J. Chem. Downloaded from www.nrcresearchpress.com by 210.87.254.5 on 09/05/12
For personal use only.

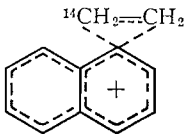
REARRANGEMENT STUDIES WITH ^{14}C
XXVI. SOLVOLYSES OF 2-(β-NAPHTHYL)-1-^{14}C-ETHYL *p*-TOLUENESULFONATE

C. C. LEE AND A. G. FORMAN

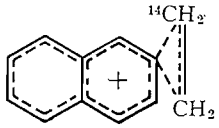
In an earlier paper (1), the results obtained from the acetolysis and formolysis of 2-(α-naphthyl)-1-^{14}C-ethyl *p*-toluenesulfonate (α-I-OTs) were reported, and it was concluded that these solvolyses involved the nonclassical ethylene-α-naphthonium ion as an intermediate. This ion was drawn as II*a* by analogy with the suggested representation of the ethylenephenonium ion by Brown *et al.* (2). Recently, Eberson, Winstein, and co-workers (3, 4) have presented very strong evidence, including the direct observation of the nuclear magnetic resonance spectrum, for the bridged ion from the 9-anthrylethyl system. These workers (3, 4) preferred a structure which was regarded as a better representation of positive-charge delocalization and from which, by analogy, the ethylene-α-naphthonium ion would be written as II*b*. In the present work, the acetolysis and formolysis of 2-(β-naphthyl)-1-^{14}C-ethyl *p*-toluenesulfonate (β-I-OTs) were studied, and the results also suggest some involvement of the ethylene-β-naphthonium ion III or its equivalent of a pair of rapidly equilibrating classical ions.



II*a*



II*b*



III

β-I-OTs was prepared from β-chloromethylnaphthalene (5) by a series of reactions analogous to those already described for the preparation of α-I-OTs (1). Acetolysis and formolysis of β-I-OTs were allowed to proceed to 50% completion; the "unreacted" β-I-OTs and the respective products, 2-(β-naphthyl)ethyl acetate and formate (β-I-OAc and β-I-OCHO), were recovered, converted into 2-(β-naphthyl)ethanol (β-I-OH), and degraded to β-naphthoic acid (IV) by procedures previously described for the α-naphthyl series (1). The radioactivity in IV gave the extents of rearrangement of the ^{14}C label from the C-1 to the C-2 positions of the ethyl chain in the various products and in the recovered β-I-OTs. The results are summarized in Table I.

The isotope position rearrangements tabulated in Table I show a trend very similar to those observed in the solvolyses of α-I-OTs (1), but the actual extents of rearrangement are somewhat lower than those obtained in the corresponding reactions with the α-naphthyl series. Thus the rearrangements in the solvolysis products from β-I-OTs are 34% and 43%, respectively, for acetolysis and formolysis, whereas the corresponding rearrangements from acetolysis and formolysis of α-I-OTs are 46% and 50% (1). This difference is not surprising when the well-known greater reactivity of the α-position than the β-position of the naphthalene nucleus towards aromatic substitution, and theoretical considerations (6) are taken into account. It is therefore expected that nonclassical ion II*b* will have somewhat greater stability than nonclassical ion III. Solvolyses of β-I-OTs will thus show a greater S_N2 component than the corresponding reactions with α-I-OTs. Hence, slightly lower extents of ^{14}C rearrangement are observed in the present studies with β-I-OTs. It is of interest to point out that a change in the same direction has also been observed in the isotope position rearrangements accompanying the nitrous acid deamination of the 2-(α-naphthyl)- and 2-(β-naphthyl)-1-^{14}C-ethylamines (5).

Can. J. Chem. Downloaded from www.nrcresearchpress.com by 210.87.254.105 on 09/05/12
For personal use only.

Can. J. Chem. Downloaded from www.nrcresearchpress.com by 210.87.254.105 on 09/05/12
For personal use only.

TABLE I

Rarrangements in solvolyses of 2-(β-naphthyl)-1-^{14}C-ethyl *p*-toluenesulfonate

Reaction	Compound assayed	Reaction product				Recovered tosylate			
		Activity* (c.p.m./mmole)		% rearrangement		Activity* (c.p.m./mmole)		% rearrangement	
		Run 1	Run 2	Run 1	Run 2	Run 1	Run 2	Run 1	Run 2
Acetolysis	β-$C_{10}H_7CH_2CH_2OH$	906	906			239	184		
	β-$C_{10}H_7COOH$	308	311	34	34	73	58	31	32
Formolysis	β-$C_{10}H_7CH_2CH_2OH$	72	77			68	82		
	β-$C_{10}H_7COOH$	32	33	43	43	0.5	0.6	0.7	0.7

*Measured by a liquid scintillation counter.

The rearrangement found in the β-I-OTs recovered from the acetolysis reaction is about 31% compared with a corresponding rearrangement of about 38% in the sulfonate recovered from the acetolysis of α-I-OTs (1). As in the case with the α-isomer, the rearrangement in the sulfonate recovered from the formolysis of β-I-OTs is almost negligible. As pointed out previously (1), these isotopic rearrangements in the recovered starting material indicate some return from an ionic intermediate, such as III, to covalent bonding. The fact that extensive return takes place in acetic acid whereas the return is almost negligible in formic acid is consistent with well-established concepts regarding the effects of reaction medium on internal return. The ionizing power and nucleophilic character of acetic acid are such that an optimum opportunity is provided for return from ionic to covalent bonding, whereas in the highly ionizing formic acid the return process cannot compete favorably with product formation (7, 8).

EXPERIMENTAL

Preparation of β-I-OTs

The reaction of ^{14}C-carbon dioxide with the Grignard reagent from β-chloromethylnaphthalene gave β-naphthylacetic acid, m.p. 142–143 °C (lit. (9) m.p. 143.1–143.4 °C), which was reduced with lithium aluminium hydride to β-I-OH, m.p. 67–68 °C (lit. (5) m.p. 67–68 °C). The alcohol was then treated with *p*-toluenesulfonyl chloride in pyridine (10) to give β-I-OTs, m.p. 75–76 °C.

Anal. Calcd. for $C_{19}H_{18}O_3S$: C, 69.91; H, 5.56; S, 9.82. Found: C, 70.01; H, 5.60; S, 9.80.

Acetolysis

A solution of 5.712 g (0.0175 mole) of β-I-OTs in 100 ml of anhydrous acetic acid was heated at 110.6 °C for one half-life (1 110 min). The resulting mixture was worked up in the same manner as described for the acetolysis of α-I-OTs (1). Both "unreacted" β-I-OTs and the reaction product, β-I-OAc, were recovered in about 80% yields based on 50% reaction. β-I-OAc was distilled at 148–153 °C and 1 mm.

Anal. Calcd. for $C_{14}H_{14}O_2$: C, 78.48; H, 6.59. Found: C, 78.66; H, 6.67.

Formolysis

A solution of 2.448 g (0.0075 mole) of β-I-OTs in 250 ml of anhydrous formic acid was heated at 56.5 °C for one half-life (1 300 min), and the resulting mixture was worked up as previously described (1). For the two runs, 0.7 and 0.8 g (57% and 65% based on 50% reaction) of β-I-OTs were recovered, and the yields of β-I-OCHO were 0.37 g and 0.42 g (48% and 54% based on 50% reaction). β-I-OCHO was distilled at 140–146 °C and 1 mm.

Anal. Calcd. for $C_{13}H_{12}O_2$: C, 77.98; H, 6.04. Found: C, 78.02; H, 6.01.

Degradation

The recovered β-I-OTs and the reaction products, β-I-OAc and β-I-OCHO, were converted into β-I-OH and then oxidized to β-naphthoic acid (IV) by the same procedures already described for the α-naphthyl series (1). A control degradation showed that these reactions did not cause any isotopic rearrangement.

ACKNOWLEDGMENT

The financial support given by the National Research Council of Canada is gratefully acknowledged.

1. C. C. Lee and A. G. Forman. Can. J. Chem. **43**, 3387 (1965).
2. H. C. Brown, K. J. Morgan, and F. J. Chloupek. J. Am. Chem. Soc. **87**, 2137 (1965).
3. L. Eberson, J. P. Petrovich, R. Baird, D. Dyckes, and S. Winstein. J. Am. Chem. Soc. **87**, 3504 (1965).
4. L. Eberson and S. Winstein. J. Am. Chem. Soc. **87**, 3506 (1965).
5. A. G. Forman and C. C. Lee. Can. J. Chem. **40**, 1130 (1962).
6. A. Streitwieser, Jr. Molecular orbital theory for organic chemists. John Wiley & Sons, Inc., New York. 1961. pp. 313–338.
7. W. G. Young, S. Winstein, and H. L. Goering. J. Am. Chem. Soc. **73**, 1958 (1951).
8. A. Streitwieser, Jr. Solvolytic displacement reactions. McGraw-Hill Book Co., New York. 1962. pp. 86–91.
9. I. Heilbron and H. M. Bunbury. Dictionary of organic compounds. Vol. III. Eyre & Spottiswoode Ltd., London. 1953. p. 571.
10. R. S. Tipson. J. Org. Chem. **9**, 235 (1944).

Received December 6, 1965.
Department of Chemistry and Chemical Engineering,
University of Saskatchewan,
Saskatoon, Saskatchewan.

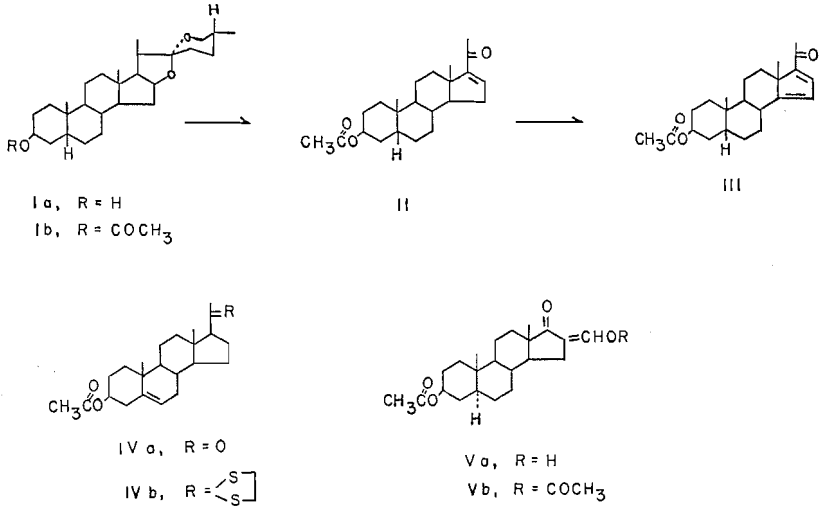
Can. J. Chem. Downloaded from www.nrcresearchpress.com by 210.87.254.105 on 09/05/12
For personal use only.

STEROIDS AND RELATED NATURAL PRODUCTS XXVI. SYNTHESIS OF 3β-ACETOXY-20-OXO-5β-PREGNA-14,16-DIENE[1,2]

GEORGE R. PETTIT[3] AND DAVID M. PIATAK[4]

A pure specimen of 3β-acetoxy-20-oxo-5β-pregna-14,16-diene, obtained by a synthetic procedure which would constitute formal total synthesis, was required as part of another problem. Although a variety of similar D-ring dienes have been prepared (1), none was considered to be suitable; hence we developed the following synthetic route.

The important total synthesis of tigogenin by Sondheimer and colleagues (2) completes, in turn, a total synthetic route (3) to smilagenin (I*a*) and allowed the latter compound to serve as starting material. Smilagenin acetate (I*b*) was degraded to 3β-acetoxy-20-oxo-5β-pregna-16-ene (II) essentially as reported by Wall,[5] and the olefin was treated with N-bromosuccinimide.[6] Dehydrohalogenation of the product by a sodium iodide procedure yielded a mixture of starting material (II) and the required diene (III). Partial purification of diene III was achieved by successive column chromatography on basic alumina and Florisil. Final purification of diene III was realized by a combination of preparative thin-layer chromatography and recrystallization procedures.



Several other methods were used in early attempts to obtain diene III; during this phase ethylenethioketal IV*b* was prepared, and regeneration of the original ketone by a mercuric chloride desulfurization (7) method was studied. In addition, a route to androstane derivative V*b* was developed.

[1]*For part XXV in this series, see G. R. Pettit, R. E. Kadunce, P. Sunder-Plassmann, and J. Occolowitz, Can. J. Chem., 43, 2872 (1965).*

[2]*This investigation was supported by Public Health Service research grants Nos. CA-04074-04 and CA-04074-07 from the National Cancer Institute, and is based on part of the Ph.D. dissertation submitted by D. M. Piatak to the Graduate School, University of Maine, Orono, Maine, June 1962.*

[3]*Present address: Department of Chemistry, Arizona State University, Tempe, Arizona.*

[4]*Present address: Worcester Foundation for Experimental Biology, Shrewsbury, Massachusetts.*

[5]*The procedure used was that described in ref. 4. More recently the overall technique has been improved (5).*

[6]*A detailed study of the reaction between N-bromosuccinimide and 20-oxo-16-pregnenes has recently been reported (6).*

Can. J. Chem. Downloaded from www.nrcresearchpress.com by 210.87.254.42 on 09/05/12
For personal use only.

Can. J. Chem. Downloaded from www.nrcresearchpress.com by 210.87.254.42 on 09/05/12
For personal use only.

EXPERIMENTAL

All solvents were redistilled, and melting points were determined on a Fisher–Johns apparatus. The new compounds reported are colorless, and the purity of each was determined by thin-layer chromatography on Kieselguhr G (E. Merck, A.G.). Optical rotation measurements (in chloroform) were determined in the laboratory of Drs. Weiler and Strauss, Oxford, England. Ultraviolet (ethanol solution) and infrared spectra were recorded by Dr. R. A. Hill, University of Maine; Dr. A. Bernhardt, Max-Planck Institut, Mülheim, Germany, provided the elemental analyses.

3β-Acetoxy-20-oxo-5β-pregna-14,16-diene (III)

In a typical experiment smilagenin acetate (I*b*, 10. 0 g) was converted into 3β-acetoxy-20-oxo-5β-pregna-16-ene (II, 3.6 g, m.p. 141–143°) essentially[7] as described by Wall and his colleagues (reported (5) m.p. 141–143°). Degradation of smilagenin acetate to ketone II was repeated a number of times, with similar results in each case. A solution of the 20-ketone (II, 2.0 g) and N-bromosuccinimide (1.24 g) in carbon tetrachloride (60 ml) was heated at reflux and irradiated for 12 min with a General Electric sunlamp (250 W). The bromination reaction was repeated a total of seven times and the reaction mixtures were combined. After succinimide was collected, the solvent was removed (*in vacuo*) and the residue dissolved in acetone (230 ml). Sodium iodide (28 g) was added and the mixture was stored at room temperature for 65 h. After dilution with water and diethyl ether, the organic layer was successively washed with 5% sodium hydrogen sulfite, 5% sodium bicarbonate, and water. Removal of solvent provided an oily residue (14.0 g) which was chromatographed, in 4:1 petroleum ether – benzene, on basic alumina (250 g, Merck "suitable for chromatography"). Elution with the same solvent followed by 1:1 petroleum ether – benzene and benzene gave a series of fractions (7.0 g) containing increasing quantities of diene III. A qualitative estimation of monoolefin II content (as evidenced by infrared spectral determination) was determined for each fraction. The fractions eluted by 9:1 to 1:1 benzene–chloroform weighed 6.1 g and represented (based on infrared spectra) principally the diene. The 6.1 g portion was reacetylated (1:1 acetic anhydride – pyridine, room temperature, 24 h), and the product was crystallized from methanol and recrystallized from benzene – petroleum ether to yield needles melting at 131–132°. However, a detectable (by infrared spectral analysis) amount of starting material (II) was still present. The crystalline, but slightly impure, diene was further purified as follows. A 0.50 g portion was dissolved in 20:1 petroleum ether – benzene and carefully chromatographed on Florisil (15.0 g; Floridine Company, Tallahassee, Florida). A 25 mg specimen of the fractions (0.173 g) eluted with 1:1 petroleum ether – benzene was subjected to preparative thin-layer chromatography on Kieselguhr G (1:1 benzene–chloroform being used as the mobile phase). The diene was located with an ultraviolet lamp (dark spot) and eluted with chloroform. The chloroform solution was filtered through a column of neutral alumina (E. Merck, A.G.); removal of solvent led to 12 mg of 3β-acetoxy-20-oxo-5β-pregna-14,16-diene (III) melting at 112–115°. Several recrystallizations from benzene–ligroin (b.p. 80–90°) gave an analytical specimen as needles melting at 118.5–119.5°; λ_{max} 310 mμ (log ε 4.15); the optical rotatory dispersion[8] in methyl alcohol (*c*, 0.015) at room temperature, $[\alpha]_{254}$ −22 000, $[\alpha]_{285}$ −27 800, $[\alpha]_{335}$ +27 800, $[\alpha]_{350}$ +20 000, $[\alpha]_{356}$ +10 000, and $[\alpha]_{440}$ +4 000;[8] $[\alpha]_D^{22}$ +374° (*c*, 1.28); ν_{max}^{KBr} 1 733, 1 638, 1 526, and 1 258 cm^{-1}.

Anal. Found: C, 77.36; H, 9.03. $C_{23}H_{32}O_3$ requires C, 77.49; H, 9.05.

The same procedure was employed to prepare a larger quantity (0.06 g) of pure diene (III).

3β-Acetoxy-pregna-5-ene 20-Ethylenethioketal (IVb)

To a warm (steam bath) solution of 3β-acetoxy-20-oxo-pregna-5-ene (IV*a*, 4.0 g) in glacial acetic acid (50 ml) – ethanedithiol (7 ml) was added boron trifluoride etherate (7 ml). The reaction mixture was slowly cooled, and the crystalline product which separated was collected and washed with methanol to yield 4.6 g (92%) of thioketal IV*b* melting at 209–211°. Recrystallization from chloroform–methanol provided a pure crystalline specimen, m.p. 211.5–212.5°, $[\alpha]_D^{18}$ −27.8° (*c*, 1.32), $\nu_{max}^{CHCl_3}$ 1 722 cm^{-1}.

Anal. Found: C, 68.99; H, 8.65; S, 15.01. $C_{25}H_{38}O_2S_2$ requires C, 69.09; H, 8.81; S, 14.73.

The original ketone was regenerated by application of the following procedure. A mixture of thioketal IV*b* (0.50 g), cadmium carbonate (2.0 g), mercuric chloride (2.0 g), water (3 ml), chloroform (3 ml), and acetone (15 ml) was allowed to stand at room temperature for 22 h. After the solution was filtered through Celite, additional chloroform was added and the mixture washed successively with water, 5% aqueous potassium iodide, and water. Removal of solvent gave 0.40 g (97%) of 3β-acetoxy-20-oxo-pregna-5-ene (IV*a*) melting at 147–150°. Recrystallization from methanol provided a specimen melting at 147–148°. Mixture melting point determination and infrared spectral comparison with an authentic specimen confirmed the product's composition.

3β-Acetoxy-16-acetoxymethylene-17-oxo-5α-androstane (Vb)

A specimen of 3β-hydroxy-16-hydroxymethylene-17-oxo-5α-androstane (V*a*, 92% yield, m.p. 222–225°) was prepared from 3β-acetoxy-17-oxo-5α-androstane (5.0 g) as described by Ruzicka (reported (8) m.p.

[7]*Substitution of chloroform for diethyl ether in the extraction step led to a more easily crystallized product.*

[8]*We thank Dr. Herman Ziffer, National Institutes of Health, U.S. Public Health Service, for providing the optical rotatory dispersion data.*

223.5–225.5°). The formyl compound (V*a*) was acetylated (see III) and the product was recrystallized from methanol to yield 3.7 g (66%, m.p. 148–149.5°) of diacetate V*b*. Recrystallization from the same solvent gave pure crystals melting at 150.5–151.5°; $[\alpha]_D^{23}$ −21.4° (*c*, 1.27); $\nu_{max}^{CHCl_3}$ 1 770, 1 726, and 1 656 cm^{-1}.

Anal. Found: C, 71.48; H, 8.67. $C_{24}H_{34}O_5$ requires C, 71.61; H, 8.51.

1. L. RUZICKA, P. A. PLATTNER, H. HEUSSER, and J. PATAKI. Helv. Chim. Acta, **29**, 936 (1946). P. A. PLATTNER, L. RUZICKA, H. HEUSSER, and E. ANGLIKER. Helv. Chim. Acta, **30**, 385 (1947); **30**, 395 (1947). P. A. PLATTNER, K. MEIER, and H. HEUSSER. Helv. Chim. Acta, **30**, 905 (1947). L. RUZICKA, P. A. PLATTNER, H. HEUSSER, and K. MEIER. Helv. Chim. Acta, **30**, 1342 (1947). P. A. PLATTNER, H. HEUSSER, and A. SEGRE. Helv. Chim. Acta, **31**, 249 (1948). A. BUTENANDT and J. SCHMIDT-THOME. Ber. **71**, 1487 (1938). E. BATRES, T. CARDENAS, J. A. EDWARDS, G. MONROY, O. MANCERA, C. DJERASSI, and H. J. RINGOLD. J. Org. Chem. **26**, 871 (1961). A. J. SOLO, H. S. SACHDEV, and S. S. H. GILANI. J. Org. Chem. **30**, 769 (1965). A. J. SOLO and B. SINGH. J. Org. Chem. **30**, 1658 (1965).
2. Y. MAZUR, N. DANIELI, and F. SONDHEIMER. J. Am. Chem. Soc. **82**, 5889 (1960).
3. R. E. MARKER, T. TSUKAMOTO, and D. L. TURNER. J. Am. Chem. Soc. **62**, 2525 (1940).
4. M. E. WALL, H. E. KENNEY, and E. S. ROTHMAN. J. Am. Chem. Soc. **77**, 5665 (1955).
5. M. E. WALL and S. SEROTA. J. Org. Chem. **24**, 741 (1959); Tetrahedron, **10**, 238 (1960).
6. R. TSCHESCHE, F. RIEMHOFER, and G. SNATZKE. Chem. Ber. **98**, 1188 (1965).
7. G. R. PETTIT and E. E. VAN TAMELEN. Org. Reactions, **12**, 405 (1962).
8. L. RUZICKA, V. PRELOG, and J. BATTEGAY. Helv. Chim. Acta, **31**, 1296 (1948).

RECEIVED OCTOBER 27, 1965.
DEPARTMENT OF CHEMISTRY,
UNIVERSITY OF MAINE,
ORONO, MAINE,
AND
DEPARTMENT OF CHEMISTRY,
ARIZONA STATE UNIVERSITY,
TEMPE, ARIZONA.

THE SYNTHESIS OF SUBSTITUTED BIURETS[1]

H. STOLLAR, R. J. RANZ, AND FRANCIS L. CHUBB

In a previous communication (1) the synthesis and pharmacology of some 1-substituted biurets were described. We now report the synthesis of a new series of mono- and poly-substituted biurets (Table I), some of which were synthesized by a novel method. This method, while being generally applicable to the synthesis of biurets, is particularly suitable for the synthesis of 1,5-disubstituted biurets.

Most of the biurets herein reported were synthesized by the reaction of nitrobiuret with a primary or secondary amine (2), or by the reaction of a 1,1-disubstituted-5-nitrobiuret (Table II) with a primary amine (3). However, there are no reports in the literature of this method having been used for the synthesis of 1,5-disubstituted biurets (4, 5). We found that the reaction of 1-methyl-5-nitrobiuret with phenethylamine gave very low yields of the required 1-methyl-5-phenethylbiuret.

The reaction of allophanic esters with amines has been used to prepare some 1,5-disubstituted biurets, but has been found to be of limited usefulness (4). When we attempted to prepare 1,5-disubstituted biurets by causing methyl-4-phenethylallophanate to react with various amines, we were successful only in the case of methylamine and benzylamine.

Another method which has been used for the synthesis of 1,5-disubstituted biurets is the condensation of an isocyanate with an O-alkyl-N-substituted isourea to yield an isobiuret,

[1]*Presented at the 150th meeting of the American Chemical Society, September 1965, Atlantic City, New Jersey.*

Can. J. Chem. Downloaded from www.nrcresearchpress.com by 210.87.254.42 on 09/05/12
For personal use only.

223.5–225.5°). The formyl compound (V*a*) was acetylated (see III) and the product was recrystallized from methanol to yield 3.7 g (66%, m.p. 148–149.5°) of diacetate V*b*. Recrystallization from the same solvent gave pure crystals melting at 150.5–151.5°; $[\alpha]_D^{23}$ −21.4° (*c*, 1.27); $\nu_{max}^{CHCl_3}$ 1 770, 1 726, and 1 656 cm^{-1}.

Anal. Found: C, 71.48; H, 8.67. $C_{24}H_{34}O_5$ requires C, 71.61; H, 8.51.

1. L. Ruzicka, P. A. Plattner, H. Heusser, and J. Pataki. Helv. Chim. Acta, **29**, 936 (1946). P. A. Plattner, L. Ruzicka, H. Heusser, and E. Angliker. Helv. Chim. Acta, **30**, 385 (1947); **30**, 395 (1947). P. A. Plattner, K. Meier, and H. Heusser. Helv. Chim. Acta, **30**, 905 (1947). L. Ruzicka, P. A. Plattner, H. Heusser, and K. Meier. Helv. Chim. Acta, **30**, 1342 (1947). P. A. Plattner, H. Heusser, and A. Segre. Helv. Chim. Acta, **31**, 249 (1948). A. Butenandt and J. Schmidt-Thome. Ber. **71**, 1487 (1938). E. Batres, T. Cardenas, J. A. Edwards, G. Monroy, O. Mancera, C. Djerassi, and H. J. Ringold. J. Org. Chem. **26**, 871 (1961). A. J. Solo, H. S. Sachdev, and S. S. H. Gilani. J. Org. Chem. **30**, 769 (1965). A. J. Solo and B. Singh. J. Org. Chem. **30**, 1658 (1965).
2. Y. Mazur, N. Danieli, and F. Sondheimer. J. Am. Chem. Soc. **82**, 5889 (1960).
3. R. E. Marker, T. Tsukamoto, and D. L. Turner. J. Am. Chem. Soc. **62**, 2525 (1940).
4. M. E. Wall, H. E. Kenney, and E. S. Rothman. J. Am. Chem. Soc. **77**, 5665 (1955).
5. M. E. Wall and S. Serota. J. Org. Chem. **24**, 741 (1959); Tetrahedron, **10**, 238 (1960).
6. R. Tschesche, F. Riemhofer, and G. Snatzke. Chem. Ber. **98**, 1188 (1965).
7. G. R. Pettit and E. E. van Tamelen. Org. Reactions, **12**, 405 (1962).
8. L. Ruzicka, V. Prelog, and J. Battegay. Helv. Chim. Acta, **31**, 1296 (1948).

Received October 27, 1965.
Department of Chemistry,
University of Maine,
Orono, Maine,
and
Department of Chemistry,
Arizona State University,
Tempe, Arizona.

THE SYNTHESIS OF SUBSTITUTED BIURETS[1]

H. Stollar, R. J. Ranz, and Francis L. Chubb

In a previous communication (1) the synthesis and pharmacology of some **1**-substituted biurets were described. We now report the synthesis of a new series of mono- and poly-substituted biurets (Table I), some of which were synthesized by a novel method. This method, while being generally applicable to the synthesis of biurets, is particularly suitable for the synthesis of 1,5-disubstituted biurets.

Most of the biurets herein reported were synthesized by the reaction of nitrobiuret with a primary or secondary amine (2), or by the reaction of a 1,1-disubstituted-5-nitrobiuret (Table II) with a primary amine (3). However, there are no reports in the literature of this method having been used for the synthesis of 1,5-disubstituted biurets (4, 5). We found that the reaction of 1-methyl-5-nitrobiuret with phenethylamine gave very low yields of the required 1-methyl-5-phenethylbiuret.

The reaction of allophanic esters with amines has been used to prepare some 1,5-disubstituted biurets, but has been found to be of limited usefulness (4). When we attempted to prepare 1,5-disubstituted biurets by causing methyl-4-phenethylallophanate to react with various amines, we were successful only in the case of methylamine and benzylamine.

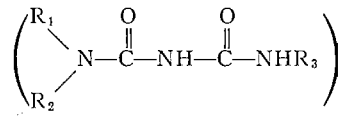
Another method which has been used for the synthesis of 1,5-disubstituted biurets is the condensation of an isocyanate with an O-alkyl-N-substituted isourea to yield an isobiuret,

[1]*Presented at the 150th meeting of the American Chemical Society, September 1965, Atlantic City, New Jersey.*

Can. J. Chem. Downloaded from www.nrcresearchpress.com by 210.87.254.105 on 09/05/12
For personal use only.

Can. J. Chem. Downloaded from www.nrcresearchpress.com by 210.87.254.105 on 09/05/12
For personal use only.

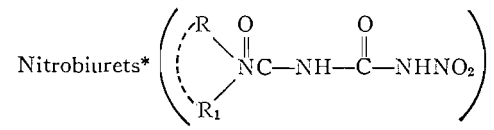
TABLE I

Substituted biurets 

FWH No.	R_1	R_2	R_3	Method of preparation*	Yield (%)	Formula	Analysis (%) Calcd. C	Calcd. H	Calcd. N	Found C	Found H	Found N	Melting point (°C)
503	CH_3	CH_3	ϕCH_2CH_2	B	9	$C_{12}H_{17}N_3O_2$	61.25	7.28	17.86	60.95	7.19	18.27	104–106
505	$(CH_2)_2O(CH_2)_2$		ϕCH_2CH_2	A, B	83, 78	$C_{14}H_{19}N_3O_3$	60.63	6.91	15.13	60.77	6.87	15.26	135–136
506	$(CH_2)_5$		ϕCH_2CH_2	A, B	65.74	$C_{16}H_{21}N_3O_2$	65.42	7.69	15.26	65.51	7.75	14.97	110–111
507	$(CH_2)_6$		ϕCH_2CH_2	B	38	$C_{16}H_{23}N_3O_2$	66.72	8.01	14.52	66.71	7.92	14.99	95–96
509	$(CH_2)_4$		ϕCH_2CH_2	B	79	$C_{14}H_{19}N_3O_2$	64.36	7.33	16.08	63.98	7.32	15.99	163–164
510	C_2H_5	C_2H_5	ϕCH_2CH_2	B	86	$C_{14}H_{21}N_3O_2$	63.86	8.04	15.96	64.22	8.17	16.05	79–80
535	C_2H_5	C_2H_5	ϕCH_2	B	80	$C_{13}H_{19}N_3O_2$	62.64	7.68	16.86	62.65	7.88	16.45	92–94
538	C_2H_5	C_2H_5	$\phi(CH_2)_4$	B	45	$C_{16}H_{26}N_3O_2$	65.95	8.65	14.42	66.36	8.65	14.09	63–64
547	C_2H_5	C_2H_5	$\phi(CH_2)_3$	B	24	$C_{15}H_{23}N_3O_2$	64.95	8.36	15.15	65.26	8.44	15.44	52–53
548	C_3H_7	C_3H_7	ϕCH_2	B	27	$C_{15}H_{23}N_3O_2$	64.95	8.36	15.15	64.72	8.48	14.98	71–72.5
549	C_3H_7	C_3H_7	$\phi(CH_2)_3$	B	21	$C_{17}H_{27}N_3O_2$	66.85	8.91	13.76	66.77	8.79	13.85	58–59
550	C_2H_7	C_3H_7	$\phi(CH_2)_4$	B	23	$C_{18}H_{29}N_3O_2$	67.68	9.15	13.15	68.05	9.33	13.42	50–50.5
567	C_2H_5	C_2H_5	p-$ClC_6H_4CH_2CH_2$	B	79	$C_{14}H_{20}N_3O_2Cl$	56.45	6.77	14.11	56.64	6.89	13.91	102–104
558	p-$ClC_6H_4CH_2CH_2$	H	H	B	81	$C_{10}H_{12}N_3O_2Cl$	49.69	5.01	17.38	49.82	4.88	17.22	174–175
560	p-$AcNHC_6H_4$	H	H	B	81	$C_{10}H_{12}N_4O_3$	50.84	5.12	23.72	50.87	5.72	23.75	>300
561	o-$AcNHC_6H_4$	H	H	B	43	$C_{10}H_{12}N_4O_3$	50.84	5.12	23.72	50.61	5.13	23.88	200
546	n-C_3H_7	n-C_3H_7	H	B	75	$C_8H_{17}N_3O_2$	51.31	9.15	22.44	51.45	9.12	22.10	130.5–132
574	ϕCH_2CH_2	C_2H_5	H	B	74	$C_{12}H_{17}N_3O_2$	61.24	7.28	17.85	61.07	7.49	18.12	154–156
579	ϕCH_2CH_2	n-C_3H_7	H	B	68	$C_{13}H_{19}N_3O_2$	62.63	7.68	16.86	62.71	7.56	16.94	119–120
580	ϕCH_2CH_2	n-C_4H_9	H	B	88	$C_{14}H_{21}N_3O_2$	63.86	8.04	15.96	63.82	8.00	16.22	93–94
528	ϕCH_2CH_2	H	CH_3	C	60	$C_{11}H_{15}N_3O_2$	59.70	6.83	19.00	59.89	6.95	19.25	119.5–120.5
529	ϕCH_2CH_2	H	ϕCH_2	C	64	$C_{17}H_{19}N_3O_2$	68.68	6.44	14.14	69.17	6.20	14.08	158–160
541	$\phi(CH_2)_3$	H	$\phi(CH_2)_3$	A	37	$C_{20}H_{26}N_3O_2$	70.78	7.43	12.38	70.82	7.45	12.57	84–85
564	$\phi(CH_2)_2$	H	n-C_4H_9	A	55	$C_{14}H_{21}N_3O_2$	63.86	8.04	15.96	63.65	8.26	15.93	89–90
570	$\phi(CH_2)_2$	H	n-C_3H_7	A	61	$C_{13}H_{19}N_3O_2$	62.63	7.68	16.86	62.37	7.70	16.65	89–90
573	ϕCH_2CH_2	H	n-C_8H_7	A	78	$C_{18}H_{29}N_3O_2$	67.67	9.15	13.15	67.48	9.17	12.95	60–61
576	ϕCH_2	H	n-C_3H_7	A	86	$C_{12}H_{17}N_3O_2$	61.24	7.28	17.85	61.20	7.40	18.26	85–87

*A, azide method; B, nitrobiuret method; C, allophanic ester method.

TABLE II

Nitrobiurets* 

R_1, R	Decomposition point (°C)	Yield of crude product
$(CH_2)_2O(CH_2)_2$	113–115	50%
$(CH_2)_4$	107–108	Quantitative
$(CH_2)_5$	107–108	Quantitative
$(CH_2)_6$	108–110	Quantitative

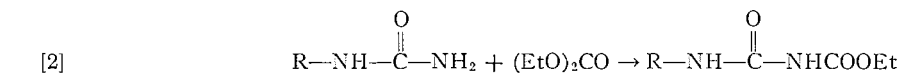
*These rather unstable compounds were used in the next step without further purification or analysis.

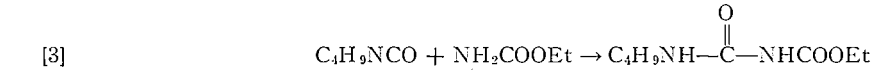
which was then hydrolyzed to the biuret (4). This method necessitates the synthesis of both the required isocyanates and isoureas, and the reported yields were low.

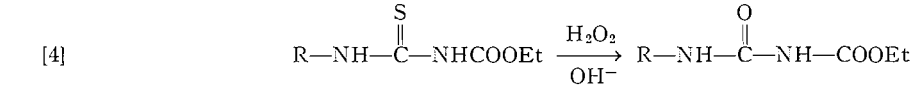
Lipschitz (6) has reported biuret to be the only product of the reaction of allophanyl azide with ammonia. We have found that 4-substituted allophanyl azides react smoothly with primary amines to yield 1,5-disubstituted biurets. In general, allophanyl azide or 4-substituted allophanyl azides react with primary or secondary amines to give high yields of the corresponding substituted biurets.

[1] 

Key intermediates required for the preparation of allophanyl azides were the corresponding allophanic esters (Table III). Three different methods of synthesis were investigated. The most convenient and generally applicable synthesis was the base-catalyzed condensation of diethyl carbonate with the appropriate substituted urea (eq. [2]) according to the procedure of a German patent (7). Ethyl 4-*n*-butylcarbamate was synthesized by the reaction of butyl isocyanate with ethyl carbamate (eq. [3]), but this method was not found to be generally applicable. A third method investigated was the oxidative desulfurization of 4-substituted-3-thioallophanic esters. Dixon and Taylor (8) reported that methyl 4,4-diphenyl-3-thioallophanate was resistant to heavy metal desulfurization. We have found that oxidative desulfurization of 4-substituted-3-thioallophanates by hydrogen peroxide (eq. [4]) worked in the case of the 4-*n*-butyl and 4-*n*-propyl derivatives, but we did not investigate the method any further since it was not as convenient as the ethyl carbonate method.

[2] 

[3] 

[4] 

The allophanic esters were then converted into hydrazides (Table IV), which were in

Can. J. Chem. Downloaded from www.nrcresearchpress.com by 210.87.254.105 on 09/05/12
For personal use only.

Can. J. Chem. Downloaded from www.nrcresearchpress.com by 210.87.254.105 on 09/05/12
For personal use only.

TABLE III

Substituted allophanates $\left(\begin{matrix} & X \\ & \| \\ RNHC—NHCOOR_1 & \end{matrix}\right)$

R	X	R_1	Method of preparation*	Yield (%)	Melting point (°C)	Formula	Analyses (%) Calcd. C	H	N	S	Found C	H	N	S
C_2H_5	O	C_2H_5	A	74	74–75†	$C_6H_{12}N_2O_3$	—	—	—	—	—	—	—	—
n-C_3H_7	O	C_2H_5	A, C	57,53	75–77	$C_7H_{14}N_2O_3$	48.26	8.10	16.09	—	47.80	8.27	15.95	—
n-C_3H_7	S	C_2H_5	D	38	45–46	$C_7H_{14}N_2O_2S$	44.16	7.41	14.72	16.85	43.70	7.39	14.37	16.78
n-C_4H_9	O	CH_3	B	50	69–70	$C_7H_{14}N_2O_3$	48.26	8.10	16.09	—	47.98	8.47	15.81	—
n-C_4H_9	O	C_2H_5	A, B, C	77, 54, 34	61	$C_8H_{16}N_2O_3$	51.04	8.56	14.89	—	51.31	8.42	15.09	—
n-C_4H_9	S	C_2H_5	D	40	38–39	$C_8H_{16}N_2O_2S$	47.03	7.90	13.72	15.70	47.03	7.76	13.57	15.91
ϕCH_2CH_2	O	C_2H_5	A	57	90	$C_{12}H_{16}N_2O_3$	60.98	6.83	11.86	—	60.76	6.92	11.75	—
ϕCH_2CH_2	S	CH_3	D	27	109–110	$C_{11}H_{14}N_2O_2S$	55.43	5.92	11.76	13.45	55.59	5.77	12.03	13.59
ϕCH_2CH_2	S	C_2H_5	D	65	92–93	$C_{12}H_{16}N_2O_2S$	57.12	6.39	11.11	12.71	56.86	6.22	11.24	12.89
$\phi(CH_2)_3$	O	C_2H_5	A	62	76.5–77	$C_{13}H_{18}N_2O_3$	62.38	7.25	11.19	—	62.43	7.27	11.01	—

*A, ethyl carbonate method; B, isocyanate method; C, oxidative desulfurization method; D, method of Elmore and Ogle (9).
†Literature (12) m.p. 72°.

turn converted into the corresponding azides (Table V). The crude azides were sufficiently pure for conversion into biurets as described above.

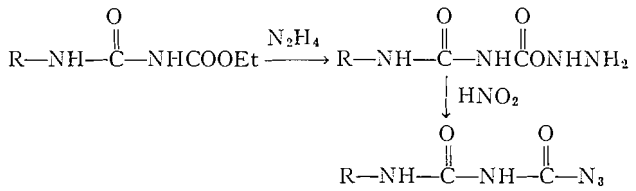
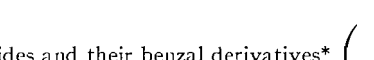
[5] 

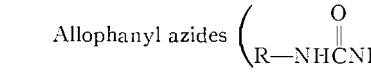
TABLE IV

Allophanyl hydrazides and their benzal derivatives* 

R	Yield (%)	Melting point (°C)	Formula	Analyses (%) Calcd. C	H	N	Found C	H	N
C_2H_5	78	146–147	$C_4H_{10}N_4O_2$	32.86	6.90	38.32	33.12	7.00	38.43
n-C_3H_7	70	154–155	$C_5H_{12}N_4O_2$						
		166–169	$C_{12}H_{16}N_4O_2$*	58.03	6.50	22.56	57.70	6.64	22.47
n-C_4H_9	70	154–155	$C_6H_{14}N_4O_2$	41.37	8.10	32.17	41.47	7.84	31.99
ϕCH_2CH_2	71	153	$C_{10}N_{14}N_4O_2$	54.04	6.35	25.22	53.96	6.74	25.36
$\phi(CH_2)_3$	77	146–146.5	$C_{11}H_{16}N_4O_2$						
		141–142	$C_{18}H_{20}N_4O_2$*	66.65	6.22	17.28	66.83	6.35	17.47

*Benzal derivatives were prepared in cases where a good analysis was not obtainable on the hydrazide.

TABLE V

Allophanyl azides 

R	Yield (%)	Melting point (°C)	Formula	Analyses (%) Calcd. C	H	N	Found C	H	N
C_2H_5	80	119–124	$C_4H_7N_5O_2$	30.58	4.49	44.59	30.75	4.78	44.74
n-C_3H_7	80	90–98	$C_5H_9N_5O_2$	35.08	5.30	40.92	35.28	5.25	41.17
n-C_4H_9	78	85–91	$C_6H_{11}N_5O_2$	38.90	5.99	37.82	38.88	6.09	38.15
ϕCH_2CH_2	94	153–155	$C_{10}H_{11}N_5O_2$	51.48	4.75	30.03	51.51	5.05	29.67
$\phi(CH_2)_3$	94	95–97	$C_{11}H_{13}N_5O_2$	53.42	5.30	28.32	53.35	5.25	28.08

EXPERIMENTAL

Melting points are uncorrected. Microanalyses were carried out by C. Daessle, 5757 Decelles, Montreal.

4-Substituted Allophanic Esters

The synthesis of ethyl 4-*n*-butylallophanate by the three methods used is given by way of illustration.

Ethyl 4-n-Butylallophanate

Procedure A.—N-Butylurea (7.3 g, 0.046 mole) and diethyl carbonate (5.9 ml, 0.048 mole) were added to a solution of 1.05 g (0.046 mole) sodium in 25 ml of absolute alcohol. After the solution was refluxed for 45 min it was evaporated to near dryness. The residue was dissolved in water and the aqueous solution was acidified with acetic acid, causing an oil to separate which soon solidified. The precipitate was filtered, and when water was added to the filtrate a second crop of product was obtained. The total yield of crude product was

Can. J. Chem. Downloaded from www.nrcresearchpress.com by 210.87.254.105 on 09/05/12
For personal use only.

5.2 g (77%), m.p. 54–60°. Recrystallization from *n*-hexane yielded a product, m.p. 60–61°, whose infrared spectrum was identical with that of the analytical sample.

Procedure B.—A mixture of 89 g (1 mole) of ethyl carbamate, 99 g (1 mole) of *n*-butyl isocyanate, and 5 drops of triethylamine was heated on the steam cone overnight. The cooled solid residue was recrystallized twice from *n*-hexane to yield 103 g (54%) of ethyl 4-*n*-butylallophanate, m.p. 55–61°. Repeated recrystallization from *n*-hexane gave the analytical sample, m.p. 61°; ν_{max}^{Nujol} 3 330, 1 730, and 1 710 cm^{-1}.

Procedure C.—To a mixture of ethyl 4-*n*-butyl-3-thioallophanate (3 g, 0.015 mole) prepared according to the procedure of Elmore and Ogle (9), 5 ml of concentrated ammonia, and 50 ml of alcohol in a three-necked flask was added 7 ml of 30% hydrogen peroxide at such a rate that the temperature was prevented from rising above 30°. After the mixture was stirred for 2 h it was made acidic with hydrochloric acid. When the solution was concentrated and cooled 1.2 g of crude product was obtained. One recrystallization from alcohol yielded 0.95 g (33.5%) of ethyl-4-*n*-butylallophanate, m.p. 57–60°, whose infrared spectrum was identical with that of the analytical sample.

Allophanyl Hydrazides

The 4-substituted allophanyl hydrazides (Table IV) were prepared according to the procedure of Audrieth and Gordon (10). Analytical samples were prepared by careful recrystallization from low-boiling solvents such as methanol–water or methylene chloride – hexane.

Allophanyl Azides

The 4-substituted allophanyl azides (Table V) were prepared according to the procedure of Audrieth and Gordon (10).

Substituted Biurets

1-Benzyl-5-n-propylbiuret (Azide Method)

A mixture of 10.7 g (0.1 mole) of benzylamine and 17.1 g (0.1 mole) of 4-*n*-propylallophanyl azide in 150 ml of benzene was stirred for 30 min at room temperature. The mixture was then heated to reflux on the steam cone. After evaporation of the solvent under reduced pressure the residue was recrystallized from water–alcohol to yield 20.2 g (86%) of 1-benzyl-5-*n*-propylbiuret, m.p. 85–87°.

Nitrobiuret Method

These biurets were prepared by the reaction of amines with nitrobiuret or a 1,1-disubstituted-5-nitrobiuret according to the procedure of Davis and Blanchard (2) as modified by Dunnigan and Close (11).

1-Methyl-5-phenethylbiuret (Allophanic Ester Method)

Methyl 4-phenethylallophanate (5 g, 0.0225 mole) was heated with an excess of anhydrous methylamine at 120–125° for 3 h in a Parr pressure reaction apparatus. After the solution was cooled, the excess amine was evaporated and the residue was recrystallized from methanol–water to yield 3.0 g (60%) of 1-methyl-5-phenethylbiuret, m.p. 105–110°.

Two recrystallizations from methanol–water gave the analytical sample, m.p. 119.5–120.5°.

1,1-Disubstituted-5-nitrobiurets

These derivatives (Table II) were prepared according to the procedure of Davis and Constan (3).

ACKNOWLEDGEMENT

The assistance of Mr. Brine Kirk is gratefully acknowledged.

1. J. D. McColl, F. L. Chubb, C. F. Lee, A. Hajdu, and J. Komlossy. J. Med. Chem. **6**, 584 (1963).
2. T. L. Davis and K. C. Blanchard. J. Am. Chem. Soc. **51**, 1801 (1929).
3. T. L. Davis and N. D. Constan. J. Am. Chem. Soc. **58**, 1800 (1936).
4. F. H. S. Curd, D. G. Davey, and D. N. Richardson. J. Chem. Soc. 1732 (1949).
5. F. Kurzer. Chem. Rev. **56**, 95 (1956).
6. W. L. Lipschitz. J. Am. Chem. Soc. **66**, 658 (1944).
7. C. Diehl. Ger. Patent No. 427,417 (April 8, 1926).
8. A. E. Dixon and J. Taylor. J. Chem. Soc. **93**, 697 (1908).
9. D. T. Elmore and J. R. Ogle. J. Chem. Soc. 1961 (1960).
10. L. F. Audrieth and P. G. Gordon. J. Org. Chem. **20**, 244 (1955).
11. D. A. Dunnigan and W. J. Close. J. Am. Chem. Soc. **75**, 3615 (1953).
12. M. C. Mauguin. Ann. Chim. Paris, **22**(8), 297 (1911).

Received November 9, 1965.
Research Laboratories,
Frank W. Horner Limited,
Montreal, Quebec.

Can. J. Chem. Downloaded from www.nrcresearchpress.com by 210.87.254.105 on 09/05/12
For personal use only.

ERRATUM: PROTON MAGNETIC RESONANCE SPECTRA OF D-GLUCOPYRANOSE POLYMERS

C. A. GLASS

(Ref. Can. J. Chem. 43, 2652 (1965))

On page 2659, line 9, the worker referred to as Hybil should read Albert Hybl.

NORTHERN REGIONAL RESEARCH LABORATORY,
U.S. DEPARTMENT OF AGRICULTURE,
PEORIA, ILLINOIS.

Canadian Journal of Chemistry. Volume 44 (1966)

Can. J. Chem. Downloaded from www.nrcresearchpress.com by 210.87.254.6 on 09/05/12
For personal use only.

Can. J. Chem. Downloaded from www.nrcresearchpress.com by 210.87.254.105 on 09/05/12
For personal use only.

Canadian Journal of Chemistry

Issued by THE NATIONAL RESEARCH COUNCIL OF CANADA

VOLUME 44 APRIL 15, 1966 NUMBER 8

ELECTRICAL PROPERTIES AND STRUCTURES OF SOLID AND LIQUID GeS, SnS, AND PbS[1]

G. HANDFIELD, M. D'AMBOISE, AND M. BOURGON

Department of Chemistry, Université de Montréal, Montreal, Quebec

Received November 2, 1965

ABSTRACT

The electrical conductivity of germanium(II) sulfide in the liquid state has been measured with a capillary-type cell. Both a-c. and d-c. methods were used. The conductivity of liquid GeS increases regularly with temperature from 1.33 Ω^{-1} cm^{-1} at 664 °C to 2.52 Ω^{-1} cm^{-1} at 705 °C. The experimental facts lead to the conclusion that GeS remains a semiconductor in the liquid state with a conduction band situated at 2.5 eV above the valence band.

The energy gaps of GeS, SnS, and PbS in the solid state are compared with those of the corresponding liquids. It is concluded that these sulfides, in the liquid state, have structures very similar to that of the solids. Liquid PbS has a structure somewhat similar to that of metals. In the case of SnS and GeS, heating and melting are accompanied by a gradual loosening of the double layers which constitute the crystals. Accumulated evidence indicates that the molecular character of SnS and GeS is increased on going from the solid to the liquid state.

INTRODUCTION

Work done in recent years (1–3) has established beyond any doubt that semiconduction can be a property of liquids and glasses as well as of solids. This experimental evidence has led to the view that the existence of energy bands is to be considered as a general property of substances in a condensed state, the structure of the bands and the width of the forbidden energy gaps being determined by the short-range order (1, 4, 5). By short-range order is meant the relative disposition around an atom of its nearest neighbors and the nature of the chemical bonds between these atoms.

It should thus be possible to obtain information, qualitative at least, about the structural changes which a solid undergoes on melting by a study of the electrical properties of substances in both the solid and liquid states. That this is the case has been shown by Ioffe and Regel (1) and other workers.

The present paper reports on the electrical properties of germanium(II) sulfide GeS in the liquid state and from this, and other available data, attempts to establish a correlation between the structures of the sulfides of the fourth group elements GeS, SnS, PbS in the solid state and their structures in the liquid state.

EXPERIMENTAL

Preparation of GeS

Three methods of preparation of GeS were investigated: precipitation from aqueous solutions of $GeCl_2$ by H_2S, high temperature reaction between GeO_2 and H_2—H_2S mixtures, and high temperature synthesis from the elements. The first method proved to be tedious and gave a product of doubtful purity. Although good crystals were obtained by the second method, the third method was finally adopted because of its convenience and simplicity. Quantitative yields were also obtained by this method.

[1]*This paper was presented in part at the 48th Annual Conference, Chemical Institute of Canada, Montreal, Quebec, June 1965.*

The germanium was obtained in powder form by hydrogen reduction of high purity GeO_2 (Sylvania Corporation). Sublimed sulfur was used. The elements reacted in Pyrex vials at 375–410 °C under vacuum. Spectrographic analysis of the final product showed traces of silicon as the only contaminant. Repeated vacuum sublimation of the sulfide eliminated this impurity.

Germanium(II) sulfide obtained under the above conditions has a metallic appearance (the powder is black), cleaves very easily to give very thin red crystals, and melts at 665 °C. X-ray powder patterns of the sublimed product were taken (114.8 mm camera, Cu radiation, Ni filter); these were strictly identical with the known X-ray powder pattern of GeS (6). Chemical analyses of the product were performed to determine possible deviations from stoichiometric proportions. This proved to be impossible. The deviations, if any, are within the experimental errors of the analytical methods.

The Conductivity Cell

The cell used for measuring the electrical conductivity was a four-terminal capillary-type cell and is shown in Fig. 1. Because of the high vapor pressure of liquid GeS, a closed cell must be used. It is made entirely of Vycor tubing. Contacts to the melt are made by means of machined high purity (AUC grade National Graphite) graphite plugs fitted into female standard joints. Necessary connections to the graphite are made by means of chromel wires held in the bottom of the wells by copper sleeves. The potential probe wires and the current wires are protected by double-bore insulated sheathing. Since preliminary measurements had shown that the resistance of GeS is rather high and since the resistance of graphite is quite low in comparison, the depth of the wells is not critical. The capillary bore is 1 mm and its length is approximately $1\frac{1}{4}$ in.

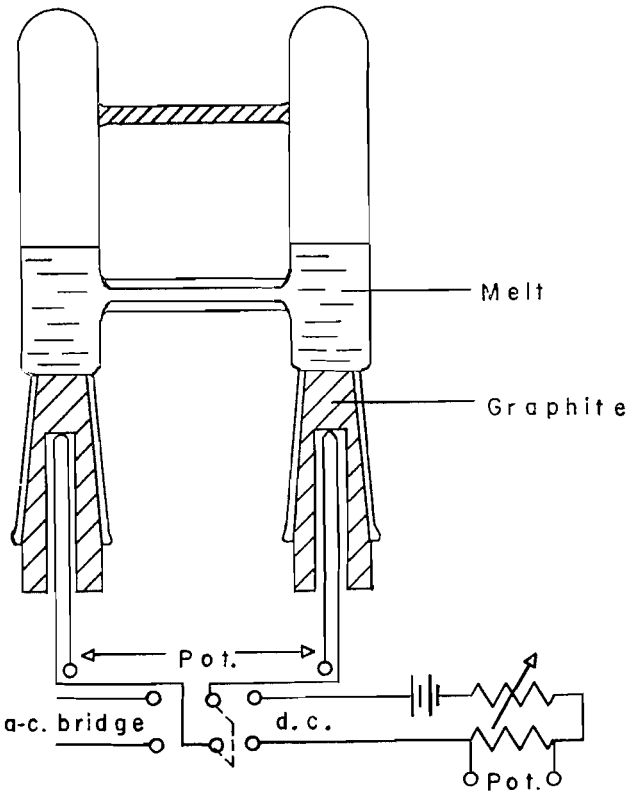


FIG. 1. Cell used for measuring the specific conductivity of GeS in the liquid state.

The cell was enclosed in a steel casing connected to ground and surmounted by steel radiation shields. Temperature measurements were made with uncalibrated chromel–alumel thermocouples suitably protected and located at a distance of 1 in. from the cell. The whole assembly was enclosed in a 4 in. × 1/2 in. × 30 in. gas-tight Rotosil fused silica tubing closed at one end and fitted at the other end with a cooling head. This head allowed passage of the necessary electrical connections and also permitted the introduction of special atmospheres in the furnace tube or the evacuation of the latter. This tube was heated by a Globar furnace

Can. J. Chem. Downloaded from www.nrcresearchpress.com by 210.87.254.105 on 09/05/12
For personal use only.

controlled by a Celectray Indicating Potentiometer Controller. The constant temperature section of the furnace was approximately 8 in. long. The maximum temperature drift in the constant temperature section of the furnace was ±0.5 °C per day. The furnace was mounted on rockers to provide thorough mixing of the sample.

The cells were calibrated at 25 °C by mercury and d-c. methods. The resistance of the graphite proved to be significant; for this reason the graphite plugs were replaced, for calibration purposes, by rubber stoppers through which copper wires were inserted. These calibrations were checked by further calibrations with KCl solutions, H_2SO_4 (30.4%) solutions, and a-c. methods. In the last case, the rubber stoppers were covered with a layer of mercury which in turn was covered with the solution used for calibration. All these measurements agreed extremely well. A typical value of the cell constant is 215 ± 0.5 cm^{-1}.

Resistance Measurements

To detect polarization effects in the cell, both d-c. and a-c. measurements were made. With the d-c. method, potential drops were measured across the potential probes of the cell, and across a precision resistor (Guildline Multiple Standard Resistor type 9200) in series with the cell, with a high precision potentiometer (Honeywell 2781). By this method the lead resistances are eliminated. The a-c. measurements were made by means of an a-c. bridge (10 to 20 000 c.p.s.) provided with an amplifier and an oscillograph as detector. The resistance of the leads was duly accounted for. All measurements were made under a purified helium atmosphere.

RESULTS

The results are shown graphically in Fig. 2, where the natural log of the specific conductivity is plotted against the inverse of the absolute temperature. The following experimental details are pertinent:

(*a*) No polarization effects could be detected; a-c. measurements (400 to 1 000 c.p.s.) and d-c. measurements agreed very well. For this reason, a-c. measurements were discontinued after some time and the reported results are those obtained from d-c. measurements.

(*b*) After each d-c. measurement, the polarity was reversed and the reading repeated to detect possible thermoelectric effects. The maximum difference observed between two such measurements was 0.2 Ω (out of a total of approximately 100 Ω), which gives a negligible error in the value of the specific conductivity.

(*c*) At the start of a run, after the sulfide had melted, it took several days for equilibrium to be attained. No final readings were taken until consecutive measurements, made after repeated mixing of the sample, gave identical results. After the initial equilibration period, the technique of measurement adopted was to increase the temperature to a given value and make repeated measurements until reproducibility of the readings indicated that thermal equilibrium had been established. The temperature was periodically lowered during the measurements and other readings taken to insure that the melt had undergone no change, decomposition or otherwise, during the heating. No such change could be detected and the measurements were quite reproducible.

(*d*) The cells often broke during the measurements; this was caused by the expansion of the graphite plugs. The results reported in this paper are those obtained during a good run where no breakage was experienced. Although a second complete run could not be achieved, sufficient results were obtained to insure that the reported data are reliable. The maximum error in the absolute values of the conductivity is believed to be 1.5%; this error is mainly due to the uncalibrated chromel–alumel thermocouples.

The specific conductivity of liquid GeS as determined in this work follows the exponential law:

$$\sigma = A \exp(-E/RT).$$

The absence of polarization effects in the melt, the exponential dependance of the conductivity on the temperature, and the positive temperature coefficient of conductivity

Can. J. Chem. Downloaded from www.nrcresearchpress.com by 210.87.254.105 on 09/05/12
For personal use only.

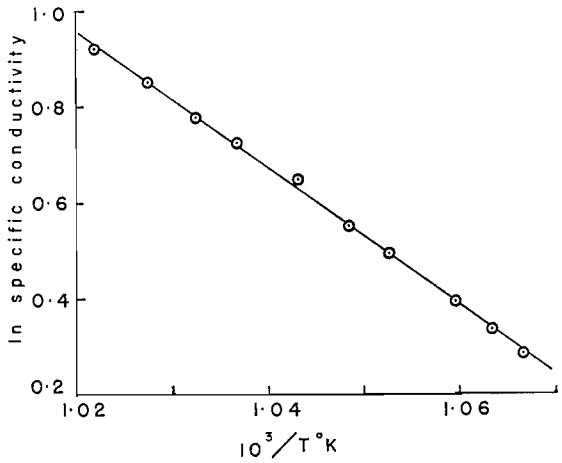


FIG. 2. Specific conductivity of liquid GeS as a function of temperature.

allow the conclusion that GeS remains a semiconductor in the liquid state in the temperature range considered. This is to be expected since other sulfides of the fourth group elements, SnS and PbS, have been reported to be a semiconductor and a metallic conductor respectively in the liquid state.

If a hole-electron equilibrium is assumed in the GeS melt, the above expression takes the form

$$\sigma = A \exp(-E_g/2RT),$$

where the value of E_g, the width of the energy gap for intrinsic conduction, has been calculated from the slope of the curve in Fig. 2 to be 2.47 $\pm$ 0.05 eV.

The only other reported values of the specific conductivity of liquid GeS are those of Velikanov (7) who found 0.02, 0.05, and 0.1 Ω^{-1} cm^{-1} at 600, 700, and 800 °C. The author states, however, that "these values are to be considered as very approximate".

DISCUSSION

The electrical conductivity of liquid SnS has been studied by Bourgon and Boutin (8) and also by Velikanov (7). The former authors reported specific conductivity values of 24 to 33.4 Ω^{-1} cm^{-1} in the temperature range 895–937 °C. From these results the value of the forbidden energy gap is calculated to be 1.7 eV. They also observed the partial dissociation of SnS at approximately 938 °C and for this reason did not extend their measurements beyond this temperature. Velikanov reports specific conductivity values of 19 to 54.6 Ω^{-1} cm^{-1} in the temperature range 885 to 1 138 °C. Examination of his results shows that there is a change in the slope of the (log σ vs. $1/T$) curve at approximately 950 °C which would seem to confirm the dissociation mentioned above. This change of slope corresponds to a decrease in the calculated energy gap from 1.3 to 1.05 eV. This decrease is consistent with a more metallic nature due to an excess of metal in the melt. Since it is believed that the work of Bourgon and Boutin was performed under more rigorous conditions, more weight is given to their value of the energy gap and the latter can be taken to be 1.7 eV in the temperature range close to the melting point.

Velikanov (7) also studied the electrical conductivity of liquid PbS. The data show that the conductivity decreases steadily from a maximum of approximately 110 Ω^{-1} cm^{-1}

Can. J. Chem. Downloaded from www.nrcresearchpress.com by 210.87.254.105 on 09/05/12
For personal use only.

in the vicinity of the melting point to 97 Ω^{-1} cm^{-1} at 1 200 °C. The negative temperature coefficient of conductivity is interpreted by the author as being indicative of metallic conduction. The value of the conductivity, however, is several orders of magnitude lower than the value typical of metals. It is quite possible therefore that PbS remains a semiconductor in the liquid state, the energy gap being very small, i.e. close to zero.

TABLE I

Energy gaps (eV) of GeS, SnS, and PbS in the solid and liquid states

	E_g(solid)				E_g(liquid)	
	Optical	References	Thermal	References	Thermal	References
GeS	1.8	(9, 11)	1.5	(9, 10)	2.47	This paper
SnS	1.1	(13)	1.2	(12)	1.7	(7, 8)
PbS	0.22	(22)	0.37	(14)	0	(7)

The energy gaps of liquid GeS, SnS, and PbS are compared in Table I with the energy gaps for intrinsic conduction of the corresponding solids. The onset of intrinsic conductivity in these solids takes place at temperatures below 300 °C and, in general, the conductivity has not been studied at temperatures greater than 500 °C except in the case of SnS (12).

Mooser and Pearson (4) have pointed out the trend in the energy gaps of the group V elements As, Sb, and Bi where the atoms are arranged in double layers (Strukturbericht A7) each atom having three nearest neighbors in its own double layer and three next nearest neighbors in the adjacent double layer. As the atomic number increases the distance between the different double layers decreases in such a way that the ratio of the distances between the nearest and next nearest neighbors approaches unity. At the same time the bond angles approach 90°. The limiting case in which the ratio of the bond lengths is 1 and the bond angles are 90° correspond to a NaCl type of structure. Thus, strong interaction between the layers leads to a metallic-type conductivity (Bi is metallic, Sb is either a metal or a semiconductor with a low energy gap), whereas weak interaction increases the molecular character (As is a semiconductor).

A similar situation prevails among the group VI elements Se, Te, and Po. Selenium and tellurium have chain structures (Strukturbericht A8) in which the ratio of the bond length inside the chains to the bond length between the chains increases from Se to Te; this increase is accompanied by a decrease of the energy gaps from 1.6 to 0.34 eV. Polonium is a metal and crystallizes with a coordination number of 6. When selenium melts the resistance increases (1, 15) as the energy gap increases to 2.31 eV. This has been interpreted as corresponding to a loosening of the bonds between the chains, this loosening having the effect of increasing the bond strength inside the chains and thus increasing the energy gap. The fact that selenium easily forms a glass on rapid cooling is consistent with the presence of a chain structure in the melt. Liquid tellurium has a chain structure (1, 16) near the melting point but the chains are destroyed on further heating to give a metallic melt. The process of fusion, in this case, is accompanied by a sudden rise in the conductivity.

The behavior of the solid sulfides GeS, SnS, and PbS is quite similar to that of the above substances. It is to be expected that the structures of these group IV–VI compounds will be related to the structures of the group V elements. This is indeed the case. PbS crystallizes in the NaCl arrangement, whereas GeS and SnS have layer-type structures

Can. J. Chem. Downloaded from www.nrcresearchpress.com by 210.87.254.105 on 09/05/12
For personal use only.

Can. J. Chem. Downloaded from www.nrcresearchpress.com by 210.87.254.105 on 09/05/12
For personal use only.

(Strukturbericht B29) reminiscent of the structure of the group V elements. That the interaction between the double layers decreases steadily from PbS to GeS is shown by the fact that GeS cleaves much more easily than SnS or PbS in a direction perpendicular to the layers. This decrease in the interlayer binding is accompanied by an increase in the value of the energy gap (see Table I).

It is interesting to compare the energy gaps of the solid sulfides with those of the corresponding liquids to obtain information on the change of structure which accompanies melting. It may be argued that no such comparison can be made, since the energy gaps of the solids were determined in a temperature range quite lower than the melting point. Solid state transformations in the upper temperature range could lead to significant changes in the values of the energy gaps. This objection is quite valid, but we believe that a correlation can be established between the structures of the solids and those of the corresponding liquids by reasoning along the following lines.

Solid state transformations in the higher temperature region have been reported for GeS, SnS, and the related compound SnSe. Dembovskii *et al.* (17) have shown that SnSe suffers a transformation of the second order, the "λ" point being situated at 540 °C. This transformation is not accompanied by a phase change, but gives rise to an anomalous Hall resistance. In the same manner, Orr and Christensen (18) have detected a minor transformation in SnS at 602 °C, while studying the heat content – temperature curve of this compound. The anomalous Hall effect reported for SnS (13) at high temperature is probably related to this change. Examination of the recently reported phase diagram of the Ge—S system (19) reveals a solid state transformation at 590 °C. In view of the fact that GeS, SnS, and SnSe are isostructural it has been suggested (17, 19) that the observed transformations are all of the second order. No such change, to our knowledge, has been reported for PbS or the related compounds PbSe and PbTe (20).

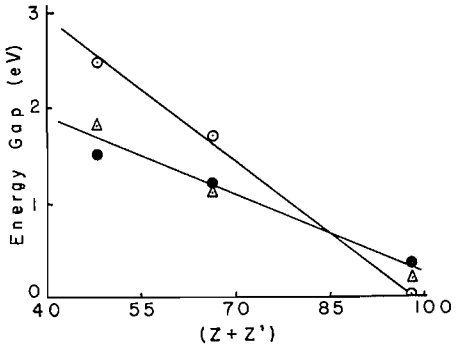


FIG. 3. Energy gap as a function of the sum of the atomic numbers of the elements in GeS, SnS, and PbS. (●) Solid (thermal), (△) solid (optical), (○) liquid.

Examination of the data in Table I reveals clearly that the energy gaps of the liquid sulfides increase regularly in a manner similar to that of the solid sulfides. The close similarity between the two trends is indicated further in Fig. 3 where the values of the energy gaps of the solids and the liquids are plotted as a function of $(Z + Z')$, the sum of the atomic numbers of sulfur and the metal in a given sulfide ($Z = 16$ is merely an additive constant for sulfides, but $Z + Z'$ is used in order to conform to usage). The value $(Z + Z')$ was chosen for comparison since this parameter has been used by some authors

(21) as a measure of the polarity of bonds and appears, together with electronegativity data, in empirical equations used for calculating values of energy gaps of solid semiconductors.

The fact that the liquid sulfides are semiconductors indicates that there must be one, two, or three dimensional continuity in the melts. This fact and the experimental evidence given above indicate that there is no essential difference between the structures of the solid sulfides and those of the corresponding liquids in the temperature range considered. In the case of PbS, all bonds are equivalent and the lower energy gap of the liquid is due to a more "chaotic" type of short-range order. In the case of SnS and GeS the transition to the liquid state is accompanied by a gradual loosening of the double layers. This loosening of the layers may well begin in the solids and is perhaps related to the minor transformations mentioned above. The absence of such transformations in PbS corroborates this view. There is probably some interaction between the layers in liquid SnS, whereas in GeS this interaction is much weaker. This conclusion is based on the high value of the energy gap of liquid GeS and on the following experimental facts.

Goryunova and Kolomiets (3) have examined the problem of vitrification in the sulfur-group compounds of phosphorus, arsenic, antimony, and bismuth. From this work, they concluded that a necessary condition for vitrification is the existence of covalent bonding in the material both in the solid state and also in the liquid state. If these covalent bonds become more metallic this would make vitrification more difficult, and if the process continued too far it would, in the limit, prevent vitrification altogether. It has been observed in our laboratory that GeS can form a reddish glass when quenched from the liquid state. To our knowledge, SnS and PbS have no glass-forming properties.

Examination of the phase diagrams of the Ge—S (19), Sn—S (20), and Pb—S (20) systems reveals that Pb and PbS show complete miscibility in the liquid state, whereas Sn and SnS show light miscibility and Ge and GeS show very light miscibility. This is to be expected if the molecular character of the melt increases from PbS to GeS. It is significant that the related compounds SnTe, PbSe, and PbTe which crystallize in the NaCl structure and give highly conducting melts show complete or high miscibility with the respective metals in the liquid state (20). SnSe on the other hand is isostructural with GeS and SnS and the phase diagram reveals light miscibility of Sn with SnSe (20).

Mention should be made finally of the change in conductivity on melting these sulfides. Accurate information on this point is difficult to obtain experimentally. It was nevertheless observed during the course of this work that there is no sudden change in the value of the conductivity of GeS on freezing the melt. While Bourgon and Boutin (8) reported a slight increase in the value of the conductivity of SnS on melting, Anderson and Morton (12) observed no such change. According to these authors there is no discontinuity in the conductivity on going from the solid to the liquid state. These facts give support to the suggestion that there is very little change on melting.

ACKNOWLEDGMENTS

The financial support of the National Research Council of Canada is gratefully acknowledged. One of us (G. H.) wishes to thank the Ministère de l'Education de la Province de Québec for assistance in the form of a bursary. Thanks are due also to Prof. Guy Perreault of the Ecole Polytechnique for determining the X-ray diagrams and to Prof. Raymond Bélair of the Département de physique, Université de Montréal, for assistance in the spectrographic analyses.

Can. J. Chem. Downloaded from www.nrcresearchpress.com by 210.87.254.105 on 09/05/12
For personal use only.

REFERENCES

1. A. E. IOFFE and A. R. REGEL. Progr. Semicond. 4, 239 (1960).
2. B. R. SUNDHEIM. Fused salts. McGraw-Hill Book Co., New York. 1964.
3. N. A. GORYUNOVA and B. T. KOLOMIETS. *In* Modern aspects of the vitreous state. Vol. 3. *Edited by* J. D. Mackenzie. Butterworths, London. 1964.
4. E. MOOSER and W. B. PEARSON. J. Electron. **1**, 629 (1956).
5. A. I. GUBANOV. Proc. Intern. Conf. Phys. Semicond. Exeter, Eng. 1962.
6. E. SHIMZAKI and T. WADA. Bull. Chem. Soc. Japan, **29**, 294 (1956).
7. A. A. VELIKANOV. Fiz. Khim. Rasplavlen. Solei i Shlakov Akad. Nauk SSSR Ural'sk. Filial Inst. Elektrokhim. Tr. Vses. Soveshch. Sverdlovsk, 1960, 454 (1962).
8. M. BOURGON and D. BOUTIN. Can. J. Chem. **39**, 915 (1961).
9. T. YABUMOTO. J. Phys. Soc. Japan, **13**, 559 (1958).
10. C. R. BETZ. Ph.D. Thesis, Northwestern University, Evanston, Illinois. 1958. University Microfilms Inc., Ann Harbor, Michigan.
11. K. F. LIDER and L. E. SOLOV'EV. Soviet Phys.-Solid State English Transl. 4, 1102 (1962).
12. J. S. ANDERSON and M. C. MORTON. Proc. Roy. Soc. London, Ser. A, **83**, 184a (1945).
13. W. ALBERS, C. HAAS, H. J. VINK, and J. D. WASSCHER. J. App. Phys. **32**, 2220 (1961).
14. R. F. BREBRICK and W. W. SCANLON. Phys. Rev. **96**, 598 (1954).
15. H. W. HENKELS. J. App. Phys. **21**, 725 (1950).
16. A. EPSTEIN and H. FRITZSCHE. Phys. Rev. **93**, 922 (1954).
17. S. A. DEMBOVSKII, B. N. EGOROV, A. S. PASHINKIN, and Y. A. POLYAKOV. Russ. J. Inorg. Chem. English Transl. **8**, 530 (1963).
18. R. L. ORR and A. U. CHRISTENSEN. J. Phys. Chem. **62**, 124 (1958).
19. LIU CH'UN-HUA and A. S. PASHINKIN. Dokl. Akad. Nauk SSSR, **151**, 1335 (1963).
20. M. HANSEN. Constitution of binary alloys. 2nd ed. McGraw-Hill Book Co., New York. 1961.
21. J. P. SUCHET. Chimie physique des semiconducteurs. Dunod, Paris. 1962.
22. W. W. SCANLON. J. Phys. Chem. Solids, **8**, 423 (1958).

Can. J. Chem. Downloaded from www.nrcresearchpress.com by 210.87.254.105 on 09/05/12
For personal use only.

THE INHIBITED AUTOXIDATION OF STYRENE

PART V. THE KINETICS AND DEUTERIUM ISOTOPE EFFECT FOR INHIBITION BY DIPHENYLAMINE, PHENYL-α-NAPHTHYLAMINE, AND PHENYL-β-NAPHTHYLAMINE[1]

I. T. BROWNLIE[2] AND K. U. INGOLD
Division of Applied Chemistry, National Research Council, Ottawa, Canada

Received November 10, 1965

ABSTRACT

The thermal oxidation of styrene inhibited by diphenylamine, phenyl-α-naphthylamine, and phenyl-β-naphthylamine has been examined. It has been shown that the autocatalysis of the diphenylamine- and phenyl-β-naphthylamine-inhibited oxidations is probably due to a reaction between the inhibitor radical and the hydroperoxide formed in the primary step of inhibition. This reaction is too slow to produce significant autocatalysis with phenyl-α-naphthylamine under the present experimental conditions.

The primary inhibition reaction involves abstraction of the amino hydrogen since its replacement by deuterium leads to a fairly large kinetic isotope effect ($k_H/k_D \sim 3$–4).

INTRODUCTION

The previous papers in this series (1) have shown that the kinetics for the inhibition of the autoxidation of styrene by phenols can be described by the following simplified reaction scheme

[1] $$I_2 \rightarrow 2I\cdot$$

[2] $$R\cdot\ (I\cdot) + O_2 \rightarrow RO_2\cdot$$

[3] $$RO_2\cdot + RH \rightarrow ROOR\cdot H$$

[5] $$RO_2\cdot + RO_2\cdot \rightarrow \text{Inactive products}$$

[6] $$RO_2\cdot + AH \rightarrow ROOH + A\cdot$$

[7] $$RO_2\cdot + A\cdot \rightarrow \text{Inactive products}$$

where I_2 represents α,α′-azo-bis-isobutyronitrile (AIBN) which was used to initiate the oxidations, RH represents the styrene, and AH the phenolic inhibitor. The chain-breaking step of inhibition, reaction [6], undoubtedly involves abstraction of the phenolic hydrogen since the overall reaction exhibits a large kinetic isotope effect ($(k_6)_{AH}/(k_6)_{AD} \sim 10$). More complicated kinetics are observed with non-hindered phenols in tetralin and in other hydrocarbons which yield a hydroperoxide rather than a polyperoxide as the main oxidation product (2–4). The complications arise mainly from the reversibility of reaction [6] (2, 4).

[−6] $$A\cdot + ROOH \rightarrow AH + RO_2\cdot$$

In addition, A· may abstract a hydrogen atom from the hydrocarbon (3) and, with certain

[8] $$A\cdot + RH \rightarrow AH + R\cdot$$

phenols, chain termination is apparently due to the coupling of phenoxy radicals (4).

[9] $$A\cdot + A\cdot \rightarrow \text{Inactive products}$$

Although these additional reactions complicate the overall kinetics of inhibition they do not disguise the fact that reaction [6] has a large deuterium isotope effect (4).

The inhibition of autoxidation by phenols can now be said to be fairly well understood, but the situation with regard to inhibition by substituted anilines is still in an extremely confused state. In the liquid phase, most workers have reported that there was no

[1]*Issued as N.R.C. No. 8846.*
[2]*National Research Council Postdoctorate Fellow 1964–1965.*

Can. J. Chem. Downloaded from www.nrcresearchpress.com by 210.87.254.6 on 09/05/12
For personal use only.

deuterium isotope effect for inhibition (5–8) or, at best, only a very small one ~1.0–1.3 (9, 10). In contrast, Shelton and co-workers have shown that in the solid phase (styrene–butadiene polymer (11, 12) and a highly purified *cis*-1,4-polyisoprene (13)) quite significant isotope effects (up to 2.1) are readily observed. Boozer and Hammond, who first reported the absence of an isotope effect, observed that the rate of oxidation of tetralin inhibited by *N*-methylaniline (or phenol) was proportional to $[I_2]^{\frac{1}{2}}/[AH]^{\frac{1}{2}}$ (6). This was attributed to the reversible formation of a complex between AH and a peroxy radical, the complex then reacting with a second peroxy radical to give inactive products. Although a good deal of subsequent work has been interpreted on the basis of this mechanism, the half-order kinetics are in fact much more readily explained by the chain transfer reactions [−6] and [8] (2–4, 14). In this connection, Bickel and Kooyman (15) have shown that both aniline and *N*-methylaniline readily undergo reaction [8] with 9,10-dihydroanthracene at 60°. However, this reaction is much slower or does not occur with *N*-phenyl-α- and -β-naphthylamines and for these two compounds the inhibited rate is proportional to $[I_2]/[AH]$ (15).

Probably the most important development in recent years towards our understanding of the overall inhibition process with amines was the discovery by Thomas and co-workers (16–18, see also ref. 19) that stable diaryl nitric oxide radicals are produced in fairly high concentrations during inhibition with diaryl amines, i.e.,

$$[10] \qquad A\cdot + RO_2\cdot \rightarrow AO\cdot + RO\cdot$$

The nitric oxide radical stops about half as many chains as the parent amine (8). Thomas and Tolman interpreted the results of their very thorough study of the diphenylamine and diphenyl nitric oxide inhibited oxidation of cumene (8) in terms of peroxy radical – inhibitor complex formation (5, 6) since the importance of reaction [−6] was not appreciated at that time. However, later attempts by Thomas to observe such complexes directly in electron spin resonance studies of cumene oxidizing in the presence of pyridine, triphenylamine, and trialkyl amines were unsuccessful (20) and can be interpreted as throwing a very considerable doubt on the existence of peroxy radical – amine complexes.

The kinetics of the inhibition of the oxidation of styrene and tetralin by 2,4,6-tri-*t*-butylaniline has been described in a recent paper from this laboratory (21). In contrast to a similarly hindered phenol this aniline appears to undergo extensive chain transfer with styrene and with tetralin hydroperoxide so that the inhibited rate has a non-integral dependence on the $[I_2]$ and [AH] concentrations. There is a pronounced deuterium isotope effect in both substrates ($k_H/k_D \geqslant 3.0$). Since this aniline is hardly a representative amine inhibitor, we decided to examine diphenylamine (DPA), *N*-phenyl-α-naphthylamine (PAN), and *N*-phenyl-β-naphthylamine (PBN) as typical inhibitors which have been studied extensively by previous workers. Styrene was chosen as the oxidizing substrate so as to prevent or at least reduce reaction [−6]. While this work was in progress, a paper by MacLachlan was published (22) which described the reaction of diphenylamine, *N*-methylaniline, and *N*,*N*′-diphenyl-*p*-phenylenediamine with the peroxy radicals formed during the pulse radiolysis of cyclohexane and ethanol. The rate of reaction was estimated from the rate of formation of a colored product which, in the case of the phenylenediamine, was shown to be the corresponding quinodiimine as would be expected (cf. 23). The colored products from the other two amines were not identified. Although this technique is obviously of great value in providing data on the overall process of inhibition, it is a rather indirect method of studying reaction [6] since the kinetics of color formation may be only indirectly connected with the rate of this reaction. As a case in point, a deuterium isotope effect of about 3.0 was found with the phenylenediamine but none was found with

Can. J. Chem. Downloaded from www.nrcresearchpress.com by 210.87.254.6 on 09/05/12
For personal use only.

diphenylamine. However, the diphenylamine would be expected to form its nitric oxide radical rapidly at the high peroxy radical concentrations produced by pulse radiolysis ($\sim 4 \times 10^{-4}$ *M*) and an isotope effect would not necessarily be observed if the rate of color formation was connected with the subsequent destruction of this radical. The observation of a deuterium isotope effect of about 3.0 with diphenylamine in the present work (see below) provides a much more logical picture of the inhibition process than one in which the isotope effect could vary from 0 to 3 for what is after all a very minor change in the structure of the inhibitor.

EXPERIMENTAL

The apparatus and general experimental technique have been described previously (1). In the present work it was frequently necessary to measure rather small initial oxidation rates. A solution of AIBN in purified *o*-dichlorobenzene was added to a thin-walled glass bucket (maximum capacity 3 ml). This bucket was hung above the reaction vessel which contained the styrene (up to 100 ml) and diphenylamine. The suspension for the bucket could be manipulated through a ground glass joint from outside the reaction vessel system in such a way as to drop the bucket into the styrene after thermal equilibrium was achieved. The bottom of the bucket broke on contact, so that the AIBN was rapidly and thoroughly mixed with the warmed styrene and true initial oxidation rates could be quite readily obtained. In general, the styrene concentration was 7.24 mole/l, i.e., 5:1 styrene:*o*-dichlorobenzene.

The inhibited rates did not normally depend on the oxygen pressure (75–750 mm) and low rates were therefore usually measured at low pressures. However, at AIBN concentrations below about 5×10^{-4} mole/l it was necessary to make allowance for the self-initiation process in which chains are started by a direct reaction of the styrene with oxygen, the rate of this reaction naturally depending on the oxygen pressure (24).

The DPA, PAN, and PBN were recrystallized from benzene–hexane and were further purified to completely colorless materials by zone-refining. This was done to eliminate impurities since these might be more efficient inhibitors which could perhaps affect initial oxidation rates at high inhibitor concentrations.

All the work reported in this paper was done at 65 °C and all oxidation rates have been corrected for nitrogen evolution and oxygen absorption by the initiator.

RESULTS AND DISCUSSION

Autocatalysis

The diphenylamine-inhibited oxidation of styrene has a quite pronounced autocatalysis. A typical oxygen absorption curve is shown in Fig. 1, curve 1 ($[I_2] = 4.33 \times 10^{-3}$ mole/l, $[AH] = 4.33 \times 10^{-3}$ mole/l). This autocatalysis is not due to consumption of the inhibitor

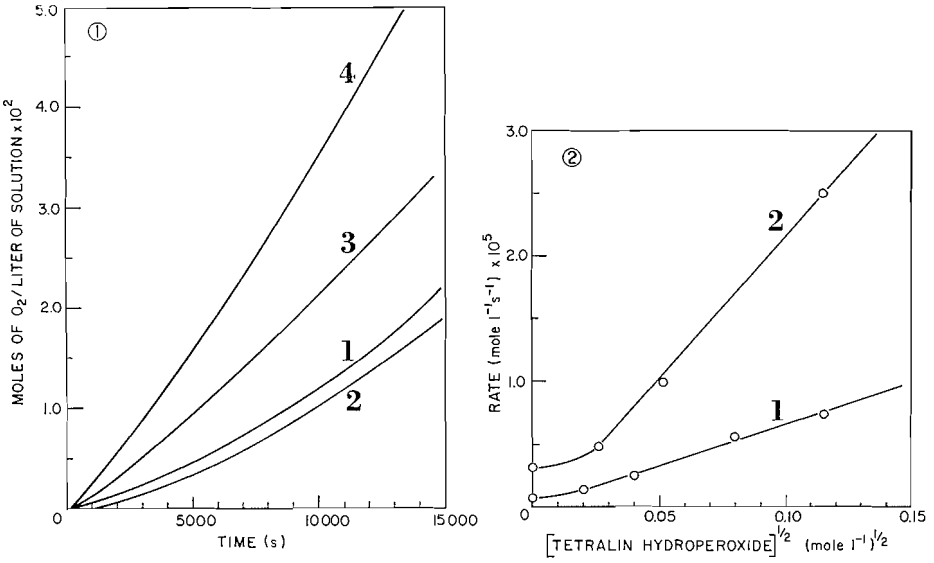


FIG. 1. Inhibited oxidation of 7.24 *M* styrene at 65 °C with 4.33×10^{-3} mole/l AIBN and 4.33×10^{-3} mole/l inhibitor. Curve 1, diphenylamine; 2, diphenylamine + H_2O; 3, diphenylamine + D_2O; 4, phenol.

FIG. 2. Inhibited oxidation rate as a function of tetralin hydroperoxide concentration with 7.24 mole/l styrene, 4.33×10^{-3} mole/l AIBN, and 4.33×10^{-3} mole/l inhibitor. Curve 1, diphenylamine; 2, phenol.

Can. J. Chem. Downloaded from www.nrcresearchpress.com by 210.87.254.6 on 09/05/12
For personal use only.

since a completely linear absorption of oxygen is observed for over 12 000 s when 2,6-di-*t*-butyl-4-methylphenol (a compound which gives simple inhibition kinetics in both styrene and tetralin (1, 4)) or phenyl-α-naphthylamine is used under identical conditions.[3] The autocatalysis observed in the phenol-inhibited oxidation of tetralin (2, 4) or cumene (2) has been shown to be due to the hydroperoxide formed in the oxidation, i.e., to reaction [−6]. A similar explanation seemed possible in the present instance since hydroperoxide will be formed both in reaction [6] and in some chain transfer reactions which are involved in the normal propagation sequence (24). If reaction [−6] occurs, the inhibited rate P should be proportional to the square root of the hydroperoxide concentration (2, 4), i.e.,

$$[I] \qquad P = \frac{ek_1k_3[RH][I_2]}{2k_6[AH]}\left\{1 + \left(1 + \frac{4k_6k_{-6}[AH][ROOH]}{ek_1k_7[I_2]}\right)^{1/2}\right\}$$

where e is the efficiency with which the AIBN initiates the oxidation.[4]

In agreement with this equation, the increase in the rate of a DPA-inhibited oxidation is found to be very roughly proportional to the square root of the amount of oxygen absorbed. This autocatalysis is not due to styrene polyperoxide since the addition of 0.2 mole/l of highly purified $[C_8H_8O_2]_n$ had very little effect on the rate of oxidation under the experimental conditions of curve 1, Fig. 1. However, the addition of tetralin hydroperoxide had a very pronounced effect on the rate and, moreover, the rate showed the expected half-order dependence on the hydroperoxide concentration (see Fig. 2). In this figure the rates at the higher hydroperoxide concentrations have been corrected to allow for chain initiation by the hydroperoxide itself (25, 26). At this temperature AIBN is about 55 times more efficient than tetralin hydroperoxide as an initiator.

Further confirmation that the autocatalysis is due to the hydroperoxide which is formed during the inhibited oxidation is provided by comparison of the measured and calculated rates after 12 000 s for curve 1, Fig. 1. Provided most of the hydroperoxide is formed in reaction [6] (which is then followed by reaction [7] or other chain-terminating steps in which hydroperoxide is not formed) then the amount of hydroperoxide produced in a given time, t, should equal half the number of reaction chains started in that time, i.e.,

$$[ROOH]_t = ek_1[I_2]t.$$

At 12 000 s, therefore,

$$[ROOH] = 0.65 \times 1.8 \times 10^{-5} \times 4.33 \times 10^{-3} \times 12\,000 = 7.2 \times 10^{-4} \text{ mole/l.}$$

If the hydroperoxide from styrene has the same effect on the rate as tetralin hydroperoxide then, from Fig. 2, this quantity of hydroperoxide should produce a rate of 1.8×10^{-6} mole/l s. This value is in perfect agreement with the measured rate at this time. This result implies that very little hydroperoxide is formed in the normal chain propagation sequence. This last conclusion is further borne out by the fact that under the experimental

[3]*Since a significant fraction of the initiator was consumed in 12 000 s, the linearity of the 2,6-di-t-butyl-4-methylphenol and PAN oxygen absorption curves implies that there is just sufficient autocatalysis to balance the loss of initiator.*

[4]*In view of the importance of reaction [10] it is possible that reaction [−6] is of less importance in determining the overall kinetics for diarylamines than for phenols. However, if reaction [10] is followed by:*

$$[-11] \qquad AO\cdot + ROOH \rightarrow AOH + RO_2\cdot$$

$$[11] \qquad RO_2\cdot + AOH \rightarrow AO\cdot + ROOH$$

then an equation that is formally similar to [I] will be obtained at long chain lengths. The referee has pointed out that in this case the k_{-6}/k_7 values given in Table I do not have quite the same meaning for the amines as for the phenols. On the other hand, if the nitric oxide radicals were mainly responsible for the autocatalysis it is difficult to see why the three amines studied in this work should show such different degrees of autocatalysis.

Can. J. Chem. Downloaded from www.nrcresearchpress.com by 210.87.254.6 on 09/05/12
For personal use only.

Can. J. Chem. Downloaded from www.nrcresearchpress.com by 210.87.254.6 on 09/05/12
For personal use only.

conditions of curve 1 ((initial rate = 7.65×10^{-7} mole/l s), pre-oxidation of the styrene with 0.25 mole/l O_2 before the addition of the diphenylamine increased the rate to only 2.3×10^{-6} mole/l s. This rate is equal to that obtained with 1.6×10^{-3} mole/l of tetralin hydroperoxide (see Fig. 2). It therefore seems likely that only $1.6 \times 10^{-3} \times 100/0.25 = 0.64\%$ of the absorbed oxygen formed hydroperoxide in the uninhibited reaction. The autocatalysis of the inhibited oxidation must arise mainly from the hydroperoxide formed in the primary inhibition process.

Since the unsubstituted phenoxy radical is known to react rapidly with hydroperoxide (2, 4) it seemed likely that phenol should also show autocatalytic behavior in styrene. Curve 4 in Fig. 1 shows that this is indeed the case although the degree of autocatalysis is rather less than for the amine under the same conditions, which probably accounts for our previous failure to observe this phenomenon (1). In Fig. 2 the phenol-inhibited rate is shown to be proportional to the square root of the added tetralin hydroperoxide concentration. The measured rate for curve 4 at 12 000 s is 4.4×10^{-6} mole/l s, in satisfactory agreement with a value of 5.0×10^{-6} mole/l s obtained from Fig. 2. Incidentally, the slope of the straight lines in this figure can be used to calculate k_{-6}/k_6k_7 (4). For phenol a value of 2.65×10^{-9} mole s/l is obtained. If k_6 is taken as 4.9×10^3 l/mole s for phenol in styrene at 65° (4), $k_{-6}/k_7 = 1.3 \times 10^{-5}$, which is rather smaller than the value of 5.15×10^{-5} obtained previously with tetralin hydroperoxide in tetralin at 65 °C (4). The lower value in styrene may be due to a decrease in k_{-6} resulting from increased hydrogen bonding between the hydroperoxide and the substrate, i.e., styrene forms stronger hydrogen bonds than aralkyl hydrocarbons with hydroxylic compounds (1). The lower extent of autocatalysis for phenol compared with diphenylamine at the same concentration may also perhaps be partly related to hydrogen bonding. That is, the more rapid oxidation with phenol will give more polyperoxide and this will tend to form strong hydrogen bonds with the hydroperoxide. For diphenylamine the results in Fig. 2 give $k_{-6}/k_6k_7 = 2.2 \times 10^{-10}$ mole s/l.

The oxygen absorption curves for the phenyl-β-naphthylamine inhibited reaction are less autocatalytic than those for DPA but more autocatalytic than those for phenol under the same conditions. The inhibited oxidation is accelerated by tetralin hydroperoxide and the rate has the expected dependence on the square root of the hydroperoxide concentration with $k_6/k_{-6}k_7 = 5.8 \times 10^{-11}$ mole s/l. Under the same experimental conditions as those used for DPA in Fig. 1, the initial PBN-inhibited rate is 3.0×10^{-7} mole/l s and the rate at 12 000 s is 6.5×10^{-7} mole/l s. The calculated rate at this time (based on a hydroperoxide concentration of 7.2×10^{-4} mole/l) is 7.3×10^{-7} mole/l s. Pre-oxidation of the styrene before the addition of the inhibitor indicated that about 0.7% of the absorbed oxygen was present as hydroperoxide.

Phenyl-α-naphthylamine was not noticeably autocatalytic under the usual experimental conditions. However, tetralin hydroperoxide did have a small accelerating effect on the inhibited reaction, k_{-6}/k_6k_7 having a value of 5.1×10^{-12} mole s/l.

Kinetics

The initial rate of the diphenylamine inhibited oxidation has been plotted in Fig. 3 as a function of the DPA concentration. At low initiator concentrations (1.3×10^{-4} mole/l) the rate is proportional to $[DPA]^{-1.0}$ but at a higher concentration (4.3×10^{-3} mole/l) this simple proportionality is only applicable to a rather limited range of DPA concentrations.[5] The decrease in order at low DPA concentrations can probably be ascribed to the

[5]*The rate over the entire DPA concentration range could be represented almost as well by a straight line of slope −0.7 as by the curve shown in Fig. 3.*

Can. J. Chem. Downloaded from www.nrcresearchpress.com by 210.87.254.6 on 09/05/12
For personal use only.

increasing importance of reaction [5] as a chain-ending process, i.e., the rate approaches a limiting value of 5×10^{-5} mole/l s as the DPA concentration approaches zero. A decrease in order at high DPA concentrations would arise if chain transfer with the styrene (reaction [8]) were important (2–4). In this case, the rate may approach a limit if chain termination occurs by reaction [9] (4) or, in theory at least (2), the rate may go through a minimum if reaction [−6] is important and chain termination occurs by reaction [7]. However, all the kinetic expressions which have so far been derived indicate that when the order in [AH] is between −1.0 and 0, then the order in $[I_2]$ will be between 1.0 and 0.5. This is not observed with diphenylamine, i.e., the rate is accurately proportional to $[I_2]^{1.0}$ over a wide range in the diphenylamine concentration (see Fig. 4). We are therefore inclined to ascribe the decrease in the kinetic order with increasing inhibitor concentration to non-ideal behavior of the diphenylamine at high concentrations, i.e., to a reduced activity coefficient for the DPA at high concentrations. However, the possibility that chain transfer contributes in a minor way to the observed behavior cannot be entirely ruled out. Moreover, there may be a contribution towards the low kinetic order from a direct chain-initiating reaction between amine and oxygen at high DPA concentrations (cf. 11–13, 27). However, such a process is probably not very important in our system since low rates were obtained in the absence of AIBN when high concentrations of DPA were added to the styrene.

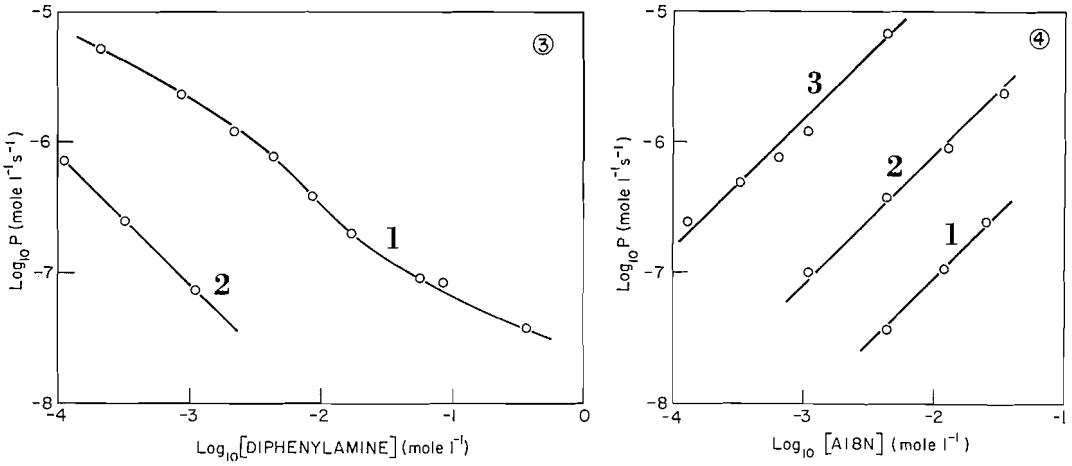


FIG. 3. Rate of oxidation of 7.24 *M* styrene initiated with AIBN as a function of the diphenylamine concentration. Curve 1, [AIBN] = 4.33×10^{-3} mole/l; 2, [AIBN] = 1.3×10^{-4} mole/l.

FIG. 4. Rate of oxidation of 7.24 *M* styrene inhibited with diphenylamine as a function of the AIBN concentration. Curve 1, 3.5×10^{-1}; 2, 8.66×10^{-3}; 3, 3.25×10^{-4} mole/l diphenylamine.

The diphenylamine-inhibited oxidation rate is first order in styrene from 7.24 to 0.72 mole/l. Under conditions where reaction [5] is completely suppressed, the overall kinetics can be represented by the simple equation (1, 4)

$$[II] \qquad P = \frac{ek_1[I_2]k_3[RH]}{k_6[AH]}$$

provided the DPA concentration is less than about 3×10^{-2} mole/l.[6] In the region where

[6]*Incidentally, the order in* [AH] *was reduced to about −0.7 by the addition of* 6×10^{-3} *mole/l of tetralin hydroperoxide. This can probably be attributed to a change from kinetics governed by eq. [II] to kinetics described by eq. [I]. It implies that the simple kinetics of eq. [II] would not be readily observed with DPA in a substrate which gave a hydroperoxide as its major oxidation product.*

this simple equation applies, the measured rates give $k_3/k_6 \approx 9.0 \times 10^{-3}$, from which $k_6 \approx 2.0 \times 10^4$ l mole^{-1} s^{-1} (taking $k_3 = 178$ l mole^{-1} s^{-1} for styrene at 65 °C (28)). This is much larger than the value of 3.3×10^2 l mole^{-1} s^{-1} at 65 °C obtained by Buchachenko *et al.* (10) for the reaction of DPA with the peroxy radicals from 2,4,6-trimethylheptane. The discrepancy may be due to the fact that trimethylheptyl peroxy radicals will be sterically more hindered than styryl peroxy radicals. In connection with our relatively high rate constant for inhibition (see Table I) it is perhaps worth pointing out that kinetic studies of the type described in this paper become more difficult as the inhibitor becomes more efficient. That is, it is necessary for a measurable amount of oxygen to be absorbed without any significant fraction of the inhibitor being used up. A very efficient inhibitor would suppress virtually all oxidation until it was completely consumed and so reaction kinetics could not be based on rates of oxygen absorption. Although this problem is not too critical for DPA in styrene, it would become important in a less readily oxidizable substrate, i.e., in a substrate for which k_3 was much smaller. The major experimental difficulty with DPA in styrene was the autocatalytic nature of the oxygen absorption curves. This necessitated the measurement of initial rates even when only a small fraction of the inhibitor was consumed during the experiment.

The kinetics described by eq. [II] seem to apply to phenyl-β-naphthylamine. That is, $P \propto [AH]^{-1.0}$ over a range from 5×10^{-4} to 2×10^{-2} mole/l PBN at AIBN concentrations of 1.3×10^{-2} and 4.3×10^{-3} mole/l. Similarly, $P \propto [I_2]^{1.0}$ over a range from 1×10^{-4} to 1×10^{-2} mole/l AIBN at a PBN concentration of 5×10^{-4} mole/l. The rate is also first order in styrene from 0.72 to 7.24 mole/l. The rate constant for inhibition is given by $k_6 = 5.0 \times 10^4$ l mole^{-1} s^{-1}. Equation [II] also applies to phenyl-α-naphthylamine over similar ranges in reactant concentrations. For this amine $k_6 = 7.0 \times 10^4$ l mole^{-1} s^{-1}.

Deuterium Isotope Effects

We have shown previously that deuterium isotope effects for reaction [6] are most easily measured by a comparison of the oxidation rates obtained with the system saturated with H_2O and with D_2O (1, 4, 21). The results of such experiments with diphenylamine as the inhibitor are shown in curves 2 and 3 in Fig. 1. The higher rate in the presence of D_2O implies that k_6 is smaller for $(C_6H_5)_2ND$ than for $(C_6H_5)_2NH$. Values of $(k_6)_H/(k_6)_D$ are given in Table I for the three amines studied in this work. Each value represents the average of at least four determinations at various initiator and inhibitor concentrations in the region where eq. [II] is valid. The isotope effect for diphenylamine contrasts with the results of MacLachlan (22) but, as was mentioned in the Introduction, the present result provides a much more logical picture of the inhibition process for amines.

The values found for k_6 are also included in Table I together with values for k_{-6}/k_7, which provides a measure of the susceptibility to autocatalysis by hydroperoxide of

TABLE I

Inhibited oxidation of styrene at 65 °C

Inhibitor	$(k_{-6}/k_6k_7) \times 10^{11}$* (mole s l^{-1})	$(k_{-6}/k_7) \times 10^5$*	$k_6 \times 10^{-3}$ (l mole^{-1} s^{-1})	$(k_6)_H/(k_6)_D$
Diphenylamine	22	0.44	20	3.0±0.5
Phenyl-β-naphthylamine	5.8	0.29	50	3.0±0.5
Phenyl-α-naphthylamine	0.51	0.036	70	4.0±0.5
2,6-Di-*t*-butyl-4-methylphenol	Very small (4)	—	17.8†	10.6 (1)
Phenol	265	1.3	4.9 (1)	~15 (1)

*With added tetralin hydroperoxide.
†Redetermined for this work.

Can. J. Chem. Downloaded from www.nrcresearchpress.com by 210.87.254.6 on 09/05/12
For personal use only.

oxidations inhibited by the three amines. The results suggest that simple first-order kinetics, eq. [II], are unlikely to be obtained with diphenylamine in any substrate in which hydroperoxide is the major oxidation product (see e.g. refs. 4–6, 8). In such a system, eq. [II] is most likely to be applicable to phenyl-α-naphthylamine (see e.g. ref. 15).

Phenols exhibit a considerably larger deuterium isotope effect in reaction [6] than is found with amines. This can probably be attributed to the fact that transfer of a hydrogen atom between two identical atoms should, in general, proceed through a transition state in which the zero-point energy of the hydrogen is lost (29). Under these conditions the isotope effect will tend to be a maximum (29). The slightly larger isotope effect found for PAN compared with the other two amines may result from some steric hindrance for hydrogen abstraction from this amine (30).

REFERENCES

1. J. A. HOWARD and K. U. INGOLD. Can. J. Chem. **40**, 1851 (1962); **41**, 1744, 2800 (1963); **42**, 1044 (1964).
2. J. R. THOMAS. J. Am. Chem. Soc. **85**, 2166 (1963); **86**, 4807 (1964).
3. L. R. MAHONEY and F. C. FERRIS. J. Am. Chem. Soc. **85**, 2346 (1963).
4. J. A. HOWARD and K. U. INGOLD. Can. J. Chem. **42**, 2324 (1964); **43**, 2724 (1965).
5. C. E. BOOZER and G. S. HAMMOND. J. Am. Chem. Soc. **76**, 3861 (1954).
6. G. S. HAMMOND, C. E. BOOZER, C. E. HAMILTON, and J. N. SEN. J. Am. Chem. Soc. **77**, 3238 (1955).
7. C. J. PEDERSEN. Ind. Eng. Chem. **48**, 1881 (1956).
8. J. R. THOMAS and C. A. TOLMAN. J. Am. Chem. Soc. **84**, 2930 (1962).
9. K. U. INGOLD and I. E. PUDDINGTON. Ind. Eng. Chem. **51**, 1319 (1959).
10. A. L. BUCHACHENKO, K. YA. KAGANSKAYA, and M. B. NEĬMEN. Kinetika i Kataliz, **2**, 161 (1961). Tr. Khim. i. Khim. Tekhnol. 4, 31 (1961).
11. J. R. SHELTON and E. T. MCDONEL. J. Polymer Sci. **32**, 75 (1958).
12. J. R. SHELTON, E. T. MCDONEL, and J. C. CRANO. J. Polymer Sci. **42**, 289 (1960).
13. J. R. SHELTON and D. N. VINCENT. J. Am. Chem. Soc. **85**, 2443 (1963).
14. W. A. WATERS and C. WICKHAM-JONES. J. Chem. Soc. 812 (1951).
15. A. F. BICKEL and E. C. KOOYMAN. J. Chem. Soc. 2217 (1957).
16. O. L. HARLE and J. R. THOMAS. J. Am. Chem. Soc. **79**, 2973 (1957).
17. J. R. THOMAS. J. Am. Chem. Soc. **82**, 5955 (1960).
18. J. C. BAIRD and J. R. THOMAS. J. Chem. Phys. **35**, 1507 (1961).
19. A. T. KORITSKII and A. F. LUKOVNIKOV. Dokl. Akad. Nauk SSSR, **147**, 1126 (1962).
20. J. R. THOMAS. J. Am. Chem. Soc. **85**, 591, 593 (1963).
21. D. V. GARDNER, J. A. HOWARD, and K. U. INGOLD. Can. J. Chem. **42**, 2847 (1964).
22. A. MACLACHLAN. J. Am. Chem. Soc. **87**, 960 (1965).
23. C. E. BOOZER, G. S. HAMMOND, C. E. HAMILTON, and J. N. SEN. J. Am. Chem. Soc. **77**, 3233 (1955).
24. A. A. MILLER and F. R. MAYO. J. Am. Chem. Soc. **78**, 1017 (1956).
25. C. WALLING and L. HEATON. J. Am. Chem. Soc. **87**, 38, 48 (1965).
26. R. HIATT, C. W. GOULD, and F. R. MAYO. J. Org. Chem. **29**, 3461 (1964).
27. W. R. YATES and J. L. IHRIG. J. Am. Chem. Soc. **87**, 710 (1965).
28. J. A. HOWARD and K. U. INGOLD. Can. J. Chem. **43**, 2729 (1965).
29. C. A. BUNTON and V. J. SHINER, JR. J. Am. Chem. Soc. **83**, 3214 (1961).
30. E. BACIOCCHI, G. ILLUMINATI, and G. SLEITER. Tetrahedron Letters, No. 23, 30 (1960).

Can. J. Chem. Downloaded from www.nrcresearchpress.com by 210.87.254.6 on 09/05/12
For personal use only.

Can. J. Chem. Downloaded from www.nrcresearchpress.com by 210.87.254.40 on 09/05/12
For personal use only.

STUDIES ON HYDROGEN–OXYGEN SYSTEMS IN THE ELECTRIC DISCHARGE

I. THE REACTIONS OF HYDROGEN ATOMS WITH HYDROGEN PEROXIDE

NORISUKE HATA[1] AND PAUL A. GIGUÈRE
Département de Chimie, Université Laval, Québec, Québec

Received September 2, 1965

ABSTRACT

Hydrogen gas partly dissociated in an electrodeless discharge was mixed downstream with hydrogen peroxide vapor at low pressure (0.1 mm Hg) in a liquid nitrogen trap. The reaction products condensed readily on the wall as a clear, yellowish glass resembling that from dissociated water vapor and other related systems. A manometric study of the warming-up process has revealed four distinct steps. The first two, in which only traces of gas are given off, look like the recombination of trapped free radicals. The major evolution of oxygen upon crystallization of the glassy deposit at 160 °K is ascribed to the decomposition of hydrogen peroxide under the influence of some unidentified species generated in the electric discharge through hydrogen. Experimental evidence for this is presented. In any case the stoichiometry cannot be reconciled with the formation of a metastable intermediate, such as the hypothetical polyoxide H_2O_4.

In the last step beginning around 215 °K more peroxide is decomposed during the eutectic melting of the solid. Qualitatively these phenomena are similar to those shown by the condensate from dissociated water vapor.

INTRODUCTION

Ever since the early investigations of Geib and Harteck (1) on the electric discharge through water vapor, considerable effort and ingenuity have been spent in attempting to elucidate the reaction occurring in this system and in other hydrogen–oxygen systems and in determining the nature of the solid products condensed therefrom; cf. ref. 2 for a review of the question up to 1961. Besides the usual techniques of chemical kinetics (3) and stoichiometry (4), a variety of physical methods have been applied to this problem, such as calorimetry (5), thermal analysis (6), magnetic susceptibility (7), electron spin resonance (8), molecular spectroscopy (4, 9), and X-ray (10) and electron diffraction (11). For all that, the situation is not completely understood, and some aspects of it, like the often postulated formation of hydrogen polyoxides (H_2O_3 and H_2O_4), are still controversial.

Previous claims for the synthesis of these hydrogen polyoxides have rested mainly on the evolution of gaseous oxygen that accompanies crystallization of the glassy condensate at 160 °K. This is particularly abundant in the system atomic hydrogen – liquid ozone (4, 12). We have suggested elsewhere (2) that the origin of this phenomenon is the decomposition of hydrogen peroxide present in the frozen condensate under the influence of some impurity introduced through the electric discharge. Accordingly, we suspected that the same effect could be reproduced, at least qualitatively, by trapping together hydrogen peroxide vapor at low pressure and a stream of hydrogen gas issuing from an electric discharge. Winkler and his co-workers (13) have shown that this same system at room temperature gives water and oxygen.

EXPERIMENTAL

The apparatus (Fig. 1) was basically the same as used before in producing deuterium peroxide (14). The inlet system was changed to take in a gas (hydrogen, Matheson, electrolytic grade) instead of a liquid (heavy water). A flowmeter, A, indicated the gas input, and the pressure was read on a mechanical manometer, B, "Molecular Vacuum Gage" (General Electric Model No. C-148 388). An aneroid manometer, C,

[1]*National Research Council Postdoctorate Fellow, 1962–1964.*

(Wallace and Tiernan, No. FA-141) served to follow the evolution of gas on warming. The effective "load" in the discharge was measured with a wattmeter in the output tank circuit of the r.f. generator. The useful range extended from a maximum of 500 W down to 300 W, at which point the discharge became unstable. A rough calibration of the wattmeter had already been made by visual comparison of the light intensity of a pair of 500 W electric bulbs, one of which was excited by the r.f. discharge. The efficiency of this type of discharge in dissociating water vapor has been discussed elsewhere (15). Since it was not essential for our purpose to know the concentration of hydrogen atoms in the discharged gas stream, no attempts were made to measure it. Here are a few relevant data (for the larger input, 26 mmoles H_2 h^{-1}): rate of flow, 75 cm s^{-1}; volume of gas put through, 1.1 l s^{-1} at the operating pressure of 0.1 mm Hg. Although the discharge was concentrated mainly inside the r.f. coil, the red glow of the Balmer lines extended all the way down the cold trap. No coating was used on the inner wall of the Pyrex discharge tube to avoid contamination of the peroxide.

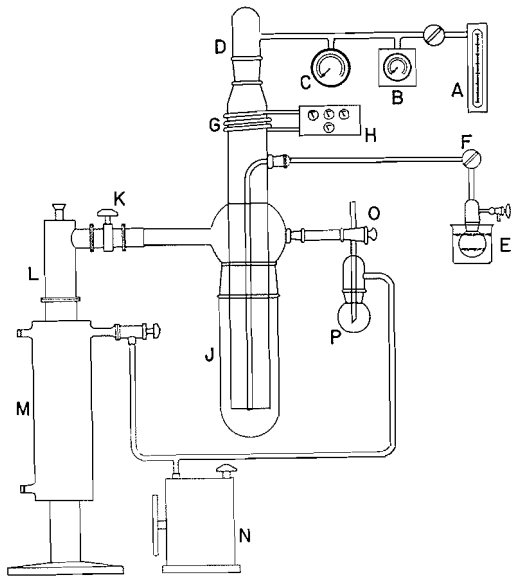


FIG. 1. Diagram of the electric discharge apparatus.

The sample of hydrogen peroxide 99.3% (Buffalo Electro-Chemical Co.) was thoroughly deaerated by repeated freezing and melting under vacuum. It was stored in a thermostated bulb, E, connected through a metering valve, F, with the inlet tube. The latter, 8 mm i.d., entered the large discharge tube laterally some 20 cm below the high-frequency coil, and terminated flush with the bottom of the discharge tube. Blank runs confirmed that the peroxide vapor in the inlet tube was in no way affected by the electric discharge. Likewise, blank runs *without the electric discharge* showed that the decomposition of hydrogen peroxide, by heterogeneous reactions through the whole series of operations, amounted to less than 5%. After a run (usually 4 h) the trapped material was isolated by closing the main valve, K, and the liquid nitrogen was removed from the Dewar flask. The temperature was measured with a tiny thermocouple, copper–constantan, cemented to the outer wall of the glass trap near the bottom. Because of the slow warming rate (0.6–0.7 deg min^{-1}), the readings must have followed closely the true temperature of the condensate except, perhaps, during the exothermic reaction at 160 °K. Once at room temperature the liquid products were distilled under reduced pressure into a small flask, P, for weighing and analysis of the peroxide content by refractive index measurement.

RESULTS

Preliminary tests indicated that it was possible to get a glassy deposit with this system provided the flow of peroxide vapor was small enough (less than 2 g h^{-1}), and was turned on only while the electric discharge in hydrogen was operating. Otherwise the peroxide froze in the inlet tube. In physical appearance this deposit was quite like that produced from dissociated water vapor and other similar systems; that is, a clear glass with a light yellow tint which was particularly noticeable at the bottom of the trap. Its behavior on warming is represented in Fig. 2 for a typical run (No. 5 in Table I). Four distinct

Can. J. Chem. Downloaded from www.nrcresearchpress.com by 210.87.254.40 on 09/05/12
For personal use only.

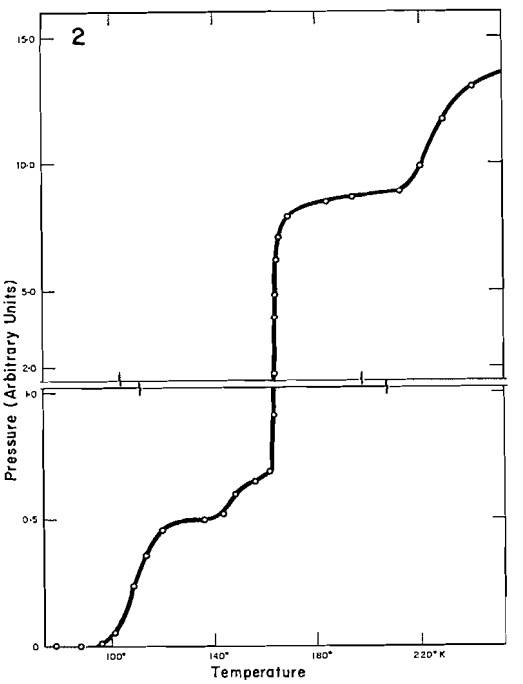
Can. J. Chem. Downloaded from www.nrcresearchpress.com by 210.87.254.40 on 09/05/12
For personal use only.

TABLE I

Experimental data for a few typical runs

Run No.	Electric power (W)	H_2 input (mmoles h^{-1})	H_2O_2 input (mmoles h^{-1})	Condensate				
				% H_2O_2	% wt. loss	H_2O_2 (mmoles h^{-1})	H_2O (mmoles h^{-1})	O_2 evolved (mmoles h^{-1})
1	300	26	9.5	89.7	6	8.1	1.7	0.01
2	350	26	14	76.5	17	9.0	5.1	0.03
3	400	26	18	57.5	23	7.8	10.9	0.05
4	400	26	52	61.0	25	23.5	28.5	0.37
5	400	2.7	48	65.7	23	24	23.5	0.42
6	500	2.7	6.5	16.4	42	0.6	6.0	~0.002
7	500	26	10.5	7.0	45	0.4	10.1	~0.001

steps are discernible. The first two correspond to very small pressure increases (note the change in pressure scale at arbitrary unit 1.0). About twice as much gas is released in step 1 (from 90 to 130 °K) as in step 2 (from 140 to 150°K). During the latter the yellow color gradually fades out. Essentially this is similar to what is observed in the dissociated water vapor system.



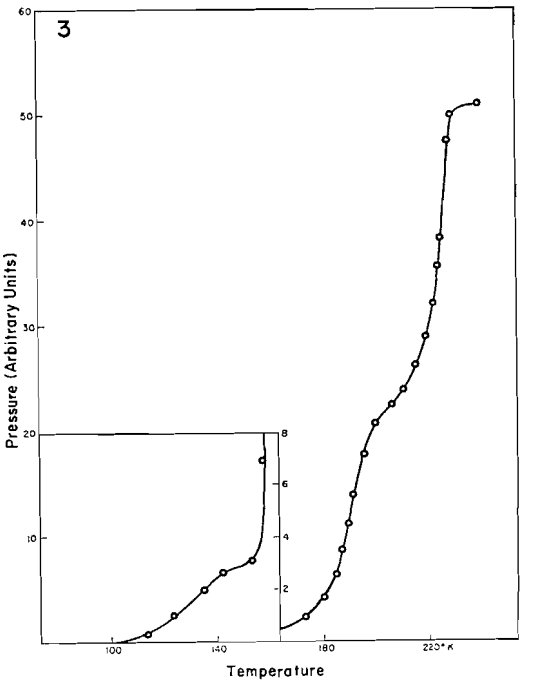


FIG. 2. Warming curve of the condensed products in the system hydrogen atoms – molecular peroxide.
FIG. 3. Warming curve of the condensate from dissociated water vapor (same pressure scale and about 80% as much condensate as in Fig. 2).

For the next step, however, the two systems differ somewhat. Although crystallization begins at the same point in both, namely 160 °K, the process is not so sharp in the case of dissociated water vapor (Fig. 3), and more oxygen, roughly three times, is evolved. Furthermore, only in the latter case does the gas have a strong ozone smell. Again in the last step quite a lot more oxygen is produced during melting of the deposit from dissociated water, and the phenomenon begins at 200 °K, some 20° lower than in the present system. The final products in both cases are rather unstable, as evidenced by streams of oxygen bubbles, even after one distillation.

Table I summarizes the most significant data for a few typical runs, in which the input of both reagents as well as the electric power were varied. The following relationships may be noted.

(*a*) The fraction of input peroxide lost as non-condensible products varies linearly with the power dissipated in the discharge (Fig. 4).

(*b*) The amounts of peroxide decomposed and of water produced (Fig. 5) increase both with the input of hydrogen atoms (runs 1–3) and that of peroxide (runs 3–4).

(*c*) The amount of oxygen evolved from the glassy deposit on crystallization depends on the input of hydrogen atoms (runs 1–3) and, to a greater extent, on the amount of hydrogen peroxide in the deposit (runs 4–5).

Can. J. Chem. Downloaded from www.nrcresearchpress.com by 210.87.254.40 on 09/05/12
For personal use only.

(*d*) Decreasing the input of molecular hydrogen in the discharge causes only minor changes in the composition of the condensate (compare runs 4–5 and 6–7).

(*e*) Increasing the ratio of hydrogen atoms to that of peroxide input, as in runs 6 and 7, leads eventually to complete destruction of the peroxide.

(*f*) The balance of material (oxygen) in all cases fits the stoichiometry of the overall reaction

[1] $$2H_2O_2 = 2H_2O + O_2$$

within the accuracy of the analyses.

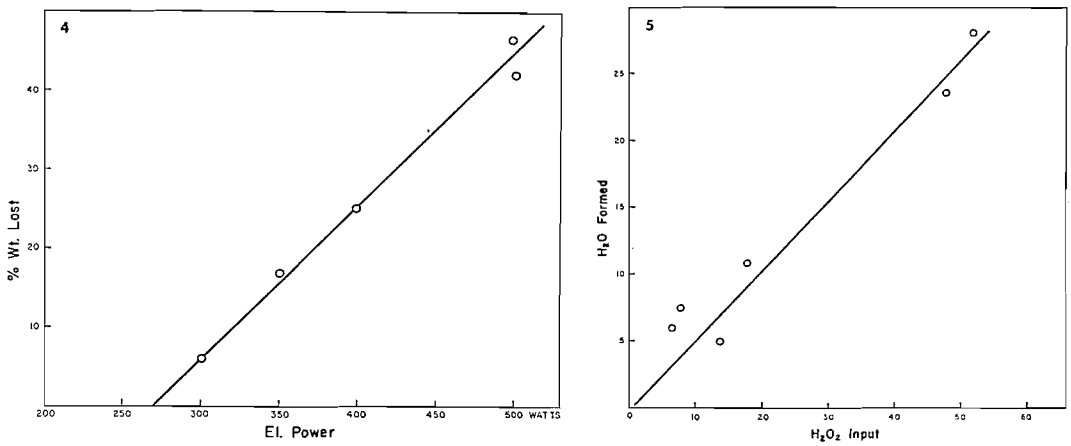


FIG. 4. Relationship between the "load" in the r.f. discharge and the fraction of input material lost.
FIG. 5. Dependence of water formation on peroxide input.

DISCUSSION

It seems appropriate to consider first the reaction kinetics in the present system, even if this was not our main purpose. The bulk of the experimental evidence from a number of related systems, in particular the much studied hydrogen–oxygen reaction (16, 17), the homogeneous decomposition of hydrogen peroxide, either alone (18–20), or in the presence of hydrogen (21, 22), leads to the following mechanism as the most important, if not the unique one, for the gas phase reactions in the present case.

[2] $$H_2O_2 + H = H_2O + OH$$

[3] $$H_2O_2 + OH = H_2O + HO_2$$

[4] $$HO_2 + HO_2 = H_2O_2 + O_2$$

On thermodynamic grounds [2] appears much more likely than the other alternative

[5] $$H_2O_2 + H = H_2 + HO_2$$

for the primary step (17). Recent kinetics studies also support this view (23). As for reaction [3] its high efficiency in chain termination process is well established. The choice between [4] and the other possibility

[6] $$HO_2 + OH = H_2O + O_2$$

for the last step is not so clear cut, but this is of little consequence here. It should be noted, however, that the steady state concentration of OH radicals was certainly very low in our system because of the presence at all times of an excess of hydrogen peroxide over hydrogen atoms. Accordingly the cold wall reaction

[7] $$OH + OH = H_2O_2,$$

Can. J. Chem. Downloaded from www.nrcresearchpress.com by 210.87.254.40 on 09/05/12
For personal use only.

which is responsible for the production of peroxide from dissociated water vapor, was unimportant. The same is true of the chain reaction

[8] $$H_2 + OH = H_2O + H.$$

On the other hand, free radicals in low concentrations were certainly trapped in the glassy condensate, and their recombination by diffusion must account for at least part of the unidentified gas evolved in the first two steps. With that hypothesis and from reaction [4], the maximum concentration of trapped HO_2 radicals turns out to be of order of a few parts per thousand, which agrees well with the results of electron spin resonance (e.s.r.) studies (8, 24). At any rate the bleaching of the yellow color in step 2 coincides with the fading away of the e.s.r. signal. Incidentally we have shown that the yellow color in our experiments was not due to atmospheric contaminations nor to impurities from the electric discharge. No yellow color was observed (and no peroxide was formed) in the glassy solid condensed from water vapor and discharged hydrogen. Similarly prolonged bombardment, up to 3 h, of a film of glassy hydrogen peroxide by discharged hydrogen failed to produce any detectable color, and when the film was warmed only minute traces of gas were given off in a continuous fashion (curve B in Fig. 6).

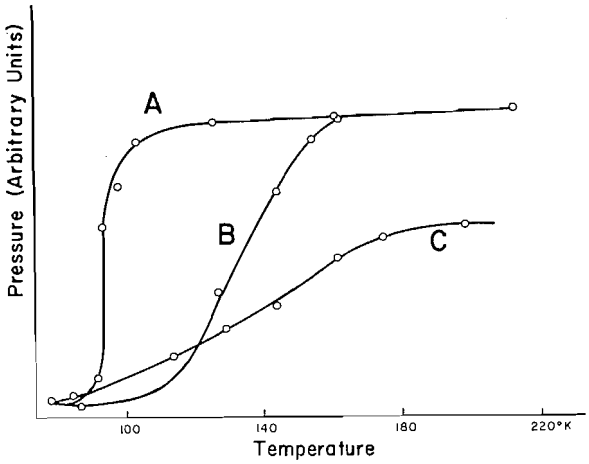


FIG. 6. Gas evolution on warming the condensed products from various systems: A, H_2O_2 and traces of SiH_4; B, glassy H_2O_2 bombarded with H atoms; C, discharge through hydrogen gas.

The most significant aspect of our results is the stoichiometry, in particular the fact that the percent loss of input material, mostly oxygen, is directly proportional to the electric power, that is the hydrogen atom input. Therefore, the bulk of the chemical action is the homogeneous decomposition of part of the hydrogen peroxide following reaction with dissociated hydrogen. This is in opposition to a proposed scheme (4, 12, 25) involving formation of a metastable intermediate by recombination of free radicals at low temperature according to the equation

[9] $$HO_2 + HO_2 = H_2O_4.$$

Presumably the decomposition of this intermediate would be the source of the gas evolved upon crystallization of the glassy deposit,

[10] $$H_2O_4 = H_2O_2 + O_2.$$

If such were the case, then the amount of evolved oxygen should be proportional, *other*

Can. J. Chem. Downloaded from www.nrcresearchpress.com by 210.87.254.40 on 09/05/12
For personal use only.

Can. J. Chem. Downloaded from www.nrcresearchpress.com by 210.87.254.40 on 09/05/12
For personal use only.

things being equal, to the input of hydrogen atoms, contrary to observation; compare, for instance, runs 1 and 7. As suggested before (2), a more rational, albeit more prosaic, explanation of these phenomena is based on the decomposition of part of the hydrogen peroxide caused by some impurities trapped from the discharged gas. The nature of that reaction is still uncertain, although from various indications it appears to be stoichiometric rather than catalytic. Indeed, various authors have found a constant ratio of evolved oxygen to residual peroxide in series of experiments with the same system and the same type of apparatus. Furthermore, the extent of decomposition is independent of the rate of warming of the condensate (25). Also the main reaction terminates rather abruptly, at least in the present case (Fig. 2). It is not ruled out, however, that some catalysis also takes place.

As for the impurities generated in the electric discharge, there is now a good deal of experimental evidence for their existence, to wit:

(*a*) Thirty-five years ago Hiedemann (26) showed that the unusual reactivity of electrically discharged hydrogen gas could be due to formation of traces of silane.

(*b*) In experiments on the trapping in a solid matrix of hydrogen atoms from discharge tubes the e.s.r. spectrum exhibited a very intense four-line signal even with the purest hydrogen gas (27). Recently the same spectrum was reproduced in the ultraviolet photolysis of silane (28).

(*c*) Redox analysis of the condensate from dissociated water vapor has shown a greater oxidizing and reducing power than that of the same material after melting (29).

(*d*) The well-known "clean up" of atomic hydrogen, leading to progressive "hardening" of hydrogen discharge tubes, has always been interpreted as a surface interaction. The same explanation was invoked even in the photochemical decomposition of hydrogen (30).

(*e*) Definite identification of traces of silane in a stream of hydrogen gas dissociated by a microwave discharge in quartz or Pyrex tubes was achieved recently by mass spectrometry (31).

(*f*) In this laboratory we have observed repeatedly that, after the preparation of large quantities of deuterium peroxide in the electric discharge, the wall of the trap always became covered with a white powder, presumably silica. What is more, this fine powder can be "cleaned up" entirely by passing for a while a stream of discharged hydrogen gas.

We propose to investigate this matter further. Already we have shown that hydrogen peroxide, frozen in liquid nitrogen along with traces of silane, reacts on warming, but in a manner entirely different from the glassy deposit (Fig. 6). Also, warming the condensed products from a prolonged (4 h) discharge in hydrogen evolves traces of an unidentified gas between 100 and 160 °K. From the present results it would appear that more contamination is produced in dissociated water, Fig. 3, (including probably some ozone) than in dissociated hydrogen (Fig. 2). According to the work of Winkler *et al.* (13) on the influence of the trapping temperature, the yield of evolved oxygen from dissociated water or hydrogen peroxide vapor increases linearly as the temperature is lowered, beginning around 120 °K. Yet the formation of peroxide in the solid begins some 30° lower. In our hypothesis this could mean that 120° is the critical trapping temperature for the impurities in these systems.

Finally, the release of oxygen in step 4 must be simply another instance of decomposition of hydrogen peroxide during melting, as reported formerly (32). Further confirmation of this is seen in the fact that in the present case, the crystalline deposit began melting at about the temperature of the lower eutectic in the binary system water–peroxide (33). In contrast, the deposit from dissociated water begins melting at a lower temperature,

around 200 °K, at the metastable eutectic (34), because no hydrogen peroxide is present in the gas phase before condensation, and the hydrate $H_2O_2 \cdot 2H_2O$ is not formed in the solid.

ACKNOWLEDGMENT

The authors are grateful to the National Research Council for generous financial support of this project.

REFERENCES

1. K. H. GEIB and P. HARTECK. Ber. **65**, 1551 (1932).
2. P. A. GIGUÈRE. ICSU Rev. **4**, 172 (1962).
3. I. I. SKOROKHODOV, L. I. NEKRASOV, N. I. KOBOZEV, and E. I. MAKAROVA. Russ. J. Phys. Chem. **35**, 443 (1961).
4. J. A. WOJTOWICZ, F. MARTINEZ, and J. A. ZALOWSKY. J. Phys. Chem. **67**, 849 (1963).
5. D. A. CSEJKA, F. MARTINEZ, J. A. WOJTOWICZ, and J. A. ZASLOWSKY. J. Phys. Chem. **68**, 3878 (1964).
6. I. I. SKOROKHODOV, L. I. NEKRASOV, and N. I. KOBOZEV. Russ. J. Phys. Chem. **35**, 994 (1961).
7. I. I. SKOROKHODOV, L. I. NEKRASOV, N. I. KOBOZEV, and V. B. EVDOKIMOV. Russ. J. Phys. Chem. **36**, 136 (1962).
8. I. I. SKOROKHODOV, V. B. GOLUBEV, L. I. NEKRASOV, V. B. EVDOKIMOV, and N. I. KOBOZEV. Russ. J. Phys. Chem. **36**, 47 (1962).
9. T. V. YAGODOVSKAYA and L. I. NEKRASOV. Russ. J. Phys. Chem. **38**, 953 (1964).
10. F. MARTINEZ, J. A. WOJTOWICZ, and J. A. ZASLOWSKY. J. Phys. Chem. **67**, 714 (1963).
11. YU. A. MAL'TSEV, I. I. SKOROKHODOV, and L. I. NEKRASOV. Russ. J. Phys. Chem. **37**, 1480 (1963).
12. N. I. KOBOZEV, I. I. SKOROKHODOV, L. I. NEKRASOV, and E. I. MAKAROVA. Zh. Fiz. Khim. **31**, 1843 (1957).
13. J. S. BATZOLD, C. LUNER, and C. A. WINKLER. Can. J. Chem. **31**, 262 (1953).
14. P. A. GIGUÈRE, E. A. SECCO, and R. S. EATON. Discussions Faraday Soc. **14**, 104 (1953).
15. E. A. SECCO. J. Chem. Phys. **23**, 1734 (1955).
16. B. LEWIS and G. VON ELBE. Combustion, flames and explosions. Academic Press, New York. 1961.
17. W. FORST and P. A. GIGUÈRE. J. Phys. Chem. **62**, 340 (1958).
18. P. A. GIGUÈRE and I. D. LIU. Can. J. Chem. **35**, 283 (1957).
19. W. FORST. Can. J. Chem. **36**, 1308 (1958).
20. D. E. HOARE, J. B. PORTHEROE, and A. D. WALSH. Trans. Faraday Soc. **55**, 548 (1959).
21. W. FORST. Can. J. Chem. **37**, 1616 (1959).
22. R. R. BALDWIN, D. BOOTH, and D. BRATTAN. Can. J. Chem. **39**, 2130 (1961).
23. R. R. BALDWIN, D. JACKSON, R. W. WALKER, and S. J. WEBSTER. Tenth Symposium (International) on Combustion. Academic Press, Inc., New York. 1965. p. 423.
24. R. LIVINGSTON, J. GHORMLEY, and H. ZELDES. J. Chem. Phys. **24**, 483 (1956).
25. E. OHARA. J. Chem. Soc. Japan, **61**, 657 (1940).
26. E. H. HIEDEMANN. Z. Physik. Chem. A, **153**, 210 (1931).
27. C. K. JEN, S. N. FONER, E. L. COCHRAN, and V. A. BOWERS. Phys. Rev. **112**, 1169 (1958).
28. E. L. COCHRAN. Intern. Symp. Free Radical Stabilization, Washington, D.C. 4, D-I-1 (1959).
29. H. M. GLADNEY and D. GARVIN. J. Phys. Chem. **66**, 1560 (1962).
30. L. B. THOMAS and W. D. GWINN. J. Am. Chem. Soc. **70**, 2643 (1948).
31. R. M. FRISTON. Private communication.
32. P. A. GIGUÈRE and P. GEOFFRION. Can. J. Res. B, **28**, 599 (1950).
33. W. C. SCHUMB, C. N. SATTERFIELD, and R. L. WENTWORTH. Hydrogen peroxide. Reinhold Publishing Corp., New York. 1955.
34. P. A. GIGUÈRE. J. Chem. Phys. **42**, 2989 (1965).

Can. J. Chem. Downloaded from www.nrcresearchpress.com by 210.87.254.40 on 09/05/12
For personal use only.

Can. J. Chem. Downloaded from www.nrcresearchpress.com by 210.87.254.105 on 09/05/12
For personal use only.

ADSORPTION OF CYCLOHEXANE AND BENZENE ON MIXED HYDROXIDES AND OXIDES OF MAGNESIUM AND ALUMINIUM

R. I. Razouk,[1] Sh. Nashed, and F. N. Antonious
Chemistry Department, Faculty of Science, Ain Shams University, Abbassia, Cairo
and
National Research Centre, Dokki, Cairo, United Arab Republic

Received April 22, 1965

ABSTRACT

Seven mixed hydroxides of magnesium and aluminium were prepared, and phase and structural changes accompanying their dehydration were investigated by differential thermal analysis, thermogravimetric analysis, and X-ray diffraction techniques. The differential thermal analysis curves possess 2 peaks corresponding to those of parent hydroxides together with a new peak, and the thermogravimetric analysis curves show slight inflections. X-ray diffraction patterns of the mixed hydroxides possess the characteristic lines of the parent hydroxides together with three to five new intense lines which might indicate the formation of a double hydroxide. When the mixed hydroxides are progressively heated they give rise to products possessing patterns which first become diffuse and ultimately pass mainly into the spinel pattern.

Adsorption isotherms of cyclohexane and benzene were measured on the mixed hydroxides and their dehydration products. Specific surface areas calculated by the application of the Brunauer, Emmett, Teller (B.E.T.) equation are in general in good agreement for the two adsorbates. The surface area increases with rise of dehydration temperature to a maximum at 500–600 °C and then decreases with further rise in temperature. This behavior is common to crystalline oxide systems and may be ascribed to the intermingling of decomposition, recrystallization, and sintering processes. Variations in the molecular ratio of the mixed oxides (as much as 20-fold), and in the method of preparation, do not much alter the surface area.

INTRODUCTION

Mixed oxides have lately become important catalysts, and the study of their surface properties is therefore of special interest in view of the close relation between the latter and catalytic activity. The mixed oxides which have been studied most extensively are silica–alumina cracking catalysts. The surface properties and reactivity of several other oxide mixtures have been investigated, but no work is known to the authors on the adsorptive properties of the $MgO–Al_2O_3$ system, although the individual components have been the subject of numerous studies.

The object of this work was to study the adsorption of cyclohexane and benzene on mixed hydroxides of magnesium and aluminium as well as on their dehydration products formed at various temperatures *in vacuo*, i.e. under continuous pumping conditions. Phase and structural changes accompanying the dehydration of the mixed hydroxides were also investigated.

EXPERIMENTAL

(i) Materials

Seven mixed hydroxides were prepared.

Mixed hydroxide I was prepared by coprecipitation from a mixture of equal volumes of 0.4 *M* aluminium nitrate solution and 0.2 *M* magnesium nitrate solution by the slow addition of an equal volume of 1.6 *M* carbonate-free sodium hydroxide solution. The precipitate was freed from nitrate ions by decantation and then by washing with 1% ammonia solution, and was finally dried at 110 °C to constant weight. Chemical analysis gave the composition $MgO.0.96Al_2O_3.4.28H_2O$.

Mixed hydroxides II–V were prepared in the same manner with appropriate concentrations of magnesium, aluminium, and hydroxyl ions. Their compositions are indicated by the following:

Mixed hydroxide II: $MgO.0.443Al_2O_3.3.21H_2O$.
Mixed hydroxide III: $MgO.2.01Al_2O_3.7.45H_2O$.
Mixed hydroxide IV: $MgO.0.336Al_2O_3.2.86H_2O$.
Mixed hydroxide V: $MgO.7.83Al_2O_3.22.11H_2O$.

[1]*Present address: Department of Physical Sciences, the American University of Cairo, Cairo, U.A.R.*

Mixed hydroxide M was prepared by mechanically mixing suspensions of $Mg(OH)_2.H_2O$ and $Al_2O_3.3H_2O$ in approximately equimolecular quantities. Magnesium hydroxide was prepared by slowly running carbonate-free 0.4 *M* sodium hydroxide solution into an equal volume of 0.2 *M* magnesium nitrate solution in the cold. Aluminium hydroxide was prepared by the slow addition of approximately 1.2 *M* ammonia solution to an equal volume of 0.4 *M* aluminium nitrate solution in the cold. Both precipitates were freed from nitrate ions by decantation and washing with 1% ammonia solution. When the parent hydroxides were dried at 110 °C they gave the composition $MgO.1.02H_2O$ and $Al_2O_3.2.91H_2O$, and the diffraction patterns of brucite and bayerite respectively. Mixed hydroxide M has the composition $MgO.1.12Al_2O_3.3.57H_2O$.

Mixed hydroxide A was obtained by the addition of 0.2 *M* magnesium nitrate solution to sodium aluminate solution prepared by the interaction of 0.4 *M* aluminium nitrate solution with 1.6 *M* carbonate-free sodium hydroxide solution in slight excess. Chemical analysis gave the composition $MgO.0.825Al_2O_3.4.3H_2O$.

Several dehydration products were prepared by heating the mixed hydroxides *in vacuo* for 5 h at suitable temperatures. The ultimate limit of vacuum during dehydration was 10^{-4} mm.

Cyclohexane and benzene were prepared in a pure state by standard methods.

(ii) Apparatus and Technique

The adsorption isotherms were determined with a conventional volumetric apparatus in which mercury cut-outs were used in place of stopcocks to eliminate contamination with grease (see, for example, ref. 1). In the procedure adopted the adsorbent was flushed with the vapor of the adsorbate and the latter was then pumped off during 3 h at a temperature 100 °C below the temperature of dehydration; this procedure was not used for the mixed oxides formed at 800 °C and 1 000 °C when degassing was conducted at 600 °C. This treatment was found satisfactory to ensure reproducible results by minimizing further loss of the water content at the lower temperatures, and sintering at the higher temperatures, when duplicate experiments were carried out.

Differential thermal analysis curves were obtained with an automatic recording apparatus supplied by Linseis, Prüfgerätebau Kg., Selb Bayern, G.F.R. Thermogravimetric analysis curves were recorded with an apparatus manufactured by Gebrüdernetzsch, ABT, Prüfgeräte, Selb, Bayern, G.F.R. In both cases the rate of heating was 6 deg per minute. X-ray diffraction patterns were obtained with a Philips 114.6 mm Debye-Scherrer powder camera with Ni-filtered Cu radiation.

RESULTS AND DISCUSSION

(i) Differential Thermal Analysis and Thermogravimetric Analysis

The results of typical experiments of differential thermal analysis and thermogravimetric analysis are illustrated in Fig. 1.

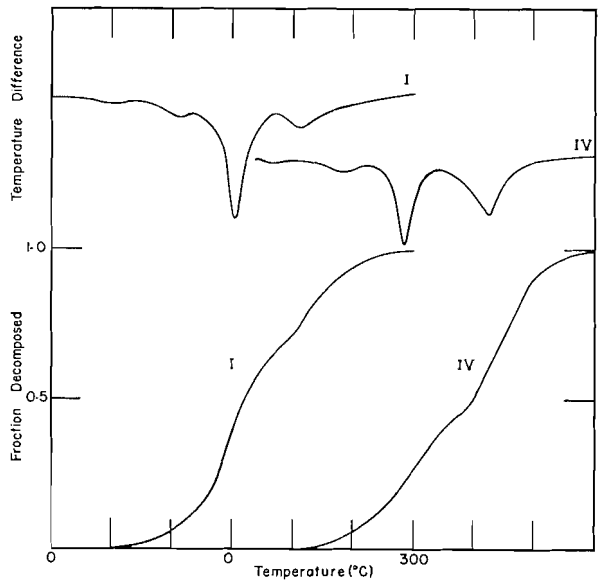


FIG. 1. Typical differential thermal analysis and thermogravimetric analysis curves. Mixed hydroxides I and IV.

Can. J. Chem. Downloaded from www.nrcresearchpress.com by 210.87.254.105 on 09/05/12
For personal use only.

Can. J. Chem. Downloaded from www.nrcresearchpress.com by 210.87.254.105 on 09/05/12
For personal use only.

PLATE I

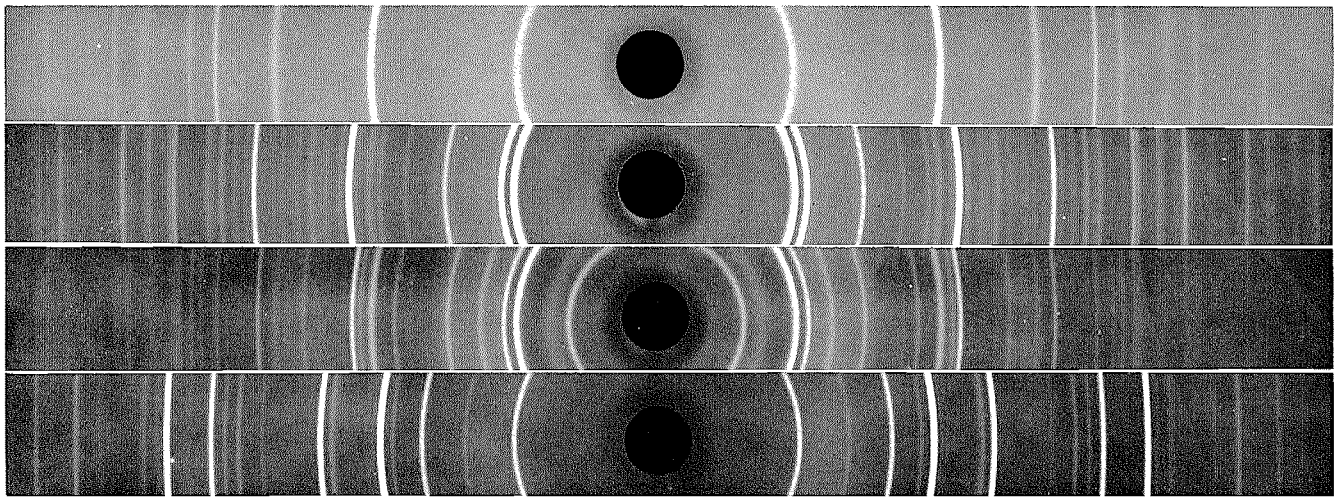


FIG. 2. Typical X-ray diffraction patterns. (*a*) Magnesium hydroxide dried at 110 °C; (*b*) aluminium hydroxide dried at 110 °C; (*c*) mixed hydroxide M dried at 110 °C; (*d*) spinel formed at 1 000 °C.

The mixed hydroxides, except mixed hydroxide V, give differential thermal analysis curves which are characterized by the presence of four endothermic peaks, namely, a very small peak at about 100 °C, a small one at 180–220 °C, and two pronounced peaks at 280–300 °C and 380–420 °C. The first peak presumably results from the loss of adsorbed water, and the last two peaks correspond to the endothermic dehydration of aluminium hydroxide (300 °C) and magnesium hydroxide (400 °C). The second peak is attributed to the dehydration of a partially formed double hydroxide (*vide infra*). The thermal effects of the last two peaks, as measured by the areas they enclose, are found to correspond approximately to the relative amounts of the parent individual hydroxides present in the mixed hydroxides. With mixed hydroxide V, however, the peak at 400 °C was masked by the strong endothermicity associated with the dehydration of the high content of aluminium hydroxide.

Thermogravimetric analysis curves exhibit small inflections marking the separate dehydration processes of the parent hydroxides of aluminium and magnesium. The position of this inflection is found to correspond nearly to the composition of the mixed hydroxide. However, when the rate of heating is increased, the dehydration processes overlap and give rise to almost continuous smooth curves.

(ii) X-Ray Investigation

X-ray diffraction patterns of the mixed hydroxides exhibit the lines characteristic of the parent individual hydroxides. Furthermore, except in the case of mixed hydroxide V, all the patterns also show three to five relatively intense lines which are not found in the patterns of the parent hydroxides or spinel $MgAl_2O_4$. The new lines give *d*-values of 7.56, 3.78, 2.58, 2.30, and 2.03 Å, and *I*-values up to 100, 80, 80, 60, and 60 respectively, but they do not appear in the patterns of intimate mixtures of dry magnesium hydroxide and aluminium hydroxide, which in fact are found to be the addition of the patterns of the two hydroxides. Typical patterns are shown in Fig. 2.

The presence of new lines in the diffraction patterns of mixed hydroxides of magnesium and aluminium might indicate the partial development of a new structure. The formation of a hydrated spinel was assumed by Abich (2) to take place when ammonia is added to a solution of equimolecular parts of magnesium and aluminium salts containing enough ammonium chloride to keep magnesium in solution. It is more likely, however, that a double hydroxide, analogous to tricalcium aluminate hexahydrate described by Flint, McMurdie, and Wells (3), is partially formed. The presence of most of the lines of the parent hydroxides in the diffraction patterns of the mixed hydroxides, as a result of incomplete reaction or excess of one component or the other, makes it difficult at present to determine the structure and the dimensions of the unit cell. However, there is indication that the double hydroxide very likely possesses a cubic lattice similar to that of $3CaO.Al_2O_3.6H_2O$. Attempts are being made at the moment to have the reaction go to completion and to grow crystals so as to enable the elucidation of the exact nature and the structure of this product.

It is worth mentioning that mixed hydroxides of magnesium and iron exhibit a similar behavior when investigated by X-rays and differential thermal analysis (4).

X-ray diffraction patterns of the products of dehydration formed at 200 °C retain some of the lines of the original mixed hydroxides, but the product formed at 300–400 °C gives practically no patterns. Diffuse lines of spinel begin to appear in the diffraction patterns of the mixed oxides prepared by dehydration at 500 °C. As the temperature of dehydration rises, the lines in the patterns become sharper, and, ultimately, the product

Can. J. Chem. Downloaded from www.nrcresearchpress.com by 210.87.254.105 on 09/05/12
For personal use only.

formed at 1 000 °C possesses very clear lines of spinel together with faint lines of periclase and γ-alumina, depending on the component present in excess of stoichiometry. The partial synthesis of spinel from magnesium and aluminium oxides by heating a mixture of equimolecular quantities above 700 °C was ascertained by Budnikov and Zlochevskaya (5). The lower temperatures of spinel formation recorded in the present investigation are ascribed to the high surface activity and intimate admixture of the two oxides.

(iii) Adsorption Measurements

Adsorption–desorption isotherms of cyclohexane and benzene were determined at 35 °C on mixed hydroxide I and its dehydration products formed by heating *in vacuo* for 5 h at eight temperatures between 200 °C and 1 000 °C, and also on mixed hydroxides II–V, M, and A, and their dehydration products prepared by heating at 600 °C *in vacuo*.

The adsorption of cyclohexane is physical in nature, and the isotherms on all the preparations and their dehydration products are type II of Brunauer's classification (6). Desorption isotherms form hysteresis loops which close at relative vapor pressures depending on the particular preparation. The hysteresis loops may be described as type A combined with little of type E of de Boer's classification (7), and thus indicate a broad pore spectrum. A typical set of isotherms is represented in Fig. 3. It is clear that the monolayer capacity increases with rise of temperature of thermal treatment to a maximum at 600 °C, and then decreases with further rise in temperature.

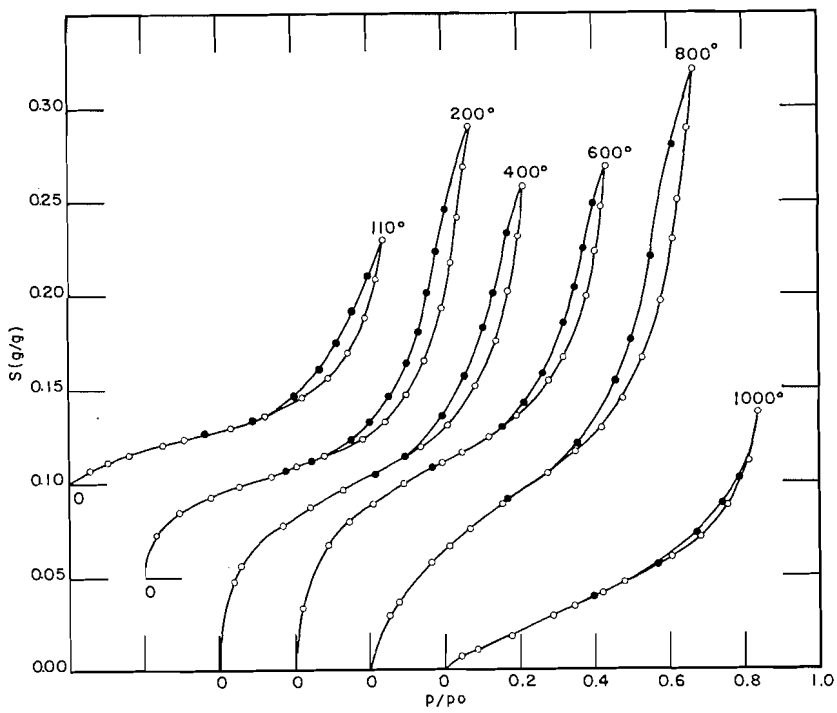


FIG. 3. Adsorption–desorption isotherms of cyclohexane vapor on mixed hydroxide I and its dehydration products formed at 200°, 400°, 600°, 800°, and 1 000 °C. Solid points represent desorption.

Adsorption isotherms of benzene vapor closely resemble those of cyclohexane. The results of typical experiments are illustrated in Fig. 4.

Adsorption values of cyclohexane and benzene vapors on the various preparations of

Can. J. Chem. Downloaded from www.nrcresearchpress.com by 210.87.254.105 on 09/05/12
For personal use only.

mixed hydroxides and their dehydration products are found to give satisfactory Brunauer, Emmett, Teller (B.E.T.) linear plots in most cases. Specific surface areas were calculated taking 39 Å² and 32.3 Å² as cross-sectional areas of cyclohexane (8) and benzene (9) respectively. Earlier work in this laboratory on oxides of magnesium (10) and iron (11) has shown that the adsorption of cyclohexane can be satisfactorily used for evaluating the specific surface area of such systems. The specific surface areas calculated from the adsorption isotherms of the two vapors are found to be in good agreement for most of the products of dehydration (Figs. 5 and 6), but some discrepancies are encountered especially with the original mixed hydroxides. It is noteworthy that the adsorption of the two vapors on the parent mixed hydroxides is found to be sensitive to slight variations in the method of preparation, and duplicate experiments gave mixed hydroxides possessing surface areas which sometimes vary by as much as 50%. But the effect is much smaller in the case of the dehydration products, and the areas are in agreement within 5–10%.

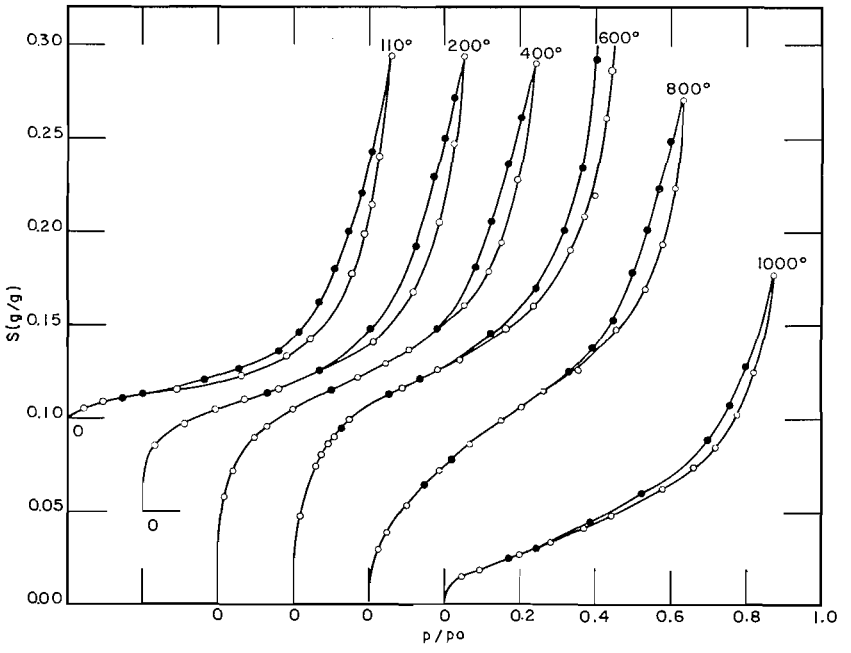


FIG. 4. Adsorption–desorption isotherms of benzene vapor on mixed hydroxide I and its dehydration products formed at 200°, 400°, 600°, 800°, and 1 000 °C. Solid points represent desorption.

The effect of the temperature of dehydration on the specific surface area of the products formed from mixed hydroxide I calculated from the adsorption isotherms of cyclohexane and benzene is shown in Fig. 5. The rise of temperature of dehydration increases the specific surface area to a maximum of about 236 m² per g obtained in the case of the product formed at 600 °C. A further rise of temperature reduces the surface area. This behavior is in harmony with the results of earlier work on the surface properties of magnesium hydroxide (10), ferric hydroxide (11), and aluminium hydroxide (12), and their dehydration products.

The development of surface area on dehydration may be attributed to (*a*) the formation of voids and cracks produced by the loss of water and the destruction of the lattice, although the solid might keep its structure for some time in the form of a pseudo-lattice, and (*b*) the breaking up of the metastable pseudo-lattice and its recrystallization into a

Can. J. Chem. Downloaded from www.nrcresearchpress.com by 210.87.254.105 on 09/05/12
For personal use only.

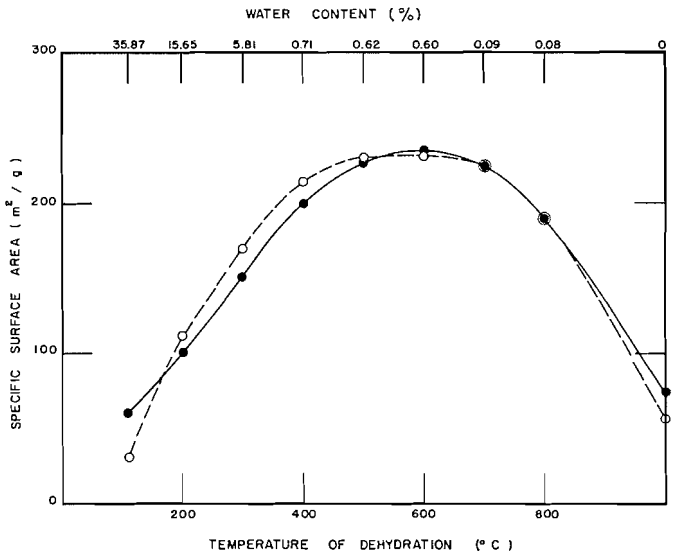


FIG. 5. Effect of temperature of thermal treatment on the specific surface area of mixed hydroxide I and its dehydration products, as calculated from the adsorption of cyclohexane (●) and benzene (○).

new structure developed in strained conditions. At the lower temperatures of dehydration, the evolution of the surface area is mainly caused by the first process, for the increase of the surface area is approximately proportional to the decrease in the water content. But at the higher temperatures of dehydration, especially between 400 °C and 600 °C, the second process predominates, and the development of the surface area is much more than that expected from the increase in the degree of dehydration, thus indicating the occurrence of activation. It is interesting to note that it is in this range of thermal treatment that diffuse lines of the spinel diffraction patterns first make their appearance.

On the other hand, the decrease in surface area which accompanies the thermal treatment above 600 °C is considered to result from sintering effects. The surface area diminishes considerably as the temperature of dehydration is raised to 1 000 °C when spinel structure becomes well developed. This is in agreement with the observation of Jander and Pfister (13) that the catalytic ability of $MgO–Al_2O_3$ mixtures in the carbon monoxide – oxygen reaction decreases strongly at 920 °C when spinel crystals are formed.

The variation of the specific surface area of the mixed hydroxides and oxides with composition is represented in Fig. 6, in which the surface area is plotted as a function of the mole % MgO in the nonvolatile content of the seven preparations. In general there is satisfactory agreement between the specific surface areas of the mixed oxides when calculated from the adsorption isotherms of cyclohexane and benzene, except in the case of mixed oxide M when the two values differ by about 20%. However, marked differences are observed in the case of the parent mixed hydroxides except mixed hydroxide M, and the surface areas calculated from the adsorption of benzene are much lower than the corresponding values calculated from the cyclohexane isotherms. It is difficult at present to find a satisfactory explanation of this result, but reference has been made to the experimental fact that the surface area of mixed hydroxides is highly sensitive to conditions of preparation. In particular, the state of the surafce might play an important role in the relative amounts adsorbed, and it is possible that on the surface of the hydroxides the molecules of cyclohexane and benzene occupy areas different from those on the dehydrated

Can. J. Chem. Downloaded from www.nrcresearchpress.com by 210.87.254.105 on 09/05/12
For personal use only.

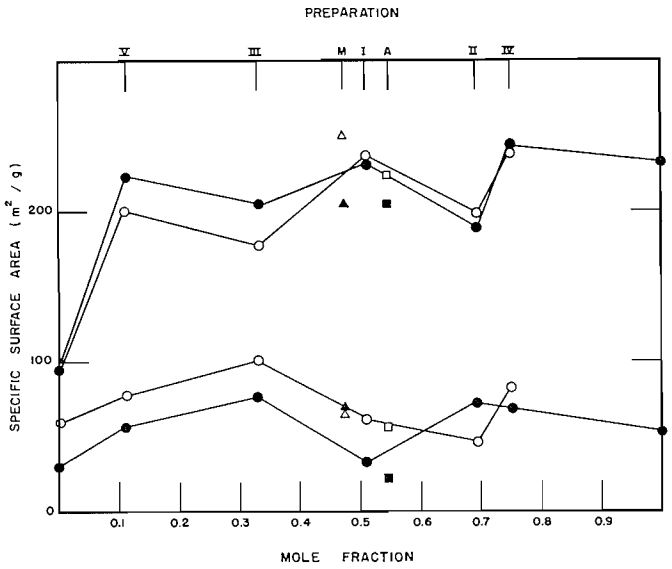


FIG. 6. Variation of the specific surface area of mixed hydroxides (lower curves) and mixed oxides (upper curves) with composition and method of preparation. Surface areas from cyclohexane adsorption: (○) mixed hydroxides and oxides I–V, (△) mixed hydroxide and oxide M, (□) mixed hydroxide and oxide A. Surface areas from benzene adsorption: (●) mixed hydroxides and oxides I–V, (▲) mixed hydroxide and oxide M, (■) mixed hydroxide and oxide A.

surface, although there appears to be no simple correlation between the calculated surface area values and the water content or nonstoichiometry of the mixed hydroxides. It is therefore important to note that the values of the specific surface area of the parent mixed hydroxides calculated from the adsorption of cyclohexane and benzene have to be considered with reserve.

Figure 6 also shows that over a range of 20-fold variation of composition (*a*) the specific surface area of the mixed oxides does not change in a regular manner with composition, (*b*) no mixed oxide of magnesium and aluminium with a markedly high surface area is formed, and (*c*) the specific surface areas of the mixed oxides formed at 600 °C are considerably higher than the values of the corresponding parent mixed hydroxides. Finally, variations in the method of preparation do not bring about basic changes in the surface properties of the mixed oxides.

ACKNOWLEDGMENT

The authors thank Dr. L. E. Copeland for valuable discussions relevant to the structure of the double hydroxide.

REFERENCES

1. R. I. RAZOUK and A. S. SALEM. J. Phys. Colloid Chem. **52**, 1208 (1948).
2. H. ABICH. Kgl. Vet. Acad. Handl. Stockholm, **6** (1842). Cited by J. W. Mellor. A comprehensive treatise of inorganic and theoretical chemistry. Vol. 5. Longmans, Green & Co., London. 1946. p. 294.
3. E. P. FLINT, H. F. MCMURDIE, and L. S. WELLS. J. Res. Natl. Bur. Std. **26**, 13 (1941).
4. R. I. RAZOUK, SH. NASHED, and F. N. ANTONIOUS. To be published.
5. P. P. BUDNIKOV and K. M. ZLOCHEVSKAYA. Ogneupory, **25**, 111 (1958).
6. S. BRUNAUER. Physical adsorption of gases and vapors. Oxford, New York. 1945. p. 150.
7. J. H. DE BOER. *In* The structure and properties of porous materials. *Edited by* D. H. Everett and F. S. Stone. Butterworths Scientific Publications, London. 1958. p. 68.
8. R. N. SMITH, C. PIERCE, and H. CORDES. J. Am. Chem. Soc. **72**, 5596 (1950).
9. H. K. LIVINGSTON. J. Colloid Sci. **4**, 447 (1949).
10. R. I. RAZOUK and R. SH. MIKHAIL. J. Phys. Chem. **61**, 886 (1957).
11. R. I. RAZOUK, R. SH. MIKHAIL, and B. S. GIRGIS. Advan. in Chem. Ser. **33**, 42 (1961).
12. R. I. RAZOUK, R. SH. MIKHAIL, and G. R. ISKANDER. J. Phys. Chem. **69**, 1805 (1965).
13. W. JANDER and H. PFISTER. Z. Anorg. Allgem. Chem. **239**, 95 (1958).

Can. J. Chem. Downloaded from www.nrcresearchpress.com by 210.87.254.105 on 09/05/12
For personal use only.

Can. J. Chem. Downloaded from www.nrcresearchpress.com by 210.87.254.42 on 09/05/12
For personal use only.

NUCLEAR RECOIL REACTIONS IN CYCLOPENTADIENYLMANGANESE TRICARBONYL[1]

T. COSTEA AND IRINA NEGOESCU
Institute of Atomic Physics, Bucharest, Romania

AND

P. VASUDEV[2] AND D. R. WILES
Chemistry Department, Carleton University, Ottawa, Canada

Received November 19, 1965

ABSTRACT

The first stages in an intensive study of Szilard–Chalmers recoil reactions in a covalent metal-organic compound are described. The radioactive manganese-56 is found, as expected, as inorganic manganese (75–80%), as the parent compound (12–20%), and as one or other of two hitherto unidentified, unstable compounds depending on whether anhydrous paper chromatography or paper ionography is used as the separation method (5–7%). Some data are given showing the effect of room-temperature annealing following irradiation at −196 °C. In particular, the yield of one of the unidentified compounds increases markedly (to ~15%) while that of the other compound remains nearly unaffected.

Thin-layer chromatography in anhydrous benzene was used as separation method in thermal annealing studies. They show two hitherto unreported phenomena: The apparent retention increases considerably and then decreases again as annealing continues, and the annealing reaction at two temperatures in the liquid and one in the solid phase are qualitatively very similar. These results are interpreted as indicating the presence of another species, the "pseudoparent", which is not distinguished chromatographically from the parent. Some discussion is given as to possible mechanisms.

It is over thirty years since the discovery by Szilard and Chalmers (1) that atoms having captured a neutron recoil with sufficient energy to break their chemical bonds. A great deal of work has been done (2, 3) in attempting to discover the nature of the chemical reactions following this recoil. However, while much has been learned about the ultimate results of the recoil, the chemistry of the process as it occurs in condensed states remains unknown in detail, largely because of the ephemeral nature of the compounds and atomic states remaining after the recoil. One tantalizing difficulty is the virtual impossibility of observing the primitive atom, since the methods of investigation used to date have always involved dissolution of the sample under observation and subsequent chemical processing. Thus the species observed are those remaining after some quite drastic changes have occurred in the physical and chemical surroundings of the recoil atoms.

One technique which has been used to approach the primitive atom more closely is that of annealing the crystals in one way or another before the chemical processing begins. Although several types of annealing, such as crushing and treatment with γ-rays, light, ultrasonic energy, and high-energy electrons, have been found to have an effect on the recovery of the recoil species, the most usual method is isothermal heating. This method has been used quite extensively, with the result that several quite fundamental hypotheses have been postulated to describe the chemical and physical influences which affect the behavior of the displaced atom. Most work on thermal annealing has been done on ionic compounds (3) and little has been reported on metal-organic compounds. The results

[1]*This work was done in part at Carleton University and at Chalk River Nuclear Laboratories (P. V.'s M.Sc. Thesis, 1965) and in part at IFA in Bucharest, where D. R. W. was a Visiting Scientist during the summer of 1965.*

[2]*Present address: University Chemical Laboratory, Lensfield Road, Cambridge, England.*

obtained so far have mostly shown simple first-order approach to a maximum value or to a pseudoplateau with a very gentle slope. The postulated mechanisms, too, have been based upon first-order kinetics, primarily diffusion mechanisms.

In an attempt to get a closer picture of the reactions occurring in at least one instance, we are undertaking a series of investigations of reactions in a single compound: cyclopentadienylmanganese tricarbonyl, $C_5H_5Mn(CO)_3$. This compound, easily obtainable in a pure state, is straightforward to work with, offers convenient nuclear properties, and presents a reasonably small variety of possible interactions which must be studied. The first stage of this study, which is described here, involves an investigation of the gross features of the recoil and its products. In particular, we were looking for other products than the parent compound and "inorganic" manganese. The second stage, also reported here, is a study of the effect of thermal treatment of neutron-irradiated cyclopentadienylmanganese tricarbonyl, and in particular a comparison of the effects in the solid and liquid states.

EXPERIMENTAL

Target Material

Cyclopentadienylmanganese tricarbonyl was obtained from Ethyl Corporation (U.S.A.) and was sublimed *in vacuo* before use. The reagents used were the purest obtainable grade.

Irradiations

Neutron irradiations were performed in the NRX reactor at Chalk River, Canada, and in the IFA reactor at Bucharest, Romania. Flux and other characteristics in the various irradiation positions used are given in Table I. Freshly-sublimed samples sealed in nylon capsules were used for most irradiations in NRX, while for

TABLE I

Characteristics of irradiation positions*

Position	Thermal flux ($n\ cm^{-2}\ s^{-1}$)	Fast flux ($n\ cm^{-2}\ s^{-1}$)	Dose rate ($rad\ h^{-1}$)	Temperature (°C)
S-6-1	1.4×10^{12}	0.2×10^{10}	1×10^{6}	50
J-Rod	0.6×10^{13}	5×10^{10}	7×10^{6}	50–90
X-Rod	1×10^{14}	2×10^{12}	90×10^{6}	100–120
Self-serve	1×10^{13}	5×10^{10}	6.5×10^{6}	50–90
CT2	1.2×10^{11}	6.3×10^{9}	4.2×10^{6}	30–50
CT3	8.8×10^{8}	3.1×10^{5}	6.4×10^{4}	25–35

*Data obtained through the courtesy of Dr. A. W. Boyd (NRX) and Ing. L. Mantescu (IFA).

low-temperature irradiations in NRX and all irradiations at IFA resublimed material was sealed *in vacuo* in quartz ampoules. Irradiations at −196 °C were done in liquid nitrogen using quartz Dewar flasks. All other irradiations were done at reactor temperature. This leaves some question as to the actual temperature of the sample during irradiation. In NRX, most irradiations lasted 1.0 min, during which time they would not likely reach the ambient temperature. In no case was the melting temperature (77 °C) of the sample reached. Irradiations in CT2 were of 3 min and in CT3 of 60 min duration.

Sample Measurement

Following chromatography or ionography, the strips were cut into small sections and the 0.845 MeV γ-ray was counted with a Na(Tl)I scintillation counter. Background, decay, and coincidence loss corrections were made.

Separation Methods

Solvent extraction was found to give very poor reproducibility, which was traced to extensive adsorption on the glass surfaces and to apparent decomposition of the $C_5H_5Mn(CO)_3$ during the extraction. This method was therefore not used in this study. We regard this adsorption, as also that in the case of ferrocene (4), as indicative of the presence of fragments of molecules (or perhaps ions or radicals) which attain a degree of chemical stability through adsorption on the glass walls.

Paper chromatography.—Ascending paper chromatography in anhydrous benzene was performed in the usual manner except that in all experiments air and moisture were carefully excluded. Whatman No. 1 paper

Can. J. Chem. Downloaded from www.nrcresearchpress.com by 210.87.254.42 on 09/05/12
For personal use only.

was used in these experiments. Many of the experiments were performed in a nitrogen-filled dry-box. The benzene used was dried over anhydrous calcium chloride overnight and filtered, and the filtrate was distilled twice over $LiAlH_4$.

Ionography (paper electrophoresis).—This separation procedure was effected using Whatman 3MM paper, with a solution of 0.2 *M* $NaClO_4$ and 0.1 *M* $HClO_4$ as background electrolyte. The irradiated compound, dissolved in alcohol containing a few drops of the background electrolyte, was spotted on paper strips 2 cm × 57 cm. These strips were clamped between Teflon-insulated, water-cooled brass plates. The d.-c. potential applied was about 500 V, giving a potential gradient of about 11 V/cm. The air-free water used was prepared by boiling redistilled water, cooling under vacuum, and storing under nitrogen.

Thin-layer chromatography.—Thin-layer chromatography in an anhydrous, oxygen-free system was used to process all samples irradiated at IFA. After irradiation, the quartz ampoules were crushed, the sample was dissolved in a few drops of dry benzene, and the vial containing the solution was tightly stoppered with a silicone serum port. This procedure was carried out entirely in a nitrogen-filled glove bag. Separation of the recoil species was done by thin-layer chromatography, using the prepared sheets of powdered SiO_2 on a polyester backing (Eastman Chromagram Sheets type K301R2). The chromatography was done in a vacuum-dried, nitrogen-filled vessel, as shown in Fig. 1. Transfer of the solution was done with syringes, allowing essentially no contact with air or moisture. The solvent used for chromatography was benzene,

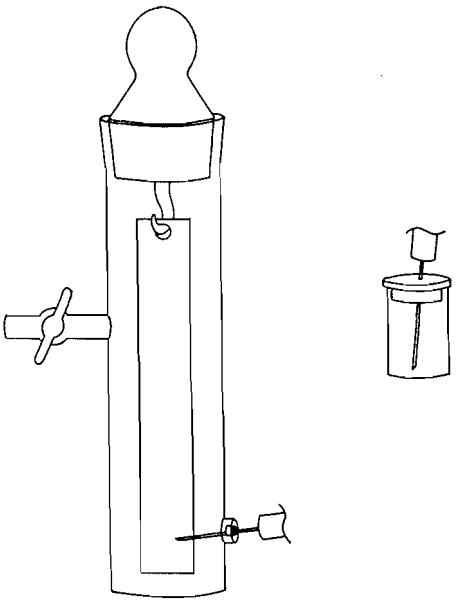


FIG. 1. Apparatus used for controlled-atmosphere chromatography.

distilled and dried over Linde No. 4A molecular sieve. Under these conditions, the resolution was good, and reproducibility in parallel runs was excellent. This technique is very quick and convenient, and we recommend it for use in all cases of chromatography of air-sensitive substances.

Annealing Experiments

Thermal treatment was done by placing the irradiated quartz ampoules into an oven adjusted to the proper temperature. The temperature was reproducible from one experiment to another to within ±0.5°. Heating and cooling times may introduce an uncertainty of ±0.1 min in the annealing times. Temperatures used ranged from 55° to 155°. Gross decomposition did not occur at any temperature, as was shown by (*a*) the absence of macroquantities of manganese in the first strips of the chromatograms and (*b*) by the sharpness of the solidification temperature following heating at temperatures above the melting point.

RESULTS

Species Observed

A typical paper chromatogram is shown in Fig. 2. The large peak at the zero position is clearly inorganic manganese, which we shall assume to be Mn^{2+}. The peak labelled $C_5H_5Mn(CO)_3$ was identified by observation of the behavior of macroscopic quantities of

Can. J. Chem. Downloaded from www.nrcresearchpress.com by 210.87.254.42 on 09/05/12
For personal use only.

the parent compound. It was also found that both manganocene and dimanganese decacarbonyl show similar behavior. Thus the purity of the species in this peak cannot be assured. The peak labelled compound A was present in all chromatograms, and although it is small in size it is statistically significant.[3] Figure 3 shows a typical ionogram. The peak labelled $C_5H_5Mn(CO)_3$ may, of course, contain other uncharged species. The ionographic behavior of Mn^{2+} was checked by the use of manganese-54 as Mn^{2+}. Again a small but distinct third peak, labelled compound B, is observed.

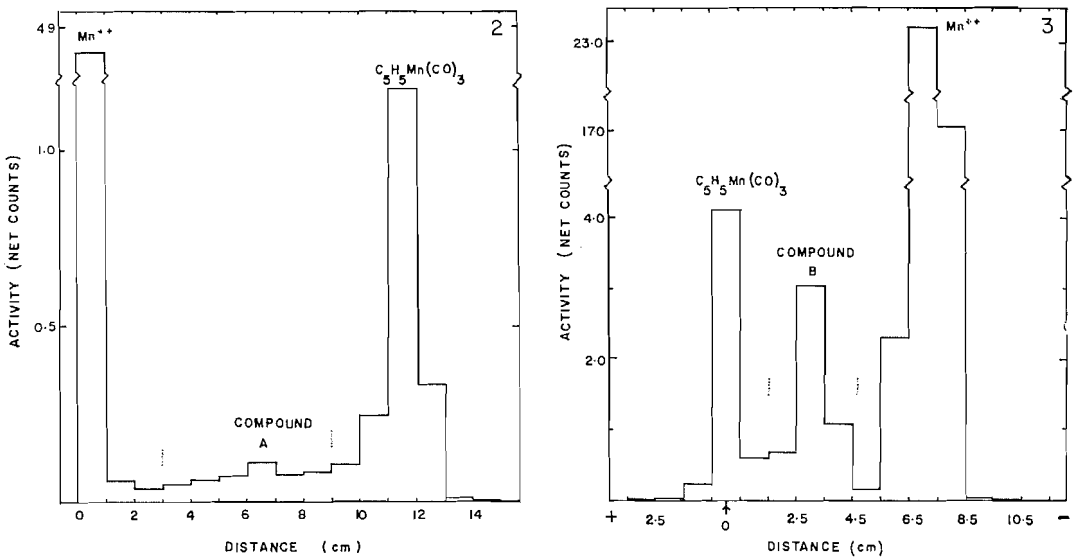


FIG. 2. Typical paper chromatogram for X-rod irradiation.
FIG. 3. Typical paper ionogram for J-rod irradiation.

The compounds A and B have not been identified as yet but some description of their nature and behaviour can be given. In the first place, compound A is likely an uncharged molecule while B seems to be a 1+ (or possibly 2+) cation. That they are related is shown by the following experiment:

The section of a paper chromatogram containing compound A was cut out, dried in nitrogen, and inserted into a paper strip for ionography; of the activity present, most appeared as Mn^{2+}, but some was found as a peak at the position of compound B, and some remained as a molecular compound at the position of the original spot. It is evident from the rapid conversion of this apparently molecular species to ionic species that compound A is unstable in water.

The chemical instability of compound B was shown by aerating a solution of the irradiated parent compound for a few minutes just before ionographic separation. Compound B all but disappeared (1.2% was found compared to 8.6% found in a simultaneous non-aerated control test). Dissolution and chromatography in hexane or in another solvent, as was done by Baumgärtner, Zahn, and Seeholzer (5) for dibenzene chromium, was not possible in this case because of the insufficient solubility of the parent compound.

No positive identification of compounds A and B can be made at present. However, it seems certain that they are constituted from remnants of the original molecule or fragments encountered on the recoil path. Identification of compounds A and B by standard

[3]*On nine observations the activity at the peak of compound A was larger than the mean of nearby activity by an average of 4.5 times the standard deviation of the nearby activity.*

Can. J. Chem. Downloaded from www.nrcresearchpress.com by 210.87.254.42 on 09/05/12
For personal use only.

methods is not possible since we have a total of only about 10^{10} molecules to work with. Since in this case alkyl manganese compounds are not stable, the only likely fragments are the cyclopentadiene ring and the carbonyl group. Some plausible compounds are suggested in Table II. It is hoped that experiments now under way using carbon-14 as an additional

TABLE II

Possible formulations for the unidentified species

Compound A	Compound B
$C_5H_5MnC_6H_6$	$Mn(CO)_3(H_2O)_3^+$
$C_6H_6Mn(CO)_3$	$C_5H_5Mn(H_2O)_3^+$
$(C_5H_5)_2Mn_2(CO)_4$	$C_5H_5Mn(CO)_{3-y}(H_2O)_y^+$

tracer will enable us soon to make unequivocal identification. A typical thin-layer chromatogram for a CT-2 or CT-3 irradiation is shown in Fig. 4. The important result to be noted immediately is the absence of compound A in the CT-2 and CT-3 experiments. The reason for this is not known, but may originate with the difference in chromatographic techniques used.

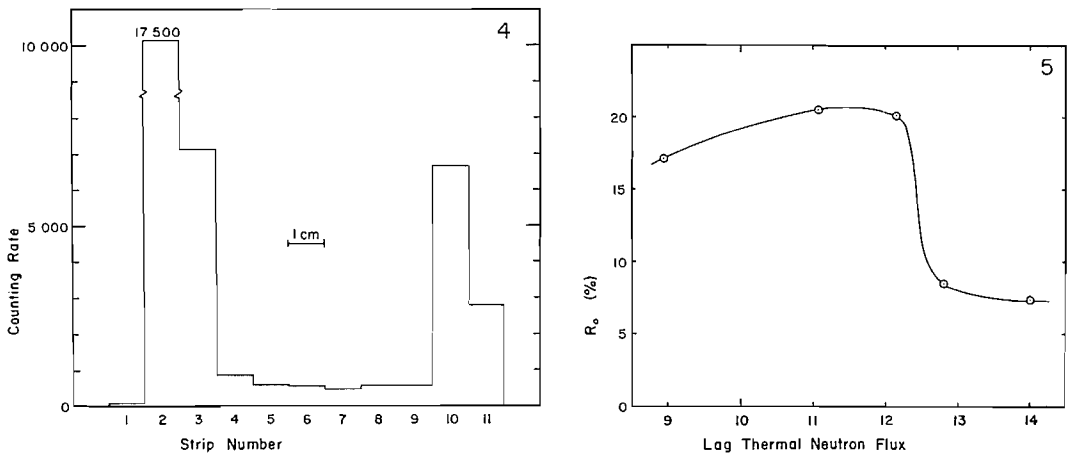


FIG. 4. Typical thin-layer chromatogram for CT2 and CT3 irradiations.
FIG. 5. Dependence of the initial parent yield (R_0) on neutron flux.

It was found in all ionograms that roughly 75–80% of the ^{56}Mn appeared as Mn^{2+}, while in the paper chromatograms and the thin-layer chromatograms a like amount was found as a benzene-insoluble species. Moreover, some 12–20% of the activity appeared as the parent compound in both types of experiment. While these amounts could not have been predicted with confidence, the results are not surprising, and are quite comparable to the results of studies on other metal-organic compounds (4–7).

The yields observed for the various species are summarized in Table III. The rather high relative uncertainties shown for compounds A and B and for $C_5H_5Mn(CO)_3$ are likely due to the chemical instability of these species in solution. One interesting feature of these data is the evident flux-dependence of the yield of the parent compound, as is shown in Fig. 5. The data are not, of course, strictly comparable, since the duration of the irradiations differed, as did the probable temperatures. Thus, the true origin of this effect cannot be identified from the present experiments. In this connection, it seems quite possible that the appearance of compound A in NRX irradiations and not in IFA experiments may be a result of a similar effect if not, in fact, the same reaction.

Can. J. Chem. Downloaded from www.nrcresearchpress.com by 210.87.254.42 on 09/05/12
For personal use only.

TABLE III

Distribution of recoil species found after irradiation (at ambient temperature) at various thermal neutron flux values; uncertainties are the mean deviations of 3–8 determinations, except for CT2, which is the mean of 2 determinations

Reactor	Position in reactor	Duration (min)	Yield (%) Mn^{2+}	A	B	$C_5H_5Mn(CO)_3$
Paper chromatography (dry benzene)						
NRX	S-6-1	15	75.9±3.0	4.0±0.7		20.1±3.0
	J-Rod	1	85.9±0.7	5.6±0.2		8.5±0.5
	X-Rod	0.1	88.4±0.9	4.2±0.9		7.4±0.1
Thin-layer chromatography (dry benzene)						
IFA	CT3	60	82.8±0.2	0		17.2±0.2
	CT2	3	79.5±1.4	0		20.5±1.4
Paper ionography (water–$NaClO_4$)						
NRX	S-6-1	15	82.3±3.8		5.0±1.1	12.7±3.4
	J-Rod	1	81.0±4.0		10.1±3.3	9.0±2.1

Thermal Annealing

The results of thermal treatment of the irradiated samples are given in Table IV and are shown in Figs. 6*a* and 6*b* for CT3 and CT2 irradiations, respectively. In considering these data it is important to note that the melting point of the starting compound is 77 °C.

TABLE IV

Values of R, the recovery of ^{56}Mn as the parent compound, by chromatography in benzene

Position in reactor	Without heating R_0 (%)	Heating at 65 °C Time (min)	R (%)	Heating at 88 °C Time (min)	R (%)	Heating at 120 °C Time (min)	R (%)	Heating for 30 min Temp.	R (%)
CT3	17.4	10	15.9	5	21.8	5	38.6		
	17.0	20	18.4	12	24.5	10	36.3		
		30	28.9	15	30.2	20	32.3		
	Av. 17.2	30	27.8	20	37.4	30	21.1		
		37	21.4	25	32.9				
		45	25.2	32	29.1				
		60	16.5	45	23.9				
				80	30.3				
CT2	19.0	10	31.5			5	28.2	55	30.2
	21.9	20	43.6			10	37.8	56	27.0
		30	19.7			20	32.3	72	17.9
	Av. 20.5	45	35.3			60	33.0	88	23.7
								98	28.6
								109	32.2
								119	30.0

Low-Temperature Irradiations

Some experiments were done in which the irradiation was carried out at liquid nitrogen temperature. Irradiations were done in the J-rod self-serve position of NRX. Chemical separation of the irradiated samples was done at 25 °C after varying lengths of time. Processing at low temperatures was attempted, but the insolubility of the target compound made such experiments impracticable. Results obtained are shown in Table V. The data of Table V are not strictly comparable to those of Table III, since the neutron flux and gamma-ray intensities were different. However, there are some striking features. In the

Can. J. Chem. Downloaded from www.nrcresearchpress.com by 210.87.254.42 on 09/05/12
For personal use only.

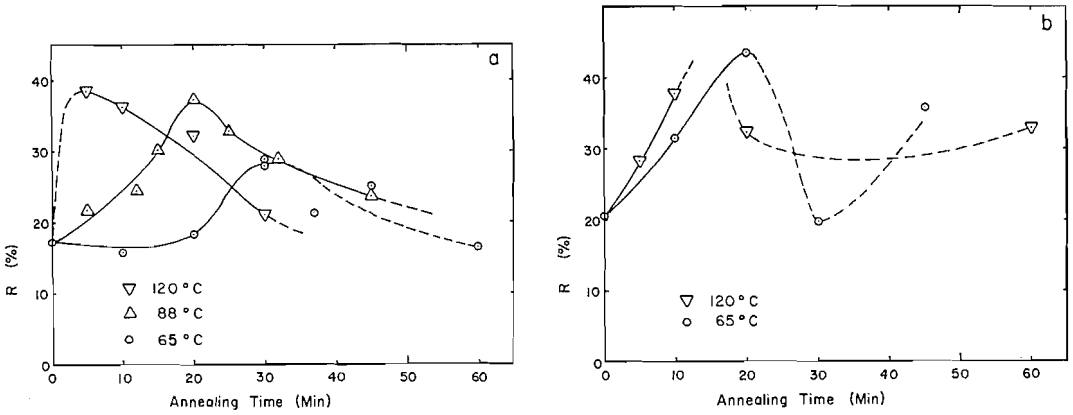


FIG. 6. Results of thermal annealing experiments (*a*) for CT3 irradiations, (*b*) for CT2 irradiations.

TABLE V

Distribution of recoil species produced by neutron irradiation at −196 °C in J-rod (self-serve) position

Annealing time at 25 °C (min)	Yield (%)			
	Mn^{2+}	A	B	$C_5H_5Mn(CO)_3$
Paper chromatography				
0	87.9	3.4		8.7
10	81.8	4.7		13.5
40	77.4	5.3		17.4
Paper ionography				
0	71.0		16.2	12.8
30	60.3		19.6	20.2

first place, the yield of the parent compound is seen to increase markedly with annealing at 25°. This result is a convincing demonstration of the importance of irradiation at controlled temperatures, since the sample temperature is undoubtedly higher than 25° under the usual irradiation conditions. The second interesting feature of these data is the distinct difference in the behavior of compounds A and B. The yield of compound A is increased somewhat on annealing, but is generally little affected either by annealing or by the temperature of irradiation. The yield of compound B, on the other hand, is greatly enhanced in the low-temperature irradiation, and seems to be further increased by the annealing. This difference suggests that these compounds, whatever their ultimate nature, arise from quite different reactions in the solid.

DISCUSSION

A number of interesting features are shown by the curves of Figs. 6*a* and 6*b*, some of which have not been observed in systems studied previously. In the first place, there is a good deal of recombination occuring in the liquid state, as is seen clearly in the results of the 88° experiments. While this is not the first time that "annealing" has been observed in the liquid state (8), it is, we believe, the first time that the solid and liquid states have been found to be so similar. Secondly, the form of the curves is not the simple first-order approach to a final value as is usually found, but shows a higher-order process which increases in rate from a slow beginning. In fact, at 65° there seems to be an

Can. J. Chem. Downloaded from www.nrcresearchpress.com by 210.87.254.42 on 09/05/12
For personal use only.

induction period of ~20 min before much change occurs. A further interesting feature is the decrease in retention which occurs after a maximum value has been reached. As the temperature of annealing is increased, the maximum value of the retention increases, and the time required to reach this maximum decreases. This fact suggests that two or more temperature-sensitive competitive reactions are in progress. In this case, of course, it cannot be a solid-state phenomenon, and is thus more likely a molecular displacement or exchange mechanism. The fact that the retention value appears in some cases to increase once more is quite interesting, but unfortunately we have too few data to be sure of this phenomenon.

It is important to note that a different batch of samples, prepared, as far as possible, in exactly the same way but stored for some months at room temperature before irradiation, gave somewhat different results. Qualitatively the trends in retention values as a function of heating time were the same, but some quantitative differences were noted. Thus, in addition to the effects reported here, there is some subtle effect due to sample history. This is a common and tantalizing observation which may result from, among other possibilities, lattice stress (9).

One important result of this work is the discovery that the results of annealing are the same in the liquid and the solid state, for samples irradiated as solids. Mechanisms currently used for explaining recombination involve processes such as short-range diffusion and electron detrapping, both of which will likely proceed to completion almost instantly on melting of the crystal. Thus, it seems that none of the existing mechanisms is likely to apply in the present case. The one exception may be the induction period seen in the 65° CT3 experiment; this induction period could well be a slow detrapping of electrons, to produce molecular or ionic species which subsequently form the species recovered.

The form of the curves, too, seems inconsistent with present mechanisms, in that the usual first-order increase in retention gives way to a more complicated shape. This complexity of shape undoubtedly indicates the occurrence of a series of consecutive and perhaps competitive reactions. After the induction period, which is discernible in only the one case, comes an increase in retention followed by a decrease to approximately the initial value. A further increase, indicated in some cases, is too uncertain to warrant much discussion.

Generally, annealing curves showing a maximum may be interpreted in terms of competitive reactions (10). These reactions may be of several kinds, including micro (11, 12) and gross (13, 14) decomposition and chemical (15, 16) and electronic (17) reduction. The decrease in retention following the maximum in the present work is very considerable, and amounts to roughly 50% in the 120° cases. The fact that this decrease is not accompanied by a corresponding gross decomposition of the sample, coupled with the observation that the same form is shown by the curves for the two phases, suggests that the decrease is due neither to decomposition nor to the type of microrecrystallization postulated by Dimotakis (12). Likewise, the two reduction processes seem not to be relevant to the present system. It is, moreover, difficult to imagine any sort of defect mechanism which would persist when the solid is melted. One is thus led to the conclusion that the observations do not represent an increase in true retention, but an increase in concentration of either an excited state of the parent molecule which decomposes on further heating, or a different compound, fleetingly stable, formed from the available fragments, and not chromatographically distinguished from the parent compound. In view of the relatively long times involved, the second of these alternatives seems the more likely. An analogous hypothesis was invoked by Miller and Dodson (18) in their work on carbon tetrachloride.

Can. J. Chem. Downloaded from www.nrcresearchpress.com by 210.87.254.42 on 09/05/12
For personal use only.

If this is the case—that the retention curves show the formation and subsequent decomposition of some compound other than the parent compound—then it is useful to speculate further about the general nature of the reactions in the solid and in the liquid. In the first place, from the similarity of retention values before and after the hump, one concludes that formation of the parent compound occurs very rapidly before the first observations and thereafter slowly, if at all, even at 120°. On the other hand, the changing values and times at the maximum apparent retention suggest that the reaction leading to the formation of this other compound, which we shall call the "pseudoparent," is quite temperature sensitive and that the decomposition reaction is slightly less so.

One can thus construct the following series of reactions:

[1] $$\text{Recoil} \rightarrow \text{Mn}^{\ddagger} + \text{fragments}$$

where $Mn^{\ddagger}$ represents a labile manganese-56 atom, perhaps recombined into an unstable molecular form, which undergoes reactions as follows.

[2] $$\text{Mn}^{\ddagger} + \text{fragments} \rightarrow \text{C}_5\text{H}_5\text{Mn}^*(\text{CO})_3$$

[3] $$\text{Mn}^{\ddagger} \xrightarrow{\text{dissolution}} \text{Mn}^{2+}$$

[4] $$\text{Mn}^{\ddagger} \xrightarrow{\text{heating}} (\text{Mn}^*)$$

The quantity (Mn*) is a postulated unstable molecular species which reacts further.

[5] $$(\text{Mn}^*) \xrightarrow{\text{dissolution}} \text{pseudoparent}$$

[6] $$(\text{Mn}^*) \xrightarrow{\text{heating}} \text{Mn}^* \xrightarrow{\text{dissolution}} \text{Mn}^{2+}$$

Reaction [4] followed by either [5] or [6] gives rise to the observed annealing effects. It appears that reaction [4] is accelerated at higher temperatures, while reaction [6] is less sensitive to heating. Unfortunately no reasonable estimates of activation energy can be made from the present data.

It is not intended to imply that (Mn*) and the stable pseudoparent are necessarily different species, although this is likely the case. It is important, moreover, to emphasize the probable role of the dissolution reactions in converting species metastable in the solid state into other species stable in solution. Doubtless this is the origin of compounds A and B.

The identities of the pseudoparent and of the metastable (Mn*) are not known. Both manganocene and dimanganese dekacarbonyl have chromatographic behavior similar to that of the parent compound. Of these, manganocene is the more likely to be the pseudoparent compound, since the probability of assembling the dekacarbonyl molecule is surely very small.

The similarity of the liquid and solid systems suggests that reaction [5] does not occur as result of diffusion back to the initial site, since diffusion processes would presumably show much greater differences between the two phases. Reaction [5] could be, among others, exchange between (Mn*) and inactive manganese atoms produced by local destruction on the recoil path.

Since the "fragments" involved in reaction [2] may quite well involve radiolysis products, or recoil-produced fragments modified by further radiolysis, the effect of flux on the initial retention and on the compounds A and B is rationalized. We thus have the generalized reaction below.

[2*a*] $$\text{Mn}^{\ddagger} + \text{fragments} \rightarrow \text{other products}$$

Can. J. Chem. Downloaded from www.nrcresearchpress.com by 210.87.254.42 on 09/05/12
For personal use only.

We are continuing our studies of recoil reactions in this compound, in an attempt to identify the molecular species produced and to isolate, if possible, reactions at the initial site from those occurring at the end of the recoil path.

In conclusion we may enumerate the species we have observed: In all cases we found activity attributable to the parent compound and to inorganic manganese. In addition, by three different techniques we have found, directly or indirectly, three other species. We call these compound A, compound B, and the pseudoparent, as observed by, respectively, paper chromatography, paper electrophoresis, and thin-layer chromatography. While it is true that the compounds we actually saw most likely are different, how they originate is unknown. Thus it may well be that all come from a single activated atomic or molecular species in the solid. There is low-temperature annealing evidence to suggest that compounds A and B may perhaps be of different origin. It is possible that compound A and the pseudoparent are the same compound, even though they show different chromatographic behavior, since the chromatographic media were different. Research programs currently under way may help to elucidate these questions.

ACKNOWLEDGMENTS

We express our gratitude to Academician H. Hulubei, Director of the Institute of Atomic Physics, Bucharest, for his support of this project and for his permission for D. R. W. to work at the Institute, and to Drs. R. H. Betts and J. P. Butler of the Chalk River Nuclear Laboratories for much assistance and advice. The President of Carleton University provided a travel grant for D. R. W. and the National Research Council of Canada provided financial assistance.

REFERENCES

1. L. Szilard and T. A. Chalmers. Nature, **134**, 462 (1934).
2. J. E. Willard. Ann. Rev. Nucl. Sci. **3**, 193 (1953).
3. G. Harbottle and N. Sutin. Advan. Inorg. Chem. Radiochem. **1**, 267 (1959).
4. N. Sutin and R. W. Dodson. J. Inorg. Nucl. Chem. **6**, 91 (1958).
5. F. Baumgärtner, U. Zahn, and J. Seeholzer. Z. Naturforsch. **15**a, 1086 (1960).
6. F. Baumgärtner and U. Zahn. Radiochim. Acta, **1**, 51 (1963).
7. G. Harbottle and U. Zahn. *In* Chemical effects of nuclear transformations. I.A.E.A. Symposium, Vienna, 1964. Vol. II. p. 133.
8. N. A. Katsanos and A. G. Varvoglis. J. Chem. Soc. 5935 (1964).
9. A. G. Maddock and J. I. Vargas. Nature, **184**, 1931 (1959).
10. T. Costea and I. Negoescu. J. Inorg. Nucl. Chem. In press. 1966.
11. P. N. Dimotakis and S. S. Kontis. Radiochim. Acta, **2**, 85 (1963).
12. P. N. Dimotakis and A. G. Maddock. J. Inorg. Nucl. Chem. **26**, 1503 (1964).
13. T. Costea, I. Dema, and A. Tipluica. Studii Cercetari Chim. **9**, 533 (1961).
14. P. N. Dimotakis and A. G. Maddock. *In* Chemical effects of nuclear transformations. I.A.E.A. Symposium, Vienna, 1961. Vol. I. p. 364.
15. N. Getoff and M. Nishikawa. Nature, **192**, 61 (1961).
16. N. Getoff and A. G. Maddock. Radiochim. Acta, **2**, 90 (1963).
17. T. Costea and I. Negoescu. Z. Physik. Chem. Frankfurt, **45**, 136 (1965).
18. J. M. Miller and R. W. Dodson. J. Chem. Phys. **18**, 865 (1950).

Can. J. Chem. Downloaded from www.nrcresearchpress.com by 210.87.254.42 on 09/05/12
For personal use only.

Can. J. Chem. Downloaded from www.nrcresearchpress.com by 210.87.254.6 on 09/05/12
For personal use only.

ABSORPTION SPECTRA AND CONFIGURATION OF SOME AMINE COMPLEXES OF COPPER(II) ACETATE

GOPAL NARAIN
Department of Chemistry, Lucknow University, Lucknow, U.P., India

Received August 31, 1965

ABSTRACT

Coordination complexes of copper(II) acetate, ammonia, aliphatic amines, and pyridine have been prepared. Molecular formulae on the basis of percentage of constituent elements were found to be $Cu(OAc)_2(am)_2$, where OAc represents acetate ion and am any amine used. Conductivity measurements in nitrobenzene and formamide indicate that the complexes are nonelectrolytes and thus it is suggested that acetate ions are also coordinated. Molecular weight measurements in the same solvents confirm this. Visible absorption measurements in formamide show a single band at about 635 mμ.

INTRODUCTION

A survey of the literature shows that a large number of amine complexes of bivalent copper have been prepared with almost all possible inorganic salts. Very little work has been done, however, with the organic salts (1, 2), although dimeric $Cu_2(OAc)_4.2H_2O$ and a number of ammonia and long chain aliphatic amine complexes of monomeric copper(II) acetate have been prepared (3–7). Since then no definite attempt towards preparation and the assignment of structures to these has been made.

The present communication relates to the synthesis and visible absorption measurements of a series of amine complexes of copper(II) acetate. The object of the work was to study whether the acetate ion, besides neutralizing the charge on the metal, is also coordinated to it.

EXPERIMENTAL

(A) Syntheses

(1) Copper(II) acetate.—This was prepared by dissolving the commercial 'neutral' salt in dilute acetic acid, filtering hot, cooling, washing the crystals well with water, and drying the air-dried solid *in vacuo* over phosphoric oxide until fresh desiccant extracted no more water.

The complexes were prepared by the following two methods:

(*X*) Finely powdered copper(II) acetate (500 mg) was placed in a calcium chloride tube fitted with a cotton wool plug at the bottom. This tube was attached to the neck of a flask containing amine, thereby exposing the blue solid to the vapors of amine for 4 h. The complex was formed, and the tube was taken out and left over calcium chloride to remove and absorb excess amine. The complex was dried over phosphorus pentoxide.

(*Y*) Copper(II) acetate (500 mg) was suspended in 15 cc of benzene. A little more than the calculated quantity of amine was added and the solution was refluxed for 2 h. The resulting complex (reaction mixture) was kept overnight and filtered the next morning. The precipitate was washed repeatedly with benzene, and dried first over calcium chloride and then over P_2O_5.

(2) Biacetato, biaminocopper(II).—Prepared by method *X*.
Anal. Found: Cu, 29.20; N, 12.75. $C_4H_{12}O_4N_2.Cu$ requires Cu, 29.47; N, 13.0.

(3) Biacetato, bi(methylamino)copper(II).—Prepared by method *X*.
Anal. Found: Cu, 26.31; N, 11.80. $C_6H_{16}O_4N_2.Cu$ requires Cu, 26.08; N, 11.5.

(4) Biacetato, bi(ethylamino)copper(II).—Prepared by method *X*.
Anal. Found: Cu, 23.50; N, 10.56. $C_8H_{20}O_4N_2.Cu$ requires Cu, 23.38; N, 10.31.

(5) Biacetato, bi(isopropylamino)copper(II).—Prepared by method *X*.
Anal. Found: Cu, 20.95; N, 9.23. $C_{10}H_{24}O_4N_2.Cu$ requires Cu, 21.2; N, 9.35.

(6) Biacetato, bi(n-propylamino)copper(II).—Prepared by method *X*.
Anal. Found: Cu, 20.86; N, 9.18. $C_{10}H_{24}O_4N_2.Cu$ requires Cu, 21.2; N, 9.35.

(7) Biacetato, bi(isobutylamino)copper(II).—Prepared by method *X*.
Anal. Found: Cu, 19.16; N, 8.73. $C_{12}H_{28}O_4N_2.Cu$ requires Cu, 19.39; N, 8.55.

(8) Biacetato, bi(n-butylamino)copper(II).—Prepared by method *X*.
Anal. Found: Cu, 19.0; N, 8.66. $C_{12}H_{28}O_4N_2.Cu$ requires Cu, 19.39; N, 8.55.

(9) Biacetato, bi(pyridino)copper(II).—Prepared by method *Y*.
Anal. Found: Cu, 18.98; N, 8.02. $C_{14}H_{16}O_4N_2.Cu$ requires Cu, 18.71; N, 8.25.

(B) Determination of Total Bases

The bases were estimated by treating 500 mg of a complex with $N/10$ sulfuric acid for $\frac{1}{2}$ h and titrating unreacted acid with $N/10$ sodium carbonate. A blank experiment was also done with 500 mg of $CuOAc_2$. The difference in volume of acids in the two cases gave the volume of acid neutralized by the amine, and the percentage was calculated on the assumption that two molecules of amine react with one molecule of acid.

(C) Molecular Weight Measurements

Molecular weights were determined by the method of freezing point depression, with nitrobenzene and formamide as solvents. Since the complexes dissolve only to a limited extent, a Beckmann thermometer with a scale of only 1 °C was used. The thermometer was extremely sensitive to supercooling and hence a modified apparatus was constructed. A glass vessel containing the freezing point tube was placed in a copper cylinder filled with water maintained at −5 °C with constant stirring by a mechanical stirrer. This cylinder was surrounded by another well-lagged copper cylinder containing ice.

(D) Conductivity Measurements

Measurements were done in nitrobenzene and formamide at a concentration of 10^{-3} M. The cell used had a cell constant = 0.0245.

(E) Purification of Solvents

Nitrobenzene was purified by steam distillation followed by distillation at reduced pressure. Formamide was distilled at reduced pressure.

(F) Spectral Measurements

The spectra were recorded on a Unicam S.P.500 spectrophotometer.

RESULTS AND DISCUSSION

The percentages of constituent elements and the synthesis of the complexes have been given in the Experimental section. The results of total base, molecular weight, conductivity, visible absorption measurements, and colors of the complexes are given in Table I.

On the basis of percentages of metal, nitrogen, and total base, the molecular formulae are $Cu(OAc)_2(am)_2$. These complexes are violet or green in color. They do not melt, but if heated or warmed with acids they decompose and become black in color. Their solubility is extremely low and they are soluble only in nitrobenzene and formamide.

The molar conductances in nitrobenzene and formamide (10^{-3} M solutions) give a value similar to that of the solvent or a value less than 1. These values indicate that the compounds are nonelectrolytes (8).

The freezing point depressions in formamide give the normal absolute value of molecular weight. These results suggest that acetate ion is also inside the coordination sphere along with amine. Therefore the formulae of the complexes are to be written as $[Cu(OAc)_2(am)_2]^0$. Thus in formamide and nitrobenzene, these compounds are monomeric and presumably planar four coordinate, if solvent interaction in the axial position is ignored.

The arrangement of any four groups around a copper(II) ion has usually been found to be planar. The stabilizing energy calculated from the energy level diagram is greater for a square planar than a tetrahedral structure and hence it is evident that unless a ligand possesses sufficient steric repulsions which can balance the decrease in crystal field stabilization energy, the tetra-coordinated complex will not take a tetrahedral configuration. Although such an arrangement is known to occur in the case of $CuCl_4^{-2}$ (9), the usual configuration for copper complexes is planar.

These complexes, which are themselves blue, violet, or green in color, dissolve in formamide to give blue solutions which exhibit a single band at about 635 mμ.

The position of this band depends on the intensity of the ligand field around the metal. Thus for the $[Cu(H_2O)_4]^{+2}$ ion the band is observed at 800 mμ. The successive replacement of water ligands by amines shifts the band from 800 mμ to 600 mμ for $[Cu(am)_4]^{+2}$. This bathochromic effect is due to the stronger ligand field environment produced around the metal, which causes the absorption band to shift to shorter wavelength.

Can. J. Chem. Downloaded from www.nrcresearchpress.com by 210.87.254.6 on 09/05/12
For personal use only.

Can. J. Chem. Downloaded from www.nrcresearchpress.com by 210.87.254.6 on 09/05/12
For personal use only.

TABLE I

Results obtained for amine complexes of copper(II) acetate

No.	Formulae*	% base		Molecular weight		Molar conductance	λ_{max} (mμ)	Color
		Observed	Calculated	Observed	Calculated			
1	$[Cu(OAc)_2(NH_3)_2]^0$	15.56	15.78	205	215.5	Nonelectrolyte†	635	Violet
2	$[Cu(OAc)_2(CH_3NH_2)_2]^0$	25.18	25.46	250	243.5	Nonelectrolyte	640	Violet
3	$[Cu(OAc)_2(C_2H_5NH_2)_2]^0$	33.36	33.15	281	271.5	Nonelectrolyte	640	Violet
4	$[Cu(OAc)_2(\text{iso-pr})_2]^0$	39.20	39.40	286	299.5	Nonelectrolyte	630	Violet
5	$[Cu(OAc)_2(n\text{-pr})_2]^0$	39.32	39.40	290	299.5	Nonelectrolyte	630	Violet
6	$[Cu(OAc)_2(\text{iso-bu})_2]^0$	44.78	44.6	335	327.5	Nonelectrolyte	635	Violet
7	$[Cu(OAc)_2(n\text{-bu})_2]^0$	44.80	44.6	333	327.5	Nonelectrolyte	635	Violet
8	$[Cu(OAc)_2(py)_2]^0$	46.38	46.54	331	339.5	Nonelectrolyte	630	Green

*OAc represents acetate ion; iso-pr, isopropylamine; *n*-pr, *n*-propylamine; iso-bu, isobutylamine; *n*-bu, *n*-butylamine; py, pyridine.
†Nonelectrolyte means the conductance value is either less than 1 or the same as that of the free solvent.

REFERENCES

1. L. TSCHUGAEFF. Ber. **38**, 2899 (1905).
2. G. SPACU and P. VOICHESCU. Z. Anorg. Allgem. Chem. **226**, 273 (1936).
3. J. N. WAN NICKERK and F. K. L. SCHOENING. Nature, **171**, 36 (1953).
4. A. R. BURKIN. J. Chem. Soc. 122 (1950).
5. H. J. S. KING. J. Chem. Soc. 2307 (1930).
6. F. K. BROOME, A. W. RALSTON, and M. H. THORNTON. J. Am. Chem. Soc. **68**, 67 (1946).
7. HERMANN GROSSMAN and GUSTAV JAGER. Z. Anorg. Chem. **73**, 48 (1912).
8. R. S. NYHOLM. J. Chem. Soc. 1714 (1957).
9. G. FELSENFELD. Proc. Roy. Soc. London, Ser. A, **236**, 506 (1956).

Can. J. Chem. Downloaded from www.nrcresearchpress.com by 210.87.254.6 on 09/05/12
For personal use only.

Can. J. Chem. Downloaded from www.nrcresearchpress.com by 210.87.254.5 on 09/05/12
For personal use only.

THE RELATIVE ACCEPTOR POWER OF BORON TRIHALIDES TOWARD ACETONITRILE BY PROTON NUCLEAR MAGNETIC RESONANCE MEASUREMENTS[1]

J. M. MILLER[2] AND M. ONYSZCHUK
Inorganic Chemistry Laboratory, McGill University, Montreal, Quebec
Received August 31, 1964

ABSTRACT

Proton nuclear magnetic resonance spectra of BF_3, BCl_3, and BBr_3 adducts of acetonitrile have been measured in nitrobenzene solution. Single peaks were observed in each case and chemical shifts relative to tetramethylsilane decreased in the order $BBr_3 > BCl_3 > BF_3$, suggesting that this is the order of acceptor activity toward acetonitrile. Linear relationships exist between methyl proton chemical shifts of $CH_3CN.BX_3$ and the heats of formation, dipole moments, and infrared vibrational shifts of the same or related adducts.

INTRODUCTION

In a previous article (1) we reported that proton nuclear magnetic resonance (n.m.r.) chemical shifts of $(CH_3)_3N.BX_3$ (where X = H, F, Cl, or Br) relative to tetramethylsilane decrease in the order $BBr_3 > BCl_3 > BH_3 > BF_3$, and that proton resonance peaks are singlets in $(CH_3)_3N.BF_3$ and $(CH_3)N.BH_3$ but quartets in $(CH_3)_3N.BCl_3$ and $(CH_3)_3N.BBr_3$. It was suggested that the quartet splitting resulted from coupling of methyl protons to ^{11}B (spin 3/2) only when there is appreciable steric hindrance to free rotation about the B—N bond, which appears from Courtauld molecular models to be true in $(CH_3)_3N.BCl_3$ and $(CH_3)_3N.BBr_3$ but not in $(CH_3)_3N.BF_3$ and $(CH_3)_3N.BH_3$. However, our failure to observe splitting of methyl protons in $(CH_3)_3N.BF_3$ was probably due to a lack of sensitivity of our spectrometer, as has been pointed out recently by Heitsch (2). He found that under high resolution the methyl proton peak consists of a decet due to coupling of protons with ^{11}B and ^{19}F nuclei. Similarly, Banister and Greenwood (3) attributed broadening of the methyl proton peak of dimeric dimethylaminoboron difluoride to ^{19}F-proton and ^{11}B-proton coupling.

To obtain more information about ^{11}B-proton coupling in boron trihalide complexes we have measured the ^1H n.m.r. spectra of $CH_3CN.BX_3$ adducts (where X = F, Cl, or Br). It was also of particular interest to determine whether proton chemical shifts could be correlated with the acceptor power order $BBr_3 > BCl_3 > BF_3$, which has been inferred from heats of formation of $CH_3CN.BX_3$ adducts (4, 5).

RESULTS AND DISCUSSION

The ^1H chemical shifts of $CH_3CN.BX_3$ adducts in nitrobenzene solution (1.0 mole %) are compared in Table I with the corresponding ^1H chemical shifts of $(CH_3)_3N.BX_3$ adducts* in nitrobenzene and chloroform solution (1.0 mole %) and with other physical

[1]*This work was supported by a grant from the Defence Research Board of Canada (grant number 9530-20, project D46-95-30-20).*
[2]*Holder of a N.R.C. bursary, 1961–1962, and N.R.C. studentships, 1962–1964.*
**After reporting our measurements on* $(CH_3)_3N.BX_3$ *adducts (1), we prepared* $(CH_3)_3N.BI_3$ *and found that its* ^1H *spectrum in chloroform solution consists of a quartet centered at 201.6 c.p.s. with a* ^{11}B—^1H *coupling constant of 3.3 c.p.s. and a profile almost the same as those previously observed for* $(CH_3)_3N.BCl_3$ *and* $(CH_3)_3N.BBr_3$. *Thus, in the series of* $(CH_3)_3N.BX_3$ *complexes, proton chemical shifts decrease in the order* $BI_3 > BBr_3 > BCl_3 > BF_3$. *It is also noteworthy that in the same series proton chemical shifts are directly proportional to* ^{11}B—^1H *coupling constants. When an attempt was made to prepare* $CH_3CN.BI_3$ *by adding* BI_3 *to a nitrobenzene solution of* CH_3CN, *an explosion occurred.*

data regarding BX_3 adducts. In the $(CH_3)_3N$ and CH_3CN series of adducts chemical shifts decrease in the order $BBr_3 > BCl_3 > BF_3$. The same order is also indicated by the heats of formation of $CH_3CN.BX_3$ and by dipole moments and infrared carbonyl shifts of related adducts. Moreover, as shown in Fig. 1, ^1H chemical shifts of $CH_3CN.BX_3$ are

TABLE I

Physical data for some BX_3 complexes

Property	Complex			Reference
	BF_3	BCl_3	BBr_3	
Methyl proton chemical shift, δ in c.p.s., for:				
$CH_3CN.BX_3$ in $C_6H_5NO_2$*	161.8	182.8	189.9	This work
$(CH_3)_3N.BX_3$ in $C_6H_5NO_2$	165.7	187.2	196.8	This work
$(CH_3)_3N.BX_3$ in $CHCl_3$	157.3	180.2	190.8	1
Heat of reaction, $-\Delta H$, kcal mole^{-1}, for:				
$CH_3CN_{(g)} + BX_{3(g)}$	26.5	33.8	—	4
$\rightarrow CH_3CN.BX_{(3s)}$	—	—	39.4	5
Dipole moment, in debyes, for:				
$(CH_3)_3N.BX_3$	4.04	5.13	5.57	6
$C_5H_5N.BX_3$	5.31	6.52	6.90	6
Infrared shift, $\Delta\gamma$(C=O), cm^{-1}, for:				
$CH_3COOC_2H_5.BX_3$	119	176	191	7
Xanthone.BX_3	138	229	253	8

*These values have not been corrected for the slight dissociation of $CH_3CN.BX_3$ that occurs in $C_6H_5NO_2$ solution.

directly proportional to: (i) heats of formation of $CH_3CN.BX_3$, (ii) dipole moments of $C_5H_5N.BX_3$ and $(CH_3)_3N.BX_3$, (iii) infrared carbonyl shifts of xanthone.BX_3. These correlations strongly suggest that all four measurements depend mainly upon the same fundamental property which we believe to be the strength of the donor–acceptor bond. It has not yet been possible to relate heats of formation, dipole moments, and carbonyl shifts directly to donor–acceptor bond strengths. In spite of this, these measurements have invariably been interpreted as indicating that the order of acceptor power is $BBr_3 > BCl_3 > BF_3$. While each of these measurements strongly suggests this order, none proves it conclusively. This is now also true of our proton chemical shifts of $CH_3CN.BX_3$ adducts. Nevertheless, we consider that the most reasonable explanation of the observed trend in proton chemical shifts of $CH_3CN.BX_3$ complexes is that the acceptor power toward acetonitrile decreases in the order $BBr_3 > BCl_3 > BF_3$.

This order also applies to N,N-dimethylformamide as reference electron-pair donor, as evident from the methyl proton resonance measurements of Kuhn and McIntyre (9). More recently, Gates, McLauchlin, and Mooney (10) measured ^{11}B chemical shifts of $L.BX_3$ complexes, where L = benzophenone, pyridine, and triethylamine, and X = F, Cl, Br, and I. They found that the difference between ^{11}B chemical shifts of complexed and free boron trihalide decreased in the order $BI_3 > BBr_3 > BCl_3 > BF_3$. This order correlates well with infrared and thermochemical data for acetophenone and pyridine complexes, respectively, strongly suggesting that this order is also that of the relative acceptor power.

Proton resonance peaks of $CH_3CN.BX_3$ complexes were sharp singlets, clearly indicating that there was little, if any, coupling of protons to ^{11}B, ^{19}F, and ^{14}N nuclei. Although ^{11}B-proton coupling was detected in $(CH_3)_3N.BX_3$ complexes, it is probably too weak to be observed in $CH_3CN.BX_3$ complexes because of the additional carbon atom between the ^1H and ^{11}B nuclei. The proton resonance peak of free CH_3CN at 123 c.p.s. was not observed in 1.0 mole % nitrobenzene solutions of $CH_3CN.BCl_3$. In the presence of a large excess of CH_3CN only a single peak occurred at 127 c.p.s. and its position varied with concentration.

Can. J. Chem. Downloaded from www.nrcresearchpress.com by 210.87.254.5 on 09/05/12
For personal use only.

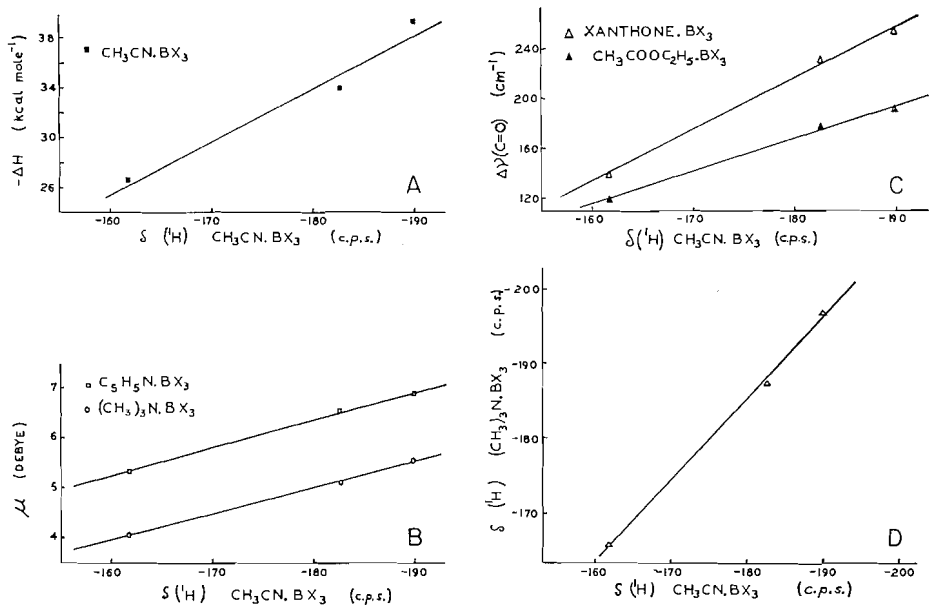


FIG. 1. Correlation of methyl proton chemical shifts of $CH_3CN.BX_3$ with: (A) heat of formation of $CH_3CN.BX_3$, (B) dipole moments of $C_5H_5N.BX_3$ and $(CH_3)_3N.BX_3$, (C) infrared carbonyl shifts of $CH_3COOC_2H_5.BX_3$ and xanthone.BX_3, and (D) ^{1}H n.m.r. shifts of $(CH_3)_3N.BX_3$.

These results confirmed that a fast exchange of BF_3 occurs between free and complexed CH_3CN. This was not true for $(CH_3)_3N.BCl_3$ in excess $(CH_3)_3N$ (1), presumably because of the greater stability of $(CH_3)_3N.BCl_3$ compared with $CH_3CN.BCl_3$ in nitrobenzene solution. Fast exchange in the $CH_3CN.BCl_3 - CH_3CN$ system would be expected to mask any splitting or broadening due to long range ^{11}B—^1H coupling.

Infrared spectra of $CH_3CN.BX_3$ complexes as 1.0 mole % solutions in nitrobenzene confirmed that they are only slightly dissociated ($< 5\%$) in this solvent. The spectrum of each complex contained a small peak at 2 250 cm^{-1} characteristic of the C≡N stretching vibration of pure CH_3CN, in addition to a strong, sharp, and narrow band due to "C≡N stretching" in complexed CH_3CN; these occurred at 2 360, 2 330, and 2 320 cm^{-1} in the BF_3, BCl_3, and BBr_3 complexes, respectively. Beattie and Gilson (11) have shown by normal coordinate analysis of $CH_3CN.BX_3$ that it is not possible to describe a pure "C≡N stretching" frequency in these complexes. It is not surprising, therefore, that "C≡N stretching" frequency shifts do not correlate with the observed ^{1}H chemical shifts.

EXPERIMENTAL

Materials

Acetonitrile complexes of BF_3, BCl_3, and BBr_3 were prepared by combining, in a standard high vacuum apparatus, the purified boron trihalide with acetonitrile previously dried over CaH_2. The component taken in excess was removed by distillation at 0° and the remaining white solid complex was pure after resublimation (for $CH_3CN.BF_3$: found m.p. 132–136°, lit. (4) 135°; for $CH_3CN.BCl_3$: found m.p. 195–201°, lit. (4) 195–200°; for $CH_3CN.BBr_3$: found m.p. 233–235°, with decomposition). Trimethylamine adducts of BF_3, BCl_3, and BBr_3 were prepared and purified as described previously (1). Nitrobenzene was purified by distillation over CaH_2. Tetramethylsilane (Anderson) was used without further purification.

Apparatus and Methods

Proton n.m.r. spectra were measured as described previously (1). Measurements were made on 1.0 mole % solutions of $CH_3CN.BX_3$ in nitrobenzene. To prevent hydrolysis of the adducts, solutions were prepared and transferred in a nitrogen-filled dry box. Measurements were also made on 1.0 mole % solutions of $(CH_3)_3N.BX_3$ in nitrobenzene. Infrared spectra were recorded on a Perkin–Elmer model 421 grating spectrometer.

Can. J. Chem. Downloaded from www.nrcresearchpress.com by 210.87.254.5 on 09/05/12
For personal use only.

ACKNOWLEDGMENTS

We thank Dr. A. Taurins and Dr. C. Stammer for the n.m.r. measurements. We are grateful to the Defence Research Board for financial assistance and to the National Research Council for the award of scholarships to one of us (J. M. M.).

REFERENCES

1. J. M. MILLER and M. ONYSZCHUK. Can. J. Chem. **42**, 1518 (1964).
2. C. W. HEITSCH. Inorg. Chem. **4**, 1019 (1965).
3. A. J. BANISTER and N. N. GREENWOOD. J. Chem. Soc. 1534 (1965).
4. A. W. LAUBENGAYER and D. B. SEARS. J. Am. Chem. Soc. **67**, 164 (1945).
5. J. M. MILLER and M. ONYSZCHUK. Can. J. Chem. **43**, 1877 (1965).
6. C. M. BAX, A. R. KATRITZKY, and L. E. SUTTON. J. Chem. Soc. 1258 (1958).
7. M. F. LAPPERT. J. Chem. Soc. 542 (1962).
8. D. COOK. Can. J. Chem. **41**, 522 (1963).
9. S. J. KUHN and J. S. MCINTYRE. Can. J. Chem. **43**, 375 (1965).
10. P. N. GATES, E. J. MCLAUCHLIN, and E. F. MOONEY. Spectrochim. Acta, **21**, 1445 (1965).
11. I. R. BEATTIE and T. GILSON. J. Chem. Soc. 2292 (1964).

Can. J. Chem. Downloaded from www.nrcresearchpress.com by 210.87.254.5 on 09/05/12
For personal use only.

Can. J. Chem. Downloaded from www.nrcresearchpress.com by 210.87.254.40 on 09/05/12
For personal use only.

THE REACTIVITY OF METAL–METAL BONDS

I. THE Sn–Sn BOND[1]

H. C. CLARK,[2] J. D. COTTON,[3] AND J. H. TSAI[4]

Department of Chemistry, University of British Columbia, Vancouver, British Columbia

Received December 15, 1965

ABSTRACT

The reactions of a series of fluorinated olefins with hexamethylditin have been investigated, under conditions which favor the formation of $(CH_3)_3Sn\cdot$ radicals. Two principal types of products have been isolated, namely (polyfluoroalkyl)trimethyltin compounds, e.g. $(CH_3)_3SnCF_2CF(R)H$, and insertion products of the type $(CH_3)_3SnCF_2CF(R)Sn(CH_3)_3$, where R = F or CF_3. These results are consistent with the formation of intermediate radicals such as $(CH_3)_3SnCF_2C(R)F\cdot$ which then participate either in hydrogen abstraction or in the formation of the insertion products. Reactions of hexamethylditin with $CF_2{=}CFH$, $CF_2{=}CH_2$, $CF_2{=}CFCl$, $CF_2{=}CFBr$, and C_2H_4 are also discussed. The direction of attack of the $(CH_3)_3Sn\cdot$ radical on the olefins indicates that the former has a high degree of nucleophilic character. A more detailed study of the reactions of the cyclic hexamers of dimethyltin and diphenyltin with tetrafluoroethylene shows that some addition does occur, but that the products are of indeterminate composition. The reaction of hexameric dimethyltin with trifluoroiodomethane has also been examined.

INTRODUCTION

Although numerous compounds have now been reported containing metal–metal bonds, few investigations have been made of the chemical reactivity of such bonds. We have become interested in such studies because of the considerable interest, from structural and theoretical viewpoints, in metal–metal bonds, and also because of the possible synthetic routes they provide to new organometallic compounds. In this paper we report on the chemical behavior of the Sn—Sn bond, as found in hexamethylditin, towards a series of fluorinated olefins; in later papers, other metal–metal bonded systems will be examined. Olefins have been chosen as the first set of standard reactants, since their high reactivity towards metal–metal bonds has been amply demonstrated, for example, by the catalytic properties of a platinum–tin complex in the homogeneous hydrogenation of ethylene and acetylene (1). The use of fluorinated olefins makes the application of ^{19}F nuclear magnetic resonance spectroscopy possible as an additional tool to follow the course of the reactions.

Hexaorganoditin compounds are well characterized, and the work of Kraus and Sessions (2) revealed the reactivity of the tin–tin bonds which they contain towards oxygen, chlorine, and sulfur. Interestingly, hexamethylditin reacts with mercury(II) chloride (2) to give mercury and trimethyltin chloride, showing the electropositive nature of the trimethyltin group. Although magnetic measurements (3) have shown that the $(CH_3)_3Sn$ group does not exist as the monomer in dilute benzene solution, other studies have provided indirect evidence of the free radical behavior of this group. Hexamethylditin is cleaved by trifluoroiodomethane (4, 5) according to the equation

$$(CH_3)_3Sn{-}Sn(CH_3)_3 + CF_3I \rightarrow (CH_3)_3SnCF_3 + (CH_3)_3SnI.$$

The most favorable conditions, requiring ultraviolet irradiation of the reactants at 25° for 6 h, are much milder than those usually required for free-radical formation from

[1]*Presented in part at the Chemical Conference, Chemical Institute of Canada, Montreal. May 1965.*

[2]*To whom correspondence should be addressed. Present address: Department of Chemistry, University of Western Ontario, London, Ontario.*

[3]*Present address: Department of Inorganic Chemistry, The University, Bristol, England.*

[4]*Present address: Exploratory Laboratory, Dow Chemical of Canada Ltd., Sarnia, Ontario.*

trifluoroiodomethane. It was thus suggested (6) that a radical–chain mechanism might be operating, probably involving homolytic fission of the Sn–Sn bond as the first step. Other workers (7) have interpreted the photolytic behavior of hexaethylditin in terms of homolytic fission of the Sn–Sn bond, in addition to rupture of the Sn–C bond, and the formation of new Sn–Sn bonds in polymeric organotin compounds.

This high reactivity of the Sn–Sn bond under free radical conditions suggested that ready addition across the olefinic double bond might also occur. This was supported by a preliminary study (8) of the reaction of hexamethylditin with tetrafluoroethylene, although the reaction products were not fully characterized.

RESULTS AND DISCUSSION

The reaction of hexamethylditin with tetrafluoroethylene was studied most fully, and in a typical reaction, equimolar quantities were irradiated with a 200 W Hanovia lamp at 75° for 4 h. Based on the recovery of hexamethylditin, the reaction was then about 60% complete. Of the ditin consumed, 13% appeared as decomposition products, mainly tetramethyltin which must result from the photochemical decomposition of hexamethylditin (7). This is consistent with the observed formation of a deeply colored, involatile residue, shown spectroscopically to contain polymeric organotin compounds. The other decomposition product, produced in as high as 28% yield, was trimethyltin fluoride, which must result from an α-fluorine atom elimination from fluorocarbontin compounds (5, 9). It was observed in all of the following reactions.

Two distinct types of products were formed as colorless liquids, namely the adducts, $(CH_3)_3Sn(CF_2CF_2)_nSn(CH_3)_3$, and polyfluoroalkyl trimethyltin compounds, $(CH_3)_3Sn(CF_2CF_2)_nH$. The compounds $(CH_3)_3Sn(CF_2CF_2)_nH$, $n = 1$ and 2, were fully characterized but the adducts could not be completely separated and were identified spectroscopically.

From a series of experiments summarized in Table I, in which controlled variations were made in the reaction conditions, several conclusions become apparent. Firstly, the extent of the reaction was approximately doubled when performed in a silica tube (transparent to radiation of wavelength $>2\,200$ Å) as compared with the use of a Pyrex tube (transparent for wavelength $>3\,000$ Å). Secondly, the reaction proceeded much further towards completion with irradiation at 75°, rather than 25°, although no reaction occurred in an experiment performed at 100° without irradiation. Thirdly, at 75° with irradiation, the yields of $(CH_3)_3SnCF_2CF_2H$ and the 1:1 adduct were markedly higher than at 25°, at which temperature the relative abundance of adducts containing several C_2F_4 units was much increased although the overall reaction was less complete.

The accelerating influence of the lower wavelength radiation is understandable in terms of the ultraviolet absorption maxima of ditin derivatives. Van der Kerk *et al.* (10) have reported a maximum at 247 mμ for hexaphenylditin, which they associated with the Sn—Sn bond system. We observe a similar maximum for hexamethylditin $\leqslant 210$ mμ, so that $(CH_3)_3Sn\cdot$ radicals may be formed under ultraviolet irradiation. If the reaction occurs principally in the gas phase, the increased rate at higher temperatures may arise from the consequent increase in the partial pressure of hexamethylditin (b.p. 182°).

The formation of the above products suggests that two principal reactions must occur, both involving the radical $(CH_3)_3SnCF_2CF_2\cdot$. It is reasonable to assume that this species is formed by the attack of $(CH_3)Sn\cdot$ radicals on tetrafluoroethylene. The resultant radical then either participates in hydrogen abstraction, presumably from methyl groups, or attacks another hexamethylditin molecule giving the 1:1 adduct and another $(CH_3)Sn\cdot$

Can. J. Chem. Downloaded from www.nrcresearchpress.com by 210.87.254.40 on 09/05/12
For personal use only.

radical. Both of these steps may alternatively be preceded by combination of $(CH_3)_3SnCF_2CF_2\cdot$ with one or more C_2F_4 molecules giving higher molecular weight radicals. The overall reactions can be described by the following scheme.

$$(CH_3)_3Sn{-}Sn(CH_3)_3 \xrightarrow{\text{ultraviolet}} 2(CH_3)_3Sn\cdot$$

Initiation: $(CH_3)_3Sn\cdot + CF_2{=}CF_2 \rightarrow (CH_3)SnCF_2CF_2\cdot$

Propagation: $(CH_3)_3SnCF_2CF_2\cdot + CF_2{=}CF_2 \rightarrow (CH_3)_3SnCF_2CF_2CF_2CF_2\cdot$, etc.

Chain transfer:

(*a*) $(CH_3)_3Sn(CF_2CF_2)_n\cdot + (CH_3)_3Sn{-}Sn(CH_3)_3 \rightarrow (CH_3)_3Sn(CF_2CF_2)_nSn(CH_3)_3 + (CH_3)_3Sn\cdot$, etc.

or

(*b*) $$(CH_3)_3Sn(CF_2CF_2)_n\cdot + \diagdown\!\!\!\!\diagup C{-}H \rightarrow (CH_3)_3Sn(CF_2CF_2)_nH + \diagdown\!\!\!\!\diagup C\cdot, \text{ etc.}$$

Clearly the higher proportion of olefin in the gas phase at 25° will favor the propagation reaction (i.e. formation of products where n is large), while in agreement with observation, the increased vapor pressure and hence higher proportion of hexamethylditin at 75° will favor the chain transfer reactions. It is possible that at much higher temperatures, the products with $n = 1$ might be formed almost exclusively, but under these more vigorous conditions, decomposition to trimethyltin fluoride and fluorocarbons would probably be extensive.

We must stress that the above evidence does not exclude a molecular, four-center type of mechanism. Moreover, assuming a radical mechanism is involved, these results provide no information on the direction of radical attack. Some such information could well be obtained by examining the reactions of hexamethylditin with unsymmetrical fluoroolefins.

In several reactions of hexamethylditin with perfluoropropene, the only observed products, apart from the photochemical decomposition products from the ditin, were 1,1,2,3,3,3-hexafluoropropyltrimethyltin, $(CH_3)_3SnCF_2CF(CF_3)H$, and 1,2-bis-(trimethyltin)hexafluoropropane, $(CH_3)_3SnCF_2(CF_3)Sn(CH_3)_3$. These colorless liquids were characterized analytically and spectroscopically, and the latter data will be described fully elsewhere. When the reaction was performed at 90° rather than 70°, the yield of the 1:1 adduct was reduced markedly because of decomposition, while at 25° the formation of this adduct was almost negligible.

The hexafluoropropyl derivative has two possible isomeric forms, namely

$$(CH_3)_3SnCF_2CF(CF_3)H \quad \text{and} \quad (CH_3)_3SnCF(CF_3)CF_2H,$$

I II

of which only isomer I was observed in four experiments. The reaction therefore proceeds by the attack of $(CH_3)_3Sn\cdot$ radicals exclusively on the $F_2C{=}$ group of the propene.

$$(CH_3)_3Sn{-}Sn(CH_3)_3 \xrightarrow{\text{ultraviolet}} 2(CH_3)_3Sn\cdot$$

$$(CH_3)_3Sn\cdot + CF_2{=}CFCF_3 \rightarrow (CH_3)_3SnCF_2CF(CF_3)\cdot$$

and

$$(CH_3)_3SnCF_2CF(CF_3)\cdot + \diagdown\!\!\!\!\diagup C{-}H \rightarrow (CH_3)_3SnCF_2CF(CF_3)H + \diagdown\!\!\!\!\diagup C\cdot \text{ etc.}$$

or

$$(CH_3)_3SnCF_2CF(CF_3)\cdot + (CH_3)_3Sn{-}Sn(CH_3)_3 \rightarrow (CH_3)_3SnCF_2CF(CF_3)Sn(CH_3)_3 + (CH_3)Sn\cdot \text{ etc.}$$

Can. J. Chem. Downloaded from www.nrcresearchpress.com by 210.87.254.40 on 09/05/12
For personal use only.

Products arising from the propagation step:

$$(CH_3)_3SnCF_2CF(CF_3)\cdot + CF_2{=}CFCF_3 \rightarrow (CH_3)_3SnCF_2CF(CF_3)CF_2CF(CF_3)\cdot \text{ etc.}$$

were not observed.

Radical addition to fluoro-olefins has been investigated by several groups of workers (11–13), and in particular the direction of addition to unsymmetrical olefins has been discussed by Haszeldine *et al.* (11). They point out that hexafluoropropene is very sensitive to nucleophilic attack, and that such attack is exclusively on the $F_2C{=}$ group. The more nucleophilic the attacking radical, therefore, the more should radical attack be oriented towards the $F_2C{=}$ group. A comparison of our results with those of Haszeldine *et al.* thus shows that the $(CH_3)_3Sn\cdot$ radical is as specific as the $(CH_3)_3Si\cdot$ and the $(CH_3)_2SiH\cdot$ radicals in directing attack to the $F_2C{=}$ group, and possesses considerable nucleophilic character.

Temperatures of 85–105° with ultraviolet irradiation favored the reaction of hexamethylditin with trifluoroethylene, leading to similar series of products, $(CH_3)_3Sn(C_2F_3H)_nH$ and $(CH_3)_3Sn(C_2F_3H)_nSn(CH_3)_3$, as well as decomposition products of the ditin. On the basis of spectroscopic evidence, products formulated as $(CH_3)_3SnCFHCF_2H$, $(CH_3)_3SnCFHCF_2CFHCF_2H$, and $(CH_3)_3SnCF_2CFHCF_2CFHSn(CH_3)_3$ were identified, and were probably formed by a series of reactions similar to those for tetrafluoroethylene and perfluoropropene, and involving radicals such as $(CH_3)_3SnCFHCF_2\cdot$ and $(CH_3)_3Sn(CFHCF_2)_nCFHCF_2\cdot$. The presence in the hydrogen abstraction products of terminal $-CF_2H$ groups rather than $-CFH_2$ groups strongly suggests that addition of $(CH_3)_3Sn\cdot$ is predominantly to the $=CFH$ group of trifluoroethylene, as for other radical additions (14, 15).

An increase in the concentration of hexamethylditin should reduce the extent of the propagation reaction

$$(CH_3)_3SnCFHCF_2\cdot + CF_2{=}CFH \rightarrow (CH_3)_3SnCFHCF_2CFHCF_2\cdot, \text{ etc.}$$

When hexamethylditin in 40% excess was irradiated with trifluoroethylene at 90°, a mixture of *both* the 1:1 adduct, $(CH_3)_3SnCFHCF_2Sn(CH_3)_3$ and the 1:2 adduct in an approximate ratio 2:1 was identified spectroscopically. Moreover, neither of these products was formed in a reaction carried out at 100° in the absence of radiation, although considerable decomposition of hexamethylditin to metallic tin, tetramethyltin, and some hydrogen was observed. Similarly, with hexamethylditin and 1,1-difluoroethylene, both hydrogen abstraction products, $(CH_3)_3Sn(CH_2CF_2)_nH$ ($n = 1$ or 2), and adducts $(CH_3)Sn(CF_2CH_2)_nSn(CH_3)_3$ were formed. Spectroscopic evidence showed conclusively that the hydrogen abstraction products contained terminal $-CF_2H$ groups, again demonstrating that the most probable mechanism involves attack of $(CH_3)_3Sn\cdot$ radicals on the CH_2 group of 1,1-difluoroethylene. This agrees with other data relating to radical attack on this olefin by $CF_3\cdot$ (16), $Br\cdot$ (17), and $PH_2\cdot$ (11).

It is clear, then, that the nucleophilic character of $(CH_3)_3Sn\cdot$ does not play too important a role in its reactions with trifluoroethylene and 1,1-difluoroethylene, since products arising from the intermediate radicals $(CH_3)_3SnCF_2CFH\cdot$ and $(CH_3)_3SnCF_2CH_2\cdot$ would otherwise have been formed. These results, however, agree with previous conclusions (11) that the difference in stability of the possible intermediate radicals is sufficient to determine the position of radical attack of the fluoro-olefin, e.g.

$(CH_3)_3SnCH_2CF_2\cdot$ formed rather than $(CH_3)_3SnCF_2CH_2\cdot$

$(CH_3)_3SnCFHCF_2\cdot$ formed rather than $(CH_3)_3SnCF_2CFH\cdot$.

Can. J. Chem. Downloaded from www.nrcresearchpress.com by 210.87.254.40 on 09/05/12
For personal use only.

With perfluoropropene the difference in stability of the two possible radicals $(CH_3)_3SnCF_2CF(CF_3)\cdot$ and $(CH_3)_3SnCF(CF_3)CF_2\cdot$ is apparently not great, so that the nucleophilic character of $(CH_3)_3Sn\cdot$ is the determining factor.

Somewhat different reactions occurred between hexamethylditin and trifluorochloroethylene or trifluorobromoethylene. With trifluorochloroethylene, only the hydrogen abstraction product, $(CH_3)_3SnCF_2CFHCl$, and secondary products such as tetramethyltin, trimethyltin chloride, and trimethyltin fluoride were formed. No adduct could be detected by careful spectroscopic examinations of the reaction mixtures. Apparently, the radical $(CH_3)_3SnCF_2CFCl\cdot$ is formed by attack of $(CH_3)_3Sn\cdot$ on the CF_2 group of CF_2CFCl. The orientation of this attack is in good agreement with other systems e.g. $CF_3\cdot$ and $CCl_3\cdot$ (18), $Br\cdot$ (19), $SiCl_3\cdot$ (15), and $PH_2\cdot$ (11). In all these cases, the direction of radical attack was attributed to the difference in stability of the radicals, $RCF_2CFCl\cdot > RCFClCF_2\cdot$, because of the powerful stabilizing effect of the chlorine atom (14). The formation of both trimethyltin chloride and trimethyltin fluoride could be due to the decomposition of either the alkyltin compounds

$$(CH_3)_3SnCF_2CFHCl \rightarrow (CH_3)_3SnF \text{ (or Cl)} + CF_2{=}CHCl \text{ (or F)}$$

or of an unstable and unobserved adduct

$$[(CH_3)_3SnCF_2CFClSn(CH_3)_3] \rightarrow (CH_3)_3SnF \text{ (or Cl)} + (CH_3)_3SnCF{=}CFCl \text{ (or F)}.$$

However, no vinyltin compounds could be identified among the products.

With trifluorobromoethylene, reaction occurred under irradiation at room temperature, to give perfluorovinyltrimethyltin, tetramethyltin, trimethyltin fluoride, and trimethyltin bromide, in addition to involatile polymeric forms of organotin compounds. Neither hydrogen abstraction products nor adducts could be detected even under these mild conditions. These results suggest the following reaction sequence.

$$(CH_3)_3Sn{-}Sn(CH_3)_3 \xrightarrow{\text{ultraviolet}} 2(CH_3)_3Sn\cdot$$

$$(CH_3)_3Sn\cdot + CF_2{=}CFBr \rightarrow [(CH_3)_3SnCF_2CFBr\cdot] \rightarrow (CH_3)_3SnCF{=}CF_2 + Br\cdot$$

$$Br\cdot + (CH_3)_6Sn_2 \rightarrow (CH_3)_3SnBr + (CH_3)_3Sn\cdot, \text{ etc.}$$

This is consistent with the ease of formation of the reactive $Br\cdot$ radical under irradiation (11, 14, 19, 20). However, an alternative sequence cannot be eliminated:

$$(CH_3)_3Sn{-}Sn(CH_3)_3 + CF_2{=}CFBr \rightarrow [(CH_3)_3SnCF_2CFBrSn(CH_3)_3] \rightarrow (CH_3)_3SnCF{=}CF_2 + (CH_3)_3\,SnBr.$$

In the reaction of tetramethyldiarsine with trifluorobromoethylene, both the adduct, $(CH_3)_2AsCF_2CFBrAs(CH_3)_2$, and its decomposition products, $(CH_3)_2AsCF{=}CF_2$ and $(CH_3)_2AsBr$, have been observed (21).

Finally, in view of the successful addition of acetylenes to organotin hydrides to give compounds of the type $R_3SnCH_2CH_2SnR_3$ (22), it was hoped that 1,2-bis(trimethyltin)-ethane might be formed by the reaction of hexamethylditin with ethylene. Even after prolonged periods of irradiation at 25°, no adducts could be detected. This is in sharp contrast to the sequence given by Haszeldine and Osborne (17) for the ease of radical attack, i.e.

$$C_2H_4 \sim CH_2{=}CHCH_3 \sim CH_3CH{=}CHCH_3 > CH_2{=}CF_2 > CF_2{-}CHCl > CF_2{=}CFCl > CF_2{=}CHCF_3 > CF_2{=}CFCF_3.$$

However, this order was established by the use of $Br\cdot$ and $CF_3\cdot$ radicals which must behave more as electrophiles than the $(CH_3)_3Sn\cdot$ radical. Although $Br\cdot$ and $CF_3\cdot$ should readily attack the electron-rich carbon atoms of ethylene, the more nucleophilic $(CH_3)_3Sn\cdot$ may very much more readily attack the electron-poor carbon atoms of tetrafluoroethylene.

Can. J. Chem. Downloaded from www.nrcresearchpress.com by 210.87.254.40 on 09/05/12
For personal use only.

Can. J. Chem. Downloaded from www.nrcresearchpress.com by 210.87.254.40 on 09/05/12
For personal use only.

In our preliminary communication (8), in addition to the reaction of hexamethylditin with tetrafluoroethylene, we described the reaction of diphenyltin with tetrafluoroethylene. Since that time, the constitution and polymeric complexities of diorganotin compounds, $[R_2Sn]_n$, have been examined by several workers. The linear polymers $[(CH_3)_2Sn]_x$ where $x = 12$–20, and the cyclic hexamer $[(CH_3)_2Sn]_6$ have been synthesized and distinguished on the basis of their infrared and proton magnetic resonance spectra (23). The constitution of the various forms of diphenyltin has been established by the work of Neumann and Konig (24) and the structural study of Olsen and Rundle (25). Since these developments have made it possible to work with homogeneous and well-defined forms of specific diorganotin compounds, we have repeated the earlier work, hoping to characterize the products more fully.

We chose to work chiefly with the cyclic hexameric forms of dimethyltin and diphenyltin. The former was obtained firstly by the method described by Brown and Morgan (23) involving the reduction by lithium aluminium hydride of dimethyltin dichloride in diethyl ether in the presence of triethylamine. The results of Brown and Morgan were readily reproduced, with respect to the general characteristics of the products and to the major features of the infrared and proton magnetic resonance spectra. It was clear, however, as Brown and Morgan had shown, that this method gives predominantly the cyclic hexamer with varying amounts of linear polymers. An alternative preparation involving the decomposition of dimethyltin dihydride with pyridine in the presence of a trace of dimethyltin dichloride was therefore also used. This method has been most recently applied by Neumann (26) to the preparation of $[(C_6H_5)_2Sn]_6$ and $[(C_2H_5)_2Sn]_6$, and the available evidence shows that formation of the cyclic hexamer $[(CH_3)_2Sn]_6$ is essentially quantitative by this method. Similarly, the cyclic hexamer of diphenyltin was obtained (24) by reduction of diphenyltin dihydride with pyridine, and for comparisons with earlier results (8), the product obtained by the reduction of diphenyltin dihydride with methanol was also used in certain reactions. This latter "white modification" was originally considered by Kuivila and Jakusik (27) to be another form of polymeric diphenyltin, but Neumann has shown it to be H—$[(C_6H_5)_2Sn]_6$—H which loses the remaining hydrogen, for example on treatment with pyridine or dimethylformamide, to give the cyclic hexamer.

Reactions of polydimethyltin with tetrafluoroethylene were carried out firstly with heating to 105°. The olefin underwent some polymerization (~25%) and extensive decomposition of the dimethyltin was observed, but no fluorocarbon-tin derivative could be detected. Ultraviolet irradiation of dimethyltin (obtained by the lithium aluminium hydride reduction method) with tetrafluoroethylene in a silica tube at 60° led to extensive polymerization of the olefin with some decomposition of the organotin, and again no fluorocarbon-tin appeared to be formed. When reactions of dimethyltin (prepared by reduction of the dihydride with pyridine) with tetrafluoroethylene were carried out in benzene solution, under ultraviolet irradiation in either Pyrex or silica reaction tubes, there was apparently some uptake of the olefin, other than in polymerization. All the products, however, were resinous substances which solidified on exposure to air. The infrared spectra showed shifts of about 30 cm^{-1} to higher frequencies for the Sn–C stretching vibrations, compared with those of dimethyltin, and also C—F stretching vibrations different from those of polymerized tetrafluoroethylene. However, no products could be obtained in a form suitable for characterization.

Similarly, from reactions of diphenyltin with tetrafluoroethylene, usually carried out in benzene solution under ultraviolet irradiation, only small quantities of yellow oils were obtained, except when the product mixtures were allowed to oxidize in air when unidentified white solids resulted. The consumption of olefin was always small compared with that

required for complete reaction with the diphenyltin, and although the infrared spectra of the oils showed features similar to those reported previously (8), identifiable substances could not be obtained. In summary, after a very careful examination, under rigorously controlled conditions, of the reactions of dimethyl- and diphenyl-tin with tetrafluoroethylene, it is clear that at best only a low proportion of the Sn—Sn bonds are broken and that identifiable species cannot be obtained. The solid material described previously (8) is presumably some type of oxidation product, in which fluorocarbon groups are present, and in which terminal hydrogen atoms of the starting material are probably replaced by chlorine atoms from the solvent.

Finally, we have examined the reaction of dimethyltin (prepared from the dihydride by reduction with pyridine) with trifluoroiodomethane under ultraviolet irradiation in a silica tube at room temperature. The less volatile fractions of the reaction mixture were shown to be mixtures, and from the infrared and proton magnetic resonance spectra, four components were identified. Two of these, from known data, were trimethyltrifluoromethyltin, and trimethyltin iodide. The remaining two were presumably dimethyl bis(trifluoromethyl)tin and dimethyltrifluoromethyltin iodide. The reaction residue contained dimethyltin diiodide. None of these could be obtained as pure compounds because of their similar volatilities and because several of them readily decomposed on gas chromatographic columns. Our evidence does confirm again, however, that trifluoroiodomethane adds across the Sn—Sn bond.

EXPERIMENTAL

Standard high vacuum techniques were used throughout these reactions for the manipulation of volatile compounds. Infrared spectra were recorded with Perkin-Elmer model 137 and model 21 spectrophotometers. Proton spectra were recorded on a Varian A60 spectrometer, and fluorine magnetic resonance spectra at 56.4 Mc s^{-1} with a Varian V-4300 spectrometer. Gas chromatographic separations were performed on a Beckman GC-2A gas chromatograph with helium as the carrier gas.

Reactants

Hexamethylditin was prepared according to the procedure described by Clark and Willis (5). Tetrafluoroethylene was prepared by the pyrolysis of Teflon chips in a silica tube at ~600° and was purified by vacuum fractionation. All other olefins were obtained commercially and were purified by vacuum fractionation.

Reactions of Hexamethylditin with Tetrafluoroethylene

(*a*) Hexamethylditin (7.0 g, 21.4 mmoles) and tetrafluoroethylene (2.2 g, 22 mmoles) in a silica tube at 75° were exposed to ultraviolet radiation for 4 h. The volatile products were separated under vacuum into fractions condensing at −196°, −126°, −78°, −46°, and 0° to leave a brown liquid in the reaction tube. The −196° fraction (0.10 mmole) was mainly tetrafluoroethylene with some perfluoropropane, both identified by infrared spectrometry and chromatography. The −126° fraction was perfluoro-1,3-butadiene (0.15 mmole; mol. wt. calcd. 162, observed 159), unambiguously identified (28) by the characteristic infrared bands at 1 780 (s), 1 330 (vs), 1 190 (s), 1 140 (s), and 965 (s) cm^{-1}. The −78° fraction was tetramethyltin (0.3 g, 1.7 mmole), identified by comparison of its gas chromatographic retention time and its infrared spectrum with those of a standard sample. The −46° fraction was separated chromatographically (preparative dinonyl phthalate column at 140°, with 15 p.s.i. of helium) into 1,1,2,2-tetrafluoroethyl trimethyltin (0.12 g, 0.45 mmole) and 1,1,2,2,3,3,4,4-octafluorobutyltrimethyltin (0.08 g, 2.22 mmole). The former was characterized analytically and by comparison of its infrared and proton magnetic resonance spectra with those of dimethylbis(tetrafluoroethyl)tin (29, 30).

Anal. Calcd. for $C_5H_{10}F_4Sn$: C, 22.6; H, 3.9; mol. wt. 265. Found: C, 22.6; H, 4.1; mol. wt. 251.

The second chromatographic fraction (retention time 6.8 min) was the octafluorobutyltrimethyltin. This was characterized by its infrared and proton magnetic resonance spectra. The latter showed, in addition to the methyl absorptions, a tripleted triplet at −5.97 p.p.m. with respect to internal TMS. This contrasts with the tripleted triplet at −5.51 p.p.m. observed for the SnC_2F_4H group. Both spectra will be discussed more fully elsewhere.

The 0° fraction was combined with the brown liquid, and distillation under reduced pressure (22 mm Hg) at 78° gave unchanged hexamethylditin (2.6 g, 37% recovery). Ether extraction of the residue left a white solid which was treated first with carbon tetrachloride followed by hot methanol. There remained a white solid (0.35 g) whose infrared spectrum was identical to that of polymerized tetrafluoroethylene. Evaporation of the methanol solution gave trimethyltin fluoride (1.3 g, 7.1 mmoles).

Anal. Calcd. for C_3H_9FSn: C, 19.8; H, 4.9. Found: C, 19.7; H, 4.03.

Can. J. Chem. Downloaded from www.nrcresearchpress.com by 210.87.254.40 on 09/05/12
For personal use only.

TABLE I

Product distribution in reactions of hexamethylditin with C_2F_4

		Expt. 1	Expt. 2	Expt. 3	Expt. 4
Reactants (mmoles)	$(CH_3)_6Sn_2$	18.3	20.8	21.9	21.4
	C_2F_4	18.5	21.7	22.0	22.0
Conditions	Carius tube	Pyrex	Pyrex	Silica	Silica
	Temperature (°C)	25	25	25	75
	Time (h)	17	60	31	4
% recovery	$(CH_3)_6Sn_2$	77	56	63	37
	C_2F_4	43	35	5	Trace
Products (mmoles)	$(CH_3)_4Sn$		0.18	0.91	1.70
	$(CH_3)_3SnCF_2CF_2H$	0.72	0.19	0.19	0.45
	$(CH_3)_3SnCF_2(CF_2)_2CF_2H$	0.85	0.27	0.27	0.22
	$(CH_3)_3SnCF_2(CF_2)_4CF_2H$*		0.43	0.43	1.30
	$(CH_3)_3SnCF_2CF_2Sn(CH_3)_3$*		Trace	0.23	0.70
	$(CH_3)_3SnCF_2(CF_2)_2CF_2Sn(CH_3)_3$*				0.55
	$(CH_3)_3SnCF_2(CF_2)_{12}CF_2Sn(CH_3)_3$	0.29	0.49	~0.1	
	$(CH_3)_3SnF$	0.44			7.1
	Polymerized C_2F_4		2 g	1 g	0.35

*Quantities of these compounds were estimated from spectroscopic (n.m.r. and infrared) and chromatographic data.

Oxygen was bubbled through the ether extract and the last trace of hexamethylditin was removed by filtration as the tin oxide. Evaporation of the ether left a viscous oil, which was separated by distillation *in vacuo* (10^{-3} mm Hg) into fractions boiling in the 40–60° (1.2 g), 60–80° (0.5 g), and >80° (~1 g) ranges. All three fractions gave complex infrared spectra which show bands attributable to C—H stretching, C—F stretching, CH_3—Sn rocking, and Sn—C stretching vibrations. No further characterization of the 60–80° and >80° fractions was achieved. The 40–60° fraction was a colorless liquid.

Anal. Calcd. for $C_8H_{18}F_4Sn_2$: C, 22.5; H, 4.25; F, 17.7. Calcd. for $C_{10}H_{18}F_8Sn_2$: C, 22.8; H, 3.42; F, 28.8. Calcd. for $C_9H_{10}F_{12}Sn$: C, 23.2; H, 2.15; F, 49.0. Found: C, 22.0; H, 3.45; F, 30.0.

The proton magnetic resonance spectrum of this fraction showed three methyl peaks at −0.42, −0.40, and −0.34 p.p.m. with respect to TMS, as well as a tripleted triplet at −6.08 p.p.m., with ^1H–^{19}F coupling constants of 51.8 and 5.1 c.p.s. The ^{19}F spectrum showed seven peaks in the region +25.8 to +53.3 p.p.m. with respect to trifluoroacetic acid, the peak at +53.3 p.p.m. being a doublet with an ^1H–^{19}F coupling constant of 52 c.p.s. This confirms the presence of a terminal $—CF_2H$ group. The infrared spectrum showed C—F stretching absorptions at 1 205 (s,br), 1 150 (s,br), 1 080 (s), 1 040 (s), and 1 020 (s). An attempted gas chromatographic separation suggested the presence of three components in the approximate ratio of 1:3:1 with retention times of 12, 21.5, and 37 min (dinonyl phthalate column), but the very low volatilities prevented a macro separation, and there was also some evidence of decomposition on the column. It seems probable from this evidence that one component was $(CH_3)_3SnCF_2(CF_2)_4CF_2H$ and that the other two could well be $(CH_3)_3SnCF_2CF_2Sn(CH_3)_3$ and $(CH_3)_3SnCF_2(CF_2)_2CF_2Sn(CH_3)_3$. Species containing longer fluorocarbon chains would give a much higher fluorine analysis and more peaks in the ^{19}F spectrum than were observed.

(*b*) Hexamethylditin (6.1 g, 18.3 mmoles) and tetrafluoroethylene (1.85 g, 18.5 mmoles) in a Pyrex Carius tube were irradiated with ultraviolet light at 25° for 17 h. Vacuum fractionation of the volatile products gave fractions which condensed at 0°, −46°, and −196°, leaving a liquid–solid mixture. The −196° fraction was tetrafluoroethylene (43% recovery). Calcd. mol. wt. 100. Found mol. wt. 100. The −46° fraction was separated chromatographically, and the components were identified, as described above, as 1,1,2,2-tetrafluoroethyltrimethyltin (0.19 g) and 1,1,2,2,3,3,4,4-octafluorobutyltrimethyltin (0.31 g). The 0° fraction was unchanged hexamethylditin (2.1 g). The involatile mixture was extracted several times with ether to leave a white solid (A), and from the ether extract more hexamethylditin was recovered by distillation (2.6 g, total recovery 77%). The white solid (A), after several extractions with hot carbon tetrachloride followed by evaporation and recrystallization from carbon tetrachloride, gave white crystals (0.3 g) with the following analytical results.

Anal. Calcd. for $C_{20}H_{18}F_{28}Sn_2$: C, 23.4; H, 1.7; F, 51.8; Sn, 23.1. Found: C, 23.1; H, 1.6; F, 51.0; Sn, 23.9.

This is consistent with a mixture of adducts averaging to the formula $(CH_3)_3Sn(C_2F_4)_7Sn(CH_3)_3$. The white solid (B) remaining after the carbon tetrachloride extraction was treated with hot methanol and left a trace (0.05 g) of a white solid whose infrared spectrum was identical with that of polymerized tetrafluoroethylene. From the methanol solution, trimethyltin fluoride (0.08 g, 0.44 mmoles) was recovered.

Other reactions were carried out with irradiation of the reactants, in Pyrex or silica tubes, over much longer periods. For example, an experiment performed with a silica tube and ultraviolet irradiation at 25° for 31 h gave the same products as in reaction (*a*) above. However, 63% of the hexamethylditin was recovered,

Can. J. Chem. Downloaded from www.nrcresearchpress.com by 210.87.254.40 on 09/05/12
For personal use only.

and while the same relative quantities of trimethyltin fluoride and polymerized C_2F_4 were isolated as in reaction (*a*), the yields of all other products were much smaller.

Reactions of Hexamethylditin with Perfluoropropene

Hexamethylditin (7.2 g, 22 mmoles) was allowed to react with perfluoropropene (3.84 g, 25.6 mmoles) in a silica tube at 70° under ultraviolet irradiation for 8 h. Vacuum fractionation gave fractions at −126°, −78°, −46°, and 0°, and a dark brown liquid–solid mixture remained in the reaction tube. The −126° fraction was shown by gas chromatography to be 95% pure perfluoropropene, with a trace of a second component. The infrared spectrum of this fraction was that of the original propene with several additional weak bands including one at 1 752 cm^{-1}. Apparently a trace of a second olefin was produced. The −78° fraction was shown chromatographically to be composed of tetramethyltin (0.75 g, 4.2 mmole) and 1,1,1,2,3,3,3-heptafluoropropane (0.1 mmole). Calcd. for C_3F_7H: mol. wt. 170. Found: mol. wt. 176. The latter was also identified by its infrared spectrum.

The −46° fraction, on chromatography (dinonylphthalate column) gave hexamethylditin and 1,1,2,3,3,3-hexafluoropropyltrimethyltin, $(CH_3)_3SnCF_2CF(CF_3)H$ (1.2 g, 3.8 mmoles).

Anal. Calcd. for $C_6H_{10}F_6Sn$: C, 22.9; H, 3.2; mol. wt. 315. Found: C, 22.7; H, 3.0; mol. wt. 305.

This was also completely characterized by its ^1H and ^{19}F magnetic resonance spectra which will be discussed fully elsewhere. The 0° fraction was identified spectroscopically as unchanged hexamethylditin (0.7 g).

Carbon tetrachloride was added to the brown reaction mixture, and oxygen was bubbled through the solution for 30 min. The white suspension (3.4 g) which formed was removed by centrifugation and from its infrared spectrum was found to be a mixture of methyltin oxides and trimethyltin fluoride. The carbon tetrachloride solution was reduced to a small volume, and transferred to a special vacuum distillation apparatus. The fraction which distilled at 40–80° and 10^{-3} mm Hg was 1,2-bis(trimethyltin)hexafluoropropane, $(CH_3)_3SnCF_2CF(CF_3)Sn(CH_3)_3$ (1.2 g, 2.5 mmoles).

Anal. Calcd. for $C_9H_{18}F_6Sn_2$: C, 22.6; H, 3.8; F, 23.85; mol. wt. 476. Found: C, 22.3; H, 3.5; F, 23.87; mol. wt. 486.

The proton magnetic resonance spectrum indicated the presence of other species, probably trimethyltin chloride formed during the oxidation in carbon tetrachloride solution, and also higher molecular weight adducts, but in amounts too small to affect the analytical figures.

A tar (~1 g) remained in the distillation apparatus and was not examined further.

Two other reactions at room temperature and under ultraviolet irradiation, were carried out in Pyrex and silica tubes for 50 and 11 h respectively. Both experiments yielded 0.1–0.15 g of the hexafluoropropyltrimethyltin but gave only a trace of the 1:1 adduct.

Reactions of Hexamethylditin with Trifluoroethylene

(*a*) Hexamethylditin (7.9 g, 24.0 mmoles) and trifluoroethylene (1.96 g, 24.0 mmoles) were irradiated at 85° in a silica tube for 4 h. By means of vacuum fractionation and gas chromatography as described above, the volatile products were shown to be trifluoroethylene (0.43 g, 22% recovery), tetramethyltin (0.35 g, 1.95 mmole), hexamethylditin, and a fraction (0.15 g) which condensed at −46°. The latter could not be purified chromatographically because of decomposition on the column, but its proton magnetic resonance spectrum showed, in addition to three methyl peaks at −0.2 (hexamethylditin), −0.25, and −0.30 p.p.m., a complex absorption centered at −5 p.p.m. with respect to internal TMS. This signal appeared essentially as a doublet with secondary splittings. Such a peak at low field, taken into account with the volatility of this fraction, suggested that the fraction contains species such as hexamethylditin, $(CH_3)_3SnCFHCF_2H$, $(CH_3)_3SnCFHCF_2CFHCF_2H$ etc., and not the bis(trimethyltin)fluorocarbon adducts.

Part of the unreacted hexamethylditin was recovered from the involatile material by distillation at 76° and 20 mm Hg (total recovery 2.7 g, 35%) and the residue was extracted with carbon tetrachloride. Oxygen was bubbled through the resulting solution to remove the last traces of hexamethylditin as tin oxides, and after removal of the solvent in a stream of dry air the remaining oil was separated by vacuum distillation into fractions which distilled in the ranges 45–60° and 60–90° respectively. In this experiment, both fractions gave identical infrared spectra and hence were combined (1 g). The proton magnetic resonance spectrum showed two methyl absorptions at −0.334 and −0.30 p.p.m. and a weak peak at −0.20 p.p.m. due to hexamethylditin, as well as an unresolved band centered at −5.0 p.p.m. This with analytical data, identified the compound as >95% pure 1,4-bis(trimethyltin)-1,1,2,3,3,4-hexafluorobutane, $(CH_3)_3SnCF_2CFHCF_2CFHSn(CH_3)_3$.

Anal. Calcd. for $C_{10}H_{20}F_6Sn_2$: C, 24.4; H, 4.1; mol. wt. 490. Found: C, 24.7; H, 3.5; mol. wt. 477.

The ^{19}F magnetic resonance spectrum showed absorptions centered at +163, +138, +52, +46, +41, +36, +31, and +25 p.p.m. with respect to trifluoroacetic acid. In the formulation

$$(CH_3)_3Sn\overset{1}{C}F_2\overset{2}{C}FH\overset{3}{C}F_2\overset{4}{C}FHSn(CH_3)_3$$

there are two types of CH_3 group, accounting for the two methyl peaks in the proton spectrum. Since the unshielding of a fluorine atom is affected by the amount of charge the F atom is able to draw from a carbon atom, the +163 and +138 p.p.m. peaks of the ^{19}F spectrum may be assigned to fluorine atoms 4 and 2 respectively. The peaks in the +25 to +52 p.p.m. region possibly result from the overlapping of the two quartets of fluorine atoms 1 and 3, which in turn arise from the asymmetry of carbon atoms 2 and 4.

Can. J. Chem. Downloaded from www.nrcresearchpress.com by 210.87.254.40 on 09/05/12
For personal use only.

(*b*) Hexamethylditin (21.0 g, 64.2 mmole, 40% excess) and the olefin (3.6 g, 46 mmole) were irradiated at 95° for 8 h. The distribution and nature of the products obtained were the same as in (*a*) except that vacuum distillation of the final oily liquid, followed by spectroscopic examination, showed the presence of several components. The fractions which distilled in the 45–60° and 60–90° ranges gave infrared and n.m.r. spectra identical with those obtained in experiment (*a*). The fraction which distilled at 35–45°, however, in addition to the peaks expected from experiment (*a*) for $(CH_3)_3SnCF_2CFHCF_2CFHSn(CH_3)_3$, showed in the proton spectrum two quartets at −6.5 p.p.m. which might be assigned to the internal proton of $(CH_3)_3SnCFHCF_2Sn(CH_3)_3$. This was consistent with the appearance in the ^{19}F spectrum of three new peaks at +160, +151, and +47 p.p.m., of which the former may be assigned to the fluorine atom of —CFH— and the lower field peaks may be components of the quartet arising from the F atoms of the $—CF_2—$ group.

Reactions of Hexamethylditin with 1,1-Difluoroethylene

Hexamethylditin (20.4 g, 62.2 mmole, 40% excess) and 1,1-difluoroethylene (2.84 g, 44.4 mmole) were exposed to ultraviolet irradiation for 7 h at 92°. Vacuum fractionation gave unreacted olefin (0.81 g, 32% recovery), tetramethyltin (0.6 g, 3.4 mmole), and a fraction which condensed at −46° in addition to involatile material. Chromatographic separation of the −46° fraction gave three components, the first of which was identified spectroscopically (31) as monofluoroethylene. Calcd. for C_2H_3F: mol. wt. 46. Found: mol. wt. 58.2. The second component (retention time 11.0 min) was tentatively identified as $CF_2HCH_2CF{=}CH_2$. Calcd. for $C_4H_5F_3$: mol. wt. 110. Found: mol. wt. 108.5. These two products must have arisen by the thermal decomposition on the column of products of the type $(CH_3)_3Sn(CH_2CF_2)_nH$. The third component was hexamethylditin.

Centrifugation of the involatile material led to the separation of a white solid (4.2 g) which was shown spectroscopically to be chiefly trimethyltin fluoride with some fluorocarbon polymers. Distillation of the remaining involatile liquid (76° at 20 mm Hg) gave hexamethylditin (12.5 g, total recovery 57%). Further distillation at 10^{-3} mm Hg gave a fraction which distilled at 30–60° to leave a brown gum as residue (3.7 g). The 30–60° fraction showed infrared absorptions associated with fluorocarbon groups at 1 380 (m), 1 188 (vs,br), 1 120 (s), 1 033 (s), 996 (s), 950 (s,br), and 876 (m,br) cm^{-1}. The ^1H and ^{19}F n.m.r. spectra showed the resonances indicated in Table II. Clearly one of the components must have a terminal $—CF_2H$ group which is responsible for the −6.3 p.p.m. ($^1H_2$ spectrum) and +34.6 p.p.m. (^{19}F spectrum) resonances (30). This, together with the fact that only three resonances of unequal intensity were observed in the ^{19}F spectrum suggested the presence of

$$\underset{\text{I}}{(CH_3)Sn\overset{1}{C}H_2\overset{2}{C}F_2\overset{3}{C}H_2\overset{4}{C}F_2H} \quad \text{and} \quad \underset{\text{II}}{(CH_3)_3SnCH_2CF_2Sn(CH_3)_3}$$

and the n.m.r. spectra can be assigned on this basis. The −1.62 p.p.m. (^1H) and +16.2 p.p.m. (^{19}F) resonances can be assigned to the internal protons and fluorine atoms respectively of II. The −1.65 p.p.m. resonance (^1H) might be assigned to the protons of $\overset{1}{C}H_2$ of I because of the similar environment to that of the internal $—CH_2—$ group of II. The −2.7 and −6.3 p.p.m. resonances in the proton spectrum may then be assigned to the $—\overset{3}{C}H_2—$ and $—\overset{4}{C}F_2H$ protons of I respectively. In the ^{19}F spectrum the +34.6 p.p.m. resonance can be assigned to the $\overset{4}{C}F_2H$ fluorine atoms leaving the +11.5 p.p.m. multiplet as arising from the $—\overset{2}{C}F_2—$ fluorine atoms.

Reactions of Hexamethylditin with Trifluorochloroethylene

(*a*) Hexamethylditin (7.6 g, 22.9 mmole) and trifluorochloroethylene (2.64 g, 22.61 mmole) were exposed to ultraviolet irradiation at 90° for 4 h. Vacuum fractionation led to the separation of unreacted olefin (1.64 g, 63%) and tetramethyltin (0.52 g, 2.8 mmole), as well as a 0° fraction which rapidly turned brown in sunlight. From the latter fraction a clear liquid was separated by centrifugation. This gave a complex infrared spectrum, while the proton magnetic resonance spectrum showed four absorptions in the CH_3 region at −0.01, −0.20, −0.33, and −0.62 p.p.m. The first, second, and last peaks can be assigned to the methyl proton resonances of tetramethyltin (32), hexamethylditin (33), and trimethyltin chloride (34). At lower field, eight lines of equal intensity were observed, centered at −6.3 p.p.m. These could be defined as a doublet–doublet–doublet pattern (J_1 = 48.5 c.p.s., J_2 = 8.1 c.p.s., and J_3 = 7.0 c.p.s.), suggesting the presence of a

$$—\overset{\alpha}{C}F_2\overset{\beta}{C}FClH$$

group in which the signal of H_β is split into a large doublet because of coupling with the F_β nucleus and each component is further split into a doubleted doublet because of interaction with the two non-equivalent F_α atoms which in turn arises from the asymmetry of the β-carbon atom. Since the relative intensity of this H_β resonance and the peak at −0.33 p.p.m. is approximately 1:10, and the chemical shift of the latter is characteristic for the $(CH_3)_3Sn$ group directly bonded to a $—CF_2—$ group (35), these resonances at −0.32 and −6.2 p.p.m. are thought to arise from the same species, probably $(CH_3)_3SnCF_2CFHCl$.

Can. J. Chem. Downloaded from www.nrcresearchpress.com by 210.87.254.40 on 09/05/12
For personal use only.

TABLE II

Nuclear magnetic resonance spectrum for ^1H and ^{19}F

		CH_3 region			Lower field region			
^1H	Chemical shift (p.p.m., TMS)	−0.3	−0.32	−0.34	−1.62	−1.65	−2.7	−6.3
	Coupling constant (c.p.s.)				Triplet 23.3	Triplet 23.5	Multiplet 15.2 6.1 4.0	Tripleted triplet 55.1 4.5 4.5
	Intensity ratio	1.0	1.5	1.5	1.5	1.0	1.0	0.5
^{19}F	Chemical shift (p.p.m., TFA)	+11.5		+16.2	+34.6			
	Coupling constant (c.p.s.)	Multiplet		Triplet 25.0	Tripleted doublet 54.5 12.0			
	Intensity ratio	1.0		1.5	1.0			

From the involatile residue, hexamethylditin (5 g, 66% recovery) and trimethyltin fluoride were isolated. Neither in this experiment, nor in a second in which the reactants were irradiated in pentane solution at 25° for 70 h, was there any evidence for the presence of adducts. In this latter experiment the identified products were again trimethyltin fluoride, trimethyltin chloride, and $(CH_3)_3SnCF_2CFHCl$.

Reactions of Hexamethylditin with Trifluorobromoethylene

Hexamethylditin (7.2 g, 21.8 mmole) and trifluorobromethylene (3.6 g, 22 mmole) were irradiated at 25° for 27 h. An orange solid appeared in the reaction tube after 10 h; after completion of the irradiation, the liquid phase turned orange on standing overnight. Vacuum fractionation gave unreacted olefin (2.7 g, 75% recovery), tetramethyltin (0.78 g, 4.4 mmole), a trace of an unidentified volatile fluorocarbon, colorless liquids which condensed at −46° and 0°, and an involatile material.

The −46° fraction was identified as trimethyl perfluorovinyltin, by comparison of its infrared spectrum and gas chromatographic retention time with those of a known sample (35).

The 0° fraction, which became yellow and finally brown on standing, was shown to contain unreacted hexamethylditin containing some tetramethyltin, both of which were also present in the involatile material. From the latter, by extraction first with carbon tetrachloride and then methanol, trimethyltin fluoride was separated. The remaining solid, from its infrared spectrum, contained fluorocarbon polymers.

From a similar experiment in which the reactants were irradiated for only 14 h, the same products were obtained.

Reaction of Hexamethylditin with Ethylene

Hexamethylditin (7.2 g, 22 mmole) and ethylene (0.62 g, 22 mmole) were irradiated in a silica tube at 25° for 1 week, with no changes in appearance. Vacuum fractionation gave unreacted ethylene (0.56 g, 90% recovery), a fraction (0.4 g) which condensed at −78°, and unreacted hexamethylditin (6.8 g, 95% recovery). Gas chromatographic examination of the −78° fraction showed it to contain 90% tetramethyltin, 5% hexamethylditin, and traces of three unidentified compounds.

Preparation of Polydimethyltin

All preparations were carried out either on the vacuum line or in closed systems under nitrogen. Manipulations of diorganotin compounds were always performed in a nitrogen-filled dry-box.

(*a*) Dry triethylamine (10 ml) was added to a slurry of dimethyltin dichloride (10.4 g) in 50 ml anhydrous ether under a nitrogen atmosphere. A slurry of lithium aluminium hydride (2.88 g) in anhydrous ether (250 ml) was added with stirring over 45 min at 0°. The mixture was stirred under nitrogen for a further $3\frac{1}{2}$ h, after which a whitish precipitate was filtered off. The ether was removed under vacuum from the yellow filtrate, which was very air-sensitive, to give an oily liquid. On standing, this liquid slowly separated, with the evolution of gas, into an upper colorless layer and a lower yellow layer. After 48 h gas evolution had ceased, and the lower yellow layer had become solid. The latter was extracted with hot benzene. Several such preparations were conducted and the proton magnetic resonance spectra of the resulting benzene solutions were in general agreement with that obtained by Brown and Morgan (23) for dodecamethylcyclohexatin.

Can. J. Chem. Downloaded from www.nrcresearchpress.com by 210.87.254.40 on 09/05/12
For personal use only.

(*b*) Dimethyltin dihydride (2.47 mmole), prepared as described previously (29), together with dimethyltin dichloride (5 mg), was stirred in pyridine (5 ml) for 3 h at 30–40°. Gas evolution gradually decreased over this period, and on removal of the pyridine, a yellow solid was obtained. From a number of such preparations, it was established that the quantity of hydrogen evolved was 92–100% of that calculated. The proton resonance spectra of benzene solutions of these products were again very similar to that reported by Brown and Morgan for the dodecamethyl cyclohexatin (after Brown and Morgan's terminology), although weak absorption peaks due to linear forms of dimethyltin were also observed.

Reactions with Tetrafluoroethylene

Typical reactions were carried out as follows:

(*a*) Dimethyltin (1.45 mmole), prepared by method (*a*) above, and tetrafluoroethylene (4.38 mmole) were sealed in a Pyrex tube and heated in the dark at 105° for 18 h. After this period, the color had changed from yellow to brown and a metallic mirror had formed. Vacuum fractionation gave unreacted tetrafluoroethylene (3.38 mmole) and tetramethyltin (0.14 mmole), identified spectroscopically. Characterization of the insoluble and involatile residue was not possible although clearly metallic tin was present.

(*b*) Dimethyltin (1.45 mmole), prepared by method (*a*) above, and tetrafluoroethylene (5.94 mmole) were sealed in a silica tube and irradiated for 30 min at 60° under a 200 W ultraviolet lamp. During this period, the tube became coated with a white powder. Vacuum fractionation gave unreacted olefin (0.96 mmole), a trace of tetramethyltin, and a trace of hexamethylditin identified by its melting point and infrared spectrum. The white residue on heating gave tetrafluoroethylene, and its infrared spectrum showed absorption bands at 1 240 (s), 1 180 (s), 636 (m), 624 (sh), 554 (m), and 523 (m) in agreement with those of a solid semipolymerized sample of tetrafluoroethylene.

(*c*) Dimethyltin (2.90 mmole), prepared by method (*b*) above, with tetrafluoroethylene (9.89 mmole), was dissolved in benzene (20 ml) in a Pyrex Carius tube. The mixture was irradiated at 45–60° for 43 h. The volatile fractions were only olefin (5.48 mmole) and benzene, and a resinous material remained. This gave an infrared spectrum which showed absorptions due to fluorocarbon groups and benzene, and moreover the doublet in the 500 cm^{-1} region characteristic of dimethyltin itself had almost disappeared, being replaced by a new doublet at 530 and 515 cm^{-1}. The product solidified rapidly in air.

(*d*) Dimethyltin (2.47 mmole), prepared from the dihydride, tetrafluoroethylene (2.56 mmole), and Spectrograde benzene (15 ml) were irradiated in a silica tube at 50–60° for 17 h to give a brown solution. Vacuum fractionation gave some tetrafluoroethylene (0.06 mmole) which was shown spectroscopically to contain also hexafluoropropene, trifluoromethane, and benzene, and left a yellow oil. Even under prolonged pumping, benzene could not be removed completely. The infrared spectrum of the product, and of those from a number of reactions, were generally similar, typically showing C—F absorptions at 1 185 (m), 1 165 (sh), 1 074 (sh), 1 060 (s), 1 020 (sh), and new Sn—C stretching absorptions at 532 (s), and 518 (sh). A molecular weight determination in benzene (vapor pressure osmometer) gave a value of 1 990. Calcd. for $[(CH_3)_2SnC_2F_4]_8$: 1 984.

Reactions of Diphenyltin with Tetrafluoroethylene

(*a*) Diphenyltin dihydride (6.85 mmole) dissolved in ether in a silica tube was decomposed with methanol (10 ml) over 30 h. Removal of ether and methanol left a yellow-white solid. Carbon tetrachloride (20 ml) and tetrafluoroethylene (16.2 mmole) were added, and the sealed tube was irradiated under a 100 W ultraviolet lamp at 30° for 47 h. The yellow color disappeared and a white solid was deposited. Vacuum fractionation of the more volatile products gave tetrafluoroethylene (12.7 mmole) and a mixture of chloroform and carbon tetrachloride. Polymerized olefin was removed from the remaining carbon tetrachloride solution by filtration and the filtrate was treated with oxygen for 1 h in an attempt to remove unreacted diphenyltin. A white solid (0.07 g) was formed, whose infrared spectrum showed no C—F absorptions, but still showed phenyl—Sn absorptions. Evaporation of the remaining solution gave a yellow oil, which showed C—F absorptions at 1 215 (s), 1 191 (s), 1 157 (s), 1 145 (sh), 1 125 (m), 1 115 (sh), and 1 105 (sh). The Sn—H absorption of the linear polymer (1 824 cm^{-1}) was not detected in the product.

(*b*) Diphenyltin dihydride (4.77 mmole) in ether was decomposed with 6 ml of pyridine in a silica tube. Pentane (12 ml) and tetrafluoroethylene (5.50 mmole) were distilled onto the hexamer, and the sealed tube was irradiated at 50° for 89 h. The volatile products were pentane and tetrafluoroethylene (3.8 mmole) containing some hexafluoropropene. The involatile residue was extracted with warm benzene, leaving insoluble polymerized olefin (1.8 mmole). Evaporation of the benzene gave a cream solid with C—F absorptions at 1 190 (m), 1 169 (m), 1 157 (sh), and 1 100 cm^{-1}. Further extraction with pentane gave a reddish gum showing stronger but broader C—F infrared absorptions centered at 1 168 and 1 101 cm^{-1}.

(*c*) Diphenyltin dihydride (4.77 mmole) in ether was decomposed with 10 ml of methanol over 48 h in a silica tube to give linear polydiphenyltin. Pentane (22 ml) and tetrafluoroethylene (10.72 mmole) were distilled in, and the sealed tube was irradiated at 30° for 90 h. The volatile products were pentane and unreacted olefin (5.22 mmole). The residue was extracted with pentane to leave on evaporation a pale-yellow oil. This showed C—F absorption bands at 1 193 (m), 1 170 (s), 1 130 (w), 1 097 (vs,br), 1 072 (m), 1 038 (w), 1 022 (w). The proton resonance spectrum of a solution in pentane of this oil showed weak, broad absorption in the range 4.6–5.2 τ suggesting the presence of $—C_2F_4H$ groups. The pentane-insoluble material could be

Can. J. Chem. Downloaded from www.nrcresearchpress.com by 210.87.254.40 on 09/05/12
For personal use only.

dissolved in benzene which on evaporation gave a cream solid with similar, but relatively weaker C—F absorptions.

In all of the above experiments, attempts to convert the oily products to solids by treatment with various solvents were unsuccessful.

Reaction of Dimethyltin with Trifluoroiodomethane

Dimethyltin (16.9 mmole), prepared by the pyridine reduction of the dihydride, was irradiated with a large excess of trifluoroiodomethane (111.5 mmole) in a silica tube at 30° for 48 h. Vacuum fractionation gave unreacted trifluoroiodomethane (103.2 mmole) and a mixture of fluorocarbon–tin compounds which condensed in traps at −78°, −46°, and −13°. White crystals remained in the reaction tube and were identified spectroscopically as dimethyltin diiodide. The components of the mixture could not be separated completely by further fractionation and gas chromatographs taken at 78° and 117° on a 30% Ucon 50 on firebrick column, showed extensive broadening and tailing of the peaks due to decomposition. However, the components could be distinguished from the infrared and proton magnetic resonance spectra as shown in Table III.

TABLE III

Identification by infrared and proton magnetic resonance spectra

Component	τ*	J for $^{119}SnCH_3$	J for ^{117}–$SnCH_3$	Sn—C stretch (cm^{-1})	Ref.
A	9.59	60.4	57.6	542, 516†	(30)
B	9.23	65.7	62.4	[557, 530]	
C	9.13	57.7	54.9	540, 511	(34, 36)
D	8.85	64.1	61.3	[552, 522]	
E				547, 511	(36)

*Relative to internal TMS.
†Observed from known sample.

On this basis, components A and C were unambiguously identified as trimethyltrifluoromethyltin and trimethyltin iodide. Since volatility appeared to decrease from A to D, and from the data in Table III, it was concluded that component B was probably dimethyl bis(trifluoromethyl)tin, and component D dimethyltrifluoromethyl tin iodide. From the infrared and n.m.r. intensities the ratio of A:B:C:D was approximately 1:10:4:40. The total amount of these products indicated that approximately 30% of the dimethyltin had been consumed.

ACKNOWLEDGMENTS

The financial support of the National Research Council, in form of grants-in-aid (to H. C. C.) and a Postdoctorate fellowship (to J. D. C.), and the award (to J. H. T.) of a Graduate Fellowship of the University of British Columbia are gratefully acknowledged. We are also grateful for gifts of chemicals from M. and T. Corporation.

REFERENCES

1. R. D. Cramer, E. L. Jenner, R. V. Lindsay, Jr., and U. G. Stolberg. J. Am. Chem. Soc. **85**, 1691 (1963).
2. C. A. Kraus and W. V. Sessions. J. Am. Chem. Soc. **47**, 2361 (1925).
3. H. Moms and P. W. Selwood. J. Am. Chem. Soc. **63**, 2509 (1941).
4. H. D. Kaesz, J. R. Phillips, and F. G. A. Stone. Chem. Ind. London, 1409 (1959).
5. H. C. Clark and C. J. Willis. J. Am. Chem. Soc. **82**, 1888 (1960).
6. R. D. Chambers, H. C. Clark, and C. J. Willis. Chem. Ind. London, 76 (1960).
7. G. A. Razavaeu, N. S. Vyazankin, Yu. I. Dergunov, and O. S. Dyachkovskaya. Dokl. Akad. Nauk SSSR, **132**, 364 (1960).
8. M. A. A. Beg and H. C. Clark. Chem. Ind. London, 140 (1962).
9. R. N. Haszeldine, M. J. Newland, and J. B. Plumb. Proc. Chem. Soc. 147 (1960).
10. W. Drenth, M. J. Janssen, and G. J. M. Van der Kerk. J. Organometal. Chem. **2**, 265 (1964).
11. G. M. Burch, H. Goldwhite, and R. M. Haszeldine. J. Chem. Soc. 1083 (1963).
12. J. F. Harris, Jr. and F. W. Stacey. J. Am. Chem. Soc. **83**, 840 (1961).
13. J. R. Case, N. H. Ray, and H. L. Roberts. J. Chem. Soc. 2070 (1961).
14. R. N. Haszeldine and B. R. Steele. J. Chem. Soc. 2800 (1957).
15. R. N. Haszeldine and J. C. Young. J. Chem. Soc. 4502 (1960).
16. R. N. Haszeldine and B. R. Steele. J. Chem. Soc. 923 (1954).
17. R. N. Haszeldine and J. E. Osborne. J. Chem. Soc. 61 (1956).
18. R. N. Haszeldine and B. R. Steele. J. Chem. Soc. 1592 (1953).
19. R. N. Haszeldine and B. R. Steele. J. Chem. Soc. 3747 (1954).

Can. J. Chem. Downloaded from www.nrcresearchpress.com by 210.87.254.40 on 09/05/12
For personal use only.

20. R. N. HASZELDINE. J. Chem. Soc. 3565 (1953).
21. W. R. CULLEN and N. K. HOTA. Can. J. Chem. **42**, 1123 (1964).
22. J. G. NOLTES and G. J. M. VAN DER KERK. Functionally substituted organotin compounds. Tin Research Institute, Middlesex, England. 1958.
23. T. L. BROWN and G. L. MORGAN. Inorg. Chem. **2**, 736 (1963).
24. W. P. NEUMANN and K. KONIG. Ann. **677**, 1 (1964).
25. D. H. OLSON and R. E. RUNDLE. Inorg. Chem. **2**, 1310 (1963).
26. W. P. NEUMANN. Ann. **677**, 12 (1964).
27. H. G. KUIVILA and E. R. JAKUSIK. J. Org. Chem. **26**, 1426 (1961).
28. D. G. WEIBLEN. *In* Fluorine chemistry. Vol. 2. *Edited by* J. H. Simons. Academic Press, Inc., New York. 1954. p. 449.
29. H. C. CLARK, S. G. FURNIVAL, and J. T. KWON. Can. J. Chem. **41**, 2889 (1963).
30. H. C. CLARK, J. T. KWON, L. W. REEVES, and E. J. WELLS. Can. J. Chem. **41**, 3005 (1963).
31. B. BAK and D. CHRISTENSEN. Spectrochim. Acta, **12**, 355 (1958).
32. H. C. CLARK, J. T. KWON, L. W. REEVES, and E. J. WELLS. Inorg. Chem. **3**, 907 (1964).
33. H. C. CLARK, J. T. KWON, L. W. REEVES, and E. J. WELLS. Can. J. Chem. **42**, 941 (1964).
34. H. SCHMIDBAUR and I. RUIDISCH. Inorg. Chem. **3**, 599 (1964).
35. A. D. BEVERIDGE, H. C. CLARK, and J. T. KWON. Can. J. Chem. **44**, 179 (1966) and references therein.
36. R. OKAWARA, D. E. WEBSTER, and E. G. ROCHOW. J. Am. Chem. Soc. **82**, 3287 (1960).

Can. J. Chem. Downloaded from www.nrcresearchpress.com by 210.87.254.40 on 09/05/12
For personal use only.

Can. J. Chem. Downloaded from www.nrcresearchpress.com by 210.87.254.42 on 09/05/12
For personal use only.

THE ENERGY OF HYDROGEN BONDING IN THE SYSTEM: ACETONE–BROMOFORM

A. N. CAMPBELL AND E. M. KARTZMARK
Department of Chemistry, University of Manitoba, Winnipeg, Manitoba
Received October 8, 1965

ABSTRACT

A study of the equilibrium freezing-point diagram for the system acetone–bromoform shows that no solid-phase compound forms between acetone and bromoform. The diagram is of the simple eutectic type, the eutectic lying at −101° and 84 mole % acetone. The enthalpies of mixing have been determined for various compositions of mixture and the numerical value of ΔH (per mole of acetone or bromoform) extrapolated to infinite excess of bromoform or of acetone, to obtain the value for completely undissociated complex. This figure is −1.3 kcal per mole of complex (assumed mole to mole). The dipole moments, excess volumes of mixing, viscosities, and total and partial vapor pressures of the system have been measured. From these data, the excess free energy and excess entropy and other thermodynamic functions have been evaluated.

INTRODUCTION

In a previous paper (1) dealing with the system acetone–chloroform, we demonstrated that an equimolar compound, stable in the solid state, at its melting point of −160°, exists, and we evaluated the energy of hydrogen bonding to be 2.7 ± 0.1 kcal. The existence of hydrogen bonding in this system, as well as in the system acetone–bromoform, has been demonstrated by nuclear magnetic resonance and infrared techniques and it has been shown qualitatively that the enthalpy of mixed association is greater in the acetone–chloroform system than in the acetone–bromoform system (2).

It was suggested to us by our colleague, Dr. H. Gesser, that it would be of interest to repeat our studies on the system acetone–bromoform and also evaluate the energy of hydrogen bonding in this system. Since a knowledge of total and partial vapor pressures enables one to calculate the excess free energies and entropies of the hydrogen bonding, we have added these determinations to those previously made.

EXPERIMENTAL

This is for the most part described in our previous communication (1), as far as the determinations of freezing point, density, viscosity, and heats of mixing are concerned. The excess volume of mixing was determined directly, since the determination from density measurements calls for a very high order of accuracy. For this purpose we used the apparatus of Brown and Smith (3), which is itself a modification and simplification of that of Keyes and Hildebrand (4). The only modification we introduced was to replace the ground glass plug by a stopcock. This apparatus works admirably and gives high accuracy, if sufficient care is taken with the calibration of the capillary. Mixtures of different compositions are obtained by varying the amount of mercury in the apparatus.

Refractive indices were determined with an Abbe refractometer, with thermostatic control. An electric sodium lamp was used as the source of illumination, so that all refractive indices refer to the sodium doublet. For our measurements of dielectric constant we used the Sargent Oscillometer, a great improvement on the somewhat crude homemade apparatus of our previous work. We enclosed the capacity cells in an air space within a liquid thermostat, so that constancy of temperature was preserved to 25° ± 0.1°. For the measurement of total vapor pressure we used a simple, large bore, mercury manometer. The apparatus for the determination of vapor composition and hence partial pressures is more complex and is described in detail in our work with Gieskes (5).

The acetone and bromoform used were both Fisher certified chemicals. It was found that distillation of bromoform, even under reduced pressure, yielded a slightly brown product. It was therefore thought better to use freshly opened bottles of the product as it came from the manufacturers. In any case, it seems to us that bromoform is more stable with time than chloroform, which requires repurification every 2 weeks. The physical constants, viz. density and refractive index, were in good agreement with the accepted values.

Can. J. Chem. Downloaded from www.nrcresearchpress.com by 210.87.254.42 on 09/05/12
For personal use only.

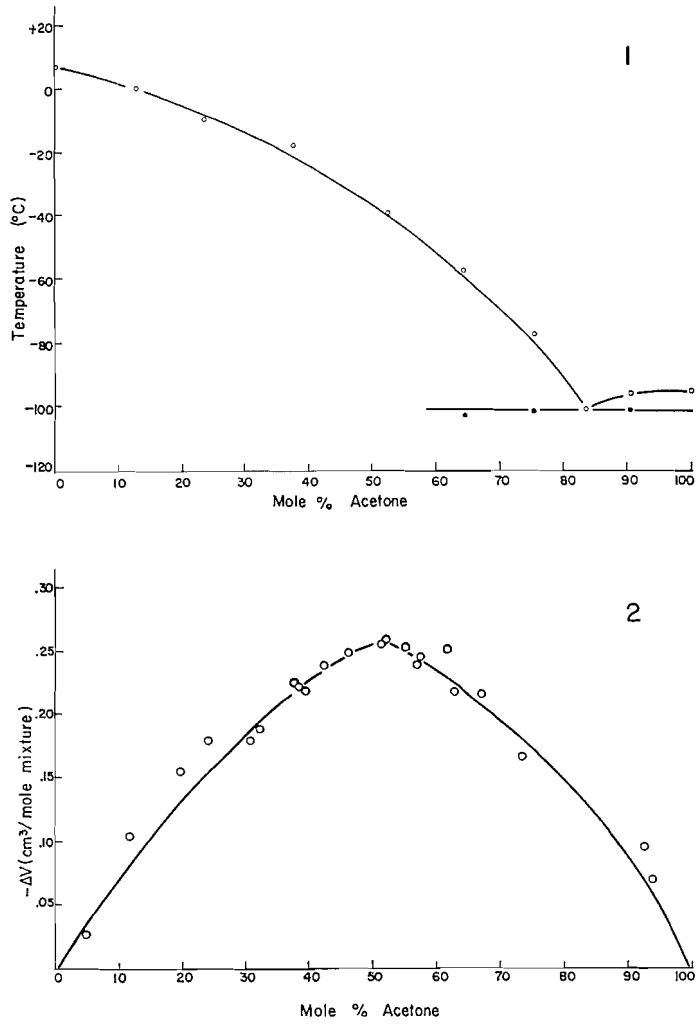


FIG. 1. Equilibrium diagram, freezing point vs. mole % acetone, for acetone-bromoform system.
FIG. 2. Plot of excess volumes of mixing vs. mole % acetone.

The equilibrium diagram, freezing point versus mole % acetone, is represented in Fig. 1. There is no indication of a compound between acetone and bromoform existing in the solid state. (Cf. the corresponding diagram in our previous publication (1).) The single eutectic lies at $-101°$ and 84 mole % acetone.

Figure 2 is a graphical representation of the excess volumes of mixing (all are negative) versus mole % acetone. A maximum contraction of about 0.25 cc occurs at about 50 mole % acetone. Figure 3 represents partial molal excess volumes, derivable from Fig. 2. They are of necessity negative. (Molal volumes are accurately obtained by adding observed excess volumes to the ideal molal volume. These are plotted against mole fraction and tangents taken to give the partial molal volume. The difference $\bar{V} - V^0$ is the excess partial molal volume.)

The relative viscosities and fluidities are reproduced in Fig. 4. The dielectric data for mixtures of acetone and bromoform are given in Table I.

Solutions were also made up containing various proportions of acetone and bromoform and a fixed quantity, namely 91 mole % of benzene. The dielectric data of these solutions are given in Table II. The "molar polarization in absence of benzene" is calculated in the usual way on the assumption that the polarizability of benzene in solution is the same as in the free state.

The figures of the last column of Table II, "molar polarization in absence of benzene", as well as the figures for molar refraction (distortion polarization, Table I) were now plotted against mole % bromoform

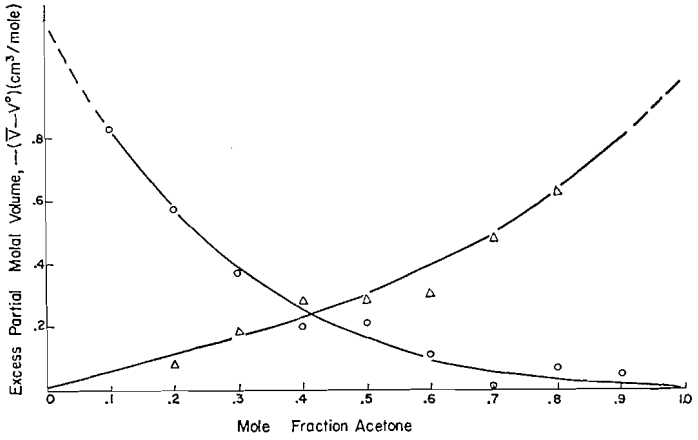


FIG. 3. Partial molal excess volumes derived from Fig. 2. (○) Acetone, (△) bromoform.

TABLE I

Dielectric constants and refractive indices of mixtures of acetone and bromoform

Composition in mole % $CHBr_3$	Dielectric constant	Density in g/ml at 25°	Molar polarization	Refractive index $n_D^{25°}$	Molar refraction	Orientation polarization
0.00	20.7	0.7854	64.16	1.3561	16.16	48.00
9.29	18.9	1.014	64.33	1.3857	17.62	46.71
16.82	17.8	1.193	64.59	1.4050	18.65	45.94
27.03	16.25	1.428	64.79	1.4313	20.10	44.69
36.47	14.95	1.635	64.98	1.4563	21.48	43.50
45.07	13.6	1.825	64.58	1.4797	22.69	41.89
55.70	12.05	2.039	64.23	1.5005	24.04	40.19
66.29	10.3	2.247	62.89	1.5229	25.43	37.46
77.00	8.45	2.451	60.51	1.5470	26.90	33.61
89.49	6.6	2.675	56.55	1.5721	28.27	28.28
100.00	4.4	2.861	46.87	1.5934	30.00	16.87

TABLE II

Dielectric constant and other data of solutions containing benzene

Actual molar composition		Composition (in absence of benzene) in mole % $CHBr_3$	Density $d_4^{o25°}$	D_K	Molar polarization of solution	Molar polarization in absence of benzene
Mole fraction acetone	Mole fraction bromoform					
0.08716	0	0	0.8667	3.282	38.07	158.21
0	0.09018	100	1.0654	2.458	28.81	49.79
0.00889	0.0816	90.18	1.0204	2.528	30.50	68.07
0.0179	0.0729	80.33	1.0023	2.616	31.66	79.04
0.0267	0.0636	70.41	0.9853	2.700	32.55	90.94
0.0345	0.0543	65.47	0.9686	2.796	33.59	102.77
0.0442	0.0451	50.49	0.9516	2.864	34.27	110.79
0.0529	0.0360	40.47	0.9345	2.946	35.09	120.43
0.0616	0.0269	30.42	0.9178	3.024	35.81	129.11
0.0698	0.0178	20.32	0.9057	3.106	36.35	136.28
0.0784	0.00889	10.18	0.8868	3.185	37.36	148.22

and interpolations made for 10 mole % intervals. Finally, the molar polarizations for each 10% bromoform were plotted against benzene content of solution (0 and 91 mole % respectively) and straight line extrapolations made to infinite dilution (100% benzene). In each case, the corresponding molar refraction was subtracted to obtain the "orientation polarization". Each solution was now treated on the (obviously incorrect) assumption that equimolecular proportions of acetone and bromoform were combined to form a

Can. J. Chem. Downloaded from www.nrcresearchpress.com by 210.87.254.42 on 09/05/12
For personal use only.

Can. J. Chem. Downloaded from www.nrcresearchpress.com by 210.87.254.42 on 09/05/12
For personal use only.

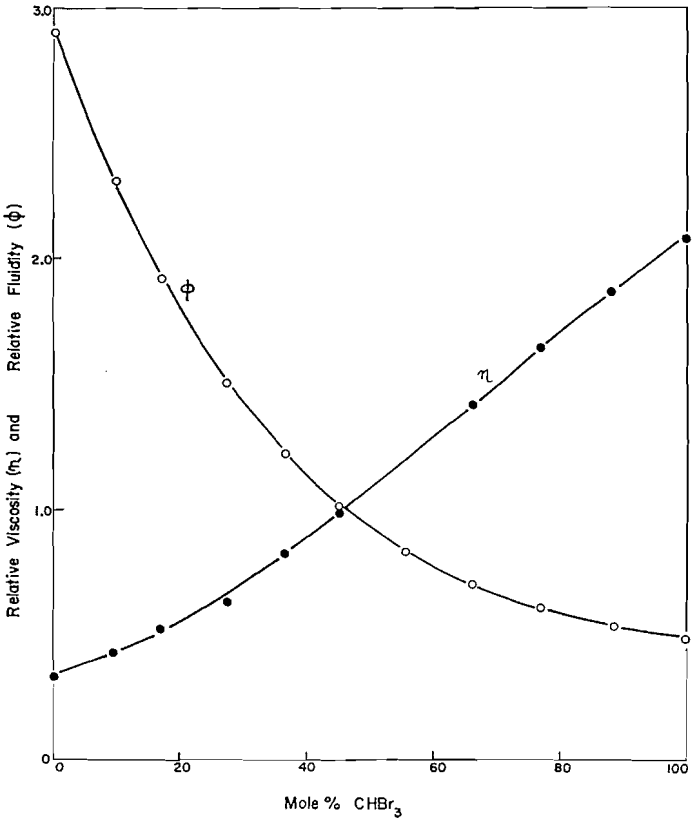


FIG. 4. Relative viscosities and fluidities vs. mole % bromoform.

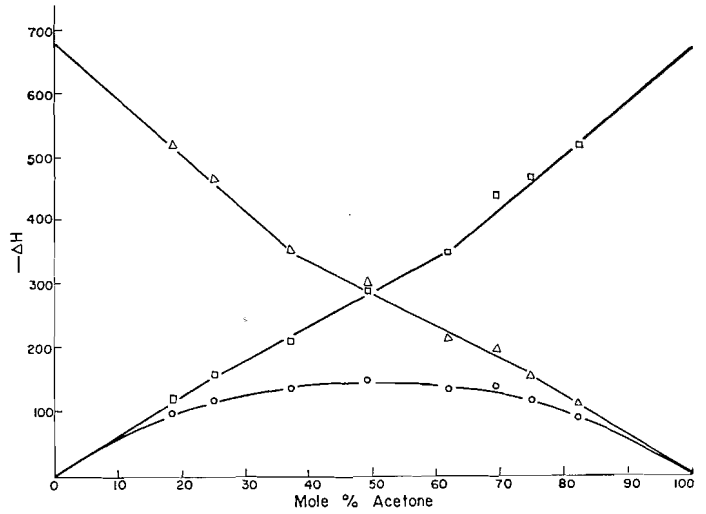


FIG. 5. Heat of mixing for system acetone–bromoform. (○) ΔH per mole mixture, (△) ΔH per mole acetone, (□) ΔH per mole bromoform.

compound and the excess (acetone or bromoform) was 'free'. Again on the assumption that the 'free' acetone or bromoform possessed the same orientation polarization as in the pure liquid state, multiplication of this figure by the mole fraction of 'free' acetone or bromoform gave the orientation polarization of a known mole fraction of 'compound'. This, when converted to mole fraction unity, gave the dipole moment of the so-called compound. The results are given in Table III.

TABLE III

Dipole moment of 'compound'

Mole % $CHBr_3$	Molar polarization at infinite dilution	Molar refraction	Orientation polarization	Dipole moment of compound in debye units
0	168	16	152	2.71
10	157	18	139	3.05
20	145	19	126	2.97
30	135	20	115	2.98
40	131	22	109	3.09
50	124	23	101	3.15
60	114	25	89	3.31
70	103	26	77	3.36
80	82	27	55	3.24
90	69	29	40	3.43
100	50	30	20	1.17
		Mean value of dipole moment = 3.18		

TABLE IV

Total and partial vapor pressures

Composition (mole % acetone)	Total pressure	Partial pressure acetone		Partial pressure bromoform	
		(Obs.)	(Ideal)	(Obs.)	(Ideal)
0.0	6.6	—	—	—	—
10.15	36.9	28.4	23.3	8.5	5.94
18.4	55.0	47.5	42.2	7.5	5.39
39.1	97.0	92.4	89.6	4.6	4.01
49.0	119.2	115.3	112.3	3.9	3.36
60.5	148.4	145.3	138.7	3.1	2.61
74.8	169.4	168.0	171.4	1.4	1.66
89.6	204.4	204.0	205.4	0.4	0.69
100.0	229.2				

The enthalpy of mixing is negative for all proportions of acetone and bromoform. The results are expressed graphically in Fig. 5, in three ways, viz. ΔH per mole of mixture (circles), ΔH per mole of acetone (triangles), and ΔH per mole of bromoform (squares).

Table IV gives the vapor pressures, total and partial, for various compositions of bromoform–acetone mixtures.

DISCUSSION

The equilibrium diagram (Fig. 1) shows that the compound between bromoform and acetone, if such exists, does not appear as a solid phase. The diagram is of the simplest type, with a eutectic at $-101°$ and at 84% acetone.

Work shortly to be published by Campbell, Kartzmark, and Chatterjee on the system acetone–chloroform, in which there is undoubted compound formation (mixed association), shows that here the excess volumes are small and negative (maximum $V^E = -0.152$ cc/mole) over the larger part of the concentration range and become slightly positive for concentrations of acetone greater than 68 mole %. In the present system, however, the excess volume is larger and negative over the whole range (-0.25 cc/mole, maximum).

Can. J. Chem. Downloaded from www.nrcresearchpress.com by 210.87.254.42 on 09/05/12
For personal use only.

On a first consideration, this behavior might be considered to indicate interaction, but if there is mixed association in this system, the equilibrium

$$CHBr_3 + (CH_3)_2O \rightleftarrows CHBr_3.(CH_3)_2O$$

must be very far to the left, for equimolar proportions. The result is more surprising, since Murthy (6) finds a weak monomer–dimer equilibrium for bromoform in cyclohexane. Presumably the dissociating effect of acetone would tend to produce expansion. Staveley's (7) work, however, indicates that the value of V^E is determined by the magnitude of other thermodynamic functions, and therefore it is not in itself conclusive evidence for compound formation. The graph of viscosity vs. composition shows negative deviation from additivity.

We have treated our dielectric data by the method outlined under Experimental and assumed the existence (by analogy with the system acetone–chloroform (1)) of a mole to mole compound, stable in the presence of infinite excess of either bromoform or acetone. Such a line of reasoning gives the dipole moment of the hypothetical compound as 3.18 D. The sum of the dipole moments of the constituents is 3.88. We found a similar decrease with the system acetone–chloroform, where a compound is undoubtedly formed. In the past, attempts were frequently made to determine the degree of dissociation of the compound from such results but it is now realized that such calculations have no validity. Nevertheless, the result may be accepted as qualitative evidence for association between the two substances.

The enthalpies of mixing, though negative, are much less than those of the corresponding system acetone–chloroform. If the line of argument of the preceding paragraph is valid, then by the method of calculation of our previous paper (1), the enthalpy of hydrogen bonding in this system becomes $-700 - 625 = -1325$ cal, say -1.3 kcal. The line of argument does seem valid because with a very large excess of either component it is almost inconceivable that the few molecules of the lesser component are not hydrogen bonded to the other component, even if the amount of 'compound' in an equimolar solution is extremely small.

When the total vapor pressures of Table IV are plotted against composition, it is seen that the mixture exhibits positive deviation from Raoult's law from 0 to 75 mole % acetone, and after that slight negative deviation. The same is of course true of the partial pressures.

Our partial pressure data, together with the heats of mixing, permit the calculation of numerous derived data. We have calculated, in Table V, the activities, activity coefficients, partial molal excess free energies, and total excess free energy (free energy of mixing). Finally, from these results, the product TS^E and the excess entropy (S^E) have been calculated. It would then be possible to obtain a great many thermodynamic relations and to 'classify' the system in various ways, but we are ourselves sceptical of the value of this kind of thing. In any case, from the data of this paper it is possible for the reader to make these calculations. We content ourselves with pointing out that while the excess entropy (entropy of mixing) is always negative and passes through a numerical maximum at 50 mole % concentration, the excess molal free energy decreases steadily with increasing acetone concentration from a value of $+203.8$ cal at 10.15 mole % acetone to a value of -37.0 cal at 89.6 mole %. A similar behavior is observed with the excess enthalpy, a quantity which is always negative. This indicates that the nature of the process when a small quantity of acetone is added to a large excess of bromoform is not the same as when a small quantity of bromoform is added to a large quantity of acetone. If it is true

Can. J. Chem. Downloaded from www.nrcresearchpress.com by 210.87.254.42 on 09/05/12
For personal use only.

Can. J. Chem. Downloaded from www.nrcresearchpress.com by 210.87.254.42 on 09/05/12
For personal use only.

TABLE V
Derived thermodynamic quantities

Mole % acetone	Acetone			Bromoform						
	α	γ	μ^E	α	γ	μ^E	G^E	H^E	TS^E	S^E
10.15	0.124	1.222	118.8	1.288	1.434	213.5	203.8	−60	−263.8	−0.884
18.4	0.207	1.125	69.7	1.136	1.392	195.9	172.7	−95	−267.7	−0.897
39.1	0.403	1.031	18.0	0.697	1.144	79.7	55.5	−140	−195.5	−0.655
49.0	0.503	1.027	15.7	0.591	1.159	87.4	52.3	−150	−202.3	−0.678
60.5	0.634	1.049	28.2	0.470	1.190	103.0	57.7	−135	−192.7	−0.646
74.8	0.733	0.980	−12.0	0.212	0.841	−102.6	−34.8	−115	−80.2	−0.269
89.6	0.890	0.993	−4.23	0.0606	0.583	−319.6	−37.0	−55	−18.0	−0.060
100.0	1.000	1.000	0	—	—	—	—	—	—	—

that bromoform in the pure state is partially dimerized, dissociation might become complete in the presence of a large excess of acetone, an effect which would not be predominant when the circumstances were reversed.

REFERENCES

1. A. N. CAMPBELL and E. M. KARTZMARK. Can. J. Chem. **38**, 652 (1960).
2. W. G. PATERSON and D. M. CAMERON. Can. J. Chem. **41**, 198 (1963). C. J. CRESWELL and A. L. ALLRED. J. Am. Chem. Soc. **85**, 1723 (1963). R. E. KAGARISE. Spectrochim. Acta, **19**, 629 (1963).
3. I. BROWN and F. SMITH. Australian J. Chem. **15**, 1 (1962).
4. D. B. KEYES and J. H. HILDEBRAND. J. Am. Chem. Soc. **39**, 2126 (1917).
5. A. N. CAMPBELL, E. M. KARTZMARK, and J. M. T. M. GIESKES. Can. J. Chem. **41**, 407 (1963).
6. A. S. N. MURTHY. Ph.D. Thesis, Indian Institute of Science, Bangalore, India. 1964.
7. L. A. K. STAVELEY, W. I. TUPMAN, and K. R. HART. Trans. Faraday Soc. **51**, 323 (1955).

Can. J. Chem. Downloaded from www.nrcresearchpress.com by 210.87.254.42 on 09/05/12
For personal use only.

Can. J. Chem. Downloaded from www.nrcresearchpress.com by 210.87.254.40 on 09/05/12
For personal use only.

THE ELECTROLYTIC CONDUCTANCES OF SODIUM CHLORATE AND OF LITHIUM CHLORATE IN WATER AND IN WATER–DIOXANE

A. N. CAMPBELL, E. M. KARTZMARK, AND B. G. OLIVER
Chemistry Department, University of Manitoba, Winnipeg, Manitoba

Received November 22, 1965

ABSTRACT

The conductances, densities, and viscosities of aqueous solutions of sodium chlorate were determined over the complete range of concentration at 25 °C and at 35 °C. An attempt was made to reproduce the results at 25 °C with the viscosity-corrected Falkenhagen–Leist and Wishaw–Stokes equations. The limiting equivalent conductances of sodium chlorate at 25 °C and 35 °C in water were also determined.

The conductances, densities, and viscosities of sodium chlorate at 25 °C and 35 °C were determined in a solvent consisting of 64.5% dioxane, 35.5% water. The limiting equivalent conductances of sodium chlorate at 25 °C and 35 °C and of lithium chlorate at 25 °C in this solvent were determined by analyzing the data with the Fuoss–Onsager equation for associated electrolytes.

Finally, conductances of sodium chlorate and lithium chlorate at 25 °C were determined in a solvent consisting of 90% dioxane, 10% water.

Because of the preoccupation of this laboratory with molten lithium chlorate and sodium chlorate, their conductances and physical properties generally (1–4), we thought an investigation of the conductivity of these salts in media of low dielectric constant, such as dioxane-water mixtures, might throw some light on the structure of the melt. The specific conductance of molten lithium chlorate is of the same order of magnitude as that of lithium chlorate in 90% dioxane.

With the method of Fuoss and Accascina (5), we have calculated the degree of association (ion-pair formation) of the two electrolytes in various dioxane–water mixtures. We also determined the conductivity of sodium chlorate in water alone, over the entire concentration range, as an obvious comparison with the work of Campbell and Paterson (6) who determined the conductance of lithium chlorate in water.

EXPERIMENTAL

Purity of Materials

Salts

Fisher Certified sodium chlorate received no other purification than drying at 120 °C for 48 h. Lithium chlorate was prepared and purified by the method of Campbell and Griffiths (7). We observed a melting point of 127.9 °C as against 127.6 °C formerly reported by Campbell and Griffiths.

Solvents

Conductance water was obtained by passing distilled water through a mixed resin demineralization column and then purging with purified nitrogen. The specific conductance of water prepared in this way was between 0.9×10^{-7} and 2×10^{-7} mhos.

Spectroscopically pure dioxane was further purified by the method of Hess and Frahm (8). After purification, the refractive index and dielectric constant were found to be 1.4202 (n_D at 25 °C) and 2.21 respectively. Frey and Gilbert (9) report a refractive index of 1.42025 and Critchfield, Gibson, and Hall (10) an identical dielectric constant.

The thermostat was controlled at 25.00 ± 0.005 °C. The conductance apparatus for exact measurement is well known. We used a Jones bridge, with an oscilloscope as detector, tuned amplifier, frequency filter, and all the usual refinements. Resistance measurements could be made to well within 1 Ω in 10 000. Pyrex glass cells of the type recommended by Jones and Bollinger (11) were used for the more concentrated solutions and a cell of the Shedlovsky type (12) for the very dilute region. Cell constants were determined from the equation for the conductances of dilute solutions of potassium chloride, at 25 °C, given by Lind, Zwolenik, and Fuoss (13), viz.

$$\Lambda = 149.93 - 94.65C^{1/2} + 58.74C \log C + 198.4C.$$

Preparation of Solutions

Concentrated Solutions

These were made up by weight and the molar concentration determined from the density and these weights.

Dilute Solutions

These solutions were prepared by successive additions of salt, in platinum cups, to a known amount of water in the conductance cell. These additions were made in a nitrogen-filled drybox to exclude carbon dioxide from the solution. In each case, at least 0.02 g of salt was weighed to the nearest μg, on a Mettler M-5 balance. Thus the weight concentration was known to 0.01%. Molar concentrations were calculated on the assumption that the density of the solution was the same as that of the pure solvent.

Viscosity

A viscometer of the Cannon and Fenske type (14), having negligible drainage and kinetic energy corrections, was calibrated with water at 25 °C and 35 °C.

RESULTS AND DISCUSSION

The direct experimental results are contained in Tables I–V.

Aqueous Solutions of Sodium Chlorate at 25 °C and 35 °C

The data of Tables I and II are expressed graphically in Fig. 1. The existence of a maximum in such curves is a fairly common phenomenon and is due either to a rapid increase in viscosity, or to ion-pair formation, or both. In the present case and in that of lithium chlorate (6), the composition of the maximum does not change with temperature. It happens also that in both cases the composition at the maximum is 5.2 *M*.

In Fig. 2, equivalent conductances, at 25 °C and 35 °C, have been plotted against the square root of concentration. These curves have the normal shape. As usual we have attempted to fit our results for 25 °C to the (viscosity-corrected) equations of Falkenhagen–Leist and Wishaw–Stokes (see ref. 6 for literature and method). The results are expressed graphically in Fig. 3. In contradistinction to the behavior of lithium chlorate, both equations reproduce the results with only fair accuracy up to about 0.1 *M*. At higher concentrations, both equations fail rather badly.

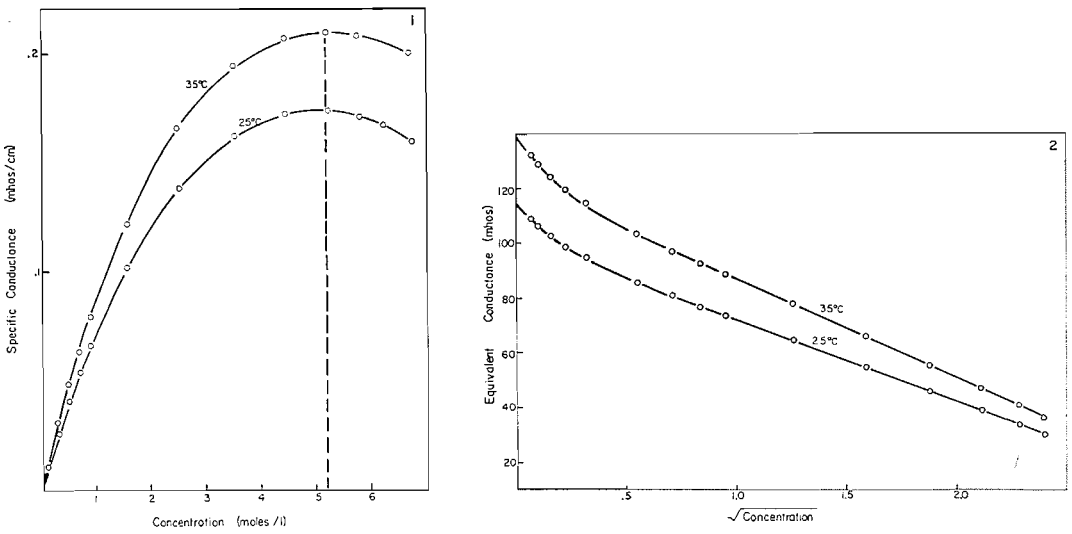


FIG. 1. Specific conductance vs. concentration of sodium chlorate in water.
FIG. 2. Equivalent conductance vs. square root of concentration for sodium chlorate in water.

Can. J. Chem. Downloaded from www.nrcresearchpress.com by 210.87.254.40 on 09/05/12
For personal use only.

Fluidity versus concentration graphs are given in Fig. 4. The graphs are linear over the entire concentration range at both temperatures.

The activation energies both of conductance and of viscosity were calculated from the formula

$$\Delta E_{\text{cond}} = \frac{2.303RT_1T_2}{T_2 - T_1} \log_{10} \frac{\Lambda_2}{\Lambda_1}$$

and the corresponding formula for ΔE_{visc} and are reproduced in Table VI. The ratio of the two energies is sensibly unity, at least in the dilute region. This effect is commonly observed with aqueous solutions. This suggests that, although conductance involves ionic migration within the solution, and viscosity is a shearing movement of the solution as a whole, there must be a resemblance between the two processes. Although it is admitted that a satisfactory conductance equation, if one is ever obtained for the concentrated region, must contain a viscosity term, in practice no advance has been made towards a theoretical solution of the problem.

The limiting equivalent conductances of sodium chlorate in water at 25 °C and 35 °C were obtained by the Kohlrausch method (Fig. 5). Experience has convinced us that this is the most reliable method, where it is applicable. For the straight line portion of the graph, the method of least squares was used to get the best slope. Λ_0 for sodium chlorate at 25 °C was thus found to be 114.7 mhos. The experimental slope of the straight line plot (87.32) was slightly greater than the Onsager tangent ($\alpha\Lambda_0 + \beta$), which has the value 86.49 $cm^2\ ohm^{-1}\ equiv^{-1}$. Our value for Λ_0 agrees exactly with the sum of the individual limiting ionic conductances, as reported in the literature (12, 15).

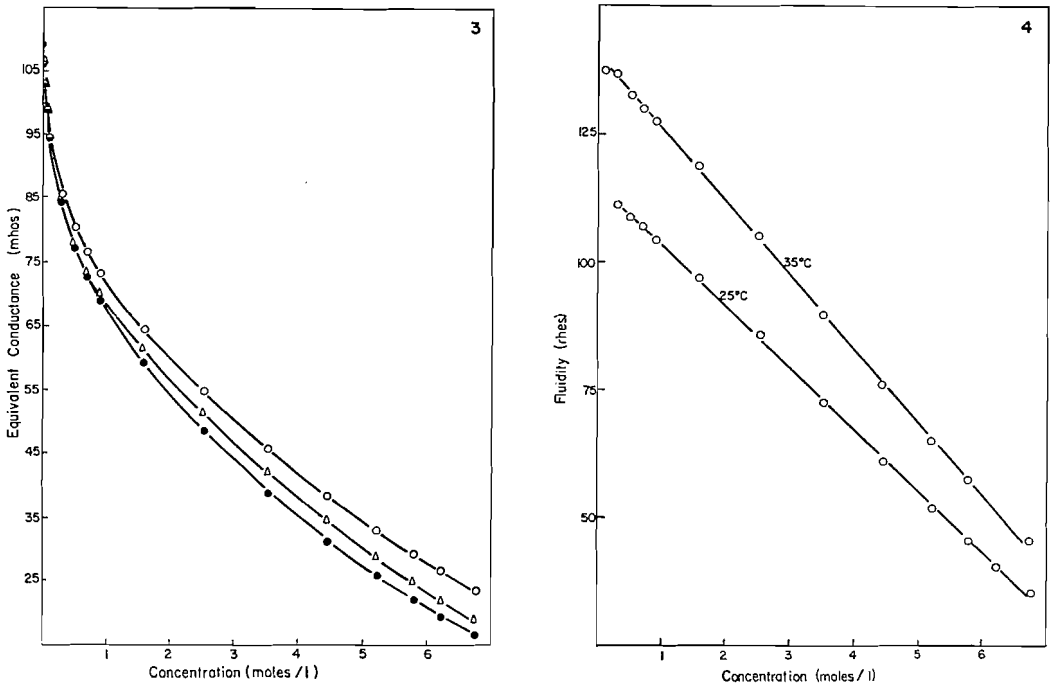


FIG. 3. Experimental and calculated conductances of sodium chlorate at 25°. (○) Experimental, (●) calculated from Wishaw–Stokes equation, (△) calculated from Falkenhagen–Leist equation.

FIG. 4. Fluidity vs. concentration for sodium chlorate in water.

Can. J. Chem. Downloaded from www.nrcresearchpress.com by 210.87.254.40 on 09/05/12
For personal use only.

Can. J. Chem. Downloaded from www.nrcresearchpress.com by 210.87.254.40 on 09/05/12
For personal use only.

TABLE I

Densities, viscosities, and conductances of aqueous solutions of sodium chlorate at 25 °C and 35 °C

Concentration (moles/l)	Density (g/ml)	Relative viscosity (water = 1.00)	Specific conductance (mhos/cm) × 10^3	Equivalent conductance (mhos)	Concentration (moles/l)	Density (g/ml)	Relative viscosity (water = 1.00)	Specific conductance (mhos/cm) × 10^3	Equivalent conductance (mhos)
Temperature = 25 °C					Temperature = 35 °C				
0.00500	0.9976	—	0.5456	109.02	0.00499	0.9945	—	0.6590	132.16
0.01000	0.9979	—	1.0628	106.24	0.00997	0.9950	—	1.2846	128.77
0.02433	0.9990	—	2.4994	102.73	0.02426	0.9959	—	3.0190	124.08
0.05030	1.0007	—	4.9720	98.85	0.05010	0.9975	—	5.9997	119.75
0.1007	1.0043	—	9.5109	94.45	0.1003	1.0011	1.011	11.460	114.26
0.3027	1.0183	1.008	25.913	85.60	0.3017	1.0149	1.029	31.150	103.25
0.5045	1.0312	1.038	40.629	80.53	0.5033	1.0286	1.048	48.747	96.85
0.7015	1.0458	1.056	53.769	76.65	0.6987	1.0418	1.070	64.397	92.15
0.9050	1.0596	1.076	66.411	73.37	0.9014	1.0554	1.091	79.694	88.41
1.5818	1.1058	1.154	101.98	64.47	1.5758	1.1016	1.168	122.17	77.53
2.5246	1.1679	1.307	138.37	54.81	2.5114	1.1618	1.319	165.39	65.86
3.5329	1.2334	1.538	161.91	45.83	3.5137	1.2267	1.541	194.11	55.24
4.4592	1.2928	1.832	171.97	38.56	4.4335	1.2863	1.828	207.17	46.73
5.2282	1.3413	2.159	173.43	33.17	5.1998	1.3340	2.133	210.11	40.41
5.7954	1.3773	2.468	170.93	29.49	5.7647	1.3700	2.422	207.91	36.07
6.2211	1.4052	2.777	167.10	26.86	6.7303	1.4300	3.056	199.57	29.65
6.7685	1.4381	3.163	161.98	23.93					

TABLE II

Specific and equivalent conductances (dilute solution) of sodium chlorate in water at 25 °C and 35 °C

Concentration (moles/l) × 10^4	Specific conductance (mhos/cm) × 10^4	Equivalent conductance (mhos)	Concentration (moles/l) × 10^4	Specific conductance (mhos cm^{-1}) × 10^4	Equivalent conductance (mhos)
Temperature = 25 °C			Temperature = 35 °C		
1.2593	0.14561	113.85	1.0510	0.14508	138.04
1.9089	0.21647	113.40	2.1589	0.29678	137.47
6.3899	0.71867	112.47	4.2876	0.58624	136.73
8.8536	0.99267	112.12	7.0978	0.96587	136.08
11.799	1.3177	111.68	10.118	1.3705	135.45
12.420	1.3866	111.64	14.312	1.9280	134.71
15.561	1.7318	111.29	20.396	2.7284	133.77
17.433	1.9362	111.06			
19.572	2.1696	110.85			
22.917	2.5328	110.52			
24.073	2.6589	110.45			

Can. J. Chem. Downloaded from www.nrcresearchpress.com by 210.87.254.40 on 09/05/12
For personal use only.

TABLE III

Densities, viscosities, and conductances of sodium chlorate in a solvent consisting of 64.5% dioxane, 35.5% water at 25 °C and 35 °C

Concentration (moles/l)	Density (g/ml)	Relative viscosity (water = 1.00)	Specific conductance (mhos/cm) × 10^4	Equivalent conductance (mhos)	Concentration (moles/l)	Density (g/ml)	Relative viscosity (water = 1.00)	Specific conductance (mhos/cm) × 10^4	Equivalent conductance (mhos)
Temperature = 25 °C					Temperature = 35 °C				
0.0014031	1.0366	2.159	0.57429	40.93	0.0014303	1.0279	2.081	0.72416	50.63
0.0023100	"	"	0.90899	39.35	0.0021182	"	"	1.0381	49.01
0.0032087	"	"	1.2254	38.19	0.0027386	"	"	1.3115	47.89
0.0040983	"	"	1.5278	37.28	0.0035743	"	"	1.6667	46.63
0.0049414	"	"	1.8061	36.55	0.0043991	"	"	2.0060	45.60
0.0069421	"	"	2.4422	35.18	0.0056772	"	"	2.5150	44.30
0.018696	1.0378	2.172	5.7920	30.98	0.018539	1.0291	2.090	7.0356	37.95
0.052085	1.0400	2.193	14.110	27.09	0.051644	1.0312	2.115	17.043	33.00
0.098176	1.0428	2.229	24.289	24.74	0.097394	1.0345	2.151	29.355	30.14
0.27866	1.0545	2.329	59.605	21.39	0.27633	1.0457	2.244	72.067	26.08
0.57568	1.0736	2.505	108.11	18.78	0.57080	1.0645	2.407	130.88	22.93
1.0290	1.1019	2.823	167.52	16.28	1.0204	1.0928	2.692	203.88	19.98
1.2681	1.1168	3.009	192.75	15.20	1.2578	1.1077	2.857	236.21	18.78

TABLE IV

Specific and equivalent conductance of sodium chlorate and of lithium chlorate in a solvent consisting of 90% dioxane, 10% water at 25 °C

Concentration (moles/l) × 10^4	Specific conductance (mhos/cm) × 10^6	Equivalent conductance (mhos)	Concentration (moles/l) × 10^4	Specific conductance (mhos/cm) × 10^6	Equivalent conductance (mhos)
Sodium chlorate			Lithium chlorate		
3.3139	0.56625	1.7087	2.7957	0.74877	2.6783
6.0631	0.80081	1.3208	5.6472	1.1237	1.9898
10.848	1.1157	1.0285	10.083	1.5822	1.5692
15.618	1.3856	0.8872	17.278	2.1966	1.2713
20.325	1.6250	0.7995	25.690	2.8316	1.1022
29.545	2.0283	0.6865	32.718	3.3261	1.0166
41.382	2.5330	0.6121	46.977	4.2820	0.9115
			168.54	12.507	0.7421

Can. J. Chem. Downloaded from www.nrcresearchpress.com by 210.87.254.40 on 09/05/12
For personal use only.

TABLE V

Specific and equivalent conductances of lithium chlorate in a solvent consisting of 64.5% dioxane, 35.5% water at 25 °C

Concentration (moles/l) × 10^4	Specific conductance (mhos cm^{-1}) × 10^4	Equivalent conductance (mhos)
10.017	0.38525	38.46
16.121	0.60002	37.22
25.743	0.92186	35.81
34.778	1.2127	34.87
43.204	1.4758	34.16
50.970	1.7126	33.60
83.699	2.6675	31.87

TABLE VI

Activation energies of conductance and of viscosity of sodium chlorate in water

Concentration (moles/l)	Activation energy of conductance (kcal/mole)	Activation energy of viscosity (kcal/mole)	$\frac{\Delta E \text{ viscosity}}{\Delta E \text{ conductance}}$
0	3.56	3.62	1.02
0.3	3.42	3.23	0.94
0.7	3.36	3.34	0.99
1.0	3.42	3.33	0.97
2.0	3.30	3.39	1.03
3.0	3.29	3.44	1.05
4.0	3.38	3.57	1.06
5.0	3.51	3.69	1.05
6.0	3.66	3.93	1.07

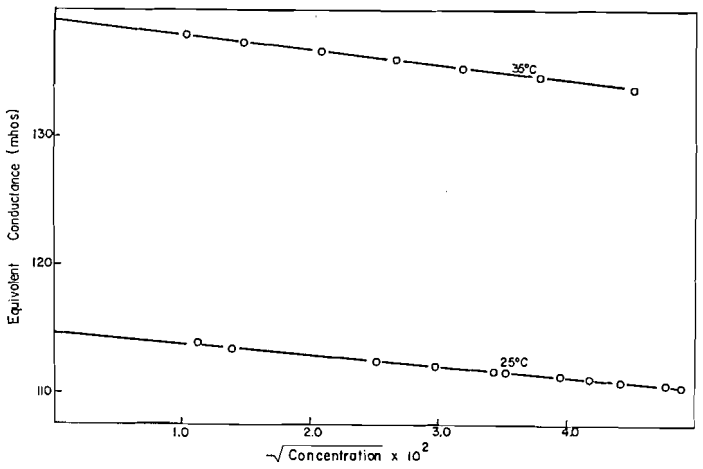


FIG. 5. Limiting equivalent conductance of sodium chlorate in water by the Kohlrausch method.

The same method applied to the 35 °C data yielded a limiting equivalent conductance 139.26 mhos. The slope of the straight line is 120.75 and the Onsager tangent 107.70. Thus, to use the language of Fuoss (16), the phoreogram of sodium chlorate at 35 °C is catabatic to the Onsager tangent, indicating ion association.

Solutions of Sodium Chlorate and of Lithium Chlorate in a Solvent Consisting of 64.5% Dioxane and 35.5% Water at 25 °C and 35 °C

Graphs of equivalent conductance versus the square root of the concentration of sodium chlorate, at 25° C and at 35 °C, and of lithium chlorate in dilute solution at 25°, are given in Fig. 6. Because of the limited solubility, the maximum in the specific conductance is no longer observed. Fluidity is plotted against concentration in Fig. 7. Table VII gives the values of the activation energies of conductivity and of viscosity. Both are greater than the corresponding energies with water as solvent. This may be connected with the fact that the dioxane molecule is much larger than the water molecule, their respective molar volumes being 85 and 18 ml. Greater energy will be required to form a "hole" in dioxane than in water. This, of course, assumes a "hole" mechanism for both conductance and viscosity.

TABLE VII

Activation energy of conductance and of viscosity of sodium chlorate in a solvent consisting of 64.5% dioxane, 35.5% water

Concentration (moles/l)	Activation energy of conductance (kcal/mole)	Activation energy of viscosity (kcal/mole)	$\frac{\Delta E \text{ viscosity}}{\Delta E \text{ conductance}}$
0	4.03	4.29	1.07
0.1	3.77	4.25	1.13
0.3	3.73	4.29	1.15
0.5	3.67	4.33	1.18
0.7	3.70	4.36	1.18
1.0	3.76	4.44	1.18
1.2	3.94	4.49	1.14

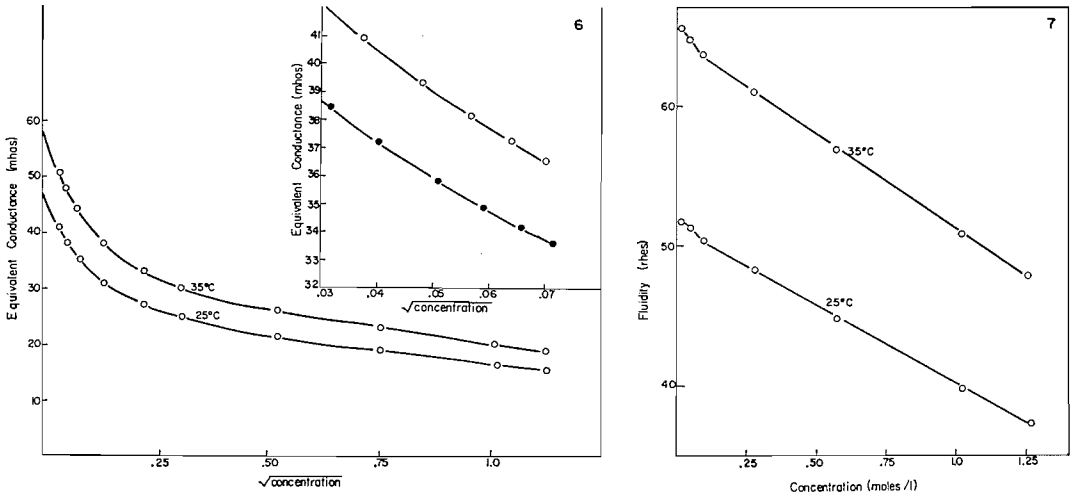


FIG. 6. Equivalent conductance vs. square root of concentration. (○) Sodium chlorate at 25° and 35°, (●) lithium chlorate at 25°.

FIG. 7. Fluidity vs. concentration of sodium chlorate in a solvent consisting of 64.5% dioxane, 35.5% water.

The limiting equivalent conductances of sodium chlorate and of lithium chlorate in this solvent were found by applying the Fuoss-Onsager equation for associated electrolytes (17). Plots of y vs. x are shown in Fig. 8. A summary of quantities derived from the Fuoss-Onsager equation is given in Table VIII.

Can. J. Chem. Downloaded from www.nrcresearchpress.com by 210.87.254.40 on 09/05/12
For personal use only.

It is no longer believed that a, the distance of closest approach, contact distance, or center-to-center distance, has a physical meaning. It is merely an empirical parameter. It can only be said that the a values (in Å units) are of the order of magnitude which might be expected for solvated ions.

TABLE VIII

Derived quantities for the mixture 64.5% dioxane, 35.5% water

Salt and temperature	D	$J(a)$	a	K_A	Λ_0
Sodium chlorate at 25 °C	23.4	1 690	3.80	16.6	46.69
Sodium chlorate at 35 °C	22.1	2 257	3.77	17.0	58.21
Lithium chlorate at 25 °C	23.4	1 724	3.93	26.2	43.10

TABLE IX

Walden products

Salt and temperature	$\Lambda_0\eta_0$ in water	$\Lambda_0\eta_0$ in 64.5% dioxane, 35.5% water
Sodium chlorate at 25 °C	1.025	0.901
Sodium chlorate at 35 °C	1.017	0.884
Lithium chlorate at 25 °C	0.923	0.832

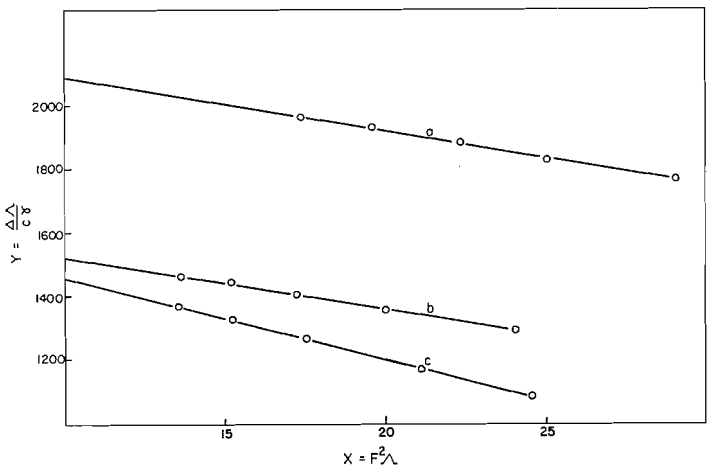


FIG. 8. Plot of y vs. x for the solvent 64.5% dioxane, 35.5% water. (a) Sodium chlorate at 35 °C, (b) sodium chlorate at 25 °C, (c) lithium chlorate at 25 °C.

In Table IX, the so-called Walden product, $\Lambda_0\eta_0$, is compared for both electrolytes in both solvents. Apparently, $\Lambda_0\eta_0$ decreases with decreasing dielectric constant.

Conductances of Sodium Chlorate and of Lithium Chlorate in a Mixture of 90% Dioxane and 10% Water at 25 °C

Plots of equivalent conductance against the square root of the concentration are presented in Fig. 9. The graphs are curved, even in the extremely dilute region. Even the y vs. x plots are curved, making it almost impossible to find Λ_0 by this method. A fair approximation to Λ_0 can be obtained, however, from Walden's rule, using the known

Can. J. Chem. Downloaded from www.nrcresearchpress.com by 210.87.254.40 on 09/05/12
For personal use only.

viscosity of the solvent. It is then possible to obtain an approximation to K_A, the association constant, by a method given by D'Aprano and Fuoss (18). According to these authors, a plot of log K_c($K_c = \Lambda_0^2F^2/\Lambda_0^2f^2C$) against C should be linear and extrapolate to K_A at zero concentration. Such plots of log K_c versus C are shown in Fig. 10. The plots are linear, except for the most dilute point. The values of K_A and Λ_0 thus obtained are presented in Table X.

TABLE X

Association constants and limiting conductances in a solvent of 90% dioxane, 10% water at 25 °C (dielectric constant = 6.07)

Salt	Λ_0 by Walden's rule	K_A (association constant)
Sodium chlorate	68.0	6.0×10^6
Lithium chlorate	62.8	2.6×10^6

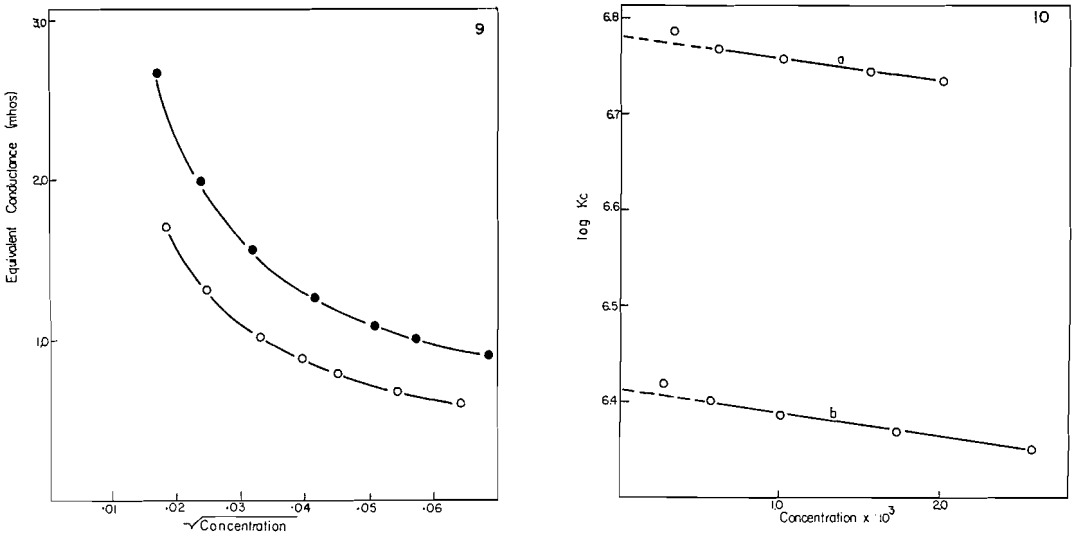


FIG. 9. Equivalent conductance vs. square root of concentration. (○) Sodium chlorate in a solvent consisting of 90% dioxane, 10% water; (●) lithium chlorate in a solvent consisting of 90% dioxane, 10% water.

FIG. 10. Log K_c vs. concentration for 90% dioxane and 10% water mixture. (*a*) Sodium chlorate at 25 °C, (*b*) lithium chlorate at 25 °C.

Figure 9 shows that in 90% dioxane, lithium chlorate has a higher conductance than sodium chlorate, at corresponding concentrations. The reverse is true in the other solvents, which contain more water.

An examination of the association constants shows that in 90% dioxane, sodium chlorate is more associated than lithium chlorate, whereas the reverse is true in 64.5% dioxane.

The original intent of this work was to throw some light on the structure of the melt. One important result emerges. The specific conductance of lithium chlorate in 90% dioxane (dielectric constant = 6.07), at 25 °C, is of the same order of magnitude as that of the anhydrous melt at 130°, both being very low. From Table X, it is obvious that the low conductance in 90% dioxane is due to ion-pair formation, very few free ions being present;

Can. J. Chem. Downloaded from www.nrcresearchpress.com by 210.87.254.40 on 09/05/12
For personal use only.

the viscosity of the solution is low. On the other hand, the low conductance of the melt, despite the fact that it is at a temperature 105 deg higher, is unquestionably due, in large part, to the enormous viscosity (6).

As far, at least, as lithium chlorate is concerned, our previous work (1–4) leads us to doubt the view that the melt is highly, or completely, ionized. We are inclined to the view that some sort of coordinate linkage exists in molten lithium chlorate.

REFERENCES

1. A. N. CAMPBELL and D. F. WILLIAMS. Can. J. Chem. **42**, 1778 (1964).
2. A. N. CAMPBELL and D. F. WILLIAMS. Can. J. Chem. **42**, 1984 (1964).
3. A. N. CAMPBELL and M. K. NAGARAJAN. Can. J. Chem. **42**, 1137 (1964).
4. A. N. CAMPBELL and M. K. NAGARAJAN. Can. J. Chem. **42**, 1616 (1964).
5. R. M. FUOSS and F. ACCASCINA. Electrolytic conductance. Interscience Publishers Inc., New York. 1959.
6. A. N. CAMPBELL and W. G. PATERSON. Can. J. Chem. **36**, 1004 (1958).
7. A. N. CAMPBELL and J. E. GRIFFITHS. Can. J. Chem. **34**, 1647 (1956).
8. K. HESS and H. FRAHM. Ber. **71**, 2627 (1938).
9. P. R. FREY and E. C. GILBERT. J. Am. Chem. Soc. **59**, 1344 (1937).
10. F. E. CRITCHFIELD, J. A. GIBSON, and J. L. HALL. J. Am. Chem. Soc. **75**, 1991 (1953).
11. C. JONES and G. M. BOLLINGER. J. Am. Chem. Soc. **53**, 411 (1931).
12. T. SHEDLOVSKY. J. Am. Chem. Soc. **54**, 1411 (1932).
13. J. E. LIND, JR., J. J. ZWOLENIK, and R. M. FUOSS. J. Am. Chem. Soc. **81**, 1557 (1959).
14. M. J. CANNON and M. R. FENSKE. Ind. Eng. Chem. Anal. Ed. **10**, 299 (1938).
15. C. B. MONK. J. Am. Chem. Soc. **70**, 3281 (1948).
16. R. M. FUOSS. J. Chem. Educ. **32**, 527 (1955).
17. R. M. FUOSS. J. Am. Chem. Soc. **81**, 2659 (1959).
18. A. D'APRANO and R. M. FUOSS. J. Phys. Chem. **67**, 1871 (1963).

Can. J. Chem. Downloaded from www.nrcresearchpress.com by 210.87.254.40 on 09/05/12
For personal use only.

Can. J. Chem. Downloaded from www.nrcresearchpress.com by 210.87.254.40 on 09/05/12
For personal use only.

THE SYSTEMS SODIUM CHLORATE – WATER – DIOXANE AND LITHIUM CHLORATE – WATER – DIOXANE, AT 25°

A. N. CAMPBELL, E. M. KARTZMARK, AND W. B. MARYK
Department of Chemistry, University of Manitoba, Winnipeg, Manitoba

Received November 22, 1965

ABSTRACT

The phase diagrams of the systems sodium chlorate – water – dioxane and lithium chlorate – water – dioxane have been determined at 25 °C.

The sodium chlorate – water – dioxane diagram is relatively simple, anhydrous sodium chlorate being the only solid phase. The occurrence of two liquid layers in contact with sodium chlorate is found between dioxane concentrations of 67.7 and 88.8%.

The lithium chlorate – water – dioxane system exhibits both complex formation and a ternary miscibility gap. The lithium chlorate hydrate, $LiClO_3.\frac{1}{4}H_2O$, exists from 0 to 2.2% dioxane. A mole to mole compound of lithium chlorate and dioxane, $LiClO_3.C_4H_8O_2$, exists from 2.2% dioxane to 100% dioxane. There exists a ternary miscibility gap between dioxane concentrations of 81.5 and 93.6%

The X-ray powder data for anhydrous lithium chlorate, its quarter hydrate, and the compound of lithium chlorate and dioxane have been obtained.

This work arose as a side issue to the work of Campbell, Kartzmark, and Oliver (1) on the conductances of sodium and of lithium chlorates in water–dioxane mixtures. It was thought that the nature of the solid phases might throw some light on the nature of the ions in solution and, indeed, the fact that lithium chlorate forms a compound with dioxane, whereas sodium chlorate does not, would indicate some difference in the solvation of the two cations in dioxane–water mixtures.

EXPERIMENTAL

Materials

Lithium chlorate was prepared by the method of Campbell and Griffiths (2). We found the melting point to be 127.9° ± 0.1° in comparison with the value of 127.8° reported by Campbell and Griffiths. Dioxane was purified by the method of Hess and Frahm (3). Our product boiled at 101.3° (p = 760 mm). The boiling point, density (d^{25} = 1.0278), and refractive index (n_D^{25} = 1.4201) were in close agreement with the results of Frey and Gilbert (4) and of Schott (5). Water distilled in an electric still and having a specific conductance of 5×10^{-6} mhos was used. The sodium chlorate was Fisher certified reagent and received no other purification than drying at 130°.

Determination of Solubility and Methods of Analysis

Both the methods of the "wet residue" and total composition of complex were used to determine the nature of the equilibrium solid phase. After separation of the saturated solution from the wet solid phase, weighed samples of both were submitted to distillation and the distillate analyzed refractometrically for dioxane content. The residue, consisting either of sodium chlorate or of lithium chlorate, was weighed. A complication occurs with lithium chlorate, in that decomposition occurs when dioxane–water mixtures of dioxane content greater than 10% are distilled from lithium chlorate. Hence, such solutions were previously diluted with a weighed amount of water to ensure a dioxane concentration less than 10%.

Since sodium chlorate is not hygroscopic, it was possible to determine the content of sodium chlorate simply by weighing the residue from distillation. The content of lithium chlorate was determined by estimating chlorate radical by a method described by Vogel (6) and by Talbot (7), in which iodine liberated from potassium iodide by the chlorate is titrated with thiosulfate.

X-Ray Powder Photographs

These were taken on anhydrous lithium chlorate, lithium chlorate quarter hydrate, and on the compound of lithium chlorate and dioxane. Because of the hygroscopic nature of the samples containing lithium chlorate, it was necessary to enclose them in fine glass capillaries and mount them in this form in the camera. The capillaries were filled in a drybox and exposed to the X-rays for a period of 10 h.

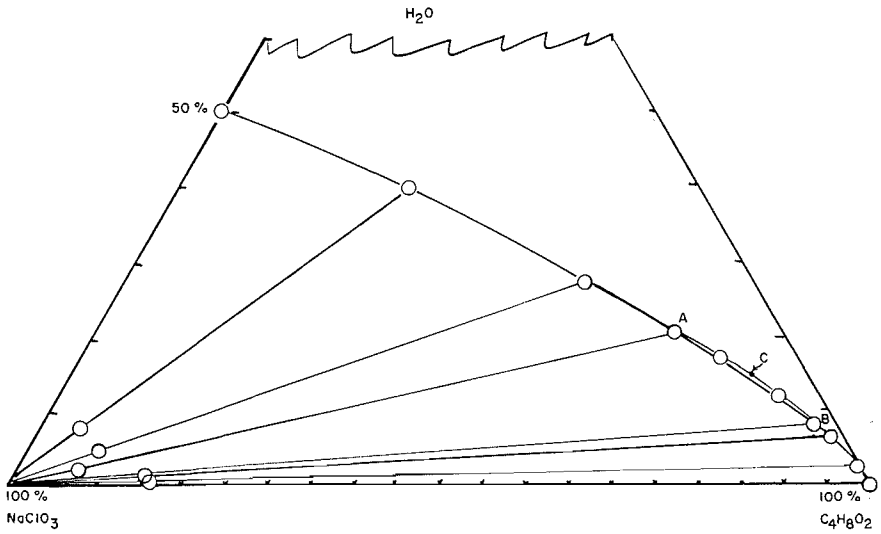


FIG. 1. The system sodium chlorate – water – dioxane, at 25 °C.

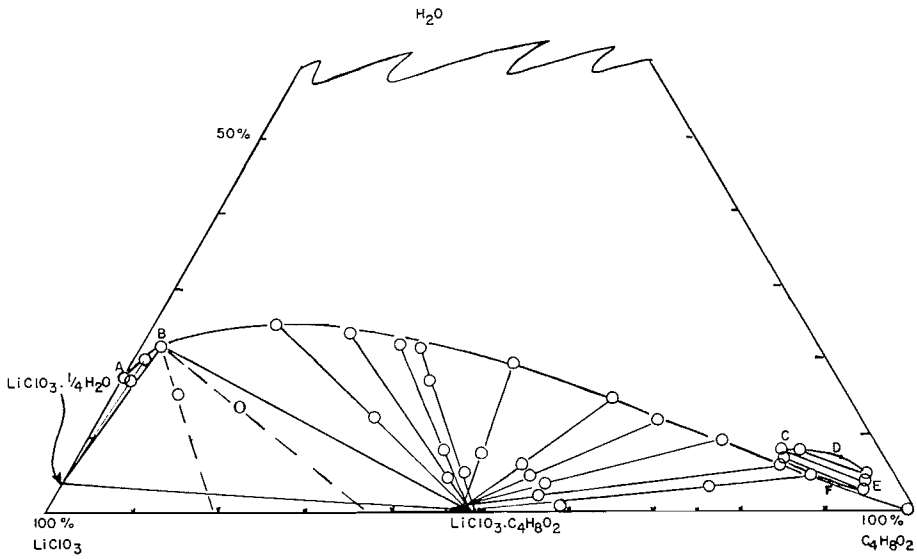


FIG. 2. The system lithium chlorate – water – dioxane, at 25 °C.

RESULTS

The system sodium chlorate – dioxane – water, at 25°, is represented graphically in Fig. 1, and the corresponding system lithium chlorate – dioxane – water, at 25°, in Fig. 2. The X-ray data have been communicated to the American Society for Testing Materials.

DISCUSSION

The sodium chlorate – dioxane – water system (Fig. 1) is relatively simple. No complex formation occurs, the only solid phase being anhydrous sodium chlorate at this temperature. Occurrence of two liquid layers in contact with solid sodium chlorate is found in that region of the diagram where the dioxane concentration is between 67.7 and 88.8%.

Can. J. Chem. Downloaded from www.nrcresearchpress.com by 210.87.254.40 on 09/05/12
For personal use only.

The triangular area, A–$NaClO_3$–B, is an invariant triangle, there being two liquid phases and a solid in equilibrium at constant temperature and pressure, and hence zero degree of freedom. The region of stable existence of two liquid layers, in the absence of solid phase, is very small; the two liquid layers disappear upon addition of a few percent of water. The plait point or critical composition is estimated to be 81.0% dioxane, 5.0% water, and 14.0% sodium chlorate.

The lithium chlorate – water – dioxane system, Fig. 2, exhibits both compound formation and a ternary miscibility gap. As the results of Campbell and Griffiths (2) indicate, a one-quarter hydrate, $LiClO_3.\frac{1}{4}H_2O$, exists at 25° in the binary system lithium chlorate – water. Our results show that the region of existence of this hydrate is very limited in the ternary system: it exists only up to concentrations of 2.2% dioxane. Point B (Fig. 2) is an isothermally invariant point, and it represents this limit. At B, the three phases in equilibrium are solid $LiClO_3.\frac{1}{4}H_2O$, solid compound ($LiClO_3.C_4H_8O_2$), and saturated solution of composition (by weight) 75.5% lithium chlorate, 2.0% dioxane, and 22.5% water. The triangular area, B–$LiClO_3.\frac{1}{4}H_2O$–$LiClO_3.C_4H_8O_2$, is thus an invariant triangle.

The rest of the continuous curve, BF (Fig. 2) represents solutions in equilibrium with a solid of composition 49.3% dioxane and 50.7% lithium chlorate, i.e. a mole to mole compound. The tie lines intersect and spread over a range of 48 to 50% dioxane; this is not surprising because of the great experimental difficulties encountered in this region. The X-ray pattern, however, gives convincing proof of the existence of this compound. A brief summary of the strongest lines is as follows: anhydrous $LiClO_3$: 3.907, 3.767, and 2.803 Å; $LiClO_3.\frac{1}{4}H_2O$: 7.865, 4.103, and 3.751 Å; compound: 4.073, 3.587, and 3.348 Å. Similar dioxanates have been found with other salts.

There exists a ternary miscibility gap in the region where the dioxane concentration is between 81.5 and 93.6%. The gap is small and the lower limit of the gap approaches so near to the solid solubility curve that it was at first difficult to determine whether the two liquids could exist in the presence of solid or not. Accordingly, a large amount of solution containing water, dioxane, and lithium chlorate and unsaturated with respect to lithium chlorate, and such that the mixture consisted of approximately equal volumes of the two liquid layers, was prepared. To this mixture anhydrous lithium chlorate was added. After the mixture was stirred briefly, the two liquid layers disappeared, solid remaining in equilibrium with a single liquid. A further quantity of the two-liquid mixture was added and the system kept at 25° for 24 h. The two liquid layers disappeared. On decanting off the homogeneous liquid and adding a minute amount of water, the two liquid layers reappeared instantaneously and remained even after prolonged stirring. It is, therefore, certain that the miscibility gap in the ternary system lithium chlorate – dioxane – water does not exist in the presence of solid phase, at 25°.

The upper critical composition point is 88.7% dioxane, 4.5% lithium chlorate, and 6.8% water; the lower critical composition point is 88.3% dioxane, 7.3% lithium chlorate, and 4.4% water.

REFERENCES

1. A. N. Campbell, E. M. Kartzmark, and B. G. Oliver. Can. J. Chem. This issue.
2. A. N. Campbell and J. E. Griffiths. Can. J. Chem. **34**, 1647 (1956).
3. K. Hess and H. Frahm. Ber. **71**, 2627 (1938).
4. P. R. Frey and E. C. Gilbert. J. Am. Chem. Soc. **59**, 1344 (1937).
5. H. Schott. J. Chem. Eng. Data, **6**, 1, 19 (1961).
6. A. I. Vogel. Textbook of quantitative inorganic analysis. Longmans, Green & Co., Inc., New York and Toronto. 1961.
7. H. P. Talbot. Quantitative chemical analysis. The Macmillan Co. of Canada, Ltd., Toronto. 1958.

Can. J. Chem. Downloaded from www.nrcresearchpress.com by 210.87.254.40 on 09/05/12
For personal use only.

Can. J. Chem. Downloaded from www.nrcresearchpress.com by 210.87.254.42 on 09/05/12
For personal use only.

A REFINEMENT OF THE CRYSTAL STRUCTURES OF $(NH_4)_2TeBr_6$ AND Cs_2TeBr_6

A. K. DAS AND I. D. BROWN
Department of Physics, Hamilton College, McMaster University, Hamilton, Ontario

Received December 1, 1965

ABSTRACT

$(NH_4)_2TeBr_6$ and Cs_2TeBr_6 crystals have the cubic K_2PtCl_6 structure with space group: $Fm3m(O_h^5)$ with $a_0 = 10.728 \pm 0.003$ Å and 10.918 ± 0.002 Å respectively. The positional coordinate of the bromine atom, and the anisotropic temperature factors of all atoms in the unit cell, have been refined for both crystals by a full matrix least-squares analysis of the three dimensional X-ray diffraction data ($R = 0.08$). The Te—Br distance, corrected for probable thermal motions of atoms forming the bond, is 2.70 ± 0.01 Å in both crystals.

INTRODUCTION

In a previous paper, one of us (I. D. B.) reported the crystal structure of K_2TeBr_6 (1), which possesses a distorted K_2PtCl_6 structure (2). To examine the influence of the cation on the bonding within the $TeBr_6^{2-}$ ion, we have now refined the structures of $(NH_4)_2TeBr_6$ and Cs_2TeBr_6, both of which possess the undistorted K_2PtCl_6 structure at room temperature.

Accurate lattice parameters for both crystals have already been determined by Swanson and his co-workers (3, 4). The unit cell and space group of $(NH_4)_2TeBr_6$ have been determined by Manojlović (5) and the structure of Cs_2TeBr_6 crystal has been reported by Bagnall *et al.* (6). In the present work, new X-ray diffraction data have been obtained and more accurate values of Te—Br bond distances are reported.

EXPERIMENTAL

Bright-red crystals of $(NH_4)_2TeBr_6$ and Cs_2TeBr_6 were prepared by methods similar to those described for K_2TeBr_6 and $(NH_4)_2TeCl_6$ in Inorganic Syntheses (7). Powder photographs of these crystals with Ni-filtered Cu radiation were used to calculate accurate lattice parameters, and their densities were measured pycnometrically with CCl_4 at 25 °C. The crystal data thus obtained are listed in Table I together with the reported lattice parameters (3, 4), which are in good agreement with the present measurements.

Visually estimated intensity data were collected from a single crystal ($0.39 \times 0.15 \times 0.08$ mm) of $(NH_4)_2TeBr_6$ in five layers parallel to the largest face (001) of the crystal with precession photographs taken with Zr-filtered Mo radiation. The intensities were corrected for the Lorentz and polarization effects but not for absorption. Because of the cubic symmetry of the crystal, some of the reflections in higher layer

TABLE I

Crystal data for $(NH_4)_2TeBr_6$ and Cs_2TeBr_6

	$(NH_4)_2TeBr_6$	Cs_2TeBr_6
System	Cubic	Cubic
Formula weight	643.2	872.9
a_0	10.728±0.003 Å (present work) 10.731 Å (ref. 3) 10.73±0.02 Å (ref. 5)	10.918±0.002 Å (present work) 10.919 Å (ref. 4) 10.910±0.005 Å (ref. 6)
V	1234.7 Å^3	1301.5 Å^3
D_m (pycnometric)	3.42±0.02 g cm^{-3}	4.43±0.02 g cm^{-3}
Z	4	4
D_x	3.46 g cm^{-3}	4.45 g cm^{-3}
Absorption coefficient for Mo K_α	230 cm^{-1}	274 cm^{-1}
Space group	$Fm3m(O_h^5)$	$Fm3m(O_h^5)$
Systematic absences hkl: $h+k$, $k+l$, $h+l = 2n+1$ (both crystals)		

lines were equivalent to those in lower layers and thus the data from different layers could be scaled to each other. However, it was not possible to scale odd and even layers together. We assumed that the crystal has the K_2PtCl_6 structure (2) and refined the positional coordinate of the bromine atom and the anisotropic temperature factors of all atoms in the unit cell by a full matrix least-squares analysis* of the three dimensional data. Each reflection was weighted individually according to an estimate of its reliability. The atomic scattering factors for all the atoms except hydrogen, which was not included in the refinement, were taken from International Tables (8). The observed and calculated structure factors are given in Table II and the atomic parameters after the final cycle of refinement are listed in Table IV. The weighted R index given by

$$R = \{\sum w(|F_o| - |F_c|)^2 / \sum w|F_o|^2\}^{1/2}$$

for these parameters was 0.079.

TABLE II

The observed and calculated structure factors for $(NH_4)_2TeBr_6$

h	k	l	$\lvert F_o\rvert$	F_c	h	k	l	$\lvert F_o\rvert$	F_c
2	0	0	376	381	6	2	2	255	−261
4	0	0	714	772	8	2	2	93	88
6	0	0	211	181	10	2	2	98	−99
8	0	0	456	393	12	2	2	89	90
10	0	0	38	45	14	2	2	31	−29
12	0	0	180	177	16	2	2	59	57
2	2	0	< 20	−19	4	4	2	278	267
4	2	0	344	313	6	4	2	< 13	10
6	2	0	29	−23	8	4	2	193	183
8	2	0	213	213	10	4	2	< 15	−3
10	2	0	26	−22	12	4	2	107	107
12	2	0	124	126	14	4	2	< 17	−4
14	2	0	< 18	−14	16	4	2	49	55
16	2	0	59	65	6	6	2	137	−149
4	4	0	540	590	8	6	2	64	56
6	4	0	178	166	10	6	2	41	−52
8	4	0	330	321	12	6	2	69	62
10	4	0	51	49	8	8	2	135	122
12	4	0	141	147	10	8	2	30	26
14	4	0	< 17	5	12	8	2	77	68
16	4	0	63	64	3	3	3	*	140
6	6	0	< 29	−15	5	3	3	118	120
8	6	0	132	129	7	3	3	107	97
10	6	0	< 16	−6	9	3	3	76	77
12	6	0	73	83	11	3	3	62	57
8	8	0	174	186	13	3	3	43	43
10	8	0	40	51	5	5	3	113	105
12	8	0	98	88	7	5	3	83	86
1	1	1	*	196	9	5	3	66	69
3	1	1	167	171	11	5	3	48	52
5	1	1	140	141	13	5	3	35	39
7	1	1	117	111	7	7	3	60	72
9	1	1	101	87	9	7	3	57	58
11	1	1	62	64	11	7	3	35	45
13	1	1	46	48	13	7	3	35	34
3	3	1	152	154	9	9	3	49	48
5	3	1	129	130	11	9	3	43	37
7	3	1	100	104	4	4	4	612	469
9	3	1	86	81	6	4	4	149	151
11	3	1	59	61	8	4	4	272	263
13	3	1	40	45	10	4	4	44	50
5	5	1	103	113	12	4	4	136	123
7	5	1	95	92	14	4	4	< 17	10
9	5	1	69	73	16	4	4	54	54
11	5	1	52	55	6	6	4	< 12	8
13	5	1	38	41	8	6	4	108	114
7	7	1	82	76	10	6	4	< 15	6
9	7	1	57	61	12	6	4	69	72
11	7	1	38	47	14	6	4	17	4
13	7	1	26	36	8	8	4	133	155
9	9	1	65	50	10	8	4	48	47
11	9	1	47	39	12	8	4	71	74
13	9	1	33	29					
2	2	2	378	−496					
4	2	2	39	31					

*Unobservable on the precession films because of beam stop.

**The program used was written in this laboratory by Mr. J. S. Stephens.*

Can. J. Chem. Downloaded from www.nrcresearchpress.com by 210.87.254.42 on 09/05/12
For personal use only.

Can. J. Chem. Downloaded from www.nrcresearchpress.com by 210.87.254.42 on 09/05/12
For personal use only.

TABLE III

The observed and calculated structure factors for Cs_2TeBr_6

h	k	l	$\lvert F_o\rvert$	F_c	h	k	l	$\lvert F_o\rvert$	F_c
2	0	0	< 35	37	4	4	2	< 59	43
4	0	0	920	1062	6	4	2	166	154
6	0	0	< 54	−5	8	4	2	< 72	45
8	0	0	526	540	6	6	2	308	−313
10	0	0	< 58	−24	8	6	2	100	109
12	0	0	216	218	10	6	2	149	−143
2	2	0	328	305	8	8	2	< 60	37
4	2	0	77	40	3	3	3	143	103
6	2	0	168	174	5	3	3	116	107
8	2	0	52	48	7	3	3	61	57
4	4	0	747	822	9	3	3	51	67
6	4	0	< 56	7	5	5	3	110	106
8	4	0	449	443	7	7	3	< 42	34
10	4	0	< 80	−14	4	4	4	703	659
12	4	0	183	182	6	4	4	< 53	14
6	6	0	115	108	8	4	4	342	365
8	8	0	263	254	10	4	4	< 60	−7
1	1	1	234	209	12	4	4	154	153
3	1	1	184	162	6	6	4	100	98
5	1	1	152	156	8	6	4	< 86	24
7	1	1	73	84	10	6	4	< 94	42
9	1	1	76	91	8	8	4	207	211
3	3	1	128	128	5	5	5	107	101
5	3	1	133	129	7	5	5	58	62
7	3	1	66	69	7	7	5	< 42	37
5	5	1	125	125	6	6	6	225	−208
7	5	1	63	72	8	6	6	73	73
7	7	1	< 59	41	10	6	6	100	−96
2	2	2	800	−815	8	8	6	< 59	21
4	2	2	264	255	7	7	7	< 42	22
6	2	2	435	−482	8	8	8	138	125
8	2	2	139	168					
10	2	2	191	−213					
12	2	2	87	91					

A similar procedure was followed in the refinement of the structure of Cs_2TeBr_6. The crystal used had the dimensions 0.23 × 0.15 × 0.06 mm. Integrated precession photographs were taken in four layers parallel to the largest face (011) of the crystal and the intensity of each reflection was measured with a microdensitometer. After refinement of the structural parameters, the weighted R index was 0.082. Table III lists the observed and calculated structure factors and Table IV the final positional coordinates and anisotropic temperature factors of Cs_2TeBr_6.

TABLE IV

Atomic parameters derived from the final least-squares refinement

Atom	Positional coordinates	Temperature factor*
$(NH_4)_2TeBr_6$ crystal		
Te in 4(*a*)†	(0,0,0; etc.)	$\beta_{11}(=\beta_{22}=\beta_{33})=42\pm1$
Br in 24(*e*)	(x,0,0; etc.) with x = 0.2499±0.0002	$\beta_{11}=37\pm2$; $\beta_{22}(=\beta_{33})=134\pm1$
N in 8(*c*)	($\frac{1}{4},\frac{1}{4},\frac{1}{4}$; etc.)	$\beta_{11}(=\beta_{22}=\beta_{33})=118\pm22$
Cs_2TeBr_6 crystal		
Te in 4(*a*)	(0,0,0; etc.)	$\beta_{11}(=\beta_{22}=\beta_{33})=69\pm4$
Br in 24(*e*)	(x,0,0; etc.) with x = 0.2468±0.0004‡	$\beta_{11}=53\pm7$; $\beta_{22}(=\beta_{33})=106\pm1$
Cs in 8(*c*)	($\frac{1}{4},\frac{1}{4},\frac{1}{4}$; etc.)	$\beta_{11}=(\beta_{22}=\beta_{33})=94\pm3$

*The anisotropic temperature factors appear in the structure factor calculation as $\exp(-10^{-4}(\beta_{11}h^2+\beta_{22}k^2+\beta_{33}l^2))$.
†See International Tables for X-ray crystallography. Vol. I, 1962. p. 338.
‡The value of x given by Bagnall *et al.* (6) is 0.24.

RESULTS AND DISCUSSION

Both crystals possess the K_2PtCl_6 structure which is based on a face-centered cubic array of the octahedral $TeBr_6^{2-}$ ions oriented with the Te—Br bonds along the principal cube axes. The cations occupy the tetrahedral holes between 4 neighboring anions and are surrounded by 12 bromine atoms, 3 from each anion.

The Te—Br bond lengths are given in Table V. A correction can be made for the apparent shortening of the bond due to thermal motion (9) on the assumption that the $TeBr_6^{2-}$ ion is librating about the central tellurium atom. If this is done, the mean Te—Br bond length in both crystals becomes 2.70 Å. Owing to the uncertainty in the absolute values of the amplitudes of thermal motion and the proper way to correct for them, the standard error in this bond distance is estimated to be about 0.01 Å. Thus, the Te—Br bond is not significantly different in two structures nor does it differ significantly from the value (2.71 Å) found in K_2TeBr_6 (1). It is apparent that the cations do not have a large influence on the structure of the anion.

TABLE V

Interatomic distances and thermal motions in M_2TeBr_6 crystals

	K_2TeBr_6*	$(NH_4)_2TeBr_6$	Cs_2TeBr_6
Interatomic distances before correction for thermal motion (Å)			
Te—Br	2.692±0.006†	2.681±0.002†	2.695±0.004†
M—Br		3.793±0.001†	3.860±0.001†
Br—Br (between anions)		3.794±0.003†	3.909±0.003†
Interatomic distances after correction for thermal motion (see text) (Å)			
Te—Br	2.71±0.01‡	2.70±0.01‡	2.70±0.01‡
M—Br		3.82±0.01‡	3.89±0.01‡
Br—Br (between anions)		3.84±0.01‡	3.94±0.01‡
Root mean square amplitudes of thermal vibration (Å)			
Te	0.15§	0.16	0.20
Br (i) along TeBr bond	0.14§	0.15	0.18
Br (ii) perpendicular to Te—Br bond	0.25§	0.28	0.25
M	0.28§	0.26	0.23
Ratio of perpendicular: parallel motion of the bromine atom	1.8	1.9	1.4

*See ref. 1.
†The error quoted is that calculated from the standard errors indicated for the cell constants and the least-squares refinement, and does not include possible systematic errors.
‡Estimated standard errors, including an allowance for possible systematic errors.
§Average values.

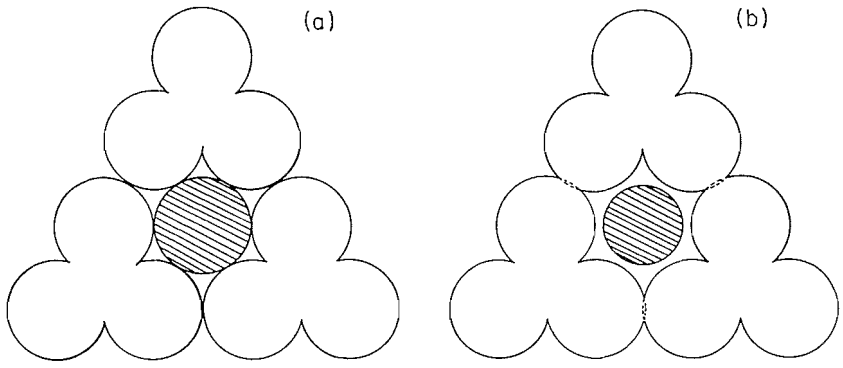


FIG. 1. Sections through the cation perpendicular to (111) direction in (*a*) Cs_2TeBr_6 and (*b*) $(NH_4)_2TeBr_6$: cation (striped circle), bromine (open circle).

The thermal corrections applied to the other interatomic distances are made on the assumption that there is no correlation between their motions. It is interesting to compare the bromine–cation distances with those predicted from the ionic radii.* The observed

**The values of the ionic radii used are:* Br, *2.10 Å;* Cs, *1.80 Å (Pauling's radii corrected for 12 coordination (10)); and* NH_4, *1.56 Å (1) (from Pauling's value of the ionic radius of rubidium (1.60 Å) reduced in accordance with the observation that crystals of* $(NH_4)_2MX_6$ (X = Cl, Br) *all have slightly smaller cells than the corresponding rubidium compounds).*

Can. J. Chem. Downloaded from www.nrcresearchpress.com by 210.87.254.42 on 09/05/12
For personal use only.

Cs—Br distance (3.89 Å) is the same as that predicted (3.90 Å) but the NH_4—Br distance (3.82 Å) is considerably longer than expected (3.66 Å). On the other hand, the Br—Br separation between anions, which one might expect to be the same in both crystals, is shorter in $(NH_4)_2TeBr_6$ (3.84 Å) than in Cs_2TeBr_6 (3.94 Å). In the latter case, the distances are determined by the fact that the cesium and bromine atoms are in contact so that the anions are just separated (Fig. 1*a*). In $(NH_4)_2TeBr_6$ it is the bromine atoms in different anions that are in contact (Fig. 1*b*). The ammonium ion is smaller than the cavity which is formed by the 12 bromine atoms which surround it, and, as discussed in a previous paper (1), this should lead to a distortion at low temperatures. At −52 °C, $(NH_4)_2TeBr_6$ transforms to a lower symmetry (11), which is probably tetragonal. A mechanism for such a distortion has been proposed by Morfee *et al.* (12) for the analogous $(NH_4)_2SnBr_6$ compound. The anions rotate about the (001) direction with alternate anions rotating in an opposite sense. Such a rotation, which has the effect of reducing the anion–cation separation, has been found at room temperature in K_2SnBr_6 (13) and K_2TeBr_6 (1). At temperatures close to the transition temperature, the $TeBr_6^{2-}$ ions would be expected to be librating with a rather large amplitude. This would be manifested in the X-ray investigation as an anisotropy in the thermal motions of the bromine atoms. Such an anisotropy is indeed observed in K_2TeBr_6 and $(NH_4)_2TeBr_6$ (Table V). It is significant that although the same anisotropy is also present in Cs_2TeBr_6, it is very much less marked. We are presently continuing this work by investigating the changes which occur in $(NH_4)_2TeBr_6$ below room temperature.

ACKNOWLEDGMENTS

We acknowledge the financial support of the National Research Council of Canada for this work. One of us (A. K. D.) wishes to thank the University of Ranchi, Bihar, India, for granting him leave of absence.

REFERENCES

1. I. D. Brown. Can. J. Chem. **42**, 2758 (1964).
2. F. J. Ewing and L. Pauling. Z. Krist. **68**, 223 (1928).
3. H. E. Swanson, N. T. Gilfrich, M. I. Cook, R. Stinchfield, and P. C. Parks. Diffraction powder patterns. Natl. Bur. Std. (U.S.) Circ. No. 539. **8**, 1957. p. 5.
4. H. E. Swanson, M. I. Cook, T. Issacs, and E. H. Evans. Diffraction powder patterns. Natl. Bur. Std. (U.S.) Circ. No. 539. **9**, 1960. p. 24.
5. L. M. Manojlović. Bull. Inst. Nucl. Sci. "Boris Kidrich" Belgrade, **7**, 79 (1957).
6. K. W. Bagnall, R. W. M. D'Eye, and J. H. Freeman. J. Chem. Soc. 3963 (1955).
7. W. C. Fernelius. Inorganic syntheses. Vol. 2. McGraw-Hill, New York. 1946. p. 189.
8. International Tables for X-Ray Crystallography. Vol. III. The Kynoch Press. Birmingham, England. 1962. Tables 3.3.1A and 3.3.1B.
9. W. R. Busing and H. A. Levy. Acta Cryst. **17**, 142 (1964).
10. L. Pauling. The nature of the chemical bond. 3rd ed. Cornell University Press, New York. 1960. pp. 511–530.
11. D. Nakamura, K. Ito, and M. Kubo. J. Am. Chem. Soc. **84**, 163 (1962).
12. R. G. S. Morfee, L. A. K. Staveley, S. T. Walters, and D. L. Wigley. Phys. Chem. Solids, **13**, 132 (1960).
13. G. Markstein and H. Nowotny. Z. Krist. **100**, 265 (1939).

Can. J. Chem. Downloaded from www.nrcresearchpress.com by 210.87.254.42 on 09/05/12
For personal use only.

Can. J. Chem. Downloaded from www.nrcresearchpress.com by 210.87.254.6 on 09/05/12
For personal use only.

MOLECULAR MOTION IN WEAK CHARGE TRANSFER COMPLEXES[1]

D. F. R. GILSON[2] AND C. A. MCDOWELL
Department of Chemistry, University of British Columbia, Vancouver, British Columbia

Received November 8, 1965

ABSTRACT

"Wide line" nuclear magnetic resonance studies of several charge transfer complexes are reported. Line width transitions and comparisons of theoretical and experimental second moments indicate that molecular rotation occurs in several of these complexes. Estimates of the barriers to reorientation in the complexes show these to be lower than those observed for the corresponding pure compounds.

INTRODUCTION

The structural details of a number of so-called "weak" charge transfer complexes in the solid state are now well known, due largely to the work of Hassel and his co-workers (1). Apart from such structural studies these complexes have received little attention when compared with the extent of electronic spectral investigations of aromatic charge transfer systems in solution (2). A notable feature of some complexes in the solid state is the occurrence of endless chains of alternating molecular species. In one such complex, between 1,4-dioxane and dinitrogen tetroxide, Groth and Hassel (3) have recently reported that a statistical distribution of the dioxane methylene group positions was evident from the X-ray data and that a proton magnetic resonance study revealed a line width transition above −40 °C. Molecular reorientation has also been observed in complexes between dioxane and silver perchlorate (4, 5) and benzene and silver perchlorate (6).

Because of the evidence we had earlier found for the rotation of the benzene molecule in the benzene–silver perchlorate complex (6) it seemed of interest to study other charge-transfer complexes by nuclear magnetic resonance methods. One would wish to know if, for example, intramolecular motions of the components of charge transfer complexes were of general occurrence. It was also obviously of some interest to discover what were the magnitudes of the potential energy barriers which controlled the extent and frequency of such intramolecular motions.

It is of interest to note that Voigt and Reid (7) have suggested that there may be a mutual rotation of the two components of the tetracyanoethylene-parasubstituted benzenes complexes in solution to account for the intensities of the charge transfer absorptions.

EXPERIMENTAL

Proton and fluorine nuclear magnetic resonance spectra were recorded at 30 Mc/s and at 40 Mc/s. The 40 Mc/s spectra were obtained using a Varian Dual Purpose spectrometer with a 12 in. magnet. While these studies were in progress a wide line spectrometer was constructed (8), employing essentially Varian units with a 6 in. magnet, and measurements were continued at 30 Mc/s.

Variable temperature control was achieved by passing around the sample either heated air or tank nitrogen cooled by liquid nitrogen or dry ice/acetone mixture. For measurements at temperatures below the lower limit of the flow system the sample was immersed directly in liquid nitrogen, air, or oxygen. Temperatures were measured with copper/constantan thermocouples placed upstream and downstream from the sample.

Complexes of 1,4-dioxane with mercuric chloride and silver perchlorate were prepared by recrystallization, the latter from acetone as described by Comyns and Lucas (9). Other complexes were prepared by weighing equimolar quantities of the components into sample tubes, which were then sealed, heated above the melting points of the components, and cooled slowly. Reagent grade chemicals were used except for hexafluorobenzene which was obtained from Imperial Smelting Co. Ltd. and further purified by vapor chromatography.

[1]*Presented in part at the 43rd Annual Conference of the Chemical Institute of Canada, Ottawa. June 1960.*
[2]*Present address: Department of Chemistry, McGill University, Montreal.*

Can. J. Chem. Downloaded from www.nrcresearchpress.com by 210.87.254.6 on 09/05/12
For personal use only.

RESULTS AND DISCUSSION

1,4-Dioxane Complexes

Experimental second moments at 77 °K and at room temperature (298 °K) are given in Table I. The theoretical intramolecular second moment of dioxane, calculated from the carbon atom positions in the bromine complex (10) and assuming a C—H bond length of 1.09 Å and tetrahedral angles, is 15.5 gauss^2. The methods used in estimating the theoretical values of the second moments were identical with those given in refs. 18, 19, 23, and 24. From the parameters obtained by Davies and Hassel in their electron diffraction study of dioxane vapor (11) a second moment of 14.5 gauss^2 is obtained. The lower value results from an increase in the C—H bond length to 1.10 Å. The second moment of the "boat" as opposed to "chair" form falls within this same range. For reorientation about the oxygen–oxygen axis the intramolecular second moment is reduced to 1.2–1.3 gauss^2. In the complexes with bromine and mercuric chloride the dioxane molecule is fixed at room temperature. The low values of the experimental second moment for the complexes with antimony trichloride and silver perchlorate show that rotation or a reorientation occurs.[3] In the latter case, rotation was suggested on the basis of the X-ray structural investigation (4). While the present studies were in progress the temperature dependences of the proton resonance line width and second moment of the benzene–silver perchlorate complex were reported by Kawamori and Sakiyama (5). Below 14 °C the dioxane molecules are fixed but above this temperature undergo rotation, first about the oxygen–oxygen axis and then isotropically. Powell (12) has suggested that rotation affords better packing in the crystal; a similar argument might apply to the antimony trichloride complex, the structure of which has not been reported.

TABLE I

Second moments of dioxane complexes

Complex	Second moment (gauss^2) At 298°K	At 77 °K
Dioxane–Br_2	18.7±0.3	18.9±0.5
Dioxane–$HgCl_2$	18.5±0.2	19.0±0.4
Dioxane–$AgClO_4$	1.5±0.2	20.9±0.4
Dioxane–$SbCl_3$	3.6±0.3	18.6±0.4

Benzene Complexes

The temperature dependences of the line width and second moment of both ^1H and ^{19}F resonances for the 1:1 benzene–hexafluorobenzene complex (13) are shown in Figs. 1 and 2. Line width and second moment transitions occurred for both resonances. The fluorine resonance line exhibited some structure over the transition temperature range of 110–145 °K, Fig. 3. As the temperature was increased, the narrow line grew in intensity at the expense of the broader component.

The calculated intramolecular second moments of benzene and hexafluorobenzene are 3.1 gauss^2 and 1.7 gauss^2, respectively. These values will be reduced by a factor $\frac{1}{4}$ for rotation about the sixfold axes, to 0.8 gauss^2 and 0.4 gauss^2. The crystal structure of this

[3]*It is difficult to decide from n.m.r. studies alone if a molecule or a group rotates continuously, or undergoes a rapid reorientation. The narrowing of nuclear magnetic resonance lines only requires frequencies of rotation (or orientation) of the order of magnitude of the line widths expressed in frequency units, i.e. usually about* 10^4–10^5 *c/s.*

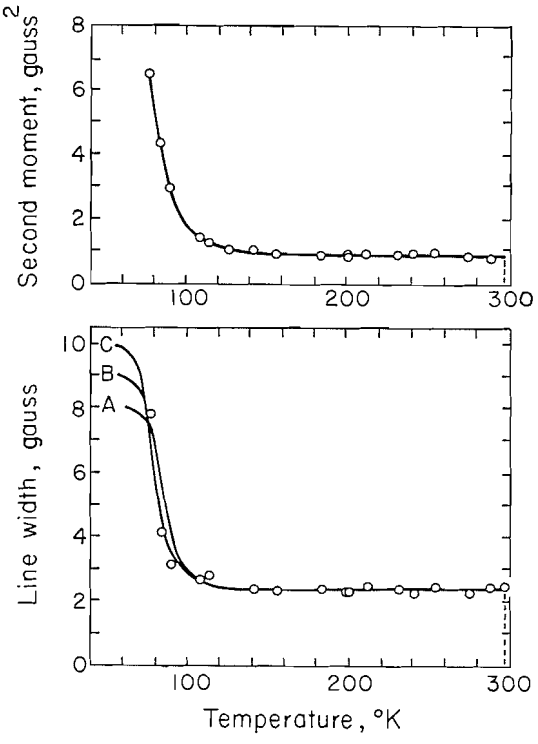


FIG. 1.

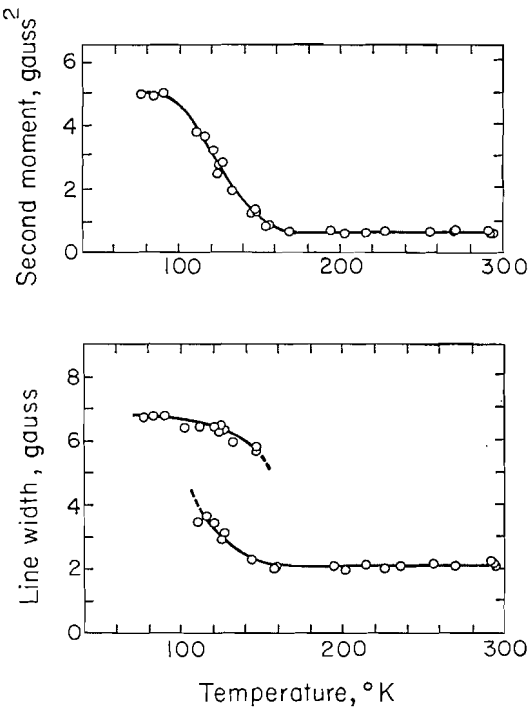


FIG. 2.

FIG. 1. Temperature dependence of the line width and second moment of the proton resonance in the complex $C_6H_6.C_6F_6$. Calculated line width dependences obtained from the following parameters.

	B (gauss)	E (kcal/mole)	$\alpha\nu_0$ (c/s)
Curve A	8.0	1.9	2.3×10^9
Curve B	9.0	1.7	1.2×10^9
Curve C	10.0	1.6	1.2×10^9

FIG. 2. Temperature dependence of the line width and second moment of the fluorine resonance in the complex $C_6H_6.C_6F_6$. Calculated line width dependences obtained from the following parameters.

	E (kcal/mole)	$\alpha\nu_0$ (c/s)
Broad line	1.5	1.0×10^7
Narrow line	1.3	1.1×10^6

complex has not been reported, but by analogy with other aromatic complexes (14) it is probable that the two molecular species are stacked alternately in columns with their molecular planes parallel. Reorientations about the sixfold axes are thus the most probable causes of the transitions. The structure shown by the ^{19}F resonance can be explained if two resonance lines are present arising from C_6F_6 molecules which are stationary and rotating, respectively.

The line width and second moment of the proton resonance of the benzene – carbon tetrabromide complex are plotted against temperature in Fig. 4. The structure of this complex is not known but probably resembles that of the *p*-xylene – carbon tetrabromide complex determined by Strieter and Templeton (15). Each aromatic ring has a bromine atom on each face and zig-zag strings of alternate carbon tetrabromide and *p*-xylene molecules run parallel to the *c* azis of the crystal. The distance from the bromine atom to the center of the aromatic ring is 3.34 Å, which is 0.2 Å less than the sum of the van der Waals radii. A transition occurs in the benzene – carbon tetrabromide complex below

Can. J. Chem. Downloaded from www.nrcresearchpress.com by 210.87.254.6 on 09/05/12
For personal use only.

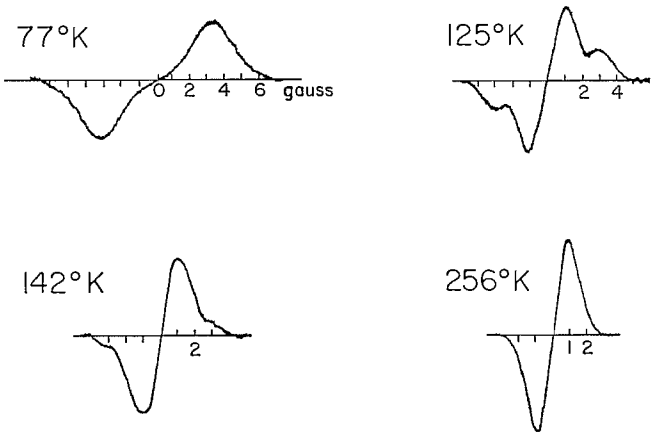


FIG. 3. Line shape derivative curves of the fluorine resonance in the complex $C_6H_6.C_6F_6$ at different temperatures.

100 °K and is not complete at 77 °K. This transition, resulting again from rotation about the sixfold axis, is probably responsible for the disappearance of the ^{81}Br nuclear quadrupole resonance between 77 and 90 °K (16).

The second moment of the proton resonance of the benzene – antimony trichloride complex increases only slightly from 0.82 ± 0.03 gauss² at room temperature to 0.86 ± 0.05 gauss² at 77 °K. The X-ray structure has not been determined, but Daasch (17) has suggested two possibilities, having C_{2v} and C_{3v} symmetry, from an infrared investigation. While the present results do not enable one to decide between these structures, the fact that reorientation still occurs at the lowest temperature studied favors the more symmetrical structure, which is preferred also by Daasch.

Mesitylene–Hexafluorobenzene Complex

The proton second moment and line width below 90 °K were 9.26 gauss² and 5.50 gauss respectively. These values decreased to 1.56 gauss² and 2.47 gauss at room temperature. The fluorine second moment and line width at 77 °K were 1.33 gauss² and 2.60 gauss, respectively, decreasing to 0.61 gauss² and 1.81 gauss at room temperature.

The calculated intramolecular second moment for a mesitylene molecule with fixed methyl groups is 19.7 gauss². It has been shown that methyl group rotation (or tunnelling) in methyl-substituted benzenes occurs down to very low temperatures (18, 19). In hexamethylbenzene the experimental second moment at 1 °K is less than the calculated value for a completely rigid molecule (20). Calculation of theoretical second moments in rotating molecules can be made using the formulae of Andrew and Eades (24). For a mesitylene molecule with rotating methyl groups the calculated intramolecular second moment becomes 4.75 gauss². At room temperature the experimental second moment is reduced to a value less than that calculated for methyl group rotation alone and therefore some further molecular motion must occur. Reorientation about the threefold axis normal to the aromatic ring is most likely. It is assumed that the second moment is this case will be reduced by a factor of $\frac{1}{4}$, i.e. that the internuclear vectors are effectively all normal to the axis of rotation, to give a value of 1.2 gauss², which is compatible with the experimental second moment.

Mesitylene itself has been studied by Andrew *et al.* (19) who report a continuous reduction in second moment from 4 °K to the melting point at 220 °K. The second moment at 220 °K was 8.0 gauss² and there is no evidence of rotation about the threefold axis. The

Can. J. Chem. Downloaded from www.nrcresearchpress.com by 210.87.254.6 on 09/05/12
For personal use only.

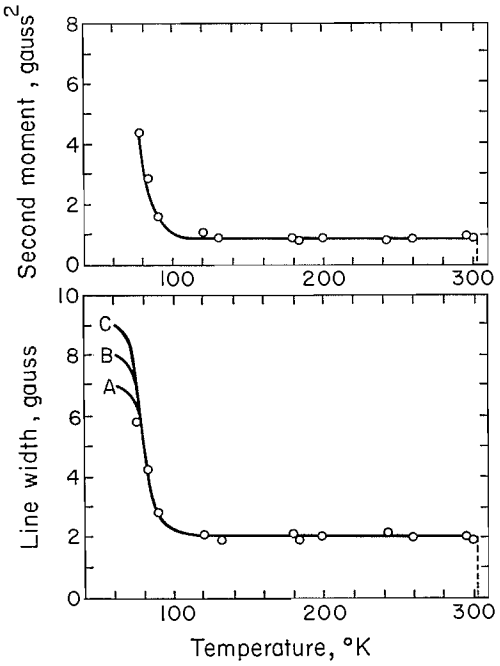


FIG. 4.

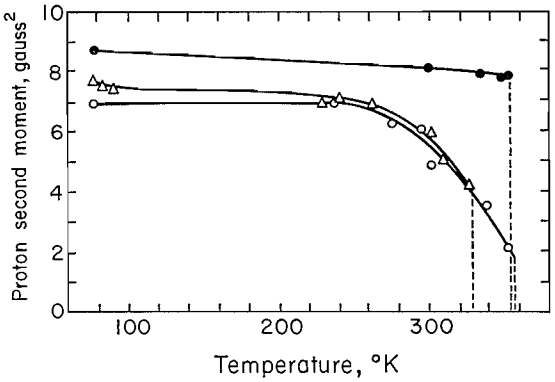


FIG. 5.

FIG. 4. Temperature dependence of the line width and second moment of the proton resonance in the comples $C_6H_6.CBr_4$. Line width dependences calculated from the following parameters.

	B (gauss)	E (kcal/mole)	$\alpha\nu_0$ (c/s)
Curve A	7.0	2.3	3.5×10^{10}
Curve B	8.0	2.1	1.9×10^{10}
Curve C	9.0	2.1	1.7×10^{10}

FIG. 5. Temperature dependence of the proton second moment of pure durene and in complexes of durene: ○, durene; △, C_6F_6–complex; ●, CBr_4–complex.

low value of the fluorine resonance second moment shows that in the complex the hexafluorobenzene molecule is still reorienting at 77 °K.

Durene Complexes

The temperature dependence of the proton second moments of durene complexes with carbon tetrabromide and hexafluorobenzene are shown in Fig. 5. The calculated rigid intramolecular contribution is 23.3 gauss^2 which is reduced to 5.7 gauss^2 by methyl group rotation. For durene itself the experimental second moment at 77 °K is 8.74 gauss^2, decreasing smoothly to 8.14 gauss^2 at 353 °K (m.p.). Thus methyl group reorientation must occur in durene and the complexes at 77 °K.

The behavior of the second moments, and also the line shapes, with temperature is remarkably similar for both of these complexes. The second moments decrease slowly as the temperature is increased from 77 °K, but then fall rapidly from 250 °K (C_6F_6) and 230 °K (CBr_4) to the melting points; 328 °K and 357 °K, respectively. The line shapes at 77 °K were simple but became quite complicated at higher temperatures. Derivative curves of the durene – hexafluorobenzene complex proton resonance absorption at different temperatures are shown in Fig. 6. This structure of the resonance absorption cannot arise from the three-spin system of a rigid methyl group since the second moments are too low. However, a similar line shape was observed previously (20) for the thiourea adduct with durene and, therefore, appears to be a property of the "isolated" durene

Can. J. Chem. Downloaded from www.nrcresearchpress.com by 210.87.254.6 on 09/05/12
For personal use only.

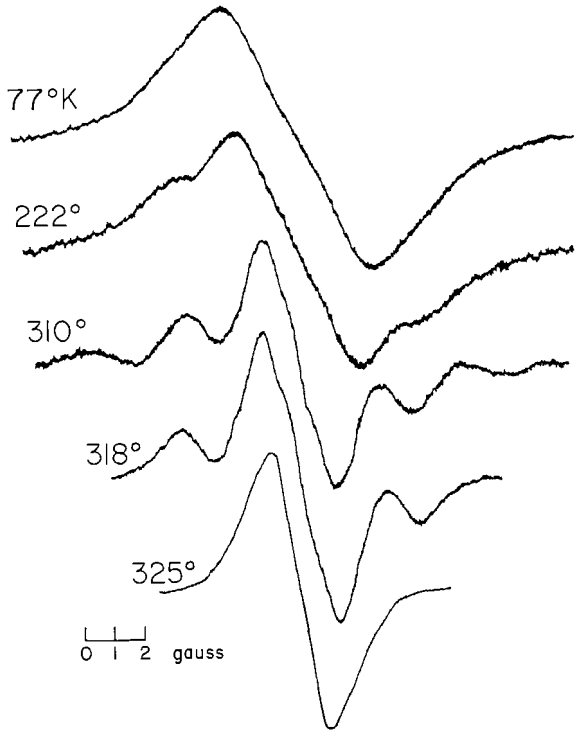


FIG. 6. Line shape derivative curves of the proton resonance in the complex durene–hexafluorobenzene at different temperatures.

molecule. The resonance line shape of pure durene does not show this structure because of the increased intermolecular dipolar interactions in the pure compound.

The reductions in second moments at higher temperatures indicate further molecular motion. This is probably some form of rotational oscillation since there is no evidence of a plateau in the second moment versus temperature plot at about 2 gauss^2. Such a plateau would be expected if the motion were complete reorientation about an axis normal to the molecular plane. These results are of interest in connection with the bromine nuclear quadrupole resonance studies of carbon tetrabromide in the durene complex (21). In this complex the resonances of the two crystallographically inequivalent bromine atoms merged together and then disappeared about 50° below the melting point of the complex. This suggested that their environment had become indentical. The nuclear magnetic and nuclear quadrupole resonance results indicate weakening of the crystal lattice with considerable disorder and molecular motion. It must be emphasised that the motions investigated by these techniques are of low frequency, $\sim 10^4$–10^5 c/s; the long range crystal structure is maintained, therefore, to a much higher temperature.

The fluorine resonance in the durene–hexafluorobenzene complex has second moments of 3.97 gauss^2 and 0.70 gauss^2 at 77 and 298 °K respectively. For a rigid molecule a total second moment of about 5 gauss^2 would be expected and thus molecular reorientation still occurs at 77 °K.

Barriers to Rotation

The line width changes can be related via the theory of Bloembergen, Purcell, and Pound (22), as modified by Gutowsky and Pake (23), to a correlation frequency, ν_c, for the motion responsible for the change.

[1] $$\nu_c = \frac{\alpha\gamma\delta H}{2\pi} \Big/ \tan\frac{\pi}{2}\frac{(\delta H)^2 - B^2}{B^2 - C^2}$$

Can. J. Chem. Downloaded from www.nrcresearchpress.com by 210.87.254.6 on 09/05/12
For personal use only.

where δH is the line width, γ is the magnetogyric ratio, B is the rigid lattice line width, and C is the limiting value of the line width above the transition. The line widths are expressed in gauss. The factor α arises from uncertainties in the limits of integration used in obtaining eq. [1] and is rather ill-defined. The correlation frequency can be used in the expression

$$[2] \qquad \nu_c = \nu_0 \exp(-E/RT)$$

to give an activation energy E for the molecular reorientation. Since α will affect ν_0 rather than E, it can be incorporated as $(\alpha\nu_0)$.

There are objections to this treatment of correlation frequencies. It assumes that a single correlation frequency, rather than a distribution, may be used to describe the motion. Changes in line shape are ignored, as are the relative magnitudes of the inter- and intra-molecular contributions to the line width. Despite these difficulties fruitful comparisons between similar systems can still be made (19, 25–29). The values of E and $\alpha\nu_0$ obtained from eqs. [1] and [2] were used to calculate theoretical line width versus temperature plots as shown in Figs. 1, 2, and 4. In the complexes of benzene with hexafluorobenzene and carbon tetrabromide the proton resonance line width had not reached a limiting rigid lattice value at 77 °K. Comparison with the benzene – silver perchlorate complex (6) and with benzene itself (24), where the rigid lattice line widths were 8.2 gauss and 9.1 gauss respectively, suggested extreme limits of 7 and 10 gauss. These limits were used to calculate possible ranges of E.

For benzene in the benzene–hexafluorobenzene complex the barrier to rotation ranged from 1.6 to 1.9 kcal/mole. For the hexafluorobenzene molecule, barriers were calculated for both the broad and narrow components of the resonance line. The values obtained were in quite close agreement, 1.3 and 1.5 kcal/mole respectively. In the benzene – carbon tetrabromide complex the barrier ranged from 2.1 to 2.3 kcal/mole depending on the value chosen for the rigid lattice line width. The barriers in these complexes may be compared with those obtained from line width changes for the pure compounds. For benzene Andrew (24) and Eades obtained 3.5 kcal/mole, and in hexafluorobenzene a line width transition between 85 and 100 °K gave a value of 4.5 kcal/mole (20). We are unable to suggest a satisfactory explanation as to why our values for these activation energies should be somewhat lower than those found by Andrew and his co-workers. It is possible, however, that the different crystal symmetries at the respective sites for rotation or reorientation may play some part in determining the magnitude of the activation energies.

ACKNOWLEDGMENTS

We wish to thank the National Research Council for grants in aid of this work.

REFERENCES

1. O. HASSEL and CHR. RØMMING. Quart. Rev. London, **16**, 1 (1962).
2. R. S. MULLIKEN and W. B. PERSON. Ann. Rev. Phys. Chem. **13**, 107 (1962).
3. P. GROTH and O. HASSEL. Acta Chem. Scand., **19**, 120 (1965).
4. R. J. PROSEN and K. N. TRUEBLOOD. Acta Cryst. **9**, 741 (1956).
5. A. KAWAMORI and M. SAKIYAMA. J. Phys. Soc. Japan, **18**, 1218 (1963).
6. D. F. R. GILSON and C. A. MCDOWELL. J. Chem. Phys. **39**, 1825 (1963).
7. E. M. VOIGT and C. REID. J. Am. Chem. Soc. **86**, 3930 (1964).
8. D. WARE. M.Sc. Thesis, University of British Columbia. 1962.
9. A. E. COMYNS and H. J. LUCAS. J. Am. Chem. Soc. **76**, 1019 (1954).
10. O. HASSEL and J. HVOSLEF. Acta Chem. Scand. **8**, 873 (1954).
11. M. DAVIS and O. HASSEL. Acta Chem. Scand. **17**, 1181 (1963).
12. H. M. POWELL. J. Inorg. Nucl. Chem. **8**, 546 (1958).
13. C. R. PATRICK and C. S. PROSSER. Nature, **187**, 1021 (1960).
14. S. C. WALLWORK. J. Chem. Soc. 494 (1961).
15. F. J. STRIETER and D. H. TEMPLETON. J. Chem. Phys. **37**, 161 (1962).

Can. J. Chem. Downloaded from www.nrcresearchpress.com by 210.87.254.6 on 09/05/12
For personal use only.

16. D. F. R. GILSON and C. T. O'KONSKI. Unpublished results.
17. L. W. DAASCH. Spectrochim. Acta, **9**, 726 (1959).
18. E. R. ANDREW. J. Chem. Phys. **18**, 607 (1950).
19. E. R. ANDREW, R. G. EADES, Z. EL SAFFAR, and J. P. LLEWELLYN. Arch. Sci. Geneva, **13**, 379 (1960).
20. D. F. R. GILSON and C. A. MCDOWELL. Unpublished results.
21. D. F. R. GILSON and C. T. O'KONSKI. J. Chem. Phys. In press. 1966.
22. N. BLOEMBERGEN, E. M. PURCELL, and R. V. POUND. Phys. Rev. **73**, 679 (1948).
23. H. S. GUTOWSKY and G. E. PAKE. J. Chem. Phys. **18**, 163 (1950).
24. E. R. ANDREW and R. G. EADES. Proc. Roy. Soc. London, Ser. A, **218**, 537 (1953).
25. G. E. PAKE. Solid state physics. Vol. 2. Academic Press Inc., New York. 1959. p. 1.
26. E. R. ANDREW, A. BRADBURY, and R. G. EADES. Arch. Sci. Geneva, **11**, 223 (1958).
27. E. R. ANDREW, A. BRADBURY, and R. G. EADES. Nature, **182**, 1659 (1958); **183**, 1802 (1959).
28. E. R. ANDREW and R. A. NEWING. Proc. Phys. Soc. London, A, **72**, 959 (1958).
29. E. R. ANDREW. Phys. Chem. Solids, **18**, 9 (1961).

Can. J. Chem. Downloaded from www.nrcresearchpress.com by 210.87.254.6 on 09/05/12
For personal use only.

Can. J. Chem. Downloaded from www.nrcresearchpress.com by 210.87.254.105 on 09/05/12
For personal use only.

THE Hg $6(^3P_1)$ PHOTOSENSITIZED DECOMPOSITION OF METHYLENECYCLOBUTANE VAPOR

G. R. De Maré, O. P. Strausz, and H. E. Gunning
Department of Chemistry, University of Alberta, Edmonton, Alberta

Received October 22, 1965

ABSTRACT

The main mode of decomposition, in which at least two biradicals are involved, is a molecular split into ethylene and allene. The pressure dependence of the reaction exhibits some unusual features which may be interpreted by a stepwise collisional removal of vibrational energy from one of the transient biradicals.

INTRODUCTION

Nangia and Benson (1) have proposed the following general mechanism for the pyrolysis of small ring compounds

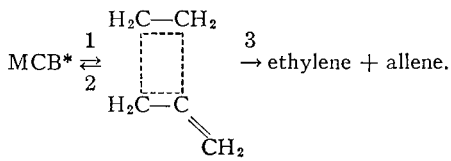
[A] $$\text{ring}^* \underset{2}{\overset{1}{\rightleftarrows}} \text{biradical} \xrightarrow{3} \text{olefin (one or more).}$$

The biradicals involved are believed to have short lifetimes (10^{-10} to 10^{-11} s); therefore their collisional deactivation at subatmospheric pressures should be unimportant.

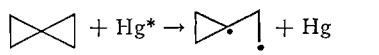
For methylenecyclobutane (MCB) this mechanism may be written

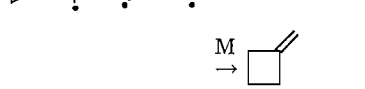
[B] $$\text{MCB}^* \underset{2}{\overset{1}{\rightleftarrows}} \text{1,4-biradical, 2-methylenebutane} \xrightarrow{3} \text{ethylene} + \text{allene.}$$

An alternate, although less likely but experimentally unrefuted mechanism is

[C] 

The 1,4-biradical, 2-methylenebutane intermediate has been postulated also in the mercury sensitization of spiropentane (2) as a precursor of the final products, ethylene + allene and methylenecyclobutane.

[D] 

[E] 

The intervention of the same biradical would also be expected in the mercury sensitization of MCB. Both sequences, [B] for the thermal reaction of MCB and [E] for the mercury sensitization of spiropentane, could be further substantiated if the nature of the mercury-photosensitized reaction of MCB would be consistent with this expectation. The present study was undertaken for this reason.

Can. J. Chem. Downloaded from www.nrcresearchpress.com by 210.87.254.105 on 09/05/12
For personal use only.

EXPERIMENTAL

The reaction system and the method used to determine the amount of light absorbed in the cell have been described in a previous paper (3).

The light intensity, measured by propane actinometry at 730 Torr propane pressure, was 1.7×10^{15} quanta/s.

MCB (Aldrich) was found to be 70% pure and was purified by several passages on the diisodecyl phthalate column previously described (3). Methylcyclobutane (MB) was prepared by the mercury-photosensitized decomposition of molecular hydrogen in the presence of MCB. It was purified by gas chromatography (g.c.) and identified by mass and nuclear magnetic resonance (n.m.r.) spectroscopy. Isoprene (IP) (Eastman) and 1,4-pentadiene (PD) (prepared by Mr. L. G. Walker of this department by the thermal decomposition of 1,5-pentanediol diacetate) were used without further purification. Nitric oxide (Matheson C.P.) and ethane-d_6 (Merck) were purified as previously described (3). Methyl mercaptan (Matheson) was purified by g.c. on the above column. Oxygen (Airco assayed reagent) was used without purification.

Analysis of the noncondensable products was identical with that described in the previous paper (3). Good resolution of the ethylene, allene, MB, IP, PD, and MCB peaks was obtained on the diisodecyl phthalate column at ambient temperature.

Ethylene and allene were identified by their mass spectra. MB, IP, and PD were identified by comparison of mass spectra and g.c. retention times with those of authentic samples.

The small quantities of MB, IP, and PD formed in the experiments makes the determination of their quantum yields very inaccurate. Thus the detector response for MCB was used, since it would not increase the experimental error involved in their determination.

RESULTS

The reaction products which were identified (with their respective quantum yields at 40 Torr substrate pressure in parentheses) are ethylene (0.50), allene (0.50), hydrogen (0.02), MB (0.004), IP (0.002), and PD (0.01). The high efficiency of the step(s) forming ethylene and allene and the low yields of hydrogen and MB suggested that the total yield of C_{10} products must be very low; this was verified experimentally.

Vinylcyclopropane, cyclopentene, and *cis*- and *trans*-1,3-pentadiene have retention times similar to that of the substrate on the column used. It was therefore imperative to show that no products were eluting with the substrate. A sample of MCB was subjected to very extensive decomposition by successive reuse after removal of the known products at reasonably short reaction times. The n.m.r. spectrum of this MCB (trapped from the g.c. effluent) was identical with the published one (4) and thus indicated that no products with combined quantum yields > ca. 0.05 were hidden under the substrate peak.

Three series of experiments were carried out.

I. The product yields were determined as a function of reaction time at a substrate pressure of 40 Torr. All yields were found to be independent of reaction time up to 90 min. Mass spectral analysis of the C_2 fraction formed in a 90 min run showed the presence of a trace of acetylene, indicating that secondary decomposition of the ethylene had begun. The hydrogen yield appeared to be slightly higher but was still within experimental error of being unchanged. The yield of IP became measurable only after 30 min reaction time.

II. The quantum yields of ethylene, allene, hydrogen, PD, and MB were examined as a function of substrate pressure at 10 min reaction time. The results are shown in Fig. 1. The yield of MB was too small to provide reliable kinetic data and it is excluded from the figure. The yields of the other products decrease sharply with increasing substrate pressure, indicating that they are formed from an excited molecule which can be deactivated.

III. The various effects of adding a few percent of nitric oxide, or methyl mercaptan, or oxygen, or a large excess of ethane-d_6 to the reaction were studied. Nitric oxide appeared to have no effect on any of the products (hydrogen was not measured). The addition of 1.3 Torr methyl mercaptan to 42 Torr MCB caused a 50% increase in $\Phi(H_2)$ to 0.033 and a

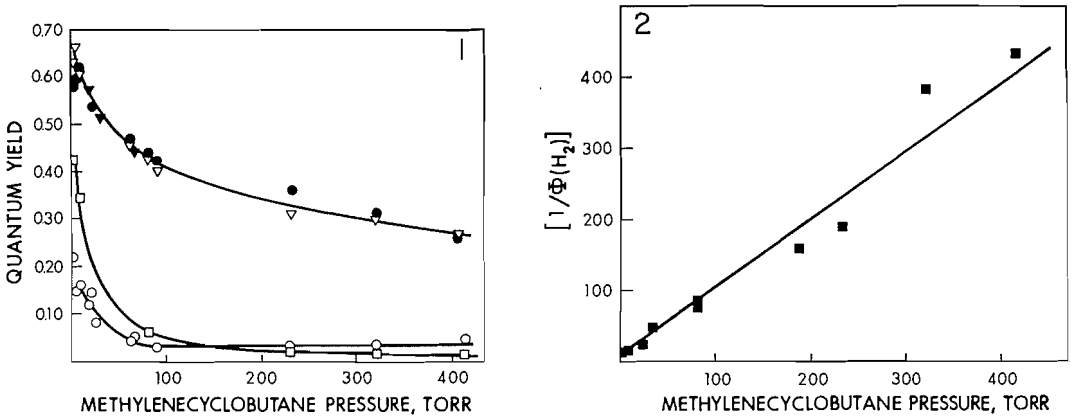


FIG. 1. Quantum yield of formation as a function of methylenecyclobutane pressure: $\Phi(C_2H_4)$, ▽; $\Phi(C_3H_4)$, ●; $5 \times \Phi(H_2)$, □; $3 \times \Phi(PD)$, ○; and $\Phi(C_2H_4) = \Phi(C_3H_4)$, ▼.
FIG. 2. $1/\Phi(H_2)$ as a function of methylenecyclobutane pressure.

ninefold increase in Φ(MB) to 0.028. The addition of 76 Torr ethane-d_6 to 6.5 Torr MCB had no effect on the product yields. This is probably due to the cancelling of two opposing effects; increased absorption due to pressure broadening of the absorption line and increased deactivation of the excited MCB. No HD was detected, indicating that either the hydrogen is formed as H_2 or that abstraction from MCB is favored by a factor of 10 or more over abstraction from ethane-d_6. Molecular oxygen was added to 42 Torr MCB in concentrations up to 45%. Competitive quenching was corrected for using σ_Q^2(MCB) = 48 Å^2 and $\sigma_Q^2(O_2)$ = 13 Å^2 (5). Transmission through the reaction vessel was measured continuously and was found to increase rapidly at higher O_2 concentrations. The yield of allene[1] was corrected for this change in absorption. The collisional deactivating efficiency of O_2 was assumed to be equal to that of MCB. After application of these three corrections the yield of allene was below the expected value by as much as 12%.[2]

DISCUSSION

The dependence of the yields of the major products of the photosensitization of methylenecyclobutane on substrate pressure indicates that the major primary step of the reaction is the formation of an excited molecule

[1] Hg 6($^3P_1$) +  → Hg 6($^1S_0$) + 

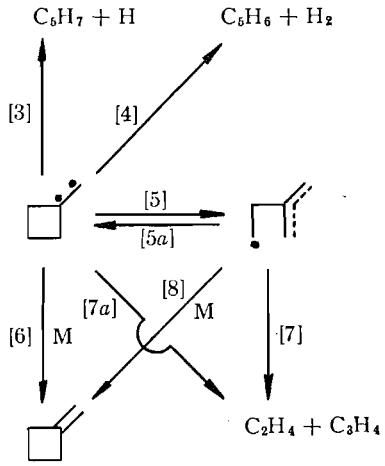
where  is a methylenecyclobutane molecule in a vibrationally excited triplet state. A second primary step which might occur is

[2] Hg 6($^3P_1$) +  → Hg 6($^1S_0$) + $C_5H_7\cdot$ + H.

[1]*Quantitative measurements of* CO, CO_2, *and* C_2H_4 *were not attempted.*
[2]*The largest decrease, 12%, was found at the highest added oxygen pressure, 45%. The decrease could be caused by the reaction of oxygen atoms with the product allene or be the effect of an error in the quenching cross-sections, or perhaps the collisional deactivating efficiency of* O_2 *is greater than that of methylenecyclobutane.*

Can. J. Chem. Downloaded from www.nrcresearchpress.com by 210.87.254.105 on 09/05/12
For personal use only.

Excluding the formation of the isomers, the species formed in steps [1] and [2] may lead to the following reactions:



and

[9] $H + \square\!\!\diagup\!\!\diagup \rightarrow \square\!\!\diagup\!\!\cdot$

[10] $\rightarrow H_2 + C_5H_7\cdot$

[11] $\square\!\!\diagup\!\!\cdot + \square\!\!\diagup\!\!\diagup \rightarrow \square\!\!\diagup + C_5H_7\cdot$

[12] $2\,\square\!\!\diagup\!\!\cdot \rightarrow \square\!\!\diagup + \square\!\!\diagup\!\!\diagup$

[13] $\square\!\!\diagup\!\!\cdot + C_5H_7\cdot \rightarrow \square\!\!\diagup + C_5H_6$

Radical–radical and radical–substrate reactions for which product evidence has not been found have been excluded. It is assumed that the biradicals will not react with the substrate to any appreciable extent.

The formation of each product will now be considered.

Hydrogen

If step [4] is neglected, steady-state treatment (s.s.t.) of the mechanism for $\Phi(H_2)$ gives

$$[14] \qquad \Phi(H_2) = \frac{\alpha}{I_a}\left(\frac{k_{10}}{k_9 + k_{10}}\right) + \frac{\beta}{I_a}\left(\frac{k_3}{k_3 + k_5 + k_6P}\right)\left(\frac{k_{10}}{k_9 + k_{10}}\right)$$

where α/I_a and β/I_a are the fractions of the primary reaction proceeding via steps [2] and [1] respectively; I_a is the absorbed light intensity and P is the substrate pressure. Thus steps [2] and [3] are kinetically distinguishable as possible sources of the H-atoms in the sensitization since $\Phi(H_2)$ from hydrogen atoms formed in [2] should be independent of substrate pressure and is therefore $\leqslant 0.002$. Thus, at low pressures (< 100 Torr) the first term of eq. [14] may be neglected. Setting $\beta/I_a \simeq 1.0$ and inverting, one obtains

$$[15] \qquad 1/\Phi(H_2) = \left(\frac{k_3 + k_5}{k_3}\right)\left(\frac{k_9 + k_{10}}{k_{10}}\right) + \left(\frac{k_9 + k_{10}}{k_3 k_{10}}\right) k_6 P.$$

Figure 2, a plot of $1/\Phi(H_2)$ vs. P, shows that a straight line fits the data within experimental error even at pressures well above 100 Torr. Step [2] will therefore be omitted from subsequent steady-state calculations.

Can. J. Chem. Downloaded from www.nrcresearchpress.com by 210.87.254.105 on 09/05/12
For personal use only.

If only [3] and [4] are considered as the possible sources of H-atoms and molecular hydrogen respectively, s.s.t. yields

$$[16] \qquad \Phi(H_2) = \left(\frac{k_3 k_{10}}{[k_3 + k_4 + k_5 + k_6 P][k_9 + k_{10}]}\right) + \left(\frac{k_4}{k_4 + k_3 + k_5 + k_6 P}\right).$$

Thus a linear dependence of $1/\Phi(H_2)$ on substrate pressure would be observed if [3] alone or [4] alone take part in the formation of hydrogen.

It may be argued that [4] should be considered as a possible step because of the absence of HD as a product of the reaction in the presence of ethane-d_6. Elimination of molecular hydrogen from the excited methylenecyclobutane should yield methylenecyclobutene and it is not likely to be important. Step [3], on the other hand, must occur. The formation of methylcyclobutane in the photosensitization of the pure substrate and the increased yields of H_2 and methylcyclobutane when methyl mercaptan (a good source of abstractable hydrogen) is added dictate the presence of H-atoms.[3] From the relative yields of hydrogen and methylcyclobutane in the methyl mercaptan experiment and from the low yields of C_{10} compounds in the pure substrate reaction, it appears that the ratio of abstraction to addition is nearly one, which is much greater than that obtained for similar reactions with other olefins (cf. the value for cyclohexene = 0.23 (6)). This high ratio for methylenecyclobutane as well as the resistance of cyclohexene to both abstraction and addition (7) explain why in the presence of ethane-d_6 and under similar conditions the mercury photosensitization of cyclohexene yields hydrogen which is 12% HD, 88% H_2, whereas the photosensitization of methylenecyclobutane yields hydrogen in which only H_2 was detectable. Steps [3] and [10] are therefore considered to be the source of H_2.

Ethylene and Allene

Step [7] satisfactorily explains the equality of $\Phi(C_2H_4)$ and $\Phi(C_3H_4)$ over the pressure range studied. Figure 3 shows the comparison of the yield of ethylene from the methylenecyclobutane photosensitization and the yield of hydrogen from the photosensitization of ethylene. Although both reactions have the same efficiency at 10 Torr substrate pressure the ethylene reaction is much more easily suppressed, indicating that the species involved in the formation of acetylene and hydrogen from ethylene are either longer lived or require fewer collisions to be deactivated than the species involved in the formation of ethylene and allene from methylenecyclobutane.

$1/\Phi(C_2H_4)$ plotted against P in Fig. 4 shows a lower than first order pressure dependence. This is an unusual feature of the methylenecyclobutane system because most of the olefinic triplet state reactions obey second order and none lower than first order kinetics.

From the general mechanism it is possible to obtain kinetic expressions by s.s.t. for $1/\Phi(C_2H_4)$ ranging from less than first order to second order on pressure, depending on the elementary steps chosen. For example, s.s.t. of a mechanism comprised of steps [5] to [7] yields

$$1/R(C_2H_4) = \frac{A + BP}{C + DP},$$

and that comprised of steps [5] to [8] yields

$$1/R(C_2H_4) = \frac{A + BP + CP^2 + DP^3}{E + FP + GP^2},$$

where $A, \ldots G$ are complex functions of the elementary rate constants.

[3]H-*atoms formed by quenching of excited mercury by* CH_3SH *could not explain the relatively small increase in* $\Phi(H_2)$ *in comparison with the increase in* Φ*(methylcyclobutane).*

Can. J. Chem. Downloaded from www.nrcresearchpress.com by 210.87.254.105 on 09/05/12
For personal use only.

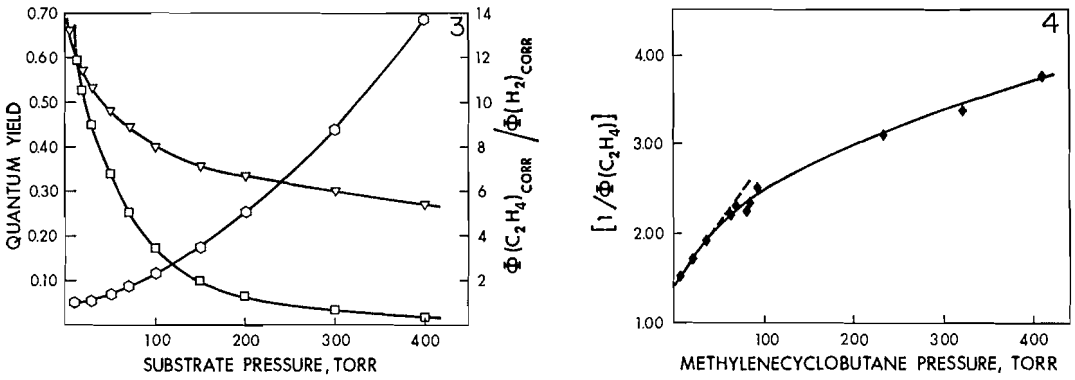


FIG. 3. Comparison of (▽) $\Phi(C_2H_4)_{corr}$ from methylenecyclobutane from Fig. 1 and (□) $\Phi(H_2)_{corr}$ from ethylene mercury photosensitization from ref. 12; also the ratio (○) $\Phi(C_2H_4)_{corr}/\Phi(H_2)_{corr}$.
FIG. 4. $1/\Phi(C_2H_4)$ as a function of methylenecyclobutane pressure.

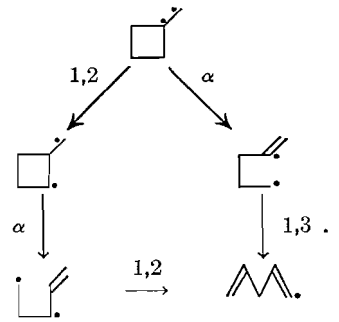
An alternative and perhaps more likely explanation for the low order of pressure dependence is a stepwise deactivation mechanism. If step [6] proceeds slower than the gas kinetic collision frequency some of the excess vibrational energy of the ethylenic triplet biradical (and perhaps of the 1,4-biradical, 2-methylenebutane) may be removed and a lowering of the overall decomposition rate will result.

The 1,4-biradical, 2-methylenebutane has also been postulated as reactive intermediate in the thermal decomposition of methylenecyclobutane (1). The reaction is truly unimolecular and the first order rate constant has been reported as $k = 2 \times 10^{15} \exp(-62/RT)$ s^{-1} (8).

If we estimate the ethylenic (π,π^*) triplet state in methylenecyclobutane to lie at ca. 70 kcal/mole, decomposition may occur even from the ground vibrational level of the triplet state ($E_a \sim 62$ kcal/mole (8)) and this could leave a vibrational energy span of over 40 kcal/mole to be removed in a number of collisions. This stepwise deactivation is contrary to the generally accepted view of a single step mechanism consistent with the kinetic behavior of all other olefinic triplet state reactions in mercury sensitization.

1,4-Pentadiene

The formation of the additional major reaction product 1,4-pentadiene from the triplet methylenecyclobutane seems to require either a 1,2 hydrogen shift followed by an α-ring cleavage and a second 1,2 hydrogen shift or, alternately, an α-ring cleavage and subsequent 1,3 hydrogen shift, as indicated by the sequence,



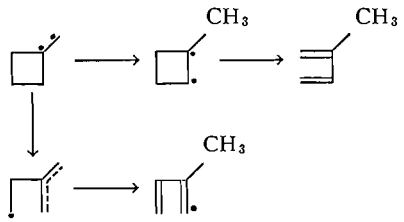
Can. J. Chem. Downloaded from www.nrcresearchpress.com by 210.87.254.105 on 09/05/12
For personal use only.

The quantum yield of PD first falls rapidly with pressure (from about 0.07 at 2 Torr to ca. 0.01 at 90 Torr) but becomes invariant between 90 and 420 Torr (cf. Fig. 1) (indicating that one of the two (or more) processes responsible for its formation is pressure dependent, the other is not). This is at variance with the general behavior of olefinic triplet state isomerization reactions, in which the isomer yield is a maximum function of pressure (whereas in the present case the percentage yield of isomer is a minimum function). The existence of this maximum in the pressure function can be rationalized in terms of the necessity for a collisional stabilization of the initially hot isomerization product. It is unlikely that the PD product in the present system does not require this pressure stabilization; its apparent lack is probably due to the overriding suppressing effect of pressure on the isomerization reaction itself. The controversy could be resolved by the assumption that PD arises only from the upper vibrational states of the triplet methylenecyclobutene, which is very efficiently relaxed by collision (with the exception of the small pressure invariant portion).

It has been suggested that internal H-atom transfers in triplet state olefins are favored in the order 1,4 > 1,3 > 1,2 (9). This order of reactivity is valid for open chain molecules, where steric, structural, or conformational hindrances are minimal. In triplet MCB 1,4 translocations could not take place because of the spacial separation of the 4-(C—H) bond and the 1-(C) p_π orbital. Even the 4 → 2 shift would not be expected to proceed readily because the 4-(C—H) sp^3 bond points away from the 2-(C) p_π orbital.

Isoprene

The formation of this minute product could proceed via a 1,3 hydrogen shift in the triplet MCB molecule before C—C bond cleavage or in the 1,4-biradical, 2-methylenebutane,



A 1,2 shift from position 3 to 2 in the triplet MCB would more likely give rise to PD and 1,2 shift in the 1,4-biradical, 2-methylenebutane from position 3 to 2 to vinylcyclopropane. (The presence of this latter compound in small quantities among the reaction products cannot be entirely ruled out (cf. Results).) The 1,2 shift seems less likely than the 1,3 shift for two reasons: firstly, because of the empirical rule (*vide supra*), and secondly, because the 1,3 shift involves the translocation of a hydrogen from a secondary to a primary position, whereas in the 1,2 shift the translocation would be from a secondary to a tertiary position (10).

Effect of Added Radical Traps

(i) Nitric Oxide

The absence of any effect on the yields of ethylene and allene again proves that nitric oxide does not react chemically with the triplet states of olefins or with biradicals. The absence of an effect on the yield of methylcyclobutane was unexpected. Perhaps the nitroso compound formed by the reaction of nitric oxide with 1-radical, methylcyclobutane is unstable or very susceptible to secondary photolysis, giving back the starting materials and thus giving the radical another chance to abstract.

Can. J. Chem. Downloaded from www.nrcresearchpress.com by 210.87.254.105 on 09/05/12
For personal use only.

(ii) Oxygen

As previously mentioned, the decrease in the yield of allene (the only product measured) was small and well within experimental error. Setser *et al.* (11) have reported a larger effect of oxygen on the ethylene reaction. Thus it appears that the triplet biradicals formed in the methylenecyclobutane reaction are more stable and also more resistant towards oxygen than the triplet biradicals in the ethylene system.

CONCLUSIONS

(i) The major primary step in the photosensitization is the formation of a vibrationally excited triplet state molecule for which the kinetic evidence indicates a stepwise deactivation mechanism.

(ii) The excited molecule decomposes by at least two modes, one of which yields H-atoms, the other 1,4-biradical, 2-methylenebutane (and a possible third mode giving $C_2H_4 + C_3H_4$ directly without the intervention of the 1,4-biradical, 2-methylenebutane).

(iii) The 1,4-biradical, 2-methylenebutane is formed with a quantum efficiency of ca. 0.70 to 0.75. The fate of the biradical is decomposition to ethylene and allene.

(iv) The identity of the final decomposition products and the interpretation of the kinetic data, although far from being free of ambiguity, lend support to the postulated mechanism for the thermal reaction of MCB (1) and the mercury photosensitization of spiropentane (2).

(v) Neither nitric oxide nor oxygen have any effect on the excited molecule or on the 1,4-biradical, 2-methylenebutane.

ACKNOWLEDGMENT

The authors gratefully acknowledge financial assistance from the National Research Council of Canada.

REFERENCES

1. P. Nangia and S. W. Benson. J. Am. Chem. Soc. **84**, 3411 (1962).
2. G. R. De Maré, L. G. Walker, O. P. Strausz, and H. E. Gunning. Can. J. Chem. **44**, 457 (1966).
3. G. R. De Maré, O. P. Strausz, and H. E. Gunning. Can. J. Chem. **43**, 1329 (1965).
4. N. S. Bhacca, D. P. Hollis, L. F. Johnson, and J. N. Shoolery. Varian Associates, NMR Spectra Catalog. Vol. I. National Press, 1962. No. 109.
5. S. Penzes, A. J. Yarwood, O. P. Strausz, and H. E. Gunning. To be published.
6. T. J. Hardwick. J. Phys. Chem. **66**, 291 (1962).
7. J. Gresser, A. Rajbenbach, and M. Szwarc. J. Am. Chem. Soc. **83**, 3005 (1961).
8. F. P. Chesick. J. Phys. Chem. **65**, 2170 (1961). P. I. Brandaur, B. Short, and S. M. E. Kellner. J. Phys. Chem. **65**, 2269 (1961).
9. M. Avrahami and P. Kebarle. J. Phys. Chem. **67**, 354 (1963). P. Kebarle and M. Avrahami. J. Chem. Phys. **38**, 700 (1963).
10. D. W. Plazcek and B. S. Rabinovitch. Can. J. Chem. **43**, 820 (1965).
11. D. W. Setser, D. W. Placzek, R. J. Cvetanović, and B. S. Rabinovitch. Can. J. Chem. **40**, 2179 (1962).
12. Kang Yang. J. Am. Chem. Soc. **86**, 3941 (1964).

Can. J. Chem. Downloaded from www.nrcresearchpress.com by 210.87.254.105 on 09/05/12
For personal use only.

Can. J. Chem. Downloaded from www.nrcresearchpress.com by 210.87.254.5 on 09/05/12
For personal use only.

THE STUDY OF HYDROGEN BONDING AND RELATED PHENOMENA BY SPECTROSCOPIC METHODS

PART IX. THE ULTRAVIOLET ABSORPTION SPECTRUM OF 3-TRIFLUOROMETHYL-2-NITROPHENOL[1]

A. Balasubramanian and W. F. Forbes
Chemistry Department, University of Waterloo, Waterloo, Ontario

AND

J. C. Dearden
Department of Pharmacy, College of Technology, Liverpool, England

Received June 18, 1965

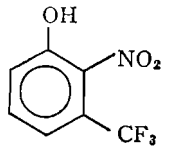
ABSTRACT

The ultraviolet and infrared spectra of 3-trifluoromethyl-2-nitrophenol (I) and of a number of reference compounds have been determined. The transitions which give rise to the observed absorption bands, as well as the effect of steric and electronic interactions on these transitions, are discussed.

Remarkable spectral changes are observed for compound I on altering the solvent from cyclohexane to polar solvents such as ether, ethanol, and water. In cyclohexane solution, there is evidence for steric interactions and for relatively weak intramolecular hydrogen bonding. In polar solvents, rupture of the intramolecular hydrogen bond occurs because solvent molecules attach themselves to the functional groups, and particularly to the phenolic OH group. This, in turn, causes the NO_2 group to be twisted out of the plane of the benzene ring.

INTRODUCTION

In a previous paper (1) it was noted that the molar absorptivities of all the main absorption bands in the electronic spectrum of 3-methyl-2-nitrophenol were drastically reduced on changing the solvent from cyclohexane to ether or ethanol. The unusual nature of this phenomenon prompted us to investigate the spectra of related compounds. One of these was 3-trifluoromethyl-2-nitrophenol (I), the spectral properties of which were even more unusual than those of 3-methyl-2-nitrophenol.



I

EXPERIMENTAL

The ultraviolet spectra were determined by standard methods using a Cary model 14 and a Beckman model DU spectrophotometer. The accuracy of λ_{max} values is estimated to be ± 1 mμ, and the precision of molar absorptivities $\pm 5\%$ or better. Absorptivity values were reproducible to $\pm 2\%$. For each compound, at least two independent sets of observations were made.

The infrared spectra were determined on a Beckman model IR 9 spectrophotometer, as previously described.[1] The solute concentration was usually between 0.01 and 0.02 *M*, unless otherwise stated.

The compounds used were normally prepared and purified by standard methods as described in the literature. Generous gifts of 3-trifluoromethyl-2-nitrophenol were received from Professor Manning A. Smith of Bucknell University and from Dr. G. C. Finger of the Illinois State Geological Survey, and of 3-methyl-4,6-di-*t*-butyl-2-nitrophenol from Dr. G. E. P. Smith, Jr. of the Firestone Tire and Rubber Company, Akron, Ohio.

[1]*Part VIII: Can. J. Chem. 42, 2674 (1964).*

THE SPECTRUM OF 3-TRIFLUOROMETHYL-2-NITROPHENOL

The ultraviolet absorption maxima of compound I and of some reference compounds are listed in Table I. The spectrum of I is shown in Fig. 1.

TABLE I

The ultraviolet absorption maxima of 3-trifluoromethyl-2-nitrophenol and of some reference compounds in cyclohexane solution. (In this and subsequent tables values in italics represent inflections)

	B-bands				*C*-band	
Compound	λ_{max} (mμ)	ϵ_{max}	λ_{max} (mμ)	ϵ_{max}	λ_{max} (mμ)	ϵ_{max}
3-Trifluoromethyl-2-nitrophenol (I)	*~230*	*4 600*	259	3 950	338	3 460
2-Nitrophenol*	*~231*	*4 000*	271	7 350	346	3 700
2-Nitroanisole*	Not detected		250	3 400	307	2 500
2-Trifluoromethylnitrobenzene	*~235*	*4 800*‡	*~272*	*1 400*‡	~335	300
3-Trifluoromethyl-4-nitrophenol	(215	10 100)	265	5 450	Shoulder	
3-Methyl-2-nitrophenol†	*~234*	*3 400*	278	6 500	351	2 900
3,4-Dimethyl-2-nitrophenol†	243	3 200	280	5 000	361	2 600
3-*t*-Butyl-2-nitrophenol	*~234*	*3 600*	271	2 500	344	850
	~241	*2 900*	*~279*	*2 200*		
Nitrobenzene†			252	9 000	*~285*	*1 500*

*Data from ref. 2.
†Data from ref. 1.
‡Band assignment doubtful.

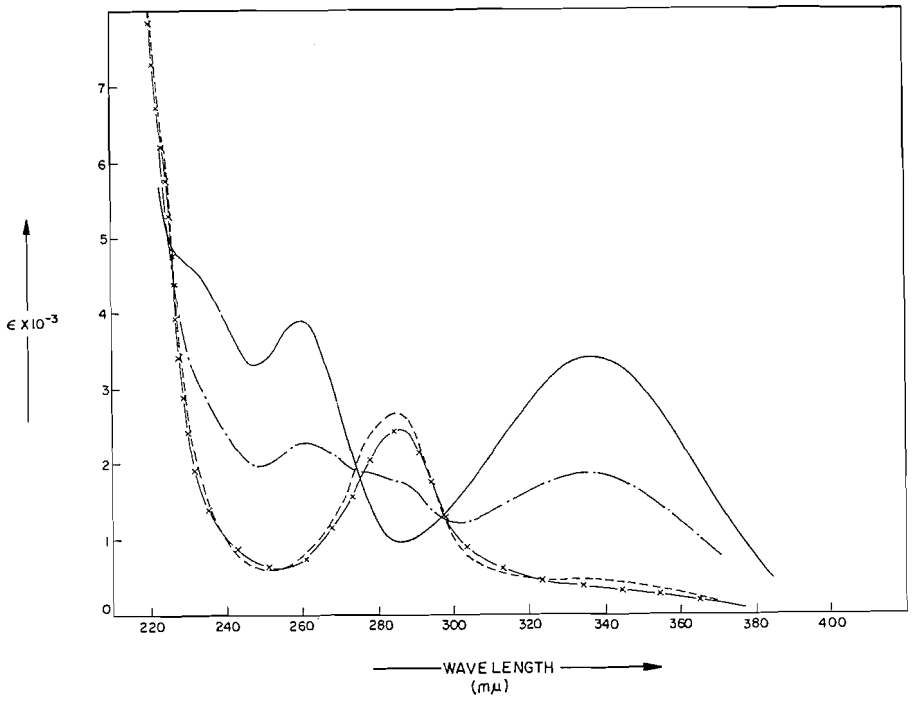


FIG. 1. The spectrum of 3-trifluoromethyl-2-nitrophenol in cyclohexane (—), in 5% ether/cyclohexane (—·—·), in ether (— — —), and in ethanol (—×—×) solutions.

The band at 259 mμ in cyclohexane solution is taken, by analogy with the spectra of nitrobenzene and 2-nitrophenol, to correspond to nitrobenzene *B*-band absorption whereas the 338 mμ band is believed, by analogy with the spectrum of 2-nitrophenol, to be a *C*-band. The latter band is not as pronounced in nitrobenzene, probably because of the greater symmetry in that molecule.

Can. J. Chem. Downloaded from www.nrcresearchpress.com by 210.87.254.5 on 09/05/12
For personal use only.

The *B*-band of I differs from that of 2-nitrophenol in two respects: it is of lower molar absorptivity, so much so that it is only slightly more intense than the *C*-band; and it occurs at appreciably shorter wavelength. The first difference, which is also observed in the other substituted nitrobenzenes listed in Table I, can be related to the well-known observation that increased steric hindrance in a molecule causes a decrease in molar absorptivity of the *B*-band, but not necessarily of the *C*-band. This explains the progressive decrease in molar absorptivity of the nitrobenzene-type *B*-band on passing from 2-nitrophenol through 3-methyl-2-nitrophenol to 3,4-dimethyl-2-nitrophenol. Since the covalent radius of fluorine (0.72 Å) is greater than that of hydrogen (0.30 Å), the CF_3 group would be expected to exert a larger steric effect on the NO_2 group than does the CH_3 group; this is, in fact, observed and even the presence of a buttressed 3-methyl group as in 3,4-dimethyl-2-nitrophenol is apparently less effective sterically than the 3-CF_3 group, as judged from the molar absorptivities given in Table I.

The inductive properties of the CF_3 group (3) presumably contribute to these spectral effects, by withdrawing electrons from the NO_2 group. As an illustration, it is pointed out that the *B*-band of 3-trifluoromethylnitrobenzene is at 247 mμ (4), while that of nitrobenzene occurs at 260 mμ (5). Such interactions would be expected to weaken the double-bond character of the *N*-aryl bond, thus increasing the transition energy of the *B*-band and in addition causing the NO_2 group to be twisted more readily out of the plane of the benzene ring. This then can account for both the observed hypsochromic displacement and for the reduced absorption intensity. The sensitivity of the nitrobenzene *B*-band to changes in double-bond character is also indicated by the spectrum of 3-trifluoromethyl-4-nitrophenol (see Table I), where the hydroxy substituent strengthens the double-bond character of the *N*-aryl bond so that a considerably more intense *B*-band is obtained (cf. also the intense *B*-band in 4-nitrophenol (5)).

In addition, the electron-withdrawing effect of the CF_3 group can cause a weakening of the intramolecular hydrogen bond in I. It may be noted that in 2-nitroanisole or 2-trifluoromethylnitrobenzene which contain no intramolecular hydrogen bond, absorption occurs at 250 mμ and near 235 mμ respectively, but that hydrogen-bonded compounds, such as 3-methyl-2-nitrophenol, absorb intensely at longer wavelength (see Table I).

The electronic, as distinct from the steric, effects of the CF_3 group have previously been discussed (cf. refs. 6–8). Concerning the spectroscopic effects of fluoro substituents, a number of workers have collected infrared data (9; cf. also 10, 11) which show that a carbon-bonded fluorine atom does not form strong hydrogen bonds of type C—F---H—O. This is also borne out by the ultraviolet spectrum of benzotrifluoride which undergoes no unusual spectral change on altering the solvent from cyclohexane to ethanol (12). Comparing the spectra of trifluoromethyl-substituted compounds with methyl-substituted analogues, there are examples where no appreciable spectral changes are observed (see refs. 13–15). If a significant spectral change is observed, the introduction of the trifluoromethyl group is frequently accompanied by a hypsochromic displacement, that is, by a spectral change similar to that observed for compound I with respect to 2-nitrophenol (12 mμ; see Table I). Part of the reason for such a displacement is presumably the electron-withdrawing effect of the trifluoromethyl substituent on neighboring atoms, and frequently the operation of steric interactions.

SOLVENT EFFECTS ON THE SPECTRUM OF 3-TRIFLUOROMETHYL-2-NITROPHENOL

The main absorption maxima of I in various solvents are given in Table II, and some of the spectra are shown in Fig. 1. The most remarkable feature of these spectra is the pronounced bathochromic displacement of the main absorption band which occurs on

Can. J. Chem. Downloaded from www.nrcresearchpress.com by 210.87.254.5 on 09/05/12
For personal use only.

passing from inert to polar solvent (see Fig. 1). Such a displacement is unusual in simple aromatic compounds in which an electron-donating substituent is not situated in the para position with respect to an electron-attracting substituent. For example, although appreciable displacements (*B*-bands, cyclohexane to ether and cyclohexane to ethanol respectively) are observed for 4-nitrophenol (13 mμ, 28 mμ) and 4-hydroxyacetophenone (7.5 mμ, 17.5 mμ), the same solvents have far less effect on the spectra of 2- and 3-disubstituted benzenes: 2-nitrophenol (0 mμ, 1.5 mμ), 3-nitrophenol (6.5 mμ, 11 mμ), 2-hydroxyacetophenone (0.5 mμ, 1 mμ), and 3-hydroxyacetophenone (3.5 mμ, 10 mμ). Next, while generally the effect of ethanol is greater than that of ether, the main absorption band of I is displaced to the same extent by ether and ethanol.

TABLE II

The ultraviolet absorption maxima of 3-trifluoromethyl-2-nitrophenol in various solvents

	B-bands				*C*-band	
Solvent	λ_{max} (mμ)	ϵ_{max}	λ_{max} (mμ)	ϵ_{max}	λ_{max} (mμ)	ϵ_{max}
Cyclohexane	*~230*	*4 600*	259	3 950	338	3 460
Chloroform			267	3 300	343	2 550
Cyclohexane containing 1% ether	*~230*	*4 300*	261	3 400	337	2 920
Cyclohexane containing 2% ether	*~230*	*3 900*	261	3 050	336 *~285*	2 450 *1 600*
Ether					286*	2 680
Ethanol					286*	2 500
Water	*~235*	Shoulder			283*	1 700
1 *N* aqueous NaOH	235	10 900	294	2 500	407	1 100

*Band assignment doubtful.

The present solvent effect can be explained by assuming that the band at 286 mμ in the spectrum of I in ethanol does not correspond to the *B*-band at 259 mμ in cyclohexane solution, but is primarily a phenol-type *C*-band, probably with some contribution from nitrobenzene-type *B*-band transitions. For 3-methyl- and 3,4-dimethyl-2-nitrophenol, the observed drastic hypochromic effect of polar solvents has previously been attributed (1) to intermolecular hydrogen bonding breaking the intramolecular hydrogen bond; consequently, the NO_2 group is free to take up the position of minimum steric stress, that is one not coplanar with the benzene ring. This non-coplanarity is further enhanced because of the increased effective size of the functional groups caused by hydrogen bonding to solvent molecules. Since the spectral changes are similar in ethanol and ether solutions, intermolecular hydrogen bonding involving the phenolic OH group is sufficient to bring about the observed changes. However, ethanol is also able to interact with the NO_2 group, which increases the effective size of that group, thereby giving rise to the slightly lower ϵ value in ethanolic solution. In either case, the conjugation between the NO_2 group and the benzene ring is reduced, and this in turn decreases the transition probability of the delocalized π-electron system of the nitrobenzene chromophore. As this loss of conjugation increases, the NO_2 group contributes less and less to the observed spectrum.

Evidence for phenol-type absorption has been noted in the spectrum of 3-methyl-2-nitrophenol in ethanol (16). For compound I (where the NO_2 group is more readily displaced from the plane of the benzene ring, and where probably the intramolecular hydrogen bond is more readily broken) it seems likely that in hydrogen-bonding solvents, conjugation of the NO_2 group with the ring is even less, leaving 3-trifluoromethylphenol as the

Can. J. Chem. Downloaded from www.nrcresearchpress.com by 210.87.254.5 on 09/05/12
For personal use only.

absorbing species. The spectrum of 3-trifluoromethylphenol in ethanol, in fact, resembles the spectrum of I in ethanol (cf. Tables II and III). The location of the band of I at 286 mμ, ϵ_{max} = 2 500 in ethanol, is, of course, typical of a *C*-band of a substituted phenol. Moreover, the spectrum of I in aqueous alkali (see Table II) is similar to that of 3-trifluoromethylphenol in alkaline medium (λ_{max} = 239 mμ, ϵ_{max} = 9 100, and λ_{max} = 298mμ, ϵ_{max} = 3 050 in 50% ethanol – 50% 0.01 *N* sodium hydroxide (17)). Evidence for phenol-type *C*-band absorption is also provided by the occurrence of only one pronounced absorption band in the 240–360 mμ region of the spectrum of compound I in ethereal or ethanolic solution (see Fig. 1); that is, the *C*-band in the region of 340 mμ, associated with *o*-nitrophenol-type absorption, has virtually disappeared. Against the interpretation of predominant phenol-type absorption, it may be argued that the observed bands are featureless (see Table II), which is characteristic of nitrobenzene *B*-band absorption (18) but not of phenolic *C*-band absorption (19). However, not all substituted-phenol spectra possess the same amount of fine structure; for example, for 2-trifluoromethylphenol in cyclohexane solution the *C*-band fine structure is less pronounced than for many other phenols (17). Hence, *both* types of transitions are believed to contribute to the observed absorption band. For example, in 3,4-dimethyl-2-nitrophenol both the nitrobenzene-type *B*-band and the phenol-type *C*-band would be expected to be near 280 mμ, and it is probable that residual *C*-band absorption, as well as *B*-band absorption, contributes to the observed absorption band. Generally, as illustrated in Table III, the spectra of related compounds fit in well with present band assignments. That is, as larger groups are substituted in the 3-position in 2-nitrophenol, there is a gradual decrease in molar absorptivity of the nitrobenzene *B*-band, while the *C*-band undergoes a variety of changes.

A similar phenomenon has been observed by Wepster (20), who showed that as the steric forces on the *N*,*N*-dimethylamino group in *p*-nitro-*N*,*N*-dimethylaniline were increased by 2- and 2,6-substitution, the absorption band corresponding to *p*-nitro-*N*,*N*-dimethylaniline steadily decreased, while that corresponding to nitrobenzene steadily increased.

It may be noted here that the *B*-band of 2-nitroanisole occurs at shorter wavelength than does that of 2-nitrophenol (see Table III) or even that of 3-nitrophenol, which occurs at λ_{max} = 258.5 mμ, ϵ = 6 100 in cyclohexane solution (2). The effect of ethanol on the *B*-band of 2-nitroanisole is a bathochromic shift of 7 mμ, typical of the effect of a polar solvent on a *B*-band (see also the spectra of 2-trifluoromethylnitrobenzene). If, however, a group such as Cl or OCH_3 is inserted in the 3-position of 2-nitroanisole, absorption occurs at some 30 mμ longer wavelength, which is ascribed to predominantly anisole-type *C*-band absorption. This seems more satisfactory than to assume that the *B*-band is displaced bathochromically by some 30 mμ (see Table III).

Next, the spectrum of 3-hydroxy-2-nitrophenol may be rationalized by assuming two intramolecular hydrogen bonds which cause this compound to absorb at longer wavelength in cyclohexane solution, both directly because of the presence of additional hydrogen bonding and indirectly by keeping the NO_2 group more planar. In ethanol, competitive intermolecular hydrogen bonding is probably not sufficient to destroy completely the intramolecular hydrogen bonds, and thus some *B*-band absorption remains.

The infrared spectra clearly show the intermolecular hydrogen bonding between the phenolic OH group and ether molecules; the data are consistent with an intramolecularly hydrogen-bonded molecule changing to an intermolecularly hydrogen-bonded molecule on addition of polar solvent (see Table IV and note the very broad absorption bands (ca. 600 cm^{-1}) suggesting overlap of different O—H stretching bands). The presence of

Can. J. Chem. Downloaded from www.nrcresearchpress.com by 210.87.254.5 on 09/05/12
For personal use only.

Can. J. Chem. Downloaded from www.nrcresearchpress.com by 210.87.254.5 on 09/05/12
For personal use only.

TABLE III

Main maxima of some substituted nitro compounds in cyclohexane and ethanol solutions

Compound	*B*-band (cyclohexane)		*C*-band (cyclohexane)		*B*-band (ethanol)		*C*-band (ethanol)			
	λ_{max} (mμ)	ϵ_{max}	λ_{max} (mμ)	ϵ_{max}	λ_{max} (mμ)	ϵ_{max}	λ_{max} (mμ)			ϵ_{max}
3-Trifluoromethylphenol	214	5 420	275	2 240	219	6 150	278			2 250
			282	2 025						
			286	1 800						
5,6-Dimethyl-2-nitrophenol	216	11 750	355	3 200	214.5	10 500	355			2 900
	292.5	7 650			297.5	7 000[f]				
2-Nitrophenol[a]	271	7 350	346	3 700	272.5	6 050	347			3 250
5-Fluoro-2-nitrophenol	211	14 700	334	4 100	209.5	14 000	334			3 250
	278	6 600			273	5 200[f]				
6-Chloro-2-nitrophenol	218	11 500	353	2 600	216.5	13 200	354			2 000
	279	5 500			277.5	4 500[c,f]				
3-Methyl-2-nitrophenol[b]	278	6 500	351	2 900			270	~340	740	1 750[c]
3,4-Dimethyl-2-nitrophenol[b]	280	5 000	361	2 600	251	1 425	275	~345	565	1 650[c]
								~359	490	
3-*t*-Butyl-2-nitrophenol	271	2 500	344	850	276.5	2 750	351–352			940
3,5-Di-*t*-butyl-2-nitrophenol	256	2 210	280	3 000[c]			273.5			2 300[c]
3-Methyl-4,6-di-*t*-butyl-2-nitrophenol	251	2 160	289	3 350[c]			271			1 840[c]
2-Nitroanisole[a]	250	3 400	307	2 500	257	3 200	319			2 350
3-Methoxy-2-nitroanisole			279	1 650[b,c]			270			3 500[c,d]
3-Chloro-2-nitroanisole[e]			282.5	1 760[c]			281			1 600[c,f]
2-Trifluoromethylnitrobenzene	~235	4 800	~335	300	244	3 700	275			Wk. shoulder
	~272	1 400					~335			450
3-Trifluoromethyl-4-nitrophenol	215	10 100			222	8 200	375			2 100
	265	5 450			291	5 600				
3-Nitrocatechol	239.5	6 150	364.5	1 760	241.5	1 700	367			550
	292	7 350			296	1 870				
3-Hydroxy-2-nitrophenol[b]	314.5	10 800	406	1 600	308	4 000	281	~370	800	2 370[c,g]

[a]Data from ref. 2.
[b]Data from ref. 1.
[c]Probably includes contributions from residual nitrobenzene *B*-band absorption.
[d]Data from ref. 21.
[e]Data from ref. 22.
[f]In methanol solution.
[g]Not reported previously.

two distinct species is also suggested by the ultraviolet spectra in cyclohexane–ether solvent mixtures which almost pass through an isosbestic point (see Fig. 1).

Two additional comments may be made. First, although intramolecular hydrogen bonding is assumed to be present in compound I in inert solution, such bonding has been assumed to be weaker than in other 2-nitrophenols. Such weakening in intramolecular hydrogen bonding is inferred from the appropriate infrared results which are shown in Table IV. Table IV shows that for compound I in carbon tetrachloride solution, the O—H stretching frequency is relatively high whereas the N—O stretching frequencies are relatively low compared with these bands in 2-nitrophenol and 3-methyl-2-nitrophenol. For 3,5-di-*t*-butyl-2-nitrophenol the O—H stretching band occurs at higher frequency, but for this compound the ultraviolet absorption spectrum in cyclohexane solution also indicates an even weaker hydrogen bond than in compound I. The infrared spectra are therefore consistent with the interpretation put forward in this paper.

TABLE IV

O—H and N—O stretching vibrations of a number of substituted nitrophenols in carbon tetrachloride solution

Compound	O—H band		Symm. N—O band		Asymm. N—O band
	"ν_{max}" (cm^{-1})	ϵ_{max}	"ν_{max}" (cm^{-1})	ϵ_{max}	"ν_{max}" (cm^{-1})
2-Trifluoromethylnitrobenzene			1 313 1 359	860 285	
3-Trifluoromethylphenol	3 609	260			
5,6-Dimethyl-2-nitrophenol	3 190	46	1 315.5 1 344	161 135	1 536.5
3-Methyl-2-nitrophenol	3 200		1 340.5 1 354.0	180 130	1 539.5
6-Chloro-2-nitrophenol	3 200	52	1 307 1 334.5	77 133	1 538.5
5-Fluoro-2-nitrophenol	3 193 3 216	73	1 327	547	1 537
2-Nitrophenol	3 245	65*	1 333 1 380	420* Weak	
3-Trifluoromethyl-2-nitrophenol (I)	3 340	80	1 306 1 352	1 000 300	1 485 1 452
I (solution containing 1% ether)†	3 200	33	1 305.5 1 332.5	600 300	
I (solution containing 2%ether)†	3 160	42			
I (solution containing 5% ether)†	3 162	70	1 305.5 1 332.5		1 487 1 455
3-Trifluoromethyl-4-nitrophenol	3 352 3 592	~15 300	1 320 1 325 Shoulder 1 351		1 538.5
3,5-Di-*t*-butyl-2-nitrophenol	3 491 3 612	20* 20	1 347 1 367	115* 155*	1 481

*No concentration dependence was observed for these bands within the concentration range 0.1–0.005 *M*.
†O—H bands are very broad (~600 cm^{-1}).

ACKNOWLEDGMENTS

The authors are indebted to Mr. H. A. Habermehl and Miss M. A. Shadbolt for competent technical assistance and discussions. Financial assistance from the National Research Council is also gratefully acknowledged.

REFERENCES

1. J. C. DEARDEN and W. F. FORBES. Can. J. Chem. **38**, 1852 (1960).
2. J. C. DEARDEN and W. F. FORBES. Can. J. Chem. **38**, 1837 (1960).
3. C. N. R. RAO, G. K. GOLDMAN, and A. BALASUBRAMANIAN. Can. J. Chem. **38**, 2508 (1960).

Can. J. Chem. Downloaded from www.nrcresearchpress.com by 210.87.254.5 on 09/05/12
For personal use only.

4. H. H. SZMANT and J. F. ANZENBERGER. J. Am. Chem. Soc. **76**, 3785 (1954).
5. W. F. FORBES. Can. J. Chem. **36**, 1350 (1958).
6. D. J. CRAM and A. S. WINGROVE. J. Am. Chem. Soc. **86**, 5490 (1964).
7. J. HINE. J. Am. Chem. Soc. **85**, 3239 (1963).
8. W. A. SHEPPARD. J. Am. Chem. Soc. **87**, 2410 (1965).
9. P. v. R. SCHLEYER and R. WEST. J. Am. Chem. Soc. **81**, 3164 (1959).
10. A. W. BAKER and W. W. KAEDING. J. Am. Chem. Soc. **81**, 5904 (1959).
11. W. F. FORBES, A. R. KNIGHT, and D. L. COFFEN. Can. J. Chem. **38**, 728 (1960).
12. M. KAMLET and H. UNGNADE. Organic electronic spectral data. Vol. I. Interscience Publishers, Inc., New York. p. 121.
13. H. SPONER and D. S. LOWE. J. Opt. Soc. Am. **39**, 840 (1949).
14. C. H. MILLER and H. W. THOMPSON. J. Chem. Phys. **17**, 845 (1949).
15. F. SMITH and L. M. TURTON. J. Chem. Soc. 1701 (1951).
16. J. C. DEARDEN. J. Org. Chem. **29**, 1821 (1964).
17. D. GRAY. U.S. Air Force, Wright-Patterson Air Force Base, Technical Documentary Report 63-355.
18. W. M. SCHUBERT, J. ROBINS, and J. L. HAUN. J. Am. Chem. Soc. **79**, 910 (1957).
19. J. C. DEARDEN and W. F. FORBES. Can. J. Chem. **37**, 1294 (1959).
20. B. M. WEPSTER. Rec. Trav. Chim. **76**, 357 (1957).
21. A. E. LUTSKII. Zh. Obshch. Khim. **19**, 282 (1945).
22. G. FAVINI. Rend. Ist. Lombardo Sci. Lettere, A: **92**, 23 (1957).

Can. J. Chem. Downloaded from www.nrcresearchpress.com by 210.87.254.5 on 09/05/12
For personal use only.

Can. J. Chem. Downloaded from www.nrcresearchpress.com by 210.87.254.40 on 09/05/12
For personal use only.

NOTES

THE PHOTOLYSIS OF PERFLUOROAZOETHANE AT ROOM TEMPERATURE

J. R. Dacey, W. C. Kent, and G. O. Pritchard[1]

This note deals with experiments carried out at room temperature and at a wavelength of 3 660 Å. The photodecomposition of simple aliphatic azo-compounds under these conditions follows a very simple mechanism in which decomposition competes with collisional deactivation steps.

$$A + h\nu = A^*$$
$$A^* \xrightarrow{k_a} \text{products } (N_2 + 2 \text{ radicals})$$
$$A^* + A \xrightarrow{k_b} A + A$$

A* represents a molecule of azo-compound with sufficient energy to decompose, and A a molecule with insufficient energy for decomposition to occur. The original investigations of Wieninger and Rice (1) on azoethane and Durham and Steacie (2) on azoisopropane showed a marked pressure dependence for Φ_{N_2}, in accord with the mechanism. These results have been substantiated in careful re-investigations of both compounds by Kutschke and his co-workers (3, 4). For azomethane $\Phi_{N_2} = 1$ below 1 atm, but above this pressure Φ_{N_2} does in fact fall below unity (5). It is generally accepted (1–5) that although the primary photochemical excitation is mainly electronic the mechanism of decomposition involves conversion into vibrational energy, with its eventual accumulation in a particular bond; thus collisional deactivation processes will increase in importance as the number of degrees of vibrational freedom in a molecule increases, in agreement with observation (1–4). We (6) have extended Φ_{N_2} determinations to hexafluoroazomethane, and found a stronger pressure dependence than was obtained with azoethane (3), which was explained by the greater number of effective oscillators in the fluorine-containing compound (6). Herein we report some experiments with perfluoroazoethane.

The apparatus and the preparation and purification of perfluoroazoethane have been previously described (7), as well as the analysis and purity checks on the N_2 and C_4F_{10} (from C_2F_5 recombination) formed in the reaction system (7). The 3 660 Å radiation was isolated by solution filters (8), and actinometry was performed by the modified Parker method (9). The transmitted intensity, when the reaction cell was under *vacuo*, was 12.3×10^{15} quanta/s.

The results of the experiments are recorded in Table I (27.5 ± 2.5 °C represents the temperature range of the experiments, and not the temperature variation in any one run). The percentage decomposition of the azo-compound was usually less than 2%, based on N_2 produced. The quantum yields of N_2 and C_4F_{10} both decrease with increasing pressure, and, except at low pressures, $\Phi_{C_4F_{10}} < \Phi_{N_2}$. This is expected because of the successive addition of two C_2F_5 radicals to the —N=N—,

$$C_2F_5N{=}NC_2F_5 \xrightarrow{C_2F_5} (C_2F_5)_2N{-}NC_2F_5 \xrightarrow{C_2F_5} (C_2F_5)_4N_2,$$

[1]*Department of Chemistry, University of California, Santa Barbara, California.*

TABLE I
Photolysis of $(C_2F_5)_2N_2$ at 27.5 ± 2.5 °C

Perfluoroazoethane pressure, cm	Time, s	Product (moles × 10^5) N_2	Product (moles × 10^5) C_4F_{10}	Φ_{N_2}	$\Phi_{C_4F_{10}}$
2.71	1 200	0.387	(0.468)	0.45	(0.55)
5.08	5 000	1.95	1.13	0.40	0.23
8.95	5 000	2.00	0.763	0.28	0.11
11.0	5 000	1.90	0.743	0.22	0.085
11.8	5 000	1.96	1.30	0.25	0.17
13.3	5 000	1.80	1.05	0.20	0.12
13.9	5 000	2.01		0.22	
14.3	5 000	1.66	0.952	0.19	0.11

to produce a hydrazine. The C_4F_{10} formed in the reaction was roughly equal to $\Delta P(V/RT)$, where ΔP was the pressure increase in the reaction volume V. This indicated the absence of tetrazine, $(C_2F_5)_6N_4$, formation, when smaller values of ΔP were observed. Tetrazine formation would not in any case be expected from steric considerations (6). In preliminary photochemical experiments with perfluoroazoethane Young and Dresdner (10) report N_2, C_4F_{10}, and a hydrazine as the only products; the hydrazine was a liquid, with boiling point about 118 °C. In the Ward-Still separation of our reaction mixture we observed a liquid product which condensed in the gas buret at a total pressure of about 1 cm at room temperature, which would be the approximate hydrazine vapor pressure at 25 °C.

After collection of the C_4F_{10} and azo-fraction at −104 °C for vapor phase chromatographic analysis, the remaining perfluoroazoethane was fractionated at −80 °C, and reused in subsequent runs. This led to a slight contamination of the perfluoroazoethane with C_4F_{10}, accounting for the high C_4F_{10} yield in the run at 2.71 cm. The main purpose of this investigation was to examine Φ_{N_2} as a function of pressure; the N_2 analyses are accurate to 1%.

In the steady state we have $1/\Phi_{N_2} = 1 + (k_b/k_a)[A]$ and a plot of $1/\Phi_{N_2}$ versus azo pressure is given in Fig. 1, where we have arbitrarily drawn the line through $1/\Phi_{N_2} = 1$ at

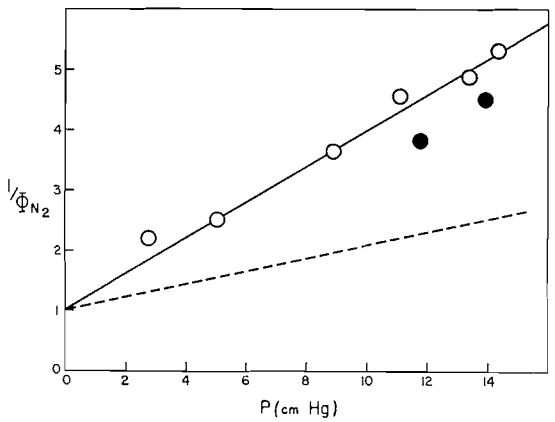


FIG. 1. (○) Plot of $1/\Phi_{N_2}$ versus pressure (cm) of perfluoroazoethane; (●) less accurate data (see text); (- -) plot for hexafluoroazomethane, ref. 6.

Can. J. Chem. Downloaded from www.nrcresearchpress.com by 210.87.254.40 on 09/05/12
For personal use only.

$P = 0$ cm. The two shaded points at higher pressures represent experiments in which the actinometer solution was underexposed for an accurate photon count. In the subsequent experiments at higher pressures the exposure time was increased by a factor of 5. The experimental slope $k_b/k_a = 5.6 \times 10^5$ cc mole^{-1}, which is $2\frac{1}{2}$ times the slope obtained for $CF_3N_2CF_3$, 2.3×10^5 cc mole^{-1} under the same conditions (6) (see Fig. 1).

The comparable values of k_b/k_a for the H-containing azo-compounds are 0.8 and 1.0×10^5 for azoethane (3, 11), 7.6×10^5 for azoisopropane (4), 9.1×10^5 for 1-propylazoethane (11), and 2.2×10^6 for azopropane (11), all in units of cc mole^{-1}. The flash photolysis work (11) appears to yield slightly bigger values than are obtained from the direct photolysis data (3, 4), for a particular molecular weight. However, unity intercepts at $P = 0$ cm were chosen in the flash work (11) for azoethane and azopropane, although the very careful direct photolysis investigations on azoethane and azoisopropane (3, 4) indicate intercepts greater than unity, leading to lesser slopes for $1/\Phi_{N_2}$ versus P. The intercepts are accounted for (3, 4) by an interval conversion process

$$A^* \rightarrow A,$$

where A is incapable of dissociation. The significant occurrence of any radiative processes has been ruled out (3, 4). It is not apparent from our data whether such a process contributes to the mechanism in perfluoroazoethane photolysis.

It is seen that the values of k_b/k_a for the azo-compounds discussed do vary in the qualitative way that would be expected from the changes in effective oscillators in the molecules. Specific values of k_a will depend, to some extent, on the C—N bond dissociation energies, which show small variations (12). Values of k_b will be a function of the collision numbers and the magnitude of the vibrational quanta transferred on collision. Any comparison of k_b/k_a values for different molecules must take these factors into account. Although not strictly valid, it is commonly assumed (1, 3, 6) that $k_b = Z$, the collision number, in evaluation of k_a, assuming collision efficiencies of unity, with respect to deactivation.

ACKNOWLEDGMENT

The generous financial assistance of the Defence Research Board of Canada, under grant 9530/13, is gratefully acknowledged. One of us (G. O. P.) thanks the National Science Foundation for assistance.

1. J. L. Weininger and O. K. Rice. J. Am. Chem. Soc. **74**, 6216 (1952).
2. R. W. Durham and E. W. R. Steacie. Can. J. Chem. **31**, 377 (1953).
3. H. Cerfontain and K. O. Kutschke. Can. J. Chem. **36**, 344 (1958).
4. R. H. Riem and K. O. Kutschke. Can. J. Chem. **38**, 2332 (1960).
5. R. E. Rebbert and P. Ausloos. J. Am. Chem. Soc. **87**, 1847 (1965).
6. J. R. Dacey, R. F. Mann, and G. O. Pritchard. Can. J. Chem. **43**, 3215 (1965).
7. G. O. Pritchard, J. R. Dacey, W. C. Kent, and C. R. Simonds. Can. J. Chem. **44**, 171 (1966).
8. M. Kasha. J. Opt. Soc. **38**, 929 (1948).
9. J. H. Baxendale and N. K. Bridge. J. Phys. Chem. **59**, 783 (1955).
10. J. A. Young and R. D. Dresdner. J. Org. Chem. **28**, 833 (1963).
11. J. O. Terry. M.Sc. Thesis, Air University, Wright-Patterson Air Force Base, Ohio. 1964.
12. E. Leventhal, C. R. Simonds, and C. Steel. Can. J. Chem. **40**, 930 (1962).

Received November 22, 1965.
Department of Chemistry,
Royal Military College of Canada,
Kingston, Ontario.

Can. J. Chem. Downloaded from www.nrcresearchpress.com by 210.87.254.40 on 09/05/12
For personal use only.

QUINOLINE N-OXIDE COMPLEXES OF TITANYL, ZIRCONYL, AND THORIUM PERCHLORATES

V. KRISHNAN AND C. C. PATEL

Heterocyclic N-oxides have recently been used as complexing agents. The complexes of quinoline N-oxide have not been investigated, however, except for a report on the preparation and magnetic susceptibility determinations of some copper complexes (1). The study on quinoline N-oxide complexes of titanyl, zirconyl, and thorium perchlorates is given here.

EXPERIMENTAL

Materials

Quinoline N-oxide dihydrate (2) and crystalline titanyl (3), zirconyl (4), and thorium (5) perchlorates were prepared as described earlier.

Preparation and Analyses of the Complexes

The complexes were prepared by mixing the respective perchlorate (1 g) dissolved in about 50 ml of anhydrous ethanol with quinoline N-oxide (3 g) in about 50 ml of the same solvent. After about 12 h, the precipitated complex was filtered off, washed with ethanol, dried over phosphorus pentoxide in vacuum, and analyzed.

Titanium, zirconium, and thorium were analyzed as their dioxides, perchlorate by Kurz's method (6), and nitrogen by the semimicro method of Dumas.

Anal. Calcd. for $TiO.5(C_9H_7NO)(ClO_4)_2$: Ti, 4.84; ClO_4, 20.13; N_2, 7.08. Found: Ti, 4.78; ClO_4, 20.04; N_2, 6.81.

Anal. Calcd. for $ZrO.6(C_9H_7NO)(ClO_4)_2$: Zr, 7.75; ClO_4, 16.91; N_2, 7.14. Found: Zr, 7.61; ClO_4, 17.02; N_2, 6.90.

Anal. Calcd. for $Th.6(C_9H_7NO)(ClO_4)_4$: Th, 15.46; ClO_4, 26.53; N_2, 5.87. Found: Th, 15.52; ClO_4, 26.41; N_2, 5.86.

PROPERTIES

All the complexes are hygroscopic. The titanyl complex is brownish yellow, zirconyl pale yellow, and thorium dark brown. The complexes are soluble in polar solvents and insoluble in nonpolar solvents. Differential thermal analysis (7) study showed that titanyl, zirconyl, and thorium complexes decompose at 210, 295, and 330 °C respectively.

The electronic absorption spectra of quinoline N-oxide dihydrate and the complexes in pure dry acetonitrile, as shown in Fig. 1, were taken with a Hilger Uvispeck spectrophotometer. The infrared spectra of the quinoline N-oxide dihydrate and the complexes were taken with a Perkin–Elmer 521, double-beam grating instrument using KBr disc technique. The results are given in Table I.

DISCUSSION

The titanyl, zirconyl, and thorium complexes decompose at 210, 295, and 330 °C respectively. These decomposition temperatures are slightly higher than the temperatures at which the respective metal perchlorates start decomposing (8, 9). It seems that the oxygen released during the decomposition of the perchlorate is responsible for the oxidation of the ligand molecules.

Quinoline N-oxide dihydrate (Fig. 1) has a π–π^* absorption maximum at 340 mμ (ϵ = 7 470). On complex formation, this band undergoes a hypsochromic shift, similar to pyridine N-oxide complexes, showing bonding through oxygen of NO. In titanyl, zirconyl, and thorium complexes, this band occurs at 335, 330, and 320 mμ respectively. This shows that the π-electrons in the N—O group of the complexes are held in the following increasing strength: titanyl < zirconyl < thorium.

Can. J. Chem. Downloaded from www.nrcresearchpress.com by 210.87.254.40 on 09/05/12
For personal use only.

Can. J. Chem. Downloaded from www.nrcresearchpress.com by 210.87.254.40 on 09/05/12
For personal use only.

TABLE I

Infrared frequencies and assignments of quinoline N-oxide dihydrate and of its complexes of titanyl, zirconyl, and thorium perchlorates

$C_9H_7NO.2H_2O$ (cm^{-1})	$[TiO.5(C_9H_7NO)](ClO_4)_2$ (cm^{-1})	$[ZrO.6(C_9H_7NO)](ClO_4)_2$ (cm^{-1})	$[Th.6(C_9H_7NO)](ClO_4)_4$ (cm^{-1})	Assignments
1 625 w	1 620 w	1 620 s	1 620 s	C=C str.
1 570 s	1 580 m	1 575 m	1 580 m	C=N str.
1 510 s	1 515 m	1 515 m	1 515 m	Ring str.
1 445 m	1 455 w	1 450 w	1 450 w	
1 395 vs	1 395 s	1 395 s	1 395 s	
1 345 w	1 355 w	1 355 w	1 355 w	
1 307 s	1 310 w	1 310 w	1 310 w	C—H in-plane def.
1 265 s	1 265 m	1 265 m	1 265 m	
1 230 vs*	1 230 m	1 230 m	1 235 m	
1 210 m	1 215 m	1 215 m	1 215 m	
1 180 w	1 180 m	1 180 m	1 180 m	
1 135 m	1 145 s	1 145 s	1 145 s	
	1 122 vs	1 125 vs	1 125 vs	N—O str.
1 190 m	1 085 vs	1 090 vs	1 090 vs	ν_3 of ClO_4
1 055 w		1 060 s	1 060 s	Ring breathing
1 015 w				
885 s	885 s	885 s	885 s	N—O bending
795 vs	805 vs	805 s	800 s	C—H out-of-plane def.
765 s				
725 m	765 s			
650 vw		765 s	765 s	
625 vw	725 m	725 m	725 m	
	625 s	635 s	638 s	ν_4 of ClO_4
		625 s	630 s	
580 w	590 m	580 wb	585 w	
565 w	565 m			
550 w		560 w	550 w	

ABBREVIATIONS: s = strong, v = very, m = medium, w = weak, str. = stretching, def. = deformation.
*C—H in-plane def. + NO stretch.

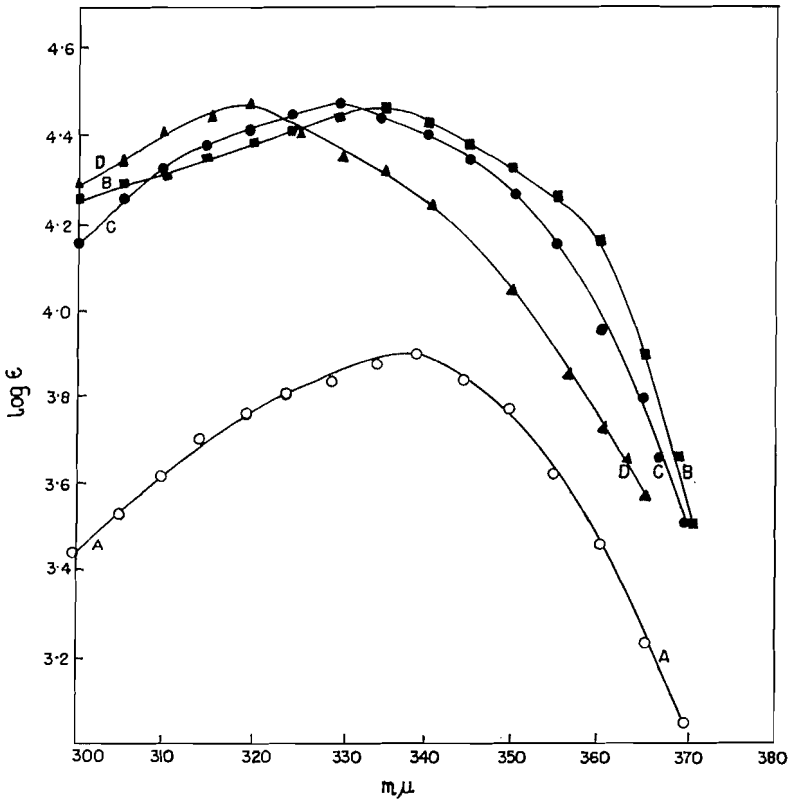


FIG. 1. Electronic absorption spectra of (A) $C_9H_7NO.2H_2O$, (B) $TiO.5(C_9H_7NO)(ClO_4)_2$, (C) $ZrO.6(C_9H_7NO)(ClO_4)_2$, and (D) $Th.6(C_9H_7NO)(ClO_4)_4$ in acetonitrile.

Earlier workers (10–14) assigned a system of infrared bands of quinoline N-oxide dihydrate to N—O stretching in the region 1 350 to 1 250 cm^{-1}. In the present study, the band at 1 230 cm^{-1} of quinoline N-oxide dihydrate is assigned to N—O stretching by comparison of the spectra of naphthalene and quinoline. In the complexes studied, this band is reduced in intensity and a strong new band appears at about 1 125 cm^{-1}. This shows that the band at 1 230 cm^{-1} of quinoline N-oxide is not due to N—O stretching only; it may be due to an overlap of CH in-plane deformation and N—O stretch. The pure N—O band for titanyl, zirconyl, and thorium complexes occurs at 1 122, 1 125, and 1 125 cm^{-1} respectively, making the comparison of the bond strength between the metal and ON< difficult. By comparison of the spectra of pyridine N-oxide (16), dipyridyl N,N′-dioxide (15), and quinoline (17), the NO bending for quinoline N-oxide is assigned at 885 cm^{-1}. This band does not undergo any shift on complex formation, as happens with the NO bending frequency of pyridine N-oxide complexes (18, 19). The perchlorate band ν_3 at 1 090 cm^{-1} and a split band ν_4 at 640 cm^{-1} of the complexes suggest a lowering of the T_d symmetry of the perchlorate, mainly due to crystal field effects.

Titanyl, zirconyl, and thorium complexes have their usual coordination numbers 6, 7, and 6 respectively.

ACKNOWLEDGMENT

The authors are thankful to Prof. M. R. A. Rao for his kind interest in this work.

Can. J. Chem. Downloaded from www.nrcresearchpress.com by 210.87.254.40 on 09/05/12
For personal use only.

1. C. M. HARRIS, E. MOKOT, S. L. LENZER, and T. N. LOCHYER. Chem. Ind. London, 151 (1962).
2. E. OCHIAI. J. Org. Chem. **18**, 548 (1953).
3. V. KRISHNAN and C. C. PATEL. Chem. Ind. London, 321 (1961).
4. P. RAMAMURTHY and C. C. PATEL. Naturwissenschaften, **22**, 693 (1961).
5. P. RAMAMURTHY and C. C. PATEL. J. Inorg. Nucl. Chem. **25**, 310 (1963).
6. E. KURZ, G. KOBER, and M. BERL. Anal. Chem. **30**, 1983 (1958).
7. N. S. K. PRASAD and C. C. PATEL. J. Indian Inst. Sci. **36**, 23 (1954).
8. V. KRISHNAN and C. C. PATEL. Indian J. Chem. **2**, 425 (1964).
9. P. RAMAMURTHY and C. C. PATEL. Indian J. Chem. **3**, 134 (1965).
10. G. TSOUCARIS. J. Chim. Phys. **58**, 619 (1961).
11. C. W. VALDEMORO. Compt. Rend. **253**, 277 (1961).
12. G. COSTA, P. BLASIMA, and G. SARTORI. Chem. Abs. **50**, 1183 (1956).
13. H. SHINDO. Chem. Abs. **55**, 19480 (1960).
14. J. HAMER and A. MACALUSO. Chem. Rev. **64**, 473 (1964).
15. A. VINICIGUERRA, P. H. SIMSON, V. KAKIUTI, and J. V. QUAGLIANO. Inorg. Chem. **2**, 286 (1963).
16. S. KIDA, J. V. QUAGLIANO, J. A. WALMSLEY, and S. Y. TYREE. Spectrochim. Acta, **19**, 189 (1964).
17. A. R. KATRIZKY and R. L. JONES. J. Chem. Soc. 2942 (1960).
18. P. RAMAMURTHY and C. C. PATEL. Can. J. Chem. **42**, 856 (1964).
19. V. KRISHNAN and C. C. PATEL. Can. J. Chem. **43**, 2685 (1965).

RECEIVED AUGUST 20, 1965.
DEPARTMENT OF INORGANIC AND PHYSICAL CHEMISTRY,
INDIAN INSTITUTE OF SCIENCE,
BANGALORE, 12, INDIA.

Can. J. Chem. Downloaded from www.nrcresearchpress.com by 210.87.254.40 on 09/05/12
For personal use only.

INVESTIGATIONS ON SOME AMINE COMPLEXES OF IRON(III) PHTHALIMIDE. INFRARED SPECTROSCOPIC MEASUREMENTS

GOPAL NARAIN

INTRODUCTION

The preparation of a series of amine complexes of iron(III) phthalimide and some preliminary investigations on them dealing with analysis, molecular weight, and conductivity have been reported (1). It has been pointed out that the nonelectrolytic nature of the complexes shows that three phthalimide ions are also coordinated along with the amine ligands and that the coordination of the phthalimide ion to the metal could be either through the negatively charged nitrogen or through the oxygen of the carbonyl group. Infrared spectroscopic measurements were obtained in order to provide further confirmation and to establish that both the amine and the phthalimide ligands are coordinated to the iron atom.

EXPERIMENTAL

The spectra were taken as Nujol mulls, on a Perkin–Elmer infrared spectrophotometer model 21 with a sodium chloride prism.

RESULTS AND DISCUSSION

The spectra were examined throughout the entire infrared range from 600 to 3 500 cm^{-1}. The various bands obtained for individual complexes are listed in Table I.

As has been mentioned earlier, it is possible that the phthalimide ion can be coordinated to the metal atom either through the nitrogen or through the oxygen of the carbonyl group. It is not expected that the infrared spectra will make a sharp distinction between these two conditions because any change in phthalimide nitrogen which is directly linked to the carbonyl group will alter the molecular environment and accordingly the frequency of the latter, even if it is not coordinated (2); but on the basis of the *Lewis* concept it is expected that the nitrogen which is negatively charged has better possibilities of being coordinated than the oxygen (3).

1. C. M. HARRIS, E. MOKOT, S. L. LENZER, and T. N. LOCHYER. Chem. Ind. London, 151 (1962).
2. E. OCHIAI. J. Org. Chem. **18**, 548 (1953).
3. V. KRISHNAN and C. C. PATEL. Chem. Ind. London, 321 (1961).
4. P. RAMAMURTHY and C. C. PATEL. Naturwissenschaften, **22**, 693 (1961).
5. P. RAMAMURTHY and C. C. PATEL. J. Inorg. Nucl. Chem. **25**, 310 (1963).
6. E. KURZ, G. KOBER, and M. BERL. Anal. Chem. **30**, 1983 (1958).
7. N. S. K. PRASAD and C. C. PATEL. J. Indian Inst. Sci. **36**, 23 (1954).
8. V. KRISHNAN and C. C. PATEL. Indian J. Chem. **2**, 425 (1964).
9. P. RAMAMURTHY and C. C. PATEL. Indian J. Chem. **3**, 134 (1965).
10. G. TSOUCARIS. J. Chim. Phys. **58**, 619 (1961).
11. C. W. VALDEMORO. Compt. Rend. **253**, 277 (1961).
12. G. COSTA, P. BLASIMA, and G. SARTORI. Chem. Abs. **50**, 1183 (1956).
13. H. SHINDO. Chem. Abs. **55**, 19480 (1960).
14. J. HAMER and A. MACALUSO. Chem. Rev. **64**, 473 (1964).
15. A. VINICIGUERRA, P. H. SIMSON, V. KAKIUTI, and J. V. QUAGLIANO. Inorg. Chem. **2**, 286 (1963).
16. S. KIDA, J. V. QUAGLIANO, J. A. WALMSLEY, and S. Y. TYREE. Spectrochim. Acta, **19**, 189 (1964).
17. A. R. KATRIZKY and R. L. JONES. J. Chem. Soc. 2942 (1960).
18. P. RAMAMURTHY and C. C. PATEL. Can. J. Chem. **42**, 856 (1964).
19. V. KRISHNAN and C. C. PATEL. Can. J. Chem. **43**, 2685 (1965).

RECEIVED AUGUST 20, 1965.
DEPARTMENT OF INORGANIC AND PHYSICAL CHEMISTRY,
INDIAN INSTITUTE OF SCIENCE,
BANGALORE, 12, INDIA.

Can. J. Chem. Downloaded from www.nrcresearchpress.com by 210.87.254.105 on 09/05/12
For personal use only.

INVESTIGATIONS ON SOME AMINE COMPLEXES OF IRON(III) PHTHALIMIDE. INFRARED SPECTROSCOPIC MEASUREMENTS

GOPAL NARAIN

INTRODUCTION

The preparation of a series of amine complexes of iron(III) phthalimide and some preliminary investigations on them dealing with analysis, molecular weight, and conductivity have been reported (1). It has been pointed out that the nonelectrolytic nature of the complexes shows that three phthalimide ions are also coordinated along with the amine ligands and that the coordination of the phthalimide ion to the metal could be either through the negatively charged nitrogen or through the oxygen of the carbonyl group. Infrared spectroscopic measurements were obtained in order to provide further confirmation and to establish that both the amine and the phthalimide ligands are coordinated to the iron atom.

EXPERIMENTAL

The spectra were taken as Nujol mulls, on a Perkin–Elmer infrared spectrophotometer model 21 with a sodium chloride prism.

RESULTS AND DISCUSSION

The spectra were examined throughout the entire infrared range from 600 to 3 500 cm^{-1}. The various bands obtained for individual complexes are listed in Table I.

As has been mentioned earlier, it is possible that the phthalimide ion can be coordinated to the metal atom either through the nitrogen or through the oxygen of the carbonyl group. It is not expected that the infrared spectra will make a sharp distinction between these two conditions because any change in phthalimide nitrogen which is directly linked to the carbonyl group will alter the molecular environment and accordingly the frequency of the latter, even if it is not coordinated (2); but on the basis of the *Lewis* concept it is expected that the nitrogen which is negatively charged has better possibilities of being coordinated than the oxygen (3).

TABLE I

Infrared bands of amine complexes

Sample No.	Complex	Infrared bands
1	Phthalimide	645 w, 715 s, 792 w, 815 w, 1 070 w, 1 090 w, 1 140 s, 1 185 w, 1 310 s, 1 380 s, 1 465 s, 1 605 w, 1 744 w, 3 180 s
2	Iron(III) phthalimide	645 w, 712 s, 855 w, 1 050 m, 1 085 m, 1 145 w, 1 180 w, 1 310 m, 1 380 s, 1 465 s, 1 605 m, 1 725 s, 1 765 m, 3 140 m
3	Triphthalimido-triaminoiron(III)	670 m, 710 s, 855 w, 1 075 m, 1 130 s, 1 185 m, 1 225 m, 1 290 s, 1 315 s, 1 460 s, 1 510 w, 1 525 m, 1 610 m, 1 705 s, 3 270 s
4	Triphthalimido-tri(methylamino)-iron(III)	675 m, 712 s, 940 m, 780 w, 855 m, 955 w, 1 070 w, 1 130 s, 1 185 s, 1 220 w, 1 265 s, 1 310 s, 1 380 s, 1 465 s, 1 105 w, 1 710 s, 3 266 m
5	Triphthalimido-tri(ethylamino)-iron(III)	675 s, 720 s, 850 m, 1 055 m, 1 075 s, 1 130 s, 1 180 s, 1 285 m, 1 310 s, 1 380 s, 1 460 s, 1 303 s, 1 605 s, 1 710 s, 3 280 s
6	Triphthalimidotri-(propylamino)iron(III)	670 m, 722 s, 855 m, 1 055 w, 1 075 m, 1 107 m, 1 180 m, 1 210 w, 1 295 w, 1 310 m, 1 380 m, 1 265 s, 1 605 m, 1 640 s, 1 715 m, 3 285 s
7	Triphthalimido-tri(butylamino)-iron(III)	670 m, 725 m, 850 w, 1 130 m, 1 180 m, 1 315 m, 1 380 s, 1 460 s, 1 510 w, 1 520 w, 1 560 w, 1 580 w, 1 703 s, 3 280 m
8	Triphthalimidotri-(dimethylamino)-iron(III)	670 m, 715 s, 740 m, 780 m, 860 m, 960 w, 1 075 s, 1 090 s, 1 140 w, 1 185 m, 1 220 w, 1 295 w, 1 305 s, 1 380 m, 1 460, 1 500 w, 1 700 s, 3 310 s
9	Triphthalimidotri-(diethylamino)iron(III)	675 m, 710 s, 740 m, 825 w, 855 s, 950 m, 1050 m, 1 090 w, 1 125 s, 1 180 s, 1 225 w, 1 265 w, 1 310 s, 1 375 s, 1 460 s, 1 605 m, 1 705 s, 3 300 m

All complexes show a single sharp absorption band in the vicinity of 3 300 cm^{-1}, which is assigned to the NH stretching frequency band. In free ammonia and in aliphatic amines the band occurs at 3 414 cm^{-1} and 3 400 cm^{-1}, respectively. This negative shift of the frequency is a result of the coordination of the amine to the iron atom, with the formation of a highly covalent M—N bond which weakens the NH bond.

The band observed in the carbonyl stretching frequency region is of interest. In phthalimide the band occurs at 1 745 cm^{-1}, in iron phthalimide it shifts to 1 725 cm^{-1}, whereas in complexes it shifts in the vicinity of 1 700 to 1 710 cm^{-1}. The cause of this negative shift of frequency appears to be the electron density at nitrogen. In the case of iron(III) phthalimide, which is supposed to possess a partial covalent character, the band shifts only by 25 cm^{-1}. The negative charge on nitrogen increases from phthalimide to iron phthalimide and to amine complexes. This increase brings about a corresponding decrease in frequency.

1. G. Narain. Z. Anorg. Allgem. Chem. Accepted for publication.
2. S. Krimm. J. Chem. Phys. **23**, 1371 (1955).
3. J. C. Bailar. Chemistry of coordination compounds. Reinhold, New York. 1956. p. 180.

Received August 31, 1965.
Department of Chemistry,
Lucknow University,
Lucknow, U.P., India.

Can. J. Chem. Downloaded from www.nrcresearchpress.com by 210.87.254.105 on 09/05/12
For personal use only.

Can. J. Chem. Downloaded from www.nrcresearchpress.com by 210.87.254.105 on 09/05/12
For personal use only.

AQUEOUS SOLUTIONS OF "SODIUM PERNITRITE" FROM ALKALINE HYDROGEN PEROXIDE AND NITRIC OXIDE

GIANNA L. PETRICONI AND HENRY M. PAPEE

Relatively little information about the formation and properties of "alkali metal pernitrites" is, at present, available in the literature. Neither "pernitrous acid" nor its alkaline salts have, so far, been isolated. Although it appears to be customary to assign the "acid" a simple peroxy-formula of the type H—O—O—N=O, it was suggested that the compound may actually be an acid nitrosyl peroxide $NO^+HO_2^-$. Solutions of "alkali-metal pernitrite" are usually prepared in the laboratory (1, 2) by the reaction of alkali nitrite dissolved in water with acidified hydrogen peroxide and by a fast alkalization of the resulting mixture. They, furthermore, can be obtained by the action of ozone on aqueous solutions of alkali azides (3), and they are also formed when aqueous alkaline nitrates, at high pH values, are photolyzed with ultraviolet light (4). Alkaline solutions of the "pernitrous acid" are known to be very powerful inorganic oxidants, since they decompose to yield free $OH^\cdot$ radicals (2, 5).

An investigation which extends work on ultraviolet photolysis of nitrates (quoted in refs. 4 and 6) is presently being carried out in this laboratory; the results obtained so far show that when solutions of concentrated alkali metal nitrates are irradiated with ultraviolet light at acid *or alkaline* pH values, gaseous oxygen and *oxides of nitrogen* are formed in the liquid and can be carried away from the solution in a stream of nitrogen. It was hence suspected that one of the mechanisms of "pernitrite" formation may proceed through the action of $OH^\cdot$ radicals on nitric oxide and (or) nitrogen dioxide in solution, and therefore an attempt was made to prepare this oxidant from hydrogen peroxide and the above-mentioned oxides of nitrogen.

When *gaseous* nitrogen dioxide is introduced, at room temperature, into aqueous solutions of hydrogen peroxide, a fast reaction of oxidation at the interphase becomes immediately visible. The bubbles of gas become almost instantly discolored as they rise through the liquid, and a dense white fog, probably due to the formation of N_2O_5, forms above the surface. The process lasts as long as hydrogen peroxide is present in solution; a similar formation of fog takes place when nitric oxide is used instead of NO_2, but no change in the color of the bubbles of gas is noticeable. The introduction, under vigorous stirring, of *nitric oxide* into solutions of about 1% hydrogen peroxide and at pH 12.5–13.5 results in the formation of fairly substantial amounts of the "pernitrous" compound (up to 6×10^{-3} mole/l), which can easily be identified by its reactions and rates of decomposition (4). This synthesis does not occur when nitrogen dioxide is used; no "pernitrite" can, in fact, be detected by analytical methods previously outlined (4), even when several milliliters of liquid and purified N_2O_4 are introduced, under stirring, into a 1% solution of H_2O_2 at a pH of 13 and at 0 °C.

The experiments aimed at establishing the best conditions at which "sodium pernitrite" could be formed from NO and H_2O_2 were carried out with reagent grade Merck's products throughout, and the nitric oxide used was prepared in a standard laboratory manner and in a closed vessel from dilute nitric acid and copper metal. The gas was passed slowly through a dry ice – acetone spiral trap, and subsequently dissolved in concentrated sulfuric acid, under vigorous stirring and in the presence of 99.9% pure oxygen, which was

simultaneously bled into the acid; concentrations of the nitrosyl-sulfuric acid thus formed (7) were evaluated by titration with permanganate (8). The acid was introduced drop-by-drop into a spherical flask which contained crushed ice made from distilled water and suspended, under strong mechanical stirring, in alkaline hydrogen peroxide. In a typical run, for example, 250 ml of 50.0% NaOH was precooled to about 0 °C in a thermostat, added with 10.0 cc of 32.5% hydrogen peroxide and with about 500 g of ice; 60 ml of ice-cold sulfuric acid which contained 3.2×10^{-2} mole of nitric oxide, as calculated on the basis of the well-known reaction

[1] $$2HNOSO_4 + H_2O \rightarrow 2H_2SO_4 + NO + NO_2,$$

was then added slowly and under stirring to the mixture described above. The resulting yellow solution was slightly warmed and brought to a volume of 1 l, at 20 °C, and the "pernitrite" determined colorimetrically. The amounts of reactants were so chosen that a fairly uniform range of pH values (13.0–13.5) could be obtained after the reactants were mixed and brought to volume and to the temperature of 20 °C; similarly, the amount of ice used was so adjusted as to maintain the reacting mixture at low temperatures until the mixing was completed.

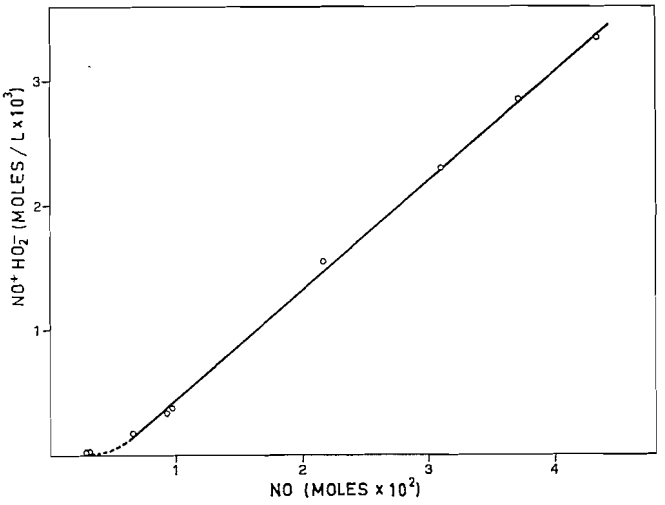


FIG. 1. Yield of "sodium pernitrite" upon addition of increasing aliquots of a nitrosyl-sulfuric acid solution in concentrated H_2SO_4 to 250 ml of NaOH at 50% containing 0.096 mole of H_2O_2. Solid line was fitted by least squares.

Figure 1 illustrates the formation, under our experimental conditions, of the "pernitrous" compound obtained when the reactants are mixed in different proportions; the process appears to be slightly inhibited at low values of NO, in agreement with previous observations by Rius and Foz (9), which indicate that decomposition of the peroxy-compound is favored by an excess of hydrogen peroxide. In fact, when 25 ml aliquots of nitrosyl-sulfuric acid solutions in concentrated H_2SO_4, containing a total of about 7×10^{-3} mole of NO, are oxidized with increasing amounts of H_2O_2 in the presence of NaOH and under conditions previously described, an increase of "pernitrite" formation is observed until the ratio of reactants $H_2O_2/NO = 10$ is arrived at; at this ratio the "pernitrous" compound reaches a concentration of 5×10^{-4} mole/l. A sharp decrease in the formation of the

Can. J. Chem. Downloaded from www.nrcresearchpress.com by 210.87.254.105 on 09/05/12
For personal use only.

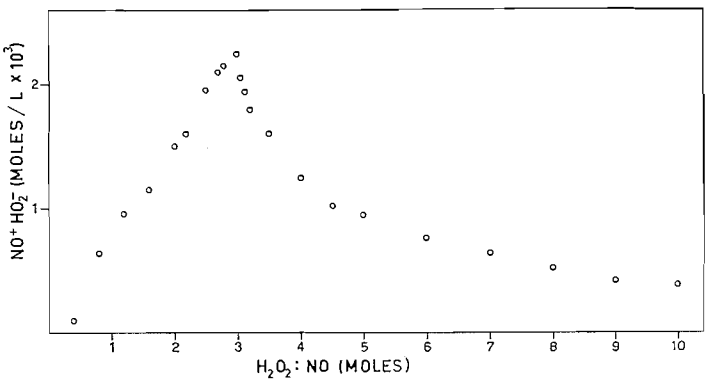


FIG. 2. Yield of "sodium pernitrite" upon reaction of a solution of nitrosyl-sulfuric acid in concentrated H_2SO_4 with alkaline hydrogen peroxide.

peroxy compound occurs as the amount of hydrogen peroxide is increased; yields of "pernitrite" are practically nil here at ratios over 35.

Figure 2 shows the result of a series of experiments which were carried out by Job's (10) method of "continuous variations"; varying amounts of hydrogen peroxide were mixed with solutions of nitrosyl-sulfuric acid under conditions analogous to those previously described except that the sum of H_2O_2 + NO was kept constant and equal to 1.26×10^{-1} mole/l. The sharp maximum in Fig. 2 suggests an optimum ratio of 3.0 for the coefficients in the overall reaction between hydrogen peroxide and components released according to eq. [1]. Changes in concentration of sodium sulfate, of solutions prepared, or the increase of the NaOH content by a factor of about 2 did not have any appreciable effect on the experimental values obtained.

In an extension of our previous work (4) which dealt with the formation of "pernitrite" during ultraviolet photolysis of alkaline nitrates in concentrated aqueous solutions, we found that substantial amounts of oxides of nitrogen (NO and NO_2) are liberated both during and after irradiation, and may be found in the gas carrier. The process can be monitored if the reaction is carried out under vigorous stirring in a closed vessel and in a fast current of nitrogen or oxygen, with unfiltered light obtained from a high-pressure mercury 450 W Hanovia immersion lamp. This result appears to us to be of some importance, in that it may extend similar reactions obtained during the radiolysis of nitric acid (11) and solutions of nitrates (12), where formation of the radical $NO_3^{\cdot}$ (see for example ref. 13 for further references) was reported, to the ultraviolet photolysis of nitrates dissolved in water. Furthermore, it appears to be relevant that this process occurs here at intensities of light which are less than those recently used by other workers for research on formation of $NO_3^{\cdot}$ in solution (14, 15). Since we have also found that formation of "pernitrite" and nitrite occurs when vapors of N_2O_5 carried in a stream of $O_2 + O_3$ and hence containing $NO_3^{\cdot}$ (16–21) are led into concentrated NaOH, it is thought that the process of "pernitrite" formation, under conditions discussed in this note, proceeds through and is due to steps which involve reactions of the transient $NO_3^{\cdot}$ radical in solution. Conversely, the acid nitrosyl peroxide $NO^+HO_2^-$ (Abel's formula for "pernitrous acid" (22)) appears to decompose, at suitable conditions, yielding $NO_3^{\cdot}$, which may be driven out of solution in a gas stream before its decomposition is completed.

We are grateful to Professor V. Caglioti for his interest in this work, and to Mr. C. Luttazzi for his technical help.

Can. J. Chem. Downloaded from www.nrcresearchpress.com by 210.87.254.105 on 09/05/12
For personal use only.

1. K. GLEU and R. HUBOLD. Z. Anorg. Allgem. Chem. **223**, 305 (1935).
2. E. HALFPENNY and P. L. ROBINSON. J. Chem. Soc. 928 (1952).
3. K. GLEU and E. ROELL. Z. Anorg. Allgem. Chem. **179**, 233 (1929).
4. H. M. PAPEE and G. L. PETRICONI. Nature, **204**, 142 (1964).
5. A. JOHNSON and A. P. LOCKETT. Proc. Chem. Soc. 218 (1960).
6. T. W. ZAWIDZKI, G. L. PETRICONI, and H. M. PAPEE. Nature, **207**, 262 (1965).
7. H. REMY. Treatise on inorganic chemistry. Vol. I. Elsevier Press, Inc., New York. 1965.
8. G. CHARLOT. Les méthodes de la chimie analytique. Masson et Cie, Paris. 1961.
9. A. RIUS and O. R. FOZ. Anales Real Soc. Espan. Fis. Quim. Madrid, Ser. B, **36**, 308 (1940).
10. P. JOB. Ann. Chim. Paris, **9**, 113 (1928).
11. A. ALLEN. Radiation chemistry of water and aqueous solutions. D. Van Nostrand Co., Inc., New York. 1961.
12. M. L. HYDE. J. Phys. Chem. **69**, 1858 (1965).
13. P. A. LEIGHTON. Photochemistry of air pollution. Academic Press, Inc., New York. 1961.
14. T. W. MARTIN, A. HENSHALL, and R. C. GROSS. J. Am. Chem. Soc. **85**, 113 (1963).
15. T. W. MARTIN, R. E. RUMMEL, and R. C. GROSS. J. Am. Chem. Soc. **86**, 2595 (1964).
16. T. M. LOWRY and R. V. SEDDON. J. Chem. Soc. 626 (1938).
17. J. H. SMITH and F. DANIELS. J. Am. Chem. Soc. **69**, 1735 (1947).
18. R. L. MILLS and H. S. JOHNSTON. J. Am. Chem. Soc. **73**, 938 (1951).
19. W. B. DE MORE and N. DAVIDSON. J. Am. Chem. Soc. **81**, 5869 (1959).
20. W. GUILLORY and H. S. JOHNSTON. J. Am. Chem. Soc. **85**, 1695 (1963).
21. W. GUILLORY and H. S. JOHNSTON. J. Chem. Phys. **42**, 2457 (1965).
22. E. ABEL. Monatsh. Chem. **83**, 1111 (1952).

RECEIVED NOVEMBER 24, 1965.
CENTRO NUCLEAZIONE AEROSOLI,
CONSIGLIO NAZIONALE DELLE RICERCHE
VIA VETTORE 4 (MONTE SACRO),
ROME, ITALY.

Can. J. Chem. Downloaded from www.nrcresearchpress.com by 210.87.254.105 on 09/05/12
For personal use only.

EVIDENCE FOR THE INFLUENCE OF TRACES OF HYDROGEN HALIDES IN HALOGEN EXCHANGE REACTIONS

MYRON J. RAND AND FREMONT REIZMAN

We have studied the kinetics of the halogen exchange between germanium tetrachloride and boron tribromide in the liquid phase at room temperature, with the $GeCl_4/BBr_3$ ratio about 10^3. Such anhydrous halide systems are of practical importance in the deposition of thin films of doped semiconductors or oxides from the vapor phase. Considerations of vapor pressure and thermodynamic stability may dictate the use of a mixed halide system, but if rapid halogen exchange occurs the low-concentration halide is essentially completely altered at equilibrium. It is thus difficult to maintain control of the dopant concentration in the reaction zone, to say nothing of the deposited film itself.

For sufficient sensitivity the progress of the exchange reaction was followed by long-path infrared spectrophotometry (1). With a 10 cm sample path 10^{-5} mole fraction boron tribromide in germanium tetrachloride can be detected, and concentration changes in the intermediates BBr_2Cl and $BBrCl_2$ may also be followed. The method permits measurement of the concentration of any component of the solution having absorption bands in the 2 to 10 μ range, including some common trace impurities detectable to a few parts per million. As a consequence it was discovered that the exchange mechanism is unexpectedly complicated. The nature of the reactions competing with direct exchange, which is the chief subject and purpose of this report, suggests that they are by no means unique to the system studied, and may indeed be rate-controlling in exchange reactions among moisture-sensitive halides.

1. K. GLEU and R. HUBOLD. Z. Anorg. Allgem. Chem. **223**, 305 (1935).
2. E. HALFPENNY and P. L. ROBINSON. J. Chem. Soc. 928 (1952).
3. K. GLEU and E. ROELL. Z. Anorg. Allgem. Chem. **179**, 233 (1929).
4. H. M. PAPEE and G. L. PETRICONI. Nature, **204**, 142 (1964).
5. A. JOHNSON and A. P. LOCKETT. Proc. Chem. Soc. 218 (1960).
6. T. W. ZAWIDZKI, G. L. PETRICONI, and H. M. PAPEE. Nature, **207**, 262 (1965).
7. H. REMY. Treatise on inorganic chemistry. Vol. I. Elsevier Press, Inc., New York. 1965.
8. G. CHARLOT. Les méthodes de la chimie analytique. Masson et Cie, Paris. 1961.
9. A. RIUS and O. R. FOZ. Anales Real Soc. Espan. Fis. Quim. Madrid, Ser. B, **36**, 308 (1940).
10. P. JOB. Ann. Chim. Paris, **9**, 113 (1928).
11. A. ALLEN. Radiation chemistry of water and aqueous solutions. D. Van Nostrand Co., Inc., New York. 1961.
12. M. L. HYDE. J. Phys. Chem. **69**, 1858 (1965).
13. P. A. LEIGHTON. Photochemistry of air pollution. Academic Press, Inc., New York. 1961.
14. T. W. MARTIN, A. HENSHALL, and R. C. GROSS. J. Am. Chem. Soc. **85**, 113 (1963).
15. T. W. MARTIN, R. E. RUMMEL, and R. C. GROSS. J. Am. Chem. Soc. **86**, 2595 (1964).
16. T. M. LOWRY and R. V. SEDDON. J. Chem. Soc. 626 (1938).
17. J. H. SMITH and F. DANIELS. J. Am. Chem. Soc. **69**, 1735 (1947).
18. R. L. MILLS and H. S. JOHNSTON. J. Am. Chem. Soc. **73**, 938 (1951).
19. W. B. DE MORE and N. DAVIDSON. J. Am. Chem. Soc. **81**, 5869 (1959).
20. W. GUILLORY and H. S. JOHNSTON. J. Am. Chem. Soc. **85**, 1695 (1963).
21. W. GUILLORY and H. S. JOHNSTON. J. Chem. Phys. **42**, 2457 (1965).
22. E. ABEL. Monatsh. Chem. **83**, 1111 (1952).

RECEIVED NOVEMBER 24, 1965.
CENTRO NUCLEAZIONE AEROSOLI,
CONSIGLIO NAZIONALE DELLE RICERCHE
VIA VETTORE 4 (MONTE SACRO),
ROME, ITALY.

Can. J. Chem. Downloaded from www.nrcresearchpress.com by 210.87.254.42 on 09/05/12
For personal use only.

EVIDENCE FOR THE INFLUENCE OF TRACES OF HYDROGEN HALIDES IN HALOGEN EXCHANGE REACTIONS

MYRON J. RAND AND FREMONT REIZMAN

We have studied the kinetics of the halogen exchange between germanium tetrachloride and boron tribromide in the liquid phase at room temperature, with the $GeCl_4/BBr_3$ ratio about 10^3. Such anhydrous halide systems are of practical importance in the deposition of thin films of doped semiconductors or oxides from the vapor phase. Considerations of vapor pressure and thermodynamic stability may dictate the use of a mixed halide system, but if rapid halogen exchange occurs the low-concentration halide is essentially completely altered at equilibrium. It is thus difficult to maintain control of the dopant concentration in the reaction zone, to say nothing of the deposited film itself.

For sufficient sensitivity the progress of the exchange reaction was followed by long-path infrared spectrophotometry (1). With a 10 cm sample path 10^{-5} mole fraction boron tribromide in germanium tetrachloride can be detected, and concentration changes in the intermediates BBr_2Cl and $BBrCl_2$ may also be followed. The method permits measurement of the concentration of any component of the solution having absorption bands in the 2 to 10 μ range, including some common trace impurities detectable to a few parts per million. As a consequence it was discovered that the exchange mechanism is unexpectedly complicated. The nature of the reactions competing with direct exchange, which is the chief subject and purpose of this report, suggests that they are by no means unique to the system studied, and may indeed be rate-controlling in exchange reactions among moisture-sensitive halides.

Can. J. Chem. Downloaded from www.nrcresearchpress.com by 210.87.254.42 on 09/05/12
For personal use only.

EXPERIMENTAL

Electronic-grade germanium tetrachloride (Sylvania Electric Products Co.) was distilled through a 15-valve Young column in a closed all-glass apparatus, with generous fore- and after-run fractions discarded. The still was continuously flushed with dry nitrogen. The receiver was the spectrophotometer cell, a 10 cm section of 30 mm outside diameter Pyrex tubing with end windows of Irtran-2 (Eastman Kodak Co.) sealed on with Araldite epoxy resin (Ciba Co.). Filler tubes near each end of the cell terminated in O-ring joints to which caps could be clamped tightly. Cell volume was about 50 cc. Cells were never entirely filled, in order that the contents could be mixed by rocking a gas bubble back and forth.

A Perkin–Elmer 221 spectrophotometer with a calcium fluoride prism was used to scan the range 2 to 9 μ. The reference beam was attenuated to produce a transmission reading near 90% in a region with no absorption bands. The spectrum of the pure germanium tetrachloride, as distilled, was taken first; there was no 2.76 μ absorption and only a trace of 3.5 μ absorption, and thus both hydroxyl and hydrogen chloride concentration were < 20 p.p.m. (1). The boron tribromide, from a freshly opened ampoule (Eagle–Picher Co.), was added under the surface of the germanium tetrachloride with a 50 μl syringe. Initial boron tribromide concentration was 0.132% by weight (0.00113 mole fraction). The reaction temperature was 24 ± 1 °C. Concentrations were followed for 150 h after mixing. The reaction vessel was the cell itself.

RESULTS

Addition of boron tribromide to germanium tetrachloride gave rise to many new absorption bands. The BBr_3 itself has several; the intermediate BBr_2Cl and $BBrCl_2$ became visible as exchange proceeded, and eventually also the bands of boron trichloride. ^{10}B–halogen (20%) and ^{11}B–halogen (80%) vibrations were easily separated. There were also two strong absorptions which could only be boron–oxygen vibrations from a hydrolysis product of boron halides. (It is impossible to keep the cell contents perfectly anhydrous, since there is slow moisture desorption from the O-ring seals or even from the glass itself. Boron tribromide is an excellent moisture scavenger, and the long-liquid-path technique is so sensitive that the minute but regularly increasing concentration of the hydrolysis product was easily seen. From its spectrum this substance is neither B_2O_3 nor H_3BO_3. It probably contains the B—O—B linkage.)

Assignment of absorption bands was made with the help of literature reports on the spectra of the boron mixed halides (2), boron trichloride (3), boron tribromide (4), and germanium tetrachloride (1). In addition the spectrum of boron trichloride (C. P. grade, Matheson Co.) dissolved in germanium tetrachloride was studied. Without exception it was found that the absorption maxima in germanium tetrachloride solution agreed closely with those reported for the pure liquid compounds, and were 0.06 to 0.10 μ higher than those for the pure vapors.

The 5 to 6.5 μ region shows the stepwise transformation of boron tribromide to boron trichloride most clearly. Spectrum changes at selected intervals are illustrated in Fig. 1.

Figure 2 summarizes concentration changes with time. The ordinate, log (I_0/I), is the absorbance, which is proportional to the concentration. Since the proportionality constant (the absorptivity) may differ for each boron species, Fig. 2 cannot be used to compare concentrations of different compounds, but it does show the relative amount of a given compound present at any time. It is evident that an exchange does occur, since boron tribromide is converted slowly to boron trichloride via BBr_2Cl and $BBrCl_2$ intermediates. But the mechanism is not solely direct exchange: HCl and HBr are involved.

DISCUSSION

If the exchange proceeded by consecutive replacements of bromine atoms, the first step, the disappearance of boron tribromide, would be pseudounimolecular and first order kinetically because of the overwhelming excess of $GeCl_4$. Thus a plot of absorbance versus time would not be linear. In fact, Fig. 2 shows a linear decrease of boron tribromide

Can. J. Chem. Downloaded from www.nrcresearchpress.com by 210.87.254.42 on 09/05/12
For personal use only.

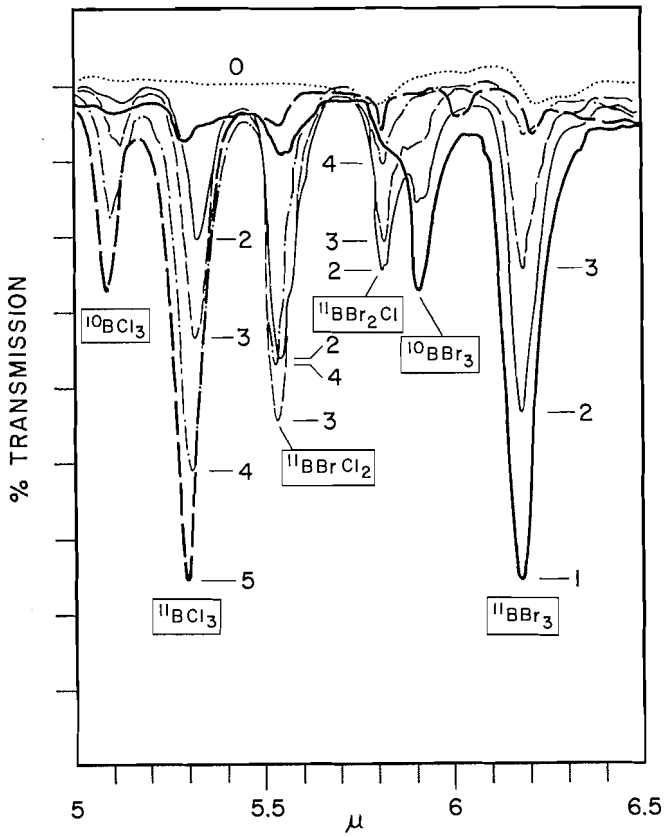


FIG. 1. Typical spectra during the reaction $GeCl_4 + BBr_3$ (1 130 p.p.m. B/Ge).

CURVE	SYMBOL	SAMPLE
0	.....	$GeCl_4$, as distilled into cell
1	———	0.15 h after mixing
2	———	29.7 h after mixing
3	— —	45.5 h after mixing
4	— · —	53.5 h after mixing
5	— —	69.7 h after mixing

concentration with time throughout. The reaction velocity is therefore independent of the reactant concentration and kinetically the reaction is of zero order. This unusual result suggests that the rate is actually determined by the amount of some catalyst present. Furthermore, a direct exchange model does not give the observed initial slopes for the intermediates, and cannot account for their rather rapid decay after slower buildup. Finally, this model has no provision at all for the behavior of HCl and HBr. While direct $GeCl_4$—BBr_3 exchange cannot be ruled out, it is certainly not the only process occurring and probably not even the dominant one.

In the "catalytic" mechanism we propose, a trace of HCl arises from

[1] $$GeCl_4 + H_2O \rightleftarrows Ge(OH)Cl_3 + HCl$$

and is the intermediary which transfers chlorine from $GeCl_4$ to BBr_3. The HCl is converted to HBr by

[2] $$BBr_3 + HCl \overset{k_1}{\rightleftarrows} BBr_2Cl + HBr$$

[3] $$BBr_2Cl + HCl \overset{k_2}{\rightleftarrows} BBrCl_2 + HBr$$

[4] $$BBrCl_2 + HCl \overset{k_3}{\rightleftarrows} BCl_3 + HBr.$$

The HBr in turn exchanges with $GeCl_4$ to regenerate the HCl by

[5] $$HBr + GeCl_4 \overset{k_4}{\rightleftarrows} HCl + GeBrCl_3$$

and the cycle continues until all the BBr_3 has been converted to BCl_3. Finally any HBr reverts to HCl and reaction ceases with the original amount of HCl (which may be very small) still present.

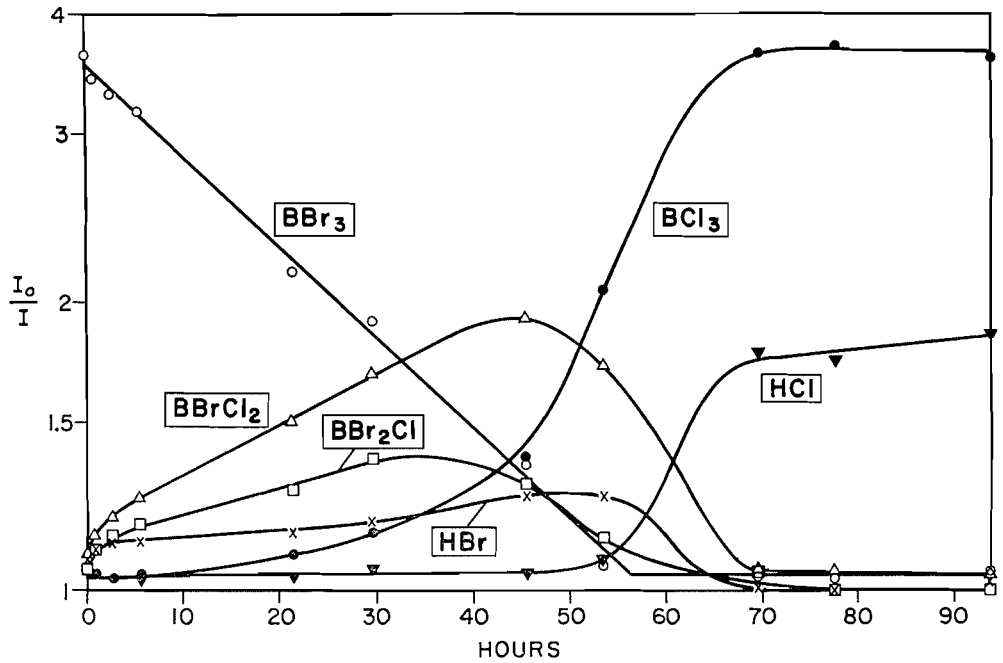


FIG. 2. Concentration changes with time. The absorption bands are: (○) $^{11}BBr_3$ ($2\nu_3$), 6.18 μ; (□) $^{11}BBr_2Cl$ ($\nu_1 + \nu_4$), 5.82 μ; (△) $^{11}BBrCl_2$ ($\nu_1 + \nu_4$), 5.55 μ; (●) $^{11}BCl_3$ ($2\nu_3$), 5.30 μ; (▼) HCl, 3.53 μ; and (×) HBr, 3.98 μ.

Rate equations were written for reactions [1]–[5], and $[HCl]_{init}$ and the four k's varied in an attempt to obtain the best fit to the experimental results. The calculated concentration curves were generated by an iterative numerical integration procedure with an IBM 1620 computer. It was soon discovered that one slight refinement to the model was advantageous. The clue is seen in the behavior of HCl in Fig. 2: the concentration continues to rise slowly after all reaction is completed. This suggests a slow, continuous injection of HCl, due perhaps to desorption of moisture from the rubber O-ring seals. Confirmation of adventitious moisture contamination is easily obtained by a blank run in which pure $GeCl_4$ is allowed to stand in the reaction cell for many days. The spectrum soon develops hydroxyl absorption which strengthens slowly and steadily. This feature was allowed for simply by adding a constant term to the equation for d[HCl]/dt, the value chosen to give the proper final slope to the HCl curve. This small correction produced a significantly better fit in the curves for both intermediates and those for BBr_3 and HBr as well.

Can. J. Chem. Downloaded from www.nrcresearchpress.com by 210.87.254.42 on 09/05/12
For personal use only.

Even with the assumption $k_1 = k_2 = k_3 = k_4$, the HCl-exchange model is able to reproduce closely many features of the experimental curves. The initial transients, the shapes and positions of maxima of the curves for the intermediates, and the shapes of the HCl and HBr curves are all accounted for. The curve for BBr_3 concentration is still not linear, but it is much more nearly so than is the exponential decay predicted by the direct $GeCl_4$—BBr_3 exchange model.

The success of the "catalytic" exchange model, together with the very low steady-state concentration of HCl, suggests that the HCl—BBr_3 reaction is rapid compared with $GeCl_4$—BBr_3, a thermodynamically and kinetically credible hypothesis.

The importance of hydrogen chloride in the exchange was demonstrated experimentally with a sample of $GeCl_4$ which had been exposed to the atmosphere: both hydroxyl and HCl contamination developed by reaction [1]. From the spectrum the HCl concentration was of the order of 100 p.p.m. Eight minutes after adding 0.1% BBr_3 the HCl content was only a fifth of its original value, and HBr had appeared prominently in the spectrum.

To support the proposed mechanism the effect of varying the initial concentration of hydrogen chloride should be studied. For convenient reaction speeds, however, the preparation and analysis of $GeCl_4$ with only a few p.p.m. HCl are required; the experimental difficulties became prohibitive.

Moisture contamination of the mixed halide system ultimately results in highly selective hydrolysis. After the 0.1% BBr_3 addition in the experiment described above, the hydroxyl band (2.76 μ) had disappeared, and strong B—O absorption developed near 7.7 μ. This reaction is believed to be

[6] $$Ge(OH)Cl_3 + BBr_3 \rightarrow GeBrCl_3 + \text{hydrolysis product } (+ HBr?)$$

so that [6] competes with [2] for the removal of BBr_3, and is evidently rapid. When germanium tetrachloride containing 1 000 p.p.m. of either boron tribromide or boron trichloride was gassed with wet nitrogen, the boron halide absorption bands completely disappeared in a few minutes.

It has not been possible to find a single mechanism which will exactly reproduce all the features illustrated in Fig. 2. The evidence is nevertheless very strong that halogen exchange between metal halides may proceed rapidly via hydrogen halide intermediates, thus masking the true exchange rate, if any. These catalysts are effective in amounts so minute that conventional purification and handling techniques may not be adequate to exclude the moisture responsible for their presence. Furthermore, one halide may be preferentially hydrolyzed (as is boron tribromide in germanium tetrachloride) so that small amounts of moisture will have a disproportionately large effect on its concentration.

ACKNOWLEDGMENT

We acknowledge with thanks the helpful comments of Ernest M. Grunwald on the reaction mechanism. The computations were programmed and carried out by Mrs. F. P. Crabtree.

1. M. J. Rand. Anal. Chem. **35**, 2126 (1963).
2. L. P. Lindeman and M. K. Wilson. J. Chem. Phys. **24**, 242 (1956).
3. R. E. Scruby, J. R. Lacher, and J. D. Park. J. Chem. Phys. **19**, 386 (1951). J. R. Lacher, R. E. Scruby, and J. D. Park. J. Am. Chem. Soc. **74**, 5292 (1952).
4. T. Wentink, Jr. and V. H. Tiensuu. J. Chem. Phys. **28**, 826 (1958).

Received October 14, 1965.
Bell Telephone Laboratories, Inc.,
Allentown, Pennsylvania.

Can. J. Chem. Downloaded from www.nrcresearchpress.com by 210.87.254.42 on 09/05/12
For personal use only.

p 925-996

Canadian Journal of Chemistry

Issued by THE NATIONAL RESEARCH COUNCIL OF CANADA

VOLUME 44 MAY 1, 1966 NUMBER 9

Can. J. Chem. Downloaded from www.nrcresearchpress.com by 210.87.254.6 on 09/05/12
For personal use only.

THE OXIDATION OF PHENOLS

III. THE STOICHIOMETRIES FOR THE OXIDATION OF SOME SUBSTITUTED PHENOLS WITH PEROXY RADICALS[1]

E. C. HORSWILL, J. A. HOWARD, AND K. U. INGOLD

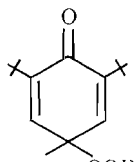
Division of Applied Chemistry, National Research Council, Ottawa, Canada

Received November 29, 1965

ABSTRACT

The stoichiometries for the oxidation of some substituted phenols with cumyl peroxy radicals at 65 °C have been measured. The results can be correlated generally with the expected phenolic oxidation products. Phenols with one or two unsubstituted ortho positions can react with more than 2 peroxy radicals per molecule. A maximum stoichiometry of 2.6 peroxy radicals was obtained with 2,4-dimethylphenol. 2,4,6-Tri-substituted phenols generally have stoichiometric factors of 2.0 or less.

It has been shown by previous workers that the oxidation of 2,6-di-*t*-butyl-4-methylphenol (BMP) with peroxy radicals requires either 2 or 3 radicals per molecule of phenol depending on whether the product is a peroxycyclohexadienone (I) (stoichiometric factor (n) = 2.0) or a stilbenequinone (n = 3.0).[2] The nature of the product depends

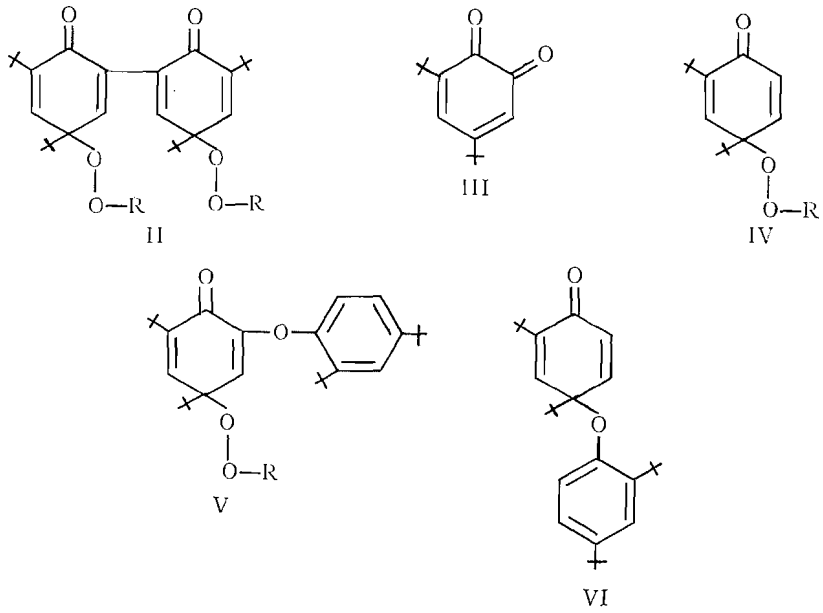


I

on the attacking peroxy radical and, probably, also on the temperature and the particular method used for the oxidation. The identification of alkyl benzoquinones and diphenoquinones as the main products formed in the oxidation of 2,6-dialkylphenols under conditions which give the peroxycyclohexadienone from BMP (1) suggests that these phenols will react with just 2 peroxy radicals per molecule. In contrast, the various fully oxidized products from 2,4-di-*t*-butylphenol (see part II in this series (2)) imply specific stoichiometric factors of 3 (compound II) and 2 (compounds III, IV, and V), whereas a simple phenoxy radical dimer (e.g. VI) would give a n value of only 1.0.

[1]*Issued as N.R.C. No. 8879.*

[2]*See part I in this series (1) for a full discussion of the previous work.*



The relative yields of the different products obviously depend on the radical concentrations and on the relative rates of the numerous radical–radical coupling reactions. The measured value of n must therefore depend on the experimental conditions. The present work, which covers a wide variety of substituted phenols, was undertaken to investigate the effect of structure on n, since this is of obvious importance in the evaluation of oxidation inhibitors. That is, both a fast reaction with peroxy radicals and a high molar efficiency are among the more important properties of a commercial antioxidant.

EXPERIMENTAL

The stoichiometries of the phenols were determined at 65 °C by the induction-period method of Boozer *et al.* (3). Pure, undiluted cumene (Phillips research grade) was generally used as the oxidizable substrate since even weak inhibitors produce quite sharp breaks in the oxygen absorption curves (4). The cumene was passed through alumina immediately before use. α,α'-Azo-bis-isobutyronitrile (AIBN) was used as the initiator at a concentration of 2.86×10^{-2} mole/l. All the phenols were carefully purified, and were generally used at a concentration of about 2.4×10^{-3} mole/l.

RESULTS AND DISCUSSION

Inhibitor stoichiometries determined by the induction-period method show variations with both the nature of the oxidizable substrate (5) and the solvent (5–7) which so far remain largely unexplained. For example, in highly polar solvents such as acetonitrile and nitromethane the usual assumption that $n = 2$ for BMP[3] would sometimes lead to the conclusion that the rate of radical production by AIBN is more than twice its rate of decomposition (6, 7). However, under a standard set of conditions in a relatively nonpolar medium (i.e. pure cumene) the induction periods for different phenols should be directly comparable. With the experimental conditions employed in this work the induction period for BMP (2.40×10^{-3} mole/l) was 8 420 s. This implies that the efficiency (e) of chain initiation from the AIBN is 0.55, provided $n = 2.0$ for BMP. The basis for this assumption was checked by measuring the yields of the isobutyronitrile peroxy and cumyl peroxy

[3]*See ref. 1 and references therein for a discussion of the experimental basis for this assumption.*

435705

Can. J. Chem. Downloaded from www.nrcresearchpress.com by 210.87.254.6 on 09/05/12
For personal use only.

derivatives of BMP, i.e. I with R = $(CH_3)_2CCN$ (hereafter referred to as IBN-1) and with R = $C_6H_5C(CH_3)_2$ (hereafter referred to as CUM-1). The analysis of compounds of this type by thin-layer chromatography has been described previously (1).

The cumene was oxidized for 9 250 s, at which point 1.5×10^{-2} mole O_2/l had been absorbed. The yields of the two products (based on the initial BMP concentration) were 21 ± 4%[4] for IBN-1 and 53 ± 9%[4] for CUM-1. Similar results were also obtained for solutions of cumene in *n*-heptane, *t*-butanol, and acetonitrile (Table I). The overall yield of compounds with structure I is similar to the previously determined yield of IBN-1 in chlorobenzene, i.e. 62–71%[5] (1), but is somewhat less than the value of 95 ± 10% found for tetralin at 40 °C (1). The difference does not seem to be due to the decomposition of IBN-1 or CUM-1 during the reaction, since both compounds were quite stable at 65° for 16 h in toluene containing both the usual concentration of AIBN and 0.2 mole of cumene hydroperoxide/l. The different yields might, however, be due to the fact that a hydrogen atom is much less readily abstracted from cumene than from tetralin. This factor might also be responsible for the measured difference in the initiation efficiencies in the two hydrocarbons (i.e. 0.55 in cumene and 0.64 in tetralin).

TABLE I

Induction periods and product yields at 65 °C ([AIBN] = 2.86×10^{-2} mole/l, [BMP] = 2.40×10^{-3} mole/l)

Solvent	Cumene concentration (moles/l)	Induction period (s)	Product yield (%)		
			IBN-1	CUM-1	Total
n-Heptane	3.6	9 050	16	52	68
None	7.2	8 420	21	53	74
t-Butanol	3.6	7 750	15	63	78
CH_3CN	3.6	5 900	15	54	69

The expected yields of IBN-1 and CUM-1 can be calculated by comparing the rate of chain initiation ($2ek_1$[AIBN] = 5.7×10^{-7} mole/l s) with the amount of oxygen absorbed by the end of the induction period (1), i.e. about 3×10^{-3} mole/l. If the rate of chain initiation equals the rate of production of isobutyronitrile peroxy radicals, then $8\,420 \times 5.7 \times 10^{-7} = 5 \times 10^{-3}$ mole of these radicals/l will have been formed in this time. The calculated yields are therefore roughly $\frac{5}{8}$ (~60%) IBN-1 and $\frac{3}{8}$ (~40%) CUM-1. The measured yield of IBN-1 is therefore much less than that predicted. The present results support our previous suggestion that isobutyronitrile peroxy radicals are not the only radicals initiating oxidation chains in systems of this type (1).

The phenol stoichiometries which are given in Tables II and III have been calculated with the assumption that $n = 2.0$ for BMP, since the yields of CUM-1 and IBN-1 indicate that it cannot differ significantly from this figure. A value of $n < 1.9$ or $n > 2.1$ indicates a significant change in the usual stoichiometry, since the induction periods were reproducible to better than 5%. The present results can be compared with the stoichiometries reported by Boozer *et al.* (3) for the following phenols in a cumene (2 ml) – chlorobenzene (4 ml) mixture at 62.5 °C: phenol and 4-*t*-butylcatechol, 2.0; *o*- and *p*-cresol, 2.2; 2,5-di-*t*-butylhydroquinone, 0.85; β-naphthol, 2.1.

[4]*95% confidence limits. These results are the average of three determinations for each of two separate experiments.*

[5]*This value is probably about 10–20% too low, as some of the IBN-1 may have been pumped off along with the chlorobenzene. A repeat of this experiment in* CCl_4 *(which was removed with a water pump after the reaction was complete) gave a yield of 80% of IBN-1. In the present work, the cumene was pumped off at 0 °C since blank experiments showed that no IBN-1 or CUM-1 was lost under these conditions.*

Can. J. Chem. Downloaded from www.nrcresearchpress.com by 210.87.254.6 on 09/05/12
For personal use only.

TABLE II

Phenol stoichiometries

Para substituents	Ortho substituents						
	None	2-Methyl	2,6-Dimethyl	2-*t*-Butyl	2,6-Di-*t*-butyl	2-Methyl-6-*t*-butyl	2-Hydroxy
None	2.1*	2.1*	2.0	2.1*	2.0*	1.9	2.3‡
Methyl	2.5*	2.6*	2.2	2.4	2.0§	2.0*	
t-Butyl	2.3†	1.9*		2.3†	1.8	1.5*	2.2*
Methoxy	2.0			2.1	2.1		
Hydroxy	1.8*			1.1*			
Chloro	1.7‡	1.7*	1.3*		1.0		
Cyano	—‖		1.7‡	—‖	2.2		

*Final rate is 85–94% of the calculated uninhibited rate.
†Final rate is 75–84% of the calculated uninhibited rate.
‡Final rate is 65–74% of the calculated uninhibited rate.
§By definition.
‖Stoichiometric factor could not be determined.

TABLE III

Phenol stoichiometries

Compound	Stoichiometry
Resorcinol	2.0*
3,5-Di-*t*-butylcatechol	2.0
2,5-Di-*t*-butylhydroquinone	—‡
2,5-Di-*t*-butyl-4-methoxyphenol	1.8
2-Methoxy-4-methylphenol	1.3*
2,6-Dimethoxyphenol	1.4
α-Naphthol	2.0†
β-Naphthol	1.8*
Propyl gallate	2.0§
Pyrogallol	2.5
Nordihydroguaiaretic acid‖	2.3¶
Compound VIII	1.4¶
Compound IX	1.4*

*Final rate is 85–94% of the calculated uninhibited rate.
†Final rate is 65–74% of the calculated uninhibited rate.
‡Stoichiometric factor could not be determined.
§See text and Fig. 1.
‖2,3-Dimethyl-1,4-bis(3,4-dihydroxyphenyl)butane.
¶Per ring.

Stoichiometric factors of 2.0 for the 2,6-dialkylphenols are not unexpected in view of the importance of benzoquinones and diphenoquinones in the products from these phenols (1). Rather surprisingly, the n factors are also quite close to 2.0 for many other compounds, such as 2-alkylphenols, resorcinol, 3,5-di-*t*-butylcatechol, *α*-naphthol, 4-methoxyphenol, and even phenol itself. The 2,4-dialkylphenols have the largest n factors, which suggests that *o*,*o*′-phenoxy radical coupling (leading to products similar to II) is important in nearly all these compounds. However, it is clear that an unsubstituted ortho position does not, in itself, insure that $n > 2.0$.

It can be seen from Table II that a *t*-butyl group in the para position is less effective than a methyl group. This phenomenon is also generally true of the inhibiting power of 2,4-di- and 2,4,6-tri-alkylphenols (8), and we have shown that it can be attributed to a combination of polar (9, 10) and steric (10) factors. In the case of 2,4,6-tri-*t*-butylphenol, the low n factor suggests that some of the initially formed phenoxy radicals couple through a molecule of oxygen to give bis-(1,3,5-tri-*t*-butyl-2,5-cyclohexadien-4-one) peroxide (cf. ref. 11).

The three phenols listed in Table II which contain a 4-methoxy group all have n factors

Can. J. Chem. Downloaded from www.nrcresearchpress.com by 210.87.254.6 on 09/05/12
For personal use only.

Can. J. Chem. Downloaded from www.nrcresearchpress.com by 210.87.254.6 on 09/05/12
For personal use only.

of about 2.0. This result emphasizes the difference between the n factor and the rate of the primary inhibition step, in which the phenolic hydrogen atom is abstracted since the p-methoxy group is highly activating for abstraction (9). In the ortho position the methoxy group reduces n to 1.3–1.4, a reduction which is probably connected with the strong internal hydrogen bond in these phenols. In contrast, catechol and 4-t-butylcatechol, which have a free OH group as well as an internal hydrogen bond, have n factors of 2.2–2.3 (see also nordihydroguaiaretic acid). With regard to catechol itself, the primary induction period, during which a negligible quantity of oxygen is absorbed, is followed by a period of retardation, during which oxygen is absorbed at a rate which is only 70% of the expected rate. This implies that one or more of the catechol oxidation products can also react with peroxy radicals, but at a very much lower rate than most phenols. Relatively low rates after the induction period were also observed with several other phenols, as is noted in Tables II and III.[6] Propyl gallate, a commonly used food antioxidant, is of particular interest in this respect. Its oxygen absorption curve is shown in Fig. 1. The initial induction period corresponds to a n factor of 2.0, but the rate after this point is only 15% of the expected rate. A second break occurs at $n = 3.0$, and the rate then rises to its uninhibited value. This general type of behavior has previously been reported by Boozer *et al.* for 2,5-di-t-butylhydroquinone in a mixture of cumene and chlorobenzene (3), and for 4-t-butylcatechol in a mixture of 1-methylcyclohexene, 2,2,4-trimethylpentene-1, and chlorobenzene (5). In both cases there were two stages to the inhibition, the first break occurring with a n factor of about 1.0. Under our conditions, the n factor of 4-t-butylcatechol was 2.2, and that of 2,5-di-t-butylhydroquinone could not be determined since the compound did not show any sharp break in its oxygen absorption curve. Both hydroquinone and 2-t-butylhydroquinone had low n factors. The low value for the latter compound (i.e. 1.1) cannot be due to the formation of an unreactive quinhydrone, since the addition of an equimolar concentration of 2-t-butyl-p-benzoquinone did not affect the stoichiometric factor of the 2-t-butylhydroquinone.

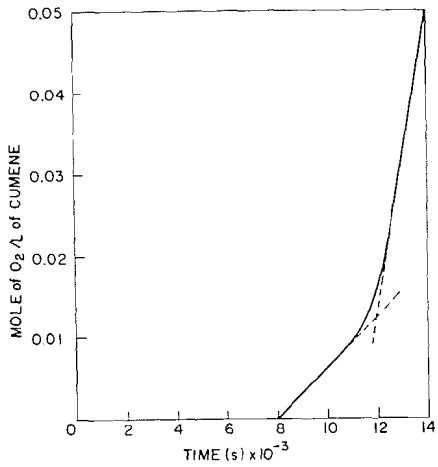


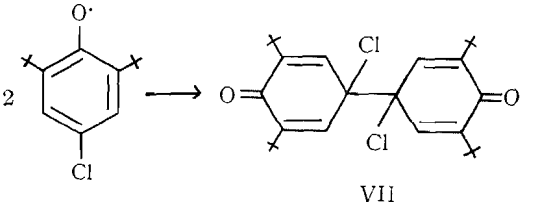
FIG. 1. Oxygen absorption by cumene containing 2.27×10^{-3} mole propyl gallate/l and 2.86×10^{-2} mole AIBN/l.

[6]*A referee has suggested that this retardation after the induction period may be connected with the formation of quinones by the beta cleavage of labile 4-substituents from 4-substituted-4-peroxy-2,5-cyclohexadien-1-ones. Most benzoquinones are retarders of autoxidation.*

Can. J. Chem. Downloaded from www.nrcresearchpress.com by 210.87.254.6 on 09/05/12
For personal use only.

Very weak inhibitors such as 4-cyanophenol and its 2-*t*-butyl derivative gave oxygen absorption curves in which the rate increased smoothly with time, thereby preventing any determination of the stoichiometric factor. Slightly stronger inhibitors, such as phenol itself, allowed oxidation to occur at a significant rate from the start of the reaction but showed a definite break after a certain time. In these cases, the induction period was taken to be the time at which a linear extrapolation of the initial and final portions of the oxygen absorption curve intersected (3).[7] In addition to phenol, the following compounds allowed a noticeable initial rate of oxygen absorption: 2-methylphenol, 2-*t*-butylphenol, 4-*t*-butylphenol, 4-chlorophenol, 2-methyl-4-chlorophenol, 2,6-dimethyl-4-chlorophenol, 2,6-di-*t*-butyl-4-chlorophenol, 2,6-dimethyl-4-cyanophenol, 2,6-di-*t*-butyl-4-cyanophenol, 3-hydroxyphenol, 2-methoxy-4-methylphenol, 2,6-dimethoxyphenol, β-naphthol, and compound IX.

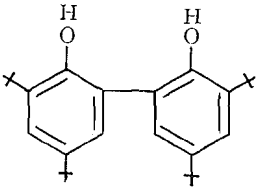
The *n* factor of 1.0 for 2,6-di-*t*-butyl-4-chlorophenol can probably be attributed to phenoxy radical coupling to give bis-(1-chloro-3,5-di-*t*-butyl-4-oxo-2,5-cyclohexadienyl-1).



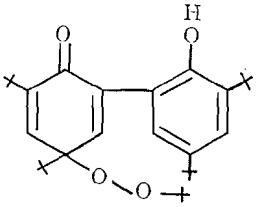
VII

This relatively stable product is easily formed from the starting phenol by oxidation with sodium ferricyanide, or from the 2,4,6-tri-*t*-butyl phenoxy radical (13). We have previously observed a similar stoichiometry in the oxidation of this phenol with *t*-butoxy radicals in CCl_4 at 122 °C (14). The fact that the other *p*-chlorophenols have low *n* factors suggests that similar products may also be formed from these compounds.

The two dimeric phenolic oxidation products prepared by the oxidation of 2,4-di-*t*-butylphenol with *t*-butyl peroxy radicals (2), i.e. compounds VIII and IX, probably



VIII



IX

owe their low *n* factors both to the steric effect of the *t*-butyl groups in the para position and to the internal hydrogen bonding of the phenolic hydrogens (2).

After this work was completed, a paper by Lloyd and Zimmerman (15) appeared which described the measurement of the induction periods in the uninitiated oxidation of cumene at higher temperatures (110–160 °C) produced by several phenols that we had also studied. The relative inhibitor stoichiometries found by these workers differ quite markedly from the values given in Table II. This is hardly surprising in view of the expected instability

[7]*This type of curve is also obtained with a strong inhibitor in a readily oxidizable substrate, e.g. styrene (12).*

at high temperatures of peroxidic products similar to I, II, IV, V, and IX. For those phenols common to both studies the following stoichiometries were obtained at 132 °C: BMP, 2.0 (assumed); 2,4-dimethyl-6-*t*-butylphenol, 4.0; 2,4,6-trimethylphenol, 3.0; 2-hydroxy-4-*t*-butylphenol, 1.7; 2-methyl-4-*t*-butylphenol, 1.6; pyrogallol, 1.5; and hydroquinone, 1.0.

REFERENCES

1. E. C. HORSWILL and K. U. INGOLD. Can. J. Chem. **44**, 263 (1965).
2. E. C. HORSWILL and K. U. INGOLD. Can. J. Chem. **44**, 269 (1965).
3. C. E. BOOZER, G. S. HAMMOND, C. E. HAMILTON, and J. N. SEN. J. Am. Chem. Soc. **77**, 3233 (1955).
4. D. V. GARDNER, J. A. HOWARD, and K. U. INGOLD. Can. J. Chem. **42**, 2847 (1964).
5. C. E. BOOZER, G. S. HAMMOND, C. E. HAMILTON, and C. PETERSON. J. Am. Chem. Soc. **77**, 3380 (1955).
6. J. A. HOWARD and K. U. INGOLD. Can. J. Chem. **42**, 1044 (1964).
7. D. G. HENDRY and G. A. RUSSELL. J. Am. Chem. Soc. **86**, 2368 (1964).
8. A. C. NIXON. *In* Autoxidation and antioxidants. Vol. II. *Edited by* W. O. Lundberg. Interscience Publishers, Inc., New York. 1962. Chap. 17. p. 728.
9. J. A. HOWARD and K. U. INGOLD. Can. J. Chem. **41**, 1744 (1963); **41**, 2800 (1963).
10. K. U. INGOLD. J. Phys. Chem. **64**, 1636 (1960).
11. G. M. COPPINGER. J. Am. Chem. Soc. **86**, 4385 (1964).
12. J. A. HOWARD and K. U. INGOLD. Can. J. Chem. **40**, 1851 (1962).
13. K. LEY, E. MÜLLER, R. MAYER, and K. SCHEFFLER. Ber. **91**, 2670 (1958).
14. K. U. INGOLD. Can. J. Chem. **41**, 2816 (1963).
15. W. G. LLOYD and R. G. ZIMMERMAN. Ind. Eng. Chem. Prod. Res. Develop. **4**, 180 (1965).

Can. J. Chem. Downloaded from www.nrcresearchpress.com by 210.87.254.6 on 09/05/12
For personal use only.

Can. J. Chem. Downloaded from www.nrcresearchpress.com by 210.87.254.42 on 09/05/12
For personal use only.

EXOCELLULAR ALGINIC ACID FROM AZOTOBACTER VINELANDII[1]

P. A. J. GORIN AND J. F. T. SPENCER
National Research Council of Canada, Prairie Regional Laboratory, Saskatoon, Saskatchewan

Received December 7, 1965

ABSTRACT

Azotobacter vinelandii produces a partly acetylated exocellular polysaccharide which consists mainly of D-mannuronic acid units and a small proportion of L-guluronic acid units. It resembles alginic acid since it contains 4-*O*-linked mannuronosyl residues and guluronosyl residues which are 4-*O*- and (or) 5-*O*-linked. The specific rotation of bacterial sodium alginate is close to that of its algal counterpart, thus suggesting that the glycosidic configurations are similar.

Several species of *Azotobacter* are known to form capsules, and some produce exocellular polysaccharides. Parikh and Jones have isolated exocellular polysaccharides from *Azotobacter indicum* and, after fractionation, obtained an acidic component which consisted predominantly of *O*-D-glucopyranuronosyl-(1 → 3)-*O*-D-glucopyranosyl-(1 → 2)-*O*-D-glycero-D-mannoheptopyranosyl repeating units (1). The capsular polysaccharides of *Azotobacter chroococcum* were isolated by Lawson and Stacey (2) and methylated, and a neutral portion of the methylated polysaccharide was hydrolyzed to 2,3,6- and 2,4,6-tri-*O*-methyl-D-glucose, 2,3-di-*O*-methyl-D-glucose, and 2,4,6-tri-*O*-methyl-D-galactose. From an acidic methylated polysaccharide fraction 2,4,6-tri-*O*-methyl-D-glucose, 2,3-di-*O*-methyl-D-glucuronic acid, and a partly methylated glucose derivative were obtained. These two methylated fragments were also obtained from the acidic exocellular polysaccharide of *Azotobacter indicum*, thus suggesting that the two acidic polysaccharides may be similar in structure.

These acidic polysaccharides differ from those formed exocellularly by *Azotobacter vinelandii*. Cohen and Johnstone reported that hydrolysis in aqueous acid gave rise to galacturonic acid, smaller amounts of D-glucose and rhamnose, and possibly a trace of mannuronolactone (3). Another component was later characterized by Claus as 2-*keto*-3-deoxygalactonic acid (4). A closely related *Azotobacter* species, *A. agilis*, did not produce exocellular slime, and it was concluded that this difference strengthened the designation of two distinct species, *A. agilis* and *A. vinelandii* (5). The composition of the capsule of *A. agilis* was different from that of the exocellular polysaccharide of *A. vinelandii* and contained galactose and rhamnose units and a thiobarbituric acid positive moiety (5). The structure of a possible exocellular polygalacturonide formed by *A. vinelandii* was of interest and required further investigation.

A. vinelandii was grown on Burk's medium, and produced exocellular polysaccharides which were isolated by precipitation with ethanol. Hydrolysis of the precipitate with hot aqueous acid gave hexuronic acid and smaller amounts of glucose, arabinose, ribose, and rhamnose on paper chromatograms. This hydrolysis pattern suggested that a polysaccharide consisting exclusively of hexuronic acid residues was present; purification was effected by precipitation from the concentrated culture filtrate by acidification with hydrochloric acid. The polyuronide was soluble in dilute aqueous sodium hydroxide and had a saponification equivalent of 152 compared with 176 required for a hexuronic acid polymer. This discrepancy was explained on examination of a solution of the polysaccharide in

[1]*Issued as N.R.C. No. 8882.*

deuterium oxide containing sodium deuteriooxide by nuclear magnetic resonance spectroscopy. A well-defined uncoupled C-methyl signal was obtained which corresponded to sodium acetate; this assignment was confirmed by preparation of S-benzyl thiouronium acetate after saponification. Based on a C-methyl analysis the polyuronide contained one acetyl group per 5.2 anhydrohexuronic acid units. Cohen and Johnstone report that exocellular polysaccharides of some strains of *A. vinelandii* contain *O*-acetyl groups (3).

The polyuronide, although not readily soluble in hot aqueous acid, could be hydrolyzed with aqueous acid after solubilization and partial degradation with 80% sulfuric acid (6). Examination of the product by paper electrophoresis in borate according to the method of Haug and Larsen (7) showed the presence of mannuronic acid and a trace of guluronic acid.[2] More evidence for two hexuronic acid components was obtained by methanolyzing the polyuronide to methyl ester methyl glycosides. These were reduced with sodium borohydride to methyl hexosides, which were hydrolyzed to mannose and a trace of gulose. Sodium borohydride reduction of the mixed hexoses gave polyols, which were acetylated to mannitol, and sorbitol hexaacetates which were present in the ratio of 11 to 1 as shown by gas–liquid chromatography (g.l.c.). Fractional crystallization of the mixture gave D-mannitol hexaacetate, which arose from mannuronic acid units in the polysaccharide.

Information on the configuration of the guluronic acid moieties at C-5 and the positions of the glycosidic linkages in the polyuronide was obtained by periodate oxidation studies. Oxidation kinetics were studied at 4° on a solution that was prepared by dissolution of the partly acetylated natural product in dilute alkali followed by adjustment of the pH to 3.7. These conditions were similar to those used by Drummond *et al.* (10), who observed that alginic acid from *Laminaria digitata* was oxidized rapidly in the initial stages. The bacterial polysaccharide rapidly consumed 0.46 mole of oxidant/sugar unit and was oxidized slowly thereafter (Table I). The uptake of periodate was only fractionally less than that for alginic acid. In a larger scale experiment the deacetylated bacterial polysaccharide was oxidized with periodate for 24 h at room temperature, and the product reduced with sodium borohydride to a polyalcohol. This was hydrolyzed to give mannuronic acid, D-erythrono-γ-lactone, and threonolactone. Erythrono-γ-lactone was isolated as crystals, and L-threonolactone was converted into a crystalline phenylhydrazide. Isolation of the L-isomer showed that the guluronic acid units have the L-configuration and are glycosidically linked in the 4- and (or) 5-positions. Similarly, the isolation of erythrono-γ-lactone shows that the oxidized mannuronosyl units are 4-*O*- and (or) 5-*O*-linked.

The immunity to oxidation of some of the uronic acid residues in alginic acid from marine sources contrasts with methylation experiments in which only the 2,3-isomer of di-*O*-methyl-D-mannuronic acid has been characterized (11). Hirst and his colleagues have considered the possibility of 3,6-lactone residues in alginic acid, but infrared absorption at

TABLE I

Periodate oxidation kinetics of alginic acids

Time (h)	1	2	5	11	23	47
Mole oxidant consumed by *A. vinelandii* polyuronide	0.27	0.38	0.45	0.47	0.50	0.56
Mole oxidant consumed by algal alginic acid	0.29	0.41	0.50	0.52	0.53	0.58

[2]*A high ratio of mannuronic acid to guluronic acid (M/G) has been found in a polysaccharide isolated from a mucoid Pseudomonas sp. by Linker and Jones (8). The alginic acids isolated from several species and samples of seaweed have M/G ratios varying from 0.37 to 1.82 (9).*

Can. J. Chem. Downloaded from www.nrcresearchpress.com by 210.87.254.42 on 09/05/12
For personal use only.

Can. J. Chem. Downloaded from www.nrcresearchpress.com by 210.87.254.42 on 09/05/12
For personal use only.

1 745 – 1 750 cm^{-1} corresponded more closely to ester linkages, which could arise from association of the carboxyl groups of one chain with the C-2 or C-3 hydroxyls of another chain (10). The presence of 1,2- or 1,3-furanosyl or 1,3-pyranosyl uronic acid units can also be considered as another possible reason for resistance to periodate oxidation. However, these linkages were shown to be absent from the bacterial polyuronide by the following methylation experiment carried out on the derived polyalcohol.

The fully methylated polyalcohol was hydrolyzed, and the hydrolysate was examined on a paper chromatogram with *p*-anisidine hydrochloride spray to give one pink spot. The product could have the 2,3-, 3,4-, 2,4-, 2,5-, or 3,5-di-*O*-methyl mannuronic acid structure. A series of characterization experiments was therefore carried out. The di-*O*-methyl mannuronic acid was converted by treatment with methanolic hydrogen chloride into methyl ester methyl mannuronosides, which were reduced with sodium borohydride. Hydrolysis of the product with acid gave a di-*O*-methyl mannose which ran more slowly than the 3,4-isomer on a paper chromatogram. Reduction of the di-*O*-methyl mannose to a di-*O*-methyl mannitol followed by oxidation with periodic acid gave 2,3-di-*O*-methyl erythrose (paper chromatogram), which could only arise from 2,3-di-*O*-methyl mannuronic acid. 2,3-Di-*O*-methyl-D-erythrose was also prepared by sodium borohydride reduction of the methyl ester of the di-*O*-methyl mannuronic acid to di-*O*-methyl mannitol, which was then oxidized with periodic acid. Sodium borohydride reduction of the *O*-methyl tetrose gave 2,3-di-*O*-methyl erythritol, which was converted into its crystalline bis-*p*-nitrobenzoate. The absence of 2,4-di-*O*-methyl arabinose as a periodic acid oxidation product eliminated 2,4- and 3,5-di-*O*-methyl mannuronic acids as possibilities. 2,5-Di-*O*-methyl and 2,4-di-*O*-methyl mannuronic acids were not present, since sodium borohydride reduction of the methylated fragment gave a di-*O*-methyl mannonic acid which did not lactonize (infrared data) when it was heated at 100° *in vacuo*. The above data therefore establish that the bacterial polyuronide polyalcohol contains only 4-*O*-pyranosyl and (or) 5-*O*-furanosyl mannuronic acid units.

Since the periodate and methylation results did not distinguish between 4-*O*-pyranosyl and 5-*O*-furanosyl uronic acid residues in the polyuronide, an attempt was made to reduce the polyuronide to a neutral polymer. The polyuronide was converted into its propionate derivative (12), which was reduced with diborane (13). Hydrolysis of the de-esterified reduction product showed that mannose units were present. Some were 1,4-*O*-linked since hydrolysis of the derived polyalcohol gave erythritol, as shown by paper chromatograms and g.l.c. of the derived acetate. Mannose was also formed, in small amounts, but was not structurally significant since it may have arisen from mannose units substituted at C-2 or C-3 by interchain ester linkages. Gulose and threitol were not detected.

Although the polyuronide from *A. vinelandii* has a higher M/G ratio than algal alginic acids, common features, such as the periodate oxidation kinetics and the presence of 4-*O*-D-mannuronosyl (14) and 4-*O*- or 5-*O*-L-guluronosyl units, indicate that the polymers are closely related.

EXPERIMENTAL

Evaporations were carried out under reduced pressure, and specific rotations were measured at 25°. Nuclear magnetic resonance spectra were obtained on a Varian HA-100 nuclear magnetic resonance spectrometer with tetramethylsilane as standard. Paper chromatography was carried out, unless otherwise stated, in solvent A (*n*-butanol–ethanol–water (40:11:19 v/v/v)) or solvent B (ethyl acetate – acetic acid – water (9:2:2 v/v/v)).

Cultural Methods for Polysaccharide Production

Azotobacter vinelandii (Canada Department of Agriculture, Ottawa, No. 534) was maintained on slants of Burk's nitrogen-free medium (15) solidified with 2% agar. Inoculum was produced in 500 ml Erlenmeyer

flasks containing 100 ml Burk's medium/flask, inoculated from the slants, and incubated for 2–3 days at 25° on a rotary shaker (eccentricity 1 inch, operated at 230 r.p.m.). These cultures were used to inoculate 3 l of Burk's medium contained in 5 l stirred fermentors, which were operated at 400 r.p.m. and 25° with an air flow rate of 1 l/min per fermentor. After 4–5 days the cultures were harvested, the cells were removed by centrifugation, and the supernatant liquid was concentrated by evaporation.

Isolation of Polyuronide

Direct precipitation from the culture medium with 3 volumes of ethanol gave a polysaccharide (0.95 g/l) containing 0.73% nitrogen. Hydrolysis with *N* sulfuric acid at 100° for 18 h gave a pink spot on paper chromatography (solvent B, *p*-anisidine hydrochloride spray) running slightly faster (R_{gal} 1.0) than that of galacturonic or glucuronic acid. Smaller amounts of sugars corresponding to glucose, arabinose, ribose, and rhamnose were detected in solvents A and B.

A pure sample of polyuronide could be obtained on evaporation of an 18 l batch of culture filtrate to 2 l and addition of concentrated hydrochloric acid (100 ml). The precipitated polyuronide (22.0 g) was washed with water and then methanol. It was insoluble in water, but dissolved in aqueous 1% sodium hydroxide to give a solution with $[\alpha]_D$ −125° (*c*, 1.0).

Hydrolysis of Polyuronide and Analysis of Components

The polyuronide had a saponification equivalent of 152 and contained 2.81% C-methyl. A spectrum in D_2O containing NaOD gave an uncoupled C-methyl signal in the nuclear magnetic resonance at 2.36 p.p.m. corresponding to sodium acetate. The polyuronide (1.19 g) was dissolved by shaking it for 18 h in water (200 ml) containing sodium hydroxide (1.0 g), and the solution was acidified with sulfuric acid and distilled. The distillate was titrated with 0.1 *N* sodium hydroxide to pH 8 and found to contain 0.89 meq of acid. The sodium salt was converted into S-benzyl thiouronium acetate, which, after two recrystallizations from water, had m.p. 148–149°; yield 51 mg. Its X-ray diffraction pattern was identical with that of an authentic specimen.

The polysaccharide (50 mg) was solubilized and partly hydrolyzed in 80% sulfuric acid (5 ml) at room temperature for 5 h. The solution was diluted with water until the sulfuric acid was 2 *N*, and hydrolysis was completed by heating the solution at 100° for 5 h. The solution was neutralized ($BaCO_3$), filtered, and evaporated to a residue which was examined by paper electrophoresis in borate buffer (7), *p*-anisidine hydrochloride being used as the spray reagent. Mannuronic acid and a trace of guluronic acid were detected as reddish-brown spots. Hydrolysis, under similar conditions, of practical alginic acid (Matheson Coleman & Bell, P6856) prepared from *Laminaria digitata* and a small amount of *Laminaria cloustoni* gave a much higher proportion of guluronic acid. Haug and Larsen (9) report M/G values of between 1.16 and 1.58 for various samples from *Laminaria digitata*.

Hydrolysis of the polyuronide was repeated on a 1 g scale and the resulting mixture of acids heated for 18 h at 100° *in vacuo*. The partly lactonized product was fractionated on a cellulose column, *n*-butanol one-quarter saturated with water being used as solvent. D-Mannurono-γ-lactone was isolated and crystallized from ethanol to give material with m.p. 160–161° and $[\alpha]_D$ +75 → +92° (18 h; constant value *c*, 1.0 in H_2O). Although the specific rotation corresponded to that of D-mannuronolactone (16), the melting point differed from those previously reported. Since the closest melting point was 145° as reported by Spoehr (16), this component was characterized by conversion of the polyuronide into D-mannitol hexaacetate.

The polyuronide (70 mg) was refluxed overnight in 5% methanolic hydrogen chloride (20 ml), and partial dissolution took place. The hydrolysate was neutralized (Ag_2CO_3), filtered, and evaporated to a syrup which consisted of a mixture of methyl ester methyl hexuronosides. This was reduced at room temperature with sodium borohydride (50 mg) in methanol (5 ml) containing 0.1 *N* methanolic sodium methoxide (0.5 ml). After 18 h the solution was evaporated and the reagents removed. The methyl glycosidic mixture was hydrolyzed with *N* hydrochloric acid (5 ml) at 100° for 3 h, neutralized (Ag_2CO_3), filtered, and evaporated to a syrup. Examination on a paper chromatogram (*p*-anisidine hydrochloride spray) in solvent B gave a spot corresponding to mannose. In methyl ethyl ketone – acetic acid – water (9:1:1 v/v/v) saturated with boric acid (10), a trace of gulose was detected.

The hexose-containing mixture was reduced with sodium borohydride (50 mg) in water (1 ml). After 3 h the reagent was removed and the mixture of polyols acetylated by heating it at 100° in acetic anhydride (5 ml) containing pyridine (5 ml). The product was examined by g.l.c. with 2% neopentyl glycol succinate on Chromosorb W (80–100 mesh) (packing A) and 2% nitrile silicone gum XE-60 on Chromosorb W (80–100 mesh) (packing B) in 8 ft × ¼ inch outside diameter copper tubes at 210°, with helium as the carrier gas. Peaks corresponding to mannitol and sorbitol hexaacetates were obtained with packing B, which can resolve the hexaacetates of galactitol (retention time (R_t) 7.3 min), sorbitol (R_t 8.0 min), and mannitol (R_t 6.0 min). For quantitative purposes packing A was used, since it gave a superior resolution of mannitol and sorbitol hexaacetates (R_t 21.5 min and 25.0 min, respectively). The g.l.c. unit was of conventional design with thermal conductivity detectors. Derivatives having retention times identical with those of the hexaacetates of mannitol (92%) and sorbitol (8%) were detected. Crystallization of the product from ethanol gave D-mannitol hexaacetate (32 mg) with m.p. and mixed m.p. 123–124° and $[\alpha]_D$ +19° (*c*, 1.3 in AcOH). Patterson and Todd (17) report m.p. 126° and $[\alpha]_D$ +18.8° (AcOH) for this compound. The X-ray diffraction pattern of the product was identical with that of D-mannitol hexaacetate.

Can. J. Chem. Downloaded from www.nrcresearchpress.com by 210.87.254.42 on 09/05/12
For personal use only.

Can. J. Chem. Downloaded from www.nrcresearchpress.com by 210.87.254.42 on 09/05/12
For personal use only.

Periodate Oxidation of the Deacetylated Polyuronide

A 100 mg sample of polyuronide was dissolved by shaking it overnight in water (20 ml) containing sodium hydroxide (0.10 g). The pH of the solution was adjusted to 3.7 and the solution made up to 50 ml. A 20 ml sample was treated with 0.1 *M* sodium metaperiodate (10 ml) at 4° and the oxidation kinetics recorded (Table I). A sample of alginic acid from *Laminaria digitata* and a little *Laminaria cloustoni* was oxidized simultaneously. The pH of the solutions after 48 h was 3.8.

Preparation and Hydrolysis of the Polyalcohol

The polyuronide (11.0 g) was shaken for 18 h in water (1 l) containing sodium hydroxide (10 g), the solution adjusted to pH 3.7 with acetic acid, and sodium metaperiodate (20 g) added. After 24 h at room temperature acetic acid (5 l) was added and the precipitated oxypolysaccharide isolated by filtration. The product was dried *in vacuo* and shaken for 3 h in water (1 l) containing sodium borohydride (10 g). The solution was adjusted to pH 7 with acetic acid and evaporated to dryness. Boric acid was removed by refluxing the residue in methanol, and the polyalcohol was precipitated by addition of 3 volumes of ethanol to an aqueous solution of the polymer; yield 9.3 g.

The polyalcohol (0.94 g) was hydrolyzed in *N* sulfuric acid (20 ml) at 100° for 3 h. The solution was neutralized ($BaCO_3$), filtered, and treated with Amberlite IR-120 to remove cations. Examination by paper electrophoresis in borate (7) with *p*-anisidine hydrochloride spray gave a reddish-brown spot corresponding to mannuronic acid and a faster moving yellow spot, possibly tetruronic acid(s). The solution was evaporated and heated at 100° *in vacuo* to promote lactonization, and the resulting syrup was examined on a paper chromatogram in solvent A (ammoniacal silver nitrate spray). Mannuronolactone, erythrono-γ-lactone ($R_{glycerol}$ 1.1), and threono-γ-lactone ($R_{glycerol}$ 1.3) were detected, and fractionation on a cellulose column (eluant: benzene–ethanol–water (300:50:1 v/v/v)) gave a mixture of erythrono- and threonolactones (0.18 g). These were separated on paper sheets (solvent A) to give erythrono-γ-lactone (34 mg) which, after crystallization from acetone, had m.p. and mixed m.p. 105°. Its X-ray diffraction pattern was identical with that of an authentic specimen. The L-threonolactone had $[\alpha]_D$ +25° (*c*, 1.0 in H_2O); it was converted into L-threonic acid phenylhydrazide, which had m.p. 160–161° when crystallized from ethanol and $[\alpha]_D$ +39° (*c*, 0.4 in MeOH). D-Threonic acid phenylhydrazide has m.p. 157° (18) and $[\alpha]_D$ −45° (*c*, 1.0 in MeOH). The X-ray diffraction pattern of the product was identical with that of D-threonic acid phenylhydrazide.

Methylation of the Polyuronide Polyalcohol

The polyalcohol (2.0 g) was methylated by dropwise addition of dimethyl sulfate (40 ml) to an aqueous solution (80 ml) containing sodium hydroxide (40 g). After 1 day this process was repeated, and the following day another methylation was carried out with dimethyl sulfate (100 ml) and sodium hydroxide (100 g) in water (200 ml). The solution was neutralized with acetic acid, dialyzed against tap water for 3 days, and evaporated. The residue was again methylated by the above methylation procedure. One-half of the product was hydrolyzed at 100° for 24 h in 4 *N* sulfuric acid (25 ml), and the solution was neutralized ($BaCO_3$) and evaporated. Examination on a paper chromatogram in solvent B showed the presence of a pink spot running at 1.2 times the rate of rhamnose (*p*-anisidine hydrochloride spray). Only traces of other spots were detected. The hydrolysate was purified on a Dowex-1 column (acetate form) and the di-*O*-methyl mannuronic acid eluted with 10% acetic acid. A pure fraction (0.28 g), which had $[\alpha]_D$ +17° (*c*, 1.2 in MeOH), and a fraction (0.21 g) containing di-*O*-methyl mannuronic acid and small amounts of impurities were isolated.

Characterization of Di-O-methyl Mannuronic Acid

The di-*O*-methyl mannuronic acid (30 mg) was treated with refluxing 3% methanolic hydrogen chloride (5 ml) for 2 h; then the solution was neutralized (Ag_2CO_3), filtered, and evaporated. The resulting methyl ester methyl mannuronosides were reduced at room temperature for 18 h in methanol (2 ml) containing 0.1 *N* methanolic sodium methoxide (0.3 ml) and sodium borohydride (30 mg). The solution was evaporated and cations were removed by the addition of Amberlite IR-120 in water. The resin was filtered off, the solution evaporated to dryness, and boric acid removed by repeated evaporations of methanol. The product, which contained methyl di-*O*-methyl mannosides, was hydrolyzed at 100° for 3 h in *N* hydrochloric acid, and the hydrolysate was neutralized (Ag_2CO_3), filtered, and evaporated to a syrup. The product gave a brown spot on a paper chromatogram in solvent A (*p*-anisidine hydrochloride spray) which ran at 0.95 times the rate of 3,4-di-*O*-methyl mannose (yellow-brown spot).

The di-*O*-methyl mannose was reduced with sodium borohydride by the method used above, and the resulting di-*O*-methyl mannitol was oxidized for 2 h in an aqueous solution (2 ml) containing periodic acid (200 mg). The oxidant was neutralized ($BaCO_3$), excess acetone added, and the solution filtered and evaporated. On a paper chromatogram (solvent A, *p*-anisidine hydrochloride spray) a yellow-brown spot was detected which ran at the same rate as that of 2,3-di-*O*-methyl erythrose (19). No 2,4-di-*O*-methyl arabinose, reported to run more slowly than the available 2,3-isomer (20), was detected.

Di-*O*-methyl-D-mannuronic acid (30 mg) in methanol (5 ml) was treated with ethereal diazomethane to give an ether-soluble methyl ester with $[\alpha]_D$ +17° (*c*, 1.8 in EtOH). It moved at 1.6 times the rate of glycerol on a paper chromatogram in solvent A and gave a pink spot with *p*-anisidine hydrochloride spray. The methyl ester was reduced with sodium borohydride in methanol (for the method see the reduction of α,β-methyl 2,3-di-*O*-methyl mannuronoside methyl ester) to give di-*O*-methyl mannitol ($[\alpha]_D$ 0° (*c*, 0.8 in EtOH)) moving

at 1.16 times the speed of glycerol in solvent A (ammoniacal silver nitrate spray). Oxidation with periodic acid gave 2,3-di-*O*-methyl erythrose as the only product detectable with *p*-anisidine hydrochloride spray. It was characterized after sodium borohydride reduction to 2,3-di-*O*-methyl erythritol. This was converted into its crystalline bis-*p*-nitrobenzoate which, when crystallized from ethyl acetate, had m.p. and mixed m.p. 178–180° and gave a X-ray diffraction pattern identical with that of an authentic specimen.

Authentic 2,3-di-*O*-methyl erythritol was prepared by sodium borohydride reduction of 2,3-di-*O*-methyl-D-erythrose (30 mg) (19). The 2,3-di-*O*-methyl erythritol was converted into its bis-*p*-nitrobenzoate (29 mg), m.p. 177–180° after crystallization from ethyl acetate.

Anal. Calcd. for $C_{20}H_{20}O_{10}N_2$: C, 53.57; H, 4.50. Found: C, 53.14; H, 4.61.

Sodium borohydride reduction of 2,3-di-*O*-methyl mannuronic acid gave 4,5-di-*O*-methyl mannonic acid, which was heated overnight at 100° *in vacuo*. No lactone was detected in the infrared, only absorption at 1 605 cm^{-1} being detected.

Diborane Reduction of the Polyuronide

The polyuronide (2.0 g) was dissolved in formamide (500 ml) by heating the mixture overnight on a steam bath; after the solution was cooled a mixture of propionic anhydride and pyridine (50 ml of each) was added with stirring. After 18 h the reaction mixture was poured into ice water (3 l), and concentrated hydrochloric acid (10 ml) was added. The precipitated polyuronide propionate (2.3 g) was isolated by centrifugation, washed with water, and dried *in vacuo*.

The propionate was reduced with diborane by using 3 times the quantities of reagents cited by Wolfrom *et al.* (21) in the reduction of acetylated heparin (1.5 g). The product was depropionated by the addition of an excess of aqueous sodium hydroxide and then dialyzed for 3 days. The polysaccharide solution was evaporated to a small volume and the reduced polysaccharide precipitated with excess ethanol. Hydrolysis of the product with 2 *N* sulfuric acid at 100° overnight gave mainly hexuronic acids on paper chromatograms. Less-intense spots corresponding to mannose and a trace amount of gulose were detected.

Periodate Oxidation of Reduced Polyuronide

The reduced polyuronide (0.20 g) was oxidized with sodium periodate (0.50 g) for 24 h in aqueous solution (20 ml) at pH 3.7. The oxidized polysaccharide was precipitated by the addition of acetic acid (150 ml) and was isolated by filtration. It was reduced to a polyalcohol for 3 h in an aqueous solution of sodium borohydride (0.20 g in 20 ml). Excess reagent was destroyed by adjusting the pH to 7 by the addition of acetic acid, the solution was evaporated to dryness, and boric acid was removed by refluxing the residue in methanol; yield 0.14 g. Hydrolysis of the polyalcohol in *N* hydrochloric acid at 100° for 18 h gave on a paper chromatogram a small amount of mannose as the only reducing sugar (*p*-anisidine hydrochloride spray). With the ammoniacal silver nitrate spray a spot corresponding to erythritol was obtained. Examination of the acetylated hydrolysate by g.l.c. at 160° with a 4 ft column of 2% nitrile silicone gum XE-60 on Chromosorb W (80–100 mesh) indicated that erythritol tetraacetate (R_t 7.9 min) was present. No threitol tetraacetate (R_t 9.7 min) was detected.

ACKNOWLEDGMENTS

The authors thank Mr. N. Gardner for technical assistance, Mr. W. C. Haid for microanalytical determinations and infrared spectroscopy, and Mr. M. Mazurek for preparing the nuclear magnetic resonance spectra. The culture of *Azotobacter vinelandii*, No. 534, was supplied by the Canada Department of Agriculture, Ottawa, Canada.

REFERENCES

1. V. M. PARIKH and J. K. N. JONES. Can. J. Chem. **41**, 2826 (1963).
2. G. J. LAWSON and M. STACEY. J. Chem. Soc. 1925 (1954).
3. G. H. COHEN and D. B. JOHNSTONE. J. Bacteriol. **88**, 329 (1964).
4. D. CLAUS. Biochem. Biophys. Res. Commun. **20**, 745 (1965).
5. G. H. COHEN and D. B. JOHNSTONE. J. Bacteriol. **88**, 1695 (1964).
6. F. G. FISCHER and H. DÖRFEL. Z. Physiol. Chem. **302**, 186 (1955).
7. A. HAUG and B. LARSEN. Acta Chem. Scand. **15**, 1395 (1961).
8. A. LINKER and R. S. JONES. Nature, **204**, 187 (1964).
9. A. HAUG and B. LARSEN. Acta Chem. Scand. **16**, 1908 (1962).
10. D. W. DRUMMOND, E. L. HIRST, and E. PERCIVAL. J. Chem. Soc. 1208 (1962).
11. E. L. HIRST, J. K. N. JONES, and W. O. JONES. J. Chem. Soc. 1880 (1939).
12. J. F. CARSON and W. D. MACLAY. J. Am. Chem. Soc. **68**, 1015 (1946).
13. F. SMITH and A. M. STEPHEN. Tetrahedron Letters, **7**, 17 (1960).
14. E. L. HIRST, E. PERCIVAL, and J. K. WOLD. J. Chem. Soc. 1493 (1964).
15. J. W. NEWTON, P. W. WILSON, and R. H. BURRIS. J. Biol. Chem. **204**, 445 (1953).
16. H. A. SPOEHR. Arch. Biochem. **14**, 153 (1947).
17. T. S. PATTERSON and A. R. TODD. J. Chem. Soc. 2876 (1929).
18. J. U. NEF, O. F. HEDENBURG, and J. W. E. GLATTFELD. J. Am. Chem. Soc. **39**, 1638 (1917).
19. R. C. HOCKETT and C. W. MAYNARD. J. Am. Chem. Soc. **61**, 2111 (1939).
20. P. ANDREWS, D. H. BALL, and J. K. N. JONES. J. Chem. Soc. 4090 (1953).
21. M. C. WOLFROM, J. R. VERCELLOTTI, and G. H. S. THOMAS. J. Org. Chem. **29**, 536 (1964).

Can. J. Chem. Downloaded from www.nrcresearchpress.com by 210.87.254.42 on 09/05/12
For personal use only.

Can. J. Chem. Downloaded from www.nrcresearchpress.com by 210.87.254.5 on 09/05/12
For personal use only.

STEROIDS AND STEROIDASES

I. LONG-RANGE EFFECTS AND THE PREPARATION OF A-HOMOSTEROIDS

J. Bryan Jones and Philip Price

Lash Miller Laboratories, Department of Chemistry, University of Toronto, Toronto, Ontario

Received October 14, 1965

ABSTRACT

The direction of the diazomethane ring enlargement of 17β-hydroxy-5α-androstan-3-one (I, R = OH) appears to be controlled by the long-range effect of the 17β-hydroxyl group, and proceeds with migration of the C_3—C_4 bond to give the A-homo-3-one III (R = OH). This is in direct contrast to the rearrangement of 5α-cholestan-3-one (I, R = C_8H_{17}), which gives the A-homoketone II (R = C_8H_{17}) as a result of C_2—C_3 bond migration. An analogous directing effect was not observed for the reaction of diazomethane with 17β-hydroxy-5β-androstan-3-one (VII). Oxidation of the A-homo-17β-alcohols gave the corresponding diones III (R = =O), X, and XI.

The need to prepare various A-homosteroids arose from the initiation of investigations designed to evaluate the electronic and structural specificities of the enzymes of steroid metabolism. The main objective of the programme is to gain further information on the mechanism of action of various steroidases, and on the structural and other features of steroids which contribute to biological activity. In addition, it is hoped that the factors responsible for the carcinogenic properties of certain steroids will become apparent.

Until recently, very little information was available concerning the stereochemical and mechanistic pathways of reactions catalyzed by steroidases. However, studies during the past 10 years by several groups have provided evidence regarding some of the steps involved in oxygenation (1, 2), isomerization of Δ^5-3-ketones (2, 3), and dehydrogenation (2).

Studies on the stereochemical pathway for Δ^1-dehydrogenation were carried out independently by several workers (2); after an elegant series of experiments, Ringold *et al.* (4) were able to describe the stereochemical pathway for the Δ^1-dehydrogenase of *Bacillus sphaericus* in terms of the mechanism summarized in Fig. 1, in which A represents an acidic or electrophilic binding site at the active center, and B a basic amino acid side chain.

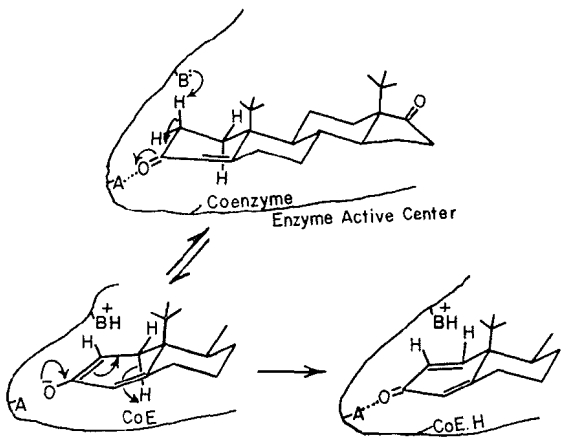


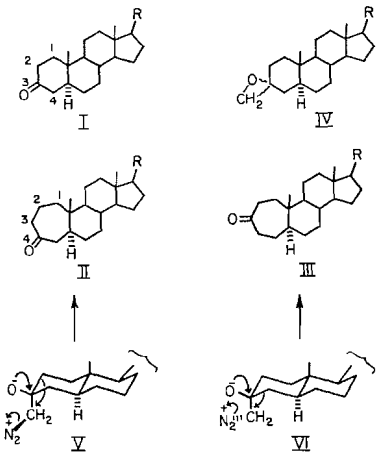
FIG. 1. Mechanism of action of Δ^1-dehydrogenase of *Bacillus sphaericus* (after Ringold *et al.* (4)).

Can. J. Chem. Downloaded from www.nrcresearchpress.com by 210.87.254.5 on 09/05/12
For personal use only.

When the present investigation was contemplated, the mechanistic pathway was not known in such detail for any other steroidase. Accordingly, the Δ^1-dehydrogenase of *Bacillus sphaericus* was selected for the initial specificity studies, as it was considered that the structural factors important in the binding and orientation of ring A of steroidal substrates at the active center could be analyzed in terms of the mechanism formulated in Fig. 1.

The aspect of structural specificity that was considered initially was the influence, on binding and catalysis, of variation of the size of ring A; thus, as the first stage of a systematic survey, the synthesis of some androstanes having ring A seven-membered has been effected.

A survey of the literature showed that, in contrast to studies on the expansion of ring D of steroids, relatively little had been reported on the preparation of A-homosteroids (5).



In 1943, Goldberg and Kirchensteiner (6) reported the enlargement of ring A of 17β-acetoxy-5α-androstan-3-one (I, R = OAc) and 5α-cholestan-3-one (I, R = C_8H_{17}) by means of the Tiffeneau–Demjanov rearrangement, which involves conversion of the ketone into the cyanohydrin, followed by reduction to the primary amine and treatment with nitrous acid. The products in both cases were the corresponding A-homo-4-ones II (R = OAc and C_8H_{17}) arising from migration of the C_2—C_3 bond of I. During the course of their investigations on A-homosteroids, Nelson and Schut (7) confirmed the tentative structural assignments of Goldberg and Kirchensteiner for A-homo-5α-cholestan-4-one (II, R = C_8H_{17}) by its synthesis via an independent route. The ring enlargement of 5α-cholestan-3-one (I, R = C_8H_{17}) with diazomethane was also studied by Nelson and Schut (7), and the major product (50% yield) was again the A-homo-4-one II (R = C_8H_{17}) resulting from C_2—C_3 bond migration as under the Tiffeneau–Demjanov reaction conditions. However, a smaller amount (10% yield) of the product of C_3—C_4 migration, A-homo-5α-cholestan-3-one (III, R = C_8H_{17}), was detected. Neither group reported the isolation of an A-homo-3-one III from the Tiffeneau route.

The formation of the same product on ring expansion from both the Tiffeneau and diazomethane reactions was expected (7), as the intermediates and reaction mechanisms involved in the rearrangement step are presumably similar (cf. refs. 8 and 9). Accordingly, in an attempt to prepare 17β-hydroxy-A-homo-5α-androstan-4-one (II, R = OH), diazomethane ring expansion conditions similar to those resulting in C_2—C_3 bond migration in the 5α-cholestane series (7) were applied to 17β-hydroxy-5α-androstan-3-one

Can. J. Chem. Downloaded from www.nrcresearchpress.com by 210.87.254.5 on 09/05/12
For personal use only.

(I, R = OH). Gas–liquid chromatographic analysis showed the product to be a mixture of at least six compounds, with one predominating to the extent of 85%. Column chromatographic purification yielded the major component, m.p. 212°, $[\alpha]_D^{24}$ −57.1°, which was obviously different from the expected product II (R = OH), m.p. 197°, $[\alpha]_D^{26}$ +112°, obtained by Goldberg and Kirchensteiner (6). The structural assignment of II (R = OH) by the latter authors was not unambiguous, but it was independently confirmed recently by the preparation of II from 17β-hydroxy-A-homo-5α-androst-1-en-4-one via catalytic hydrogenation (10). The infrared absorption at 1 695 cm^{-1} of the product whose melting point was 212° indicated the presence of a seven membered ring carbonyl, and the elemental analysis and molecular weight (mass spectrum) were in accord with an A-homo-ketone structure. This evidence led inescapably to the conclusion that in the diazomethane ring enlargement of 17β-hydroxy-5α-androstan-3-one (I, R = OH), in contrast to the 5α-cholestane series (which differs only in the nature of the substituent at C_{17}), C_3—C_4 bond migration predominates to give the A-homo-3-one III (R = OH). The many attempts to isolate II (R = OH), the product of C_2—C_3 migration, from the reaction mixture were all unsuccessful. Gas–liquid chromatographic analyses of the reaction mixture showed that the amount of each of the other products expected, the A-homo-4-one II (R = OH), the epoxide IV (R = OH), and A-bishomo compounds, was not greater than 3%.

Investigation of the optical rotatory dispersion (o.r.d.) curve of III (R = OH) confirmed its structure. A comparison of its o.r.d. curve, which shows a strongly negative Cotton effect, with that of A-homo-5α-cholestan-4-one (II, R = C_8H_{17})* is given in Fig. 2*a*.

The observed strongly negative Cotton effect (*a* = −91) of III (R = OH) is in agreement with that quoted (*a* = −60) in ref. 11 for A-homo-5α-cholestan-3-one (III, R = C_8H_{17}). The o.r.d. of 17β-hydroxy-A-homo-5α-androstan-4-one has not been reported, but the circular dichroism spectrum (10) shows a positive maximum, as would be expected by analogy with the positive Cotton effect observed for the o.r.d. curve of II (R = C_8H_{17}).

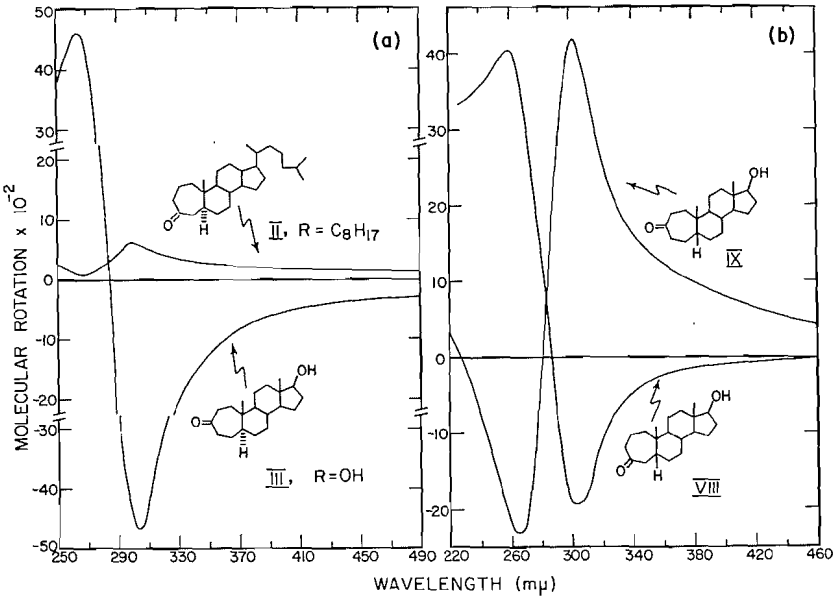


FIG. 2.

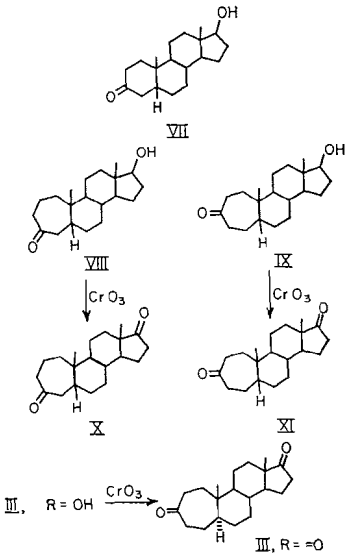
**We thank Drs. G. D. Meakins and D. J. Morris, University of Oxford, for providing us with a pure sample of this compound.*

That the change in the direction of ring enlargement is due to the effect of the hydroxyl group alone, and is not in some way associated with differences between the androstane and cholestane skeletons, has been confirmed by the observation that, for 5α-androstan-3-one (I, R = H), diazomethane ring enlargement proceeds mainly with C_2—C_3 migration, as in the cholestane series, to give 80% of A-homo-5α-androstan-4-one (II, R = H) (a = +94) (12).

The marked influence of the hydroxyl group at C_{17} on the direction of diazomethane ring enlargement appears to be another example of the long-range effects that substituents may exert across widely separated areas of the steroid nucleus (13). As the direction of ring enlargement is almost completely reversed when the polar hydroxyl group replaces the nonpolar substituents at C_{17}, this effect is one of the most powerful yet observed.

At present, the factors determining the direction of ring enlargement, in both the diazomethane and Tiffeneau reactions, are not well defined. Explanations for the differences in bond migration, based either on equatorial nucleophilic attack of the steroid-3-ketone leading to one migration, and axial addition to the other, or on differences in conformations of the intermediate arising by axial attack of the nucleophile, e.g. V and VI for C_2—C_3 and C_3—C_4 migration, respectively, are not completely satisfactory. The latter rationale is suggested from a consideration of the data available on the stereochemistry of additions of nucleophiles, with steric dimensions similar to those of diazomethane and cyanide ions, to cyclohexanones in general (14). It seems probable that axial addition (product development control (15)) should predominate; further experiments designed to provide information on this point, and on the nature of the long-range effect exerted by the hydroxyl group on the nucleophilic addition and subsequent rearrangement steps, are in progress.

As A-homo-androstanes with an A/B *cis* ring fusion were also required for the specificity studies, the reaction of 17β-hydroxy-5β-androstan-3-one (VII) with diazomethane was carried out. Ring expansion to the A-homo compounds occurred in 72% yield, but no overriding influence of the 17β-hydroxyl on the direction of migration was observed in this reaction and the products of both C_2—C_3 and C_3—C_4 migration, VIII and IX,



Can. J. Chem. Downloaded from www.nrcresearchpress.com by 210.87.254.5 on 09/05/12
For personal use only.

respectively, were formed in equivalent amounts. The properties of 17β-hydroxy-A-homo-5β-androstan-3-one (IX) were in agreement with those reported by Müller (11) for IX obtained by hydrogenation of 17β-hydroxy-A-homo-androst-4*a*-en-3-one. The o.r.d. curve showed a positive Cotton effect (Müller reports a positive circular dichroism curve), whereas that for the isomeric A-homo-4-one VIII showed a strongly negative Cotton effect (see Fig. 2*b*). Oxidation of both alcohols with chromium trioxide gave the corresponding diones X and XI in quantitative yields. Oxidation of 17β-hydroxy-A-homo-5α-androstan-3-one (III, R = OH) with chromium trioxide also gave the corresponding diketone III (R = =O) in good yield.

Since enzymes are, in general, stereospecific in their catalytic action, before any meaningful specificity and inhibition studies of the A-homo-androstanes with the Δ^1-dehydrogenase of *Bacillus sphaericus* can be carried out, it is necessary to establish the conformation of the seven-membered ring. A discussion of the conformation of ring A of A-homosteroids will be reported shortly.

EXPERIMENTAL

Infrared spectra were obtained on a Beckmann model 11 spectrometer, and optical rotations on a Bendix–Ericsson polarimeter. Optical rotary dispersions were measured on a Jasco–Durrum ORD 5 spectropolarimeter. Melting points were determined on a Fisher–Johns apparatus and are corrected. All solvents for column chromatography were distilled before use; alumina refers to British Drug Houses chromatographic alumina deactivated by shaking with 5% of its own weight of 10% acetic acid. Gas–liquid chromatographic analyses were effected with columns containing 3.8% SE 30 on silanized "Diatoport S" and 1% QF-1 on silanized "Chromosorb G" by using a F and M model 400 biomedical unit. Merck silica gel G was used as the thin-layer chromatography adsorbent, and benzene – 50% ether as the developing solvent. The spots were visualized by spraying the chromatograms with 50% aqueous toluene – *p*-sulfonic acid followed by heating them at 100°. All compounds that are described were purified until no impurity could be detected by thin-layer chromatography or by gas–liquid chromatography on both SE 30 and QF-1 columns.

17β-Hydroxy-5α-androstan-3-one (I, R = OH)

17β-Hydroxyandrost-4-en-3-one was reduced with lithium in liquid ammonia as described by Brutcher and Bauer (16). The crude product (80% yield) was purified by column chromatography on alumina prepared in petroleum ether, b.p. 40–60°, and was eluted with benzene. Recrystallization from acetone gave needles, m.p. 181–182° (lit. m.p. 181.5–182.5° (17)).

Reaction of 17β-Hydroxy-5α-androstan-3-one with Diazomethane

Potassium hydroxide (14.2 g) followed by 17β-hydroxy-5α-androstan-3-one (10 g) was dissolved in methanol (400 ml) and anhydrous ether (300 ml). N-Nitrosomethylurea (10.6 g) was added in portions during 20 min to the stirred, cooled (0°) solution; after the addition was complete, stirring was continued for a further 5 h. Hydrochloric acid (200 ml, 2 *N*) was then added, the mixture filtered, and the solid material washed well with ether. The combined filtrate and ether washings were concentrated under reduced pressure to remove the organic solvents, and the resulting mixture was extracted with ether (3 × 75 ml). The ether solution was washed with water (50 ml), dried ($MgSO_4$), and evaporated. The residual solid (10.8 g) was chromatographed on alumina (300 g), and elution with benzene – 10% ether gave 17β-hydroxy-A-homo-5α-androstan-3-one (III, R = OH) (8.4 g). Repeated chromatography followed by recrystallization from acetone gave needles (5.1 g), m.p. 212–213°, $[\alpha]_D^{25}$ −57.1° (*c*, 0.7 in $CHCl_3$); $\nu_{max}^{CHCl_3}$ 3 600 (hydroxyl) and 1 695 cm^{-1} (seven membered ring carbonyl); nuclear magnetic resonance ($CDCl_3$) δ 0.73 and 0.80 (C_{18}, C_{19}, CH_3, singlets), 1.9 (OH, singlet), and 3.65 p.p.m. (C_{17}—α-H, triplet); o.r.d. (Fig. 2*a*) (*C*, 0.004 in CH_3OH) 24°; $[\phi]_{700}$ −166°; $[\phi]_{589}$ −227°; $[\phi]_{304}$ −4 489°; $[\phi]_{260}$ +4 599°; $[\phi]_{220}$ +444°.

Anal. Calcd. for $C_{20}H_{32}O_2$ (304.5): C, 78.90; H, 10.59. Found: C, 78.88; H, 10.51; mol. wt. (mass spectrum) 304.

A-Homo-5α-androstan-3,17-dione (III, R = =O)

17β-Hydroxy-A-homo-5α-androstan-3-one (450 mg) was dissolved in the minimum amount of acetone (60 ml), and 8 *N* chromic acid (Jones' reagent (18)) was added dropwise to the stirred, cooled (5°) solution until the solution just retained the brown-orange color of the chromic acid. After the mixture was stirred for a further 30 min at 5°, it was poured into water (600 ml) and extracted with ether (3 × 100 ml). The combined ether extracts were washed first with saturated sodium bicarbonate and then with water, and dried ($MgSO_4$). Evaporation of the ether gave a solid (450 mg) which, on recrystallization from hexane,

Can. J. Chem. Downloaded from www.nrcresearchpress.com by 210.87.254.5 on 09/05/12
For personal use only.

yielded A-homo-5α-androstan-3,17-dione as needles (430 mg), m.p. 112.5–113.5°, $[\alpha]_D^{25}$ 22.5° (*c*, 0.8 in $CHCl_3$); $\nu_{max}^{CHCl_3}$ 1 735 (five membered ring carbonyl) and 1 698 cm^{-1} (seven membered ring carbonyl).

Anal. Calcd. for $C_{20}H_{30}O_2$ (302.5): C, 79.42; H, 9.99. Found: C, 79.20; H, 9.96; mol. wt. (mass spectrum) 302.

17β-Hydroxy-5β-androstan-3-one (VII)

17β-Hydroxy-5β-androstan-3-one was prepared in 95% yield by catalytic hydrogenation of 17β-hydroxy-androst-4-en-3-one in the presence of potassium hydroxide, based on the procedure described by Djerassi *et al.* (19). After purification by chromatography on alumina and recrystallization from cyclohexane, a product with m.p. 141–142° was obtained (lit. m.p. 139–141° (20)).

Reaction of 17β-Hydroxy-5β-androstan-3-one with Diazomethane

Potassium hydroxide (3.6 g) was added to 17β-hydroxy-5β-androstan-3-one (5 g) in methanol (200 ml) and anhydrous ether (150 ml), and the resulting solution was cooled to 0°. N-Nitrosomethylurea (2.7 g) was added, with stirring, during 20 min, and the cold mixture was stirred for a further 5 h at 0°. Hydrochloric acid (50 ml, 2 *N*) was then added, and the insoluble material filtered off and washed with ether. The combined filtrate and ether washings were evaporated under reduced pressure, and the residue was extracted with ether (3 × 50 ml). The ether solution was washed with water (50 ml), dried ($MgSO_4$), and evaporated, and the crude product (5.0 g) was then chromatographed on alumina (500 g). Elution with benzene – 1% ether gave 17β-hydroxy-A-homo-5β-androstan-4-one (VIII) (1.6 g) which, after repeated recrystallization from *n*-hexane, gave needles, m.p. 172.5–173°, $[\alpha]_D^{25}$ 12.7° (*c*, 0.8 in $CHCl_3$); $\nu_{max}^{CHCl_3}$ 3 597 and 3 436 (hydroxyl), and 1 695 cm^{-1} (seven membered ring carbonyl); o.r.d. (Fig. 2*b*) (*C*, 0.004 in CH_3OH) 24°; $[\phi]_{700}$ +1°; $[\phi]_{589}$ 44°; $[\phi]_{303}$ −1 932°; $[\phi]_{260}$ +4 049°; $[\phi]_{220}$ +3 660°.

Anal. Calcd. for $C_{20}H_{32}O_2$ (304.5): C, 78.90, H, 10.59. Found: C, 78.87; H, 10.46.

Subsequent elution with benzene – 10% ether gave 17β-hydroxy-A-homo-5β-androstan-3-one (IX) (1.6 g). Repeated recrystallization from *n*-hexane gave needles, m.p. 162–162.5° (lit. m.p. 156–157° (11)), $[\alpha]_D^{25}$ 84.8° (*c*, 0.6 in $CHCl_3$); $\nu_{max}^{CHCl_3}$ 3 597 and 3 436 (hydroxyl), and 1 698 cm^{-1} (seven membered ring carbonyl); o.r.d. (Fig. 2*b*) (*C*, 0.003 in CH_3OH) 24°; $[\phi]_{700}$ +150°; $[\phi]_{589}$ +177°; $[\phi]_{302}$ +4 160°; $[\phi]_{264}$ −2 314°; $[\phi]_{220}$ +362°.

Anal. Calcd. for $C_{20}H_{32}O_2$ (304.5): C, 78.90; H, 10.59. Found: C, 78.93; H, 10.43.

A-Homo-5β-androstan-4,17-dione (X)

17β-Hydroxy-A-homo-5β-androstan-4-one (150 mg) was dissolved in acetone (10 ml), and 8 *N* chromic acid (Jones' reagent (18)) was added dropwise, with stirring, to the cooled (ice bath) solution until a permanent brown color remained. After the solution was stirred for a further 30 min, it was poured into water (100 ml) and extracted with ether (3 × 50 ml). The ethereal extract was washed with saturated sodium bicarbonate and then with water. The dried ($MgSO_4$) ether solution was evaporated and the residue (150 mg) was recrystallized several times from petroleum ether (b.p. 40–60°) to give A-homo-5β-androstan-4,17-dione as needles (98 mg), m.p. 127–128°, $[\alpha]_D^{21}$ 85.7° (*c*, 0.25 in $CHCl_3$); $\nu_{max}^{CHCl_3}$ 1 733 (five membered ring carbonyl) and 1 695 cm^{-1} (seven membered ring carbonyl).

Anal. Calcd. for $C_{20}H_{30}O_2$ (302.5): C, 79.42; H, 9.99. Found: C, 79.36; H, 9.95.

A-Homo-5β-androstan-3,17-dione (XI)

17β-Hydroxy-A-homo-5β-androstan-3-one (150 mg) was oxidized with Jones' reagent as described above to give a quantitative yield of A-homo-5β-androstan-3,17-dione, which, after several recrystallizations from petroleum ether (b.p. 40–60°), gave rhombs (94 mg), m.p. 80–81° (lit. m.p. 87–88° (11)), $[\alpha]_D^{24}$ 150.7° (*c*, 0.35 in $CHCl_3$); $\nu_{max}^{CHCl_3}$ 1 736 (five membered ring carbonyl) and 1 698 cm^{-1} (seven membered ring carbonyl).

Anal. Calcd. for $C_{20}H_{30}O_2$ (302.5): C, 79.42; H, 9.99. Found: C, 79.53; H, 9.94.

ACKNOWLEDGMENTS

Financial support of this work by the National Research Council, the National Cancer Institute of Canada, and the Petroleum Research Fund is gratefully acknowledged. We also thank Dr. A. D. Cross for a generous gift of 17β-hydroxy-androst-4-en-3-one, and Dr. D. B. MacLean for the mass spectra.

REFERENCES

1. M. Hayano. *In* Oxygenases. *Edited by* O. Hayaishi. Academic Press, Inc., New York. 1962. p. 181 *et seq.*
2. P. Talalay. Ann. Rev. Biochem. **34**, 347 (1965).
3. S. K. Malhotra and H. J. Ringold. J. Am. Chem. Soc. **87**, 3228 (1965).
4. H. J. Ringold, M. Hayano, and V. Stefanovic. J. Biol. Chem. **238**, 1960 (1963).
5. N. L. Wendler. *In* Molecular rearrangements. *Edited by* P. de Mayo. Interscience Publishers, Inc., New York. 1964. Part 2. p. 1019 *et seq.*

Can. J. Chem. Downloaded from www.nrcresearchpress.com by 210.87.254.5 on 09/05/12
For personal use only.

6. M. W. GOLDBERG and H. KIRCHENSTEINER. Helv. Chim. Acta, **26**, 288 (1943).
7. N. A. NELSON and R. N. SCHUT. J. Am. Chem. Soc. **81**, 6486 (1959).
8. P. A. S. SMITH and D. R. BAER. *In* Organic reactions. Vol. 11. *Edited by* R. Adams. John Wiley & Sons, Inc., New York. 1960. p. 157 *et seq.*
9. C. D. GUTSCHE. *In* Organic reactions. Vol. 8. *Edited by* R. Adams. John Wiley & Sons, Inc., New York. 1954. p. 364 *et seq.*
10. G. SNATZKE, B. ZEEH, and E. MÜLLER. Tetrahedron, **20**, 2937 (1964).
11. N. A. NELSON. *Quoted by* G. SNATZKE, B. ZEEH, and E. MÜLLER. Tetrahedron Letters, 1425 (1963).
12. J. B. JONES and J. M. ZANDER. To be published.
13. E. L. ELIEL, N. L. ALLINGER, S. J. ANGYAL, and G. A. MORRISON. Conformational analysis. Interscience Publishers, Inc., New York. 1965. pp. 345–350.
14. A. V. KAMERNITZKY and A. A. AKHREM. Tetrahedron, **18**, 705 (1962). E. L. ELIEL, N. L. ALLINGER, S. J. ANGYAL, and G. A. MORRISON. Conformational analysis. Interscience Publishers, Inc., New York. 1965. pp. 112–120.
15. W. G. DAUBEN, G. J. FONKEN, and D. S. NOYCE. J. Am. Chem. Soc. **78**, 2579 (1956).
16. F. V. BRUTCHER and W. BAUER. J. Am. Chem. Soc. **84**, 2236 (1962).
17. L. RUZICKA and H. KÄGI. Helv. Chim. Acta, **20**, 1557 (1937).
18. K. BOWDEN, I. M. HEILBRON, E. R. H. JONES, and B. C. L. WEEDON. J. Chem. Soc. 39 (1946).
19. C. DJERASSI, R. YASHIN, and G. ROSENKRANZ. J. Am. Chem. Soc. **74**, 422 (1952).
20. R. E. MARKER and E. ROHRMANN. J. Am. Chem. Soc. **62**, 900 (1940).

Can. J. Chem. Downloaded from www.nrcresearchpress.com by 210.87.254.5 on 09/05/12
For personal use only.

Can. J. Chem. Downloaded from www.nrcresearchpress.com by 210.87.254.40 on 09/05/12
For personal use only.

PREPARATION AND REACTIONS OF SOME PYRRYLTHIOL ESTERS

E. Bullock, T.-S. Chen, and C. E. Loader
Department of Chemistry, Memorial University, St. John's, Newfoundland
Received December 16, 1965

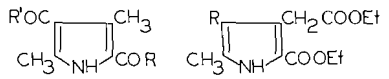
ABSTRACT

Two syntheses and some reactions of pyrrylthiol esters are described. The value of the thiol ester residue as a protecting group in the synthesis of complex pyrroles and their derivatives is considered. A simplified synthesis of a pyrrole related to the uroporphyrins is reported.

The synthesis of complex pyrromethanes and porphyrins requires the use of protecting groups. The literature contains numerous examples, but among the most favored groups are the carboxylic esters of ethyl (e.g. ref. 1), benzyl (e.g. ref. 2), and *t*-butyl (e.g. ref. 3) alcohols. One disadvantage of the ester grouping is that it is frequently necessary to remove it by de-esterification and decarboxylation, to free the specific pyrrole ring position for further synthetic operations.

When considering methods of simplifying classical syntheses of pyrroles and pyrromethanes, we investigated the properties of pyrrylthiol esters. The thiol ester group is potentially valuable since it is easily converted into formyl by treatment with an appropriate grade of Raney nickel.

Pyrrylthiol esters can readily be prepared by ring synthesis, and ethyl acetothiolacetate can be used in Knorr-type syntheses wherever the oxygen analogue has been employed. To test the scope of the synthesis, the three possible thiol ester variants on the Knorr pyrrole (I*a*–I*c*) were prepared. It might be expected that the use of zinc dust in the condensation step would lead to some desulfurization and reduced yields. However, a



Ia R = SEt; R' = OEt
Ib R = OEt; R' = SEt
Ic R = R' = SEt

IIa R = CH_2CH_2COOEt
IIb R = COSEt
IIc R = CHO
IId R = CH=CHCOOEt

comparison between a modified Knorr method (2) and the variant with sodium dithionite as reducing agent (4) showed that the former gave superior yields, which were comparable with those obtained in the synthesis of the analogous oxygen compound.

A second successful synthesis of pyrrylthiol esters involves the use of preformed pyrrole rings. Phenyl isothiocyanate reacts with alkylated pyrroles in α- or β-positions to give very high yields of thiocarbanilides (5). By analogy with the thiobenzanilides, the pyrrylthiocarbanilides were readily S-alkylated by dimethyl sulfate (with or without added base), or by alkyl halides and base. Hydrolysis of the S-alkylthioanilides with very dilute mineral acid gave good yields of the corresponding thiol esters. The products isolated by this method were difficult to purify for analysis (possibly as a result of partial hydrolysis), but behaved as expected in subsequent reactions.

Conversions of the thiol ester group into hydroxymethyl (6) or into aldehyde (7) have been reported. By use of the appropriate grade of Raney nickel we have converted

pyrrylthiol esters into the corresponding formyl derivatives. To obtain simple products it is necessary to prepare the nickel strictly according to the published method (8).

As an example of the use of a thiol ester in synthesis we have prepared a pyrrole (II*a* (9)) related to the uroporphyrins. A Knorr-type condensation of ethyl acetothiolacetate with nitrosated diethyl acetonedicarboxylate (10) gave the thiol ester II*b*. The product was desulfurized with W-2 Raney nickel by a novel technique to give the aldehyde II*c* in about 80% yield. Condensation of II*c* with ethyl hydrogen malonate in pyridine (11) gave a good yield of the acrylic ester II*d*, and this was reduced almost quantitatively to II*a* by hydrogen over Adams' catalyst.

Pyrrylthiol esters behave very much like their oxygen analogues. They are generally colorless and can be purified by crystallization or sublimation. Ethyl 2,4-dimethylpyrrole-5-thiolcarboxylate was compared closely with the corresponding ester, and in some of the common reactions of pyrrole synthesis (e.g. acylation, formylation, and Houben–Hoesch reaction) gives yields and products analogous to those obtained from the oxygen compound.

EXPERIMENTAL

Infrared spectra were recorded on a Perkin–Elmer 237B instrument, ultraviolet spectra on a Beckmann DK-2A, and nuclear magnetic resonance (n.m.r.) spectra on a Varian A-60. Melting points were taken in capillaries and are uncorrected. Analyses are by A. Bernhardt (Mülheim, Germany). Ultraviolet spectra were recorded for solutions in 95% ethanol. Petroleum ether refers to the fraction boiling at 60–80 °C.

Ethyl Acetothiolacetate

Two methods of preparation were used. Claisen condensation (12) of ethyl thiolacetate (13) gave a reasonable yield, but a preparation from diketene is simpler.

(*a*) Ethanethiol (100 g) and anhydrous sodium acetate (0.5 g) were mixed in ligroin (300 ml, b.p. 80–90°); diketene (135 g; T. Schuchardt GMBH, Munich) was added dropwise over 4 h. The reagents were protected against moisture and allowed to stand overnight at room temperature. The solvent was removed by distillation under reduced pressure, and the ester isolated by fractional distillation. The fraction distilling at 92–94° and 12 mm weighed 89 g (38%). This reaction is accompanied by the formation of a large amount of dehydracetic acid.

(*b*) Ethanethiol (15 g) and triethylamine (3 drops) were dissolved in ligroin (100 ml) and treated dropwise with diketene (21 g), with stirring, under gentle reflux. After the solution had been allowed to stand at room temperature overnight, it was poured into ice water. The layers were separated and the aqueous layer was washed twice with ether. The combined organic phases were washed with warm (30–35°) sodium bicarbonate solution and then with water, and dried over anhydrous magnesium sulfate. The solvent was removed under reduced pressure and the thiol ester (19.5 g, 55%) was distilled at 92–94° and 12 mm.

Ethyl 2,4-Dimethyl-3-ethylthiolcarbonylpyrrole-5-carboxylate (Ib)

(*a*) To ethyl acetoacetate (1.3 g) in acetic acid (1.2 ml) was added sodium nitrite (0.7 g, in the minimum volume of water) dropwise, with stirring. The stirring was continued for another 4 h at room temperature, after which the solution was neutralized (Universal indicator paper) with 20% sodium hydroxide solution. Ethyl acetothiolacetate (1.4 g) was added, followed by sodium dithionite (2.6 g (4)), the mixture being kept neutral (by adding 20% caustic soda) and the temperature of the solution being maintained at about 40 °C. After addition of the dithionite the mixture was stirred for another hour at 40 °C and then made alkaline to phenolphthalein. After the solution had stood for 12 h, crystals separated out. The mixture was diluted with water and extracted with ether (3 × 25 ml). The ether extract was washed and dried (Na_2SO_4), and evaporation of the solvent gave a gummy solid which slowly crystallized. Recrystallization from ethanol–water gave colorless needles (0.85 g, 40%), m.p. 112–113 °C, identical with the material described in method *b* below.

(*b*) Sodium nitrite (0.22 g) in water (0.3 ml) was added dropwise to a solution of ethyl acetoacetate (0.4 g) in acetic acid (0.9 ml) at 5 °C, with stirring. The solution was left to stand for 1 h, and then added dropwise to a stirred mixture of ethyl acetothiolacetate (0.41 g), acetic acid (1.4 ml), and zinc dust (0.6 g) at 60°. The temperature of the mixture rose to 100°; this temperature was maintained (steam bath) for 1½ h, and the mixture left to stand overnight at room temperature. The product was isolated as in method *a* above and yielded colorless needles (0.45 g, 57%), m.p. 112–113 °C after crystallization from chloroform – petroleum ether. The product was sublimed (100° at 15 mm) for analysis. Ultraviolet absorption, maxima at 231, 247, and 285.5 mμ ($\log_{10} \epsilon_{max}$ 4.28, 4.16, and 4.14, respectively). The infrared spectrum (KCl disk) showed maxima (*inter alia*) at 1 634 and 1 669 cm^{-1}.

Anal. Calcd. for $C_{12}H_{17}NO_3S$: C, 56.44; H, 6.71; N, 5.49; S, 12.59. Found: C, 56.14; H, 6.65; N, 5.37; S, 12.34.

Can. J. Chem. Downloaded from www.nrcresearchpress.com by 210.87.254.40 on 09/05/12
For personal use only.

Can. J. Chem. Downloaded from www.nrcresearchpress.com by 210.87.254.40 on 09/05/12
For personal use only.

Ethyl 2,4-Dimethyl-3-ethoxycarbonylpyrrole-5-thiolcarboxylate (Ia)

This compound was prepared by method *b* above, on the same scale. In this case the ethyl acetothiolacetate was nitrosated and added to ethyl acetoacetate in the reducing mixture. The product formed very pale yellow needles when crystallized from chloroform – petroleum ether, m.p. 143–144 °C (0.51 g, 60%). Ultraviolet absorption, maxima at 232 and 302 mμ ($\log_{10} \epsilon_{max}$ 4.27 and 4.35, respectively). The infrared spectrum (KCl disk) included peaks at 1 675 and 1 619 cm^{-1}.

Anal. Calcd. for $C_{12}H_{17}NO_3S$: C, 56.44; H, 6.71; N, 5.49; S, 12.59. Found: C, 56.26; H, 6.53; N, 5.60; S, 12.45.

Diethyl 2,4-Dimethylpyrrole-3,5-dithiolcarboxylate (Ic)

The dithiol ester was prepared by method *b* above, except that in this case both halves of the potential pyrrole ring were derived from ethyl acetothiolacetate. The product formed colorless needles, m.p. 107–108 °C (0.59 g, 66%) when crystallized from chloroform – petroleum ether. Ultraviolet absorption, maxima at 237 and 308 mμ ($\log_{10} \epsilon_{max}$ 4.26 and 4.38, respectively). The infrared spectrum (KCl disk) included maxima at 1 650 and 1 594 cm^{-1}.

Anal. Calcd. for $C_{12}H_{17}NO_2S_2$: C, 53.10; H, 6.32; N, 5.16. Found: C, 53.05; H, 6.23; N, 5.30.

Methyl 2-Methylpyrrole-5-thiolcarboxylate

2-Methylpyrrole-5-thiocarbanilide (12 g (5)) was rapidly stirred with caustic soda (3 *N*, 24 ml) and dimethyl sulfate (7 ml) on a steam bath. The two-phase mixture was cooled and treated with ammonium hydroxide (6 *N*, 30 ml) to decompose excess dimethyl sulfate. The mixture was extracted with ether (3 × 50 ml), and the combined extracts were washed with water and dried (Na_2SO_4). Removal of the ether gave a yellowish oil which was crude 2-methylpyrrole-5-(S-methyl)-thiocarbanilide (12 g). This material was used without purification.

The oily product (above) was suspended in hydrochloric acid (1 *N*, 240 ml) and stirred at 100° for 2 h. Crystalline material was deposited and removed (after the mixture had been cooled in ice) by filtration. The filtrate was again heated until no more crystalline material accumulated. The combined precipitates (6.5 g, 75% based on the thioanilide) were recrystallized from chloroform – petroleum ether to give colorless needles, m.p. 126–127°. A sample was sublimed for analysis. Ultraviolet absorption, maxima at 283 and 311.5 mμ ($\log_{10} \epsilon_{max}$ 4.34 and 3.67, respectively). Infrared absorptions (Nujol mull) included a band at 1 620 cm^{-1}. The n.m.r. spectrum (CH_2Cl_2) showed peaks at τ 3.02 and 4.15 (pseudo triplets, ring proton absorptions), 7.58 (S-methyl), and 7.67 (ring methyl).

Anal. Calcd. for C_7H_9NOS: C, 54.17; H, 5.81; N, 9.02; S, 20.66. Found: C, 54.19; H, 5.90; N, 9.20; S, 20.57.

Ethyl 2-Methylpyrrole-5-thiolcarboxylate

This compound was prepared in a manner similar to the above, except for the formation of the S-ethyl-thiocarbanilide. 2-Methylpyrrole-5-thiocarbanilide (6 g (5)) was added to a stirred mixture of sodium hydroxide solution (3 *N*, 24 ml) and ethyl bromide (4 ml). The mixture was boiled under reflux for 4 h, cooled, and extracted with ether (3 × 30 ml). The ether extract was worked up as above to give an almost quantitative yield of the crude S-ethylthioanilide. This compound could be crystallized from aqueous ethanol or chloroform – petroleum ether to give yellow plates, m.p. 49.5–51°, but this was unnecessary for a successful preparation of the ester. The S-ethyl thioanilide (3 g) was hydrolyzed in the same way as the S-methyl compound to give the ethyl thiol ester as colorless needles (1.8 g, 84%), m.p. 88–90 °C. The infrared spectrum showed a maximum at 1 616 cm^{-1} (thiol ester carbonyl).

By analogous reactions, 2,4-dimethylpyrrole-5-(S-ethyl)-thiocarbanilide, m.p. 69.5–70.5°, and ethyl 2,4-dimethylpyrrole-5-thiolcarboxylate, m.p. 111.5–113°, were prepared.

Methyl 2-Methyl-3-formylpyrrole-5-thiolcarboxylate

Methyl 2-methylpyrrole-5-thiolcarboxylate (2.8 g) was added to a cooled mixture of dimethylformamide (6 g) and phosphorus oxychloride (2 ml) while the temperature was maintained below 0°. The red solution was warmed on an oil bath at 35° for 30 min (aldimine hydrochloride begins to crystallize at this point), cooled, and poured into an ice-cold solution of sodium hydroxide (4 g) in water (8 ml). After 10 min the solution was brought to pH 6 with cold 3 *N* hydrochloric acid, and after 10 min more the pinkish precipitate was filtered off. Crystallization of the aldehyde from aqueous ethanol gave off-white needles (2.78 g, 85%), m.p. 179–181°. Ultraviolet spectrum, maxima at 229, 272.5, and 307 mμ ($\log_{10} \epsilon_{max}$ 4.30, 4.04, and 4.26, respectively).

Anal. Calcd. for $C_8H_9NO_2S$: C, 52.50; H, 4.96. Found: C, 52.25; H, 4.98.

Methyl 2,4-dimethyl-3-formylpyrrole-5-thiolcarboxylate, m.p. 145–146°, was prepared in an analogous manner.

Methyl 2-methyl-3-(ethylglyoxalyl)pyrrole-5-thiolcarboxylate, m.p. 167.5–169°, was prepared by a Houben–Hoesch reaction (14) between ethyl cyanoformate and methyl 2-methylpyrrole-5-thiolcarboxylate.

Ethyl 2,4-Dimethyl-3-acetylpyrrole-5-thiolcarboxylate

(*a*) Ethyl 2,4-dimethylpyrrole-5-thiolcarboxylate (0.25 g) in a mixture of acetic acid (2 ml) and acetic anhydride (1 ml) was treated with 70% perchloric acid (5 drops). After 15 min the reddish solution was

poured into ice-cold water. The solid precipitate was collected and crystallized from aqueous ethanol to give colorless crystals, m.p. 123–124°, in an almost quantitative yield. Infrared bands (Nujol mull) at 1 666 and 1 594 cm^{-1} (*inter alia*).

Anal. Calcd. for $C_{11}H_{15}NO_2S$: C, 58.64; H, 6.48; N, 6.22; S, 14.23. Found: C, 58.54; H, 6.75; N, 6.41; S, 14.14.

(*b*) A Knorr-type, ring synthesis reaction between nitrosated ethyl acetothiolacetate (see above) and acetylacetone gave a product identical (melting point, mixed melting point, and spectra) with that prepared by method *a* above.

Desulfurization Experiments

W-2 Raney nickel (8) was used as the standard desulfurization material. It was deactivated with boiling acetone for various periods of time, depending on the activity required. In a typical batchwise desulfurization, Raney nickel (2.8 g) was deactivated by refluxing it with acetone (6 ml) for 1 h. Methyl 2-methylpyrrole-5-thiolcarboxylate (0.25 g) was added, followed by acetone (2 ml) and water (2 ml). The mixture was boiled under reflux for another hour, cooled, and filtered through diatomite. Removal of the solvent *in vacuo* yielded an oily product which rapidly crystallized when treated with a drop of methanol. The crystalline product, 2-methyl-5-formylpyrrole, after sublimation, had m.p. 68.5–69.5° (lit. (15) m.p. 68°) and formed an oxime, m.p. 151–152° (lit. (15) m.p. 153°). The n.m.r. spectrum (CCl_4) showed absorptions at τ 0.69 (singlet, formyl), 3.13 and 3.98 (pseudo triplets, ring protons), and 7.57 (singlet, methyl).

Diethyl Acetonedicarboxylate

The commercial acid (Eastern Chemical Corp., Pequannock, New Jersey) was esterified (10) in very high (81.5%) yield, b.p. 119–124° at 6 mm.

Ethyl 5-Carbethoxy-4-carbethoxymethyl-2-methylpyrrole-3-thiolcarboxylate (IIb)

Freshly distilled amyl nitrite (57 g) was added during 1 h at 20° to a stirred, cooled mixture of ethyl acetonedicarboxylate (97 g) and concentrated hydrochloric acid (0.8 ml). The mixture was allowed to warm up to room temperature spontaneously, and then was heated at 40° for 2 h. The mixture was treated with sodium acetate (1.0 g) and then added (over 30 min) to a vigorously stirred mixture of ammonium acetate (75 g), acetic acid (500 ml), ethyl acetothiolacetate (70 g), and zinc dust (25 g) which was cooled in ice water. During the addition of the nitroso compound, zinc dust (50 g) was added in small portions. After the initial temperature rise had ceased, the reaction mixture was slowly heated to 90°, with continued stirring, during 2 h. The hot solution was decanted from excess zinc into stirred ice water (6 l). The zinc was washed with a little hot 50% acetic acid, and the washings were added to the aqueous mixture. After 2 h the precipitate was collected, washed with 50% aqueous ethanol (200 ml), and crystallized from absolute ethanol to yield colorless, flat prisms (75 g, 48%), m.p. 102–103°. The n.m.r. spectrum (CCl_4) showed absorptions at τ −0.27 (broad, NH), 5.73 and 5.88 (O—CH_2, quartets), 5.81 (—CH_2—CO), 7.02 (S—CH_2, quartet), 7.69 (CH_3), and 8.63, 8.69, and 8.76 (ester CH_3, triplets).

Anal. Calcd. for $C_{15}H_{21}O_5NS$: C, 55.04; H, 6.47; N, 4.29; S, 9.80. Found: C, 55.10; H, 6.47; N, 4.40; S, 9.68.

Ethyl 2-Methyl-3-formyl-4-carbethoxymethylpyrrole-5-carboxylate (IIc)

(*a*) W-2 Raney nickel (50 g) was added to acetone (150 ml) and heated under reflux for 2 h with magnetic stirring. A solution of the above thiol ester (IIb, 3.72 g) in acetone (100 ml) and methanol (50 ml) was added, and the mixture was refluxed for another 2 h. The catalyst was removed and the filtrate evaporated to dryness *in vacuo*. The residue was recrystallized from methanol to give white needles (2.16 g, 71%), m.p. 153–154.5° (lit. (9) m.p. 154°).

(*b*) When the foregoing reaction was repeated with the thiol ester (IIb, 0.75 g) and Urushibara nickel-B (10 g (16)), the aldehyde IIc was again isolated (0.52 g, 85%), m.p. 153–154.5°.

(*c*) W-2 Raney nickel (65 g) and silica gel (100 g) were mixed well and packed into a chromatographic column (25 × 500 mm). Acetone (100 ml) was allowed to percolate through the column at about 2–3 ml/min. The exterior of the column was warmed with a water jacket at 50°, and a solution of the thiol ester (IIb, 4.95 g) in methanol (180 ml) and acetone (20 ml) was run through the column at about 2 ml/min. Fractions were collected and the amount of aldehyde present in each was estimated from the n.m.r. spectrum. When the emerging solution showed gross contamination with starting material and a by-product, the earlier fractions were combined and yielded almost pure aldehyde (3.1 g, 77%) as white needles, m.p. 153–154.5°.

Ethyl 3-Carbethoxymethyl-4-(2′-carbethoxyvinyl)-5-methylpyrrole-2-carboxylate (IId)

A mixture of the foregoing aldehyde (IIc, 3.0 g), ethyl hydrogen malonate (1.8 g), pyridine (10 ml), and piperidine (8 drops) was heated at 90° for 6 h, and then refluxed for another 3 h. The mixture was poured into ice water and neutralized with dilute hydrochloric acid. After 3 h the precipitate was collected, washed with water, and recrystallized from aqueous methanol and then hexane to give colorless prisms, m.p. 88–89° (2.3 g). The filtrate and mother liquors were combined and extracted with ether to yield a further crop of the vinyl ester (0.5 g, total yield 74%).

Anal. Calcd. for $C_{17}H_{23}O_6N$: C, 60.51; H, 6.88; N, 4.16. Found: C, 60.45; H, 6.85; N, 4.14.

The n.m.r. spectrum (CCl_4) showed absorptions at τ −0.25 (broad, NH), 2.40 and 4.10 (olefinic CH, AB quartet, J = 16.5 c.p.s.), 5.77 (quartet, O—CH_2), 6.01 (singlet, —CH_2—CO), 7.71 (CH_3), and 8.68 (triplet,

Can. J. Chem. Downloaded from www.nrcresearchpress.com by 210.87.254.40 on 09/05/12
For personal use only.

ester CH_3). The ester signals were not resolved in the spectrum of this compound and the signals for the $O—CH_2—CH_3$ groups are broad. Integrated areas for all the peaks are in accord with structure II*d*.

Ethyl 3-Carbethoxymethyl-4-(2'-carbethoxyethyl)-5-methylpyrrole-2-carboxylate (IIa)

A solution of the vinyl ester (II*d*, 2.0 g) in 95% ethanol (50 ml) was shaken for 1 h with Adams' catalyst (50 mg) under hydrogen (at 50 lb/sq. in.) at room temperature. The platinum was removed and the solvent distilled off *in vacuo*. The residue was crystallized from cyclohexane to give white needles (1.91 g, 95%), m.p. 63–64° (lit. (9) m.p. 63.5°).

ACKNOWLEDGMENTS

The authors are grateful to Memorial University for a teaching fellowship (awarded to C. E. L.), and to the National Research Council for financial support.

REFERENCES

1. H. FISCHER and H. ORTH. Chemie des Pyrrols. Vols. I and II*a*. Akademische Verlagsgesellschaft, Leipzig. 1937. Numerous examples.
2. S. F. MACDONALD. J. Chem. Soc. 4176 (1952).
3. E. BULLOCK, A. W. JOHNSON, E. MARKHAM, and K. B. SHAW. J. Chem. Soc. 1430 (1958).
4. A. TRIEBS, R. SCHMIDT, and R. ZINSMEISTER. Chem. Ber. **90**, 79 (1957).
5. E. BULLOCK and R. J. ABRAHAM. Can. J. Chem. **37**, 1391 (1959).
6. A. V. MCINTOSH, JR., A. M. SEARCY, E. M. MEINZER, and R. H. LEVIN. J. Am. Chem. Soc. **71**, 3317 (1949).
7. G. B. SPERO, A. V. MCINTOSH, JR., and R. H. LEVIN. J. Am. Chem. Soc. **70**, 1907 (1948).
8. R. MOZINGO. *In* Organic syntheses. Collective Vol. III. E. C. Horning (*Editor*). John Wiley & Sons, Inc., New York. 1947. p. 181.
9. S. F. MACDONALD. J. Chem. Soc. 4184 (1952).
10. R. ADAMS and H. M. CHILES. *In* Organic syntheses. Collective Vol. I. H. Gilman (*Editor*). John Wiley & Sons, Inc., New York. 1947. p. 237.
11. W. A. M. DAVIES, A. R. PINDER, and I. G. MORRIS. Tetrahedron, **18**, 405 (1962).
12. M. W. CRONYN. J. Am. Chem. Soc. **77**, 3033 (1955).
13. R. B. BAKER and E. E. REID. J. Am. Chem. Soc. **51**, 1567 (1929).
14. S. F. MACDONALD and R. J. STEDMAN. Can. J. Chem. **33**, 458 (1955).
15. H. FISCHER. Ber. **61**, 1074 (1928).
16. Y. URUSHIBARA. Bull. Chem. Soc. Japan, **27**, 480 (1954).

Can. J. Chem. Downloaded from www.nrcresearchpress.com by 210.87.254.40 on 09/05/12
For personal use only.

Can. J. Chem. Downloaded from www.nrcresearchpress.com by 210.87.254.5 on 09/05/12
For personal use only.

ÉTUDE QUANTITATIVE DES RÉACTIONS D'OZONOLYSE

II. OZONATION DU *trans*-STILBÈNE

S. FLISZÁR, D. GRAVEL ET E. CAVALIERI
Département de Chimie, Université de Montréal, Montréal, Québec

Reçu le 10 décembre 1965

ABSTRACT

The ozonolysis of 1 mole of *trans*-stilbene (in CCl_4) by a stream of O_2–O_3 leads to the formation of 0.677 mole of stilbene ozonide, 0.468 mole of benzaldehyde, and 0.089 mole of benzaldehyde diperoxide. This ratio, observed for 80–100% ozonizations, is independent of the olefin concentration, the ozone flow rate, and the temperature (in the range 25–45 °C). These observations are explained, if one assumes that the reaction between two zwitterions can follow two courses: (*a*) formation of a dimer peroxide (55%), and (*b*) elimination of oxygen with the formation of two molecules of benzaldehyde (45%).

Depuis que Criegee *et al.* (1) ont décrit la préparation de l'ozonide du *trans*-stilbène, l'ozonation de cette oléfine a fait l'objet de plusieurs travaux (2); on a notamment pu mettre en évidence que la production de fortes proportions d'aldéhyde benzoïque accompagne la formation de l'ozonide (3).

Par ailleurs on a pu montrer que la formation d'ozonides est toujours accompagnée de la production d'aldéhydes. Ainsi, par exemple, on a pu reconnaître et doser l'aldéhyde benzoïque (ozonation du styrène (4)), le formol (ozonation du styrène (4), de l'estragole (4), de l'*o*-méthyleugénol (5) et de l'eugénol (6)), l'aldéhyde acétique (ozonation des anétholes *cis* et *trans* (4*b*), de l'*o*-méthylisoeugénol (7, 4*b*) et de l'isoeugénol (6)), à côté des aldéhydes aromatiques correspondants. De même, le glyoxylate d'éthyle a pu être mis en évidence lors de l'ozonation de trois esters oléfiniques: les maléate, fumarate et cinnamate d'éthyle (8). Il est à souligner que cette production d'aldéhydes se manifeste toujours dès le début de la réaction d'ozonation, et que nous avons vérifié que la présence d'aldéhydes dans le mélange réactionnel ne peut être attribuée à une scission des ozonides. Ces observations peuvent être expliquées en admettant qu'une partie des molécules zwitterion engendrées lors de la scission de l'ozonide primaire[1] réagit avec d'autres molécules zwitterion pour former des peroxydes; ainsi, une partie de l'aldéhyde engendré lors de la scission de l'ozonide primaire n'étant pas consommé par le zwitterion pour donner l'ozonide stable, cette proportion d'aldéhyde se retrouve finalement dans le mélange réactionnel.

Nous nous proposons, dans nos travaux, d'étudier plus en détail le comportement du zwitterion et la formation de peroxydes par la polymérisation de molécules zwitterion. Dans le cas du stilbène, on peut montrer par des expériences très simples que les fragments carbonylé et zwitterion jouissent d'une indépendance marquée (en regard d'un "mécanisme de cage" proposé par Criegee (10)), appuyant ainsi bien les vues de Criegee (11) sur la scission de l'ozonide primaire.

Une première série d'expériences a permis de déterminer, à différents degrés d'avancement de la réaction, les quantités d'aldéhyde benzoïque et d'ozonide formés lors de l'ozonation de 20 ml de solution d'oléfine 0.1 *M* dans CCl_4 (Fig. 1). Ainsi, à 25 °C, on obtient pour le rapport aldéhyde formé/ozonide formé la valeur 0.20 mmole/0.13 mmole = 1.54 pour un degré d'avancement de la réaction d'environ 13.5%; ce rapport décroît à 0.75 (pour 76.5% de réaction) et, pour l'ozonation complète, à 0.59. Le fait que l'aldéhyde se forme

[1]*Le mécanisme d'ozonolyse de Criegee est brièvement résumé en réf. 9.*

principalement au début de la réaction montre clairement, d'une part, que la probabilité de réaction associée à une rencontre entre deux molécules zwitterion pour former un peroxyde est avantagée par rapport à la probabilité de réaction se rapportant à une rencontre entre une molécule zwitterion et une molécule d'aldéhyde pour donner l'ozonide, et, d'autre part, que les fragments zwitterion et aldéhyde issus de la scission de l'ozonide primaire sont en large mesure indépendants. On note, en effet, que les rendements en ozonide, très faibles en début de réaction, vont en augmentant avec l'avancement de la réaction (~37% à 6% de réaction et ~75% à la fin de la réaction) du fait que l'accumulation progressive de l'aldéhyde favorise la formation de l'ozonide.

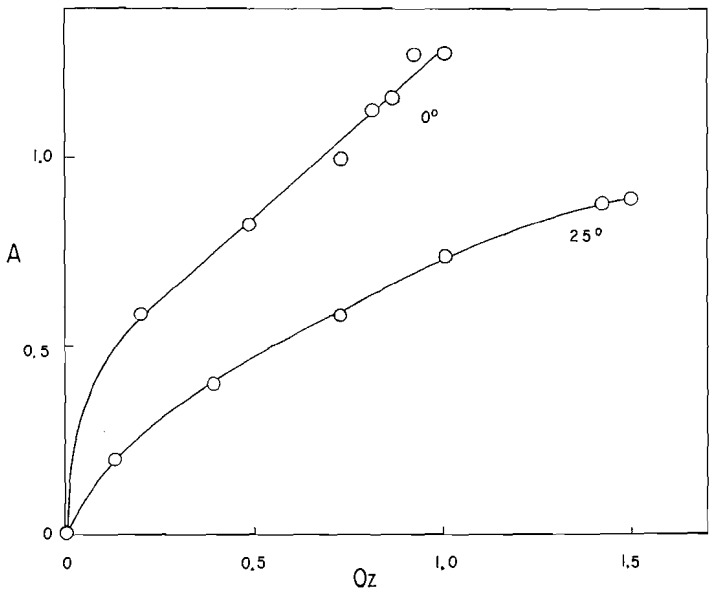


FIG. 1.

Ce phénomène est encore plus accusé aux basses températures. On note, en effet, à 0 °C (Fig. 1) les grandes proportions d'aldéhyde formé au début de la réaction, contrastant avec la production relativement faible d'ozonide; ainsi on a un rendement en ozonide de seulement 31% (rapporté à l'oléfine consommée) pour une consommation de 32% de l'oléfine initialement présente, ce rendement en ozonide étant encore bien plus faible aux phases initiales de la réaction.[2]

Nous nous sommes d'ailleurs assurés que la forte production d'aldéhyde benzoïque n'est pas due à une décomposition des produits engendrés par l'ozonation: ozonide et peroxyde dimère (I). Une solution 0.05 *M* d'ozonide de *trans*-stilbène dans CCl_4, chauffée à reflux pendant 5 h, ne montre que des traces d'aldéhyde benzoïque; une solution 0.05 *M* (dans CCl_4) de diperoxyde de benzaldéhyde (I), chauffée pendant 5 h à reflux, n'a pas engendré d'aldéhyde benzoïque en quantité décelable. Ces constatations sont importantes, particulièrement en ce qui touche la stabilité du diperoxyde de benzaldéhyde, lorsqu'on examine les bilans de production d'aldéhyde.

[2]*Les valeurs reproduites dans la Fig. 1 pour l'ozonation à* 0 °C *ont été obtenues au moyen de deux séries d'expériences indépendantes; dans d'autres cas (pour des raisons que nous n'avons pas pu éclaircir) les rendements en ozonide ont été encore bien plus faibles.*

Can. J. Chem. Downloaded from www.nrcresearchpress.com by 210.87.254.5 on 09/05/12
For personal use only.

En vue de faciliter la discussion, définissons le rapport: r = (aldéhyde plus ozonide formés)/stilbène consommé, qui représente la quantité totale d'aldéhyde (soit sous forme libre, soit sous forme d'ozonide) engendré par mole d'oléfine ozonée. Or, dans toutes les expériences d'ozonation du stilbène, on trouve $r > 1$ ($r = 1.19$ à 25° et $r = 1.14$ à 0° dans les expériences rapportées à la Fig. 1) bien que l'ozonolyse du stilbène engendre en un premier temps des quantités égales d'aldéhyde et de zwitterion, soit 1 mole de chaque produit par mole d'oléfine consommée (Tableau I).

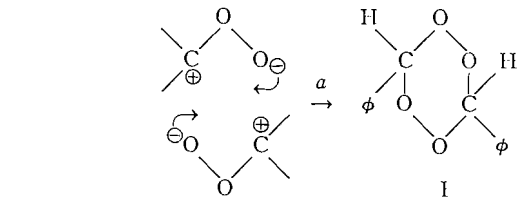
TABLEAU I

Ozonation de 2.0 mmoles de stilbène dans 20 ml de CCl_4 à 25 °C, en présence de CH_3OH (0.5 M)

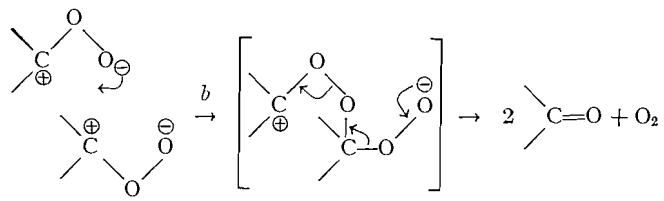
O_3 consommé	Stilbène consommé	ϕ CHO formé	Hydroperoxide formé
0.53	0.51	0.50	0.52
1.08	1.09	1.08	1.10
1.48	1.49	1.49	1.50
1.85	1.83	1.84	1.82

NOTONS: Débit O_3: 0.046 mmole/min. Les quantités sont indiquées en millimoles.

Par conséquent, puisque ni l'ozonide ni le diperoxyde de benzaldéhyde ne se décomposent pour engendrer de l'aldéhyde benzoïque, et puisqu'au départ (à la suite de la scission de l'ozonide primaire) il se forme 1 mole d'aldéhyde par mole d'oléfine consommée, on est conduit à admettre que la formation excessive de benzaldéhyde intervient au stade de la réaction entre zwitterions,[3] cette réaction pouvant soit engendrer un peroxyde dimère (I) par la voie a, soit aboutir à la formation d'aldéhyde benzoïque avec élimination d'oxygène par la voie b.



I



II

On note la similitude de ces conclusions avec celles exposées au sujet de l'ozonation du tétraphényléthylène (9), sauf que pour cette dernière oléfine la décomposition en composé carbonylé ne prenait d'importance qu'aux températures plus élevées (~80 °C) ou encore en présence d'un agent réducteur (I^- en solution acétique), tandis que dans le cas du

[3] *Une possibilité de réaction entre deux molécules d'ozonide primaire, qui (du point de vue de la stoïchiométrie) pourraient engendrer quatre molécules d'aldéhyde et une molécule d'oxygène, ne semble pas devoir être retenue, du fait de la très grande instabilité des ozonides primaires.*

Can. J. Chem. Downloaded from www.nrcresearchpress.com by 210.87.254.5 on 09/05/12
For personal use only.

Can. J. Chem. Downloaded from www.nrcresearchpress.com by 210.87.254.5 on 09/05/12
For personal use only.

stilbène cette décomposition spontanée est très rapide, même à 25 °C. Ceci peut être interprété en observant que la présence dans l'intermédiaire II de deux atomes d'hydrogène (cas du stilbène) en lieu de deux noyaux phényles (cas du tétraphényléthylène) diminue la délocalisation des charges positive et négative dans cet intermédiaire, favorisant ainsi le mécanisme de type "push–pull" représenté en II.

En vue d'évaluer en quelles proportions la voie *b* est suivie, nous avons procédé à une série de déterminations, résumées dans le Tableau II.

On remarque que, même sujets à quelques fluctuations, les rendements en ozonide sont inférieurs aux températures $\leqslant 0°$ par rapport aux températures plus élevées ($\geqslant 25°$); dans tous les cas les valeurs calculées pour r sont supérieures à l'unité, et proches de 1.14 pour les températures $\geqslant 25°$. Ces chiffres représentent en fait un grand excès de production d'aldéhyde, par rapport à la production qui aurait été observée en absence d'un mécanisme de décomposition (voie *b*). Par exemple, l'ozonation complète à 25° de 20 ml de solution 0.1 *M* de stilbène a engendré 1.40 mmoles d'ozonide; donc $2.00 - 1.40 = 0.60$ mmole de benzaldéhyde n'ont pas été utilisées pour la formation de l'ozonide et devraient se retrouver dans le mélange réactionnel; en fait, on trouve 0.88 mmole d'aldéhyde, soit près de 50% de plus que la quantité attendue.

Pour évaluer le pourcentage de zwitterion se décomposant en aldéhyde plus oxygène par rapport à la totalité du zwitterion non utilisé pour la formation d'ozonide, on a avantage à procéder comme suit, ce calcul tenant compte de l'ensemble des résultats obtenus.

Posons (en millimoles) A = aldéhyde et Oz = ozonide formés pour S = stilbène consommé; f = proportion de zwitterion se décomposant en aldéhyde plus oxygène par rapport à la quantité de zwitterion non utilisé pour former l'ozonide. En absence d'un mécanisme de décomposition, le bilan d'ozonation s'écrirait comme suit: 1 mmole de stilbène ozoné $\rightarrow Oz/S$ (ozonide) + $(1 - Oz/S)$ (aldéhyde) + $(1 - Oz/S)$ (zwitterion). La quantité d'aldéhyde formé par millimole de stilbène ozoné étant A/S, l'excès $A/S - (1 - Oz/S)$ représente l'aldéhyde formé par décomposition de zwitterion, soit le nombre de millimoles de zwitterion que s'est décomposé par millimole de stilbène ozoné, donc pour $1 - Oz/S$ millimole de zwitterion non utilisé pour la formation d'ozonide. Alors, par définition, $f = (A/S + Oz/S - 1)/(1 - Oz/S)$, une expression que peut s'écrire comme suit: $S/A = [1/(f + 1)] + Oz/A$.

La Fig. 2, qui reproduit les valeurs de S/A et de Oz/A calculées d'après les résultats résumés dans le Tableau II, montre bien que la relation que nous venons de déduire est satisfaite pour $f \simeq 0.45$; en trait pointillé est indiqué le résultat auquel on aurait du s'attendre pour $f = 0$, c'est-à-dire s'il n'y avait pas de formation d'aldéhyde à partir de zwitterion.

Le calcul de f a été effectué sur les résultats (Tableau II) se rapportant aux expériences faites aux températures $\geqslant 25°$ et $\leqslant 45°$; l'estimé des déviations relatives nous a conduit à rejetter les 2 valeurs marquées d'un astérisque, manifestement entachées d'erreurs expérimentales (Fig. 2), et à accepter les autres 11 résultats,[4] d'après lesquels $f = 0.451$ avec l'écart type 0.0166; exprimé avec une limite de confiance de 95%, on obtient $f = 0.451 \pm 0.037$. Pour simplifier la discussion nous admettrons $f = 0.45$, ce qui signifie qu'environ 45% du zwitterion n'ayant pas réagi avec l'aldéhyde pour former l'ozonide se décompose en aldéhyde benzoïque plus oxygène (voie *b*), les autres 55% se retrouvant sous forme de diperoxyde de benzaldéhyde. Ce dernier point est confirmé par des expériences exposées plus loin.

[4]*Concernant les règles pour le rejet de valeurs douteuses, voir, par exemple, réf. 11, p. 173.*

Can. J. Chem. Downloaded from www.nrcresearchpress.com by 210.87.254.5 on 09/05/12
For personal use only.

TABLEAU II

Ozonation de 20 ml de solutions de stilbène 0.1 et 0.2 *M* dans CCl_4

Temperature (°C)	Concentration stilbène	Débit O_3	% ozonation	Stilbène consommé	ϕ CHO formé	Ozonide formé	Rendement en ozonide	r
−20	0.1	0.060	93.0	1.86	1.69	0.54	29	1.20
−10	0.1	0.115	84.5	1.69	1.82	0.31	18	1.26
0	0.1	0.058	99.0	1.98	1.42	0.92	46	1.14
0	0.1	0.111	86.0	1.72	2.27	0.18	10.5	1.42
25	0.1	0.061	100.0	2.00	0.88	1.40	70.0	1.14
25	0.2	0.062	94.5	3.77	1.83	2.64	70.0	1.13
25	0.1	0.114	83.2	1.66	0.78	1.09	65.7	1.13
25	0.2	0.116	79.3	3.17	1.46	2.23	70.4	1.16
35	0.1	0.059	96.5	1.93	0.88	1.32	68.5	1.14
35	0.1	0.057	94.5	1.88	0.84	1.29	68.6	1.14
35	0.2	0.064	99.0	3.95	1.80	2.70	68.5	1.14
35*	0.1	0.128	89.0	1.78	0.80	1.11	62.5	1.07
35	0.2	0.110	77.0	2.17	1.18	1.39	64.0	1.18
45	0.1	0.060	97.5	1.95	0.92	1.28	65.5	1.13
45	0.2	0.058	93.5	3.74	1.76	2.52	67.5	1.14
45*	0.2	0.125	97.0	3.88	1.90	2.84	73.2	1.22
45	0.2	0.120	97.4	3.89	1.96	2.58	66.4	1.16

NOTONS: Débit O_3: millimole/minute. Les quantités (stilbène, ϕCHO et ozonide formés) sont indiquées en millimoles.

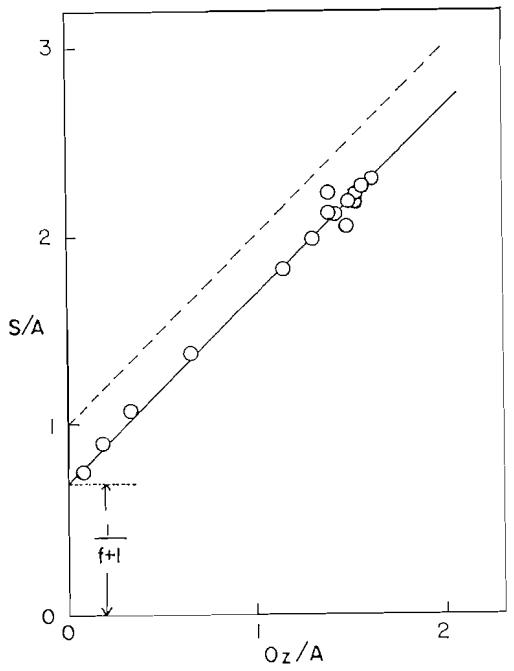


FIG. 2.

En ce qui concerne les rendements en ozonide (rapportés aux quantités d'oléfine consommée), l'analyse statistique des résultats du Tableau II ne permet pas de conclure à une différence significative de ces rendements à 25°, 35° et 45°. Par conséquent, sans faire de distinction quant à la température, le calcul conduit au résultat suivant, exprimé avec une limite de confiance de 95%: rendement en ozonide (rapporté à l'oléfine consommée) = 67.7 ± 1.3%, pour une consommation de 80–100% de l'oléfine initialement présente.

D'après les résultats obtenus, le bilan de l'ozonation du stilbène, en solution dans du CCl_4, s'établit donc comme suit, aux températures comprises entre 25 et 45 °C: 1.0 mole d'oléfine engendre 1.0 mole d'ozonide primaire, qui se scinde en 1.0 mole d'aldéhyde benzoïque plus 1.0 mole de zwitterion. C'est le processus de Criegee, confirmé par les expériences effectuées en présence de CH_3OH. Dans une deuxième étape, 0.677 mole de zwitterion réagit avec une égale quantité d'aldéhyde benzoïque pour former 0.677 mole d'ozonide; restent donc 0.323 mole de benzaldéhyde et 0.323 mole de zwitterion non utilisés. Finalement, 45% du zwitterion non utilisé pour former l'ozonide réagit selon la voie *b* avec formation de 0.145 mole de benzaldéhyde, et 55% réagit selon la voie *a* en engendrant un peroxyde stable. Il s'est ainsi formé complessivement 0.323 + 0.145 = 0.468 mole d'aldéhyde benzoïque[5] par mole de stilbène ozoné, soit près de 1.45 fois la quantité attendue en absence d'une décomposition du zwitterion.

Nous nous sommes encore assurés de la constance de f dans le cas de réactions moins avancées, alors que les rendements en ozonide sont inférieurs à 67.7% (Tableau III). De même nous avons dosé approximativement le diperoxyde de benzaldéhyde en l'isolant de solutions ozonées à 100% et en le séparant de l'ozonide par des recristallisations fractionnées dans du CH_3OH; dans trois expériences nous avons ainsi obtenu des rendements correspondant à 55, 65 et 69% par rapport à la quantité attendue, soit 0.089 mmole par

[5]*Ce rendement en aldéhyde benzoïque peut être obtenu directement en formant la moyenne des quantités A/S observées dans les 11 expériences retenues dans l'établissement de ce bilan.*

Can. J. Chem. Downloaded from www.nrcresearchpress.com by 210.87.254.5 on 09/05/12
For personal use only.

millimole de stilbène ozoné; des rendements variant entre 50 et 70% ont été également obtenus lors de l'isolement de ce diperoxyde à partir de mélanges artificiels d'ozonide et de diperoxyde. Ces observations portent à croire que les 55% du zwitterion non engagé dans la formation d'ozonide engendrent (du moins en majeure partie) du diperoxyde de benzaldéhyde.

TABLEAU III

Ozonation de 20 ml de solution 0.1 *M* de *trans*-stilbène à 25 °C

S	*A*	*Oz*	*f*
0.268	0.20	0.13	0.442
0.673	0.40	0.40	0.460
1.134	0.58	0.73	0.435

NOTONS: *S*, *A* et *Oz*: millimoles.

Quant aux expériences effectuées aux températures $\leqslant 0$ °C, on note $r > 1$ (donc qu'il y a une décomposition du zwitterion en benzaldéhyde) et que les rendements en ozonide sont inférieurs à ceux trouvés aux températures $\geqslant 25$ °C. Ces expériences étant toutesfois difficilement reproductibles, nous nous limiterons pour l'instant à ces constatations.

PARTIE EXPÉRIMENTALE

La technique d'ozonation, le dosage de l'ozone et des hydroperoxydes ont été décrits précédemment (9). L'aldéhyde benzoïque et l'ozonide ont été dosés par voie spectrographique infrarouge d'après les densités optiques de la bande de vibration du groupement carbonyle à 1 705 cm^{-1} pour l'aldéhyde et de la bande à 1 053 cm^{-1} de l'ozonide (3); l'ozonide[6] (p.f. 74 °C) ayant servi à l'établissement des courbes de calibration a été préparé selon Criegee (1). Les dosages du *trans*-stilbène (Eastman Kodak, scintillation grade) ont été effectués par spectrophotométrie en ultraviolet à 312 mμ; nous nous sommes assurés que cette bande disparaît complètement par ozonation à 100%. Le diperoxyde de benzaldéhyde isolé du mélange réactionnel (et purifié par plusieures cristallisations fractionnées dans du CH_3OH) a été reconnu identique par son point de fusion et le point de fusion du mélange à un échantillon préparé selon réf. 12, p.f. 202 °C, confirmant ainsi une expérience de Criegee (1). Ce produit possède dans son spectre infrarouge (en solution dans du CCl_4) deux bandes faibles vers 1 023 et 1 006 cm^{-1}, et n'absorbe pas à 1 053 cm^{-1}; par conséquent sa présence ne gêne nullement les mesures d'intensité de la forte bande de l'ozonide (1 053 cm^{-1}).

REMERCIEMENTS

Nous sommes reconnaissants à M. le Professeur C. Sandorfy, Directeur du Laboratoire de Spectroscopie chimique, pour toutes les facilités qu'il nous accorde dans nos recherches expérimentales. Nous remercions également M. G. Bélanger de son assistance technique précieuse, et le Conseil National de Recherches du Canada pour une subvention qui a permise ces recherches.

BIBLIOGRAPHIE

1. R. CRIEGEE, A. KERCKOV ET H. ZINKE. Chem. Ber. **88**, 1878 (1955).
2. S. MARVEL et V. NICHOLS. J. Org. Chem. **6**, 296 (1941). E. BRINER, E. DALLWIGK et M. RICCA. Helv. Chim. Acta, **41**, 1390 (1958).
3. E. BRINER, C. CHRISTOL, H. CHRISTOL et S. FLISZÁR. Helv. Chim. Acta, **44**, 1088 (1961).
4. (*a*) E. BRINER, S. FLISZÁR et M. RICCA. Helv. Chim. Acta, **42**, 749 (1959). (*b*) E. BRINER, C. CHRISTOL, H. CHRISTOL, S. FLISZÁR et G. ROSSETTI. Helv. Chim. Acta, **46**, 2249 (1963).
5. E. BRINER et S. FLISZÁR. Helv. Chim. Acta, **42**, 2063 (1959).
6. E. BRINER et S. FLISZÁR. Helv. Chim. Acta, **42**, 1310 (1959).
7. E. BRINER et E. DALLWIGK. Helv. Chim. Acta, **39**, 1446 (1956). E. DALLWIGK et E. BRINER. Helv. Chim. Acta, **39**, 1826 (1956).
8. E. BRINER, S. FLISZÁR et G. P. ROSSETTI. Helv. Chim. Acta, **47**, 2041 (1964).
9. S. FLISZÁR, D. GRAVEL et E. CAVALIERI. Can. J. Chem. **44**, 67 (1966).
10. R. CRIEGEE. Record Chem. Progr. Kresge-Hooker Sci. Lib. **18**, 111 (1957).
11. N. ARLEY et K. RANDER BUCH. Introduction to the theory of probability and statistics. John Wiley & Sons, Inc., New York. 1953.
12. A. BAEYER et V. VILLIGER. Chem. Ber. **33**, 2484 (1900).

[6]*La géométrie de cet ozonide n'ayant pas encore été établie de manière certaine, nous reviendrons sur ce sujet lors d'un prochain travail.*

Can. J. Chem. Downloaded from www.nrcresearchpress.com by 210.87.254.5 on 09/05/12
For personal use only.

Can. J. Chem. Downloaded from www.nrcresearchpress.com by 210.87.254.105 on 09/05/12
For personal use only.

THE STEREOSELECTIVE ADDITION OF DIHALOCARBENES TO *cis,trans,trans*-CYCLODODECA-1,5,9-TRIENE AND THE SYNTHESIS OF CYCLOTRIDECANONE

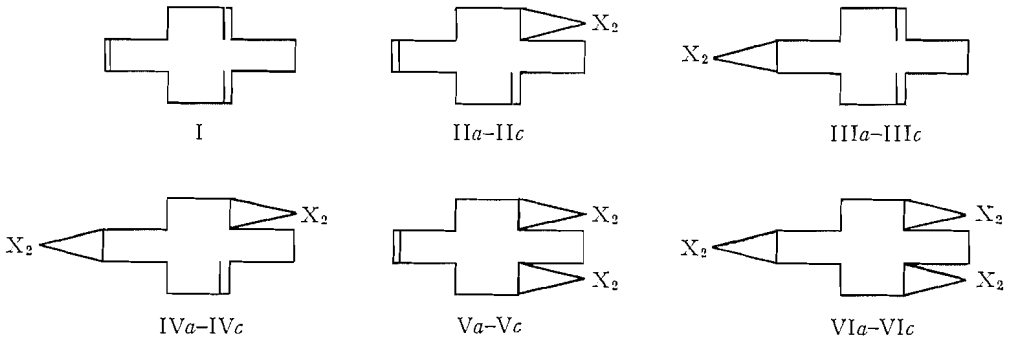
H. NOZAKI, S. KATÔ, AND R. NOYORI
Department of Industrial Chemistry, Kyôto University, Kyôto, Japan
Received December 21, 1965

ABSTRACT

The addition reactions of dibromo- and dichloro-carbenes to *cis,trans,trans*-cyclododeca-1,5,9-triene (I) followed a stereoselective scheme analogous to that of other reagents forming a three-membered ring on addition to an olefinic bond. The carbenes attacked preferentially one of the *trans* double bonds of I and then added to the *cis* double bond of the resulting bicyclic *cis,trans* dienes. Skattebøl's ring cleavage of dihalocarbene adducts of *cis*-cyclododecene as well as of the monoadducts of I, followed by several steps, gave cyclotridecanone in fairly good yields.

In a continuation of the work on 12-membered homocyclic systems (1), the addition reactions of dihalocarbenes to *cis,trans,trans*-cyclododeca-1,5,9-triene (I) and *cis*-cyclododecene (VII) were examined, and the resulting adducts were transformed into cyclotridecanone in fair yields.

The chemistry of the addition of dihalocarbenes to the triene I is described first.[1] Treatment of the triene I with bromoform and potassium *t*-butoxide gave a mixture of the monoadducts (II*a*, III*a*) of dibromocarbene as a viscous oil. Similarly, reaction of the triene I with dichlorocarbene, as produced by thermal decomposition of sodium trichloroacetate in diglyme or by treatment of chloroform with potassium *t*-butoxide, gave the corresponding adducts (II*b*, III*b*) in good yields. Reduction of these dihalocarbene adducts with metallic sodium dissolved in liquid ammonia (3) yielded an isomeric mixture of bicyclo[10.1.0]tridecadienes (II*c*, III*c*) smoothly. Reduction of all of the dihalomethylena-



a X = Br *b* X = Cl *c* X = H

tion products yielded a mixture of mono- (II*c*, III*c*), bis- (IV*c*, V*c*), and tris-cyclopropane derivatives (VI*c*). All of the halogen-free cyclopropanes were identified by comparison of the retention times on gas–liquid chromatography (g.l.c.) with those of the specimen

[1]*Preferential addition of dichlorocarbene to a trans double bond of I was very recently recorded independently (2).*

previously synthesized by means of the Simmons–Smith reaction (1*b*). The isomer distributions of the cyclopropane hydrocarbons should be regarded as reflecting those of the parent dihalocarbene adducts and are summarized in Table I.

TABLE I

Stereoselectivity of the addition of dihalocarbenes to *cis,trans,trans*-cyclododeca-1,5,9-triene

Carbene	Method of generation	Reaction temperature (°C)	Monoadduct II/III	Bisadduct* IV/V
CBr_2	$CHBr_3$–KOBu-*t*	−10 to 25	89:11	84:16
CCl_2	$CHCl_3$–KOBu-*t*	−5 to 25	91:9	87:13
CCl_2	CCl_3COONa	80 to 90	85:15	72:28
$(ICH_2)_2Zn \cdot ZnI_2$†		35	97:3	81:19

*The ratios were calculated on the basis of the peak areas in g.l.c. (high-vacuum silicone grease (2 m), He). Polyethylene glycol 6000 treated with silver nitrate as the stationary phase gave practically the same results.
†The results obtained in the previous work (1*b*) are reproduced.

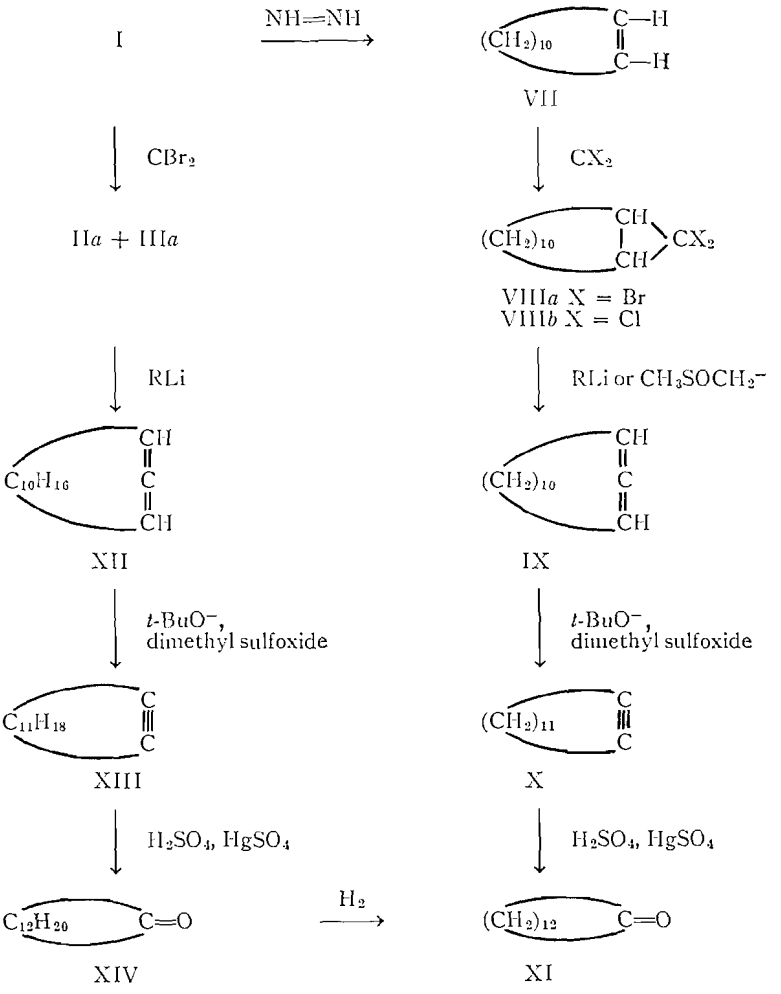
The *trans* double bond of the triene I appears to be much more susceptible to the electrophilic attack of dihalocarbenes, even the selectivity being comparable to that of the Simmons–Smith reagent (4). Further attack of the carbene on the respective monoadducts occurs at the *cis* bond rather than at the *trans* bond, with poorer preference. Such a behavior of carbenes is closely analogous to that previously observed in the epoxidation (5) and the Simmons–Smith reaction (1*b*), all proceeding with closure of a three-membered ring. In contrast, however, the recorded *cis* additions of the triene I that yield monocyclic products, viz. diimide reduction, etc., occur predominantly at the *trans* bonds even in the second stage of the addition.[2]

The next problem is concerned with the synthesis of cyclotridecanone (XI) (6) from the triene I via the dihalocarbene monoadducts. Diimide reduction (1*a*) of the triene I gives selectively *cis*-cyclododecene (VII), which has been used as the starting material in the first synthesis. Treatment of VII with dibromocarbene as produced from bromoform and potassium *t*-butoxide gave the adduct VIII*a* as an oil in 70% yield based on the amount of VII consumed. Ring enlargement by the method of Skattebøl (7) resulted in the formation of cyclotrideca-1,2-diene (IX) in 76% yield. The corresponding dichlorocarbene adduct VIII*b* could also be dehalogenated with *n*-butyllithium to give IX, whereas methyllithium proved to be inactive toward VIII*b*. Treatment of the dibromocarbene adduct VIII*a* with sodium methylsulfinyl carbanion (8) in dimethyl sulfoxide gave the allene IX in 46% yield. These samples of the allene IX were found to be contaminated with 10–20% of the acetylenic isomer X,[3] but IX was so easily autoxidized that this could not be isolated in an analytically pure form. The oily product consisting largely of IX was immediately subjected to isomerization caused by potassium *t*-butoxide in dimethyl sulfoxide, to yield cyclotridecyne (X). Other bases such as potassium *t*-butoxide in *t*-butanol, potassium hydroxide in ethanol, methyllithium, and basic alumina failed to effect this isomerization.[4]

The cyclic allene IX showed characteristic infrared absorptions at 1 950 and 870 cm^{-1}, whereas the cycloalkyne X showed no absorption around 2 200 cm^{-1}. Hydration of X by the action of dilute sulfuric acid containing mercuric sulfate gave the desired ketone XI as a crystalline solid, m.p. 26–30°. The yield of XI based on I amounted to about 25%.

[2]*Previous data were summarized in ref. 1b.*
[3]*The analysis was performed by g.l.c. (polyethylene glycol 6000 treated with silver nitrate, He). For acetylene formation as by-products in this kind of reaction, see ref. 7.*
[4]*For allene–acetylene equilibration in cyclic systems, see ref. 9.*

Can. J. Chem. Downloaded from www.nrcresearchpress.com by 210.87.254.105 on 09/05/12
For personal use only.



In the second process, a similar sequence of reactions was applied to the dibromocarbene monoadducts (II*a*, III*a*) of the triene I; cyclotridecadienone (XIV) was obtained in about a 20% yield based on I. Final catalytic reduction of XIV upon palladium–charcoal gave XI in an almost quantitative yield.

Although the yields of XI that were realized were not very high, the ready availability of the starting material I and the simplicity of each preparative step would give the present routes precedence over the known ones (6).

EXPERIMENTAL

All temperatures were uncorrected. Microanalyses were performed at the Elemental Analyses Centre, Kyôto University.

13,13-Dibromo-trans-bicyclo[10.1.0]trideca-cis-4,trans-8-diene (IIa)

To a stirred mixture of I (57.0 g; 0.35 mole), potassium *t*-butoxide (77.5 g; 0.70 mole), and dry *n*-hexane (40 ml) was added freshly distilled bromoform (127 g; 0.50 mole) at −10 to 0° during 4 h under a nitrogen atmosphere. After an additional 5 h of stirring at room temperature, the mixture was treated with water and extracted with methylene chloride. Distillation *in vacuo* gave the unchanged triene I (18 g) and then the dibromocarbene adduct (a mixture of II*a* and III*a*) (58.5 g; 73% yield based on the amount of the triene I

Can. J. Chem. Downloaded from www.nrcresearchpress.com by 210.87.254.105 on 09/05/12
For personal use only.

consumed) as a viscous oil, b.p. 103–107° at 0.07 mm. Infrared absorptions (neat): 970 s (*trans* double bon d and 700 cm^{-1} (a closely separated twin peak, *cis* double bond).

Anal. Calcd. for $C_{13}H_{18}Br_2$: C, 46.7; H, 5.4. Found: C, 46.8; H, 5.7.

13,13-Dichloro-trans-bicyclo[10.1.0]trideca-cis-4,trans-8-diene (IIb)

To a slurry of potassium *t*-butoxide (33.6 g; 0.30 mole) in the triene I (32.4 g; 0.20 mole) and dry *n*-hexane (30 ml) kept at −5 to 0°, freshly distilled chloroform (36.0 g; 0.30 mole) was added dropwise during 3 h under a nitrogen atmosphere; the mixture was then allowed to stand at room temperature for 20 h. Distillation *in vacuo* gave the unchanged triene I (9.5 g) and the dichlorocarbene monoadduct (a mixture of II*b* and III*b*) (31.5 g; 91% yield based on the amount of I consumed) as a colorless oil, b.p. 115–118° at 1 mm. Infrared absorptions (neat): 970 (*trans* double bond) and 700 cm^{-1} (*cis* double bond).

Anal. Calcd. for $C_{13}H_{18}Cl_2$: C, 63.7; H, 7.4. Found: C, 63.9; H, 7.6.

A mixture of the triene I (8.1 g; 0.05 mole) and dried sodium trichloroacetate (14.8 g; 0.08 mole) in anhydrous diglyme (30 ml) was heated at 80–90° until the evolution of carbon dioxide had ceased. The reaction mixture was treated as usual and distilled *in vacuo* to give the dichlorocarbene adduct (a mixture of II*b* and III*b*) (6.4 g; 83% yield based on the amount of I consumed), b.p. 112–117° at 1 mm, besides the unchanged triene I (3.0 g).

Reduction of the Dihalocarbene Adducts with Sodium in Liquid Ammonia (3)

To a solution of metallic sodium (2.3 g; 0.1 g-atom) in liquid ammonia (80 ml) kept at −60°, an ethereal solution containing the dichlorocarbene monoadduct (a mixture of II*b* and III*b*) (4.9 g; 0.02 mole) was added dropwise during 30 min; the mixture was then stirred for an additional 5 h. After treatment with ammonium hydroxide solution, the mixture was extracted with ether. Distillation *in vacuo* gave a mixture of *cis*- and *trans*-bicyclo[10.1.0]tridecadiene (II*c* and III*c*) (3.1 g; 88% yield), b.p. 110–113° at 10 mm. A similar treatment of the isomeric mixture of the dibromocarbene adducts (II*a* and III*a*) gave the hydrocarbon mixture (II*c* and III*c*) in 86% yield.

The g.l.c. analyses of the cyclopropane hydrocarbons II*c* and III*c* of various origins are given in Table I.

Dehalogenation of the distillation residue of the dihalocarbene monoadducts or of the crude addition products directly without isolation of each component gave a hydrocarbon mixture, which was subjected to g.l.c. analyses. The isomer distributions of the bis-cyclopropane fraction (IV*c*, V*c*) are given in Table I. Traces of the tris-cyclopropane fraction (VI*c*) were definitely detected.

13,13-Dibromo-cis-bicyclo[10.1.0]tridecane (VIIIa)

To a suspension of potassium *t*-butoxide (77.5 g; 0.70 mole) in *cis*-cyclododecene (VII) (1*a*) (57.8 g; 0.35 mole) and dry *n*-hexane (40 ml) cooled at −10°, freshly distilled bromoform (127 g; 0.50 mole) was added dropwise, with stirring, during 4 h; the mixture was then allowed to stand at room temperature for 5 h. The reaction was carried out under a nitrogen atmosphere, and the addition at temperatures below 0°. The reaction mixture was treated with water and extracted with methylene chloride. The combined extracts were washed with 2 *N* hydrochloric acid, sodium bicarbonate solution, and water; dried over calcium chloride; and concentrated *in vacuo*. Distillation of the residue gave unchanged cyclododecene (17.5 g) and the dibromocarbene adduct VIII*a* (59.4 g; 70% yield based on the amount of olefin VII consumed) as a viscous pale-yellow oil, b.p. 110–115° at 0.08 mm.

Anal. Calcd. for $C_{13}H_{22}Br_2$: C, 48.2; H, 6.6. Found: C, 48.4; H, 6.5.

13,13-Dichloro-cis-bicyclo[10.1.0]tridecane (VIIIb)

A suspension of potassium *t*-butoxide (prepared from 6.0 g (0.15 g-atom) of potassium and freed from *t*-butanol) in *cis*-cyclododecene (VII) (24.9 g; 0.15 mole) and *n*-hexane (20 ml) was kept below 10° under nitrogen. To this, chloroform (17.8 g; 0.15 mole) was added dropwise, with stirring, during 3 h. After the reaction mixture was allowed to stand at room temperature for 1 h, it was treated with water and extracted with *n*-hexane. The extracts were combined, washed, dried, and concentrated *in vacuo*. Distillation of the residual oil gave the dichlorocarbene adduct VIII*b* (23.2 g; 81% based on the amount of VII consumed), b.p. 94–98° at 0.1 mm, besides unchanged VII (5.5 g).

Anal. Calcd. for $C_{13}H_{22}Cl_2$: C, 62.7; H, 8.9. Found: C, 62.9; H, 8.9.

Cyclotrideca-1,2-diene (IX) by Debromination of VIIIa with Methyllithium

To a solution of the *gem*-dibromide VIII*a* (67.6 g; 0.20 mole) in anhydrous ether (200 ml) kept below −40° under a nitrogen atmosphere, an ethereal solution of methyllithium (50 ml; 0.20 mole) was added, with stirring, during 3 h. Then the mixture was stirred at room temperature for an additional 3 h. Distillation of the product *in vacuo* gave crude IX (27.0 g; 76% yield), b.p. 83–85° at 3 mm. Infrared absorptions (neat): 1 950 and 870 cm^{-1}. Gas chromatography ($AgNO_3$ – polyethylene glycol 6000, He) showed that this contained ca. 20% of the acetylenic isomer X. The relative retention times of IX and X were 1.00 and 1.25 min, respectively. Microanalyses did not give reproducible results, probably because of the high sensitivity of the products to air.

Cyclotrideca-1,2-diene (IX) by Debromination of VIIIa with Sodium Methylsulfinyl Carbanion[5]

Sodium methylsulfinyl carbanion solution was prepared by dissolving sodium hydride (1.5 g; 0.06 mole)

[5]*This procedure was based on the successful debromination of 9,9-dibromobicyclo[6.1.0]-4-nonene observed by Mr. T. Aratani of this laboratory independently from Professor Gardner's group (8c).*

Can. J. Chem. Downloaded from www.nrcresearchpress.com by 210.87.254.105 on 09/05/12
For personal use only.

in freshly distilled dimethyl sulfoxide (30 ml) under a nitrogen atmosphere according to Corey and Chaykovsky (*8a*). A solution of the *gem*-dibromide VIII*a* (10.0 g; 0.03 mole) in dimethyl sulfoxide (10 ml) was added dropwise during 30 min with cooling (an ice-water bath), when an exothermic reaction occurred. The reaction mixture was allowed to stand overnight at room temperature, diluted with water, and extracted with several portions of *n*-hexane. The extracts were washed with water until neutral, dried over sodium sulfate, and concentrated *in vacuo*. Distillation of the residual oil gave crude IX of 85% purity (2.4 g; 46% yield), b.p. 84–87° at 3 mm.

Cyclotrideca-1,2-diene (IX) by Dechlorination of VIIIb with n-Butyllithium

To a solution of the dichlorocarbene adduct VIII*b* (6.0 g; 0.02 mole) in anhydrous ether (60 ml) kept at −40° under nitrogen was added an ethereal solution containing *n*-butyllithium (50 ml; 0.04 mole) during 1 h; the mixture was then allowed to stand overnight. The product was purified by passing it through an alumina column, and then distilled to give crude IX (3.2 g; 75% yield), b.p. 83–86° at 3 mm, whose content as estimated by g.l.c. was ca. 83%.

Cyclotridecyne (X)

To a solution of potassium *t*-butoxide (3.3 g; 0.03 mole) in freshly distilled dimethyl sulfoxide (70 ml) was added in one portion the crude IX (5.6 g; 0.03 mole) as obtained above. The reaction mixture was stirred under a nitrogen atmosphere at room temperature for 12 h, diluted with water, and extracted with *n*-hexane. Distillation *in vacuo* gave cyclotridecyne (X) (5.0 g; 89% yield) as a colorless oil, b.p. 84–86° at 3 mm. The absence of infrared absorptions at 1 950 and 870 cm^{-1} indicated complete conversion, which was also confirmed by g.l.c.

Anal. Calcd. for $C_{13}H_{22}$: C, 87.6; H, 12.4. Found: C, 87.5; H, 12.4.

The allene–acetylene interconversion with potassium *t*-butoxide could not be effected in refluxing *t*-butanol.

Cyclotrideca-1,2,cis-6,trans-10-tetraene (XII)

A solution of the *gem*-dibromide II*a* (68.5 g; 0.21 mole) in dry ether (200 ml) was cooled at −30° under nitrogen, and an ethereal solution containing methyllithium (100 ml; 0.42 mole) was added during 3 h. The mixture was stirred at room temperature for an additional 3 h and treated with water. Distillation *in vacuo* gave the crude allene (mainly XII) (21.7 g; 60% yield) as a colorless oil, b.p. 84–85° at 3 mm. Infrared absorptions (neat): 1 950 and 870 (allenic linkage), 960 (*trans* double bond), and 700 cm^{-1} (a doublet, *cis* double bond). Although the allene XII was fairly sensitive to air and could not be obtained in an analytically pure form, gas chromatography indicated the presence of less than 5% impurities. The crude allene was subjected immediately to the following isomerization.

Cyclotrideca-5,9-dien-1-yne (XIII)

To a solution of potassium *t*-butoxide (8.0 g; 0.07 mole) in dimethyl sulfoxide (200 ml) under nitrogen was added the allene XII (8.0 g; 0.05 mole) in one portion; then the mixture was stirred at room temperature for 12 h, poured into water, and extracted with *n*-hexane. Distillation *in vacuo* gave the dienyne XIII (6.2 g; 78%) as a colorless oil, b.p. 84–86° at 3 mm. Complete isomerization was shown by the disappearance of the 1 950 and 870 cm^{-1} bands in the infrared spectrum. Gas–liquid chromatography ($AgNO_3$ – polyethylene glycol 6000, He) gave several peaks, one of which accounted for ca. 70%. The mixture, however, gave correct analyses for XIII. Infrared absorptions (neat) at 970 s (*trans* double bond) and 690 cm^{-1} (*cis* double bond) suggested XIII consisting of mainly the *cis,trans* isomer.

Anal. Calcd. for $C_{13}H_{18}$: C, 89.6; H, 10.4. Found: C, 89.4; H, 10.6.

Prolonged treatment in this medium caused further isomerization to give a complex mixture, the infrared spectrum of which showed a strong new band at 740 cm^{-1} and no absorption in the 960–970 cm^{-1} region.

Cyclotridecadienone (XIV)

To a solution of the acetylenic hydrocarbon XIII (9.2 g; 0.05 mole) in 80% ethanol (150 ml) was added mercuric sulfate (1 g) and a few drops of concentrated sulfuric acid. The mixture was heated at reflux under vigorous stirring for 10 h, cooled, diluted with water, and extracted with ether. Distillation *in vacuo* gave a colorless oil (7.8 g), b.p. 85–100° at 3 mm, which was subjected to chromatography on an alumina column. Elution with *n*-hexane gave unchanged XIII (3.7 g), and elution with a 1:1 mixture of benzene and ether gave cyclotrideca-4,8- (and (or) -5,9-) dienone(s) (3.5 g; 58% yield based on the amount of XIII consumed) as a colorless oil. Redistillation *in vacuo* gave an analytical sample, b.p. 107–110° at 6 mm. Infrared absorptions (neat): 1 720 (ketone), 970 (*trans* double bond), and 690 cm^{-1} (*cis* double bond). Gas–liquid chromatography ($AgNO_3$ – polyethylene glycol 6000, He) gave a broad single peak. These data may suggest that the ketone XIV thus obtained consisted largely of a *cis,trans* dienone.

Anal. Calcd. for $C_{13}H_{20}O$: C, 81.2; H, 10.5. Found: C, 81.5; H, 10.5.

The ketone XIV gave a 2,4-dinitrophenylhydrazone, m.p. 117–118° when crystallized from ethanol.

Anal. Calcd. for $C_{19}H_{24}N_4O_4$: C, 61.3; H, 6.5. Found: C, 61.4; H, 6.6.

Cyclotridecanone (XI) by Hydration of Cyclotridecyne (X)

To a solution of cyclotridecyne (X) (16.6 g; 0.09 mole) in 60% dioxane (200 ml) containing mercuric sulfate (1.0 g) was added a few drops of concentrated sulfuric acid; then the mixture was heated at reflux for 10 h under vigorous stirring. Distillation of the ethereal extracts *in vacuo* gave a colorless oil (14.3 g), b.p.

Can. J. Chem. Downloaded from www.nrcresearchpress.com by 210.87.254.105 on 09/05/12
For personal use only.

80–100° at 3 mm, which was subjected to chromatography on an alumina column. Elution with *n*-hexane gave unchanged X (5.1 g), and then elution with a 1:1 mixture of benzene and ether gave cyclotridecanone (8.2 g; 65% yield based on the amount of X consumed), m.p. 26–30° (lit. (6*d*) m.p. 26–29°). The following derivatives of XI were prepared: oxime, m.p. 102–103° (lit. (6*a*) m.p. 106°); semicarbazone, m.p. 210–211° (lit. (6*a*) m.p. 208°); and 2,4-dinitrophenylhydrazone, m.p. 114–115° (lit. (6*e*) m.p. 118–119°). All gave correct analyses.

The attempted hydration of the allene IX (10) under similar conditions gave the ketone XI in very poor yield.

Cyclotridecanone (XI) by Hydrogenation of XIV

An ethanolic solution of the dienone XIV was shaken with 10% palladium on charcoal in a hydrogen atmosphere at ordinary pressure to give cyclotridecanone XI in a nearly quantitative yield. Identification was established by comparing the infrared spectrum and gas chromatogram with those of the above specimen.

ACKNOWLEDGMENTS

The authors thank Professor K. Sisido for help and encouragement. They are also indebted to Mr. H. Katô for technical assistance.

REFERENCES

1. (*a*) H. Nozaki and R. Noyori. J. Org. Chem. **30**, 1652 (1965). (*b*) H. Nozaki, M. Kawanisi, and R. Noyori. J. Org. Chem. **30**, 2216 (1965). (*c*) H. Nozaki, Y. Nisikawa, Y. Kamatani, and R. Noyori. Tetrahedron Letters, 2161 (1965). (*d*) H. Nozaki, T. Mori, and R. Noyori. Tetrahedron. In press.
2. J. M. Locke and E. W. Duck. Chem. Ind. London, 1727 (1965).
3. O. M. Nefedov and N. N. Novitskaya. Dokl. Akad. Nauk SSSR, **152**, 629 (1963); Chem. Abstr. **60**, 1609 (1964).
4. E. P. Blanchard and H. E. Simmons. J. Am. Chem. Soc. **86**, 1337 (1964).
5. L. I. Zakharkin and V. V. Korneva. Dokl. Akad. Nauk SSSR, **132**, 1078 (1960); Chem. Abstr. **54**, 20918 (1960).
6. (*a*) L. Ruzicka, M. Stoll, and H. Schinz. Helv. Chim. Acta, **9**, 249 (1926). (*b*) K. Ziegler. Ber. **67A**, 139 (1934). (*c*) M. Stoll. Helv. Chim. Acta, **30**, 1837 (1947). (*d*) N. J. Leonard and C. W. Shimelpfenig, Jr. J. Org. Chem. **23**, 1708 (1958). (*e*) E. Müller and M. Bauer. Liebigs Ann. Chem. **654**, 92 (1962). (*f*) W. Kirchhof, W. Stumpf, and W. Franke. Liebigs Ann. Chem. **681**, 32 (1965).
7. L. Skattebøl. Acta Chem. Scand. **17**, 1683 (1963).
8. (*a*) E. J. Corey and M. Chaykovsky. J. Am. Chem. Soc. **87**, 1345 (1965). (*b*) C. G. Cardenas, A. N. Khafaji, C. L. Osborn, and P. D. Gardner. Chem. Ind. London, 345 (1965). (*c*) C. L. Osborn, T. C. Shields, B. A. Shoulder, C. G. Cardenas, and P. D. Gardner. Chem. Ind. London, 766 (1965).
9. W. R. Moore and H. R. Ward. J. Am. Chem. Soc. **87**, 86 (1965).
10. A. V. Fedorova and A. A. Petrov. Zh. Obshch. Khim. **32**, 1755 (1962); Chem. Abstr. **58**, 3307 (1963).

Can. J. Chem. Downloaded from www.nrcresearchpress.com by 210.87.254.105 on 09/05/12
For personal use only.

Can. J. Chem. Downloaded from www.nrcresearchpress.com by 210.87.254.42 on 09/05/12
For personal use only.

POLAROGRAPHIC HALF-WAVE POTENTIALS OF SOME 1,4-NAPHTHOQUINONES[1]

D. J. Currie and H. L. Holmes

Chemistry Section, Defence Research Board, Suffield Experimental Station, Ralston, Alberta

Received September 8, 1965

ABSTRACT

The half-wave potentials for the reduction of 103 substituted 1,4-naphthoquinones were measured in 75% v/v aqueous ethanol containing buffer components. In general, if two constants were assigned, one characteristic of monosubstitution and the other characteristic of disubstitution, it was possible, by assuming additivity of the constants, to predict the half-wave potentials of the compounds within the experimental accuracy of the polarographic method.

INTRODUCTION

The effect of substituents on the polarographic half-wave potentials or the oxidation–reduction potentials (1) of substituted 1,4-naphthoquinones has been the subject of several recent papers (2, 3). Our interest in the bacteriostatic activity of substituted 1,4-naphthoquinones as related to half-wave potentials prompted this further investigation, emphasis being placed on the 1,4-naphthoquinones formed when amines and thiols react with the naphthoquinones. At the same time, an attempt was made to find a relationship between structure and half-wave potential for disubstituted 1,4-naphthoquinones.

EXPERIMENTAL

The polarograms of the 1,4-naphthoquinones and related compounds, the preparation and purity of which will be reported elsewhere, were recorded on a Sargent model XV polarograph; the experimental technique was essentially the same as that of Vladimertsev and Stromberg (2). Stock solutions of the naphthoquinones were made up in ethanol, and determinations were made on 25 ml samples of a 75% v/v aqueous ethanolic solution, 8×10^{-4} *M* in the reducible substance, containing buffer components as the supporting electrolyte. Two buffer solutions were used: (*i*) 0.10 *M* acetic acid and 0.10 *M* sodium acetate, and (*ii*) 0.10 *M* ammonium hydroxide and 0.10 *M* ammonium chloride. The pH values of the ethanolic buffers as measured with a glass electrode were 6.60 and 8.70 units, respectively. The half-wave potentials at two pH values measured against a saturated calomel electrode were used to check the change of half-wave potential with pH. The cell resistance with the ethanolic acetic buffer was ~6 800 Ω, and with the ethanolic ammonium buffer ~5 200 Ω. Methylene blue thiocyanate (0.001%) was used as a maximum suppressor. The drop mass, *m*, was 2.68 mg/s and the drop time, *t*, was 3.27 s in both buffers; from these figures $m^{\frac{2}{3}}t^{\frac{1}{6}} = 2.35\ \text{mg}^{\frac{2}{3}}\ \text{s}^{-\frac{1}{2}}$.

RESULTS

The half-wave potentials, $E_{\frac{1}{2}}$, of some 2-substituted and 2,3-disubstituted 1,4-naphthoquinones, of 6-methyl-1,4-naphthoquinones, and of 6,7-dimethyl-1,4-naphthoquinones in both buffers are tabulated in Tables I–III. The half-wave potentials of some related compounds are shown in Table IV. These tables have been placed in The Depository of Unpublished Data.[2] The values are the average of at least two successive determinations on the same sample, and the differences in the two determinations rarely exceeded 5 mV. On different samples the accuracy was $\sim\pm 10$ mV; moreover, $E_{\frac{1}{2}\ \text{acetic buffer}} - E_{\frac{1}{2}\ \text{ammonia buffer}}$ except for the hydroxy derivatives varied by the same amount.

Where duplication of compounds exists, the values of the half-wave potentials obtained by Vladimertsev and Stromberg (2) agree well with those of this work. The diffusion

[1]*Issued as Suffield Technical Paper No. 318, D.R.B. project No. D52-20-20-28.*

[2]*Photocopies of Tables I–IV may be obtained, upon request, from: The Depository of Unpublished Data, National Science Library, National Research Council, Ottawa, Canada.*

currents for soluble 1,4-naphthoquinones were somewhat variable, the values lying between 3 and 6 μA. The results were not corrected for the iR drop across the cell,[3] and therefore a combined error of $\sim\pm 25$ mV is placed on the values reported in the tables.

DISCUSSION

The effects of substituents on the half-wave potentials of quinones have been discussed by Zuman (3), and although the theoretical basis for his treatment is well founded, the use of σ constants is of little help in accurately predicting the half-wave potentials of disubstituted 1,4-naphthoquinones. The assignment of shifts of oxidation–reduction potentials, m, for substituents in monosubstituted derivatives was done by Fieser and Fieser (4). An examination of the results obtained in this work revealed that the shifts in the half-wave potentials of disubstituted 1,4-naphthoquinones, $E_{\frac{1}{2}\,XY}$, from that of the unsubstituted 1,4-naphthoquinone, $E_{\frac{1}{2}\,H}$, were not the algebraic sum of the shifts for the substituents in monosubstituted derivatives, i.e. $E_{\frac{1}{2}\,XY} \neq E_{\frac{1}{2}\,H} + m_X + m_Y$. However, it was also observed, for example, that the sum of half the shifts in the half-wave potentials of 2,3-dimethoxy- and 2,3-dimethyl-1,4-naphthoquinone is very close to the shift observed for 2-methyl-3-methoxy-1,4-naphthoquinone. Similarly, the sum of the shifts in the half-wave potentials of 2-methyl-3-*n*-butylamino- and 2-methyl-3-*n*-butylthio-1,4-naphthoquinone minus the shift in the half-wave potential of 2,3-dimethyl-1,4-naphthoquinone is close to the shift observed for 2-*n*-butylamino-3-*n*-butylthio-1,4-naphthoquinone. After a consideration of other such combinations, it was apparent that, by assigning another constant characteristic of disubstitution, d, to a substituent, and by assuming the relationship $E_{\frac{1}{2}\,XY} = E_{\frac{1}{2}\,H} + d_X + d_Y$, the half-wave potentials of disubstituted 1,4-naphthoquinones could be predicted, in general, to within ± 0.025 V, i.e. within experimental error.

The constants for substituents on the benzene ring were assumed to be additive and independent of substituent effects on the quinonoid side of the naphthoquinone, i.e. $E_{\frac{1}{2}} = E_{\frac{1}{2}\,H} + m$ or $\sum d$ (2- or 2- and 3-substituted) + m or $\sum d$ (6- or 6- and 7-substituted), thereby allowing the prediction of the half-wave potentials of 6-methyl- and 6,7-dimethyl-1,4-naphthoquinones. The empirical values of m and d for various substituents are given in Table V. The observed and calculated values of the shifts of half-wave potential with respect to 1,4-naphthoquinone are given in Tables I–III.

A correlation performed on 90 compounds yielded ($E_{\frac{1}{2}\,X}$ or $E_{\frac{1}{2}\,XY}$) $- E_{\frac{1}{2}\,H} = 0.98(m$ or $\sum d) - 1.5$, where $E_{\frac{1}{2}}$, m, and d are expressed in millivolts. The regression coefficient was 0.99, and the standard errors of the estimate and the regression coefficient were 14 and 0.02, respectively.

The necessity for the two constants m and d seems to be due only to neighboring substituent interactions not directly involving, but indirectly affecting, the carbonyl or hydroxy groups.

This type of approach can be extended to the oxidation potentials of 1,4-naphthoquinones with other substituents. Moreover, a cursory examination of a series of 1,4-benzoquinones reveals that, by using m and d, it is possible to predict their oxidation–reduction potentials with reasonable success by assuming that each side of the quinonoid ring can be treated independently as either mono- or di-substituted, e.g. $E_{\frac{1}{2}}$ (2,5,6-trisubstituted) = $E_{\frac{1}{2}\,H} + m$ (2-substituted) + $\sum d$ (5,6-disubstituted). This is in agreement

[3]*The Russian workers (2) did not correct their results for the iR drop across the cell. The correspondence between the standard oxidation–reduction potentials determined by the polarographic method and those determined by the potentiometric method is made worse if such a correction is applied.*

Can. J. Chem. Downloaded from www.nrcresearchpress.com by 210.87.254.42 on 09/05/12
For personal use only.

TABLE V

Empirical shifts in the half-wave potentials of substituted 1,4-naphthoquinones

Substituent	m (mV)	d (mV)
2- or 2- and 3-substituted		
n-C_4H_9NH	−286 (−252)*	−218
NH_2	−208 (−210)	−215
C_6H_5NH	−201 (—)	−124
HO	— (−128)	—
CH_3O	−119 (−131)	−54
CH_3	−55 (−76)	−60
CH_3CONH	−60 (−67)	−14
CH_3S	−121 (—)	—
n-C_4H_9S	−48 (—)	−21
C_6H_5S	−57 (—)	−18
C_6H_5	−40 (−32)	−30
CH_3CO_2	+24 (−9)	—
H	0 (0)	0
Br	+8 (—)	−3
Cl	+24 (+24)	+9
SO_3K	+86 (+69)	+64
$C_6H_5SO_2$	+136 (+121)	+55
6- or 6- and 7-substituted		
CH_3	−40 (—)	−20

*In parentheses are the values obtained for the substituent or a related group by a potentiometric method (4).

with the assumptions concerning the independent additivity of the substituent constants for substituents on the fused benzene ring of the 1,4-naphthoquinones.

REFERENCES

1. L. I. Smith, I. M. Kolthoff, S. Wawzonek, and P. M. Ruoff. J. Am. Chem. Soc. **63**, 1018 (1941).
2. I. F. Vladimertsev and A. G. Stromberg. J. Gen. Chem. USSR Engl. Transl. **27**, 1110 (1957); Chem. Abstr. **53**, 4232 (1959).
3. P. Zuman. Collection Czech. Chem. Commun. **27**, 2035 (1962); Chem. Abstr. **57**, 16321 (1962).
4. L. F. Fieser and M. Fieser. J. Am. Chem. Soc. **57**, 491 (1935).

Can. J. Chem. Downloaded from www.nrcresearchpress.com by 210.87.254.42 on 09/05/12
For personal use only.

Can. J. Chem. Downloaded from www.nrcresearchpress.com by 210.87.254.5 on 09/05/12
For personal use only.

POLAROGRAPHIC HALF-WAVE POTENTIALS OF SOME β-NITROSTYRENES AND RELATED COMPOUNDS[1]

R. F. SILVER AND H. L. HOLMES

Chemistry Section, Defence Research Board, Suffield Experimental Station, Ralston, Alberta

Received September 8, 1965

ABSTRACT

The polarographic half-wave potentials of a number of β-nitrostyrenes, β-nitropropenylbenzenes, and β-nitrobutenylbenzenes have been determined in aqueous ethanolic solution at an apparent pH of 6.54. A linear relationship exists between these values and Hammett sigma constants, but not with their ultraviolet absorption maxima or with their dipole moments.

The polarographic wave of 11 diethyl benzalmalonates, under the same conditions, was masked by the hydrogen wave.

Nitro groups are reducible at the dropping-mercury cathode, and their half-wave potentials depend upon the solvent[2] and upon whether it is an isolated or an aromatic nitro group. Holleck and Jannakoudakis (2) state that the nitro group of β-nitrostyrene shows some properties characteristic of the above two classes.

In an acid medium nitroalkanes exhibit only one polarographic wave, which varies little with pH (−0.75 to −0.89 V over a range of 5 pH units); at pH 4.5 a second wave starts at −1.5 V which is obscured by the hydrogen wave (1). In an alkaline medium the diffusion current of the nitroalkanes falls with time because of equilibration with the non-reducible *aci*-form (1). Reduction of the nitro group at the dropping-mercury electrode is an irreversible, four-electron process which leads to the respective hydroxylamine. The second wave, at more negative potentials, involves the reduction of the alkylhydroxylammonium ion to the alkylammonium ion and is a two-electron process (1).

Aromatic nitro compounds, except for the *o*- and *p*-nitroanilines, the *o*- and *p*-nitrophenols, and the *o*- and *p*-dinitrobenzenes, behave similarly, except that the half-wave potential changes linearly with pH over at least part of the pH scale. At pH < 5 nitrobenzene gives two waves involving four electrons and two electrons to give the respective phenylhydroxylamine and aniline.[3] The exceptions noted above are abnormal, because the resulting phenylhydroxylamine can lose water to give a reducible quinonoid structure (1, 3). Introduction of one or two methyl groups into the benzene ring has little effect upon the half-wave potential of the nitrobenzene unless the two methyl groups are both ortho to the nitro group (see Table II),[4] when the half-wave potential is shifted to more negative values (1). Such effects are noted when the functional group, such as nitro, can undergo a marked mesomerism with the aromatic ring, and when both the functional group and the ortho substituents are bulky (1, 4). The nitro group then should, and does, behave more like an aliphatic nitro group toward polarographic reduction (1). It has been stated (4) that differences in the half-wave potentials of ortho- and para-substituted members of this series give an insight into the nature and extent of certain types of ortho

[1]*Issued as Suffield Technical Paper No. 319, D.R.B. project No. D52-20-20-28.*

[2]*In 50% ethanol the half-wave potentials of the nitrotoluenes are approximately 0.35 V more negative than when 8% aqueous ethanol is the solvent (1).*

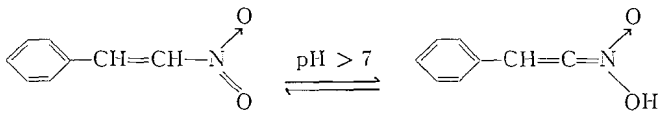
[3]*The nitro group of the 2-nitrofurans and 2-nitrothiophenes behaves similarly (25–28). The order of increasing difficulty of reduction is 2-nitrofuran < 2-nitrothiophene < nitrobenzene (23–25).*

[4]*Tables I and II have been placed in The Depository of Unpublished Data. Photocopies may be obtained, upon request, from: The Depository of Unpublished Data, National Science Library, National Research Council, Ottawa, Canada.*

effects. The half-wave potentials of para-substituted nitrobenzenes appear to bear a linear relationship with Hammett sigma constants (1, 5). Differences in the half-wave potentials of certain ortho- and meta-substituted derivatives have been ascribed to differences in the reduction mechanism rather than to hydrogen bonding (4).

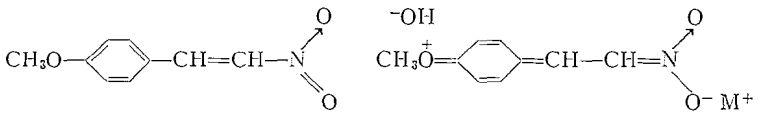
Phenylhydroxylamine is the reduced form of the polarographically reversible system nitrosobenzene $\rightleftharpoons$ phenylhydroxylamine (6–8). The reduction of nitrosobenzene is a two-electron process (6, 7, 9) in which the half-wave potential is dependent upon pH. The shift per pH unit in water is 0.053 V (8) to 0.058 V (7) whereas in ethanol it is 0.0603 V (7). The reduction of an aromatic nitroso group occurs at a much more positive half-wave potential than does an aromatic nitro group (1, 7), and it has been stated (8) that the position of the nitroso group in substituted nitrosobenzenes has no effect upon its half-wave potential.

Between pH 1 and pH 11 β-nitrostyrene is reduced by a four-electron, one-step process, and over the pH range 1–3 a second, two-electron process occurs (2, 11). In analogy with nitrobenzene the half-wave potential of β-nitrostyrene in 10% aqueous methanol varies linearly with pH over the pH range 1–7 (2, 10), and against the saturated calomel electrode can be expressed as $E_{\frac{1}{2}} = -0.023 - 0.063\text{pH}$ (2). Above pH 7 the half-wave potential is constant at about −0.46 V. Holleck and Jannakoudakis (2) considered that the four-electron process led to β-hydroxylaminostyrene and the two-electron process to β-aminostyrene, whereas Masui and Sayo (10, 11) have advanced evidence that the reduction product of the four-electron process was the oxime of phenylacetaldehyde, a product isolated also from the reverse lithium aluminium hydride reduction of β-nitrostyrene (12). The two-electron process is considered to be the reduction of the derived oxime to β-hydroxylaminoethylbenzene (10). The observation that oximes are reduced directly to an amine (13) by a four-electron process (13–17) would appear to negate the process advanced by Masui and Sayo for the reduction of β-nitrostyrene. At pH 7 the waves for β-nitrostyrene decreased with time and three new ones appeared. These new waves were identified as waves of a polymer (−0.7 V against the saturated calomel electrode), of nitromethane (−0.9 V), and of benzaldehyde (−1.4 V) (2). Besides these, it is claimed that the non-reducible *aci*-form (II) of nitrostyrene (I) is formed in an alkaline medium (2).



I II

The energy required to form a cumulated system of double bonds as in structure II must cast some doubt on such a structure. The non-reducible form of 4-methoxy-β-nitrostyrene (III) might better be represented by structure IV.



III IV

If the non-reducible *aci*-form is represented by IV, then it would appear that electron-donating groups in the ortho and para positions should, and do, make reduction more difficult. In fact, Platford and Kerr (18) have shown that, when potassium chloride (pH 7.2) and tetramethylammonium bromide (pH 7.5) are the electrolytes, the half-wave

Can. J. Chem. Downloaded from www.nrcresearchpress.com by 210.87.254.5 on 09/05/12
For personal use only.

potentials for two of the waves of the substituted β-nitrostyrenes vary linearly with Hammett sigma constants. In the present work, a buffered acid medium (pH 6.54) was used and only one wave appears. Except for the aryl nitro derivatives, the half-wave potentials of the β-nitrostyrenes, the β-nitropropenylbenzenes, and the β-nitrobutenylbenzenes vary linearly with sigma constants (20, 21).

One difference appears in the half-wave potentials of the ortho- and para-substituted β-nitropropenylbenzenes and β-nitrobutenylbenzenes on the one hand, and the β-nitrostyrenes on the other. Except for the small fluoro group, the half-wave potentials of the C_2-substituted β-nitropropenylbenzenes are considerably more negative than the C_4-substituted analogues. The reverse is true for the β-nitrostyrenes. This may reflect a certain degree of interference between the ortho substituent and the beta methyl group in the β-nitropropenylbenzenes. This is particularly evident with the 2,4- and 2,6-dichloro derivatives of β-nitrostyrene and β-nitropropenylbenzene. Similar effects are also present to a lesser extent in the β-nitrobutenylbenzenes.

Since the ultraviolet absorption maxima for the β-nitrostyrenes and β-nitropropenylbenzenes do not bear a linear relationship to Hammett sigma constants,[5] then a linear relationship between polarographic half-wave potentials and ultraviolet absorption maxima is not to be expected. Indeed, no linear relationship was observed. This agrees with the observation of Wheeler and Covarrubias (19) that no simple relationship exists between these two properties for the substituted cinnamic acids. The same appears to be true when the half-wave potentials of the β-nitrostyrenes and β-nitropropenylbenzenes are plotted against their dipole moments (22).

The half-wave potentials of the nitrobenzenes (Table II) are more negative than those of their vinylogs (Table I). Also the half-wave potential of β-nitroethylbenzene is much more negative than that of β-nitrostyrene. The identical values for the half-wave potentials of β-nitrostyrene dibromide and β-bromo-β-nitrostyrene suggest that the former is readily converted into the latter in the acetate buffer. Because of the greater participation of a furyl group in conjugation over that of a phenyl group, the half-wave potential of 2-(2′-nitrovinyl)-furan should be, and is, more negative than that of β-nitrostyrene (10). In fact, the half-wave potential of 2-(2′-nitrovinyl)-furan is identical with that of 4-methoxy-β-nitrostyrene. The value for 9-nitromethylenefluorene is surprisingly low.

The polarographic reduction of diethyl benzalmalonates in a buffered aqueous ethanolic solution has already been studied (29, 30). Under the conditions used for the β-nitrostyrenes it is found that the polarographic wave is masked by the hydrogen wave.

EXPERIMENTAL

The polarograms of the β-nitrostyrenes, β-nitropropenylbenzenes, β-nitrobutenylbenzenes, and diethyl benzalmalonates were recorded in a Sargent model XV polarograph and against a saturated calomel electrode. The compound (5×10^{-5} mole) was dissolved in 40 ml of ethanol, and to 16 ml of this solution was added 6.25 ml of sodium acetate – acetic acid buffer (pH 4.67) and 0.25 ml of 0.01% ethanolic methylene blue solution. The solution, when diluted to 25 ml with ethanol, had an apparent pH of 6.54 against a glass electrode.

The solution was deaerated by bubbling nitrogen through it for 10 min before the polarogram was recorded at 25 °C. A second polarogram was recorded on the same solution after a second 10 min sweep with nitrogen. The half-wave potentials recorded in Tables I and II are the averages of values obtained from the two polarograms. The half-wave potentials listed in Tables I and II are accurate to ±0.004 V.

Under the conditions employed here, the polarograms of the diethyl benzalmalonates were masked by the hydrogen wave and no half-wave potentials could be determined. Multiwave polarograms were obtained for the β-nitrostyrenes and their β-alkyl homologues when they contained an aryl nitro group. The additional half-wave potentials are listed in parentheses in Tables I and II.[4]

[5] *Unpublished work in this laboratory.*

Can. J. Chem. Downloaded from www.nrcresearchpress.com by 210.87.254.5 on 09/05/12
For personal use only.

The diffusion currents for the β-nitrostyrenes, the β-nitropropenylbenzenes, and the β-nitrobutenylbenzenes fell, respectively, between 8.32×10^{-6} and 12.16×10^{-6} A, 6.88×10^{-6} and 15.28×10^{-6} A, and 8.32×10^{-6} and 11.04×10^{-6} A. The diffusion currents for 9-nitromethylenefluorene, β-bromo-β-nitrostyrene, and β-nitrostyrene dibromide were 5.36×10^{-6} A, 17.36×10^{-6} A, and 13.92×10^{-6} A, respectively.

REFERENCES

1. I. M. KOLTHOFF and J. J. LINGANE. Polarography. Interscience Publishers, Inc., New York. 1952.
2. L. HOLLECK and D. JANNAKOUDAKIS. Z. Naturforsch. **16b**, 396 (1961); Chem. Abstr. **56**, 9876 (1962).
3. I. F. VLADIMERTSEV and A. G. STROMBERG. Zh. Obshch. Khim. **27**, 1029 (1957).
4. P. ZUMAN. Collection Czech. Chem. Commun. **27**, 648 (1962); Chem. Abstr. **58**, 13448 (1963).
5. E. IMOTO, R. MOTOYAMA, and H. KAKIUCHI. Nippon Kagaku Zasshi, **77**, 812 (1956); Chem. Abstr. **52**, 9066 (1958).
6. J. W. SMITH and J. G. WALLER. Trans. Faraday Soc. **46**, 290 (1950).
7. R. M. ELOFSON and J. G. ATKINSON. Can. J. Chem. **34**, 4 (1956).
8. L. HOLLECK and H. J. EXNER. Naturwissenschaften, **39**, 159 (1952); Chem. Abstr. **47**, 3716 (1953).
9. W. KEMULA and R. SIODA. Bull. Acad. Polon. Sci. Ser. Sci. Chim. **10**, 107 (1962); Chem. Abstr. **57**, 7015 (1962).
10. M. MASUI and H. SAYO. Pharm. Bull. Tokyo, **4**, 332 (1956); Chem. Abstr. **51**, 9370 (1957).
11. M. MASUI, H. SAYO, and Y. NOMURA. Pharm. Bull. Tokyo, **4**, 337 (1956); Chem. Abstr. **51**, 9370 (1957).
12. R. T. GILSDORF and F. F. NORD. J. Am. Chem. Soc. **74**, 1837 (1952).
13. C. CALZOLARI and C. FURLANI. Ann. Triest. Cura Univ. Trieste, Sez. 2, **21**, 47 (1951); Chem. Abstr. **47**, 4220 (1953).
14. C. CALZOLARI and C. FURLANI. Boll. Sci. Fac. Chim. Ind. Bologna, **12**, 50 (1954); Chem. Abstr. **49**, 5157 (1955).
15. C. CALZOLARI and C. FURLANI. Ann. Triest. Cura Univ. Trieste, Sez. 2, **22–23**, 43 (1953); Chem. Abstr. **49**, 938 (1955).
16. H. J. GARDNER and W. P. GEORGANS. J. Chem. Soc. 4180 (1956).
17. N. TYUTYULKOV and V. PALIKAROV. Compt. Rend. Acad. Bulgare Sci. **15**, 399 (1962); Chem. Abstr. **59**, 1286 (1963).
18. R. F. PLATFORD and K. A. KERR. Suffield Technical Paper No. 231 (1962).
19. O. H. WHEELER and C. B. COVARRUBIAS. J. Org. Chem. **28**, 2015 (1963).
20. H. H. JAFFÉ. Chem. Rev. **53**, 191 (1953).
21. M. S. NEWMAN. Steric effects in organic chemistry. John Wiley & Sons, Inc., New York. 1956. p. 619.
22. V. N. VASILEVA, V. V. PEREKALIN, and V. G. VASILEV. Zh. Obshch. Khim. **31**, 2175 (1961).
23. E. IMOTO, R. MOTOYAMA, and H. KAKIUCHI. Bull. Naniwa Univ. **A3**, 203 (1955); Chem. Abstr. **49**, 15557 (1955).
24. E. IMOTO, R. MOTOYAMA, and H. KAKIUCHI. Nippon Kagaku Zasshi, **77**, 804 (1956); Chem. Abstr. **52**, 9066 (1958).
25. J. STRADINŠ and S. HILLERS. Latvijas PSR Zinatnu Akad. Vestis, **2**, 95 (1960); Chem. Abstr. **55**, 27257 (1961).
26. J. STRADINŠ, S. HILLERS, and Y. K. YUR'EV. Dokl. Akad. Nauk SSSR, **129**, 816 (1959); Chem. Abstr. **54**, 6363 (1960).
27. J. STRADINŠ and S. HILLERS. Latvijas PSR Zinatnu Akad. Vestis, 121 (1958); Chem. Abstr. **53**, 7827 (1959).
28. J. STRADINŠ, S. HILLERS, and A. DZENE. Latvijas PSR Zinatnu Akad. Vestis, **12**, 71 (1959); Chem. Abstr. **54**, 20085 (1960).
29. M. BARGAIN. Compt. Rend. **255**, 1948 (1962).
30. M. BARGAIN. Thesis, University of Rennes, Rennes, France. 1962.

Can. J. Chem. Downloaded from www.nrcresearchpress.com by 210.87.254.5 on 09/05/12
For personal use only.

Can. J. Chem. Downloaded from www.nrcresearchpress.com by 210.87.254.42 on 09/05/12
For personal use only.

PARTITION COEFFICIENTS OF SOME CONJUGATED HETEROENOID COMPOUNDS AND 1,4-NAPHTHOQUINONES[1]

D. J. CURRIE, C. E. LOUGH, R. F. SILVER, AND H. L. HOLMES
Chemistry Section, Defence Research Board, Suffield Experimental Station, Ralston, Alberta

Received September 8, 1965

ABSTRACT

The concept of additive constants to predict the partition coefficient of a compound has been developed and applied to 244 compounds. Some of the limitations of such a concept are discussed.

INTRODUCTION

In a series of recent papers, Fujita, Iwasa, and Hansch (1–3) have developed a new substituent constant, π, derived from partition coefficients. They used as the reference system 1-octanol–water, a system which, although useful in correlating biological activity with chemical constitution, is not altogether satisfactory in assessing the effects of very polar groupings in systems with a less-polar phase. The constant π was defined by these authors as $\pi = \log K_X - \log K_H$, where K_H is the partition coefficient of benzene or a monosubstituted benzene between two solvents, and K_X is that for a derivative. Our results indicate that values of π can be given more general significance and can be used to predict within an order of magnitude the partition coefficients of a variety of different compounds. Although no attempt was made in this work to examine the effect of the electronic environment of the same grouping in different compounds, an attempt was made to deal with neighboring group effects. An empirical approach has been used throughout, and therefore, like the Hammett σ constants, succeeding determinations of partition coefficients may change the values of π reported here.

EXPERIMENTAL

The concentrations of the compounds partitioned, the preparation and purity of which will be reported elsewhere, were determined on a Cary model 15 spectrophotometer. The solvents used were Fisher spectranalyzed cyclohexane, Fisher certified reagent 1-octanol, and distilled water. When the two phases were 1-octanol and water, the 1-octanol was saturated with distilled water, and the distilled water was saturated with 1-octanol. When cyclohexane and water were used, no prior equilibration was felt to be necessary. The volume ratios of the two phases were 1:50, 1:1, or 50:1 (organic phase : aqueous phase), and were chosen so that, in general, there was a measurable difference in the optical density of the solution (initially 10^{-3} to 10^{-4} M in the compound) before and after partitioning. Only the concentration of the sample in one phase was measured, this phase being the one which easily dissolved the compound; the concentration in the other phase was calculated by difference.

The partition coefficients were calculated from the expression $K = C_{\text{organic phase}}/C_{\text{water}}$ and the compounds were assumed to be neither associated nor dissociated in either phase. Each determination was done at least twice, the phases remaining in contact for 10 min and 30 min, with periods of shaking of 10 min and 15 min, respectively. The difference between the two log K values rarely exceeded 0.06 log unit, and the average value of these determinations is recorded. The temperature at which partitioning was done was 25 $\pm$ 5 °C.

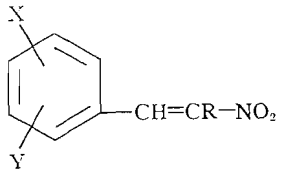
RESULTS

Table I gives the logarithm of the partition coefficients in the cyclohexane–water system of 36 β-nitrostyrenes, 40 β-nitropropenylbenzenes, and 20 β-nitrobutenylbenzenes. The partition coefficients of 33 compounds more or less related to the nitrostyrenes, and the partition coefficients of 86 substituted 1,4-naphthoquinones are tabulated in Tables II and

[1]*Issued as Suffield Technical Paper No. 317, D.R.B. project No. D52-20-20-28.*

TABLE I

Partition coefficients of β-nitrostyrenes in the system cyclohexane–water at 25 ± 5 °C



		R = H		R = CH_3		R = C_2H_5	
X	Y	Log K	$\sum\pi - 1.30$	Log K	$\sum\pi - 1.30$	Log K	$\sum\pi - 1.30$
H	H	+1.80	+1.80	+2.69	+2.45	~+3.45	+3.10
2-CH_3	H	+2.40	+2.45	+2.98	+3.10	+3.61	+3.75
4-CH_3	H	+2.42	+2.45	+3.00	+3.10	+3.10	+3.75
4-$(CH_3)_2CH$	H	+3.82	+3.75	+3.52	+4.40	~+2.89	+5.05
2-F	H	+1.94	+2.05	+2.67	+2.70	—	—
3-F	H	+1.74	+1.90	~+2.57	+2.55	—	—
4-F	H	+1.61	+1.85	+2.47	+2.50	—	—
2-Cl	H	+2.52	+2.60	+3.31	+3.25	+3.23	+3.90
3-Cl	H	+2.33	+2.35	+2.63	+3.00	+4.40	+3.65
4-Cl	H	+2.24	+2.25	+2.97	+2.90	~+3.19	+3.55
2-Br	H	+2.44	+2.50	+3.01	+3.15	—	—
3-Br	H	~+2.48*	+2.40	+3.05	+3.05	—	—
4-Br	H	+2.33	+2.30	—	—	—	—
3-OH	H	−1.36	−1.40	—	—	—	—
4-OH	H	−1.60	−1.70	—	—	—	—
2-CH_3O	H	~+2.15	+2.15	+2.61	+2.80	~+2.88	+3.45
3-CH_3O	H	+1.89	+2.00	+2.63	+2.65	+2.88	+3.30
4-CH_3O	H	~+1.73	+1.70	+2.33	+2.35	~+2.49	+3.00
2-C_2H_5O	H	—	—	+3.07	+3.45	—	—
2-NO_2	H	+0.89	+0.80	+1.52	+1.45	—	—
3-NO_2	H	+1.01	+0.95	+1.62	+1.60	—	—
4-NO_2	H	+0.72	+0.95	+1.59	+1.60	+2.39	+2.25
3-CN	H	—	—	+1.18	+1.20	—	—
4-CN	H	—	—	+1.18	+1.20	—	—
4-$(CH_3)_2N$	H	+1.94	+2.00	+2.56	+2.65	—	—
4-CH_3O_2C	H	—	—	+2.30	+2.30	—	—
2-Cl	4-Cl	+2.76	+3.05	+3.61	+3.70	+4.4	+4.35
2-Cl	6-Cl	+3.12	+3.40	+4.40	+4.05	—	—
3-Cl	4-Cl	+2.68	+2.80	+3.36	+3.45	+4.4	+4.10
2-F	5-NO_2	+0.87	+1.20	—	—	—	—
4-F	5-NO_2	+0.31	+1.00	—	—	—	—
2-Cl	5-NO_2	+1.49	+1.75	+2.46	+2.40	—	—
2-Br	5-NO_2	+1.66	+1.65	—	—	—	—
5-Cl	2-CH_3O	—	—	+3.02	+3.35	—	—
5-Br	2-CH_3O	—	—	+2.92	+3.40	—	—
4-OH	3-CH_3O	~+0.04	+0.30	+0.77	+0.95	+1.57	+1.60
4-OH	3-C_2H_5O	—	—	+1.49	+1.60	~+2.24	+2.25
2-CH_3O	3-CH_3O	+1.93	+1.85	+2.57	+2.50	+3.22	+3.15
2-CH_3O	4-CH_3O	+2.04	+2.05	~+2.54	+2.70	+2.68	+3.35
2-CH_3O	5-CH_3O	~+1.79	+2.35	+2.49	+3.00	+2.68	+3.65
3-CH_3O	4-CH_3O	+0.88	+1.40	+1.71	+2.05	~+2.17	+2.70
3-C_2H_5O	4-C_2H_5O	—	—	~+2.45	+3.35	—	—
CH_2 (O-3, O-4)		+1.41	+1.40	~+2.06	+2.05	+2.65	+2.70
2-(C_4H_4)-3		+3.38	+3.25	+2.84	+3.90	—	—
3-(C_4H_4)-4		—	—	+2.82	+3.90	—	—
5-Bromo derivative of 3-CH_3O, 4-CH_3O		—	—	+2.63	+2.65	—	—

*The sign "~" indicates that the variation in the measured log K values exceeded 0.06 log unit.

Can. J. Chem. Downloaded from www.nrcresearchpress.com by 210.87.254.42 on 09/05/12
For personal use only.

TABLE II

Partition coefficients of related compounds in the system cyclohexane–water

Compound	Log K	$\sum \pi - 1.30$
Benzyl alcohol	−0.62	−1.15
Benzaldehyde	+1.13	+1.15
Benzalacetophenone	~+3.94	+3.35
Nitromethane	−0.93	−1.60
β-Nitroethylbenzene	+1.81	+1.80
β-Bromo-β-nitrostyrene	+2.76	+2.70
Ethyl α-carbethoxy-β-anilino-β-phenylpropionate	+4.22	+3.95
1-Phenyl-1-*p*-toluidino-2-nitroethane	+2.93	+3.20
Dibenzylamine	+0.66	+4.60
Diethyl benzalmalonate	+3.26	+3.45
Ethyl benzalcyanoacetate	+2.63	+2.60
4-Nitro-5-phenyl-1-cyclohexene	+3.60	+4.40
Cinnamalmalononitrile	+1.87	+2.40
Cinnamonitrile	+1.53	+1.50
2-(β-Nitrovinyl)-furan	+1.01	+1.15
2-(β-Nitrovinyl)-thiophene	+1.46	+1.25
9-Nitromethylenefluorene	+4.4	+4.55
4-Hydroxybenzalmalononitrile	−2.15	−1.75
4-Hydroxy-3-methoxybenzalmalononitrile	+0.30	+0.25
2,4-Dimethoxybenzalmalononitrile	+2.02	+2.00
3,4-Dimethoxybenzalmalononitrile	+1.05	+1.35
α-Methylbenzalmalononitrile	+1.56	+2.40
α-Phenylbenzalmalononitrile	+3.52	+4.50
Phenanthrenequinone	+1.39	—
5-Methyl-1,4-naphthoquinone	+1.84	—
2,3-Dichloro-5-methyl-1,4-naphthoquinone	~+2.49	+3.25
2,6,7-Trimethyl-3-anilino-4-phenylimino-1-naphthoquinone	⩾+4.0	—
6-Methyl-1,4-naphthoquinone	+1.82	+1.85
2-Anilino-6-methyl-1,4-naphthoquinone*	+3.05	+3.20
2,3-Dichloro-6-methyl-1,4-naphthoquinone	+3.06	+3.25
2-Chloro-3-anilino-6-methyl-1,4-naphthoquinone*	+4.22	+3.05
Ethyl γ-phenylbutyrate	⩾+3.80	+3.90
Ethyl α-phenylbutyrate	⩾+3.80	+3.90

*These compounds may be 7-methyl and not 6-methyl derivatives.

III, respectively. The effect of increasing the length of an alkyl chain on the partition coefficient is shown in Table IV (26 compounds).

In addition to the results given above, the partition coefficients of 41 of the compounds were measured in the 1-octanol–water system, and the results are given in Table V.

DISCUSSION

The System Cyclohexane–Water

The assumption was made that the logarithm of the partition coefficient of any compound could be expressed as the algebraic sum of the π values of the component groupings of the molecule (eq. [1]).

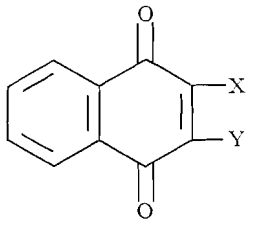
$$[1] \qquad \log K = m \sum \pi + b$$

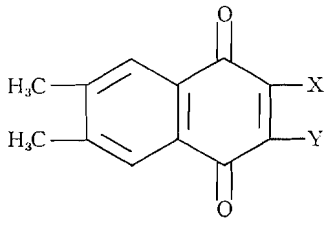
Our results were empirically fitted to this expression with $m = 1$ and $b = -1.30$, and the self-consistent π values of the component groupings that were derived are given in Table VI. This table made possible the calculation of the partition coefficient of many of the compounds (see example 1). It was soon apparent, however, that when two polar groupings were attached to the same carbon atom, or to adjacent carbon atoms, the calculated values of the partition coefficients did not agree with the measured values. To obviate this, an

Can. J. Chem. Downloaded from www.nrcresearchpress.com by 210.87.254.42 on 09/05/12
For personal use only.

TABLE III

Partition coefficients of 1,4-naphthoquinones in the system cyclohexane–water at 25 ± 5 °C



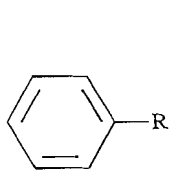


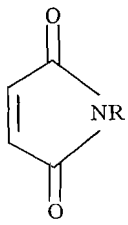
X	Y	Log K	$\sum\pi - 1.30$	Log K	$\sum\pi - 1.30$
H	H	+1.26	+1.20	~+2.17	+2.50
CH_3	H	+1.88	+1.85	~+2.72	+3.15
C_6H_5	H	+3.62	+3.95	+4.22	+5.25
Cl	H	+1.91	+1.90	+2.98	+3.20
Br	H	+2.12	+2.10	+3.41	+3.40
OCH_3	H	~+0.48	+1.35	—	—
CH_3O_2C	H	+1.12	+1.05	—	—
NH_2	H	−1.90	−1.10	—	—
CH_3CONH	H	+0.13	−3.20	—	—
NHC_4H_9	H	+2.39	+2.40	—	—
NHC_6H_5	H	+2.63	+2.55	+2.70	+3.85
SCH_3	H	+1.87	+1.45	—	—
SC_4H_9	H	+3.43	+3.40	⩾+4.7	+4.70
SC_6H_5	H	⩾+4.4	+3.55	+3.96	+4.85
SO_3K	H	—	—	−2.48	−2.50
$SO_2C_6H_5$	H	+1.50	+1.20	+2.23	+2.50
$COCH_3$	H	+0.67	−0.30	—	—
CH_3	CH_3	+2.70	+2.50	+3.48	+3.80
CH_3	C_6H_5	+3.52	+4.60	—	—
Vitamin K_1		+3.27	+14.20	—	—
CH_3	Cl	+2.61	+2.55	+3.74	+3.85
CH_3	Br	+2.85	+2.75	+4.00	+4.05
CH_3	OH	+0.79	−1.65	~+1.58	−0.35
CH_3	OCH_3	+2.31	+2.00	+3.37	+3.30
CH_3	NHC_4H_9	+2.92	+3.05	—	—
CH_3	NHC_6H_5	+4.22	+3.20	+4.7	+4.50
CH_3	SC_4H_9	+4.70	+4.05	+4.4	+5.35
CH_3	SC_6H_5	⩾+4.7	+4.20	⩾+4.4	+5.50
C_6H_5	C_6H_5	⩾+4.4	+6.70	—	—
C_6H_5	Br	⩾+4.4	+4.85	⩾+4.7	+6.15
C_6H_5	OH	+0.49	+0.45	—	—
C_6H_5	NHC_4H_9	⩾+4.7	+5.15	⩾+4.7	+6.45
C_6H_5	NHC_6H_5	⩾+4.4	+5.30	⩾+4.0	+6.60
Cl	Cl	~+2.56	+2.60	+2.91	+3.90
Cl	NH_2	+0.41	+0.50	~+1.47	+1.80
Cl	$(CH_3)_2N$	+1.24	+1.20	—	—
Cl	NHC_4H_9	+2.64	+2.25	—	—
Cl	NHC_6H_5	+1.56	+2.40	+3.22	+3.70
Cl	SC_4H_9	⩾+4.4	+3.75	—	—
Br	Br	+2.84	+3.00	—	—
Br	CH_3O	~+2.17	+2.00	—	—
Br	NH_2	+0.72	+0.70	—	—
Br	NHC_4H_9	+2.67	+2.45	—	—
Br	NHC_6H_5	+2.00	+2.60	+2.32	+3.90
CH_3O	CH_3O	+1.09	+1.00	~+1.76	+2.30
NH_2	CH_3CONH	−1.30	−2.10	−0.72	−0.80
NH_2	SC_4H_9	~+2.23	+1.65	—	—
CH_3CONH	CH_3CONH	−2.31	−2.60	−1.31	−1.30
CH_3CONH	NHC_4H_9	~+0.49	−0.35	—	—
CH_3CONH	NHC_6H_5	−0.71	−0.20	—	—
CH_3CONH	SC_4H_9	+1.28	+1.15	—	—
NHC_4H_9	SC_4H_9	~+3.44	+3.40	—	—
NHC_6H_5	$NHC_6H_4CH_3$-4	+4.00	+3.10	—	—
NHC_6H_5	$NHC_6H_4OCH_3$-4	~+2.30	+2.10	—	—
NHC_6H_5	SC_4H_9	+4.40	+3.55	⩾+4.4	+4.85
NHC_6H_5	SO_3K	~−4.7	−2.45	—	—
NHC_6H_5	$SO_2C_6H_5$	~+2.45	+2.55	—	—
SC_4H_9	SC_4H_9	~+3.45	+4.90	—	—

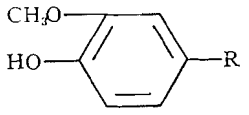
Can. J. Chem. Downloaded from www.nrcresearchpress.com by 210.87.254.42 on 09/05/12
For personal use only.

TABLE IV

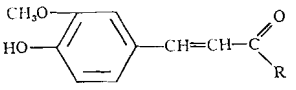
Partition coefficients in the system cyclohexane–water; effect of increase in length of the alkyl chain

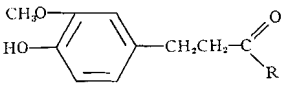


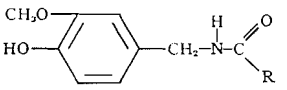




R	Log K	$\sum\pi - 1.30$	Log K	$\sum\pi - 1.30$	Log K	$\sum\pi - 1.30$
H	+2.36	+2.35	−2.61	−2.55	—	—
CH_3	+3.12	+2.35	−0.82	−0.80	~+0.76	+0.85
C_2H_5	⩾+4.4	+2.75	−0.04	−0.15	—	—
n-C_3H_7	⩾+4.4	+3.40	—	—	—	—
n-C_4H_9	⩾+4.4	+4.05	~+1.23	+1.15	+2.56	+2.55
n-C_5H_{11}	—	—	—	—	+2.24	+3.20
n-C_6H_{13}	—	—	+2.62	+2.45	⩾+3.93	+3.85
n-C_8H_{17}	—	—	⩾+4.4	+3.75	—	—
n-C_9H_{19}	—	—	⩾+4.4	+4.40	—	—







R	Log K	$\sum\pi - 1.30$	Log K	$\sum\pi - 1.30$	Log K	$\sum\pi - 1.30$
CH_3	−0.31	−0.25	−0.21	−0.25	−3.9	−3.55
C_2H_5	+0.41	+0.40	+0.35	+0.40	−3.9	−2.90
C_3H_7	+0.95	+1.05	+0.81	+1.05	—	—
C_5H_{11}	—	—	—	—	−0.95	−0.95
C_8H_{17}	—	—	—	—	+0.72	+0.50

interaction parameter, π interaction, was assigned, where possible, to each polar group and was used in the expression shown in eq. [2].

$$[2] \qquad \log K = \sum \pi + \sum \pi \text{ interaction} - 1.30$$

The assumption was made that each interacting group could be assigned its own constant, i.e. that

$$\pi \text{ interaction}_{CXY} = \pi \text{ interaction}_{CXCY} = \pi \text{ interaction}_X + \pi \text{ interaction}_Y.$$

The use of eq. [2] is demonstrated in example 2.

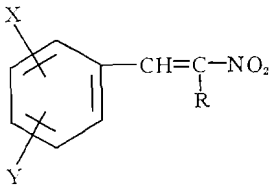
The principle of additivity of π values was applied to the π values of several classes of functional groupings, i.e. it was possible to derive generalized π constants for the groupings OR, C(O)R, C(O)OR, OC(O)R, SR, NHR, and NR_2 where R = alkyl or aryl. The application of this concept is treated in examples 3 and 4. When R = hydrogen, the measured log K values were understandably different from those predicted by the generalized constants, and appropriate constants were defined for the $—NH_2$ and —OH functions. The reaction of water with these groupings to form $—NH_3^+$ and $—O^-$ is expected to nullify the use of the π values reported here, i.e. for the compounds 2-methyl-3-hydroxy- and 2,6,7-trimethyl-3-hydroxy-1,4-naphthoquinone. The same is true for the functions RNH— and R_2N— and the species RNH_2^+— and R_2NH^+—, i.e. for dibenzylamine.

Can. J. Chem. Downloaded from www.nrcresearchpress.com by 210.87.254.42 on 09/05/12
For personal use only.

TABLE V

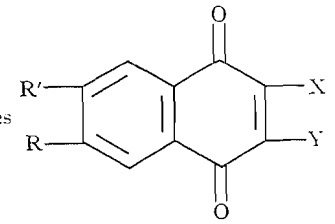
Partition coefficients in the system 1-octanol–water

A. β-Nitrostyrenes



X	Y	R	Log K	$\sum\pi - 1.30$
H	H	H	+2.11	+1.80
4-CH_3	H	H	~+2.28	+2.45
2-Cl	H	H	+2.85	+2.60
3-Cl	H	H	+2.57	+2.35
4-Cl	H	H	+2.44	+2.25
3-OH	H	H	+2.07	−1.40
4-OH	H	H	+2.12	−1.70
3-CH_3O	H	H	~+2.30	+2.00
2-NO_2	H	H	+1.80	+0.80
3-NO_2	H	H	+1.82	+0.95
4-NO_2	H	H	+1.89	+0.95
4-$(CH_3)_2N$	H	H	+2.67	+2.00
2-Cl	4-Cl	H	+2.53	+3.05
2-Cl	5-NO_2	H	+2.23	+1.75
4-OH	3-CH_3O	H	+1.88	+0.30
H	H	CH_3	+2.52	+2.45
H	H	C_2H_5	+2.86	+3.10

B. 1,4-Naphthoquinones



X	Y	R	R′	Log K	$\sum\pi - 1.30$
H	H	H	H	+1.71	+1.20
CH_3	H	H	H	+2.20	+1.85
C_6H_5	H	H	H	⩾+4.4	+3.95
Cl	H	H	H	+2.15	+1.90
OH	H	H	H	+1.38	−2.30
OCH_3	H	H	H	~+1.35	+1.35
NH_2	H	H	H	+1.88	−1.10
$NHC(O)CH_3$	H	H	H	+1.29	−3.20
NHC_4H_9	H	H	H	+3.11	+2.40
NHC_6H_5	H	H	H	+2.84	+2.55
SC_4H_9	H	H	H	~+3.29	+3.40
SO_3K	H	H	H	−1.08	−3.80
$SO_2C_6H_5$	H	H	H	~+2.14	+1.20
H	H	CH_3	H	+2.10	+1.85
H	H	CH_3	CH_3	~+2.49	+2.50
CH_3	OH	H	H	+1.20	−1.65
CH_3	OCH_3	H	H	~+2.14	+2.00
Cl	NH_2	H	H	+2.12	+0.50
Cl	NHC_4H_9	H	H	+4.26	+2.25
Cl	NHC_6H_5	H	H	+4.22	+2.40
$NHC(O)CH_3$	NHC_6H_5	H	H	+1.73	−0.20
$NHC(O)CH_3$	SC_4H_9	H	H	+2.07	+1.15
NHC_6H_5	SO_3K	H	H	−0.99	−2.45
NHC_6H_5	$SO_2C_6H_5$	H	H	+3.38	+2.55

Can. J. Chem. Downloaded from www.nrcresearchpress.com by 210.87.254.42 on 09/05/12
For personal use only.

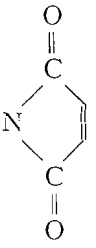
TABLE VI

π values in the system cyclohexane–water

X	π_X in C_6H_4XR (R = alkyl) Ortho	Meta	Para	π_X in RCH(X)R or RCH_2X or CH_3X*	π interaction
H	0	0	0	0	None
CH_3	+0.65	—	+0.65	+0.65	None
C_6H_5	—	—	—	+2.75‡	None
(C_4H_4)†	+1.45	+1.45		—	None
F	+0.25	+0.10	+0.05	—	0.00
Cl	+0.80	+0.55	+0.45	+0.70	0.00
Br	+0.70	+0.60	+0.50	+0.90	0.00
OH	—	−3.20	−3.50	−3.50	+2.05
OR*	−0.30	−0.45	−0.75	−0.50	−0.25
NO_2	−1.00	−0.85	−0.85	−0.95	0.00
CN	—	−1.25	−1.25	−1.25	+0.75
CHO	—	—	—	−1.20	None used
COR	—	—	—	−2.15	None used
CO_2R and OCOR	—	—	—	−0.80	−0.15
(OCH_2O)†	—	−0.40		—	—
NR_2	—	—	−1.10	−2.00	None used
NH_2	—	—	—	−2.30	+0.90
NHR	—	—	—	−1.40	−0.85
NHCOR	—	—	—	−5.05	+2.50
SR	—	—	—	−0.40	−0.35
SO_3K	—	—	—	−5.00	None used
SO_2R	—	—	—	−2.75	None used

*R = alkyl or aryl.
†These are bifunctional groups attached in the positions indicated between the two columns.
‡In compounds containing the structure C_6H_5X and $C_6H_5CH_2X$ where $X \neq$ alkyl and where, in addition, no alkyl groups are directly attached to the ring, π_{phenyl} = +3.65 and +3.00, respectively.

1,4-Naphthoquinone presented special difficulties in the choice of component groups, and it was decided to give this compound its own π value of +2.50. The interaction parameter for the carbonyl groups in the naphthoquinone series was assumed to be zero; with a few notable exceptions, e.g. 2-acetamido-1,4-naphthoquinone, this assumption appeared to be justified. It is recognized, however, that our method of calculation of the π values may partially have obscured this interaction. A deviation from the additivity of π interaction values for X and Y might be expected in systems in which three or more groups are involved, e.g. —CXYZ, —CX—CYZ, and —CXCYCZ— (see, however, example 5).

Compounds of the form  were given a π value of −0.15, and again no attempt was made to separate the components. The compound in which R = H was treated separately and given a π value of −1.25.

The gross agreement between our results and those of Fujita, Iwasa, and Hansch implies that the π values derived in this work for compounds of the form $XC_6H_4CH{=}C{=}$ would apply equally well to compounds of the form $XC_6H_4CH_2$— or XC_6H_5. A comparison of the logarithm of the partition coefficients of benzene, monosubstituted benzenes, and benzyl derivatives with the calculated values indicated that a more positive π value for the phenyl group in these compounds would be more appropriate. Therefore, in compounds

Can. J. Chem. Downloaded from www.nrcresearchpress.com by 210.87.254.42 on 09/05/12
For personal use only.

containing the structure C_6H_5X and $C_6H_5CH_2X$ where X $\neq$ alkyl and where, in addition, no alkyl groups are directly substituted on the phenyl ring, different values of π_{phenyl} were used. The logarithms of the partition coefficients of benzene (+2.36), phenol (−0.85), aniline (+0.01), nitrobenzene (+1.69), benzonitrile (+1.15), and ethylbenzoate (+1.40) in cyclohexane–water are accommodated by $\pi_{phenyl} = +3.65$. The values for phenylacetonitrile (+1.31), ethyl phenylacetate (+2.40), and some compounds in Table IV are accommodated by $\pi_{phenyl} = +3.00$. This effect is also present to an extent in the 6-methyl- and 6,7-dimethyl-1,4-naphthoquinones. In these two series, the calculated values were derived from the expression $\pi_{1,4\text{-naphthoquinone}} + \pi_{methyl}$ (or $2\pi_{methyl}$) − 1.30.

The π value for benzene, expressed as $6\pi_{methyl} - 12\pi_{hydrogen} - 1.30 = +2.60$, is even more positive than that indicated by the measured value of log K; therefore, since the logarithms of the partition coefficients of hydrocinnamonitrile (+1.35), ethyl hydrocinnamate (+3.11), and other examples in Table IV show that unsaturation has little effect on the partition coefficient, a term involving a different neighboring group effect has been incorporated in π_{phenyl}. This effect, which gives rise to different values of π_{phenyl} in compounds of the form $C_6H_5(CH_2)_nX$, is likely to be associated with the ease of solvation, and therefore the flexibility of the aralkyl system as a whole. The value of the partition coefficient of 4-nitro-5-phenyl-1-cyclohexene and the values of $\pi_{C_4H_4}$ for naphthalene derivatives are in accord with this explanation. The partition coefficient of vitamin K_1 is much less than the estimated value, and in solution the long hydrocarbon chain is flexible enough to blanket some of the functional groups of the molecule. Because of insufficient data on related compounds, no estimates were made of the $\sum \pi - 1.30$ values of phenanthrenequinone or 2,6,7-trimethyl-3-anilino-4-phenylimino-1-naphthoquinone.

A correlation yielding $\log K = 0.907(\sum \pi - 1.30) + 0.07$ was performed on 223 compounds, excluding those log K values expressed, for example, as $\geqslant +4.4$ and omitting dibenzylamine, 2-methyl-3-hydroxy-1,4-naphthoquinone, 2,6,7-trimethyl-3-hydroxy-1,4-naphthoquinone, vitamin K_1, and those compounds for which no π values were calculated. The regression coefficient was 0.95, and the standard errors of the estimate and of the regression coefficient were 0.50 and 0.02, respectively. Although an examination of Table VI indicates that, in general, the π values for a given substituent on an alkyl or alkenyl chain or in any position on a phenyl ring are for all practical purposes the same, nevertheless the inequalities which are apparent indicate that the electronic environment of a substituent cannot be ignored completely.

The System 1-Octanol–Water

The π values derived for the cyclohexane–water system were of limited value in predicting the partition coefficients of compounds in the 1-octanol–water system. A comparison of the π values of Fujita, Iwasa, and Hansch (2) with those derived in this work shows that the agreement is excellent for all but the polar groups. It is apparent, therefore, that either different parameters for polar groups have to be used for other solvent systems (the 1-octanol–water π values of Fujita, Iwasa, and Hansch were partially successful in correlating our data in this system without the use of interaction parameters), or a linear relationship has to be scrapped in favor of a continuous nonlinear one. The latter is perhaps more convenient, since other solvent pairs are likely to be investigated.

Examples

(1) 2-Chloro-β-nitropropenylbenzene

$\log K = \sum \pi - 1.30$

Can. J. Chem. Downloaded from www.nrcresearchpress.com by 210.87.254.42 on 09/05/12
For personal use only.

$$= \sum (3\pi_{\text{methyl}} + \pi_{\text{phenyl}} + \pi_{\text{nitro}} + \pi_{o\text{-chloro}} - 5\pi_{\text{hydrogen}}) - 1.30$$
$$= 3(+0.65) + 2.75 - 0.95 + 0.80 - 5(0) - 1.30$$
$$= +3.25 \text{ (calculated)}.$$

The measured value of K gives a value of $\log K = +3.31$.

(2) 4-Hydroxy-3-methoxybenzalmalononitrile

$$\log K = \sum \pi + \sum \pi \text{ interaction} - 1.30$$
$$= \sum (2\pi_{\text{methyl}} + 2\pi_{\text{cyano}} + \pi_{\text{phenyl}} + \pi_{p\text{-hydroxy}} + \pi_{m\text{-methoxy}} - 7\pi_{\text{hydrogen}}) + \sum (\pi \text{ interaction}_{\text{hydroxy}} + \pi \text{ interaction}_{\text{methoxy}} + 2\pi \text{ interaction}_{\text{cyano}}) - 1.30$$
$$= 2(+0.65) + 2(-1.25) + 2.75 - 3.50 + 0.20 - 7(0) + 2.05 - 0.25 + 2(+0.75) - 1.30$$
$$= +0.25 \text{ (calculated)}.$$

The measured value of K gives a value of $\log K = +0.30$.

(3) n-Butylamino Group

$$\pi_{n\text{-butylamino}} = \pi_{\text{NHR}} + 4\pi_{\text{methyl}} - 3\pi_{\text{hydrogen}}$$
$$= -1.40 + 4(+0.65) - 3(0)$$
$$= +1.20.$$

(4) Furfuryl Group

$$\pi_{\text{furfuryl}} = \pi_{\text{OR}} + 4\pi_{\text{methyl}} - 8\pi_{\text{hydrogen}}$$
$$= -0.50 + 4(+0.65) - 8(0)$$
$$= +2.10.$$

(5) Ethyl α-Carbethoxy-β-anilino-β-phenylpropionate

$$\log K = \sum \pi + \sum \pi \text{ interaction} - 1.30$$
$$= 6\pi_{\text{methyl}} + 2\pi_{\text{C(O)OR}} + 2\pi_{\text{phenyl}} + \pi_{\text{NHR}} - 6\pi_{\text{hydrogen}} + 2\pi \text{ interaction}_{\text{C(O)OR}} + \pi \text{ interaction}_{\text{NHR}} - 1.30$$
$$= 6(+0.65) + 2(-0.80) + 2(+2.75) - 1.40 - 6(0) + 2(-0.15) - 0.85 - 1.30$$
$$= +3.95 \text{ (calculated)}.$$

The measured value of K gives a value of $\log K = +4.22$.

ACKNOWLEDGMENTS

The authors thank Dr. G. Feniak for supplying samples of all the compounds in Table IV with the exception of benzene and the monoalkylbenzenes, and Dr. J. B. Reesor for his suggestions concerning the apparent differences in π_{phenyl} for aryl derivatives. Mrs. A. Linderman assisted in the measurement of the partition coefficients, and Mr. D. Park and Mr. F. McClusky assisted with the computations.

REFERENCES

1. C. HANSCH and T. FUJITA. J. Am. Chem. Soc. **86**, 1616 (1964).
2. T. FUJITA, J. IWASA, and C. HANSCH. J. Am. Chem. Soc. **86**, 5175 (1964).
3. J. IWASA, T. FUJITA, and C. HANSCH. J. Med. Chem. **8**, 150 (1965).

Can. J. Chem. Downloaded from www.nrcresearchpress.com by 210.87.254.42 on 09/05/12
For personal use only.

Can. J. Chem. Downloaded from www.nrcresearchpress.com by 210.87.254.42 on 09/05/12
For personal use only.

THE SPECIFICITY OF HYDROGEN BOND FORMATION BETWEEN DERIVATIVES OF NUCLEIC ACID BASES AND SOME ANALOGUES[1]

J. PITHA[2] AND R. NORMAN JONES
Division of Pure Chemistry, National Research Council of Canada, Ottawa, Canada

AND

P. PITHOVA
Institute of Organic Chemistry and Biochemistry, Czechoslovak Academy of Sciences, Prague, Czechoslovakia

Received December 23, 1965

ABSTRACT

Hydrogen bonding between pairs of derivatives of the base constituents of nucleic acids and their analogues has been studied in chloroform solution by infrared spectrophotometry. The strongest interactions occur between derivatives of guanine and cytosine. The introduction of the additional ring nitrogen atom in the pharmacologically active 5-azacytosine and 6-azacytosine derivatives does not change the complexing behavior. The positions of the N—H stretching bands in the infared spectra indicate that these complexes have a structure similar to that of the complexes formed between the corresponding pairs of bases in the naturally occurring desoxyribonucleic acid chain.

INTRODUCTION

The stability of double-stranded nucleic acids depends on the interplay of van der Waals and electrostatic interactions and on selective hydrogen bonding between specific pairs of purine and pyrimidine base units. There is considerable interest in the incorporation of other bases into nucleic acids; to understand the biochemical and pharmacological action of these groups, means must be devised to distinguish among the different types of stabilizing forces. It is particularly important to isolate the stabilizing effects of specific hydrogen bonding; this may be done by examining model structures in which these forces may be expected to predominate.

In proteins, the ability of amide–amide hydrogen bonds to stabilize specific conformations of peptides has been demonstrated by studies in nonpolar solvents (1, 2); the same methods can be applied to nucleic acids. Although the overall environment of the complexing groups in a nonpolar solvent differs from that in a biologically active system, the more immediate environment of the hydrogen bonds is not necessarily so different; in aqueous media the structurally functional hydrogen bonds tend to be shielded from surrounding water molecules by the skeletal structure.

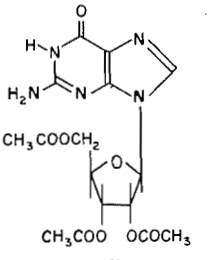
In nucleic acids, interactions between the stacked base groups not only shield the hydrogen bonds, but also actively stabilize the structures. Ts'o *et al.* (3) have shown that the attractions between the stacked base units can be studied in dilute aqueous solution, where the hydrogen bonding between bases is least effective. Conversely, the hydrogen bonding forces should dominate in nonpolar media.

The insolubility of the free bases, and of their simpler derivatives and analogues, restricts studies of this kind. Krackov *et al.* (4), in a search for more soluble model substances, used 2-pyridone and its sulfur and selenium analogues to investigate specific hydrogen bonding in benzene and dioxane solutions. They were able to show that specific complexing did occur in these compounds, and although the analogy with the natural

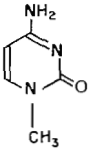
[1]*Issued as N.R.C. No. 8904.*
[2]*National Research Council Postdoctorate Fellow.*

nucleoside bases is somewhat remote, their results lend support to the conventional picture of hydrogen bond stabilization in nucleic acid systems. More recently, while our own work was in progress, Hamlin *et al.* (5) have shown spectroscopically that complex formation occurs between 9-ethyladenine and 1-cyclohexyluracil in deuteriochloroform solution.

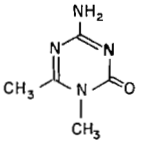
In this paper we demonstrate specific hydrogen bonding between 2′,3′,5′-tri-*O*-acetylguanosine (I) and 1-methylcytosine (II) in chloroform. The introduction of an additional nitrogen atom into the cytosine ring to form 5-aza- and 6-aza-cytosine derivatives is of considerable interest, since these compounds have been shown to possess cancerostatic and bacteriostatic activity (6, 7). We have been able to show that derivatives of these bases (III, IV) complex specifically with 2′,3′,5′-tri-*O*-acetylguanosine (I), and that the complexes have a structure similar to that of the complexes formed between I and II.



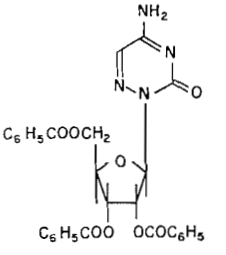
I



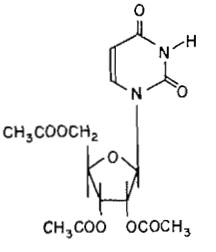
II



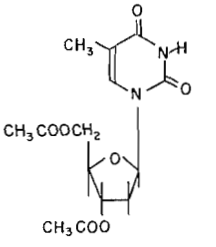
III



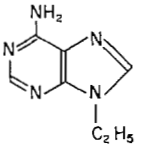
IV



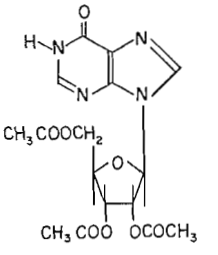
V



VI



VII



VIII

Can. J. Chem. Downloaded from www.nrcresearchpress.com by 210.87.254.42 on 09/05/12
For personal use only.

Can. J. Chem. Downloaded from www.nrcresearchpress.com by 210.87.254.42 on 09/05/12
For personal use only.

EXPERIMENTAL

The preparation of the substances I–VIII used in this investigation has been described (Table I). Complex formation was detected by infrared spectrophotometry with 2 cm long, brass-walled cells having sodium chloride windows, thermostatted at 32°. The spectra were measured over the range 3 570 – 3 330 cm^{-1}, limited by the chloroform cutoff. A Perkin–Elmer model 521 spectrophotometer was used, with the wavenumber scale calibrated against ammonia vapor (8) and the transmittance scale checked with rotating sectors. The chloroform solvent was freed from antioxidants and dried by shaking with phosphorus pentoxide followed by distillation. Chloroform prepared in this manner is unstable and develops a band at 3 486 cm^{-1}, presumably by photolysis in the spectrometer beam or catalysis from the metal cell walls. Solutions were prepared by boiling the solvent and solute together under reflux, and residual traces of water were removed by isothermal distillation. Molal concentrations in the range 1.2×10^{-4} to 2.5×10^{-4} *m* were employed. The solubility of I is less than 1.2×10^{-4} *m*, at 25°, but supersaturated solutions were readily obtained. The solubility of II is also very low and its solutions are light sensitive, resulting in the deposition of a precipitate which is probably a hydrochloride. This can be avoided by careful handling of the solution and the use of freshly prepared chloroform.

RESULTS

The solutions of the individual substances exhibited the absorption bands listed in Table I, which are typical of the N—H stretching vibrations (9, 11). In compounds II–VIII these bands were narrow; their peak intensity – concentration dependence followed

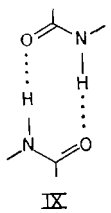
TABLE I

Band positions of N—H stretching vibrations (chloroform solutions)

Substance	ν_{max} (cm^{-1})	Method of preparation
I	3 510, 3 408	Ref. 23
II	3 531, 3 418	Ref. 24
III	3 541, 3 423	Ref. 25
IV	3 521, 3 405	Ref. 26
V	3 489	Ref. 27
VI	3 492	Ref. 28
VII	3 523, 3 414	*
VIII	3 484	Ref. 23

*Obtained from Cyclo Chemical Company, Los Angeles.

Beer's law within the accuracy of the measurements. This excluded any significant degree of self-association over the concentration range examined. The spectrum of I did show slight asymmetry on the low wavenumber side of both bands at room temperature, but



IX

the peak absorbances remained linearly dependent on the concentration over the accessible range (7.3×10^{-5} to 2.2×10^{-4} *m*). Complexing through hydrogen bonding to the N—H groups of primary amines would be expected to produce a new band within the measured wavenumber range. Complexes not involving primary amino groups, such as the dimerization V → IX, would yield new bands outside the measured range, but this should be accompanied by the disappearance or diminution of the bands of free species. It is known that such complexes are only formed at concentrations higher by several orders of magnitude than those used in our experiments (5, 10).

The spectra of binary solutions of I–V, I–VI, I–VII, II–V, II–VI, II–VII, II–VIII, IV–VIII, V–VI, V–VII, and VI–VII were examined in varied proportions at a total concentration of 1.5×10^{-4} *m*, and exhibited only the bands of the monomeric species. The spectra of binary solutions of I–II, I–III, and I–IV, however, when measured in the same concentration range, each exhibited one prominent new band at 3 489, 3 488, and 3 472 cm^{-1}, respectively. The system I–III was studied over the temperature range 30–45°, and the band showed reversible intensity changes typical of an equilibrium system. It is inferred that the new band is associated with the spectrum of a complex, and is the higher N—H stretching vibration of a hydrogen-bonded primary amine group, the lower component of which is obscured by chloroform absorption (11). Analysis of the band intensities showed that, within the limits of experimental precision, only 1:1 complexes are formed. The spectral changes for the I–II system are illustrated in Fig. 1, and the continuous variation graph (12) for the I–IV pair is shown in Fig. 2. The corresponding spectra and graphs for the other pairs are qualitatively similar. Since the intensity of the bands associ-

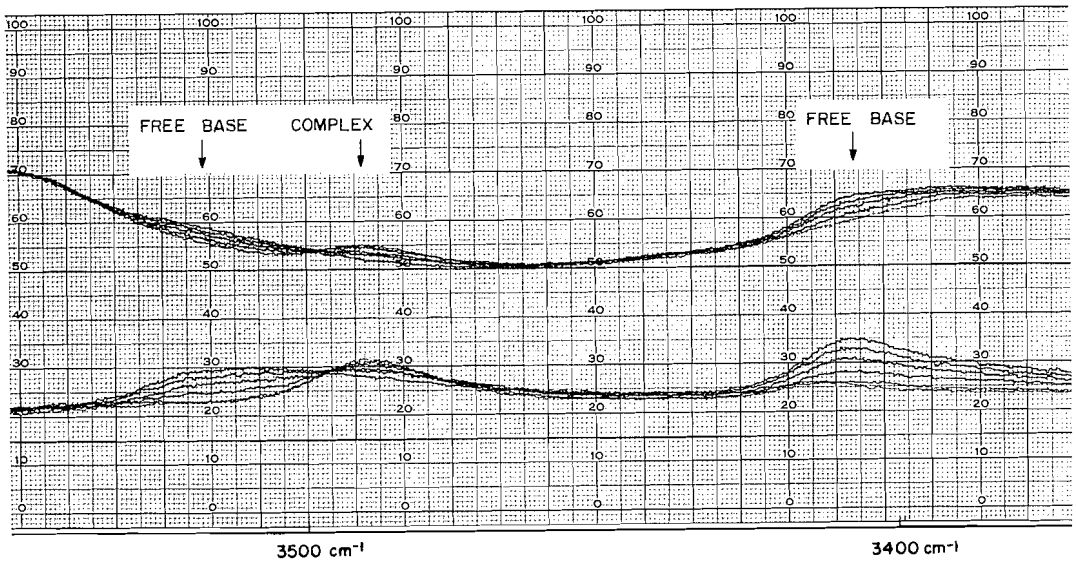


FIG. 1. Infrared spectra in chloroform solution. Formation of complex between guanine and cytosine derivatives (I–II). Upper spectra obtained without compensation; lower spectra compensated for chloroform absorption. Total molality 1.5×10^{-4}; molal proportions of I are 100%, 90%, 80%, 70%, 60%, and 50%; temperature 32 °C; path length 2 cm.

ated with the free amino groups of both components diminishes on complex formation, it is presumed that both amino groups participate in complex formation. The instability of the solutions prevented an accurate evaluation of the equilibrium constants, but the analysis by the continuous variation method suggested values of the order of 10^5 l $mole^{-1}$ for the equilibrium constant of the I–II system, and a somewhat lower value for the I–IV system. Under the conditions of our experiments we should have been able to observe complex formation, provided the equilibrium constant was not less than 10^4 l $mole^{-1}$. These findings are consistent with those of Hamlin *et al.* (5), who reported that the equilibrium constant for complex formation between 9-ethyladenine and 1-cyclohexyluracil is of the order of 10^3. In our experiments the system most closely corresponding to this is V–VII, in which the cyclohexyl group of Hamlin's uracil derivative is replaced by 2′,3′,5′-tri-*O*-acetylribose; as stated above, we failed to detect complex formation under our experimental

Can. J. Chem. Downloaded from www.nrcresearchpress.com by 210.87.254.42 on 09/05/12
For personal use only.

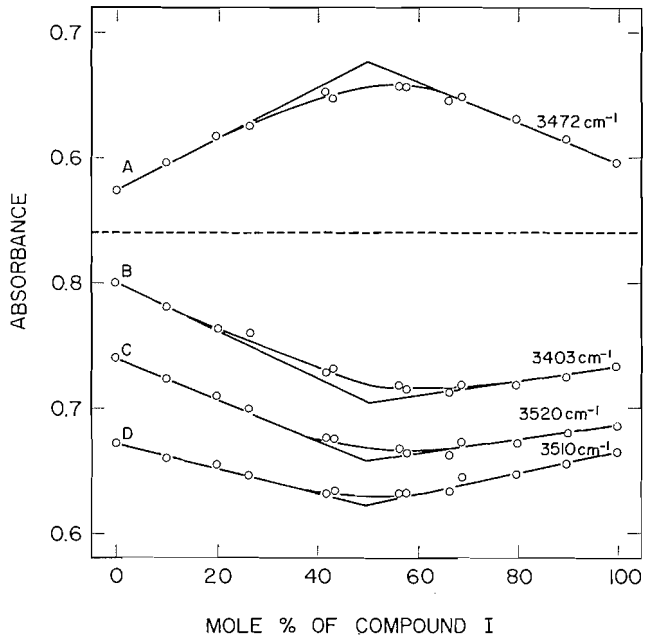
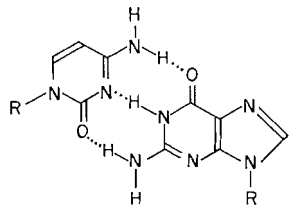


FIG. 2. Continuous variation graph for the I–IV mixture. The absorbance values are for measurements obtained without compensation. Total molality 2.5×10^{-4}.

conditions for this system, which would indicate that the equilibrium constant must be less than 10^4.

DISCUSSION

Since the amino groups of both the guanine and cytosine moieties are involved in the guanine–cytosine type complexes (I–II, II–III, and I–IV), these would appear to have structure X as in desoxyribonucleic acid. This mode of association is apparently very



X

stable, and has been shown to occur in crystalline complexes modelled on the guanine–cytosine base pair (13–15). Studies on polynucleotides (16) indicate that 2:1 complexing can also occur, but this is unlikely at the high dilutions we used; in no case did we observe any evidence for it.

Equilibrium constants of the order of 10^5 l mole^{-1} indicate that the structural stability of these complexes is remarkably high. Three hydrogen bonds are formed per pair, and the presence of all three seems to be essential, since replacement of the guanosine derivative (I) by the corresponding inosine derivative (VIII) reduced the stability of the complex below our limit of detection. The extremely high stability of the guanine–cytosine type

Can. J. Chem. Downloaded from www.nrcresearchpress.com by 210.87.254.42 on 09/05/12
For personal use only.

complexes may be illustrated by the fact that the equilibrium constant for simple dimeric association of the amide group in ϵ-caprolactam is 1.5 l mole^{-1} (1); for complex formation between aniline and dimethylacetamide an equilibrium constant of 6.0 l mole^{-1} has been reported (17). Substitution in the ring system of complexing pairs can induce large changes in other physical behavior: thus aza substitution at position 6 in cytidine lowers the basicity by a factor of 10 (18); nevertheless, the complexing facility remains virtually unchanged.

This evidence for the high stability of guanine–cytosine pairs, as contrasted with adenine–uracil or adenine–thymine pairs, is consistent with the generally accepted view, based on experimental studies of nucleic acids and on quantum mechanical calculations (19). One might infer from our results that the aza analogues should be incorporated extensively into nucleic acids, but this is not supported by experiment. 6-Azacytidine is known to inhibit enzyme reactions that precede the nucleic acid synthesis (6), and the ability of 5-azacytidine to be incorporated is partially concealed by its rapid hydrolysis (20–22). Nevertheless, we see that 5-azacytidine type substances do exhibit a specificity to complex with guanine; this offers some support for the hypothesis (20) that the cancerostatic and bacteriostatic actions of 5-azacytidine involve modification of the nucleic acid structure. This might be brought about by its hydrolysis subsequent to its incorporation into the nucleic acid chain. Lastly, it must be remembered that the formation of specific hydrogen bonds is only one factor determining nucleic acid stability, and differences in the interactions between adjacent stacked base groups must also be considered.

ACKNOWLEDGMENTS

We thank Prof. Šorm for his interest in this work, and Dr. Škoda, Dr. Žemlicka, and Dr. Piskala for their helpful discussions.

REFERENCES

1. J. S. Franzen and R. E. Stephens. Biochemistry, **2**, 1321 (1963).
2. J. S. Franzen and B. C. Franzen. J. Phys. Chem. **68**, 3898 (1964).
3. P. O. P. Ts'o, I. S. Melvin, and A. C. Olson. J. Am. Chem. Soc. **85**, 1289 (1963).
4. M. H. Krackov, C. M. Lee, and H. G. Mautner. J. Am. Chem. Soc. **87**, 982 (1965).
5. R. M. Hamlin, R. C. Lord, and A. Rich. Science, **148**, 1734 (1965).
6. R. E. Handschumacher, J. Škoda, and F. Šorm. Collection Czech. Chem. Commun. **28**, 2983 (1963).
7. F. Šorm, A. Piskala, A. Čihak, and J. Vesely. Experientia, **20**, 202 (1964).
8. I.U.P.A.C. tables of wavenumbers for the calibration of infra-red spectrometers. Butterworths, London. 1961.
9. J. Pitha and S. Vašičkova. Collection Czech. Chem. Commun. **30**, 1792 (1965).
10. J. Pitha and J. Beranek. Collection Czech. Chem. Commun. **28**, 1507 (1963).
11. P. J. Krueger. Can. J. Chem. **42**, 201 (1964).
12. F. J. C. Rossoti and H. Rossoti. The determination of stability constants. McGraw-Hill Book Co., Inc., New York. 1961.
13. A. E. V. Haschemeyer and H. M. Sobell. Nature, **202**, 69 (1964).
14. E. J. O'Brien. J. Mol. Biol. **7**, 107 (1963).
15. H. M. Sobel, K. Tomita, and A. Rich. Proc. Natl. Acad. Sci. U.S. **49**, 885 (1963).
16. F. Pochon and A. M. Michelson. Proc. Natl. Acad. Sci. U.S. **53**, 1425 (1965).
17. F. Takahashi and N. C. Li. J. Phys. Chem. **69**, 2950 (1965).
18. J. Beranek and F. Šorm. Collection Czech. Chem. Commun. **28**, 469 (1963).
19. B. Pullman and A. Pullman. Quantum biochemistry. Interscience Publishers, Inc., New York. 1963.
20. P. Pithova, A. Piskala, J. Pitha, and F. Šorm. Collection Czech. Chem. Commun. **30**, 2801 (1965).
21. P. Pithova, V. Fučik, S. Zadražil, Z. Šormova, and F. Šorm. Collection Czech. Chem. Commun. **30**, 2879 (1965).
22. M. Jurovčik, K. Raška, Z. Šormova, and F. Šorm. Collection Czech. Chem. Commun. **30**, 3370 (1965).
23. H. Bredereck and A. Martini. Chem. Ber. **80**, 401 (1947).
24. G. W. Kenner, C. B. Reese, and A. R. Todd. J. Chem. Soc. 855 (1955).
25. A. Piskala and J. Gut. Collection Czech. Chem. Commun. **28**, 1681 (1963).
26. J. Žemlicka, J. Smrt, and F. Šorm. Tetrahedron Letters, 397 (1962).
27. D. M. Brown, A. R. Todd, and S. Varadarajan. J. Chem. Soc. 2388 (1956).
28. R. E. Beltz and D. W. Visser. J. Am. Chem. Soc. **77**, 736 (1955).

Can. J. Chem. Downloaded from www.nrcresearchpress.com by 210.87.254.42 on 09/05/12
For personal use only.

Can. J. Chem. Downloaded from www.nrcresearchpress.com by 210.87.254.105 on 09/05/12
For personal use only.

STRUCTURAL COMPONENTS IN METHYL VINYL SULFONE MODIFIED COTTON CELLULOSE[1]

S. P. ROWLAND, V. O. CIRINO, AND A. L. BULLOCK

Southern Regional Research Laboratory, Southern Utilization Research and Development Division, Agricultural Research Service, United States Department of Agriculture, New Orleans, Louisiana

Received January 5, 1966

ABSTRACT

Methylsulfonylethyl cellulose was prepared at a low degree of substitution (0.11), which is conventional for the chemical modification of cotton, by the Michael addition of methyl vinyl sulfone to cotton fabric. The distribution of substituents in the anhydroglucose units was determined by hydrolysis of the molecular chain to glucose units, selective concentration of the substituted glucose components, gas–liquid chromatographic analyses of the methylsulfonylethylglucoses, and comparison with authentic samples of 2-*O*-, 3-*O*-, and 6-*O*-methylsulfonylethylglucoses in the form of trimethylsilyl ethers. The validity of each of these steps for quantitative analyses has been examined. The ratio of the 2-*O*-, 3-*O*-, and 6-*O*-monomethylsulfonylethylglucoses was found to be 0.20:0.03:1.0. No evidence was found for the presence of di- or tri-substituted glucoses.

INTRODUCTION

The sites of reaction and the distributions of substituents on the 2-*O*, 3-*O*-, and 6-*O*-positions of the anhydroglucose units of cellulose have been well characterized for a number of etherification reactions, primarily methylation (1, 2), ethylation (3), hydroxyethylation (4), carboxymethylation (5), and carbamoylethylation (6). However, aside from studies of trimethylolmelamine-treated (7) and divinyl sulfone treated cottons (8), etherifications which are of interest in the chemical modification and cross-linking of cotton cellulose have received little attention, and in neither of these cases has the distribution of substituents been delineated.

Unambiguous characterizations of the structural components of chemically modified celluloses depend upon molecular degradation of the polymer to glucose units, quantitative recovery of the components, and identification of the modified glucoses. The direct approach to identification of the structural components, which has been applied very successfully by Croon and co-workers (1–5) for celluloses modified to a degree of substitution in the range of 0.5–1 or higher, becomes more demanding when applied to chemically modified cottons for which the cross-linking or modifying agent seldom exceeds 10% of the composition or an apparent average degree of substitution of 0.15.

This paper describes the substituent group distribution resulting from the base-catalyzed Michael addition reaction of methyl vinyl sulfone with cotton cellulose under conditions approximating those for cross-linking cotton with divinyl sulfone. Special attention is devoted to the development of techniques having a degree of general applicability for the facile characterization of chemically modified cottons, and to the verification of the quantitative validity of these techniques. Gas–liquid chromatography has been employed extensively throughout this study.

EXPERIMENTAL

Materials

The cotton cellulose was in the form of desized, scoured, bleached 80 × 80 print cloth weighing 3.3 oz./yd. Methyl vinyl sulfone was obtained from K and K Laboratories, Incorporated,[2] β-cellobiose (white label

[1]*Presented in part before the Joint Chromatography Symposium of the Division of Cellulose, Wood, and Fiber Chemistry and the Division of Carbohydrate Chemistry at the winter meeting of the American Chemical Society, Phoenix, Arizona, January 1966.*

[2]*Naming a company and (or) product by the Department of Agriculture does not imply approval or recommendation of the product to the exclusion of others which may also be suitable.*

grade) from Eastman Kodak Company, α-glucose from the National Bureau of Standards, trimethylchlorosilane from General Electric Company, and hexamethyldisilazane from Peninsular Chemresearch. Reagent grade pyridine was dried over sodium hydroxide pellets. The syntheses of authentic samples of 2-*O*-, 3-*O*-, and 6-*O*-monomethylsulfonylethylglucoses are described elsewhere (9).

Apparatus

The gas–liquid chromatographic unit was a F & M model 1609 equipped with a hydrogen flame ionization detector. The gas–liquid chromatographic columns were based on a solid phase of acid-washed dimethyldichlorosilane-treated Chromosorb W of 80–100 mesh from Johns–Mansville Corporation. The liquid phases consisted of SE-52, Apiezon M, XE-60, and QF-1 from Wilkens Instrument and Research, Incorporated. The columns were prepared in ¼ inch outside diameter tubing and are identified as follows: 3% SE-52, 6 ft stainless steel column; 10% Apiezon M, 2 ft aluminium column; 8.5% XE-60, 2 ft aluminium column; and 3% QF-1, 5.5 ft aluminium column.

Procedure

Methyl Vinyl Sulfone Modified Cotton Cellulose

Methyl vinyl sulfone was caused to react with cotton print cloth under conditions generally similar to those described by Tesoro and Oroszlan (10). The extent of reaction was measured by weight gain and sulfur analysis (Schoeniger combustion method (11)). The samples of methylsulfonylethyl cellulose which were studied contained 1.97% sulfur (ca. 6.5% weight gain), corresponding to a degree of substitution of 0.11.

Hydrolysis of Cottons to Glucose and Substituted Glucoses

Cotton celluloses were hydrolyzed with sulfuric acid by the general procedure of Hägglund (12) as modified by Abend (8). One gram of fabric from a supply of material homogenized as small (ca. 0.25 cm^2) squares was covered with 15 g of 72% sulfuric acid and was subjected to mild agitation at room temperature under an atmosphere of nitrogen for 8 h. The homogeneous solution was diluted to 7.7 *N* with 20 ml of distilled water, and mild agitation was continued under a nitrogen blanket for 16–20 h. At this time the solution was diluted to 1.5 *N* with 120 ml of water and refluxed for 6 h under nitrogen. Barium hydroxide was utilized to adjust the pH between 5.6 and 6.0, the barium sulfate was removed, the filtrate was concentrated under vacuum below 40 °C, and the concentrate was freeze-dried to a solid product.

Hydrolyses of cotton celluloses with 90% formic acid by the procedure of McGilvray (13) was accomplished with 42 ml of formic acid for 2 g of air-dried fabric. After a 5 h period on a boiling water bath, insoluble cellulose (A-1) was removed by centrifugation and filtration. The filtrate was evaporated to dryness and the evaporation process was repeated three times (or until all the free formic acid was removed), with the addition of ca. 50 ml of water each time. The product which contained formate groups was hydrolyzed to free saccharides (B-1) by reflux for 4 h with 1 *N* or 2 *N* sulfuric acid. Neutralization and removal of acid were conducted as described above. The cellulose fraction (A-1) which remained undissolved after the 5 h treatment in formic acid was retreated with fresh formic acid (42 ml) for 9 h and subsequently hydrolyzed to the free saccharide (B-2) with dilute sulfuric acid. A 2.02 g sample of unmodified cotton yielded 0.2920 g of fraction B-1 and 0.2380 g of B-2. A 2.0157 g sample of methylsulfonylethyl cellulose yielded 0.3279 g of fraction B-1 and 0.2416 g of fraction B-2. Insoluble fraction A-1 contained 0.93% sulfur. A 2.0101 g sample of methylsulfonylethyl cellulose, ball-milled to show a completely noncrystalline X-ray diffractogram, yielded only the soluble fraction B-1.

Removal of Glucose from Chemically Modified Glucoses

A 1.0 g sample of the hydrolysate of cotton fabric was dissolved in 20 ml of water together with 0.2 g of dried yeast. Fermentation was allowed to proceed at ambient temperature until no more microbubbles appeared. The solution was filtered and freeze-dried to a solid product. The hydrolyzed cotton or glucose yielded less than 0.1 g of residual nonvolatile product; methylsulfonylethyl cellulose yielded 0.25 g of product.

Gas–Liquid Chromatographic Analyses

Trimethylsilyl ethers of saccharides were prepared for gas–liquid chromatographic analyses by the method of Sweeley *et al.* (14), which employs approximately 10 mg of sample, 1.0 ml of anhydrous pyridine, 0.2 ml of hexamethyldisilazane, and 0.1 ml of trimethylchlorosilane. Heating for 5–15 min at 90–95 °C was necessary to insure conversion of cellobiose into the trimethylsilyl ether.

RESULTS

Hydrolysis and Concentration of Structural Components from Modified Cotton

During these studies it was found that gas–liquid chromatography of methylsulfonylethylglucoses (either as pure isomers or as hydrolysates from methylsulfonylethyl cellulose) in the form of trimethylsilyl ethers required high temperatures for both the injection port and the columns. Column temperatures in the range of 190–250 °C produced the

Can. J. Chem. Downloaded from www.nrcresearchpress.com by 210.87.254.105 on 09/05/12
For personal use only.

best results. Although a variety of liquid phases was investigated, only the following were found to be suitable: SE-52, Apiezon M, XE-60, and QF-1. The limitation of other more polar columns was the inability to desorb the methylsulfonylethylglucoses at suitable operating temperatures and (or) the tendency to catalyze rearrangement of the blocking groups introduced into these molecules for synthesis purposes (9, 15).

Direct hydrolyses of cotton and wood celluloses to glucose have been achieved under a variety of conditions (12), but invariably with the requirement of a strong acid, unless the modified cellulose was uniquely soluble in the hydrolyzing medium. The process commonly employed in preceding studies involves dissolution in 72% sulfuric acid at room temperature followed by hydrolysis of the cellulose at higher levels of dilution. This procedure, when applied to cotton under an inert atmosphere, yielded a light-colored hydrolysate. The effectiveness of the hydrolysis in our hands is indicated by chromatograms of the trimethylsilyl ethers of the hydrolysate of the unmodified cotton cellulose (curve A, Fig. 1). Chromatograms of pure glucose and cellobiose are shown for comparison

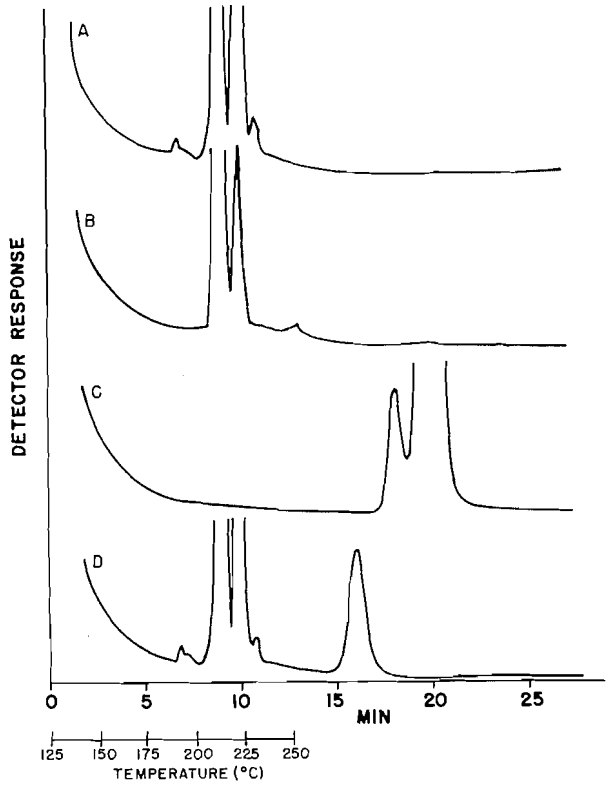


FIG. 1. Chromatograms of trimethylsilyl derivatives on SE-52 liquid phase with temperature of column programmed at 10 °C/min from 125 to 250 °C. Curve A is the hydrolysate of cotton; curve B is α-glucose; curve C is β-cellobiose; curve D is the hydrolysate of methylsulfonylethyl cellulose.

(curves B and C). Comparison of the peaks and retention times for the cotton hydrolysate with those of glucose and cellobiose indicates that the hydrolysate contains no cellobiose or higher oligomer. Glucose is indicated in a high state of purity, with the traces of impurities in minute peaks at retention times of $6\frac{3}{4}$ and 11 min.

Can. J. Chem. Downloaded from www.nrcresearchpress.com by 210.87.254.105 on 09/05/12
For personal use only.

Can. J. Chem. Downloaded from www.nrcresearchpress.com by 210.87.254.105 on 09/05/12
For personal use only.

This hydrolytic procedure, when applied to methylsulfonylethyl cellulose, results in total hydrolysis and high recovery of the hydrolysate (97–100% of theory) without significant loss in sulfur content (93–100% recovery). Chromatograms of the trimethylsilyl ethers of the hydrolysate of methylsulfonylethyl cellulose are shown in curve D of Fig. 1. In addition to the major peak corresponding to glucose, a new peak is observed intermediate in retention time between those of glucose and cellobiose. The new peak is attributed to methylsulfonylethylglucoses; no evidence for methyl vinyl sulfone or methyl 2-hydroxyethyl sulfone was found in the chromatogram of the hydrolysate.

Since Croon and Lindberg (1) observed a decrease in optical rotation amounting to 3–5% for methyl ethers of glucose treated under conditions very similar to those employed in this study, the effect of 72% sulfuric acid upon the individual methylsulfonylethylglucoses (see later section) has been examined together with the effect of milder conditions of hydrolysis for methylsulfonylethyl cellulose. McGilvray (13) found that a completely methylated cellulose was hydrolyzed much faster in 90% formic acid than under the more drastic conditions involving sulfuric acid. No demethylation occurred when he subjected 2,3,6-tri-*O*-methylglucose to this hydrolytic procedure.

When the formic acid hydrolysis was applied to cotton, 14% of the cellulose was dissolved in the period (5 h) which McGilvray found to be sufficient to hydrolyze methyl cellulose completely. An additional 9 h of hydrolysis solubilized 12% of the original cotton, leaving aggregates of material not unlike hydrocellulose (16). The soluble fraction of cellulose was found by gas–liquid chromatography to be present as a complex mixture of formates of glucose and higher saccharides. Upon hydrolysis with 1 *N* sulfuric acid, this formate fraction showed the presence of minor amounts of cellobiose together with major amounts of glucose.

Methylsulfonylethyl cellulose was hydrolyzed selectively in 90% formic acid; 53% of the sulfur-containing components was removed in 26% of the total sample. Ball-milled methylsulfonylethyl cellulose was solubilized completely and hydrolyzed rapidly without selectivity, under the same conditions used in the reaction with formic acid. Hydrolysis of solubilized carbohydrate formates with 2 *N* sulfuric acid was employed to remove formate groups and to convert cellobiose and higher saccharides into glucose units. Chromatograms of this hydrolysate showed a ratio of peak areas of modified glucoses to glucose equivalent, within experimental variation, to the ratio observed for the product from hydrolysis with 72% sulfuric acid. This indicates that the loss of methylsulfonylethyl substituents during hydrolysis is small, if it occurs at all.

To establish the extent to which the peaks under consideration as methylsulfonylethylglucoses from hydrolyzed methylsulfonylethyl cellulose represent complete detection of these components in gas–liquid chromatography, the response of the flame ionization detector to glucose and to 3-*O*-methylsulfonylethylglucose (9) was calibrated against cellobiose as an internal standard (17). By applying correction factors (1.07 for glucose and 2.0 for 3-*O*-methylsulfonylethylglucose) to specific peak areas before normalization of the total peak areas, it appears that the methylsulfonylethylglucose fraction constitutes 15.2% of the hydrolysate. This is in good agreement with the expectation, on the basis of sulfur analysis together with the reasonable assumption that only monosubstitution occurs within the anhydroglucose unit, that modified glucose components amount to 15.6% of the hydrolysate.

The small fraction of modified glucoses in the hydrolysate imposes limitations upon the resolution of peaks of the unknown components. Fermentation proved to be the simplest

and most effective method for removal of the unmodified glucose. Except for the appearance of glycerol and traces of components near the retention time for glucose, the chromatograms of the concentrate were free of interference in the region of the methylsulfonylethylglucose fraction. Chromatograms and analyses indicate that the methylsulfonylethylglucoses constitute 70% of the concentrate. The effectiveness of removal of glucose is apparent from curves A and B of Fig. 2.

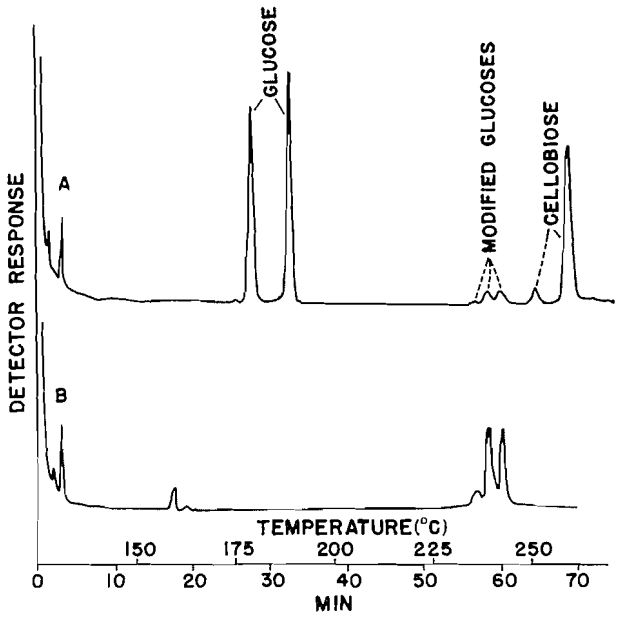


FIG. 2. Chromatograms of trimethylsilyl derivatives on SE-52 liquid phase programmed at 2 °C/min from 125 to 250 °C. Curve A is the hydrolysate of methylsulfonylethyl cellulose containing cellobiose as an internal reference; curve B is the concentrate of the hydrolysate after fermentation.

2-O-, 3-O-, and 6-O-Monomethylsulfonylethylglucoses

Individual samples of 2-*O*-, 3-*O*-, and 6-*O*-methylsulfonylethylglucoses, whose syntheses are described elsewhere (9), were subjected to the 72% sulfuric acid treatment employed for the hydrolysis of cottons; no detectable change was observed in the chromatograms, confirming earlier evidence for the complete stability of the ether linkage between the glucose and methylsulfonylethyl groups.

Methylsulfonylethylglucoses in the form of trimethylsilyl ethers were characterized by gas–liquid chromatography on several columns with glucose or cellobiose as internal reference for relative retention values (Table I). In each case the methylsulfonylethylglucose was resolved into two peaks representing anomeric forms. To facilitate comparisons of the relative retention values for the anomeric forms of the pure methylsulfonylethylglucoses, we have assigned to the reference materials relative retention values which are consistent with a relative retention value of 1.0 for the peak of the second anomer of 6-*O*-methylsulfonylethylglucose. Ratios of the areas of the two anomeric peaks were characteristic for each position isomer and are as follows: 2-*O*-methylsulfonylethylglucose, 0.43:0.57; 3-*O*-methylsulfonylethylglucose, 0.50:0.50; and 6-*O*-methylsulfonylethylglucose, 0.49:0.51.

Can. J. Chem. Downloaded from www.nrcresearchpress.com by 210.87.254.105 on 09/05/12
For personal use only.

TABLE I

Relative retention values for methylsulfonylethylglucoses*

Compound	Column:† SE-52	Apiezon M	XE-60	QF-1
Glucose	0.08	0.057	—	—
	0.106	0.088		
Cellobiose	1.56	1.55	0.125	0.21
	2.47		0.217	0.30
2-*O*-MSEG‡	0.702	0.68	0.63	0.65
	0.851	0.84	0.76	0.755
3-*O*-MSEG	0.537	0.449	0.40	0.49
	0.83	0.77	0.685	0.72
6-*O*-MSEG	0.833	0.78	0.784	0.88
	1.00	1.00	1.00	1.00

*The internal standards are assigned fractional relative retention values such that the value for the peak of the second anomer of 6-*O*-methylsulfonylethylglucose is 1.0.
†XE-60 operated isothermally at 190 °C; all others at 200 °C.
‡MSEG is methylsulfonylethylglucose.

Ratio of Isomeric Monomethylsulfonylethylglucoses in Methylsulfonylethyl Cellulose

Chromatograms of the concentrated methylsulfonylethylglucose fraction from the hydrolysis of methylsulfonylethyl cellulose with 72% sulfuric acid are reproduced in Fig. 3 together with markers which designate positions at which the anomers of the pure

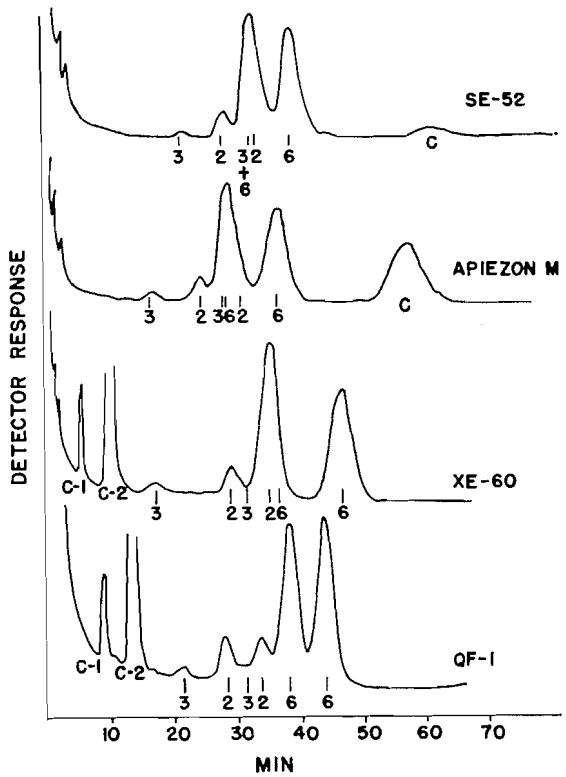


FIG. 3. Chromatograms of the trimethylsilyl derivatives of the concentrate from the hydrolysis of methylsulfonylethyl cellulose with 72% sulfuric acid. Isothermal operation; XE-60 operated at 190 °C; all other columns operated at 200 °C. Vertical markers indicate the positions of peaks of anomers of the individual 2-*O*-, 3-*O*-, and 6-*O*-monomethylsulfonylethylglucoses. Cellobiose (C) is an internal standard.

Can. J. Chem. Downloaded from www.nrcresearchpress.com by 210.87.254.105 on 09/05/12
For personal use only.

monomethylsulfonylethylglucoses appear in the chromatogram. On SE-52 and Apiezon M columns, one anomer of each isomeric substituted glucose is resolved separately, and the other anomers (i.e. the second anomer of 2-*O*- and 3-*O*- together with the first anomer of 6-*O*-methylsulfonylethylglucose) are unresolved and appear together in a single peak. The separation is less satisfactory on the XE-60 column and most effective on the QF-1 column, where only the second anomeric peak of the 3-*O*-methylsulfonylethylglucose is secluded between two other peaks.

The ratio of peak areas (product of retention time and peak height) on QF-1 for the 2-*O*-, 3-*O*-, and 6-*O*-isomers is 0.20:0.03:1.0. The ratios obtained from gas–liquid chromatography on SE-52, Apiezon M, and XE-60, if the ratios of the peak areas for the anomers of each individual position isomer are taken into consideration, are 0.21:0.03:1.0, 0.21:0.036:1.0, and 0.17:0.03:1.0. The ratios of peak areas from triangulation or planimetry measurements were generally less consistent, extending over the following range: 0.18–0.25 : 0.03–0.06 : 1.0. We conclude that the best data are represented in the ratio 0.20:0.03:1.0, which is preferably expressed with the value of unity assigned to the 6-*O*-methylsulfonylethylglucose. The assignment of a value of unity to the 3-*O*-isomer, which is present in the smallest amount and subject to the largest inaccuracies, accentuates errors and impedes comparisons.

DISCUSSION

The base-catalyzed reaction of an alcohol with an activated olefin is a reversible nucleophilic attack of an alkoxide ion on the vinyl group (18, 19). The mechanism of the reaction of methyl vinyl sulfone with an alkoxide ion is considered to be similar to that of acrylonitrile in cyanoethylation or acrylamide in carbamoylethylation. The distribution of methylsulfonylethyl groups among the 2-*O*-, 3-*O*-, and 6-*O*-positions of the anhydroglucose unit in the ratio 0.20:0.03:1.0 is similar to that which Touzinsky (6) has reported recently (Table II) for carbamoylethyl groups from calculations of equilibrium constants by a modification of Spurlin's equations (20).

TABLE II

Distributions of substituents in cellulose ethers

Reagent	Ratio of substituents			Reference
	2	3	6	
Methyl vinyl sulfone	0.20	0.03	1.0	—
Acrylamide	0.47	0.05	1.0	6
Methyl chloride	2.5	0.5	1.0	2
Dimethyl sulfate	1.75	0.5	1.0	1
Ethyl chloride	2.25	0.5	1.0	3
Sodium chloroacetate	0.8	0.4	1.0	5
Ethylene oxide	0.3	0.1	1.0	4

In contrast to the major reaction at the 6-hydroxyl group for these Michael reactions involving small molecular species, the related reactions of large molecules proceeding through similar activated sulfone intermediates with cellulose are less well defined; Stamm (21) has indicated that reaction of a dye, 1-amino-9,10-dihydro-4[*p*[(2-sulfatoethyl)sulfonyl]anilino]9,10-dioxo-2-anthracenesulfonic acid, with cellulose or α-methylglucoside occurs mainly at the 2-hydroxyl group, a conclusion reached on the basis of the structure of methylglucoses isolated subsequent to complete methylation and removal of the dye substituent. Chekalin (22), studying the same reaction with rayon, cellobiose, and

Can. J. Chem. Downloaded from www.nrcresearchpress.com by 210.87.254.105 on 09/05/12
For personal use only.

Can. J. Chem. Downloaded from www.nrcresearchpress.com by 210.87.254.105 on 09/05/12
For personal use only.

α-methylglucoside and employing diagnostic reactions with triphenylmethyl chloride, periodate, and phenylhydrazine, found evidence for 65–75% of the substituent in the 6-*O*-position, with the major portion of the rest in the 2-*O*-position. It is not clear, therefore, to what extent molecular size, conditions of reaction, or methods of analyses have contributed to these differences.

The marked preference of methyl vinyl sulfone for reaction at the 6-hydroxyl group is distinctly different from the results of nucleophilic substitution reactions involving an alkyl halide or sulfate with cellulose in the presence of alkali (see Table II). Since the Michael reaction is reversible, the distribution of substituents among the different types of hydroxyl groups is controlled by the relative equilibria of the individual reactions. On the other hand, the nucleophilic substitution reactions with alkyl halides are not reversible; the distribution of substituents in the latter case is controlled by the rates of reactions. In these rate-controlled reactions the 2-hydroxyl group is the predominant point of attack. It is interesting, also, that the ratios of distribution of substituent groups between the 2- and 3-hydroxyls for methylsulfonylethylation (1.0:0.15) and carbamoethylation (1.0:0.11) appear to be generally different from those observed for rate-controlled reactions (1.0 : 0.20–0.33). An exception is carboxymethylation (1.0:0.5), for which the relative reactivity at the 3-position appears to be uniquely high among nucleophilic substitution reactions with cellulose; this reaction is also unique in that an electrostatic interference is indicated between substituent and reagent at the 2- and 3-positions for polysubstitution of an anhydroglucose unit (5).

It is now recognized that reactions employed for the modification or cross-linking of cotton cellulose may be rate controlled or equilibrium controlled, and that each class of reaction may exhibit a different pattern of distribution of substituents among the hydroxyl groups of the anhydroglucose unit. It further appears that each specific reagent may differ from another of the same class, but that the contribution of steric and electronic factors of the reagent, solubility of reagent, and conditions of reaction remain to be clarified.

ACKNOWLEDGMENTS

The authors are indebted to Mr. C. H. Mack and Mr. E. R. Cousins for technical contributions. We thank Mr. P. F. Pittman for analyses and Mr. G. I. Pittman for preparation of the line drawings.

REFERENCES

1. I. Croon and B. Lindberg. Svensk Papperstid. **60**, 843 (1957).
2. I. Croon. Svensk Papperstid. **61**, 919 (1958).
3. I. Croon and E. Flamm. Svensk Papperstid. **61**, 963 (1958).
4. I. Croon and B. Lindberg. Svensk Papperstid. **59**, 794 (1956).
5. I. Croon and G. B. Purves. Svensk Papperstid. **62**, 876 (1959).
6. G. F. Touzinsky. J. Org. Chem. **30**, 426 (1965).
7. J. J. Willard, R. Turner, and R. F. Schwenker, Jr. Textile Res. J. **35**, 564 (1965).
8. T. Abend, O. A. Stamm, and H. Zollinger. Helv. Chim. Acta. In press.
9. A. L. Bullock, V. O. Cirino, and S. P. Rowland. To be published.
10. A. C. Tesoro and A. Oroszlan. Textile Res. J. **33**, 93 (1963).
11. I. Lysyj and J. E. Zarembo. Microchem. J. **3**, 173 (1959).
12. E. Hägglund. *In* Chemistry of wood. Academic Press, Inc., New York. 1951. p. 100.
13. D. I. McGilvray. J. Chem. Soc. 2577 (1953).
14. C. C. Sweeley, R. Bentley, M. Maketa, and W. W. Wells. J. Am. Chem. Soc. **85**, 2497 (1963).
15. C. T. Bishop, F. P. Copper, and R. K. Murray. Can. J. Chem. **41**, 2245 (1963).
16. O. A. Battista. Am. Scientist, **53**, 151 (1965).
17. S. D. Nogare and R. S. Juvet, Jr. Gas liquid chromatography, theory and practice. Interscience Publishers, Inc., New York. 1962. p. 220.
18. B. A. Feit and A. Zilkha. J. Org. Chem. **28**, 406 (1963).
19. H. A. Bruson. Org. Reactions, **5**, 79 (1949).
20. H. M. Spurlin. J. Am. Chem. Soc. **61**, 2222 (1939).
21. O. A. Stamm. Helv. Chim. Acta, **46**, 3019 (1961); Textil-Rundschau, **19**, 245 (1964).
22. M. A. Chekalin. Tekstil'n. Prom. **21**, 40 (1961); **23**, 67 (1963).

Can. J. Chem. Downloaded from www.nrcresearchpress.com by 210.87.254.6 on 09/05/12
For personal use only.

CARCINOGENICITY OF LACTONES

I. THE REACTION OF 4-METHYLBUTENO- AND 4-METHYLBUTANO-γ-LACTONES WITH PRIMARY AMINES

J. Bryan Jones and John M. Young

Lash Miller Laboratories, Department of Chemistry, University of Toronto, Toronto, Ontario

Received December 1, 1965

ABSTRACT

As the first stage in the investigations of the mechanisms of action of carcinogenic lactones, the reactions of 4-hydroxypent-2-enoic acid lactone (II, R = CH_3), which is a carcinogen, and of the non-carcinogenic 4-hydroxypent-3-enoic (III, R = CH_3) and 4-hydroxypentanoic (IV, R = CH_3) acid lactones with methylamine and benzylamine have been studied. As expected, the carcinogenic lactone reacts to give the Michael addition products, whereas both inactive lactones undergo ring opening by nucleophilic attack at the carbonyl group. From the relative rates of reaction of the amines with the lactones it is concluded that the induction of tumors by II (R = CH_3) does not involve alkylation of biological primary alkylamino groups. The proton magnetic resonance spectra of the products enable the different reaction pathways to be distinguished readily, and may provide the basis for rapid physicochemical screening of alkylation agents that are potential carcinogens.

The wide range of biological activity exhibited by lactones has been well known for many years (1). In particular, unsaturated lactones are able to inhibit selectively both tissue growth and seed germination, and many of them possess antibiotic, cardiac, anthelmintic, hemorrhagic, and insecticidal activity (1). Recently, their ability to act as chemical carcinogens was also demonstrated (2).

In contrast to the extensive data on the biological effects of unsaturated lactones, of which refs. 1 and 2 are merely illustrative, there appears to be relatively little known about the chemical mechanisms of action involved. As the active lactones are all alkylating agents, their biological effect is probably due to an in vivo modification of the nucleophilic groups either of proteins (including enzymes) or of deoxyribonucleic (DNA) and ribonucleic (RNA) acids (2–4). However, many of the studies which have been carried out (1, 2) in attempts to verify this supposition, and to determine the nature of the most reactive biological nucleophile and hence the probable in vivo site of alkylation, were of necessity carried out without the aid of modern spectroscopic analytical methods. As a result, many conclusions have been drawn which cannot be regarded as satisfactory when the often rather meagre data are reexamined from the standpoint of the current knowledge of the mechanisms of organic and biochemical reactions.

Accordingly, a systematic survey of the reactions of a series of active lactones, representing a wide variation of biological effects, with the nucleophilic groups present in proteins and in DNA and RNA has been initiated. It is hoped that such a study of all the possible sites of alkylation and a determination of their mechanism of reaction with the active lactones, together with a comparison of the *relative* rates of combination, will enable the probable site of alkylation in the cell to be identified.

The results reported in this communication represent the preliminary investigations in the aspect of this programme concerned with the carcinogenesis of certain unsaturated lactones (2). This area is of importance for several reasons. Lactones, which have subsequently been shown to be carcinogenic, are in widespread use as antibiotics, food preservatives, sterilization agents, etc., and a knowledge of their reaction with proteins and nucleic acids would result in an increased margin of safety in their application. Also,

apart from being of interest with regard to current theories of chemical carcinogenesis (3–5), the results of this survey could enable guidelines to be laid down for distinguishing carcinogenic from non-carcinogenic alkylating agents on a chemical basis. This would obviate the tedious and expensive biological testing which at present precludes the examination of many potential carcinogens in general use.

Before 1961, the examination of lactones as carcinogens had largely been neglected, apart from fairly extensive studies on β-propiolactone (2). Since then, largely due to Dickens and Jones (2), a broad range of lactones and related compounds has been evaluated. Dickens and Jones were able to demonstrate a correlation between carcinogenic activity and structure, and they classified the various types into groups on this basis, as illustrated in Diagram 1. Compounds of the structural type represented by groups 1 and 2 were found to be carcinogenic whereas the related lactones of group 3 failed to produce tumors.

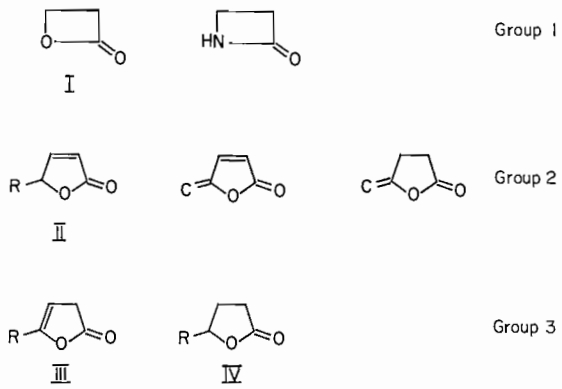


DIAGRAM 1.

The reactions of β-propiolactone (I) (group 1) with nucleophiles have been well documented (2–4, 6). Nucleophilic attack with a wide variety of nucleophiles occurs exclusively at the β-carbon atom, with alkyl–oxygen fission to give β-substituted propionic acids (V) as shown in Diagram 2. In contrast, the data available on the corresponding reactions of the lactones of groups 2 and 3 are very limited. Lactones II (R = CH_3), III (R = CH_3), and IV (R = CH_3) were selected as typical examples of the carcinogenic and non-carcinogenic compounds of these groups. The possible pathways for the reactions of these lactones with nucleophiles are summarized in Diagram 2.

The nucleophile considered first was the primary amino group. The NH_2 group is present in the DNA and RNA bases (adenine, guanine, and cytosine) and is the basic terminal group of all open-chain proteins. In addition, it is present in the side chain of the basic amino acids lysine (an essential amino acid), hydroxylysine, ornithine, and α,ε-diaminopimelic acid. To simplify the interpretation of the proton magnetic resonance (p.m.r.) spectra of the products of the first experiments, and thereby facilitate the elucidation of the reaction pathways, simple primary amines were used as models for the nucleic acid bases and for peptides containing the primary amino group.

The reactions of the simplest model amine, methylamine, with lactones II (R = CH_3), III (R = CH_3), and IV (R = CH_3) have been studied widely (7–11). However, the results obtained from these independent investigations were not consistent with one another, and different conclusions regarding the structures of several of the products were

Can. J. Chem. Downloaded from www.nrcresearchpress.com by 210.87.254.6 on 09/05/12
For personal use only.

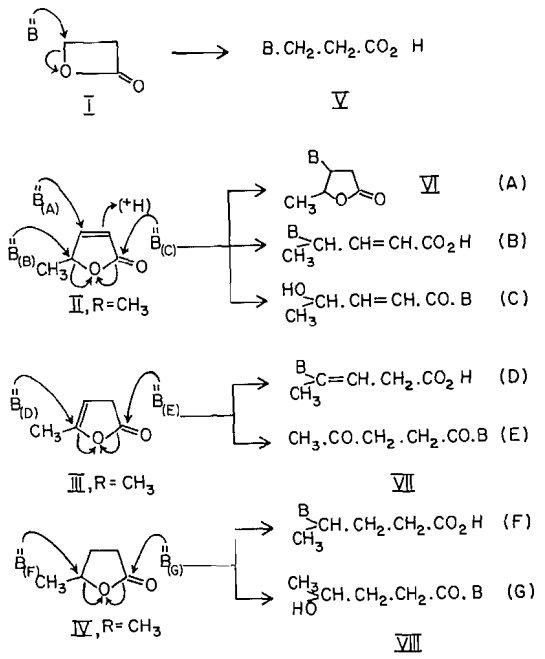


DIAGRAM 2.

drawn by the various groups. In view of the importance of the above reactions with respect to the objectives of this study, they have been reinvestigated to resolve the controversies regarding the nature of the products and the reaction pathways involved.

When aqueous methylamine and 4-hydroxypent-2-enoic acid lactone (β-angelica lactone)[1] (II, R = CH_3) were mixed in equivalent amounts at 20°, reaction occurred during 25 min to give a product which, when worked up at temperatures below 20°, was shown by p.m.r. to contain 80% of the Michael addition product VI (B = $NHCH_3$). It was not possible to obtain a pure sample of VI (B = $NHCH_3$) because, when the temperature was raised, and particularly during distillation, a reverse Michael reaction occurred to give a mixture containing the starting lactone II (R = CH_3) as the major component. These results contrast with those of Lukes *et al.* (*7c*), who reported that methylamine and the lactone II (R = CH_3) did not react by addition across the double bond but gave, instead, the 3-pyrroline-2-one X. However, the readiness with which VI (B = $NHCH_3$) undergoes a reverse Michael reaction on distillation accounts for the absence of this compound in the products obtained by Lukes from reactions carried out at elevated temperatures for relatively extended periods.

The reaction of 4-hydroxypent-3-enoic acid lactone (α-angelica lactone)[1] (III, R = CH_3) with methylamine proceeded rapidly at 0° in aqueous solution. When the reaction mixture was worked up at temperatures below 20° a product was obtained, the infrared (1 685 cm^{-1}, pyrrolidinone carbonyl) and p.m.r. (Fig. 1*a*) spectra of which were consistent with structure XI (R = CH_3). This shows that the initial attack by methylamine is at the carbonyl group of III (R = CH_3), and that the intermediate keto amide VII (B = $NHCH_3$) which is produced cyclizes spontaneously to the pyrrolidinone. These results confirm the most

[1]*Many difficulties have arisen in the literature (2, 7–11) from the anomalous α and β nomenclature of angelica lactones. Systematic nomenclature has been used in this communication to avoid further confusion.*

Can. J. Chem. Downloaded from www.nrcresearchpress.com by 210.87.254.6 on 09/05/12
For personal use only.

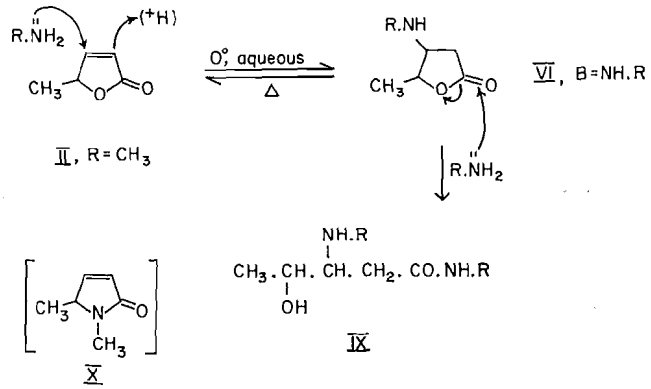


DIAGRAM 3.

recent conclusions reached by Lukes *et al.* (7*c*) in a review of his own and other data. Attempts made to dehydrate XI (R = CH_3) by distillation and by acid catalysis resulted in the formation of unresolvable mixtures. The presence of the pyrrolinone XII, reported by Lukes *et al.* (7*c*) to be formed under these conditions, was excluded by the absence of olefinic proton peaks in the p.m.r. spectrum.

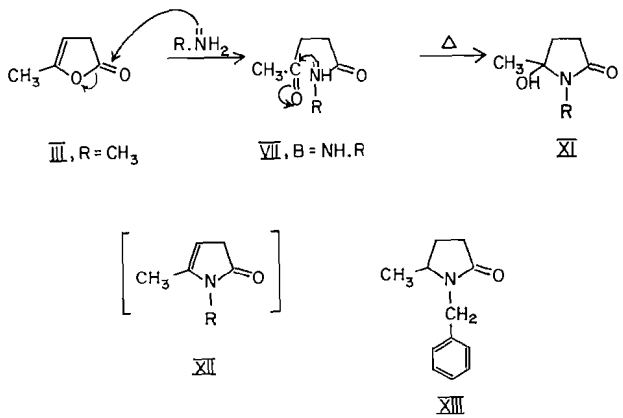


DIAGRAM 4.

In contrast to the extremely rapid reactions of the unsaturated lactones with methylamine, that of 4-hydroxypentanoic acid lactone (IV, R = CH_3) was slow. Isolation of the hydroxyamide VIII (B = $NHCH_3$) as the major product showed that nucleophilic attack at the carbonyl group had occurred (p.m.r. spectrum in Fig. 1*b*).

Because of the complications encountered when methylamine was used as a model biological nucleophile, other primary amines were considered. An amine of sufficient steric bulk to prevent cyclization of the initial products to pyrrolidine derivatives was desirable, and it was felt that aniline might satisfy this condition. Aniline possessed the added advantage that its protons would be sufficiently far downfield in the p.m.r. spectra of the products that no overlap with lactone-derived protons would occur. However, it was found that aniline and the lactones II (R = CH_3) and IV (R = CH_3) did not react, even when heated to 180°. This was not unexpected, because aniline, with a pK_a of 4.69,

Can. J. Chem. Downloaded from www.nrcresearchpress.com by 210.87.254.6 on 09/05/12
For personal use only.

Can. J. Chem. Downloaded from www.nrcresearchpress.com by 210.87.254.6 on 09/05/12
For personal use only.

is approximately one million times less basic than a typical primary alkylamine (12). The reaction of aniline with the β,γ-unsaturated lactone III (R = CH_3) yielded the keto amide VII (B = NHC_6H_5) as reported by Walton (8) and by Lukes and his collaborators (7*b*). No cyclization to the pyrrolidinone XI (R = C_6H_5) was observed.

The model nucleophile finally adopted was benzylamine, which combined aliphatic amine reactivity with the advantage that the aromatic protons would not cause confusion in the interpretation of the p.m.r. spectra. Also, the increase in steric dimensions from those of methylamine was found to be effective in inhibiting to a large extent the cyclization of the products. The reactions were first carried out under nonaqueous conditions to facilitate product identification, since there was evidence from some of the methylamine experiments that secondary reactions with water had delayed formulation of the primary product. Subsequently, the reactions were repeated in aqueous solutions approximating in vivo biological conditions more closely. When reactions occurred very slowly at or below 37° (human body temperature) the mixtures were heated until reaction did occur. This was done to obtain an estimate of the relative rates at which the active and inactive lactones reacted. (Even when a distinction between active and inactive lactones can be made on the basis of different mechanisms of reaction, the relative rates at which alkylations occur may well be of greater biological significance.)

As for methylamine, the reaction of benzylamine with the α,β-unsaturated lactone II (R = CH_3) resulted in the formation of the Michael addition product VI (B = $NHCH_2C_6H_5$) (p.m.r. spectrum in Fig. 1*c*), under both nonaqueous and aqueous conditions. When the reaction was carried out for 15 min at 20° the yield of VI (B = $NHCH_2C_6H_5$) reached 75% (before purification), but when the reactants were kept for longer periods at room temperature, increasing amounts of the amino amide IX (R = $CH_2C_6H_5$) (p.m.r. spectrum in Fig. 1*d*) were produced. In contrast to the Michael addition product formed in the analogous methylamine reaction, the benzylamino lactone VI (B = $NHCH_2C_6H_5$) could be distilled, and when pure was stable indefinitely. On suspension in water it gradually equilibrated to give a 1:1 mixture of IX (R = $CH_2C_6H_5$) and the starting lactone II (R = CH_3), presumably by a reverse Michael reaction as indicated in Diagram 3. (An alternative pathway involving opening of the lactone ring as the first step followed by addition of methylamine to the resulting α,β-unsaturated amide could also account for the formation of IX (R = $CH_2C_6H_5$), but this route is considered to be less credible than that suggested in Diagram 3.) Lukes *et al.* (7*c*) reported only the formation of the secondary product IX (R = $CH_2C_6H_5$). When 2 equivalents of benzylamine was mixed with the lactone II (R = CH_3), a 90% yield of IX (R = $CH_2C_6H_5$) was isolated.

Since most biological processes, particularly those involving enzymes, are stereospecific (13), the stereochemistry of the addition to the double bond is of interest in that it gives an indication of the preferred direction of approach of the nucleophile. Infrared spectroscopic and chemical evidence enabling the configurations of the diastereomers of lactones VI (B = $NHCH_3$) and VI (B = $NHCH_2C_6H_5$) to be distinguished has been presented by Lukes *et al.* (7*c*). However, the compounds were not obtained directly from addition of the amine across the double bond of the lactone II, and, for the benzylamine products, the results were not unambiguous, as it was necessary to assign configurations mainly by analogy with those proposed for the methylamine addition compounds. To clarify this biologically important point, the hydrobromide and hydrochloride salts of the benzylamino lactone VI (B = $NHCH_2C_6H_5$) were prepared and are currently being examined by X-ray diffraction.

Can. J. Chem. Downloaded from www.nrcresearchpress.com by 210.87.254.6 on 09/05/12
For personal use only.

Lukes *et al.* (7*c*) reported that the β,γ-unsaturated lactone III (R = CH_3) reacted with benzylamine to give the keto benzylamide VII (B = $NHCH_2C_6H_5$). The yield obtained was only 18%, and thus the keto amide could not be regarded as the major product under the conditions applied. A reinvestigation of this reaction confirmed that the first step in the reaction of lactone III (R = CH_3) with benzylamine, under both nonaqueous and aqueous conditions, was nucleophilic attack at the carbonyl group (path E, Diagram 2). The reaction mixture was found to contain the keto amide VII (B = $NHCH_2C_6H_5$) (p.m.r. spectrum in Fig. 1*e*) as reported by Lukes *et al.* (7*c*), together with varying amounts of the cyclized product, the benzylpyrrolidinone XI (R = $CH_2C_6H_5$). When the temperature was maintained at 0–5° during reaction and work-up, the keto benzylamide VII (B = $NHCH_2C_6H_5$) was obtained in yields of up to 90%. Purification by standard recrystallization from benzene greatly diminished the proportion of keto amide, and from the filtrates was recovered an oil which was shown to be the pyrrolidinone XI (R = $CH_2C_6H_5$) by its p.m.r. spectrum (Fig. 1*f*). The AB pattern at δ 4.42 p.p.m. was found to be characteristic of the benzyl methylene protons in the cyclized products. The difference in chemical shifts of the benzyl methylene protons arises from the asymmetric environment produced by the nitrogen atom with three dissimilar substituents. The cyclic structure appears to restrict the inversion of nitrogen sufficiently that the AB pattern is observable at room temperature in contrast to the analogous open-chain compounds, such as N-benzyl-O,N-dimethylhydroxylamine, for which Griffith and Roberts observed an AB-type spectrum only when it was cooled to −40° (14). The keto benzylamide VII (B = $NHCH_2C_6H_5$) was shown by its infrared spectra (1 723 cm^{-1}, 1 670 cm^{-1}, no hydroxyl absorption) to exist in the open-chain form both in the solid state and in freshly prepared solution in various solvents. When the solutions were kept at room temperature gradual equilibration with the pyrrolidinone occurred. Refluxing in water produced a 1:1 mixture of open-chain and cyclic forms. Partial equilibration also occurred during the attempted purification of both isomers by chromatography and by distillation. For this reason it was not possible to obtain a completely pure sample of 1-benzyl-5-hydroxy-5-methylpyrrolidin-2-one (XI, R = $CH_2C_6H_5$).

As with methylamine, nucleophilic attack by benzylamine on the saturated lactone IV (R = CH_3) occurred at the carbonyl group to give the hydroxybenzylamide VIII (B = $NHCH_2C_6H_5$) (p.m.r. spectrum in Fig. 1*g*). The reaction was extremely slow at room temperature under nonaqueous conditions, and proceeded only a little more rapidly when water was present. A measure of the rate was provided by the fact that the reaction was incomplete even after the reaction mixture had been refluxed under aqueous conditions for 48 h. In an attempt to ascertain the conditions necessary to achieve complete reaction, the lactone IV (R = CH_3) and benzylamine were heated at 190° for several days. These vigorous conditions resulted in much decomposition, but some starting lactone was always recovered. On one occasion a trace amount of 1-benzyl-5-methylpyrrolidin-2-one (XIII), arising from cyclization of the hydroxyamide VIII (B = $NHCH_2C_6H_5$), was formed. Restriction of nitrogen inversion (imposed by cyclization) was again indicated by the appearance of the benzyl methylene protons as an AB quartet in the p.m.r. spectrum (Fig. 1*h*).

CONCLUSIONS

From the above results it is apparent that, as expected, there is a marked difference in the mode of reaction of the carcinogenic and non-carcinogenic lactones with the amino group. Both inactive lactones, III (R = CH_3) and IV (R = CH_3), react by nucleophilic

Can. J. Chem. Downloaded from www.nrcresearchpress.com by 210.87.254.6 on 09/05/12
For personal use only.

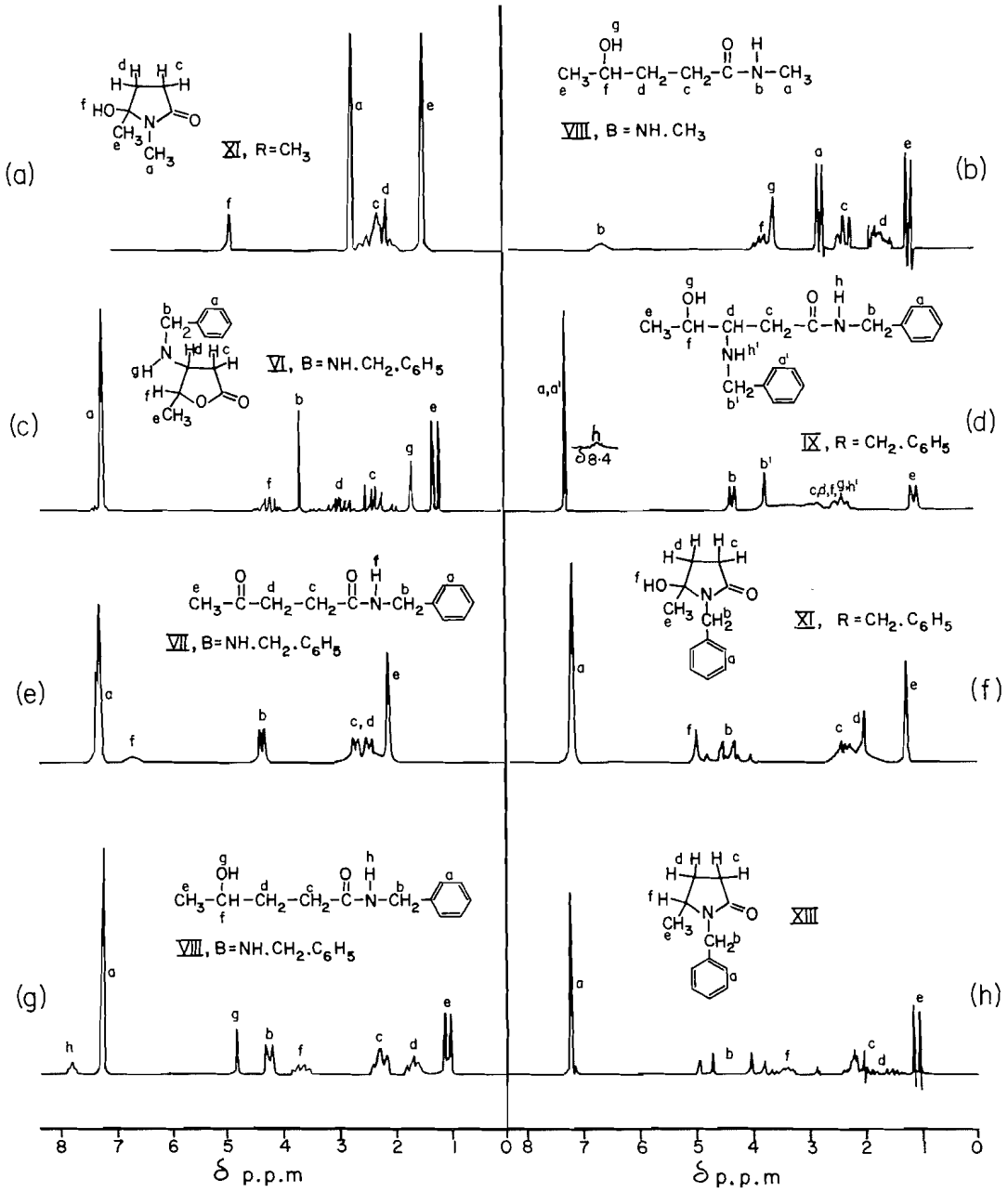


FIG. 1. Comparison of the p.m.r. spectra of products from carcinogenic (II, R = Me) and non-carcinogenic (III (R = Me) and IV (R = Me)) lactones.

attack at the carbonyl group (paths E and G, respectively, Diagram 2) whereas the active lactone II (R = CH_3) undergoes Michael addition preferentially (path A, Diagram 2).

The terminal and side-chain amino groups present in peptides and proteins have pK_a's of 7.5 to ~11 (12) and, in the lower range of physiological pH, the amino groups

would be present mainly as their conjugate acids. However, many enzymes (13) are active at pH > 8, at which sufficient concentrations of the non-protonated amino groups would be available for alkylation by such facile reagents as II (R = CH_3) and III (R = CH_3). A qualitative comparison of the relative rates of the reactions studied gives the order of reactivity as III $\geqslant$ II $\ggg$ IV. The fact that the *inactive* lactone III (R = CH_3) reacts most rapidly is regarded as evidence against the amino group being an important in vivo site at which the carcinogenic lactones effect their modification. This was not an unexpected result, because the role of a nucleophile at the active site of an enzyme has not yet been ascribed to the primary amino group (13). The model amines studied cannot be regarded as representative of this group in the nucleic acid bases. However, studies with other carcinogenic alkylating agents (4) have not implicated the primary amino groups of adenine, guanine, and cytosine.[2] The reactions of the DNA and RNA bases and associated compounds with the active and inactive lactones will be reported in a future communication.

It might well be significant that treatment of the biologically active lactone with amines yields an unstable Michael addition product which appears to be capable of undergoing a reverse reaction, whereas the inactive lactones give rise to the much more stable amide derivatives.

The p.m.r. spectra of the various products reproduced in Fig. 1 show how readily they enable the different mechanisms of reaction to be distinguished. They give hope that this approach may eventually provide the basis of a rapid non-biological screening method for distinguishing carcinogenic from non-carcinogenic alkylating agents.

EXPERIMENTAL

The p.m.r. spectra were obtained at 60 mc.p.s. with tetramethylsilane as internal standard; the melting points were determined on a Fisher–Johns apparatus and are corrected. All solvents used for chromatography were redistilled; aqueous solutions were prepared from carbon dioxide free, distilled water which was saturated with nitrogen before use.

4-Hydroxypent-3-enoic Acid Lactone (III, R = CH_3)

The commercial product (Aldrich Chemical Co.) was redistilled, b.p. 48–50° at 10 mm (lit. (15) b.p. 52° at 10 mm); $\nu_{max}^{CCl_4}$ 1 806 and 1 687 cm^{-1} (lactone carbonyl); p.m.r. (CCl_4) δ 1.97 (3H, essentially singlet), 3.10 (2H, multiplet), and 5.15 p.p.m. (1H, multiplet).

4-Hydroxypent-2-enoic Acid Lactone (II, R = CH_3)

Isomerization of 4-hydroxypent-3-enoic acid lactone with triethylamine as described by Thiele (15) gave the lactone II (R = CH_3) in 70% yield, b.p. 99–100° at 18 mm (lit. (19) b.p. 89° at 15 mm); $\nu_{max}^{CCl_4}$ 1 782 and 1 765 cm^{-1} (lactone carbonyl); p.m.r. (CCl_4) δ 1.41 (3H, doublet, J = 6.5 c.p.s.), 5.10 (1H, multiplet), 6.01 (1H, doublet, J = 5.5 c.p.s.), and 7.58 p.p.m. (1H, multiplet).

Reaction of 4-Hydroxypent-2-enoic Acid Lactone with Aqueous Methylamine

Methylamine (1.13 g of a 29% aqueous solution, 1 mole) was added dropwise, with stirring, during 5 min at 0° to 4-hydroxypent-2-enoic acid lactone (1.96 g, 1 mole); the mixture was allowed to warm to room temperature and then stirred for a further 15 min. The solution was rotary evaporated at room temperature to give a yellow oil (2.5 g), shown by the p.m.r. spectrum to contain 80% of 4-hydroxy-3-methylaminopentanoic acid lactone (VI, B = $NHCH_3$): δ 1.32 (CH_3, doublet, J = 6.5 c.p.s.), 1.95 (N—H, singlet), 2.05–3.25 (C_2,C_3—H, complex multiplet), 2.32 (N—CH_3, singlet), and 4.32 p.p.m. (C_4—H, multiplet). A pure sample of the amino lactone could not be obtained since, on distillation, a facile reverse Michael reaction occurred to give the starting lactone II (R = CH_3).

Reaction of 4-Hydroxypent-3-enoic Acid Lactone with Aqueous Methylamine

4-Hydroxypent-3-enoic acid lactone (5 g, 1 mole) was cooled to 0°, and methylamine (5.4 g of a 29% aqueous solution, 1 mole) was added dropwise, with stirring, during 10 min. The aqueous solvent was then removed by rotary evaporation at 20° to give an orange solid (6.5 g), shown by infrared and p.m.r. spectra

[2]*The pK_a of this group in nucleosides and related compounds is in the range 1.6–4.4.*

Can. J. Chem. Downloaded from www.nrcresearchpress.com by 210.87.254.6 on 09/05/12
For personal use only.

to contain 95% of 1,5-dimethyl-5-hydroxypyrrolidin-2-one (XI, R = CH_3). A sample that had been recrystallized five times from ether yielded colorless rhombs, m.p. 69° (lit. (7*a*) m.p. 71°); $\nu_{max}^{CHCl_3}$ 3 610, 3 440 – 3 330 (hydroxyl), and 1 685 cm^{-1} (pyrrolidinone carbonyl); p.m.r. ($CDCl_3$) (Fig. 1*a*) δ 1.48 (3H, singlet), 1.9–3.0 (4H, multiplet), 2.79 (3H, singlet), and 5.65 p.p.m. (1H, singlet).

Reaction of 4-Hydroxypentanoic Acid Lactone with Aqueous Methylamine

4-Hydroxypentanoic acid lactone (1 g, 1 mole) and methylamine (0.57 g of a 29% aqueous solution, 1 mole) were kept at 20° for 3 h. The mixture was then concentrated *in vacuo* and distilled to give 4-hydroxy-N-methylpentanoamide (VIII, B = $NHCH_3$) (1 g), b.p. 104° at 0.1 mm; $\nu_{max}^{CHCl_3}$ 3 490 and 3 330 (hydroxyl, amide) and 1 668 cm^{-1} (amide carbonyl); p.m.r. ($CDCl_3$) (Fig. 1*b*) δ 1.19 (3H, doublet, J = 6.5 c.p.s.), 1.4–2.0 (2H, complex multiplet), 2.1–2.6 (2H, complex multiplet), 2.78 (3H, doublet, J = 5 c.p.s.), 3.5–4.0 (1H, complex multiplet), and 6.6 p.p.m. (1H, broad multiplet).

Anal. Calcd. for $C_6H_{13}NO_2$ (129.2): C, 55.78; H, 10.15; N, 10.85. Found: C, 55.59; H, 9.99; N, 10.52.

N-Phenyl-4-oxopentanoamide (VII, B = NHC_6H_5)

Aniline (0.94 g, 1 mole) and 4-hydroxypent-3-enoic acid lactone (0.98 g, 1 mole) were heated to 180° for 5 min. Recrystallization of the mixture from benzene – petroleum ether (b.p. 70–90°) gave the anilide (1.36 g) as needles, m.p. 101° (lit. (7*b*, 11) m.p. 101°); $\nu_{max}^{CHCl_3}$ 3 480 (amide), 1 720 (ketone carbonyl), and 1 695 cm^{-1} (amide carbonyl); p.m.r. ($CDCl_3$) δ 2.15 (3H, singlet), 2.69 (4H, quartet, J = 4.5 c.p.s.), 7.0–7.7 (5H, multiplet), and 8.4 p.p.m. (1H, broad multiplet).

Reaction of 4-Hydroxypent-2-enoic Acid Lactone (II, R = CH_3) with Benzylamine

A. Nonaqueous Conditions

4-Hydroxypent-2-enoic acid lactone (2.95 g, 1 mole) and benzylamine (3.22 g, 1 mole) were kept at 20° for 2 h. The mixture was then distilled and the fraction boiling at 134–138° and 0.04 mm was collected to give 3-benzylamino-4-hydroxypentanoic acid lactone (0.87 g); $\nu_{max}^{CCl_4}$ 3 350 (amino hydrogen) and 1 785 cm^{-1} (γ-lactone carbonyl); p.m.r. (CCl_4) (Fig. 1*c*) δ 1.24 (3H, doublet, J = 6 c.p.s.), 1.67 (1H, singlet), 2.32 and 2.98 (2H and 1H, ABX multiplet), 3.64 (2H, singlet), 4.24 (1H, multiplet), and 7.20 p.p.m. (5H, singlet).

Anal. Calcd. for $C_{12}H_{15}NO_2$ (205.3): C, 70.22; H, 7.36; N, 6.82. Found: C, 70.20; H, 7.41; N, 7.02.

The hydrobromide was obtained by treatment with aqueous hydrobromic acid. Recrystallization from methanol gave rhombs, m.p. 186°.

Anal. Calcd. for $C_{12}H_{16}BrNO_2$ (286.2): C, 50.37; H, 5.72; Br, 27.93; N, 4.90. Found: C, 50.67; H, 5.82; Br, 28.27; N, 5.03.

The hydrochloride was prepared in an analogous manner, separating as rhombs from ethanol, m.p. 179–181° (lit. (7*c*) m.p. 179–181°).

B. Aqueous Conditions

4-Hydroxypent-2-enoic acid lactone (2 g) was dissolved in water (2 ml) and a solution of benzylamine (2.16 g, 1 mole) in water (2 ml) was added dropwise, with magnetic stirring, during 5 min at 20°. Stirring was continued for a further 10 min, the solvent was then removed by rotary evaporation at 20°, and the crude product (3.9 g) was chromatographed on Florisil (120 g). Elution with chloroform–acetone (3:1) followed by distillation yielded 3-benzylamino-4-hydroxypentanoic acid lactone as a colorless oil (1.4 g), b.p. 136° at 0.12 mm, the properties of which were identical with those described above.

3-Benzylamino-4-hydroxy-N-benzylpentanomide (IX, R = $CH_2C_6H_5$)

A. A solution of 4-hydroxypent-2-enoic acid lactone (1 g, 1 mole) and benzylamine (2.13 g, 2 moles) in water (2 ml) was heated to 80° for 10 min, and the water was then removed in a rotary evaporator. The resulting white solid (3 g) was recrystallized from benzene to give 3-benzylamino-4-hydroxy-N-benzylpentanoamide as needles (2.7 g), m.p. 126.5–127° (lit. (7*c*) m.p. 127–128°); $\nu_{max}^{CHCl_3}$ 3 460 (hydroxyl, amide NH) and 1 668 cm^{-1} (amide carbonyl); p.m.r. (dimethyl sulfoxide-d_6) (Fig. 1*d*) δ 1.06 (3H, doublet, J = 6.5 c.p.s.), 2.3 (4H, multiplet), 2.78 (1H, multiplet), 3.27 (1H, multiplet), 3.72 (2H, singlet), 4.28 (2H, doublet, J = 6 c.p.s.), 7.24 (10H, singlet), and 8.48 (1H, multiplet).

Anal. Calcd. for $C_{19}H_{24}N_2O_2$ (312.4): C, 73.05; H, 7.74; N, 8.97. Found: C, 73.18; H, 7.91; N, 9.08.

B. A suspension of 3-benzylamino-4-hydroxypentanoic acid lactone (0.5 g) in water (2 ml) was kept at room temperature (20°) for 2 weeks. The solid that was produced was filtered off (0.23 g) and recrystallized from benzene to give the amino amide IX (R = $CH_2C_6H_5$) as needles (0.1 g), the properties of which were identical with those of the sample obtained above.

Reaction of 4-Hydroxypent-3-enoic Acid Lactone (III, R = CH_3) with Benzylamine

A. Nonaqueous Conditions

A mixture of 4-hydroxypent-3-enoic acid lactone (1 g, 1 mole) and benzylamine (1.06 g, 1 mole) was kept at 20° for 1 h. The N-benzyl-4-oxopentanoamide (VII, B = $NHCH_2C_6H_5$) (2.06 g) that was produced was then recrystallized from benzene to give needles (1.29 g), m.p. 79.5–80° (lit. (7*c*) m.p. 82–83°); $\nu_{max}^{CHCl_3}$ 3 550 (amide NH), 1 723 (ketone carbonyl), and 1 670 cm^{-1} (amide carbonyl); p.m.r. ($CDCl_3$) (Fig. 1*e*) δ 2.10 (3H, singlet), 2.55 (4H, A_2B_2 quartet, J = 5.5, 9.0, and 5.5 c.p.s.), 4.32 (2H, doublet, J = 6 c.p.s.), 6.59 (1H, broad multiplet), and 7.25 p.p.m. (5H, singlet).

Can. J. Chem. Downloaded from www.nrcresearchpress.com by 210.87.254.6 on 09/05/12
For personal use only.

B. Aqueous Conditions

Benzylamine (3.24 g, 1 mole) in water (5 ml) was cooled to 0°, and a suspension of 4-hydroxypent-3-enoic acid lactone (2.97 g, 1 mole) in water (5 ml) was added dropwise, with stirring, during 15 min. The mixture was then rotary evaporated at 20° and the yellow solid (6 g) was recrystallized from benzene. N-Benzyl-4-oxopentanoamide separated as needles (3.5 g) which were identical in all respects with the sample obtained above under nonaqueous conditions. Evaporation of the benzene mother liquid yielded an oil (2.4 g), which was estimated spectroscopically to contain 80% of the cyclized product 1-benzyl-5-hydroxy-5-methylpyrrolidin-2-one; $\nu_{max}^{CHCl_3}$ 3 400 (hydroxyl) and 1 680 cm^{-1} (pyrrolidinone carbonyl); p.m.r. ($CDCl_3$) (Fig. 1*f*) δ 1.26 (3H, singlet), 1.85–2.70 (4H, complex multiplet), 6.42 (2H, AB quartet, J_{AB} = 15.7 c.p.s., $\nu_A - \nu_B$ = 24.4 c.p.s.), 5.01 (1H, singlet), and 7.19 p.p.m. (5H, singlet). The crude product decomposed on distillation, and all attempts to effect purification by chromatography were unsuccessful because partial equilibration of the open-chain (VII, B = $NHCH_2C_6H_5$) and cyclic (XI, R = $CH_2C_6H_5$) isomers occurred on the column.

A pure sample of the keto amide VII (B = $NHCH_2C_6H_5$), m.p. 80°, underwent 50% conversion into the pyrrolidinone XI (R = $CH_2C_6H_5$) when it was refluxed in water for 2 days.

Reaction of 4-Hydroxypentanoic Acid Lactone with Benzylamine

A. Nonaqueous Conditions

4-Hydroxypentanoic acid lactone (5 g, 1 mole) and benzylamine (6.2 g, 1 mole) were heated at 140° under nitrogen for 48 h. The product was dissolved in chloroform (50 ml), and the chloroform solution was washed with 2 *N* hydrochloric acid (25 ml), then with saturated aqueous sodium hydrogen carbonate (25 ml), and finally with water (10 ml). The dried ($MgSO_4$) solution was evaporated and the red oil (6.3 g) was chromatographed on Florisil. Elution with benzene–acetone (20:1) followed by distillation gave N-benzyl-4-hydroxypentanoamide (3.8 g), b.p. 179–180° at 0.02 mm; $\nu_{max}^{CHCl_3}$ 3 490 and 3 350 (hydroxyl, amide NH) and 1 668 cm^{-1} (amide carbonyl); p.m.r. ($CDCl_3$) (Fig. 1*g*) δ 1.05 (3H, doublet, J = 6 c.p.s.), 1.68 (2H, triplet, J = 6.5 c.p.s.), 2.25 (2H, triplet, J = 6.5 c.p.s.), 3.67 (1H, quartet, J = 6 c.p.s.), 4.24 (2H, doublet, J = 6 c.p.s.), 4.81 (1H, singlet), 7.17 (5H, singlet), and 7.74 p.p.m. (1H, broad multiplet).

Anal. Calcd. for $C_{12}H_{17}NO_2$ (207.3): C, 69.54; H, 8.27; N, 6.76. Found: C, 69.33; H, 8.24; N, 6.57.

On one occasion, after the above hydroxybenzylamide was heated at 190° for 3 days, some cyclization to 1-benzyl-5-methylpyrrolidin-2-one was observed; $\nu_{max}^{CHCl_3}$ 1 670 cm^{-1} (pyrrolidinone carbonyl); p.m.r. ($CDCl_3$) (Fig. 1*h*) δ 1.09 (3H, doublet, J = 6 c.p.s.), 1.20–2.45 (4H, complex multiplet), 3.10–3.65 (1H, complex multiplet), 4.37 (2H, AB quartet, J_{AB} = 15.0 c.p.s., $\nu_A - \nu_B$ = 53.4 c.p.s.), and 7.19 p.p.m. (5H, singlet).

B. Aqueous Conditions

Benzylamine (5.4 g, 1 mole) and 4-hydroxypentanoic acid lactone (5 g) were refluxed in water (10 ml) under nitrogen for 48 h. Work-up as described above gave N-benzyl-4-hydroxypentanoamide (5.4 g), b.p. 173–174° at 0.015 mm, identical with the product obtained above under nonaqueous conditions.

ACKNOWLEDGMENTS

We express our appreciation to the National Cancer Institute of Canada for their generous support of this work. The award of a Province of Ontario Graduate Fellowship to one of us (J. M. Y.) is gratefully acknowledged.

REFERENCES

1. L. J. Haynes. Quart. Rev. London, **2**, 46 (1948).
2. F. Dickens and H. E. H. Jones. Brit. J. Cancer, **15**, 85 (1961); **17**, 100 (1963); **17**, 691 (1963). F. Dickens. Brit. Med. Bull. **20**, 96 (1964).
3. W. C. J. Ross. Biological alkylating agents. Butterworths, London. 1962.
4. P. Brookes and P. D. Lawley. Brit. Med. Bull. **20**, 91 (1964).
5. D. B. Clayson. Chemical carcinogenesis. J. & A. Churchill, Ltd., London. 1962.
6. J. J. Roberts and G. P. Warwick. Biochem. Pharmacol. **12**, 1441 (1963).
7. (*a*) R. Lukes and V. Prelog. Collection Czech. Chem. Commun. **1**, 119 (1929). (*b*) R. Lukes and Z. Linhartova. Collection Czech. Chem. Commun. **25**, 502 (1960). (*c*) R. Lukes, Z. Koblicova, and K. Blaha. Collection Czech. Chem. Commun. **28**, 2183 (1963).
8. E. Walton. J. Chem. Soc. 438 (1940).
9. N. H. Cromwell and K. E. Cook. J. Am. Chem. Soc. **80**, 4573 (1958).
10. K. E. Schulte and J. Reisch. Arch. Pharm. **292**, 125 (1959).
11. M. Semonsky, A. Cerny, B. Kakac, and V. Subrt. Collection Czech. Chem. Commun. **28**, 3278 (1963).
12. J. Clark and D. D. Perrin. Quart. Rev. London, **18**, 295 (1964). J. Steinhardt and S. Beychok. *In* The proteins. Vol. II. 2nd ed. *Edited by* H. Neurath. Academic Press, Inc., New York. 1964. pp. 162–164.
13. M. Dixon and E. C. Webb. *In* The enzymes. 2nd ed. Longmans, Green & Co., Ltd., London. 1964. Chap. VI.
14. D. L. Griffith and J. D. Roberts. J. Am. Chem. Soc. **87**, 4089 (1965).
15. J. Thiele. Ann. **319**, 144 (1902).

Can. J. Chem. Downloaded from www.nrcresearchpress.com by 210.87.254.6 on 09/05/12
For personal use only.

SYNTHESIS OF 6′-SUBSTITUTED MALTOSES

G. G. S. DUTTON AND K. N. SLESSOR[1]
Department of Chemistry, University of British Columbia, Vancouver, British Columbia
Received November 9, 1964

ABSTRACT

Derivatives of maltose substituted at position 6′ have been prepared by the replacement of a 6′-*O*-*p*-toluenesulfonate ester by various reagents. Tritylation of 1,6-anhydro-β-maltose followed by acetylation and detritylation yielded 2,3,2′,3′,4′-penta-*O*-acetyl-1,6-anhydro-β-maltose, which gave the 6′-*O*-*p*-toluenesulfonate in good yield. Replacement of the sulfonate ester with iodide led to a derivative from which 6′-deoxy-maltose was prepared by reduction, acetolysis, and deacetylation. 6′-Deoxy-6′-mercapto-maltose was prepared by replacement of the sulfonate with thiolacetate followed by acetolysis and deacetylation. 6′-Amino-6′-deoxy-maltose was prepared in low yield by azide replacement of the sulfonate, deacetylation, reduction, and mild acid hydrolysis.

Attempts to prepare 6-substituted derivatives from benzyl 4′,6′-*O*-benzylidene-β-maltoside were unsuccessful. The possible explanations for the unreactivity of position 6 are discussed.

Specifically substituted disaccharides are important not only as reference compounds in partial hydrolyses of substituted polysaccharides (1–3), but also as substrates in studies on the action of carbohydrases. The information gained in such specificity studies may be useful when applied to the action of these enzymes on oligo- and poly-saccharides.

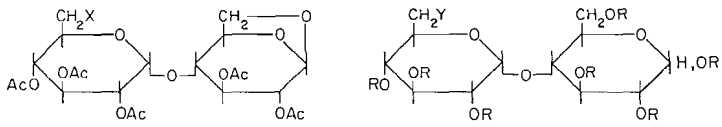
Because of the difficulty of synthesizing α-linked glucosidic disaccharides from their monosaccharide constituents, the modification of a naturally occurring disaccharide containing an α-linkage was undertaken. Maltose was chosen for two reasons. Firstly, this disaccharide is the most common α-linked glucopyranosyl glucose, and secondly, information obtained in specificity studies would be of interest in the interpretation of the action of enzymes on starches. An earlier paper (4) described the catalytic oxidation of benzyl β-maltoside to yield maltobiouronic acid (4-*O*-[α-D-glucopyranosyluronic acid]-D-glucose).

The preparation of specifically substituted derivatives is dependent on the use of reagents which show high selectivity in their reactions. Thus, sulfonation (*p*-toluenesulfonyl or methanesulfonyl chloride in pyridine) of 1,6-anhydro-β-maltose gave a complex mixture of products, as shown by thin-layer chromatography. Tritylation, however, yielded only the 6′-*O*-trityl derivative. Acetylation of this material followed by detritylation with aqueous acetic acid gave a pentaacetate with only the 6′-hydroxyl free (III). Subsequent *p*-toluenesulfonation yielded 2,3,2′3′,4′-penta-*O*-acetyl-1,6-anhydro-6′-*O*-*p*-toluenesulfonyl-β-maltose in high yield (IV).

Replacement of the sulfonate with iodide followed by reduction gave the 6′-deoxy derivative (VI). Acetolysis with 1% sulfuric acid as the catalyst permitted opening of the 1,6-anhydro ring without cleavage of the disaccharide linkage. Deacetylation yielded 6′-deoxy-maltose (VII), which was characterized as the β-hepta-acetate (VIII). Acid hydrolysis yielded glucose and material chromatographically identical with 6-deoxy-D-glucose prepared by the method of Fischer and Zach (5). Sodium borohydride reduction followed by hydrolysis yielded two compounds, which were identified chromatographically as 6-deoxy-D-glucose and sorbitol. Although benzyl 6′-deoxy-β-maltoside has been prepared (6), the free sugar was not reported.

[1]*Present address*: *Biochemistry Department, Royal Free Hospital, London W.C.1.*

Can. J. Chem. Downloaded from www.nrcresearchpress.com by 210.87.254.105 on 09/05/12
For personal use only.



(I) X = OAc
(II) X = OTr
(III) X = OH
(IV) X = OTs
(V) X = I
(VI) X = H
(IX) X = SAc
(XII) X = N_3

6'-Derivatives of 1,6-anhydro-β-maltose

(VII) Y = H, R = H
(VIII) Y = H, R = Ac
(X) Y = SAc, R = Ac
(XI) Y = SH, R = H
(XIII) Y = NH_2, R = H

6'-Derivatives of maltose

Replacement of the sulfonate with thiolacetate (7) yielded the 6′-*S*-acetyl derivative (IX) which, upon acetolysis, gave hepta-*O*-acetyl-6′-*S*-acetyl-6′-deoxy-α-maltose (X). Deacetylation with sodium methoxide in methanol gave a product which oxidized very rapidly in contact with air. The free thiol was regenerated by the addition of excess 2-mercaptoethanol. Hydrolysis of 6′-deoxy-6′-mercapto-maltose yielded two compounds chromatographically identical with D-glucose and 6-deoxy-6-mercapto-D-glucose (8). Hydrolysis of the borohydride-reduced disaccharide gave 6-deoxy-6-mercapto-glucose and sorbitol, as indicated by paper chromatography.

Replacement of the sulfonate with azide yielded 2,3,2′,3′,4′-penta-*O*-acetyl-1,6-anhydro-6′-azido-6′-deoxy-β-maltose (XII). Reduction of the azide in this molecule led to an amorphous mixture, presumably caused by *O*- to *N*-migration of the acetates. Deacetylation followed by reduction led to the desired 6′-amino-1,6-anhydro-6′-deoxy-β-maltose. The ability of the 6-amino group to hinder acid hydrolysis (9) would be expected to stabilize the glycosidic linkage of a 6-amino-glucose, which has, in fact, been reported by Cramer and co-workers (10). Thus mild acid hydrolysis should open the 1,6-anhydro ring without cleavage of the disaccharide, thereby yielding 6′-amino-6′-deoxy-maltose. After hydrolysis of the amino anhydride with 0.15 *N* hydrochloric acid for 13 h at 100°, chromatography indicated the presence of two ninhydrin-positive materials, the slower of which gave a positive test with *p*-anisidine trichloroacetate spray and was shown to be 6′-amino-6′-deoxy-maltose (XIII). The faster running, ninhydrin-positive material was chromatographically identical with the starting material. *p*-Anisidine trichloroacetate spray revealed, in addition to 6′-amino-6′-deoxy-maltose, a relatively large proportion of glucose. Both sprays, however, failed to indicate the presence of any 6-amino-6-deoxy-glucose, which should have been produced in an amount equal to that of glucose by hydrolysis of the disaccharide.

It has been suggested that these results may indicate that 6-amino-6-deoxy-D-glucose is more easily destroyed by acid than is D-glucose (11). Such degradations of amino sugars are known. For example, Paulsen has reported the ease with which 5-amino-5-deoxy sugars are transformed into pyridine derivatives (12).

Attempts to prepare 6-substituted derivatives of maltose by preferential reaction of the single, free, primary hydroxyl group on benzyl 4′,6′-*O*-benzylidene-β-maltoside were unsuccessful. *p*-Toluenesulfonation yielded three major products, as indicated by thin-layer chromatography. Two of these products travelled at a rate corresponding to that of monotosylates, the other travelling at a rate corresponding to that of a ditosylate. Methanesulfonation yielded a mixture of starting material and monosubstituted material. Disubstituted material was formed when reaction times were increased. Tritylation was attempted, and thin-layer chromatography indicated that no reaction had occurred even after 3 days at room temperature.

Can. J. Chem. Downloaded from www.nrcresearchpress.com by 210.87.254.105 on 09/05/12
For personal use only.

The isolation of both uronic acids from the catalytic oxidation of methyl β-maltoside (13) is contrasted with the isolation of only maltobiouronic acid from the oxidation of benzyl β-maltoside (4, 14). Partial tritylation of either maltose or benzyl β-maltoside leads to the 6′-*O*-trityl derivative (6, 15). The acid chromate oxidation of position 6 was found to be much more difficult than the oxidation of position 6′ in the synthesis of pseudo-cellobiouronic and cellobiouronic acids (16). Results presented in this work further demonstrate the difference in reactivity of the two primary hydroxyl groups in maltose.

Whereas a disaccharide may appear to be composed of two identical sugar residues, it must be realized that the glcycose residue is substituted (e.g. at C-4 in maltose and cellobiose) whereas the glycosyl portion is not. It therefore follows that seemingly identical positions in the two residues may well be subjected to different electronic effects and hence have different reactivities.

In addition, the presence of a bulky aglycone in the β-anomeric position may exert a marked steric effect upon substitution at position 6. For these reasons the selectivity normally associated with certain typical monosaccharide reactions may undergo marked change when applied to disaccharides.

EXPERIMENTAL

Evaporations were carried out under reduced pressure at a bath temperature of 40–45°. Optical rotations are equilibrium values measured on a Bendix–Ericson ETL-NPL automatic polarimeter (type 143A) at 21 ± 2°. Molecular weights were determined on a M.S.9 spectrometer. Melting points quoted are uncorrected. Chromatograms were run by the descending technique in the following solvents: (*a*) ethyl acetate – acetic acid – formic acid – water (18:3:1:4), (*b*) 1-butanol–ethanol–water (4:1:5), and (*c*) ethyl acetate – acetic acid – water (18:7:8). The sulfonate replacement reactions and acetolyses of 1,6-anhydro rings were followed by thin-layer chromatography on silica gel with solvent *d* (ethyl ether – toluene (2:1)).

Sugars were detected on paper chromatograms by the *p*-anisidine trichloroacetate spray (17) for reducing sugars and the periodate–permanganate spray (18) for nonreducing sugars. Detection of sugars on thin-layer plates was accomplished by spraying the plates with concentrated sulfuric acid and heating them at 150–200°.

1,6-Anhydro-β-maltose

To a suspension of hexa-*O*-acetyl-1,6-anhydro-β-maltose (19) (7 g, 1) in methanol (95 ml) was added a solution of 0.1 *M* sodium methoxide in methanol (5 ml). After 4 h the acetate had dissolved, and after a further 14 h the solution was neutralized with Amberlite IR 120 (H^+) ion-exchange resin. The solution was filtered and evaporated to give a sirup which was dissolved in refluxing methanol (50 ml). The hot solution was thinned with ethyl acetate (100 ml) and allowed to cool. The crystals (3.2 g) were filtered off, and then recrystallized in the same manner to give 1,6-anhydro-β-maltose, m.p. 156–158°, $[\alpha]_D$ 108° (*c*, 7.3 in H_2O) (lit. (20) m.p. 150°, $[\alpha]_D$ 79°).

Anal. Calcd. for $C_{12}H_{20}O_{10}$: C, 44.44; H, 6.17. Found: C, 44.02; H, 5.93.

1,6-Anhydro-6′-O-trityl-β-maltose

To 1,6-anhydro-β-maltose (2.2 g, powdered and dried over P_2O_5 *in vacuo*) was added freshly distilled pyridine (25 ml). The mixture was warmed to effect solution and cooled to room temperature. Recrystallized trityl chloride (2.85 g, 1.5 mole equivalents) was added and the solution was left at room temperature for 5 h. The pyridine solution was added dropwise to ice water (500 ml) with continuous stirring. The mixture was then extracted with chloroform (2 × 100 ml), and the chloroform extracts were amalgamated and filtered through Celite. The clear solution was thinned with an equal volume of petroleum ether (30–60°) and the precipitate (1.9 g) collected by filtration. The trityl ether was recrystallized three times from ethanol–water (1:2, 75 ml/g) to yield 1,6-anhydro-6′-*O*-trityl-β-maltose melting at 141–142°, $[\alpha]_D$ 40.8° (*c*, 2.53 in MeOH).

Anal. Calcd. for $C_{31}H_{34}O_{10}\cdot H_2O$: C, 63.70; H, 6.16. Found: C, 63.78; H, 6.26.

Penta-O-acetyl-1,6-anhydro-6′-O-trityl-β-maltose (II)

To 1,6-anhydro-6′-*O*-trityl-β-maltose (1.5 g) dissolved in pyridine (15 ml) was added acetic anhydride (15 ml), and the solution was left overnight at room temperature. Dropwise addition of the acetylation solution to ice water (1 000 ml) gave the acetylated ether (2.2 g). Recrystallization from ethanol–water (3:1, 50 ml/g) gave penta-*O*-acetyl-1,6-anhydro-6′-*O*-trityl-β-maltose melting at 101–102°, $[\alpha]_D$ 55.0° (*c*, 1.55 in $CHCl_3$).

Anal. Calcd. for $C_{41}H_{44}O_{15}$: C, 63.40; H, 5.67. Found: C, 62.98; H, 5.67.

Can. J. Chem. Downloaded from www.nrcresearchpress.com by 210.87.254.105 on 09/05/12
For personal use only.

2,3,2′,3′,4′-Penta-O-acetyl-1,6-anhydro-β-maltose (III)

Penta-*O*-acetyl-1,6-anhydro-6′-*O*-trityl-β-maltose (1 g) was dissolved in 80% aqueous acetic acid (40 ml) and the solution was kept for 3 h at 50°. To the warm solution was added water (90 ml), and the mixture was kept at 5° for 18 h. The precipitate was collected by filtration and washed with 25% aqueous acetic acid (10 ml). The combined filtrates were evaporated to a sirup. Crystals (665 mg) were obtained by dissolving the sirup in hot 2-propanol (25 ml). Recrystallization from the same solvent (40 ml/g) gave 2,3,2′,3′,4′-penta-*O*-acetyl-1,6-anhydro-β-maltose melting at 82–83°, $[\alpha]_D$ 43.4° (*c*, 2.43 in $CHCl_3$).

Anal. Calcd. for $C_{22}H_{30}O_{15}$: C, 49.44; H, 5.62; mol. wt. 534. Found: C, 49.50; H, 5.70; mol. wt. 534.

Penta-O-acetyl-1,6-anhydro-6′-O-p-toluenesulfonyl-β-maltose (IV)

To the pentaacetate (4 g) dissolved in dry pyridine (18 ml) was added *p*-toluenesulfonyl chloride (7.5 g). After 5 h at room temperature, water (3 drops) was added to hydrolyze excess *p*-toluenesulfonyl chloride and the solution was poured into ice water (80 ml). This mixture was extracted with chloroform (3 × 100 ml), and the chloroform extracts were combined and washed with water (7 × 100 ml). The solution was dried with calcium chloride, filtered, and evaporated to give a sirup which, when dissolved in hot 2-propanol (155 ml), gave the crystalline tosylate (4.25 g). Recrystallization from the same solvent (36 ml/g) gave penta-*O*-acetyl-1,6-anhydro-6′-*O*-*p*-toluenesulfonyl-β-maltose melting at 170–171°, $[\alpha]_D$ 55.7° (*c*, 1.00 in $CHCl_3$).

Anal. Calcd. for $C_{29}H_{36}O_{17}S$: C, 50.58; H, 5.23; S, 4.65. Found: C, 50.48; H, 5.11; S, 4.36.

Penta-O-acetyl-1,6-anhydro-6′-deoxy-6′-iodo-β-maltose (V)

To a solution of the 6′-*O*-*p*-toluenesulfonate (1.2 g) in *N*,*N*-dimethylformamide (50 ml) was added finely powdered sodium iodide (4 g). The solution was heated on a steam bath for 1½ h. The cooled solution was diluted with water (100 ml), and extracted with chloroform (4 × 50 ml). The combined chloroform extracts were washed with water (6 × 100 ml), dried over calcium chloride, filtered, and evaporated. The sirup that was obtained was dissolved in hot 2-propanol (100 ml), from which crystals (1.04 g) were obtained. Recrystallization from the same solvent (100 ml/g) gave penta-*O*-acetyl-1,6-anhydro-6′-deoxy-6′-iodo-β-maltose melting at 194–195°, $[\alpha]_D$ 42.0° (*c*, 1.03 in $CHCl_3$).

Anal. Calcd. for $C_{22}H_{29}O_{14}I$: C, 40.99; H, 4.50. Found: C, 41.09; H, 4.58.

Penta-O-acetyl-1,6-anhydro-6′-deoxy-β-maltose (VI)

To a solution containing penta-*O*-acetyl-1,6-anhydro-6′-deoxy-6′-iodo-β-maltose (0.5 g) and pyridine (0.1 ml) in ethanol (10 ml) was added 10% palladium on charcoal (0.5 g). The mixture was kept at 60° and a stream of hydrogen was introduced through a capillary. After 4 h the catalyst was filtered off and the solution evaporated. The resulting sirup was dissolved in chloroform (30 ml), and the solution was washed with 1% sodium thiosulfate (15 ml) and finally with water (4 × 30 ml). The chloroform solution was dried over calcium chloride and evaporated to give a faintly yellow sirup. The sirup was dissolved in hot 2-propanol (25 ml) and the solution, when cooled, gave the crystalline deoxy sugar (252 mg). Recrystallization from 2-propanol (40 ml/g) gave penta-*O*-acetyl-1,6-anhydro-6′-deoxy-β-maltose melting at 141–142°, $[\alpha]_D$ 44.5° (*c*, 0.86 in $CHCl_3$).

Anal. Calcd. for $C_{22}H_{30}O_{14}$: C, 50.96; H, 5.77. Found: C, 50.87; H, 5.89.

6′-Deoxy-maltose (VII)

Penta-*O*-acetyl-1,6-anhydro-6′-deoxy-β-maltose (485 mg) was dissolved in the acetolysis mixture (10 ml; sulfuric acid – acetic anhydride – acetic acid, 1:70:30). The optical rotation changed from 89.2° (5 min) to 138.8° (2 h), after which time it was constant. The flask was cooled in ice after 3 h and ice (5 g) was added. The sulfuric acid was neutralized by the addition of 1% barium acetate, and the precipitate was removed by centrifugation. The solution was evaporated to give a sirup which was evaporated to dryness with ethanol (3 × 10 ml). The hepta-*O*-acetate could be obtained as an amorphous powder on precipitation from alcohol–water. The sirupy acetate was dissolved in methanol (10 ml), and a solution of 0.1 *M* sodium methoxide in methanol (2 ml) was added. After 17 h at room temperature the solution was neutralized with Amberlite IR 120 (H^+), filtered, and evaporated to a sirup. The sirup, which was chromatographically pure, could not be induced to crystallize even after chromatography on Dowex 50WX2 (Li^+) ion-exchange resin (21). After hydrolysis of a sample of the sugar with 2 *N* sulfuric acid, the presence of glucose and material identical with 6-deoxy-glucose (5) was indicated by chromatography. A second sample, which had been reduced with sodium borohydride before hydrolysis, consisted of sorbitol and 6-deoxy-glucose. The 6′-deoxy-maltose had $[\alpha]_D$ 112.7° (*c*, 2.77 in H_2O).

Anal. Calcd. for $C_{12}H_{22}O_{10}\cdot H_2O$: C, 41.86; H, 6.93. Found: C, 41.39; H, 6.96.

Hepta-O-acetyl-6′-deoxy-β-maltose (VIII)

A portion of the 6′-deoxy-maltose (23.3 mg) was dissolved in pyridine (1 ml), and acetic anhydride (4 ml) was added. The solution was left for 30 h at room temperature, poured into ice water (40 ml), and extracted with chloroform (3 × 30 ml). The combined chloroform extracts were washed thoroughly with water (6 × 50 ml), dried over calcium chloride, filtered, and evaporated. The resulting sirup was dissolved in hot ethanol (2 ml) and the solution, when cooled, yielded crystalline hepta-*O*-acetyl-6′-deoxy-β-maltose, m.p. 183–185°, $[\alpha]_D$ 64° (*c*, 0.68 in $CHCl_3$).

Anal. Calcd. for $C_{26}H_{36}O_{17}$: C, 50.32; H, 5.80. Found: C, 50.58; H, 6.12.

Can. J. Chem. Downloaded from www.nrcresearchpress.com by 210.87.254.105 on 09/05/12
For personal use only.

Penta-O-acetyl-6′-S-acetyl-1,6-anhydro-6′-deoxy-β-maltose (IX)

To a solution of penta-*O*-acetyl-1,6-anhydro-6′-*O*-*p*-toluenesulfonyl-β-maltose (500 mg) in *N*,*N*-dimethylformamide was added potassium thiolacetate (220 mg). The mixture was heated on a steam bath for half an hour. To the cooled solution was added water (50 ml), and the mixture was extracted with chloroform (4 × 50 ml). The combined chloroform extracts were thoroughly washed with water (7 × 100 ml), dried over calcium chloride, filtered, and evaporated to a sirup. The sirup was dissolved in hot 2-propanol (45 ml), and the solution, when cooled, gave crystals (300 mg) of the *S*-acetate. Recrystallization of this material from 2-propanol (80 ml/g) yielded penta-*O*-acetyl-6′-*S*-acetyl-1,6-anhydro-6′-deoxy-β-maltose melting at 219–220°, $[\alpha]_D$ 34.6° (*c*, 0.72 in $CHCl_3$).

Anal. Calcd. for $C_{24}H_{32}O_{15}S$: C, 48.66; H, 5.41; S, 5.41. Found: C, 48.74; H, 5.57; S, 5.24.

Hepta-O-acetyl-6′-S-deoxy-α-maltose (X)

Penta-*O*-acetyl-6′-*S*-acetyl-1,6-anhydro-6′-deoxy-β-maltose (150 mg) was dissolved in the acetolysis mixture (3 ml; sulfuric acid – acetic anhydride – acetic acid, 1:70:30). After 3 h at room temperature the solution was added dropwise to ice water (25 ml). The white powder so obtained was filtered and a portion recrystallized from ethanol–water (1:3, 100 ml/g). Further recrystallization did not remove a small amount of the β-anomer which was shown to be present by thin-layer chromatography in solvent *d*. Hepta-*O*-acetyl-6′-*S*-acetyl-6-deoxy-α-maltose had m.p. 73–75° and $[\alpha]_D$ 113° (*c*, 0.79 in $CHCl_3$).

Anal. Calcd. for $C_{28}H_{38}O_{18}S$: C, 48.42; H, 5.49. Found: C, 48.67; H, 5.79.

6′-Deoxy-6′-mercapto-maltose (XI)

To hepta-*O*-acetyl-6′-*S*-acetyl-6′-deoxy-α-maltose (120 mg) in methanol (4 ml) was added a solution of 0.1 *M* sodium methoxide in methanol (1 ml). After the solution had been kept at room temperature overnight, it was neutralized with Amberlite IR 120 (H^+), filtered, and evaporated to a sirup. Chromatography in solvent *a* indicated two products (R_f 0.018 and 0.23), which were the disulfide and free thiol, respectively. When excess 2-mercaptoethanol and 1 drop of concentrated ammonia were added, only the more mobile compound was present. Chromatography of the acid hydrolysate of 6′-deoxy-6′-mercapto-maltose indicated the presence of glucose and 6-deoxy-6-mercapto-glucose. Borohydride reduction followed by hydrolysis yielded sorbitol and 6-deoxy-6-mercapto-glucose. Attempts to crystallize the chromatographically pure disaccharide were unsuccessful. Insufficient material was recovered to obtain suitable analyses. The 6′-deoxy-6′-mercapto-maltose had $[\alpha]_D$ 137.6° (*c*, 2.02 in H_2O).

Penta-O-acetyl-1,6-anhydro-6′-azido-6′-deoxy-β-maltose (XII)

Penta-*O*-acetyl-1,6-anhydro-6′-*O*-*p*-toluenesulfonyl-β-maltose (1.5 g) dissolved in *N*,*N*-dimethylformamide (75 ml) was heated on a steam bath with sodium azide (1.5 g) for 1 h. The cooled solution was poured into an equal volume of water and the mixture was extracted with chloroform (4 × 100 ml). The combined chloroform extracts were thoroughly washed with water (8 × 200 ml), dried over calcium chloride, filtered, and evaporated to a sirup. The sirup was dissolved in hot 2-propanol, and the solution was cooled to give crystals (1.06 g) of the 6′-azide. Recrystallization from the same solvent (50 ml/g) yielded penta-*O*-acetyl-1,6-anhydro-6′-azido-6′-deoxy-β-maltose melting at 151–152°, $[\alpha]_D$ 47.9° (*c*, 2.53 in $CHCl_3$).

Anal. Calcd. for $C_{22}H_{29}O_{14}N_3$: C, 47.23; H, 5.19; N, 7.51; mol. wt. 559. Found: C, 47.68; H, 5.34; N, 7.38; mol. wt. 559.

6′-Amino-6′-deoxy-maltose (XIII)

To a solution of penta-*O*-acetyl-1,6-anhydro-6′-azido-6′-deoxy-β-maltose (560 mg) in methanol (20 ml) was added 0.1 *M* sodium methoxide in methanol (4 ml). After 18 h at room temperature, the solution was neutralized with Amberlite IR 120 (H^+) and evaporated to a sirup which plainly showed an infrared absorption band near 2 100 cm^{-1} characteristic of the azide group (22). The sirup was dissolved in ethanol (15 ml), and 10% palladium on charcoal (300 mg) was added. The mixture was maintained at 65° while a fine stream of hydrogen was bubbled through the solution. After 45 min the solution was made slightly acidic with 3% hydrogen chloride in methanol and the hydrogenation was continued for a further 2 h. The catalyst was removed by filtration, and the solution was evaporated to give a chromatographically pure sirup, R_f 0.054 (solvent *b*, detected with ninhydrin). This material was dissolved in 0.015 *N* hydrochloric acid and heated in a sealed tube for 13 h at 100°. The hydrolysate was neutralized with silver carbonate, filtered, and adjusted to pH 5 with 0.3 *N* hydrochloric acid. Chromatography in solvent *b* indicated only two ninhydrin-positive materials, R_f 0.041 and 0.054. However, *p*-anisidine trichloroacetate spray indicated the presence of glucose, the material showing R_f 0.041, and slower running degradation products. The presence of glucose was indicated by comparison with standards in solvent systems *a*, *b*, and *c*, and also by thin-layer chromatography (23). Preparative paper chromatography on Whatman 3MM paper in solvent *b* gave a small amount (10 mg) of the R_f 0.041 material. Hydrolysis of a sample of this material yielded glucose and 6-amino-6-deoxy-glucose, identical with material prepared by the method of Cramer and co-workers (10). This indicated that the R_f 0.041 material was 6′-amino-6′-deoxy-maltose, $[\alpha]_D$ 88° (*c*, 0.3 in H_2O).

Anal. Calcd. for $C_{12}H_{23}O_{10}N \cdot HCl$: N, 3.70. Found: N, 3.97.

The very low yield prevented any attempts to prepare suitable derivatives.

Can. J. Chem. Downloaded from www.nrcresearchpress.com by 210.87.254.105 on 09/05/12
For personal use only.

ACKNOWLEDGMENTS

We are grateful to the National Research Council for financial support, and one of us (K. N. S.) thanks the council for the award of a studentship. We are also indebted to Mrs. C. Jenkins of this department and Dr. A. Bernhardt, Mulheim (Ruhr), Germany, for analyses, and to Mr. F. Bloss for the molecular weight determinations.

REFERENCES

1. B. J. Bines and W. J. Whelan. Chem. Ind. London, 997 (1960).
2. M. L. Wolfrom, M. I. Taha, and D. Horton. J. Org. Chem. **28**, 3553 (1963).
3. R. L. Whistler and D. G. Medcalf. Arch. Biochem. Biophys. **105**, 1 (1964).
4. G. G. S. Dutton and K. N. Slessor. Can. J. Chem. **42**, 1110 (1964).
5. E. Fischer and K. Zach. Chem. Ber. **45**, 3761 (1912).
6. B. Helferich and W. Speicher. Ann. **579**, 106 (1953).
7. J. H. Chapman and L. N. Owen. J. Chem. Soc. 579 (1950).
8. M. Akagi, S. Tejima, and M. Haga. Chem. Pharm. Bull. Tokyo, **10**, 562 (1962).
9. R. W. Jeanloz and A. M. C. Rapin. J. Org. Chem. **28**, 2978 (1962).
10. F. Cramer, H. Otterbach, and H. Springmann. Chem. Ber. **92**, 384 (1959).
11. J. K. N. Jones. Private communication.
12. H. Paulsen. Ann. **665**, 166 (1963).
13. D. Abbot and H. Weigel. J. Chem. Soc. 5157 (1965).
14. Y. Hirasaka. Yakugaku Zasshi, **83**, 960 (1963).
15. Y. Hirasaka, I. Matsunaga, K. Umemoto, and M. Sukegawa. Yakugaku Zasshi, **83**, 966 (1963).
16. I. Johanson, B. Lindberg, and O. Theander. Acta Chem. Scand. **17**, 2019 (1963).
17. L. Hough, J. K. N. Jones, and W. H. Wadman. J. Chem. Soc. 1702 (1950).
18. R. U. Lemieux and H. F. Bauer. Anal. Chem. **26**, 920 (1954).
19. L. Asp and B. Lindberg. Acta Chem. Scand. **6**, 941 (1952).
20. P. Karrer and C. Kamienski. Hevl. Chim. Acta, **15**, 739 (1932).
21. J. K. N. Jones, R. A. Wall, and A. O. Pittet. Can. J. Chem. **38**, 2285 (1960).
22. R. D. Guthrie and D. Murphy. J. Chem. Soc. 5288 (1963).
23. G. W. Hay, B. A. Lewis, and F. Smith. J. Chromatog. **11**, 479 (1963).

Can. J. Chem. Downloaded from www.nrcresearchpress.com by 210.87.254.105 on 09/05/12
For personal use only.

Can. J. Chem. Downloaded from www.nrcresearchpress.com by 210.87.254.6 on 09/05/12
For personal use only.

CARBONYL AND THIOCARBONYL COMPOUNDS

X. SYNTHETIC EXPERIMENTS WITH COUMARIN-2-THIONE AND BENZOXANTHIONES

N. LATIF AND I. FATHY
National Research Center, Dokki, Cairo, United Arab Republic

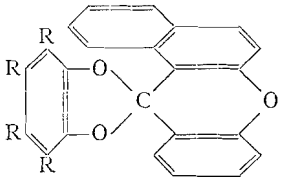
Received July 6, 1965

ABSTRACT

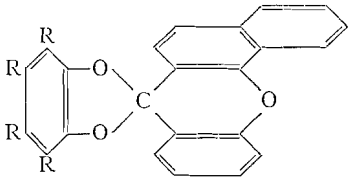
The benzoxanthene ethers I*a*–II*b* are obtained in good yields by the action of tetrachloro- and tetrabromo-*o*-benzoquinone on 1,2- and 3,4-benzoxanthione, respectively. The benzopyran analogues III*a*–III*b* are obtained by the interaction of the corresponding haloquinone and coumarin hydrazone. The latter, which is now readily obtained by the action of hydrazine hydrate on coumarin-2-thione, condenses with thioketones to give coumarin azines. The benzopyran ethers III*a* and III*b* are cleaved by malononitrile, cyanoacetic ester, hydrazine hydrate, phenylhydrazine, and benzoylhydrazine, yielding the unsaturated nitriles (V*a*–V*b*) and the corresponding hydrazones, respectively.

1,2-Benzoxanthione reacts with 9-diazoxanthene, diphenyldiazomethane, and diphenylenediazomethane to give the ethylene sulfides VI–VIII, respectively. However, coumarin-2-thione reacts with the diazo compounds in a different manner; it gives the ethylenes X and XI directly, together with the symmetrical thiiranes XII and XIII, in the cases of diphenyldiazomethane and 9-diazoxanthene, respectively, whereas the cyclopropane derivative XIV is produced in the case of diphenylenediazomethane. XIV is also obtained by the photochemical interaction of coumarin itself and the diazo compound.

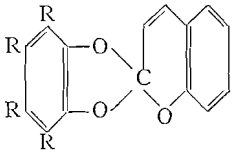
Tetrahalo-*o*-benzoquinones react with xanthione and thioxanthione to give the corresponding methylene ethers (1, 2). It is now shown that benzoxanthiones readily undergo this quinone–thione reaction to give the analogous benzoxanthene ethers. Thus, I*a*–II*b* are obtained, in good yield, by the action of tetrachloro- and tetrabromo-*o*-benzoquinone on 1,2- and 3,4-benzoxanthione, respectively, in boiling dry benzene. The products are identical with the benzoxanthene ethers previously obtained by the reaction of 1,2- and 3,4-benzoxanthone hydrazone with the corresponding tetrahalo-*o*-benzoquinone (3, 4). When the reaction was applied to coumarin-2-thione, tetrachloro-*o*-benzoquinone gave the spiropyran III*a* (1), whereas tetrabromoquinone oxidized the thione mainly to



I*a*, R = Cl
I*b*, R = Br



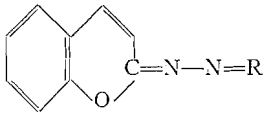
II*a*, R = Cl
II*b*, R = Br



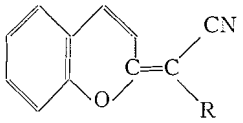
III*a*, R = Cl
III*b*, R = Br

coumarin. Both III*a* and III*b* are now readily obtained by the interaction of coumarin hydrazone with the corresponding tetrahalo-*o*-benzoquinone, possibly through the intermediate formation of an unstable diazo derivative (5). Although hydrazine hydrate opens the lactone ring of coumarin (6), it condenses readily with coumarin-2-thione to give coumarin hydrazone. The latter reacts with thioketones, e.g. thiobenzophenone, thiofluorenone, xanthione, and 1,2-benzoxanthione, to give the coumarin azines IV*a*–IV*d*, respectively, which are identical with the products obtained by the condensation of coumarin-2-thione with the corresponding ketohydrazones. The structure given for III*b*

is based on analogy, and is supported by the following facts: (*i*) it is colorless and does not contain sulfur, (*ii*) it is hydrolyzed by mineral acids to give coumarin and tetrabromocatechol, and (*iii*) its infrared spectrum lacks the stretching frequency band characteristic of the lactone carbonyl group.



IV*a*, R = diphenylmethylene
IV*b*, R = diphenylene
IV*c*, R = xanthylene
IV*d*, R = 1,2-benzoxanthylene

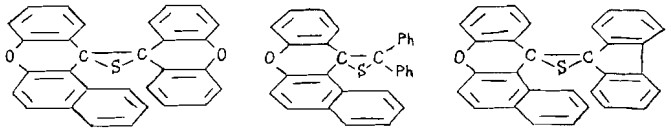


V*a*, R = CN
V*b*, R = $COOC_2H_5$

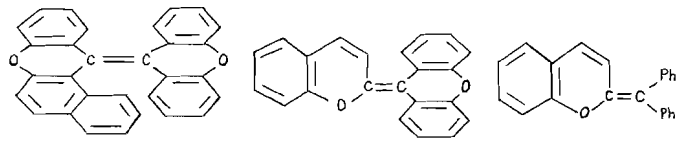
The ethers III*a* and III*b* are cleaved by active hydrogen compounds to yield the corresponding unsaturated benzopyran derivatives and tetrahalocatechol. Thus, III*a* reacts readily with hydrazine hydrate, phenyl- and benzoyl-hydrazine, malononitrile, and cyanoacetic ester to give coumarin hydrazone, phenyl- and benzoyl-hydrazone, and the unsaturated nitriles V*a* and V*b*, respectively, possibly through a β-elimination process of an intermediate semiether (7). A similar uncatalyzed cleavage of xanthene ethers by active hydrogen compounds has been reported (3, 7). Authentic samples of the products are obtained by condensing coumarin-2-thione with the appropriate active hydrogen compound.

Reaction of 1,2-Benzoxanthione and Coumarin-2-thione with Diazo Compounds

9-Diazoxanthene reacts with xanthione, thioxanthione (8), and 3,4-benzoxanthione (4) to give the corresponding ethylene sulfides. It is now found that 1,2-benzoxanthione reacts with 9-diazoxanthene and diphenyl- and diphenylene-diazomethane in a similar manner to give the ethylene sulfides VI–VIII. However, coumarin-2-thione reacts with the diazo compounds in a different manner. Thus, diphenyldiazomethane and 9-diazoxanthene give the ethylenes X and XI directly, together with the symmetrical thiiranes XII and XIII, respectively, whereas 9-diazofluorene gives the cyclopropane derivative XIV. Constitution of the sulfides VI–VIII is based on analogy (4, 8), lack of color, and the fact that, upon treatment with copper powder, the corresponding ethylene is obtained, e.g. VI gives IX. The structures of X and XI are supported by analytical data, lack of the stretching frequency band characteristic of the lactone carbonyl group in their infrared spectra, and the fact that they are readily cleaved by thionyl chloride or sulfur. Thus, for example,

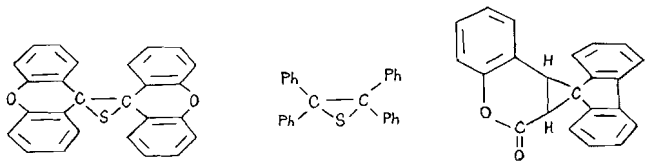


VI VII VIII

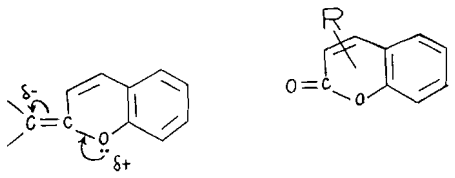


IX X XI

Can. J. Chem. Downloaded from www.nrcresearchpress.com by 210.87.254.6 on 09/05/12
For personal use only.



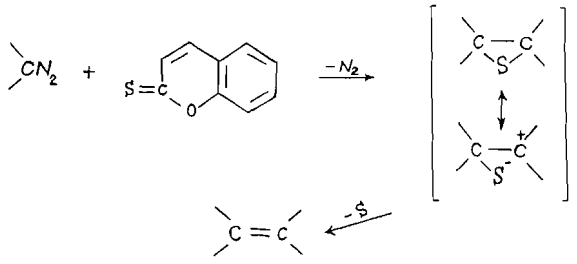
XII XIII XIV



R = 9-fluorenyl

XV XVI

the ethylene X gives coumarin and xanthone when it is allowed to react with boiling thionyl chloride, and gives coumarin-2-thione and xanthione upon fusion with sulfur. It has been reported (9) that, at higher temperatures, certain ethylenes, such as dixanthylene and dithioxanthylene, acquire ionic betaine structures which are susceptible to cleavage by thionyl chloride or sulfur. It is assumed, in the case of X and XI, that the presence of an unshared electron pair on the oxygen of the benzopyran residue enhances the stabilization of heteropolar structures (cf. XV) through resonance. Production of the ethylenes X and XI in this reaction may proceed through the intermediate formation of an unstable ethylene sulfide (cf. Reaction Scheme 1), which splits off sulfur under the reaction conditions. The latter reacts immediately with the diazo compound to give the symmetrical thiiranes XII and XIII, respectively. 9-Diazoxanthene and diphenyldiazomethane react with sulfur, at room temperature, to give XII and XIII in good yields (8), whereas 9-diazofluorene undergoes this reaction very slowly.



REACTION SCHEME 1.

The structure of XIV is supported by the fact that the product is soluble in aqueous alkali, and by its infrared spectrum, which shows a strong stretching frequency band at 5.75 μ (Nujol) characteristic of the carbonyl group of a saturated δ-lactone (cf. ref. 10). Nuclear magnetic resonance spectral data also exclude the possible structure XVI; the two protons attached to the cyclopropane ring gave rise to the AB system around δ 3.5 p.p.m.

Can. J. Chem. Downloaded from www.nrcresearchpress.com by 210.87.254.6 on 09/05/12
For personal use only.

Can. J. Chem. Downloaded from www.nrcresearchpress.com by 210.87.254.6 on 09/05/12
For personal use only.

EXPERIMENTAL

Melting points were not corrected. Microanalyses were performed by A. Bernhardt, Germany, and by the Microanalysis Unit, National Research Center, Cairo. Infrared spectra were measured on a Perkin–Elmer infracord 137, and the nuclear magnetic resonance spectra were recorded on a Varian A-60 spectrometer.

Preparation of 9,9-(Tetrachloro-o-phenylenedioxy)1,2-benzoxanthene (Ia)

A solution of tetrachloro-*o*-benzoquinone (1 g) and 1,2-benzoxanthione (1 g) in dry benzene (20 ml) was heated under reflux for 3 h, filtered while hot, and evaporated to dryness under reduced pressure. A few milliliters of ether was added to the residue, and the solid that formed was filtered off, washed with acetone, and crystallized from xylene to give 9,9-(tetrachloro-*o*-phenylenedioxy)1,2-benzoxanthene (I*a*) (1.35 g), m.p. 333–334 °C (undepressed when admixed with an authentic sample (3)). Its infrared spectrum was identical with that of an authentic sample.

Preparation of 9,9-(Tetrabromo-o-phenylenedioxy)1,2-benzoxanthene (Ib)

Tetrabromo-*o*-benzoquinone (2 g) and 1,2-benzoxanthione (1.4 g) were allowed to react as in the case of the chloro analogue. The product that was obtained (2.52 g) was recrystallized from benzene to give 9,9-(tetrabromo-*o*-phenylenedioxy)1,2-benzoxanthene (I*b*), m.p. 344 °C (decomp.). Its infrared spectrum is identical with that of an authentic sample (3).

Preparation of 9,9-(Tetrachloro-o-phenylenedioxy)3,4-benzoxanthene (IIa)

Tetrachloro-*o*-benzoquinone (1 g) and 3,4-benzoxanthione (1 g) were allowed to react together as in the case of I*a*. The product that was obtained was crystallized from benzene to give II*a* (1.04 g) as colorless crystals, m.p. 305 °C (undepressed when admixed with an authentic sample (4)). The product and the authentic sample have identical infrared spectra.

When the reaction was carried out with tetrabromo-*o*-quinone, 9,9-(tetrabromo-*o*-phenylenedioxy)3,4-benzoxanthene (II*b*) was obtained as colorless crystals, m.p. 306 °C (decomp.). Its infrared spectrum is identical with that of an authentic sample (4).

Preparation of Coumarin Hydrazone

A solution of coumarin-2-thione (11) (2 g) and hydrazine hydrate (99–100%; 0.6 ml) in absolute alcohol (50 ml) was heated under reflux for 3 h. The solution was filtered while hot and evaporated to dryness under reduced pressure, and the residue was extracted with boiling petroleum ether (40–60°). The extract was concentrated and cooled, and the solid that separated out was recrystallized from methanol to give coumarin hydrazone (1.3 g) as yellow crystals, m.p. 85–86 °C.

Anal. Calcd. for $C_9H_8ON_2$: C, 67.50; H, 5.00; N, 17.5. Found: C, 67.78; H, 4.94; N, 17.69.

Preparation of 2,2-(Tetrachloro-o-phenylenedioxy)benzopyran (IIIa)

Coumarin hydrazone (0.8 g) was added in portions, at room temperature (25 °C), to a dry ethereal solution of tetrachloroquinone (2.5 g). After each addition, a reaction, with evolution of gas, occurred. When all the hydrazone had been added, the reaction mixture was evaporated to dryness under reduced pressure. A few milliliters of acetone was added to the residue that was obtained, and the solid that separated out was recrystallized from the same solvent to give 2,2-(tetrachloro-*o*-phenylenedioxy)benzopyran (III*a*) (1.2 g), m.p. 214 °C (undepressed when admixed with an authentic sample (1)). The filtrate was evaporated to dryness and extracted with methanol, and the extract was poured onto ice-cold water, and acidified. The solid that formed was dried and added to acetic anhydride, and the mixture was heated under reflux for 30 min and then poured onto ice. The solid that separated out was crystallized from methanol, and proved to be the diacetate of tetrachlorocatechol (melting point and mixed melting point).

Preparation of 2,2-(Tetrabromo-o-phenylenedioxy)benzopyran (IIIb)

Tetrabromo-*o*-benzoquinone (2.1 g) and coumarin hydrazone (0.4 g) were allowed to react as in the case of III*a*. The solid that was obtained was crystallized from acetone to give III*b* (0.65 g) as colorless crystals, m.p. 222–224 °C.

Anal. Calcd. for $C_{15}H_6O_3Br_4$: Br, 57.70. Found: Br, 56.91.

Hydrolysis of IIIb

The cyclic ether (0.2 g) was added to a solution of concentrated hydrochloric acid (specific gravity 1.19; 1 ml) in dioxane (5 ml), and the mixture was heated under reflux for 30 min and poured onto ice. The precipitate that formed was filtered off, dried, and shown to be tetrabromocatechol (identified as its diacetate). The filtrate was left to evaporate slowly at room temperature (25 °C). The colorless crystals that formed were recrystallized from petroleum ether (30–50°), and proved to be coumarin (m.p. and mixed m.p. 70 °C).

Preparation of Coumarin Azines

General Procedure A

A mixture of coumarin hydrazone (0.01 mole), the thioketone (0.01 mole), and yellow mercuric oxide

(2 g) in absolute alcohol (30 ml) was boiled under reflux for 3 h. The reaction mixture was filtered while hot, concentrated, and left to cool. The precipitate that formed was filtered off and recrystallized from the appropriate solvent (Table I).

General Procedure B

A suspension of coumarin-2-thione (0.01 mole), the appropriate ketohydrazone (0.01 mole), and yellow mercuric oxide (2 g) in absolute alcohol (30 ml) was heated under reflux for 6 h, filtered while hot, and cooled. The azines IV*a*–IV*e* were obtained, and proved to be identical with the products obtained from procedure A.

TABLE I

Reaction of coumarin hydrazone with thioketones

Thioketone used	Coumarin azine, color, and yield	Solvent of crystallization	Melting point (°C)	Analysis (%)
Thiobenzophenone*	IV*a*, yellow, 60%	Acetone	157–158	Calcd. for $C_{22}H_{16}N_2O$: C, 81.48; H, 4.93; N, 8.61. Found: C, 81.50; H, 5.07; N, 8.90.
Thiofluorenone*	IV*b*, orange-yellow, 65%	Acetone	170–171	Calcd. for $C_{22}H_{14}N_2O$: C, 81.98; H, 4.38; N, 8.69. Found: C, 81.92; H, 4.78; N, 8.79.
Xanthione	IV*c*, orange-yellow, 45%	Benzene	176–177	Calcd. for $C_{22}H_{14}N_2O_2$: C, 78.1; H, 4.14; N, 8.28. Found: C, 77.98; H, 4.13; N, 8.64.
1,2-Benzoxanthione	IV*d*, orange-yellow, 42%	Acetone–alcohol	140–141	Calcd. for $C_{26}H_{16}N_2O_2$: C, 80.41; H, 4.12; N, 7.21. Found: C, 80.34; H, 4.42; N, 7.56.

*The reaction was carried out in a carbon dioxide atmosphere.

Preparation of Coumarin Benzoylhydrazone

A mixture of coumarin-2-thione (0.5 g), benzoylhydrazine (0.5 g), yellow mercuric oxide (1 g), and absolute alcohol (20 ml) was boiled under reflux for 6 h. The reaction mixture was filtered while hot, concentrated, and cooled. The product that separated out (0.48 g) was recrystallized from acetone to give coumarin benzoylhydrazone as pale yellow crystals, m.p. 160–161 °C.

Anal. Calcd. for $C_{16}H_{12}N_2O_2$: C, 72.72; H, 4.54; N, 10.60. Found: C, 72.40; H, 4.66; N, 11.06.

Preparation of 2H-1-Benzopyran-Δ2,α-malononitrile (Va)

A mixture of the thione (1 g), malononitrile (0.5 g), and yellow mercuric oxide (1 g) in dry toluene (20 ml) was heated under reflux for 6 h and filtered while hot. The solution was concentrated and cooled, and the solid that separated out was crystallized from benzene to give V*a* (0.92 g) as yellow crystals, m.p. 167–168 °C.

Anal. Calcd. for $C_{12}H_6N_2O$: C, 74.22; H, 3.09; N, 14.43. Found: C, 74.43; H, 3.23; N, 14.82.

Preparation of 2H-1-Benzopyran-Δ2,α-cyanoacetic Ester (Vb)

Coumarin-2-thione and ethyl cyanoacetate were allowed to react as above, when V*b* was obtained as yellow crystals (from methanol), m.p. 141–142 °C.

Anal. Calcd. for $C_{14}H_{11}NO_2$: C, 69.71; H, 4.57; N, 5.80. Found: C, 70.22; H, 4.59; N, 6.04.

Reaction of 2,2-(Tetrachloro-o-phenylenedioxy)benzopyran (IIIa) with Hydrazine Hydrate

A mixture of III*a* (0.5 g) and hydrazine hydrate (99–100%; 0.2 ml) in alcohol (30 ml) was heated under reflux for 3 h, filtered while hot, and evaporated to dryness under reduced pressure. The residue was extracted with boiling petroleum ether (40–60°), and the extract was concentrated and cooled. The product that separated out (0.15 g) was shown to be coumarin hydrazone (m.p. and mixed m.p. 85°). The residue, after extraction with petroleum, was shown to contain tetrachlorocatechol as usual.

Reaction of IIIa with Phenylhydrazine

The reaction was carried out as above, and the solution was left to cool. Coumarin phenylhydrazone (0.23 g), m.p. 143 °C (undepressed when admixed with an authentic sample (11)), was obtained.

When benzoylhydrazine was used instead of phenylhydrazine, coumarin benzoylhydrazone, m.p. 160 °C (0.35 g), was obtained.

Reaction of IIIa with Malononitrile

The cyclic ether III*a* (0.5 g) and malononitrile (0.25 g) in ethanol (25 ml) were heated under reflux for

Can. J. Chem. Downloaded from www.nrcresearchpress.com by 210.87.254.6 on 09/05/12
For personal use only.

6 h. The solid which separated when the solution was allowed to cool was recrystallized from benzene to give 2*H*-1-benzopyran-Δ2,α-malononitrile (*Va*) (0.2 g), m.p. 167–168 °C.

When the reaction was carried out in *n*-butanol with cyanoacetic ester, *Vb* was similarly obtained.

Reaction of Diazo Compounds with 1,2-Benzoxanthione

The thione (0.01 mole) was added in portions to the ethereal solution of the diazo compound. A vigorous reaction, with evolution of gas, took place after each addition. When all the thione had been added, the reaction mixture was left at room temperature (25 °C) for 30 min. The product that separated out was filtered off, washed with ether, and crystallized from acetone to give the corresponding episulfide as colorless crystals (Table II).

Action of Copper Bronze on VI

The episulfide VI (0.5 g) and copper bronze (0.3 g) in xylene (20 ml) were heated under reflux for 1 h. The reaction mixture was filtered while hot, concentrated, and cooled, and the product that separated out was recrystallized from benzene to give the ethylene IX as colorless crystals, m.p. 312–314 °C, in an almost theoretical yield.

Anal. Calcd. for $C_{30}H_{18}O_2$: C, 87.78; H, 4.42. Found: C, 86.94; H, 4.41.

TABLE II

Reaction of 1,2-benzoxanthione with diazo compounds

Diazo compound	Episulfide, % yield, and melting point	Analysis (%)
9-Diazoxanthene	VI, 90%, 188–190°	Calcd. for $C_{30}H_{18}O_2S$: C, 81.44; H, 4.07; S, 7.23. Found: C, 80.98; H, 4.24; S, 7.47.
Diphenyldiazomethane	VII, 80%, 168–170°	Calcd. for $C_{30}H_{20}OS$: C, 84.11; H, 4.67; S, 7.47. Found: C, 84.06; H, 4.54, S, 7.99.
9-Diazofluorene	VIII, 85%, 184–186°	Calcd. for $C_{30}H_{18}OS$: C, 84.5; H, 4.22; S, 7.5. Found: C, 83.87; H, 4.44; S, 6.54.

Reaction of 9-Diazoxanthene with Coumarin-2-thione

Coumarin-2-thione (0.95 g) was added to a solution of 9-diazoxanthene (1.45 g) in dry ether (30 ml), and the reaction mixture was left for 1 h at room temperature (25 °C). The product that separated out was crystallized from acetone as colorless crystals (0.6 g), which were proved to be dispiro(xanthene-9,2′-thiirane-3′,9″-xanthene) (XII) (m.p. and mixed m.p. 206°). The filtrate was evaporated to dryness under reduced pressure, and a few milliliters of methanol was added. The solid that separated out was filtered off and recrystallized from methanol–acetone to give X (0.7 g) as orange-yellow crystals, m.p. 137 °C.

Anal. Calcd. for $C_{22}H_{14}O_2$: C, 85.16; H, 4.51. Found: C, 84.86; H, 4.24.

Reaction of X with Thionyl Chloride

A solution of X (0.5 g) in thionyl chloride (10 ml) was heated under reflux for 6 h, left to cool, and poured onto ice. The solid that formed was filtered off, washed with water, and crystallized from methanol to give xanthone (m.p. and mixed m.p. 174°). The aqueous filtrate was left to evaporate slowly at room temperature, and the colorless crystals that separated out were recrystallized from petroleum ether (40–60°) and proved to be coumarin (m.p. and mixed m.p. 70°).

Reaction of X with Sulfur

A mixture of X (0.8 g) and powdered sulfur (0.15 g) was heated for 2 h at 270–275° (bath temperature), while a stream of dry carbon dioxide was passed through. The reaction mixture was left to cool and then extracted with methanol, the extract was concentrated and cooled, and the product that separated out (0.17 g) was proved to be coumarin-2-thione (melting point and mixed melting point). The alcohol-insoluble residue was crystallized from benzene, and proved to be xanthione (melting point and mixed melting point) (0.23 g).

Reaction of Diphenyldiazomethane with Coumarin-2-thione

The reaction was carried out as in the case of 9-diazoxanthene. The colorless product which separated out after 30 min was filtered off, and proved to be epithiotetraphenylethane (XIII) (m.p. and mixed m.p. 178°). The mother liquor was left overnight, and a yellow product separated out. It was recrystallized from acetone to give XI as yellow crystals, m.p. 132 °C.

Anal. Calcd. for $C_{22}H_{16}O$: C, 89.18; H, 5.4. Found: C, 89.11; H, 5.6.

Can. J. Chem. Downloaded from www.nrcresearchpress.com by 210.87.254.6 on 09/05/12
For personal use only.

Reaction of 9-Diazofluorene with Coumarin-2-thione

A solution of 9-diazofluorene (1.9 g) and coumarin-2-thione (1.6 g) in dry ether (30 ml) was kept at room temperature for 24 h. The product that separated out was recrystallized from acetone to give XIV (1.2 g) as colorless crystals, m.p. 286 °C. The product is soluble in 5% aqueous sodium hydroxide solution.

Anal. Calcd. for $C_{22}H_{14}O_2$: C, 85.16; H, 4.51. Found: C, 85.16; H, 4.56.

Photochemical Reaction of 9-Diazofluorene and Coumarin

A solution of equimolecular amounts of 9-diazofluorene and coumarin in dry benzene was exposed to sunlight for 15 days (May), in a pyrex glass tube which was sealed, while a stream of carbon dioxide was passed through the mixture. The product that separated out was recrystallized from acetone, and proved to be XIV (m.p. and mixed m.p. 286 °C). Its infrared spectrum was identical with that of an authentic sample.

ACKNOWLEDGMENTS

The authors thank Professor F. G. Baddar, Faculty of Science, A'in Shams University, Cairo, for determination of the infrared spectra, and Dr. U. Scheidegger, Research Chemist, Varian AG, Switzerland, for determination of the nuclear magnetic resonance spectrum.

REFERENCES

1. N. LATIF and I. FATHY. Can. J. Chem. **37**, 863 (1959).
2. N. LATIF, I. FATHY, N. MISHRIKY, and A. ATALLAH. J. Org. Chem. **25**, 1618 (1960).
3. N. LATIF and I. FATHY. Can. J. Chem. **43**, 1246 (1965).
4. A. MUSTAFA, N. LATIF, and H. EL NAMAKY. Rec. Trav. Chim. In press.
5. N. LATIF, I. FATHY, and N. MISHRIKY. J. Org. Chem. **24**, 1883 (1959).
6. A. DARAPSKY, H. BERGER, and A. NEUHAUS. J. Prakt. Chem. **147**, 145 (1936).
7. N. LATIF, I. FATHY, and N. MISHRIKY. Can. J. Chem. **42**, 1736 (1964).
8. N. LATIF and I. FATHY. J. Org. Chem. **27**, 1633 (1962).
9. A. SCHÖNBERG, A. ISMAIL, and W. ASKER. J. Chem. Soc. **442**, (1946).
10. L. J. BELLAMY. The infrared spectra of complex molecules. John Wiley & Sons, Inc., New York. 1958. p. 179. R. JONES and B. GALLAGHER. J. Am. Chem. Soc. **81**, 5246 (1959).
11. F. TIEMANN. Ber. **19**, 1661 (1886).

Can. J. Chem. Downloaded from www.nrcresearchpress.com by 210.87.254.6 on 09/05/12
For personal use only.

Can. J. Chem. Downloaded from www.nrcresearchpress.com by 210.87.254.42 on 09/05/12
For personal use only.

NOTES

CHEMISTRY OF TETRAHYDROFURANONE DERIVATIVES II. A CONVENIENT PROCEDURE FOR THE SYNTHESIS OF 3-ALKYL-SUBSTITUTED FURANS[1]

M. A. GIANTURCO AND P. FRIEDEL

A variety of isoprenoid products of plant origin contain a 3-alkyl-substituted furan nucleus (1, 2). Moreover, this structural unit has recently been found to be present in dendrolasin, an odorous substance isolated from ants; this appears to be the first furan derivative ever found in the animal kingdom (3, 4).

Although a few of these natural products have been synthesized (1, 5–7), no convenient procedure for the preparation of 3-alkyl-substituted furans seems to have been reported in the literature. In fact, the best synthesis of compounds of this class appears to be the one based upon the reaction of 3-furoyl chloride with the appropriate alkylcadmium, followed by Wolff–Kischner reduction of the resulting ketone (4, 8).

However, the above procedure is laborious and inefficient, primarily because of the unavailability of a good synthetic method for 3-furoic acid. Prugh has recently reported (9), indeed, that the method of Gronowitz, which leads to 3-furoic acid in 5% overall yield, is the best of the published procedures for the synthesis of this key intermediate (1, 10–12).

The present note describes a convenient approach to 3-alkyl-substituted furans, by a method which should be of fairly general applicability and does not require the preparation of 3-furoic acid.

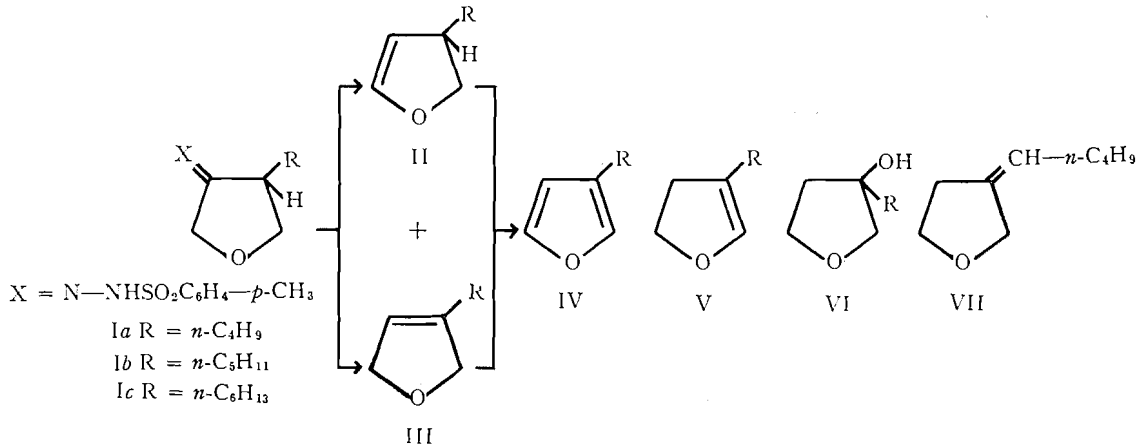
In a previous communication (13), it has been shown that high yields of mixtures of 2,3- and 2,5-dihydrofurans are obtained when the tosylhydrazones of the now easily available tetrahydrofuranones (14) are treated with sodium dissolved in ethylene glycol (Bamford–Stevens reaction). The ratios of the 2,3- and 2,5-isomers were found to depend upon the position of the alkyl substituent on the ring, being approximately 8:1 and 24:1, respectively, when the tosylhydrazones of 2-methyltetrahydrofuran-3-one and 2-methyltetrahydrofuran-4-one were reacted, and approximately 2:1 when the reaction was carried out with the 3-methyltetrahydrofuran-4-one derivative.

In the course of the present work, application of the Bamford–Stevens reaction to the tosylhydrazones of 3-*n*-butyl-, 3-*n*-pentyl-, and 3-*n*-hexyl-tetrahydrofuran-4-one (I*a*–I*c*) has led to the isolation of the appropriate mixtures of dihydrofurans in yields higher than 90%; in all three cases, the ratios II*a*/III*a*, II*b*/III*b*, and II*c*/III*c* were approximately 3:2.

Subsequent treatment of each of the three above dihydrofuran mixtures with 2,3-dichloro-5,6-dicyano-1,4-benzoquinone gave, after 45 min at room temperature, the corresponding furans (IV) in yields slightly higher than 50%. Besides the solvent (benzene), the desired furan, and traces of starting materials, no other volatile product could be detected in the reaction mixtures by gas–liquid partition chromatography. When the reaction was followed chromatographically to determine its optimal time, it was found that yields of at least 40% could actually be obtained after only 10 to 15 min. Reaction

[1]*For part I of this series, see ref. 13.*

times longer than 1 h, or the use of other quinones as dehydrogenating agents (*o*-chloranil, *p*-chloranil, and phenanthrenequinone) did not improve the yields.



To establish definitely which one of the two isomers (II or III) is best suited for the conversion into the corresponding furan, the mixture of II*b* and III*b* obtained from I*b* was separated into its components by preparative gas–liquid partition chromatography, and II*b* and III*b* were treated separately with 2,3-dichloro-5,6-dicyano-1,4-benzoquinone. Although the maximum yield of 3-*n*-pentylfuran (IV*b*) which could be obtained from 3-*n*-pentyl-2,3-dihydrofuran (II*b*) was somewhat lower than 50%, the reaction of 3-*n*-pentyl-2,5-dihydrofuran (III*b*) with the above quinone at room temperature for 1 h resulted in the formation of IV*b* in yields higher than 80%.

When the ease of quinone dehydrogenation of the third possible type of 3-alkyl-substituted dihydrofuran was tested by reacting 4-*n*-pentyl-2,3-dihydrofuran (V*b*) with 2,3-dichloro-5,6-dicyano-1,4-benzoquinone, it was found that this isomer gave only extremely low yields of the corresponding furan (IV*b*).

4-*n*-Pentyl-2,3-dihydrofuran (V*b*) was isolated by preparative gas–liquid partition chromatography from the mixture obtained by copper sulfate dehydration of 3-hydroxy-3-*n*-pentyltetrahydrofuran (VI*b*). The above mixture, unsuitable for quinone dehydrogenation to IV*b*, was found to contain 30% V*b*; the remaining 70% consisted of an unidentified compound, accompanied by some III*b* (infrared evidence). The unidentified substance, which co-chromatographs with III*b* on two columns of different polarity, may be the product (VII) of the loss of water between the OH and the extranuclear α-methylene of VI*b*.

These results suggest an explanation for Wynberg's previous report (15) that 3-alkyl-2,5-dihydrofurans are extremely stable in the presence of dehydrogenating agents. Since the starting materials employed by the above investigator had been prepared by the method of Yur'ev *et al.* (16), i.e. iodine-catalyzed dehydration of 3-alkyl-3-hydroxytetrahydrofurans, it seems probable, in fact, that they were not 3-alkyl-2,5-dihydrofurans but rather mixtures analogous to the one obtained in this laboratory by copper sulfate dehydration of VI*b*.

In view of the above, it appears that the position of the double bond in the ring and that of the substituent with respect to the double bond play a dominant role in determining the success or failure of the quinone dehydrogenation of 3-alkyl-substituted dihydrofurans to the corresponding furan.

Can. J. Chem. Downloaded from www.nrcresearchpress.com by 210.87.254.42 on 09/05/12
For personal use only.

A full account of our attempts to employ quinone dehydrogenation of dihydrofurans for the synthesis of monoalkyl- and polyalkyl-substituted furans will be reported in due time. However, the data given in the Experimental section are typical of the general procedure.

EXPERIMENTAL

The infrared data refer to dilute CCl_4 solutions of the compounds; only the most significant bands are reported. The nuclear magnetic resonance spectra were measured at 60 Mc.p.s., with tetramethylsilane as internal standard. Only the seven most intense mass spectral peaks are reported (ionizing voltage, 150 eV; source temperature, 150°). Retention times (R_T) refer to the following chromatographic conditions: 6 m × $\frac{3}{8}$ inch SE-30 column, 30% on 45–60 mesh Chromosorb W, 200°, 120 cc He/min.

Potassium Salt of 3-Carbomethoxytetrahydrofuran-4-one

To a 13.2 g portion of 85% powdered KOH dissolved in 3 ml H_2O and 45 ml 96% ethanol was added, with stirring and external ice cooling, 28.8 g (0.2 mole) of freshly distilled 3-carbomethoxytetrahydrofuran-4-one, prepared as previously described (14). After the addition of 10 ml ether, the pasty precipitate was centrifuged out immediately, washed once with 10 ml ice-cold 96% ethanol and then with 40 ml ether, and vacuum-dried to yield 36.4 g (100%) of crude product. The material so obtained was suitable for further reactions.

3-n-Pentyl-3-carbomethoxytetrahydrofuran-4-one

To a stirred suspension of the above potassium salt (36.4 g, 0.2 mole) in dimethyl sulfoxide (300 ml) was added, in one lot and at room temperature, *n*-pentyl iodide (79.2 g, 0.4 mole). After all the material had dissolved (30 min), stirring was continued for an additional 3 h (negative $FeCl_3$ test); the solution was then poured into ice water (300 ml), salted, and extracted with ether. Distillation yielded, after a forerun consisting chiefly of *n*-pentyl iodide, 35.94 g (84% yield) of the alkylated ester. A sample that was redistilled for analysis had the following physical properties: b.p. 78–79° at 0.2 mm; $n_D^{22.3}$ 1.4555; infrared: $\lambda_{C=O}$ at 5.62 and 5.72 μ.

Anal. Calcd. for $C_{11}H_{18}O_4$: C, 61.66; H, 8.47. Found: C, 61.62; H, 8.46.

3-n-Pentyltetrahydrofuran-4-one

A stirred solution of the above ester (33.5 g, 0.156 mole) in a mixture of 150 ml 20% H_2SO_4 and 150 ml acetic acid was refluxed until the theoretical amount of carbon dioxide had evolved (4 h). After cooling, the solution was brought to pH 10 with NaOH, salted, and extracted with ether. The usual work-up and distillation yielded, after a small forerun, 20.15 g of ketone (82.7% yield). A sample that was redistilled for analysis had the following physical properties: b.p. 78° at 6 mm; $n_D^{25.3}$ 1.4426; infrared: $\lambda_{C=O}$ at 5.65 μ, λ_{C-O-C} at 9.38 μ.

Anal. Calcd. for $C_9H_{16}O_2$: C, 69.19; H, 10.32. Found: C, 68.95; H, 10.32.

3-n-Pentyl-2,3-dihydrofuran (IIb) and 3-n-Pentyl-2,5-dihydrofuran (IIIb)

The tosylhydrazone (m.p. 115–116°) of the above ketone was obtained in 80% yield by the usual procedure (13). Heating the solution of this derivative in diethylene glycol (in which sodium had previously been dissolved) according to the previously described procedure (13) gave a mixture of II*b* and III*b* (57.5% II*b* and 42.5% III*b*, by gas–liquid partition chromatography) in 94.3% yield. The mixture (b.p. 45–60° at 12.5 mm) was used as such for conversion into IV*b*; its components, separated from each other by preparative gas–liquid partition chromatography, had the physical properties given below.

3-n-Pentyl-2,3-dihydrofuran (IIb)

R_T 10.5 min; n_D^{28} 1.4372; infrared: 3.22 (w), 6.18 (s), 6.22 (m), 6.80 (s), 8.78 (vs), 10.83 μ (s); nuclear magnetic resonance: absorptions at δ = 0.88 (triplet, 3H), 1.28 (8H), 2.85 (broad signal, 1H), 3.65 to 4.45 (complex multiplet of sharp lines, 2H), 4.80 (triplet, 1H), 6.15 (triplet, 1H); mass spectrum: m/e = 69 (100%), 41 (17%), 140 (molecular ion, 9%), 39 (8%), 27 (6%), 70 (6%), 68 (5%).

Anal. Calcd. for $C_9H_{16}O$: C, 77.09; H, 11.50. Found: C, 76.85; H, 11.47.

3-n-Pentyl-2,5-dihydrofuran (IIIb)

R_T 14.2 min; n_D^{28} 1.4480; infrared: 6.00 (w), 6.80 (m), 9.30 (vs), 11.08 μ (vs); nuclear magnetic resonance: absorptions at δ = 0.91 (deformed triplet, 3H), 1.36 (band envelope, 6H), 2.08 (distorted triplet, 2H), 4.44 (complex multiplet, 4H), 5.4 (1H); mass spectrum: m/e = 69 (100%), 41 (96%), 55 (83%), 39 (53%), 29 (50%), 27 (48%), 56 (37%), 140 (molecular ion, 16%).

Anal. Calcd. for $C_9H_{16}O$: C, 77.09; H, 11.50. Found: C, 76.85; H, 11.59.

3-n-Pentylfuran (IVb)

To a stirred and cooled suspension of 2,3-dichloro-5,6-dicyano-1,4-benzoquinone (12.95 g, 0.057 mole) in anhydrous benzene (50 ml) was added, in small portions, the mixture of II*b* and III*b* described above (7.98 g, 0.057 mole). After the mixture was stirred for 1 h, it was centrifuged, the solid was washed with 250 ml pentane, and the combined solutions were passed through a 30 cm × 2 cm column of neutral alumina, which was then washed with more pentane. The bulk of the solvents was distilled off at normal pressure

Can. J. Chem. Downloaded from www.nrcresearchpress.com by 210.87.254.42 on 09/05/12
For personal use only.

through an efficient column. A vacuum was then applied and IV*b* was obtained in 52% yield as the fraction boiling at 77–79° and 83 mm (146–148° at 760 mm); R_T 9.1 min; $n_D^{25.5}$ 1.4445; infrared: 6.38 (w), 6.62 (m), 6.80 (m), 8.58 (s), 9.38 (m), 9.73 (s), 11.43 μ (s); mass spectrum: m/e = 82 (100%), 81 (50%), 95 (20%), 138 (molecular ion, 18%), 53 (11%), 27 (7%), 41 (7%).

Anal. Calcd. for $C_9H_{14}O$: C, 78.21; H, 10.21. Found: C, 78.37; H, 10.50.

4-n-Pentyl-2,3-dihydrofuran (Vb)

Heating the previously described (16) 3-*n*-pentyl-3-hydroxytetrahydrofuran (V*b*) over anhydrous $CuSO_4$ at 160–180° (bath temperature), while the dehydration products were being swept out in a stream of nitrogen through a short column, yielded a mixture containing 30% V*b* (see text). This compound, separated by preparative gas–liquid partition chromatography from the accompanying III*b* and from another unidentified substance (which co-chromatographs with III*b*), had the following physical properties: R_T 12.2 min; n_D^{25} 1.4452; nuclear magnetic resonance: absorptions at δ = 0.91 (distorted triplet, 3H), 1.10 to 1.70 (band envelope, 6H), 2.02 (2H), 2.47 (broadened triplet, 2H), 4.20 (triplet, 2H), 5.92 (1H); mass spectrum: m/e = 83 (100%), 55 (20%), 41 (17%), 140 (molecular ion, 12%), 27 (11%), 39 (10%).

Anal. Calcd. for $C_9H_{16}O$: C, 77.09; H, 11.50. Found: C, 77.00; H, 11.35.

1. F. M. Dean. Naturally occurring oxygen ring compounds. Butterworths, London. 1963.
2. A. P. Dunlop and F. N. Peters. The furans. Reinhold Publishing Corp., New York. 1953.
3. A. Quilico, F. Piozzi, and M. Pavan. Tetrahedron, **1**, 177 (1957).
4. A. Quilico, P. Grunanger, and F. Piozzi. Tetrahedron, **1**, 186 (1957).
5. T. Reichstein, A. Zschokke, and A. Georg. Helv. Chim. Acta, **14**, 1370 (1931).
6. A. J. Birch, R. A. Massey-Wintropp, S. E. Wright, K. Matsura, and H. D. Sutherland. Chem. Ind. London, 902 (1954).
7. T. Kubota and T. Matsura. Chem. Ind. London, 521 (1956).
8. P. Grunanger and F. Piozzi. Gazz. Chim. Ital. **89**, 897 (1959).
9. J. D. Prugh. Ph.D. Thesis, University of Washington, Seattle, Washington. 1964.
10. S. Gronowitz and G. Sorlin. Arkiv Kemi, **19**, 515 (1962).
11. H. Gilman and R. R. Burtner. J. Am. Chem. Soc. **55**, 2903 (1933).
12. E. Sherman and E. D. Amstutz. J. Am. Chem. Soc. **72**, 2195 (1950).
13. M. A. Gianturco, P. Friedel, and V. Flanagan. Tetrahedron Letters, **23**, 1847 (1965).
14. M. A. Gianturco, P. Friedel, and A. S. Giammarino. Tetrahedron, **20**, 1763 (1964).
15. H. Wynberg. J. Am. Chem. Soc. **80**, 364 (1957).
16. Yu. K. Yur'ev, E. M. Lukina, and T. K. Korobitsyna. Zh. Obshch. Khim. **24**, 1238 (1954).

Received November 8, 1965.
Fundamental Research Department,
The Coca-Cola Company,
Linden, New Jersey.

A GENERAL METHOD OF PREPARATION OF SUBSTITUTED 2-HYDROXY-1,4-QUINONES

T. R. Kasturi and T. Arunachalam

6-Methoxy-1-naphthol (I), required in connection with a projected synthesis of oxasteroids, has earlier been prepared in very low yield either by the dehydrogenation of 6-methoxy-1-tetralone (II) with sulfur (1) or by the diazotization of 6-methoxy-1-naphthylamine (III) (2, 3). Hence, an alternative simple and better method of preparation of I was desirable.[1]

Recently, Crowshaw and his co-workers (4) reported the conversion of an unsaturated cyclic ketone (IV) into the corresponding phenol (V) by treating the former with potassium *t*-butoxide in *t*-butanol, in an atmosphere of oxygen. Mechanistic considerations[2] suggested that a similar reaction with 6-methoxy-1-tetralone (II) may give rise to the naphthol I. When compound II was treated with potassium *t*-butoxide in *t*-butanol, in an atmosphere

[1]*We have already synthesized I by a simple method which will be published later.*
[2]*We thank Dr. N. A. J. Rogers of the University of Birmingham for helpful discussions.*

Can. J. Chem. Downloaded from www.nrcresearchpress.com by 210.87.254.42 on 09/05/12
For personal use only.

through an efficient column. A vacuum was then applied and IV*b* was obtained in 52% yield as the fraction boiling at 77–79° and 83 mm (146–148° at 760 mm); R_T 9.1 min; $n_D^{25.5}$ 1.4445; infrared: 6.38 (w), 6.62 (m), 6.80 (m), 8.58 (s), 9.38 (m), 9.73 (s), 11.43 μ (s); mass spectrum: m/e = 82 (100%), 81 (50%), 95 (20%), 138 (molecular ion, 18%), 53 (11%), 27 (7%), 41 (7%).

Anal. Calcd. for $C_9H_{14}O$: C, 78.21; H, 10.21. Found: C, 78.37; H, 10.50.

4-n-Pentyl-2,3-dihydrofuran (Vb)

Heating the previously described (16) 3-*n*-pentyl-3-hydroxytetrahydrofuran (V*b*) over anhydrous $CuSO_4$ at 160–180° (bath temperature), while the dehydration products were being swept out in a stream of nitrogen through a short column, yielded a mixture containing 30% V*b* (see text). This compound, separated by preparative gas–liquid partition chromatography from the accompanying III*b* and from another unidentified substance (which co-chromatographs with III*b*), had the following physical properties: R_T 12.2 min; n_D^{25} 1.4452; nuclear magnetic resonance: absorptions at δ = 0.91 (distorted triplet, 3H), 1.10 to 1.70 (band envelope, 6H), 2.02 (2H), 2.47 (broadened triplet, 2H), 4.20 (triplet, 2H), 5.92 (1H); mass spectrum: m/e = 83 (100%), 55 (20%), 41 (17%), 140 (molecular ion, 12%), 27 (11%), 39 (10%).

Anal. Calcd. for $C_9H_{16}O$: C, 77.09; H, 11.50. Found: C, 77.00; H, 11.35.

1. F. M. Dean. Naturally occurring oxygen ring compounds. Butterworths, London. 1963.
2. A. P. Dunlop and F. N. Peters. The furans. Reinhold Publishing Corp., New York. 1953.
3. A. Quilico, F. Piozzi, and M. Pavan. Tetrahedron, **1**, 177 (1957).
4. A. Quilico, P. Grunanger, and F. Piozzi. Tetrahedron, **1**, 186 (1957).
5. T. Reichstein, A. Zschokke, and A. Georg. Helv. Chim. Acta, **14**, 1370 (1931).
6. A. J. Birch, R. A. Massey-Wintropp, S. E. Wright, K. Matsura, and H. D. Sutherland. Chem. Ind. London, 902 (1954).
7. T. Kubota and T. Matsura. Chem. Ind. London, 521 (1956).
8. P. Grunanger and F. Piozzi. Gazz. Chim. Ital. **89**, 897 (1959).
9. J. D. Prugh. Ph.D. Thesis, University of Washington, Seattle, Washington. 1964.
10. S. Gronowitz and G. Sorlin. Arkiv Kemi, **19**, 515 (1962).
11. H. Gilman and R. R. Burtner. J. Am. Chem. Soc. **55**, 2903 (1933).
12. E. Sherman and E. D. Amstutz. J. Am. Chem. Soc. **72**, 2195 (1950).
13. M. A. Gianturco, P. Friedel, and V. Flanagan. Tetrahedron Letters, **23**, 1847 (1965).
14. M. A. Gianturco, P. Friedel, and A. S. Giammarino. Tetrahedron, **20**, 1763 (1964).
15. H. Wynberg. J. Am. Chem. Soc. **80**, 364 (1957).
16. Yu. K. Yur'ev, E. M. Lukina, and T. K. Korobitsyna. Zh. Obshch. Khim. **24**, 1238 (1954).

Received November 8, 1965.
Fundamental Research Department,
The Coca-Cola Company,
Linden, New Jersey.

A GENERAL METHOD OF PREPARATION OF SUBSTITUTED 2-HYDROXY-1,4-QUINONES

T. R. Kasturi and T. Arunachalam

6-Methoxy-1-naphthol (I), required in connection with a projected synthesis of oxasteroids, has earlier been prepared in very low yield either by the dehydrogenation of 6-methoxy-1-tetralone (II) with sulfur (1) or by the diazotization of 6-methoxy-1-naphthylamine (III) (2, 3). Hence, an alternative simple and better method of preparation of I was desirable.[1]

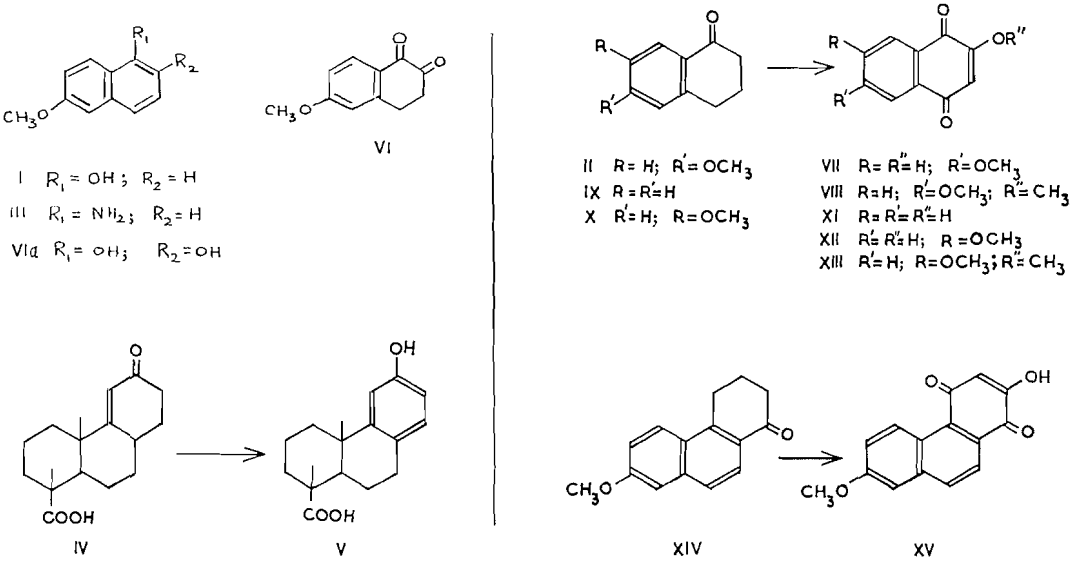
Recently, Crowshaw and his co-workers (4) reported the conversion of an unsaturated cyclic ketone (IV) into the corresponding phenol (V) by treating the former with potassium *t*-butoxide in *t*-butanol, in an atmosphere of oxygen. Mechanistic considerations[2] suggested that a similar reaction with 6-methoxy-1-tetralone (II) may give rise to the naphthol I. When compound II was treated with potassium *t*-butoxide in *t*-butanol, in an atmosphere

[1]*We have already synthesized I by a simple method which will be published later.*
[2]*We thank Dr. N. A. J. Rogers of the University of Birmingham for helpful discussions.*

Can. J. Chem. Downloaded from www.nrcresearchpress.com by 210.87.254.42 on 09/05/12
For personal use only.

of oxygen, it rapidly absorbed 2 moles of oxygen per mole of ketone II to give a high-melting, yellow, crystalline solid in 80% yield. This product was different from the expected naphthol I or the α-diketone[3] VI, which could presumably be isolated as 1,2-dihydroxy-6-methoxynaphthalene (VI*a*).

The above-mentioned yellow solid dissolved readily in sodium bicarbonate solution to give a red solution, and its elemental analysis corresponded to $C_{11}H_8O_4$. It showed peaks at 3 257 (enolic OH), 1 669 (C=O), 1 645 (C=C), and 840 and 794 cm^{-1} (trisubstituted double bond) in the infrared spectrum; in the electronic spectral region it showed λ_{max} at 278 and 294 mμ with high intensity, and a broad absorption around 380 mμ. In the presence of alkali the band at 380 mμ was shifted to a longer wavelength at 470 mμ which is characteristic of 2-hydroxy-1,4-quinones (8). The aforementioned solid, on methylation with diazomethane, gave the corresponding methyl ether, analyzed as $C_{12}H_{10}O_4$. Based on the foregoing data, the yellow solid was assigned the structure of 2-hydroxy-6-methoxy-1,4-naphthaquinone (VII), and the corresponding ether that shown by VIII.



The melting point of the yellow solid was undepressed on admixture with an authentic sample of VII prepared by an unambiguous method (9), and the infrared spectra of the two were superimposable. The authentic sample VII obtained by us via the method of Buu-Hoi and Cagniant (9) melted at 217–218°, though the melting point reported by these authors was only 197–200°.

With a view to finding out the generality of this reaction,[4] we carried out the oxygenation with α-tetralone (IX), 7-methoxy-1-tetralone (X), and 7-methoxy-1-keto-1,2,3,4-tetrahydrophenanthrene (XIV), when good yields of the corresponding quinones, viz. 2-hydroxy-1,4-naphthaquinone (XI), 2-hydroxy-7-methoxy-1,4-naphthaquinone (XII), and 2-hydroxy-7-methoxy-1,4-phenanthrequinone (XV), were obtained, as proved by the ultraviolet and infrared absorption data given in Table I. The spectral data of the methyl ethers VIII and XIII, corresponding to the 2-hydroxyquinones VII and XII, respectively, are also recorded in Table I.

[3]*Oxygenation of ketones under these conditions is known to give α-diketones (5–7).*

[4]*This reaction was not applied to cyclohexenone, as Dr. N. A. J. Rogers and his co-workers are presently engaged in this study (4).*

Can. J. Chem. Downloaded from www.nrcresearchpress.com by 210.87.254.42 on 09/05/12
For personal use only.

TABLE I

Infrared and electronic spectra of 2-hydroxy-1,4-quinone derivatives

Compound	Infrared (Nujol), ν_{max} (cm^{-1})	Electronic spectra in ethanol		Electronic spectra in ethanol + alkali	
		λ_{max} (mμ)	log ϵ	λ_{max} (mμ)	log ϵ
VII	3 257	278	4.2083	276	4.2072
	1 669	294	4.1921	293	4.1503
	1 645	380	3.0892	470	3.3096
	840				
	794				
XI	3 268	232	4.1354	270	4.3087
	1 681	270	4.3269	480	3.2223
	1 645	390	3.0329		
	806				
	787				
XII	3 300	264	4.3815	264	4.3898
	1 669	272	4.4109	272	4.4134
	1 640	292	3.8719	296	3.8695
	833	340	3.7279	345	3.7536
	800	450	2.8265	465	3.4922
VIII	1 672	266	4.2174	—	—
	1 653	292	4.1867		
	833	378	3.5203		
	794				
XIII	1 684	262	4.3217	—	—
	1 647	288	4.0503		
	840	334	3.4104		
	800				
XV	3 344	237	4.4947	238	4.4840
	1 661	302	4.2890	304	4.2752
	1 626	353	3.9753	358	3.9635
	826			500	2.8198
	794				

In agreement with the generality of this reaction, Anderson and his co-workers (10) have recently also reported the formation of 2-hydroxy-5,6,7,8-tetramethoxy-1,4-naphthaquinone under similar conditions from 5,6,7,8-tetramethoxy-1-tetralone in 28% yield. Therefore, we feel that this is a general and simple method for the preparation of 2-hydroxy-1,4-quinones.[5,6]

EXPERIMENTAL[7]

2-Hydroxy-6-methoxy-1,4-naphthaquinone (VII)

A solution of 0.704 g (0.004 mole) of 6-methoxy-1-tetralone (II) (11) in 10 ml of dry *t*-butanol was added to a solution of potassium *t*-butoxide prepared from 0.39 g (0.01 g-atom) of potassium in 12 ml of dry *t*-butanol; the resulting solution was stirred at room temperature in an atmosphere of oxygen for 2 h, at the end of which period the initial rapid absorption of oxygen had ceased. The absorption of oxygen corresponded to 2 moles per mole of II. The mixture was acidified with 4 *N* hydrochloric acid and then extracted with ether. The ether extract was washed with 10% sodium bicarbonate solution; the alkali extract, on acidification, gave 0.65 g (80%) of VII, which was crystallized from ethanol as yellow needles, m.p. 217–218° (lit. m.p. 197–200° (9)).

Anal. Calcd. for $C_{11}H_8O_4$: C, 64.70; H, 3.95. Found: C, 64.70; H, 3.99.

[5]*Prof. Thomson and his co-workers have also found this reaction to be a general one (private communication). We thank Prof. Thomson, Aberdeen, Scotland, for giving us this information before its publication, and also for his valuable comments on this manuscript.*

[6]*This oxygenation reaction may be a normal ketone autoxidation in basic solution in the presence of oxygen, and may proceed via the α-diketone VI.*

[7]*All melting points are uncorrected. The ultraviolet spectra were determined in ethanol on a Beckmann DU spectrophotometer. The infrared spectra were recorded with a Perkin–Elmer model 137 B infracord spectrophotometer. The microanalyses were carried out by Mr. B. R. Seetharamia of our department, and by the CIBA Research Centre, India.*

Can. J. Chem. Downloaded from www.nrcresearchpress.com by 210.87.254.42 on 09/05/12
For personal use only.

The above reaction was repeated with 0.704 g (0.004 mole) of 6-methoxy-1-tetralone (II) in 10 ml of *t*-butanol containing potassium *t*-butoxide (0.005 mole) prepared from 0.19 g of potassium and 6 ml of *t*-butanol; 0.308 g (37.8%) of VII, m.p. 217–218°, and 0.325 g of II, m.p. 76–77°, were obtained.

2-Hydroxy-1,4-naphthaquinone (XI)

A solution of 0.292 g (0.002 mole) of α-tetralone (IX) in 5 ml of dry *t*-butanol was added to a solution of potassium *t*-butoxide prepared from 0.234 g (0.006 g-atom) of potassium in 8 ml of dry *t*-butanol; the reaction was carried out as before to give 0.215 g (61.8%) of XI, which was crystallized from ethanol as brown needles, m.p. 190–191° (lit. m.p. 188–190° (12)).

Anal. Calcd. for $C_{10}H_6O_3$: C, 68.96; H, 3.47. Found: C, 68.93; H, 3.73.

2-Hydroxy-7-methoxy-1,4-naphthaquinone (XII)

The foregoing oxygenation was carried out with 0.704 g (0.004 mole) of 7-methoxy-1-tetralone (X) (13), in a solution of potassium *t*-butoxide prepared from 0.39 g of potassium in 12 ml of dry *t*-butanol, to yield 0.61 g (74.8%) of XII, which was crystallized from ethanol as light-brown needles, m.p. 214–215° (lit. m.p. 214° (14), 220–222° (15)).

Anal. Calcd. for $C_{11}H_8O_4$: C, 64.70; H, 3.95. Found: C, 64.75; H, 3.94.

2-Hydroxy-7-methoxy-1,4-phenanthrequinone (XV)

The above reaction was repeated with a solution of 0.340 g of 7-methoxy-1-keto-1,2,3,4-tetrahydrophenanthrene (XIV) (16) in 5 ml of *t*-butanol, in the presence of a solution of potassium *t*-butoxide prepared from 0.156 g of potassium in 6 ml of dry *t*-butanol, to yield 0.3 g (78%) of XV (9),[8] which was crystallized from ethanol as orange needles, m.p. 226–227°.

Anal. Calcd. for $C_{15}H_{10}O_4$: C, 70.86; H, 3.96. Found: C, 70.81; H, 3.98.

2,6-Dimethoxy-1,4-naphthaquinone (VIII)

An ethereal solution of diazomethane, prepared from 0.5 g of nitrosomethylurea, was added to a chilled solution of 0.204 g of VII with occasional swirling, and the mixture was left at 0° for 0.5 h. The excess of diazomethane was decomposed with acetic acid, and the ether layer was separated and washed with 5% sodium hydroxide and water. Removal of the ether gave 0.2 g (91%) of VIII, which was crystallized from ethanol as yellow needles, m.p. 232–233°.

Anal. Calcd. for $C_{12}H_{10}O_4$: C, 66.05; H, 4.62. Found: C, 66.11; H, 4.71.

2,7-Dimethoxy-1,4-naphthaquinone (XIII)

Similarly, 0.204 g of XII was methylated with an ethereal solution of diazomethane to give 0.2 g (91%) of XIII, which was crystallized from ethanol as light-brown needles, m.p. 217–218°.

Anal. Calcd. for $C_{12}H_{10}O_4$: C, 66.05; H, 4.62. Found: C, 66.25; H, 4.74.

ACKNOWLEDGMENTS

The authors thank Prof. D. K. Banerjee for his keen interest in this problem and for his helpful suggestions. We are grateful to Dr. T. R. Govindachari of the CIBA Research Centre for providing the microanalytical data of a few compounds reported here. We also thank Dr. S. R. Ramadas for helpful discussions. One of the authors (T. A.) thanks the Indian Institute of Science, Bangalore, for the award of a predoctorate fellowship.

1. A. J. Shand and R. H. Thomson. Tetrahedron, **19**, 1919 (1963).
2. G. Schroeter. Ber. **63**, 1308 (1930).
3. R. J. W. Byrde, D. F. Downing, and D. Woodcock. Biochem. J. **72**, 344 (1959).
4. K. Crowshaw, R. C. Newstead, and N. A. J. Rogers. Tetrahedron Letters, **33**, 2307 (1964).
5. E. J. Bailey, D. H. R. Barton, J. Elks, and J. F. Templeton. J. Chem. Soc. 1578 (1962). D. H. R. Barton and D. W. Jones. J. Chem. Soc. 3563 (1965).
6. H. R. Nace. J. Org. Chem. **29**, 1677 (1964).
7. G. A. Russell and E. R. Talaty. Science, **148**, 1217 (1965). G. A. Russell and E. T. Strom. J. Am. Chem. Soc. **86**, 744 (1964). G. A. Russell and E. R. Talaty. J. Am. Chem. Soc. **86**, 5345 (1964).
8. G. Patterson. Acta Chem. Scand. **18**, 2303 (1964).
9. Buu-Hoi and P. Cagniant. Compt. Rend. **214**, 87 (1942).
10. H. A. Anderson, J. Smith, and R. H. Thomson. J. Chem. Soc. 2141 (1965).
11. G. Stork. J. Am. Chem. Soc. **69**, 576 (1947).
12. P. Pfeiffer and T. Hesse. J. Prakt. Chem. **158**, 315 (1941).
13. H. Plimmer, W. F. Short, and P. Hill. J. Chem. Soc. 694 (1938).
14. J. F. Garden and R. H. Thomson. J. Chem. Soc. 2483 (1957).
15. L. F. Fieser and R. H. Brown. J. Am. Chem. Soc. **71**, 3615 (1949).
16. G. Stork. J. Am. Chem. Soc. **69**, 2936 (1947).

Received December 6, 1965.
Department of Organic Chemistry,
Indian Institute of Science,
Bangalore, India.

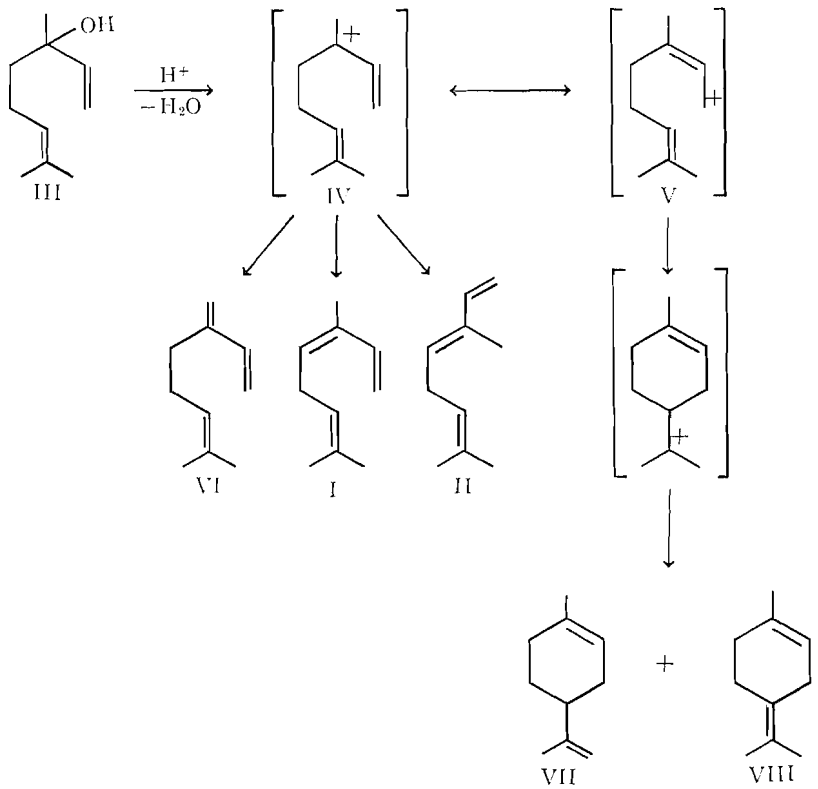
[8]*The authors have not reported the melting point of XV.*

Can. J. Chem. Downloaded from www.nrcresearchpress.com by 210.87.254.42 on 09/05/12
For personal use only.

PREPARATION OF *cis*- AND *trans*-OCIMENE FROM CATALYTIC PYROLYSIS OF LINALYL ACETATE

BERNARD M. MITZNER,[1] SEYMOUR LEMBERG, AND ERNST T. THEIMER

cis-Ocimene (I) and *trans*-ocimene (II) have recently been reported as occurring in nature (1, 2).[2] They can be prepared in the laboratory by the acid-catalyzed dehydration of linalool (III), presumably by the mechanism shown in Reaction Scheme 1. This rationale allows for formation of dipentene (VII), myrcene (VI), and terpinolene (VIII). The products of a typical linalool dehydration are shown in Table I.



REACTION SCHEME 1.

Unfortunately, the dehydration of linalool is not a practical method for the preparation of quantities of pure *cis*- and *trans*-ocimene, since it is extremely difficult to separate the ocimene from the dipentene via distillation.

The thermal pyrolysis of linalyl acetate (IX) has been investigated by the authors, but temperatures in excess of 300° are necessary to crack the ester, and under these

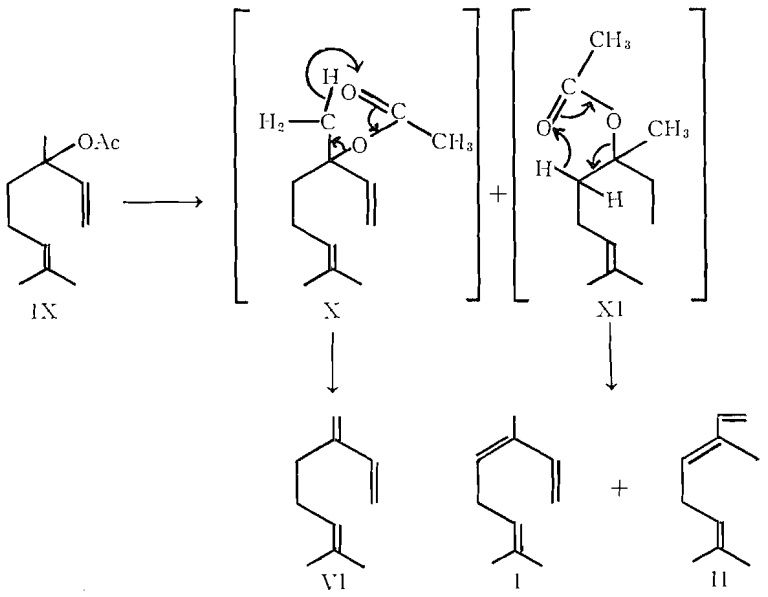
[1]*Present address: International Flavors & Fragrances Inc., 521 W 57th St., New York, New York.*
[2]*Unreported work performed in 1959 in the laboratories of International Flavors & Fragrances Inc., Union Beach, New Jersey.*

Can. J. Chem. Downloaded from www.nrcresearchpress.com by 210.87.254.5 on 09/05/12
For personal use only.

TABLE I

Linalool dehydration		Linalyl acetate pyrolysis	
Compound	%	Compound	%
Myrcene (VI)	32.3	Myrcene (VI)	43
Dipentene (VII)	23.3	*cis*-Ocimene (I)	20
cis-Ocimene (I)	13.7	*trans*-Ocimene (II)	35
trans-Ocimene (II)	25.5	Dipentene (VII)	2 (approximately)
Terpinolene (VIII)	5.3		

conditions the *cis*-ocimene is quickly converted into alloocimene (3) and relatively large quantities of dipentene are formed. We have, however, developed a catalytic pyrolysis procedure that allows linalyl acetate, in the vapor state and in contact with acid-washed Chromosorb, to undergo catalytic pyrolysis. The path of the reaction can be rationalized as shown in Reaction Scheme 2. By this proposed mechanism, myrcene (VI), *cis*-ocimene



REACTION SCHEME 2.

(I), and *trans*-ocimene (II) are formed as the major products. The actual percentages of terpenes are recorded in Table I.

EXPERIMENTAL

Catalytic Pyrolysis

The thermal catalytic pyrolysis of linalyl acetate is carried out by passing linalyl acetate through a copper tube ($\frac{3}{4}$ inch outside diameter × $\frac{11}{16}$ inch inside diameter, packed with 40–60 mesh Chromosorb P (acid washed and supplied by Johns–Manville Co.), and heated to 140 °C) at a rate of 5 ml/min, with a nitrogen flow rate of 250 ml/min. The resulting pyrolysate is neutralized with K_2CO_3 and distilled via a 4 ft protruded packed column.

Gas chromatographic measurements were carried out with a copper column ($\frac{1}{4}$ inch outside diameter × $\frac{3}{16}$ inch inside diameter, 10 ft long, and packed with 10% Carbowax 20M on 60–80 mesh silane-treated Celite) at a column temperature of 100 °C and an inlet pressure of 20 p.s.i., with a helium flow rate of 90 ml/min.

Procedure temperatures of only 140–150 °C are required.

Can. J. Chem. Downloaded from www.nrcresearchpress.com by 210.87.254.5 on 09/05/12
For personal use only.

Because of the relatively low amount of dipentene formed (approximately 2%) quantities of *cis*- and *trans*-ocimene can be prepared as described and can be distilled pure. (See Fig. 1 for a comparison of the vapor phase chromatographic curves of the dehydration and pyrolysis.)

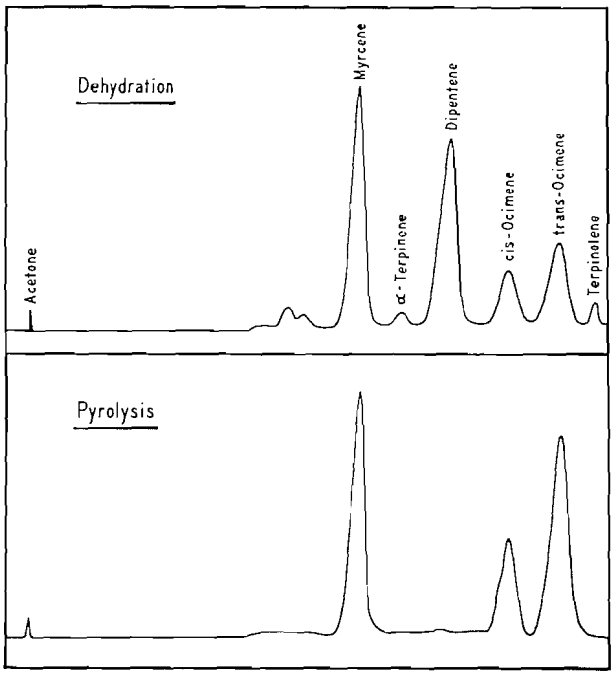


FIG. 1. Gas–liquid chromatographic comparison of the elimination reactions.

Dehydration of Linalool

A mixture of 175 g $KHSO_4$ (analytical grade) and 3 000 g linalool (99% pure as indicated by vapor phase chromatography) was heated and stirred at 128–160 °C liquid temperature, under a vacuum of 150 mm Hg, in a flask fitted with a thermometer, stirrer, and 6 inch distillation column. In this manner, 2 715 g of oil and 278 g of water were collected. The oil was fractionated via a 28 inch P.P. column; the ocimene-rich section, b.p. 70–72 °C at 60 mm Hg, n_D^{20} 1.478, amounted to 773 g and had the analysis shown in Table I.

1. Y. R. NAVES and P. TULLEN. Helv. Chim. Acta, **43**, 1619 (1960); **44**, 316 (1961).
2. H. FARNOW and F. PORSCH. Dragoco Rept. **8**, 75 (1961).
3. J. WOLINSKY, B. CHOLLAR, and M. D. BAIRD. J. Am. Chem. Soc. **84**, 2775 (1962).

RECEIVED OCTOBER 14, 1965.
INTERNATIONAL FLAVORS & FRAGRANCES INC.,
UNION BEACH, NEW JERSEY.

SYNTHESIS OF CHLORINATED 2-(3-BENZOFURANYL)PHENOLS

E. C. M. COXWORTH

An interest in *o*-hydroxybenzophenones prompted us to repeat the reaction of β,β-dichloro-α,α-bis(3,5-dichloro-2-hydroxyphenyl)ethane with potassium hydroxide in refluxing methanol, which was reported by Riemschneider and his co-workers (1) to

Can. J. Chem. Downloaded from www.nrcresearchpress.com by 210.87.254.5 on 09/05/12
For personal use only.

Because of the relatively low amount of dipentene formed (approximately 2%) quantities of *cis*- and *trans*-ocimene can be prepared as described and can be distilled pure. (See Fig. 1 for a comparison of the vapor phase chromatographic curves of the dehydration and pyrolysis.)

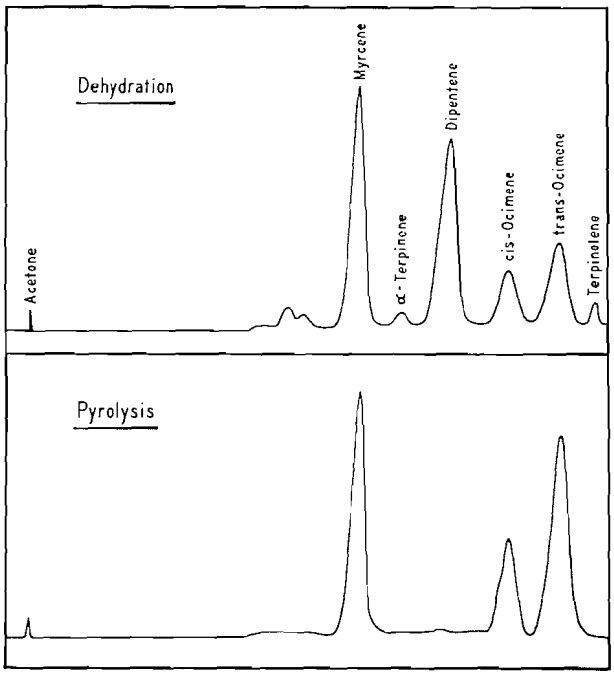


FIG. 1. Gas–liquid chromatographic comparison of the elimination reactions.

Dehydration of Linalool

A mixture of 175 g $KHSO_4$ (analytical grade) and 3 000 g linalool (99% pure as indicated by vapor phase chromatography) was heated and stirred at 128–160 °C liquid temperature, under a vacuum of 150 mm Hg, in a flask fitted with a thermometer, stirrer, and 6 inch distillation column. In this manner, 2 715 g of oil and 278 g of water were collected. The oil was fractionated via a 28 inch P.P. column; the ocimene-rich section, b.p. 70–72 °C at 60 mm Hg, n_D^{20} 1.478, amounted to 773 g and had the analysis shown in Table I.

1. Y. R. NAVES and P. TULLEN. Helv. Chim. Acta, **43**, 1619 (1960); **44**, 316 (1961).
2. H. FARNOW and F. PORSCH. Dragoco Rept. **8**, 75 (1961).
3. J. WOLINSKY, B. CHOLLAR, and M. D. BAIRD. J. Am. Chem. Soc. **84**, 2775 (1962).

RECEIVED OCTOBER 14, 1965.
INTERNATIONAL FLAVORS & FRAGRANCES INC.,
UNION BEACH, NEW JERSEY.

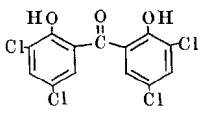
SYNTHESIS OF CHLORINATED 2-(3-BENZOFURANYL)PHENOLS

E. C. M. COXWORTH

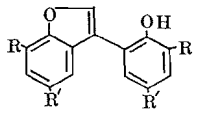
An interest in *o*-hydroxybenzophenones prompted us to repeat the reaction of β,β-dichloro-α,α-bis(3,5-dichloro-2-hydroxyphenyl)ethane with potassium hydroxide in refluxing methanol, which was reported by Riemschneider and his co-workers (1) to

Can. J. Chem. Downloaded from www.nrcresearchpress.com by 210.87.254.105 on 09/05/12
For personal use only.

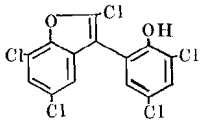
yield 2,2′-dihydroxy-3,3′,5,5′-tetrachlorobenzophenone (I). The product we obtained (A) conformed with that of Riemschneider with respect to melting point and the melting points of its acetate and its methyl ether. However, the analytical and spectroscopic data led us to conclude that the product A is actually 2-(5,7-dichloro-3-benzofuranyl)-4,6-dichlorophenol (II*a*).



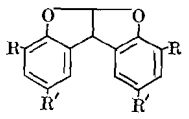
I



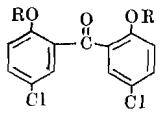
II a R=R′=Cl
II b R=H, R′=Cl



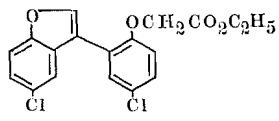
III



IV a R=R′=Cl
IV b R=H, R′=Cl



V a R=$CH_2CO_2C_2H_5$
V b R=CH_2CO_2H



VI

The following evidence led us to the conclusion that A has structure II*a* and not structure I.

(*i*) The analytical data for the experimental product A and its acetate and methyl ether are in good agreement with those for II*a* and its derivatives; they do not agree with those for I and its derivatives. Riemschneider and his co-workers (1) found a percentage chlorine for A close to the calculated value for I, but since II*a* has a similar percentage chlorine, this analytical data will not distinguish between the two structures.

(*ii*) The nuclear magnetic resonance spectrum of the acetate of A had peaks at 7.89 τ (singlet, 3H), 2.61 τ (doublet, 2H), 2.49 τ (triplet, 2H), and 2.22 τ (singlet, 1H). On the basis of the acetate of structure II*a* these peaks may be assigned, respectively, to an acetate CH_3, benzene H's, benzene H's, and the H on the α-carbon of the furan ring. The diacetate of structure I would be expected to show peaks for six acetate H's and four benzene H's, and no other peaks.

(*iii*) The ultraviolet spectrum of A showed λ_{max} 296, 287, and 253 mμ, but there was no absorption in the region 325–450 mμ where *o*-hydroxybenzophenones have been reported (2) to show a strong absorption maximum. In corroboration of this, a sample of 5,5′-dichloro-2,2′-dihydroxybenzophenone (3) had λ_{max} 344, 259, and 223 mμ. (Attempts to synthesize 2,2′-dihydroxy-3,3′,5,5′-tetrachlorobenzophenone by the unambiguous route (3) used to synthesize 5,5′-dichloro-2,2′-dihydroxybenzophenone were not successful.)

(*iv*) The infrared spectrum of A had absorption bands at 1 610 and 1 582 cm^{-1} but only of medium intensity, and a sharp band in the OH stretching region at 3 500 cm^{-1} suggestive of an unchelated phenolic hydroxyl group. In contrast, 5,5′-dichloro-2,2′-dihydroxybenzophenone had an intense, broad band at 1 630 – 1 615 cm^{-1} (both the position and intensity being typical of chelated *o*-hydroxyphenyl ketones (4)), and a broad hydroxyl peak at 3 340 cm^{-1}.

When the literature was now checked for references concerning the synthesis of 2-(3-benzofuranyl)phenols, it was found that Riemschneider and Lange (5) had reported recently that treatment of α,α-bis(3,5-dichloro-2-hydroxyphenyl)-β,β,β-trichloroethane

Can. J. Chem. Downloaded from www.nrcresearchpress.com by 210.87.254.105 on 09/05/12
For personal use only.

with refluxing aqueous potassium hydroxide gave the potassium salt of 4,6-dichloro-2-(2,5,7-trichloro-3-benzofuranyl)phenol (III). However, in their report, no mention was made of previous reactions of this kind.

One other relevant synthesis of 2-(3-benzofuranyl)phenols was noted. Dischendorfer (6) had reported that treatment of the inner acetal of bis(2-hydroxy-1-naphthyl)acetaldehyde with hot alcoholic sodium hydroxide, or with acetic acid containing hydrochloric acid, gave 4-(2-hydroxy-1-naphthyl)naphtho[2′,1′,2,3]furan. Now, in the original paper which prompted our investigation, Riemschneider (1) had reported that the phenolic product A mentioned previously could also be obtained by treatment of the inner acetal of bis(3,5-dichloro-2-hydroxyphenyl)acetaldehyde (IV*a*) with either hot alcoholic potassium hydroxide or hot 10% sulfuric acid. Our proposal that the phenolic product A has the structure II*a* thus makes the reactions of the acetal IV*a* with acid or base analogous to the reactions described by Dischendorfer (6). The inner acetal IV*a* was obtained by treating β,β-dichloro-α,α-bis(3,5-dichloro-2-hydroxyphenyl)ethane with cold alcoholic potassium hydroxide (1). The acetal may thus be considered a possible intermediate in the reaction of this dichloroethane compound with hot alcoholic potassium hydroxide, which leads directly to II*a*.

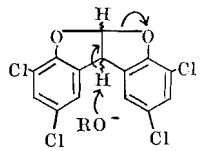
Since II*a* could not be prepared by the unambiguous route of Moshfegh *et al.* (3), it was of interest to determine the effect of hot alcoholic potassium hydroxide on the known acetal IV*b* (1), since the product from this reaction could be compared directly with the available 5,5′-dichloro-2,2′-dihydroxybenzophenone. The benzophenone was not obtained from this reaction; the product (B) which was obtained is considered to be the benzofuranyl phenol II*b*, on the basis of analytical and spectroscopic data (see Experimental section). The structure of II*b* was proven by the independent synthesis of the carbethoxymethyl ether in the following fashion, the method of approach being modelled on the work of Johnson and Robertson (7):

The reaction of 5,5′-dichloro-2,2′-dihydroxybenzophenone (3) with ethyl bromoacetate gave the diester V*a*, which was converted readily into the diacid V*b*. Ring closure of V*b* was effected by heating the diacid in acetic anhydride containing sodium acetate. The crude product from the ring closure, apparently a mixture of anhydride and acid (ν 1 850 and 1 780 cm^{-1}, with a prominent shoulder at 1 750 cm^{-1}), was converted directly into the desired ethyl ester by refluxing in ethylene chloride containing ethanol and a trace of toluenesulfonic acid. The ethyl ester VI so obtained was identical (by mixed melting point and infrared spectrum) with the product obtained by treating the experimental product B with ethyl bromoacetate.

The reactions of acetals such as IV*a* with acids to yield enol ethers, of which II*a* would be a special type, are well known (10). However, the reactions of acetals with bases, as exemplified by the transformation IV*a* → II*a* (as the potassium salt), seems more unusual, since acetals are generally considered not to react with bases. Some ethers have been reported to undergo E2-type elimination reactions in the presence of strong bases such as NaPh in aprotic solvents (11), but the types of base and solvent are quite different from the reagents employed in the reactions under consideration here. It is suggested that a possible mechanism for these base–acetal reactions is a normal E2 elimination process, which would be favored in this type of acetal by the following characteristics: the considerable acidity of the β-hydrogen, the stabilization of the incipient double bond by the benzofuran system being formed, the ease of accommodation of the negative charge on the leaving phenoxide ion, and the favorable geometry. By analogy to the physostigmine ring system (12), the ring fusion between the two dihydrofuran rings in acetals such as IV*a*

Can. J. Chem. Downloaded from www.nrcresearchpress.com by 210.87.254.105 on 09/05/12
For personal use only.

is probably *cis*. Thus the β-hydrogen and the acetal oxygen would be in a *trans* relationship to each other, favorable for an E2 elimination to occur.



Further work on the reaction of these types of acetals with base is in progress. This will include attempts to distinguish between the E2 elimination process and the alternative E1*cb* process.

EXPERIMENTAL

The infrared spectra were all recorded as Nujol mulls. The ultraviolet spectra were measured in methanol. The nuclear magnetic resonance spectra were all taken in carbon tetrachloride, with tetramethylsilane as internal standard. Melting points are uncorrected.

Reaction of β,β-Dichloro-α,α-bis(3,5-dichloro-2-hydroxyphenyl)ethane with Potassium Hydroxide in Refluxing Methanol

This reaction was carried out as described by the previous authors (1). The product obtained (A) had m.p. 185–187° (reported (1) m.p. 185–186°).

Anal. Calcd. for $C_{13}H_6Cl_4O_3$ (I): C, 44.40; H, 1.72. Calcd. for $C_{14}H_6Cl_4O_2$ (II*a*): C, 48.31; H, 1.73. Found: C, 48.16; H, 1.83.

The acetate of A had m.p. 128.5–130.5° (reported (1) m.p. 126°).

Anal. Calcd. for $C_{17}H_{10}Cl_4O_5$ (diacetate of I): C, 46.9; H, 2.31; mol. wt. 436. Calcd. for $C_{16}H_8Cl_4O_3$ (acetate of II*a*): C, 49.26; H, 2.06; mol. wt. 390. Found: C, 49.37; H, 2.21; mol. wt. 402.

The methyl ether of A had m.p. 107.5–108.5° (reported (1) m.p. 107°).

Anal. Calcd. for $C_{15}H_{10}Cl_4O_3$ (dimethyl ether of I): C, 47.4; H, 2.65. Calcd. for $C_{15}H_8Cl_4O_2$ (methyl ether of II*a*): C, 49.8, H, 2.22. Found: C, 49.6; H, 2.40.

The nuclear magnetic resonance spectrum of the methyl ether of A showed peaks at 6.40 τ (singlet, 3H), 2.57 τ (multiplet, 3H), 2.41 τ (doublet, 1H), and 1.97 τ (singlet, 1H). On the basis of the methyl ether of II*a*, these peaks were assigned, respectively, to a methoxy CH_3, benzene H's, a benzene H, and the H on the α-carbon of the furan ring.

Reaction of the Inner Acetal IVb with Potassium Hydroxide (Preparation of B)

The inner acetal IV*b* was prepared as described by previous authors (1). The acetal (0.584 g) in ethylene glycol (9.0 g) containing potassium hydroxide (1 g) was heated at 100–115° for 3 h with occasional swirling. The resultant clear yellow solution was cooled and diluted with water (30 ml), and the solution was filtered. The filtrate was acidified with hydrochloric acid and the resultant oil extracted with benzene. The benzene solution was washed three times with water, and then film evaporated to remove benzene and moisture. The residue was a viscous oil (0.586 g) that crystallized to a product of m.p. 80–92°. Recrystallization from *n*-hexane gave prisms, m.p. 89–91°, but further crystallizations from *n*-hexane gave needles, m.p. 109.5–110° (B). The compound had the following ultraviolet spectrum: λ_{max} 293 (ε 8 200), 285 (ε 7 400), 260 (ε 12 800), 254 (ε 15 000), 248 (ε 14 950), and 242 mμ (ε 15 800); λ_{min} 289 (ε 6 900), 278 (ε 6 490), 259 (ε 12 300), 252 (ε 13 800), and 246 mμ (ε 14 000). The general shape of this spectrum was similar to that of the spectrum of II*a*. The infrared spectrum showed peaks at 1 619, 1 600, 1 580, and 3 520 cm^{-1}, all of medium intensity.

Anal. Calcd. for $C_{14}H_8O_2Cl_2$ (II*b*): C, 60.23; H, 2.88. Found: C, 60.46; H, 3.13.

The acetate was prepared by refluxing product B for 3 h in acetic anhydride containing sodium acetate. The acetate of B had m.p. 119–120°; the nuclear magnetic resonance spectrum of the acetate had peaks at 8.04 τ (singlet, 3H), 2.41–2.98 τ (multiplet, 6H), and 2.31 τ (singlet, 1H), assigned, respectively, on the basis of the acetate of II*b*, to an acetate CH_3, benzene H's, and the H on the α-carbon of the furan ring.

Anal. Calcd. for $C_{16}H_{10}O_3Cl_2$ (acetate of II*b*): C, 59.8; H, 3.14. Found: C, 59.6; H, 3.16.

The carbethoxymethyl ether of B was prepared by the same method as was used to prepare V*a*. The product had m.p. 132–133°, mixed m.p. with authentic VI 131.5–133.5°. The infrared spectrum was identical with that of VI.

5,5′-Dichloro-2,2′-dihydroxybenzophenone

The procedures and relative molar quantities of reagents that were used were according to the method of Moshfegh *et al.* (3). However, the methyl ether was used instead of the ethyl ether as a protecting group. Thus, 5,5′-dichloro-2,2′-dihydroxydiphenylmethane was converted into 5,5′-dichloro-2,2′-dimethoxydiphenylmethane (8), which was oxidized to 5,5′-dichloro-2,2′-dimethoxybenzophenone (9). The dimethoxy-

Can. J. Chem. Downloaded from www.nrcresearchpress.com by 210.87.254.105 on 09/05/12
For personal use only.

benzophenone was demethylated to give the desired 5,5′-dichloro-2,2′-dihydroxybenzophenone, m.p. 151.5–153.5° (reported (2) m.p. 152–155°); λ_{max} 344, 259, and 223 mμ; λ_{min} 290 and 245 mμ.

5,5′-Dichloro-2,2′-dihydroxybenzophenone, Bis(carbethoxymethyl Ether) (Va)

In 100 ml dry acetone were placed 5,5′-dichloro-2,2′-dihydroxybenzophenone (2.69 g, 0.0095 mole), ethyl bromoacetate (5.0 g, 0.030 mole), and freshly ground anhydrous potassium carbonate (8.3 g, 0.060 mole). The mixture was refluxed, with the exclusion of atmospheric moisture, for 5 h. The reaction mixture was cooled and filtered, and the filtrate was film evaporated to remove the acetone. The residue from the film evaporation was dissolved in diethyl ether (40 ml) and filtered to remove the insoluble material; the insoluble material was washed with diethyl ether (10 ml). The combined filtrates were film evaporated to remove the solvents. The gummy residue from the film evaporation was stirred with *n*-hexane (20 ml) to yield a white solid, which was removed by filtration, washed with *n*-hexane, and dried to yield 3.14 g (73.5%) of *Va*, m.p. 86.5–87.5°. Recrystallization from *n*-hexane gave colorless plates, m.p. 88.5–89.5°, ν 1 770 and 1 675 cm^{-1}.

Anal. Calcd. for $C_{21}H_{20}Cl_2O_7$: C, 55.39; H, 4.42. Found: C, 55.30; H, 4.47.

5,5′-Dichloro-2,2′-dihydroxybenzophenone, Bis(carboxymethyl Ether) (Vb)

The diester *Va* (2.63 g, 0.0058 mole) was refluxed for 45 min in a mixture of ethanol (100 ml) and water (70 ml) containing potassium hydroxide (4.5 g). The solution was then film evaporated to remove most of the ethanol. After removal of the ethanol the solution was cooled, filtered, and extracted once with diethyl ether. The aqueous layer was then acidified with dilute hydrochloric acid to precipitate the product as a white solid. The product was removed by filtration, washed with water, and dried to yield 2.14 g (93%) of *Vb*, m.p. 217–218°, ν 1 752 (intense shoulder at 1 729) and 1 684 cm^{-1}. Recrystallization from ethanol–water gave material of m.p. 218–221°.

Anal. Calcd. for $C_{17}H_{12}Cl_2O_7$: C, 51.14; H, 3.03. Found (crude product): C, 51.34; H, 3.37.

Ring Closure of Vb and Preparation of 2-(5-Chloro-3-benzofuranyl)-4-chlorophenol Carbethoxymethyl Ether (VI)

The diacid *Vb* (2.03 g, 0.0051 mole), acetic anhydride (20 ml), and fused sodium acetate (5.0 g) were mixed, and the mixture was then refluxed (bath temperature 150–155°) for 50 min. After the reaction mixture was cooled, it was poured into water (200 ml) and stirred for 2 h. The white precipitate so formed was removed by filtration, washed with water, and dried. This material (1.86 g) had m.p. 85–98°; ν 1 850 and 1 780 (anhydride) with a prominent shoulder at 1 750 (acid), and 1 619 and 1 576 cm^{-1}, no bands between 1 750 – 1 620 cm^{-1}. The product was partially soluble in dilute sodium hydroxide.

The crude product (0.45 g) was dissolved in ethylene dichloride (10 ml) containing ethanol (1.3 ml) and toluenesulfonic acid (30 mg), and the solution refluxed for 6 h. The solution was cooled, diluted with chloroform, washed with water and then sodium bicarbonate, and dried over sodium sulfate. Film evaporation left a crystalline product, 0.41 g, m.p. 125–131°. Recrystallization from *n*-hexane gave VI, m.p. 132–133°; ν 1 759, 1 618, and 1 572 cm^{-1}.

Anal. Calcd. for $C_{18}H_{14}Cl_2O_4$ (VI): C, 59.19; H, 3.86. Found: C, 58.96; H, 3.98.

ACKNOWLEDGMENTS

The author is indebted to Dr. J. D. Davis for determining and interpreting the nuclear magnetic resonance spectra. Microanalyses were performed by the Prairie Regional Laboratories of the National Research Council.

1. R. Riemschneider, I. Ahrlé, W. Cohnen, and E. Heilman. Chem. Ber. **92**, 900 (1959).
2. J. Van Allen and J. F. Tinker. J. Org. Chem. **19**, 1243 (1954).
3. A. Moshfegh, S. Fallab, and H. Erlenmeyer. Helv. Chim. Acta, **40**, 1157 (1957).
4. L. J. Bellamy. Infra-red spectra of complex molecules. Methuen & Co., Ltd., London. 1958.
5. R. Riemschneider and D. Lange. Chem. Ber. **97**, 300 (1964).
6. O. Dischendorfer. Monatsh. **73**, 45 (1940).
7. P. C. Johnson and A. Robertson. J. Chem. Soc. 2381 (1950).
8. H. E. Faith. J. Am. Chem. Soc. **72**, 837 (1950).
9. A. S. Hussey and I. J. Wilk. J. Am. Chem. Soc. **72**, 830 (1950).
10. Chem. Abstr. **54**, 19534 (1960); **55**, 7288 (1961); **55**, 27030 (1961).
11. D. V. Banthorpe. Elimination reactions. Elsevier Pub. Co., Ltd., London. 1963. p. 99.
12. B. Robinson. Chem. Ind. London, 218 (1963).

Received December 8, 1965.
Chemistry Division,
Saskatchewan Research Council,
Saskatoon, Saskatchewan.

Can. J. Chem. Downloaded from www.nrcresearchpress.com by 210.87.254.105 on 09/05/12
For personal use only.

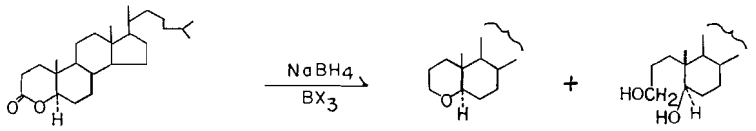
STEROIDS AND RELATED NATURAL PRODUCTS XXIX. SODIUM BOROHYDRIDE – BORON TRIHALIDE REDUCTION OF 3-OXO-4-OXA-5α-CHOLESTANE[1]

GEORGE R. PETTIT[2] AND WILLIAM J. EVERS

A variety of esters have conveniently been reduced to the corresponding ether derivatives by a complex metal hydride – boron trifluoride (1) or diborane – boron trifluoride (1*g*) reagent. In the metal hydride procedure, the required diborane was generated from a large excess of boron trifluoride. Since the generally useful Lewis acid, aluminium chloride, in combination with sodium borohydride, failed (1*g*) to effect ester → ether conversion, it was desirable to determine whether other boron halides would replace or prove to be superior to boron trifluoride. To explore this area, 3-oxo-4-oxa-5α-cholestane (I) was again (1*g*) selected for model experiments.

Reduction of lactone I to 4-oxa-5α-cholestane (II) was previously accomplished with lithium aluminium hydride – boron trifluoride (1*g*, 1*i*).[3] Here, the more practical sodium borohydride – boron trifluoride procedure (1*e*) was first utilized for transforming lactone I into tetrahydropyran II. Reduction was conducted during a 2 h period at ice-bath temperature to approximate the conditions that were anticipated to be necessary with boron tribromide and boron triiodide. Depending on the mode of initiating the reaction, yields of pure tetrahydropyran II varied from 44 to 58%. The best conversion into ether II was obtained by adding the lactone – boron trifluoride mixture to the hydride (see ref. 1*e*).

Under similar conditions, with boron trichloride in place of the trifluoride, the yields of ether II varied from 3 to 64%. When the reduction was repeated with boron tribromide and again with boron triiodide, conditions approximating those giving the poorest result (hexane–diglyme solvent system) with boron trichloride were used to decrease the concomitant attack on both solvent and product.[4] Comparably poor yields (less than 5%) of ether II were obtained in both cases. Boron triiodide rapidly attacked diethylene glycol dimethyl ether, and a substantial quantity of 1,2-diiodoethane accompanied the expected products. The experiments did demonstrate, however, that the presence of fluorine or boron trifluoride was not a necessary requirement of ester → ether reduction.



I II III

The preceding experiments also suggested that other periodic group III*a* hydrides or related hydrides from groups IV*a* or V*a* in combination with a boron halide might prove to be unique, and perhaps useful, reducing agents. Of the various possibilities, preliminary

[1]*For part XXVIII in this series, see G. R. Pettit, J. C. Knight, and W. Evers, Can. J. Chem., 44, 807 (1966).*
[2]*Present address: Department of Chemistry, Arizona State University, Tempe, Arizona.*
[3]*The ether (II) has also been prepared from diol III by phosphorus oxychloride (1i) or p-toluenesulfonyl chloride (1i and 2) cyclization techniques.*
[4]*Boron tribromide and boron triiodide have been recommended for cleaving ethers (3).*

Can. J. Chem. Downloaded from www.nrcresearchpress.com by 210.87.254.42 on 09/05/12
For personal use only.

examination of stannane (group IV*a*) and phosphine (group V*a*) was undertaken. Phosphine has already been used for reduction of aromatic nitro compounds (4), and of the two appeared to be the more promising. Under reaction conditions analogous to those employed in the case of diborane – boron trifluoride, neither phosphine nor stannane with boron trifluoride reduced lactone I. Reaction of such hydride systems as diborane–phosphine with various other functional groups, or under more vigorous conditions with esters, offers interesting possibilities but was not considered of further importance in evaluating the ester → ether reaction.

In summary, diborane in combination with a boron trihalide yields a hydride reagent unique in its manner of attacking esters.[5]

EXPERIMENTAL[6]

Sodium Borohydride – Boron Trihalide Reduction of 3-Oxo-4-oxa-5α-cholestane (I)

A. Boron Trifluoride

Boron trifluoride etherate (2.4 g) in diglyme (10 ml) was added over a 15 min period to a cold (ice bath) solution of lactone I (0.20 g) and sodium borohydride (0.04 g) in diglyme (15 ml). Before the slow addition of water (10 ml) followed by 2 *N* hydrochloric acid (10 ml), stirring (with cooling) was continued for an additional 2 h. The mixture was extracted with diethyl ether, and the combined ethereal extracts were washed with water and concentrated to a crystalline residue. A hexane solution of the crude product was chromatographed on activated alumina (6.0 g). After elution with the same solvent (200 ml) and recrystallization of the resulting fraction from hexane, a 0.09 g yield (44%) of 4-oxa-5α-cholestane melting at 90–91.5° was obtained. Melting points of 90–91° and 93–94° have been reported (1*h*–1*i*, 2*b*) for ether II.

In an earlier experiment, the usual technique (I*e*), i.e. adding a mixture of the lactone (I) and boron trifluoride etherate to the hydride solution, was employed and a 58% yield of ether II was obtained.

B. Boron Trichloride

To a cool (ice bath) solution composed of sodium borohydride (0.20 g), lactone I (2.0 g), and diglyme (20 ml) was added, with stirring, over a 15 min period a solution of boron trichloride (18.5 g, The Matheson Company, Inc., chemically pure grade) in hexane (8 ml). After 2 h, water (40 ml) was added, and the mixture extracted with diethyl ether. The combined ethereal extracts were washed successively with water, 10% sodium bicarbonate, and water. Removal of solvent *in vacuo* led to a semicrystalline residue, which was dissolved in benzene and chromatographed on activated alumina. Elution with the same solvent gave a 0.34 g fraction. Continued elution with chloroform–methanol (20:1) led to 0.49 g of diol III. Two recrystallizations from methanol yielded a sample of the diol (III) melting at 137.5–138.5°. A melting point of 136–137° has been reported (1*g*, 2*b*). Concurrently, the benzene fraction (0.34 g) was rechromatographed on activated alumina, and the substance that was eluted with hexane was recrystallized from the same solvent to yield ether II (0.07 g) melting at 91–91.5°.

In another experiment boron trichloride (10 g) was condensed at 0° and allowed to evaporate into a reaction flask containing a cool (ice bath) solution of lactone I (1.0 g) in diglyme (30 ml). Next, a solution of sodium borohydride (0.1 g) in diglyme (15 ml) was added, with stirring, over a 20 min period. One hour later the mixture was diluted with water (70 ml) and extracted with diethyl ether. The combined ethereal extracts were washed with water and concentrated *in vacuo* to a crystalline solid. Isolation of tetrahydropyran II (0.64 g, m.p. 91.5–92.5°) was conducted essentially as described in the preceding paragraph.

C. Boron Tribromide

To a cool (ice bath) solution of sodium borohydride (0.20 g) and lactone I (2.0 g) in diglyme (15 ml) was added, during 15 min, a solution of boron tribromide (37 g, Metro Industries) in hexane (20 ml). After the addition was complete, stirring with cooling was continued for 2 h; then the products were isolated as

[5]*Diborane (alone) reacts with esters to yield hemiacetal derivatives*[1] *(1g), and in combination with aluminium chloride (1g) results in reduction to the alcohol level, as generally observed in the case of lithium aluminium hydride. The useful variation in reducing properties offered by diborane and derived reagents suggests that a procedure utilizing diborane will eventually replace many of the now commonly employed metal hydride techniques. The recent introduction of commercial (Metal Hydrides Division, Ventron Corp.) 1 M diborane in tetrahydrofuran solution has greatly simplified experimentation utilizing diborane.*

[6]*A description of reagents, solvents, and chromatographic techniques has been summarized in the introduction to the Experimental section of part XXVIII in this series.*[1]

A Kofler melting point apparatus was used for melting point determinations (corrected). Optical rotation (chloroform solution) and microanalytical values were determined, respectively, in the laboratories of Dr. P. Demoen, Janssen Pharmaceutica, Beerse, Belgium, and Dr. A. Bernhardt, Mülheim, Germany. The infrared spectra (potassium bromide) were recorded by Dr. R. A. Hill, University of Maine, Orono, Maine.

The identity of each substance isolated from the reduction reaction sequences was established by mixture melting point determination and infrared spectral comparison with an authentic specimen.

Can. J. Chem. Downloaded from www.nrcresearchpress.com by 210.87.254.42 on 09/05/12
For personal use only.

illustrated in experiment B. After two recrystallizations from hexane, ether II weighed 0.03 g and melted at 91–91.5°. In addition, a 0.45 g specimen, m.p. 135–137°, of diol III was isolated.

D. Boron Triiodide

The preceding experiment (C) was repeated with boron triiodide (6.0 g) in hexane (20 ml) and a solution composed of lactone I (0.2 g), sodium borohydride (0.04 g), and diglyme (12 ml). In this case the lactone-containing mixture was added dropwise to the boron triiodide solution to insure an excess of halide. Upon contact, an immediate and vigorous reaction was observed. The crude crystalline product was isolated essentially as described in experiment A, and triturated with hexane. The hexane solution was chromatographed on activated alumina. Elution with the same solvent gave 1,2-diiodoethane (0.73 g, m.p. 81.5–82°)[7] and 0.02 g of impure (m.p. 55–63°) ether II. After three recrystallizations from acetone, the latter specimen melted at 88–90.5° and weighed 5 mg.

Attempted Reduction of 3-Oxo-4-oxa-5α-cholestane (I)

(a) Phospine – Boron Trifluoride

Phosphine generated (5) by treating lithium aluminium hydride with phosphorous trichloride (11.0 g), in diethyl ether, was swept with nitrogen during 2.5 h into a reaction mixture composed of lactone I (1.0 g), boron trifluoride etherate (11 g), and diethyl ether (20 ml). The experiment was performed (see above) at ice-bath temperature and terminated by sweeping the system with nitrogen and slowly adding water (20 ml). The aqueous phase was discarded and the ethereal layer was successively washed with water, potassium carbonate (10%), and water. Removal of solvent gave 0.82 g of lactone I melting at 115–117°.

(b) Stannane – Boron Trifluoride

The attempted reaction between lactone I (1.0 g), boron trifluoride etherate, and stannane (generated (6) by allowing stannic chloride (3.4 g) in diethyl ether (40 ml) to react with lithium aluminium hydride (0.6 g) in diethyl ether (40 ml) at −40°) was conducted at ice-bath temperature as described in experiment *a* for phosphine – boron trifluoride. In this example, a 0.92 g recovery of starting material melting at 116–118° was observed.

ACKNOWLEDGMENTS

This investigation was supported in part by Public Health Service research grants CA-04074-06 and CA-04074-07 from the National Cancer Institute, and by Smith, Kline, and French Laboratories. Grateful acknowledgment is also extended by G. R. P. to Professor Carl Djerassi and the Department of Chemistry, Stanford University, for providing facilities during the initial preparation of this manuscript.

1. (*a*) A. D. Cross, F. A. Kincl, and A. Bowers. U.S. Patent No. 3,150,140 (September 22, 1964); Chem. Abstr. **61**, 16131 (1964).
(*b*) G. W. Moersch, T. P. Culbertson, D. F. Morrow, E. L. Wittle, R. R. Humphrey, W. A. Neuklis, M. E. Butler, and M. M. Creger. J. Med. Chem. **7**, 741 (1964).
(*c*) R. Pappo and C. Jung. U.S. Patent No. 3,101,349 (August 2, 1963); Chem. Abstr. **60**, 597 (1964).
(*d*) G. R. Pettit, A. K. Das Gupta, and U. R. Ghatak. Steroids, **1**, 137 (1963).
(*e*) G. R. Pettit and D. M. Piatak. J. Org. Chem. **27**, 2127 (1962).
(*f*) G. R. Pettit, B. Green, T. R. Kasturi, and U. R. Ghatak. Tetrahedron, **18**, 953 (1962).
(*g*) G. R. Pettit and T. R. Kasturi. J. Org. Chem. **26**, 4557 (1961).
(*h*) G. R. Pettit and T. R. Kasturi. J. Org. Chem. **26**, 4553 (1961).
(*i*) N. J. Doorenbos and M. T. Wu. J. Org. Chem. **26**, 4550 (1961).
(*j*) G. R. Pettit and T. R. Kasturi. J. Org. Chem. **25**, 875 (1960).
(*a*) L. F. Fieser, T. Goto, and B. K. Bhattacharyya. J. Am. Chem. Soc. **82**, 1700 (1960).
(*b*) J. T. Edward and P. F. Morand. Can. J. Chem. **38**, 1325 (1960).
3. R. D. Youssetyeh and Y. Mazur. Chem. Ind. London, 609 (1963).
4. S. A. Buckler, L. Doll, F. K. Lind, and M. Epstein. J. Org. Chem. **27**, 794 (1962). A. C. Bellaart. Rec. Trav. Chim. **83**, 718 (1964). A. C. Bellaart. Tetrahedron, **21**, 3285 (1965).
5. N. L. Paddock. Nature, **167**, 1070 (1951).
6. A. E. Finholt, A. C. Bond, Jr., K. E. Wilzbach, and H. I. Schlesinger. J. Am. Chem. Soc. **69**, 2692 (1947).

Received December 15, 1965.
Department of Chemistry,
University of Maine,
Orono, Maine,
and
Department of Chemistry,
Arizona State University,
Tempe, Arizona.

[7]*An authentic sample obtained from Aldrich Chemical Company melted at 81.5–82° after recrystallization from diethyl ether.*

Can. J. Chem. Downloaded from www.nrcresearchpress.com by 210.87.254.42 on 09/05/12
For personal use only.

THERMAL ISOMERIZATION OF HEXACHLOROCYCLOPROPANE

W. F. HALE

The thermal decomposition of hexachlorocyclopropane (I) has been examined to study the effect of halogen substitution on the isomerization of cyclopropane and, in addition, as a possible route to polydichloromethylene. Considerable literature exists (1 and references therein) concerning the nature of the thermal isomerization of cyclopropanes to propenes. Although not supported by unequivocal evidence, it has been generally assumed that the transition state possesses some diradical character. Since it was known (2) that substitution of halogen for hydrogen stabilizes methyl radicals, ring opening of I with linear coupling to form a polymer was considered to be possible. Recently, a similar approach was outlined (3) in the attempted preparation of polydiphenylmethylene via hexaphenylcyclopropane.

Several recent reports (4) have discussed the preparation and properties of I. We have found that the addition of dichlorocarbene to tetrachloroethylene according to the procedure of Fields and Meyerson (4*c*) is a convenient synthetic method providing about a 10% yield of I.

Pyrolyses were carried out in the vapor phase in a flow system under reduced pressure. A weighed quantity of I was sublimed into a flowing stream of argon, which served as the carrier gas. The mixed vapor stream was then allowed to pass through an electrically heated furnace in an unpacked Vycor tube under the conditions indicated in Table I.

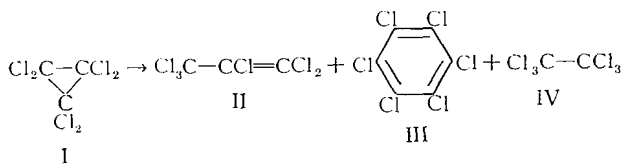
TABLE I

Pyrolysis of hexachlorocyclopropane

Temperature (°C)	Pressure (mm)	Flow rate (g/h)	Product distribution				
			I	II	III	IV	V*
200	2.8	0.33	100	—	—	—	—
300	100	0.50	20	80	—	—	—
400	2.8–4.0	1.00	—	100	—	—	—
500	3.0–4.0	0.20	—	35	30	25	10

*Unresolved mixture with infrared bands characteristic of CCl_4 and $Cl_2C{=}CCl_2$.

The products (as shown in the equation) were identified by physical properties, infrared spectra, and gas chromatography. As previously noted by Tobey and West (4*d*), I was stable at 200 °C. At 300 and 400 °C, facile conversion into hexachloropropene (II) occurred,[1] with no evidence of polymer formation. This result parallels the structural isomerization observed with cyclopropane (1,5,6) and, to a lesser extent, hexafluoro-



[1]*Fields and Meyerson (4c) noted 15% conversion into II when the inlet system for a mass spectrum determination was set at 250 °C.*

Can. J. Chem. Downloaded from www.nrcresearchpress.com by 210.87.254.40 on 09/05/12
For personal use only.

cyclopropane (7) at somewhat higher temperatures. At 500 °C, additional compounds were found which could have resulted from rearrangement, decomposition, and coupling reactions (8) of either the initially generated II or I directly. Again, products of the direct coupling of hexachlorotrimethylene, such as perchlorocyclohexane and polydichloromethylene, were not detected. It would appear that either chlorine substitution does not sufficiently stabilize the proposed diradical intermediate or the transition state has little diradical character.

Attempts to trap the intermediate by inclusion of maleic anhydride or styrene in the sublimate were unsuccessful. Starting materials and II were recovered from pyrolyses at 250 and 400 °C in a flow system. Treatment of I in a sealed tube at 200 °C with maleic anhydride or tetracyanoethylene yielded only starting materials and II.

EXPERIMENTAL

Melting points were measured in a Thomas–Hoover bath and are uncorrected. Infrared spectra were obtained on a Beckman IR-5 spectrophotometer. Gas chromatographic separations were accomplished with a F. and M. No. 502 dual-column instrument equipped with a 4 m column of QF-1 fluorosilicone (liquid phase) on 80 × 100 mesh, acid-washed, dimethyldichlorosilane-treated Johns–Manville Chromosorb P (height equivalent to a theoretical plate, ~0.6 mm).

Hexachlorocyclopropane (I)

The decomposition of sodium trichloroacetate in dimethoxyethane in the presence of tetrachloroethylene according to the procedure of Fields and Meyerson (4*c*) gave a 10.2% yield of I, m.p. 102.5–104° (reported (4*d*) m.p. 102.5–103.5°).

Pyrolysis of Hexachlorocyclopropane (I)

All pyrolyses were carried out in a horizontally oriented, 74 cm × 2.4 cm inside diameter Vycor tube which was heated in the center portion with a 27 cm Hevi-Duty Heating Equipment Co. electric furnace. The pyrolysis temperatures listed in Table I were recorded by a chrome–alumel thermocouple in the center of the furnace. No packing was used in the tube and an argon sweep was provided through a capillary opening before the sublimation zone. Samples of I (1.00 g per run) were contained in a combustion boat in the sublimation zone, which was maintained at 40–120 °C (depending on the pressure and desired flow rate) with an externally wrapped heating tape. A water-cooled condenser and a dry ice trap were connected in series to the Vycor tube following the furnace such that the air-cooled zone for product condensation was about 20 cm in length. The pyrolysis products which collected in the various cool zones were characterized as follows: I by melting point, mixed melting point, infrared spectrum, and gas chromatographic retention time; II by boiling point, refractive index (n_D^{20} 1.5491; reported (9) n_D^{20} 1.5491), infrared spectrum, and gas chromatographic retention time; III by melting point (223°; reported (10) m.p. 226–227°), mixed melting point, and infrared spectrum; IV by melting point (185–186°; reported (10) m.p. 187°) and infrared spectrum; and V by characteristic infrared absorption bands.

1. D. W. Setser and B. S. Rabinovitch. J. Am. Chem. Soc. **86**, 564 (1964). H. M. Frey and C. D. Marshall. J. Chem. Soc. 191 (1965).
2. C. Walling. Free radicals in solution. John Wiley & Sons, Inc., New York. 1957. pp. 50–51.
3. B. S. Gorton. J. Org. Chem. **30**, 648 (1965).
4. (*a*) D. Seyferth, R. J. Minasz, A. J. H. Treiber, J. M. Burlitch, and S. R. Dowd. J. Org. Chem. **28**, 1163 (1963).
   (*b*) W. R. Moore, S. E. Krikorian, and J. E. La Prade. J. Org. Chem. **28**, 1404 (1963).
   (*c*) E. K. Fields and S. Meyerson. J. Org. Chem. **28**, 1915 (1963).
   (*d*) S. W. Tobey and R. West. J. Am. Chem. Soc. **86**, 56 (1964).
5. T. S. Chambers and G. B. Kistiakowsky. J. Am. Chem. Soc. **56**, 399 (1934).
6. W. E. Falconer, T. E. Hunter, and A. F. Trotman-Dickenson. J. Chem. Soc. 609 (1961).
7. R. D. Chambers, H. C. Clark, and C. J. Willis. J. Am. Chem. Soc. **82**, 5298 (1960).
8. J. A. Krynitsky and H. W. Carhart. J. Am. Chem. Soc. **71**, 816 (1949).
9. M. Prober. J. Am. Chem. Soc. **76**, 4189 (1954).
10. Handbook of chemistry and physics. Chemical Rubber Publishing Co., Cleveland, Ohio. 1964.

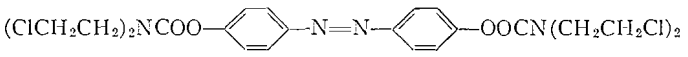
Received January 14, 1966.
Research and Development Department,
Plastics Division, Union Carbide Corporation,
Bound Brook, New Jersey.

Can. J. Chem. Downloaded from www.nrcresearchpress.com by 210.87.254.40 on 09/05/12
For personal use only.

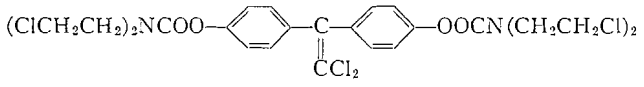
POTENTIAL ANTICANCER AGENTS
III. URETHANE-TYPE NITROGEN MUSTARDS OF SOME SYNTHETIC ESTROGENS

I. NICULESCU-DUVĂZ, V. FEYNS, E. GRANT, AND E. TĂRNĂUCEANU

While studying the anticancer activity of the urethane-type nitrogen mustards, we prepared a number of compounds of this type from synthetic estrogens, with the purpose of establishing a relationship between the estrogenic activity of the bis-hydroxyphenyl derivatives and the anticancer action of their nitrogen mustard carbamates. Since compounds I and II that had previously been prepared (1) exhibited 50–60% inhibitions on Walker carcinosarcoma 256 (2), it seemed to be of interest to extend the series of these substances.



I

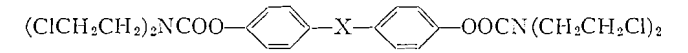


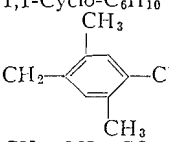
II

The urethane-type nitrogen mustards were obtained by condensation of the bis-hydroxyphenyl derivatives with di-(2-chloroethyl)-carbamyl chloride in pyridine (3) followed, after pyridine removal, by crystallization from ethanol. The nitrogen mustards thus obtained are summarized in Table I.

TABLE I

New urethane-type nitrogen mustards



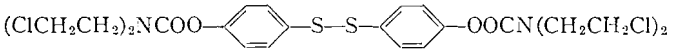
X	Melting point (°C)	Yield (%)	ν_{max}* carbamate group† (cm^{-1})	Analysis (%) Calcd. C	Calcd. H	Calcd. N	Found C	Found H	Found N
$CH_2—CH_2$	101.5–102	80.5	1712	52.36	5.09	5.09	52.06	5.12	5.08
$C(CH_3)_2$	180–181	36.6	1730	53.19	5.32	4.96	53.00	5.39	4.96
$C(CH_3)(C_2H_5)$	120–120.5	50.4	1725	53.97	5.53	4.84	54.19	5.49	4.66
$C(C_2H_5)_2$	98	52.0	1725	54.73	5.74	4.72	54.52	5.81	4.75
1,1-Cyclo-C_5H_8	105–106	72.4	1712	54.91	5.42	4.74	54.97	5.56	4.80
1,1-Cyclo-C_6H_{10}	89	51.8	1720	55.63	5.62	4.64	55.56	5.70	4.74
	133–134	22.1	1725	58.71	5.50	4.28	58.69	5.49	4.51
CH=CH—CO	89–90	33.5	1724	52.08	4.51	4.84	52.10	4.54	5.01
CH=N	91	38.0	1722	50.27	4.55	7.65	50.27	4.54	7.58
CH=N—N=CH	148	85.0	1712	50.00	4.52	9.72	50.03	4.70	9.70
S—S	46–47	34.7	1725	45.05	4.09	4.77	45.10	4.30	4.76
SO_2‡	114–115	50.0	1715 1740	45.05	4.09	4.77	44.99	4.06	4.73

*Infrared spectra were determined on a UR 10 Zeiss-Jena-DDR spectrophotometer, in KBr disks.
†Amide I band.
‡Carbamate groups are in 2,4′ positions.

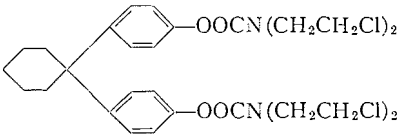
Can. J. Chem. Downloaded from www.nrcresearchpress.com by 210.87.254.40 on 09/05/12
For personal use only.

Some of the carbamates prepared in this way were obtained as gums which could not be purified by crystallization. Column chromatography on alumina was employed, the urethane group not being split as reported by Nogrady for N-di-(2-chloroethyl)-D-1-glucopyranosyl carbamate (4).

Thus, in the case of bis(4-(N,N-di-(2-chloroethyl)-carbamyl)phenyl)disulfide (III), after pyridine removal, the residue was extracted first with benzene and then with benzene – methylene chloride mixtures (from 1:1 to 1:9). The extracts were chromatographed over alumina. The carbamate was recovered from the light-yellow benzene eluate, the other fractions containing small quantities of unidentified dark-colored resinous substances. The chromatography of 1,1-bis(4-(N,N-di-(2-chloroethyl)-carbamyl)phenyl)-cyclohexane (IV) was similarly performed, except that residue extraction, column development, and elution were carried out with benzene and benzene–methanol mixtures (from 99:1 to 90:10). Here also, the carbamate was found in the benzene eluate.

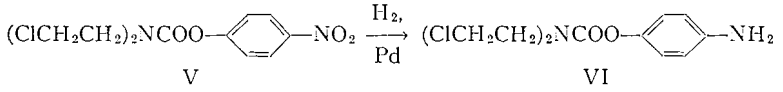


III

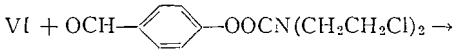


IV

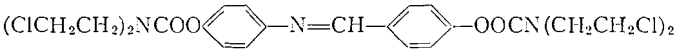
For the same reason (an impossibility to purify), 1,2-bis(4-(N,N-di-(2-chloroethyl)-carbamyl)phenyl)methylenimine (VIII) was synthesized according to the reaction sequence shown in Reaction Scheme 1.



V VI



VII



VIII

REACTION SCHEME 1.

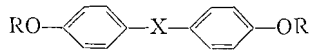
The carbamates of *p*-hydroxynitrobenzene (V) and *p*-hydroxybenzaldehyde (VII) were prepared by common procedures (3); amine VI was obtained in good yield by the catalytic hydrogenation of the nitro derivative V with palladium chloride on carbon at room temperature.

Biological evaluation of the compounds is in progress. The estrogenic activity of some of the bis-*p*-hydroxyphenyl derivatives used as precursors in the present work and in ref. 1, and the antitumor activity of their bis(N,N-di-(2-chloroethyl)carbamyl) derivatives against Walker carcinosarcoma 256 are shown in Table II. Mention should also be made that preliminary tests showed compounds V and VI (not tabulated) to be inactive against Walker carcinosarcoma 256.

Can. J. Chem. Downloaded from www.nrcresearchpress.com by 210.87.254.40 on 09/05/12
For personal use only.

TABLE II

Biological activities*



X	Estrogenic activity† (R = H)	% inhibition against Walker carcinosarcoma 256‡ (R = $OCN(CH_2CH_2Cl)_2$)	References for the estrogenic activity
CH=CH (*trans*)	++	21	5, 6
CH_2—CH_2	++	22	6
CH=CH—CO	+	29	6
CH_2	+	30	7
$C(CH_3)_2$	+	36	7
$CH(CCl_3)$	+	0	8
C ‖ CCl_2	+	52	9
—	+	7, 3	6
N=N	+	59	6
O	+	35	5
S	+	36	6
CH=N	−	T/C > 1§	6
SO_2	−	13	6
2,4′-SO_2	?	30	—
SO	?	25	—
CO	?	0	—
CH=N—N=CH	?	T/C > 1	—

*The table includes derivatives reported in ref. 1.
†Estrogenic activity: ++, 1–100 mg/kg body weight (rat); +, 100 – 1 000 mg/kg body weight; −, over 1 000 mg/kg body weight.
‡Doses of 50 mg/kg body weight (rat) every 2 days, beginning with the 7th day after tumor transplantation up to the 23rd day.
§T = tumor weight (treated animals); C = tumor weight (control animals).

Structural evidence for the new compounds was provided by infrared absorbtion spectra.

EXPERIMENTAL

4-(N,N-Di-(2-chloroethyl)-carbamyl)nitrobenzene (V)

Di-(2-chloroethyl)-carbamyl chloride (7.8 g, 0.038 mole) in 20 ml of pyridine was added to 5 g (0.036 mole) of *p*-nitrophenol. After the solution was allowed to stand for 3 days at room temperature, pyridine hydrochloride separated out and was filtered off. The filtrate was evaporated to dryness *in vacuo* to give a residue, which was triturated with toluene and again evaporated to dryness *in vacuo*. The procedure was repeated 3 times until all the pyridine had been removed; 9.2 g (83%) of V was obtained (after recrystallization from ethanol, m.p. 85–86 °C). Infrared (KBr): ν_{max} carbamate (amide I band) 1 732 cm^{-1}.

Anal. Calcd. for $C_{11}H_{12}Cl_2N_2O_4$: C, 42.99; H, 3.90; N, 9.12. Found: C, 42.97; H, 3.94; N, 9.09.

4-(N,N-Di-(2-chloroethyl)-carbamyl)benzaldehyde (VII) was similarly prepared. The residue after pyridine was removed failed to crystallize and was extracted with benzene; the benzene solution was evaporated to dryness *in vacuo* to give the desired product (viscous yellow oil) of analytical purity. Infrared: ν_{max} carbamate (amide I band) 1 735 cm^{-1}.

Anal. Calcd. for $C_{12}H_{13}Cl_2NO_3$: C, 49.65; H, 4.48; N, 4.82. Found: C, 49.65; H, 4.50; N, 4.78.

4-(N,N-Di-(2-chloroethyl)-carbamyl)aniline (VI)

V (7.9 g, 0.026 mole) was dissolved in 250 ml ethanol and hydrogenated in the presence of 2 g of 5% palladium chloride on carbon catalyst at atmospheric pressure and room temperature, the theoretical amount of hydrogen (1 730 ml) being consumed during 4 h. The catalyst was filtered off and the solvent was removed by distillation under reduced pressure. The residue was dissolved in ether, and dry hydrogen chloride was passed into the solution to give 7.3 g (91%) of the hydrochloride of VI (m.p. 182–183 °C). Infrared (KBr): ν_{max} carbamate (amide band I) 1 730 cm^{-1}.

Anal. Calcd. for $C_{11}H_{15}Cl_3N_2O_2$: C, 42.10; H, 4.78; N, 8.93. Found: C, 42.14; H, 4.80; N, 8.98.

1,2-Bis(4-(N,N-di-(2-chloroethyl)-carbamyl)phenyl)methylenimine (VIII)

Aldehyde VII (3.3 g, 0.011 mole) was added to a solution of 2.9 g (0.011 mole) of amine VI in 110 ml of ethanol. After the solution was allowed to stand for 2 days at room temperature with occasional shaking, a solid was collected and recrystallized from ethanol to give 2.2 g (38%) of pure VIII (see Table I).

Can. J. Chem. Downloaded from www.nrcresearchpress.com by 210.87.254.40 on 09/05/12
For personal use only.

SUMMARY

The synthesis of new urethane-type nitrogen mustards from the following bis-hydroxyphenyl derivatives is reported: 1,2-bis(*p*-hydroxyphenyl)ethane; 2,2-bis(*p*-hydroxyphenyl)-propane; 2,2-bis(*p*-hydroxyphenyl)butane; 3,3-bis(*p*-hydroxyphenyl)pentane; 1,1-bis-(*p*-hydroxyphenyl)cyclopentane; 1,1-bis(*p*-hydroxyphenyl)cyclohexane; 2,5-bis(*p*-hydroxybenzyl)-*p*-xylene; *p*,*p*′-dihydroxychalcone; 1,2-bis(*p*-hydroxyphenyl)methylenimine; *p*,*p*′-dihydroxybenzalazine; 1,2-bis(*p*-hydroxyphenyl)disulfide; 2,4′-dihydroxydiphenyl sulfone.

Antitumor activities against Walker carcinosarcoma 256 are given for some of the new compounds.

ACKNOWLEDGMENTS

The authors thank Mr. Filip Chiraleu for performing infrared measurements and Miss Maria Stănescu for technical assistance. The cancerostatic screening was done by Dr. V. Dobre. We thank him for making the screening data available to us.

1. E. GRANT and I. NICULESCU-DUVĂZ. Can. J. Chem. **43**, 1227 (1965).
2. V. DOBRE, C. NEACSU, and I. NICULESCU-DUVĂZ. Sci. Symp. Institutul de Cercetări Chimico-Farmaceutice 4th, Bucharest, Rumania, May 1965.
3. T. NOGRADY, M. K. VAGI, and V. W. ADAMKIEWICZ. Can. J. Chem. **40**, 2126 (1962).
4. T. F. NOGRADY. J. Org. Chem. **26**, 4177 (1961).
5. C. W. EMMENS. J. Endocrinol. **2**, 444 (1941).
6. D. SCHMAHL. Arzneimittel-Forsch. **7**, 211 (1957).
7. N. R. CAMPBELL. Proc. Roy. Soc. London, Ser. B, **129**, 528 (1940).
8. A. L. FISCHER, A. H. KEASTLING, and F. W. SCHNELER. Proc. Soc. Exptl. Biol. Med. **81**, 439 (1952).
9. O. COSTACHEL, I. NICULESCU-DUVĂZ, V. FEYNS, and C. NEACSU. Natl. Symp. Cancer Chemotherapy 1st, Bucharest, Rumania, November 1965.

RECEIVED OCTOBER 28, 1965.
DEPARTMENT OF ORGANIC SYNTHESIS AND PHYSICAL CHEMISTRY,
ONCOLOGICAL INSTITUTE,
BUCHAREST, RUMANIA.

Can. J. Chem. Downloaded from www.nrcresearchpress.com by 210.87.254.40 on 09/05/12
For personal use only.

Can. J. Chem. Downloaded from www.nrcresearchpress.com by 210.87.254.40 on 09/05/12
For personal use only.

Canadian Journal of Chemistry

Issued by THE NATIONAL RESEARCH COUNCIL OF CANADA

VOLUME 44 MAY 15, 1966 NUMBER 10

A GRAVIMETRIC STUDY OF HYDRATION OF POLYNUCLEOTIDES[1]

MICHAEL FALK

Atlantic Regional Laboratory, National Research Council, Halifax, Nova Scotia

Received December 6, 1965

ABSTRACT

The hydration of soluble ribonucleic acid, of two forms of polyriboadenylic acid, and of nucleohistone was determined gravimetrically as a function of relative humidity (r.h.). The curves are smooth functions of r.h., similar to those obtained earlier for deoxyribonucleic acid. The general similarity of the hydration curves of the polynucleotides so far investigated is in agreement with the suggestion that the ionic phosphate groups are the primary hydration sites in polynucleotides. The hydration data fit the Brunauer–Emmett–Teller equation up to about 75% r.h. and the Harkins–Jura equation at higher values. Both equations yield a value of about 2.0 molecules of H_2O per nucleotide for the "monolayer content" for all the polynucleotides investigated.

INTRODUCTION

Polynucleotides are highly hygroscopic. For example, deoxyribonucleic acid (DNA) takes up its own weight of water at 90% relative humidity (r.h.); its degree of hydration rapidly tends to infinity as r.h. increases towards 100%. The study of the degree of hydration as a function of r.h. is particularly important in view of the structural changes that occur in many polynucleotides at certain values of r.h. Such structural changes are well known for DNA (1–3) and have recently been observed also for ribonucleic acid (RNA) (4) and for several synthetic polynucleotides (5). The knowledge of hydration of nucleic acids in the solid state is additionally useful because it appears to be related to their hydration in aqueous solution, which is of importance in biology. There is a correlation between the hydration of DNA in the solid state (6) and in solution (7–9).

In the present study the hydration of soluble RNA, of two forms of polyriboadenylic acid (poly-A), and of nucleohistone was measured gravimetrically as a function of r.h. and was compared with the hydration of DNA, measured earlier by the same technique (6).

EXPERIMENTAL

Materials

Poly-A was purchased as the potassium salt from the California Corporation for Biochemical Research, Los Angeles. This material had been prepared by the method of Beers (10). The material as received was in the "neutral" form, corresponding to pH 7. The "acid" form was prepared by titration of a concentrated aqueous solution with HCl to pH 4, followed by lyophilization. The absorption spectra were identical with the previously published infrared (11) and ultraviolet (12) spectra of the two forms of poly-A. The X-ray diffraction patterns of fibers made from the samples at pH 7 and pH 4 agreed with those reported in the literature (13, 14).

Soluble RNA from yeast was prepared by the method of Holley (15) and was the sodium salt. The infrared and ultraviolet spectra were identical with those recorded in this laboratory for many samples of soluble RNA from several sources (4, 5) and with the spectra reported elsewhere (16, 17).

Nucleohistone, isolated from calf thymus, was purchased from the California Corporation for Biochemical Research. Its infrared spectrum was identical with that reported by Bradbury *et al.* (18).

[1]*Issued as N.R.C. No. 8920.*

Methods

Several specimens of each sample, 30 to 50 mg, were exposed to atmospheres of constant r.h. and were weighed to within 0.05 mg until constant weights were obtained, which usually required 3 to 6 days. The constant relative humidity was maintained by a saturated solution of an appropriate salt contained in a Petri dish. The r.h. values for most of the solutions were taken from the data of Wink and Sears (19) and were estimated to be accurate to ±0.5% or better. The temperature was kept at 21.0 ± 0.4°, except for a part of the study on poly-A in which it was controlled to ±1°. Several cycles of hydration and dehydration were performed for each specimen. At the end of each series of measurements the dry weight was obtained by drying to constant weight in a vacuum of 10^{-3} Torr at 25, 50, and 80°. None of the samples showed any additional loss of weight between 50 and 80° and it was assumed for the purpose of the calculations that all of the adsorbed water was expelled from the samples.

RESULTS AND DISCUSSION

The results, averaged from several hydration–dehydration cycles, are presented in Table I as moles water per mole nucleotide. The average deviation was ±0.15 mole H_2O per mole. To convert weights to moles the following molecular weights "per nucleotide" were used: DNA, 331; nucleohistone, 662; poly-A at pH 4, 403; poly-A at pH 7, 367; RNA, 345. The above values for DNA, nucleohistone, and RNA are based on 1:1:1:1 base ratios (they are not very sensitive to the exact value of the ratios) and the value for calf-thymus nucleohistone on the assumption of a 50% DNA content (20, 21); the value for poly-A at pH 4 was based on the assumption of the addition of 1 mole of HCl per adenylate unit. The values of hydration for nucleohistone are plotted in Fig. 1.

TABLE I

Hydration and dehydration of polynucleotides in moles H_2O per mole of nucleotide

Relative Humidity(%)	RNA		Poly-A, pH 7		Poly-A, pH 4		Nucleohistone		DNA (ref. 6)	
	Hyd.	Dehyd.	Hyd.	Dehyd.	Hyd.	Dehyd.	Hyd.	Dehyd.	Hyd.	Dehyd.
5.0	0.70	1.27	1.51	1.98	1.03	1.49	1.36	1.86	1.32	
11.0	1.27	1.78	1.59	2.25	1.21		1.66	2.34	1.68	1.99
23.0	1.72	2.26	2.42	2.88	1.83	2.42	2.43	3.21	2.32	
33.1	2.17		2.56		2.42		3.06		3.06	
38.8	2.46	3.01	2.89	4.09	2.39	2.96	3.33	4.52	3.37	4.23
48.8	3.16		3.55	4.22	2.73	3.20	4.15		4.23	
59.0	4.24	4.45	4.25	4.97	3.36		5.43	6.16	5.33	6.44
65.2	4.72	5.02	4.55		3.84	4.13	5.99	6.65	6.09	
75.5	6.49		5.86		5.17	5.26	8.38		8.42	
86.6	9.94		8.44		10.88	9.88	12.18		13.12	
93.2	15.64		13.03		18.45		18.06		20.73	

Hydration of Different Polynucleotides

The curves of hydration and dehydration were smooth functions of relative humidity for all the compounds investigated and had the same form as the corresponding curves for DNA (6). The absence of distinct plateaux, such as occur for some compounds of low molecular weight which contain the phosphate group (22), indicates the absence of well-defined hydrates. Hydration–dehydration hysteresis occurred for all of the substances investigated and was of the order of 1 mole H_2O per mole nucleotide, as indicated in Table I. The discussion which follows neglects hysteresis and is based on the data for hydration, which are more extensive than for dehydration.

The polynucleotides listed in Table I differ from one another in their secondary structure and in the nature of the cation. The general similarity of their hydration curves is therefore in agreement with the suggestion that the hydration of polynucleotides is largely controlled by the phosphate groups (1, 3, 22, 23), and is not strongly affected by the

Can. J. Chem. Downloaded from www.nrcresearchpress.com by 210.87.254.40 on 09/05/12
For personal use only.

nature of the cation and by the detailed secondary structure. The similarity of the hydration curves of the sodium and lithium salts of DNA (6) also shows that the hydration is not strongly dependent upon the cation.

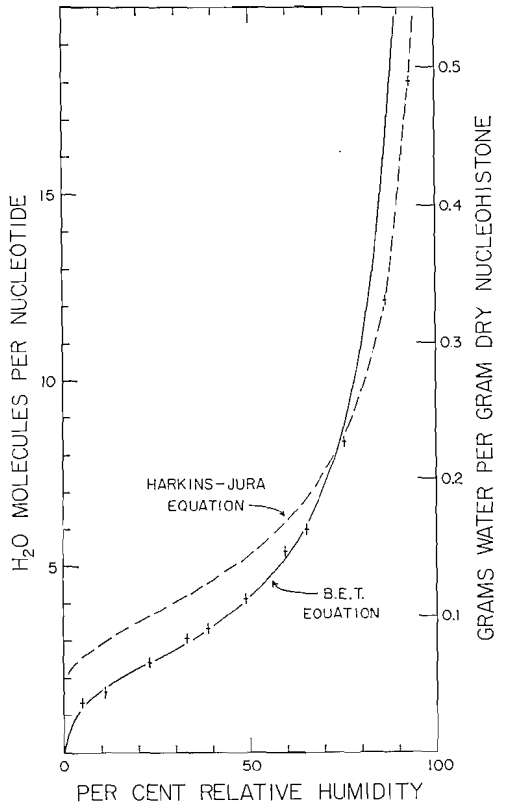


FIG. 1. Plot of the values of hydration for nucleohistone.

The small differences in the hydration of the individual polynucleotides are too complex to be interpreted in detail, but may be at least partly due to the differences of accessibility of the phosphate groups to water. For example, the hydration of polynucleotide double helices may be expected to be higher than that of the single-stranded structures as a result of the efficient way in which the phosphate groups are exposed to water on the outside of the double helix. This expectation is fulfilled in the case of RNA, which has an incomplete double helix and a lower hydration than native DNA. The hydration of denatured DNA, which also has an incomplete double helix, is about the same as that of RNA (5). On the other hand, the hydration of the pH 4 form of poly-A (which is known to be a double helix) would be expected to be higher than that of the pH 7 form of poly-A (which is known to be single-stranded), but below about 80% r.h. it is actually lower.

DNA in the form of sodium salt undergoes reversible structural transitions at about 80% r.h. (2) and at about 65% r.h. (3). These transitions do not cause detectable discontinuities in the hydration curve of DNA. It would be of interest to determine whether the structural transitions in RNA (4) and in the pH 4 form of poly-A (5), which occur near 98% r.h., affect the hydration curves of these compounds in a discontinuous manner.

Can. J. Chem. Downloaded from www.nrcresearchpress.com by 210.87.254.40 on 09/05/12
For personal use only.

However, the determination of hydration above about 93% r.h. is difficult and has not been attempted in the present study.

The Brunauer–Emmett–Teller and Harkins–Jura Equations

It is of interest to test the present data for a fit with the Brunauer–Emmett–Teller (B.E.T.) equation (24). This equation is of the form $A = BCx/(1 - x + Cx)(1 - x)$, where A is the total amount of water adsorbed at relative humidity x, and B and C are adjustable parameters which have some physical significance (6). The hydration data for all the substances investigated fit the B.E.T. equation within experimental error up to about 75% r.h. At higher relative humidities the observed hydration is lower than that calculated, as shown for nucleohistone in Fig. 1. For all four polynucleotides investigated, the best fit with the B.E.T. equation corresponds to the following approximate values of the two parameters: $B = 1.9$ H_2O molecules per nucleotide and $RT \ln C = 1.8$ kcal/mole. These values are of the same magnitude as those obtained for DNA (6).

It is also of interest to test the data for a fit with the Harkins–Jura equation (25, 26). This equation is applicable to a liquid-like phase condensed upon a solid surface of limited area and has previously been shown to fit the hydration of proteins (27, 28) and of cellulose (29) at high r.h. In the present notation this equation is of the form $\log x = D - B^2/A^2$, where D is an adjustable parameter and x, A, and B are the same as in the B.E.T. equation. The present hydration data were found to fit the Harkins–Jura equation above about 75% r.h. (Attempts to find a Harkins–Jura fit below 75% r.h. lead to a negative value of D, and hence to imaginary values of A over some part of the range.) At lower relative humidities the observed hydration is lower than that calculated from the parameters D and B found at high r.h. This is shown for nucleohistone in Fig. 1. The values of the parameter B, the "monolayer content", derived from the high relative-humidity portion of the hydration data, are about 2 molecules of H_2O per nucleotide for the various polynucleotides. The data for the sodium salt of DNA (6) gave $B = 2.3$. The agreement between the values of the parameter B derived from the data at lower r.h. by the B.E.T. equation and at higher r.h. by the Harkins–Jura equation is within 20% for the various polynucleotides. This agreement is interesting as the two equations are based on very different physical models and make use of different portions of the hydration data. It appears that strong binding of approximately 2 water molecules to each phosphate group may be common to all polynucleotides, and may be largely independent of the cation.

The part of the hydration curves up to about 75% r.h., which fits the B.E.T. equation, probably corresponds to the adsorption of further layers of water molecules, also largely around the phosphate groups. The part of the curves at higher r.h., which fits the Harkins–Jura equation, probably corresponds to a gradual transition of the adsorbed layer to a condensed film with properties which approach those of liquid water.

ACKNOWLEDGMENTS

I wish to thank Professor R. F. Beers for a sample of poly-A, Professor R. W. Holley for the sample of RNA, Dr. J. T. Finch for recording and interpreting X-ray diffraction patterns of two samples of poly-A, and Dr. Karl A. Hartman, Jr. for the preparation of one sample of pH 4 poly-A. The work on poly-A was begun at the Spectroscopy Laboratory, Massachusetts Institute of Technology, and was supported by a grant (No. A-2262 (C3) from the National Institutes of Health) to Professor R. C. Lord.

Can. J. Chem. Downloaded from www.nrcresearchpress.com by 210.87.254.40 on 09/05/12
For personal use only.

REFERENCES

1. R. E. FRANKLIN and R. G. GOSLING. Acta Cryst. **6**, 673 (1953).
2. M. H. F. WILKINS. J. Chim. Phys. **58**, 891 (1961).
3. M. FALK, K. A. HARTMAN, JR., and R. C. LORD. J. Am. Chem. Soc. **85**, 391 (1963).
4. M. FALK. Can. J. Chem. **43**, 3151 (1965).
5. M. FALK. Unpublished results.
6. M. FALK, K. A. HARTMAN, JR., and R. C. LORD. J. Am. Chem. Soc. **84**, 3843 (1962).
7. J. H. WANG. J. Am. Chem. Soc. **77**, 258 (1955).
8. J. E. HEARST. Proc. Nat. Acad. Sci. U.S. **47**, 825 (1961).
9. J. E. HEARST. Biopolymers, **3**, 57 (1965).
10. R. F. BEERS. Biochem. J. **66**, 686 (1957).
11. R. S. MORGAN and E. R. BLOUT. J. Am. Chem. Soc. **81**, 4625 (1959).
12. J. R. FRESCO and P. DOTY. J. Am. Chem. Soc. **79**, 3928 (1957).
13. A. RICH, D. R. DAVIES, F. H. C. CRICK, and J. D. WATSON. J. Mol. Biol. **3**, 71 (1961).
14. R. S. MORGAN and R. BYRNE. J. Mol. Biol. **1**, 188 (1959).
15. R. W. HOLLEY. Biochim. Biophys. Res. Commun. **10**, 186 (1963).
16. G. B. B. M. SUTHERLAND and M. TSUBOI. Proc. Roy. Soc. London, Ser. A, **239**, 446 (1957).
17. D. VOET, W. B. GRATZER, R. A. COX, and P. DOTY. Biopolymers, **1**, 193 (1963).
18. E. M. BRADBURY, W. C. PRICE, G. R. WILKINSON, and G. ZUBAY. J. Mol. Biol. **4**, 50 (1962).
19. W. A. WINK and R. R. SEARS. Tappi, **33**, 96A (1960).
20. E. CHARGAFF. *In* The nucleic acids. Vol. I. *Edited by* E. Chargaff and J. N. Davidson. Academic Press, New York, 1955. p. 318.
21. M. H. F. WILKINS, G. ZUBAY, and H. R. WILSON. J. Mol. Biol. **1**, 179 (1959).
22. M. FALK. Can. J. Chem. **43**, 314 (1965).
23. M. FALK, K. A. HARTMAN, JR., and R. C. LORD. J. Am. Chem. Soc. **85**, 387 (1963).
24. S. BRUNAUER, P. H. EMMETT, and E. TELLER. J. Am. Chem. Soc. **60**, 309 (1938).
25. W. D. HARKINS and G. JURA. J. Am. Chem. Soc. **66**, 1366 (1944).
26. S. C. LIANG. J. Phys. and Colloid Chem. **55**, 1410 (1951).
27. H. B. DUNFORD and J. L. MORRISON. Can. J. Chem. **32**, 558 (1954).
28. H. B. DUNFORD and J. L. MORRISON. Can. J. Chem. **33**, 904 (1955).
29. J. L. MORRISON and M. A. DZIECIUCH. Can. J. Chem. **37**, 1379 (1959).

Can. J. Chem. Downloaded from www.nrcresearchpress.com by 210.87.254.40 on 09/05/12
For personal use only.

Can. J. Chem. Downloaded from www.nrcresearchpress.com by 210.87.254.105 on 09/05/12
For personal use only.

ABSOLUTE RATE CONSTANTS FOR HYDROCARBON AUTOXIDATION

III. α-METHYLSTYRENE, β-METHYLSTYRENE, AND INDENE[1]

J. A. HOWARD AND K. U. INGOLD

Division of Applied Chemistry, National Research Council, Ottawa, Canada

Received December 21, 1965

ABSTRACT

Absolute rate constants for the copolymerization of α-methylstyrene and oxygen have been measured from 13 to 50 °C. The propagation and termination rate constants can be represented by

$$k_p = (6.6 \pm 0.7) \times 10^6 \exp(-(8\,070 \pm 800)/RT) \text{ l mole}^{-1} \text{ s}^{-1}$$
$$k_t = (1.6 \pm 0.7) \times 10^8 \exp(-(3\,700 \pm 1\,600)/RT) \text{ l mole}^{-1} \text{ s}^{-1}.$$

Experiments with 2,6-di-*t*-butyl-4-methylphenol at 65 °C have shown that $C_6H_5C(CH_3):CH_2$ and $C_6H_5C(CD_3):CD_2$ have the same propagation rate constant but that chain termination involves a deuterium isotope effect $(k_t)_H/(k_t)_D \simeq 1.5$.

Absolute rate constants for the copolymerization of oxygen with β-methylstyrene and with indene at 30 °C showed that a significant fraction of the oxidation chains were terminated by a kinetically first order process (rate constant k_x). The rate constants for β-methylstyrene and indene at 30 °C are $k_p = 51$ and 142 l mole^{-1} s^{-1}, $k_t = 1.6 \times 10^7$ and 2.5×10^7 l mole^{-1} s^{-1}, and $k_x = 0.61$ and 1.2 s^{-1}, respectively. The propagation rate constant for indene can be separated into a rate constant for the copolymerization with oxygen ($k_{add} = 128$ l mole^{-1} s^{-1}) and a rate constant for hydrogen atom abstraction ($k_{abstr} = 14$ l mole^{-1} s^{-1}). In the presence of heavy water the first order process for indene had a deuterium isotope effect $(k_x)/(k_x)_{D_2O} \simeq 3$.

INTRODUCTION

The effects of temperature and solvents on the absolute rate constants for the autoxidation of styrene, i.e., for its copolymerization with oxygen, were described in the first paper in this series (1). The second paper gave the absolute rate constants for four deuterium-labelled styrenes and a number of ring-substituted styrenes (2). The present paper extends this work to α- and β-methylstyrene and indene. Both α-methylstyrene and indene have been shown to copolymerize with oxygen in thermally initiated oxidations (3, 4). α-Methylstyrene is of particular interest since it yields a tertiary peroxy radical. The mechanism of chain termination for compounds giving tertiary peroxy radicals has been under very active study in the past 2 or 3 years (5–9) but absolute rate constants have been measured in only a few cases, i.e., for chain propagation (k_p) and chain termination (k_t) in the autoxidation of cumene (9–12) and 2,4,6-trimethyl heptane (13) and for the mutual destruction of *t*-butylperoxy radicals derived from *t*-butylhydroperoxide (9). α-Methylstyrene is also interesting in that the rate of the α,α′-azo-bis-isobutyronitrile (AIBN) thermally initiated oxidation has been reported to increase very noticeably as the oxygen pressure is increased, e.g., the rate at 50° with 0.01 mole/l AIBN is 0.076, 0.12, and 0.13 mole l^{-1} h^{-1} at 100, 750, and 3 200 mm oxygen pressure, respectively (3). This variation in the rate with the oxygen pressure has been attributed to a contribution from crossed chain termination, involving aralkyl ($R^\cdot$) and aralkylperoxy ($RO_2^\cdot$) radicals, to the overall rate of chain termination at oxygen pressures below 3 200 mm (3).

This paper describes the effects of temperature on the absolute rate constants for the oxidation of α-methylstyrene. The results of a few measurements on the deutero-α-methylstyrene, $C_6H_5C(CD_3):CD_2$, are also included. In addition, the inhibition with 2,6-di-*t*-butyl-4-methylphenol (BMP) of the thermally initiated autoxidation of α-methylstyrene has been studied.

[1]*Issued as N.R.C. No. 8892.*

Can. J. Chem. Downloaded from www.nrcresearchpress.com by 210.87.254.105 on 09/05/12
For personal use only.

EXPERIMENTAL

The experimental technique and theory of the rotating sector method has been described previously (1, 2). α,α'-Azo-bis-cyclohexylnitrile (ACHN) was used as the photo-initiator. The deutero-α-methylstyrene, $C_6H_5C(CD_3):CD_2$, was obtained from Merck, Sharp and Dohme of Canada, Limited. Mass spectrometric analysis showed it to be 89% $C_9H_5D_5$ and 11% $C_9H_6D_4$.

Indene (Eastman) was purified by crystallization and distillation. β-Methylstyrene (Aldrich) was purified by distillation.

It is nearly impossible to assign a specific error to each of the absolute rate constants reported in this paper and in the other papers in this series. We have previously discussed the sources of some of the errors involved in rotating sector measurements (1). The errors will be increased under the following circumstances: (i) when there are concurrent first and second order chain termination reactions, (ii) when the reaction is autocatalytic or autoretarding, and (iii) when the chain length is relatively short. On the whole, it is probably safe to assume that all the values for k_t should be accurate to within a factor of 2 and all the values for k_p should be accurate to within ±50%. Under ideal conditions, and when a large number of measurements have been made (as for all our work on deuterium-labelled hydrocarbons), the results should be a great deal more accurate.

RESULTS AND DISCUSSION

Uninhibited Oxidation of α-Methylstyrene

The ACHN-photosensitized oxidation of α-methylstyrene is self-retarding.[2] That is, the rate decreases as the reaction proceeds to a greater extent than can be accounted for by the consumption of ACHN and the hydrocarbon. This has also been observed in the AIBN thermally initiated oxidation (3) but the effect is more pronounced in the photochemical reaction, apparently because a reaction product absorbs some of the 365 mμ initiating radiation. Thus, for example, the oxidation of 1.78 mole/l of α-methylstyrene in chlorobenzene containing 6.7×10^{-3} mole/l ACHN with 0.04 mole/l O_2 increased the ultraviolet absorption at this frequency by a factor of more than 4. This increase in absorption can probably be attributed to the acetophenone which is formed in large amounts in both the thermal (3) and photochemical[3] oxidation. This problem renders the determination of absolute rate constants rather difficult, it being necessary to correct for the changing rate of chain initiation during each experiment.

The results given in Table I contrast with those of Miller and Mayo in that oxygen pressure in the range 100–680 mm had no significant effect on the oxidation rate or, more correctly,[4] on $k_p/(2k_t)^{1/2}$. The lower temperature of the present experiments as well as the smaller pressure range which was covered probably accounts for this discrepancy.

At 40 and 50 °C, α-methylstyrene showed no sign of the first order chain-terminating process that was observed in styrene at these temperatures (1, 2). Its absence reinforces our previous conclusion, drawn from studies of the deuterium isotope effect (2), that the α-hydrogen atom in styrene is involved in this process.

The rate constants in Table I can be represented by:

$$k_p/(2k_t)^{1/2} = (3.5 \pm 0.2) \times 10^2 \exp(-(6\,170 \pm 300)/RT)\ (\text{l mole}^{-1}\ \text{s}^{-1})^{1/2}$$
$$k_p = (6.6 \pm 0.7) \times 10^6 \exp(-(8\,070 \pm 800)/RT)\ \text{l mole}^{-1}\ \text{s}^{-1}$$
$$k_t = (1.6 \pm 0.7) \times 10^8 \exp(-(3\,700 \pm 1\,600)/RT)\ \text{l mole}^{-1}\ \text{s}^{-1}.$$

[2]*In the absence of ACHN the photo-oxidation is autocatalytic but very slow, the rate being only about 1/6 of that found for styrene under similar conditions, c.f., the self-initiated thermal oxidation (3).*

[3]*For example, the absorption of 0.1 mole/l O_2 in a photochemical autoxidation of 1.78 mole/l of α-methylstyrene in chlorobenzene at 50° and 680 mm O_2 gave a 70% yield of acetophenone and a 16% yield of a methanol insoluble polymer, $(C_9H_{10}O_2)_n$. These yields are based on the assumption that 0.1 mole/l of the α-methylstyrene had reacted. The chain length in this oxidation was about 80.*

The α-methylstyrene was only very slightly oxidized during most of our kinetic measurements (<0.01 mole/l O_2.) We have therefore assumed that the small amounts of formaldehyde which must have been formed in the reaction did not interfere with the determination of k_t and k_p for the α-methylstyrene.

[4]*Throughout this work the measured rate of chain termination is taken to be $2k_t$ since two oxidation chains are ended, i.e.,*

$$RO_2\cdot + RO_2\cdot \xrightarrow{2k_t} \textit{Inactive products.}$$

TABLE 1

Absolute rate constants for the autoxidation of 1.78 *M* α-methylstyrene in chlorobenzene

Temperature (°C)	Oxygen pressure (mm)	$(k_p/(2k_t)^{1/2}) \times 10^2$ $(l\ mole^{-1}\ s^{-1})^{1/2}$	k_p $(l\ mole^{-1}\ s^{-1})$	$k_t \times 10^{-5}$ $(l\ mole^{-1}\ s^{-1})$
13	100	0.62	5	4
13	200	0.68	6	3
13	680	0.65*	4*	2*
30	680	1.3	7	2
30	680	1.3*†	10*†	3*†
40	300	1.5	17	6
40	680	1.6	12	3
50	680	2.3	28	7

*Average of two independent experiments each consisting of not less thant hree separate determinations of k_t.
†With 0.57 *M* α-methylstyrene.

The small activation energy for the chain termination of tertiary peroxy radicals is in agreement with the recent electron spin resonance studies of Thomas (9) on the chain-terminating interaction of *t*-butylperoxy radicals ($E = 10.2 \pm 1$ kcal/mole) and cumylperoxy radicals ($E = 0 \pm 1$ kcal/mole from the oxidation of cumene and 2 ± 1 kcal/mole from the decomposition of cumene hydroperoxide). Vichutinskii (12) has also reported obtaining an activation energy of 2.3 ± 0.3 kcal/mole for the mutual destruction of cumylperoxy radicals, the reaction being followed by the method of chemiluminescence. The actual rate constant for the chain termination is larger than for *t*-butylperoxy radicals ($k_t = 3.1 \times 10^2$ l mole^{-1} s^{-1} at 30 °C (9)), cumylperoxy radicals[5] ($k_t = 1.9 \times 10^4$ l mole^{-1} s^{-1}), or the peroxy radicals from 2,4,6-trimethylheptane ($k_t = 1.8 \times 10^5$ l mole^{-1} s^{-1} at 40–80° (13)). It is, perhaps, specifically worth pointing out that the rate of oxidation of α-methylstyrene is about twice as great as the rate of oxidation of styrene under comparable conditions even though both k_p and k_t are smaller for the former compound than for the latter.[6] It is clear that structural influences on oxidation rates cannot be easily interpreted unless both rate constants are known.

The deutero-α-methylstyrene, $C_6H_5C(CD_3):CD_2$, oxidized slightly more rapidly at 30° than the undeuterated compound ($k_p/(2k_t)^{1/2} = 1.6 \times 10^{-2}$ (l mole^{-1} s^{-1})$^{1/2}$). At this temperature the measured rate constants (5 and 5×10^4 l mole^{-1} s^{-1} for k_p and k_t, respectively, at a $C_6H_5C(CD_3):CD_2$ concentration of 0.57 mole/l) indicated an unbelievably large isotope effect for both propagation and termination. A rather different experimental approach involving measurement of the rates of oxidation at 65 °C in the presence of 2,6-di-*t*-butyl-4-methylphenol (see below) indicated that $(k_p)_H/(k_p)_D = 1.0 \pm 0.05$. This suggests that the entire variation in $k_p/(2k_t)^{1/2}$ is due to a change in k_t. That is, $(k_t)_H/(k_t)_D = (1.6)^2/(1.3)^2 = 1.5$, this isotope effect being calculated from oxidations with a chain length of 15 for the normal and 18.5 for the deutero-α-methylstyrenes (see ref. 7). These isotope effects are in fair agreement with the values obtained by Boozer *et al.* (14) from the oxidation of cumene and $C_6H_5C(CD_3)_2H$, i.e., $rate_H/rate_D \simeq 0.88$. This deuterium

[5]*This value is derived from the results of Melville and Richards (10) and Vichutinskii (12). Melville and Richards give values for $2k_t$ of 2.8 and 3.3×10^4 l mole^{-1} s^{-1} at 50 and 65 °C, respectively. These values have been corrected by a factor of 1/0.6 to allow for the fact that the efficiency of chain initiation from ACHN is not equal to 1.0, i.e., $(k_t)_{50°} = 2.8/(0.6 \times 2.0) = 2.35 \times 10^4$ l mole^{-1} s^{-1}. Extrapolation to 30 °C gives $k_t = 1.88 \times 10^4$ l mole^{-1} s^{-1}. Vichutinskii's value for $2k_t$ of 3.3×10^4 l mole^{-1} s^{-1} at 20 °C combined with this activation energy also gives $k_t = 1.88 \times 10^4$ l mole^{-1} s^{-1} at 30 °C. Howard and Robb's (11) value is significantly higher than this, i.e., 9×10^4 l mole^{-1} s^{-1} at 56 °C.*

In connection with these calculations, extrapolation of Thomas' data (9) and Vichutinskii's data (12) to 60 °C gives $k_t = 1.42 \times 10^8$ l mole^{-1} s^{-1} for t-butylperoxy radicals and $k_t = 2.65 \times 10^4$ l mole^{-1} s^{-1} for cumylperoxy radicals. The ratio of these two rate constants is 18.7, in excellent agreement with the ratio of 16 determined by Traylor and Russell at this temperature (7).

[6]*For example, for styrene at 30 °C $k_p = 41$ l mole^{-1} s^{-1} and $k_t = 2.1 \times 10^7$ l mole^{-1} s^{-1} (1).*

Can. J. Chem. Downloaded from www.nrcresearchpress.com by 210.87.254.105 on 09/05/12
For personal use only.

isotope effect in chain termination has been explained by Traylor and Russell (7) as arising from a secondary isotope effect in the reaction,

$$C_6H_5C(CH_3)_2O\cdot \rightarrow CH_3\cdot + C_6H_5COCH_3$$

and a primary isotope effect in the reaction

$$CH_3OO\cdot + ROO\cdot \rightarrow CH_2O + O_2 + ROH.$$

Inhibited Oxidation of α-Methylstyrene

In previous communications from this laboratory (15) we have shown that the highly hindered phenol 2,6-di-*t*-butyl-4-methylphenol (BMP) inhibits the AIBN thermally initiated oxidation of styrene and tetralin with very simple overall kinetics. The self-termination reaction of two peroxy radicals is replaced by hydrogen atom abstraction from the phenol, AH, i.e.,

$$RO_2\cdot + AH \xrightarrow{k_{inh}} ROOH + A\cdot$$

the oxidation rate, P, being given by

$$P = \frac{R_i k_p[RH]}{2k_{inh}[AH]}$$

where R_i is the rate of chain initiation and RH represents the substrate. It is inconceivable that deuteration of the substrate could have any significant effect on k_{inh}. A comparison of the BMP-inhibited rates of oxidation of a deuterated and undeuterated substrate should therefore reveal any isotope effect in k_p.

The BMP-inhibited oxidation of pure α-methylstyrene at 65 °C showed the expected first order kinetics. That is, at an AIBN concentration of 3×10^{-3} mole/l, $P \propto [AH]^{-1.0}$ in the range $10^{-4} - 5 \times 10^{-3}$ mole/l, and at a BMP concentration of 1.2×10^{-3} mole/l, $P \propto [AIBN]^{1.0}$ in the range $3 \times 10^{-4} - 3 \times 10^{-2}$ mole/l. The measured rates gave $k_p/k_{inh} = 2.7 \times 10^{-3}$ for neat α-methylstyrene and 5.0×10^{-3} for 1.78 *M* α-methylstyrene in chlorobenzene. Extrapolation of the data in Table I gives $(k_p)_{65°} = 40$ l mole^{-1} s^{-1}. Hence, $k_{inh} = 8.0 \times 10^3$ l mole^{-1} s^{-1} for α-methylstyrene in chlorobenzene and 1.5×10^4 l mole^{-1} s^{-1} for neat α-methylstyrene (if it is assumed that k_p is unaffected by the chlorobenzene, see Part IV).

The normal and deutero-α-methylstyrene were compared in dilute solution (1.87 *M*) in dimethylsulfoxide (DMSO) as a solvent. This procedure was employed because DMSO increases the inhibited rate by a factor of about 5 compared with chlorobenzene and it thus made possible the accurate measurement of inhibited rates with only 1 ml of the α-methylstyrenes. This accelerating effect of the DMSO is chiefly due to a reduction in k_{inh} since the solvent effect on k_p is quite small (see Part IV). Using 2×10^{-3} mole/l AIBN and 1.5×10^{-3} mole/l BMP, we obtained identical oxygen absorption curves for the two compounds. Within the limit of accuracy of the measurements $(k_p)_H/(k_p)_D = 1.0 \pm 0.05$ (see footnote[7]).

β-Methylstyrene

The oxidation of this compound does not appear to have been studied previously. Benzaldehyde was one of the main products (~40%) from the photochemically initiated

[7]*This result contrasts with the small positive isotope effect of 1.05–1.27 obtained by Boozer et al. (14) from the rates of the 4-nitrophenol- and 2,4-dichlorophenol-inhibited oxidation of cumene and* $C_6H_5C(CD_3)_2H$ *and also contrasts with the small positive isotope effect of (~10–20%) from our absolute measurements of* k_p *for styrene,* $C_6H_5CD{:}CH_2$ *and* $C_6H_5CD{:}CD_2$ *(2).*

Can. J. Chem. Downloaded from www.nrcresearchpress.com by 210.87.254.105 on 09/05/12
For personal use only.

oxidation of a 0.89 *M* solution in chlorobenzene at 30 °C. It is presumably formed together with acetaldehyde, by the depolymerization of an oxygen–β-methylstyrene copolymer. The polymer could be precipitated from benzene with petroleum ether.

β-Methylstyrene oxidizes more rapidly than styrene. The presence of a kinetically first order chain termination process (rate constant k_x) in addition to the usual bimolecular termination renders the accurate determination of k_p and k_t quite difficult. We have previously observed concurrent first and second order termination processes in the oxidation of styrene (1, 2). However, the first order process is a more important source of chain termination in β-methylstyrene and, moreover, its importance increases slightly as the oxidation proceeds. The measured rate constants for styrene and β-methylstyrene at 30 °C are compared in Table II. The slightly larger value of k_p for the latter compound suggests that electron release by the methyl group more than outweighs the expected steric effect which would tend to hinder the addition of the peroxy radical.

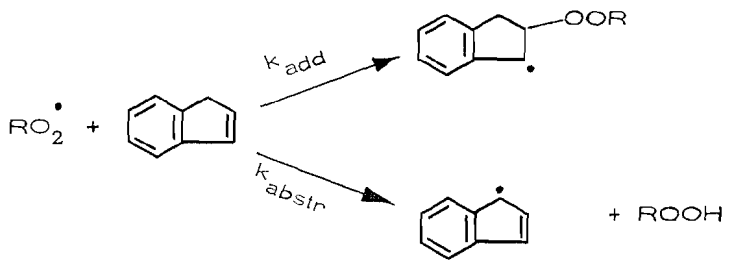
TABLE II

Absolute rate constants for styrenes in chlorobenzene at 30 °C

Substrate	Concentration (mole l^{-1})	k_p ($l\ mole^{-1}\ s^{-1}$)	$k_t \times 10^{-7}$ ($l\ mole^{-1}\ s^{-1}$)	k_x (s^{-1})
Styrene (ref. 1)	2.01	41	2.1	0.24
β-Methylstyrene	0.89	51	1.6	0.61
Indene	0.67	142	2.5	1.24

Indene

The AIBN thermally initiated oxidation of indene involves both addition and abstraction by the chain-propagating peroxy radicals (4). Addition gives a 1:1 copolymer of indene and oxygen (rate constant k_{add}) while abstraction results in chain transfer and the formation of a hydroperoxide (rate constant k_{abstr}).



In the present experiments at 30° with photochemical initiation of a 0.67 *M* solution of indene in chlorobenzene 10% of the absorbed oxygen is present as readily titratable hydroperoxide (4), i.e., $k_{add}/k_{abstr} = 9$.

There is a very pronounced first order chain termination process which renders the accurate determination of k_p and k_t for indene extremely difficult. At 30 °C the measured rate constants for 0.67 *M* indene in chlorobenzene were $k_p = 85\ l\ mole^{-1}\ s^{-1}$, $k_t = 8.2 \times 10^6\ l\ mole^{-1}\ s^{-1}$, and $k_x = 1.24\ s^{-1}$. If the first order process had been neglected an apparent $k_t = 4 \times 10^8$ would have been obtained.

We have shown previously that the first order process in styrene is strongly suppressed by the addition of heavy water (2).[8] With this in mind, absolute rate constants were

[8]*This was attributed to the replacement of readily abstractable, labile hydrogen atoms by much less readily abstractable deuterium atoms. The suggested mechanism involves hydroxylation of aromatic nuclei by hydroxyl radicals to give, eventually, phenols which are primarily responsible for the first order termination.*

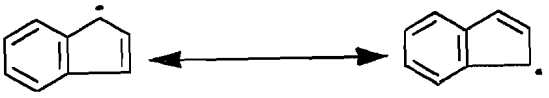
Can. J. Chem. Downloaded from www.nrcresearchpress.com by 210.87.254.105 on 09/05/12
For personal use only.

measured for indene under the same conditions as above except that a large excess of D_2O was added to the reactants. The following values were obtained: $k_p = 142$ l mole^{-1} s^{-1}; $k_t = 2.5 \times 10^7$ l mole^{-1} s^{-1}, and $k_x = 0.34$ s^{-1}. Neglect of the first order process would give $k_t = 6.7 \times 10^7$ l mole^{-1} s^{-1}. These propagation and bimolecular termination rate constants are probably a great deal more reliable than those obtained in the absence of D_2O since the first order termination has become much less important. They are compared with the constants for styrene and β-methylstyrene in Table II. The deuterium isotope effect on k_x, i.e., $k_x/(k_x)_{D_2O} \approx 3$ is in fair agreement with the value of $\geqslant 4.5$ found previously for styrene at 50 °C (2).

The overall propagation rate constant, k_p, can be divided into two parts, i.e.,

$$k_{add} = 142 \times 0.9 = 128 \text{ l mole}^{-1} \text{ s}^{-1}$$
$$k_{abstr} = 142 \times 0.1 = 14 \text{ l mole}^{-1} \text{ s}^{-1}.$$

Indene is about three times as reactive as styrene towards the addition of the corresponding peroxy radicals. This enhanced reactivity can probably be at least partly attributed to the fact that electron release by the methylene group is not accompanied by an opposing steric effect as was the case in β-methylstyrene. The rate constant for hydrogen abstraction is about 40% larger than the value found for allylbenzene at this temperature (see Part IV). This is probably caused by the greater stability of the indenyl radical which results from the two resonance structures (4).



REFERENCES

1. J. A. Howard and K. U. Ingold. Can. J. Chem. **43**, 2729 (1965).
2. J. A. Howard and K. U. Ingold. Can. J. Chem. **43**, 2737 (1965).
3. F. R. Mayo and A. A. Miller. J. Am. Chem. Soc. **80**, 2480 (1958).
4. G. A. Russell. J. Am. Chem. Soc. **78**, 1035, 1041 (1956).
5. P. D. Bartlett and T. G. Traylor. J. Am. Chem. Soc. **85**, 2407 (1963).
6. A. Factor, C. A. Russell, and T. G. Traylor. J. Am. Chem. Soc. **87**, 3692 (1965).
7. T. G. Traylor and C. A. Russell. J. Am. Chem. Soc. **87**, 3698 (1965).
8. R. Hiatt and T. G. Traylor. J. Am. Chem. Soc. **87**, 3766 (1965).
9. J. R. Thomas. J. Am. Chem. Soc. **87**, 3935 (1965).
10. H. W. Melville and S. Richards. J. Chem. Soc. 944 (1954).
11. J. A. Howard and J. C. Robb. Trans. Faraday Soc. **59**, 1590 (1963).
12. A. A. Vichutinskii. Dokl. Akad. Nauk SSSR, **157**, 150 (1964).
13. A. L. Buchachenko, K. Ya. Kaganskaya, M. B. Neiman, and A. A. Petrov. Kinetika i Kataliz, **2**, 44 (1961).
14. C. E. Boozer, B. W. Ponder, J. C. Trisler, and C. E. Wightman III. J. Am. Chem. Soc. **78**, 1506 (1956).
15. J. A. Howard and K. U. Ingold. Can. J. Chem. **40**, 1851 (1962); **42**, 2324 (1964).

Can. J. Chem. Downloaded from www.nrcresearchpress.com by 210.87.254.105 on 09/05/12
For personal use only.

Can. J. Chem. Downloaded from www.nrcresearchpress.com by 210.87.254.6 on 09/05/12
For personal use only.

ABSOLUTE RATE CONSTANTS FOR HYDROCARBON AUTOXIDATION

IV. TETRALIN, CYCLOHEXENE, DIPHENYLMETHANE, ETHYLBENZENE, AND ALLYLBENZENE[1]

J. A. HOWARD AND K. U. INGOLD

Division of Applied Chemistry, National Research Council, Ottawa, Canada

Received December 21, 1965

ABSTRACT

Absolute rate constants have been measured for the autoxidation of five hydrocarbons under a variety of conditions. The propagation (k_p) and termination (k_t) rate constants at 30 °C (in l mole^{-1} s^{-1}) are: tetralin in chlorobenzene 6.3 and 3.8×10^6 respectively, cyclohexene in chlorobenzene 6.1 and 2.8×10^6, diphenylmethane 4.8 and 8.0×10^7, ethylbenzene 0.11 and 2.0×10^7, and allylbenzene 10 and 2.2×10^8. Measurements on tetralin, α-methylstyrene, and allylbenzene in different solvents indicate that the effect of solvents on oxidation rates is mainly connected with changes in the rate of termination rather than propagation. Experiments with α,α-d_2-diphenylmethane gave isotope effects $k_H/k_D \sim 5.1$ for k_p and ~ 1.4 for k_t. The rate constant for hydrogen atom abstraction from 2,6-di-*t*-butyl-4-methylphenol by peroxy radicals decreases in the order expected if steric effects are important, i.e., primary peroxy > secondary peroxy > tertiary peroxy radical.

The co-oxidation method of estimating chain termination constants is criticized on the grounds that it can only be used to distinguish the fairly large changes in k_t commonly encountered between hydrocarbons giving tertiary peroxy radicals and those giving secondary or primary radicals.

The effect of hydrocarbon structure on bimolecular chain termination rate constants is reviewed. There is a gradation in k_t from $\sim 2 \times 10^8$ l mole^{-1} s^{-1} for primary peroxy radicals, through the range 8×10^7 to 1×10^6 for secondary radicals, to the range from 3×10^5 to 3×10^2 for tertiary peroxy radicals.

INTRODUCTION

The present paper extends our measurements of absolute rate constants for autoxidation from substances which copolymerize with oxygen (1, 2) to substances from which a benzylic and (or) allylic hydrogen atom is abstracted. Attention has again been devoted to deuterium isotope effects on the propagation and termination rate constants (k_p and k_t) with measurements being made on perdeutero tetralin and α,α-d_2-diphenylmethane. Solvent effects on k_p and k_t for tetralin suggest that the increase in oxidation rates in polar solvents is due more to a decrease in k_t than to an increase in k_p. The present data are in quite good agreement with previous determinations of k_t for cyclohexene (3–5) and tetralin (6).

The propagation and termination rate constants for allylbenzene have been measured. This compound is particularly interesting in that the initially formed benzyl radical isomerizes to a cinnamyl radical. Chain termination must involve the mutual interaction of cinnamyl peroxy radicals (7).

$$C_6H_5CH_2CH{=}CH_2 \xrightarrow{RO_2\cdot} C_6H_5\dot{C}HCH{=}CH_2 \rightarrow C_6H_5CH{=}CH\dot{C}H_2 \xrightarrow{O_2} C_6H_5CH{=}CHCH_2OO\cdot$$

The rates of oxidation of mixtures of tetralin and allylbenzene have been measured at 65 °C. The present results illustrate the difficulties which are inherent in this method of comparing rate constants for chain termination.

The 2,6-di-*t*-butyl-4-methylphenol inhibited oxidation of several substrates in chlorobenzene and dimethyl sulfoxide (DMSO) has been examined. It was found that the rate constant for inhibition depends on the nature of the peroxy radical.

[1]*Issued as N.R.C. No. 8893.*

The rate constants for bimolecular chain termination found in the present work have been combined with other reliable values from the literature to give an overall picture of the variation in k_t with hydrocarbon structure.

EXPERIMENTAL

Perdeuterotetralin was obtained from Merck, Sharpe and Dohme. Analysis by mass spectrometry gave 83.5% $C_{10}D_{12}$, 14.0% $C_{10}D_{11}H$, and 2.5% $C_{10}D_{10}H_2$. We are indebted to Dr. L. C. Leitch for a generous sample of α,α-d_2-diphenylmethane ($C_{13}D_2H_{10}$ 91%, $C_{13}DH_{11}$ 9%). None of the hydrocarbons used in this work contained more than 0.5% of impurities as determined by vapor phase chromatography.

All the absolute rate constants given in the tables are averages of at least two independent experiments consisting of not less than two, and usually three or four, measurements of k_t.

RESULTS AND DISCUSSION

Tetralin

Absolute rate constants for the autoxidation of pure tetralin from 13 to 50 °C and of 1.69 *M* tetralin in chlorobenzene from 22 to 50 °C are presented in Table I. At temperatures of 30 °C and above, the reaction shows fairly pronounced autocatalysis which is due to thermal, rather than photochemical, decomposition of tetralin hydroperoxide. This increasing thermal contribution to chain initiation as the reaction proceeds complicates the determination of k_p and k_t. Two methods were employed to overcome this difficulty. Firstly, a fresh sample of tetralin was used for each rate measurement. Secondly, a number of rate measurements were made in a single run, but the thermal contribution was determined after each pair of photochemical experiments, i.e., repeated rate measurements were made in the order, (i) steady illumination, (ii) intermittent illumination, (iii) no illumination. This second method gave somewhat more reproducible results but the agreement between the two methods was quite satisfactory. No kinetically first order chain terminating process could be detected at any temperature (1, 2) and the rate was independent of the oxygen pressure in the range 100–700 mm.

TABLE I

Absolute rate constants for the autoxidation of tetralin

Tetralin concentration (moles/l)	Temp. (°C)	$(k_p/(2k_t)^{1/2}) \times 10^3$ $(l\ mole^{-1}\ s^{-1})^{1/2}$	k_p $(l\ mole^{-1}\ s^{-1})$	$k_t \times 10^6$ $(l\ mole^{-1}\ s^{-1})$
7.34	13	1.14	2.2	1.9
1.69*	22	1.66	3.8	2.6
7.34	30	2.2	6.2	3.8
1.69*	30	2.3	6.4	3.8
7.34	40	2.8	8.5	5.0
1.69*	40	3.4	7.6	2.5
7.34	50	4.0	13.6	6.0
1.69	50	4.0	12.9	5.3

*In chlorobenzene.

Since the absolute rate constants appear to be identical in pure tetralin and in the chlorobenzene solution, the results of both sets of measurements were combined to determine the temperature coefficients.

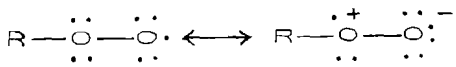
$$k_p/(2k_t)^{1/2} = (44 \pm 2) \exp -(6\,000 \pm 300)/RT\ (l\ mole^{-1}\ s^{-1})^{1/2}$$
$$k_p = (5.7 \pm 0.6) \times 10^6 \exp -(8\,300 \pm 800)/RT\ l\ mole^{-1}\ s^{-1}$$
$$k_t = (4.3 \pm 1.5) \times 10^9 \exp -(4\,300 \pm 1\,500)/RT\ l\ mole^{-1}\ s^{-1}$$

The measured activation energy for termination may be too large because of the uncertainties in k_t at the higher temperatures. The average value of k_t over the whole

Can. J. Chem. Downloaded from www.nrcresearchpress.com by 210.87.254.6 on 09/05/12
For personal use only.

temperature range is 4×10^6 l mole^{-1} s^{-1}, in moderately good agreement with Bamford and Dewar's estimate of 1.1×10^7 l mole^{-1} s^{-1} at 25 °C.

Current interest in solvent effects on rates of hydrocarbon autoxidation (see e.g. 1, 8, 9) prompted us to examine the effect of *n*-decane, acetonitrile, and DMSO on the absolute rate constants for the oxidation of tetralin at 30 °C. The data are given in Table II together with the results obtained for α-methylstyrene in DMSO and chlorobenzene and for allylbenzene in DMSO and as the pure material. The data suggest that the solvents influence k_t to a much greater extent than k_p. This result contrasts with our previous results in styrene at 13 °C (1).[2] It lends support to Hendry and Russell's proposal (9) that the solvent effect is connected with the fact that peroxy radicals have some polar character in their ground state, i.e.,



which is destroyed in termination. It is possible that some of the variation in k_t with the different solvents may be due to changes in the viscosity of the medium. However, this effect is probably not very large since acetonitrile has a lower viscosity than chlorobenzene and DMSO a higher viscosity.

The use of DMSO as a solvent in autoxidations may appear somewhat unusual in view of the well known reactions between sulfur-containing compounds and hydroperoxides which were first described by Denison (10). However, DMSO does not affect the yield of hydroperoxide formed during the oxidation of tetralin at 65 °C (see Table III). The slightly greater than theoretical yields of hydroperoxide noted in this table are almost certainly due to the oxidation that occurs after the absorption measurements are completed while the sample is being removed from the reaction vessel for analysis. It is clear that DMSO acts as an "inert" solvent under the conditions of these experiments.

In a preliminary experiment a small sample of the perdeuterotetralin was oxidized at 65 °C. The rate was unexpectedly low, being only about 8% of the rate for normal tetralin[3] instead of an expected 20% (11). Only three very minor impurities totalling less than 0.5% were detected in the deuterotetralin by gas chromatography on a 150 ft Golay capillary column at 120 °C. However, when the deuterotetralin was washed with concentrated D_2SO_4 the acid layer turned black. The washing was repeated many times until the acid layer became only a pale yellow. The deuterotetralin was then washed with D_2O, passed through alumina, dried with calcium hydride, and distilled. The final product ($C_{10}D_{12}$ 76.8%, $C_{10}D_{11}H$ 19.8%, $C_{10}D_{10}H_2$ 3.4%) showed no detectable impurities by gas chromatography and had an identical ultraviolet spectrum to that of undeuterated tetralin. However, the result of all this "purification" was to *reduce* the rate at 65° to only 5% of the value for pure tetralin. Rotating sector experiments on this "purified" material at 30 °C and a chain length of about 5 ([RD] = 7.34 mole/l) gave the following.

$$k_p/(2k_t)^{1/2} = 5.7 \times 10^{-5}\ \text{l}^{1/2}\ \text{mole}^{-1/2}\ \text{s}^{-1/2}$$
$$k_p = 1.1 \times 10^{-1}\ \text{l mole}^{-1}\ \text{s}^{-1}$$
$$k_t = 2.0 \times 10^{6}\ \text{l mole}^{-1}\ \text{s}^{-1}$$

[2]*However, DMSO was not used as a solvent in the styrene experiments and a great deal of the observed variation in rate with solvent was due to a change in the rate of chain initiation, R_i. Thus, at 13 °C, $k_p/(2k_t)^{1/2}$ was constant in benzene, chlorobenzene, and acetonitrile (2.7×10^{-3} l$^{1/2}$ mole$^{-1/2}$ s$^{-1/2}$) although it was slightly smaller in t-butylbenzene (2.3×10^{-3}) and quite a bit smaller in n-decane (1.2×10^{-3}). In DMSO the rate of chain initiation is lower than in chlorobenzene (see Table II).*

[3]*The oxidation was initiated with 5.72×10^{-2} mole/l AIBN. The rates were 5.35×10^{-5} and 4.5×10^{-6} mole l^{-1} s^{-1} for $C_{10}H_{12}$ and $C_{10}D_{12}$ respectively.*

Can. J. Chem. Downloaded from www.nrcresearchpress.com by 210.87.254.6 on 09/05/12
For personal use only.

Can. J. Chem. Downloaded from www.nrcresearchpress.com by 210.87.254.6 on 09/05/12
For personal use only.

TABLE II

Solvent effects on absolute rate constants for hydrocarbon autoxidation at 30 °C

Substrate	Concentration (mole l^{-1})	Solvent	$R_i \times 10^7$* (mole l^{-1} s^{-1})	$(k_p/(2k_t)^{1/2}) \times 10^3$ (l $mole^{-1}$ $s^{-1})^{1/2}$	k_p (l $mole^{-1}$ s^{-1})	$k_t \times 10^{-5}$ (l $mole^{-1}$ s^{-1})
Tetralin	1.69	*n*-Decane	1.30	1.6	4.6	40
		Chlorobenzene	2.62	2.3	6.4	38
		Acetonitrile	2.71	5.6	10	16
		DMSO	1.35	5.4	6.6	7.6
α-Methylstyrene	1.78	Chlorobenzene	2.62	13	10	3.0
		DMSO	1.35	24	13	1.5
Allylbenzene	7.56	None	1.3	0.49	10	2 200
	1.74	DMSO	1.35	1.2	10	370

*R_i measured before each run with 2,6-di-*t*-butyl-4-methylphenol in the relevant solvent.

TABLE IV

Absolute rate constants for the autoxidation of cyclohexene at 30 °C

Solvent	Cyclohexene concentration (mole l^{-1})	Experimental method	$(k_p/(2k_t)^{1/2}) \times 10^3$ (l $mole^{-1}$ $s^{-1})^{1/2}$	k_p (l $mole^{-1}$ s^{-1})	$k_t \times 10^{-6}$ (l $mole^{-1}$ s^{-1})	$k_{inh} \times 10^{-3}$ (l $mole^{-1}$ s^{-1})	Reference
None	9.86	Rotating sector	1.8				This work
C_6H_5Cl	1.90	Rotating sector	2.5	6.1	2.8	13.5	This work
None	9.86	Rotating sector	1.3*	1.3*	0.48	—	(3)
None	9.86	Thermocouple	2.0†	2.5†	0.8	3.0†	(4)
None	9.86	Thermocouple	1.8‡	2.6‡	1.0	5.6‡	(5)

*Extrapolated from 15 °C.
†Extrapolated from 40 °C.
‡Extrapolated from 56 °C.

TABLE III

Hydroperoxide yields in the oxidation of tetralin with 0.01 mole/l AIBN at 65 °C

Tetralin concentration (mole l^{-1})	Solvent	Rate $\times 10^6$ (mole l^{-1} s^{-1})	$[O_2] \times 10^2$ absorbed (mole l^{-1})	$[ROOH] \times 10^2$ produced* (mole l^{-1})	$([ROOH]/[O_2]) \times 100$
7.34	None	21.6	8.6	8.8	102
2.0	C_6H_5Cl	7.42	2.35	2.4	102
2.0	DMSO	14.3	2.36	2.4	102

*Sample refluxed in isopropanol containing potassium iodide and acetic acid for 10 min under nitrogen. The liberated iodine was titrated with sodium thiosulfate. Recrystallized tetralin hydroperoxide titrated to about 98% of theory. There was no significant blank correction when chlorobenzene and DMSO were treated with 0.01 *M* AIBN and oxygen at 65 °C for the same lengths of time as the corresponding tetralin oxidations.

The isotope effect on k_p (>50) is completely out of line with previous work on the isotope effect in a similar oxidation (11) and with our own results for diphenylmethane which are described below. Under these circumstances the observed isotope effect on k_t (~ 2) can hardly be meaningful. We can only suppose that some undetected and hard to remove impurity was present in the deuterotetralin.

Cyclohexene

The photochemically initiated autoxidation of cyclohexene at 30 °C showed fairly pronounced autocatalysis which was mainly due to the thermal decomposition of the hydroperoxide. For this reason, the absolute rate constants were measured on a dilute solution of cyclohexene in chlorobenzene. There was no detectable first order chain termination.

In Table IV the propagation and termination rate constants obtained in this work are compared with previously reported values for pure cyclohexene (which have been extrapolated to 30 °C). The rate constant for the reaction of cyclohexenylperoxy radicals with 2,6-di-*t*-butyl-4-methylphenol at 30 °C are also compared in this table.

$$RO_2\cdot + AH \xrightarrow{k_{inh}} ROOH + A\cdot \text{ (see footnote [4])}$$

On the whole, the agreement between different workers is quite satisfactory.

Diphenylmethane

The oxidation of this compound is autocatalytic at 30 °C. There is no detectable first order chain termination. Absolute rate constants for the pure unlabelled and pure α,α-d_2-diphenylmethane are given in Table V. The deuterium isotope effects for $k_p/(2k_t)^{1/2}$, k_p, and k_t are all of the expected order of magnitude (11). The isotope effect for termination (~ 1.4) provides further support for the view that one of the α-hydrogen atoms is abstracted in the chain-terminating interaction of secondary peroxy radicals (1, 11).

Ethylbenzene

Although this compound is quite resistant to oxidation at 30 °C it was found that a

[4]*Since the reaction of the phenoxy radical with* $RO_2\cdot$, *i.e.*,

$$RO_2\cdot + A\cdot \rightarrow ROOA$$

is very rapid, two chains are terminated for each primary step of inhibition. The inhibited rate P_{inh} *is therefore given by (12)*

$$P_{inh} = (k_p[RH]R_i)/(2k_{inh}[AH]).$$

The values of k_{inh} *quoted in refs. 4 and 5 have therefore been divided by 2 after extrapolating to 30 °C.*

Can. J. Chem. Downloaded from www.nrcresearchpress.com by 210.87.254.6 on 09/05/12
For personal use only.

TABLE V

Absolute rate constants for the autoxidation of diphenylmethane at 30 °C

	$(k_p/(2k_t)^{1/2}) \times 10^4$ (l mole^{-1} s^{-1})$^{1/2}$	k_p (l mole^{-1} s^{-1})	$k_t \times 10^7$ (l mole^{-1} s^{-1})
$(C_6H_5)_2CH_2$	3.8	4.8	8.0
$(C_6H_5)_2CD_2$	0.88	0.94	5.7
k_H/k_D	4.3	5.1	1.4

reasonable chain length (~13) could be obtained by reducing the light intensity to 13% of its maximum value. In the pure hydrocarbon at 30 °C

$$k_p/(2k_t)^{1/2} = 2.0 \times 10^{-4} \text{ (l mole}^{-1} \text{ s}^{-1})^{1/2}$$
$$k_p = 1.1 \text{ l mole}^{-1} \text{ s}^{-1}$$
$$k_t = 1.6 \times 10^7 \text{ l mole}^{-1} \text{ s}^{-1}.$$

This chain termination rate constant is in good agreement with the value of $(9.5 \pm 2.0) \times 10^6$ l mole^{-1} s^{-1} reported by Tsepalov and Shlyapintokh (13) using the rotating sector method in the range 50–90° and is in even better agreement with the value of $(2.0 \pm 0.3) \times 10^7$ l mole^{-1} s^{-1} reported by Vichutinskii (14) using the chemiluminescence method in the range 30–60 °C.

Allylbenzene

Absolute rate constants for the oxidation of allylbenzene at 30 °C have been given in Table II for the pure hydrocarbon and for a 1.74 *M* solution in DMSO. The reaction was neither autocatalytic nor autoretarding and there was no detectable first order chain termination.

It is clear that the comparatively low rate of oxidation of allylbenzene is not due to a low rate of propagation but instead is due to the very high rate of termination of the *primary* cinnamyl peroxy radicals.

The differences found in this work for the chain termination rate constants of allylbenzene and the three secondary hydrocarbons was a little unexpected. It led us to re-examine a currently popular indirect method of estimating chain termination rate constants known as competitive oxidation.

Competitive Oxidations

In 1955 Russell published a paper on the competitive oxidation of cumene and tetralin which was of fundamental importance to the whole field of autoxidation (15). Russell found that mixtures of cumene and tetralin, containing only small amounts of the more reactive compound, tetralin, are oxidized at rates considerably below those observed for either of the pure hydrocarbons. This decrease in the rate stems from the fact that a relatively high concentration of tetralylperoxy radicals is formed in solutions containing mostly cumene. Tetralylperoxy radicals terminate much more readily than cumylperoxy radicals and a lower rate of oxidation is observed for the mixture than for pure cumene because of the lowered steady-state concentration of peroxy radicals. Small amounts of other reactive hydrocarbons that produce secondary peroxy radicals were also shown to retard the oxidation of cumene. The limitations of this method for estimating k_t were clearly realized at this time, although they seem to have been overlooked in recent years. That is, a well defined minimum rate can only be obtained when the second hydrocarbon has a larger k_t *and* is oxidized at a greater rate than the first. It must therefore have a

Can. J. Chem. Downloaded from www.nrcresearchpress.com by 210.87.254.6 on 09/05/12
For personal use only.

Can. J. Chem. Downloaded from www.nrcresearchpress.com by 210.87.254.6 on 09/05/12
For personal use only.

very much larger k_p. If this condition is not met, plots of rate against mixture composition may be curved but they will not exhibit a minimum.

Russell's original observation that primary and secondary peroxy radicals terminate more rapidly than tertiary has been repeatedly confirmed. However, the co-oxidation method seems quite incapable of distinguishing even the grossest variations in k_t for hydrocarbons giving primary and secondary peroxy radicals. For example, Balacéanu and co-workers (16, 17) have based a fairly extensive compilation of k_t values on the fine details of a large number of co-oxidation rate curves. Cumene, cyclohexene, and tetralin were used as reference hydrocarbons with values of $2k_t$ taken (from the literature) to be 3×10^4 (18), 1×10^6 (3), and 2 (or 4) $\times 10^7$ (6) l mole^{-1} s^{-1}, respectively. However, the data we have presented above show that k_t is virtually the same for cyclohexene and tetralin. One might perhaps be tempted to be wise after the event and draw this same conclusion from the almost linear co-oxidation rate vs. composition curve which is shown for these two hydrocarbons in ref. 16*a*, except for the fact that hydrocarbons with widely different k_t's also give nearly linear plots. Thus, Balacéanu (16*d*) has taken Tsepalov and Shlyapintokh's recent measurement of $2k_t$ for ethylbenzene (i.e., 1.9×10^7 l mole^{-1} s^{-1} (13) see above) to confirm the validity of the co-oxidation method of estimating k_t since ethylbenzene and tetralin ($2k_t$ taken as 2×10^7 (6)) give an exactly linear relation between rate and mixture composition. In conjunction with our present value of k_t for tetralin this linear relation actually provides one of the best pieces of evidence that the co-oxidation method of estimating k_t is not at all accurate. Further evidence along these lines is provided by Balacéanu's conclusion that $2k_t > 2 \times 10^7$ l mole^{-1} s^{-1} for cyclohexane (16*d*); a direct determination by McCarthy and Maclachlan, using a pulse radiolysis method, gave $2k_t = 2.8 \times 10^6$ l mole^{-1} s^{-1} (19). This latter value is in line with our own determination of $2k_t$ for cyclohexene and tetralin (two other hydrocarbons with six membered rings, see below). It would appear that the co-oxidation method is too insensitive to detect any but the very largest changes in the chain termination rate constants.

To check this conclusion we have examined the co-oxidation of tetralin ($k_t \approx 4 \times 10^6$ l mole^{-1} s^{-1}) and allylbenzene ($k_t \approx 2 \times 10^8$ l mole^{-1} s^{-1}). Russell (20) has shown that there is little or no curvature in the plots of rate against concentration for the oxidation of mixtures of indan with the following compounds at 90 °C (0.02 *M* *t*-butyl perbenzoate as initiator): dibenzyl ether, tetralin, allylbenzene, diphenylmethane, and methyl phenylacetate, these compounds being arranged in order of decreasing rate with indan lying between tetralin and allylbenzene. In spite of the very large differences in k_t we should therefore not expect much curvature in the co-oxidation of tetralin and allylbenzene, nor in fact do we find very much (see Fig. 1).

Inhibited Oxidations at 65 °C

The hindered phenol, 2,6-di-*t*-butyl-4-methylphenol (AH), inhibits the oxidation of hydrocarbons by replacing the normal bimolecular chain termination process by the following reactions.

$$RO_2\cdot + AH \xrightarrow{k_{inh}} ROOH + A\cdot$$

$$RO_2\cdot + A\cdot \xrightarrow{fast} ROOA$$

The inhibited rate, P_{inh}, can be very simply represented.

$$P_{inh} = k_p[RH]\frac{R_i}{2k_{inh}[AH]}$$

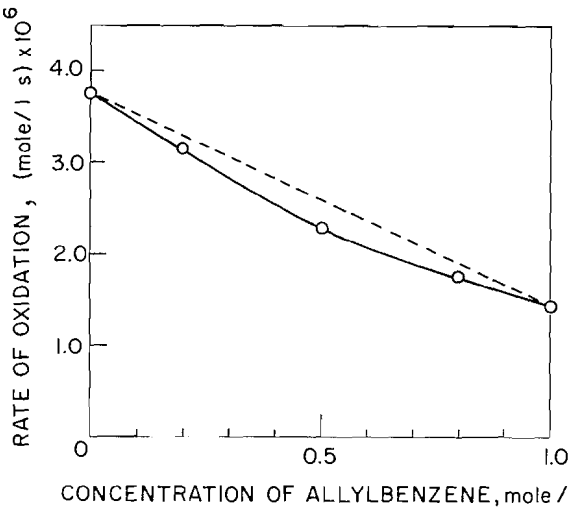


FIG. 1. The co-oxidation of tetralin and allylbenzene in *o*-dichlorobenzene at 65 °C with 0.01 mole/l AIBN as initiator. The total reactant concentration was kept at 1.0 *M* to reduce purely solvent effects on the rate which might be brought about by changes in the relative concentrations of the two reactants. The measured rate has been corrected for nitrogen evolution by the AIBN.

It follows that, for the same rate of chain initiation, the ratio of the inhibited rate to the uninhibited rate (P_0) is given by the following equation.

$$\frac{P_{\text{Inh}}}{P_0} = \left(\frac{R_i}{2}\right)^{1/2} \frac{k_t^{1/2}}{k_{\text{Inh}}[\text{AH}]}$$

We have previously suggested (1, 21) that, in a given solvent (8), k_{Inh} might be nearly independent of the nature of the peroxy radical. If k_{Inh} is indeed constant then measurement of P_{Inh}/P_0 will give k_t directly provided both the inhibited and the uninhibited[5] reactions conform to the simple kinetic equations. This method of obtaining k_t looked promising for compounds for which the rotating sector method could not be readily applied, e.g., fluorene, which absorbs quite strongly at 365 mμ, and dibenzyl ether, which is strongly autoretarding in chlorobenzene.

Several readily oxidizable compounds were examined at 65 °C as 2.0 *M* solutions in chlorobenzene (Table VI) and DMSO (Table VII). These solvents were used to reduce any variation in the strength or extent of phenol–solvent hydrogen bonding from one substrate to another. In calculating the data for these tables the rate constant for decomposition of AIBN was taken to be 1.8×10^{-5} s^{-1} and its efficiency of chain initiation[6] was taken to be 0.65. The first five substrates in the two tables have been arranged in order of decreasing k_t. It is quite clear that k_{Inh} is not independent of the nature of the peroxy radical. In fact, the results suggest a steric effect on the reaction rate since k_t decreases from the primary radical (allylbenzene), through the secondary radials to the tertiary radical (α-methylstyrene). The rather low value of k_{Inh} for α-methylstyrene in chlorobenzene, which is obtained from k_t at 30 °C, may be due to the relatively large activation energy for termination observed with this compound (2).

[5]*Obviously this method will not give k_t for styrene (1) or indene (2) since the uninhibited oxidations are terminated by both first and second order processes.*

[6]*This is smaller than the value of 0.8 used previously in chlorobenzene which partly accounts for the lower values of $k_p/(2k_t)^{1/2}$ for styrene and α-methylstyrene compared with the previously given values of $k_p/k_t^{1/2}$ (8) The remaining difference is probably due to the higher substrate concentrations employed in the present work.*

Can. J. Chem. Downloaded from www.nrcresearchpress.com by 210.87.254.6 on 09/05/12
For personal use only.

Can. J. Chem. Downloaded from www.nrcresearchpress.com by 210.87.254.6 on 09/05/12
For personal use only.

TABLE VI

Oxidation in chlorobenzene at 65 °C for 2.0 M oxidizable substrate with 2.4×10^{-3} mole/l AIBN and 1.0×10^{-3} mole/l 2,6-di-*t*-butyl-4-methylphenol

Substrate	$(k_p/(2k_t)^{1/2}) \times 10^3$ (l mole^{-1} s^{-1})$^{1/2}$	$(k_p/k_{inh}) \times 10^3$	$k_t^{1/2}/k_{inh}$ (mole s l^{-1})$^{1/2}$	$k_{inh} \times 10^3$ calculated from: (1) k_p at 65°* (l mole^{-1} s^{-1})	$k_{inh} \times 10^3$ calculated from: (2) k_t at 30°† (l mole^{-1} s^{-1})
Allylbenzene	2.4	2.3	0.67	—	22.1
Diphenylmethane	1.0	1.0	0.72	—	12.4
Styrene	(9.7)‡	10.0	(0.73)‡	17.8	—‡
Tetralin	7.7	1.8	0.17	13.4	11.5
α-Methylstyrene	25.4	5.0	0.14	8.0	3.9
Fluorene	3.0	1.6	0.38		
Dibenzyl ether	27.7§	10.6	0.27		

*Obtained by extrapolation of k_p from lower temperatures using the appropriate Arrhenius equations for 2.0 M (or weaker) solutions of the hydrocarbon in chlorobenzene. That is, at 65 °C k_p = 178 l mole^{-1} s^{-1} for styrene (1), k_p = 24.2 l mole^{-1} s^{-1} for tetralin (the value of 16.4 used in a previous paper (22) is in error), k_p = 39.8 l mole^{-1} s^{-1} for α-methylstyrene (2).

†Obtained with the following values of k_t (in l mole^{-1} s^{-1}): allylbenzene 2.2×10^8, diphenylmethane 8×10^7, tetralin 3.8×10^6 (this work), α-methylstyrene 3×10^5 (2).

‡Includes concurrent first order chain termination and therefore k_{inh} cannot be calculated from k_t at 30 °C.

§Autoretarding.

TABLE VII

Oxidations in dimethyl sulfoxide at 65 °C for 2.0 *M* oxidizable substrate with 2.4×10^{-3} mole/l AIBN and 1.0×10^{-3} mole/l 2,6-di-*t*-butyl-4-methylphenol

Substrate	$(k_p/(2k_t)^{1/2} \times 10^3$ (l mole^{-1} s$^{-1})^{1/2}$	$(k_p/k_{inh}) \times 10^5$	$k_t^{1/2}/k_{inh}$ (mole s l$^{-1})^{1/2}$	$k_{inh} \times 10^{3*}$ (l mole^{-1} s^{-1})
Allylbenzene	4.3	12	2.0	2.5
Diphenylmethane	1.8	2.9	1.2	—
Styrene	34.3	60	1.2	—
Tetralin	15.7	8.3	0.38	2.3
α-Methylstyrene	32.6†	26	0.56	0.69
Fluorene‡	8.3	13	1.1	
Dibenzyl ether	15.8†	35	1.6	

*Calculated from the k_t values at 30 °C given in Table II.
†Autocatalytic.
‡1.0 *M* solution.

While it is obviously impossible to assign accurate k_t values by this method it does provide rough numbers which seem fairly reasonable. Thus, taking $k_{inh} = 1.2 \times 10^4$ l mole^{-1} s^{-1} in chlorobenzene for compounds which give a secondary peroxy radical, we obtain $k_t = 2.1 \times 10^7$ l mole^{-1} s^{-1} for fluorene (in good agreement with the values found for styrene (1) and indene (2) in chlorobenzene) and $k_t = 1.0 \times 10^7$ l mole^{-1} s^{-1} for dibenzyl ether. Similarly, taking $k_{inh} = 2 \times 10^3$ l mole^{-1} s^{-1} in DMSO we obtain $k_t = 5 \times 10^6$ l mole^{-1} s^{-1} for fluorene (cf. allylbenzene and tetralin in DMSO, Table II) and $k_t = 1.0 \times 10^7$ for dibenzyl ether. The results suggest that k_t for dibenzyl ether is relatively unaffected by the solvent.

Summary of Bimolecular Chain Termination Constants for Hydrocarbon Autoxidation

The bimolecular chain termination rate constants found in the present work have been combined in Table VIII with values from our previous work (1, 2) and with other reliable values from the literature so as to give an overall picture of the variation in k_t with hydrocarbon structure. Rate constants for alcohols and aldehydes have not been included because there are too few values presently available for useful comparisons to be made with the hydrocarbons. Octene-1 has been placed with allylbenzene since it almost certainly gives mainly primary peroxy radicals (22). The value given in the table was obtained by the pulse radiolysis of octene-1 in the presence of oxygen (19). However, when this technique is used for a compound in which the hydrogen atoms are not all equivalent, some question must always remain as to whether the peroxy radicals whose decay kinetics are observed are the same as the peroxy radicals formed in the thermal chain process. The anomalous position of octene-1 in Table VIII strongly suggests that this pulse radiolysis value for k_t is at least an order of magnitude too small.

Table VIII does not include the numerous k_t values reported by Bateman and co-workers (3, 23–25) for olefinic hydrocarbons since, where comparison is possible, their values are very much smaller than those found by other workers. For example, they give values of 4.8×10^5 and $0.8–1.5 \times 10^5$ l mole^{-1} s^{-1} for cyclohexene (3) and octene-1 (23) respectively. In addition, their internal consistency was not very good, e.g., the reported values of k_t for ethyl linoleate vary from 1.5×10^5 (23, 24) to 1.5×10^7 l mole^{-1} s^{-1} (25) and the values reported for digeranyl vary almost as much. Table VIII includes a recent determination of k_t for the simplest peroxy radical, namely the hydroperoxy radical, HOO· (26).

The results in Table VIII show that there is a continuous gradation in k_t over a range of about 10^6 as the peroxy radical is changed from the primary cinnamylperoxy (from

Can. J. Chem. Downloaded from www.nrcresearchpress.com by 210.87.254.6 on 09/05/12
For personal use only.

allylbenzene), through the secondaries, to the tertiary butylperoxy radical. The data for the secondary peroxy radicals suggest that k_t has a median value of about 2×10^7 for fairly unhindered benzylic peroxy radicals. This value is enhanced in diphenylmethane, presumably because the radical center is activated by a second phenyl group and is depressed in tetralin because the radical center is part of a six membered ring. In the latter case, steric hindrance to chain termination is expected since the peroxy (or alkoxy) group in one radical must be in the highly unfavorable axial position (19). This is, of course, also true of cyclohexene and cyclohexane. In this connection it is interesting to note that Robb and Shahin (27) obtained low k_t values for three methyl cyclohexenes, viz. 4.3×10^5, 1.7×10^6, and 1.4×10^6 l mole^{-1} s^{-1} for the 1-methyl-, 4-methyl-, and 4,5-dimethyl-cyclohexenes. Incidentally, our own attempt to measure k_t for cyclohexane was frustrated by its low rate of oxidation. The idea that steric factors may be important in chain termination provides a tentative explanation for the very high k_t value found for allylbenzene since steric effects would be at a minimum for this primary peroxy radical. The high k_t value for this compound may also be partly due to the greater resonance stabilization which is possible for the cinnamyl system relative to the benzyl system.

The variation in k_t for the tertiary peroxy radicals can probably be attributed to variations in the stabilities of their alkoxy radicals. That is, the termination of tertiary peroxy radical chains seems to proceed mainly through the formation and subsequent β-scission of the corresponding alkoxy radicals (30). The radical ejected in the β-scission adds oxygen to form a primary (or secondary) peroxy radical which can terminate chains much more readily than the main chain carrying tertiary peroxy radicals (15).

TABLE VIII

Bimolecular chain termination rate constants for hydrocarbon autoxidation (data refer to pure hydrocarbon or to the hydrocarbon in chlorobenzene solution)

Parent hydrocarbon		k_t* (l mole^{-1} s^{-1})	References
	H_2	1.0×10^6†	(26)
Primary radicals	Allylbenzene	2.2×10^8	This work
	Octene-1	4.6×10^6‡	(19)
Secondary radicals	Diphenylmethane	8.0×10^7	This work
	Indene	2.5×10^7	(2)
	Styrene	2.1×10^7	(1)
	m-, *p*-Subst. styrenes	2.2–5.4×10^7§	(1)
	Fluorene	2.0×10^7‖	This work
	Ethylbenzene	1.6×10^7	This work (13, 14)
	Tetralin	3.8×10^6	This work
	Cyclohexene	2.8×10^6	This work (3–5, 27)
	Cyclohexane	1.4×10^6‡	(19)
Tertiary radicals	α-Methylstyrene	3.0×10^5	(2)
	2,4,6-Trimethylheptane	1.8×10^5¶	(28)
	Cumene	1.9×10^4	(14, 18)
	Isobutane	3.1×10^2	(29)

*Generally measured at or near 30 °C. The rate constants have been extrapolated to 30 °C for the last two hydrocarbons in the table since the activation energy for chain termination is known for these compounds.
†Radiolysis of concentrated aqueous solutions of hydrogen peroxide at 10–25 °C.
‡Radiolysis at room temperature.
§At 40 °C.
‖Indirect measurement. See text.
¶In range 40–80 °C.

REFERENCES

1. J. A. HOWARD AND K. U. INGOLD. Can. J. Chem. **43**, 2729, 2737 (1965).
2. J. A. HOWARD AND K. U. INGOLD. Can. J. Chem. In press. 1966.
3. L. BATEMAN and G. GEE. Proc. Roy. Soc. London, Ser. A, **195**, 391 (1948).
4. J. C. ROBB and M. SHAHIN. J. Inst. Petrol. **44**, 283 (1958).

Can. J. Chem. Downloaded from www.nrcresearchpress.com by 210.87.254.6 on 09/05/12
For personal use only.

5. J. A. HOWARD and J. C. ROBB. Trans. Faraday Soc. **59**, 1590 (1963).
6. C. H. BAMFORD and M. J. S. DEWAR. Proc. Roy. Soc. London, Ser. A, **198**, 252 (1949).
7. L. BATEMAN. Quart. Rev. London, **8**, 147 (1954).
8. J. A. HOWARD and K. U. INGOLD. Can. J. Chem. **42**, 1044, 1250 (1964).
9. D. G. HENDRY and G. A. RUSSELL. J. Am. Chem. Soc. **86**, 2368 (1964).
10. G. H. DENISON, Jr. Ind. Eng. Chem. **36**, 477 (1944).
11. G. A. RUSSELL. J. Am. Chem. Soc. **79**, 3871 (1957).
12. J. A. HOWARD and K. U. INGOLD. Can. J. Chem. **40**, 1851 (1962).
13. V. F. TSEPALOV and V. YA. SHLYAPINTOKH. Dokl. Akad. Nauk SSSR, **124**, 883 (1959). Kinetika i Kataliz, **6**, 870 (1962).
14. A. A. VICHUTINSKII. Dokl. Akad. Nauk SSSR, **157**, 150 (1964).
15. G. A. RUSSELL. J. Am. Chem. Soc. **77**, 4583 (1955).
16. J. ALAGY, G. CLÉMENT, and J. C. BALACÉANU. Bull. Soc. Chim. France, (*a*) 1325 (1959); (*b*) 1495 (1960); (*c*) 1303 (1961); (*d*) 1792 (1961).
17. C. PARLANT, I. SÉRÉE DE ROCH, and J. C. BALACÉANU. Bull. Soc. Chim. France, 3161 (1964).
18. H. W. MELVILLE and S. RICHARDS. J. Chem. Soc. 944 (1954).
19. R. L. MCCARTHY and A. MACLACHLAN. J. Chem. Phys. **35**, 1625 (1961). Trans. Faraday Soc. **57**, 1107 (1961).
20. G. A. RUSSELL. J. Am. Chem. Soc. **78**, 1047 (1956).
21. J. A. HOWARD and K. U. INGOLD. Can. J. Chem. **43**, 2724 (1965).
22. S. J. Moss and H. STEINER. J. Chem. Soc. 2372 (1965).
23. L. BATEMAN and G. GEE. Trans. Faraday Soc. **47**, 155 (1951).
24. L. BATEMAN, J. L. BOLLAND, and G. GEE. Trans. Faraday Soc. **47**, 274 (1951).
25. L. BATEMAN, G. GEE, A. L. MORRIS, and W. F. WATSON. Discussions Faraday Soc. **10**, 250 (1951).
26. D. J. CURRIE and F. S. DAINTON. Trans. Faraday Soc. **61**, 1156 (1965).
27. J. C. ROBB and M. SHAHIN. Trans. Faraday Soc. **55**, 1753 (1959).
28. A. L. BUCHACHENKO, K. YA. KAGANSKAYA, M. B. NEIMAN, and A. A. PETROV. Kinetika i Kataliz, **2**, 44 (1961).
29. J. R. THOMAS. J. Am. Chem. Soc. **87**, 3935 (1965).
30. T. G. TRAYLOR and C. A. RUSSELL. J. Am. Chem. Soc. **87**, 3698 (1965).

Can. J. Chem. Downloaded from www.nrcresearchpress.com by 210.87.254.6 on 09/05/12
For personal use only.

Can. J. Chem. Downloaded from www.nrcresearchpress.com by 210.87.254.5 on 09/05/12
For personal use only.

A CRITIQUE OF PAULI REPULSIONS AND MOLECULAR GEOMETRY

R. F. W. BADER[1] AND H. J. T. PRESTON
Burke Chemical Laboratories, Department of Chemistry, McMaster University, Hamilton, Ontario

Received July 30, 1965

ABSTRACT

A theoretical method, which allows one to determine the effect of the Pauli exclusion principle on the electron density distribution, is used to test the concepts underlying the electron pair repulsion theory of molecular geometry. It is shown that pictures of overlapping orbitals frequently do not correspond to the actual effect which the Pauli principle has on the three-dimensional charge density. An alternative electrostatic approach, involving the concept of a binding region for a polyatomic molecule, is proposed to account for the observed molecular geometries.

INTRODUCTION

A theory of molecular geometry has been advanced "on the idea that the arrangement of all the electron pairs (bonding pairs and lone pairs) in the valency shell of the central atom is determined by the operation of the Pauli exclusion principle (1)". This theory relates the electron distribution in three-dimensional space and thus the molecular geometry to "Pauli repulsions" between pairs of electrons, the pairs being in bond or lone pair orbitals. Lone pairs of electrons, since they are considered to be in the field of principally one nucleus, are considered as occupying a more diffuse orbital than the bonding electron pairs. Thus one speaks of lone pair – lone pair repulsions as being greater than lone pair – bond repulsions which in turn are more important than bond–bond repulsions. It is the purpose of the present work to find a theoretical basis for the concept of "Pauli repulsions" when applied in this manner.

The Pauli principle in its most general form demands that a wave function be antisymmetric with respect to permuting the space and spin coordinates of all the electrons present in the system. When an orbital approximation to the wave function is employed, the demands of the Pauli principle are met if no more than two electrons with opposite spins are placed in any one space orbital when these orbitals form an *orthogonal* set. Indeed, within the orbital approximation, this is an alternative statement of the Pauli principle. The important feature for the present discussion is that the Pauli principle demands that the set of orbitals, atomic or molecular, used to describe the system be orthogonal,

$$\int \phi_i \phi_j \, d\tau = \delta_{ij}. \qquad [1]$$

Thus for a system of N electrons requiring a minimal set of $N/2$ space orbitals (or $(N + 1)/2$ if N is odd), the Pauli principle is in reality an orthogonality restraint imposed in an $(N/2)$- or $((N + 1)/2)$-dimensional mathematical space. This is the source of confusion regarding "Pauli repulsions" which are treated as occurring in the three-dimensional physical space of the molecular system. To state that the Pauli principle gives rise to repulsions between filled orbitals in three-dimensional space is *not* the same as requiring these orbitals to be orthogonal in the many-dimensional space required to define the orbitals. The only function of the electronic coordinates which can be pictured in three-dimensional space is the one-electron density distribution, not the orbitals. Thus to determine what effect the Pauli principle has on molecular shape or the electronic

[1]*A. P. Sloan Research Fellow.*

arrangement in physical space, one must ask the question "what effect does the requirement of orthogonality of the orbitals in the many-dimensional orbital space have on the electron density distribution of three-dimensional space?" The answer to this problem is not obvious and does not in general follow from pictures of colliding orbitals in physical space. It is possible to formulate a technique which does show the effect of the orthogonality requirements of the Pauli principle on the three-dimensional electron density distribution. We shall illustrate this method with a number of examples.

The one-electron density distribution is the probability of finding electronic charge at some point in real space. Thus it is obtained by first squaring the total wave function

$$\psi^*\psi \, d\tau_1 \, d\tau_2, \ldots d\tau_N$$

which then gives the N-electron density function. This function gives the probability of electron 1 being in its volume element $d\tau_1$ when simultaneously electron 2 is in its volume element $d\tau_2$, etc. This is a function in $3N$-dimensional space. If this expression is integrated over the coordinates of all the electrons but one, we will have the probability of any one electron being at some point in its three-dimensional space. Since all the electrons are equivalent, multiplication of the integral by N gives the total one-electron density at each point in space designated by $\rho(\bar{r})$

$$[2] \qquad \rho(\bar{r}) = N \int \psi^*\psi \, d\tau_2 \, d\tau_3 \ldots d\tau_N$$

It is the density $\rho(\bar{r})$ which is responsible for the scattering of X-rays and electrons and which determines the electrical properties of the molecule such as the dipole moment and the electric field and field gradients within the molecule. For a molecule in a stationary state, the electron density distribution can be interpreted as a *static* distribution of negative charge, rather than as a probability function. For an orbital approximation to a wave function, eq. [2] takes the particularly simple form

$$[3] \qquad \rho(\bar{r}) = \sum_i n_i \phi_i^2$$

where the ϕ_i's are an orthogonal set of orbitals and the n_i's are the occupation numbers equal to one or two.

When the orbitals are orthogonal, the Pauli principle is satisfied and there are no Pauli repulsion effects. To determine the effect of the Pauli principle on a wave function or a density, one must start with an orbital set which is orthogonal because of some restraint. The restraint may be artificial or be the result of a large separation between the orbitals. Then the effects of the nonorthogonality are determined when the restraint is removed. For example, we may consider the effects of the Pauli exclusion principle on the electron density distribution obtained when two helium atoms approach one another. Let ϕ_a and ϕ_b be doubly occupied atomic orbitals on atoms a and b. When the atoms are widely separated, the overlap between the orbitals is zero and the electron density is then simply

$$\rho_0 = 2(\phi_a^2 + \phi_b^2).$$

The same expression would hold for the density for small values of the internuclear distance if the orbitals did not overlap. However, since they do overlap, the Pauli exclusion principle demands the corrected form

$$[4] \qquad \rho = \rho_0 + \Delta\rho.$$

The quantity $\Delta\rho$ is the change in the electron density which arises from the orthogonality

Can. J. Chem. Downloaded from www.nrcresearchpress.com by 210.87.254.5 on 09/05/12
For personal use only.

requirements of the Pauli exclusion principle. Longuet-Higgins and Salem (2)[2] have shown that when ρ is expressed in the form of eq. [4], $\Delta\rho$ has the form

$$\Delta\rho = -4S\phi_a\phi_b + 2S^2(\phi_a^2 + \phi_b^2) \quad [5]$$

where S is the overlap integral between ϕ_a and ϕ_b. Expression [5] for $\Delta\rho$ is correct to the order S^2 and goes to zero as S goes to zero. It is seen that $\Delta\rho$ is negative in some parts of space, giving a total density ρ less than that of the original atomic densities, and positive, in others, giving in these regions a total density which is greater than the original atomic densities. The integration of ρ over all space must yield the total number of electrons, four in this case, and this is given by the integration of ρ_0 itself. Thus the integration of $\Delta\rho$ must yield zero,

$$\int \Delta\rho \, d\bar{r} = 0.$$

The positive and negative regions of $\Delta\rho$ exactly balance so that the decrease in density in certain regions from the value given by ρ_0 must be equal to the increase over the ρ_0 values in other regions. The quantity $\Delta\rho$ thus gives a three-dimensional picture of the charge density which is transferred relative to the original set of orbitals because of the operation of the Pauli principle. In this simple example where ϕ_a, ϕ_b, and S are all positive, the expression for $\Delta\rho$ shows that charge of total amount $4S^2$ must be removed from regions where ϕ_a and ϕ_b overlap and transferred to regions where ϕ_a^2 and ϕ_b^2 are large. Figure 1 shows a plot of $\Delta\rho$ in the molecular plane. The plot shows dramatically the operation of the Pauli exclusion principle on two overlapping, doubly filled orbitals, or if one wishes, the effect of Pauli repulsions. Wherever the overlap of the original atomic orbitals is large, $\Delta\rho$ is negative, showing that electron density has migrated away from this region. The density is transferred to the regions behind each nucleus. The region between the nuclei is one of low potential energy, and is the region where charge density must be concentrated to achieve a stable chemical bond. This is the origin of the Pauli repulsions. The operation of the Pauli exclusion principle requires that density be removed from the region of low potential energy and be placed in less favored regions. The electronic energy is thus raised above that of the separated atoms and a repulsive force results. Thus while there are no Pauli repulsive forces as such, the Pauli exclusion principle does place restraints on the distribution of the electronic charge and this in turn determines the electronic energy of the system.

Actually, the energy is not related to the one-electron density distribution in any simple way.[3] However, the forces acting on the nuclei are explicable in terms of classical electrostatics and are determined by the one-electron density distribution (4). Therefore, the change in stability brought about by the charge which is transferred as a result of the Pauli principle is best discussed in terms of the forces acting on the nuclei. For example, in the case of the two He atoms, it is easily shown[4] that for any finite value of the internuclear separation the density distribution obtained from the overlap of the original atomic densities ρ_0 results in net forces of repulsion on both nuclei. For a diatomic molecule one can define a region, called the binding region, in which charge must be concentrated

[2] *The general theorem for $\Delta\rho$ was contributed by H. C. Longuet-Higgins.*

[3] *The energy is determined by the second-order or two-electron probability distribution (3).*

[4] *According to Gauss' law the electric field resulting from a spherical charge distribution acts as though all the charge were concentrated at its origin, and only that charge within the sphere defined by the bond length is effective. Thus for any finite value of the internuclear distance, where each nucleus has penetrated the density of the other, each experiences a force of repulsion due to two units of positive charge and an attractive force equivalent to something less than two negative charges.*

Can. J. Chem. Downloaded from www.nrcresearchpress.com by 210.87.254.5 on 09/05/12
For personal use only.

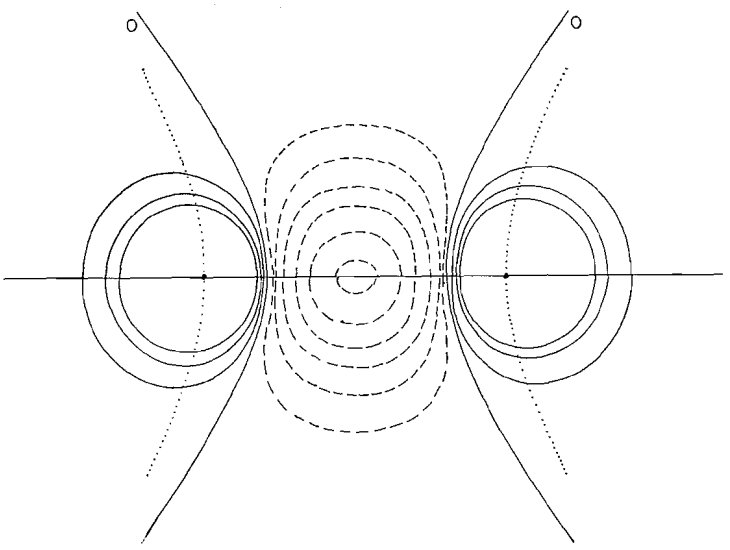


FIG. 1. A plot of $\Delta\rho$ for two He atoms at an internuclear separation of 2.5 atomic units (a.u.). The solid contours represent positive $\Delta\rho$ values, increasing in steps of 0.002 a.u. from the zero line. The dashed contours are negative $\Delta\rho$ values, decreasing in steps of 0.002 a.u. from the zero line. The dotted lines through the nuclei are the boundary curves which separate the binding and antibinding regions.

to overcome the nuclear forces of repulsion and achieve electrostatic equilibrium (5). This region is illustrated in Fig. 1 for a homonuclear diatomic molecule. Any charge density placed between the two boundary curves exerts an attractive force on both nuclei along the axis. Any charge outside these two curves exerts a greater force on one nucleus than on the other and leads to a separation of the molecule into atoms. Charge density on the boundary curves exerts equal forces on both nuclei along the bond axis. It is evident from Fig. 1 that $\Delta\rho$ is primarily negative in the binding region and positive in the antibinding regions. Since the sum of the original atomic densities, ρ_0, was insufficient to bind the nuclei, the density transferred because of the operation of the Pauli exclusion principle $\Delta\rho$ will clearly lead to an increase in the force of repulsion on both nuclei. That is, $\Delta\rho$ leads to a decrease in the charge density in the binding region over that present in the original atomic distribution which was itself insufficient to balance the forces of nuclear repulsion.

In this simple example of two He atoms, the form of $\Delta\rho$ fits in well with the concept of "Pauli repulsions" as they are usually applied (1). In a sense the orbitals do collide. However, it should be remembered that the resulting instability is an electrostatic one, resulting from the forced migration of charge from the binding region and the consequent increase in the nuclear forces of repulsion. For more complicated examples with more orbitals the analogy of $\Delta\rho$ with that of colliding orbitals in real space breaks down.

The expression for $\Delta\rho$ (2) and the concept of a binding region (6) can be extended to a polyatomic system. For any molecular system we can first determine $\Delta\rho$, the charge which is transferred because of the Pauli principle, and secondly, determine what effect this transfer of charge has on the stability of the system by noting whether or not it corresponds to an accumulation in the binding region. The general expression for $\Delta\rho$ for doubly occupied orbitals is (2)

$$[6] \qquad \Delta\rho = \sum_{i<j} \left(-4S_{ij}\phi_i\phi_j + 2S_{ij}^2[\phi_i^2 + \phi_j^2]\right)$$

Can. J. Chem. Downloaded from www.nrcresearchpress.com by 210.87.254.5 on 09/05/12
For personal use only.

and the total density is

$$\rho = 2 \sum_i \phi_i^2 + \Delta\rho. \qquad [7]$$

There is a contribution to $\Delta\rho$ from every pair of overlapping orbitals which is identical in form to that obtained for the two He atoms. The form of $\Delta\rho$ is determined by the initial choice for the set of orbitals ϕ_i. If they are chosen as an orthogonal set, then $\Delta\rho$ is zero at every point in space. However, in discussions of chemical bonding, comparisons between different systems are often employed, either between the separated atoms and the molecule, or between different members of an isoelectronic series. For example, we may consider the classic case of the ten-electron Ne atom and what effect the Pauli principle has on the relationship between its electron density distribution and that of the isoelectronic molecules H_2O, NH_3, and CH_4.

An Analysis of the Assumed Pauli Repulsions in H_2O and NH_3

Sidgwick and Powell (7) were the first to point out that molecules with four pairs of electrons in the valency shell were either tetrahedral in shape (CH_4) or were related to the basic tetrahedral geometry, e.g., the nearly tetrahedral bond angles found in NH_3 and H_2O. Lennard-Jones demonstrated (8) that the antisymmetrization requirements of the Pauli principle forces the electrons of an inert gas atom, such as neon, to dispose themselves so that those of the same spin subtend tetrahedral angles at the nucleus. He also showed that there was no correlation between the two tetrahedra resulting from the electrons with α and β spin. Pople (9) postulated that as one considered the withdrawal of successive protons from the Ne nucleus to form HF, H_2O, NH_3, and CH_4 respectively, the motion of the two tetrahedra would become correlated so as to concentrate a pair of electrons with opposite spin along each bond to a hydrogen atom. In this way the electron densities in these molecules were directly related to the tetrahedral hybridization (sp^3) of Ne and thus one accounted for the nearly tetrahedral bond angles in NH_3 and H_2O.[5] In their original paper Gillespie and Nyholm (1) also consider the orbital descriptions of H_2O and NH_3 to be sp^3 and related to that of Ne. They accounted for the fact that the bond angle in NH_3 is actually slightly less than tetrahedral by postulating that the repulsions between the lone pair and bond orbitals is greater than those between the bond orbitals themselves. Similarly in the case of H_2O, the extraction of two protons from the Ne nucleus changes the four equivalent orbitals into two lone pairs and two bonding pairs. Here the lone pair – lone pair "repulsion" causes an even greater decrease in the originally tetrahedral angle between the bonding pairs. In both these examples the important assumptions are the essentially tetrahedral arrangement of the electron pairs and the effects of the Pauli repulsions on these pairs as the original equality of the orbitals is perturbed by the change in the number of bonded protons. We shall investigate the physical basis of this theory by first determining $\Delta\rho$ and comparing this with the assumed repulsions between the orbitals, and secondly, by determining the stability of the tetrahedral density arrangement by means of the concept of a binding region. It will be shown that the polarizations made necessary by the presence of the protons are indeed of crucial importance.

In Ne the electron density is given by (ignoring the inner 1s electrons)

$$\rho = 2 \sum_i \phi_i^2$$

[5]*Sinanoglu has pointed out that to consider these molecules as distortions from the basic tetrahedron of* Ne *is a gross oversimplification. Such a theory "recognizes only the exclusion principle-type hybridization (in* Ne*), but not the polarization-type hybridization due to the protons (10)".*

Can. J. Chem. Downloaded from www.nrcresearchpress.com by 210.87.254.5 on 09/05/12
For personal use only.

Can. J. Chem. Downloaded from www.nrcresearchpress.com by 210.87.254.5 on 09/05/12
For personal use only.

where each ϕ_i may be considered as an sp^3 hybrid orbital. These form an orthogonal set and $\Delta\rho$ is zero. The density ρ is of course spherical. We now consider the effects of perturbing this density distribution by extracting three protons from the Ne nucleus, one into each of three of the sp^3 hybrids. This results in a tetrahedral NH_3 molecule and destroys the orthogonality between the original Ne orbitals. The resulting $\Delta\rho$ will be directly determined by the effects of the Pauli exclusion principle arising from this nonorthogonality. The final molecular density distribution for tetrahedral NH_3 expressed in terms of equivalent molecular orbitals is

$$\rho = 2(\phi_1^2 + \phi_{b1}^2 + \phi_{b2}^2 + \phi_{b3}^2) + \Delta\rho_{1b} + \Delta\rho_{bb}.$$

Where ϕ_1 is an original unperturbed Ne orbital (the lone pair) and the ϕ_{bi} are bonding orbitals of the form[6]

$$\phi_{bi} = \lambda[(1/2)s + (\sqrt{3}/2)p_i] + \mu h_i ,$$

λ/μ being a polarity factor and p_i a nitrogen 2p orbital directed at the hydrogen orbital h_i. The term in brackets defines an sp^3 orbital. The λ/μ ratio must be unity or less to obtain the correct order of magnitude for the molecular dipole moment (11) and was taken as one in the present calculations. In any event, the variation of this ratio over a wide range of reasonable values does not alter the conclusions discussed below. Since the total $\Delta\rho$ is constructed of terms from pairs of overlapping orbitals, we may divide it into contributions, one due to the lone pair orbital overlapping with the bonding orbitals and one due to the bond orbitals overlapping each other. In this way we may determine separately the lone pair – bond "repulsions" and the bond–bond "repulsions". These two expressions have the forms respectively

$$\Delta\rho_{1b} = -4S_{b1}\left(\sum_i \phi_1\phi_{bi}\right) + 2S_{b1}^2\left(\sum_i (\phi_{bi}^2 + \phi_1^2)\right) \qquad [8]$$

$$\Delta\rho_{bb} = -4S_{bb}\left(\sum_{i<j} \phi_{bi}\phi_{bj}\right) + 2S_{bb}^2\left(2\sum_i \phi_{bi}^2\right) \qquad [9]$$

where S_{b1} and S_{bb} are the overlap integrals between the lone pair orbital and a bond orbital and between two bond orbitals respectively. Figure 2 is a plot of $\Delta\rho_{1b}$. The figure shows that the charge migration which results from the finite overlap of the lone pair and bonding orbitals corresponds to a depletion in the density above the N nucleus and to its accumulation below, between the three hydrogen nuclei. The reason for the form of the charge migration is easy to understand in terms of the nonorthogonalities. The whole of S_{b1} arises from the overlap of ϕ_1 with the hydrogen orbitals in the ϕ_{bi} only, since the nitrogen sp^3 orbital contributions to the ϕ_{bi} are still orthogonal to the sp^3 orbital which comprises ϕ_1.

$$S_{b1} = \mu[(1/2)S_2 - (1/2\sqrt{3})S_3].$$

(S_2 and S_3 are respectively the overlap integrals of a 2s and 2p on nitrogen with a hydrogen orbital.) S_{b1} in this case equals +0.06381. Since S_{b1} is positive, the first set of terms in eq. [8] will decrease the density where the product $\phi_1\phi_{bi}$ is positive and increase it where this product is negative. The orbital ϕ_1, since it has a 2p orbital contribution, is positive above the nitrogen and negative below it. The second term in $\Delta\rho_{b1}$ is positive in all regions.

[6]*The atomic orbitals employed in the calculations of the density distributions are Slater functions. We have previously demonstrated (6) that the use of Slater functions rather than the Hartree-Fock expressions does not alter the appearance or the general characteristics of the calculated electron density plots.*

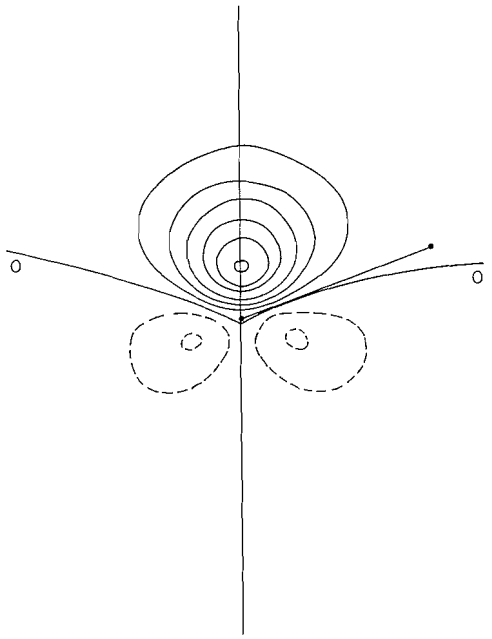


FIG. 2. A plot of the density shift, $\Delta\rho_{lb}$, due to the interaction of the lone pair with the bonding orbitals in tetrahedral NH_3. This and the subsequent diagrams are plotted in the plane parallel to the threefold symmetry axis and along an N–H bond. The vertical line is the threefold symmetry axis. The $\Delta\rho_{lb}$ contours increase and decrease in steps of 0.01 a.u. from the zero line.

Figure 3 shows a plot of $\Delta\rho_{bb}$, the density which is transferred because of the nonorthogonality between the bonding orbitals. This plot is close to the reverse of that found for $\Delta\rho_{lb}$, as it shows a decrease in density in the region below the N nucleus and its concentration above. The bond–bond interaction is greater than the bond – lone pair interaction, however, since the value of S_{bb} (0.1284) is greater than that of S_{b1}. The nonorthogonality between two bonding orbitals is again due entirely to the hydrogens,

$$S_{bb} = \mu^2 S_1 + 2\lambda\mu[(1/2)S_2 - (1/2\sqrt{3})S_3],$$

the first term arising from the overlap of two hydrogen orbitals and the second from the overlap of the hydrogen in one orbital with the sp^3 hybrid from another. The bonding orbitals will overlap one another most strongly in the region between all four nuclei and thus $\Delta\rho_{bb}$ is negative in this region. The net result of the lone pair – bond and bond–bond overlap is shown in Fig. 4 which is a plot of the total charge migration as determined by the orthogonality requirements of the Pauli principle. Charge density is removed from above and below the N nucleus along the symmetry axis and is concentrated in the region of each H nucleus. Figure 4 thus shows the effect of the Pauli exclusion principle on the three-dimensional electron density distribution for the NH_3 molecule when this distribution is related to an idealized tetrahedral one. The question now to be asked is whether the form of $\Delta\rho$ is such that it will lead to a decrease in the tetrahedral bond angle. In order that the bond angle decrease, electron density must be concentrated in the region below the nitrogen nucleus, between the three hydrogen nuclei. Such a charge migration would exert attractive forces on the three protons, drawing them together. The form of $\Delta\rho$ does not meet this requirement. There is a greater amount of charge placed above the

Can. J. Chem. Downloaded from www.nrcresearchpress.com by 210.87.254.5 on 09/05/12
For personal use only.

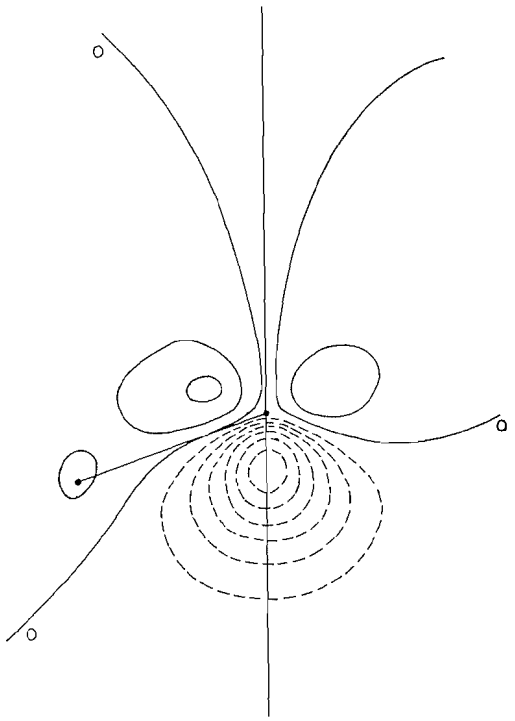


FIG. 3. A plot of the density shift, $\Delta\rho_{bb}$, due to the bond–bond interactions in tetrahedral NH_3. The contours are in steps of 0.01 a.u.

proton along the H—N bond axis than below it and the charge is depleted in regions between all four nuclei. Thus one finds that the basic assumptions of the electron pair repulsion theory are not met. The interactions between the bonding orbitals are larger than those involving the lone pair orbital, and the overall migration of the charge density due to the "Pauli repulsions" is such as to lead to an increase rather than the predicted decrease in the tetrahedral bond angle.

The application of this type of analysis to the water molecule leads to similar conclusions. Consider first the distribution to be tetrahedral in character and derived from neon by the removal of two protons from the neon nucleus. Since the two lone pair orbitals in the resulting water molecule would remain orthogonal, $\Delta\rho_{11}$, the density transferred because of the overlap of the two lone pair orbitals would be zero. Thus there are no Pauli repulsions at all between the lone pairs in the water molecule when its electron density is related to that of neon. The same result would be obtained by relating the density distribution to that of methane. The fact that the two lone pair orbitals in the water molecule overlap one another when pictured in three-dimensional space does not preclude the possibility that their total overlap is still zero, i.e.

$$\int \phi_{11}\phi_{12}\,d\tau = 0.$$

Thus a pair of electrons can coexist in both orbitals with no shift in electron density as the Pauli exclusion principle is satisfied. The electron density distribution in certain regions

Can. J. Chem. Downloaded from www.nrcresearchpress.com by 210.87.254.5 on 09/05/12
For personal use only.

of real space will contain contributions from both of the lone pair orbitals. This is permissible as long as the orbitals are orthogonal in the orbital space.[7] The forms of $\Delta\rho_{1b}$ and $\Delta\rho_{bb}$ are similar to those calculated for ammonia, resulting in a total charge migration which would increase rather than decrease the tetrahedral bond angle. In addition, there is no charge migration due to the interaction of the lone pairs. i.e. $\Delta\rho_{11}$ is zero. Thus the concept that the bond angle in the water molecule is less than the tetrahedral value because of Pauli repulsions between the lone pairs is incorrect.

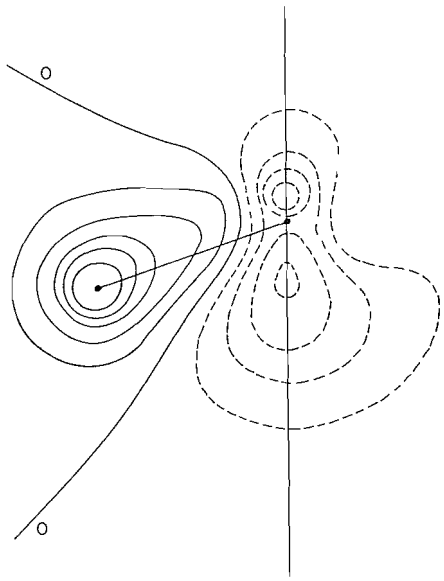


FIG. 4. A plot of the total charge migration as required by the Pauli exclusion principle for tetrahedral NH_3 with sp^3 hybridization. The contours are in steps of 0.002 a.u.

The identification of "Pauli repulsions" between filled orbitals with shifts in the electronic charge density has demonstrated that their interpretation in terms of overlapping orbitals in real space can be misleading. In the simple case of two He atoms where the overlapping orbitals are centered on different atoms, the form of $\Delta\rho$ does fit in with the simple interpretation. However, when a number of the orbitals are centered on one nucleus, such as in H_2O or NH_3, this is no longer true. The order of magnitude of the shifts $\Delta\rho_{bb} > \Delta\rho_{1b} > \Delta\rho_{11}$ is in contradiction with the proposals of the electron pair repulsion theory and, more important, $\Delta\rho_{11}$ is actually zero. The latter point is especially important in emphasizing that the overlap of orbitals when pictured in real space does not preclude the possibility they are orthogonal and hence satisfy the Pauli principle. Furthermore, the density shift arising from the requirements of the Pauli principle as calculated for the tetrahedral distribution does not predict a decrease in the tetrahedral bond angle. Thus the second basic assumption of the theory, that the electron density distribution in these molecules can be related to a tetrahedrally oriented set of orbitals, is incorrect. This conclusion is necessary not only because $\Delta\rho$ does not lead to a decrease in the bond angle, but for an even more fundamental one. The concept of a binding region discussed previously for a diatomic molecule can be extended to a polyatomic molecule (6). One can

[7]*Lone pair – lone pair Pauli repulsions will never exist between equivalent lone pair orbitals centered on the same nucleus. They will always be orthogonal by definition.*

Can. J. Chem. Downloaded from www.nrcresearchpress.com by 210.87.254.5 on 09/05/12
For personal use only.

determine a spatial region in a polyatomic molecule in which the electron density binds all the nuclei simultaneously and is the region in which electron density must be concentrated in order to achieve electrostatic equilibrium in terms of the forces exerted on the nuclei. We shall demonstrate below that tetrahedral density distributions for water and ammonia do not concentrate density in the binding region, and for this reason are unacceptable.

Analysis of the Charge Distributions for H_2O and NH_3 in Terms of Their Binding Regions

The binding region for the ammonia molecule is indicated by the dotted line in Fig. 5. It is derived on the basis that the charge distribution for the ammonia molecule must reflect the threefold symmetry of the nuclear framework. Thus one must consider the forces exerted on the nuclei by a symmetrically equivalent set of charge points in deriving the binding region. This set of symmetrically equivalent points reduces to a single one for charge along the threefold axis, to a set of three for charge in the symmetry planes, and to a set of six for charge placed in any other regions. Any such set of symmetrically equivalent charge points placed below the boundary curve will exert forces on the nuclei such as to decrease all of the internuclear separations. Charge density outside of this boundary curve will tend to separate the molecule into either a diatomic molecule and two atoms or into four atoms.[8] Charge density must be concentrated in the binding region if the molecule is to achieve electrostatic equilibrium. The existence and shape of the binding region and the necessity of concentrating charge in this region illustrates the importance of the requirements imposed on the density distribution by the presence of the protons. The shape of the binding region will in fact determine the polarization-type hybridization induced by the protons which was referred to by Sinanoglu (10).

The question as to how much charge must be placed in the binding region can be determined by choosing a standard distribution which is known to be insufficient from the point of view of the amount of charge it places in the binding region. The density difference between the molecular charge distribution of interest and this standard one is then determined. A distribution with a positive difference in the binding region is a possible one. A distribution with a negative difference in the binding region is unacceptable since it places less charge density in the binding region than does the standard distribution which is known to be insufficient in this regard. The standard density distribution is the one obtained by placing the nuclei at the positions they have in the molecule, each with its original atomic charge distribution. By arguments similar to those employed in the case of the approach of the two He atoms, there are net forces of repulsion acting on all the nuclei for a charge distribution composed of the overlap of atomic charge densities. This is a general result (6). We shall label this type of density difference $\Delta\rho_m$ to distinguish it from the $\Delta\rho$ due to the Pauli principle.

$$\Delta\rho_m = \rho(\text{molecule}) - \rho(\text{atomic})$$

Figure 5 shows a plot of $\Delta\rho_m$ for the tetrahedrally based density distribution for NH_3. There is less charge density between every pair of nuclei than in that obtained from the simple overlap of atomic densities. Thus there would be large forces of repulsion acting on all the nuclei. In particular, the large accumulation of charge density above the nitrogen and its depletion below would result in large forces tending to increase the bond

[8]*One can also construct a binding region by considering the forces exerted on the nuclei by only a single charge point at a time. The binding region thus obtained is equivalent to the superposition of all the possible diatomic boundary curves. Such a region has been given previously for the water molecule (6) and corresponds to the region between all three nuclei defined by an angular boundary curve subtended at the oxygen nucleus with an angle less than the bond angle. A similar less extended binding region for an ammonia molecule would be pyramidal in shape, enclosed within the region of all four nuclei with its apex at the nitrogen nucleus.*

Can. J. Chem. Downloaded from www.nrcresearchpress.com by 210.87.254.5 on 09/05/12
For personal use only.

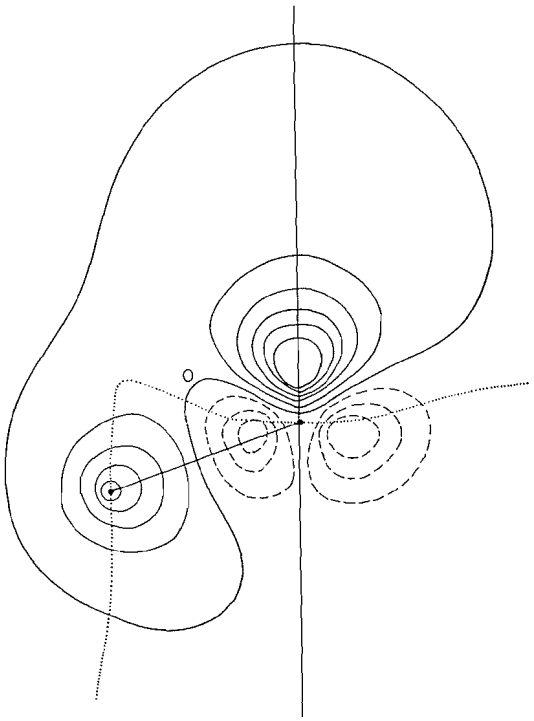


FIG. 5. A plot of $\Delta\rho_m$ (molecular density – atomic density) for tetrahedral NH_3 with sp^3 hybridization. The contours are in steps of 0.05 a.u. in this and the following diagram. The dotted line divides the binding region (below the line) from the antibinding region.

angle. Thus not only does the form of $\Delta\rho$, the density shift due to Pauli repulsions, predict an increase in the bond angle for a tetrahedral distribution, but the form of the distribution itself predicts even larger forces of repulsion on the nuclei.

A plot of $\Delta\rho_m$ for a tetrahedral density distribution for the water molecule has been given previously (6) and illustrates the same general features as those noted for the ammonia molecule. The value of $\Delta\rho_m$ is negative in the binding region and in the regions between all three nuclei, and is large and positive in the antibinding region above the oxygen nucleus. The large decrease in the electron density in the binding regions found for the tetrahedral distributions is due to the sp^3 hybridization assumed for the lone pair electrons. When an sp^3 hybrid orbital is squared, there is a contribution to the electron density of $(\sqrt{3}/2)sp$ per electron. This term is positive above the nodal plane of the p orbital (where it leads to an increase in the electron density) and negative below it (where it leads to a decrease in ρ). In Ne the four cross terms are all equally weighted and a spherical density distribution is obtained. In ammonia, the lone pair orbital contributes a term $\sqrt{3}sp_l$, which increases the density in the antibinding region above the nitrogen nucleus at the expense of density in the binding region. However, the density in a bonding orbital is shared between the nitrogen (a fraction equal to $\lambda^2 \sim 0.5$) and a hydrogen (a fraction equal to μ^2). Thus the bonding orbitals in ammonia contribute $3\lambda^2\sqrt{3}sp_i$ rather than the $3\sqrt{3}sp_i$ necessary to *just* balance the charge migration due to the lone pair. It is clear that hybridization of the lone pair must be reduced and must approach pure s character in order to concentrate charge density in the binding region in the water and ammonia molecules. At the same time, the demands of the Pauli principle require the

Can. J. Chem. Downloaded from www.nrcresearchpress.com by 210.87.254.5 on 09/05/12
For personal use only.

bonding orbitals to acquire more p character from the nitrogen or the oxygen as the lone pair becomes more s-like. Figure 6 is a plot of $\Delta\rho_m$ for the ammonia molecule in which the molecular density possesses a lone pair in a pure 2s orbital and the bonding orbitals are close to pure 2p in character from the nitrogen. The bonding orbitals contain a small amount of 2s character but it is of negative sign. This distribution does accumulate charge density in the binding region and does balance all of the forces exerted on the nuclei (11). In addition, the values calculated for the other physical properties which depend upon the one-electron density are in excellent agreement with experiment. A density distribution for the water molecule which does concentrate density in the binding region and which does balance the forces on all the nuclei is similar in character to that found for the ammonia molecule (12). The oxygen contributions to the bond orbitals are of almost pure 2p character and the lone pair orbitals are sp hybrids. (The lone pair may also be viewed as one orbital of pure 2s character and another of pure 2p, perpendicular to the molecular plane.) A plot of $\Delta\rho_m$ for this type of distribution for the water molecule has been given previously (6).

One can envisage a whole spectrum of possible hybridizations for the nitrogen and oxygen atoms in the ammonia and water molecules, extending from the one extreme of sp^3 hybrids to the other in which the lone pair is pure 2s (and in water, a second of pure 2p, perpendicular to the molecular plane) and the bonds pure 2p. The analysis of the resulting charge distributions in terms of the amount of charge shifted to the binding region has shown that only the latter of the extremes of hybridization is satisfactory in this respect. Thus a theory which assumes that the charge distribution in these molecules arises from a perturbed neon-like distribution will be unsatisfactory as the unperturbed density is chosen from the wrong end of the hybridization spectrum. Rather, the charge distribution should be considered as arising from a perturbation of the original ground state electronic densities for the nitrogen and oxygen atoms. This is, of course, more realistic on energetic grounds as well. In both the water and ammonia molecules an orbital angle less than the bond angle is necessary to concentrate density in the binding region and along the bonds in three-dimensional space. In a sense one must have "bent orbitals" in these molecules in order to obtain chemical bonds in terms of the density distribution in real space.

Interestingly enough, the acceptable density distributions for the H_2O and NH_3 molecules (with the 2s lone pairs) concentrate density above the heavy nucleus to almost identical extents as do the distributions with sp^3 lone pairs. However, in the distributions with the 2s lone pair this increase is not due to the lone pair. The lone pair density, in fact, cancels out in the determination of $\Delta\rho_m$ as the 2s orbital is unchanged from the atomic distribution. Instead, the increase in $\Delta\rho_m$ above the nitrogen or oxygen nucleus arises from the density contained in the bonding orbitals. A 2p orbital concentrates density on both sides of the nucleus it is centered on. Thus bonds formed from 2p orbitals will necessarily place density above and below the nitrogen nucleus. In addition, the negative 2s character found in the bonding orbitals also contributes to this build-up of charge above the heavy nucleus. However, the fact that there is an increase in the electron density above the nitrogen and oxygen nuclei over that found in the atomic cases indicates that the ammonia and water molecules do possess directed lone pairs. In fact an excellent definition of a lone or unshared pair would be the concentration of electron density in an antibinding region. The fact that the positive $\Delta\rho_m$ values in the antibinding regions arise from the density in the bonding orbitals is irrelevant. An infinite number of choices as to the forms of the orbitals is possible and to express the density (which is invariant to an

Can. J. Chem. Downloaded from www.nrcresearchpress.com by 210.87.254.5 on 09/05/12
For personal use only.

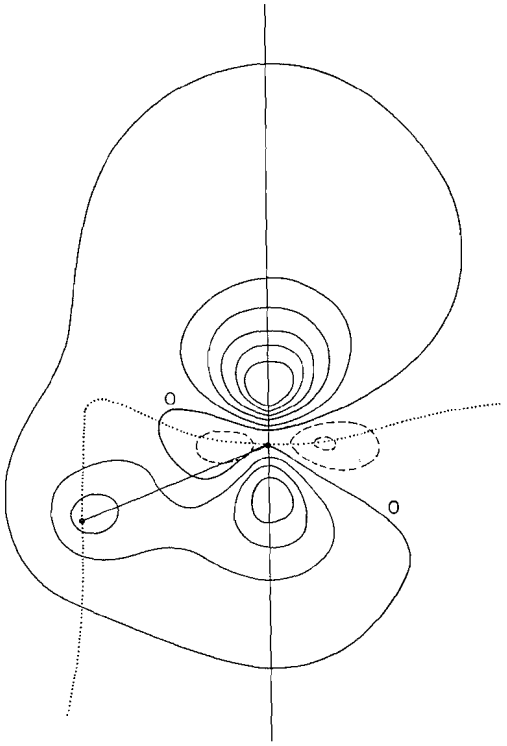


FIG. 6. A plot of $\Delta\rho_m$ for NH_3 with the experimental bond angle of 107.3° for the density distribution which balances all the forces on the nuclei and has the correct dipole moment (11).

orthonormal change in the basis set) in terms of equivalent orbitals as done here is but one of many possibilities. Only the total density distribution is of significance and the concentration of charge density in the antibonding region, where by definition it plays no role in binding the nuclei together, must correspond to the existence of a lone pair. The results of self-consistent field (S.C.F.) calculations, when expressed in terms of equivalent orbitals (11, 12), exhibit the same characteristics as determined by the present considerations of concentrating density in the binding regions. Thus one finds for these variationally determined functions that the bonding orbitals are primarily of 2p character with negative 2s contributions, that the orbital angle is less than the bond angle, and that the lone pairs approach the limiting 2s form. This has also been pointed out by Peters (13) for the diatomic hydride functions of Ransil (14). Ruedenberg and Edmiston (15) have shown that when the molecular orbitals describing these wave functions are transformed into a new set, one which minimizes the overall interorbital coulombic and exchange interactions, bonding orbitals are obtained which now contain 2p and 2s character of the same sign and the lone pair orbitals are directed behind the heavy nucleus. However, the definition of a lone pair orbital is now changed, for the orbitals labelled as lone pairs by Ruendenberg no longer consist of atomic orbitals centered only on the heavy atom. Rather, they contain contributions from the hydrogen orbitals as well, with negative coefficients. In fact, Ruedenberg ascribes the origin of nonbonded interactions to the antibonding nature of these lone pair orbitals. A definition of a lone pair based on the final density distribution avoids the ambiguities associated with an orbital definition. There is but one density distribution but many possible orbital descriptions of it.

Can. J. Chem. Downloaded from www.nrcresearchpress.com by 210.87.254.5 on 09/05/12
For personal use only.

Can. J. Chem. Downloaded from www.nrcresearchpress.com by 210.87.254.5 on 09/05/12
For personal use only.

One can give an electrostatic interpretation as to why the ammonia and water molecules are pyramidal and bent, respectively. In a planar ammonia molecule the unshared pair of electrons would necessarily be placed in a 2p orbital perpendicular to the plane of the molecule. A p_π orbital is very inefficient at screening a nucleus, since density is placed above and below the bond axis or the molecular plane. By bending the bonds out of the plane the lone pair takes on an increasing amount of s character. The electrons in a 2s orbital are much more efficient at screening a nucleus, since the density is distributed spherically about it. In addition, the 2s orbital is easily polarized (by the admixture of 2p) to place density in the binding region below the nitrogen nucleus in a pyramidal molecule. Thus the total density between the nuclei obtained from s–p hybrid bonds and a p_π lone pair in the planar molecule is *less* than that obtained from bonds composed of p orbitals and a 2s lone pair for the pyramidal geometry. In the case of the water molecule one lone pair remains in a p_π orbital (perpendicular to the molecular plane) whether the molecule is linear or bent. The second lone pair, however, changes from a p_π orbital in the linear case through a range of s–p hybridizations to the limiting form of an s orbital when the bonding orbitals are pure p and the molecule is bent. Again one finds that to achieve maximum screening of the heavy nucleus and to achieve the maximum electron density along the bonds, the bonding orbitals must be approximately pure p orbitals and one lone pair must be placed in an s orbital. This corresponds to the bent geometry. The $\Delta\rho_m$ plots for the tetrahedral density distributions again illustrate the importance of considering the total density distribution. The sp^3 bonding orbitals in a tetrahedral density distribution for NH_3 or H_2O do concentrate a maximum amount of density along the bonds. However, the orthogonality restraints of the Pauli exclusion principle demand that the lone pair must be strongly s–p hybridized when the bonds are s–p hybrids. The result of the forced hybridization of the lone pair is the removal of more density from the binding region and from between the nuclei than was concentrated by the sp^3 bonding orbitals. The net effect is a distribution which places less charge density between the nuclei than that obtained from the simple overlap of the atomic densities. Thus the presence or absence of lone pairs does affect the geometry of a molecule, but not in the sense of exerting Pauli repulsions. Rather, the geometry can be interpreted as being determined by the molecule attaining a density distribution which provides a maximum screening of the nuclei and places a maximum of electron density along the bonds.

We have shown that the effects of the Pauli exclusion principle on the density distributions of simple molecules is not what is commonly pictured. However, one is still faced with the fact that the electron pair repulsion theory is remarkably successful. In recent papers Gillespie (see for example ref. 16) has purposely avoided any reference to the degree of hybridization. Instead, the distortions from the most probable arrangement of a given number of initially equivalent pairs of electrons is determined by arguments based on the relative sizes of the orbitals. Thus orbitals which are lone pairs in the molecule become more diffuse and less directional and occupy a larger volume of space. In terms of the argument put forward in this paper this would correspond to an increase in the s character of the lone pair orbitals. Similarly the bonding orbitals are stated to be contracted and polarized by the presence of the ligands. This description coincides with the predicted increase in the p character of the bonding orbitals found here. However, the present approach arrives at these conclusions by a determination of which distribution places the maximum density in the binding region, and not by arguments based on orbital repulsions. It will be of interest to determine whether or not the parallelism between the two approaches noted above will continue to hold in the non-hydride molecules as well.

ACKNOWLEDGMENT

The authors are indebted to Professor R. J. Gillespie for the many valuable discussions held with him regarding this work.

REFERENCES

1. R. J. GILLESPIE and R. S. NYHOLM. Quart. Rev. London, **11**, 339 (1957). R. J. GILLESPIE. J. Am. Chem. Soc. **82**, 5978 (1960).
2. L. SALEM. Proc. Roy. Soc. London, Ser. A, **264**, 379 (1961).
3. PER-OLOV LÖWDIN. Advan. Chem. Phys. **2**, 207 (1959).
4. J. HELLMANN. Einführung in die Quantencheme. Deutiche and Co., Leipzig, Germany. 1937. R. P. FEYNMAN. Phys. Rev. **56**, 340 (1939).
5. T. BERLIN. J. Chem. Phys. **19**, 208 (1951).
6. R. F. W. BADER. J. Am. Chem. Soc. **86**, 5070 (1964).
7. H. M. POWELL and N. V. SIDGWICK. Proc. Roy. Soc. London, Ser. A, **176**, 153 (1940).
8. J. E. LENNARD-JONES. J. Chem. Phys. **20**, 1024 (1952).
9. J. A. POPLE. Quart. Rev. London, **11**, 291 (1957).
10. O. SINANOGLU. Advan. Chem. Phys. **6**, 315 (1964).
11. R. F. W. BADER and G. A. JONES. J. Chem. Phys. **38**, 2791 (1963).
12. R. F. W. BADER and G. A. JONES. Can. J. Chem. **41**, 2251 (1963).
13. D. PETERS. J. Chem. Soc. 2003 (1963).
14. B. J. RANSIL. Rev. Mod. Phys. **32**, 245 (1960).
15. C. EDMISTON and K. RUEDENBERG. J. Chem. Phys. **43**, S97 (1965).
16. R. J. GILLESPIE. J. Chem. Educ. **40**, 295 (1963).

Can. J. Chem. Downloaded from www.nrcresearchpress.com by 210.87.254.5 on 09/05/12
For personal use only.

Can. J. Chem. Downloaded from www.nrcresearchpress.com by 210.87.254.6 on 09/05/12
For personal use only.

SORPTION OF HYDROGEN AND OXYGEN BY CADMIUM OXIDE

M. J. D. Low and A. M. Kamel
School of Chemistry, Rutgers, The State University, New Brunswick, New Jersey

Received May 31, 1965

ABSTRACT

The sorptions of hydrogen and of oxygen on freshly prepared and on gas-treated cadmium oxide were measured from 0 to 250 °C. The data suggest that hydrogen chemisorption predominates near 26°, where it is the precursor of water formed on the surface. Surface reduction occurs at temperatures as low as 50°. At least two types of oxygen sorption exist. The isobar has a minimum near 50°. Chemisorption occurs below 50° and the sorption kinetics indicates the presence of two types. The incorporation of oxygen into the bulk may account for the observed increased sorption above 150°.

SORPTION OF HYDROGEN AND OXYGEN BY CADMIUM OXIDE

The relatively large deviations from stoichiometry of cadmium oxide and its behavior as degenerate electronic semiconductor have prompted a considerable amount of work on the electronic properties of that substance. Some effects of oxygen pressure on conductivity or thermoelectric power have been noted, but quantitative sorption experiments have not been reported. In view of the importance of surface effects to semiconductor behavior, and the possibility of comparison of data with those of zinc oxide, we have undertaken the present study.

EXPERIMENTAL DETAILS

Gas sorptions were measured by following the decrease in pressure within a high-vacuum system of conventional design equipped with mercury and dibutylphthalate manometers. Hydrogen was purified by diffusion through hot palladium. Tank oxygen was passed over hot CuO and through a trap filled with glass wool at −196°. Helium and nitrogen were purified by passage through glass-wool-filled traps at −196°. Water was degassed by alternate freezing and thawing *in vacuo*.

A reproducible adsorbent was prepared by the decomposition of $CdO{\cdot}1.65H_2O$ to $CdO_{0.80}$ *in vacuo* (1). A sample of the hydroxide was placed in the sample chamber of the adsorption system and evacuated at room temperature. A furnace, preheated to 500°, was then placed around the sample chamber. A pressure of approximately 10^{-5} mm Hg was reached within about 15 min. The furnace was removed after 40 min, a second preheated furnace was installed, and the sample was then held at some previously chosen temperature. Dead spaces were measured by the expansion of helium. The nitrogen B.E.T. surface area (2) of the oxide prepared as described remained constant at 5.2 m^2/g *in vacuo* for 12 h. The analysis of several samples yielded the formula $CdO_{0.80}$ and indicated that the decomposition of the hydroxide was complete (1). Amounts of gas sorbed are given as ml N.T.P./g $CdO_{0.80}$.

EXPERIMENTS AND RESULTS

To obtain information about sorption on gas-treated as well as on freshly prepared surfaces, several series of experiments were made. Each series was isothermal, and was made with a freshly prepared sample weighing ~1 g. In one series, an adsorbent sample was prepared as described, and was then exposed to hydrogen at an initial pressure of 206 mm Hg. The isothermal gas sorption was followed for some time. Each of the plots of Fig. 1 of the amount sorbed, q, versus time shows such data. After some time, marked with arrow N in Fig. 1, a Tesla coil discharge was started in the tubing near the sample chamber. The discharge was stopped at time F, and the hydrogen uptake followed for a further period. The sample chamber was then opened to the pumps for 15 min. Oxygen at an initial pressure of 188 mm Hg was then introduced, and the sorption was followed for some time. Oxygen uptake data are shown in the plots of Fig. 2. At time N, a Tesla coil discharge was started and continued to time F. The experiment was stopped after a further period of time, and the sample was discarded. This sequence of operations was

then repeated with a freshly prepared sample at each of the temperatures given in Figs. 1 and 2.

The surface area of a sample was occasionally measured after the 15 min degassing prior to exposure to oxygen. The total amounts of hydrogen sorbed in ml N.T.P. and the surface areas in m^2/g were: 0, 5.2; 0.394, 5.1; 1.098, 4.5; 1.579, 4.6; and 2.278, 4.9, respectively.

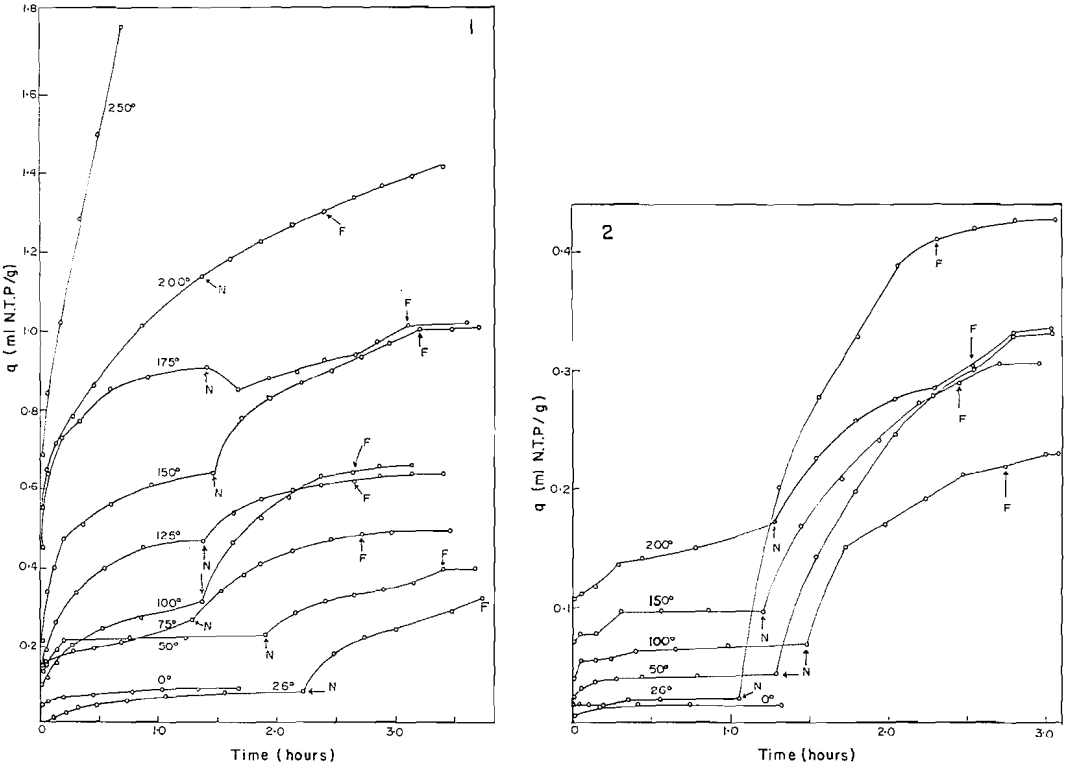


FIG. 1. Hydrogen sorption on fresh surfaces.
FIG. 2. Oxygen sorption on hydrogen-treated surfaces.

As the changes in surface areas were small, and therefore no major changes in adsorbent texture occurred, the possible effects of small changes in area brought about by interaction of the oxide with hydrogen were disregarded.

Some of the data of Fig. 1 are shown in Fig. 3 as plots of amounts of hydrogen sorbed after various specific times as functions of temperature. As the q vs. t plots below 200° of Fig. 1 show that gas sorptions were nearing completion after ~1 h, the 60 min plot of Fig. 3 approximates an initial-pressure isobar, and can be taken to be analogous to a true isobar. The general shape of the plot indicates at least two modes of sorption, a change in the nature of the uptake being indicated by the minimum near 26°.

A second series of experiments on hydrogen sorption by oxygen-treated surfaces was made as follows. A freshly prepared adsorbent sample was exposed to oxygen at an initial pressure of 188 mm Hg, and the isothermal sorption was followed (Fig. 4). The sample was then degassed for 15 min and exposed to hydrogen at an initial pressure of 206 mm Hg (Fig. 5). The adsorbent was then discarded. This sequence was repeated with freshly prepared samples at each of the temperatures indicated in Figs. 4 and 5. The data of Fig. 4 are replotted in Fig. 6 in the manner described for hydrogen sorption.

Can. J. Chem. Downloaded from www.nrcresearchpress.com by 210.87.254.6 on 09/05/12
For personal use only.

Can. J. Chem. Downloaded from www.nrcresearchpress.com by 210.87.254.6 on 09/05/12
For personal use only.

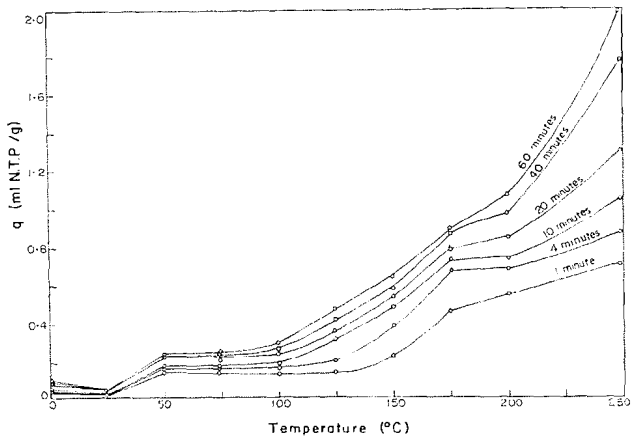
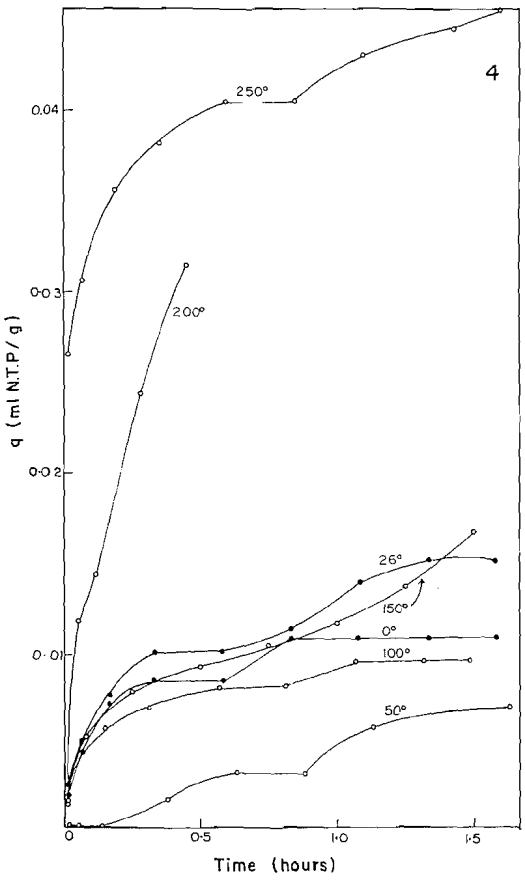


FIG. 3. Hydrogen sorption on fresh surfaces.



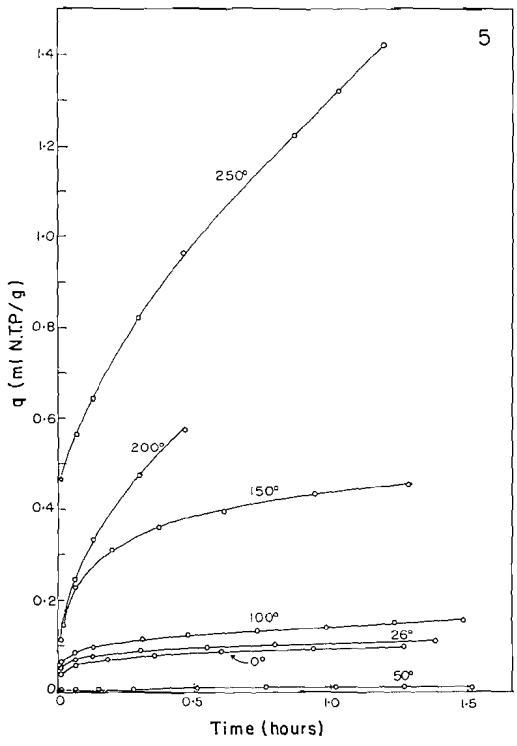


FIG. 4. Oxygen sorption on fresh surfaces.
FIG. 5. Hydrogen sorption on oxygen-treated surfaces.

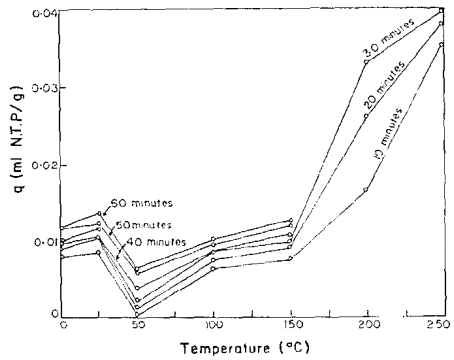


FIG. 6. Oxygen sorption on fresh surfaces.

Pretreatment of the adsorbent with one gas had marked effects on the subsequent uptake of a second gas. The potential desorption of a fraction of the first gas during the pumping step between the two gas sorptions precludes a quantitative treatment, but useful comparisons can be made. Corresponding data of Figs. 1 and 5 show that treatment of the adsorbent with oxygen caused marked changes in the subsequent hydrogen sorption, the pretreatment effects being noticeable mainly as changes in the initial rapid gas sorption. The effects were complex. For example, on computing the change in hydrogen sorption after 30 min caused by oxygen pretreatment, there was a decrease of about 10 ml H_2/g per ml of oxygen pre-adsorbed at $\geq 50°$. There was little change at 0°, but an increase of 4 ml H_2/g per ml of oxygen pre-adsorbed occurred at 26°. The changes in the hydrogen sorption caused by small amounts of pre-adsorbed oxygen (these being taken as the final values of each of the plots of Fig. 4) especially up to $\sim$100°, cause the initial-pressure isobar for hydrogen sorption on the oxygen-treated adsorbent to resemble that of the oxygen isobar of Fig. 6. Similar complex changes in oxygen sorption were caused by hydrogen pretreatment. Comparison of corresponding data of Figs. 2 and 4 shows the oxygen sorption to be enhanced by the hydrogen treatments. The rapid initial oxygen sorption was increased by an order of magnitude, and small increases occurred in the slow sorption. The enhancement, however, was inefficient. The oxygen sorption after 30 min, for example, was increased by $\sim$0.07 ml O_2/g per ml of hydrogen pre-sorbed.

A number of other experiments were made, each with a fresh sample of adsorbent. Voluminous and irreversible oxygen sorptions such as those of Fig. 2 could be caused by Tesla coil discharges during oxygen sorption on clean surfaces. Oxygen sorption did not cause a change in surface areas. Some other experiments were made with hydrogen-treated surfaces. In one experiment, a 1 g sample of fresh adsorbent was exposed to hydrogen at 30 cm Hg and 26° and was heated to 250° in 30 min. A total of 0.904 ml of hydrogen had been taken up when 250° was reached. The sample was then degassed for 15 min at 250° to $\sim 3 \times 10^{-6}$ mm Hg and cooled to 50°. Hydrogen at 31 cm Hg and 50° was introduced but was not taken up. The sample was then raised to 100° in the presence of the gas, but no sorption was found. The sample was then degassed at 100° for 15 min and heated to 150°. Some sorption of hydrogen then occurred. The adsorbent was then heated to 200° in the presence of hydrogen. A further sorption of hydrogen occurred, but the sorption was smaller than that occurring with a freshly prepared surface, i.e., exposure to hydrogen deactivated the surface.

Similar experiments were made with water-treated surfaces. For example, a fresh

Can. J. Chem. Downloaded from www.nrcresearchpress.com by 210.87.254.6 on 09/05/12
For personal use only.

sample was exposed for 2 min to water vapor at 8 mm Hg. After pumping for 15 min to a pressure of about 3×10^{-6} mm Hg to remove excess water, the sample was exposed to oxygen, all steps being carried out at 26°. It was not possible to measure the amount of water taken up (3). Comparison of results with those of oxygen sorption on fresh surfaces showed that water pretreatment had an enhancing effect on oxygen sorption. The total oxygen uptake was increased by ~80% at 26° and 100°, but voluminous initial sorptions similar to those observed with hydrogen-treated surfaces were not found. Other experiments showed that hydrogen sorption was almost totally inhibited by pre-adsorbed water.

Numerous attempts were made to obtain infrared spectra of the surface species at room temperature, using a Perkin-Elmer model 521 spectrophotometer. The relatively high conductivity and consequent high infrared absorption as well as the high light scattering of the pressed oxide pellets and evaporated films did not permit meaningful transmission measurements to be made in many cases. Samples transmitting about 2% of the incident radiation could on occasion be prepared but, in numerous trials, surface OH and CdH groups analogous to OH and ZnH groups found on ZnO surfaces (4) were never observed. This indicates that such groups, if formed, are few in number or have a transient existence on the surface.

DISCUSSION

The hydrogen sorption below the temperature region of the minimum of the isobar of Fig. 3 is ascribed predominantly to chemisorption. This is based on the low probability of physical adsorption at such relatively high temperatures and, more significantly, on the enhancement of oxygen sorption by hydrogen pretreatment. This effect indicates that below the isobar minimum at least a portion of the hydrogen must have been strongly bound to the surface in order to be able to affect the subsequent sorption of oxygen. The relatively rapid increase in q from 26° to 50°, the relatively small difference between q at 50° and at 75°, and the increasing coverage with time at $\geq 50°$ indicate a second process. Some evidence for this comes from the shape of the plots of Fig. 1. The 50° plot quickly rises to an almost constant q value. The sorption at 75° occurs more slowly but continues to a higher value than at 50°, indicating a decline in predominance of one process and transition to a second one, as do the more rapid and voluminous sorptions at $\geq 100°$.

The various data show that strong interactions occurred between hydrogen and the oxide over the entire temperature range studied. This supplements rather than conflicts with the statement (5) that cadmium oxide reduction starts at 95° and that bulk reaction occurs at 120°, or the similar observation (6) that reduction begins in the range 221–254°, based on experiments designed to establish the reduction threshold through the detection of free water. Failure to detect unbound water, however, does not exclude the possibility that reduction had occurred but the water formed was retained by the oxide surface, as suggested by the present data. For example, hydrogen sorption was inhibited by water and also by hydrogen treatment of the surface until the temperature was raised, so that water desorption could occur near 150° as indicated by previous work (7), thus suggesting a self-poisoning of hydrogen sorption through the formation of water at low temperatures. Also, as it had been shown that temperatures in the vicinity of 200° were required to degass cadmium oxide prior to surface area measurements (1, 7), it is likely that the decline and subsequent increase in surface areas on hydrogen treatment were an artifact: water formed at low temperatures could partially block the pore system of the adsorbent and thus cause an apparent reduction in area until desorption took place. Also, water as well as hydrogen enhanced oxygen sorption, again suggesting the formation of water at low temperatures.

Can. J. Chem. Downloaded from www.nrcresearchpress.com by 210.87.254.6 on 09/05/12
For personal use only.

The various effects are in agreement with a postulated mechanism involving a chemisorption predominant near 26°, which is the precursor to water formation on the surface. Chemisorbed hydrogen could be slowly converted to adsorbed water, some water formation occurring as low as 50°. The surface mobility of hydrogen atoms or ions and of bound water species as well as the rate of conversion or reduction is increased with increasing temperature, most of the water formed being retained by the surface below ~150°.

The shapes of the plots of Fig. 6 indicate that at least two processes were involved in the sorption of oxygen between 0° and 250°. As the sorption of oxygen influenced the subsequent hydrogen sorption, the region of the isobar below 50° can be ascribed to an oxygen chemisorption, at least in part. Similarly, a second chemisorption can be invoked to account for the region of the isobar above 50°. The plots of Fig. 4, however, with the exception of the short experiment at 200°, show the rate of oxygen sorption to decelerate markedly and then to accelerate after a short period of quiescence. A second deceleration then occurs below 150°. The general kinetic behavior indicates the occurrence of two processes and points to a conversion of one chemisorption into a second type. The dual effect of oxygen in enhancing hydrogen sorption at 26° but inhibiting it at higher temperature also suggests two modes of oxygen sorption. The relatively more voluminous oxygen sorption above 150° as shown by Figs. 4 and 6 may involve a diffusion of oxide ions from the surface into the bulk of the adsorbent to fill vacancies in the anion sublattice. Support for this comes from the work of Haul, Just, and Dümbgen (8, 9), who studied the disorder and oxygen transport in cadmium oxide by measuring the ^{16}O–^{18}O exchange between gaseous oxygen and cadmium oxide crystals from 630° to 855°. Their results furnished strong evidence for a transport mechanism involving vacancies in the anion sublattice. However, the exact nature of the surface species and the mechanism of the enhancing effect of the discharges, as well as a detailed explanation of the various poisoning effects, are unknown and speculative in the absence of simultaneous measurements of gas sorption and electronic behavior of the adsorbent.

ACKNOWLEDGMENTS

Partial support for this work by the Government of the United Arab Republic by means of a Fellowship for A. M. K., The Petroleum Research Fund grant 1247-A3, National Science Foundation grant GP1434, and spectroscopic work by K. Brown, are gratefully acknowledged.

REFERENCES

1. M. J. D. Low and A. M. Kamel. J. Phys. Chem. **69**, 450 (1965).
2. S. Brunauer, P. H. Emmett, and E. Teller. J. Am. Chem. Soc. **59**, 1558 (1937).
3. M. J. D. Low and H. A. Taylor. J. Phys. Chem. **63**, 1317 (1959).
4. R. P. Eischens, H. A. Pliskin, and M. J. D. Low. J. Catalysis, **1**, 180 (1962).
5. G. Gallo and M. Del Guerra. Ann. Chim. Rome, **41**, 51 (1951).
6. V. A. Romanov, V. M. Drozdova, and G. A. Shif. Uch. Zap. Leningr. Gos. Univ. No. 150, Ser. Khim. Nauk, **10**, 79 (1951).
7. M. J. D. Low and A. M. Kamel. Can. J. Chem. **42**, 2907 (1964).
8. R. Haul and D. Just. J. Appl. Phys. **33**, 487 (1962).
9. R. Haul, D. Just, and G. Dümbgen. Reactivity of solids. Proc. 4th Intern. Symp. Reactivity Solids, 4th Amsterdam, 1960. *Edited by* J. H. de Boer. Elsevier Publ. Co., Inc., Amsterdam. 1961. pp. 65ff.

Can. J. Chem. Downloaded from www.nrcresearchpress.com by 210.87.254.6 on 09/05/12
For personal use only.

Can. J. Chem. Downloaded from www.nrcresearchpress.com by 210.87.254.6 on 09/05/12
For personal use only.

THE DIELECTRIC CONSTANT OF ETHYL CHLORIDE ADSORBED ON POROUS SILICA GLASS TREATED TO REMOVE SILANOL GROUPS

R. SHIGEISHI[1] AND R. MCINTOSH
Department of Chemistry, Queen's University, Kingston, Ontario
Received November 4, 1965

ABSTRACT

The real and imaginary parts of the complex dielectric constant of the composite system ethyl chloride adsorbed on porous glass have been determined over a range of temperature, namely −20 to −190 °C in the frequency range 1 000 to 4 000 Mc/s. The porous glass was treated to remove the majority of the silanol groups. The dielectric constants of the adsorbate are also reported. The major finding was that removal of the silanol groups eliminated the second linear section (of lower slope) of the usual plots. The behavior of the polar adsorbate is then shown to be quite similar to that of polar adsorbates on nonporous rutile. Loss curves as functions of frequency and temperature are given and discussed. There is insufficient evidence to discriminate between Debye-type loss and that of an oscillator or resonator.

A method is given of obtaining the dielectric parameters from the standing wave data with greater accuracy than can be obtained from use of Von Hippel plots.

INTRODUCTION

Almost from the earliest publications concerning the dielectric behavior of adsorbates in such solids as silica gel and porous glass, there has been reported the existence of two linear sections of the primary data as a function of quantity adsorbed (1–6). The relative slopes of these two sections of the dielectric constant or capacitance change plots have depended upon the adsorbate in some instances. Thus Higuti (2) reported the second linear section to have the higher slope for propanol in titania gel, except at the highest temperature of his experiments when that section had the lower slope. For the system nitrobenzene – silica gel the slope of the second section was the higher (3). McIntosh, Johnson, Hollies, and McLeod (4) found the second linear section to have the lower slope for ethyl chloride and butane, among other adsorbates, using silica gel as adsorbent. Kurbatov (5) reported the same situation for water and acetone in silica gel. As further experience was gained and it was learned that the temperature coefficients of these slopes might differ, attention was directed to the underlying cause of the sudden change of dielectric property rather than to the absolute value of the polarization which is directly related to the value of these slopes. A frequent suggestion was that the change of dielectric behavior corresponded with the completion of the first layer of adsorbate, which was expected to be firmly bound and to have reduced orientational polarizability in comparison with bulk liquid or higher layers. This explanation could account for a change to a higher slope, but did not seem to offer a reason for a change to a lower slope. Moreover, the position of the abrupt change of slope did not correlate particularly well with the monolayer volume, V_m, deduced from the usual Brunauer, Emmett, Teller plots. In this respect, and in the fact that the second linear section frequently had a lower slope, the behavior of adsorbates in rigid gels differed from the behavior of adsorbates on the nonporous adsorbent rutile, which until very recently was the only nonporous adsorbent examined (7). Because of the poor correlation between V_m and the kink of the relevant plots and because a nonpolar adsorbate such as butane behaved similarly to polar adsorbates, McIntosh, Rideal, and Snelgrove (8) suggested that the phenomenon is probably universal in porous adsorbents and also pointed out that an abrupt change of the density of the adsorbate could account for the

[1]*Present Address: Inorganic Chemistry Laboratory, Oxford University, Oxford, England.*

Can. J. Chem. Downloaded from www.nrcresearchpress.com by 210.87.254.6 on 09/05/12
For personal use only.

experimental results. This latter explanation was soon proved untenable because the required density was too low to permit adsorption of the quantities taken up by porous glass (9).

Another relevant fact to be considered in explaining the dielectric behavior was the observed shift of the position of change of slope with the water content of a silica gel (8); still another that the activation energy of the process causing dielectric loss was shown by Waldman (10) in Professor Freymann's laboratory to change abruptly at the volume adsorbed corresponding to the B.E.T. monolayer volume. However, all the relevant facts and suggestions need not be repeated here. It is sufficient to summarize the situation by pointing out that at least three reasonable explanations have been offered. The first was the completion of the first layer of adsorbate. The second was the onset of capillary condensation. The third was a new environment of the adsorbate in which the electrical field experienced by the adsorbate differed from that to which molecules in the initial adsorption range were exposed.

While the information referred to above was being accumulated through dielectric studies, evidence of the existence of chemisorbed hydroxyl groups was being obtained by the determination of infrared spectra (11, 12). Such adsorbed groups, called silanol groups, were found to have an influence on the spectra of adsorbates, and in turn to have their own spectra perturbed by adsorbate (13). Means to remove these silanol groups were invented. Thus heating to high temperatures such as 800 °C with pumping was shown to be quite effective. The treatment of the glass with a fluoride and subsequent heating and evacuation also proved valuable (14).

In the present study a porous glass sample which had been evacuated at 800 °C and had not appreciably sintered was used as the adsorbent and ethyl chloride as the adsorbate. A temperature range from −20 to −190 °C was utilized along with a frequency range of 1 000 to 4 000 Mc/s. These conditions served to extend the observations of Chapman and McIntosh (15) and at the same time permitted the examination of a silica glass substrate from which most of the silanol groups had been removed. The treatment is shown to have eliminated the second linear region of lower slope in the dielectric plots. Moreover, results at these frequencies and temperatures are now quite similar to those found for polar adsorbates on nonporous rutile. As it is believed that improvements in the experimental techniques of measuring the dielectric constants are also worth describing, these are reported. An improved procedure of converting the standing wave data to the real and imaginary parts of the complex dielectric constant was also developed and is given in Appendix I.

EXPERIMENTAL

Dielectric constants were obtained by the shorted coaxial line method described by Von Hippel (16). In essence, a standing wave is established in a coaxial line by propagating an electromagnetic wave between two concentric channels of a coaxial cell containing the dielectric sample and terminated by a metallic short. Determination of the node position and the voltage standing wave ratio yields the dielectric constant of the adsorbate–adsorbent system.

The coaxial cell along with the ancillary components of the inner and outer cell housings are shown in Fig. 1. The dimensions of the coaxial cell and of the tapers leading to the UG30C/U connector were chosen to present an impedance of 50.0 Ω to the microwave.

The inner cell housing fitted over the coaxial cell and the connector and was gasketed to the main brass plate with indium. Evacuation and admission of gas to the sample were accomplished by a narrow Monel Metal tube and a pinhole in the outer conductor. A 5 in. diameter outer cell housing was gasketed with indium to the top plate. The region between the inner and outer cell housings was evacuated through glass to metal Kovar seals soldered to the brass plate.

To obtain desired temperatures in the cell, heating coils were wrapped around a copper cylinder placed around the bottom of the inner cell housing, which was filled with brass filings to improve thermal conduction.

Can. J. Chem. Downloaded from www.nrcresearchpress.com by 210.87.254.6 on 09/05/12
For personal use only.

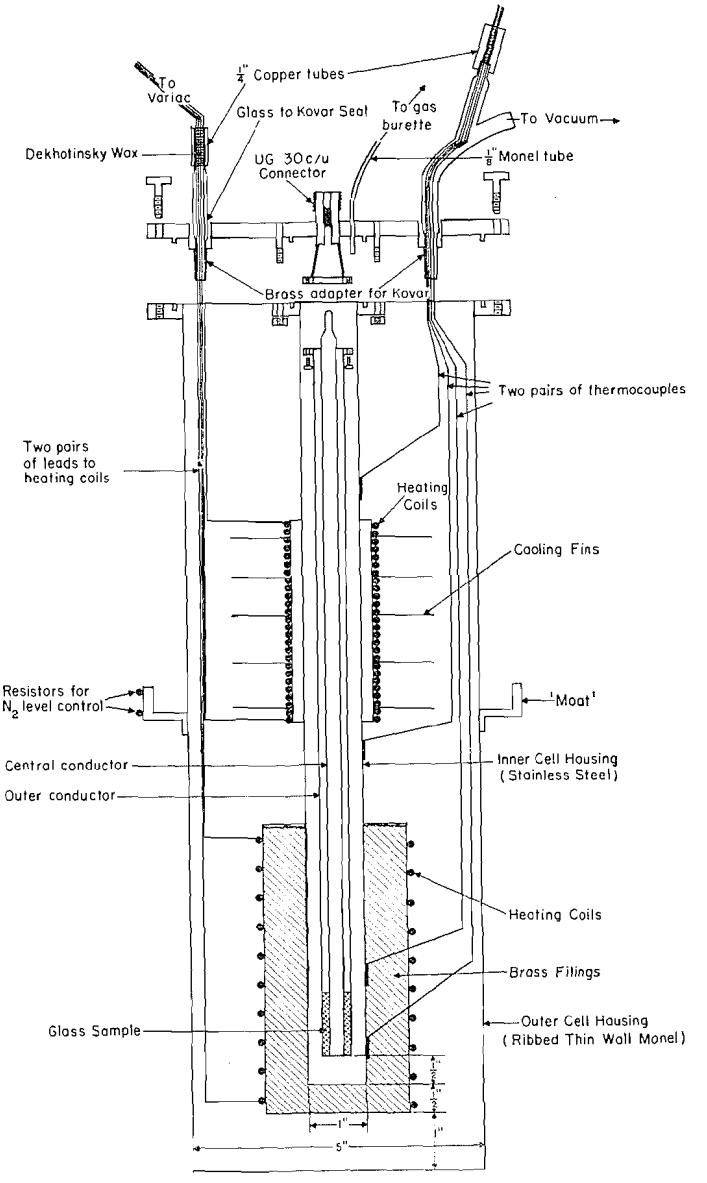


FIG. 1. Coaxial dielectric cell and jackets.

Another heating jacket was placed somewhat higher on the housing. This second heating jacket provided heating coils and in addition circular copper vanes. When no current was passed through this heater, the vanes had the effect of making the top part of the cell cooler than the bottom. By adjusting the currents in the heating coils temperature gradients spanning the length of the porous glass sample were reduced to less than 0.5 °C.

Temperatures were measured by copper–constantan thermocouples placed at various points along the inner cell housing. They gave the temperature of the sample, the temperature gradient along the sample, and the temperature gradients spanning the entire cell. The latter measurements were required in the calculation of the quantities adsorbed. Both the thermocouples and the leads to the heating coils were passed into the vacuum region via copper tubes soldered to the Kovar of the glass-to-metal seal. The glass end was joined to another glass-to-metal seal which was soldered into the brass plate. A vacuum seal was obtained by filling the channels in the copper tubes with Dekhotinsky wax.

A large Dewar placed around the entire cell contained liquid nitrogen as the coolant. The level of the liquid nitrogen in the Dewar was automatically controlled between two desired levels by a device which regulated the solenoid valve through which the air to the storage vessels of liquid nitrogen passed (17). Two carbon resistors which formed a part of the controlling device were strapped one above the other to a rectangular funnel-shaped device designated 'moat'. The controller worked in such a way that the level of the liquid nitrogen never rose above the height of the top resistor and never fell below that of the bottom resistor. The 'moat' kept the level of the liquid nitrogen in contact with the outer cell housing at a constant level despite the fall and rise of the liquid nitrogen level in the Dewar. By these means the temperature could be controlled to ±0.3 °C.

Admissions of gas to the sample were made when the sample was at −20 °C. The temperature of the sample was then adjusted to that desired and appropriate corrections were applied for adsorption from the gas phase when these were significant. A standard gas burette and mercury manometer system were employed and need not be described.

The ethyl chloride, obtained in cylinders from the Matheson Co., contained water as its main impurity. This was removed by slowly passing the ethyl chloride from the cylinder through ~20 ft of glass tubing which contained particles (activated Linde type 13X) acting as a molecular sieve into a distillation trap kept at 0.0 °C. The molecular sieve had previously been heated to 180 °C and evacuated for 3 d. The ethyl chloride was then subjected to trap-to-trap distillations.

Adsorbed water and the majority of surface hydroxyl groups were eliminated from the adsorbent by placing the porous glass sample (Corning glass No. 7930) in a Vycor tube connected to a vacuum rack. A heating jacket of Kanthal A was placed around this tube, and the sample was heated to 800 °C and evacuated for 5 h. An amount of ethyl chloride sufficient to immerse the glass was condensed into the cooled Vycor tube, and the tube was closed off and removed from the vacuum line. It was subsequently placed in a dry-box along with the coaxial cell and a polyethylene bag. When the humidity in the dry-box had dropped to zero, the Vycor tube was broken, the sample was taken out and inserted into the cell, and the cell was placed in the polyethylene bag. The cell was mounted as quickly as possible in a dry nitrogen atmosphere and slowly evacuated at room temperature.

To determine the extent of removal of hydroxyl groups, infrared spectra were taken of thin glass samples placed in a quartz cell and evacuated at temperatures between 25 and 850 °C. To determine whether the procedure for loading the cell was effective in preventing hydroxyl groups from the water in the atmosphere reforming during the short time the sample was exposed to the atmosphere, spectra were taken of samples accorded the same treatment as the actual sample used except that they were not immersed in liquid ethyl chloride.

The general procedure for obtaining the dielectric data has been outlined previously (18). The coaxial lines were manufactured by Hewlett-Packard. Amplification of signals was achieved by a Guildline photocell amplifier and the microwave signals were rectified by matched silicon crystal diodes of the type 1N21CM.

An extensive calibration of the empty cell was done for the frequency and temperature ranges employed in the measurements for the adsorbate–adsorbent system. These calibrations were required since the short position changed with the temperature of the cell. The empty cell showed a small loss and the ambient temperature affected the node positions. Furthermore, corrections were applied to the rectified signal outputs to account for contact potentials in the external d.-c. circuit.

ARITHMETIC PROCEDURE

The relation between the primary data and the propagation factor of the adsorbate–adsorbent system is

$$\frac{\tanh \gamma_2 d}{\gamma_2 d} = -j\frac{\lambda_1}{2\pi d}\left[\frac{\frac{E_{\min}}{E_{\max}} - j\tan\frac{2\pi X_0}{\lambda_1}}{1 - j\frac{E_{\min}}{E_{\max}}\tan\frac{2\pi X_0}{\lambda_1}}\right] = C\,e^{-j\zeta}$$

where $E_{\min}/E_{\max}$ is the inverse standing wave ratio, λ_1 the wave length, d the length of the glass sample, X_0 the distance of the first minimum from the surface of the glass (defined as the position $X = 0$), and γ_2 the propagation factor; C and ζ are found from the primary data. Thus if $\gamma_2 d = Te^{j\tau}$, T and τ can be evaluated from charts drawn by Von Hippel (16). It can then be shown that

$$\frac{\epsilon^*}{\epsilon_v} = -\left(\frac{\lambda_1}{2\pi d}\right)^2 (T\,e^{j\tau})^2$$

Can. J. Chem. Downloaded from www.nrcresearchpress.com by 210.87.254.6 on 09/05/12
For personal use only.

where ϵ^* is the complex dielectric constant of the composite system and ϵ_v that of free space.

To overcome the errors inherent in this procedure which were pointed out by McCowan, a program for the 1620 IBM computer was written which obtained T and τ accurately. See Appendix I.

RESULTS

The infrared spectra of thin glass samples which were evacuated at temperatures between 25 and 800 °C are shown in Fig. 2*a*. The relatively sharp peak at 3 760 cm^{-1} obtained for glass heated to 800 °C is attributed to the fundamental stretching frequency of a surface OH group which is oriented in such a way that it cannot interact with its surroundings (12, 19). The broad band obtained for glass evacuated at lower temperatures is attributed to a composite spectrum of the peak at 3 760 cm^{-1} and one at a lower frequency. The latter peak is thought to be caused by a hydrogen bonding of the OH groups among themselves.

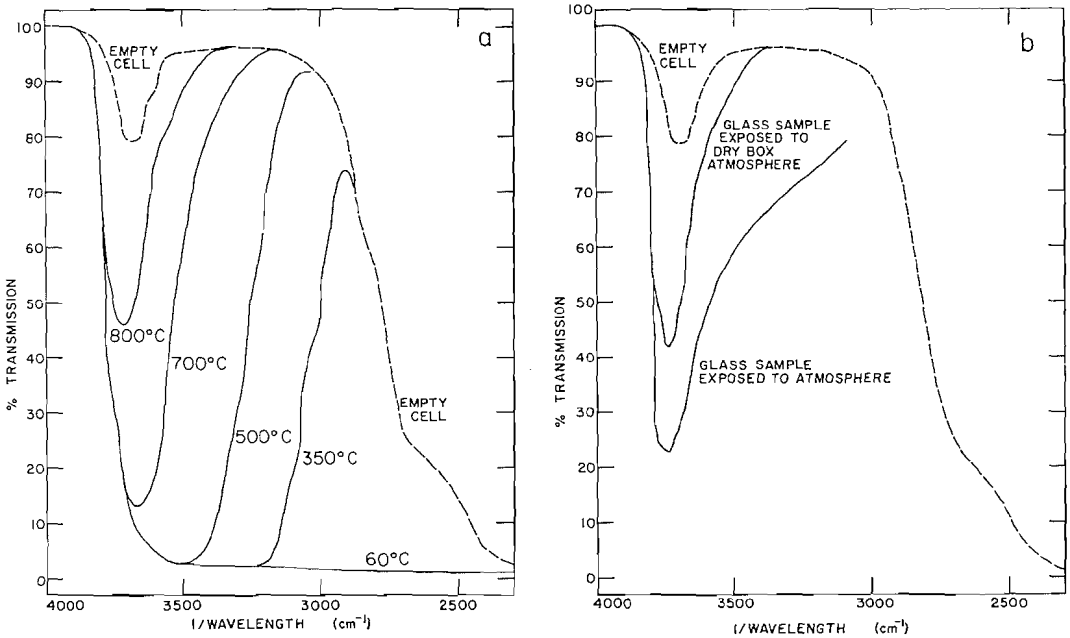


FIG. 2. Infrared spectra of glass samples (*a*) evacuated at several temperatures (*b*) exposed to atmosphere of dry-box and of room.

Figure 2*b* shows the spectra of glass samples heated to 800 °C and exposed for 30 min to the atmosphere inside and outside the dry-box used to transfer the actual sample to the cell. The spectrum for the former case reveals no significant increase of the peak height or width and hence this method was effective in preventing OH groups from reforming on the surface.

An isotherm is shown in Fig. 3. This is typical for ethyl chloride adsorbed on porous glass except for the initial amounts adsorbed (18). For glass containing hydroxyl groups there is initially a sharp rise in amount adsorbed with equilibrium pressure. The lesser adsorption at low pressure of the treated sample is another indication of the greatly reduced OH content of the glass and indicates a lesser heat of adsorption.

Can. J. Chem. Downloaded from www.nrcresearchpress.com by 210.87.254.6 on 09/05/12
For personal use only.

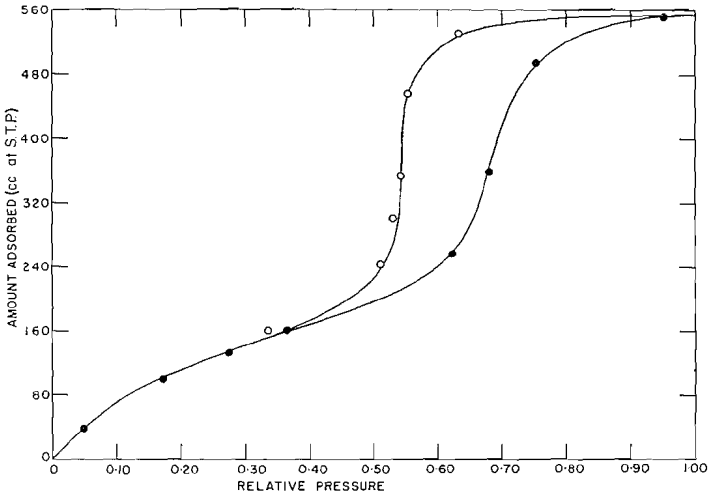


FIG. 3. Adsorption isotherm at −20 °C of ethyl chloride in porous silica glass from which silanol groups have been removed.

Both parts of the dielectric constant for the bare glass (ϵ_0', ϵ_0'') indicate that there is no consistent variation with frequency. At any temperature the smallest and largest values of ϵ_0' differ by approximately 4%. The deviation from the mean is 1%. The ϵ_0'' values, although showing a relatively large overall fluctuation with frequency, are divided into two groups. For the four lowest frequencies there is little or no loss, the highest value being 0.005. At the three highest frequencies ϵ_0'' is three to four times this value.

It is felt that these changes with frequency are not significant but are a reflection of a frequency-dependent error inherent in the cell and the measuring apparatus. These arise from cell and line characteristics which vary with frequency and from the frequency-dependent corrections applied in the calculations to account for the attenuation in the line and its coaxial fittings. A similar but larger fluctuation was reported by McCowan (18) in his work which encompassed the same frequency range and employed General Radio coaxial lines. It had been hoped that the use of improved Hewlett-Packard lines would eliminate these fluctuations. Unfortunately they have only been reduced. These fluctuations, however, would be expected to be less important as the dielectric constant of the system increased since the corrections would be a smaller percentage of the total measured change.

The variation of ϵ_0' and ϵ_0'' with temperature is consistent. Both quantities rise as the temperature is decreased. The change in ϵ_0' in going from −20 to −191 °C is approximately 2%. The preceding remarks apply equally to the dielectric constant of the glass phase (ϵ_1' and ϵ_1'') obtained by the Böttcher method (20).

Figures 4a, 4b, 5a, and 5b show typical plots of ϵ' and ϵ'' as a function of volume adsorbed.

Three points of particular interest are shown by these plots. First, the dielectric isotherms at −20 and −60 °C and the three lowest frequencies at −100 °C show only one linear section. Second, those for −140 °C and the remaining frequencies at −100 °C show two linear sections with the second having a higher slope than the first. These observations are in contrast to previous results for the same adsorbent–adsorbate system where a kink was found at all temperatures and the second linear section had a lower slope

Can. J. Chem. Downloaded from www.nrcresearchpress.com by 210.87.254.6 on 09/05/12
For personal use only.

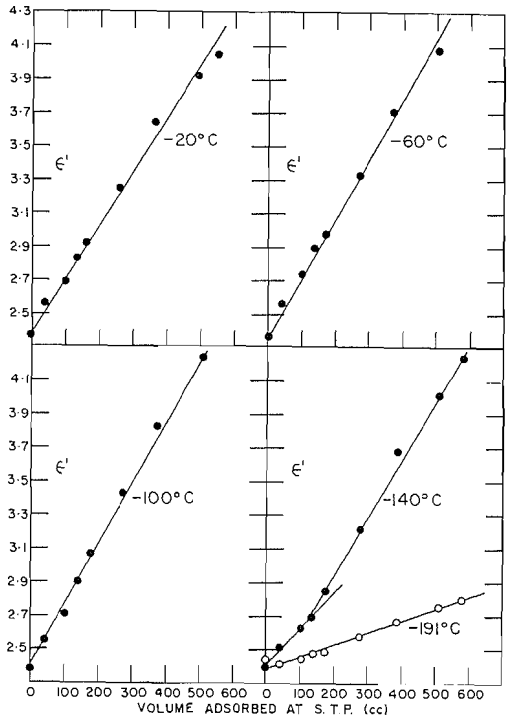


FIG. 4a.

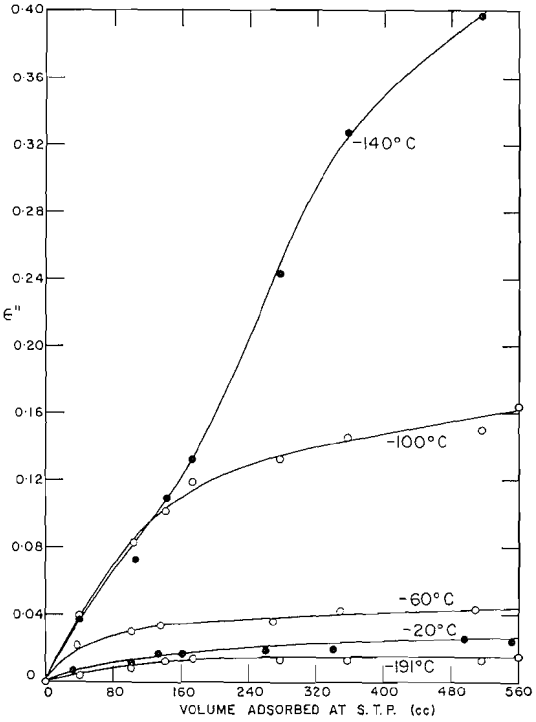


FIG. 4b.

FIG. 4. (*a*) ϵ' (composite system) and (*b*) ϵ'' (composite system) as a function of volume adsorbed for various temperatures and 1 000 Mc/s.

than the first. Third, the plots at −191 °C show that ϵ' for the first admission always falls below that of the glass alone and from this point increases linearly with the volume adsorbed. This is confirmation of a similar observation first made by Chapman (15) in the frequency range 3 kc/s to 4 Mc/s. In that case, however, the anomalous behavior began at approximately −170 °C.

Evidence of dispersion at all temperatures is given by the ϵ'' versus volume adsorbed plots in Figs. 4*b* and 5*b*. At high temperatures these show a rapid rise for initial amounts adsorbed followed by a region of less rapid rise as the amount adsorbed is increased. As the temperature is lowered the curves tend to become linear till at −140 °C the behavior is reversed from that at high temperatures. Here, the slope of the curve is less for the initial amounts than for the later quantities adsorbed. Hence at the higher temperatures the multilayers are showing less loss than the monolayer while at −140 °C this is reversed.

Plots of ϵ' and ϵ'' versus temperature, Figs. 6*a* and 6*b*, show the existence of loss peaks for the composite system which shift to lower temperatures as the amount adsorbed is increased. This is accompanied by a similar shift in the peaks of ϵ' versus temperature.

The dielectric behavior of the adsorbate itself is shown in typical plots of ϵ_2' and ϵ_2'' versus temperature for 100, 300, and 500 cc adsorbed (Figs. 7*a*, 7*b*, 8*a*, and 8*b*). These show more explicitly the difference in behavior of the initial and later amounts adsorbed; the loss for the initial amounts shows a peak while for greater quantities adsorbed the loss continues to increase as the temperature is lowered. From the former plots a definite negative temperature coefficient for ϵ_2' can be seen. Its value $d\epsilon_2'/dT = -0.01$, although

Can. J. Chem. Downloaded from www.nrcresearchpress.com by 210.87.254.6 on 09/05/12
For personal use only.

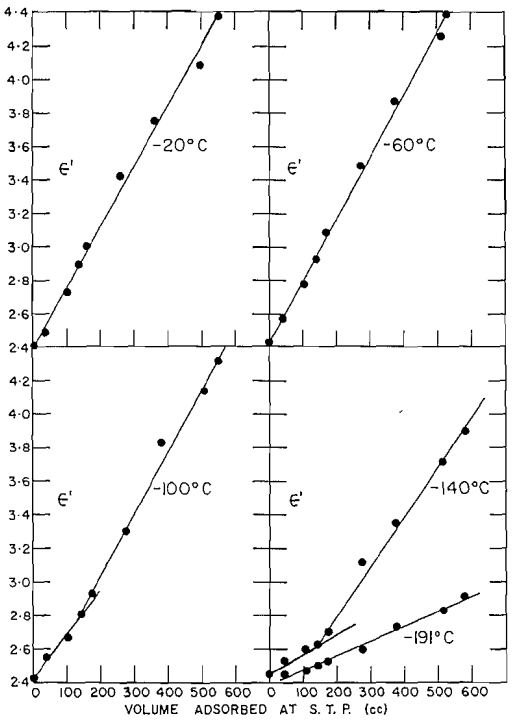


FIG. 5a.

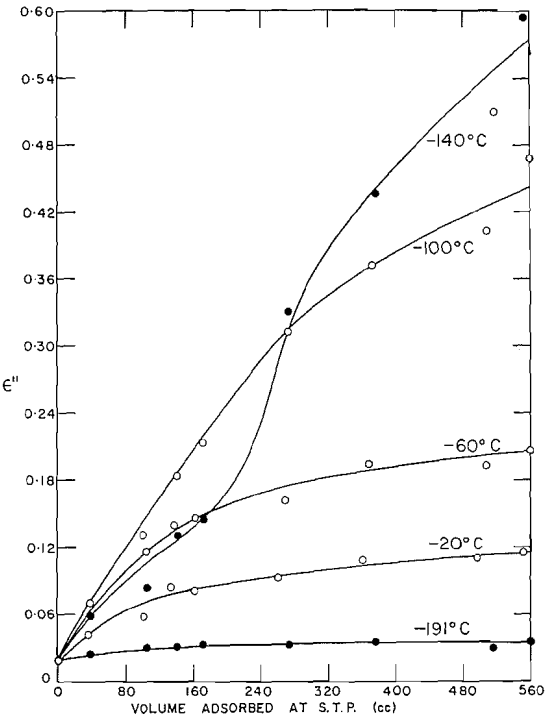


FIG. 5b.

FIG. 5. (*a*) ϵ' (composite system) and (*b*) ϵ'' (composite system) as a function of volume adsorbed for various temperatures and 4 000 Mc/s.

well below that for liquid ethyl chloride (−0.05), agrees well with that reported by Chapman. In his investigation, however, the multilayers showed a temperature coefficient almost twice that for the monolayer. In this research the difference was smaller.

Although the frequency range is limited and the results not as consistent as those obtained with temperature as a variable, plots were drawn of ϵ_2'' versus frequency for 100 and 300 cc adsorbed. These are shown in Figs. 9*a* and 9*b*.

DISCUSSION

The mean value of the real part of the dielectric constant of the glass phase is 3.41, in good agreement with the values obtained by both Chapman and Petrie (3.4 and 3.6) for glass samples evacuated at 350 and 120 °C respectively. Although the value is low compared with that for fused silica (3.75), this is not surprising in view of the fact that the Böttcher method of extraction is not completely satisfactory. McCowan obtained the high value of 5.2. His sample, however, was evacuated at 60 °C, and at this temperature porous glass contains physically adsorbed water, which is polar and may be expected to contribute to the dielectric polarization. This could explain the high result.

The shape of the initial part of the isotherms, the small heat of adsorption, and the high loss values for initial amounts adsorbed are evidence that ethyl chloride prefers the OH to the Si or O sites. Previous work on systems such as ammonia-porous glass (21) indicates that a hydrogen bond is formed between the surface hydroxyl groups and the ammonia. Evidence presented here suggests that the chlorine of the ethyl chloride and the silanol group may form a bond.

Can. J. Chem. Downloaded from www.nrcresearchpress.com by 210.87.254.6 on 09/05/12
For personal use only.

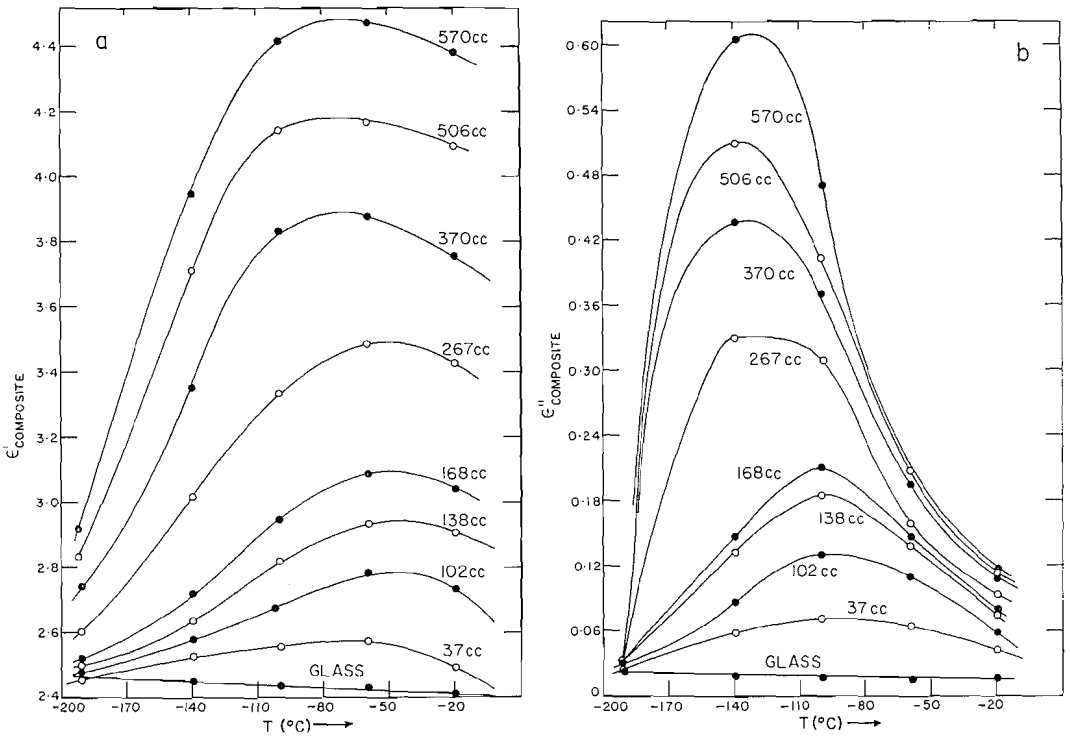


FIG. 6. (*a*) ϵ' (composite system) and (*b*) ϵ'' (composite system) as a function of temperature for several quantities adsorbed and a frequency of 4 000 Mc/s.

The marked effect of such a complex on the dispersion characteristics of the adsorbent–adsorbate system is clear from the data at −191 °C. At this temperature ϵ' is less after the first admission of gas than for the glass alone. Consistent with this apparent anomaly is the high value of the loss for the adsorbate. At such low temperatures it would be expected that the dipoles would be immobile and that the dielectric constant of the adsorbate would have a value given by $\epsilon' = \Delta\epsilon + n^2$, where n is the refractive index and $\Delta\epsilon$ is the elastic displacement of the dipoles. Since the first term is very small, ϵ' should be approximately equal to the square of the refractive index. The value of n^2 was 2.3 as estimated from tables of molar refraction while that of ϵ_2' at −191 °C was 2.44. Hence the dipoles are not free to rotate and the adsorbed ethyl chloride should show no loss. It was found, however, that the average value for ϵ_2'' for the first admission was 0.17 (bulk ethyl chloride shows no loss at −191 °C). It can then be inferred that the complex has different dispersion properties than adsorbed ethyl chloride and that this complex might explain the apparent anomaly at −191 °C.

Further evidence that the complex is responsible for the anomaly was obtained by Chapman (15) from his work on *n*-butane which would not form a hydrogen bond with the OH group adsorbed on porous glass at −180 °C. In this case ϵ' was always larger than that for glass alone and the adsorbate showed no loss.

The elimination of the kink point in the plot of ϵ' versus volume adsorbed for the higher temperatures is a significant observation. The occurrence of a kink and especially the lower slope of the second linear section for porous adsorbents have never been satisfactorily explained. Although no definite answer is given here, certain worthwhile suggestions may be offered with regard to its occurrence.

Can. J. Chem. Downloaded from www.nrcresearchpress.com by 210.87.254.6 on 09/05/12
For personal use only.

Can. J. Chem. Downloaded from www.nrcresearchpress.com by 210.87.254.6 on 09/05/12
For personal use only.

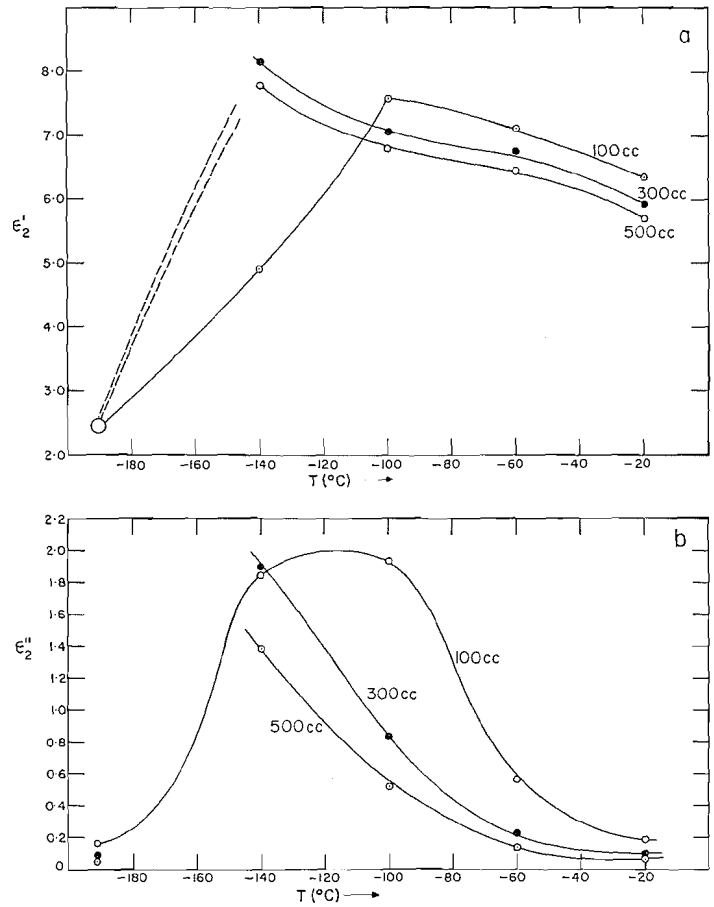


FIG. 7. The variation of (*a*) the real part and (*b*) the imaginary part of the dielectric constant of adsorbate with temperature for a measuring frequency of 1 000 Mc/s.

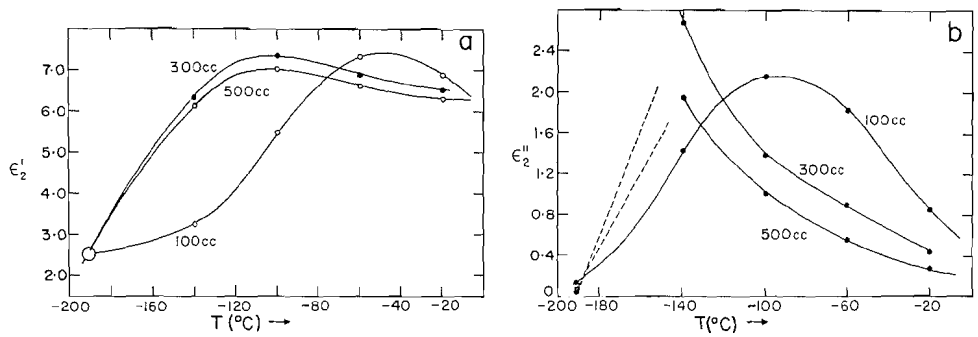


FIG. 8. The variation of (*a*) the real part and (*b*) the imaginary part of the dielectric constant of adsorbate with temperature for a measuring frequency of 4 000 Mc/s.

Two linear sections in the Böttcher equation imply a combination of one or more of three things, occurring at the kink point. These are a change in the adsorbate density, a change in the polarizability of the adsorbate, or a change in the internal field. From studies on *n*-butane on porous glass Petrie (9) was able to conclude that the density change

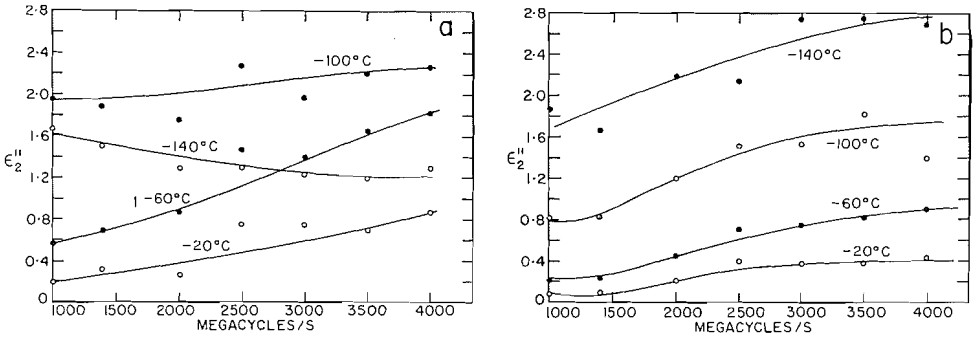


FIG. 9. The imaginary part of the dielectric constant of the adsorbate as a function of frequency for several temperatures and (*a*) 100 cc adsorbed (*b*) 300 cc adsorbed.

was not responsible, since the low density required to bring values of polarization up to those of the first section was not consistent with the available pore volume. She also reasoned that there was no cause for the polarizability to undergo a sudden large change. At first glance, the fact that ethyl chloride may form a complex with OH groups could be a possible answer since the complex may have a different polarizability from adsorbed ethyl chloride. However, since *n*-butane on porous glass also shows two linear sections this again must be discarded. The cause of the second linear section must therefore be due to a change in the internal field.

It has been shown recently by Yates (22) that nonporous rutile has bound to its surface OH groups which have a somewhat different absorption peak than those adsorbed on silica, namely 3 680 cm^{-1} rather than 3 760 cm^{-1}. Also, there appears to be a greater variation in the number and absorption frequency of the OH groups on the rutile. Nevertheless, one would suppose that such groups would also be capable of forming hydrogen bonds with appropriate adsorbates. One should therefore attempt to compare the dielectric behavior on the three adsorbents which are, nonporous rutile containing OH groups, porous glass containing OH groups, and porous glass with most of the OH groups removed. By so doing one would seek to answer the question whether or not the number of hydroxyl groups is responsible for the different behaviors or whether the hydroxyl groups must be associated with a porous structure to bring about the effects. Unfortunately the relative numbers of OH groups on the surfaces of the adsorbents are not known and an unequivocal answer to the query is not possible. At the same time some analysis and discussion is warranted.

In summary, a nonpolar adsorbate on rutile shows a single dielectric constant over the range of adsorption up to 3 or 4 V_m, and thus there is no indication of a changed local field over the range of adsorption studied. All polar adsorbates show two values of dielectric constant. The first region shows the lower value and one which changes little with temperature. The second region shows a dielectric constant more nearly equal to that of bulk liquid and its temperature coefficient is negative. The sudden change from one value to the other occurs at an amount adsorbed corresponding quite well with V_m. Thus, first-layer material has been interpreted as quite firmly bound and as undergoing oscillatory motion.

The OH-free porous glass shows a dielectric constant for ethyl chloride independent of coverage at temperatures down to about −100 °C, and of value about 6.5 to 7.5 throughout the temperature range whereas bulk liquid varies from 12.1 to 19.3. This range for

Can. J. Chem. Downloaded from www.nrcresearchpress.com by 210.87.254.6 on 09/05/12
For personal use only.

adsorbate agrees with the values of ethyl chloride along the first linear section of porous glass having many OH groups on the surface (15) and for adsorbate within the first adsorbed layer on rutile (23). Thus on all three surfaces the first quantities of ethyl chloride appear to be firmly bound and have the small temperature coefficient of dielectric constant associated with oscillators. As the quantity of adsorbed ethyl chloride is increased on the OH-free porous glass, there is no evidence of greater orientational freedom. Thus the matter adsorbed above the beginning of the hysteresis loop is still only one layer in thickness or the pore structure is reducing its rotational freedom.

The ethyl chloride adsorbed below the hysteresis loop is less firmly bound on the OH-free surface than on the porous glass containing OH groups as is shown by the shape of the isotherm or the lower value of C obtained from B.E.T. plots. This is further evidence that apparent dielectric constants are quite insensitive to changes in the heat of adsorption, which must be the case for a constant value during the filling of the first layer.

As the temperature of the OH-free surface is lowered, it is seen that dispersion begins in the adsorbate below the hysteresis loop for the comparatively high measuring frequencies employed in this investigation. Thus the binding of this material to the surface is stronger than that of the "capillary-condensed" material. The plots for these lower temperatures now resemble those for nonporous rutile and ethyl chloride, although it must be remembered that the adsorbate taken on at higher relative pressures does not behave like bulk liquid as is the case for multilayer material on rutile.

Ethyl chloride adsorbed above the inception of the hysteresis loop on glass containing OH groups has a low apparent dielectric constant. Since the heat of adsorption for the low range of adsorption is increased by the presence of the OH groups without reducing the apparent value of the dielectric constant, the reduction of ϵ_2 for the capillary-condensed material remains unexplained. The effect is apparently not related to orientational contributions to the polarization because it is found also with normal butane. Hydroxyl groups on rutile do not prevent high values of dielectric constant for the adsorbate in the higher layers. One is therefore led to speculate that in some way hydroxyl groups in the porous solid create within the pores an internal field which leads to a lesser apparent value of polarization.

In reaching the conclusion above, it is clear that the different nature of OH groups on the rutile and silica surfaces has been ignored. The unknown effect of the relative number of OH groups situated on the two surfaces has also been neglected. Neither of these two simplifications is strictly justifiable. However, the experimental effect arising from the three factors is a gross effect, and the gross difference between adsorbents is the porosity of the glass. It is therefore possible to associate this difference, namely the porosity (in conjunction with OH groups), with the experimental observation.

At low temperatures, both the appearance of a second linear section with a slope larger than the first (ϵ' versus volume adsorbed) and the increased loss for the later quantities adsorbed are interesting since these observations have never been made for porous glass. These facts and the plots of ϵ_2' and ϵ_2'' versus temperature for 100, 300, and 500 cc adsorbed show that the dielectric properties of the initial and later quantities adsorbed are different. A qualitative explanation of this in terms of the strength of binding to the surface may be made.

Dielectric loss is due to a phase difference between the polarization and the electric field. If the dipole cannot follow the field at high frequency, at low temperature, or because of some hindering mechanism, such a phase difference results and dielectric loss occurs. Thus the initial amounts adsorbing on the high-energy sites should have a larger relaxation time and should show loss at lower frequencies and higher temperatures than the adsorbate

Can. J. Chem. Downloaded from www.nrcresearchpress.com by 210.87.254.6 on 09/05/12
For personal use only.

taken up at the higher relative pressures. It must be noted here that this case is complicated by the fact that much of this high initial loss is due to the complex between ethyl chloride and the residual OH groups. These complexes have different dispersion properties than ethyl chloride adsorbed on Si and O sites, as is shown by the drop in ϵ' for the composite system at -191 °C below that of the glass alone and was shown earlier by Chapman (15).

When the temperature is lowered, the movement of the dipoles becomes more restricted and the loss will rise for all quantities adsorbed until at some temperature it is a maximum. Lowering the temperature still further will then decrease the loss since the adsorbate will approach the condition where orientation of dipoles is negligible. The quantities adsorbed on the high-energy sites show a maximum at a higher temperature then matter adsorbed on sites of lower binding energy. In Figs. 7*b* and 8*b* it is seen that for 100 cc adsorbed the maximum occurs at approximately -100 to -120 °C depending on the frequency, while for 300 and 500 cc the loss is still rising at -140 °C and does not show a maximum. Similarly ϵ_2' should show a maximum at higher temperatures for initial amounts adsorbed. This is seen in Figs. 7*a* and 8*a*. Furthermore, below the temperature at which ϵ_2'' has a maximum for 100 cc adsorbed the difference in ϵ_2' between initial and later quantities adsorbed should become larger, since ϵ_2'' for the former has passed its maximum while it is still rising for the latter. When the difference in ϵ_2' values between initial and later quantities adsorbed becomes sufficiently large, it is manifest in the appearance of a kink in the primary plots of ϵ' versus volume adsorbed, with the second section having a higher slope.

Despite the limitations of the frequency range it can be seen that the temperature of the maximum of ϵ_2' and ϵ_2'' shifts to lower values as the frequency is lowered. This is to be expected since at constant temperature the dipole can follow the field more easily when the frequency is lower so that the loss will be lower. In addition, a noticeable difference in ϵ_2' values between initial and later quantities adsorbed occurs at lower temperatures for lower frequencies. For example, a comparison of the curves for 4 000 and 1 000 Mc/s shows that for the former, a relatively large difference is noted at -100 °C, while for the latter, such a comparable difference does not occur till -140 °C. Thus at -100 °C only the higher frequencies show a kink in the plots of ϵ' versus volume adsorbed. At -140 °C the difference is large for all frequencies and hence all plots show kinks. It is surprising, however, that at -100 °C the division of the frequencies that show kinks and those that do not is so sharp. No doubt this is in part caused by the judgment that must be exercised in deciding whether a kink exists or not since the kinks are not as clear as they are at -140 °C.

Chapman's results also show the shifting of the loss to lower temperatures as the volume adsorbed is increased. He did not observe the marked rise in values for later quantities adsorbed because of the high concentration of OH groups and the fact that the losses in his case never showed a maximum when plotted against temperature. Although the temperature range he employed was large, he used low frequencies so that significant losses did not occur till -130 °C. Thus the conditions of the investigation were comparable to those above -60 °C in this work.

The curves for ϵ_2' in Figs. 7*a* and 8*a* show that ϵ_2' is smaller for larger amounts adsorbed at the high temperatures. This observation is not consistent with the explanations just offered, since the orientational polarization should increase with amount adsorbed. Whether ϵ_2' rises or falls with quantity adsorbed is dependent on which of two methods is used to compute these values from given data. A discussion of this point need not be given here, as the results differ significantly only in this one respect. In view of the earlier discussion the procedure giving increasing values of ϵ_2' with amount adsorbed seems preferable.

Plots of ϵ_2'' versus frequency for 100 and 300 cc adsorbed are shown in Figs. 9*a* and 9*b*.

Can. J. Chem. Downloaded from www.nrcresearchpress.com by 210.87.254.6 on 09/05/12
For personal use only.

It is evident that the amount of scatter in the values of ϵ_2'' at any temperature is much larger than in comparable plots of ϵ_2'' versus temperature at constant frequency. However, definite trends can be seen which are consistent with the conclusions reached from ϵ_2'' versus temperature plots. Thus for 300 cc adsorbed and for the higher temperatures the loss curves seem to be far removed from the loss peaks while at the lower temperatures the loss curves are closer to the peaks, i.e. the loss peaks have shifted to lower frequencies for the lower temperatures. At all temperatures the frequency maximum is beyond the range used in this work. The absence of loss peaks precludes any conclusions regarding the mode of motion of the adsorbate from these data. The fact that ϵ_2'' increases for decreasing temperature can be explained by a shift in the peak position of the Debye type of dispersion curve or equally by the increased peak level of resonance absorption (24).

The plots for 100 cc adsorbed are more interesting. The curve at -140 °C indicates that at this temperature the loss peak occurs at a frequency lower than 1 000 Mc/s while the curve at -100 °C indicates that a loss peak occurs in the frequency range employed here.

Of the three criteria one might wish to use to discriminate between resonant and Debye-type systems, only two appear to be available because of the limited range of frequency employed in the measurement. The first is the absolute value of the real part of the dielectric constant ϵ_2'. It is appreciably less than that of bulk liquid at equivalent temperatures, but much greater than expected for distortion polarization alone. The second is the temperature coefficient of ϵ_2', which is smaller than for liquid. Both these findings are consistent with the behavior of rotational oscillators. The shape of the loss curves as a function of frequency and the changes in these curves with temperature are not well enough defined to provide useful evidence. When it is recalled that a Debye loss curve stretches over about six decades in the frequency, the small factor of four in frequency in the present investigation is seen to represent too small a section of the curve. On the basis of present evidence, therefore, it would seem that a description of the adsorbed ethyl chloride as a rotational oscillator is still acceptable on a provisional basis.

ACKNOWLEDGMENT

The authors are very much indebted to Professor R. A. Stairs, Trent University, Peterborough, for suggesting the method of obtaining ϵ' and ϵ'' from the standing wave data, and for outlining a less rigorous procedure, which itself was not successful but which led to the method described in Appendix I.

APPENDIX I

The Evaluation of ϵ' and ϵ'' from the Experimentally Determined Characteristics of the Standing Wave

Von Hippel (16) develops the equation

$$\frac{\tanh \gamma_2 d}{\gamma_2 d} = \frac{(-j\lambda_1/2\pi d)(E_{\min}/E_{\max} - j \tan (2\pi X_0/\lambda_1)}{1 - j(E_{\min}/E_{\max}) \tan (2\pi X_0/\lambda_1)}$$

where γ_2 is the complex propagation factor of the wave in medium 2, d is the thickness of the sample, X_0 its distance from the first minimum of the standing wave, and λ_1 the wavelength in the air part of the guide. The right-hand side may be expressed as $C \exp(-j\zeta)$ where C and ζ are obtained from experimental data. The term $\gamma_2 d$ may be expressed as $T \exp(j\tau)$. Charts provided by Von Hippel (16) give values of T and τ for values of C and ζ. Knowing T and τ we may evaluate ϵ' and ϵ'' from the definition of γ_2 and the relations which thus exist, namely

$$\epsilon' = -KT^2 \cos 2\tau$$
$$\epsilon'' = KT^2 \sin 2\tau$$

Can. J. Chem. Downloaded from www.nrcresearchpress.com by 210.87.254.6 on 09/05/12
For personal use only.

where $K = \epsilon_0\lambda_1^2/(2\pi d)^2$ and ϵ_0 is here the dielectric constant of vacuum.

The value of K arises in the following way:

$$\gamma = \alpha + j\beta = j\omega(\epsilon\mu)^{1/2},$$

where α is the attenuation factor and β the phase factor of the standing wave. In the coaxial line system, where the air part of the guide is designated as medium 1 and the dielectric as medium 2,

$$z_1 = (\mu_1/\epsilon_1)^{1/2} \text{ and } z_1\gamma_1 = j\omega\mu_1.$$

Similarly

$$z_2\gamma_2 = j\omega\mu_2$$

and for nonmagnetic materials this means $z_1\gamma_1 = z_2\gamma_2$.

$$\gamma_2^2/\gamma_1^2 = \epsilon_2/\epsilon_1.$$

For medium 1, assumed lossless,

$$\gamma_1 = j\beta_1 = j2\pi/\lambda_1$$

and

$$\epsilon_1 = \epsilon_1' = \epsilon_0.$$

Hence

$$\epsilon_2 = -\gamma_2^2\lambda_1^2\epsilon_0/4\pi^2.$$

Since we have defined

$$\gamma_2 d = T\exp(j\tau),$$
$$\gamma_2^2 = T^2(\cos 2\tau + j\sin 2\tau)/d^2,$$

so that

$$\epsilon_2 = -\lambda_1^2\epsilon_0 T^2(\cos 2\tau + j\sin 2\tau)/(2\pi d)^2$$

and

$$K = \lambda_1^2\epsilon_0/(2\pi d)^2.$$

Because of the forms of the functions, interpolation between curves on the charts is not always easy and some accuracy of the primary data is readily lost. A solution may be obtained to the equation below which can be programmed for an IBM 1620 computer.

$$[\tanh(T\exp(j\tau)) - C\exp(-j\zeta)T\exp(j\tau)]^2 = 0$$

Calling $\tanh(T\exp j\tau) = u + jv$ and $C\exp(-j\zeta)T\exp(j\tau) = x + jy$, we wish to solve the equation

$$G = (u - x)^2 + (v - y)^2 = 0,$$

where

$$u = \frac{\sinh(2T\cos\tau)}{\cosh(2T\cos\tau) + \cos(2T\sin\tau)} \qquad v = \frac{\sin(2T\sin\tau)}{\cosh(2T\cos\tau) + \cos(2T\sin\tau)}$$

$$x = CT(\cos(\tau - \zeta)) \qquad y = CT(\sin(\tau - \zeta))$$

G is thereby given by the equation

$$G = C^2T^2 + \frac{\cosh(2T\cos\tau) - \cos(2T\sin\tau)}{\cosh(2T\cos\tau) + \cos(2T\sin\tau)} - 2CT\frac{[\cos(\tau - \zeta)\sinh(2T\cos\tau) + \sin(\tau - \zeta)\sin(2T\sin\tau)]}{\cosh(2T\cos\tau) + \cos(2T\sin\tau)}.$$

Since any values other than the best ones cause the function G to increase, it was assumed that the function could be represented as a paraboloid of the form

$$G = A(T - T_0)^2 + B(T - T_0)(\tau - \tau_0) + D(\tau - \tau_0)^2$$

Can. J. Chem. Downloaded from www.nrcresearchpress.com by 210.87.254.6 on 09/05/12
For personal use only.

near the values T_0 and τ_0 which are the best values of the solution of the equation. The quantities A, B, D, may be eliminated and T_0 and τ_0 evaluated through the relations

$$\tau_0 = \tau - \left(\frac{\partial^2 G}{\partial T \partial \tau} \cdot \frac{\partial G}{\partial T} - \frac{\partial^2 G}{\partial T^2} \cdot \frac{\partial G}{\partial \tau}\right) \Big/ \left[\left(\frac{\partial^2 G}{\partial T \partial \tau}\right)^2 - \frac{\partial^2 G}{\partial \tau^2} \cdot \frac{\partial^2 G}{\partial T^2}\right]$$

$$T_0 = T - \left(\frac{\partial^2 G}{\partial T \partial \tau} \cdot \frac{\partial G}{\partial \tau} - \frac{\partial^2 G}{\partial \tau^2} \cdot \frac{\partial G}{\partial T}\right) \Big/ \left[\left(\frac{\partial^2 G}{\partial T \partial \tau}\right)^2 - \frac{\partial^2 G}{\partial \tau^2} \cdot \frac{\partial^2 G}{\partial T^2}\right].$$

Preliminary values of T and τ are read from the charts and first values of τ_0 and T_0 obtained. The process is repeated until values of τ_0 and T_0 within acceptable limits of the answer are obtained.

Analytical expressions for the first and second derivatives of the function G are very cumbersome. An attempt to obtain a solution by approximating these derivatives through small increments in the G function due to small increments in τ and T was not successful, as the computer gave answers which oscillated in value. It thus became mandatory to use the exact functions for these terms; these are set out below.

Derivatives of the Function G with respect to T and τ

$$\frac{\partial G}{\partial T} = [4(AD) - 2C(AX)(AA) - 4CT(AB)]\frac{1}{(AA)^2} + 2C^2T$$

$$\frac{\partial G}{\partial \tau} = [4T(AE) - 2CT(AF)(AA) + 4CT^2(AC)]\frac{1}{(AA)^2}$$

$$\frac{\partial^2 G}{\partial T \partial \tau} = [4(AE)(AA) - 2C(AF)(AA)^2 - 8T[\sin Q \sinh P(AA) - 2(AD)(AG)] + 4CT(AC)(AA) - 8CT^2[-(AZ)(AA) + 2(AB)(AG)]]\frac{1}{(AA)^3}$$

$$\frac{\partial^2 G}{\partial T^2} = [8(\cos Q \cosh P)(AA) - 16(AD)(AH) - 8C(AB)(AA) - 8CT[(AY)(AA) - 2(AB)(AH)]]\frac{1}{(AA)^3} + 2C^2$$

$$\frac{\partial^2 G}{\partial \tau^2} = [-4T(AD)(AA) + 8T^2[\cos Q \cosh P(AA) + 2(AE)(AG)] + 2CT(AX)(AA)^2 - 4CT^2(AB)(AA) - 8CT^3[(AY)(AA) - 2(AC)(AG)]]\frac{1}{(AA)^3}$$

$$(AA) = (\cosh P + \cos Q)$$
$$(AB) = (\cos Z + \cos Z \cos Q \cosh P + \sin Z \sin Q \sinh P)$$
$$(AC) = (\sin Z + \sin Z \cos Q \cosh P - \cos Z \sin Q \sinh P)$$
$$(AD) = (\sin \tau \sin Q \cosh P + \cos \tau \cos Q \sinh P)$$
$$(AE) = (\cos \tau \sin Q \cosh P - \sin \tau \cos Q \sinh P)$$
$$(AF) = (\sin Q \cos R - \sin R \sinh P)$$
$$(AG) = (\sin \tau \sinh P + \cos \tau \sin Q)$$
$$(AH) = (\cos \tau \sinh P - \sin \tau \sin Q)$$
$$(AX) = (\sin Q \sin R + \cos R \sinh P)$$
$$(AY) = (\cos R \cos Q \sinh P - \sin R \sin Q \cosh P)$$
$$(AZ) = (\cos R \sin Q \cosh P + \sin R \cos Q \sinh P)$$

where $P = 2T \cos \tau \qquad Q = 2T \sin \tau \qquad R = \tau - \zeta$

Can. J. Chem. Downloaded from www.nrcresearchpress.com by 210.87.254.6 on 09/05/12
For personal use only.

REFERENCES

1. I. HIGUTI. Bull. Inst. Phys. Chem. Res. Tokyo, **21**, 1138 (1942).
2. I. HIGUTI. Sci. Rept. Res. Inst. Tohoku Univ. Ser. A, **33**, 99 (1949).
3. I. HIGUTI. Sci. Rept. Res. Inst. Tohoku Univ. Ser. A, **33**, 174 (1949).
4. R. McINTOSH, H. S. JOHNSON, N. HOLLIES, and L. McLEOD. Can. J. Res. B, **25**, 566 (1947).
5. L. N. KURBATOV. J. Phys. Chem. USSR, **24**, 899 (1950).
6. G. EBERT and G. LANGHAMMER. Kolloid-Z. **174**, 5 (1961).
7. E. W. CHANNEN and R. McINTOSH. Can. J. Chem. **33**, 172 (1955).
8. R. McINTOSH, E. K. RIDEAL, and J. A. SNELGROVE. Proc. Roy. Soc. London, Ser. A, **208**, 292 (1951).
9. S. E. PETRIE and R. McINTOSH. Can. J. Chem. **35**, 183 (1957).
10. M. WALDMAN. J. Phys. Radium, **17**, 426 (1956).
11. A. N. SIDOROV. J. Phys. Chem. USSR, **30**, 183 (1956).
12. M. FOLMAN and D. J. C. YATES. Trans. Faraday Soc. **54**, 1684 (1958).
13. D. J. C. YATES, N. SHEPPARD, and C. L. ANGELL. J. Phys. Chem. **23**, 1980 (1955).
14. I. D. CHAPMAN and M. L. HAIR. J. Catalysis, **2**, 145 (1963).
15. I. D. CHAPMAN and R. McINTOSH. Can. J. Chem. **40**, 92 (1962).
16. A. VON HIPPEL. Dielectrics and waves. John Wiley & Sons, Inc., New York. 1954. Dielectric materials and applications. John Wiley & Sons, Inc., New York. 1954.
17. M. S. FRED and E. G. RAUH. Rev. Sci. Instr. **21**, 258 (1950).
18. J. D. McCOWAN and R. McINTOSH. Can. J. Chem. **39**, 425 (1961).
19. R. S. McDONALD. J. Am. Chem. Soc. **79**, 850 (1957).
20. C. J. F. BÖTTCHER. Rec. Trav. Chim. **64**, 47 (1945).
21. D. FIAT, M. FOLMAN, and U. GARBATSKI. Proc. Roy. Soc. London, Ser. A, **260**, 409 (1960).
22. D. J. C. YATES. J. Phys. Chem. **65**, 746 (1961).
23. S. E. PETRIE, R. McINTOSH, and E. W. CHANNEN. Can. J. Chem. **35**, 1534 (1957).
24. H. FRÖHLICH. Theory of dielectrics. The Clarendon Press, Oxford. 1949. p. 99 *et seq.*

Can. J. Chem. Downloaded from www.nrcresearchpress.com by 210.87.254.6 on 09/05/12
For personal use only.

REACTION OF $N_2(A^3\Sigma_u^+)$ WITH ATOMIC NITROGEN[1]

ROBERT A. YOUNG
Stanford Research Institute, Menlo Park, California

Received October 26, 1965

ABSTRACT

Attempts to measure the actual lifetime of $N_2(A^3\Sigma_u^+)$ in active nitrogen resulted only in a very small upper limit of $\approx 5 \times 10^{-4}$ s. This result is consistent with quenching of the $A^3\Sigma_u^+$ state by atomic nitrogen in an atom–atom interchange process,

$$N + N_2(A^3\Sigma_u^+, v = 0) \rightarrow N_2(X^1\Sigma_g^+, v = 25) + N,$$

having a rate coefficient of $\gtrsim 2 \times 10^{-10}$ cm^3/molecule s. It is suggested that similar processes are involved in determining the distribution of excited states observed in atom association.

I. INTRODUCTION

Although Berkowitz *et al.* (1) showed that atomic nitrogen was the predominant reactive species in active nitrogen, several investigators (2) studying chemical reactions in discharged nitrogen have found it necessary to hypothesize other energy-rich species. In almost all instances this additional component of active nitrogen has been assumed to be the $A^3\Sigma_u^+$ state of N_2. However, emission from this state has never been detected in the reacting gas. In fact, spectrographic tests for its presence have been avoided except in one case (3) in which none was detected.

Usually these chemical reaction studies are done near the discharge ($\approx$0.1 s in travel time) which forms active nitrogen. It is known that large quantities of vibrationally excited N_2 exist just beyond the discharge (4) ($\approx$0.05 s) and probably are the major energy reservoir powering the pink nitrogen afterglow (5). Furthermore, their collisional deactivation rate coefficient (6) is $\approx 10^{-16}$ cm^3/s. In the light of this information it would appear that vibrationally excited N_2 is responsible for most of the observed chemical effects which require an excited species other than atomic nitrogen.

Experiments have indicated that the $A^3\Sigma_u^+$ state of N_2 has a radiative lifetime of $\tau \approx 20$ s and is not deactivated by nitrogen (7) ($k_Q < 10^{-18}$ cm^3/s). If this is correct there should be a detectable concentration of $A^3\Sigma_u^+$ molecules maintained by the recombination of atomic nitrogen. The flux of the 1st positive band of nitrogen whose lower state is $A^3\Sigma_u^+$ represents a lower bound to this rate of population. For example, if radiation is the only loss of $N_2(A^3\Sigma_u^+)$, and the recently measured (8) chemiluminescent recombination rate of N is applied to a steady state situation with [N] $\approx 10^{15}$ atoms/cm^3 and [N_2] $\approx 10^{17}$ molecules/cm^3, then

$$k[N]^2 = 10^{-17}[10^{15}]^2 = \frac{1}{\tau}[N_2(A^3\Sigma_u^+)]$$

and gives $[N_2(A^3\Sigma_u^+) = 2 \times 10^{14}$ molecules/cm^3 emitting 10^{13} photons/s cm^3 in the Vegard–Kaplan bands. If, however, processes other than radiation remove this species, then its steady state density will be lower and fewer metastable molecules could survive from the discharge to cause chemical effects.

It is of crucial interest to spectroscopically verify the presence or absence of large amounts of $N_2(A^3\Sigma_u^+)$ in discharge nitrogen within $\approx$0.1 s of the discharge and to obtain

[1]*This work was supported by the U.S. Army Research Office, Durham, through Contract No. DA-31-124-ARO(D)-104.*

Can. J. Chem. Downloaded from www.nrcresearchpress.com by 210.87.254.5 on 09/05/12
For personal use only.

some limits on its rate of removal in a typical experimental situation. As the environment near the discharge is complicated by the pink glow, a study of the concentration further from the discharge seems more likely to give results analyzable into elementary processes. This experiment was performed.

II. EXPERIMENT

Nitrogen of various purities (starting from gas purified by passing over heated Ti–Zr turnings to which known amounts of impurities were added) was passed through a 100 W microwave discharge in a flow system previously described (9). The gas was viewed after ≈0.5 s through the quartz window of a 10 cm diameter, 100 cm long tube by a crossed-grating echelle spectrograph of ≈6 Å/mm plate factor and $f/1.0$ aperture. The nitrogen atoms were measured by NO titration and the spectrograph was calibrated for intensity when [O] = [N] by obtaining spectrograms of the NO bands excited in the process

[1] $$N + O + (M) \rightarrow NO^* + (M)$$

whose rate has been previously measured (9). Hence each experiment consisted of the following steps: (*a*) establish a stable pressure and determine the purity of the flowing gas, (*b*) establish a stable discharge (the microwave oscillator was incorporated into a power supply which regulated the cathode current to 0.1%), (*c*) titrate with NO to obtain $[N]_0$, (*d*) re-establish the conditions before titration, (*e*) time the long spectrographic exposure, (*f*) adjust the NO flow until [N] = (O), (*g*) take a sequence of timed spectrographic exposures, and (*h*) titrate with NO to again obtain $[N]_0$.

III. DATA REDUCTION

If reciprocity failure of the film (103 a-0) is not considered, if the time necessary to obtain an image of the (0,5) Vegard–Kaplan band (one of the strongest from $v' = 0$) is t_1, and if the exposure time to obtain an equally dense image of the $\gamma(0,3)$ NO band is t_2, then

$$I_{VK}(0,5) \approx k_1(\gamma(0,3))\frac{[N]_0^2}{4}\frac{t_2}{t_1} = \frac{[N_2(A^3\Sigma_u^+)_{v=0}]}{\tau}\frac{I_{VK}'(0,5)}{\sum_{v''} I_{VK}'(0,v'')}$$

where $I_{VK}'(0,v'')$ are the intensities of these bands in any uniform set of arbitrary units. A lower bound to the rate of $A^3\Sigma_u^+$ formation is the rate of emission of the first positive bands. This can be represented as

$$P = k_2[N]^2$$

where k_2 refers[2] to

[2] $$N + N + (M) \rightarrow N_2 + (M) + h\nu$$

If the rate of loss of $N_2(A^3\Sigma_u^+, v = 0)$ is $(A/\tau)[N_2(A^3\Sigma_u^+, v = 0)]$, then in a steady state

[3] $$fk_2[N]_0^2 \approx \frac{A}{\tau}\left(\frac{\tau\sum_{v''} I_{VK}'(0,v')}{I_{VK}'(0,5)}\right)k_1(\gamma(0,3))\frac{[N]_0^2}{4}\frac{t_2}{t_1}$$

or

[4] $$\frac{A}{\tau} \gtrsim \left(\frac{4k_2}{k_1(\gamma(0,3))}\right)\left(\frac{t_1}{t_2}\right)(f)\left(\frac{I_{VK}'(0,5)}{\tau\sum_{v''} I_{VK}'(0,v'')}\right)$$

where f is the fraction of all radiation which eventually leads to $A^3\Sigma_u^+$, $v = 0$, and $A/\tau = 1/\tau + k_Q[Q]$: k_Q is the rate coefficient for a reaction between Q and $N_a(A^3\Sigma_u^+)$. The last parenthesis of eq. [4] is $\approx 1/6\tau$ (11).

[2] *Young and Black (8) report values of* $k_{N_2} = 8 \times 10^{-18} + 1.2 \times 10^{-34}[N_2]$ *cm³/molecule-s;* $k_{N_2} = 5 \times 10^{-16} + 3.8 \times 10^{-33}[IIe]$.

Can. J. Chem. Downloaded from www.nrcresearchpress.com by 210.87.254.5 on 09/05/12
For personal use only.

If vibrational relaxation occurs before emission, $f \approx 1$. If electronic deactivation occurs more rapidly than vibrational relaxation, then $f \approx 0.3$ (12). Assuming the latter, we have

$$[5] \qquad \frac{A}{\tau} \gtrsim \frac{10^{-2}k_2}{k_1(\gamma(0,3))}\frac{t_1}{t_2}.$$

Corrections must still be applied because of film reciprocity failure.

Note that the actual value of [N] is not involved in eq. [5] because of the calibration procedure used. For a similar reason the spatial distribution of [N] and [O] is relatively unimportant—decay down the tube affects both the production rate and calibration of the spectrograph. If $A/\tau < 10$, this equation will not be applicable because a steady state has not yet been established.

IV. RESULTS

Under no circumstances were the Vegard–Kaplan bands ever observed in active nitrogen. The longest exposure was 240 h in 1% N_2 in He at 6 mm Hg with [N] $\approx 10^{13}$ atoms/cm^3 and [O] $\approx 10^{11}$. The $\gamma(0,3)$ band was detected in 1 min. Exposures of 50 h in 100% N_2 at 2 mm Hg with [N] $\approx 10^{15}$ atoms/cm^3 and [O] $\approx 10^{13}$ were also unsuccessful in obtaining any record of the Vegard–Kaplan bands when the $\gamma(0,3)$ NO band was detected in 30 s for [N] = [O]. Other combinations of parameters gave a similar result. Equation [5] gives $A/\tau \gtrsim 2.5 \times 10^2$/s for the 50 h exposure after correction for reciprocity failure (≈ 5), and substitution of $k_2 \approx 2 \times 10^{-17}$ cm^3/molecule s (8), $k_1\gamma(0,3) \approx 10^{-18}$ cm^3/molecule s.[3] Similar treatment of the 240 h exposure gives $A/\tau \gtrsim 2 \times 10^3$ with $k_2 = 1.3 \times 10^{-15}$, $k_1(0,3) \cong 10^{-18}$, and a correction factor of 10 for reciprocity failure. These results indicate that significant vibrational relaxation probably does not occur before electronic deactivation; hence the $v' = 0$ level of the $A^3\Sigma_u^+$ state is significantly populated only by direct emission from the $B^3\pi_g$ state.

V. DISCUSSION

The large value of A/τ derived from our measurements must be due to a gas collision process—diffusion of $N_2(A^3\Sigma_u^+)$ to the walls of the flow system cannot account for the measured A/τ, nor can such a large value result from an incomplete approach to a steady state. Since N_2 and He are inefficient quenchers of $N_2(A^3\Sigma_u^+)$, the most likely reaction removing this species is

$$[6] \qquad N + N_2(A^3\Sigma_u^+, v = 0) \rightarrow N_2(X^1\Sigma, v = 25) + N$$

i.e., atom–atom interchange. The maximum lower bound to the rate of this process can then be deduced from the He experiment

$$\frac{A}{\tau} \approx 2 \times 10^3 = k_6[N] = k_6[10^{13}]$$

i.e., $k_6 \gtrsim 2 \times 10^{-10}$ cm^3/s.

For any reaction other than [6] to account for the measured A/τ requires the presence of an unsuspected impurity in concentrations at least comparable to that of atomic nitrogen and probably much higher in view of the large value found for k_6. From past experience (8–10) this is considered extremely unlikely.

A review of the literature (7, 13) pertaining to observations of the Vegard–Kaplan bands revealed an inverse correlation of these bands and significant concentrations of

[3] *Young and Sharpless (10) report values of*

$$k\gamma(0,3) = 8.2 \times 10^{-19} + 2.4 \times 10^{-36}[N_2];\ k\gamma(0,3) = 8.2 \times 10^{-19} + 5 \times 10^{-37}[He].$$

Can. J. Chem. Downloaded from www.nrcresearchpress.com by 210.87.254.5 on 09/05/12
For personal use only.

nitrogen atoms. Reaction [6] implies just this. The correlation found between a high intensity of the Vegard–Kaplan bands and the need for high purity nitrogen probably is due to the correlation between high purity and low atom production (14) rather than to direct quenching by impurities.

Reaction [6] is probably fast since selection rules are less restrictive for atom–atom interchange than in other processes and large internuclear distance changes between reactants and products are anticipated since this is a reaction coordinate. Reaction [6] may be another example where excess energy goes into vibration of a newly formed bond (15).

For initial vibrational levels higher than $v' = 6$ other electronic states (16) may be formed in reaction [6], although at room temperature one would expect as major products those states whose potential well was outside the reactant's potential well. The distribution of product states will, of course, be determined by the level structure of the unstable N_3 collision complex and the initial levels populated.

Other excited N_2 molecules can probably undergo reactions similar to [6], i.e.,

$$N + N_2(\alpha) \rightarrow N_2(\beta) + N$$

where energy and momentum are conserved but large changes in internuclear distance can occur. Such mechanisms are probably extremely important in determining the observed population of excited states in active nitrogen. Furthermore, since this mechanism may lead preferentially to the electronic ground state, it may account for the small number of electronically excited molecules found in atomic association in nitrogen, oxygen (10), and other diatomic molecules.

ACKNOWLEDGMENTS

The importance of atom-atom interchange reactions in removing $N_2(A^3\Sigma_u^+)$ was jointly realized by Dr. D. M. Hunten of the Kitt Park National Observatory and the author. I wish to thank Dr. Hunten for a stimulating discussion of it.

REFERENCES

1. J. Berkowitz, W. A. Chupka, and G. B. Kistiakowsky. J. Chem. Phys. **25**, 457 (1956).
2. E. Fersht and R. A. Back. Can. J. Chem. **43**, 1899 (1965) and additional references cited in this article; R. A. Young, R. L. Sharpless, and R. S. Stringham. J. Chem. Phys. **40**, 117 (1964).
3. H. B. Dunford, E. R. V. Milton, and D. L. Walen. Can. J. Chem. **42**, 2504 (1964).
4. Y. Tanaka, F. R. Innes, A. S. Jursa, and M. Nakamura. J. Chem. Phys. **42**, 1183 (1965).
5. C. E. Beale, Jr. and H. P. Broida. J. Chem. Phys. **31**, 1030 (1959). R. A. Young. J. Chem. Phys. **36**, 2854 (1962).
6. J. E. Morgan, L. F. Phillips, and H. I. Schiff. Discussions Faraday Soc. **33**, 118 (1962).
7. E. C. Zipf. J. Chem. Phys. **38**, 2034 (1963). J. F. Noxon. J. Chem. Phys. **36**, 926 (1962). W. R. Brennan. Studies in active nitrogen. Ph.D. Thesis, Dept. of Chemistry, Harvard University. Sept. 1964. K. L. Wray. J. Chem. Phys. To be published.
8. R. A. Young and G. Black. To be published.
9. R. A. Young and R. L. Sharpless. Discussion Faraday Soc. **33**, 228 (1962).
10. R. A. Young and R. L. Sharpless. J. Chem. Phys. **39**, 1071 (1963).
11. R. W. Nicholls. J. Res. Natl. Bur. Std. **A6**, 5451 (1961).
12. K. Bayes. The spectrum of active nitrogen. Thesis, Harvard University. 1959.
13. A. Lofthus. The molecular spectrum of N_2. Spectroscopic Rept. No. 3. Dept. of Physics, University of Oslo, Blindern, Norway, 1960 and references cited in this publication. R. E. Miller. J. Chem. Phys. **43**, 1695 (1965).
14. R. A. Young. J. Chem. Phys. **69**, 1963 (1965).
15. J. C. Polanyi. J. Chem. Phys. **31**, 1338 (1959).
16. F. R. Gilmore. Memorandum RM-4034-PR. The RAND Corp., Santa Monica, California. June 1964.

Can. J. Chem. Downloaded from www.nrcresearchpress.com by 210.87.254.5 on 09/05/12
For personal use only.

CHARGE TRANSFER IN THE RADIOLYSIS OF BINARY HYDROCARBON MIXTURES[1]

J. A. STONE, A. R. QUIRT,[2] AND O. A. MILLER
Research Chemistry Branch, Atomic Energy of Canada Limited, Chalk River, Ontario
Received October 5, 1965

ABSTRACT

The radiolysis of dilute solutions of ethane-d_6, propane-d_8, and *n*-butane-d_{10} in liquid hydrocarbons at 195 °K results in the production of D_2 and HD in amounts which are determined by the relative ionization potentials of solvent and solute. Solvents of higher ionization potential enhance the production of D_2 and HD from deuterated solutes of lower ionization potential. When the ionization potentials are in the reverse order the yields are diminished. This solute–solvent interaction, which is ionic in nature, is a general phenomenon in the radiolysis of mixtures of saturated hydrocarbons in the liquid phase and is consistent with charge transfer between solvent and solute.

INTRODUCTION

The radiolysis of saturated hydrocarbons yields hydrogen as a major product. The use of deuterated hydrocarbons (cyclohexane-d_{12} and methylcyclohexane-d_{14}) as aids to the study of the mechanism of hydrogen formation has been described by Dyne and Denhartog (1). They showed that the yield of deuterium (HD + D_2) from dilute solutions (~5 electron %) of a deuterated hydrocarbon in a hydrocarbon solvent was not governed solely by the concentration of the deuterated species. The solvent exerted a major effect on the yields, e.g., with *n*-pentane as solvent the yield of D_2 was ten times and the yield of HD was eight times greater than when *n*-decane was the solvent. Hardwick (2) showed that this effect of solvent could be correlated with the relative ionization potentials of the deuterated solute molecules and the solvent molecules. Taking the standard value as the yield of D_2 from a dilute solution of cyclohexane-d_{12} in cyclohexane, enhanced yields of D_2 were observed for solvents with ionization potentials greater than that of cyclohexane, while diminished yields were observed for solvents of lower ionization potential. This correlation with ionization potential was interpreted by Hardwick in terms of a charge transfer mechanism. However, the ionization potentials of the two deuterated hydrocarbons used by Dyne and Denhartog, methylcyclohexane-d_{14} (9.85 ± 0.03 eV) and cyclohexane-d_{12} (9.88 ± 0.02 eV) are essentially the same (3), while the range in ionization potentials of the hydrocarbon solvents used is small (~0.5 eV). The lower hydrocarbons, ethane, propane, and *n*-butane, have wide and clear-cut differences in ionization potentials, viz. ethane 11.65 eV, propane 11.08 eV, and *n*-butane 10.63 eV (4). Using these hydrocarbons as solvents and their deuterated analogues as solutes, we have determined that this effect of solvent on the radiolysis of dilute solutions of hydrocarbon solute is a general phenomenon in the radiolysis of saturated hydrocarbons in the liquid phase. However, although our results are qualitatively in agreement with Hardwick's theory, we did not obtain quantitative agreement with the simple theory.

For the series of hydrocarbons chosen the most convenient temperature for carrying out experiments in the liquid phase is that of a solid CO_2/ethanol mixture (195 °K).

[1]*Issued as A.E.C.L. No. 2414.*
[2]*Summer Student A.E.C.L., 1964.*

Can. J. Chem. Downloaded from www.nrcresearchpress.com by 210.87.254.105 on 09/05/12
For personal use only.

Can. J. Chem. Downloaded from www.nrcresearchpress.com by 210.87.254.105 on 09/05/12
For personal use only.

EXPERIMENTAL

Materials and Sample Preparation

The deuterated hydrocarbons, ethane-d_6, propane-d_8, and n-butane-d_{10}, all with a minimum isotopic purity of 98 atom % D, were from Merck Sharp & Dohme of Canada Ltd. The hydrocarbons ethane, propane, butane, cyclopentane, n-hexane, and methylcyclohexane were Phillips Research Grade.

Solutions of from 1.5 to 18 electron % deuterated hydrocarbon were made up in protiated hydrocarbons so that the liquid sample sizes were ~1.5–2.0 ml at 195 °K. The hydrocarbons were degassed by trap-to-trap distillation before being passed into the irradiation vessels. These were cylindrical Pyrex tubes 4 ml in volume with long necks (15 cm of narrow-bore tubing) which were sealed off at their upper ends after the sample was introduced.

Irradiation and Product Analysis

The samples were irradiated at 195 °K in a ^{60}Co γ-source at a dose rate of 2.3×10^{22} eV/l h (as measured in the Fricke dosimeter taking $G(Fe^{3+}) = 15.5$) to a total dose of 4.6×10^{22} eV/l. The cells were opened for analysis by breaking the narrow neck of the sample tube by means of flexible bellows attached to the analytical vacuum line. The hydrogen produced was removed from the frozen samples and measured by conventional methods. Solid nitrogen traps ensured that only hydrogen and methane were collected and measured. The total hydrogen content and the isotopic composition of this hydrogen were determined mass spectrometrically.

RESULTS

The yields of hydrogen from the radiolysis of liquid ethane, propane, and n-butane at 195 °K and a total dose of 4.6×10^{22} eV/l are shown in Table I.

TABLE I

Hydrogen yields from liquid ethane, propane, and n-butane at 195 °K (4.6×10^{22} eV/l)

Hydrocarbon	$G(H_2)$
Ethane	3.75±0.15
Propane	4.25±0.25
n-Butane	4.00±0.15

Gillis (5) found that $G(H_2)$ for liquid ethane at 195 °K was constant over the dose range $2 \times 10^{22} - 10 \times 10^{22}$ eV/l. The value of 3.75 in Table I is consistent with the value of 3.60 given by Gillis for 3 MeV X-rays. However, he reported a value of 3.36 for ^{60}Co gammas but could offer no explanation for the difference between the two values.

The addition of small quantities (from 1.5 to ~4.5 electron %) of the deuterated hydrocarbons to any of the above hydrocarbons resulted in the production of HD and D_2 in addition to H_2. In these very dilute solutions the yields of HD and D_2 were, within experimental error, linear up to ~4.5 electron % of deuterated solute. In the case of n-butane-d_{10} in ethane, which system showed the highest yields of D_2 and HD for a given electron fraction of deuterated solute, this linearity did not extend much above 3 electron % solute. Typical results are shown in the first two figures. Figure 1 shows the D_2 yields from dilute solutions of n-butane-d_{10} in ethane, propane, n-butane, cyclopentane, methylcyclohexane, and n-hexane. Figure 2 shows the corresponding HD yields.

Using the notation of Dyne and Denhartog (1), $G(D_2)$ extrapolated to 100 electron % deuterated hydrocarbon will be defined as $G_1(D)$ while the corresponding extrapolated value of $G(HD)$ will be defined as $g(HD)$. The results for all experiments in which low concentrations of deuterated solutes in protiated solvents were used are summarized in Table II. The ionization potentials, P_1, of the various solvents shown in the fifth column are from photoionization determinations of Watanabe (4).

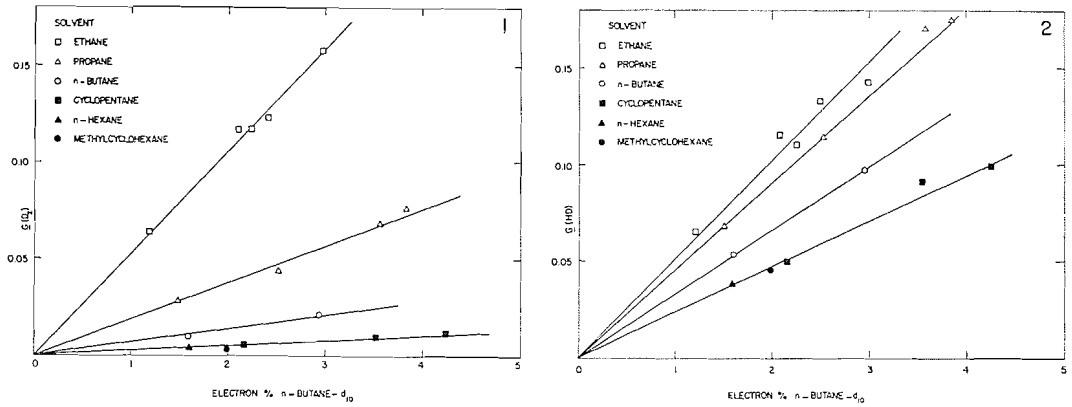


FIG. 1. D_2 yields from dilute solutions of n-butane-d_{10} in various hydrocarbons at 195 °K.
FIG. 2. HD yields from dilute solutions of n-butane-d_{10} in various hydrocarbons at 195 °K.

TABLE II

G_i(D) and g(HD) for deuterated solutes in protiated solvents

Solute	Solvent	G_i(D)	g(HD)	P_i of solvent, eV
C_2D_6	C_2H_6	0.75	2.40	11.65
C_2D_6	C_3H_8	0.35	2.18	11.08
C_3D_8	C_2H_6	3.05	4.73	11.65
C_3D_8	C_3H_8	0.50	3.25	11.08
C_3D_8	n-C_4H_{10}	0.35	2.40	10.63
n-C_4D_{10}	C_2H_6	5.28	5.17	11.65
n-C_4D_{10}	C_3H_8	1.92	4.57	11.08
n-C_4D_{10}	n-C_4H_{10}	0.70	3.33	10.63
n-C_4D_{10}	c-C_5H_{10}	0.28	2.40	10.09

The results of single experiments with n-butane-d_{10} in n-hexane and methylcyclohexane (shown in Figs. 1 and 2) were essentially the same as those obtained with cyclopentane as solvent.

As the concentration of solute is increased, the HD and D_2 yield curves must depart from linearity. This is shown in Figs. 3 and 4 where the yields of D_2 and HD from all three deuterated solutes in ethane as solvent are plotted over the solute concentration range 1–18 electron %.

To gain further insight into the mechanism of the solvent–solute interaction two further experiments were performed.

(i) The addition of 0.32 electron % ammonia to a solution containing 3.8 electron % n-butane-d_{10} in ethane reduced G(HD) to 0.114 from 0.190 and $G(D_2)$ to 0.053, also from 0.190.

(ii) The addition of 0.98 electron % sulfur hexafluoride to a solution of 3.00 electron % n-butane-d_{10} in ethane in the liquid phase at 195 °K resulted in a lowering of the total hydrogen yield from 3.75 to 2.36. This lowered yield was composed of $G(H_2) = 2.25$, G(HD) = 0.091, and $G(D_2) = 0.024$.

DISCUSSION

A true measure of the effect of solvent on the radiolytic yields of D_2 and HD could be obtained if it were possible to measure these yields in a system where no solvent–solute interaction of the type under study occurred. Such a system probably does not exist.

Can. J. Chem. Downloaded from www.nrcresearchpress.com by 210.87.254.105 on 09/05/12
For personal use only.

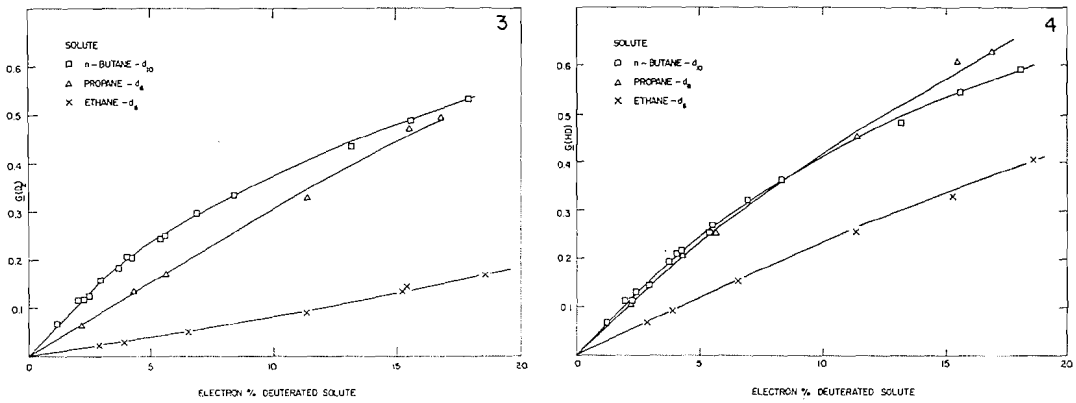


FIG. 3. D_2 yields from n-butane-d_{10}, propane-d_8, and ethane-d_6 in ethane at 195 °K.
FIG. 4. HD yields from n-butane-d_{10}, propane-d_8, and ethane-d_6 in ethane at 195 °K.

However Table II shows that when a deuterated solute is irradiated in the corresponding protiated hydrocarbon e.g. n-butane-d_{10} in n-butane, then the values of $G_1(D)$ and $g(HD)$ are similar for the three solutes used. $G_1(D)$ ranges from 0.50 to 0.75 and $g(HD)$ from 2.40 to 3.33. For purposes of comparison between the different solutes, we have therefore taken these values of $G_1(D)$ and $g(HD)$ as the standard values, e.g. for propane-d_8 the standard values are 0.50 and 3.25. Any deviations from these standard values with change of solvent will be used to assess the effect of solvent on the radiolysis of the deuterated solute. By this choice of standard states we do not wish to imply that the systems used to define the states are ideal and obey the "mixture law". The similarity of the standard values for all these deuterated solutes is indicative of similar modes of hydrogen formation. Intercomparisons of the radiolysis of these three deuterated solutes in different solvents should therefore be meaningful.

$G_1(D)$ and $g(HD)$ for all three deuterated solutes depart significantly from their standard values with change of solvent. Table III shows the differences, $\Delta G_1(D)$ and $\Delta g(HD)$, between the values of $G_1(D)$ and $g(HD)$ in a given solvent and the standard values for the solute used. The values of ΔP_i, the difference in ionization potential between solvent and solute, are given in the last column. We have computed these differences on the assumption that the ionization potential of a deuterated molecule is the same as that of the corresponding protiated molecule. The limitation of this assumption is discussed later.

An immediate general conclusion is that the results are consistent with Hardwick's prediction: when the solvent has the higher ionization potential, $\Delta G_1(D)$ and $\Delta g(HD)$

TABLE III

Changes in $G_1(D)$ and $g(HD)$ with change of solvent

Solute	Solvent	$\Delta G_1(D)$	$\Delta g(HD)$	ΔP_i, eV
C_2D_6	C_2H_6	0	0	0
C_2D_6	C_3H_8	−0.40	−0.22	−0.57
C_3D_8	C_2H_6	2.55	1.48	0.57
C_3D_8	C_3H_8	0	0	0
C_3D_8	n-C_4H_{10}	−0.15	−0.85	−0.45
n-C_4D_{10}	C_2H_6	4.58	1.84	1.02
n-C_4D_{10}	C_3H_8	1.22	1.24	0.45
n-C_4D_{10}	n-C_4H_{10}	0	0	0
n-C_4D_{10}	c-C_5H_{10}	−0.42	−0.93	−0.54

Can. J. Chem. Downloaded from www.nrcresearchpress.com by 210.87.254.105 on 09/05/12
For personal use only.

are both positive, but when the solute has the higher ionization potential, they are both negative.

Three facts lead us to the conclusion that the observed solvent–solute interaction is ionic in nature.

(i) The relative ionization potentials of solvent and solute tell whether "activation" or "deactivation" of the deuterated solute occurs.

(ii) The enhanced yields of D_2 and HD from *n*-butane-d_{10} in ethane are depressed by the addition of ammonia, which is known to have a very high proton affinity in the gas phase (6) and has also been shown to be effective in inhibiting the cationic polymerization of cyclopentadiene in the liquid phase via a proton transfer mechanism (7). Williams (8) has discussed the competition between proton transfer and charge neutralization in the case of the radiolysis of liquid cyclohexane containing ammonia-d_3. His arguments should be equally applicable to the present case with the additional possibility of charge transfer between hydrocarbon molecular ions and ammonia (photoionization potential = 10.23 eV (4)).

(iii) The addition of sulfur hexafluoride, an efficient electron scavenger (9), depresses $G(H_2)$ for ethane but at the same time inhibits the effect of this solvent on the radiolytic production of D_2 and HD from *n*-butane-d_{10}. For 0.98 electron % SF_6, $G_1(D) = 0.80$ and $g(HD) = 3.03$. Even allowing for a reduction in total hydrogen yield from 3.75 to 2.36, these values are much closer to the standard values for *n*-butane-d_{10} ($G_1(D) = 0.70$ and $g(HD) = 3.33$) than those obtained in the absence of SF_6 ($G_1(D) = 5.28$, $g(HD) = 5.17$).

In the region of low solute concentration shown in Figs. 1 and 2, G(total hydrogen) i.e. $G(H_2 + HD + D_2)$ remained constant within experimental error and was equal to $G(H_2)$ for the pure solvent. At higher solute concentrations G(total hydrogen) did decrease measureably as might be expected since $G(D_2 + HD)$ for the pure deuterated solutes was ~3.1. The enhanced yields of HD and D_2 found in the "activating" solvents are therefore obtained at the expense of H_2 production from the solvent. The enhanced yields do not arise from excited solvent species which do not lead to hydrogen formation in the radiolysis of the pure solvent. These results are qualitatively in agreement with Hardwick's mechanism outlined by reactions [1] to [6] i.e. charge transfer competing with charge neutralization. Charge transfer is assumed to occur with 100% efficiency when the appropriate reactants collide, i.e. it is governed by the normal laws of diffusion in the liquid phase.

[1] $$R_1H \rightsquigarrow R_1H^+ + e$$

[2] $$R_2D \rightsquigarrow R_2D^+ + e$$

[3] $$R_1H^+ + R_2D \rightarrow R_1H + R_2D^+$$

[4] $$R_2D^+ + R_1H \rightarrow R_2D + R_1H^+$$

[5] $$R_1H^+ + e \rightarrow [R_1H]^* \rightarrow H_2 \text{ or HD}$$

[6] $$R_2D^+ + e \rightarrow [R_2D]^* \rightarrow D_2 \text{ or HD}$$

Reactions [5] and [6] are written to show that the solvent–solute interaction we are studying affects both the first and second order yields of hydrogen i.e. affects both H_2 and D_2 produced in first order processes and H_2 and HD produced in second order processes (we neglect a second order yield of D_2 at the low concentrations of deuterated solutes employed). Dyne (10) has concluded that the enhanced yields of D_2 and HD from cyclohexane-d_{12} in various solvents arise from a common precursor, namely, the

Can. J. Chem. Downloaded from www.nrcresearchpress.com by 210.87.254.105 on 09/05/12
For personal use only.

cyclohexane-d_{12} molecular ion. The effect of ammonia and sulfur hexafluoride on the yields of HD and D_2 from *n*-butane-d_{10} in ethane is consistent with such a designation.

Reactions [1] and [2] have been written with the implication that only molecular ions are of importance in the solvent–solute interaction. Fragment ions of general formula $C_nH^+_{2n+1}$ have ionization potentials too low for charge transfer with solvent molecules to be exothermic.

Reactions [3] and [4] are of course mutually exclusive for a given solvent–solute system, only that reaction which is exothermic being allowed.

The results may be conveniently divided into two groups (see Table III) according to whether (*a*) the solvent increases $G_1(D)$ and $g(HD)$ above the standard values (activating solvents) or (*b*) the solvent decreases $G_1(D)$ and $g(HD)$ below the standard values (deactivating solvents).

(a) Activating Solvents

Only three systems were studied in which activation of the solute occurred, viz, *n*-butane-d_{10} in ethane, *n*-butane-d_{10} in propane, and propane-d_8 in ethane. These were of course the only systems used in which the solvent had the higher ionization potential. The results are qualitatively consistent with the charge transfer mechanism outlined by eqs. [1]–[6] but are not quantitatively in agreement with such a simple mechanism.

In an activating solvent an electron is transferred to the solvent ion from the solute, which is in low concentration (reaction [3]). Charge transfer as outlined by reactions [1] to [6] will depend simply upon the diffusion rates of the reacting species and the sign of the difference in ionization potential between solvent and solute. The absolute magnitude of the difference in ionization potential plays no part. The results obtained are not consistent with such a simple behavior.

(i) It would be expected that two deuterated solutes irradiated in the same activating solvent would yield very similar values of $G_1(D)$ and $g(HD)$. However, *n*-butane-d_{10} gives higher yields of D_2 and HD ($G_1(D) = 5.28$ and $g(HD) = 5.17$) than does propane-d_8 ($G_1(D) = 3.05$ and $g(HD) = 4.73$) in the same solvent, ethane. It would appear then that charge transfer to *n*-butane-d_{10} is about twice as efficient as to propane-d_8. The greater diffusion rate of propane-d_8 in ethane should actually lead to slightly higher values of $G_1(D)$ and $g(HD)$ than those for *n*-butane-d_{10} (the plotting of Figs. 1 and 2 in terms of electron fraction compensates for the difference in geometrical size between the two solute molecules).

(ii) $G(D_2 + HD)$ is much greater for the radiolysis of *n*-butane-d_{10} in ethane than in propane. The diffusion rates of the reactants in ethane will be greater than those of the reactants in propane but this will probably not be sufficient to account for the large difference in yields.

(iii) Throughout this discussion we have assumed that the ionization potential of a deuterated molecule is exactly the same as that of the corresponding protiated molecule. This is certainly not the case for methane and methane-d_4 which have photoionization potentials of 12.71 and 12.87 eV respectively (11). The ionization potentials of the deuterated molecules we used have not been determined but presumably they show similar small differences from those of the corresponding protiated hydrocarbons. This means that in theory any protiated hydrocarbon should be a deactivating solvent for the corresponding deuterated hydrocarbon. However, we have shown that for all three deuterated hydrocarbons the values of $G_1(D)$ and $g(HD)$ can be reduced in deactivating solvents below the standard values. This implies that small differences in ionization

Can. J. Chem. Downloaded from www.nrcresearchpress.com by 210.87.254.105 on 09/05/12
For personal use only.

potential (~0.1 eV) may not be sufficient to ensure that charge transfer occurs at every collision.

Libby (12) has discussed the role of the Franck–Condon principle in determining the rates of electron transfer between aqueous ions in different valence states. On the basis of his argument, resonance charge exchange between a hydrocarbon ion and the same hydrocarbon molecule, both in the ground state, is forbidden (13). Vibrational excitation of the ion will help to overcome the Franck–Condon restriction as will a difference in ionization potential between electron donor and acceptor molecules. Most ions will be formed in vibrationally excited states but relaxation soon occurs. The extent to which charge transfer occurs in a given system will therefore be governed by the difference in ionization potential of donor and acceptor molecules and the extent of vibrational excitation of the ion at the instant that charge transfer occurs.

In activating solvents at low solute concentrations the absolute difference in ionization potential will play the major role in overcoming the Franck–Condon restriction. Since relaxation is rapid, the contribution from ionic excitation assumes importance only as the concentration of the solute increases. Figures 3 and 4 show that at low solute concentrations $G(D_2 + HD)$ for *n*-butane-d_{10} in ethane is greater than that for propane-d_8 in ethane because of the more favorable difference in ionization potentials. At ~20 electron % solute, when each solvent molecule is in contact with at least one solute molecule, charge transfer can occur before ionic relaxation. In this case the values of $G(D_2 + HD)$ are practically the same for both systems. Similarly, the difference in yield of $(D_2 + HD)$ for low concentrations of *n*-butane-d_{10} in propane and ethane reflects the differences in ionization potential between solvent and solute, ionic excitation playing a minor role. These results are in agreement with those reported by Guarino and Hamill (14), who found that the degree of positive charge transfer from an organic glass to different solutes in low concentration depended upon the magnitudes of the differences in ionization potential between solvent and solute.

(b) Deactivating Solvents

In the deactivating solvents used, charge transfer from solute to solvent is always favored, since the difference in ionization potential is significant ($\leqslant$0.45 eV) and the vibrationally excited solute ion is surrounded by eligible electron donors. Charge transfer therefore readily competes with charge neutralization. Figures 1 and 2 show that when *n*-butane-d_{10} is irradiated in solvents of lower ionization potential the yields of HD and D_2 are practically the same regardless of the solvent. That the yield of D_2, which is produced in a first order reaction, is not zero in these deactivating solvents means that it must be produced in a process (or processes) not susceptible to charge transfer, e.g. molecular elimination from excited, non-ionized molecules.

As stated before, a protiated hydrocarbon solvent should be a deactivating solvent for the corresponding deuterated solute. However, deactivation is not complete. Even though excitation of the solute ion favors charge transfer, the free energy requirements are not fully met in all cases. It would appear that in deactivating solvents, for small differences in ionization potential between solvent and solute, the degree of charge transfer is dependent to a great extent on the absolute magnitude of ΔP_1. When $\Delta P_1 \simeq 0.45$ eV this dependence vanishes.

ACKNOWLEDGMENTS

It is a pleasure to acknowledge the many helpful discussions with Dr. P. J. Dyne. Drs. Betts and Sagert are thanked for comments on the earlier drafts of this paper.

Can. J. Chem. Downloaded from www.nrcresearchpress.com by 210.87.254.105 on 09/05/12
For personal use only.

REFERENCES

1. P. J. DYNE and J. DENHARTOG. Can. J. Chem. **40**, 1616 (1962).
2. T. J. HARDWICK. J. Phys. Chem. **66**, 2132 (1962).
3. R. I. REED. Ion production by electron impact. Academic Press, Inc., New York. 1962. p. 9.
4. K. WATANABE. J. Chem. Phys. **26**, 542 (1957).
5. H. A. GILLIS. J. Phys. Chem. **67**, 1399 (1963).
6. M. S. B. MUNSON. J. Am. Chem. Soc. **87**, 2332 (1965).
7. M. A. BONIN, W. R. BUSLER, and T. F. WILLIAMS. J. Am. Chem. Soc. **87**, 199 (1965).
8. T. F. WILLIAMS. J. Am. Chem. Soc. **86**, 3954 (1964).
9. R. A. LEE and D. A. ARMSTRONG. Nature, **200**, 552 (1963).
10. P. J. DYNE. Can. J. Chem. **43**, 1080 (1965).
11. V. H. DIBELER, M. KRAUSS, R. M. REESE, and F. N. HARLLEE. J. Chem. Phys. **42**, 3791 (1965).
12. W. F. LIBBY. J. Phys. Chem. **56**, 863 (1952).
13. S. Z. TOMA and W. H. HAMILL. J. Am. Chem. Soc. **86**, 1478 (1964).
14. J. P. GUARINO and W. H. HAMILL. J. Am. Chem. Soc. **86**, 777 (1964).

Can. J. Chem. Downloaded from www.nrcresearchpress.com by 210.87.254.105 on 09/05/12
For personal use only.

Can. J. Chem. Downloaded from www.nrcresearchpress.com by 210.87.254.42 on 09/05/12
For personal use only.

EXCESS VOLUMES, VAPOR PRESSURES, AND RELATED THERMODYNAMIC PROPERTIES OF THE SYSTEM ACETONE–CHLOROFORM–BENZENE, AND ITS COMPONENT BINARY SYSTEMS

A. N. Campbell, E. M. Kartzmark, and R. M. Chatterjee
Department of Chemistry, University of Manitoba, Winnipeg, Manitoba

Received October 28, 1965

ABSTRACT

The volume changes on mixing of the three binary mixtures, acetone–chloroform, benzene–chloroform, acetone–benzene, and the ternary mixture, acetone–chloroform–benzene, and their molar refractivities and viscosities, were determined.

Determinations of total and partial vapor pressures were made. The systems acetone–chloroform and benzene–chloroform show negative deviations from Raoult's law. The system acetone–benzene shows positive deviations.

The excess Gibbs free energies of mixing have been calculated for all systems. By combining these data with previously measured heats of mixing (1), the excess entropy has also been calculated. The curves representing zero excess volume, zero heat of mixing, zero excess free energy of mixing, and zero excess viscosity as functions of composition in the ternary system do not coincide. It, therefore, must be concluded that they result from compensating effects and do not represent ideality.

INTRODUCTION

Campbell, Kartzmark, and Friesen (1) found a curve of zero heat of mixing in the system acetone–chloroform–benzene at 25°. We have now determined the volume changes on mixing to find whether the curve of zero volume of mixing coincided in composition with the former curve. The total and partial vapor pressures were determined at 25°. These measurements in conjunction with the previous heat of mixing data complete the thermodynamic description of the system. The excess Gibbs free energy and the product TS^E, where S^E is the excess entropy, are obtained by standard methods. Since a compound is known to be formed in the system acetone–chloroform, it was thought advisable to determine also the densities, refractive indices, and viscosities over the whole ternary system.

EXPERIMENTAL

Purification of Materials

Acetone

Spectranalyzed acetone (A.C.S.) from the Fisher Scientific Company was dried with calcium chloride and then subjected to distillation after adding potassium permanganate to remove any nonaqueous impurities. The distillate collected was again dried by means of calcium chloride and distilled once again without adding potassium permanganate. Care was taken to avoid unnecessary exposure to air and freshly distilled acetone was used for each measurement.

Chloroform

Chloroform (A.C.S.) from the Fisher Scientific Company was purified to remove ethanol. Repeated extraction with concentrated sulfuric acid and final washing with distilled water removed ethanol completely. Chloroform was dried over anhydrous calcium chloride and then finally distilled from anhydrous phosphorus pentoxide, twice, in air. The purified reagent was stored in the dark. The sample purified in this manner could not be kept for more than a week. Fresh treatments were made every week.

Benzene

Thiophene-free benzene (A.C.S.) from the Fisher Scientific Company was frequently shaken with concentrated sulfuric acid until the yellow color in the acid layer disappeared. It was then washed with a solution of sodium bicarbonate and water, and the product then dried with anhydrous sodium sulfate and sodium. Finally it was distilled twice from sodium.

Method of Analysis

Theoretically, the composition of a ternary mixture may be obtained from a knowledge of any two physical properties. It is necessary first to prepare calibration curves of the physical properties for all proportions,

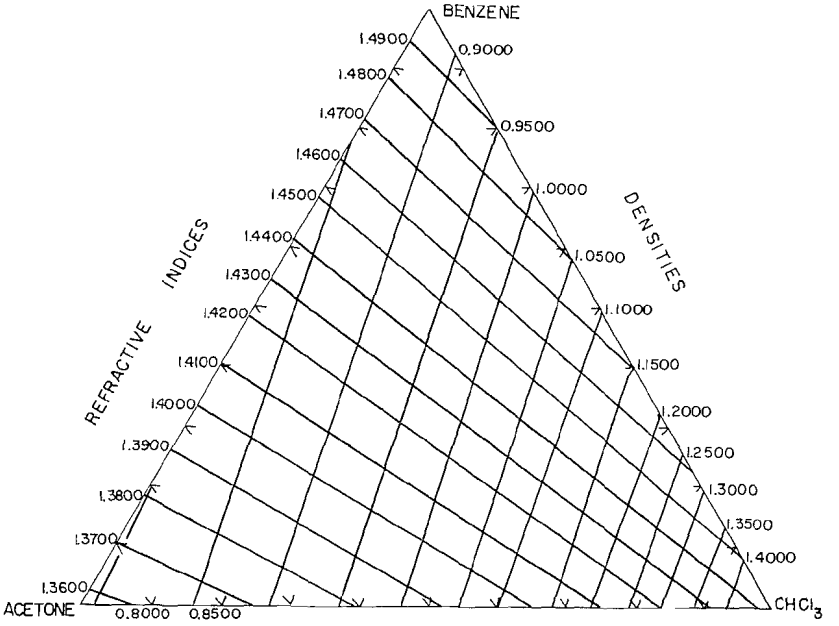


FIG. 1. Curves of equal density and refractive index. System acetone–chloroform–benzene at 25 °C.

and express the results on a triangular diagram in the form of curves of equal values. In practice, the physical quantities chosen must: (*a*) be easily and accurately determinable, (*b*) vary largely for small changes in concentration, and (*c*) exhibit a graphical behavior such that curves of the different properties intersect one another at a sharp angle. We found refractive index and density to satisfy these requirements. Figure 1 reproduces the data. Our densities are accurate to ±0.0001 g/cc. Densities and refractive indices were measured on 55 ternary mixtures as well as on 47 binary mixtures, in order to obtain the calibration plot of Fig. 1. The accuracy of the refractive index measurements was ±0.0001.

Volume Change on Mixing

The change in volume on mixing is very small and attempts to determine this from density measurements result in serious error. We therefore used the method of Brown and Smith (2), which measures V^E directly. We modified their apparatus by introducing a 2 mm bore stopcock at the filling end of the apparatus, instead of the ground stopper used by them. The advantage of this is that several cells are no longer required to cover the whole composition range, since with the stopcock the mercury can be adjusted at different levels in the two limbs. The accuracy of the method is about ±0.003 cc/mole.

Vapor Pressure, Vapor Composition, and Partial Pressure

The air saturation method was used for the determination of the composition of the equilibrium vapor but not for the determination of total vapor pressure, since the precautions to be taken and the corrections applied are extensive when the method is used for this purpose. Total vapor pressure was therefore determined manometrically, to ±0.1 mm. Details of the method are given in a paper by Campbell, Kartzmark, and Gieskes (3).*

Viscosity

Viscosities were determined with Cannon- and Fenske-type viscometers.

Refractive Index and Molar Refraction

An Abbe refractometer with temperature control at 25° ± 0.1° and a sodium arc lamp were used.

RESULTS

The experimental data are so extensive that they have been compiled in the following tables which are to be found in the depository.†

**For more complete details see the M.Sc. theses of J. M. T. M. Gieskes (1962) and R. M. Chatterjee (1965), University of Manitoba.*

†Photocopies of Tables I–V may be obtained, upon request, from the Depository of Unpublished Data, National Science Library, National Research Council, Ottawa, Canada.

Can. J. Chem. Downloaded from www.nrcresearchpress.com by 210.87.254.42 on 09/05/12
For personal use only.

Table I. Excess volumes in binary systems at 25 °C.

Table II. Partial molar volumes in the binary systems.

Table III. Excess volume data for the system acetone–chloroform–benzene at 25 °C.

Table IV. Viscosity data at 25 °C in the system acetone–benzene–chloroform.

Table V. Partial pressures obtained with Von Zawidski's treatment in the system acetone–chloroform at 25 °C.

Excess Volume

The quantities $\bar{V}^E = (\bar{V} - \bar{V}^0)$ have an uncertainty of ± 0.01 cc/mole.

To find the excess volumes for the ternary system, solutions of chloroform and of acetone in a fixed amount of benzene were mixed. In this way, we found V^E's for pseudobinary systems containing respectively 0.10, 0.20, 0.25, 0.30, 0.40, 0.50, 0.60, and 0.70 mole fraction benzene. From these and the data for the true binary systems, it is possible to calculate two curves of zero excess volume of mixing. These are shown in Fig. 2, on which also the curve of $G^E = 0$, as well as the curve of $H^E = 0$, are expressed as dotted curves.

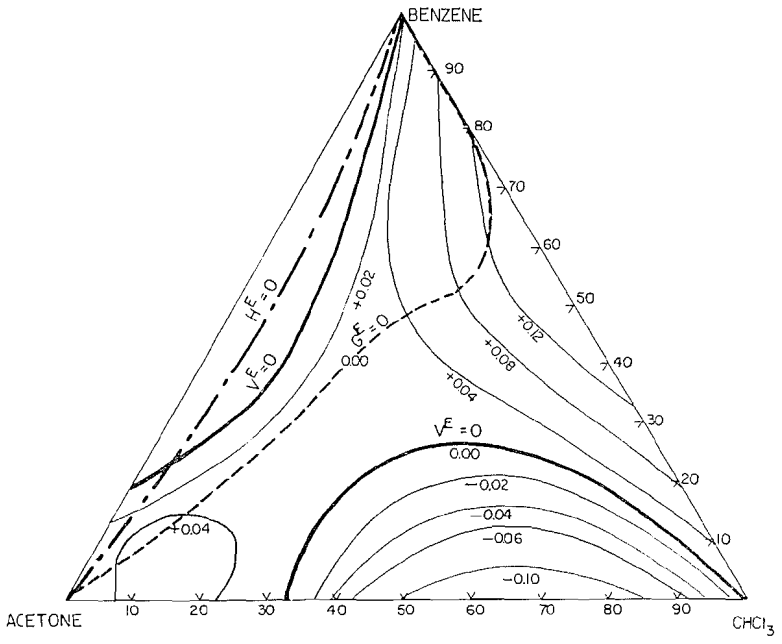


FIG. 2. Curves of equal excess volume. System acetone–benzene–chloroform at 25 °C.

Viscosity

Figure 3 is a ternary plot of lines of equal excess viscosity, including that of $\eta^E = 0$.

Vapor Pressure

For the calculations of activity coefficients and total excess free energies in Table VI the following formulae were used:

$$\mu^E_{\text{acetone}} = RT \ln \frac{P_{\text{acetone}}}{x_{\text{acetone}} P^0_{\text{acetone}}}$$

$$G^E = x_{\text{acetone}} \mu^E_{\text{acetone}} + x_{\text{chloroform}} \mu^E_{\text{chloroform}}$$

Can. J. Chem. Downloaded from www.nrcresearchpress.com by 210.87.254.42 on 09/05/12
For personal use only.

Can. J. Chem. Downloaded from www.nrcresearchpress.com by 210.87.254.42 on 09/05/12
For personal use only.

TABLE VI

Total and partial pressures and derived thermodynamic quantities at 25 °C

Liquid mole % X	Total pressure (mm Hg)	Partial pressure X (mm Hg)	Activity coefficient (γ)		G^E (cal/mole)	H^E (1) (cal/mole)	TS^E (cal/mole)
A. Acetone – chloroform (X)							
			Acetone	Chloroform			
0.00	226.5	0.0	1.000	—	—	—	—
8.95	217.5	10.8	1.0023	0.6123	−25.0	−103.8	−78.8
17.61	205.8	22.6	0.9817	0.6508	−53.8	−194.0	−140.2
31.66	185.0	39.4	0.9406	0.6311	−111.2	−336.8	−225.6
40.00	175.0	54.5	0.8867	0.6910	−130.4	−395.2	−264.8
52.50	165.0	79.2	0.7975	0.7650	−147.0	−451.2	−304.2
65.01	162.5	108.5	0.6813	0.8463	−142.5	−464.0	−321.5
72.86	167.5	129.5	0.6183	0.9013	−122.2	−422.7	−300.5
88.62	182.5	170.0	0.4833	0.9728	−63.4	−212.8	−149.4
100.00	197.2	197.2	—	1.000	—	—	—
B. Benzene (X) – Chloroform							
			Benzene	Chloroform			
0.00	197.2	0.00	—	1.000	—	—	—
19.93	176.0	19.4	1.0246	0.9916	−1.1	−71.0	−69.9
40.15	152.0	36.2	0.9489	0.9811	−19.3	−102.5	−83.2
55.07	134.0	49.2	0.9404	0.9570	−31.7	−106.0	−74.3
66.73	121.5	61.3	0.9670	0.9176	−30.3	−86.0	−55.7
75.84	111.5	70.0	0.9717	0.8709	−32.7	−65.8	−33.1
83.46	105.8	78.2	0.9863	0.8464	−23.1	−46.7	−23.6
90.01	101.9	85.6	1.0011	0.8278	−10.6	−29.0	−18.4
94.96	97.5	89.5	0.9922	0.8048	−10.9	−14.0	−3.1
100.00	95.0	95.0	1.000	—	—	—	—
C. Acetone – benzene (X)							
			Acetone	Benzene			
0.00	226.5	0.0	1.000	—	—	—	—
12.51	218.0	19.6	1.0011	1.6491	37.7	14.2	−23.5
25.00	210.1	35.2	1.0296	1.4824	71.3	27.1	−44.2
36.52	201.0	47.4	1.0684	1.3664	92.5	38.6	−53.9
55.50	184.0	63.3	1.1975	1.2007	107.7	45.0	−62.7
71.50	165.0	74.3	1.4049	1.0940	95.4	33.3	−62.1
82.49	148.1	83.7	1.6236	1.0681	82.5	22.1	−60.4
88.62	133.5	87.5	1.7847	1.0395	59.5	14.8	−44.7
95.00	116.2	93.0	2.0480	1.0306	38.2	6.7	−31.5
100.00	95.0	95.0	—	1.0000	—	—	—

TABLE VII

Total and partial pressures and derived thermodynamic quantities for the system acetone–chloroform–benzene at 25 °C

Liquid (mole %)		Total pressure	Partial pressure (mm Hg)		Activity coefficient (γ)			G^E
Acetone	Benzene	(mm Hg)	Acetone	Benzene	Acetone	Benzene	Chloroform	(cal/mole)
44.9	22.8	173.1	97.1	29.4	0.9548	1.3574	0.7316	−30.8
32.2	42.5	153.9	71.9	48.8	0.9857	1.2087	0.6652	−16.2
57.9	28.0	183.8	130.1	36.8	0.9921	1.3836	0.6078	+9.5
47.0	40.4	173.0	108.5	49.1	1.0191	1.2795	0.6198	+28.4
41.4	10.4	166.0	78.5	13.1	0.8372	1.3260	0.7828	−96.1
40.4	54.7	169.1	99.1	63.2	1.0829	1.2163	0.7041	+72.4
35.4	52.8	160.6	80.6	64.1	1.0051	1.2780	0.6831	+51.2
48.9	33.4	175.6	111.3	41.4	1.0049	1.3048	0.6559	+9.9
14.1	67.6	134.0	33.8	73.2	1.0582	1.1400	0.7481	+25.7
11.1	51.5	138.8	23.9	54.4	0.9505	1.1120	0.8203	−14.8
24.1	59.1	146.9	57.4	65.5	1.0514	1.1666	0.7244	+29.1
69.6	22.9	198.5	158.6	30.6	1.0060	1.4065	0.6293	+28.1
80.1	10.0	206.5	180.3	14.2	0.9938	1.4950	0.6152	−7.7
6.9	78.8	123.1	18.2	83.5	1.1594	1.1155	0.7587	+33.7
88.0	7.8	215.0	199.3	10.3	1.0000	1.3897	0.6524	+4.6
28.8	51.2	153.2	69.5	57.8	1.0653	1.1885	0.6565	+13.3

The H^E values of Campbell and Kartzmark (4) and the values of TS^E calculated from $TS^E = H^E - G^E$ have been obtained.

These three excess quantities for acetone–chloroform are represented graphically in Fig. 4. The partial pressure data have been treated by the Zawidzki method (5). For the calculation of the constants α and β the total pressure data were used and approximations applied until the values satisfied the experimental results. Observed and calculated partial pressures were compared. Figures 5 and 6 show the excess thermodynamic functions in the systems benzene–chloroform and acetone–benzene. Table VII gives the total and partial pressures for the system benzene–acetone–chloroform and the activity coefficients and total excess Gibbs free energy for the system. From the data for total excess Gibbs free energy, the curve of $G^E = 0$ has been interpolated and is given in Fig. 2.

DISCUSSION

A. The System Acetone–Chloroform

Volume contraction on mixing occurs up to about 68 mole % acetone, after which V^E changes sign. A maximum value of V^E of $+0.05$ cm³/mole occurs at 86 mole % acetone and a minimum of -0.152 cm³/mole at 32 mole % acetone. The partial molal excess volume of acetone passes through a maximum and that of chloroform through a minimum when the molar ratio is approximately unity. These results are in agreement with those of Hubbard (6).

This system shows marked positive deviation of viscosity with a maximum at 60 mole % chloroform. The total vapor pressure also shows the greatest deviation at this concentration. Beckmann and Faust (7) agree with our viscosity findings but state that the maximum disappears at higher temperatures. Our data for compositions of equilibrium liquid and vapor show that this system exhibits azeotropic behavior at 25°. The strong negative deviations from Raoult's law imply that G^E is strongly negative, as is found to be the case.

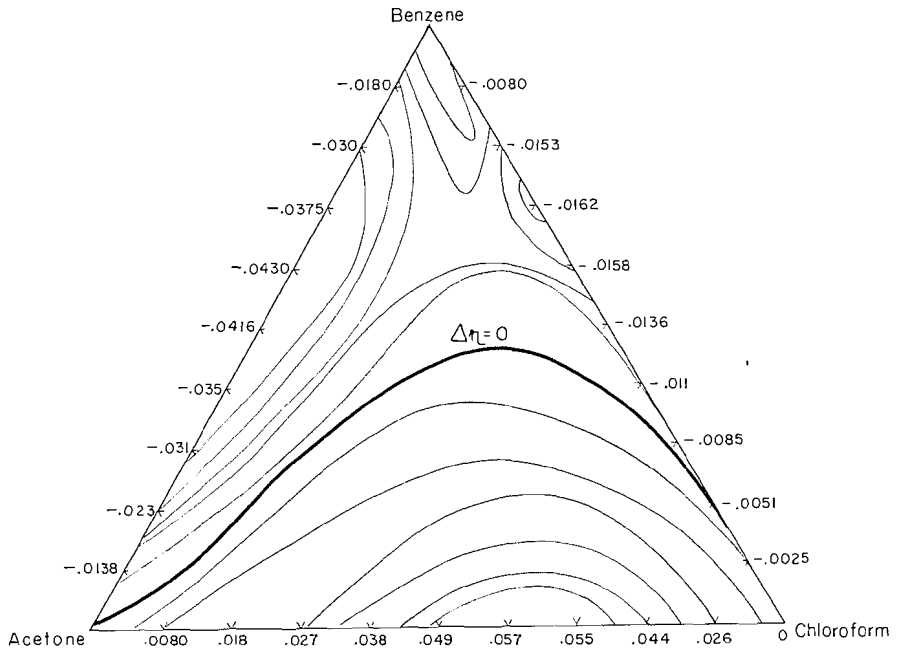


FIG. 3. Curves of equal excess viscosity in system acetone–benzene–chloroform at 25 °C.

Can. J. Chem. Downloaded from www.nrcresearchpress.com by 210.87.254.42 on 09/05/12
For personal use only.

Can. J. Chem. Downloaded from www.nrcresearchpress.com by 210.87.254.42 on 09/05/12
For personal use only.

Figure 4 shows that the curves for all thermodynamic excess functions are unsymmetrical. Haase (8) has pointed out that experimental results in general seem to indicate that the function $V^E(x)$ has a behavior similar to that of $S^E(x)$. Clearly this is not true of the system acetone–chloroform. Gieskes (9) has recently reported a similar deviation in the system acetic acid – chloroform and Scott *et al.* (10) for the system 1-hydro-*n*-perfluoroheptane – acetone. Scott and his co-workers observed a very large positive V^E and a negative S^E.

Campbell and Kartzmark (4) have proved the existence of a 1:1 compound between acetone and chloroform and it is probably the formation of this compound that accounts for the negative deviation from Raoult's law and the considerable heat of mixing. The contraction of volume on mixing, however, can scarcely be attributed to this cause, since Campbell and Kartzmark (in press) find a much more pronounced negative V^E in the system bromoform–acetone, where the tendency to compound formation is certainly less, whereas Stavely, Tupman, and Hart (11) and Hubbard (6) found that for the present system the volume contraction increases with rising temperature, despite the fact that the dissociation of the compound must also increase.

B. The System Benzene–Chloroform

This system exhibits an increase of volume on mixing. The excess partial molar volume curves are not symmetrical.

The viscosity shows a minimum at 33 mole % chloroform but no conclusion can be drawn from this.

When the results of Table VI are plotted it is apparent that there is no azeotropic point in this system, but a slight negative deviation from Raoult's law. According to Reeves and Schneider (12) large total shift of the chloroform proton signal in benzene solution is indicative of complex formation between chloroform and the aromatic hydrocarbon, but Campbell, Kartzmark, and Friesen (1) failed to detect compound formation in the solid state in their study of the freezing point diagram.

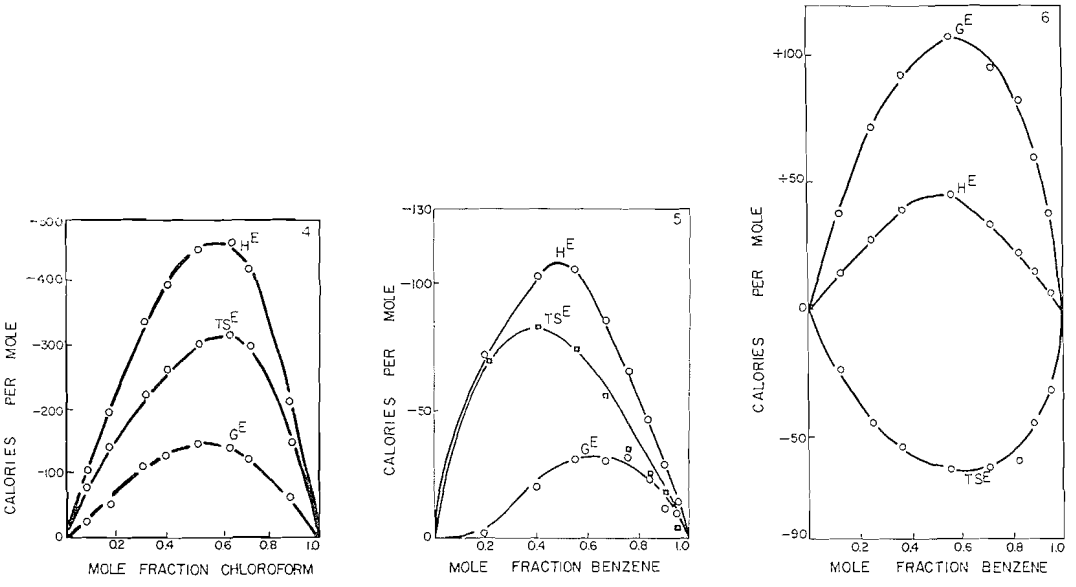


FIG. 4. Excess thermodynamic functions. System acetone–chloroform at 25 °C.
FIG. 5. Excess thermodynamic functions. System benzene–chloroform at 25 °C.
FIG. 6. Excess thermodynamic functions. System acetone–benzene at 25 °C.

All the thermodynamic functions of Fig. 5 are negative but V^E is positive throughout. Our values are in disagreement with the results of Schmidt (13) who used a pycnometric method.

C. The System Acetone–Benzene

This system shows contraction on mixing up to relatively high acetone concentration, followed by expansion over a small region of concentration: the region of positive V^E has not previously been observed. The results of Harms (14), of McCombie, Roberts, and Scarborough (15), and of Ebersole (16), as well as measurements of Brown and Smith (17), are in reasonably good agreement with ours. None, however, has observed the region of positive ΔV. In the case of Brown and Smith, who used the same direct method as ourselves, this is due to their not having pushed their measurements beyond 88.8 mole % acetone.

The viscosity shows negative deviation from straight line behavior. When the data of Table VI are plotted, in the usual way, it is apparent that the vapor pressures show positive deviation from Raoult's law, but no azeotrope.

D. The System Acetone–Chloroform–Benzene

Figure 2 shows that in the ternary system there are two curves, along which the excess volume, V^E, is equal to zero. The curve of zero heat of mixing obtained by Campbell, Kartzmark, and Friesen (1) does not coincide with either of the $V^E = 0$ curves. Neither semi-ideality nor pseudo-ideality exists in this system. The existence of curves of zero excess volume must be due to opposing deviations from ideality in the constituent binary systems. The partial and total vapor pressures show both negative and positive deviation (Table VII). The excess Gibbs free energy has been calculated and the interpolated curve of $G^E = 0$ appearing in Fig. 2 shows the compensating effects of the binary systems. The concentrations for which $G^E = 0$ do not coincide either with those for which $H^E = 0$ or $V^E = 0$ or $\eta^E = 0$. The obvious conclusion is that the $V^E = 0$, $H^E = 0$, $G^E = 0$, and $\eta^E = 0$ curves occur in the ternary system as a result of compensating effects of the respective functions in the respective binary systems. Since they do not coincide, the system cannot be considered as even semi-ideal. The ternary freezing point diagram of Campbell, Kartzmark, and Friesen (1) shows that the compound between acetone and chloroform continues to exist in the ternary system.

The excess viscosity is plotted in Fig. 3 in the form of curves of equal excess viscosity. A curve of $\eta^E = 0$ is shown. The excess viscosity is defined as the actual viscosity minus the $\sum x_i \eta_i^0$, where x_i = mole fraction and η_i^0 = viscosity of pure liquid.

REFERENCES

1. A. N. CAMPBELL, E. M. KARTZMARK, and H. FRIESEN. Can. J. Chem. **39**, 735 (1961).
2. I. BROWN and F. SMITH. Australian J. Chem. **15**, 1 (1962).
3. A. N. CAMPBELL, E. M. KARTZMARK, and J. M. T. M. GIESKES. Can. J. Chem. **41**, 407 (1963).
4. A. N. CAMPBELL and E. M. KARTZMARK. Can. J. Chem. **38**, 652 (1960).
5. J. VON ZAWIDZKI. Z. Physik. Chem. Leipzig, **35**, 129 (1900).
6. J. C. HUBBARD. Phys. Rev. **30**, 740 (1910).
7. E. BECKMANN and O. FAUST. Z. Physik. Chem. Leipzig, **89**, 235 (1914).
8. R. HASSE. Thermodynamik der Mischphasen. Springer, Berlin. 1956.
9. J. M. T. M. GIESKES. Can. J. Chem. **43**, 2448 (1965).
10. D. L. ANDERSON, R. A. SMITH, D. B. MEYERS, S. A. ALLEY, A. G. WILLIAMSON, and R. L. SCOTT. J. Phys. Chem. **66**, 621 (1962).
11. L. A. K. STAVELEY, W. I. TUPMAN, and K. R. HART. Trans. Faraday Soc. **51**, 323 (1955).
12. L. W. REEVES and W. G. SCHNEIDER. Can. J. Chem. **35**, 251 (1957).
13. G. C. SCHMIDT. Z. Physik. Chem. Leipzig, **121**, 221 (1926).
14. H. HARMS. Z. Physik. Chem. Leipzig, **B41**, 321 (1938).
15. H. MCCOMBIE, H. M. ROBERTS, and H. A. SCARBOROUGH. J. Chem. Soc. 753 (1925).
16. M. R. EBERSOLE. J. Phys. Chem. **5**, 239 (1901).
17. I. BROWN and F. SMITH. Australian J. Chem. **15**, 9 (1962).

Can. J. Chem. Downloaded from www.nrcresearchpress.com by 210.87.254.42 on 09/05/12
For personal use only.

Can. J. Chem. Downloaded from www.nrcresearchpress.com by 210.87.254.42 on 09/05/12
For personal use only.

THE KINETICS OF THE THERMAL DECOMPOSITION OF PYRITE

A. W. COATS[1] AND NORMAN F. H. BRIGHT
Mineral Sciences Division, Mines Branch, Department of Mines and Technical Surveys, Ottawa, Canada
Received December 16, 1965

ABSTRACT

The kinetics of the thermal decomposition of purified pyrite to pyrrhotite and sulfur in a dynamic argon atmosphere have been studied over the temperature range 600 to 653 °C. The reaction was followed by the rate of weight loss as indicated by a quartz spring balance and also by the rate of progression of the pyrite/pyrrhotite interface into a cylindrical, compressed, polycrystalline pellet. The temperature coefficient of the reaction was found to be 69.5 ± 5.9, 64.7 ± 3.3, and 66.9 ± 5.1 kcal mole^{-1}, when the results were processed in three different ways. The pyrite/pyrrhotite interface was found to progress at a linear rate into the pellet at a given temperature; equations were derived to express the variation of reaction rate with temperature. Attempts to follow the early nucleation stage of the decomposition, using massive mineral crystals, proved unsuccessful.

INTRODUCTION

The thermal decomposition of the mineral pyrite (FeS_2) to yield pyrrhotite (FeS_{1+z}) and sulfur has been made the subject of many investigations (1–13); this work has recently been reviewed by Kullerud and Yoder (1). Most studies have been made by measuring sulfur vapor pressure values (p_S) under equilibrium conditions over a range of temperatures. The enthalpy, ΔH, of the reaction, obtained from these measurements, has given values ranging from 39 to 104 kcal mole^{-1} for various investigators, most values lying in the 65 to 85 kcal mole^{-1} range. Most workers employed static conditions at less than 1 atm pressure; Kullerud and Yoder (1), however, extended their measurements to higher pressures. The only investigation to be made under the dynamic conditions of a flow of inert gas appears to be that of Udintseva and Chufarov (12), who used both single crystals and polycrystalline cubes of pyrite.

The difficulties associated with the study of this reaction arise from two sources: (*a*) variability of composition of the resultant pyrrhotite, which is a nonstoichiometric body; Bog and Rosenqvist (9) expressed the reaction by the equation

$$\left(\frac{2}{1-x}\right) FeS_2 \rightarrow \left(\frac{2}{1-x}\right) FeS_{1+z} + S_{2(g)} \qquad [1]$$

for temperatures of 500 to 550 °C, where x varies with temperature; (*b*) Wunderlich (13) has pointed out that the degree of association of the sulfur also varies with temperature, higher pressures and lower temperatures of reaction favoring the formation of S_8 and S_6 molecules over the S_2 indicated in eq. [1].

In the present study, the conditions employed were those of constant gas flow similar to those that might be expected to obtain in an industrial manufacturing process for sulfur from pyrite. The aim of this work was to determine the kinetic parameters for the reaction of small, polycrystalline cylindrical pellets of pyrite that would approximate in size the pieces of ore that would be used in the industrial process. In addition, this type of study was amenable to the same type of analytical treatment as that employed by McKewan (14) in the reduction of iron oxide pellets by hydrogen.

[1]*NRC Postdoctorate Fellow (1964–1965), assigned to the Mines Branch, Department of Mines and Technical Surveys, Ottawa; present address: High-Temperature Chemistry Division, Central Electricity Research Laboratories, Cleave Road, Leatherhead, Surrey, England.*

Initially, an attempt was made to study the nucleation processes occurring in the very earliest stages of the decomposition; no success was, however, achieved in this objective. This work is mentioned in the Appendix.

EXPERIMENTAL TECHNIQUE AND RESULTS

The pyrite used in this work was a mineral sample from Eastman, Quebec. It was crushed, washed with dilute acid to remove any pyrrhotite, and then washed with water. The product ($-40 + 100$ mesh) was found to contain an appreciable amount of quartz. Accordingly, it was crushed to -200 mesh and the quartz removed as far as possible by heavy-liquid separation with tetrabromoethane. The final product, on analysis, corresponded to the formula $FeS_{1.99}$; spectrographic analysis showed no significant impurity other than 0.3% Si, presumably as unliberated quartz. The powder was pressed into cylindrical pellets of 0.25 in. diameter and height at 160 000 lb in^{-2}. The pellets weighed approximately 0.86 g, corresponding to a bulk density of about 4.27 g cm^{-3} or about 85% theoretical density. The apparatus in which the decomposition was studied consisted of a vertical quartz tube, a portion of which was heated by a Kanthal-wound furnace. Temperatures were maintained constant in the hot zone of the furnace to within ± 0.5 °C, both in respect of location and of time. Samples were suspended in a light quartz stirrup at the end of a fine platinum wire, the upper end of which was attached to a calibrated helical quartz spring of sensitivity 5.39 cm g^{-1}. This spring was well above the top of the furnace and was, in turn, attached to a fine gold chain that was used for raising and lowering the sample by a suitable windlass mechanism. The extension of the spring was measured with a cathetometer. Sample temperatures were measured with a Pt : Pt 10% – Rh thermocouple, sheathed in a fine quartz tube and placed not more than 0.25 in. below the sample and still well within the hot zone of the furnace. Argon flows of approximately 180 ml min^{-1} were used in the decomposition runs. The gas flow was maintained for 10 min before the pellet was lowered into the hot zone of the furnace; at the completion of a run, the sample was raised out of the hot zone and the gas flow maintained for 15 min before opening the apparatus.

Pellets were sectioned laterally, mounted, and polished by the usual metallographic procedures. A partly decomposed pellet exhibited a well-defined reaction interface having surfaces parallel to the external faces of the pellets. The diameter of the unreacted material was measured at two locations at right angles on both top and bottom faces of the sectioned surface; the mean of these four values was taken to represent the extent to which the decomposition had proceeded. Cathetometer readings were taken at regular 5 min intervals, so that the change in reading formed a measure of the bulk rate of decomposition.

The results were treated in two ways:

(*a*) Straight lines were obtained when the diameter of unreacted pyrite was plotted against time for a given temperature. An Arrhenius plot of $\log_{10} k_0$ against $1/T$ °K, where k_0 is the velocity of advance of the interface in cm min^{-1} at a temperature of T °K, also gave a straight line. Least squares treatment was applied to this plot to obtain the equation of the best line through the points. The equation obtained was:

$$\log_{10} k_0 = 14.3 - \frac{15.18 \times 10^3}{T}. \qquad [2]$$

(*b*) In McKewan's treatment (14), eq. [3] was assumed and, from it, eq. [4] was derived for spherical and for cylindrical pellets with equal height and diameter,

$$dw/dt = k_1 A \qquad [3]$$

$$r_0 d_0[1 - (1 - R)^{1/3}] = k_2 t, \qquad [4]$$

Can. J. Chem. Downloaded from www.nrcresearchpress.com by 210.87.254.42 on 09/05/12
For personal use only.

where dw/dt = rate of weight loss, A = interfacial area between reactant and product, r_0 = initial radius of pellet, d_0 = initial density of pellet, k_1 and k_2 = rate constants, t = time, R = fraction of reactant decomposed at time t, = (% wt. lost at time t)/(% wt. lost at end of reaction) ($0 < R < 1$).

In the present work, results were available to test the validity of eqs. [3] and [4]. In eq. [3], dw/dt is directly proportional to the difference in successive cathetometer readings (Δx), taken at 5 min intervals. A, the area of the interface between the pyrite and the pyrrhotite, is directly proportional to the square of the diameter (d^2) of the unreacted pyrite in the case where the initial height and diameter are equal and where the height and diameter of the unreacted material remain equal throughout the reaction, i.e. where the rate of progress of the reaction into the pellet can be considered as isotropic. This requirement was, in fact, satisfied in the present case, as evidenced by many observations of the height and diameter of unreacted material made on sectioned pellets at various stages during the course of the decomposition. Thus, a plot of Δx against d^2 for various temperatures should give a series of straight lines of slope k_1, where k_1 varies with temperature according to an Arrhenius equation. Again, applying a least squares fit to the values of log k_1 plotted against $1/T$ °K, the following equation was obtained.

$$[5] \qquad \log_{10} k_1 = 12.8 - \frac{14.14 \times 10^3}{T}.$$

In eq. [4], values of R can be calculated from the weight of the pellet at a known time; this can be obtained either by direct weighing after a known reaction time or, alternatively, by computation from the cathetometer readings. In this work, the former method was used. In the calculation of R, a value of 23.0% was taken as the total percentage weight loss in the reaction. The use of this value will be further commented upon later. Plots of $[1 - (1 - R)^{1/3}]$ against t gave straight lines of slope k_2, where k_2 varies with temperature according to an Arrhenius equation. As in the other cases, the application of the least squares method to the plot yielded the equation

$$[6] \qquad \log_{10} k_2 = 14.0 - \frac{14.63 \times 10^3}{T}.$$

DISCUSSION OF RESULTS

A calculation of the activation energy (E) from eqs. [2], [5], and [6] gave the following results:

METHOD	E (KCAL MOLE^{-1})
From diameter–time plot (eq. [2])	69.5±5.9
From area-of-interface plot (eq. [5])	64.7±3.3
From weight-loss plot (eq. [6])	66.9±5.1

The tolerance values quoted here were calculated for 90% confidence limits (15). From these results, it would appear that there is no significant difference in the value of E obtained from the three different plots.

In the terms of absolute rate theory, where the rate constant k_3 is given by the equation

$$[7] \qquad k_3 = \frac{kT}{h} e^{\Delta S/R} e^{-\Delta H/RT},$$

where the symbols have their usual significance, the value of E should be equivalent to ΔH. A comparison of the values obtained in the present work with those of earlier workers shows that the values of Bog and Rosenqvist (9) and of D'Or (5) fall within the 90% confidence limits obtained in this work.

Can. J. Chem. Downloaded from www.nrcresearchpress.com by 210.87.254.42 on 09/05/12
For personal use only.

Of the two methods used to determine the kinetic parameters of the reaction, that based on the direct measurement of the unreacted material appears to be simple to perform and involves no assumptions. The method can show whether the interface is advancing at a linear rate; however, many experimental runs would be required. The method based on the work of McKewan, on the other hand, can be evaluated from far fewer experiments, since the weight changes can be obtained directly from the changes in the extension of the quartz spring or from some similar method. However, this method does incorporate a number of assumptions, e.g. that the rate is proportional to the interfacial area (eq. [3]), and that the stoichiometry of the reaction is exactly known. A complete verification of the validity of eq. [3] would require practically the same quantity of results as would be needed for the former method; however, if eq. [4] is found to hold, then this would constitute a verification of the validity of eq. [3]. In this particular reaction, the exact stoichiometry is *not* known, since the composition of the resultant pyrrhotite is a function of temperature. In this work, the value of 23.0% decomposition, which was taken as representing the end point of the reaction, had to be an approximation. This was based upon the form of the decomposition/time curves and showed that the reaction was completed after 75 min at the highest temperatures studied, and that the sample weight at this time corresponded to a 23.0% loss. This value of 23.0% would imply a formula approximating to Fe_7S_8 for the reaction product, pyrrhotite. This is reasonable when the known range of composition of this compound is considered.

CONCLUSIONS

1. The temperature coefficient of the decomposition of pyrite in a dynamic argon atmosphere is 69.5 ± 5.9, 64.7 ± 3.3, and 66.9 ± 5.1 kcal $mole^{-1}$ when the experimental results are processed in three different ways.
2. The equations of McKewan can be used to represent this decomposition reaction.
3. The pyrite/pyrrhotite interface advances at a linear rate; equations were obtained expressing the variations of the reaction rate with temperature.

ACKNOWLEDGMENTS

The authors would like to express their thanks to the scientific and technical staff of the Mineral Sciences Division, Mines Branch, for help and advice at various stages of the investigation. One of us (A. W. C.) wishes to express his thanks to the National Research Council of Canada for the grant of a Postdoctorate Research Fellowship.

The authors would also like to express their gratitude for useful discussions to Dr. T. R. Ingraham, Extraction Metallurgy Division, Mines Branch, who, with his collaborators, has, in recent years, studied the kinetics of thermal decomposition of numerous polycrystalline inorganic compounds employing the "advancing interface" technique.

APPENDIX

Preliminary Investigation of the Nucleated Decomposition of Natural Pyrite Crystals

At the commencement of this investigation, we hoped to study the decomposition of pyrite by investigating the rate of development of nuclei of decomposition on the surfaces of crystals of the mineral and also the rate of growth of these nuclei, possibly in various crystallographic directions. We hoped to correlate this information with the bulk rate of decomposition as determined by other methods, described in the main portion of this paper. There was also the possibility that the rates of decomposition in various directions could be correlated with the crystal structure in the same way as was done by one of us (N. F. H. B.) (16) for the dehydration of certain salt hydrates several years ago.

Can. J. Chem. Downloaded from www.nrcresearchpress.com by 210.87.254.42 on 09/05/12
For personal use only.

The study was conducted on small natural pyrite crystals (approximately 0.25 in. cubes). The crystals were heated *in vacuo* and observed with a low-power microscope. No individual nuclei could be observed up to a temperature of 550 °C but, on removal of the crystal from the vacuum enclosure after cooling, it was obvious that some decomposition had taken place, since the crystal was then black in color in contrast to its original brassy hue. Oblique illumination of the crystal with colored light also failed to reveal the formation of any discrete nuclei on heating.

On closer examination, blue-grey areas which appeared at first to increase and then to decrease in size could be observed. This effect could possibly be due to interference colors caused by a very thin film of pyrrhotite over the surface of the crystal, the appearance and disappearance of the colors being associated with the varying film thickness.

Other problems encountered with the use of natural pyrite crystals were: inhomogeneity of the interior of the crystal, the presence of impurities, and the variation in weight, size, and composition from crystal to crystal. These problems could best be eliminated by using polycrystalline, pelletized material. As no discrete nuclei had been observed, the aim of the work thereafter was directed towards studying the kinetics of the post-nucleation reaction.

This preliminary work did, however, imply that the surface of the crystal was very quickly covered by a thin film of reaction product and that the formation and growth of individual nuclei was unlikely to be the rate-controlling step in the decomposition, but rather the rate of movement of the pyrite/pyrrhotite interface into the crystal.

The fact that the polycrystalline pellets used in the main portion of this study had 85% of theoretical density implies that the amount of open porosity in the pellets must have been small. It is, then, not surprising that the rate of movement of the pyrite/pyrrhotite interface in both the single crystal and compressed polycrystalline pellet should be the rate-controlling step in the decomposition, and that similar kinetics, therefore, would govern both cases.

REFERENCES

1. G. KULLERUD and H. S. YODER. Econ. Geol. **54**, 533 (1959).
2. E. T. ALLEN and R. H. LOMBARD. Am. J. Sci. **43**, 175 (1917).
3. H. KAMURA. Chem. Met. Eng. **24**, 437 (1921).
4. M. G. RAEDER. Kgl. Norske Videnskab. Selskabs Forh. **11**, 151 (1929).
5. L. D'OR. J. Chim. Phys. **28**, 377 (1931).
6. R. JUZA, W. BILTZ, and K. MEISEL. Z. Anorg. Allgem. Chem. **205**, 273 (1932).
7. F. DE RUDDER. Bull. Soc. Chim. France, 1225 (1936).
8. T. ROSENQVIST. J. Iron Steel Inst. London, **176**, 37 (1954).
9. S. BOG and T. ROSENQVIST. Trans. Faraday Soc. **55**, 1565 (1959).
10. F. W. DICKSON, L. D. SHIELDS, and G. C. KENNEDY. Econ. Geol. **57**, 1021 (1962).
11. P. TOULMIN III and P. B. BARTON, JR. Geochim. Cosmochim. Acta, **28**, 641 (1964).
12. V. S. UDINTSEVA and G. I. CHUFAROV. J. Appl. Chem. USSR English Transl. **14**, 3 (1941).
13. G. WUNDERLICH. Z. Elektrochem. **56**, 218 (1952).
14. W. M. MCKEWAN. Trans. AIME, **212**, 791 (1958).
15. W. J. DIXON and F. J. MASSEY. Introduction to statistical analysis. 2nd ed. McGraw-Hill Book Company, Inc., New York. 1957. Chap. 11.
16. N. F. H. BRIGHT and W. E. GARNER. J. Chem. Soc. 1872 (1934).

Can. J. Chem. Downloaded from www.nrcresearchpress.com by 210.87.254.42 on 09/05/12
For personal use only.

Can. J. Chem. Downloaded from www.nrcresearchpress.com by 210.87.254.40 on 09/05/12
For personal use only.

THE SULFURIC ACID SOLVENT SYSTEM

PART VII. SOLUTIONS OF SOME TIN(IV) AND LEAD(IV) COMPOUNDS

R. J. GILLESPIE AND R. KAPOOR
Department of Chemistry, McMaster University, Hamilton, Ontario

AND

E. A. ROBINSON
Department of Chemistry, University of Toronto, Toronto, Ontario

Received November 15, 1965

ABSTRACT

Solutions of tetramethyl tin, trimethyl tin sulfate, di-*n*-butyl tin diacetate, tetraphenyl tin, and triphenyl tin hydroxide in 100% sulfuric acid have been investigated by cryoscopic and conductimetric methods. Tetramethyl tin reacts with sulfuric acid with the evolution of methane and the formation of trimethyl tin hydrogensulfate. Trialkyl tin hydrogensulfates and dialkyl tin dihydrogensulfates behave as strong bases. It is probable that the cationic species formed are protonated hydrogensulfates rather than "stannonium" ions. Phenyl-substituted tin compounds are cleaved in sulfuric acid with the formation of benzene sulfonic acid and the complex hexa(hydrogensulfato) stannic acid, $H_2Sn(HSO_4)_6$, and its anions. Lead tetraacetate gives yellow solutions containing hexa(hydrogensulfato) plumbic acid, $H_2Pb(HSO_4)_6$, and its anions.

INTRODUCTION

Little work has been reported previously concerning the behavior of stannic compounds dissolved in sulfuric acid. Stannic oxide and stannic sulfate are almost insoluble in concentrated sulfuric acid. Salts of sulfatostannic acid, $H_2Sn(SO_4)_3$, have, however, been prepared by several workers. Weinland and Kuhl (1) prepared $K_2Sn(SO_4)_3$ by evaporating a solution containing 1 mole of stannic acid and 1.5 moles of potassium sulfate in sulfuric acid. They also prepared a number of other related salts such as $Rb_2Sn(SO_4)_3$ and $PbSn(SO_4)_3.3H_2O$. The potassium and calcium salts were also obtained by Druce (2) by the reaction of a chlorostannate, e.g. K_2SnCl_6 with sulfuric acid. He also prepared complex sulfatostannates of the anilinium and related cations. More recently Brubaker (3) has studied solutions of Sn(IV) in aqueous solutions of sulfuric acid of various strengths. He concluded that in dilute aqueous acid tin is present as a cation such as Sn^{4+} or SnO^{2+} (presumably solvated) and in very strong acid as an anion $Sn(SO_4)_3^{2-}$. There appears to have been no previous investigation of the cryoscopic and conductimetric behavior of organotin compounds in 100% sulfuric acid.

The preparation of plumbic sulfate, $Pb(SO_4)_2$, has been reported by several workers. For example, it was prepared by Brauner (4) from PbF_4 and concentrated sulfuric acid and by Hutchinson and Pollard (5) from lead tetraacetate and sulfuric acid. In the present work $Pb(SO_4)_2$ was prepared by the latter method and in agreement with the results of Hutchinson and Pollard and other early workers it was found to be only slightly soluble in sulfuric acid and dilute oleums. The more usual method of preparation of $Pb(SO_4)_2$ is by the electrolysis of sulfuric acid with lead electrodes (6). Dolezalek and Finkh (7), and Esche (8), suggested that the solutions in sulfuric acid from which $Pb(SO_4)_2$ is obtained, and the greenish-yellow solutions obtained by the electrolysis of sulfuric acid using lead electrodes, contain "hydrotrisulfato" plumbic acid, $H_2Pb(SO_4)_3$, since the potassium and ammonium salts, $K_2Pb(SO_4)_3$ and $(NH_4)_2Pb(SO_4)_3$, could be obtained from the solutions. Elbs and Fischer (6) prepared several insoluble alkali metal

salts such as $K_2Pb(SO_4)_3$ by treating an acid solution of $Pb(SO_4)_2$ with a solution of the metal sulfate in sulfuric acid. We have prepared the potassium salt and confirmed its very low solubility in 100% sulfuric acid.

The results of the present cryoscopic and conductimetric measurements on solutions of lead tetraacetate in sulfuric acid have already been reported in a preliminary communication (9); they are given now in detail.

EXPERIMENTAL

The freezing-point depression and electrical conductivities of solutions were measured by methods described previously (10–12). *Tetramethyl tin* was prepared by the method of Edgill and Ward (13) from methyl magnesium iodide and stannic chloride in *n*-butyl ether as solvent. It was purified by fractional distillation (b.p. 77.2 °C, $n_D^{25} = 1.4410$). *Trimethyl tin sulfate*, $[(CH_3)_3Sn]_2SO_4$, was prepared by dissolving tetramethyl tin in 100% sulfuric acid. Methane was evolved and addition of a small amount of water to the solution precipitated the sulfate, which was filtered off and washed with acetone and then with dry ether. *Di-n-butyl diacetate* was a sample obtained from Allbright and Wilson Ltd. *Tetraphenyl tin* was prepared by the method of Chambers and Scherer (14) by the reaction of phenyl zinc chloride with stannic chloride in toluene as solvent and under an inert atmosphere. The crude product was extracted with ether to remove chlorostannanes and recrystallized from toluene (m.p. 225–226°). *Triphenyl tin hydroxide* was prepared from the chloride (Eastman Kodak) by hydrolysis in alkaline solution. The product was extracted into ether and crystallized from the ether solution by cooling to ice temperature. It was recrystallized from petroleum ether (m.p. 118–120°). *Lead Tetraacetate* was obtained from the G. F. Smith Co. and was recrystallized from a mixture of acetic acid and acetic anhydride (m.p. 176°). The preparation of the 100% sulfuric acid solvent has been described previously (10, 11).

RESULTS AND DISCUSSION

The results of the freezing-point and conductivity measurements are given in Table I in the form of values at round concentrations. These were obtained by interpolation from plots of the results of at least two separate experiments on each compound in each of which a number of separate additions of the solute were made. Values of ν, the total number of moles of particles (molecules or ions) formed by the reaction of 1 mole of solute with sulfuric acid, were obtained from the expression

$$\nu = \Theta(1 + 0.002\Theta - 0.098\, ms)/6.12\, m_d/m$$

where Θ is the freezing-point depression calculated from the hypothetical freezing-point of undissociated sulfuric acid, i.e. 10.625°, m is the molality of the solute, m_d is the molality of the self-dissociation products, and s is the number of moles of solvent used up in the reaction of 1 mole of the solute (15). Values of γ, the number of moles of hydrogensulfate ions formed by the ionization of 1 mole of solute, were obtained by comparing the concentrations of solutions of the solute with those of an appropriate fully ionized reference base such as $KHSO_4$, H_2O, or CH_3CO_2H (15).

Tetramethyl Tin and Trimethyl Tin Sulfate

Tetramethyl tin dissolves rapidly in sulfuric acid with the evolution of methane according to the equation

$$[1] \qquad (CH_3)_4Sn + H_2SO_4 = (CH_3)_3Sn.HSO_4 + CH_4 \quad .$$

A similar reaction has been observed between tetramethyl tin and concentrated aqueous solutions of hydrogen halides (16).

A concentrated solution of tetramethyl tin in 100% sulfuric acid was prepared and the reaction allowed to go to completion. The solution was then added to 100% sulfuric acid in the conductimetric and cryoscopic cells. Values of ν and γ slightly greater than 2.0 and 1.0 respectively were obtained, in substantial agreement with the formation of trimethyl tin hydrogensulfate according to eq. [1] and its ionization to give a trimethyl tin cation

$$(CH_3)_3Sn.SO_4H = (CH_3)_3Sn^+ + HSO_4^-, \quad \nu = 2.0, \gamma = 1.0,$$

Can. J. Chem. Downloaded from www.nrcresearchpress.com by 210.87.254.40 on 09/05/12
For personal use only.

TABLE I

Cryoscopic and conductimetric measurements and calculated ν and γ values for solutions in 100% H_2SO_4

m	f.p. (°C)	Θ	ν	$10^2\varkappa$ (ohm^{-1} cm^{-1})	γ	$\nu - \gamma$
$(CH_3)_4Sn$						
0.04	10.051	0.574	1.81	1.435	1.1	
0.06	9.779	0.846	1.99	1.670	1.0	
0.08	9.490	1.135	2.08	1.900	1.0	
0.10	9.204	1.421	2.13	—	—	
0.12	8.925	1.700	2.14	—	—	
0.14	8.647	1.978	2.16	—	—	
0.16	8.362	2.263	2.18	—	—	
0.18	8.083	2.542	2.18	—	—	
$[(CH_3)_3Sn]_2SO_4$						
0.02	10.007	0.618	4.16	1.364	2.1	
0.03	9.846	0.779	3.94	1.574	1.9	
0.04	9.571	1.054	4.05	1.763	1.9	
0.05	9.312	1.313	4.03	1.936	1.8	
0.06	9.043	1.582	4.07	—	—	
0.08	8.508	2.117	4.08	—	—	
0.10	7.880	2.645	4.08	—	—	
$(n\text{-}C_4H_9)_2Sn(OOCH_3)_2$						
0.01	—	—	—	1.258	3.2	
0.02	—	—	—	1.655	3.1	
0.03	—	—	—	2.075	3.1	
0.04	—	—	—	2.437	3.0	
0.05	—	—	—	2.762	2.9	
$(C_6H_5)_4Sn$						
0.010	9.900	0.725	10.1	1.172	2.6	
0.015	9.572	1.053	10.5	1.292	2.5	
0.020	9.243	1.382	10.5	1.430	2.4	
0.025	8.918	1.707	10.5	1.572	2.3	
0.030	8.590	2.035	10.4	1.721	2.3	
$(C_6H_5)_3Sn.OH$						
0.010	9.900	0.725	10.4	1.160	—	
0.015	9.600	1.025	10.3	1.270	2.3	
0.020	9.304	1.321	10.1	1.404	2.3	
0.025	8.993	1.632	10.0	1.550	2.3	
0.030	8.686	1.939	9.9	1.688	2.2	
0.035	8.380	2.245	9.9	1.817	2.2	
0.040	—	—	—	1.942	2.1	
$Pb(OOC.CH_3)_4$						
0.005	10.184	0.441	8.22	1.107	3.43	5.39
0.010	9.983	0.642	8.12	1.240	3.22	4.90
0.015	9.768	0.857	7.92	1.402	3.04	4.88
0.020	9.550	1.075	7.74	1.585	2.84	4.90
0.025	9.328	1.297	7.61	1.617	2.74	4.87
0.030	9.106	1.519	7.53	1.901	2.66	4.87
0.035	8.880	1.745	7.45	2.062	2.60	4.85
0.040	8.650	1.975	7.45	2.231	2.56	4.89
0.045	8.430	2.195	7.39	2.395	2.54	4.85
0.050	8.205	2.420	7.33	2.556	2.51	4.82
0.055	7.980	2.645	7.25	2.722	2.50	4.75

assuming that all of the methane produced in reaction [1] is evolved from the solution. The fact that the observed values of ν and γ are slightly greater than predicted can be explained by the production of small amounts of methane sulfonic acid and water.

$$CH_4 + 2H_2SO_4 = CH_3SO_3H + H_3O^+ + HSO_4^-$$

For trimethyl tin sulfate the experimental results are $\nu = 4$ and $\gamma = 2$, in agreement with the ionization

$$[(CH_3)_3Sn]_2SO_4 + H_2SO_4 = 2(CH_3)_3Sn^+ + 2HSO_4^-,$$

and confirm the results for tetramethyl tin.

Can. J. Chem. Downloaded from www.nrcresearchpress.com by 210.87.254.40 on 09/05/12
For personal use only.

Can. J. Chem. Downloaded from www.nrcresearchpress.com by 210.87.254.40 on 09/05/12
For personal use only.

On the basis of the cryoscopic and conductimetric measurements alone it is not possible to distinguish between solvated species such as $(CH_3)_3Sn.SO_4H_2^+$ and $(CH_3)_3Sn(SO_4H_2)_2^+$ and the "stannonium" ion $(CH_3)_3Sn^+$. In aqueous solution it has been shown that trialkyl tin cations exist in solvated forms, e.g. $R_3SnOH_2^+$, rather than as the planar R_3Sn^+ ion. The formation of the latter would lead to racemization of optically active methyl ethyl *n*-propyl tin sulfate, and it has been shown that no racemization occurs, since the camphorsulfonate has been resolved from aqueous solution (16). Recently, infrared studies of solid trimethyl tin salts such as the perchlorate, nitrate, and carbonate have led to the conclusion that these compounds do not contain $(CH_3)_3Sn^+$ cations (17–19) and that the anions are covalently bound to tin to give a five-coordinated trigonal bipyramidal configuration around tin. X-ray studies of $(CH_3)_3SnF$ show that there is a trigonal bipyramidal coordination of tin in a structure involving fluorine bridges (20). It has also been reported (18) that the tetrafluoroborate ion in $(CH_3)_3SnBF_4$ is covalently bound to tin in a polymeric chain structure containing five-coordinated tin. Henceforth in this paper we will write all alkyl tin cations in their more probable solvated forms.

Di-n-butyl Tin Diacetate

This compound reacts with sulfuric acid to give 3 hydrogen sulfate ions per solute molecule ($\gamma = 3$). Reaction according to the equation

$$(n\text{-Bu})_2Sn(OAc)_2 + 4H_2SO_4 = (n\text{-Bu})_2Sn(HSO_4)_2 + 2AcOH_2^+ + 2HSO_4^-,$$

for which $\gamma = 2$, might be expected by analogy with the behavior of dialkyl silicon compounds (12), but the observed γ value of 3 is consistent only with the formation of a singly charged tin cation, e.g.

$$(n\text{-Bu})_2Sn(OAc)_2 + 5H_2SO_4 = [(n\text{-Bu})_2Sn(HSO_4)_2]H^+ + 2AcOH_2^+ + 3HSO_4^- \quad .$$

Ionization to give a doubly charged cation is also inconsistent with the experimental results.

$$(n\text{-Bu})_2Sn(OAc)_2 + 6H_2SO_4 = [(n\text{-Bu})_2Sn(HSO_4)_2]H_2^{2+} + 2AcOH_2^+ + 4HSO_4^-, \quad \gamma = 4.0.$$

Similar reactions in which tin anions are formed are also inconsistent with the conductimetric results.

$$R_2Sn(OAc)_2 + 4H_2SO_4 = R_2Sn(HSO_4)_3^- + 2AcOH_2^+ + HSO_4^-, \quad \gamma = 1.0,$$

$$R_2Sn(OAc)_2 + 4H_2SO_4 = R_2Sn(HSO_4)_4^{2-} + 2AcOH_2^+, \quad \gamma = 0.$$

Tetraphenyl Tin and Triphenyl Tin Hydroxide

The cryoscopic and conductimetric results are only explicable if complete cleavage of the Sn—C bonds occurs. Thus the reaction of aryl tin compounds is quite similar to that of aryl silicon compounds (12). The experimental ν and γ values for triphenyl tin hydroxide of 10.4–9.9 and 2.3–2.1 respectively are in reasonably good agreement with the formation of $HSn(HSO_4)_6^-$ and $Sn(HSO_4)_6^{2-}$.

$$Ph_3Sn.OH + 13H_2SO_4 = H_2Sn(HSO_4)_6 + 3PhSO_3H + 4H_3O^+ + 4HSO_4^-, \quad \nu = 12, \gamma = 4,$$

$$Ph_3Sn.OH + 12H_2SO_4 = HSn(HSO_4)_6^- + 3PhSO_3H + 4H_3O^+ + 3HSO_4^-, \quad \nu = 11, \gamma = 3,$$

$$Ph_3Sn.OH + 11H_2SO_4 = Sn(HSO_4)_6^{2-} + 3PhSO_3H + 4H_3O^+ + 2HSO_4^-, \quad \nu = 10, \gamma = 2.$$

For tetraphenyl tin ν has an approximately constant value of 10.5 and γ decreases from 2.6 to 2.3 with increasing concentration.

These results are in approximate agreement with the formation of $HSn(HSO_4)_6^-$ and

$Sn(HSO_4)_6^{2-}$ according to the following equations

$$Ph_4Sn + 14H_2SO_4 = H_2Sn(HSO_4)_6 + 4PhSO_3H + 4H_3O^+ + 4HSO_4^-, \quad \nu = 13, \gamma = 4,$$

$$Ph_4Sn + 13H_2SO_4 = HSn(HSO_4)_6^- + 4PhSO_3H + 4H_3O^+ + 3HSO_4^-, \quad \nu = 12, \gamma = 3,$$

$$Ph_4Sn + 12H_2SO_4 = Sn(HSO_4)_6^{2-} + 4PhSO_3H + 4H_3O^+ + 2HSO_4^-, \quad \nu = 12, \gamma = 2.$$

The low value of ν suggests that some polymerization of the sulfato tin anion may be occurring as was previously found for the $Si(HSO_4)_6^{2-}$ anion (12). However, it is not clear why there is no indication of polymerization in the results obtained with triphenyl tin hydroxide. Because of the large ν values and the variety of probable products it is not possible to interpret these results with complete certainty. $H_2Sn(HSO_4)_6$ is clearly a relatively strong acid of the sulfuric acid solvent system but it is not possible to give any quantitative estimate of its strength.

Lead Tetraacetate

Both ν and γ vary with increasing concentration of solute, from 8.2 to 7.5 and 3.4 to 2.5 respectively, over the concentration range 0.005 *m* to 0.055 *m*.

The results are consistent with the reaction of lead tetraacetate to give a solution containing hexa(hydrogensulfato) plumbic acid, $H_2Pb(HSO_4)_6$, and its anions.

$$Pb(OAc)_4 + 10H_2SO_4 = H_2Pb(HSO_4)_6 + 4AcOH_2^+ + 4HSO_4^-, \quad \nu = 9, \gamma = 4,$$

$$Pb(OAc)_4 + 9H_2SO_4 = HPb(HSO_4)_6^- + 4AcOH_2^+ + 3HSO_4^-, \quad \nu = 8, \gamma = 3,$$

$$Pb(OAc)_4 + 8H_2SO_4 = Pb(HSO_4)_6^{2-} + 4AcOH_2^+ + 2HSO_4^-, \quad \nu = 7, \gamma = 2.$$

An estimate of the dissociation constants of the acid $H_2Pb(HSO_4)_6$ was obtained from the conductivity data in the following manner. For very dilute solutions it was assumed that the concentration of $Pb(HSO_4)_6^{2-}$ is negligible. We then have

$$[H_2Pb(HSO_4)_6] = \gamma - 3 \text{ and } [HPb(HSO_4)_6^-] = 4 - \gamma.$$

Hence the limiting value at low concentrations for $K_{b_1} = [HPb(HSO_4)_6^-]/[H_2Pb(HSO_4)_6][HSO_4^-]$ was found to be 48 moles kg^{-1}. For relatively concentrated solutions it was assumed that the concentration of un-ionized acid is small so that to a good approximation

$$[HPb(HSO_4)_6^-] = \gamma - 2 \text{ and } [Pb(HSO_4)_6^{2-}] = 3 - \gamma.$$

Hence the mean value of $K_{b_2} = [Pb(HSO_4)_6^{2-}]/[HPb(HSO_4)_6^-][HSO_4^-]$ was found to be 7.4 moles kg^{-1}.

The acid dissociation constants K_{a_1} and K_{a_2} of hexa(hydrogensulfato) plumbic acid are related to the basic dissociation constant K_{b_1} and K_{b_2} by the relationship

$$K_a = K_b K_{ap}$$

where K_{ap} is the autoprotolysis constant of sulfuric acid. K_{ap} has the value 2.4×10^{-4} $mole^2\ kg^{-2}$ at 25 °C (22). Thus for $H_2Pb(HSO_4)_6$

$$K_{a_1} = 1.2 \times 10^{-2} \text{ mole kg}^{-1}$$

and

$$K_{a_2} = 1.8 \times 10^{-3} \text{ mole kg}^{-1}, \text{ at 25 °C.}$$

These values are slightly different from those reported earlier (9) because of the use of an improved value for K_{ap}. The first dissociation constant of $H_2Pb(HSO_4)_6$ is of a similar magnitude to the acid dissociation constant of $H_2S_2O_7$ (21).

Can. J. Chem. Downloaded from www.nrcresearchpress.com by 210.87.254.40 on 09/05/12
For personal use only.

Solutions containing hexa(hydrogensulfato) plumbic acid are not stable above $\sim 100°$; decomposition occurs to give oxygen and a precipitate of plumbous sulfate.

$$H_2Pb(HSO_4)_6 \rightarrow PbSO_4 + H_2S_2O_8 + 3H_2SO_4$$

$$2H_2S_2O_8 \rightarrow 2H_2S_2O_7 + O_2$$

Lead tetraacetate was also found to be soluble in selenic, fluorosulfuric, and chlorosulfuric acids, giving yellow solutions which may contain the acids $H_2Pb(HSeO_4)_6$, $H_2Pb(FSO_3)_6$, and $H_2Pb(ClSO_3)_6$ respectively. On heating all the solutions decomposed, the yellow color faded, and oxygen was evolved. Plumbic oxide, PbO_2, precipitated by adding lead tetraacetate to water and dried at 120° was found to be insoluble in sulfuric acid. However, slightly moist PbO_2 was found to dissolve slowly on warming with sulfuric acid to give a yellow solution.

ACKNOWLEDGMENTS

We thank the National Research Council of Canada and the Ontario Research Foundation for financial assistance.

REFERENCES

1. R. F. WEINLAND and H. KUHL. Z. Anorg. Chem. **54**, 244 (1907).
2. J. G. F. DRUCE. Chem. News, **128**, 33 (1924).
3. R. C. H. BRUBAKER. J. Am. Chem. Soc. **77**, 5265 (1955).
4. B. BRAUNER. Z. Anorg. Chem. **7**, 11 (1894).
5. A. HUTCHINSON and W. POLLARD. J. Chem. Soc. **69**, 221 (1896).
6. K. ELBS and F. FISCHER. Z. Elektrochem. **7**, 343 (1901).
7. F. DOLEZALEK and K. FINKH. Z. Anorg. Chem. **50**, 82 (1906); **51**, 320 (1906).
8. W. ESCHE. Chem. Ztg. **27**, 297 (1903).
9. R. J. GILLESPIE and E. A. ROBINSON. Proc. Chem. Soc. 147 (1957).
10. R. J. GILLESPIE, J. V. OUBRIDGE, and C. SOLOMONS. J. Chem. Soc. 1804 (1957).
11. R. J. GILLESPIE, E. D. HUGHES, and C. K. INGOLD. J. Chem. Soc. 2504 (1950).
12. R. H. FLOWERS, R. J. GILLESPIE, and E. A. ROBINSON. Can. J. Chem. **41**, 2464 (1963).
13. W. F. EDGILL and C. H. WARD. J. Am. Chem. Soc. **76**, 1169 (1954).
14. R. F. CHAMBERS and P. C. SCHERER. J. Am. Chem. Soc. **48**, 1054 (1926).
15. R. J. GILLESPIE and E. A. ROBINSON. *In* Non-aqueous solvent systems. *Edited by* T. C. Waddington. Academic Press, New York. 1965. pp. 132 and 148.
16. G. E. COATES. Organo-metallic compounds. Wiley, New York. 1960.
17. R. OKAWARA, B. J. HATHAWAY, and D. E. WEBSTER. Proc. Chem. Soc. 13 (1963).
18. B. J. HATHAWAY and D. E. WEBSTER. Proc. Chem. Soc. **14** (1963).
19. H. C. CLARK and R. J. O'BRIEN. Inorg. Chem. **2**, 1020 (1963).
20. H. C. CLARK, R. J. O'BRIEN, and J. TROTTER. Proc. Chem. Soc. 85 (1963).
21. S. J. BASS, R. J. GILLESPIE, and E. A. ROBINSON. J. Chem. Soc. 821 (1960).
22. R. J. GILLESPIE, E. A. ROBINSON, and C. SOLOMONS. J. Chem. Soc. 4320 (1960).

Can. J. Chem. Downloaded from www.nrcresearchpress.com by 210.87.254.40 on 09/05/12
For personal use only.

Can. J. Chem. Downloaded from www.nrcresearchpress.com by 188.143.235.115 on 09/06/12
For personal use only.

THE SULFURIC ACID SOLVENT SYSTEM

PART VIII. SOLUTIONS OF SOME PHOSPHORUS(V) AND VANADIUM(V) COMPOUNDS

R. J. GILLESPIE AND R. KAPOOR
Department of Chemistry, McMaster University, Hamilton, Ontario

AND

E. A. ROBINSON
Department of Chemistry, University of Toronto, Toronto, Ontario

Received November 15, 1965

ABSTRACT

It is shown that a number of phosphates ionize in sulfuric acid to give the $P(OH)_4^+$ ion. Triphenyl phosphine and triethyl phosphate are fully protonated but phosphorus oxyfluoride and phosphorus oxychloride are shown to be nonelectrolytes.

Ammonium metavanadate and vanadium pentoxide give the acid $H[VO(HSO_4)_4]$ and there is evidence that the dimer $H[V_2O_3(HSO_4)_6]$ and possibly higher polymers are present in increasing amounts with increasing concentration.

PHOSPHORUS(V) COMPOUNDS

Arlman (1) prepared the compound $H_3PO_4.HClO_4$ and suggested that it was an ionic perchlorate $P(OH)_4^+.ClO_4^-$. To obtain more definite evidence for $P(OH)_4^+$, and other possible oxy-cations of phosphorus, we have investigated solutions of KH_2PO_4, $K_4P_2O_7$, $Na_2H_2P_2O_7$, $K_5P_3O_{10}$, $Na_5P_3O_{10}$, $(C_6H_5)_3PO$, $(C_2H_5O)_3PO$, POF_3, and $POCl_3$ in sulfuric acid by cryoscopic and conductimetric measurements.

The results of the cryoscopic and conductimetric studies are given in Table I, and the conductivities are plotted in Fig. 1. They show that all the phosphates are converted quantitatively to the $P(OH)_4^+$ ion according to the following equations:

[1] $$KH_2PO_4 + 2H_2SO_4 = P(OH)_4^+ + K^+ + 2HSO_4^-, \quad \nu = 4, \gamma = 2,$$

[2] $$K_4P_2O_7 + 7H_2SO_4 = 2P(OH)_4^+ + 4K^+ + HS_2O_7^- + 5HSO_4^-, \quad \nu = 12, \gamma = 5,$$

[3] $$Na_2H_2P_2O_7 + 5H_2SO_4 = 2P(OH)_4^+ + 2Na^+ + HS_2O_7^- + 3HSO_4^-, \quad \nu = 8, \gamma = 3,$$

[4] $$M_5P_3O_{10} + 10H_2SO_4 = 3P(OH)_4^+ + 5M^+ + 2HS_2O_7^- + 6HSO_4^-, \quad \nu = 16, \gamma = 6.$$

The polyphosphates all dehydrate sulfuric acid to give the $P(OH)_4^+$ ion and there is no evidence that any other cation of phosphorus is present in the solutions. Triphenyl phosphine and triethyl phosphate are protonated to give the cations $(C_6H_5)_3POH^+$ and $(C_2H_5O)_3POH^+$, respectively.

[5] $$(C_6H_5)_3PO + H_2SO_4 = (C_6H_5)_3POH^+ + HSO_4^-, \quad \nu = 2, \gamma = 1,$$

[6] $$(C_2H_5O)_3PO + H_2SO_4 = (C_2H_5O)_3POH^+ + HSO_4^-, \quad \nu = 2, \gamma = 1.$$

Phosphorus oxyfluoride and phosphorus oxychloride both behave as nonelectrolytes, although solutions of the former are not completely stable.

VANADIUM(V) COMPOUNDS

Early workers obtained a compound having the composition $V_2O_5.3SO_3$, or $(VO)_2(SO_4)_3$, from solutions of vanadium pentoxide in concentrated sulfuric acid (2). Hayek and Engelbrecht (3) reported the formation of $V_2O(SO_4)_4$ from the reaction of $VOCl_3$ with SO_3. Woolf (4) formulated this compound as $(VO)_2S_4O_{13}$. More recently Mishra and Symons

(5) have studied solutions of V_2O_5 in 65% oleum and in sulfuric acid. In 65% oleum they state that their results are consistent with the reaction

[7] $$V_2O_5 + 9H_2S_2O_7 = 2VO(HS_2O_7)_3 + 6H_2SO_4$$

and exclude the formation of species such as VO_2^+ and $V(OH)_4^+$. In sulfuric acid their conductivity measurements give approximately 2.4 for γ, the number of hydrogensulfate ions formed from 1 molecule of V_2O_5, and they conclude that this results from a combination of the reactions:

[8] $$V_2O_5 + 9H_2SO_4 = 2VO(HSO_4)_3 + 3H_3O^+ + 3HSO_4^-$$

and

[9] $$V_2O_5 = 5H_2SO_4 = 2VO(OH)(HSO_4)_2 + H_3O^+ + HSO_4^-.$$

We now report the results of cryoscopic and conductimetric measurements on solutions of ammonium metavanadate and vanadium pentoxide in 100% sulfuric acid and dilute oleum.

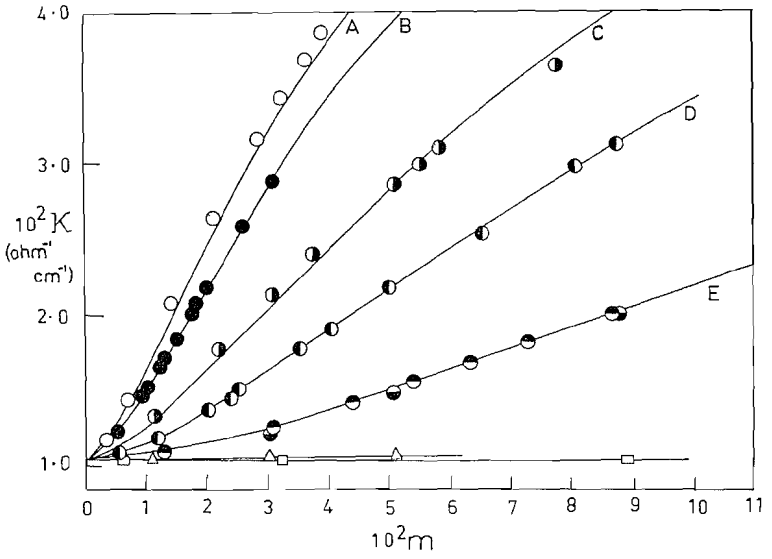


FIG. 1. Electrical conductivities of solutions of phosphorus(V) compounds at 25 °C. (A) $6KHSO_4$, (B) $5KHSO_4$, (C) $3NaHSO_4$, (D) $2KHSO_4$, (E) $KHSO_4$, (○)$K_5P_3O_{10}$, (●) $K_4P_2O_7$, (◑) $Na_2H_2P_2O_7$, (◐) KH_2PO_4, (◓) $(C_6H_5)_3PO$, (◒) $(C_2H_5O)_3PO$, (△) POF_3, (□) $POCl_3$.

Solutions in 100% H_2SO_4

The freezing-point results for ammonium metavanadate (Table II) show that ν is approximately 6. At first sight this might be taken to indicate an ionization similar to that of potassium nitrate (6, 7), i.e.

[10] $$KNO_3 + 3H_2SO_4 = K^+ + NO_2^+ + H_3O^+ + 3HSO_4^-$$

[11] $$NH_4VO_3 + 3H_2SO_4 = NH_4^+ + VO_2^+ + H_3O^+ + 3HSO_4^- \quad .$$

However, this ionization cannot account for the fact that the value of ν is initially greater than 6 and decreases with increasing concentration to a value that is definitely less than 6, nor for the observation that the conductivity results (Table II) give a γ value that is considerably less than the expected value of 3 and decreases with increasing concentration.

Can. J. Chem. Downloaded from www.nrcresearchpress.com by 188.143.235.115 on 09/06/12
For personal use only.

TABLE I

Cryoscopy and conductivity measurements for solutions of phosphorus(V) compounds with calculated ν and γ values

Solute	$10^2 m$	f.p. (°C)	ν	$10^2 \mathscr{K}$ (ohm^{-1} cm^{-1})	γ
$K_4P_2O_7$	0.8	9.940	11.7	1.365	
	1.2	9.670	11.6	1.616	
	1.6	9.396	11.9	1.91	
	2.0	9.116	11.7	2.19	5
	2.4	8.825	11.8	2.46	
	2.8	8.502	11.9	2.65	
	3.2	8.175	12.1	—	
KH_2PO_4	2.0	9.981	4.2	1.351	
	3.0	9.750	4.1	1.625	
	4.0	9.523	4.0	1.902	
	5.0	9.296	4.0	2.17	2
	6.0	9.067	4.0	2.43	
	7.0	8.834	3.9	2.70	
	8.0	8.601	3.9	2.97	
	9.0	8.395	3.9	—	
	10.0	8.136	3.9	—	
$Na_2H_2P_2O_7$	1.5	9.813	7.9	1.425	
	2.0	9.582	7.9	1.661	
	2.5	9.349	7.9	1.865	3
	3.0	9.118	7.9	2.07	
	3.5	8.887	7.9	2.28	
	4.0	8.654	7.8	2.49	
$K_5P_3O_{10}$	0.5	10.018	16.0	1.38	
	1.0	9.590	15.7	1.70	
	1.5	9.128	15.7	2.13	6
	2.0	8.658	15.6	2.55	
	2.5	8.188	15.5	2.95	
$Na_5P_3O_{10}$	0.5	10.015	16.0	1.25	
	1.0	9.585	15.7	1.61	
	1.5	9.128	15.7	2.01	6
	2.0	8.635	15.8	2.38	
	2.5	8.146	15.7	2.73	
$(C_6H_5)_3PO$	4.0	10.005	2.0	1.354	
	5.0	9.881	2.0	1.497	
	6.0	9.748	2.1	1.641	1
	7.0	9.615	2.1	1.784	
	8.0	9.478	2.1	1.920	
	9.0	9.343	2.1	—	
$(C_2H_5O)_3PO$	4.0	10.032	1.9	1.344	
	6.0	9.813	1.9	1.614	
	8.0	9.550	2.0	1.898	1
	10.0	9.273	2.0	2.15	
	12.0	8.997	2.1	2.42	
	14.0	8.721	2.1	2.68	
$POCl_3$	5.0	10.064	1.0	1.033	
	10.0	9.755	1.0	1.023	
	15.0	9.428	1.0	1.013	0
	20.0	9.100	1.0	1.002	
	25.0	8.770	1.0	0.992	
POF_3	1.0	10.313	1.1	1.046	
	2.0	10.226	1.2	1.047	0
	3.0	10.142	1.2	1.047_5	

Can. J. Chem. Downloaded from www.nrcresearchpress.com by 188.143.235.115 on 09/06/12
For personal use only.

Since vanadium is known to form numerous compounds of the type VOX_3, it seems reasonable to postulate the following reaction

[12] $$NH_4VO_3 + 6H_2SO_4 = NH_4^+ + VO(HSO_4)_3 + 2H_3O^+ + 3HSO_4^-$$

for which $\nu = 7$ and $\gamma = 3$. It is possible that $VO(HSO_4)_3$ is a weak acid in which case the following equilibrium would be set up,

[13] $$VO(HSO_4)_3 + HSO_4^- \leftrightharpoons VO(HSO_4)_4^- \quad .$$

Complete formation of the $VO(HSO_4)_4^-$ anion would give the overall reaction

[14] $$NH_4VO_3 + 6H_2SO_4 = NH_4^+ + VO(HSO_4)_4^- + 2H_3O^+ + 2HSO_4^-$$

for which $\nu = 6$ and $\gamma = 2$.

The anion $VO(HSO_4)_4^-$ is derived from the acid $H[VO(HSO_4)_4]$, which differs from $VO(HSO_4)_3$ only by a solvent molecule. The formula $H[VO(HSO_4)_4]$ probably represents the neutral species in solution better than does $VO(HSO_4)_3$.

The equilibrium constant for [13] is given by

[15] $$K_b = [HVO(HSO_4)_4][HSO_4^-]/[VO(HSO_4)_4^-] = (\gamma - 2)\gamma m/(3 - \gamma).$$

Using the results from 0.01 to 0.05 m NH_4VO_3 we find $K_b = (2.9 \pm 0.2) \times 10^{-2}$ mole kg^{-1}, and since

[16] $$K_a = [VO(HSO_4)_4^-][H_3SO_4^+]/[HVO(HSO_4)_4],$$

we have

[17] $$K_a = K_{ap}/K_b = 0.8 \times 10^{-2} \text{ mole kg}^{-1}$$

for the acid dissociation constant of $HVO(HSO_4)_4$ at 25°, since K_{ap} has the value 2.4×10^{-4} $mole^2$ kg^{-2} at this temperature (8).

TABLE II

Freezing points and conductivities of solutions of NH_4VO_3 and V_2O_5 in 100% H_2SO_4 with calculated ν and γ values

Compound	$10^2 m$	f.p. (°C)	ν	$10^2 \mathscr{K}$ (ohm^{-1} cm^{-1})	γ	$\nu - \gamma$
NH_4VO_3	1	10.125	6.31	1.228	2.50	3.81
	2	9.798	6.18	1.475	2.43	3.75
	3	9.462	5.99	1.748	2.30	3.69
	4	9.118	5.89	2.024	2.25	3.64
	5	8.772	5.81	2.300	2.18	3.63
	6	8.420	5.74	2.575	2.15	3.59
V_2O_5	1	10.111	6.68	1.156	2.15	4.53
	2	9.788	6.19	1.338	1.92	4.27
	3	9.456	5.92	1.520	1.71	4.21
	4	9.128	5.74	1.700	1.61	4.13
	5	8.808	5.56	1.886	1.55	4.06
	6	8.490	5.38	2.067	1.50	3.88

The above equilibria require that $(\nu - \gamma) = 4.0$ and the observed results are in fair agreement with this. However, ν decreases to values of less than 6, γ to values less than 2, and $\nu - \gamma$ is always somewhat less than 4 and decreases with increasing concentration. The simplest explanation of this is that the dimeric species $V_2O_3(HSO_4)_4$ and its anion

Can. J. Chem. Downloaded from www.nrcresearchpress.com by 188.143.235.115 on 09/06/12
For personal use only.

$V_2O_3(HSO_4)_5^-$, or their solvated forms, are formed in increasing amounts at higher concentrations. The corresponding equations are

[18] $2NH_4VO_3 + 9H_2SO_4 = [VO(HSO_4)_2]_2O + 2NH_4^+ + 3H_3O^+ + 5HSO_4^-, \quad \nu = 5.5, \gamma = 2.5, (\nu - \gamma) = 3,$

and

[19] $2NH_4VO_3 + 9H_2SO_4 = V_2O_3(HSO_4)_5^- + 2NH_4^+ + 3H_3O^+ + 4HSO_4^-, \quad \nu = 5.0, \gamma = 2.0, (\nu - \gamma) = 3.$

The results of the cryoscopic and conductimetric measurements on solutions of vanadium pentoxide in 100% H_2SO_4 (Table II) can be accounted for by reactions similar to those proposed for ammonium metavanadate. The value of ν decreases from 6.7 in dilute solutions to 5.4 at higher concentrations, whereas the conductimetric γ factor decreases from approximately 2.0 to about 1.5 over the same concentration range. The results are reasonably consistent with the formation of $HVO(HSO_4)_4$ in equilibrium with $VO(HSO_4)_4^-$, i.e. with reaction according to the equations

[20] $V_2O_5 + 11H_2SO_4 = 2HVO(HSO_4)_4 + 3H_3O^+ + 3HSO_4^-, \quad \nu = 8, \gamma = 3, (\nu - \gamma) = 5,$

and

[21] $V_2O_5 + 9H_2SO_4 = 2VO(HSO_4)_4^- + 3H_3O^+ + HSO_4^-, \quad \nu = 6, \gamma = 1, (\nu - \gamma) = 5.$

In this case the equilibrium constant for [13] is given by

[22] $$K_b = (\gamma - 1)\gamma m/(3 - \gamma),$$

and using the results from 0.01 to 0.05 m V_2O_5, we find $K_b = (2.9 \pm 0.2) \times 10^{-2}$ and hence $K_a = 0.8 \times 10^{-2}$ mole kg^{-1}, in excellent agreement with the value found from the ammonium vanadate results.

However, ν decreases below 6 and $\nu - \gamma$ is somewhat smaller than expected and also decreases with increasing concentration. Again these results are consistent with the formation of an increasing amount of dimer with increasing concentration.

[23] $V_2O_5 + 6H_2SO_4 = V_2O_3(HSO_4)_4 + 2H_3O^+ + 2HSO_4^-, \quad \nu = 5, \gamma = 2, \nu - \gamma = 3,$

[24] $V_2O_5 + 6H_2SO_4 = V_2O_3(HSO_4)_5^- + 2H_3O^+ + HSO_4^-, \quad \nu = 4, \gamma = 1, \nu - \gamma = 3.$

Solutions in Dilute Oleum

The freezing points of solutions of NH_4VO_3 and V_2O_5 in dilute oleum, which are shown in Table III and Fig. 2, lend support to the above conclusions.

The freezing point rises on addition of NH_4VO_3 to oleum and the slope of the freezing-point curve corresponds to $\Delta\nu = -1$, as expected for the reaction

[25] $$NH_4VO_3 + \underbrace{3H_2S_2O_7}_{\nu \simeq (3 \times 1.3)} = \underbrace{NH_4^+ + HVO(HSO_4)_4 + HS_2O_7^-}_{\nu = 3} \qquad \Delta\nu \simeq -1 \ .$$

Since 1 mole of NH_4VO_3 reacts with 3 moles of $H_2S_2O_7$ to give $HVO(HSO_4)_4$, and since the initial concentration of $H_2S_2O_7$ in the experiment was 0.30 m, the freezing point would be expected to rise until the concentration $m_{NH_4VO_3} = 0.30/3 = 0.10\ m$, and at this point the freezing-point depression should correspond to $\nu = 3$. The maximum is observed experimentally at 0.095 m, which is very close to the expected value, and the freezing-point depression gives $\nu = 3.1$, in good agreement with the formation of $HVO(HSO_4)_4$. Similarly on addition of V_2O_5 to oleum the freezing point rises and the slope of the curve corresponds to $\Delta\nu = -2$, in accord with the reaction

[26] $$V_2O_5 + \underbrace{3H_2S_2O_7}_{\nu \simeq (3 \times 1.3)} + 2H_2SO_4 = \underbrace{2HVO(HSO_4)_4}_{\nu = 2} \qquad \Delta\nu \simeq -2 \ .$$

Can. J. Chem. Downloaded from www.nrcresearchpress.com by 188.143.235.115 on 09/06/12
For personal use only.

On addition of ammonium metavanadate to dilute oleum the conductivity decreases and passes through a minimum when the ratio of the number of moles of added NH_4VO_3 to the initial number of moles of $H_2S_2O_7$ = r = 0.35 to 0.36 (Table III and Fig. 2).

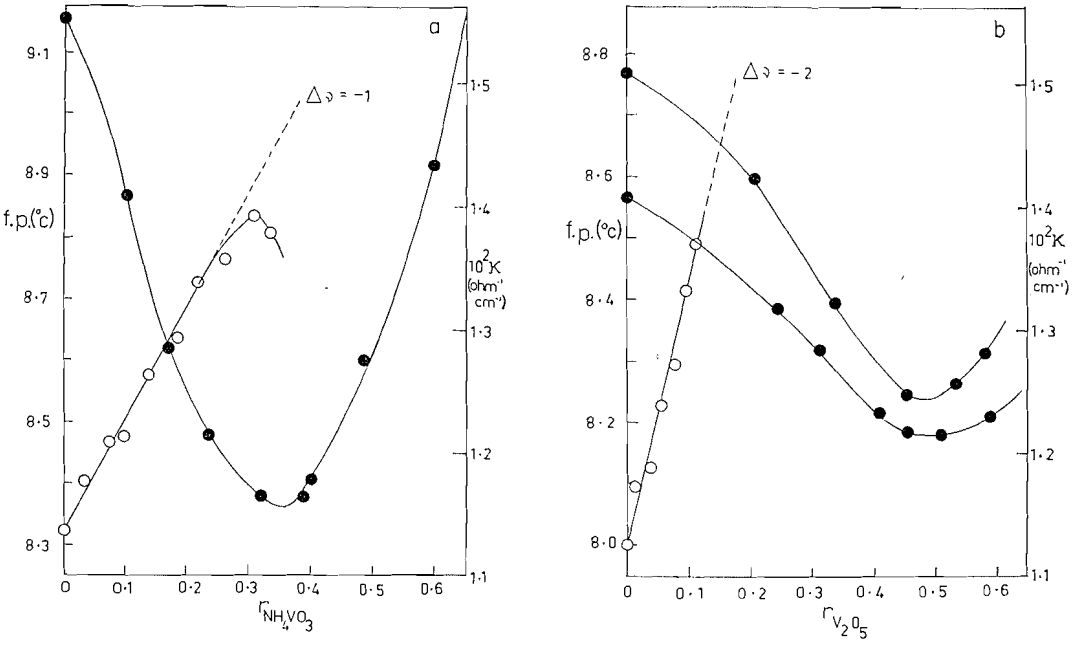


FIG. 2. Freezing points (○), and conductivities (●), of solutions of (*a*) NH_4VO_3, and (*b*) V_2O_5, in dilute oleum.

Ammonium metavanadate behaves in sulfuric acid as

[27] $$2H_2O + NH_4HSO_4 + HVO(HSO_4)_4$$

(see eq. [14]), and we can look at the titration in terms of adding these species to a solution containing $H_2S_2O_7$. Thus the following reactions are expected to occur,

[28] $$H_2O + H_2S_2O_7 = 2H_2SO_4$$

[29] $$NH_4HSO_4 + H_2S_2O_7 = NH_4^+ + HS_2O_7^- + H_2SO_4$$

[30] $$NH_4HSO_4 + HVO(HSO_4)_4 = NH_4^+ + VO(HSO_4)_4^- + H_2SO_4 \quad .$$

If the initial concentration of $H_2S_2O_7$ is n_a, and n_b moles of NH_4VO_3 are added to give a conductivity minimum ($r = n_b/n_a$), then $2n_b$ moles of $H_2S_2O_7$ are used up in reaction [28], leaving $n_a - 2n_b$ moles of $H_2S_2O_7$ to take part in reaction [29]. Suppose n_c moles of NH_4HSO_4 react with $H_2S_2O_7$ in reaction [29] to give a conductivity minimum, then since the conductivity minimum occurs at r = 0.56 in the titration of a strong base with $H_2S_2O_7$ (9),

[31] $$n_c/(n_a - 2n_b) = 0.56.$$

Thus $n_b - n_c$ moles of NH_4HSO_4 are left to give a conductivity minimum in reaction [30].

A conductivity minimum is predicted at r = 0.44 in the titration of a weak acid, K_a 1×10^{-2}, with a strong base (9), i.e.

[32] $$(n_b - n_c)/n_b = 0.44, \text{ i.e. } n_c = 0.56n_b.$$

Can. J. Chem. Downloaded from www.nrcresearchpress.com by 188.143.235.115 on 09/06/12
For personal use only.

TABLE III

Freezing points and conductivities of solutions of NH_4VO_3 and V_2O_5 in dilute oleum

NH_4VO_3		V_2O_5	
r	f.p. (°C)	r	f.p. (°C)
Initial molality of $H_2S_2O_7$ = 0.30		Initial molality of oleum = 0.34	
0.000	8.323	0.000	8.001
0.034	8.403	0.015	8.095
0.075	8.467	0.038	8.128
0.099	8.476	0.057	8.227
0.138	8.577	0.081	8.294
0.186	8.636	0.098	8.413
0.217	8.727	0.122	8.490
0.263	8.764		
0.309	8.834		
0.336	8.808		
NH_4VO_3		V_2O_5	
r*	$10^2\,\mathcal{K}$ (ohm^{-1} cm^{-1})	r*	$10^2\,\mathcal{K}$ (ohm^{-1} cm^{-1})
Initial molality of $H_2S_2O_7$ = 0.110		Initial molality of $H_2S_2O_7$ = 0.079	
0.000	1.552	0.000	1.407
0.104	1.408	0.247	1.317
0.388	1.164	0.314	1.284
0.600	1.434	0.409	1.233
0.653	1.572	0.456	1.217
0.695	1.697	0.514	1.211
		0.584	1.230
		0.771	1.377
Initial molality of $H_2S_2O_7$ = 0.110		Initial molality of oleum = 0.100	
0.000	1.552	0.000	1.510
0.170	1.285	0.207	1.424
0.235	1.214	0.338	1.321
0.320	1.164	0.459	1.248
0.401	1.178	0.534	1.256
0.483	1.276	0.582	1.282
0.616	1.597		

*r = ratio of moles of NH_4VO_3 or V_2O_5 to initial $H_2S_2O_7$.

Thus from eqs. [31] and [32] we have

[33] $$n_b/n_a = 0.33,$$

which is close to the observed minimum.

Addition of V_2O_5 to dilute oleum also gives a minimum in the conductivity–concentration curve at $r = n_b/n_a = 0.48$ to 0.50 (Table III and Fig. 2).

V_2O_5 behaves in sulfuric acid as

[34] $$3H_2O + 2HVO(HSO_4)_4$$

(see eq. [20]) and we can consider the titration in terms of adding these species to $H_2S_2O_7$. The following reactions will occur,

[35] $$H_2O + H_2S_2O_7 = 2H_2SO_4$$

and

[36] $$HVO(HSO_4)_4 + H_2O = H_3O^+ + VO(HSO_4)_4^- \quad .$$

Can. J. Chem. Downloaded from www.nrcresearchpress.com by 188.143.235.115 on 09/06/12
For personal use only.

If the initial concentration of $H_2S_2O_7$ is n_a it will react with n_a moles of water, so that at the conductivity minimum, when n_b moles of V_2O_5 have been added, the system contains $2n_b$ moles of $HVO(HSO_4)_4$ and $3n_b - n_a$ moles of water.

For the titration of a weak acid, such as $HVO(HSO_4)_4$ ($K_a \simeq 1 \times 10^{-2}$), with water a conductivity minimum is expected at $r = n_{H_2O}/n_{HA}$, the number of moles of added water to moles of acid = 0.42 (9) so that for an initial concentration of the acid $HVO(HSO_4)_4 = 2n_b$

[37] $$n_{H_2O}/n_{HVO(HSO_4)_4} = (3n_b - n_a)/2n_b = 0.42.$$

Hence $$r = n_b/n_a = 0.46,$$

which is quite close to the observed minimum.

Thus in both the titration of NH_4VO_3 with dilute oleum and in the titration of V_2O_5 with dilute oleum the positions of the conductivity minima are consistent with the formation of $HVO(HSO_4)_4$, a weak acid with $K_a \simeq 1 \times 10^{-2}$ mole kg^{-1}, and thus confirm the previous results.

The results obtained in oleum do not give any evidence for the dimer $V_2O_3(HSO_4)_4$. This is consistent with the fact that the equilibrium

[38] $$2VO(HSO_4)_3 + H_2O \leftrightharpoons V_2O_3(HSO_4)_4 + 2H_2SO_4$$

would be expected to lie well over to the left-hand side in oleum.

EXPERIMENTAL

The method of carrying out cryoscopic and conductivity measurements and the methods of calculating ν and γ have been described previously (10).

V_2O_5 and NH_4VO_3 were commercial samples of at least 99% purity (Anderson Chemical Company) and the phosphorus compounds were also obtained from commercial sources (Alpha Inorganics Inc.). The compounds were dried at 120°.

ACKNOWLEDGMENTS

We thank the National Research Council of Canada for generous financial assistance.

REFERENCES

1. E. J. ARLMAN. Rec. Trav. Chim. **56**, 919 (1937).
2. J. W. MELLOR. A comprehensive treatise of inorganic chemistry and theoretical chemistry. Vol. IV. Longmans, Green & Co., Inc., New York and Toronto. 1939. p. 821.
3. E. HAYEK and A. ENGELBRECHT. Monatsh. **80**, 640 (1949).
4. A. A. WOOLF. Chem. Ind. London, 4113 (1954).
5. H. C. MISHRA and M. C. R. SYMONS. J. Chem. Soc. 4411 (1962).
6. R. J GILLESPIE, J. GRAHAM, E. D. HUGHES, C. K. INGOLD, and E. R. A. PEELING. J. Chem. Soc. 2504 (1950).
7. D. J. MILLEN. J. Chem. Soc. 2600 (1950).
8. R. J. GILLESPIE, E. A. ROBINSON, and C. SOLOMONS. J. Chem. Soc. 4320 (1960).
9. R. H. FLOWERS, R. J. GILLESPIE, and E. A. ROBINSON. Can. J. Chem. **38**, 1363 (1960).
10. R. J. GILLESPIE, R. KAPOOR, and E. A. ROBINSON. Can. J. Chem. This issue.

Can. J. Chem. Downloaded from www.nrcresearchpress.com by 188.143.235.115 on 09/06/12
For personal use only.

Can. J. Chem. Downloaded from www.nrcresearchpress.com by 210.87.254.5 on 09/05/12
For personal use only.

AUTOMATIC DIRECT ANALYSIS OF A_2B_2 NUCLEAR MAGNETIC RESONANCE SPECTRA

T. K. Lim, A. Taurins, and M. A. Whitehead
Theoretical Chemistry Laboratory, McGill University, Montreal, Quebec
Received December 3, 1965

ABSTRACT

A method for complete direct analysis of A_2B_2 n.m.r. spectra is described. The number of possible combinations of spectral lines is reduced from 1 663 200 to 128 by classifying the lines into six pairs. The method is equally effective in analyzing both overlapping and non-overlapping line systems. The n.m.r. spectra of phenazine, 2,3-dimethylquinoxaline, thianthrene, naphthalene, and *o*-dichlorobenzene are analyzed; they give theoretical spectra which agree well with the observed spectra.

INTRODUCTION

The interpretation of A_2B_2 n.m.r. spectra has been discussed (1–3) for cases in which the chemical shift and the coupling constants are of comparable size, so that strong coupling is possible. With the spin coupling constants given as J_{AA}, J_{AB}, etc., two constants K and M were defined as $K = J_{AA} + J_{BB}$ and $M = J_{AA} - J_{BB}$ and the assumption was made that $K = -M$.

When the solution of the secular equation was considered in detail, practical equations correlating the spectrum and parameters were developed, and these gave analyses of A_2B_2 spectra which reproduced the experimental spectra quite well (4–9). When the 24 spectral lines do not overlap, the computer program by Whitman (10) can be used to solve the spectra, but it presents ambiguities in choosing and extracting the experimental lines, especially when they are closely spaced.

The method described herein extends the correlation between the spectrum and parameters, and permits a complete direct mechanical analysis of A_2B_2 spectra. The number of possible combinations of spectral lines is reduced from 1 663 200 to 128, by classifying six pairs of lines instead of four groups. Assigning six pairs is much easier, and since these lines are close together or overlapping, less ambiguities occur than when four groups are considered. The present method also allows several best assignments for each compound, thus avoiding the influence of experimental errors.

THEORY

An A_2B_2 system, under the selection rule, gives a symmetrical theoretical spectrum of 28 lines, of which 4 are combination transitions corresponding to the change of spin of three or four nuclei simultaneously. This type of transition is always weak, and can be neglected. The remaining 12 possible transitions of the half spectrum are summarized in Fig. 1 (1–4).

The 24 fundamental transitions are summarized in Fig. 2 according to their components of angular momentum, while the corresponding transition energies and intensities are shown in Table I.

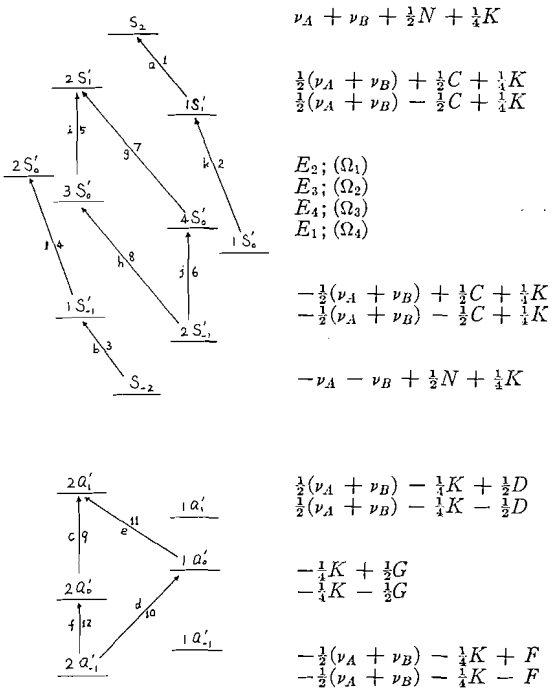


FIG. 1. The 12 permitted transitions and corresponding energies of the A_2B_2 half-spectrum. The numbers are the Pople notation, while the letters are the Dischler notation.

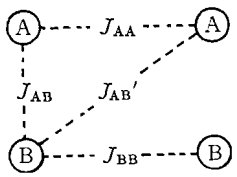
TABLE I

Summary of transitions and intensities

		Transitions	Energies relative to center (c/s)	Intensities*
a	1	$1S_1' \rightarrow S_2$	$(C+N)/2$	$1-N/C$
b	3	$S_{-2} \rightarrow 1S_{-1}'$	$(C-N)/2$	$1+N/C$
c†	9	$2a_0 \rightarrow 2a_1'$	$(D+G)/2$	$\sin^2(\theta-\Psi)$
d†	10	$2a_{-1} \rightarrow 1a_0'$	$(F+G)/2$	$\cos^2(\theta+\chi)$
e†	11	$1a_0 \rightarrow 2a_1'$	$(D-G)/2$	$\cos^2(\theta-\Psi)$
f†	12	$2a_{-1} \rightarrow 2a_0'$	$(F-G)/2$	$\sin^2(\theta+\chi)$
g	7	$4S_0 \rightarrow 2S_1'$	$\frac{1}{2}C+\frac{1}{4}K-\Omega_3$	$[(A_{31}+A_{32})\cos\Phi + (A_{32}+A_{34})\sin\Phi]^2$
h	8	$2S_{-1}' \rightarrow 3S_0'$	$\frac{1}{2}C-\frac{1}{4}K+\Omega_2$	$[(A_{22}+A_{24})\cos\Phi - (A_{21}+A_{22})\sin\Phi]^2$
i	5	$3S_0' \rightarrow 2S_1'$	$\frac{1}{2}C+\frac{1}{4}K-\Omega_2$	$[(A_{21}+A_{22})\cos\Phi + (A_{22}+A_{24})\sin\Phi]^2$
j	6	$2S_{-1}' \rightarrow 4S_0'$	$\frac{1}{2}C-\frac{1}{4}K+\Omega_3$	$[(A_{32}+A_{34})\cos\Phi - (A_{31}+A_{32})\sin\Phi]^2$
k	2	$1S_0' \rightarrow 1S_1'$	$-\frac{1}{2}C+\frac{1}{4}K-\Omega_4$	$[(A_{43}+A_{44})\cos\Phi - (A_{41}+A_{42})\sin\Phi]^2$
l	4	$1S_{-1}' \rightarrow 2S_0'$	$-\frac{1}{2}C-\frac{1}{4}K+\Omega_1$	$[(A_{11}+A_{12})\cos\Phi + (A_{12}+A_{14})\sin\Phi]^2$

*The total sum of intensity of the half-spectrum is 8.
†If M takes negative value, then D and F interchange and i, e, c, and d lines interchange as well as e and f lines.

In the figures and tables, the following nomenclature is used: A and B are the protons, and J_{AA}, J_{AB}, etc. are the spin coupling constants,



Can. J. Chem. Downloaded from www.nrcresearchpress.com by 210.87.254.5 on 09/05/12
For personal use only.

$$N = J_{AB} + J_{AB}', \qquad K = J_{AA} + J_{BB} \geqslant 0,$$
$$L = J_{AB} - J_{AB}' \geqslant 0, \qquad M = J_{AA} - J_{BB} \geqslant 0;$$
$$\nu_0\delta = |\nu_A - \nu_B|,$$

where ν_A and ν_B are the line frequencies in the absence of spin coupling and $\nu_0\delta$ is the chemical shift in cycles per second.

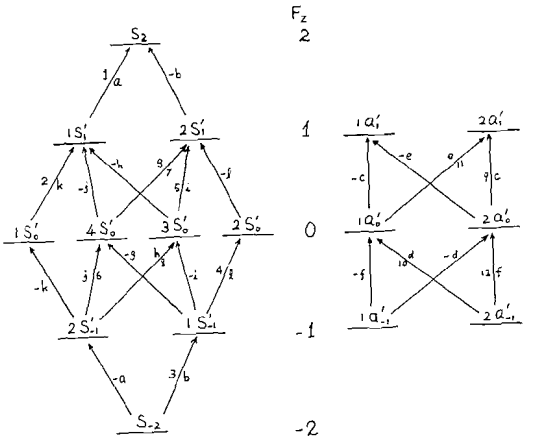


FIG. 2. The 24 possible transitions of the A_2B_2 system according to their components of angular momentum. The symmetric transitions are shown on the left half of the figure and the antisymmetric transitions on the right.

$$C = \sqrt{[(\nu_0\delta)^2 + N^2]}$$
$$D = \sqrt{[(\nu_0\delta + M)^2 + L^2]}$$
$$F = \sqrt{[(\nu_0\delta - M)^2 + L^2]}$$
$$G = \sqrt{(M^2 + L^2)}.$$

Four angles are defined in terms of which the energies E_n and wave functions ζ_n of the system can be expressed.

$$\sin\theta = \sqrt{[(1/2)(1 - M/G)]}$$
$$\sin\chi = \sqrt{\{(1/2)[1 - (\nu_0\delta - M)/F]\}}$$
$$\sin\Psi = \sqrt{\{(1/2)[1 - (\nu_0\delta + M)/D]\}}$$
$$\sin\Phi = \sqrt{[(1/2)(1 - \nu_0\delta/C)]}\,\frac{N}{|N|}.$$

The Ω_i s in Fig. 3 are the eigenvalues of the 4×4 S_0 submatrix, whereas the A_i s are their corresponding eigenvectors; by definition, $\Omega_1 \geqslant \Omega_2 \geqslant \Omega_3 \geqslant \Omega_4$ (4).

In the interpretation of A_2B_2 spectra by Pople *et al.* (2), the difficulty of solving the 4×4 S_0 submatrix was avoided by making all the interpretations from transitions other than those involving S_0 states, and by assuming that $K = -M$. The correlations between spectrum and parameters are as follows:

[1] $$N = a - b$$

[2] $$\nu_0\delta = \sqrt{(4ab)}$$

[3] $$c + e = \sqrt{[(\nu_0\delta + M)^2 + L^2]}$$

[4] $$c - e = \sqrt{(M^2 + L^2)}$$

Can. J. Chem. Downloaded from www.nrcresearchpress.com by 210.87.254.5 on 09/05/12
For personal use only.

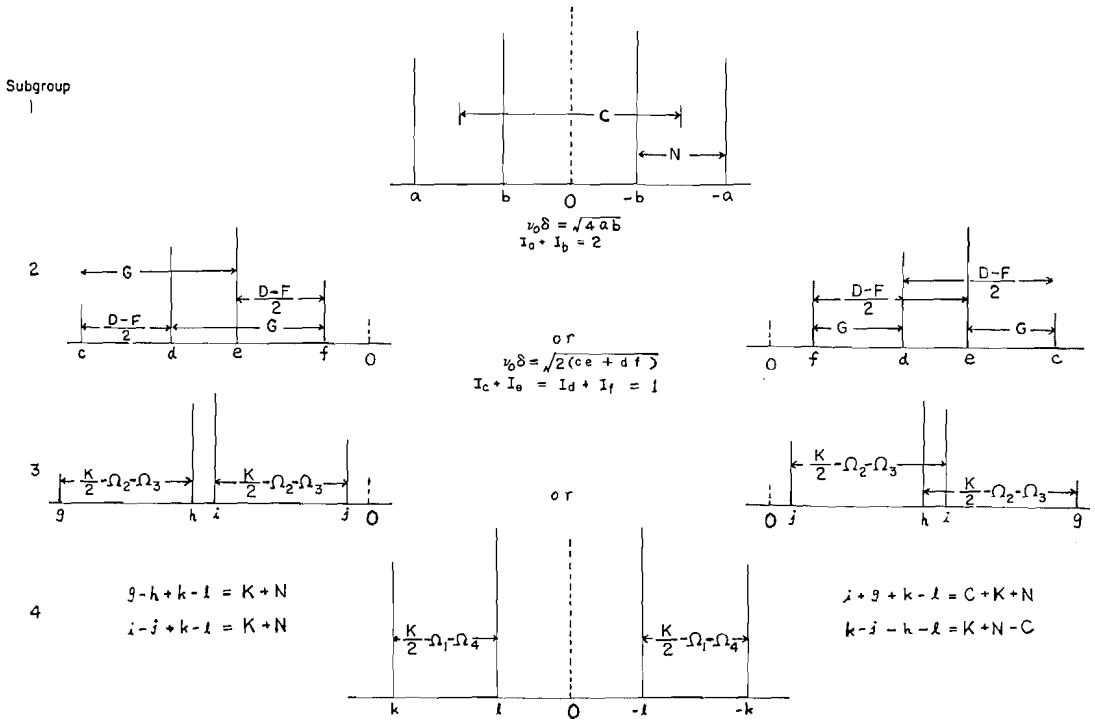


FIG. 3. The correlation of lines and parameters of the A_2B_2 spectrum.

$$M = \frac{2ce}{\nu_0\delta} - \frac{\nu_0\delta}{2} \quad [5]$$

$$L = \sqrt{[(c-e)^2 - M^2]} \quad [6]$$

$$K = -M. \quad [7]$$

Dischler *et al.* (4, 5) avoided the assumption that $K = -M$, by dividing the half-spectrum into four groups and expressing K explicitly. The resulting correlations were:

$$N = a - b \quad [1]$$

$$\nu_0\delta = \sqrt{(4ab)} = \sqrt{[2(ce + df)]} \quad [8]$$

$$M = \frac{ce - df}{\nu_0\delta} \quad [9]$$

$$L = \sqrt{[(c-e)^2 - M^2]} = \sqrt{[(d-f)^2 - M^2]} \quad [10]$$

$$K = k - l - N + \tfrac{1}{2}(g - h + i - j) \quad [11]$$

$$c \geqslant d \geqslant e \geqslant f \quad [12]$$

$$g \geqslant h \geqslant i \geqslant j \quad [13]$$

$$I_a : I_b = b : a \quad [14]$$

$$I_a + I_b = 2 \quad [15]$$

Can. J. Chem. Downloaded from www.nrcresearchpress.com by 210.87.254.5 on 09/05/12
For personal use only.

[16] $$I_c + I_e = I_d + I_f = 1$$

[17] $$2 \geqslant I_g + I_h + I_i + I_j \geqslant 1$$

[18] $$2 \leqslant I_k + I_c \leqslant 3$$

where eqs. [14] through [18] are intensity correlations: eqs. [12] and [13] are incorrect, for Dischler's equations (5, 6) are:

$$c - e = d - f \geqslant 0 = G,$$
$$c + f = d + e \geqslant 0 = \tfrac{1}{2}(D + F),$$
$$c - d = e - f \geqslant 0 = \tfrac{1}{2}(D - F).$$

Hence while it is true that $c \geqslant d$ and $e \geqslant f$, the relationship between d and e is not specified and d could be greater than, equal to, or less than e. This is also true of h and i. We shall therefore use eqs. [12a] and [13a] in this paper.

[12a] $$c \geqslant d, \qquad e \geqslant f$$

[13a] $$g \geqslant h, \qquad i \geqslant j$$

These four characteristic groups possess 4, 8, 8, and 4 lines, respectively, and can be further divided symmetrically into A and B parts with an equal number of lines. The assignment of the groups is given in Fig. 3.

To correlate the lines and parameters, the mean value of equivalent sets is taken rather than the absolute value of either set (5), and the half-spectrum is divided into six pairs. The correlation between these six pairs and the four groups is given in Fig. 4.

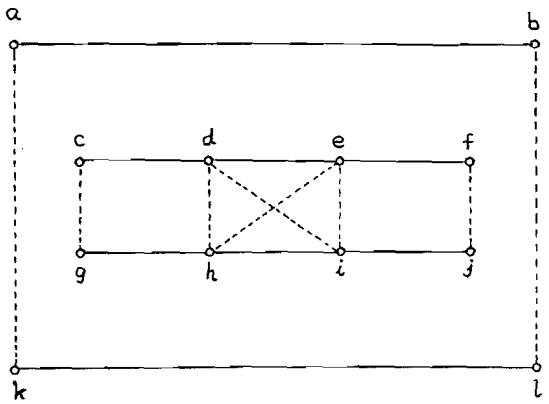


FIG. 4. Correlation between the classification of six pairs of lines in the present work and the four groups of Dischler. Each solid line represents one group while each dashed line represents one pair. The pairing in the center part of the figure should be either $d \ldots h$ and $e \ldots i$ or $d \ldots i$ and $e \ldots h$.

The possible permutations of the assignment of each spectrum using four groups are $2^3 \cdot C_2^{12} \cdot C_4^{10} \cdot C_4^6 = 1\,663\,200$; the number reduces to $2^7 = 128$ using six pairs. This greatly facilitates the interpretation and the calculation of the spectrum.

Besides the arrangement shown in Fig. 3, the possibility also exists of interchanging a and b, and k and l simultaneously, since N is positive or negative according to whether a is greater or less than b. Interchange of d and e, and h and i, is also possible, since we have the possibility of h greater or less than i depending on their values. Thus there are four possible arrangements similar to that in Fig. 3, all of which must be calculated separately and compared with the experimental results, as they cannot be distinguished in the course of the computer program.

Can. J. Chem. Downloaded from www.nrcresearchpress.com by 210.87.254.5 on 09/05/12
For personal use only.

The complete set of equations becomes:

$$[19] \qquad \nu_0\delta = \frac{\sqrt{(4ab)} + \sqrt{[2(ce - df)]}}{2}$$

$$[20] \qquad C = (\tfrac{1}{4})(2a + 2b + g + h + i + j)$$

$$[21] \qquad N = \pm\sqrt{[C^2 - (\nu_0\delta)^2]}$$

$$[9] \qquad M = \frac{ce - df}{\nu_0\delta}$$

$$[22] \qquad K = k - l - N + \frac{C}{2} + \frac{1}{4}(g - 3h + i - 3j)$$

$$[23] \qquad L = \sqrt{\left[\left(\frac{c - e + d - f}{2}\right)^2 - M^2\right]}$$

$$[12a] \qquad c \geqslant d, \qquad e \geqslant f$$

$$[13a] \qquad g \geqslant h, \qquad i \geqslant j$$

with the same intensity correlation equations, eqs. [14–18], as before.

The change to equations [12*a*] and [13*a*] is made because there is no reason to assume that d must be greater than e, or that h must be greater than i. For example if G is less than $(D - F)/2$, then e must be greater than d (Fig. 3 subgroup 2). Equation [10] was replaced by eq. [23] because if $c - e$ is equal to $d - f$, then it is more reasonable to adjust the experimental error by considering all the 4 lines in group 2 rather than only two lines. Equation [22] was used to adjust the experimental error. This equation is easy to derive from Fig. 3 by adding or subtracting the expressions of subgroup 4.

The method used to assign the six pairs of lines in the spectrum is as follows (see Fig. 3).

Step 1.—The first pair assigned has the highest intensity of the six pairs and, depending on whether N is positive or negative, will consist of the lines b and l or a and k.

Step 2.—Another intense pair of lines is then chosen and will consist of the two lines not assigned to the first pair, namely a and k or b and l. The intensity of this pair and of the pair assigned below in step 6 is often very close. Therefore the intensity sum is of importance. The total intensity of one line from step 1 and one line from step 2 should equal 2, the sum of the remaining two lines being nearly 2. Furthermore from eq. [8] it is known that this second pair of lines should be two or three pairs away from the first pair.

Step 3.—The innermost lines (those nearest to the center of the spectrum) are then assigned as the lines f and j; they are generally of low intensity.

Step 4.—The outermost lines (those furthest from the center of the spectrum) are assigned as c and g; they are the least intense lines.

Step 5.—The remaining two pairs are of medium to high intensity; one pair lies between the two high intensity lines assigned in steps 1 and 2 above and possesses several possible assignments such as (d,h) or (d,i) for $i > h$ or $h > i$ when $e > d$, or such as (e,h) or (e,i) for $i > h$ or $h > i$ when $d > e$.

Step 6.—The only remaining pair of lines will also possess several possible assignments such as (e,h) or (e,i) when $e \geqslant d$ and (d,h) or (d,i) when $d > e$.

The initial assignment of the lines under these conditions is arbitrary, but the computer program considers each arbitrary assignment and calculates the correct assignment.

Can. J. Chem. Downloaded from www.nrcresearchpress.com by 210.87.254.5 on 09/05/12
For personal use only.

Can. J. Chem. Downloaded from www.nrcresearchpress.com by 210.87.254.5 on 09/05/12
For personal use only.

MECHANICAL CALCULATION

The computer program for the IBM 7040 was coded for complete direct analysis of A_2B_2 spectra. There are 128 possible permutations of the 12 lines in each spectrum. Defining

$$\Delta_i = |\sqrt{[2(c_i e_i + d_i f_i)]} - \sqrt{(4a_i b_i)}|,$$

where the subscript i stands for the ith permutation, then the permutation with the smallest Δ_i is chosen as the best assignment. To avoid the influence of experimental error, the permutation j, if any, is also considered as a "possible best" permutation if the difference $\Delta_j - \Delta_i$ is within the range of 0.02 c/s. (This value is adjustable when necessary.) After the "possible best" permutations have been assigned, four different cases, (1) $N > 0$ and $h > i$, (2) $N > 0$ and $i > h$, (3) $N < 0$ and $h > i$, and (4) $N < 0$ and $i > h$, are considered simultaneously. Note that the cases for $d > e$ or $e > d$ have been automatically defined during the sorting procedure of the "possible best" assignments. Before calculating these four cases, the parameters K, L, M, N and the chemical shift $\nu_0\delta$ are calculated from the required equations given above. When the values of the chemical shift and the parameters have been calculated, a subprogram consisting of

(i) the calculation of the Hamiltonian matrix,

(ii) the diagonalization,

(iii) the sorting of the energy levels and their corresponding eigenvectors, and

(iv) the calculation of intensities and positions is used for each case, and the calculated results are listed and compared with the observed spectrum. The corresponding values of chemical shifts, parameters, and coupling constants for the four cases are printed. Finally, the theoretical and experimental spectra can be plotted if desired.

RESULTS AND DISCUSSION

The method has been used to investigate the spectra of the following A_2B_2 compounds: phenazine, 2,3-dimethylquinoxaline, thianthrene, naphthalene, and *o*-dichlorobenzene. The theoretical calculations compare well with the observed spectra. Only the spectrum of *o*-dichlorobenzene does not involve the overlap of the spectral lines, so that the method was tested on both overlapping line and non-overlapping line systems, and appears equally valid for both systems. See Tables II and III.

The spectra of phenazine, 2,3-dimethylquinoxaline, thianthrene, and naphthalene were measured on the Varian A-60 spectrometer in these laboratories; the *o*-dichlorobenzene spectrum is from the published work of Whitman (10).

The experimentally observed spectra are not labelled in the tables; this is because the lines take the sequence of letters appropriate to the case to which the observed spectra is being compared.

As stated, the calculations were made in two main steps (i) the calculation of the parameters $\nu_0\delta$, J_{AA} etc. and (ii) the calculation of the frequencies and intensities. The formulae for calculating the frequencies and intensities are essentially the same as in the Dischler method and therefore the results should be nearly the same, as they are. The most important difference between this method and that of Dischler is that this method provides a possible way of carrying out a mechanical calculation of all the parameters, so that all possible assignments can be fully considered and analyzed; this seems very difficult to do in Dischler's method. Pople's method using the $K = -M$ approximation usually gives worse correlation results for a few lines although generally the results seem good. Table IV gives the comparable results from these three methods, all the calculations being made on the same spectra, in this laboratory, using the formulae in the text.

Can. J. Chem. Downloaded from www.nrcresearchpress.com by 210.87.254.5 on 09/05/12
For personal use only.

TABLE II

Comparison of possible assignments in *o*-dichlorobenzene, where there is no overlap of lines

	Energies relative to center (c/s)				Intensities† (total sum = 8)					
	$N > 0$		$N < 0$			$N > 0$		$N < 0$		
Δ_i (c/s)	$h > i$	$i > h$	$h > i$	$i > h$	Obs.*	$h > i$	$i > h$	$h > i$	$i > h$	Obs.
0.249	(*g*) 17.023	(*g*) 18.299	(*g*) 17.356	(*g*) 18.509	17.380	0.050	0.033	0.051	0.038	0.044
	(*c*) 16.450	(*c*) 16.450	(*c*) 16.450	(*c*) 16.450	16.710	0.049	0.049	0.049	0.049	0.046
	(*a*) 13.936	(*a*) 13.936	(*b*) 13.936	(*b*) 13.936	13.780	0.059	0.059	0.059	0.059	0.560
	(*k*) 13.306	(*k*) 13.433	(*l*) 12.768	(*l*) 12.739	13.300	0.490	0.476	0.545	0.548	0.516
	(*h*) 9.631	(*i*) 8.688	(*h*) 11.051	(*i*) 7.182	10.040	0.636	0.671	0.489	0.873	0.481
	(*d*) 9.906	(*d*) 9.906	(*d*) 9.906	(*d*) 9.906	9.700	0.589	0.589	0.589	0.589	0.562
	(*i*) 8.456	(*h*) 9.400	(*i*) 7.036	(*h*) 10.906	8.390	0.662	0.682	0.863	0.512	0.698
	(*e*) 6.850	(*e*) 6.850	(*e*) 6.850	(*e*) 6.850	6.800	0.951	0.951	0.951	0.951	0.964
	(*b*) 4.151	(*b*) 4.151	(*a*) 4.151	(*a*) 4.151	4.130	1.541	1.541	1.541	1.541	1.559
	(*l*) 3.521	(*l*) 3.506	(*k*) 4.119	(*k*) 4.442	3.540	1.829	1.837	1.425	1.177	1.834
	(*j*) 1.064	(*j*) −0.211	(*j*) 0.731	(*j*) −0.421	0.720	0.331	0.300	0.627	0.852	0.312
	(*f*) 0.306	(*f*) 0.306	(*f*) 0.306	(*f*) 0.306	0.410	0.411	0.411	0.411	0.411	0.425
0.258	(*g*) 17.292	(*g*) 18.291	(*g*) 17.389	(*g*) 18.284	17.380	0.048	0.035	0.053	0.042	0.044
	(*c*) 16.569	(*c*) 16.569	(*c*) 16.569	(*c*) 16.569	16.710	0.051	0.051	0.051	0.051	0.046
	(*a*) 13.811	(*a*) 13.811	(*b*) 13.811	(*b*) 13.811	13.780	0.466	0.466	0.466	0.466	0.560
	(*k*) 13.358	(*k*) 13.471	(*l*) 12.743	(*l*) 12.718	13.300	0.483	0.470	0.546	0.548	0.516
	(*h*) 9.668	(*i*) 8.520	(*h*) 11.047	(*i*) 7.080	9.700	0.638	0.686	0.488	0.875	0.562
	(*d*) 10.081	(*d*) 10.081	(*d*) 10.081	(*d*) 10.081	10.040	0.569	0.569	0.569	0.569	0.481
	(*i*) 8.335	(*h*) 9.483	(*i*) 6.956	(*h*) 10.922	8.390	0.680	0.673	0.686	0.508	0.698
	(*e*) 6.799	(*e*) 6.799	(*e*) 6.799	(*e*) 6.799	6.800	0.949	0.949	0.949	0.949	0.964
	(*b*) 4.191	(*b*) 4.191	(*a*) 4.191	(*a*) 4.191	4.130	1.534	1.534	1.534	1.534	1.559
	(*l*) 3.594	(*l*) 3.581	(*k*) 4.270	(*k*) 4.535	3.540	1.807	1.813	1.363	1.170	1.834
	(*j*) 0.710	(*j*) −0.289	(*j*) 0.614	(*j*) −0.281	0.720	0.343	0.320	0.683	0.856	0.312
	(*f*) 0.311	(*f*) 0.311	(*f*) 0.311	(*f*) 0.311	0.410	0.431	0.431	0.431	0.431	0.425

*The order of the observed lines is governed by the assignment of the lines in the correct column of N and h,i values. Thus since $N > 0$ and $h > i$ are the correct assignments, the observed lines are labelled *g*, *c*, *a*, *k*, *h*, *d*, *i*, *e*, *b*, *l*, *j*, and *f*. This leaves two choices within the experimental error, but when $\Delta_i = 0.249$ $h_{theory} = 9.631$, $h_{exp} = 10.040$ and $d_{theory} = 9.906$ while $d_{exp} = 9.700$; when $\Delta_i = 0.258$ the sequence is correct.

†Sequence of line designations as in appropriate column of energies.

Can. J. Chem. Downloaded from www.nrcresearchpress.com by 210.87.254.5 on 09/05/12
For personal use only.

TABLE III

Comparison of possible cases for spectra with line overlap

Energies relative to center (c/s)					Intensities† (total sum = 8)				
$N > 0$		$N < 0$			$N > 0$		$N < 0$		
$h > i$	$i > h$	$h > i$	$i > h$	Obs.*	$h > i$	$i > h$	$h > i$	$i > h$	Obs.
2,3-Dimethylquinoxaline									
(g) 19.481	(g) 21.103	(g) 19.144	(g) 20.753	19.000	0.060	0.038	0.071	0.049	0.424
(c) 17.966	(c) 17.966	(c) 17.966	(c) 17.966	18.000	0.080	0.080	0.080	0.080	
(a) 16.191	(a) 16.191	(b) 16.191	(b) 16.191	16.500	0.545	0.545	0.545	0.545	1.356
(k) 15.629	(k) 15.726	(l) 15.261	(l) 15.233		0.574	0.564	0.609	0.612	
(h) 12.011	(i) 10.502	(h) 13.076	(i) 9.392	12.000	0.678	0.775	0.568	0.884	1.372
(d) 12.139	(d) 12.139	(d) 12.139	(d) 12.139		0.643	0.643	0.643	0.643	
(i) 10.239	(h) 11.748	(i) 9.174	(h) 12.858	10.000	0.760	0.728	0.864	0.605	1.037
(e) 8.866	(e) 8.866	(e) 8.866	(e) 8.866	8.800	0.920	0.920	0.920	0.920	0.570
(b) 6.059	(b) 6.059	(a) 6.059	(a) 6.059	6.000	1.455	1.455	1.455	1.455	2.438
(l) 5.473	(l) 5.455	(k) 5.818	(k) 5.963		1.636	1.642	1.490	1.415	
(j) 2.769	(j) 1.147	(j) 3.106	(j) 1.497	3.000	0.292	0.252	0.398	0.435	0.804
(f) 3.029	(f) 3.039	(f) 3.039	(f) 3.039		0.357	0.357	0.357	0.357	
Phenazine									
(g) 20.873	(g) 23.036	(g) 21.416	(g) 23.632	21.400	0.091	0.051	0.083	0.050	0.150
(c) 20.153	(c) 20.153	(c) 30.153	(c) 20.153	20.200	0.097	0.097	0.097	0.097	0.165
(a) 18.245	(a) 18.245	(b) 18.245	(b) 18.245	18.000	0.601	0.601	0.601	0.601	1.500
(k) 17.757	(k) 17.852	(l) 17.485	(l) 17.452		0.626	0.617	0.650	0.653	
(h) 14.397	(i) 12.095	(h) 15.021	(i) 11.364	14.500	0.658	0.823	0.612	0.898	1.250
(d) 14.335	(d) 14.335	(d) 14.335	(d) 14.335		0.655	0.655	0.655	0.655	
(i) 11.678	(h) 13.980	(i) 11.054	(h) 14.711	11.800	0.790	0.733	0.868	0.665	1.700
(e) 10.703	(e) 10.703	(e) 10.703	(e) 10.703	10.800	0.903	0.903	0.903	0.903	
(b) 7.830	(b) 7.803	(a) 7.830	(a) 7.830	7.800	1.399	1.399	1.399	1.399	2.400
(l) 7.321	(l) 7.295	(k) 7.604	(k) 7.744		1.519	1.525	1.429	1.376	
(j) 5.202	(j) 3.039	(j) 4.659	(j) 2.443	5.000	0.316	0.250	0.358	0.358	0.850
(f) 4.885	(f) 4.885	(f) 4.885	(f) 4.885		0.345	0.345	0.345	0.345	
Thianthrene									
(g) 17.197	(g) 18.791	(g) 17.222	(g) 18.664	17.700	0.045	0.028	0.051	0.035	0.244
(c) 16.661	(c) 16.661	(c) 16.661	(c) 16.661	16.700	0.045	0.045	0.045	0.045	
(a) 13.722	(a) 13.722	(b) 13.722	(b) 13.722	13.700	0.484	0.484	0.484	0.484	1.145
(k) 13.182	(k) 13.334	(l) 12.676	(l) 12.644		0.510	0.492	0.564	0.567	
(h) 9.595	(i) 8.743	(h) 10.872	(i) 7.397	10.200	0.669	0.708	0.523	0.881	1.375
(d) 9.854	(d) 9.854	(d) 9.854	(d) 9.854		0.618	0.618	0.618	0.618	
(i) 8.505	(h) 9.357	(i) 7.228	(h) 10.703	8.200	0.699	0.717	0.868	0.552	0.799
(e) 7.061	(e) 7.061	(e) 7.061	(e) 7.061	7.200	0.955	0.955	0.955	0.955	0.671
(b) 4.378	(b) 4.378	(a) 4.378	(a) 4.378	4.200	1.516	1.516	1.516	1.516	2.588
(l) 3.785	(l) 3.785	(k) 4.325	(k) 4.682		1.773	1.781	1.430	1.166	
(j) 0.903	(j) −0.691	(j) 0.878	(j) −0.564	0.500	0.304	0.273	0.563	0.799	1.179
(f) 0.254	(f) 0.524	(f) 0.254	(f) 0.254		0.382	0.382	0.382	0.382	

*The observed lines carry the line designations of the appropriate theoretical case.
†Sequence of line designations as in appropriate column of energies.

TABLE IV

Comparison of theoretical and experimental spectra

	Energies relative to center (c/s)				Intensities (total sum = 8)			
	Dischler*	Pople*	Present	Obs.	Dischler*	Pople*	Present	Obs.
o-Dichlorobenzene								
(*g*)	16.671	17.03	17.292	17.380	0.053	0.05	0.048	0.045
(*c*)	16.388	16.71	16.569	16.710	0.044	0.05	0.051	0.046
(*a*)	14.228	13.78	13.811	13.780	0.419	0.46	0.466	0.560
(*k*)	13.293	13.25	13.358	13.300	0.468	0.48	0.483	0.516
(*h*)	9.460	9.59	9.668	9.700	0.603	0.63	0.638	0.562
(*d*)	9.662	9.93	10.081	10.040	0.575	0.58	0.569	0.481
(*i*)	8.543	8.32	8.335	8.390	0.592	0.67	0.680	0.698
(*e*)	6.618	6.80	6.799	6.800	0.956	0.95	0.949	0.964
(*b*)	3.775	4.13	4.191	4.130	1.581	1.54	1.534	1.559
(*l*)	3.069	3.52	3.594	3.540	1.936	1.82	1.807	1.834
(*j*)	1.332	0.88	0.710	0.720	0.345	0.34	0.343	0.312
(*f*)	−0.108	0.02	0.311	0.410	0.425	0.42	0.431	0.425
2,3-Dimethylquinoxaline								
(*g*)	19.382	18.54	19.481	19.000	0.062	0.09	0.060	0.424
(*c*)	17.966	18.00	17.966	18.00	0.080	0.09	0.080	
(*a*)	16.191	16.50	16.191	16.500	0.545	0.53	0.545	1.356
(*k*)	15.623	15.85	15.629		0.575	0.57	0.574	
(*h*)	12.031	12.51	12.011	12.000	0.674	0.61	0.678	1.372
(*d*)	12.139	12.39	12.139		0.643	0.62	0.643	
(*i*)	10.219	9.99	10.239	10.000	0.758	0.73	0.760	1.037
(*e*)	8.866	8.80	8.866	8.800	0.920	0.91	0.920	0.0570
(*b*)	6.059	6.00	6.059	6.000	1.455	1.47	1.455	2.438
(*l*)	5.475	5.41	5.473		1.635	1.65	1.636	
(*j*)	2.868	3.96	2.769	3.000	0.295	0.36	0.292	0.804
(*f*)	3.039	3.19	3.039		0.357	0.38	0.357	
Phenazine								
(*g*)	20.983	20.63	20.873	21.400	0.088	0.08	0.091	0.150
(*c*)	20.153	20.20	20.153	20.200	0.097	0.08	0.097	0.165
(*a*)	18.289	18.00	18.245	18.000	0.599	0.60	0.601	1.500
(*k*)	17.790	17.47	17.757		0.625	0.63	0.626	
(*h*)	14.381	14.07	14.397	14.500	0.661	0.68	0.658	1.250
(*d*)	14.335	13.91	14.335		0.655	0.69	0.655	
(*i*)	11.719	11.73	11.678	11.800	0.790	0.79	0.790	1.700
(*e*)	10.703	10.80	10.703	10.800	0.903	0.92	0.903	
(*b*)	7.811	7.80	7.830	7.800	1.401	1.40	1.399	2.400
(*l*)	7.293	7.28	7.321		1.523	1.52	1.519	
(*j*)	5.117	5.17	5.202	5.000	0.312	0.29	0.316	0.850
(*f*)	4.885	4.51	4.885		0.345	0.31	0.345	
Thianthrene								
(*g*)	17.275	17.43	17.197	17.700	0.043	0.03	0.045	0.244
(*c*)	16.661	16.70	16.661	16.700	0.045	0.03	0.045	
(*a*)	13.722	13.70	13.722	13.700	0.484	0.47	0.484	1.145
(*k*)	13.189	12.73	13.182		0.509	0.53	0.510	
(*h*)	9.581	8.90	9.595	10.200	0.672	0.74	0.669	1.375
(*d*)	9.854	8.94	9.854		0.618	0.72	0.618	
(*i*)	8.519	9.00	8.505	8.200	0.699	0.67	0.699	0.799
(*e*)	7.061	7.20	7.061	7.200	0.955	0.97	0.955	0.671
(*b*)	4.378	4.20	4.378	4.200	1.516	1.53	1.516	2.588
(*l*)	3.784	3.51	3.785		1.773	1.84	1.773	
(*j*)	0.825	0.48	0.903	0.500	0.302	0.20	0.304	1.179
(*f*)	0.254	−0.56	0.254		0.382	0.28	0.382	
Naphthalene								
(*g*)	20.673	20.24	20.575	21.500	0.078	0.08	0.080	0.126
(*c*)	20.124	20.00	20.124	20.000	0.080	0.08	0.080	
(*a*)	17.725	17.20	17.725	17.200	0.596	0.62	0.596	1.212
(*k*)	17.232	16.87	17.228		0.622	0.64	0.623	
(*h*)	13.799	13.77	13.821	13.728	0.679	0.68	0.675	1.238
(*d*)	13.728	13.73	13.728		0.679	0.68	0.679	
(*i*)	11.451	11.22	11.429	11.700	0.795	0.82	0.793	1.672
(*e*)	10.474	10.50	10.474	10.500	0.920	0.92	0.920	
(*b*)	7.525	7.80	7.525	7.800	1.404	1.38	1.404	2.820
(*l*)	7.007	7.38	7.008		1.531	1.47	1.530	
(*j*)	4.577	4.75	4.675	4.000	0.295	0.30	0.298	0.824
(*f*)	4.078	44.23	4.078		0.321	0.32	0.321	

*Calculated from the mean value method of Dischler and Pople's formulae as given in the text.

Can. J. Chem. Downloaded from www.nrcresearchpress.com by 210.87.254.5 on 09/05/12
For personal use only.

The calculation on *o*-dichlorobenzene gives two possible best assignments within the limit $\Delta_i < 0.3$ c/s. Their chemical shifts and coupling constants are given in Table V as A and B.

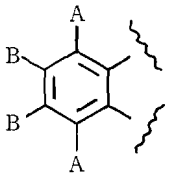
It should be noted that equations

$$K = J_{AA} + J_{BB} \geqslant 0, \qquad M = J_{AA} - J_{BB} \geqslant 0$$

are used in this paper instead of Pople's equations

$$K = J_{AA} + J_{BB} \geqslant 0, \qquad M = J_{AA} - J_{BB} \leqslant 0.$$

Therefore Pople's assumption of $K = -M$ (i.e., $J_{AA} = 0$) becomes $K = M$ (i.e. $J_{BB} = 0$) when the equations of this new method are used. This results in the exchange of the nuclei A and B. For example, the positions of nuclei A and B in *o*-disubstituted benzene for Pople's paper and the present paper are respectively



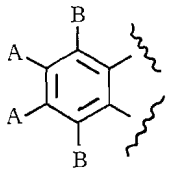
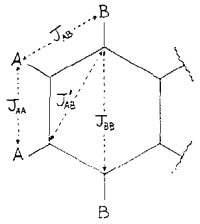


TABLE V

Assignments of chemical shift and coupling constants



Compounds	$\nu_0\delta$	J_{AA}	J_{BB}	J_{AB}	J_{AB}'
(A) *o*-Dichlorobenzene	15.212	7.300	0.092	8.063	1.720
(B) *o*-Dichlorobenzene	15.217	7.483	0.286	8.114	1.506
(C) 2,3-Dimethylquinoxaline	19.809	6.836	0.675	8.407	1.726
(D) Phenazine	23.904	6.295	0.202	8.819	1.596
(E) Thianthrene	15.502	7.542	0.115	7.713	1.631
(F) Naphthalene	23.098	6.738	0.036	8.572	1.629

A and the first part of Table II are calculated with $\Delta_i = 0.249$ c/s, while B and the second part of Table II are calculated with $\Delta_i = 0.258$ c/s. The comparison of the theoretical and experimental results are given in Table II. It is clear that the results for the $N > 0$ and $h > i$ case are preferable. Although the theoretical results of both assignments are within the range of experimental error, assignment B in Table V is preferable because the h and d lines are in the same sequence of energies in the theoretical and experimental spectra, whereas in assignment A in Table V the h and d lines are in the reverse sequence of energies in the experimental and theoretical spectra. These are the cases $N > 0$ and $h > i$ in Table II.

In the other four compounds, only one best assignment is found for each compound: 2,3-dimethylquinoxaline $\Delta_i = 0.182$ c/s, phenazine $\Delta_i = 0.412$ c/s, naphthalene $\Delta_i = 0.135$ c/s, and thianthrene $\Delta_i = 0.662$ c/s, and their spectra all have overlapping lines.

Can. J. Chem. Downloaded from www.nrcresearchpress.com by 210.87.254.5 on 09/05/12
For personal use only.

The assignments of these compounds are given in Table III. In all cases the best assignment requires $N > 0$ and $h > i$ as was assumed by Dischler.

The experimental spectra of 2,3-dimethylquinoxaline, phenazine, and thianthrene, as well as the theoretically calculated spectra, are shown in Figs. 5–7.

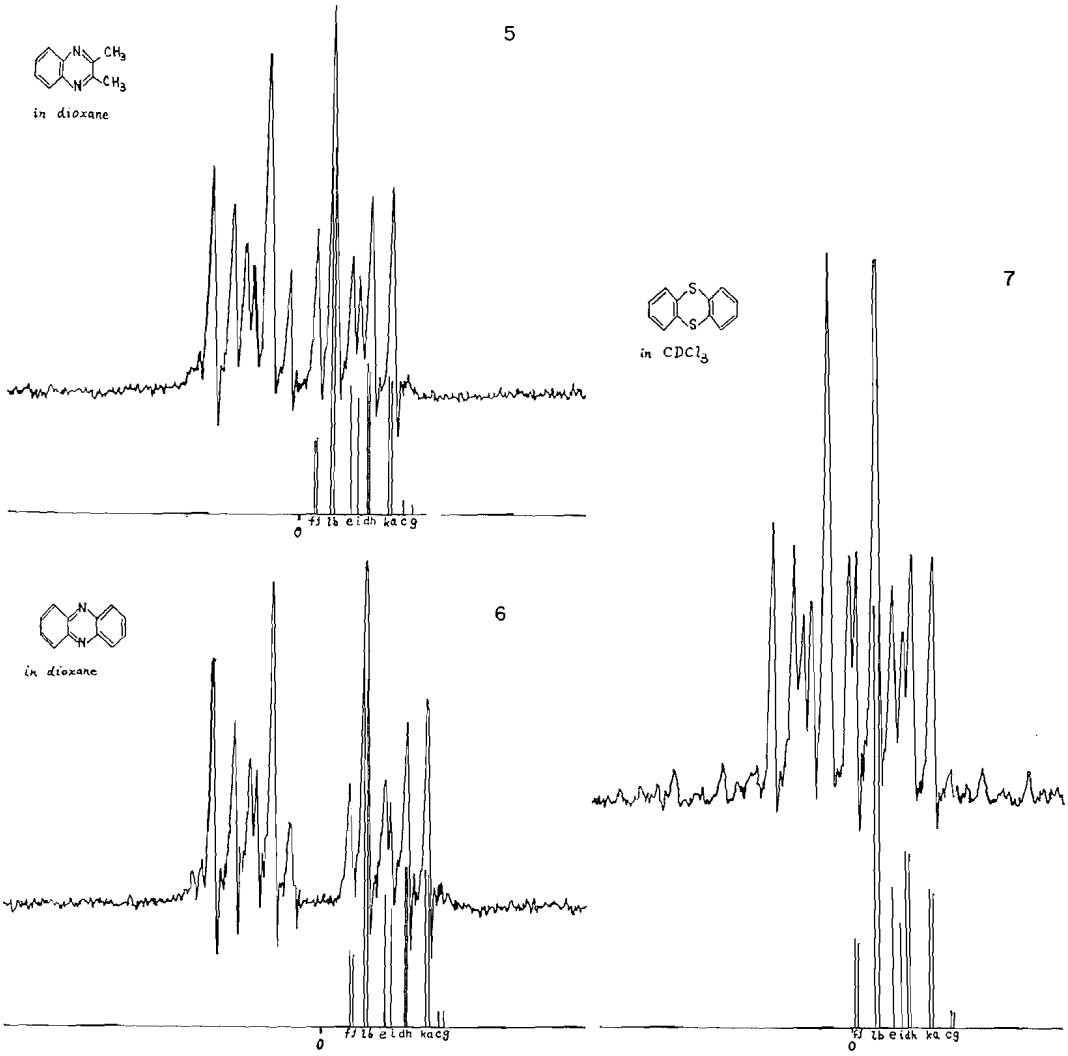


FIG. 5. Experimental and theoretical spectra of 2,3-dimethylquinoxaline.
FIG. 6. Experimental and theoretical spectra of phenazine.
FIG. 7. Experimental and theoretical spectra of thianthrene.

ACKNOWLEDGMENTS

We wish to thank the National Research Council of Canada for financial support of this research, and the McGill Computing Centre for use of its facilities. We wish to thank the referees for helpful comments.

Can. J. Chem. Downloaded from www.nrcresearchpress.com by 210.87.254.5 on 09/05/12
For personal use only.

REFERENCES

1. H. M. McCONNELL, A. D. McLEAN, and C. A. REILLY. J. Chem. Phys. **23**, 1152 (1955).
2. J. A. POPLE, W. G. SCHNEIDER, and H. J. BERNSTEIN. Can. J. Chem. **35**, 1060 (1957).
3. J. A. POPLE, W. G. SCHNEIDER and H. J. BERNSTEIN. High-resolution nuclear magnetic resonance. McGraw-Hill Book Co., of Canada, Ltd., Toronto. 1959.
4. B. DISCHLER and G. ENGLERT. Z. Naturforsch. **16a**, 1180 (1961).
5. B. DISCHLER and W. MAIER. Z. Naturforsch. **16a**, 318 (1961).
6. D. M. GRANT, R. C. HIRST, and H. S. GUTOWSKY. J. Chem. Phys. **40**, 1909 (1964).
7. D. M. GRANT, R. C. HIRST, and H. S. GUTOWSKY. J. Chem. Phys. **38**, 470 (1963).
8. P. F. COX. J. Am. Chem. Soc. **85**, 380 (1963).
9. C. N. R. RAO and VENKATESWARLU. Proc. Indian Acad. Sci. Sect. A, **54**, 1 (1961).
10. D. R. WHITMAN. J. Chem. Phys. **36**, 2085 (1962).

Can. J. Chem. Downloaded from www.nrcresearchpress.com by 210.87.254.5 on 09/05/12
For personal use only.

Can. J. Chem. Downloaded from www.nrcresearchpress.com by 210.87.254.40 on 09/05/12
For personal use only.

NOTES

DIMETHYLTRIFLUOROACETYLARSINE AND RELATED COMPOUNDS

W. R. Cullen and G. E. Styan

Although fluoroacyl derivatives of transition metals have been known for some time, little work has been done on the analogous derivatives of other metals and metalloids (1). Therefore, since compounds with Sn—Sn and As—As bonds are readily cleaved by fluoroalkyl iodides to give fluoroalkyl derivatives of tin or arsenic (2–4),

$$CF_3I + (CH_3)_3Sn{-}Sn(CH_3)_3 \rightarrow (CH_3)_3SnCF_3 + ISn(CH_3)_3,$$

it was of interest to see whether these bonds would react similarly with active trifluoroacetyl derivatives of the type $CF_3C(O)X$.

Tetramethyldiarsine is readily cleaved by trifluoroacetyl chloride at 20° to give a good yield of the pale-yellow liquid dimethyltrifluoroacetylarsine. With trifluoroacetic anhydride, however, the main products are dimethyltrifluoromethylarsine and dimethyltrifluoroacetoxyarsine.

$$(CH_3)_2As{-}As(CH_3)_2 \xrightarrow{CF_3C(O)Cl} (CH_3)_2AsC(O)CF_3 + ClAs(CH_3)_2$$

$$(CH_3)_2As{-}As(CH_3)_2 \xrightarrow[[CF_3C(O)]_2O]{} (CH_3)_2AsCF_3 + (CH_3)_2AsOOCCF_3 + CO$$

The last reaction may proceed through initial formation of the trifluoroacetyl compound followed by decarbonylation.

$$(CH_3)_2AsC(O)CF_3 \rightarrow (CH_3)_2AsCF_3 + CO$$

This process occurs slowly on heating the pure trifluoroacetylarsine but the reason for its ready occurrence in the anhydride reaction is obscure.

In the transition metal field it has been found that the fluoroacyl derivatives usually decarbonylate when heated, giving the fluoroalkyl compound, and some are so unstable that they cannot be isolated at ordinary temperatures (1).

$$LiCo(CO)_4 + CF_3C(O)Cl \rightarrow CF_3Co(CO)_4 + CO + LiCl$$

Apparently a similar situation is found when trifluoroacetyl iodide is mixed with hexamethylditin. Carbon monoxide is evolved and the main products are trimethyltrifluoromethyltin and, probably, trimethyltin iodide.

$$CF_3C(O)I + (CH_3)_3Sn{-}Sn(CH_3)_3 \rightarrow (CH_3)_3SnCF_3 + CO + ISn(CH_3)_3$$

The reaction of the ditin compound with trifluoroacetic anhydride at 60° follows a different route, the main products being tetramethyltin (instead of $(CH_3)_3SnCF_3$ or $(CH_3)_3SnC(O)CF_3$), trimethyltin trifluoroacetate, and carbon monoxide. The tetramethyltin does not arise through thermal decomposition of trimethyltrifluoromethyltin, since this yields trimethyltin fluoride and difluorocarbene (2).

Irradiation of a mixture of trifluoroacetyl chloride and hexaethylditin gives triethyltin chloride and diethyltin dichloride as the major tin-containing products. In this case the acid chloride seems to be acting mainly as a source of halogen. Similar reactions of

hexaethylditin with compounds such as benzoyl chloride and ethyl bromide have been described (5, 6).

We have also found that dimethyltrifluoroacetylarsine is obtained in low yield by reacting dimethylarsine with trifluoroacetyl chloride.

$$(CH_3)_2AsH + CF_3C(O)Cl \rightarrow (CH_3)_2AsC(O)CF_3 + HCl$$

Other products including chlorodimethylarsine are obtained. Dimethylarsine and acetyl chloride are reported to react similarly (7).

EXPERIMENTAL

The techniques used in this investigation have been described previously (4) and all known compounds were identified, at least, by their infrared spectra.

Reaction of Tetramethyldiarsine with Trifluoroacetyl Chloride

The diarsine (5.4 g) and trifluoroacetyl chloride (7.7 g) were left at 20° for 3 days. Unreacted acetyl chloride (4.5 g) was recovered. The remaining material could not be separated by distillation and all came over in the range 98–101°. Separation was effected by vapor phase chromatography (v.p.c.) (10 ft dinonyl phthalate column at 100°). Some dimethyltrifluoromethylarsine (~ 0.5 g) was collected and identified by its molecular weight of 174 (calcd. 174). The second component, a pale-yellow liquid (~ 4.3 g, 96% yield), was identified as *dimethyltrifluoroacetylarsine.*

Anal. Calcd. for $C_4H_6AsF_3O$: C, 23.8; H, 3.0; As, 37.1; F, 28.2. Found: C, 23.7; H, 3.1; As, 36.9; F, 28.5.

Infrared spectrum (vapor): 3 024 (m), 2 940 (m), 2 832 (w), 1 839 (w), 1 720 (s), 1 431 (m), 1 277 (vs), 1 204 (vs), 1 161 (vs), 909 (vs), 854 (m), 727 (s) cm^{-1}. Nuclear magnetic resonance data: ^1H spectrum, singlet at 1.00 p.p.m. downfield from external tetramethylsilane; ^{19}F spectrum, singlet at 0.38 p.p.m. downfield from external trifluoroacetic acid. The third component (~ 3.6 g) was identified as chlorodimethylarsine.

A sample of the acetylarsine was heated to 120° (18 h) and some decomposition took place. After 17 h at 150° decomposition was more extensive (~ 20%) and the major product was found to be dimethyltrifluoromethylarsine. The acetylarsine seemed to decompose readily on a mercury surface.

Reaction of Tetramethyldiarsine with Trifluoroacetic Anhydride

The diarsine (5.3 g) and the anhydride (8.0 g) were left at 20° for 28 days. A noncondensable gas was produced which was identified as carbon monoxide by its molecular weight of 28 (calcd. 28.0). Distillation of the least volatile fraction gave dimethyltrifluoromethylarsine, b.p. 56–60° (lit. 58° (8)), and dimethyltrifluoroacetoxyarsine, b.p. 136° (lit. 136–137° (9)) (4.3 g, 78% yield).

Reaction of Dimethylarsine with Trifluoroacetyl Chloride

The arsine (1.1 g) and acid chloride (4.6 g) were left at 20° (10 days). Trap-to-trap distillation gave hydrogen chloride (0.3 g) and unreacted trifluoroacetyl chloride (2.6 g). The least volatile fraction (1.5 g) could not be separated into its constituents by this means, but v.p.c. (10 ft dinonyl phthalate column at 110°) gave three main components. The first was identified as dimethyltrifluoroacetylarsine; the second was a mixture of compounds containing C, H, As, F, and O; the third was identified as chlorodimethylarsine. The relative area of the three peaks on the chromatogram was 1:4:2 in order of elution.

Reaction of Hexamethylditin with Trifluoroacetyl Iodide

The iodide (6.25 g) and the ditin compound (4.3 g) were left at 20° for 4 h. Noncondensable gas was evolved. Trap-to-trap distillation gave a trace of fluoroform, trifluoroiodomethane (0.5 g), trifluoroacetyl iodide (2.4 g), tetramethyltin (0.6 g), and trimethyltrifluoromethyltin (2.3 g, 74% yield). The tin compounds were also identified by comparison of their retention times on 6 ft silicone and 10 ft Apiezon J v.p.c. columns with those of authentic samples. The involatile residue was found to contain 46.5% iodine, determined as silver iodide (calcd. for $(CH_3)_3SnI$: I, 45.3%).

Reaction of Hexamethylditin with Trifluoroacetic Anhydride

When the tin compound (6.0 g) and the anhydride (4.8 g) were heated at 60° (15 h), a considerable amount of carbon monoxide of molecular weight 28 (calcd. 28) was produced. The volatile contents of the tube consisted of a trace of fluoroform, trifluoroacetyl fluoride (0.5 g) of molecular weight 116 (calcd. 116), unreacted anhydride (1.0 g), and tetramethyltin (2.5 g) of molecular weight 178 (calcd. 179). The tetramethyltin was also identified by its retention times as described in the preceding experiment. The solid residue (5.6 g) was identified as slightly impure trimethyltin trifluoroacetate, m.p. 90–100° decomp. (lit. m.p. 122–124° decomp. (10)).

Anal. Calcd. for $C_5H_9F_3SnO_2$: C, 21.7; H, 3.2. Found: C, 21.1; H, 2.8.

Can. J. Chem. Downloaded from www.nrcresearchpress.com by 210.87.254.40 on 09/05/12
For personal use only.

Reaction of Hexaethylditin with Trifluoroacetyl Chloride

Hexaethylditin (9.7 g) and the acetyl chloride (12 g) were irradiated with ultraviolet light (10 cm from a 100 W G.E. lamp) for 66 h. The least volatile fraction contained only triethyltin chloride (~ 7 g) and diethyltin dichloride (~ 4.5 g), which were separated by v.p.c. (Ucon Polar column at 135°). Ethane (0.4 g) was also isolated.

ACKNOWLEDGMENTS

Financial assistance from the National Research Council of Canada is gratefully acknowledged. We also wish to thank M and T Chemicals Inc. for gifts of tin compounds.

1. P. M. Treichel and F. G. A. Stone. Advan. Organomet. Chem. **1**, 143 (1964).
2. H. C. Clark and C. J. Willis. J. Am. Chem. Soc. **82**, 1888 (1960).
3. H. D. Kaesz, J. R. Phillips, and F. G. A. Stone. J. Am. Chem. Soc. **82**, 6228 (1960).
4. W. R. Cullen. Can. J. Chem. **38**, 439 (1960).
5. G. A. Razuvaev, N. S. Vyazankin, E. N. Gladyshev, and I. A. Borodavko. J. Gen. Chem. USSR English Transl. **32**, 2123 (1963).
6. G. A. Razuvaev, Yu. I. Deryunov, and N. S. Vyazankin. J. Gen. Chem. USSR, English Transl. **32**, 2481 (1963).
7. H. Albers, W. Künzel, and W. Schuler. Ber. **85**, 239 (1952).
8. R. N. Haszeldine and B. O. West. J. Chem. Soc. 699 (1956).
9. W. R. Cullen and L. G. Walker. Can. J. Chem. **38**, 472 (1960).
10. H. G. Kuivila, W. Rahman, and R. H. Fish. J. Am. Chem. Soc. **87**, 2835 (1965).

Received January 5, 1966.
Chemistry Department,
University of British Columbia,
Vancouver, British Columbia.

A NEW SYNTHESIS OF GERMYL IODIDE

James E. Griffiths and Alexander L. Beach

The versatility of silyl iodide in the preparative chemistry of the silicon hydrides arises from its position far to the left in MacDiarmid's silver salt conversion series (1). Attempts to establish such a series for the preparation of germyl compounds have been frustrated in part by the relatively poor stability of some of the materials (2). It has not always been clear, however, whether this is a problem of intrinsic instability (2) or of impurity-catalyzed decomposition.* In any case, the availability of a convenient synthesis of germyl iodide seems desirable if the chemistry of the germyl group is to be studied effectively. Although it is true that the germane iodine reaction produces germyl iodide (3–5), it is also generally true that the germane–halogen reaction is highly exothermic and rather difficult to control. A new method is presented here which takes advantage of the pseudo-halogen nature of trifluoromethyl iodide and effectively circumvents the disadvantages of the other method.

Trifluoromethyl iodide and germane react at a range of temperatures (25 to 235 °C) in a sealed tube forming germyl iodide and fluoroform. The reaction is very slow at room temperature taking up to 2 months to proceed to an appreciable extent but proceeds at a convenient rate near 130 °C. Some conversion of germyl iodide into less desirable products (probably GeH_2I_2, $GeHI_3$, and GeI_4 since no H_2 or HI was detected) occurs at these elevated temperatures but condensation of the products outside of the hot zone can quite

**Apiezon greases appear to promote decomposition of germyl compounds, whereas polymeric chlorofluorocarbon greases and waxes give much better results.*

Can. J. Chem. Downloaded from www.nrcresearchpress.com by 210.87.254.40 on 09/05/12
For personal use only.

Reaction of Hexaethylditin with Trifluoroacetyl Chloride

Hexaethylditin (9.7 g) and the acetyl chloride (12 g) were irradiated with ultraviolet light (10 cm from a 100 W G.E. lamp) for 66 h. The least volatile fraction contained only triethyltin chloride (~ 7 g) and diethyltin dichloride (~ 4.5 g), which were separated by v.p.c. (Ucon Polar column at 135°). Ethane (0.4 g) was also isolated.

ACKNOWLEDGMENTS

Financial assistance from the National Research Council of Canada is gratefully acknowledged. We also wish to thank M and T Chemicals Inc. for gifts of tin compounds.

1. P. M. Treichel and F. G. A. Stone. Advan. Organomet. Chem. **1**, 143 (1964).
2. H. C. Clark and C. J. Willis. J. Am. Chem. Soc. **82**, 1888 (1960).
3. H. D. Kaesz, J. R. Phillips, and F. G. A. Stone. J. Am. Chem. Soc. **82**, 6228 (1960).
4. W. R. Cullen. Can. J. Chem. **38**, 439 (1960).
5. G. A. Razuvaev, N. S. Vyazankin, E. N. Gladyshev, and I. A. Borodavko. J. Gen. Chem. USSR English Transl. **32**, 2123 (1963).
6. G. A. Razuvaev, Yu. I. Deryunov, and N. S. Vyazankin. J. Gen. Chem. USSR, English Transl. **32**, 2481 (1963).
7. H. Albers, W. Künzel, and W. Schuler. Ber. **85**, 239 (1952).
8. R. N. Haszeldine and B. O. West. J. Chem. Soc. 699 (1956).
9. W. R. Cullen and L. G. Walker. Can. J. Chem. **38**, 472 (1960).
10. H. G. Kuivila, W. Rahman, and R. H. Fish. J. Am. Chem. Soc. **87**, 2835 (1965).

Received January 5, 1966.
Chemistry Department,
University of British Columbia,
Vancouver, British Columbia.

A NEW SYNTHESIS OF GERMYL IODIDE

James E. Griffiths and Alexander L. Beach

The versatility of silyl iodide in the preparative chemistry of the silicon hydrides arises from its position far to the left in MacDiarmid's silver salt conversion series (1). Attempts to establish such a series for the preparation of germyl compounds have been frustrated in part by the relatively poor stability of some of the materials (2). It has not always been clear, however, whether this is a problem of intrinsic instability (2) or of impurity-catalyzed decomposition.* In any case, the availability of a convenient synthesis of germyl iodide seems desirable if the chemistry of the germyl group is to be studied effectively. Although it is true that the germane iodine reaction produces germyl iodide (3–5), it is also generally true that the germane–halogen reaction is highly exothermic and rather difficult to control. A new method is presented here which takes advantage of the pseudo-halogen nature of trifluoromethyl iodide and effectively circumvents the disadvantages of the other method.

Trifluoromethyl iodide and germane react at a range of temperatures (25 to 235 °C) in a sealed tube forming germyl iodide and fluoroform. The reaction is very slow at room temperature taking up to 2 months to proceed to an appreciable extent but proceeds at a convenient rate near 130 °C. Some conversion of germyl iodide into less desirable products (probably GeH_2I_2, $GeHI_3$, and GeI_4 since no H_2 or HI was detected) occurs at these elevated temperatures but condensation of the products outside of the hot zone can quite

*Apiezon greases appear to promote decomposition of germyl compounds, whereas polymeric chlorofluorocarbon greases and waxes give much better results.

Can. J. Chem. Downloaded from www.nrcresearchpress.com by 210.87.254.6 on 09/05/12
For personal use only.

likely minimize this effect. Although the latter point has not been demonstrated directly in the sealed tube experiments subsequent work under different conditions leads one to this conclusion. The reaction is quite rapid above 200 °C forming germyl iodide, fluoroform, and copious amounts of yellow-orange solids which may well include GeI_4. No hydrogen or hydrogen iodide was produced.

For larger scale preparations, several experiments have shown that a flow system through a heated container also is feasible and affords a more convenient method for synthesis. If a mixture of germane and CF_3I is passed through a heated glass bulb (195 to 260 °C) at moderate pressure (nominally 10 cm Hg) at various flow rates, the yield of GeH_3I varies between 15 and 37% based upon the CF_3I consumed. The lowest yield reflects a low flow rate of reactants or, in other words, the longer the desired product is in the hot zone, the greater its decomposition.

EXPERIMENTAL AND RESULTS

Trifluoromethyl iodide,* germane (6), and germane-d_4 (7) were prepared by standard methods and were purified by fractional vaporization and condensation in an all glass vacuum system. Criteria of purity were molecular weight (±1), tensimetric homogeneity (±0.3 mm Hg), and the absence of impurity bands in the infrared spectrum. The last was recorded on a Beckman IR-12 spectrophotometer.

In a typical experiment, 2.01 mmoles of GeD_4 and 1.00 mmoles of CF_3I were sealed in an evacuated tube and heated at 130 °C for 2 h. Yellow solid deposits appeared on the tube walls. Reactants and products were individually separated by repeated fractional condensation and vaporization in U-type vacuum traps maintained at −45 °C to separate GeD_2I_2 and less volatile products, −95 °C to isolate GeD_3I, −126 °C to stop CF_3I, and at −196 °C to recover GeD_4 and CF_3D. The deuterium compound GeD_4 rather than GeH_4 was used for many of the experiments so that infrared spectra could be employed to monitor the effectiveness of the separations of products and reactants. The deformation modes of the GeD_3 group (ν_2 and ν_5) or ν_4 of GeD_4 do not overlap with other absorption bands and in the spectrum of CF_3D a strong doublet band well isolated from all others appears at 974 cm^{-1} (8). The latter served as a useful criterion for establishing to what extent CF_3D and GeD_4 were separated. Since the initial separation was not entirely successful, the contents of the trap which had been cooled to −196 °C (see above) were repeatedly passed through a trap held at −160 °C into a trap cooled to −196 °C until the former fraction contained only CF_3D and the latter contained mainly GeD_4 with a small amount of CF_3D. By making up known mixtures an infrared calibration was possible.

The result of all of the vacuum manipulations was to collect 0.33 mmole of GeD_3I (molecular weight, 206, calcd. 205.5; vapor pressure at 20.2 °C, 56 mm), 0.373 mmole of CF_3I (molecular weight 195.9, calcd. 195.9), 0.629 mmole of CF_3D, and 0.746 mmole of GeD_4. Molecular weight measurements on mixtures of CF_3D and GeD_4 are not useful criteria of purity. The conversion into GeD_3I based upon initial amounts of GeD_4 and CF_3I was 17 and 31% respectively. Based upon reactants actually used up in the reaction the yields were 82 and 53% respectively. Solid deposits left in the reaction tube and traces of volatile materials trapped at −45 °C were not treated further. It is assumed that the bulk of this was germanium tetraiodide.

Separations and identification of various compounds in all subsequent experiments were done similarly and details are not given except when necessary.

When 1.01 mmoles of GeD_4 and 2.00 mmoles of CF_3I were heated together in a sealed tube at 135 to 140 °C during 4.5 h, 0.216 mmole of GeD_3I, 0.401 mmole of CF_3D, 0.746

Peninsular Chemresearch Inc., Gainesville, Florida.

Can. J. Chem. Downloaded from www.nrcresearchpress.com by 210.87.254.6 on 09/05/12
For personal use only.

mmole of GeD_4, and 1.60 mmoles of CF_3I were recovered, representing a yield of GeD_3I of 85 or 54% respectively based upon the amounts of GeD_4 or CF_3I actually used up in the reaction.

When 8.1 mmoles of GeH_4 and 8.8 mmoles of CF_3I were heated rapidly to about 230 to 240 °C, reaction proceeded vigorously with immediate deposition of bright orange solids. After about 40 min at these temperatures, 1.00 mmole of GeH_3I (molecular weight, 203, calcd. 202.5; vapor pressure at 19.1 °C, 53 mm) could still be recovered but only about 1 mmole of unconsumed CF_3I remained. The only other volatile product was CF_3H. All of the germane was used.

Several flow system experiments are reported in which products were removed from the hot zone and two types of glass apparatus were used. In the first an equimolar mixture (16 mmoles) of GeH_4 and CF_3I was passed through a 1 in. diameter glass tube at 185 °C at a flow rate of 5 mmoles/h. No products were detected but at 220 °C a small amount (0.1 mmole) of GeH_3I (identified by its infrared spectrum) could be isolated. No solid deposits were noted. In this type of experiment, however, the gases passed through the hot zone at very low pressure and the results are not particularly reproducible.

In the next series of experiments the reactant gases were passed through a 1 l glass bulb heated with a heating mantle and fitted with inlet and outlet tubes. Instead of allowing the gases to pass slowly through the hot zone at low pressure, a nominal pressure of 5 or 10 cm Hg was maintained and the overall flowrate was much increased. The results are summarized in Table I. The GeH_3I and CF_3I were isolated after the reaction, but CF_3H was not separated from GeH_4 because of the great deal of effort required to separate them.

TABLE I

Flow reaction of GeH_4 with CF_3I

Taken*		Recovered*		Temp.	Flow rate	Pressure
GeH_4	CF_3I	GeH_3I	CF_3I	(°C)	(mmole/min)	(cm Hg)
6.16	5.37	0.6 (201.9)†	3.84 (196.6)†	195	1.15	10.0
4.36	4.63	0.5 (202.1)	1.51 (196.3)	225	0.30	10.0
9.71	9.74	1.5 (201.9)	5.37 (196.6)	260	0.97	5.1

*Amounts in mmoles.
†Observed molecular weights in parenthesis.

In summary, germyl iodide can be conveniently prepared by methods outlined above and is moderately stable in a static system at temperatures near 135 °C. A flow system with the reactants at moderate pressures (5 to 10 cm Hg) and rather high temperatures (200 to 260 °C) offers some advantages over the sealed hot tube method. Specifically, rapid removal of products from the hot zone and better control of the total pressure is easier to accomplish. Furthermore, the limited data available in this work indicate that further scale-up of the reaction would be profitable and also that germyl iodide is not nearly as unstable thermally as was previously thought.

1. A. G. MacDiarmid. Quart. Rev. London, **10**, 208 (1956).
2. T. N. Srivastava, J. E. Griffiths, and M. Onyszchuk. Can. J. Chem. **40**, 739 (1962).
3. S. Sujishi. XVIIth Intern. Congr. Pure Appl. Chem. Munich, 1959.
4. T. D. Goldfarb and S. Sujishi. J. Am. Chem. Soc. **86**, 1679 (1964).
5. D. E. Freeman, K. H. Rhee, and M. K. Wilson. J. Chem. Phys. **39**, 2908 (1963).
6. J. E. Griffiths. Inorg. Chem. **2**, 375 (1963).
7. L. M. Dennis, R. B. Corey, and R. W. Moore. J. Am. Chem. Soc. **46**, 657 (1924).
8. W. F. Edgell and C. E. May. J. Chem. Phys. **22**, 1808 (1954).

Received August 23, 1965.
Bell Telephone Laboratories, Incorporated,
Murray Hill, New Jersey.

Can. J. Chem. Downloaded from www.nrcresearchpress.com by 210.87.254.6 on 09/05/12
For personal use only.

REACTIONS OF ACTIVE NITROGEN WITH ORGANIC SUBSTRATES. IV. ISOPRENE[1]

TERUKYO HANAFUSA[2] AND NORMAN N. LICHTIN

Can. J. Chem. Downloaded from www.nrcresearchpress.com by 210.87.254.40 on 09/05/12
For personal use only.

Some time ago we (1) communicated the very limited results of an initial cursory examination of the reaction of isoprene with active nitrogen. This reaction has now been subjected to more extensive investigation but, because of its complexity and in spite of considerable effort, relatively few conclusive results have been obtained and the investigation has been terminated.

Reactions were carried out in a fast flow system at autogenous temperature (ca. 60°), at pressures of 2.0 to 2.5 Torr and linear flow rates of 4.0 to 4.6 m s^{-1}. The molar ratio of isoprene to $N(^4S)$ was 10 ± 2. The use of a large excess of isoprene minimizes secondary attack of active nitrogen on the products. A glow discharge supported by 2 450 Mc microwaves was used to generate the reagent and the pyrex walls of the system were not poisoned.

Products were divided into three categories (2) on the basis of volatility. Those trapped at −78° but volatile at 10^{-2} Torr and 60° are hereafter designated as "monomeric"; those trapped at −78° but not volatile at 10^{-2} Torr and 60° are called "polymeric"; and those trapped at −196° but not at −78° are called "degradative". Gas chromatography was employed to isolate and purify individual products (cf. Experimental). Except for HCN, quantitative yields were not determined.

Nine compounds besides recovered isoprene were identified in the "degradative" fraction. Propane, the least abundant of these, was identified only by its gas-chromatographic retention time. Hydrogen cyanide was identified by its reaction with test paper (American Cyanamide Co.) and was determined quantitatively by titration of the total "degradative" product by Liebig's method (cf. ref. 3). The other seven were identified by comparison of both their infrared spectra and gas-chromatographic retention times with those of authentic samples. The most prominent "degradative" hydrocarbon under the conditions employed is propylene. Ethylene appears to be the next most abundant, whereas yields of ethane, acetylene, propyne, 2-methylbutene-1, and 1,3-butadiene are smaller. All of these products except 2-methylbutene-1 are degradative in the structural sense. The present data are too few to provide an independent test of the mechanistic model which has been suggested (2, 4) to rationalize products of the reaction of active nitrogen with butadiene. They are, however, not inconsistent with the postulate that they are formed as a result of various modes of decomposition of complexes of substrate with $N^4(S)$.

All the "degradative" products obtained from isoprene except 2-methylbutene-1 were also obtained in the reaction with 1,3-butadiene. This compound probably is formed by addition of hydrogen to isoprene. 1,3-Butadiene may have been formed directly in the decomposition of the primary adduct, along with $CN + H_2$ or $HCN + H$, or indirectly by combination of molecular fragments analogous to the "resynthesis" of propylene (5).

With the concentration of $N(^4S)$ (as determined by emission titration with NO (6)) equal to $6 \pm 1 \times 10^{-7}$ *M*, 27% of N was converted to HCN. This percentage conversion

[1]*Research supported principally by the U.S. Army Research Office (Durham) under grant No. 31-124-G171. The technical assistance of Mr. M. S. Puar in some of this work was supported by grant No. 702A of the Petroleum Research Fund of the American Chemical Society.*

[2]*Present address: The Institute of Scientific and Industrial Research, Osaka University, Osaka, Japan.*

is, within experimental precision, identical with the values found for butadiene (4) and propylene (7) under similar conditions with substrate in excess over N(^{4}S). The weight ratio of the yield of HCN to the total yield of monomeric products to the total yield of polymeric products was approximately 1.2:1:1.2.

The "monomeric" fraction contained at least 16 compounds, only 4 of which were unequivocally identified by infrared spectrometry, 3 by comparison of their spectra with those of authentic samples and the fourth, *beta*-methylpyrrole, by comparison with data in the literature (8). The formation of the latter product from isoprene is analogous to the formation of pyrrole from 1,3-butadiene. This compound constitutes a much smaller fraction of the total monomeric product from isoprene than does pyrrole from 1,3-butadiene, however. Its relative yield based on peak areas uncorrected for differences in area factors is only about 8% compared with the value of 26% found for pyrrole. The reason for this difference is not apparent. The reaction of isoprene also provides a small yield of pyrrole (2% on the above basis). In view of the large excess of isoprene employed and the small yield of 1,3-butadiene, it is improbable that this product is formed by secondary attack on butadiene. Presumably it is formed from the initial addition complex (2, 4) with loss of a methyl group.

Ammonia constituted about 3% of the "monomeric" product. It has not been detected among the products from 1,3-butadiene and its formation in significant yield is apparently associated with the presence of a methyl group in the molecule. Enhancement of ammonia yields is associated with the presence of methyl groups in a number of other substrates (9, 10) and has been explained (9) on the basis of simultaneous abstraction of two or three hydrogen atoms from one methyl group.

The fourth product, 1-cyanoisoprene, was isolated from the products of one experiment but not from those of several others. This compound is the analog of the *cis*-1-cyanobutadiene-1,3 obtained from 1,3-butadiene. These products presumably arise from attack of the cyanogen radical on substrate.

In spite of extensive gas chromatography of fractions of the "monomeric" product and, in a few cases, of mass-spectrometric analysis,* no other pure product was isolated and identified. One unresolved fraction appeared to contain primary amines, on the basis of infrared bands at 3 300 – 3 400 cm^{-1}. A number of fractions contained one or more unsaturated nitriles, on the basis of infrared absorptions in the 2 215 – 2 235 cm^{-1} region.

Examination of the "polymeric" product involved fractionation on the basis of solubility and volatility under vacuum, vapor phase chromatography, ultraviolet and infrared spectrometry, elemental analysis, and attempted formation of picrates as described under Experimental. All five fractions which were obtained had very similar infrared spectra. Absorption bands observed at 2 800 – 3 000, 1 450, and 1 375 cm^{-1} are presumably due to aliphatic CH_2 and CH_3; those near 2 200 cm^{-1} indicate the presence of nitrile groups. Broad absorption at 3 200 – 3 300 and bands around 1 625 – 1 650 suggest the presence of amino groups. This suggestion is consistent with the solubility of several fractions (all which were tested) in 2 *M* aqueous HCl. Elemental analyses of two fractions (cf. Experimental) correspond to the atomic ratios $C_{3.0}H_{4.3}N_{1.00}$ and $C_{3.0}H_{5.0}N_{1.00}$ respectively. C, H, and N constituted only 89.2 wt. % of the former fraction and 79.9 wt. % of the latter, however. Gas chromatography on Carbowax 20 M at 75–200° of two CCl_4-soluble fractions indicated that both were complex mixtures of many components, but the possibility that fragmentation of the "polymer" took place on the column was not investigated.

*For which we are grateful to the Eastern Research Laboratory of the Dow Chemical Company.

Can. J. Chem. Downloaded from www.nrcresearchpress.com by 210.87.254.40 on 09/05/12
For personal use only.

Can. J. Chem. Downloaded from www.nrcresearchpress.com by 210.87.254.40 on 09/05/12
For personal use only.

EXPERIMENTAL

Apparatus and procedures were essentially the same as previously described (2, 4). The pyrex walls of the system were not poisoned but were conditioned before each experiment by evacuating overnight with a mercury diffusion pump and then by passing molecular nitrogen for 20 min at the pressure of the experiment and active nitrogen for 30 min before isoprene was introduced into the reactor 30 cm downstream from the glow discharge. The flow rate of isoprene was controlled by thermostatting its reservoir.

Emission titration of active nitrogen with NO (6) was carried out to a visual end point periodically during the course of the work. The selectivity of the NO titration for $N(^4S)$ is still controversial (11–13) but the uncertainty inherent in this controversy (12) only has the effect of rendering the ratios of isoprene to $N(^4S)$ quoted in this paper minimum possible values of the true quantities: i.e. there is no question that isoprene was in large excess.

An F and M model 500 instrument equipped with a model 720 temperature-programmed oven was used for most of the gas chromatography reported here. Some preliminary separations of "monomeric" products were carried out on a Aerograph Autoprep model A-700.

The "degradative" fraction was separated into its components on an 8 ft × $\frac{1}{4}$ in. outside diameter diisodecyl phthalate column at room temperature with a helium flow of 20 cc min^{-1}. The separated fractions were collected at −196° and rechromatographed on an 8 ft × $\frac{1}{4}$ in. outside diameter silica gel column temperature programmed from 50 to 250 °C at 4 deg min^{-1} with a helium flow rate of 30 cc min^{-1}. Individual fractions were rechromatographed to homogeneity as needed. Each purified fraction was transferred to a 10 cm gas cell for measurement of its infrared spectrum on a Perkin–Elmer model 237 instrument.

The "monomeric" fraction was first chromatographed on an 8 ft preparative silicone 550 column programmed at 50 to 200 °C at 2.9 deg min^{-1} with a helium flow rate of 40 cc min^{-1}. This procedure cleanly separated out NH_3 and the small portion of the recovered isoprene collected in the "monomeric" fraction. The other, poorly resolved fractions were individually rechromatographed on an 8 ft preparative Carbowax 20 M column programmed from 50 to 200 °C at 2.9 deg min^{-1} with a helium flow rate of 40 cc min^{-1}. The components corresponding to individual peaks were collected and their infrared spectra measured in CCl_4 solution in a 2 mm cell on a Perkin–Elmer model 237 spectrometer.

The "polymeric" fraction was extracted with refluxing methylene chloride and the insoluble residue was completely dissolved by refluxing pyridine. The solvents were then removed by distillation under reduced pressure. The methylene chloride soluble fraction was then extracted with CCl_4. The tan insoluble residue melted at 116–128°, was soluble in chloroform, ethanol, acetone, and 2 *M* aqueous HCl, as well as in methylene chloride and pyridine. Its infrared spectrum was measured in Nujol mull and in methylene chloride solution. Its elemental analysis was C, 58.9; H, 7.36; N, 23.0. A picrate formed by reaction with picric acid in ethanol did not have a sharp melting point. After removal of solvent from the carbon tetrachloride extract, the residue was fractionally distilled at 0.07 Torr to yield two fractions, b.p. 75–82° and 82–105°. The two fractions were then gas chromatographed on a 6 ft × $\frac{1}{4}$ in. Carbowax 20 M column programmed from 75 to 200 °C at 4 deg min^{-1} with a helium flow rate of 30 cc min^{-1}. Infrared spectra of the two fractions and the residue from distillation were determined with liquid films. The 75–82° fraction had an ultraviolet absorption maximum at 206–210. The dark pyridine-soluble fraction of the "polymeric" product was found to be soluble in glacial acetic acid and 2 *M* aqueous HCl. Its infrared spectrum was determined in Nujol. Its elemental analysis was C, 52.3; H, 7.28; N, 20.3. The material had a wide melting range above 130°.

Nitrogen was Matheson Co. prepurified grade. Isoprene was Matheson Co. research grade. Solvents were reagent or spectroscopic grade. Authentic 1-cyanoisoprene was prepared by the method of Snyder (14).

1. A. Tsukamoto and N. N. Lichtin. J. Am. Chem. Soc. **82**, 3798 (1960).
2. A. Tsukamoto and N. N. Lichtin. J. Am. Chem. Soc. **84**, 1601 (1962).
3. M. Kolthoff and E. B. Sandell. Textbook of quantitative inorganic analysis. McMillan Co., New York. 1956. pp. 458–460.
4. A. Fujino, S. Lundsted, and N. N. Lichtin. J. Am. Chem. Soc. **88**, 775 (1966).
5. P. T. Hinde, Y. Titani, and N. N. Lichtin. Radiation Res. **25**, 198 (1965).
6. P. Harteck, G. Mannella, and R. R. Reeves. J. Chem. Phys. **29**, 608 (1958).
7. Y. Shinozaki, R. Shaw, and N. N. Lichtin. J. Am. Chem. Soc. **86**, 341 (1964).
8. R. E. Lancaster, Jr. and C. A. van der Werf. J. Org. Chem. **23**, 1208 (1954).
9. H. A. Dewhurst and G. D. Cooper. J. Am. Chem. Soc. **82**, 4220 (1960).
10. J. L. Weininger. J. Phys. Chem. **65**, 941 (1961); J. Am. Chem. Soc. **83**, 3388 (1961).
11. A. A. Westenberg and N. de Haas. J. Chem. Phys. **40**, 3087 (1964).
12. E. Fersht and R. A. Back. Can. J. Chem. **43**, 1899 (1965).
13. J. T. Herron. J. Phys. Chem. **69**, 2736 (1965).
14. H. R. Snyder, J. M. Stewart, and R. L. Moyers. J. Am. Chem. Soc. **71**, 1055 (1949).

Received January 5, 1966.
Chemistry Department,
Boston University,
Boston, Massachusetts.

Can. J. Chem. Downloaded from www.nrcresearchpress.com by 210.87.254.40 on 09/05/12
For personal use only.

THE COPPER/SELENIUM SYSTEM

R. D. HEYDING

The copper-rich region of the copper/selenium phase diagram is well established (1), and room temperature phase relationships at higher selenium concentrations have been reported by Borchert and Patzak (2). Apparently no comprehensive examination has been made of the selenium-rich region, although the 'hypothetical' diagram proposed by Gattow and Schneider (3) is remarkably accurate. The crystal structures of the compounds stable at room temperature are known, with the exception of the low temperature Cu_2Se modifications. The structure of Cu_2Se reported by Borchert (4) was not observed by Boettcher *et al.* (5) or by Kotovich and Frank-Kamenetskii (6). Boettcher, on the other hand, observed seven distinct electron diffraction patterns for thin films of $Cu_{1.9}Se$ between 20 and 320 °C.

A series of alloys with 27 to 70 atomic % selenium have been prepared in our laboratory and examined by differential thermal analysis (d.t.a.) and by room temperature and high temperature X-ray diffraction techniques. A phase diagram to 880 °C has been obtained, crystal structures have been examined, and enthalpies of transformation have been estimated.

EXPERIMENTAL

Samples were prepared by the reaction of copper and selenium (both Asarco 59) in sealed evacuated Vycor tubes in the usual manner. When the formation reactions were complete, specimens were annealed for various periods depending on the rate at which apparent equilibrium was attained, and either slowly cooled in the annealing furnace or quenched in ice/water mixtures.

One gram samples for d.t.a. were sealed *in vacuo* in Vycor tubes with reentrant thermocouple wells. Nickel sponge was used as the standard specimen. Heating rates (not programmed) were between 2° and 3 deg/min, and free cooling rates varied from 5 deg/min at 800 °C to 3 deg/min at 130 °C. Indium (39_5), cadmium (59), zinc (69), and antimony (69) as primary standards, and sulfur (59) and selenium (59) as secondary standards, were used to calibrate the instrument with respect to temperature and the area of the differential signal. The high vapor pressure of selenium at the strain point of Vycor imposed an upper limit of 880 °C on the analysis.

Diffraction patterns of three specimens (Cu_2Se, Cu_3Se_2, and CuSe) were obtained in a 19 cm Unicam high temperature Debye–Scherrer camera. Room temperature powder patterns were obtained in 11.46 cm cameras. Nickel-filtered copper radiation ($\lambda_{K\alpha}$ = 1.54050 Å) was used throughout.

RESULTS AND DISCUSSION

The phase diagram is shown in Fig. 1. Transformation temperatures are considered to be accurate to ±1 °C. The monotectic at 523 °C is inferred; no direct evidence was sought for the two phase liquid field.

The diselenide $CuSe_2$ melts peritectically at 342 °C, forming CuSe and a liquid phase. The reverse reaction is slow. On cooling through the transformation point at 3 deg/min, less than 10% of the stoichiometric quantity of $CuSe_2$ is formed. The compound has the C18 marcasite structure reported by Gattow (7), although the unit cell volume of our specimens is 5% smaller than that of Gattow's single crystal (cf. Table I).

The monoselenide CuSe undergoes a rapid and reversible polymorphic transformation at 53 °C, and decomposes at 382 °C to $Cu_{2-x}Se$ and a liquid phase. The low temperature modification, αCuSe, has the B18 covellite structure. The diffraction data are in good agreement with published intensities and cell dimensions for klockmannite (8, 9). The high temperature modification, βCuSe, has been indexed on an orthorhombic cell (Table I) based on observed splittings in low order αCuSe reflections. In this setting the transformation appears to involve a small decrease in the a/b ratio from the orthohexagonal

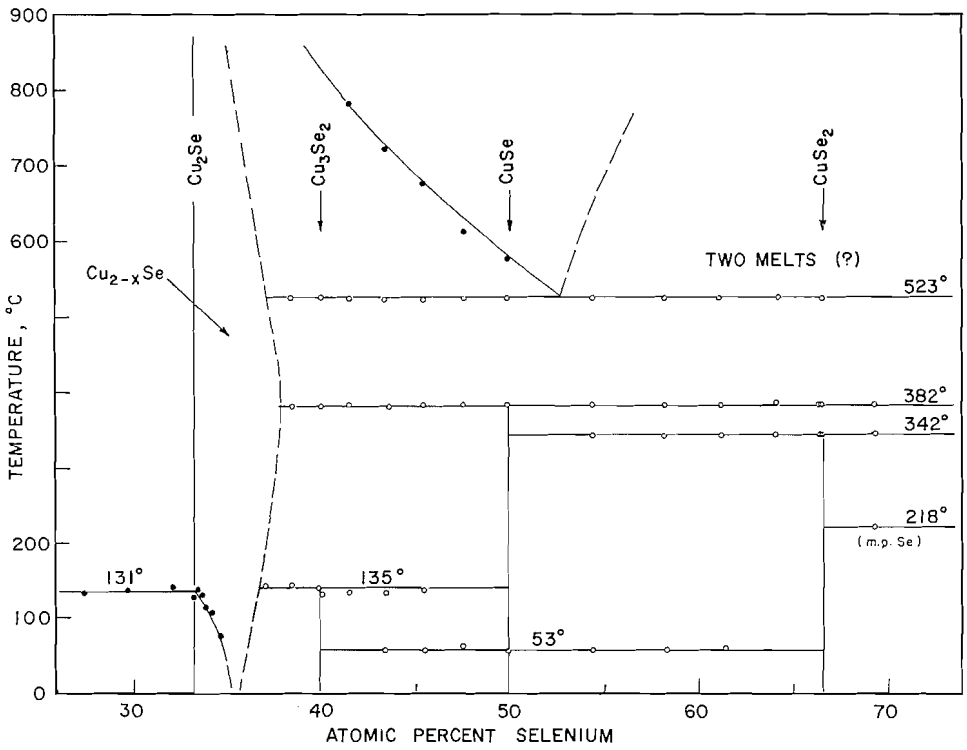


FIG. 1. Phase diagram of the copper/selenium system: (○) differential thermal signal, heating cycle; (●) differential thermal signal, cooling cycle.

value. The high temperature diffraction patterns of this compound were of indifferent quality, and it must be emphasized that this assignment is tentative.

The compound Cu_3Se_2 disproportionates at 135 °C to $Cu_{2-x}Se$ and βCuSe. The reaction of the latter two compounds below 135 °C to form Cu_3Se_2 is exceedingly slow. On the other hand, specimens with this composition quenched rapidly from 360 °C contain Cu_3Se_2 and, in many instances, only traces of the end-members. Normally one would infer from these observations that Cu_3Se_2 is a high temperature phase. However, careful examination of specimens of Cu_3Se_2 in the high temperature camera has confirmed the disproportionation at 135 °C, the $Cu_{2-x}Se/\beta$CuSe field between 135 and 382 °C, and the $Cu_{2-x}Se$/liquid field above 382 °C. (Once heated above 135 °C, the Cu_3Se_2 phase did not reappear in the camera.) Moreover, specimens in this concentration range showed consistent d.t.a. patterns before and after long annealing periods between 300 and 390 °C in the d.t.a. furnace itself.

It is uncommon for a phase to appear on quenching from well above its stability field when the rate of transformation just below the transformation temperature is very slow. In this instance an explanation can be based on the assumption that the selenium-rich limit of the homogeneous $Cu_{2-x}Se$ phase moves to higher selenium concentrations with increasing temperature, as indicated by the dotted line in Fig. 1. On quenching from the $Cu_{2-x}Se/\beta$CuSe field, Cu_3Se_2 may be formed by a precipitation mechanism imposed by the decreasing number of Cu vacancies in the $Cu_{2-x}Se$ solid solution.

The tetragonal unit cell dimensions of Cu_3Se_2 obtained in quenched specimens are only slightly smaller than those of the mineral umangite (10).

Can. J. Chem. Downloaded from www.nrcresearchpress.com by 210.87.254.40 on 09/05/12
For personal use only.

TABLE I

Unit cell dimensions of copper/selenium compounds at 26 °C

Composition	System	Space group	a (Å)	b (Å)	c (Å)
$Cu_{1.84}Se$*	Cubic	$Fm3m$	$5.764_8 \pm 0.001$		
$Cu_{1.80}Se$	Cubic	$Fm3m$	$5.759_4 \pm 0.001$		
$Cu_{1.70}Se$†	Cubic	$Fm3m$	5.743 ± 0.002		
Cu_3Se_2‡	Tetragonal	$P4/mnm$	6.394 ± 0.005		4.269 ± 0.005
αCuSe	Hexagonal	$P6_3/mmc$	3.940 ± 0.003		17.216 ± 0.005
βCuSe§	Orthorhombic (?)	—	$6.81_3 \pm 0.01$	$4.01_5 \pm 0.01$	$17.09_5 \pm 0.02$
$CuSe_2$	Orthorhombic	$Pnnm$	$5.01_7 \pm 0.01$	$6.19_8 \pm 0.01$	3.741 ± 0.005

*In the presence of αCu_2Se.
†In the presence of αCuSe.
‡In the presence of $Cu_{2-x}Se$ and CuSe.
§Specimen temperature 63 ± 2 °C.

The cubic C1 $Cu_{2-x}Se$ phase has a very narrow homogeneity range at room temperature centered at ca. $Cu_{1.8}Se$, within the limits $0.18 \leq x \leq 0.25$ (Table I). When x is zero, the cubic phase is not stable below 131 °C. Between 131 and 440 °C no phases other than the cubic C1 phase were observed in the high temperature camera.

The symmetry of the low temperature Cu_2Se phase (which will be called αCu_2Se in accord with the nomenclature used for other low temperature 2:1 IB/VIA compounds) is not yet known. The diffraction pattern is in substantial agreement with that recorded by Kotovich (6), provided the cubic $Cu_{2-x}Se$ reflections are deducted from the Kotovich pattern. The reflections cannot be indexed using the tetragonal cell proposed by Borchert (4). The compound does not appear to be isomorphous with Cu_2S III (11), αCu_2Te (12), Ag_2S (13), or αAg_2Se (14), or, indeed, any of the copper and silver chalicides in the same composition region.

Recently Sharma (15) studied thin films of Cu_2Se and failed to observe a transformation at 110 °C reported in an early paper by Rahlfs (16). Sharma suggested that if the transformation occurs in films it must do so at much higher temperatures than in bulk specimens. Since the film was cubic at room temperature and was therefore $Cu_{1.8}Se$ and not Cu_2Se as Sharma believed, no transformation was to be expected below ca. 900 °C. The structural properties of the film and of our bulk specimens appear to be identical.

The enthalpies associated with the transformations have been estimated from the areas of the d.t.a. signals observed during the transformations. These data are compared in Table II with values calculated from room temperature enthalpies of formation reported by Gattow and Schneider (3). Even with very generous allowances for the semiquantitative d.t.a. data, the agreement is so unsatisfactory that some discussion is required.

TABLE II

Enthalpies of transformations in the Cu/Se system

Compound	ΔH_f^{298}* (kcal/mole)	Transformation	T (°C)	Products	$\Delta H_{calcd}{}^T$† (kcal/mole)	$\Delta H_{obs}{}^T$‡ (kcal/mole)
αCu_2Se	−13.01	α,β	131	$Cu_{2-x}Se$	—	$+4.9 \pm 1.0$
Cu_3Se_2	−23.64	Decomposition	135	$Cu_{2-x}Se$ + βCuSe	$+0.3 \pm 2.5$	$+4.6 \pm 0.9$
αCuSe	-9.4_5	α,β	53	βCuSe	—	$+0.33 \pm 0.09$
βCuSe	—	Decomposition	382	$Cu_{2-x}Se$ + Se (1)	$+2.3 \pm 0.8$	$+3.4 \pm 0.8$
$CuSe_2$	−10.3	Decomposition	342	βCuSe + Se (1)	$+2.4 \pm 1.0$	$+2.9 \pm 0.7$

*Gattow and Schneider (3).
†Calculated from ΔH_f^{298}, with ΔH_{liq} for Se = +1.30 kcal/mole, and assuming ΔH_{trans} α,βCuSe = +0.33 kcal/mole; $C_p\,dT$ terms neglected. Uncertainties in $\Delta H_{calcd}{}^T$ indicate the result of a 5% uncertainty in ΔH_f^{298}.
‡Estimated from the area of the differential thermal signal during the transformation.

Can. J. Chem. Downloaded from www.nrcresearchpress.com by 210.87.254.40 on 09/05/12
For personal use only.

Obviously small errors in the enthalpies of formation will invoke disproportionately large errors in calculated heats of reaction. Gattow and Schneider obtained their data by direct calorimetric determination of heats of reaction of powdered copper and selenium. Incomplete reaction in the calorimeter was observed in several instances, particularly in the Cu_3Se_2 composition range. It is difficult to estimate what uncertainties incomplete reaction might impose on the results. The uncertainties assigned in Table II for purposes of comparison are based on an uncertainty of 5% in the enthalpies of formation. With this assumption the calculated and observed heats of decomposition of $CuSe_2$ and βCuSe are within the assigned limits. The enthalpy of formation of Cu_3Se_2 is based on an assumption which implies that the disproportionation of Cu_3Se_2 involves little or no change in enthalpy. (The value of 0.3 kcal/mole in Table II arises solely from the α,βCuSe transition.) This supposition is not supported by d.t.a. The quantities of Cu_3Se_2 formed in the calorimeter may have been less than the authors appreciated.

The enthalpy of the $\alpha Cu_2Se/Cu_{2-x}Se$ transformation is larger than one would expect for a simple polymorphic change. It is quite possible that the low temperature phase is not a polymorphic form of the cubic $Cu_{2-x}Se$ phase, but a new phase, slightly richer in copper than the tentative formula indicates.

Powder diffraction patterns of $CuSe_2$ and βCuSe have been submitted to the ASTM Index, and to the Depository of Unpublished Data.*

ACKNOWLEDGMENTS

I am indebted to Prof. F. A. Hames, Department of Metallurgy, for the use of his high temperature camera, and to Mr. V. Lawetz for assistance in preparing samples and obtaining diffraction patterns. An operating grant from the Ontario Research Foundation is gratefully acknowledged.

NOTE ADDED IN PROOF: In a recent paper, Gattow (17) has reported the atom positions in $CuSe_2$, and has given 350 °C as the temperature at which this compound decomposes.

1. M. HANSEN and K. ANDERKO. Constitution of binary alloys. 2nd ed. McGraw-Hill Book Co., Inc., New York and London. 1958.
2. W. BORCHERT and I. PATZAK. Heidelberger Beitr. Mineral. Petrog. **4**, 434 (1955).
3. G. GATTOW and A. SCHNEIDER. Z. Anorg. Allgem. Chem. **286**, 296 (1956).
4. W. BORCHERT. Z. Krist. **106**, 5 (1945).
5. A. BOETTCHER, G. HAASE, and H. TREUPEL. Z. Angew. Phys. **7**, 478 (1955).
6. V. A. KOTOVICH and V. A. FRANK-KAMENETSKII. Uch. Zap. Leningr. Gos. Univ. Ser. Geol. Nauk, **8**, 135 (1957).
7. G. GATTOW. Naturwissenschaften, **52**, 258 (1965).
8. J. W. EARLY. Am. Mineralogist, **34**, 435 (1949).
9. L. G. BERRY. Am. Mineralogist, **39**, 504 (1954).
10. L. G. BERRY. X-Ray powder data file. 8th Set. 1958. Card 8-279. Special technical publication 480G. A.S.T.M. Philadelphia.
11. S. DJURLE. Acta Chem. Scand. **12**, 1415 (1958).
12. K. VAN CON and H. RODOT. Compt. Rend. **260**, 1908 (1965).
13. H. E. SWANSON, M. I. COOK, E. H. EVANS, and J. H. DEGROOT. Natl. Bur. Std. Circ. No. 539, 10, 51 (1960).
14. Z. G. PINSKER, C. L. CHOU, R. M. IMAMOV, and E. L. LAPIDUS. Soviet Phys. Cryst. English Transl. **10**, 225 (1965).
15. S. K. SHARMA. Nature, **206**, 187 (1965).
16. P. RAHLFS. Z. Physik. Chem. Leipzig, **B31**, 157 (1936).
17. G. GATTOW. Z. Anorg. Allgem. Chem. **340**, 312 (1965).

RECEIVED DECEMBER 23, 1965.
DEPARTMENT OF CHEMISTRY,
QUEEN'S UNIVERSITY,
KINGSTON, ONTARIO.

Photocopies of deposited material may be obtained upon request to: Depository of Unpublished Data, National Science Library, National Research Council, Ottawa, Canada.

Can. J. Chem. Downloaded from www.nrcresearchpress.com by 210.87.254.40 on 09/05/12
For personal use only.

Can. J. Chem. Downloaded from www.nrcresearchpress.com by 210.87.254.6 on 09/05/12
For personal use only.

THE REACTION OF HYDROGEN AND ETHYLENE IN THE GAS PHASE

M. C. LIN

Recent measurements of the chain initiation and termination steps in the thermal decomposition of ethane (1) led to the conclusion that the combination of ethyl radicals was the main termination step and that the unimolecular decomposition of the ethyl radical was in its pressure-dependent region in the range of temperatures and pressures covered by the experiments. On the basis of these facts the mechanism for the homogeneous hydrogenation of ethylene in a similar region of temperature and pressure was reexamined, and a mechanism is proposed which is consistent with the new values for the rates of the elementary reactions.

Early work by Pease (2) showed that with mixtures of hydrogen and ethylene in the ratio 3:1 the main product was ethane and its rate of formation was first order with respect to both hydrogen and ethylene. The rate constant for the formation of ethane was given by the expression

$$k = 5.90 \times 10^{13}\, e^{-44800/RT} \text{cc mole}^{-1}\, \text{s}^{-1}$$

in the temperature range 475–550 °C. It is apparently well established that the reaction occurs by a free radical chain mechanism. For example, from the reaction of D_2 with C_2H_4 at temperatures between 550 and 660 °C large amounts of C_2H_3D were formed, and C_2H_5D and $C_2H_4D_2$ were the major deuterated ethanes produced (3). The following mechanism was proposed by Rice and Herzfeld (4):

[1] $$H_2 + C_2H_4 \rightarrow H + C_2H_5$$

[2] $$C_2H_5 + H_2 \rightarrow H + C_2H_6$$

[3] $$H + C_2H_4 \rightarrow C_2H_5$$

[4] $$H + C_2H_5 \rightarrow C_2H_6 \text{ or } H_2 + C_2H_4 \quad .$$

The rate of production of ethane is then

[5] $$d[C_2H_6]/dt = (k_1k_2k_3/k_4)^{1/2}[H_2][C_2H_4].$$

This expression is, however, inconsistent with the measurements of the related elementary reactions in the thermal decomposition of ethane in the following ways:

(*a*) The chain termination step

[6] $$C_2H_5 + C_2H_5 \rightarrow C_4H_{10} \text{ or } C_2H_4 + C_2H_6$$

can be shown to be faster than reaction [4] under the conditions of the experiments. If the chain length is long, the relative rates of reactions [4] and [6] may be expressed as follows

[7] $$R_4/R_6 = [H]/[C_2H_5] = k_2[H_2]/k_3[C_2H_4],$$

where k_4 is assumed to be equal to k_6. Neither k_2 nor k_3 is well known but they may be calculated from the rate constants of the reverse reactions and the corresponding equilibrium constants. For 900 °K the following data were used: $K_2 = k_{-2}/k_2 = 1.4 \times 10^3$ (5); $K_3 = k_{-3}/k_3 = 6.2 \times 10^{-10}$ mole/cc (5); $k_{-2} = 7.6 \times 10^{10}$ cc/mole s (6); $k_{-3} = 1.1 \times 10^4$ s^{-1} at 500 mm (1). Thus

[8] $$R_4/R_6 = 3.1 \times 10^{-6}\, [H_2]/[C_2H_4].$$

The combination of ethyl radicals must therefore be the predominant chain-ending step.

(*b*) The overall activation energy predicted by eq. [5] may be calculated by using the following values, in kcal/mole: $E_1 = 66.5$; $E_2 = 12.5$ (both calculated from taking $D(C_2H_5—H) = 97.5$, $D(H—H) = 103.2$, and $E_{-2} = 6.8$ (6)); $E_4 = 0$. E_3 may be obtained from the measured value for E_{-3}, the activation energy for reaction [−3], combined with the heat of the reaction $C_2H_5 \rightleftharpoons C_2H_4 + H$ of 38.6 kcal/mole (5). The decomposition of the ethyl radical has been shown to be pressure dependent at temperatures from 430–620 °C and pressures below 600 mm (1, 7). The order of the decomposition is about 1.4 at 600 mm and 1.7 at 60 mm. E_{-3} was found to be 32.7 kcal/mole over the range of pressures and temperatures studied (1). Thus

$$E_3 = 32.7 - 38.6 = -5.9 \text{ kcal/mole}$$

and

$$E_{\text{overall}} = \tfrac{1}{2}(E_1 + E_2 + E_3 - E_4) = 36.5 \text{ kcal/mole},$$

which is much lower than the value of 44.8 kcal/mole obtained by Pease.

To overcome these difficulties the following mechanism is proposed in which initiation occurs by the bimolecular reaction of ethylene and termination by the combination of ethyl radicals, i.e.

[9] $$C_2H_4 + C_2H_4 \rightarrow C_2H_3 + C_2H_5$$

[2] $$C_2H_5 + H_2 \rightarrow C_2H_6 + H$$

[3] $$H + C_2H_4 \rightarrow C_2H_5$$

[6] $$C_2H_5 + C_2H_5 \rightarrow C_4H_{10} \text{ or } C_2H_4 + C_2H_6 \quad .$$

The rate of ethane production is then

[10] $$d[C_2H_6]/dt = k_2(k_9/k_6)^{1/2}[C_2H_4][H_2].$$

The reaction is thus correctly predicted to be first order in both ethylene and hydrogen.

The activation energy of reaction [9] may be estimated by assuming a value of 103 ± 3 kcal/mole for $D(C_2H_3—H)$ (8). If E_{-9} is taken as 0 then $E_9 = 64$ kcal/mole. Thus $E_{\text{overall}} = E_2 + \frac{1}{2}(E_9 - E_6) = 44.5$ kcal/mole. This is in agreement with the experimental value.

ACKNOWLEDGMENT

The author would like to express his indebtedness to Dr. M. H. Back for continued discussions and also to Professor K. J. Laidler for valuable comments.

1. M. C. Lin and M. H. Back. Can. J. Chem. **44**, 505 (1966).
2. R. N. Pease. J. Am. Chem. Soc. **54**, 1877 (1932).
3. R. E. Varnerin and J. S. Dooling. J. Am. Chem. Soc. **78**, 1119 (1956).
4. F. O. Rice and K. F. Herzfeld. J. Am. Chem. Soc. **56**, 284 (1934).
5. S. W. Benson. The foundations of chemical kinetics. McGraw-Hill Book Co., Inc., New York and London. 1960.
6. M. R. Berlie and D. J. LeRoy. J. Chem. Phys. **20**, 200 (1952).
7. J. H. Purnell and C. P. Quinn. Proc. Roy. Soc. London, Ser. A, **270**, 267 (1962).
8. B. E. Knox and H. B. Palmer. Chem. Rev. **61**, 247 (1961).

Received December 6, 1965.
Department of Chemistry,
University of Ottawa,
Ottawa, Canada.

Can. J. Chem. Downloaded from www.nrcresearchpress.com by 210.87.254.6 on 09/05/12
For personal use only.

Can. J. Chem. Downloaded from www.nrcresearchpress.com by 210.87.254.105 on 09/05/12
For personal use only.

Canadian Journal of Chemistry

Issued by THE NATIONAL RESEARCH COUNCIL OF CANADA

VOLUME 44 JUNE 1, 1966 NUMBER 11

CONFIGURATION OF DIELS–ALDER ADDUCT OF FURAN AND ACETYLENE DICARBOXYLIC ACID[1]

J. KALLOS AND P. DESLONGCHAMPS[2]

Research Laboratory, Department of Pathology, St. Mary's Memorial Hospital, Montreal, Quebec

Received December 9, 1965

ABSTRACT

The configuration of the Diels–Alder adduct (I) of furan and acetylene dicarboxylic acid was established by chemical and spectroscopic methods and found to be *exo–exo* (II*a*).

In 1931, Diels and Alder (1) reported the preparation of an adduct (I) obtained by reacting furan (2 moles) with acetylene dicarboxylic acid (1 mole). Theoretically this adduct could have three possible configurations: *exo–exo* (II*a*), *endo–exo* (III), or *endo–endo* (IV). This communication presents experimental evidence that the stereochemistry of this adduct is *exo–exo*.

Diels and Olsen (2) obtained a dibromodilactone by reacting the diester of the adduct (I) with bromine in chloroform; they proposed a planar formula (V) for this dibromodilactone but did not present any proof for the configuration of the adduct. However, if the dibromodilactone derivative possesses the Diels–Olsen formula (V), the configuration of the adduct has to be *exo–exo* (II*a*).

In 1948, Woodward and Bear (3) showed that bromolactonization of the carboxylic acid derivatives of 7-oxa-bicyclo[2.2.1]hept-2-ene occurs with the *exo* type (VII) as well as the *endo* type (VI). They also showed that the *exo* compound reacts via a Wagner–Meerwein rearrangement as shown (VIII). In view of these findings the planar formula suggested for the dibromodilactone required further investigation. In fact, three formulae are possible for this compound; these are as represented in IX, X, and XI.

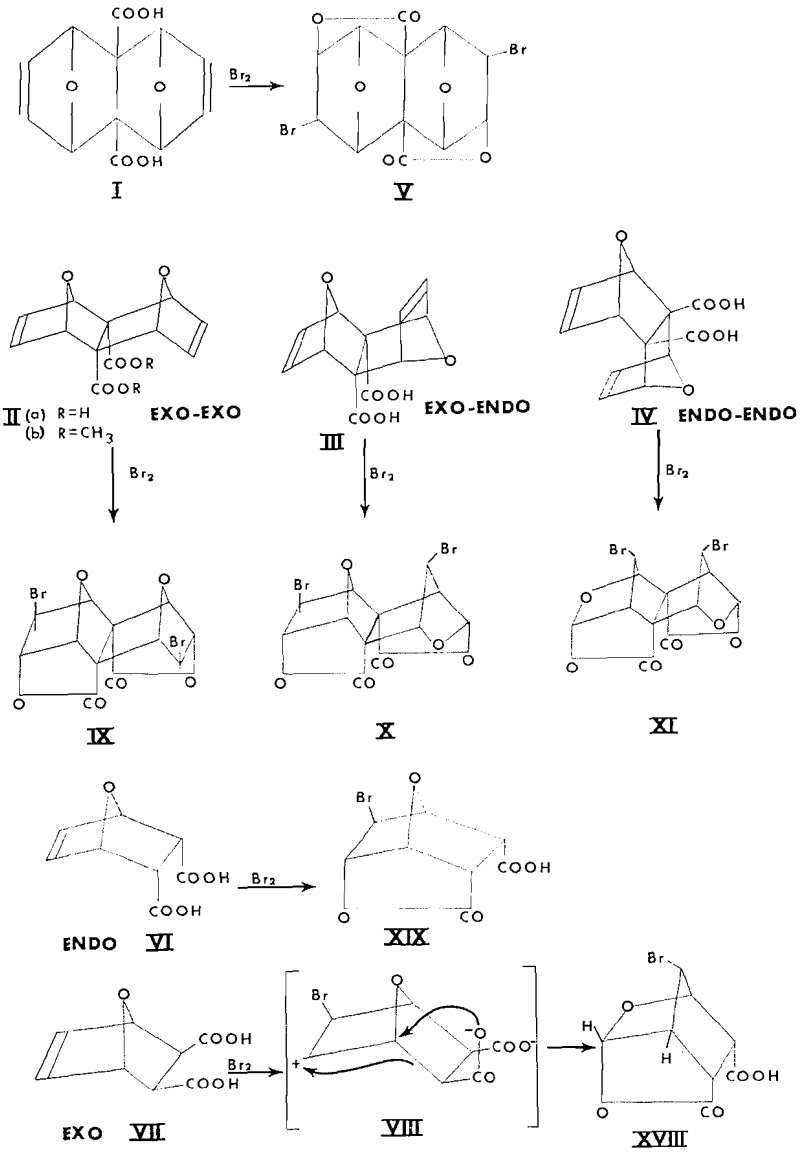
In 1961, iodolactonization of the diacid I was investigated by Stockman (4). He concluded that the adduct was a mixture of 4% *exo–exo* (II*a*) and 96% *endo–exo* (III). However, his argument is based on the specificity of iodolactonization, which in our view cannot be conclusive.

The stereochemistry of the adduct was elucidated by the following sequence of reactions. Iodolactonization (5) of the diacid II*a* in potassium carbonate solution with iodine gave iodolactone acid XII*a*; infrared: 1 775 and 1 715 cm^{-1}. On esterification with diazomethane the corresponding iodolactone acid methyl ester (XII*b*) was formed; infrared: 1 785 and 1 745 cm^{-1}. Iodolactonization usually occurs only with *endo* derivatives (5). This was confirmed when the iodolactone acid XII*a* was reconverted into the starting diacid II*a* by zinc – acetic acid treatment. This eliminated the possibility of the *endo–endo* configuration.

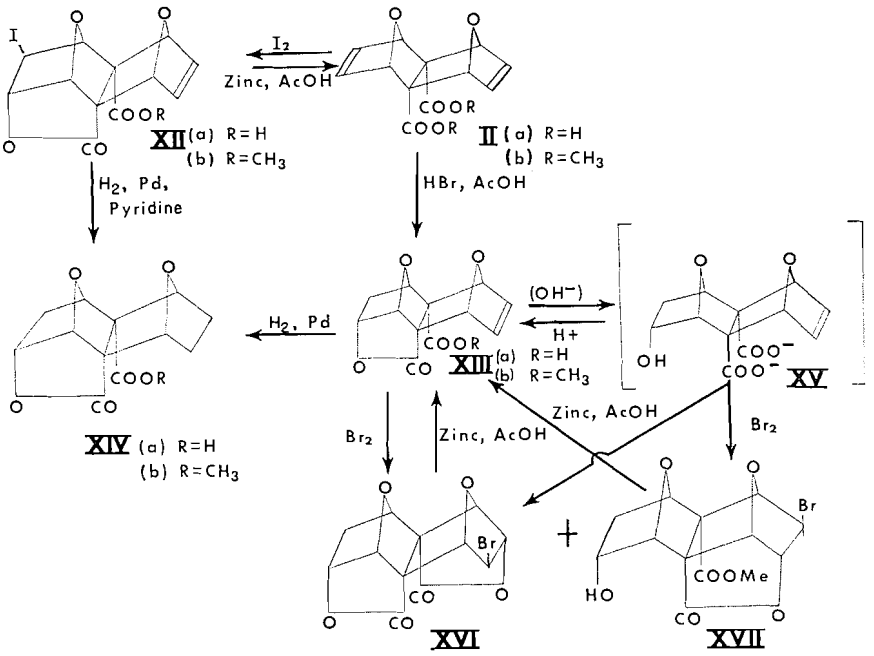
[1]*This paper has been presented in part at the Congrès de l'Association Canadienne-Française pour l'Avancement des Sciences, Montreal, Quebec, 1962.*

[2]*Present address: Département de Chimie, Université de Montréal, Montréal, Québec.*

Can. J. Chem. Downloaded from www.nrcresearchpress.com by 210.87.254.105 on 09/05/12
For personal use only.



The diacid II*a* was transformed into the lactone acid XIII*a* by the action of hydrobromic acid in acetic acid solution; infrared: 1 765 – 1 770 and 1 715 – 1 735 cm^{-1}. On esterification with diazomethane the corresponding lactone acid methyl ester (XIII*b*) was obtained; infrared: 1 780 and 1 720 – 1 740 cm^{-1}. The fact that no rearrangement occurs during lactonization was proven by a direct correlation of lactone acid XIII*a* with iodolactone acid methyl ester XII*b*. Hydrogenation of lactone acid XIII*a* yielded the dihydrolactone acid XIV*a* which, after esterification, gave dihydrolactone acid methyl ester XIV*b*; carbonyl absorption: 1 790 and 1 730 – 1 750 cm^{-1}. The same compound (XIV*b*) was obtained from a hydrogenolysis of iodolactone acid methyl ester XII*b* with Raney nickel – pyridine and was shown to be identical in every respect.



Lactone acid XIII*a* was saponified with methanolic potassium hydroxide, and the resulting dipotassium salt (XV) was brominated. Two compounds were isolated: an insoluble bromodilactone (XVI) (infrared: 1 785 cm^{-1}) and a bromohydroxylactone acid, obtained as its methyl ester (XVII) (infrared: 3 390, 1 765, and 1 745 cm^{-1}). As expected, the bromodilactone derivative (XVI) was also obtained by a direct bromination of lactone acid XIII*a*. In this manner, monolactone acid derivatives XIII*a* and XVII were obtained; these have a lactone across one or the other bicyclic ring system with the same carboxyl group.

That no skeletal rearrangement occurs during the bromolactonization was shown by the following: the hydroxylactone acid methyl ester XVII was transformed into lactone acid methyl ester XIII*b* by the action of zinc – acetic acid; the insoluble bromodilactone XVI yielded lactone acid XIII*a* after treatment with zinc – acetic acid.

The nuclear magnetic resonance spectra of two model compounds were first examined. The first one (XVIII), the rearranged bromolactone from *exo*, gave two interesting signals as expected: a proton at 8.42 τ and the proton of the hemiacetal at 3.92 τ. The second compound (XIX), the bromolactone from *endo*, did not have proton signals in these positions. Since hemiacetal protons are in a distinct position in the nuclear magnetic resonance spectrum, these findings indicate that this method can be used to differentiate between the *exo* and the *endo* forms after bromolactonization.

The nuclear magnetic resonance spectra of the soluble lactones were examined. For iodolactone acid methyl ester XII*b* in CF_3COOD, the two olefinic hydrogens appeared, respectively, as doublets (J = 6 c.p.s.) at 3.05 and 3.50 τ; from 4.40 to 4.82 τ, a complex multiplet evaluated for five hydrogens corresponded to the lactone hydrogen (—COO—*CH*$\langle$) and the four bridgehead ether protons, and at 5.82 τ a singlet for one hydrogen represented the proton of the $\rangle$CHI group. Finally, a singlet (three hydrogens) attributed to the methoxyl resonance was found at 6.34 τ.

Can. J. Chem. Downloaded from www.nrcresearchpress.com by 210.87.254.105 on 09/05/12
For personal use only.

Lactone acid methyl ester XIII*b* in $CDCl_3$ exhibited two separate doublets ($J = 6$ c.p.s.) at 3.09 and 3.62 τ, representing the two olefinic protons, and a complex multiplet from 4.77 to 5.50 τ integrating for five hydrogens, which represented the lactone proton and the four bridgehead ether protons. The methoxyl group appeared as a singlet (three hydrogens) at 6.34 τ, and the methylene group is shown as a broad singlet at 8.02 τ.

Hydroxybromolactone acid methyl ester XVII in CF_3COOD showed a complex multiplet of six protons from 4.33 to 5.23 τ attributed to the four bridgehead ether protons, the lactone proton, and the secondary alcohol groups (>CH—OH). The methoxyl and the hydrogen of the >CH—Br group appeared together as a singlet with a slight shoulder at 6.04 τ (four hydrogens), and the methylene group was shown as a broad singlet integrating for two protons at 7.92 τ. All three spectra showed no signal in the hemiacetal absorption region.

In conclusion, we first have proved the structure of the diacid II*a* by a series of chemical transformations, and then have independently confirmed it by nuclear magnetic resonance spectral analysis.

During this work, reactions of the dibromodilactone derivative IX were investigated. From the reaction of phenylmagnesium bromide on the dibromodilactone, two compounds were isolated: 1,1-diphenyl-1,4-butanediol (6) and 1-phenyl-1,4-butanediol (7). This unusual fragmentation might be explained by a retro Diels–Alder reaction to give furan which then reacted with the Grignard reagent to yield the two diols. This was confirmed by reacting the Grignard reagent with furan, which yielded the same two diols. The zinc – acetic acid reaction of the insoluble dibromodilactone IX resulted in the formation of succinic acid in a high yield. Clearly, this also indicates a retro Diels–Alder reaction to give acetylene dicarboxylic acid which was then hydrogenated to succinic acid.

EXPERIMENTAL

Melting points were recorded on a Kofler micro hot stage melting point apparatus and are uncorrected. The infrared spectra were measured on a Perkin–Elmer "Infra Cord" spectrophotometer. The nuclear magnetic resonance spectra were measured with tetramethylsilane as internal standard.

Hexahydro-1,4;5,8-dioxonaphthalene-9,10-dicarboxylic Acid (IIa) (2–6)

A modified procedure of the Diels and Alder method was employed. Acetylene dicarboxylic acid (15 g, 132 mmoles) and furan (20.5 g, 307.5 mmoles) were dissolved in ether (75 ml) and the solution was left at room temperature for 2 weeks, after which the material crystallized out. The crystals were filtered off and washed with isopropyl alcohol (95%) and finally with ether (14.3 g, 65% yield, m.p. 157–160 °C).

The analytical sample was prepared by recrystallization from isopropyl alcohol (90%), m.p. 160–162 °C (reported m.p. 158 °C (1)).

Anal. Calcd. for $C_{10}H_{10}O_6$: C, 57.60; H, 4.02. Found: C, 57.55, 57.35; H, 3.92, 3.82.

Diacid Dimethyl Ester IIb

(a) From Diacid IIa

The diacid (250 mg, 1 mmole) was dissolved in methanol and the solution cooled in an ice–salt bath. An excess of diazomethane in ether was added and the solution was immediately evaporated *in vacuo*. The crystalline material (278 mg) was recrystallized from ethanol, m.p. 154–156 °C (reported m.p. 148 °C (1)).

Anal. Calcd. for $C_{14}H_{14}O_6$: C, 60.04; H, 5.07; O, 34.50. Found: C, 59.95; H, 5.21; O, 34.70.

(b) From Iodolactone Acid XIIa

To the iodolactone acid (48.7 mg, 0.13 mmole) dissolved in glacial acetic acid (5 ml) was added zinc dust (76 mg), and the mixture was magnetically stirred at room temperature for 1 h. Then, a second portion of zinc (33 mg) was added. After 1 h, the undissolved material was filtered off and the solution evaporated to dryness. The foamy residue was dissolved in water (15 ml) and stirred with Amberlite IR-120 (H^+) resin (7.5 g) for 1 h, after which the resin was removed by filtration and the solution evaporated *in vacuo* with a water bath (temperature 35 °C). The material (37 mg) was esterified in methanol with diazomethane at a low temperature (0 °C), and the resulting mixture was purified by preparative thin-layer chromatography with silica gel G as absorbent and methanol in chloroform (1%) as eluent; the spots were developed with iodine in chloroform (0.5%).

Can. J. Chem. Downloaded from www.nrcresearchpress.com by 210.87.254.105 on 09/05/12
For personal use only.

The band in the chromatogram having a R_f value from 0.25 to 0.50 was eluted. It gave a crystalline compound (17.4 mg, 55% yield, m.p. 154–156 °C) which was recrystallized from ethanol. A mixed melting point with the compound obtained by procedure *a* showed no depression, and its infrared curve was also identical.

Iodolactone Acid XIIa

The diacid (850 mg, 4.0 mmoles) was dissolved in water (5 ml) and neutralized with sodium hydroxide (20%). Sodium bicarbonate solution (5%, 8 ml), methanol (1 ml), and water (5 ml) were added. To this mixture, an iodine solution (6.1 ml; 5 g of iodine and 10 g of KI in 30 ml of water) was added dropwise, with stirring.

After acidification (to Congo) with hydrochloric acid (3 *N*), crystallization occurred. The crystals were filtered off, washed with water, and dried (1.03 g, 80% yield, m.p. 200–205 °C (decomp.)). The analytical sample was prepared by crystallization from methanol, m.p. 205–210 °C.

Anal. Calcd. for $C_{12}H_9O_6I$: C, 38.30; H, 2.41; O, 25.50; I, 33.80. Found: C, 38.34; H, 2.52; O, 25.53; I, 33.85.

Iodolactone Acid Methyl Ester XIIb

Iodolactone acid (400 mg, 1.06 mmoles) was partly dissolved in methanol (15 ml), cooled in an ice bath, and magnetically stirred. The mixture was saturated with an ethereal solution of diazomethane. After 15 min, it was evaporated to dryness *in vacuo* and a crystalline material was obtained. The analytical sample was prepared by recrystallization from ethyl acetate or acetonitrile, m.p. 231–233 °C.

Anal. Calcd. for $C_{13}H_{11}O_6I$: C, 40.00; H, 2.83. Found: C, 40.14; H, 3.07.

Lactone Acid XIIIa

The diacid (5 g, 2 mmoles) was dissolved in a solution of hydrobromic acid in acetic acid (100 ml of a saturated solution of hydrobromic acid in acetic acid mixed with 200 ml of acetic acid) while cooled in an ice bath. The reaction mixture was stirred at room temperature for 1.5 h. The hydrobromic acid was removed *in vacuo* (water pump) and the acetic acid distilled off. The dried black crystalline material was dissolved in a minimum amount of methanol and allowed to crystallize in the cold. The crystals were filtered off and washed with methanol (2.575 g, 51.5% yield, m.p. 242–245 °C).

Anal. Calcd. for $C_{12}H_{10}O_6$: C, 57.6; H, 4.00; neutral equiv. 250.2. Found: C, 57.41; H, 4.15; neutral equiv. 246.

Lactone Acid Methyl Ester XIIIb

(a) From Lactone Acid XIIIa

Lactone acid (300 mg, 0.6 mmole) was dissolved in methanol (10 ml) and cooled in an ice bath. To this solution was added an excess of diazomethane in ether. The solvent was evaporated and the residue was crystallized from methanol (235 mg, m.p. 248–250 °C).

Anal. Calcd. for $C_{13}H_{12}O_6$: C, 59.10; H, 4.58. Found: C, 59.34, 58.95; H, 4.59, 4.70.

(b) From Bromodilactone XVI

Bromodilactone (60 mg, 0.182 mmole) was mixed with glacial acetic acid (8 ml) and zinc dust (78 mg), and refluxed for 3 h. Another portion of zinc dust was added and refluxing was continued for another 3 h. The solution was filtered and evaporated to dryness (101 mg). The residue was dissolved in water (10 ml) and stirred with Amberlite IR-120 (H^+) resin (4 g). After the resin was filtered off, the aqueous solution was evaporated to dryness. This material was dissolved in methanol (10 ml), cooled in an ice bath, and esterified with diazomethane. After evaporation, a crystalline material was obtained. This material was purified by preparative thin-layer chromatography with silica gel G as absorbent and methanol in chloroform (3%) as eluent.

The material having a R_f value from 0.64 to 0.77 was eluted. Its infrared spectrum was identical with that of an authentic sample (from procedure *a*). After crystallization from methanol, it had m.p. 248–250 °C. The material showed no depression on a mixed melting point determination.

(c) From Bromohydroxylactone Acid Methyl Ester XVII

Bromohydroxylactone acid methyl ester (15.4 mg, 0.042 mmole) was dissolved in acetic acid (2 ml) and mixed with zinc dust (24 mg). This mixture was refluxed for 3 h, then another portion of zinc dust (38 mg) was added, and refluxing was continued for an extra 3 h. The acetic acid solution was filtered and evaporated to dryness. The residue was dissolved in water (3 ml) and extracted with five portions of chloroform (5 ml). The dried chloroform solutions were evaporated to dryness (9.1 mg).

This material was purified by preparative thin-layer chromatography as described in procedure *b*. The resulting crystalline material (3 mg, m.p. 248–250 °C) was shown to be identical with an authentic sample (from procedure *a*) by comparison of infrared spectra. Also, the material showed no depression on a mixed melting point determination.

Dihydrolactone Acid Methyl Ester XIVb

(a) From Lactone Acid XIIIa

Lactone acid (92 mg, 0.35 mmole) was dissolved in methanol (25 ml) and hydrogenated with pre-reduced platinum oxide (20 mg). The hydrogen consumption stopped after 6 min, the catalyst was removed by filtration, and the solvent was evaporated to dryness. The residue was dissolved in methanol and esterified with an

Can. J. Chem. Downloaded from www.nrcresearchpress.com by 210.87.254.105 on 09/05/12
For personal use only.

ethereal solution of diazomethane. The solution was evaporated to yield a crystalline material (92 mg). After recrystallization from methanol, it had m.p. 260–262 °C.

Anal. Calcd. for $C_{13}H_{13}O_6$: C, 58.7; H, 4.95. Found: C, 58.76, 58.52; H, 5.13, 5.18.

(b) From Iodolactone Acid Methyl Ester XIIb

Iodolactone acid methyl ester (60 mg, 0.154 mmole) was dehalogenated and hydrogenated in ethanol (75 ml) in the presence of pyridine (0.06 ml) and Raney nickel (about 300 mg) for 4 h in an atmosphere of hydrogen at normal pressure. The solution was filtered and evaporated to dryness. The solid mixture (46.6 mg) was purified by preparative thin-layer chromatography with silica gel G as absorbent and methanol in chloroform (1%) as eluent. The material (R_f value 0.5) was eluted (36.5 mg) and crystallized from methanol, m.p. 252–255 °C. The infrared spectrum of this compound was identical with that of the compound from procedure *a*. A mixed melting point determination showed no depression.

Bromodilactone XVI

(a) From Lactone Acid XIIIa

Lactone acid (165 mg, 0.66 mole) was dissolved in a sodium bicarbonate solution (1.91 mmoles, 11 ml), cooled in an ice bath, and stirred magnetically. Bromine was added until a persistent bromine color remained. The reaction was left for 50 min at room temperature. The solution was acidified with dilute hydrochloric acid (to Congo); the resulting precipitate was filtered off, washed with water and then methanol, and dried (180 mg, 84% yield). Recrystallization from dimethylformamide gave the analytical sample, m.p. 355–365 °C.

Anal. Calcd. for $C_{12}H_9O_6Br$: C, 43.8; H, 2.75; O, 29.2; Br, 24.3. Found: C, 43.91; H, 2.79; O, 28.98; Br, 24.31.

(b) Bromodilactone XVI and Bromohydroxylactone Acid Methyl Ester XVII from the Dipotassium Salt XV

Lactone acid (250 mg, 1 mmole) was mixed with methanol (60 ml) containing potassium hydroxide (179 mg, 3.2 mmoles). This mixture was refluxed until all the solid was dissolved (0.5 h), and then left for 2 h. This solution was evaporated *in vacuo* and water (20 ml) was added. To this solution was added an excess of bromine (0.1 ml, 298 mg, 1.88 mmoles). After the solution was stirred at room temperature (30 min), the resulting precipitate was filtered off, washed with boiling water, and dried (87.5 mg). A mixed melting point determination with bromodilactone from the previous experiment showed no depression. The infrared spectrum was also identical.

The mother liquor was acidified (to Congo) with hydrochloric acid solution (*N*) and extracted overnight with ether. The dried ether solution was evaporated to dryness (173.2 mg). This material was partly dissolved in methanol, saturated with an ethereal solution of diazomethane, and then evaporated to dryness (174.7 mg). The resulting crystalline mixture was separated by chromatography with silica gel (5.1 g). Elution with chloroform in benzene (25%) yielded two fractions (40 mg and 91 mg). The second fraction (91 mg) was recrystallized from acetonitrile (48.3 mg, m.p. 250–255 °C (melts, resolidifies at 275°, and remelts at 330–340 °C)).

Anal. Calcd. for $C_{13}H_{13}O_7Br$: C, 43.30; H, 3.60; O, 31.1; Br, 22.10. Found: C, 43.48, 43.22; H, 3.71, 3.69; O, 31.07; Br, 22.09.

Dibromodilactone IX

The diacid (1 g, 4.03 mmoles) was dissolved in an aqueous solution (50 ml) of sodium bicarbonate (715 mg, 8.50 mmoles). This solution was cooled in an ice bath and bromine (1.3 g, 8.2 mmoles) was added until a persistent bromine color remained. This solution was acidified (to Congo) with hydrochloric acid (*N*), and when cooled, crystallization occurred. The crystals were filtered off and washed with water, methanol, and ether (1.59 g, 97% yield). The compound was recrystallized from dimethylformamide or ethyl acetate. It sublimed slowly from 300 to 360 °C.

Anal. Calcd. for $C_{12}H_8O_6Br_2$: C, 35.4; H, 1.98; Br, 39.3. Found: C, 35.47; H, 2.04; Br, 39.01.

Zinc – Acetic Acid Reaction on Dibromodilactone IX

Dibromodilactone (400 mg, 0.98 mmole) was mixed with glacial acetic acid (100 ml) and zinc dust (150 mg), and the mixture refluxed for 11 h. After the second (200 mg), the fourth (400 mg), and the fifth hour (400 mg), fresh portions of zinc dust were added. The zinc residue was removed by filtration and the solution evaporated to dryness. The foamy residue (1.4 g) was dissolved in water (40 ml). A portion (20 ml) of this aqueous solution was mixed with Amberlite IR-120 (H^+) resin (5 g). After removal of the resin by filtration, the aqueous solution was evaporated to dryness *in vacuo* (water bath temperature 35 °C) and yielded a crystalline residue (46.7 mg). After sublimation *in vacuo*, a crystalline material (34 mg, 60% yield, m.p. 185 °C) was obtained and identified as succinic acid by comparison of its infrared spectrum with that of an authentic sample. Also, a mixed melting point determination showed no depression.

Grignard Reaction on Dibromodilactone IX

The phenylmagnesium bromide reagent was prepared in the usual way by mixing magnesium turnings (729 mg, 30.0 mg-atoms) with bromobenzene (4.70 g, 30.0 mmoles) in dry ether (10 ml.). A solution of dibromodilactone (204 mg, 0.5 mmole) in dry tetrahydrofuran (130 ml) was dropped slowly into the Grignard reagent solution and the reaction mixture was refluxed for 1 day with magnetic stirring. The tetrahydrofuran

Can. J. Chem. Downloaded from www.nrcresearchpress.com by 210.87.254.105 on 09/05/12
For personal use only.

solvent was replaced by benzene by the distillation technique. This benzene solution was cooled in an ice bath and an ammonium chloride solution (25%, 5 ml) was dropped in slowly. The benzene layer was separated, and the aqueous solution was acidified with hydrochloric acid and extracted with ether. The benzene–ether phase was washed with sodium hydroxide solution (*N*) and water. The dried organic phase was evaporated to dryness (1.09 mg). This mixture was chromatographed on Florisil (25 g).

Elution with benzene yielded a compound (550 mg) which was identified as biphenyl. Elution with benzene–chloroform (50%) gave a compound (108 mg) which was crystallized from toluene (50.2 mg), m.p. 106–107 °C. This crystalline material was found to be 1,1-diphenyl-1,4-butanediol by comparison of its infrared curve with that of an authentic sample (6). Also, a mixed melting point showed no depression.

Elution with pure chloroform yielded a semicrystalline material (120 mg) which was mixed with a solution of chloroform – carbon tetrachloride (1:9) and the insoluble crystals filtered off (73.1 mg). Recrystallization from toluene yielded a compound with m.p. 60–64 °C. The infrared spectrum of this compound was identical with that of 1-phenyl-1,4-butanediol (7). A mixed melting point determination showed no depression.

Grignard Reaction on Furan

This experiment was performed under the exact conditions described above, except that dibromodilactone was replaced by furan (300 mg). The same work-up gave both compounds: 1,1-diphenyl-1,4-butanediol (10 mg) and 1-phenyl-1,4-butanediol (90 mg).

REFERENCES

1. O. DIELS and K. ALDER. Ann. **490**, 243 (1931).
2. O. DIELS and S. OLSEN. J. Prakt. Chem. **156**, 285 (1940).
3. R. B. WOODWARD and H. BEAR. J. Am. Chem. Soc. **70**, 1161 (1948).
4. H. STOCKMAN. J. Org. Chem. **26**, 2025 (1961).
5. C. S. RONDESVEDT and C. V. DER NOOY. J. Am. Chem. Soc. **77**, 4878 (1955).
6. C. WEIZMAN and F. BERGMAN. J. Am. Chem. Soc. **60**, 2647 (1938).
7. R. L. LETSINGER and D. F. POLLART. J. Am. Chem. Soc. **78**, 6079 (1956).

Can. J. Chem. Downloaded from www.nrcresearchpress.com by 210.87.254.105 on 09/05/12
For personal use only.

Can. J. Chem. Downloaded from www.nrcresearchpress.com by 210.87.254.105 on 09/05/12
For personal use only.

CHEMISTRY AND SYNTHESIS OF SOME DIHYDRO-2*H*-1,4-BENZOTHIAZINE DERIVATIVES

RAJ NANDAN PRASAD[1] AND KARIN TIETJE
Research Department, Abbott Laboratories Limited, Montreal, Quebec

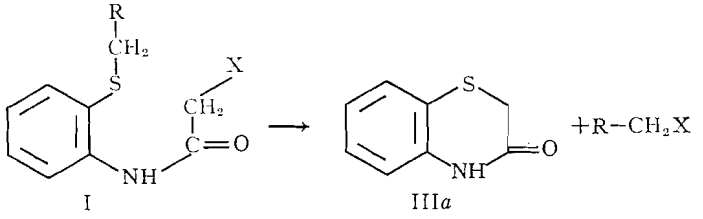
Received October 13, 1965

ABSTRACT

The formation of 3-oxo-3,4-dihydro-2*H*-1,4-benzothiazine (III*a*) by cyclization of alkyl 2-haloacetamidophenyl sulfides (I) was investigated; it is proposed that the reaction proceeds via a six-membered sulfonium halide. The preparation of 4-alkyl derivatives of III*a* and of 4-alkyl and 4-acyl derivatives of its reduction product 3,4-dihydro-2*H*-1,4-benzothiazine (V*a*) is described. Acylation of V*a* was shown to proceed without opening of the thiazine ring. Preparation of the O-benzoyl, N-benzoyl, and O,N-dibenzoyl derivatives of 2-(β-hydroxyethylmercapto)aniline (VIII) has permitted clarification of the confusion in the literature with respect to the derivatives of V*a* and VIII. Compound XVIII, the 1,1-dioxide of III*a*, undergoes C-alkylation at the 2-position when treated with alkyl halides, rather than O-alkylation as previously suggested.

The formation of 3-oxo-3,4-dihydro-2*H*-1,4-benzothiazine (III*a*) when the distillation of 2-(α-chloroacetamido)phenyl methyl sulfide (I*a*) was attempted was reported recently by Davis *et al.* (1). It was observed in this laboratory that the reaction is general for 2-(α-chloroacetamido)phenyl alkyl (and aralkyl) sulfides (Table I), and that when the

TABLE I



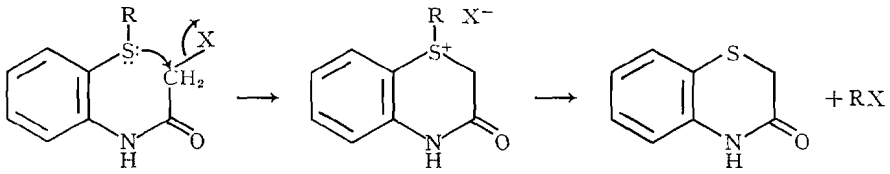
I III*a*

Compound No.	R	X	Method	% yield of products III*a*	% yield of products RCH_2X
I*a*	H	Cl	A	65*	—
I*b*	CH_3	Cl	A	61	—
I*c*	CH_3CH_2	Cl	A	30	—
I*d*	$CH_3CH_2CH_2$	Cl	A	26	—
I*e*	C_6H_5	Cl	A	64	76
I*f*	$C_6H_5CH_2$	Br	B	50	88
I*f*	$C_6H_5CH_2$	Br	C	51	43†
I*g*	$C_6H_5CH_2$	I	D	24	—
I*g*	$C_6H_5CH_2$	I	E	49	49
I*g*	$C_6H_5CH_2$	I	F	17	22
I*g*	$C_6H_5CH_2$	I	G	48	57
I*g*	$C_6H_5CH_2$	I	H	70	48

*See ref. 1.
†The halide that was isolated was phenethyl iodide.
NOTE: A, heating at 180–200 °C, under water aspirator pressure; B, heating at 140–180 °C, under water aspirator pressure (8 mm); C, refluxed for 3 h with an equivalent amount of sodium iodide in acetone; D, refluxed for 3 h in acetone only; E, refluxed for 3 h with an equivalent amount of sodium bromide in acetone; F, stirred at room temperatu re for 3 h in dimethyl sulfoxide; G, stirred in dimethyl sulfoxide at 60° for 3 h; H, stirre d in dimethyl sulfoxide at 60° for 3 h with an equivalent amount of sodium bromide.

[1]*To whom inquiries concerning this paper should be sent.*

aralkyl group was benzyl or phenethyl, the corresponding halide was isolated in good yield. This suggests the possibility that the elimination of these halides proceeds through a six-membered cyclic sulfonium halide (II).



I II IIIa

Refluxing 2-(α-bromoacetamido)phenyl phenethyl sulfide (I*f*) with an equivalent amount of sodium iodide in acetone gave III*a* in 51% yield. Instead of phenethyl bromide, however, phenethyl iodide was obtained in 43% yield as the second product. 2-(α-Iodoacetamido)phenyl phenethyl sulfide was prepared in 78% yield by stirring the bromo compound with an equivalent amount of sodium iodide in acetone at room temperature for 20 min. The iodo derivative, when it was refluxed in acetone for 3 h, gave only a 20% yield of III*a*; however, when sodium bromide was added the yield was increased to 49%.

The reaction probably proceeds in two stages. In the slow or rate-determining step, the sulfonium ion (II) is formed. The rate of sulfonium ion formation appears to be dependent on the polarity of the solvent. Because charged moieties are being formed in the transition state, the addition of sodium bromide can be expected to accelerate the reaction by providing additional charge stabilization (2).

Distillation of 2-(α-chloroacetamido)anisole under similar conditions proceeded normally with no decomposition or elimination of methyl chloride, thus showing the lesser nucleophilic reactivity of oxygen compared with that of sulfur.

The 2-(α-haloacetamido)phenyl alkyl or aralkyl sulfides (I) were prepared according to the method of Davis *et al.* (1) from 2-alkyl- or 2-aralkyl-mercaptoanilines (Table II).

The 6-chloromethyl (3) and 6-trifluoromethyl (4) derivatives (III*b* and III*c*) were prepared by reductive cyclization of the corresponding *o*-nitrophenylthioglycolic acids (5, 6). It was found that the reduction was more conveniently performed with sodium hydrosulfite than with the other reagents previously described in the literature.

Treatment of III with alkyl or aralkyl halides in alcoholic potassium hydroxide or in dimethylformamide containing sodium hydroxide gave the new N-alkyl or N-aralkyl derivatives (IV) (Table III). When III*a* was allowed to react with ethyl chloroacetate, the use of sodamide gave better results than the standard method with sodium hydride.

The reduction of III*a* with $LiAlH_4$ in ether by the procedure of Angelini *et al.* (7) gave 3,4-dihydro-2*H*-1,4-benzothiazine (V*a*) in 80% yield, but was unsatisfactory for large-scale preparation because of the low solubility of III*a* in ether. The use of tetrahydrofuran according to the procedure of Hromatka *et al.* (8) repeatedly resulted in a violent and uncontrollable reaction towards the end of the addition period; when the addition was performed at reflux temperature, the reduction could be accomplished without difficulty. III*b* was reduced smoothly by $LiAlH_4$ in ether solution to V*b* (9). III*c* was more conveniently reduced with diborane in tetrahydrofuran solution to V*c*.

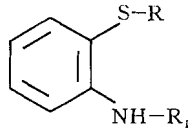
Several of the N-alkyl derivatives (IV) were reduced by $LiAlH_4$ in ether to give the N-alkyl dihydrobenzothiazines (VI) (Table IV). The carbethoxymethyl substituent in IV*d* was reduced during the reaction to a β-hydroxyethyl group (VI*c*).

Can. J. Chem. Downloaded from www.nrcresearchpress.com by 210.87.254.105 on 09/05/12
For personal use only.

Can. J. Chem. Downloaded from www.nrcresearchpress.com by 210.87.254.105 on 09/05/12
For personal use only.

TABLE II

o-Substituted aminophenyl sulfides



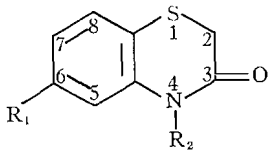
Compound No.	R	R_1	Melting, °C, or boiling, °C (mm), point	Solvent*	% yield	Formula	% analyses: Calcd. C	H	N	S	X†	Found C	H	N	S	X†
	i-C_3H_7	H	78–80 (0.55)‡	—	86	$C_9H_{13}NS$	64.62	7.83	8.38	—	—	64.68	7.98	8.46	—	—
	$CH_2CH_2C_6H_5$	H	150 (0.2)	—	81	$C_{14}H_{15}NS$	73.32	6.59	6.11	—	—	73.14	6.62	6.20	—	—
Ie	$CH_2C_6H_5$	$COCH_2Cl$	53–54	E + PE	63	$C_{15}H_{14}ClNOS$	61.73	4.84	4.80	—	12.15 (Cl)	61.79	4.85	4.96	—	12.17 (Cl)
If	$CH_2CH_2C_6H_5$	$COCH_2Br$	60–62	E + PE	61	$C_{16}H_{16}BrNOS \cdot \frac{1}{2}H_2O$	53.48	4.77	3.90	—	22.24 (Br)	53.93	4.94	4.47	—	22.24 (Br)
Ig	$CH_2CH_2C_6H_5$	$COCH_2I$	83–84	E + PE	78	$C_{16}H_{16}INOS$	48.37	4.06	3.53	—	31.94 (I)	48.50	4.09	3.72	—	32.22 (I)
Ih	CH_3	$COCH_2Br$	67–68.5	E + PE	45.6	$C_9H_{10}BrNOS$	41.55	3.88	5.39	12.32	30.72 (Br)	41.50	3.97	5.19	12.49	30.95 (Br)
Ii	CH_3	$COCH_2CH_2Cl$	70–71	E + PE	61	$C_{10}H_{12}ClNOS$	52.28	5.27	6.10	13.96	15.43 (Cl)	52.30	5.31	6.06	13.81	15.61 (Cl)
Ij	CH_3	$COCHCl_2$	96–97	E + PE	80	$C_9H_9Cl_2NOS$	43.21	3.63	5.60	12.82	28.34 (Cl)	43.10	3.65	5.68	12.56	28.46 (Cl)
X	CH_2CH_2OH	COC_6H_5	88.5–90§	E + M	68	$C_{15}H_{15}NO_2S$	65.90	5.53	5.13	11.73	—	65.97	5.37	4.92	11.67	—
XI	$CH_2CH_2OCOC_6H_5$	H	44.5–46	A + W	69.6	$C_{15}H_{15}NO_2S$	65.90	5.53	5.12	11.73	—	65.92	5.68	5.04	12.09	
			176–180			$C_{15}H_{16}NO_2S \cdot HCl$	58.14	5.21	4.32	10.35	11.45 (Cl)	58.23	5.28	4.42	10.59	11.15 (Cl)
XII	CH_2CH_2OH	$CONHC_6H_3Cl_2$	156–157	E	68.6	$C_{15}H_{14}Cl_2N_2O_2S$	50.42	3.95	7.84	8.97	19.85 (Cl)	50.72	4.08	8.07	8.99	19.74 (Cl)
XIII	$CH_2CH_2OCOC_6H_5$	$CONHC_6H_3Cl_2$	153–154	A	34.8	$C_{22}H_{18}Cl_2N_2O_3S$	57.28	3.93	6.07	6.95	15.37 (Cl)	57.01	4.25	5.87	6.76	15.30 (Cl)
XIV	$CH_2CH_2OCOCH_3$	$COCH_3$	184–186 (1.1)	—	96	$C_{12}H_{15}NO_3S$	56.89	5.97	5.53	12.66	—	56.85	5.91	5.63	12.88	—
XV	CH_2CH_2OH	$COCH_3$	176 (0.5)	—	96	$C_{10}H_{13}NO_2S$	56.85	6.20	6.63	15.18		57.07	6.43	6.70	15.01	

*Recrystallization solvents: E, ether; PE, petroleum ether (30–60°); A, ethanol; W, water; M, methanol.
†The particular halogen analyzed is indicated in parentheses.
‡n_D^{25} 1.5808.
§96% yield from IX and potassium hydroxide in dilute ethanol; lit. (14) m.p. 75°.

Can. J. Chem. Downloaded from www.nrcresearchpress.com by 210.87.254.105 on 09/05/12
For personal use only.

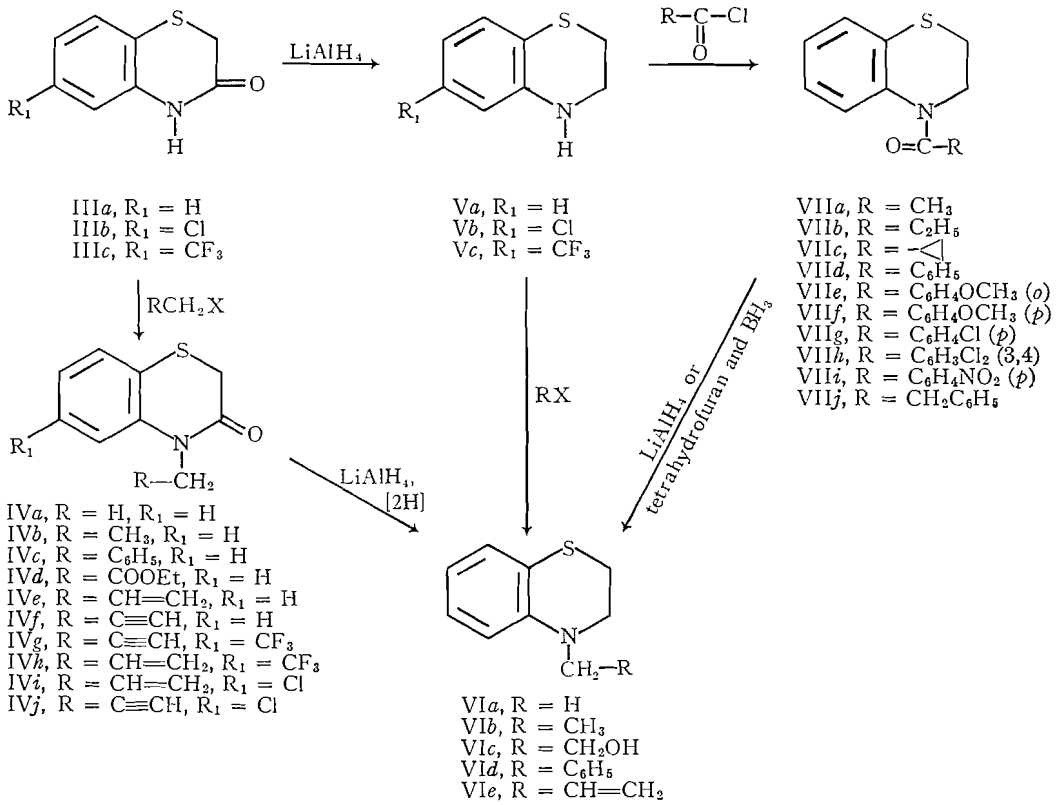
TABLE III

3,4-Dihydro-3-oxo-substituted-2*H*-1,4-Benzothiazines



Compound No.	R_1	R_2	Melting, °C, or boiling, °C (mm), point	% yield	Solvent*	Formula	% analyses: Calcd. C	H	N	S	X†	Found C	H	N	S	X†	Method
IV*b*	H	C_2H_5	182–190 (12)	54‡	—	—											B
IV*c*	H	$CH_2C_6H_5$	84.5–85.5	62§	A	$C_{15}H_{13}NOS$	70.55	5.13	5.59		—	70.66	5.24	5.58			A, B
IV*d*	H	$CH_2COOC_2H_5$	48.5–50.5	19	E + PE	$C_{12}H_{13}NO_3S$	57.35	5.21	5.58	—	—	57.24	5.28	5.75	—	—	
IV*e*	H	$CH_2CH{=}CH_2$	124 (0.3)	63.5	—	$C_{11}H_{11}NOS$	64.36	5.40	6.83	—	—	64.40	5.37	7.07	—	—	A‖
IV*f*	H	$CH_2{-}C{\equiv}CH$	111–112	59	A + W	$C_{11}H_9NOS$	65.00	4.46	6.89	—	—	64.80	4.54	6.92	—	—	A‖
IV*g*	F_3C	$CH_2{-}C{\equiv}CH$	72–76	62	PE	$C_{12}H_8F_3NOS$	53.13	2.97	5.16	—	21.02 (F)	52.85	2.89	5.38	—	20.64 (F)	A‖
IV*h*	F_3C	$CH_2CH{=}CH_2$	124 (0.65)	82	—	$C_{12}H_{10}F_3NOS$	52.72	3.69	5.13	—	20.86 (F)	52.85	3.79	5.21	—	20.58 (F)	A‖
IV*i*	Cl	$CH_2CH{=}CH_2$	52–55	25	PE	$C_{11}H_{10}ClNOS$	55.11	4.21	5.84	—	14.80 (Cl)	54.95	4.01	5.87	—	15.24 (Cl)	A‖
IV*j*	Cl	$CH_2{-}C{\equiv}CH$	78.5–80.5	23	PE	$C_{11}H_8ClNOS$	55.58	3.39	5.89	—	14.92 (Cl)	55.37	3.07	6.00	—	14.82 (Cl)	A‖

*Recrystallization solvents: A, ethanol; E, ether; PE, petroleum ether (30–60°); W, water.
†The particular halogen analyzed is indicated in parentheses.
‡The distilled product was cloudy; hence it was reduced to VI*b* without elemental analysis.
§The yield varied depending on the method used: 42% by method A and 62% by method B.
‖The halide that was used was allyl or propargyl bromide.



REACTION SCHEME 1.

Treatment of the unsubstituted dihydrobenzothiazine (V*a*) with acyl halides and pyridine in ether gave a number of new N-acyl dihydrobenzothiazines (VII) (Table IV).

The N-benzoyl derivative (VII*d*) was reduced by diborane to the corresponding N-benzyl derivative (VI*d*). This reduction could not be effected by $LiAlH_4$, which caused cleavage of the benzoyl group (cf. Nystrom and Brown (10)).

In contrast, the N-acetyl derivative (VII*a*) was readily converted by $LiAlH_4$ into the N-ethyl derivative (VI*b*).

An alternative approach to the N-alkyl derivatives (VI) was the direct alkylation of V*a*; this method was applied successfully in the preparation of the N-benzyl and N-methyl derivatives.

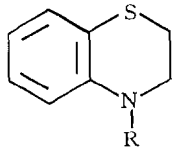
It is interesting to note that none of the acylation reactions of V*a* showed signs of thiazine ring opening. Acylation of several substituted 3,4-dihydro-2*H*-1,4-benzothiazines in an alkaline medium has also been reported by Lowrie (11) to occur without ring opening. The suggestion that the heterocyclic ring in dihydrobenzothiazines is readily opened (12, 13) would thus appear to be incorrect. Some of the confusion in the earlier literature arises from the reported synthesis of V*a* (Fusco and Palazzo (14)) from *o*-nitrochlorobenzene and 2-mercaptoethanol. Fusco and Palazzo isolated the dibenzoyl derivative (IX) when their product was benzoylated, and therefore concluded that ring cleavage had occurred; however, it has been shown (8, 15) that their initial product was, in fact, 2-(β-hydroxyethylmercapto)aniline (VIII). The interconversions of the O-benzoyl,

Can. J. Chem. Downloaded from www.nrcresearchpress.com by 210.87.254.105 on 09/05/12
For personal use only.

Can. J. Chem. Downloaded from www.nrcresearchpress.com by 210.87.254.105 on 09/05/12
For personal use only.

TABLE IV

3,4-Dihydro-4-substituted-2*H*-1,4-benzothiazines



Compound No.	R	Melting, °C, or boiling, °C (mm), point	% yield*	Solvent†	Formula	% analyses									
						Calcd.					Found				
						C	H	N	S	X‡	C	H	N	S	X‡
V*a*	H	37–38,§ 116–118 (0.5)	62		C_8H_9NS	63.53	6.00	9.26	21.21	—	63.36	6.06	9.13	21.37	—
				M + B	$C_8H_9NS{\cdot}HCl$‖	51.19	5.37	7.47	17.08	18.89 (Cl)	51.37	5.34	7.27	17.11	18.86 (Cl)
VI*a*	CH_3	100 (0.4)	65.5¶		$C_9H_{11}NS$**	65.42	6.71	8.48	19.40	—	65.36	6.70	8.71	19.72	—
VI*b*	C_2H_5	104 (0.17)	76.5		$C_{10}H_{13}NS$	66.99	7.31	7.81	17.89	—	67.27	7.10	7.73	17.63	—
VI*c*	CH_2CH_2OH	151 (0.4)	60		$C_{10}H_{13}NOS$	61.50	6.71	7.18	16.42	—	61.20	6.73	7.54	15.95	—
VI*d*	$CH_2C_6H_5$	96.5–97.5	80††	A + W	$C_{15}H_{15}NS$	74.64	6.27	5.81	13.29	—	74.80	6.20	5.67	13.39	—
VI*e*	$CH_2{-}CH{=}CH_2$	102–103 (0.3)	47		$C_{11}H_{13}NS$	69.06	6.85	7.32	—	—	68.72	6.62	7.73	—	—
VII*a*	$COCH_3$	55–57	59	E + PE	$C_{10}H_{11}NOS$	62.14	5.74	7.25	16.59	—	62.35	5.73	7.32	16.78	—
VII*b*	$COCH_2CH_3$	52–53	67	E + PE	$C_{11}H_{13}NOS$	63.73	6.32	6.76	15.47	—	63.90	6.44	6.78	15.76	—
VII*c*	CO—◁	70–71.5	62	M + W	$C_{12}H_{13}NOS$	65.72	5.97	6.39	14.62	—	65.67	5.87	6.47	14.44	—
VII*d*	COC_6H_5	88–89.5	74	E + PE	$C_{15}H_{13}NOS$	70.55	5.13	5.49	12.56	6.26 (O)	70.35	5.04	5.70	12.73	5.88 (O)
VII*e*	$COC_6H_4OCH_3$ (*o*)	141.5–142.5	61	A + W	$C_{16}H_{15}NO_2S$	67.34	5.30	4.91	11.24	—	67.11	5.38	5.11	11.25	—
VII*f*	$COC_6H_4OCH_3$ (*p*)	127–128	69	A + W	$C_{16}H_{15}NO_2S$	67.34	5.30	4.91	11.24	—	67.23	5.42	4.83	11.28	—
VII*g*	COC_6H_4Cl (*p*)	101–103	94	A + W	$C_{15}H_{12}ClNOS$	62.16	4.18	4.83	11.07	12.24 (Cl)	62.13	4.23	4.69	11.21	12.03 (Cl)
VII*h*	$COC_6H_3Cl_2$ (3,4)	101.5–103	72	A + W	$C_{15}H_{11}Cl_2NOS$	55.56	3.42	4.32	9.89	21.87 (Cl)	55.45	3.37	4.15	10.22	21.75 (Cl)
VII*i*	$COC_6H_4NO_2$ (*p*)	186.5–188.5	89	A + B	$C_{15}H_{12}N_2O_3S$	59.98	4.03	9.33	10.68	—	60.26	4.30	9.13	10.79	—
VII*j*	$COCH_2C_6H_5$	73–74	90	A + W	$C_{16}H_{15}NOS$	71.35	5.61	5.20	11.90	—	71.48	5.65	5.06	11.72	—
XXII*a*	$CONHC_6H_3Cl_2$ (3,4)	160–161	99	A	$C_{15}H_{12}Cl_2N_2OS$	53.10	3.57	8.26	9.45	20.90 (Cl)	53.41	3.50	8.17	9.28	20.43 (Cl)
XXII*b*	$CONHCH_3$	116–117.5	18	M + E	$C_{10}H_{12}N_2OS$	57.65	5.81	13.45	15.40	—	57.66	5.85	13.36	15.21	—
XXII*c*	$CONHC_2H_5$	81.5–82.5	27	E + PE	$C_{11}H_{14}N_2OS$	59.43	6.35	12.61	14.42	—	59.83	6.07	12.68	14.74	—
XXII*d*	$CONHC_6H_5$	110–111	65	PE	$C_{15}H_{12}N_2OS$	65.18	7.29	10.14	11.60	—	65.18	7.15	10.18	11.81	—
XXII*e*	$CONHC_{10}H_{17}$	171–172	94	B	$C_{19}H_{16}N_2OS$	71.22	5.03	8.75	10.00	—	70.96	4.86	8.72	10.18	—

*Yields given are those of the crude solid or the once-distilled liquid.

†Recrystallization solvents: A, ethanol; B, benzene; E, ether; M, methanol; PE, petroleum ether (30–60°); W, water.

‡The particular element analyzed is indicated in parentheses.

§For reported physical data, see refs. 7–9, 23, and 28.

‖The pinkish-white hydrochloride (m.p. 162–165 °C) was obtained from V*a* and dry HCl gas, in ether containing a little methanol. Fusco and Palazzo (14) report that the hydrochloride salt was hygroscopic and gave no melting point, etc.

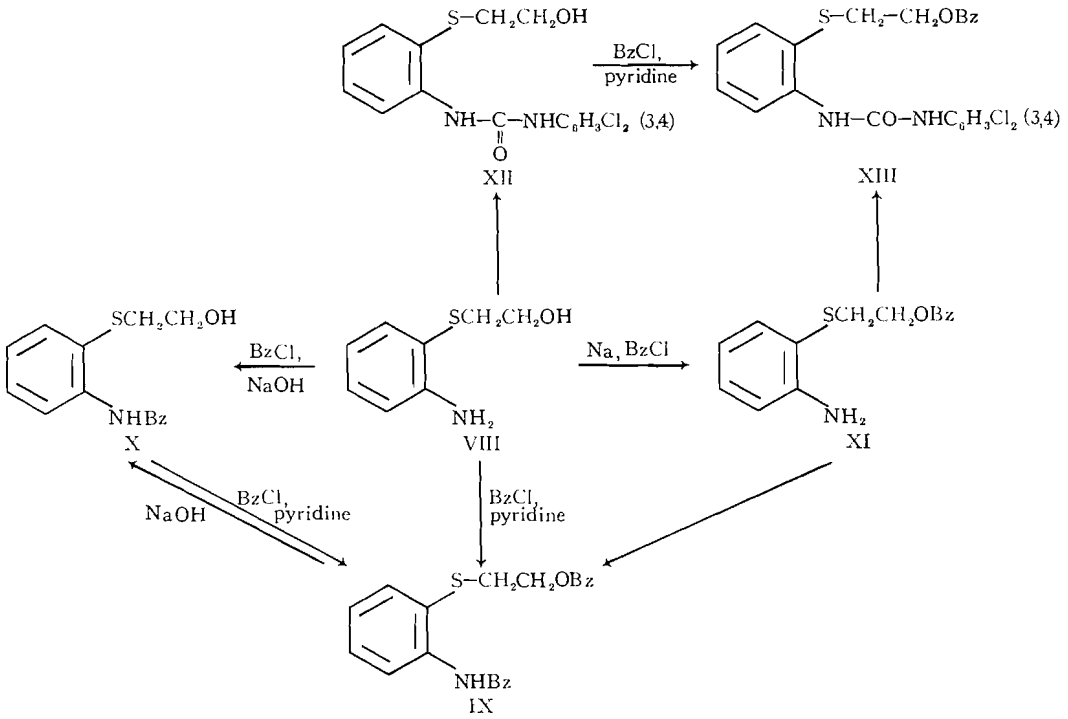
¶65.5% from IV*a* and $LiAlH_4$.

**Formed a picrate, m.p. 132–133° (decomp.) when crystallized from aqueous ethanol.

Anal. Calcd. for $C_9H_{11}NS{\cdot}C_6H_3N_3O_7$: C, 45.68; H, 3.58; N, 14.21. Found: C, 45.82; H, 3.79; N, 14.16.

††Yield varied from 0 to 80% depending on the method used: 80% from IV*c* and diborane; 70% from VII*d* and diborane; 0% from VII*d* and $LiAlH_4$; 52% from V*a*, benzyl chloride, and potassium iodide.

N-benzoyl, and O,N-dibenzoyl derivatives of VIII are shown in Reaction Scheme 2. The O-benzoyl derivative (XI) may be prepared by the gradual addition of 1 equivalent of benzoyl chloride to a suspension of the sodium salt of VIII in toluene.



REACTION SCHEME 2.

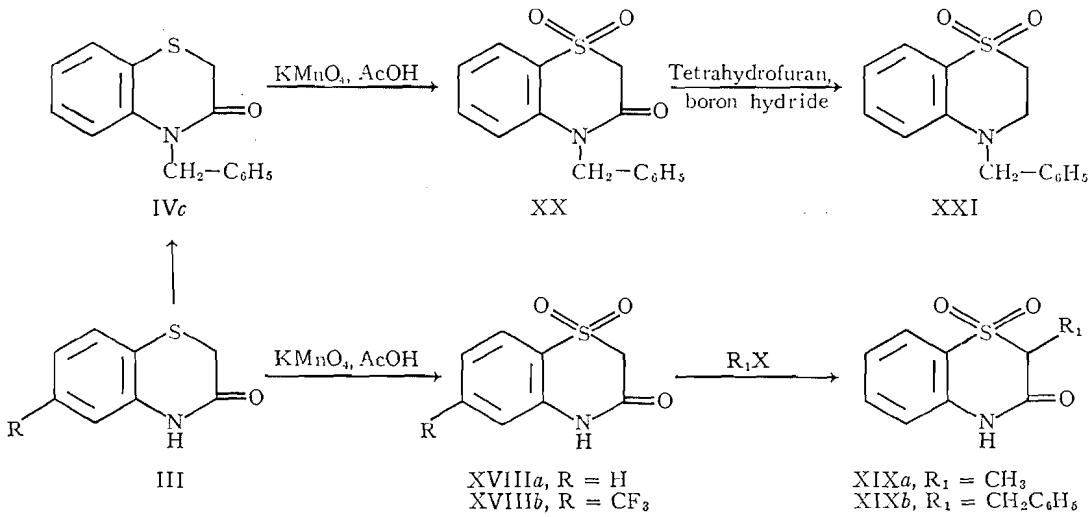
Reaction of XI with 3,4-dichlorophenylisocyanate gives XIII, which could also be obtained from XII and benzoyl chloride. Refluxing VIII with acetic anhydride gave the N,O-diacetyl derivative (XIV) in a quantitative yield. The latter, when boiled with aqueous alcoholic potassium hydroxide for 5 min, gave 2-(β-hydroxyethylmercapto)-acetanilide (XV) in 96% yield.

Nitrosation of V*a* gave 3,4-dihydro-4-nitroso-2*H*-1,4-benzothiazine (XVI) as an oil, which was reduced to 4-amino-3,4-dihydro-2*H*-1,4-benzothiazine (XVII) (characterized as the hydrochloride). The two methylene groups of XVII gave signals centered at τ 6.36 and 6.85 in the nuclear magnetic resonance spectra (in dimethyl sulfoxide). This establishes that nitrosation of V*a* does not involve thiazine ring opening.

Oxidation of III*a* with potassium permanganate in glacial acetic acid gave the sulfone XVIII*a*, which was previously prepared by Claasz (16) by the reductive cyclization of 2-nitrobenzenesulfonylacetic acid. The compound shows strong infrared absorption bands at 3 300 and 1 700 cm^{-1}, which suggests the predominance of the oxo form (XVIII*a*). The sulfone could not be reduced by diborane or $LiAlH_4$. However, the 4-benzyl sulfone (XX) (prepared from IV*c* and potassium permanganate) could be reduced by diborane to 4-benzyl-3,4-dihydro-2*H*-1,4-benzothiazine-1,1-dioxide (XXI).

Benzylation of XVIII*a* in the presence of a base gave a benzyl derivative (XIX*b*) which was different from XX. Infrared absorption bands indicated the presence of NH (3 200 cm^{-1}) and C=O (1 680 cm^{-1}) groups in XIX*b*. The nuclear magnetic resonance spectrum

Can. J. Chem. Downloaded from www.nrcresearchpress.com by 210.87.254.105 on 09/05/12
For personal use only.



REACTION SCHEME 3.

(in deuteriochloroform) showed the expected singlet at low field (τ 0.25) for the NH hydrogen (which disappeared on treatment with deuterium oxide), and a typical ABX pattern with a quadruplet centered at τ 5.79 for a methine group and a multiplet centered at τ 6.64 for a methylene group. Thus benzylation of XVIII*a* caused substitution on the 2-carbon atom to give 2-benzyl-3-oxo-3,4-dihydro-2*H*-1,4-benzothiazine-1,1-dioxide (XIX*b*).

Methylation of XVIII*a* with methyl iodide in a basic medium produced the known (Claasz (17)) methyl derivative (XIX*a*). The infrared absorption spectrum of XIX*a* had peaks at 1 670 cm^{-1} (C=O) and 3 220 cm^{-1} (NH). Its nuclear magnetic resonance spectrum (in dimethyl sulfoxide) had a signal at τ 0.22 (NH) which disappeared when D_2O was added, as well as a quadruplet at τ 5.25 and a doublet at τ 8.50 which indicated the presence of a CH—CH_3 grouping.

On the basis of this evidence, the methylation product of XVIII*a* has the structure XIX*a*. The original suggestion by Claasz that the methylation of XVIII*a* gives the O-alkylated product, 3-methoxy-2*H*-1,4-benzothiazine-1,1-dioxide, is therefore incorrect.

EXPERIMENTAL

Melting points, determined with a Thomas Hoover capillary melting point apparatus, are corrected. Infrared spectra were obtained with a Beckman IR-8 spectrophotometer. Analyses were carried out by the Abbott Microanalytical Laboratory, Chicago, Illinois.

2-Phenethylmercaptoaniline

Phenethyl bromide (185.0 g, 1.0 mole) was added dropwise to a solution of 2-aminobenzenethiol (125.1 g, 1.0 mole) and sodium hydroxide (44.0 g, 1.1 moles) in 90% ethanol (700 ml) at a rate sufficient to maintain a gentle reflux. After the addition was complete the reaction mixture was refluxed for an additional hour. The solution was concentrated to half its volume, and the residue was diluted with water and extracted with ether. The ethereal extract was washed with water, dried, and distilled to give the product, b.p. 149–155° at 0.2 mm, yield 185.0 g (81%). The analytical sample distilled at 150° and 0.2 mm.

The above method was used for the preparation of 2-isopropylmercaptoaniline and the known 2-methylmercaptoaniline (1), 2-ethylmercaptoaniline (18), 2-*n*-propylmercaptoaniline (19), 2-*n*-butylmercaptoaniline (18), and 2-benzylmercaptoaniline (1, 20).

2-(α-Haloacetamido)phenyl Alkyl or Aralkyl Sulfides (I)

All compounds in this series were made according to the method of Davis *et al.* (1), and are recorded in Table II.

Can. J. Chem. Downloaded from www.nrcresearchpress.com by 210.87.254.105 on 09/05/12
For personal use only.

2-(α-Iodoacetamido)phenyl Phenethyl Sulfide (Ig)

A solution of sodium iodide (8.6 g, 0.057 mole) in acetone (200 ml) was stirred with a solution of I*f* (20.0 g, 0.057 mole) in acetone (70 ml) for 20 min at room temperature. The precipitated sodium bromide (5.6 g, 97%) was removed by filtration, and the filtrate was evaporated under reduced pressure in a bath at 30° to give the product melting at 82.5–84°. One crystallization from ether – petroleum ether (30–60°) gave the analytical sample, m.p. 83–84°.

6-Chloro-3-oxo-3,4-dihydro-2H-1,4-benzothiazine (IIIb)

Sodium hydrosulfite (15.6 g, 0.09 mole) was added in portions to a solution of 4-chloro-2-nitrophenylthioglycolic acid (7.4 g, 0.03 mole) (which was being stirred at 45°) in water (500 ml) containing sodium hydroxide (5.2 g, 0.13 mole). The reaction was exothermic and the temperature was held at 90° for 5 min after the addition of the hydrosulfite was complete. The hot reaction solution was treated with norite, filtered, and acidified while hot to give 4.0 g (66%) of the product, m.p. 205–206°; infrared absorption (Nujol mull): 3 200 cm^{-1} and 1 655 cm^{-1}.

4-Methyl-3-oxo-3,4-dihydro-2H-1,4-benzothiazine (IVa)

Method A, Table III

A solution of III*a* (40.0 g, 0.242 mole) (22–25), methyl iodide (52.0 g, 0.40 mole), and potassium hydroxide (13.6 g, 0.243 mole) in ethanol (400 ml) was refluxed for 5 h. The mixture was filtered and the filtrate was evaporated to dryness. The residue was extracted with ether (leaving some unchanged starting material), and the ether solution was washed with aqueous sodium thiosulfate, dried, and evaporated. The product was obtained by distillation, b.p. 119–122° at 0.5 mm, m.p. 53.5–55.5° (lit. (26) m.p. 55–56°).

4-Benzyl-3-oxo-3,4-dihydro-2H-1,4-benzothiazine (IVc)

Method B, Table III

A solution of III*a* (33.0 g, 0.2 mole) in dimethylformamide (200 ml) was added to a suspension of sodium hydride (9.6 g, 50% NaH, 0.2 mole) in dimethylformamide (100 ml) without external cooling, and the mixture was stirred for 90 min. A solution of benzyl chloride (25.3 g, 0.2 mole) in benzene (50 ml) was added dropwise without external cooling, and the temperature was held at 100° for 1 h.

The reaction mixture was diluted with water, and extracted with benzene (200 ml). The benzene extract was evaporated and crystallized from petroleum ether to give the product, m.p. 84–85°, yield 31.5 g (62%).

4-Carbethoxymethyl-3-oxo-3,4-dihydro-2H-1,4-benzothiazine (IVd)

A suspension of sodium amide (23.0 g, 0.623 mole) in toluene (1 300 ml) and a solution of III*a* (100 g, 0.605 mole) were mixed and refluxed for 17 h. Ethyl chloroacetate (85.5 g, 0.7 mole) was then added to the cooled reaction mixture, followed by further refluxing for 4.5 h.

The reaction mixture was cooled and diluted with water (500 ml). The organic layer was separated, washed with water, dried, and distilled to give 29.0 g (19%) of the product, b.p. 148–158° at 0.2–0.3 mm, which solidified on standing. The analytical sample was obtained by crystallization from ether – petroleum ether (30–60°), m.p. 48.5–50.5°.

3,4-Dihydro-2H-1,4-benzothiazine (Va)

The procedure of Hromatka *et al.* (8) was modified by performing the addition of the 3-oxo compound (III*a*) to the $LiAlH_4$ in tetrahydrofuran at reflux temperature instead of 0°, thereby preventing a violent reaction at the end of the addition period.

6-Trifluoromethyl-3,4-dihydro-2H-1,4-benzothiazine (Vc)

3-Oxo-6-trifluoromethyl-3,4-dihydro-2*H*-1,4-benzothiazine (III*c*, m.p. 200–202° (lit. (4) m.p. 185–186°)) was reduced with diborane by the procedure described below for the preparation of VI*d*, yield 67%, m.p. 88–89° when crystallized from petroleum ether.

Anal. Calcd. for $C_9H_8F_3NS$: C, 49.31; H, 3.65; N, 6.39. Found: C, 49.11; H, 3.57; N, 6.40.

4-(β-Hydroxyethyl)-3,4-dihydro-2H-1,4-benzothiazine (VIc)

IV*d* (21.7 g, 0.086 mole) in ether (200 ml) was added dropwise to a suspension of $LiAlH_4$ (7.27 g, 0.19 mole) in ether (500 ml) at a rate sufficient to maintain a gentle reflux. After the addition was complete (1 h), the mixture was refluxed for an additional 2 h, and cooled; then ethyl acetate (34 g, 0.38 mole) was added dropwise, followed by water (58 ml). The precipitate was filtered, and the filtrate dried and distilled to give the product, b.p. 125–143° at 0.15–0.18 mm, yield 13.3 g (79%). The analytical sample distilled at 151° and 0.4 mm.

Reduction of IV*a*, IV*b*, and IV*e* by the above procedure gave VI*a*, VI*b*, and VI*e*, respectively.

4-Benzyl-3,4-dihydro-2H-1,4-benzothiazine (VId)

A solution of IV*c* (12.75 g, 0.05 mole) in tetrahydrofuran (100 ml) was added dropwise to a 1 *M* diborane (27) solution (100 ml) in tetrahydrofuran, and the temperature was held at 0°. The reaction mixture was then refluxed for 1 h, cooled, hydrolyzed by 10% aqueous hydrochloric acid (60 ml), and concentrated to one-fourth of its volume. The residue was made strongly alkaline and extracted with chloroform. The chloroform

Can. J. Chem. Downloaded from www.nrcresearchpress.com by 210.87.254.105 on 09/05/12
For personal use only.

extract was washed with water, dried, and evaporated to give the product, m.p. 90–93°, yield 7.4 g (62%). Crystallization from ether – petroleum ether (30–60°) gave the analytical sample, m.p. 96.5–97.5°.

Another method for the preparation of VI*d* was by refluxing a mixture of V*a* (7.55 g, 0.05 mole), benzyl chloride (6.32 g, 0.05 mole), and potassium iodide (8.3 g, 0.05 mole) in absolute ethanol (200 ml) for 16 h, filtering the hot mixture, and evaporating the filtrate. The residue, on crystallization from ether–petroleum ether (30–60°), gave the product, yield 6.35 g (52%).

VI*a* was similarly obtained (66% yield, b.p. 104° at 0.17 mm) by refluxing V*a* (30.2 g, 0.2 mole), methyl iodide (42.63 g, 0.3 mole), and anhydrous potassium carbonate (15.2 g, 0.11 mole) in methanol (300 ml) for 4.5 h.

4-Benzoyl-3,4-dihydro-2H-1,4-benzothiazine (VIId)

Benzoyl chloride (14.1 g, 0.1 mole) in ether (50 ml) was added, with stirring, to a solution of V*a* (15.1 g, 0.1 mole) in ether (250 ml) containing pyridine (8.3 g, 0.105 mole) at −5°. After the reaction mixture was stirred for 4 h at room temperature, it was filtered and the filtrate washed with 10% aqueous hydrochloric acid and water. The dried ethereal extract was evaporated and the residue crystallized from ether – petroleum ether (30–60°) to give the product, m.p. 86–89°, yield 19.0 g (79%). One recrystallization from the same solvent gave the analytical sample, m.p. 88–89.5°; infrared absorption (Nujol mull): 1 645 cm^{-1} (C=O).

All other 4-acyl derivatives of V*a* were synthesized by this method, and all had the characteristic infrared absorption band in the 1 635 – 1 660 cm^{-1} region.

The 4-benzoyl derivative was also obtained under Schotten–Baumann conditions, but the yield was somewhat inferior.

Reduction of VIIa and VIId

VII*a* was reduced by $LiAlH_4$ in ether by the procedure described for the reduction of IV*d*. For the reduction of VII*d*, however, the procedure employing diborane, described for the reduction of IV*c*, had to be followed.

4-Amino-3,4-dihydro-2H-1,4-benzothiazine (XVII)

Sodium nitrite (13.8 g, 0.2 mole) in 20 ml water was added to V*a* (30.2 g, 0.2 mole) in 5% hydrochloric acid (250 ml) at −5°. The solution was basified and extracted with chloroform, and the chloroform solution was washed with water and saturated sodium chloride, dried, and evaporated. The nitrosated product (XVI) could not be distilled without decomposition; accordingly, it was reduced with $LiAlH_4$ in ether in the usual way. The 4-amino derivative thus obtained was treated with hydrogen chloride in ether to give the hydrochloride, m.p. 174° (decomp.) when crystallized from methanol.

Anal. Calcd. for $C_8H_{11}ClN_2S$: C, 47.37; H, 5.47; N, 13.83; S, 15.82; Cl, 17.49. Found: C, 47.81; H, 5.61; N, 13.27; S, 15.26; Cl, 17.63.

2-(β-Hydroxyethylmercapto)aniline (VIII) (9, 21)

Treatment of 2-aminobenzenethiol with ethylene oxide in the presence of alcoholic potassium hydroxide gave VIII in an almost quantitative yield. Culvenor *et al.* (21) claimed to have prepared V*a* by this reaction.

2-(β-Acetoxyethylmercapto)acetanilide (XIV)

A mixture of VIII (46.0 g, 0.275 mole) and acetic anhydride (100 ml) was slowly distilled for 2 h at atmospheric pressure in a bath at 150–170°. The residue was fractionally distilled to give the product, b.p. 184–186° at 1.1 mm, as a colorless liquid which slowly solidified on standing. The product, when refluxed with 5% dilute ethanolic potassium hydroxide, gave 2-(β-hydroxyethylmercapto)acetanilide (XV), b.p. 176° at 0.5 mm.

2-(β-Benzoxyethylmercapto)benzanilide (IX) (14)

Benzoyl chloride (13.3 g, 0.094 mole) was added dropwise to VIII (8.0 g, 0.047 mole) in pyridine (180 ml), and the mixture was stirred overnight at room temperature. Dilution with water yielded the crude product, which was purified by crystallization from methanol, m.p. 81–83°, yield 14.0 g (78%); infrared absorption (Nujol mull): 3 390 cm^{-1} (NH), 1 725 cm^{-1} (ester), and 1 685 cm^{-1} (C=O).

The same product was obtained by the reaction of either X or XI with benzoyl chloride in pyridine, as described above.

2-(β-Hydroxyethylmercapto)benzanilide (X)

Benzoyl chloride (8.3 g, 0.059 mole) was added to a stirred mixture of VIII (10.0 g, 0.059 mole) in 100 ml of 3.3% aqueous potassium hydroxide solution. After being stirred vigorously for 10–15 min, the mixture was extracted with ether. The ethereal extract was washed with water and evaporated, and the residue was crystallized from ether to give 11.0 g (68%) of the product, m.p. 88.5–90°; infrared absorption (Nujol mull): 3 430 cm^{-1}, 3 330 cm^{-1}, and 1 665 cm^{-1}.

2-(β-Benzoxyethylmercapto)aniline (XI)

A solution of VIII (17.0 g, 0.1 mole) in toluene (100 ml) was added to a vigorously stirred mixture of sodium (2.3 g, 0.1 mole) in 300 ml boiling toluene, under a dry nitrogen atmosphere. After the addition was complete (15 min), the mixture was refluxed for 1½ h and then cooled to room temperature, and benzoyl chloride (14.0 g, 0.1 mole) in toluene (50 ml) was slowly added. The mixture was stirred for another 30 min

Can. J. Chem. Downloaded from www.nrcresearchpress.com by 210.87.254.105 on 09/05/12
For personal use only.

at room temperature, and then 200 ml water was added at 15°. The organic layer was separated, washed with water, dried, and evaporated under reduced pressure in a bath below 40°. Part of the oily residue was dissolved in ether, and hydrogen chloride was added to give the product as the hydrochloride, m.p. 176–180°.

The free base was obtained from the hydrochloride as a viscous, honey-colored liquid which solidified (m.p. 43–46°) when it was allowed to stand overnight. Recrystallization from warm ethanol gave the analytical sample, m.p. 44.5–46°; infrared absorption (Nujol mull): 3 460 cm^{-1}, 3 360 cm^{-1} (primary sorpamine), and 1 710 cm^{-1} (ester).

N-(2-(β-Hydroxyethylmercaptophenyl))-N'-(3',4'-dichlorophenyl)urea (XII)

3,4-Dichlorophenylisocyanate (18.8 g, 0.1 mole) in ether (500 ml) was added to VIII (15.1 g, 0.1 mole) in ether (500 ml); after the mixture had been stirred for 1 h at room temperature, it was refluxed for over 2½ h. The crude product (24.5 g) was filtered off and crystallized from acetone–ether, m.p. 156–157°; infrared absorption (Nujol mull): 3 550 cm^{-1} (OH), 3 330 cm^{-1} (NH), and 1 700 cm^{-1} (C=O).

N-(2-(β-Benzoxyethylmercaptophenyl))-N'-(3',4'-dichlorophenyl)urea (XIII)

A solution of XI (2.0 g, 0.0073 mole) in ether was mixed with an equivalent amount (1.4 g) of 3,4-dichlorophenylisocyanate in ether. The clear solution was refluxed for 30 min and then left for 2 days at room temperature. The crystalline solid (1.7 g, 50%) was filtered off and crystallized from 15 ml absolute ethanol to give the product, yield 0.9 g, m.p. 153–154°; infrared absorption (Nujol mull): 3 350 cm^{-1} (NH), 3 280 cm^{-1} (NH), 1 720 cm^{-1} (ester), and 1 655 cm^{-1} (amide).

The same product (XIII) was also obtained from XII (10.0 g, 0.028 mole) and benzoyl chloride (3.9 g, 0.028 mole) in pyridine.

4-(3',4'-Dichlorophenylcarbamyl)-3,4-dihydro-2H-1,4-benzothiazine (XXIIa)

Equivalent amounts of V*a* and 3,4-dichlorophenylisocyanate in benzene were refluxed for 1½ h, and then the solvent was removed to give the product in a quantitative yield. One recrystallization from 360 ml boiling ethanol gave colorless needles, m.p. 159–161°; infrared absorption (Nujol mull): 3 260 cm^{-1} and 1 655 cm^{-1}. The mixed melting point of XXII with XII was 128–146°.

Other ureas (XXII*b*–XXII*e*) were similarly prepared by refluxing equivalent amounts of V*a* and the corresponding isocyanate for 1½ h in ether. The final products were isolated by the addition of petroleum ether (30–60°) to the reaction solution.

3-Oxo-3,4-dihydro-2H (4H) -1,4-benzothiazine-1,1-dioxide (XVIIIa)

A solution of III*a* (33.0 g, 0.2 mole) in glacial acetic acid (500 ml) was added to potassium permanganate (45 g, 0.28 mole) in water (1 000 ml) over a 15 min period. The temperature was allowed to rise to 42° during the addition. After 1.5 h at room temperature, sodium bisulfite (24.0 g, 0.23 mole) was added at 15–20°. The solution was concentrated to 200 ml under reduced pressure, and the product separated out when the concentrate was cooled, yield 31.9 g (81%), m.p. 195–202°. Recrystallization from methanol–benzene raised the melting point to 208–209° (lit. (16) m.p. 207–208°); infrared absorption (KBr pellet): 3 300 cm^{-1} (NH) and 1 700 cm^{-1} (C=O).

The 6-trifluoromethyl analogue (XVIIIb) was prepared in the same way, m.p. 256–257° (decomp.) when crystallized from acetone – petroleum ether, yield 60%.

Anal. Calcd. for $C_9H_6F_3NO_3S$: C, 40.75; H, 2.26; F, 21.50; S, 12.07. Found: C, 40.94; H, 2.53; F, 21.54; S, 12.29.

The 4-benzyl derivative (XX) was similarly prepared from IV*c*, m.p. 140–141° when crystallized from chloroform – petroleum ether, yield 64%.

Anal. Calcd. for $C_{15}H_{13}NO_3S$: C, 62.71; H, 4.52; N, 4.87; O, 16.72. Found: C, 63.03; H, 4.66; N, 5.18; O, 16.37.

2-Benzyl-3-oxo-3,4-dihydro-2H-1,4-benzothiazine-1,1-dioxide (XIXb)

A solution of XVIII*a* (9.85 g, 0.05 mole) in 50% aqueous ethanol (50 ml) containing sodium hydroxide (2.0 g, 0.05 mole) was refluxed for 1 h. The cooled reaction mixture was extracted first with petroleum ether (to remove unreacted benzyl chloride) and then with ether. The ethereal extract was washed with water, dried, and evaporated. The residue was crystallized from ether – petroleum ether (30–60°) to give 9.0 g (62%) of the product, m.p. 144–147°. Two recrystallizations from the same solvent gave the analytical sample, m.p. 147–148°; infrared absorption (Nujol mull): 3 200 cm^{-1} and 1 685 cm^{-1}.

Anal. Calcd. for $C_{15}H_{13}NO_3S$: C, 62.71; H, 4.52; N, 4.77; S, 11.15. Found: C, 62.69; H, 4.50; N, 4.64; S, 11.31.

4-Benzyl-3,4-dihydro-2H-1,4-benzothiazine-1,1-dioxide (XXI)

Treatment of 4-benzyl-3-oxo-3,4-dihydro-2*H*-1,4-benzothiazine-1,1-dioxide with diborane in tetrahydrofuran as described for the preparation of VI*d* gave the product, m.p. 127–128° when crystallized from aqueous methanol, yield 60%.

Anal. Calcd. for $C_{15}H_{15}NO_2S$: C, 65.93; H, 5.49; N, 5.12; O, 11.72; S, 11.72. Found: C, 65.86; H, 5.31; N, 5.18; O, 11.94; S, 11.57.

Can. J. Chem. Downloaded from www.nrcresearchpress.com by 210.87.254.105 on 09/05/12
For personal use only.

ACKNOWLEDGMENTS

We express our appreciation to Professor Z. Valenta, Chemistry Department, University of New Brunswick, Fredericton, for valuable suggestions and advice. We further acknowledge several helpful and stimulating discussions with Dr. James H. Short and Dr. D. L. Garmaise. We especially thank the latter for his invaluable help in the preparation of the manuscript.

REFERENCES

1. C. S. DAVIS, G. L. JENKINS, A. M. KNEVEL, and C. PAGET. J. Pharm. Sci. **51**, 840 (1962).
2. C. K. INGOLD. Structure and mechanism in organic chemistry. Cornell University Press, Ithaca, New York. 1953. p. 360.
3. J. POLLAK, E. REISZ, and Z. KAHANI. Monatsh. Chem. **49**, 213 (1928); Chem. Abstr. **22**, 3658 (1928).
4. YU. E. GERASIMENKO, S. M. SHEIN, G. G. BAKULINA, A. P. CHEREPIVSKAYA, G. V. SEMENYUK, and L. M. YAGUPOL'SKII. J. Gen. Chem. USSR Engl. Transl. **32**, 1849 (1962).
5. G. TRAVERSO and C. B. RIOLO. Ann. Chim. Rome, **45**, 668 (1955).
6. G. M. BADGER, D. J. CLARK, W. DAVIES, and K. T. H. FARRER. J. Chem. Soc. 2624 (1957).
7. C. ANGELINI, G. GRANDOLINI, and L. MIGNINI. Ann. Chim. Rome, **46**, 235 (1956).
8. O. HROMATKA, M. VACULNY, J. AUGL, and K. WILSCHKE. Monatsh. Chem. **88**, 822 (1957).
9. K. FUJII. J. Pharm. Soc. Japan, **77**, 355 (1957); Chem. Abstr. **51**, 12102 (1957).
10. R. F. NYSTROM and W. G. BROWN. J. Am. Chem. Soc. **70**, 3738 (1948).
11. H. S. LOWRIE. U.S. Patent No. 2,947,744 (August 2, 1960); Chem. Abstr. **55**, 583 (1961).
12. R. C. ELDERFIELD. Heterocyclic compounds. Vol. 6. R. C. Elderfield (*Editor*). John Wiley & Sons, Inc., New York. 1957. p. 617.
13. G. R. RAMAGE, E. H. RODD, and J. K. LANDQUIST. Chemistry of carbon compounds. Vol. IVC. E. H. Rodd (*Editor*). Elsevier Press, Inc., New York. 1960. p. 1510.
14. R. FUSCO and G. PALAZZO. Gazz. Chim. Ital. **81**, 735 (1951).
15. J. F. KERWIN, J. E. MCCARTY, and C. A. VANDER WERF. J. Org. Chem. **24**, 1719 (1959).
16. M. CLAASZ. Ber. **45**, 747 (1912).
17. M. CLAASZ. Ber. **49**, 350 (1916).
18. R. F. PARCELL. U.S. Patent No. 2,836,594 (May 27, 1958); Chem. Abstr. **52**, 20215 (1958).
19. R. F. PARCELL. U.S. Patent No. 2,836,595 (May 27, 1958); Chem. Abstr. **52**, 20215 (1958).
20. F. GIALDI and A. BARUFFINI. Farmaco Pavia Ed. Sci. **12**, 206 (1957); Chem. Abstr. **51**, 12858 (1957).
21. C. C. J. CULVENOR, W. DAVIES, and N. S. HEATH. J. Chem. Soc. 278 (1949).
22. O. UNGER and G. GRAFF. Ber. **30**, 2393 (1897).
23. N. A. LANGLET. Bihang till Svenska Vet.-Akad. Handlingar, **22**(11), No. 1, 8–10 (1896). F. K. Beilstein. Handbuch der Organischen Chemie. Vol. 27. 4th ed. Verlag von Julius Springer, Berlin. 1937. p. 34.
24. O. UNGER and G. GRAFF. Ber. **30**, 2393 (1897).
25. A. W. HOFMANN. Ber. **13**, 1234 (1880).
26. A. I. KIPRIANOV and Z. N. PAZENKO. J. Gen. Chem. USSR Engl. Transl. **21**, 163 (1951).
27. H. C. BROWN and P. HEIM. J. Am. Chem. Soc. **86**, 3566 (1964).
28. J. CYMERMAN-CRAIG, W. P. ROGERS, and G. P. WARWICK. Australian J. Chem. **8**, 252 (1955). J. K. KIRCHNER and E. J. ALEXANDER. J. Am. Chem. Sec. **81**, 1721 (1959).

Can. J. Chem. Downloaded from www.nrcresearchpress.com by 210.87.254.105 on 09/05/12
For personal use only.

Can. J. Chem. Downloaded from www.nrcresearchpress.com by 210.87.254.5 on 09/05/12
For personal use only.

THE ALKALOIDS OF PAPAVERACEOUS PLANTS

LV. A NEW ALKALOID, ESCHSCHOLTZIDINE, AND ITS STRUCTURE

RICHARD H. F. MANSKE AND KJU HI SHIN
Research Laboratories, Dominion Rubber Co. Ltd., Guelph, Ontario

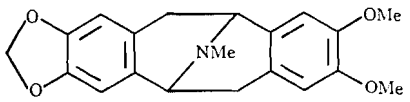
Received February 10, 1966

ABSTRACT

A very small amount of a new alkaloid, eschscholtzidine, present in *E. californica*, was shown to be eschscholtzine in which a methylenedioxy group is replaced by two methoxyls.

The present authors have recorded the isolation of a number of alkaloids from *Eschscholtzia californica* Cham. (1). The fraction which yielded eschscholtzine has now yielded a new base, eschscholtzidine, which so far has not been crystallized either free or in the form of salts. It was ultimately purified by means of column chromatography, and its purity checked by the thin-layer technique (R_f 0.51 on silica gel with cyclohexane–chloroform–diethylamine (7:2:1)).

That this alkaloid was related to eschscholtzine (2) was suspected because of its chemical behavior and its source. The nuclear magnetic resonance spectrum confirmed this close relation, and in fact indicated the structure shown by I.



I

Its nuclear magnetic resonance spectrum was superposable on that of eschscholtzine, except that now two methoxyls (τ 6.18 (3H) and 6.27 (3H)) and a methylenedioxy group (τ 4.23 (2H)) were evident. Hence it appeared to have structure I. This was readily confirmed by first demethylenating the alkaloid to the corresponding dihydroxy base followed by methylation with diazomethane. The product was identical with a specimen of argemonine kindly supplied by Dr. T. O. Soine.

EXPERIMENTAL

The final mother liquors, from which no further alkaloids could be crystallized either as free bases or as salts (hydrochloride, nitrate, and hydrobromide) (from 270 kg of *E. californica*), were combined, dissolved in dilute hydrochloric acid, and filtered. The solution was then extracted with several portions of chloroform. The alkaloids were regenerated from the fraction that was extracted with chloroform, dissolved in ether, and dried with potassium hydroxide.

The solution was then passed through a long column of alumina (250 g, pH 8.15, activity 0.98) and eluted with dry ether. The first fraction colored on exposure to air and was discarded. The large middle fraction was again passed through a second column, and its middle fraction proved to be chromatographically pure; yield 3 g. For analysis a portion was distilled at 180° and 1 mm.

Anal. Calcd. for $C_{20}H_{21}O_4N$: C, 70.78; H, 6.24; N, 4.13. Found: C, 70.65; H, 5.88; N, 3.92.

It is optically active ($[\alpha]_D^{24}$ +194.2° (*c*, 1.56 in methanol)). This value is almost exactly equal to the arithmetic mean between the values for argemonine and eschscholtzine. The ultraviolet spectrum shows λ_{max}^{EtOH} 291 mμ (log ϵ 4.08).

Conversion into Argemonine

A solution of 0.4 g of eschscholtzidine in 10 ml of 58% sulfuric acid plus 1 g of phloroglucinol was heated to boiling and digested on a steam bath for 1 h. The cooled and diluted solution was filtered and the filtrate was

extracted with three successive portions of ether, basified with ammonia, and again exhausted with ether. The residue from the latter ether extract was dissolved in methanol and left overnight with an excess of ethereal diazomethane. Removal of the solvent left a residue which was extracted with dilute aqueous oxalic acid; then the filtered solution was thoroughly extracted with ether. The aqueous phase was then basified with ammonia and extracted once more with ether. The residue from the latter extract was a colorless oil which crystallized at once when seeded with a crystal of argemonine. When recrystallized from dry ether the base consisted of colorless, stout polyhedra which melted sharply at 155°;* in admixture with a specimen of argemonine it melted at 154–155°.

NOTE ADDED IN PROOF: The phenolic alkaloid melting at 254° but not further characterized, reported as present in *E. californica* (1), has been identified as bisnorargemonine (m.p. 256°, mixed m.p. 254°), a specimen of which was kindly supplied by Dr. T. O. Soine. The infrared spectra of the two alkaloids in potassium bromide pellets were superimposable; λ_{max}^{EtOH} 288.5 mμ.

REFERENCES

1. R. H. F. MANSKE and K. H. SHIN. Can. J. Chem. **43**, 2180 (1965).
2. R. H. F. MANSKE, K. H. SHIN, A. R. BATTERSBY, and D. F. SHAW. Can. J. Chem. **43**, 2183 (1965).

**Melting points are corrected.*

Can. J. Chem. Downloaded from www.nrcresearchpress.com by 210.87.254.5 on 09/05/12
For personal use only.

Can. J. Chem. Downloaded from www.nrcresearchpress.com by 210.87.254.105 on 09/05/12
For personal use only.

EFFECT OF INTRAMOLECULAR HYDROGEN BONDING ON IONIZATION CONSTANTS OF SUBSTITUTED SALICYLIC ACIDS

G. E. DUNN AND FEI-LIN KUNG
Chemistry Department, University of Manitoba, Winnipeg, Manitoba

Received December 14, 1965

ABSTRACT

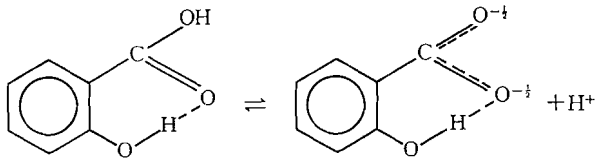
Ionization constants at 25 °C have been determined by a spectrophotometric method for 17 substituted salicylic acids. These have been fitted to the simple Hammett relationship and to the extended one proposed by Jaffe, which takes into account the transmission of substituent effects by the *o*-hydroxy group. The results with Jaffe's equation show that substituent effects on acidity are transmitted only slightly, if at all, through the intramolecular hydrogen bond of a chelate ring. Possible interpretations of the results are discussed.

Salicylic acid is well known to be a decidedly stronger acid than benzoic or the other monohydroxybenzoic acids. The relevant ionization constants are shown in Table I, where it may be seen that the second *o*-hydroxy group in 2,6-dihydroxybenzoic acid has an even greater effect than the first. Since the hydroxy group normally has a strong resonance effect of electron release, a hydroxy group in the ortho position might have been expected

TABLE I
Ionization constants of hydroxybenzoic acids in water at 25 °C (1)

Substituent	$K \times 10^5$	$K/K_{benzoic}$
Benzoic	6.30	1.0
m-Hydroxy	8.33	1.32
p-Hydroxy	2.62	0.42
o-Hydroxy	105	16.7
2,6-Dihydroxy	6 000	952

to decrease the strength of a benzoic acid just as it does when in the para position. The anomalous increase in acid strength produced by an *o*-hydroxy group is commonly attributed to intramolecular hydrogen bonding between the phenolic hydroxyl and the carboxyl group (2–8). Among the hydroxybenzoic acids, chelation is possible only for the ortho isomer and, since it would be expected to be stronger in the anion than in the unionized acid, it should stabilize the anion more than it does the acid and so cause increased ionization.



If the above argument is correct, then a substituent in the 4- or 5-position of salicylic acid should influence the ionization constant by two paths. For example, an electron-withdrawing group, such as nitro, in the 5-position should exert its normal acid-strengthening influence on the carboxyl group by way of the usual combination of

inductive, field, and resonance effects, as in the corresponding nitrobenzoic acid. This effect would be represented in terms of the Hammett relationship (9) by

$$[1] \qquad \log K/K_0 = \rho_1\sigma_1,$$

where K is the ionization constant of 5-nitrosalicylic acid, K_0 is that of salicylic acid, σ_1 is the Hammett substituent constant for the *m*-nitro group, and ρ_1 is Hammett's reaction constant for the ionization of salicylic acids under the conditions concerned. Second, the substituent should have a similar but larger effect on the acidity of the phenolic group, thus increasing the strength of the chelating hydrogen bond and so exerting a further acid-strengthening influence on the carboxyl group. This second effect would be represented by

$$[2] \qquad \log K/K_0 = \rho_2\sigma_2^-,$$

where σ_2^- is the Hammett *p*-nitro substituent constant for use with phenols and amines (Hammett's σ^*), and ρ_2 is a Hammett reaction constant representing the susceptibility of the ionization of salicylic acids to subsequent influences by way of the chelate hydrogen bond. Jaffe (10) has shown that influences through the two paths should be additive, so that the overall effect of a substituent should be given by

$$[3] \qquad \log K/K_0 = \rho_1\sigma_1 + \rho_2\sigma_2^-.$$

He found (10) that, in the case of the salicylic acids, eq. [3] was not an improvement over eq. [1]. Jaffe attributed this to the fact that the six substituents for which data were available (11) were such that σ_1 and σ_2 are linearly related, so that for these substituents eqs. [1] and [3] become indistinguishable. He proposed that eqs. [1] and [3] can be distinguished only when the correlation coefficient between σ_1 and σ_2 is less than 0.9.

Since there was available in our laboratory a collection of sixteen 4- and 5-substituted salicylic acids prepared in connection with a study of their decarboxylation (12), it appeared to be worthwhile to determine their ionization constants, both for comparison with their rates of decarboxylation and for a test of eq. [3]. The fact that the correlation constant between σ_1 and σ_2^- for the 16 acids is 0.723 makes them particularly suitable for the latter purpose. The present paper reports the results of these determinations.

EXPERIMENTAL

Materials

The 5-methyl-, 4-nitro-, 5-nitro-, 4-hydroxy, 5-hydroxy-, 5-bromo-, 4-ethoxy-, 5-chloro-, and 5-iodosalicylic acids, as well as salicylic acid itself, were commercial products. The 4-methoxy- and 5-methoxysalicylic acids were prepared by methylating the corresponding hydroxy acids (12). All the acids were purified to constant melting point by one or more recrystallizations from water or aqueous ethanol; the melting points reported are for the recrystallized acids. All melting points were determined with a Hershberg melting point apparatus (13) by using calibrated Anschütz thermometers, and are expressed in degrees Centigrade.

3-Methylsalicylic Acid

A product sold commercially under the name 2,4-cresotic acid (m.p. 166.8–168.0°) and consequently supposed to be 4-methylsalicylic acid (2-hydroxy-4-methylbenzoic acid) was found to have an ionization constant which, according to the Hammett parameters derived from the other salicylic acids, was inconsistent with its supposed structure. Decarboxylation of the acid with copper powder in hot quinoline gave a cresol which was converted into the dibromo derivative by the usual method (14). This derivative produced no depression in the melting point when mixed with the dibromo derivatives prepared from an authentic sample of *o*-cresol. The "2,4-cresotic acid" must therefore have its methyl and hydroxyl groups ortho to each other. Its large ionization constant (0.962×10^{-3}) shows that the carboxyl and hydroxyl groups are also ortho to each other, so that the acid must be 3-methylsalicylic acid (2-hydroxy-3-methylbenzoic acid). Melting points of the *p*-bromophenacyl, *p*-nitrobenzyl, acetyl, and dinitro derivatives confirm this structure. Its ionization constant is therefore reported in Table III under the heading 3-methylsalicylic acid.

Can. J. Chem. Downloaded from www.nrcresearchpress.com by 210.87.254.105 on 09/05/12
For personal use only.

4-Methylsalicylic Acid

This acid was prepared by treating 4-methylanthranilic acid with nitrous acid. A solution of 7.6 g of 4-methylanthranilic acid in 33 ml concentrated sulfuric acid and 45 ml water was cooled to 0–5° and stirred while 4 g sodium nitrite in 10 ml water was added dropwise over a period of 10 min. The mixture was stirred for another 15 min, and then poured into 200 ml boiling water. When this solution was cooled, 4-methylsalicylic acid precipitated out; after two recrystallizations from water 1.1 g (14.5%) melting at 177.0–177.8° (lit. (15) m.p. 172°) was recovered.

4-Cyanosalicylic Acid

This acid was prepared from 4-aminosalicylic acid by the Sandmeyer reaction. A solution of 10.0 g of 4-aminosalicylic acid in 30 ml of concentrated sulfuric acid and 60 ml water was cooled to 0–5° and stirred while 20 g sodium nitrite in 100 ml water was added slowly until the mixture gave a positive test with starch–iodide paper. The cold solution was poured into 200 ml water containing 14.5 g cuprous cyanide and enough potassium cyanide to keep the latter in solution. The mixture was warmed to 60° for half an hour, and then filtered. The residue was extracted with three 200 ml portions of ether, and 4-cyanosalicylic acid was recovered from the ether. After several recrystallizations from water the yield was 0.2 g (2%) melting at 228.0–229.0° (lit. (16) m.p. 227–229°).

5-Cyanosalicylic Acid

This compound has not previously been reported in the literature. The cyano group was introduced by the method of Friedman and Schechter (17). A solution of 11.9 g 5-iodosalicylic acid and 4.65 g cuprous cyanide in 50 ml dimethylformamide was refluxed for 2 days. The resulting brown mixture was cooled and poured into a solution of 10 g ferric chloride hexahydrate in 30 ml concentrated hydrochloric acid and 30 ml water. This mixture was heated on a steam bath for half an hour, and then extracted with three 200 ml portions of ether. The extract was washed with aqueous sodium bisulfite, dried, and evaporated. The residue, after several recrystallizations from water, yielded 3.1 g (43%) of 5-cyanosalicylic acid melting at 224.0–225.0°. The characteristic nitrile band in the infrared spectrum of the acid was present at 2 230 cm^{-1}.

Anal. Calcd. for $C_8H_5NO_3$: C, 58.90; H, 3.09; N, 8.59. Found: C, 58.90; H, 3.12; N, 8.77.

Method

A spectrophotometric method was chosen for the determination of the ionization constants because it had been used previously in this laboratory on anthranilic acids (18) and could be extended, if desired, to include the overlapping ionization constants of the zwitterionic aminosalicylic acids.

For the ionization of a monoprotic acid in water,

$$HB \rightleftarrows H^+ + B^-,$$

the ionization constant may be expressed by

$$K = \frac{[H^+][B^-]}{[HB]},$$

where the quantities in brackets represent molar concentrations or, at high ionic strengths, activities. If the total concentration of acid (ionized plus un-ionized) is C, then

$$K = \frac{[H^+][B^-]}{C - [B^-]} = \frac{[H^+](C - [HB])}{[HB]},$$

so that

$$[B^-] = \frac{KC}{[H^+] + K} \quad \text{and} \quad [HB] = \frac{C[H^+]}{[H^+] + K}.$$

Since hydronium ion does not absorb in the visible or ultraviolet regions, the total absorbance, A, of the equilibrium solution of HB is given by

$$A = A_{HB} + A_B,$$

where A_{HB} is the absorbance of the equilibrium concentration of un-ionized acid HB, and A_B is the absorbance of the equilibrium concentration of anion B^-. For a 1 cm cell the Beer–Lambert relationship converts the preceding equation into

$$A = \epsilon_{HB}[HB] + \epsilon_B[B^-],$$

where ϵ = molar absorptivity.

When the expressions for [HB] and $[B^-]$ derived above are introduced, this becomes

$$A = C \times \frac{\epsilon_{HB}[H^+] + \epsilon_B K}{[H^+] + K}. \qquad [4]$$

Can. J. Chem. Downloaded from www.nrcresearchpress.com by 210.87.254.105 on 09/05/12
For personal use only.

Since A, $[H^+]$, and C are observable quantities, eq. [4] contains only three unknowns: K, ϵ_{HB}, and ϵ_B.

In principle, ϵ_{HB} and ϵ_B can be determined experimentally by measurements made in strongly acidic and strongly basic solutions, respectively. However, these strongly acidic and basic solutions will have much larger ionic strengths than are necessary in the equilibrium region, and it is desirable to make all measurements at the same low ionic strength. Hence, in the present work the absorbances were measured at one wavelength for several (usually 16) different values of $[H^+]$ in the equilibrium region at an ionic strength of 0.01, and all three unknowns were obtained by fitting the data to eq. [4] by the least squares method (19). All measurements were made at the same total concentration of a substituted salicylic acid, so that the actual value of C is unimportant provided it is such as to give absorbances suitable for measurement. It varied from acid to acid, but averaged about 10^{-4} M.

The apparatus and procedure for choosing appropriate wavelengths, concentrations, and pH ranges, as well as for making the measurements of pH and absorbances, are the same as those previously described (18).

RESULTS

Figure 1 shows the ultraviolet absorption spectra of salicylic and 5-nitrosalicylic acids at pH values of about 0, 3, and 9. The spectra of all the other acids resembled that of salicylic

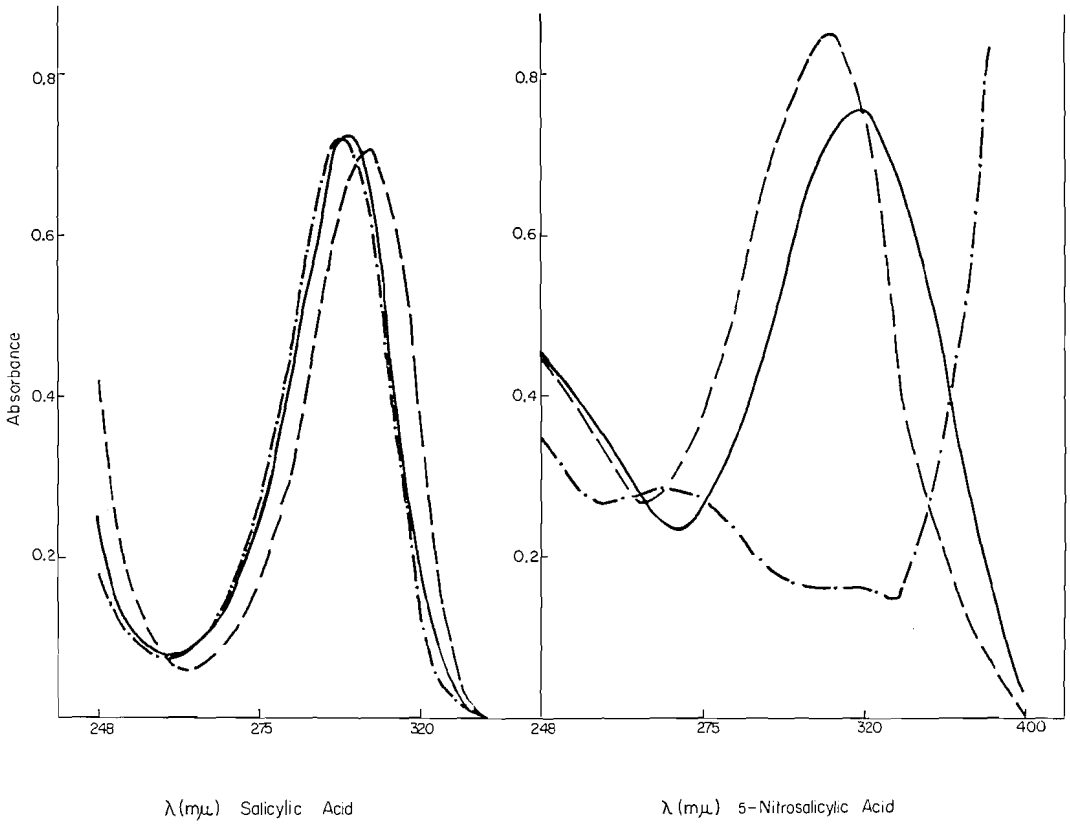


FIG. 1. Effect of pH on the ultraviolet spectra of salicylic acids. LEGEND: —, formate buffer (pH ~ 3); — —, 1 N hydrochloric acid; —·—, ammonia buffer (pH ~ 9).

acid, with small shifts in wavelength and absorptivity as the substituents varied. The 5-nitro acid is distinctly different from the others, no doubt because the p-nitro substituent activates the phenolic group to the point where it is significantly ionized at pH 9.

The absorbance and pH data obtained for salicylic and 5-nitrosalicylic acids are reported in Table II. In Fig. 2, the experimental points are compared with the curves calculated by using the data of Table II to solve eq. [4]. The measurements in 1 N hydrochloric acid and ammonia buffers (shown as the first and last items of Table II) were used to provide the

Can. J. Chem. Downloaded from www.nrcresearchpress.com by 210.87.254.105 on 09/05/12
For personal use only.

TABLE II

Variation of absorbance with pH for salicylic and 5-nitrosalicylic acids at 25 °C and $\mu = 0.010$

Salicylic acid, 2.5×10^{-4} M			5-Nitrosalicylic acid, 0.9×10^{-4} M		
Buffer*	pH	A (313 mμ)	Buffer*	pH	A (310 mμ)
1.0 N HCl	—	0.653	1.0 N HCl	—	0.946
HCl	0.649	0.652	HCl	0.652	0.938
HCl	1.115	0.648	HCl	1.145	0.933
HCl	1.538	0.639	HCl	1.562	0.924
HCl	2.065	0.617	HCl	2.082	0.902
HCl	2.291	0.593	HCl	2.285	0.890
HCl	2.489	0.570	HCl	2.474	0.880
ACl	2.702	0.533	ACl	2.691	0.869
ACl	2.897	0.500	ACl	2.884	0.858
ACl	3.075	0.470	ACl	3.060	0.854
ACl	3.276	0.432	ACl	3.276	0.850
ACl	3.482	0.405	ACl	3.497	0.846
F	3.628	0.387	F	3.658	0.845
F	3.817	0.369	F	3.860	0.844
F	3.999	0.357	F	4.130	0.843
A	4.970	0.328	A	4.995	0.840
A	5.832	0.328	A	5.815	0.840
NH_3	9	0.328	NH_3	9	0.194

*F = formate, A = acetate, ACl = chloroacetate.

preliminary estimates of $C\epsilon_{HB}$ and $C\epsilon_B$ required for fitting eq. [4]. They were not included among the points to be fitted because they were obtained at ionic strengths greater than 0.01, but they are reported for comparison with the values of $C\epsilon_{HB}$ and $C\epsilon_B$ obtained from eq. [4]. For salicylic acid they may be compared with the calculated values $C\epsilon_{HB} = 0.653$

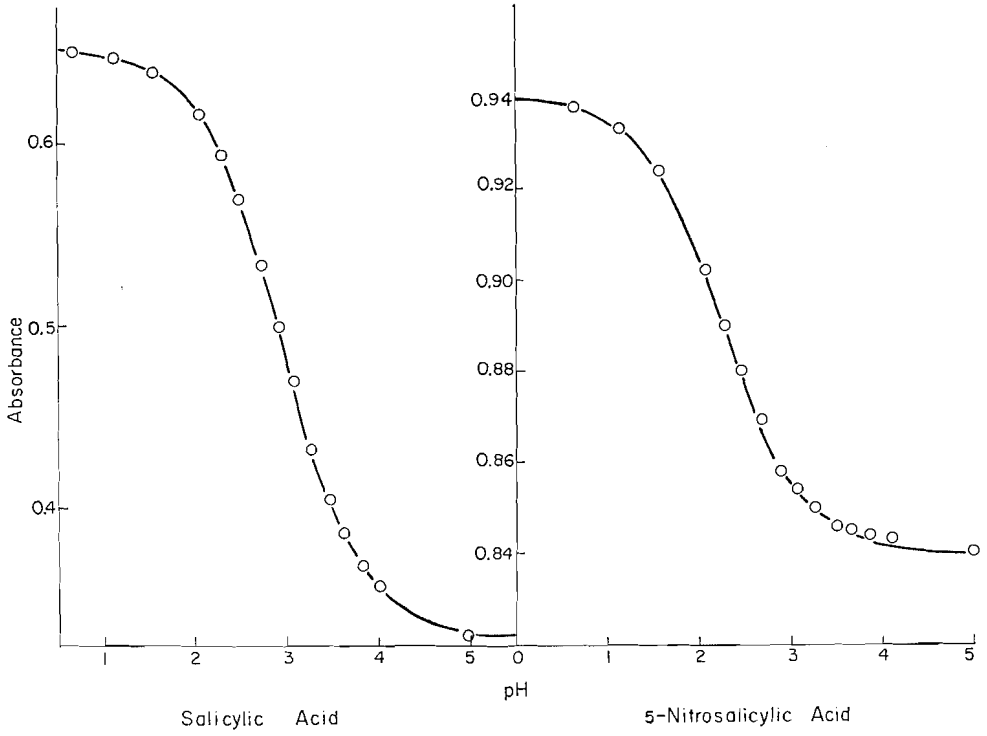


FIG. 2. Determination of ionization constants. LEGEND: O, experimental points; —, line calculated from eq. [4] by using the least squares values of K, $C\epsilon_{HB}$, and $C\epsilon_B$.

Can. J. Chem. Downloaded from www.nrcresearchpress.com by 210.87.254.105 on 09/05/12
For personal use only.

$\pm$ 0.005 and $C\epsilon_B = 0.328 \pm 0.003$; the agreement is equally good for all the other acids except the 5-nitro acid. For this acid eq. [4] gives $C\epsilon_{HB} = 0.940 \pm 0.008$ and $C\epsilon_B = 0.840 \pm 0.004$, which are in good agreement with the data of Table II at pH $\sim$ 0 and 6, respectively, but not with that in ammonia. This is further evidence that the phenolic group of 5-nitrosalicylic acid is significantly ionized at pH $\sim$ 9.

Table III shows the ionization constants of the various substituted salicylic acids and their standard deviations obtained from the least squares fit of the data to eq. [4]. Also

TABLE III

Ionization constants of substituted salicylic acids at 25 °C

Substituent	λ (mμ)	Concentration $\times 10^4$ M	$K \times 10^3$		
			μ = 0.010	Thermodynamic	Literature
4-OCH_3	305	1.4	0.532±0.018	0.494±0.017	
4-OH	255	0.4	0.635±0.009	0.591±0.008	0.505 (21); 0.605 (22)
4-OC_2H_5	305	1.6	0.679±0.021	0.630±0.020	
4-CH_3	308	1.8	0.830±0.037	0.770±0.034	0.72 (23)
5-CH_3	325	2.5	1.002±0.033	0.931±0.030	0.86 (23)
3-CH_3	318	2.4	1.033±0.031	0.962±0.029	1.018 (23); 1.00 (11)
None	313	2.5	1.107±0.031	1.02±0.03	1.05 (24); 1.06 (25)
5-OH	337	2.2	1.117±0.036	1.04±0.02	1.08 (21)
5-OCH_3	342	2.0	1.239±0.032	1.15±0.03	
4-Br	315	2.0	1.991±0.079	1.85±0.07	
5-Cl	325	3.0	2.148±0.111	1.99±0.10	1.97 (26); 2.35 (27); 2.23 (25)
5-I	325	3.0	2.153±0.094	2.00±0.09	
5-Br	328	3.0	2.618±0.086	2.43±0.08	2.44 (27); 2.40 (21); 2.20 (25)
5-CN	270	2.5	4.519±0.180	4.19±0.16	
4-CN	334	2.0	4.808±0.181	4.46±0.16	
5-NO_2	310	0.9	5.188±0.170	4.82±0.16	7.59 (27); 8.00 (28)
4-NO_2	288	0.8	5.309±0.406	4.93±0.36	5.88 (27)

shown are the wavelengths and concentrations at which the absorbance and pH measurements were made. The last column of Table III gives literature values for the ionization constants of those acids for which they are available. For comparison with these, thermodynamic ionization constants were estimated from our observed ionization constants by multiplying each by 0.929, the activity of the unsubstituted salicylate ion at an ionic strength of 0.010 reported by Kielland (20).

It is seen that our calculated thermodynamic ionization constants agree reasonably well with the literature values except for the nitro acids. Here the 4-nitro acid is stronger than the 5-nitro, where previous workers found the opposite order. The earlier results were obtained by a conductometric method, and it appears that they could be too high because of the phenolic ionization which our spectra show to be strongly activated in the 5-nitro acid by the *p*-nitro group. It may be noted that only one of the literature values was considered to be sufficiently reliable to be included in the I.U.P.A.C. tabulations of dissociation constants, although all but one were available when the compilation was made (1).

DISCUSSION

Jaffe has proposed (10) that eqs. [1] and [3] can be distinguished only when σ_1 and σ_2 have a correlation coefficient less than 0.9. For the 16 acids used in the present work, this correlation coefficient is 0.723. The σ values were taken from Hine's tables (8) by using σ^- for σ_2 when dealing with the 5-nitro and 5-cyano acids.

The data of Table III were fitted by the least squares method (19) to eq. [1] in the form

$$\log K = \rho_1\sigma_1 + \log K_0.$$

Can. J. Chem. Downloaded from www.nrcresearchpress.com by 210.87.254.105 on 09/05/12
For personal use only.

Since the standard deviations of log K were very similar for all substituents, the points were weighted equally. The calculated value of ρ_1 is 0.889 ± 0.061, and of log K_0 is -2.989 ± 0.025 (observed, -2.991 ± 0.013). The external estimate of error* (s_{ext}) is 0.0524. Figure 3 shows the data and the calculated line as a plot of log K against σ_1. The fit appears to be as good as that found in most other Hammett plots.

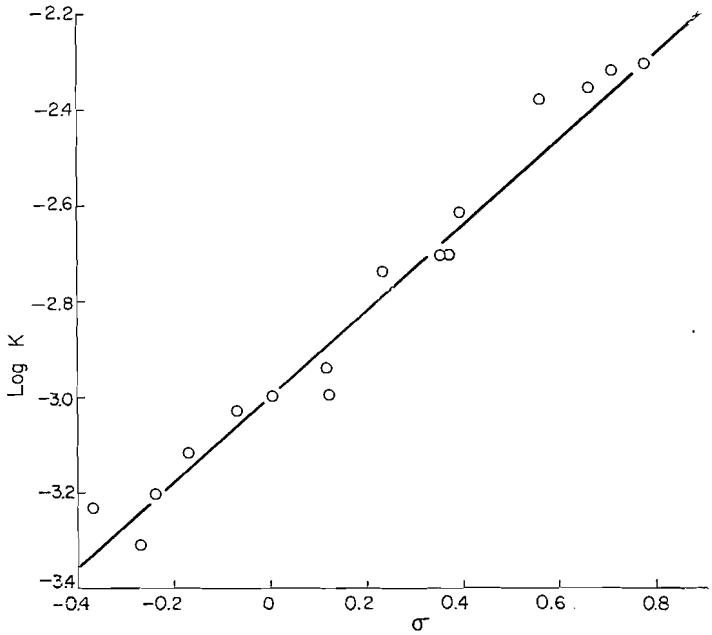


FIG. 3. Hammett plot of σ vs. the data from Table III.

The least squares fit (19) of the same data to eq. [3] in the form

$$\log K = \rho_1\sigma_1 + \rho_2\sigma_2 + \log K_0$$

gives $\rho_1 = 0.820 \pm 0.038$, $\rho_2 = 0.101 \pm 0.046$, log $K_0 = -2.997$, and $s_{ext} = 0.0454$. It is seen that ρ_2 is very small (only about double its standard deviation). The Student's t test (19) indicates that ρ_2 differs from zero only at the 95% confidence level (conditions under which Jaffe considers eq. [3] to be not significantly better than eq. [1] (10)). Consequently, we may conclude that the electronic effects of substituents upon the ionization constants of salicylic acids are transmitted only very slightly, if at all, through the phenolic hydroxyl group.

The reason for the failure of the chelate ring to transmit a substituent effect to the carboxyl group is not obvious. Comparison of the ionization constants reported in Table III with those in Table I shows that the range of ionization constants produced by changing substituents in salicylic acid is one-fourth as large as the difference in the ionization constants of salicylic and *p*-hydroxybenzoic acids. If the latter difference is produced entirely by chelation, it is surprising that the former one is independent of chelation. Several possible interpretations present themselves, but none is unequivocal.

For example, it might be argued that the variation in phenolic acidity produced by substituents is not large enough to affect the strength of the intramolecular hydrogen bond

The external estimate of error, s_{ext}, is given by $s_{ext}^2 = \sum (y - \bar{y})^2/n$, where y is log K observed, $\bar{y}$ is log K calculated from the equation, and n is the degrees of freedom ($n = 14$ for eq. [1] and 13 for eq. [3]).

Can. J. Chem. Downloaded from www.nrcresearchpress.com by 210.87.254.105 on 09/05/12
For personal use only.

significantly. Rubin and Panson (29), however, have shown that substituents in phenols do produce significant changes in the strength of intermolecular hydrogen bonds with pyridine. The ρ value for this complex formation in carbon tetrachloride is about +1. It would therefore seem probable that substituents should have a significant effect on the strength of chelation in salicylic acids.

An extension of the above argument suggests that an electronic effect which makes the phenolic group more acidic (strengthening chelation) will make the carboxylate group less basic (weakening chelation), so that the intramolecular hydrogen bond will be little affected by substituents. No doubt these opposing effects do exist, but they strengthen the expectation that the data should fit eq. [3] rather than eq. [1]. This can perhaps best be seen by considering them in an equation of the Hammett form. The total effect of a substituent on the ionization constant of a substituted salicylic acid would then involve three terms, which could be represented by

$$\log K/K_0 = \rho_1\sigma_1 + \rho_2\sigma_2 + \rho_3\sigma_3. \qquad [5]$$

The first term ($\rho_1\sigma_1$) corresponds to the usual substituent effect found in benzoic acids, the second term represents the substituent effect on the acidity of the phenolic group, and the third term represents the effect of the substituent on the basicity of the carboxylate ion. Since the first and third terms represent processes taking place at the carboxyl group, σ_1 applies to both; but since the second term represents the acidity of the phenolic group, σ_2 is different. For example, a 4-substituted acid has $\sigma_1 = \sigma_p$ and $\sigma_2 = \sigma_m$, whereas a 5-substituted acid will require $\sigma_1 = \sigma_m$ and $\sigma_2 = \sigma_p$. Hence, eq. [5] reduces to

$$\log K/K_0 = (\rho_1 + \rho_3)\sigma_1 + \rho_2\sigma_2,$$

which is equivalent to eq. [3]. Furthermore, since ρ_3 will be negative and ρ_1 positive, some cancellation will occur between ρ_1 and ρ_3, and this will tend to diminish the importance of the "direct" route for substituent influence in comparison with the "indirect" one via the intramolecular hydrogen bond.

Another obvious way to explain the absence of an "indirect" substituent effect is to suppose that in aqueous solution intramolecular hydrogen bonding is replaced by intermolecular hydrogen bonds between anion and solvent. The probability of the survival of chelate hydrogen bonds in aqueous solutions of carboxylic acids has been debated much (30, 32), but remains uncertain. Concerning salicylate ion, there is very little evidence, except that from ionization constants. Voroshin and Vlasov interpret the ultraviolet spectrum of sodium salicylate as indicating the presence of a chelate hydrogen bond in ethanol solution (31), and Chapman *et al.* reach similar conclusions from an infrared study of sodium salicylate in heavy water (32). Certainly, it is very difficult to account for the enhanced ionization of *o*-hydroxybenzoic acid over the para acid without recourse to chelation in the anion. It is true that other benzoic acids having bulky ortho substituents show a similarly enhanced ionization in aqueous solution, as shown in Table IV, and this is usually attributed to destabilization of the un-ionized acid by steric interference, with conjugation between the carboxylic group and the aromatic ring (4, 5, 8, 30, 33). However, the hydroxy group is much smaller than any of the other ortho groups which increase benzoic acid ionization, and its effect is larger. It is possible that in aqueous solution solvation of the phenolic group may increase its effective size, but whether this could be large enough to account for the enhanced acidity of salicylic acids is, at present, impossible to say. Further work on the transmission of substituent effects through chelation is in progress.

Can. J. Chem. Downloaded from www.nrcresearchpress.com by 210.87.254.105 on 09/05/12
For personal use only.

TABLE IV

Ionization constants of substituted benzoic acids in water at 25 °C (1)

	$K \times 10^5$	
Substituent	Ortho	Para
None	6.30	6.30
Methyl	12.35	4.24
Ethyl	16.1	4.44
Isopropyl	23.15	4.43
t-Butyl	29.1	3.98
Fluoro	54.1	7.22
Chloro	119.8	10.32
Bromo	140	9.95
Iodo	137	—

ACKNOWLEDGMENT

The authors are grateful to the National Research Council for a grant in aid of this project.

REFERENCES

1. G. KORTÜM, W. VOGEL, and K. ANDRUSSOW. Dissociation constants of organic acids in aqueous solution. Butterworths, London. 1961.
2. W. BAKER. J. Chem. Soc. 1687 (1934).
3. G. E. K. BRANCH and D. L. YABROFF. J. Am. Chem. Soc. **56**, 2568 (1934).
4. C. K. INGOLD. Structure and mechanism in organic chemistry. Cornell University Press, Ithaca, New York. 1953. pp. 744–749.
5. H. C. BROWN, D. H. MCDANIEL, and O. HÄFLIGER. *In* Determination of organic structures by physical methods. Vol. I. *Edited by* E. A. BRAUDE and F. C. NACHOD. Academic Press, Inc., New York. 1955. pp. 603–629.
6. E. S. GOULD. Mechanism and structure in organic chemistry. Henry Holt & Co., New York. 1959. p. 30.
7. G. C. PIMENTEL and A. L. MCLELLAN. The hydrogen bond. W. H. Freeman & Co., San Francisco. 1960. p. 182.
8. J. HINE. Physical organic chemistry. 2nd ed. McGraw-Hill Book Co., Inc., New York. 1962. p. 100.
9. L. P. HAMMETT. Physical organic chemistry. McGraw-Hill Book Co., Inc., New York. 1940.
10. H. H. JAFFE. J. Am. Chem. Soc. **76**, 4261 (1954).
11. J. SHORTER and F. J. STUBBS. J. Chem. Soc. 1180 (1949).
12. G. E. DUNN and E. G. JANZEN. Unpublished work.
13. E. B. HERSHBERG. Ind. Eng. Chem. Anal. Ed. **8**, 312 (1936).
14. R. L. SHRINER, R. C. FUSON, and D. Y. CURTIN. The systematic identification of organic compounds. 4th ed. John Wiley & Sons, Inc., New York. 1960.
15. T. MUKAI, M. KUNORI, H. KISHI, T. MUROI, and K. MATSUI. Proc. Japan Acad. **27**, 410 (1951).
16. H. BRETSCHNEIDER and W. KLOTZER. Monatsh. Chem. **82**, 13 (1951).
17. L. FRIEDMAN and H. SCHECHTER. J. Org. Chem. **26**, 2522 (1961).
18. P. LEGGATE and G. E. DUNN. Can. J. Chem. **43**, 1158 (1965).
19. W. E. DEMING. Statistical adjustment of data. John Wiley & Sons, Inc., New York. 1944.
20. J. KIELLAND. J. Am. Chem. Soc. **59**, 1677 (1937).
21. J. KENDALL. Medd. Kgl. Vetenskapakad. Nobelinst. **2**, 38 (1913); Chem. Abstr. **8**, 1044 (1914).
22. C. T. ABICHANDANI and K. K. F. JATKAR. J. Indian Chem. Soc. **16**, 385 (1939).
23. F. STOHMANN and H. LANGBEIN. J. Prakt. Chem. **50**, 399 (1894).
24. L. J. MINNICK and M. J. KILPATRICK. J. Phys. Chem. **43**, 259 (1939).
25. Z. L. ERNST and J. MENASHI. Trans. Faraday Soc. **59**, 230 (1963).
26. A. COPPADORO. Gazz. Chim. Ital. **32**, 542 (1902).
27. L. G. BRAY, J. F. J. DIPPY, R. C. HUGHES, and J. W. LAXTON. J. Chem. Soc. 2405 (1957).
28. G. MAGNANINI. Gazz. Chim. Ital. **21**, 215 (1891).
29. J. RUBIN and G. S. PANSON. J. Phys. Chem. **69**, 3089 (1965).
30. D. H. MCDANIEL and H. C. BROWN. Science, **118**, 370 (1953). R. E. DODD, R. E. MILLER, and W. F. K. WYNNE-JONES. J. Chem. Soc. 2790 (1961), and references therein.
31. E. M. VOROSHIN and V. G. VLASOV. Zh. Obsch. Khim. **30**, 3004 (1960).
32. D. CHAPMAN, D. R. LLOYD, and R. H. PRINCE. J. Chem. Soc. 550 (1964).
33. G. S. HAMMOND and D. H. HOGLE. J. Am. Chem. Soc. **77**, 338 (1954). G. FERGUSON and J. M. ROBERTSON. *In* Advances in physical organic chemistry. Vol. I. *Edited by* V. Gold. Academic Press, Inc., New York. 1963. pp. 241–242, and references therein.

Can. J. Chem. Downloaded from www.nrcresearchpress.com by 210.87.254.105 on 09/05/12
For personal use only.

Can. J. Chem. Downloaded from www.nrcresearchpress.com by 210.87.254.40 on 09/05/12
For personal use only.

CYANOESTERS AND DINITRILES

I. SYNTHESIS OF MALONONITRILES FROM METHYLENE ETHERS

N. LATIF AND N. MISHRIKY
National Research Center, Dokki, Cairo, United Arab Republic

Received July 13, 1965

ABSTRACT

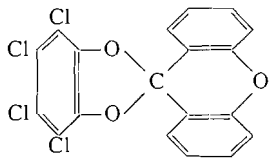
α-(9-Fluorenylidene) malononitrile (V) is obtained by the interaction of malononitrile and 9,9-(tetrachloro-*o*-phenylenedioxy) fluorene (II) in boiling *n*-butanol. Whereas fluorenone phenyl- or benzoyl-hydrazone is similarly obtained by the action of the corresponding hydrazine on II, the latter also undergoes reductive cleavage by hydrazine hydrate to give fluorene and tetrachlorocatechol. The heteropolar structures of methylene ethers are stressed.

Methyl-, ethyl-, isopropyl-, and benzyl-magnesium halides react readily with V to give the 9-dicyanomethyl-9-alkylfluorenes (VII*b*–VII*e*), respectively, which give, upon oxidation with alkaline potassium permanganate, the corresponding 9-alkylfluorene-9-carboxylic acids.

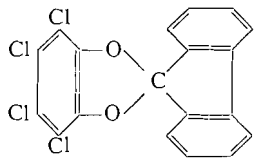
α-(9-Xanthenylidene) malononitrile (VI*a*) reacts similarly with alkylmagnesium halides to give the corresponding 9-xanthenylmalononitriles (VIII*b*–VIII*d*). However, V and VI are reduced by isobutylmagnesium iodide to give 9-fluorenyl- (VII*a*) and 9-xanthenyl-malononitrile (VIII*a*), respectively.

Whereas the infrared spectra of unsaturated malononitriles and cyanoesters show strong absorption in the 4.5 μ region, the spectra of the saturated analogues lack this absorption.

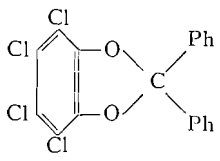
It has been reported throughout (1) that 9,9-(tetrachloro-*o*-phenylenedioxy) xanthene (I), in contrast to the fluorene analogue II, is cleaved readily by active hydrogen compounds in boiling ethanol to give the corresponding xanthenes. Cleavage of II is now brought about readily when the reaction is carried out in the higher boiling *n*-butanol. Thus, when II



I

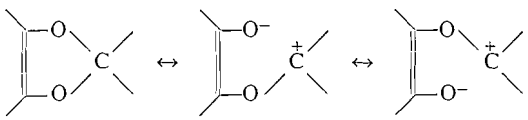


II



III

is refluxed with malononitrile, α-(9-fluorenylidene) malononitrile (V) is produced together with tetrachlorocatechol. With phenyl- or benzoyl-hydrazine, the corresponding fluorenone hydrazone is produced, possibly through the intermediate formation of an unstable open-chain ether by a β-elimination process (1). However, in contrast to other analogous methylene ethers previously investigated, II also undergoes reductive cleavage by hydrazine hydrate, yielding fluorene and tetrachlorocatechol, on prolonged boiling in *n*-butanol. The diphenylmethylene analogue III is not attacked by active hydrogen compounds under similar conditions. It is assumed that the methylene ether is a resonance



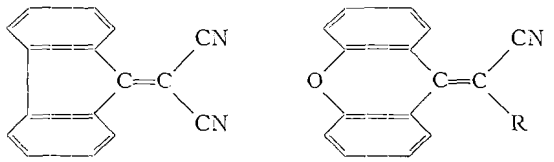
IV*a* IV*b* IV*c*

hybrid of various structures (2) (cf. IV), and the reaction proceeds through the nucleophilic attack of the active hydrogen compound. In the case of I, the heteropolar structure (IV*b* or IV*c*) is greatly stabilized by the strong resonance of the carbonium ion having

the unshared electron pair on the oxygen of the xanthene residue. In the case of II, the heteropolar structures contribute largely to the actual state of the molecule at higher temperatures.

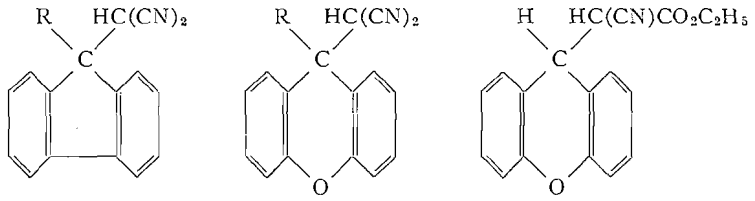
Reaction of Alkylmagnesium Halides on Unsaturated Dinitriles

In an attempt to prepare substituted malononitriles for biological purposes and spectral investigation, the action of Grignard reagents on the unsaturated malononitriles (V and VI*a*) has been investigated. It is found that V reacts with methyl-, ethyl-, isopropyl-, and benzyl-magnesium halides to give 9-dicyanomethyl-9-methyl- (VII*b*), 9-dicyanomethyl-9-ethyl- (VII*c*), 9-dicyanomethyl-9-isopropyl- (VII*d*), and 9-dicyanomethyl-9-benzyl-



V

VI*a*, R = CN
VI*b*, R = $COOC_2H_5$



VII*a*, R = H
VII*b*, R = CH_3
VII*c*, R = C_2H_5
VII*d*, R = iso-C_3H_7
VII*e*, R = $CH_2C_6H_5$

VIII*a*, R = H
VIII*b*, R = CH_3
VIII*c*, R = C_2H_5
VIII*d*, R = iso-C_3H_7
VIII*e*, R = $CH_2C_6H_5$

IX

fluorene (VII*e*), respectively, in good yields. The analogous α-9-xanthenylmalononitriles VIII*b*, VIII*c*, and VIII*d* are similarly obtained by the action of the corresponding alkylmagnesium halides on α-(9-xanthenylidene) malononitrile (VI*a*). However, it is found that the latter is reduced by the action of isobutylmagnesium iodide in ether to give, in good yield, 9-dicyanomethylxanthene (VIII*a*), which is identical with the product obtained by the action of malononitrile on xanthydrol (3). V is similarly reduced by isobutylmagnesium iodide to give 9-dicyanomethylfluorene (VII*a*). Hook and Robinson (4) have reported the isolation of some α-cyano-β-alkylbutyric esters as reduction products from the reaction of alkylidene cyanoesters with Grignard reagents in the presence of cuprous iodide. The α-substituted malononitriles (VII*a*–VII*e* and VIII*a*–VIII*d*) are colorless, whereas V and VI are highly colored. Their infrared spectra do not show the frequency bands characteristic of NH or C=O groups, and thus support the structures given and exclude the possibility of 1,2-addition of the Grignard reagents to the cyano group. The 9-dicyanomethyl-9-alkylfluorenes or 9-dicyanomethyl-9-alkylxanthenes are oxidized by potassium permanganate to the corresponding 9-alkylfluorene- or 9-alkylxanthene-9-carboxylic acids, in good yields, and thus provide a new method for preparing these biologically important acids.[1] 1,4-Addition of Grignard reagents to unsaturated nitriles has previously been recorded (5);

[1]*Aminoesters of fluorene- and xanthene-9-carboxylic acids proved to have remarkable spasmolytic and related activities (6).*

Can. J. Chem. Downloaded from www.nrcresearchpress.com by 210.87.254.40 on 09/05/12
For personal use only.

however, as far as we are aware, nothing has been published on the action of these reagents on arylidene malononitriles.

When the infrared spectra of the substituted malononitriles were investigated, it was found that the spectra of the unsaturated derivatives V and VI*a* showed strong absorption in the 4.5 μ region characteristic of the cyano group (7), whereas the saturated analogues VII and VIII do not show absorption in this region. Similarly, the spectrum of the unsaturated cyanoester VI*b* shows strong absorption whereas that of the saturated analogue IX lacks absorption in this region.[2] Kitson and Griffith (8) have reported that the introduction of an oxygenated group into the molecule results in a quenching of the C≡N absorption intensity to a remarkable extent, or even in the absence of the frequency band characteristic of the cyano group when the oxygenated group is attached to the same carbon atom as the nitrile. It is clear, now, that monosubstituted malononitriles, where the same carbon atom is bonded to two cyano groups, also exhibit this quenching property, provided that, in all cases, this carbon atom is saturated. In the spectra of the unsaturated analogues where the rotation of the carbon atom is not free, strong absorption in the 4.5 μ region is observed.

EXPERIMENTAL

Melting points were not corrected. Infrared spectra were measured on a Perkin–Elmer infracord spectrophotometer, model 137 (Nujol).

Reaction of 9,9-(Tetrachloro-o-phenylenedioxy) Fluorene (II) with Hydrazine Hydrate

A mixture of the cyclic ether (1 g) and hydrazine hydrate (98–100%, 1 ml) in *n*-butanol (10 ml) was refluxed for 20 h and filtered while hot. The solid which separated out when the solution cooled (0.5 g) proved to be unchanged II. The mother liquor was evaporated to dryness, and the residue was crystallized from ethanol to give fluorene (0.12 g), m.p. 114 °C (undepressed when admixed with an authentic sample).

Reaction of II with Phenylhydrazine

The reaction was carried out as above with 1 g of II, 1 g of phenylhydrazine, and a reflux period of 3 h. The solution was filtered while hot, concentrated, and left to cool. The solid that separated out (0.3 g), m.p. 150–151 °C, proved to be fluorenone phenylhydrazone (melting point and mixed melting point).

Reaction of II with Benzoylhydrazine

The reaction was carried out as above with 1 g of II and 0.6 g benzoylhydrazine. The product that was obtained was recrystallized from alcohol to give fluorenone benzoylhydrazone (0.6 g), m.p. 171 °C (undepressed when admixed with an authentic sample (9)).

*Preparation of 9-Dicyanomethyl-9-methylfluorene (VII*b*)*

α-(9-Fluorenylidene) malononitrile (V) (2 g) was added slowly to an ethereal solution of methylmagnesium iodide (from magnesium (0.7 g) and methyl iodide); the mixture was refluxed for 3 h, cooled, decomposed with ice and dilute hydrochloric acid, and extracted with ether. The dried ethereal extract was evaporated to dryness, a few milliliters of methanol was added to the oily residue, and the mixture was cooled. The solid that formed was crystallized from methanol to give 9-dicyanomethyl-9-methylfluorene (VII*b*) as colorless crystals, m.p. 107 °C (yield 1.2 g).[3]

Anal. Calcd. for $C_{17}H_{12}N_2$: C, 83.6; H, 4.9; N, 11.5. Found: C, 83.2; H, 4.5; N, 11.8.

Oxidation of VIIb

A hot saturated solution of potassium permanganate was added dropwise to a suspension of the product (VII*b*) (0.5 g) in a solution of sodium hydroxide (2 *N*, 50 ml) heated on the water bath. The addition was continued until the pink color persisted; then the reaction mixture was heated on the boiling water bath for 30 min, left to cool, and filtered. The filtrate was acidified with dilute hydrochloric acid and the product that separated out was crystallized from methanol to give 9-methylfluorene-9-carboxylic acid, m.p. 170 °C (10).[3]

*Preparation of 9-Dicyanomethyl-9-ethylfluorene (VII*c*)*

The dinitrile V (2 g) was allowed to react with ethylmagnesium iodide (from 0.7 g of magnesium) as above. The dried ethereal extract was left to evaporate slowly at room temperature, and the solid that separated out was crystallized from methanol to give 9-dicyanomethyl-9-ethylfluorene (VII*c*) (1 g) as colorless prisms, m.p. 117 °C.[3]

Anal. Calcd. for $C_{18}H_{14}N_2$: C, 83.7; H, 5.4; N, 10.8. Found: C, 84.0; H, 5.5; N, 10.5.

[2]*Spectra of both malononitrile and cyanoacetic ester show absorption.*
[3]*This experiment is described in the Ph.D. thesis of one of us (N. L.).*

Can. J. Chem. Downloaded from www.nrcresearchpress.com by 210.87.254.40 on 09/05/12
For personal use only.

Oxidation of VIIc

The substance was oxidized as above. The colorless product that was obtained was crystallized from petroleum ether (60–80°) to give 9-ethylfluorene-9-carboxylic acid (11), m.p. 145 °C.[3]

Anal. Calcd. for $C_{16}H_{14}O_2$: C, 80.6; H, 5.9. Found: C, 80.3; H, 5.8.

Preparation of 9-Dicyanomethyl-9-isopropylfluorene (VIId)

This was prepared from V and isopropylmagnesium bromide as above. The dried ethereal extract was concentrated and cooled. The crystals that separated out were filtered off and recrystallized from methanol to give VII*d* as colorless needles (0.9 g), m.p. 159 °C.

Anal. Calcd. for $C_{19}H_{16}N_2$: C, 83.8; H, 5.9; N, 10.3. Found: C, 84.2; H, 6.0; N, 10.1.

When VII*d* was oxidized with potassium permanganate, 9-isopropylfluorene-9-carboxylic acid was obtained as colorless crystals (from benzene), m.p. 204 °C.

Anal. Calcd. for $C_{17}H_{16}O_2$: C, 80.9; H, 6.4. Found: C, 81.1; H, 6.0.

Preparation of 9-Dicyanomethyl-9-benzylfluorene (VIIe)

The reaction between V and benzylmagnesium chloride was carried out as above. The dried ethereal extract was left to evaporate slowly at room temperature. The solid that formed was extracted with warm petroleum ether (40–60°) and the residue was crystallized from petroleum ether (60–80°) to give VII*e* as colorless crystals, m.p. 141 °C.[3]

Anal. Calcd. for $C_{23}H_{16}N_2$: C, 86.2; H, 5.0; N, 8.7. Found: C, 86.3; H, 4.9; N, 8.9.

Preparation of 9-Dicyanomethyl-9-methylxanthene (VIIIb)

The reaction between methylmagnesium iodide (from 0.7 g magnesium) and α-(9-xanthenylidene) malononitrile (VI*a*) (2.4 g) was carried out as usual. The ethereal extract was evaporated to dryness and a few drops of methanol was added to the oily residue. The solid that formed was crystallized from cyclohexane to give VIII*b* as colorless rods (1.1 g), m.p. 128 °C.

Anal. Calcd. for $C_{17}H_{12}N_2O$: C, 78.4; H, 4.7; N, 10.8. Found: C, 78.7; H, 4.7; N, 10.4.

When VIII*b* (1 g) was oxidized as above, 9-methylxanthene-9-carboxylic acid was obtained (0.5 g), m.p. 206 °C (12).

Anal. Calcd. for $C_{15}H_{12}O_3$: C, 75.0; H, 5.0. Found: C, 75.3; H, 4.9.

Preparation of 9-Dicyanomethyl-9-ethylxanthene (VIIIc)

The reaction was carried out as above with ethylmagnesium iodide and VI*a*. VIII*c* was obtained as colorless prisms (from *n*-hexane), m.p. 97–98 °C.

Anal. Calcd. for $C_{18}H_{14}N_2O$: C, 78.8; H, 5.1; N, 10.2. Found: C, 79.2; H, 5.2; N, 10.0.

Preparation of 9-Dicyanomethyl-9-isopropylxanthene (VIIId)

Isopropylmagnesium bromide and VI*a* were allowed to react as above. The ethereal extract was evaporated to dryness. The residue was recrystallized from *n*-hexane several times to give VIII*d* as colorless rods, m.p. 92–94 °C (yield 0.8 g).

Anal. Calcd. for $C_{19}H_{16}N_2O$: C, 79.2; H, 5.6; N, 9.7. Found: C, 79.9; H, 5.7; N, 9.7.

Reduction of α-(9-Xanthenylidene) Malononitrile (VIa)

Isobutylmagnesium iodide (from magnesium (0.7 g) and isobutyl iodide (3.4 ml)) and VI*a* (2.4 g) were allowed to react together as usual. The dried ethereal extract was concentrated and cooled, and the solid that separated out was crystallized from methanol to give 9-xanthenylmalononitrile (VIII*a*) (1 g) as colorless rods, m.p. 186–188 °C (undepressed when admixed with an authentic sample (3)). When the reaction was carried out with V instead of VI*a*, 9-fluorenylmalononitrile (VII*a*) was obtained as colorless leaflets (from petroleum ether, 50–75°), m.p. 152 °C.

Anal. Calcd. for $C_{16}H_{10}N_2$: C, 83.5; H, 4.4; N, 12.2. Found: C, 83.3; H, 4.5; N, 12.8.

REFERENCES

1. N. Latif, I. Fathy, and N. Mishriky. Can. J. Chem. **42**, 1736 (1964).
2. R. Parker and N. Isaacs. Chem. Rev. **59**, 737 (1959).
3. E. Sawicki and V. Oliverio. J. Org. Chem. **21**, 183 (1956).
4. W. Hook and R. Robinson. J. Chem. Soc. 152 (1944).
5. M. Kharash and O. Reinmuth. Grignard reactions of nonmetallic substances. Constable & Co., Ltd., London. 1954. p. 767.
6. R. Burtner and J. Cusic. J. Am. Chem. Soc. **65**, 1582 (1943). A. Goldberg and A. Wragg. J. Chem. Soc. 453 (1960).
7. L. J. Bellamy. The infrared spectra of complex molecules. John Wiley & Sons, Inc., New York. 1958. p. 266.
8. R. Kitson and N. Griffith. Anal. Chem. **24**, 334 (1952).
9. G. Reddelien. Ber. **54**, 3121 (1921); Chem. Abstr. **16**, 1761 (1922).
10. F. Anet and P. Bavin. Can. J. Chem. **34**, 991 (1956).
11. W. Wisclicenus and W. Mocker. Ber. **46**, 2772 (1913).
12. J. Conant and B. Garvey. J. Am. Chem. Soc. **49**, 2599 (1927).

Can. J. Chem. Downloaded from www.nrcresearchpress.com by 210.87.254.40 on 09/05/12
For personal use only.

Can. J. Chem. Downloaded from www.nrcresearchpress.com by 210.87.254.6 on 09/05/12
For personal use only.

STRUCTURE OF A GALACTURONAN FROM SUNFLOWER PECTIC ACID[1]

V. ZITKO[2] AND C. T. BISHOP
Division of Biosciences, National Research Council, Ottawa, Canada

Received January 12, 1966

ABSTRACT

Fractions of sunflower pectic acid containing 89.8%, 94.2%, and 91.4% of D-galacturonic acid were carboxyl reduced as their methyl or ethylene glycol esters by potassium borohydride. Critical assessment of the effects of three different solvents (water, 80% aqueous dimethyl sulfoxide, and 80% aqueous methanol) on the efficiency of reduction showed that the latter solvent was best. The reductions caused a decrease in the degree of polymerization from 270 to 21. Measurement of the rates of hydrolysis of partially reduced pectic acids containing 90%, 41.6%, 19.9%, 11.0%, and 0.65% of D-galacturonic acid showed that the rate of hydrolysis was directly related to the proportion of galacturonosidic linkages present. Methylation and hydrolysis of the carboxyl-reduced pectic acid fractions yielded 2,3,4,6-tetra-*O*-methyl-D-galactose and 2,3,6-tri-*O*-methyl-D-galactose in an approximate molar ratio of 1:20. Results of the periodate oxidation of the carboxyl-reduced pectic acid supported the conclusion inferred from the methylation results that the pectic acid was a linear polymer of $1 \rightarrow 4$ linked α-D-galacturonic acid units.

There has been considerable evidence that the main structural feature of pectin is a linear chain of $1 \rightarrow 4$ linked α-D-galacturonic acid units (1–3). However, in most of the early work (1) the pectins examined were of uncertain homogeneity, and in one of the later investigations (2) there was evidence that the product examined was a mixture of closely related acidic polysaccharides. In the most recent work reported (3), it was shown that pectin from the bark of amabilis fir could be fractionated to yield a galacturonan which contained no neutral sugars. This galacturonan was shown to be a linear polysaccharide of $1 \rightarrow 4$ linked α-D-galacturonic acid units. However, the report of some $1 \rightarrow 3$ linkages in a galacturonoxyloglycan from mountain pine pollen (4) indicates that linkages other than $1 \rightarrow 4$ may occur in some galacturonans.

Sunflower seed heads provide an excellent source of galacturonan, which is obtained in good yield and relatively free of other polysaccharides (5). A previous publication (6) described the fractionation of pectic acids from sunflowers and other sources into two acidic polysaccharides: a galacturonan to which neutral sugars were attached glycosidically, and a galacturonan which yielded only D-galacturonic acid on hydrolysis. The present paper describes the structural investigation of the latter polyuronide.

Three of the fractions obtained from sunflower pectic acid (6) were chosen for this investigation: (I) the polysaccharide precipitated by 0.14 *M* sodium acetate, containing 89.8% of D-galacturonic acid and having $[\alpha]_D$ +280° and $[\eta]$ 256; (II) the polysaccharide precipitated by 0.12 *M* sodium acetate and reprecipitated by 0.14 *M* sodium acetate, containing 94.2% of D-galacturonic acid and having $[\alpha]_D$ +300° and $[\eta]$ 215; (III) the polysaccharide precipitated by 0.14 *M* sodium acetate and reprecipitated by 0.12 *M* sodium acetate, containing 91.4% of D-galacturonic acid and having $[\alpha]_D$ +291° and $[\eta]$ 200.

On moving-boundary electrophoresis polysaccharide I showed a main peak with a small shoulder. Polysaccharides II and III each showed a single, symmetrical peak under the same conditions of electrophoresis.

[1]*Issued as N.R.C. No. 8952.*
[2]*National Research Council Postdoctorate Fellow, 1964–1966.*

Because pectic acids are resistant to methylation and are subject to degradation under the strongly alkaline conditions used, the polysaccharides described above were each reduced to yield neutral galactans. This procedure has been used frequently in structural polysaccharide chemistry (2, 3, 7–9), but there has been no critical assessment of the conditions used. In the present study, both methyl and ethylene glycol esters of the galacturonans were used as starting materials and were reduced by potassium borohydride in 80% aqueous methanol, in water, or in 80% aqueous dimethyl sulfoxide. Because of weight changes caused by partial reduction and partial de-esterification of galacturonic acid units in the galacturonan during reduction, the direct analytical results did not permit valid comparisons. Comparisons can be made, however, with the proportions of reduced to de-esterified galacturonic acid units, and of reduced to original ester content. These proportions and recoveries on a theoretical basis are shown in Table I.

TABLE I

Reduction of esterified galacturonan

Reduction	A*	B*	Yield (% of theory)
Methyl ester of polysaccharide I			
1. In 80% aqueous methanol	0.835	0.620	90
2. In 80% aqueous methanol	0.720	0.550	90
3. In 80% aqueous methanol	0.630	0.410	92
4. In 80% aqueous methanol	0.577	0.320	88
In water†	0.580	0.580	67
In 80% aqueous dimethyl sulfoxide‡	0.720	0.719	69
Ethylene glycol ester of polysaccharide I			
In 80% aqueous methanol	0.723	0.576	94
In water	0.670	0.670	79

*A = reduced galacturonic acid/reduced + de-esterified galacturonic acid; B = reduced galacturonic acid/original esterified galacturonic acid.
†The starting product for this reduction had been reduced twice in 80% aqueous methanol.
‡The starting product for this reduction had been reduced three times in 80% aqueous methanol.

The results showed that reductions in 80% aqueous methanol were the most efficient; de-esterification was suppressed, a reasonably high proportion of the galacturonic acid units was reduced, and recoveries were good. In water, a high proportion of galacturonic acids was reduced but there was also considerable de-esterification and recoveries were low, undoubtedly because of the degradation of esterified galacturonan in alkaline media (10). In 80% aqueous dimethyl sulfoxide, de-esterification was greatly suppressed, and the highest proportion of reduced groups was obtained when a partially reduced product was taken for the reduction. These advantages were offset by the low recovery; indeed, when this solvent was used for the first reduction of a fully esterified galacturonan, complete degradation occurred and no product precipitable by methanol could be obtained. Reductions were only slightly more efficient with methyl esters than with ethylene glycol esters.

Another factor in these reductions was the efficiency of esterification. A heterogeneous esterification with diazomethane in ether can be used until the galacturonan is about 80% reduced. After that only 78% of the remaining carboxyl groups could be esterified, and at the next stage (galacturonic acid content, 11%) no more than 45%, even when the substrate was freeze-dried to provide a large surface area. Esterification with ethylene or propylene oxide gave good results but the products, when precipitated by organic solvents, tended to form gels which were difficult to handle. There was no evidence of hydroxyalkylation of alcohol groups by these reagents. Residual carboxyl groups in highly reduced galacturonans can be esterified effectively with diazomethane in dimethyl

Can. J. Chem. Downloaded from www.nrcresearchpress.com by 210.87.254.6 on 09/05/12
For personal use only.

sulfoxide. In this procedure the esterified product need not be isolated before reduction, which can be done immediately afterwards in the same solution. A preparation containing 1.7% of D-galacturonic acid residues was obtained from one containing 6.8% in a yield of 54% by this procedure. Two esterifications and reductions were required to decrease the D-galacturonic acid content from 7.8% to 0.65%, with a recovery of 45%, when water was used as the solvent.

In summary, the best procedure for borohydride reduction of pectic acid methyl ester is heterogeneous esterification with diazomethane followed by borohydride reduction in 80% aqueous methanol until the product contains less than 20% of galacturonic acid. At that stage, both esterification and reduction can be carried out in 80% aqueous dimethyl sulfoxide to give the fully reduced product. In our hands, reduction of pectic acid by the diborane method (11) was incomplete and caused considerable degradation. Reduction of di-*O*-acetyl polyuronide methyl esters by lithium borohydride (12), reported while the present manuscript was in preparation, may offer a better route to carboxyl-reduced polysaccharides; however, possible degradative effects of the latter method have not been investigated.

Throughout this work, samples of polysaccharide I which were carboxyl reduced to varying extents became available, and their relative resistances to acid hydrolysis were determined. Rate constants were determined for acid hydrolysis (13, 14) with 0.5 *N* sulfuric acid in 95% (v/v) aqueous dimethyl sulfoxide at 100 °C. Plots of ln $(1 - \alpha)$ against time (α = percentage of hydrolysis) were linear. Figure 1 shows a plot of the rate constants as functions of the D-galacturonic acid content. There is a linear increase in rate constant with decreasing D-galacturonic acid content, indicating that the rate of acid hydrolysis is an additive property of the amounts of more resistant galacturonoside linkages (15) and less resistant galactoside linkages.

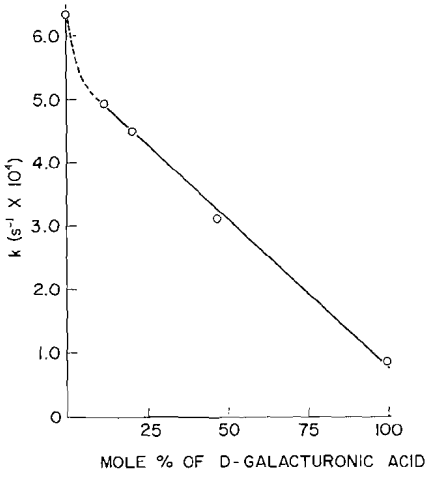


FIG. 1. Relation between rates of hydrolysis and D-galacturonic acid content for partially reduced pectic acid.

Reduction of polysaccharide I provided, in an overall yield of 37%, an α-galactan which contained 0.65% of D-galacturonic acid. The galactan had $[\alpha]_D$ +232° and showed a single, unsymmetrical peak on moving-boundary electrophoresis. The galactan contained 5.47% methoxyl and, on hydrolysis, yielded galactose and small amounts of two other components, which were probably 3-*O*- and 6-*O*-methyl-D-galactose. The *O*-methyl

Can. J. Chem. Downloaded from www.nrcresearchpress.com by 210.87.254.6 on 09/05/12
For personal use only.

groups were a result of methylation by diazomethane during the esterification steps. A portion of the hydrolysate was methylated (16) and examined by gas–liquid chromatography (17). The only products found were the methyl glycosides of 2,3,4,6- and 2,3,5,6-tetra-*O*-methyl-D-galactose. Another portion of the hydrolysate was demethylated (18), and examination by paper chromatography showed that galactose was the only sugar present. The foregoing results established conclusively that the pectic acid was a polymer formed from D-galacturonic acid units exclusively.

Polysaccharides II and III were reduced in the same way as polysaccharide I but, because they were not available in as large a quantity, these two fractions were not analyzed during the reduction steps.

The three, reduced fractions were methylated by successive application of the procedures of Haworth (19), Falconer and Adams (20), and Purdie (21). The methylated products were isolated by precipitation with light petroleum and were purified, where necessary, by chromatography on silica gel. These procedures yielded the following main methylated polysaccharides: from polysaccharide I, yield 63%, methoxyl 45.2%, $[\alpha]_D$ +214°; from polysaccharide II, yield 55%, methoxyl 32.8%, $[\alpha]_D$ +126°; and from polysaccharide III, yield 16%, methoxyl 43.1%, $[\alpha]_D$ +146°. Hydrolysis of each of these methylated products yielded 2,3,4,6-tetra-*O*-methyl- and 2,3,6-tri-*O*-methyl-D-galactose, as shown by paper, thin-layer, and gas–liquid chromatography; the two compounds were also characterized by preparation of their crystalline derivatives. The fully methylated polysaccharide I also yielded small amounts of 2,3,5,6-tetra-*O*-methyl-D-galactose and di-*O*-methyl-D-galactoses. The latter consisted of at least three isomers, each amounting to less than 1.5% of the total hydrolysis products.

In addition to the main methylated products described above, methylation of polysaccharides I, II, and III provided some minor methylated products which were soluble in light petroleum or were separated from the main products by chromatography on silica gel. Each of these minor products had lower methoxyl contents (24% to 29%) and lower specific rotations (+60° to +70°). However, each of these minor products yielded 2,3,4,6-tetra-*O*-methyl- and 2,3,6-tri-*O*-methyl-D-galactose on hydrolysis; the only other methylated sugar found was a small amount of 2,3,5,6-tetra-*O*-methyl-D-galactose in the light petroleum soluble fraction from the methylation of polysaccharide I. The ratio of tetra- to tri-*O*-methyl-D-galactose was about 1:20 for each of these products. The lower methoxyl contents and specific rotations of the minor products from the methylation of the polysaccharides indicated the presence of considerable amounts of impurities. These impurities must have been polymeric artifacts, because no compounds other than the methylated galactoses mentioned above were detected in the hydrolysates by any of the chromatographic procedures. It is likely that these polymeric artifacts were formed during the reductions and methylations, which caused extensive degradation; the initial degree of polymerization of polysaccharide I was 270 (from the limiting viscosity number), whereas the methylated products had a degree of polymerization of 21 based on the ratio of tetra- to tri-*O*-methyl-D-galactose.

When reduced polysaccharide I was oxidized by periodate, it consumed 0.82 mole of oxidant per monomer unit, with production of 0.09 mole of formic acid. The oxidized polysaccharide I was reduced and hydrolyzed (22). Examination of the acetylated hydrolysis products by gas–liquid chromatography (17) showed the presence of the following components: ethylene glycol diacetate, glycerol triacetate, two unidentified compounds, and threitol tetraacetate. The latter compound was characterized as its tetra-*p*-nitrobenzoate (23). The molar ratio of the last four components was 9.5:3:22:266; the amount of ethylene glycol diacetate was not determined because ethylene glycol was added to the

Can. J. Chem. Downloaded from www.nrcresearchpress.com by 210.87.254.6 on 09/05/12
For personal use only.

oxidation to destroy excess periodate. An α-(1 → 4)-galactan should consume 1.00 mole of periodate per monomer unit, if one ignores the end groups. The observed value of 0.82 mole per mole is low, probably because of the 5.47% of methoxyl groups introduced during esterification. This may also account for the two unidentified components (retention times 1.17 and 2.15 min) in the hydrolysate described above. Traces of galactitol were found in the hydrolysate by paper chromatography, but the amounts were insignificant. The ratio of glycerol to threitol (1:28) from the periodate-oxidized product was close to the ratio of tetra- to tri-*O*-methyl-D-galactose (1:20) found in the methylated polysaccharides, indicating that the major degradation of the polysaccharide occurred during the reduction of the galacturonan methyl ester and not during the methylation.

The results of methylation and periodate oxidation showed that the polysaccharide fractions precipitated from sunflower pectic acid by low concentrations of sodium acetate were linear galacturonans formed by α-(1 → 4) linkages. Because the polyuronides suffered extensive degradation during reduction to neutral galactans, the possibility that some labile units or linkages were cleaved cannot be overlooked. Such a process may well account for the isolation of 2,3,5,6-tetra-*O*-methyl-D-galactose among the methylation products from polysaccharide I; units of D-galactose, split off during degradation, would be methylated preferentially in the furanose ring form (24). However, it is likely that the degradation of the polyuronides was a random process and would not be specific for glycosidic linkages other than α-(1 → 4). The linear α-(1 → 4) structure assigned to the degraded galactan may therefore be regarded as fairly representative of the galacturonan from which it was derived. The galacturonans from apples, citrus fruits, and sugar beets should also have similar structures, because of their close resemblance to sunflower galacturonan in both specific rotation and electrophoretic mobility (6).

EXPERIMENTAL

Paper chromatograms were run on Whatman No. 1 paper by the descending method in the following solvent systems (by volume): A, ethyl acetate – pyridine – water (10:4:3); B, ethyl acetate – acetic acid – formic acid – water (18:3:1:4); C, butanone half saturated with water; D, butan-1-ol–ethanol–water (4:1:5) (upper layer).

Paper electrophoreses were run on Whatman 3MM paper in 0.10 *M* sodium tetraborate at a potential gradient of 25–30 mA (25). A Tiselius-type, Spinco model H apparatus was used for moving-boundary electrophoresis; the buffer was 0.05 *M* sodium tetraborate (26). A Pye argon chromatograph was used for gas–liquid chromatography (17); the column packings were: (*a*) 10% Carbowax 6000 on Chromosorb W, 100–120 mesh, 164 °C, and (*b*) 15% polyphenyl ether on Gas Chrom A, 100–120 mesh, 190 °C. Retention times are given relative to that of methyl 2,3,4,6-tetra-*O*-methyl-β-D-glucoside unless otherwise stated. Thin-layer chromatograms were run on Adsorbosil 1 with benzene–acetone (4:6) as the developing solvent. Preparative thin-layer chromatograms were run on 0.8 mm layers of Adsorbosil 1, and the separated components were detected by a template technique (27). The *p*-anisidine hydrochloride (28) and alkaline silver nitrate (29) spray reagents were used to detect glycoses and alditols, respectively. Methods of analysis of galacturonans were described previously (6). Solvents were evaporated at 35–37 °C under diminished pressure, melting points are corrected, and specific rotations were measured at room temperature (24–26 °C).

Isolation of Polysaccharides

Sunflower pectic acid was prepared as previously described (5, 6). It was dissolved in water at pH 6.0, and 2.0 *M* sodium acetate was added to a concentration of 0.14 *M* sodium acetate. The precipitate which formed was washed with acidified 60% aqueous ethanol (5 ml of concentrated hydrochloric acid per l), and then with 60% aqueous ethanol until free of chlorides; it was then dried by solvent exchange with ethanol and ether. The precipitation by sodium acetate was repeated once to yield polysaccharide I (galacturonic acid, 89.8%; $[\alpha]_D$ +280° (*c*, 0.5 in water); $[\eta]$ 256; yield, 51% of the pectic acid; electrophoretic mobility, $\mu = 12.6 \times 10^{-5}$ cm^2 V^{-1} s^{-1}).

Polysaccharide II (galacturonic acid, 94.2%; $[\alpha]_D$ +300° (*c*, 0.5 in water); $[\eta]$ 215) and polysaccharide III (galacturonic acid, 91.4%; $[\alpha]_D$ +291° (*c*, 0.5 in water); $[\eta]$ 200) were isolated as described previously (6).

Reduction of Polysaccharide I

Polysaccharide I (20 g) was esterfied by dispersion in methanol which contained concentrated sulfuric acid to a concentration of 2 *N*. The mixture was kept at 0 to 2 °C for 19 days and yielded a product (21.2 g)

Can. J. Chem. Downloaded from www.nrcresearchpress.com by 210.87.254.6 on 09/05/12
For personal use only.

with a degree of esterification (percentage of galacturonic acid units esterified) of 87.3%. The ester (21 g) was suspended in 80% aqueous methanol (1 000 ml), and potassium borohydride (22 g) was added in small portions with vigorous stirring. After 18 h the product was filtered off, washed with 80% aqueous methanol, and dried by solvent exchange; yield, 17.4 g; degree of esterification, 48.8%; galacturonic acid, 42.7%.

The above preparation was esterified by diazomethane in ether (30) at 0 to 2 °C for 24 h. The resulting product (17 g; degree of esterification, 88.5%) was reduced by potassium borohydride (12 g) as described above to yield partially reduced polysaccharide I (15 g); degree of esterification, 41.6%; galacturonic acid, 19.0%. Another esterification by diazomethane and then reduction yielded a product (11.2 g) with a degree of esterification of 38.5%; galacturonic acid, 11.0%. This product was dissolved in water, freeze-dried, and esterified with diazomethane; after 1 week the degree of esterification was 45%. Reduction yielded a polysaccharide (8.8 g) with a degree of esterification of 21%; galacturonic acid, 7.8%. This product was esterified with ethylene oxide in water (3) for 6 days at room temperature. The ester was recovered by precipitation with acetone; yield, 8.7 g; degree of esterification, 99.0%. Reduction by potassium borohydride (2.5 g) in water (550 ml) yielded a product (5.2 g) with a degree of esterification of 0%; galacturonic acid, 4.3%. Esterification with ethylene oxide and reduction were repeated once more to yield reduced polysaccharide I (3.9 g); degree of esterification, 0%; galacturonic acid, 0.65%; methoxyl, 5.47%; $[\alpha]_D$ +232° (*c*, 0.5 in 95% aqueous dimethyl sulfoxide); electrophoretic mobility, $\mu = 3.04 \times 10^{-5}$ cm^2 V^{-1} s^{-1}.

The following alternative procedures for esterification and reduction were examined.

(i) Reduction of Ethylene Glycol Ester of Polysaccharide I

Polysaccharide I was esterified with aqueous ethylene oxide as described above; degree of esterification, 96.5%. The ester (0.7 g) was reduced by potassium borohydride (0.7 g) in 80% aqueous methanol (50 ml); yield, 0.53 g; degree of esterification, 43.2%; galacturonic acid, 35.1%.

Another sample of the ethylene glycol ester (0.65 g) was reduced by potassium borohydride (0.65 g) in water (50 ml); yield, 0.39 g; degree of esterification, 0%; galacturonic acid, 29.7%.

(ii) Esterification and Reduction in Dimethyl Sulfoxide

Partially esterified, partially reduced polysaccharide I (1 g; degree of esterification, 45%; galacturonic acid, 11%) was dissolved in dimethyl sulfoxide (75 ml); potassium borohydride (0.5 g) in water (25 ml) was added. The solution was stirred overnight and was then poured into four volumes of acidified methanol. The precipitated polysaccharide was washed with methanol and dried by solvent exchange; yield, 0.69 g; degree of esterification, 10.7%; galacturonic acid, 6.8%. This sample was dissolved in dimethyl sulfoxide, and ethereal diazomethane (2 ml) was added dropwise, with vigorous stirring, over 2 h. A solution of potassium borohydride (0.1 g) in dimethyl sulfoxide (10 ml) and water (5 ml) was then added and the solution was stirred overnight. The reduced polysaccharide was recovered as above; yield, 0.37 g; degree of esterification, 0%; galacturonic acid, 1.7%.

Polysaccharide I (1 g) was esterified in dimethyl sulfoxide by ethereal diazomethane as described above to yield a product (1 g) with a degree of esterification of 91.6%. When this product was reduced by potassium borohydride in dimethyl sulfoxide, no methanol-insoluble material could be recovered.

(iii) Reduction in Water

A solution of partially reduced polysaccharide I (2 g; degree of esterification, 78%; galacturonic acid, 19.9%) in water (200 ml) was added dropwise to a solution of potassium borohydride (2.5 g) in water (250 ml). The solution was stirred overnight and the reduced polysaccharide was then recovered by precipitation with acidified methanol; yield, 1.32 g; degree of esterification, 0%; galacturonic acid, 10.1%.

Reductions of Polysaccharides II and III

Polysaccharide II (0.75 g) was esterified with aqueous ethylene oxide (12.7%, 250 ml) and reduced by potassium borohydride to yield a partially reduced polysaccharide II (0.6 g). Two further reductions of the propylene glycol ester yielded the carboxyl-reduced polysaccharide II used for structural studies. The small amount (0.24 g) of this product precluded analysis for ester and galacturonic acid.

Polysaccharide III (6.5 g) was converted into its ethylene glycol ester between each reduction. It was reduced twice in 80% aqueous methanol and three times in water to yield carboxyl-reduced polysaccharide III (1.84 g); galacturonic acid, 5.8%.

Rates of Hydrolysis

The ethylene glycol esters of polysaccharide I and a series of partially reduced products containing 41.6%, 19.9%, 11.0%, and 0.65% of galacturonic acid were hydrolyzed by 0.5 *N* sulfuric acid in 95% aqueous dimethyl sulfoxide on a boiling water bath. The degree of hydrolysis was determined polarimetrically (14).

Periodate Oxidation of Carboxyl-Reduced Polysaccharide I

Carboxyl-reduced polysaccharide I (301 mg; galacturonic acid, 0.65%) was dissolved in water (40 ml), 0.1 *M* sodium metaperiodate (40 ml) was added, and the volume was adjusted to 100 ml with water. Aliquots (2 ml) were removed at intervals for an estimation of the periodate (31) and formic acid (32) content. Periodate consumption was 0.79, 0.80, and 0.82 mole per monomer unit after 17, 24, and 40 h, respectively. Formic acid production after 40 h was 0.09 mole per monomer unit. Ethylene glycol was added to the oxidation reaction to destroy excess periodate, and the solution was then deionized with exchange resins. Potassium

Can. J. Chem. Downloaded from www.nrcresearchpress.com by 210.87.254.6 on 09/05/12
For personal use only.

borohydride (0.2 g) was added to the deionized solution and the reduction was left for 24 h. Excess borohydride was destroyed by cation-exchange resin, and boric acid was removed by repeated addition and evaporation of methanol. The syrupy residue was hydrolyzed with 0.5 *N* sulfuric acid on a boiling water bath for 4 h. The hydrolysate was neutralized with barium carbonate, barium salts were filtered off, and potassium borohydride (0.2 g) was added to the filtrate. The reduction was worked up as described above to yield a syrup (2.9 g). Part of this product was acetylated by acetic anhydride – pyridine (1:1) at 65 °C for 1 h and examined by gas–liquid chromatography (column *b*); the following components were found (retention times relative to that of glycerol triacetate): ethylene glycol diacetate (0.83), glycerol triacetate (1.00), two unidentified compounds (1.17, 2.15), and threitol tetraacetate (4.21). The rest of the reduced hydrolysate was examined by paper chromatography (solvents A and B), which showed the presence of threitol and traces of galactitol. Threitol (30 mg) was isolated by preparative paper chromatography in solvent B and was converted into tetra-*O*-(*p*-nitrobenzoyl)-D-threitol (23), m.p. 210 °C.

Anal. Calcd. for $C_{32}H_{20}O_{16}N_4$: C, 53.4; H, 3.1; N, 7.8. Found: C, 53.3; H, 3.3; N, 7.9.

Methylation of Carboxyl-Reduced Polysaccharide I

Carboxyl-reduced polysaccharide I (1.01 g; galacturonic acid, 0.65%) was methylated with dimethyl sulfate (20 ml) and 30% aqueous sodium hydroxide (50 ml) (19); four additions of reagents were made. The partially methylated product (1.05 g) was isolated by extraction into chloroform, and methylated by dimethyl sulfate (10 ml) and solid sodium hydroxide (10 g) in tetrahydrofuran (20); two additions of reagents were made. After extraction into chloroform the methylated product was precipitated by light petroleum (b.p. 30–60 °C) and gave a precipitated (680 mg) and a soluble fraction (354 mg). Both fractions showed hydroxyl absorption in the infrared. The two fractions were combined and methylated twice with methyl iodide and silver oxide (21). The product was again precipitated with light petroleum to yield an insoluble (633 mg) and a soluble (350 mg) fraction. The insoluble product had $[\alpha]_D$ +214° (*c*, 1.0 in chloroform) and a methoxyl content of 45.2%; the soluble fraction had $[\alpha]_D$ +60.5° (*c*, 1.9 in chloroform) and a methoxyl content of 25.8%. Methanolysis of each fraction by 4% methanolic hydrogen chloride at 100 °C for 12 h yielded identical products, as shown by gas–liquid chromatography (column *a*).

The fraction (633 mg) that was insoluble in light petroleum was hydrolyzed (33). Paper chromatography of the hydrolysate in solvent D showed the presence of components with the following mobilities relative to that of 2,3,4,6-tetra-*O*-methyl-D-galactose: 1.14 (very weak), 1.00, 0.82 (very strong), 0.59 (trace), and 0.18 (very weak). The methylated sugars in the hydrolysate were resolved by preparative thin-layer chromatography to give the following five fractions (in decreasing order of mobility).

Fraction 1

The syrup (66 mg) contained 2,3,5,6-tetra-*O*-methyl-D-galactose and an unidentified compound of high mobility on both paper and gas–liquid chromatograms. Rechromatography on thin layers yielded a syrup (18 mg) which had the same chromatographic mobility as an authentic sample of 2,3,5,6-tetra-*O*-methyl-D-galactose; demethylation (18) yielded galactose. The sample was oxidized by bromine, esterified by methanolic hydrogen chloride, and treated with ammoniacal methanol; the resulting amide failed to crystallize.

Fraction 2

This fraction (77 mg) contained a mixture of 2,3,4,6-tetra- and 2,3,6-tri-*O*-methyl-D-galactose. Methanolysis and gas–liquid chromatography showed the presence of components with retention times of 1.57, 3.06, 3.36, 3.93, and 4.16 on column *a*. Further purification by thin-layer chromatography yielded pure samples of the tetra-*O*-methyl (27 mg) and tri-*O*-methyl (34 mg) derivatives. 2,3,4,6-Tetra-*O*-methyl-D-galactose yielded a crystalline anilide (34), m.p. 194–196 °C, unchanged on admixture with an authentic sample.

Fraction 3

The syrup (429 mg) showed only one component corresponding to 2,3,6-tri-*O*-methyl-D-galactose on paper chromatography (solvent C). Gas–liquid chromatography of the methyl glycosides showed components with retention times of 3.06, 3.36, 3.93, and 4.16, corresponding to the anomeric methyl furanosides and pyranosides of 2,3,6-tri-*O*-methyl-D-galactose. Oxidation with bromine yielded 2,3,6-tri-*O*-methyl-D-galactono-(1 → 4)-lactone (35), m.p. 96–97 °C, $[\alpha]_D$ −41° → −32° (*c*, 1.26 in water). A syrup obtained from the mother liquors from the above crystallization contained a mixture of (1 → 4)- and (1 → 5)-lactones as shown by its infrared spectrum (36). This sample was esterified by methanolic hydrogen chloride and was then converted into the amide (37), m.p. 128–129 °C, unchanged on admixture with an authentic sample of 2,3,6-tri-*O*-methyl-D-galactonamide.

Fraction 4

This syrup (18 mg) contained at least three different compounds, as shown by thin-layer chromatography and by gas–liquid chromatography of the methyl glycosides; it was not examined further.

Fraction 5

This material (19 mg) was recovered from the starting line of the thin-layer chromatograms. Methanolysis and gas–liquid chromatography showed that 2,3,6-tri-*O*-methyl-D-galactose was the main product.

The portion of methylated, carboxyl-reduced polysaccharide I that was soluble in light petroleum (350 mg) was fractionated further by chromatography on silica gel to yield three products: the first (90 mg), eluted by chloroform, had $[\alpha]_D$ −3.5° (*c*, 0.9 in chloroform); the second (142 mg), eluted by chloroform–methanol

Can. J. Chem. Downloaded from www.nrcresearchpress.com by 210.87.254.6 on 09/05/12
For personal use only.

(98:2), had $[\alpha]_D$ +76° (*c*, 1.4 in chloroform) and a methoxyl content of 28.9%; the third (45 mg), eluted by chloroform–methanol (75:25), had $[\alpha]_D$ +160° (*c*, 0.9 in chloroform) and a methoxyl content of 37.8%. Methanolysis and gas–liquid chromatography showed that each of these products contained the same methylated sugars as were present in the light petroleum insoluble fraction. The fraction with $[\alpha]_D$ +76° was found to contain methyl 2,3,5,6-tetra-*O*-methyl-D-galactosides before hydrolysis.

Methylation of Carboxyl-Reduced Polysaccharide II

Carboxyl-reduced polysaccharide II (207 mg) was methylated by the procedures of Haworth (19) and Purdie (21) to yield a product (114 mg) with $[\alpha]_D$ +126° (*c*, 2.28 in chloroform) and a methoxyl content of 32.8%; there was negligible hydroxyl absorption in the infrared. Paper chromatography (solvents C and D) and gas–liquid chromatography (columns *a* and *b*) of a hydrolysate and a methanolysate, respectively, showed the presence of only two compounds: 2,3,4,6-tetra-*O*-methyl-D-galactose and 2,3,6-tri-*O*-methyl-D-galactose in a molar ratio of 1:20 as determined by gas–liquid chromatography.

Methylation of Carboxyl-Reduced Polysaccharide III

Carboxyl-reduced polysaccharide III (1.6 g) was methylated by the procedures of Haworth (19) and Purdie (21) to yield light petroleum insoluble (608 mg) and soluble (472 mg) fractions. The latter, $[\alpha]_D$ +64° (*c*, 2.3 in chloroform), was not examined further. The fraction that was insoluble in light petroleum was chromatographed on silica gel to yield, first, a fraction (258 mg) eluted by chloroform–methanol (98:2) ($[\alpha]_D$ +146° (*c*, 1.29 in chloroform); methoxyl, 43.1%), and second, a fraction (167 mg) eluted by chloroform–methanol (95:5) ($[\alpha]_D$ +152° (*c*, 1.1 in chloroform); methoxyl, 39.0%). Each of these fractions contained only 2,3,4,6-tetra-*O*-methyl-D-galactose and 2,3,6-tri-*O*-methyl-D-galactose, as shown by paper chromatography (solvents C and D) of hydrolysates and gas–liquid chromatography (columns *a* and *b*) of methanolysates. The ratios of tetra- to tri-*O*-methyl-D-galactose were 1:24 and 1:36, respectively, in these two fractions.

REFERENCES

1. E. L. Hirst and J. K. N. Jones. Advan. Carbohydrate Chem. **2**, 235 (1946).
2. G. O. Aspinall and A. Canas-Rodriguez. J. Chem. Soc. 4020 (1958).
3. S. S. Bhattacharjee and T. E. Timell. Can. J. Chem. **43**, 758 (1965).
4. H. O. Bouveng. Acta Chem. Scand. **19**, 953 (1965).
5. C. T. Bishop. Can. J. Chem. **33**, 1521 (1955).
6. V. Zitko and C. T. Bishop. Can. J. Chem. **43**, 3206 (1965).
7. G. O. Aspinall. Methods Carbohydrate Chem. **5**, 397 (1965).
8. T. E. Timell and A. Jabbar-Mian. Tappi, **44**, 788 (1961).
9. U. K. Sen Gupta and A. Das. Bull. Chem. Soc. Japan, **38**, 1074 (1965).
10. B. Vollmert. Makromol. Chem. **5**, 110 (1950).
11. F. Smith and A. M. Stephen. Tetrahedron Letters, 17 (1960).
12. D. A. Rees and J. W. B. Samuel. Chem. Ind. London, 2008 (1965).
13. W. Kuhn. Ber. **63**, 1503 (1930).
14. K. Freudenberg, W. Kuhn, W. Dürr, F. Bolz, and G. Steinbrunn. Ber. **63**, 1510 (1930).
15. S. C. McKee and E. E. Dickey. J. Org. Chem. **28**, 1561 (1963).
16. R. Kuhn, H. Trischmann, and I. Löw. Angew. Chem. **67**, 32 (1955).
17. C. T. Bishop. Advan. Carbohydrate Chem. **19**, 95 (1964).
18. L. Hough and R. S. Theobald. Methods Carbohydrate Chem. **2**, 203 (1963).
19. W. N. Haworth. J. Chem. Soc. **107**, 8 (1915).
20. E. L. Falconer and G. A. Adams. Can. J. Chem. **34**, 338 (1956).
21. T. Purdie and J. C. Irvine. J. Chem. Soc. **83**, 1021 (1903).
22. G. W. Hay, B. A. Lewis, and F. Smith. Methods Carbohydrate Chem. **5**, 381 (1965).
23. A. M. Unrau. Can. J. Chem. **42**, 916 (1964).
24. H. G. Walker and R. M. McCready. Can. J. Chem. **41**, 3133 (1963).
25. A. B. Foster. Advan. Carbohydrate Chem. **12**, 81 (1957).
26. D. H. Northcote. Biochem. J. **58**, 353 (1954).
27. C. T. Bishop, M. B. Perry, F. Blank, and F. P. Cooper. Can. J. Chem. **43**, 30 (1965).
28. L. Hough, J. K. N. Jones, and W. H. Wadman. J. Chem. Soc. 1702 (1950).
29. W. E. Trevelyan, D. P. Procter, and J. S. Harrison. Nature, **166**, 444 (1950).
30. B. Vollmert. Chemiker Ztg. **74**, 50 (1950).
31. G. Neumuller and E. Vasseur. Arkiv Kemi, **5**, 235 (1953).
32. G. W. Hay, B. A. Lewis, and F. Smith. Methods Carbohydrate Chem. **5**, 357 (1965).
33. I. Croon, G. Herrström, G. Kull, and B. Lindberg. Acta Chem. Scand. **14**, 1338 (1960).
34. J. C. Irvine and D. McNicoll. J. Chem. Soc. **97**, 1449 (1910).
35. W. N. Haworth, E. L. Hirst, and M. Stacey. J. Chem. Soc. 2481 (1932).
36. S. A. Barker, E. J. Bourne, R. M. Pinhard, and D. H. Whiffen. Chem. Ind. London, 658 (1958).
37. P. Andrews, L. Hough, and J. K. N. Jones. J. Chem. Soc. 806 (1954).

Can. J. Chem. Downloaded from www.nrcresearchpress.com by 210.87.254.6 on 09/05/12
For personal use only.

Can. J. Chem. Downloaded from www.nrcresearchpress.com by 210.87.254.40 on 09/05/12
For personal use only.

STEROIDS AND RELATED NATURAL PRODUCTS

XXX. SELECTIVE REDUCTION OF ESTERS. PART A. BENZOATES[1]

GEORGE R. PETTIT,[2] BRIAN GREEN, GEORGE L. DUNN,[3] PETER HOFER, AND WILLIAM J. EVERS

Department of Chemistry, University of Maine, Orono, Maine, and Department of Chemistry, Arizona State University, Tempe, Arizona

Received January 5, 1966

ABSTRACT

Previously, reagents such as sodium borohydride – boron trifluoride were shown to be capable of reducing typical aliphatic esters and lactones to the corresponding ether derivatives. Under the same reaction conditions, a variety of benzoate esters (*Ib*, *IIb*, III, and V) were essentially unaffected. Resistance to attack was illustrated by conversion, with sodium borohydride – boron trifluoride, of 3-oxo-17β-benzoyloxy-5α-androstane (III) into 3β-hydroxy-17β-benzoyloxy-5α-androstane (IV) and of reserpine (V) into alcohol VI. With aryl–carbon–oxygen bonds of the ketone VII or alcohol IX*a* type, reaction with sodium borohydride – boron trifluoride was shown, in general, to cause reductive fission of the benzyl–oxygen linkage (e.g. X → XI). An exception was noted in the case of tertiary benzyl alcohols containing an available β-hydrogen (e.g. IX*c*). Here, dehydration to yield, for example, olefin XII*b* appears to be the more favorable reaction course. The marked difference in the reactivity of sodium borohydride – boron trifluoride toward benzoyl–oxygen vs. benzyl–oxygen bonds has been demonstrated.

Previous applications of diborane – boron halide[1] reagents for direct conversion of esters into ethers have involved a variety of aliphatic-type esters and lactones. In general, conversion into the ether derivative increased substantially as the alcohol segment of the ester varied from primary to tertiary.[4] Two phenyl esters, however, were found (1) to undergo only hydrogenolysis to the corresponding alcohol derivatives. More recently, Eliel and Daignault (2) have extended the reduction reaction to thiol esters and have obtained good yields of the corresponding thioethers. The present investigation was undertaken to determine whether the mesomeric effect of the aromatic ring in a benzoate-type ester would decrease the basicity[5] of the carbonyl group enough to substantially reduce the rate of reduction, or whether attack would proceed by one or more of the

[1] *For part XXIX in this series, see G. R. Pettit and W. J. Evers, Can. J. Chem., 44, 1097 (1966). The present study is based on part of the Ph.D. dissertation submitted by G. L. Dunn to the Graduate School, University of Maine, Orono, Maine, July 1962.*

[2] *Present address: Department of Chemistry, Arizona State University, Tempe, Arizona.*

[3] *NDEA Predoctorate Fellow, 1960–1962.*

[4] *Dr. J. S. E. Holker and his colleagues have extended the reduction reaction to several steroid ring-D lactones derived from primary alcohols, and have obtained good yields of the corresponding tetrahydropyrans. We are grateful to Dr. Holker for providing us with this information before publication. One unsuccessful attempt to reduce a γ-lactone derived from a tertiary alcohol has also been noted (3a). Interestingly, extended platinum – perchloric acid catalyzed hydrogenation of 3β-acetoxy-5α-lanost-8-ene has been found to yield 3β-ethoxy-5α-lanostane (3b). We thank Professor J. T. Edward for bringing a similar, but unpublished, example to our attention. Both observations seem to be related to the recently reported (3c) preparation of ethers by reductive (platinum-catalyzed) condensation of alcohol–ketone mixtures.*

[5] *The increased π-bond overlap resulting from phenyl–carbonyl conjugation would be expected to inhibit association with boron trifluoride (compare with eq. [i]).*

[i] $$\mathrm{Ar{-}\overset{\displaystyle O}{\overset{\|}{C}}{-}OR \xrightarrow{BF_3} Ar{-}\overset{\displaystyle \ominus OBF_3}{\overset{|}{\underset{\displaystyle \oplus}{C}}}{-}OR \leftrightarrow Ar{-}\overset{\displaystyle \ominus OBF_3}{\overset{|}{\underset{\displaystyle \oplus}{C}}}{=}OR}$$

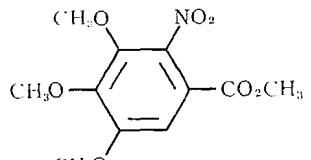
The reaction sequence illustrated in part by eq. [i] is assumed (4) to represent an important step in the reduction of esters to ethers by diborane – boron trihalide reagents.

following pathways: (*a*) reduction to the corresponding benzyl ether, or (*b*) hydrogenolysis to the corresponding alcohol derivatives.[6]

Subjecting 24-benzoyloxy-5β-cholane (I*b*, prepared from alcohol I*a*), in diethylene glycol dimethyl ether (diglyme) containing sodium borohydride, to treatment with boron trifluoride (in tetrahydrofuran) under conditions (1 h at ice-bath temperature and 1 h at room temperature) normally employed[1] in the ester → ether reduction sequence led to unreacted benzoate I*b* (79% recovery) accompanied by alcohol I*a* (20% yield). Extending the same reaction procedure to 3β-benzoyloxy-5α-cholestane (II*b*) gave comparable results: unreacted ester and alcohol II*a*. Under the same conditions 3β-cyclohexylcarbonyloxy-5α-cholestane (II*c*) was easily converted, in reasonable yield (50%), into ether II*d*. Comparing the benzoate and cyclohexanecarboxylate esters of alcohol II*a* provided a vivid illustration of differences in the reaction course.

Reduced reactivity of the benzoate esters toward sodium borohydride – boron trifluoride suggested that other more reactive carbonyl groups might be reduced selectively in their presence. Accordingly, two examples were studied. First, 3-oxo-17β-benzoyloxy-5α-androstane (III) was reduced (68% yield) with sodium borohydride – boron trifluoride to 3β-hydroxy-17β-benzoyloxy-5α-androstane (IV*a*). The remaining reaction product consisted primarily of diol IV*b* (20% yield). Sodium borohydride reduction of ketone III to alcohol IV*a* confirmed the structural and stereochemical assignments. The predominant formation of the C-3 equatorial alcohol when sodium borohydride – boron trifluoride is used is consistent with an earlier observation by Jones (9) involving diborane – boron trifluoride reduction of 4-*t*-butylcyclohexanone.[7] A second example of selective reduction, namely, conversion of reserpine (V) into alcohol VI, was of more practical importance.

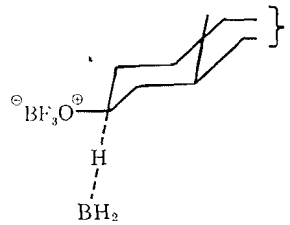
[6]*Brown and Subba Rao reported (5) that reaction between sodium borohydride – boron trifluoride etherate (in diglyme) and ethyl benzoate, as well as two derivatives, proceeded slowly, but the products were not ascertained. During the same period, a similar study with diborane was summarized (6), and a potentially important observation concerning the unreactivity of diborane toward acid halides (5, attributable to the electron-withdrawing effect of the halogen, thereby reducing attack by the Lewis acid diborane) was noted. The amine borane derived from pyridine and diborane, however, appears to resemble a borohydride, and has been shown (7) to reduce benzoyl chloride easily to benzoyl alcohol.*



ii

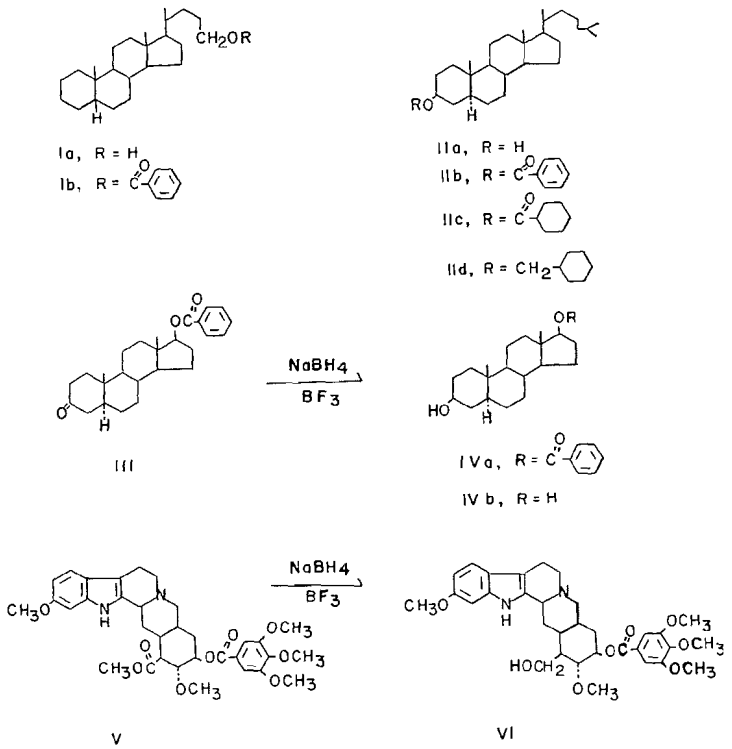
Again, in 1960, Tarbell and his colleagues reduced methyl benzoate (ii) to the corresponding benzyl alcohol (68% yield) with sodium borohydride – aluminium chloride (known to generate diborane), and the same alcohol was obtained in excellent conversion (93%) from the corresponding carboxylic acid by employing sodium borohydride – boron trifluoride (8).

[7]*Diborane or diborane – boron trifluoride reduction of 4-t-butylcyclohexanone yielded, in each case, approximately 15–16% of the thermodynamically less stable (cis) axial alcohol. Interestingly, trimethylamine borane – boron trifluoride gave 46–52% yields of the axial alcohol. The stereochemical course of ketone reduction by diborane (10) appears, in general, to favor equatorial alcohol formation, and in the case of ketone III may proceed via an intermediate such as iii.*



iii

Can. J. Chem. Downloaded from www.nrcresearchpress.com by 210.87.254.40 on 09/05/12
For personal use only.



When reduction was attempted, in normal fashion, by adding a mixture of boron trifluoride and the alkaloid to sodium borohydride, a solid boron trifluoride – reserpine adduct separated from solution. Subsequently, a procedure based on adding boron trifluoride etherate to a mixture of reserpine and sodium borohydride provided alcohol VI. The results of infrared spectral and elemental analytical determinations supported structural assignment VI. Preferential reduction at the carbomethoxy group provides, in effect, a new means of further modifying the hypotensive and central nervous system activity of reserpine.[8]

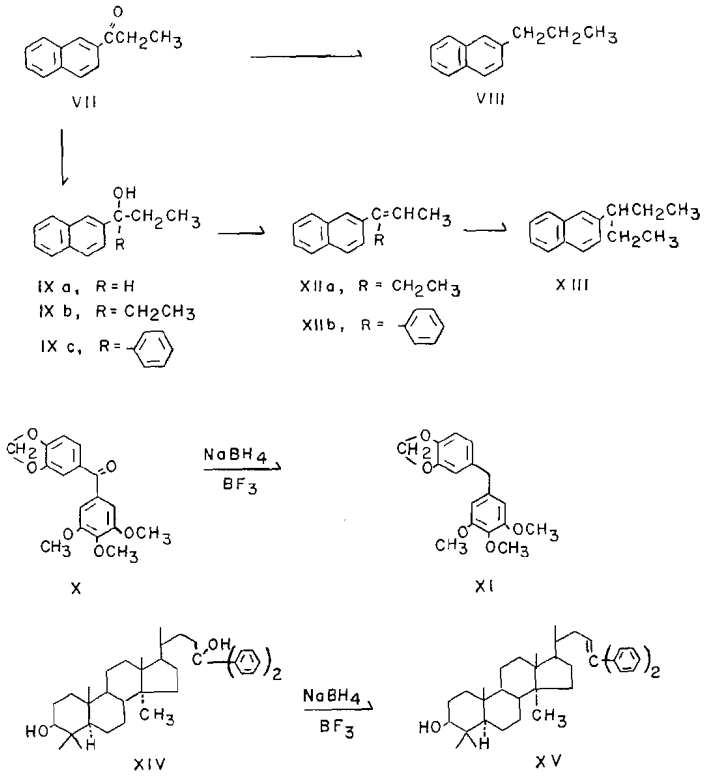
At this point, the investigation was expanded to encompass effects of boron trifluoride – sodium borohydride on other types of benzyl–oxygen linkages.[9] Allowing both 2-naphthylethyl ketone (VII) and the corresponding alcohol (IX*a*) to react with boron trifluoride – sodium borohydride as in the case of, for example, benzoate I*b* yielded (good overall conversion) in both cases the product of complete hydrogenolysis: 2-(*n*-propyl)naphthalene (VIII). Benzyl alcohol IX*a* was obtained by lithium aluminium hydride reduction of ketone VII, and an authentic specimen of hydrocarbon VIII was prepared by catalytic hydrogenation (VII → VIII). Under similar conditions, diaryl ketone X was easily reduced to 3,4-methylenedioxyphenyl-3,4,5-trimethoxyphenylmethane (XI).[10]

[8]*Consult ref. 11 for leading literature citations pertinent to this point.*

[9]*A preliminary account of this study has been summarized in ref. 12. During the same period Venkataraman and his colleagues (13) reported boron trifluoride – sodium borohydride to be useful for the reduction of anthraquinones to anthracenes, and indicated that the reagent was also convenient for the analogous reduction of chromones and chromanones. Longer treatment with diborane was observed to give comparable results. Later, two additional examples (14) of the reaction with respect to chromanones were reported. Proposed mechanisms for this type of reduction reaction have been summarized (13b, 14b).*

[10]*It should be noted that other metal hydride techniques, particularly with aluminium chloride – lithium aluminium hydride, have been employed successfully for reductive cleavage of benzyl–oxygen bonds in various aryl ketones and in benzylic and allylic alcohols (see ref. 15 and footnotes 2 and 3 in ref. 12).*

Can. J. Chem. Downloaded from www.nrcresearchpress.com by 210.87.254.40 on 09/05/12
For personal use only.



One limit to the utility of the hydrogenolysis reaction was found during routine extension to several tertiary-type benzylic alcohols. Treating ketone VII with ethylmagnesium bromide provided tertiary alcohol IX*b*. From the reaction between alcohol IX*b* and boron trifluoride – sodium borohydride, only a mixture of *cis* and *trans* olefins corresponding to structure XII*a* was isolated. The olefin mixture was not further characterized, but was instead hydrogenated in the presence of palladium on charcoal to hydrocarbon XIII. The latter compound (XIII) was identical with a specimen prepared in an unequivocal manner (acid-catalyzed dehydration followed by hydrogenation) from alcohol IX*b*. The analogous preparation (VII and phenylmagnesium bromide) of diaryl tertiary alcohol IX*c* and subsequent reaction with the hydride reagent yielded olefin XII*b*. The crystalline hydrocarbon was readily characterized and shown to be identical with a sample prepared by hydrochloric acid catalyzed dehydration of alcohol IX*c*. A reaction course terminating in dehydration was again encountered with tertiary alcohol XIV. Reaction with boron trifluoride – sodium borohydride gave only olefin XV, a substance previously characterized in our laboratory. The possibility of dehydration catalyzed by boron trifluoride taking precedence came into question when a solution of alcohol IX*b* in diglyme (containing sodium borohydride) was slowly treated with boron trifluoride etherate; the same result ensued (production of olefin XII*a*). These experiments also suggest that hydroboration of olefins such as XII and XV is a relatively slow process, or that they (the olefins) arise at a terminal stage.[11] In this regard, boron trifluoride – sodium borohydride reduction

[11]*Olefins are known to arise during lithium aluminium hydride reduction of certain aryl ketones; for example, see ref. 15a.*

Can. J. Chem. Downloaded from www.nrcresearchpress.com by 210.87.254.40 on 09/05/12
For personal use only.

of triphenylcarbinol gave, as expected, triphenylmethane; however, no further effort was made to delineate the mechanism (13*b*, 14*b*) of olefin formation.

The preceding experiments served to extend the scope of reduction reactions with boron trifluoride – sodium borohydride to selective reduction in the presence of a benzoate ester, and with certain limitations (tertiary benzyl alcohols bearing an available β-hydrogen substituent) to reductive fission of benzyl–oxygen bonds. Later, carbonate-type esters were found to be similar to benzoates in their resistance to attack by boron trifluoride – sodium borohydride; a summary of these observations will appear in a later paper.

EXPERIMENTAL[12]

24-Benzoyloxy-5β-cholane (Ib)

To a cool (ice bath) solution of 24-hydroxy-5β-cholane (I*a*, 1.2 g) in pyridine (7 ml, distilled from potassium hydroxide) was added benzoyl chloride (1 ml). After 8 h at room temperature, the mixture was poured into water (50 ml) and extracted with diethyl ether. The combined ethereal extracts were washed successively with saturated sodium bicarbonate solution, water, 5% hydrochloric acid, and water. Removal of solvent *in vacuo* yielded a pale-yellow oil (1.7 g), which was dissolved in petroleum ether and chromatographed on a column of acid-washed alumina (30 g). Elution with petroleum ether and 3:1 petroleum ether – benzene gave a colorless oil, 1.4 g, 90%; ν_{max}^{neat} 1 720, 1 600, 1 580, 1 260, and 706 cm^{-1}. Crystallization from methanol – diethyl ether gave 1.35 g of crystals melting at 44–45°. After three recrystallizations from the same solvent mixture, an analytical specimen displayed the same melting point and had $[\alpha]_D^{20}$ +18.5° (*c*, 1.27). A thin-layer chromatogram (10:1 petroleum ether – ethyl acetate as the mobile phase) showed one spot.

Anal. Calcd. for $C_{31}H_{46}O_2$: C, 82.61; H, 10.29. Found: C, 82.25; H, 10.67.

Attempted Sodium Borohydride – Boron Trifluoride Reduction of 24-Benzoyloxy-5β-cholane (Ib)

A solution of ester I*a* (1.0 g) in tetrahydrofuran (20 ml) containing boron trifluoride etherate (7.5 ml) was added to a cool (ice bath) solution of sodium borohydride (0.17 g) in 20 ml of dry diglyme. Stirring was continued for 1 h at ice-bath temperature, and during a second hour while the solution was being heated at reflux. The solution was cooled (ice bath) and cautiously treated with 2 *N* hydrochloric acid, followed by dilution with water and extraction with diethyl ether. The combined ethereal extracts were washed with saturated sodium bicarbonate solution and water, and concentrated *in vacuo* to a colorless oil (1.2 g). A solution of the oily product in petroleum ether was chromatographed on acid-washed alumina (30 g). The petroleum ether and 1:1 petroleum ether – benzene fractions provided 0.79 g, m.p. 44–45°, of ester I*a*.[13] A fraction eluted with chloroform crystallized from methanol as needles (0.15 g, 20%) melting at 127–129°. The latter product proved[13] to be 24-hydroxy-5β-cholane (I*a*).

3β-Benzoyloxy-5β-cholestane (IIb)

Conversion of 3β-hydroxy-5α-cholestane (5.0 g) into benzoate ester II*b* by employing benzoyl chloride (8 ml) in dry pyridine (40 ml) was accomplished essentially as noted with ester I*b*. The crude product recrystallized from diethyl ether – methanol as colorless needles weighing 5.2 g and melting at 137–138° to an opaque liquid which cleared at 158–159° (ref. 17 reports m.p. 133–135° to 152–156°).

Attempted Reduction of 3β-Benzoyloxy-5α-cholestane (IIb)

Method A: Sodium Borohydride – Boron Trifluoride

A 1.0 g sample of ester II*b* was subjected to treatment with sodium borohydride (0.16 g) in the presence of boron trifluoride etherate (7.5 g) as described above for benzoate ester I*b*. A thin-layer chromatogram of the product indicated a two-component mixture. The first substance isolated weighed 0.92 g and proved[13] to be starting material (II*b*). The remaining product was found to contain, on the basis of comparative thin-layer chromatograms, 3β-hydroxy-5α-cholestane. No substance corresponding to ether II*d* was detected.

[12]*Acid-washed alumina refers to a Merck (Rahway) product. The petroleum ether employed was a fraction boiling at 65–70°. A summarized description of other general methods, solvents, reagents, and chromatographic procedures used in the present study appears in an introduction to the Experimental section of part XXVIII in this series (see G. R. Pettit, J. C. Knight, and W. J. Evers, Can. J. Chem., 44, 807 (1966)).*

Melting points reported for analytical specimens were recorded on a Kofler melting point apparatus. All other melting point determinations were performed with open Kimble glass capillaries in a silicone oil bath and are uncorrected. The purity of all analytical samples (colorless in each case) was confirmed by thin-layer chromatography on silica gel G, and the plates were developed with concentrated sulfuric acid.

Proton magnetic resonance (see ref. 16), ultraviolet (ethanol solution, Perkin–Elmer model 400 spectrometer), infrared spectra (potassium bromide, unless otherwise noted) and gas chromatographic data were provided by Dr. R. A. Hill (University of Maine). Specific rotation values (chloroform solution) were determined in the laboratories of Drs. Weiler and Strauss, Oxford, England, and P. Demoen, Janssen Pharmaceutica, Beerse, Belgium. Elemental analytical data was provided by Dr. A. Bernhardt, Max-Planck Institut, Mülheim, Germany.

[13]*The identity of this substance was established by mixture melting point determination and infrared spectral comparison with an authentic sample.*

Can. J. Chem. Downloaded from www.nrcresearchpress.com by 210.87.254.40 on 09/05/12
For personal use only.

Method B: Lithium Aluminium Hydride – Boron Trifluoride

The preceding experiment (A) was repeated with lithium aluminium hydride (0.16 g) in place of sodium borohydride and with tetrahydrofuran (40 ml total) as solvent (1). The principal product, 0.80 g, was starting material,[13] and the residual mixture consisted largely of ester II*b* accompanied by a small amount of alcohol II*a*. A thin-layer chromatographic study of the mixture failed to reveal ether II*d*.

3β-Cyclohexylcarbonyloxy-5α-cholestane (IIc)

Method A

Platinum oxide (0.2 g) was added to a solution of commercial cholesteryl benzoate (8.7 g) and 70% perchloric acid (3 drops) in tetrahydrofuran (200 ml), and the mixture was shaken under a slight positive pressure of hydrogen for 2 h. At this time, an aliquot sample displayed a strong tetranitromethane test; thus, another 0.5 g quantity of platinum oxide was added and hydrogenation continued. Five hours later, hydrogen absorption appeared to be complete, and catalyst was removed by filtration. Dilution with water led to a solid which crystallized from chloroform–methanol as colorless needles, 4.2 g, m.p. 161–162°. An additional 0.62 g, m.p. 159–161°, of cyclohexylcarbonyloxy ester II*c* was obtained by recrystallization of the second and third crystal crops.

Method B

The cyclohexylcarbonyloxy ester II*c* of alcohol II*a* (0.5 g) was prepared from the acid chloride (by employing 10 ml of thionyl chloride, reflux for 1.5 h) derivative of cyclohexanecarboxylic acid (1.0 g) in pyridine (5 ml) as summarized with ester I*b*. The pale-yellow solid crystallized from chloroform–methanol as colorless needles, 0.5 g, m.p. 160–161° (ref. 18 reports m.p. 158.5–159°). The identical composition of both esters (obtained by methods A and B) was confirmed.[13]

3β-Cyclohexylmethyleneoxy-5α-cholestane (IId)

Reduction of cyclohexylcarbonyloxy ester II*c* (1.0 g in 50 ml of tetrahydrofuran) with sodium borohydride (0.19 g in 20 ml of diglyme) and boron trifluoride (12 ml) was accomplished by the procedure illustrated with ester I*a*. A petroleum ether solution of crude product was chromatographed on activated alumina (30 g). Elution with the same solvent (400 ml) gave a fraction (0.43 g) which crystallized from chloroform–methanol as colorless blades, 0.40 g, m.p. 157.5–158.5°. Further recrystallization from the same solvent mixture gave an analytical specimen with an unchanged melting point and with $[\alpha]_D^{20}$ +15.2° (*c*, 1.212); ν_{max} 2 900, 1 470, 1 450, 1 380, and 1 120 (broad) cm^{-1}.

Anal. Calcd. for $C_{34}H_{60}O$: C, 84.23; H, 12.47; O, 3.30. Found: C, 84.14; H, 12.39; O, 3.65.

Continued elution with chloroform gave 0.57 g of alcohol II*a*.

3-Oxo-17β-benzoyloxy-5α-androstane (III)

After one recrystallization from methanol, the pale-yellow solid (7.5 g, m.p. 150–160°) obtained from 3-oxo-17β-hydroxy-5α-androstane (7.0 g) and benzoyl chloride (6 ml) in pyridine (40 ml) was dissolved in 1:1 petroleum ether – benzene and chromatographed on acid-washed alumina. An initial fraction (0.45 g, m.p. 150–160°) eluted with the same solvent mixture was discarded, and subsequent fractions through 5:1 benzene–chloroform were collected. The colorless solid weighed 6.3 g (66%) and melted at 196–199°. Four recrystallizations from acetone gave an analytical sample in the form of rods, m.p. 201–202° (ref. 19 reports m.p. 201–202°), $[\alpha]_D^{20}$ +73.1° (*c*, 1.30); ν_{max} 1 710, 1 280, and 720 cm^{-1}.

Anal. Calcd. for $C_{26}H_{34}O_3$: C, 79.14; H, 8.68. Found: C, 79.11; H, 8.33.

3β-Hydroxy-17β-benzoyloxy-5α-androstane (IVa)

Method A

Reduction of ketone III (1.0 g) in diglyme (25 ml) – tetrahydrofuran (25 ml) with sodium borohydride (0.19 g) – boron trifluoride etherate (7.7 ml) was conducted as described for benzoate ester I*b*. The crude viscous oil was chromatographed on acid-washed alumina, and fractions eluted by benzene yielded a solid (0.73 g) melting at 170–180°. One recrystallization from acetone – petroleum ether gave colorless plates weighing 0.68 g (68%, m.p. 201–202°). Further recrystallization from the same solvent mixture gave a pure specimen melting at 202–203°, $[\alpha]_D^{20}$ +53.4° (*c*, 1.25).

Anal. Calcd. for $C_{26}H_{36}O_3$: C, 78.74; H, 9.15. Found: C, 78.99; H, 8.87.

The column was next eluted with chloroform and the resulting fraction allowed to crystallize from benzene – petroleum ether. The specimen of 3β,17β-dihydroxy-5α-androstane (IV*b*) that was obtained weighed 0.15 g (20%) and melted at 164–165° (ref. 20 reports m.p. 164°).

Method B

The preceding experiment (see method A) was repeated, omitting boron trifluoride etherate and tetrahydrofuran. The crude viscous oil (0.95 g) crystallized upon trituration with methanol to yield 0.90 g of crude alcohol IV*a* melting at 175–185°. A 0.10 g sample was purified as described above by column chromatography on acid-washed alumina (3 g). The fraction eluted by 5:1 benzene–chloroform yielded 0.08 g of alcohol IV*a* melting at 202–203°; ν_{max} 3 400, 1 710, 1 280, and 715 cm^{-1}. The specimen of alcohol IV*a* prepared by method B was identical[13] with that obtained by method A.

Sodium Borohydride – Boron Trifluoride Reduction of Reserpine (V)

In a typical experiment, reserpine (15.0 g) was dissolved in hot (100–110°) diglyme (750 ml) and, after the solution was cooled (ice bath), sodium borohydride (5.6 g) was added. Next, a solution composed of boron

Can. J. Chem. Downloaded from www.nrcresearchpress.com by 210.87.254.40 on 09/05/12
For personal use only.

Can. J. Chem. Downloaded from www.nrcresearchpress.com by 210.87.254.40 on 09/05/12
For personal use only.

trifluoride etherate (190 ml) and tetrahydrofuran (190 ml) was added dropwise over a 30 min period. Before the cool (20°) solution was cautiously treated with 2 *N* hydrochloric acid (250 ml), stirring was continued for 3 h at ice-bath temperature and for 1 h at reflux. The pH of the mixture was adjusted to 8–9 with ammonium hydroxide, and the solution was diluted with water and extracted with chloroform. After removal of solvent the red viscous oil was triturated with diethyl ether, and the yellow solid (10.5 g, giving a green Beilstein test) was collected, dissolved in methanol (475 ml) – concentrated hydrochloric acid (25 ml), and heated at reflux for 30 min. Concentration to a volume of ca. 200 ml and cooling (ice bath) provided 5.0 g of a straw-colored solid, decomposition point 265°, which recrystallized from 95% ethanol as cream-colored plates decomposing at 265°. Two additional recrystallizations from the same solvent did not change the appearance or decomposition point of *alcohol VI hydrochloride*, $[\alpha]_D^{22}$ −76.5° (*c*, 1.2); ν_{max} 3 400, 3 150, 2 600, and 1 708 cm^{-1} (in reserpine, the bands at 1 709 and 1 720 cm^{-1} correspond, respectively, to benzoate and methoxycarbonyl absorption).

Anal. Calcd. for $C_{32}H_{41}O_8N_2Cl$: C, 62.27; H, 7.00; Cl, 5.75; N, 4.54; O, 20.74. Found: C, 61.87; H, 6.58; Cl, 6.01; N, 4.76; O, 21.16.

A suspension of the hydrochloride in water – diethyl ether was shaken with 1 *N* sodium hydroxide. The mixture was diluted with benzene, and the upper phase was washed with water and concentrated. When the concentrate was allowed to stand at room temperature, *alcohol VI* separated from solution as rosettes of colorless needles, decomposition point 134–144° (Kofler block m.p. 144–148°). The free base (VI) was pure as evidenced by a thin-layer chromatogram, but quickly became yellow and impure on exposure to air and light. A pure specimen was preserved in the dark and exhibited $[\alpha]_D^{20}$ −55.7° (*c*, 0.88) and ν_{max} 3 400, 1 709, and 1 130 cm^{-1}.

Anal. Calcd. for $C_{32}H_{40}O_8N_2$: C, 66.20; H, 6.94; N, 4.83; O, 22.05. Found: C, 65.99; H, 6.88; N, 4.93; O, 21.95.

2-(n-Propyl)naphthalene (VIII)

Method A

By using the procedure outlined for the attempted reduction of benzoate *Ib*, a sample of 2-naphthylethyl ketone (3.0 g, VII (21)) was reduced with sodium borohydride (1.3 g) – boron trifluoride etherate (80 g). A solution of the crude product in petroleum ether was chromatographed on activated alumina (80 g). Elution with the same solvent yielded 2.2 g of a colorless mobile oil, b.p. 134° at 20 mm; λ_{max} 225, 276, and 319 mμ (log ε 4.23, 3.90, and 2.73). The ultraviolet spectrum of 2-methylnaphthalene has been reported (22) to be λ_{max} 220, 276, and 319 mμ (log ε 4.02, 3.68, and 2.71). Homogeneity of the hydrocarbon was confirmed by vapor phase chromatography. The *picrate* derivative (prepared in 95% ethyl alcohol) crystallized from ethanol as yellow needles, m.p. 89–91°. Boiling points of 273–274° at 760 mm and 135° at 12 mm have been reported (23) for hydrocarbon VIII, and the *picrate* derivative has been found (23*a*) to melt at 90–92°.

Method B

A solution of 2-naphthylethyl ketone (3.0 g) in tetrahydrofuran (20 ml) was reduced with lithium aluminium hydride (6.0 g) in tetrahydrofuran (50 ml) during 3 h at room temperature. The mixture was cautiously treated with 2 *N* sulfuric acid and extracted with chloroform. Removal of solvent from the combined chloroform extracts gave a nearly quantitative yield of 1-(2-naphthyl)propanol (IX*a*), b.p. 162° at 20 mm, ν_{max}^{neat} 3 480 cm^{-1}. A 0.92 g specimen of alcohol IX*a* was reduced by the sodium borohydride (0.38 g) – boron trifluoride etherate (22 g) technique as noted above in method A. After chromatographic purification, a 0.57 g quantity of 2-(*n*-propyl)naphthalene was isolated. The product (VIII) displayed the same ultraviolet spectrum as material prepared by method A, and both the hydrocarbon (VIII) and alcohol (IX*a*) precursor were pure as evidenced by vapor phase chromatography.

Method C

An authentic specimen of hydrocarbon VIII was prepared by catalytic (0.5 g of 10% palladium on charcoal) hydrogenation (4 h with a slightly positive pressure) of 2-naphthylethyl ketone (3.0 g) in methanol (100 ml). After catalyst and solvent were removed, the pale-yellow oily product was distilled *in vacuo*. The pure sample of hydrocarbon VIII (2.7 g) displayed ultraviolet and infrared (neat) spectra and vapor phase chromatographic behavior identical with those observed for the products from methods A and B. The *picrate* derivative, m.p. 89–91°, was identical[13] with the corresponding derivative described as part of method A.

3,4-Methylenedioxyphenyl-3,4,5-trimethoxyphenylmethane (XI)

Sodium borohydride (0.24 g) – boron trifluoride etherate (16 g) reduction of 3,4-methylenedioxy-3′,4′,5′-trimethoxybenzophenone (X, 1.0 g (12)) was performed as noted above (see VIII, method A). The product (XI, 0.58 g, m.p. 56–58°) crystallized from petroleum ether as colorless plates. Two recrystallizations from the same solvent provided an analytical sample melting at 55.5–56°.

Anal. Calcd. for $C_{17}H_{18}O_5$: C, 67.54; H, 6.00; O, 26.46. Found: C, 67.89; H, 5.94; O, 26.18.

3-Hydroxy-3-(2-naphthyl)pentane (IXb)

A solution of 2-naphthylethyl ketone (16.3 g) in diethyl ether (125 ml) was added during 30 min to a solution prepared from diethyl ether (35 ml), ethyl bromide (16 g), and magnesium (3.6 g). Twenty minutes later, reaction was complete and the mixture was treated with water (20 ml) followed by 10% aqueous sulfuric acid (100 ml). The ethereal layer was separated and successively washed with water, aqueous

potassium carbonate, and water. After removal of solvent, the residue was distilled through a 6 inch Vigreux column to yield 7.7 g of tertiary alcohol IX*b* boiling at 105–106° (0.08–0.09 mm); ν_{max}^{neat} 3 400, 3 010, 2 950, 2 900, 2 840, 1 598, 1 505, 1 460, 1 375, 1 270, 1 155, 1 132, 965, 915, 900, 860, 820, and 750 cm^{-1}.

Anal. Calcd. for $C_{15}H_{18}O$: C, 84.07; H, 8.46; O, 7.14. Found: C, 83.99; H, 8.22; O, 7.63.

3-(2-Naphthyl)pentane (XIII)

Method A

Reaction between 3-hydroxy-3-(2-naphthyl)pentane (2.0 g) and sodium borohydride (0.70 g) – boron trifluoride etherate (30 g) was attempted and the product isolated as was, for example, ketone VII. Again, when the reaction was repeated with a total reaction time of only 20 min, the following results were observed. A thin-layer chromatogram (hexane as the mobile phase) of the crude oily product indicated a major component (assumed to be olefin XII*a*) as a mixture of the two geometrical isomers, accompanied by a number of more polar materials. The presence of starting material was not detected. A solution of the product in hexane was chromatographed on activated alumina. Elution with the same solvent gave 1.14 g of an oily fraction displaying two spots (believed to be the geometrical isomers of olefin IX*a*) on a thin-layer chromatogram (hexane as the mobile phase). The olefin mixture was dissolved in hexane (20 ml) and hydrogenated (under a slightly positive pressure) in the presence of 10% palladium on charcoal (0.05 g). Next, the solution was filtered and chromatographed on activated alumina (35 g). Elution with hexane gave 1.1 g of 3-(2-naphthyl)pentane (XIII); ν_{max}^{neat} 3 010, 2 950, 2 900, 2 840, 1 600, 1 509, 1 460, 1 375, 890, 858, 820, and 750 cm^{-1}; proton magnetic resonance response ($CDCl_3$ solution): triplet (J = 7 c.p.s.) at 0.76 and complex signals at 1.40–1.87, 2.14–2.52, and 6.85–7.53 δ.

Anal. Calcd. for $C_{15}H_{18}$: C, 90.85; H, 9.15. Found: C, 90.81; H, 9.13.

Method B

A solution of alcohol IX*b* (1.6 g) in methanol (15 ml) containing 1 drop of concentrated hydrochloric acid was heated at reflux for 30 min. After dilution with water, the mixture was extracted with diethyl ether. The ethereal extract was washed with water and concentrated to an oily residue. A thin-layer chromatogram (hexane as the mobile phase) of the olefin mixture (XII*a*) displayed two principal spots with R_f values identical with those observed for the olefin described in method A (see above), and a number of lesser and more polar components. The crude olefin was partially purified by column chromatography and the mixture of geometrical isomers subjected to catalytic hydrogenation as described in the preceding experiment (see method A). Final purification was again achieved by column chromatography with hexane as solvent and eluent to yield 0.68 g hydrocarbon XIII as a colorless oil.

Anal. Found: C, 90.88; H, 9.13.

The infrared (neat) and proton magnetic resonance spectra of hydrocarbon VIII prepared by methods A and B were identical.

1-(2-Naphthyl)-1-phenylpropanol (IXc)

Conversion of 2-naphthylethyl ketone (5.0 g) into tertiary alcohol IX*c* was accomplished with the Grignard reagent prepared from magnesium (3.8 g) and bromobenzene (23 g) in tetrahydrofuran solution (80 ml). Except for a 2 h period at reflux and final dilution of the reaction mixture with saturated ammonium chloride solution, the reaction and isolation of crude alcohol were carried out as illustrated in the case of tertiary alcohol IX*a*. A pure specimen of alcohol IX*c* (4.9 g) crystallized from diethyl ether – petroleum ether as prismatic needles melting at 91–92°.

Anal. Calcd. for $C_{19}H_{18}O$: C, 86.98; H, 6.92. Found: C, 87.07; H, 7.04.

1-(2-Naphthyl)-1-phenyl-prop-1-ene (XIIb)

Method A

A sample of 1-(2-naphthyl)-1-phenylpropanol (IX*c*, 1.5 g) was treated with sodium borohydride (0.43 g) – boron trifluoride etherate (24 g) and the product isolated as summarized in the case of alcohol IX*b*. A solution of the crude olefin in hexane was chromatographed on activated alumina (40 g). The fraction eluted with hexane weighed 0.95 g (XII*b*) and crystallized from diethyl ether – petroleum ether as colorless prisms (0.35 g) melting at 104–106°; λ_{max} 239, 248, 276, 286, and 297 mμ (log ϵ 4.67, 4.64, 4.06, and 3.94); ν_{max} 3 000, 2 850, 1 500, 1 490, 1 440, 1 360, 900, 850, 825, 818, 770, 755, and 700 cm^{-1}; proton magnetic resonance response ($CDCl_3$ solution): doublet (J = 7 c.p.s. (CH_3)) at 1.78, quartet (J = 7 c.p.s. (=CH—)) at 6.33, and complex signals from 7.25 to 7.85 (12 aromatic H) δ.

Anal. Calcd. for $C_{19}H_{16}$: C, 93.40; H, 6.60. Found: C, 93.59; H, 6.73.

Method B

The acid-catalyzed dehydration of alcohol IX*c* (1.5 g) in methanol (30 ml) containing concentrated hydrochloric acid (2 ml) and isolation of olefin were executed as described for alcohol IX*b*. Recrystallizing the crude product (1.4 g) from diethyl ether – petroleum ether led to 0.40 g of hydrocarbon XII*b* melting at 104–106°. The ultraviolet spectra of olefin XII*b* prepared by methods A and B were identical, and both specimens were shown[13] to represent the same substance.

3β-Hydroxy-24,24-diphenyl-4,4,14α-trimethyl-5α-23-cholane (XV)

The sodium borohydride (0.008 g) – boron trifluoride etherate (0.46 g) reagent was allowed to react with 3β,24-dihydroxy-24,24-diphenyl-4,4,14α-trimethyl-5α-cholane (0.06 g, XIV) and the product isolated as

Can. J. Chem. Downloaded from www.nrcresearchpress.com by 210.87.254.40 on 09/05/12
For personal use only.

summarized for alcohol IXc. Crystallizing the crude material from chloroform–acetone gave 0.045 g of colorless crystals melting at 237–239°. Recrystallization from the same solvent led to a pure sample of olefin XV melting at 244–246° (ref. 24 reports m.p. 244–247°). Olefin XV was identical[13] with an authentic sample.

Triphenylmethane

Triphenylcarbinol (1.0 g) was easily reduced by sodium borohydride (0.29 g) – boron trifluoride etherate (16 g) as noted above for ketone VII. A solution of the crude hydrocarbon in hexane was chromatographed on activated alumina. Elution with the same solvent gave 0.66 g of triphenylmethane, which crystallized from diethyl ether – methanol as colorless needles (0.36 g) melting at 93–94°. The hydrocarbon was identical[13] with an authentic sample.

ACKNOWLEDGMENTS

The investigation was supported in part by Public Health Service research grants Nos. CA-04074-04 to CA-08705-01 from the National Cancer Institute, and by Smith, Kline, and French Laboratories. We are also indebted to Professor C. Djerassi and the Department of Chemistry, Stanford University, for providing one of us (G. R. P.) with facilities during the initial preparation of this manuscript. Technical assistance provided by P. A. Whitehouse with several related experiments is also gratefully acknowledged.

REFERENCES

1. G. R. PETTIT and D. M. PIATAK. J. Org. Chem. **27**, 2127 (1962).
2. E. L. ELIEL and R. A. DAIGNAULT. J. Org. Chem. **29**, 1630 (1964).
3. (*a*) S. RAKHIT and M. GUT. J. Org. Chem. **29**, 229 (1964).
   (*b*) J. D. CHANLEY and T. MEZZETTI. J. Org. Chem. **29**, 228 (1964).
   (*c*) M. VERZELE, M. ACKE, and M. ANTEUNIS. J. Chem. Soc. 5598 (1963).
4. G. R. PETTIT and T. R. KASTURI. J. Org. Chem. **26**, 4557 (1961).
5. H. C. BROWN and B. C. SUBBA RAO. J. Am. Chem. Soc. **82**, 681 (1960).
6. H. C. BROWN and W. KORYTNYK. J. Am. Chem. Soc. **82**, 3866 (1960).
7. E. M. FEDNEVA. Zh. Obshch. Khim. **30**, 2818 (1960).
8. K. I. H. WILLIAMS, S. E. CREMER, F. W. KENT, E. J. SEHM, and D. S. TARBELL. J. Am. Chem. Soc. **82**, 3982 (1960).
9. W. M. JONES. J. Am. Chem. Soc. **82**, 2528 (1960).
10. H. C. BROWN and D. B. BIGLEY. J. Am. Chem. Soc. **83**, 3166 (1961). W. M. JONES and H. E. WISE, JR. J. Am. Chem. Soc. **84**, 997 (1962).
11. G. R. PETTIT and A. B. NEILL. Can. J. Chem. **42**, 1764 (1964).
12. G. R. PETTIT, B. GREEN, P. HOFER, D. C. AYRES, and P. J. S. PAUWELS. Proc. Chem. Soc. 357 (1962).
13. (*a*) D. S. BAPAT, B. C. SUBBA RAO, M. K. UNNI, and K. VENKATARAMAN. Tetrahedron Letters, 15 (1960).
   (*b*) C. J. SANCHORAWALA, B. C. SUBBA RAO, M. K. UNNI, and K. VENKATARAMAN. Indian J. Chem. **1** 19 (1963).
14. (*a*) H. B. BHAT and K. VENKATARAMAN. Tetrahedron, **19**, 77 (1963).
   (*b*) W. J. WECHTER. J. Org. Chem. **28**, 2935 (1963).
15. (*a*) K. T. POTTS and D. R. LILJEGREM. J. Org. Chem. **28**, 3202 (1962).
   (*b*) J. H. BREWSTER, H. O. BAYER, and S. F. OSMAN. J. Org. Chem. **29**, 110 (1964).
   (*c*) J. H. BREWSTER and H. O. BAYER. J. Org. Chem. **29**, 116 (1964).
   (*d*) E. L. ELIEL. Record Chem. Progr. Kresge-Hooker Sci. Lib. **22**, 129 (1961).
16. G. R. PETTIT, J. A. SETTEPANI, and R. A. HILL. Can. J. Chem. **43**, 1792 (1965).
17. CH. TAMM and R. ALBRECHT. Helv. Chim. Acta, **42**, 2177 (1959). W. BERGMANN, M. KITA, and D. J. GIANCOLA. J. Am. Chem. Soc. **76**, 4974 (1954).
18. J. W. COOK and M. F. C. PAIGE. J. Chem. Soc. 336 (1944).
19. L. RUZICKA and M. W. GOLDBERG. Helv. Chim. Acta, **19**, 99 (1936).
20. J. FAJKOS. Chem. Listy, **52**, 1780 (1958); Chem. Abstr. **53**, 5344 (1959).
21. C. DJERASSI and G. R. PETTIT. J. Org. Chem. **22**, 393 (1957).
22. R. N. JONES. J. Am. Chem. Soc. **67**, 2127 (1945).
23. (*a*) S. H. MORRELL, G. B. PICKERING, and J. C. SMITH. J. Inst. Petrol. **34**, 677 (1948); Chem. Abstr. **43**, 2608 (1949).
   (*b*) H. KÖLBEL. Brennstoff-Chem. **30**, 73 (1949); Chem. Abstr. **44**, 2217 (1950).
24. G. R. PETTIT, P. HOFER, W. J. BOWYER, T. R. KASTURI, R. C. BANSAL, R. E. KADUNCE, and B. GREEN. Tetrahedron, **19**, 1143 (1963).

Can. J. Chem. Downloaded from www.nrcresearchpress.com by 210.87.254.40 on 09/05/12
For personal use only.

Can. J. Chem. Downloaded from www.nrcresearchpress.com by 210.87.254.42 on 09/05/12
For personal use only.

STEROIDS AND RELATED NATURAL PRODUCTS

XXXI. SELECTIVE REDUCTION OF ESTERS. PART B. CARBONATES[1]

GEORGE R. PETTIT[2] AND WILLIAM J. EVERS[3]

Department of Chemistry, University of Maine, Orono, Maine, and Department of Chemistry, Arizona State University, Tempe, Arizona

Received January 26, 1966

ABSTRACT

Direct reduction of several pivalate esters to neopentyl ethers has been accomplished with boron trifluoride – sodium borohydride. The utility of the reduction reaction was illustrated with esters I*c*, II*b*, and IV*a*. Under the same conditions, a selection (I*d*, II*d*, and IV*a*) of carbonate esters was found to be relatively resistant to reduction. In this respect, the carbonate esters resembled benzoate esters, and selective reduction of a ketone (II*d*) or another ester (IV*a* → IV*b*) in their presence was possible. For comparison, one xanthate ester (I*e*) was allowed to react with boron trifluoride – sodium borohydride, and only the corresponding alcohol (I*a*) was isolated. Raney nickel desulfurization of xanthate I*a* was shown to provide alcohol I*a* and hydrocarbon I*f* as principal products.

Prior studies of ester → ether reduction reactions with diborane – boron trifluoride type reagents indicated that the alcohol segment of the ester influences the yield of ether while the carbonyl portion can influence the ease of reduction. For example, a series of otherwise equivalent *n*-, *s*-, and *t*-butyl esters, when allowed to react with boron trifluoride – sodium borohydride, were transformed to the corresponding ethers with marked increments in yield (7–76%) as alkyl branching adjacent to the ester alcohol group increased (2). Under the same conditions, benzoate esters were found to be essentially unaffected (1). To define further the scope of these observations and to increase biological knowledge of steroidal ethers (e.g. see ref. 3), we have examined the reaction between boron trifluoride – sodium borohydride and several pivalate- and carbonate-type esters.

Appropriate esters derived from primary alcohol I*a* were chosen for initial model experiments. The requirements for 24-hydroxy-5β-cholane (I*a*) were conveniently met by modifying a prior route (see ref. 2 for leading literature citations) to this substance. Cholic acid was oxidized to dehydrocholic acid by a modification of the Jones' chromic acid technique, and after Wolff–Kishner reduction, the 5β-cholanic acid was reduced with commercial diborane in tetrahydrofuran.[4] Treating alcohol I*a* in pyridine solution with pivaloyl chloride gave ester I*b*. Previous experience (2) suggested that reduction of pivalate I*b* would provide neopentyl ether I*c* in approximately 10% yield, and indeed 13% conversion was realized. Although the actual reagent used in this experiment was diborane – boron trifluoride,[5] all subsequent reduction reactions were carried out with a boron trifluoride – sodium borohydride reagent.[6] Next, pivalate ester II*b*, prepared from

[1]*For part XXX in this series, refer to ref. 1. The present contribution is based on part of the Ph.D. dissertation submitted by W. J. Evers to the Graduate School, University of Maine, Orono, Maine, December 1964.*

[2]*Present address: Department of Chemistry, Arizona State University, Tempe, Arizona.*

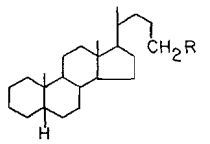
[3]*NDEA Predoctorate Fellow, 1960–1963.*

[4]*Carboxylic acids may even be reduced selectively by diborane in the presence of ketones (4a). For example, by employing a calculated amount of diborane, levulinic acid has been reduced to 4-oxopentanol (4b).*

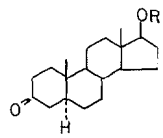
[5]*Reaction between diborane, boron trichloride, and diethyl ether or tetrahydrofuran has been shown to yield a dichloroborane etherate with the composition* $HCl_2B \cdot OR_2$ *or, when a limited amount of boron trichloride is used, a monochloroborane etherate* ($H_2ClB \cdot OR_2$) *(5). At room temperature, chloroborane etherate was found to reduce (rapidly) certain ketones, but did not affect esters such as ethyl acetate (compare with ref. 6). Interestingly, Brown and Tierney (5a) did not detect a similar reaction between diborane and boron trifluoride. Boron trifluoride etherate has recently been expressed (5b) as* $F_2B[O(CH_2CH_3)_2]_2BF_4$.

[6]*The present series of experiments was performed by adding a solution of sodium borohydride in diglyme to the ester – boron trifluoride mixture. Except for possible lower overall ester → ether conversion (cf. ref. 2), no other important differences were noted when this "reverse" technique was used.*

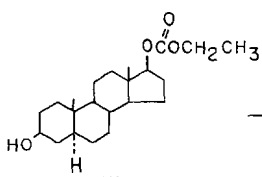
3-oxo-17β-hydroxy-5α-androstane and trimethylacetyl chloride, was reduced by boron trifluoride – sodium borohydride in diglyme–tetrahydrofuran. The product was subjected to oxidation with an 8 *N* chromic acid reagent, and neopentyl ether II*c* was isolated in 55% yield. The oxidation step eliminated separation of the 3β- and 3α-hydroxy epimers formed during reduction. Interestingly, when reduction was repeated with diethyl ether in place of tetrahydrofuran, only 17% conversion into ether II*c* was noted and 21% of ester II*b* was recovered. The lower yield suggests that the rate of reduction is temperature dependent, but this point was not pursued further. Reduction of the pivalate esters illustrates a new and convenient route to neopentyl ethers[7] and further confirms that alkyl branching adjacent to the carbonyl moiety has little influence on the yield of corresponding ether(s).



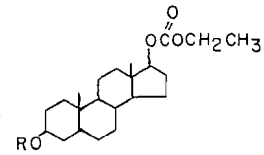
Ia, R=OH
Ib, R=OCOC(CH$_3$)$_3$
Ic, R=OCH$_2$C(CH$_3$)$_3$
Id, R=OCOCH$_2$CH$_3$
Ie, R=OCSCH$_3$
If, R=H



IIa, R = H
IIb, R = COC(CH$_3$)$_3$
IIc, R = CH$_2$C(CH$_3$)$_3$
IId, R = C-OCH$_2$CH$_3$



III



IVa, R = COC(CH$_3$)$_3$
IVb, R = CH$_2$C(CH$_3$)$_3$

Extending the reduction reaction to ethyl carbonate I*d*, prepared from alcohol I*a* and ethyl chloroformate,[8] was expected either to yield a methylenedioxy derivative or to provide an example of relative unreactivity.[9] In practice, ester I*d* was essentially unaffected (98% recovery), and when an attempt at reduction was repeated with boron trichloride (6*b*) in place of boron trifluoride, carbonate I*d* was recovered in 92% yield. Also, 3-oxo-17β-ethoxycarbonyloxy-5α-androstane (II*d*) was prepared and reduced, and the product reoxidized as with ester II*b*; a significant quantity (33%) of the starting ketoester was recovered. Decreased reactivity of carbonate ester II*d* was then demonstrated by a selective reduction sequence. Ketone II*d* was reduced by sodium borohydride in methanol

[7]*Recently, Eliel and Daignault (6a) have applied the lithium aluminium hydride – boron trifluoride reagent to reduction of thiol esters and have, for example, converted cyclohexyl thiopivalate into cyclohexyl neopentyl sulfide (33% yield).*

[8]*A recent review of reactions between chloroformates and alcohols has been prepared (7).*

[9]*If one assumes a molecular orbital picture for carbonate esters with the carbonyl group in an extended π bond overlap system, a reduced rate of reaction with diborane – boron trifluoride, as already experienced with benzoate esters (1), might be predicted.*

Can. J. Chem. Downloaded from www.nrcresearchpress.com by 210.87.254.42 on 09/05/12
For personal use only.

to a mixture of the corresponding C-3 epimeric alcohols. The more polar constituent, assumed to be equatorial alcohol III, was isolated by column chromatography and treated with trimethylacetyl chloride in pyridine. Applying the same reduction conditions (see II*b*) to diester IV*a* gave a mixture composed principally of neopental ether IV*b* and starting material (IV*a*) in essentially equal amounts (approximately 20% each). Results of the preceding reduction reactions suggest that carbonate esters, like benzoate esters, will, in general, display reduced reactivity.

The possibility that xanthate-type esters might be of greater utility than carbonates was discounted when thiocarbonate I*e* was found to yield (82%) alcohol I*a*. Since the fate of the alkoxy group during Raney nickel desulfurization of xanthate esters has, to our knowledge, not been determined (8), the present series of experiments was concluded by subjecting xanthate I*e* to desulfurization with an acid-washed (8*c*) W-4 Raney nickel. The major product was alcohol I*a* accompanied by 5β-cholane (I*f*).[10]

EXPERIMENTAL

All solvents were redistilled. A description of reagents and pretreatment of several solvents used in the present study appears in the Experimental sections of two prior contributions (1, 6*b*). Diborane (1 *M*) in tetrahydrofuran was employed as received from Metal Hydrides Division, Ventron Corp. Except for column chromatographic grade (0.02–0.5 mm) silica gel (E. Merck, A.G.) and Mallinckrodt chemical silicic acid (100 mesh), all other chromatographic and thin-layer techniques have been noted in refs. 1 and 6*b*.

After a crude reaction product had been partitioned between solvent and aqueous phase, the solvent layer was dried over anhydrous sodium sulfate or potassium carbonate. Each analytical sample was colorless, and its melting point was determined on a Kofler melting point apparatus. Unless otherwise indicated, the remaining melting points were determined in open Kimble glass capillary tubes immersed in a silicone oil bath. Optical rotation measurements (in the laboratory of Dr. C. Janssen, Beerse, Belgium) were conducted in chloroform solution. Infrared (in potassium bromide) and proton magnetic resonance (on a Varian Associates model A-60 nuclear magnetic resonance spectrometer) spectra were recorded by Dr. R. A. Hill, University of Maine. Elemental analyses were provided by Dr. A. Bernhardt, Mülheim, Germany.

3,7,12-Trioxo-5β-cholanic Acid

A solution of cholic acid (62 g) in acetic acid (370 ml) – acetone (1.5 l) was treated (room temperature, stirring) with an 8 *N* chromic acid reagent (9) until the orange color persisted for 15 min. Excess chromic acid was reduced with methanol, and solvent was removed (steam bath, *in vacuo*) until a precipitate began to separate. The solid was redissolved by adding acetic acid and the resulting solution was diluted with approximately 2 l of water. The solid product was collected, washed with water, and recrystallized from methanol (300 ml) to yield 40 g of dehydrocholic acid melting at 234–237° (ref. 10 reports m.p. 237–238°). The product was used without further purification for reduction.

24-Hydroxy-5β-cholane (Ia)

Commercial 1 *M* diborane in tetrahydrofuran (15 ml) was added to 5β-cholanic acid (2.7 g) in the same solvent (28 ml) at room temperature. Sixteen hours later the solution was diluted with water (15 ml) and diethyl ether (100 ml). The ethereal phase was separated, washed with water, and evaporated. The solid residue was recrystallized from ethyl acetate to give alcohol I*a* (2.2 g), m.p. 129.5–131° (ref. 10 reports m.p. 130.5–132.5°).

24-(2,2-Dimethyl)propionyloxy-5β-cholane (Ib)

A reaction mixture prepared from pyridine (16 ml), 24-hydroxy-5β-cholane (2.2 g), and 5 ml of 2,2-dimethylpropionyl chloride (11) was allowed to remain at room temperature for 1 h. After dilution with water (20 ml) – diethyl ether (60 ml), the ethereal solution was washed successively with water, 10% hydrochloric acid, and water. Removal of solvent (*in vacuo*) gave a viscous residue (2.3 g) which was crystallized from acetone–methanol to yield 1.8 g, m.p. 59.5–61.5°. Two recrystallizations from the same solvent system gave an analytical specimen as plates melting at 63–64°, $[\alpha]_D^{20}$ +9° (*c*, 5.63); ν_{max} 1 730, 1 282, and 1 158 cm^{-1}.

Anal. Calcd. for $C_{29}H_{50}O_2$: C, 80.86; H, 11.56; O, 7.43. Found: C, 81.34; H, 11.85; O, 6.90.

24-(2,2-Dimethyl)propoxy-5β-cholane (Ic)

Diborane (1 *M*) in tetrahydrofuran (4 ml) was added to pivalate ester I*b* (0.90 g) in tetrahydrofuran (10 ml) – boron trifluoride etherate (10 ml) and the solution was heated at reflux for 1 h. After it was cooled

[10]*Hydrocarbon If may have arisen by a Chugaev-type elimination leading to 5β-chol-23-ene, which would undergo ready hydrogenation in the presence of Raney nickel catalyst.*

Can. J. Chem. Downloaded from www.nrcresearchpress.com by 210.87.254.42 on 09/05/12
For personal use only.

water was added and the mixture extracted with hexane. The combined hexane extracts were chromatographed on activated alumina. Elution with the same solvent gave 0.12 g of neopentyl ether I*c*, which was recrystallized from acetone as plates melting at 69.5–70°, $[\alpha]_D^{20}$ +17° (*c*, 1.21), ν_{max} 1 120 cm^{-1}.

Anal. Calcd. for $C_{29}H_{52}O$: C, 83.58; H, 12.58. Found: C, 83.57; H, 12.46.

*3-Oxo-17β-(2,2-dimethyl)propionyloxy-5α-androstane (II*b*)*

Except for a 2 day reaction period at room temperature, 3-oxo-17β-hydroxy-5α-androstane (II*a*, 2.0 g) in pyridine (15 ml) – diethyl ether (20 ml) was converted into pivalate II*b* with pivaloyl chloride (5 ml) as noted for ester I*b*. Recrystallizing the product from ethyl acetate – ethanol yielded 1.4 g of ester II*b* melting at 199–200° (Fisher–Johns melting point apparatus). A pure sample was recrystallized from acetone–methanol as waxy needles, m.p. 194.5–196°, $[\alpha]_D^{20}$ +28° (*c*, 7.15); ν_{max} 1 720, 1 282, 1 171, and 1 032 cm^{-1}.

Anal. Calcd. for $C_{24}H_{38}O_3$: C, 76.96; H, 10.22; O, 12.82. Found: C, 76.94; H, 10.10; O, 12.86.

*3-Oxo-17β-(2,2-dimethyl)propoxy-5α-androstane (II*c*)*

Sodium borohydride (0.16 g) in diethylene glycol dimethyl ether (diglyme, 6 ml) was added to an ice-cold solution of pivalate II*b* (0.51 g) in tetrahydrofuran (20 ml) – boron trifluoride etherate (8 ml). Before the mixture was heated at reflux for 1 h, cooling was continued for 50 min. Next, water was added and the mixture extracted with chloroform. The combined extracts were washed with water and solvent removed *in vacuo*. Residual solid (0.47 g) was dissolved in acetone (50 ml) and treated with an 8 *N* chromic acid reagent (9) until the orange color remained for 5 min. After dilution with water (50 ml) and extraction with chloroform, removal (*in vacuo*) of solvent yielded 0.38 g of crystalline residue. A solution of the residue in benzene–chloroform (7:3) was chromatographed on activated alumina (13 g). Elution with the same solvent mixture gave 0.28 g of neopentyl ether II*c*. A thin-layer chromatogram (13:3 hexane – diethyl ether as the mobile phase) of the product displayed only one spot, and recrystallization from ethanol–water yielded 0.20 g melting at 189–191.5°. A second recrystallization from acetone gave crystals with the same melting point. The analytical sample exhibited $[\alpha]_D^{20}$ +13° (*c*, 0.73) and ν_{max} 1 715, 1 145, 1 119, and 1 102 cm^{-1}.

Anal. Calcd. for $C_{24}H_{40}O_2$: C, 79.94; H, 11.18; O, 8.88. Found: C, 79.80; H, 11.20; O, 8.82.

When the reduction was repeated with 0.27 g of pivalate ester II*b* and diethyl ether (20 ml) in place of tetrahydrofuran, only 0.047 g, m.p. 188–191°, of neopentyl ether II*c* was obtained. Continued elution of the column chromatogram with chloroform gave 0.06 g of starting ester II*b* melting at 193–195°.

*24-Ethoxycarbonyloxy-5β-cholane (I*d*)*

Ethylchloroformate (6 ml) was added during a 10 min period to 24-hydroxy-5β-cholane (I*a*, 2.0 g) in pyridine (15 ml) – benzene (40 ml). After the solution had stood for 5 min at room temperature, water (20 ml) was added, the aqueous phase discarded, and the benzene solution washed with 2 *N* hydrochloric acid and water. The benzene solution was concentrated to an oily residue, which was dissolved in 1:1 hexane–benzene and chromatographed on activated alumina (60 g). Elution with the same solvent mixture gave an oil which crystallized on standing. Recrystallization from methanol–acetone yielded 1.9 g melting at 69.5–72°. Three recrystallizations from the same solvent system gave a pure specimen as plates, m.p. 69.5–72°, $[\alpha]_D^{22}$ +28° (*c*, 1.23); ν_{max} 1 742, 1 250, 1 030, 1 010, 995, 953, 875, 859, and 792 cm^{-1}.

Anal. Calcd. for $C_{27}H_{46}O_2$: C, 77.45; H, 11.07; O, 11.46. Found: C, 77.74; H, 11.05; O, 11.47.

*Attempted Diborane – Boron Trihalide Reduction of 24-Ethoxycarbonyloxy-5β-cholane (I*d*)*

Procedure A

Reaction between carbonate ester I*d* (0.5 g) and sodium borohydride (0.11 g) – boron trifluoride etherate (13 g) was attempted essentially as described for ester II*b*, except that the hour at reflux (increased reductive cleavage) was not employed. After recrystallization from acetone–methanol, the product weighed 0.43 g, m.p. 69.5–71°, and was identical with ester I*d*.

Procedure B

The experimental approach summarized in procedure A was repeated with boron trichloride (7 ml) in place of boron trifluoride etherate. Here, reaction was carried out with diglyme (20 ml) as solvent and 0.59 g of carbonate ester I*d*. The product,[11] 0.50 g, m.p. 69.5–71°, was carbonate I*d*.

*3-Oxo-17β-ethoxycarbonyloxy-5α-androstane (II*d*)*

Preparation of ethyl carbonate II*d* (10 g crude yield, m.p. 129–136°) was accomplished by the method summarized above for obtaining ester I*d*, with appropriately adjusted quantities of reagents. The analytical specimen was recrystallized from 95% ethanol as fine plates, m.p. 138–139°, $[\alpha]_D^{22}$ +27° (*c*, 4.76); ν_{max} 1 738, 1 710, 1 270, 1 020, 992, 972, 890, 879, and 790 cm^{-1}.

Anal. Calcd. for $C_{22}H_{34}O_4$: C, 72.89; H, 9.45; O, 17.65. Found: C, 72.80; H, 9.20; O, 17.86.

*Reaction of 3-Oxo-17β-ethoxycarbonyloxy-5α-androstane (II*d*) with Sodium Borohydride – Boron Trifluoride*

Ketone II*d* (1.1 g) was allowed to react with the boron trifluoride – sodium borohydride reagent as noted with pivalate ester II*b*. The crude product (1.1 g) was reoxidized with 8 *N* chromic acid reagent (cf. II*b*),

[11]*Identification was supported by the results of mixture melting point determination and infrared spectral comparison.*

Can. J. Chem. Downloaded from www.nrcresearchpress.com by 210.87.254.42 on 09/05/12
For personal use only.

Can. J. Chem. Downloaded from www.nrcresearchpress.com by 210.87.254.42 on 09/05/12
For personal use only.

and a solution of the oxidation product (0.85 g) in 17:3 benzene–chloroform was chromatographed on activated alumina (15 g). Elution with the same solvent mixture gave 0.33 g of starting carbonate ester (II*d*). Two recrystallizations from hexane gave 0.26 g of carbonate ester II*d* melting at 136–137°.[11] Continued elution with more polar solvents gave fractions with a combined weight of 0.39 g, but each was shown (by thin-layer chromatography) to contain substances considerably more polar than ester II*d*. The mixtures were not further separated.

3β-Hydroxy-17β-ethoxycarbonyloxy-5α-androstane (III)

A solution composed of 3-oxo-17β-ethoxycarbonyloxy-5α-androstane (II*d*, 8.0 g), sodium borohydride (3.0 g), and methanol (350 ml) was allowed to remain at room temperature for 3 h. After dilution with *N* hydrochloric acid (250 ml) and water (750 ml), the aqueous mixture was extracted repeatedly with diethyl ether. The combined extracts were washed with water and concentrated to a crystalline residue (6.0 g). A thin-layer chromatogram (1:1 hexane – diethyl ether as the mobile phase) of the residue indicated the presence of two substances with very similar R_f values: presumably the 3α- and 3β-isomers. A solution of the mixture in hexane – diethyl ether (3:2) was chromatographed on silica gel (430 g). A fraction eluted with the same solvent mixture gave 1.1 g of the more polar (on a thin-layer chromatogram) component. Two recrystallizations from hexane–chloroform and one from acetone led to a pure specimen of the 3β-isomer III, m.p. 132–133°, $[\alpha]_D^{20}$ +6° (*c*, 1.33); ν_{max} 3 500, 1 750, 1 740, 1 265 (broad), 1 050, 1 030, 1 014, 975, 881, and 790 cm^{-1}.

Anal. Calcd. for $C_{22}H_{36}O_4$: C, 72.49; H, 9.95; O, 17.56. Found: C, 72.52; H, 9.84; O, 17.56.

3β-(2,2-Dimethyl)propionyloxy-17β-ethoxycarbonyloxy-5α-androstane (IVa)

Alcohol III (0.16 g) was converted into pivalate ester IV*a* as described for ester II*b*. After recrystallization from 95% ethanol, ester IV*a* weighed 0.12 g and melted at 114–117°. A second recrystallization from the same solvent gave an analytical specimen as leaflets, m.p. 116–117°, $[\alpha]_D^{20}$ −10.9° (*c*, 1.83); ν_{max} 1 740, 1 720, 1 280 (broad with shoulders at 1 290 and 1 260), 1 172, 1 010, 969, 881, and 792 cm^{-1}.

Anal. Calcd. for $C_{27}H_{44}O_5$: C, 72.28; H, 9.88; O, 17.83. Found: C, 72.51; H, 10.01; O, 17.44.

3β-(2,2-Dimethyl)propoxy-17β-ethoxycarbonyloxy-5α-androstane (IVb)

Reduction of 3β-(2,2-dimethyl)propionyloxy-17β-ethoxycarbonyloxy-5α-androstane (IV*a*, 0.54 g) with boron trifluoride etherate (15 ml) – sodium borohydride (0.14 g) in tetrahydrofuran (25 ml) – diglyme (7 ml) was performed essentially as described for ester II*b*. However, 15 min at ice-bath temperature and 45 min at reflux were employed here. A solution of crude product (0.52 g) in hexane–benzene (1:1) was chromatographed on activated alumina (15 g). The same solvent eluted 0.1 g of neopentyl ether IV*b*, which was crystallized from ethanol–water as fine needles, m.p. 98–99°, $[\alpha]_D^{20}$ 0.0°; ν_{max} 1 740, 1 270, 1 109 (shoulder at 1 100), 1 018 (shoulder at 1 005), 980, 880, and 795 cm^{-1}.

Anal. Calcd. for $C_{27}H_{46}O_4$: C, 74.60; H, 10.59; O, 14.70. Found: C, 74.74; H, 10.59; O, 14.64.

A fraction eluted by 19:1 benzene–chloroform weighed 0.12 g and was identical[11] with starting diester IV*a*. Continued elution with 9:1 chloroform–methanol gave 0.23 g of a mixture of two alcohols (indicated by thin-layer chromatography), apparently arising from ester cleavage; these alcohols were not further characterized.

24-Methylthiolthiocarbonyloxy-5β-cholane (Ie)

A mixture of toluene (200 ml), 24-hydroxy-5β-cholane (I*a*, 15 g), and potassium (1.7 g) was heated at reflux for 16 h. After the solution was cooled to room temperature, carbon disulfide (5 g) was added, followed in 1 h by methyl iodide (5 ml). When a total of 4 h had elapsed, the solution was filtered and the solvent concentrated *in vacuo* to a red oil. The residue in hexane–benzene (1:1) was passed through a column of silicic acid to yield a yellow oil, which crystallized, m.p. 84–87°, upon trituration with methanol. When a thin-layer chromatogram (hexane as the mobile phase) indicated the presence of impurities, a 1.5 g portion of the product in hexane was chromatographed on acid-washed alumina (45 g). Of five fractions eluted by hexane–benzene (9:1), the fourth was pure as evidenced by a thin-layer chromatogram (hexane as the mobile phase); this fraction was recrystallized from 2-propanol–hexane to yield 0.35 g of needles melting at 87.5–89°, $[\alpha]_D^{20}$ +17.4° (*c*, 1.55); ν_{max} 1 379, 1 249, 1 225, 1 118, and 1 060 cm^{-1}.

Anal. Calcd. for $C_{26}H_{44}OS_2$: C, 71.50; H, 10.15; O, 3.66; S, 14.68. Found: C, 71.97; H, 10.10; O, 3.81; S, 14.08.

Reaction of 24-Methylthiolthiocarbonyloxy-5β-cholane (Ie) with Boron Trifluoride – Sodium Borohydride

Xanthate I*e* (2.0 g) was allowed to react with boron trifluoride (22 ml) – sodium borohydride (0.50 g) as described for ketone II*b*. A solution of crude product (1.6 g) in benzene–chloroform (4:1) was chromatographed on activated alumina. Elution with the same solvent gave 1.3 g of 24-hydroxy-5β-cholane (I*a*) melting at 130–131° after one recrystallization from ethyl acetate.[11]

Reaction of 24-Methylthiolthiocarbonyloxy-5β-cholane (Ie) with W-4 Raney Nickel

A sample (from 40 g of Raney nickel alloy) of W-4 Raney nickel (12) was washed successively with 0.4% acetic acid (2 × 500 ml), water (4 × 500 ml), 95% ethanol (2 × 100 ml), ethanol (3 × 150 ml), and tetrahydrofuran (3 × 150 ml). After the final washing, a mixture of xanthate I*e* (1.0 g) in tetrahydrofuran

(250 ml) and the nickel was heated at reflux for 14 h. The nickel residue was collected and washed with tetrahydrofuran (50 ml), and the combined filtrates were evaporated *in vacuo*. Chromatographing the crude product (0.96 g) in hexane on activated alumina and eluting with the same solvent gave 0.29 g of 5β-cholane melting at 91–92° (homogeneous on a thin-layer chromatogram with hexane as the mobile phase). Recrystallization from acetone gave 0.21 g, m.p. 91–92° (ref. 13 reports m.p. 90–91°); ν_{max} 2 950, 2 840, 1 450 (shoulder at 1 465), and 1 379 cm^{-1}; proton magnetic resonance (deuteriochloroform solution): broad response from 0.5 to 2.1 δ with methyl group signals at 0.65, 0.91, and 1.25 δ.

A series of fractions eluted by 13:7 hexane–benzene were found by thin-layer chromatography to consist of two or more components in small amounts, and were not further separated. However, the fraction eluted by chloroform provided 0.34 g of 24-hydroxy-5β-cholane[11] which melted at 130–131° after one recrystallization from ethyl acetate.

ACKNOWLEDGMENTS

This investigation was supported by Public Health Service research grants Nos. CA-04074-06 to CA-08705-01 from the National Cancer Institute, and in part by The Upjohn Co. We also thank Professor C. Djerassi and the Department of Chemistry, Stanford University, for providing facilities for one of us (G. R. P.) during the initial preparation of this manuscript.

REFERENCES

1. G. R. PETTIT, B. GREEN, G. L. DUNN, P. HOFER, and W. J. EVERS. Can. J. Chem. This issue.
2. G. R. PETTIT and D. M. PIATAK. J. Org. Chem. **27**, 2127 (1962).
3. G. FALCONI, G. BRUNI, and A. ERCOLI. Steroids, **5**, 211 (1965).
4. (*a*) H. C. BROWN and W. KORYTNYK. J. Am. Chem. Soc. **82**, 3866 (1960).
   (*b*) B. C. SUBBA RAO and G. P. THAKER. Current Sci. India, **32**, 404 (1963); Chem. Abstr. **60**, 438 (1964).
5. (*a*) H. C. BROWN and P. A. TIERNEY. J. Inorg. Nuclear Chem. **9**, 51 (1959).
   (*b*) T. A. SHCHEGOLEVA, V. D. SHELUDYAKOV, and B. M. MIKHAILOV. Dokl. Akad. Nauk SSSR, **152**, 888 (1963); Chem. Abstr. **60**, 6455 (1964).
   (*c*) W. GERRARD. The organic chemistry of boron. Academic Press, Inc., New York. 1961. p. 217.
6. (*a*) E. L. ELIEL and R. A. DAIGNAULT. J. Org. Chem. **29**, 1630 (1964).
   (*b*) G. R. PETTIT and W. J. EVERS. Can. J. Chem. **44**, 1097 (1966).
7. N. MATZNER, R. T. KURKJY, and R. J. COTTER. Chem. Rev. **64**, 645 (1964).
8. (*a*) D. A. LIGHTNER and C. DJERASSI. Chem. Ind. London, 1236 (1962).
   (*b*) D. H. R. BARTON, M. V. GEORGE, and M. TOMOEDA. J. Chem. Soc. 1967 (1962).
   (*c*) G. R. PETTIT and E. E. VAN TAMELEN. *In* Organic reactions. Vol. 12. *Edited by* A. C. Cope. John Wiley & Sons, Inc., New York. 1962.
9. K. BOWDEN, I. M. HEILBRON, E. R. H. JONES, and B. C. L. WEEDON. J. Chem. Soc. 39 (1946).
10. F. WESSELY and W. SWOBODA. Monatsh. Chem. **82**, 437 (1951).
11. H. C. BROWN. J. Am. Chem. Soc. **60**, 1325 (1938).
12. H. ADKINS and A. A. PAVLIC. J. Am. Chem. Soc. **69**, 3039 (1947).
13. R. T. BLICKENSTAFF and F. C. CHANG. J. Am. Chem. Soc. **80**, 2726 (1958).

Can. J. Chem. Downloaded from www.nrcresearchpress.com by 210.87.254.42 on 09/05/12
For personal use only.

Can. J. Chem. Downloaded from www.nrcresearchpress.com by 210.87.254.42 on 09/05/12
For personal use only.

STEREOCHEMICAL STUDIES

VI. REACTIONS OF 3β-HYDROXY-4-OXA-5α-ESTRANE AND 3α,17β-DIHYDROXY-4-OXA-5α-ESTRANE

J. T. EDWARD AND J.-M. FERLAND
Department of Chemistry, McGill University, Montreal, Quebec

Received November 1, 1965

ABSTRACT

The configurations at the 3 positions of 3β-hydroxy-4-oxa-5α-estrane and of 3α,17β-dihydroxy-4-oxa-5α-estrane were assigned from a study of the anomerizations of these compounds in aqueous tetrahydrofuran. 3α-Chloro-4-oxa-5α-estrane solvolyzed in alkaline methanol to give a mixture of 3α- and 3β-methoxy-4-oxa-5α-estrane, the former predominating. The difference in the solvolytic behavior of 3α-chloro-4-oxa-5α-steroids and of α-glycosyl halides is discussed.

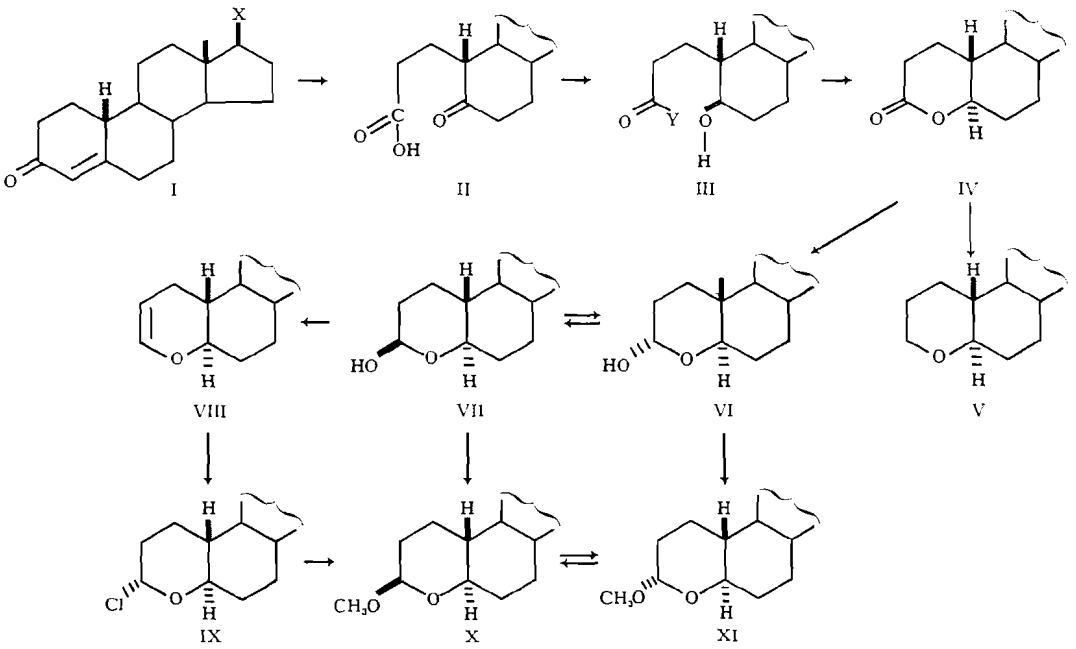
The solvolysis of 3α-chloro-4-oxa-5α-cholestane in buffered or alkaline alcohols gives 3-alkoxy derivatives with predominant retention of configuration (1). The solvolysis of acylglycosyl halides, on the contrary, generally gives a product of inverted configuration (2) if participation by neighboring groups is avoided (3, 4) and if there is not excessive hindrance to approach of the substituting molecule (5). A possible explanation for the behavior of the steroidal chloroether was considered to be the shielding of the β face of ring A by the angular methyl group (1). Although the shielding of this ring is believed to be less complete than the shielding of rings C and D (6), it has been invoked frequently to explain cases of preferential reaction of ring A on its α face; a recent example is the hydroboration of Δ^1-, Δ^2-, Δ^3-, and Δ^4-cholestenes (7).

To test this possibility, we have synthesized a chloroether (IX, X = H) lacking the angular methyl group, and have studied the stereochemistry of its solvolysis in methanol.

Synthetic Routes

The synthetic route to the desired chloroether IX (X = H) is outlined in Reaction Scheme 1. The three-stage preparation from estrone of the unsaturated ketone I (X = H) is described in the literature (8). Ozonolysis of this ketone gave the keto acid II (X = H), which was reduced with sodium borohydride to the hydroxy acid III (X = H, Y = OH). On acidification, the latter formed the lactone IV (X = H). The α configuration at the 5 position of the lactone was indicated by its nuclear magnetic resonance (n.m.r.) spectrum (discussed in ref. 9), and by the negative shift in molecular rotation (Table I) when it was hydrolyzed in alkaline solution (10, 11). Hydrogenation of the lactone over platinum in acetic acid containing a small amount of perchloric acid gave the ether V (X = H), whereas reduction with lithium aluminium hydride (cf. refs. 1 and 12) or diborane (cf. ref. 13) gave the cyclic hemiacetal VII (X = H). The evidence for the β configuration of the hydroxyl group of the crystalline hemiacetal is discussed below. An examination of the ultraviolet and infrared spectra of the hemiacetal in solution and in the solid state revealed no detectable amount of hydroxyaldehyde present (cf. ref. 1).

Dehydration of the hemiacetal with phosphorus oxychloride in pyridine yielded the dihydropyran VIII (X = H), which in ether solution added hydrogen chloride (cf. refs. 1 and 14) to give the reactive chloroether IX (X = H). This reaction is known to be reversible (1, 15), and the sample of chloroether sent for analysis lost hydrogen chloride completely when allowed to stand, and analyzed as the dihydropyran. However, the



REACTION SCHEME 1.

freshly prepared chloroether used in our experiments was free from the dihydropyran, as shown by the absence from its n.m.r. spectrum of characteristic peaks at 3.74 τ (doublet, J 6.0 c.p.s.) and 4.47 τ (triplet, J 6.0 c.p.s.) caused by the 3- and 2-hydrogen atoms, respectively, of VIII (X = H). Instead, the spectrum showed a single one-proton peak at 3.77 τ having a half-width of 6 c.p.s., diagnostic of an equatorial hydrogen (16, p. 154; 17). Furthermore, the infrared spectrum showed a band at 581 cm^{-1} characteristic of an axial chlorine atom (18), and no trace of the peaks at 3 058 and 1 652 cm^{-1} found in the spectrum of the dihydropyran.

The α configuration of the chlorine atom indicated by these spectral data was in accord with the molecular rotation of the compound. The 3β-chloroether should have about the same molecular rotation as the parent ether V (X = H), and the 3α-chloroether should have a more positive molecular rotation (1, 19, 20). The chloroether obtained in our work did indeed have a more positive molecular rotation (Table II), although much less than anticipated from the rotation of 3α-chloro-4-oxa-6α-cholestane (1). This may indicate a small deformation in ring A when the angular methyl group is present (cf. ref. 21); Brewster (19) has already drawn attention to this possibility.

TABLE I

Molecular rotation ($[M]_D$) values of lactones and of compounds derived from them

Lactone	$[M]_D$	Derived compound	$[M]_D$	$\Delta[M]_D$
IV, X = H*	+166°	III; X = H, Y = O⁻*	+70°	−96°
IV, X = OH*	+193°	III; X = OH, Y = O⁻*	+8°	−185°
IV, X = OH†	+200°	III; X = OH, Y = NH_2†	+56°	−154°

*In methanol–water (99:1 v/v).
†In methanol.

Can. J. Chem. Downloaded from www.nrcresearchpress.com by 210.87.254.42 on 09/05/12
For personal use only.

TABLE II

Molecular rotation ($[M]_D$) values of 3-substituted 4-oxa-5α-steroids

3-Substituent	Compound	$[M]_D$ (calcd.)	$[M]_D$ (obs.)	Solvent*
4-Oxa-5α-cholestanes (ref. 1)				
(Hydrogen)		(+190°)	+190°	THF
α-Hydroxy		+360°	+356°	THF–H_2O (9:1 v/v)
β-hydroxy		+160°	—	
α-Methoxy		+465°	+460°	THF–MeOH (1:1 v/v)
β-Methoxy		+75°	+73°	THF–MeOH (1:1 v/v)
4-Oxa-5α-estranes				
(Hydrogen)	V, X = H	(+94°)	+93°	$CHCl_3$
			+95°	THF
α-Hydroxy	VI, X = H	+264°	—	
β-Hydroxy	VII, X = H	+64°	+67°	THF–H_2O (9:1 v/v)
			+62°	$CHCl_3$
α-Methoxy	XI, X = H	+369°	+363°	THF–MeOH (1:1 v/v)
			+348°	$CHCl_3$
β-Methoxy	X, X = H	−21°	−24°	THF–MeOH (1:1 v/v)
			−23°	$CHCl_3$
α-Chloro	IX, X = H	> +94°	+210°	$CHCl_3$
17β-Hydroxy-4-oxa-5α-estranes				
(Hydrogen)	V, X = OH	(+111°)	+111°	$CHCl_3$
α-Hydroxy	VI, X = OH	+281°	+273°	Dioxane (26)
			+203°	THF–H_2O (9:1 v/v)
β-Hydroxy	VII, X = OH	+81°	—	

*THF = tetrahydrofuran.

This axial configuration of the chlorine atom was expected; the compound having equatorial chlorine would be less stable, because of the "anomeric effect" (1, 3, 15, 21–25), and would be expected to isomerize easily to the axial compound. For the same reason, glycosyl halides are generally more stable when the halogen is in an axial orientation (2, 3, 20, 24, 26), and frequently the equatorial halide is so unstable as to elude isolation. For compound IX (X = H), the data of Lemieux and Hayami (24) indicate that the 3β isomer, if in equilibrium with the 3α isomer, would be present to the extent of about 5%. Such an amount would be close to the limit of detection by our spectroscopic methods.

An attempt was made to synthesize 17β-acetoxy-3α-chloro-4-oxa-5α-estrane (IX, X = OAc) by a similar reaction sequence, starting with commercially available 19-nortestosterone acetate (I, X = OAc). This attempt succeeded as far as the hemiacetal VI (X = OH), but was frustrated by our failure to prepare a crystalline diacetate of this hemiacetal. The 5α configuration of the lactone IV (X = OH), and of the compounds derived from it, was indicated by its n.m.r. spectrum (9) and by the sign of the rotational shift when the lactone ring was opened to form the hydroxyamide (III; X = OH, Y = NH_2) or the sodium salt of the hydroxy acid (III; X = OH, Y = O^-) (Table I).

After most of this work was completed (27), Pettit *et al.* (28) described the synthesis of the lactone IV (X = OAc) by direct oxidation of 19-nortestosterone acetate with persulfuric acid, and its further conversion into the hemiacetal VI (X = OH). We had also used persulfuric acid to oxidize nortestosterone to the hydroxylactone IV (X = OH) in low yield (27). This reaction would be expected, on the basis of Pettit's mechanism (13) and of the known stereospecificity of the Baeyer–Villiger reaction (29), to yield a 5α-lactone, and hence may be construed as further evidence for the configurations shown in Reaction Scheme 1.

Can. J. Chem. Downloaded from www.nrcresearchpress.com by 210.87.254.42 on 09/05/12
For personal use only.

During the present work it was found that δ-lactones such as IV (X = H or OH) and others (see Experimental) were hydrogenolyzed over Adams' catalyst in acetic acid containing a small amount of perchloric acid to yield cyclic ethers.* The rate of the reaction varied greatly with different batches of catalyst. With any one batch it was strongly dependent on the concentration of perchloric acid, as shown in Table III. This unexpected

TABLE III

Effect of addition of differing volumes of 70% perchloric acid to the solvent acetic acid (5 ml) on the rate of absorption of hydrogen by 4-oxa-5α-cholestan-3-one*

Volume of perchloric acid (ml)	Initial rate (ml/min)
0	0.13
0.02	0.58
0.03	0.78
0.05	0.47
0.06	0.44
0.12	0.36

*Conditions: 20 mg lactone, 10 mg prereduced platinum oxide, magnetic stirring.

reaction accounts for the low yields of lactones sometimes obtained (e.g. refs. 11 and 31) from the hydrogenation of keto acids in acetic acid. Thus hydrogenation of II (X = OH) with 1 mole of hydrogen yielded a mixture of lactone IV (X = OH), ether V (X = OH), and starting material; hydrogenation with an excess of hydrogen gave the ether in good yield. The stereochemistry of this hydrogenation is discussed in ref. 9.

Solvolysis of 3α-Chloro-4-oxa-5α-estrane in Alkaline Methanol

Solvolysis of the chloroether IX (X = H) in alkaline methanol gave a mixture from which two isomeric methoxy compounds (X and XI; X = H) were isolated. The configurations of these methoxy compounds were shown by their differing n.m.r. spectra. For both compounds the peak at lowest field must be due to the anomeric 3-hydrogen atom, and numerous studies (17, 32) have shown that this peak is at higher field and has a greater width when the hydrogen atom is axial than when it is equatorial. Consequently, the isomer having this peak at 5.46 τ (half-width 4 c.p.s.) must be the 3α-methoxy derivative (XI, X = H), and the isomer having it at 5.83 τ (half-width 16 c.p.s.) must be the 3β-methoxy derivative (X, X = H). The latter peak was a poorly resolved quartet. These values of chemical shift and half-width agree closely with those found for the anomeric protons of 2-methoxy-4-methyltetrahydropyran (25).

These configurations were also indicated by the molecular rotations of the compounds, which agreed well with the values calculated by Brewster's method (19) (Table II). The calculations made use of group parameters (Table IV) that were slightly altered from Brewster's parameters to give better agreement between the calculated and observed rotations of 4-oxa-5α-steroids,† including compounds from previous studies (1, 15).

The proportions of 3-methoxy anomers obtained from the solvolysis of the chloroether IX (X = H) were: 78% of the α anomer (XI, X = H) and 22% of the β anomer (X, X = H). These are almost the proportions in which the 3α- and 3β-benzyloxy derivatives

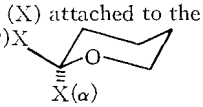
*A preliminary account of this reaction has been published (30).

†The superiority, for our purposes, of the revised parameters in Table IV may be explained by the particular solvents used in our studies. Brewster's calculations take no account of the effect of solvent, although obviously the extent to which a group is solvated will affect its torsional asymmetry and hence its effect on molecular rotation. The large effect of changing solvent is apparent from the data in Table I, ref. 1.

Can. J. Chem. Downloaded from www.nrcresearchpress.com by 210.87.254.42 on 09/05/12
For personal use only.

TABLE IV

Contributions to molecular rotation of groups (X) attached to the tetrahydropyran ring in the conformation:



Group X	Brewster's parameters	Revised parameters
α-Hydroxyl	+100	+170
β-Hydroxyl	0	−30
α-Methoxyl	+205	+275
β-Methoxyl	−105	−115

were formed in the solvolysis of 3α-chloro-4-oxa-5α-cholestane in benzyl alcohol. The exact proportions of 3α- and 3β-methoxy derivatives formed from the solvolysis of the latter chloroether in methanol are not known, although the 3α-methoxy derivative clearly preponderated (1).

It thus becomes apparent that the angular methyl group at the 10 position has little or no effect on the stereochemistry of the displacement reactions of 3-chloro-4-oxa-5α-steroids. It would seem that the intermediate oxocarbonium ion (see ref. 1 for a detailed discussion of the mechanism) has an inherent tendency to react on its α rather than its β face. A similar tendency is shown by 19-nor-5α-steroids having a 3:4 double bond in adding diborane (33), although the absence of the angular methyl group makes the preference for reaction on the α face less complete (7). Various speculations based on stereoelectronic considerations may be advanced to explain this behavior (34), but discussion is best deferred until more experimental data have been accumulated.

If oxocarbonium ions derived from chlorotetrahydropyrans in the C1 conformation (35) have this tendency to react on their α face, the question arises: why do the ions derived from most α-glycosyl halides in this conformation react with alcohols on their β face? A possible explanation lies in the greater reactivity of the latter oxocarbonium ions, destabilized by many electron-withdrawing methoxy or acetoxy groups. For this reason these ions ("encumbered ions") will react with alcohol before the halide ion formed by rupture of the carbon–halogen bond has diffused away and while it is still blocking the α face.

Acid-Catalyzed Mutarotation of 3α- and 3β-Methoxy-4-oxa-5α-estrane

Although 3α- and 3β-methoxy-4-oxa-5α-estrane are stable in neutral or alkaline solution, in acidic methanol either one is rapidly converted into an equilibrium mixture, shown by its optical rotation to contain 67% of the 3α and 33% of the 3β compound (Fig. 1). About the same proportions (65% of 3α, 35% of 3β) were obtained by reaction of the hemiacetal VII (X = H) with methanol containing 3% hydrogen chloride, neutralization, and isolation of the products by chromatography. As expected (36), the 3β isomer, having the equatorial methoxyl group, was eluted more slowly than the 3α compound from the chromatographic column.

The proportions of the α and β anomers are about the same as those found from the equilibration of 3-alkoxy-4-oxa-5α-cholestanes (15).

Mutarotation of 3β-Hydroxy-4-oxa-5α-estrane and 3α,17β-Dihydroxy-4-oxa-5α-estrane

The optical rotation of 3β-hydroxy-4-oxa-5α-estrane (VII, X = H) dissolved in chloroform did not change when the solution was allowed to stand. However, in 90% (v/v) aqueous tetrahydrofuran the rotation increased, following a first-order rate equation (Fig. 2). This indicated a partial conversion into 3α-hydroxy-4-oxa-5α-estrane (VI,

Can. J. Chem. Downloaded from www.nrcresearchpress.com by 210.87.254.42 on 09/05/12
For personal use only.

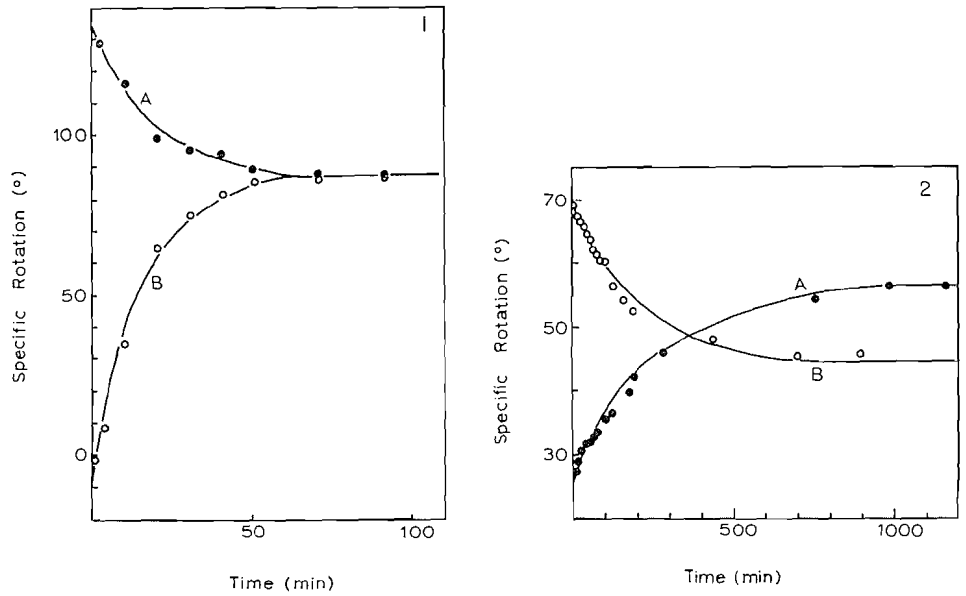


FIG. 1. Change in specific rotation of 3α- (A) and 3β-methoxy-4-oxa-5α-estrane (B) in methanol–tetrahydrofuran (1:1 v/v) containing 0.012 *M* hydrogen chloride at 24 ± 0.5°. Points: experimental; curves: theoretical for first-order reactions having $k = 0.063$ min^{-1}.

FIG. 2. Change in specific rotation of (A) 3β-hydroxy-4-oxa-5α-estrane and (B) 3α,17β-dihydroxy-4-oxa-5α-estrane in tetrahydrofuran–water (9:1 v/v) at 24 ± 0.5°. Points: experimental; curves: theoretical for first-order reactions having rate constants of (A) 0.0044 min^{-1} and (B) 0.0052 min^{-1}.

X = H), known from Hudson's rules of isorotation (37; cf. also ref. 19) to have a higher rotation. The molecular rotation of the 3α compound, estimated by Brewster's method (19) with the revised parameters of Table IV, is given in Table II. If this value is accepted, it may be calculated that the equilibrium mixture contains 41% of the 3α and 59% of the 3β isomer at equilibrium.

These results received a rough confirmation from n.m.r. analysis of equilibrated material isolated at a low temperature as quickly as possible (and so, it was hoped, with as little change in composition as possible during the isolation process). In pure, dry dimethyl sulfoxide this isolated material showed unresolved multiplets* at 3.83 and 4.26 τ caused by hydroxyl hydrogens, since they disappeared on treatment of the solution with deuterium oxide, and peaks at 5.00 and 5.56 τ caused by 3β and 3α protons. Pure 3β-hydroxy-4-oxa-5α-estrane showed only the peaks at 3.83 and 5.56 τ. The relative areas of peaks in the spectrum of the mixture indicated that it contained 38% of the 3α-hydroxy and 62% of the 3β-hydroxy anomers.

The chemical shifts of the anomeric hydroxyls are at higher field than the values for the anomeric hydroxyls of the common monosaccharides in dimethyl sulfoxide (39), as should be expected from the presence of many electron-withdrawing hydroxyl groups in the latter, but have the same order: axial hydroxyls absorb at higher field than equatorial hydroxyls. Thus, both n.m.r. data and optical rotation show the crystalline hemiacetal to have the 3β-hydroxy structure (VII, X = H). On the other hand, the crystalline hemiacetal isolated from the reduction of IV (X = OH) has the 3α-hydroxy structure (VI, X = OH). This is apparent from its molecular rotation (Table II), and from the

**The anomeric hydroxyl, perhaps because of its greater acidity, differs in this respect from the hydroxyl of secondary alcohols, which in dimethyl sulfoxide gives rise to a doublet (38).*

Can. J. Chem. Downloaded from www.nrcresearchpress.com by 210.87.254.42 on 09/05/12
For personal use only.

decrease in optical rotation of a solution in tetrahydrofuran–water (90:10 v/v) when it is allowed to stand (Fig. 2). If the calculated value shown in Table II for the molecular rotation of the 3β isomer is accepted, the final rotation indicates the equilibrium mixture to consist of 43% of the 3α and 57% of the 3β isomer.

The 3-hydroxy-4-oxa-5α-estranes thus differ from 3-hydroxy-4-oxa-5α-cholestane, in which the 3α isomer predominates at equilibrium (1). (If the revised molecular rotation for 3β-hydroxy-4-oxa-5α-cholestane given in Table II is accepted, the equilibrium mixture contains 61% of the 3α isomer, and not 55% as reported earlier (1).) However, the differences (in terms of free energy differences) are small, and may reflect slight changes in the shape of ring A brought about by the presence of the angular methyl group.

The predominance at equilibrium of the 3α-methoxy over the 3β-methoxy isomer is more decisive in both the 4-oxa-5α-cholestane and the 4-oxa-5α-estrane series. This predominance of the α isomer has also been noted in the mutarotation of methyl glycosides; in contrast, in the mutarotation of the parent sugars the β isomer may predominate (16, p. 411). It is apparent that in these equilibria the hydroxyl group behaves as a "larger" group than the methoxyl group, probably because of solvent interactions (25).

EXPERIMENTAL

Melting points were determined in a Gallenkamp apparatus and are corrected. Optical rotations were measured with a Carl Zeiss automatic polarimeter with chloroform as solvent. Infrared spectra were determined on a Perkin–Elmer 337 grating spectrophotometer with 1 mm sodium chloride cells and carbon tetrachloride as solvent. Nuclear magnetic resonance spectra were recorded on a Varian A-60 instrument with carbon tetrachloride as solvent. Woelm alumina was used for column chromatography, and Merck A.G. silica gel for thin- and thick-layer chromatography. Magnesium sulfate was used to dry all solvent extracts before concentration.

5-Oxo-3,5-seco-4-norestran-3-oic Acid (II, X = H)

A solution of 3-oxoestra-4-ene (I, X = H) (20 g (8)) in glacial acetic acid (300 ml) and ethyl acetate (300 ml) was cooled in an ice bath while being treated with oxygen containing ozone for 1.5 h. The solution was allowed to warm to room temperature, an aqueous 10% solution of hydrogen peroxide (60 ml) was added, and the mixture was left overnight. It was diluted with ether (2 l) and washed with water to remove acetic acid and hydrogen peroxide; the acidic product was then dissolved in 2% sodium hydroxide solution. Acidification of this solution gave an oil which was dissolved in ether and crystallized from hexane to give colorless crystals (13.9 g, 64%), m.p. 116–119°. After recrystallization several times from hexane – methylene chloride it melted at 117–119°, $[\alpha]_D^{20}$ −8.84° (*c*, 1.08).

Anal. Calcd. for $C_{17}H_{26}O_3$: C, 73.34; H, 9.41. Found: C, 73.12; H, 9.20.

3-Oxo-4-oxa-5α-estrane (IV, X = H)

The keto acid II (X = H) (4.00 g) in ethanol (300 ml) – water (100 ml) was treated with sodium borohydride (2.00 g) in water (20 ml) for 3 h at room temperature. The reaction mixture was poured into ice water, acidified with concentrated hydrochloric acid, and extracted with ether. Evaporation of the ether gave a solid which was crystallized from methanol–water to give a first crop (2.01 g), m.p. 128–130°, and a second crop (0.52 g), m.p. 125–129°; total yield, 70%. Two more recrystallizations from methanol–water gave an analytical sample, m.p. 135–136°, $[\alpha]_D^{24}$ +92.3° (*c*, 0.72), ν_{max} 1 748 cm^{-1}.

Anal. Calcd. for $C_{17}H_{26}O_2$: C, 77.82; H, 9.99. Found: C, 77.74; H, 9.98.

4-Oxa-5α-estrane (V, X = H)

3-Oxo-4-oxa-5α-estrane (0.200 g) in acetic acid (15 ml) containing 70% perchloric acid (0.05 ml) was hydrogenated over platinum oxide (0.105 g) until there was no further uptake of hydrogen. The solution was filtered, diluted with ether, washed with 2% sodium hydroxide solution and with water, and dried. Evaporation of the ether left a solid which crystallized from methanol–ether as needles (0.162 g, 89% yield), m.p. 74–76°, $[\alpha]_D^{24}$ +37.5° (*c*, 1.08).

Anal. Calcd. for $C_{17}H_{28}O$: C, 82.20; H, 11.36. Found: C, 81.88; H, 10.86.

3β-Hydroxy-4-oxa-5α-estrane (VII, X = H)

(a) With Diborane

Diborane generated from sodium borohydride (5.00 g) and boron trifluoride etherate (27 ml) in diethylene glycol dimethyl ether (100 ml) was passed in a stream of nitrogen through dry tetrahydrofuran and then into a solution of lactone IV (X = H) (2.05 g) in dry tetrahydrofuran (100 ml). After 3 h the solution was poured

Can. J. Chem. Downloaded from www.nrcresearchpress.com by 210.87.254.42 on 09/05/12
For personal use only.

into ice water and extracted with ether. The oily residue from the extract was chromatographed on neutral alumina. Elution with benzene–ether (70:30 v/v) removed a solid (0.982 g, 49%) melting at 138–142°; on recrystallization from hexane – methylene chloride this solid melted at 143–144°, $[\alpha]_D^{24}$ +62.4° (*c*, 1.11), ν_{max} 3 610 cm^{-1}.

Anal. Calcd. for $C_{17}H_{28}O_2$: C, 77.22; H, 10.67. Found: C, 76.96; H, 10.40.

(b) With Lithium Aluminium Hydride

Lithium aluminium hydride (58 mg) in anhydrous, peroxide-free tetrahydrofuran (50 ml) was added under nitrogen over a period of 5 min to a stirred solution of lactone IV (X = H) (2.00 g) in tetrahydrofuran (50 ml) cooled by an ice bath. The mixture was allowed to warm to room temperature and stirred for another 60 min. It was then poured into cold 1 *N* sulfuric acid (100 ml). A white solid precipitated and was removed by filtration, washed with water, and dissolved in ether. The ether solution was dried ($MgSO_4$) and evaporated, and the residue crystallized from hexane as a white solid (1.47 g, 74%), m.p. 139–142°. A recrystallized sample was shown by mixed melting point and infrared spectrum to be identical with the 3β-hydroxy-4-oxa-5α-estrane obtained above.

4-Oxa-5α-estra-2-ene (VIII, X = H)

A solution of 3β-hydroxy-4-oxa-5α-estrane (0.500 g) and phosphorus oxychloride (1.5 ml) in pyridine (5 ml) was refluxed for 1 h. The solution was cooled, diluted with water, and extracted with ether. The ethereal solution, on evaporation, gave an oily residue which crystallized from methanol–ether as plates (0.382 g, 81%), m.p. 59–62°. Recrystallization raised the melting point to 61–63°, $[\alpha]_D^{24}$ +125° (*c*, 0.66), ν_{max} 3 058 and 1 652 cm^{-1}, ϵ_{210} 5 000 (in cyclohexane; end absorption only).

Anal. Calcd. for $C_{17}H_{26}O$: C, 82.87; H, 10.64. Found: C, 83.13; H, 10.18.

3α-Chloro-4-oxa-5α-estrane (IX, X = H)

A solution of 4-oxa-5α-estra-2-ene (0.300 g) in anhydrous ether (20 ml) saturated with dry hydrogen chloride was kept under nitrogen for 2 h. Evaporation of the ether by a jet of dry nitrogen left crystals which sintered at 78°, m.p. 84–88°, $[\alpha]_D^{24}$ +74.0° (*c*, 1.00), ν_{max} 580 cm^{-1}. The compound contained chlorine, and was used immediately, without purification. A sample sent for analysis appeared to have decomposed to starting material.

3α- and 3β-Methoxy-4-oxa-5α-estrane (X and XI; X = H)

(a) From 3β-Hydroxy-4-oxa-5α-estrane

A solution of the hemiacetal VII (X = H) (0.360 g) in a mixture of anhydrous ether (15 ml) and anhydrous methanol (15 ml) containing 3% hydrogen chloride was refluxed for 30 min. To the cooled solution was added excess silver carbonate (40) (3 g), with stirring. The silver salts were removed by filtration and washed with anhydrous ether. The filtrate and washings, evaporated at reduced pressure, left an oil which was chromatographed on alumina (50 g, neutral, grade II). Elution with hexane removed 3α-methoxy-4-oxa-5α-estrane (XI, X = H) (0.234 g), m.p. 59–62°. This was purified by thick-layer chromatography to give a solid, m.p. 61–63°, $[\alpha]_D^{24}$ −8.2° (*c*, 0.75).

Anal. Calcd. for $C_{18}H_{30}O_2$: C, 77.65; H, 10.86. Found: C, 77.61; H, 10.42.

Elution with hexane–benzene (80:20 v/v) removed the 3β isomer (X, X = H) (0.116 g) which, after purification by thick-layer chromatography, melted at 79–81°, $[\alpha]_D^{24}$ +125° (*c*, 0.71).

Anal. Calcd. for $C_{18}H_{30}O_2$: C, 77.65; H, 10.86. Found: C, 77.97; H, 10.64.

(b) From 3α-Chloro-4-oxa-5α-estrane

Sodium (70 mg) was dissolved in absolute methanol (15 ml), and the 3α-chloro compound (IX, X = H) (0.250 g) was added. The solution was refluxed for 1 h, and the solvent then removed under reduced pressure. The residue was treated with water (15 ml) and ether (30 ml), and the ether layer was washed with water, dried, and evaporated. The oil thus obtained was chromatographed on alumina (50 g, neutral, grade II). Elution with hexane removed the 3α compound (XI, X = H) (0.179 g, 78%), m.p. 59–62°, identical (mixed melting point and infrared spectrum) with the 3α compound described above. Elution with hexane–benzene (80:20 v/v) removed the 3β compound (X, X = H) (0.050 g, 22%) as an oil. Thick-layer chromatography of this oil gave a solid which was identical (mixed melting point and infrared spectrum) with the 3β-methoxy compound described above.

17β-Hydroxy-5-oxo-3,5-seco-4-norestran-3-oic Acid (II, X = OH)

19-Nortestosterone acetate (I, X = OAc) (1.007 g) dissolved in ethyl acetate (60 ml) was treated with oxygen containing 6% ozone for 1 h at room temperature. Hydrogen peroxide (10%, 6 ml) and methanol (10 ml) were then added and the mixture was left overnight. It was concentrated to half volume, diluted with ether, and extracted with 2% sodium hydroxide. The alkaline extract, after standing for 12 h, was acidified and the keto acid dissolved in ether. Removal of the ether gave a crystalline solid (0.813 g, 95%), m.p. 85–92°. Two crystallizations from acetone–hexane gave the pure keto acid (II, X = OH), m.p. 108–109°, $[\alpha]_D^{24}$ +1.8° (*c*, 0.449), $\nu_{max}^{CHCl_3}$ 3 538 and 1 710 cm^{-1}.

Anal. Calcd. for $C_{17}H_{26}O_4$: C, 69.36; H, 8.90. Found: C, 69.27; H, 8.79.

Can. J. Chem. Downloaded from www.nrcresearchpress.com by 210.87.254.42 on 09/05/12
For personal use only.

Can. J. Chem. Downloaded from www.nrcresearchpress.com by 210.87.254.42 on 09/05/12
For personal use only.

17α-Acetoxy-5-oxo-3,5-seco-4-norestran-3-oic Acid (II, X = $OCOH_3$)

Potassium carbonate (0.28 g) in water (4 ml) was added, with vigorous stirring, to a solution of 19-nortestosterone acetate (0.500 g) in *t*-butanol–water azeotrope (30 ml), followed by 5 ml of a solution prepared from sodium metaperiodate (2 g) and water (25 ml), and then 0.5 ml of 0.8% aqueous potassium permanganate. The rest of the periodate was added at a rate of 5 ml/min for 2 min and then 2 ml/min for 5 min. Permanganate solution was added as necessary to maintain the purple color.

After 1 h excess permanganate was destroyed with sodium bisulfite. The solution was concentrated at reduced pressure to 30 ml, cooled to 4°, acidified with ice-cold 50% sulfuric acid, and extracted with ether. The ethereal extract was washed with sodium bisulfite until free from iodine, and then with water. Evaporation gave an oil (0.446 g) which was chromatographed on 3% deactivated silica gel. Elution with ether removed a crystalline fraction (0.068 g, 12%), m.p. 80–89°, which, after two recrystallizations from methanol–water, gave keto acid II (X = $OCOCH_3$), m.p. 114–115°, $[\alpha]_D^{24}$ −3.8° (*c*, 0.457), ν_{max} 1 708 and 1 733 cm^{-1} (lit. (41) m.p. 113–115°, $[\alpha]_D^{28}$ −4.08°).

Anal. Calcd. for $C_{19}H_{28}O_5$: C, 67.83; H, 8.39. Found: C, 67.52; H, 8.33.

17β-Hydroxy-3-oxo-4-oxa-5α-estrane (IV, X = OH)

(a) With Sodium Borohydride

A mixture of keto acid II (X = OH) (1.00 g) in 25% aqueous ethanol (50 ml), and of sodium borohydride (1.00 g) in water (15 ml), was left overnight and then heated under reflux until decomposition of the borohydride was complete. The solution was acidified to pH 3, concentrated under reduced pressure to half volume, and diluted with ice-cold water. After 12 h a crystalline solid (0.404 g, 52%), m.p. 105–115°, was collected. Recrystallization from ethyl ether yielded pure 17β-hydroxy-3-oxo-4-oxa-5α-estrane, m.p. 131–132°, $[\alpha]_D^{24}$ +70.1° (*c*, 0.502), $\nu_{max}^{CHCl_3}$ 3 630 and 1 725 cm^{-1} (lit. (28) m.p. 132–134°, $[\alpha]_D^{20}$ +78.9°).

Anal. Calcd. for $C_{17}H_{26}O_3$: C, 73.31; H, 9.41. Found: C, 73.09; H, 9.13.

(b) With Lithium Aluminium Tri-t-butoxy Hydride

Keto acid II (X = OH) (0.972 g) dissolved in tetrahydrofuran (15 ml) was added to a suspension of lithium aluminium tri-*t*-butoxy hydride (4.0 g) in the same solvent (15 ml). The mixture was left at 0° for 30 min and at room temperature for 60 min, and then was poured into an excess of dilute hydrochloric acid. When allowed to stand overnight the solution deposited a solid (0.575 g, 61%) which, after recrystallization from ethyl ether, melted at 131–132°, $[\alpha]_D^{24}$ +70.1° (*c*, 0.504), $\nu_{max}^{CHCl_3}$ 3 630 and 1 725 cm^{-1}.

(c) With Potassium Persulfate

A solution of 19-nortestosterone acetate (0.999 g) in glacial acetic acid (22 ml) was treated with a mixture of potassium persulfate (1.3 g) and sulfuric acid (1.4 g) in acetic acid (22 ml) according to procedures already described (28). The product, after saponification with potassium hydroxide in aqueous dioxane, was obtained as an oil (0.158 g) which crystallized from ethyl ether, m.p. 131–132°, $[\alpha]_D^{24}$ +70.4° (*c*, 0.517), identical by mixed melting point and infrared spectrum with the product obtained in experiments *a* and *b* above.

5β,17β-Dihydroxy-3,5-seco-4-norestran 3-Carboxamide (III; X = OH, Y = NH_2)

A solution of 17β-hydroxy-3-oxo-4-oxa-5α-estrane (0.200 g) in methanol (20 ml) saturated with ammonia deposited needles of the hydroxyamide (III; X = OH, Y = NH_2) (0.165 g) which, after recrystallization from methanol, melted at 298–300°, $[\alpha]_D^{24}$ +18.8° (*c*, 0.461 in methanol); ν_{max}^{KBr} 3 465, 3 360, 3 180, 1 680, and 1 610 cm^{-1}.

Anal. Calcd. for $C_{17}H_{29}O_3N$: C, 69.11; H, 9.90; N, 4.74. Found: C, 69.31; H, 9.73; H, 4.91.

On treatment with dilute hydrochloric acid the amide regenerated the lactone (IV, X = OH), identified by melting point, mixed melting point, infrared spectrum, and optical rotation.

17β-Hydroxy-4-oxa-5α-estrane (V, X = OH)

(a) From Reduction of 17β-Hydroxy-3-oxo-4-oxa-5α-estrane with Lithium Aluminium Hydride – Boron Trifluoride

17β-Hydroxy-3-oxo-4-oxa-5α-estrane (0.262 g) dissolved in boron trifluoride – ether complex (0.840 g) was added to a suspension of lithium aluminium hydride (0.080 g) in ether (50 ml). The mixture was left at 0° for 1 h, refluxed for 2 h, and poured into an excess of dilute hydrochloric acid. The aqueous mixture was extracted with ether, and the extract washed with 2% sodium hydroxide and with water. Evaporation of the ether gave a crystalline solid (0.216 g, 86%), m.p. 166–168°, raised by two recrystallizations from ether to 173–175°, $[\alpha]_D^{24}$ +42.8° (*c*, 0.492) (lit. (26) m.p. 175–176°, $[\alpha]_D^{20}$ +28.8°).

Anal. Calcd. for $C_{17}H_{28}O_2$: C, 77.22: H, 10.67. Found: C, 77.15; H, 10.63.

(b) From Hydrogenation of 17β-Hydroxy-3-oxo-4-oxa-5α-estrane

17β-Hydroxy-3-oxo-4-oxa-5α-estrane (0.200 g) dissolved in glacial acetic acid (15 ml) was hydrogenated over Adams' catalyst (0.090 g) until no more hydrogen was absorbed (2 h). The catalyst was removed by filtration and the product, worked up as above, was obtained as a white crystalline solid (0.185 g, 90%), m.p. 173–175°, identical (mixed melting point, infrared spectrum, and optical rotation) with the product obtained above. The same compound was obtained in 87% yield by hydrogenation of the lactone in acetic acid (15 ml) containing 70% perchloric acid (0.1 ml), hydrogenation now being complete in 45 min.

(c) From Hydrogenation of 17β-Hydroxy-5-oxo-3,5-seco-4-norestran-3-oic Acid

Keto acid II (X = OH) (0.831 g) in glacial acetic acid (15 ml) was hydrogenated over Adams' catalyst (0.420 g) at room temperature and pressure. After 48 h, 3.7 moles of hydrogen/mole of keto acid had been absorbed. The catalyst was removed by filtration and the filtrate diluted with ether. The ether solution was washed with 2% aqueous sodium hydroxide and water. Evaporation gave colorless needles (0.545 g, 74%), m.p. 168–172°, raised by recrystallization from ether to 173–175°, $[\alpha]_D^{21}$ +42.6° (*c*, 0.496), $\nu_{max}^{CHCl_3}$ 1 103 and 1 093 cm^{-1}.

Hydrogenation of 17β-Hydroxy-5-oxo-3,5-seco-4-norestran-3-oic Acid with 1 Mole of Hydrogen

In the presence of Adams' catalyst (0.420 g), keto acid II (X = OH) (1.142 g) dissolved in glacial acetic acid (15 ml) absorbed the theoretical amount of hydrogen after 2½ h at room temperature and pressure. The catalyst was removed by filtration, and the filtrate diluted with ether and washed with 2% sodium hydroxide solution. The ether solution, on evaporation, gave an oil (0.142 g, 14%) that slowly crystallized and which, after recrystallization, was identified (melting point, mixed melting point, and infrared spectrum) as 17β-hydroxy-4-oxa-5α-estrane.

The sodium hydroxide solution was acidified and extracted with ether. The ether solution was washed with 5% sodium carbonate and with water, and dried. Evaporation of the ether gave an oil (0.487 g) which was chromatographed over activated silica gel. The fractions (0.287 g, 26%) eluted with benzene–ether (50:50 v/v) crystallized from ether to give 17β-hydroxy-3-oxo-4-oxa-5α-estrane, m.p. 125–129°, $[\alpha]_D^{21}$ +67.6° (*c*, 0.492), identified by mixed melting point, thin-layer chromatography, and infrared spectrum.

The sodium carbonate solution, after acidification, gave the starting keto acid II (X = OH) (0.456 g, 40%).

Preparation of Tetrahydropyrans by Hydrogenolysis of δ-Lactones

(a) 4-Oxa-5α-cholestane

3-Oxo-4-oxa-5α-cholestane (0.200 g) in acetic acid (15 ml) containing 70% perchloric acid (0.1 ml) was hydrogenated over Adams' catalyst (0.090 g) for 45 min. The product was obtained, after crystallization from methanol, as plates (0.187 g, 92%), m.p. 89–90°, $[\alpha]_D^{23}$ +43.4° (*c*, 0.577), identified as 4-oxa-5α-cholestane (12) by mixed melting point and infrared spectrum.

(b) 4-Oxa-5β-cholestane

Similar hydrogenation of 3-oxo-4-oxa-5β-cholestane (0.200 g) gave 4-oxa-5β-cholestane (0.175 g, 89%), m.p. 51–52°, $[\alpha]_D^{23}$ +3.5° (*c*, 0.629), identified by comparison (mixed melting point and infrared spectrum) with an authentic specimen (12).

(c) 1-Oxadecalin

2-Oxo-1-oxadecalin (42) (1.688 g), on hydrogenation, gave an oil (1.421 g, 80%), b.p. 184–185°, n_D^{27} 1.9686, ν_{max} 1 098 cm^{-1}.

Anal. Calcd. for $C_9H_{16}O$: C, 77.09; H, 11.50. Found: C, 76.51; H, 11.23.

3α,17β-Dihydroxy-4-oxa-5α-estrane (VI, X = OH)

Lactone IV (X = OH) (2.2 g) was reduced with diborane according to Pettit *et al.* (28) to give the hemiacetal (0.8 g), m.p. 196–199°. After several recrystallizations from ether – ethyl acetate it had m.p. 202–205°, $[\alpha]_D^{21}$ +62° (*c*, 0.98) (lit. (28) m.p. 204–207°).

ACKNOWLEDGMENTS

We are grateful to Ayerst, McKenna and Harrison, Ltd., and to Wyeth Inc. for generous gifts of estrone and nortestosterone, respectively; to Professor G. R. Pettit for helpful discussions; and to the National Research Council for financial support.

REFERENCES

1. J. T. EDWARD, P. R. MORAND, and I. PUSKAS. Can. J. Chem. **39**, 2069 (1961).
2. L. J. HAYNES and F. H. NEWTH. Advan. Carbohydrate Chem. **10**, 207 (1955).
3. R. U. LEMIEUX. Molecular rearrangements. *Edited by* P. de Mayo. Interscience Publishers, Inc., New York. 1964. Part II. p. 735.
4. R. U. LEMIEUX and C. BRICE. Can. J. Chem. **30**, 295 (1952); **33**, 109 (1955); **34**, 1006 (1956).
5. A. J. RHIND-TUTT and C. A. VERNON. J. Chem. Soc. 4637 (1960).
6. L. F. FIESER. Experientia, **6**, 312 (1950). T. F. GALLAGHER and T. H. KRITCHEVSKY. J. Am. Chem. Soc. **72**, 882 (1950). L. F. FIESER and M. FIESER. Steroids. Reinhold Publishing Corp., New York. 1959. p. 14.
7. M. NUSSIM, Y. MAZUR, and F. SONDHEIMER. J. Org. Chem. **29**, 1120 (1964).
8. K. J. SAX, R. H. BLANK, P. H. EVANS, JR., L. I. FELDMAN, and C. E. HOLMLUND. J. Org. Chem. **29**, 2351 (1964).
9. J. T. EDWARD and J.-M. FERLAND. Can. J. Chem. **44**, 1311 (1966).
10. W. KLYNE. Chem. Ind. London, 1198 (1954).
11. J. T. EDWARD and P. F. MORAND. Can. J. Chem. **38**, 1325 (1960).

Can. J. Chem. Downloaded from www.nrcresearchpress.com by 210.87.254.42 on 09/05/12
For personal use only.

12. G. E. ARTH. J. Am. Chem. Soc. **75**, 2413 (1953).
13. G. R. PETTIT and T. R. KASTURI. J. Org. Chem. **26**, 4557 (1961).
14. D. G. JONES and A. W. G. TAYLOR. Quart. Rev. London, **4**, 195 (1950).
15. J. T. EDWARD and I. PUSKAS. Can. J. Chem. **40**, 711 (1962).
16. E. L. ELIEL, N. L. ALLINGER, S. J. ANGYAL, and G. A. MORRISON. Conformational analysis. Interscience Publishers, Inc., New York. 1965.
17. R. U. LEMIEUX, R. K. KULLNIG, H. J. BERNSTEIN, and W. G. SCHNEIDER. J. Am. Chem. Soc. **79**, 1005 (1957); **80**, 6098 (1958).
18. L. J. BELLAMY. The infrared spectra of complex molecules. John Wiley & Sons, Inc., New York. 1960. p. 331.
19. J. H. BREWSTER. J. Am. Chem. Soc. **81**, 5475 (1959); **81**, 5483 (1959).
20. W. KORYTNYK. J. Chem. Soc. 650 (1959).
21. M. GORODETSKY and Y. MAZUR. Tetrahedron Letters, **4**, 227 (1964).
22. R. U. LEMIEUX and N. J. CHU. American Chemical Society Meeting, San Francisco, California, April 13–18, 1958. Abstr. Papers. N. J. CHU. Ph.D. Thesis, University of Ottawa, Ottawa, Canada. 1959. p. 97.
23. C. T. BISHOP and F. P. COOPER. Can. J. Chem. **41**, 2742 (1963).
24. R. U. LEMIEUX and J. I. HAYAMI. Can. J. Chem. **43**, 2162 (1965).
25. C. B. ANDERSON and D. T. SEPP. Chem. Ind. London, 2054 (1964).
26. B. CAPON, P. M. COLLINS, A. A. LEVY, and W. G. OVEREND. J. Chem. Soc. 3242 (1964).
27. J.-M. FERLAND. M.Sc. Thesis, McGill University, Montreal, Quebec. 1963.
28. G. R. PETTIT, A. K. DAS GUPTA, and U. R. GHATAK. Steroids, **1**, 137 (1963).
29. K. MISLOW and J. BRENNER. J. Am. Chem. Soc. **75**, 2319 (1953).
30. J. T. EDWARD and J.-M. FERLAND. Chem. Ind. London, 975 (1964).
31. R. B. TURNER. J. Am. Chem. Soc. **72**, 579 (1950).
32. R. W. LENZ and J. P. HEESCHEN. J. Polymer Sci. **51**, 247 (1961). V. S. R. RAO and J. F. FOSTER. J. Phys. Chem. **67**, 951 (1963). J. M. VAN DER VEEN. J. Org. Chem. **28**, 564 (1963).
33. L. CAGLIOTTI, G. CAINELLI, G. MAINA, and A. SELVA. Tetrahedron, **20**, 957 (1964).
34. J.-M. FERLAND. Ph.D. Thesis, McGill University, Montreal, Quebec. 1965. p. 17.
35. R. E. REEVES. J. Am. Chem. Soc. **72**, 1499 (1950).
36. K. SAVARD. J. Biol. Chem. **202**, 457 (1953).
37. C. S. HUDSON. J. Am. Chem. Soc. **31**, 66 (1909).
38. O. L. CHAPMAN. J. Am. Chem. Soc. **86**, 1256 (1964).
39. B. CASER, M. REGGIANI, G. G. GALLO, and A. VIGEVARIC. Tetrahedron Letters, **39**, 2839 (1964).
40. C. M. MCCLOSKEY and G. H. COLEMAN. Org. Syn. **25**, 53 (1945).
41. J. A. HARTMAN, A. J. TOMASEWSKI, and A. S. DREIDING. J. Am. Chem. Soc. **78**, 5662 (1956).
42. H. O. HOUSE, H. BABAD, R. B. TOOTHILL, and A. W. NOLTES. J. Org. Chem. **27**, 4141 (1962).

Can. J. Chem. Downloaded from www.nrcresearchpress.com by 210.87.254.42 on 09/05/12
For personal use only.

Can. J. Chem. Downloaded from www.nrcresearchpress.com by 210.87.254.6 on 09/05/12
For personal use only.

STEREOCHEMICAL STUDIES

VII. HYDROGENATION OF SOME STEROIDAL KETONES OVER ADAMS' CATALYST

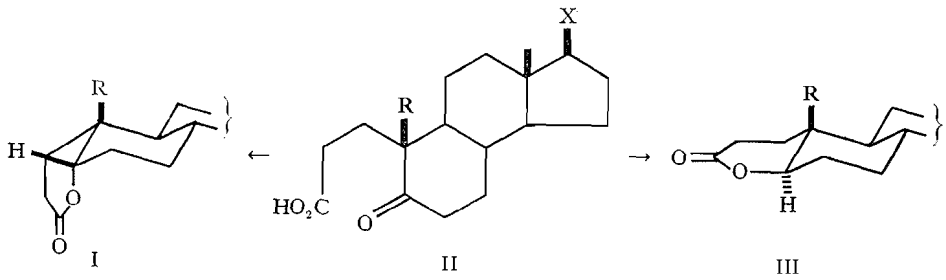
J. T. EDWARD AND J.-M. FERLAND
Department of Chemistry, McGill University, Montreal, Quebec

Received November 1, 1965

ABSTRACT

The influence of the acidity of the solvent on the proportions of axial and equatorial alcohols obtained by hydrogenation of some steroidal ketones was investigated.

The hydrogenation of cyclic ketones over platinum in acetic acid generally gives axial alcohols (1, 2). This has been explained by the greater ease of adsorption of the ketone onto the catalyst from its less-hindered (equatorial) side, the hydrogen from the catalyst then being added to this side to produce the axial alcohol (3–6). Accordingly, it was expected that hydrogenation in acetic acid of keto acids of the general formula II would give *cis* lactones (I) in preference to *trans* lactones (III). This proved to be true for hydrogenation of Windaus' keto acid II (R = Me, X = C_8H_{17}) (7, 8); however, hydro-



I II III

genation of the keto acid II (R = H, X = OH) gave predominantly the *trans* lactone (9). It appeared, paradoxically, that the presence of the angular 19-methyl group made it easier for the catalyst to approach the top side of the molecule and add hydrogen to the carbonyl group.

A chair conformation of ring B of the keto acid II (R = Me, X = C_8H_{17}) and a boat conformation of ring B of the keto acid II (R = H, X = OH) offered a possible explanation of this curious result. Boat conformations have been postulated for some steroidal and triterpene ketones (10, 11), although in some cases the evidence for these conformations is contentious (11).

However, in the present case the optical rotatory dispersion curves indicated ring B to be in the chair form in both keto acids. The amplitude ([*A*]) predicted from the octant rule (12) for the Cotton effect of the keto acid II (R = H, X = OH) would be strongly negative if ring B were in the chair form, and weakly negative if it were in the boat form; in fact, it was strongly negative ([*A*] = −98). Similarly, the amplitude predicted for the keto acid II (R = Me, X = C_8H_{17}) would be weakly positive if ring B were in the chair form, and weakly negative if it were in the boat form; in fact, it was weakly positive ([*A*] = +14).

It was evident that hydrogenation of II (R = H, X = OH) in acetic acid gave predominantly the equatorial alcohol. Since the proportions of epimeric alcohols that are

obtained vary slightly with the sample of catalyst used, it became of interest to test our catalyst and reaction conditions with 3-oxo-5α-cholestane, previously studied by Vavon and Jakubowicz (13). At the same time, 3-oxolanost-8-ene (in which ring A has been claimed to assume the boat conformation (10)) and the keto acids II (R = Me, X = OCOPh) and II (R = H, X = OAc) were studied, in an attempt to discern the effect of structural changes on the proportions of axial and equatorial alcohols formed.

Effect of Acidity of Solvent on Rate and Stereochemistry of Hydrogenation

Vavon and Jakubowicz (13) obtained 50% of the 3α alcohol when 3-oxo-5α-cholestane was hydrogenated over platinum in butyl ether, 60% when it was hydrogenated in acetic acid, and 75% when it was hydrogenated in butyl ether containing hydrochloric acid. They used a melting point – composition diagram to determine the proportions of isomers in their product; this analytical method is unlikely to be very accurate. By the nuclear magnetic resonance (n.m.r.) method of analysis described below, we found that hydrogenation of 3-oxo-5α-cholestane with our catalyst gave only 35% of the 3α alcohol. It is apparent that hydrogenation in acetic acid does not always give the axial alcohol as the chief product. However, by adding small amounts of hydrochloric acid to the solvent it was possible to increase the proportion of axial alcohol, so that it effectively became the sole product of hydrogenation. The results are summarized in Table I. It is evident that steroidal ketones differ in the extent to which they yield axial alcohols on hydrogenation in acetic acid, but that for all of them the proportion of axial alcohol obtained goes up progressively when hydrochloric acid is added to the solvent.

TABLE I

Proportions (%) of α alcohols from hydrogenations of ketones in acetic acid containing varying amounts of mineral acid

Ketone	Hydrochloric acid:* 0%	2%	10%	Perchloric acid,† 10%
3-Oxo-5α-cholestane	35	>95	>95	62
3-Oxolanost-8-ene	33	70	>95	45
II; R = Me, X = C_8H_{17}	42	59	70	45
II; R = Me, X = OCOPh	45	62	75	52
II; R = H, X = OH	21	33	79	45
II; R = H, X = OAc	40	65	90	—

*37% aqueous hydrochloric acid; percentages are by volume.
†70% aqueous perchloric acid.

The mechanism by which hydrochloric acid achieves this effect is obscure. It does not seem to be related to the rate of hydrogenation, as shown by the varying effect upon the latter of adding hydrochloric acid (Table II). The depressing effect of large amounts of hydrochloric acid upon the rate was due to the water being added. The use of acetic acid containing 2% hydrogen chloride (added as the dry gas) caused the time required for the hydrogenation of 3-oxo-5α-cholestane to drop to 4 min; use of acetic acid containing 10% hydrogen chloride caused it to drop to 3 min. In both cases, only the 3α alcohol could be detected in the product.

The addition of 70% aqueous perchloric acid was very effective in accelerating the rate of hydrogenation (Table II), but less effective in increasing the proportion of axial alcohol (Table I). This casts doubt on Brewster's suggestion (4) that the axial alcohol is formed by a hydride transfer from the catalyst to the protonated ketone, since the acetic acid

Can. J. Chem. Downloaded from www.nrcresearchpress.com by 210.87.254.6 on 09/05/12
For personal use only.

TABLE II

Time (in minutes) required for complete hydrogenation of ketones in acetic acid containing varying amounts of aqueous mineral acid

Ketone	Hydrochloric acid:* 0%	2%	10%	Perchloric acid,† 10%
3-Oxo-5α-cholestane	8	5	20	4
3-Oxolanost-8-ene	15	12	20	10
II; R = Me, X = C_8H_{17}	11	17	18	6
II; R = Me, X = OCOPh	10	7	16	7
II; R = H, X = OAc	24	15	40	—

*37% aqueous acid.
†70% aqueous acid.

containing 10% of aqueous (70%) perchloric acid should be considerably more acidic than acetic acid containing 10% of aqueous (37%) hydrochloric acid.

The use of trifluoroacetic acid (14) in place of acetic acid as solvent caused the time required for the hydrogenation of 3-oxo-5α-cholestane to drop to 4 min, and the proportion of the 3α alcohol to rise to 62%. On the other hand, addition of 2% of sodium acetate to acetic acid lengthened the time to 17 min, and caused the proportion of the 3α alcohol to drop to 21%. The evidence for a relation between the acidity of the solvent and the proportion of axial alcohol formed is indisputable, but specific effects of different acids seem also to be involved. This general effect of acidity of solvent, although it has been known for a long time (13), is sometimes forgotten. Thus, a recent paper on the hydrogenation of ketoquinolizidines (15) attributed the greater proportion of axial alcohol obtained with an acidic solvent solely to protonation of the nitrogen so that it was prevented from "anchoring" the molecule on the catalyst.

Effect of Substrate Structure on Rate and Stereochemistry of Hydrogenation

It is evident from the results in Table I that the proportion of axial alcohol formed in the hydrogenation of the keto acid II (R = H, X = OH), the fact provoking the present studies, is unusually low, but that this proportion can be raised to respectable levels by addition of enough hydrochloric acid to the acetic acid. The 17β-hydroxy group apparently militates against formation of the axial alcohol, as shown by comparison with the results for II (R = H, X = OAc). No plausible reason can be advanced for this behavior. In comparison, the effects of the flanking 19-methyl group of II (R = Me, X = C_8H_{17} or OCOPh) seem to be minor. A study of the effect of the 17-hydroxyl group on the stereochemistry of hydrogenation of ketone groups at other positions would be desirable.

The results for 3-oxolanost-8-ene, very similar to those for 3-oxo-5α-cholestane, indicate only a minor effect from the two flanking methyl groups. The configuration of the resulting alcohols is best explained by postulating a chair rather than a boat conformation of ring A (cf. refs. 10 and 11).

Proof of Configurations of Hydrogenation Products

The configurations of the epimeric alcohols obtained by the hydrogenation of 3-oxo-5α-cholestane (10), 3-oxolanost-8-ene (16, 17), and Windaus' keto acid (II; R = Me, X = C_8H_{17}) (8) have already been established. The chemical shift of the proton at the epimeric center is at lowest field in the spectrum, and differs for each epimer in the direction already expected (18–20) for axial and equatorial protons, the axial being at higher field, as shown in Table III. A second difference lies in the half-widths of the peaks, those

Can. J. Chem. Downloaded from www.nrcresearchpress.com by 210.87.254.6 on 09/05/12
For personal use only.

TABLE III

Chemical shifts (τ) and half-widths ($w/2$, in cycles per second) of n.m.r. peaks of epimeric protons of alcohols, acetates, and lactones

Compound	Equatorial proton		Axial proton	
	τ	$w/2$	τ	$w/2$
Known configuration				
3-Hydroxy-5α-cholestane	6.20	8	6.71	17
3-Acetoxy-5α-cholestane	5.14	7	5.46	22
3-Hydroxylanost-8-ene	5.60	4.5	5.93	11
3-Acetoxylanost-8-ene	4.82	6	5.50	22
3-Oxo-4-oxacholestane (I and III; R = Me, X = C_6H_{17})	5.87	3	6.11	10
Uncertain configuration				
17β-Benzoyloxy-3-oxo-4-oxaandrostane (I and III; R = Me, X = OCOPh)	5.22	3.5	6.00	10
17β-Hydroxy-3-oxo-4-oxaestrane (I and III; R = H, X = OH)	5.57	6	6.39	10
17β-Acetoxy-3-oxo-4-oxaestrane (I and III; R = H, X = OAc)	5.53	*	6.00	12

*The half-width was not measurable because of overlapping of the peak with that of 17β-acetoxy protons.

from axial protons being about three times as great as those from equatorial protons (Table III). This is also in line with expectation (18, 21).

These differences may be used to assign configurations to hydrogenation products of uncertain configuration. Atwater and Ralls (22) reduced 17β-benzoyloxy-5-oxo-3,5-seco-4-norandrostan-3-oic acid (II; R = Me, X = OCOPh) with sodium borohydride to a mixture of lactones, tentatively formulated as 3-oxo-17β-benzoyloxy-4-oxa-5α-androstane (III; R = Me, X = OCOPh) for the major product and as the 5β epimer (I; R = Me, X = OCOPh) for the minor product. These structures are confirmed by the positions and widths of the peaks at lowest field. Similarly, the lactones obtained from the hydrogenation of 17β-hydroxy-5-oxo-3,5-seco-4-norestran-3-oic acid (II; R = H, X = OH) may be assigned structures I and III (R = H, X = OH).

An analytical method for mixtures of epimers based on the n.m.r. spectra of the compounds is described in the Experimental section.

The configurations assigned on the basis of n.m.r. spectra were confirmed by measurements of the molecular rotations of the lactones and of the sodium salts of the hydroxy acids derived from them, obtained by placing the lactones in methanolic sodium hydroxide. The direction of the shift in rotation (Table IV) was in the direction predicted by the

TABLE IV

Molecular rotation ($[M]_D$) values of lactones and of sodium salts of the corresponding hydroxy acids in different solvents

Formula	Lactone			Hydroxy acid		
	$CHCl_3$	Aqueous methanol†	pH 3	pH 6	Alkaline solution	$\Delta[M]_D$*
I (R=CH_3, X=OCOPh)	+237°	+234°	+228°	+411°	+380°‡	−183°
I (R=H, X=OH)	+32°	+29°	+29°	+77°	+71°‡	−48°
III (R=CH_3, X=OCOPh)	+399°	+394°	+380°	+287°	+285°§	+93°
III (R=H, X=OH)	+160°	+153°	+151°	+104°	+104°‖	+47°

*$\Delta[M]_D = [M]_D$ (pH 3) − $[M]_D$ (pH 6).
†Methanol–water (99:1 v/v).
‡0.2 *M* NaOH in methanol–water (98:2 v/v).
§1 *M* NaOH in methanol–water (98:2 v/v).
‖0.5 *M* NaOH in methanol–water (98:2 v/v).

Can. J. Chem. Downloaded from www.nrcresearchpress.com by 210.87.254.6 on 09/05/12
For personal use only.

Klyne–Hudson "lactone rule" (23). The *trans* lactones III (R = Me, X = OCOPh) and III (R = H, X = OH) were more slowly attacked by alkali than the corresponding *cis* lactones, and required stronger alkali (see Table IV) to hydrolyze them in a convenient time. Neutralization of the solution of sodium salts to pH 6 caused almost no change in rotation, but acidification to pH 3 caused the rotation (in the 2–3 min required for measurement) to become that of the original lactone. Obviously, recyclization to the lactone was rapid.

EXPERIMENTAL

Materials

3-Oxo-5α-cholestane was a commercial product. 3-Oxolanost-8-ene (24), 5-oxo-3,5-seco-4-norcholestan-3-oic acid (II; R = Me, X = C_8H_{17}) (25), 17β-benzoyloxy-5-oxo-3,5-seco-4-norandrostan-3-oic acid (II; R = Me, X = OCOPh) (22), 17β-hydroxy-5-oxo-3,5-seco-4-norestran-3-oic acid (II; R = H, X = OH) (9), and 17β-acetoxy-5-oxo-3,5-seco-4-norestran-3-oic acid (II; R = H, X = OAc) (9, 26) were prepared by methods described in the literature. Johnson, Matthey and Mallory platinum oxide was used as catalyst; small differences were noted in the activity of different samples, but all results listed in any table were obtained with the same sample, so that comparative results are not affected.

General Hydrogenation Procedure

The ketone (200 mg) in acetic acid or acidified acetic acid (10 ml) was hydrogenated in an all-glass apparatus with a magnetic stirrer over prereduced platinum oxide (100 mg) at room temperature and atmospheric pressure. After absorption of hydrogen had ceased, the solution was filtered and diluted with ether. After several washings with water and with 5% sodium carbonate solution, the ether was evaporated and the crude product dissolved in carbon tetrachloride (3-hydroxy-5α-cholestane, 3-hydroxylanost-8-ene, and 3-oxo-4-oxacholestane) or deuteriochloroform (17β-benzoyloxy-3-oxo-4-oxaandrostane, 17β-hydroxy-3-oxo-4-oxaestrane, and 17β-acetoxy-3-oxo-4-oxaestrane) for n.m.r. analysis. It was found that hydrogenation in acetic acid containing perchloric acid or more than 2% (v/v) hydrochloric acid (37%) was accompanied by partial acetylation of hydroxyl groups. In these cases, the product was completely acetylated with acetic anhydride – pyridine before n.m.r. analysis.

The crude lactones obtained by hydrogenation of the keto acids were shown by thin-layer chromatography to contain only traces of ether resulting from further hydrogenolysis (27).

Analytical Procedure

The proportions of axial and equatorial alcohols obtained in hydrogenations were found by measuring with a planimeter the areas of the peaks caused by the epimeric protons. The accuracy of the method was tested by applying it to synthetic mixtures of lactones I and III (R = Me, X = C_8H_{17}) and of lactones I and III (R = H, X = OAc), made up from known weights of the pure compounds. The results showed the method to have an accuracy of about ±2%. However, when the minor constituent was present to the extent of less than 5%, it was impossible to measure the area of the n.m.r. peak with any confidence.

17β-Acetoxy-3-oxo-4-oxa-5β-estrane (I; R = H, X = OAc)

17β-Acetoxy-5-oxo-3,5-seco-4-norestran-3-oic acid (9, 26) (0.321 g) was hydrogenated over platinum oxide (0.155 g) in acetic acid (25 ml), and the product worked up as above. Crystallization of the crude product from ether–acetone gave a first crop of crystalline 17β-acetoxy-3-oxo-4-oxa-5α-estrane (58 mg, 18% yield), m.p. 210–212°, $[\alpha]_D^{26}$ +50.1° (*c*, 0.92 in chloroform) (lit. (28) m.p. 210–212°, $[\alpha]_D^{22}$ +46.9°).

A second crop crystallized as needles (0.127 g, 42% yield), m.p. 159–164°. Two recrystallizations from ether–acetone yielded pure 17β-acetoxy-3-oxo-4-oxa-5β-estrane, m.p. 169–170°, $[\alpha]_D^{26}$ +10.0° (*c*, 0.79), $\nu_{max}^{CHCl_3}$ 1 738 cm^{-1}.

Anal. Calcd. for $C_{19}H_{28}O_4$: C, 71.21; H, 8.88. Found: C, 71.06; H, 8.59.

The 5β lactone was also obtained by hydrogenation of the keto acid (1.00 g) in 90:10 glacial acetic acid – concentrated hydrochloric acid (50 ml) over platinum oxide (0.502 g). The crude product crystallized from ether–acetone as needles (0.672 g), shown by mixed melting point and infrared spectrum to be identical with the 5β lactone obtained above.

ACKNOWLEDGMENTS

We are grateful to Prof. W. Klyne and Dr. P. M. Scopes for measurement of optical rotatory dispersion, and to the National Research Council for financial support.

REFERENCES

1. R. L. BURWELL. Chem. Rev. **57**, 895 (1957).
2. D. H. R. BARTON. J. Chem. Soc. 1027 (1953).
3. R. P. LINSTEAD, W. E. DOERING, W. E. DAVIS, S. B. LEVINE, and R. R. WHETSTONE. J. Am. Chem. Soc. **64**, 1985 (1942).
4. J. H. BREWSTER. J. Am. Chem. Soc. **76**, 6361 (1954).

Can. J. Chem. Downloaded from www.nrcresearchpress.com by 210.87.254.6 on 09/05/12
For personal use only.

5. R. J. WICKER. J. Chem. Soc. 2165 (1956).
6. E. L. ELIEL. Stereochemistry of carbon compounds. McGraw-Hill Book Co., Inc., New York. 1962. p. 328.
7. R. B. TURNER. J. Am. Chem. Soc. **72**, 579 (1950).
8. J. T. Edward and P. F. Morand. Can. J. Chem. **38**, 1325 (1960).
9. J. T. EDWARD and J.-M. FERLAND. Can. J. Chem. **44**, 1299 (1966).
10. J. S. E. HOLKER and W. B. WHALLEY. Proc. Chem. Soc. 464 (1961). M. BALSUBRAMANIAM. Chem. Rev. **62**, 591 (1962).
11. N. L. ALLINGER and M. A. DAROOGE. J. Am. Chem. Soc. **84**, 4561 (1962). N. L. ALLINGER, J. ALLINGER, and M. A. DAROOGE. J. Am. Chem. Soc. **86**, 4061 (1964). M. J. T. ROBINSON and W. B. WHALLEY. Tetrahedron, **19**, 2123 (1963).
12. W. MOFFITT, R. B. WOODWARD, A. MOSCOWITZ, W. KLYNE, and C. DJERASSI. J. Am. Chem. Soc. **82**, 4013 (1961).
13. G. VAVON and B. JAKUBOWICZ. Bull. Soc. Chim. France, **53**, 581 (1933).
14. P. E. PETERSON and C. CASEY. J. Org. Chem. **29**, 2325 (1964).
15. C. P. RADER, G. E. WICKS, R. L. YOUNG, and H. S. AARON. J. Org. Chem. **29**, 2252 (1964).
16. L. F. FIESER and M. FIESER. Steroids. Reinhold Publishing Corp., New York. 1959. pp. 28, 367, and 377.
17. R. E. MARKER, E. L. WITTLE, and L. W. MIXOM. J. Am. Chem. Soc. **59**, 1368 (1937). R. E. MARKER and E. L. WITTLE. J. Am. Chem. Soc. **59**, 2289 (1937).
18. R. U. LEMIEUX, R. K. KULLNIG, H. J. BERNSTEIN, and W. G. SCHNEIDER. J. Am. Chem. Soc. **80**, 6098 (1958).
19. A. A. BOTHNER-BY and C. NAAR-COLIN. Ann. N.Y. Acad. Sci. **70**, 1833 (1958).
20. E. L. ELIEL and M. H. GIANNI. Tetrahedron Letters, **3**, 97 (1962).
21. M. KARPLUS. J. Chem. Phys. **30**, 11 (1959).
22. N. W. ATWATER and J. W. RALLS. J. Am. Chem. Soc. **82**, 2011 (1960).
23. W. KLYNE. Chem. Ind. London, 1198 (1954).
24. A. WINDAUS. Z. Physiol. Chem. **190**, 51 (1930). H. WIELAND, H. PASEDACH, and A. BALLAUF. Ann. **529**, 68 (1937).
25. J. T. EDWARD, D. HOLDER, W. H. LUNN, and I. PUSKAS. Can. J. Chem. **39**, 599 (1961).
26. J. A. HARTMAN, A. J. TOMASEWSKI, and A. S. DREIDING. J. Am. Chem. Soc. **78**, 5662 (1956).
27. J. T. EDWARD and J.-M. FERLAND. Chem. Ind. London, 975 (1964).
28. G. R. PETTIT, A. G. DAS GUPTA, and U. R. GHATAK. Steroids, **1**, 137 (1963).

Can. J. Chem. Downloaded from www.nrcresearchpress.com by 210.87.254.6 on 09/05/12
For personal use only.

Can. J. Chem. Downloaded from www.nrcresearchpress.com by 210.87.254.40 on 09/05/12
For personal use only.

STEREOCHEMICAL STUDIES

VIII. SYNTHESIS OF *cis*-1-OXA-10-METHYLDECAL-2-ONE

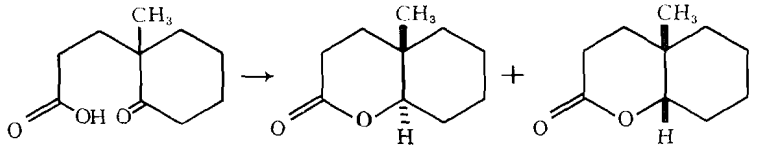
J. T. EDWARD AND J.-M. FERLAND
Department of Chemistry, McGill University, Montreal, Quebec

Received November 4, 1965

ABSTRACT

9-Methylhydrindan-1-one was obtained as a mixture (80% *trans*, 20% *cis*) in four steps from 10-methyl-$\Delta^{1,9}$-octal-2-one. In the presence of alkali it epimerized to *cis*-9-methylhydrindan-1-one containing less than 1% of the *trans* isomer. Oxidation of this *cis* ketone with peroxytrifluoroacetic acid gave *cis*-1-oxa-10-methyldecal-2-one.

House and Schellenbaum (1) reduced 3-(1′-methyl-2′-oxocyclohexyl)propionic acid (I) with sodium borohydride and obtained, after acidification of the product, a neutral material. From the nuclear magnetic resonance (n.m.r.) spectrum of this material they concluded that it was made up of *trans*- (II) and *cis*-1-oxa-10-methyldecal-2-one (III) in the ratio 35:65. A broad multiplet (one proton) centered at about 4.0 τ was attributed to



the C-9 hydrogens of II and III. Sharp, unsplit peaks at 9.05 τ and 8.95 τ (total area three protons; relative areas 35:65) were attributed to the angular methyl groups of the *trans* (II) and *cis* (III) isomers, respectively, by analogy with the positions of the peaks of angular methyl groups in the spectra of *trans* and *cis* decalols (2). The isomers could not be separated completely by vapor phase chromatography.

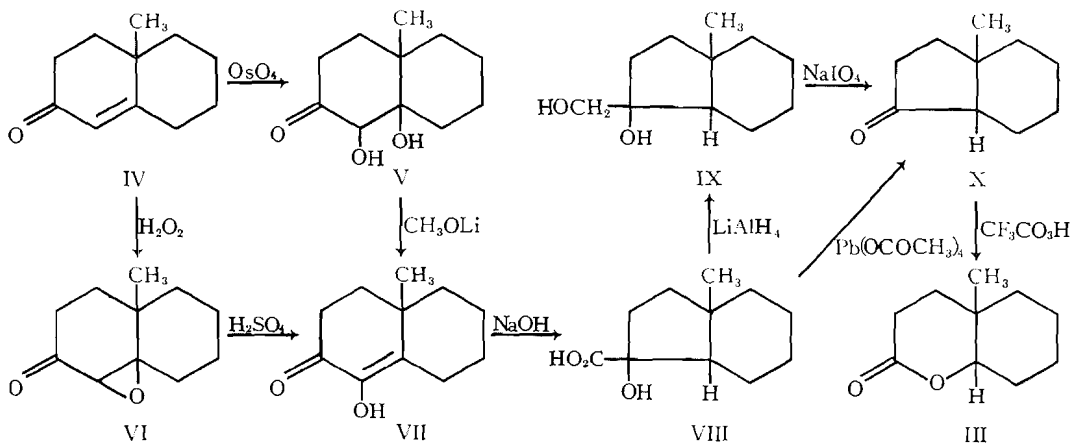
We have repeated this work and confirmed most of House and Schellenbaum's observations. The n.m.r. spectrum of our product had peaks at 8.94 τ and 9.03 τ; however, the peak at lowest field was a triplet at 5.93 τ (4.07 δ), and not at 4.0 τ. A peak at 5–6 τ for the C-9 hydrogens of II and III is to be expected from previous studies of δ-lactones (3).

Hydrogenation of the keto acid I over Adams' catalyst in acetic acid gave a lactone mixture, indicated by its n.m.r. spectrum to be made up of II and III in the proportions 2:1. This ratio was not affected by addition of hydrochloric acid to the acetic acid solvent (cf. ref. 3).

For stereochemical studies the pure isomers II and III were required, and consequently a stereospecific synthesis of (±)-III was carried out by the route outlined in Reaction Scheme 1. The stereochemistry of the various intermediates (all (±) mixtures) is not shown in this scheme, but is discussed below, separately for each compound.

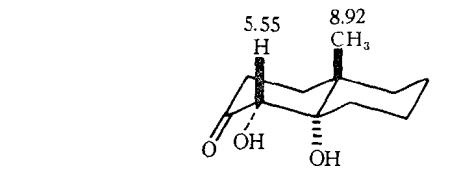
1,9-Dihydroxy-10-methyldecal-2-one (V)

Osmium tetroxide hydroxylates a double bond *cis* (4), and consequently oxidation of the unsaturated ketone IV would be expected to yield a mixture of the diastereoisomeric diols V*a* and V*b*. This expectation was realized. Although the solid product of the reaction had a sharp melting point after one recrystallization, its n.m.r. spectrum showed it to be a

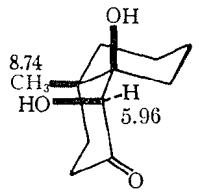


REACTION SCHEME 1.

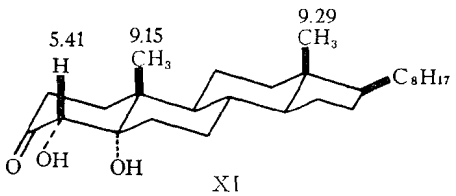
mixture of V*a* and V*b* in the proportions 70:30. Two peaks at lowest field, at 5.55 τ and 5.96 τ, had a total area equivalent to one proton, and could be assigned to the protons at the 1 position of V*a* and V*b*. The two peaks at highest field, at 8.92 τ and 8.74 τ, with a total area equivalent to three protons, could be assigned to the angular methyl groups. In both cases the relative areas of the peaks were 70:30. The assignment of these peaks to the individual isomers V*a* and V*b* as shown in the formulae comes from a comparison with the n.m.r. spectra of the known compounds, 4α,5α-dihydroxycholestan-3-one (XI) and



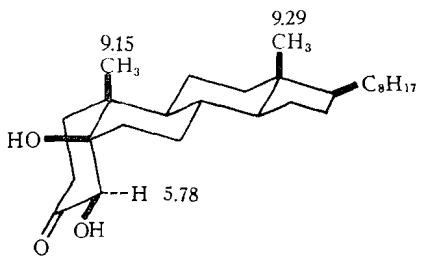
V*a*



V*b*



XI



XII

4β,5β-dihydroxycholestan-3-one (XII) (5, 6). The various peaks of these spectra may be assigned on the basis of the known n.m.r. spectra of steroids (7), and the chemical shifts of the relevant peaks are shown in the formulae XI and XII. It is apparent that the *cis* decalone is either in the non-steroid conformation of V*b* (cf. refs. 2 and 8), or in a conformation in which one of the rings has become a twist-boat (9).

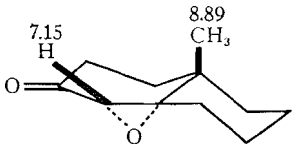
These results indicate the *trans* isomer V*a* to be the chief product from the oxidation of

Can. J. Chem. Downloaded from www.nrcresearchpress.com by 210.87.254.40 on 09/05/12
For personal use only.

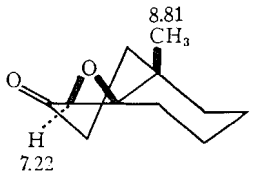
IV by osmium tetroxide, probably because the β-methyl group shields the β face of the molecule. Similarly, the oxidation of testosterone under the same conditions has been found to yield 70% of the 4α,5α-diol (10). However, when a mixture of osmium tetroxide and hydrogen peroxide was used to oxidize IV, the proportion of V*a* in the product decreased to 40%, again paralleling the behavior of steroidal compounds (6).

1,9-Epoxy-10-methyldecal-2-one (VI)

Oxidation of the unsaturated ketone IV with alkaline hydrogen peroxide according to published procedures (11, 12) gave a liquid product, indicated by its n.m.r. spectrum to contain two compounds. Two sharp peaks at highest field (8.89 τ and 8.81 τ; relative areas 1:2), having a total area equivalent to three protons, may be assigned with reasonable certainty (cf. ref. 8) to the angular methyl groups of the *trans* (VI*a*) and *cis* (VI*b*) isomers, respectively. The peaks at lowest field (7.15 τ and 7.22 τ; relative areas 1:2), corresponding to one proton, are then assigned to the protons on the 1 position, as shown below. This



VI*a*



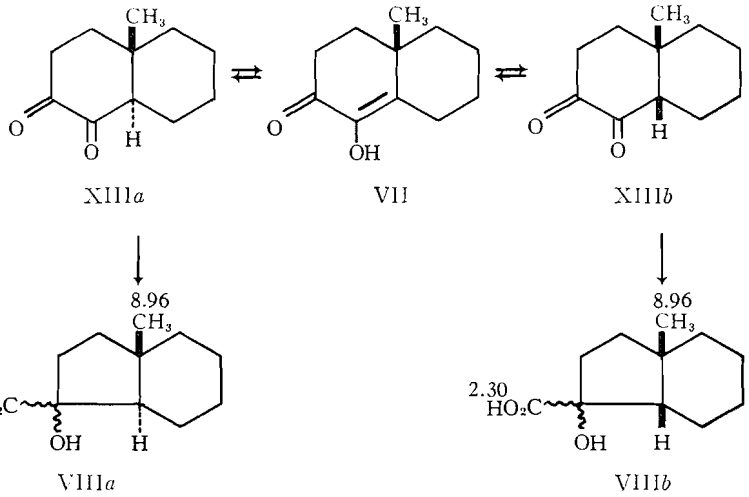
VI*b*

ratio of 2:1 for the *cis* and *trans* isomers in the product agrees with the ratio of 70:30 obtained by Shaw and Stevenson (12) from the oxidation of cholest-4-ene-3-one.

Treatment of the epoxide mixture with sulfuric acid in acetic acid (cf. ref. 13) or of the diolones (V) with lithium methoxide in methanol (cf. ref. 6) yielded the diosphenol (VII), which gave a characteristic blue color with ferric chloride.

1-Hydroxy-9-methylhydrindan-1-carboxylic Acid (VIII)

Diosphenols undergo a benzilic acid type rearrangement in alkali (14, 15), presumably because of a small amount of diketone in equilibrium with diosphenol. In the present instance, the diketone can have either a *trans* (XIII*a*) or *cis* (XIII*b*) fusion of the rings (Reaction Scheme 2). It seems to be likely (cf. ref. 16) that both diones have about the



XIII*a* VII XIII*b*

VIII*a* VIII*b*

REACTION SCHEME 2.

Can. J. Chem. Downloaded from www.nrcresearchpress.com by 210.87.254.40 on 09/05/12
For personal use only.

same stability, and so are present in roughly equal amounts, but that the *trans* compound XIII*a* reacts more rapidly with hydroxide ion, because of the better solvation possible for the highly charged intermediate (17) leading from XIII*a* to VIII*a*. In fact, it proved to be impossible to determine the proportions of *trans* (VIII*a*) and *cis* (VIII*b*) products from the n.m.r. spectrum of the hydroxy acid, which showed only a single peak for the carboxyl (2.30 τ) and methyl (8.96 τ) protons; however, the products from the next stage of the synthesis showed the ratio of *trans* (VIII*a*) to *cis* (VIII*b*) to be about 80:20.

9-Methylhydrindan-1-one (X)

Lead tetraacetate oxidation of the hydroxy acid VIII gave 9-methylhydrindan-1-one (X). The n.m.r. spectrum of this compound showed two peaks at 8.81 τ and 9.21 τ, with a total area equivalent to three protons and with relative areas of 20:80. As shown below, these are due to the angular methyl groups of the *cis* and *trans* forms of X.

Because it was feared that some epimerization could have taken place under the acidic conditions of lead tetraacetate oxidation, the preparation of 9-methylhydrindan-1-one was carried out by an alternative route which avoided acidic conditions. The mixture of hydroxy acids (VIII) was reduced with lithium aluminium hydride to a mixture of diols (IX), which was then oxidized with sodium metaperiodate in neutral solution (14). Again, the ratio of *trans* to *cis* was shown by n.m.r. to be 80:20.

Treatment of this *cis*–*trans* mixture with sodium hydroxide in methanol gave a product showing a peak at 8.81 τ (three protons) and no peak at 9.21 τ. Evidently, under these conditions conversion of the *trans* into the *cis* compound was almost complete, because the n.m.r. spectrum would have revealed the *trans* compound if it had been present to the extent of more than about 1%. This isomerization took place very readily: after 2 days in a Pyrex container, the proportion of *cis* isomer had risen to 70%, and after 2 months to 90%.

These results are in accord with expectation. Although the proportion of *cis*- to *trans*-hydrindan-1-one at equilibrium is 75:25 (18), the addition of an angular methyl group would be expected to increase this ratio considerably (16, 19).

cis-1-Oxa-10-methyldecal-2-one (III)

The Baeyer–Villiger oxidation of *cis*-9-methylhydrindan-1-one (X) gave *cis*-1-oxa-10-methyldecal-2-one (III). This reaction proceeds with retention of configuration of the migrating groups (20) and almost always, as in the present case, involves migration of the more alkylated of the two carbons flanking the carbonyl group (21). The n.m.r. spectrum of the lactone III showed a sharp methyl peak (three protons) at 8.93 τ and a triplet ($J \sim 3.5$ c.p.s.) at 5.93 τ (one proton) caused by the proton at the 9 position. This confirms House's assignment of the methyl peak at lower field to III (1).

EXPERIMENTAL

Hydrogenation of 3-(1′-Methyl-2′-oxocyclohexyl)propionic Acid (I)

3-(1′-Methyl-2′-oxocyclohexyl)propionic acid (I) (2.014 g) in glacial acetic acid (2 ml) was hydrogenated over platinum oxide (0.794 g) at room temperature and atmospheric pressure. After 1½ h, uptake of hydrogen ceased. The solution was diluted with ether, filtered, and washed with 2% sodium hydroxide solution and with water. Distillation gave 1-oxa-10-methyldecal-2-one, b.p. 95–96° at 0.3 mm, n_D^{21} 1.4909 (lit. (1) b.p. 102–104° at 0.8 mm, n_D^{26} 1.4916).

Anal. Calcd. for $C_{10}H_{16}O_2$: C, 71.39; H, 9.59. Found: C, 71.26; H, 9.56.

1,9-Dihydroxy-10-methyldecal-2-one (V)

(a) With Osmium Tetroxide

A solution of 10-methyl-$\Delta^{1,9}$-octal-2-one (IV) (1.1 g) in pyridine (150 ml) was stirred at room temperature for 2½ h with osmium tetroxide (1.79 g). The black mixture was then stirred for 10 min with a solution of sodium bisulfite (2.8 g) in water (40 ml) and pyridine (30 ml). This mixture was extracted with ether, and

Can. J. Chem. Downloaded from www.nrcresearchpress.com by 210.87.254.40 on 09/05/12
For personal use only.

the ether solution dried (K_2CO_3). Removal of the ether at reduced pressure left a black oil which was filtered through silica gel (20 g). Washing the silica gel with chloroform and concentration of the chloroform gave a brown solid (1.05 g), m.p. 85–89°, which, after several recrystallizations from hexane, was obtained as colorless needles, m.p. 90–92°; $\nu_{max}^{CCl_4}$ 3 580, 3 460, and 1 738 cm^{-1}.

Anal. Calcd. for $C_{11}H_{18}O_3$: C, 66.64; H, 9.15. Found: C, 66.52; H, 8.99.

(b) With Osmium Tetroxide – Hydrogen Peroxide

Osmium tetroxide (2 g) was added to a solution of 10-methyl-$\Delta^{1,9}$-octal-2-one (15 g) in ether (200 ml), and the mixture allowed to stand in the dark for 5 h. Hydrogen peroxide (30%, 30 ml) was then added slowly and the mixture was stirred at room temperature for 4 days. Portions of hydrogen peroxide (10 ml) were added when the solution darkened. The excess of hydrogen peroxide was removed, and the ether solution was washed with water and then treated with a slow stream of hydrogen sulfide for 30 min. The solution was filtered, washed with 2% sodium bicarbonate and with water, and dried. The oily residue obtained on evaporation was chromatographed on silica gel. Benzene–ether (75:25 v/v) eluted an oily, crystalline material (8.2 g) which crystallized from hexane as a colorless solid, m.p. 90–92°. The compound was identical (mixed melting point and infrared spectrum) with the material prepared above, but its n.m.r. spectrum showed different proportions of the isomers V*a* and V*b*.

1,9-Epoxy-10-methyldecal-2-one (VI)

10-Methyl-$\Delta^{1,9}$-octal-2-one (29.7 g) in methanol (500 ml) was treated at 0° with ice-cold 30% hydrogen peroxide (308 ml) and then with ice-cold 10% sodium hydroxide solution (103 ml). The solution was kept at 0° for 48 h, and then diluted with water and extracted with ether. The ether solution was washed with water, dried, and evaporated, and the residue distilled to give 1,9-epoxy-10-methyldecal-2-one as an oil (22.5 g), b.p. 96–98° at 0.75 mm, n_D^{20} 1.4992; $\nu_{max}^{CCl_4}$ 1 720, 922, and 858 cm^{-1}.

Anal. Calcd. for $C_{11}H_{16}O_2$: C, 73.30; H, 8.95. Found: C, 73.27; H, 8.71.

1-Hydroxy-10-methyl-$\Delta^{1,9}$-octal-2-one (VII)

(a) From 1,9-Dihydroxy-10-methyldecal-2-one (V)

A solution of 4 *M* lithium methoxide in methanol (85 ml) was added to 1,9-dihydroxy-10-methyldecal-2-one (3.38 g) in methanol (200 ml), and the mixture was boiled under reflux for 2 h. The cooled solution was acidified to pH 3 with concentrated hydrochloric acid, diluted with a large excess of water, and extracted with ether. The ether was evaporated and the residue distilled to give an oil (2.3 g), b.p. 86–90° at 1.5 mm, which slowly crystallized. After recrystallization from hexane the diosphenol was obtained as a colorless solid, m.p. 84–85°, λ_{max}^{EtOH} 276 mμ (ϵ_{max} 20 000); $\nu_{max}^{CCl_4}$ 3 485, 1 720, 1 685, and 1 665 cm^{-1}.

Anal. Calcd. for $C_{11}H_{16}O_2$: C, 73.30; H, 8.95. Found: C, 73.38; H, 8.97.

(b) From 1,9-Epoxy-10-methyldecal-2-one (VI)

The epoxide (20 g) in glacial acetic acid (375 ml) containing concentrated sulfuric acid (37.5 ml) was left at room temperature for 24 h. The black solution was diluted with ice water (3 l) and neutralized with sodium bicarbonate. A solid separated and was distilled to give an oil, b.p. 90–100° at 2.8 mm, which slowly crystallized. After recrystallization from hexane the solid melted at 84–85°, and was shown by mixed melting point and ultraviolet and infrared spectra to be identical with the compound described in the preceding section.

1-Hydroxy-9-methylhydrindan-1-carboxylic Acid (VIII)

A solution of 1-hydroxy-10-methyl-$\Delta^{1,9}$-octal-2-one (3.9 g) in methanol (50 ml) and 5% aqueous sodium hydroxide (500 ml) was kept at 100° for 16 h under nitrogen. The cooled solution was acidified to pH 3 and extracted with ether, and the ether in turn extracted with 5% aqueous sodium bicarbonate. The latter solution was acidified and extracted with ether. Evaporation of the ether gave an oil which slowly crystallized. Recrystallization from hexane gave plates of the hydroxy acid (VIII) (2.11 g), m.p. 108–111°. Two more crystallizations from hexane raised the melting point to 112–113°; $\nu_{max}^{CCl_4}$ 3 575, 1 724, 1 448, and 1 272 cm^{-1}.

Anal. Calcd. for $C_{11}H_{18}O_3$: C, 66.69; H, 9.15. Found: C, 66.67; H, 8.91.

1-Hydroxymethyl-9-methylhydrindan-1-ol (IX)

Under dry nitrogen, a solution of 1-hydroxy-9-methylhydrindan-1-carboxylic acid (1.2 g) in ether (25 ml) was added, with stirring, over 15 min to a suspension of lithium aluminium hydride (1.5 g) in ether (100 ml). The mixture was refluxed for 2 h, and then water (5 ml) and 10% aqueous sodium hydroxide (4 ml) were added dropwise, with continued stirring. The inorganic precipitate was removed by filtration and washed with ether. The filtrate and washings, on concentration, gave the diol as an oil (1.1 g) which could not be crystallized.

9-Methylhydrindan-1-one (X)

(a) From 1-Hydroxy-9-methylhydrindan-1-carboxylic Acid (VIII)

A solution of the hydroxy acid (6.1 g) and lead tetraacetate (40 g) in methanol (200 ml) was left at room temperature overnight. The solution was concentrated, diluted with water, and extracted with ether. The ether solution was washed with 5% sodium bicarbonate and water, dried, and concentrated. Distillation of the residue (3.6 g) gave an oil (2.6 g), b.p. 60–68° at 1.3 mm, n_D^{20} 1.4804, $\nu_{max}^{CCl_4}$ 1 760 cm^{-1}. The n.m.r. spectrum showed this material to be a mixture of the *cis* and *trans* isomers.

Anal. Calcd. for $C_{10}H_{16}O$: C, 78.89; H, 10.59. Found: C, 78.62; H, 11.06.

Can. J. Chem. Downloaded from www.nrcresearchpress.com by 210.87.254.40 on 09/05/12
For personal use only.

(b) From 1-Hydroxymethyl-9-methylhydrindan-1-ol (IX)

The diol (1.0 g) in methanol (50 ml) was treated with sodium metaperiodate (2 g) in water (40 ml), followed by sufficient 5% aqueous sodium bicarbonate to adjust the pH of the mixture to about 6. The suspension was stirred overnight at room temperature. The methanol was removed at reduced pressure, and the residual mixture extracted with ether. The residue, after removal of the ether, was distilled to give an oil, b.p. 62–68° at 1.4 mm, n_D^{21} 1.4800, having an infrared spectrum identical with that of the ketone mentioned above.

cis-9-Methylhydrindan-1-one

The mixture of *trans-* and *cis*-9-methylhydrindan-1-one obtained above (3.0 g) was dissolved in 2.7% methanolic sodium hydroxide (220 ml) and left overnight. The solution was then acidified, diluted with water, concentrated at reduced pressure, and extracted with ether. Distillation of the residue from the ether gave *cis*-9-methylhydrindan-1-one as an oil (2.7 g), b.p. 70° at 1.25 mm, n_D^{20} 1.4812, $\nu_{max}^{CCl_4}$ 1 760 cm^{-1}.

Anal. Calcd. for $C_{10}H_{16}O$: C, 78.89; H, 10.59. Found: C, 78.81; H, 10.59.

cis-1-Oxa-10-methyldecal-2-one (III)

A solution of trifluoroperoxyacetic acid, prepared from trifluoroacetic anhydride (13 ml) and 90% hydrogen peroxide (2.6 ml) in methylene chloride (100 ml) (22), was added over a period of 1 h to a stirred solution of *cis*-9-methylhydrindan-1-one (2.6 g) in methylene chloride (160 ml) containing a suspension of disodiohydrogen phosphate (9 g). Stirring was continued for 2 h at room temperature. After dilution with ether and filtration, the solution was washed with 5% aqueous sodium bicarbonate and water, and dried. Slow distillation of the residue from evaporation of the ether gave starting material (0.23 g), b.p. 78–80° at 2.5 mm, followed by the lactone (III) (1.36 g), b.p. 130–134° at 2.5 mm, n_D^{20} 1.4892, $\nu_{max}^{CCl_4}$ 1 737 and 1 210 cm^{-1}.

Anal. Calcd. for $C_{10}H_{16}O_2$: C, 71.39; H, 9.59. Found: C, 71.11; H, 9.46.

ACKNOWLEDGMENT

Grateful acknowledgment is made to the National Research Council for financial support.

REFERENCES

1. H. O. House and M. Schellenbaum. J. Org. Chem. **28**, 34 (1963).
2. J. I. Musher. J. Am. Chem. Soc. **83**, 1146 (1961).
3. J. T. Edward and J.-M. Ferland. Can. J. Chem. **44**, 1311 (1966).
4. E. L. Eliel. Stereochemistry of carbon compounds. McGraw-Hill Book Co., Inc., New York. 1962. p. 357.
5. A. Butenandt and H. Woltz. Ber. **71**, 1483 (1938).
6. J. F. Eastham, G. B. Miles, and C. A. Krauth. J. Am. Chem. Soc. **81**, 3114 (1959).
7. J. M. Shoolery and M. T. Rogers. J. Am. Chem. Soc. **80**, 5121 (1958).
8. W. Klyne. Experientia, **12**, 119 (1956).
9. P. Geneste and G. Lamaty. Bull. Soc. Chim. France, 2439 (1964). C. Djerassi, J. Burakevitch, J. W. Chamberlin, D. Elad, T. Toda, and G. Stork. J. Am. Chem. Soc. **86**, 465 (1964).
10. C. Djerassi, L. B. High, T. T. Grossnickle, R. Ehrlich, J. A. Moore, and R. B. Scott. Chem. Ind. London, 474 (1955).
11. H. J. Ringold, E. Batres, D. Mancera, and G. Rosenkranz. J. Org. Chem. **21**, 1432 (1956).
12. J. I. Shaw and R. Stevenson. J. Chem. Soc. 3549 (1955).
13. K. Heusler, J. Kalvoda, P. Wieland, G. Anner, and D. A. Wettstein. Helv. Chim. Acta, **45**, 2575 (1962).
14. R. Hirschmann, G. A. Bailey, R. Walker, and J. M. Chemerda. J. Am. Chem. Soc. **81**, 2822 (1959). J. F. Biellmann and M. Ragic. Bull. Soc. Chim. France, 441 (1962). P. K. Grant and N. R. Hill. Australian J. Chem. **17**, 66 (1964).
15. H. R. Nace and M. Inaba. J. Org. Chem. **27**, 4024 (1962).
16. A. S. Dreiding. J. Org. Chem. **20**, 905 (1955). W. Klyne. Experientia, **12**, 119 (1956).
17. C. K. Ingold. Structure and mechanism in organic chemistry. Bell & Sons, Ltd., London. 1953. p. 345.
18. H. O. House and G. H. Rasmusson. J. Org. Chem. **28**, 31 (1963).
19. R. B. Turner. J. Am. Chem. Soc. **74**, 2118 (1952). J. F. Biellmann, D. Francetić, and G. Ourisson. Tetrahedron Letters, **18**, 4 (1960).
20. R. B. Turner. J. Am. Chem. Soc. **72**, 879 (1950). K. Mislow and J. Brenner. J. Am. Chem. Soc. **75**, 2319 (1953).
21. W. E. Doering and L. Speers. J. Am. Chem. Soc. **72**, 5515 (1950). S. L. Friess and N. Farnham. J. Am. Chem. Soc. **72**, 5518 (1950). M. F. Murray, B. A. Johnson, R. R. Pederson, and A. C. Ott. J. Am. Chem. Soc. **78**, 981 (1956). J. Meinwald and E. Frauenglass. J. Am. Chem. Soc. **82**, 5235 (1960). R. R. Sauers and G. P. Ahearn. J. Am. Chem. Soc. **83**, 2759 (1961). R. R. Sauers and J. A. Beisler. J. Org. Chem. **29**, 210 (1964).
22. G. R. Pettit, B. Green, T. R. Kasturi, and U. R. Ghatak. Tetrahedron, **18**, 953 (1962).

Can. J. Chem. Downloaded from www.nrcresearchpress.com by 210.87.254.40 on 09/05/12
For personal use only.

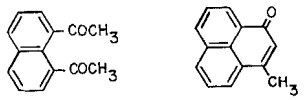
Can. J. Chem. Downloaded from www.nrcresearchpress.com by 210.87.254.40 on 09/05/12
For personal use only.

NOTES

1,8-DIACETYLNAPHTHALENE AND 3-METHYLPHENALENONE

D. F. TAVARES AND J. P. BORGER

This note describes a preparation of 1,8-diacetylnaphthalene (I), which was required in another problem, and the subsequent formation of 3-methylphenalenone (II). The usual



I II

method for the preparation of I involves cleavage of 1,2-dimethylacenaphthene-1,2-diol by lead tetraacetate (1). A modified chromic acid oxidation was found to be successful and more convenient.[1]

If 1,2-dimethylacenaphthene-1,2-diol was first dissolved in warm acetic acid and then cooled to room temperature, and 1 equivalent of chromic anhydride in water added, followed immediately by addition of water, 1,8-diacetylnaphthalene (I) was obtained in yields of 85–90%, which compare favorably with those obtained with lead tetraacetate (70–75%, in our hands).

If, on the other hand, 1.5 moles of chromic anhydride was used per mole of diol at 75° and water added after 10 min, the product was 3-methylphenalenone (II) in yields of 84–90%. At room temperature the use of this same excess of chromic anhydride yielded, after 10 min, 52% of I and 28% of II. Treatment of I in hot acetic acid with an excess of chromic acid to produce II in a quantitative yield established that I was a precursor of II.[2] Though a very facile cyclization of I, with piperidine, to form II is known (1), the acid-catalyzed cyclization has not been reported.

EXPERIMENTAL

All melting points are uncorrected; infrared spectra were determined in dilute chloroform solution with a Perkin–Elmer model 421 spectrophotometer; nuclear magnetic resonance spectra were measured at 100 Mc/s in deuteriochloroform, with tetramethylsilane as internal standard ($\tau = 10$); microanalyses were performed by Dr. C. Daessle, Montreal.

1,2-Dimethylacenaphthene-1,2-diol

The procedure is that of Maxim (3), with modification. Powdered acenaphthenequinone (15 g) was added in small portions to methylmagnesium iodide (50 g methyl iodide and 8.5 g magnesium) in anhydrous ether (100 ml), and the mixture was heated under reflux for 7 h. After hydrolysis with either 10% sulfuric acid or aqueous ammonium chloride solution, the combined, dried ($MgSO_4$) ether extracts were evaporated under reduced pressure. The residue of mixed *cis*- and *trans*-diols was crystallized from acetone and then chloroform to yield 4.0 g (23%) of *cis*-diol, m.p. 193–194° (lit. m.p. 187–189° (3)), as thick colorless plates from acetone, and 10.4 g (59%) of *trans*-diol, m.p. 186–187° (lit. m.p. 182–183° (3)), as fine white needles from chloroform.

[1]*For the preparation of large quantities of I, the lead tetraacetate method (1) requires large quantities of solvent (benzene).*

[2]*The formation of II is readily explained as an intramolecular acid-catalyzed aldol condensation. In the excellent review by Reid (2), 1,8-diacylnaphthalenes were not considered as precursors for phenalenones. In the particular case of II, the synthesis outlined here would appear to be the one of choice.*

1,8-Diacetylnaphthalene (I)

A mixture of *cis*- and *trans*-diols (6.4 g) was dissolved in acetic acid (175 ml) with heating, and then cooled to room temperature. Chromic anhydride (3.1 g) in water (30 ml) was added dropwise, as rapidly as possible and with good mixing, followed immediately by rapid dropwise addition of cold water, with good mixing, to precipitate I. Crystallization from acetone gave 8.1 g (89%) of colorless plates, m.p. 174–175° (lit. m.p. 171–172° (1)). The infrared spectrum showed carbonyl absorption at 1 683 cm^{-1}.

3-Methylphenalenone (II)

To a hot solution (75°) of diol (6.8 g) as described above was added an excess of chromic anhydride (4.7 g) in water (50 ml). The solution was kept at 75° for 10 min, and then cold water was added slowly, with stirring, to give II as pale-yellow crystals. After crystallization from an acetone–water mixture and then from ethanol the melting point was 151–152° (lit. m.p. 152° (1)); yield 5.4 g (90%). The infrared spectrum showed carbonyl absorption at 1 640 cm^{-1}. The nuclear magnetic resonance spectrum showed three methyl protons at 7.46 τ, one olefinic proton at 3.40 τ, and six aromatic protons (multiplet, 1.4–2.5 τ).

Anal. Calcd. for $C_{14}H_{10}O$: C, 86.56; H, 5.24. Found: C, 86.56, 87.00; H, 4.91, 5.22.

ACKNOWLEDGMENTS

We thank Mr. Glen Bigam for the 100 Mc/s nuclear magnetic resonance spectra, and the National Research Council of Canada for financial support.

1. R. Criegee, L. Kraft, and B. Rank. Ann. **507**, 159 (1933).
2. D. H. Reid. Quart. Rev. London, **19**, 274 (1965).
3. N. Maxim. Bull. Soc. Chim. France, **45**, 1137 (1929).

Received February 1, 1966.
Department of Chemistry,
University of Alberta,
Calgary, Alberta.

CONCERNING *cis*- AND *trans*-3-THIOCYANOPROPENAL AND THE SYNTHESIS OF ISOTHIAZOLE

R. Raap

The isothiazole ring system has received much attention lately and several methods leading to its synthesis have been developed (1). Recently, Wille *et al.* (2) reported the preparation of isothiazole by the reaction of either 3-thiocyanopropenal or sodium propenal-3-thiosulfate with liquid ammonia. This method is the most practical laboratory synthesis of this interesting compound, but full experimental details have not yet been reported. As stated by Slack and Wooldridge (3) (citing a personal communication from Wille), success is dependent on the reaction of the *cis* adducts with ammonia. The purpose of this publication is to supply practical details for obtaining optimal yields of isothiazole from both the thiocyanate and the thiosulfate.

When a solution of propynal in acetone was added to an aqueous solution of thiocyanic acid at 0°, an almost quantitative yield of 3-thiocyanopropenal, m.p. 93–94°, was obtained. The structural assignment was fully supported by the infrared spectrum and by the elemental analysis. However, when this compound was allowed to react with liquid ammonia, only a tar resulted, from which not a trace of isothiazole could be isolated. On examination of the compound's nuclear magnetic resonance spectrum (Table I), a coupling constant of 15 c.p.s. between the olefinic protons was revealed, indicating a *trans* relationship (4, 5). Attempts to isomerize *trans*-3-thiocyanopropenal (III) to the *cis* isomer were

Can. J. Chem. Downloaded from www.nrcresearchpress.com by 210.87.254.40 on 09/05/12
For personal use only.

1,8-Diacetylnaphthalene (I)

A mixture of *cis*- and *trans*-diols (6.4 g) was dissolved in acetic acid (175 ml) with heating, and then cooled to room temperature. Chromic anhydride (3.1 g) in water (30 ml) was added dropwise, as rapidly as possible and with good mixing, followed immediately by rapid dropwise addition of cold water, with good mixing, to precipitate I. Crystallization from acetone gave 8.1 g (89%) of colorless plates, m.p. 174–175° (lit. m.p. 171–172° (1)). The infrared spectrum showed carbonyl absorption at 1 683 cm^{-1}.

3-Methylphenalenone (II)

To a hot solution (75°) of diol (6.8 g) as described above was added an excess of chromic anhydride (4.7 g) in water (50 ml). The solution was kept at 75° for 10 min, and then cold water was added slowly, with stirring, to give II as pale-yellow crystals. After crystallization from an acetone–water mixture and then from ethanol the melting point was 151–152° (lit. m.p. 152° (1)); yield 5.4 g (90%). The infrared spectrum showed carbonyl absorption at 1 640 cm^{-1}. The nuclear magnetic resonance spectrum showed three methyl protons at 7.46 τ, one olefinic proton at 3.40 τ, and six aromatic protons (multiplet, 1.4–2.5 τ).

Anal. Calcd. for $C_{14}H_{10}O$: C, 86.56; H, 5.24. Found: C, 86.56, 87.00; H, 4.91, 5.22.

ACKNOWLEDGMENTS

We thank Mr. Glen Bigam for the 100 Mc/s nuclear magnetic resonance spectra, and the National Research Council of Canada for financial support.

1. R. Criegee, L. Kraft, and B. Rank. Ann. **507**, 159 (1933).
2. D. H. Reid. Quart. Rev. London, **19**, 274 (1965).
3. N. Maxim. Bull. Soc. Chim. France, **45**, 1137 (1929).

Received February 1, 1966.
Department of Chemistry,
University of Alberta,
Calgary, Alberta.

CONCERNING *cis*- AND *trans*-3-THIOCYANOPROPENAL AND THE SYNTHESIS OF ISOTHIAZOLE

R. Raap

The isothiazole ring system has received much attention lately and several methods leading to its synthesis have been developed (1). Recently, Wille *et al.* (2) reported the preparation of isothiazole by the reaction of either 3-thiocyanopropenal or sodium propenal-3-thiosulfate with liquid ammonia. This method is the most practical laboratory synthesis of this interesting compound, but full experimental details have not yet been reported. As stated by Slack and Wooldridge (3) (citing a personal communication from Wille), success is dependent on the reaction of the *cis* adducts with ammonia. The purpose of this publication is to supply practical details for obtaining optimal yields of isothiazole from both the thiocyanate and the thiosulfate.

When a solution of propynal in acetone was added to an aqueous solution of thiocyanic acid at 0°, an almost quantitative yield of 3-thiocyanopropenal, m.p. 93–94°, was obtained. The structural assignment was fully supported by the infrared spectrum and by the elemental analysis. However, when this compound was allowed to react with liquid ammonia, only a tar resulted, from which not a trace of isothiazole could be isolated. On examination of the compound's nuclear magnetic resonance spectrum (Table I), a coupling constant of 15 c.p.s. between the olefinic protons was revealed, indicating a *trans* relationship (4, 5). Attempts to isomerize *trans*-3-thiocyanopropenal (III) to the *cis* isomer were

Can. J. Chem. Downloaded from www.nrcresearchpress.com by 210.87.254.40 on 09/05/12
For personal use only.

TABLE I

Nuclear magnetic resonance spectral parameters for *cis* and *trans*-propenals

	δ, τ			J (c.p.s.)		
	H^1	H^2	H^3	$J_{1,2}$	$J_{2,3}$	$J_{1,3}$
cis-3-Thiocyanopropenal*	0.18§	2.62‖	3.16§	2	9	0
trans-3-Thiocyanopropenal*	0.35§	3.31‖	2.63§	6.5	15	0
trans-3-*p*-Nitrothiophenoxypropenal*†	0.42§	3.74‖	2.20§	7.5	15.5	0
Sodium *cis*-propenal-3-thiosulfate‡	0.37‖	3.43‖	2.10‖	3	9.5	1

*In $CDCl_3$ solution.
†The phenyl group protons appear as two doublets of an AB quartet at 1.65 and 2.27 (J = 9 c.p.s.).
‡In D_2O solution.
§Doublet.
‖Quartet.

unsuccessful. Therefore, a search was made for conditions which would favor the formation and preservation of the *cis* isomer during the addition of the thiocyanic acid to the propynal. An optimum yield of *cis*-3-thiocyanopropenal was obtained when an aqueous solution of thiocyanic acid was *slowly* added to a solution of propynal in acetone at −10 to −15°. A mixture of the isomeric 3-thiocyanopropenals precipitated readily as the compounds formed (78% yield), and consisted predominantly (85–90%) of the *cis* isomer. When higher temperatures were employed the isomer ratio changed drastically in favor of the *trans* isomer.

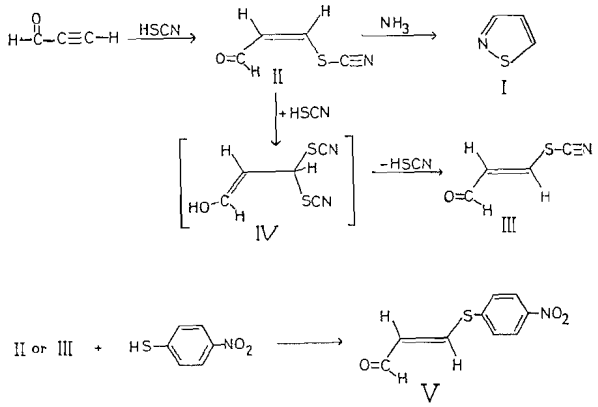
cis-3-Thiocyanopropenal, m.p. 62–64°, could be purified by recrystallization. The assigned structure was fully supported by the infrared and nuclear magnetic resonance (Table I) spectra, the elemental analysis, and the compound's chemical behavior. The coupling constant, $J_{2,3}$ = 9 c.p.s., for the olefinic protons requires the *cis* relationship (4, 5). The compound was completely isomerized to the *trans* isomer ($J_{2,3}$ = 15 c.p.s.) when it was heated for 1 h at 100°.

In contrast to the *trans* isomer, *cis*-3-thiocyanopropenal reacted with liquid ammonia to give isothiazole (22% yield).

The results indicated that, similar to the addition of thiocyanic acid to propiolamides (5), the addition of thiocyanic acid to propynal proceeded in the usual *trans* manner and actually gave rise to *cis*-3-thiocyanopropenal, which, however, readily isomerized to the *trans* isomer under the reaction conditions. Thiocyanic acid was found to be responsible for this rapid isomerization. Acid alone did not cause the rapid isomerization, since II was recovered in high yield when left for 1 h in contact with either dilute sulfuric acid in aqueous acetone or with trifluoroacetic acid in ether solution, at room temperature. Also, when ammonium thiocyanate was added to a solution of II in aqueous acetone, no isomerization could be detected after 15 min at room temperature. However, when a few drops of dilute sulfuric acid was added to the latter solution, the isomerization to III was complete within a few minutes. The isomerization probably proceeds by way of the intermediate IV, which decomposes to the thermodynamically more stable *trans* isomer III. Evidence in support of this contention was provided by the observation that both *cis*- and *trans*-3-thiocyanopropenal react readily at room temperature with *p*-nitrothiophenol in ethyl acetate to give *trans*-3-*p*-nitrothiophenoxypropenal (V). Surely, the diadducts rather than the propynal were intermediate in these transformations.

Isothiazole can most conveniently be prepared from sodium *cis*-propenal-3-thiosulfate. The latter compound was obtained in 65% yield by the addition of an aqueous solution of sodium thiosulfate to a solution of propynal in aqueous acetone containing an equivalent

Can. J. Chem. Downloaded from www.nrcresearchpress.com by 210.87.254.40 on 09/05/12
For personal use only.



amount of acetic acid. The nuclear magnetic resonance spectrum (Table I) revealed a coupling constant ($J_{2,3}$) of 9.5 c.p.s. for the olefinic protons. The thiosulfate adduct reacted with liquid ammonia to give a 61% yield of isothiazole.

EXPERIMENTAL

All temperatures are uncorrected. Infrared spectra were obtained on a Perkin–Elmer model 421 spectrophotometer. Nuclear magnetic resonance spectra were measured with a Varian Associates model A-60 spectrometer, with tetramethylsilane as a reference. Microanalyses were performed by Dr. G. Weiler and Dr. F. B. Strauss, Microanalytical Laboratory, Oxford, England.

trans-3-Thiocyanopropenal (III)

An aqueous solution of thiocyanic acid was prepared by the addition of 160 ml of 3 *N* aqueous sulfuric acid to a solution (cooled in ice) of potassium thiocyanate (44.4 g, 0.457 mole) in 200 ml of water. The stirred solution was cooled in ice, and propynal (24.7 g, 0.457 mole) in 75 ml of acetone was added dropwise in 20 min. After the addition was complete, the stirring and cooling were continued for 40 min. The product, 50.0 g (97%) of white needles, m.p. 88–92°, was gathered by filtration, washed with ice water, and air-dried. The compound was recrystallized from benzene, m.p. 93–94°.

Anal. Calcd. for C_4H_3NOS: C, 42.46; H, 2.67; S, 28.34. Found: C, 42.44; H, 2.70; S, 28.45.

The infrared spectrum (in $CHCl_3$) showed strong bands at 2 180, 1 694, 1 572, 1 110, and 942 cm^{-1}. The nuclear magnetic resonance spectral parameters are reported in Table I.

cis-3-Thiocyanopropenal (II)

An aqueous solution of thiocyanic acid was prepared by the addition of 170 ml of 3 *N* hydrochloric acid to an ice-cold solution of potassium thiocyanate (48.5 g, 0.50 mole) in 220 ml of water. The solution was cooled in ice and then added dropwise to an efficiently stirred solution (maintained at −10 to −15°) of propynal (30.0 g, 0.55 mole) in 90 ml of acetone. The product precipitated during the addition, which was completed in approximately 1 h. The mixture was kept at −10 to −15° for an additional 30 min before the product was gathered by filtration and washed with ice water. The dried white solid, 43.9 g (78%), m.p. 50–56°, according to the nuclear magnetic resonance spectrum, consisted of 85–90% of *cis*-3-thiocyanopropenal (II) and 10–15% of the *trans* isomer (III). The pure *cis* isomer, m.p. 62–64°, was obtained after two recrystallizations from a 1:3 acetone–water mixture.

Anal. Calcd. for C_4H_3NOS: C, 42.46; H, 2.67; S, 28.34. Found: C, 42.51; H, 2.88; S, 28.60.

The infrared spectrum (in $CHCl_3$) had strong bands at 2 180, 1 670, 1 540, 1 110, 970, and 870 cm^{-1}, and the nuclear magnetic resonance spectral parameters are given in Table I. Whereas II is soluble in either ether or benzene in the cold, the *trans* isomer (III) is almost completely insoluble.

Conversion of cis-3-Thiocyanopropenal into the trans Isomer under the Influence of Thiocyanic Acid

Aqueous sulfuric acid (3 *N*, 1 ml) was added to a solution of potassium thiocyanate (0.50 g, 5 mmoles) in 25 ml of water. This mixture was then added to a solution of *cis*-3-thiocyanopropenal (1.13 g, 10 mmoles) in 10 ml of acetone. The reaction mixture was left at room temperature for 15 min, whereafter it was diluted with 20 ml of water and cooled. The precipitate was filtered off and air-dried to give 0.62 g of white solid, m.p. 87–91°. The melting point was not depressed by *trans*-3-thiocyanopropenal, and the infrared spectra were superimposable.

Can. J. Chem. Downloaded from www.nrcresearchpress.com by 210.87.254.40 on 09/05/12
For personal use only.

trans-3-p-Nitrothiophenoxypropenal (V)

A mixture of 3-thiocyanopropenal (0.50 g, 4.4 mmoles) (either the *cis* or *trans* isomer) and *p*-nitrothiophenol (0.80 g, 5.1 mmoles) in 25 ml of ethyl acetate was left at room temperature for 1 h. The solution was next washed with a 5% aqueous sodium carbonate solution and dried. Removal of the solvent yielded 0.80 g (87%) of a yellow-colored solid, m.p. 109–115°. An analytical sample of fine yellow needles melting at 118–119° was obtained after two recrystallizations from ethyl acetate.

Anal. Calcd. for $C_9H_7NO_3S$: C, 51.67; H, 3.37; S, 15.33. Found: C, 51.80; H, 3.64; S, 15.39.

The nuclear magnetic resonance spectral parameters which require the *trans* configuration are reported in Table I. The infrared spectrum (in $CHCl_3$) had strong bands at 1 672, 1 562, 1 520, 1 345, 1 120, 945, and 853 cm^{-1}.

Sodium cis-Propenal-3-thiosulfate

A solution of sodium thiosulfate pentahydrate (505 g, 2.0 moles) in 600 ml of water was added dropwise in 1 h to a stirred mixture of propynal (97 g, 1.8 moles), acetic acid (111 g, 1.8 moles), water (370 ml), and acetone (185 ml). During the addition the temperature of the reaction mixture was kept at −5 to 0°. A white solid precipitated readily. After the addition was completed, the mixture was kept for an additional 30 min at 0°; then 400 ml of cold acetone was added and the white solid was filtered off and dried. The product amounted to 228 g (65%). The nuclear magnetic resonance spectral parameters are given in Table I.

Isothiazole (I)

(*a*) 3-Thiocyanopropenal (100 g, 0.89 mole; consisting of approximately 85% *cis* and 15% *trans* isomer) was added in portions, with stirring, to 500 ml of liquid ammonia at approximately −60°. The reaction mixture was left at this temperature for a few hours and was then allowed to come to room temperature. The dark-colored residue was steam-distilled until approximately 350 ml of distillate had been collected. The isothiazole layer was separated and the aqueous solution extracted with five 40 ml portions of ether. The combined organic layers were dried and fractionally distilled to give 14.0 g (22%, based on *cis*-3-thiocyanopropenal) of isothiazole, b.p. 111–112° at 700 mm (lit. (6) b.p. 113° at 770 mm).

(*b*) Sodium *cis*-propenal-3-thiosulfate (486 g, 2.56 moles) was added to liquid ammonia (approximately 1 l). The resulting mixture was stirred for a few hours at −60°, and then the ammonia was allowed to evaporate. Enough water was added to the residue to dissolve all the white solid material. The mixture was then extracted with four 150 ml portions of ether. The combined ether extracts were dried and fractionally distilled to give 133 g (61%) of isothiazole, b.p. 111–112° at 700 mm.

ACKNOWLEDGMENTS

The author thanks Professor R. U. Lemieux for guidance and advice in the conduct of this research, and Mr. P. K. Wolfert for technical assistance.

1. R. Slack and K. R. H. Wooldridge. *In* Advances in heterocyclic chemistry. Vol. 4. *Edited by* A. R. Katritzky. Academic Press, Inc., New York. 1965. p. 107.
2. F. Wille, L. Capeller, and A. Steiner. Angew. Chem. Intern. Ed. Engl. **1**, 335 (1962); Angew. Chem. **74**, 467 (1962).
3. R. Slack and K. R. H. Wooldridge. *In* Advances in heterocyclic chemistry. Vol. 4. *Edited by* A. R. Katritzky. Academic Press, Inc., New York. 1965. p. 110.
4. L. M. Jackman. Applications of nuclear magnetic resonance spectroscopy in organic chemistry. Pergamon Press, New York. 1959. pp. 83–89.
5. W. D. Crow and N. J. Leonard. J. Org. Chem. **30**, 2660 (1965).
6. A. Adams and R. Slack. J. Chem. Soc. 3061 (1959).

Received February 2, 1966.
R & L Molecular Research Ltd.,
Edmonton, Alberta.

SOME NEW ROUTES FOR THE SYNTHESIS OF AROMATIC FLUORINE COMPOUNDS

H. L. Sharma, V. N. Sharma, and R. L. Mital

One of the important methods for the synthesis of aromatic fluorine compounds involves the exchange of fluorine for some other halogen atom (1–3), for some other univalent functional group like the hydroxyl, or for oxygen in the carbonyl and carboxyl groups (4).

Can. J. Chem. Downloaded from www.nrcresearchpress.com by 210.87.254.40 on 09/05/12
For personal use only.

trans-3-p-Nitrothiophenoxypropenal (V)

A mixture of 3-thiocyanopropenal (0.50 g, 4.4 mmoles) (either the *cis* or *trans* isomer) and *p*-nitrothiophenol (0.80 g, 5.1 mmoles) in 25 ml of ethyl acetate was left at room temperature for 1 h. The solution was next washed with a 5% aqueous sodium carbonate solution and dried. Removal of the solvent yielded 0.80 g (87%) of a yellow-colored solid, m.p. 109–115°. An analytical sample of fine yellow needles melting at 118–119° was obtained after two recrystallizations from ethyl acetate.

Anal. Calcd. for $C_9H_7NO_3S$: C, 51.67; H, 3.37; S, 15.33. Found: C, 51.80; H, 3.64; S, 15.39.

The nuclear magnetic resonance spectral parameters which require the *trans* configuration are reported in Table I. The infrared spectrum (in $CHCl_3$) had strong bands at 1 672, 1 562, 1 520, 1 345, 1 120, 945, and 853 cm^{-1}.

Sodium cis-Propenal-3-thiosulfate

A solution of sodium thiosulfate pentahydrate (505 g, 2.0 moles) in 600 ml of water was added dropwise in 1 h to a stirred mixture of propynal (97 g, 1.8 moles), acetic acid (111 g, 1.8 moles), water (370 ml), and acetone (185 ml). During the addition the temperature of the reaction mixture was kept at −5 to 0°. A white solid precipitated readily. After the addition was completed, the mixture was kept for an additional 30 min at 0°; then 400 ml of cold acetone was added and the white solid was filtered off and dried. The product amounted to 228 g (65%). The nuclear magnetic resonance spectral parameters are given in Table I.

Isothiazole (I)

(*a*) 3-Thiocyanopropenal (100 g, 0.89 mole; consisting of approximately 85% *cis* and 15% *trans* isomer) was added in portions, with stirring, to 500 ml of liquid ammonia at approximately −60°. The reaction mixture was left at this temperature for a few hours and was then allowed to come to room temperature. The dark-colored residue was steam-distilled until approximately 350 ml of distillate had been collected. The isothiazole layer was separated and the aqueous solution extracted with five 40 ml portions of ether. The combined organic layers were dried and fractionally distilled to give 14.0 g (22%, based on *cis*-3-thiocyanopropenal) of isothiazole, b.p. 111–112° at 700 mm (lit. (6) b.p. 113° at 770 mm).

(*b*) Sodium *cis*-propenal-3-thiosulfate (486 g, 2.56 moles) was added to liquid ammonia (approximately 1 l). The resulting mixture was stirred for a few hours at −60°, and then the ammonia was allowed to evaporate. Enough water was added to the residue to dissolve all the white solid material. The mixture was then extracted with four 150 ml portions of ether. The combined ether extracts were dried and fractionally distilled to give 133 g (61%) of isothiazole, b.p. 111–112° at 700 mm.

ACKNOWLEDGMENTS

The author thanks Professor R. U. Lemieux for guidance and advice in the conduct of this research, and Mr. P. K. Wolfert for technical assistance.

1. R. Slack and K. R. H. Wooldridge. *In* Advances in heterocyclic chemistry. Vol. 4. *Edited by* A. R. Katritzky. Academic Press, Inc., New York. 1965. p. 107.
2. F. Wille, L. Capeller, and A. Steiner. Angew. Chem. Intern. Ed. Engl. **1**, 335 (1962); Angew. Chem. **74**, 467 (1962).
3. R. Slack and K. R. H. Wooldridge. *In* Advances in heterocyclic chemistry. Vol. 4. *Edited by* A. R. Katritzky. Academic Press, Inc., New York. 1965. p. 110.
4. L. M. Jackman. Applications of nuclear magnetic resonance spectroscopy in organic chemistry. Pergamon Press, New York. 1959. pp. 83–89.
5. W. D. Crow and N. J. Leonard. J. Org. Chem. **30**, 2660 (1965).
6. A. Adams and R. Slack. J. Chem. Soc. 3061 (1959).

Received February 2, 1966.
R & L Molecular Research Ltd.,
Edmonton, Alberta.

SOME NEW ROUTES FOR THE SYNTHESIS OF AROMATIC FLUORINE COMPOUNDS

H. L. Sharma, V. N. Sharma, and R. L. Mital

One of the important methods for the synthesis of aromatic fluorine compounds involves the exchange of fluorine for some other halogen atom (1–3), for some other univalent functional group like the hydroxyl, or for oxygen in the carbonyl and carboxyl groups (4).

Can. J. Chem. Downloaded from www.nrcresearchpress.com by 210.87.254.42 on 09/05/12
For personal use only.

A survey of the literature reveals that only a few references (5–7) deal with the methods for the synthesis of fluoronitrobenzenes via exchange of fluorine for some other halogen atom, and that practically no work has been done on their synthesis via exchange of fluorine for the *p*-toluenesulfonic ester group, though the latter method has been worked out for the synthesis of alkyl fluorides (8, 9).

The present note describes some new routes for the synthesis of fluoronitrobenzenes via exchange of fluorine for another halogen atom or for a *p*-toluenesulfonic ester group.

Several workers have shown that picryl and 2,4-dinitrophenyl carbonium ions are stabilized by heterocyclic bases (10, 11). Thus, when polynitrohalogenobenzenes are treated with pyridine or α-, β-, or γ-picoline, polynitrophenylpyridinium or polynitrophenyl-α-, -β-, or -γ-picolinium halides are obtained. It has been observed by us that these yield fluoronitrobenzenes when treated with anhydrous potassium fluoride in dry dimethylformamide or nitrobenzene.

Polynitrophenylpyridinium or polynitrophenyl-α-, -β-, or -γ-picolinium *p*-toluenesulfonates were obtained by treating polynitrophenyl *p*-toluenesulfonates with pyridine or α-, β-, or γ-picoline, and it has been found that these, under the conditions mentioned above, yield fluoronitrobenzenes. Even polynitrophenyl *p*-toluenesulfonates were successfully converted into fluoronitrobenzenes under these conditions. Thus this method provides a new route for the synthesis of fluoronitrobenzenes from polynitrophenols.

The exchange of fluorine in all these compounds has been found to be much easier in dimethylformamide than in nitrobenzene. This could be explained on the basis of the findings of Miller and Parker (12), who observed that there is a lower degree of solvation of F^- ions in dipolar aprotic solvents.

EXPERIMENTAL

Nitrophenyl p-Toluenesulfonates

4,6-Dinitro-3-methylphenyl, 2,6-dinitrophenyl, and 2,4-dinitrophenyl *p*-toluenesulfonates were prepared by the methods reported earlier (13–15).

Nitrophenylpyridinium and Nitrophenyl-α-, -β-, or -γ-picolinium Halides or p-Toluenesulfonates

A mixture of halogenonitrobenzene (0.01 mole) or nitrophenyl *p*-toluenesulfonate (0.01 mole) and one of the heterocyclic bases such as pyridine or α-, β-, or γ-picoline (0.012 mole) was heated at 90–95° in dry toluene (ca. 15 ml) under reflux for 4 h. The mixture was cooled, and the resulting solid was filtered off, washed successively with benzene and ether, and dried. The compounds are listed in Table I.

Only 2,6-dinitrochlorobenzene did not react with α-picoline, probably because the nitro groups hindered the approach of the attacking reagent.

Preparation of Fluoronitrobenzenes

(i) From Nitrophenylpyridinium or Nitrophenyl-α-, -β-, or -γ-picolinium Halides or p-Toluenesulfonates

(a) Reaction in dimethylformamide.—A mixture of nitrophenylpyridinium or nitrophenyl-α-, -β-, or -γ-picolinium halide or *p*-toluenesulfonate (0.01 mole) (as the case may be) and anhydrous potassium fluoride (0.012 mole) in dry dimethylformamide (ca. 20 ml) was heated at 110–115° for 1½ h. Dimethylformamide was removed under reduced pressure, and the residue was refluxed with 25 ml of ethanolic hydrochloric acid (1:1 v/v) for ½ h. The solution was then diluted with water (ca. 100 ml) and extracted with benzene. Removal of benzene by distillation yielded the fluoronitrobenzene.

(b) Reaction in nitrobenzene.—The same procedure was followed as described above, except that the reaction mixture was refluxed at 210° for 3 h.

(ii) From Nitrophenyl p-Toluenesulfonates

(a) Reaction in dimethylformamide.—A mixture of anhydrous potassium fluoride (0.015 mole) and nitrophenyl *p*-toluenesulfonate (0.01 mole) in dry dimethylformamide (ca. 25 ml) was heated at 150° for 2½ h. After dilution with water, the isolated product was extracted with benzene. Removal of benzene by distillation yielded the fluoronitrobenzene.

(b) Reaction in nitrobenzene.—A mixture of anhydrous potassium fluoride (0.015 mole) and the nitrophenyl *p*-toluenesulfonate (0.01 mole) in nitrobenzene (ca. 20 ml) was refluxed for 3½ h. The mixture was cooled and filtered, and the residue was washed well with hot toluene. The combined filtrate and washings were dried and vacuum-distilled to yield the fluoronitrobenzenes.

These compounds are listed in Table II.

Can. J. Chem. Downloaded from www.nrcresearchpress.com by 210.87.254.42 on 09/05/12
For personal use only.

Can. J. Chem. Downloaded from www.nrcresearchpress.com by 210.87.254.42 on 09/05/12
For personal use only.

TABLE I

Characteristics of nitrophenylpyridinium and nitrophenyl-α-, -β-, and -γ-picolinium halides and *p*-toluenesulfonates

Halogenonitrobenzene or nitrophenyl *p*-toluenesulfonate used	Heterocyclic base used	Product formed	% yield	Molecular formula	Melting point (°C)	% Cl	
						Found	Calcd.
1-Chloro-2,4-D	Pyridine	2,4-Dp (I)	95	$C_{11}H_8ClN_3O_4$	184*	12.59	12.61
	α-Picoline	2,4-Dα (II)	90	$C_{12}H_{10}ClN_3O_4$	183*	12.04	12.01
	β-Picoline	2,4-Dβ (III)	92	$C_{12}H_{10}ClN_3O_4$	195*	12.04	12.01
	γ-Picoline	2,4-Dγ (IV)	92	$C_{12}H_{10}ClN_3O_4$	163*	12.02	12.01
1-Chloro-2,6-D	Pyridine	2,6-Dp (V)	90	$C_{12}H_8ClN_3O_4$	183	12.58	12.61
	α-Picoline	—	—	—	—	—	—
	β-Picoline	2,6-Dβ (VI)	86	$C_{12}H_{10}ClN_3O_4$	176	12.03	12.01
	γ-Picoline	2,6-Dγ (VII)	86	$C_{12}H_{10}ClN_3O_4$	172	12.03	12.01
1-Chloro-2,4,6-T	Pyridine	2,4,6-Tp (VIII)	95	$C_{11}H_7ClN_4O_6$	121*	10.86	10.87
	α-Picoline	2,4,6-Tα (IX)	86	$C_{12}H_9ClN_4O_6$	118*	10.41	10.42
	β-Picoline	2,4,6-Tβ (X)	92	$C_{12}H_9ClN_4O_6$	118*	10.43	10.42
	γ-Picoline	2,4,6-Tγ (XI)	92	$C_{12}H_9ClN_4O_6$	115*	10.41	10.42
1-Chloro-3-methyl-2,4,6-T	Pyridine	3-Methyl-2,4,6-Tp (XII)	89	$C_{12}H_9ClN_4O_6$	177	10.41	10.42
	α-Picoline	3-Methyl-2,4,6-Tα (XIII)	80	$C_{13}H_{11}ClN_4O_6$	172	10.02	10.01
	β-Picoline	3-Methyl-2,4,6-Tβ (XIV)	86	$C_{13}H_{11}ClN_4O_6$	174	10.02	10.01
	γ-Picoline	3-Methyl-2,4,6-Tγ (XV)	90	$C_{13}H_{11}ClN_4O_6$	162	10.03	10.01
1-*p*-Toluenesulfonyl-2,4-D	Pyridine	2,4-DpT (XVI)	90	$C_{18}H_{15}N_3O_7S$	249	7.65†	7.67†
	α-Picoline	2,4-DαT (XVII)	90	$C_{19}H_{17}N_3O_7S$	208	7.39†	7.42†
	β-Picoline	2,4-DβT (XVIII)	92	$C_{19}H_{17}N_3O_7S$	243	7.39†	7.42†
	γ-Picoline	2,4-DγT (XIX)	92	$C_{19}H_{17}N_3O_7S$	223	7.41†	7.42†

*Literature (10) m.p. 186, 184, 197, 163, 121, 117, 119, and 114 °C, respectively.

†Percentage of sulfur.

NOTE: D = dinitrobenzene; T = trinitrobenzene; Dp, Dα, Dβ, and Dγ = dinitrophenylpyridinium and dinitrophenyl-α-, -β-, and -γ-picolinium chlorides, respectively; Tp, Tα, Tβ, and Tγ = trinitrophenylpyridinium and trinitrophenyl-α-, -β-, and -γ-picolinium chlorides, respectively; DpT, DαT, DβT, and DγT = dinitrophenylpyridinium and dinitrophenyl-α-, -β-, and -γ-picolinium *p*-toluenesulfonates, respectively.

Can. J. Chem. Downloaded from www.nrcresearchpress.com by 210.87.254.42 on 09/05/12
For personal use only.

TABLE II

Characteristics of fluoronitrobenzenes

Reactant used	Fluoronitrobenzene formed	Melting or boiling point (°C)	% yield*	Molecular formula	% N	
					Found	Calcd.
I, II, III, IV, XVI, XVII, XVIII, XIX, or 2,4-dinitrophenyl *p*-toluenesulfonate	1-Fluoro-2,4-D	135†	80	$C_6H_3FN_2O_4$	15.02	15.05
V, VI, VII, or 2,6-dinitrophenyl *p*-toluenesulfonate	1-Fluoro-2,6-D	61‡	75	$C_6H_3FN_2O_4$	15.01	15.05
VIII, IX, X, or XI	1-Fluoro-2,4,6-T	126§	80	$C_6H_2FN_3O_6$	19.02	19.04
XII, XIII, XIV, or XV	1-Fluoro-3-methyl-2,4,6-T	86‖	81	$C_7H_4FN_3O_6$	17.09	17.14
4,6-Dinitro-3-methylphenyl *p*-toluenesulfonate	1-Fluoro-3-methyl-4,6-D	78¶	70	$C_7H_5FN_2O_4$	13.88	14.00

*The average % yields obtained from various reactants are reported here.
†Literature (6) b.p. 138 °C at 2 mm.
‡Literature (16) m.p. 63 °C.
§Literature (17) m.p. 128 °C.
‖Literature (19) m.p. 88 °C.
¶Literature (18) m.p. 78–79 °C.
NOTE: D = dinitrobenzene, T = trinitrobenzene.

ACKNOWLEDGMENTS

The authors express their sincere thanks to Dr. R. M. Kasliwal, Principal, S.M.S. Medical College, Jaipur, and Prof. R. C. Mehrotra, Head of the Chemistry Department, University of Rajasthan, Jaipur, for providing the necessary facilities.

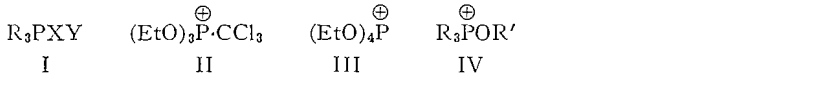
1. H. SCHROEDER. J. Am. Chem. Soc. **82**, 4115 (1960).
2. K. WALLENFELS and W. DRABER. Chem. Ber. **90**, 2819 (1957).
3. J. FERNANDEZ BOLAÑOS, W. G. OVEREND, A. SYKES, J. C. TATLOW, and E. H. WISEMAN. J. Chem. Soc. 4003 (1960).
4. W. R. HASEK, W. C. SMITH, and V. A. ENGLEHARDT. J. Am. Chem. Soc. **82**, 543 (1960).
5. H. G. COOK and B. C. SAUNDERS. Biochem. J. **41**, 558 (1947).
6. G. C. FINGER and C. W. KRUSE. J. Am. Chem. Soc. **78**, 6034 (1956).
7. H. B. GOTTLIEB. J. Am. Chem. Soc. **58**, 532 (1936).
8. W. F. EDGELL and L. PARTS. J. Am. Chem. Soc. **77**, 4899 (1955).
9. E. D. BERGMANN and I. SHAHAK. Chem. Ind. London, 157 (1958).
10. G. GROCHOWSKI and K. OKON. Biul. Wojskowej Akad. Tech. **10** (111–112), 68 (1961).
11. G. GROCHOWSKI and K. OKON. Biul. Wojskowej Akad. Tech. **11** (121–122), 45 (1962).
12. J. MILLER and A. J. PARKER. J. Am. Chem. Soc. **83**, 117 (1961).
13. S. M. SANE and S. S. JOSHI. J. Indian Chem. Soc. **5**, 299 (1928).
14. S. M. SANE and S. S. JOSHI. J. Indian Chem. Soc. **9**, 60 (1932).
15. R. L. DATTA and P. VARMA. J. Am. Chem. Soc. **41**, 2043 (1919).
16. R. E. PARKER and T. O. REED. J. Chem. Soc. 3149 (1962).
17. N. N. VOROZHTSOV and G. G. YAKOBSON. Zh. Obshch. Khim. **31**, 3705 (1961).
18. G. C. FINGER, F. H. REED, and R. T. LEO. Illinois State Geol. Sur. Circ. **199**, 15 (1955).
19. A. OSTASZYNSKI and W. TUSZKO. Roczniki Chem. **35**, 1243 (1961).

RECEIVED JANUARY 19, 1966.
DEPARTMENT OF PHARMACOLOGY,
S.M.S. MEDICAL COLLEGE,
AND
DEPARTMENT OF CHEMISTRY,
UNIVERSITY OF RAJASTHAN,
JAIPUR, INDIA.

SUGAR ESTERS
III. NEW REAGENT FOR DEOXYHALO SUGAR PREPARATION

J. B. LEE AND T. J. NOLAN

The need to prepare deoxyhalo analogues of certain sugar-containing natural products, together with the potential synthetic applications of deoxyhalo sugars, has prompted our examination of a number of possible routes to these compounds (1), including various modifications of Rydon's reagents (2). The latter reagents, of the type I (R = aryloxy or alkoxy, X = alkyl or halide, Y = halide), in principle offer ready means for conversion of



I II III IV

alcohols into halides. In practical use with natural products, we have found the original conditions used by Rydon to be unsatisfactory with respect to either yield, need for vigorous conditions, or necessitating tedious processes. These difficulties have been overcome by modification of the original conditions or reagents (3), but a need still exists for a reagent which would act rapidly in mild, essentially neutral, conditions.

Crofts and Downie (4) describe the reaction of triethyl phosphite with ethanol and carbon tetrachloride to give ethyl chloride, chloroform, and triethyl phosphate. Since

Can. J. Chem. Downloaded from www.nrcresearchpress.com by 210.87.254.42 on 09/05/12
For personal use only.

ACKNOWLEDGMENTS

The authors express their sincere thanks to Dr. R. M. Kasliwal, Principal, S.M.S. Medical College, Jaipur, and Prof. R. C. Mehrotra, Head of the Chemistry Department, University of Rajasthan, Jaipur, for providing the necessary facilities.

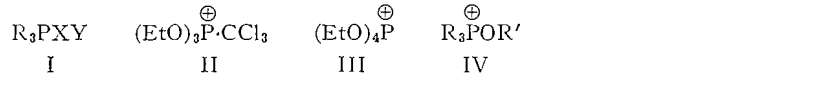
1. H. SCHROEDER. J. Am. Chem. Soc. **82**, 4115 (1960).
2. K. WALLENFELS and W. DRABER. Chem. Ber. **90**, 2819 (1957).
3. J. FERNANDEZ BOLAÑOS, W. G. OVEREND, A. SYKES, J. C. TATLOW, and E. H. WISEMAN. J. Chem. Soc. 4003 (1960).
4. W. R. HASEK, W. C. SMITH, and V. A. ENGLEHARDT. J. Am. Chem. Soc. **82**, 543 (1960).
5. H. G. COOK and B. C. SAUNDERS. Biochem. J. **41**, 558 (1947).
6. G. C. FINGER and C. W. KRUSE. J. Am. Chem. Soc. **78**, 6034 (1956).
7. H. B. GOTTLIEB. J. Am. Chem. Soc. **58**, 532 (1936).
8. W. F. EDGELL and L. PARTS. J. Am. Chem. Soc. **77**, 4899 (1955).
9. E. D. BERGMANN and I. SHAHAK. Chem. Ind. London, 157 (1958).
10. G. GROCHOWSKI and K. OKON. Biul. Wojskowej Akad. Tech. **10** (111–112), 68 (1961).
11. G. GROCHOWSKI and K. OKON. Biul. Wojskowej Akad. Tech. **11** (121–122), 45 (1962).
12. J. MILLER and A. J. PARKER. J. Am. Chem. Soc. **83**, 117 (1961).
13. S. M. SANE and S. S. JOSHI. J. Indian Chem. Soc. **5**, 299 (1928).
14. S. M. SANE and S. S. JOSHI. J. Indian Chem. Soc. **9**, 60 (1932).
15. R. L. DATTA and P. VARMA. J. Am. Chem. Soc. **41**, 2043 (1919).
16. R. E. PARKER and T. O. REED. J. Chem. Soc. 3149 (1962).
17. N. N. VOROZHTSOV and G. G. YAKOBSON. Zh. Obshch. Khim. **31**, 3705 (1961).
18. G. C. FINGER, F. H. REED, and R. T. LEO. Illinois State Geol. Sur. Circ. **199**, 15 (1955).
19. A. OSTASZYNSKI and W. TUSZKO. Roczniki Chem. **35**, 1243 (1961).

RECEIVED JANUARY 19, 1966.
DEPARTMENT OF PHARMACOLOGY,
S.M.S. MEDICAL COLLEGE,
AND
DEPARTMENT OF CHEMISTRY,
UNIVERSITY OF RAJASTHAN,
JAIPUR, INDIA.

SUGAR ESTERS
III. NEW REAGENT FOR DEOXYHALO SUGAR PREPARATION

J. B. LEE AND T. J. NOLAN

The need to prepare deoxyhalo analogues of certain sugar-containing natural products, together with the potential synthetic applications of deoxyhalo sugars, has prompted our examination of a number of possible routes to these compounds (1), including various modifications of Rydon's reagents (2). The latter reagents, of the type I (R = aryloxy or alkoxy, X = alkyl or halide, Y = halide), in principle offer ready means for conversion of



alcohols into halides. In practical use with natural products, we have found the original conditions used by Rydon to be unsatisfactory with respect to either yield, need for vigorous conditions, or necessitating tedious processes. These difficulties have been overcome by modification of the original conditions or reagents (3), but a need still exists for a reagent which would act rapidly in mild, essentially neutral, conditions.

Crofts and Downie (4) describe the reaction of triethyl phosphite with ethanol and carbon tetrachloride to give ethyl chloride, chloroform, and triethyl phosphate. Since

Can. J. Chem. Downloaded from www.nrcresearchpress.com by 210.87.254.5 on 09/05/12
For personal use only.

triethyl phosphite and carbon tetrachloride have been shown (5) to give diethyl trichloromethyl phosphonate, which is not attacked by alcohols under these conditions (4), it is likely that ethanol is reacting with an intermediate of type II to give III (plus chloroform), the latter intermediate (III) breaking down in an Arbusov-type (e.g. see ref. 6) reaction. We considered that, if we could induce an alcohol to react to form an analogous intermediate of type IV (where R'OH was the original alcohol), in which no competition for the halide ion in the final Arbusov reaction is possible (a condition satisfied when the R groups are aryl or alkyl, but not when they are alkoxy groups), then formation of the required halide should proceed readily.

We therefore examined the reaction of triphenylphosphine with alcohols in excess carbon tetrachloride. Model reactions with aliphatic primary and secondary alcohols proceeded in good yield, the reaction proceeding rapidly at the reflux temperature (approximately 80 °C) of the solution.

We then investigated the stability of acetal, ether, and ester groups (commonly used as protecting groups in the carbohydrate field) towards the reagent. For example, when 2,2-dimethyl-4-hydroxymethyl-1,3-dioxolane was heated under reflux with an equimolar amount of triphenylphosphine in excess carbon tetrachloride, the reaction was complete in 1 h, and a high yield (>80%) of the 4-chloromethyl derivative (correct analysis, identical in infrared and proton magnetic resonance spectra with authentic material) was obtained.

Under similar conditions (1 mole triphenylphosphine, excess carbon tetrachloride, reflux) the following ethers and esters were converted in high yield into the halo compound without effect upon the protecting groups: 2-acetoxyethanol, 4-acetoxybutanol, glycolic aldehyde diethylacetal, 2-hydroxyethyl ethyl ether, 2-hydroxyethyl methyl ether, 2-hydroxyethyl butyl ether, and 2-hydroxyethyl stearate.

The absence of rearrangement of the carbon skeleton of alcohols under the reaction conditions was confirmed by the conversion of neopentanol and 3-hydroxymethylheptane into neopentyl chloride and 3-chloromethylheptane, respectively, in good yield, their identity being confirmed by comparison with authentic material, and the absence of rearrangement being confirmed by examination of their proton magnetic resonance spectra.

When Rydon's reagents (e.g. triphenyl phosphite methiodide) are applied to sugars or polyols having two free hydroxyl groups sterically situated next to one another, the formation of phosphonate esters occurs in preference to halide formation (3). We showed that this disadvantage was eliminated by the use of our modified reagent.

Thus ethanediol reacted with triphenylphosphine and carbon tetrachloride to give a good yield of dichloroethane, together with some ethylene chlorohydrin. Similar behavior was observed with the butanediols.

In view of these observations, we proceeded to examine the reaction of 1,2;3,4-di-*O*-isopropylidene-α-D-galactopyranose with triphenylphosphine in excess carbon tetrachloride. From the reaction mixture we obtained, in good yield, 1,2;3,4-di-*O*-isopropylidene-6-deoxy-6-chloro-α-D-galactopyranose together with a little 1,2;3,4-di-*O*-isopropylidene-6-deoxy-5,6-didehydro-β-L-arabinohexopyranose.

We are examining the utility of this reaction in the preparation of other halo sugars and halopolyols.

To separate the sugar derivatives obtained in this and other work, we have applied the new technique of 'dry column' chromatography, which combines the selectivity of the thin-layer technique with the larger scale of normal column chromatography, without the

Can. J. Chem. Downloaded from www.nrcresearchpress.com by 210.87.254.5 on 09/05/12
For personal use only.

disadvantages of cumbersome apparatus and large amounts of support needed for large-scale layer chromatography, or of large volumes of solvent required in normal column chromatography.

EXPERIMENTAL

Proton magnetic resonance spectra were measured with a Perkin–Elmer 40 Mc.p.s. instrument. Infrared spectra were measured on Unicam SP 100 and SP 200 instruments. Thin-layer chromatography used Kieselgel HF_{254} support. The solvents used were: A, 9:1 benzene–methanol; B, benzene; C, 19:1 benzene–methanol. Gas–liquid chromatography with a Perkin–Elmer 452, Shandon FB 4, or Wilkins Autoprep instrument employed Silicone, Carbowax, Apiezon L, or dinonyl phthalate (supported on Celite) liquid phases in 2 m columns. Materials were in most cases purified commercial samples. 1,2;3,4-Di-*O*-isopropylidene-α-D-galactopyranose was prepared by the method of Tipson (7). Melting and boiling points are uncorrected. We are indebted to P. Borda for microanalyses.

Typical Procedures

2,2-Dimethyl-4-chloromethyl-1,3-dioxolane

To a solution of triphenylphosphine (26 g) in carbon tetrachloride (15 ml) was added 2,2-dimethyl-4-hydroxymethyl-1,3-dioxolane (15 ml), and the solution was warmed under reflux on a water bath. After the initial vigorous reaction had moderated, the mixture was heated under reflux for a further 15 min. The mixture was fractionated under reduced pressure, and the fraction boiling at 64–78° at 17 mm was collected and redistilled at atmospheric pressure to give a fraction (13 g, b.p. 156–159°) identical in infrared and proton magnetic resonance spectra with authentic material (8).

2-Chloroethyl Methyl Ether

A mixture of redistilled 2-hydroxyethyl methyl ether (b.p. 122–124°, 7.2 g), dry triphenylphosphine (26 g), and anhydrous carbon tetrachloride (17 g) was warmed gently under reflux. A vigorous reaction ensued, and when this had moderated the mixture was kept at 80 °C for a further 10 min, and was then fractionated to give chloroform (contaminated with small amounts of carbon tetrachloride and chloroether) and 2-chloroethyl methyl ether (b.p. 92–94°, n_D^{18} 1.4108, 7.3 g), identical in retention (Silicone column, 50°) on gas–liquid chromatography, and in infrared and proton magnetic resonance spectra with authentic material.

1,2;3,4-Di-O-isopropylidene-6-deoxy-6-chloro-α-D-galactopyranose

A solution of 1,2;3,4-di-*O*-isopropylidene-α-D-galactopyranose (6.5 g) and triphenylphosphine (6.56 g) in carbon tetrachloride (25 ml) was heated under reflux for 3 h. The solution was cooled, and the solid which had crystallized was separated and shown (by thin-layer chromatographic, spectral, and melting point comparison) to be triphenylphosphine oxide. Solvent was removed from the filtrate *in vacuo*, and the oily residue was extracted with ether (6 × 50 ml) to leave, as residue, a further amount of triphenylphosphine oxide.

TABLE I

Compound	Product* (physical constants)
2-Acetoxyethanol	2-Chloroethyl acetate (b.p. 144–146°)
4-Acetoxybutanol	4-Chlorobutyl acetate (b.p. 85–90° at 15 mm)
Glycolic aldehyde diethylacetal	Chlorodiethylacetal (b.p. 148–155°, n_D^{21} 1.4160)
2-Hydroxyethyl ethyl ether	2-Chloroethyl ethyl ether (b.p. 107–109°, n_D^{20} 1.4118)
2-Hydroxyethyl butyl ether	2-Chloroethyl butyl ether (b.p. 132–138°)
2-Hydroxyethyl stearate	2-Chloroethyl stearate (m.p. 47–49°)
Neopentyl alcohol	Neopentyl chloride (b.p. 80–83°)
1,3-Butanediol	1,3-Dichlorobutane (b.p. 130–135°, n_D^{20} 1.4458)
1,2-Butanediol	1,2-Dichlorobutane (b.p. 125–130°)
2,3-Butanediol	2,3-Dichlorobutane (b.p. 112–114°, n_D^{20} 1.4496)

*Comparisons of spectra with authentic material, and comparisons of gas–liquid chromatographic behavior, were made in each case.

Can. J. Chem. Downloaded from www.nrcresearchpress.com by 210.87.254.5 on 09/05/12
For personal use only.

Ether was removed from the extracts at the pump, and the clear yellow syrup that remained was subjected to 'dry column' chromatography upon Kieselgel HF_{254} (eluted with solvent B), the eluted fractions (1 ml fractions) being examined by thin-layer chromatography (solvents A and B).

1,2;3,4-Di-*O*-isopropylidene-6-deoxy-6-chloro-α-D-galactopyranose was obtained as a pale-yellow syrup showing only one component on thin-layer chromatography (Kieselgel HF_{254}; solvents A, B, and C) and on gas–liquid chromatography (Apiezon L column, 200 °C). This component analyzed correctly and had a correct infrared spectrum for the expected product.

Dichloroethane

A solution of carbon tetrachloride (50 ml) containing triphenylphosphine (26.5 g) was heated under reflux, with stirring, with ethanediol (3.1 g) for 12 h. The mixture was fractionated on a Silicone column to give ethylene chlorhydrin (n_D^{17} 1.4427, 0.8 g) and 1,2-dichloroethane (n_D^{18} 1.4458, 2.7 g), the products being identical in infrared spectra and in behavior on gas–liquid chromatography with authentic compounds.

Other Reactions

These are summarized in Table I.

1. J. B. LEE. Tetrahedron, **12**, 226 (1961). J. B. LEE and M. M. EL SAUI. Chem. Ind. London, 839 (1960).
2. H. N. RYDON and S. R. LANDAUER. J. Chem. Soc. 2224 (1953).
3. J. B. LEE, T. J. NOLAN, and M. M. EL SAUI. Chem. Ind. London. In press.
4. P. C. CROFTS and I. M. DOWNIE. J. Chem. Soc. 2559 (1963).
5. T. KAMAI and Z. S. EGOROVA. Zh. Obshch. Khim. **16**, 1521 (1946). G. KOSSALAPOFF. J. Am. Chem. Soc. **12**, 347 (1958).
6. P. C. CROFTS. Quart. Rev. London, **12**, 347 (1958).
7. R. S. TIPSON. *In* Methods in carbohydrate chemistry. *Edited by* R. L. Whistler. Academic Press, Inc., New York. 1963. p. 247.
8. E. FISCHER and B. PFÄHLER. Ber. **53**, 1608 (1920).

RECEIVED NOVEMBER 30, 1965.
DEPARTMENT OF CHEMISTRY,
LOUGHBOROUGH COLLEGE OF TECHNOLOGY,
LOUGHBOROUGH, LEICESTERSHIRE, ENGLAND.

STEREOCHEMISTRY OF *o*-SUBSTITUTED FORMANILIDES

IAN D. RAE

INTRODUCTION

The degree of coplanarity achieved by a benzene ring and its conjugated substituents has been the subject of close scrutiny in recent years, and X-ray crystallographic results suggest that complete coplanarity is rarely achieved in the crystalline state (1–5). Non-coplanarity implies loss of resonance energy (6), which is presumably offset by the energy gain from relief of steric compression or improved molecular packing in the crystal. Some recent results for solutions have revealed non-coplanarity in aromatic solutes where solute–solvent interactions may provide compensation for the resonance energy lost by rotation of substituents about the bonds joining them to the ring. On the basis of dipole moment measurements in dioxane, it has been proposed that the carboxamido group of benzamide lies in a plane inclined at 37° to that of the benzene ring (7). Again, proton magnetic resonance measurements in pyridine have revealed that the amide and ring planes in N-methylacetanilide are orthogonal (2).

Some substituted formanilides have now been examined by proton magnetic resonance spectroscopy to measure the effects of ring substituents and the nature of the solvent on the orientation of the formamido group with respect to the aromatic ring. The *cis* (I) and *trans* (II) forms of formanilide have been shown to coexist in deuteriochloroform solution

Can. J. Chem. Downloaded from www.nrcresearchpress.com by 210.87.254.5 on 09/05/12
For personal use only.

Ether was removed from the extracts at the pump, and the clear yellow syrup that remained was subjected to 'dry column' chromatography upon Kieselgel HF_{254} (eluted with solvent B), the eluted fractions (1 ml fractions) being examined by thin-layer chromatography (solvents A and B).

1,2;3,4-Di-*O*-isopropylidene-6-deoxy-6-chloro-α-D-galactopyranose was obtained as a pale-yellow syrup showing only one component on thin-layer chromatography (Kieselgel HF_{254}; solvents A, B, and C) and on gas–liquid chromatography (Apiezon L column, 200 °C). This component analyzed correctly and had a correct infrared spectrum for the expected product.

Dichloroethane

A solution of carbon tetrachloride (50 ml) containing triphenylphosphine (26.5 g) was heated under reflux, with stirring, with ethanediol (3.1 g) for 12 h. The mixture was fractionated on a Silicone column to give ethylene chlorhydrin (n_D^{17} 1.4427, 0.8 g) and 1,2-dichloroethane (n_D^{18} 1.4458, 2.7 g), the products being identical in infrared spectra and in behavior on gas–liquid chromatography with authentic compounds.

Other Reactions

These are summarized in Table I.

1. J. B. LEE. Tetrahedron, **12**, 226 (1961). J. B. LEE and M. M. EL SAUI. Chem. Ind. London, 839 (1960).
2. H. N. RYDON and S. R. LANDAUER. J. Chem. Soc. 2224 (1953).
3. J. B. LEE, T. J. NOLAN, and M. M. EL SAUI. Chem. Ind. London. In press.
4. P. C. CROFTS and I. M. DOWNIE. J. Chem. Soc. 2559 (1963).
5. T. KAMAI and Z. S. EGOROVA. Zh. Obshch. Khim. **16**, 1521 (1946). G. KOSSALAPOFF. J. Am. Chem. Soc. **12**, 347 (1958).
6. P. C. CROFTS. Quart. Rev. London, **12**, 347 (1958).
7. R. S. TIPSON. *In* Methods in carbohydrate chemistry. *Edited by* R. L. Whistler. Academic Press, Inc., New York. 1963. p. 247.
8. E. FISCHER and B. PFÄHLER. Ber. **53**, 1608 (1920).

RECEIVED NOVEMBER 30, 1965.
DEPARTMENT OF CHEMISTRY,
LOUGHBOROUGH COLLEGE OF TECHNOLOGY,
LOUGHBOROUGH, LEICESTERSHIRE, ENGLAND.

STEREOCHEMISTRY OF *o*-SUBSTITUTED FORMANILIDES

IAN D. RAE

INTRODUCTION

The degree of coplanarity achieved by a benzene ring and its conjugated substituents has been the subject of close scrutiny in recent years, and X-ray crystallographic results suggest that complete coplanarity is rarely achieved in the crystalline state (1–5). Non-coplanarity implies loss of resonance energy (6), which is presumably offset by the energy gain from relief of steric compression or improved molecular packing in the crystal. Some recent results for solutions have revealed non-coplanarity in aromatic solutes where solute–solvent interactions may provide compensation for the resonance energy lost by rotation of substituents about the bonds joining them to the ring. On the basis of dipole moment measurements in dioxane, it has been proposed that the carboxamido group of benzamide lies in a plane inclined at 37° to that of the benzene ring (7). Again, proton magnetic resonance measurements in pyridine have revealed that the amide and ring planes in N-methylacetanilide are orthogonal (2).

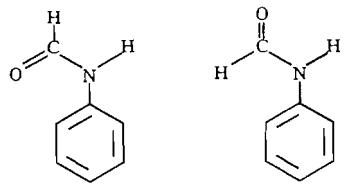
Some substituted formanilides have now been examined by proton magnetic resonance spectroscopy to measure the effects of ring substituents and the nature of the solvent on the orientation of the formamido group with respect to the aromatic ring. The *cis* (I) and *trans* (II) forms of formanilide have been shown to coexist in deuteriochloroform solution

Can. J. Chem. Downloaded from www.nrcresearchpress.com by 210.87.254.40 on 09/05/12
For personal use only.

(8), and signals arising from both types of formyl proton are readily identifiable in the proton magnetic resonance spectrum because of the difference in coupling with the amide proton (J_{cis} ca. 2 c/s, J_{trans} ca. 11 c/s). If the formamido group itself remains planar and rotation is permitted about the bond joining the nitrogen and the aromatic ring, it is clear that the magnetic environment of formyl protons in the *trans* form (II) will change appreciably as rotation proceeds. Measurements from Dreiding models (or trigonometrical calculation) and use of the data of Johnson and Bovey (9) show that the changes in shielding of the formyl proton by the aromatic ring are dependent on the angle of rotation (ϕ) as follows ($\phi = 0$ for completely planar molecules).

Angle of rotation (ϕ)	0°	30°	45°	60°	90°
Relative shielding (p.p.m.)					
cis	0	0.01	0.02	0.05	0.08
trans	0	0.18	0.21	0.43	0.63

Since it had also been shown that the formyl proton resonances of formanilide were almost independent of concentration (8), the chemical shift of a *trans* formyl proton was seen as an excellent probe for investigating rotation about the Ar—N bond in formanilides. It was proposed to effect such a rotation by means of substituents placed ortho to the



I II

formamido group; also, to preserve the simplicity of the calculated relationship, it was necessary to choose substituents with low anisotropy and minimum electronic effect on the benzene ring. Halogen atoms and alkyl groups fulfilled both these conditions (10, 11), and the investigation was therefore confined to formanilides bearing substituents of these types. Further, the choice of solvents was influenced by the following factors: (*i*) the need to avoid the highly specific shielding effects of aromatic solvents (12, 13), (*ii*) the retention of slow exchange of the amide protons so that formyl proton signals might be clearly identified by means of coupling constants, and (*iii*) the solubility of formanilides. This last factor was doubly important since the ratio of *trans* to *cis* forms decreased markedly at low concentrations (cf. ref. 8); when the solubility of a formanilide was too low, only the *cis* form could be observed in solution.

RESULTS AND DISCUSSION

The *cis* formyl proton resonances (not recorded here) showed the small variation expected, thus confirming that the formyl protons may be regarded as electronically insulated from the aromatic ring. The *trans* proton resonances, however, showed a much greater variation with structure; they are recorded in the tables and form the basis for the discussion.

The results in Table I for dimethyl sulfoxide solutions are compatible with a model where the formamido group lies in the ring plane when no hindering substituents are present, and is orthogonal to the ring plane when both the 2′- and 6′-positions of the ring are occupied by substituents. In deuteriochloroform, the change in chemical shift of the formyl protons when two flanking substituents are introduced is somewhat smaller and

Can. J. Chem. Downloaded from www.nrcresearchpress.com by 210.87.254.40 on 09/05/12
For personal use only.

leads to a calculated value of about 65° for the interplane angle ϕ. If this figure has any reality, the effect of solvent may be rationalized in terms of an increase in the "effective size" of the formamido group as outlined later in this section, but the paucity of data deters speculation.

TABLE I

Chemical shift of *trans* formyl protons for 4′- and 2′,6′-substituted formanilides

	Chemical shift (δ)	
Substituent	$CDCl_3$	CH_3SOCH_3
None	8.62	8.65
4′-Methyl	8.67	8.55
4′-Chloro	8.67	8.62
4′-Bromo	8.67	8.63
Mean of above values	8.66	8.61
2′,6′-Dimethyl	8.20	7.85
2′,6′-Dichloro	—*	8.02
2′,6′-Dibromo	—†	7.95
2′-Chloro-6′-methyl	8.17	7.95

*cis form predominates (>95%).
†Insufficiently soluble.

In the other solvents tried, the resonances for the 2′,6′-disubstituted formanilides could not be identified clearly, but 2′-substituted cases could be handled effectively; the data are reported in Table II. In each solvent the resonance positions for formanilide and three 4′-substituted formanilides were averaged to give a value for the coplanar standard ($\phi = 0$), and time-average values for the angles of rotation of 2′-substituted formanilides were computed on this basis. The varying limits of error result from the nonlinear dependence of shielding on ϕ and are based on an estimated error in the measurement of the chemical shift differences of 0.03 p.p.m.

TABLE II

Chemical shift of *trans* formyl protons and calculated angle ϕ for 2′-substituted formanilides

	$CDCl_3$		CH_3COCH_3		CH_3OH		CH_3SOCH_3	
Substituent	δ	ϕ	δ	ϕ	δ	ϕ	δ	ϕ
Planar standard	8.62	0	8.76	0	8.24	0	8.61	0
2′-Methyl	8.42	35±9°	8.50	50±3°	7.97	51±3°	8.22	58±2°
2′-Chloro	8.68	0	8.70	4±2°	8.12	12±4°	—*	
2′-Bromo	8.63	0	8.67	8±4°	8.10	16±6°	—*	
2′-Iodo	8.53	10±3°	8.52	48±3°	8.00	48±3°	—*	
2′,5′-Dimethyl	8.53	10±3°	8.40	57±2°	8.02	45±4°	8.25	57±2°

*Either predominantly *cis* isomer in solution, or coincident signal at 8.25 p.p.m. ($\phi = 57 \pm 2°$).

The data of Table II reveal a tendency towards increasing ϕ as the size of the 2′-substituent increases, and also as the solvent is changed from deuteriochloroform through methanol and acetone to dimethyl sulfoxide. The dependence of ϕ on steric factors is not unexpected, although the effect of a 2′-methyl group seems disproportionally large in view of the accepted covalent radii (14) of the chlorine and bromine atoms and the methyl group (1.80, 1.95, and 2.0 Å, respectively). In a study of N-substituted formanilides, a similar progressive increase in ϕ with the bulk of the N-alkyl substituent has been noted (15).

Can. J. Chem. Downloaded from www.nrcresearchpress.com by 210.87.254.40 on 09/05/12
For personal use only.

The dependence of ϕ on the nature of the solvent gives a solvent order which follows the dipole moment of the solvent molecules rather than the bulk property dielectric constant (see Experimental). In the more polar solvents it is proposed that a closer association of solvent molecules with the dipolar formamido group greatly increases its steric requirements and thus leads to higher ϕ values.

EXPERIMENTAL

No new compounds were employed in this study. With the exception of formanilide itself, which was commercially available, and 2′-methyl- and 2′,5′-dimethyl-formanilides, which were kindly supplied by Dr. L. Marion, the formanilides were prepared by the action of boiling 98% formic acid (16) or cold 4:1 formic acid – acetic anhydride (17) on the appropriately substituted anilines. The properties of the purified formanilides agreed with those reported in the literature (16, 18, 19), and further confirmation of their identity was obtained from infrared and proton magnetic resonance spectra.

Dielectric constants for the liquid state at 25° are: chloroform (20), 4.8; acetone (20), 20.7; methanol (20), 32.6; dimethyl sulfoxide (21), 45.5. Dipole moments for solutions in benzene (22) are: chloroform, 1.1; methanol, 1.6; acetone, 2.4; dimethyl sulfoxide, 3.9.

Proton magnetic resonance spectra were recorded for approximately 5% solutions on a Varian A-60 spectrometer at 25°. Tetramethylsilane was used as an internal (deuteriochloroform, acetone) or external (methanol, dimethyl sulfoxide) standard.

ACKNOWLEDGMENTS

The author thanks Dr. D. G. Gillies for discussion and communication of unpublished results, and Dr. L. Marion for generous samples of formanilides. This work was commenced during the tenure of a Postdoctorate Award at the National Research Council, Ottawa.

1. C. J. Brown and D. E. C. Corbridge. Acta Cryst. **7**, 711 (1954).
2. B. F. Pedersen and B. Pedersen. Tetrahedron Letters, 2995 (1965).
3. A. T. McPhail and G. A. Sim. J. Chem. Soc. 227 (1965).
4. C. J. Brown and R. Sodanaga. Acta Cryst. **18**, 158 (1965).
5. R. E. Long, R. A. Sparks, and K. N. Trueblood. Acta Cryst. **18**, 932 (1965).
6. L. L. Ingraham. *In* Steric effects in organic chemistry. M. S. Newman. John Wiley & Sons, Inc., New York. 1956. p. 479.
7. M. J. Arony, R. J. W. LeFevre, and A. N. Singh. J. Chem. Soc. 3179 (1965).
8. A. J. R. Bourn, D. G. Gillies, and E. W. Randall. Tetrahedron, **20**, 1811 (1964).
9. C. E. Johnson and F. A. Bovey. J. Chem. Phys. **29**, 1012 (1958).
10. G. S. Reddy and J. H. Goldstein. J. Chem. Phys. **38**, 2736 (1963).
11. H. H. Jaffé. Chem. Rev. **53**, 191 (1953).
12. R. E. Klinck and J. B. Stothers. Can. J. Chem. **40**, 1071 (1962).
13. R. M. Moriarty. J. Org. Chem. **28**, 1296 (1963).
14. J. A. A. Ketelaar. Chemical constitution. 2nd ed. Elsevier Press, Inc., New York. 1958. p. 201.
15. D. G. Gillies and E. W. Randall. Unpublished observations.
16. N. V. Philips Gloeilampenfabriehen. Fr. Patent No. 1,341,781 (November 2, 1963); Chem. Abstr. **60**, 5402*h* (1964).
17. J. C. Sheehan and D.-D. H. Yang. J. Am. Chem. Soc. **80**, 1154 (1958).
18. G. R. Pettit, M. V. Kalnins, T. M. H. Lin, E. G. Thomas, and K. Parent. J. Org. Chem. **26**, 2563 (1961).
19. F. J. Smith and E. Jones. A scheme of qualitative organic analysis. Blackie & Son, Ltd., London. 1953. pp. 136–138 and 261–263.
20. Handbook of chemistry and physics. 44th ed. Chemical Rubber Publishing Co., Cleveland, Ohio. 1964. p. E31.
21. J. J. Lindberg and R. Hakalax. Finska Kemistsamfundets Medd. **71**, 97 (1962); Chem. Abstr. **59**, 3395*c* (1963).
22. A. L. McClellan. Tables of experimental dipole moments. W. H. Freeman & Co., San Francisco. 1963.

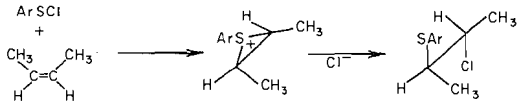
Received February 16, 1966.
Department of Chemistry,
University of Toronto,
Toronto, Ontario.

Can. J. Chem. Downloaded from www.nrcresearchpress.com by 210.87.254.40 on 09/05/12
For personal use only.

THE INFLUENCE OF TEMPERATURE ON THE STEREOCHEMISTRY OF THE ADDITION OF *p*-CHLOROBENZENESULFENYL CHLORIDE TO *cis*- AND *trans*-2-BUTENE

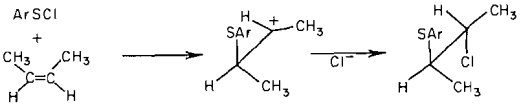
GEORGE H. SCHMID AND VALERIA M. CSIZMADIA[1]

The mechanism of the reaction of an arylsulfenyl chloride with an olefin has been postulated by Kharasch (1) to involve a cyclic sulfonium ion intermediate (I).



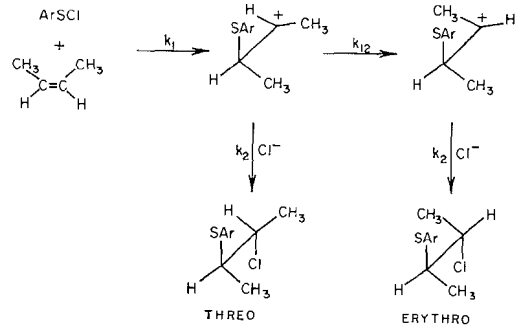
I

This intermediate has been invoked to account for the observed *trans* addition. Evidence that such an intermediate is capable of formation has been obtained by Pettitt and Helmkamp (2) and by Eliel (3). These results do not rule out the formation of an open carbonium ion (II) as an intermediate.



II

trans Addition will be favored because of the steric hindrance of the sulfur group and its substituent. This intermediate would retain its stereochemical integrity if the rate of rotation about the carbon–carbon single bond to form the isomeric carbonium ion is slower than the rate of attack by chloride ion. This mechanism is illustrated in Reaction Scheme 1. The bimolecular step is a reaction between ions of different charge. Such



REACTION SCHEME 1.

reactions have been shown to have extremely fast rates (4), and in addition, energy barriers to rotation in the range of 10 kcal are known (5). Thus, this mechanism cannot be rejected arbitrarily. A method to distinguish between these two mechanisms is to study the effect of temperature on the stereochemistry of the product of the addition of an arylsulfenyl chloride to a *cis* and *trans* olefin. The system chosen for study was the addition of *p*-chlorobenzenesulfenyl chloride to *cis*- and *trans*-2-butene.

[1]*Holder of a Province of Ontario Government Fellowship, 1965–1966.*

Can. J. Chem. Downloaded from www.nrcresearchpress.com by 210.87.254.40 on 09/05/12
For personal use only.

Consider the kinetic scheme for the addition to *cis*-2-butene as illustrated in Reaction Scheme 1. The rates of formation of the threo isomer and the erythro isomer are given by eqs. [1] and [2], respectively.

$$[1] \qquad \frac{\mathrm{d[threo]}}{\mathrm{d}t} = \frac{k_1[cis\ \text{olefin}][\mathrm{ArSCl}]}{1 + (k_{12}/(k_2[\mathrm{Cl^-}]))}$$

$$[2] \qquad \frac{\mathrm{d[erythro]}}{\mathrm{d}t} = \frac{k_1[cis\ \text{olefin}][\mathrm{ArSCl}]}{(k_2[\mathrm{Cl^-}]/k_{12}) + 1}$$

Elimination of time as a variable (6) and integration gives eq. [3].

$$[3] \qquad \frac{[\text{erythro}]}{[\text{threo}]} = \frac{k_{12}}{k_2[\mathrm{Cl^-}]}$$

The relation between the [erythro]/[threo] ratio at any two temperatures is given by eq. [4].

$$[4] \qquad \frac{([\text{erythro}]/[\text{threo}])_{T_1}}{([\text{erythro}]/[\text{threo}])_{T_2}} = L = (k_{12}/k_2)_{T_1}(k_2/k_{12})_{T_2}$$

Replacement of the rate constants by the Arrhenius equation gives eq. [5].

$$[5] \qquad L = \frac{\exp \frac{E_a^{12}}{R}\left(\frac{1}{T_2} - \frac{1}{T_1}\right)}{\exp \frac{E_a^{2}}{R}\left(\frac{1}{T_2} - \frac{1}{T_1}\right)}$$

This can be simplified to eq. [6].

$$[6] \qquad \log L = \frac{E_a^{12} - E_a^{2}}{2.303R}\left(\frac{1}{T_2} - \frac{1}{T_1}\right)$$

Equation [6] predicts that the ratio L will depend upon the relative activation energies of the two processes and the temperature range chosen to study the product composition. From eq. [6] it is possible to calculate the change in temperature necessary to observe a value of 5 for L if the difference in activation energies is but 2.0 kcal/mole. A temperature range of 150 degrees is predicted. Thus, eq. [6] gives a convenient method of testing the open carbonium ion mechanism. If the energy of activation of rotation is greater than the energy of activation of the bimolecular reaction by at least 2 kcal/mole, a significant change in the [erthyro]/[threo] ratio should be observed as the temperature of the reaction is increased over a range of 150 degrees.

The experimental results of the stereochemistry of the addition of *p*-chlorobenzenesulfenyl chloride to *cis*- and *trans*-2-butene in 1,1,2,2-tetrachloroethane over a temperature range of 180 degrees are given in Table I. The product composition was determined by vapor phase chromatography, which cleanly separated the *dl*-erythro and *dl*-threo isomers. Addition of oxygen, to suppress any free-radical reaction, had no effect upon the product composition. Control experiments showed that a minimum of 0.05% of one isomer could be detected in the presence of the other. The nearly constant 0.5% of threo isomer in the addition to *trans*-2-butene is due to *cis*-2-butene being an impurity in the starting material. The *cis*-2-butene contained less than 0.05% of *trans*-2-butene.

From the data in Table I it is clear that the ratio L given by eq. [4] has a value of 1. Therefore, if eq. [6] is to be consistent with the experimental observations, then $E_a^{12} = E_a^{2} = E$. This means that the difference in rates must be due to the pre-exponential factors.

Can. J. Chem. Downloaded from www.nrcresearchpress.com by 210.87.254.40 on 09/05/12
For personal use only.

TABLE I

Observed temperature effect on product stereochemistry

Temperature (°C)	*cis*-2-Butene		*trans*-2-Butene	
	dl-Erythro	*dl*-Threo	*dl*-Erythro	*dl*-Threo
−34	0.05	99.95	99.44	0.56
0	0.05	99.95	99.55	0.45
25	0.05	99.95	99.49	0.51
50	0.05	99.95	99.46	0.54
75	0.05	99.95	99.56	0.44
100	0.05	99.95	99.49	0.51
146	0.05	99.95	99.54	0.46

Equation [7] is obtained by substitution of the Arrhenius equations for k_{12} and k_2 into eq. [3], and relates the [erythro]/[threo] ratio and the pre-exponential factors.

$$[7] \qquad \frac{[\text{erythro}]}{[\text{threo}]} = \frac{A_{12}\exp(-E/RT)}{A_2\exp(-E/RT)[\text{Cl}^-]} = \frac{A_{12}}{A_2[\text{Cl}^-]}$$

Experimentally, the [erythro]/[threo] ratio is given by eq. [8].

$$[8] \qquad \frac{[\text{erythro}]}{[\text{threo}]} = \frac{0.05}{99.95} = 5 \times 10^{-4} = \frac{A_{12}}{A_2[\text{Cl}^-]}$$

For eq. [8] to be true, the product of the pre-exponential factor A_2 and the chloride ion must be 5×10^4 times the pre-exponential factor A_{12}. This seems to be unlikely. The concentration of chloride ion will be so small (approximately 10^{-8} mole/l) that, even if the pre-exponential factor is among the highest known (10^{19} l moles/s (4)), the product of the two will still be approximately equal to or less than a normal pre-exponential factor for a unimolecular process (10^{10} to 10^{12}/s) involving rotation (7). Thus, for an open carbonium ion mechanism to account for the observed results, it is necessary not only that the activation energies of the rotation and bimolecular steps be identical but also that the pre-exponential factor for the bimolecular step be extremely high.

It seems to be clear that the cyclic sulfonium ion intermediate mechanism originally postulated by Kharasch (1) and supported by the work of Pettitt and Helmkamp (2) and Eliel (3) explains more easily and more satisfactorily not only the *trans* addition but also the absence of a temperature effect upon the stereochemistry of the product.

EXPERIMENTAL

All melting and boiling points are uncorrected. Vapor phase chromatography was performed on a Wilkens Instruments model 705 chromatograph with helium as a carrier gas.

Bis-(4-chlorobenzene)disulfide

In a 2 l Erlenmeyer flask equipped with a magnetic stirrer were placed 1 000 ml of distilled water, 86.7 g (0.60 mole) of *p*-chlorothiophenol, and 24.0 g (0.60 mole) of sodium hydroxide. The crystalline *p*-chlorothiophenol dissolved as a fluffy precipitate of sodium *p*-chlorothiophenoxide was formed. To the mixture was added 450 ml of 3% hydrogen peroxide at such a rate that the temperature of the reaction mixture did not exceed 30 °C. The light-yellow disulfide precipitated as it was formed. After the addition of the hydrogen peroxide, the reaction mixture was stirred overnight at room temperature. The crystals were filtered, and washed with warm tap water and then distilled water until the filtrate was alkaline free. Recrystallization from 95% ethyl alcohol gave a 95% yield of pale-yellow plates, m.p. 73.0–73.5 °C (lit. m.p. 71–71.5 °C (8)).

p-Chlorobenzenesulfenyl Chloride

This compound was prepared by the method of Lawson and Kharasch (9) in 81% yield, b.p. 33–34 °C at 0.22 mm (lit. b.p. 86–90 °C at 5 mm (10)). The purity of the material was determined by the method of Kharasch and Wald (11) and found to be 99.8 ± 1%.

Can. J. Chem. Downloaded from www.nrcresearchpress.com by 210.87.254.40 on 09/05/12
For personal use only.

Reaction of p-Chlorobenzenesulfenyl Chloride with cis- and trans-2-Butene

The reaction was carried out in the dark in a 250 ml, three-necked, round-bottomed flask equipped with a thermometer, a $CaCl_2$ drying tube, a gas inlet tube, and a dry ice – acetone condenser. 1,1,2,2-Tetrachloroethane (40 ml) was placed in the flask and brought to the desired temperature by a liquid ammonia bath, water bath, or oil bath. During this time, dry nitrogen gas was bubbled through the solution. After the desired temperature had been reached, 0.6 g (0.0035 mole) of *p*-chlorobenzenesulfenyl chloride was added to the reaction vessel. As soon as the temperature of the reaction mixture returned to its former value, the butene gas was bubbled in slowly. The reaction was rapid and exothermic. The temperature of the reaction mixture rose by 2–4 °C at the beginning of the reaction. The reaction was judged to be complete upon disappearance of the yellow color of the *p*-chlorobenzenesulfenyl chloride. The time for complete reaction was 1 to 5 min, depending upon the temperature. The flask was removed from the bath and the reaction mixture was analyzed directly by vapor phase chromatography. The *dl*-erythro and *dl*-threo isomers were cleanly separated on a ¼ inch by 13 ft column of 5% Carbowax on Chromosorb G. The yield of product was determined at 25 °C by the same procedure, except that methylene chloride was used as solvent. The solvent was removed under reduced pressure to constant weight. The residue, representing a 99% yield, was shown by vapor phase chromatography to consist of one isomer.

Quantitative Determination of Threo- and Erythro-3-chloro-2-butyl-p-Chlorobenzenesulfide

Two stock solutions were prepared: one containing 60.1 mg of the pure threo isomer in 1.0 ml of 1,1,2,2-tetrachloroethane and another containing 60.6 mg of the pure erythro isomer in 1.0 ml of 1,1,2,2-tetrachloroethane. The pure erythro isomer was prepared from a sample of research grade *trans*-2-butene not previously available to us. By means of microliter syringes, several mixtures of known quantities of each component were prepared. These mixtures were analyzed by vapor phase chromatography under the identical conditions used to analyze the reaction product mixtures. It was found that the limit of detection was 0.05% of one component in the presence of the other.

ACKNOWLEDGMENT

The authors are grateful to the National Research Council of Canada for financial aid.

1. N. KHARASCH and C. M. BUESS. J. Am. Chem. Soc. **71**, 2724 (1949).
2. D. J. PETTITT and G. K. HELMKAMP. J. Org. Chem. **29**, 2702 (1964).
3. E. L. ELIEL, L. A. PILATO, and V. G. BADDING. J. Am. Chem. Soc. **84**, 2377 (1962).
4. A. A. FROST and R. G. PEARSON. Kinetics and mechanism. John Wiley & Sons, Inc., New York. 1953. Chap. 7. p. 113.
5. D. THOMPSON, R. NEWMARK, and C. SEDERHOLM. J. Chem. Phys. **37**, 411 (1962).
6. S. W. BENSON. J. Chem. Phys. **20**, 1605 (1952).
7. A. ALLERHAND and H. S. GUTOWSKY. J. Chem. Phys. **41**, 2115 (1964).
8. A. H. NATHAN and M. T. BOGERT. J. Am. Chem. Soc. **63**, 2363 (1941).
9. D. D. LAWSON and N. KHARASCH. J. Org. Chem. **24**, 858 (1959).
10. M. B. SPARKE, J. L. CAMERON, and N. KHARASCH. J. Am. Chem. Soc. **75**, 4907 (1953).
11. N. KHARASCH and M. M. WALD. Anal. Chem. **27**, 996 (1955).

RECEIVED JANUARY 6, 1966.
DEPARTMENT OF CHEMISTRY,
UNIVERSITY OF TORONTO,
TORONTO, ONTARIO.

Can. J. Chem. Downloaded from www.nrcresearchpress.com by 210.87.254.40 on 09/05/12
For personal use only.

Can. J. Chem. Downloaded from www.nrcresearchpress.com by 210.87.254.5 on 09/05/12
For personal use only.

Canadian Journal of Chemistry

Issued by THE NATIONAL RESEARCH COUNCIL OF CANADA

VOLUME 44 JUNE 15, 1966 NUMBER 12

PARACHORS AND OTHER PROPERTIES OF ORGANOTINS

ROBERT C. PUTNAM

Research Laboratory, M & T Chemicals Inc., Rahway, New Jersey

Received February 1, 1966

ABSTRACT

The parachors of a group of organotins were measured and compared with calculated values using both atomic constants and bond constants to obtain corresponding values for tin. The variation was found to be lower for the first method. The parachors were found to be about 8 times the molar refractions and could be approximately predicted from calculated molar refractions.

The refrachors of the organotins were calculated and a suitable series of additive constants devised to approximate the found values. Excellent correlation was obtained between the order of refrachors corrected for molecular weight and the order of dispersions as expressed by the Nu (ν) values. An initial indication of alternation in methylene group increments for both molar refraction and Nu values was found. For a constant dispersion ratio (Q value) the refractive indices for the F and C lines of hydrogen were calculated.

For many years, chemists have searched for ways to correlate physical properties with structure. The prediction of structure from physical properties and the prediction of physical properties from structure have been goals long sought, but only poorly realized.

It has been evident that more than one physical property will be needed, since all efforts using only one constant have ended far from the mark. The most promising combination of properties and the one most fruitful in results has been the parachor. This constant has been the subject of innumerable studies, and its value is generally available in most fields of chemistry. It is the purpose of this paper to present some new data in the field of organometallics relative to the parachor and certain other properties of organotins.

The parachor is a constant of great utility in studies on structures of closely related compounds. It has both additive and constitutive properties. It is affected by unsaturation, branching, rings, and hydrogen bonds and is related to several other constants. Over 2 000 parachors are listed in a review article by Quayle (1). A. I. Vogel has published more than 40 papers in which the parachor holds an important place.

The parachor was introduced by Sugden (2) in 1924 and may be defined as

$$P = M\gamma^{1/4}/D,$$

where M is the molecular weight, γ is the surface tension, and D is the density of the liquid.

The compounds investigated were certain organotins whose constants are given in Table I. The densities were determined on a Fisher–Davidson gravitometer at 25 °C and the surface tensions on a Fisher surface tensiometer at 25 °C with corrections applied according to the method of Zuidema and Waters (3). The compounds had purities exceeding 99%, most being 99.7 to 100% pure.

TABLE I
Physical constants of organotins

	D_4^{25}	γ^{25}	M
Me_4Sn	1.280	19.7	178.8
Et_4Sn	1.181	25.9	234.9
Pr_4Sn	1.092	24.5	291.0
iPr_4Sn	1.117	25.7	291.0
Bu_4Sn	1.040	26.2	347.1
iBu_4Sn	1.045	24.5	347.1
Vi_4Sn	1.254	24.1	226.8
Me_3EtSn	1.251	21.6	192.7
Me_3PrSn	1.206	22.2	206.9
Me_3iPrSn	1.198	21.4	206.9
Me_3ViSn	1.277	21.3	190.7
$Me_3CyhexSn$	1.216	25.3	247.0
$Me_3\phi Sn$	1.326	28.9	240.9

The parachors were determined and compared with calculated values in order to determine the constancy of a value for tin in the organotins. The constants used for the calculated values were mainly Sugden's (4), since they gave the most consistent results. They were C, 4.8; H, 17.1; C=C, 23.2; ring, 6.1; branch, −5.7. (A ring is also a branch.)

The values obtained are shown in Table II.

TABLE II
Parachors obtained using atomic constants

	P found	Calcd. Sn
Me_4Sn	295	70.6
Et_4Sn	451	70.6
Pr_4Sn	593	57.0
iPr_4Sn	588	74.4
Bu_4Sn	757	64.6
iBu_4Sn	739	69.4
Vi_4Sn	401	64.6
Me_3EtSn	333	69.6
Me_3PrSn	372	69.6
Me_3iPrSn	372	69.6
Me_3ViSn	322	69.6
$Me_3CyhexSn$	456	70.4
$Me_3\phi Sn$	422	69.4

The values for tin are quite consistent considering the structural differences represented. The average value found for Sn was 69.4, omitting tetrapropyl tin. The standard error of the mean was 1.1% of the mean, and the latter's value was 69.4 ± 1.7 (95%), omitting tetrapropyl tin.

Values for the parachor of tin have been previously reported by Kadomtzeff (5); these values showed a much greater variation and suggested a possible alternation with the number of carbon atoms. There appears to be no clear indication of an alternation of the parachors of tin in the few *n*-tetra-alkyl tins considered here. The abnormally low value found for tin in tetrapropyl tin suggests that there may be some anomaly in its structure. The parachor for tin would be 68, in line with the other values, if half the propyl groups were considered to be branched. Since parachors are very sensitive to structural differences, this implies the existence of a factor requiring another adjusting constant. Tetrapropyl tin has a feature not present in the lower homologues. The *n*-propyl group can have either of

Can. J. Chem. Downloaded from www.nrcresearchpress.com by 210.87.254.5 on 09/05/12
For personal use only.

two internal torsional configurations, *trans* or *gauche*, with respect to orientation about the C_1C_2 bond. This isomerism is independent of the arrangement between alkyl groups or of interaction between them (6). The complexity of the spectrum of the compound is due in part to this factor and indicates that both forms are present in the liquid state.

When compared at temperatures where surface tensions are equal, parachors of compounds are proportional to molar volumes at those temperatures. If we assume that the presence of two forms affects the molar volume, then we can account for the anomaly in the parachor.

Instead of using additive atomic constants for computing the parachor, one may use bond constants. Those developed by Vogel and co-workers (7) for alkyl groups, and also the individual values from their work, were used to compute the parachors minus the Sn—C linkages in order to compare with the found values and to show the possible constancy of the Sn—C bond. The individual values obtained by Vogel *et al.* are: C—H, 17.85; C—C, 4.30; C=C, 28.5; C_{ar}—C_{ar}, 16.5; C—C (cyclohexane), 4.5.

Their values were established for 20 °C but have been applied without correction to the present work which was done at 25 °C. The error involved in the values is less than one part per thousand.

TABLE III

Parachors obtained using bond constants

	P		
	Found	Calcd. minus Sn—C	Sn—C
Me_4Sn	295	213	20.5
Et_4Sn	451	373	19.5
Pr_4Sn	593	533	15.0
iPr_4Sn	588	526	15.4
Bu_4Sn	757	692	16.2
iBu_4Sn	739	686	13.2
Vi_4Sn	401	328	18.2
Me_3EtSn	333	253	20.0
Me_3PrSn	372	293	19.7
Me_3iPrSn	372	291	20.1
Me_3ViSn	322	242	20.0
$Me_3CyhexSn$	456	383	18.3
$Me_3\phi Sn$	422	348	18.5
			Mean 18.0

The calculated parachors excluding the Sn—C bonds are listed in Table III with corresponding calculated values for the latter bond.

The standard error of the mean was 3.6% of the mean, and the latter's value was 18.0 ± 1.4 (95%).

MOLAR REFRACTIONS

The parachors of the organotins investigated were found to bear a constant relationship to the determined molar refractions. The average value of the ratio is 7.91. Since calculated molar refractions using Vogel (7) bond refractions closely approximate the found values, one may estimate the parachors from the calculated molar refractions. The pertinent data are listed in Table IV. The average ratio of parachor to calculated molar refraction is 7.95. As an approximation the parachor may be considered to be 8 times the calculated molar refraction. The bond refraction values used for the calculated molar refraction were those given by Vogel for alkyl groups (7) and the following (8): C—C, 1.296; Sn—C, 4.16; C—H, 1.676; Sn—C (ar.), 3.78; C=C, 4.17; C—C (ar.), 2.688; C—C (cyclohexane), 1.27.

Can. J. Chem. Downloaded from www.nrcresearchpress.com by 210.87.254.5 on 09/05/12
For personal use only.

TABLE IV

Parachors and molar refractions

	P found	N found	P/N found	N calcd.	P/N calcd.
Me_4Sn	295	36.73	8.03	36.66	8.05
Et_4Sn	451	55.38	8.14	55.24	8.16
Pr_4Sn	593	74.59	7.95	73.92	8.02
iPr_4Sn	588	74.38	7.91	73.96	7.95
Bu_4Sn	757	93.37	8.10	92.40	8.19
iBu_4Sn	739	93.46	7.91	92.52	7.99
Vi_4Sn	401	52.99	7.57	53.43	7.51
Me_3EtSn	333	41.32	8.06	41.30	8.06
Me_3PrSn	372	46.25	8.04	45.97	8.09
Me_3iPrSn	372	46.47	8.01	45.98	8.09
Me_3ViSn	322	40.69	7.91	40.85	7.88
$Me_3CyhexSn$	456	58.79	7.76	57.71	7.90
$Me_3\phi Sn$	422	56.45	7.48	56.24	7.51
			Average 7.91		Average 7.95

Vogel's constants pertain to 20 °C, whereas all measurements here were at 25 °C. The error involved is less than one part per thousand. The refractions refer to the sodium D line.

Since $P = M\gamma^{1/4}/D$ and $N = \dfrac{n^2 - 1}{n^2 + 2} \cdot \dfrac{M}{D}$ (N = molar refraction)

$$P/N = \gamma^{1/4} \Big/ \frac{n^2 - 1}{n^2 + 2}$$

and the values listed under P/N represent this ratio.

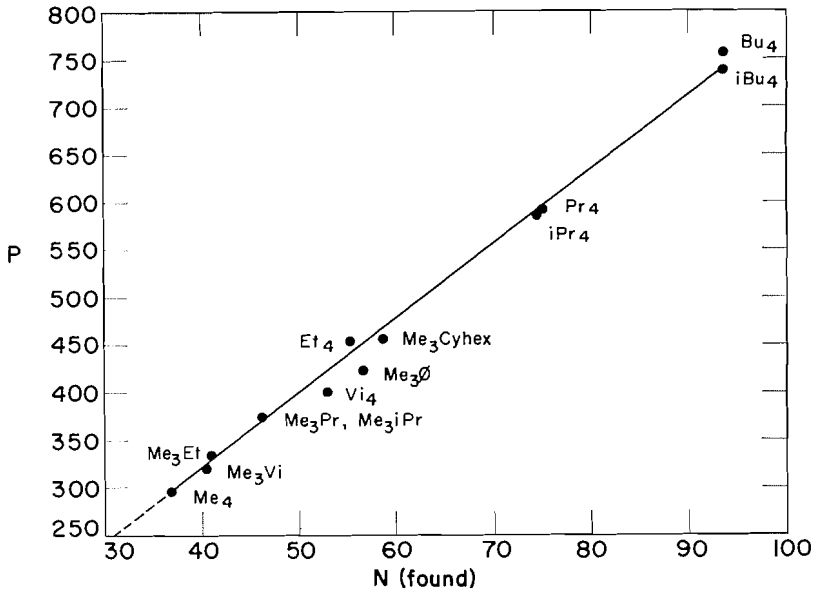


FIG. 1. Plot of parachor versus molar refraction.

Lagemann and Dunbar (9) discussed various relationships pertaining to the physical properties of liquids, and from their constants the following equation applying to *n*-alkanes may be derived,

$$P = 8.488N + 17.29,$$

Can. J. Chem. Downloaded from www.nrcresearchpress.com by 210.87.254.5 on 09/05/12
For personal use only.

relating parachor and molar refraction. From a plot of the data relating to the alkyl tins, the corresponding equation in this field is:

$$P = 7.83N \text{ (calcd.)} + 7.3.$$

The per cent differences between the calculated and found values using the latter equation are approximately the same as those obtained using the relationship:

$$P = 7.95N \text{ (calcd.)}.$$

A plot of the parachor versus the found molar refraction is shown in Fig. 1.

REFRACHOR

The refrachor is a physical constant proposed by Joshi and Tuli (10) and is defined as

$$F = -P \log (n_D - 1),$$

where P is the parachor and n is the refractive index. It is very sensitive to structural variations and has the advantage that it combines both internal and external factors. They proposed a set of atomic, structural, and group refrachors. When these were applied to the tin compounds under study and compared with the determined refrachors, the values for tin were not found to be constant, viz.:

Compounds	F(Sn)
Me_4Sn	21.79
Et_4Sn	30.83
Pr_4Sn	36.98
iPr_4Sn	43.94
Bu_4Sn	34.74

When the following values were assigned to the bonds, reasonable agreement between found and calculated refrachors was obtained as shown in Table V: Sn—C, 38.4; C=C, 5; C—H, −4.3; branch, −2; C—C, 20.6; sat. ring, −48. (A ring is one branch.)

TABLE V

Refrachors of organotin compounds

	F found	F calcd.
Me_4Sn	105.5	102
Et_4Sn	148.3	150
Pr_4Sn	193.5	198
iPr_4Sn	185.9	190
Bu_4Sn	247.2	246
iBu_4Sn	239.1	238
Me_3EtSn	115.8	114
Me_3PrSn	128.4	126
Me_3iPrSn	128.8	126
$Me_3CyhexSn$	140.7	141
Me_3ViSn	109.4	107
$Me_3\phi Sn$	106.4	106
Vi_4Sn	121.5	122

The values show a mean deviation of two units on a whole number basis.

Since the parachor has been shown to have an average value of 7.91 times the measured molar refraction, this means that for the compounds studied the refrachor has the following average value:

$$F = -7.91N \log (n_D - 1)$$

Can. J. Chem. Downloaded from www.nrcresearchpress.com by 210.87.254.5 on 09/05/12
For personal use only.

Can. J. Chem. Downloaded from www.nrcresearchpress.com by 210.87.254.5 on 09/05/12
For personal use only.

ABBE NUMBER

The Abbe number or Nu (ν) value is a measure of the optical dispersion based on the determination of the refractive index using the D line of sodium, the C or red line of hydrogen, and the F or blue line of hydrogen. It is often characteristic of a given class of compounds and shows a greater variation within a class than the refractive index. It is defined as:

$$\nu = (n_D - 1)/(n_F - n_C).$$

It has been found that the compounds under study when arranged in order of decreasing ν correlate exactly with the order obtained by dividing the refrachor by the molecular weight. As shown in Table VI there was only one exception, trimethyl cyclohexyl tin.

TABLE VI

Specific refrachors and ν values of organotin compounds

	$100F/M$	ν
Bu_4Sn	71.21	45.5
iBu_4Sn	68.89	44.6
Pr_4Sn	66.48	41.5
iPr_4Sn	63.90	39.3
Et_4Sn	63.15	39.1
Me_3iPrSn	62.22	38.1
Me_3PrSn	62.05	37.7
Me_3EtSn	60.09	37.2
Me_4Sn	59.02	35.1
Me_3ViSn	57.37	33.5
$Me_3CyhexSn$	56.95	40.3
Vi_4Sn	53.58	30.2
$Me_3\phi Sn$	47.72	29.8

TABLE VII

Dispersion values and refractive indices of organotin compounds

	n_D	$n_F - n_C$	n_C'	n_F'	$(n_F - n_C)\frac{10^4}{D}$
Me_4Sn	1.4388	0.01250	1.4352	1.4478	97.6
Et_4Sn	1.4689	0.01199	1.4655	1.4775	101.5
Pr_4Sn	1.4718	0.01137	1.4685	1.4799	104.1
Bu_4Sn	1.4715	0.01036	1.4685	1.4789	99.6
iPr_4Sn	1.4828	0.01195	1.4796	1.4916	107.0
iBu_4Sn	1.4747	0.01065	1.4717	1.4823	101.9
Me_3EtSn	1.4490	0.01208	1.4456	1.4576	96.5
Me_3ViSn	1.4573	0.01366	1.4534	1.4670	106.9
$Me_3\phi Sn$	1.5337	0.01790	1.5285	1.5465	134.9
Me_3iPrSn	1.4507	0.01182	1.4473	1.4591	98.6
Vi_4Sn	1.4977	0.01647	1.4930	1.5094	131.3
Me_3PrSn	1.4517	0.01197	1.4483	1.4603	99.2
$Me_3CyhexSn$	1.4914	0.01218	1.4879	1.5001	100.2

A plot of F/M versus ν (in Fig. 2) shows reasonable correlation. The only important deviations are the two cyclic compounds, trimethyl phenyl and trimethyl cyclohexyl tin. Most of the compounds fall on or near a straight line whose equation is

$$Y = 1.154X + 18.8$$

where $Y = 100\ F/M$ and $X = \nu$.

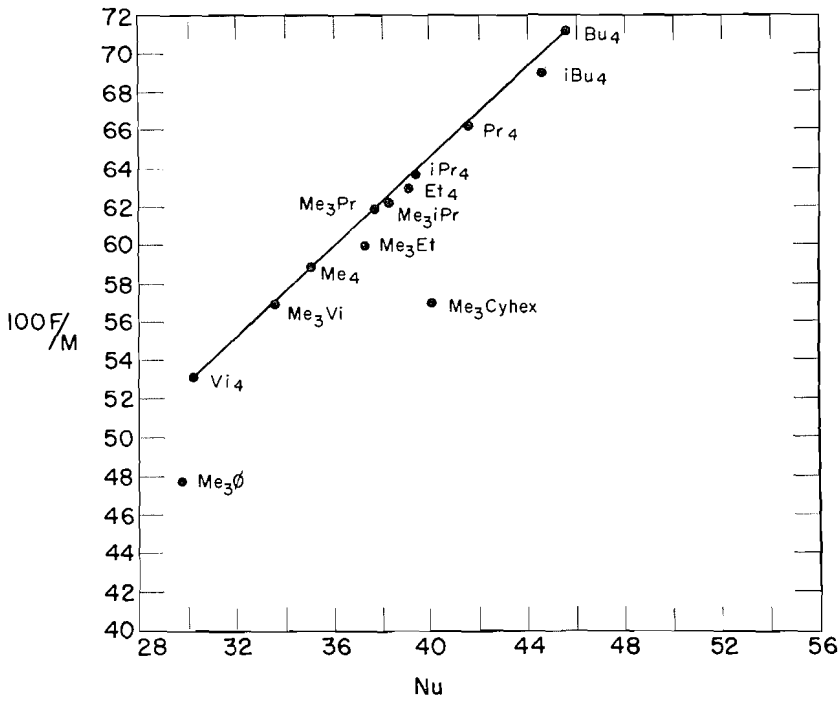


FIG. 2. Plot of F/M versus ν.

METHYLENE GROUP INCREMENTS

Work by Jones *et al.* (11) has indicated an alternation in the molar refraction increment in the *n*-tetra-alkyl tin series, and an initial indication of this is shown here for the lower members, the values being slightly different if the correction for air density (d) is included. The same effect is indicated by the ν values.

	Using $D - d$	Using D	ν
Me—Et	4.69	4.68	1.0
Et—Pr	4.78	4.79	0.6
Pr—Bu	4.69	4.67	1.0

Q VALUE

The Q value has been defined by Waldmann (12) as the ratio of the dispersions shown:

$$Q = (n_D - n_C)/(n_F - n_C).$$

Measurements on 100 organic materials gave an average value of $Q = 0.286$. The extremes varied from $+12$ to -10%, but most values deviated less than 5%. If we assume the stated value for Q, the individual calculated values n_F' and n_C' may be obtained from the measured values of n_D and the dispersion $n_F - n_C$. The data are given in Table VII. The average value of the mean specific dispersion times 10^4, omitting the unsaturated compounds, is 100.6.

REFERENCES

1. O. R. QUAYLE. Chem. Rev. **53**, 439 (1953).
2. S. J. SUGDEN. J. Chem. Soc. **125**, 1177 (1924).
3. H. H. ZUIDEMA and G. W. WATERS. Anal. Chem. **13**, 312 (1941).
4. S. J. SUGDEN. J. Chem. Soc. 1550 (1935).

Can. J. Chem. Downloaded from www.nrcresearchpress.com by 210.87.254.5 on 09/05/12
For personal use only.

5. I. KADOMTZEFF. Compt. Rend. **226**, 407 (1948).
6. P. TAIMSALU and J. L. WOOD. Trans. Faraday Soc. **59**, 1754 (1963).
7. A. VOGEL, W. CRESSWELL, G. JEFFERY, and J. LEICESTER. J. Chem. Soc. 514 (1952).
8. A. VOGEL, W. CRESSWELL, and J. LEICESTER. J. Phys. Chem. **58**, 174 (1954).
9. R. I. LAGEMANN and W. S. DUNBAR. J. Phys. Chem. **49**, 428 (1945).
10. S. S. JOSHI and G. D. TULI. J. Chem. Soc. 837 (1951).
11. W. JONES, D. EVANS, T. GULWELL, and D. GRIFFITHS. J. Chem. Soc. 39 (1935).
12. H. WALDMANN. Helv. Chim. Acta, **21**, 1053 (1938).

Can. J. Chem. Downloaded from www.nrcresearchpress.com by 210.87.254.5 on 09/05/12
For personal use only.

Can. J. Chem. Downloaded from www.nrcresearchpress.com by 210.87.254.42 on 09/05/12
For personal use only.

REACTIONS OF THERMAL ENERGY IONS

II. RATES OF SOME HYDROGEN TRANSFER ION–MOLECULE REACTIONS[1]

A. G. HARRISON,[2] A. IVKO,[3] AND T. W. SHANNON[4]

Department of Chemistry, University of Toronto, Toronto, Ontario

Received December 20, 1965

ABSTRACT

The rate constants for the ion–molecule reactions forming the protonated molecule in CH_3CN, H_2, CH_4, and CH_3OCH_3, the equivalent reactions in the deuteriated species, and the reactions forming COD^+ in CO–CD_4 mixtures have been measured at thermal energies and at 10.5 V/cm repeller field strength. For H_2, HD, D_2 and the reactions in CO–CD_4 mixtures the rate constant for the thermal reaction is approximately 0.3–0.5 that of the 10.5 V/cm rate constant. For all other cases the ratio of rate constants is approximately unity as predicted by the ion-induced dipole model. The absolute values of the rate constants in most cases are considerably lower than predicted by theory.

INTRODUCTION

Although mass spectrometric studies of gaseous ion–molecule reactions have provided much qualitative information of interest in radiation chemistry and other fields, they have provided little reliable quantitative data on the rates of reaction of thermal energy ions. In conventional mass spectrometric methods the reactant ions undergo acceleration by the electric field required to withdraw the ions from the ionization chamber, with the result that the measured kinetic data represent an appropriately weighted average for reactant ions with velocities ranging from zero to the final exit velocity. Estimation of the rate constants for thermal energy ions thus requires a knowledge of the dependence of the cross section on the electric field (or ion velocity), and this information does not appear to be easily obtainable.

For ion–molecule reactions where the interaction is determined by ion-induced dipole forces Gioumousis and Stevenson (1) have derived the following expression for the macroscopic (or observed) cross section, Q.[5]

$$Q = 2\pi \left(\frac{2M_1\alpha e^2}{\mu}\right)^{1/2} \left(eEl\right)^{-1/2} \qquad [1]$$

where M_1 is the mass of the ion, α is the polarizability of the neutral species, μ is the reduced mass of the colliding pair, e is the electronic charge, E is the field strength, and l is the path length of the reactant ion. They have also shown that the rate constant, k, is given by

$$k = \left(\frac{eEl}{2M_1}\right)^{1/2} Q \qquad [2]$$

and is, in this case, independent of field strength. Such a result has been obtained experimentally for a number of systems by Stevenson and colleagues (1, 2) although Field *et al.* (3–5) have found the cross section to follow an E^{-1} dependence for both simple

[1] *Part I is considered to be Can. J. Chem. 43, 159 (1965).*

[2] *Alfred P. Sloan Fellow 1962–1964.*

[3] *Exchange student 1964–1965. Present address: Department of Chemistry, Byelorussian State University, Minsk, U.S.S.R.*

[4] *Present address: Department of Chemistry, Purdue University, Lafayette, Indiana.*

[5] *The variable Q is given experimentally by* $Q = (I_s/I_p)l$ [m] *where* I_s *is the secondary ion current,* I_p *is the reactant ion current, l is the path length of the reactant ion, and* [m] *is the concentration of neutral species.*

and complex systems. Hamill and colleagues (6–10) have shown for several systems that the energy dependence changes with ion velocity. Recently Giese and Maier (11), using a preselected ion beam of known energy, have reported that the velocity dependence of the cross section for reactions involving H^+ transfer differs from that for reactions involving H transfer. The discrepancies in the results obtained by conventional techniques probably result from instrumental problems. This is particularly true at low field strengths where space charge and discrimination effects can become more serious.

Since it thus appears that conventional studies have not yielded reliable data for the reactions of thermal energy ions, several groups (12–15) recently have undertaken studies of ion–molecule reactions using pulsing techniques which permit the direct measurement of the rates of reaction of thermal energy ions. In this technique a short pulse of electrons is admitted to a field-free ion source to produce the reactant ions by electron impact. A known (and variable) time later, a second pulse is applied, either to the ion repeller or to the draw-out plate, which removes for mass analysis both the primary ions and those formed by bimolecular reactions. In the time interval between the two pulses the ions react under field-free conditions, and from the variation with this time of the product/reactant ion ratios, the rate of reaction under thermal conditions can be obtained.

In a continuation of our studies of the reactions of thermal energy ions we report in the present paper the determination of the rate constants for a number of hydrogen transfer ion-molecule reactions. We have also compared the thermal rate constants with those obtained at 10.5 V/cm repeller field strength to obtain some indication of the variation of rate constant with field strength.

EXPERIMENTAL

The apparatus and experimental techniques for determining the thermal rate constants have been described previously (15). Cross sections at 10.5 V/cm were determined in the usual manner or, where more than one reaction contributed to the product ion, by the ratio-plot technique outlined earlier (16). The cross sections were converted to rate constants by eq. [2].

All chemicals were reagent grade and, with the exception of the labelled methanes, showed no detectable impurities in the mass spectra. Deuterium gas was obtained from The Matheson Co., Inc., while the other labelled samples were supplied by Merck, Sharp & Dohme of Canada Ltd. The mass spectra of the labelled methanes showed the presence of air impurity ranging up to 5%.

RESULTS AND DISCUSSION

The thermal rate constants, k(pulse), are compared in Table I with the rate constants obtained from the 10.5 V/cm data by eq. [2]. The thermal data for the methanes have been presented previously (15) as have the 10.5 V/cm data for the CO–CD_4 mixture (16), D_2, and CH_3CN (17). Each rate constant is an average of three or more determinations.

[3] $$D_2^+ + D_2 \rightarrow D_3^+ + D$$

[4a] $$HD^+ + HD \rightarrow \begin{cases} H_2D^+ + D \\ HD_2^+ + H \end{cases}$$

[5] $$H_2^+ + H_2 \rightarrow H_3^+ + H$$

[6] $$CH_4^+ + CH_4 \rightarrow CH_5^+ + CH_3$$

[7a] $$CH_3D^+ + CH_3D \rightarrow \begin{cases} CH_4D^+ + CH_2D \\ CH_3D_2^+ + CH_2 \end{cases}$$

Can. J. Chem. Downloaded from www.nrcresearchpress.com by 210.87.254.42 on 09/05/12
For personal use only.

[8a] $CH_2D_2^+ + CH_2D_2 \rightarrow CH_3D_2^+ + CHD_2$

[8b] $CH_2D_2^+ + CH_2D_2 \rightarrow CH_2D_3^+ + CH_2D$

[9a] $CHD_3^+ + CHD_3 \rightarrow CH_2D_3^+ + CD_3$

[9b] $CHD_3^+ + CHD_3 \rightarrow CHD_4^+ + CHD_2$

[10] $CD_4^+ + CD_4 \rightarrow CD_5^+ + CD_3$

[11] $CD_4^+ + CO \rightarrow COD^+ + CD_3$

[12] $CO^+ + CD_4 \rightarrow COD^+ + CD_3$

[13] $CH_3CN^+ + CH_3CN \rightarrow CH_3CNH^+ + CH_2CN$

[14] $(CH_3)_2O^+ + (CH_3)_2O \rightarrow (CH_3)_2OH^+ + CH_3OCH_2$

[15a] $CD_3OCH_3^+ + CD_3OCH_3 \rightarrow CD_3OCH_3H^+ + CD_3OCH_2$

[15b] $CD_3OCH_3^+ + CD_3OCH_3 \rightarrow CD_3OCH_3D^+ + CH_3OCD_2$

TABLE I

Rate constants for hydrogen transfer reactions

Reaction No.	k(pulse) (cm^3 molecule^{-1} s^{-1}) $\times 10^{10}$	k(10.5 V/cm) (cm^3 molecule^{-1} s^{-1}) $\times 10^{10}$	k(pulse)/k(10.5 V/cm)
[3]	5.8	15.0	0.38
[4a]	3.8	8.4	0.45
[4b]	2.9	6.9	0.42
[5]	5.9	13.3	0.44
[6]	6.12	7.58	0.81
[7a]	4.47	5.86	0.76
[7b]	1.30	1.73	0.75
[8a]	2.70	4.18	0.65
[8b]	2.16	3.36	0.65
[9a]	1.64	2.30	0.71
[9b]	3.36	4.90	0.69
[10]	4.71	6.35	0.74
[11]	1.96	5.22	0.38
[12]	2.67	5.57	0.48
[13]	18.7	21.5	0.87
[14]	9.49	8.24	1.15
[15a]	5.36	4.76	1.13
[15b]	4.39	4.13	1.07

For D_2, HD, and H_2, k(pulse) is considerably lower than k(10.5 V/cm), the ratio varying between 0.38 and 0.45. For H_2 and D_2, our results are in good agreement with the results of Ryan and Futrell (14) who reported k(pulse) = 4.73×10^{-10} for D_2, k(pulse) = 6.6×10^{-10} for H_2, and a ratio k(pulse)/k(10 V/cm) = 0.33 for both systems. As they have pointed out, these systems are unique in that the product and reactant ions differ by >50% in mass so that mass discrimination effects are difficult to avoid in the zero field work; furthermore, it is not possible to correct for these effects as was done for the methanes (15). Typical examples of the experimental results for the hydrogen isotopes are shown in Figs. 1 and 2 and it is apparent that mass discrimination effects are important, particularly in the H_2 and HD systems. For D_2 (Fig. 1) the ratio $I_{D_3^+}/I_{D_2^+}$ was linear with delay time to approximately 1 μs, following which an upward curvature was

Can. J. Chem. Downloaded from www.nrcresearchpress.com by 210.87.254.42 on 09/05/12
For personal use only.

observed undoubtedly due to mass discrimination. For H_2 and HD, much more serious discrimination effects were observed and it was necessary to work with very short ionizing pulses ($\leqslant 0.1$ μs) and to limit the total delay time. As shown in Fig. 2 the plots of the ion current ratio versus delay time break upward after approximately 0.16 μs delay time. As would be expected the $I_{H_2D^+}/I_{HD^+}$ curve is linear over a longer region than that of $I_{HD_2^+}/I_{HD^+}$. We have taken the slopes of the initial linear portions to obtain the thermal rate constants.

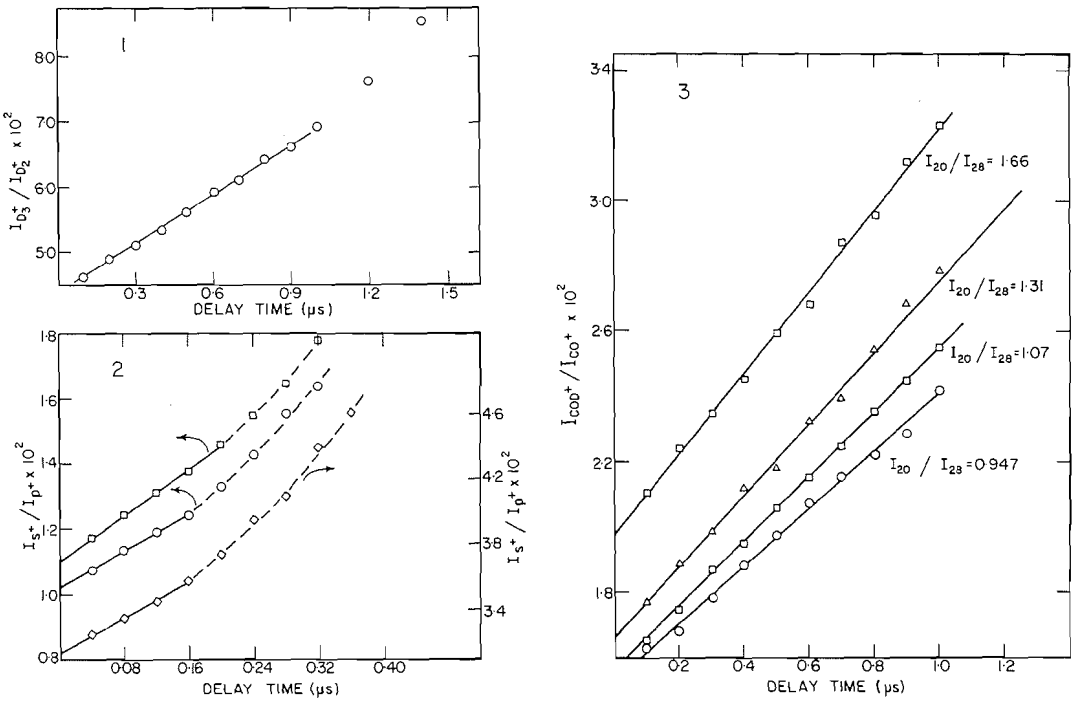


FIG. 1. Typical results for reaction $D_2^+ + D_2 \rightarrow D_3^+ + D$.
FIG. 2. Typical results for reactions in H_2 and HD: □, $I_{H_2D^+}/I_{HD^+}$ versus t in HD; ○, $I_{HD_2^+}/I_{HD^+}$ versus t in HD; ◇, $I_{H_3^+}/I_{H_2^+}$ versus t in H_2.
FIG. 3. Typical results for formation of COD^+ in CO–CD_4 mixtures.

Discrimination effects due to the higher thermal velocity of the reactant ion should vary considerably in this series since M_{s^+}/M_{p^+} varies from 1.33 (H_2D^+/HD^+) to 1.67 (HD_2^+/HD^+). The good agreement of the measured rate constants for the various isotopic reactions suggests that this is not a significant error. Further, such discrimination, if significant, would lead to erroneously high rate constants. Such considerations lead us to believe that the result k(pulse)/k(10.5 V/cm) ≈ 0.40 is not seriously in error.

The results obtained for the hydrogen transfer reactions in the methane series yield k(pulse)/k(10.5 V/cm) in the range 0.65–0.80. This result is not significantly lower than the ratio k(thermal)/k(10 V/cm) = 0.92 obtained for the reaction in CH_4 by Ryan and Futrell (18) using a modified pulsing technique.

It has been shown previously (16) that the formation of COD^+ in CO–CD_4 mixtures is the result of both reactions [11] and [12], and the cross sections and derived rate constants at 10.5 V/cm field strength have been reported. For the two concurrent reactions studied by the present pulsing techniques the secondary ion current observed after a time

Can. J. Chem. Downloaded from www.nrcresearchpress.com by 210.87.254.42 on 09/05/12
For personal use only.

delay, t, can be expressed as the sum of two independent contributions, neglecting small differences in collection efficiencies

$$[16] \qquad I_{COD^+} = (k_{11}[CO]I_{CD_4^+} + k_{12}[CD_4]I_{CO^+})t + C$$

where C is a constant reflecting the COD^+ originating by reaction occurring during the ionizing and withdrawal pulses. Rearrangement of the above equation, as follows,

$$[17] \qquad \frac{I_{COD^+}}{I_{CO^+}} = \left[k_{11}[CO]\frac{I_{CD_4^+}}{I_{CO^+}} + k_{12}[CD_4]\right]t + C$$

shows that the slope of the I_{COD^+}/I_{CO^+} versus t plots should be a function of the primary ion current ratio $I_{CD_4^+}/I_{CO^+}$, for constant source concentration. Typical results are shown in Fig. 3 for $[CO] = 2.30 \times 10^{13}$ molecules cm^{-3} and $[CD_4] = 2.05 \times 10^{13}$ molecules cm^{-3}. The $I_{CD_4^+}/I_{CO^+}$ ratio was varied by changing the ionizing electron energy and, over the range of delay times used, remained constant for constant electron energy. The slopes of the lines, such as those in Fig. 3, are plotted in Fig. 4 against the $I_{CD_4^+}/I_{CO^+}$ ratio. Although the scatter is fairly large, a reasonable straight line is obtained which yields, by least squares analysis, the values of k_{11}(pulse) and k_{12}(pulse) recorded in Table I. Although these values are obviously subject to large errors, there seems to be little doubt that the thermal rate constants are significantly lower than the 10.5 V/cm rate constants.

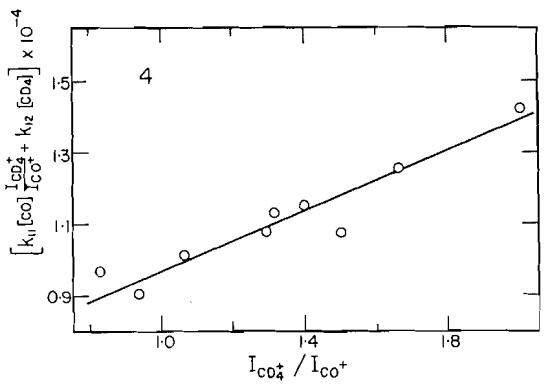


FIG. 4. Analysis of results for CO–CD_4 mixtures.

Typical results obtained in the study of reaction [13] are shown in Fig. 5. In this case the relatively high mass and small percentage mass difference permitted delay times up to 3 μs without any indication of mass discrimination. In view of the high rate constant for this reaction the rate constant was evaluated from the plot of

$$\log\left[1 + \frac{I_{CH_3CNH^+}}{I_{CH_3CN^+}}\right] \text{ versus } t.$$

The average of six determinations gave k(pulse) $= 18.7 \pm 2.1 \times 10^{-10}$ cm^3 $molecule^{-1}$ s^{-1}, only slightly lower than k(10.5 V/cm) $= 21.5 \pm 2.1 \times 10^{-10}$ cm^3 $molecule^{-1}$ s^{-1}. The ratio of rate constants is thus approximately unity.

In CH_3OCH_3 an abundant formation of the protonated ion $(CH_3)_2OH^+$ was observed. The ratio $I_{(CH_3)_2OH^+}/I_{(CH_3)_2O^+}$ was found to increase with increasing electron energy indicating occurrence of further reactions in addition to reaction [14]. The mass spectrum

Can. J. Chem. Downloaded from www.nrcresearchpress.com by 210.87.254.42 on 09/05/12
For personal use only.

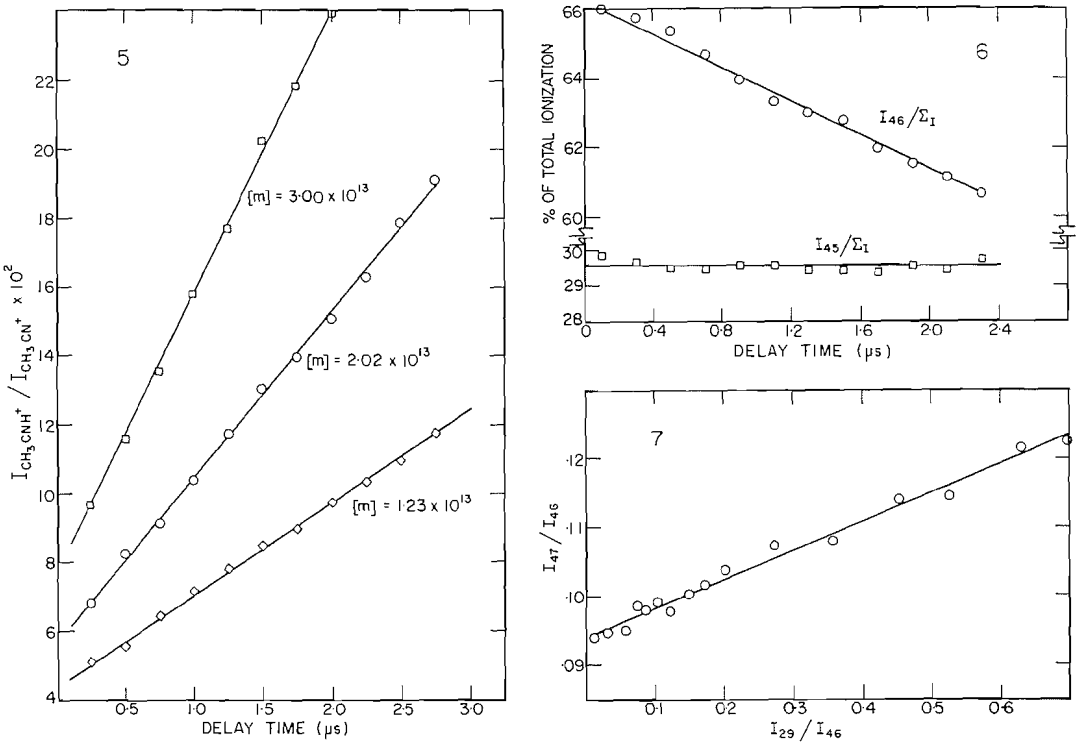


FIG. 5. Experimental results for the reaction $CH_3CN^+ + CH_3CN \rightarrow CH_3CNH^+ + CH_2CN$ where [m] refers to concentration of neutral species in molecules cm^{-3}.
FIG. 6. Ion intensities as a function of delay time for CH_3OCH_3.
FIG. 7. Plot of $I_{(CH_3)_2OH^+}/I_{(CH_3)_2O^+}$ versus $I_{CHO^+}/I_{(CH_3)_2O^+}$ for the CH_3OCH_3 system.

shows three major primary ions which must be considered as possible reactants in the following reactions.

[14] $$(CH_3)_2O^+ + (CH_3)_2O \rightarrow (CH_3)_2OH^+ + CH_3OCH_2$$

[18] $$CH_3OCH_2^+ + (CH_3)_2O \rightarrow (CH_3)_2OH^+ + ?$$

[19] $$CHO^+ + (CH_3)_2O \rightarrow (CH_3)_2OH^+ + CO$$

The occurrence of reaction [14] and the non-occurrence of reaction [18] was indicated by the ratio-plot technique (16) at low electron energies although the data were not very accurate due to the small range of ion current ratios which could be covered before the CHO^+ made a significant contribution. To provide further evidence the behavior of the $CH_3OCH_3^+$ and $CH_3OCH_2^+$ ion currents with delay time were examined at low energies where only these two ions and the $(CH_3)_2OH^+$ ion were significant. As shown in Fig. 6, $I_{CH_3OCH_2^+}$ remains a constant % of the total ion current with increasing reaction time while $I_{CH_3OCH_3^+}$ decreases as a percentage of the total. We thus conclude that reaction [14] occurs but that reaction [18] does not. At higher electron energies the occurrence of reaction [19] in addition to reaction [14] is indicated by the ratio plot (Fig. 7) obtained at 10.5 V/cm field strength. From such ratio plots we obtained $Q_{14} = 47.5 \times 10^{-16}$ cm^2 $molecule^{-1}$ and $Q_{19} = 27.5 \times 10^{-16}$ cm^2 $molecule^{-1}$ corresponding to rate constants of 8.24×10^{-10} cm^3 $molecule^{-1}$ s^{-1} and 5.66×10^{-10} cm^3 $molecule^{-1}$ s^{-1} respectively for the two reactions. In Fig. 8 we show typical results for variation of $I_{(CH_3)_2OH^+}/I_{CH_3OCH_3^+}$ with

Can. J. Chem. Downloaded from www.nrcresearchpress.com by 210.87.254.42 on 09/05/12
For personal use only.

delay time and it can be seen that the slope is much greater at 50 eV than at 10 eV nominal electron energy where the CHO^+ ion was absent from the spectrum. From the low energy data k_{14}(pulse) was found to be 9.49×10^{-10} cm^3 molecule^{-1} s^{-1}. Analysis of the results for the rate of disappearance of $CH_3OCH_3^+$ gave rate constants in good agreement. From the 50 eV data one arrives at a rough estimate k_{19}(pulse) $\approx 8 \times 10^{-10}$ cm^3 molecule^{-1} s^{-1}. It should be emphasized that at 50 eV further reactions in addition to [14] and [19] may occur (e.g. reaction of CH_3O^+) with consequent errors in the rate constant for reaction of CHO^+. Figure 8 also shows typical results obtained for the transfer reactions in CH_3OCD_3 at electron energies where the CHO^+ and CDO^+ ions were absent from the spectrum. At 50 eV both the rate of formation of $CD_3OCH_3H^+$ and $CD_3OCH_3D^+$ were considerably higher, again indicating reaction of other ions. As shown in Table I for the reactions studied in the ethers, k(pulse)/k(10.5 V/cm) is slightly above unity.

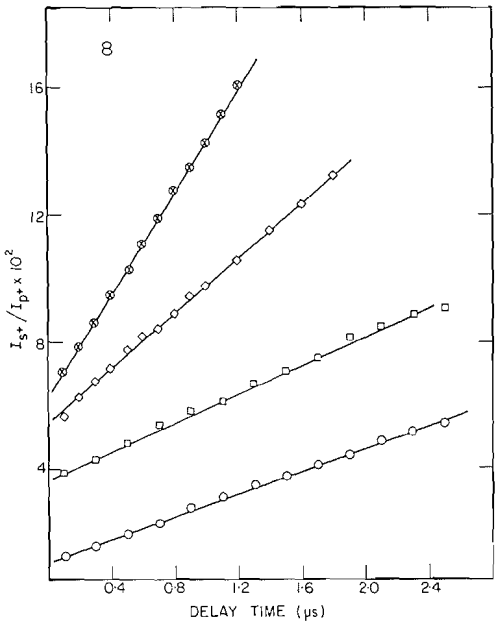


FIG. 8. Experimental results for dimethyl ether: ⊗, $I_{(CH_3)_2OH^+}/I_{(CH_3)_2O^+}$ versus t at 50 eV for CH_3OCH_3; ◇, $I_{(CH_3)_2OH^+}/I_{(CH_3)_2O^+}$ versus t at 10 eV for CH_3OCH_3; □, $I_{CH_3OCD_3H^+}/I_{CH_3OCD_3^+}$ versus t at 10 eV for CD_3OCH_3; ○, $I_{CH_3OCD_3D^+}/I_{CH_3OCD_3^+}$ versus t at 10 eV for CD_3OCH_3.

In summary, the thermal rate constants for the self-reactions in H_2, HD, and D_2 and for the reactions leading to COD^+ in CO–CD_4 mixtures are significantly lower than the rate constants obtained at 10.5 V/cm. The differences would appear to be outside the limits of error and thus we conclude that the ion-induced dipole model does not adequately describe these systems. For most of the remaining reactions listed in Table I, k(pulse)/k(10.5 V/cm) < 1. Since random experimental errors would not be expected to give ratios below unity, such a result must either be significant or due to some systematic error. In an examination of possible systematic errors we can immediately eliminate errors of ion source concentration since the thermal and 10.5 V/cm data usually were determined with a close time relationship so that flow characteristics and hence ion source concentrations did not vary. Discrimination effects in the pulsing experiments

Can. J. Chem. Downloaded from www.nrcresearchpress.com by 210.87.254.42 on 09/05/12
For personal use only.

either due to the higher thermal velocity of the primary ion or due to diffusion of secondary ions initially formed outside the ionizing volume into the ionizing volume (18) cannot account for the results for two reasons. Firstly, such discrimination effects cannot be important in the present work since usually $<20\%$ of the primary ions were lost at the longest delay times used and, secondly, such discrimination effects, if significant, would lead to erroneously high thermal rate constants and hence to ratios of rate constants greater than unity rather than less. On the other hand, a systematic error leading to the observed results could occur if the inherent mass spectrometer collection efficiency for secondary ions were lower in the pulsing mode than during continuous ion repulsion. The magnitude of such an effect cannot be assessed but would probably depend on the kinetic energy of the secondary ion and its position of formation.

INTRAMOLECULAR ISOTOPE EFFECTS

The results for HD, CD_3OCH_3, and the partially deuteriated methanes provide information in intramolecular H/D isotope effects in hydrogen transfer reactions. The isotope effects, summarized in Table II, are relatively small. At thermal energies it is probable

TABLE II

H–D isotope effects

Reactants	k_H/k_D(pulse)	k_H/k_D(10.5 V/cm)
$HD^+ + HD$	1.31	1.22
$CH_3D^+ + CH_3D$	1.15	1.14
$CH_2D_2^+ + CH_2D_2$	1.25	1.25
$CHD_3^+ + CHD_3$	1.46	1.41
$CD_3OCH_3^+ + CD_3OCH_3$	1.22	1.15

that the reactions proceed through formation of an intermediate collision complex and these small isotope effects undoubtedly arise in the decomposition of this complex. The good agreement of the isotope effects observed at 10.5 V/cm field strength with those observed at thermal energies suggests that there is no change in reaction mechanism over this energy range. It is interesting to note that the results for the deuteriated methanes show an apparent increase in the isotope effect with increasing deuterium substitution. Such an effect might be expected since increased deuterium substitution will increase the total non-fixed energy of the collision complex and thus lead to a more rapid H transfer process compared to the D transfer process. A similar effect is observed (19) in the fragmentation of the methane parent ion where increasing deuterium substitution leads to an increased probability of rupture of the C—H bond. For all the reactions studied it is impossible by the present techniques to determine whether the reaction proceeds by a neutral atom or a positive ion transfer process; thus more detailed consideration of these isotope effects does not appear justified. Further work is in progress to study the intramolecular isotope effects in neutral atom and positive ion transfer reactions.

COMPARISON OF EXPERIMENTAL AND THEORETICAL RATE CONSTANTS

For the ion-induced dipole model of ion–molecule reactions it has been shown (20) that the rate constant k is given by

$$k = 2\pi e \left(\frac{\alpha}{\mu}\right)^{1/2}, \qquad [20]$$

Can. J. Chem. Downloaded from www.nrcresearchpress.com by 210.87.254.42 on 09/05/12
For personal use only.

where the symbols are as defined previously. The experimental rate constants are compared in Table III with the values calculated by eq. [20]. For the reaction in CH_3CN

TABLE III

Comparison of experimental and calculated rate constants

Reactants	k(pulse) (cm^3 $molecule^{-1}$ s^{-1}) $\times 10^{10}$	k(10.5 V/cm) (cm^3 $molecule^{-1}$ s^{-1}) $\times 10^{10}$	k(calc)* (cm^3 $molecule^{-1}$ s^{-1}) $\times 10^{10}$
$H_2^+ + H_2$	5.9	13.3	20.8
$D_2^+ + D_2$	5.8	15.0	14.5
$CH_4^+ + CH_4$	6.12	7.58	13.36
$CD_4^+ + CD_4$	4.71	6.35	11.86
$CD_4^+ + CO$	1.96	5.22	9.51
$CO^+ + CD_4$	2.67	5.87	10.97
$CH_3CN^+ + CH_3CN$	18.7	21.5	11.0
$CH_3OCH_3^+ + CH_3OCH_3$	9.49	8.24	11.15

*k calculated on basis of ion-induced dipole interactions only.

the experimentally measured rate constants are considerably higher than the calculated value presumably because of the neglect of ion–dipole forces in calculating the rate constant. A similar neglect probably invalidates the calculations in the dimethyl ether case as well. For the other cases, where ion–dipole interactions should be negligible, it is found that the measured rate constants are markedly lower than predicted by theory. This indicates that a rather large proportion of the ion–molecule collisions does not lead to the protonated species. Whether this is due to reversion to reactants (transmission coefficient <1) or to competing reactions, such as charge exchange, is not known. It might be noted that for the self-reactions the charge exchange reaction is a resonance process and might be expected to occur with a relatively high cross section.

ACKNOWLEDGMENTS

The authors are indebted to the National Research Council for financial support of this work and for the award of a Studentship (1964–1965) to T. W. S.

REFERENCES

1. G. Gioumousis and D. P. Stevenson. J. Chem. Phys. **29**, 294 (1958).
2. D. P. Stevenson and D. O. Schissler. J. Chem. Phys. **29**, 282 (1958).
3. F. H. Field, J. L. Franklin, and F. W. Lampe. J. Am. Chem. Soc. **79**, 2419 (1957).
4. F. H. Field, J. L. Franklin, and F. W. Lampe. J. Am. Chem. Soc. **79**, 2665 (1957).
5. F. H. Field and F. W. Lampe. J. Am. Chem. Soc. **80**, 5583 (1958).
6. N. Boelrijk and W. H. Hamill. J. Am. Chem. Soc. **84**, 730 (1962).
7. R. F. Pottie, A. J. Lorquet, and W. H. Hamill. J. Am. Chem. Soc. **84**, 529 (1962).
8. L. P. Theard and W. H. Hamill. J. Am. Chem. Soc. **84**, 1134 (1962).
9. D. A. Kubose and W. H. Hamill. J. Am. Chem. Soc. **85**, 125 (1963).
10. T. F. Moran and W. H. Hamill. J. Chem. Phys. **39**, 1413 (1963).
11. C. F. Giese and W. B. Maier. J. Chem. Phys. **39**, 739 (1963).
12. V. L. Tal'roze and E. L. Frankevich. Russ. J. Phys. Chem. English Transl. **34**, 1275 (1960).
13. C. W. Hand and H. von Weyssenhoff. Can. J. Chem. **42**, 195 (1964); **42**, 2385 (1964).
14. K. R. Ryan and J. H. Futrell. J. Chem. Phys. **42**, 824 (1965).
15. T. W. Shannon, F. Meyer, and A. G. Harrison. Can. J. Chem. **43**, 159 (1965).
16. T. W. Shannon and A. G. Harrison. J. Chem. Phys. **43**, 4201 (1965).
17. T. W. Shannon and A. G. Harrison. J. Chem. Phys. **43**, 4206 (1965).
18. K. R. Ryan and J. H. Futrell. J. Chem. Phys. **43**, 3009 (1965).
19. D. O. Schissler, S. O. Thompson, and J. Turkevitch. Discussions Faraday Soc. **10**, 46 (1951).
20. M. A. Eliason and J. O. Hirschfelder. J. Chem. Phys. **30**, 1426 (1959).

Can. J. Chem. Downloaded from www.nrcresearchpress.com by 210.87.254.42 on 09/05/12
For personal use only.

Can. J. Chem. Downloaded from www.nrcresearchpress.com by 210.87.254.40 on 09/05/12
For personal use only.

A METHOD FOR THE DETERMINATION OF WATER IN NONPOLAR LIQUIDS; THE SOLUBILITY OF WATER IN BENZENE

D. C. MOULE AND W. M. THURSTON
Research Chemistry Branch, Atomic Energy of Canada Limited, Chalk River, Ontario
Received February 8, 1966

ABSTRACT

A new method is described for the analysis of water in nonpolar organic liquids. It is based on an isotope dilution procedure and involves the exchange of the water present in the sample with D_2O. The change in isotopic composition of the D_2O is determined by infrared difference spectroscopy. The method appears to be accurate to $\pm 0.8\%$.

The principal advantage of this method is that the difficult problem of calibration with organic–water standards is avoided. It is restricted, however, to solvents which have a low solubility in water and do not have exchangeable hydrogens.

A series of solubility measurements were carried out for H_2O in C_6H_6 from 10 to 60 °C. The data were fitted to the usual interpolation equation $\ln (f/x) = -A/T + B \ln T + C$, and the thermodynamic functions of solution, ΔG, ΔH, ΔC_p, and ΔS, were computed for the transfer of 1 mole of water from the benzene phase to the vapor phase.

INTRODUCTION

A review of the profusion of papers published on water analysis indicates that there has been real difficulty in the determination of water solubility in hydrocarbons to an accuracy approaching 1%. This is partly because it is extremely difficult to prepare exact water concentrations in the organic materials used to calibrate and test an analytical method, and also because it is difficult to avoid contamination of the samples by atmospheric water, during and at the end point of an analysis. Methods which use tritiated water as a tracer may introduce errors associated with the tritium isotope effect, which are not easily accounted for.

We have developed an isotope dilution method for the determination of the solubility of H_2O in organic solvents which avoids some of these difficulties. It is based on a precision method for the determination of H_2O in D_2O which has recently been developed in these laboratories (1). Essentially, a quantity of benzene saturated with light water at a constant temperature is equilibrated with a known amount of heavy water and the change in heavy water concentration is determined by infrared difference spectroscopy. Water solubility is calculated from the concentration change in the heavy water, the quantities of heavy water and benzene involved, and a blank correction.

EXPERIMENTAL

1. *Materials*

Reagent grade benzene (Fisher Certified) was fractionally distilled twice and dried over molecular sieve (Linde No. 4A). Light water from the Ottawa River (0.0146 mole % D_2O) (2) was redistilled from alkaline permanganate. The reactor grade heavy water, 99.82 wt. % D_2O, used in this experiment had a specific conductance of $5 \times 10^{-6}\ \Omega^{-1}\ cm^{-1}$ and was not purified further.

2. *Saturation of Benzene with Water*

In a typical experiment, 5 ml H_2O and 25 ml dry benzene were placed in a 50 ml volumetric flask, which was closed with a Teflon stopper and inserted into a constant temperature bath. Samples were agitated in the thermostat for 12 h to ensure that equilibrium between the two phases was complete. Before the benzene phase was decanted, the samples were left for another 24 h in the bath to allow the liquid layers to separate completely. The temperature was measured by a platinum resistance thermometer and controlled to ±0.02 °C.

3. Isotope Exchange

About 15 ml saturated benzene were withdrawn quickly from the thermostated liquid into a 30 ml hypodermic syringe (Multifit, Luer Lock) to which was added 2–10 ml reference D_2O solution, taken from the heavy water storage reservoir. The needle tip of the syringe was capped with a rubber stopper and the liquid phases agitated for 4 h on a wrist-action shaker until the isotope exchange between the H_2O dissolved in the benzene phase, and the D_2O phase, was complete. The weight of the benzene and heavy water phases was determined by weighing the syringe and contents during the sampling process.

It was necessary to soak the inside of the syringes with D_2O for 24 h before use, in order to eliminate H_2O absorbed on the surface of the glass by exchange with D_2O. After this treatment, syringes were dried in a vacuum oven and stored in a desiccator until required.

4. The Infrared Cell

Only a brief description of the infrared cell will be given here as complete details are given elsewhere (1). The cell was designed primarily to reduce temperature differences between the sample and reference compartments, which can be a serious limitation in infrared liquid analysis. A novel feature of the cell design was the union of the reference (A) and sample (B) compartments into a single cell (C), as illustrated in Fig. 1.

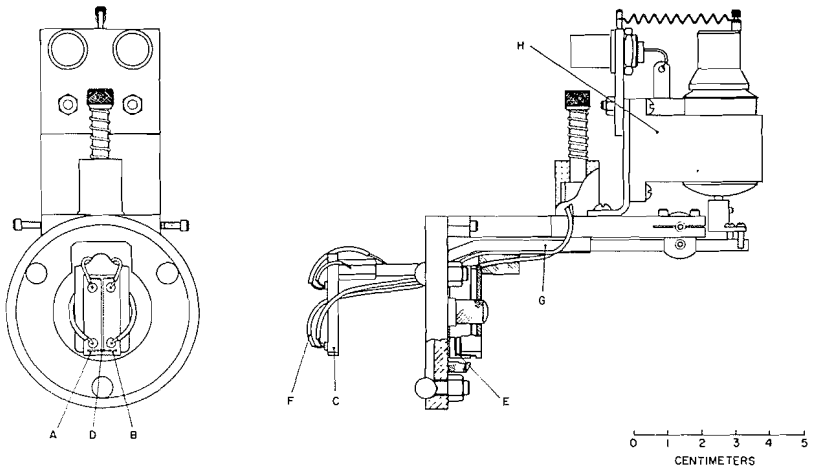


FIG. 1. The infrared cell.

Sample and reference compartments were formed between common sapphire windows and separated by a silver–epoxy divider (D). This arrangement allowed the liquids in the two compartments to come quickly to thermal equilibrium even though the cell was not at the temperature of the spectrometer. To reduce heating of the sample by the infrared radiation a bandpass filter (E) was inserted into the light beam. Sample and reference solutions were introduced into the cell compartments through Teflon leads (F) by displacing the heavy water within the cell out through the outlet tube (G). To measure the difference in optical density between sample and reference solutions, the compartments were interchanged in the front beam of the spectrometer by the motor drive (H). As the spectrometer operated on time drive, at fixed frequency, a square wave was traced on the chart paper. Ordinate scale expansion was used to magnify the amplitude of the square wave trace and thereby increase the precision to which the absorbance difference between the sample and reference compartments could be measured. The concentration of the unknown sample was calculated from the optical density difference between the sample and reference solution, the calibration factor, and the concentration of the reference solution.

5. Heavy Water Containers

Considerable care was given to the development of apparatus and techniques for the preparation, storage, and transfer of the heavy water standard solutions, as the accuracy of the analytical method is limited by the stability of the deuterium content of the heavy water. The containers for the heavy water standards, shown in Fig. 2, were of vacuum tight construction. The vessel consisted of a stainless steel beaker (A) closed at the top by a steel plate (B). Heavy water was introduced into the containers through a brass filling cap (C), which was sealed by O-ring (D). The vessel and contents were pressurized with helium to prevent atmospheric moisture from entering the system. Samples were removed from the containers by opening valve (E), the pressure within the vessel forcing the heavy water out through lead (I).

A cross section of the two-way valve is illustrated in Fig. 2. It was constructed mainly from brass and consisted of two grease-free metal valves joining side arms (J) and (K) to common arm (I). The side arm of

Can. J. Chem. Downloaded from www.nrcresearchpress.com by 210.87.254.40 on 09/05/12
For personal use only.

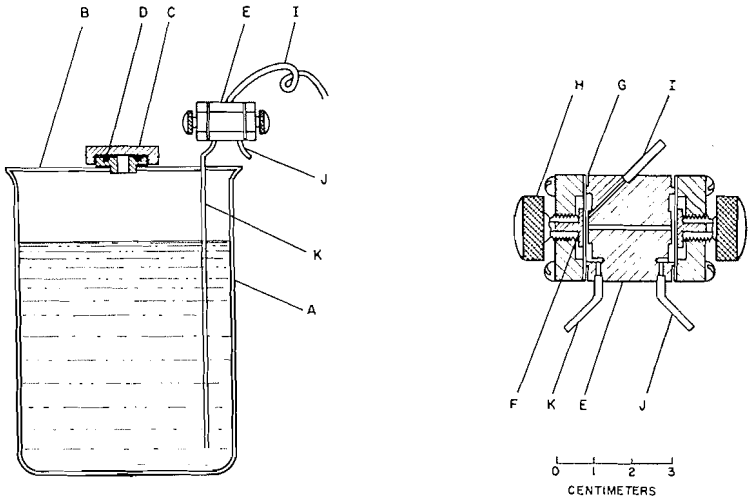


FIG. 2. Containers for storing heavy water reference and standard solutions.

the valve was closed to the outlet lead by tightening thumb screw (H) which applied pressure to disc (F) and forced neoprene diaphragm (G) into the valve seat. The rubber diaphragm was found to be sufficiently elastic to open the valve when the pressure from the thumb screw was released. The inside of the valve, and the Teflon tube (I) which lead to the infrared cell could be alternately flushed from side arm (J) with dry nitrogen and heavy water before the standard solution was withdrawn from the storage container.

Three 1-l vessels were constructed to contain the heavy water standard solutions (heavy water which had been diluted by the addition of 0.22–0.24 wt. % H_2O) and one 3-l vessel to hold the heavy water reference solution (undiluted heavy water, 99.82 wt. % D_2O).

6. Preparation of the D_2O Standard Solutions

The containers for the heavy water storage were carefully cleaned, dried, and treated with aliquots of heavy water over a period of several days to eliminate traces of light water. In a light-water-free atmosphere, 500 g D_2O was carefully weighed into each of the three standard solution containers. At about the same time 2 l D_2O was added to the reference solution vessel. The heavy water in the storage containers was degassed, pressurized slightly above 1 atm with helium, and then left for a week with intermittent shaking to allow the isotopic composition of the water to reach a constant value. The heavy water samples were compared against each other by infrared difference analysis to check for possible contamination by traces of water introduced during the cleaning and filling process. No evidence of heavy water degradation was found. Three heavy water standard solutions were prepared by adding weighed amounts of H_2O (1.1–1.2 g) to 500 g of the D_2O reference solution to give standard solutions of 0.2201, 0.2297, and 0.2401 wt. % H_2O relative to the undiluted reference solution.

7. Procedure for Filling the Infrared Cell

At least 24 h before an analysis the compartments of the infrared cell were filled with undiluted D_2O (reference solution) to offset the memory effect associated with H_2O absorbed on the metal and sapphire inside surfaces of the cell. Before the heavy water container was connected to the infrared cell, outlet lead (I) of Fig. 2 was dried with a stream of dry nitrogen introduced through side arm (J). The Teflon leads of the reference compartment of the infrared cell and the outlet lead from the heavy water standard container were connected by a length of hypodermic needle in such a fashion as to minimize air pockets at the junction. The valve of the heavy water container was slowly opened and the standard solution allowed to displace the liquid in the cell. Usually ~1 ml of heavy water flushed slowly through the cell compartment was sufficient to bring the isotopic concentration of the water in the cell to the concentration of the heavy water standard. It was necessary to reduce the helium pressure in the heavy water storage containers to ~1.01 atm in order to eliminate the formation of micro bubbles in the infrared cell created by the degassing of helium under the action of the infrared light. The flow of heavy water into the system was assisted by elevating the heavy water reservoir several feet above the infrared cell.

The unknown samples resulting from the equilibration of moist benzene with heavy water were removed from the wrist action shaker (see Section 3) and injected from the hypodermic syringes directly into the sample compartment of the infrared cell. A minimum of 0.5 ml of sample was used for each determination.

Can. J. Chem. Downloaded from www.nrcresearchpress.com by 210.87.254.40 on 09/05/12
For personal use only.

8. Spectrometer Conditions

For the optical density measurements a Perkin-Elmer model 21 infrared spectrometer operated at a fixed frequency of 3 400 cm^{-1}, a slit width of 300 μ, and a time drive of 2 cm/min was used. Reference and sample cell compartments were interchanged in the front beam of the spectrometer about every 20 s, for a 5 min period. A variable density spiral filter (1) was inserted into the back beam of the spectrometer to compensate for absorption from the cell and its contents. The band pass filter transmitted at a frequency of 3 380 cm^{-1} with a full-width at half-maximum of 260 cm^{-1}. When scale expansion of 10 times was used, ordinate pen displacement of 5 cm or less was found to be directly proportional to optical density.

9. Experimental Procedure and Calculation of Data

The experimental procedure and the treatment of observed data may be illustrated from the results of a typical experiment shown in Table I. The second and third columns give the relative isotopic composition of

TABLE I

Results of a typical experiment to determine the solubility of light water in benzene at 24.54 °C

Run	Sample compartment (wt % H_2O)	Reference compartment (wt % H_2O)	$I_S - I_R$ (mm pen displacement) 1	2	3	Av.
1	0.2401	0.2401	6.0	7.0	7.0	6.7
2	0.2297	0.2201	65.4	63.4	65.4	64.7
3	0.2401	0.2297	76.9	76.4	76.9	76.7
4	Unknown	0.2201	87.4	84.4	85.4	85.7

the heavy water solutions in the sample and reference compartments of the infrared cell. The remaining columns list the optical density differences, in mm of pen displacement for 10× scale expansion between sample and reference compartments for three successive interchanges of the compartments in the front beam of the spectrometer. In run 1 the reference and sample compartments were filled with identical heavy water standard solutions. The observed infrared absorption, referred to as the cell constant, resulted from a mismatch in path length, geometry, and window transparency. To determine the slope of the Beer's law plot or the calibration factor, a comparison was made in runs 2 and 3 of the optical density difference between sets of heavy water standards. From the data of run 4, the concentration of a heavy water sample resulting from the exchange of 13.487 g benzene saturated with water at 24.54 °C with 4.236 g heavy water reference solution was determined.

The solubility of light water in benzene in parts per million by weight is given as

$$S = \left\{\left[I_S(C_u) - I_R(C_1) - I_C\right]\left[\frac{C_2 - C_1}{I_S(C_2) - I_R(C_1) - I_C}\right] + C_1\right\}\frac{\mathrm{wt}(C_u)}{\mathrm{wt}(C_6H_6)} \times 10^4,$$

where I_R and I_S refer to the optical densities of the reference and sample compartments, and C_1 and C_2 to the concentrations of a pair of standard heavy water solutions; C_u is the concentration of the heavy water resulting from the exchange of wt(C_u) grams of reference solution with wt.(C_6H_6) grams of moist benzene.

The cell constant $I_C = I_S(C_1) - I_R(C_1)$ which is determined in run 1 was found to be constant within the experimental error over the range of heavy water solutions employed. It did, however, tend to vary from day to day and was checked periodically during a set of runs. Run 2 comparing standard solution 0.2201 wt. % H_2O with standard solution 0.2297 wt. % gave a value of 1.65×10^{-4} wt. % H_2O per mm pen displacement for the calibration factor $[C_2 - C_1]/[I_S(C_2) - I_R(C_1) - I_C]$. Run 3 in a similar fashion yielded a value of 1.48×10^{-4}. The solubility of water in benzene at 24.54 °C was calculated to be 730.3 p.p.m. from the solubility equation and the data in Table I, run 4.

10. Blank Correction

It was necessary to correct for traces of light water and benzene contamination in the heavy water samples and for possible isotopic exchange between C_6H_6 and D_2O which were introduced during the sampling and exchange procedures. Blank samples were prepared by equilibrating dry benzene that had been pre-equilibrated with heavy water, with standard heavy water solution. When the blank samples were analyzed, the light water concentration of the blank was found to have increased by 0.59%. It was therefore necessary to divide the calculated solubility by the correction factor 1.0059.

11. Estimation of the Errors

A temperature uncertainty of 0.05 °C causes an error of 0.17% in the solubility results. The temperature, however, is known and controlled to within 0.02 °C. The optical density difference between the sample and reference cell-compartments can be measured to ±0.5 mm pen displacement (Table I) which limits sensitivity of the method to 0.03%. The accuracy to which the protium concentration of an unknown D_2O sample can be

Can. J. Chem. Downloaded from www.nrcresearchpress.com by 210.87.254.40 on 09/05/12
For personal use only.

determined is limited by the uncertainty in the concentration of the heavy water standards and is estimated from runs 2 and 3 to be 0.23%.

A standard deviation of 0.8% was obtained from a series of eight solubility measurements at 24.54 °C which indicates that the major component in the experimental uncertainty arises from contamination of heavy water sample by atmospheric moisture prior to the spectroscopic analysis.

RESULTS AND DISCUSSION

Results for the solubility of light water in benzene in parts per million by weight over the range 10 to 50 °C are recorded in Table II. Each value is the mean of three determinations and is estimated to be accurate to ±0.8% (Section 11).

TABLE II

The solubility of water in benzene as a function of temperature

T (°C)	S (p.p.m. by weight)	ln (f/x)
9.44	442.5	8.4527
14.98	530.2	8.6370
20.10	639.2	8.7786
24.54	726.0	8.9177
29.52	848.0	9.0521
34.88	1017.1	9.1821
40.06	1177.8	9.3159
43.78	1333.7	9.3796
49.45	1570.6	9.5033

An interpolation equation (ref. 3) of the form

$$\ln (f/x) = -A/T + B \ln T + C,$$

where x is the solubility of water in benzene expressed as mole fraction and f is the fugacity of the water vapor above the saturated solution, was fitted to the observed results. Fugacities were obtained from the second virial coefficient (4) and the vapor pressure data for water (5) which was corrected for the finite solubility of benzene in the aqueous phase (3). A least squares fit of the values of ln (f/x) listed in Table II to the interpolation equation gave $A = 5\,566.32\ °K^{-1}$, $B = -10.575$, and $C = 87.8429$ with a residual mean squared deviation of 0.5%. From the interpolation equation the thermodynamic quantities $\Delta G(298.16) = -5\,285$ cal mole^{-1}, $\Delta H(298.16) = 4\,793$ cal mole^{-1}, $\Delta S = 33.80$ cal deg^{-1} mole^{-1}, and $\Delta C_p = -21.00$ cal deg^{-1} mole^{-1} were obtained for the transfer of 1 mole of water from the benzene phase at unit mole fraction to the vapor phase at a fugacity of 1 mm.

The observed solubilities are plotted as a function of temperature in Fig. 3 along with the available literature data. Examination of Fig. 3 reveals that although there is considerable scatter in the combined data of Kirschenbaum (Karl Fischer titration) (6), Hill (silver perchlorate method) (7), and Grosschuff (turbidity method) (8), the overall agreement with our results may be considered to be reasonable.

The present results are also in excellent agreement with the recent tritium isotope tracer studies of Jones and Monk (9), providing an adjustment is made to their data to correct for the tritium isotope effect. If the fractionation factor $\alpha_1 = [(H_2O)/(HTO)]_{benz}/[(H_2O)/(HTO)]_{liq}$ is known for the equilibrium

$$(\text{water})_{liq} \overset{\alpha_1}{\rightleftarrows} (\text{water})_{benz}$$

Can. J. Chem. Downloaded from www.nrcresearchpress.com by 210.87.254.40 on 09/05/12
For personal use only.

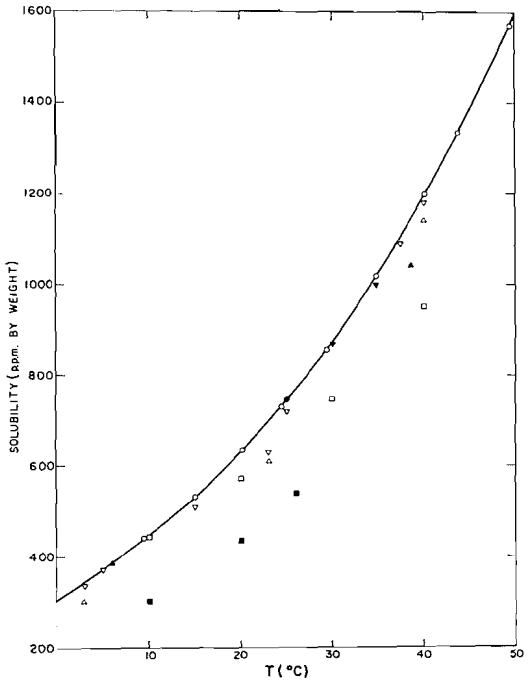


FIG. 3. Plot of the solubility of H_2O in C_6H_6 (parts per million by weight) against the temperature in degrees centigrade. ○ This research; □ Rosenbaum and Walton (15); ▽ Hill (7); △ Grosschuff (8); ■ Joris and Taylor (13); ▲ Kirshenbaum (6); ▼ Jones and Monk (as corrected) (9).

the solubility of H_2O in benzene is obtained as the product of α_1 and the observed solubility of HTO in benzene. Alternatively, given the fractionation factors $\alpha_2 = [(H_2O)/(HTO)]_{vap}/[(H_2O)/(HTO)]_{liq}$ and $\alpha_3 = [(H_2O)/(HTO)]_{benz}/[(H_2O)/(HTO)]_{vap}$ for the equilibrium

$$(water)_{liq} \overset{\alpha_2}{\rightleftarrows} (water)_{vap} \overset{\alpha_3}{\rightleftarrows} (water)_{benz}$$

then $\alpha_1 = \alpha_2 \cdot \alpha_3$. Values of α_2 are well known over the liquid range for water and at 25 °C α_2 is 1.11 (10). Although the fractionation factor α_3 has not been determined directly it may be estimated from the solubility relationships in the (H_2O–D_2O–C_6H_6) system. From the assumption that the isotope effect depends only on the molecular weight (11) it follows that $\alpha_3 = [(H_2O)/(D_2O)]_{benz}/[(H_2O)/(D_2O)]_{vap}$. We have measured (12) the solubility of D_2O in benzene by a method similar to the one described here. The solubility data for D_2O in benzene combined with the present results gave a value of $\alpha_3 = 1.05$. Therefore, $\alpha_1 = 1.16$ and the results of Jones and Monk must be increased by 16% to correct for the isotope effect. The excellent fit of the corrected points to our interpolation equation is shown in Fig. 3.

The results of Taylor and co-workers (13) are somewhat lower than those reported here. These authors absorbed the tritiated water saturated in benzene with calcium oxide and then exchanged the tritium with ethanol vapor for counting. It has been suggested (14), however, that incomplete exchange or isotope fractionation could be responsible for the low values obtained in this experiment.

The other work which is seriously out of line with the present study is that of Rosenbaum and Walton (15) who measured the volume of hydrogen liberated on the addition of

Can. J. Chem. Downloaded from www.nrcresearchpress.com by 210.87.254.40 on 09/05/12
For personal use only.

calcium hydride to the moist benzene. Perryman (16) has found that the volume of hydrogen evolved is considerably lower than the value predicted by the reaction stoichometry, and has suggested that the method be calibrated with distilled water.

The principal advantage of the present method is that the difficult problem of calibration with water–organic standards is avoided since the heavy water reference solutions used in the infrared difference analysis were prepared as primary standards. The method also eliminates a correction for isotope effects as water is determined directly as H_2O. The chief limitation of the method is that it is restricted to solvents which have a low solubility in water and do not have exchangeable hydrogens. The method also is not rapid as the analyses are normally of several days' duration.

ACKNOWLEDGMENTS

The authors wish to express their thanks to Dr. R. H. Betts for suggesting this problem.

REFERENCES

1. W. H. STEVENS and W. M. THURSTON. To be published.
2. W. H. STEVENS and W. M. THURSTON. Unpublished results.
3. F. FRANKS, M. GENT, and H. H. JOHNSON. J. Chem. Soc. 2716 (1963).
4. J. P. MCCULLOUGH, R. E. PENNINGTON, and G. WADDINGTON. J. Am. Chem. Soc. **74**, 4439 (1952).
5. E. WHALLEY. Proc. Conf. Thermodyn. Transport Properties Fluids, London, 1957. p. 15.
6. I. KIRSHENBAUM. Physical properties and analysis of water. McGraw-Hill Book Co., Inc., New York and London. 1951.
7. A. E. HILL. J. Am. Chem. Soc. **45**, 1143 (1923).
8. E. GROSSCHUFF. Z. Elektrochem. **17**, 348 (1911).
9. J. R. JONES and C. B. MONK. J. Chem. Soc. 2633 (1963).
10. YA. D. ZEL'VENSKII, V. A. SHALYGIN, V. S. TATARINSKII, and D. A. NIKOLGEV. At. Energ. USSR, **18**, 46 (1965).
11. J. BIGELEISEN. J. Chem. Phys. **28**, 695 (1958).
12. D. C. MOULE. To be published.
13. G. G. JORIS and H. S. TAYLOR. J. Chem. Phys. **16**, 45 (1948).
14. J. WING and W. H. JOHNSTON. J. Am. Chem. Soc. **79**, 864 (1957).
15. C. K. ROSENBAUM and J. H. WALTON. J. Am. Chem. Soc. **52**, 3568 (1930).
16. P. W. PERRYMAN. Analyst, **70**, 45 (1945).

Can. J. Chem. Downloaded from www.nrcresearchpress.com by 210.87.254.40 on 09/05/12
For personal use only.

Can. J. Chem. Downloaded from www.nrcresearchpress.com by 210.87.254.6 on 09/05/12
For personal use only.

ORGANIC COMPOUNDS OF SAMARIUM

II. REACTIONS OF SAMARIUM ISOPROPOXIDE WITH ETHYL ACETOACETATE

B. S. SANKHLA AND R. N. KAPOOR
Department of Chemistry, University of Jodhpur, Jodhpur, India

Received October 20, 1965

ABSTRACT

The reactions of samarium isopropoxide with ethyl acetoacetate have been carried out in benzene medium in different stoichiometric ratios and the compounds of the type $Sm(OPr^i)_2$(Etacac), $Sm(OPr^i)(Etacac)_2$, and $Sm(Etacac)_3$ have been isolated in quantitative yields. However, the reaction of samarium isopropoxide with excess of the acetoacetic ester lead to the formation of $Sm(Etacac)_3$.Etacac, which on heating under reduced pressure at 110 °C for $1\frac{1}{2}$ h loses its addition molecule of ester. The reactions are exothermic and the amount of heat liberated also increases with the increase in the concentration of the ester.

The interchange reactions of the products $Sm(OPr^i)_2(Etacac)$ and $Sm(OPr^i)(Etacac)_2$ with *t*-butyl alcohol have also been carried out; they are endothermic reactions. The compounds $Sm(OBu^t)_2(Etacac)$ and $Sm(OBu^t)(Etacac)_2$ have been obtained in quantitative yields from the reaction mixture. All the products are stable up to 200 °C at 0.5 mm, but at higher temperature they decompose to deep-red solids. Molecular weight determinations show that they are dimeric in nature.

INTRODUCTION

Recently the reactions of the alkoxides of aluminium (1), lanthanum, neodymium (2), praseodymium (3), titanium (4), niobium (5), tantalum (6), and uranium (7) with bidentate ligands have been carried out with interesting results regarding their volatility and coordination number. A survey of the literature reveals that no such type of work has been carried out with samarium alkoxides. It was, therefore, considered of interest to carry out the reaction of samarium isopropoxide with ethyl acetoacetate.

Kapoor *et al.* (8) were the first to report the synthesis of samarium alkoxides by a sodium alkoxide method. The reactions of samarium isopropoxide with ethyl acetoacetate may be represented by the following general equation:

$$Sm(OPr^i)_3 + n\text{Etacac} \rightarrow Sm(OPr^i)_{3-n}(Etacac)_n + nPr^iOH \ (n = 1, 2, \text{or } 3).$$

The experimental technique consists of adding the required amount of ethylacetoacetate to the solution of samarium isopropoxide in benzene, whereupon an exothermic reaction takes place. The reaction mixture was refluxed for about 5 h during which time the liberated isopropyl alcohol was collected azeotropically. The compounds were obtained on removal of the excess solvent under reduced pressure, 0.5 mm at 60 °C. From the analyses of the products formed, the reactions may be represented by the equations shown on the following page.

All these products are faint-yellow or deep-yellow crystalline solids, soluble in benzene.

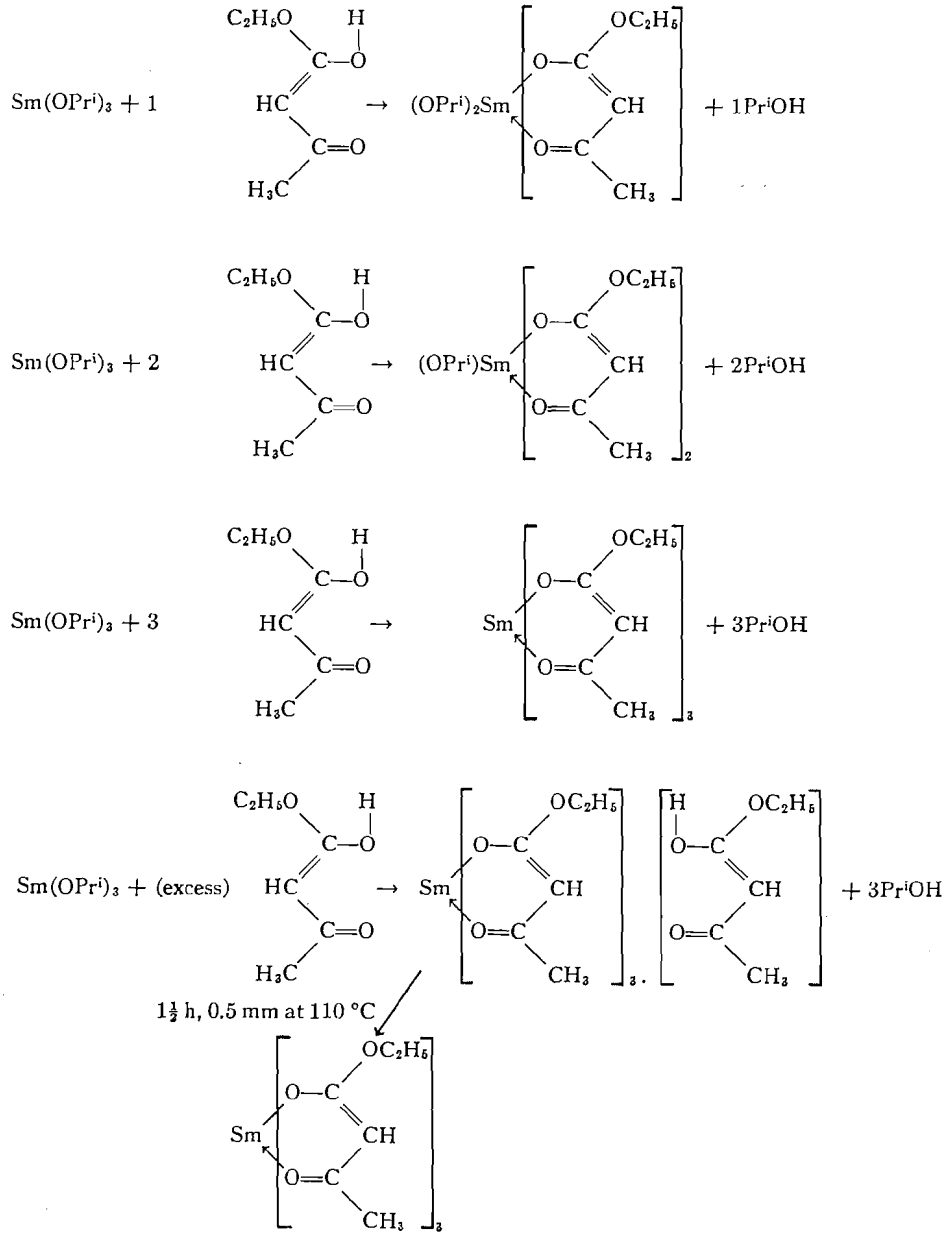
The mixed isopropoxy ethyl acetoacetate derivatives were found to interchange their isopropoxy group on treatment with *t*-butyl alcohol, which can be represented as follows:

$$Sm(OPr^i)_2(Etacac) + 2Bu^tOH \rightarrow Sm(OBu^t)_2(Etacac) + 2Pr^iOH,$$

$$Sm(OPr^i)(Etacac)_2 + 1Bu^tOH \rightarrow Sm(OBu^t)(Etacac)_2 + 1Pr^iOH.$$

These reactions are endothermic and the corresponding *t*-butoxy derivatives, which are faint-yellow crystalline solids, can be obtained from their benzene solution in quantitative yields.

Can. J. Chem. Downloaded from www.nrcresearchpress.com by 210.87.254.6 on 09/05/12
For personal use only.



The thermal stability studies of these compounds have been studied. All these derivatives are stable to heat at low temperatures (200 °C at 0.5 mm), but when attempts were made to sublime them at higher temperatures (270–280 °C at 0.5 mm), they decomposed to deep-red solids.

The determination of molecular weights of these compounds in refluxing benzene suggests that they are dimeric in nature. In the mono- and di-derivatives, samarium shows the coordination number 6, and in tri-derivatives, it shows coordination number 8.

Can. J. Chem. Downloaded from www.nrcresearchpress.com by 210.87.254.6 on 09/05/12
For personal use only.

TABLE I

Reactions of samarium isopropoxide with ethylacetoacetate

Alkoxide (g)	Ethyl acetoacetate (g)	Molar ratio	Product, its state and weight	Molecular weight		Amount of alcohol in azeotrope (g)		Analysis			
								Metal (%)		Isopropoxy (%)	
				Found	Calcd.	Found	Calcd.	Found	Calcd.	Found	Calcd.
1.225	0.486	1:1	$Sm(OPr^i)_2(Etacac)$ faint-yellow crystalline solid (1.46 g)	814	794	0.224	0.225 (for 1 mole)	37.80	37.85	29.50	29.70
1.277	1.015	1:2	$Sm(OPr^i)(Etacac)_2$ faint-yellow crystalline solid (1.81 g)	971	934	0.467	0.467 (for 2 moles)	32.91	32.20	12.11	12.62
1.254	1.494	1:3	$Sm(Etacac)_3$ yellow crystalline solid (2.12 g)	1 094	1 074	0.682	0.689 (for 3 moles)	27.80	27.99	—	—
0.940	3.553	1:excess	$Sm(Etacac)_3$.Etacac deep-yellow crystalline solid (1.93 g), changing to $Sm(Etacac)_3$ on heating at 110 °C under reduced pressure (0.5 mm) for 1½ h	—	—	0.509	0.517 (for 3 moles)	22.64	22.56	—	—
				999	1 074	—	—	27.92	27.99	—	—

TABLE II

Interchange with tertiary butyl alcohol

Compound (g)	*t*-Butyl alcohol (g)	Product, its state and weight	Molecular weight		Amount of alcohol in azeotrope (g)		Metal analysis (%)	
			Found	Calcd.	Found	Calcd.	Found	Calcd.
$Sm(OPr^i)_2(Etacac)$ (1.024)	7.92	$Sm(OBu^t)_2(Etacac)$ faint-yellow crystalline solid (1.19 g)	848	850	0.311	0.308	35.12	35.30
$Sm(OPr^i)(Etacac)_2$ (1.325)	6.02	$Sm(OBu^t)(Etacac)_2$ faint-yellow crystalline solid (1.41 g)	995	962	0.169	0.170	31.02	31.23

Can. J. Chem. Downloaded from www.nrcresearchpress.com by 210.87.254.6 on 09/05/12
For personal use only.

EXPERIMENTAL

Samarium isopropoxide was prepared by the sodium isopropoxide method (8) and was analyzed before use for samarium and isopropoxy contents. Ethyl acetoacetate (L. Light & Co.) was dried by reflux over aluminium isopropoxide and then distillation at 180 °C. Benzene (B.D.H. A.R.) was dried over sodium wire and then obtained by azeotropic fractionation in the presence of a little ethanol. *t*-Butyl alcohol (B.D.H.) was dried by careful distillation over the corresponding sodium alkoxide.

An all-glass apparatus with interchangeable standard joints was used throughout, special precautions being taken to exclude moisture from the system. Fractionations were carried out in a column packed with Raschig rings and fitted to a total condensation variable-takeoff stillhead. Molecular weights were determined ebulliometrically with a Gallenkamp semimicro ebulliometer.

Samarium was estimated by igniting the organic compounds and converting to the sesquioxide (Sm_2O_3). Isopropoxy constituents of the mixed isopropoxy acetoacetate derivatives were determined by estimating the isopropyl alcohol in the ternary azeotrope (benzene – water – isopropyl alcohol) by oxidation with normal dichromate solution in 12.5% sulfuric acid (9).

Reaction of Samarium Isopropoxide with Ethyl Acetoacetate in Benzene (Molar Ratio 1:1)

Ethyl acetoacetate (0.486 g) was allowed to react with samarium isopropoxide (1.225 g) in benzene (52 g); the reaction was exothermic. The binary azeotrope of benzene–isopropanol was collected at 72 °C, after refluxing the reaction mixture at 115–120 °C for 5 h. The excess benzene was removed under reduced pressure (0.5 mm at 60 °C). A faint-yellow crystalline solid was obtained. Yield 1.46 g. Found: isopropyl alcohol in the azeotrope, 0.224 g; Sm, 37.80%; OPr^i, 29.5%. Calcd. for $Sm(OPr^i)_2(Etacac)$: replacement of 1 mole requires 0.225 g isopropyl alcohol; Sm, 37.85%; OPr^i, 29.7%.

Other reactions of samarium isopropoxide with ethyl acetoacetate are given in Table I.

Reaction of Samarium Diisopropoxy Monoethyl Acetoacetate with t-Butyl Alcohol (Excess)

t-Butyl alcohol (7.92 g) was admitted to a solution of samarium diisopropoxy monoethyl acetoacetate (1.024 g) in benzene (45 g). The reaction was endothermic. After the mixture was refluxed slowly for about 5 h, the isopropanol–benzene azeotrope was collected slowly at 72 °C, and finally the *t*-butanol–benzene azeotrope at 74 °C. The excess benzene was also collected along with the azeotrope until the temperature reached 80 °C. After the compound was dried under reduced pressure, 0.5 mm at 60 °C, a faint-yellow crystalline solid was obtained. Yield 1.10 g. Found: isopropyl alcohol in the azeotrope, 0.311 g; replacement of 2 moles requires 0.308 g. Calcd. for $Sm(OBu^t)_2(Etacac)$: Sm, 35.30%. Found: Sm, 35.12%.

The interchange reactions with *t*-butyl alcohol are given in Table II.

ACKNOWLEDGMENT

The authors thank Prof. R. C. Mehrotra, Head of the Chemistry Department, and Dean, Faculty of Science, Rajasthan University, Jaipur, for valuable criticism, and Dr. S. N. Misra for helpful suggestions. We also thank Prof. R. C. Kapoor, Head of the Chemistry Department, and Dean, Faculty of Science, Jodhpur University, Jodhpur, for providing laboratory facilities; and the Ministry of Education, Government of India, for providing a research scholarship to B. S. S.

REFERENCES

1. R. K. Mehrotra and R. C. Mehrotra. Can. J. Chem. **39**, 795 (1961).
2. T. N. Misra. Ph.D. Thesis, Rajasthan University, Jaipur, India. 1963.
3. S. N. Misra. Ph.D. Thesis, Rajasthan University, Jaipur, India. 1964.
4. D. M. Puri and R. C. Mehrotra. J. Less-Common Metals, **3**, 253 (1961).
5. R. C. Mehrotra and P. N. Kapoor. J. Less-Common Metals, **7**, 176, (1964).
6. R. C. Mehrotra and P. N. Kapoor. J. Less-Common Metals, **7**, 453, (1964).
7. A. M. Bhandari and R. N. Kapoor. Can. J. Chem. This issue.
8. B. S. Sankhla, R. N. Kapoor, and S. N. Misra. Chem. Ind. London, 382 (1965).
9. D. C. Bradley and W. Wardlaw. J. Chem. Soc. 3450 (1950).

Can. J. Chem. Downloaded from www.nrcresearchpress.com by 210.87.254.42 on 09/05/12
For personal use only.

THERMAL DECOMPOSITION OF MOLECULAR COMPLEXES

IV. FURTHER STUDIES OF THE β-QUINOL CLATHRATES

H. G. McAdie
Department of Physical Chemistry, Ontario Research Foundation, Toronto, Ontario
Received January 21, 1966

ABSTRACT

The endothermal decomposition of 18 β-quinol clathrates has been studied by thermoanalysis, calorimetry, and X-ray diffraction, and the decomposition process shown to be

$$3\ \beta\text{-quinol}.x\text{M (s)} \rightarrow 3\ \alpha\text{-quinol (s)} + x\text{M (g)},$$

For those symmetrical guest molecules (M) which do not distort the β-quinol cavities from their normal dimensions, both temperatures and enthalpies of clathrate decomposition increase with increasing volume of the guest molecule. For those unsymmetrical guest species which require distortion of the cavities along their c-axis, temperatures and enthalpies of decomposition tend to decrease as the initial distortion required to accommodate the guest increases. Thermal stability of β-quinol clathrates is thus strongly influenced both by the size and shape of the guest molecule.

The mechanism of thermal decomposition is suggested to involve a combination of the loss of stabilizing guest–wall interactions, together with increased thermal motion of the interpenetrating networks of hydrogen-bonded quinol molecules.

An earlier paper in this series (1) described the thermal decomposition of four β-quinol clathrates, demonstrating that the endothermal loss of a given guest species from within the host β-quinol network occurs over a considerable temperature range. Thermal decomposition was shown to follow the general process

$$\text{clathrate (s)} \rightarrow \text{quinol (s)} + \text{guest (g)},$$

which occurs below the melting point of the host quinol. It was apparent that the size and shape of the guest species exerted considerable influence upon the thermal stability of the corresponding β-quinol clathrate and the present studies were undertaken to investigate further this influence of size and shape, through examination of a wide range of clathrates, and to clarify some details of the thermal decomposition process. A preliminary report of findings was made elsewhere (2).

EXPERIMENTAL

Clathrate Preparation

Reagent or C.P. grade materials were used throughout this work without further purification.

Clathrates of MeOH, HCOOH, and MeCN were prepared by slow crystallization from solutions of quinol in these solvents, saturated at 70 °C. The clathrates were filtered on sintered glass and air dried, the formic acid clathrate being dried over KOH (3).

Clathrates of H_2S, and SO_2, were prepared by passing these gases at about 2 atm pressure through stirred solutions of quinol in water, saturated at room temperature. The products were dried over KOH, the SO_2 clathrate having the yellow color previously reported (4). Clathrates of HCl, and HBr, were prepared by the same technique except that ether was used as solvent and the filtered products were washed sparingly with ether prior to drying over KOH.

Clathrates of the guest species listed in Table I were prepared with an Autoclave Engineers, Inc., 300 cc stainless steel autoclave equipped with a Magnedrive stirring unit and operable to 5000 p.s.i. at 650 °F. Approximately 66 gm of quinol and 100 ml of ethanol were placed in the autoclave and subjected to the initial pressures of guest species shown in Table I. In most cases these represented the maximum available supply pressure. The supply was then sealed off and the autoclave heated to 85–90 °C, followed by slow cooling overnight with continuous stirring. The products were filtered quickly and air dried.

TABLE I

Preparation of clathrates

Guest	Initial pressure (p.s.i.g.)
N_2	1 750
Ar	1 300
N_2O	600
CO	800
CO_2	700
CH_4	825
C_2H_2	200
C_2H_4	800
C_2H_6	500

Clathrates of MeCl and MeBr were prepared (5) by adding dry quinol to the autoclave, or to a 250 cc heavy-walled pyrex bomb, and condensing about 100 ml of the respective materials into the vessels at −75 °C. The vessels were sealed and heated to above 60 °C before slow cooling overnight. The MeBr clathrate initially possessed an orange tint which disappeared on drying in air.

α-Quinol was prepared by crystallization from ethanol according to the procedure of Evans and Richards (6). After drying, the material was heated for several hours at 150 °C to ensure the absence of β-quinol and solvent.

β-Quinol was also prepared as described (6), with air-free *n*-propanol as solvent. A seed crystal of the MeOH clathrate was used to facilitate crystallization, and the material was studied as soon as possible after preparation.

Analysis

The fraction of cavities within each clathrate occupied by guest molecules was determined by dissolving known weights of clathrate in ethanol and drying to constant weight at 40 °C. At this temperature loss in weight is due entirely to liberation of the guest species on dissolution of the clathrate, whereas higher temperatures resulted in some weight loss over long periods due to sublimation of the quinol.

Debye–Scherrer powder patterns were obtained with Cu K_α radiation. Patterns of samples heated to various temperatures were obtained by loading X-ray capillaries with about 2 mm depth of sample, and packing the tubes into the differential thermal analysis (DTA) block so that their open ends projected above the block. At the required temperature the tubes were sealed with a small flame and quickly removed to the X-ray camera.

Differential Thermal Analysis

Previous work (1) made no provision for atmosphere control within the DTA sample. To prevent access of air as well as to remove volatiles directly, the sample was purged continuously by an inert atmosphere using a modified version of the Stone dynamic atmosphere (7) sample block made of Inconel (Fig. 1). Reference

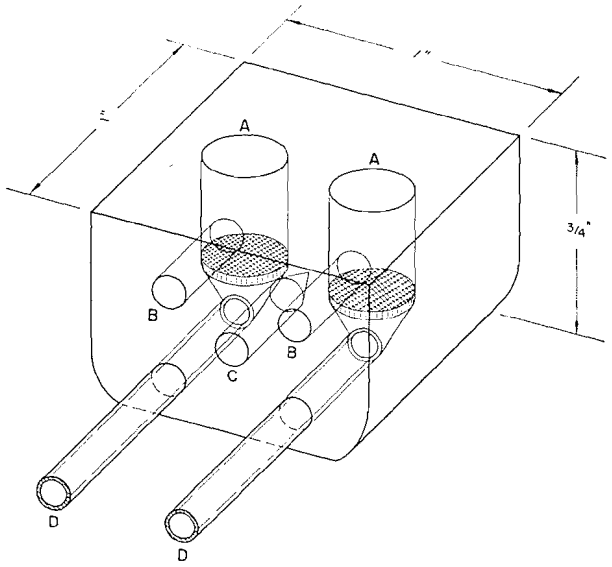


FIG. 1. Dynamic atmosphere DTA block.

Can. J. Chem. Downloaded from www.nrcresearchpress.com by 210.87.254.42 on 09/05/12
For personal use only.

alumina, and samples diluted to 20% by weight in the same material, were packed in cavities A, the differential thermocouples entering through B. Sample and reference cavities were purged with separately controlled streams of dry nitrogen entering through tubes D, and passing through porous discs which formed the base of the cavities, at a flow rate of 6 cc min^{-1}. Differential temperature was amplified by a Leeds and Northrup 9835-B d-c. microvolt amplifier and fed into a Philips PR 2210A millivolt recorder. The usual display sensitivity was 0.8 $\mu V\ cm^{-1}$ chart width, with higher sensitivities being available. Block temperature was measured by a separate, calibrated, iron–constantan thermocouple located at C. A horizontal tubular-type furnace was employed and manually programmed at 3 °C min^{-1}.

All peak temperatures reported have been corrected to a value of 172.7 °C for the peak of the quinol fusion endotherm. Peak areas were estimated by tracing curves on semi-transparent graph paper and counting squares.

Calorimetry

Samples (0.5 gm) of clathrate were dissolved in 600 gm of 0.001 *N* HCl at 25 °C in a twin-type heat of solution calorimeter (8) calibrated against samples of potassium chloride.

Heats of solution of the individual pure guest species were obtained from standard tables (9), or were calculated from solubility data (10–12).

RESULTS

Thermograms

A typical differential thermogram for each of the β-quinol clathrates studied appears in Fig. 2. As the temperature increased, three main thermal effects were observed:

(i) a broad endotherm corresponding to the decomposition of the clathrate, i.e. liberation of the guest species from within the host β-quinol lattice, accompanied by the reversion of the residual quinol to the α-quinol crystal structure as shown by X-ray diffraction;

(ii) a relatively sharp endotherm due to the fusion of the residual α-quinol;

(iii) a broad, variable, endotherm which is associated with the volatilization of the molten quinol spread over the surface of the diluent alumina.

This latter peak was not observed previously (1) because sufficient air was present under the static atmosphere conditions then employed to permit oxidation and general exothermal degradation of the molten quinol. In the present work, the dynamic nitrogen atmosphere both prevents the access of air and purges any volatiles from the sample as they occur.

On the basis of heats of decomposition determined earlier (1) the thermal decomposition process was reported to produce solid β-quinol. It has now been possible to obtain X-ray diffraction patterns of samples heated through the clathrate decomposition endotherm. These patterns show the previous conclusions to be in error, and that the thermal decomposition of the clathrate produces residual quinol having the α crystal structure. Thus the thermal decomposition process may be represented as

$$3\ \beta\text{-quinol}.x\text{M (s)} \rightarrow 3\ \alpha\text{-quinol (s)} + x\text{M (g)}$$

for the clathrate where x moles of guest M are present.

That the first endotherm corresponds to loss of the guest species, accompanied by destruction of the β-quinol lattice, was further confirmed by simultaneous DTA–TGA (thermogravimetric analysis). Figure 3 shows the experimental record for the N_2 clathrate obtained for an undiluted sample heated in nitrogen at 4 °C min^{-1}. It may be noted that both DTA and TGA base lines begin to deviate prior to the decomposition endotherm and first rapid loss of weight. This represents the onset of sublimation of the host quinol at a measurable rate, and complicates any attempt to calculate decomposition kinetics and accompanying activation energies from TGA data. Decomposition of the clathrate through sublimation of the host lattice may be likened to dissolution of the clathrate in a solvent, i.e. the physical removal of quinol walls from about the guest molecule. However, the thermal decomposition process is complete at temperatures below which the rate of sublimation of quinol is sufficient to account for the decomposition, and the possibility of another mechanism will be discussed shortly.

Can. J. Chem. Downloaded from www.nrcresearchpress.com by 210.87.254.42 on 09/05/12
For personal use only.

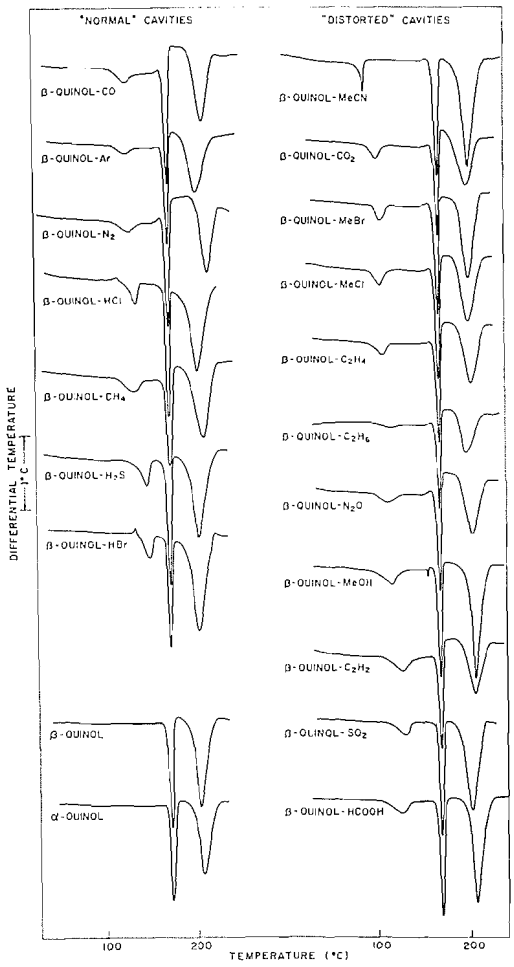


FIG. 2. Differential thermograms of β-quinol clathrates.

Two other minor thermal effects have been observed (Fig. 2). For the HCl and HBr clathrates a distinct indication of exothermal activity prior to the decomposition endotherm was found. This could suggest a small direct interaction of these guest species with the walls of the β-quinol clathrate cavities. Such exothermal activity was not observed with clathrates of the larger molecules MeCl and MeBr.

The other minor thermal effect has been observed only in the methanol clathrate. A small endotherm, equivalent to an enthalpy change of about $+0.2$ kcal mole^{-1} quinol, was found just prior to the quinol fusion endotherm, but X-ray diffraction patterns of samples heated to temperatures on either side of this endotherm showed only the α-quinol. Unfortunately, all X-ray diffraction patterns reported here were obtained ultimately at room temperature, and it is possible that the true structures prevailing before and after this endotherm have not been determined. In a further experiment, the methanol clathrate was decomposed isothermally at 120 °C and the residue of α-quinol (by X-ray diffraction) examined by DTA. No trace of the clathrate decomposition endotherm was observed, but a well-defined small endotherm was obtained just prior to quinol fusion. Because of the

Can. J. Chem. Downloaded from www.nrcresearchpress.com by 210.87.254.42 on 09/05/12
For personal use only.

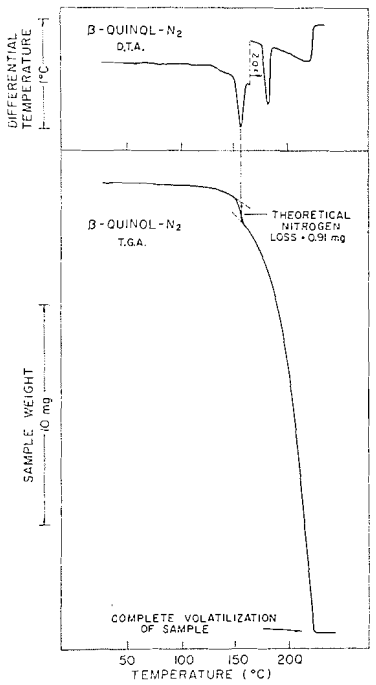


FIG. 3. Simultaneous DTA–TGA of the β-quinol–N_2 clathrate in N_2 atmosphere.

proximity of this endotherm to the onset of the quinol fusion, it has not been possible with the present equipment to verify whether a reversible process is associated with the small endotherm.

Thermograms of α- and β-quinol are also included in Fig. 2 and appear to be identical.

Decomposition Temperatures

Although clathrates of several of the guest species studied were prepared having more than one ratio of guest:host molecules, for brevity only those having the highest fraction of available cavities occupied are considered in Tables II and III. All decomposition temperatures reported are based on a peak temperature for the quinol fusion endotherm of 172.7 °C.

With some clathrates a small apparent increase in the average temperature of the clathrate decomposition peak (t_d) was found as the fraction of occupied cavities increased. Such increases in t_d were never more than 3 °C for an increase of 10% in the cavities occupied. It is possible to interpret these apparent changes in decomposition temperatures with composition on a purely kinetic basis, the clathrate having more cavities occupied requiring a somewhat longer time to reach the *rate* of decomposition represented by the peak of the decomposition endotherm. In dynamic techniques such as DTA, two competing rate processes are always present: the rate of the change under study, and the rate at which the conditions of the study themselves change.

Decomposition temperatures obtained in the present work were somewhat higher than reported previously (1) (Tables II and III), principally because of the conditions of the DTA experiment, viz. static vs. dynamic inert atmosphere. For the MeOH and MeCN clathrates, decomposition in a static atmosphere block allowed the accumulation of the

Can. J. Chem. Downloaded from www.nrcresearchpress.com by 210.87.254.42 on 09/05/12
For personal use only.

Can. J. Chem. Downloaded from www.nrcresearchpress.com by 210.87.254.42 on 09/05/12
For personal use only.

TABLE II

Properties of "normal" clathrates

Guest	% occupied cavities	Principal d-spacings (Å) (22)			Clathrate cell dimensions (4)		Thermal decomposition			Literature		$\alpha \times 10^{24}$ (cm^3)	ΔH_{sub} (kcal mole^{-1} guest) (9)
		3.89 (100)	4.40 (60)	4.80 (30)	a (Å)	c (Å)	t_d (°C)	ΔH_d (kcal mole^{-1} guest)	$\Delta H_d'$ (kcal mole^{-1} guest)	t_d (1) (°C)	$-\Delta H_f^0$ (3, 13) (kcal mole^{-1} guest)		
Ar	80.00	3.85 (10)	4.35 (6)	4.80 (6)	—	—	127.1	6.3	4.9	—	5.5	1.68	1.84
N_2	81.17	3.85 (10)	4.36 (7)	4.80 (6)	—	—	128.4	6.8	4.7	114.5	5.3	1.76	1.56
CO	71.93	3.86 (10)	4.36 (8)	4.79 (8)	—	—	126.6	6.9	6.5	—	—	1.98	1.80
CH_4	73.81	3.86 (10)	4.37 (8)	4.79 (8)	—	—	129.4	9.5	8.6	—	6.7	2.60	2.18
HCl	75.89	3.85 (10)	4.36 (8)	4.81 (8)	16.55	5.46	139.9	10.0	8.6	—	8.7	2.63	4.62
HBr	86.76	3.86 (10)	4.37 (4)	4.79 (4)	16.57	5.48	151.0	8.4	10.4	—	9.7	3.36	4.79
H_2S	96.05	3.86 (10)	4.37 (7)	4.81 (7)	16.58	5.49	150.9	10.4	10.0	—	—	3.65	5.51

TABLE III

Properties of "distorted" clathrates

Guest	% occupied cavities	Principal d-spacings (Å) (22)			Clathrate cell dimensions (4)		Thermal decomposition			Literature		b (cc mole^{-1})	ΔH_{sub} (kcal mole^{-1} guest) (9)
		3.89 (100)	4.40 (60)	4.80 (30)	a (Å)	c (Å)	t_d (°C)	ΔH_d (kcal mole^{-1} guest)	$\Delta H_d'$ (kcal mole^{-1} guest)	t_d (1) (°C)	$-\Delta H_f^0$ (3, 13) (kcal mole^{-1} guest)		
C_2H_2	87.56	3.86 (10)	4.26 (8)	4.81 (9)	16.63	5.46	131.6	9.5	8.2	—	—	0.0514	5.10
C_2H_6	44.36	3.86 (9)	4.36 (9)	4.77 (10)	—	—	115.1	7.5	7.8	—	—	0.0638	4.20
C_2H_4	44.04	3.90 (10)	4.39 (9)	4.80 (9)	—	—	108.5	11.3	10.7	—	—	0.0571	4.04
MeOH	98.10	3.90 (10)	4.41 (9)	4.82 (8)	16.56	5.55	122.3	9.2	9.8	116.5	10.5	0.0670	9.34
SO_2	53.65	3.91 (10)	4.40 (8)	4.79 (8)	16.49	5.60	134.5	10.4	9.7	—	—	0.0564	7.72
HCOOH	80.70	3.91 (10)	4.44 (8)	4.77 (5)	16.42	5.65	135.7	8.7	11.2		11.7	—	8.35
CO_2	75.09	3.91 (10)	4.48 (6)	4.70 (6)	16.17	5.82	103.3	7.1	9.4	101.0	9.4	0.0427	8.02
N_2O	76.08	3.93 (10)	4.49 (7)	4.70 (7)	—	—	119.2	6.4	9.5	—	—	0.0442	5.52
MeCl	52.31	3.95 (10)	4.49 (7)	4.71 (6)	—	—	105.5	11.3	8.4	—	—	0.0648	6.69
MeBr	75.70	3.95 (10)	4.41 (6)	4.78 (3)	—	—	96.5	6.4	8.2	—	—	0.0928	7.26
MeCN	92.36	4.01 (10)	4.64 (8)	5.03 (8)	15.95	6.24	100.8	7.6	9.0	80.0	7.5	0.1168	9.96

vaporized guest species, both of which in the liquid state are excellent solvents for quinol. One might reasonably expect both these materials in the vapor state to promote destruction of the β-quinol lattice under conditions where they were not removed promptly. In the case of the nitrogen clathrate, decomposition under 1 atm N_2 would be expected to occur at a slightly higher temperature than under the lesser, but unknown, pressure which prevailed in the static block. The decomposition temperature of the CO_2 clathrate is not appreciably different under the two techniques.

Palin and Powell (4) have reported that the formic acid clathrate melts at 160 °C. There is no evidence from the present studies to support this observation, and no indication that the host quinol melts at other than its normal temperature in this case.

Heats of Decomposition

From differential thermograms the heats of decomposition in kcal mole^{-1} *guest*, were estimated as previously (1). The average values are reported as ΔH_d (at t_d) in Tables II and III, and were generally reproducible to ±10% over a series of thermograms of clathrates having different fractions of occupied cavities.

It was also possible to calculate heats of decomposition of the clathrates, $\Delta H_d'$ (at 25 °C), from experimental heats of solution in 0.001 *N* HCl as follows

3 β-quinol.xM (s) → 3 α-quinol (aq.) + xM (aq.)	$+\Delta H_1$
3 α-quinol (aq.) → 3 α-quinol (s)	$-\Delta H_2$
xM (aq.) → xM (g)	$-\Delta H_3$
3 β-quinol.xM (s) → 3 α-quinol (s) + xM (g)	$+\Delta H_4$

$$\Delta H_d' = \Delta H_4/x$$

where ΔH_1 = experimental heat of solution of clathrate (kcal per 3 moles quinol), ΔH_2 = experimental heat of solution of 3 moles of α-quinol (kcal), ΔH_3 = heat of solution of x moles gaseous guest (kcal), ΔH_4 = heat of decomposition of clathrate (kcal per 3 moles quinol).

The heat of solution of α-quinol prepared by the method of Evans and Richards (6) was found to be +4.78 ± 0.03 kcal mole^{-1}, which compares favorably with their value of +4.7 kcal mole^{-1}. In certain cases x moles of guest exceeds the solubility of that substance at 1 atm, so that ΔH_3 then represents the enthalpy change to form a solution saturated with respect to guest under 1 atm pressure.

Since one of the objectives in this work was to produce clathrates with a large fraction of cavities occupied by guest species, no attempt was made to produce a systematic range of compositions. The observations of Evans and Richards (6) that the heats of solution of argon and oxygen clathrates are directly proportional to the fraction of available cavities filled was assumed to hold true for the other clathrates reported here.

For the clathrates of HBr, HCOOH, CO_2, N_2O, MeBr, and MeCN, $\Delta H_d'$ is significantly more endothermal than ΔH_d. Although the two quantities are measured at different temperatures, the temperature coefficient is not likely to be large, and this difference suggests secondary exothermal reaction between the liberated guest species and the residual quinol, or alumina diluent, prior to being completely purged from the system.

DISCUSSION

The spatial limitations imposed by the geometry of the clathrate cavity severely limit the choice of potential guest molecules. Thus, with few exceptions, it is not possible to compare two clathrates in which several parameters of the guest molecules have not been

Can. J. Chem. Downloaded from www.nrcresearchpress.com by 210.87.254.42 on 09/05/12
For personal use only.

altered, and it becomes difficult to define the influence of any single parameter upon the thermal stability of β-quinol clathrates generally.

The thermal stability of these clathrates depends, among other factors, upon the initial distortion of the clathrate cavity required to accommodate the particular guest species. In cases for which the cell dimensions have been reported (4), present data indicate decreasing decomposition temperature and heat of decomposition with increasing initial distortion of the clathrate cavity as shown by its c-dimension (Fig. 4). A linear relationship has been fitted to these data to illustrate the overall trend, recognizing that with the many accompanying differences in guest parameters, and in their interaction with the β-quinol lattice, it would be fortuitous if such a linear relationship is entirely correct.

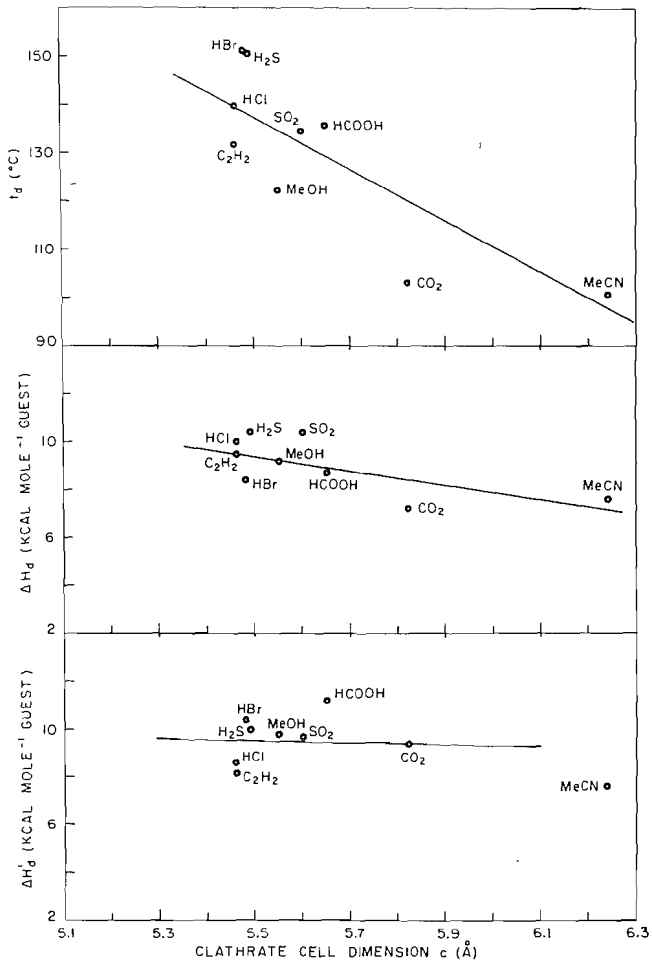


FIG. 4. Thermal stability of clathrates in relation to distortion of the clathrate cavity.

Two broad classes of β-quinol clathrates may then be considered: (i) those in which the clathrate cavity is essentially undistorted in accommodating the guest species, and (ii) those in which it is distorted. In Tables II and III guest species are therefore grouped on the basis of their influence upon the lattice parameters of the clathrate cell, determined from present diffraction patterns, and from available cell dimensions (4). The "normal" or

Can. J. Chem. Downloaded from www.nrcresearchpress.com by 210.87.254.42 on 09/05/12
For personal use only.

undistorted cavity can accommodate those guest species listed in Table II without significant alteration in its dimensions. For simplicity these species may be considered to be generally spherical in shape, and to occupy a proportion of the available cavity volume in relation to their molecular volume. "Distorted" cavities result when the species shown in Table III are incorporated into the β-quinol lattice. Again for simplicity, these may be considered to be roughly "dumbbell" in shape. Not only will the length of the dumbbell vary from guest to guest, hence altering the extent to which the clathrate cavity is distorted, but the overall volume of the guest molecule in relation to the available cavity volume will vary, affecting its packing within the cavity.

"Normal" Clathrates

Since the group of clathrates in Table II have virtually the same cell dimensions, differences in thermal stability may be attributed to differences in the interaction of individual guest molecules with the cavity walls, arising not only from differences in the chemical nature of the various species but also from differences in the fraction of available cavity volume occupied by each guest. Further, since the environment of guest molecules is not strictly symmetrical (14), because of the grouping of oxygen atoms of the quinol at the poles of the cavity and carbon atoms at the equators, this may tend to give rise to preferred orientations of guest molecules within the cavities.

As a measure of the volume of these symmetrical guest molecules, the molar polarizability, α, calculated from refractive index (15) and vapor density (16) data is considered. Figure 5 shows that decomposition temperatures and heats of decomposition increase approximately linearly with the polarizability of these spherical guest molecules or, approximately, with the extent to which the available cavity volume is occupied. There is a maximum, as well as minimum, limit to which the undistorted cavity can be filled, and between these limits increasing thermal stability reflects increasing interaction of the guest with the cavity walls imparting increased stability to the entire lattice structure. These interactions are mainly van der Waals type, but differences due to the electronic structure of the guest species will result in different contributions from such effects as dipole–dipole interactions with the cavity walls. These should be relatively small since most of the guest molecules are small and relatively nonpolar. In a future paper it is hoped to present data for a series of the rare gas clathrates in which essentially only the volume of the guest molecule will vary.

In Fig. 5 heats of decomposition obtained from DTA and from heats of solution have been compared on a common basis with heat of formation data from the literature (1, 3, 13). A reasonable correlation was found in both cases, the calorimetric data showing somewhat less scatter than those obtained from DTA.

Although the magnitude of the guest–host interactions is considerably greater than the magnitude of guest–guest interactions, in the pure solid for instance, one might expect the thermal stability of β-quinol clathrates to be proportional to the heat of sublimation of the pure guest (3, 9). This is demonstrated in Fig. 6, indicating further that at least a portion of the forces which must be overcome by the guest molecule prior to escaping from the clathrate cavity are similar to those which must be overcome in removing individual molecules from their respective pure solids.

"Distorted" Clathrates

A group of guest species which generally distort the β-quinol clathrate cavity from its normal dimensions are listed in Table III. This comprises a very heterogeneous group of substances, about the only common feature being the more or less "dumbbell" shape of

Can. J. Chem. Downloaded from www.nrcresearchpress.com by 210.87.254.42 on 09/05/12
For personal use only.

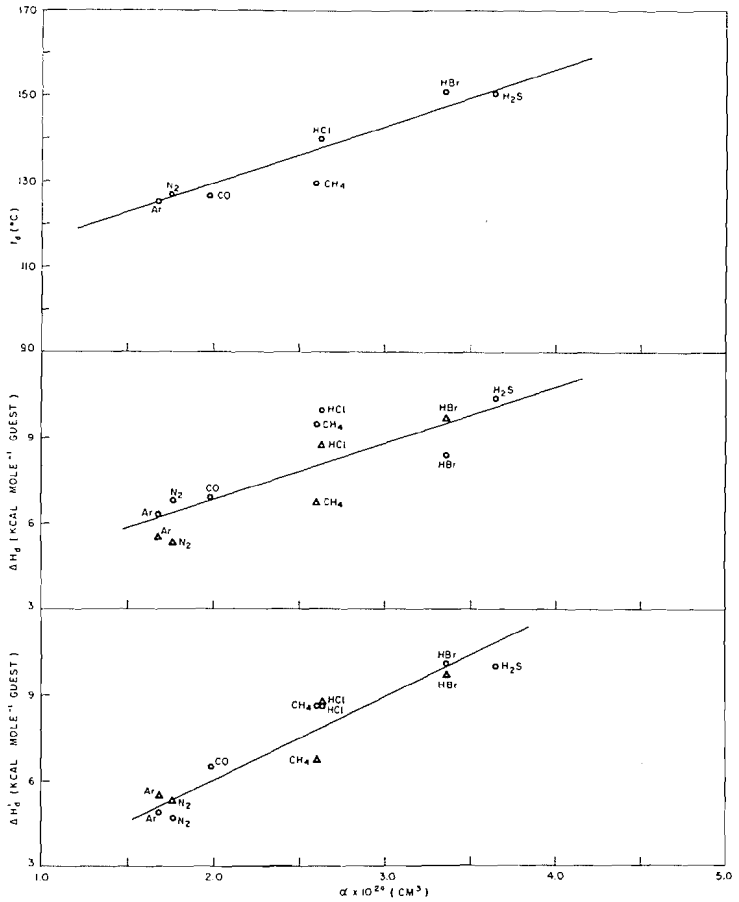


FIG. 5. Thermal stability of "normal" clathrates as a function of guest size: (○) present data, (△) literature data.

the molecules. For this reason the use of molar polarizability as a measure of molecular volume is not longer valid, and the van der Waals covolume, b, has been chosen as a measure of this parameter. As indicated by Fig. 7, there is a trend toward *decreasing* thermal stability with increasing molecular size. For the species investigated, increasing molecular size is generally accompanied by increasing extension of the cavity along its c-axis (Table III), complicated by differences in the overall fraction of available cavity volume occupied after the distortion. Such differences may be expected to be significant when comparing, for example, acetylene and methyl bromide and to contribute to differences in packing within the cavities. Another factor which contributes to the considerable scatter of data in Fig. 7 is the variation in the electronic structure among the different guest species.

The structures of the C_2H_2 and MeOH clathrates appear to be slightly anomalous, in that whereas one cell dimension is larger than normal for the undistorted case there is no compensating decrease in the other dimension as would be expected from the trellis-like architecture of the cell.

Despite an almost threefold difference in van der Waals b, CO_2 and MeCN form clathrates of remarkably similar thermal stability. CO_2 produces considerable distortion

Can. J. Chem. Downloaded from www.nrcresearchpress.com by 210.87.254.42 on 09/05/12
For personal use only.

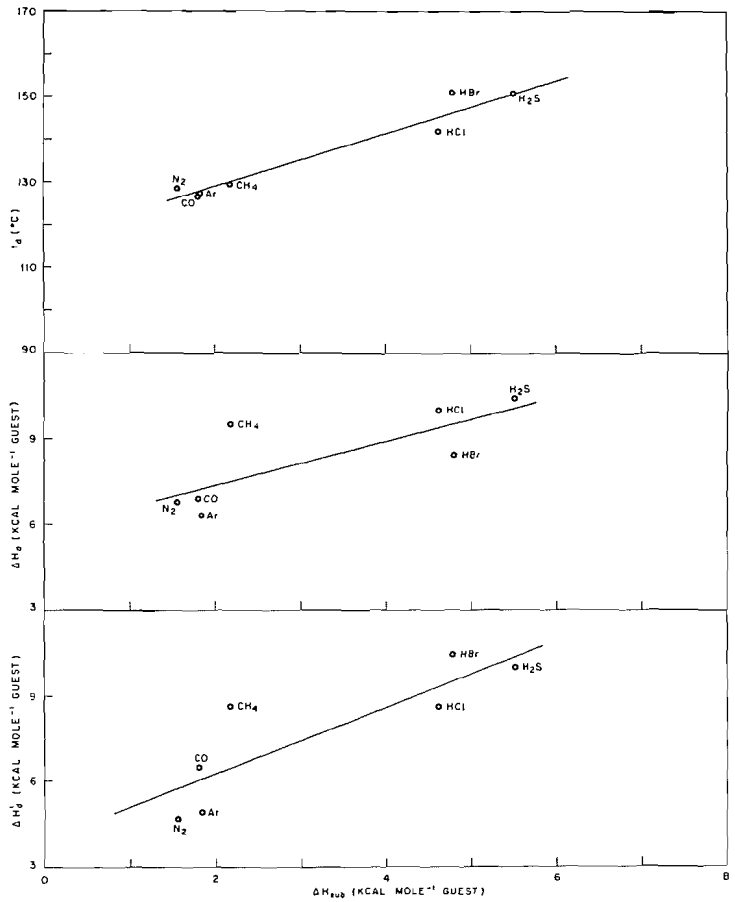


FIG. 6. Thermal stability of "normal" clathrates in relation to heat of sublimation of guest.

of the lattice and there appears to be a possible reduction in the O—H . . . O hydrogen-bond lengths in the quinol network from 2.8 to 2.72 Å (4) accompanying the packing of this guest molecule into the cavity. In the case of MeCN (17) a puckering of the hydrogen-bonded oxygen hexagons has been suggested.

From the relatively similar size and thermal stability of CO_2, N_2O, and their clathrates, one might suspect a packing situation prevails in the case of N_2O similar to that postulated for CO_2. These two clathrates are similar in other respects: (i) both guest species have roughly linear molecules with an axial length of about 5.2 Å (18, 19), and (ii) although increased pressure of guest during clathrate formation generally results in an increased fraction of the available cavities being filled, both N_2O and CO_2 are exceptional in that after a maximum of about 75% cavities filled has been reached further increase in pressure of guest during formation reduces the number of cavities occupied (18).

For those species which distort the clathrate cavity, the relation of thermal stability to heat of sublimation of the pure guest is poor, the scatter preventing any real conclusions from being drawn. It is interesting that for this group the heats of clathrate decomposition more nearly approximate the heats of sublimation of the pure guest, indicating that the removal of an individual guest molecule from the distorted clathrate cell is roughly

Can. J. Chem. Downloaded from www.nrcresearchpress.com by 210.87.254.42 on 09/05/12
For personal use only.

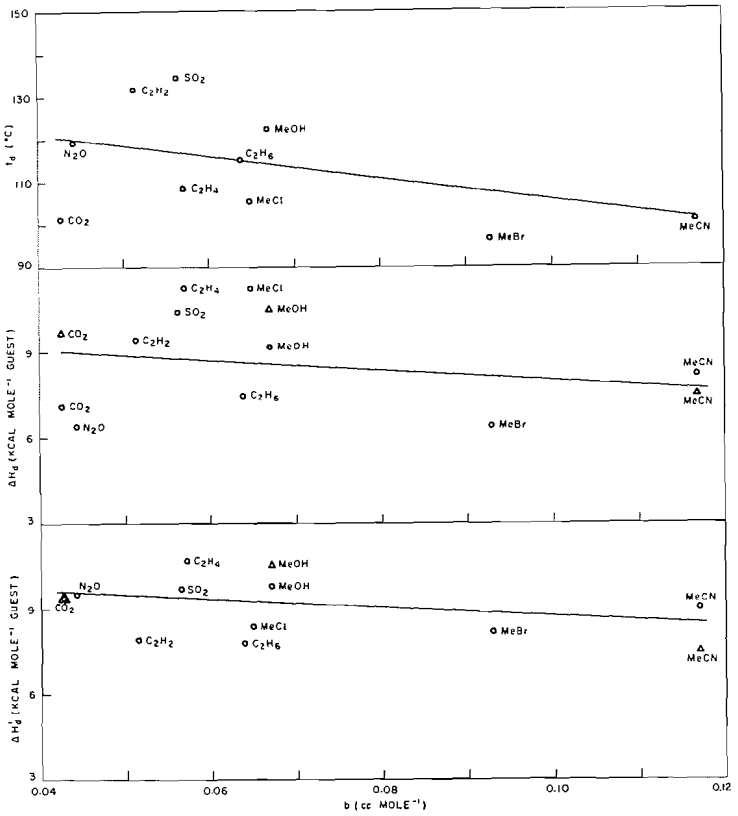


FIG. 7. Thermal stability of "distorted" clathrates as a function of guest size: (○) present data, (△) literature data.

equivalent to removal of that molecule from its pure solid state although the detailed nature of the interactions may be somewhat different in the two cases.

Comment

The size and shape of the guest molecule have a more pronounced effect upon the temperature at which the clathrate decomposes than upon the accompanying enthalpy change, suggesting that lattice vibration may play a significant role. In the clathrate structure there are no "holes" through which a guest molecule may escape from the cavity without approaching the walls closer than normal van der Waals distances; thus a high activation energy is required. Unfortunately, incipient sublimation of the quinol complicates calculation of experimental activation energies for thermal decomposition from TGA data. The fact that clathrates do decompose thermally, and do liberate guest molecules at temperatures well below the melting point of quinol where the rate of sublimation of quinol is measurable but not appreciable, requires (i) overcoming guest – cavity wall interactions and (ii) an opening of sufficient size to permit egress of the guest. It has been well established (14, 20, 21) that most guest species are capable of a considerable degree of motion within the clathrate cavity, even at low temperature, dependent upon the closeness of fit between cavity and guest. This motion may be expected to increase with temperature accompanied by a decrease in the extent to which the clathrate lattice is stabilized by interactions with the guest molecules in the cavities. At temperatures where these interactions have been overcome the contribution of the guest molecules to the stability of the

Can. J. Chem. Downloaded from www.nrcresearchpress.com by 210.87.254.42 on 09/05/12
For personal use only.

clathrate is virtually lost. Concurrently the interpenetrating quinol networks have acquired increasing energy of thermal motion and will vibrate with respect to one another at an increased frequency. The amplitude of these vibrations will also increase to the extent that there is general stretching of the O—H . . . O hydrogen bonds at the poles of the cavities, and the networks become somewhat more flexible with respect to one another. This combination of loss of the stabilizing influence of the guest upon the β-quinol structure, plus increased overall lattice vibration, results in destruction of the clathrate cavities with liberation of the individual guest molecules.

Thus, for an undistorted cavity, increasing the fraction of available cavity volume occupied by the guest molecule, or otherwise increasing the guest–wall interaction, will result in increased clathrate stability. Conversely, increasing distortion of the cavity by other types of guest species may be expected to overcome any increased stabilization of the lattice (due to dipole–dipole interactions or the like) rather readily, and loss of such internal stabilization will facilitate hydrogen-bond rearrangements at decreasing temperatures. It should be emphasized that these decomposition temperatures represent not thermodynamic transition points but temperatures at which the rates of the associated phenomena become measurable.

ACKNOWLEDGMENTS

The technical assistance of Miss Joan E. Price and Mr. D. E. King is gratefully acknowledged. It is also a pleasure to acknowledge the kindness of Mr. H. P. Vaughan, Mettler Instrument Corp., for performing the simultaneous DTA–TGA work described.

This research has been sponsored by a research grant to the Ontario Research Foundation from the Province of Ontario, received through the Department of Economics and Development.

REFERENCES

1. H. G. McADIE. Can. J. Chem. **41**, 2137 (1963).
2. H. G. McADIE. *In* Thermal analysis '65. *Edited by* J. P. Redfern. Macmillan, London. 1965. p. 68.
3. D. F. EVANS and R. E. RICHARDS. Proc. Roy. Soc. London, Ser. A, **223**, 238 (1954).
4. D. E. PALIN and H. M. POWELL. J. Chem. Soc. 815 (1948).
5. B. E. BRYANT. U.S. Patent No. 3,076,742 (February, 1963).
6. D. F. EVANS and R. E. RICHARDS. J. Chem. Soc. 3932 (1952).
7. R. L. STONE and H. F. RASE. Anal. Chem. **29**, 1273 (1957).
8. H. G. McADIE. Mater. Res. Std. **4**, 413 (1964).
9. Natl. Bur. Std. U.S. Circ. 500. Selected values of chemical thermodynamic properties. 1952.
10. A. SEIDELL. Solubilities of inorganic and metal organic compounds. 3rd ed. and supplement. Van Nostrand, New York. 1940, 1952.
11. A. SEIDELL. Solubilities of organic compounds. 3rd ed. Van Nostrand, New York. 1941.
12. G. P. HAIGHT, JR. Ind. Eng. Chem. **43**, 1827 (1951).
13. W. C. CHILD, JR. Quart. Rev. London, **18**, 321 (1964).
14. N. R. GREY and L. A. K. STAVELEY. Mol. Phys. **7**, 83 (1963).
15. J. R. PARTINGTON. An advanced treatise on physical chemistry. Vol. IV. Longmans, New York. 1953.
16. HANDBOOK OF CHEMISTRY AND PHYSICS. 44th ed. Chemical Rubber Publishing Co., Cleveland, Ohio. 1963.
17. S. C. WALLWORK and H. M. POWELL. J. Chem. Soc. 4855 (1956).
18. G. PEYRONEL and G. BARBIERI. Intern. Symp. Chem. Coord. Compds., Rome, 1958.
19. R. M. HEXTER and T. D. GOLDFARB. J. Inorg. Nucl. Chem. **4**, 171 (1957).
20. G. L. STEPAKOFF and L. V. COULTER. Phys. Chem. Solids, **24**, 1435 (1963).
21. M. DAVIES and W. C. CHILD, JR. Spectrochim. Acta, **21**, 1195 (1965).
22. AMERICAN SOCIETY FOR TESTING MATERIALS. Index to X-ray powder data file (1964).

Can. J. Chem. Downloaded from www.nrcresearchpress.com by 210.87.254.42 on 09/05/12
For personal use only.

Can. J. Chem. Downloaded from www.nrcresearchpress.com by 210.87.254.40 on 09/05/12
For personal use only.

A PARAMAGNETIC RESONANCE STUDY OF HINDERED DIARYLMETHYL RADICALS AND RELATED COMPOUNDS

I. ANALYSIS OF THE SPECTRA

H. R. FALLE[1] AND F. C. ADAM
Department of Chemistry, University of Alberta, Calgary, Calgary, Alberta
Received April 30, 1965

ABSTRACT

Several ortho-substituted radicals of the benzhydryl type and a variety of diaryl ketyls have been studied through the nuclear hyperfine structure of their electron spin resonance spectra. A strong similarity is found between the spectra of a given ketyl and its hydrocarbon analogue. This suggests that when ketones are reduced, a very tight ion pair is formed between the ketyl anion and its cation. Although the coupling constants of the protons vary with different reducing agents, larger variations are observed when bulky groups are substituted into ortho positions. These larger changes are attributed to a forced internal rotation of the phenyl rings. The distortion results from the steric repulsion between the ortho groups. The effect of 'buttressing' of ortho methyl groups is also studied. Deuterium and ^{13}C substitutions have been effected in some of the compounds.

INTRODUCTION

The underlying purpose of this study was to determine the effect that ortho substituents have on the proton hyperfine structure of the electron spin resonance (e.s.r.) spectra of various compounds with a benzhydryl skeleton. Molecular models of the parent compound, diphenylmethyl, show that two of the four ortho protons are in positions which should give rise to large steric repulsions when the two rings are held in a coplanar configuration. The other pair of ortho protons is not constrained in this way, and steric interactions should not occur unless the carbon–carbon bond angles are severely distorted from the normal sp^2 hybrid angles of 120°. For convenience in the following text, the sterically hindered pairs of ortho groups will be termed the "inner" groups and those at the sterically inactive positions the "outer" groups. This distinction is unique for the diarylmethyl radicals, because for triphenylmethyl derivatives both inner and outer groups are sterically involved, whereas for the benzyl radical neither of the ortho protons is particularly effective in introducing steric repulsions.

The e.s.r. spectrum of triphenylmethyl may be analyzed in terms of six equivalent ortho protons, six meta protons, and three para protons (1). The implied threefold axis of symmetry would result if the steric strain at the ortho sites were relieved by symmetrical rotation of the three phenyl rings about the central bonds, resulting in a propellor configuration. Nuclear magnetic resonance (n.m.r.) studies of the carbanion and carbonium ions of diphenyl and triphenylmethyl derivatives support this conclusion because similar shifts are found for equivalent protons in each ring of these compounds (2, 3). The optical spectra of the ions also suggest a symmetrical structure for both diphenyl and triphenyl derivatives. The inferences here are less clear-cut, and the suggestion has been made that the optical spectrum results from transitions which do not involve all of the phenyl rings (4). This conclusion is based mostly on the lack of a bathochromic shift due to extension of conjugation in proceeding from the monophenyl to the triphenyl ions of this series. It has been shown theoretically (5) that this behavior is to be expected, and calculations

[1]*Present address: Department of Chemistry, Cambridge University, Cambridge, England.*

based on the transition intensities (6) appear to favor a structure in which all rings present contribute equally to the conjugation of the molecule.

It will therefore be assumed that the stable form of the radicals under consideration is of the form depicted in Fig. 1*a* rather than the unsymmetrical rotomer in Fig. 1*b*. Although this assumption leaves the question of the possible non-equivalence of the ortho substituents, the matter is not critical to the following discussion.

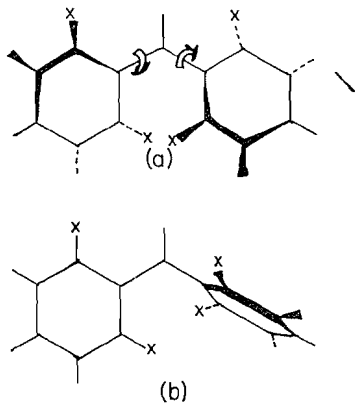


FIG. 1. Angular distortions of diphenylmethyl radicals. (*a*) Symmetrical, both rings rotated; (*b*) unsymmetrical, one of the four possible rotomers. The symbol X represents any sterically hindering group.

As can be seen from Fig. 1*a*, as the size of the ortho group, X, is increased, the additional steric strain may be partly relieved by rotation about the central carbon–carbon bonds. This will decrease the conjugation between the central carbon and each of the rings, with the result that the odd electron density will be confined more closely to the central position. In the extreme case of very large hindering groups, the phenyl rings would be held perpendicular to the plane of the central group. In all naivety it could be assumed that the unpaired electron would then be completely localized in the 2p orbital of the extracyclic carbon atom. According to the well-known formulation of McConnell (7), the coupling constant (a_i) of the ith aryl-type proton is given by the relationship

$$a_i = \rho_i Q(\mathrm{H})$$

where ρ_i is the spin density at the adjoining sp^2 hybridized carbon atom and $Q(\mathrm{H})$ is a constant of the order of 25 Oe. For the localized electron considered above, $\rho = 1$, so the hyperfine splitting of the lone proton on this central carbon atom would be ~ 25 Oe. There would be no hyperfine splittings from the ring protons. Smaller hindering groups would give smaller internal rotations, and greater delocalization of the unpaired spin density. Thus the lone proton splittings would decrease, whereas the contributions of the ring protons to the hyperfine spectrum would increase as the coplanar configuration is approached.

Unfortunately, the hydrocarbon radicals corresponding to diphenylmethyl dimerize more or less completely, unless wholly substituted in the ortho positions by fairly bulky groups (8). To obtain spectra for compounds with smaller hindering groups, the study has been extended to include the ketyls of the analogous substituted benzophenones, with which similar effects might be expected to occur.

Kinetic studies on the racemization of optically active biphenyls (9) have indicated that the size of a hindering ortho group may be effectively increased by "buttressing" this

Can. J. Chem. Downloaded from www.nrcresearchpress.com by 210.87.254.40 on 09/05/12
For personal use only.

group with bulky substituents in the meta position. As applied to the situation under consideration here, 'buttressed' ortho groups should lead to a decrease in the ring-splitting constants by increasing the internal angle of rotation. Accordingly, compounds of this sort have been included in the present study.

EXPERIMENTAL

A variety of methylated and methoxylated benzophenones has been prepared. These appear in Table I, along with the source, or method of preparation, and the shorthand notation which will be used in this paper. The hydrocarbon radicals were obtained from the corresponding ketones by reduction to the carbinol with lithium aluminium hydride in ether solution. This carbinol was treated with dry HCl gas in acetyl chloride. On completion of the reaction, the solvent was removed on a vacuum line and replaced by toluene, along with a small amount of triethylamine (10). The chloride was reduced with amalgamated silver.

In addition to the precursors listed in Table I, the isotopically labeled species 4,4′-dideutero-2,3,6,2′,3′,6′-octamethylbenzophenone (i.e. dideutero diduryl ketone or DDK-d^2) and centrally substituted ^{13}C diduryl ketone (DDK-^{13}C) were prepared. Durene was dibrominated in chloroform at −10 °C and partially lithiated with *n*-butyl lithium in ether. Excess D_2O was added and the resulting monodeuterobromodurene isolated. The magnesium grignard of this material was then prepared in tetrahydrofuran. Half of it was carbonated with dry ice, hydrolyzed, and treated with thionyl chloride. To this product was added the remaining grignard, hydrolysis giving the desired ketone.

TABLE I

Diphenyl ketones and precursors of the diphenylmethyl radicals

Compound	Symbol	Source	Melting point (uncorrected) (°C)
Benzophenone (diphenyl ketone)	DPK	Eastman	—
4,4′-Dimethylbenzophenone (ditolyl ketone)	DTK	Eastman	—
2,6,2′,6′-Tetramethylbenzophenone (dixylyl ketone)	DXK	Reference 8	127–129
2,4,6,2′,4′,6′-Hexamethylbenzophenone (dimesityl ketone)	DMK	Reference 8	135–138
2,3,5,6,2′,3′,5′,6′-Octamethylbenzophenone (diduryl ketone)	DDK	Reference 8	153–155
4,4′-Dimethoxybenzophenone (dianisyl ketone)	DAK	MCB*	—
2,6,2′,6′-Tetramethoxybenzophenone (tetramethoxydiphenyl ketone)	TMK	Reference 12	204–205

*Mathieson, Coleman and Bell.

^{13}C substitution was effected with gaseous $^{13}CO_2$ from 55.9 atom % $Ba^{13}CO_3$ (Isomet Corporation, Palisades, N.J.) and concentrated sulfuric acid, using a vacuum-line preparation. The gas was frozen in a thick-walled pyrex cell containing normal durylmagnesium bromide in tetrahydrofuran. This cell was then sealed off from the vacuum line and heated for 2 days on a steam bath. Hydrolysis of the product gave tetramethyl benzoic acid-^{13}C, which could then be treated as above to give DDK-^{13}C.

The spectra of the radical species were obtained with a TE_{011} tunable cylindrical cavity in a modified Strand Labs X-band spectrometer and a Harvey Wells magnet (L-128) system. Field modulation was at 6.2 kc/s. The magnetic field sweep had a nonlinearity of about a half a percent so that after each spectrum was run, the field was retraced at fixed microwave frequency and the spectrum of peroxylamine disulfonate superimposed on the sample spectrum. The hyperfine constants were determined from the averaged values of the field standard values. Low temperature spectra were obtained in a similar manner by the standard technique of blowing cold nitrogen gas past the sample in a quartz dewar insert set in the cavity. The ketyl spectra reported were obtained at room temperature, in dimethyoxyethane, whereas the hydrocarbon radicals spectra were taken in toluene at −60 °C. Electrolytic reductions were done in acetonitrile solution, with tetra *n*-propylammonium perchlorate as the supporting electrolyte and tungsten wire for the electrodes. The samples were prepared under vacuum. Three metals sodium, potassium, and calcium were also used as reductants. The first two were distilled into the system under vacuum by standard techniques (11), whereas calcium was cleaned as well as possible with emery paper and flamed thoroughly after introduction to the sample cell. The reductions with calcium were very slow and took several days at low temperatures, in some cases.

Can. J. Chem. Downloaded from www.nrcresearchpress.com by 210.87.254.40 on 09/05/12
For personal use only.

Can. J. Chem. Downloaded from www.nrcresearchpress.com by 210.87.254.40 on 09/05/12
For personal use only.

RESULTS

The analyses of the hyperfine spectra result in the coupling constants appearing in Tables II and III. The notation which is used follows from the notation used for the ketones in Table I. For example, DMKK-e is taken to mean 'dimesitylketone ketyl-produced electrolytically' and DMKK-Ca is the ketyl resulting from calcium metal reduction. DMM stands for dimesityl methyl, the neutral hydrocarbon species.

TABLE II

Coupling constants of the protons at various ring positions for the ketyls of the diphenyl ketone series of compounds

Compound	Coupling constants (Oe)			
	a_p	a_o	a_m	a_{metal}
DPKK-Ca	3.46	2.77	1.01	—
DPKK-Na	3.45	2.60	0.88	1.16
DPKK-K	3.44	2.55	0.86	0.24
DPKK-e	3.54	2.78	0.95	—
DTKK-Ca	3.53*	2.80	1.04	—
DTKK-Na	3.59*	2.68	0.98	—
DTKK-K	3.60*	2.67	0.97	0.25
DTKK-e	3.54*	2.81	1.03	—
DAKK-e	0.29†	2.86	0.97	—
TMKK-e	3.57	—†	0.82	—
DXKK-Ca	2.52	1.49*	1.07	—
DXKK-Na	2.50	1.59*	0.95	0.16
DXKK-K	2.50	1.59*	0.93	—
DXKK-e	2.72	1.63*	0.85	—
DMKK-Ca	2.54*	1.49*	1.07	—
DMKK-Na	2.62*	1.59*	1.02	0.1
DMKK-K	2.62*	1.60*	1.02	—
DMKK-e	2.89*	1.63*	0.93	—
DDKK-e	2.34	1.97*	1.42*	—

*Methyl protons.
†Methoxyl protons.

TABLE III

Splitting constants for methyl-substituted diphenyl methyl radicals

Compound	Coupling constants (Oe)			
	a_p	a_o	a_m	a_{1p}
DXM	3.27	2.18*	1.47	16.1
DMM	3.38*	2.15*	1.45	15.7
DDM	2.80	3.04*	2.16*	15.9

*Methyl protons.

The precise analysis of these compounds becomes very difficult and less certain as the number of ring substituents increases because of the proliferation of protons resulting from multiple methylations. To simplify the process the assumption has been made that if the substitution of methyl or methoxyl groups is made in sterically inactive positions, these substitutions do not materially change the spin distribution in the conjugated system, so that the magnitude of the splitting constants does not change from the order found in the parent ketyl of benzophenone. This latter spectrum is readily analyzed as being due to a triplet and two quintet splittings. The largest splitting is that of the triplet, and is due to the pair of para protons. This assignment is verified in the para-methylated and para-methoxylated derivatives of benzophenone, DTKK and DAKK, where the

triplet has been replaced by septets in both cases. In the spectrum of DAKK, the methoxyl splittings are very small, whereas for DTKK the methyl proton splittings are only slightly larger than the ring protons that have been replaced. The remaining two quintet splittings are due to the ortho and meta protons and do not change markedly as a result of either of these substitutions. This fact lends support to the contention that the spin densities are not markedly changed by substitution at unhindered sites. Alternatively, these substitutions produce only small perturbations to the ground state wave functions. It also appears that freely rotating methyl groups give splitting constants a_i(Me) which follow the approximate relationship (13)

$$a_i(\mathrm{Me}) = \rho_i Q(\mathrm{Me}),$$

where Q(Me) is but slightly larger than the value for ring protons (25 Oe) and ρ_i is the unperturbed spin density at the substitution site. Although on somewhat doubtful theoretical ground (14) this formulation will be assumed to hold in the present work.

It remains to be decided which of the two quintet splittings of DPKK is due to the ortho protons. If the spectrum of TMKK is considered, a large triplet splitting is obtained. Each line is further split by a single quintet. The ortho protons have been replaced by methoxyl groups from which no splittings were found. Contributions from these protons were unresolved within the rather broad lines ($\sim$ 0.4 Oe) of the absorption spectrum. The triplet splitting is similar to that of the para protons in DPKK, and the remaining quintet splitting corresponds to the smaller of the quintet splittings in DPKK. This latter structure is therefore assigned as due to the meta protons, and the larger quintet splittings in DPKK as due to the ortho protons. Thus the magnitudes of the splittings fall in the order $a_p > a_o > a_m$ for DPKK and its derivatives. This order does not appear to change when the ortho positions are completely methylated. The 13 line progressions due to these protons are quite apparent in the spectra of the ketyls of both DMK and DXK. Since the spectrum of DXKK-Ca is fairly well resolved it is possible to locate the subsidiary triplet and quintet due to para and meta ring protons. In the case of DMKK-Ca, essentially the same meta quintet splitting is found, along with the expected para methyl proton septet. Again the methyl proton splitting is only slightly larger than that of a ring proton at the same position. As with DTKK (compared to DPKK), para methylation would not be expected to alter the spin distribution in the ring nor effect the 'steric size' of the ortho group.

The spectrum of DDKK was not so amenable to the above cut-and-try method of analysis. The lines which appear in the spectrum may be interpreted in terms of two sets of 12 equivalent protons. The outer components of the triplet due to the para protons are of relatively lower intensity and appear to coincide with the progression of lines arising from the central component. As a result of this overlap a para proton coupling constant cannot be obtained except from a consideration of the relative intensities of the lines. Since the coincidences are probably not exact, this procedure would not give rise to an unequivocal assignment. On the other hand the ortho and meta methyl proton splitting constants must be considered anomalously large. This may result from the fact that these buttressed methyl groups interact very strongly; they may be interlocked in such a way as to allow only a concerted motion or may even be twisted out of the plane of the phenyl ring. In either case a different coupling constant from that obtained for freely rotating groups might be expected. For this reason, the para proton coupling constant would appear to be a more satisfactory index of the spin densities in the ring than would be the more readily available methyl splittings. Accordingly the para-deuterated DDKK was prepared.

Can. J. Chem. Downloaded from www.nrcresearchpress.com by 210.87.254.40 on 09/05/12
For personal use only.

Can. J. Chem. Downloaded from www.nrcresearchpress.com by 210.87.254.40 on 09/05/12
For personal use only.

The spectrum of this derivative was considerably different than that of the normal ketyl. The envelope of the hyperfine lines was symmetrical and bell shaped in the former case, but serrate in the latter. The 0.32 Oe spacing between adjacent lines was the same in both spectra. A number of possibilities exist. Firstly the deuterium splitting (1:2:3:2:1) may be very small compared to the linewidth. In this case one would expect the same symmetrical spectrum, or a 1:2:1 repetition of this symmetrical spectrum, for the normal derivative. Neither will give the characteristic spectrum observed. On the other hand, if the deuterium splitting corresponds to the 0.32 Oe interval (or a multiple of it), the symmetrical spectrum could result from the fivefold repetition of the basic 169 line pattern due to the ortho and meta methyl protons, with the coupling constants cited. Furthermore the proton coupling constant would be expected to be about $6\frac{1}{2}$ times the 0.32 Oe splitting, or an integral multiple of it. With this information it was possible to select the 'most likely' para proton coupling constant which appears in Table II. The ortho and meta coupling constants are assigned so that $a_o > a_m$ and correspond to the order found with the other compounds, but the reverse assignment may in fact be appropriate.

The spectra of the neutral hydrocarbon radicals are characterized by a large doublet splitting due to the lone central proton. However, the splitting is not so large as to prevent overlapping of the hyperfine components from the doublet states. This fact, along with a lack of symmetry between the high field and low field side of the spectrum, made the location of the central lines of the two halves of the spectrum rather uncertain. A striking similarity is to be observed between the intensity pattern of the ketyls and that of the corresponding neutral radicals. In fact the latter spectrum looks very much like the sum of two ketyl spectra displaced by the doublet separation. Comparison of the ketyl spectrum with that of the hydrocarbon radical leads to an assignment of the doublet splitting that is considerably more trustworthy than would have been obtained from the hydrocarbon data alone. The essential difference between the spectra of the two types of compound appears to be only in the doublet splitting and the fact that the coupling constants of the hydrocarbons are slightly larger than those of the ketyls. The assignments for the neutral radicals are set out in Table III. The same procedure was used in the case of DDM as was used for the corresponding ketyl; the para coupling constants were obtained from the comparison of the dideutero and the normal compound.

The lack of symmetry between the high and low field sides of the spectrum mentioned above was found in several of the cases studied. The situation with regard to the alteration of line intensities in these compounds is rather more difficult to cope with than in simpler spectra, where g value and residual dipolar anisotropies or intermolecular motional effects (15) serve to broaden the lines and so reduce the peak-to-peak amplitudes. The further complications arise because most of the lines observed result from the overlap of several transitions between different nuclear substates. The resulting line depends therefore not only on the width of the composite members but also on the degree of overlap. This complex matter is not considered further at present. However, to compare computed and observed spectra, an attempt was made to reduce intensity variation effects in the observed spectra by averaging the high and low field peak heights. This procedure will not yet give a true representation of the relative peak heights since these quantities will still be dependent upon the degree of superposition, and upon the intensities of the various components giving rise to the observed line. Plotted spectra corresponding to the suggested coupling constants have been drawn up for each of the compounds studied and have been compared to the averaged experimental intensities. Quite good agreement is found. While the computed intensities are generally somewhat higher than those observed, there is extremely

good agreement between the intensity patterns. The same procedure has been carried out for other assignments which correspond to other possible molecular arrangements. For instance, spectra have been computed for the situations where there is coupling in one ring only, or in two rings unequally, or where different inner and outer group splittings are assumed. In no case was the fit with the experimental data nearly as good as given by the results cited, nor was such reasonable internal consistency of the results obtained.

One further observation may be made about the spectrum of DMM. The spectrum of this compound and its analysis agree with that reported by Chestnut and Sloan (16) and, apart from intensity alteration effects, agree very closely with the calculated values. The line widths in this spectrum are of the order of 0.08 Oe, and in none of the lines is there the slightest indication of a splitting of the ortho lines due to differences between the inner and outer groups. It is also apparent that the methyl groups in this compound rotate freely, even in the sterically restrictive sites occupied by the inner groups.

The ^{13}C splitting for DDM-^{13}C was found to be 24.8 Oe, which compares very closely with the value of 24.5 Oe obtained by Adam and Weissman (17) for DMM-^{13}C. The spectrum of the corresponding diduryl ketyl was also taken, but although the resulting spectrum was different from the normal material, it proved impossible to analyze. However, from the increased width of the spectrum, an upper limit of some 15 Oe can be placed on the ^{13}C coupling constant in this compound.

DISCUSSION

As was outlined in the Introduction, it should be possible to assess gross changes in the molecular structure of diphenylmethyl radicals by a study of the proton hyperfine structure. In particular, substitution into the ortho positions should result in an increase in spin density at the central position and a decrease in the total density in the rings as a result of the decreased electronic coupling between the central position and the rings. It is hoped that the substitutions themselves do not produce changes in spin distribution and electron–proton interactions which are sufficient to mask any effects which are due to the steric factors alone. Since the spin density at the central position would be the least affected by perturbations within the rings, the lone proton splittings, and, to a lesser extent, the ^{13}C splittings, should therefore be the most reliable index of what is happening in the molecule as a result of chemical substitution. When the three compounds DXM, DMM, and DDM are compared on this basis, little change is observed in the lone proton splitting. The ^{13}C coupling constants for DMM and DDM are also very similar. One is forced to conclude that neither *p*-methylation nor buttressing of the sterically hindered groups produces much change in the interannular orientation. The ring densities for DXM and DMM are also quite similar. On the other hand DDM has coupling constants which show that considerable changes have occurred; apparently the buttressed groups affect each other much more than they do the remainder of the molecule. Although the para coupling constant decreases, it is suggested in this case that this results from distortion of the phenyl ring rather than from any large change in the dihedral angles of the ring relative to the central position.

The hydrocarbon results cannot be directly compared to those obtained with the ketyls because of the presence of the oxygen function and its possible interaction with the outer groups. With the absence of the lone proton one has to rely on the coupling constants of the ring substituents to indicate the distribution of spin within the ketyl radical. If xanthone ketyl (XKK) is considered in addition to the remaining examples of Table II, then a series of compounds is obtained which vary considerably in the disposition of the

Can. J. Chem. Downloaded from www.nrcresearchpress.com by 210.87.254.40 on 09/05/12
For personal use only.

two rings bonded to the ketone function. Xanthone ketyl (XKK-Ca) has splitting constants $a_o \approx a_p \approx 3.9$ Oe, and should be approximately planar by virtue of the oxygen bridge between the two rings. For DPKK-Ca, the value for a_p has dropped to 3.46 Oe, and for DXKK-Ca, to 2.52 Oe. The value of 2.34 Oe obtained for the buttressed form may or may not be real, since the coupling constant anomalies parallel those of its hydrocarbon analogue, which is also suspect. In any case this is the order predicted in the Introduction; as a result of steric repulsive forces, the odd electron population in the rings has decreased, planar > ortho hydrogens > ortho methyls. Whereas the meta coupling constants do not seem appreciably changed, the ortho values show a parallel decrease: XKK (3.9 Oe) > DPKK (2.77 Oe) > DXKK (1.49 Oe).

Attention must be drawn to the DAKK spectrum. The para coupling constant shows an increase over DPKK even though the ortho hydrogens have been replaced by methoxyl groups. It is not known whether this is due to a spin redistribution caused by the multiple substitution, or whether methoxyl has an intrinsically small steric effect in this particular situation where the methyl groups can get out of each other's way.

From the results in Table II, it can be seen that for each of the ketone samples for which the reducing agent is sodium, hyperfine coupling to that nucleus ($I = 3/2$) occurs. It is much smaller in the orthomethylated compounds than in the case of DPKK. The reverse situation would normally have been expected if the metal ion is associated with the oxygen atom which is, in turn, in a region of relatively higher spin density as a result of ortho methylation. This suggests that the ortho methyl groups interfere with the formation of a 'normal' bond between the metal and the oxygen atom. While the presence of metal nuclear coupling is strongly suggestive of a tight ion pair, there must be considerable difference in the structure of these complexes to give the order of magnitude variation which is observed. A further peculiarity may be observed in a comparison of the magnitudes of the splittings for various metals. Other recent work (18) reports lithium splittings for some of these compounds. For DPKK, $a_{Li}/a_{Na} = 0.37$, whereas for DTKK, $a_{Li}/a_{Na} = 0.36$. The ratio of the nuclear moments $\mu_{Li}/\mu_{Na} = 1.47$. Similarly from Table II, $a_{Na}/a_K = 4.8$, whereas $\mu_{Na}/\mu_K = 5.68$ for the same compounds. Thus the more electropositive elements have relatively higher spin densities, all other factors constant. Arguments based on relative ionic character for the metal–oxygen bond, or the length of the bond, and so on, all appear to favor a higher spin density with the more electronegative metal atoms. Sodium also has a relatively larger coupling constant compared to magnesium (19).

A further trend may be noticed within the sequence of splitting constants observed for a particular ketone. The values in Table II may be arranged in the arbitrary order $N(iPr)_4^{1+}$, Ca^{2+}, Na^{1+}, K^{1+} (which probably corresponds to the ionization potentials). For the metal reductions, the ring proton coupling constant for a given ketone decreases, or at worst remains unchanged, in the above order. On the other hand if the substituent is a methyl proton, the coupling constants increase in the same sequence.

Finally, reference should be made to the observation that in the spectra studied no evidence has been found which would indicate that there is any difference between the coupling constants of the inner and outer groups. Furthermore no differences appear to exist between the protons of each methyl group in these sterically restricted situations. Whereas it is reasonable to suppose that these methyl groups are free to rotate about the carbon–carbon axis even in severely hindered environments, there is no simple explanation of the apparent equivalence of the different groups. They are not related by symmetry, and exist in very different spin localities. This is especially true of the ketyls, where any

Can. J. Chem. Downloaded from www.nrcresearchpress.com by 210.87.254.40 on 09/05/12
For personal use only.

spin density on the oxygen atom would almost certainly be felt by the outer group. On the other hand the protons of the inner group are held close to the spin concentration of the adjacent ring. It is possible that these different sites may exchange places with sufficient rapidity to average out any field differences. The lack of high and low field symmetry may be a token of such an internal motion. The possibility of such an oscillation occurring at low energies of activation will be discussed in the second paper of this series.

ACKNOWLEDGMENTS

The authors wish to express their gratitude to the National Research Council for the purchase of the magnet system, and for financial support (H. A. F.) during the course of the work.

REFERENCES

1. P. Brovetto and S. Ferroni. Nuovo Cimento, **5**, 142 (1957).
2. T. Schaefer and W. G. Schneider. Can. J. Chem. **41**, 966 (1963).
3. V. R. Sandel and H. H. Freedman. J. Am. Chem. Soc. **85**, 2328 (1963).
4. N. C. Deno. J. Am. Chem. Soc. **73**, 3644 (1951).
5. R. Grinter and S. F. Mason. Proc. Chem. Soc. 386 (1961).
6. E. K. Ng and F. C. Adam. Can. J. Chem. **42**, 810 (1964).
7. H. M. McConnell. J. Chem. Phys. **24**, 632 (1956).
8. J. Coops, W. T. Nauta, M. J. E. Ernsting, and R. C. Faber. Rec. Trav. Chim. **59**, 1109 (1940).
9. R. Adams and G. C. Finger. J. Am. Chem. Soc. **61**, 2828 (1939).
10. D. C. Reitz. Ph.D. Thesis, Washington University, St. Louis, Missouri. 1959.
11. T. R. Tuttle. Ph.D. Thesis, Washington University, St. Louis, Missouri. 1957.
12. G. Wittig and U. Pockels. Ber. **72**, 89 (1958).
13. A. D. McLachlan. Mol. Phys. **1**, 234 (1958).
14. J. P. Colpa and J. R. Bolton. Mol. Phys. **6**, 273 (1963).
15. J. H. Freed and G. K. Fraenkel. J. Chem. Phys. **40**, 1815 (1964).
16. D. B. Chestnut and G. J. Sloan. J. Chem. Phys. **35**, 443 (1961).
17. F. C. Adam and S. I. Weissman. Abstracts, 133rd Meeting, American Chemical Society, San Francisco. 1958.
18. R. Tanikaga, K. Maruyama, and R. Goto. Bull. Chem. Soc. Japan, **38**, 144 (1965).
19. N. Hirota. J. Chem. Phys. **37**, 1884 (1962).

Can. J. Chem. Downloaded from www.nrcresearchpress.com by 210.87.254.40 on 09/05/12
For personal use only.

Can. J. Chem. Downloaded from www.nrcresearchpress.com by 210.87.254.42 on 09/05/12
For personal use only.

A STUDY OF HINDERED DIARYLMETHYL RADICALS

II. THE BENZHYDRYL MODEL

F. C. ADAM AND H. R. FALLE[1]

Department of Chemistry, University of Alberta, Calgary, Calgary, Alberta

Received July 30, 1965

ABSTRACT

This paper presents a model in which internal rotations of diphenylmethyl radical types effectively average out differences between the ortho and the meta substituent pairs in each ring. The process involves a very low energy of activation even though π-electron bonds are broken. The model is supported by valence bond (VB) and Huckel molecular orbital (HMO) calculations, and comparison is made with experimentally determined quantities wherever this is possible. Certain cases in which transannular pseudosymmetry has not been found are also discussed in relation to the above model.

INTRODUCTION

In this paper, a model will be developed to describe some of the phenomena which are observed with diarylmethyl systems. Of particular interest will be those molecules with a benzhydryl radical skeleton substituted with various saturated groups which do not formally extend the conjugated length of the system. A sequence of compounds with this property has been reported in an earlier paper (1), herein referred to as I, which describes the electron paramagnetic resonance (e.p.r.) spectra of a number of substituted diphenylmethyl hydrocarbon radicals and the spectra of the ketyls of the analagously substituted benzophenone derivatives. Strong similarities were observed between the proton hyperfine coupling constants of corresponding members of these two classes of compounds. Nuclear hyperfine structure for the counterion was found in a number of the ketyl spectra, suggesting that tight ion pairs are formed in these compounds. This observation, along with the similarities in the proton hyperfine structure, leads to the conclusion that the ketyls might profitably be studied as perturbed benzhydryl radicals, rather than as ketonic anion radicals perturbed by the electrostatic interaction with the counterion (2). Thus one basic model may be used to describe both types of radicals.

The sequence of compounds studied in I shows that substitutions at different positions in the rings produce markedly different effects. Whereas saturated para substituents such as methyl or methoxyl do not greatly change the coupling constants of the other ring protons, ortho substituents have the effect of reducing considerably the net spin density in the rings. The latter conclusion may be deduced from the hyperfine splittings by the well-known McConnell relationship (3) for ring protons, or that of McLachlan (4) for methyl groups. These relationships state that the coupling constants are proportional to the spin densities at the site of substitution, so that $a_i(\mathrm{H, or\ Me}) = \rho_i Q(\mathrm{H, or\ Me})$ where Q is a constant. According to the results of I, the value of Q for methyl protons is only slightly larger than its value for ring protons ($\sim$ 25 Oe).

The reason for the ortho substitution effect may be most readily seen from Fig. 1*a*. Introduction of bulky ortho groups at the 3, 3′, 7, and 7′ positions force internal rotation about the 1–2 extracyclic bonds. In this way the ortho groups can avoid one another and reduce the non-bonding repulsive forces between them. This loss in planarity occurs at the expense of the delocalization energy of the conjugated system, since the internal rotation

[1]*Present address: Department of Chemistry, Cambridge University, Cambridge, England.*

is accompanied by a decrease in exchange interaction (or overlap) between the central atom 1, and the ring carbon atoms at 2 and 2′. Thus the eventual ground state configuration will be that in which further rotation of the rings results in a loss of resonance energy greater than the gain in terms of the steric repulsion energy. The most likely configuration need not be the symmetrical rotomer where each ring has rotated through equal and opposite angles; it may even be a configuration in which one ring is perpendicular to the plane defined by the central carbon atom and the atoms of other rings (5). An acceptable model of the system would have to discriminate between these two extreme possibilities. The bulk of the evidence favors the former alternative (6), and the text immediately following will be based on this premise.

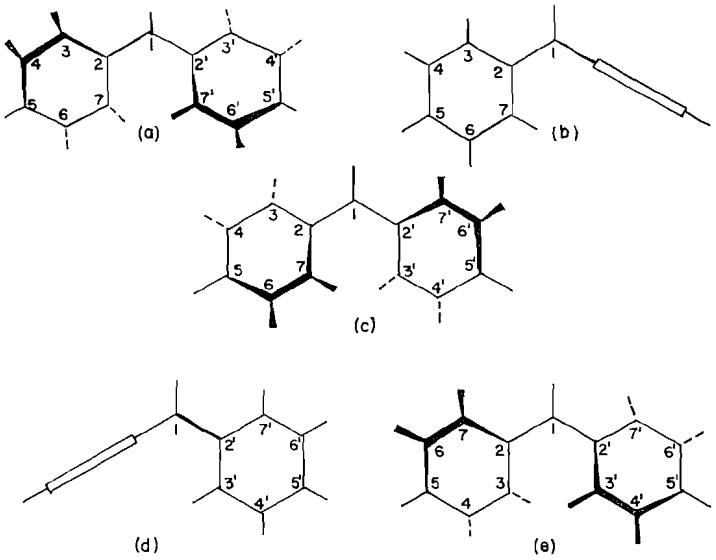


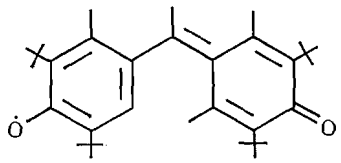
FIG. 1.

As may be seen from Fig. 1, ortho substituents at 3 and 3′ will not be particularly effective in introducing steric repulsion, unless there is also some fairly bulky substituent on the carbon atom at 1. The inner and outer groups are not related in the symmetry group (C_2) of the molecule. The 'outer' groups at 3 and 3′ are considerably further apart than the 'inner' group substituents at 7 and 7′ so that on complete ortho methylation of the benzhydryl skeleton, the protons of the inner methyl groups lie very close to the carbon atoms of the opposite rings, whereas the 'outer' methyl group protons point out and away from the center of the molecule. In the 20-odd radicals studied in I, a variety of ortho substituents was used as the hindering groups, but yielded the same coupling constants for both inner and outer groups. The equivalence of these groups seems even more unusual when it is considered in relation to the behavior of certain other radicals of different molecular structure. A number of species is known in which hyperfine structure is obtained from nuclei that are separated from the centers of electron spin density by a number of σ bonds (7, 8). The nuclear-electronic interactions appear to depend more critically upon the distance and position of the nucleus (or of the orientation of the σ bond involving the nucleus) relative to the orbital containing the unpaired electron spin. The peculiarities of the σ-bond system joining the centers do not seem to be at all important. Whereas the inner groups of a benzhydryl system are in a position to interact with the electron spin density in the π orbitals of the opposite ring, the outer groups are not.

Can. J. Chem. Downloaded from www.nrcresearchpress.com by 210.87.254.42 on 09/05/12
For personal use only.

The similarity between inner and outer groups is not restricted to studies involving the benzhydryl radicals. A similar situation is found in the nuclear magnetic resonance (n.m.r.) spectrum of the diphenylmethyl carbanion. In this case the inner and outer protons exhibit identical chemical shifts (9), although it seems unlikely that the inner protons should lie in a region which would give, in effect, a zero ring current contribution from the opposite phenyl ring (10).

There are, however, a few instances in which an apparent difference between inner and outer groups is known to be measurable. One is found in the recent work of Hyde and Maki (11) who have obtained an electron-nuclear double resonance (ENDOR) signal from the ortho ring protons of Coppinger's radical.



The signal is a doublet with a separation of about 0.06 Oe. This difference may be presumed to be between inner and outer ortho protons, rather than a difference arising from a lack of symmetry between the two rings. The resolution of the spectrum of dimesitylmethyl radical in I was only slightly larger than this value (0.08 Oe), yet no detectable broadening or splitting could be observed for the ortho lines. On the basis of the foregoing considerations, a much larger splitting than 0.06 Oe might have been expected for the latter compound if for no other reason than that the protons are much closer to the opposite ring than they are in Coppinger's radical.

Differences between the inner and outer proton hyperfine coupling constants are also observed in the electron spin resonance (e.s.r.) spectra of ortho-bridged benzophenone ketyl compounds. These are exemplified by the ketyl of xanthone which has an oxygen atom bridge between the two rings. The proton hyperfine spectrum may be explained in terms of a quartet of triplets so that the inner and outer protons are not equivalent in this compound. The observed difference probably does not result from the hetero atom substitution, since the proton coupling constants are not sensibly dependent upon the particular bridging group; the ketyl of thioxanthone has hyperfine coupling constants similar to those of the xanthone ketyl (12). It is apparent that the dichotomy with regard to inner and outer ortho group splittings persists when inner and outer meta protons are considered. It is hoped that some of the diversity in behavior may be explained by a model which will be discussed in the following sections.

THE BENZHYDRYL MODEL

For magnetic nuclei of the same molecule to exhibit the same hyperfine coupling constants, it is necessary that the totality of interactions with the unpaired electron distribution be identical for each nucleus. This may result simply from the requirements of molecular symmetry, so that the nuclei are situated in identical potential fields. Equivalence can also be observed under conditions where the nuclei are exchanged over non-equivalent positions in space. As long as the rate of exchange is rapid enough to average out completely the differences in potential energy during the measurement, the nuclei will appear to be equivalent. One example of such an averaging process is exhibited by the methyl protons studied in I. Although the protons interact instantaneously with the unpaired spin in an unsymmetrical way, rotation about the symmetry axis of these methyl groups is rapid enough to average the differences. There appear to be three equivalent

Can. J. Chem. Downloaded from www.nrcresearchpress.com by 210.87.254.42 on 09/05/12
For personal use only.

Can. J. Chem. Downloaded from www.nrcresearchpress.com by 210.87.254.42 on 09/05/12
For personal use only.

protons. The motion persists at very low temperatures (13) and in sterically unfavorable environments (1). The observed similarity between the coupling constants of inner and outer groups in the benzhydryl system would result from a similar process provided there were some mechanism by which these inner and outer groups could exchange positions. The situation would be considerably more complicated in this case, since such a process requires the breaking of π bonds, which for most conjugated systems involves very high activation energies. One would normally expect a very low exchange rate for such a process. However, the benzhydryl system is somewhat unique in that it is composed of two highly conjugated systems coupled together; if by some means the delocalization energy which is lost in one half of the molecule is gained by the other half during a distortion of the nuclear framework, then a considerable number of configurations may be possible in which there is little change in the total π-electron energy of the molecule. Consider the symmetrical isomer of Fig. 1*a*. The ortho groups are held apart by repulsive forces, and the same dihedral angle, θ, exists between the normal to each ring and the axis of the $2p\pi$ orbital of the central carbon atom. The molecule would have a resonance energy dependent to some extent upon this dihedral angle. Suppose now that the left-hand ring were to assume a coplanar configuration with the central carbon atom. The dihedral angle (θ_1) for the 1–2 bond would reduce to zero. The ortho groups of the second ring would be forced further out of the plane by steric forces, and the dihedral angle (θ_2) for the 1–2′ bond would approach the maximum value of 90°, as depicted in Fig. 1*b*. The system would now have the resonance energy of a planar benzyl radical plus that of an isolated benzene ring. If now the rotation were to be continued in the same direction, so that the group at 7, originally below the plane, were now to lie above the plane, then a symmetrical isomer would again be obtained as in Fig. 1*c*. The difference between the rotomers of Fig. 1*a* and Fig. 1*c* is that the inner and outer groups of the right-hand ring have exchanged positions. Further rotation in the same direction will result in the exchange of the inner and outer groups of the left-hand ring. This is shown in Figs. 1*d* and 1*e*.

The inner and outer groups at both ortho and meta positions are exchanged by this mechanism, and the question immediately arises concerning the amount of energy which must be expended in order to effect the exchange. It is easy to see that at least part of the delocalization energy lost to the out-of-plane ring may be compensated for by the increased resonance of the highly stable benzyl residue. The question then becomes one of determining the resonance energies for the systems benzyl plus benzene, and for benzhydryl. This is equivalent to finding the relationship between these energies and the dihedral angle θ, or equivalently the exchange energy of the 1–2 and 1–2′ π-electron bonds. Other interactions between the electrons in different rings may be neglected, as may the interactions of electrons on non-neighboring atoms. Values for the delocalization energy may then be obtained by simple valence bond (VB) or Huckel molecular orbital (HMO) techniques. The calculations are simple and straightforward, and one may set up appropriate secular equations in which the 1–2 and 1–2′ interactions are expressed in terms of the nearest neighbor interactions. Thus for the HMO treatment, $\beta_{12} = \gamma\beta_{\text{ring}}$, while for VB determinations, $\alpha_{12} = \gamma\alpha_{\text{ring}}$; β and α have their usual meaning (14). The parameter γ will have different meanings in the two methods, but will depend upon the 1–2 bond distance as well as upon the dihedral angle θ. In either case,

$$\gamma = f(r)g(\theta).$$

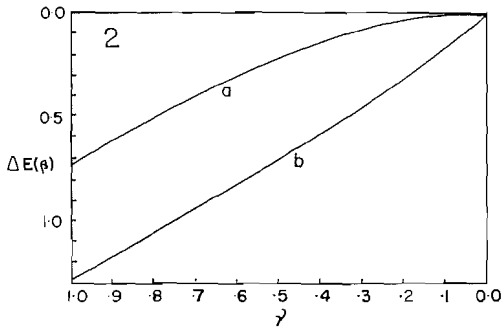
Although $g(\theta)$ may be taken to be $\cos\theta$ in a HMO treatment, it will be $\cos^2\theta$ in the VB method. The function $f(r)$ is a little more complicated, although theoretical estimates

Can. J. Chem. Downloaded from www.nrcresearchpress.com by 210.87.254.42 on 09/05/12
For personal use only.

could be used if the bond lengths were known for these radical systems. However, both the HMO and VB treatments suggest that since the mobile bond order (or double bond character) is somewhat less than for normal benzene ring bonds, the 1–2 bond is somewhat elongated in these systems. Thus all that can be said is that $1 > f(r) > 0$. As will be seen an estimate of this parameter may be made in certain cases.

RESULTS

The results of HMO calculations appear in Fig. 2, and those of the VB calculations in Fig. 3. The π-electron delocalization energies are shown as functions of γ for both the symmetrical rotomer of the benzhydryl radical and the unsymmetrical rotomer corresponding to ω-phenyl benzyl radical. The latter is the transition state for the exchange process which switches the inner and outer groups of the benzhydryl system. The desired information is the low energy transition states available to a given symmetrical radical. Suppose this symmetrical molecule has inner ortho substituents of a size which requires the dihedral angles θ_1 and θ_2, at the 1–2 and 1–2′ bonds respectively, to accommodate their combined steric volumes. A certain bond length will also be pertinent to the given molecule, so that $\gamma_1 = f(r_1)\cos^2\theta_1 = f(r_2)\cos^2\theta_2 = \gamma_2$ or $\gamma_1 = \gamma_2$. This is denoted by γ in Fig. 3, and is the same for both extracyclic bonds. If now the rings were allowed to rotate as suggested in Fig. 1, the value of γ for the benzyl part of the system would increase and the γ value for the other bond would decrease. In the transition state, the bond extracyclic to the perpendicular ring would have a value $\gamma = 0$, by virtue of the cosine dependency. For the benzyl fragment, $\gamma = f(r)\cos^2\theta = \gamma' = f(r)$. γ' has also been indicated in Fig. 3. It pertains to the transition state whose energy is the same as that of symmetrical form, and therefore corresponds to a pure rotational isomer involving no energy of activation. The same symmetrical radical could exchange through a higher



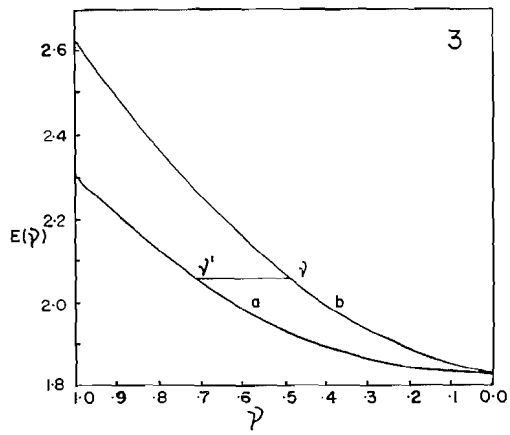


FIG. 2. Plot of $\Delta E(\beta)$ versus γ from HMO calculation.
FIG. 3. Plot of $E(\gamma)$ versus γ from VB calculation.

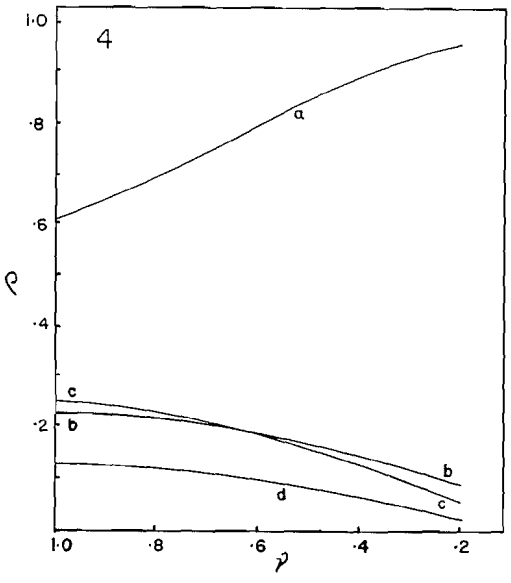
energy transition state (i.e. a benzyl fragment with a smaller γ') but this would require the addition of energy to the system. It is also possible that the bond distance might shorten during the rotation, so that a given symmetrical radical could proceed through any of the transition states with a larger value of γ'. In this case the energy required to compress the σ bond must be supplied. All things considered, the range of γ' values which must be taken into account is probably fairly small. It may readily be seen that

$\gamma/\gamma' = \cos^2\theta$, where θ is the equilibrium angle dictated by the size of the ortho group. Similar considerations apply to the molecular orbital (MO) results in Fig. 2, but in this case $\gamma/\gamma' \approx \cos\theta$. From the same figure it may be seen that any symmetrical radical, with $f(r) \approx 1$, and a dihedral angle $\theta \gtrsim 60°$, may pass to the other symmetrical isomers with no energy of activation. By the same token, a planar radical ($\gamma = 1.0$) would require an energy of activation of 0.6 in units of β, or about 46.3 kcal/mole. As is apparent in both Figs. 2 and 3, the benzhydryl system is more stable than the corresponding benzyl fragment for any specific value of γ.

While neither of the above methods can lay any claim to great accuracy, it is encouraging that they predict similar trends. The variety of possible transition states is predicted to be smaller by the VB method.

The calculations may be extended to compute the spin densities for the symmetrical benzhydryl radicals. The VB results are shown in Fig. 4. They predict negative spin densities at the meta and bridgehead positions, and for the planar radicals ($\gamma = 1.0$), the ortho spin density is positive and larger than that at the para position. As γ decreases, the ortho densities decrease more rapidly than the para densities, with the result that they are the same at $\gamma = 0.65$. Thereafter the para position has the larger spin density. This is the region which applies to most of the radicals of I. The wave functions become badly behaved at about $\gamma = 0.1$, as has been reported by McLachlan (15). This probably results from the rather stringent constraints used in the VB treatment, but when many effects are collapsed into a single parameter, it is not surprising that peculiar effects should be predicted under certain circumstances. The fact remains that the trends predicted for the spin densities are indeed observed, and the range of applicability apparently goes from the planar ketyl radicals to the buttressed ortho methyl derivatives of the benzhydryl radicals.

The HMO predictions of spin densities as obtained by the McLachlan method (16) are a little less successful, at least in a system using only two adjustable parameters. The ortho spin densities are uniformly predicted to be greater than the para densities at all



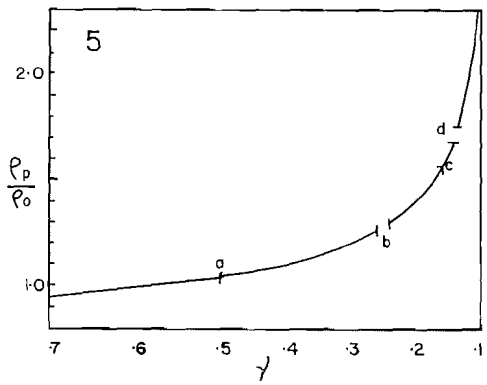


FIG. 4. Plot of ρ vs. γ for VB results.
FIG. 5. Computed ratios of spin densities as a function of γ.

Can. J. Chem. Downloaded from www.nrcresearchpress.com by 210.87.254.42 on 09/05/12
For personal use only.

values of γ. On the other hand, the general magnitudes are predicted fairly well if the value of the SCF mixing parameter, λ, is chosen correctly. The same cannot be said for the VB treatment. For instance for the ortho-methylated benzhydryl radicals, the observed 16 Oe splitting for the lone central proton corresponds to a spin density of about 0.64 and a γ value of ~ 0.9, as estimated from Fig. 4. For the same molecule a para proton splitting of 3.3 Oe is obtained. This corresponds to a spin density of ~ 0.13 and is supposed to occur at $\gamma = 0.3$. Clearly γ is a single-valued parameter, so that the results are inconsistent. It is likely that the poor quantitative agreement results from the neglect of many high energy long bond and ionic structures in the formalism used. According to the results of Simonetta (17) for the benzene molecule, these latter may amount to some 20% of the total. The wave function may be written in the form $\psi = a\psi(\text{covalent}) + b\psi(\text{ionic})$. If the covalent and ionic functions are considered to be orthogonal, then $a^2 + b^2 = 1$. The effect of the ionic structures is to 'steal' spin density from the covalent structures and to redistribute it more or less equally throughout the molecule. Thus the high spin density site at the central carbon atom will be decreased by a^2. This loss will be added to all of the sites of spin density (i.e. about $b^2/13$ at each carbon atom). The additive term is quite small, but would be important at the meta and bridgehead positions of negative spin density. At the other sites, this small term may be neglected, and the constant scaling factor may be eliminated by comparing the ratios of the computed spin densities. Thus ρ_p/ρ_o may be compared to the experimentally obtained ratio of the splitting constants a_p/a_o, and should lead to a more realistic value of γ. The use of such a ratio has the added advantage that it is independent of the particular value of Q which might pertain to the group under consideration as long as the substituents are the same at both positions. The computed ratios of spin density appear as a function of γ in Fig. 5. Four regions are marked off on this curve, and these correspond to the range of values of the ratios of the coupling constants a_p/a_o obtained in I for the various ketyls of xanthone, benzophenone, dimesityl ketone, and finally for the hydrocarbon, dimesitylmethyl. The ratio a_p/a_o for the calcium ketyl of xanthone was found to be 1.04, as indicated in Fig. 5 (12). The ketyl of xanthone is approximately planar because of the ortho oxygen bridge. The value of γ given from the above ratio is 0.5. Since the dihedral angle in this molecule is approximately zero, then $\gamma = f(r) = 0.5$. This value corresponds to rather a long bond, since the exchange integral is reduced to about 50% of that found in the phenyl rings. With the other derivatives, further elongation of this bond might be expected to occur as rotation about the 1–2 bond further weakens the π linkage. Thus $f(r) = 0.5$ represents a maximum value, and, no further information being available, must be used for the remaining compounds. It is easily found from Fig. 5 that $\cos^2\theta$ is therefore 0.5, 0.30, and 0.34 for the ketyls of benzophenone, dimesityl ketone, and dimesitylmethyl respectively. These values correspond to maximum dihedral angles of 45°, 58°, and 57° for these compounds. The distance between ortho protons at the 45° configuration is somewhat greater than the van der Waals diameter for hydrogen atoms (18), suggesting that $f(r) < 0.5$. On the other hand the distance between the centers of the carbon atoms in the 60° configuration is somewhat less than twice the CH bond lengths plus the van der Waals diameter of hydrogen. It appears the e.s.r. spectroscopy is not a very good method for predicting the constants of molecular geometry, at least in systems as complicated as the benzhydryl radicals.

DISCUSSION

The physical observations which have been made for the benzhydryl systems become more understandable on the basis of a model which allows rotation about the extracyclic bonds of these compounds. In one respect the benzhydryl system is quite different from

Can. J. Chem. Downloaded from www.nrcresearchpress.com by 210.87.254.42 on 09/05/12
For personal use only.

the other arylmethyl systems. In triphenylmethyl, for instance, all six ortho protons are in positions allowing steric interactions. In order for this molecule to execute an internal rotation similar to that presently being discussed, it would be necessary for two of the rings to assume perpendicular configurations simultaneously. This is a much less favorable proposition from the energetic point of view, but there appears to be a small range of equilibrium angles at large distortions where such would be possible. Because of the high symmetry of this molecule there are no 'inner' and 'outer' protons as such, and one could not use the present method to detect such a process. On the other hand, with the benzyl-type radicals such as the ketyls of benzaldehyde, there exists no axis of symmetry in the molecule, so that the pairs of ortho protons or meta protons are not equivalent. In this case, the rotation of the extracyclic ketyl group must involve the rupture of a π bond. There is no compensation for the loss in delocalization energy, and the process must then be one of high energy and low probability. This is reflected in the observations of Steinberger and Fraenkel (19) regarding the ketyl anions of this compound. For the free ion, the presence of a localized negative charge on the oxygen atom changes the electron distribution in the nearby ring, and hence the spin densities. Thus the two ortho splitting constants are different. Apparently when the ion associates, this coulombic interaction vanishes, and a second species is obtained which corresponds more closely to the benzyl-type systems mentioned here. The pseudosymmetry in this case results not from rotational averaging, but from the lack of a strong unsymmetrical potential field.

An attempt may now be made to explain the differences found between inner and outer groups in the xanthone ketyls and in Coppinger's radical. In the case of the xanthone ketyls, the two rings cannot rotate. The oxygen atom which bridges two of the ortho positions constrains the molecule to a fixed configuration. Coppinger's radical on the other hand exists largely in one of the two equivalent resonant forms illustrated in the Introduction; the lone proton splitting in this compound is only about 6 Oe as compared with the 15–16 Oe splitting found for the other diphenylmethyl derivatives. The quinoidal structure implies that the 1–2 bonds in this compound are shorter, being perhaps nearly the same as those in the aromatic rings. As a result the stable configuration is considerably 'more planar' than the remaining benzhydryl compounds, suggesting that a considerable amount of energy is required to effect the counter-rotation of the rings. The value of $f(r) \approx 0.5$ obtained from the xanthyl ketyls would appear to support this contention. If the value of $f(r) = 1$, and the same angular dependence as found for benzophenone, is taken, then with the curves of Fig. 2 one finds that an activation energy of $\sim 0.25\ \beta$ is required (i.e. ~ 20 kcal/mole).

The general trends observed for the compounds studied in I appear to fit in well with the present model. When there are no restraining influences such as interannular bridges, or exceptionally stable quinoidal ground states, the molecules apparently undergo a low energy libation which results in the appearance of a pseudosymmetry for the substituent pairs in each phenyl ring. For the ketyls, where there is a bulky oxygen-counterion substituent on the central position, the internal rotation may be hampered in that this group must also participate in the concerted motion. This may account in part for the relatively broad spectral lines of these compounds compared to the hydrocarbon species which have no large substituent at the central atom.

The ratios a_p/a_o compare very well to the ρ_p/ρ_o determined from the VB theory. The compounds lie in positions which are much as might be expected. The larger the hindering groups, the larger is the observed ratio. The insensitivity of the lone proton and ^{13}C splittings to buttressing of the ortho groups, which was mentioned in I, is also understandable. The spin density at carbon atom 1, upon which these splittings depend,

Can. J. Chem. Downloaded from www.nrcresearchpress.com by 210.87.254.42 on 09/05/12
For personal use only.

changes relatively little as γ varies in the region of small γ. On the other hand, the spin densities at the ring sites are very sensitive to the γ value, as may be seen from a comparison of Figs. 4 and 5.

Although better quantitative agreement might have been hoped for, it is apparent that much more sophisticated computational techniques will be required. These appear to be prohibitively difficult for the present system of compounds. However, one cannot deny the excellence of the qualitative agreement.

ACKNOWLEDGMENTS

The authors would like to thank Dr. A. H. Reddoch for a preprint of his paper, and Mr. C. R. Kepford of this laboratory for his unstinting help. We would also like to recognize the enormous assistance that Mr. M. Williams of the University Computing Centre has given. Thanks are also due to the National Research Council of Canada for financial assistance (H. R. F.) during the process of this investigation.

REFERENCES

1. H. R. Falle and F. C. Adam. Can. J. Chem. This issue.
2. A. H. Reddoch. J. Chem. Phys. **43**, 225 (1965).
3. H. M. McConnell. J. Chem. Phys. **24**, 632 (1956).
4. A. D. McLachlan. Mol. Phys. **1**, 234 (1958).
5. N. C. Deno. J. Am. Chem. Soc. **73**, 3644 (1951).
6. E. K. Ng and F. C. Adam. Can. J. Chem. **42**, 810 (1964).
7. R. W. Fessenden and R. H. Schuler. J. Chem. Phys. **38**, 773 (1963).
8. F. C. Adam, W. C. Hoell, and D. A. Stiles. Can. J. Chem. To be published.
9. V. R. Sandel and H. H. Freedman. J. Am. Chem. Soc. **85**, 2328 (1963).
10. J. A. Pople, W. G. Schneider, and H. J. Bernstein. High-resolution nuclear magnetic resonance. McGraw-Hill Book Co. of Canada, Ltd., Toronto. 1959.
11. J. S. Hyde and A. H. Maki. J. Chem. Phys. **40**, 3117 (1964).
12. C. R. Kepford and F. C. Adam. Can. J. Chem. To be published.
13. C. Heller. J. Chem. Phys. **36**, 175 (1962).
14. R. Daudel, R. Lefebvre, and C. Moser. Quantum chemistry. Interscience Publishers, New York. 1959.
15. A. D. McLachlan. J. Chem. Phys. **32**, 1488 (1960).
16. A. D. McLachlan. Mol. Phys. **3**, 233 (1960).
17. N. Simonetta. J. Chim. Phys. **49**, 68 (1952).
18. L. Pauling. Nature of the chemical bond. Cornell University Press, Ithaca, N.Y. 1960.
19. N. Steinberger and E. K. Fraenkel. J. Chem. Phys. **40**, 723 (1964).

Can. J. Chem. Downloaded from www.nrcresearchpress.com by 210.87.254.42 on 09/05/12
For personal use only.

Can. J. Chem. Downloaded from www.nrcresearchpress.com by 210.87.254.40 on 09/05/12
For personal use only.

STUDIES OF METAL COMPLEXES OF PYRIDINE DERIVATIVES

THE EFFECTS OF COORDINATION UPON INFRARED INTENSITY OF THE FUNCTIONAL GROUP IN β-CYANOPYRIDINE

D. G. Brewer and Patrick T. T. Wong

Department of Chemistry, University of New Brunswick, Fredericton, New Brunswick

Received November 25, 1965

ABSTRACT

The infrared intensity of the C≡N group in β-cyanopyridine complexes with some first-row transition metal ions (Zn(II), Cu(II), Ni(II), Co(II), Fe(II), and Mn(II)) in aqueous solution has been measured. The coordination between the nitrogen atom on the pyridine ring and these metal ions exerts a marked change in the magnitude of the band intensity of the functional group. This can be interpreted in terms of a simple molecular orbital model and the relative magnitudes of σ-bonding and π-bonding involved in the complexes. A "coordination constant" is introduced for this system, and a linear correlation between these constants and the C≡N band intensities of the metal complexes is obtained from both the experimental data and theoretical considerations.

INTRODUCTION

The intensities of the infrared absorption band associated with the C≡N functional group vibration in aliphatic and aromatic cyanides have been studied to a considerable extent (1–5). In particular, studies of the C≡N band infrared intensities in a number of substituted benzonitriles showed that substituents on the ring exerted a pronounced effect on the magnitude of the functional group intensity; electron-releasing substituents enhanced the functional group intensity, whereas electron-attracting substituents lowered the intensity.

The correlation of the intensity variations in substituted benzonitriles with the so-called "substitution constants" (6) has also been studied. The results suggest that there is an essentially linear relation between the logarithm of the intensity and the substitution constant for both meta- and para-substituted compounds in various solvents.

In the present investigation, the intensities of the C≡N band in heterocyclic cyanides were studied. β-Cyanopyridine was chosen as a starting point for these studies. An attempt has been made to determine the effects of coordination between the nitrogen atom on the pyridine ring and some first-row transition metal ions on the C≡N band intensity. A simple molecular orbital model is presented; this model is used to give a quantitative treatment of the data for the system, for which purpose a "coordination constant" is introduced.

EXPERIMENTAL

Materials

β-Cyanopyridine, supplied by the L. Light and Co. Ltd., was recrystallized three times from ether – petroleum ether (60–68°) mixture.

Pyridine, reagent grade supplied by British Drug Houses (Canada) Ltd., was dried over potash overnight and then redistilled twice.

3-Pyridinol, supplied by Aldrich Chemical Co. Inc., was recrystallized twice in absolute alcohol and then purified by sublimation.

Most of the transition metal salts were nitrates supplied by the G. Frederick Smith Chem. Co., and were recrystallized from water several times.

Deuterium oxide was obtained from Merck Sharp and Dohme of Canada Ltd., and had an assay of 99.7% D_2O.

Carbonate-free potassium hydroxide solution for the pH titration was prepared by the method of Schwarzenbach (7).

Infrared Absorption Spectra

In the present study a Perkin-Elmer model 21 spectrometer was employed. The spectra were determined in aqueous solution with matched calcium fluoride cells (platinum foil spacers, 0.025 mm).

For all the intensity measurements, the slit width was held at a constant value to eliminate the error caused by the variations of slit width in each measurement. The resolution knob was set at 23.

The solution in the reference cell had a composition equal to that in the sample cell except for a certain amount of pyridine exchanged for β-cyanopyridine in the latter. In this way an almost complete compensation for the water absorption was obtained in the spectral region under investigation, 2 000 – 2 500 cm^{-1}.

The intensity of the C≡N band was estimated according to Ramsay's method (8). The intensity is given by

$$A = (1/CL)\ (1/2)\ 2.303 \Delta V_{1/2} \log\ (T_0/T)_{max}$$

where $\Delta V_{1/2}$ is the half-intensity width of the C≡N band, $\log\ (T_0/T)_{max}$ is the observed absorbance at band maximum, C is the total concentration of the ligand expressed in moles per liter of solution, and L is the cell length in cm.

All measurements for C≡N band intensities of β-cyanopyridine complexes were carried out using a 2:1 ratio for metal ion and ligand concentrations.[1]

The intensities of C≡N functional group, measured for β-cyanopyridine in the presence and absence of the first-row transition metal ions in the solution, are listed in Table I.

TABLE I

C≡N band intensities of β-cyanopyridine and its metal complexes

	A (10^3 $mole^{-1}$ l cm^{-2})	$A^{1/2}$ (10 $mole^{-1}$ l cm^{-2})
Ligand	7.57	8.70
Mn(II) complex	7.40	8.60
Ni(II) complex	6.07	7.79
Co(II) complex	5.67	7.53
Zn(II) complex	5.16	7.19
Cu(II) complex	3.54	5.95
Fe(II) complex	7.93	8.90

pH Titration

A Beckman model GS meter with glass and calomel electrodes was used to record the pH. The electrode system of the pH meter was calibrated against standard buffers supplied by British Drug Houses (Canada) Ltd.

Titrations were carried out in a 300 ml Berizeleus beaker closed by a rubber stopper with holes to accommodate a microburet, nitrogen inlet and outlet tubes, and the electrodes. The running nitrogen was washed beforehand by passing through Fieser's Solution, sodium hydroxide, and concentrated sulfuric acid.

The ionic strength was maintained constant by using 0.1 N KNO_3 as a supporting electrolyte. The concentration of 3-pyridinol used was 10^{-3} M and the concentration ratio of ligand to metal ion was 5:1. All measurements were made at a temperature of 25.0 °C in a thermostated bath.

Both the acid dissociation constants and the coordination constants of the metal complexes are shown in Table II.

TABLE II

Acid dissociation constants and coordination constants of 3-pyridinol and its metal complexes in aqueous solution at 25 °C

	k_{HA}	$\alpha \equiv \log k_{HA(ML)} - \log k_{HA(L)}$
Ligand	3.52×10^{-9}	0.00
Mn(II) complex	3.79×10^{-9}	0.03
Ni(II) complex	4.16×10^{-9}	0.07
Co(II) complex	4.33×10^{-9}	0.09
Zn(II) complex	4.50×10^{-9}	0.11
Cu(II) complex	5.49×10^{-9}	0.19

[1]*A study of the* C—N *and* C=N *band intensities of the pyridine ring in* D_2O *solution showed that both band intensities increased with increasing metal ion concentration and their intensities became constant when metal ion concentrations reached twice that of the ligand concentration.*

Can. J. Chem. Downloaded from www.nrcresearchpress.com by 210.87.254.40 on 09/05/12
For personal use only.

Can. J. Chem. Downloaded from www.nrcresearchpress.com by 210.87.254.40 on 09/05/12
For personal use only.

RESULTS AND DISCUSSION

Infrared Intensities

The C≡N band infrared intensities of β-cyanopyridine and its complexes of the first-row transition metal ions, Zn(II), Cu(II), Ni(II), Co(II), Fe(II), and Mn(II), were determined. The data in Table I show that the C≡N band intensity of β-cyanopyridine is enhanced when it forms a complex with ferrous ion, whereas the C≡N band intensities are lowered when it forms complexes with other first-row transition metal ions, Zn(II), Cu(II), Ni(II), Co(II), and Mn(II). The data also indicate that coordination between β-cyanopyridine and different metal ions gives different C≡N band intensities, and the relative magnitude of the C≡N band intensities follows the order:

$$\text{Zn(II)} > \text{Cu(II)} < \text{Co(II)} < \text{Ni(II)} < \text{Mn(II)} < \text{Ligand} < \text{Fe(II)}.$$

Comparing with Irving's order of stability for the complexes of these metal ions (9), the positions of Co(II) and Fe(II) are unexpected.

These observed results can be understood by a simple molecular orbital approach. For this purpose the energy levels of this system are required. The delocalized molecular orbital functions of pyridine can be written as (10):

$$\Psi_1 = 0.4208(\varphi_1 + \varphi_5) + 0.3540(\varphi_2 + \varphi_4) + 0.3219\varphi_3 + 0.5400\varphi_6$$

$$\Psi_2 = 0.1815(\varphi_1 + \varphi_5) - 0.3610(\varphi_2 + \varphi_4) - 0.6113\varphi_3 + 0.5475\varphi_6$$

$$\Psi_3 = 0.4970(\varphi_1 + \varphi_5) + 0.5030(\varphi_2 - \varphi_4)$$

$$\Psi_4 = 0.3383(\varphi_1 + \varphi_5) + 0.2728(\varphi_2 - \varphi_4) - 0.5893\varphi_3 - 0.5244\varphi_6$$

$$\Psi_5 = 0.5030(\varphi_1 + \varphi_5) - 0.4970(\varphi_2 - \varphi_4)$$

$$\Psi_6 = 0.4189(\varphi_1 + \varphi_5) - 0.4156(\varphi_2 + \varphi_4) + 0.4188\varphi_3 - 0.3662\varphi_6$$

where the φ's are Slater atomic orbitals. The energy level diagram of both pyridine and the C≡N group is shown in Fig. 1, in which the energies of the highest occupied orbitals were taken as equal to the first ionization potentials (10–18), and the energies of the lowest vacant orbitals were estimated approximately from a combination of the highest occupied levels and the experimental data of $\pi \rightarrow \pi^*$ or $n \rightarrow \pi^*$ absorption spectra (5, 19).

The interaction between the delocalized π-orbitals in the ring and the localized π-orbitals in the C≡N group presumably involves the highest occupied molecular orbital in the ring, H_{Py}, and the lowest vacant molecular orbital in the C≡N group, V_{CN}, rather than the orbitals H_{CN} and V_{Py}, since the energy difference between the former two is

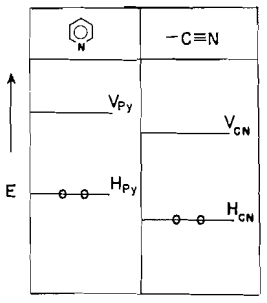


FIG. 1. The energy level diagram of pyridine and cyanide system.

much smaller than that of the latter two. Also, H_{CN} of the C≡N group is a non-bonding orbital predominantly localized on the nitrogen atom and is thus far from the pyridine ring. The interaction between the V_{CN} and H_{Py} orbitals gives two new orbitals which may be considered as a linear combination, $\Phi = a\phi_P \pm b\phi_{CN}$, and results in a migration of electrons from the pyridine ring towards the C≡N group. In addition, an interaction between V_{Py} and V_{CN} orbitals is also expected, since they are very close in energy and the interaction is symmetry allowed.

By means of this simple molecular orbital model, the effect of coordination on the C≡N band intensities of β-cyanopyridine may be interpreted. The coordination between pyridine derivatives and metal ions involves both σ-bonding and π-bonding contributions (20–23), which produce opposite effects on the C≡N band intensity; viz. σ-bonding lowers the C≡N band intensity, whereas π-bonding enhances the C≡N band intensity. The σ-bond in the metal complexes is formed by withdrawing the non-bonding electron pair from the pyridine ring to the metal ion. This lowers the H_{Py} energy level and the energy difference between H_{Py} and V_{CN} increases. Therefore the magnitude of the interaction between H_{Py} and V_{CN} is decreased, as is the electron density in $\Phi = a\phi_P + b\phi_{CN}$, and the dipole moment of the C≡N group is lowered. The π-bond is formed by the back donation of d electrons to the V_{Py} orbital. The interaction between V_{Py} and V_{CN} will also cause an electronic migration from the ring to the C≡N group and hence the dipole moment of the C≡N group is increased; thus the C≡N band intensity is increased. Moreover, the H_{Py} energy level is raised by the π-bonding, resulting in an increased interaction between H_{Py} and V_{CN}, and consequently an enhanced C≡N band intensity.

In complexes of pyridine and its derivatives, the relative magnitude of σ-bonding was deduced by F. A. Cotton to be much higher than that of π-bonding (20), and therefore the net effect of the σ-bonding and π-bonding in β-cyanopyridine complexes with Zn(II), Cu(II), Ni(II), Co(II), and Mn(II) is to lower the C≡N band intensity.

However, the intensity in the Fe(II) β-cyanopyridine complex was found to be higher than that of the free ligand. It seems probable that a polynuclear complex is formed in this system. A series of solutions with a constant concentration of the ligand and an increasing concentration of Fe(II) ion was prepared. Deuterium oxide (D_2O) was used for the preparation of all these solutions to avoid the interfering absorption bands of the H_2O molecule in the C—N, C=N region of the pyridine ring, 1 350 – 1 700 cm^{-1}. At equilibrium, the intensities of both the C—N and C=N bands of the pyridine ring should be increased by increasing the Fe(II) concentration (24, 25). The opposite results obtained in this laboratory suggest the presence of a polynuclear complex in this system.

In this polynuclear complex, Fe(II) ion could coordinate not only with the nitrogen atom on the pyridine ring, but also with the nitrogen atom on the nitrile group. This latter bond can be interpreted as resulting from the formation of a σ-molecular orbital between the occupied non-bonding orbital on the nitrogen atom and the vacant Fe atomic orbitals (26). This interaction lowers the energies of the π-orbitals in the C≡N group, and results in decreasing the energy difference between the V_{CN} orbital and the H_{Py} orbital and thus in increasing the interaction between these two orbitals. Therefore the C≡N band intensity of this system should be much higher.

The relative magnitude of the C≡N group infrared intensities in the β-cyanopyridine complexes studied were observed to be as follows:

$$Cu(II) < Zn(II) < Co(II) < Ni(II) < Mn(II).$$

Can. J. Chem. Downloaded from www.nrcresearchpress.com by 210.87.254.40 on 09/05/12
For personal use only.

Can. J. Chem. Downloaded from www.nrcresearchpress.com by 210.87.254.40 on 09/05/12
For personal use only.

According to earlier work (27), the relative magnitude of a σ-bond in a particular complex for the first-row transition metals can be estimated from the second ionization potentials of the metals. An estimate of the relative magnitude of π-bond in a particular complex for the first-row transition metals can be obtained from the first ionization potential of these metals. The lower the first ionization potential of a metal, the higher the relative magnitude of a π-bond in its metal complex. This suggestion is based on Pauling's electroneutrality rule of coordination (28); that is, when a metal ion forms a complex, its positive charge will be almost neutralized by the donation of electrons from the surrounding ligands. Therefore the "back donation" can be considered to have occurred from a neutral metal, and the magnitude of this back donation must be related to the first ionization potential. Moreover, this suggestion is supported by a comparison of the stabilities of some first-row transition metal complexes of the two classes of ligands (20) with the first and second ionization potentials (see Table III).

The first class of ligands, such as ammonia, ethylenediamine, etc., can act only as a donor in complex formation and thus only a σ-bond is present in their metal complexes. The second class of ligands, such as pyridine and its derivatives, cyanide, etc., coordinate with metal ions through both σ-bonding and π-bonding.

The second ionization potentials of the first-row transition metals in Table III show the relative magnitude of σ-bond in a particular complex is

$$\text{Cu(II)} > \text{Ni(II)} > \text{Zn(II)} > \text{Co(II)} > \text{Fe(II)} > \text{Mn(II)}.$$

Therefore the relative stability of the first-class complexes of these metal ions should follow the same order. The stability constants listed in Table III show this same result.

The first and second ionization potential data in Table III predict that the σ-bond magnitude in Zn(II) complexes with class two ligands is close to that in Co(II) complexes, whereas the π-bond magnitude in the same Zn(II) complexes is much lower than that in Co(II) complexes. Therefore the second class complexes of Co(II) should be more stable than those of Zn(II) and the stability of the first class complexes of Co(II) should be close to, or a little lower than, those of Zn(II). Similarly we may predict that the stability of Fe(II) complexes of both the first- and second-class ligands are lower than those of Co(II) complexes. Also, the Fe(II) complexes of the first-class ligands should be more stable than the corresponding Mn(II) complexes, whereas those of second-class ligands must be close to or a little lower in stability than those of the Mn(II) complexes. The first ionization potentials of Cu, Ni, and Mn are very similar, but the second ionization potential of Cu is much higher than those of Ni and Mn, and that of Ni is in turn much higher than that of Mn. Thus, we may predict that the relative stabilities of both the first- and second-class complexes of these three metal ions are mainly determined by the relative magnitude of σ-bonding in their complexes, and follow the order:

$$\text{Cu(II)} > \text{Ni(II)} > \text{Mn(II)}.$$

The stability constants of the first- and second-class complexes listed in Table III support the correlation between the relative magnitude of π-bonding in a particular complex of the first-row transition metals and the first ionization potentials of these metals.

From these studies we may conclude that the relative magnitudes of σ-bonding and π-bonding in β-cyanopyridine complexes for these first-row transition metal ions follow

Can. J. Chem. Downloaded from www.nrcresearchpress.com by 210.87.254.40 on 09/05/12
For personal use only.

TABLE III

The ionization potentials of the first-row transition metals (ref. 32) and the stability constants of some first- and second-class metal complexes (ref. 33)

Metals	First ionization potential (V)	Second ionization potential (V)	First-class ligands (σ)			Second-class ligands (σ, π)		
			Ammonia	Ethylenediamine		Pyridine	8-Hydroxyquinoline	
			log K_1	Log K_1	Log β_2	log K_1	Log K_1	Log β_2
Cu(II)	7.723	20.20	4.15	10.55	19.60	2.52	13.49	26.22
Ni(II)	7.633	18.13	2.79	7.66	14.06	1.78	11.44	21.38
Zn(II)	9.391	17.89	2.37	—	11.07	0.95	9.95	18.86
Co(II)	7.860	17.30	2.11	5.86	10.66	1.14	10.55	19.66
Fe(II)	7.896	16.50	1.40	4.28	7.53	0.71	9.83*	10.84*
Mn(II)	7.432	15.70	0.80	2.73	4.79	—	10.30*	20.40*

*In 75% dioxane–water, i.e., under conditions different from those for the other 8-hydroxyquinoline metal complexes.

the order:

σ-bond, $\quad$ Cu(II) > Ni(II) > Zn(II) ≈ Co(II) > Fe(II) > Mn(II),

π-bond, $\quad$ Zn(II) < Fe(II) ≈ Co(II) < Cu(II) < Ni(II) < Mn(II).

Since π-bonding contributions enhance, and σ-bonding contributions diminish, the C≡N band intensity, the observed order in the β-cyanopyridine complexes can now be interpreted.

The position of Zn(II), Cu(II), Ni(II), and Mn(II) are related to Irving's order (9), and agree with predictions made on the basis of σ- and π-bonding contributions. However, the position of Co(II) is perhaps unusual. The first ionization potential of cobalt is much higher than that of nickel, and even higher than that of copper. This means the relative magnitude of π-bonding in the Co(II) complex is lower than that in the Ni(II) complex. The net effect of both σ- and π-bonding effects results in the C≡N band intensity in the Co(II) complex being a little lower than that in the Ni(II) complex.

The intensity data in Table I also show that the intensity of the Co(II) complex is higher than that of Zn(II) complex. Again, from the ionization potential data we may expect the relative magnitude of the π-bond in Co(II) complex to be higher than that in Zn(II) complex, whereas the magnitudes of σ-bond in complexes of these two metal ions are almost the same. Thus the higher C≡N band intensity in Co(II) complex is expected.

Coordination Constant

The C≡N band intensities of substituted benzonitriles have been correlated with the Hammett constant (6). The effects of coordination on the free energy change involved in some functional groups of pyridine derivatives have been studied, and a coordination constant, similar to the Hammett constant, was introduced. The coordination constant is defined by

$$\alpha \equiv \log k_{ML} - \log k_{L},$$

where k_L is the acid dissociation constant of 3-pyridinol in H_2O at 25 °C, and k_{ML} is the acid dissociation constant of the metal complex of 3-pyridinol.

The acid dissociation constants of some metal 3-pyridinol complexes were determined by pH titrations of 3-pyridinol solution in the presence of metal ion, and are listed in Table II together with the coordination constants.

The formation of the monohydroxo complexes of these metal ions in aqueous solution have some influence on the equilibria being studied, although all titrations were carried out in a region where no precipitation of the metal hydroxide took place. An equation for the calculation of the acid dissociation constant taking account of this hydrolysis was deduced as in Appendix I.

If C_{HA} and C_M represent the total concentration of 3-pyridinol and metal ion, respectively, C_{KOH} represents the total concentration of KOH added and k_{L_mMOH} represents the dissociation constant of the monohydroxo complex, the acid dissociation constant may be calculated from the relationship

$$k_{HA} = \frac{[H^+]\{C_{KOH} - [OH^-] - (C_{M^{++}}[OH^-]/k_{L_mMOH^+} + [OH^-])\}}{C_{HA} - \{C_{KOH} - [OH^-] - (C_{M^{++}}[OH^-]/k_{L_mMOH^+} + [OH^-])\}}.$$

Correlation Between the Infrared Intensities and the Coordination Constants

When the square root of the measured intensity or the log (intensity) was plotted against the coordination constant, a straight line was obtained (Fig. 2).

Can. J. Chem. Downloaded from www.nrcresearchpress.com by 210.87.254.40 on 09/05/12
For personal use only.

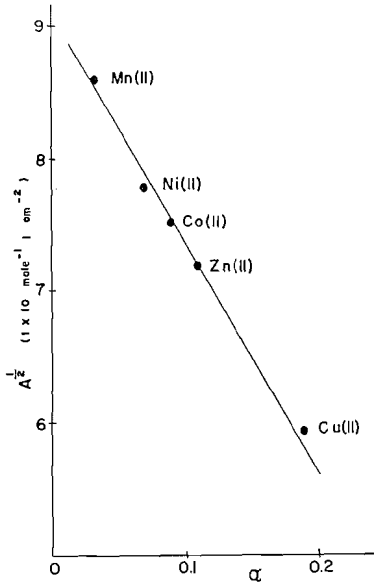


FIG. 2. A plot of square root of C≡N band intensities of β-cyanopyridine complexes vs. coordination constants.

As has been done for the substituted benzonitrile systems (5), this correlation can be predicted by a direct calculation (Appendix II) of the C≡N band infrared intensity based on the simple molecular orbital model.

The final equation of Appendix II correlated the square root of the intensity with the coordination constant:

$$A^{1/2} = \left[\left(\frac{N^2\pi}{3\,000\,c^2m}\right)^{1/2}\left(\frac{\partial\mu_0}{\partial q}\right)_{q=0}\right] + \left[\left(\frac{2exr^nE_LP}{GS}\right)\left(\frac{N^2\pi}{3\,000\,c^2m}\right)^{1/2}\right] - \left[\left(\frac{2exr^nP\gamma RT}{GS}\right)\left(\frac{N^2\pi}{3\,000\,c^2m}\right)^{1/2}\right]\alpha.$$

All the values inside the bracketed terms in this equation are constants. Therefore α is linearly related to $A^{1/2}$, as obtained experimentally.

APPENDIX I

For the equilibrium

$$(H_2O)_mMOH^+ \rightleftharpoons (H_2O)_nM^{++} + OH^-,$$

$$k_{(H_2O)_mMOH^+} = \frac{[(H_2O)_nM^{++}][OH^-]}{[(H_2O)_mMOH^+]}.$$

For the equilibrium

$$A_mMOH^+ \rightleftharpoons A_nM^{++} + OH^-,$$

where A is a ligand,

$$k_{A_mMOH^+} = \frac{[A_nM^{++}][OH^-]}{[A_mMOH^+]}.$$

Assume[2]

$$k_{(H_2O)_mMOH^+} = k_{A_mMOH^+} = k_{L_mMOH^+}.$$

[2]*A 10-fold change in order of magnitude of this constant leads to about 2–3% error in the k_{HA} of the most hydrolyzed copper complex.*

Can. J. Chem. Downloaded from www.nrcresearchpress.com by 210.87.254.40 on 09/05/12
For personal use only.

Can. J. Chem. Downloaded from www.nrcresearchpress.com by 210.87.254.40 on 09/05/12
For personal use only.

Then

[1] $$k_{L_mMOH^+} = \frac{[L_nM^{++}][OH^-]}{[L_mMOH^+]},$$

where

$$[L_nM^{++}] = [(H_2O)_nM^{++}] + [A_nM^{++}],$$

$$[L_mMOH^+] = [(H_2O)_mMOH^+] + [A_mMOH^+].$$

For

$$(HA)_t \rightleftharpoons (A^-)_t + H^+,$$

[2] $$k_{HA} = \frac{[(A^-)_t][H^+]}{[(HA)_t]},$$

where

$$[(HA)_t] = n[(HA)_nM^{++}] + m[(HA)_mMOH^+] + [HA],$$

$$[(A^-)_t] = n[A_nM^{++}] + m[A_mMOH^+] + [A^-].$$

Materials balance:

[3] $$C_{HA} = [(HA)_t] + [(A^-)_t],$$

[4] $$C_{M^{++}} = [L_nM^{++}] + [L_mMOH^+],$$

[5] $$C_{KOH} = [OH^-] + [L_mMOH^+] + [(A^-)_t],$$

and from [4]

[6] $$[L_nM^{++}] = C_{M^{++}} - [L_mMOH^+].$$

Substitution of [6] into [1] gives

[7] $$[L_mMOH^+] = \frac{C_{M^{++}}[OH^-]}{k_{L_mMOH^+} + [OH^-]},$$

and from [3]

[8] $$[(HA)_t] = C_{HA} - [(A^-)_t].$$

Substitution of [8] into [2] gives

[9] $$[(A^-)_t] = \frac{C_{HA} - k_{HA}}{[H^+] + k_{HA}},$$

and substitution of [9] and [7] into [5] gives

$$k_{HA} = \frac{[H^+]\{C_{KOH} - [OH^-] - (C_{M^{++}}[OH^-]/k_{L_mMOH^+} + [OH^-])\}}{C_{HA} - \{C_{KOH} - [OH^-] - (C_{M^{++}}[OH^-]/k_{L_mMOH^+} + [OH^-])\}}.$$

APPENDIX II

The integrated infrared intensity was found to be related to molecular properties according to (31)

[10] $$A = \frac{\pi N}{3\,000\,c^2 m}\left(\frac{\partial \mu}{\partial q}\right)^2_{q=0}$$

where A represents the integrated intensity in units of mole^{-1} l cm^{-1}, N is Avogadro's number, c is the velocity of light, m is the reduced mass, $(\partial\mu/\partial q)_{q=0}$ represents the first derivative of the dipole moment change, and q is the displacement coordinate along the C≡N bond axis.

The molecular orbital formed by the interaction can be expressed as

$$\Phi = a\phi_P + b\phi_{CN}.$$

The dipole moment of the C≡N group is

$$\mu = \mu_0 + 2b^2ex,$$

where $2b^2ex$ represents the moment arising from the migration of charge from ϕ_P to ϕ_{CN}, x represents the distance separating the charge centers and μ_0 represents all other contributions to the moment, which keeps constant before and after β-cyanopyridine coordinates with the first-row transition metal ions. Then,

$$[11] \qquad \left(\frac{\partial\mu}{\partial q}\right)_{q=0} = \left(\frac{\partial\mu_0}{\partial q}\right)_{q=0} + 2b^2e\left(\frac{\partial x}{\partial q}\right)_{q=0} + 2ex\left(\frac{\partial b^2}{\partial q}\right)_{q=0}.$$

The quantity $\partial x/\partial q$ is very small, and the second term in eq. [11] can be dropped.

The energy of orbital Φ can be written as

$$E = \frac{\int \Phi^* H \Phi \mathrm{d}t}{\int \Phi^2 \mathrm{d}t} = \frac{\int (a\phi_P + b\phi_{CN}) H (a\phi_P + b\phi_{CN})\mathrm{d}t}{\int (a\phi_P + b\phi_{CN})^2 \mathrm{d}t}$$

$$= \frac{a^2\int \phi_P H \phi_P \mathrm{d}t + 2ab\int \phi_P H \phi_{CN}\mathrm{d}t + b^2\int \phi_{CN} H \phi_{CN}\mathrm{d}t}{a^2\int \phi_P{}^2\mathrm{d}t + 2ab\int \phi_P\phi_{CN}\mathrm{d}t + b^2\int \phi_{CN}{}^2\mathrm{d}t}.$$

Let

$$\int \phi_P H \phi_P \mathrm{d}t = H_{PP}, \quad \int \phi_{CN} H \phi_{CN}\mathrm{d}t = H_{CN}, \quad \int \phi_P H \phi_{CN}\mathrm{d}t = H_{PCN},$$

$$\int \phi_P{}^2\mathrm{d}t = \int \phi_{CN}{}^2\mathrm{d}t = 1, \quad \int \phi_P\phi_{CN}\mathrm{d}t = 0.$$

One obtains

$$E = \frac{a^2H_{PP} + 2abH_{PCN} + b^2H_{CN}}{a^2 + b^2}.$$

Then

$$[12] \qquad \frac{\partial E}{\partial a} = a(H_{PP} - E) + b(H_{PCN}) = 0,$$

$$[13] \qquad \frac{\partial E}{\partial b} = a(H_{PCN}) + b(H_{CN} - E) = 0.$$

From [12] and [13]

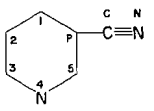
$$[14] \qquad b = \frac{[H_{CN} - H_{PP}] - [(H_{PP} - H_{CN})^2 + 4(H_{PCN})^2]^{1/2}}{2/a[H_{PCN}]}.$$

If the atoms in β-cyanopyridine are labeled as in the diagram below, it follows that

$$[15] \qquad H_{PCN} = \int \phi_P H \phi_{CN}\mathrm{d}t$$

$$= \int (C_1\varphi_1 + C_2\varphi_2 + C_3\varphi_3 + C_4\varphi_4 + C_5\varphi_5 + C_P\varphi_P) H (C_C\varphi_C + C_N\varphi_N)\mathrm{d}t$$

$$= \int C_P\varphi_P H C_C\varphi_C \mathrm{d}t = C_PC_C\int \varphi_C H \varphi_P \mathrm{d}t = C_CC_P\beta.$$



Since

$$[16] \qquad a^2 + b^2 = 1,$$

combination of [14], [15], and [16] gives

$$b^2 = \frac{(H_{CN}-H_{PP})^2 - 2(H_{PP}-H_{CN})[H_{PP}-H_{CN})^2 + 4C_C{}^2C_P{}^2\beta^2]^{1/2} + [H_{PP}-H_{CN})^2 + 4C_C{}^2C_P{}^2\beta^2]}{(2C_CC_P\beta)^2 + (H_{CN}-H_{PP})^2 - 2(H_{PP}-H_{CN})[H_{PP}-H_{CN})^2 + 4C_C{}^2C_P{}^2\beta^2]^{1/2} + [(H_{PP}-H_{CN})^2 + 4C_C{}^2C_P{}^2\beta^2]}.$$

Can. J. Chem. Downloaded from www.nrcresearchpress.com by 210.87.254.40 on 09/05/12
For personal use only.

Can. J. Chem. Downloaded from www.nrcresearchpress.com by 210.87.254.40 on 09/05/12
For personal use only.

Then

$$[17]\quad (\partial b^2/\partial q)_{q=0} = -\Big(4C_C^2C_P^2\beta^2\{(H_{CN}-H_{PP})^2-(H_{CN}-H_{PP})[(H_{PP}-H_{CN})^2+4C_C^2C_P^2\beta^2]^{1/2}+2C_C^2C_P^2\beta^2\}(\partial H_{CN}/\partial q)_{q=0}\Big)\Big/\Big(\{16C_C^4C_P^4\beta^4+8C_C^2C_P^2\beta^2(H_{CN}-H_{PP})^2-8C_C^2C_P^2\beta^2(H_{CN}-H_{PP})\times[(H_{PP}-H_{CN})^2+4C_C^2C_P^2\beta^2]^{1/2}+(H_{CN}-H_{PP})^4+(H_{CN}-H_{PP})^3-2(H_{CN}-H_{PP})^3[(H_{PP}-H_{CN})^2+4C_C^2C_P^2\beta^2]^{1/2}\}\times[(H_{PP}-H_{CN})^2+4C_C^2C_P^2\beta^2]^{1/2}\Big).$$

In the LCAO model of C≡N bond (29), $(\partial H_{CN}/\partial q)_{q=0}$ can be written as

$$\left(\frac{\partial H_{CN}}{\partial q}\right)_{q=0} = -0.62\left(\frac{\partial \beta_{CN}}{\partial q}\right)_{q=0}.$$

Since $\beta_{CN} = k_{CN}\beta_{CC}$ and since $(\partial\beta_{CC}/\partial q)_{q=0}$ is approximately linear with a value of 6.25 eV/Å (30), the value of $(\partial H_{CN}/\partial q)_{q=0}$ can be easily calculated; suppose it to be P.

Let the coefficient of $(\partial H_{CN}/\partial q)_{q=0}$ in eq. [17] equal Q, then

$$[18]\qquad \left(\frac{\partial b^2}{\partial q}\right)_{q=0} = QP.$$

Combination of [10], [11], and [18] gives

$$[19]\qquad A^{1/2} = \left[\left(\frac{N^2\pi}{3\,000\,c^2m}\right)^{1/2}\left(\frac{\partial \mu_0}{\partial q}\right)_{q=0}\right] - \left[2ex\left(\frac{N^2\pi}{3\,000\,c^2m}\right)^{1/2}\right]QP.$$

Suppose that a process, such as protonation or hydration, occurs at the C≡N group of β-cyanopyridine. The activation energy which is contributed from electrostatic effects involved in this process can be written as E_L and E_{ML} for β-cyanopyridine and its metal complexes, respectively. In a particular process, E_L is a constant, whereas E_{ML} is varied with change of metal ion in the complex. E_{ML} arises from the interaction of the electrophile with the partial charge on the C≡N group, and can be written as

$$[20]\qquad E_{ML} = -\frac{2(b^2+\Delta b^2)G}{r^n},$$

where G and n are values depending on the nature of the electrophile (ion or dipole) attacking at the C≡N group, r represents the distance between the centers of the C≡N group and the electrophile in the transition state, and Δb^2 represents the change in the π-electronic interaction in the transition state from that in the ground state. From eq. [17]

$$[21]\qquad \Delta b^2 = -Q\Delta H_{CN}.$$

Substitution of [21] into [20] gives

$$[22]\qquad E_{ML} = -\frac{GQ}{r^n}\left[\frac{2\delta^2}{Q(1+\delta^2)} - 2\Delta H_{CN}\right],$$

where

$$\delta = \frac{(H_{CN}-H_{PP}) - [(H_{PP}-H_{CN})^2+4C_C^2C_P^2\beta^2]^{1/2}}{2C_CC_P\beta}.$$

In eq. [22] the bracketed term is very small, and ΔH_{CN} and $2\delta^2/Q(1+\delta^2)$ are changed in the opposite direction with complex formation, so that we may assume that this term is a constant,

$$\left[\frac{2\delta^2}{Q(1+\delta^2)} - 2\Delta H_{CN}\right] \equiv S.$$

Then

$$E_{ML} = -\frac{GQS}{\gamma^n}. \qquad [23]$$

Since the usual linear relation of free energy (6) is valid for the system being studied,[3] it follows that

$$\gamma\alpha = -\frac{E_{ML} - E_L}{RT}, \qquad [24]$$

where γ is a constant characteristic of the functional group, the attacking electrophile, and the reaction medium. Combination of [23], [24], and [19] gives

$$A^{1/2} = \left[\left(\frac{N^2\pi}{3\,000\,c^2m}\right)^{1/2}\left(\frac{\partial\mu_0}{\partial q}\right)_{q=0}\right] + \left[\left(\frac{2exr^nE_LP}{GS}\right)\left(\frac{N^2\pi}{3\,000\,c^2m}\right)^{1/2}\right] - \left[\left(\frac{2exr^nP\gamma RT}{GS}\right)\left(\frac{N^2\pi}{3\,000\,c^2m}\right)^{1/2}\right]\alpha.$$

ACKNOWLEDGMENTS

We wish to thank Dr. F. Grein for useful discussions on theoretical aspects and the Organic Research Section of the University of New Brunswick for use of the infrared spectrometer. We are grateful to the National Research Council for financial support of this research.

REFERENCES

1. P. Sensi and G. G. Gallio. Gazz. Chim. Ital. **85**, 235 (1955).
2. H. W. Thompson and G. Steel. Trans. Faraday Soc. **52**, 1451 (1956).
3. T. L. Brown. J. Am. Chem. Soc. **80**, 794 (1958).
4. P. J. Krueger and H. W. Thompson. Proc. Roy. Soc. London, Ser. A, **250**, 22 (1959).
5. T. L. Brown. J. Phys. Chem. **64**, 1798 (1960).
6. H. H. Jaffe. Chem. Rev. **53**, 221 (1953).
7. G. Schwarzenbach. Helv. Chim. Acta, **31**, 339 (1948).
8. D. A. Ramsay. J. Am. Chem. Soc. **74**, 72 (1952).
9. H. Irving and R. J. P. Williams. Nature, **162**, 746 (1948).
10. S. Mataga and N. Mataga. Z. Physik. Chem. Frankfurt, **13**, 140 (1957).
11. S. Nagakura and J. Tanaka. J. Chem. Phys. **22**, 236 (1954).
12. J. A. Culter. J. Chem. Phys. **16**, 136 (1948).
13. J. Omara and H. Baba. J. Phys. Soc. Japan, **10**, 317 (1955).
14. H. Baba, I. Omura, and K. Higasi. Bull. Chem. Soc. Japan, **29**, 521 (1956).
15. A. Hustrulid, P. Kusch, and J. T. Tate. Phys. Rev. **54**, 1037 (1938).
16. K. Watanaba. J. Chem. Phys. **26**, 542 (1957).
17. F. Mostafa and M. Kasha. J. Chem. Phys. **34**, 334 (1961).
18. M. R. Basila and R. J. Clancy. J. Phys. Chem. **67**, 1551 (1963).
19. S. F. Mason. J. Chem. Soc. 493 (1962).
20. F. A. Cotton. J. Am. Chem. Soc. **83**, 351 (1961).
21. H. C. A. King, E. Koros, and S. M. Nelson. J. Chem. Soc. 5449 (1963).
22. H. C. A. King, E. Koros, and S. M. Nelson. J. Chem. Soc. 4832 (1964).
23. S. M. Nelson and T. M. Shepherd. Inorg. Chem. **4**, 813 (1965).
24. S. Froaeus and R. Larsson. Acta Chem. Scand. **16**, 1433 (1962).
25. S. Froaeus and R. Larsson. Acta Chem. Scand. **14**, 1364 (1960).
26. T. L. Brown. J. Am. Chem. Soc. **83**, 4175 (1961).
27. M. Calvin and N. C. Melchior. J. Am. Chem. Soc. **70**, 3270 (1948).
28. S. Mataga and N. Mataga. Z. Phys. Chem. Frankfurt, **33**, 374 (1962).

[3]*This is supported by a study of free energy change due to coordination involved in some β-substituted pyridine derivatives in this laboratory.*

Can. J. Chem. Downloaded from www.nrcresearchpress.com by 210.87.254.40 on 09/05/12
For personal use only.

29. L. E. ORGEL, T. L. COTTRELL, W. DICK, and L. E. SUTTON. Trans. Faraday Soc. **47**, 113 (1951).
30. J. D. MORRISON. J. Chem. Phys. **19**, 1305 (1951); **20**, 1021 (1952).
31. G. M. BARROW. Introduction to molecular spectroscopy. McGraw-Hill Book Co., Inc., New York. 1962. p. 76.
32. N. A. LANGE. Handbook of Chemistry. 9th ed. Handbook Publishers Inc., Sandusky, Ohio. 1956. p. 111.
33. K. B. YATAIMIRSKŬ and V. P. VASIL'EV. Instability constants of complex compounds. The Pergamon Press, Ltd., London. 1960. p. 94. J. BJERRUM, G. SCHWARZENBACH, and L. G. SILLEN. Stability constants of metal-ion complexes. Part I. Organic Ligands. The Chemical Society, London. 1956. pp. 5, 27, 66.

Can. J. Chem. Downloaded from www.nrcresearchpress.com by 210.87.254.40 on 09/05/12
For personal use only.

Can. J. Chem. Downloaded from www.nrcresearchpress.com by 210.87.254.40 on 09/05/12
For personal use only.

THE COLLISION RATE IN A DILUTE CLASSICAL GAS

R. J. C. BROWN
Chemistry Department, Queen's University, Kingston, Ontario
Received January 26, 1966

ABSTRACT

The result given by Maxwell and by Boltzmann for the collision rate in a dilute classical gas has been widely accepted. Investigation of a stochastic model for the collisions indicates that the collision rate averaged over a macroscopic period of time is about 3% lower than the original result.

INTRODUCTION

One of the basic quantities of the classical kinetic theory of gases is the collision rate, and the result of Maxwell (1) and Boltzmann (2) has been widely accepted since it was first proposed (3, 4). This situation is in contrast with that of the mean free path, for which a number of different definitions and results have been given; as a result of these differing opinions, the mean free path is given an extended discussion in many textbooks while the collision rate is presented as if no ambiguity existed in its definition. The present work attempts to approach the collision problem by regarding the collisions of a single molecule as a stochastic process; it is shown that the collision rate averaged over a long period of time differs from the usual result given, and that the difference is analogous to that between the mean free paths calculated by Maxwell and by Tait (3).

COLLISION PROBABILITIES

Consider a gas of identical hard sphere molecules of mass m and diameter σ in thermal equilibrium at a temperature T, having a number density N molecules cm^{-3}. The velocity of a molecule selected at random in the gas is a random variable having the usual Maxwell–Boltzmann distribution (4): the probability that the velocity lies in the range $\boldsymbol{v}$ to $\boldsymbol{v} + \mathrm{d}\boldsymbol{v}$ is $F_1(\boldsymbol{v})\ \mathrm{d}\boldsymbol{v}$, where

$$[1] \qquad F_1(\boldsymbol{v}) = (\beta/\pi)^{3/2} \exp\{-\beta(v_x^2 + v_y^2 + v_z^2)\} \text{ and } \beta = m/2kT.$$

Suppose that a molecule having a particular velocity $\boldsymbol{v}$ is selected in the gas at the origin of time, $t = 0$; the next collision of this molecule is to be considered. The other molecules in the gas can be divided into groups such that each group contains molecules having essentially the same velocity; the number density of a group of molecules having velocities in the range $\boldsymbol{v}_1$ to $\boldsymbol{v}_1 + \mathrm{d}\boldsymbol{v}_1$ is $NF_1(\boldsymbol{v}_1)\ \mathrm{d}\boldsymbol{v}_1$. One can ask, what is the probability that the particular molecule considered collides with a molecule belonging to the specified group in the very short time interval between the times t, $t + \Delta t$? The probability is easily obtained if the gas is observed from a reference frame moving with velocity $\boldsymbol{v}_1$; the observer then sees the single molecule moving with velocity $\boldsymbol{w} = \boldsymbol{v} - \boldsymbol{v}_1$ through a group of almost stationary molecules whose centers are distributed at random. A collision occurs if the center of any one of the stationary molecules lies inside a particular cylindrical region of volume $\pi\sigma^2 w.\Delta t$, and the probability that this occurs is $\pi\sigma^2 w.\Delta t.NF_1(\boldsymbol{v}_1)\ \mathrm{d}\boldsymbol{v}_1$. Considering now all groups of molecules, the total probability that a collision occurs is

$$[2] \qquad \mu(v)\Delta t = N\pi\sigma^2\langle w|v\rangle.\Delta t,$$

where

$$\langle w|v\rangle = \int |\boldsymbol{v} - \boldsymbol{v}_1| F_1(\boldsymbol{v}_1)\, d\boldsymbol{v}_1 = (\pi\beta)^{-1/2}(\beta^{1/2}v)^{-1}\psi(\beta^{1/2}v), \quad [3]$$

and

$$\psi(x) = x\, e^{-x^2} + (2x^2 + 1) \int_0^x e^{-y^2}\, dy. \quad [4]$$

The quantity $\langle w|v\rangle$ is the average relative speed of two molecules in the gas, given that the speed of one of them is v. The following points may be noted in connection with the result [2]:

(i) It is implicitly assumed that Δt is small enough that the probability of more than one collision in the interval Δt is negligible, for the result is obtained formally by applying the theorem of total probability.

(ii) It is not meaningful to ask, "how many collisions per second are made by a molecule having velocity $\boldsymbol{v}$?" since the speed of the molecule changes at every collision. Conservation of energy and momentum require that the relative speed of the colliding molecules is the same after as before the collision; however, the molecules which were considered as stationary in the above argument were not rigidly fixed in space, and hence after the collision the speed of the incoming molecule relative to the rest of the group is altered and the probability associated with the second collision is different.

(iii) Since the speed of the molecule is specified, the interval of time Δt corresponds to an interval of path length $\Delta l = v.\Delta t$ and the probability that a collision occurs in this interval is

$$\mu'(v).\Delta l = N\pi\sigma^2\langle w|v\rangle.\Delta l/v. \quad [5]$$

COLLISIONS AS A STOCHASTIC PROCESS

The collisions which a molecule suffers occur at random times and can be regarded as events in a stochastic process; the probability law governing the distribution of collisions in time is given by eq. [2]. The probability density $\mu(v)$ is constant between collisions, but whenever a collision occurs, the speed of the molecule changes and hence the probability density changes to a new random value.

Define the probabilities $g_n(t)$ and $f_n(t).\Delta t$ by the following:

$g_n(t) = P\{n$ collisions in an interval of time $t\}$
$= P\{n, t\}$

$f_n(t).\Delta t = P\{1$ collision in an interval of time Δt *given* that n collisions occurred in the preceding interval of time $t\}$
$= P\{1, \Delta t|n, t\}$.

Let $F_2(v)$ be the distribution function for the speed of a molecule in a gas:

$$F_2(v) = 4\pi(\beta/\pi)^{3/2}v^2 \exp(-\beta v^2). \quad [6]$$

Then

$$g_0(t) = \int_0^\infty P\{0, t|v\} F_2(v)\, dv = \int_0^\infty e^{-\mu(v)\,t} F_2(v)\, dv, \quad [7]$$

Can. J. Chem. Downloaded from www.nrcresearchpress.com by 210.87.254.40 on 09/05/12
For personal use only.

since when v is specified, the "next" collision is distributed as in a Poisson process (5). For $n > 0$,

$$g_n(t) = \sum_{t_1=0}^{t} P\{n\text{th collision occurs between } t_1 - \Delta t_1 \text{ and } t_1\text{; and no collisions occur between } t_1 \text{ and } t\}$$
$$= \sum_{t_1=0}^{t} P\{n\text{th collision occurs between } t_1 - \Delta t_1 \text{ and } t_1\} \times P\{\text{no collisions occur between } t_1 \text{ and } t\}$$

since these two events are statistically independent. The first factor in each term of this expression can be further expanded using conditional probabilities:

$P\{n\text{th collision occurs between } t_1 - \Delta t_1 \text{ and } t_1\}$
$= P\{1 \text{ collision between } t_1 - \Delta t_1 \text{ and } t_1\text{; and } n-1 \text{ collisions between 0 and } t_1 - \Delta t_1\}$
$= P\{1 \text{ collision between } t_1 - \Delta t_1 \text{ and } t_1 | n-1 \text{ collisions between 0 and } t_1 - \Delta t_1\}$
$\times P\{n-1 \text{ collisions between 0 and } t_1 - \Delta t_1\}$
$= f_{n-1}(t_1 - \Delta t_1)\Delta t_1 . g_{n-1}(t_1 - \Delta t_1).$

Collecting these expressions and taking the limit as $\Delta t_1 \to 0$, one obtains the result

[8] $$g_n(t) = \int_0^t f_{n-1}(t_1) g_{n-1}(t_1) g_0(t - t_1)\, dt_1.$$

A differential equation involving the functions f_n and g_n may be obtained as follows: first it is noted that the probability of more than one collision occurring in a very short interval Δt is at least of order $(\Delta t)^2$ and hence

[9] $$P\{0, \Delta t | n, t\} + P\{1, \Delta t | n, t\} \cong 1.$$

The time development of $g_n(t)$ is governed by the expansion

$$P\{n, t + \Delta t\} = P\{n, t; 0, \Delta t\} + P\{n-1, t; 1, \Delta t\}$$
$$= P\{0, \Delta t | n, t\} P\{n, t\} + P\{1, \Delta t | n-1, t\} P\{n-1, t\},$$

and upon introducing eq. [9], and taking the limit as $\Delta t \to 0$, the following equation results:

[10a] $$\frac{dg_n(t)}{dt} = -f_n(t) g_n(t) + f_{n-1}(t) g_{n-1}(t).$$

For $n = 0$, the above argument yields

[10b] $$\frac{dg_0(t)}{dt} = -f_0(t) g_0(t).$$

Equations [7], [8], and [10] may now be solved for successive values of n, yielding the set of functions $\{g_n\}$ from which the average number of events in a time interval t, $\bar{n}(t)$, may be calculated:

[11] $$\bar{n}(t) = \sum_{n=0}^{\infty} n g_n(t).$$

This result is also obtainable by use of a suitable generating function,

[12] $$G(t, z) = \sum_{n=0}^{\infty} g_n(t) z^n,$$

Can. J. Chem. Downloaded from www.nrcresearchpress.com by 210.87.254.40 on 09/05/12
For personal use only.

since

$$\bar{n}(t) = \left[\frac{\partial G(t, z)}{\partial z}\right]_{z=1} \quad [13]$$

Now

$$\frac{\partial G}{\partial t} = \sum_{n=0}^{\infty} \frac{\mathrm{d}g_n}{\mathrm{d}t} z^n$$

$$= \sum_{n} (-f_n g_n + f_{n-1} g_{n-1}) z^n$$

$$= (z - 1) \sum_{n=0}^{\infty} f_n g_n z^n,$$

and using this result and eq. [8] in the definition of $G(t, z)$, there results

$$G(t, z) = g_0(t) + \sum_{n=1}^{\infty} z^n \int_0^t f_{n-1}(t_1) g_{n-1}(t_1) g_0(t - t_1)\, \mathrm{d}t_1,$$

$$= g_0(t) + \frac{z}{z - 1} \int_0^t \frac{\partial G(t_1, z)}{\partial t_1} g_0(t - t_1)\, \mathrm{d}t_1.$$

Introducing the Laplace transform denoted by

$$\phi^*(s) = \int_0^{\infty} \phi(t)\, \mathrm{e}^{-st}\, \mathrm{d}t$$

and using the convolution theorem, one obtains

$$G^*(s, z) = g_0^*(s) + \frac{z}{z - 1} g_0^*(s)[sG^*(s, z) - G(0, z)].$$

Since

$$G(0, z) = 1,$$

$$G^*(s, z) = \frac{g_0^*(s)}{1 + z[sg_0^*(s) - 1]},$$

and hence from eq. [13],

$$\bar{n}^*(s) = \frac{1}{s^2 g_0^*(s)} - \frac{1}{s}.$$

The formal result for $\bar{n}(t)$ is

$$\bar{n}(t) = \frac{1}{2\pi i} \int_{c-i\infty}^{c+i\infty} \frac{\mathrm{e}^{ts}\, \mathrm{d}s}{s^2 g_0^*(s)} - 1 \quad [14]$$

where the integration path lies to the right of the poles of the integrand, and

$$g_0^*(s) = \int_0^{\infty} \frac{F_2(v)\, \mathrm{d}v}{s + \mu(v)}. \quad [15]$$

The function $g_0^*(s)$ is non-zero and analytic everywhere in the complex s-plane except on the negative real axis to the left of $s = -2N\pi\sigma^2(\pi\beta)^{-1/2}$. Hence the contour in eq. [14] can be completed with any simple curve in the negative half-plane which excludes the real axis to the left of $s = -2N\pi\sigma^2(\pi\beta)^{-1/2}$, and then the only contribution to the integral over the whole contour is the residue at the double pole at the origin,

$$\frac{tg_0^*(0) - g_0^{*\prime}(0)}{[g_0^*(0)]^2}.$$

Can. J. Chem. Downloaded from www.nrcresearchpress.com by 210.87.254.40 on 09/05/12
For personal use only.

The integral around the curve can be shown to vanish as $t \to \infty$ since the real part of s is negative, and hence

$$\lim_{t\to\infty} \frac{\bar{n}(t)}{t} = \frac{1}{g_0^*(0)} = \frac{1}{\langle 1/\mu \rangle} \tag{16}$$

since

$$g_0^*(0) = \int_0^\infty \frac{F_2(v)}{\mu(v)}\,dv = \langle 1/\mu \rangle. \tag{17}$$

On the other hand, for a very small value of t, $g_n(t)$ becomes vanishingly small for $n > 1$, and from the definition [11] of $\bar{n}(t)$,

$$\bar{n}(t) \cong g_1(t) \cong 1 - g_0(t) \cong \langle \mu \rangle t$$

$$\text{i.e.} \quad \lim_{t\to 0} \frac{\bar{n}(t)}{t} = \langle \mu \rangle \tag{18}$$

where

$$\langle \mu \rangle = \int_0^\infty \mu(v) F_2(v)\,dv. \tag{19}$$

Hence for this process, $\bar{n}(t)/t$ has different limiting values for very large and very small values of t. The average time from any arbitrary origin until the "next" collision is

$$\langle t_1 \rangle = \int_0^\infty t f_0(t) g_0(t)\,dt$$

$$= \int_0^\infty g_0(t)\,dt$$

$$= \langle 1/\mu \rangle, \tag{20}$$

which is exactly analogous to Tait's mean free path.

COLLISION RATE AND MEAN FREE PATH

The limiting value of the collision rate as $t \to \infty$ can be written explicitly using eqs. [2] and [3] in [17]:

$$\lim_{t\to\infty} \frac{\bar{n}(t)}{t} = \frac{N\pi\sigma^2\beta^{-1/2}}{I_3} \tag{21}$$

where

$$I_n = 4\int_0^\infty \frac{x^n \exp(-x^2)}{\psi(x)}\,dx. \tag{22}$$

The total number of collisions per cm^3 made by all molecules is obtained by multiplying the result [21] by $N/2$, the factor of $\frac{1}{2}$ being due to double counting of each collision.

The limiting value of the collision rate as $t \to 0$ is identical to the usual result quoted:

$$\lim_{t\to 0} \frac{\bar{n}(t)}{t} = N\pi\sigma^2\langle w \rangle$$

$$= N\pi\sigma^2\beta^{-1/2}(8/\pi)^{1/2}. \tag{23}$$

The status of the result [23] is clear: it is valid only for a period of time so short that $\bar{n}(t) \sim 0$, and except in a gas at exceedingly low pressures, such a period of time is very short.

Can. J. Chem. Downloaded from www.nrcresearchpress.com by 210.87.254.40 on 09/05/12
For personal use only.

The mean free path may also be discussed using the above stochastic model, using the probability density $\mu'(v)$ defined in eq. [5]; the number of collisions per cm of path length is

$$[24] \qquad \lim_{l\to\infty} \frac{\bar{n}(l)}{l} = \frac{1}{\langle 1/\mu' \rangle} = \frac{N\pi\sigma^2}{I_4}.$$

A mean free path may be defined as the inverse of this quantity, and is identical to the mean free path defined by Tait (6), as might be expected from eq. [20]; the Maxwell mean free path (3) may be obtained as the limit of $\bar{n}(l)/l$ as $l \to 0$. Thus the two collision rates defined above are entirely analogous to the two mean free paths.

Boltzmann calculated (6) the value of I_4 as 0.677464, which agreed in the first three figures with the result of Tait (7). The values of $I_{\bar{n}}$ for $n = 2$ up to $n = 6$ have been computed using Simpson's rule; the interval of subdivision was decreased until convergence to 8 decimal places was obtained, and only the basic arithmetic operations (using 22 digits) were employed in evaluating the exponential and error functions. The results are shown in Table I, and comparison with the usual results shows that the proposed collision rate [21] is smaller than the result [23] by about 3%.

TABLE I

The integral I_n
$(\pi/8)^{1/2} = 0.6266571$
$(1/2)^{1/2} = 0.7071068$

n	I_n
2	0.80336908
3	0.65051102
4	0.67746223
5	0.83826485
6	1.18235152

ACKNOWLEDGMENTS

This work was carried out during a Summer Associateship at Queen's University; computations were performed at Queen's University Computing Centre.

REFERENCES

1. J. C. MAXWELL. Scientific papers. Dover Publications, New York. 1952.
2. L. BOLTZMANN. Lectures on gas theory. *Translated by* S. G. Brush. University of California Press. 1964.
3. SIR JAMES JEANS. Introduction to the kinetic theory of gases. Cambridge University Press, London. 1962.
4. S. CHAPMAN and T. G. COWLING. The mathematical theory of non-uniform gases. Cambridge University Press, London. 1939.
5. E. PARZENS. Stochastic processes. Holden-Dav Inc., San Francisco. 1962.
6. L. BOLTZMANN. Wien. Ber. **96**, 905 (1887).
7. P. G. TAIT. Trans. Roy. Soc. Edinburgh, **33**, 74 (1886).

Can. J. Chem. Downloaded from www.nrcresearchpress.com by 210.87.254.40 on 09/05/12
For personal use only.

Can. J. Chem. Downloaded from www.nrcresearchpress.com by 210.87.254.42 on 09/05/12
For personal use only.

THE PHOTOLYTIC AND PHOTOSENSITIZED DECOMPOSITION OF CHLOROFORM[1]

I. UNGER AND G. P. SEMELUK
Department of Chemistry, University of New Brunswick, Fredericton, New Brunswick

Received November 22, 1965

ABSTRACT

The photolysis of $CHCl_3$, in the vapor phase, was carried out using the 1 849 Å line of Hg as the exciting radiation. The photosensitized reaction was also studied using benzene as a photosensitizer. In the latter case, the exciting wavelength was the 2 537 Å line of mercury, which $CHCl_3$ does not absorb.

The study was primarily concerned with establishing the initial steps of the direct photolysis and photosensitized reactions. Experimental observations rule out a molecular detachment of HCl in both the direct photolysis and photosensitized reactions at the wavelength used. The initial step of the photolysis appears to be a carbon–chlorine bond cleavage, but in the photosensitized reaction a carbon–hydrogen bond break is indicated as the primary step. It is concluded that in neither case does dissociation take place from the ground electronic state.

INTRODUCTION

Of the halogenated compounds those containing a carbonyl group have received the most attention. Very recently Majer and Simons published an excellent review of the photochemistry of halogenated compounds (2). Alkyl iodides have been studied more extensively than the other haloalkanes, perhaps because they are so easily dissociated. In the case of iodides it is now believed that two primary processes occur at different wavelengths; e.g., in ethyl iodide (3)

$$C_2H_5I \rightarrow \cdot C_2H_5 + I \text{ (at long wavelengths)}$$
$$\rightarrow C_2H_4 + HI \text{ (at shorter wavelengths)}$$

A molecular detachment mechanism has been suggested in the photodissociation of haloethylenes (4), although a radical mechanism may also be involved. More recently, the polyhalomethanes have been examined in an attempt to produce dichloro- and dibromocarbenes and to photograph their spectra (5). The photolysis of chloroform was studied by Hill (6), who identified only one product, HCl. Chloroform was photolyzed alone and in the presence of oxygen, hydrogen, and nitrogen. For chloroform alone the quantum yield was 3.99, and was not changed by the presence of hydrogen. Nitrogen increased the quantum yield to 23, while oxygen accelerated the reaction still more markedly.

Hill proposed the primary step of the reaction to be

[1] $$CHCl_3 \xrightarrow{h\nu} \cdot CHCl_2 + Cl$$

or

[2] $$CHCl_3 \xrightarrow{h\nu} \cdot CCl_3 + H$$

Shilov and Sabirova (7–9) have shown that in the pyrolysis of $CHCl_3$ the primary step of the reaction is

[3] $$CHCl_3 \rightarrow :CCl_2 + HCl$$

It is also interesting to note that in the radiolysis of $CHCl_3$ (10) the possibility of $:CCl_2$ formation by a "molecular mechanism" was used to explain the formation of one of the

[1]*Abstracted from the Ph.D. thesis (1963) of I. Unger. A preliminary report on this work has appeared as a note (1). In this communication we wish to present more extensive data as well as some experimental details.*

minor products, C_2Cl_4. On considering the above, it becomes evident that the primary step in the photolysis of $CHCl_3$ may be any one of reactions [1], [2], [3] or even the energetically less likely reaction [4].

$$[4] \qquad CHCl_3 \xrightarrow{h\nu} :CHCl + Cl_2$$

Neither should one exclude the possibility that more than one of the above reactions may participate in the initial dissociation.

Until recently, mercury has been used exclusively as a photosensitizer, but organic compounds are now becoming prominent as photosensitizers (11–13) perhaps because of the greater range of energies available and the broader knowledge of energy states of organic compounds made possible by the advent of flash photolysis. Ishikawa and Noyes (14) were able to show by an indirect method that all the benzene molecules which are excited by 2 537 Å radiation and do not fluoresce cross over to the triplet state, i.e., about 78%. This thesis has received support from the work of Cundall and Palmer (15) who used benzene to sensitize the isomerization of butene-2 and concluded that it was the triplet state of the benzene which sensitized this isomerization. We felt it was of interest to investigate the photolysis of chloroform, the possibility of a benzene-sensitized decomposition in a region of the spectrum where $CHCl_3$ does not absorb, and to perhaps relate the above dissociations to specific excited states, in the light of modern concepts and with the aid of modern instrumentation.

EXPERIMENTAL

Materials

C.P. chloroform was purified according to the method described by Vogel (16), degassed thoroughly, and stored in hermetically sealed ampoules under vacuum. Chloroform thus treated was found to be chromatographically pure and did not show any signs of decomposition even when stored for prolonged periods of time. Fisher Certified Thiophene-Free Spectranalyzed benzene was found to be chromatographically pure and was used without any further purification. Butenes and ethylene were Phillips Research Grade hydrocarbons, and *cis*- and *trans*-1,2-dimethyl-2,2-dichlorocyclopropane were prepared by the method described by Doering and Hoffman (17) and purified by several distillations. The fraction of *cis*-1,2-dimethyl-2,2-dichlorocyclopropane collected had a boiling point of 127–128 °C, while that of *trans*-1,2-dimethyl-2,2-dichlorocyclopropane collected had a boiling point of 121–122 °C. The 1,1-dichlorocyclopropane was prepared according to the method given by Stevens (18) and purified by distillation.

Pharmaceutical hydrogen (mercury-free), obtained from the Linde Air Products Co., was passed over hot finely divided copper to remove traces of oxygen and then passed through a phosphorus pentoxide drying tower. Linde nitrogen was treated in the same manner. Canadian Industries Limited anhydrous ammonia was purified by bulb-to-bulb distillation *in vacuo*.

The vacuum system was conventional but mercury-free, consisting essentially of three sections—storage, analytical, and reaction. Photolyses were carried out in a quartz cell 25 mm in diameter and 50 mm long and equipped with Suprasil windows. Pressure measurements were made using a Pyrex spiral gauge as a null instrument.

The lamp used for experiments at 1 849 Å was a custom made Hanovia low-pressure mercury arc, adjusted for optimum emission at 1 849 Å. A small heating tape, near the window of the lamp, was used to prevent mercury condensation on the window. This lamp was also used for experiments at 2 537 Å, in which case a Corning No. 9863 filter, 2 mm thick, effectively removed 1 849 Å radiation. For experiments in the presence of olefins a high-pressure mercury–xenon arc, Hanovia No. 908 B1 was used in conjunction with a Baird Atomic interference filter having a maximum transmission at 2 150 Å. Light emitted by the low-pressure mercury arc was monitored with a one stage platinum phototube (constructed at the N.R.C. laboratories in Ottawa) in conjunction with a Keithley electrometer. This phototube is insensitive to wavelengths above 2 100 Å.

When $CHCl_3$ or $CHCl_3$ plus a condensible were being studied, the reactants were admitted to the cell, frozen in the side arm of the cell, and then flash-vaporized, a half hour being allowed for efficient mixing. When $CHCl_3$ plus N_2 or H_2 were being studied, a period of 3 h was allowed for mixing following flash evaporation of the chloroform, since in this case mixing was much slower. After photolysis the products and reactants were collected in the analytical section. Hydrogen chloride was distilled into a trap containing sodium bicarbonate, and the carbon dioxide produced was collected in a short ampoule of 1 mm internal diameter, which was then detached while under vacuum and set aside to await analysis. The remaining

Can. J. Chem. Downloaded from www.nrcresearchpress.com by 210.87.254.42 on 09/05/12
For personal use only.

products and reactants were collected in a similar ampoule. In the benzene-photosensitized runs the dark-colored residue which was occasionally deposited on the window of the cell was removed by flaming the cell to a dull red, first in the presence of air and finally in the presence of hydrogen.

Most of the analyses were carried out using a model 500 F and M Linear Temperature Programmed Gas Chromatograph. An F and M SI-4 solid sample injector was used for ampoule injection. All the chlorinated hydrocarbon products were analyzed on a 10 ft column containing 10% silicone oil on 60/80 mesh Chromosorb W, temperature-programed from 65 to 225 °C at a rate of 15 deg/min, with a hydrogen carrier gas flow rate of 1 cc/s. A 3 ft 40/60 mesh silica gel column, at 105 °C, was used for carbon dioxide determination. A 12 ft column packed with 20% diisodecyl phthalate on 60/80 Chromosorb W held at 125 °C was used to identify chlorinated cyclopropanes. Hydrogen was determined on a 4 ft 40/60 mesh molecular sieve 5A column operating at room temperature, with a nitrogen carrier gas flow rate of 0.5 cc/s.

Actinometry

Ammonia was chosen as the chemical actinometer. Although an absolute quantum yield with it is uncertain because of the lack of data below 2 100 Å, it has some singular advantages (19). It is easily purified, the products of the reaction are H_2 and N_2 in the ratio 3:1 (at any extent of decomposition in a static system) and it is transparent to 2 537 Å radiation while absorbing 1 849 Å radiation strongly.

Wiig (20, 21) has calculated the quantum yield of NH_3 decomposition at 1 atm for a cell of the same geometry as the one used in the present study to be 0.163 at 2 100 Å. Our quantum yields are based on this value. It seems unlikely that the quantum yield of NH_3 decomposition at 1 849 Å will be sufficiently different from that at 2 100 Å to require a change in our interpretation of the chloroform photolysis. On the contrary, the available data (22) suggests that the quantum yield of NH_3 decomposition could be the same at both wavelengths, since the initial steps of the decomposition, the products, and the product ratios are nearly the same at both wavelengths. Should this not be the case, then our results may be corrected when an absolute value for ammonia photolysis at 1 849 Å is determined.

RESULTS AND DISCUSSION

Direct Photolysis

To establish whether the photolysis proceeds via a molecular mechanism, [3] and [4], or a radical mechanism, [1] and [2], numerous experiments were performed in the presence of olefins. If a biradical were formed in the first step, then in the presence of olefins one would expect a dichloro- or monochloro-cyclopropane among the products. When the photolysis was carried out in the presence of *cis*- or *trans*-butene-2, no evidence for the formation of the above-mentioned compounds could be obtained. The reactions of $:CH_2$ are fairly well characterized (23, 24) and are known to be very rapid. Those of heavier biradicals are not too well known and may be quite different. Frey (25) found that $CH_3CH:$ did not add to the double bond in *cis*- and *trans*-butene-2 but did react with propylene; he tentatively ascribed the reason to steric hindrance. One would, therefore, expect $:CCl_2$ to be even less reactive to *cis*- and *trans*-butene-2 than $CH_3CH:$ and for this reason several experiments were carried out in the presence of ethylene, which has the added advantage that its long wave limit of absorption is lower than that of any other olefin (26). None of these experiments showed any cyclopropanes among the products even when performed in a large excess of nitrogen.

Further evidence ruling out the molecular mechanism was obtained by performing photolyses in the presence of large amounts of H_2 and N_2 which should yield CCl_2H_2 and C_2Cl_4, respectively, if $:CCl_2$ is formed initially in a "hot" state according to the reactions

[5] $$:CCl_2^{**} + H_2 \rightarrow :CCl_2^{*} + H_2$$

[5a] $$:CCl_2^{*} + H_2 \rightarrow CCl_2H_2$$

[6] $$CCl_2^{**} + N_2 \rightarrow :CCl_2^{*} + N_2$$

[6a] $$2{:}CCl_2^{*} \rightarrow C_2Cl_4$$

Our observations indicate that the photolysis of $CHCl_3$ proceeds through an initial carbon–chlorine bond cleavage. Table I summarizes our results for varying $CHCl_3$

Can. J. Chem. Downloaded from www.nrcresearchpress.com by 210.87.254.42 on 09/05/12
For personal use only.

pressure. No products other than $C_2H_2Cl_4$, C_2HCl_5, C_2Cl_6 and HCl were detected. The mechanism (for small percentage conversions) can be described by

[1] $$CHCl_3 \xrightarrow{h\nu} \cdot CHCl_2 + Cl$$

[7] $$Cl + CHCl_3 \rightarrow HCl + \cdot CCl_3$$

[8] $$\cdot CHCl_2 + \cdot CCl_3 \rightarrow C_2HCl_5$$

[9] $$2 \cdot CHCl_2 \rightarrow C_2H_2Cl_4$$

[10] $$2 \cdot CCl_3 \rightarrow C_2Cl_6$$

TABLE I

Products, product ratios, and quantum yield of decomposition of $CHCl_3$ at various $CHCl_3$ pressures (λ = 1 849 Å, T = 27 °C, irradiation time = 30 min)

P_{CHCl_3} (cm Hg)	$[C_2H_2Cl_4]$ (10^8 moles)	$[C_2HCl_5]$ (10^8 moles)	$[C_2Cl_6]$ (10^8 moles)	$[C_2HCl_5]/[C_2H_2Cl_4]$	$[C_2Cl_6]/[C_2H_2Cl_4]$	Φ
2.2	7.3	13.8	4.4	1.89	0.603	0.37
4.4	6.9	14.7	5.8	2.10	0.827	0.40
6.6	9.1	17.7	6.5	1.94	0.707	0.48
1.1	5.3	12.3	4.9	2.30	0.911	0.37
0.55	4.7	8.3	3.4	1.77	0.725	0.30
8.8	10.1	19.9	9.0	1.98	0.88	0.54
16.7	10.7	21.6	10.2	2.02	0.947	0.58
12.8	10.2	18.4	7.4	1.80	0.681	0.49
4.4	8.3	16.4	7.2	1.98	0.875	0.46
2.2	7.6	15.1	5.9	1.92	0.770	0.42
13.9	9.2	19.8	10.1	2.15	1.09	0.54

If [7] is sufficiently rapid, then the steady state concentration of CCl_3 and $CHCl_2$ radicals will be equal and on a purely statistical basis it would be expected that C_2HCl_5, $C_2H_2Cl_4$, and C_2Cl_6 would be formed in the ratio 2:1:1 (27), which would be modified slightly for mass differences among these radicals, but changed more significantly if the activation energies for [8], [9], and [10] were different. The expected relationship between these activation energies $E_{10} > E_9 \geqslant E_8$ (27) is roughly confirmed by our observations, as shown in Table I.

An initial carbon–hydrogen bond rupture is shown to be unlikely by the absence of H_2 among the products and can be corroborated by photolyzing in the presence of an excess of H_2. If [1] applies, then this reaction would be followed rapidly by

[11] $$Cl + H_2 \rightarrow HCl + H$$

and then by

[12] $$H + CHCl_3 \rightarrow HCl + \cdot CHCl_2$$

or

[13] $$H + CHCl_3 \rightarrow H_2 + \cdot CCl_3$$

Hardwick (28) gives k_{12}/k_{13} as 7.3. Thus there would be an increase in the steady state concentration of $CHCl_2$ radicals relative to that of CCl_3 radicals and the product ratios should change in favor of $C_2H_2Cl_4$. In the case of carbon–hydrogen bond rupture, however, little change would be expected. The product ratios did indeed change significantly in the presence of H_2 (Fig. 1) though the quantum yield was very little affected (Fig. 2). Nitrogen, on the other hand, reduced the quantum yield slightly (Fig. 3) but hardly altered the product ratios (Fig. 4). The slight increase in favor of C_2Cl_6 in the presence of N_2 is also consistent with our mechanism, since if [1] is the first step of the sequence, the $CHCl_2$

Can. J. Chem. Downloaded from www.nrcresearchpress.com by 210.87.254.42 on 09/05/12
For personal use only.

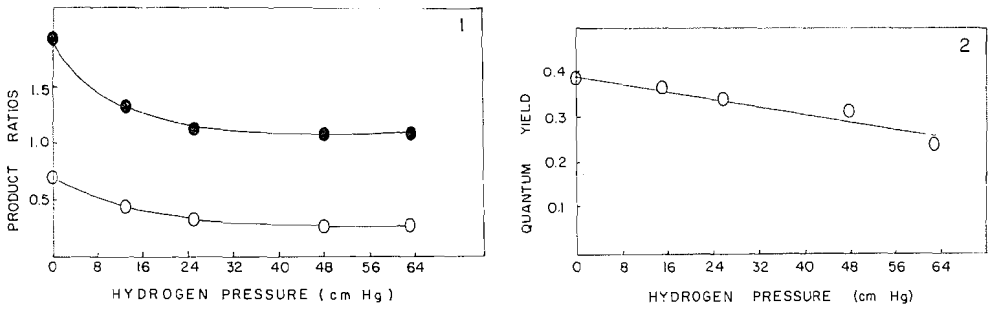


FIG. 1. Dependence of product ratios on hydrogen pressure: ●, $[C_2HCl_5]/[C_2H_2Cl_4]$; ○, $[C_2Cl_6]/[C_2H_2Cl_4]$.
FIG. 2. Quantum yield variation with hydrogen pressure.

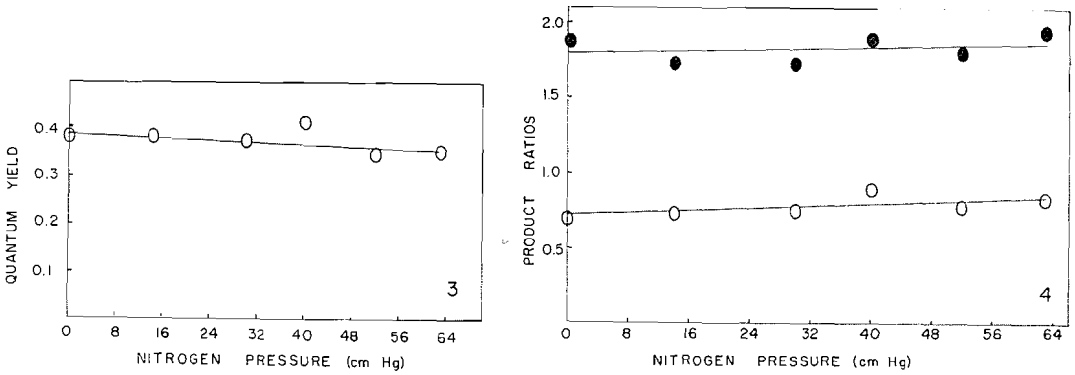


FIG. 3. Quantum yield variation with nitrogen pressure.
FIG. 4. Dependence of product ratios on nitrogen pressure: ●, $[C_2HCl_5]/[C_2H_2Cl_4]$; ○, $[C_2Cl_6]/[C_2H_2Cl_4]$.

radical is produced in the "hot" state, whereas the CCl_3 radical is not produced in a "hot" state. In the presence of N_2 some of the excess energy possessed by $CHCl_2$, which would otherwise be partly available for activation energy during a collision, would be removed and the amount of $C_2H_2Cl_4$ relative to C_2Cl_6 should decrease. This thesis is supported by data obtained at elevated temperatures, listed in Table II. Under these conditions the products arising from "hot" radicals should not be as strongly favored over those stemming from "cold" radicals and the product ratios should therefore change in favor of C_2Cl_6, as is illustrated in Fig. 5.

TABLE II

Variation of products with temperature and added quenching gas
(λ = 1 849 Å, irradiation time = 30 min)

T (°C)	P_{CHCl_3} (cm Hg)	P_{N_2} (cm Hg)	$[C_2H_2Cl_4]$ (10^8 moles)	$[C_2HCl_5]$ (10^8 moles)	$[C_2Cl_6]$ (10^8 moles)
130	8.4	0	9.1	20.8	10.5
130	14.0	0	9.1	20.1	10.6
130	2.2	0	7.5	17.3	8.8
80	2.2	30	7.6	14.2	7.5
130	2.2	30	6.2	12.6	7.7
130	2.2	30	6.5	14.2	7.8
27	2.2	0	7.3	13.8	4.4
27	2.2	0	7.6	15.1	5.9
27	2.2	30	7.7	13.2	5.7

Can. J. Chem. Downloaded from www.nrcresearchpress.com by 210.87.254.42 on 09/05/12
For personal use only.

To make the mechanism a little more detailed, though by no means complete, the following reactions must be considered:

[14] $$CHCl_3 + h\nu \rightarrow CHCl_3^*$$

[15] $$CHCl_3^* \rightarrow CHCl_3 + h\nu$$

[16] $$CHCl_3^* + CHCl_3 \rightarrow 2CHCl_3$$

[17] $$CHCl_3^* + M \rightarrow CHCl_3 + M$$

[18] $$CHCl_3^* \rightarrow \cdot CHCl_2 + Cl\cdot$$

It is perhaps unusual to include [15], [16], and [17] in the scheme since in this spectral region chloroform apparently gives a continuous absorption band (29), and so implies that it finds itself in at least a repulsive part of the upper electronic state. The possibility exists, of course, that the band does have structure and that its appearance is the result of spectrographic insensitivity to small intensity differences, but it is also possible that the theoretical basis for understanding the relationship between dissociation and electronic spectra of polyatomic molecules is much less secure than it is for diatomic molecules. For example, fluorescence is observed when CF_4 is excited by radiation of about 900 Å, even though CF_4 absorption is continuous in this region (30).

It should be noted that the quantum yield of chloroform decomposition is significantly different from 2, the value which one would expect if dissociation took place from a completely repulsive state under the pressure conditions of this study. Although it is possible that our quantum yield is in error due to experimental shortcomings and to an incorrect value for the quantum yield of NH_3 dissociation, a careful consideration of the sources of error leads us to believe that any adjustment would likely result in a lower value than we report.

According to the proposed mechanism the quantum yield for the disappearance of $CHCl_3$ will be given by

[19] $$\Phi = \frac{2k_{18}}{k_{18} + k_{15} + k_{16}[CHCl_3] + k_{17}[M]}$$

In the presence of foreign gas, for constant $CHCl_3$ pressure, the denominator of [19] increases as foreign gas pressure increases and the quantum yield therefore decreases. This is graphically confirmed in Figs. 2 and 3, which also suggests that hydrogen is a more efficient quencher of excited $CHCl_3$ than is nitrogen, a behavior which has been observed in many other cases (31).

There is an apparent increase in the quantum yield of decomposition with increasing $CHCl_3$ pressure. There are several possible explanations for this phenomenon (wall quenching, dissociation from some state other than the one initially excited, etc.). We prefer to reserve judgement on this point until more accurate data become available.

Thus, the evidence presented here strongly supports an initial carbon–chlorine bond rupture and is in line with the view of Mulliken (32) that the continuous absorption band of $CHCl_3$, with maximum at 1 750 Å (29) is due to the excitation of an electron from a non-bonding orbital on the chlorine atom to a sigma carbon–chlorine antibonding orbital.

Benzene-Sensitized Photolysis

Chloroform and benzene when present separately in the cell did not show any detectable signs of decomposition when irradiated with 2 537 Å radiation, but when both were present simultaneously, chloroform decomposition did occur. The major organic products determined were hexachloroethane, methylene chloride, α,α,α-trichlorotoluene, and pentachloroethane. Much smaller quantities of tetrachloroethylene and tetrachloroethane were

Can. J. Chem. Downloaded from www.nrcresearchpress.com by 210.87.254.42 on 09/05/12
For personal use only.

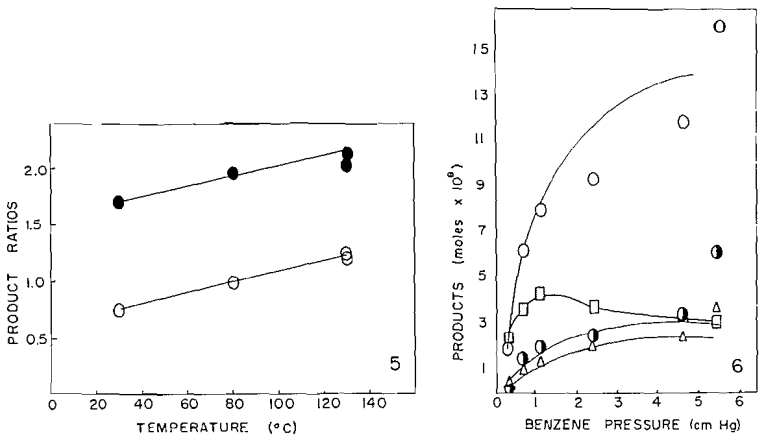


FIG. 5. Dependence of product ratios on temperature: ●, $[C_2HCl_5]/[C_2H_2Cl_4]$; ○, $[C_2Cl_6]/[C_2H_2Cl_4]$.
FIG. 6. Product dependence on benzene pressure: ○, $[C_2Cl_6]$; □, $[CH_2Cl_2]$; ◑, $[CCl_3{\cdot}C_6H_5]$; △, $[C_2HCl_5]$.

also found, but chlorobenzene and biphenyl which were expected products could not be detected in any experiment. The dependence of major organic products on benzene pressure is shown in Fig. 6. The inorganic products consisted of hydrogen chloride and, in marked contrast to the direct photolysis case, hydrogen. The quantitative determination of the inorganics has been more difficult and much less accurate, but it appears that hydrogen chloride production approximately parallels the production of methylene chloride.

In devising a mechanism for this reaction, the choice of radical reactions has been strongly influenced by the product distribution, and particularly by the absence of chlorobenzene among the products. This we have interpreted to mean that abstraction by phenyl radicals is not important in this system and that chlorine atoms do not significantly participate in the reaction.

Our results, then, are consistent with a mechanism based on a carbon–hydrogen bond split in $CHCl_3$ following energy transfer from an excited benzene molecule. In the following mechanism which is based on reactions of excited benzene discussed by Noyes (33), B represents benzene in the ground electronic state, $^1B^I$ represents electronically excited singlet benzene, $^3B^I_v$ represents electronically excited triplet benzene in a high vibrational energy-level, $^3B^I_0$ represents electronically excited triplet benzene in the ground vibrational level, M = $CHCl_3$ + B represents an 'energy-removing body', k_i represents the rate constant of the ith step in the mechanism, and T_a represents the absorbed intensity.

[20] $$B + h\nu \rightarrow {}^1B^I \qquad I_a$$

[21] $$^1B^I \rightarrow B + h\nu$$

[22] $$^1B^I + B \rightarrow 2B$$

[23] $$^1B^I \rightarrow {}^3B^I_v$$

[24] $$^3B^I_v + M \rightarrow {}^3B^I_0 + M$$

[25] $$^3B^I_0 + M \rightarrow B + M$$

[26] $$^3B^I_v + CHCl_3 \rightarrow B + \cdot CCl_3 + H$$

or

[26a] $$^1B^I + CHCl_3 \rightarrow B + \cdot CCl_3 + H$$

Can. J. Chem. Downloaded from www.nrcresearchpress.com by 210.87.254.42 on 09/05/12
For personal use only.

[12] $H + CHCl_3 \rightarrow HCl + HCCl_2$

[13] $H + CHCl_3 \rightarrow H_2 + \cdot CCl_3$

[27] $H + B \rightarrow H_2 + \cdot C_6H_5$

[10] $2\cdot CCl_3 \rightarrow C_2Cl_6$

[28] $\cdot CHCl_2 + H \rightarrow CH_2Cl_2$

[29] $\cdot C_6H_5 + H \rightarrow B$

[30] $\cdot C_6H_5 + \cdot CCl_3 \rightarrow C_6H_5CCl_3$

[8] $\cdot CHCl_2 + \cdot CCl_3 \rightarrow C_2HCl_5$

If reaction [26] is responsible for the initial step of the decomposition of $CHCl_3$, then the steady state concentration of the triplet is given by

$$[31] \qquad [^3B^I_v] = \frac{k_{23}I_a}{\{(k_{24} + k_{21})[CHCl_3] + k_{24}[B]\}\{k_{21} + k_{23} + k_{22}[B]\}}$$

On the other hand if reaction [26*a*] is responsible, the steady state concentration of the singlet is given by

$$[32] \qquad [^1B^I] = \frac{I_a}{k_{21} + k_{23} + k_{26a}[CHCl_3] + k_{22}[B]}$$

If the sensitization rate is represented in general by $k_x[B^*][CHCl_3]$ where $k_x[B^*]$ is to be replaced by $k_{26a}[^1B^I]$ for singlet activation and by $k_{26}[^3B^I_v]$ for triplet activation, then the steady state concentration of hydrogen atoms is given by

$$[33] \qquad [H] = \frac{k_x[B^*][CHCl_3]}{(k_{12} + k_{13})[CHCl_3] + k_{27}[B] + k_{28}[CCl_2H\cdot] + k_{29}[C_6H_5\cdot]}$$

By using the average rate of formation of $C_2H_2Cl_4$ during the photolysis time, and a reasonable recombination rate constant of 10^{10} l mole^{-1} s^{-1}, it can be shown that $k_{28}[CCl_2H\cdot] \sim 0.1$. A similar evaluation of the production of C_2Cl_6 and $CCl_3\cdot C_6H_5$ indicates that $k_{29}[C_6H_5\cdot]$ will be no greater than $k_{28}[CCl_2H\cdot]$. On the other hand, from other similar reactions of hydrogen atoms (34, 35), and the known ratio k_{12}/k_{13} (28), it can be estimated that $k_{12} + k_{13}$ will have a value of $\sim 10^7$ l mole^{-1} s^{-1}. It would be expected that k_{27} would be somewhat smaller than k_{13} (36), so that under the experimental conditions we estimate that

$$(k_{12} + k_{13})[CHCl_3] + k_{27}[B] \sim 10^4$$

and therefore it may be assumed that

$$[34] \qquad [H] = \frac{k_x[B^*][CHCl_3]}{(k_{12} + k_{13})[CHCl_3] + k_{27}[B]}$$

The solutions for the remaining radicals and for the rates of formation of the products are now straightforward and give, for example

$$[35] \qquad \frac{d[C_2Cl_6]}{dt} = \frac{k_{13}k_x[B^*][CHCl_3]}{(k_{12} + k_{13}) + k_{27}[B]/[CHCl_3]}$$

A considerably more bulky expression results for the rate of formation of CH_2Cl_2, whose characteristic is that the denominator contains a higher order polynomial in [B] than does [35]. Simple substitution for $k_x[B^*]$ into these equations will yield two expressions for each

Can. J. Chem. Downloaded from www.nrcresearchpress.com by 210.87.254.42 on 09/05/12
For personal use only.

rate depending on whether $^3B^I_v$ or $^1B^I$ causes sensitization. Both possible mechanisms of energy transfer predict

(*a*) the rate of formation of CH_2Cl_2 and C_2Cl_6 have maxima with respect to benzene pressure;

(*b*) at low benzene pressure the rate of production of C_2Cl_6 and CH_2Cl_2 should be the same;

(*c*) the maxima for CH_2Cl_2 occurs at lower benzene pressures than that for C_2Cl_6.

These predictions are qualitatively confirmed by the results, except at higher benzene pressure where the experimental conditions are complicated by the formation of heavy products which deposit on the cell windows. At present most of the rate constants in the above expressions are unknown and it is, therefore, impossible to determine which energy transfer mechanism is operative. However, data are available which narrow the possibilities.

Ground state decomposition of $CHCl_3$ proceeds via molecular elimination of HCl (7) and is incompatible with our observations. The dissociation of $CHCl_3$ must then take place in an excited singlet or an excited triplet state. We have previously discussed (1) the possibilities of either of these states being responsible for the reaction. The long lifetime of the benzene triplet (37) and its greater abundance, combined with the lack of an ultraviolet absorption spectrum for $CHCl_3$ at 2 537 Å leading to a singlet state (spin allowed), would favor photosensitization by the triplet.

It is interesting to note that work in this laboratory (G. P. Semeluk and A. K. Basak, unpublished results) with CH_2Cl_2 also indicates an initial carbon–chlorine bond cleavage in photolysis, and that both the benzene- and hexafluorobenzene-photosensitized reactions proceed via a carbon–hydrogen bond rupture. The possibility that hexafluorobenzene-sensitized decomposition of $CHCl_3$ will result in a much simpler sequence of reactions, as it does for CH_2Cl_2 (38), is being investigated.

ACKNOWLEDGMENTS

This work was supported by grants and the gift of some equipment from the National Research Council. One of us (I. U.) wishes to thank Canadian Industries Limited for a fellowship.

REFERENCES

1. G. P. Semeluk and I. Unger. Nature, **198**, 853 (1963).
2. J. R. Majer and J. P. Simons. *In* Advances in photochemistry. Vol. 2. *Edited by* W. Albert Noyes, Jr., George S. Hammond, and J. N. Pitts, Jr. Interscience Publishers, New York. 1964. p. 137.
3. B. A. Thrush. Proc. Roy. Soc. London, Ser. A, **243**, 555 (1958).
4. M. H. J. Wijen. J. Am. Chem. Soc. **83**, 4109 (1961).
5. J. P. Simons and A. J. Yarwood. Trans. Faraday Soc. **59**, 90 (1963).
6. D. G. Hill. J. Am. Chem. Soc. **54**, 32 (1932).
7. A. E. Shilov and R. D. Savirova. Dokl. Akad. Nauk SSSR, **114**, 1058 (1957).
8. A. E. Shilov and R. D. Sabirova. Zh. Fiz. Khim. **33**, 1365 (1959).
9. A. E. Shilov and R. D. Sabirova. Zh. Fiz. Khim. **34**, 408 (1960).
10. M. Ottolenghi and G. Stein. Radiation Res. **14**, 281 (1961).
11. R. Kopocky, G. S. Hammond, and P. A. Leermakers. J. Am. Chem. Soc. **84**, 1015 (1962).
12. G. S. Hammond, J. Saltiel, A. A. Lamola, N. J. Turro, J. S. Bradshaw, D. O. Cowan, R. C. Counsell, V. Vogt, and C. Dalton. J. Am. Chem. Soc. **86**, 3197 (1964).
13. B. N. Shelimov, N. V. Fok, and V. V. Voevodshii. Dokl. Akad. Nauk SSSR, **144**, 596 (1962).
14. H. Ishikawa and W. A. Noyes, Jr. Chem. Phys. **37**, 583 (1962).
15. R. B. Cundall and T. F. Palmer. Trans. Faraday Soc. **56**, 1211 (1960).
16. A. I. Vogel. Textbook of practical organic chemistry. Longmans, Green and Co., London. 1948. p. 174.
17. W. E. Doering and A. K. Hoffman. J. Am. Chem. Soc. **76**, 6162 (1954).
18. P. G. Stevens. J. Am. Chem. Soc. **68**, 620 (1946).
19. W. C. Kreye and R. A. Marcus. J. Chem. Phys. **37**, 419 (1962).
20. E. O. Wiig. J. Am. Chem. Soc. **57**, 1559 (1935).
21. E. O. Wiig. J. Am. Chem. Soc. **59**, 827 (1937).

Can. J. Chem. Downloaded from www.nrcresearchpress.com by 210.87.254.42 on 09/05/12
For personal use only.

22. J. R. McNesby, I. Tanaka, and H. Okabe. J. Chem. Phys. **36**, 605 (1962).
23. J. A. Bell. Progress in physical organic chemistry. Vol. 2. Interscience Publishers, New York. 1964. p. 1.
24. W. B. DeMore and S. W. Benson. Advances in photochemistry. Vol. 2. Interscience Publishers, New York. 1964. p. 219.
25. H. M. Frey. Chem. Ind. London, 218 (1962).
26. L. C. Jones and L. W. Taylor. Anal. Chem. **27**, 228 (1955).
27. A. F. Trotman-Dickenson. Ann. Rept. Progr. Chem. (Chem. Soc. London), **55**, 36 (1958).
28. T. J. Hardwick. J. Phys. Chem. **66**, 2246 (1962).
29. C. R. Zobel and A. B. F. Duncan. J. Am. Chem. Soc. **77**, 2611 (1955).
30. G. R. Cook and B. K. Ching. J. Chem. Phys. **43**, 1794 (1965).
31. P. Pringsheim. Fluorescence and phosphorescence. Interscience Publishers, New York. 1949.
32. R. S. Mulliken. Phys. Rev. **47**, 413 (1935).
33. W. A. Noyes, Jr. Proc. Acad. Sci. Lisbon, 3 (1964).
34. A. F. Trotman-Dickenson. Gas kinetics. Butterworths, London. 1955. Chap. 4.
35. V. N. Kondrat'ev. Chemical kinetics of gas reactions. Engl. transl. Addison-Wesley Publishing Co., Inc., Reading, Mass. 1964. Chap. 4.
36. W. Fielding and H. O. Pritchard. J. Phys. Chem. **66**, 821 (1962).
37. E. C. Lim. J. Chem. Phys. **36**, 3497 (1962).
38. A. K. Basak, G. P. Semeluk, and I. Unger. J. Phys. Chem. **70**, 1337 (1966).

Can. J. Chem. Downloaded from www.nrcresearchpress.com by 210.87.254.42 on 09/05/12
For personal use only.

THE REACTION OF METHANESULFONIC ACID WITH SULFUR TRIOXIDE

E. A. ROBINSON AND V. SILBERBERG
Lash Miller Chemical Laboratories, University of Toronto, Toronto, Ontario
Received December 14, 1965

ABSTRACT

The reaction of sulfur trioxide with methanesulfonic acid has been studied by examination of the nuclear magnetic resonance (n.m.r.) and Raman spectra of solutions containing up to 0.8 stoichiometric mole fraction of SO_3.

At relatively low SO_3 concentrations the polysulfonic acid $CH_3S_2O_6H$ is formed initially and reacts with excess methane sulfonic acid to give methanesulfonic anhydride.

$$CH_3S_2O_6H + CH_3SO_3H \rightleftharpoons (CH_3)_2S_2O_5 + H_2SO_4$$

$CH_3S_2O_6H$ and CH_3SO_3H exchange protons and SO_3 rapidly and a single methyl resonance peak only is observed for these species in the n.m.r. spectrum. A separate methyl resonance is observed for $(CH_3)_2S_2O_5$ at relatively low concentrations of SO_3, but at higher concentrations the peak merges with that due to CH_3SO_3H and $CH_3S_2O_6H$ because of the rapid equilibration of $(CH_3)_2S_2O_5$ with $H_2S_2O_7$.

$$(CH_3)_2S_2O_5 + H_2S_2O_7 \rightleftharpoons 2CH_3S_2O_6H$$

At higher concentrations of SO_3 it is likely that the system contains polymers of the three series $CH_3S_{n+1}O_{3n+3}H$, $(CH_3)_2S_{n+2}O_{3n+5}$, and $H_2S_{n+1}O_{3n+4}$ in rapid equilibrium. Free SO_3 is not found in the system at concentrations less than 60 mole %.

INTRODUCTION

In previous work it was shown that, at room temperature, solutions of sulfur trioxide in sulfuric acid, fluorosulfuric acid, or chlorosulfuric acid, contain the corresponding polysulfuric acids (1, 2).

$$H_2SO_4 + nSO_3 \rightleftharpoons H_2S_{n+1}O_{3n+4}$$

$$HSO_3F + nSO_3 \rightleftharpoons HS_{n+1}O_{3n+3}F$$

$$HSO_3Cl + nSO_3 \rightleftharpoons HS_{n+1}O_{3n+3}Cl$$

With the H_2SO_4–SO_3 system direct evidence was obtained for the formation of $H_2S_2O_7$ and $H_2S_3O_{10}$ by comparison of the Raman spectra with the spectra of the isoelectronic polysulfuryl fluorides $S_2O_5F_2$ and $S_3O_8F_2$, and detailed examination of the spectra provided strong support for the formation of $H_2S_4O_{13}$ and higher polysulfuric acids (1). Similarly for the HSO_3F–SO_3 and HSO_3Cl–SO_3 systems evidence was obtained from the Raman spectra for the formation of HS_2O_6F, HS_3O_9F, HS_2O_6Cl, HS_3O_9Cl, and higher polyacids (2). The fluorine nuclear magnetic resonance (n.m.r.) spectra of solutions of SO_3 in fluorosulfuric acid were also investigated. A single ^{19}F resonance only was observed which shifted to lower field as the concentration of SO_3 was increased and which was attributed to the rapid exchange of protons and SO_3 between the various polyacids $HS_{n+1}O_{3n+3}F$ (2). Addition of polysulfuryl fluorides, such as $S_2O_5F_2$ or $S_3O_8F_2$, to solutions of SO_3 in HSO_3F gave additional fluorine resonances in the n.m.r. spectra, and there was no evidence for any exchange between the polysulfuryl fluorides and the fluoro-polysulfuric acids. Thus it was clear that polysulfuryl fluorides were not present in the HSO_3F–SO_3 system at room temperature. However, when sulfuric acid and fluorosulfuric acid were heated to 100 °C in sealed tubes for several hours the n.m.r. measurements showed that polysulfuryl fluorides $S_nO_{3n-1}F_2$ (with n at least as high as 7) were formed.

Can. J. Chem. Downloaded from www.nrcresearchpress.com by 210.87.254.105 on 09/05/12
For personal use only.

In recent work van Wazer and his co-workers (3) have shown that dimethylsulfate and SO_3 react to give a liquid mixture of methoxy-terminated polysulfates, $CH_3O(SO_3)_nCH_3$, where n has values at least as high as 9. For each species a separate line was observed in the n.m.r. spectrum.

Complex formation between organic sulfonic acids and SO_3 was first postulated by Vicary and Hinshelwood (4) who found that the rate of sulfonation of nitrobenzene by sulfur trioxide was explicable if a 1:1 complex was postulated. Later work by Wadsworth and Hinshelwood (5) gave evidence that similar complexes are probably formed between the sulfonic acids of *p*-nitrotoluene and chlorobenzene, respectively, and SO_3.

The Raman spectrum of a solution of SO_3 in methanesulfonic acid has been examined previously by Sandeman (6) who compared the spectrum with those of solutions of SO_3 in sulfuric acid. He concluded that a complex acid, $CH_3S_2O_6H$, with structure similar to that of $H_2S_2O_7$ is formed. Sandeman also examined the phase diagram of the CH_3SO_3H–SO_3 system and obtained a freezing point maximum at the composition 21% SO_3 by weight. He assumed that this was due to a complex in which two molecules of methanesulfonic acid are hydrogen bonded to each $CH_3S_2O_6H$ molecule.

The present results are interpreted to show that both the polyacid $CH_3S_2O_6H$ and methanesulfonic anhydride, $(CH_3)_2S_2O_5$, are formed at low concentrations of SO_3 and the anhydride exchanges only slowly with the other components of the system under these conditions. At higher concentrations of SO_3 the anhydride is in rapid equilibrium with $H_2S_2O_7$ and higher polysulfuric acids which result from the reaction of SO_3 with the sulfuric acid formed in [2].

At very high concentrations of SO_3 it is probable that polysulfuryl compounds of the series $CH_3S_{n+1}O_{3n+3}H$, $H_2S_{n+1}O_{3n+4}$, free SO_3, and perhaps $(CH_3)_2S_{n+2}O_{3n+5}$ are in equilibrium.

RESULTS AND DISCUSSION

The results of the n.m.r. studies interpolated at round concentrations from large scale plots of the data are shown in Table I, and Figs. 1 and 2 show the original measurements. All chemical shifts are shown in c.p.s. relative to external tetramethylsilane.

Nuclear Magnetic Resonance Spectra

Whereas in the methylsulfate–SO_3 system van Wazer and co-workers (3) observed methyl resonances due to each of the species $CH_3O(SO_3)_nCH_3$, $9 \geqslant n \geqslant 1$, in the CH_3SO_3H–SO_3 system only two methyl resonance peaks were observed at concentrations less than 36 mole % SO_3. At SO_3 concentrations greater than this the two peaks collapsed to a single peak.

Pure methanesulfonic acid has its methyl resonance at 186.5 c.p.s. (relative to tetramethylsilane). On addition of SO_3 this peak gradually shifts to lower field with increasing concentration of SO_3. In the most dilute solution studied (4.35 mole % SO_3) the peak was at 187.8 c.p.s. A second peak was found in the spectrum of this solution, in the methyl region, at 202.4 c.p.s. This can be reasonably attributed to the methyl resonance of methanesulfonic anhydride since a dilute solution of $(CH_3)_2S_2O_5$ in methanesulfonic acid gave a single methyl resonance peak at 202.0 c.p.s. in addition to the methyl resonance peak of the acid. These resonances were observed immediately on mixing (in less than ca. 5 min) and were unchanged after several days. Furthermore the peak widths at half height were less than 1 c.p.s. Moreover it has been shown (E. A. Robinson, unpublished results) by cryoscopic and conductimetric measurements that $(CH_3)_2S_2O_5$ behaves as a nonelectrolyte in CH_3SO_3H, and a solution of the anhydride in chloroform gave a single

Can. J. Chem. Downloaded from www.nrcresearchpress.com by 210.87.254.105 on 09/05/12
For personal use only.

TABLE I

Nuclear magnetic resonance spectra of solutions of sulfur trioxide and methanesulfonic acid

Mole % SO_3	Chemical shifts, c.p.s.†				
	$CH_3(1)$		$CH_3(2)$	—OH	R*
0	186.5		(202.0)	628.5	—
2	187.2		—	629.0	0.05
4	187.8		202.4	629.0	0.10
6	188.2		203.2	629.2	0.15
8	189.0		203.8	629.4	0.19
10	189.6		204.4	629.6	0.24
14	191.0		205.2	630.0	0.34
18	192.4		205.8	630.8	0.44
22	194.0		206.2	632.0	0.54
26	195.8		206.3	633.4	0.64
30	198.0		206.2	635.6	0.73
34	201.0		206.0	638.0	0.82
36	202.8		205.4	638.8	—
37		203.6		639.0	—
38		204.2		638.8	—
40		205.2		638.4	—
45		207.8		636.6	—
50		209.4		634.0	—
55		211.0		631.0	—
60		212.2		628.0	—
65		213.2		625.0	—
70		214.0		619.0	—
80		215.6		608.0	—

*R = ratio of areas of $CH_3(2)$ and $CH_3(1)$ peaks = $\frac{1}{2}[(CH_3)_2S_2O_5]:([CH_3SO_3H] + [CH_3S_2O_6H])$.
†Relative to external tetramethylsilane, uncorrected for changes in diamagnetic susceptibilities.

methyl resonance at 203.0 c.p.s. (relative to internal tetramethylsilane). Thus it appears that SO_3 reacts rapidly with CH_3SO_3H to give methanesulfonic anhydride.

The shift of the methyl resonance of CH_3SO_3H to lower field (curve A, Fig. 1*a*), and the shift of the acid proton (Fig. 1*b*), which is reminiscent of the behavior of the proton resonance in the HSO_3F–SO_3, HSO_3Cl–SO_3, and H_2SO_4–SO_3 systems (1, 2), is consistent with the simultaneous formation of the polyacid $CH_3S_2O_6H$. This suggests that the initial reaction of SO_3, at low concentrations, is to give $CH_3S_2O_6H$,

[1] $$CH_3SO_3H + SO_3 \rightleftharpoons CH_3S_2O_6H,$$

and that methanesulfonic anhydride is formed as a result of the reaction

[2] $$CH_3S_2O_6H + CH_3SO_3H \rightleftharpoons (CH_3)_2S_2O_5 + H_2SO_4.$$

A single methyl resonance only is observed for the acid species CH_3SO_3H and $CH_3S_2O_6H$, which shows that there is rapid exchange of protons and of SO_3 between them. The separate peak that is observed for the anhydride implies that the equilibrium established in [2] leads to only very slow exchange of the species involved.

On further addition of SO_3 to the system the resonance peak attributed to $(CH_3)_2S_2O_5$ ($CH_3(2)$) shifts *slightly* to lower field. It is at 205.4 c.p.s. in a solution containing 36 % SO_3. It would thus seem likely that the higher anhydrides, $(CH_3)_2S_3O_8$, $(CH_3)_2S_4O_{11}$, etc., are formed in the system by comparison with, for example, the $(CH_3O)_2SO_2$–SO_3 system where the following approximate shifts were observed: $(CH_3O)_2S_2O_5$, 247.5 c.p.s.; $(CH_3O)_2S_3O_8$, 252.0 c.p.s.; and $(CH_3O)_2S_4O_{11}$, 254.1 c.p.s. (3). Over the same concentration range the lower field methyl resonance peak ($CH_3(1)$) shifts towards that of the anhydride. At 36 mole % SO_3 it is at 202.8 c.p.s. The shift in the $CH_3(1)$ resonance peak is consistent with

Can. J. Chem. Downloaded from www.nrcresearchpress.com by 210.87.254.105 on 09/05/12
For personal use only.

the formation of $CH_3S_2O_6H$, and perhaps higher polyacids which exchange protons and SO_3 rapidly among themselves but *not* with the polyanhydrides. (Both the $CH_3(1)$ and the $CH_3(2)$ resonance peaks remain sharp up to 36 % SO_3.) However, on the basis of the above interpretation exchange of SO_3 between the methyl-polysulfuric acids and the polyanhydrides would certainly have been expected since they must exchange rapidly among themselves. It must therefore be concluded that the obvious interpretation of the results is incorrect and an alternative explanation must be sought.

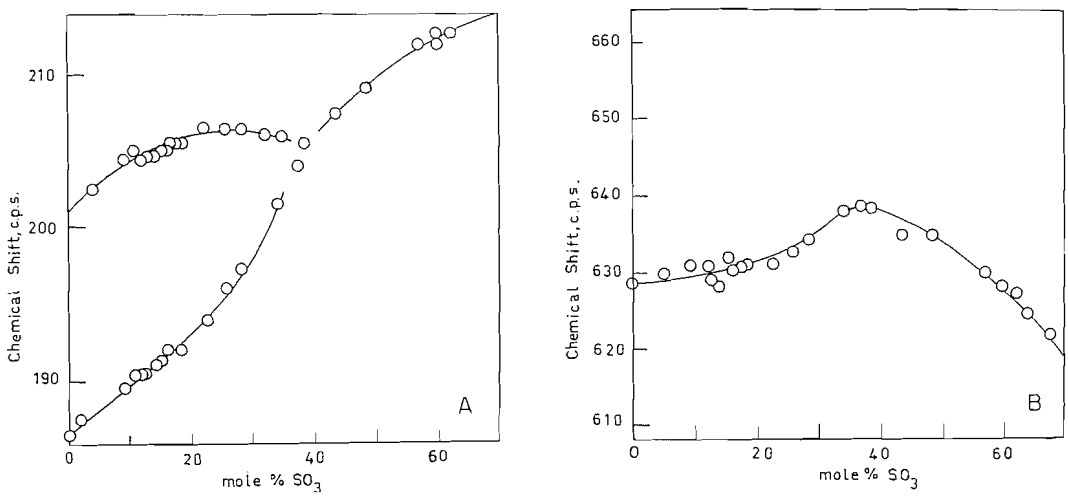


FIG. 1. Nuclear magnetic resonance shifts: (*a*) CH_3 protons, (*b*) —OH protons.

New evidence comes from the Raman spectra (see later) which significantly do not show the distinctive pattern of two lines in the 700 cm^{-1} region characteristic of the formation of a trisulfuryl compound (1) until the composition 40.2 % SO_3 is reached. Thus it would appear that trisulfuryl compounds are not present at lower concentrations in any appreciable amounts.

The difficulty appears to arise from the impossibility of using tetramethylsilane as an internal reference in this system because of its reaction.* Thus the chemical shifts quoted in Table I are uncorrected for changes in the diamagnetic susceptibilities of the solutions. Whereas the $CH_3(1)$ peak shifts quite rapidly to low field on the addition of SO_3, that due to $CH_3(2)$ shifts only very slowly to low field and indeed shows the reverse trend near 36 mole % SO_3 (Fig. 1*a*). It thus seems probable that $CH_3(2)$ is due solely to $(CH_3)_2S_2O_5$ and that its apparent shift is illusory. Indeed if we assume that this is so, and use $CH_3(2)$ as an internal reference from which to measure $CH_3(1)$ shifts, the results are explicable in terms of an equilibrium between CH_3SO_3H, $CH_3S_2O_6H$, $(CH_3)_2S_2O_5$, and H_2SO_4 at concentrations less than 36 mole % SO_3.

If reaction [1] followed by reaction [2] were the only reactions occurring then R (the ratio of the areas of the $CH_3(2)$ and $CH_3(1)$ peaks) would be expected to change as in curve A (Fig. 2). Only at low SO_3 concentrations are the results consistent with this model which supports writing reaction [2] as an equilibrium. If we assume that all the SO_3 in the system reacts with CH_3SO_3H to give $CH_3S_2O_6H$ which is then partly converted to $(CH_3)_2S_2O_5$ the value of R can then be used to calculate the concentrations of the species in the system (Table II). These give a value for the equilibrium constant of reaction [2] of 0.6 ± 0.1.

**Methanesulfonyl fluoride was found to be equally unsuitable.*

Can. J. Chem. Downloaded from www.nrcresearchpress.com by 210.87.254.105 on 09/05/12
For personal use only.

TABLE II

Calculation of the equilibrium constant for eq [2] (*A*) and the chemical shift of $CH_3S_2O_6H$ (*B*)

(*A*) Calculation of the equilibrium constant for eq. [2]

$[SO_3]_s$*	$[CH_3SO_3H]_s$*	*R*†	$[(CH_3)_2S_2O_5]$	$[CH_3SO_3H]$	$[CH_3S_2O_6H]$	$[H_2SO_4]$	*K*‡
5	95	0.12	5.0	84.8	0.0	5.0	—
10	90	0.24	8.7	72.3	1.3	8.7	0.8
15	85	0.36	11.2	58.7	3.7	11.2	0.6
20	80	0.48	13.0	47.0	7.0	13.0	0.5
25	75	0.60	14.1	35.9	10.9	14.1	0.5
30	70	0.72	14.6	25.3	15.3	14.6	0.6
35	65	0.84	14.8	15.1	20.2	14.8	0.7
						Mean	0.6±0.1

(*B*) Chemical shift of $CH_3S_2O_6H$

$[SO_3]_s$	Chemical shift§	$(\delta - \delta_1)$	*M*‖	$M(\delta - \delta_1)$	$[CH_3S_2O_6H]$
5	186.7	0.2	84.8	18.0	0.0
10	187.2	0.7	72.6	50.3	1.3
15	187.8	1.2	62.5	77.8	3.7
20	189.1	2.6	54.0	140.4	7.0
25	190.9	4.4	49.9	219.6	10.9
30	193.8	7.3	40.7	297.1	15.3
35	198.5	12.0	35.3	423.6	20.2

*Stoichiometric concentrations [ ]$_s$; all concentrations in mole %.
†Ratio of areas of $CH_3(2)$ and $CH_3(1)$ peaks = $\frac{1}{2}[(CH_3)_2S_2O_5]:([CH_3SO_3H] + [CH_3S_2O_6H])$.
‡$K = [(CH_3)_2S_2O_5][H_2SO_4]/[CH_3SO_3H][CH_3S_2O_6H]$.
§Relative to $(CH_3)_2S_2O_5$.
‖$[CH_3SO_3H] + [CH_3S_2O_6H]$.

The chemical shifts for $CH_3(1)$ measured from $CH_3(2)$ are shown in Table II. If $CH_3(1)$ is due solely to the exchange between CH_3SO_3H and $CH_3S_2O_6H$, then we can write

$$[3] \qquad [CH_3SO_3H]\delta_1 + [CH_3S_2O_6H]\delta_2 = ([CH_3SO_3H] + [CH_3S_2O_6H])\delta,$$

which is more conveniently expressed as

$$[4] \qquad ([CH_3SO_3H] + [CH_3S_2O_6H])(\delta - \delta_1) = [CH_3S_2O_6H](\delta_2 - \delta_1),$$

where δ is the observed chemical shift, δ_1 is the chemical shift of CH_3SO_3H, and δ_2 is the chemical shift of $CH_3S_2O_6H$ (all shifts relative to that of $(CH_3)_2S_2O_5$ at 202.0 c.p.s.). Thus a plot of the left-hand side of eq. [4] versus $[CH_3S_2O_6H]$ should be a straight line with slope equal to $(\delta_2 - \delta_1)$. The data is shown in Table II and is plotted in Fig. 3. It gives a good straight line with a slope of 21 c.p.s., i.e. $\delta_2 = 207.5$ c.p.s. The magnitude of this chemical shift seems reasonable by comparison with those of the CH_3 groups in CH_3SO_3H, 186.5; $CH_3SO_2CH_3$, 178.0; and $(CH_3)_2S_2O_5$, 202.0 c.p.s. Thus below 36 mole % SO_3 it seems very likely the CH_3SO_3–SO_3 system contains principally the species CH_3SO_3H, $CH_3S_2O_6H$, $(CH_3)_2S_2O_6$, and H_2SO_4 in equilibrium.

At 37 mole % SO_3 the $CH_3(1)$ and $CH_3(2)$ peaks collapse into a single broad peak which continues to shift to lower field as the concentration of SO_3 increases. Clearly some additional species is now present which enables the exchange process between $CH_3S_2O_6H$ and $(CH_3)_2S_2O_5$ to become rapid. The most likely species is $H_2S_2O_7$ formed by the reaction of SO_3 with the H_2SO_4 resulting from reaction [2], i.e.

$$[5] \qquad (CH_3)_2S_2O_5 + H_2S_2O_7 \rightleftharpoons 2CH_3S_2O_6H.$$

Above 40 mole % SO_3 the single CH_3 resonance becomes sharp again and continues to move to lower field, showing that exchange is now rapid. It can probably now be attributed

Can. J. Chem. Downloaded from www.nrcresearchpress.com by 210.87.254.105 on 09/05/12
For personal use only.

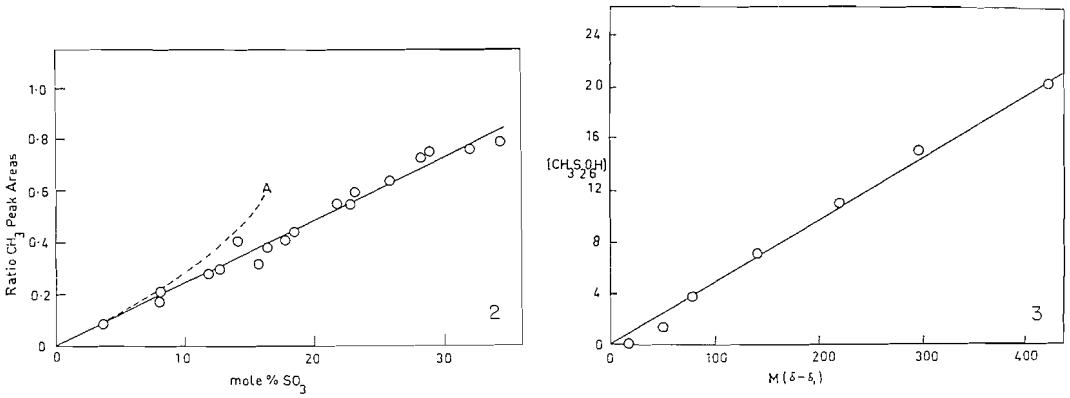


FIG. 2. Ratio of areas (R) of high- and low-field CH_3 peaks.
FIG. 3. Chemical shift plot to give $\delta_{CH_3S_2O_6H}$.

to a mixture of polyacids, $CH_3S_{n+1}O_{3n+3}H$, and polyanhydrides, $(CH_3)_2S_{n+2}O_{3n+5}$, in rapid equilibrium with each other and with polysulfuric acids, $H_2S_{n+1}O_{3n+4}$.

When samples were heated to 100 °C for several hours no change occurred in their n.m.r. spectra.

Raman Spectra

The above conclusions are supported by an analysis of the Raman spectra of solutions of SO_3 in CH_3SO_3H (Table III).

Sandeman (6) compared the Raman spectrum of a mixture of composition $3CH_3SO_3H$-SO_3 to that of disulfuric acid and showed that the spectra were similar in many respects. He claimed that these similarities support the proposal that $CH_3S_2O_6H$ is formed in the system. However, since many of the features of the spectra of $CH_3S_2O_6H$, structure I, and methanesulfonic anhydride, structure II, are expected to be similar a very careful examination of the results is necessary in order to unambiguously determine the nature of the products of the reaction.



I II

No evidence was found in the present work for the complex $CH_3S_2O_6H.2CH_3SO_3H$.

In the most dilute SO_3 solution studied (9.5 mole % SO_3) (Table III), new Raman lines were observed at 150, 263, 310, 370, 567, 661, 798, 890, 913, 1 200, 1 230, 1 380, and 2 775 cm^{-1} in addition to the frequencies of methanesulfonic acid. The new lines are to be compared with lines in the Raman spectrum of methanesulfonic anhydride (ref. 7 and E. A. Robinson, unpublished results) at 264, 308, 359, 572, 664, 800, 886, 1 209, and 1 384 cm^{-1}, and clearly show that this species is formed in the CH_3SO_3H–SO_3 system. The additional lines at 913, 1 230, and 2 775 cm^{-1} may probably be attributed to the polyacid $CH_3S_2O_6H$: 913 cm^{-1}, S—OH stretch; 1 230 cm^{-1}, SO_2 symmetric stretch; 2 775 cm^{-1}, C—H stretch. Many of the frequencies attributed to $(CH_3)_2S_2O_5$ are also doubtlessly common to $CH_3S_2O_6H$.

Can. J. Chem. Downloaded from www.nrcresearchpress.com by 210.87.254.105 on 09/05/12
For personal use only.

TABLE III

The Raman spectra of solutions of SO_3 in methanesulfonic acid* (frequencies in cm^{-1})

Mole % SO_3							
0	9.5	25.7	40.2	61.0	88.9	SO_3	$(CH_3)_2S_2O_5$†
—	150(1/2)	148(1/2)	148(1)	150(1)	—	147	—
—	—	—	175(1)	170(1)	165(1)	—	—
—	—	—	230(1/2)	231(1)	230(1)	—	—
—	263(1/2)	263(2)	266(4)	266(3)	265(1)	243	264(3)
—	—	—	—	—	288(5)	290	—
—	310(1/2)	308(2)	311(5)	303(6)	315(3)	—	308(4)
338(4)	335(4)	330(3)	329(3)	—	—	322	339(2)
—	370(1/2)	370(1)	369(1)	369(2)	370(5)	368	359(2)
480(2)	480(2)	482(1)	481(2)	478(3)	483(2)	480	457/77(1)
506(3)	504(3)	507(3)	512(4)	510(5)	504(3)		510(4)
535(5)	535(5)	535(3)	535(2)	540(1)	529(6)	534	537(4)
—	567(1/2)	564(1)	569(2)	—	545(1)	560	572(0)
—	—	—	—	—	640(4)	657	612(0)
—	661(1)	661(2)	661(2)	661(2)	664(5)	665	664(4)
—	690(1/2)	696(1)	695(2)	695(4)	—	698	—
—	—	—	735(1/2)	732(2)	735(1)	—	—
772(7)	770(7)	767(5)	768(3)	770(1)	765(6)	773	774(5)
—	798(1/2)	795(2)	795(2)	798(2)	—	—	800(2)
—	890(2)	880(1)	890(2)	—	887(2)	860	886(0)
904(3)	898(2)	900(2)	—	—	—	—	—
—	913(1/2)	913(2)	910(2)	910(2)	—	—	—
—	—	—	955(1)	950(2)	—	—	—
985(1)	990(1)	996(2)	997(3)	994(1/2)	993(2)	—	996(4)
—	—	—	—	—	1 007(1)	1 018	—
—	—	—	—	1 075(1/2)	1 070(7)	1 070	1 070(1/2)
1 123(4)	1 138(5)	1 145(2)	1 145(1)	—	1 135(2)	1 162	1 148(3)
1 174(2)	1 179(3)	1 163(2)	1 160(2)	1 170(2)	—	—	1 186(4)
—	1 200(1)	1 200(4)	1 200(6)	1 202(6)	1 200(1)	—	1 209(5)
—	1 230(1/2)	1 230(1)	1 225(3)	1 225(6)	1 222(2)	1 231	—
—	—	—	1 240(1)	1 240(2)	1 253(5)	—	—
1 265(1)	1 270(1/2)	—	—	—	1 270(5)	1 271	1 272(0)
1 350(2)	1 346(1)	1 340(1)	1 340(1)	1 337(1)	1 337(1)	—	—
—	—	—	—	—	1 360(2)	—	—
—	1 380(1)	1 376(2)	1 390(1)	1 380(1/2)	1 393(5)	1 390	1 384(3)
1 420(4)	1 420(4)	1 415(3)	1 416(2)	1 423(1)	1 433(1)	—	1 430(4)
—	—	1 450(1/2)	1 460(1)	1 470(1)	1 456(1)	—	—
—	—	—	—	—	1 489(3)	1 489	—
—	—	—	—	—	—	1 515	—
—	2 775(1)	2 765(6)	2 760(6)	2 765(4)	2 777(3)	—	—
—	—	2 486(1)	2 840(1)	2 850(1)	2 857(1/2)	—	—
2 945(6)	2 948(6)	2 922(5)	2 910(5)	2 925(5)	2 932(5)	—	2 948(6)
3 015(1)	3 020(2)	3 010(2)	3 020(1)	3 017(1)	3 019(1)	—	—
3 030(4)	3 035(4)	3 020(3)	3 035(4)	3 030(4)	3 035(4)	—	3 035(5)

*Relative intensities in parenthesis.
†Robinson and Silberberg, unpublished experiments.

Additional lines appear in the spectrum of the 25.9 mole % SO_3 solution at 564, 1 450, and 2 846 cm^{-1} and in the spectrum of the 40.2 mole % SO_3 solution at 175, 230, 735, 955, and 1 240 cm^{-1}. The appearance of two lines near 700 cm^{-1} (695 and 735 cm^{-1}) is diagnostic of a trisulfuryl compound, and additional low frequency lines (cf. 170 and 230 cm^{-1}) are also expected for such a species (1). The absorption at 950 cm^{-1} can probably be assigned to the S—OH stretching frequency of $CH_3S_3O_9H$ and 1 240 and 1 460 cm^{-1} to the SO_2 symmetric and asymmetric stretching frequencies of this species.

In the 60.1 mole % SO_3 solution a very sharp line, which is diagnostic of SO_3 monomer (1), appears weakly at 1 075 cm^{-1} and shows that monomeric SO_3 is present in low concentration. There is no evidence that free SO_3 is present in any of the solutions of lower concentration. The spectrum of the 88.9 mole % SO_3 solution is complex and shows many

Can. J. Chem. Downloaded from www.nrcresearchpress.com by 210.87.254.105 on 09/05/12
For personal use only.

additional lines that are diagnostic of SO_3 monomer and trimer (1). Presumably polymers higher than $CH_3S_2O_6H$ and $(CH_3)_2S_2O_5$ are present at relatively high mole % SO_3 since the lines assigned to the SO_2 stretching frequencies gradually move to higher frequencies (1 253 and 1 433 cm^{-1} in 88.9 mole % SO_3) (1).

EXPERIMENTAL

Sulfur trioxide was obtained by distillation of Sulphan B (Allied Chemical Corporation).

Methanesulfonic acid, m.p. 19.85 °C, was prepared by distillation of the commercial acid under reduced pressure followed by equilibration of the slightly aqueous acid so obtained with methanesulfonic anhydride.

Methanesulfonic anhydride, m.p. 70 °C, was obtained by dehydration of methanesulfonic acid. CH_3SO_3H and thionyl chloride were refluxed together for several hours and the excess thionyl chloride distilled off. The anhydride was recrystallized from anhydrous ether (8).

All the CH_3SO_3H–SO_3 solutions were made up by weight and they were handled in a dry box. Nuclear magnetic resonance measurements were performed at 35 °C on tightly stoppered samples with a Varian A-60 spectrometer. The Raman spectra were recorded photographically with a Hilger E 612 spectrometer in conjunction with a Toronto mercury arc lamp. The spectra were measured by comparison with a standard iron arc by means of a Joyce Loebl microdensitometer.

ACKNOWLEDGMENTS

Professor R. J. Gillespie and Mr. J. Bacon of McMaster University are thanked for helpful discussions, and the latter for his technical assistance in preliminary measurements.

We are indebted to the National Research Council of Canada, the Ontario Research Foundation, the Allied Chemical Corporation, and the University of Toronto for financial assistance.

REFERENCES

1. R. J. GILLESPIE and E. A. ROBINSON. Can. J. Chem. **40**, 658 (1962).
2. R. J. GILLESPIE and E. A. ROBINSON. Can. J. Chem. **40**, 675 (1962).
3. J. R. VAN WAZER, D. GRANT, and C. DUNGAN. J. Am. Chem. Soc. **87**, 3333 (1965).
4. D. R. VICARY and C. N. HINSHELWOOD. J. Chem. Soc. 1372 (1939).
5. K. D. WADSWORTH and C. N. HINSHELWOOD. J. Chem. Soc. 469 (1944).
6. I. SANDEMAN. J. Chem. Soc. 1135 (1953).
7. A. SIMON and H. KRIEGSMANN. Chem. Ber. **89**, 2378 (1956).
8. L. N. OWEN and S. P. WHITELAW. J. Chem. Soc. 3723 (1953).

Can. J. Chem. Downloaded from www.nrcresearchpress.com by 210.87.254.105 on 09/05/12
For personal use only.

Can. J. Chem. Downloaded from www.nrcresearchpress.com by 210.87.254.6 on 09/05/12
For personal use only.

KINETICS OF THE ABSTRACTION OF HYDROGEN ATOMS FROM HYDROGEN SULFIDE BY TRIFLUOROMETHYL RADICALS

N. L. ARTHUR AND T. N. BELL
Department of Physical and Inorganic Chemistry, University of Adelaide, South Australia
Received January 27, 1966

Trifluoromethyl radicals generated from the photolysis of hexafluoroacetone abstract hydrogen atoms from hydrogen sulfide.

$$CF_3 + H_2S \rightarrow CF_3H + SH$$

The rate constant of this reaction measured by comparing the rate with that for the recombination of trifluoromethyl radicals ($k = 2.3 \times 10^{13}$ cc mole^{-1} s^{-1}) is given by,

$$k = 10^{11.65\pm0.16}\, e^{-(3880\pm260)/RT} \text{ cc mole}^{-1}\text{ s}^{-1}.$$

INTRODUCTION

Free radicals interact rapidly with the S—H hydrogen atom of thiols, this transfer reaction being of importance in polymer chemistry. A knowledge of the rate constants of this type of reaction is of interest. The rate constant for the abstraction of hydrogen from HSH by trifluoromethyl has been measured and is compared with available information on the relevant systems, CH_3–HBr (2), CF_3–HBr (3), CH_3–HSH (4, 5), where the bond being attacked in the substrate molecule has similar properties.

EXPERIMENTAL

Materials

(*a*) Hydrogen sulfide, generated from ferrous sulfide and sulfuric acid, was fractionated through traps at −78°, −96°, −145°, and −196°. The fraction collecting at −145° was thoroughly degassed and stored in a blackened bulb.

(*b*) Hexafluoroacetone from a cylinder (Allied Chemical Corporation) was fractionated as above. The fraction condensing at −145° was thoroughly degassed at that temperature to remove traces of trifluoromethane and hexafluoroethane.

Apparatus

Photolysis experiments were carried out in a quartz reaction vessel (illuminated volume 173 ml) fitted with plane parallel windows which was suspended in a tubular furnace (37 cm long) fitted with quartz end windows. Radiation was through a Hanovia S500 mercury arc filtered with Corning filters, color specification 0-53 and 7-54. Light intensity was measured with an RCA 935 photocell and spot galvanometer. Temperature measurement was through six chromel–alumel thermocouples attached along the cell walls. Pressures in the reaction vessel were measured with a Pyrex spiral gauge used as a null instrument. The reaction vessel was connected through stainless steel Hoke 413 valves to the analytical and storage sections. The analytical section was fitted with Springham greaseless stopcocks.

In operation, either fresh mixtures of the two reactants or measured quantities of each reactant admitted singly were introduced into the reaction vessel. In the latter case a mixing time of 15 min was allowed.

After reaction the non-condensible products were measured in a gas burette and subsequently analyzed by gas chromatography. The condensible products were collected in a U trap, allowed to warm up, and then swept onto a ¼ in. absorption column sectioned with 30 cm alumina, 9 cm silver nitrate – ethylene glycol on firebrick, and 9 cm alumina, all 60–80 mesh. Nitrogen carrier at a flow rate 20 ml/min was used. The eluent was collected during a time of 10 min in a trap packed with glass wool. This trap was then evacuated and the eluent was transferred into a side arm, which could be sealed off ready for gas chromatographic analysis.

Using this method all reactants and products except trifluoromethane and hexafluoroethane were absorbed on the column. In the course of time two extra peaks appeared in the chromatographic analysis, at which stage hydrogen sulfide had reached the silver nitrate packing as determined by blackening of this phase. Removal of the silver nitrate packing resulted in elimination of these extra peaks whence it was concluded that a reaction between silver nitrate and hydrogen sulfide was occurring, possibly giving oxides of nitrogen. Consequently the absorption column was replaced by one consisting of alumina alone, this absorbent being sufficiently retentive to absorb the small quantities of hydrogen sulfide used.

Gas chromatographic analysis of the non-condensible fraction was carried out on a charcoal 2 m column (60–80 mesh) at 25°. Hydrogen was detected using nitrogen as carrier, and carbon monoxide was estimated with hydrogen carrier (flow rate 50 ml/min).

After the treatment described above, the condensible products were analyzed for CF_3H and C_2F_6 on an alumina column (60–80 mesh, length 1 m) with hydrogen carrier at a flow rate of 60 ml/min and temperature of 25°.

RESULTS AND DISCUSSION

The photolysis of hexafluoroacetone is described (6) by the equation

[1] $$(CF_3)_2CO \rightarrow 2CF_3 + CO,$$

the actual mass balance C_2F_6/CO being approximately 0.95 under our experimental conditions (7). The slight discrepancy may well be due to the addition of trifluoromethyl radicals to the carbonyl bond to yield $(CF_3)_3COCF_3$ (8). On the basis of the formation of trifluoroacetyl halides when hexafluoroacetone is photolyzed in the presence of bromine and chlorine, Tucker and Whittle concluded that the primary photolytic step yields the trifluoroacetyl radical (9). The instability of this radical is such, however, that in the absence of large amounts of radical scavengers, eq. [1] adequately describes the photolysis of hexafluoroacetone. The product of trifluoroacetyl radical scavenging in this work, namely trifluoroacetaldehyde, was not detected, but because of the difficulty of the analysis this does not constitute proof of the absence of this reaction.

A possible complication in the present work through the photolysis of hydrogen sulfide was considered; accordingly, hydrogen sulfide at 14 mm and 95° was photolyzed for 45 min with the filtered radiation used in the rate determinations. No hydrogen was detected; hence the photolysis of hydrogen sulfide may be ignored.

Experiments wherein hydrogen sulfide (1 mm) and hexafluoroacetone (39 mm) were heated for 9 min at 94°, were carried out to check for a possible dark reaction. Analyses for CO, C_2F_6, and CF_3H proved negative.

The volatile products from the photolysis of HFA/H_2S mixtures were analyzed by the method outlined in the Experimental section. The non-condensible products contained hydrogen and carbon monoxide, while the volatile products passing through the alumina absorption column consisted of hexafluoroethane and trifluoromethane. The efficiency of the abstraction process was such that the hexafluoroethane only became measurable at low concentrations of hydrogen sulfide.

The observed products may be accounted for in terms of the following reactions.

[1] $$(CF_3)_2CO \xrightarrow{h\nu} 2CF_3 + CO$$

[2] $$2CF_3 \rightarrow C_2F_6$$

[3] $$CF_3 + H_2S \rightarrow CF_3H + SH$$

[4a] $$SH + SH \nearrow H_2 + S_2$$

[4b] $$SH + SH \searrow H_2S + S$$

Darwent and Roberts (10), from work on the photolysis of hydrogen sulfide, concluded that $k_{4a}/k_{4b} \sim 0.15$.

The expected mass balance,

$$CO = \tfrac{1}{2}CF_3H + C_2F_6,$$

is seen from Table I not to hold, there being a deficiency of CF_3 radicals of some 18%. The formation of $(CF_3)_3COCF_3$ cannot account for this deficiency, but the efficiency of reaction [3] will lead to the formation of a relatively large number of SH radicals. Thus the occurrence of a hetero radical recombination step is highly probable.

Can. J. Chem. Downloaded from www.nrcresearchpress.com by 210.87.254.6 on 09/05/12
For personal use only.

TABLE I

Photolysis of hexafluoroacetone with hydrogen sulfide

T (°C)	Photolysis time (min)	P (mm)		Rate of formation (10^4 μmole/min)				Log $k_3/k_2^{\frac{1}{2}}$
		H_2S	$(CF_3)_2CO$	CO	H_2	C_2F_6	CF_3H	
63	12	0.91	38.9	nm*	nm	3.2	224	2.447
73	12	0.92	40.6	nm	nm	6.3	359	2.522
73.5	15	1.05	44.0	nm	nm	6.9	419	2.510
81.5	15	1.05	44.0	329	27	8.6	538	2.579
87.5	9	1.05	43.7	392	30	11.0	623	2.596
99	6	1.00	42.4	nm	nm	7.7	625	2.716
100.5	9	1.05	43.8	476	8	10.0	737	2.698
100.5	6	1.04	43.6	433	17	9.3	658	2.678

*nm = not measured.

[5] $$CF_3 + SH \rightarrow CF_3SH$$

If reaction [5] plays a significant part in the reaction scheme, the expected mass balance is given by,

$$CO = \tfrac{1}{2}CF_3H + C_2F_6 + \tfrac{1}{2}CF_3SH,$$

which would account for $CO > \frac{1}{2}CF_3H + C_2F_6$ in these experiments.

If the CF_3H and C_2F_6 arise solely from [2] and [3] then,

$$k_3/k_2^{1/2} = R_{CF_3H}/R_{C_2F_6}^{1/2}[H_2S].$$

Thus measurement of R_{CF_3H} and $R_{C_2F_6}$ leads to a determination of $k_3/k_2^{1/2}$. In the absence of data to the contrary, it is assumed that the disproportionation reaction corresponding to [5] can be neglected as a source of CF_3H.

The results of the rate measurements are shown in Table I. A maximum temperature of 100° and maximum pressure of hydrogen sulfide of 1 mm ensured sufficient hexafluoroethane for analysis. Even so, the % reaction based on the ratio of the amount of CF_3H formed to H_2S present was somewhat higher than normal, being 5–8%. An Arrhenius plot of log $k_3/k_2^{1/2}$ against $1/T$ is shown in Fig. 1. Evaluation of the data by the method of least

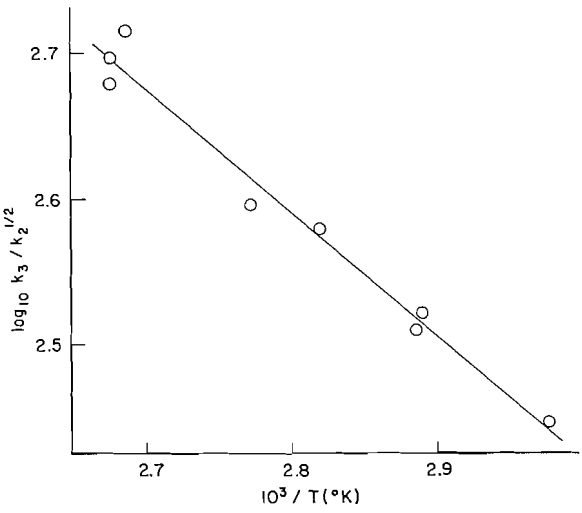


FIG. 1. Arrhenius plot of log $k_3/k_2^{1/2}$ against $1/T$.

Can. J. Chem. Downloaded from www.nrcresearchpress.com by 210.87.254.6 on 09/05/12
For personal use only.

squares leads to $E_3 - \frac{1}{2}E_2 = 3.88 \pm 0.26$ kcal mole^{-1}. Using the value of $k_2 = 2.3 \times 10^{13}$ cm^3 mole^{-1} s^{-1} derived by Ayscough (1) for the recombination of trifluoromethyl radicals, and assuming $E_2 = 0$, leads to $\log A_3 = 11.65 \pm 0.16$. Thus the rate constant for the abstraction of H atoms from H_2S by CF_3 radicals is given by,

$$k_3 = 10^{11.65 \pm 0.16}\, e^{-(3880 \pm 260)/RT} \text{ cc mole}^{-1} \text{ s}^{-1}.$$

Using a collision diameter of 5 Å for CF_3 (assumed), and 4.6 Å for H_2S (calculated), the collision number for CF_3–H_2S collisions is 2.7×10^{14} cc mole^{-1} s^{-1}. Thus a steric factor of 1.6×10^{-3} is operative for reaction [3]. This is similar to the steric factors involved in hydrogen abstraction from many organic systems, and may be considered normal.

The high rate of reaction is thus due to the low activation energy which is considerably less than that for similar reactions of hydrocarbons. The ease of removal of the S—H hydrogen is well known, and Kerr and Trotman-Dickenson (11) have estimated an activation energy range of 4.9 to 5.6 kcal for removal of this hydrogen by methyl radicals from a series of thiols (*t*-butyl to methyl).

The reaction of methyl with hydrogen sulfide is more directly comparable, and Imai and Toyama have made two determinations of this abstraction. The first (4), based on product analysis from the acetone–H_2S system, gave $k_6 = 10^{11.4}\, e^{-2600/RT}$ cc mole^{-1} s^{-1}.

[6] $$CH_3 + H_2S \rightarrow CH_4 + SH$$

The second determination (5), where acetaldehyde was photolyzed in the presence of hydrogen sulfide, may be considered less reliable in that an overall rate of reaction based on pressure change was measured. The Arrhenius parameters of [6] were determined in comparison with the abstraction of hydrogen from acetaldehyde, reaction [7].

[7] $$CH_3 + CH_3CHO \rightarrow CH_4 + CH_3CO$$

A number of determinations of [7] have been made (12) allowing a range of possible values for E_6 between 2.8 and 4.0 kcal; A_6/A_7 was given as 1.7 ± 0.5. Reasonable agreement between the values for k_6 derived from the two methods is apparent, and the values are of the same order of magnitude as that for abstraction by trifluoromethyl.

Hydrogen bromide has a bond length 1.41 Å and bond strength 88 kcal; hydrogen sulfide has a bond length 1.34 Å, but its bond strength is a matter of some conjecture, reported values being: 92 ± 2 (13*a*), 95.3 (13*b*), 89 ± 4 (13*c*), $\leqslant 90.6$ (13*d*). A figure around 90 kcal might appear reasonable in view of these results. Thus it would be in order to compare hydrogen abstraction from HBr with that from H_2S, bearing in mind the different polarity of the H—Br bond compared with the S—H bond. Dipole moments are $\mu_{HBr} = 0.78 \times 10^{18}$ e.s.u. and $\mu_{H_2S} = 1.1 \times 10^{18}$ e.s.u.; hence for the S—H component $\mu = 0.79 \times 10^{18}$ e.s.u.

Assuming that iodine atom abstraction from I_2 has zero activation energy, Tucker and Whittle (3) find an activation energy for [8] of 3 kcal,

[8] $$CF_3 + HBr \rightarrow CF_3H + Br,$$

while for the corresponding methyl reaction, Fettis and Trotman-Dickenson (2) find $E_9 = 1.4$ kcal.

[9] $$CH_3 + HBr \rightarrow CH_4 + Br$$

The order of the magnitudes of the activation energies for [8] and [9] are very similar to those for the corresponding abstractions from H_2S. Compared to hydrogen abstraction from hydrocarbons, there is an inversion of the order of activation energies for methyl and

Can. J. Chem. Downloaded from www.nrcresearchpress.com by 210.87.254.6 on 09/05/12
For personal use only.

trifluoromethyl attack. This is considered (3) to arise through the polarity of the HBr system causing a repulsion with the attacking CF_3 radical.

If $E_{CH_3-H_2S} \sim 2.6$ kcal and $E_{CF_3-H_2S} \sim 3.9$ kcal, this argument could well be applied in the H_2S system.

ACKNOWLEDGMENTS

We are grateful to the ICIANZ for a Postgraduate Fellowship to N. L. Arthur.

REFERENCES

1. P. B. Ayscough. J. Chem. Phys. **33**, 1566 (1955).
2. G. C. Fettis and A. F. Trotman-Dickenson. J. Chem. Soc. 3037 (1961).
3. B. G. Tucker and E. Whittle. Trans. Faraday Soc. **61**, 866 (1965).
4. N. Imai and O. Toyama. Bull. Chem. Soc. Japan, **33**, 652 (1960).
5. N. Imai and O. Toyama. Bull. Chem. Soc. Japan, **33**, 1120 (1960).
6. P. B. Ayscough and E. W. R. Steacie. Proc. Roy. Soc. London, Ser. A, **234**, 476 (1956).
7. A. N. Strachan, R. K. Boyd, and K. O. Kutschke. Can. J. Chem. **42**, 1345 (1964).
8. A. S. Gordon. J. Chem. Phys. **36**, 1330 (1962).
9. B. G. Tucker and E. Whittle. Trans. Faraday Soc. **61**, 484 (1965).
10. B. de B. Darwent and R. Roberts. Proc. Roy. Soc. London, Ser. A, **216**, 344 (1953).
11. J. A. Kerr and A. F. Trotman-Dickenson. J. Chem. Soc. 3322 (1957).
12. J. A. Kerr and A. F. Trotman-Dickenson. Progress in reaction kinetics. Vol. 1. The Pergamon Press, Ltd., London. 1961. p. 117.
13. (*a*) D. P. Stevenson. Trans. Faraday Soc. **49**, 867 (1953).
    (*b*) J. L. Franklin and H. E. Lumpkin. J. Am. Chem. Soc. **74**, 1023 (1952).
    (*c*) A. Sehon. J. Am. Chem. Soc. **74**, 4722 (1952). A. Sehon and B. de B. Darwent. J. Am. Chem. Soc. **76**, 4806 (1954).
    (*d*) T. F. Palmer and F. P. Lossing. J. Am. Chem. Soc. **84**, 4661 (1962).

Can. J. Chem. Downloaded from www.nrcresearchpress.com by 210.87.254.6 on 09/05/12
For personal use only.

Can. J. Chem. Downloaded from www.nrcresearchpress.com by 210.87.254.5 on 09/05/12
For personal use only.

RELATION BETWEEN ELECTRONS AND HOLES, AND THE VECTOR-COUPLING COEFFICIENTS FOR $p^m f^q$ AND $d^n f^q$ CONFIGURATIONS

GULZARI L. MALLI
Department of Chemistry, University of Alberta, Edmonton, Alberta
Received January 25, 1966

ABSTRACT

The electrostatic energy of an atomic state arising from a configuration involving holes differs by ΔW from the energy expression of the same state arising from the configuration involving electrons where ΔW can be expressed in terms of Slater's integrals.

General formulas for ΔW are given for the $p^m f^q$ and $d^n f^q$ configurations. In addition, the vector-coupling (VC) coefficients useful for atomic self-consistent field (SCF) calculations are presented for all the states arising from the $p^m f^q$ and $d^n f^q$ configurations.

THEORETICAL DEVELOPMENT

Shortley (1) has shown that, aside from an array of coefficients common to the entire configuration, the energy expression of a state belonging to the configuration $l^{4l+2-N} l'^{4l'+2-N'}$ (involving holes) is given by the same equation as that for the *same* state arising from the configuration $l^N l'^{N'}$ (involving electrons); where N and N' are the number of electrons (occupation numbers) in the (nl) and (n'l') shells respectively.

In a previous publication (2) general formulas were given for these arrays of coefficients for atomic configurations consisting of all the possible combinations of s, p, and d shells, and for a single f shell.

In this section, we give the general formulas for any combination of p and f shells, and d and f shells. The necessity for considering the pf and df shells arises from the observation of Condon and Shortley (3) that 4f6p and 4f5d configurations occur for La(II).

For general theoretical development and notation we refer the reader to the previous publication (2).

For brevity, if we consider an atomic configuration then the energy expression of an atomic state (4) ^{2S+1}L is expressed as

$$E(^{2S+1}L) = E_{\text{Core}} + E_{\substack{\text{Core}\\ \text{open}}} + E_{\text{O}} + W(^{2S+1}L). \qquad [1]$$

$W(^{2S+1}L)$ is the only term which distinguishes the various states arising from the same configuration. Expressions for all the terms are given in the previous publication (2).

Let us now consider the configuration where *holes replace electrons in open shells only*, and the closed shell core is arbitrary; then for the same atomic state viz ^{2S+1}L the energy expression $E(^{2S+1}L)$ can be expressed by an equation analogous to eq. [1].

The term $\bar{W}(^{2S+1}L)$ depends upon the state only; and so if we define

$$\Delta W = \bar{W}(^{2S+1}L) - W(^{2S+1}L), \qquad [2]$$

we obtain

$$\Delta W = \sum_{k\neq 0}^{2(l_i,l_j)<} \Delta f^k F^k(n_i l_i, n_j l_j) - \sum_{k=|l_i-l_j|}^{l_i+l_j} \Delta g^k G^k(n_i l_i, n_j l_j). \qquad [3]$$

The ΔW of eq. [3] can be derived by evaluating the *difference* between the energies of *any two corresponding states* of the configuration with electrons and holes; however, a very convenient *state* to choose for this purpose is the state of highest total angular momentum

and highest multiplicity (in that order) since its wave function can be represented by a single Slater determinant. Thus it was found by a method analogous to that of a previous paper (2) that ΔW for $p^m f^q$ and $d^n f^q$ can be represented by *two* very simple formulas, namely:

$$[4] \quad \Delta W(p^{6-m}f^{14-q}) = (m-3)[(2/5)F^2(pp) + (3/5)G^2(pf) + (4/9)G^2(pf)] + (q-7)[(4/15)F^2(ff) + (2/11)F^4(ff) + (100/429)F^6(ff) + (9/35)G^2(pf) + (4/21)G^4(pf)]$$

TABLE I

Vector-coupling coefficients for the pf configuration

State	K_{pf2}	K_{pf4}	J_{pf2}
^1D	3/25	4/9	−4/25
^3D	9/175	−20/63	−4/25
^1F	−3/35	10/63	1/5
^3F	9/35	−2/63	1/5
^1G	3/5	2/27	−1/5
^3G	−3/7	10/189	−1/5

TABLE II

Vector-coupling coefficients (in addition to those in Table I) *common to all the states* arising from the pf configuration

$K_{pp0} = -5/3$	$K_{ff0} = -13/7$
$K_{pp2} = 2/15$	$K_{ff2} = 4/105$
	$K_{ff4} = 2/77$
	$K_{ff6} = 100/3003$

TABLE III

Vector-coupling coefficients for the df configuration

State	K_{df1}	K_{df3}	K_{df5}	J_{df2}	J_{df4}
^1P	1/7	4/21	10/21	−8/35	−2/21
^3P	1/35	−4/35	−30/77	−8/35	−2/21
^1D	−3/35	−8/35	20/77	−2/35	1/7
^3D	9/35	32/105	−40/231	−2/35	1/7
^1F	3/7	10/63	80/693	11/105	−2/21
^3F	−9/35	−26/315	−20/693	11/105	−2/21
^1G	−17/35	82/315	40/693	1/7	2/63
^3G	23/35	−58/315	20/693	1/7	2/63
^1H	33/35	32/315	340/7623	−2/21	−1/231
^3H	−27/35	−8/315	320/7623	−2/21	−1/231

TABLE IV

Vector-coupling coefficients (in addition to those in Table III) *common to all the states* arising from the df configuration

$K_{dd0} = -9/5$	$K_{ff0} = -13/7$
$K_{dd2} = 2/35$	$K_{ff2} = 4/105$
$K_{dd4} = 2/35$	$K_{ff4} = 2/77$
	$K_{ff6} = 100/3003$

Can. J. Chem. Downloaded from www.nrcresearchpress.com by 210.87.254.5 on 09/05/12
For personal use only.

TABLE V

Vector-coupling coefficients for the p^5f^{13} configuration

State	K_{pf2}	K_{pf4}	J_{pf2}
^1D	3/1625	4/585	−4/1625
^3D	9/11375	−4/819	−4/1625
^1F	−3/2275	2/819	1/325
^3F	9/2275	−2/4095	1/325
^1G	3/325	2/1755	−1/975
^3G	−3/455	2/2457	−1/975

TABLE VI

Vector-coupling coefficients (in addition to those in Table V) *common to all the states* arising from the p^5f^{13} configuration

$K_{pp0} = -1/15$	$K_{ff0} = -1/91$
$K_{pp2} = 2/375$	$K_{ff2} = 4/17745$
	$K_{ff4} = 2/13013$
	$K_{ff6} = 100/507507$

TABLE VII

Vector-coupling coefficients for the d^9f^{13} configuration

State	K_{df1}	K_{df3}	K_{df5}	J_{df2}	J_{df4}
^1P	−151/2275	−8/325	−82/3003	−8/2275	−2/1365
^3P	−31/455	−8/273	−122/3003	−8/2275	−2/1365
^1D	−159/2275	−212/6825	−92/3003	−2/2275	1/455
^3D	−21/325	−4/175	−16/429	−2/2275	1/455
^1F	−141/2275	−514/20475	−296/9009	11/6825	−2/1365
^3F	−33/455	−118/4095	−316/9009	11/6825	−2/1365
^1G	−173/2275	−482/20475	−304/9009	1/455	2/4095
^3G	−133/2275	−622/20475	−4/117	1/455	2/4095
^1H	−123/2275	−76/2925	−3364/99099	−2/1365	−1/15015
^3H	−183/2275	−44/1575	−3368/99099	−2/1365	−1/15015

TABLE VIII

Vector-coupling coefficients (in addition to those in Table VII) *common to all the states* arising from the d^9f^{13} configuration

$K_{dd0} = -1/45$	$K_{ff0} = -1/91$
$K_{dd2} = 2/2835$	$K_{ff2} = 4/17745$
$K_{dd4} = 2/2835$	$K_{ff4} = 2/13013$
	$K_{ff6} = 100/507507$

$$[5]\ \Delta W(d^{10-n}f^{14-q}) = (n-5)[(2/7)F^2(dd) + (2/7)F^4(dd) + (3/5)G^1(df) + (4/15)G^3(df) + (10/33)G^5(df)] + (q-7)[(4/15)F^2(ff) + (2/11)F^4(ff) + (100/429)F^6(ff) + (3/7)G^1(df) + (4/21)G^3(df) + (50/231)G^5(df)],$$

where $1 \leqslant m \leqslant 2$, $1 \leqslant n \leqslant 4$, and $1 \leqslant q \leqslant 6$.

VECTOR-COUPLING COEFFICIENTS

In a previous paper (5) general formulas were derived for the vector-coupling (VC) coefficients useful in atomic self-consistent-field (SCF) calculations; and tables of the (VC) coefficients for all the states arising from any combination of s, p, and d shells and a single f shell were prepared and are available elsewhere (6).

Can. J. Chem. Downloaded from www.nrcresearchpress.com by 210.87.254.5 on 09/05/12
For personal use only.

We refer the reader to the paper (5) mentioned above for further details. We merely quote here the results; namely, that the vector-coupling coefficients $J_{\lambda\mu\nu}$ and $K_{\lambda\mu\nu}$ are given by the following expressions:

$$[6] \qquad \begin{cases} J_{\lambda\mu 0} = 0, \\ J_{\lambda\mu\nu} = -f^{\nu}(\lambda,\mu)/N_{\lambda}N_{\mu}, \quad \nu \neq 0 \end{cases}$$

$$[7] \qquad \begin{cases} K_{\lambda\lambda 0} = A_{\lambda\lambda 0} - 2/N_{\lambda}, \\ K_{\lambda\lambda\nu} = A_{\lambda\lambda\nu} + 4f^{\nu}(\lambda,\lambda)N_{\lambda}^{2}, \quad \nu \neq 0 \\ K_{\lambda\mu\nu} = A_{\lambda\mu\nu} + 2g^{\nu}(\lambda,\mu)/N_{\lambda}N_{\mu}, \quad \lambda \neq \mu \end{cases}$$

where the coefficients $A_{\lambda\mu\nu}$ are defined (7) as follows: viz

$$[8] \qquad A_{\lambda\mu\nu} = \frac{A_{\lambda+\mu-\nu}\, A_{\mu+\nu-\lambda}\, A_{\lambda+\nu-\mu}}{(\lambda+\mu+\nu+1)A_{\lambda+\mu+\nu}}$$

and

$$A_{\rho} = \frac{\rho!}{[(\rho)!]^{2}}$$

where ρ is always an even integer.

The eqs. [6] through [8] were used to derive the coefficients $J_{\lambda\mu\nu}$ from existing tabulations (3) of the Slater coefficients $f^{\nu}(\lambda,\mu)$ and $g^{\nu}(\lambda,\mu)$ for the pf and df configurations. The Slater coefficients for p^5f^{13} and d^9f^{13} were obtained from those of pf and df respectively by using the relations [4] and [5] respectively.

The results for the p^mf^q and d^nf^q configurations are presented in Tables I–VIII.

REFERENCES

1. G. H. SHORTLEY. Phys. Rev. **40**, 185 (1932).
2. G. L. MALLI. Phys. Rev. **135**, A978 (1964).
3. E. U. CONDON and G. H. SHORTLEY. The theory of atomic spectra. Cambridge University Press, Cambridge, England. 1957. pp. 204, 206.
4. J. C. SLATER. Phys. Rev. **34**, 1293 (1929).
5. G. L. MALLI and J. P. OLIVE. J. Chem. Phys. **43**, 861 (1965).
6. G. L MALLI. Ph.D. Thesis, University of Chicago, Chicago, Illinois. 1964.
7. C. C. J. ROOTHAAN *et al.* Rev. Mod. Phys. **32**, 187 (1960).

Can. J. Chem. Downloaded from www.nrcresearchpress.com by 210.87.254.5 on 09/05/12
For personal use only.

IONIZATION POTENTIALS OF ALKYL FREE RADICALS AND *n*-ALKANES THROUGH $C_{17}H_{36}$ BY ENERGY-CALIBRATED MOLECULAR ORBITAL METHODS[1]

CHARLES E. MELTON AND HUBERT W. JOY

Chemistry Division and Metals and Ceramics Division, Oak Ridge National Laboratory, Oak Ridge, Tennessee

Received February 9, 1966

ABSTRACT

Ionization potentials are calculated by simple energy-calibrated molecular orbital techniques for the normal alkanes through $C_{17}H_{36}$ and for some normal and branched alkyl free radicals. A model is formulated which allows the computations to be extended to extremely large molecules by using "radical" orbitals as well as atomic orbitals in the expansion scheme. Auto-ionization levels as well as ionization potentials are calculated for the radicals. Computed and observed values are in good agreement where recent experimental data are available.

INTRODUCTION

Molecular orbital (MO) approaches to the properties of saturated hydrocarbons have been summarized recently by Pople and Santry (1), and some new calculations of their ionization potentials by the bond orbital (BO) method of Hall (2) have recently been made by Fueki (3). However, the reliability of these and other calculations and the validity of the models on which they are based is open to some question because their calibrations and comparisons were made on older experimental data which is well known to be of poor quality. In recent years several new and improved experimental techniques (4–8) have been used to obtain ionization potentials which may be accurate enough to eliminate some of the various models (9–13). Hence another semiempirical calculation seems not out of place, particularly if it uses new models and techniques.

In previous publications we have described a general model and a simple energy-calibrated molecular orbital scheme which was used to calculate ionization potentials and excitation levels for several free radicals (14), and ionization potentials for some simple halides (15). In this work we present similar results for some other free radicals, and the results of an extension of the approach to the ionization potentials of normal alkanes, this latter scheme being the same as the one applied to the halides. We consider the work an effort to determine the limits of reliability of the very simplest molecular orbital ideas in a context where the most adequate (obtained by least-squares fitting to experimental data on a computer) values of its parameters are used, and where attention is restricted to only one molecular property. We do not propose it as a contribution to molecular orbital theory per se; we offer it instead as a practical technique which we hope will provide good values of molecular orbital parameters and useful values of observable molecular properties.

MODELS

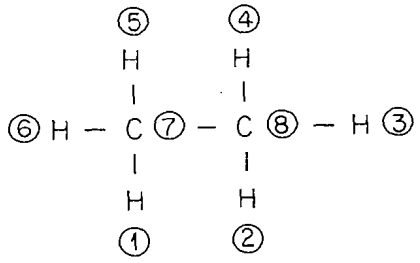
We here outline the structure of the secular equations which we used in the calculations on the *n*-alkanes, and the halides (15). The models for the radicals have already been described (14). Our problem is to assign values to the matrix elements of the usual (16) LCAO–MO (linear combination of atomic orbital – molecular orbital) secular equation

$$|H_{ij} - S_{ij}E| = 0 \qquad i,j = 1, \ldots, N,$$

[1]*Research sponsored by the U.S. Atomic Energy Commission under contract with Union Carbide Corporation.*

Can. J. Chem. Downloaded from www.nrcresearchpress.com by 210.87.254.6 on 09/05/12
For personal use only.

where $H_{ij} = \int \chi_i H \chi_j \, d\tau$, $S_{ij} = \int \chi_i \chi_j \, d\tau$, and χ_i is one of an N-membered set of atomic orbital wave functions, and H is some effective one-electron hamiltonian, in such a way as to obtain the minimum number of adjustable parameters and the minimum adjustment of them which will adequately correlate the ionization potentials of a set of similar molecules. After some experimentation with several physically more appealing alternatives we found that a model which takes the molecules to be planar and which invokes only one orbital per constituent atom is actually the most suitable for obtaining a set of transferable parameters. Within this model we use the ordinary approximations of zero off-diagonal overlap ($S_{ij} = \delta_{ij}$) and zero nonadjacent hamiltonian interaction to allow the secular equation for any n-alkane to be made up from seven different non-zero elements, all of which are found in the calculation for ethane,



,

whose secular equation is here of order 8. In an effort to give the maximum physical significance to the molecular orbital parameters

$$\alpha_i \equiv H_{ii} = \int \chi_i H \chi_i \, d\tau \quad \text{(coulomb integral)}$$

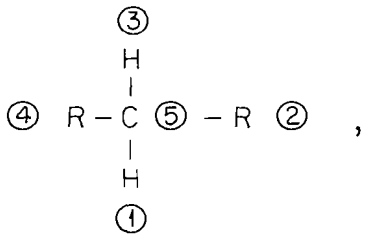
and

$$\beta_{ij} \equiv H_{ij} = \int \chi_i H \chi_j \, d\tau \quad \text{(resonance integral)},$$

we recognize that four of them may be identified as "independently known physical properties" and assigned fixed values, $\alpha_H = \alpha_1 = \ldots = \alpha_6$ = ionization potential of hydrogen, $\alpha_C = \alpha_7 = \alpha_8$ = ionization potential of carbon, $\beta_{CH}{}^0 = \beta_{17} = \ldots = \beta_{67}$ = C—H bond dissociation energy, $\beta_{CC}{}^0 = \beta_{78}$ = C—C bond dissociation energy. Thus the three allowed non-bonding interactions become the only adjustable parameters, $\beta_{HH}{}^1 = \beta_{16} = \ldots = \beta_{56}$ = interaction of adjacent hydrogens on the same carbon, $\beta_{HH}{}^2 = \beta_{12} = \beta_{45}$ = interaction of adjacent hydrogens on neighboring carbons, $\beta_{CH}{}^1 = \beta_{18} = \ldots = \beta_{58}$ = interaction of a hydrogen with an adjacent carbon. Values of these adjustable parameters are determined by the energy-calibration techniques (14), wherein the energy of the highest occupied molecular orbital is made equal to the (negative of the) ionization potential of the molecule used for calibration. We have in fact found a value for $\beta_{HH}{}^1$ from calibration on methane and values for $\beta_{HH}{}^2$ and $\beta_{CH}{}^1$ from calibration on ethane. These parameters are now fixed at this point and no further adjustments in them are made in treating the rest of the n-alkanes.

To try to keep the size of the secular equations within bounds when extending the approach to larger n-alkanes we have invoked the approximation of representing the molecular orbitals as linear combinations of atomic and "radical" orbitals (LCARO), where we introduce radical orbitals to replace hydrogen orbitals as needed. For example, we may treat pentane as methane with ethyl radicals in place of two of the hydrogens,

Can. J. Chem. Downloaded from www.nrcresearchpress.com by 210.87.254.6 on 09/05/12
For personal use only.



and make a calibration run to determine $\beta_{HR}^1 = \beta_{12} \ldots = \beta_{14}$ = interaction of hydrogen and ethyl on the same carbon, using for $\alpha_R = \alpha_2 = \alpha_4$ = ionization potential of ethyl, either an experimental or energy-calibrated value for the radical, and taking $\beta_{CR}^0 = \beta_{CC}^0$. Then, as usual, once a value for the interaction is found in one simple case it is fixed for all other cases. Nonane may be treated in a similar manner as methane with two attached butyl radicals. Thus the LCARO approximation greatly extends the upper limit on the size of molecules for which these calculations can be made. One merely needs to make calibration runs on the constituent radicals to find α_R values and on the first members of a series to find β_{HR}^1 values.

In the calculations on the halides (15) we also used planar models with one atomic orbital per constituent atom, and took ionization potentials for α values and bond dissociation energies for bonding β values. We made five calibration runs to obtain the non-bonding β values β_{HH}^1, β_{FF}^1, β_{ClCl}^1, β_{HF}^1, β_{HCl}^1, and assumed $\beta_{FCl}^1 = \beta_{ClCl}^1$.

In the next section we give our computed simplest-planar-model ionization potentials and our corresponding best sets of transferable molecular orbital parameters. We note here that, in every case we tried, more complex models which removed the restriction of planarity, or which allowed for non-nearest neighbor interactions, or which invoked more than one orbital per constituent atom or radical, led to sets of parameters which were significantly less transferable.

RESULTS AND DISCUSSION

In Table I we list, for the radicals (14), halides (15), and *n*-alkanes, the molecular orbital parameter values which were used as inputs to our calculations and those which were obtained as outputs from the calibration runs. In the calculations on the radicals we used several different values of α_C corresponding to various auto-ionization levels in carbon to obtain, as before (14), possible auto-ionizations in the radicals. In the other calculations we used only the lowest ionization potential of carbon. We were unable to find a single set of non-bonding H—H interactions common to all three cases, but this is not unexpected since these interactions would seem to be most dependent on intramolecular environment. For convenience in computation and tabulation we have made all elements (and thus all roots) in the secular equations positive (instead of negative, ref. 14). This does not affect the results except in a shift of the energy scale.

Alkyl Radicals

Calculated ionization potentials and auto-ionization levels for *n*-pentyl, *s*-propyl, *i*-butyl, *s*-butyl, and *t*-butyl free radicals are given in Tables II–VI together with available experimental results (5, 17). We also show all roots of the secular equations for each different value of α_C. They represent the ionization spectra as predicted by our models. The calculated values for ionization potentials tend to be lower than the electron impact values obtained by conventional techniques. This is not surprising, since experimental

Can. J. Chem. Downloaded from www.nrcresearchpress.com by 210.87.254.6 on 09/05/12
For personal use only.

Can. J. Chem. Downloaded from www.nrcresearchpress.com by 210.87.254.6 on 09/05/12
For personal use only.

TABLE I

Molecular orbital parameter values used and obtained for radicals, halides, and *n*-alkanes

Parameter values, eV					
Independent		Calibrated		LCAO	LCARO
		Radicals			
α_C	11.26	β_{HH}^1	2.37		
	12.13	β_{HH}^2	2.37		
	12.84	β_{CH}^1	2.42		
	13.11				
	14.86				
α_H	13.53				
		Halides			
α_C	11.26	β_{HH}^1	0.99		
α_H	13.53	β_{FF}^1	0.85		
α_F	17.42	β_{ClCl}^1	0.76		
α_{Cl}	13.01	β_{HF}^1	1.11		
α_{Xe}	12.08	β_{HCl}^1	0.96		
β_{CH}^0	4.50	β_{FCl}^1	0.77		
β_{CF}^0	4.48				
β_{CCl}^0	3.40				
β_{XeF}^0	1.50				
β_{XeCl}^0	1.25				
		Alkanes			
α_C	11.26	β_{HH}^1		1.89	1.14
α_H	13.53	β_{HH}^2		0.26	0.10
β_{CH}^0	4.50	β_{CH}^1		0.31	0.28
β_{CC}^0	3.50	$\beta_{H(C_2H_5)}^1$			0.28
		$\beta_{H(C_4H_9)}^1$			0.28

TABLE II

Ionization potentials and auto-ionizing levels of the *n*-pentyl free radical

Calculated ionization potentials and auto-ionizing levels, eV				
$C(^2P_{1/2})$	$C(2p^3\ ^1D)$	$C(3s\ ^5p)$	$C(2p^3\ ^3S)$	$C(2p^3\ ^1P)$
7.7				
	8.0			
		8.2	8.2	8.3
8.6	8.7	8.8	8.8	
9.0	9.0	9.0	9.0	9.0
10.5	10.6	10.7	10.8	
10.8	10.9	10.9	10.9	10.9
				11.1
13.2	13.3	13.4	13.4	13.5
13.5	13.5	13.5	13.5	13.7
15.9	16.0	16.1	16.1	
16.2	16.2	16.2	16.2	16.2
				16.4
17.8	17.9	18.0	18.0	18.0
18.1	18.1	18.1	18.1	18.4
18.7	18.8	18.8	18.8	19.0

TABLE III

Ionization potentials and auto-ionizing levels of the *s*-propyl free radical

Ionization potentials and auto-ionizing levels, eV					
	Calculated				
Experimental*†	$C(^2P_{1/2})$	$C(2p^3\ ^1D)$	$C(3s\ ^5P)$	$C(2p^3\ ^3S)$	$C(2p^3\ ^1P)$
7.52, 7.9	7.5				
8.1		7.9	8.1	8.2	
8.6					8.6
	9.5	9.5	9.6	9.7	
	10.1	10.1	10.1	10.1	10.0
	13.1	13.3	13.4		
	13.5	13.5	13.5	13.5	13.5
	16.9	17.0	17.2	17.2	17.0
					17.5
	18.4	18.5	18.6	18.7	
					19.2

*Reference 5.
†Reference 17.

TABLE IV

Ionization potentials and auto-ionizing levels of the *i*-butyl free radical

Ionization potentials and auto-ionizing levels, eV					
Experimental, direct*	Calculated				
	$C(^2P_{1/2})$	$C(2p^3\ ^1D)$	$C(3s\ ^5P)$	$C(2p^3\ ^3S)$	$C(2p^3\ ^1P)$
8.35	7.80				
		8.0			
			8.1		
				8.2	8.3
	8.8	8.9	9.0	9.1	
	9.3	9.3	9.3	9.3	9.3
					9.4
	11.4	11.5	11.6	11.7	11.8
	11.9	11.9	12.0	12.0	12.3
	14.6	14.8	14.9	14.9	
	15.2	15.2	15.3	15.3	15.1
					15.5
	17.5	17.5	17.7	17.7	17.7
	17.8	17.8	17.8	17.8	18.2
	18.8	18.8	18.8	18.8	19.0

*Reference 17.

values obtained by electron impact by conventional techniques are usually higher than the "true" or adiabatic ionization potentials. Experimental (obtained by RPD (retarding potenial difference)) (5, 8) and calculated auto-ionization levels for *s*-propyl are in excellent agreement over the limited range of the experimental data.

Normal Alkanes

Ionization potentials for the normal alkanes through heptadecane are given in Table VII. The calculated values are in excellent agreement with experimental ionization potentials measured by photon impact (18, 19) over the limited range of the experimental values. Electron impact values are not tabulated since most of the available data obtained by conventional techniques (20) tend to be higher and less reliable than the photon impact

Can. J. Chem. Downloaded from www.nrcresearchpress.com by 210.87.254.6 on 09/05/12
For personal use only.

TABLE V

Ionization potentials and auto-ionizing levels of the *s*-butyl free radical

Ionization potentials and auto-ionizing levels, eV					
	Calculated				
Experimental*	$C(^2P_{1/2})$	$C(2p^3\ ^1D)$	$C(3s\ ^5P)$	$C(2p^3\ ^3S)$	$C(2p^3\ ^1P)$
7.93	7.6				
		8.0			
			8.2	8.2	
					8.5
	9.0	9.1	9.2	9.2	
	9.4	9.4	9.4	9.4	9.4
					9.5
	11.5	11.6	11.7	11.8	
	11.9	12.0	12.0	12.0	11.9
					12.2
	14.8	14.9			
	15.1	15.1	15.0	15.0	15.1
			15.2	15.2	15.4
	17.4	17.5	17.6	17.6	
	17.6	17.6	17.7	17.7	17.7
					18.0
	18.5	18.6	18.6	18.7	
					19.0

*Reference 17.

TABLE VI

Ionization potentials and auto-ionizing levels of the *t*-butyl free radical

Ionization potentials and auto-ionizing levels, eV					
	Calculated				
Experimental, direct*	$C(^2P_{1/2})$	$C(2p^3\ ^1D)$	$C(3s\ ^5P)$	$C(2p^3\ ^3S)$	$C(2p^3\ ^1P)$
7.42	7.3				
		7.7	7.8		
				7.9	8.1
	8.6	8.7	8.8	8.8	
	9.1	9.1	9.1	9.1	9.1
					9.2
	11.6		11.7	11.7	11.7
	11.7	11.8	11.8	11.9	
					12.1
	14.8	14.9	15.0	15.0	
	15.3	15.3	15.3	15.3	15.3
	17.7	17.8			
	17.9	17.9	17.9	17.9	17.9
				18.0	
					18.3
	18.9	18.9	19.0	19.0	
					19.4

*Reference 17.

data. Results from these calculations, for the heavier alkanes, indicate that the ionization potential for the homologous series decreases very slowly with increasing mass above decane.

CONCLUSIONS

It is interesting to compare our results with Fueki's (3), which were obtained from Hall's (2) "linear combination of bond orbital" (LCBO) (or "equivalent orbital") approach (21) (Table VIII). At first glance it would seem that there is little to choose between LCAO

Can. J. Chem. Downloaded from www.nrcresearchpress.com by 210.87.254.6 on 09/05/12
For personal use only.

TABLE VII

Ionization potentials of some normal alkane hydrocarbons using LCAO and LCARO molecular orbitals

Compound		Ionization potentials, eV			
		Experimental	Calculated*	Calculated†	Calculated‡
Methane	CH_4	13.0§	13.0‖		
Ethane	C_2H_6	11.65§	11.65‖		
Propane	C_3H_8	11.08§	11.28		
Butane	C_4H_{10}	10.63§	10.50		
Pentane	C_5H_{12}	10.33¶	10.25	10.25‖	
Hexane	C_6H_{14}	10.17¶	10.12	10.15	
Heptane	C_7H_{16}	10.06¶	10.07	10.05	
Octane	C_8H_{18}			10.03	
Nonane	C_9H_{20}			10.02	10.02‖
Decane	$C_{10}H_{22}$			9.95	9.95
Hendecane	$C_{11}H_{24}$			9.93	9.93
Dodecane	$C_{12}H_{26}$			9.93	9.93
Tridecane	$C_{13}H_{28}$				9.92
Tetradecane	$C_{14}H_{30}$				9.92
Pentadecane	$C_{15}H_{32}$				9.91
Hexadecane	$C_{16}H_{34}$				9.91
Heptadecane	$C_{17}H_{36}$				9.89

*LCAO.
†LCARO (R = C_2H_5).
‡LCARO (R = C_4H_9).
§Reference 18. Photon impact.
‖Calibration points.
¶Reference 19.

TABLE VIII

Comparison of calculated and observed ionization potentials

	Calculated and observed ionization potentials, eV		
	Experimental*	LCBO†(Fueki)	LCAO‡(this work)
Stable compounds			
Methane	13.0	13.16	13.0§
Ethane	11.65	11.65	11.65§
Propane	11.08	11.00	11.28
Butane	10.63	10.68	10.50
Pentane	10.33	10.50	10.25
Hexane	10.17	10.40	10.12
Heptane	10.06	10.35	10.07
Octane		10.30	10.03
Alkyl radicals			
Methyl	9.82¶	9.95	9.82§
Ethyl	8.25‖	8.68	8.25§
n-Propyl	8.15	8.61	8.20
s-Propyl	7.5	8.14	7.5
n-Butyl		8.6	8.0
i-Butyl		8.57	7.8
s-Butyl		8.11	7.6
t-Butyl		7.8	7.3
n-Pentyl		8.6	7.7

*References 4 and 20. Photon impact.
†LCBO linear combination of bond orbitals (or "equivalent orbitals"). Reference 3.
‡LCAO linear combination of atomic orbitals.
§Calibration points.
‖Electron impact retarding potential difference method.
¶Reference 5.

and LCBO techniques, but it must be remembered that it is usually more difficult to give an "independent" physical interpretation to, as well as to find adequate values for, the α's and the β's when they are thought of as bond interactions rather than atom interactions. The LCBO α for a C—H bond must be related to the observed first ionization potential

Can. J. Chem. Downloaded from www.nrcresearchpress.com by 210.87.254.6 on 09/05/12
For personal use only.

and an estimated second ionization potential for methane, whereas the LCAO α for a C atom is simply its observed ionization potential. In addition, we can use (empirical) "independent" bond energy terms for the LCAO β's which describe bonding interactions, and then take recourse in data fitting only for non-bonding interactions. By contrast, all Fueki's LCBO β's must be obtained by data fitting. Because LCAO methods make more adequate use of physical quantities determined elsewhere, they may be said to use fewer adjustable parameters. Thus it would appear that they provide a simpler and more practical technique for correlating ionization potentials in a series of related molecules.

REFERENCES

1. J. A. POPLE and D. P. SANTRY. Mol. Phys. **7**, 269 (1964).
2. G. G. HALL. Proc. Roy. Soc. London, Ser. A, **205**, 541 (1951).
3. K. FUEKI. J. Phys. Chem. **68**, 2656 (1964).
4. K. WATANABE, T. NAKAYAMA, and J. MOTTL. J. Quant. Spectr. Radiative Transfer, **2**, 369 (1962).
5. C. E. MELTON and W. H. HAMILL. J. Chem. Phys. **41**, 3464 (1964).
6. G. HERZBERG and J. SHOOSMITH. Can. J. Phys. **34**, 523 (1956).
7. C. E. BRION. J. Chem. Phys. **40**, 2995 (1964).
8. R. E. FOX, W. M. HICKAM, T. KJELKAAS, and D. J. GROVE. Phys. Rev. **84**, 859 (1951).
9. G. G. HALL. Trans. Faraday Soc. **49**, 113 (1953) and earlier papers.
10. R. S. MULLIKEN. Phys. Rev. **115**, 1225 (1959) and earlier papers.
11. A. STREITWIESER, JR. J. Am. Chem. Soc. **82**, 4123 (1960).
12. J. L. FRANKLIN. J. Chem. Phys. **22**, 1304 (1954).
13. J. LENNARD-JONES and G. G. HALL. Trans. Faraday Soc. **48**, 581 (1952).
14. C. E. MELTON and H. W. JOY. J. Chem. Phys. **42**, 1986 (1965).
15. C. E. MELTON and H. W. JOY. J. Chem. Phys. **42**, 2982 (1965).
16. J. D. ROBERTS. Molecular orbital calculations. W. A. Benjamin, Inc., New York. 1962.
17. F. P. LOSSING and J. B. DE SOUSA. J. Am. Chem. Soc. **81**, 281 (1959).
18. K. WATANABE. J. Chem. Phys. **26**, 542 (1957).
19. K. WATANABE. Private communication to Price, Bralsford, Harris, and Ridley. Spectrochim. Acta, **14**, 45 (1959).
20. R. W. KISER. Tables of ionization potentials. TID-6142. USAEC. 1960. p. 3.
21. R. DAUDEL, R. LEFEBVRE, and C. MOSER. Quantum chemistry. Interscience Publishers Inc., New York. 1959. p. 90 ff.

Can. J. Chem. Downloaded from www.nrcresearchpress.com by 210.87.254.6 on 09/05/12
For personal use only.

Can. J. Chem. Downloaded from www.nrcresearchpress.com by 210.87.254.105 on 09/05/12
For personal use only.

NOTES

DECARBOXYLATION OF STRONG ACIDS BY METAL ACETYLACETONATES

NEIL R. FETTER

INTRODUCTION

In a study of the reactions of carboranes with beryllium acetylacetonate, an attempt was made to prepare beryllium *o*-carboranylcarboxylic acid compounds from beryllium acetylacetonate and 1-methyl-2-*o*-carboranylcarboxylic acid with the elimination of acetylacetone. However, it was found that decarboxylation occurred and *o*-methylcarborane was formed.

The decarboxylations of trichloroacetate (1), trinitrobenzoate (2), and trifluoroacetate (3) anions in several solvents have been described by Verhoek and co-workers. The decarboxylations followed first order kinetics with respect to the anion concentration and occurred at mild temperatures, except with sodium trifluoroacetate, which required temperatures near 180 °C.

Because of the poor solubility of the carborane carboxylic acids in common solvents, the decarboxylations described below were conducted as melt reactions. The chloroacetic acids were treated with zinc acetylacetonate under similar conditions to see whether other strong carboxylic acids would behave similarly.

EXPERIMENTAL

Apparatus and Reagents

The zinc and beryllium acetylacetonates were obtained from Chemicals Procurement Laboratories, College Point, N.Y., and used without further purification.

The 1,2-*o*-carboranyldicarboxylic acid, $HOOC(C_2B_{10}H_{10})COOH$, was obtained from the Olin Mathieson Chemical Corp. through the courtesy of Dr. Theodore Heying. The 1-methyl-2-*o*-carboranylcarboxylic acid, $CH_3(C_2B_{10}H_{10})COOH$, was prepared from *o*-methyl carborane by reaction with butyllithium to form $CH_3(C_2B_{10}H_{10})Li$, followed by reaction with CO_2 and acidification (4). The crude product was recrystallized from CCl_4 before use. The chloroacetic acids were obtained from the Matheson, Coleman, and Bell Corp. and were used without further treatment.

The reactions were carried out on a standard high vacuum apparatus equipped with a Toepler pump for evolved gas measurement. The reaction vessel was a 50 ml, round-bottom flask, attached to a −20 °C cold finger to permit refluxing, connected to the vacuum line. In a typical experiment, approximately 1 g each of metal acetylacetonate and the carboxylic acid were heated under 200 mm of dry nitrogen at approximately 200 °C for about 3 h until gas evolution ceased.

After the reaction, the nitrogen was pumped off and the condensables, including CO_2, were retained in a −196 °C trap. The trap temperature was raised to −78 °C and the CO_2 was measured. The composition of the remaining condensables was determined by examination of the liquid phases with a Varian A-60 nuclear magnetic resonance spectrometer and the vapors with an infrared spectrophotometer. The crude products that remained in the reaction flasks were sublimed under vacuum (0.01 mm) at 75–80 °C onto a −20 °C cold finger where a solid carborane was deposited. The products were identified from infrared spectral comparison with authentic samples, melting point, and elemental analyses, which were performed by the Schwarzkopf Analytical Laboratories, Woodside, N.Y.

The results of the experimental work are summarized in Table I.

DISCUSSION

As can be seen from the data in Table I, the decarboxylation of $CH_3(C_2B_{10}H_{10})COOH$ and $HOOC(C_2B_{10}H_{10})COOH$ is quantitative with $Be(AcCHAc)_2$ and nearly so with $Zn(AcCHAc)_2$; however, recovery of a pure product was difficult when $Be(AcCHAc)_2$ was used, because unreacted portions of it co-sublimed with the carboranes.

TABLE I

Decarboxylation of strong acids by metal acetylacetonates

Carboxylic acid (mmoles)	Metal acetylacetonate (mmoles)	Reaction T (°C)	CO_2 evolved (mmoles)	Other products (mmoles)
$CH_3C(B_{10}H_{10})CCOOH$ (3.42)	$Zn(AcCHAc)_2$ (4.00)	205	3.49	$CH_3C(B_{10}H_{10})CH$ (2.56) M.p. 205–210 °C; lit. m.p. 214–217 °C Anal. Calcd.: C, 22.81; H, 8.91; B, 68.33 Found: C, 23.08; H, 8.81; B, 68.12 Acetone (0.932)
$HOOCC(B_{10}H_{10})CCOOH$ (3.88)	$Zn(AcCHAc)_2$ (7.98)	205	6.40	$HC(B_{10}H_{10})CH$ (1.13) M.p. 285–290 °C; lit. m.p. 294–296 °C Infrared spectrum matched authentic spectrum Acetone (1.94) Acetylacetone (2.90)
CCl_3COOH (10.80)	$Zn(AcCHAc)_2$ (11.5)	155	7.82	Chloroform (4.5) Acetone (0.72) Acetic acid (0.72)
$CHCl_2COOH$ (10.75)	$Zn(AcCHAc)_2$ (11.10)	200	2.09	Acetone (6.00)
$CH_2ClCOOH$ (22.80)	$Zn(AcCHAc)_2$ (22.60)	210	2.29	Acetone (11.7) Methyl chloride (1.25) Acetylacetone (1.00)
CF_3COOH (14.42)	$Zn(AcCHAc)_2$ (18.10)	195	No reaction	
C_6H_5COOH (5.48)	$Zn(AcCHAc)_2$ (5.57)	215	No reaction	
$CH_3C(B_{10}H_{10})CCOOH$ (4.45)	$Be(AcCHAc)_2$ (4.55)	190	4.10	Acetylacetone (0.184) Sublimate: mixture of $Be(AcCHAc)_2$ and $CH_3(C_2B_{10}H_{10})H$ (1.04 g) Anal. Found: B, 32.80; Be, 2.75
$HOOCC(B_{10}H_{10})CCOOH$ (2.37)	$Be(AcCHAc)_2$ (5.12)	200	4.47	Acetylacetone (0.455) Sublimate: mixture of $Be(AcCHAc)_2$ and carborane (0.470 g) Anal. Found: B, 17.84; Be, 3.55

To be sure that autodecarboxylation did not occur, samples of $CH_3(B_{10}H_{10}C_2)COOH$, $HOOC(B_{10}H_{10}C_2)COOH$, and Cl_3CCOOH were heated to 205 °C; no CO_2 evolution was observed.

Decarboxylations of the chloroacetic acids with $Zn(AcCHAc)_2$ were carried out to determine the effect of decreasing acid strength on the carbon dioxide yields. The carbon dioxide values obtained from Cl_3CCOOH, $CHCl_2COOH$, and $CH_2ClCOOH$ were 72.3, 19.4, and 9.3 mole % respectively, indicating that the ability of $Zn(AcCHAc)_2$ to effect decarboxylation depends upon the acids' strengths, whose pK_a values in water are 0.70, 1.48, and 2.85 (5), respectively. The quantitative decarboxylation of the carborane carboxylic acids suggests they are strong, with dissociation constants of 10^{-1} or larger.

Can. J. Chem. Downloaded from www.nrcresearchpress.com by 210.87.254.105 on 09/05/12
For personal use only.

The pK_a value of 1-methyl-2-*o*-carboranylcarboxylic acid has been reported (4) to be 2.74 in 50% aqueous ethanol, but insolubility of the carboranylcarboxylic acid in water has prevented measurement in this medium. Benzoic acid is apparently too weak to be affected by metal acetylacetonates.

The inability to decarboxylate trifluoroacetic acid at 195 °C is not readily explainable; however, the larger activation energy for the decarboxylation of trifluoroacetate ion (42.0 kcal/mole) vs. trichloroacetate ion (31.6 kcal/mole) in the same solvent, as reported by Verhoek (3), suggests that 195 °C may have been too low to decarboxylate trifluoroacetic acid in the presence of zinc acetylacetonate.

It is apparent from the variety of condensables obtained at −78 °C that the reaction mechanism is probably not a first order decarboxylation of the acid anions. For example, the reaction of the carborane carboxylic acid with $Be(AcCHAc)_2$ yielded acetylacetone as the primary condensable, but with $Zn(AcCHAc)_2$, acetone was obtained. Also, the decarboxylation of $Cl_2CHCOOH$ yielded no dichloromethane and $ClCH_2COOH$ produced only 5.5 mole % of the methyl chloride possible.

Although the evolution of acetylacetone or acetone would indicate the presence of the carborane carboxylic acid salts such as $CH_3(B_{10}H_{10}C_2)COOBeAcCHAc$, these compounds were not isolated because the evolution of acetylacetone and carbon dioxide occurred at approximately the same temperatures.

ACKNOWLEDGMENT

The author wishes to thank Drs. Peter J. Slota, Jr. and Charles P. Haber of this laboratory for their assistance and suggestions. This work was supported in part by the Office of Naval Research.

1. F. H. VERHOEK. J. Am. Chem. Soc. **56**, 571 (1934).
2. F. H. VERHOEK. J. Am. Chem. Soc. **61**, 186 (1939).
3. I. AUERBACH, F. H. VERHOEK, and A. L. MENNE. J. Am. Chem. Soc. **72**, 299 (1950).
4. D. GRAFSTEIN and J. DVORAK. Inorg. Chem. **2**, 1128 (1963).
5. HANDBOOK OF CHEMISTRY AND PHYSICS. 45th ed. Chemical Rubber Publishing Co., Cleveland, Ohio. pp. D-77.

RECEIVED JANUARY 20, 1966.
U.S. NAVAL ORDNANCE LABORATORY,
CORONA, CALIFORNIA.

CHEMICAL DEACTIVATION BY HYDROCARBONS IN THE PHOTOLYSIS OF HEXAFLUOROACETONE[1]

S. N. KHANNA[2] AND K. O. KUTSCHKE

In a previous discussion (1) a distinction was made between the mode of action of "inert" gases, such as CO_2, C_4F_{10}, etc., and of a hydrocarbon (isobutane) in causing a reduction of the quantum yield, ϕ, for the photodecomposition of hexafluoroacetone. Experiments with the inert gases had been done by Ayscough and Steacie (2). They showed

[1]*Issued as N.R.C. No. 8966.*
[2]*National Research Council of Canada Postdoctorate Fellow, 1962–1964. Present address: Dominion Rubber Company, Guelph, Ontario.*

Can. J. Chem. Downloaded from www.nrcresearchpress.com by 210.87.254.105 on 09/05/12
For personal use only.

The pK_a value of 1-methyl-2-*o*-carboranylcarboxylic acid has been reported (4) to be 2.74 in 50% aqueous ethanol, but insolubility of the carboranylcarboxylic acid in water has prevented measurement in this medium. Benzoic acid is apparently too weak to be affected by metal acetylacetonates.

The inability to decarboxylate trifluoroacetic acid at 195 °C is not readily explainable; however, the larger activation energy for the decarboxylation of trifluoroacetate ion (42.0 kcal/mole) vs. trichloroacetate ion (31.6 kcal/mole) in the same solvent, as reported by Verhoek (3), suggests that 195 °C may have been too low to decarboxylate trifluoroacetic acid in the presence of zinc acetylacetonate.

It is apparent from the variety of condensables obtained at −78 °C that the reaction mechanism is probably not a first order decarboxylation of the acid anions. For example, the reaction of the carborane carboxylic acid with $Be(AcCHAc)_2$ yielded acetylacetone as the primary condensable, but with $Zn(AcCHAc)_2$, acetone was obtained. Also, the decarboxylation of $Cl_2CHCOOH$ yielded no dichloromethane and $ClCH_2COOH$ produced only 5.5 mole % of the methyl chloride possible.

Although the evolution of acetylacetone or acetone would indicate the presence of the carborane carboxylic acid salts such as $CH_3(B_{10}H_{10}C_2)COOBeAcCHAc$, these compounds were not isolated because the evolution of acetylacetone and carbon dioxide occurred at approximately the same temperatures.

ACKNOWLEDGMENT

The author wishes to thank Drs. Peter J. Slota, Jr. and Charles P. Haber of this laboratory for their assistance and suggestions. This work was supported in part by the Office of Naval Research.

1. F. H. VERHOEK. J. Am. Chem. Soc. **56**, 571 (1934).
2. F. H. VERHOEK. J. Am. Chem. Soc. **61**, 186 (1939).
3. I. AUERBACH, F. H. VERHOEK, and A. L. MENNE. J. Am. Chem. Soc. **72**, 299 (1950).
4. D. GRAFSTEIN and J. DVORAK. Inorg. Chem. **2**, 1128 (1963).
5. HANDBOOK OF CHEMISTRY AND PHYSICS. 45th ed. Chemical Rubber Publishing Co., Cleveland, Ohio. pp. D-77.

RECEIVED JANUARY 20, 1966.
U.S. NAVAL ORDNANCE LABORATORY,
CORONA, CALIFORNIA.

CHEMICAL DEACTIVATION BY HYDROCARBONS IN THE PHOTOLYSIS OF HEXAFLUOROACETONE[1]

S. N. KHANNA[2] AND K. O. KUTSCHKE

In a previous discussion (1) a distinction was made between the mode of action of "inert" gases, such as CO_2, C_4F_{10}, etc., and of a hydrocarbon (isobutane) in causing a reduction of the quantum yield, ϕ, for the photodecomposition of hexafluoroacetone. Experiments with the inert gases had been done by Ayscough and Steacie (2). They showed

[1]*Issued as N.R.C. No. 8966.*
[2]*National Research Council of Canada Postdoctorate Fellow, 1962–1964. Present address: Dominion Rubber Company, Guelph, Ontario.*

Can. J. Chem. Downloaded from www.nrcresearchpress.com by 210.87.254.42 on 09/05/12
For personal use only.

Can. J. Chem. Downloaded from www.nrcresearchpress.com by 210.87.254.42 on 09/05/12
For personal use only.

that, in the absence of added gas, ϕ decreased as the concentration of ketone, [A], increased and that it approached a limiting value, ϕ_∞, at sufficiently large [A]. The deactivation experiments were done with a fixed concentration, $[A]_1$, of ketone, corresponding in the absence of added gases to a quantum yield of ϕ', and yielded values of the quantum yield, ϕ_M, which decreased as the concentration, [M], of added gas was increased. The mechanism evolved (1) predicted that a plot of ϕ'/ϕ_M vs. [M] should rise from unity at [M] = 0 with a finite initial slope which decreased as the limiting value, ϕ'/ϕ_∞, of the function was approached at large [M]. The mechanism assumed that the inert gas acted only as a catalyst in the degradation of the vibrational energy in the excited singlet state; this mode of action can be termed physical deactivation. The limited data available were consistent with this prediction and a procedure was outlined to evaluate q, the efficiency of the inert gas as an agent for the transfer of vibrational energy relative to that for the ketone.

A few data with isobutane as the added species yielded a value of q greatly in excess of unity. It was suggested that a chemical reaction occurred between some excited state of the ketone and the added hydrocarbon; this reaction is designated as chemical deactivation. The present note reports additional data which support the hypothesis that chemical deactivation occurs.

Experiments were done in the usual type of apparatus. Light from a 550 W Hanovia Type A mercury arc was rendered approximately parallel and the group of lines near 3 130 Å was isolated by the combination of filters described by Kasha (3). The light beam just filled the cylindrical fused quartz cell (10 cm long, 5 cm diameter). All experiments with added gases were done at 79 °C with $[A]_1$ = 10.0 mm. Quantum yields were determined by acetone actinometry; values of ϕ' (= 0.70) and of ϕ_∞ (= 0.29) agreed closely with those obtained earlier (1, 2). Analysis was confined to the measurement of the amount of carbon monoxide formed. The data are shown in Fig. 1 as plots of ϕ'/ϕ_M vs. [RH] for the three hydrocarbons. The ordinate origin has been shifted for each gas to improve the clarity; the horizontal broken lines to the right of the figure indicate the position of ϕ'/ϕ_∞ (= 2.4) for the various ordinate origins.

The data have been treated in the manner outlined (1) to evaluate $q_{i\text{-}C_4H_{10}} = 1.6$, $q_{C_6H_{14}} = 2.9$, and $q_{C_6H_6} = 1.5$. All exceed unity but by rather smaller factors than did the $q_{i\text{-}C_4H_{10}} \simeq 30$ obtained earlier (1) when shorter wavelengths were used for excitation. It should also be noted that values of ϕ'/ϕ_M greatly in excess of ϕ'/ϕ_∞ are obtained even at moderate concentration of the hydrocarbons. This latter observation is strong evidence in favor of a chemical reaction of an excited molecule.

The nature of the chemical reaction cannot be specified with certainty at this time. The correlation which exists between the respective values of q and the number of tertiary hydrogen atoms on the two paraffins suggests that the reaction might be

$$A^* + RH \rightarrow AH + R \qquad [1]$$

where A* represents an excited state of the ketone molecule. In view of the slowness of reactions like [1] when free radicals attack benzene, it seems unreasonable to postulate [1] as the reaction involved in the present system when benzene is the added gas. By analogy with the reactions of free radicals, it is suggested that an addition reaction, [2], possibly followed by some rearrangement, operates in this case.

$$A^* + C_6H_6 \rightarrow AC_6H_6 \qquad [2]$$

A search for products of the species formed in [1] and [2] has not been made although such an investigation is an obvious extension of this work.

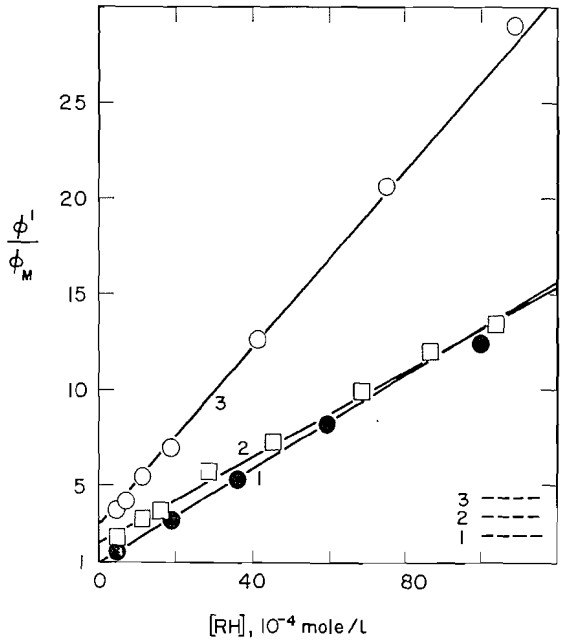


FIG. 1. Plots of ϕ'/ϕ_M vs. [RH]: (1) isobutane, (2) benzene, (3) 2,3-dimethylbutane. The ordinate origin is shifted upward by 1 unit for each successive plot. Broken lines to the right indicate the position of ϕ'/ϕ_∞ for each ordinate origin.

It also is impossible to identify A* on the basis of the data available. It is observed that plots of ϕ_M/ϕ' vs. $[RH]^{-1}$ pass through the origin within experimental error. However, this would be predicted if any of the excited states discussed previously (1) is involved. It seems reasonable to identify A* with the state designated $^3A_0$ in the previous discussion. Additional studies of the light emission will be of assistance in answering this question and these have been undertaken.

It should be noted that when a reaction like [1] or [2] is included in the mechanism, the procedure outlined previously (1) to evaluate q is no longer valid. This is a consequence of the fact that $S_M°$ then contains terms which cannot be evaluated by measurements of S_K' (see reference (1) for definitions of $S_M°$ and S_K'). It appears probable that the discrepancy between the value of $q_{t\text{-}C_4H_{10}}$ reported here and that reported earlier arises from differences in the degree of validity of the procedure used for the evaluation of q for the two sets of experimental conditions.

One final point should be made. It is conceivable that the phenomenon observed does not involve a reaction of the excited state of the ketone but rather involves a reaction such as [3] with an addition-type reaction occurring when unsaturated species are present.

[3] $$CF_3\dot{C}{=}O + RH \rightarrow CF_3CHO + R$$

Support for this suggestion is derived from the recent observation of CF_3COBr as a product of the photolysis of hexafluoroacetone in the presence of bromine (4). Although it is not possible to exclude this suggestion it should be noted that in the presence of relatively large amounts of isobutane the yield of C_2F_6 is negligible and the ratio CF_3H/CO is approximately 1.7 (5). Although this is smaller than the value of 2 expected if each CF_3CO radical decomposed, the decrement from 2 is explicable in terms of known reactions of CF_3

Can. J. Chem. Downloaded from www.nrcresearchpress.com by 210.87.254.42 on 09/05/12
For personal use only.

radicals with the isobutene unavoidably produced in this system. Pearson and Szwarc (6) have discussed this point. Moreover, it should be noted that any reaction which inhibits the formation of CO from CF_3CO radicals leads to an expected increase in CF_3H/CO and cannot explain the observed decrement. It is concluded, therefore, that the lifetime of CF_3CO radicals with respect to decomposition is small enough to prevent the occurrence of a reaction such as [3] even at concentrations of hydrocarbon near atmospheric pressure.

Thus it seems reasonable to conclude that chemical deactivation is the most likely explanation of the phenomenon observed here. It would be desirable, however, to obtain analytical data to confirm or refute this conclusion.

1. A. N. Strachan, R. K. Boyd, and K. O. Kutschke. Can. J. Chem. **42**, 1345 (1964).
2. P. B. Ayscough and E. W. R. Steacie. Proc. Roy. Soc. London, Ser. A, **234**, 476 (1956).
3. M. Kasha. J. Opt. Soc. Am. **38**, 929 (1948).
4. B. G. Tucker and E. Whittle. Trans. Faraday Soc. **61**, 484 (1965); Proc. Chem. Soc. 93 (1963).
5. A. N. Strachan and S. A. McIntosh. Unpublished work in these laboratories.
6. J. M. Pearson and M. Szwarc. Trans. Faraday Soc. **60**, 553 (1964).

Received February 4, 1966.
Division of Pure Chemistry,
National Research Council,
Ottawa, Canada.

Can. J. Chem. Downloaded from www.nrcresearchpress.com by 210.87.254.42 on 09/05/12
For personal use only.

ORGANIC COMPOUNDS OF URANIUM. PART I. REACTIONS OF URANIUM PENTAETHOXIDE WITH β-KETOESTERS

A. M. Bhandari and R. N. Kapoor

The reaction between alkoxides of aluminium (1), neodymium (2), praseodymium (3), titanium (4), niobium (5), tantalum (6), and samarium (B. S. Sankhla and R. N. Kapoor, private communication), and bidentate ligands like β-diketones and β-ketoesters have recently been studied in these and other laboratories with interesting results regarding the volatility and coordination number of the products. No reference appears to be available in the literature on the preparation of β-ketoester derivatives of pentavalent uranium. It was therefore considered of interest to carry out reactions between β-ketoesters and uranium pentaethoxide.

A systematic study was made of the reactions of uranium pentaethoxide with β-ketoesters (methyl acetoacetate and ethyl acetoacetate) in different stoichiometric ratios in benzene solution. The ethanol produced in these reactions was fractionated azeotropically and estimated by an oxidation method (7). It was found that the reaction proceeded comparatively easily up to the replacement of two ethoxy groups, but thereafter became very slow and required a larger amount of the β-ketoester. The final product appeared to be $(EtO)_2U(lig)_3$. All of the derivatives, $(EtO)_xU(lig)_{5-x}$ (where $x = 2$, 3, or 4), were dark-brown liquids or pasty solids. The viscosity increased as more ethoxy groups were replaced. These derivatives could be distilled under reduced pressure. In all of them the uranium was found to be pentavalent.

Description of the products of the reactions of uranium pentaethoxide with methyl acetoacetate and ethyl acetoacetate in different stoichiometric ratios are given in Table I.

On the basis of the analyses of the products formed, the various reactions of uranium pentaethoxide with β-ketoesters may be represented by the following equations, which probably involve an S_N2 type of mechanism (R = the methyl or ethyl group).

radicals with the isobutene unavoidably produced in this system. Pearson and Szwarc (6) have discussed this point. Moreover, it should be noted that any reaction which inhibits the formation of CO from CF_3CO radicals leads to an expected increase in CF_3H/CO and cannot explain the observed decrement. It is concluded, therefore, that the lifetime of CF_3CO radicals with respect to decomposition is small enough to prevent the occurrence of a reaction such as [3] even at concentrations of hydrocarbon near atmospheric pressure.

Thus it seems reasonable to conclude that chemical deactivation is the most likely explanation of the phenomenon observed here. It would be desirable, however, to obtain analytical data to confirm or refute this conclusion.

1. A. N. STRACHAN, R. K. BOYD, and K. O. KUTSCHKE. Can. J. Chem. **42**, 1345 (1964).
2. P. B. AYSCOUGH and E. W. R. STEACIE. Proc. Roy. Soc. London, Ser. A, **234**, 476 (1956).
3. M. KASHA. J. Opt. Soc. Am. **38**, 929 (1948).
4. B. G. TUCKER and E. WHITTLE. Trans. Faraday Soc. **61**, 484 (1965); Proc. Chem. Soc. 93 (1963).
5. A. N. STRACHAN and S. A. MCINTOSH. Unpublished work in these laboratories.
6. J. M. PEARSON and M. SZWARC. Trans. Faraday Soc. **60**, 553 (1964).

RECEIVED FEBRUARY 4, 1966.
DIVISION OF PURE CHEMISTRY,
NATIONAL RESEARCH COUNCIL,
OTTAWA, CANADA.

Can. J. Chem. Downloaded from www.nrcresearchpress.com by 210.87.254.5 on 09/05/12
For personal use only.

ORGANIC COMPOUNDS OF URANIUM. PART I. REACTIONS OF URANIUM PENTAETHOXIDE WITH β-KETOESTERS

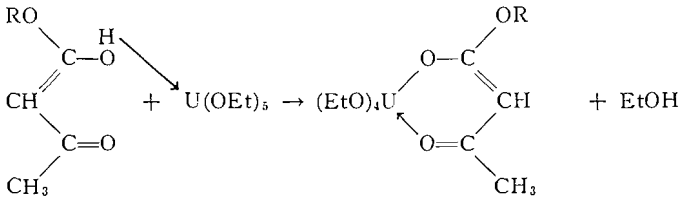
A. M. BHANDARI AND R. N. KAPOOR

The reaction between alkoxides of aluminium (1), neodymium (2), praseodymium (3), titanium (4), niobium (5), tantalum (6), and samarium (B. S. Sankhla and R. N. Kapoor, private communication), and bidentate ligands like β-diketones and β-ketoesters have recently been studied in these and other laboratories with interesting results regarding the volatility and coordination number of the products. No reference appears to be available in the literature on the preparation of β-ketoester derivatives of pentavalent uranium. It was therefore considered of interest to carry out reactions between β-ketoesters and uranium pentaethoxide.

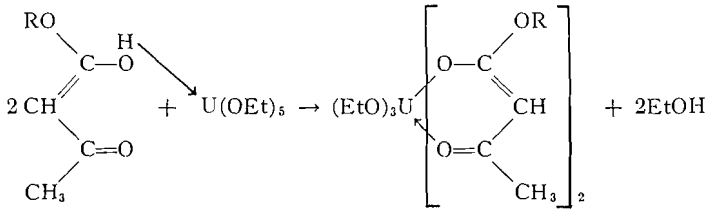
A systematic study was made of the reactions of uranium pentaethoxide with β-ketoesters (methyl acetoacetate and ethyl acetoacetate) in different stoichiometric ratios in benzene solution. The ethanol produced in these reactions was fractionated azeotropically and estimated by an oxidation method (7). It was found that the reaction proceeded comparatively easily up to the replacement of two ethoxy groups, but thereafter became very slow and required a larger amount of the β-ketoester. The final product appeared to be $(EtO)_2U(lig)_3$. All of the derivatives, $(EtO)_xU(lig)_{5-x}$ (where $x = 2$, 3, or 4), were dark-brown liquids or pasty solids. The viscosity increased as more ethoxy groups were replaced. These derivatives could be distilled under reduced pressure. In all of them the uranium was found to be pentavalent.

Description of the products of the reactions of uranium pentaethoxide with methyl acetoacetate and ethyl acetoacetate in different stoichiometric ratios are given in Table I.

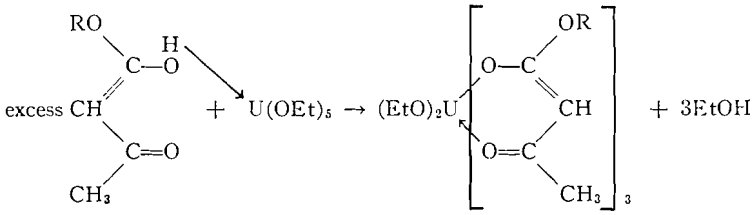
On the basis of the analyses of the products formed, the various reactions of uranium pentaethoxide with β-ketoesters may be represented by the following equations, which probably involve an S_N2 type of mechanism (R = the methyl or ethyl group).



(I)



(II)



(III)

The non-replacement of the fourth ethoxy group of uranium pentaethoxide, even in the presence of an excess of β-ketoesters, could be ascribed either to steric hindrance or to a saturated coordination state (coordination number 8) of compound III.

EXPERIMENTAL

Materials

Uranium pentaethoxide was prepared by the method described by Gilman and co-workers (8), and was distilled before use. Methyl acetoacetate and ethyl acetoacetate were dried by refluxing over aluminium isopropoxide, and distilled at 168–170 °C and 180 °C, respectively. Benzene (B.D.H.) was dried over sodium wire then subjected to azeotropic fractionation in the presence of a little ethanol.

Apparatus

All glass apparatus with interchangeable standard joints was used throughout, special precautions being taken to exclude moisture from the system. Fractionations were carried out in a column packed with Raschig rings and fitted to a total condensation variable takeoff still head.

Analytical Methods

Uranium was estimated as U_3O_8. The ethoxy constituent of the compounds was estimated by hydrolysis, and determination by chromic acid oxidation of the ethanol collected in the ternary azeotrope (7). The valency of the uranium was determined by double oxidation with ceric sulfate, as described by Bradley *et al.* (9).

Reactions

Reaction of Uranium Pentaethoxide with Methyl Acetoacetate in Molar Ratio of 1:1 in Benzene

Methyl acetoacetate (0.43 g) was added to uranium pentaethoxide (1.70 g) in benzene (60 g). The reaction mixture was refluxed for 4 h. The binary azeotrope of benzene–ethanol was collected slowly between 68 to 80 °C. The benzene was slowly distilled at 80 °C. When the mixture cooled, a dark-brown solution was obtained. When the excess solvent was removed under reduced pressure at room temperature, a dark-brown liquid (1.89 g) was left. The azeotrope collected between 68 and 80 °C was found to contain 0.17 g ethanol (calcd. for 1 mole = 0.17 g). The product was distilled under reduced pressure (b.p. 140–141 °C at 0.5 mm) and analyzed.

Can. J. Chem. Downloaded from www.nrcresearchpress.com by 210.87.254.5 on 09/05/12
For personal use only.

Can. J. Chem. Downloaded from www.nrcresearchpress.com by 210.87.254.5 on 09/05/12
For personal use only.

TABLE I

Reactions of uranium pentaethoxide with methyl acetoacetate and with ethyl acetoacetate

Reactants			Ethanol in azeotrope (g)				Results of analysis of product				
							Metal			Ethoxy	
(*a*) Alkoxide (g)	(*b*) β-Ketoester (g)	Molar ratio (*a*/*b*)	Found	Calcd.	Distillation conditions	Product, its state and amount	Valency	Found (%)	Calcd. (%)	Found (%)	Calcd. (%)
With β-ketoester as methyl acetoacetate											
1.70	0.43	1:1	0.17	0.17*	140–141 °C at 0.5 mm	$U(OEt)_4(Meacac)$ brown liquid (1.89 g)	5.0	44.53	44.66	33.50	33.78
2.15	1.08	1:2	0.41	0.43†	152–153 °C at 0.6 mm	$U(OEt)_3(Meacac)_2$ brown viscous liquid (2.75 g)	5.0	39.17	39.48	22.39	22.39
1.26	0.95	1:3	0.24	0.25†	155–156 °C at 0.8 mm	$U(OEt)_3(Meacac)_2$ brown viscous liquid (1.61 g)	5.01	39.40	39.48	22.17	22.39
2.04	2.04	1:4	0.33	0.40†	154 °C at 0.7 mm	$U(OEt)_3(Meacac)_2$ brown viscous liquid (2.62 g)	5.0	39.08	39.48	21.91	22.39
1.26	1.60	1:5	0.35	0.37‡	—	$U(OEt)_2(Meacac)_3$ brown paste (1.82 g)	5.0	35.03	35.37	13.30	13.38
With β-ketoester as ethyl acetoacetate											
0.99	0.26	1:1	0.92	0.98*		$U(OEt)_4(Etacac)$ brown paste (1.08 g)	5.0	43.28	43.51	32.76	32.91
1.74	1.46	1:3	0.32	0.35†		$U(OEt)_3(Etacac)_2$ orange-brown paste (2.22 g)	5.0	37.56	37.72	21.14	21.39
1.49	2.09	1:5	0.41	0.44‡		$U(OEt)_2(Etacac)_3$ orange-brown pasty solid (2.18 g)	5.02	32.89	33.29	12.46	12.59

*For 1 mole.
†For 2 moles.
‡For 3 moles.

ACKNOWLEDGMENT

The authors thank Prof. R. C. Mehrotra, Head of the Department of Chemistry and Dean of the Faculty of Science, University of Rajasthan, Jaipur, for valuable criticism, and Prof. R. C. Kapoor, Head of the Department of Chemistry and Dean of the Faculty of Science, University of Jodhpur, for providing laboratory facilities. One of the authors (A. M. B.) is grateful to the Council of Scientific & Industrial Research, New Delhi, for the award of a Junior Research Fellowship during the tenure of which this work was carried out.

1. R. K. Mehrotra and R. C. Mehrotra. Can. J. Chem. **39**, 795 (1961).
2. T. N. Misra. Ph.D. Thesis, Rajasthan University, Jaipur, India. 1963.
3. S. N. Misra. Ph.D. Thesis, Rajasthan University, Jaipur, India. 1965.
4. D. M. Puri and R. C. Mehrotra. J. Less-Common Metals, **3**, 253 (1961).
5. R. C. Mehrotra and P. N. Kapoor. J. Less-Common Metals, **7**, 176 (1964).
6. R. C. Mehrotra and P. N. Kapoor. J. Less-Common Metals, **7**, 453 (1964).
7. D. C. Bradley and W. Wardlaw. J. Chem. Soc. 3450 (1950).
8. R. G. Jones, E. Bindschadler, G. Karmas, F. A. Yoeman, and H. Gilman. J. Am. Chem. Soc. **78**, 4287 (1956).
9. D. C. Bradley, B. N. Chakravarti, and A. K. Chatterjee. J. Inorg. Nucl. Chem. **3**, 367 (1957).

Received October 14, 1965.
Department of Chemistry,
University of Jodhpur,
Jodhpur, India.

RARE-EARTH PICOLINATE AND PICOLINATE-N-OXIDE COMPLEXES

P. G. Manning

Stepwise stability constants for rare-earth picolinate and rare-earth picolinate-N-oxide complexes (Fig. 1) have been reported in two recent publications (1, 2). The *n*-dentate characters of the two ligands were discussed, but no unequivocal conclusions were drawn.

It has been shown in earlier publications (3, 4) that the magnitudes of ratios (P) of stepwise stability constants are useful in elucidating the structures of metal complexes, and in this paper the P values for the picolinate and picolinate-N-oxide systems are analyzed. The stepwise stability constant is defined as

$$b_m = [ML_m]/[ML_{m-1}][L],$$

where M and L are metal and ligand ions respectively. The ratios are given by

$$b_1{:}b_2 = P = S \times T \times R,$$

where S is a statistical factor calculable from a knowledge of the number of available cation sites and ligand groups, T is a measure of the electrostatic repulsion between the bound ligand (in ML_1) and the ligand about to bind (L_2), and R covers any change in the nature of the metal–ligand bonding in the first and second stages of ion association. The S, T, and R factors have been described in detail in earlier publications (3, 4). For the α-hydroxymonocarboxylate complexes of rare-earth, cupric, and zinc ions $T = 1.6$ and $R = 1.0$ (3), and it was postulated that a T value $= 1.6$ is valid for singly charged ligands binding to transition metal or rare-earth ions. This T value also holds for some transition metal halide and amino acid complexes (5).

Can. J. Chem. Downloaded from www.nrcresearchpress.com by 210.87.254.5 on 09/05/12
For personal use only.

ACKNOWLEDGMENT

The authors thank Prof. R. C. Mehrotra, Head of the Department of Chemistry and Dean of the Faculty of Science, University of Rajasthan, Jaipur, for valuable criticism, and Prof. R. C. Kapoor, Head of the Department of Chemistry and Dean of the Faculty of Science, University of Jodhpur, for providing laboratory facilities. One of the authors (A. M. B.) is grateful to the Council of Scientific & Industrial Research, New Delhi, for the award of a Junior Research Fellowship during the tenure of which this work was carried out.

1. R. K. Mehrotra and R. C. Mehrotra. Can. J. Chem. **39**, 795 (1961).
2. T. N. Misra. Ph.D. Thesis, Rajasthan University, Jaipur, India. 1963.
3. S. N. Misra. Ph.D. Thesis, Rajasthan University, Jaipur, India. 1965.
4. D. M. Puri and R. C. Mehrotra. J. Less-Common Metals, **3**, 253 (1961).
5. R. C. Mehrotra and P. N. Kapoor. J. Less-Common Metals, **7**, 176 (1964).
6. R. C. Mehrotra and P. N. Kapoor. J. Less-Common Metals, **7**, 453 (1964).
7. D. C. Bradley and W. Wardlaw. J. Chem. Soc. 3450 (1950).
8. R. G. Jones, E. Bindschadler, G. Karmas, F. A. Yoeman, and H. Gilman. J. Am. Chem. Soc. **78**, 4287 (1956).
9. D. C. Bradley, B. N. Chakravarti, and A. K. Chatterjee. J. Inorg. Nucl. Chem. **3**, 367 (1957).

Received October 14, 1965.
Department of Chemistry,
University of Jodhpur,
Jodhpur, India.

RARE-EARTH PICOLINATE AND PICOLINATE-N-OXIDE COMPLEXES

P. G. Manning

Stepwise stability constants for rare-earth picolinate and rare-earth picolinate-N-oxide complexes (Fig. 1) have been reported in two recent publications (1, 2). The *n*-dentate characters of the two ligands were discussed, but no unequivocal conclusions were drawn.

It has been shown in earlier publications (3, 4) that the magnitudes of ratios (P) of stepwise stability constants are useful in elucidating the structures of metal complexes, and in this paper the P values for the picolinate and picolinate-N-oxide systems are analyzed. The stepwise stability constant is defined as

$$b_m = [ML_m]/[ML_{m-1}][L],$$

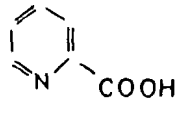
where M and L are metal and ligand ions respectively. The ratios are given by

$$b_1{:}b_2 = P = S \times T \times R,$$

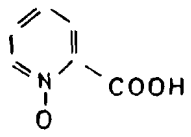
where S is a statistical factor calculable from a knowledge of the number of available cation sites and ligand groups, T is a measure of the electrostatic repulsion between the bound ligand (in ML_1) and the ligand about to bind (L_2), and R covers any change in the nature of the metal–ligand bonding in the first and second stages of ion association. The S, T, and R factors have been described in detail in earlier publications (3, 4). For the α-hydroxymonocarboxylate complexes of rare-earth, cupric, and zinc ions $T = 1.6$ and $R = 1.0$ (3), and it was postulated that a T value $= 1.6$ is valid for singly charged ligands binding to transition metal or rare-earth ions. This T value also holds for some transition metal halide and amino acid complexes (5).

Can. J. Chem. Downloaded from www.nrcresearchpress.com by 210.87.254.105 on 09/05/12
For personal use only.

P values for the presently studied systems may be calculated in the following manner. For a monodentate ligand binding to a six-coordinate rare-earth ion $S = 2 \times 6/5 = 2.40$. Table I lists P, S, and T values for monodentate and bidentate ligands associating with 6- and 8-coordinate cations. The experimentally determined P values are listed in Table II.



Picolinic acid



Picolinic acid-N-Oxide

FIG. 1.

TABLE I

Calculation of P values

	6-Coordinated		8-Coordinated*	
	Monodentate ligand	Bidentate ligand	Monodentate ligand	Bidentate ligand
S	2.4	4.8	2.3	3.5
T	1.6	1.6	1.6	1.6
P	3.85	7.7	3.7	5.6

*Dodecahedral structure. Also $S = 3.4$ for cube arrangement and bidentate ligandcy.

TABLE II

Log P(obs.) values for rare-earth complexes

Metal	Picolinate (1)	Picolinate (2)	N-Oxide (2)
La	0.80	1.11	0.77
Ce	0.92	1.53	
Pr	0.74	0.99	0.49
Nd	0.84	0.93	0.76
Sm	0.70	0.86	
Eu	0.66	0.87	0.65
Gd	0.78	0.70	0.66
Tb	0.68		
Dy	0.70	0.74	0.45
Ho	0.72		
Er	0.70		
Tm	0.74	1.14	0.47
Yb	0.74	0.90	0.55
Lu	0.70	1.43	0.64
Average P(obs.)	5.6	10	4.0

The P(calcd.) and P(obs.) are indicative of a monodentate picolinic acid-N-oxide. The pK_a value (3.31) for this ligand is of the same order as the pK_a values for the α-hydroxymonocarboxylic acids studied earlier. For a much weaker acid, however, the metal–ligand bond may have a lifetime greater than that of a metal–water bond, and chelation would then occur. The P(obs.) values for the picolinic acid ($pK = 5.34$) complexes are consistent with bidentate ligandcy (Tables I and II). Thompson's (1) P(obs.) values indicate an 8-coordinate cation whereas the data of Yoneda and co-workers (2) support a 6-coordinate structure. If we omit the two "wild" P(obs.) values for Ce and Lu picolinates, as determined by Yoneda and co-workers (2), the P(obs.) and P(calcd.)

Can. J. Chem. Downloaded from www.nrcresearchpress.com by 210.87.254.105 on 09/05/12
For personal use only.

values are in good agreement. Thompson's (1) data are extremely consistent, however, so that an unequivocal decision as to the coordination number of rare-earth ions cannot be reached. It is apparent, nevertheless, that the independent derivation of P values for the picolinate system should resolve the argument.

Yoneda and co-workers (2) suggested that the greater stability of the picolinate-N-oxide complexes relative to the acetate species was indicative of bidentate ligandcy. However, it was postulated in a recent publication (4) that the rare-earth acetates were ion pairs, and the greater stability of the picolinate-N-oxide complexes, therefore, is not proof of bidentate ligandcy.

The author is grateful to the referees for the interesting suggestion that the coordination number of the rare-earth ions depends on the nature of the medium. The data analyzed here could be interpreted in terms of an 8-coordinate structure in 0.1 M KNO_3 (ref. 1) and a 6-coordinate structure in 2.0 M $NaClO_4$ (ref. 2). An earlier examination of the rare-earth α-hydroxymonocarboxylate system (3) indicated that these ligands were monodentate. The S values for the 8- and 6-coordinate structures (2.3 and 2.4 respectively) were too close to give any information on the rare-earth coordination number.

T values seem to show little dependence upon ionic strength. In the α-hydroxymonocarboxylate system (3), experimental data determined at ionic strengths of 0.1 and 2.0 were analyzed with reasonable facility. Furthermore, T values for the cupric acetates (3) also seemed to be independent of ionic strength, at least within experimental error.

1. L. C. THOMPSON. Inorg. Chem. **3**, 1319 (1964).
2. H. YONEDA, G. R. CHOPPIN, J. L. BEAR, and A. J. GRAFFEO. Inorg. Chem. **4**, 244 (1965).
3. P. G. MANNING. Can. J. Chem. **43**, 3258 (1965).
4. P. G. MANNING. Can. J. Chem. **43**, 3476 (1965).
5. P. G. MANNING. Can. J. Chem. To be published.

RECEIVED DECEMBER 15, 1965.
MINERAL PHYSICS SECTION,
MINES BRANCH,
DEPARTMENT OF MINES AND TECHNICAL SURVEYS,
OTTAWA, CANADA.

THE SIGN, TEMPERATURE, AND SOLVENT DEPENDENCE OF THE PROTON COUPLING CONSTANT AND CHEMICAL SHIFT IN α-CHLOROACRYLONITRILE

K. A. MCLAUCHLAN, L. W. REEVES, AND T. SCHAEFER

Solvent dependent geminal proton coupling constants, J, appear to decrease algebraically as the dielectric constant of the medium increases (1–4). Some workers (4) suggest a linear dependence of J on the reaction field (5) of the medium, whereas others (2) suggest specific interactions of solute molecules with donor or acceptor atoms in the solvent molecules. Further experiments are here reported on the solvent and temperature dependence of J and the chemical shift of the protons in α-chloroacrylonitrile. The sign of J is shown to be opposite to that of $J(^{13}C—H)$ in this molecule (see Experimental) and is taken as negative in the discussion that follows.

Temperature and Solvent Dependence of J

From Table I it is seen that in methylcyclohexane and toluene J increases appreciably as the temperature increases. The increase of J in methylcyclohexane may indicate that

Can. J. Chem. Downloaded from www.nrcresearchpress.com by 210.87.254.105 on 09/05/12
For personal use only.

values are in good agreement. Thompson's (1) data are extremely consistent, however, so that an unequivocal decision as to the coordination number of rare-earth ions cannot be reached. It is apparent, nevertheless, that the independent derivation of P values for the picolinate system should resolve the argument.

Yoneda and co-workers (2) suggested that the greater stability of the picolinate-N-oxide complexes relative to the acetate species was indicative of bidentate ligandcy. However, it was postulated in a recent publication (4) that the rare-earth acetates were ion pairs, and the greater stability of the picolinate-N-oxide complexes, therefore, is not proof of bidentate ligandcy.

The author is grateful to the referees for the interesting suggestion that the coordination number of the rare-earth ions depends on the nature of the medium. The data analyzed here could be interpreted in terms of an 8-coordinate structure in 0.1 M KNO_3 (ref. 1) and a 6-coordinate structure in 2.0 M $NaClO_4$ (ref. 2). An earlier examination of the rare-earth α-hydroxymonocarboxylate system (3) indicated that these ligands were monodentate. The S values for the 8- and 6-coordinate structures (2.3 and 2.4 respectively) were too close to give any information on the rare-earth coordination number.

T values seem to show little dependence upon ionic strength. In the α-hydroxymonocarboxylate system (3), experimental data determined at ionic strengths of 0.1 and 2.0 were analyzed with reasonable facility. Furthermore, T values for the cupric acetates (3) also seemed to be independent of ionic strength, at least within experimental error.

1. L. C. THOMPSON. Inorg. Chem. **3**, 1319 (1964).
2. H. YONEDA, G. R. CHOPPIN, J. L. BEAR, and A. J. GRAFFEO. Inorg. Chem. **4**, 244 (1965).
3. P. G. MANNING. Can. J. Chem. **43**, 3258 (1965).
4. P. G. MANNING. Can. J. Chem. **43**, 3476 (1965).
5. P. G. MANNING. Can. J. Chem. To be published.

RECEIVED DECEMBER 15, 1965.
MINERAL PHYSICS SECTION,
MINES BRANCH,
DEPARTMENT OF MINES AND TECHNICAL SURVEYS,
OTTAWA, CANADA.

THE SIGN, TEMPERATURE, AND SOLVENT DEPENDENCE OF THE PROTON COUPLING CONSTANT AND CHEMICAL SHIFT IN α-CHLOROACRYLONITRILE

K. A. MCLAUCHLAN, L. W. REEVES, AND T. SCHAEFER

Solvent dependent geminal proton coupling constants, J, appear to decrease algebraically as the dielectric constant of the medium increases (1–4). Some workers (4) suggest a linear dependence of J on the reaction field (5) of the medium, whereas others (2) suggest specific interactions of solute molecules with donor or acceptor atoms in the solvent molecules. Further experiments are here reported on the solvent and temperature dependence of J and the chemical shift of the protons in α-chloroacrylonitrile. The sign of J is shown to be opposite to that of $J(^{13}C—H)$ in this molecule (see Experimental) and is taken as negative in the discussion that follows.

Temperature and Solvent Dependence of J

From Table I it is seen that in methylcyclohexane and toluene J increases appreciably as the temperature increases. The increase of J in methylcyclohexane may indicate that

Can. J. Chem. Downloaded from www.nrcresearchpress.com by 210.87.254.105 on 09/05/12
For personal use only.

self-association of solute molecules decreases as the temperature increases, but a corresponding change in the chemical shift is not observed. In toluene, association with solvent molecules is indicated since, at −80 °C, J is smaller than in the pure compound at 35 °C (1) and also smaller than in methylcyclohexane whose dielectric constant is nearly the same as that of toluene. The association with toluene molecules may be of a dipole–induced dipole type as discussed by Schneider (6). In both acetonitrile and dimethylformamide the temperature dependence of J is either very small or zero, although the chemical shift changes are appreciable.

Watts and Goldstein (4) suggest that the change in J parallels the reaction field of the medium as measured by the function $Z(\epsilon) = (\epsilon - 1)/(2\epsilon + 2.5)$. Their extrapolation of J to the limit $Z(1) = 0$ is based on the points for cyclohexane and dimethylformamide as solvents at 35 °C. They obtain $J = -1.4$ c/s. $Z(\epsilon)$ changes by only 0.02 to 0.03 for methylcyclohexane and toluene over the temperature range in Table I, but the $Z(\epsilon)$ dependence of J appears to be linear in both solvents. However, an extrapolation of such a plot to $Z(1) = 0$ yields $J = -0.7$ to -0.9 c/s, indicating the very approximate validity of such extrapolations.

*Temperature and Solvent Dependence of the Chemical Shift**

A graph of the mean chemical shift of the protons in Table I versus temperature indicates that at high temperatures the mean chemical shift approaches a common value, probably that in tetramethylsilane at infinite dilution (4). From this viewpoint it is natural that the largest changes in shift for a given temperature interval occur for those solvents (toluene and dimethylformamide) in which the low temperature value of the shift deviates most from the value in tetramethylsilane.

In toluene the ring-current effect, together with decreasing solute–solvent association, accounts for the large low-field shift observed as the temperature increases. In acetonitrile and dimethylformamide the shift changes are appreciable and as expected, if hydrogen bonds with the solvent molecules are being broken as the temperature increase shifts the equilibrium towards the non-bonded species. The shift change in acetonitrile is less than in dimethylformamide. In acetonitrile as solvent there is a *positive* contribution to the hydrogen bond shift of a proton donor by the magnetic anisotropy of the cyano group (7). It opposes the larger but comparable negative contribution from the electric field effect. Hence the total shift on hydrogen bonding may well be less than in dimethylformamide, where the anisotropy of the carbonyl group probably reinforces the low-field electric field shift. If the hydrogen bond energy is comparable in the two solvents, the relative temperature dependence of the shift in the two solvents appears reasonable.

Graphs of shift versus $Z(\epsilon)$ in the solvents toluene, acetonitrile, and dimethylformamide are linear for each solvent, but the $Z(\epsilon)$ dependence is much greater than that obtained by Watts and Goldstein (4) for different solvents at 35 °C. For the three solvents above it is very probable that there is an association with the solvent which is strongly temperature dependent. Correlations with $Z(\epsilon)$ are therefore of limited utility.

The reaction field model is valid only for a solute molecule in a medium which in no way interacts with solute molecules at the molecular level but simply presents a continuum of certain dielectric properties. For protons which are normally exposed to direct contact with solvent molecules, the reaction field model is probably realistic only for solvents of low dielectric constant. This was pointed out originally by Buckingham (5), but since then

**The low-field shift is consistently assigned to the proton trans to the chlorine atom for reasons discussed by Watts and Goldstein (4).*

Can. J. Chem. Downloaded from www.nrcresearchpress.com by 210.87.254.105 on 09/05/12
For personal use only.

Can. J. Chem. Downloaded from www.nrcresearchpress.com by 210.87.254.105 on 09/05/12
For personal use only.

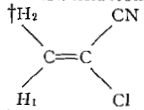
TABLE I

Solvent and temperature dependence of the chemical shift* and proton coupling constant of α-chloroacrylonitrile

	Solvent											
	Methylcyclohexane			Toluene			Acetonitrile			Dimethylformamide		
	−58 °C	40 °C	72 °C	−80 °C	40 °C	72 °C	−40 °C	40 °C	72 °C	−58 °C	40 °C	72 °C
$-J$(H—C—H), c/s	2.60±0.02	2.40±0.02	2.36±0.02	2.84±0.04	2.61±0.02	2.53±0.02	3.04±0.02	3.00±0.03	2.97±0.03	3.11±0.03	3.15±0.03	3.13±0.02
$\nu(H_1)$†, p.p.m.	5.868	5.874	‡	4.657	5.166	5.234	6.351	6.273	6.241	6.798	6.527	6.462
$\nu(H_2)$†, p.p.m.	6.006	6.974	‡	4.697	5.222	5.292	6.479	6.389	6.351	6.992	6.701	6.624
ϵ§	2.15‖	1.99‖	1.94‖	2.62	2.345	2.275	48.0	34.0	28.4	50.5	34.3	29.0
$Z(\epsilon)$¶	0.169	0.153	0.148	0.209	0.187	0.181	0.477	0.468	0.462	0.478	0.468	0.463

*To low field from internal tetramethylsilane, with a precision of ±0.002 p.p.m.

†



.

‡Because of its high volatility, locking to the tetramethylsilane resonance peak was impossible. However, the shift change from −58 to 40 °C is very small so that the shift change from 40 to 72 °C will be almost negligible.

§Dielectric constant.

‖For cyclohexane (see Experimental).

¶$Z(\epsilon) = (\epsilon - 1)/(2\epsilon + 2.5)$.

this qualification has been largely ignored. Temperature studies are probably a good test of the model's validity for any particular solute–solvent system.

EXPERIMENTAL

Samples of α-chloroacrylonitrile were prepared as approximate 5% v/v solutions in the four solvents in Table I. Cyclohexane itself was not used because of its high melting point. Small amounts of tetramethylsilane were added to serve as an internal reference and locking signal. The proton resonance spectrum of each sample was recorded at three temperatures on an HA-100 Varian spectrometer. The temperature extremes depended on the liquid range of the solvent and were measured with an accuracy of 1 deg C by calibration with a methanol sample. Dielectric constant data are given in Table I for the pure solvents and were taken from refs. 8–11. The dielectric constant of methylcyclohexane at 20° is the same as that of cyclohexane (9, 10) and is here assumed to be that of cyclohexane at the other temperatures.

The sign of J was determined by a heteronuclear "tickling" (12) experiment performed on a modified Varian D.P.60 spectrometer operating at 56.4 Mc/s in the proton region. The modifications, which have been described elsewhere (13), consisted firstly in stabilizing the field/frequency ratio by a feedback loop operated from the signal of the internal reference compound. The probe was tuned both to the ^1H and ^{13}C (ca. 14.18 Mc/s) resonance frequencies and irradiating power was obtained at the lower frequency from a Rohde and Schwarz frequency synthesizer. The behavior observed in the "tickling" experiments was consistent only with the directly bonded ^{13}C—H coupling being of opposite sign to the geminal proton–proton coupling.

ACKNOWLEDGMENTS

L. W. R. and T. S. thank the Basic Physics Division for guest-worker facilities and the National Research Council, Ottawa, for financial aid. This work forms part of the research program of the National Physical Laboratory and is published by permission of the Director.

1. V. S. Watts, G. S. Reddy, and J. H. Goldstein. J. Mol. Spectry. **11**, 325 (1963).
2. P. Bates, S. Cawley, and S. S. Danyluk. J. Chem. Phys. **40**, 2415 (1964).
3. B. L. Shapiro, S. J. Ebersole, and R. M. Kopchik. J. Chem. Phys. **39**, 3154 (1963); J. Mol. Spectry. **11**, 326 (1963).
4. V. S. Watts and J. H. Goldstein. J. Chem. Phys. **42**, 228 (1965).
5. A. D. Buckingham. Can. J. Chem. **38**, 300 (1960).
6. W. G. Schneider. J. Phys. Chem. **66**, 2653 (1962).
7. P. J. Berkeley and M. W. Hanna. J. Am. Chem. Soc. **86**, 2990 (1964).
8. R. E. Gray (*Editor*). American institute of physics handbook. 2nd ed. McGraw-Hill Book Company, New York. 1963.
9. G. W. C. Kaye and T. H. Laby (*Editors*). Table of physical and chemical constants. 12th ed. Longmans, Green and Company, London. 1959.
10. A. Aihara and M. Davies. J. Colloid Sci. **11**, 671 (1956).
11. G. R. Leader and J. G. Gormley. J. Am. Chem. Soc. **73**, 5731 (1951).
12. R. Freeman and W. A. Anderson. J. Chem. Phys. **37**, 2053 (1962).
13. K. A. McLauchlan, L. W. Reeves, and D. H. Whiffen. Mol. Phys. In press.

Received January 19, 1966.
Physical Chemistry Laboratory,
South Parks Road,
Oxford, England.

AN IMPROVED PREPARATION, ANALYSIS, AND SOME PROPERTIES OF TETRAOXYGEN DIFLUORIDE[1]

A. G. Streng

Tetraoxygen difluoride, O_4F_2, is the fourth member of the oxygen fluorides series and like all the other members of the group is a high energy oxidizer. Tetraoxygen difluoride was first synthesized in 1958 and isolated in 1960 (1, 2). Since then, the method of

[1]*This paper describes a part of work performed for the Office of Naval Research, Contract Nonr 3085(01).*

Can. J. Chem. Downloaded from www.nrcresearchpress.com by 210.87.254.105 on 09/05/12
For personal use only.

this qualification has been largely ignored. Temperature studies are probably a good test of the model's validity for any particular solute–solvent system.

EXPERIMENTAL

Samples of α-chloroacrylonitrile were prepared as approximate 5% v/v solutions in the four solvents in Table I. Cyclohexane itself was not used because of its high melting point. Small amounts of tetramethylsilane were added to serve as an internal reference and locking signal. The proton resonance spectrum of each sample was recorded at three temperatures on an HA-100 Varian spectrometer. The temperature extremes depended on the liquid range of the solvent and were measured with an accuracy of 1 deg C by calibration with a methanol sample. Dielectric constant data are given in Table I for the pure solvents and were taken from refs. 8–11. The dielectric constant of methylcyclohexane at 20° is the same as that of cyclohexane (9, 10) and is here assumed to be that of cyclohexane at the other temperatures.

The sign of J was determined by a heteronuclear "tickling" (12) experiment performed on a modified Varian D.P.60 spectrometer operating at 56.4 Mc/s in the proton region. The modifications, which have been described elsewhere (13), consisted firstly in stabilizing the field/frequency ratio by a feedback loop operated from the signal of the internal reference compound. The probe was tuned both to the ^1H and ^{13}C (ca. 14.18 Mc/s) resonance frequencies and irradiating power was obtained at the lower frequency from a Rohde and Schwarz frequency synthesizer. The behavior observed in the "tickling" experiments was consistent only with the directly bonded ^{13}C—H coupling being of opposite sign to the geminal proton–proton coupling.

ACKNOWLEDGMENTS

L. W. R. and T. S. thank the Basic Physics Division for guest-worker facilities and the National Research Council, Ottawa, for financial aid. This work forms part of the research program of the National Physical Laboratory and is published by permission of the Director.

1. V. S. Watts, G. S. Reddy, and J. H. Goldstein. J. Mol. Spectry. **11**, 325 (1963).
2. P. Bates, S. Cawley, and S. S. Danyluk. J. Chem. Phys. **40**, 2415 (1964).
3. B. L. Shapiro, S. J. Ebersole, and R. M. Kopchik. J. Chem. Phys. **39**, 3154 (1963); J. Mol. Spectry. **11**, 326 (1963).
4. V. S. Watts and J. H. Goldstein. J. Chem. Phys. **42**, 228 (1965).
5. A. D. Buckingham. Can. J. Chem. **38**, 300 (1960).
6. W. G. Schneider. J. Phys. Chem. **66**, 2653 (1962).
7. P. J. Berkeley and M. W. Hanna. J. Am. Chem. Soc. **86**, 2990 (1964).
8. R. E. Gray (*Editor*). American institute of physics handbook. 2nd ed. McGraw-Hill Book Company, New York. 1963.
9. G. W. C. Kaye and T. H. Laby (*Editors*). Table of physical and chemical constants. 12th ed. Longmans, Green and Company, London. 1959.
10. A. Aihara and M. Davies. J. Colloid Sci. **11**, 671 (1956).
11. G. R. Leader and J. G. Gormley. J. Am. Chem. Soc. **73**, 5731 (1951).
12. R. Freeman and W. A. Anderson. J. Chem. Phys. **37**, 2053 (1962).
13. K. A. McLauchlan, L. W. Reeves, and D. H. Whiffen. Mol. Phys. In press.

Received January 19, 1966.
Physical Chemistry Laboratory,
South Parks Road,
Oxford, England.

AN IMPROVED PREPARATION, ANALYSIS, AND SOME PROPERTIES OF TETRAOXYGEN DIFLUORIDE[1]

A. G. Streng

Tetraoxygen difluoride, O_4F_2, is the fourth member of the oxygen fluorides series and like all the other members of the group is a high energy oxidizer. Tetraoxygen difluoride was first synthesized in 1958 and isolated in 1960 (1, 2). Since then, the method of

[1]*This paper describes a part of work performed for the Office of Naval Research, Contract Nonr 3085(01).*

Can. J. Chem. Downloaded from www.nrcresearchpress.com by 210.87.254.42 on 09/05/12
For personal use only.

preparation of O_4F_2 has been improved (3) and a number of its properties have been determined

METHOD OF PREPARATION OF TETRAOXYGEN DIFLUORIDE

Like O_2F_2 and O_3F_2, tetraoxygen difluoride is prepared from the elements in a high-voltage electric-discharge apparatus, but at much milder conditions. The reaction proceeds in accordance with the equation:

[1] $$2O_2 + F_2 \rightarrow O_4F_2 \quad .$$

The apparatus is shown in Fig. 1.

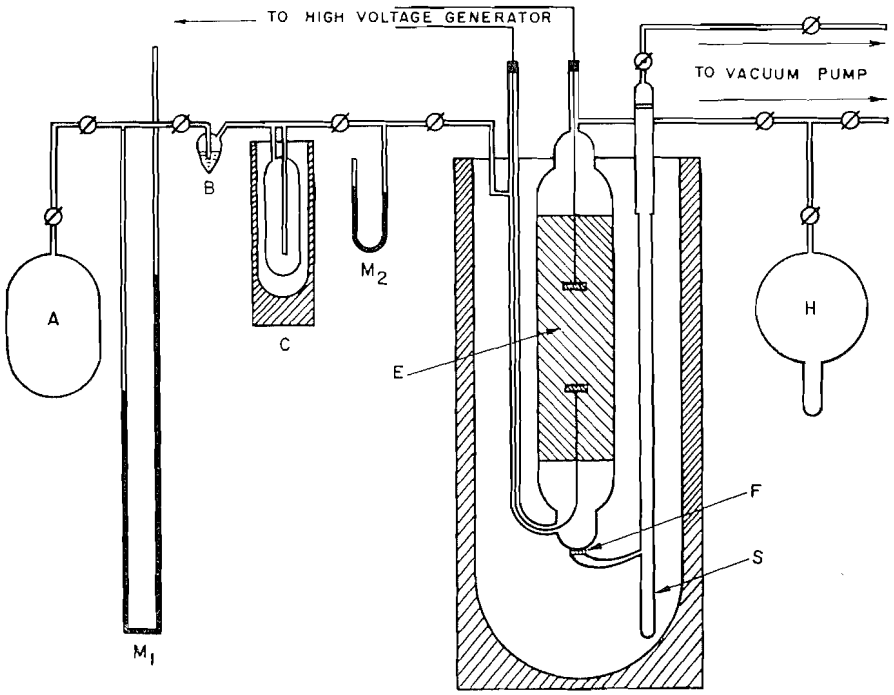


FIG. 1.

A 2:1 (by volume) mixture of oxygen and fluorine is fed from the stainless steel cylinder, A, through the flowmeter, B, containing Kel-F oil No. 3, and through the trap, C, cooled with Dry Ice, into the reaction vessel, E, cooled to 60–70 °K. M_1 and M_2 are the manometers for measuring the gas pressure in cylinder A and in reaction vessel E, respectively. They are filled with mercury covered with Kel-F oil No. 3.

A high voltage electric discharge is established in the reaction vessel between the copper electrodes which are fixed 4.5 cm apart. The discharges varied from 4 to 6 mA at 1 000 – 1 500 V; the power input should not exceed 6 W.

In distinction to the Pyrex glass reaction vessel (1, 2) used earlier, the main part of the reaction vessel in the new apparatus is made of copper. Copper was chosen as the material for the reaction zone walls because of its high thermal conductivity, since it is important to quench rapidly the O_4F_2 formed and thus avoid its decomposition.

The reaction vessel is 3 cm in diameter and 18 cm long. Its total volume, including connection tubes, is about 280 cm^3. Before use for preparation of O_4F_2, the reaction vessel and the whole apparatus must be prefluorinated.

Can. J. Chem. Downloaded from www.nrcresearchpress.com by 210.87.254.42 on 09/05/12
For personal use only.

The feed rate of the $2O_2 + F_2$ mixture is adjusted so that the pressure in the reaction vessel is maintained below 15 mm Hg and is usually about 2 cm^3/min. Under these conditions normally all the oxygen–fluorine mixture is consumed and the O_4F_2 formed condenses on the walls of the reaction vessel. The maximum yield of O_4F_2 is about 3 mg/min. Flask H is for measuring and sampling the unreacted gas, in case all the gas fed is not consumed.

The product obtained can be either melted by warming the cooling bath to about 85 °K or dissolved and rinsed down (with an appropriate solvent), filtered through glass filter F, and collected in tube S. Carbon tetrafluoride (Freon-14) or oxygen difluoride can be used as solvents for O_4F_2. If commercially available Freon-14 is used, it is advisable to treat it (before use as a solvent for O_4F_2) with fluorine at room temperature to eliminate possible traces of oxidizable impurities.

Pure tetraoxygen difluoride or its solutions are stored cooled in liquid nitrogen.

The amount of SiF_4, usually formed as a by-product during preparation of O_4F_2, was reduced in the new reaction vessel to 2–4% by weight with respect to the amount of the tetraoxygen difluoride produced. Tetraoxygen difluoride is an explosive compound. Thus, corresponding safety precautions must be taken in its preparation, storage, and handling.

CHEMICAL ANALYSIS OF TETRAOXYGEN DIFLUORIDE

For chemical analysis, tetraoxygen difluoride is decomposed into oxygen and fluorine by warming it slowly to room temperature. The gas evolved is measured and analyzed for O_2 and F_2.

Fluorine can be determined by the Moissan method, namely by reaction with dry metallic mercury in a gas burette at room temperature. The gas mixture must be shaken with mercury until the volume of the remaining gas is constant. Fluorine reacts with mercury quantitatively, forming solid mercury fluorides, HgF and HgF_2. Thus, the decrease of the gas volume indicates the amount of F_2 present. This figure is then checked to determine the amount of F^- formed by reacting the mercury fluorides with a known amount of a standard solution of NaOH, in accordance with the equations

[2] $$Hg_2F_2 + 2NaOH \rightarrow 2NaF + Hg_2O + H_2O$$

or

[3] $$HgF_2 + 2NaOH \rightarrow 2NaF + HgO + H_2O \quad .$$

In any case, the amount of sodium hydroxide consumed corresponds to the amount of F_2 present. The excess NaOH is back-titrated with standard HCl. The residual gas (after absorption of F_2 with Hg) is analyzed for oxygen by absorption of O_2 with an alkaline pyrogallol solution. The decrease in the volume of gas indicates the amount of O_2 present. Fluorine may be determined also by reaction with dry potassium iodide

[4] $$F_2 + 2KI \rightarrow 2KF + I_2$$

and subsequent titration of the iodine evolved by a standard solution of $Na_2S_2O_3$.

The accuracy of the analysis depends upon the size of the sample and the accuracy of the measurements.

PROPERTIES OF TETRAOXYGEN DIFLUORIDE

Some of the properties of O_4F_2 have been described in earlier publications (1, 4–8). Additional characteristics are given here.

Thermal Stability

At 90 °K tetraoxygen difluoride decomposes with about a 16 day half-life to trioxygen difluoride and oxygen. Trioxygen difluoride decomposes, in turn, at 90–115 °K to O_2F_2 and

Can. J. Chem. Downloaded from www.nrcresearchpress.com by 210.87.254.42 on 09/05/12
For personal use only.

finally to O_2 and F_2. Pure O_4F_2, or its solidified solutions containing about 1 mole % of O_4F_2 in CF_4, has been kept at liquid nitrogen temperature for weeks without noticeable decomposition. O_4F_2 explodes at fast warming.

Vapor Pressure

In addition to the two values (5) obtained earlier, the vapor pressure of tetraoxygen difluoride at 90 °K was found to be 0.25 mm Hg.

Melting and Boiling Points

The melting point of O_4F_2 was found to be 82 ± 2 °K. The extrapolated normal boiling point of O_4F_2 is 194 °K. The compound decomposes completely below this temperature.

Solubility

Solid O_4F_2 is practically insoluble in liquid nitrogen at 77 °K, and in liquid argon at 85 °K, i.e. the solubility is less than 0.01 mole % (the limit of our detection). In liquid oxygen at 77 °K the solubility of O_4F_2 is about 0.05 mole %.

Carbon tetrafluoride (Freon-14) dissolves appreciable amounts of O_4F_2 at 90 °K (melting point of CF_4 = 89.2 °K). The solution containing 1 mole % of O_4F_2 is reddish brown. Reddish brown solutions of O_4F_2 have been obtained also in $CClF_3$ (Freon-13) at 90 °K. Mixtures of CF_4 with 50% $CClF_3$ (by volume, liquid), or with 3% O_2, or with 6% N_2, or with 15% NF_3, dissolve about 1 mole % of O_4F_2 at 77 °K.

Tetraoxygen difluoride is readily soluble in liquid oxygen difluoride, OF_2. At 77 °K, the solubility is about 2% by weight; at 90 °K, OF_2 dissolves 5% by weight (or 3 moles %), or more, of O_4F_2.

Reaction with Ozone

At 116 °K (melting point of Freon-12), tetraoxygen difluoride decomposes and, if there is contact with concentrated ozone, both explode.

Reaction with Tetrafluorohydrazine

With N_2F_4, tetraoxygen difluoride (dissolved in OF_2) reacts at 77 °K producing O_2F_2, NF_3, and oxygen.

Reaction with Xenon

If a mixture of tetraoxygen difluoride with xenon (prepared at 77 °K) is warmed slowly to 195 °K, O_4F_2 decomposes and a part of its decomposition products reacts with xenon forming xenon fluorides.

ACKNOWLEDGMENTS

Acknowledgment is due to Mrs. L. V. Streng for assistance in the experimental work and to Dr. A. V. Grosse for valuable suggestions.

1. A. V. Grosse, A. G. Streng, and A. D. Kirshenbaum. J. Am. Chem. Soc. **83**, 1004 (1961).
2. A. G. Streng and A. V. Grosse. First Annual Progress Report for the Office of Naval Research, Contract Nonr 3085(01). Research Institute of Temple University, Philadelphia, Pa. January 3, 1961.
3. A. G. Streng and A. V. Grosse. Fifth Annual Progress Report for the Office of Naval Research, Contract Nonr 3085(01). Research Institute of Temple University, Philadelphia, Pa. January 5, 1965.
4. A. G. Streng. Chem. Rev. **63**, 607 (1963).
5. I. J. Solomon. Report No. IITRT-C227-6, IIT Research Institute, Chicago, Illinois. February 19, 1964.
6. A. G. Streng and L. V. Streng. J. Phys. Chem. **69**, 1079 (1965).
7. A. Arkell. J. Am. Chem. Soc. **87**, 4057 (1965).
8. A. D. Kirshenbaum and A. G. Streng. An electron paramagnetic resonance study of oxygen fluorides. II. Tetraoxygen difluoride. J. Am. Chem. Soc. In press.

Received February 15, 1966.
Research Institute of Temple University,
Philadelphia, Pennsylvania.

Can. J. Chem. Downloaded from www.nrcresearchpress.com by 210.87.254.42 on 09/05/12
For personal use only.

COMPLEXES OF ALKYL AND ARYL CYANIDES. PART III.[1] THE FAR-INFRARED SPECTRA (500–200 CM^{-1}) AND ASSIGNMENT OF THE METAL–NITROGEN STRETCHING FREQUENCY IN COMPLEXES WITH PALLADIUM(II), PLATINUM(II), AND RHODIUM(III) HALIDES

R. A. WALTON[2]

In a recent study (2) of the infrared spectra (4 000 – 265 cm^{-1}) of the methyl and phenyl cyanide complexes of palladium(II) and platinum(II) halides, no bands were observed which could be assigned to the ν(Pd—N) and ν(Pt—N) modes. Similarly, ν(M—N) modes have not been observed in studies on the far-infrared spectra of alkyl cyanide complexes of a variety of metal halides (3–5). However, Evans and Lo (6) have assigned ν(Zn—N) to a strong band at 174 cm^{-1} in the infrared spectrum of $ZnCl_2.2MeCN$, and recently, Farha and Iwamoto (7) have examined the infrared spectra of several cyanopyridine complexes of copper(I), silver(I), and gold(I) perchlorates and, in the case of the nitrogen-bonded 2-cyanopyridine complexes, observed a new band in the 480–520 cm^{-1} region. This they point out is in the region where Lott (unpublished observations, quoted in ref. 7) has assigned ν(M—N) modes.

Although "metal–nitrogen" stretching vibrations have been assigned in several ammine (8, 9) and pyridine (10) complexes of the platinum metals, no such modes have yet been reported for the alkyl and aryl cyanide complexes of these metals. The present note reports the far-infrared spectra of several of these complexes in the 500–200 cm^{-1} region.

EXPERIMENTAL

Spectra were recorded in Nujol mulls between polythene plates on a Grubb-Parsons DM4 spectrophotometer which was calibrated with the spectrum of water vapor. The frequencies quoted are probably accurate to ± 2 cm^{-1}. The platinum(II) and palladium(II) were prepared as previously described (2) by the method of Hofmann and Bugge (11). Analytical data for the ethyl cyanide complexes, which were not reported previously (2), are shown below.

Dichlorobispropionitrileplatinum(II). Yellow crystals. Anal. Found: C, 20.30; H, 2.64; N, 7.60. $PtCl_2.2C_3H_5N$ requires C, 19.15; H, 2.68; N, 7.45.

Dibromobispropionitrileplatinum(II). Yellow crystals. Anal. Found: C, 15.72; H, 2.11; N, 6.64. $PtBr_2.2C_3H_5N$ requires C, 15.49; H, 2.17; N, 6.02.

For both complexes, the analytical data is consistent with the presence of a trace of "free" ligand, which was not readily removed on pumping *in vacuo*.

The alkyl cyanide complexes of rhodium(III) were those samples described in Part II of this series (1).

RESULTS AND DISCUSSION

Although metal–nitrogen stretching modes occur around 500 cm^{-1} in a variety of ammine complexes (8, 9), in other systems, e.g. metal halide – pyridine (py) complexes (10), these vibrations may occur as low as 200 cm^{-1}. Table I lists the principal infrared absorption bands recorded in the region 500–200 cm^{-1}. In addition, the infrared spectra of the 2,2-bipyridyl complexes MX_2.bipy, where M = Pd(II) or Pt(II) and X = Cl or Br, have been examined in this region and are included in Table I.

Durig *et al.* (12) have reported that for $PdCl_2$.bipy, the ν(Pd—N) modes occur as weak bands at 479 and 446 cm^{-1}. These workers also assigned ν(Pd—N) vibrations to bands $\sim$ 460 cm^{-1} in *cis*- and *trans*-$PdCl_2.2py$, whereas such modes are invariably found near

[1]*For Part II see ref. 1.*

[2]*Present address: Department of Chemistry, Massachusetts Institute of Technology, Cambridge 39, Massachusetts, U.S.A.*

Can. J. Chem. Downloaded from www.nrcresearchpress.com by 210.87.254.6 on 09/05/12
For personal use only.

TABLE I

Principal infrared absorption bands in the region 500–200 cm^{-1} for the alkyl cyanide complexes of palladium(II), platinum(II), and rhodium(III)

$PtCl_2.2MeCN$	353 s,* 344 s,* 310 sh,* 270–250 w,br, 226 m
$PtBr_2.2MeCN$	313 m,* 303 sh,* 277 w, 238 s,† 227 sh,† 213 m-s
$PtCl_2.2EtCN$	428 w, 397 m, 338 s,† 316 m-w, ~285 sh
$PtBr_2.2EtCN$	376 vw, 307 vw, 242 s,† 225 sh†
$PdCl_2.2PhCN$	415 m,* 364 s,* 308 m-s,* 281 s,* 247 m
$PtCl_2.2PhCN$	353 s,* 341 s,* 301 m-s,* ~270 sh
$PtBr_2.2PhCN$	240 s,† 234 s†
$RhCl_3.3PhCN$	421 w, 401 w, 384 m-w, 365 sh, 353 s, 325 m, 285 s
$RhCl_3.3MeO.CH_2CH_2.CN$	448 m-s, 385 w, ~360 sh, 347 s, ~335 sh, 275 m,br
$PdCl_2.bipy$	441 w, 409 s,* 352 sh,* 341 vs,* 320 m,* 275 m, 244 m, ~200‡
$PtCl_2.bipy$	410 s,* 383 vw, 347 s,* 333 s,* 289 m-w,* 256 m-w, ~200‡
$PtBr_2.bipy$	430 m, 410 s,* 370 w,* 285 w, 265 w, 235 s,† 224 s,† 209 m

ABBREVIATIONS: s = strong; sh = shoulder; w = weak; br = broad; m = medium; v = very.
*Similar band observed in an earlier study (see ref. 2).
†Platinum–halogen stretching vibration.
‡At the limit of the measurements.

200 cm^{-1} in pyridine complexes of transition metal halides (10). In the present study, a weak band was observed at 441 cm^{-1} in the spectrum of $PdCl_2.bipy$, but the presence of a band of similar intensity at 479 cm^{-1} could not be confirmed. These weak bands may arise from ligand vibrations activated by coordination, whereas medium-strong bands at ~410 cm^{-1}, observed in the complexes $MX_2.bipy$, are almost certainly the modified ligand vibration which occurs at ~400 cm^{-1} in free bipyridyl. The infrared spectra of the 2,2′-bipyridyl complexes also revealed bands at ~280, ~255, and ~200 cm^{-1}, which may be associated with the metal–nitrogen stretching vibrations. However, in other systems (13), such modes have not been observed above 200 cm^{-1}. These bands are unlikely to arise from modified ligand vibrations since no such absorptions are observed in the spectra of the free ligand (2, 13) or other bipyridyl complexes (4, 13, 14). The expected *cis*-planar configuration of the bromide complex $PtBr_2.bipy$ was confirmed by the observation of ν(Pt—Br) at 235 and 224 cm^{-1}; for a *cis*-planar configuration two such modes (symmetry $A_1 + B_1$) are expected.

In none of the alkyl cyanide complexes (Table I) were bands observed above 350 cm^{-1} which could be assigned to ν(M—N), thus contradicting the observations of Lott (unpublished observations, quoted in ref. 7). However, for the palladium(II) and platinum(II) complexes several bands, other than those assigned to ν(M—X), were observed between 350 and 200 cm^{-1} (see also ref. 2). Their number and position depended upon the particular halide and cyanide, and their assignment as ν(M—N) was not generally in keeping with the known stereochemistry of the complexes. Thus *trans*-$PdCl_2.2PhCN$, for which one ν(Pd—N) mode is predicted, had bands at 308 (m-s),* 281 (s),* and 247 (m-w)* cm^{-1}, whereas *cis*-$PtCl_2.2PhCN$ had only one band at 301 (m-s) cm^{-1} (with a weak shoulder at ~270 cm^{-1}) in the same region of the spectrum. Similarly, this difficulty was not resolved for the rhodium(III) complexes, $RhCl_3.3RCN$ (1), which in all cases had a single band below 290 cm^{-1}. Also, a comparison of the analogous chloride and bromide complexes of platinum(II) did not reveal bands which were independent of halogen, although most complexes had a band in the region 320–300 cm^{-1} which could possibly arise from the metal–nitrogen stretching vibration. In fact, in the case of $PtBr_2.2EtCN$ and $PtBr_2.2Ph$ CN, no prominent bands were observed below 350 cm^{-1} other than those due to ν(Pt—Br), although $PtBr_2.2EtCN$ had a very weak absorption at 307 cm^{-1}.

**m = medium; s = strong; w = weak.*

Can. J. Chem. Downloaded from www.nrcresearchpress.com by 210.87.254.6 on 09/05/12
For personal use only.

Bands in the 320–200 cm^{-1} region are unlikely to arise from ligand modes activated by coordination, since neither the infrared nor Raman spectra of the free ligands (15–17) reveal bands in this region. Also, since these bands are not independent of halogen for a particular metal ion, they cannot be associated with pure metal–nitrogen stretching vibrations. Thus the present study indicates that none of the infrared absorption bands above 200 cm^{-1} can be unambiguously assigned to ν(M—N). However, these modes may well occur below 200 cm^{-1}, as reported for $ZnCl_2.2MeCN$ (6).

ACKNOWLEDGMENT

The award of a D.S.I.R. Postdoctorate fellowship is gratefully acknowledged.

1. B. F. G. Johnson and R. A. Walton. J. Inorg. Nucl. Chem. In press. 1966.
2. R. A. Walton. Spectrochim. Acta, **21**, 1795 (1965).
3. I. R. Beattie, G. P. McQuillan, L. Rule, and M. Webster. J. Chem. Soc. 1514 (1963).
4. I. R. Beattie and M. Webster. J. Chem. Soc. 3507 (1964).
5. R. J. H. Clark. Spectrochim. Acta, **21**, 955 (1965).
6. J. C. Evans and G. Y. S. Lo. Spectrochim. Acta, **21**, 1033 (1965).
7. F. Farha and R. T. Iwamoto. Inorg. Chem. **4**, 844 (1965).
8. H. Poulet, P. Delorme, and J. P. Mathieu. Spectrochim. Acta, **20**, 1855 (1964).
9. K. Nakamoto. Infrared spectra of inorganic and co-ordination compounds. John Wiley, New York. 1963. p. 146.
10. R. J. H. Clark and C. S. Williams. Inorg. Chem. **4**, 350 (1965).
11. K. A. Hofmann and G. Bugge. Ber. **40**, 1772 (1907).
12. J. R. Durig, R. Layton, D. W. Sink, and B. R. Mitchell. Spectrochim. Acta, **21**, 1367 (1965).
13. R. J. H. Clark. J. Chem. Soc. 1377 (1963).
14. R. A. Walton. Ph.D. Thesis, University of Southampton, Southampton, England. 1964.
15. P. Venkateswarlu. J. Chem. Phys. **19**, 293 (1951); **20**, 923 (1952).
16. N. E. Duncan and G. J. Janz. J. Chem. Phys. **23**, 434 (1955).
17. J. H. S. Green. Spectrochim. Acta, **17**, 607 (1961).

Received January 27, 1966.
Department of Chemistry,
University of Manchester,
Manchester, England.

Can. J. Chem. Downloaded from www.nrcresearchpress.com by 210.87.254.6 on 09/05/12
For personal use only.

Can. J. Chem. Downloaded from www.nrcresearchpress.com by 210.87.254.40 on 09/05/12
For personal use only.

Canadian Journal of Chemistry

Issued by THE NATIONAL RESEARCH COUNCIL OF CANADA

VOLUME 44 JULY 1, 1966 NUMBER 13

REACTIONS OF SUGAR CHLOROSULFATES

VII. SOME CONFORMATIONAL ASPECTS

A. G. COTTRELL,[1] E. BUNCEL, AND J. K. N. JONES

Department of Chemistry, Queen's University, Kingston, Ontario

Received January 13, 1966

ABSTRACT

The reaction of sulfuryl chloride with several 1,6-anhydro-hexosans has yielded crystalline, fully chlorosulfated derivatives. Replacement of the chlorosulfate moieties by chlorodeoxy groups could not be achieved under the reaction conditions employed. This non-reactivity is discussed in terms of steric interactions in the transition state for substitution.

An examination of some chloro-substituted sugar chlorosulfates confirmed that an axial chlorodeoxy group in a glycopyranoside deactivates a neighboring equatorial chlorosulfate group and thus prevents further chlorodeoxy groups being introduced into such positions. Methyl α-D-altropyranoside, methyl α-L-rhamnopyranoside, methyl α-D-lyxopyranoside, L-rhamnose, and D-lyxose were reacted with sulfuryl chloride. The resulting products were those expected if these sugars reacted primarily in the C1 conformation.

INTRODUCTION

Previous work (1–5) has shown that the reaction of sulfuryl chloride with carbohydrates containing free hydroxyl groups gives derivatives containing both chlorodeoxy and chlorosulfate moieties, and that these products are formed via fully chlorosulfated derivatives. The chlorodeoxy groups are derived by the nucleophilic displacement (S_N2) of certain of the chlorosulfate groups by chloride ion. Kinetic studies carried out with model alkyl chlorosulfates have shown the remarkable facility with which the OSO_2Cl moiety can act as a leaving group (6).

It has been shown in the previous work carried out with hexopyranoses and hexopyranosides that the OSO_2Cl group at C-6 is the most reactive and is readily converted into a chlorodeoxy group. Preferential displacement at C-6 in hexopyranosides has been noted previously, for instance, with the tosyl derivatives (7).

Whether a secondary chlorosulfate group is replaced by the chloride ion depends on the conformation of the pyranoside of which it forms a part. Several steric factors have been demonstrated to affect adversely the replacement and may be summarized as: (*i*) 1,3-diaxial interactions to the approach of the chloride ion; (*ii*) deactivation of the C-2 position by anomeric chloro and methoxyl groups; and (*iii*) deactivation of an equatorial chlorosulfate ester group vicinal to an axial substituent which itself is resistant to substitution. The relevance of these factors to the synthesis of a fully chlorinated sugar glycoside was considered recently (8).

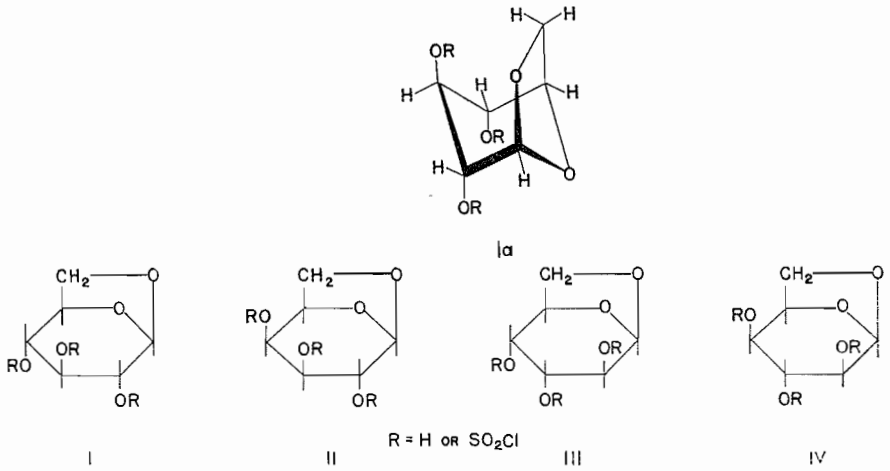
The present paper reports on a number of topics. For the first time, chlorosulfates of 1,6-anhydro-hexopyranoside derivatives have been investigated, with the view that the

[1]*Present address: Imperial Chemical Industries Ltd., Mond Division Research Laboratories, Runcorn Heath, Cheshire, England.*

rigidity of these structures would impose stringent conditions on the substitution process. Secondly, a number of sugars have been examined in which chloro substituents were introduced into certain specific positions to learn more about steric and electronic effects in these substitution processes. Lastly, experiments have been performed with the aim of obtaining further information about the preferred conformation of certain sugars. Thus D-lyxose and D-altrose were considered by Reeves (9) to exist in both C1 and 1C conformations, but other workers (10, 11) have disagreed. It was considered that an examination of chlorosulfate substitution in these compounds might provide a chemical approach to this problem.

The Reaction of 1,6-Anhydro-hexosans

The following hexosans were studied: 1,6-anhydro-β-D-glucopyranose (I, R = H, or I*a*, R = H (conformational formula)), 1,6-anhydro-β-D-galactopyranose (II, R = H), 1,6-anhydro-β-D-altropyranose (III, R = H), and 1,6-anhydro-β-D-idopyranose (IV, R = H). The product obtained in each case was a crystalline 2,3,4-trichlorosulfate (I–IV, R = SO_2Cl). Treatment of the trichlorosulfates with pyridine hydrochloride in chloroform solution failed to introduce chlorodeoxy groups into the molecules under the conditions employed. Since substitution does not occur in any of the cases, it must be



concluded that the steric interactions are too great throughout or, of course, that the reaction conditions employed were not at an optimum. Another factor may contribute to the lower reactivity of the chlorosulfates of these bicyclic systems relative to that of the simple hexopyranosides, namely, that re-hybridization from sp^3 to sp^2 requisite for substitution (12) may be disfavored by the rigidity of this bicyclic system.

The Reaction of Some Substituted Methyl Glycopyranosides

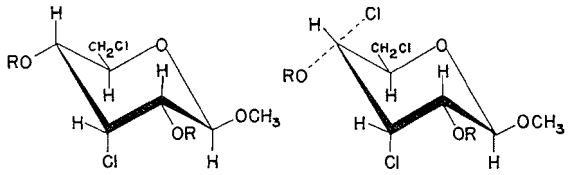
When methyl α- and β-D-glucopyranosides were treated with sulfuryl chloride in pyridine, 4,6-dichloro-substituted derivatives were obtained which were resistant to further substitution (5). In the case of the methyl β-D-glycosidic derivative, in which the anomeric methoxyl group is equatorial, the resistance to further substitution was explained as being due to the deactivating effect of the axial chlorodeoxy group at C-4. It was decided in the current work to examine whether a chlorodeoxy group at C-3 would have the same deactivating effect. The known methyl 3-chloro-3-deoxy-β-D-allopyranoside

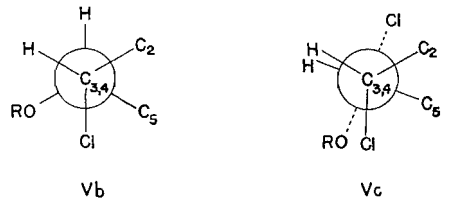
Can. J. Chem. Downloaded from www.nrcresearchpress.com by 210.87.254.40 on 09/05/12
For personal use only.

Can. J. Chem. Downloaded from www.nrcresearchpress.com by 210.87.254.40 on 09/05/12
For personal use only.

was prepared from methyl 4,6-*O*-benzylidene-β-D-glucopyranoside. The methyl 3-chloro-3-deoxy-β-D-allopyranoside (V) was then treated with sulfuryl chloride in the usual way. The product was a syrup which, on dechlorosulfation, gave a crystalline compound that was most probably methyl 3,6-dichloro-3,6-dideoxy-β-D-allopyranoside. Elemental analysis showed the formation of a dichlorodideoxy compound, and periodate oxidation results indicated that the chlorodeoxy groups were at the C-3 and C-6 positions. The D-allo configuration is assumed, since in all cases examined hitherto the chlorodeoxy groups were observed to be introduced with inversion (3–5).

The observation that no further substitution by chloride ion occurred under these standard conditions to form a trichlorotrideoxy derivative indicates a deactivating effect of the axial chloro group at C-3. This is further evidence that an axial substituent which cannot itself be replaced deactivates a vicinal, equatorial chlorosulfate ester group. A possible explanation for this is shown in formulae V–V*c*. To introduce a chlorodeoxy





group at C-4 by S_N2 reaction, the transition state V*a* would have to be formed (13). The end-on representation of V and V*a*, viewed along the C-3, C-4 axis, is shown in V*b* and V*c*, and it is seen that steric interaction in V*c* between the chlorodeoxy group on C-3 and the large chlorosulfate group on C-4 would strongly hinder S_N2 reaction at C-4.

The Reaction of Methyl α-L-Rhamnopyranoside and L-Rhamnose

Methyl α-L-rhamnopyranoside has the anomeric methoxyl group on C-1 and the hydroxyl group on C-2 axially oriented, since its preferred conformation is 1C (9). The product obtained from its reaction with sulfuryl chloride in pyridine was a crystalline trichlorosulfate, and no further substitution could be obtained even when it was heated in chloroform solution with pyridine hydrochloride. A chlorodeoxy group might perhaps be introduced into methyl α-L-rhamnopyranoside at C-2 since this chlorosulfate group is axially oriented, by analogy with cyclohexyl derivatives where it is known that axial substituents are displaced at a faster rate than corresponding equatorial substituents. The axial methoxyl group at C-1 would further hinder substitution at C-2.

To verify the latter effect, L-rhamnose itself was reacted with sulfuryl chloride and pyridine. The product from this reaction was a crystalline compound which analyzed as (β?)-L-rhamnosyl chloride 2,3,4-trichlorosulfate. Treatment of this trichlorosulfate with pyridine hydrochloride yielded a syrup which, after dechlorosulfation, had the R_f value and chlorine content expected for a dichlorodideoxy compound. A periodate oxidation

showed no uptake of reagent within 2 days, as expected for 2,4-dichloro-2,4,6-trideoxy-L-galactose which would result if it is assumed that inversion takes place in the normal manner when the chlorodeoxy groups are introduced. The only other possible structure which would not be affected by periodate is a 2,3-dichloro-2,3,6-trideoxy compound, but the formation of the compound is unlikely on the basis of previous results.

The Reactions of Methyl α-D-Altropyranoside, Methyl α-D-Lyxopyranoside, and D-Lyxose

Glycosides and free sugars in the D-altropyranose and D-lyxopyranose configurations have been reported as existing in the C1 and 1C conformations.

Methyl 6-chloro-6-deoxy-α-D-altropyranoside was obtained from methyl α-D-altropyranoside after it was reacted with sulfuryl chloride in pyridine followed by dechlorosulfation. This is the product that would be formed if the glycoside reacted in the C1 conformation, since in this conformation the C-2 and C-3 hydroxyl groups are axially oriented. In the 1C conformation the OR (R = H or SO_2Cl) group at C-4 would be axially oriented, as would be also the CH_2Cl group on C-5. Substitution of the axial chlorosulfate group at C-4 is therefore prevented by the neighboring axial CH_2Cl group.

Proof of the structure of the methyl 6-chloro-6-deoxy-α-D-altropyranoside was given by its elemental analysis and periodate oxidation. The periodate oxidation of this compound was somewhat unusual. The consumption of 2 moles of periodate and the release of 1 mole of formic acid were consistent with the chlorodeoxy group being on C-6. However, unlike the periodate oxidation of the corresponding gluco compound, the rate of production of formic acid was much less than half the uptake of periodate during the first 6 h of the oxidation, and it was not until the reaction had been proceeding for about 1 day that the number of moles of formic acid released became approximately half the number of moles of periodate consumed. If an internal hemiacetal is postulated as an intermediate, these results may be explained.

Methyl α-D-lyxopyranoside in the C1 conformation has the axial glycosidic methoxyl group at C-1 and also an axial substituent at C-2. This situation is directly analogous to the situation in methyl α-D-mannopyranoside and methyl α-L-rhamnopyranoside, which also have axial groups at C-1 and C-2. Methyl α-D-mannopyranoside was shown to yield methyl 6-chloro-6-deoxy-α-D-mannopyranoside 2,3,4-trichlorosulfate when reacted with sulfuryl chloride (5). It was found in the present study that the reaction between methyl α-D-lyxopyranoside and sulfuryl chloride yielded methyl α-D-lyxopyranoside 2,3,4-trichlorosulfate; no chlorodeoxy groups could be introduced by reacting the product further with pyridine hydrochloride. However, if methyl α-D-lyxopyranoside reacted in the 1C conformation, the product might well be the same, since in this conformation the C-3 and C-4 hydroxyl groups would be axial.

To extend the analogy with the manno conformation further, it was decided to examine the reaction of D-lyxose with the sulfuryl chloride – pyridine mixture. D-Mannose had been found to yield a 6-chloro-6-deoxy-trichlorosulfate which, when reacted with pyridine hydrochloride, gave a trichlorotrideoxy compound whose methyl glycoside was assigned the structure methyl 2,4,6-trichlorotrideoxy-β-D-galactopyranoside (compare with L-rhamnose) (5). D-Lyxose also gave a chloro-trichlorosulfate derivative when reacted with sulfuryl chloride, and reaction with pyridine hydrochloride followed by treatment with sodium iodide solution now gave a syrup which was shown by thin-layer chromatography and chlorine analysis to be a dichlorodideoxy sugar. Periodate oxidation showed no uptake of periodate after 48 h, so that the compound was probably 2,4-dichloro-2,4-dideoxy-L-arabinose if the sugar is assumed to react in the pyranose form. The other possibility,

Can. J. Chem. Downloaded from www.nrcresearchpress.com by 210.87.254.40 on 09/05/12
For personal use only.

2,3-dichloro-2,3-dideoxy-D-ribose, is considered to be unlikely, since the D-ribose configuration is known to undergo readily further substitution at C-4 (14). This indicates that D-lyxopyranose reacts primarily in the C1 conformation, as does D-mannopyranose. If it were in the 1C conformation, there would be an axial chlorosulfate at both C-3 and C-4 and an equatorial chlorosulfate group at C-2. This situation would be unlikely to lead to further introduction of chlorodeoxy groups.

EXPERIMENTAL[2]

Thin-layer chromatograms were run by the ascending technique on glass plates which had been coated with silica gel G and dried at 150–160° for 2 h. The following solvent systems were used: (*a*) benzene–methanol (10:1), (*b*) benzene–methanol (20:1), (*c*) benzene–methanol (50:1), and (*d*) benzene–isopropanol (2:1). The sugars were detected on chromatograms by spraying them with sulfuric acid and subsequent heating of the plate in an oven at 110°.

Three general procedures were used. (A) Sulfuryl chloride[3] was added dropwise to the stirred pyridine–chloroform reaction mixtures, cooled in an acetone – solid carbon dioxide bath (approximately −70°), and maintained at this temperature for 2 h, after which time the mixtures were allowed to come to room temperature and held at that temperature for 1 to 2 h. The products were then isolated in the usual way (1–5). (B) The experiment was repeated, except that the mixture was left for 8–12 h before the products were isolated. (C) If thin-layer chromatography (t.l.c.) indicated that further reaction had taken place, then the product was heated with pyridine hydrochloride in dry chloroform to complete, as far as the configuration would allow, the formation of chlorodeoxy groups.

Tetra-*n*-butylammonium chloride could be used as an alternative source of chloride ions to effect displacement (see below).

The Preparation of 1,6-Anhydro Sugars

1,6-Anhydro-β-D-glucopyranose was obtained by the pyrolytic distillation of starch (15) but with the following modification. The dry starch was mixed with copper powder to improve heat transfer through the decomposing starch, and a layer of glass wool was placed above the charge to reduce frothing. The yield was about 40 g from 150 g of starch (26.8%).

1,6-Anhydro-3,4-*O*-isopropylidene-β-D-galactopyranose was prepared from α-lactose monohydrate (16) except that copper powder was mixed with the charge to improve heat transfer through the decomposing lactose. 1,6-Anhydro-3,4-*O*-isopropylidene-β-D-galactopyranose (10 g) was dissolved in water, and the solution was treated with 8 g of Amberlite IR-120 (H^+) resin for 1½ h on a water bath at 70° and then filtered. The product, after evaporation, was recrystallized from alcohol–water (80:20). The yield of 1,6-anhydro-D-galactopyranose, m.p. 220°, was practically quantitative.

1,6-Anhydro-β-D-altropyranose was prepared as follows. A solution of syrupy methyl α-D-altropyranoside (17) in 200 ml of 6% hydrochloric acid was refluxed for 2 h. The solution was neutralized with lead carbonate and filtered, and the lead ions were removed from the filtrate as lead sulfide. The filtered solution was then deionized to yield 10.5 g of syrup. The syrup (6 g) was separated on a cellulose column (63 × 5 cm). The eluting solvent was butan-1-ol half saturated with water. The first fraction was nonreducing in character, and crystallized as long, needle-shaped crystals upon evaporation of the solvent. The relative speed of movement on paper of D-altrose and 1,6-anhydro-β-D-altropyranose is not great but was sufficient to follow the separation without difficulty. In solvent system *e* (ethyl acetate – acetic acid – formic acid – water (18:3:1:4 by volume)) the R_{Rh} of D-altrose was 0.70, and of 1,6-anhydro-β-D-altropyranose 0.95. The yield of 1,6-anhydro-β-D-altropyranose was 2 g (63%), and of D-altrose 1.5 g (58%), characterized as the penta-acetate (17). The yields are based on a 53:47 ratio of anhydro compound to free sugar. 1,6-Anhydro-β-D-altropyranose analyzed as the anhydrous sugar.

Anal. Calcd. for $C_6H_{10}O_5$: C, 44.4; H, 6.22. Found: C, 44.4; H, 6.07.

No definite melting point has previously been reported for 1,6-anhydro-β-D-altropyranose. The melting point of the above sample was 133°, with slight preliminary sintering. It had $[\alpha]_D$ −210° (*c*, 1.0 in water). A sample of 1,6-anhydro-β-D-altropyranose was also obtained from Dr. N. K. Richtmyer; this had a melting point and a mixed melting point with the above sample of 133°. The infrared spectrographs of the two samples were also identical. Dr. Richtmyer's sample was believed to have been the monohydrate before it was stored.

1,6-Anhydro-β-D-glucopyranose 2,3,4-Trichlorosulfate

1,6-Anhydro-β-D-glucopyranose (2 g, 0.012 mole) in dry pyridine (8 ml, 0.099 mole) and dry chloroform (25 ml) was treated with sulfuryl chloride (5 ml, 0.061 mole) and the product isolated according to

[2]*For details see refs. 1–5.*

[3]*The amount of sulfuryl chloride used to make the chlorosulfate ester was 1.5 to 2 moles per hydroxyl group. The pyridine – sulfuryl chloride ratio was in the range 1.5 to 2 moles per mole.*

Can. J. Chem. Downloaded from www.nrcresearchpress.com by 210.87.254.40 on 09/05/12
For personal use only.

procedure A. Recrystallization from chloroform–petrol gave colorless needles, 3.6 g (66%), m.p. 144–146°, $[\alpha]_D$ −17° (*c*, 1.0 in chloroform).

Anal. Calcd. for $C_6H_7Cl_3O_{11}S_3$: C, 15.7; H, 1.54; Cl, 23.2; S, 21.0. Found: C, 15.6; H, 1.66; Cl, 23.1; S, 21.3.

The product gave a positive test for chlorosulfate groups. The infrared spectrum exhibited very sharp peaks at 1 200 and 1 435 cm^{-1} characteristic of chlorosulfate groups (18).

A small amount of crystalline 1,6-anhydro-β-D-glucopyranose 2,3,4-trichlorosulfate was dissolved in methanol (5 ml), and barium carbonate (1 g) was added. One drop of *N* sodium iodide solution was added to dechlorosulfate the product; after 8 h the liquor was co-chromatographed against 1,6-anhydro-β-D-glucopyranose on a paper run in solvent *f* (butan-1-ol–ethanol–water (3:1:1 v/v/v)). The only sugar detected was 1,6-anhydro-β-D-glucopyranose.

The reaction between 1,6-anhydro-β-D-glucopyranose and sulfuryl chloride was carried out according to procedure B. The only chloroform-soluble product obtained was 1,6-anhydro-β-D-glucopyranose 2,3,4-trichlorosulfate.

1,6-Anhydro-β-D-glucopyranose 2,3,4-trichlorosulfate (2 g, 0.043 mole) in dry chloroform (20 ml) and pyridine hydrochloride (2 g, 0.012 mole) was treated according to procedure C. The white crystals so obtained (0.6 g (40.0%)) were found to be identical with the starting material. A small amount of a reducing product (0.012 g) was also obtained but could not be identified.

1,6-Anhydro-β-D-galactopyranose 2,3,4-Trichlorosulfate

1,6-Anhydro-β-D-galactopyranose (1.5 g, 0.0093 mole) in dry pyridine (6 ml, 0.075 mole) and dry chloroform was reacted with excess sulfuryl chloride (4 ml, 0.049 mole) (procedure A). The product was recrystallized from chloroform – petrol (b.p. 35–60°) to give colorless needles, 1.7 g (40%), m.p. 105–106°, $[\alpha]_D$ −27° (*c*, 1.0 in chloroform). The material gave a positive test for chlorosulfate groups and the infrared spectrum exhibited very sharp peaks at 1 418 and 1 183 cm^{-1} corresponding to OSO_2Cl groups (18).

Anal. Calcd. for $C_6H_7Cl_3O_{11}S_3$: C, 15.7; H, 1.54; S, 21.1; Cl, 23.2. Found: C, 15.4; H, 1.64; S, 20.8; Cl, 23.0.

Procedure B gave 1,6-anhydro-β-D-galactopyranose 2,3,4-trichlorosulfate in somewhat lower yield.

1,6-Anhydro-β-D-altropyranose 2,3,4-Trichlorosulfate

1,6-Anhydro-β-D-altropyranose (0.67 g, 0.0041 mole) in pyridine (3 ml, 0.038 mole) and dry chloroform (10 ml) was treated with an excess of sulfuryl chloride (2 ml, 0.025 mole) according to procedure A. The product was recrystallized from chloroform – petrol (b.p. 40–65°) as white needles, 0.74 g (40%), m.p. 143°, $[\alpha]_D^{25}$ −130° (*c*, 0.1 in chloroform). It gave a positive test for chlorosulfate groups and the infrared spectrum exhibited very sharp peaks corresponding to OSO_2Cl groups.

Anal. Calcd. for $C_6H_7Cl_3O_{11}S_3$: C, 15.7; H, 1.54; Cl, 23.2; S, 21.1. Found: C, 15.3; H, 1.4; Cl, 23.0; S, 21.0.

Procedure B gave 1,6-anhydro-β-D-altropyranose 2,3,4-trichlorosulfate in somewhat lower yield.

1,6-Anhydro-β-D-idopyranose 2,3,4-Trichlorosulfate[4]

1,6-Anhydro-β-D-idopyranose (1.01 g from 2.0 g of the triacetate) in pyridine (4.5 ml) and dry chloroform (12.0 ml) was converted into the trichlorosulfate by addition of sulfuryl chloride (2.2 ml) to the mixture (procedure A). The crystalline product had m.p. 164–165° and $[\alpha]_D$ −41° (*c*, 1.8 in methanol).

Anal. Calcd. for $C_6H_7Cl_3O_{11}S_3$: C, 15.7; H, 1.54; Cl, 23.2; S, 21.1. Found: C, 16.1; H, 1.83; Cl, 22.9; S, 21.1.

Procedure C gave starting material as the main product. Some small quantities of other unidentified sugar derivatives were also produced.

Methyl 3,6-Dichloro-3,6-dideoxy-β-D-allopyranoside

Methyl 3-chloro-3-deoxy-β-D-allopyranoside (1.4 g, 0.007 mole), prepared from methyl 4,6-*O*-benzylidene-β-D-glucopyranoside, in pyridine (6 ml, 0.0075 mole) and chloroform was treated with sulfuryl chloride according to procedure A. The product was a syrup (2 g (88%)) which solidified but could not be recrystallized. Dechlorosulfation with sodium iodide gave a crystalline product which, after two recrystallizations, was shown to be pure by t.l.c. in solvent *f* (as used for paper chromatography), R_f 0.59, yield 1.0 g (75%), $[\alpha]_D$ −45°, m.p. 145–156° with some decomposition.

Anal. Calcd. for $C_7H_{12}Cl_2O_4$: C, 36.4; H, 5.23; Cl, 30.7. Found: C, 36.6; H, 5.37; Cl, 30.5.

Periodate oxidation of the methyl 3,6-dichloro-3,6-dideoxy-β-D-allopyranoside, determined in the usual way (19, 20), showed no consumption of periodate during 24 h.

Methyl α-L-Rhamnopyranoside 2,3,4-Trichlorosulfate

Methyl α-L-rhamnopyranoside (31) (0.5 g, 0.003 mole) in anhydrous pyridine (3 ml, 0.038 mole) and dry chloroform (10 ml) was treated with sulfuryl chloride (2 ml, 0.025 mole) (procedure A). The crystalline product was recrystallized from chloroform–petrol, 0.9 g (64%), m.p. 112–113°, $[\alpha]_D$ −2° (*c*, 1.0 in chloroform). Infrared analysis and the aniline–pyridine spray test confirmed the presence of chlorosulfate groups.

[4]*This experiment was carried out by Mr. S. S. Ali.*

Can. J. Chem. Downloaded from www.nrcresearchpress.com by 210.87.254.40 on 09/05/12
For personal use only.

Anal. Calcd. for $C_7H_{11}Cl_3O_{11}S_3$: C, 17.8; H, 2.3; Cl, 22.5; S, 20.0. Found: C, 18.1; H, 2.1; Cl, 22.5; S, 20.1.

A portion of the above crystals (0.5 g, 0.002 mole) in chloroform and anhydrous pyridine hydrochloride (0.5 g, 0.044 mole) was treated according to procedure C. The melting point (112–113°) of the product (0.3 g) was undepressed on admixture with the starting compound.

(β?)-L-Rhamnosyl Chloride 2,3,4-Trichlorosulfate

L-Rhamnose (8 g, 0.05 mole) (dehydrated by heating it at 50° in a vacuum oven for several hours) in pyridine (30 ml) and chloroform (85 ml) was treated with 17 ml of sulfuryl chloride (procedure A). The crystalline product was recrystallized from chloroform – petrol (b.p. 40–60°), 8.5 g (35%), m.p. 140°, $[\alpha]_D$ +57.8° (*c*, 0.1 in chloroform).

Anal. Calcd. for $C_6H_8Cl_4O_{10}S_3$: C, 15.1; H, 1.69; Cl, 29.7; S, 20.1. Found: C, 14.8; H, 1.69; Cl, 29.6; S, 20.5.

The trichlorosulfate (5 g) was dissolved in a minimum of dry chloroform which contained an excess of pyridine hydrochloride, and the solution was heated for 12 h. The product, after dechlorosulfation, contained a major component with R_f 0.67 (solvent *e*). It was purified by preparative thin-layer chromatography and then distilled. The syrupy product had $[\alpha]_D$ −45° (*c*, 1.0 in chloroform).

Anal. Calcd. for $C_6H_{10}Cl_2O_3$: Cl, 35.3. Found: Cl, 35.8.

Periodate oxidation of the dichlorodideoxy compound showed no consumption of periodate during 48 h.

Methyl 6-Chloro-6-deoxy-α-D-altropyranoside 2,3,4-Trichlorosulfate

Methyl α-D-altropyranoside (1 g, 0.0052 mole) in anhydrous pyridine (5 ml, 0.062 mole) and chloroform (20 ml) was treated with sulfuryl chloride (3 ml, 0.037 mole) (procedure A). The crystalline product was recrystallized from chloroform–petrol to give colorless prisms, 2.1 g (79.5%), m.p. 156°, $[\alpha]_D$ +99.2° (*c*, 0.97 in chloroform).

Anal. Calcd. for $C_7H_{10}Cl_4O_{11}S_3$: C, 16.5; H, 1.98; Cl, 27.9; S, 18.9. Found: C, 16.8; H, 2.04; Cl, 28.1; S, 19.0.

Methyl 6-Chloro-6-deoxy-α-D-altropyranoside

The above crystals (2 g) were dissolved in methanol and dechlorosulfated with sodium iodide as previously described. The colorless syrup (1 g (60%)) was shown by t.l.c. to be one component with R_f 0.25 in solvent *b*, $[\alpha]_D$ +101° (*c*, 0.92 in chloroform).

Anal. Calcd. for $C_7H_{13}ClO_5$: C, 39.5; H, 6.16; Cl, 16.7. Found: C, 39.3; H, 6.07; Cl, 16.7.

Periodate Oxidation of Methyl 6-Chloro-6-deoxy-α-D-altropyranoside

A sample of the glycoside (39 mg) was oxidized in the usual way (20). The results are shown in Table I.

TABLE I

Periodate oxidation of methyl 6-chloro-6-deoxy-α-D-altropyranoside

Time	Periodate uptake (moles per mole)	Formic acid released (mole per mole)
20 min	0.99	0.19
1 h	1.24	0.29
3 h	1.36	0.37
6½ h	1.53	0.58
10 h	1.65	0.66
23 h	1.91	0.91
34 h	1.94	0.97
48 h	1.95	0.97
96 h	1.95	0.97

Methyl α-D-Lyxopyranoside 2,3,4-Trichlorosulfate

Methyl α-D-lyxopyranoside (21) (2 g, 0.012 mole) in anhydrous pyridine (10 ml, 0.02 mole) and chloroform (25 ml) was treated with sulfuryl chloride (6 ml, 0.074 mole) (procedure A). The crystalline product was methyl α-D-lyxopyranoside 2,3,4-trichlorosulfate, 3.3 g (60%). It was recrystallized from chloroform – petrol (b.p. 35–60°). The colorless plates had m.p. 129–130° and $[\alpha]_D$ −7° (*c*, 1.0 in chloroform).

Anal. Calcd. for $C_6H_9Cl_3O_{11}S_3$: C, 15.8; H, 1.96; Cl, 23.1; S, 20.8. Found: C, 15.8; H, 1.98; Cl, 23.5; S, 20.6.

A portion of the crystals (1 g, 0.006 mole) obtained from the previous experiment was treated according to procedure C. The crystalline product, 0.52 g (52%), m.p. 129–130°, was indistinguishable from the starting material.

Can. J. Chem. Downloaded from www.nrcresearchpress.com by 210.87.254.40 on 09/05/12
For personal use only.

D-Lyxosyl Chloride 2,3,4-Trichlorosulfate

D-Lyxose (2 g, 0.013 mole) in anhydrous pyridine (10 ml, 0.12 mole) and chloroform (25 ml) was treated with sulfuryl chloride (6 ml, 0.074 mole) according to procedure A and gave colorless crystals, 3 g (52%), m.p. 94–96°, $[\alpha]_D$ +20.4° (*c*, 1.0 in chloroform).

Anal. Calcd. for $C_5H_6Cl_4O_{10}S_3$: C, 13.0; H, 1.30; Cl, 30.6; S, 20.7. Found: C, 13.1; H, 1.37; Cl, 30.4; S, 20.6.

The Reaction of D-Lyxosyl Chloride 2,3,4-Trichlorosulfate with Pyridine Hydrochloride

The crystals (1.5 g, 0.003 mole) (above) in anhydrous chloroform and pyridine hydrochloride (1.3 g, 0.012 mole) gave (procedure C) a syrupy product containing several substances. A positive test for chlorosulfate groups was obtained. The syrup was dechlorosulfated with sodium iodide. A syrup was obtained which was shown by t.l.c. to contain one main substance, R_f 0.53 and R_{Rh} 2.5 in solvent *b*, and several minor substances. A small amount of the main substance was purified by t.l.c. followed by vacuum distillation. It had $[\alpha]_D$ +39.8°.

Anal. Calcd. for $C_5H_{10}Cl_2O_3$: Cl, 37.9. Found: Cl, 35.6.

Methyl 2-Chloro-2-deoxy-β-D-galactopyranoside[5]

Methyl 2-chloro-2-deoxy-β-D-galactopyranoside 2,3,4-triacetate (2.1 g, 0.007 mole), prepared from triacetyl D-galactal (22) in 19% yield according to the procedure of Lemieux and Fraser-Reid (23) except that silver carbonate was used in place of silver acetate, was dissolved in anhydrous methanol (25 ml) and cooled to 5°. It was de-*O*-acetylated catalytically with a cold, freshly prepared solution of sodium methoxide in the usual way. The methyl 2-chloro-2-deoxy-β-D-galactopyranoside, 0.95 g (72%), had m.p. 145–147° (mixed m.p. with a sample obtained from Dr. R. U. Lemieux 144–146°) and $[\alpha]_D$ +25° (*c*, 0.88 in water).

Methyl 2,3,4,6-Tetrachloro-2,3,4,6-tetradeoxy-β-D-alloside[5]

Methyl 2-chloro-2-deoxy-β-D-galactopyranoside (1.28 g, 0.006 mole) in pyridine (6 ml, 0.075 mole) and dry chloroform (24 ml) was treated with sulfuryl chloride (2.5 ml, 0.030 mole) (procedure A). The syrupy product (1 g) contained, as shown by t.l.c., one major component, R_f 0.94, and small amounts of two other components with R_f 0.83 and 0.75 (solvent *a*). Tests indicated that there was probably a small amount of material present containing the OSO_2Cl group. The syrup (1 g) in anhydrous chloroform and pyridine hydrochloride (0.5 g) was reacted according to procedure C and gave a syrupy product (0.85 g (54%)) which contained a single component, R_f 0.93 in solvent *a* and 0.62 in solvent *d* (t.l.c.). The volatile component was purified by vacuum distillation at 0.15 mm. The aniline–pyridine test for chlorosulfate groups was negative. The infrared spectrograph showed the absence of any hydroxyl peaks and confirmed the absence of any chlorosulfate groups.

Anal. Calcd. for $C_7H_{10}Cl_4O_2$: C, 31.4; H, 3.76; Cl, 52.9; OMe, 11.6. Found: C, 31.7; H, 3.7; Cl, 52.4; OMe, 11.9.

The Use of Tetra-n-butylammonium Chloride as a Source of Chloride Ions instead of Pyridine Hydrochloride

Methyl α-D-Glucopyranoside 2,3,4,6-Tetrachlorosulfate

Methyl α-D-glucopyranoside (10 g, 0.051 mole) was treated with sulfuryl chloride (26 ml, 0.32 mole) and pyridine in chloroform solution at −70° for 2 h. The mixture was allowed to warm up rapidly to −30° so that it became less viscous, while at this temperature an ice-cold 70% solution of sulfuric acid (500 ml) was added to the reaction mixture, with stirring. This modified method gave a considerably improved yield of the tetrachlorosulfate, 24 g (80%), m.p. 111–114°.

Methyl 4,6-Dichloro-4,6-dideoxy-α-D-galactopyranoside

The above material (2 g, 0.034 mole) in dry chloroform and anhydrous tetra-*n*-butylammonium chloride (2.06 g, 0.072 mole) was heated on a water bath at 50–60° for 5 h. From the chloroform solution was isolated a syrup which gave a positive test for chlorosulfate groups (aniline–pyridine test). The syrup was dechlorosulfated with sodium iodide to give a crystalline product, 0.70 g (85%), which, after recrystallization from chloroform–petrol, had m.p. 156–157°, undepressed on admixture with methyl 4,6-dichloro-4,6-dideoxy-α-D-galactopyranoside (3, 4).

The previous experiment was repeated with a mole ratio of tetrachlorosulfate to tetra-*n*-butylammonium chloride of 1:4.4. The reaction was left for 24 h on the water bath at 50°. The only chloroform-soluble product obtained was methyl 4,6-dichloro-4,6-dideoxy-α-D-galactopyranoside 2,3-dichlorosulfate.

ACKNOWLEDGMENTS

The authors thank the National Research Council, Queen's University, and the Ontario Research Foundation for financial assistance. Dr. N. K. Richtmyer is thanked for a gift of 1,6-anhydro-D-idosan triacetate.

[5]*A short account of these reactions has been given (8).*

Can. J. Chem. Downloaded from www.nrcresearchpress.com by 210.87.254.40 on 09/05/12
For personal use only.

REFERENCES

1. P. D. Bragg, J. K. N. Jones, and J. C. Turner. Can. J. Chem. **37**, 1412 (1960).
2. J. K. N. Jones, M. B. Perry, and J. C. Turner. Can. J. Chem. **38**, 1122 (1960).
3. H. J. Jennings and J. K. N. Jones. Can. J. Chem. **40**, 1408 (1962).
4. H. J. Jennings and J. K. N. Jones. Can. J. Chem. **41**, 1151 (1963).
5. H. J. Jennings and J. K. N. Jones. Can. J. Chem. **43**, 2372 (1965).
6. E. Buncel and J. P. Millington. Proc. Chem. Soc. 406 (1964); Can. J. Chem. **43**, 547 (1965); **43**, 556 (1965).
7. J. W. H. Oldham and J. K. Rutherford. J. Am. Chem. Soc. **54**, 366 (1932).
8. A. G. Cottrell, E. Buncel, and J. K. N. Jones. Chem. Ind. London, 552 (1966).
9. R. E. Reeves. Advan. Carbohydrate Chem. **6**, 107 (1951).
10. G. R. Barker and D. F. Shaw. J. Chem. Soc. 584 (1959).
11. H. Spedding. Advan. Carbohydrate Chem. **19**, 23 (1964).
12. H. C. Brown. J. Chem. Soc. 1248 (1956).
13. E. L. Eliel. The stereochemistry of carbon compounds. McGraw-Hill Book Co., Inc., New York. 1962. Chap. 8. p. 225.
14. S. S. Ali and T. J. Mepham. Unpublished results.
15. R. B. Ward. Methods in carbohydrate chemistry. Vol. II. Academic Press, Inc., New York. 1962. p. 396.
16. R. M. Hann and C. S. Hudson. J. Am. Chem. Soc. **64**, 2435 (1942).
17. N. K. Richtmyer and C. S. Hudson. J. Am. Chem. Soc. **63**, 1727 (1941).
18. E. A. Robinson. Can. J. Chem. **39**, 247 (1961).
19. G. Neumüller and E. Vasseur. Arkiv Kemi, **5**, 235 (1953).
20. D. M. W. Anderson, C. T. Greenwood, and E. L. Hirst. J. Chem. Soc. 225 (1955).
21. F. P. Phelps and C. S. Hudson. J. Am. Chem. Soc. **48**, 503 (1926).
22. B. Helferich, E. N. Mulcahy, and H. Ziegler. Ber. **87**, 233 (1954).
23. R. U. Lemieux and B. Fraser-Reid. Can. J. Chem. **42**, 532 (1964).

Can. J. Chem. Downloaded from www.nrcresearchpress.com by 210.87.254.40 on 09/05/12
For personal use only.

THE TRANSMISSION OF POLAR EFFECTS

IV. THE KINETICS OF ESTERIFICATION WITH DIAZODIPHENYLMETHANE OF SUBSTITUTED HETEROCYCLIC CARBOXYLIC ACIDS[1]

KEITH BOWDEN[2] AND D. C. PARKIN[2]

Department of Pure and Applied Chemistry, Royal College of Advanced Technology, Salford, Lancashire, England

Received December 30, 1965

ABSTRACT

The rate coefficients for the reaction with diazodiphenylmethane, in ethanol at 30.0°, of a number of substituted indole-2-carboxylic acids, indole-3-carboxylic acids, coumarin-3-carboxylic acids, coumarilic acids, and N-phenylglycines have been determined. The effect of substitution is assessed by use of adapted Hammett and Dewar–Grisdale relations. The relations give good correlations for oxygen-ring heterocyclic systems, and the relative ability of the systems to transmit π-electron effects has been determined. An anomalous perturbing effect appears to operate in the indole-carboxylic acid systems.

Can. J. Chem. Downloaded from www.nrcresearchpress.com by 210.87.254.5 on 09/05/12
For personal use only.

INTRODUCTION

The transmission of polar effects in heterocyclic systems has been reviewed recently by Jaffé and Jones (1). In particular, the ionization of carboxylic acids and the rates of the hydrolysis of the corresponding esters have been employed usefully. The esterification of carboxylic acids by diazodiphenylmethane has been employed successfully in investigating the transmission of polar effects (2–5). Other workers (6, 7) have extended this technique recently to simple heterocyclic systems. In the present studies we have made a series of measurements of the transmission of the polar effects of substituents in a benzenoid ring fused to a heterocyclic ring having a carboxylic acid group. The reaction chosen was that of the acids with diazodiphenylmethane, and the analysis of the substituent effects was made by use of linear free energy relations.

EXPERIMENTAL

Materials

The carboxylic acids used in this study were synthesized by standard methods or obtained commercially. The 6-nitroindole-3-carboxylic acid was prepared by nitration of the unsubstituted acid by the method of Majima and Kotake (8). The indole-3-carboxylic acids were prepared by the reaction of the substituted indole with methylmagnesium iodide, followed by reaction with solid carbon dioxide (9). The indole-2-carboxylic acids were obtained commercially. The coumarin-3-carboxylic acids were synthesized by the Knoevenagel reaction from diethyl malonate and a substituted salicylaldehyde, followed by acid hydrolysis (10). The coumarilic acids were prepared by Perkin's method from substituted coumarins (11). The reaction of a substituted aniline with ethyl bromoacetate was employed to prepare the N-phenylglycines (12).

The acids were recrystallized to a constant melting point and had melting points identical with or close to those in the literature. Neutralization equivalents were determined for the indole-carboxylic and coumarilic acids and were found to be within 1% of the theoretical values. The N-phenylglycines were difficult to prepare with satisfactory neutralization equivalents. This is probably due to their liability to decarboxylation (12). Neutralization equivalents were measured just before a rate determination and were between 1 and 4% high. These values were then used to calculate the rates. No apparent decrease in acid present over the reaction time at the reaction temperature was found. The coumarin-3-carboxylic acids appear to undergo alkaline ring fission and slowly reacted with alkali in excess of 1 equivalent.

Pure ethanol, b.p. 78.3° (lit. b.p. 78.3° (13)), was prepared by Smith's method (14). Solutions of diazodiphenylmethane, prepared as before (3, 15), were stored in a refrigerator. The solutions were all stored with careful exclusion of atmospheric moisture.

[1]*For part III in this series, see K. Bowden, Can. J. Chem., 44, 661 (1966).*

[2]*Present address: Department of Chemistry, University of Essex, Colchester, Essex, England.*

Measurements

The rate coefficients were determined, at 30 ± 0.05°, as described previously (3, 15), using a Unicam S.P.500 spectrophotometer. An approximately 5- or 10-fold excess of acid was used (0.015 or 0.03 *M*). The reaction was then studied as a first-order process by using eq. [i], where k is the second-order rate

$$k = k_1/a \qquad [i]$$

coefficient, k_1 is the observed first-order rate coefficient, and a is the acid concentration. The rate coefficients for a given acid obtained at either concentration were within the experimental reproducibility. The faster nitro acids were inconveniently fast for the latter method, and the reaction was studied as a second-order process. Equation [ii] was then used to calculate the rate coefficient k, where a is the initial concentration of the

$$k = \frac{2.303}{t(a - Rb)} \log \frac{b(a - Rx)}{a(b - x)} \qquad [ii]$$

acid, b the initial concentration of diazodiphenylmethane, and x the concentration of diazodiphenylmethane that has reacted at time t. R is the amount of diazodiphenylmethane consumed in the reaction with acid to give the ester compared with the total amount consumed. The ratio was determined as described previously (16), by a titration method. The values of R that were obtained were 0.56 ± 0.02 (indole-2-carboxylic acids), 0.59 ± 0.02 (indole-3-carboxylic acids), 0.59 ± 0.01 (coumarilic acids), and 0.59 ± 0.02 (N-phenylglycines). There is thus little change for these non-proximate substituents, as noted previously for similar systems (2, 17). Recent mechanistic studies (17) have demonstrated the meaningfulness of the rate coefficients. The results are summarized in Table I.

TABLE I

Rate coefficients for substituted carboxylic acids in diazodiphenylmethane in ethanol at 30.0°

Substituent	k	Substituent	k
Indole-2-carboxylic acid (III)		Coumarilic acid (VI)	
5-Me	1.64	5-OMe	6.51
H	1.76	5-Me	7.94
5-OMe	1.80	H	9.98
5-Cl	2.57	5-Cl	13.8
5-Br	2.65	5-Br	14.9
6-NO_2	13.4	5-NO_2	28.2
Indole-3-carboxylic acid (IV)		Coumarin-3-carboxylic acid (V)	
5-OMe	3.09	6-Me	5.85
5-Me	3.27	H	6.83
H	5.17	6-Cl	9.23
5-Cl	11.1	6-Br	9.69
5-Br	12.1	6-NO_2	13.9
6-NO_2	22.9		
N-Phenylglycine			
H	3.07		
4-Cl	3.18		
3-Cl	3.85		
3-NO_2	3.95		
4-NO_2	4.31		

NOTE: The rate coefficients, k (l mole^{-1} min^{-1}), are reproducible to ±3% or better and are the mean of at least two determinations.

DISCUSSION

State of Acids in Solution

It has been shown that the normal acid form (I) of N-phenylglycines, in aqueous solution, exists in equilibrium with a zwitterionic form (II) (12). This becomes increasingly important as the electron-withdrawing capacity of the substituent decreases. The present

$$\underset{\text{I}}{RNHCH_2CO_2H} \rightleftharpoons \underset{\text{II}}{R\overset{+}{N}H_2CH_2CO_2^-}$$

measurements have been made in ethanol, where the tendency to the zwitterionic behavior is *greatly* reduced.[3] The substituted acids employed in this study are the least susceptible to this behavior, and it seems likely that the acids are completely in the form (I). Pyridine

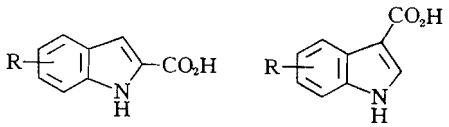
[3]*See ref. 21, footnote on p. 424.*

Can. J. Chem. Downloaded from www.nrcresearchpress.com by 210.87.254.5 on 09/05/12
For personal use only.

carboxylic acids exist predominantly as the zwitterionic species in aqueous solution (18), and apparently successful measurements have been made on the reaction of these acids with diazodiphenylmethane in ethanol (7).

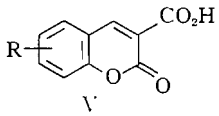
Linear Free Energy Relations

The systems under study are shown below (III to VI). Jaffé (1, 19) has adapted the Hammett equation (eq. [iii]) (20) to correlate the transmission of substituent effects

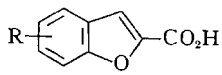


III

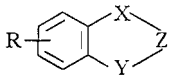
IV



V



VI



VII

through the two links X and Y to a reactive site Z (VII). The effect is then described by eq. [iv], where the substituent constants σ_X and σ_Y are the appropriate Hammett meta

[iii] $$\log (k/k_0) = \rho\sigma$$

[iv] $$\log (k/k_0) = \rho_X\sigma_X + \rho_Y\sigma_Y$$

or para σ values for the position of the substituent R in relation to the link X or Y. The reaction constants ρ_X and ρ_Y describe the transmission by the links X and Y. The correlations were obtained by using the latter equation with the substituent constants recommended by McDaniel and Brown (21), and are shown in Table II.

A treatment similar to that of Dewar and Grisdale (22) can be used to analyze the results (3). The relative rates are assessed in terms of a field effect (F) and a π-inductive–resonance effect (M), as shown in eq. [v], where r_{ij} is the distance between the reactive group and

[v] $$\log (k/k_0) = \rho_D(F/r_{ij} + Mq_{ij})$$

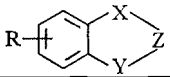
the carbon atom bonded to it (measured in units of benzene carbon–carbon bond distances) and q_{ij} is the formal charge at the site produced by the substituent. The reaction constant found is ρ_D. The values of r_{ij} can be calculated for our systems, and are also shown in Table III. The values of q_{ij} are obtained, in this method, from the correlation itself, since these values are not available for these heterocyclic rings. The relation, as used here, has q_{ij} as an adjustable parameter.

However, these two treatments are basically similar. The substituent effect in the Dewar–Grisdale treatment has an a priori separation of the field and π-electron effects. This separation was made from the σ values of meta- and para-substituents. The Jaffé relation deals with the substituent as having a dual meta- and para-type nature. The parameters ρ_D and q_{ij} obtained by the former method can be compared usefully with those of the reference benzene system. On the other hand, the Jaffé treatment appears to imply transmission only via the links. The parameters ρ_X and ρ_Y are of more limited significance, and their relative values are very dependent on the substituents with quite different meta and para σ values, e.g. MeO. It seems likely that the total reaction constant ($\rho_X + \rho_Y$) is of more significance, in comparison to the reference benzene system, than the ratio ρ_X/ρ_Y.

Can. J. Chem. Downloaded from www.nrcresearchpress.com by 210.87.254.5 on 09/05/12
For personal use only.

Can. J. Chem. Downloaded from www.nrcresearchpress.com by 210.87.254.5 on 09/05/12
For personal use only.

TABLE II

Hammett equation analysis* of reactivity for the system 

System	X	Y	Z	Reaction	ρ_X	S_X	ρ_Y	S_Y	$-\log k_0$	r	n	Reference
Coumarilic (VI)	CH	O	C—CO_2H	Esterification†	−0.02	0.01	0.62	0.01	−1.00	0.999	6	This work
Coumarilic (VI)	CH	O	C—CO_2H	Ionization‡	0.23	0.03	0.93	0.02	4.41	0.999	7	1, 23
Coumarilic (VI)	CH	O	C—CO_2Et	Ester hydrolysis§	0.81	0.12	1.00	0.10	1.24	0.998	6	1, 23
Coumarin-3-carboxylic (V)	CH	—CO—O	C—CO_2H	Esterification†	0.13	0.01	0.31	0.01	−0.82	1.000	5	This work
Indole-2-carboxylic (III)	CH	NH	C—CO_2H	Esterification†	0.46	0.28	0.54	0.35	−0.25	0.980	6	This work
Indole-2-carboxylic (III)	CH	NH	C—CO_2H	Ionization‡	0.82	0.10	0.46	0.09	5.18	0.996	8	1, 23
Indole-2-carboxylic (III)	CH	NH	C—CO_2Et	Ester hydrolysis§	0.49	0.02	0.66	0.01	2.64	0.998	6	1, 23
Indole-3-carboxylic (IV)	—	=CH—NH	C—CO_2H	Esterification†	0.23	0.13	0.78	0.10	−0.71	0.997	7	This work
Indole-3-carboxylic (IV)	—	=CH—NH	C—CO_2H	Ionization‡	0.31	0.23	0.42	0.11	7.04	0.998	6	9
N-Phenylglycine¶	—	NH	—CH_2—CO_2H	Esterification†	—	—	0.180	0.030	−0.49	0.934	5	This work
N-Phenylglycine¶	—	NH	—CH_2—CO_2H	Ionization‖	—	—	0.359	0.022	4.00	0.972	10	12

*S_X and S_Y are the respective standard deviations; r is the correlation coefficient; and n is the number of substituents studied.
†Esterification by diazodiphenylmethane in ethanol at 30.0° (ρ (benzoic acids) = 0.94 (2)).
‡Ionization in 50% aqueous ethanol at 25° (ρ (benzoic acids) = 1.57 (25)).
§Alkaline hydrolysis of ethyl esters in 85% ethanol–water at 35.0° (ρ (ethyl benzoates) = 2.56 at 25.0° (25)).
‖Ionization in water at 25° (ρ (benzoic acids) = 1.00 (25)).
¶Using σ^n (25).

Can. J. Chem. Downloaded from www.nrcresearchpress.com by 210.87.254.5 on 09/05/12
For personal use only.

The correlations (eqs. [iv] and [v]) have also been applied to data available for the pK values of the acids (series III, IV, and V) (1, 9, 23) in 50% aqueous ethanol and for the rates of the alkaline hydrolysis of the ethyl esters (series III and IV) (1, 23) in 85% ethanol–water. Jaffé (1) has previously made these correlations by using eq. [iv] for the latter data, and minor variations are caused by our use of different σ values (21). The furoic acid system has also been analyzed by applying eq. [v] to the pK_a values of 5-substituted-2-furoic acids in water and to the esterification of the acids with diazodiphenylmethane in ethanol (6). The N-phenylglycine system was also analyzed by using the normal Hammett equation (Table II). The results in Tables II and III cannot be compared directly because, whereas eq. [iv] applies to all substituents, eq. [v] is specific for any one position.

In all cases a satisfactory fit is obtained, *but* the standard deviation is particularly high for the results in Table II and for the indole-carboxylic acids in general. The results in Table II obtained by using the Jaffé relation show a confused picture, with the ratio of ρ_X to ρ_Y varying considerably; in view of the limits of the certainty, any conclusions are difficult to make. Although the total value of $(\rho_X + \rho_Y)$ in comparison to the reference system seems to give a more meaningful interpretation of the results, the conclusions can more clearly be drawn from the results of the Dewar–Grisdale relation in Table III.

The results for the latter correlations are very interesting. The Dewar–Grisdale reaction constant ρ_D should be comparatively constant for any stated reaction. The factor r_{ij} should, to a large extent, compensate for the change in situation of the substituent. The ρ_D values obtained for the coumarilic, coumarin-3-carboxylic, and furoic acid systems compare well with the reaction constant for the reference benzoic acid system. The transmission of the π-electron effects (q_{ij}) indicates the following order of efficiency: *trans*-acrylic (1, 2)[4] > furoic (2, 5) > benzoic (1, 4) > coumarilic (2, 5) > coumarin-3-carboxylic (3, 6).

The indole-carboxylic acids present a somewhat confusing picture. The ρ_D values, especially, are quite different from those expected. The variations are also not systematic. The results for the esterification of the indole-2-carboxylic acids and the ester hydrolysis of the latter system are reasonable, but the ionization reaction for both systems is particularly confused. It would appear that, in the indole system, there are interactions which perturb these relations.

It was therefore of interest to know the Hammett reaction constants for meta- and para-substituted N-phenylglycine and phenoxyacetic acids. The phenoxyacetic acids have already been studied in their esterification with diazodiphenylmethane and their ionization in water, where the reaction constants were equal to 0.247 and 0.341, respectively (24). In the present study, the rates of esterification of N-phenylglycines were measured. The correlation gives ρ equal to 0.180 and is shown in Table II. The correlation coefficient is *quite poor* for the esterification of the N-phenylglycines. Since our original study, the ionization of substituted N-phenylglycines has been studied (12) and the pK_a values of the acids estimated when they are ionizing as a normal acid (I). This correlation is also shown in Table II, and ρ equals 0.359. It thus seems to be quite possible that the effect of the proximate $\rangle$NH group may affect the application of these relations, e.g. by a hydrogen-bonding interaction (1). This latter explanation is not applicable to the indole-3-carboxylic acid system. Another possibility is that the zwitterionic behavior exists for

[4]*The value of q_{ij} for this system has been found to be between 0.25 and 0.30 (3).*

Can. J. Chem. Downloaded from www.nrcresearchpress.com by 210.87.254.5 on 09/05/12
For personal use only.

TABLE III

Dewar–Grisdale equation analysis*

System	Reaction	i	j	r_{ij}	ρ_D	S	q_{ij}	S	$-\log k_0$	r	n	Reference
Coumarilic (VI)	Esterification†	2	5	3.3	0.99	0.00	0.09	0.00	−1.00	0.999	6	This work
Coumarilic (VI)	Ionization†	2	5	3.3	1.65	0.01	0.10	0.00	4.33	1.000	5	1, 23
Coumarilic (VI)	Ester hydrolysis†	2	5	3.3	2.45	0.02	0.10	0.00	1.07	0.999	5	1, 23
Coumarin-3-carboxylic (V)	Esterification†	3	6	3.5	0.86	0.00	0.02	0.00	−0.82	1.000	5	This work
Furoic	Esterification†,‡	2	5	1.6	0.79	0.00	0.17	0.00	−0.63	1.000	5	6
Furoic	Ionization†,§	2	5	1.6	1.10	0.01	0.20	0.00	3.15	1.000	6	6
Indole-2-carboxylic (III)	Esterification†	2	5	3.3	0.87	0.00	0.02	0.00	−0.25	0.999	5	This work
Indole-2-carboxylic (III)	Ionization†	2	5	3.3	2.59	0.05	0.03	0.00	5.17	0.999	5	1, 23
Indole-2-carboxylic (III)	Ionization†	2	6	3.3	0.67	0.00	0.01	0.00	5.27	1.000	4	1, 23
Indole-2-carboxylic (III)	Ester hydrolysis†	2	5	3.3	1.85	0.01	0.07	0.00	2.75	0.999	5	1, 23
Indole-3-carboxylic (IV)	Esterification†	3	5	2.7	1.85	0.01	0.07	0.00	−0.71	0.999	5	This work
Indole-3-carboxylic (IV)	Ionization†	3	5	2.7	0.91	0.09	0.08	0.01	7.02	0.999	4	9

*S is the standard deviation; r is the correlation coefficient; and n is the number of substituents studied.
†See Table II.
‡Esterification by diazodiphenylmethane in ethanol at 25.0° (ρ (benzoic acids) = 0.94 at 30.0° (25)).
§Ionization in water at ambient temperature (ρ (benzoic acids) = 1.00 at 25° (26)).

indole-carboxylic acids and persists even in aqueous ethanol and ethanol. A likely explanation is the occurrence of specific changes in electronic interactions which preclude the simple interpretations of the relations used here.

Our conclusions from this study are that (*a*) the equation of Jaffé (eq. [iv]) presents a satisfactory correlation of the data, although the physical significance of the reaction constants is in question; (*b*) the Dewar–Grisdale relation (eq. [v]) (as used herein) produces a useful correlation when applied to substitution in a single position; and (*c*) both treatments are empirical in nature and it is difficult to evaluate them on the limited data available.

REFERENCES

1. H. H. JAFFÉ and H. L. JONES. *In* Advances in heterocyclic chemistry. *Edited by* A. R. Katritzky. Academic Press, Inc., New York. 1964. p. 209.
2. K. BOWDEN, N. B. CHAPMAN, and J. SHORTER. Can. J. Chem. **42**, 1979 (1964).
3. K. BOWDEN. Can. J. Chem. **43**, 3354 (1965).
4. R. A. M. O'FERRALL and S. I. MILLER. J. Am. Chem. Soc. **85**, 2440 (1963).
5. J. D. S. RITTER and S. I. MILLER. J. Am. Chem. Soc. **86**, 1507 (1964).
6. W. K. KWOK, R. A. M. O'FERRALL, and S. I. MILLER. Tetrahedron, **20**, 1913 (1964).
7. D. M. DIMITRIJEVIC, Z. D. TADIC, and M. D. MUSKATIROVIC. Glasnik Hem. Drustva Beograd, **28**, 83 (1963); **27**, 397 (1962). Z. D. TADIC, M. M. MISIC, and D. M. DIMITRIJEVIC. Glasnik Hem. Drustva Beograd, **27**, 407 (1962); Chem. Abstr. **60**, 14346 (1964); **60**, 15698 (1964).
8. R. MAJIMA and M. KOTAKE. Ber. **63**, 2237 (1930).
9. M. S. MELZER. J. Org. Chem. **27**, 496 (1962).
10. L. L. WOODS and J. SAPP. J. Org. Chem. **30**, 312 (1965).
11. R. C. FUSON, J. W. KNEISLEY, and E. W. KAISER. Org. Syn. Collective Vol. **3**, 209 (1955).
12. A. BRYSON, N. R. DAVIES, and E. P. SERJEANT. J. Am. Chem. Soc. **85**, 1933 (1963).
13. A. WEISBERGER. Techniques of organic chemistry. Vol. VII. 2nd ed. Interscience Publishers, Inc., New York. 1955.
14. A. I. VOGEL. Practical organic chemistry. 3rd ed. Longmans, Green & Co., Ltd., London. 1956. p. 168.
15. A. BUCKLEY, N. B. CHAPMAN, and J. SHORTER. J. Chem. Soc. 178 (1963).
16. N. B. CHAPMAN, J. SHORTER, and J. H. P. UTLEY. J. Chem. Soc. 1291 (1963).
17. K. BOWDEN, A. BUCKLEY, N. B. CHAPMAN, and J. SHORTER. J. Chem. Soc. 3380 (1964).
18. F. J. MILLERO, J. C. AHLUWALIA, and L. G. HEPLER. J. Phys. Chem. **68**, 3435 (1964).
19. H. H. JAFFÉ. J. Am. Chem. Soc. **76**, 4261 (1954).
20. H. H. JAFFÉ. Chem. Rev. **53**, 191 (1953).
21. D. H. MCDANIEL and H. C. BROWN. J. Org. Chem. **23**, 420 (1958).
22. M. J. S. DEWAR and P. J. GRISDALE. J. Am. Chem. Soc. **84**, 3539 (1962); **84**, 3548 (1962).
23. Y. OTSUJI and H. H. JAFFÉ. 137th Meeting, American Chemical Society, Cleveland, Ohio, April 1960. Abstr. Papers, p. 760.
24. K. BOWDEN. Can. J. Chem. **41**, 2781 (1963).
25. H. VAN BEKKUM, P. E. VERKADE, and B. M. WEPSTER. Rec. Trav. Chim. **78**, 815 (1959).

Can. J. Chem. Downloaded from www.nrcresearchpress.com by 210.87.254.5 on 09/05/12
For personal use only.

Can. J. Chem. Downloaded from www.nrcresearchpress.com by 210.87.254.40 on 09/05/12
For personal use only.

ORGANIC AND BIOLOGICAL SPECTROCHEMICAL STUDIES

XXIII. CONFORMATION OF THE *p*-DIMETHOXYBENZENE CATION RADICAL IN CONCENTRATED SULFURIC ACID[1]

W. F. FORBES AND P. D. SULLIVAN

Department of Chemistry, University of Waterloo, Waterloo, Ontario

Received January 5, 1966

ABSTRACT

The electron spin resonance spectrum of the *p*-dimethoxybenzene cation radical in concentrated sulfuric acid is interpreted in terms of *cis–trans* isomerism. Empirical molecular orbital calculations support these assignments. The two isomers are found to possess slightly different "*g*" values, Δg (*cis* − *trans*) being ca. 1.8×10^{-5}.

Nuclear magnetic resonance and ultraviolet data show that the radical exists in equilibrium with the neutral non-radical species at room temperature, but that sulfonation occurs at higher temperatures. Nuclear magnetic resonance and electron spin resonance data of solutions of *p*-dimethoxybenzene in D_2SO_4 show that rapid exchange of the ring protons occurs.

INTRODUCTION

As part of an electron spin resonance (e.s.r.) study of some substituted aromatic compounds in 98% sulfuric acid, the cation radicals of *p*-dimethoxybenzene have been investigated. The relevant spectrum, and a partial interpretation, have previously been reported by Zweig *et al.* (1). The present paper represents a continuation of this work; in addition, the species formed are also investigated by nuclear magnetic resonance (n.m.r.) and ultraviolet spectroscopy. The results are divided into sections. Sections I and II describe the n.m.r. and ultraviolet work, respectively, section III summarizes the e.s.r. data, section IV gives the appropriate molecular orbital calculations, and section V represents a discussion of line widths and *g* value data.

EXPERIMENTAL

A commercially available sample of *p*-dimethoxybenzene was recrystallized and gave only one band on vapor phase chromatography. The concentrated sulfuric acid was best-grade commercially available 98% sulfuric acid. Dideuteriosulfuric acid was a commercially available sample (Merck).

The e.s.r. spectra were determined on a JES-3BX e.s.r. spectrometer at 100 kc/s modulation utilizing a field selector unit. The *g* values were obtained by simultaneously inserting in the cavity a solution of peroxylamine disulfonate with the sample under investigation. Parameters used for peroxylamine disulfonate were $g = 2.0055$[2] and $a_N = 13.07$ G. The magnetic field was also calibrated against a n.m.r. probe, and values of the splitting constants are believed to be accurate to ±0.5%. Radical concentrations were estimated by over-modulating the signal and comparing it, under the same conditions, with a standard diphenylpicrylhydrazyl (DPPH) sample of known spin concentration.

The e.s.r. spectra were determined in ca. 0.2 *M* solution, ca. 0.04 ml of which was inserted in a glass capillary tube which was then placed in the TE_{011} cavity of the spectrometer. This concentration was found to give minimum line width, consistent with a good ratio of signal to noise. All spectral traces represent the first derivative of the actual absorption curves.

The n.m.r. spectra were obtained on a JNM-3H-10 n.m.r. spectrometer, with 0.5 *M* solutions of *p*-dimethoxybenzene in concentrated H_2SO_4 or concentrated D_2SO_4.

The ultraviolet absorption spectra were determined by standard methods in 1 cm cells on a Beckman model DU and a Cary model 14 spectrophotometer. The accuracy of the λ_{max} values is estimated to be ±2 mμ.

[1]*For part XXII in this series, see E. J. Moriconi, J. P. St. George, and W. F. Forbes, Can. J. Chem., 44, 759 (1966).*

[2]*The g values were measured relative to peroxylamine disulfonate, taking g absolute = 2.005500. A recent, more accurate study by Fraenkel (2) for the anthracene positive ion gives g = 2.00256 ± 0.000006, whereas our work leads to a g value of 2.002506 ± 0.000012. The present g values may therefore be in error by −0.00006.*

The e.s.r. spectra were simulated on an IBM 7040 computer, with a modified program kindly supplied by Dr. Lawrence C. Snyder of the Bell Telephone Laboratories. The output data from the IBM 7040, in the form of punched cards, were taken to an IBM 1710 computer and thence to a plotter.

Molecular orbital calculations were carried out by the self-consistent field method of McLachlan (3) on an IBM 7040 computer with a program kindly supplied by Dr. J. M. Fritsch (4) of the University of Kansas.

RESULTS AND DISCUSSION

I. Nuclear Magnetic Resonance Spectra

At room temperature in concentrated sulfuric acid, the n.m.r. spectrum consists of two broad absorption bands, of an approximate intensity ratio 3:2 (see Fig. 1*a*), together with some high-field bands caused by sulfuric acid (not shown). The two broad bands are assigned to the OCH_3 protons and ring protons, respectively. The band broadening is due to the presence of a free electron in the system which causes a perturbation of energy levels (cf. ref. 5). When the temperature is raised (see Figs. 1*b* and 1*c*) the lines sharpen, approximately in a manner parallel with the decrease in the e.s.r. signal intensity. If the temperature is maintained at 90 °C, the free radical decays, as shown by the disappearance of the e.s.r. signal and the appearance of a well-resolved n.m.r. spectrum.

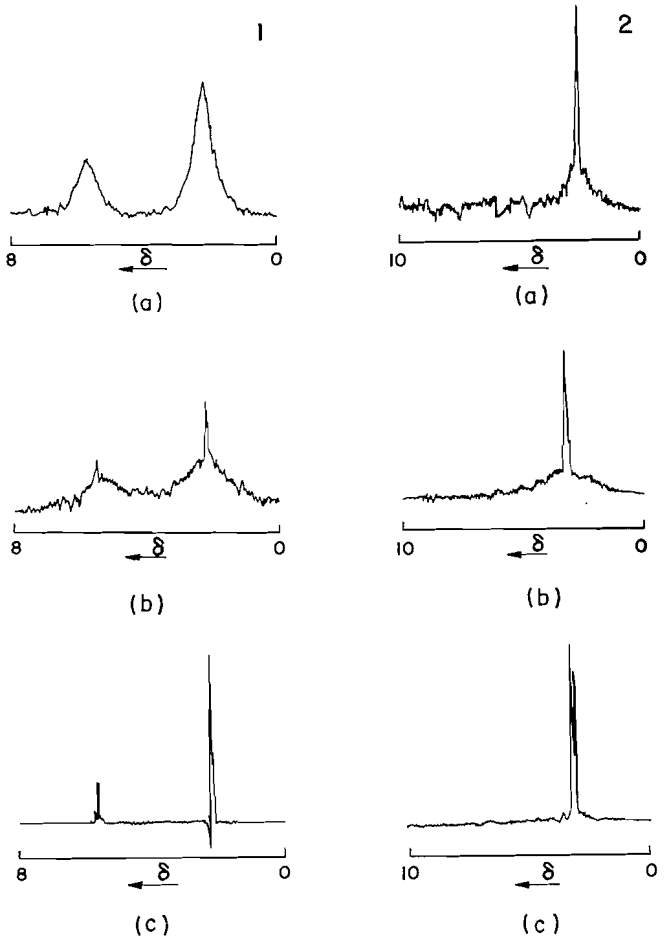
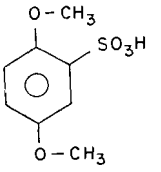


FIG. 1. Nuclear magnetic resonance spectra of *p*-dimethoxybenzene in concentrated sulfuric acid (*a*) at room temperature, (*b*) at 65 °C, and (*c*) at 90 °C after standing for 1 h.

FIG. 2. Nuclear magnetic resonance spectra of *p*-dimethoxybenzene in D_2SO_4 at room temperature (*a*) immediately after dissolution, (*b*) after standing for 3 h, and (*c*) after standing for 1 day.

Can. J. Chem. Downloaded from www.nrcresearchpress.com by 210.87.254.40 on 09/05/12
For personal use only.

The species formed is the sulfonic acid (I), which can be isolated from the acid solution (6). Moreover, the ultraviolet and n.m.r. spectra of the heated solution are identical with the corresponding spectra of a solution of I in sulfuric acid.



I

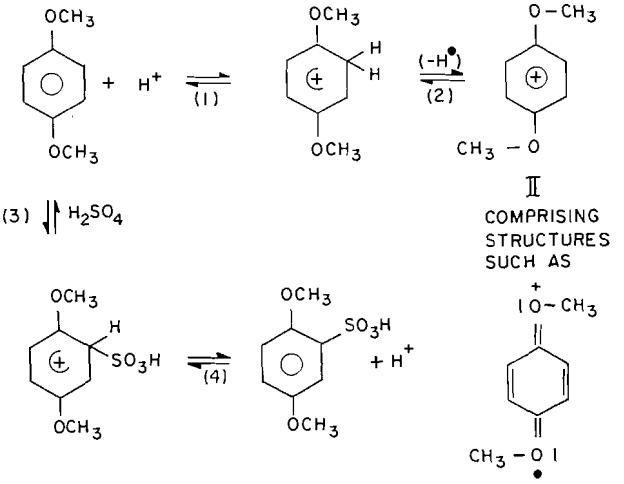
In D_2SO_4 solution (see Figs. 2*a*–2*c*) the ring proton absorption disappears, indicating rapid H–D exchange of the ring protons.

When this solution is allowed to stand at room temperature, the absorption ascribed to the OCH_3 protons splits into a doublet (see Fig. 2*c*), suggesting again that sulfonation is taking place.

II. Ultraviolet Spectra

The spectrum of a solution of *p*-dimethoxybenzene in concentrated sulfuric acid shows intense bands at 280 mμ which are ascribed to *p*-dimethoxybenzene and to the sulfonic acid (I), and bands at 434 and 460 mμ which are ascribed to free-radical and (or) protonated species. By using the radical concentration obtained from e.s.r. data (0.025%), the molar absorptivity of these latter bands was found to be of the order of 5 000 (cf. the maximal absorption at 445 mμ for the durosemiquinone cation radical in concentrated sulfuric acid (7)).

The n.m.r. and ultraviolet data are consistent with the reactions shown below. At room temperature, reaction 1 is fast and reversible, whereas reaction 2, crudely represented as a one-step reaction, seems to be rate determining for the formation of the radical (II). Reactions 3 and 4 predominate as the temperature is increased. As judged from the intensity of the e.s.r. signal, species II contributes only about 0.025% to the postulated equilibrium at 20 °C. There is no evidence from the n.m.r. or ultraviolet data for secondary



Can. J. Chem. Downloaded from www.nrcresearchpress.com by 210.87.254.40 on 09/05/12
For personal use only.

reactions such as diphenyl formation, although admittedly, *p,p'*-dimethoxydiphenyl in concentrated sulfuric acid did not give rise to an e.s.r. spectrum under our conditions (unpublished information).

III. Electron Spin Resonance Spectra

The e.s.r. spectrum (Fig. 3*a*) was found to contain a maximum of 87 lines at room temperature. By using increased modulation and carefully studying the wings of the spectrum, it was found that the spectrum could be represented as the sum of two species (A and B), possessing the following splitting constants (given in parentheses).

Species A	Species B
Six equivalent protons (3.45 G)	Six equivalent protons (3.33 G)
Two equivalent protons (2.99 G)	Two equivalent protons (2.68 G)
Two equivalent protons (1.49 G)	Two equivalent protons (1.81 G)

A spectrum computed by using these constants and assuming a displacement of 0.03 G between the two centers (see section V) is shown in Fig. 3*b*. By analogy with the e.s.r. spectrum of the anion radical of 1,4-diacetylbenzene (8) and of the durosemiquinone cation radical (9), where *cis–trans* isomerism has previously been postulated, the present

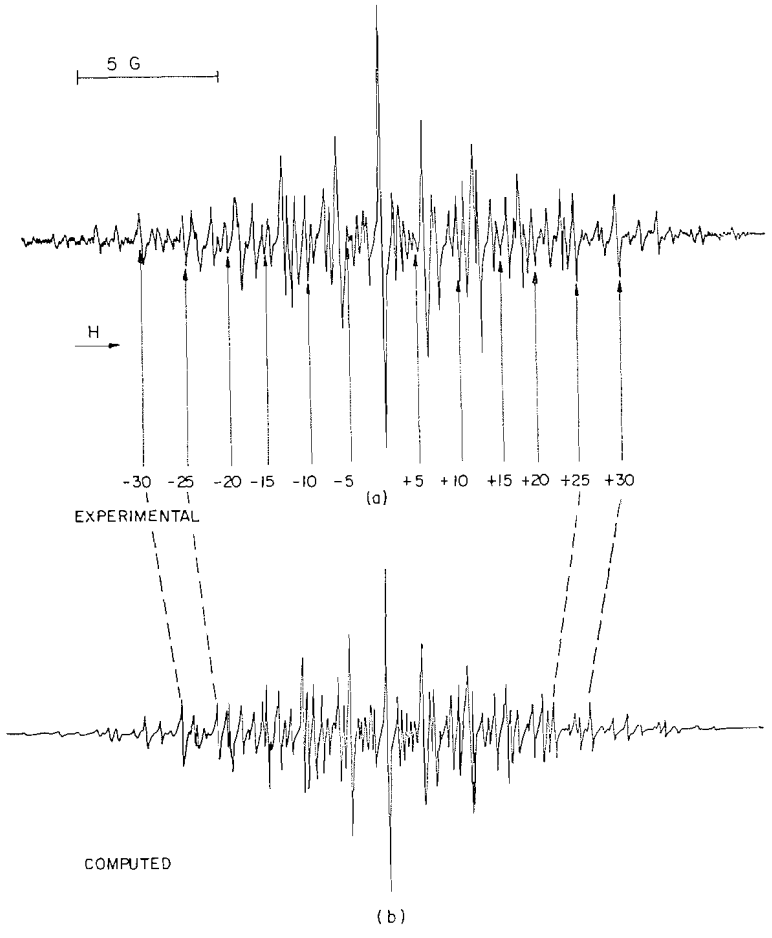
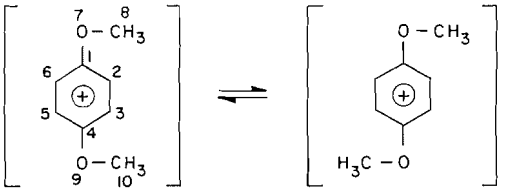


FIG. 3. (*a*) Electron spin resonance spectrum of a 0.2 *M* solution of *p*-dimethoxybenzene in concentrated sulfuric acid at room temperature. Lines are numbered as shown, proceeding from the center line. (*b*) A spectrum computed by using coupling constants as given in the text.

Can. J. Chem. Downloaded from www.nrcresearchpress.com by 210.87.254.40 on 09/05/12
For personal use only.

two species are associated with the *cis* and *trans* isomers of the *p*-dimethoxybenzene cation radical (II*a* and II*b*).



II a II b

An attempt to solve the problem of assigning splitting constants to the appropriate isomer was made by investigating line intensities. Lines 10 and 15 from the center of the spectrum (Fig. 3*a*) were found to belong to species B with no appreciable overlap from species A, whereas lines 11, 20, and 25 could be associated with species A. Theoretical intensities were then calculated and compared with the average of the experimental intensities; from this, the ratio of species A to species B was obtained. At +22 °C, this ratio was 1.19:1.00 (cf. Table II). Since the *trans* isomer would be expected to be more stable, species A is assumed to correspond to the *trans* form (see also a later discussion).

Effect of Temperature

Figures 4*a* and 4*b* show the changes of the e.s.r. spectrum with temperature. The changes were found to be reversible up to 80 °C for short periods of time. It is possible to explain the changes by using the model proposed by Bolton and Carrington (9) for the durosemiquinone cation. At room temperature, since both *cis* and *trans* forms are observed, τ (the lifetime of a particular conformation) must be large compared with $1/\Delta\omega$, where

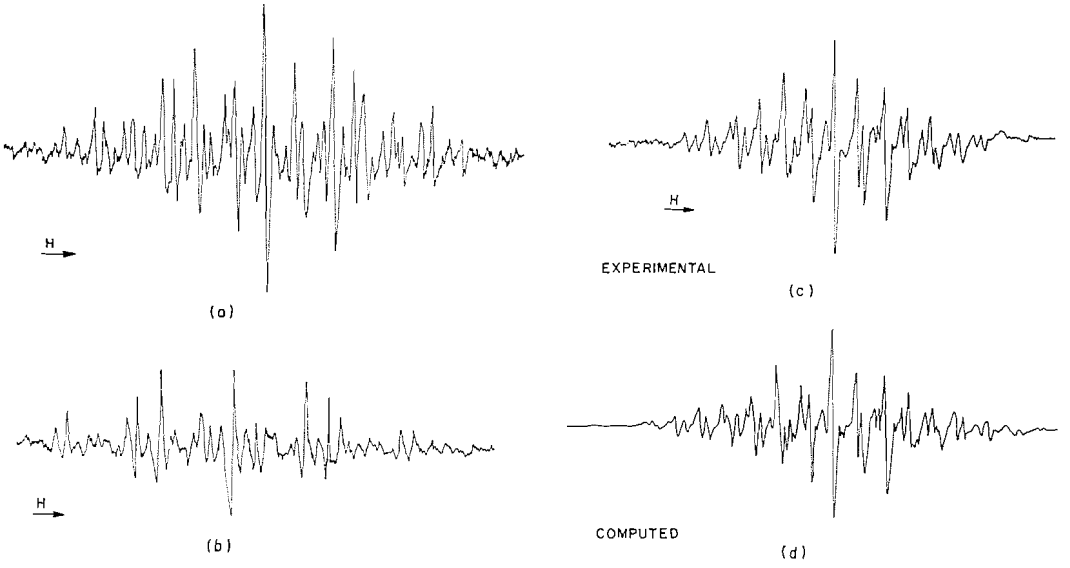


FIG. 4. (*a*) Electron spin resonance spectrum of a 0.2 *M* solution of *p*-dimethoxybenzene in concentrated sulfuric acid at 54 °C. (*b*) The same spectrum at 68 °C. (*c*) Electron spin resonance spectrum of a 0.2 *M* solution of *p*-dimethoxybenzene in a 50:50 (by volume) mixture of concentrated sulfuric acid and trifluoroacetic acid at room temperature. (*d*) A spectrum computed by using coupling constants given in the text and a line-width parameter of 0.25 G.

Can. J. Chem. Downloaded from www.nrcresearchpress.com by 210.87.254.40 on 09/05/12
For personal use only.

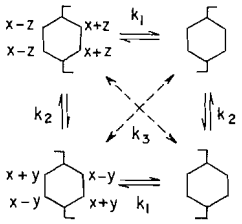


FIG. 5. Schematic representation of *cis* and *trans* forms of *p*-dimethoxybenzene at different temperatures.

$\Delta\omega$ is the frequency separation between corresponding lines of the separate isomers. Under these conditions, $k_1 \simeq k_2 \gg k_3$, and k_1 and k_2 must be slow compared with τ. Since the smallest frequency separation between the isomers corresponds to that between the OCH_3 protons (i.e. 0.12 G), a lower limit can be placed on the lifetimes of the *cis* and *trans* isomers, namely, ca. 3.0×10^{-6} s. As the temperature increases, k_1 and k_2 also increase and τ decreases. Since $\Delta\omega$ for the ring protons corresponds to $\tau = 2.4 \times 10^{-7}$ s, an intermediate state should exist with $\tau \simeq 10^{-6}$ s, when an uncertainty in the energy levels of the OCH_3 protons causes the lines from these protons to coalesce, whereas the lines caused by the ring protons are still discernible as *cis* and *trans* forms. This is shown in Fig. 4*a* (compare with the computed spectrum shown in Fig. 4*d*, which assumes a general broadening of each line to a half-width of 0.25 G, and a 50:50 ratio of the *cis* and *trans* isomers).

At still higher temperatures, τ approaches 10^{-7} s, thus leading to a condition when line-width alternation for the ring protons could occur (9, 10).

It has been shown theoretically that line-width alternation for four ring protons results in a broadening of the lines for which $\tilde{M}_{H(ring)} = \pm 1$;[3] hence, sharp lines at $\tilde{M}_{H(ring)} = \pm 2, 0$ would be expected. τ will be less than $1/\Delta\omega$ for the OCH_3 protons, and hence the splitting caused by these protons will be seen as the average of the *cis* and *trans* splittings (i.e. 3.39 G). The average splitting from the ring protons is 2.24 G, and sharp lines are therefore expected at ca. ± 4.48 G from the center of the spectrum, and broad lines at ca. ± 2.24 G. Figure 4*b* shows that the above predictions are being approached, since narrow lines at ± 4.48 G are actually observed. In addition, as the lines from the OCH_3 protons coalesce, the intensity of the outer lines (e.g. ± 12, ± 13, $\tilde{M}_{OCH_3} = \pm 1$, $\tilde{M}_{H(1)} = \tilde{M}_{H(2)} = 0$) should increase relative to that of the center line. The ratio of the intensities between line numbers ± 12 and the central line at room temperature is 2.18:1 (calculated 2.67:1), whereas at +68 °C the ratio between lines ± 12 and ± 13 (which have coalesced to one line) and the central line is 1.75:1 (calculated 1.33:1). The differences between the calculated and experimental ratios may be partly due to overlapping of lines and (or) differences in half-width, which makes the accurate determination of amplitudes difficult.

It is interesting to note that *p*-dimethoxybenzene is only just approaching line-width alternation for the ring protons at +70 °C, whereas the durosemiquinone cation shows this condition at +10 °C (9). As a first approximation, one might consider the barrier to rotation about the —C(ring)—O— bond to be similar in both molecules because steric

[3]*The field direction components of the nuclear spin angular momenta (M_{OCH_3}, $M_{H(1)}$, and $M_{H(2)}$) can have the following values: $M_{OCH_3} = \pm 3, \pm 2, \pm 1, 0$; $M_{H(1)} = \pm 1, 0$; $M_{H(2)} = \pm 1, 0$. Line positions can be specified in terms of 'spectral index' numbers: $\tilde{M}_{OCH_3}$, $\tilde{M}_{H(1)}$, and $\tilde{M}_{H(2)}$. The quantities are equal in magnitude to the respective quantum numbers, but are always defined so as to be positive on the high-field side of the spectrum. The spectral index numbers are identical with the absolute values if the splitting constant is negative, but $\tilde{M}_i = -M_i$ if a_i is positive (see ref. 18).*

Can. J. Chem. Downloaded from www.nrcresearchpress.com by 210.87.254.40 on 09/05/12
For personal use only.

Can. J. Chem. Downloaded from www.nrcresearchpress.com by 210.87.254.40 on 09/05/12
For personal use only.

interactions are similar. Moreover, the total spin density on the ring is approximately equal: $a_{CH_3} = 2.10$ G (9) and $a_{H(average)} = 2.24$ G (this paper). $1/\Delta\omega$ would therefore be expected to possess the same order of magnitude for both molecules. The main contribution causing the difference between the two molecules is therefore probably the relative rates (k_1 and k_2) of isomerization; i.e. for durosemiquinone k_1 and k_2 are greater than k_1, k_2 for *p*-dimethoxybenzene, presumably because of the differences in double bond character of the O-nuclear bond and (or) the differences in mass of the OH and OCH_3 groups.

The spectrum has also been recorded in a 50:50 mixture of trifluoroacetic and sulfuric acid (Fig. 4*c*); this spectrum can again be well represented by the simulated spectrum (Fig. 4*d*), which has an individual line-width parameter of 0.25 G (cf. the value of 0.075 G used in Fig. 3*b* in simulating the spectrum at room temperature).

The spectrum in D_2SO_4 is shown in Fig. 6*a*. It consists of seven groups of lines possessing fine structures. Since the spectrum is again slightly asymmetrical, and the fine structure within each group is not identical, this is consistent with the existence of *cis* and *trans* isomerism. The n.m.r. data show the ring protons to have exchanged, and the fine structure of the spectrum is therefore interpreted in terms of deuterium splittings. Such splitting gives a larger number of lines (the deuterium nucleus has a spin of 1), and the splitting caused by deuterium is approximately equal to 1/6.5 times the splitting caused by the proton. Figure 6*b* shows a simulated spectrum of *p*-dimethoxybenzene in D_2SO_4 with the following parameters (splitting constants in parentheses).

Species A		Species B	
Six equivalent protons	(3.45 G)	Six equivalent protons	(3.33 G)
Two equivalent deuterons	(0.482 G)	Two equivalent deuterons	(0.432 G)
Two equivalent deuterons	(0.242 G)	Two equivalent deuterons	(0.292 G)

IV. Molecular Orbital Calculations

The results of molecular orbital calculations are shown in Table I. Spin densities (ρ_1 (calcd.)) on the ring protons were calculated by choosing parameters which were consistent with normal interactions (11) and gave values which agreed approximately with the spin densities on the ring protons (ρ_1 (exptl.)); the latter were obtained from the splitting constants via McConnell's equation (12). Normally, such calculations on systems

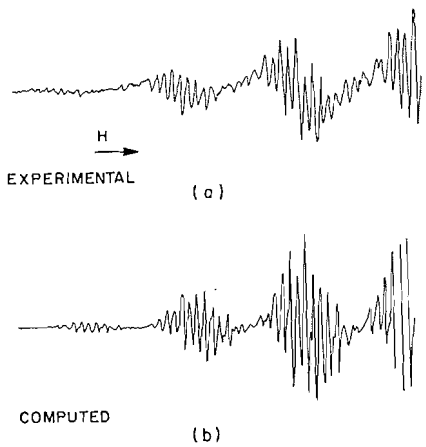
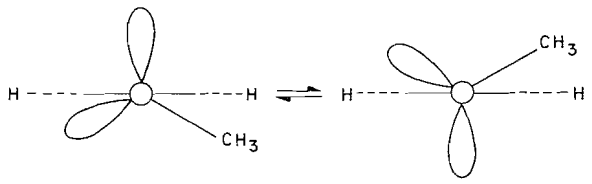


FIG. 6. (*a*) Electron spin resonance spectrum of a 0.2 *M* solution of *p*-dimethoxybenzene in D_2SO_4. (*b*) A spectrum computed by using coupling constants as given in the text. Only half the spectrum is shown.

Can. J. Chem. Downloaded from www.nrcresearchpress.com by 210.87.254.40 on 09/05/12
For personal use only.

of this type will produce an equivalent amount of spin density on each of the ring positions. To rationalize the observed asymmetry in the ring splittings, an empirical approach was employed. Stone and Maki (13), in their treatment of the terephthalaldehyde anion, took into account two effects, which they called the α and β effects. The α effect was considered to be an electrostatic effect across space on the carbon atoms of the ring. In the present system, it was assumed that the OCH_3 protons may have a residual δ^+ charge and hence will change the Coulomb integrals of carbon atoms 2 and 3 in the *cis* isomer (II*a*), but of carbon atoms 2 and 5 in the *trans* isomer (II*b*). Incidentally, the sign of the α effect is now opposite to that in the terephthalaldehyde anion, where the effect was ascribed to a large negative charge on the oxygen atom.

The β effect is assumed to reflect the tendency for overlap between carbon atoms 2 and 8 (and between carbon atoms 3 and 10) in the *cis* isomer. In the *trans* isomer, the tendency for overlap is between carbon atoms 2 and 8 (and between carbon atoms 5 and 10). This effect is thought to be small, compared with the α effect in this system, but in any case would be expected to lead to an asymmetry in the same direction as the α effect. In our calculations, only the α effect was considered. This seems to be justified, because significant spin density changes were obtained only if an exceptionally large β effect was assumed.



III IV

It may next be noted that interactions with the lone pair of electrons on the oxygen atoms have been ignored since their interactions with the ring hydrogens are probably small. This follows because the p orbitals presumably spend most of their time in a direction at right angles to the plane of the ring (cf. ref. 14). The equilibrium position for the CH_3 group will therefore tend to be in the plane of the ring, as shown in structures III and IV.

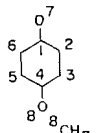
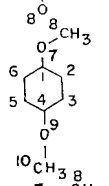
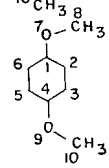
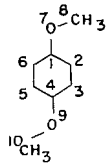
In Table I, the calculated spin density for the *p*-benzosemiquinone cation[4] is first used to obtain a proportionality constant between a_{OH} and ρ_o; i.e. $a_{OH}/\rho_o = Q_o$, giving $Q_o = 3.44/0.114 \approx 30$. This Q_o value is then used to estimate approximate spin densities for the oxygen atom of the OCH_3 group (values in parentheses in Table I). These spin density values are only estimates, since there is little theoretical justification to apply Q_o values obtained from the hydroquinone system to the *p*-dimethoxybenzene system (cf. the Q value variations obtained from the data reported for various quinones (15)). The calculated spin density values on the ring positions for the *cis* isomer agree to within $\sim$10% with the experimentally obtained values, whereas those for the *trans* isomer agree to within $\sim$1%. This indicates that some other interaction contributes to the observed spin densities in the *cis* isomer.

It may next be noted that the molecular orbital calculations indicate that the CH_3 splittings should be approximately equal in the *cis* and *trans* isomers (spin densities

[4]*Hydroquinone in concentrated sulfuric acid exists in equilibrium with the semiquinone cation radical; the concentration of this radical was calculated from the e.s.r. spectrum to be ca. 0.006%.*

TABLE I

Experimental and calculated parameters for the *p*-dimethoxybenzene cation radical, with the hydroquinone cation radical as the reference substance

Systems*	Positions	ρ_i (calcd.)	ρ_i (exptl.)†	a_i (exptl.) (G)	E (calcd.)‡	g value§
	1	0.206				
	2	0.091	0.098	2.36¶	-0.390β	2.0034_5
	7	0.114		3.44¶		± 0.00003
	1	0.187				
	2	0.090	0.094	2.24**	-0.342β	
	7	0.127	(0.113)‖	3.39**		
	8	0.006				
	1	0.181				
	2	0.101	0.112	2.68		
	5	0.084	0.075	1.81	-0.3623β	
	7	0.128	(0.110)‖	3.33		
	8	0.007				2.0036_5
						± 0.00003
	1	0.181				
	2	0.062	0.062	1.49		
	3	0.123	0.124	2.99	-0.3602β	
	7	0.127	(0.115)‖	3.45		
	8	0.007				

*Parameters used were $h_{OO} = 2.00$, $k_{CO} = 1.30$, $h_{CH_3-CH_3} = 3.00$, $k_{O-CH_3} = 0.70$ (using the heteroatom model for the CH_3 groups and O—X (X = CH_3), giving $k_{XX} = 3.00$ and $k_{OX} = 0.70$ (cf. ref. 11)); $h_{CC(2)} = h_{CC(3)} = 0.10$ for *cis*, $h_{CC(2)} = h_{CC(5)} = 0.10$ for *trans*.

†Experimental ring proton spin densities (calculated from $a_i = \rho_i Q$, where $Q = 24$).

‡Energy of lowest unfilled orbital (calculated).

§See Experimental section.

‖Experimental spin densities of oxygen are estimated by assuming a relation $a_{OCH_3} = \rho_O Q$ for CH_3 splittings, with a Q value of 30 (from the hydroquinone spectrum).

¶Values taken from ref. 15.

**Values given are averages of experimentally obtained *cis* and *trans* splittings.

0.128 vs. 0.127), whereas in practice it is found that *trans* > *cis* (splittings 3.45 vs. 3.33 G; see Table I). This is probably because steric effects have been neglected, which would presumably be greater in the *cis* form, leading to an out-of-plane movement of the C(ring)—OMe bond and hence a decrease in the coupling to the OCH_3 protons. If it is assumed that this coupling is related to the angle of twist about the C(ring)—O bond by a $\cos^2\theta$ relationship (16), this leads to a value of $\theta = 7°$ (if one assumes $\cos^2\theta = 3.33/3.45$) for the equilibrium position of the *cis* isomer relative to that of the *trans* isomer.

The difference in energy between the *cis* and *trans* forms is calculated to be -0.0021β (see Table I). Therefore, if $\beta \approx 2$ eV, $\Delta E = 100$ cal/mole, which may be compared with the value of 110 cal/mole obtained from the experimental ratio of the two isomers at 22 °C.

V. Line Widths and g Value Variations

Closer inspection of Fig. 3*a* shows that, for example, lines 7 and 8, 12 and 13, and 24 and 25 appear to be better resolved on the low-field side than on the high-field side. If these lines are studied under slow-sweep conditions, the results show (Table II and Figs. 7*a*–7*d*) that the spectra of the two isomers are slightly displaced relative to one another, suggesting that $g_{trans} > g_{cis}$. The theory of g values (17) shows that they can

Can. J. Chem. Downloaded from www.nrcresearchpress.com by 210.87.254.40 on 09/05/12
For personal use only.

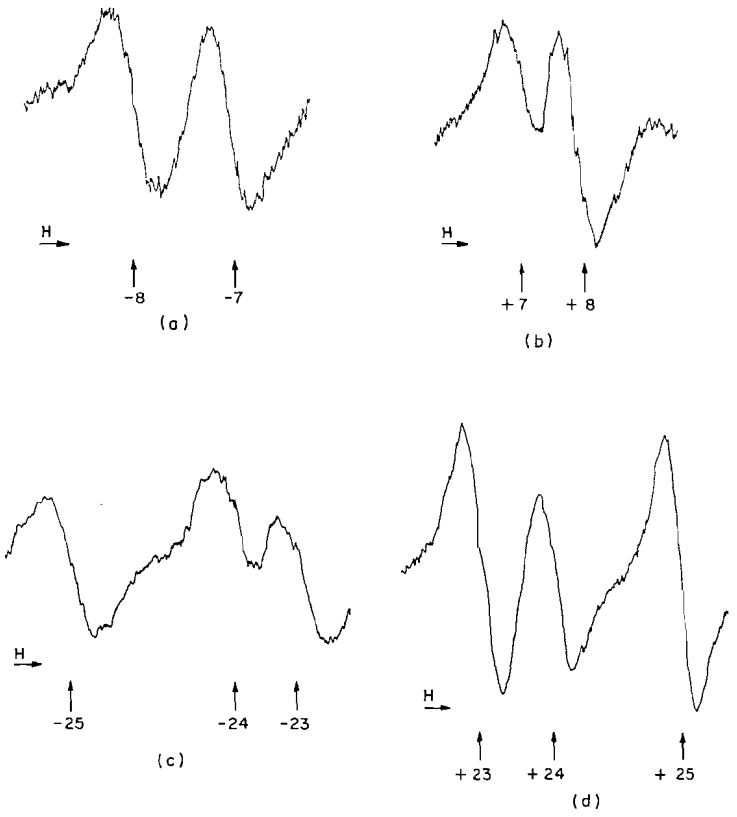


FIG. 7. Sections of the electron spin resonance spectrum (Fig. 3*a*) at low and high fields. Lines are numbered as in Fig. 3*a*.

be considered as the sum of a number of parameters. Since Δg (hydroquinone $-$ *p*-dimethoxybenzene) ≈ 0.0002 (see Table I), Δg (II*a* $-$ II*b*) would be expected to be much smaller, outside the limits of direct measurement. As a first approximation, *g* values for the *cis* and *trans* forms would be expected to be the same. However, since the splitting from the OCH_3 protons in the two isomers (3.33 and 3.45 G) is significantly different, probably because of steric interactions, the same interactions may also explain the *g* value difference. This follows, since, when the equilibrium value of θ is altered, some of the contributions to *g* would decrease and hence g_{cis} may be less than g_{trans}, as observed. From Table II the difference between the centers of the *cis* and *trans* isomers was calculated to be 0.029 ± 0.010 G as follows. Separation between $+7$, $+8$, and -7, -8 (see Figs. 7*a* and 7*b*) was found to be 0.098 G and 0.172 G on the high- and low-field sides, respectively. Hence, one line is shifted relative to the other by 0.074 G, corresponding to a displacement of the centers of 0.037 G. The average displacement of the centers as calculated from Table II was 0.029 ± 0.010 G, corresponding to Δg (*cis* $-$ *trans*) of 0.000018, an order of magnitude lower than the minimum difference which can be observed directly.

From Table II and from a separate line-width analysis it was found that, in almost every case, the low-field lines are broader than their high-field counterparts (the effect was temperature dependent, being more pronounced at low temperature, because of the

Can. J. Chem. Downloaded from www.nrcresearchpress.com by 210.87.254.40 on 09/05/12
For personal use only.

Can. J. Chem. Downloaded from www.nrcresearchpress.com by 210.87.254.40 on 09/05/12
For personal use only.

TABLE II

Line-width data for pairs of lines in *cis* and *trans* isomers (II*a* and II*b*)

Line No. (see Figs. 3 and 7)	Isomer	Spectral index numbers $\tilde{M}_{OCH_3}$	$\tilde{M}_{H(1)}$	$\tilde{M}_{H(2)}$	Half-width (G)	Relative amplitude (cm) (A)	Relative calculated amplitude (A′)	Ratio* A/A′	Splitting between pairs of lines: Line numbers	Calculated splitting (G)	Experimental splitting (G)
+7	*cis*	0	0	+1	0.069	3.9	20	0.255	+7, +8	0.15	0.098
−7	*cis*	0	0	−1	0.070	6.3			−7, −8	0.15	0.172
+8	*trans*	+1	−1	+1	0.071	7.8	22.5	0.306			
		+1	+1	−1							
−8	*trans*	−1	+1	−1	0.089	6.0					
		−1	−1	+1							
+12	*cis*	+1	0	0	0.069	9.1	30	0.297	+12, +13	0.12	0.126
−12	*cis*	−1	0	0	0.087	8.7			−12, −13	0.12	0.190
+13	*trans*	+1	0	0	0.067	14.2	30	0.473			
−13	*trans*	−1	0	0	0.082	10.2					
+23	*trans*	+1	+1	0	0.083	6.0	15	0.293	+23, +24	0.22	0.164
−23	*trans*	−1	−1	0	0.093	2.8			−23, −24	0.22	0.125
+24	*cis*	+2	0	0	0.071	4.1	12	0.254	+24, +25	0.24	0.270
−24	*cis*	−2	0	0	0.068	2.0			−24, −25	0.24	0.315
+25	*trans*	+2	0	0	0.067	6.1	12	0.388	+23, +25†	0.46	0.444
−25	*trans*	−2	0	0	0.093	3.1			−23, −25	0.46	0.440

*Ratios correspond to *trans/cis* 1.35:1.0 (cf. 1.20:1.0 from well-resolved lines).
†Splitting between two *trans* lines should be constant on high- and low-field sides.

higher viscosity of the solution). Such line-width variations are well known (18, 19), and appropriate theories have been developed (10, 20). Unfortunately, because of lines overlapping, it has not been possible to carry out a complete line-width analysis. However, by analogy with other work (10, 20), it would seem to be plausible that the line-width variation is related linearly with the quantum number associated with the OCH_3 protons. Specific attention has not been paid to the anisotropic intramolecular dipolar g tensor interactions for the OCH_3 group from a theoretical point of view. Such interactions would be expected to result in the observed linear variation of line width across the spectrum. The linear variation of line width caused by a CH_3 group has been noted before, and has also been observed in a number of other related compounds (21 and unpublished information), when broad low-field lines were also found.

The results may be summarized in the following assignment of splitting constants, which can interpret completely the observed e.s.r. spectrum of *p*-dimethoxybenzene in concentrated sulfuric acid.

trans isomer	*cis* isomer
$a_{OCH_3} = +3.45$ G	$a_{OCH_3} = +3.33$ G
$a_{H(2,5)} = -2.99$ G	$a_{H(2,3)} = -2.68$ G
$a_{H(3,6)} = -1.49$ G	$a_{H(5,6)} = -1.81$ G

The isotropic splitting constants of the OCH_3 protons are considered to be positive, since a hyperconjugative mechanism is favored (22, 23).

ACKNOWLEDGMENTS

The authors are indebted to Drs. J. M. Fritsch and L. C. Snyder for computer programs, and to Mr. Paul Riehm and Mr. J. Robinson for assistance with computer problems and with some of the ultraviolet studies. The financial assistance of the National Research Council is also gratefully acknowledged.

REFERENCES

1. A. Zweig, W. G. Hodgson, and W. H. Jura. J. Am. Chem. Soc. **86**, 4124 (1964).
2. B. G. Segal, M. Kaplan, and G. K. Fraenkel. J. Chem. Phys. **43**, 4191 (1965).
3. A. D. McLachlan. Mol. Phys. **3**, 233 (1960).
4. J. M. Fritsch, T. P. Layloff, and R. N. Adams. J. Am. Chem. Soc. **87**, 1724 (1965).
5. C. S. Johnson. J. Chem. Phys. **39**, 2111 (1963).
6. W. Baker and C. Evans. J. Chem. Soc. 372 (1938).
7. E. J. Land and G. Porter. Proc. Chem. Soc. 84 (1960).
8. P. H. Rieger and G. K. Fraenkel. J. Chem. Phys. **37**, 2811 (1962).
9. J. R. Bolton and A. Carrington. Mol. Phys. **5**, 161 (1962).
10. J. H. Freed and G. K. Fraenkel. J. Chem. Phys. **39**, 326 (1963).
11. A. Streitwieser, Jr. Molecular orbital theory for organic chemists. John Wiley & Sons, Inc., New York. 1962. Chap. 5.
12. H. M. McConnell. J. Chem. Phys. **24**, 764 (1956).
13. E. W. Stone and A. H. Maki. J. Chem. Phys. **38**, 1999 (1963).
14. A. Balasubramanian, J. C. Dearden, W. F. Forbes, and N. F. Cheetham. Can. J. Chem. **43**, 2603 (1965).
15. J. R. Bolton, A. Carrington, and J. dos Santos-Veiga. Mol. Phys. **5**, 465 (1962).
16. M. C. R. Symons. *In* Advances in physical organic chemistry. *Edited by* V. Gold. Academic Press, Inc., New York. 1963. p. 325.
17. A. J. Stone. Mol. Phys. **6**, 509 (1963).
18. B. L. Barton and G. K. Fraenkel. J. Chem. Phys. **41**, 695 (1964).
19. J. R. Bolton and G. K. Fraenkel. J. Chem. Phys. **41**, 944 (1964).
20. A. Carrington and H. C. Longuet-Higgins. Mol. Phys. **5**, 447 (1962).
21. N. Steinberger and G. K. Fraenkel J. Chem. Phys. **40**, 723 (1964).
22. M. C. R. Symons. Tetrahedran, **18**, 333 (1962).
23. J. P. Colpa and E. Deboer. Mol. Phys. **7**, 333 (1964).

Can. J. Chem. Downloaded from www.nrcresearchpress.com by 210.87.254.40 on 09/05/12
For personal use only.

Can. J. Chem. Downloaded from www.nrcresearchpress.com by 210.87.254.6 on 09/05/12
For personal use only.

RÉACTIONS DE L'ÉPOXYSTYRÈNE AVEC LA GLYCINE ET SES DÉRIVÉS

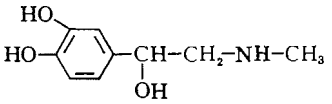
CASIMIR BERSE ET KRZYSZTOF JANKOWSKI
Département de Chimie, Université de Montréal, Montréal, Québec

Reçu le 5 janvier 1966

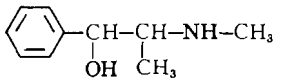
RÉSUMÉ

La présente publication décrit une étude de l'ouverture du noyau oxirannique de l'époxystyrène par la glycine et ses dérivés. Les réactions ont été effectuées dans des conditions douces sans catalyseur. Les produits des réactions ont été isolés et identifiés, soit sous forme de dérivés de la dicéto-2,5 piperazine (formés par condensation des intermédiaires), soit sous forme de lactone (formée par réaction entre le carboxyle de l'acide aminé et la fonction alcool formée par ouverture de l'époxystyrène). Les structures des composés obtenus ont été déterminées. Le mécanisme de la réaction est discuté.

Il est connu qu'un grand nombre de composés qui contiennent les groupements aminé et hydroxyle possèdent une activité pharmacodynamique, par exemple, l'adrénaline ou l'éphédrine, qui sont des amino alcools aromatiques.



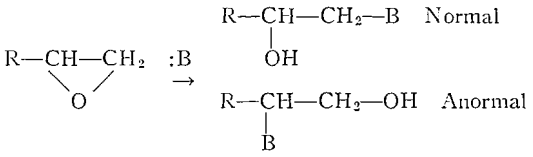
Adrénaline



Éphédrine

La recherche de nouveaux produits avec une activité semblable à été effectuée souvent utilisant la méthode d'ouverture des époxydes avec des amines aliphatiques et aromatiques (1). Nous avons donc pensé que les produits qui se forment dans la réaction d'ouverture des époxydes par les acides aminés pourraient posséder une activité pharmacodynamique particulière.

Les acides aminés libres ont assez rarement été utilisés pour ouvrir des époxydes. Kiprianov (2) et ses collaborateurs ont effectué l'ouverture de l'époxycyclohexène, de l'époxyéthylène et de l'époxybutylène avec certains dérivés de la glycine; Maekawa (3) a fait l'ouverture de l'époxyéthylène avec l'alanine. L'ouverture des époxydes donne presque toujours deux produits, qui ont été nommés par Krussuski (4) comme normal et anormal dépendant de la direction d'attaque de la fonction aminée sur le noyau oxirannique.



Les essais d'ouverture des époxydes avec les acides aminés libres n'ont pas donné, conformément à l'attente, de produits car la basicité du groupement aminé n'était pas suffisante pour ouvrir l'époxyde dans la réaction sans catalyseur. Nous avons donc utilisé des acides aminés dont le groupement carboxylique était protégé soit sous forme d'ester ou de sel sodé.

L'ouverture de l'époxystyrène avec le glycinate d'éthyle fournit quatre composés qui ont été isolés par cristallisation fractionnée: (*i*) la dicéto-2,5 piperazine (VIII), p.f. 260°,

provenant de la condensation de deux molécules de glycinate d'éthyle; (*ii*) la bis-(hydroxy-2 phényl-2 éthyl)-1,4 dicéto-2,5 piperazine (III), p.f. 275°; (*iii*) la (hydroxy-2 phényl-2 éthyl)-1 (hydroxy-2 phényl-1 éthyl)-4 dicéto-2,5 piperazine (IV), p.f. 206°; (*iv*) la lactone de la N-(hydroxy-2 phényl-2 éthyl) glycine (VI), p.f. 120–121°.

Les quatre produits ont été identifiés soit par hydrolyse, soit par synthèse et spectroscopie infrarouge.

La séparation des quatre produits a été effectuée par chromatographie sur alumine. Les résultats obtenus sont identiques avec ceux de la séparation par cristallisation. Deux autres produits possibles dans cette réaction (la bis-(hydroxy-2 phényl-1 éthyl)-1,4 dicéto-2,5 piperazine (V) et la lactone de la N-(hydroxy-2 phényl-1 éthyl) glycine (VII)) n'ont pu être isolés, ni par cristallisation ni par chromatographie.

Les structures des quatre composés ont été établies de la façon suivante. Le composé VIII a été identifié par synthèse par condensation de deux molécules de la glycine (5). Le composé III a été identifié par synthèse et hydrolyse. Le chloroacétate d'éthyle chauffé avec l'hydroxy-2 phényl-2 éthylamine (XI) donne le produit III, p.f. 275°, et le produit VI, p.f. 120–121°. L'hydrolyse du produit III par l'acide chlorhydrique concentré donne 80% de chlorhydrate de N-(hydroxy-2 phényl-2 éthyl) glycine (XIV), p.f. 186°. Ce dernier a été obtenu par la réaction du produit XI avec l'acide chloroacétique. La libération d'acide chlorhydrique à partir du produit XIV donne la N-(hydroxy-2 phényl-2 éthyl) glycine (IX), p.f. 210°. L'hydrolyse du produit III par l'acide chlorhydrique concentré dans l'éthanol donne 20% de chlorhydrate de N-(hydroxy-2 phényl-2 éthyl) glycinate d'éthyle (X), p.f. 165°. Le composé X libéré de son chlorhydrate donne le produit III. L'hydrolyse du produit III par une solution d'hydroxyde de sodium à 10% donne le composé IX, qui a été transformé par élimination d'eau dans le benzène en lactone VI et par la décarboxylation en N-(hydroxy-2 phényl-2) méthylamine (XV), p.f. 45°, identique avec le produit obtenu par l'action de la méthylamine sur l'époxystyrène.

La lactone VI a été hydrolysée et le produit IX a été obtenu. L'estérification du produit IX en présence d'acide chlorhydrique gazeux dans l'éthanol donne le produit X.

Le produit IV a été synthétisé à partir d'un mélange de 50% d'hydroxy-2 phényl-2 éthylamine (XI) et 50% d'hydroxy-2 phényl-1 éthylamine (XII); ce mélange étant mis en réaction avec le chloroacétate d'éthyle. Dans cette réaction il se forme aussi le produit III. L'hydrolyse du produit IV par l'acide chlorhydrique concentré donne le mélange de chlorhydrates suivants: 22% de chlorhydrate de N-(hydroxy-2 phényl-2 éthyl) glycine (XIV), p.f. 186°, et 26% de chlorhydrate de N-(hydroxy-2 phényl-1 éthyl) glycine (XIII), p.f. 152°.

Ce produit est identique avec le produit XIV déjà décrit. Le produit XIII est identique avec le produit obtenu par la réaction de XII avec l'acide chloroacétique. Ces données ont été confirmées par la chromatographie sur plaques minces. L'hydrolyse du produit IV par l'acide chlorhydrique concentré dans l'éthanol donne 11% du composé X; l'hydrolyse du produit IV par l'hydroxyde de sodium donne 18% du produit IX. Les autres produits de ces deux dernières hydrolyses n'ont pas été isolés.

La structure de la lactone de la N-(hydroxy-2 phényl-2 éthyl) glycine (VI) a été déterminée par la synthèse. Le produit XI chauffé avec le chloroacétate d'éthyl donne la lactone VI. Dans cette réaction le produit III se forme en majorité.

Le produit IX a été lactonisé dans le benzène anhydre et a donné le produit VI. Le produit IX laissé dans l'éthanol à 0° donne des petites quantités du produit III.

L'ouverture de l'époxystyrène avec le glycinate d'éthyle donne 20.9% de produit cristallin, dont 85.4% résulte de l'ouverture normale et 11% de l'ouverture anormale. Le

Can. J. Chem. Downloaded from www.nrcresearchpress.com by 210.87.254.6 on 09/05/12
For personal use only.

Can. J. Chem. Downloaded from www.nrcresearchpress.com by 210.87.254.6 on 09/05/12
For personal use only.

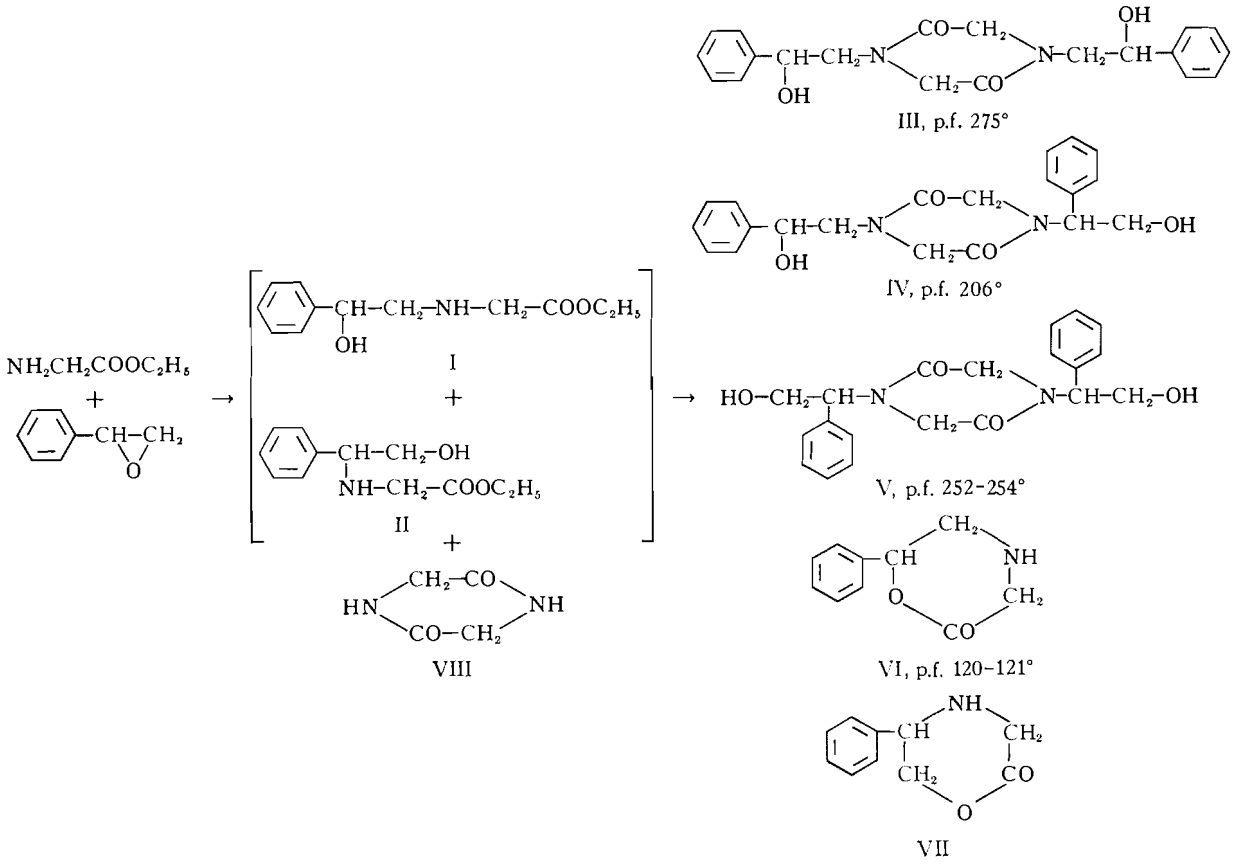


SCHÉMA 1.

Can. J. Chem. Downloaded from www.nrcresearchpress.com by 210.87.254.6 on 09/05/12
For personal use only.

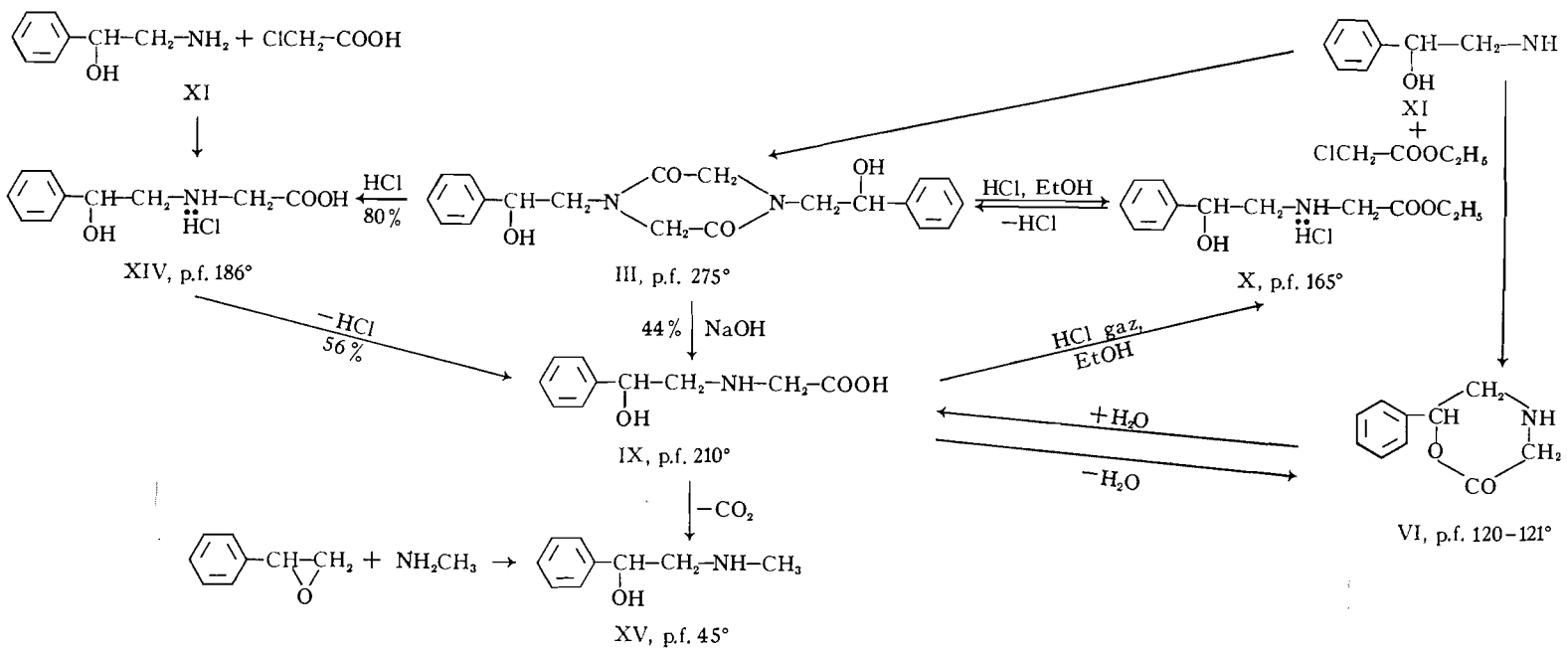


SCHÉMA 2.

Can. J. Chem. Downloaded from www.nrcresearchpress.com by 210.87.254.6 on 09/05/12
For personal use only.

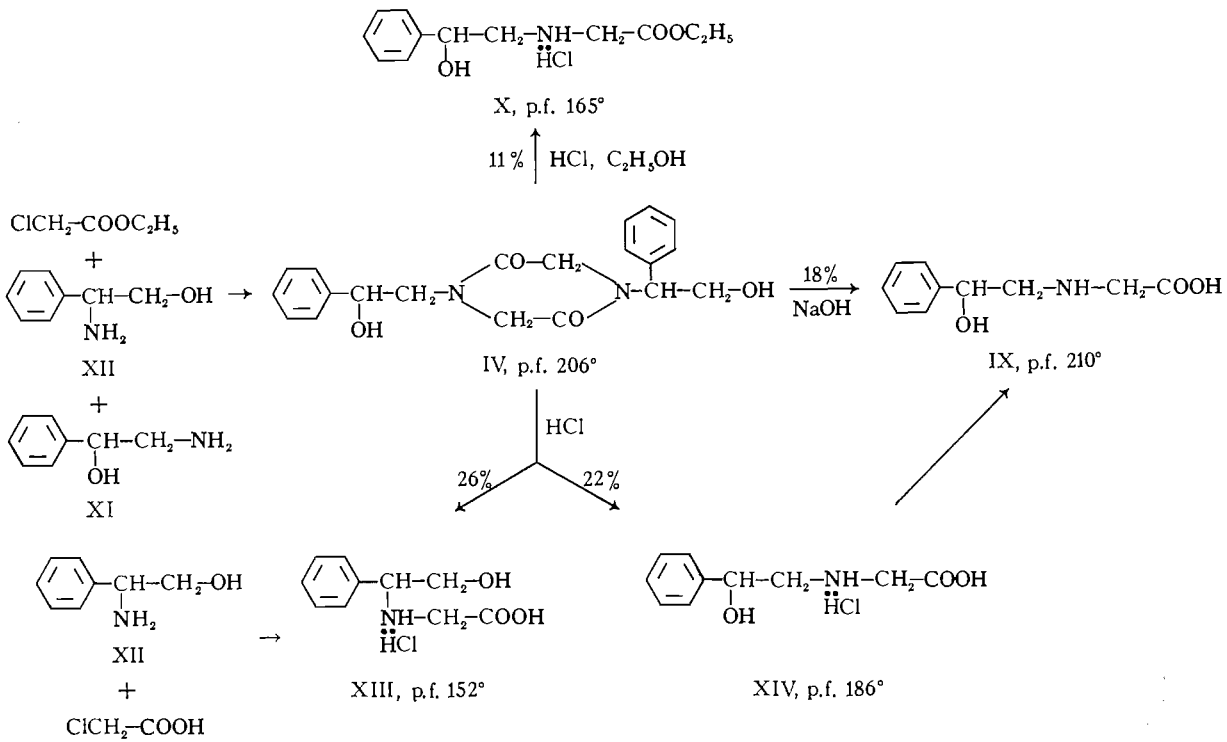


SCHÉMA 3.

rapport des produits normaux sur le produit anormal est 8:1. Les autres produits de la réaction sont très probablement des polymères. Le fait que les produits III et IV contiennent le même élément structurel, N-(hydroxy-2 phényl-2 éthyl) glycine (IX), a été établi comme suit. La quantité des produits IX, X ou XIV formés par hydrolyse du composé IV est environ deux fois plus petite que dans le cas de l'hydrolyse du composé III.

Mannich et Thiele (6) ont fait la réaction entre le produit XI et le chloroacétate d'éthyle en isolant seulement le produit VI, p.f. 121°, auquel ils ont attribué la structure III. Le spectre infrarouge du composé, p.f. 275°, montre à 1 635 cm^{-1} une bande carbonyle, suggérant la structure III pour ce produit.

Dans le cas du composé, p.f. 120–121°, une bande carbonyle à 1 720 cm^{-1} suggère la structure VI pour ce produit.

Pour compléter cette série de réactions nous avons fait la synthèse du produit V en condensant le chloroacétate d'éthyle avec le produit XII. Le produit attendu, p.f. 252°, fut isolé.

La glycine libre ne donne pas de produits d'ouverture dans la réaction avec l'époxystyrène. Aussi la dicéto-2,5 piperazine (VIII) ne réagit pas avec l'époxystyrène. Dans ces deux réactions on peut isoler seulement des produits de départ. Le glycinate de sodium (XVI) chauffé avec l'époxystyrène dans le diméthylformamide donne une petite quantité de produit IX, qui a été identifié d'après le point de fusion mixte et par son spectre infrarouge.

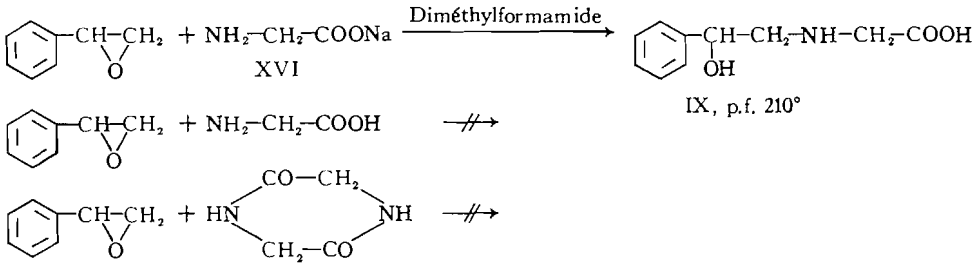


SCHÉMA 4.

Les résultats mentionnés plus haut permettent de supposer que le mécanisme réactionnel d'ouverture de l'époxystyrène est le suivant: les composés N-(hydroxy-2 phényl-2 éthyl) glycinate d'éthyle (I), qui correspondent à l'ouverture normale, et N-(hydroxy-2 phényl-1 éthyl) glycinate d'éthyle (II) (anormale) sont formés comme les intermédiaires qui à leur tour dimérisent pour donner les produits III et IV. Le produit VI est formé par lactonisation du composé I. Le deuxiéme mécanisme qu'on pourrait proposer serait la formation du dicéto-2,5 piperazine (VIII) qui réagira ensuite avec l'époxystyrène. Ce mécanisme peut être réfuté parce que la réaction entre dicéto-2,5 piperazine (VIII) avec l'époxystyrène ne donne que les produits de départ.

Il faut lier l'existance d'ouvertures normale et anormale au cours de la réaction avec la formation d'éthanol. La présence de l'éthanol comme solvant permet toujours la formation de deux produits d'ouverture des époxydes (7).

L'absence des produits V et VII il faut expliquer que l'hydroxyester II, qui pourrait donner par la dimérisation le produit V et par la lactonisation le produit VII, se forme avec un petit rendement. A la présence des plus grandes quantités du hydroxyesther I il réagit plus facilement avec les molécules du produit I que du produit II.

Can. J. Chem. Downloaded from www.nrcresearchpress.com by 210.87.254.6 on 09/05/12
For personal use only.

Can. J. Chem. Downloaded from www.nrcresearchpress.com by 210.87.254.6 on 09/05/12
For personal use only.

PARTIE EXPÉRIMENTALE

Les points de fusion ont été déterminés dans l'appareil de Kofler et ne sont pas corrigés. Les spectres infrarouges ont été déterminés dans l'appareil de Beckman modèle IR-8 (en N-oil). Les analyses sont de J. Maciak, Indianapolis, de C. Daesslé, Montréal, et de nous-mêmes (micro-Kjeldahl). Les solvants ont été purifiés d'après les méthodes généralement utilisés. L'identité des composés dans la Partie Expérimentale a été prouvée par points de fusions mixtes et par superposition des spectres infrarouges.

Ouverture de l'époxystyrène avec le glycinate d'éthyle

Le glycinate d'éthyle (20.6 g, 0.20 mole) (8) et l'époxystyrène (24 g, 0.20 mole) ont été portés à reflux pendant 12 h. Le mélange refroidie à 0° donne les cristaux qui ont été triturés dans l'éthanol absolu et filtrés. Le précipité (9.3 g, 20.9%) a été cristallisé d'éthanol absolu. Les quatre fractions ont été séparées.

Fraction	Point de fusion	Rendement
a	260° (sublimation)	0.20 g, 2.2%
b	275°	6.98 g, 74.0%
c	206°	2.04 g, 22.0%
d	120–121°	0.037 g, 0.4%

(*a*) Le produit cristallisé d'éthanol–eau a été identifié comme dicéto-2,5 piperazine (VIII). Le spectre infrarouge est identique avec celui de la littérature (5).

Anal. Calc. pour $C_4H_6O_2N_2$ (114.10): N, 24.55. Trouvé: N, 23.90.

(*b*) Le produit cristallisé d'éthanol a été identifié comme bis-(hydroxy-2 phényl-2 éthyl)-1,4 dicéto-2,5 piperazine (III). Le spectre infrarouge: 1 635 cm^{-1} et 3 350 cm^{-1}.

Anal. Calc. pour $C_{20}H_{22}O_4N_2$ (354.39): C, 67.77; H, 6.25; N, 7.89. Trouvé: C, 68.03; H, 6.10; N, 8.23.

(*c*) Le produit cristallisé d'éthanol a été identifié comme (hydroxy-2 phényl-2 éthyl)-1 (hydroxy-2 phényl-1 éthyl)-4 dicéto-2,5 piperazine (IV). Le spectre infrarouge: 1 635 cm^{-1}, 3 350 cm^{-1} et 3 180 cm^{-1}.

Anal. Calc. pour $C_{20}H_{22}O_4N_2$ (354.39): C, 67.77; H, 6.25; N, 7.89. Trouvé: C, 67.69; H, 6.24; N, 8.21.

(*d*) Le produit cristallisé d'éthanol–eau a été identifié comme lactone de N-(hydroxy-2 phényl-2 éthyl) glycine (VI). Le spectre infrarouge: 1 720 cm^{-1} et 1 100 cm^{-1}.

Anal. Calc. pour $C_{10}H_{11}O_2N$ (177.19): N, 7.89. Trouvé: N, 7.67.

Hydrolyse acide du produit III

Une solution de bis-(hydroxy-2 phényl-2 éthyl)-1,4 dicéto-2,5 piperazine (III) (1.7 g, 0.005 mole) dans l'acide chlorhydrique concentré (20 ml) a été chauffée à reflux pendant 5 h. La solution a été évaporée *in vacuo* et le résidu a été cristallisé d'éthanol; rendement de chlorhydrate de N-(hydroxy-2 phényl-2 éthyl) glycine (XIV) 1.78 g (80%), p.f. 186°. Le spectre infrarouge: 1 650 cm^{-1}.

Anal. Calc. pour $C_{10}H_{14}O_3NCl$ (231.67): C, 51.83; H, 6.17; N, 6.13. Trouvé: C, 52.22; H, 6.07; N, 5.83.

Une solution de produit XIV (1.1 g, 0.005 mole) dans le diméthylformamide (20 ml) et la quantité équimoléculaire de triéthylamine ont été chauffées au bain-marie pendant 1 h et refroidies à 0° pendant 4 h. Le précipité de chlorhydrate de triéthylamine a été filtré et la solution a été triturée avec l'éther. La N-(hydroxy-2 phényl-2 éthyl) glycine (IX) a été filtrée et recristallisée d'éthanol; rendement 560 mg (56%), p.f. 210°. Le spectre infrarouge: 1 610 cm^{-1} et 1 570 cm^{-1}.

Anal. Calc. pour $C_{10}H_{13}O_3N$ (195.21): C, 61.55; H, 6.71; N, 7.17. Trouvé: C, 60.92; H, 6.82; N, 7.10.

Hydrolyse acide du produit IV

Une solution de (hydroxy-2 phényl-2 éthyl)-1 (hydroxy-2 phényl-1 éthyl)-4 dicéto-2,5 piperazine (IV) (500 mg, 0.0015 mole) dans l'acide chlorhydrique concentré (25 ml) a été chauffée pendant 5 h. Le mélange a été évaporé *in vacuo* et le résidu a été cristallisé d'acétone. Les deux produits ont été séparés par la cristallisation fractionnée.

(*a*) Chlorhydrate de N-(hydroxy-2 phényl-2 éthyl) glycine (XIV), rendement 152 mg (22%), p.f. 186°.

Anal. Calc. pour $C_{10}H_{14}O_3NCl$ (231.67): N, 6.13. Trouvé: N, 6.02.

(*b*) Chlorhydrate de N-(hydroxy-2 phényl-1 éthyl) glycine (XIII), rendement 180 mg (26%), p.f. 152°.

Anal. Calc. pour $C_{10}H_{14}O_3NCl$ (231.67): C, 51.83; H, 6.17; N, 6.13. Trouvé: C, 52.04; H, 6.41; N, 6.00.

La chromatographie sur couche mince dans le butanol – eau – acide acétique (4:4:1) donne les résultats suivants: R_f du produit XIII, 0.48; R_f du produit XIV, 0.71; R_f du mélange après l'hydrolyse, 0.48 et 0.70.

Le produit XIV a été libéré de son chlorhydrate dans le diméthylformamide avec le triéthylamine dans les mêmes conditions que déjà décrit. Le produit IX a été isolé; rendement 28 mg (22%), p.f. 209–210° (identique avec le produit IX obtenu par l'hydrolyse acide du produit III).

Hydrolyse acide du produit III dans l'éthanol

La bis-(hydroxy-2 phényl-2 éthyl)-1,4 dicéto-2,5 piperazine (III) (350 mg, 0.001 mole) dans l'éthanol (40 ml) a été chauffée avec l'acide chlorhydrique concentré (10 ml) à reflux pendant 5 h. La solution a été

évaporée *in vacuo*. Le chlorhydrate de N-(hydroxy-2 phényl-2 éthyl) glycinate d'éthyl (X) a été isolé. Le produit a été cristallisé d'éthanol–éther; rendement 208 mg (40%), p.f. 165°. Le spectre infrarouge: 1 730 cm^{-1}.

Anal. Calc. pour $C_{12}H_{18}O_3NCl$ (259.73): N, 5.39. Trouvé: N, 5.22.

Le titrage du produit avec $AgNO_3$ 0.1 *N* donne 13.8% HCl (théorie 14.1% HCl).

Hydrolyse acide du produit IV dans l'éthanol

L'(hydroxy-2 phényl-2 éthyl)-1 (hydroxy-2 phényl-1 éthyl)-4 dicéto-2,5 piperazine (IV) (272 mg, 0.007 mole) dans l'éthanol (30 ml) a été chauffée avec l'acide chlorhydrique concentré (10 ml) à reflux pendant 5 h. La solution a été évaporée *in vacuo*. Le produit X a été isolé et le composé cristallisé d'éthanol–éther; rendement 22 mg (11%), p.f. 163–165°.

Le produit X est identique avec celui obtenu par l'hydrolyse acide du produit III dans l'éthanol. Le spectre infrarouge: 1 730 cm^{-1}.

Anal. Calc. pour $C_{12}H_{18}O_3NCl$ (259.73): N, 5.39. Trouvé: N, 5.17.

Hydrolyse alcaline du produit III

La bis-(hydroxy-2 phényl-2 éthyl)-1,4 dicéto-2,5 piperazine (III) (350 mg, 0.001 mole) dans l'hydroxyde de sodium à 10% (25 ml) a été chauffée à reflux pendant 12 h. La solution a été lavée avec l'éther. Le résidu a été acidifié avec l'acide chlorhydrique concentré et évaporé *in vacuo*. Le résidu a été chauffé avec l'éthanol absolu (25 ml) pendant 1 h, et le chlorure de sodium a été séparé par filtration. La solution a été évaporée *in vacuo*. Le produit a été libéré de son chlorhydrate dans le diméthylformamide par la triéthylamine; rendement 171 mg (44%), p.f. 208–210°. Le spectre infrarouge est identique avec celui du produit IX.

Hydrolyse alcaline du produit IV

L'(hydroxy-2 phényl-2 éthyl)-1 (hydroxy-2 phényl-1 éthyl)-4 dicéto-2,5 piperazine (IV) (90 mg, 0.00025 mole) dans l'hydroxyde de sodium à 10% (10 ml) a été chauffée pendant 12 h à reflux. La procédure a été la même que décrite plus haut. Le produit IX a été isolé; rendement 9 mg (18%), p.f. 208–209°.

Bis-(hydroxy-2 phényl-2 éthyl)-1,4 dicéto-2,5 piperazine (III)

A une solution de chlorhydrate de N-(hydroxy-2 phényl-2 éthyl) glycinate d'éthyl (X) (250 mg, 0.001 mole) dans le diméthylformamide (20 ml), la triéthylamine a été ajoutée. Le mélange a été chauffé ½ h au bain-marie. Après avoir refroidi à 0°, le précipité de chlorhydrate de triéthylamine a été filtré. L'éther a été ajouté à la solution et le mélange a été agité pendant 2 h dans la température de la pièce. Le produit cristallise pendant 24 h à 0°; rendement 48 mg (27%), p.f. 275–276°. Le produit est identique avec le produit III isolé dans la réaction d'ouverture de l'époxystyrène.

Hydroxy-2 phényl-2 éthylamine (XI)

La solution de bisulfite de sodium (104 g, 1 mole) dans l'eau (500 ml) a été agitée avec le benzaldéhyde (106 g, 1 mole) jusqu'à ce que le composé d'addition se forme.[1] Une solution de l'hydroxyde de sodium (46 g, 1.1 moles) dans l'eau (200 ml) en présence du nitrométhane (66 g, 1.1 moles) a été ajoutée goutte à goutte à la solution de bisulfite de benzaldéhyde. Le mélange a été agité pendant 1 h à la température de la pièce, et abandonné pendant la nuit dans la même température. Le produit a été séparé par l'extraction avec l'éther. La couche éthérée a été lavée avec la solution saturée de bisulfite de sodium et séchée avec $MgSO_4$ anhydre. Après l'évaporation d'éther *in vacuo* le résidu a été distillé; rendement 23 g (14%), p.é. 120–123° à 3 mm Hg (litt. (10) p.é. 163–165° à 15 mm Hg).

A une solution d'hydroxy-2 phényl-2 nitroéthane (23 g, 0.15 mole) dans l'éthanol à 95% (90 ml), l'acide sulfurique à 33% (300 ml) et le zinc (80 g)[2] ont été ajoutés. Le mélange a été agité pendant 14 h à la température de la pièce et l'excès de l'hydroxyde de sodium à 25% a été ajouté. Le produit a été extrait avec l'éther; la solution éthérée a été séchée avec K_2CO_3 et évaporée *in vacuo*. Le résidu a été distillé à 144–147° et 6 mm; rendement du produit XI 7.1 g (38%) (litt. (12) p.é. 136–137° à 5 mm Hg).

Hydroxy-2 phényl-2 éthylamine (XI) et hydroxy-2 phényl-1 éthylamine (XII)

Le mélange des produits XI et XII a été séparé avec le rendement de 25% d'après la méthode décrite par Castro et ses collaborateurs (12).

Bis-(hydroxy-2 phényl-2 éthyl)-1,4 dicéto-2,5 piperazine (III) et lactone de N-(hydroxy-2 phényl-2 éthyl) glycine (VI)

Une solution du produit XI (7 g, 0.05 mole) dans l'éthanol (40 ml) a été chauffée avec le chloroacétate d'éthyle (6 g, 0.05 mole) pendant 12.5 h. L'éthanol a été évaporé *in vacuo*. Le résidu a été lavé avec l'éther, la solution saturée de K_2CO_3 et l'eau. Les deux produits formés ont été séparés par cristallisation.

(*a*) Le produit III; rendement 650 mg (8%), p.f. 275–276°.

Anal. Calc. pour $C_{20}H_{22}O_4N_2$ (354.4): C, 67.77; H, 6.25; N, 7.89. Trouvé: C, 67.85; H, 6.23; N, 7.67.

(*b*) Le produit VI; rendement 125 mg (1.5%), p.f. 120°.

Anal. Calc. pour $C_{10}H_{11}O_2N$ (177.2): C, 67.77; H, 6.25; N, 7.89. Trouvé: C, 67.57; H, 6.33; N, 7.74.

Ils sont identiques avec les composés III et VI de l'ouverture de l'époxystyrène.

[1]*La méthode de Kamlet (9).*

[2]*La préparation est analogue à celle de Hoover et Hass (11).*

Can. J. Chem. Downloaded from www.nrcresearchpress.com by 210.87.254.6 on 09/05/12
For personal use only.

Bis-(hydroxy-2 phényl-2 éthyl)-1,4 dicéto-2,5 piperazine (III)

Une solution du produit XI (3.6 g, 0.025 mole) et du chloroacétate d'éthyle (3.0 g, 0.025 mole) dans le diméthylformamide (50 ml) a été chauffée avec la triéthylamine (2.5 g, 0.025 mole) au bain-marie pendant 2 h. Après avoir refroidi à 0°, le précipité du chlorhydrate de triéthylamine a été filtré et la solution évaporée *in vacuo* (60°). Le résidu a été cristallisé de l'éthanol absolu. Le produit obtenu (rendement 212 mg (5.3%), p.f. 273–275°) est identique avec le produit III.

Bis-(hydroxy-2 phényl-2 éthyl)-1,4 dicéto-2,5 piperazine (III), lactone de N-(hydroxy-2 phényl-2 éthyl) glycine (VI), N-(hydroxy-2 phényl-2 éthyl) glycine (IX) et chlorhydrate de N-(hydroxy-2 phényl-2 éthyl) glycine (XIV)

Une solution du produit XI (1.5 g, 0.01 mole) et d'acide chloroacétique (0.8 g, 0.01 mole) dans l'éthanol (20 ml) a été chauffée au bain-marie pendant 5 h. L'éthanol a été évaporé *in vacuo*. Le résidu a été lavé avec la solution saturée de K_2CO_3. Les quatre produits (IX, VI, III et XIV) ont été séparés par la cristallisation dans l'éthanol–eau; rendement respectif: 240 mg (11%), 82 mg (4%), 25 mg (1.2%) et 338 mg (13%).

Lactone de N-(hydroxy-2 phényl-2 éthyl) glycine (VI)

Une solution du produit IX (55 mg, 0.0025 mole) dans le benzène anhydre (50 ml) a été chauffée à reflux pendant 2 h. Les cristaux ont été dissous et le chauffage a été continué pendant 1 h. Le benzène a été évaporé *in vacuo* et le produit VI a été cristallisé d'acétate d'éthyle; rendement 28 mg (56%), p.f. 118–120°. Le spectre infrarouge: 1 723 cm^{-1} et 1 107 cm^{-1}.

Anal. Calc. pour $C_{10}H_{11}O_2N$ (177.2): N, 7.89. Trouvé: N, 7.58.

N-(Hydroxy-2 phényl-2 éthyl) glycine (IX)

Une solution du produit VI (120 mg, 0.006 mole) dans l'hydroxyde de sodium à 20% (10 ml) a été chauffée pendant 10 h à 60–70°. Le produit a été extrait avec l'éther; la solution éthérée a été acidifiée avec l'acide chlorhydrique concentré et évaporée *in vacuo*. Le résidu a été trituré avec l'éthanol absolu et le chlorure de sodium a été séparé par filtration; puis la solution a été évaporée *in vacuo* et le résidu lavé avec la solution saturée de K_2CO_3 et avec l'eau (25 ml). Le produit a été cristallisé de l'éthanol; rendement 18 mg (13%), p.f. 207–208°. Il est identique avec le produit IX.

Hydroxy-2 phényl-1 éthylamine (XII)

Une solution de phényl-2 glycine (13 g, 0.09 mole) dans l'éthanol absolu (400 ml) a été refroidie à 0° et l'acide chlorhydrique anhydre a été absorbé jusqu'à dissolution des cristaux. La solution a été chauffée pendant 2 h à reflux, abandonnée pendant 12 h à la température de la pièce et évaporée *in vacuo*. Le chlorhydrate de phényl-2 glycinate d'éthyle a été cristallisé d'éthanol–éther; rendement 10.5 g (57%), p.f. 199° (litt. (12) p.f. 197–198°).

Une solution du chlorhydrate de phényl-2 glycinate d'éthyle (10.5 g, 0.005 mole) dans l'éthanol absolu (50 ml) a été traitée avec l'éthanolate de sodium à 10% (50 ml), et le mélange a été chauffé pendant 1 h. Après refroidissement le chlorure de sodium a été filtré. La solution éthanolique a été évaporée *in vacuo* et distillé à 116–119° et 2 mm Hg; rendement 6.8 g (77%) (litt (12) p.é. 110–113° à 1.3–1.7 mm Hg).

Une solution de phényl-2 glycinate d'éthyl (8.6 g, 0.04 mole) dans l'éther absolu (15 ml) a été ajoutée à la solution du hydrure double de lithium et d'aluminium (2.3 g) dans l'éther absolu (100 ml). Le mélange a été chauffé pendant 1 h à reflux et l'eau a été ajoutée. La phase éthérée a été séparée et le résidu a été extrait deux fois avec l'éther. Les extractes éthérées combinées ont été séchés avec K_2CO_3 anhydre. L'éther a été évaporé *in vacuo* et le produit XII a été distillé à 140–145° et 6–7 mm Hg; rendement 3.6 g (54%) (litt. (12) p.é. 141–142° à 6 mm Hg).

Le composé XII a aussi été obtenu par réduction de l'oxime de la ω-hydroxyacétophénone avec l'amalgame de sodium. Les rendements ont été semblables à ceux décrits par Reiheln (13) et Gabriel (14).

Bis-(hydroxy-2 phényl-1 éthyl)-1,4 dicéto-2,5 piperazine (V)

Une solution du produit XII (6.06 g, 0.045 mole) dans l'éthanol (90 ml) a été chauffée à reflux avec le chloroacétate d'éthyle (4.8 g, 0.09 mole) pendant 12 h. La solution a été évaporée *in vacuo*, lavée de façon habituelle, séchée et évaporée à sec. Le résidu a été cristallisé plusieurs fois de l'éthanol; rendement 30 mg (0.5%), p.f. 252–254°. Le spectre infrarouge: 1 630 cm^{-1} et 3 182 cm^{-1}.

Anal. Calc. pour $C_{20}H_{22}O_4N_2$ (354.39): C, 67.77; H, 6.25; N, 7.89. Trouvé: C, 67.62; H, 6.38; N, 7.60.

Chlorhydrate de N-(hydroxy-2 phényl-1 éthyl) glycine (XIII)

Une solution du produit XII (1.4 g, 0.1 mole) dans l'éthanol absolu (25 ml) a été chauffée avec l'acide chloroacétique à reflux pendant 10 h. La solution a été évaporée et cristallisée de l'éthanol et ensuite de l'acétone; rendement 1.4 g (61%), p.f. 152°.

Anal. Calc. pour $C_{10}H_{14}O_3NCl$ (231.679): C, 51.84; H, 6.17; N, 6.17. Trouvé: C, 52.04; H, 6.41; N, 6.00.

N-(Hydroxy-2 phényl-2 éthyl) méthylamine (XV)

Le produit IX (0.25 g, 0.0008 mole) a été chauffé avec l'hydroxyde de sodium (0.1 g) jusqu'à ce que le dégagement du CO_2 ait été terminé (12 min). L'eau (15 ml) a été ajoutée et le produit a été séparé par extraction avec l'éther (3 × 15 ml). La solution éthérée a été séchée et évaporée à sec. Le produit XV a été cristallisé de l'éthanol–éther; rendement 21 mg (20%), p.f. 42–43° (litt. (15) p.f. 44–45°).

Can. J. Chem. Downloaded from www.nrcresearchpress.com by 210.87.254.6 on 09/05/12
For personal use only.

N-(Hydroxy-2 phényl-2 éthyl) méthylamine (XV)

Une solution de la méthylamine (6 g, 0.05 mole) à 50% dans l'eau a été chauffée avec l'époxystyrène (5 g, 0.04 mole) à reflux pendant 5 h. La solution a été extraite avec l'éther. L'extrait éthéré a été séché sur carbonate de potassium anhydre et saturé avec l'acide chlorhydrique gazeux anhydre. Le précipité a été séparé par filtration, lavé avec l'éther et repris dans l'hydroxyde de sodium à 1%. La solution alcaline a été extraite à l'éther. L'extrait éthéré a été séché sur carbonate de potassium anhydre et évaporé *in vacuo*. Le produit a été cristallisé de l'éthanol–éther; rendement 29 mg (3.9%), p.f. 41–44°. Il est identique avec le produit XV obtenu par décarboxylation du produit IX.

(Hydroxy-2 phényl-2 éthyl)-1 (hydroxy-2 phényl-1 éthyl)-4 dicéto-2,5 piperazine (IV)

Une solution du produit XI (0.5 g, 0.0036 mole) et du produit XII (0.5 g, 0.0036 mole) dans l'éthanol (25 ml) a été chauffée à reflux pendant 4 h avec le chloroacétate d'éthyle (0.65 g, 0.007 mole). La solution a été évaporée *in vacuo* et triturée avec l'éther, avec la solution saturée de carbonate de potassium et avec l'eau. Le résidu a été cristallisé et les deux produits ont été isolés: le produit III, rendement 52 mg (8%); le produit IV, rendement 17 mg (2.5%). Ils sont identiques avec les produits III et IV isolés dans la réaction d'ouverture de l'époxystyrène.

N-(Hydroxy-2 phényl-2 éthyl) glycine (IX)

Une solution de l'époxystyrène (10 g, 0.008 mole) avec le glycinate de sodium (XVI) (9 g, 0.009 mole) dans le diméthylformamide (100 ml) a été chauffée à reflux pendant 3 h. Le produit a été précipité avec l'éther et séparé par filtration. Le produit a été repris dans l'eau (40 ml), acidifié avec l'acide chlorhydrique concentré et évaporé *in vacuo*. Le résidu a été repris dans l'éthanol (25 ml) et le chlorure de sodium a été séparé par filtration. Le produit IX a été libéré de son chlorhydrate avec la triéthylamine dans le diméthylformamide; rendement 362 mg (2%), p.f. 209°. Il est identique avec le produit obtenu par l'hydrolyse acide du produit III.

Condensation de la glycine avec l'époxystyrène

Une suspension de la glycine (7.5 g, 0.01 mole) dans l'éthanol à 95% (100 ml) a été chauffée à reflux avec l'époxystyrène (12 g, 0.01 mole) pendant 12 h. Les trois produits ont été isolés: la dicéto-2,5 piperazine (VIII), rendement 1.2 g (30%), p.f. 260°; le phénylglycole, rendement 1.0 g (24%), p.f. 65.5°; la glycine, rendement 4.0 g (53%), p.f. 190°.

Condensation de la dicéto-2,5 piperazine (VIII) avec l'époxystyrène

Le produit VIII (1.1 g, 0.01 mole) a été chauffé à reflux avec l'époxystyrène (1.2 g, 0.01 mole) pendant 18 h. Le produit VIII a été isolé inchangé; rendement 0.9 g (82%). La fraction polymérique de l'époxystyrène a été aussi isolé; rendement 0.7 g (60%).

REMERCIEMENTS

Les auteurs remercient le Conseil National de Recherches et l'Université de Montréal pour l'aide financière apportée sous forme d'octroi de recherches et de bourse d'étude.

BIBLIOGRAPHIE

1. V. GRIGNARD. Traité de chimie organique. Vol. XII. Masson et Cie, Paris. 1941. p. 538.
2. A. KIPRIANOV et G. KIPRIANOV. Chem. Abstr. **26**, 108 (1932); **24**, 1082 (1930); **25**, 5143 (1931); **22**, 3134 (1928).
3. K. MAEKAWA et S. TSUMURA. Chem. Abstr. **51**, 2917 (1957).
4. K. KRASSUSKY. Compt. Rend. **146**, 236 (1908). R. E. PARKER et N. S. ISAACS. Chem. Rev. **59**, 737 (1959).
5. H. SCHOTT, J. LARKIN, L. ROCKLAND et M. DUNN. J. Org. Chem. **12**, 490 (1947). H. SANNIER. Bull. Soc. Chim. France, 487 (1942). H. LENORMANT. Bull. Soc. Chim. France, 33 (1948).
6. C. MANNICH et E. THIELE. Arch. Pharm. **253**, 181 (1915).
7. R. E. PARKER et B. W. ROCKETT. J. Chem. Soc. 2569 (1965).
8. E. FISHER. Ber. **34**, 436 (1901).
9. J. KAMLET. U.S. Patent No. 2,151,517 (March 21, 1939).
10. K. W. ROSENMUND. Ber. **46**, 1034 (1913).
11. F. HOOVER et H. HASS. J. Org. Chem. **12**, 506 (1947).
12. A. CASTRO, D. BRAIN, H. FISHER et R. FULLER. J. Org. Chem. **19**, 1444 (1954).
13. H. REIHELN et W. SAPPER. Ann. **534**, 247 (1938).
14. S. GABRIEL et J. COLMAN. Ber. **47**, 1867 (1914).
15. G. MENSCHIKOV. J. Gen. Chem. USSR Engl. Transl. **13**, 801 (1943).

Can. J. Chem. Downloaded from www.nrcresearchpress.com by 210.87.254.6 on 09/05/12
For personal use only.

Can. J. Chem. Downloaded from www.nrcresearchpress.com by 210.87.254.42 on 09/05/12
For personal use only.

STUDIES ON PLANTS

XI. ALKALOIDS OF ASPIDOSPERMA SPEGAZZINII[1,2]

ORFEO O. ORAZI, RENÉE A. CORRAL, AND MARTA E. STOICHEVICH
Facultad de Química y Farmacia, Universidad Nacional de La Plata, La Plata, Argentina

Received December 17, 1965

ABSTRACT

Extraction of the trunk bark of *Aspidosperma spegazzinii* Molf. ex Meyer yielded ajmaline and two quaternary alkaloids. One of the latter, characterized as the tetraphenylboride salt, was found to be identical with the N_b-metho derivative of akuammidine. Methylation of the phenolic group of the second quaternary alkaloid (named spegatrine) followed by thermal degradation led to the corresponding nor-base, which was identified as lochnerine; therefore, the structure and absolute stereochemistry of spegatrine are given by formula I. A confirmation was provided by N_b-methylation of sarpagine to spegatrine.

Five species of the genus *Aspidosperma* (Apocynaceae) may currently be recognized in the Argentinian flora, namely, *A. quebracho-blanco*, *A. chakensis*, *A. australe*, *A. polyneuron*, and the more recently described *A. spegazzinii* Molf. ex Meyer (1). Unlike the other species, no alkaloids have yet been isolated from *A. spegazzinii*, a tree 10–15 m high, indigenous to Argentina and Paraguay, and referred to by the vernacular names "quina" or "paratudo". The plant material examined in the present work (the trunk bark of old trees) was collected in Río Iguazú, Parque Nacional Iguazú (Misiones, Argentina).

The alcoholic extract of the bark was separated into tertiary bases and quaternary chlorides. The tertiary bases consisted of a mixture of several alkaloids, from which ajmaline was isolated and identified as the ethanol solvate (about 0.3% yield based on dried bark).

The new alkaloid spegatrine (I), the major component (0.25% yield based on dried bark) of the quaternary alkaloidal fraction, was characterized as the crystalline chloride and perchlorate salts. Analytical data give the empirical formula $C_{20}H_{25}N_2O_2$ for the cation and indicate the presence of one N-methyl group, three active hydrogens, and no methoxyl groups. The nuclear magnetic resonance spectrum of the chloride of I, with a doublet centered at δ 1.80 p.p.m. (3H) and an unresolved multiplet at δ 5.95 p.p.m. (1H), suggests the existence of one ethylidene grouping. The quaternary nature of I and the number of active hydrogens require the presence of two OH groups and one NH group.

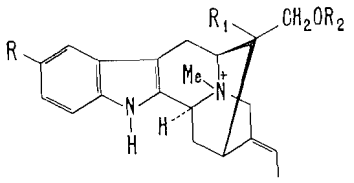
One of the oxygen atoms of I belongs to a phenolic function, as established by the following data. The chloride of I gives positive color reactions with aqueous ferric chloride and diazotized sulfanilic acid, and its ultraviolet spectrum suffers a bathochromic shift on addition of base; in addition, it may be methylated to compound II, which analyzes for one methoxyl group and shows identical ultraviolet absorption in neutral and basic media.

Acetylation of I gives compound III, which may easily be reconverted into the starting material. The acetylated product gave inconsistent results when subjected to repeated acetyl group analysis; however, the presence of infrared bands at 3 390 (NH) and 1 754 cm^{-1} (broad, ester carbonyls) coupled with the absence of amide absorption indicates that it is the O,O-diacetyl derivative of I rather than the O,N-diacetyl or O,O,N-triacetyl

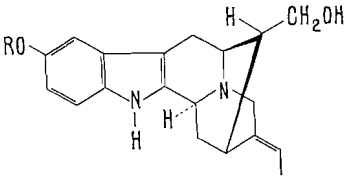
[1]*Part of the doctoral thesis (1965) of M. E. S. is included in this paper.*
[2]*For part X in this series, see R. A. Corral and O. O. Orazi, Tetrahedron, in press.*

derivatives. Furthermore, when going from compound I to III, the nuclear magnetic resonance absorption in the range δ 2.10–2.70 p.p.m. shows the appearance of two sharp peaks (δ 2.25 and 2.50 p.p.m.) and an area increase corresponding to approximately six protons.

Thermal decomposition of the chloride of II gives, besides methyl chloride, its genuine nor-base as proved by a methylation experiment. Analytical and mass spectrometric data on the nor-base establish the molecular formula $C_{20}H_{24}N_2O_2$ and the presence of two active hydrogens and one methoxyl group; the Herzig–Meyer analysis also indicated one N-methyl group, but, as observed in several other instances (2), this is a fictitious result.



	R	R_1	R_2
I	OH	H	H
II	OCH_3	H	H
III	AcO	H	Ac
VI	H	CO_2Me	H



IV R = H
V R = CH_3

The ultraviolet absorption of the nor-base is typical of an indole chromophore, and its mass spectrum shows intense M-1 and M-31 peaks; these peaks suggest a tetrahydro-β-carboline structure and the presence of a primary alcoholic function, respectively (3). Moreover, all the strong peaks (Fig. 1) are displaced by 14 mass units from those of sarpagine (IV) (4).

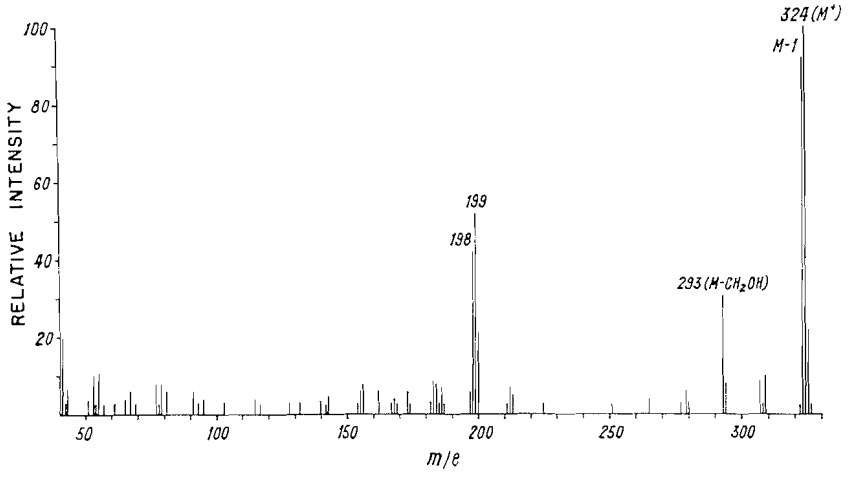


FIG. 1. The mass spectrum of the nor-base of II, inserted in the ion source; only peaks of intensity higher than 2% are plotted.

The nor-base was identical in all respects with the alkaloid lochnerine (10-O-methyl-sarpagine), the structure and absolute stereochemistry of which are shown in V (5); therefore, formula I is a complete description for the spegatrine ion. This result was confirmed by N_b-methylation of sarpagine (IV), the quaternary chloride that was obtained being identical with spegatrine chloride.

Can. J. Chem. Downloaded from www.nrcresearchpress.com by 210.87.254.42 on 09/05/12
For personal use only.

Can. J. Chem. Downloaded from www.nrcresearchpress.com by 210.87.254.42 on 09/05/12
For personal use only.

The foregoing structural elucidation also demonstrates that the ion II, characterized as the perchlorate salt, must be identical with the quaternary alkaloid lochneram, which was obtained as the iodide and tetraphenylboride salts (6).

The other quaternary alkaloid isolated from *A. spegazzinii*, characterized as the crystalline tetraphenylboride salt and then converted into the amorphous chloride salt, was available in much lesser amounts (0.01% yield based on dried bark). However, structure VI was brought into consideration by its co-occurrence with I and by the following data: ultraviolet absorption almost coincident with that of macusine-A (7); the tetraphenylboride salt shows infrared bands at 3 532, 3 357, and 1 728 cm^{-1} ascribable to alcoholic OH (ultraviolet measurements exclude the phenol group), indole NH, and CO_2Me (one methoxyl by analysis) groups, respectively; the presence of an ethylidene group according to the nuclear magnetic resonance spectrum (multiplets for one methyl group and one hydrogen at δ 1.78 and 5.9 p.p.m., respectively); the optical rotation of the chloride salt ($[\alpha]_D$ +12° (in water)) in comparison with those of macusine-A ($[\alpha]_D$ −58° (in water)) and the nonnatural akuammidine methoiodide ($[\alpha]_D$ +16° (in methanol)) (7, 8).

Methylation of akuammidine under the conditions used for the nor-base of II and sarpagine (IV) led to a quaternary tetraphenylboride salt identical (mixture melting points and superimposable infrared curves) with the sample obtained from the plant; the corresponding amorphous chlorides showed concordant chromatographic mobility, ultraviolet absorption, and optical rotation. The structure and absolute stereochemistry shown in VI are firmly established for the N_b-methylakuammidine cation (9) prepared by methylation of the natural tertiary base (8).

The complete formula VI has recently been assigned to the crystalline alkaloid macusine-C chloride, isolated from *Strychnos toxifera* bark (5); however, the sign and magnitude of the optical rotation ($[\alpha]_D$ −61° (in water)) indicate that it is not identical with the akuammidine methochloride here obtained.

The quaternary alkaloids found in *A. spegazzinii* belong to the sarpagine structural type; two tertiary bases of the same type, polyneuridine and normacusine-B, have recently been isolated from another *Aspidosperma* species (2*b*). On the other hand, the occurrence in this genus of alkaloids with the ajmaline skeleton is unprecedented; besides the biogenetic significance, this may be interesting from the chemical taxonomy viewpoint because of the peculiar anatomy of the *A. spegazzinii* bark (1*c*).

EXPERIMENTAL

Melting points were determined in sealed capillaries and are not corrected; all of the evaporations were carried out under reduced pressure. The ultraviolet spectra in neutral, acidic, or basic medium were recorded with 50% alcohol as the solvent; unless otherwise noted, the infrared spectra were taken in Nujol mulls. The nuclear magnetic resonance spectra were measured in trifluoroacetic acid at 60 Mc/s, the δ values (parts per million) being expressed downfield from internal $SiMe_4$ (δ = 0). The detection of spots in paper chromatograms and electrophoreses was made by fluorescence under ultraviolet light and by iodoplatinate reagent. The microanalyses were performed by Dr. A. Bernhardt (Mülheim, Germany) on samples dried, unless otherwise stated, to a constant weight (100° and a high vacuum) immediately before analysis.

Extraction of Alkaloids

The dried trunk bark (1 kg) of *Aspidosperma spegazzinii* Molf. ex Meyer was ground and extracted during 4 h with boiling 96% alcohol (4 l), with mechanical stirring; the liquid was separated by filtration and the process repeated three times. The combined alcoholic extracts, after concentration to a volume of 300 ml, were diluted at 0° with acetic acid (100 ml) in water (600 ml). The mixture was left in the refrigerator and then filtered; after addition of chloroform (250 ml), the aqueous layer was adjusted (ice bath) to pH 11 with aqueous sodium hydroxide.

The chloroform was decanted, and repeated extractions were made (15 × 100 ml) until the tertiary bases were completely separated. The total chloroform extracts, washed with water and dried over magnesium sulfate, gave, upon evaporation to dryness, the fraction of crude *tertiary alkaloids* (23 g).

The aqueous layer was acidified with 6 *N* hydrochloric acid to pH 2 and the quaternary alkaloids were precipitated by adding an excess of concentrated Mayer's reagent (10). The precipitate (22 g) was suspended in methanol (400 ml) and a current of hydrogen sulfide passed through until the Mayer complex had completely decomposed. The filtered methanolic solution was concentrated and passed successively through Dowex-3 (base form, 100 g) and Dowex-2 chloride (80 g); the eluate was adjusted to pH 6.5 by addition of 0.1 *N* hydrochloric acid, and subsequent removal of the solvent gave the fraction of crude *quaternary chlorides* (13 g).

Isolation of Ajmaline

A chloroform solution of the crude tertiary bases (1 g) was filtered through a column of neutral alumina (activity V, 10 g). Evaporation of the eluate left a solid (0.9 g), which was dissolved in hot absolute ethanol (2.5 ml); to obtain a very crystalline material the solution was allowed to stand undisturbed for several days and gradually cooled down to −10°. Thus was separated 125 mg of ajmaline ethanol solvate, m.p. 194–196° with apparent melting at 125° (gas evolution). A sample that was dried at 130° and 10^{-3} Torr melted at 194–196° without modification at lower temperatures.

The earlier procedure followed for the ajmaline isolation was based on adsorption chromatography. The crude tertiary bases (2 g) were fractionated over neutral alumina (activity II, 200 g); elution was carried out with benzene, benzene–chloroform (9:1 to 1:4), chloroform, and chloroform – absolute ethanol (24:1 to 1:4), and 200 samples (20 ml each) were collected. Eluates 124–167 from chloroform – absolute ethanol (15:1 to 5:1) contained essentially a single alkaloid, as indicated by paper chromatography; upon crystallization from absolute ethanol, 200 mg of ajmaline ethanol solvate, m.p. 191–193° (gas evolution at 125°), was obtained.

An analytical sample was prepared by repeated recrystallizations from the same solvent and dried at 76° and 10^{-3} Torr; $[\alpha]_D^{25}$ +130° (*c*, 1.11 in chloroform); λ_{max} 248 (log ϵ 3.96) and 291 mμ (log ϵ 3.50), λ_{min} 226 (log ϵ 3.58) and 271 mμ (log ϵ 3.20).

Anal. Calcd. for $C_{20}H_{26}N_2O_2 \cdot C_2H_5OH$: C, 70.93; H, 8.66; N, 7.52; O, 12.89; one OC_2H_5, 12.09; one $(N)CH_3$, 4.05; three active H, 0.81. Found: C, 71.23; H, 8.60; N, 7.67; O, 12.86; OC_2H_5, 12.02; $(N)CH_3$, 3.83; active H, 0.81; mol. wt. (by mass spectrum) 326 (calcd. for $C_{20}H_{26}N_2O_2$, 326.42).

An authentic specimen of ajmaline was recrystallized several times from absolute ethanol; it melted, showing the same behavior as the above samples. The identity was ascertained by chromatographic mobility, mixture melting point, and coincidence of the infrared absorptions.

Isolation of Quaternary Alkaloids

The first successful isolation of the alkaloids described below was attained by subjecting the crude quaternary chlorides to preparative paper chromatography; water-saturated methyl ethyl ketone plus 5% methanol was used as the developing solvent, and ultraviolet light and iodoplatinate reagent were used for detection of the bands. Fractionation attempts on powdered cellulose columns gave poorer results.

The work-up of subsequent batches was as follows. The mixture of crude chlorides (5 g) was chromatographed through a column of neutral alumina (activity III, 500 g); the elution was made with chloroform–methanol mixtures, methanol, 90% ethanol, and finally 80% ethanol, and 180 samples (20 ml each) were collected.

The weight distribution and paper chromatography (with the above-mentioned solvent system) showed the presence of several alkaloids; fractions 19–48 (800 mg) and the last 10 fractions (containing only a few milligrams) gave weak spots of mixtures of alkaloids. The most important fractions were fractions 62–101 (from chloroform–methanol (6:1 to 4:1), 250 mg) and fractions 102–170 (chloroform–methanol (4:1 to 90% ethanol), 1.9 g); each group of fractions gave principally a single alkaloid spot, the R_f values of which were 0.45 and 0.32, respectively.

N_b-Methylakuammidine (VI) Tetraphenylboride

(*a*) The combined fractions 62–101 were rechromatographed over neutral alumina (activity III, 25 g) with chloroform–methanol mixtures (19:1 to 1:1). The alkaloidal material of R_f 0.45 (130 mg) eluted with chloroform–methanol (7:1) was dissolved in water and mixed with an aqueous solution of sodium tetraphenylboride.

The precipitated salt (165 mg) was purified on an adsorption column of neutral alumina (activity II, 8 g); the fractions eluted with chloroform–acetone (19:1) were pure when examined by paper chromatography (150 mg). It was further purified by crystallization from alcohol to a constant melting point of 203–205° (decomp.); ν_{max} 3 532, 3 357, and 1 728 cm^{-1}.

Anal. Calcd. for $C_{22}H_{27}N_2O_3 \cdot (C_6H_5)_4B$: C, 80.45; H, 6.90; N, 4.08; one OCH_3, 4.52. Found: C, 80.63; H, 6.75; N, 3.99; OCH_3, 3.90.

This tetraphenylboride was identical with that obtained in experiment *b*, as shown by mixture melting point and complete coincidence of their infrared spectra (KBr).

The pure salt was converted into the corresponding chloride by means of Dowex-2 chloride with methanol as solvent. The resulting solid showed $[\alpha]_D^{20}$ +12° (*c*, 2.05 in water); in neutral or 0.01 *N* NaOH λ_{max} 219 (log ϵ 4.70), 271 (log ϵ 3.87), 277 (inflection) (log ϵ 3.86), and 288 mμ (log ϵ 3.75), λ_{min} 241 (log ϵ 3.55) and 285 mμ (log ϵ 3.72); ν_{max} 1 732 cm^{-1} (ester carbonyl).

Can. J. Chem. Downloaded from www.nrcresearchpress.com by 210.87.254.42 on 09/05/12
For personal use only.

(*b*) *From akuammidine.*—A solution of this base (25 mg) in a mixture of methanol (1.5 ml) and methyl iodide (1 ml) was heated in a sealed tube during 10 h at 100° in the dark (cf. ref. 8). After evaporation to dryness, the residue was dissolved in methanol and passed through Dowex-2 chloride. The crude chloride, after being washed with chloroform (2 × 1 ml) to remove unreacted akuammidine (2 mg, identified by paper chromatography), was purified by alumina chromatography as in experiment *a* and then transformed into the tetraphenylboride salt (39 mg); the latter was recrystallized from alcohol to a constant melting point of 203–205° (decomp.).

The amorphous chloride, prepared from the purified tetraphenylboride salt by ionic exchange, exhibited the same chromatographic mobility (R_f 0.45) as the sample obtained in experiment *a* when run on the same paper (water-saturated methyl ethyl ketone plus 5% methanol); $[\alpha]_D^{19}$ +13° (*c*, 1.01 in water); λ_{max} 219 (log ϵ 4.64), 270 (log ϵ 3.88), 276 (inflection) (log ϵ 3.86), and 288 mμ (log ϵ 3.74), λ_{min} 245 (log ϵ 3.68) and 285 mμ (log ϵ 3.70).

Spegatrine (I) Salts

The material of fractions 102–170, obtained from the alumina chromatogram of the crude quaternary alkaloids, was crystallized twice from absolute ethanol to give 1.1 g of spegatrine chloride, m.p. 283° (decomp.), increased to 294° (decomp.) by repeated recrystallizations. Its homogeneity was verified by paper chromatography with several solvent systems and by paper electrophoreses with buffers of pH 3 and pH 8.

It showed $[\alpha]_D^{17}$ +38° (*c*, 1.00 in methanol); in neutral or 0.3 *N* HCl λ_{max} 272 (log ϵ 3.87) and 296 mμ (inflection) (log ϵ 3.63), λ_{min} 245 mμ (log ϵ 3.43); in 0.01 *N* NaOH λ_{max} 270 (log ϵ 3.81), 309 (log ϵ 3.43), and 320 mμ (inflection) (log ϵ 3.34), λ_{min} 253 (log ϵ 3.66) and 293 mμ (log ϵ 3.34).

Anal. Calcd. for $C_{20}H_{25}N_2O_2Cl$: C, 66.56; H, 6.98; N, 7.76; O, 8.87; Cl, 9.83; one OCH_3, 8.60; one $(N)CH_3$, 4.17; three active H, 0.84. Found: C, 65.78; H, 7.08; N, 7.70; O, 8.52; Cl^-, 10.35; OCH_3, 0.61; $(N)CH_3$, 5.13; active H, 0.78.

Hot aqueous solutions of spegatrine chloride and magnesium perchlorate were mixed, thereby precipitating spegatrine perchlorate, constant m.p. 271° (decomp.) after several recrystallizations from butanol.

Anal. Calcd. for $C_{20}H_{25}N_2O_2 \cdot ClO_4$: C, 56.53; H, 5.93; N, 6.59; O, 22.60; Cl, 8.35. Found: C, 56.66; H, 6.02; N, 6.55; O, 22.55; Cl, 8.25.

10-O-Methylspegatrine (II) Perchlorate

A solution of spegatrine (I) chloride (100 mg) in methanol (2 ml) was mixed with anhydrous potassium carbonate (80 mg), and to the stirred solution was added dimethyl sulfate (125 mg) in portions.

After 12 h, the methanolic phase was decanted and evaporated to dryness. The residue was dissolved in water and a solution of ammonium reineckate (in water – acetic acid (2:1)) added; the precipitated reineckate salt was then converted into the corresponding chloride by ionic exchange. Purification by alumina chromatography (neutral, activity IV, elution with chloroform–methanol mixtures) provided the chromatographically pure quaternary chloride (100 mg), which was transformed into the perchlorate by adding an excess of magnesium perchlorate in water.

There was obtained 105 mg that, after repeated recrystallizations from butanol, melted at 147–150° (decomp.); the homogeneity was assessed by paper chromatograms and electrophoreses as indicated for the chloride of I. The perchlorate of II had $[\alpha]_D^{18}$ +45° (*c*, 1.03 in methanol); in neutral, acidic, or basic medium λ_{max} 272 (log ϵ 3.86), 291 (inflection) (log ϵ 3.63), and 303 mμ (inflection) (log ϵ 3.51), λ_{min} 245 mμ (log ϵ 3.44).

Anal. Calcd. for $C_{21}H_{27}N_2O_2 \cdot ClO_4$: C, 57.47; H, 6.20; N, 6.38; O, 21.87; Cl, 8.08; one OCH_3, 7.07; one $(N)CH_3$, 3.43. Found: C, 57.60; H, 6.33; N, 6.38; O, 21.32; Cl, 7.58; OCH_3, 6.72; $(N)CH_3$, 2.96.

10,17-O,O-Diacetylspegatrine (III) Perchlorate

A mixture of spegatrine (I) chloride (100 mg) and acetic anhydride (4 ml) was magnetically stirred at 90° for 10 h; the resulting solution was evaporated, and the solid residue was dissolved in water and mixed with a hot aqueous solution of magnesium perchlorate. The crude quaternary perchlorate (130 mg, m.p. 152–156°) was purified from alcohol to a constant melting point of 155–159°. It was homogeneous according to paper chromatograms and electrophoreses; $[\alpha]_D^{15}$ +34° (*c*, 1.89 in methanol); λ_{max} 223 (log ϵ 4.38), 268 (log ϵ 3.91), and 291 mμ (inflection) (log ϵ 3.73), λ_{min} 258 mμ (log ϵ 3.88); ν_{max} 3 390 and 1 754 (broad) cm^{-1}.

Anal. Calcd. for $C_{24}H_{29}N_2O_4 \cdot ClO_4$: C, 56.64; H, 5.74; N, 5.50; O, 25.15; Cl, 6.97. Found: C, 56.89; H, 5.78; N, 5.46; O, 25.14; Cl, 7.06.

A solution of the perchlorate of III (10 mg) in 2 *N* hydrochloric acid (1 ml) was maintained for 1 h at 90°; evaporation to dryness yielded a material which, when dissolved in methanol, was passed through Dowex-2 chloride. The eluted material was identified as spegatrine chloride by its chromatographic mobility and infrared absorption.

Degradation of 10-O-Methylspegatrine (II) Chloride

This salt, obtained above as an intermediate in the preparation of the corresponding perchlorate, was subjected to thermal degradation according to a literature technique (11).

It was heated (10 batches; in total, 330 mg) in a vacuum sublimation apparatus introduced into a bath at 250° and 10^{-4} Torr; the temperature was then increased to 280° in 1 h and the bath was maintained at this temperature for another hour.

Can. J. Chem. Downloaded from www.nrcresearchpress.com by 210.87.254.42 on 09/05/12
For personal use only.

The evolved gaseous product was condensed in an air–liquid trap and identified as practically pure methyl chloride by gas chromatographic and infrared absorption comparisons with an authentic specimen.

The combined sublimed material was extracted with several portions of chloroform; the extract was washed with water and dried, and the solvent was removed, leaving a residue (275 mg) which was purified either by column or thick-layer chromatography with thin-layer chromatograms (alumina Fluka D5F, chloroform–cyclohexane (1:1) plus 1% absolute ethanol) for analytical purposes.

In the former procedure the material (100 mg) was passed over neutral alumina (activity II, 10 g), elution being carried out with chloroform-cyclohexane (1:1) followed by the same system enriched with absolute ethanol. The main fraction (from eluant containing 0.5% ethanol, R_f 0.60) was homogeneous, and upon crystallization from methanol – ethyl ether gave 35 mg, m.p. 192–194°, increased to 204–205° by further recrystallizations. Similar results were obtained by the thick-layer procedure with chloroform–cyclohexane (1:1) plus 1% absolute ethanol as the solvent system.

The nor-base had $[\alpha]_D^{20}$ +70° (*c*, 0.62 in alcohol); λ_{max} 227 (log ϵ 4.50) and 278 mμ (log ϵ 3.94), λ_{min} 215 (log ϵ 4.47) and 250 mμ (log ϵ 3.48).

Anal. Calcd. for $C_{20}H_{24}N_2O_2$: C, 74.04; H, 7.46; N, 8.64; O, 9.86; two active H, 0.62; mol. wt. 324.41. Found: C, 73.53; H, 7.47; N, 8.94; O, 10.42; active H, 0.64; mol. wt. (by mass spectrum) 324.

A sample was dried *in vacuo* at 56°, but not quantitatively.

Anal. Calcd. for $C_{20}H_{24}N_2O_2 \cdot H_2O$: C, 70.15; H, 7.65; N, 8.18; O, 14.02; one OCH_3, 9.06. Found: C, 70.20; H, 7.42; N, 8.11; O, 14.07; OCH_3, 8.88.

The nor-base was identical with an authentic sample of the alkaloid lochnerine, as shown by mixture melting point and infrared spectra (KBr); furthermore, the values of the ultraviolet absorption and optical rotation (12) are virtually coincident.

The nor-base (10 mg) and methyl iodide (0.3 ml) in methanol (0.15 ml) were heated in a sealed tube at 100° for 10 h in the dark. Evaporation of the solution was followed by passage of the residue in methanol through Dowex-2 chloride; the material recovered from the eluate (11 mg) did not contain starting compound, as shown by a paper chromatogram.

The chloride salt was transformed into the perchlorate by magnesium perchlorate in water. The crude salt (13 mg) was crystallized from butanol, m.p. 148–150°, undepressed when admixed with a sample of the above 10-O-methylspegatrine (II) perchlorate. This identity was confirmed by coincidence of the chromatographic mobilities in several systems and of the infrared curves.

Spegatrine (I) Chloride from Sarpagine (IV)

Sarpagine was methylated as described above for the nor-base. The crude quaternary chloride was purified on neutral alumina (100 times by weight, activity III), chloroform–methanol mixtures (19:1 to 2:1) being used as eluants. The major fraction, coming from chloroform–methanol (4:1), gave a single spot on a paper chromatogram; crystallization from absolute ethanol gave N_b-methosarpagine chloride (68% yield) melting at 293° (decomp.); $[\alpha]_D^{20}$ +37° (*c*, 0.96 in methanol).

Anal. Calcd. for $C_{20}H_{25}N_2O_2Cl$: N, 7.76. Found: N, 7.86.

The quaternary salt thus obtained was identical with spegatrine chloride, as demonstrated by paper chromatographic behavior, mixture melting point, and superimposable ultraviolet and infrared spectra.

ACKNOWLEDGMENTS

The authors are grateful to the late Prof. J. F. Molfino, who supplied the plant material and made the corresponding botanical identification; and to Prof. M. G. Escalante (La Plata) for confirming the identification by an anatomicohistological study of the trunk bark. The generous support of the Consejo Nacional de Investigaciones Científicas y Técnicas (Argentina) is gratefully appreciated. Thanks are due to Prof. V. Deulofeu (Buenos Aires) and Prof. J. Le Men and Dr. L. Olivier (Paris), who kindly supplied samples of ajmaline, lochnerine, and akuammidine, respectively. The authors are also indebted to Prof. C. Djerassi (Stanford) for the mass spectra.

REFERENCES

1. (*a*) T. Meyer. Lilloa, **23**, 29 (1950). (*b*) R. E. Woodson. Ann. Missouri Botan. Garden, **38**, 119 (1951). (*c*) M. G. Escalante and M. N. Marcó. Bol. Soc. Botan. Arg. **10**, 129 (1963).
2. (*a*) S. McLean, K. Palmer, and L. Marion. Can. J. Chem. **38**, 1547 (1960). (*b*) L. D. Antonaccio, N. A. Pereira, B. Gilbert, H. Vorbrueggen, H. Budzikiewicz, J. M. Wilson, L. J. Durham, and C. Djerassi. J. Am. Chem. Soc. **84**, 2161 (1962).
3. H. Budzikiewicz, C. Djerassi, and D. H. Williams. Structure elucidation of natural products by mass spectrometry. Vol. I. Holden-Day, Inc., San Francisco. 1964. Chap. 5.
4. G. Spiteller, C. Brunné, K. Heyns, and H. F. Grützmacher. Z. Naturforsch. **17b**, 856 (1962).
5. A. R. Battersby and D. A. Yeowell. J. Chem. Soc. 4419 (1964).

Can. J. Chem. Downloaded from www.nrcresearchpress.com by 210.87.254.42 on 09/05/12
For personal use only.

6. W. ARNOLD, F. BERLAGE, K. BERNAUER, H. SCHMIDT, and P. KARRER. Helv. Chim. Acta, **41**, 1505 (1958).
7. A. R. BATTERSBY, R. BINKS, H. S. HODSON, and D. A. YEOWELL. J. Chem. Soc. 1848 (1960).
8. T. A. HENRY. J. Chem. Soc. 2759 (1932).
9. S. SILVERS and A. TULINSKY. Acta Cryst. **16**, 579 (1963).
10. L. RETI. *In* The alkaloids. Vol. IV. R. H. F. Manske and H. L. Holmes (*Editors*). Academic Press, Inc., New York. 1954. p. 26.
11. H. BICKEL, E. GIESBRECHT, J. KEBRLE, H. SCHMIDT, and P. KARRER. Helv. Chim. Acta, **37**, 553 (1954).
12. W. ARNOLD, W. VON PHILIPSBORN, H. SCHMIDT, and P. KARRER. Helv. Chim. Acta, **40**, 705 (1957).

Can. J. Chem. Downloaded from www.nrcresearchpress.com by 210.87.254.42 on 09/05/12
For personal use only.

Can. J. Chem. Downloaded from www.nrcresearchpress.com by 210.87.254.5 on 09/05/12
For personal use only.

CHOLLA GUM

II. STRUCTURE OF THE UNDEGRADED CHOLLA GUM[1]

V. M. PARIKH[2] AND J. K. N. JONES
Department of Chemistry, Queen's University, Kingston, Ontario

Received February 17, 1966

ABSTRACT

Cholla gum (*Opuntia fulgida*) has partially been degraded to yield several oligosaccharides and a degraded polymer. The structure of the degraded polymer was reported in an earlier paper.[1] Six of the oligosaccharides formed have been isolated in a pure state and identified. They are (*i*) 6-*O*-β-D-galactopyranosyl-D-galactose, (*ii*) 3-*O*-β-D-galactopyranosyl-D-galactose, (*iii*) 3-*O*-α-L-arabinofuranosyl-L-arabinose, (*iv*) 5-*O*-β-D-xylopyranosyl-L-arabinose, (*v*) 3-*O*-β-D-galactopyranosyl-L-arabinose (?), and (*vi*) a new trisaccharide *O*-β-D-xylopyranosyl-(1 → 5)-*O*-α-L-arabinofuranosyl-(1 → 3)-L-arabinose. The purified gum was subjected to Smith-type degradation, and the results of this experiment are compared with the methylation studies carried out earlier. On the basis of all this information plus the suggested structure for the degraded gum, it is proposed that the repeating unit of the polysaccharide consists of a total of 36 sugar residues with a backbone of 1 → 6 linked galactose residues.

In a previous paper (1) the results of the analysis of cholla gum (*Opuntia fulgida*) (Table I) and a probable structure (Diagram 1) of the repeating unit of the degraded gum were reported.

TABLE I
Analysis of cholla gum

Observations	Observed values
Ash	0.7%
Nitrogen	Absent
Methoxyl	Absent
Optical rotation	−86.2° (*c*, 1.8 in water)
Equivalent weight	1 734 (acidimetric)
Uronic anhydride	10.15% (acidimetric)
L-Arabinose	51.6% (18 moles)
D-Galactose	31.7% (9 moles)
D-Xylose	15.0% (5 moles)
L-Rhamnose	2–3% (1 mole)
D-Galacturonic acid	11.2% (3 moles)

In an earlier investigation, Anderson *et al.* (2) and Sands and Klass (3) isolated an aldobiouronic acid from this gum and identified it as D-galacturonosido-L-rhamnose. The presence of a second aldobiouronic acid, viz. 3-*O*-(β-D-galactopyranosyluronic acid)-D-galactose, was reported by us in part I (1). An investigation of the gum by the methylation procedure was carried out by Brown *et al.* (4), who were able to isolate, from the hydrolysate of the methylated gum, the following sugars: (*i*) 2,3,5-tri-*O*-methyl-L-arabinose (4 parts), (*ii*) 2,3,4-tri-*O*-methyl-D-xylose (2 parts), (*iii*) 2,3-di-*O*-methyl-L-arabinose (1 part), (*iv*) 2,4-di-*O*-methyl-D-galactose (3 parts), (*v*) L-arabinose (1 part), and (*vi*) 2-*O*-methyl-D-galacturonic acid (1 part). In the present communication we report the results of the partial hydrolysis and the Smith-type degradation of the gum and suggest a possible structure of the gum. Partial hydrolysis of the gum with cold acid produced

[1]*For part I in this series, see ref. 1.*
[2]*Present address: Department of Chemistry, Notre Dame University, Nelson, British Columbia.*

several oligosaccharides, six of which have been isolated and identified. A new trisaccharide, viz. *O*-β-D-xylopyranosyl-(1 → 5)-*O*-α-L-arabinofuranosyl-(1 → 3)-L-arabinose, was isolated and characterized.

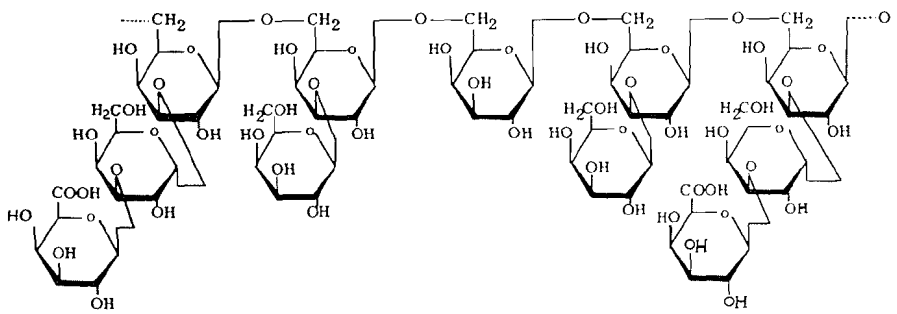


DIAGRAM 1. Proposed structure of the degraded gum.

Partial hydrolysis of the gum in cold 6 *N* sulfuric acid led to the isolation of a mixture of oligo- and mono-saccharides which was separated from the degraded gum by dialysis. Chromatographic examination showed the mixture to be composed of L-arabinose (ca. 60–65%), D-xylose (ca. 20–25%), D-galactose (ca. 5%), and several di- and oligosaccharides (total 8–10%). Most of the arabinose was crystallized from the mixture, and the rest was then removed almost completely on a cellulose column. The mixture of oligosaccharides thus obtained was further separated into six different oligosaccharides (Table II).

TABLE II

Neutral oligosaccharides from cholla gum

Oligosaccharide	Quantity (g)	R_{gal}	Color with *p*-anisidine hydrochloride spray
6-*O*-β-D-Galactopyranosyl-D-galactose	1.06	0.48	Yellow
3-*O*-β-D-Galactopyranosyl-D-galactose	0.158	0.62	Brownish-yellow
3-*O*-α-L-Arabinofuranosyl-L-arabinose	0.024	1.42	Red
5-*O*-β-D-Xylopyranosyl-L-arabinose	0.223	1.30	Pink
3-*O*-β-D-Galactopyranosyl-L-arabinose	0.018	0.76	Reddish-yellow
O-β-D-Xylopyranosyl-(1 → 5)-*O*-α-L-arabinofuranosyl-(1 → 3)-L-arabinose	0.098	1.20	Red

All of the above oligosaccharides, except *O*-β-D-xylopyranosyl-(1 → 5)-*O*-α-L-arabinofuranosyl-(1 → 3)-L-arabinose, have been reported earlier in the literature. The isolation of only two galactobioses and their identification as 1 → 6 and 1 → 3, β-linked disaccharides may be compared with the isolation of only 2,4-di-*O*-methyl-D-galactose residues from the methylated polymer by Brown *et al.* (4), and is consistent with the observation that the galactose residues in gums are usually 1 → 3 and (or) 1 → 6 linked. The isolation of trimethyl, dimethyl, and unsubstituted L-arabinose residues from the methylated polymer by Brown *et al.* had earlier indicated that the gum was a highly branched molecule with L-arabinose residues involved in several types of linkages. The isolation of four different oligosaccharides containing L-arabinose residues, in the present work, confirmed the variety of L-arabinose linkages. Because of the small amount of material available, the identification of 3-*O*-α-L-arabinofuranosyl-L-arabinose was based mainly on its optical rotation, its chromatographic mobility, and the ease with which it was hydrolyzed to

Can. J. Chem. Downloaded from www.nrcresearchpress.com by 210.87.254.5 on 09/05/12
For personal use only.

produce only L-arabinose. An attempt to prepare a phenylosazone of the disaccharide resulted in the production of L-arabinose phenylosazone. The optical rotation of the disaccharide (−4°) was in close agreement with that reported for 3-*O*-α-L-arabinofuranosyl-L-arabinose, which was isolated by Smith and Stephen (5) from *Virgilia oroboides* gum. On the basis of this evidence and on the basis of the identification of a trisaccharide, *O*-β-D-xylopyranosyl-(1 → 5)-*O*-α-L-arabinofuranosyl-(1 → 3)-L-arabinose, a partial hydrolysis of which could produce 3-*O*-α-L-arabinofuranosyl-L-arabinose, it was assumed that the arabinobiose under study was the same as that isolated by Smith and Stephen (5). Although a very small quantity of this disaccharide was obtained from the hydrolysate of the gum, it has been possible to assign structural significance to it, particularly in view of the isolation of the new trisaccharide, which is discussed later.

The isolation and identification of 5-*O*-β-D-xylopyranosyl-L-arabinose from peach and cholla gum was earlier reported by Andrews and his co-workers (6). Since the methylation studies (4) have indicated that all the D-xylose residues in the gum occupy terminal positions, at least some of the L-arabinose residues form a layer underneath the outer D-xylopyranose residues. More information regarding the arabinose-containing part of the gum was obtained by the isolation of a trisaccharide which, on further mild hydrolysis, gave L-arabinose and 5-*O*-β-D-xylopyranosyl-L-arabinose. The trisaccharide was so unstable that a sample stored at 0° for 8–10 weeks decomposed partially into L-arabinose and the disaccharide mentioned above. Complete hydrolysis of a part of the pure trisaccharide by warm 1 *N* sulfuric acid produced L-arabinose and D-xylose in the ratio 2:1, respectively. When a part of the trisaccharide was reduced by sodium borohydride and hydrolyzed, xylose, arabinose, and arabinitol were obtained, thereby showing that one L-arabinose residue formed the reducing end of the trisaccharide. The trisaccharide and its fully methylated derivative had high negative optical rotations. Methanolysis and hydrolysis of the methylated trisaccharide gave a mixture containing equal proportions of 2,3,4-tri-*O*-methyl-D-xylose, 2,3-di-*O*-methyl-L-arabinose, and 2,4-di-*O*-methyl-L-arabinose. A small amount of another sugar, probably 2,5-di-*O*-methyl-L-arabinose, was also detected. The three major sugars were separated chromatographically and were identified by their physical constants and by conversion into their respective *N*-phenylglycosylamines. The fourth sugar was extracted from the chromatogram in a quantity insufficient for further study. However, on the basis of the rate at which it moved on the chromatograms, this sugar is believed to be 2,5-di-*O*-methyl-L-arabinose. Its presence was not unexpected, because the terminal L-arabinose residue could exist in solution as either a pyranose or a furanose sugar. The linkage between D-xylopyranose and L-arabinofuranose residues was established to be of the β-type by Andrews and his co-workers (6). Application of Hudson's rules of isorotation (7) demanded that the nature of the glycosidic linkage between two arabinose residues in the trisaccharide be considered as of the α-type. Thus, on the basis of this evidence, the trisaccharide was identified as *O*-β-D-xylopyranosyl-(1 → 5)-*O*-α-L-arabinofuranosyl-(1 → 3)-L-arabinose (Diagram 2).

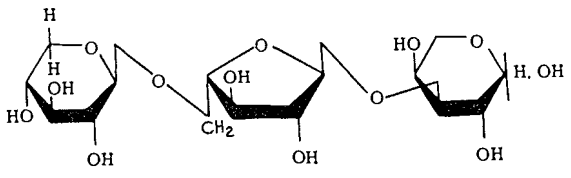


DIAGRAM 2. Neutral trisaccharide, *O*-β-D-xylopyranosyl-(1 → 5)-*O*-α-L-arabinofuranosyl-(1 → 3)-L-arabinose, from cholla gum.

Can. J. Chem. Downloaded from www.nrcresearchpress.com by 210.87.254.5 on 09/05/12
For personal use only.

A disaccharide containing D-galactose and L-arabinose was also obtained in very small yield in the present study. It was not possible to prepare a crystalline derivative of this disaccharide, but on the basis of the melting range of the crude material and optical rotation of this compound it was tentatively identified as 3-*O*-β-D-galactopyranosyl-L-arabinose. The structural significance of this disaccharide is not clear, since its isolation was found not to be consistent with other observations, such as investigations of the structure of the degraded gum and Smith-type degradation of the polymer. Its origin might possibly be attributed to an acid reversion, although formation of a β-D-linked disaccharide by acid reversion has rarely been encountered.

Periodate Oxidation Studies

Oxidation of the polysaccharide by sodium metaperiodate was almost complete within 24 h, during which time the gum had consumed 0.73 mole of the oxidant and had released 0.14 mole of formic acid per average anhydro sugar unit. When the periodate-oxidized polymer was reduced by sodium borohydride and a small portion of the resulting polyalcohol was hydrolyzed, the hydrolysate was found chromatographically to be a mixture of seven components, among which those corresponding to D-galactose, L-rhamnose, D-galacturonic acid, and L-arabinose could easily be located. No spot corresponding to the presence of xylose was noticed. All the components of the hydrolysate were identified and estimated chromatographically (Table III).

TABLE III

Products of Smith-type degradation of cholla gum

Product	Approximate percentage	Product	Approximate percentage
D-Galactose	30±2	L-Arabinose	5–6
Glycerol	25±2	Ethylene glycol	5–6
Glycolaldehyde	20±2	L-Rhamnose	2–3
D-Galacturonic acid	10±2		

When the polyalcohol was partially hydrolyzed by cold 1 *N* sulfuric acid and the hydrolysate poured into ethanol, a sticky precipitate was obtained which was repeatedly extracted with hot ethanol. The precipitated material and the ethanol extracts were now separately hydrolyzed by hot dilute acid and the hydrolysates were examined chromatographically. The hydrolysate of the precipitated material contained D-galactose (ca. 70%), D-galacturonic acid (ca. 20%), and L-rhamnose (ca. 5%) with trace quantities of L-arabinose, glycerol, glycolaldehyde, and ethylene glycol. Hydrolysis of the alcohol-soluble syrup yielded mainly glycerol (ca. 50%) and glycolaldehyde (ca. 40%) together with L-arabinose (8–10%), ethylene glycol (8–10%), and trace quantities of L-rhamnose, D-galacturonic acid, and D-galactose.

The results obtained in the present investigations were found to be consistent with the results of the methylation studies of the polymer by Brown *et al.* (4). On the basis of all these results plus the suggested structure of the degraded gum (Diagram 1), it is proposed that one of many possible structures for the repeating unit of the polymer is as shown in Diagram 3.

DISCUSSION

Although the structure proposed in Diagram 3 explains a number of experimental results, it must be emphasized that it is just one of the several possible structures for the repeating unit of the polymer.

Can. J. Chem. Downloaded from www.nrcresearchpress.com by 210.87.254.5 on 09/05/12
For personal use only.

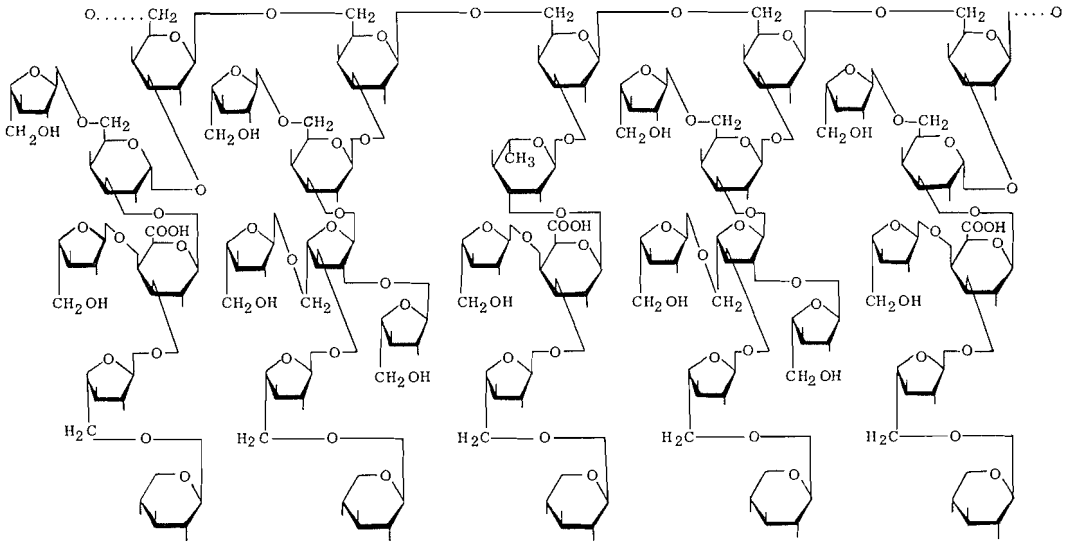


DIAGRAM 3. Proposed structure of cholla gum.

The analysis of the gum is given in Table I and is in fair agreement with a repeating unit of 36 sugar residues: 18 of L-arabinofuranose, 9 of D-galactopyranose, 5 of D-xylopyranose, 3 of D-galactopyranosyluronic acid, and 1 of L-rhamnose.

Methylated cholla gum (Diagram 3) gave, on hydrolysis, the methylated sugar derivative listed in Table IV. The quantities of methylated sugars anticipated from the hydrolysis of the methylated polymer are also in fair agreement with those isolated. The periodate results (a consumption of 0.73 mole of the oxidizing agent with the concomitant production of 0.14 mole of formic acid per average anhydro sugar residue) also support the above results. Further support for the proposed structure (Diagram 3) is obtained when the products resulting from the Smith-type periodate degradation of the gum are analyzed (Table V). It will be noted that all the D-xylose and most of the L-arabinose have been oxidized.

TABLE IV

A comparison of the methylation results with those expected according to the proposed structure

Product	Quantity (moles) expected according to the proposed structure	Quantity (moles) isolated experimentally (4)
2,4-Di-*O*-methyl-D-galactose	9	9
2,3,4-Tri-*O*-methyl-D-xylose	5	6
2-*O*-Methyl-D-galacturonic acid	3	3
2,3,5-Tri-*O*-methyl-L-arabinose	11	12
2,3-Di-*O*-methyl-L-arabinose	5	3
L-Arabinose (unsubstituted)	2	3
2,4-Di-*O*-methyl-L-rhamnose	1	Nil

The isolation of the trisaccharide (Diagram 2) gives an idea of the sequence of sugars from the end groups (D-xylopyranose) towards the inner portion of the molecule. Again it must be emphasized that the proposed structure of the gum (Diagram 3) is only one of many possibilities. Further work will be necessary before a specific structure can be advanced for cholla gum.

Can. J. Chem. Downloaded from www.nrcresearchpress.com by 210.87.254.5 on 09/05/12
For personal use only.

TABLE V

Comparison of the Smith-type degradation results with those calculated on the basis of the proposed structure

Substance	Quantity (%) expected according to the methylation studies	Quantity (%) obtained experimentally	Quantity (%) expected according to the proposed structure
D-Galactose	28.6	30±2	28.4
Glycerol	24.4	25±2	25.8
Glycolaldehyde	22.2	20±2	22.1
D-Galacturonic acid	10.3	10±2	10.2
L-Arabinose	8.0	5–6	5.3
Ethylene glycol	6.6	5–6	5.3
L-Rhamnose	Nil	2–3	2.9

Nature of Linkages and Optical Rotation

The proposed structure of the gum shows that the repeating unit of the gum is composed of a total of 36 sugar residues which are linked as follows: β-linked D-galactose (7 moles), α-linked D-galactose (2 moles), β-linked D-galacturonic acid (3 moles), α-linked L-rhamnose (1 mole), α-linked L-arabinose (18 moles), and β-linked D-xylopyranose (5 moles). The optical rotation of the polysaccharide, calculated on the basis of these data by the application of Hudson's rules (7), was found to agree reasonably well with the experimental value (−86°) for the gum.

EXPERIMENTAL

Methods

Paper chromatography was carried out on Whatman No. 1 filter paper with the following solvent systems (by volume): (*a*) butan-1-ol–ethanol–water (3:1:1); (*b*) butan-1-ol–ethanol–water (5:1:4), top layer cleared by addition of a minimum of ethanol; (*c*) ethyl acetate – acetic acid – formic acid – water (18:3:1:4); (*d*) butan-1-ol–pyridine–water–benzene (5:3:3:1); (*e*) ethyl acetate – pyridine – water (10:4:3); and (*f*) butan-1-ol–ethanol–water (1:1:1). The spray reagents used were: (*i*) alkaline silver nitrate (8), and (*ii*) *p*-anisidine hydrochloride (9). Whatman 3 MM paper and columns packed with Whatman cellulose powder by the wet method were used for the separation of sugar mixtures. Optical rotations were observed in water, unless otherwise stated. All solutions were concentrated under reduced pressure at 40–45°.

Partial Hydrolysis of the Gum and Isolation of Neutral Oligosaccharides

The gum (100 g) was purified and hydrolyzed by cold dilute sulfuric acid as described in part I (1). The hydrolysate was neutralized with barium carbonate, filtered, and dialyzed against distilled water (3 × 4 l). The dialyzate, on concentration, yielded a mixture of mono- and oligo-saccharides (58.0 g). The chromatographic examination of the mixture revealed the presence of arabinose (60–65%), xylose (20–25%), galactose (ca. 5%), and several di- and oligo-saccharides (8–10%). The syrup was thinned with methanol seeded with L-arabinose, and was kept overnight at 0°, during which L-arabinose (19 g) crystallized out and was separated by filtration. Another crop of L-arabinose (5.8 g) subsequently crystallized out from the filtrate on concentration. The residual mixture (30.2 g) was found to contain L-arabinose (ca. 30%), D-xylose (ca. 30%), D-galactose (ca. 10%), and a mixture of at least four oligosaccharides (total ca. 20%). Attempts were made to remove monosaccharides from the mixture by carrying out the separation, on the basis of the molecular weights of the sugars, on columns containing Dowex-50-2 (Li salt) and eluting the sugars with water. These attempts, however, proved to be unsuccessful.

The syrupy mixture (29 g) was therefore divided into three equal portions and each portion (ca. 10 g) was passed through large cellulose columns (90 × 13 cm), butan-1-ol saturated with water being used as the solvent. The process of separation was extremely slow, and a mixture of L-arabinose and D-xylose was eluted from the column only after 4.8 l of the eluant had been collected from each column. The elution of the mixture of L-arabinose and D-xylose continued for a period of 7 days, during which time 4 l of the eluant was collected from each column. The total weight of the mixture of arabinose and xylose collected from the three columns was found to be 18.6 g. Elution of arabinose and xylose was followed by 1 l of the sugar-free eluant, after which D-galactose was eluted from the column; the elution was continued for a period of 5 days, during which time 3 l of the effluent containing a total of 2.8 g of galactose was collected.

At this stage the solvent system for chromatography was changed to butan-1-ol–ethanol–water (1:1:1 v/v/v), 4 l of which eluted all the oligosaccharides from each column in the form of a mixture (total 3.45 g). Chromatographic examination of this mixture in solvents *a*, *c*, *e*, and *f* revealed the presence of only trace quantities of monosaccharides, viz. arabinose, xylose, and galactose with at least five to six oligosaccharides.

Can. J. Chem. Downloaded from www.nrcresearchpress.com by 210.87.254.5 on 09/05/12
For personal use only.

The constituents of the mixture were separated chromatographically on 3 MM paper with solvent *e*. Their R_{gal} values in solvent *e*, yields, and identities are given in Table II. Higher oligosaccharides (R_{gal} 0.2), which were present only in trace quantities, were not examined and are not recorded.

Identification of the Oligosaccharides

Fraction 1: 6-O-β-D-Galactopyranosyl-D-galactose

This material (1.06 g) was chromatographically pure and showed R_{gal} values of 0.16, 0.48, and 0.65 in solvents *c*, *e*, and *f*, respectively. It crystallized from methanol–acetone (1:1 v/v) to give waxy, highly hygroscopic crystals which crumbled to an amorphous powder when kept in a desiccator. The white amorphous powder melted over a broad range of 98–106° and was therefore recrystallized from methanol. The colorless needles thus obtained softened at 98–99°, almost melted at 118°, but resolidified, when heated further, at 124–128°. The resolidified material melted, when heated further, at 169–171°.

The disaccharide reduced Fehling's solution and had $[\alpha]_D^{23}$ +26 → +35.2° (48 h) (*c*, 1.5 in water). On complete hydrolysis by 2 *N* sulfuric acid at 98° for 6 h, it produced only D-galactose (detected chromatographically). Its phenylosazone, prepared by heating the solution of the disaccharide (150 mg) in ethanol (5 ml) with freshly distilled phenylhydrazine (170 mg), sodium acetate (80 mg), and glacial acetic acid (105 mg) on a boiling water bath for 1 h, melted with decomposition at 201–202°. Freudenberg *et al.* (10), who have synthesized this disaccharide by the Köenigs–Knorr method (11), reported the following constants for the disaccharide and its phenylosazone: disaccharide, m.p. 115° and $[\alpha]_D^{17}$ +25.1 → +34.1° (48 h) (*c*, 3.20 in water); phenylosazone, m.p. 207° with decomposition.

Duplicate samples of the desiccated anhydrous disaccharide (38 mg each) were dissolved in distilled water (5 ml each). Sodium metaperiodate solution (0.3 *M*, 1 ml) was added to each flask, and the solutions were made up to 25 ml with distilled water and kept in the dark. The periodate uptake was determined by the thiosulfate method with phosphate buffer (12), and the formic acid by titration with standard sodium hydroxide solution (screened methyl red indicator) after addition of ethylene glycol. Found: periodate uptake 4.97 moles and formic acid yield 3.04 moles per mole.

Fraction 2: 3-O-β-D-Galactopyranosyl-D-galactose

This disaccharide (158 mg) was obtained in the form of a chromatographically pure syrup and had R_{gal} values of 0.27, 0.62, and 0.75 in solvents *c*, *e*, and *f*, respectively. It crystallized on trituration with ether–methanol (2:1 v/v), and had m.p. 159–161° and $[\alpha]_D^{23}$ +72 → +62° (10 h) (*c*, 1.0 in water). Hydrolysis of the disaccharide gave only galactose (detected chromatographically). The literature values (13) for 3-*O*-β-D-galactopyranosyl-D-galactose isolated from *Acacia pycnantha* gum are: m.p. 159–160.5° and $[\alpha]_D$ +62° (*c*, 0.58 in water).

Periodate oxidation of the disaccharide was carried out in the same manner as described for fraction 1, taking 35 mg duplicate samples for the experiments. Found: periodate uptake 3.02 moles and formic acid yield 0.96 mole per mole of the disaccharide.

Fraction 3: 3-O-α-L-Arabinofuranosyl-L-arabinose

A very small quantity (24 mg) of this disaccharide was isolated in the form of a colorless syrup having $[\alpha]_D^{23}$ −4° (*c*, 0.5 in water) and R_{gal} values of 1.2 and 1.42 in solvents *c* and *e*, respectively. It gave a pink spot on chromatograms sprayed with *p*-anisidine hydrochloride and also with the tetraazolium red reagent. It was hydrolyzed readily by 1 *N* sulfuric acid when heated to 98° for 3 h to give only L-arabinose. The attempted synthesis of its phenylosazone gave an impure crystalline material which melted at 184–200°. These crystals were probably those of L-arabinose phenylosazone. The optical rotation and the R_{gal} values of this disaccharide are in fair agreement with those reported for 3-*O*-α-L-arabinofuranosyl-L-arabinose isolated from *Virgilia oroboides* gum, by Smith and Stephen (5). The optical rotation reported for this disaccharide is 0°. The anomer of this disaccharide was isolated from a number of gums (14–16) and is reported to have $[\alpha]_D$ +94°.

Fraction 4: 5-O-β-D-Xylopyranosyl-L-arabinose

This fraction (223 mg) was obtained as a chromatographically pure, light-yellow syrup and had R_{gal} values of 0.92 and 1.30 in solvents *c* and *e*, respectively. The disaccharide could not be crystallized. When the chromatograms were sprayed with *p*-anisidine hydrochloride and warmed, the disaccharide was detected as an initial yellow spot which rapidly turned pink when heated further. On complete hydrolysis by 1 *N* sulfuric acid it produced arabinose and xylose in equal proportions. It had $[\alpha]_D^{23}$ −38° (*c*, 1.4 in water). A crystalline phenylosazone of the disaccharide, prepared in the usual manner, melted at 214° (decomp.) and had $[\alpha]_D^{23}$ +51° (*c*, 0.8 in pyridine–ethanol (3:2 v/v)). A portion of the osazone, on hydrolysis by 2 *N* sulfuric acid, gave only xylose and no arabinose. Andrews and his co-workers (6) have isolated 5-*O*-β-D-xylopyranosyl-L-arabinose from this gum and from cherry gum, and the constants reported by them are: disaccharide, $[\alpha]_D$ −34° (*c*, 6.0 in water); phenylosazone, $[\alpha]_D$ +48° (*c*, 0.25 in pyridine–water (3:2 v/v)) and m.p. 216°.

Fraction 5: 3-O-β-D-Galactopyranosyl-L-arabinose

The very small quantity (18 mg) of this fraction that was obtained solidified when kept at 0°, but several attempts to recrystallize the solid proved to be unsuccessful. The waxy material melted at 193–202°. It reduced Fehling's solution and was chromatographically pure, having R_{gal} values of 0.46 and 0.76 in solvents

Can. J. Chem. Downloaded from www.nrcresearchpress.com by 210.87.254.5 on 09/05/12
For personal use only.

c and *e*, respectively. On hydrolysis with 2 *N* sulfuric acid it produced galactose and arabinose in equal proportions. It had $[\alpha]_D$ +64° (*c*, 0.48 in water). Further examination of this material was not possible because of the very small amount available. However, on the basis of the available data the material appears to be 3-*O*-β-D-galactopyranosyl-L-arabinose. The literature values for this disaccharide are: m.p. 200–201° and $[\alpha]_D$ +60° (*c*, 1.8 in water) for the disaccharide isolated from *Albizzia zygia* (17); m.p. 204–205° and $[\alpha]_D$ +97 → +67° (2 h) (*c*, 0.45 in water) for the disaccharide isolated from *Anogeissus schimperi* gum (16).

Fraction 6: O-β-D-Xylopyranosyl-(1 → 5)-O-α-L-arabinofuranosyl-(1 → 3)-L-arabinose

This syrupy fraction (98 mg) was chromatographically pure when isolated, and showed a red spot with *p*-anisidine hydrochloride reagent. However, when the syrup was kept for a few weeks it decomposed, and the chromatographic examination of the fraction revealed it to be a mixture of the original material (80%) and two minor fractions (ca. 10% each). The minor fractions had the same chromatographic mobility as did fraction 4 (i.e. 5-*O*-β-D-xylopyranosyl-L-arabinose) and L-arabinose, respectively. The mixture was therefore separated chromatographically by passing its aqueous solution through a column containing Sephadex G-25, medium grain (45 × 5 cm). The pure material thus obtained had $[\alpha]_D^{24}$ −74.2° (*c*, 1.1 in water), and R_{gal} 1.2 in solvent *e*. Addition of a mixture of methanol and acetone to this syrup precipitated an amorphous solid melting at 131–140°. Hydrolysis of this material on a boiling water bath by 1 *N* sulfuric acid produced only arabinose and xylose in the proportion 2:1.

A small portion of the material (8 mg) in water (3 ml) was reduced by sodium borohydride (1%, 5 ml). The solution was passed through an ion-exchange column containing layers of Amberlite IR-120 (H^+ form) and Duolite A-4 (OH^- form), and the material thus obtained was hydrolyzed by 1 *N* sulfuric acid. Chromatographic examination of the hydrolysate showed that it contained equal proportions of xylose, arabinose, and arabinitol.

The rest of the material (40 mg) was dissolved in water (3 ml), and cooled to 0°; dimethyl sulfate (2 ml) followed by sodium hydroxide solution (30%, a few drops until the pH reached 9) was added and the solution was stirred until it became nonreducing. The solution was then brought to room temperature, and dimethyl sulfate (5 ml) and sodium hydroxide (8 ml) were simultaneously added dropwise over a period of 1 h. The excess dimethyl sulfate was decomposed by heating the mixture to 65–70° and the solution was brought to pH 7 by addition of dilute sulfuric acid. The methylated sugar thus obtained (42 mg) by extraction with chloroform was found to be chromatographically pure and had $[\alpha]_D$ −91.6° (*c*, 0.574 in chloroform). The infrared spectrum of the syrup in chloroform did not show any absorption in the hydroxyl region.

Hydrolysis of the methylated material by dilute sulfuric acid and chromatographic examination of the neutralized hydrolysate in solvent *a* revealed that four partially methylated sugars were produced. Three of these sugars travelled parallel, respectively, to authentic samples of 2,3,4-tri-*O*-methyl-D-xylose, 2,3-di-*O*-methyl-L-arabinose, and 2,4-di-*O*-methyl-L-arabinose. The fourth sugar, which was present in only trace quantities (3–5%), travelled slightly faster than authentic 2,4-di-*O*-methyl-L-arabinose and was believed to be 2,5-di-*O*-methyl-L-arabinose, since the four sugars gave red spots on chromatograms sprayed with *p*-anisidine hydrochloride but none showed up when the chromatograms were sprayed with tetraazolium red reagent (18). The three components of the syrup were chromatographically separated on Whatman 3 MM filter paper with solvent *a* and were examined as follows.

Fraction 6A: 2,3,4-tri-O-methyl-D-xylose.—This fraction (11 mg) was a chromatographically pure syrup and was indistinguishable from an authentic sample of 2,3,4-tri-*O*-methyl-D-xylose. It had $[\alpha]_D^{22}$ +22° (equilibrium value) (*c*, 0.72 in water). Its *N*-phenylglycosylamine was prepared by treatment with aniline in ethanol. The crystalline derivative melted at 98–99° and had $[\alpha]_D^{22}$ −85 → +48° (*c*, 0.81 in ethanol). The literature values for 2,3,4-tri-*O*-methyl-D-xylose (19) and for its *N*-phenylglycosylamine (20) are: sugar, m.p. 91–92° and $[\alpha]_D$ +64 → +18° (in water); *N*-phenylglycosylamine, m.p. 102° and $[\alpha]_D$ −84 → +47°.

Fraction 6B: 2,3-di-O-methyl-L-arabinose.—This fraction (9 mg) was a chromatographically pure syrup and had $[\alpha]_D^{22}$ +98° (*c*, 0.52 in water). Conversion into its *N*-phenylglycosylamine in the usual manner gave tiny colorless crystals having m.p. 137–139° (undepressed). The literature values (21) for 2,3-di-*O*-methyl-L-arabinose and for its *N*-phenylglycosylamine derivative are: sugar, $[\alpha]_D$ +101° (in water); its *N*-phenylglycosylamine, m.p. 137–139°.

Fraction 6C: 2,4-di-O-methyl-L-arabinose.—This syrup was chromatographically pure and had $[\alpha]_D$ +116° (*c*, 0.52 in water). The *N*-phenylglycosylamine of the sugar, prepared in the usual manner and recrystallized from ethanol, had m.p. 143–145° (undepressed). The literature values (22) for 2,4-di-*O*-methyl-L-arabinose and for its *N*-phenylglycosylamine derivative are: sugar, $[\alpha]_D$ +129° (in water); its *N*-phenylglycosylamine, m.p. 145–146°.

ACKNOWLEDGMENTS

The authors thank Drs. B. A. Erukoff and K. Folkers for the gift of cholla gum. They also thank the National Research Council of Canada for a grant (N.R.C. T-19), Queen's University for financial assistance, and Dr. E. Buncel for helpful discussions.

Can. J. Chem. Downloaded from www.nrcresearchpress.com by 210.87.254.5 on 09/05/12
For personal use only.

REFERENCES

1. V. M. PARIKH and J. K. N. JONES. Can. J. Chem. **44**, 327 (1966).
2. E. ANDERSON, L. SANDS, and N. STURGIS. Am. J. Pharm. **97**, 589 (1925).
3. L. SANDS and R. KLASS. J. Am. Chem. Soc. **51**, 3441 (1929).
4. F. BROWN, E. L. HIRST, and J. K. N. JONES. J. Chem. Soc. 1761 (1949).
5. F. SMITH and A. M. STEPHEN. J. Chem. Soc. 4892 (1961).
6. P. ANDREWS, D. H. BALL, and J. K. N. JONES. J. Chem. Soc. 4090 (1953).
7. C. S. HUDSON. J. Am. Chem. Soc. **31**, 66 (1909).
8. W. E. TREVELYAN, D. P. PROCTER, and J. S. HARRISON. Nature, **166**, 444 (1950).
9. L. HOUGH, J. K. N. JONES, and W. H. WADMAN. J. Chem. Soc. 1702 (1950).
10. K. FREUDENBERG, A. WOLF, E. KNOPF, and S. H. ZAHEER. Chem. Ber. **61**, 1743 (1928).
11. W. KÖENIGS and E. KNORR. Ber. **34**, 957 (1901).
12. G. NEUMÜLLER and E. VASSEUR. Arkiv Kemi, **5**, 235 (1953).
13. E. L. HIRST and A. S. PERLIN. J. Chem. Soc. 2622 (1954).
14. P. ANDREWS, L. HOUGH, and D. B. POWELL. Chem. Ind. London, 658 (1956).
15. G. O. ASPINALL, E. L. HIRST, and A. NICOLSON. J. Chem. Soc. 1697 (1959).
16. G. O. ASPINALL and T. B. CHRISTENSEN. J. Chem. Soc. 3461 (1961).
17. D. W. DRUMMOND and E. PERCIVAL. J. Chem. Soc. 3908 (1961).
18. K. WALLENFELS. Naturwiss. **37**, 491 (1950).
19. S. K. CHANDA, E. L. HIRST, and E. G. V. PERCIVAL. J. Chem. Soc. 1289 (1950).
20. R. A. LAIDLAW and E. G. V. PERCIVAL. J. Chem. Soc. 528 (1950).
21. F. SMITH. J. Chem. Soc. 753 (1939).
22. J. K. N. JONES. J. Chem. Soc. 1672 (1953).

Can. J. Chem. Downloaded from www.nrcresearchpress.com by 210.87.254.5 on 09/05/12
For personal use only.

Can. J. Chem. Downloaded from www.nrcresearchpress.com by 210.87.254.40 on 09/05/12
For personal use only.

LIGNANS OF WESTERN RED CEDAR (THUJA PLICATA DONN)

IV. THUJAPLICATIN AND THUJAPLICATIN METHYL ETHER[1]

HAROLD MACLEAN[2] AND KOJI MURAKAMI[3]

Forest Products Laboratory, Department of Forestry of Canada, Vancouver, British Columbia

Received February 17, 1966

ABSTRACT

In addition to the already known plicatic acid and plicatin, five new lignans have been separated by thin-layer and column chromatography from the hot-water extractive of western red cedar (*Thuja plicata* Donn) heartwood, and two chemical structures have been identified. These are 2-(4″-hydroxy-3″,5″-dimethoxybenzyl)-3-(4′-hydroxy-3′-methoxybenzyl)-butyrolactone (thujaplicatin methyl ether) (I) and 2-(3″,4″-dihydroxy-5″-methoxybenzyl)-3-(4′-hydroxy-3′-methoxybenzyl)-butyrolactone (thujaplicatin) (II). The former is the first known example of a lignan containing a guaiacyl and a syringyl nucleus and the first example of a syringyl-group lignan isolated from a conifer. Proof of structure by synthesis, degradation, analysis, and various spectra is presented. The other components which apparently belong to this lignan series are still being investigated.

In previous papers (1–3) the structures of the lignans plicatic acid and plicatin, the main components of the hot-water extractive of western red cedar heartwood, were presented. Development of adequate thin-layer and preparative chromatographic systems has permitted the detection and separation of five new components of much lower concentration (Scheme 1), all of which appear to be related lignans. The structure of two of these components is reported in this paper. Investigation of the chemistry of the remaining compounds is continuing.

Because the first lignan of this series to be identified was the methyl ether of the second, and there are indications that the other lignans will also be derivatives of the second, the common names assigned are thujaplicatin methyl ether for I and thujaplicatin for II. The numbering and chemical naming systems follow the review of Hearon and MacGregor (4). The chemical names proposed by Freudenberg and Weinges (5) are given at the end of the discussion of each lignan.

Thujaplicatin Methyl Ether (I)

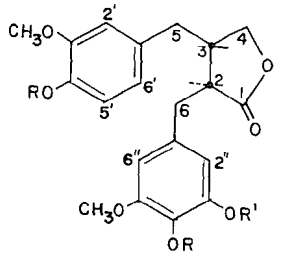
This compound gave approximately equal yields of vanillin and syringaldehyde on nitrobenzene oxidation (6). Analytical data obtained for this lignan and its di-*O*-methyl ether (III) were satisfactory; infrared spectra were as expected, showing no hydroxyl band after methylation. The ultraviolet spectrum of I had a maximum at 281 mμ shifting to 293 mμ in alkaline solvent. Nuclear magnetic resonance (n.m.r.) spectra with integrals accounted for all proton species in the dimethyl ether (III) and the diacetate (IV), the spectrum of the parent lignan being unsatisfactory because of low solubility in deuteriochloroform.

Synthesis of the dimethyl derivative (III) was accomplished by condensing (±)-3-(3′,4′-dimethoxybenzyl)-butyrolactone (V) (7) in sodium methoxide with 3,4,5-trimethoxybenzaldehyde (8, 9) to yield (±)-2-(3″,4″,5″-trimethoxybenzylidene)-3-(3′,4′-dimethoxybenzyl)-butyrolactone (VI) (10), the double bond of which was reduced by hydrogen over

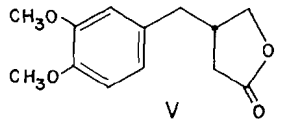
[1]*Previous papers in this series were entitled "Polyoxyphenols of Western Red Cedar (Thuja plicata Donn)".*

[2]*Research Officer, Forest Products Laboratory, Department of Forestry of Canada, Vancouver, British Columbia.*

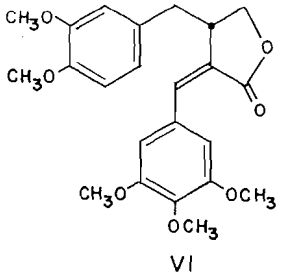
[3]*National Research Council Postdoctorate Fellow, 1963–1965. Present address: Faculty of Agriculture, Shinshu University, Ina, Nagano-ken, Japan.*



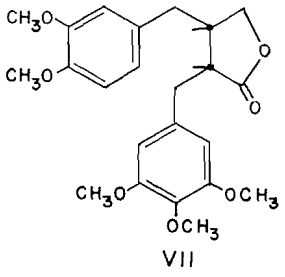
I R = H, R' = CH_3
II R = R' = H
III R = R' = CH_3
IV R = CH_3CO, R' = CH_3



V



VI



VII

a palladium chloride catalyst in methanol to the *cis* form of (±)-2-(3″,4″,5″-trimethoxybenzyl)-3-(3′,4′-dimethoxybenzyl)-butyrolactone (VII). This hydrogenation is directly analogous to Schrecker and Hartwell's conversion of savinin into (+)-isohinokinin (*cis* configuration) and the subsequent base-catalyzed epimerization to (−)-hinokinin (*trans* epimer) (11, 12). The *cis* epimer VII, which differed from the natural di-*O*-methyl ether III (shown by infrared and n.m.r. spectral comparison and by thin-layer R_f values), was dissolved in methanolic potassium hydroxide for 4 days at room temperature to yield, on acidification and purification, the *trans* epimer (±)-*trans*-2-(3″,4″,5″-trimethoxybenzyl)-3-(3′,4′-dimethoxybenzyl)-butyrolactone (III).

Additional evidence for the *cis–trans* configurations is indicated by comparing their Dreiding stereomodels and n.m.r. spectra. In the *trans* configuration, the four C5—C6 benzyl protons have free rotation and appear in the n.m.r. spectra as a singlet whereas the C2—C3 *trans* protons appear as a doublet at 7.03 and 7.10 τ. In the *cis* epimer, the rotation of the benzyl protons is sterically hindered, which, in conjunction with the 0° dihedral angle's larger coupling constant (13) for the C2—C3 protons, shows an unresolvable complex pattern totalling six protons in the 6.5 to 8.5 τ region of the n.m.r. spectra, as expected for the two overlapping ABX systems.

The *trans* epimer III was identical with natural di-*O*-methyl thujaplicatin methyl ether (III) as shown by ultraviolet, infrared, and n.m.r. spectral comparison. Although several crystals of the synthetic material had the same melting point as the natural product, the major part melted approximately 20° lower, which is indicative of a racemic mixture of individual crystals of each of the two enantiomers of the *trans* configuration (14). Thujaplicatin methyl ether (I) is therefore *trans*-2-(4″-hydroxy-3″,5″-dimethoxybenzyl)-3-(4′-hydroxy-3′-methoxybenzyl)-butyrolactone (4,4′-dihydroxy-3,3′,5′-trimethoxy-lignan-olid (9,9′) by the nomenclature of Freudenberg and Weinges (5)).

This is the first known lignan containing both a guaiacyl and a syringyl nucleus as well as the first isolated from a conifer containing a syringyl nucleus.

Thujaplicatin (II)

This compound has not been crystallized, but methylation of a chromatographically pure sample by diazomethane in methanol gave a good yield of tri-*O*-methyl thujaplicatin (III), identical with the product from the methylation of thujaplicatin methyl ether, di-*O*-methyl thujaplicatin methyl ether (III), as shown by mixed melting point, optical rotation, and infrared spectral comparison. The presence of a pyrocatechol group was indicated by a lower R_f value when chromatographed in butanol – acetic acid – water

Can. J. Chem. Downloaded from www.nrcresearchpress.com by 210.87.254.40 on 09/05/12
For personal use only.

(60:15:25 v/v/v) on molybdic acid treated paper rather than on untreated paper. Since nitrobenzene oxidation yielded only vanillin, and alkaline permanganate oxidation of the triethyl ether, prepared by diethyl sulfate and anhydrous potassium carbonate in acetone, produced 3,4-diethoxy-5-methoxybenzoic and 4-ethoxy-3-methoxybenzoic acids, this lignan was shown to be 2-(3″,4″-dihydroxy-5″-methoxybenzyl)-3-(4′-hydroxy-3′-methoxybenzyl)-butyrolactone (II) (4,3′,4′-trihydroxy-3,5′-dimethoxy-lignan-olid (9,9′) by the nomenclature of Freudenberg and Weinges (5)).

EXPERIMENTAL

Melting points were taken on a Fisher–Johns apparatus and are uncorrected. Carbon, hydrogen, and methoxyl analyses were performed by Clark Microanalytical Laboratories, Urbana, Illinois. The n.m.r. spectra were measured in deuteriochloroform with tetramethylsilane as internal reference ($\tau = 10$) on a Varian A.60 instrument at the Chemistry Department of the University of British Columbia. Ultraviolet spectra were taken in ethanol on a Beckman DK-2 spectrometer. Infrared spectra were taken as KBr disks, unless otherwise specified, on a Baird-Atomic KM-1 spectrometer. Molecular weights were determined on a Mechrolab osmometer, model 301A, with benzil and β-conidendrin as reference compounds. Thin-layer chromatography (t.l.c.) used silica gel G (Merck) as adsorbent with benzene–ethanol – acetic acid (100:10:1), unless otherwise shown, as developer, and with nitric acid – sulphuric acid (1:1) – heat and ultraviolet light as detectors. Preparative-layer chromatography (p.l.c.) used 2 mm layers of silica gel G and GF 254 (2:1) with ultraviolet light as detector and the t.l.c. developing solvent, unless otherwise indicated. All developing solvent mixtures are on a volume basis.

Fractionation of Extractive

As shown in Scheme 1, western red cedar heartwood meal (1 kg, moisture-free basis) ground to pass a 4 mm screen was extracted with water (8 l) for 5 h at 100 °C. The aqueous extract, after cooling, was extracted with chloroform (3 × 500 ml), and the aqueous layer retained for future work. The chloroform extract was evaporated to a light-colored oil (7.9 g) and triturated with petroleum ether (65–110 °C) (2 × 300 ml) to remove residual steam volatiles (thujaplicins, thujic acid, methyl thujate, etc.); the insoluble residue was subjected to silica gel column chromatography with benzene–isopropanol (100 : 2–5) as eluting solvent. Fractions were monitored by t.l.c. The fractions collected were: R_f 0.30, thujaplicatin methyl ether I (790 mg); R_f 0.25 (430 mg); R_f 0.21, thujaplicatin II (110 mg); and R_f 0.20 and 0.17 overlapping (2.5 g).

Thujaplicatin Methyl Ether (I)

Crude I (790 mg) was chromatographed first on a cellulose column to remove contaminating phenolic materials which have a low R_f value in carbonic acid paper chromatography, and then subjected to p.l.c. (R_f 0.30). The product reclaimed from the silica gel was crystallized from diethyl ether and recrystallized from acetone–water, m.p. 167–167.5 °C, $[\alpha]_D^{25}$ −48.7° (*c*, 3.94 in acetone).

Anal. Calcd. for $C_{21}H_{24}O_7$: C, 64.94; H, 6.23; OCH_3, 23.97; mol. wt. 388. Found: C, 64.86, 65.02; H, 6.06, 6.20; OCH_3, 24.02, 23.89; equiv. wt. (by back-titration) 380; mol. wt. 390.

Nitrobenzene oxidation according to Pepper and Siddiqueullah (6) yielded vanillin (3.5%) and syringaldehyde (4.2%). Spectra: λ_{min} 258 mμ (log ε 3.17), λ_{max} 281 mμ (log ε 3.60); in 0.025 *M* sodium ethoxide, λ_{min} 279 mμ (log ε 3.80), λ_{max} 293 mμ (log ε 3.86); ν_{max} 3 380 (phenol) and 1 747 (lactone) cm^{-1}.

To improve the solubility in deuteriochloroform and to remove the phenolic protons for a better n.m.r. spectrum, thujaplicatin methyl ether (150 mg) was acetylated with acetic anhydride (10 ml) in pyridine (30 ml) for 4 h at room temperature and purified by p.l.c. to yield the noncrystalline diacetate IV (130 mg). Spectra: ν_{max} no hydroxyl band, 1 753 (broad, lactone and acetoxy) cm^{-1}; n.m.r. 3.06 (1H-C5′, doublet, $J = 8.5$ c.p.s.), 3.39 (1H-C2′, doublet, $J = 1.8$ c.p.s.), 3.40 (1H-C6′, quartet, $J = 1.8$ and 8.5 c.p.s.), 3.57 (2H-C2″,6″, singlet), 5.75–6.20 (2H-C4, multiplet), 6.24 (9H-methoxyl, singlet), 7.07 (2H-C2,3, doublet), 7.39 (4H-C5,6, broad singlet), 7.70 (3H-acetyl, singlet), and 7.73 τ (3H-acetyl, singlet).

Di-O-methyl Thujaplicatin Methyl Ether (III)

A suspension of thujaplicatin methyl ether (I) (100 mg) in methanol (1 ml) was treated with excess diazomethane in ether for 24 h at room temperature. The oily product (110 mg) was recovered by vacuum evaporation, purified by p.l.c. (R_f 0.54), and crystallized from ether by seeding with tri-*O*-methyl thujaplicatin (III) (later shown to be the identical compound). Recrystallization from ether gave colorless plates, m.p. 102–103 °C, $[\alpha]_D^{24}$ −37.4° (*c*, 0.64 in chloroform), R_f 0.24 (t.l.c., developed with benzene – ether – acetic acid (70:30:1)).

Anal. Calcd. for $C_{23}H_{28}O_7$: C, 66.34; H, 6.78; OCH_3, 37.26. Found: C, 66.10; H, 6.44; OCH_3, 37.00.

Spectra: λ_{max} 278 mμ (log ε 3.54); ν_{max} no hydroxyl band, 1 763 (lactone, 1 762 in chloroform) cm^{-1}; n.m.r. 3.21 (1H-C5′, doublet, $J = 8.5$ c.p.s.), 3.41 (1H-C6′, quartet, $J = 1.7$ and 8.5 c.p.s.), 3.44 (1H-C2′, doublet, $J = 1.8$ c.p.s.), 3.59 (2H-C2″,6″, singlet), 5.8–6.2 (2H-C4, multiplet), 6.17 (15H-methoxyl, singlet), 7.07 (2H-C2,3, doublet), and 7.41 τ (4H-C5,6, broad singlet).

Can. J. Chem. Downloaded from www.nrcresearchpress.com by 210.87.254.40 on 09/05/12
For personal use only.

Can. J. Chem. Downloaded from www.nrcresearchpress.com by 210.87.254.40 on 09/05/12
For personal use only.

SCHEME 1. Fractionation of chloroform extract of hot-water extractive of western red cedar heartwood (asterisk denotes development with benzene – ethanol – acetic acid (100:10:1 v/v/v) on silica gel).

Synthesis of Di-O-methyl Thujaplicatin Methyl Ether (III)

(±)-3-(3′,4′-Dimethoxybenzyl)-butyrolactone (3.1 g), prepared by the method of Rothe and Zimmer (7), b.p. 204–206 °C at 2 mm Hg, η_D^{20} 1.5416, was condensed with prepared 3,4,5-trimethoxybenzaldehyde (8, 9) (2.55 g), with sodium methoxide (0.73 g) in benzene (24 ml) as catalyst, in a stoppered bottle at room temperature for 6 days with occasional shaking according to the procedure of Zimmer *et al.* (10), except that the final neutral product was purified by p.l.c. with benzene – ethanol – acetic acid (100:10:1) (R_f 0.64), and crystallized from ethanol to yield (±)-2-(3″,4″,5″-trimethoxybenzylidene)-3-(3′,4′-dimethoxybenzyl)-butyrolactone (VI) (700 mg), m.p. 117–118 °C.

Anal. Calcd. for $C_{23}H_{26}O_7$: C, 66.67; H, 6.28; OCH_3, 37.44. Found: C, 66.71, 66.47; H, 6.30, 6.01; OCH_3, 37.20, 37.36.

Spectra: λ_{max} 314 mμ (log ε 4.26); ν_{max} 1 730 (lactone) and 1 635 (double bond) cm^{-1}.

This product, VI (200 mg), was hydrogenated in methanol (30 ml) with palladium chloride (100 mg) as catalyst. The catalyst was filtered off with Celite and washed with methanol. The filtrates were evaporated *in vacuo*, and the product was purified by p.l.c. with benzene – ether – acetic acid (70:30:1) (R_f 0.26) and crystallized from ether to yield (±)-*cis*-2-(3″,4″,5″-trimethoxybenzyl)-3-(3′,4′-dimethoxybenzyl)-butyrolactone (VII) (130 mg) (11, 12), m.p. 143–145 °C.

Anal. Calcd. for $C_{23}H_{28}O_7$: C, 66.34; H, 6.78; OCH_3, 37.26. Found: C, 66.18; H, 6.94; OCH_3, 37.11.

Spectra: λ_{max} 278 mμ (log ε 3.56); ν_{max} 1 752 (lactone, 1 763 in chloroform) cm^{-1}; n.m.r. 3.14–3.62 (3H-C2′,5′,6′, multiplet), 3.44 (2H-C2″,6″, singlet), 5.95 (2H-C4, doublet), 6.15 (15H-methoxyl, singlet), and 6.5–8.5 τ (6H, unresolved).

This *cis* lactone was dissolved in 4% methanolic potassium hydroxide (10 ml) and kept at room temperature for 4 days. After acidification with acetic acid and refluxing for 2 h to ensure lactonization, the solvent was removed by vacuum evaporation. The residue was dissolved in chloroform, washed with sodium carbonate and water, reclaimed by vacuum evaporation, purified by p.l.c. with benzene – ether – acetic acid (70:30:1) (R_f 0.24), and crystallized from ether to yield (±)-*trans*-2-(3″,4″,5″-trimethoxybenzyl)-3-(3′,4′-dimethoxybenzyl)-butyrolactone (III) (70 mg (64% yield)), m.p. (after drying at high vacuum (54 °C) to remove ether from crystals) 80.5–81.5 °C (several small crystals melted much higher at 102–103 °C (14))

Anal. Calcd. for $C_{23}H_{28}O_7$: C, 66.34; H, 6.78; OCH_3, 37.26. Found: C, 66.49; H, 6.97; OCH_3, 37.39.

The ultraviolet, infrared (KBr disk and $CHCl_3$), and n.m.r. spectra were identical with those of natural di-*O*-methyl thujaplicatin method ether (III).

Thujaplicatin (II)

Crude II (110 mg) from the extractive fractionation was chromatographed first on a cellulose column with dilute carbonic acid elution to remove contaminating materials which have a low R_f value in paper chromatography, and then by p.l.c. to yield amorphous II (50 mg). Repeated attempts at crystallization in a variety of solvents failed. Nitrobenzene oxidation of thujaplicatin (II) (6) yielded only vanillin (2.3%). Methylation as previously described produced a tri-*O*-methyl thujaplication in 78% yield, identical, as shown by mixed melting point, optical rotation, and infrared spectrum, with di-*O*-methyl thujaplicatin methyl ether (III).

Thujaplicatin (II) (180 mg) was refluxed in acetone (10 ml) containing anhydrous potassium carbonate with diethyl sulfate (0.4 ml) for 10 h, and purified by p.l.c. to yield amorphous tri-*O*-ethyl thujaplicatin (60 mg). Spectrum: ν_{max} no hydroxyl band, 1 756 (lactone) cm^{-1}. Alkaline permanganate oxidation was carried out as in previous work (2) to yield 3,4-diethoxy-5-methoxybenzoic and 4-ethoxy-3-methoxybenzoic acids, identified by mixed melting point and infrared spectral comparison with authentic samples (2).

ACKNOWLEDGMENT

We thank Dr. L. D. Hall, University of British Columbia, for helpful discussions concerning the nuclear magnetic resonance spectra.

REFERENCES

1. J. A. F. Gardner, G. M. Barton, and H. MacLean. Can. J. Chem. **37**, 1703 (1959).
2. J. A. F. Gardner, B. F. MacDonald, and H. MacLean. Can. J. Chem. **38**, 2387 (1960).
3. J. A. F. Gardner, E. P. Swan, S. A. Sutherland, and H. MacLean. Can. J. Chem. **44**, 52 (1966).
4. W. M. Hearon and W. S. MacGregor. Chem. Rev. **55**, 957 (1955).
5. K. Freudenberg and K. Weinges. Tetrahedron, **15**, 115 (1961).
6. J. M. Pepper and M. Siddiqueullah. Can. J. Chem. **39**, 390 (1961).
7. J. Rothe and H. Zimmer. J. Org. Chem. **24**, 586 (1959).
8. H. C. Brown and R. F. McFarlin. J. Am. Chem. Soc. **78**, 252 (1956).
9. I. A. Pearl and F. F. Darling. J. Org. Chem. **22**, 1266 (1957).
10. H. Zimmer, J. Rothe, and J. M. Holbert. J. Org. Chem. **25**, 1234 (1960).
11. A. W. Schrecker and J. L. Hartwell. J. Am. Chem. Soc. **76**, 4896 (1954).
12. R. D. Haworth and J. R. Atkinson. J. Chem. Soc. 797 (1938).
13. N. S. Bhacca and D. H. Williams. Applications of nuclear magnetic resonance spectroscopy in organic chemistry. Holden-Day, Inc., San Francisco. 1964. p. 50.
14. E. L. Eliel. Stereochemistry of the carbon compounds. McGraw-Hill Book Co., Inc., New York. 1962. p. 44.

Can. J. Chem. Downloaded from www.nrcresearchpress.com by 210.87.254.40 on 09/05/12
For personal use only.

Can. J. Chem. Downloaded from www.nrcresearchpress.com by 210.87.254.105 on 09/05/12
For personal use only.

HYDROGENOLYSIS BY LITHIUM ALUMINIUM HYDRIDE – ALUMINIUM CHLORIDE OF ETHER SOLUTIONS OF CAMPHOR ETHYLENE KETAL AND NORCAMPHOR ETHYLENE KETAL

W. W. Zajac, Jr.,[1] B. Rhee, and R. K. Brown
Department of Chemistry, University of Alberta, Edmonton, Alberta

Received March 3, 1966

ABSTRACT

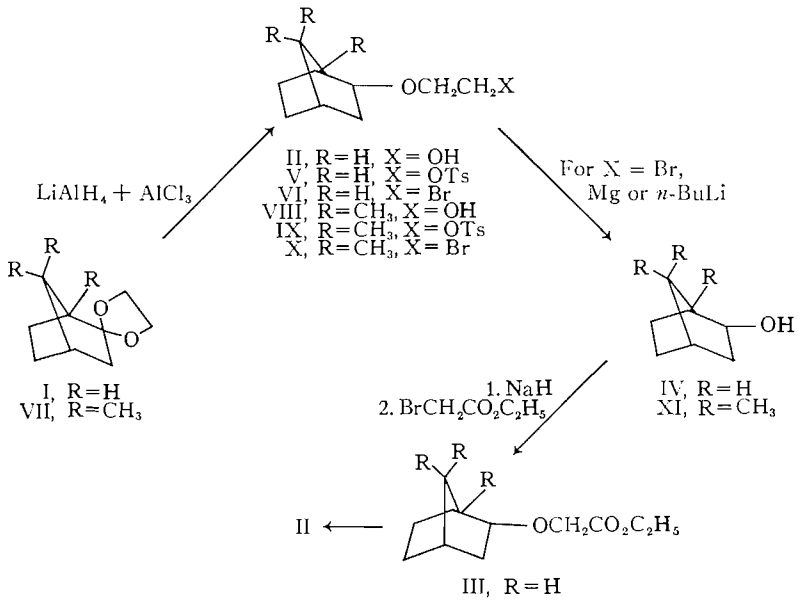
The lithium aluminium hydride – aluminium chloride reductive cleavage of norcamphor ethylene ketal yields 2-(2-*endo*-norbornyloxy)ethanol in ⩾98% yield, whereas the similar reduction of camphor ethylene ketal gives 2-(2-isobornyloxy)ethanol in 78% yield and 2-(2-bornyloxy)ethanol in 22% yield. These are the products arising from steric approach control.

INTRODUCTION

As part of an investigation of the hydrogenolysis of acetals and ketals (1–3), we have examined the reductive cleavage by lithium aluminium hydride – aluminium chloride of ether solutions of the ethylene ketals of norcamphor and camphor. This paper describes the results of this work.

RESULTS AND DISCUSSION

The hydrogenolysis of norcamphor ethylene ketal, I, by the mixed reagent $LiAlH_4$–$AlCl_3$ was carried out according to the published procedure (3). Of the two isomeric products (II*a* and II*b*, Reaction Scheme 1) which may result from this cleavage, the 2-(2-*endo*-norbornyloxy)ethanol, II*a*, was the exclusive product. This was proven by independent syntheses of both II*a* and II*b* as well as by degradation of the hydrogenolysis product, II, to 2-norborneol by a method which avoided isomerization of the 2-norborneol so formed.



Reaction Scheme 1. *a* = *endo* isomer and *b* = *exo* isomer in each case.

[1]*On sabbatical leave from Villanova University, Villanova, Pennsylvania, U.S.A.*

Can. J. Chem. Downloaded from www.nrcresearchpress.com by 210.87.254.105 on 09/05/12
For personal use only.

The synthesis of the two possible reduction products, II*a* and II*b*, was accomplished by lithium aluminium hydride reduction of the ethyl esters of 2-*endo*- and 2-*exo*-norbornyloxyacetic acid (III*a* and III*b*). The latter were prepared by reaction of the sodium salt of authentic 2-*endo*- and 2-*exo*-norborneol, IV*a* and IV*b*, with ethyl bromoacetate. Unfortunately, neither the isomeric esters III*a* and III*b* nor the hydroxyethers II*a* and II*b* could be separated by gas–liquid chromatography[2] using a variety of conditions and columns. However, the nuclear magnetic resonance spectra of the hydroxyethers II*a* and II*b* were sufficiently different to be clearly distinguishable. An examination of the nuclear magnetic resonance spectrum of the reduction product of the ketal I showed that most, if not all, of the hydrogenolysis product had the *endo* configuration II*a*. Compounds II*a* and II*b* show complex absorptions in the τ 8–9 region caused by the ring protons on carbons 3, 5, 6, and 7. The carbon 2 proton (*endo* or *exo*) absorbs in the τ 5.8–6.0 region but its identification is obscured by the absorption of the methylene protons (—OCH_2CH_2O—), which absorb in the same region. However, for the *endo* compound II*a*, the bridgehead protons on carbon 1 and carbon 4 give rise to *two* unresolved multiplets centered at τ 7.63 and τ 7.87 with half-widths of 8 c.p.s. and 11 c.p.s., respectively. The *exo* compound gives rise to only *one* unresolved multiplet centered at τ 7.83 with a half-width of 14 c.p.s.

To determine if a significant amount of the *exo* hydroxyether II*b* had actually been formed but been missed in the analytical method employed, the hydrogenolysis product II was degraded to the alcohol(s) IV, which are known to be separable quantitatively by gas–liquid chromatography (4–8). The key step in the degradation sequence was the elimination of the 2-norbornyloxy group from the bromoether VI with either magnesium (9) or *n*-butyllithium (10). That the degradation sequence of reactions truly reflects the proportion of *endo* isomer in the reduction product II was established by subjecting a synthetic mixture of known amounts of the *endo* and *exo* hydroxyethers II to the degradation reaction sequence. The proportion of *endo* and *exo* norborneols obtained agreed within $\pm 2\%$ of the proportion of *endo* and *exo* hydroxyethers in the synthetic starting mixture. The conditions of the degradation also exclude the possibility of a change in the configuration of the norborneol formed. Authentic *exo* or *endo* alcohol (IV) was found to remain unchanged under similar reaction conditions.

The product of the degradation of the material obtained by hydrogenolysis of the ketal I was shown by gas–liquid chromatography to consist of only one substance, identical in all respects with 2-*endo*-norborneol (IV*a*). Hence, the $LiAlH_4$–$AlCl_3$ reductive cleavage of the ketal I produces $\geqslant 98\%$ of the *endo* hydroxyether II*a*.

The hydrogenolysis of the ethylene ketal of camphor was carried out in the same manner as that for the norcamphor ketal. Degradation of the reduction product (VIII) was accomplished by the same reaction sequence as employed for II, i.e. VIII $\rightarrow$ IX $\rightarrow$ X $\rightarrow$ XI (Reaction Scheme 1). The borneol (XI*a*) and isoborneol (XI*b*) could also be analyzed quantitatively by gas–liquid chromatography (4, 5, 8, 11, 12). According to the results obtained from the degradation, the product of the reduction of the ethylene ketal of camphor is a mixture of $78 \pm 2\%$ of the hydroxyether with the *exo* configuration (VIII*b*) and $22 \pm 2\%$ of the hydroxyether with the *endo* configuration (VIII*a*).

The preceding results permit the conclusion that the hydride species enters from the least hindered side of the ketals I and VII. Since the hydroxyethers obtained from the $LiAlH_4$–$AlCl_3$ reductive cleavage of cyclic acetals and ketals are stable to our reaction conditions (1–3 and references therein), we are dealing with a case of steric approach

[2]*Although the individual, pure isomers II*a *and II*b *showed slightly different retention times (ca. 0.2 min) under some conditions, mixtures of the two isomers gave only one broad peak.*

control. The hydrogenolysis reactions studied in this investigation are analogous to the reduction of norcamphor and camphor to 2-norborneol (>90% *endo* isomer) and isoborneol (i.e. the *exo* isomer, >80%), respectively, with $LiAlH_4$ alone (5, 13, 14) or with $LiAlH_4$ in the presence of $AlCl_3$ (8) under kinetically controlled conditions, in that the course of reaction is governed by steric approach control (15).

This work presents a clear case in which steric factors are of predominant importance in controlling the approach of the *reducing species* during the hydrogenolysis of acetals and ketals (cf. refs. 16–18).

EXPERIMENTAL

All boiling points and melting points are uncorrected. Infrared spectra were obtained on a Perkin–Elmer model 421 spectrophotometer. Nuclear magnetic resonance spectra were obtained on a Varian Associates A-60 spectrometer with tetramethylsilane as an internal standard. In all cases the integrated nuclear magnetic resonance spectra were consistent with the assigned structures of the compounds. Gas chromatographic analysis was carried out on an Aerograph model A-700 instrument with a 20 ft by $\frac{1}{4}$ inch column packed with 25% Carbowax 20M on Gas Chrom P.

Norcamphor ethylene ketal was synthesized in 91% yield from norcamphor and ethylene glycol according to the method of Salmi (19), b.p. 78–80° at 14 mm, η_D^{25} 1.4319.

Anal. Calcd. for $C_9H_{14}O_2$: C, 70.09; H, 9.15. Found: C, 69.65; H, 8.52.

Camphor ethylene ketal was synthesized in 67% yield from camphor and ethylene glycol according to the method of Salmi (19), b.p. 64° at 1.5 mm, η_D^{25} 1.4770.

Anal. Calcd. for $C_{12}H_{20}O_2$: C, 73.43; H, 10.27. Found: C, 73.47; H, 10.08.

Ethyl (2-exo-norbornyloxy)acetate was synthesized in 50% yield from 2-*exo*-norborneol, sodium hydride, and ethyl bromoacetate in benzene according to the procedure of Leffler and Calkins (20), b.p. 77° at 1 mm, η_D^{25} 1.4162.

Anal. Calcd. for $C_{11}H_{18}O_3$: C, 66.64; H, 9.15. Found: C, 66.46; H, 9.04.

Ethyl (2-endo-norbornyloxy)acetate was synthesized in 53% yield from 2-*endo*-norborneol, sodium hydride, and ethyl bromoacetate in benzene according to the procedure of Leffler and Calkins (20), b.p. 80° at 1 mm, η_D^{25} 1.4160.

Anal. Calcd. for $C_{11}H_{18}O_3$: C, 66.64; H, 9.15. Found: C, 66.42; H, 8.93.

2-(2-exo-Norbornyloxy)ethanol was synthesized in 60% yield by the reduction of the *exo* ester with lithium aluminium hydride in ether (21), b.p. 71° at 1 mm, η_D^{25} 1.4812.

Anal. Calcd. for $C_9H_{16}O_2$: C, 69.19; H, 10.13. Found: C, 68.55; H, 10.08.

2-(2-endo-Norbornyloxy)ethanol was synthesized in 67% yield by the reduction of the *endo* ester with lithium aluminium hydride in ether (21), b.p. 72° at 1 mm, η_D^{25} 1.4815.

Anal. Calcd. for $C_9H_{16}O_2$: C, 69.19; H, 10.13. Found: C, 69.17; H, 10.26.

This compound is identical with the hydrogenolysis product of norcamphor ethylene ketal.

Hydrogenolysis of Norcamphor Ethylene Ketal

This was carried out with lithium aluminium hydride and aluminium chloride in ether according to the method of Leggetter and Brown (1). The product was obtained in 95% yield. The tosylate of the reduction product was synthesized in 95% yield from *p*-toluenesulfonyl chloride in pyridine according to the method of Wiberg and Lowry (22), m.p. 49–51°.

Anal. Calcd. for $C_{16}H_{22}O_4S$: C, 61.91; H, 7.13. Found: C, 61.75; H, 7.06.

The *p*-toluenesulfonate was converted into the bromide with lithium bromide in acetone according to the method of Wiberg and Lowry (22). The bromide was used without further purification (98% purity by gas–liquid chromatography).

Degradation of Norcamphor Ethylene Ketal Reduction Product

(a) Grignard Method

The bromide (9.0 mmoles) in 100 ml of ether was added dropwise to a mixture of ether and magnesium turnings (9.0 mmoles). The reaction mixture was heated under reflux for 20 h. The mixture was cooled in an ice bath, and 30 ml of 2% ammonium chloride solution was added dropwise. The ether layer was removed and combined with the ether extracts of the aqueous phase. The dried ($MgSO_4$) ether solution was concentrated, whereupon the residue solidified. The residue was dissolved in a small quantity of chloroform and analyzed by gas–liquid chromatography, at a column temperature of 130° and a helium flow rate of 190 ml/min. The retention time of the product 2-*endo*-norborneol was 24.4 min. 2-*exo*-Norborneol had a retention time of 22.6 min under identical conditions. The only other product present in the reaction mixture was unreacted starting material, to the extent of 37%.

(b) n-Butyllithium Method

In a nitrogen atmosphere, 5 ml of a solution of 15% *n*-butyllithium in hexane was added dropwise to a stirred solution of 8.2 mmoles of the bromide in 50 ml of ether. The solution was stirred overnight, and 30 ml

Can. J. Chem. Downloaded from www.nrcresearchpress.com by 210.87.254.105 on 09/05/12
For personal use only.

of ice water was added cautiously. The ether layer was separated and combined with the ether extracts of the aqueous phase. The dried ($MgSO_4$) ether solution was concentrated, whereupon the residue solidified. The residue was dissolved in a small quantity of chloroform and analyzed by gas–liquid chromatography as described above. The major product was 2-*endo*-norborneol. Unreacted starting material was present to the extent of 13%.

Hydrogenolysis of Camphor Ethylene Ketal

This was carried out with lithium aluminium hydride and aluminium chloride in ether according to the procedure of Leggetter and Brown (1). The product was obtained in 93% yield, b.p. 75–77° at 1.5 mm.

Anal. Calcd. for $C_{12}H_{22}O_2$: C, 72.68; H, 11.18. Found: C, 73.20; H, 11.00.

The tosylate of the reduction product was prepared according to the method of Wiberg and Lowry (22) in 98% yield. This was converted into the bromide (yield 95%) according to published directions (22). The bromide was treated with *n*-butyllithium according to the procedure described above for the degradation of the norcamphor ethylene ketal reduction product. The reaction mixture was subjected to gas–liquid chromatographic analysis, at a column temperature of 150° and a helium flow rate of 90 ml/min. The retention time of isoborneol was 32.6 min, and of borneol 36.2 min. The product consisted of 78% isoborneol and 22% borneol. Unreacted starting material was present to the extent of 11%.

REFERENCES

1. B. E. Leggetter and R. K. Brown. Can. J. Chem. **41**, 2671 (1963).
2. B. E. Leggetter and R. K. Brown. Can. J. Chem. **42**, 990 (1964).
3. B. E. Leggetter and R. K. Brown. Can. J. Chem. **43**, 1030 (1965).
4. R. R. Sauers and G. T. Kwiatkowski. J. Org. Chem. **27**, 4049 (1962).
5. G. F. Wilcox, M. Sexton, and M. F. Wilcox. J. Org. Chem. **28**, 1079 (1963).
6. C. M. DePuy and P. R. Storey. Tetrahedron Letters, **1**, 20 (1959).
7. W. M. Jones. J. Org. Chem. **26**, 3606 (1961).
8. E. L. Eliel and D. Nasipuri. J. Org. Chem. **30**, 3809 (1965).
9. L. C. Swallen and C. E. Boord. J. Am. Chem. Soc. **52**, 651 (1930).
10. G. Wittig and G. Harborth. Ber. **77B**, 306 (1944).
11. W. Huckel and O. Fechtig. Ann. **652**, 81 (1962).
12. G. Valkanas and N. Iconomou. Helv. Chim. Acta, **46**, 1089 (1963).
13. P. Hirsjarvi. Ann. Acad. Sci. Fennicae, Ser. A II, **81**, 16 (1957); Chem. Abstr. **52**, 11091 (1958).
14. R. Howe, E. C. Friedrick, and S. Winstein. J. Am. Chem. Soc. **87**, 379 (1965).
15. W. G. Dauben, G. J. Fonken, and D. S. Noyce. J. Am. Chem. Soc. **78**, 2579 (1956).
16. E. L. Eliel, V. G. Badding, and M. N. Rerick. J. Am. Chem. Soc. **84**, 2371 (1962).
17. B. E. Leggetter and R. K. Brown. Can. J. Chem. **42**, 1005 (1963).
18. E. L. Eliel, B. E. Novak, R. A. Daignault, and V. G. Badding. J. Org. Chem. **30**, 2441 (1965).
19. E. J. Salmi. Ber. **71**, 1803 (1938).
20. M. T. Leffler and A. E. Calkins. *In* Organic syntheses. Collective Vol. III. John Wiley & Sons, Inc., New York. 1955. p. 544.
21. R. F. Nystrom and W. G. Brown. J. Am. Chem. Soc. **69**, 1197 (1947).
22. K. B. Wiberg and B. R. Lowry. J. Am. Chem. Soc. **85**, 3188 (1963).

Can. J. Chem. Downloaded from www.nrcresearchpress.com by 210.87.254.105 on 09/05/12
For personal use only.

Can. J. Chem. Downloaded from www.nrcresearchpress.com by 210.87.254.5 on 09/05/12
For personal use only.

THE SYNTHESIS OF SOME IODOPHTHALAZINES AND PHTHALAZINECARBONITRILES

ARTHUR HIRSCH AND DEMETRIUS G. ORPHANOS
Canadian Technical Tape Ltd., Montreal, Quebec
Received February 21, 1966

ABSTRACT

1-Iodo- and 1,4-diiodo-phthalazines were obtained by treating the corresponding chloro compounds with a solution of sodium (or potassium) iodide in acetone containing hydrogen iodide. These iodophthalazines, on reaction with copper cyanide in pyridine, gave the relevant phthalazinecarbonitriles.

INTRODUCTION

The preparation of 1,4-diiodophthalazine (VI) has not been described in the literature. It was reported that 1-iodophthalazine (II) can be obtained, in unspecified yield, from the corresponding chloro compound I by the action of boiling hydriodic acid, either alone or in the presence of red phosphorus. However, in our hands, these procedures gave unsatisfactory results.

Attempts to prepare the iodophthalazines II and VI by (*a*) treating the corresponding phthalazinones with phosphorus triiodide or (*b*) the action of sodium (or potassium) iodide on the relevant chloro compounds in acetone were not successful. However, halogen exchange occurred readily when a significant quantity of hydrogen iodide was present in the latter reaction mixture. Attempts to effect the same reaction by merely using a solution of hydrogen iodide in acetone proved to be fruitless.

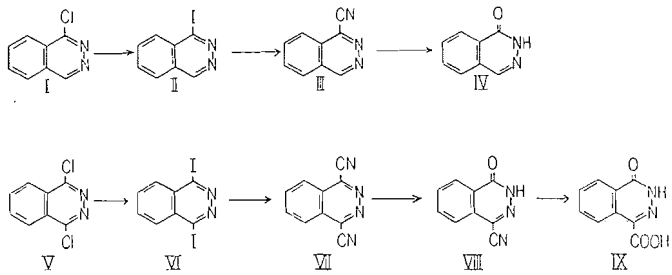
A survey of the literature reveals no previous preparation of phthalazinecarbonitriles. Earlier attempts[1] to obtain these substances from the chloro- or bromo-phthalazines via the halogen–nitrile exchange method were unsuccessful.

It has now been possible to prepare 1-phthalazinecarbonitrile (III) and 1,4-phthalazinedicarbonitrile (VII) by heating the corresponding iodo compounds with copper cyanide in pyridine for a few minutes.

The infrared spectrum of III showed a very weak nitrile absorption at 2 240 cm^{-1}, whereas such an absorption was not present in the infrared spectrum of VII. It has been shown that this band is not always evident in the infrared spectra of a variety of nitrogen heterocyclic compounds (2, 3) or in aromatic nitriles with ortho and para electron-withdrawing groups (4).

Anomalous results were obtained on the attempted hydrolysis of the nitriles III and VII. When III was refluxed in 10% sodium hydroxide solution, ammonia was constantly evolved for 5 h. This observation suggested that normal hydrolysis of III to the corresponding 1-phthalazinecarboxylic acid was taking place. However, all attempts to isolate the suspected carboxylic acid were unsuccessful and no evidence for its presence could be found. In all cases, 1(2*H*)-phthalazinone (IV) and a viscous unidentifiable oily material were isolated. Since it was found that IV is quite stable under similar alkaline reaction conditions, it appears to be more likely that the 1-phthalazinecarboxylic acid decomposes as fast as it forms, thereby giving rise to oily products.

[1]*In those attempts a wide variation of solvents (pyridine, quinoline, all three picolines, dimethylformamide, dimethyl sulfoxide, and glycol) and cyanidation agents (potassium cyanide, sodium cyanide, silver cyanide, and copper cyanide) were used to no avail.*



On the other hand, alkaline treatment of the dicarbonitrile VII, at room temperature for 15 min, resulted in a quantitative yield of 4-cyano-1(2*H*)-phthalazinone (VIII). The resulting cyanophthalazinone, on further alkaline treatment, under heating, was quantitatively hydrolyzed to the corresponding 1(2*H*)-phthalazinone-4-carboxylic acid (IX), which had previously been prepared by a direct route (5–8). The cyanophthalazinone VIII, aside from its conversion into the known IX, was also confirmed by elemental analysis and its infrared spectrum (absorption at 2 240 cm^{-1}).

The enhanced susceptibility of a cyano group to displacement by nucleophiles has been described in many instances (9–11), and the conversion of III and VII into IV and VIII, respectively, should not be altogether unexpected.

The rapid displacement of the 1- (or 4-) cyano group in 1,4-phthalazinedicarbonitrile (VII) is explicable only by assuming that the intermediate in this nucleophilic aromatic substitution would derive stabilization from the electron-withdrawing benzene ring and the 4- (or 1-) cyano group, in addition to stabilization attributable to the azine group.

Carbonitriles III and VII, on treatment with concentrated sulfuric acid or 36% hydrochloric acid at 25° for 24 h, remained unaffected. Extensive decomposition of the starting material occurred after 2 h if temperatures of over 60 °C were applied.

For identification purposes, the infrared spectra of II and VI are presented in Figs. 1 and 2, respectively.

EXPERIMENTAL

Melting points are uncorrected. Analyses were carried out by Dr. C. Daessle, Montreal, Quebec. Infrared absorption spectra were determined with a Perkin–Elmer model 337 spectrophotometer from Nujol mulls.

1,4-Dichlorophthalazine (V)

The procedure described previously by this laboratory was slightly modified (12). 2,3-Dihydro-1,4-phthalazinedione (16.2 g, 0.1 mole) and phosphorus pentachloride (85 g) were thoroughly mixed in an ordinary 6 fl. oz carbonated beverage bottle equipped with a magnetic stirring bar. The bottle was sealed with the appropriate metallic cap and placed in a cool oil bath. The temperature of the bath[2] was gradually brought up to about 180°. At this temperature the solid reaction mixture was slowly liquefied, and as soon as agitation became effective, the temperature of the oil bath was lowered to 140–150° and maintained there for 4 h. After the reaction bottle was cooled to room temperature,[3] it was refrigerated for a few hours and then carefully opened in a hood. The product was isolated as described in the original procedure (12). The yield and melting point were the same.

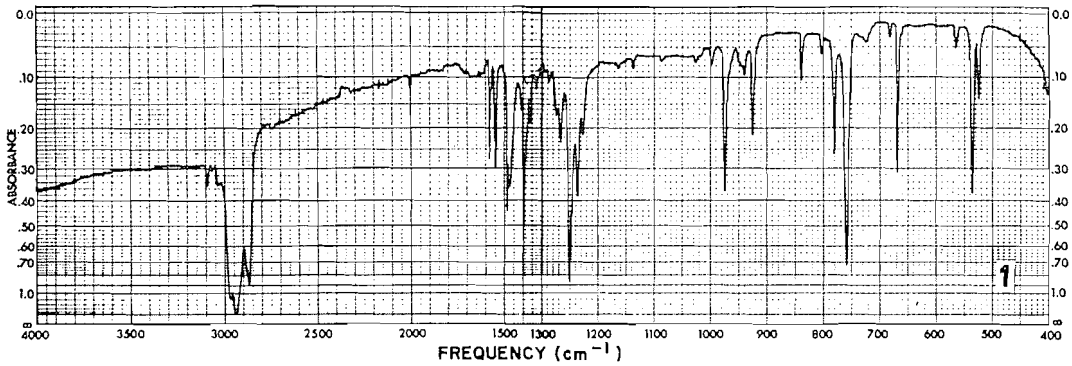
1-Iodophthalazine (II)

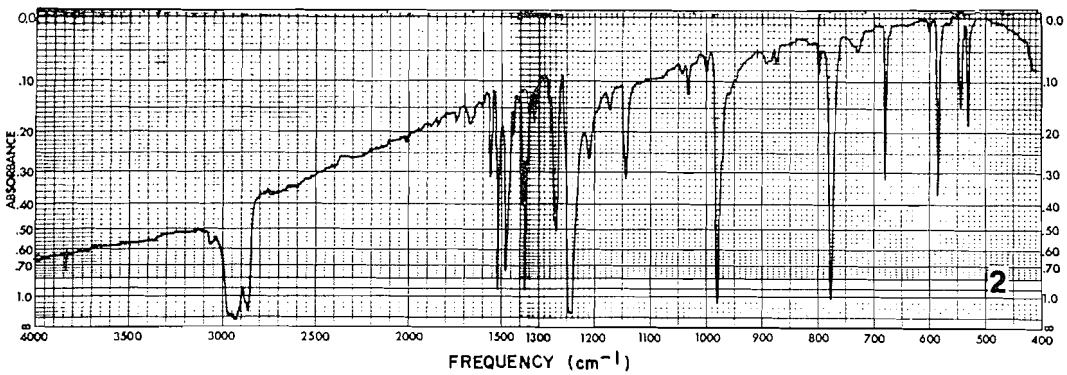
To a stirred mixture of potassium or sodium iodide (30 g), 1-chlorophthalazine (16.5 g) (13), and acetone (300 ml), a 50% aqueous solution of hydroiodic acid (20 ml) was added. The resulting yellow mixture was stirred at room temperature for 18 h. The canary-yellow precipitate was obtained by filtration, washed with diethyl ether, and dried *in vacuo*. This acidic product was apparently the hydroiodide salt. It was dissolved in ice-cold water (1 l), stirred for 15 min, and then neutralized carefully with dilute ammonium hydroxide. The faint-yellowish solid was collected, washed with cold water followed by petroleum ether,

[2]*The temperature of the oil bath should not be permitted to rise over 190° because of the explosion hazard. In any event, it should be recognized that any sealed glass vessel of this type constitutes a potential bomb and must be handled with extreme caution.*

[3]*The reaction bottle is removed from the oil bath when the latter has reached room temperature.*

Can. J. Chem. Downloaded from www.nrcresearchpress.com by 210.87.254.5 on 09/05/12
For personal use only.





FIGS. 1 and 2.

and dried *in vacuo*. It weighed 22.5 g (88%) and melted at 78° with decomposition (reported (1) m.p. 78°) 1-Iodophthalazine undergoes slow decomposition at room temperature to an amorphous yellow powder. This decomposition can be retarded by storing the substance in a freezer.

1,4-Diiodophthalazine (VI)

To a stirred mixture of potassium or sodium iodide (25 g), 1,4-dichlorophthalazine (9.95 g, 0.05 mole), and acetone (300 ml), a 50% aqueous solution of hydroiodic acid (20 ml) was added. The resulting yellow mixture was stirred at room temperature for 18 h. The canary-yellow solid was collected, washed with a little acetone followed by diethyl ether, and dried *in vacuo*. This acidic product was apparently the hydroiodide salt. It was dissolved in distilled water (2 l) and stirred until the initial yellow color of the solid had been discharged (about 1 h). The white solid was collected, washed with distilled water until the washing was no longer acidic, and dried *in vacuo*.

It melted at 156–157° with decomposition and was pure enough to be used for the next step, yield 14.5 g (76%). 1,4-Diiodophthalazine was crystallized from methylene chloride as hard white prisms melting at 161° with decomposition.

Anal. Calcd. for $C_8H_4I_2N_2$: C, 25.16; H, 1.05; N, 7.33; I, 66.45. Found: C, 25.35; H, 0.98; N, 7.53; I, 66.61.

1-Phthalazinecarbonitrile (III)

1-Iodophthalazine (12.8 g, 0.05 mole) was thoroughly mixed with copper cyanide (4.48 g, 0.05 mole). To this mixture was added dry pyridine (75 ml), and the resulting greenish suspension was placed in a preheated (110–120°) oil bath and kept there for 10 min under vigorous stirring. The black-colored reaction mixture was poured into chilled water (500 ml) and stirred for a few minutes.

Diethyl ether (500 ml) and some ice were added to lower the temperature to about 5–10°. To this chilled mixture, with vigorous stirring, dilute hydrochloric acid was added slowly until a pH of 2 was attained. Stirring was continued for an additional 20 min. (The aqueous layer must be maintained at all times at a pH of 2.)

The clear yellowish ether layer was separated and the aqueous layer extracted twice with 300 ml of diethyl ether each. The combined ether extracts were washed with water until neutral, dried over $MgSO_4$, shaken

Can. J. Chem. Downloaded from www.nrcresearchpress.com by 210.87.254.5 on 09/05/12
For personal use only.

with charcoal, and filtered. The colorless filtrate, upon removal of the solvent under reduced pressure, left a white crystalline product melting at 148–149° and weighing 1.35 g (17.3%).

1-Phthalazinecarbonitrile was recrystallized from diethyl ether as fine white needles melting at 156–157°. The infrared spectrum showed a very weak, but sharp absorption at 2 240 cm^{-1} (C≡N).

Anal. Calcd. for $C_9H_5N_3$: C, 69.67; H, 3.25; N, 27.08. Found: C, 69.94; H, 3.43; N, 27.03.

1,4-Phthalazinedicarbonitrile (VII)

This substance was prepared by a procedure similar to that applied above for the preparation of 1-phthalazinecarbonitrile. Thus, from the reaction of 1,4-diiodophthalazine (19.1 g, 0.05 mole) and copper cyanide (9 g, 0.1 mole) in pyridine (80 ml) was obtained 3.2 g of 1,4-phthalazinedicarbonitrile. It melted at 201–204°, and recrystallization from diethyl ether gave yellowish shiny crystals melting at 204–205°. The infrared spectrum showed no evidence of the C≡N stretching frequency.

Anal. Calcd. for $C_{10}H_4N_4$: C, 66.66; H, 2.23; N, 31.10. Found: C, 66.87; H, 2.32; N, 31.39.

4-Cyano-1(2H)-phthalazinone (VIII)

To a solution of 1,4-phthalazinedicarbonitrile (1.8 g) in dioxane (5 ml), 10 ml of a 20% sodium hydroxide solution was added. The resulting orange-colored solution was stirred for 15 min at room temperature. The yellow suspension was dissolved in 80 ml of water. The clear yellow solution was extracted with diethyl ether to remove ether-soluble impurities. The alkaline layer was weakly acidified with dilute hydrochloric acid. The yellowish precipitate was collected on filter paper, washed with water, and dried. It melted at 269–270° and weighed 1.49 g. This material was dissolved in tetrahydrofuran, shaken with charcoal, and filtered. Removal of the solvent under reduced pressure left a white solid melting at 270°. The infrared spectrum showed characteristic bands at 3 175, 3 100, 2 240, 1 715, and 1 645 cm^{-1}.

Anal. Calcd. for $C_9H_5N_3O$: C, 63.16; H, 2.95; N, 24.55. Found: C, 63.46; H, 3.21; N, 24.46.

1(2H)-Phthalazinone-4-carboxylic Acid (IX) from 4-Cyano-1(2H)-phthalazinone (VIII)

A mixture of 4-cyano-1(2*H*)-phthalazinone (0.5 g), 4% sodium hydroxide solution (8 ml), and methanol (25 ml) was refluxed until evolution of ammonia ceased (tested with wet red litmus paper) (about 7 days). The yellowish solution was filtered and the filtrate concentrated to about 10 ml under reduced pressure. The remaining alkaline solution was cautiously acidified with dilute hydrochloric acid, and the precipitated white solid was collected, washed with diethyl ether, and dried. It melted at 234° with foaming, and weighed 0.51 g. 1(2*H*)-Phthalazinone-4-carboxylic acid was recrystallized from a mixture of methanol and dioxane (3:1) as hard white crystals melting at 236° with foaming (reported (5) m.p. 232°).

Alternatively, the substance can be prepared directly from 1,4-phthalazinedicarbonitrile under conditions identical with those described above. The time for the hydrolysis can be reduced to a few hours if a more concentrated sodium hydroxide solution is used and no methanol is present. In the latter case, the yield of pure product is much lower and its purification is achieved with difficulty. The infrared spectrum displayed characteristic absorptions at 3 250, 3 170, 1 680, and 1 640 cm^{-1}.

Anal. Calcd. for $C_9H_6O_3N_2$: C, 56.84; H, 3.18; N, 14.73. Found: C, 56.92; H, 3.01; N, 14.76.

1(2H)-Phthalazinone (IV) from 1-Phthalazinecarbonitrile (III)

1-Phthalazinecarbonitrile (0.2 g) in 10% sodium hydroxide solution (25 ml) was refluxed for 5 h. During this time ammonia was constantly evolved. The alkaline reaction solution was weakly acidified with dilute hydrochloric acid and then extracted with methylene chloride. The extract was dried over $MgSO_4$, decolorized with charcoal, and filtered. The colorless filtrate, upon removal of the solvent, left a semisolid material which, on trituration with a few milliliters of diethyl ether, separated out as a white crystalline material melting at 184–185°, yield 0.052 g. Its infrared spectrum was identical with that displayed by an authentic sample of 1(2*H*)-phthalazinone, and a mixed melting point with the latter compound showed no depression.

ACKNOWLEDGMENT

We thank the National Research Council of Canada for financial support of this work, under the Industrial Research Grant Programme.

REFERENCES

1. S. GABRIEL. Ber. **36**, 3373 (1903).
2. E. TAYLOR and C. JEFFORD. J. Am. Chem. Soc. **84**, 3744 (1962).
3. T. SCHWAN and H. TIECKELMAN. J. Heterocyclic Chem. 1, 201 (1964).
4. P. SENSI and G. GALLO. Gazz. Chim. Ital. **85**, 224 (1955).
5. A. DARAPSKY and P. HEINRICHS. J. Prakt. Chem. **146**, 307 (1936).
6. K. FRANKEL. Ber. **33**, 2808 (1900).
7. R. VON ROTHENBURG. J. Prakt. Chem. **51**, 140 (1895).
8. K. ADACHI. J. Pharm. Soc. Japan, **75**, 1423 (1955); Chem. Abstr. **50**, 10105 (1956).
9. T. SCHWAN and H. TIECKELMAN. J. Heterocyclic Chem. **2**, 202 (1965).
10. G. DAVES, D. O'BRIEN, L. LEWIS, and C. CHENG. J. Heterocyclic Chem. **1**, 130 (1964).
11. H. YAMANAKA. Chem. Pharm. Bull. Tokyo, **7**, 508 (1959); Chem. Abstr. **54**, 18537 (1960).
12. A. HIRSCH and D. ORPHANOS. Can. J. Chem. **43**, 2708 (1964).
13. V. BRASYUNAS and A. PODZHYUNAS. Med. Prom. SSSR, **13**, 38 (1950); Chem. Abstr. **53**, 16144 (1959).

Can. J. Chem. Downloaded from www.nrcresearchpress.com by 210.87.254.5 on 09/05/12
For personal use only.

THE PHOTOINITIATED HALOGENATION REACTIONS OF N-BROMOACETANILIDE AND N-BROMO-2,4,6-TRICHLOROACETANILIDE[1]

DENNIS D. TANNER AND EUGENE PROTZ
Department of Chemistry, University of Alberta, Edmonton, Alberta
Received June 30, 1965

ABSTRACT

The photoinduced rearrangement reaction of N-bromoacetanilide to *p*-bromoacetanilide in carbon tetrachloride was found to have a quantum efficiency approaching unity, and evidence is presented to indicate a chain component to the reaction process whose product-determining species is either the mesomeric acetanilide radical or the bromine atom. It was demonstrated that small variations in the solvent composition affected the product ratio of *p*- to *o*-bromoacetanilide. The reaction of N-bromoacetanilide in carbon tetrachloride with added toluene was found to be a long-chain process producing *p*-bromoacetanilide as well as acetanilide and benzyl bromide. The bromination of toluene by N-bromo-2,4,6-trichloroacetanilide was shown to proceed by a chain mechanism involving the bromine radical as the chain-propagating species, and this mechanism is used as a model to explain the reaction of N-bromoacetanilide in dilute carbon tetrachloride solutions of toluene.

INTRODUCTION

Because of the current interest in hydrogen abstraction reactions of divalent nitrogen (1–3), an investigation of the photoinitiated reactions of N-bromoacetanilide and N-bromo-2,4,6-trichloroacetanilide has been undertaken.

The ionic counterpart of the photoinitiated rearrangement of N-haloacetanilide to *p*-haloacetanilide, the Orton rearrangement, has been studied extensively by numerous groups of workers[2] (5–7), and has long been established to proceed, both in protic and aprotic solvents, by an acid-catalyzed intermolecular mechanism.

The photoinitiated rearrangement of N-chloroacetanilide has been studied by Blanksma (8), Mathews and Williamson (9), Chattaway and Orton (10), and Hodges (11). These workers have established that in aprotic solvents the reaction is accelerated by light, and that in the solvents cyclohexane, toluene, and decalin the main product of the reaction is not *p*-chloroacetanilide, but acetanilide itself. In the reactions which produced acetanilide, it was assumed that the higher boiling liquid fractions from the reaction mixtures were chlorinated solvents. Hodges has shown the rearrangement of N-chloroacetanilide to have a quantum efficiency of 5 in carbon tetrachloride, and that, in that solvent, traces of diacetylhydrazobenzene could be isolated.

The presence of nitrogen radical coupling products in the photolysis of N-chloroacetanilide suggested to us the possibility of nitrogen radical abstraction in the reaction of N-haloacetanilide with solvent.

To provide an adequate mechanistic explanation for the above results, and because of our interest (1) in hydrogen abstraction reactions, the present study was undertaken.

DISCUSSION AND RESULTS

We have found that carbon tetrachloride solutions of N-bromoacetanilide at 80° undergo a light-catalyzed reaction to produce as the major product *p*-bromoacetanilide. The solutions remain unchanged under these conditions in the absence of light for well over three half-lives of the light-catalyzed reaction.

[1]*This work was presented at the 48th national meeting of the Chemical Institute of Canada, Organic Chemistry Section, June 1965.*
[2]*For a summary up to 1951, see ref. 4.*

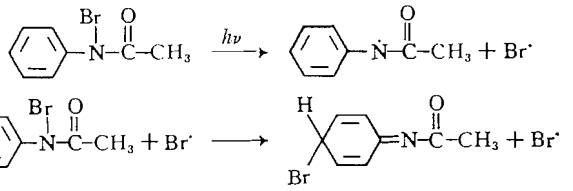
Can. J. Chem. Downloaded from www.nrcresearchpress.com by 210.87.254.40 on 09/05/12
For personal use only.

Can. J. Chem. Downloaded from www.nrcresearchpress.com by 210.87.254.40 on 09/05/12
For personal use only.

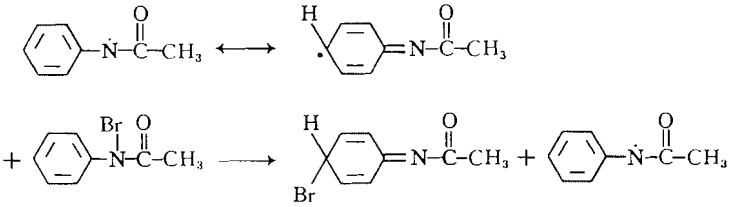
Three distinct light-catalyzed, free-radical mechanisms seem to be plausible for the N to C rearrangement of N-bromoacetanilide.

Mechanisms 1 and 2 are chain reactions for which the chain-propagation steps are shown. Mechanism 1 is a unique 1,5-displacement of a bromine atom by a bromine radical, whereas in mechanism 2 the chain-propagating species is the mesomeric carbon–nitrogen radical. Mechanism 3 depicts a reaction path which proceeds by a non-chain process to yield products by geminate cage recombination.

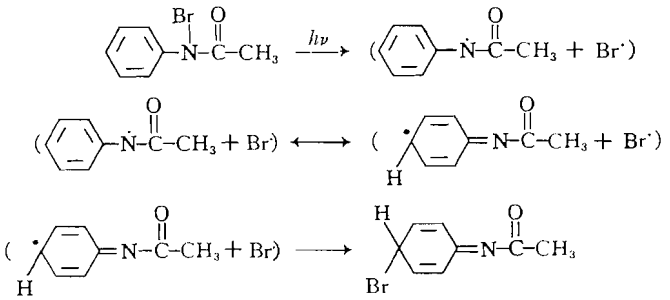
1.



2.

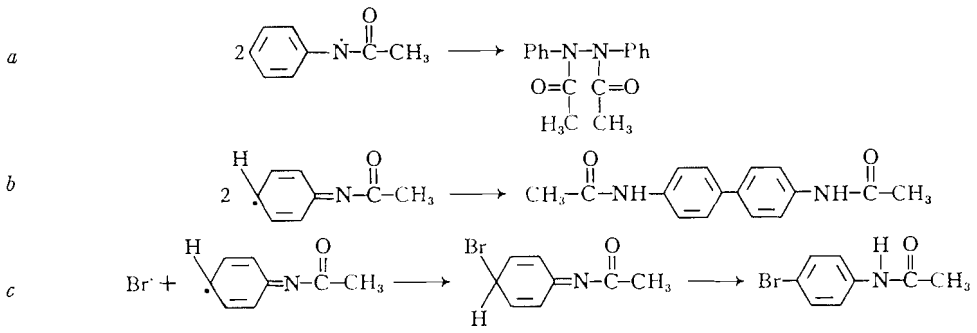


3.



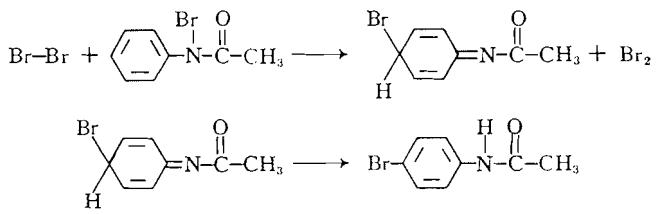
Trace initiation experiments with benzoyl peroxide and azobisisobutyronitrile, and inhibition experiments with oxygen, gave inconclusive results about the chain or non-chain nature of the radical reaction, but the failure of these experiments established that the rearrangement reaction was not a long-chain process. Investigation of the quantum efficiencies for the disappearance of N-bromoacetanilide showed ($\Phi = 1.1 \pm 0.2$) the reaction to be a very short chain process indeed. The photolysis has a chain length which approaches unity, indicating a chain component to the mechanism since cage reactions of such high quantum efficiency are not very probable (12).

The products of the photoinduced decomposition of N-bromoacetanilide in carbon tetrachloride were *p*-bromoacetanilide, 78%; *o*-bromoacetanilide, 7%; acetanilide, ~5%; N,N′-diacetyl-4,4′-diaminobiphenyl, 3%; possibly diacetylhydrazobenzene; and traces of products resulting from dibromination. Since the chain length is so short, the formation of coupling products (reactions *a–c*) is feasible for all three of the proposed pathways, and could arise from the fate of the initiation products in mechanisms 1 and 2 or by escape from the solvent cage with subsequent recombination as in mechanism 3.



Further evidence against cage recombination was obtained from the observation that small amounts of added toluene (5–15%) can change the mechanism to a relatively longer chain process which is capable of trace initiation by benzoyl peroxide and in which the ortho to para ratio of bromoacetanilides is different from that when the reaction is run in 100% carbon tetrachloride. That the rearrangement is also involved in this chain reaction is evident from the observation that less than 9 mole % (per mole of N-bromoacetanilide) of the toluene reacted, and that the major product (>70%) was *p*-bromoacetanilide. Such marked effects are not likely to be observed if the reaction proceeded primarily by cage recombination.

The possibility existed that after preliminary initiation a subsequent ionic reaction took place as shown below, which would be indistinguishable from a free-radical chain.



When the photoinitiated reaction, both with and without added toluene, was stopped after approximately 15% completion by placing the reaction in the dark, the titer for the active bromine was found to remain constant for more than three half-lives of the rearrangement reaction. It therefore seems unlikely that, under our conditions, ionic reactions could determine a significant part of the reaction course.

We have shown bromine to be the chain-carrying species in the reaction of N-bromo-2,4,6-trichloroacetanilide (I) with toluene (see the next section). If this chain process is a suitable model for the reaction of N-bromoacetanilide with solvent, then the rearrangement of N-bromoacetanilide with added toluene, a process capable of trace initiation, can be assumed to be a rearrangement carried out in the presence of a low steady-state concentration of bromine. When the photorearrangement was carried out in a mixture of 15% toluene in carbon tetrachloride, the ortho to para ratio of bromoacetanilides decreased by 11% in comparison with the ortho to para ratio for the rearrangement carried out in pure carbon tetrachloride. In the reaction with added toluene, the product mixture contained, in addition to the normal products (>70% *p*-bromoacetanilide), acetanilide and benzyl bromide. An accompanying decrease in the amount of toluene that was originally added was observed (5–8 mole % per mole of N-bromoacetanilide). A change in the

Can. J. Chem. Downloaded from www.nrcresearchpress.com by 210.87.254.40 on 09/05/12
For personal use only.

ortho to para ratio when the reaction is run under conditions where a steady-state concentration of bromine is present, i.e. with added toluene, can be interpreted as being due to a change in the mechanism for the formation of ortho- and para-brominated acetanilide.[1] Since bromine or acetanilide radicals are the product-determining species in the rearrangement, and the ortho to para ratio is concentration independent, a change in this ratio is equivalent to a change in the product-determining species. An alternative explanation for the change in the product ratio entails the formation of solvated radicals whose positional selectivity differs from the uncomplexed species. An investigation of the medium effects during the rearrangement reaction clearly substantiates this latter explanation. Photolysis of N-bromoacetanilide in carbon tetrachloride solutions containing chemically unreactive aromatic substrates had marked effects on the product ratio of *o*- to *p*-bromoacetanilide (Table I). The decrease in the amount of *o*-bromoacetanilide compared with the para-brominated isomer is consistent with complex formation between radicals and aromatic solvents (13–15). Steric considerations would predict a decrease in the ortho to para ratio by a bulkier, complexed, product-determining radical whether it were the acetanilide or the bromine radical. Although the structure of this complex cannot be defined, it is, at least in the case of the nitrobenzene–radical complex, most likely to involve the acetanilide radical, since complex formation between nitrobenzene and bromine radicals would not be favored (15).

TABLE I

Solvent effects on the product ratio of *o*- to *p*-bromoacetanilide

Solvent	% difference in ortho to para ratio‡	Number of experiments
100% CCl_4	0.0	4 to 12*
15% benzene in CCl_4	5±2	4
5% nitrobenzene in CCl_4	7±5	3
15% toluene in CCl_4	11±4	12
15% chlorobenzene in CCl_4	13±3	4
10% nitrobenzene in CCl_4	18±8	3
15% nitrobenzene in CCl_4	42±5 (43±5)†	6

*Standard experiments were run with each batch of N-bromoacetanilide used, because the purity of the reagent varied from 94 to 100%.
†Batches of differing purity gave different absolute numbers but the same percentage differences.
‡Experimental errors refer to standard deviations from average values.

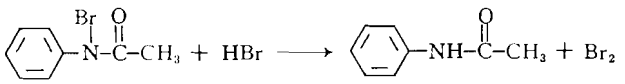
The reaction with added toluene was found to be initiated by trace amounts of azobisisobutyronitrile or benzoyl peroxide as well as by light. Trace initiation indicated the involvement of a long-chain process. The propagation reactions most readily envisaged for the reaction with solvent are those involving bromine atom abstraction, 4, or hydrogen abstraction by the mesomeric acetanilide radical, 5.

To differentiate between mechanisms 4 and 5, measurements of the relative reactivities towards hydrogen abstraction from a number of meta- and para-substituted toluenes were attempted. Recently, relative reactivity data for bromine atom abstraction from substituted toluenes has become available where both bromine and N-bromosuccinimide were the sources of bromine atoms (16, 17, 19), and a comparison with values for the abstraction reaction of N-bromoacetanilide with these substrates was undertaken. Under the desired reaction conditions, 0.3 *M* in toluene and 0.2 *M* in brominating agent, it was found that less than 10% of the reaction proceeded by hydrogen abstraction from toluene. To eliminate the rearrangement process and maximize the amount of abstraction taking

Can. J. Chem. Downloaded from www.nrcresearchpress.com by 210.87.254.40 on 09/05/12
For personal use only.

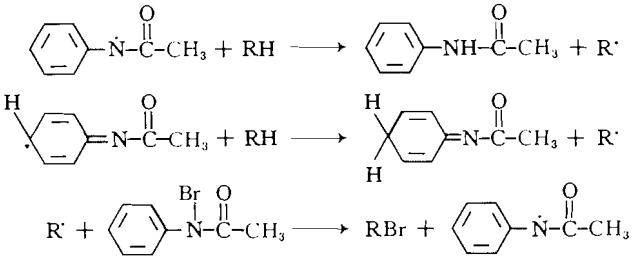
Can. J. Chem. Downloaded from www.nrcresearchpress.com by 210.87.254.40 on 09/05/12
For personal use only.

4. $Br\cdot + RH \longrightarrow HBr + R\cdot$



$$R\cdot + Br_2 \longrightarrow RBr + Br\cdot$$

5. or



place, N-bromo-2,4,6-trichloroacetanilide (I) was used in place of N-bromoacetanilide. N-Bromo-2,4,6-trichloroacetanilide has the advantage that the ortho and para positions are blocked from rearrangement, and the abstraction reaction proceeds to completion.

The products for the photoinitiated decomposition of 0.275–0.300 *M* N-bromo-2,4,6-trichloroacetanilide in a 0.15–0.3 *M* solution of toluene in carbon tetrachloride were found to be benzyl bromide and 2,4,6-trichloroacetanilide. No indication of ring bromination products of toluene was detectable by vapor-phase chromatography.

N-Bromo-2,4,6-trichloroacetanilide was found to be stable under the reaction conditions (80° in a solution of carbon tetrachloride and toluene), and its reaction with toluene could be initiated by trace amounts of azobisisobutyronitrile or benzoyl peroxide. Photoinitiation gave reactions which were identical with those using trace initiation, and the former was therefore the method of choice.

Relative rates for hydrogen abstraction by N-bromo-2,4,6-trichloroacetanilide between toluene and substituted toluenes coincided very closely with the reactivity data present in the literature for bromine atom extraction (Table II).

A plot of the logarithm of the relative reactivities vs. σ^+ values[3] (Hammett correlation $\log k/k_0 = \rho\sigma$) shows $\rho = -1.52$ (correlation coefficient $r = 0.970$), which is in good

TABLE II

Relative reactivities (per H) of substituted toluenes toward radical abstraction at 80° in CCl_4*

	Source of radicals		
Substituent	Br_2	N-Bromosuccinimide	I
p-OCH_3	9.04 (17)	11.7±0.7 (16)	8.34±0.27 (3)
p-CH_3	2.41 (17)	2.56±0.17 (16) 2.62 (16)	2.60±0.06 (4)
m-CH_3		1.52±0.05 (16)	1.23±0.05 (5)
H (standard)	1.00	1.00	1.00
p-Br		0.94±0.03 (16)	0.49±0.03 (3)
m-Cl			0.254±0.007 (5)
m-Br	0.224 (17)	0.24 (16)	0.229±0.09 (3)
m-CN		0.11 (16)	0.062±0.007 (3)

*Our results, unless indicated by reference numbers (columns 2 and 3); numbers in parentheses in column 4 show the number of independent experiments. Experimental errors are average deviations from the mean.

[3]*The σ^+ values were taken from ref. 18.*

agreement with the values $\rho = -1.38$ (16) and $\rho = -1.46$ and -1.36 (17) previously reported in the literature for bromine atom abstraction (Fig. 1).

The excellent correlation between the relative reactivity data for N-bromo-2,4,6-trichloroacetanilide and the reactivity data in the literature indicates that the reaction of I with solvent proceeds by way of the bromine atom chain, which has been established for other N-halogenating reagents (16, 17, 19) (mechanism 4).

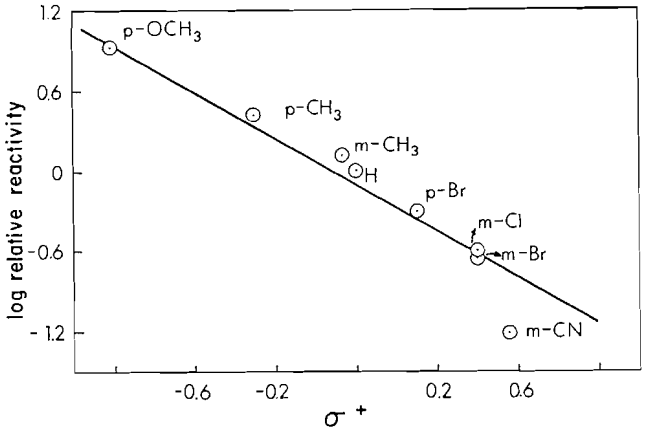


FIG. 1. Hammett $\rho\sigma$ correlation for N-bromo-2,4,6-trichloroacetanilide bromination of substituted toluenes (σ^+ = correlation, $\rho = -1.52$, and $r = 0.970$).

EXPERIMENTAL

Materials

The carbon tetrachloride used was residue-free, spectral grade Eastman reagent and its purity was checked by gas–liquid chromatography (g.l.c.) before use. Substituted toluenes were commercial materials. Before use they were distilled, the physical constants were determined, and their purity was checked by g.l.c. N-Bromoacetanilide was prepared by the method of Slosson (20) and could be obtained in 70.0–99% purity. The purity of the material was checked by iodometric titration (21). Different batches gave identical results, regardless of purity, for quantum efficiency, stability in solution, and reactivity. The product studies were carried out on material which was 99.0% pure as determined by titration. N-Bromo-2,4,6-trichloroacetanilide was prepared as pale-yellow crystals in 99.7–100% purity, as determined by iodometric titration, by using the method of Israel *et al.* (22) for the synthesis of N,2,4,6-tetrabromoacetanilide. After reaction of N-bromo-2,4,6-trichloroacetanilide in solution with added toluene, 2,4,6-trichloroacetanilide could be isolated from the reaction mixture in good yield. Different batches gave identical results for stability and relative reactivities.

Reactions of N-Bromoacetanilide and N-Bromo-2,4,6-trichloroacetanilide

The reactions were run in Pyrex cells or ampuls which had been degassed by the freeze–thaw method. Initiation experiments were carried out in the absence of light with 1–2% solutions of benzoyl peroxide or azobisisobutyronitrile. Inhibition experiments with oxygen were run in ampuls which contained atmospheric concentrations of oxygen. When irradiation was used to initiate the reaction, the light source was a Hanovia medium-pressure mercury arc (model No. 30620). All reactions of N-bromoacetanilide and N-bromo-2,4,6-trichloroacetanilide were run at 80.0 ± 0.1°, except for quantum efficiency experiments which were run at 28 ± 2°. All light-catalyzed reactions were determined by titration to be stable in the dark for over three half-lives of the light-catalyzed reactions. The average time required for the light-catalyzed reactions was approximately 4 h for the reaction of N-bromoacetanilide in carbon tetrachloride, and approximately 1 h for the reactions of N-bromoacetanilide in carbon tetrachloride with 5–15% added toluene. The photoinitiated reactions of N-bromo-2,4,6-trichloroacetanilide were irradiated for approximately 3 h for completion of the reaction.

Quantum Efficiency Measurements

Quantum yields were measured by uranyl oxalate actinometry according to the method of Forbes and Leighton (23). The apparatus and procedures used were essentially those described by Masson *et al.* (24). A Hanovia, model 30620, medium-pressure mercury arc was used as the light source. The filter used was an Eastman Kodak, No. 2B, Wratten gelatin filter, which transmits wavelengths longer than 4 000 Å. Because

Can. J. Chem. Downloaded from www.nrcresearchpress.com by 210.87.254.40 on 09/05/12
For personal use only.

of the wavelength of light used (>4 000 Å), a 20 cm actinometer cell was employed to measure the intensity of the light source. The actinometer cell was then replaced by a 1P28 photomultiplier tube whose output could be read directly from a 1 mV Sargent recorder. The filter employed was selected to alleviate the necessity to correct for the absorption of traces of products absorbing at longer wavelengths (trace absorbance was seen up to 3 700 Å). The quantum yield value used for uranyl oxylate at these wavelengths was 0.57 (23). The terminal absorbance of N-bromoacetanilide in the region 4 000 to 4 400 Å was sufficient, under our conditions, for the photolysis to proceed at a convenient rate to be measured.

Three independent determinations showed $\Phi = 1.1$, with a standard deviation of 0.2.

Expt.	% conversion	Φ
1	38	1.5
2	52	1.0
3	14	0.81

Reaction Products of N-Bromoacetanilide Photolysis

Sealed, degassed Pyrex ampuls of carbon tetrachloride, 0.324 *M* in N-bromoacetanilide (99.0% pure by titration), were placed in a thermostated water bath at 80.0° in the absence of light until they reached the bath temperature. The ampuls were then exposed to the irradiation of a Hanovia medium-pressure mercury arc for 4½ h. The pale-yellow solution turned amber and then a light brown on completion of the reaction. The amber color was shown not to be molecular bromine, since an amber-colored ampul could be shown not to contain a titratable amount of bromine. Attempts to identify the colored intermediate were unsuccessful.

After irradiation the ampuls were opened and the solvent was removed, leaving a light-brown residue. The products from the reaction were characterized and quantitatively determined in the following manner.

Diacetylhydrazobenzene

Mass spectral analysis of the product mixture showed a parent peak at *m/e* of 268 mass units. Under the operating conditions (220°), no introduction of a standard sample of N,N′-diacetyl-4,4′-diaminobiphenyl could be obtained (i.e. no ions observed), whereas an authentic sample of diacetylhydrazobenzene was easily introduced and showed a parent peak of 268 mass units. The cracking pattern of the reaction mixture was consistent with that of authentic diacetylhydrazobenzene. Retention times by thin-layer chromatography were consistent with the presence of diacetylhydrazobenzene, but attempts to isolate the compound from the reaction mixture were unsuccessful.

p-Bromoacetanilide

The major product, *p*-bromoacetanilide, was identified by its g.l.c. and thin-layer chromatography retention times. It was isolated by fractional recrystallization of the product mixture from ethanol, and its melting point and mixture melting point were identical with that of *p*-bromoacetanilide.

o-Bromoacetanilide

The retention times from thin-layer chromatography and g.l.c. indicated the presence of *o*-bromoacetanilide. Preparative thin-layer chromatographic separation of the reaction mixture, with 1.25 mm silica gel GF treated plates and a solvent system of ether – chloroform – ethyl acetate (1:1:0.8), allowed the isolation of pure *o*-bromoacetanilide after extraction from the silica gel with acetone. The melting point and mixed melting point showed the compound to be *o*-bromoacetanilide.

N,N′-Diacetyl-4,4′-diaminobiphenyl

Preparative thin-layer chromatography of 225 mg of the reaction mixture isolated 11 mg (5%) of N,N′-diacetyl-4,4′-diaminobiphenyl. The melting point (345°) was in agreement with the literature value (25), and the mixture melting point with an authentic sample showed no depression.

Products of Dibromination

Traces of products of dibromination could easily be detected in the mass spectrum of the reaction mixture. The characteristic isotopic ratios for bromine indicated a dibrominated anilinium ion (*m/e* 252, 250, and 248 mass units).

Acetanilide

Thin-layer and g.l.c. retention times indicated the presence of acetanilide. The yield (5.0%) of acetanilide was determined by adding to a weighed amount of the reaction mixture a weighed amount of an internal standard, octadecane. Analysis of the mixture by g.l.c. allowed a determination of the area ratios. The mole ratios were then calculated from a standard calibration curve, which had been determined by analysis of mixtures of known concentration analyzed under the identical conditions.

Ratio Measurements of o- and p-Bromoacetanilide

The ratio of *o*- to *p*-bromoacetanilide was determined quantitatively by g.l.c. analysis of a mixture of a weighed amount of the reaction mixture and weighed quantities of octadecane. The mole ratios were calculated from standard calibration curves. Twenty-four independent experiments were carried out: 12 reactions with 0.234 *M* N-bromoacetanilide in carbon tetrachloride and 12 reactions with 15% added toluene. The volatile components of the reaction mixture were removed and the residue dried. The analysis was carried out on acetone solutions of the dried residue. Triple analyses were carried out on each reaction mixture. The differences between the reaction mixtures, with and without added toluene, were consistent and

Can. J. Chem. Downloaded from www.nrcresearchpress.com by 210.87.254.40 on 09/05/12
For personal use only.

showed a decrease in the ortho to para ratio of 11.0 ± 4.5%. The usual formula for propagation of errors was employed (26). The ratio measurements of *o*- to *p*-bromoacetanilide with other aromatic substrates were done in a similar manner, and the results are tabulated in Table II.

Competitive Brominations

Individual experiments consisted of weighing N-bromo-2,4,6-trichloroacetanilide into small Pyrex ampuls, adding aliquots of standard carbon tetrachloride solutions of substrates and internal standard, vacuum degassing the tubes, and sealing them. A typical reaction mixture was 0.23 *M* in brominating agent, 0.19 *M* in toluene, 0.24 *M* in the desired para- or meta-substituted toluene, and 0.10 *M* in Freon 113 or 0.23 *M* in chlorobenzene. Reactions were placed in a thermostat at 80° in the absence of light, and after temperature equilibration they were exposed to the irradiation of a Hanovia medium-pressure mercury arc. The reactions were usually complete within 1½ h. The tubes were cooled, opened, and subjected to g.l.c. analysis on the Aerograph, model 202, linear-temperature programmer with either a 10 ft silicone SF-96 on firebrick column or a 10 ft column packed with diethylene glycol succinate on firebrick. Gas–liquid chromatographic analyses were carried out in triplicate, comparing peak areas before and after reaction with that of the internal standard as in previously reported work (16, 27, 28).

Calculation of Relative Reactivities

Relative reactivities were calculated via the method described by Walling *et al.* (16), either directly or, where substrate reactivity differed greatly, by successive comparison of suitable pairs. Indirect comparisons were used for the *p*-methoxytoluene value (*p*-methoxytoluene–*p*-xylene = 3.21 ± 0.04 (3)) and for the *m*-cyanotoluene value (*m*-cyanotoluene–*m*-bromotoluene = 0.269 ± 0.02 (4)). Experimental errors are average deviations from the mean, and when successive comparisons were required to give the results in Table I, the usual statistical procedure for the propagation of errors was employed (26). Disappearance of substrate by paths other than hydrogen abstraction, i.e. nuclear bromination, were ruled out, because an examination of g.l.c. traces failed to show detectable amounts of these products.

ACKNOWLEDGMENTS

The authors thank the National Research Council of Canada and the University of Alberta for their generous support of this work.

REFERENCES

1. D. D. Tanner. J. Am. Chem. Soc. **86**, 4674 (1964), and references therein.
2. J. C. Martin and J. H. Incremona. 149th Meeting, American Chemical Society, April 1965. Abstr. Papers.
3. R. C. Petterson and A. Wambsgans. J. Am. Chem. Soc. **86**, 1648 (1964).
4. C. K. Ingold. Structure and mechanism in organic chemistry. Cornell University Press, Ithaca, New York. 1953. pp. 604–610.
5. P. J. Couzens. Ph.D. Thesis, University of London, London, England. 1959
6. J. M. W. Scott and M. J. S. Dewar. J. Chem. Soc. 1445 (1957).
7. J. M. W. Scott and J. G. Martin. Can. J. Chem. **43**, 732 (1965).
8. M. J. J. Blanksma. Rec. Trav. Chim. **20**, 366 (1902); **22**, 290 (1903).
9. J. H. Mathews and R. V. Williamson. J. Am. Chem. Soc. **45**, 2574 (1923).
10. F. D. Chattaway and K. J. P. Orton. Proc. Chem. Soc. **18**, 200 (1902).
11. F. W. Hodges. J. Chem. Soc. 240 (1933).
12. T. C. Vogt, Jr. and W. H. Hamill. J. Phys. Chem. **67**, 292 (1963). C. S. Wu, G. S. Hammond, and J. M. Wright. J. Am. Chem. Soc. **82**, 5386 (1960). G. S. Hammond, C. S. Wu, O. D. Trapp, J. Warkentin, and R. T. Keys. J. Am. Chem. Soc. **82**, 5394 (1960).
13. M. L. Poutsma and R. L. Hinman. J. Am. Chem. Soc. **86**, 3807 (1964).
14. C. Walling and P. J. Wagner. J. Am. Chem. Soc. **86**, 3368 (1964).
15. G. A. Russell. J. Am. Chem. Soc. **80**, 4987 (1958).
16. C. Walling, A. L. Rieger, and D. D. Tanner. J. Am. Chem. Soc. **85**, 3129 (1963).
17. R. E. Pearson and J. C. Martin. J. Am. Chem. Soc. **85**, 3142 (1963).
18. H. C. Brown and Y. Okamoto. J. Am. Chem. Soc. **80**, 4979 (1958).
19. G. A. Russell and K. M. Desmond. J. Am. Chem. Soc. **85**, 3129 (1963).
20. E. E. Slosson. Ber. **28**, 3266 (1895).
21. T. Waugh. NBS, its reactions and uses. Arapahoe Chemicals Inc., Boulder, Colorado. 1951.
22. G. C. Israel, A. W. N. Tuck, and F. G. Soper. J. Chem. Soc. 547 (1945).
23. G. S. Forbes and W. G. Leighton. J. Am. Chem. Soc. **52**, 3139 (1930).
24. C. R. Masson, V. Boekelheide, and W. A. Noyes, Jr. Technique of organic chemistry. Vol. 2. A. Weisberger (*Editor*). Interscience Publishers, Inc., New York. 1963.
25. R. B. Carlin and E. A. Swakon. J. Am. Chem. Soc. **77**, 966 (1955).
26. C. A. Bennett and N. L. Franklin. Statistical analysis in chemistry and the chemical industry. John Wiley & Sons, Inc., London. 1954.
27. C. Walling and A. L. Rieger. J. Am. Chem. Soc. **85**, 3134 (1963).
28. C. Walling and W. H. Helmreich. J. Am. Chem. Soc. **81**, 1144 (1959).

Can. J. Chem. Downloaded from www.nrcresearchpress.com by 210.87.254.40 on 09/05/12
For personal use only.

Can. J. Chem. Downloaded from www.nrcresearchpress.com by 210.87.254.6 on 09/05/12
For personal use only.

THE REACTION OF *n*-BUTYLAMINE AND BENZYLAMINE WITH SOME β-NITROSTYRENES, DIETHYL BENZALMALONATES, AND CINNAMALMALONONITRILES[1,2]

C. E. Lough and D. J. Currie

Chemistry Section, Defence Research Board, Suffield Experimental Station, Ralston, Alberta

Received September 8, 1965

ABSTRACT

The relative rates of reaction of *n*-butylamine with 27 β-nitrostyrenes, 36 β-nitropropenylbenzenes, 20 β-nitrobutenylbenzenes and 7 related compounds, 11 diethyl benzalmalonates, and 4 cinnamalmalononitriles were measured in dioxane solution at 25 °C. In addition, the slower rates of reaction of benzylamine with 15 of these compounds were measured under identical conditions. The pseudo first order rate constants, $k_{overall}$, for all the reactions were adequately represented by the expression

$$k_{overall} = [RNH_2]^2/(A[RNH_2] + B),$$

where A and B are constants which, in general, could be correlated with Hammett sigma constants. A nitro group substituted in the ortho position or chlorines substituted in both ortho positions gave anomalous rate constants in some series but not in others. A mechanism is proposed for the amine additions.

INTRODUCTION

There are many factors which are of importance in determining the reactivity of amines with α,β-unsaturated systems. The qualitative effects of the nucleophilicity of the amine, of the steric factors associated with the amine, and of substituents on the phenyl ring and β-carbon atom of β-nitrostyrenes upon the product yields of amine–β-nitrostyrene reactions have previously been discussed.[3] For example, *o*-chloro-β-nitrostyrene will react with *p*-phenylenediamine but not with aniline, *m*-toluidine, or *p*-toluidine (1*a*). Moreover, the product yields from the addition of aromatic amines to 3-nitro-6-iodo-β-nitrostyrene appear to decrease in the order phenylhydrazine > *p*-toluidine > *m*-anisidine > *m*-toluidine > aniline > *o*-anisidine > *o*-toluidine (1*b*); therefore, in the absence of steric factors (which are operative with *o*-anisidine and *o*-toluidine), the more basic the amine, the more likely the reaction. The effects of substitution on the phenyl ring of β-bromo-β-nitrostyrenes and β-nitrostyrenes upon the product yields for a given amine reaction are such that a general correlation of the rate of reaction with Hammett sigma constants is indicated; electron-donating substituents oppose reaction and electron-withdrawing substituents favor reaction (1*a*–1*k*). Since a β-methyl group inhibits reaction whereas a β-bromine enhances reaction, the inductive effect of a substituent on the β-carbon of β-nitrostyrene is also important.

When water was a component of the solvent system, the aromatic amine adducts hydrolyzed and some polymer formation was noted. In anhydrous solvents, polymerization was unimportant and the adducts were relatively stable (1*j*). When allowed to stand, however, many of the colorless adducts became colored.

Proof of the mode of addition of aniline to β-nitrostyrene has been presented;[3] the same nitroamine is obtained from this reaction (1*j*) as is obtained from the reaction of

[1]*Issued as Suffield Technical Paper No. 320, D.R.B. project No. D52-20-20-28.*

[2]*This paper was presented in part at the 16th Defence Research Board Symposium, Ottawa, Canada, December 2–4, 1964.*

[3]*H. L. Holmes, unpublished work in this laboratory based on the research listed in ref. 1.*

benzylidene aniline and nitromethane (2). Addition products have been isolated from the reaction of benzylamine with β-nitropropenylbenzene (3), and by analogy with the above reaction it would be expected that aliphatic amines would add 1,4; nevertheless, this has not been established.

Southwick and Anderson (3) have shown that, when equimolar quantities of morpholine and β-nitropropenylbenzene react in anhydrous benzene – petroleum ether solution, two diastereomeric adducts are obtained. The unstable racemic erythro adduct is formed first, followed by the stable racemic threo adduct. The primary erythro form is probably converted into the stable threo form through the anion of the *aci*-nitro form in the presence of excess amine, or through the *aci*-form itself in ethanolic solution. When 2 mole equivalents of the stronger base pyrrolidine was used in the reaction in anhydrous ether, the pyrrolidinium salt of the *aci*-nitro form was isolated. These workers account for the primary formation of the unstable erythro adduct by steric factors favoring the approach of a proton donor on the side of the hydrogen-bonded, six-membered ring remote from the phenyl group. The present work has demonstrated that the transition state for the reactions of primary amines in anhydrous dioxane solutions involves one molecule of the unsaturated compound and two molecules of the amine. The second molecule of the amine may either form a salt as in the case of pyrrolidine, or be the hydrogen transfer agent in the conversion of the *aci*-nitro form into the nitro form. Steric factors governing the position of the second molecule of the amine for hydrogen transfer would favor the primary formation of the erythro racemate. This amine could then catalyze the conversion of this primary adduct into the stable racemate having the threo configuration.

Addition products indicating 1,4 addition have been isolated from the reaction of aromatic amines with diethyl benzalmalonate (4, 5), and 1,4 adducts are expected with *n*-butylamine. The products from the cinnamalmalononitrile reactions are assumed to arise by a 1,4 addition, although the possibility of 1,6 addition cannot be excluded.

EXPERIMENTAL

The preparation and purity of the unsaturated compounds will be described elsewhere. Fisher certified reagent dioxane was purified by the method of Fieser (6), and *n*-butylamine and benzylamine were purified by distillation from sodium hydroxide.

The experimental technique was essentially the same as that of Platford *et al.* (7). Dioxane solutions of the compound and the amine were mixed, and the solution, initially 5×10^{-4} to 5×10^{-3} *M* in the compound and 10^{-3} to 2 *M* in the amine, was transferred to a quartz absorption cell. The reaction of the unsaturated compound with *n*-butylamine or benzylamine destroys the long-wavelength ultraviolet absorption maximum and provides a method for following the reaction rate. The early runs were performed on a Beckman DU spectrophotometer equipped with a Spectracord recording attachment, and later runs were performed on a Cary model 15 spectrophotometer. When the Spectracord was used, successive spectra were recorded at appropriate time intervals; when the Cary instrument was used, the changes in optical density were recorded continuously as a function of time. The slower reactions were carried out in glass-stoppered flasks in a constant-temperature bath and aliquots taken to record the spectral data. The cell holder or compartment and bath were thermostatted at 25 ± 1 °C.

RESULTS

A plot of the logarithm of the change in the optical density at the long-wavelength absorption maximum of β-nitrostyrene (βNS) versus time during the reaction with excess *n*-butylamine (RNH_2) in dioxane showed that, although the rate of disappearance of β-nitrostyrene was first order with respect to β-nitrostyrene for a large portion of the reaction, the reaction did not go to completion but attained equilibrium, the position of which was dependent on the initial amine concentration. Unreacted β-nitrostyrene appeared to be the only absorbing species at equilibrium. The pseudo first order rate

Can. J. Chem. Downloaded from www.nrcresearchpress.com by 210.87.254.6 on 09/05/12
For personal use only.

constants, $k_{overall}$, that were calculated for the initial portion of the reaction are defined by the expression

$$-d[\beta NS]/dt = k_{overall}[\beta NS] = k[RNH_2]^x[\beta NS].$$

A plot of log $k_{overall}$ versus log $[RNH_2]$ can be used to determine the amine exponent x. For the reactions of β-nitrostyrene and substituted β-nitrostyrenes, the best straight line through the experimental points yielded non-integral values of x between 1.0 and 2.0. Moreover, these log-log plots were not strictly linear, and it soon became obvious that the apparent amine exponent was decreasing with increasing amine concentrations. This, and the desire to normalize the data, prompted the fitting of the results to the expression

$$k_{overall} = [RNH_2]^2/(A[RNH_2] + B),$$

where A and B are constants. The units of $k_{overall}$ are second^{-1} when A is in molar seconds and B is in molar^2 seconds. The values of A and B given in Table I and thus defined adequately represent the rate data for the reactions of *n*-butylamine with substituted β-nitrostyrenes, β-nitropropenylbenzenes, and β-nitrobutenylbenzenes over the range of amine concentrations used. A limited number of compounds related to β-nitrostyrenes were also examined, and the rate data for the reactions of *n*-butylamine and also benzylamine were treated in the same manner (Table II). The reactions of substituted β-nitrostyrenes with benzylamine yielded the A and B constants given in Table III. The A and B constants for the reactions of diethyl benzalmalonates and cinnamalmalononitriles with *n*-butylamine are presented in Table IV. These tables have been placed in The Depository of Unpublished Data.[4] In general, only three values of $k_{overall}$ with different amine concentrations were employed to determine the constants.

DISCUSSION

The reaction rates for compounds of the form $C_6H_5CH{=}CRNO_2$, as measured by the A and B constants, were used to assess the relative reactivities of these compounds; Figs. 1 and 2 show plots of most of these constants versus Hammett sigma constants. The mechanism for the reaction which we propose is based on the following.

A bimolecular, quasi six membered ring intermediate has been suggested in the mechanism for the addition of amines to α,β-unsaturated ketones (8) and β-nitropropenylbenzene (3). Moreover, Southwick and Anderson (3) present evidence for the involvement of two amine molecules, since in a study of the addition of secondary amines to β-nitropropenylbenzene a second amine formed the *aci*-nitro salt.[5]

The product may either remain as the salt or add a proton to give the 1,4 adduct depending on the reaction conditions, as outlined in the Introduction. If $-d[\beta NS]/dt = k_2[complex][RNH_2]$ and $-d[complex]/dt = 0$, it can be shown that

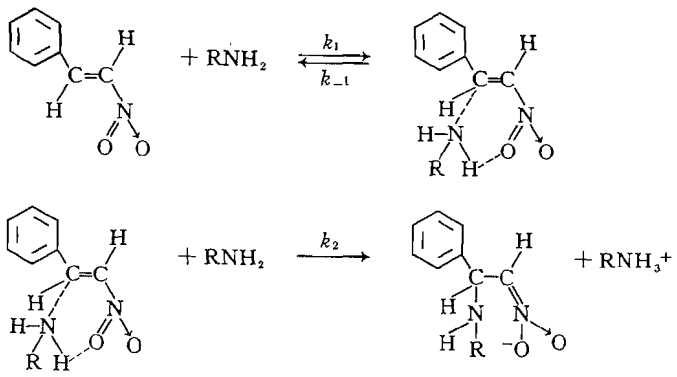
$$-d[\beta NS]/dt = \{[RNH_2]^2/([RNH_2]/k_1 + k_{-1}/k_1k_2)\}[\beta NS],$$

and the constants A and B which were used to normalize the data can therefore be related to $1/k_1$ and k_{-1}/k_1k_2, respectively. When the constants for the reactions of *n*-butylamine

[4] *Photocopies of Tables I–V may be obtained, upon request, from: The Depository of Unpublished Data, National Science Library, National Research Council, Ottawa, Canada.*

[5] *The reactions of the secondary amines di-n-butylamine (0.3 to 4.7 M) and morpholine (2×10^{-2} to 5×10^{-1} M) with β-nitrostyrene and β-nitropropenylbenzene (10^{-3} M) in dioxane at 25 °C were, in fact, second order with respect to the amine, and for the reactions of seven β-nitropropenylbenzenes (βNPB) with morpholine, log ($k_{R_2NH} \times 10^2$) = $+1.34\sigma + 0.03$, where k_{R_2NH} (in molar^{-2} second^{-1}) is defined by $-d[\beta NPB]/dt = k_{R_2NH}[\beta NPB][R_2NH]^2$. The correlation coefficient (r) was +0.89, and the standard errors of the correlation coefficient (Δr) and the estimate (Δestimate) were +0.31 and +0.21, respectively. The rate constants appear in Table V.*[4]

Can. J. Chem. Downloaded from www.nrcresearchpress.com by 210.87.254.6 on 09/05/12
For personal use only.



with β-nitrostyrene and β-nitropropenylbenzene[6] are compared, it is seen that the presence of the methyl group *cis* to the phenyl group (9) slows down the rate of the reaction which forms the complex (greater A constants) by either hindering the approach of the amine to the alpha carbon or by reducing the positive charge on this carbon through an inductive effect, or both. The presence of this methyl group tends to prevent the phenyl ring from fully participating in resonance, its bulk causing the phenyl ring and the unsaturated linkage to assume a non-planar configuration (10). This reduced resonance participation would result in a reduction of the electronic effects associated with the substituents, and the ρ value for the reaction which forms the complex or for the A constants should be, and indeed is, less for the β-nitropropenylbenzenes than for the β-nitrostyrenes. It has been suggested[7] that the positive nature of the beta carbon atom in aryl nitro β-nitrostyrenes is evidenced by amine reaction on the terminal methylene of 4-nitrostyrene (12). In aryl nitro β-nitrostyrenes the opposed or cross-conjugated system probably reduces the positive charge on the alpha carbon atom and the rate of the complex formation reaction to a value close to that for the parent compound. In Figs. 1 and 2 the solid line was drawn from correlations omitting the A constants for these aryl nitro β-nitrostyrenes; the broken line accommodates these derivatives. Because of steric inhibition of resonance, the cross conjugation in aryl nitro β-nitropropenylbenzenes would be minimized, and so the correlations included these derivatives. The B constants are not subject to the aryl-substituted nitro group effects shown by the A constants in the β-nitrostyrene series, but weakly exhibit the effects of electronic isolation of the benzene ring in the β-nitropropenylbenzene series. Since $B = k_{-1}/k_1k_2$, in the β-nitrostyrenes either the effects of aryl substituents on k_{-1} parallel those on k_1 or the variation in k_2 compensates for the variation in k_1. The constants for the reactions of the β-nitrobutenylbenzenes with *n*-butylamine are very similar to those for the β-nitropropenylbenzenes, and the effects noted above appear to have reached a maximum with the methyl group.

The inductive effect of the bromine atom in the similarly constituted (10) β-bromo-β-nitrostyrene must override any steric effect, since the A and B constants for the reaction of this compound are less than those for β-nitrostyrene. Neither the greater conjugative

[6]*For the β-nitrostyrenes* $\log A = -0.793\sigma + 0.48$, $r = -0.87$, $\Delta r = +0.09$, *and* Δ*estimate* $= +0.23$, *and* $\log (B \times 10) = -2.12\sigma + 0.28$, $r = -0.97$, $\Delta r = +0.10$, *and* Δ*estimate* $= +0.25$. *A correlation omitting all aryl nitro derivatives gave* $\log A = -1.16\sigma + 0.42$, $r = -0.91$, $\Delta r = +0.13$, *and* Δ*estimate* $= +0.19$. *For the β-nitropropenylbenzenes, if the 2-nitro and 2,6-dichloro derivatives are omitted,* $\log A = -0.276\sigma + 1.97$, $r = -0.63$, $\Delta r = +0.06$, *and* Δ*estimate* $= +0.14$, *and* $\log B = -1.28\sigma + 1.30$, $r = -0.88$, $\Delta r = +0.12$, *and* Δ*estimate* $= +0.29$. *For the β-nitrobutenylbenzenes* $\log A = -0.255\sigma + 1.83$, $r = +0.30$, $\Delta r = +0.20$, *and* Δ*estimate* $= +0.24$, *and* $\log B = -1.51\sigma + 1.34$, $r = -0.81$, $\Delta r = +0.27$, *and* Δ*estimate* $= +0.32$.

[7]*H. L. Holmes, private discussions.*

Can. J. Chem. Downloaded from www.nrcresearchpress.com by 210.87.254.6 on 09/05/12
For personal use only.

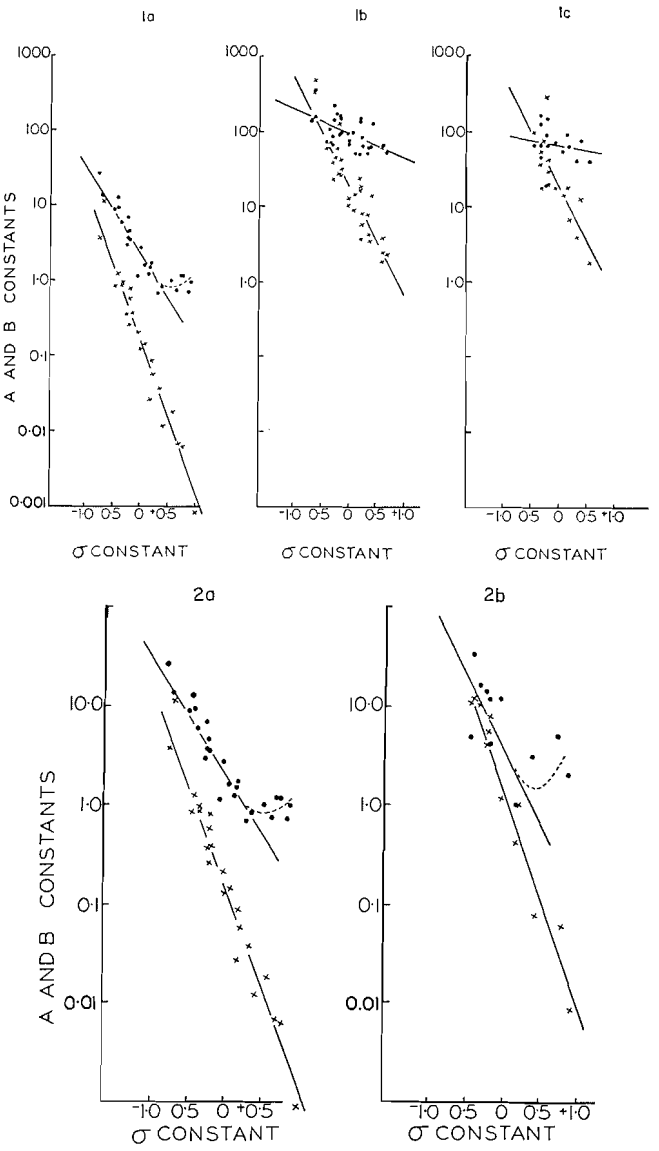


FIG. 1. A plot of the rate constants A (●) and B (×) for the reaction of n-butylamine with (*a*) β-nitrostyrenes, (*b*) β-nitropropenylbenzenes, and (*c*) β-nitrobutenylbenzenes versus sigma constants. The sigma constants for monosubstituted derivatives were taken from Taft (13). The constants for disubstituted derivatives were calculated as the algebraic sum of the constants for the component groups (11).

FIG. 2. A plot of the rate constants A (●) and B (×) for the reactions of β-nitrostyrenes with (*a*) n-butylamine and (*b*) benzylamine versus sigma constants.

effect of the α-naphthyl, α-furfuryl, or α-thienyl groups nor the steric effect of the *peri* hydrogen in the α-naphthyl group in the β-nitrostyrene analogues markedly altered the reaction constants. In the β-nitropropenylbenzene analogues the steric effect of the *peri* hydrogen in the α-naphthyl group greatly reduced the reaction rate ($A = 270$, $B = 47.0$) over that of the β-naphthyl isomer ($A = 90$, $B = 6.7$).

Can. J. Chem. Downloaded from www.nrcresearchpress.com by 210.87.254.6 on 09/05/12
For personal use only.

Can. J. Chem. Downloaded from www.nrcresearchpress.com by 210.87.254.6 on 09/05/12
For personal use only.

The reactions with benzylamine[8] and aniline demonstrate that the basicity of the amine determines the magnitude of the A and B constants: the more basic the amine, the faster the reaction and the smaller the numerical value of these constants. The steric factors associated with benzylamine do not appear to be significantly different from those associated with *n*-butylamine (Fig. 2).

The nature of the solvent exerts a pronounced effect on the apparent amine exponent, and for a given compound over a given range of amine concentrations it appears to be possible to alter this exponent from 1 to 2 by the proper choice of solvent. Aniline was reacted with a series of β-nitrostyrenes at 25 °C in 20% ethanol – 80% aqueous phosphate buffer (Sörensen, pH 7). The reactions were pseudo first order with respect to the β-nitrostyrenes with excess aniline during the initial stages of the reaction, and the amine exponent was unity.[9] If the kinetics of the reactions of aromatic amines in dioxane are the same as those for aliphatic amines, then water and hydroxylic solvents may be usurping the role of the second amine. The reactions of aniline, *p*-toluidine, and *o*-toluidine with β-nitrostyrene in ethanol–water showed that differences in the basicity and the steric effects of these amines had a minor effect on the rate of reaction.

The values of the A and B constants for the reactions of *n*-butylamine with substituted diethyl benzalmalonates[10] are intermediate between those of the corresponding β-nitrostyrenes and β-nitropropenylbenzenes or β-nitrobutenylbenzenes. The cross conjugation apparent in the aryl nitro β-nitrostyrenes does not operate to the same extent in the analogous β-nitropropenylbenzenes and diethyl benzalmalonates because of restricted rotation of the benzene ring; thus the A constants of the 4-nitro derivatives in the latter two classes of compounds are similar to those of the 3-nitro isomers.

The A and B constants for 2-nitro-β-nitropropenylbenzene ($A = 210$, $B = 450$; β-nitropropenylbenzene, $A = 76, B = 12$) and for diethyl 2-nitrobenzalmalonate ($A = 70$, $B = 1.55$; diethyl benzalmalonate, $A = 20$, $B = 0.37$) fall above the trend lines and are much greater than the constants for the parent compounds. Since any electronic interaction of the nitro group with the pendant methyl group in the β-nitropropenylbenzenes is unlikely, steric hindrance to nucleophilic attack caused by the bulky ortho substituent, *and* the non-planar configuration of the benzene ring and the ethylenic linkage appear to be the dominant causes of the reduced reaction rates. The constants for 2,6-dichloro-β-nitropropenylbenzene ($A = 220$, $B = 620$) were abnormal whereas those for 2-nitro-β-nitrostyrene ($A = 1.1, B = 0.0064$; β-nitrostyrene, $A = 1.1$, $B = 0.20$) and 2,6-dichloro-β-nitrostyrene ($A = 1.5$, $B = 0.019$) fell on the trend lines. A diminution in reaction rate is manifested to a lesser extent in other ortho-substituted β-nitropropenylbenzenes, β-nitrobutenylbenzenes, and diethyl benzalmalonates, but not in ortho-substituted β-nitrostyrenes.

The products of the reaction between cinnamalmalononitrile and *n*-butylamine absorb at 280 mμ, and therefore 1,4 addition is indicated. Separation of the *cis* phenyl and cyano groups in benzalmalononitrile by another ethenoid linkage minimizes the mechanical interference between the styryl system and the *cis* cyano group, and although there are insufficient data to discuss adequately these compounds, the Hammett plot would appear

[8]*For the β-nitrostyrenes* $\log A = -0.692\sigma + 0.75$, $r = -0.52$, $\Delta r = +0.36$, *and* $\Delta\text{estimate} = +0.51$, *and* $\log B = -2.43\sigma + 0.25$, $r = -0.98$, $\Delta r = +0.14$, *and* $\Delta\text{estimate} = +0.22$. *A correlation omitting aryl nitro derivatives gave* $\log A = -1.57\sigma + 0.65$, $r = -0.69$, $\Delta r = +0.58$, *and* $\Delta\text{estimate} = +0.47$.

[9]*For the reactions of eight β-nitrostyrenes with aniline,* $\log (k \times 10^2) = +1.99\sigma + 0.52$, $r = +0.95$, $\Delta r = +0.28$, *and* $\Delta\text{estimate} = +0.22$, *where the second-order rate constant, k (in* $\text{molar}^{-1}\ \text{second}^{-1}$*), is defined by* $-d[\beta NS]/dt = k[C_6H_5NH_2][\beta NS]$. *The rate constants are given in Table V.*[4]

[10]*The correlation omitting the 2-nitro derivative gave* $\log A = -1.11\sigma + 1.39$, $r = -0.95$, *and* $\Delta r = \Delta\text{estimate} = +0.13$, *and* $\log (B \times 10) = -2.42\sigma + 0.71$, $r = -0.79$, $\Delta r = +0.66$, *and* $\Delta\text{estimate} = +0.68$.

to be applicable. As expected, the rate constants for the 2-nitro derivative do not exhibit any anomalous effects. Therefore, in the amine reactions of conjugated heteroenoid compounds in which free rotation of the phenyl ring is unlikely, diortho substitution or ortho substitution by groups of sufficient bulk can greatly reduce the rate of the complex formation reaction (k_1) and, in addition, may either increase the rate of the reverse reaction (k_{-1}) or decrease the rate of the reaction leading to the final product (k_2).

ACKNOWLEDGMENTS

The authors thank Mr. W. C. Carpenter and Mr. D. Park for computational assistance; Drs. G. Feniak and H. L. Holmes for supplying samples of the substituted β-nitrostyrenes, β-alkyl-β-nitrostyrenes, and diethyl benzalmalonates; Mr. P. J. R. Bryant of the Chemical Defence Experimental Establishment, Porton, England, for the gift of the substituted cinnamalmalononitriles; and Dr. J. B. Reesor, Dr. H. L. Holmes, and Prof. J. B. Hyne for their helpful discussions concerning these reactions.

REFERENCES

1. (*a*) D. E. WORRALL. J. Am. Chem. Soc. **60**, 2845 (1938).
   (*b*) D. E. WORRALL and F. BENNINGTON. J. Am. Chem. Soc. **62**, 493 (1940).
   (*c*) D. E. WORRALL and J. FINKEL. J. Am. Chem. Soc. **61**, 2969 (1939).
   (*d*) D. E. WORRALL and H. T. WOLOSINSKI. J. Am. Chem. Soc. **62**, 2449 (1940).
   (*e*) D. E. WORRALL and F. BENNINGTON. J. Am. Chem. Soc. **60**, 2844 (1938).
   (*f*) D. E. WORRALL. J. Am. Chem. Soc. **60**, 2841 (1938).
   (*g*) D. E. WORRALL and F. COHEN. J. Am. Chem. Soc. **66**, 842 (1944).
   (*h*) D. E. WORRALL and A. TATILIBAUM. J. Am. Chem. Soc. **64**, 1739 (1942).
   (*i*) D. E. WORRALL. J. Am. Chem. Soc. **43**, 919 (1921).
   (*j*) D. E. WORRALL. J. Am. Chem. Soc. **49**, 1598 (1927).
   (*k*) J. LEOVENICH and H. GERBER. Ber. **63**, 1707 (1930).
   (*l*) C. MANNICH, K. HANDKE, and K. ROTH. Ber. **69**, 2112 (1936).
2. C. D. HURD and J. S. STRONG. J. Am. Chem. Soc. **72**, 4813 (1950).
3. P. L. SOUTHWICK and J. E. ANDERSON. J. Am. Chem. Soc. **79**, 6222 (1957).
4. R. BLANK. Ber. **28**, 146 (1895).
5. I. GOLDSTEIN. Ber. **28**, 1450 (1895).
6. L. F. FIESER. Experiments in organic chemistry. 2nd ed. D. C. Heath & Co., Boston. 1941. p. 368.
7. R. F. PLATFORD, E. E. BERTRAM, C. E. LOUGH, and H. L. HOLMES. Suffield Technical Paper No. 231 (1962).
8. N. H. CROMWELL and D. J. CRAM. J. Am. Chem. Soc. **65**, 301 (1943).
9. G. DREHFAHL and G. HENBLEIN. Chem. Ber. **93**, 497 (1960).
10. V. N. V. VASILEVA, V. V. PEREKALIN, and V. G. VASILEV. Zh. Obshch. Khim. **31**, 2175 (1961).
11. J. F. J. DIPPY and S. R. C. HUGHES. Tetrahedron, **19**, 1527 (1963).
12. W. J. DALE and G. BUELL. J. Org. Chem. **21**, 45 (1956).
13. R. W. TAFT. Steric effects in organic chemistry. *Edited by* M. S. Newman. John Wiley & Sons, Inc., New York. 1956. pp. 571 and 619.

Can. J. Chem. Downloaded from www.nrcresearchpress.com by 210.87.254.6 on 09/05/12
For personal use only.

Can. J. Chem. Downloaded from www.nrcresearchpress.com by 210.87.254.42 on 09/05/12
For personal use only.

2-ALKOXY-3-HYDROXYTETRAHYDROPYRANS AND 2-ALKOXY-3-HYDROXYTETRAHYDROFURANS

I. PREPARATION, STRUCTURE, AND SOME DERIVATIVES[1]

F. SWEET AND R. K. BROWN

Department of Chemistry, University of Alberta, Edmonton, Alberta

Received March 10, 1966

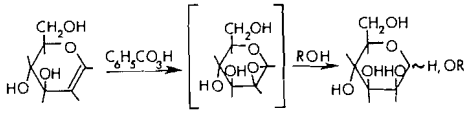
ABSTRACT

Oxidation of 2,3-dihydrofuran or 2,3-dihydropyran with peroxybenzoic acid or *m*-chloroperoxybenzoic acid in the presence of an alcohol has produced, respectively, *trans*-2-alkoxy-3-hydroxytetrahydrofurans in 59 to 64% yield and *trans*-2-alkoxy-3-hydroxytetrahydropyrans in 65 to 80% yield. In the presence of acids, these acetals isomerize readily to give an equilibrated mixture of *cis* and *trans* isomers.

INTRODUCTION

Simple models of pyranosides and furanosides which possessed, in addition to the anomeric hydroxyl or alkoxy group, only one hydroxyl group in the ring (and that specifically on C_2) were required for a study of the influence of substituents on the selective hydrogenolysis of acetals and ketals (1). The dihydroxylation of α,β-unsaturated ethers was considered to be a means to this end.

This approach has been used by several workers, but yields in general were not satisfactory. Glycals (2), which are α,β-unsaturated cyclic ethers, have in a number of cases been oxidized by peroxybenzoic acid to give, first, what is believed to be an intermediate epoxide. Under the reaction conditions this was rapidly converted into either a reducing sugar or a glycoside in the presence of water or an alcohol or a carboxylic acid (2–4) (Reaction Scheme 1).



R = H, alkyl, or benzoyl

REACTION SCHEME 1.

In a similar reaction, Bergmann *et al.* (5) showed that oxidation of 2-methyl-5,6-dihydropyran with peroxybenzoic acid provided the diol 2-methyl-2,3-dihydroxytetrahydropyran, isolated by these authors as the acyclic compound 4-hydroxy-4-aceto-1-butanol. Methanolysis of a dimer of this compound, obtained if the above product was isolated by distillation at 60° rather than 30°, gave 2-methyl-2,3-dimethoxytetrahydropyran.

Barker *et al.* (6) oxidized 5,6-dihydropyran with peroxybenzoic acid and obtained 2-benzoyloxy-3-hydroxytetrahydropyran, to which they tentatively assigned the *trans* configuration.

Recently (7), a mixture of hydrogen peroxide and a nitrile has been used to convert *n*-butyl vinyl ether in methanol into *n*-butyl β-hydroxy-α-methoxyethyl ether in 33% yield. Here also, the intermediate was considered to be an epoxide.

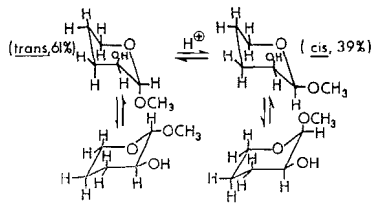
[1]*From the work of F. Sweet to be submitted to the Department of Chemistry, University of Alberta, Edmonton, as part of the requirements for the degree of Doctor of Philosophy.*

Can. J. Chem. Downloaded from www.nrcresearchpress.com by 210.87.254.42 on 09/05/12
For personal use only.

RESULTS AND DISCUSSION

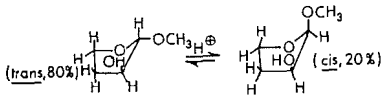
With the work mentioned above as a basis, we have obtained a simple and more productive route to 2-alkoxy-3-hydroxytetrahydropyrans and 2-alkoxy-3-hydroxytetrahydrofurans, using either peroxybenzoic acid or *m*-chloroperoxybenzoic acid to oxidize dihydropyran or dihydrofuran dissolved in the appropriate alcohol. The results of these experiments are shown in Tables I and II. In all cases the nuclear magnetic resonance (n.m.r.) spectra of the compounds were consistent with the structures designated. Oxidation of *n*-butyl vinyl ether by this modified method gave a 92% yield of pure *n*-butyl β-hydroxy-α-methoxyethyl ether.

The proposal of initial formation of an intermediate epoxide as in Reaction Scheme 1 (5) is supported by the fact that the reaction product is almost exclusively the *trans*-2-alkoxy-3-hydroxytetrahydropyran or *trans*-2-alkoxy-3-hydroxytetrahydrofuran. This is in agreement with the known preferred *trans* opening of the epoxide ring (8). Since we have not yet been able to isolate the proposed epoxide intermediate, it is not certain that it actually does occur in this reaction. However, to account for the *trans* product, either such an intermediate must be formed or, alternatively, an "epoxide-like" transition state must be involved. Evidence for the *trans* assignment is shown below and is supported by n.m.r. data. A detailed account of this and the conformational preference of the structures is given in part II in this series.[2]



REACTION SCHEME 2.

If the reaction mixture, obtained from the epoxidation and alcoholysis of the α,β-unsaturated cyclic ether, was worked up immediately after completion of the reaction (about 12 to 14 h), the *trans* isomer was obtained, as shown by gas–liquid chromatography, contaminated by less than 1% of the *cis* isomer. If the reaction mixture stood for 2 days at room temperature before work-up, the amount of *cis* contaminant increased to about 5–10%, showing that isomerization had taken place, no doubt caused by the presence of the benzoic acid.[3] When pure *trans*-2-methoxy-3-hydroxytetrahydropyran, obtained by gas–liquid chromatography, was dissolved in the appropriate alcohol containing some *p*-toluenesulfonic acid, an equilibrium mixture (39:61) of *cis* and *trans* isomers was obtained. The same proportion of *cis* and *trans* isomers was found when pure *cis* isomer was equilibrated under the same conditions (Reaction Scheme 2). In a similar manner, the acid-catalyzed isomerization of *trans*-2-methoxy-3-hydroxytetrahydrofuran gave an equilibrium mixture of *cis* and *trans* isomers in the ratio of 20:80 (Reaction Scheme 3).



REACTION SCHEME 3.

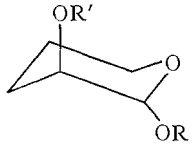
[2]*F. Sweet and R. K. Brown, in preparation.*

[3]*These acetals are hydrolyzed and isomerized extremely easily, and can be preserved only in glassware carefully cleaned under alkaline conditions.*

Can. J. Chem. Downloaded from www.nrcresearchpress.com by 210.87.254.42 on 09/05/12
For personal use only.

TABLE I

trans-2-Alkoxy-3-hydroxytetrahydropyrans from the reaction of *m*-chloroperbenzoic or perbenzoic acid with 5,6-dihydropyran in alcohol (ROH)



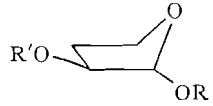
Substituent		Boiling point (melting point)	Refractive index, η_D (temperature)	% analysis						% yield
				Calcd.			Found			
R	R′			C	H	N	C	H	N	
CH_3	H	56° at 2 mm	1.4548 (23.5°)	54.53	9.15		54.58	9.18		76–82
CH_3	DNB*	(132–133°)		47.86	4.33	8.59	48.21	4.49	8.42	
CH_3	CH_3	110–111° at 110 mm	1.4318 (25°)	57.51	9.65		57.40	9.63		85
C_2H_5	H	63° at 2.5 mm	1.4506 (25°)	57.51	9.65		57.65	9.65		65
C_2H_5	DNB	(116–117°)		49.42	4.74	8.23	49.70	4.77	8.30	
C_2H_5	CH_3	46–47° at 5.2 mm	1.4322 (25°)	59.98	10.07		60.00	9.90		81
i-C_3H_7	H	63–64° at 2 mm	1.4467 (26.5°)	59.98	10.07		59.71	9.93		74
i-C_3H_7	DNB	(96–97°)		50.85	5.12	7.91	51.02	5.02	8.05	
i-C_3H_7	CH_3	92–93° at 30 mm, 56–57° at 7 mm	1.4299 (25°)	62.04	10.41		62.26	10.31		80
t-C_4H_9	H	62° at 1.5 mm	1.4487 (25°)	62.04	10.41		62.15	10.21		80
t-C_4H_9	DNB	(86–88°)		52.17	5.47	7.61	52.13	5.52	7.68	
t-C_4H_9	CH_3	61–62° at 7 mm	1.4322 (25°)	63.80	10.71		63.86	10.51		86
The *cis* isomer										
CH_3	H	62° at 2.2 mm‡	1.4517 (25°)	54.52	9.16		54.40	9.04		†
CH_3	DNB	(88°)		47.86	4.33	8.59	47.70	4.23	8.46	

*DNB = 3,5-dinitrobenzoyl.
†Obtained by separation of an equilibrated solution of *cis* and *trans* isomers.
‡Micro-determination.

Can. J. Chem. Downloaded from www.nrcresearchpress.com by 210.87.254.42 on 09/05/12
For personal use only.

TABLE II

trans-2-Alkoxy-3-hydroxytetrahydrofurans from the reaction of *m*-chloroperbenzoic acid or perbenzoic acid with 4,5-dihydrofuran in alcohol (ROH)



Substituent		Boiling point (melting point)	Refractive index, η_D^{25}	% analyses						% yield
				Calcd.			Found			
R	R′			C	H	N	C	H	N	
CH_3	H	68–70° at 7 mm	1.4421	50.84	8.53		50.72	8.68		59
CH_3	DNB*	(89–90°)		46.16	3.87	8.97	46.59	3.90	8.68	
CH_3	CH_3	57° at 21 mm	1.4201	54.53	9.15		54.87	8.92		93
C_2H_5	H	64–65° at 2.5 mm	1.4415	54.53	9.15		54.45	8.95		59
C_2H_5	DNB	(93–94°)		47.86	4.33	8.59	47.97	4.32	8.82	
C_2H_5	CH_3	71–72° at 26 mm	1.4214	57.51	9.65		57.83	9.58		86
i-C_3H_7	H	79–80° at 4 mm	1.4373	57.51	9.65		57.56	9.55		58
i-C_3H_7	DNB	(102–103°)		49.42	4.74	8.23	49.32	4.72	8.09	
i-C_3H_7	CH_3	52° at 10 mm	1.4196	59.98	10.07		60.05	9.98		92
t-C_4H_9	H	68° at 1.5 mm	1.4422	59.98	10.07		59.73	10.07		64
t-C_4H_9	DNB	(100°)		50.85	5.12	7.91	50.70	5.18	8.01	
t-C_4H_9	CH_3	46° at 6.5 mm	1.4242	62.04	10.41		61.77	10.21		88
The *cis* isomer										
CH_3	H	48° at 15 mm	1.4410	50.84	8.53		50.73	8.33		†
CH_3	DNB	(87°)		46.16	3.87	8.97	46.64	3.96	8.48	

*DNB = 3,5-dinitrobenzoyl.
†Obtained by separation of an equilibrated solution of *cis* and *trans* isomers.

Can. J. Chem. Downloaded from www.nrcresearchpress.com by 210.87.254.42 on 09/05/12
For personal use only.

The *trans* and *cis* assignments of the two isomeric 2-methoxy-3-hydroxytetrahydropyrans are supported by the n.m.r. signals for the respective anomeric protons. That for the *trans* isomer occurs as a doublet at τ 5.80 (J = 5.2 c.p.s.) whereas that for the *cis* isomer is a doublet centered at τ 5.43 (J = 3.2 c.p.s.). It is known that axial protons show signals at higher field than do those occupying an equatorial position (9). Furthermore, the coupling constant of 3.2 c.p.s. agrees with the axial–equatorial relation of the C_1 and C_2 protons found for *both* conformations of the *cis* isomer, and that of 5.2 c.p.s. is in agreement with an "average" signal obtained from two conformations of the *trans* isomer, one of which has a *trans* diaxial relation for the C_1C_2 protons, the other conformer having these two protons located diequatorially (9) (Reaction Scheme 2).

The *trans*-2-methoxy-3-hydroxytetrahydrofuran gave a singlet at τ 5.22 for the anomeric proton (unresolved even at high resolution). The signal for the anomeric proton of the *cis* isomer was a doublet centered at τ 5.05 (J = 6.3 c.p.s.). These figures support the *trans* and *cis* configurational assignments.

A more detailed discussion of the conformational arrangements will be given in part II in this series.[2]

EXPERIMENTAL

Melting points are uncorrected.

Analyses were carried out with a Burrell K-2 Kromo-Tog on a 2.5 m column packed with either 25% Carbowax 20 M on Gas Chrom P (60–80 mesh) or 20% butanediol succinate on Chromosorb B. Helium was used as the carrier gas at a flow rate of 60 ml/min, and the column temperature was 150°.

Separation of *cis* and *trans* isomers was accomplished with an Aerograph autoprep, model A-700, using a column packed with 25% Carbowax 20 M on Gas Chrom P (temperature 175°) and helium as the carrier gas at a flow rate of 110 ml/min. The equilibrium mixtures of *cis* and *trans* isomers were analyzed by gas–liquid chromatography on the butanediol succinate column by comparison of peak areas with those obtained from known and carefully weighed mixtures. These figures are consistent with those obtained by n.m.r. analyses.

Elemental analyses were carried out by Miss Darlene Roberts, Department of Chemistry, University of Alberta, Edmonton, and by Dr. C. Daessle, 5757 Decelles Avenue, Montreal.

Nuclear magnetic resonance spectra (in $CDCl_3$) were obtained with a Varian A-60 spectrometer. A Perkin–Elmer model 421 grating spectrophotometer was used to obtain infrared spectra of $CHCl_3$ solutions of the compounds.

4,5-Dihydrofuran was prepared, according to a modification (10) of published directions (11), by the base-catalyzed isomerization of commercially available 2,5-dihydrofuran. Fractional distillation in a spinning-band column gave an incomplete separation of the two isomers, as shown by gas–liquid chromatographic and n.m.r. spectroscopic analysis of each fraction. A 4 ft column packed with stainless-steel saddles gave an excellent separation. The 4,5-dihydrofuran boiled at 52.5° and 695 mm, η_D^{20} 1.4228, η_D^{25} 1.4204 (lit. b.p. 53–55° at 745, η_D^{20} 1.4200 (10); b.p. 54.3° at 760 mm, η_D^{20} 1.4282 (12)). The 2,5-dihydrofuran boiled at 63–65° and 700 mm, η_D^{25} 1.4292, η_D^{20} 1.4309.

General Procedure for the Preparation of 2-Alkoxy-3-hydroxytetrahydropyrans and 2-Alkoxy-3-hydroxytetrahydrofurans

To a cold (−10° to −5°) solution of 0.35 mole of commercial 5,6-dihydropyran or 4,5-dihydrofuran (10) in 350 ml of anhydrous alcohol[4] was added, over a period of 25 min with stirring, a suspension of 0.26 mole of peroxybenzoic acid (13) or *m*-chloroperoxybenzoic acid (FMC Corporation, 500 Roosevelt Avenue, Cartaret, New Jersey) in 150 ml of dry chloroform. The temperature during this addition was maintained at −10° to −5°. Stirring was continued at −5° for 15 min after complete addition of the oxidant. The cooling bath was then removed and the reaction mixture was stirred at room temperature overnight. The chloroform, alcohol, and excess dihydropyran (dihydrofuran) were removed under reduced pressure with a rotary evaporator and a water bath at 50°. The residue, consisting of a mixture of benzoic acid or *m*-chlorobenzoic acid and the 2-alkoxy-3-hydroxytetrahydropyran (2-alkoxy-3-hydroxytetrahydrofuran), was shaken vigorously with 400 ml of chloroform, and the mixture then cooled to 0° and filtered under suction. The benzoic acid residue in the funnel was washed twice with 25 ml portions of cold chloroform. The combined chloroform extracts and mother liquor were extracted with 10% aqueous sodium carbonate. Since these alcohols are water soluble, the aqueous sodium carbonate solution was saturated with sodium chloride and extracted in turn with chloroform to recover any of the alcohol. The combined chloroform extracts were dried (Na_2SO_4), filtered, and then freed from solvent (rotary evaporator). The colorless residue was

[4]*For the preparation of the t-butoxy analogue, the dihydropyran (dihydrofuran) was dissolved in a mixture of t-butyl alcohol (225 ml) diluted with chloroform (125 ml) to prevent solidification of the alcohol at these low temperatures.*

fractionally distilled under reduced pressure in a spinning-band column. The results are shown in Tables I and II.

The n.m.r. spectra (in deuteriochloroform) and the infrared spectra (in chloroform) of each product were consistent with the structures assigned.

The 3,5-dinitrobenzoates were prepared by the addition of 1.5 g of commercial 3,5-dinitrobenzoyl chloride to a solution of 500 mg of the alcohol in 5 ml of dry pyridine. The solution was heated in a water bath at 85° for 15 min and cooled, and then the bulk of the pyridine was removed by rotary evaporation. The residue, dissolved in diisopropyl ether or in chloroform, was washed successively with 5 ml quantities of water, 5% aqueous sodium carbonate, and water. The ether was removed, and the resultant glassy material was crystallized three times from aqueous methanol and simultaneously decolorized with charcoal. The solid was dried overnight in a vacuum desiccator at room temperature and 0.3 mm pressure.

2-Alkoxy-3-methoxytetrahydropyrans (2-Alkoxy-3-methoxytetrahydrofurans)

The alcohols were methylated by the silver oxide – methyl iodide procedure with dimethylformamide as solvent (14), or by the reaction of sodium hydride with a solution of the alcohol and methyl iodide in 1,2-dimethoxyethane. The latter method is similar to procedures which have appeared recently (15, 16). A typical experiment, with appropriate modifications, is described below for the methylation of 2-*t*-butoxy-3-hydroxytetrahydropyran. The pyran (16.0 g, 0.092 mole) was dissolved in 100 ml of 1,2-dimethoxyethane[5] containing 14.2 g (0.10 mole) of methyl iodide. The solution, in a 300 ml, three-necked flask equipped with a magnetic stirrer, an efficient condenser, and a thermometer, was cooled to 10° and four equal portions (total of 2.4 g, 0.10 mole) of sodium hydride[6] were added, with stirring, while the reaction mixture was kept at 5–10°. The mixture was then stirred for 2 h while it came to room temperature. The 1,2-dimethoxyethane was removed by distillation at atmospheric pressure until one-quarter of the volume of the mixture remained. The addition of 100 ml of dry diethyl ether precipitated the bulk of the sodium iodide. The filtered solution was freed from ether, and the residue was distilled in a spinning-band column to give 14.9 g (86%) of material boiling at 61–62° and 7 mm, n_D^{25} 1.4322.

The physical constants for the methylated compounds are shown in Tables I and II.

Isomerization of trans- and cis-2-Methoxy-3-hydroxytetrahydropyrans

A solution of pure *trans*-2-methoxy-3-hydroxytetrahydropyran in dry methanol containing a catalytic amount of concentrated hydrochloric acid was refluxed for 2 h. Analysis by gas–liquid chromatography indicated an equilibrium mixture of 61% *trans* and 39% *cis* isomers. Pure *cis*-2-methoxy-3-hydroxytetrahydropyran subjected to the same conditions gave the same proportion of *trans* and *cis* isomers.

The alcoholic solution of the equilibrated mixture was stirred with an excess of solid sodium carbonate as a suspension for half an hour until carbon dioxide evolution ceased. The solution was then filtered and freed from solvent on a rotary evaporator. The residue was dissolved in chloroform, washed with aqueous sodium carbonate (10%), dried (Na_2SO_4), filtered, and then freed from solvent. The isomers were separated with an Aerograph autoprep. It was more convenient to inject the mixture as a solution in an equal volume of solvent ($CHCl_3$), since the injector unit had a holdup of about 2–3 ml.

The *trans*- and *cis*-2-methoxy-3-hydroxytetrahydrofurans were isomerized in a similar manner.

ACKNOWLEDGMENT

The authors thank the National Research Council for financial support during the development of this work.

REFERENCES

1. B. E. LEGGETTER and R. K. BROWN. Can. J. Chem. **42**, 990 (1964).
2. B. HELFERICH. Advan. Carbohydrate Chem. **7**, 209 (1952).
3. H. B. WOOD and H. G. FLETCHER, JR. J. Am. Chem. Soc. **79**, 3234 (1957).
4. P. A. LEVENE and A. L. RAYMOND. J. Biol. Chem. **88**, 513 (1930).
5. M. BERGMANN, A. MIEKELEY, and F. STATHER. Ber. **56**, 2255 (1923).
6. S. A. BARKER, J. S. BRIMACOMBE, A. B. FOSTER, D. H. WHIFFEN, and G. ZWEIFEL. Tetrahedron, **7**, 10 (1959).
7. G. B. PAYNE, P. H. DEMING, and P. H. WILLIAMS. J. Org. Chem. **26**, 659 (1961).
8. R. E. PARKER and N. S. ISAACS. Chem. Rev. **59**, 737 (1959).
9. R. U. LEMIEUX, R. K. KULLNIG, H. J. BERNSTEIN, and W. G. SCHNEIDER. J. Am. Chem. Soc. **80**, 6098 (1958).
10. E. L. ELIEL, B. E. NOWAK, R. A. DAIGNAULT, and V. G. BADDING. J. Org. Chem. **30**, 2441 (1965).
11. R. PAUL, M. L. A. FLUCHAIRE, and G. COLLARDEAU. Bull. Soc. Chim. France, 668 (1950).
12. M. L. A. FLUCHAIRE and G. COLLARDEAU. U.S. Patent No. 2,556,325 (June 12, 1951); Chem. Abstr. **46**, 1046 (1952).
13. L. S. SILBERT, E. SIEGEL, and D. SWERN. Org. Syn. **43**, 93 (1963).
14. R. KUHN, H. T. TRISCHMANN, and I. LOW. Angew. Chem. **67**, 32 (1955).
15. M. E. TATE and C. T. BISHOP. Can. J. Chem. **41**, 1801 (1963).
16. E. D. M. EADES, D. H. BALL, and L. LONG, JR. J. Org. Chem. **30**, 3949 (1965).

[5]*Ansul ether 121, treated with lithium aluminium hydride and subsequently distilled from the hydride.*

[6]*Sodium hydride (4.3 g of 56% suspension) from Metal Hydrides Corporation was washed with 1,2-dimethoxyethane to remove the mineral oil. This gave 2.4 g of sodium hydride.*

Can. J. Chem. Downloaded from www.nrcresearchpress.com by 210.87.254.42 on 09/05/12
For personal use only.

Can. J. Chem. Downloaded from www.nrcresearchpress.com by 210.87.254.6 on 09/05/12
For personal use only.

BORON SULFIDE AS A SOURCE OF ACYLOXYBORANE

J. M. LALANCETTE, F. BESSETTE, AND J. M. CLICHE
Department of Chemistry, Faculty of Sciences, University of Sherbrooke, Sherbrooke, Quebec
Received March 9, 1966

ABSTRACT

Triacyloxyboranes ($(RCO_2)_3B$) are obtained in good yields by the action of organic acids on boron sulfide or on *o*-thioboric acid esters.

We have reported previously that functional groups bearing labile hydrogens, such as alcohols (1), mercaptans (2), and amines (3), react with boron sulfide to form B—O, B—S, and B—N bonds, respectively. Besides this sensitivity towards protons, boron sulfide can also react with aldehydic or ketonic carbonyls at room temperature to give the corresponding thioaldehydes or thioketones. Under more energetic conditions deoxygenation has been noted with esters (4). With *o*-thioboric acid esters, carbonyls are readily transformed into their corresponding thioacetals at room temperature (5). A study has been undertaken to determine the reactivity of the acid function towards boron sulfide and *o*-thioboric acid esters, the carbonyl group or the hydroxyl group or both being able a priori to react according to the pattern outlined above.

We have found that both aliphatic and aromatic organic acids react smoothly with boron sulfide to give the corresponding triacyloxyboranes (eq. [1]).

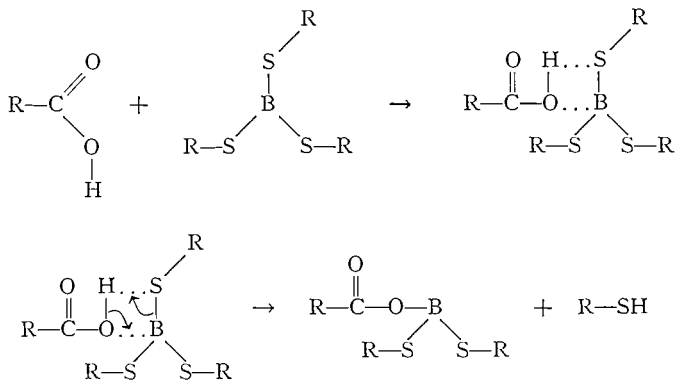
[1] $$6RCOOH + B_2S_3 \rightarrow 2(RCOO)_3B + 3H_2S$$

The triacyloxyborane is also obtained if an *o*-thioboric acid ester is used instead of boron sulfide (eq. [2]). We have noted that the carbonyl group is not affected by the *o*-thioboric acid ester.

[2] $$3RCOOH + (R'S)_3B \rightarrow (RCOO)_3B + 3R'SH$$

The mechanism of this reaction should call for the formation of a complex between the electron-poor boron atom and the acidic group, these groups being good acceptors and good donors, respectively. The formation of this complex should be facilitated by the assistance of hydrogen bonding between neighboring sulfur and hydrogen atoms. By subsequent electron shift, the rupture of the B—S bond and the formation of the B—O bond would follow (eq. [3]).

[3]



This S_N2 mechanism is much more attractive than the alternative S_N1 type, which would call for preliminary ionization of the B—S bond to give $=B^+$ and RS^-, a very unlikely step in view of the partial double bond character of the B—S bond induced by strong back-coordination of the electron pairs of the sulfur toward the boron atom.

Boron Acetates

These new methods of formation of acyloxyboranes offer interesting evidence concerning the structure of "boron acetate" obtained by the action of various acetylating agents on boric acid, and shed some light on the structural problems encountered with these compounds.

The first authors to report the formation of "boron acetate" indicated a triacetate structure for their compound (6, 7): $(CH_3COO)_3B$. This formulation has been challenged by Dimroth (8) and more recently by Gerrard (9), who favor a "pyro" structure for this compound: $(CH_3COO)_2B—O—B(CH_3COO)_2$. Gerrard, in his monograph on organoboron compounds (10), has been very categoric in rejecting the existence of the triacetate structure, indicating that he could not reproduce the experiments leading to the formation of the compound reported as the triacetate (m.p. 120°), obtaining instead (with a 99.3% yield in one case) a substance melting at 147–148°, the pyroacetate.

We agree that the product melting at 147–148° is in fact the pyroacetate, but we believe that it is formed from the triacetate by thermal decomposition.

The triacetate is produced by the reaction of acetic acid on boron sulfide or an *o*-thioborate, but cannot be obtained pure because it decomposes spontaneously and rather rapidly to give the "pyro" form (eq. [4]).

$$[4] \qquad 2(CH_3CO_2)_3B \rightarrow (CH_3CO_2)_2B—O—B(CO_2CH_3)_2 + (CH_3CO_2)_2O$$

The temperature and duration of contact seem to be the two factors determining the proportions of these two substances in the ultimate reaction mixture. The relative proportions of the tri- and tetra-acetates given by the reaction have been estimated by boron analysis. With the formation of boron acetate from boron sulfide or *o*-thioborates, the ultimate production of the tetraacetate cannot be explained without the transient existence of the triacetate, if the extreme sensitivity of the B—S bond towards labile protons is taken into account. This sensitivity is illustrated by the very fast reactions observed between alcohols, mercaptans, and boron sulfide. In the case of boron trifluoroacetate, the loss of trifluoroacetic anhydride has been observed at 100° under a vacuum (11), which indicates the feasibility of eq. [4].

Using special acetylating techniques, we have succeeded in reproducing a boron acetate melting at 120°, as reported by Ahmad (7). This material has a molecular weight of 325, not too far from the value for the tetraacetate. When kept in a desiccator, over KOH, it slowly loses acetic acid or acetic anhydride, which is absorbed by the base. After 2 weeks, the melting point has reached the correct value for the tetraacetate and the evolution of acetic fragments has stopped. In view of these results, we believe that the "triacetate" obtained by Ahmad was in fact the tetraacetate, which had retained acetic anhydride upon crystallization.

EXPERIMENTAL*

Reaction of Benzoic Acid with Boron Sulfide

A solution of 40 g (0.33 mole) of benzoic acid in 100 ml of anhydrous benzene was refluxed for 26 h in the presence of a suspension of boron sulfide (6.5 g, 0.055 mole). The reaction was accompanied by evolution

**Melting points were taken in sealed capillary tubes and are not corrected. Infrared measurements were made on a Perkin–Elmer spectrometer, model 125, with KBr cells.*

Can. J. Chem. Downloaded from www.nrcresearchpress.com by 210.87.254.6 on 09/05/12
For personal use only.

of H_2S. The crude mixture was filtered while hot, and after it was cooled, white crystals separated out, m.p. 195–197° (after recrystallization from benzene), yield 76% (reported (12) m.p. 145°). A sample of this material was analyzed by water hydrolysis and subsequent titration of the benzoic acid to a phenolphthalein end point, followed by addition of mannitol and titration of the boric acid to a phenolphthalein end point.

Anal. Calcd. for $(C_6H_5CO_2)_3B$: $C_6H_5CO_2$, 97.1; B, 2.9; mol. wt. 374.2. Found: $C_6H_5CO_2H$, 97; B, 3.0; mol. wt. (obtained by cryoscopy in ethylene dibromide) 396.

Ethylene dibromide had shown near ideal behavior in molecular weight determinations of *m*-dinitrobenzene and acetanilide. Infrared ($CHCl_3$): no bands in the region of 3 500 cm^{-1}; bands at 1 688 (very strong), 1 602 (medium), 1 420 (strong), 1 333 (very strong), and 1 282 cm^{-1} (strong).

By a similar technique, boron tripropionate (m.p. 110–113°) and boron tricinnamate (m.p. 160°) were obtained.

Anal. Calcd. for $C_{27}H_{21}O_6B$: cinnamic acid, 97.57; B, 2.40. Found: cinnamic acid, 97.2; B, 2.1.

Anal. Calcd. for $C_9H_{15}O_6B$: propionic acid, 95.22; B, 4.70. Found: propionic acid, 95.2; B, 5.0.

Reaction of Acetic Acid with Boron Sulfide

A method similar to the above was used except for the time of contact, which was 30 min instead of several hours. A mixture of two products was obtained after crystallization from glacial acetic acid, the first product melting at 120° and the second at 137–138°. Variations in the ratio of the two compounds (the tri- and pyro-acetates) have been estimated by boron analysis of the crude mixture obtained initially after the mixture was washed with dry petroleum ether to remove any excess of acetic acid.

Anal. Calcd. for $(CH_3CO_2)_3B$: B, 5.76. Calcd. for $(CH_3CO_2)BOB(CH_3CO_2)_2$: B, 7.87. Found: after a reaction period of 30 min B, 6.2; after a reaction period of 2 h B, 6.9; after a reaction period of 24 h B, 7.5.

Reaction of Acetic Acid with o-Thioboric Acid Esters

A mixture of 8.0 g (0.034 mole) of isopropyl *o*-thioborate and 25 ml (excess) of acetic acid was refluxed under a nitrogen atmosphere for 90 min. The excess of acetic acid was distilled under reduced pressure and the residue recrystallized from acetic acid. Two fractions melting at 120° and 146–148° were obtained. Similar mixtures were obtained by a prolonged contact at room temperature or a short reflux time, with *n*-butyl *o*-thioborate and acetic acid.

Acetylation of Boric Acid

A suspension of 5.0 g (0.081 mole) of boric acid in 30 g (0.29 mole, slight excess) of acetic anhydride was refluxed under a dry nitrogen atmosphere and with good stirring. The reaction took place suddenly, almost explosively, and the solid material dissolved completely. The reaction mixture was immediately cooled in an ice bath and a white solid crystallized out. This solid was filtered under a dry atmosphere, thoroughly washed with anhydrous ethyl ether, and kept for 1 h under a vacuum. The melting point was then 120°. A 5.7336 g sample of this material was kept for 2 weeks in a desiccator in the presence of KOH pellets. After a loss of 0.1905 g the weight remained constant and the melting point was then 145–147°. The increase in the weight of KOH was 0.1902 g. A molecular weight determination on the fresh material melting at 120° (cryoscopy in bromoform) was 325 ± 30; the calculated molecular weight for $(CH_3CO_2)_2BOB(CH_3CO_2)_2$ is 274. Molecular weight determinations of boron acetates proved to be a very delicate task because of their extreme sensitivity towards moisture.

ACKNOWLEDGMENTS

The authors thank the National Research Council of Canada and the Defence Research Board of Canada for financial assistance.

REFERENCES

1. J. M. LALANCETTE. Can. J. Chem. **42**, 2356 (1964).
2. J. BRAULT and J. M. LALANCETTE. Can. J. Chem. **42**, 2903 (1964).
3. S. JERUMANIS and J. M. LALANCETTE. J. Org. Chem. In press.
4. S. JERUMANIS and J. M. LALANCETTE. Can. J. Chem. **42**, 1928 (1964).
5. F. BESSETTE, J. BRAULT, and J. M. LALANCETTE. Can. J. Chem. **43**, 307 (1965).
6. A. PICTET and G. KARL. Bull. Soc. Chim. France, **3**, 1114 (1908).
7. T. AHMAD and M. H. KHUNDKAR. Chem. Ind. London, 248 (1954).
8. O. DIMROTH. Liebigs Ann. Chem. **446**, 97 (1925).
9. W. GERRARD and M. WHEELANS. Chem. Ind. London, 758 (1954).
10. W. GERRARD. The organic chemistry of boron. Academic Press, Inc., New York. 1961. p. 51.
11. E. L. MUETTERTIES. U.S. Patent No. 2,782,233 (February 19, 1957).
12. T. AHMAD, S. Z. HAIDER, and M. H. KHUNDKAR. J. Appl. Chem. London, **4**, 543 (1954).

Can. J. Chem. Downloaded from www.nrcresearchpress.com by 210.87.254.6 on 09/05/12
For personal use only.

Can. J. Chem. Downloaded from www.nrcresearchpress.com by 84.22.46.98 on 09/08/12
For personal use only.

A 5-PHOSPHAFULVENE WITTIG REAGENT[1]

M. B. HOCKING
Exploratory Research Laboratory, Dow Chemical of Canada, Limited, Sarnia, Ontario

Received November 18, 1965

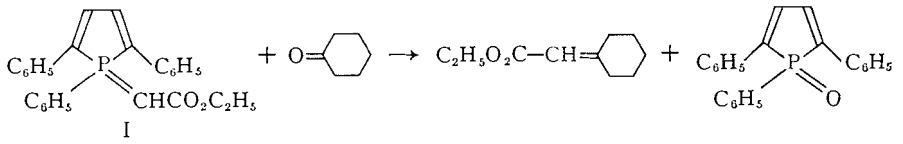
ABSTRACT

1,2,5-Triphenyl-1-carbethoxymethylenephosphole (I), a fairly stable isolable phosphorane, has been shown to undergo Wittig reactions with cyclohexanone, benzaldehyde, and acetaldehyde under a variety of conditions. Both the reactivity and stereoselectivity of I are less than the corresponding properties of triphenylcarbethoxymethylenephosphorane (II); these properties may be useful in certain applications.

INTRODUCTION

A new 1-phosphafulvene (I) has now been found to undergo Wittig reactions, and this capability has been examined to discover the latent advantages, if any, of this reagent over the analogous, more conventional triphenylphosphine Wittig reagent.

The carbethoxymethylene ligand was selected for the investigation of reactivity because of the adequacy of published work (2–4) on the reaction of triphenylcarbethoxymethylenephosphorane (II) with several aldehydes and ketones under widely differing conditions. The latter is also a stable phosphorane which does not require preparation *in situ*.



I

(Similarly, $(C_6H_5)_3P{=}CHCO_2C_2H_5$ (II))

The work was conducted in two phases, the first to give only indications of the reactivity of the phosphafulvene (I) relative to that of the triphenylphosphine phosphorane (II), whose reactivity is well established (see Tables I and II), and the second to determine any differences in the ratios of *cis* and *trans* olefins formed in reactions where geometrical isomerism is possible.

EXPERIMENTAL

Melting points and boiling points are not corrected. Benzene was dried by boiling it with $LiAlH_4$ for 2 h, and then was distilled. Ethanol was dried by the method of Lund and Bjerrum (5) and distilled to yield material containing less than 15 p.p.m. water. Acetonitrile containing 0.67% water was simply distilled, since the presence of a small percentage of polar impurity would not be detrimental. Acetaldehyde, benzaldehyde, and cyclohexanone were distilled immediately before use. Analyses were carried out by Dr. L. E. Swim and associates, The Dow Chemical Company, Midland, Michigan, and Dr. C. Daessle, Montreal, Quebec.

Ultraviolet spectroscopic data were obtained on a Unicam SP.700 recording spectrophotometer (for some of the phosphafulvene decomposition data) and on a Beckman DK-2 ratio recording spectrophotometer. Infrared data were recorded on Unicam SP.100 or Beckman IR-9 spectrophotometers. Proton resonance information was obtained on a Varian A-60 instrument fitted with a phase-detector integrator.

Phosphafulvene (I)

Several preparations of this compound were carried out as previously described (1) without interference from the reported complication, and analyses were considerably improved when carried out within 4 days of preparation.

Anal. Calcd. for $C_{26}H_{23}O_2P$: C, 78.4; H, 5.8; P, 7.8. Found: C, 78.6, 78.5; H, 5.4, 5.8; P, 7.8, 7.9.

The methyl ester of I, melting at 167–170°, was also prepared in a strictly analogous way.

Anal. Calcd. for $C_{25}H_{21}O_2P$: C, 78.1; H, 5.5; P, 8.1. Found: C, 77.8, 78.1; H, 5.3, 5.3; P, 8.1, 8.1.

[1]*Contribution No. 138 from the Exploratory Research Laboratory.*

Can. J. Chem. Downloaded from www.nrcresearchpress.com by 84.22.46.98 on 09/08/12
For personal use only.

It was not stable for long periods in the atmosphere (see the ultraviolet data), but kept satisfactorily in a desiccator (KOH). Distillation of 5.5 g of decomposed phosphafulvene failed to yield any diethyl fumarate or maleate (4). However, a small quantity of a hydrocarbon, m.p. 207–208°, was obtained (b.p. 200° at 0.04 mm), whose analysis and molecular weight corresponded to a formula of the type $C_{25}H_{16-18}$ or $C_{26}H_{18}$, but no correspondence with known compounds could be found (6) for the spectral properties (λ_{max}^{hexane} 274 mμ, ϵ_{molar} 43 500, mol. wt. 321).

Confirmation of the structure of the phosphafulvene (I) was obtained by hydrobromination back to the phosphonium salt. Excess gaseous HBr was passed into a solution of the phosphafulvene (1.0 g) in benzene (50 ml), thereby causing a yellow oil to separate. The mixture was purged with nitrogen for 15 min, the benzene decanted, and crystals obtained (1.15 g, 96%) from the oil in fresh benzene (50 ml). This salt, m.p. 128–132°, gave an infrared spectrum identical with that of the salt prepared directly from the phosphole (m.p. 167–168°). It was also completely soluble in water, and with aqueous base this solution yielded the starting phosphafulvene (m.p. and mixed m.p. 151–156°).

Reactivity Investigations

Cyclohexylideneacetic Acid via Phosphafulvene (I)

From an initial attempt in boiling benzene for 24 h on a 0.01 *M* scale with an excess of cyclohexanone in a nitrogen atmosphere, 93% of the Wittig reagent was recovered unchanged and no ethyl cyclohexylideneacetate could be isolated. A pressure reaction without solvent, however, was more successful.

The phosphafulvene (5.0 g) and cyclohexanone (6.25 g) were placed in a glass-lined stainless-steel reaction vessel which was then thoroughly flushed with nitrogen and closed. This was heated at 170° for 10 h. After the vessel was cooled to room temperature, the contents, which had partly crystallized, were rinsed into a suction filter with ethanol. The chunky yellow crystals of phosphole oxide (2.5 g) melted at 231–236°, which was raised to 232–236° after one recrystallization from ethyl acetate. Dilution of the filtrate with hexane caused small yellow needles to form (0.2 g, m.p. 178–183°) which, on recrystallization from chloroform, gave a melting point and mixed (with 1,2,5-triphenylphosphole) melting point of 183–185°. Solvents were stripped from the final filtrate by distillation on a boiling water bath, and the excess cyclohexanone (b.p. 48° at 15 mm) was subsequently removed by reducing the pressure. The dark gummy distillation residue was saponified in aqueous ethanolic sodium hydroxide, the excess alcohol was distilled off, the remaining mixture was diluted further with water, and the aqueous suspension was extracted with ether. The aqueous phase was acidified to pH 3 with HCl, and the oil which separated was extracted with ether. Evaporation of the ether gave 1.0 g of crude product. Distillation of this gum (90–146° bath at 0.05 mm) gave 169 mg (10%) of pure cyclohexylideneacetic acid, m.p. 81–88°, which, after one recrystallization from hexane, melted at 89–91° (lit. (7) m.p. 90–91.5°) and analyzed well.

Anal. Calcd. for $C_8H_{12}O_2$: C, 68.6; H, 8.6. Found: C, 68.9; H, 8.3.

Ethyl Cinnamate via Phosphafulvene

(a) At 80°.—The phosphafulvene (8.0 g) and freshly distilled benzaldehyde (2.1 g) in ethanol (90 ml) were boiled under reflux in a dry nitrogen atmosphere for 2 h. Crystals of the phosphole oxide (5.0 g, m.p. 236–239°) were filtered from the cooled reaction solution and washed with fresh ethanol. The ethanol was distilled from the combined filtrate and washings through a 50 cm Snyder column on a water bath under a very slightly reduced pressure. A further 0.6 g of phosphole oxide (m.p. 229–236°) was obtained from the residual oil on dilution with a small amount of hexane. The hexane solution was transferred to a small distilling flask and the hexane evaporated off. Distillation yielded ethyl cinnamate (2.7 g, 76%) at 262–269° (lit. (14) b.p. 265–267°) after a small forerun. The identity of the product was confirmed by comparison of its infrared spectrum with that of an authentic sample.

(b) At room temperature (23°).—The quantities of reagents used and the procedure were the same as in method *a* above, except that when the reagents were mixed the reaction mixture was left at room temperature for 48 h. Work-up as described in method *a* above yielded a total of 2.92 g (82%) of ethyl cinnamate and 6.5 g (98%) of the phosphole oxide.

Stereochemical Investigations

Preparation of the Ethyl Crotonates

(i) Ethyl trans-crotonate.—This was prepared by a method similar to that of Vogel (8). From 100 g of the crotonic acid was obtained 73 g of distilled product, b.p. 137–137.5° (lit. (8) b.p. 136.5°). The room temperature proton nuclear magnetic resonance (n.m.r.) spectrum in CCl_4 with tetramethylsilane as internal standard further established its purity and identity.

$$\underset{a}{CH_3}\text{—}\underset{b}{CH}\text{=}\underset{c}{CH}\text{—}\overset{\overset{O}{\|}}{\underset{}{C}}\text{—}O\text{—}\underset{d}{CH_2}\text{—}\underset{e}{CH_3}$$

The details were: vinyl proton (*b*) at δ 6.87 (1H, pair of overlapping quartets, J_{ba} = 6.4 and J_{bc} = 14.5 c.p.s.), vinyl proton (*c*) at δ 5.75 (1H, pair of quartets, J_{ca} = 1.5 and J_{cb} = 14.5 c.p.s.), ester methylene protons (*d*) at δ 4.08 (2H, quartet, J_{de} = 7.0 c.p.s.), vinylic methyl protons (*a*) at δ 1.83 (3H, pair of doublets, J_{ac} = 1.5 and J_{ab} = 6.4 c.p.s.), and ester methyl protons (*e*) at δ 1.22 (3H, triplet, J_{ed} = 7.0 c.p.s.).

(ii) Ethyl cis-crotonate.—*cis*-Crotonic acid[2] containing about 5% (by n.m.r.) of the *trans* isomer was cooled in an ice bath, and ice-cold 2.03 *N* ammonium hydroxide (10 ml) was added with stirring. Fifty milliliters of the ice-cold 0.4 *N* aqueous silver nitrate was then added in subdued light, with stirring, and the precipitated silver salt filtered off and dried (2.04 g). Ethyl iodide (2.5 ml) was added to a suspension of this silver salt in benzene (50 ml) and the mixture, shielded from light, was boiled under reflux for 1 h. (A preliminary run established that less time was insufficient.) The coagulated silver iodide was filtered off and the solvent evaporated from the filtrate to leave 1.0 g (52%) of a pale-yellow oil. Nuclear magnetic resonance established that this oil was ethyl crotonate, and the ratio of *cis* to *trans* was found to be 95:5, the same as in the starting acid.

The details of the n.m.r. spectrum, which was measured with the same solvent, internal standard, and conditions as for ethyl *trans*-crotonate, were: vinyl proton (*b*) at δ 6.26 (1H, pair of overlapping quartets, J_{ba} = 6.8 and J_{bc} = 11.1 c.p.s.), vinyl proton (*c*) at δ 5.72 (1H, pair of quartets, J_{ca} = 1.5 and J_{cb} = 11.1 c.p.s.), ester methylene protons (*d*) at δ 4.10 (2H, quartet, J_{de} = 7.0 c.p.s.), vinylic methyl protons (*a*) at δ 2.10 (3H, pair of doublets, J_{ac} = 1.5 and J_{ab} = 6.8 c.p.s.), and ester methyl protons (*e*) at δ 1.22 (3H, triplet, J_{ed} = 7.0 c.p.s.).

Analysis of cis–trans Mixtures of Ethyl Crotonates

To determine the *cis–trans* ratios of mixed ethyl crotonates by n.m.r. the resonance of protons on the vinylic methyl groups were used, for two reasons. Firstly, the bands caused by this resonance appeared at shifts which differed sufficiently between the *cis* and the *trans* isomers to enable integration of the peak areas for each individually, and secondly, this resonance was caused by a sufficiently high proportion of the protons in the molecules to still give an indication of the presence of as low as 3% of one of the isomers in the presence of the other. In one or two of the analyses an additional single resonance band appeared at 1.97 p.p.m., the cause of which could not be established. However, this was separated from the resonance bands being integrated for analysis by placing this portion of the spectrum on a sweep width of 100 cycles; integration could then be effected without interference from this trace impurity. Traces of 1,2,5-triphenylphosphole-1-oxide or triphenylphosphine oxide present in some of the samples analyzed had no effect on the accuracy of the ratio, since all the protons in these molecules resonate at much lower field strengths.

Parallel Wittig Reactions

1. In Boiling Benzene

(*a*) The phosphafulvene (6.0 g) and acetaldehyde (3.5 ml) in benzene (100 ml) were boiled together under reflux, with protection from atmospheric moisture, for 80 min. Further 3.5 ml portions of acetaldehyde were added at 40 min and 80 min reaction time. When the mixture was allowed to cool to room temperature crystals of the phosphole oxide (3.89 g) separated and were filtered off. The solvent was evaporated from the filtrate on a rotary evaporator with a 30 cm reflux head, using a water bath at 30° for heating and an aspirator vacuum. Residual oily yellow crystals remained which were washed with a few small portions of ether, dried, and identified (m.p. 230–233°) as a further crop of the phosphole oxide (0.89 g, total recovered 97%).

The ether was evaporated off and the residual oil (0.83 g), of which 0.67 g (39%) was ethyl crotonate, was examined by n.m.r., establishing a ratio of *cis* to *trans* of 23:77.

(*b*) As a control experiment in an attempt to demonstrate the lack of equilibration or fractionation of the isomeric crotonates the reaction was repeated with an initial addition of 0.190 g of ethyl *cis*-crotonate and on a smaller scale, but otherwise as described in method *a*. The use of 4 g of phosphafulvene and 2 ml portions of acetaldehyde gave a total of 0.68 g of crotonates, of which 33.5% was *cis*. This corresponded to a yield from the reaction of 0.49 g (43%), of which 8% was *cis*.

(*c*) The phosphorane (II) (6.0 g), acetaldehyde (10.5 ml, total), and benzene (100 ml) were reacted and worked up as described in method *a* above. Most of the triphenylphosphine oxide (4.39 g, 92%) was isolated and a yield of 1.62 g (82%) of ethyl crotonate obtained, of which 11% was *cis*.

2. In Boiling Ethanol

(*a*) The phosphafulvene (7.96 g) and acetaldehyde (2 ml) in ethanol (250 ml) were boiled under reflux for 1 h, with protection from atmospheric moisture. Two milliliter portions of acetaldehyde were added after 20 min and 40 min reaction time. The solvent and ester product were stripped off in a rotary evaporator, and the residual yellow crystals washed with a small quantity of ether and dried to yield 6.38 g (97%) of the phosphole oxide, m.p. 233–237°. The ethanol was then distilled from the ethyl crotonate through a 70 cm Vigreux column (70° bath at 120 mm). The yield of crotonate was 0.50 g (22%), of which 17% was *cis*.

(*b*) As a control experiment in a polar, protonating solvent the reaction described in method *a* above was carried out in essentially the same way, but with 0.118 g of ethyl *cis*-crotonate in addition to the quantities of reagents specified. The total ester recovery was 0.917 g (20% *cis*), of which that produced in the reaction was 0.79 g (35%) and 8% ethyl *cis*-crotonate.

(*c*) The phosphorane (II) (6.69 g) and acetaldehyde (6 ml, total) in ethanol (250 ml) were reacted and worked up as described in method *a* above. Triphenylphosphine oxide (5.17 g, 93%) was isolated and 0.44 g (19%) of ethyl crotonate obtained, of which 7% was *cis*.

[2]*Purchased from K. and K. Laboratories, Inc., Plainview, New York.*

Can. J. Chem. Downloaded from www.nrcresearchpress.com by 84.22.46.98 on 09/08/12
For personal use only.

(*d*) For a reproducibility test the reaction described in method *c* above was repeated with the same quantities. After the mixture was refluxed for 1 h the solvent was distilled through a 70 cm Vigreux column (70° bath at 120 mm). After the oily colorless crystalline residue was washed with petroleum ether (3 × 15 ml, b.p. 30–50°), the crystals were filtered off and dried to yield 5.45 g (98%) of triphenylphosphine oxide, m.p. 151–156°. The petroleum ether was distilled from the filtrate through a 70 cm Vigreux column (70° bath at 120 mm) to yield 0.24 g (12%) of ethyl crotonate, of which 6% was *cis*.

3. In Boiling Acetaldehyde

(*a*) The phosphafulvene (6.0 g) and acetaldehyde (150 ml) were boiled under reflux in a 40° water bath, with protection from atmospheric moisture, for 50 min. Initially most of the phosphafulvene was in solution, and during the reaction the solution became more yellow in color, accompanied by the precipitation of a yellow solid. The excess acetaldehyde was distilled (30° bath at 400 mm) through a 70 cm Vigreux column, and the residual yellow solid was washed free of oil with small portions of petroleum ether (b.p. 30–50°) and filtered off under suction. The yellow solid (4.68 g, 95%) was phosphole oxide, m.p. 233–237°. After the petroleum ether had been evaporated from the filtrate (same conditions as acetaldehyde) the residual yellow oil was distilled (b.p. $\simeq$ 40° at 10 mm), using a water bath at 80° and a receiver cooled to −15°. The yield was 0.59 g (35%), of which 26% was *cis*.

(*b*) The phosphorane (II) (5.23 g) and acetaldehyde (130 ml), in which the former was completely soluble, were boiled together under reflux in a 40° bath for 50 min. The work-up, which was carried out as described in method *a* above, yielded 4.00 g (93%) of triphenylphosphine oxide (m.p. 151–155°) and 0.56 g (33%) of ethyl crotonate, of which 8% was *cis*.

4. In Boiling Acetonitrile

(*a*) The phosphorane (II) (6.96 g) and acetaldehyde (2 ml) in acetonitrile (250 ml) were boiled together under reflux for 1 h. Additional 2 ml portions of acetaldehyde were added after 20 min and 40 min reaction time. Solvent and excess acetaldehyde were removed through a 70 cm Vigreux column (80° bath at 240 mm). The residual oil was distilled, keeping the pot temperature below 80° and the receiver at −15°, to yield 1.15 g of ethyl crotonate, of which 8% was *cis*. Crystallization of the solid distillation residue from benzene yielded 4.98 g (90%) of triphenylphosphine oxide, m.p. 153–156°.

(*b*) The phosphafulvene (I) (7.96 g) and acetaldehyde (2 ml) in wet acetonitrile as used in method *a* above gave no detectable yield of crotonates. However, when carried out on the same molar scale in dry acetonitrile (<20 p.p.m. water, by two treatments with P_2O_5 followed by distillation from the same drying agent) with the methyl ester of the phosphafulvene (I) a 14% yield of crotonates was obtained, of which 7% was *cis*.

5. Effect of Temperature

(*a*) The phosphafulvene was reacted and worked up essentially as described in section 2*a* above, except that the reaction was carried out at 23°, with stirring, for 24 h. The 0.54 g (24%) of ethyl crotonate obtained consisted of less than 3% *cis* ester.

(*b*) An experiment similar to the above, with the phosphorane (II) on the same scale as described in section 2*b* above, yielded 0.70 g (31%) of the mixed esters, of which 10% was ethyl *cis*-crotonate.

6. Equilibration Tests

One milliliter of a solution of ethyl *trans*-crotonate in benzene (50% by volume) was placed in each of three n.m.r. tubes. Nothing was added to the first, phosphole oxide (2 mg) was added to the second, and acetaldehyde (2 drops) and phosphafulvene (4 mg) were added to the third. One milliliter of another solution of mixed ethyl *cis*- and *trans*-crotonates (30.5% *cis*) in benzene (50% by volume) was placed in each of four n.m.r. tubes. To one tube nothing was added, to another phosphole oxide (2 mg) was added, to the third phosphole oxide (2 mg) and phosphafulvene (4 mg) were added, and to the fourth phosphole oxide (2 mg), phosphafulvene (4 mg), and acetaldehyde (2 drops) were added.

All seven tubes were then heated at 75° for 2½ h, followed by a further period of 64 h. Each tube was examined visually and by n.m.r. after each interval of heating. To those tubes starting with added acetaldehyde a further addition of the starting quantity was made after 2½ and 40 h heating, and to those starting with phosphafulvene a further 4 mg addition was made to each at 40 h. The ratio of *cis* ester to *trans* ester in each of the tubes remained the same throughout the test. However, all except one of the tubes starting as yellow solutions (containing added phosphole oxide and (or) phosphafulvene) became colorless by the end of the test, but did not after the short heating period. The one which retained most of its color contained the *trans* ester, acetaldehyde, and phosphafulvene.

RESULTS

Cyclohexanone seemed to be an ideal reagent for reactivity comparisons between the phosphafulvene (I) and the triphenylphosphine phosphorane (II). The latter reacts with cyclohexanone only slowly or under forcing conditions, yet gives better yields (9) than when it reacts with other ketones, whereas aldehydes form olefins with II so readily that a minor reluctance for the phosphafulvene to react would not be apparent.

Can. J. Chem. Downloaded from www.nrcresearchpress.com by 84.22.46.98 on 09/08/12
For personal use only.

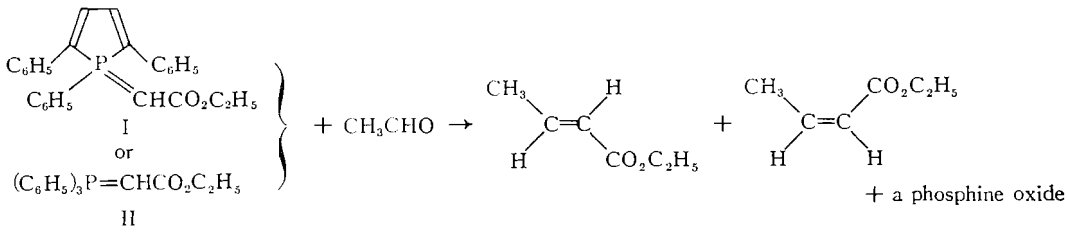
Can. J. Chem. Downloaded from www.nrcresearchpress.com by 84.22.46.98 on 09/08/12
For personal use only.

The phosphafulvene reacted with cyclohexanone only under the most stringent conditions used with II, to give a similar yield of crude ethyl cyclohexylideneacetate, as indicated in Table I. Conditions of intermediate severity were insufficient to cause any detectable reaction.

Benzaldehyde reacted readily with the phosphafulvene in ethanol both at room temperature and in the boiling solvent, to give yields of ethyl cinnamate comparable to those obtained by others with II (Table II). No attempt was made to analyze the resulting ethyl cinnamate for *cis* and *trans* isomers, since Bergelson (15, 16) had already found the Wittig reagent II to yield virtually 100% ethyl *trans*-cinnamate regardless of conditions or additives.

Though the affinity of the phosphafulvene towards carbonyl reagents has been shown to be qualitatively somewhat lower than that of the triphenylphosphine phosphorane, experience indicates that the phosphafulvene is less stable towards atmospheric conditions. In the air fairly rapid decomposition of the phosphafulvene to 1,2,5-triphenylphosphole-1-oxide occurs, as shown by changes in the ultraviolet absorption and melting point with time (Table III). Also, it should be mentioned here that the phosphafulvene is much more sensitive to hydrolytic decomposition by moist solvents than II, as evidenced by difficulties in recrystallization (1), and by the lack of any detectable product from a reaction with the phosphafulvene in acetonitrile containing 0.67% water, conditions which little affected the phosphorane II.

Stereochemical investigations with the new Wittig reagent, it was felt, should be interesting for two reasons. The bulk of the phosphorus ligands in the phosphafulvene, though quantitatively similar to that of the three phenyls in triphenylphosphine, is unsymmetrically disposed about the phosphorus, as displayed by Stuart–Briegleb models. The other



point of difference is that the phosphorus in the phosphafulvene is in a more strained configuration than that in the triphenylphosphine phosphorane, which may in itself alter the ratio of geometrical isomers obtained in reactions with the former.

Two unsymmetrical ketones, ethyl methyl ketone and acetophenone (excess as solvent), have been found (9) to give mixtures of *cis* and *trans* isomers with II, but no accurate quantitative data were obtained. More recently, Russian workers (15) found that the steric course of the reaction of II and benzaldehyde was predominantly to ethyl *trans*-cinnamate, and was relatively unaffected by environment. House and his co-workers (17) have since published the results of clean-cut stereochemical investigations of the products from reactions of II (as the methyl ester) and acetaldehyde under a wide variety of conditions.

Originally, acetaldehyde was chosen by us for experiments to demonstrate the stereochemistry of the phosphafulvene, with the intention of using low-temperature vapor-phase chromatography for analysis of the *cis* to *trans* ratio. After this work was initiated, House (17) was successful in using vapor-phase chromatography to analyze analogous

TABLE I

Yields of ethyl cyclohexylideneacetate obtained via cyclohexanone and II, or the phosphafulvene (I)

$Ph_3P{=}CHCO_2C_2H_5$ (II)					Phosphafulvene (I)			
Reference	Solvent	Temperature	Time	% yield	Solvent	Temperature	Time	% yield
10	Ethanol	Room temperature	7 days	44				
11	Benzene	—	4 h	95	Benzene	Boiling	24 h	0
12	Benzene or toluene	Boiling	—	25				
13	None	150°	—	30*				
9	Excess cyclohexanone	170°	10 h	60†	Excess cyclohexanone	170°	10 h	57 crude, 10 pure†

*With 2-methylcyclohexanone.
†Isolated as the acid after saponification of the crude product.

TABLE II

Yields of ethyl cinnamate from benzaldehyde and II, or the phosphafulvene (I)

$Ph_3P{=}CHCO_2C_2H_5$ (II)					Phosphafulvene (I)			
Reference	Solvent	Temperature	Time	% yield	Solvent	Temperature	Time	% yield
14	Ethanol	Room temperature	48 h	77*	Ethanol	Room temperature	48 h	82
15	Benzene	Boiling	8 h	73	Ethanol	Boiling	2 h	76
15	Dimethylformamide	Room temperature	48 h	78*				

*With generation of Wittig reagent *in situ*.

TABLE III

Atmospheric decomposition of phosphafulvene (I) with time*

Atmospheric exposure	20 h		48 h		50 days		80 days		150 days	Pure phosphole oxide	
Melting point	161–163°						216–227°		220–233°	237–239°	
Ultraviolet absorption	λ_{max}	ϵ_{molar}	λ_{max}	ϵ_{molar}	λ_{max}	ϵ_{molar}	λ_{max}	ϵ_{molar}		λ_{max}	ϵ_{molar}
	222†	33 500	223	30 600	222†	25 000	221	23 200	—	222	20 900
	238	20 600	239	19 300	240	17 900	241	17 750		242	16 400
	384	14 600	385	14 900	392	15 850	396	16 700		397	16 950

*The spectra were measured in absolute ethanol at accurate concentrations of the order of 10 mg/l. The wavelengths are quoted in millimicrons.
†Not a definite maximum, extinction coefficient at this wavelength.

Can. J. Chem. Downloaded from www.nrcresearchpress.com by 84.22.46.98 on 09/08/12
For personal use only.

cis–trans ester systems. However, a preliminary examination of ethyl *cis*- and *trans*-crotonates by proton n.m.r. established this method as being suitable for accurately determining the relative percentage of each in a mixture. Both the phosphafulvene (I) and the triphenylphosphine phosphorane (II) gave fair yields of mixed isomers of ethyl crotonate under identical conditions. By analysis of the integrals of the n.m.r. quadruplet caused by the respective vinylic methyl protons in the mixtures of *cis* and *trans* isomers, the relative amounts of each isomer were calculated.

Though under some conditions the triphenylphosphine phosphorane yielded a greater proportion of ethyl *cis*-crotonate than did the phosphafulvene, the tendency was to a product containing a greater proportion of *cis* ester from the phosphafulvene (Table IV). The insensitivity of the stereospecificity of II to solvent polarity was confirmed by our experiments in acetonitrile, a non-protonating polar solvent. This finding agrees with that of the Russian workers (16), and that found by House (17) with the methyl ester of II for *non-protonating* polar solvents. However, this insensitivity of II to solvent polarity cannot directly be applied to Wittig reactions of the phosphafulvene on the basis of our results.

TABLE IV

Effect of Wittig reagent, solvent, and temperature on yield and *cis* to *trans* ratio of ethyl crotonate from acetaldehyde

Solvent	Reaction temperature and type	$Ph_3P{=}CHCO_2C_2H_5$ (II)		Phosphafulvene (I)	
		Total yield	% *cis*	Total yield	% *cis*
Benzene	80°	82	11	39	24
Benzene	80°, control	—	—	43	8
Ethanol	79°	19, 12	7, 6	22	17
Ethanol	79°, control	—	—	35	8
Ethanol	23°	31	10	24	3
Acetaldehyde	21°	33	8	35	26
Acetonitrile	80°	50*	8*	14†	7†

*Reaction was carried out in solvent containing 0.67% water.
†The methyl ester of phosphafulvene (I).

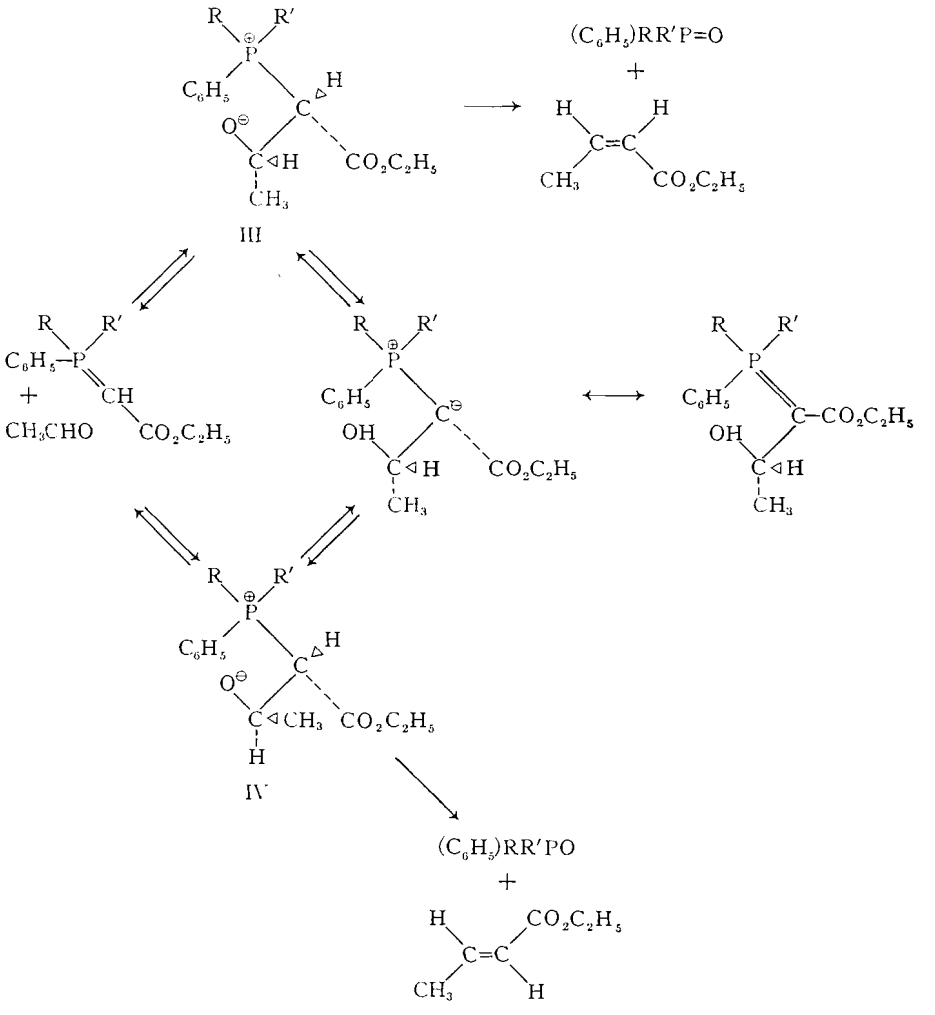
DISCUSSION

Important contributions to the mechanism outlined in Reaction Scheme 1 (4) have been made by many authors. Speziale and Bissing (18), for instance, have presented evidence to support the reversible formation of betaines from stable phosphoranes. Others have shown that both the inductive effect of the ylid substituents (19–21) of the phosphorane and the inductive effects of the other substituents on phosphorus (22, 23) play important roles, the first by changing the acidity of the α-hydrogen on the ylid, and the second by affecting the oxygen affinity of phosphorus. The recent X-ray determinations of the geometry of several phosphorus ylids (24 and references therein), particularly the findings revealing that the ylid α-carbon has little anionic character in at least the carbonyl- or sulfonyl-stabilized ylids (25),[3] also are relevant to any consideration of mechanistic pathways in the Wittig reaction.

The decreased stereoselectivity of the phosphafulvene can be attributed to one, or more, of several factors. If the main features of the mechanism (4) are accepted, slower equilibration of the two stereoisomeric betaines III*a* and IV*a* over III*b* and IV*b* will lead to a more nearly statistical distribution of *cis* and *trans* olefin product for the phosphafulvene, as

[3]*K. W. Ratts, personal communication.*

Can. J. Chem. Downloaded from www.nrcresearchpress.com by 84.22.46.98 on 09/08/12
For personal use only.



REACTION SCHEME 1. Pathways for betaine interconversion and decomposition.

found. Faster decomposition of the betaines III*a* and IV*a*, as they are formed, over the betaines III*b* and IV*b* would have the same net effect on the ratio of *cis* to *trans* olefin as slower equilibration.

Our stereochemical control experiments demonstrate that either equilibration or fractionation, or both, must have been occurring in our experiments with the phosphafulvene. Also, our small-scale tests failed to elucidate the cause of the suspected equilibration; yet equilibration is almost certainly the explanation of the low *cis* yields in the control reactions rather than fractionation, since there was only a decrease in the percentage of the *cis* isomer, not a simultaneous decrease in the yield. However ineffective the small-scale tests were in demonstrating equilibration, perhaps because of the relatively low proportion

Can. J. Chem. Downloaded from www.nrcresearchpress.com by 84.22.46.98 on 09/08/12
For personal use only.

of additive to ester compared with the proportions present in the actual reactions, they did demonstrate a further consideration. Apparently, both the *cis* and the *trans* esters undergo Diels–Alder reactions with the phosphole oxide (1), as evidenced by the loss of color. However, the *cis* ester apparently, and not surprisingly, reacts faster than the *trans* ester (see Experimental). This preferential loss of *cis* ester could help to explain the low yields of the *cis* isomer in our control experiments, but probably only partly, since between $2\frac{1}{2}$ and 64 h was required for 2–8 mg of phosphole oxide to react completely with excess ester. At least the indications from the control experiments are that actually higher percentages of *cis* ester are formed than are indicated in Table IV.

Because of the conflict between the results of our control experiments and our other stereochemical results, there is little point in applying these to any mechanistic discussion of the Wittig reaction. However, empirical considerations may explain the higher *cis* yields obtained with the phosphafulvene. For instance, the 25% lower P=O bond dissociation energy for the phosphoryl group in pentaphenylphosphole-1-oxide as opposed to that in triphenylphosphine oxide (26) discourages the suggestion of faster decomposition for the intermediate betaines III*a* and IV*a*. On the other hand, in the respective intermediate betaines the apparent greater ease with which the oxygen anion can approach the phosphonium ion (Stuart–Briegleb models) in III*a* or IV*a* rather than in III*b* or IV*b* counteracts the suggestion based on bond dissociation energy. The greater of the foregoing effects (charge magnitude or the extent of charge delocalization) decides the relative rates of betaine decomposition according to its contribution to the overall scheme.

Since at least the reactive phosphoranes showed an enhancement of the *cis* to *trans* ratio when the polarity of the solvent was increased, we were hopeful of observing an enhancement of this ratio with the phosphafulvene. Unfortunately, no significant solvent effect was observed. Even in ethanol, with which we expected a significant *cis* effect based on the findings of House (17), a decrease, if anything, in the *cis* to *trans* ratio occurred. Several workers (3, 27) have reported that the higher the temperature at which a Wittig reaction is carried out the greater the yield of the *trans* olefin. Therefore, it was thought that this lack of a noticeable *cis* enhancement in ethanol in our experiments may be explicable on the basis of a temperature effect, since House and his co-workers (17) carried out their reactions at room temperature, whereas our initial experiments were at 80°. To prove this and to help explain the high percentage of *cis* ester obtained from the phosphafulvene reaction in acetaldehyde, Wittig reactions were repeated with the phosphafulvene and the phosphorane (II) in ethanol, but at room temperature. A slight *cis* enhancement was noticed with II, but only a trace of *cis* ester, if any, was obtained with the phosphafulvene. Therefore, a temperature effect alone cannot be the explanation for either our not finding any solvent effect, or for the high percentage of *cis* ester obtained from the phosphafulvene in acetaldehyde. Indeed, these experiments gave us yet another unanswered question: why should carrying out the phosphafulvene reaction at room temperature give us such a change in the isomer ratio?

Synthetic utility of this phosphafulvene Wittig includes the preparation of *cis* olefins not readily accessible by alternative methods. Another very specific possible application is the employment of successive Wittig reactions in placing different ligands on an aldehydic carbonyl and a ketonic carbonyl in the same molecule. A phosphafulvene Wittig reagent will probably give the product involving replacement of only the aldehydic oxygen, after which a triphenylphosphine Wittig reagent can be employed for replacement of the more hindered carbonyl oxygen, a sequence of reactions not as yet demonstrated to be within the capability of conventional Wittig reagents alone.

Can. J. Chem. Downloaded from www.nrcresearchpress.com by 84.22.46.98 on 09/08/12
For personal use only.

ACKNOWLEDGMENTS

The author thanks Mr. H. D. Mak and Dr. J. S. McIntyre for measuring the n.m.r. spectra, and Mr. D. J. Peterson for obtaining many of the infrared and ultraviolet spectra.

REFERENCES

1. I. G. M. CAMPBELL, R. C. COOKSON, M. B. HOCKING, and A. N. HUGHES. J. Chem. Soc. 2184 (1965).
2. J. LEVISALLES. Bull. Soc. Chim. France, 1021 (1958). U. SCHÖLLKOPF. Angew. Chem. **71**, 260 (1959).
3. S. TRIPPETT. *In* Advances in organic chemistry. Vol. I. Interscience Publishers, Inc., New York. 1960. p. 83.
4. S. TRIPPETT. Quart. Rev. London, **XVII**, 406 (1963).
5. H. LUND and J. BJERRUM. Chem. Ber. **62**, 2801 (1931). H. LUND. J. Am. Chem. Soc. **74**, 3188 (1952).
6. M. J. KAMLET (*Editor*). Organic electronic spectral data. Vol. I. Interscience Publishers, Inc., New York. 1960. H. E. UNGNADE (*Editor*). Organic electronic spectral data. Vol. II. Interscience Publishers, Inc., New York. 1960. J. P. PHILLIPS and F. C. NACHOD (*Editors*). Organic electronic spectral data. Vol. IV. Interscience Publishers, Inc., New York. 1963.
7. H. SCHMID and P. KARRER. Helv. Chim. Acta, **XXXI**, 1067 (1948).
8. G. H. JEFFERY and A. I. VOGEL. J. Chem. Soc. 658 (1948).
9. G. FODOR and I. TÖMÖSKÖZI. Tetrahedron Letters, 579 (1961).
10. S. SUGASAWA and H. MATSUO. Chem. Pharm. Bull. Tokyo, **8**, 819 (1960).
11. C. RÜCHARDT, S. EICHLER, and P. PANSE. Angew. Chem. **75**, 858 (1963).
12. S. TRIPPETT and D. M. WALKER. Chem. Ind. London, 990 (1961).
13. H. T. OPENSHAW and N. WHITAKER. Proc. Chem. Soc. 454 (1961).
14. G. WITTIG and W. HAAG. Chem. Ber. **88**, 1654 (1955).
15. L. D. BERGELSON, V. A. VAVER, L. I. BARSUKOV, and M. M. SHEMYAKIN. Izv. Akad. Nauk SSSR Otd. Khim. Nauk, 1053 (1963); Bull. Acad. Sci. USSR Div. Chem. Sci. Engl. Transl. 957 (1963).
16. L. D. BERGELSON, V. A. VAVER, L. I. BARSUKOV, and M. M. SHEMYAKIN. Dokl. Akad. Nauk SSSR, **143**, 111 (1962); Proc. Acad. Sci. USSR Chem. Sect. Engl. Transl. **143**, 148 (1962).
17. H. O. HOUSE, V. K. JONES, and G. A. FRANK. J. Org. Chem. **29**, 3327 (1964).
18. A. J. SPEZIALE and D. E. BISSING. J. Am. Chem. Soc. **85**, 1888 (1963).
19. H. O. HOUSE and G. H. RASMUSSON. J. Org. Chem. **26**, 4278 (1961).
20. R. KETCHAM, D. JAMBOTKAR, and L. MARTINELLI. J. Org. Chem. **27**, 4666 (1962).
21. P. A. CHOPARD and R. F. HUDSON. Tetrahedron Letters, 2357 (1965).
22. H. J. BESTMANN and O. KRATZER. Chem. Ber. **95**, 1894 (1962).
23. A. W. JOHNSON and V. L. KYLLINGSTAD. J. Org. Chem. **31**, 334 (1966).
24. P. J. WHEATLEY. J. Chem. Soc. 5785 (1965).
25. A. J. SPEZIALE and K. W. RATTS. 150th Meeting, American Chemical Society, September 1965. Abstr. p. S120.
26. A. F. BEDFORD, D. M. HEINEKEY, I. T. MILLAR, and C. T. MORTIMER. J. Chem. Soc. 2932 (1962).
27. A. MONDON. Ann. Chem. **603**, 115 (1957).

Can. J. Chem. Downloaded from www.nrcresearchpress.com by 84.22.46.98 on 09/08/12
For personal use only.

Can. J. Chem. Downloaded from www.nrcresearchpress.com by 210.87.254.40 on 09/05/12
For personal use only.

NOTES

A CONVENIENT METHYLATION PROCEDURE

U. E. Diner, F. Sweet, and R. K. Brown

The use of the more powerful solvents dimethylformamide and (or) dimethyl sulfoxide has permitted one-step complete methylation in good yield, with either silver oxide – methyl iodide or methyl sulfate – barium oxide (hydroxide), of a number of polyhydroxy compounds (1). This is a distinct improvement over the silver oxide – methyl iodide (2) or methyl sulfate – sodium hydroxide (3) procedures, which often required tedious, repeated methylations to produce the fully alkylated products. A recent report (4) illustrates rapid permethylation of a glycolipid and a polysaccharide by methyl iodide in the presence of the methylsulfinyl carbanion (5) obtained from the reaction of sodium hydride with dimethyl sulfoxide.

We wish to draw attention to a methylating procedure which we have employed for some time, and which is rapid and quite broadly applicable, resulting in a clean reaction providing consistently excellent yields of readily isolable, fully methylated material. It involves the addition of sodium hydride to a solution of the hydroxy compound in 1,2-dimethoxyethane, or in dimethylformamide if the solubility of the compound is low in 1,2-dimethoxyethane, or in a mixture of the two solvents. Methyl iodide is added shortly after, or it may be present advantageously in the solution before, the addition of the sodium hydride to the reaction mixture. Yields are above 80%.

A similar procedure has been reported by Eades *et al.* (6) for the preparation of 1,5-anhydro-2,3,4,6-tetra-*O*-methyl-D-mannitol with tetrahydrofuran as solvent, and by Tate and Bishop (7) for the preparation of benzyl ethers with excess benzyl chloride as solvent.

The convenience and utility of this method prompted us to point out the work noted in the last two papers as well as our own experience. Details of our procedure are illustrated by the following two examples.

6-Methoxymethyl-5,6-dihydropyran

To a solution of 6-hydroxymethyl-5,6-dihydropyran[1] (68.4 g, 0.6 mole) and methyl iodide (99.5 g, 0.7 mole) in 350 ml of dried ($LiAlH_4$), distilled 1,2-dimethoxyethane, all contained in a 1 l, three-necked flask equipped with a condenser, dropping funnel, drying tube, and magnetic stirrer, was added 15.6 g (0.65 mole) of sodium hydride[2] over a period of 30 min. Vigorous hydrogen evolution took place after addition of each of the small portions of the hydride. Heat was evolved and sodium iodide precipitated. Ten minutes after the last of the hydride had been added, a further quantity (10 ml) of methyl iodide was added and the solution stirred at room temperature for 1 to 2 h. The 1,2-dimethoxyethane and excess methyl iodide were removed by distillation at atmospheric pressure until the volume was reduced to one-third. Anhydrous ether (60 ml) was added, whereupon more sodium iodide precipitated. The mixture was filtered, the sodium iodide was washed

[1]*Kindly donated by J. A. Craig, Shell of Canada Limited, Winnipeg, Manitoba.*

[2]*The sodium hydride (Metal Hydrides Corporation) was a 56% suspension in mineral oil. The oil was washed out with ether and the hydride obtained by filtration. Satisfactory results were obtained if this was kept covered during the interval of addition to the solution.*

with 20 ml of ether, and the combined washings and filtrate were distilled at atmospheric pressure to remove the bulk of the solvent. Residual 1,2-dimethoxyethane was removed at 100 mm pressure with a spinning-band fractionating column. Further distillation gave the product boiling at 83–84° and 65 mm, yield 70 g (91%), η_D^{27} 1.4400.

Anal. Calcd. for $C_7H_{12}O_2$: C, 65.60; H, 9.44. Found: C, 65.41; H, 9.30.

Methyl 2,3,4,6-Tetra-O-methyl-α-D-glucopyranoside

Into a three-necked flask equipped with an efficient condenser and a mechanical stirrer was placed anhydrous methyl α-D-glucopyranoside (9.7 g, 0.05 mole) dissolved in a mixture of 130 ml of dry dimethylformamide and 70 ml of 1,2-dimethoxyethane (previously dried and distilled from $LiAlH_4$). Methyl iodide (32.5 g, 0.23 mole) was added and the solution cooled to −10° by immersion of the flask for a time in a dry ice – acetone bath. About half of the sodium hydride[2] (total amount: 4.8 g, 0.02 mole) was added in small portions over a period of 7–8 min to the stirred solution. A gentle evolution of gas occurred and the reaction temperature rose slowly. Then the rest of the hydride was added all at once. When the temperature reached 30°, the reaction became vigorous, whereupon the flask was immersed in the dry ice – acetone bath. A maximum temperature of 60° was reached and maintained for about 5 min, and then dropped rapidly. The cooling bath was removed, and then the mixture was stirred for a time (total reaction time ~1 h) and finally poured cautiously into 600 ml of water containing 100 g of dissolved sodium chloride. The resulting mixture was extracted with chloroform (5 × 100 ml). The combined extracts were dried (Na_2SO_4) and freed of solvents by rotary evaporation and finally by distillation under vacuum at 2 mm with a bath temperature of 70 °C. The crude residue (11.5 g, 92%), when analyzed by gas–liquid chromatography on a 6 ft column of 20% butanediol succinate on Gas Chrom P (60–80 mesh) at 200° with a helium flow rate of 70 ml/min, consisted of only two substances: dimethylformamide (~4% on a molar basis) and the fully methylated glucoside. Removal of the residual dimethylformamide was accomplished by passage of the crude product through a column of Woelm neutral alumina (150 g), using successively the eluants (200 ml of each) benzene–pentane (7:4), benzene–chloroform (1:1), and benzene–chloroform (1:3). The sequence of increasing polarity of eluants was used to avoid the possibility of elution of the contaminating dimethylformamide. The higher polarity was required to remove the last portion of the pentamethyl glucoside from the strongly adsorbing column. When British Drug Houses alumina was used, the eluant benzene–pentane (7:4) was sufficient to remove selectively all of the glucoside. The resulting pure methyl 2,3,4,6-tetra-*O*-methyl-α-D-glucoside (10.5 g, 84%) was identical in all respects with an authentic sample (3, 8). The infrared spectrum (neat) showed no absorption in the 3 600 – 3 300 cm^{-1} region (OH).

ACKNOWLEDGMENT

This work was supported by a grant from the National Research Council of Canada.

1. K. Wallenfels, G. Bechtler, R. Kuhn, H. Trischmann, and H. Egge. Angew. Chem. Intern. Ed. Engl. **2**, 515 (1963).
2. J. Purdie and J. C. Irvine. J. Chem. Soc. **83**, 1021 (1903).
3. W. N. Haworth. J. Chem. Soc. **107**, 8 (1915).
4. S. Hakomori. J. Biochem. Tokyo, **55**, 205 (1964).
5. E. J. Corey and M. Chaykovsky. J. Am. Chem. Soc. **87**, 1345 (1965).
6. E. D. M. Eades, D. H. Ball, and L. Long, Jr. J. Org. Chem. **30**, 3949 (1965).
7. M. E. Tate and C. T. Bishop. Can. J. Chem. **41**, 1801 (1963).
8. J. Purdie and J. C. Irvine. J. Chem. Soc. **85**, 1059 (1904).

Received March 8, 1966.
Department of Chemistry,
University of Alberta,
Edmonton, Alberta.

Can. J. Chem. Downloaded from www.nrcresearchpress.com by 210.87.254.40 on 09/05/12
For personal use only.

FACILE METHYLATION OF HUMIC ACIDS FROM ORGANIC SOILS[1]

HIROKAZU MORITA

The application of classical techniques of organic chemistry to the structural elucidation of soil humic acid has been fraught with difficulties because of the intractable, labile features of the macromolecule. Partial amelioration has been sought in the conversion of the natural product into stable derivatives. The presence of polyphenolic functions in the compound (1) makes methylation an obvious choice for derivatization.

Existing methylation techniques, however, suffer from various shortcomings; none are satisfactory for the humic acid isolated from organic soils. We now describe an efficacious methylation procedure which has lead to promising results. The procedure, moreover, appears to be applicable to other polyphenolic materials.

The experiment described below is based on the one described by McCredie (2) for the one-step methylation of galactomannan with dimethyl sulfate and powdered sodium hydroxide in dioxane or dimethyl sulfoxide. In our hands, the best results were obtained with dimethyl sulfoxide as the solvent.

The advantage of the methylation procedure described herein is evident when the results are compared with those obtained by five successive Haworth methylations under conditions whereby gallic acid is completely methylated (3). Permethylation according to this procedure gave a methylated humic acid containing 16.59% methoxyl, whereas the more direct procedure involving an initial methylation in aqueous alkali followed by a methylation in dimethyl sulfoxide gave a product whose methoxyl content was 21.78%.

The importance of the solvent for an efficient methylation of humic acid is demonstrated by experiments in which dimethyl sulfoxide was replaced by other organic solvents. For example, in tetrahydrofuran and dimethylformamide the derivative had methoxyl values of 15.88% and 8.06%, respectively.

The infrared absorption spectra of the potassium bromide disks and Nujol mulls, as well as the attenuated total reflectance spectra, of the methylated humic acid containing 23.85% methoxyl showed a weak absorption at 3 400 cm^{-1}, indicating the presence of residual hydroxyl groups or absorbed moisture.

Modified Haworth methylations in organic media have been known for some time in carbohydrate chemistry (4). The utility of these procedures with phenolic materials appears to have been overlooked. The efficacy of methylations undertaken in dimethyl sulfoxide has been observed in this laboratory with unsaturated and polyphenolic acids which are fully methylated in one operation. For example, *p*-coumaric, caffeic, gallic, and *m*-digallic acids are smoothly converted into the corresponding dimethyl, trimethyl, tetramethyl, and hexamethyl derivatives.

EXPERIMENTAL

Starting Material

The soil samples, which were obtained from Alfred, Ontario, have been described earlier (5). The humic acid was isolated by a method described by Smith and Lorimer (6) involving five successive extractions with 0.2 *M* sodium hydroxide. The final freeze-dried product gave the following elemental analysis: C, 55.88%; H, 5.88%; N, 2.04%; OCH_3, 2.24%.

Methylation

Humic acid (1 g) was dispersed in 12% aqueous sodium hydroxide (20 ml) under nitrogen; after the addition of potassium borohydride (0.3 g), the reactants were set aside overnight, with continuous stirring.

[1]*Contribution No. 192 from the Soil Research Institute.*

Can. J. Chem. Downloaded from www.nrcresearchpress.com by 210.87.254.6 on 09/05/12
For personal use only.

To the reduced material cooled in a cold-water bath, 30% aqueous sodium hydroxide (17.5 ml) and dimethyl sulfate (17.5 ml) were added in portions and alternately over 6 h. Stirring, under nitrogen, was continued throughout the addition of the reagents and overnight.

Next, water (50 ml) was added to the reaction mixture and the aqueous solution heated on a steam bath for 1 h. After the methylation mixture was cooled in ice, it was acidified with 6 *N* sulfuric acid. The resulting light-brown precipitate was separated by centrifugation, thoroughly washed with water, freeze-dried, and finally dried *in vacuo*.

The partly methylated humic acid was dispersed in dimethyl sulfoxide (60 ml) (spectro grade, Eastman Kodak) and cooled. Then powdered sodium hydroxide (5.5 g) was added. The mixture was stirred under nitrogen, and dimethyl sulfate (12.5 ml) was added in portions periodically over 6 h. Stirring was continued overnight at room temperature.

The isolation of the permethylated product was accomplished by initially adding water (60 ml) to the reaction mixture to dissolve the alkali. The alkaline solution was then neutralized with 6 *N* sulfuric acid. Finally, the precipitate was isolated by centrifugation, washed thoroughly with water, freeze-dried, and dried *in vacuo*. The methylated derivative (1 g) gave the following analysis: C, 62.90%; H, 7.06%; N, 0.88%; OCH_3, 21.78%. A second methylation in dimethyl sulfoxide gave a product containing 23.85% methoxyl. The methoxyl contents of the methylated humic acids reported in the literature (1) have generally been less than 20%.

The substitution of an equal volume of tetrahydrofuran for dimethyl sulfoxide gave, after two successive methylations, a product whose elemental analysis showed C, 58.62%; H, 5.97%; N, 1.37%; OCH_3, 15.88%. When dimethylformamide was used, the methylated product contained C, 57.45%; H, 5.77%; N, 1.80%; OCH_3, 8.06%.

Haworth Methylation

Humic acid (1 g) was treated with potassium borohydride and methylated as described above. Subsequent methylations in aqueous media consisted of alternate additions of 30% aqueous sodium hydroxide (17.5 ml) and dimethyl sulfate (12.5 ml) to a solution of the partly methylated derivative in 0.3 *M* sodium hydroxide (50 ml), the reagents being added, with stirring, under nitrogen. The work-up and isolation of the product were performed as outlined in the previous methylation. Three methylations were carried out in this manner.

The final methylation was carried out by dissolving the partly methylated derivative in a solution of sodium hydroxide (3 g) and sodium carbonate (8 g) in water (50 ml), and adding dimethyl sulfate (12.5 ml) according to the procedure outlined for the preparation of methyl 3,4,5-trimethoxybenzoate (3). The resulting product gave the following analyses: C, 60.13%; H, 6.44%; OCH_3, 16.58%.

ACKNOWLEDGMENTS

The author gratefully acknowledges the technical assistance of Mr. W. G. Montgomery. The analyses were carried out by Mr. G. F. Morris of the Analytical Research Service, Canada Department of Agriculture, Ottawa.

1. M. M. Kononva. Soil organic matter. The Pergamon Press, Ltd., London. 1961.
2. R. J. McCredie. Ph.D. Thesis, Purdue University, Lafayette, Indiana. 1958.
3. M. U. Tsao. J. Am. Chem. Soc. **73**, 5495 (1951).
4. B. Lindberg and B. Wickerg. Acta Chem. Scand. **8**, 569 (1954).
5. H. Morita. J. Org. Chem. **27**, 1079 (1962).
6. D. G. Smith and J. W. Lorimer. Can. J. Soil Sci. **44**, 76 (1964).

Received March 9, 1966.
Soil Research Institute,
Canada Department of Agriculture,
Ottawa, Canada.

SELECTIVE REDUCTION OF SUBSTITUTED ALDONOLACTONES TO ALDOSE DERIVATIVES

R. K. Hulyalkar[1]

Substituted aldonolactones were reduced with sodium borohydride and acetic acid in nonaqueous media to aldose derivatives. To examine whether the diborane produced by the reaction of sodium borohydride and acetic acid was responsible for this reduction,

[1]*Present address: Polymer Corporation Limited, Sarnia, Ontario.*

Can. J. Chem. Downloaded from www.nrcresearchpress.com by 210.87.254.6 on 09/05/12
For personal use only.

To the reduced material cooled in a cold-water bath, 30% aqueous sodium hydroxide (17.5 ml) and dimethyl sulfate (17.5 ml) were added in portions and alternately over 6 h. Stirring, under nitrogen, was continued throughout the addition of the reagents and overnight.

Next, water (50 ml) was added to the reaction mixture and the aqueous solution heated on a steam bath for 1 h. After the methylation mixture was cooled in ice, it was acidified with 6 *N* sulfuric acid. The resulting light-brown precipitate was separated by centrifugation, thoroughly washed with water, freeze-dried, and finally dried *in vacuo*.

The partly methylated humic acid was dispersed in dimethyl sulfoxide (60 ml) (spectro grade, Eastman Kodak) and cooled. Then powdered sodium hydroxide (5.5 g) was added. The mixture was stirred under nitrogen, and dimethyl sulfate (12.5 ml) was added in portions periodically over 6 h. Stirring was continued overnight at room temperature.

The isolation of the permethylated product was accomplished by initially adding water (60 ml) to the reaction mixture to dissolve the alkali. The alkaline solution was then neutralized with 6 *N* sulfuric acid. Finally, the precipitate was isolated by centrifugation, washed thoroughly with water, freeze-dried, and dried *in vacuo*. The methylated derivative (1 g) gave the following analysis: C, 62.90%; H, 7.06%; N, 0.88%; OCH_3, 21.78%. A second methylation in dimethyl sulfoxide gave a product containing 23.85% methoxyl. The methoxyl contents of the methylated humic acids reported in the literature (1) have generally been less than 20%.

The substitution of an equal volume of tetrahydrofuran for dimethyl sulfoxide gave, after two successive methylations, a product whose elemental analysis showed C, 58.62%; H, 5.97%; N, 1.37%; OCH_3, 15.88%. When dimethylformamide was used, the methylated product contained C, 57.45%; H, 5.77%; N, 1.80%; OCH_3, 8.06%.

Haworth Methylation

Humic acid (1 g) was treated with potassium borohydride and methylated as described above. Subsequent methylations in aqueous media consisted of alternate additions of 30% aqueous sodium hydroxide (17.5 ml) and dimethyl sulfate (12.5 ml) to a solution of the partly methylated derivative in 0.3 *M* sodium hydroxide (50 ml), the reagents being added, with stirring, under nitrogen. The work-up and isolation of the product were performed as outlined in the previous methylation. Three methylations were carried out in this manner.

The final methylation was carried out by dissolving the partly methylated derivative in a solution of sodium hydroxide (3 g) and sodium carbonate (8 g) in water (50 ml), and adding dimethyl sulfate (12.5 ml) according to the procedure outlined for the preparation of methyl 3,4,5-trimethoxybenzoate (3). The resulting product gave the following analyses: C, 60.13%; H, 6.44%; OCH_3, 16.58%.

ACKNOWLEDGMENTS

The author gratefully acknowledges the technical assistance of Mr. W. G. Montgomery. The analyses were carried out by Mr. G. F. Morris of the Analytical Research Service, Canada Department of Agriculture, Ottawa.

1. M. M. Kononva. Soil organic matter. The Pergamon Press, Ltd., London. 1961.
2. R. J. McCredie. Ph.D. Thesis, Purdue University, Lafayette, Indiana. 1958.
3. M. U. Tsao. J. Am. Chem. Soc. **73**, 5495 (1951).
4. B. Lindberg and B. Wickerg. Acta Chem. Scand. **8**, 569 (1954).
5. H. Morita. J. Org. Chem. **27**, 1079 (1962).
6. D. G. Smith and J. W. Lorimer. Can. J. Soil Sci. **44**, 76 (1964).

Received March 9, 1966.
Soil Research Institute,
Canada Department of Agriculture,
Ottawa, Canada.

SELECTIVE REDUCTION OF SUBSTITUTED ALDONOLACTONES TO ALDOSE DERIVATIVES

R. K. Hulyalkar[1]

Substituted aldonolactones were reduced with sodium borohydride and acetic acid in nonaqueous media to aldose derivatives. To examine whether the diborane produced by the reaction of sodium borohydride and acetic acid was responsible for this reduction,

[1]*Present address: Polymer Corporation Limited, Sarnia, Ontario.*

Can. J. Chem. Downloaded from www.nrcresearchpress.com by 210.87.254.5 on 09/05/12
For personal use only.

2,3;5,6-di-*O*-isopropylidene-D-gulono-1,4-lactone was treated with diborane in tetrahydrofuran according to Brown and Subba Rao (1, 2). It was found that the original product was recovered. Reduction did not occur, probably owing to the steric hindrance of the substituent groups. Treatment of 2,3;5,6-di-*O*-isopropylidene-D-gulono-1,4-lactone with diborane in the presence of acetic acid did not cause any reduction.

The reduction of 2,3;5,6-di-*O*-isopropylidene-D-gulono-1,4-lactone, 2,3-*O*-isopropylidene-D-gulono-1,4-lactone, 2,3-*O*-isopropylidene-D-ribono-1,4-lactone, and 2,4-dihydroxy-3,3-dimethylbutanoic acid 1,4-lactone was effected in ether or tetrahydrofuran solution containing a suspension of sodium borohydride to which the calculated amount of acetic acid was added, to yield 75 to 80% of the corresponding derivatives of D-gulose, D-ribose, and butanal.

The new procedure offers an improved method for the reduction of substituted aldonolactones to aldose derivatives over the classical method involving reduction, in aqueous media, of aldonolactones with sodium amalgam (3, 4) or sodium borohydride under controlled pH conditions (5). It also offers a new and easy method for the preparation of substituted aldoses which are difficult to synthesize by other routes, particularly 2,3-*O*-isopropylidene derivatives.

EXPERIMENTAL

2,3;5,6-Di-O-isopropylidene-D-gulose

To a stirred mixture of 2,3;5,6-di-*O*-isopropylidene-D-gulono-1,4-lactone (200 mg) and sodium borohydride (190 mg) in anhydrous ether (50 ml), glacial acetic acid (0.5 ml) in ether (10 ml) was added over 30 min. After 2½ h at room temperature, acetone (2 ml) was added and stirring was continued for 30 min. Sodium hydroxide (4.5 ml, 2 *N*) was then added followed by a saturated sodium chloride solution (10 ml). The ether layer was removed, dried (anhydrous Na_2SO_4), and filtered, and the filtrate concentrated. The residue was crystallized from an ether – light petroleum ether (40–60°) mixture to yield 2,3;5,6-di-*O*-isopropylidene-D-gulose (140 mg, 70%), which had m.p. 114–115° and $[\alpha]_D$ −6.3° (*c*, 0.9 in water) (6).

Anal. Calcd. for $C_{12}H_{20}O_6$: C, 55.4; H, 7.7. Found: C, 55.2; H, 7.9.

The hydrolyzed di-*O*-isopropylidene-D-gulose, when subjected to paper chromatographic analysis, showed a single spot having chromatographic behavior identical with that of authentic D-gulose.

2,3-O-Isopropylidene-D-gulose

To a stirred suspension of sodium borohydride (190 mg) in dry tetrahydrofuran (80 ml) containing 2,3-*O*-isopropylidene-D-gulono-1,4-lactone (200 mg), glacial acetic acid (0.45 ml) in tetrahydrofuran (5 ml) was added over 1 h at room temperature. After 3½ h acetone (2 ml) was added. After 15 min the solid material was filtered off and the filtrate was concentrated to a syrup. A chromatographic examination of the hydrolyzed (*N* sulfuric acid, 1 h at 100°) syrup showed three spots having chromatographic behavior identical with that of authentic D-gulose, D-gulono-1,4-lactone, and L-glucitol. D-Gulose was estimated by the colorimetric phenol – sulfuric acid method (7) to constitute 80% of the product.

2,3-O-Isopropylidene-D-ribose

To a stirred solution of 2,3-*O*-isopropylidene-D-ribono-1,4-lactone (600 mg) in anhydrous ether (50 ml), sodium borohydride (600 mg) and glacial acetic acid (1.5 ml) in ether (15 ml) were added simultaneously over 1 h. After 3 h acetone (6 ml) was added and stirring was continued for 30 min. The solid was removed by filtration and washed with ethyl acetate. The filtrate was evaporated to dryness, and the residue was dissolved in water (15 ml) and deionized by passing it through Amberlite IR-120 (H^+) and Duolite A_4 (OH^-) resins. The eluate was concentrated to a syrup (450 mg). The hydrolyzed syrup, when subjected to paper chromatographic analysis, showed two spots having chromatographic behavior identical with that of authentic D-ribose and ribitol, ribose (75%) being the main product.

N-Phenyl-D-ribopyranosylamine

The syrup (320 mg) containing D-ribose and ribitol was dissolved in water (2 ml), and aniline (200 mg) in ethanol (4 ml) was added. After the mixture was shaken for 10 min, it was kept at 5° for 18 h. The crystalline *N*-phenyl-D-ribopyranosylamine was collected by filtration and washed with cold ethanol (250 mg), m.p. 115–117°, $[\alpha]_D$ +63° → +48° (*c*, 1.1 in pyridine) (8, 9).

2,4-Dihydroxy-3,3-dimethylbutanal

To a stirred mixture of sodium borohydride (2 g) and pantoyllactone (2,4-dihydroxy-3,3-dimethylbutanoic acid 1,4-lactone) (2 g) in absolute ether (200 ml) was added acetic acid (5 ml) in ether (15 ml) over 4½ h. Powdered potassium carbonate (2.5 g) and acetone (10 ml) were added to the reaction mixture and the solid materials were removed by filtration. The concentrated filtrate was extracted with chloroform. Removal of

Can. J. Chem. Downloaded from www.nrcresearchpress.com by 210.87.254.5 on 09/05/12
For personal use only.

the solvent gave a syrup (1.6 g) which failed to crystallize. The syrup was treated with 2,4-dinitrophenylhydrazine reagent (10) to yield the crystalline 2,4-dinitrophenylhydrazone derivative of 2,4-dihydroxy-3,3-dimethylbutanal, which, on recrystallization from an acetic acid – ether mixture and from benzene, gave a product (320 mg) which had m.p. 173–174°.

Anal. Calcd. for $C_{12}H_{16}O_6N_4$: C, 46.1; H, 5.2; N, 18.0. Found: C, 45.9; H, 5.6; N, 18.3.

*Attempted Reduction of 2,3;5,6-Di-O-isopropylidene-*D*-gulono-1,4-lactone with Diborane and with Diborane in the Presence of Acetic Acid*

Diborane was generated (1) by treating boron trifluoride etherate (4.1 g, 0.03 mole) and sodium borohydride (0.7 g, 0.02 mole), and was passed through a solution of 2,3;5,6-di-*O*-isopropylidene-D-gulono-1,4-lactone (0.51 g, 0.002 mole) in tetrahydrofuran (50 ml) over 40 min under an atmosphere of nitrogen. The reaction mixture was allowed to stand at room temperature for 2½ h. Ethanol (5 ml) was added to destroy the excess of diborane. The solution was evaporated to dryness and the residue was recrystallized from an ether – light petroleum ether (40–60°) mixture to yield the starting material (0.4 g), m.p. 153–154°. The mixed melting point with the starting material was undepressed.

The above diborane reduction was repeated with tetrahydrofuran containing 0.1 ml of acetic acid as the solvent. Starting material was recovered from this reaction.

ACKNOWLEDGMENTS

The author thanks Dr. J. K. N. Jones and Dr. M. B. Perry for their interest in the work.

1. H. C. Brown and B. C. Subba Rao. J. Org. Chem. **22**, 1135 (1957).
2. H. C. Brown and B. C. Subba Rao. J. Am. Chem. Soc. **82**, 681 (1960).
3. E. Fischer. Ber. **22**, 2206 (1889).
4. N. Sperber, H. E. Zaugg, and W. M. Sandstrom. J. Am. Chem. Soc. **69**, 915 (1947).
5. M. L. Wolfrom and H. B. Wood. J. Am. Chem. Soc. **73**, 2933 (1951).
6. K. Iwadare. Bull. Chem. Soc. Japan, **18**, 226 (1943).
7. F. Smith. Methods Biochem. Analy. **3**, 182 (1956).
8. R. L. Whistler and J. N. B. Miller. *In* Methods in carbohydrate chemistry. Vol. I. *Edited by* R. L. Whistler and M. L. Wolfrom. Academic Press, Inc., New York. 1962. p. 81.
9. G. A. Howard, G. W. Kenner, B. Lythgoe, and A. R. Todd. J. Chem. Soc. 855 (1946).
10. F. Wild. Characterisation of organic compounds. 2nd ed. Cambridge University Press, London. 1958. p. 114.

Received February 9, 1966.
Department of Chemistry,
Queen's University,
Kingston, Ontario.

NUCLEAR MAGNETIC RESONANCE STUDY OF 2,3-QUINOXALINEDICARBOXALDEHYDE AND ITS CYCLIC MONOHYDRATE[1]

Emil J. Moriconi, James W. Young,[2] Thomas E. Brady, and Albert J. Fritsch

The formation of stable isolable hydrates of aldehydes and ketones requires the presence of a strong, electronegative atom bonded to the α-carbon (as in chloral, glyoxal, glyoxalic and mesoxalic acids, hexafluoroacetone, and triketoindane). Recently, we reported the preparation of 2,3-quinoxalinedicarboxaldehyde (I), which was isolated in the presence of water as the cyclic monohydrate II (1). In I, the electronic effects of the ring aza-atoms must enhance the additive power of the carbonyl groups such that reaction with water is rapid and complete. Since 2-quinoxalinecarboxaldehyde does not form a hydrate (2), the driving force for cyclic monohydrate formation must come not only from the severe dipole–dipole repulsions in I but also from the stability of the five-membered ring in II.

[1]*Taken in part from the Ph.D. thesis of A. J. Fritsch, S.J., February 1965.*
[2]*National Science Foundation Undergraduate Research Participant.*

Can. J. Chem. Downloaded from www.nrcresearchpress.com by 210.87.254.5 on 09/05/12
For personal use only.

the solvent gave a syrup (1.6 g) which failed to crystallize. The syrup was treated with 2,4-dinitrophenylhydrazine reagent (10) to yield the crystalline 2,4-dinitrophenylhydrazone derivative of 2,4-dihydroxy-3,3-dimethylbutanal, which, on recrystallization from an acetic acid – ether mixture and from benzene, gave a product (320 mg) which had m.p. 173–174°.

Anal. Calcd. for $C_{12}H_{16}O_6N_4$: C, 46.1; H, 5.2; N, 18.0. Found: C, 45.9; H, 5.6; N, 18.3.

*Attempted Reduction of 2,3;5,6-Di-O-isopropylidene-*D*-gulono-1,4-lactone with Diborane and with Diborane in the Presence of Acetic Acid*

Diborane was generated (1) by treating boron trifluoride etherate (4.1 g, 0.03 mole) and sodium borohydride (0.7 g, 0.02 mole), and was passed through a solution of 2,3;5,6-di-*O*-isopropylidene-D-gulono-1,4-lactone (0.51 g, 0.002 mole) in tetrahydrofuran (50 ml) over 40 min under an atmosphere of nitrogen. The reaction mixture was allowed to stand at room temperature for 2½ h. Ethanol (5 ml) was added to destroy the excess of diborane. The solution was evaporated to dryness and the residue was recrystallized from an ether – light petroleum ether (40–60°) mixture to yield the starting material (0.4 g), m.p. 153–154°. The mixed melting point with the starting material was undepressed.

The above diborane reduction was repeated with tetrahydrofuran containing 0.1 ml of acetic acid as the solvent. Starting material was recovered from this reaction.

ACKNOWLEDGMENTS

The author thanks Dr. J. K. N. Jones and Dr. M. B. Perry for their interest in the work.

1. H. C. Brown and B. C. Subba Rao. J. Org. Chem. **22**, 1135 (1957).
2. H. C. Brown and B. C. Subba Rao. J. Am. Chem. Soc. **82**, 681 (1960).
3. E. Fischer. Ber. **22**, 2206 (1889).
4. N. Sperber, H. E. Zaugg, and W. M. Sandstrom. J. Am. Chem. Soc. **69**, 915 (1947).
5. M. L. Wolfrom and H. B. Wood. J. Am. Chem. Soc. **73**, 2933 (1951).
6. K. Iwadare. Bull. Chem. Soc. Japan, **18**, 226 (1943).
7. F. Smith. Methods Biochem. Analy. **3**, 182 (1956).
8. R. L. Whistler and J. N. B. Miller. *In* Methods in carbohydrate chemistry. Vol. I. *Edited by* R. L. Whistler and M. L. Wolfrom. Academic Press, Inc., New York. 1962. p. 81.
9. G. A. Howard, G. W. Kenner, B. Lythgoe, and A. R. Todd. J. Chem. Soc. 855 (1946).
10. F. Wild. Characterisation of organic compounds. 2nd ed. Cambridge University Press, London. 1958. p. 114.

Received February 9, 1966.
Department of Chemistry,
Queen's University,
Kingston, Ontario.

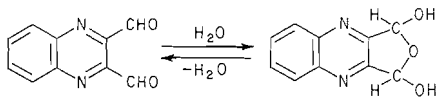
NUCLEAR MAGNETIC RESONANCE STUDY OF 2,3-QUINOXALINEDICARBOXALDEHYDE AND ITS CYCLIC MONOHYDRATE[1]

Emil J. Moriconi, James W. Young,[2] Thomas E. Brady, and Albert J. Fritsch

The formation of stable isolable hydrates of aldehydes and ketones requires the presence of a strong, electronegative atom bonded to the α-carbon (as in chloral, glyoxal, glyoxalic and mesoxalic acids, hexafluoroacetone, and triketoindane). Recently, we reported the preparation of 2,3-quinoxalinedicarboxaldehyde (I), which was isolated in the presence of water as the cyclic monohydrate II (1). In I, the electronic effects of the ring aza-atoms must enhance the additive power of the carbonyl groups such that reaction with water is rapid and complete. Since 2-quinoxalinecarboxaldehyde does not form a hydrate (2), the driving force for cyclic monohydrate formation must come not only from the severe dipole–dipole repulsions in I but also from the stability of the five-membered ring in II.

[1]*Taken in part from the Ph.D. thesis of A. J. Fritsch, S.J., February 1965.*
[2]*National Science Foundation Undergraduate Research Participant.*

Can. J. Chem. Downloaded from www.nrcresearchpress.com by 210.87.254.5 on 09/05/12
For personal use only.



I II

This seems to be the first reported instance of the isolation and interconversion of an aromatic *o*-dialdehyde and its cyclic monohydrate in which 1 equivalent of water is chemically bound.[3] We now report on the structure and interconversion of I and II as determined by nuclear magnetic resonance (n.m.r.).

Compound II was prepared in 60% yield by the dimethyl sulfoxide (DMSO) oxidation of 2,3-bis(bromomethyl)quinoxaline. In the infrared (KBr), II showed no C=O band, but did display a strong, sharp, bonded OH absorption at 3.18 μ. The insolubility of II in the conventional solvents used to distinguish between inter- and intra-molecularly hydrogen-bonded OH groups precluded such measurements. Further, Dreiding models showed no special preference for either the *cis* or *trans* isomer. The *cis* isomer, however, would permit the formation of a weak intramolecular O—H · · · O bond. Compound II lost water when it was heated, and melted at 176.5–177° (decomp.). Sublimation of II at 110–120° and 2 mm then gave, as expected, I, m.p. 177–178° (decomp.); recrystallization of I from boiling water led to II as the only isolable product. Compound I showed a strong, sharp C=O band at 5.81 μ (KBr). Both I and II displayed typical quinoxaline absorption in the ultraviolet (1): I, $\lambda_{max}^{absolute\ EtOH}$ 238 mμ (ϵ 28 100) and 322 mμ (ϵ 9 100); and II, $\lambda_{max}^{95\%\ EtOH}$ 238 mμ (ϵ 30 400) and 322 mμ (ϵ 8 100).

Five n.m.r. spectra (60 Mc.p.s.) are compiled in Fig. 1. The spectrum (A) of I dissolved in DMSO-d_6 showed an aromatic multiplet centered at δ = 8.00 and aldehyde protons as a sharp singlet at δ = 10.28, with an intensity ratio of 2:1. In spectrum C, I was dissolved in DMSO and diluted with water; its spectrum displayed an aromatic multiplet centered at δ = 8.12, a pair of doublets centered at δ = 6.39 and 6.35, and a three-peak pattern centered at δ = 7.36, in the relative area ratio 2:1:1. Each of the doublets was assigned to a methine proton coupled with its respective hydroxyl proton; the appearance of a pair of doublets could be accounted for by the presence of a 1:1 *cis–trans* hydrate mixture in solution. The pattern centered at δ = 7.36 (assigned to OH protons) would then also be a pair of doublets (arising from OH being split by the CH) merging to appear as a triplet. In spectrum B, I was dissolved in DMSO-d_6 and diluted 40% by volume with D_2O. As expected, the aromatic multiplet (δ = 8.12, four protons) remained but the OH resonances had disappeared as a result of deuterium exchange. Also, the CH protons, no longer coupled, appeared as a pair of singlets (δ = 6.63 and 6.36, intensity ratio 1:1), each assignable to the pair of CH protons in each isomer of the 1:1 *cis–trans* mixture. Thus, the n.m.r. data suggested that solutions of I in DMSO with D_2O (spectrum B) and H_2O (spectrum C) consisted of 1:1 equilibrium mixtures of *cis* and *trans* hydrate.

Spectrum D, which is that of II dissolved in DMSO-d_6, showed, in addition to the aromatic multiplet (four protons), two doublets centered at δ = 7.36 (OH, two protons, J = 8 c.p.s.) and 6.48 (CH, two protons, J = 8 c.p.s.). The appearance of this simple AB pattern suggested that recrystallization of II from water had led to the isolation of only the single, and probably less soluble, *cis* or *trans* isomer. When the n.m.r. sample of spectrum D was diluted 40% by volume with D_2O, spectrum B was again obtained.

Finally, hydrate II was recrystallized from boiling D_2O, and the precipitated white, crystalline solid was separated and dried at room temperature for several days *in vacuo*.

[3]*Compare with the three examples of aliphatic cyclic monohydrate formation mentioned in ref. 3.*

Can. J. Chem. Downloaded from www.nrcresearchpress.com by 210.87.254.5 on 09/05/12
For personal use only.

Can. J. Chem. Downloaded from www.nrcresearchpress.com by 210.87.254.5 on 09/05/12
For personal use only.

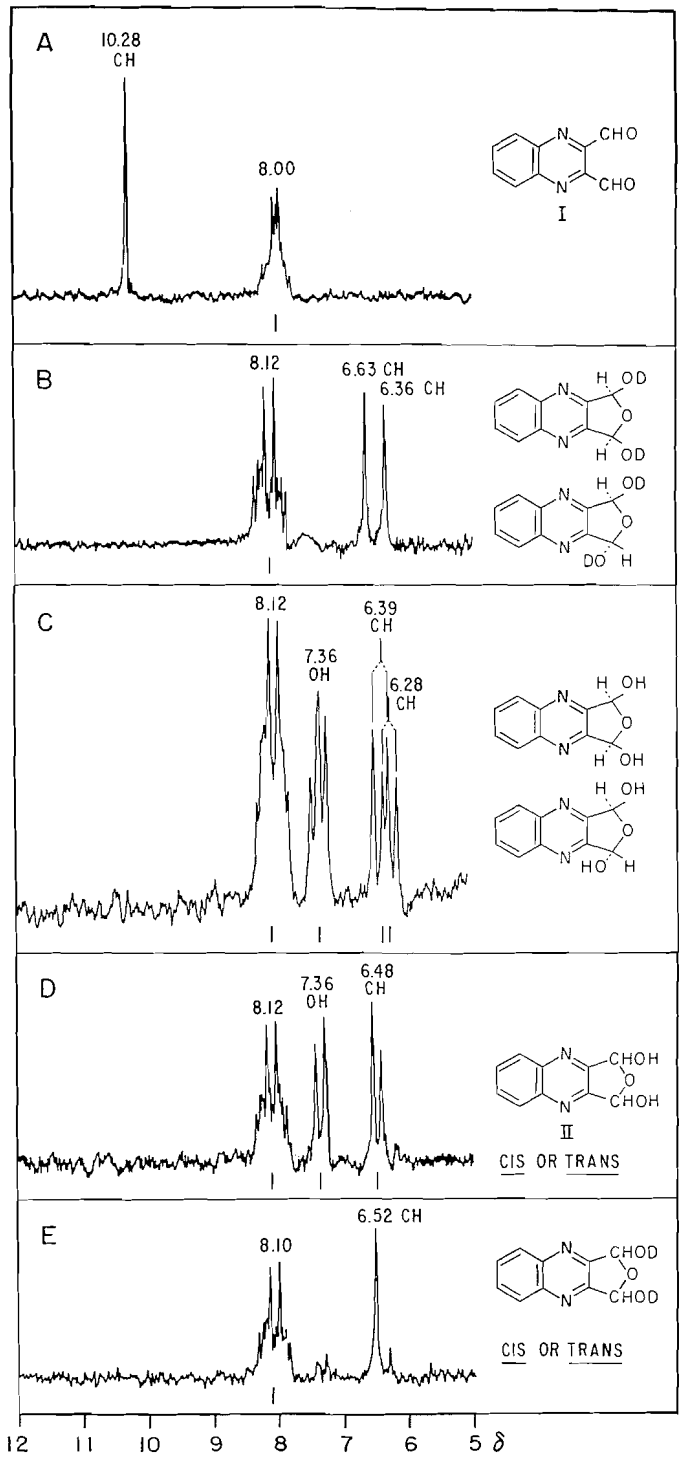


FIG. 1. All spectra were determined on a Varian A-60 spectrometer with tetramethylsilane as an internal reference. Spectrum A, I in DMSO-d_6; spectrum B, sample for spectrum A diluted 40% by volume with deuterium oxide; spectrum C, I in DMSO and diluted 40% by volume with water; spectrum D, II in DMSO; spectrum E, II recrystallized from deuterium oxide and dissolved in DMSO-d_6.

The n.m.r. spectrum of this material in DMSO-d_6 is recorded in spectrum E. The appearance of a sharp CH singlet at $\delta = 6.52$ confirmed the selective precipitation of only one of the two possible geometric isomers. As expected then, dilution of this last n.m.r. sample with D_2O led again to spectrum B.

ACKNOWLEDGMENTS

The authors thank the Directorate of Chemical Sciences, Air Force Office of Scientific Research, for their support of this research under grants AF-AFOSR-62-18 and 488-64, and acknowledge the assistance of a National Science Foundation grant GP-1482 to the Department of Chemistry towards the purchase of a n.m.r. spectrometer.

1. E. J. Moriconi and A. J. Fritsch, S.J. J. Org. Chem. **30**, 1542 (1965).
2. A. Kjaer. Acta. Chem. Scand. **2**, 455 (1948).
3. R. Criegee, L. Kraft, and B. Rank. Ann. **507**, 194 (1933). H. E. Carter, R. K. Clark, Jr., S. R. Dickman, Y. H. Loo, P. S. Skell, and W. A. Strong. Science, **103**, 540 (1946). R. B. Woodward, T. Fukunaga, and R. C. Kelly. J. Am. Chem. Soc. **86**, 3165 (1964).

Received November 5, 1965.
Department of Chemistry,
Fordham University,
New York, New York.

AMÉLIORATION DE LA SYNTHÈSE DES DI- ET TRI-BROMHYDRINES DU PENTAÉRYTHRITOL

M. Saucier, C. Sauriol et R. L. Salvador

Un besoin de quantités appréciables des di- et tri-bromhydrines du pentaérythritol comme matières premières pour la synthèse de nouveaux composés cycliques nous incita à mettre au point une méthode mieux adaptée à la préparation de grandes quantités de ces dérivés bromés. Nous nous sommes principalement inspirés de la méthode proposée par Cheymol et ses collaborateurs (1) pour la synthèse de la tribromhydrine du pentaérythritol, laquelle est une modification de la méthode de Govaert et Beyaert (2) pour éviter l'opération en vase clos. Nous avons modifié cette méthode de façon à travailler avec le gaz bromhydrique anhydre en milieu acétique et à pression atmosphérique. Cette technique nous a permis de réduire le temps de réaction de 60 h à 20 h et d'obtenir des rendements plus élevés, soit 90% au lieu de 68% de la tribromhydrine du pentaérythritol V. Ces modifications nous ont aussi permis de préparer le dérivé dibromé VI en 12 h avec des rendements de l'ordre de 85%.

Les différentes étapes de la synthèse des dérivés di- et tri-bromés sont montrées dans le Schéma Réactionnel 1. La première étape (A) consiste en la transformation du pentaérythritol I en tétraacétate II ; en effet, la substitution des acétates par le brome se fait plus facilement que la substitution directe de la fonction hydroxylique (3, 4). Il n'est pas utile d'isoler le tétraacétate ainsi formé car il se trouve déjà dans le milieu réactionnel nécessaire à la bromuration. La deuxième étape (B) consiste en la bromuration du tétraacétate II. Quoique les deux premiers bromes se fixent assez facilement (IV), la substitution par le brome du troisième groupe acétate se fait difficilement (III). Cependant, en opérant en milieu acétique saturé d'acide bromhydrique, et en maintenant un flot constant d'acide bromhydrique, on peut ainsi obtenir des conditions aussi favorables qu'en tube scellé. La

Can. J. Chem. Downloaded from www.nrcresearchpress.com by 210.87.254.5 on 09/05/12
For personal use only.

The n.m.r. spectrum of this material in DMSO-d_6 is recorded in spectrum E. The appearance of a sharp CH singlet at $\delta = 6.52$ confirmed the selective precipitation of only one of the two possible geometric isomers. As expected then, dilution of this last n.m.r. sample with D_2O led again to spectrum B.

ACKNOWLEDGMENTS

The authors thank the Directorate of Chemical Sciences, Air Force Office of Scientific Research, for their support of this research under grants AF-AFOSR-62-18 and 488-64, and acknowledge the assistance of a National Science Foundation grant GP-1482 to the Department of Chemistry towards the purchase of a n.m.r. spectrometer.

1. E. J. Moriconi and A. J. Fritsch, S.J. J. Org. Chem. **30**, 1542 (1965).
2. A. Kjaer. Acta. Chem. Scand. **2**, 455 (1948).
3. R. Criegee, L. Kraft, and B. Rank. Ann. **507**, 194 (1933). H. E. Carter, R. K. Clark, Jr., S. R. Dickman, Y. H. Loo, P. S. Skell, and W. A. Strong. Science, **103**, 540 (1946). R. B. Woodward, T. Fukunaga, and R. C. Kelly. J. Am. Chem. Soc. **86**, 3165 (1964).

Received November 5, 1965.
Department of Chemistry,
Fordham University,
New York, New York.

AMÉLIORATION DE LA SYNTHÈSE DES DI- ET TRI-BROMHYDRINES DU PENTAÉRYTHRITOL

M. Saucier, C. Sauriol et R. L. Salvador

Un besoin de quantités appréciables des di- et tri-bromhydrines du pentaérythritol comme matières premières pour la synthèse de nouveaux composés cycliques nous incita à mettre au point une méthode mieux adaptée à la préparation de grandes quantités de ces dérivés bromés. Nous nous sommes principalement inspirés de la méthode proposée par Cheymol et ses collaborateurs (1) pour la synthèse de la tribromhydrine du pentaérythritol, laquelle est une modification de la méthode de Govaert et Beyaert (2) pour éviter l'opération en vase clos. Nous avons modifié cette méthode de façon à travailler avec le gaz bromhydrique anhydre en milieu acétique et à pression atmosphérique. Cette technique nous a permis de réduire le temps de réaction de 60 h à 20 h et d'obtenir des rendements plus élevés, soit 90% au lieu de 68% de la tribromhydrine du pentaérythritol V. Ces modifications nous ont aussi permis de préparer le dérivé dibromé VI en 12 h avec des rendements de l'ordre de 85%.

Les différentes étapes de la synthèse des dérivés di- et tri-bromés sont montrées dans le Schéma Réactionnel 1. La première étape (A) consiste en la transformation du pentaérythritol I en tétraacétate II ; en effet, la substitution des acétates par le brome se fait plus facilement que la substitution directe de la fonction hydroxylique (3, 4). Il n'est pas utile d'isoler le tétraacétate ainsi formé car il se trouve déjà dans le milieu réactionnel nécessaire à la bromuration. La deuxième étape (B) consiste en la bromuration du tétraacétate II. Quoique les deux premiers bromes se fixent assez facilement (IV), la substitution par le brome du troisième groupe acétate se fait difficilement (III). Cependant, en opérant en milieu acétique saturé d'acide bromhydrique, et en maintenant un flot constant d'acide bromhydrique, on peut ainsi obtenir des conditions aussi favorables qu'en tube scellé. La

Can. J. Chem. Downloaded from www.nrcresearchpress.com by 210.87.254.5 on 09/05/12
For personal use only.

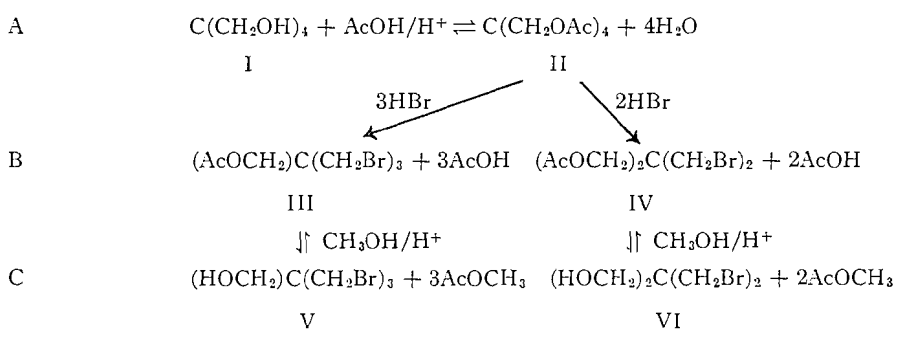


SCHÉMA RÉACTIONNEL 1.

troisième étape (C) consiste en la régénération des fonctions hydroxyliques. Cette réaction s'effectue par transestérification à l'aide de l'alcool méthylique anhydre (5). La formation de la dibromhydrine VI nécessite des conditions réactionnelles moins vigoureuses. Pour prévenir la formation du dérivé tribromé V, il est important de ne pas opérer avec un trop grand excès d'acide bromhydrique. L'excès requis est de l'ordre de 10 à 12%. Celui-ci contribue à combler le déficit d'acide bromhydrique provenant de l'évaporation par chauffage de la réaction.

PARTIE EXPÉRIMENTALE

Les points de fusion ont été déterminés au capillaire dans un appareil electrothermal à bloc d'aluminium et ne sont pas corrigés.

Tribromhydrine du pentaérythritol

Dans un ballon de 5 l à encolures multiples, muni d'un refrigérant dont l'extrémité supérieure est reliée à un système de trappes contenant de l'acide acétique glacial, on ajoue 544 g (4 moles) de pentaérythritol et 3 200 ml d'acide acétique glacial. On relie ensuite le ballon à un cylindre d'acide bromhydrique anhydre et on porte le mélange à l'ébullition pendant 20 h, tout en maintenant à un fort débit le flot d'acide bromhydrique. Le temps de chauffage écoulé, on évapore l'acide acétique sous pression réduite. On reprend le résidu par 800 ml de toluène que l'on évapore de même. Cette dernière opération a pour but d'entraîner azéotropiquement l'eau de la réaction. On ajoute alors au résidu 1 350 ml d'alcool méthylique anhydre, on y dissout une quantité catalytique d'acide bromhydrique anhydre et on distille lentement à pression atmosphérique. L'azéotrope d'acétate de méthyl – alcool méthylique passe à 53.8 °C. On poursuit cette distillation jusqu'à obtention de la quantité théorique d'acétate de méthyl soit environ 375 ml du mélange azéotropique. On élimine ensuite l'alcool méthylique résiduel par distillation rapide sous vide. On dissout alors le résidu solide dans 5 l de toluène bouillant et on traite au charbon décolorant (Darco G-60). On obtient, par refroidisement, comme produit secondaire, 60 g (6%) de bis-bromométhyl-2,2-propanediol-1,3, que l'on recrystallise dans le toluène, p.f. 109–110 °C (litt. (6) p.f. 110 °C).

On évapore le filtrat et on recrystallise le résidu dans le cyclohexane. On obtient ainsi 1 165 g (90%) de bis-bromométhyl-2,2-bromo-3-propanol-1, p.f. 68–69 °C (litt. (6) p.f. 70–71 °C).

Dibromhydrine du pentaérythritol

On prépare la dibromhydrine du pentaérythritol dans un ballon de 5 l comme pour le dérivé tribromé à partir de 4 moles de pentaérythritol dans 3 200 ml d'acide acétique glacial. On porte le mélange à l'ébullition et on sature avec l'acide bromhydrique anhydre jusqu'à obtention d'un gain de poids de 720 g, soit un excès de 72 g calculé pour deux bromes. On cesse alors l'addition d'acide bromhydrique et on continue le chauffage pendant 8 à 10 h. Après environ 4 h, on évalue par pesée la perte d'acide bromhydrique et on compense par une nouvelle addition du gaz jusqu'à obtention de l'excès initial. On poursuit alors le chauffage jusqu'à la fin de la réaction. On élimine l'acide acétique sous vide et on traite le résidu de la même façon que pour la tribromhydrine. La transestérification achevée, on dissout le residu solide dans le toluène à chaud, on traite au charbon et on obtient, par refroidissement, 890 g (85%) de bis-bromométhyl-2,2-propanediol-1,3, p.f. 109–110 °C.

REMERCIEMENT

Les auteurs remercient le Conseil National de Recherches pour leur aide financière sous forme de bourses et d'octroi.

Can. J. Chem. Downloaded from www.nrcresearchpress.com by 210.87.254.5 on 09/05/12
For personal use only.

1. J. CHEYMOL, P. CHABRIER, J. SEYDEN-PENNE et G. THIBODEAU. Bull. Soc. Chim. France, 1268 (1964).
2. F. GOVAERT et M. BEYAERT. Natuurw. Tijdschr. Ghent, **22**, 73 (1940).
3. W. H. PERKIN, JR. et J. L. SIMONSEN. J. Chem. Soc. 855 (1905).
4. A. LITHERLAND et F. G. MANN. J. Chem. Soc. 1588 (1938).
5. M. BEYAERT et M. HANSENS. Natuurw. Tijdschr. Ghent, **22**, 249 (1940).
6. E. BERLOW, R. H. BARTH et J. E. SNOW. American Chemical Society monograph No. 136. Reinhold Publishing Corp., New York. 1958. p. 104.

REÇU LE 16 MARS 1966.
LABORATOIRE DE CHIMIE MÉDICINALE,
FACULTÉ DE PHARMACIE,
UNIVERSITÉ DE MONTRÉAL,
MONTRÉAL, QUÉBEC.

Can. J. Chem. Downloaded from www.nrcresearchpress.com by 210.87.254.5 on 09/05/12
For personal use only.

PYROLYSIS OF DIMETHYLETHANOLAMINE OXIDE MONOHYDRATE

GARSON P. SHULMAN[1]

The pyrolysis of dimethylethanolamine oxide was selected as a means of generating acetaldehyde at moderate temperatures from a nonvolatile and relatively nonreactive precursor. The decomposition of trialkylamine oxides to olefin and dialkylhydroxylamine (Cope reaction) is known to proceed in good yield via a cyclic intramolecular transition state (1). The pyrolysis of some N,N-dimethyl-2-hydroxy-cycloalkylamine oxides has been reported (2). These give allylic alcohol and ketone (via enol), in a ratio ranging from 5:1 to 20:1, where stereochemical factors permit competitive elimination. Since only elimination toward the hydroxyl group is possible in dimethylethanolamine oxide, one would predict that the vinyl alcohol – acetaldehyde tautomeric system would be the principal product unless the rate of elimination were so slow that deoxygenation (3) or oxazoline formation (2) became significant. An explosion occurred during the initial preparative-scale pyrolysis. Experiments were then directed toward determination of the products and kinetics of the reaction to ascertain the cause of the violent reaction, and to see whether decomposition could be effected via a controlled reaction.

EXPERIMENTAL

Preparation of Amine Oxides

A mixture of 75 ml of isopropyl alcohol and 75 ml of 50% hydrogen peroxide was placed in a flask thermostatted at 50°. With vigorous stirring, 1.0 mole of amine was added dropwise. The homogeneous mixture was maintained at 50° for several hours; then stirring was resumed and volatile material was removed under reduced pressure. The products were analyzed for amine and amine oxide by nonaqueous acidimetric titration (3). The reaction times and analyses are shown in Table I.

TABLE I

Synthesis of amine oxides

Amine	Reaction time (h)	Product analysis (%)		
		Amine	Amine oxide*	Active oxygen
$Me_2NCH_2CH_2OH$	5	0	103	0.62
$Me_2NCH_2CH_2OAc$	20	2	104	0
$Me_2NCMe_2CH_2OH$	22	70†	30†	0

*As monohydrate.
†Relative mole percent.

[1]*Present address: Research Department, The Martin Company, Baltimore, Maryland.*

1. J. CHEYMOL, P. CHABRIER, J. SEYDEN-PENNE et G. THIBODEAU. Bull. Soc. Chim. France, 1268 (1964).
2. F. GOVAERT et M. BEYAERT. Natuurw. Tijdschr. Ghent, **22**, 73 (1940).
3. W. H. PERKIN, JR. et J. L. SIMONSEN. J. Chem. Soc. 855 (1905).
4. A. LITHERLAND et F. G. MANN. J. Chem. Soc. 1588 (1938).
5. M. BEYAERT et M. HANSENS. Natuurw. Tijdschr. Ghent, **22**, 249 (1940).
6. E. BERLOW, R. H. BARTH et J. E. SNOW. American Chemical Society monograph No. 136. Reinhold Publishing Corp., New York. 1958. p. 104.

REÇU LE 16 MARS 1966.
LABORATOIRE DE CHIMIE MÉDICINALE,
FACULTÉ DE PHARMACIE,
UNIVERSITÉ DE MONTRÉAL,
MONTRÉAL, QUÉBEC.

Can. J. Chem. Downloaded from www.nrcresearchpress.com by 210.87.254.42 on 09/05/12
For personal use only.

PYROLYSIS OF DIMETHYLETHANOLAMINE OXIDE MONOHYDRATE

GARSON P. SHULMAN[1]

The pyrolysis of dimethylethanolamine oxide was selected as a means of generating acetaldehyde at moderate temperatures from a nonvolatile and relatively nonreactive precursor. The decomposition of trialkylamine oxides to olefin and dialkylhydroxylamine (Cope reaction) is known to proceed in good yield via a cyclic intramolecular transition state (1). The pyrolysis of some N,N-dimethyl-2-hydroxy-cycloalkylamine oxides has been reported (2). These give allylic alcohol and ketone (via enol), in a ratio ranging from 5:1 to 20:1, where stereochemical factors permit competitive elimination. Since only elimination toward the hydroxyl group is possible in dimethylethanolamine oxide, one would predict that the vinyl alcohol – acetaldehyde tautomeric system would be the principal product unless the rate of elimination were so slow that deoxygenation (3) or oxazoline formation (2) became significant. An explosion occurred during the initial preparative-scale pyrolysis. Experiments were then directed toward determination of the products and kinetics of the reaction to ascertain the cause of the violent reaction, and to see whether decomposition could be effected via a controlled reaction.

EXPERIMENTAL

Preparation of Amine Oxides

A mixture of 75 ml of isopropyl alcohol and 75 ml of 50% hydrogen peroxide was placed in a flask thermostatted at 50°. With vigorous stirring, 1.0 mole of amine was added dropwise. The homogeneous mixture was maintained at 50° for several hours; then stirring was resumed and volatile material was removed under reduced pressure. The products were analyzed for amine and amine oxide by nonaqueous acidimetric titration (3). The reaction times and analyses are shown in Table I.

TABLE I
Synthesis of amine oxides

Amine	Reaction time (h)	Product analysis (%)		
		Amine	Amine oxide*	Active oxygen
$Me_2NCH_2CH_2OH$	5	0	103	0.62
$Me_2NCH_2CH_2OAc$	20	2	104	0
$Me_2NCMe_2CH_2OH$	22	70†	30†	0

*As monohydrate.
†Relative mole percent.

[1]*Present address: Research Department, The Martin Company, Baltimore, Maryland.*

Pyrolysis of Dimethylethanolamine Oxide Monohydrate

A 25 g sample was placed in a vacuum distillation apparatus, with the receiving flask cooled by dry ice – acetone. Heating with a microburner was continued until the temperature reached 110°. The temperature rose rapidly to about 180°; then the flask exploded.

A 0.5 g sample was placed in a flask fitted with a stopcock and a rubber seal. The flask was evacuated, a 10 ml hypodermic syringe (lightly greased) was inserted through the seal, and then the sample was heated with a microburner until the syringe was filled. The contents were immediately injected into the gas chromatograph (6 ft silicone oil column at 80°). Three peaks, identified as water, acetaldehyde, and dimethylhydroxylamine (by retention times), were obtained. These identities were confirmed by mass spectrometry of the eluted samples after degradation in a Perkin–Elmer pyrolysis unit at 200°. Because the water peak showed extensive tailing, a rigorous quantitative determination was not attempted. From peak areas, a molar ratio of water to acetaldehyde to dimethylhydroxylamine of about 2:1:1 was estimated.

The rate of reaction was determined at 127.5° in the manner described previously (3, 4). A rate constant of $(2.8 \pm 0.2) \times 10^{-5}$ s^{-1} was obtained.

A 3 μl sample was pyrolyzed in a duPont model 900 differential thermal analysis (DTA) apparatus (5) at a heating rate of 20°/min. The DTA curve is shown in Fig. 1.

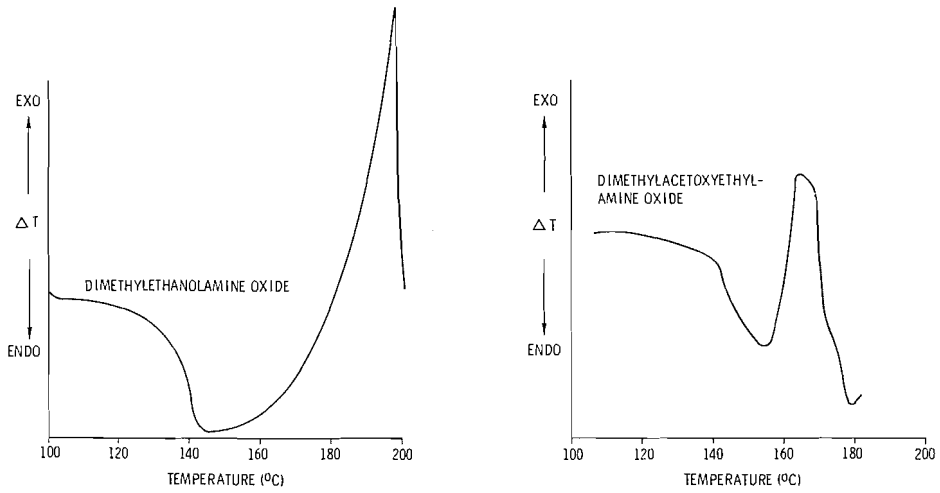


FIG. 1. DTA of dimethylethanolamine oxide and dimethyl-2-acetoxyethylamine oxide.

A 6.78 mg sample was placed in the tungsten crucible of the Knudsen cell inlet of a Bendix time-of-flight mass spectrometer and heated at a rate of 14°/min. Spectra were recorded at 1 min intervals; then the heights of peaks characteristic of each product were plotted versus temperature. The mass spectrometric thermal analysis (MTA) curve is shown in Fig. 2. The activation energies for the formation of each product were derived from the linear portion of semilogarithmic plots of peak height versus reciprocal temperature (water 6.2, acetaldehyde 32, dimethylhydroxylamine 36, and dimethylethanolamine 20 kcal $mole^{-1}$).

Differential Thermal Analysis of Dimethyl-2-acetoxyethylamine Oxide Monohydrate

A DTA taken on a 3 μl sample at a heating rate of 20°/min is shown in Fig. 1.

Pyrolysis of 2-Dimethyloxamino-2-methyl-1-propanol

A 5.0 g sample was added dropwise to a distilling flask (at 150 ± 5°) which formed part of a microdistillation apparatus. Gas chromatographic analysis (6 ft silicone oil column at 80°) of the distillate showed four components: dimethylhydroxylamine, water, and a 23:1 ratio of methallyl alcohol to isobutyraldehyde.

DISCUSSION

The expected products from the pyrolysis of dimethylethanolamine oxide monohydrate, i.e. water, dimethylhydroxylamine, and acetaldehyde, were observed gas chromatographically. Based on the mass spectra of the products, characteristic peaks of m/e 17 for water, 29 (CHO) for acetaldehyde, and 58 for dimethylhydroxylamine were selected for

Can. J. Chem. Downloaded from www.nrcresearchpress.com by 210.87.254.42 on 09/05/12
For personal use only.

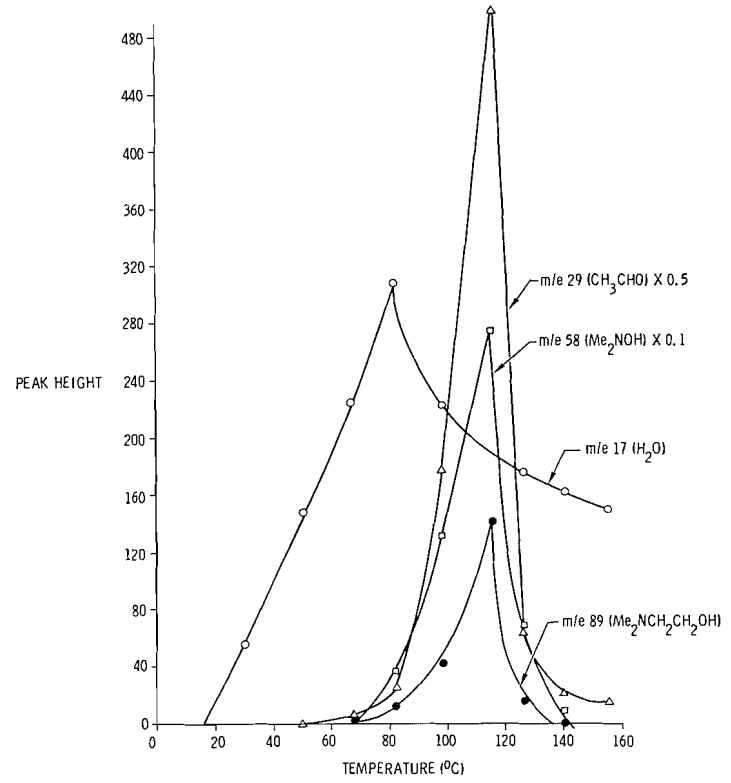


FIG. 2. MTA of dimethylethanolamine oxide.

the MTA.[2] The only identifiable peaks observed in the MTA in addition to those from fragmentation of the three principal products were peaks characteristic of an amine with a molecular ion at *m/e* 89. This must be dimethylethanolamine formed by deoxygenation of the amine oxide. No corresponding increase in the *m/e* 32 or 34 peaks was observed; hence, deoxygenation does not proceed with liberation of oxygen or hydrogen peroxide.

It is also possible to derive activation parameters from the MTA data. Based on the assumption that, in the rapidly pumped vacuum system of the mass spectrometer, the intensity of the characteristic ion is proportional to the rate of production of a species, a plot of log peak height versus reciprocal temperature should be linear as long as the concentration of the reactant is essentially unchanged. For olefin formation, an activation energy of 34 ± 2 kcal mole^{-1} was observed, based on the average for acetaldehyde and dimethylhydroxylamine; for deoxygenation the value is 20 kcal mole^{-1}, and for dehydration 6.2 kcal mole^{-1}. These values agree well with those of 36.3 and 20.6 kcal mole^{-1} determined for corresponding reactions of dimethyllaurylamine oxide. The activation energy for dehydration is in the range which one would expect for breaking a hydrogen bond.

It is clear from the MTA curve (Fig. 2) that dehydration precedes elimination, as has been postulated previously based on kinetic evidence (6). The DTA (Fig. 1) also shows

[2]*The m/e 18 peak for water was off scale. The m/e 43 peak was a major dimethylhydroxylamine fragment, and was therefore not characteristic for acetaldehyde. Only a minor molecular ion (61) peak was observed for dimethylhydroxylamine. The spectra of dialkylhydroxylamines will be reported subsequently.*

Can. J. Chem. Downloaded from www.nrcresearchpress.com by 210.87.254.42 on 09/05/12
For personal use only.

a two-stage reaction: an endotherm (dehydration) followed by an exotherm (degradation). Dimethylethanolamine oxide decomposition releases several times more energy than decomposition of its acetate ester. This extra energy must be derived from the isomerization of vinyl alcohol to acetaldehyde.

There seems to be a marked effect of pressure on the reaction. The preparative pyrolysis became uncontrollable at about 110°, and the maximum rate in the MTA is observed at 115°. In contrast, the DTA shows degradation occurring at 140–200°, and a slow rate of reaction was measured at 127.5° under atmospheric pressure. The enhanced rate *in vacuo*, which leads to an uncontrollable reaction on a preparative scale, is no doubt due to the greater use of removing water from the hydrate and the resulting rapid decomposition of anhydrous amine oxide, as shown by Sahyun and Cram (6).

Determination of the relative rates of aldehyde and allylic alcohol formation was accomplished by the competitive intramolecular reaction of 2-dimethyloxamino-2-methyl-1-propanol. The 23:1 ratio of methallyl alcohol to isobutyraldehyde shows that elimination of the methylol hydrogen is slower than that of the methyl hydrogen. If one compensates for the number of hydrogens of each type available (6:2), elimination toward a methylol group is about one-eighth as fast as that toward methyl. The corresponding factor for secondary alcohol – methylene competition ranges from 0.1 to 0.4 (2).

ACKNOWLEDGMENTS

I thank Dr. D. N. Gray, Miss M. Connor, and Messrs. P. Ellgen, R. Bunting, H. W. Lochte, and J. J. Flynn for assistance in various phases of this work.

1. A. C. Cope. *In* Organic reactions. Vol. 11. John Wiley & Sons, Inc., New York. 1960. p. 317.
2. A. C. Cope, E. Ciganek, and J. Lazar. J. Am. Chem. Soc. **84**, 2591 (1962).
3. G. P. Shulman and W. E. Link. J. Am. Oil Chemists' Soc. **41**, 329 (1964).
4. G. P. Shulman, P. Ellgen, and M. Connor. Can. J. Chem. **43**, 3459 (1965).
5. R. H. Müller. Anal. Chem. **35**, 103A (1963).
6. M. R. V. Sahyun and D. J. Cram. J. Am. Chem. Soc. **85**, 1263 (1963).

Received February 7, 1966.
Research Laboratories,
Archer-Daniels-Midland Co.,
Minneapolis, Minnesota,
and
Research Department,
The Martin Company,
Baltimore, Maryland.

ERRATUM: THE OCCURRENCE OF 2,3-DIBROMOBENZYL ALCOHOL 4,5-DISULFATE, DIPOTASSIUM SALT, IN POLYSIPHONIA LANOSA

J. H. Hodgkin, J. S. Craigie, and A. G. McInnes

(Ref. Can. J. Chem. 44, 74 (1966))

On page 74, lines 4–7 of the Introduction should read "-benzaldehyde has been shown to occur in *Polysiphonia morrowii* (3), and two other compounds (believed to be brominated sulfonated hydroxybenzoic acids) with the empirical formulae $C_7H_2O_9S_2Br_2K_2$

Can. J. Chem. Downloaded from www.nrcresearchpress.com by 210.87.254.42 on 09/05/12
For personal use only.

a two-stage reaction: an endotherm (dehydration) followed by an exotherm (degradation). Dimethylethanolamine oxide decomposition releases several times more energy than decomposition of its acetate ester. This extra energy must be derived from the isomerization of vinyl alcohol to acetaldehyde.

There seems to be a marked effect of pressure on the reaction. The preparative pyrolysis became uncontrollable at about 110°, and the maximum rate in the MTA is observed at 115°. In contrast, the DTA shows degradation occurring at 140–200°, and a slow rate of reaction was measured at 127.5° under atmospheric pressure. The enhanced rate *in vacuo*, which leads to an uncontrollable reaction on a preparative scale, is no doubt due to the greater use of removing water from the hydrate and the resulting rapid decomposition of anhydrous amine oxide, as shown by Sahyun and Cram (6).

Determination of the relative rates of aldehyde and allylic alcohol formation was accomplished by the competitive intramolecular reaction of 2-dimethyloxamino-2-methyl-1-propanol. The 23:1 ratio of methallyl alcohol to isobutyraldehyde shows that elimination of the methylol hydrogen is slower than that of the methyl hydrogen. If one compensates for the number of hydrogens of each type available (6:2), elimination toward a methylol group is about one-eighth as fast as that toward methyl. The corresponding factor for secondary alcohol – methylene competition ranges from 0.1 to 0.4 (2).

ACKNOWLEDGMENTS

I thank Dr. D. N. Gray, Miss M. Connor, and Messrs. P. Ellgen, R. Bunting, H. W. Lochte, and J. J. Flynn for assistance in various phases of this work.

1. A. C. Cope. *In* Organic reactions. Vol. 11. John Wiley & Sons, Inc., New York. 1960. p. 317.
2. A. C. Cope, E. Ciganek, and J. Lazar. J. Am. Chem. Soc. **84**, 2591 (1962).
3. G. P. Shulman and W. E. Link. J. Am. Oil Chemists' Soc. **41**, 329 (1964).
4. G. P. Shulman, P. Ellgen, and M. Connor. Can. J. Chem. **43**, 3459 (1965).
5. R. H. Müller. Anal. Chem. **35**, 103A (1963).
6. M. R. V. Sahyun and D. J. Cram. J. Am. Chem. Soc. **85**, 1263 (1963).

Received February 7, 1966.
Research Laboratories,
Archer-Daniels-Midland Co.,
Minneapolis, Minnesota,
and
Research Department,
The Martin Company,
Baltimore, Maryland.

ERRATUM: THE OCCURRENCE OF 2,3-DIBROMOBENZYL ALCOHOL 4,5-DISULFATE, DIPOTASSIUM SALT, IN POLYSIPHONIA LANOSA

J. H. Hodgkin, J. S. Craigie, and A. G. McInnes

(Ref. Can. J. Chem. 44, 74 (1966))

On page 74, lines 4–7 of the Introduction should read "-benzaldehyde has been shown to occur in *Polysiphonia morrowii* (3), and two other compounds (believed to be brominated sulfonated hydroxybenzoic acids) with the empirical formulae $C_7H_2O_9S_2Br_2K_2$

Can. J. Chem. Downloaded from www.nrcresearchpress.com by 210.87.254.5 on 09/05/12
For personal use only.

and $C_7H_3O_{10}S_2BrK_2$ have been isolated from *Polysiphonia lanosa* and *Halopitys incurvus* (2)."

On page 78, ref. 1 should read "M. Peguy. Intern. Seaweed Symp. 4th, Biarritz, France. 1964. p. 366."

ATLANTIC REGIONAL LABORATORY,
NATIONAL RESEARCH COUNCIL,
HALIFAX, NOVA SCOTIA.

Can. J. Chem. Downloaded from www.nrcresearchpress.com by 210.87.254.5 on 09/05/12
For personal use only.

Can. J. Chem. Downloaded from www.nrcresearchpress.com by 210.87.254.105 on 09/05/12
For personal use only.

Canadian Journal of Chemistry

Issued by THE NATIONAL RESEARCH COUNCIL OF CANADA

VOLUME 44 JULY 15, 1966 NUMBER 14

CHÉLATES DU GERMANIUM(IV) AVEC LA TROPOLONE, LE MALTOL, LA LAWSONE ET LA TRICHLOROHYDROXY *p*-BENZOQUINONE[1]

I. PROPRIÉTÉS ACIDES-BASES DES α-HYDROXYCÉTONES

A. BEAUCHAMP[2] ET R. L. BENOIT

Département de Chimie, Université de Montréal, Montréal, Québec

Reçu le 14 décembre 1965

RÉSUMÉ

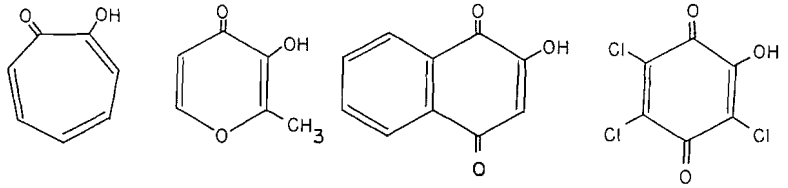
Les constantes de dissociation k_1 des α-hydroxycétones HL tropolone, maltol, lawsone et trichlorohydroxy *p*-benzoquinone sont déterminées en milieu de force ionique 0.50; les valeurs des pk_1 obtenues sont respectivement: 6.67 ± 0.04; 8.36 ± 0.03; 4.00 ± 0.04; 1.05 ± 0.04. La formation d'acides conjugués H_2L^+ en milieu fortement acide est également étudiée et les valeurs des constantes pk_2 basées sur la fonction d'acidité H_0 sont: −0.53 ± 0.10; −0.71 ± 0.10; −5.6 ± 0.2; −8.8 ± 1.0.

ABSTRACT

The acidity constants k_1 of the following α-hydroxyketones HL tropolone, maltol, lawsone, and trichlorohydroxy *p*-benzoquinone have been determined at ionic strength 0.50 (HCl, NaCl). The values of pk_1 are respectively: 6.67 ± 0.04; 8.36 ± 0.03; 4.00 ± 0.04; 1.05 ± 0.04. The formation of conjugated acids H_2L^+ in strongly acidic media has also been studied. The values of pk_2 defined in terms of the acidity function H_0 are: −0.53 ± 0.10; −0.71 ± 0.10; −5.6 ± 0.2; −8.8 ± 1.0.

INTRODUCTION

En vue d'une étude des chélates de la tropolone (I), du maltol (II), de la lawsone (III) et de la trichlorohydroxy *p*-benzoquinone (TCHQ) (IV) avec le germanium(IV), nous avons examiné en premier lieu les propriétés acides–bases de ces α-hydroxycétones HL. Les valeurs des constantes des équilibres acides–bases sont requises pour caractériser les chélates en solution et permettent d'établir des corrélations entre les propriétés basiques des atomes d'oxygène coordinés et la stabilité des chélates.



I II III IV

Il s'est révélé nécessaire de redéterminer les valeurs des constantes d'acidité k_1, celles relevées dans la littérature correspondant au milieu eau–dioxanne (1) ou à des forces ioniques différentes (2–8). A notre connaissance, la formation des acides conjugués H_2L^+

[1]*Tiré d'une communication présentée lors du 48ième Congrès de l'Institut de Chimie du Canada, tenu à Montréal les 31 mai – 2 juin 1965.*

[2]*Boursier du Conseil National de Recherches 1964–1965 et de l'Hydro-Québec 1965–1966.*

n'a été étudiée précédemment que dans le cas de la tropolone (2). Nous avons donc déterminé les constantes de dissociation k_2 de ces acides H_2L^+.

PARTIE EXPÉRIMENTALE

Réactifs

Tropolone.—Le produit brut a été sublimé à 25–30° (0.5 Torr) et il a un p.f. 49–50° (litt. (5) 49–50°). L'analyse élémentaire (Galbraith Lab.) indique 68.59% C, 4.86% H (calc. pour $C_7H_6O_2$: 68.84% C, 4.95% H). La densité optique des solutions est sensible à la présence d'air dissous, particulièrement en milieu basique. Les solutions ont été préparées immédiatement avant l'expérience, avec de l'eau bouillie et saturée d'azote et les mesures ont été faites sous atmosphère d'azote.

Maltol.—Le produit de Aldrich Chemical Co., sublimé deux fois à 60 ± 5° (0.2–1.5 Torr), a un p.f. 159° (litt. (9) 158–160°) et l'analyse élémentaire indique 57.09% C, 4.83% H (calc. pour $C_6H_6O_3$: 57.15% C, 4.80% H). Les solutions-mères neutres ou peu acides sont conservées au maximum 5 jours durant lesquels la densité optique reste constante.

Lawsone.—Le produit de Aldrich Chemical Co. a un p.f. 195–196° (décomp.) (litt. (10) 195–196° (décomp.). Le titrage par NaOH du produit dissous dans l'acétone à 50% indique une pureté de 99.6 ± 0.4%. Le produit a été utilisé sans autre purification.

TCHQ.—Le produit a été préparé à partir du chloranil, selon la méthode suggérée par Hancock *et al.* (11). Le produit de la réaction a été extrait par CH_2Cl_2 et le solvant a été évaporé: l'acide chloranilique présent comme impureté dans le produit ainsi traité à trois reprises (p.f. 197–198°, litt. (11) 198–199°) est inférieur à 0.7%, comme l'indique l'examen du spectre d'une solution à pH 4 dans la région de 325 mμ. Les solutions-mères ont été préparées en milieu acide, immédiatement avant l'expérience.

Les autres produits utilisés sont des réactifs purs pour analyse.

Technique expérimentale

Les mesures de densité optique ont été effectuées au moyen des spectrophotomètres Zeiss QII et Bausch & Lomb 505, avec une gamme de cuvettes de quartz dont l'épaisseur varie de 0.20 à 10.0 mm.

La concentration des ions H^+ a été mesurée au moyen d'un potentiopHmètre Radiometer 4, avec des électrodes de verre et de calomel – KCl saturé. La linéarité de l'électrode a été vérifiée dans l'intervalle $2.0 \leqslant -\log [H^+] \leqslant 9.2$, et des solutions de concentration $[H^+]$ connue et de force ionique 0.50 (NaCl–HCl) ont servi à la standardisation.

Toutes les expériences ont été effectuées à 25.0 ± 0.2°.

RÉSULTATS EXPÉRIMENTAUX ET DISCUSSION

(A) Détermination des constantes de dissociation k_1 de HL

Deux méthodes ont été utilisées.

(a) Spectrophotométrie

Dans les Figs. 1–4, on donne pour chacun des composés, les spectres des diverses espèces L^-, HL et H_2L^+, obtenus en opérant dans des conditions d'acidité appropriées. Les spectres des espèces L^- et HL présentent des différences importantes qui permettent de déterminer k_1 par spectrophotométrie.

Dans chacun des cas, la densité optique est mesurée à plusieurs longueurs d'onde. La concentration totale du composé C_L est maintenue constante ($1–3 \times 10^{-4}$ M), de même que la force ionique (0.50 (NaCl + HCl)). On varie l'acidité au moyen de HCl, NH_3 ou NaOH concentrés (tropolone, maltol) ou en ajoutant à une solution acide des volumes croissants de solution plus basique de même concentration C_L (lawsone, TCHQ).

On définit ϵ_L, le coefficient d'extinction molaire moyen, tel que $\epsilon_L = A_s/C_L$, où A_s est la densité optique correspondant à une épaisseur de 1.00 cm. La constante d'acidité k_1, définie de la façon habituelle, peut être calculée d'après l'équation

$$[1] \qquad -\log [H^+] = pk_1 + \log \frac{\epsilon_1 - \epsilon_L}{\epsilon_L - \epsilon_0}$$

où ϵ_0 et ϵ_1 sont les coefficients d'extinction molaire de L^- et HL, obtenus respectivement à $-\log [H^+] \sim pk_1 + 3$ et $pk_1 - 3$. L'équation [1] est celle d'une droite de pente unité, dont l'ordonnée à l'origine est égale à pk_1. On donne dans le Tableau I les valeurs de la pente et

Can. J. Chem. Downloaded from www.nrcresearchpress.com by 210.87.254.105 on 09/05/12
For personal use only.

Can. J. Chem. Downloaded from www.nrcresearchpress.com by 210.87.254.105 on 09/05/12
For personal use only.

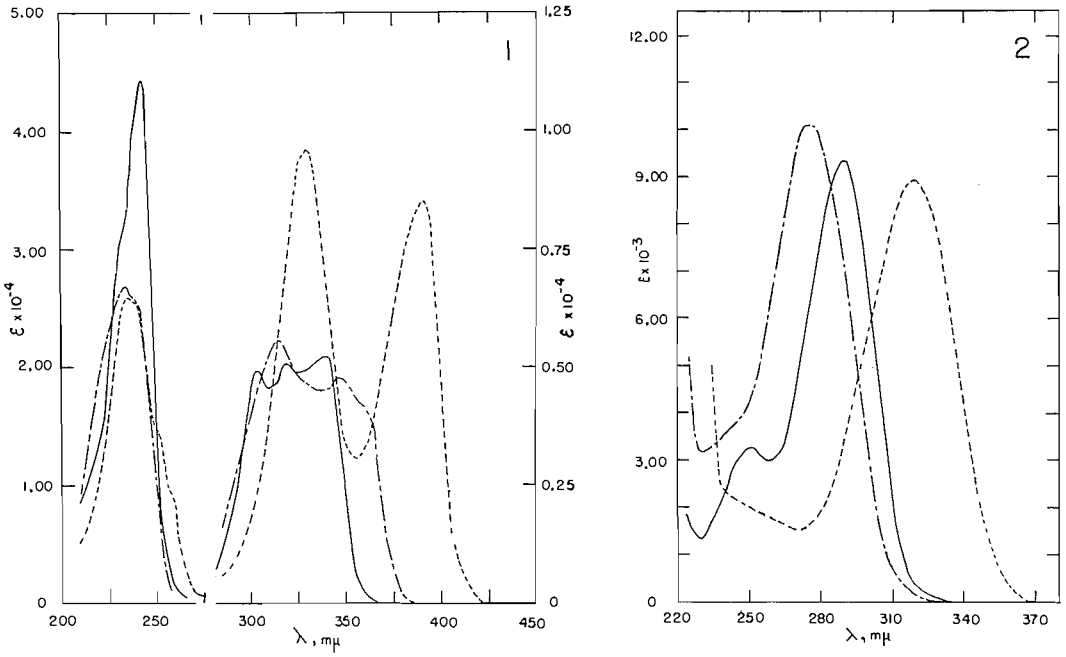


FIG. 1. Spectres de la tropolone: (--) L^- (NaOH 0.1 *M*); (-·—·-) HL (pH 2.1); (—) H_2L^+ (HCl 10.8 *M*).
FIG. 2. Spectres du maltol: (--) L^- (NaOH 0.4 *M*); (-·—·-) HL (pH 4.6); (—) H_2L^+ (HCl 10.8 *M*).

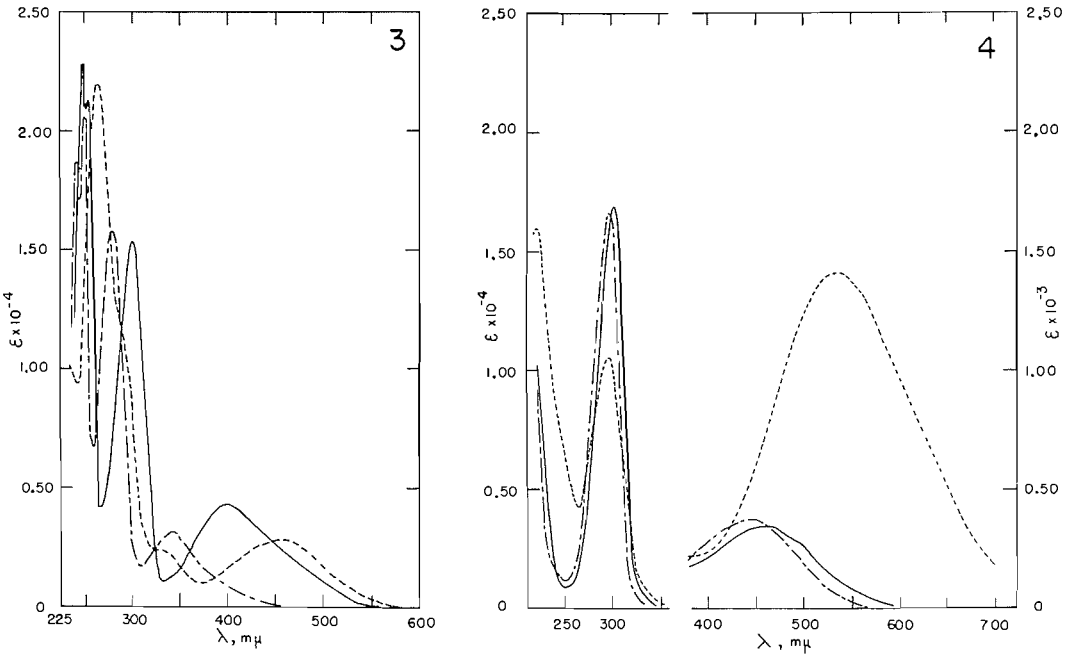


FIG. 3. Spectres de la lawsone: (--) L^- (NaOH 0.04 *M*); (-·—·-) HL (HCl 0.50 *M*); (—) H_2L^+ (H_2SO_4 86%).
FIG. 4. Spectre de la TCHQ: (--) L^- (pH 3.8); (-·—·-) HL (H_2SO_4 60%); (—) HL + H_2L^+ (H_2SO_4 86%).

de pk_1 obtenues à partir de cette équation, ainsi que les régions de longueurs d'onde où les mesures ont été effectuées. Les constantes k_1 sont définies à partir des concentrations.

TABLEAU I

Résultats des déterminations de pk_1

	Pente	λ, mμ	pk_1 Potentiométrie	pk_1 Spectrophotométrie
Tropolone	1.02±0.04	330, 335, 380–390	6.70±0.04	6.64±0.03
Maltol	1.03±0.03	260–276, 285–315	8.36±0.03	8.37±0.03
Lawsone	1.05±0.04	310, 420–500	4.02±0.04	3.97±0.04
TCHQ		500–600, 320–325	1.05±0.04	

Le coefficient ϵ_1 de TCHQ ne peut être obtenu directement, puisqu'en milieu HCl 0.50 M il existe une proportion importante de L^-. On a toutefois mesuré ϵ_0 à $-\log [H^+] = 3.8$, puis A_s en fonction de l'acidité entre $0.50 \geqslant [H^+] \geqslant 10^{-3.8}$. La constante k_1 a été déterminée graphiquement à partir de la pente de la droite correspondant à l'équation:

$$[2] \qquad A_s = \epsilon_1 C_L + k_1 \frac{\epsilon_0 C_L - A_s}{[H^+]}.$$

La valeur de pk_1 ainsi obtenue est égale à 1.05 ± 0.04.

(b) Potentiométrie

Les résultats précédents ont été confirmés par potentiométrie. On a déterminé les courbes de neutralisation par NaOH de solutions diluées (0.5 à 1.0×10^{-3} M) de maltol, de tropolone et de lawsone. On donne dans le Tableau I les valeurs de pk_1 obtenues d'après l'équation [3], $[Na^+]$ étant la concentration de soude ajoutée.

$$[3] \qquad -\log [H^+] = pk_1 + \log \frac{[Na^+] + [H^+]}{C_L - [Na^+] - [H^+]}$$

Les courbes de neutralisation de TCHQ sont telles que les valeurs de $-\log [H^+]$ diminuent régulièrement avec le temps au voisinage du point équivalent. On n'a donc pas utilisé de méthode potentiométrique dans ce cas.

On note un bon accord entre les résultats des méthodes spectrophotométrique et potentiométrique. Les valeurs données dans la littérature pour des milieux ioniques différents sont généralement voisines (2, 6, 8). Dans le cas de la lawsone, la valeur obtenue par Zozulya et Peshkova (7) ($pk_1 = 2.38$) n'est pas confirmée.

(B) Détermination des constantes de dissociation k_2 de H_2L^+

Les α-hydroxycétones étudiées peuvent également, en milieu très acide, accepter un proton sur l'oxygène du carbonyle pour former un acide conjugué H_2L^+. Les constantes de dissociation k_2 de H_2L^+ ont été déterminées par spectrophotométrie. On a mesuré l'extinction de solutions de concentration C_L constante, en des milieux de concentration H_2SO_4 variable. Les valeurs de pk_2 sont obtenues d'après l'équation

$$[4] \qquad H_0 = pk_2 - \log \frac{\epsilon_2 - \epsilon_L}{\epsilon_L - \epsilon_1} = pk_2 - \log R'.$$

L'acidité est ici définie au moyen de la fonction d'acidité H_0, dont les valeurs sont données par Paul et Long (12). ϵ_2 et ϵ_1 sont les coefficients d'extinction molaire de H_2L^+ et HL respectivement et le rapport R' est tel que $R' = [H_2L^+]/[HL]$.

Can. J. Chem. Downloaded from www.nrcresearchpress.com by 210.87.254.105 on 09/05/12
For personal use only.

Il est difficile de connaître avec précision les valeurs de ϵ_1 et ϵ_2 pour chaque concentration H_2SO_4, puisque ces valeurs varient quelque peu avec la nature du milieu. De telles variations sont souvent observées au cours de mesures de ce genre.

On a déterminé pour chacun des composés le spectre d'absorption à diverses concentrations de H_2SO_4. On a choisi, après examen des courbes donnant ϵ_L en fonction de H_0, les longueurs d'onde qui semblent les moins influencées par les changements de milieu, c'est-à-dire celles qui donnent une courbe comportant deux branches relativement horizontales. On obtient ϵ_1 et ϵ_2 à partir de points expérimentaux situés vers $H_0 = pk_2 \pm 2.3$ et on calcule pour toutes ces longueurs d'onde le facteur $\log R'$. La valeur moyenne de $\log R'$ pour toutes les longueurs d'onde choisies est portée sur la Fig. 5. L'équation [4] correspond à une droite de pente -1 et l'ordonnée à l'origine donne la valeur pk_2. Les résultats obtenus à partir de ces droites sont donnés dans le Tableau II, pour la tropolone, le maltol et la lawsone. Les valeurs calculées en utilisant la méthode de Davis et Geissman (13) sont identiques à celles du Tableau II. L'emploi de HCl au lieu de H_2SO_4 pour la mesure de la constante k_2 du maltol n'introduit pas de différences appréciables (-0.66 ± 0.10).

TABLEAU II

Résultats des déterminations de pk_2

	Pente	pk_2	λ, mμ
Tropolone	-1.01 ± 0.05	-0.53 ± 0.10	260–274, 290–300
Maltol	-1.18 ± 0.05	-0.71 ± 0.10	356–364
Lawsone	-1.19 ± 0.07	-5.6 ± 0.2	256, 275, 305–310, 400–420
TCHQ		$-8.8 \pm 1.$	500

La valeur obtenue par Dyrssen (2) pour l'ion tropolonium ($pk = 0.03$) correspond à une force ionique 3 ($HClO_4$, $NaClO_4$); ce résultat est comparable au nôtre ($pk_2 = -0.53$) si l'on considère de plus que l'acidité est définie de façon différente. La stabilité relativement grande du cation est reliée à des effets de résonance importants. Cook (14) a montré, par examen de spectres infra-rouges de sels de pyrilium, que la fixation du proton a lieu sur l'oxygène du groupe carbonyle des γ-pyrones. L'acide conjugué du maltol, comme celui de la tropolone, est stabilisé par résonance.

On note sur le spectre de la TCHQ, donné sur la Fig. 4, pour H_2SO_4 86%, un épaulement vers 500 mμ qui correspond vraisemblablement à H_2L^+. Les spectres à concentrations d'acide sulfurique inférieures présentent des variations régulières entre 15 et 65%: la solution reste jaune, avec un maximum d'absorption vers 445 mμ, mais ε varie quelque peu (435 à 360); dans l'ultra-violet, la bande se déplace de quelques mμ sans changement notable d'intensité. Ces variations sont peu importantes et du même type que celles qu'on retrouve avec la tropolone, le maltol et la lawsone et qui ont été notées par Handa (15) pour une série de composés quinoniques: elles ne correspondent apparemment pas à un changement de nature des espèces. La détermination de k_2 de TCHQ impliquerait l'emploi de milieux H_2SO_4 très concentrés (> 96%) dans lesquels le composé est peu stable. En supposant que l'épaulement observé pour la solution dans H_2SO_4 86% ($H_0 = -7.8$) correspond à une formation $1\% \leqslant H_2L \leqslant 50\%$, on peut conclure que pk_2 de TCHQ se situe dans l'intervalle -7.8 à -9.8. La TCHQ, comme la lawsone, est probablement protonée sur l'oxygène en position 4 (—OH étant en position 2): la stabilisation par résonance de tels cations serait plus grande que pour l'espèce protonée sur l'oxygène en position 1 (6).

Can. J. Chem. Downloaded from www.nrcresearchpress.com by 210.87.254.105 on 09/05/12
For personal use only.

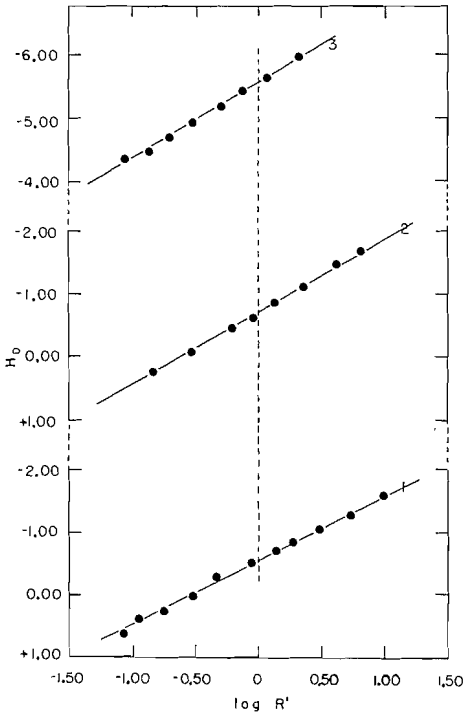


FIG. 5. Détermination des constantes k_2 de la tropolone, du maltol et de la lawsone. (1) Tropolone; (2) maltol; (3) lawsone.

Les quinones sont généralement peu basiques: anthraquinone (pk −7.5), naphtoquinone (−7.2) (15). Biedermann (16) déduit de la mesure des potentiels de l'électrode de quinhydrone en milieu acide, la formation d'un cation HL^+ de la *p*-benzoquinone, avec un pk = −1.0. Handa (15) prétend au contraire que la *p*-benzoquinone est détruite dans les milieux H_2SO_4 concentrés où elle pourrait accepter un proton. La présence d'une proportion importante de l'acide conjugué H_3L^+ de la dichloro-2,5 dihydroxy-3,6 *p*-benzoquinone (acide chloranilique H_2L) en milieu $HClO_4$ 1 *N* a été récemment avancée par Nazarenko et Flyantikova (17). Nous avons toutefois mesuré les spectres, entre 200–700 mμ, du composé dissous dans l'acétone et le dioxanne, solvants peu polaires dans lesquels l'acide chloranilique est vraisemblablement sous forme de l'espèce H_2L. Ces spectres sont semblables à ceux que l'on obtient pour le même composé dissous dans H_2SO_4 40% ce qui semble indiquer que le cation H_3L^+ ne se forme qu'en milieu très acide. Schwarzenbach et Suter (18) ont d'ailleurs étudié, par une méthode analogue à la nôtre, les propriétés basiques de la dihydroxy-2,5 *p*-benzoquinone et donnent pk = −7.0.

BIBLIOGRAPHIE

1. N. J. CLARK et B. R. WILLEFORD. J. Am. Chem. Soc. **79**, 1296 (1957).
2. D. DYRSSEN. Acta Chem. Scand. **8**, 1394 (1954).
3. Y. OKA, M. UMEHARA et T. NOZOE. Nippon Kagaku Zasshi, **83**, 1197 (1962); C.A. **59**, 9389.
4. B. E. BRYANT, W. C. FERNELIUS et B. E. DOUGLAS. J. Am. Chem. Soc. **75**, 3784 (1953).
5. J. W. COOK, A. R. GIBB, R. A. RAPHAEL et A. R. SOMERVILLE. J. Chem. Soc. 503 (1951).
6. M. G. ETTLINGER. J. Am. Chem. Soc. 72, 3085 (1950).
7. A. P. ZOZULYA et V. M. PESHKOVA. Russ. J. Inorg. Chem. English Transl. **4**, 168 (1959).
8. K. WALLENFELS et K. FRIEDRICH. Chem. Ber. **93**, 3070 (1960).
9. K. YAMADA. Bull. Chem. Soc. Japan, **35**, 1323 (1962).

Can. J. Chem. Downloaded from www.nrcresearchpress.com by 210.87.254.105 on 09/05/12
For personal use only.

10. L. F. FIESER. J. Am. Chem. Soc. **70**, 3165 (1948).
11. J. W. HANCOCK, C. E. MORRELL et D. RHUM. Tetrahedron Letters, 987 (1962).
12. M. A. PAUL et F. A. LONG. Chem. Rev. **57**, 1 (1957).
13. C. T. DAVIS et T. A. GEISSMAN. J. Am. Chem. Soc. **76**, 3507 (1954).
14. D. COOK. Can. J. Chem. **41**, 505 (1963).
15. T. HANDA. Bull. Chem. Soc. Japan, **28**, 483 (1955).
16. G. BIEDERMANN. Acta Chem. Scand. **10**, 1340 (1956).
17. V. A. NAZARENKO et G. V. FLYANTIKOVA. Zh. Obshch. Khim. **35**, 211 (1965).
18. G. SCHWARZENBACH et H. SUTER. Helv. Chem. Acta, **24**, 617 (1941).

Can. J. Chem. Downloaded from www.nrcresearchpress.com by 210.87.254.105 on 09/05/12
For personal use only.

Can. J. Chem. Downloaded from www.nrcresearchpress.com by 210.87.254.6 on 09/05/12
For personal use only.

CHÉLATES DU GERMANIUM(IV) AVEC LA TROPOLONE, LE MALTOL, LA LAWSONE ET LA TRICHLOROHYDROXY *p*-BENZOQUINONE[1]

II. NATURE ET STABILITÉ DES CHÉLATES

A. BEAUCHAMP[2] ET R. L. BENOIT

Département de Chimie, Université de Montréal, Montréal, Québec

Reçu le 25 février 1966

RÉSUMÉ

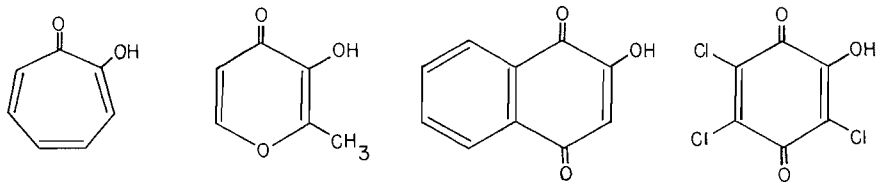
On a étudié par spectrophotométrie la formation de chélates entre le germanium(IV) et une série d'α-hydroxycétones (HL). Avec la tropolone et le maltol, on a mis en évidence la présence d'espèces $Ge(OH)_2L_2$ et GeL_3^+ et déterminé les constantes d'équilibre correspondantes β_2 et β_3. Les composés $Ge(OH)_2(tropolonate)_2.2H_2O$, $Ge(tropolonate)_3ClO_4$ et $Ge(maltolate)_3ClO_4$ ont été isolés à l'état solide. Aucun complexe n'a été observé avec la lawsone et la trichlorohydroxy *p*-benzoquinone. On examine les relations entre la stabilité des chélates, la nature du germanium(IV) en solution et les propriétés acides–bases des α-hydroxycétones.

ABSTRACT

The formation of chelates between germanium(IV) and a series of α-hydroxyketones (HL) has been examined spectrophotometrically. Tropolone and maltol have been shown to give the species $Ge(OH)_2L_2$ and GeL_3^+; the corresponding equilibrium constants β_2 and β_3 have been determined. The following solid compounds have been isolated: $Ge(OH)_2(tropolonate)_2.2H_2O$, $Ge(tropolonate)_3ClO_4$, and $Ge(maltolate)_3ClO_4$. There was no evidence of complex formation with lawsone and trichlorohydroxy *p*-benzoquinone. Relations are discussed between the chelate stability, the state of germanium(IV) in solution, and the acid–base properties of the α-hydroxyketones.

INTRODUCTION

Les complexes du germanium(IV) avec la dichloro-2,5 dihydroxy-3,6 *p*-benzoquinone (acide chloranilique) ont fait l'objet d'une étude antérieure (1). On examine maintenant la formation de complexes avec les quatre autres α-hydroxycétones cycliques simples de formules suivantes:



On a voulu préciser le comportement des deux α-hydroxyquinones, lawsone et TCHQ, afin d'effectuer des comparaisons avec la dichloro-2,5 dihydroxy-3,6 *p*-benzoquinone et son analogue non-chloré (1). En ajoutant à cette étude deux autres α-hydroxycétones, la tropolone et le maltol, on s'est proposé de rechercher une relation entre les propriétés acides–bases de ces ligands et la stabilité des complexes formés avec le germanium. On pourrait s'attendre à obtenir une relation analogue à celle établie par Fernelius *et al.* (2) entre les constantes d'acidité d'hydroxycétones et les constantes de stabilité des chélates d'ions métalliques M^{2+}.

[1]*Tiré d'une communication présentée lors du 48ième Congrès de l'Institut de Chimie du Canada, tenu à Montréal, les 31 mai – 2 juin 1965.*

[2]*Boursier du Conseil National de Recherches 1964–1965 et de l'Hydro-Québec 1965–1966.*

Kimura *et al.* (3), Oka et Matsuo (4) et Kanno (5) ont déjà noté que la présence de germanium(IV) modifie les spectres de certaines hydroxycétones de la famille des fluorones, naphtoquinones, coumarines, tropones et flavones. Des chélates solides ont été récemment isolés par réaction de $GeCl_4$ avec la tropolone (6). Les réactions de la tropolone, du maltol et de la lawsone avec plusieurs cations M^{2+} ont été caractérisées par d'autres auteurs (2, 7, 8).

PARTIE EXPÉRIMENTALE

Les solutions de germanium(IV) environ 4×10^{-2} *M* sont préparées par dissolution de bioxyde GeO_2 de haute pureté, fourni par le "Germanium Research Center" et dosées par titrage potentiométrique avec de la soude non-carbonatée en présence de mannitol.

Les autres réactifs et la technique expérimentale sont décrits dans l'article précédent.

RÉSULTATS EXPÉRIMENTAUX

Les composés étudiés comportent une ou plusieurs bandes d'absorption dans la région 200–800 mμ et les réactions avec le germanium(IV) ont été caractérisées au moyen de méthodes spectrophotométriques.

I. Chélates avec la tropolone et le maltol

La formation de chélates lors de l'addition de GeO_2 à des solutions peu acides (pH 4) de tropolone ou de maltol (HL) s'accompagne de modifications dans les spectres d'absorption des ligands. La présence de germanium affecte de façon importante les diverses bandes d'absorption de la tropolone (Fig. 1) et déplace le maximum du maltol de 275 mμ vers 290 mμ (Fig. 2). Lorsque deux espèces absorbantes seulement sont présentes, les spectres peuvent présenter des points isobestiques; ainsi cinq tels points sont présents dans les spectres de la tropolone, deux dans ceux du maltol.

En milieu plus acide (HCl 0.50 *M*) les spectres sont différents et l'influence de l'acidité sur la formation de chélates a d'abord été considérée. La densité optique A_s d'une solution de

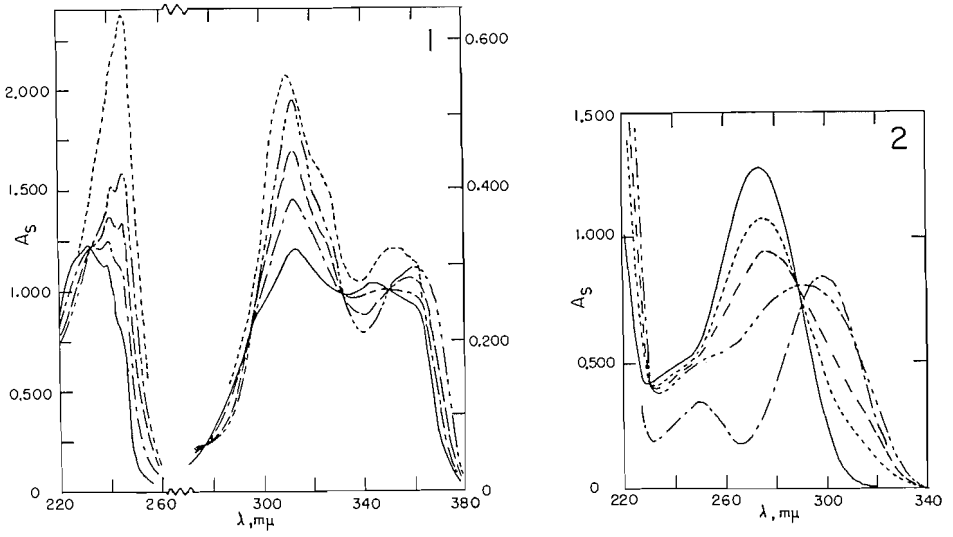


FIG. 1. Spectres de la tropolone en présence de germanium(IV). $C_L = 2.30 \times 10^{-3}$ *M*; pH = 4.0 ± 0.1; NaCl = 0.50 *M*; e (épaisseur) = 0.20 cm. (—) $C_M = 0$; (-·—·-) $C_M = 3.54 \times 10^{-1}$ *M*; (— — —) $C_M = 7.04 \times 10^{-1}$ *M*; (— · · · — · · · —) $C_M = 1.06 \times 10^{-2}$ *M*; (--) $C_L = 2.86 \times 10^{-3}$ *M*, HCl = 0.50 *M*, $C_M = 2.86 \times 10^{-2}$ *M*.

FIG. 2. Spectres du maltol en présence de germanium(IV). $C_L = 7.13 \times 10^{-3}$ *M*; pH = 4.00 ± 0.03; NaCl = 0.50 *M*; e = 0.20 cm. (—) $C_M = 0$; (--) $C_M = 3.42 \times 10^{-3}$ *M*; (— —) $C_M = 8.33 \times 10^{-3}$ *M*; (— · · · · · —) $C_M = 2.92 \times 10^{-2}$ *M*; (-·—·-) $C_L = 4.91 \times 10^{-3}$ *M*, HCl = 0.484 *M*, $C_M = 3.34 \times 10^{-2}$ *M*.

Can. J. Chem. Downloaded from www.nrcresearchpress.com by 210.87.254.6 on 09/05/12
For personal use only.

maltol et de GeO_2 a été mesurée pour des milieux d'acidité variable. Les concentrations totales du ligand ($C_L = 1.88 \times 10^{-3}\ M$) et du germanium ($C_M = 4.08 \times 10^{-2}\ M$) sont maintenues constantes, ainsi que la force ionique (HCl + NaCl = 0.50 M). Les résultats obtenus pour plusieurs longueurs d'onde sont donnés sur la Fig. 3. Dans un domaine d'acidité compris entre $2.5 \leqslant -\log [H^+] \leqslant 6$, l'acidité est sans effet sur les équilibres, comme l'indique la valeur constante de la densité optique. A $-\log [H^+] > 6$, les équilibres sont modifiés par la neutralisation du maltol ($pk_1 = 8.38$) et de l'acide germanique ($pk_1 = 9.2$). Les variations d'extinction observées pour $-\log [H^+] < 2.5$ ne peuvent s'expliquer seulement par la formation du cation H_2L^+, puisqu'à $-\log [H^+] = 1$, par exemple, le ligand est protoné à moins de 2%. Il se forme donc, en milieu acide, d'autres chélates dont la concentration dépend de l'acidité. La tropolone se comporte de façon analogue: les spectres ne dépendent pas de l'acidité dans le domaine $3 \leqslant -\log [H^+] \leqslant 6$. Les chélates présents en milieu peu acide ont d'abord été caractérisés, en opérant à $-\log [H^+] = 3.5$–4.5.

(a) Chélates formés en milieu peu acide

La méthode de variations continues permet dans les cas simples de déterminer la composition de complexes. Des mesures ont été effectuées à plusieurs longueurs d'onde et les courbes donnant $\Delta A_s = A_s - \epsilon_L C_L$ en fonction du rapport $C_L/(C_M + C_L)$ sont représentées sur la Fig. 4, ϵ_L étant le coefficient d'extinction molaire du ligand à l'acidité choisie. Toutes les courbes correspondant à un milieu peu acide présentent un maximum pour un rapport $C_L/(C_M + C_L)$ voisin de 0.67. Ces résultats indiquent que le maltol et la tropolone forment avec le germanium des chélates de type M_mL_{2m}. Comme il a été vérifié par la suite que l'indice de polymérisation m est égal à 1, la réaction suivante rend compte des faits observés:

$$[1] \qquad Ge(OH)_4 + 2HL \rightleftarrows Ge(OH)_2L_2 + 2H_2O \qquad \beta_2 = \frac{[Ge(OH)_2L_2]}{[Ge(OH)_4][HL]^2}.$$

De plus, les résultats de la Fig. 3 ayant indiqué que l'acidité est sans effet sur les équilibres dans ce domaine, on peut conclure que les —OH liés au germanium ne possèdent pas de propriétés acides–bases notables.

L'absence de quantités appréciables d'espèces de stoechiométrie différente, suggérée par l'observation de points isobestiques (Figs. 1 et 2) et par la valeur constante de l'abscisse du maximum des courbes de variations continues (Fig. 4), est confirmée par la méthode des rapports molaires. On mesure l'extinction de solutions de tropolone de concentration constante et élevée en présence de quantités croissantes de GeO_2. Les résultats obtenus sont donnés sur la Fig. 5, où on porte ΔA_s en fonction du rapport C_M/C_L. Les deux droites de pentes 0 et $2\Delta A_{s(max)}$ se coupent à un rapport C_M/C_L égal à 0.50, ce qui est caractéristique de la présence d'une seule espèce ML_2. Des proportions importantes de chélate ML_3 conduiraient à une courbure pour $C_M/C_L < 0.50$, tandis que des variations de ΔA_s seraient observées pour $C_M/C_L > 0.50$, dans le cas où il y aurait formation de ML ou d'espèces polynucléaires.

Les constantes d'équilibre β_2 ont été déterminées par la méthode de McConnell–Davidson modifiée, décrite antérieurement (1). On mesure la densité optique de solutions de tropolone ou de maltol à concentration C_L constante, en faisant varier la concentration du germanium. On porte ensuite sur la Fig. 6, $(\Delta A_s/C_M)^{1/2}$ en fonction de ΔA_s. La concentration C_M est généralement telle que $C_M \gg C_L$ et l'approximation $C_M \sim [M]$ est justifiée. Les valeurs des constantes β_2 et des coefficients d'extinction molaire ϵ_2 de ML_2 sont calculées à partir de la pente et de l'ordonnée à l'origine des droites de la Fig. 6. On

Can. J. Chem. Downloaded from www.nrcresearchpress.com by 210.87.254.6 on 09/05/12
For personal use only.

Can. J. Chem. Downloaded from www.nrcresearchpress.com by 210.87.254.6 on 09/05/12
For personal use only.

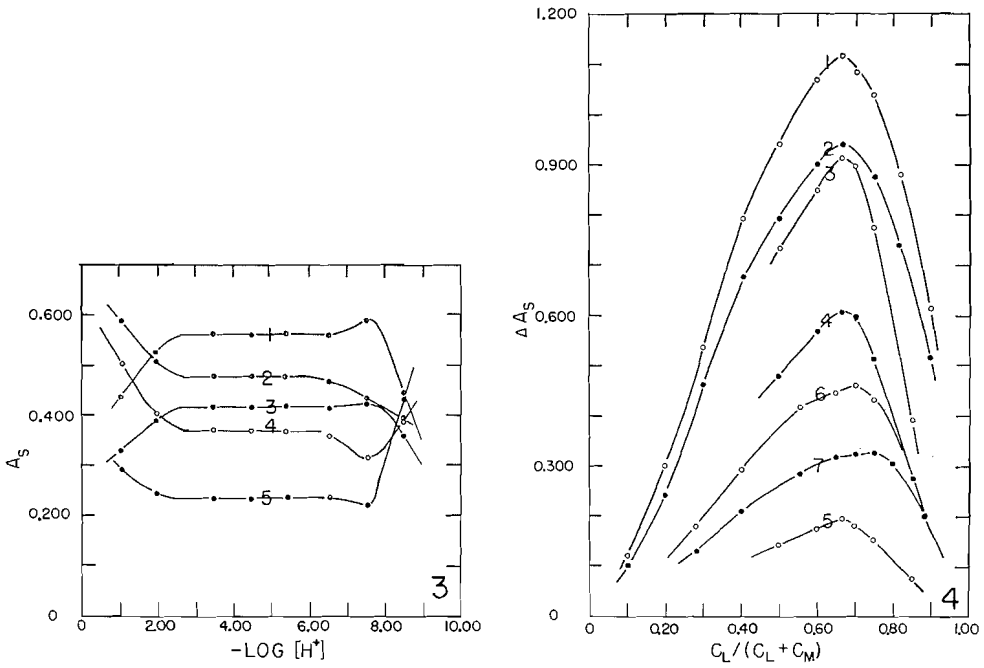


FIG. 3. Influence de l'acidité sur la formation des chélates du germanium(IV) avec le maltol. $C_L = 1.883 \times 10^{-3}$ M; $C_M = 4.08 \times 10^{-2}$ M; (NaCl + HCl) = 0.502 M; e = 0.50 mm. (1) 276 mμ; (2) 295 mμ; (3) 260 mμ; (4) 305 mμ; (5) 315 mμ.

FIG. 4. Méthode de variations continues. Maltol: $(C_M + C_L) = 4.17 \times 10^{-3}$ M; NaCl = 0.50 M; $-\log [H^+] = 4.43 \pm 0.03$; e = 0.20 cm. (1) 305 mμ; (2) 315 mμ. Maltol: $(C_M + C_L) = 2.50 \times 10^{-3}$ M; HCl = 0.502 M; e = 0.20 cm. (3) 265 mμ; (4) 315 mμ. Tropolone: $(C_M + C_L) = 3.20 \times 10^{-3}$ M; NaCl = 0.50 M; $-\log [H^+] = 3.51 \pm 0.02$; e = 0.20 cm. (5) 375 mμ; (6) 252 mμ; (7) 280 mμ.

TABLEAU I

Résultats des déterminations des constantes d'équilibre

	$\log \beta_2$	pk_1	pk_2	$p(k_1k_2)$	$\log \beta_2^0/K_{Ge}''$
Tropolone (HL)	8.03	6.67	−0.53	6.14	21.37
Maltol (HL)	3.90	8.36	−0.71	7.65	20.62
Lawsone (HL)	⩽3.0	4.00	−5.6	−1.6	⩽11.0
TCHQ (HL)	⩽1.4	1.05	−8.8	−9.7	⩽3.5
DHQ (H_2L)	9.1* (17)	5.18 (18)	2.71† (18)	7.89	19.5
Acide chloranilique (H_2L)	6.57* (1)	2.37 (1)	0.66† (1)	3.03	11.31

$^*\beta_2 = \dfrac{[Ge(OH)_2L_2^{2-}]}{[Ge(OH)_4][HL^-]^2}$.

$\dagger k_2 = \dfrac{[H^+][HL^-]}{[H_2L]}$.

obtient pour la tropolone $\beta_2 = 10^{8.03 \pm 0.05}$ et pour le maltol $\beta_2 = 10^{3.90 \pm 0.04}$ (Tableau I). On a vérifié par ailleurs que les fonctions analogues correspondant à ML, ML_3 et M_mL_{2m} où $m \neq 1$ conduisent à des courbes avec les résultats expérimentaux obtenus.

(b) Chélates formés en milieu acide

L'existence d'autres équilibres en milieu acide est suggérée par les spectres dans HCl 0.50 M (Figs. 1 et 2) et par les variations de l'extinction pour $-\log [H^+] < 2.5$ (Fig. 3). L'abscisse des maxima des courbes de variations continues du maltol à cette acidité

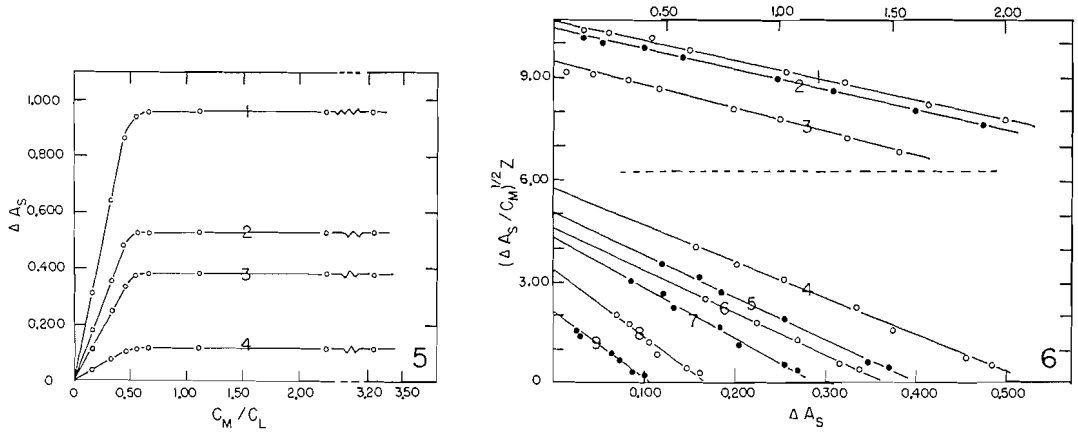


FIG. 5. Méthode des rapports molaires pour le système germanium(IV)–tropolone. $C_L = 6.41 \times 10^{-3}$ M; NaCl = 0.50 M; $-\log [H^+] = 4.34 \pm 0.05$; e = 0.20 cm. (1) 256 mμ; (2) 314 mμ; (3) 370 mμ; (4) 380 mμ.

FIG. 6. Méthode McConnell–Davidson modifiée. Maltol: $Z = 1$; $C_L = 9.97 \times 10^{-4}$ M; NaCl = 0.50 M; $-\log [H^+] = 4.02 \pm 0.03$. (1) 305 mμ; (2) 310 mμ; (3) 315 mμ. Tropolone: $Z = 10$; $C_L = 2.81 \times 10^{-5}$ M; NaCl = 0.50 M; $-\log [H^+] = 4.34 \pm 0.05$. (4) 249 mμ; (5) 252 mμ; (6) 245 mμ; (7) 254 mμ; (8) 256 mμ; (9) 314 mμ.

varient entre 0.65 et 0.75 selon la longueur d'onde. Un autre chélate est donc vraisemblablement formé en milieu acide, selon la réaction:

$$[2] \qquad Ge(OH)_4 + 3HL + H^+ \rightleftarrows GeL_3^+ + 4H_2O \qquad \beta_3 = \frac{[GeL_3^+]}{[Ge(OH)_4][HL]^3[H^+]}.$$

Les constantes d'équilibre β_3 ont été déterminées par spectrophotométrie, en utilisant une réaction compétitive avec le fer(III).

L'ion ferrique forme avec la tropolone (9) et les hydroxy-3 pyrones-4 (10) des chélates colorés qui absorbent entre 450 et 600 mμ, région où les chélates du germanium n'interfèrent pas. Les équilibres entre le germanium et ces ligands peuvent être étudiés indirectement en mesurant l'extinction due aux chélates du fer. Les résultats d'une expérience type, effectuée à 515 mμ, sont représentés sur la Fig. 7. La concentration totale de fer(III) est maintenue constante ($C_{Fe} = 7.04 \times 10^{-4}$ M) ainsi que l'acidité (HCl = 0.50 M). La densité optique est mesurée en fonction de la concentration de maltol ajoutée et on porte le rapport $Y = A_s/C_{Fe}$ en fonction de cette concentration C_L (courbe 1). Les mesures sont répétées pour des solutions qui contiennent en plus une concentration C_M de germanium(IV) (courbes 3 et 4). Cette méthode est comparable à la méthode "ferri" utilisée couramment en potentiométrie (11). On peut démontrer qu'à une valeur donnée de Y, la concentration de ligand libre [L] est constante et le nombre moyen de ligands par germanium $\bar{n}_M$ est calculable d'après l'équation $C_L' - C_L^0 = \bar{n}_M C_M$, où C_L' et C_L^0 sont les concentrations de ligand ajoutées à la solution ferrique en présence et en absence de germanium respectivement. La concentration de HCl étant constante et telle que $C_{Cl} \gg C_{Fe}$, la formation de complexes chlorhydriques du fer ne gêne pas. On obtient ainsi des paires de valeurs ($\bar{n}_M$, Y). La concentration [L] correspondant à chacune des valeurs de Y est obtenue par la méthode des solutions correspondantes (11). On détermine une autre courbe en l'absence de germanium en utilisant une concentration différente C_{Fe} (courbe 2) et on calcule [L] d'après l'équation $C_L = [L] + \bar{n}_{Fe} C_{Fe}$. A partir des paires de valeurs ($\bar{n}_M$, [L]) ainsi

Can. J. Chem. Downloaded from www.nrcresearchpress.com by 210.87.254.6 on 09/05/12
For personal use only.

obtenues, on trace la courbe de formation $\bar{n}_M = f(-\log [L])$ du système germanium(IV)–maltol à HCl 0.50 *M*. Ces résultats, de même que ceux qui correspondent à d'autres longueurs d'onde, sont donnés sur la Fig. 8. Les courbes calculées à partir de $\beta_2^* = 10^{4.4\pm0.8}$ et $\beta_3^* = 10^{7.74\pm0.06}$ donnent le meilleur accord avec les points expérimentaux.

Dans le cas de la tropolone, les conditions expérimentales ont été choisies de façon à obtenir la portion de la courbe de formation dans la région $\bar{n}_M = 2$ (Fig. 8). La constante β_1 d'un chélate ML étant négligeable, la valeur de β_3^* peut être calculée à partir de l'équation:

$$\beta_3^*[L]^3_{\bar{n}_M=2} = 2.$$

La valeur β_3^* $10^{13.0\pm0.1}$ est obtenue pour la tropolone. La constante β_2^* $10^{8.7\pm0.9}$ estimée au moyen des autres points expérimentaux est obtenue avec une mauvaise précision puisque la concentration de chélate ML_2 est très inférieure à celle de ML_3 dans les conditions de l'expérience.

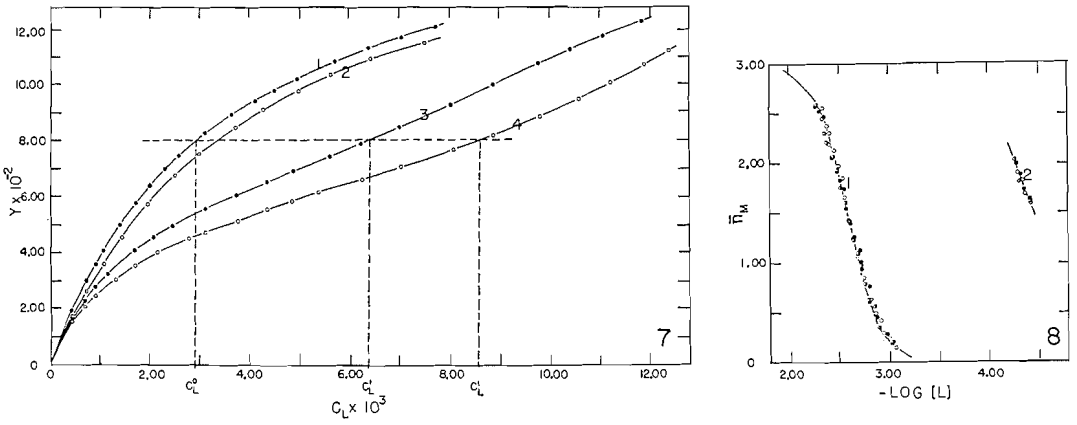


FIG. 7. Méthode compétitive Fe(III)/Ge(IV) – maltol. HCl = 0.50 *M*; e = 1.00 cm; 515 mμ. (1) $C_{Fe} = 7.04 \times 10^{-4}$ *M*, $C_M = 0$; (2) $C_{Fe} = 1.409 \times 10^{-3}$ *M*, $C_M = 0$; (3) $C_{Fe} = 7.04 \times 10^{-4}$ *M*, $C_M = 3.57 \times 10^{-3}$ *M*. (4) $C_{Fe} = 7.04 \times 10^{-4}$ *M*, $C_M = 7.14 \times 10^{-3}$ *M*.

FIG. 8. Courbes de formation des chélates du germanium(IV) en milieu HCl 0.50 *M*. (1) Maltol: (○) 530 mμ, (●) 515 mμ, (◑) 500 mμ; (2) tropolone: (○) 545 mμ, (●) 525 mμ, (◑) 480 mμ.

Les valeurs des constantes β_3 sont calculées à partir des constantes apparentes β_3^*, valables en milieu HCl 0.50 *M*, d'après la relation

$$\beta_3 = \beta_3^*(1 + (10^{-H_0}/k_2))/[H^+]$$

où k_2 est la constante d'acidité de l'acide conjugé H_2L^+, déterminée précédemment en se basant sur la fonction d'acidité H_0: $pk_2 = -0.71$ pour le maltol, -0.53 pour la tropolone; $[H^+] = 0.50$, $H_0 = 0.99$. Les constantes sont $\beta_3 = 10^{8.05\pm0.07}$ (maltol); $10^{13.3\pm0.1}$ (tropolone).

(c) Chélates solides

Quelques espèces identifiées en solution ont été isolées dans des composés solides. L'évaporation d'une solution aqueuse de GeO_2 et de tropolone (1:2 respectivement) a fourni un solide blanc de composition $Ge(OH)_2(tropolonate)_2.2H_2O$. Le germanium a été estimé gravimétriquement par calcination du chélate en GeO_2 et la tropolone a été analysée par spectrophotométrie à 330 mμ et 390 mμ sur une solution basique (NaOH 0.04 *M*). Ce composé est à rapprocher de $GeCl_2(tropolonate)_2$ isolé par réaction de la tropolone avec $GeCl_4$ (6). Dans ces mêmes conditions, le chélate $Ge(OH)_2(maltolate)_2$, dont la constante de stabilité est faible, n'est pas obtenu à l'état pur. Le spectre ultra-violet

Can. J. Chem. Downloaded from www.nrcresearchpress.com by 210.87.254.6 on 09/05/12
For personal use only.

d'une solution dans CH_2Cl_2 du mélange recueilli après évaporation, comporte un maximum vers 275 mμ, caractéristique du maltol, et un léger épaulement vers 300 mμ qui correspond vraisemblablement à un chélate. La présence d'une espèce complexe dans ce mélange est également indiquée par le spectre infra-rouge.

L'addition de $HClO_4$ (jusqu'à 1 *M*) à une solution de GeO_2 et de tropolone ou de maltol (1:3) (GeO_2:ligands) précipite des composés de formules $Ge(tropolonate)_3ClO_4$ et $Ge(maltolate)_3ClO_4$. Une bande vers 1 100 cm^{-1}, caractéristique de l'ion ClO_4^-, est observée et la bande —OH des ligands vers 3 400 cm^{-1} est absente dans les spectres infra-rouges des composés obtenus. D'autres sels de l'ion complexe $[Ge(tropolonate)_3]^+$ ont été isolés par Muetterties et Wright (6).

Les spectres ultra-violets de $Ge(OH)_2(tropolonate)_2.2H_2O$, $Ge(tropolonate)_3ClO_4$ et $Ge(maltolate)_3ClO_4$ ont été mesurés en solution dans CH_2Cl_2. Ils diffèrent peu de ceux qui ont été observés en solution aqueuse pour $Ge(OH)_2(tropolonate)_2$, $[Ge(tropolonate)_3]^+$ et $[Ge(maltolate)_3]^+$ respectivement, les faibles déplacements des maxima étant attribuables à des effets de solvant.

II. Réactions avec la lawsone et la TCHQ

Place (12) a étudié les réactions de $GeCl_4$ avec la lawsone et la TCHQ en milieu anhydre: dans des conditions où $GeCl_4$ donne lieu à la formation de chélates avec l'acide chloranilique et la dihydroxy-2,5-*p*-benzoquinone, aucun produit n'a été obtenu avec la lawsone et la TCHQ. L'absence de réaction entre le GeO_2 (3×10^{-5} *M*) et la lawsone (2.9×10^{-4} *M*) dans l'éthanol à 25% a été notée par Kimura (3). Nous nous sommes assurés que la lawsone et la TCHQ ne donnent pas de réaction détectable avec le germanium(IV) en solution aqueuse.

La présence d'une forte concentration de GeO_2 (2.9×10^{-2} *M*) dans une solution de lawsone (7.3×10^{-4} *M*) à pH 3.8 ou HCl 0.50 *M* est sans effet sur le spectre d'absorption. La lawsone est peu soluble à pH < 4 et aucun accroissement de sa solubilité n'a été noté en présence de GeO_2. A ces mêmes acidités, les spectres de solutions saturées de lawsone en présence de GeO_2(4×10^{-2} *M*) sont identiques à ceux qu'on obtient pour une solution saturée dans l'eau.

L'influence de GeO_2 sur le spectre de solutions concentrées de TCHQ (2.3×10^{-3} *M*) dans HCl 1 *M* et 0.1 *M* a été considérée. La présence de germanium (2.3×10^{-2} *M*) donne lieu à un léger épaulement dans le spectre vers 330 mμ. Cet épaulement est sans doute dû au chélate du germanium avec l'acide chloranilique présent comme impureté (0.7%) dans le produit de départ. Ceci est confirmé par le fait que les valeurs de la densité optique vers 330 mμ peuvent être expliquées quantitativement à l'aide des constantes d'équilibre et des coefficients d'extinction des chélates avec l'acide chloranilique (1).

Compte tenu de la précision de nos méthodes de détection, on peut donner pour les constantes hypothétiques de chélates du germanium avec la lawsone et la TCHQ les limites supérieures suivantes: lawsone, $\beta_2 \leqslant 10^3$; TCHQ, $\beta_2 \leqslant 10^{1.4}$.

DISCUSSION

La tropolone et le maltol réagissent avec le germanium(IV) en solution aqueuse pour former, suivant l'acidité, deux types de complexes, fort probablement des chélates, comportant soit deux, soit trois molécules de ligands par atome de germanium.

Les formules $Ge(OH)_2(tropolonate)_2$ et $Ge(OH)_2(maltolate)_2$, suggérées pour les chélates présents en milieu peu acide, rendent compte de la stoechiométrie et des propriétés observées. Cependent, l'étude des équilibres en solution ne permet pas de distinguer entre

Can. J. Chem. Downloaded from www.nrcresearchpress.com by 210.87.254.6 on 09/05/12
For personal use only.

les formules $Ge(OH)_2L_2$ et $GeOL_2$. L'étude du spectre infra-rouge du chélate solide dont la composition correspond à $Ge(OH)_2(tropolonate)_2.2H_2O$ n'a pas permis de mettre en évidence sans ambiguïté l'existence de groupes Ge—OH. La bande large vers 3 450 cm^{-1} pourrait être due à la fois à des vibrations de ces —OH et des molécules d'eau. Par ailleurs, les fréquences correspondant aux groupes Ge—O—H, Ge=O et Ge—O—C ne sont pas connues avec certitude. Clark *et al.* (13) attribuent à la vibration Ge—O—C une bande vers 940 cm^{-1}, observée dans les spectres de chélates du germanium avec des acides α-hydroxycarboxyliques, mais nous n'avons pas observé de telle bande dans les chélates de la tropolone et du maltol. Toutefois, comme on ne connaît apparemment pas de complexes comportant le groupe Ge=O (14), la formule $Ge(OH)_2L_2$ est retenue de préférence à $GeOL_2$. Elle est à rapprocher de $GeCl_2L_2$, formule du composé récemment obtenu en faisant réagir $GeCl_4$ avec la tropolone en milieu anhydre (6). L'étude effectuée ne permet pas par ailleurs de conclure quant à l'isomérie *cis–trans* de ces chélates.

On ne connait que peu de cations complexes du germanium(IV): $[GeOx_3]^+$ (où Ox^- est l'anion de l'hydroxy-8 quinoléine) présent dans $GeOx_3FeCl_4$ et stable dans certains solvants, semble avoir été le premier signalé (15). Nous avons mis en évidence l'existence des espèces $[Ge(tropolonate)_3]^+$ et $[Ge(maltolate)_3]^+$ en milieu acide et ces cations ont été isolés à l'état solide sous forme de perchlorates. Les composés sont vraisemblablement du même type que les sels $[Ge(tropolonate)_3]X$ (où $X = Cl^-$ ou tropolonate$^-$) isolés par Muetterties et Wright (6).

Les chélates du maltol et de la tropolone avec les ions métalliques sont généralement de stabilité voisine (7, 8). Il peut donc paraître surprenant que dans le cas du germanium, la constante d'équilibre β_2 du chélate de la tropolone ($\beta_2 = 10^{8.03}$) est beaucoup plus élevée que celle du composé du maltol ($\beta_2 = 10^{3.90}$). Ceci est dû au fait que la réaction [1] n'est pas strictement comparable à la réaction d'un ion métallique tel que M^{2+}, soit

$$[3] \qquad M^{2+} + 2L^- \rightleftarrows ML_2.$$

La réaction de formation de $Ge(OH)_2L_2$ formellement analogue à l'équation [3] est:

$$[4] \qquad Ge(OH)_2^{2+} + 2L^- \rightleftarrows Ge(OH)_2L_2 \qquad \beta_2^0 = \frac{[Ge(OH)_2L_2]}{[Ge(OH)_2^{2+}][L^-]^2}.$$

On peut relier le cation hypothétique $Ge(OH)_2^{2+}$ à l'acide germanique $Ge(OH)_4$ par l'équilibre:

$$[5] \qquad Ge(OH)_4 + 2H^+ \rightleftarrows Ge(OH)_2^{2+} + 2H_2O \qquad K_{Ge}'' = \frac{[Ge(OH)_4][H^+]^2}{[Ge(OH)_2^{2+}]}.$$

la constante K_{Ge}'' inconnue étant extrêmement élevée. La constante de stabilité observée β_2 se trouve ainsi reliée à β_2^0 par l'équation

$$[6] \qquad \beta_2^0 = K_{Ge}''\beta_2/K_a^2$$

où K_a est la constante d'acidité du ligand. On obtient maintenant pour β_2^0 des valeurs voisines pour les chélates du germanium avec la tropolone ($K_{Ge}'' \times 10^{21.43}$) et le maltol ($K_{Ge}'' \times 10^{20.62}$) comme dans le cas des ions M^{2+}.

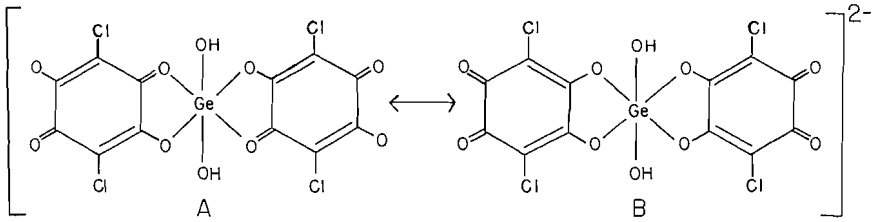
Dans les conditions habituellement imposées par les solubilités de GeO_2 et des ligands et par les méthodes d'étude, la formation d'un complexe ML_2 du germanium n'est observable que si sa constante d'équilibre est telle que $\beta_2 \geqslant 1$. On peut voir, d'après l'équation [6], que la formation de chélates $Ge(OH)_2L_2$ avec les hydroxycétones et autres composés du même type ne sera détectable que si $\beta_2^0 K_a^2 \geqslant K_{Ge}''$. Ainsi, lorsque les réactions [3] et [4] sont

Can. J. Chem. Downloaded from www.nrcresearchpress.com by 210.87.254.6 on 09/05/12
For personal use only.

thermodynamiquement favorables, la réaction avec le germanium peut ne pas être observée à cause de la grande valeur de K_{Ge}'', c'est-à-dire de la grande stabilité du "complexe" $Ge(OH)_4$. Comme les facteurs qui influencent la stabilité des chélates de $Ge(OH)_2^{2+}$ et des ions M^{2+} sont vraisemblablement analogues, il ressort que les ligands les plus aptes à "réagir" avec le germanium seront ceux qui conduisent à des chélates très stables avec les cations métalliques. Ainsi, les chélates de la lawsone avec plusieurs cations étant beaucoup moins stables que ceux de la tropolone et du maltol (2, 7, 8), on comprend pourquoi le germanium ne donne pas de réaction avec la lawsone.

L'absence de chélates de type ML avec le germanium, déjà notée dans le cas de l'acide chloranilique (1), l'oxine* et ses dérivés†, se trouve ainsi confirmée. L'instabilité des chélates ML est apparemment aussi reliée à la grande stabilité du "complexe" $Ge(OH)_4$ en milieu aqueux.

De nombreux auteurs ont cherché à relier la stabilité de complexes formés avec des ligands voisins, à la basicité des ligands telle que mesurée par les pk de l'acide conjugué. Les résultats obtenus sont insuffisants pour pouvoir conclure à l'existence d'une relation, analogue à celle notée par Fernelius *et al.* (2), entre la stabilité des chélates $Ge(OH)_2L_2$ et le pk_1 du groupe hydroxy, c'est-à-dire la basicité de l'oxygène phénolique. Cependant, dans le cas de ligands bidentés, tels que les α-hydroxycétones, il semblerait que la basicité des deux atomes d'oxygène coordinés $-\overset{|}{\underset{|}{C}}-O^-$ et $\diagdown C{=}O \diagup$ soit à considérer et on pourrait la caractériser par p(k_1k_2) (16). On note que les anions du maltol et de la tropolone, ligands qui conduisent à des complexes du germanium(IV) relativement stables, possèdent des propriétés basiques assez prononcées, comme l'indiquent les valeurs de p(k_1k_2). Selon les valeurs des constantes β_2^0, la tropolone conduit à des chélates légèrement plus stables que le maltol, en dépit de propriétés basiques inférieures: la stabilité "anormalement" grande du chélate de la tropolone avec l'ion Cu^{2+} a également été notée (7).



La lawsone et la TCHQ qui ne donnent pas de réaction détectable avec le germanium (IV), possèdent au contraire des oxygènes nettement moins basiques. La constante pk_2 semble d'ailleurs correspondre à la protonation de l'oxygène en position 4: le carbonyle susceptible de conduire à un chélate serait probablement même moins basique que ne l'indiquent les valeurs des constantes pk_2.

Il est cependant surprenant que l'acide chloranilique et la dihydroxy-2,5 benzoquinone (DHQ), deux autres hydroxyquinones qui ont des propriétés acides–bases apparemment comparables à celles de la lawsone et de la TCHQ (1, 18), conduisent à des chélates stables avec le germanium(IV). Pour ces deux dihydroxyquinones (H_2L), les acidités fortes des chélates $Ge(OH)_2L_2H_2$ et dans une certaine mesure l'absence de chélates polynucléaires (1) suggèrent une redistribution électronique dans le chélate, conduisant à la coordination d'un

P. Clerc. Thèse de Doctorat, Université de Montréal, Montréal, P.Q. En preparation.
†J. Tsau. Thèse de Maîtrise, Université de Montréal, Montréal, P.Q. En preparation.

Can. J. Chem. Downloaded from www.nrcresearchpress.com by 210.87.254.6 on 09/05/12
For personal use only.

deuxième oxygène phénolique, selon la structure prédominante B. La faible contribution d'une telle structure résonante pour la TCHQ et la lawsone expliquerait ainsi l'instabilité des chélates avec ces deux hydroxyquinones. On est alors conduit à suggérer que la basicité des oxygènes cétoniques de l'acide chloranilique et de la DHQ ($pk_{C=O} = -7.0$) (18) ne représente pas leur tendance à la coordination, mais que celle-ci correspondrait mieux au pk du deuxième groupe —OH. Il est intéressant de constater que les valeurs de log β_2^0/K_{Ge}'' et de $p(k_1k_2)$ de la DHQ diffèrent alors peu de celles du maltol. Les valeurs de log β_2^0/K_{Ge}'', pk_1, pk_2 et $p(k_1k_2)$ correspondant aux α-hydroxycétones étudiées sont rassemblées dans le Tableau I.

REMERCIEMENTS

Nous exprimons notre reconnaissance au Conseil National de Recherches qui nous a accordé un soutien financier sous forme d'une bourse (A. B.) et d'un octroi de recherches (R. L. B.). Nous sommes également reconnaissants à l'Hydro-Québec pour l'octroi d'une bourse (A. B.). Nous remercions le "Germanium Research Center" qui nous a fourni gracieusement l'oxyde de germanium.

BIBLIOGRAPHIE

1. A. Beauchamp et R. L. Benoit. Can. J. Chem. **42**, 2161 (1964).
2. H. Kido, W. C. Fernelius et C. G. Haas. Anal. Chim. Acta, **23**, 116 (1960).
3. K. Kimura, K. Saito et M. Asada. Bull. Chem. Soc. Japan, **29**, 635 (1956).
4. Y. Oka et S. Matsuo. Sci. Rept. Tohoku Univ. First Ser. **8**, 532 (1956).
5. T. Kanno. Sci. Rept. Tohoku Univ. First Ser. **11**, 145 (1959).
6. E. L. Muetterties et C. M. Wright. J. Am. Chem. Soc. **86**, 5132 (1964).
7. B. E. Bryant, W. C. Fernelius et B. E. Douglas. J. Am. Chem. Soc. **75**, 3784 (1953).
8. N. J. Clark et B. R. Willeford. J. Am. Chem. Soc. **79**, 1296 (1957).
9. Y. Oka et S. Matsuo. Sci. Rept. Tohoku Univ. First Ser. **10**, 299 (1958).
10. W. A. E. McBryde et G. F. Atkinson. Can. J. Chem. **39**, 510 (1961).
11. F. J. C. Rossotti et H. Rossotti. The determination of stability constants. McGraw-Hill Book Co., New York. 1961. pp. 162, 282.
12. J. Place. Thèse de Doctorat, Université de Montréal, Montréal, P.Q. 1964.
13. E. R. Clark, N. H. Davies et A. V. Jones. J. Inorg. Nucl. Chem. **27**, 1611 (1965).
14. I. Lindqvist. Inorganic adduct molecules of oxo-compounds. Academic Press Inc., New York. 1963. p. 16.
15. R. L. Benoit. Ann. Acfas, **28**, 49 (1962).
16. Z. L. Ernst et J. Menashi. Trans. Faraday Soc. **59**, 2838 (1963).
17. A. Beauchamp. Thèse de Maîtrise, Université de Montréal, Montréal, P.Q. 1964.
18. G. Schwarzenbach et H. Suter. Helv. Chim. Acta, **24**, 617 (1941).

Can. J. Chem. Downloaded from www.nrcresearchpress.com by 210.87.254.6 on 09/05/12
For personal use only.

Can. J. Chem. Downloaded from www.nrcresearchpress.com by 210.87.254.5 on 09/05/12
For personal use only.

ENERGETICS OF FORMATION OF SOME OXYGENATED IONS AND THE PROTON AFFINITIES OF CARBONYL COMPOUNDS

A. G. HARRISON,[1] A. IVKO,[2] AND D. VAN RAALTE
Department of Chemistry, University of Toronto, Toronto, Ontario
Received February 14, 1966

ABSTRACT

The energetics and mechanism of formation of ions of *m/e* 31, 45, and 59 from a number of alcohols, ethers, and esters have been studied. The following ionic heats of formation have been obtained: $CH_2{=}OH^+$, 176 kcal/mole; CH_3O^+, 213 kcal/mole; $CH_3CH{=}OH^+$, 145 kcal/mole; $CH_2{=}OCH_3^+$, 170 kcal/mole; $(CH_3)_2C{=}OH^+$, 125 kcal/mole; $CH_3CH_2CH{=}OH^+$, 131 kcal/mole; $CH_3CH{=}OCH_3^+$, 135 kcal/mole; $CH_2{=}OC_2H_5^+$, 144 kcal/mole. It is concluded that with the exception of CH_3O^+ the alkoxy ions probably are not formed by electron impact processes. The gas-phase proton affinities of a number of carbonyl compounds are estimated.

INTRODUCTION

The mass spectra of alcohols, ethers and, to a lesser extent, esters show prominent ions of general formula $C_nH_{2n+1}O^+$ appearing at *m/e* ratios of 31, 45, 59, 73, etc. The heats of formation of these ions and in many cases the structures are not known with certainty. During a recent study of the energetics of some gaseous oxygenated ions Munson and Franklin (1) have presented some results pertaining to the ions of *m/e* 31 and 45. During an extensive study (2–4) of the energetics and mechanism of ion formation in alcohols and esters, and related recent studies of ethers, we have accumulated a considerable body of data concerning ions of *m/e* 31, 45, and 59. This data both supplements the data reported by Munson and Franklin and serves, in some cases, to clarify points raised by their work. In addition, this data when combined with the data of Munson and Franklin (1) and others (5–9), permits more reliable estimates of the gas-phase proton affinities of a number of carbonyl compounds.

EXPERIMENTAL

Mass spectra and appearance potentials were measured with an AEI MS-2 mass spectrometer either as originally described (10) or as recently modified (11). Mass spectra were recorded at 50 V electron energy and 7–10 V/cm repeller field strength. Appearance potentials were measured in the usual manner (12) using xenon or krypton, admitted with the gas of interest, to calibrate the energy scale.

All chemicals were commercial samples of highest available purity and showed no detectable impurities in the mass spectra. The deuteriated samples studied were obtained from Merck, Sharp and Dohme, Montreal.

RESULTS AND DISCUSSION

Energetics of Formation and Structure of m/e = 31

The appearance potentials and resultant ionic heats of formation for *m/e* = 31 from a number of alcohols, ethers and esters are summarized in Table I. As can be seen there is reasonable agreement of the reported appearance potentials and therefore we have computed the ionic heats of formation using the unweighted average in each case with the exception of isopropyl alcohol where we have used the appearance potential obtained in the present work.

The first nine compounds listed in Table I give mutually consistent values for the ionic heat of formation suggesting a common structure, which we take to be $CH_2{=}OH^+$, and

[1]*Alfred P. Sloan Fellow 1962–1964. All correspondence should be addressed to this author.*
[2]*Exchange student 1964–1965. Present address: Department of Chemistry, Byelorussian State University, Minsk, U.S.S.R.*

leading to $\Delta H_f(CH_2{=}OH^+) = 176 \pm 3$ kcal/mole. This "best" value is only slightly higher than the value of 174 kcal/mole proposed by Munson and Franklin (1). The suggested structure, $CH_2{=}OH^+$, was first proposed by Cummings and Bleakney (13) and is supported by the observation of $CD_2{=}OH^+$ as the major fragment ion in the spectra of CD_3OH (14) and CH_3CD_2OH (15).

The neutral fragments postulated in column 5 require comment on the proposed fragmentation paths for some of the molecules. The proposed fragmentation path for isopropyl alcohol,

[1] $$(CH_3)_2CHOH^+ \rightarrow H + (CH_3)_2C{=}OH^+ \rightarrow CH_2OH^+ + C_2H_4,$$

is supported by the observation that in $(CD_3)_2CHOH$ the fragment ion appears as CD_2OH^+ which indicates loss of the secondary hydrogen in the rearrangement reaction. We suggest that the reaction may proceed through formation of a cationated cyclopropane as suggested (16) for a number of similar fragmentations.

The formation of $m/e = 31$ in the formate esters has been discussed previously (2) where it was shown by deuterium labelling that the formyl hydrogen was retained in the ion in all cases. This suggests, for methyl formate, the ionic structure $CH_2{=}OH^+$ with the neutral fragments assigned in Table I. The alternative formation of $CH_3O^+ + CHO$ would require a considerable rearrangement to be consistent with the labelling results.

Simple bond rupture in $CH_3OC_2H_5$ would be expected to lead to CH_3O^+ ($m/e = 31$) with C_2H_5 as the neutral fragment. That this does not occur is shown by the fact that in $CD_3OC_2H_5$ the fragment ion moves exclusively to $m/e = 33$ which indicates retention of only two deuteriums. The fragment ion is obviously formed by the rearrangement reaction

[2] $$CD_3OC_2H_5^+ \rightarrow D + CD_2OH^+ + C_2H_4.$$

There was no evidence that this was a two-step fragmentation i.e. there was no $(M{-}D)^+$ in the spectrum. This type of rearrangement has been postulated previously (17) to explain a number of prominent ions in the spectra of ethers including formation of $CH_2{=}OH^+$ in diethyl ether.

In contrast to the above cases the $m/e = 31$ ions from dimethyl ether, methyl acetate, and methyl nitrite lead to $\Delta H_f(m/e = 31) = 213 \pm 3$ kcal/mole. The high value and the structure of the molecules suggest that this heat of formation refers to the CH_3O^+ ion.

In summary, the ion of $m/e = 31$ has two possible structures, $CH_2{=}OH^+$ and CH_3O^+, with heats of formation of 176 and 213 kcal/mole respectively. The high heat of formation of CH_3O^+ means that fragmentation to form this ion is not a favorable route energetically and hence this ion is formed in relatively low abundance. A large intensity at $m/e = 31$ in a mass spectrum will thus usually indicate the $CH_2{=}OH^+$ structure for the ion rather than CH_3O^+. This is strikingly indicated in the mass spectrum of methyl formate and methyl ethyl ether where direct bond fission to yield CH_3O^+ does not occur but rather rearrangement to form $CH_2{=}OH^+$.

Energetics of Formation and Structure of $m/e = 45$

Deuterium-labelling studies and the structure of the molecules considered suggest three possible structures $CH_3CH{=}OH^+$, $CH_2{=}OCH_3^+$, and $CH_3CH_2O^+$ for the ion of $m/e = 45$. There is no evidence pointing to a fourth possible structure $HOCH_2CH_2^+$. The appearance potential data for $m/e = 45$ from a number of compounds are summarized in Table II. In this case the agreement of the reported appearance potentials is much poorer and we have chosen to calculate all ionic heats of formation using the appearance potentials measured in this laboratory.

Can. J. Chem. Downloaded from www.nrcresearchpress.com by 210.87.254.5 on 09/05/12
For personal use only.

Appearance potentials of $m/e = 45$ from ethyl alcohol, isopropyl alcohol, *s*-butyl alcohol, and diethyl ether lead to ionic heats of formation in mutual agreement and an average value of 145 ± 3 kcal/mole. The structure of the ion in this case is presumably $CH_3CH{=}OH^+$ as indicated by the loss of D in the spectra CH_3CD_2OH (15), CD_3 in the spectra of $(CD_3)_2CHOH$, and the ethyl group without isotopic mixing in the spectra of labelled *s*-butyl alcohols (18). We would suggest that the $m/e = 45$ ion from diethyl ether has the structure $CH_3CH{=}OH^+$ rather than $C_2H_5O^+$ as suggested by Munson and Franklin (1) and that it is formed by the rearrangement reaction

[3] $$[CH_3{-}CH{-}OH{-}CH_2{-}CH_2]^+ \rightarrow CH_3CHOH^+ + H + C_2H_4$$

although no deuterium labelling has been carried out to confirm this.

For ethyl and isopropyl formates, deuterium labelling (2) has shown formyl hydrogen retention indicating the fragmentation reaction

[4] $$CH_3{-}\underset{\displaystyle R}{\underset{|}{C}}H{-}O{-}\overset{\displaystyle O}{\overset{\|}{C}}{-}H^+ \rightarrow R + CO + CH_3CH{=}OH^+ \ (R = H \text{ or } CH_3)$$

with the indicated structure for the ion rather than the $CH_3CH_2O^+$ structure postulated by Munson and Franklin (1). It is clear that the calculated ionic heats of formation are anomalously high which indicates that the fragmentation processes involve excess energy. From consideration of the structure of the neutral molecule, the ion formed from dimethyl ether, methyl ethyl ether, and dimethoxymethane should have the structure $CH_2{=}OCH_3^+$. The alternative fragmentation in methyl ethyl ether leading to $CH_3CH_2O^+$ was shown not to occur by the shift of the ion to $m/e = 48$ in the spectrum of $CD_3OC_2H_5$. The appearance potentials lead to a consistent value of $\Delta H_f(CH_2{=}OCH_3^+) = 170 \pm 3$ kcal/mole, considerably higher than $\Delta H_f(CH_3CH{=}OH^+) = 145 \pm 3$ kcal/mole. That the ions do indeed have different structures is indicated by differences in their further fragmentation reactions, the most striking difference being the fragmentation to form H_3O^+. It has been shown previously (3) that alcohols of the general formula $CH_3CH(R)OH$ form H_3O^+ upon electron impact by the fragmentation sequence

[5] $$CH_3CH(R)OH^+ \rightarrow R + CH_3CH{=}OH^+ \rightarrow H_3O^+ + C_2H_2.$$

The second step of this sequence is confirmed by observation of a metastable at $m/e = 8.03$. The ethers CH_3OCH_3 and $CH_3OC_2H_5$ show no H_3O^+ fragment ion and no metastable at 8.03 although the $m/e = 45$ ion is the most abundant ion in the mass spectra at 50 eV. Further fragmentation of $CH_2{=}OCH_3^+$ leads predominately to CH_3^+ and CHO^+.

The only molecule investigated which possibly forms the $CH_3CH_2O^+$ ion on electron impact is ethyl acetate where $m/e = 45$ is of rather low abundance. The reported appearance potentials are in reasonable agreement and suggest an ionic heat of formation of about 160 kcal/mole. When compared with $\Delta H_f(CH_3O^+) = 213$ kcal/mole, this value appears to be much too low to correspond to the ethoxy cation. For example, the corresponding sulfur-containing ions CH_3S^+ and $C_2H_5S^+$ have heats of formation of 222 and 213 kcal/mole respectively (19). It is thus probable that rearrangement to a thermodynamically more favorable structure has occurred. No reliable value for $\Delta H_f(CH_3CH_2O^+)$ can be established from present electron impact data.

Energetics of Formation of $m/e = 59$

The ion of $m/e = 59$ can have many possible structures, and the present work consists only of a preliminary examination of the energetics of formation of some of the most prominent ions. The nominal structures of these ions, given in column 2 of Table III, are

Can. J. Chem. Downloaded from www.nrcresearchpress.com by 210.87.254.5 on 09/05/12
For personal use only.

Can. J. Chem. Downloaded from www.nrcresearchpress.com by 210.87.254.5 on 09/05/12
For personal use only.

TABLE I

Energetics of formation of m/e 31

Molecule	Appearance potential (eV) This lab	Appearance potential (eV) Literature	ΔH_f(molecule) (kcal/mole)	Neutral fragments	ΔH_f(m/e 31) (kcal/mole)
CH_3OH	12.1	11.8(13), 12.2(5), 11.8(26)	−48.1(28)	H	177
C_2H_5OH	11.6	11.3(13), 11.6(5), 11.3(1)	−56.2(28)	CH_3	176
n-C_3H_7OH	11.5	11.1(1), 11.6(5), 11.1(27)	−61.9(28)	C_2H_5	174
i-C_3H_7OH	13.5	12.5(5)	−65.4(28)	$H+C_2H_4$	181
s-C_4H_9OH	12.5		−70.1(28)	$CH_3+C_2H_4$	174
$CH_3OC_2H_5$	12.9		−52.1(7)	$H+C_2H_4$	180
$(C_2H_5)_2O$	12.1		−60.4(28)	$CH_3+C_2H_4$	174
$HCOOCH_3$	12.4(2)	12.1(1), 12.4(6), 12.0(9)	−81(9)	H+CO	174
$HCOOCH(CH_3)_2$	13.4_5(2)		−97(7)	$H+CO+C_2H_4$	174
$HCOOC_2H_5$	12.0(2)	12.2(6), 12.4(8)	−88(28)	CH_3+CO	187
CH_3OCH_3	12.3	12.1(1), 12.5(6), 12.6(7)	−44.3(28)	CH_3	210
CH_3COOCH_3		12.5(9), 12.7(1), 12.9(6)	−99.5(9)	CH_3CO	212
CH_3ONO		11.0(1)		NO	217

TABLE II

Energetics of formation of m/e 45

Molecule	Appearance potential (eV) This lab	Appearance potential (eV) Literature	ΔH_f(molecule) (kcal/mole)	Neutral fragments	ΔH_f(m/e 45) (kcal/mole)
C_2H_5OH	10.9	10.9(1), 11.1(13), 11.0(5), 11.7(29)	−56(28)	H	143
i-C_3H_7OH	10.5	10.9(5), 11.4(30)	−65(28)	CH_3	144
s-C_4H_9OH	10.4		−70(28)	C_2H_5	146
$(C_2H_5)_2O$	11.8	12.3(1), 12.5(7)	−60(28)	$H+C_2H_4$	147
$HCOOC_2H_5$	11.5_5(2)	11.4(1), 11.7(6), 11.7(9), 11.6(31)	−88(7)	H+CO	152
$HCOOCH(CH_3)_2$	11.5(2)		−97(9)	CH_3+CO	162
CH_3OCH_3	11.5_5	11.0(1), 11.5(7), 11.4(26)	−44(28)	H	170
$CH_3OC_2H_5$	10.9_6		−52(7)	CH_3	168
$(CH_3O)_2CH_2$	11.1		−83(33)*	CH_3O	173
$CH_3COOC_2H_5$	10.8	10.8(1), 10.8(7), 11.2(9), 11.4(32)	−107(9)	CH_3CO	153

*Estimated by bond energy scheme.

Can. J. Chem. Downloaded from www.nrcresearchpress.com by 210.87.254.5 on 09/05/12
For personal use only.

TABLE III

Energetics of formation of m/e 59

Molecule	Nominal ion structure	Appearance potential (eV)		ΔH_f(molecule) (kcal/mole)	Neutral fragments	ΔH_f(ion) (kcal/mole)
		This lab	Lit.			
$(CH_3)_3COH$	$(CH_3)_2C{=}OH^+$	10.2	10.0(25)	−75(28)	CH_3	128, 125
$C_2H_5C(CH_3)_2OH$	$(CH_3)_2C{=}OH^+$	10.0		−79(28)	C_2H_5	125
$HCOOCH(CH_3)_2$	$(CH_3)_2C{=}OH^+$	12.1(2)		−97(9)	H+CO	156?
n-C_3H_7OH	$C_2H_5CH{=}OH^+$		11.2(5)	−62(28)	H	144
$CH_3CH(OH)C_2H_5$	$C_2H_5CH{=}OH^+$	10.7		−71(28)	CH_3	143
$CH_3OC_2H_5$	$CH_3CH{=}OCH_3^+$	10.3		−52(7)	H	135
$(C_2H_5)_2O$	$CH_2{=}OC_2H_5^+$	10.3		−60(28)	CH_3	144
$CH_3COOCH(CH_3)_2$	$(CH_3)_2CHO^+$	10.6_5	11.0(9)	−116(9)	CH_3CO	141, 152
$CH_3COO(CH_2)_2CH_3$	n-$C_3H_7O^+$		11.6_4(9)	−113(9)	CH_3CO	166
$DCOO(CH_2)_2CH_3$	n-$C_3H_7O^+$		11.2_2(7)	−94(9)	DCO	164

TABLE V

Proton affinities of carbonyl compounds in the gas phase

R	ΔH_f(RCHO)	ΔH_f(RCH=OH$^+$)	Proton affinity RCHO*	ΔH_f(RCOOH)	ΔH_f(RCOOH$_2^+$)	Proton affinity RCOOH*
H	−27.7(7)	176±3	161±3	−90(7)	113±3	162±3
CH_3	−39.8(7)	145±3	180±3	−104(7)	75±3	184±3
C_2H_5	−48.7(7)	144?	172?	−110(7)	65±3	190±3

*Calculated using $\Delta H_f(H^+)$ = 365 kcal/mole, ref. 19.

based primarily on consideration of the structure of the neutral molecule and, obviously, a much more extensive investigation, including deuterium tracer studies, is desirable. The results do suggest some variation of ionic heat of formation with structure. From the present data one estimates $\Delta H_f(CH_3)_2C{=}OH^+ = 125$ kcal/mole and $\Delta H_f(CH_3CH_2\text{-}CH{=}OH^+) = 144$ kcal/mole. As will be shown in the following section, the former estimate appears reasonable but the latter value is probably 10–15 kcal/mole high.

The results in Table III also yield $\Delta H_f(CH_3CH{=}OCH_3^+) = 135$ kcal/mole and $\Delta H_f(CH_2{=}OC_2H_5^+) = 144$ kcal/mole, values which appear reasonable in comparison with $\Delta H_f(CH_2{=}OCH_3^+) = 170$ kcal/mole. These ions correspond in structure to cationated aldehydes; using well-established heats of formation (19, 20) and the above ionic heats of formation one can estimate values of 64 kcal/mole and 87 kcal/mole for the methyl ion affinity of formaldehyde and acetaldehyde respectively. The change in going from formaldehyde to acetaldehyde is also observed in the proton affinities calculated in the next section where the effect is of the same approximate magnitude. This suggests that the ionic heats of formation given above are not in serious error.

The heats of formation calculated for the ions with nominally the *n*-propoxy and isopropoxy structure again appear to be too low by comparison with CH_3O^+ which suggests rearrangement.

Proton Affinities of Carbonyl Compounds in the Gas Phase

The ions $CH_2{=}OH^+$, $CH_3CH{=}OH^+$, and $CH_3CH_2CH{=}OH^+$ can be considered (in the absence of rearrangement) as the ions formed on protonation of formaldehyde, acetaldehyde, and propionaldehyde respectively. It is of interest to use the thermochemical data on these ions to calculate the proton affinities of these aldehydes and to compare the proton affinities with those of the corresponding carboxylic acids. The proton affinity of X is given by the exothermicity of the reaction

$$H^+(g) + X(g) = HX^+(g) \qquad [6]$$

and hence a knowledge of $\Delta H_f(HX^+)$ is necessary for the calculation.

For the carboxylic acids the heat of formation of the protonated species, $RCOOH_2^+$, can be established from appearance potential studies of this ion which is observed as a rearrangement ion in the mass spectra of ethyl and higher esters. For some of the simpler esters extensive studies have been made of the mechanism (2, 4, 6, 8, 21–23) and energetics (1, 2, 4, 7–9) of this rearrangement reaction. The relevant data leading to estimates of $\Delta H_f(RCOOH_2^+)$ for R = H, CH_3, and C_2H_5 are summarized in Table IV. For the ethyl esters the neutral fragment generally has been assumed to be the vinyl radical and the calculations have been made using $\Delta H_f(\text{vinyl}) = 65$ kcal/mole (24). For the *n*-propyl and isopropyl esters both Munson and Franklin (1) and Harrison and Jones (4) have pointed out that the data are not reasonable if the neutral fragment is assumed to be the allyl radical but do give reasonable ionic heats of formation if an alternative structure of the C_3H_5 neutral fragment is considered. It has been pointed out (4) that the deuterium-labelling studies with isopropyl esters are consistent with a cyclopropyl structure for the C_3H_5 neutral. Accordingly the calculations have been made assuming $\Delta H_f(C_3H_5) = 53$ kcal/mole (1).

As can be seen in Table IV the ionic heats of formation calculated on this basis for the $CH_3COOH_2^+$ and $C_2H_5COOH_2^+$ ions from ethyl and propyl esters show reasonable internal agreement for each species. In the subsequent calculations (Table V) we have used the unweighted average of all determinations for these ions. For the formate esters the appearance potentials of $HCOOH_2^+$ from the propyl esters lead to considerably lower

Can. J. Chem. Downloaded from www.nrcresearchpress.com by 210.87.254.5 on 09/05/12
For personal use only.

TABLE IV

Appearance potentials and heats of formation of $RCOOH_2^+$ ions

RCOOR′	ΔH_f(RCOOR′) (kcal/mole)	Appearance potential $RCOOH_2^+$ (eV)		$\Delta H_f(RCOOH_2^+)$ (kcal/mole)	
		This lab	Lit.	This lab	Lit.
$HCOOC_2H_5$	−88(7)	11.60	11.3(1)	114	107
			11.64(6)		115
			11.73(8)		117
$HCOOCH(CH_3)_2$	−97(9)	10.87		94	
$HCOO(CH_2)_2CH_3$	−94(9)		11.0(1)		104
$CH_3COOC_2H_5$	−107(9)	10.80	10.75(7)	77	76
			10.95(8)		80
			11.0(34)		82
			10.8(1)		77
$CH_3COO(CH_2)_2CH_3$	−113(9)		10.48(9)		76
			10.5(1)		76
$CH_3COOCH(CH_3)_2$	−116(9)	10.42	10.72(9)	71	78
$C_2H_5COOC_2H_5$	−114(9)	10.67	10.77(8)	67	69
			10.4(1)		61
$C_2H_5COOCH(CH_3)_2$	−123(9)	10.40		64	

ionic heats of formation than the average value obtained from the ethyl esters. The agreement is better in this case if the C_3H_5 neutral fragment is assumed to have the allyl structure, but it is unlikely that the fragmentation mechanism would be different for the ethyl and higher esters. Because of this inconsistency we have adopted for $\Delta H_f(HCOOH_2^+)$ the average value obtained from appearance potential measurements on ethyl formate.

Table V presents the calculations of the proton affinities of RCHO and RCOOH where R = H, CH_3, and C_2H_5. The results suggest that the proton affinities of H_2CO and HCOOH are identical as are the proton affinities of CH_3CHO and CH_3COOH. This agreement offers some support for our assignment of $\Delta H_f(HCOOH_2^+)$. The results also suggest that the proton affinity of C_2H_5CHO is considerably less than that of C_2H_5COOH and also less than the proton affinity of CH_3CHO. This is unlikely and indicates that our estimate of $\Delta H_f(CH_3CH_2CH{=}OH^+)$ is high by 10–15 kcal/mole. A more reasonable estimate would appear to be $\Delta H_f(CH_3CH_2CH{=}OH^+)$ = 131 kcal/mole leading to a proton affinity for C_2H_5CHO = 185 kcal/mole.

In addition to the proton affinities in Table V we estimate, from $\Delta H_f((CH_3)_2C{=}OH^+)$ = 125 kcal/mole (Table III), the proton affinity of acetone to be 188 kcal/mole. This value is slightly higher than that for acetaldehyde in agreement with the observation by Munson (25) that the ion–molecule reaction

[7] $$CH_3CH{=}OH^+ + (CH_3)_2C{=}O \rightarrow CH_3CHO + (CH_3)_2C{=}OH^+$$

occurs with a large rate constant. Since this indicates that the reaction has no activation energy the reaction cannot be endothermic and hence the proton affinity of acetone must be equal to or greater than that of acetaldehyde.

Throughout this paper we have written the protonated acid as $RCOOH_2^+$. We do not intend to imply by this symbolism that protonation necessarily occurs on the hydroxylic oxygen rather than the carbonyl oxygen. The present studies provide no information on the site of protonation.

ACKNOWLEDGMENTS

The authors are indebted to the Advisory Committee on Scientific Research, University of Toronto, and to the National Research Council of Canada for financial support of this work.

Can. J. Chem. Downloaded from www.nrcresearchpress.com by 210.87.254.5 on 09/05/12
For personal use only.

REFERENCES

1. M. S. B. MUNSON and J. L. FRANKLIN. J. Phys. Chem. **65**, 3191 (1964).
2. D. VAN RAALTE and A. G. HARRISON. Can. J. Chem. **41**, 2054 (1963).
3. D. VAN RAALTE and A. G. HARRISON. Can. J. Chem. **41**, 3118 (1963).
4. A. G. HARRISON and E. G. JONES. Can. J. Chem. **43**, 960 (1965).
5. L. FRIEDMAN, F. A. LONG, and M. WOLFSBERG. J. Chem. Phys. **27**, 613 (1957).
6. A. B. KING and F. A. LONG. J. Chem. Phys. **29**, 374 (1958).
7. R. R. BERNECKER and F. A. LONG. J. Phys. Chem. **65**, 1565 (1961).
8. E. W. GODBOLE and P. KEBARLE. Trans. Faraday Soc. **58**, 1897 (1962).
9. C. E. BRION and W. J. DUNNING. Trans. Faraday Soc. **59**, 647 (1963).
10. J. M. S. TAIT, T. W. SHANNON, and A. G. HARRISON. J. Am. Chem. Soc. **84**, 4 (1962).
11. T. W. SHANNON, F. MEYER, and A. G. HARRISON. Can. J. Chem. **43**, 159 (1965).
12. A. G. HARRISON and T. W. SHANNON. Can. J. Chem. **40**, 1730 (1962).
13. C. S. CUMMINGS and W. BLEAKNEY. Phys. Rev. **58**, 787 (1940).
14. J. H. BAXENDALE and R. G. SEDGWICK. Trans. Faraday Soc. **57**, 2157 (1961).
15. J. MOMIGNY. Bull. Soc. Roy. Sci. Liege, **24**, 111 (1965).
16. H. M. GRUBB and S. MEYERSON. *In* Mass spectrometry of organic ions. *Edited by* F. W. McLafferty Academic Press, New York. 1963. Chap. 10.
17. F. W. MCLAFFERTY. Anal. Chem. **29**, 1782 (1957).
18. W. H. MCFADDEN, M. LOUNSBURY, and A. L. WAHRHAFTIG. Can. J. Chem. **36**, 990 (1958).
19. F. H. FIELD and J. L. FRANKLIN. Electron impact phenomena and the properties of gaseous ions. Academic Press, Inc., New York. 1957.
20. F. D. ROSSINI, D. D. WAGMAN, W. H. EVANS, W. H. LEVINE, and I. JAFFE. Natl. Bur. Standards, Circ. No. 500. 1952.
21. F. W. MCLAFFERTY and M. C. HAMMING. Chem. Ind. London, 1366 (1958).
22. D. R. BLACK, W. H. MCFADDEN, and J. W. CORSE. J. Phys. Chem. **68**, 1237 (1964).
23. W. BENZ and K. BIEMANN. J. Am. Chem. Soc. **86**, 2375 (1964).
24. A. G. HARRISON and F. P. LOSSING. J. Am. Chem. Soc. **82**, 519 (1960).
25. M. S. B. MUNSON. J. Am. Chem. Soc. **87**, 2332 (1965).
26. R. W. TAFT, R. H. MARTIN, and F. W. LAMPE. J. Am. Chem. Soc. **87**, 2490 (1965).
27. T. KAMBARA. J. Phys. Soc. Japan, **5**, 31 (1950).
28. J. H. S. GREEN. Quart. Rev. London, **15**, 125 (1961).
29. T. KAMBARA and I. KANOMATA. Proc. Phys. Soc. Japan, **4**, 71 (1949).
30. T. KAMBARA. J. Phys. Soc. Japan, **5**, 36 (1950).
31. R. R. BERNECKER. Ph.D. Thesis, Cornell University. 1961.
32. S. S. FRIEDLAND and R. E. STRAKNA. J. Phys. Chem. **60**, 815 (1956).
33. J. D. COX. Tetrahedron, **18**, 1337 (1962).
34. A. G. SHARKEY *et al.* Private communication to ref. 8.

Can. J. Chem. Downloaded from www.nrcresearchpress.com by 210.87.254.5 on 09/05/12
For personal use only.

AN IMPROVED METHOD OF HYDROGEN ISOTOPIC EXCHANGE WITH DEUTERIUM SULFATE, AND THE PREPARATION OF 9,10-ANTHRAQUINONE-d_8[1]

BRUNO LUNELLI AND CESARE PECILE
Institute of Physical Chemistry, University of Padua, Padua, Italy
Received February 22, 1966

ABSTRACT

An apparatus and improved conditions are described for using easily and efficiently sulfuric acid-d_2 as a deuterating agent. The preparation of 9,10-anthraquinone-d_8 with a high deuterium content is reported.

In a study of the vibrational spectrum of anthraquinone,[2] it was necessary to prepare anthraquinone-d_8 with high deuterium content. A careful consideration of the possible methods (1) convinced us that isotopic exchange would be the most convenient if a proper exchange agent could be found. The high stability of anthraquinone to concentrated sulfuric acid suggested the use of sulfuric acid-d_2.

Several deuterated aromatic compounds have been prepared by exchange with D_2SO_4 (2–7), but the operating conditions and yields are not always satisfactory. An examination of the methods used indicates that the disadvantages of using sulfuric acid-d_2 are to an important extent related to its activity as a sulfonating agent. Conditions for the isotopic exchange of a particular compound with sulfuric acid-d_2 are a concentration of the acid and a temperature at which the sulfonation rate is considerably lower than the exchange rate (5, 6). Such conditions are often attained at comparatively low temperatures and concentrations of sulfuric acid-d_2. These conditions (8) and the low solubility of the compound in sulfuric acid-d_2 (7) lead to low exchange rates. It is therefore necessary to use long exchange time and to renew the acid several times.

Because sulfonation is a reversible reaction, however, these difficulties can be avoided. The exchange can be allowed to take place at high temperature and high concentration of sulfuric acid. Under these conditions the exchange rate is high. After the exchange, the reaction mixture can be treated to hydrolyze the sulfonic acids formed. Because the solubility of many aromatic compounds is low in dilute, but appreciable in concentrated sulfuric acid, the presence of an organic solvent is not necessary (4, 6).

To apply this technique, we used an apparatus in which it is possible to obtain a gradient of both temperature and sulfuric acid concentration. The required quantity of sulfuric acid-d_2 was quite small. The method gave the fully deuterated product in high yield and isotopic purity, as shown by mass spectral analysis.

In our opinion, the procedure here described permits extension of the use of sulfuric acid-d_2, which is easy to handle, as a deuterating agent for aromatic compounds that do not undergo irreversible reactions (e.g. oxidation) under exchange conditions.

EXPERIMENTAL

Starting Materials

The anthraquinone used was a C. Erba (Milan) RP product, and the deuterium oxide was a Fluka "purissimum" product with a deuterium content of 99.7%.

[1]*This investigation was supported by the Consiglio Nazionale delle Ricerche (C.N.R., Rome).*
[2]*C. Pecile and B. Lunelli. To be published.*

Preliminary Experiments on the Exchange between Anthraquinone and Sulfuric Acid-d_2

An appreciable amount of anthraquinone dissolves in sulfuric acid of concentration higher than 80% (9), and gives oxonium salts (10). Sulfonation requires somewhat drastic conditions (11), and monosubstitution takes place principally in the β position, or in the α position if mercury salts are present. At temperatures above 230 °C, there is appreciable disulfonation and oxidation to polyhydroxylated compounds (11, 12).

Since for several aromatic compounds the exchange rates of hydrogen isotopes are appreciable at concentrations and temperatures lower than those required for sulfonation (2–7), we kept 500 mg of anthraquinone, dissolved in 5 ml of 95% D_2SO_4 (in D_2O), at 160 °C overnight. The infrared spectrum of the recovered anthraquinone (m.p. 286 °C, recrystallyzed from benzene) indicated that exchange had taken place and that no anthraquinone-d_0 was present.

To obtain larger quantities of deuterated anthraquinone, we allowed exchange and desulfonation to take place separately, in successive steps. Anthraquinone (2 g), deuterium oxide (5.5 ml), and sulfuric acid-d_2 (6.6 ml) were introduced into one arm of an inverted Y-shaped glass tube, which was then sealed under vacuum. The arm containing the mixture was heated until 5 ml of distillate had been collected in the other arm, kept at 0 °C. The arm containing the solution of anthraquinone in concentrated sulfuric acid was then kept for 20 min at 160 °C, cooled to room temperature, and poured slowly into the water which had distilled.

The same procedure[3] was repeated 4 times on the thick suspension obtained, then the apparatus was opened, 200 mg of mercury oxide were introduced, and the procedure was repeated 5 times more. Finally the whole apparatus was kept at 140 °C for 2 h, then opened; the anthraquinone was filtered off, and recrystallized from benzene. The series of 10 distillations, with introduction of mercury oxide after the fifth, was repeated twice more on the same sample, each time with fresh deuterium sulfate and deuterium oxide. At the end of these operations, 1.1 g of recrystallized anthraquinone, m.p. 286 °C, were obtained. With the quantities of reagents that were used, if we assume that the partition coefficient for deuterium between anthraquinone and sulfuric acid is 1 (6), the anthraquinone obtained in this experiment should have had a deuterium content of 99.7%. Its infrared spectrum, however, showed a number of weak bands which, when compared with the

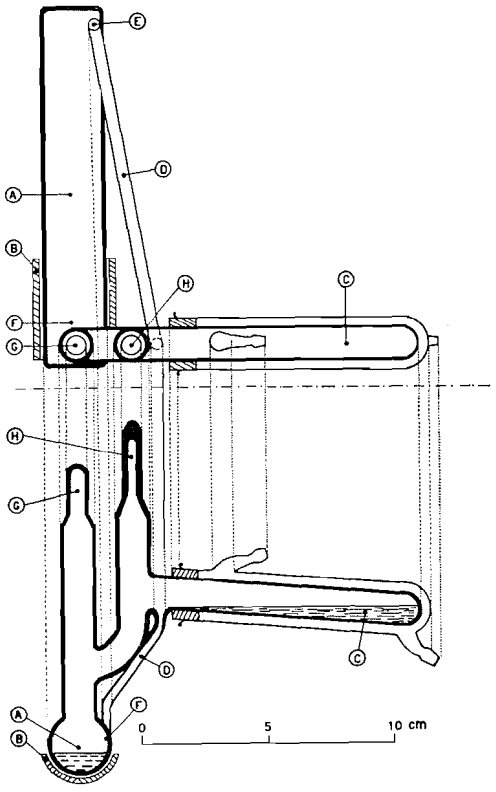


FIG. 1. Apparatus for the preparation of 9,10-anthraquinone-d_8.

[3]*At the beginning of each distillation, the concentration of sulfuric acid is low, and desulfonation takes place: at the end, the concentration is high, and both exchange and sulfonation of anthraquinone occur.*

spectra of the anthraquinone obtained at intermediate stages of the exchange, were recognized as having originated from partially deuterated anthraquinones.

This indication of low isotopic purity implied either that the partition coefficient for deuterium between anthraquinone and sulfuric acid-d_2 is less than 1, or that equilibrium distribution had not been attained. The latter seems more probable, since when the solution of anthraquinone in concentrated sulfuric acid is poured into the water, anthraquinone separates in finely divided form giving a thick suspension. This might limit mixing and therefore hydrogen isotope exchange between sulfuric acid and water. Moreover, since the partial rate factors for the exchange between anthraquinone and sulfuric acid were not known, the period allowed for exchange might have been too short.

These disadvantages and the long time required by this procedure induced us to seek another method. We designed an apparatus in which exchange sulfonation and desulfonation could take place at the same time, the reactions occurring in two separate parts of the apparatus.

Apparatus and Operating Conditions

The apparatus is made of borosilicate glass tubing. Figure 1 is a diagram of it.

The mixture of anthraquinone, deuterium sulfate, and deuterium oxide is placed in tube A. A small flame is placed under piece B (made of aluminium sheet 3 mm thick) and the water vapor produced condenses in C, which is cooled by flowing water. The condensate then flows down tube D and through E enters tube A, where it mixes with the solution of anthraquinone in sulfuric acid.

By varying the inclination of condenser C, it is possible to regulate the quantity of water held in it. An increase in the quantity of water held in C results in an increase in the concentration of the sulfuric acid in A, which causes the temperature of the mixture to rise. When the system reaches a steady state, there is a gradient of both temperature and sulfuric acid concentration from E to F. Near F, where the acid is concentrated, exchange and sulfonation of the anthraquinone occur; near E at the same time desulfonation of anthraquinone and exchange between sulfuric acid and water occur.

Several experiments were made with this apparatus to establish the proper operating conditions. It was found that the presence of mercury salts reduces considerably the quantity of recovered anthraquinone but

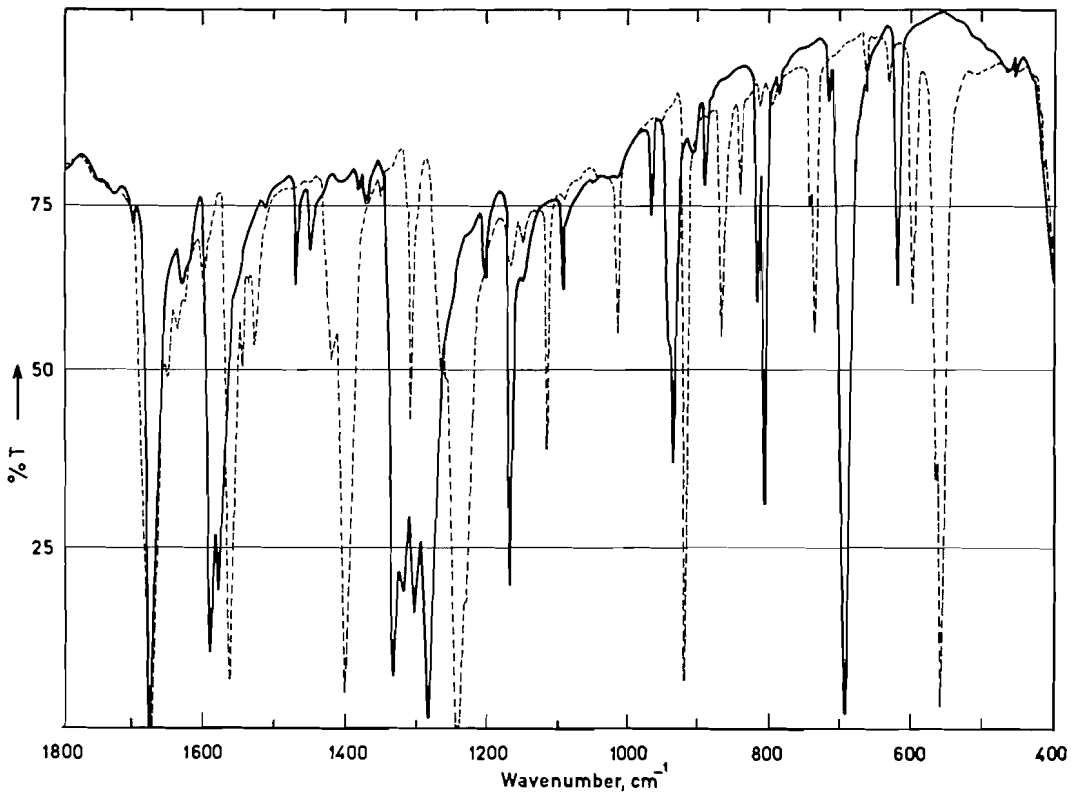


FIG. 2. Infrared spectra of 9,10-anthraquinone-d_0 (solid line) and 9,10-anthraquinone-d_8 (broken line) in KBr pellets (1 mg + 200 mg KBr). The spectra were measured on a Beckman model IR9 spectrometer.

has no influence on the degree of deuteration, and that an exchange period of 2½ h is sufficient for the attainment of equilibrium in hydrogen isotope distribution.

Preparation of Anthraquinone-d_8

An apparatus with the dimensions indicated in Fig. 1 was thoroughly degassed under vacuum, filled with dry nitrogen, and placed in a dry box. Anthraquinone (2 g) was melted in a thin glass tube, which was then broken; the compound was thus obtained free from moisture and in the form of a cylinder. It was introduced into the apparatus through tube G, which was then sealed. Deuterium oxide (5.4 ml) and deuterium sulfate (6.6 ml) were put in through tube H with a long hypodermic needle. The apparatus was immersed in liquid nitrogen and evacuated, and tube H was sealed. The apparatus was removed from the dry box, and heated for 2½ h. Because of the relatively high vapor pressure of anthraquinone at the temperatures of operation, it was necessary to discontinue heating every 30 min, and melt with a flame the anthraquinone which had sublimed on the walls. The indicated period of 2½ h does not include the time during which heating was stopped for this. The apparatus was then allowed to stand for 2 h at 130 °C in an oil bath, cooled to room temperature, and opened at G. The mixture of anthraquinone and 70% sulfuric acid was poured onto a sintered glass funnel in which a 3 mm layer of powdered glass had been placed, and filtered with suction. The product was washed repeatedly with sodium bicarbonate solution until the filtrate was no longer acid. Then it was dried, and crystallized twice from benzene with the addition of a little active charcoal. By this procedure, a yield of 1.8 g, m.p. 286 °C was obtained.

The procedure was repeated two more times. Finally, 1.4 g (yield 70%) of product, m.p. 286.8–287.2 (corr.) was obtained. The infrared spectrum is shown in Fig. 2 together with that of the light compound. The infrared spectrum of the product obtained after two exchanges differs from that indicated in Fig. 2 only by the presence of a few weak additional bands. The intensities of the C—H and the C—D stretching bands is very low and do not permit an estimate of the degree of deuteration.

The mass spectrometric analysis of the final product, made by Merck Sharp and Dohme of Canada Ltd., gave anthraquinone-d_8 95.38%, anthraquinone-d_7 4.62%, total deuterium 99.42%.

ACKNOWLEDGMENTS

The technical aid of Miss Miranda Zanetti is gratefully acknowledged.

REFERENCES

1. A. I. SHATENSHTEIN. Isotopic exchange and the replacement of hydrogen in organic compounds. Consultant Bureau, New York. 1962.
2. C. K. INGOLD, C. G. RAISIN, and C. L. WILSON. J. Chem. Soc. 1637 (1936).
3. W. P. PERSON, G. C. PIMENTEL, and O. SCHNEPP. J. Chem. Phys. **23**, 230 (1955).
4. E. R. LIPPINCOTT and E. J. O'REILLY. J. Chem. Phys. **23**, 238 (1955).
5. R. N. RENAUD, D. KOVACHIC, and L. C. LEITCH. Can. J. Chem. **39**, 21 (1961).
6. A. P. BEST and C. L. WILSON. J. Chem. Soc. 239 (1946).
7. V. GOLD and F. A. LONG. J. Am. Chem. Soc. **75**, 4543 (1953).
8. V. GOLD and D. P. N. SATCHELL. J. Chem. Soc. 3619 (1955).
9. P. J. SOKOLOW and V. P. DREVING. Z. Chim. Promysl. **5**, 412 (1928); cf. Chem. Abstr. **22**, 3889 (1928).
10. T. HANDA. Bull. Chem. Soc. Japan, **35**, 1361 (1962).
11. K. LAUER and R. ODA. J. Prakt. Chem. Ser. 2, **142**, 258 (1935).
12. GER. PATENT No. 162,035 (March 19, 1904, Bayer and Co.); cf. Chem. Central-Bl. **II**, 864 (1905).

Can. J. Chem. Downloaded from www.nrcresearchpress.com by 210.87.254.40 on 09/05/12
For personal use only.

PREPARATION AND CHARACTERIZATION OF SOME BINARY AND TERNARY METAL COMPLEXES OF IMIDAZOLE AND AMINO ACIDS[1]

G. N. Rao and N. C. Li
Duquesne University, Pittsburgh, Pennsylvania
Received February 21, 1966

ABSTRACT

Five new ternary metal complexes containing imidazole and glycylglycine or amino acid have been prepared and characterized by proton magnetic resonance and infrared spectral studies. Seven new binary metal complexes have also been prepared and studied. The isolation of $Cd(imidazole)_6Cl_2.H_2O$ and $Ni(imidazole)_6.Cl_2.4H_2O$ provides evidence that the coordination number of these metal ions to imidazole in the solid state is six. The visible spectra of the Ni(II) complexes of amino acid and imidazole show that all these are octahedral in aqueous solution.

INTRODUCTION

The imidazole group of histidine is biologically of great importance, since it plays an important part in the binding of metallic ions to proteins and in the buffer action of proteins (1, 2). Koltun, Fried, and Gurd (3) measured the rates of hydrolysis of *p*-nitrophenyl acetate in the presence of imidazole (Im), $CuCl_2$, and glycylglycinate (GG), and calculated equilibrium constant for the reaction $CuGG + Im = CuGGIm$. These authors have pointed out that Cu(II) ion may bridge the N-terminus of a protein polypeptide chain to a side-chain imidazole group, so that studies on mixed imidazole–peptide complexes may serve to some degree as model for the protein complexes. From the effects of metal–peptide complexes on the imidazole catalysis of mutarotation of glucose and glucosamine, Tang and Li (4) reported the formation of ternary cadmium and nickel complexes containing imidazole and glycylglycinate. They found that the equilibrium constants for the reaction $MGG^+ + Im = MGGIm^+$ are $10^{2.78}$ and $10^{3.16}$ for M = Cd(II) and Ni(II), respectively.

In view of the importance of metal complexes containing imidazole and amino acid or peptide, we have prepared several binary and ternary metal complexes containing these biologically important ligands in the solid state, and have carried out proton magnetic resonance and absorption spectral studies on them. The results are presented in this paper.

EXPERIMENTAL

Materials

Imidazole and glycylglycine (from Aldrich Chemical Co.), and the amino acids (from Fisher Scientific Co.), were used without further purification. The other chemicals were of analytical reagent grade. Cadmium and nickel were analyzed by complexometric titration with EDTA; chloride by the Volhard titration method. Analysis for carbon, hydrogen, and nitrogen was done by A. Bernhardt, Germany.

Preparation of solid complexes

The following compounds have not been reported previously.

Cd(GG)(Im)(Cl)

To 0.01 mole of $CdCl_2.2\frac{1}{2}H_2O$ dissolved in 30 ml of water was added 30 ml of an aqueous solution containing 0.01 mole of sodium glycylglycinate. To this solution was added 30 ml of an aqueous solution containing 0.01 mole of imidazole, and the mixture was heated on a water bath for 1 h and filtered. The filtrate was evaporated to a volume of 25 ml and then placed in a refrigerator. The white precipitate formed was filtered, washed with water, and dried in a vacuum desiccator over P_2O_5.

Anal. Calcd. for $CdC_7H_{11}O_3N_4Cl$: Cd, 32.39; C, 24.21; H, 3.20; N, 16.15; Cl, 10.22. Found: Cd, 32.45; C, 24.11; H, 3.35; N, 15.98; Cl, 10.39.

[1]*This investigation was supported by a National Science Foundation grant, No. GB-4065.*

Cd(GG)(Im)$_2$(OH)

Cadmium hydroxide was prepared by mixing 0.02 mole of NaOH with 0.01 mole of $CdCl_2.2\frac{1}{2}H_2O$ in water, washing the precipitate formed with water, and centrifuging. The cadmium hydroxide formed in this manner was mixed with 0.01 mole of glycylglycine and 0.02 mole of imidazole in 100 ml of water, and digested on a water bath for 2 h. The mixture was then cooled and filtered to remove unreacted cadmium hydroxide. The filtrate was evaporated to a volume of 30 ml and then placed in a refrigerator. The white solid formed was filtered, washed with water, and dried in a vacuum desiccator over P_2O_5.

Anal. Calcd. for $CdC_{10}H_{16}O_4N_6$: Cd, 28.34; C, 30.25; H, 4.07; N, 21.19. Found: Cd, 28.48; C, 30.23; H, 4.27; N, 21.06.

Cd(GG)(Im)(NO_3).H_2O

This compound was prepared in the same way as Cd(GG)(Im)(Cl), except that cadmium nitrate was used instead of cadmium chloride.

Anal. Calcd. for $CdC_7H_{13}O_7N_5$: Cd, 28.71; C, 21.46; H, 3.34; N, 17.89. Found: Cd, 28.74; C, 21.60; H, 3.34; N, 17.69.

Cd(GG)$_2$.H_2O

0.01 mole of cadmium hydroxide was added to 100 ml of water containing 0.02 mole of glycylglycine, and the mixture was digested on a water bath for 2 h. After filtering off the unreacted cadmium hydroxide, the filtrate was evaporated to 30 ml and cooled. The white precipitate formed was filtered, washed with water, and dried in a vacuum desiccator over P_2O_5.

Anal. Calcd. for $CdC_8H_{16}O_7N_4$: Cd, 28.63. Found: Cd, 28.80.

Cd(asparaginate)$_2$

0.01 mole of cadmium oxide was mixed with 0.02 mole of the amino acid in 100 ml of water, and heated on a water bath until the oxide dissolved. The solution was filtered and the filtrate cooled. Ethanol was added to facilitate separation of the solid. The white precipitate formed was filtered, washed with water, and dried in air.

Anal. Calcd. for $CdC_8H_{14}O_6N_4$: Cd, 30.01; C, 25.63; H, 3.77; N, 14.96. Found: Cd, 30.11; C, 25.81; H, 3.89; N, 14.92.

Cd(α-alaninate)$_2$

This compound was prepared in the same way as Cd(asparaginate)$_2$.

Anal. Calcd. for $CdC_6H_{12}O_4N_2$: Cd, 38.96; C, 24.96; H, 4.19; N, 9.71. Found: Cd, 39.16; C, 24.83; H, 4.04; N, 9.90.

Cd(β-alaninate)$_2$

This compound was prepared in the same way as Cd(α-alaninate)$_2$, except that an excess (>0.02 mole) of the amino acid was necessary.

Anal. Calcd. for $CdC_6H_{12}O_4N_2$: Cd, 38.96; C, 24.96; H, 4.19; N, 9.71. Found: Cd, 38.91; C, 24.86; H, 4.04; N, 9.63.

Cd(Im)$_6$(Cl)$_2$.H_2O

To 0.01 mole of $CdCl_2.2\frac{1}{2}H_2O$ dissolved in 30 ml of warm water, was added 0.07 mole of imidazole in 30 ml of water, slowly with stirring. A white precipitate was obtained immediately and the mixture was digested on a water bath for 1 h and filtered. The white crystals were washed with water and ethanol, and dried in air.

Anal. Calc. for $CdC_{18}H_{26}ON_{12}Cl_2$: Cd, 18.44; C, 35.43; H, 4.30; N, 27.57; Cl, 11.64. Found: Cd, 18.40; C, 35.29; H, 4.32; N, 27.36; Cl, 11.46.

Ni(asparaginate)$_2$

0.01 mole of $NiCO_3$ was mixed with 0.02 mole of the amino acid in 100 ml of water and heated on a water bath for 1 h. The solution was evaporated to a volume of 20 ml and kept in a refrigerator. The blue crystals obtained were filtered, washed with water, and dried in a vacuum desiccator over P_2O_5.

Anal. Calcd. for $NiC_8H_{14}O_6N_4$: Ni, 18.29; C, 29.92; H, 4.40; N, 17.46. Found: Ni, 18.35; C, 30.49; H, 4.65; N, 17.65.

Ni(Im)$_6$.(Cl)$_2$.4H_2O

0.01 mole of $NiCl_2$ and 0.06 mole of imidazole were dissolved in 100 ml of water and evaporated on a water bath to about 20 ml. Blue-violet crystals appeared after the solution stood 4 d. The crystals were filtered, washed with water and ethanol, and dried in air.

Anal. Calcd. for $NiC_{18}H_{32}O_4N_{12}Cl_2$: Ni, 9.62; C, 35.41; H, 5.29; N, 27.55. Found: Ni, 9.56; C, 35.60; H, 5.43; N, 27.79.

Ni(glycinate)$_2$.(Im)$_2$

0.01 mole of $NiCO_3$, 0.02 mole of the amino acid, and 0.02 mole of imidazole were mixed in 100 ml of water and heated for 1 h on a water bath. The solution was then evaporated to a volume of 20 ml and let stand for 2 d. The violet crystals formed were filtered, washed with water and ethanol, and dried in a vacuum desiccator over P_2O_5.

Anal. Calcd. for $NiC_{16}H_{16}O_4N_6$: Ni, 15.49; C, 34.99; H, 4.71; N, 24.50. Found: Ni, 15.47; C, 35.23; H, 4.81; N, 24.38.

Can. J. Chem. Downloaded from www.nrcresearchpress.com by 210.87.254.40 on 09/05/12
For personal use only.

Ni(α-alaninate)$_2$.(Im)$_2$.H$_2$O

This compound was prepared in the same way as Ni(glycinate)$_2$(Im)$_2$.

Anal. Calcd. for $NiC_{12}H_{22}O_5N_6$: Ni, 14.43; C, 37.02; H, 5.70; N, 21.61. Found: Ni, 14.37; C, 37.14; H, 5.94; N, 21.85.

Instrumental

A Varian Associates Model A-60 n.m.r. spectrometer was used for proton magnetic resonance studies. Chemical shifts were measured with respect to tetramethylsilane (TMS) and are quoted as p.p.m. All lines are downfield from TMS. Infrared spectra were obtained with a Perkin-Elmer, model 137 spectrophotometer using Nujol mulls. Absorption spectra were taken on a Cary model 14 spectrophotometer with 5 cm cells.

RESULTS AND DISCUSSION

(A) Proton Magnetic Resonance and Infrared Studies

The proton magnetic resonance spectra of imidazole in 99.8% D_2O show a simple first-order AX_2 pattern consisting of two peaks in the intensity ratio 1:2. The more intense peak, at 7.6 p.p.m. for pH $\sim$ 8, is assigned to the single proton in the 2-position, while the other, at 6.9 p.p.m., is assigned to the two protons in the 4,5-positions. The protons in the 4- and the 5-position are equivalent because rapid NH proton exchange takes place with the solvent, and therefore only give rise to one line as observed. The NH proton does not give rise to a separate line because of the exchange (5).

At pH 3.5, the peak due to the 4,5-CH protons moves downfield to 7.6 p.p.m., while the peak due to the 2-CH proton moves to 8.2 p.p.m. At the lower pH, the imidazole is protonated and an electron redistribution results from the inductive electron-withdrawal operating at the 3-nitrogen position and causes a downfield shift of the proton signals.

The proton magnetic resonance spectra of Cd(GG)(Im)(Cl), Cd(GG)(Im)$_2$(OH), and Cd(GG)(Im)(NO_3).H$_2$O in 99.8% D_2O (a small amount of acid was added, pH $\sim$ 3.0, in order to facilitate solution of the ternary complexes) show four peaks at 4.0, 4.1, 7.8, and 8.5 p.p.m. The peaks at 4.0 and 4.1 p.p.m. (of equal intensity) are assigned to the protons of the two non-equivalent CH_2 groups in glycylglycine, because an acid solution of glycylglycine shows two peaks at these positions. The two peaks, 7.8 and 8.5 p.p.m., always in the intensity ratio 2:1, are ascribed to the 2-CH and the 4,5-CH protons, respectively, in the imidazole moiety of the ternary complexes.

The relative intensities of the peaks at 4.0, 4.1, 7.8, and 8.5 p.p.m. are in the ratios: 2:2:2:1, 2:2:2:1, and 1:1:2:1 for Cd(GG)(Im)(Cl), Cd(GG)(Im)(NO_3).H$_2$O, and Cd(GG)(Im)$_2$(OH), respectively. These are as expected since in Cd(GG)(Im)(Cl) and Cd(GG)(Im)(NO_3).H$_2$O, the ratio of GG to Im is 1:1, whereas in Cd(GG)(Im)$_2$(OH), the corresponding ratio is 1:2.

The infrared spectra of Cd(GG)(ImCl), Cd(GG)(Im)(NO_3).H$_2$O, and Cd(GG)(Im)$_2$-(OH) have been obtained. The general feature is an overlap of the spectra of the glycylglycinate and imidazole components. The N—H stretching band (2) at 3 125 cm^{-1} for imidazole persists in the spectra of the three ternary complexes, indicating that imidazole does not bind to cadmium(II) by way of the 1-nitrogen atom. By noting the similarity of the complex formation constants of imidazole and N-methylimidazole with Cu(II) and Cd(II), Li, White, and Doody (6) proposed that the binding site in imidazole is the 3-nitrogen atom. By comparing data on the N-methylimidazole complex with the imidazole complex of Ag(I), Bauman and Wang (7) came to the same conclusion regarding the site of complex formation of the imidazole molecule. It is interesting to note that in the infrared absorption spectra of the metal imidazolates which Bauman and Wang prepared, the highest frequency is around 1 600 cm^{-1}. In the metal imidazolates, therefore, the N—H stretching band is missing.

Can. J. Chem. Downloaded from www.nrcresearchpress.com by 210.87.254.40 on 09/05/12
For personal use only.

(B) Visible and Ultraviolet Spectral Studies

The absorption spectra of nickel(II) complexes of amino acids, glycylglycine, imidazole, and of ternary Ni(II) complexes of amino acids and imidazole, show four bands in the region of 9 700 to 28 000 cm^{-1}, as listed in Table I. These results may be interpreted in the light of the ligand field theory and Ni(II) can be shown to be in octahedral coordination, as follows:

Ballhausen (8) has derived the following equations for calculating the frequency of bands in the spectra of octahedral nickel(II) complexes

$$\nu_1 = 10Dq \quad [1]$$

$$\nu_2 = (9/5)(10Dq) \quad [2]$$

$$\nu_3 = 17\,000 + (6/5)(10Dq), \quad [3]$$

where ν is the frequency of the absorption band in cm^{-1} and $10Dq$ is the crystal field splitting parameter. Though the value of $10Dq$ for a particular configuration can be calculated from quantum mechanics, it is usually determined from the frequency of the first absorption band in the visible spectrum, eq. [1]. The frequencies of the remaining bands may then be calculated from eqs. [2] and [3], respectively, and if the calculated and observed frequencies agree, then the complex would be octahedral since the equations were obtained on the basis of this symmetry.

TABLE I

Spectra of Ni(II) complexes in water*

Complex	ν_1	ϵ_1	ν_2	ϵ_2	ν_3	ϵ_3	ν_2/ν_1
$Ni(glycinate)_2.2H_2O$	9 720†	7.16	16 050	5.60	27 100	9.4	1.65
	9 720‡		17 450		28 660		
	8 910		16 040		27 690		
$Ni(\alpha\text{-alaninate})_2$	9 850†	7.46	15 970	5.00	26 670	9.4	1.62
	9 850‡		17 730		28 820		
	8 860§		15 950		27 636		
$Ni(asparaginate)_2$	9 810†	6.92	16 340	4.60	27 930	12.8	1.67
	9 810‡		17 660		28 780		
	9 070§		16 320		27 880		
$Ni(GG)_2$	9 720†	7.16	16 130	4.80	27 030	8.5	1.66
	9 720‡		17 490		28 660		
	8 950§		16 120		27 740		
$Ni(Im)_6(Cl)_2.4H_2O$	9 780†	3.70	16 130	6.24	26 600	11.4	1.65
	9 780‡		17 600		29 510		
	8 950§		16 110		27 990		
$Ni(glycinate)_2.(Im)_2$	9 820†	6.12	16 500	5.80	27 060	9.9	1.68
	9 820‡		17 680		28 790		
	9 160§		16 490		27 990		
$Ni(\alpha\text{-alaninate})_2.(Im)_2.H_2O$	9 830†	6.40	16 580	5.90	27 250	10.2	1.69
	9 830‡		17 700		28 800		
	9 200§		16 560		28 040		

*A very weak band at 13 000 cm^{-1} (molar extinction coefficients $\epsilon < 2.0$) was observed for each of the nickel complexes.
†Values observed.
‡Values obtained from eqs. [1–3].
§Values obtained from eqs. [4–6].

Sharma, Mathur, and Biswas (9) modified Ballhausen's equations by introducing the correction factor, X, which accounts for perturbations due to higher energy transitions on the lowest energy transition. The equations become

$$X\nu_1 = 10Dq \quad [4]$$

$$\nu_2 = (9/5)(10Dq) = (9/5)(X\nu_1) \quad [5]$$

$$\nu_3 = 17\,000 + (6/5)(10Dq) = 17\,000 + (6/5)(X\nu_1). \quad [6]$$

Can. J. Chem. Downloaded from www.nrcresearchpress.com by 210.87.254.40 on 09/05/12
For personal use only.

As an example of the use of these equations, $X = (5/9)(\nu_2/\nu_1) = (5/9)1.65$ for the spectrum of the Ni(glycinate)$_2$.2H$_2$O. The corrected value of $10Dq$ is therefore 8 910 cm^{-1}. If this value of $10Dq$ is used to calculate ν_2 and ν_3, the experimental and calculated values are in good agreement.

Jorgensen (10) has indicated that for octahedral nickel complexes there are in general four bands in the regions 8 000 – 11 000, 12 000 – 13 000, 15 000 – 19 000, and 25 000 – 29 000 cm^{-1}. The data of Table I show that there are indeed four bands in the nickel complexes listed, although the intensity of the band in the 12 000 – 13 000 region is very weak. The agreement between the calculated and observed frequencies, ν_2 and ν_3, in the spectra of the nickel complexes listed in Table I indicates that they are all octahedral.

Another characteristic feature of octahedral symmetry is the small molar extinction coefficients of the bands (of the order of 1–30) (10) and the ratio of ν_2/ν_1 is 1.8 (from eqs. 1 and 2). The values of the molar extinction coefficients and the ratio of ν_2/ν_1 in Table I again indicate the octahedral configuration.

Sharma, Mathur, and Biswas (9) have shown that if the nickel(II) complexes are tetrahedral, the first band would occur at $\nu_1 = 10Dq'$ (tetrahedral) $= (4/9)10Dq$ (octahedral) (11). In Table I, $10Dq$ is about 9 000. The first absorption band therefore should have occurred at about 4 000 cm^{-1} if the complexes were tetrahedral. Since no band is observed at 4 000 cm^{-1}, tetrahedral configuration can be ruled out. The spectra of the nickel glycinate and α-alaninate complexes in Table I cannot be compared with those reported by Jorgensen (12) and by Sharma, Mathur, and Biswas (9), since their spectra refer to triglycinate and tri-α-alaninate, respectively, while the present spectra refer to the diglycinate and di-α-alaninate complexes.

General Conclusion

The isolation and characterization of three solid ternary cadmium complexes containing glycylglycine and imidazole lend support to the finding of Tang and Li (4) on the existence of Cd(GG)(Im)$^+$ species in solution. The isolation of Ni(Im)$_6$Cl$_2$.4H$_2$O in the pure solid state supports the assumption of Li, Chu, Fujii, and White (13) that Ni(Im)$_6^{2+}$ exists in solution. The isolation of Cd(Im)$_6$(Cl)$_2$.H$_2$O in the pure solid state provides proof of the coordination number of six of cadmium in the solid state. Although Li, White, and Doody (6) find that the highest-order Cd(II) complex of imidazole is four, i.e., Cd(Im)$_4^{2+}$ in solution, other investigators have reported coordination number of six for cadmium in solution, when ligands are amines (14) and amino acids (15, 16). Proton magnetic resonance and infrared spectra are useful in the characterization of the ternary complexes. The visible spectra of binary Ni(II) complexes of amino acids, glycylglycine, imidazole, and ternary Ni(II) complexes of amino acids and imidazole, show that all these are octahedral in aqueous solution.

REFERENCES

1. F. R. N. Gurd and P. E. Wilcox. Advan. Protein Chem. **11**, 312 (1956).
2. D. Garfinkel and J. T. Edsall. J. Am. Chem. Soc. **80**, 3807 (1958).
3. W. L. Koltun, M. Fried, and F. R. N. Gurd. J. Am. Chem. Soc. **82**, 233 (1960).
4. P. Tang and N. C. Li. J. Inorg. Nucl. Chem. **26**, 1606 (1964).
5. R. J. Gillespie, A. Grimison, J. H. Ridd, and R. F. M. White. J. Chem. Soc. 3228 (1958).
6. N. C. Li, J. M. White, and E. Doody. J. Am. Chem. Soc. **76**, 6219 (1954).
7. J. E. Bauman, Jr. and J. C. Wang. Inorg. Chem. **3**, 368 (1964).
8. C. J. Ballhausen. Rec. Trav. Chim. **75**, 665 (1956).
9. V. S. Sharma, H. B. Mathur, and A. B. Biswas. Indian J. Chem. **2**, 5 (1964).
10. C. K. Jorgensen. Acta Chem. Scand. **10**, 887 (1956).
11. T. D. Dunitz and L. E. Orgel. J. Phys. Chem. Solids, **3**, 20 (1957).
12. C. K. Jorgensen. Acta Chem. Scand. **9**, 1362 (1955).
13. N. C. Li, T. L. Chu, C. T. Fujii, and J. M. White. J. Am. Chem. Soc. **77**, 859 (1955).
14. B. E. Douglas, H. A. Laitinen, and J. C. Bailar, Jr. J. Am. Chem. Soc. **72**, 2484 (1950).
15. G. Nageswara Rao and R. S. Subrahmanya. Proc. Indian Acad. Sci. Sect. A, **60**, 165 (1964).
16. N. C. Li, J. M. White, and R. L. Yoest. J. Am. Chem. Soc. **78**, 5218 (1956).

Can. J. Chem. Downloaded from www.nrcresearchpress.com by 210.87.254.40 on 09/05/12
For personal use only.

Can. J. Chem. Downloaded from www.nrcresearchpress.com by 210.87.254.6 on 09/05/12
For personal use only.

A SPECTROPHOTOMETRIC STUDY OF HEXA-, PENTA-, AND TETRA-COORDINATED HALOGENOCOPPER(II) COMPLEXES IN ACETONE – HYDROHALIC ACID MIXTURES

G. H. FAYE[1]

Mineral Sciences Division, Department of Mines and Technical Surveys, Ottawa, Canada

Received January 11, 1966

ABSTRACT

A spectrophotometric study of the Cu(II) – acetone – hydrochloric (hydrobromic) acid systems has revealed that at relatively high ratios of halide:copper there is a probable equilibrium between four-, five-, and six-coordinate halogenocopper(II) complexes. A distorted tetrahedral species is favored at the highest ratios. Ligand field bands of pseudo-octahedral monohalogenocopper(II) complexes and, in the visible region, a charge transfer band of the six-coordinate complex, $[CuCl_4(ac)_2]^{2-}$, have been identified. The results of the present work point to the important role of the solvent in determining the geometries and absorption spectra of the complexes, a factor that seems to have been misinterpreted by some previous workers.

INTRODUCTION

It is known that the tetrahalogenocopper(II) ion exists as a tetragonally distorted tetrahedron in crystalline solids such as Cs_2CuCl_4 (1), $[Ph_3MeAs]_2CuCl_4$ and $[Ph_3MeAs]_2CuBr_4$ (2), in molten chlorides (3, 4) and in certain aqueous and organic solvent media (5, 6). The structural information on the solids has been obtained largely through X-ray diffraction work and, on the solutions (including melts), by comparisons of the absorption spectra of the complexes in the two states of matter. In general, however, the absorption spectra of solutions of the halogen complexes of Cu(II) have been difficult to interpret because of "solvent effects" (7) and because of charge transfer bands arising in the visible region (8). In several cases these problems have led to the proposal of complexes that the present author finds difficult to reconcile with his own findings.

As a basis for discussion of previous work, it can be recalled that 3d transition metal complexes in solution exhibit absorption bands from the near ultraviolet to the near infrared region of the energy spectrum. Bands in the high energy region, with absorption coefficients, ϵ_{max}, $> \sim 500$ l/mole cm and oscillator strengths, f, $> \sim 10^{-2}$, are probably of the charge transfer type (ligand $\rightarrow$ metal), whereas bands in the visible to near infrared with $\epsilon_{max} < \sim 500$ l/mole cm and $< \sim 10^{-2}$ are the ligand field d–d bands.

Cu(II) has a d^9 configuration, which in a cubic field, gives rise to a single band due to the transition $T_{2g} \rightleftarrows E_g$. In an approximately octahedral field such as that in $Cu(OH_2)_6^{2+}$, this transition occurs at 12 500 cm^{-1} (800 mμ) (9). In a tetrahedral field, the transition should occur at a frequency less than 10 000 cm^{-1} because the ligand field splitting (Δ) for a tetrahedral complex should be about half as great as that for an octahedral complex (10). Felsenfeld (11), using theoretical considerations based on a tetrahedral model for $CuCl_4^{2-}$, showed that the complex should have a d–d band at 5 768 cm^{-1}.

Helmholz and Kruh (1) have shown that $CuCl_4^{2-}$ in crystalline Cs_2CuCl_4 is a flattened tetrahedron. These workers compared the absorption spectra (in the 10 000 – 45 000 cm^{-1} region) of a mull of powdered Cs_2CuCl_4 and that of an aqueous solution of cupric chloride, and concluded that the structure of the aqueous ion was not the same as that in the crystal. Both spectra obtained by Helmholz and Kruh show charge transfer bands ($> 2 \times 10^{-2}$) above 20 000 cm^{-1}, but the only d–d band resolved was that of the solution

[1]*Senior Scientific Officer, Analytical Chemistry Sub-division, Mineral Sciences Division, Mines Branch, Department of Mines and Technical Surveys, Ottawa, Canada.*

at about 13 000 cm^{-1} ($\sim$ 770 mμ). It will be evident later in the paper that this band probably should have been drawn with a maximum near 11 000 cm^{-1}; but in either case, according to the criteria outlined above, one may be led to conclude that copper probably did not exist in the solution mainly as a tetrahedral complex. It may be noted, however, that in a theoretical paper on the intensities of spectral bands in tetrahedral complexes, Ballhausen and Liehr (12) state that they considered the "$CuCl_4^{2-}$" complex in solution to be rigorously tetrahedral.

Antipova-Karataeva and Nainshtein (7) studied the spectra of solutions of cupric chloride in acetone and noted a relatively intense band at about 21 000 cm^{-1} (475 mμ), which they attributed to a solvated complex of low symmetry and implied that it contained less than four chlorines per copper. Because of the attempted structure assignment, it would appear that Antipova-Karataeva and Vainshtein considered this maximum to be due to a d-orbital transition because charge transfer bands do not readily permit such assignments.

Gažo (13) also observed the maximum at 21 000 cm^{-1} and showed that it was due to a tetrachloro complex; however, he did not identify the band as being either charge transfer or d–d in character. It will be shown later in this paper that it is a charge transfer band.

Furlani and Morpurgo (6) obtained the spectra of nitromethane solutions of certain salts of the general formula R_2CuCl_4, and under some conditions these show an absorption peak at 21 900 cm^{-1}. Furlani and Morpurgo attribute this charge transfer band to a "solvolysis product" and imply that the complex contained less than four chlorines per copper (a conclusion similar to that of Antipova-Karataeva and Vainshtein).

In nitromethane solutions of R_2CuX_4 (X = Cl or Br) containing excess X^-, the spectra measured by Furlani and Morpurgo show broad bands with maxima at 8 000 – 9 000 cm^{-1} and these are considered to be the d–d bands of pseudo-tetrahedral tetrahalogeno complexes. However, in the spectra of similar solutions not containing excess halide, maxima appear at 11 500 – 12 000 cm^{-1} and Furlani and Morpurgo assign these to distorted square planar solvolysis products, i.e. di- and (or) tri-halide species such as CuX_2L_2.

Gill and Nyholm (2) studied the complexes $[Ph_3MeAs]_2CuCl_4$ and $[Ph_3MeAs]_2CuBr_4$ but did not publish their crystal or solution spectra. However, they did indicate that they found absorbance maxima for "$CuCl_4^{2-}$" and "$CuBr_4^{2-}$" in nitromethane solutions at 11 200 and 11 500 cm^{-1} respectively, with corresponding ϵ_{max} values of 88 and 122 l/mole cm. From the arguments presented earlier, the above spectral data suggest that the two complexes, in solution, were of approximately octahedral symmetry. Gill and Nyholm suggest that in nitromethane solution a tetrahedral arrangement is not at all certain for their tetrahalogen complexes.

Barnes and Hume (5) have established the existence of the distorted tetrahedral $CuBr_4^{2-}$ ion in both aqueous and organic solvents and this has been considered to be the only example of such a geometry for Cu(II) complexes in liquid solutions (4). According to Barnes and Hume, the d–d band of the purple tetrabromo complex has its maximum at 9 100 cm^{-1} (1 100 mμ) with ϵ_{max} = 160, both parameters in the accepted range for tetrahedral (approximately) complexes.

Barnes and Hume also investigated a green complex which in acetone solutions was found to have its d–d band at about 11 400 cm^{-1} (880 mμ) with ϵ_{max} = 160. Apparently the green complex had been studied previously by Yatsimirskii and Malkova (14), who concluded that it was $CuBr_4^{2-}$. However, Barnes and Hume consider the species to be the five-coordinate entity, $CuBr_3^-$.2solvent. As we will see later, it is probably a pseudo-octahedral tetrabromo complex.

Can. J. Chem. Downloaded from www.nrcresearchpress.com by 210.87.254.6 on 09/05/12
For personal use only.

From the foregoing it is evident that further experimental work is required to elucidate the spectra and structure of the halogenocopper(II) complexes, especially in coordinating solvents such as acetone. The present paper describes studies directed to that end.

It will be shown that in acetone solutions, containing an excess of Cl^- or Br^-, an equilibrium exists between octahedral and tetrahedral (both distorted) tetrahalogenocopper-(II) complexes, the four-coordinate species being favored in solutions having the highest halide ion activity. The experimental evidence, although not conclusive, suggests that a five-coordinate (probably pentachloro) complex participates in the overall equilibrium.

The important role of solvent molecules as "primary" ligands is indicated in the present study where the six-coordinate complexes are considered to be $[CuCl_4(ac)_2]^{2-}$ and $[CuBr_4(ac)_2]^{2-}$. Information on monohalogenocopper(II) species has been obtained and it seems that these are more thermodynamically stable than the higher halogeno pseudo-octahedral complexes.

EXPERIMENTAL

Stock Solution of $CuCl_2.2H_2O$ in Acetone

This was prepared by dissolving an accurately weighed quantity of analyzed (37.5% Cu) reagent grade $CuCl_2.2H_2O$ in the required volume of reagent grade acetone. Recent studies in this laboratory have shown that in such solutions the coordination sphere of the dissolved copper species changes with time through the formation of monochloro complexes. For example, after approximately 5 days a green gelatinous material containing Cu(II) and Cl^- in a 1:1 ratio is produced in solutions that were originally 10^{-2} to 10^{-3} *M* in Cu(II). Thus to avoid complications due to the formation of such material, freshly prepared solutions only were used in the present studies.

Stock Solution of $Cu(ClO_4)_2$ in Acetone

This was prepared by dissolving high-purity copper turnings in concentrated nitric acid, evaporating the resulting solution just to dryness, and then treating the salt with several milliliters of concentrated perchloric acid. The solution was evaporated until copper perchlorate had crystallized and nearly all free perchloric acid had been driven off. After the solution had cooled, the residue was treated with acetone and several drops of concentrated perchloric acid (just sufficient to produce a clear solution) and diluted to a known volume with acetone.

Apparatus

All spectrophotometric measurements were made with a Beckman DK-2 recording spectrophotometer equipped with matched 1 cm cells.

Experimental Procedure

Most sample solutions were prepared by mixing aliquots of the appropriate copper stock solution with aliquots of either concentrated hydrochloric or hydrobromic acids, or of solutions of known concentration of each acid in acetone. The resulting mixtures were diluted to 25 ml with acetone, cooled to room temperature, and examined spectrophotometrically. In obtaining the spectra, copper-free reference solutions containing all ingredients in the same concentration as the corresponding samples were used.

During the course of the experimental work it was established that the spectra were reproducible except, as noted in the text, under conditions where Cu(II) was reduced to Cu(I) by Br^-.

It is known that at room temperature concentrated hydrochloric acid reacts relatively slowly with acetone; however, this did not complicate the present study. For example, it was found that absorbance values of the spectra of solutions in which $[Cl^-]/[Cu^{2+}] \sim 8$ decreased by 10% in 5 h, whereas in the same period the decrease in absorbance was 1–3% for solutions in which $[Cl^-]/[Cu^{2+}]$ ranged from approximately 150 to 600.

Because of the high absorbance of the solvent medium, the spectra could not be examined above approximately 31 000 cm^{-1} ($\sim$ 320 mμ) or below approximately 6 000 cm^{-1} ($\sim$ 1 700 mμ).

Extinction coefficients (ϵ_{max}) were calculated using total copper concentrations.

RESULTS AND DISCUSSION

Chlorocopper(II) Complexes in Acetone–Hydrochloric Acid Solutions: Monochlorocopper(II) Complex

From the spectra in Fig. 1 it is evident that as the ratio of the total molar concentrations of Cl^- to Cu^{2+} is increased from 0 to about 1.3 there is a gradual increase in the intensity of the d–d band and a shift of the band maximum from 12 500 to about 12 200 cm^{-1}

Can. J. Chem. Downloaded from www.nrcresearchpress.com by 210.87.254.6 on 09/05/12
For personal use only.

(820 mμ). In the mole ratio range 1.3 to 2.5 (not shown), the intensity increase continues and there is a sudden shift of the maximum to 11 500 cm^{-1} (870 mμ), at which value it remains constant up to a ratio of approximately 20:1 (see B of Fig. 2).

Absorbance data from Fig. 1, together with that from additional spectra, have been plotted against $[Cl^-]/[Cu^{2+}]$ in Fig. 3*a* and from this it is clear that Cu(II) and chlorine are present in a 1:1 ratio in the complex with d–d band maximum at 12 200 cm^{-1} (820 mμ).

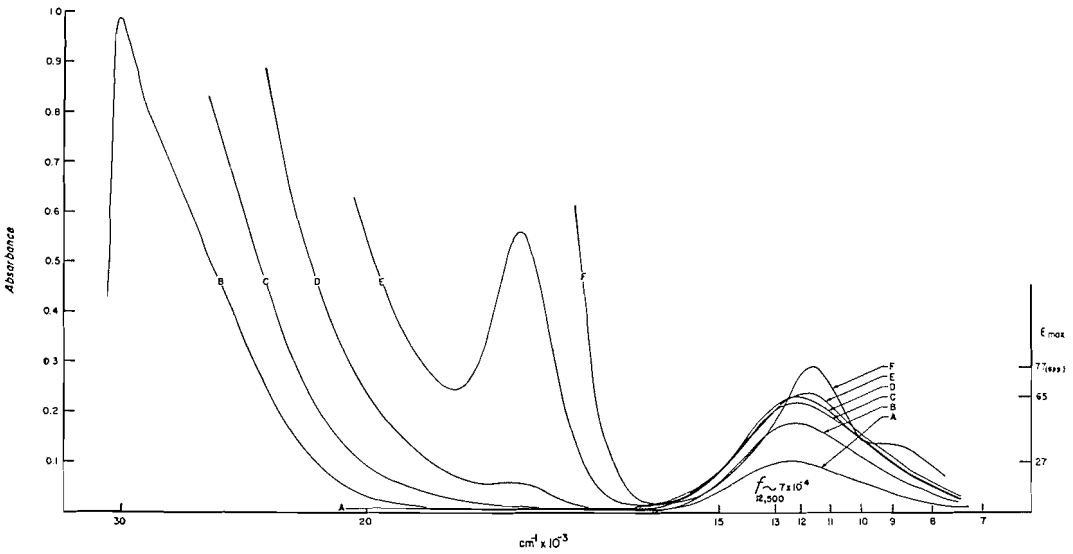


FIG. 1. Spectra of octahedral complexes. $[Cu]_{total} = 3.76 \times 10^{-3}$ *M*; $[Cl^-]/[Cu^{2+}]$ = (A) 0, (B) 0.64, (C) 0.96, (D) 1.28, (E) 1.92, and (F) 3.20.

In the interpretation of these spectral changes, it is assumed that spectrum A in Fig. 1 is that of a distorted (Jahn–Teller effect) octahedral complex $[Cu(OH_2)_4(ac)_2]^{2+}$ (where ac = acetone). Friedman and Plane (15) have shown that such a complex is present in acetone solutions of copper perchlorate containing small amounts of water. Since no free water was added to the initial system in the present work, it is possible that more than two molecules of acetone were present in the inner coordination sphere. However, the acetone used may well have contained as much as 0.05% water and because $\epsilon_{max} = 27$ l/mole cm at 12 500 cm^{-1} is similar to the value given by Friedman and Plane for $[Cu(OH_2)_4(ac)_2]^{2+}$, it is reasonable to assume that this is the complex responsible for the 12 500 cm^{-1} band. It is worth noting here that $[Cu(OH_2)_4(ac)_2]^{2+}$ has its d–d band maximum at the same energy as $Cu(OH_2)_6^{2+}$ because of the similar ligand fields of acetone and water (15).

From the above considerations it can be concluded that the monochlorocopper(II) complex is probably $[CuCl(OH_2)_3(ac)_2]^+$, or in the extreme, $[CuCl(ac)_5]^+$. Because acetones are preponderant in the system, it is felt that water molecules in the coordination sphere are replaced preferentially by chlorines. The decrease of approximately 300 cm^{-1} in Δ_{oct} accompanying the introduction of a chlorine into the coordination sphere is consistent with its position in the spectrochemical series.

At energies higher than approximately 20 000 cm^{-1} certain spectra in Figs. 1 and 2 show bands which, because of their intensity (and energy), are considered to be of the charge transfer type. Because these bands arise with chloride ligandcy it is reasonable to

Can. J. Chem. Downloaded from www.nrcresearchpress.com by 210.87.254.6 on 09/05/12
For personal use only.

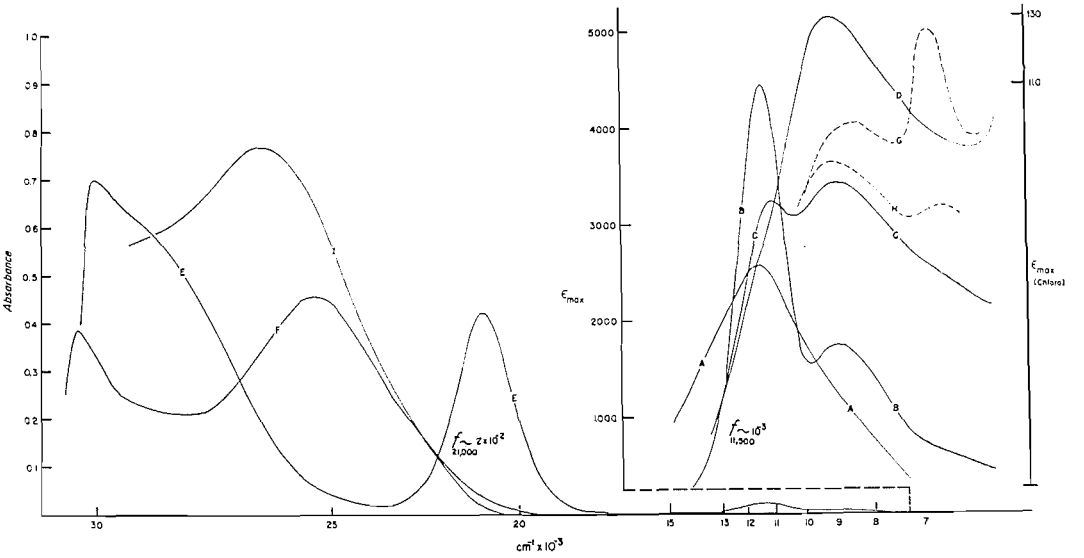


FIG. 2. Spectra of tetrahedral complexes.

	$[Cu^{2+}]_{total}$	$[Cl^-]/[Cu^{2+}]$
(A)	8×10^{-3} *M*	2
(B)	,,	8
(C)	,,	120
(D)	,,	610
(E)	2×10^{-4}	26 } note change of scale for ϵ_{max}
(F)	,,	12 000 }
(G)	$> 4 \times 10^{-3}$ *M*, acetone solution, 3.3 *M* in HBr	
(H)	2.5×10^{-3} *M*, 8.2 *M* HBr (aqueous)	
(I)	2×10^{-4} *M*, $CuCl_2.2H_2O$ in 12 *M* HCl.	

assume that they are due to electronic transitions from ligand orbitals to orbitals centered on coppers. It is to be noted that the band at approximately 21 000 cm^{-1} (475 mμ) is not apparent until $[Cl^-]/[Cu^{2+}]$ exceeds 1:1; this band will be discussed more fully later in the paper.

Equilibrium Involving Four-, Five-, and Six-Coordinate Complexes

Pseudo-Octahedral Complex

Figure 3*b* shows the variation in absorbance at 11 500 cm^{-1} (see also B of Fig. 2) with the ratio $[Cl^-]/[Cu^{2+}]$; the plot indicates that the absorbing species contains four chlorines per copper. There seems to be little doubt that the complex is approximately octahedral and thus it can be formulated as $[CuCl_4(ac)_2]^{2-}$. From Fig. 1 it is evident that Δ_{oct} of this species is 1 000 cm^{-1} smaller than that of $[Cu(OH_2)_4(ac)_2]^{2+}$, i.e. an average decrease of 250 cm^{-1} for each chlorine.

The band maxima between 12 200 and 11 500 cm^{-1} in Fig. 1 are probably due to distorted octahedral complexes containing two and three chlorines per copper.

The oscillator strength, *f*, of the 11 500 cm^{-1} transition is approximately 10^{-3}, as calculated from the expression $f = 4.6 \times 10^{-9}\ \epsilon_{max}\ \nu^{1/2}$ ($\nu^{1/2}$ is the band width where $\epsilon_\nu = \frac{1}{2}\epsilon_{max}$) (16), and this is appropriate for an octahedral complex (cf. $\sim 7 \times 10^{-4}$ for $[Cu(OH_2)_4(ac)_2]^{2+}$).

The value of the oscillator strength and the relatively high degree of symmetry of the band at 11 500 cm^{-1} are indicative of a complex of high octahedral symmetry, one in

Can. J. Chem. Downloaded from www.nrcresearchpress.com by 210.87.254.6 on 09/05/12
For personal use only.

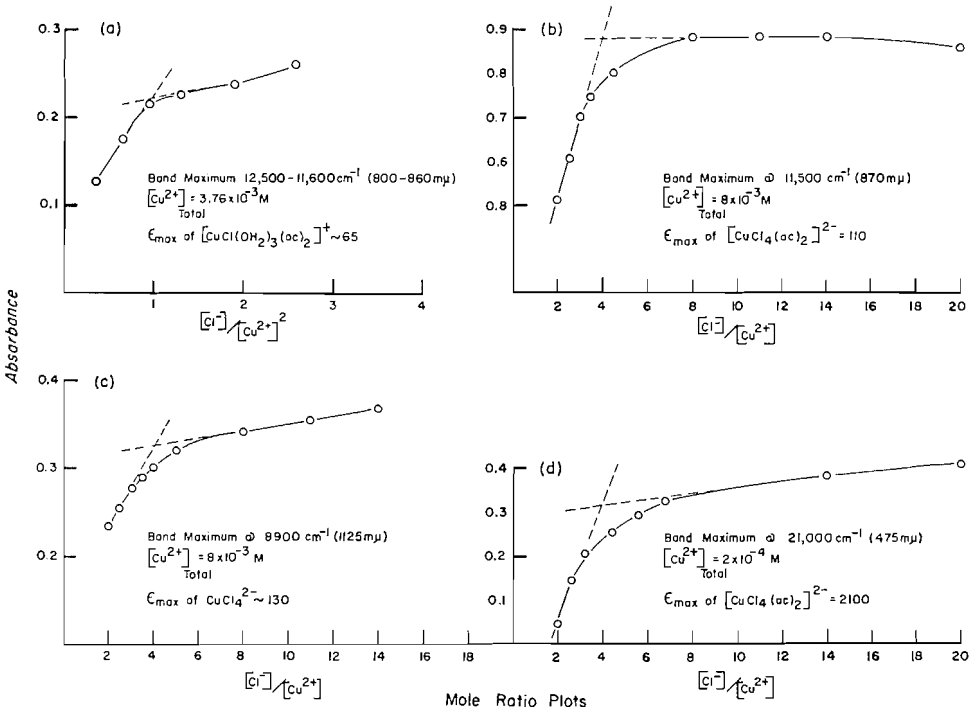


FIG. 3. Mole ratio plots.

which the four halide ions bind in a square plane. This is in accord with the previous findings that singly charged ligands are similarly bound (17).

Pseudo-Tetrahedral Complex

Spectrum B in Fig. 2 shows that even at relatively low values of $[Cl^-]/[Cu^{2+}]$, an appreciable proportion of the copper in the system is present as a species with an absorbance maximum at approximately 8 900 cm^{-1}. As indicated by the mole ratio plot in Fig. 3*c*, this band is also due to a 4:1 complex. The d-orbital splitting interval, Δ, for this complex is appreciably less than that for the pseudo-octahedral species described above, but it is larger than that calculated ($\sim$ 5 800 cm^{-1}) from theoretical considerations based on a tetrahedral model (11). It is known (1, 3, 6) that in certain systems $CuCl_4^{2-}$ is distorted, tending toward a planar structure; because of this distortion a value greater than Δ_{tetr} is to be expected for the complex. Therefore, it is reasonable to assume that the 8 900 cm^{-1} band is due to a complex having distorted tetrahedral symmetry. The change in absorbance at 8 900 and 11 500 cm^{-1} with variation in chloride ion concentration strongly suggests the existence of an equilibrium between the four- and six-coordinate species.

The asymmetry of the 8 900 cm^{-1} band (see D, especially in Fig. 2) indicates that there is one or more components at lower energies (the result of factors that cause further splitting of the d-orbital energy levels). As we will see later, the d–d band of tetrahedral $CuBr_4^{2-}$ (G and H in Fig. 2) in acetone media can be resolved into two peaks and there is reason to believe that the spectrum of $CuCl_4^{2-}$ would be analogous if it could be examined at sufficiently low energy. By extrapolation of spectrum D it is estimated that the low energy peak would lie between 5 500 and 6 000 cm^{-1}. Such a spectrum would be very similar to that of $CuCl_4^{2-}$ in Cs_2CuCl_4 at room temperature, in which Ferguson (18) found

Can. J. Chem. Downloaded from www.nrcresearchpress.com by 210.87.254.6 on 09/05/12
For personal use only.

two major peaks at 9 050 and 5 550 cm^{-1}. (At 20 °K, Ferguson observed four d–d bands for the complex and made transition assignments for each.)

Close inspection of spectra B, C, and D of Fig. 2 reveals that the band maximum near 9 000 cm^{-1} (1 100 mμ) shifts slightly to higher energies in solutions that are relatively

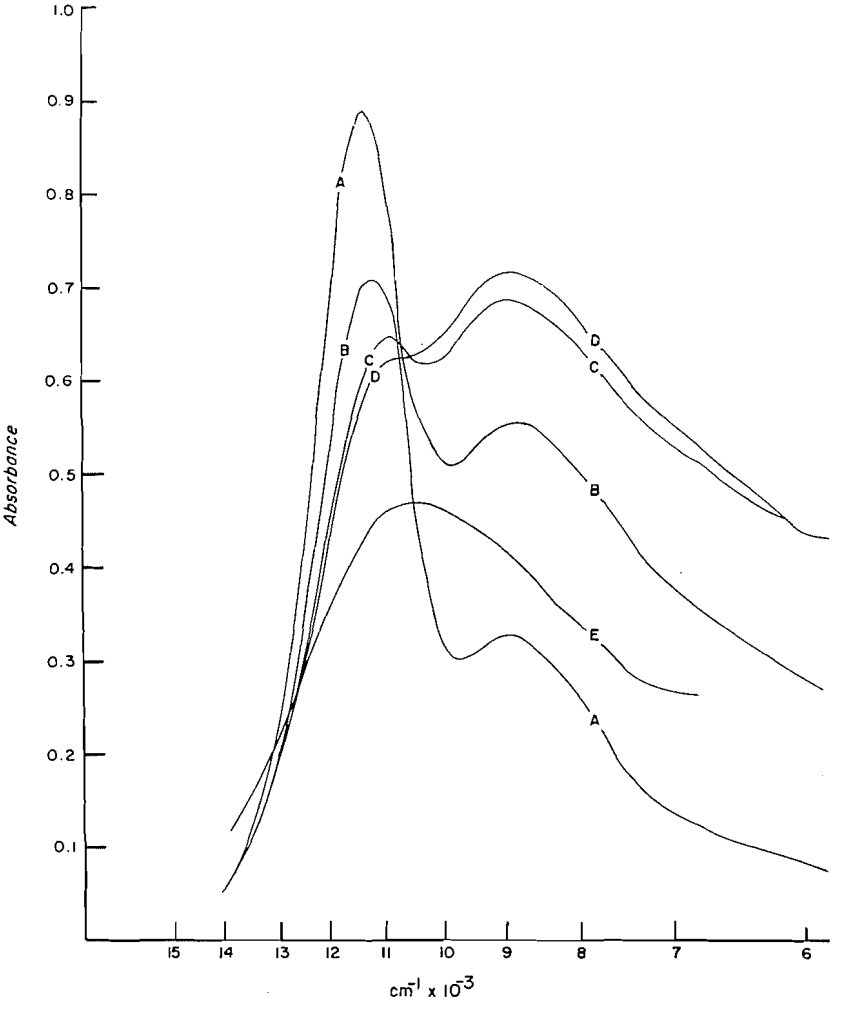


FIG. 4. d–d bands of hexa-, penta-, and tetra-coordinated species. $[Cu^{2+}]_{total} = 8 \times 10^{-3}$ *M*; $[Cl^-]/[Cu^{2+}]$ = (A) 8, (B) 62, (C) 120, (D) 154, and (E) 2×10^{-3} *M* solution of $CuCl_2.2H_2O$ in 12 *M* HCl.

concentrated with respect to hydrochloric acid (i.e. $> \sim 2$ *M*). This behavior is to be expected because such solutions contain enough water (from 12 *M* HCl) for it to compete effectively with chlorines for sites in the complex and thus the "blue shift" possibly represents the formation of a distorted tetrahedral complex having fewer than four chlorines per copper.

Evidence for Five-Coordinate Complex

At first glance, the shoulder in both spectra C and D of Fig. 4 appears to be a "remnant" of the d–d band of $[CuCl_4(ac)_2]^{2-}$. However, its maximum in D lies approximately 800 cm^{-1} lower than that of the six-coordinate complex, and, as we will see later (Fig. 5), its intensity is not consistent with the extinction coefficient of the band for $[CuCl_4(ac)_2]^{2-}$. Spectra C

Can. J. Chem. Downloaded from www.nrcresearchpress.com by 210.87.254.6 on 09/05/12
For personal use only.

and D in Fig. 4 intersect at an isobestic point at approximately 10 600 cm^{-1} and this clearly indicates that the shoulder is not due to the distorted tetrahedral complex. Therefore, from the above evidence, it seems necessary to invoke the existence of a third complex to account for the shoulder.

From Fig. 5 (the calculation of the values on the abscissa to be explained later) it is evident that when the total concentration of hydrochloric acid in the solution is 1–1.3 *M* (i.e. when $[Cl^-]/[Cu^{2+}]$ is 120–160) approximately 30% of Cu(II) is present as the pseudo-octahedral species $[CuCl_4(ac)_2]^{2-}$ with d–d band maximum at 11 500 cm^{-1}. The limiting value of the absorbance for this band is 0.89 (Figs. 2 and 3*b*) and therefore, in the mole ratio range mentioned above, it would be expected that the absorbance at the band maximum would be approximately 0.3 in the absence of other species absorbing appreciably at the same energy. However, the absorbance of the shoulder at 10 500 – 11 000 cm^{-1} in spectra C and D of Fig. 4 is over twice as high and this can be accounted for by the presence of a complex of appreciable intensity other than the six- and four-coordinate species already characterized.

It is tempting to postulate the existence of a five-coordinate complex (possibly pentachloro) as an "intermediate" in the overall structural transition from approximately octahedral $[CuCl_4(ac)_2]^{2-}$ to distorted tetrahedral $CuCl_4^{2-}$.

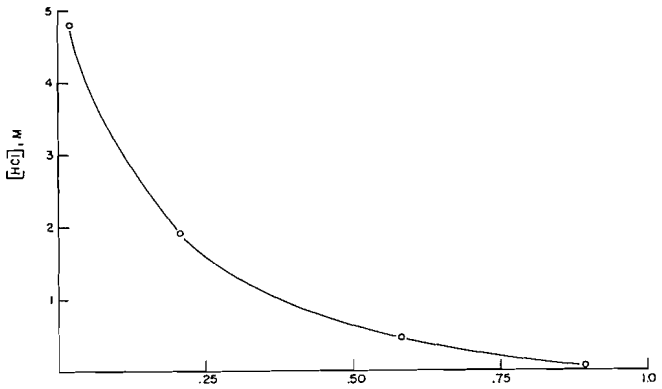


FIG. 5. Fraction of total copper present as $[CuCl_4(ac)_2]^{2-}$.

The $CuCl_5^{3-}$ ion (trigonal bipyramidal) has been identified in certain crystalline solids and its absorption spectrum shows a charge transfer band at approximately 27 000 cm^{-1} (19) and d–d bands at 10 400 and 8 200 cm^{-1} (20), the former being comparable to the shoulder of spectrum D at 10 700 cm^{-1}.

If it is assumed that the five-coordinate complex proposed in the present work is essentially trigonal bipyramidal, then consideration of a d-orbital splitting scheme for such a structure indicates that two bands due to the dx^2-y^2, $dxy \rightarrow dz^2$ and dxz, $dyz \rightarrow dz^2$ transitions should occur in the spectrum (21). It is also reasonable to expect that the band resulting from the latter transition (the higher energy of the two) should lie between those of the distorted octahedral and tetrahedral tetrachloro complexes. If the 10 700 cm^{-1} shoulder is taken to be due to the dx^2-y^2, $dxy \rightarrow dz^2$ transition, then the band due to the dxz, $dyz \rightarrow dz^2$ transition can be calculated to lie at approximately 8 500 cm^{-1}; however, at this energy it would be largely obscured by the band due to the pseudo-tetrahedral tetrachloro complex in spectra C and D of Fig. 4.

Of considerable interest are the spectra of solutions of $CuCl_2.2H_2O$ in 12 *M* HCl shown

Can. J. Chem. Downloaded from www.nrcresearchpress.com by 210.87.254.6 on 09/05/12
For personal use only.

in Figs. 2(I) and 4(E). These show, respectively, a charge transfer band at approximately 27 000 cm^{-1} and a d–d band at approximately 10 500 cm^{-1}; thus one is led to conclude that, in the solutions studied, an appreciable proportion of the copper probably existed as $CuCl_5^{3-}$. The asymmetry of the d–d band may be due to the dx^2-y^2, $dxy \rightarrow dz^2$ transition in $CuCl_5^{3-}$ and (or) to a "contribution" from the distorted $CuCl_4^{2-}$.

Charge Transfer Bands

Charge transfer bands in the spectra of the tetrachlorocopper(II) complexes in the visible to near ultraviolet region are shown in Fig. 2 (E and F).

The mole ratio plot in Fig. 3*d* indicates that the complex responsible for the 21 000 cm^{-1} (475 mμ) band has four chlorines per copper and this is in agreement with the findings of Gažo (13) but not those of Furlani and Morpurgo (6). Because the band rises and falls in concert with the d–d band at 11 500 cm^{-1}, it can be concluded that it is due to the complex $[CuCl_4(ac)_2]^{2-}$. From the estimated limiting value of the absorbance ($\sim$ 0.42) and the total copper concentration indicated in Fig. 3*d*, ϵ_{max}, at 21 000 cm^{-1}, is calculated to be approximately 2 100 l/mole cm. With this value together with absorbance readings at various hydrochloric acid concentrations, the proportion of the total copper in the system that is present as $[CuCl_4(ac)_2]^{2-}$ has been calculated from absorbance/2100$[Cu^{2+}]_{total}$. Figure 5 shows how this varies with the hydrochloric acid concentration.

Figure 2 shows that the 21 000 cm^{-1} band virtually disappears at high Cl^- concentrations and is replaced by a new charge transfer band at approximately 25 000 cm^{-1}. The new band is similar to, but of slightly lower energy than, that observed for chlorocopper(II) complexes at very high Cl^- concentration (9–12 *M*) in aqueous solutions. It is probable that the band is analogous to that found at 24 800 cm^{-1} by Ferguson (18) in the spectrum of tetrahedral $CuCl_4^{2-}$ in Cs_2CuCl_4.

The wedge-shaped band with a maximum between 30 000 and 32 000 cm^{-1} (and which appears to contain several components) also seems to be associated with the octahedrally coordinated complexes, for it appears at low $[Cl^-]/[Cu^{2+}]$ ratios and decreases in intensity in accord with the 21 000 and 11 500 cm^{-1} bands of $[CuCl_4(ac)_2]^{2-}$ at high ratios.

Bromocopper(II) Complexes in Acetone – Hydrobromic Acid Solutions

A brief spectrophotometric study was made of bromocopper(II) complexes formed in the copper perchlorate – acetone – hydrobromic acid (8.2 *M*) system. The following are some of the findings obtained with experimental techniques similar to those described earlier and their interpretation:

(*a*) When $[Br^-]/[Cu^{2+}] < \sim 1$, a relatively stable six-coordinate complex, $[CuBr(OH_2)_3(ac)_2]^+$, is formed. The d–d band of this complex has its maximum at 12 000 cm^{-1} (835 mμ) and $\epsilon_{max} \sim 60$ l/mole cm.

(*b*) Rapid reduction of Cu(II) to Cu(I) by Br^- occurs when $[Br^-]/[Cu^{2+}]$ is in the range 1–150 (i.e. when [HBr] = 0.01–1.5 *M*) and thus it is possible to obtain only semi-quantitative spectral data, at best. However, the transient spectra of the green solutions produced under these conditions show a low-intensity band between 11 800 and 11 100 cm^{-1} (845–900 mμ). By analogy to the chloride system, it is felt that absorption in this region is due to pseudo-octahedral species containing from two to four bromines per copper and these complexes are unstable with respect to cuprous complexes (probably tetrahedral).

Barnes and Hume (5) found a band maximum at about 11 000 cm^{-1} in the spectrum of the green species in acetone solutions and they ascribed this band to the complex "$CuBr_3^-$.2 solvent". In view of the present findings, it seems more probable that the complex is $[CuBr_4(ac)_2]^{2-}$.

Can. J. Chem. Downloaded from www.nrcresearchpress.com by 210.87.254.6 on 09/05/12
For personal use only.

(*c*) At high hydrobromic acid concentrations (1.5 to at least 3.5 *M*) a purple complex, presumably tetrahedral $CuBr_4^{2-}$ (5), is formed. Compared with the six-coordinate 1:2, 1:3, and 1:4 bromo complexes the purple species seems to be relatively stable to reduction by Br^-.

The d–d bands (G and H of Fig. 2) of the $CuBr_4^{2-}$ complex show two peaks that lie somewhat closer together in acetone – hydrobromic acid solutions than in 8.2 *M* hydrobromic acid. The peaks are similar to those observed in the spectrum of $CuCl_4^{2-}$ in $CsCuCl_4$ (18).

(*d*) The spectra of acetone solutions of Cu(II) containing hydrobromic acid in intermediate concentrations reveal maxima at both approximately 11 000 and 8 400 cm^{-1} thus suggesting that the system is directly analogous to that of the chlorocopper(II) complexes, i.e. there is an equilibrium between six- and four-coordinate tetrabromocopper(II) complexes.

It is noteworthy that the ligand field bands of the octahedral and the high-energy component of the band of tetrahedral bromocopper complexes appear at lower energies than those of the corresponding chloro complexes and this is to be expected from the position of the halogens in the spectrochemical series.

Previously it was mentioned that octahedral bromocopper(II) complexes containing more than one bromine are unstable with respect to reduction to cuprous species. The reduction process also results in the formation of a tetrahedral structure (22) in which Cu(I) exists as a d^{10} ion with all electrons occupying relatively stable orbitals. It is probable that charge transfer processes in $[CuBr_4(ac)_2]^{2-}$ are more efficient than in $[CuCl_4(ac)_2]^{2-}$ since the lowest energy charge transfer bands observed for these complexes appear at approximately 15 000 and 21 000 cm^{-1} respectively; this accounts for the greater stability of the pseudo-octahedral tetrachlorocopper(II) species with respect to reduction of copper.

TABLE I

Correlation of spectral data and structure of chloro- and bromo-copper(II) complexes

Absorbing species	Maximum of d–d band (cm^{-1})	Approx. ϵ_{max} (l/mole cm)	Structure	Source
$CsCd_{1-x}(Cu)_2Cl_3(CuCl_6^{4-})$	12 400	—	Distorted octahedron	(3)
$[Cu(OH_2)_4(ac)_2]^{2+}$	12 500	27	,,	This work
$[CuCl(OH_2)_3(ac)_2]^{+}$	12 200	65	,,	,,
$[CuBr(OH_2)_3(ac)_2]^{+}$	12 000	60	,,	,,
$[CuCl_4(ac)_2]^{2-}$	11 500	110	,,	,,
$[CuBr_4(ac)_2]^{2-}$	~11 000	—	,,	,,
$CuBr_3^-$.2 solvent (acetone)	~11 400	160	Trigonal bipyramid	(5)
$CuCl_4^{2-}$ in LiCl–KCl at 800 °C	9 000	—	Distorted tetrahedron	(3)
$CuCl_4^{2-}$ in Cs_2CuCl_4	9 050 and		,,	(18)
	5 550		,,	(18)
$CuCl_4^{2-}$ in acetone–HCl	8 900 and	130	,,	This work
	5 500–6 000	~100	,,	,,
$CuBr_4^{2-}$ in acetone–HBr	8 400 and	100–150	,,	,,
	6 900	100–150	,,	,,
$CuBr_4^{2-}$ in various coordinating solvents	9 100	160	,,	(5)
$[R_4N]_2CuBr_4$	9 100		,,	(5)
$[Co(NH_3)_6][CuCl_5]$	10 400 and		Trigonal bipyramid	(20)
	8 200		,,	(20)
$CuCl_5^{3-}$ in acetone–HCl (tentative)	~10 700			This work

Can. J. Chem. Downloaded from www.nrcresearchpress.com by 210.87.254.6 on 09/05/12
For personal use only.

Comparison of Spectra of Halogenocopper(II) Complexes in Acetone Solution with Those in Chloride Melts and Crystalline Solids

For comparison purposes, spectral and structural data from the present study and from various other sources, previously cited, are listed in Table I.

The results of the present study, indicating an equilibrium between six- and four-coordinate tetrachloro (bromo) Cu(II) complexes in an acetone medium, are similar to those of Gruen and McBeth (3), who studied the absorption spectra of Cu^{2+} in LiCl–KCl melts. However, Gruen and McBeth did not find evidence for, or postulate the presence of, a five-coordinate complex participating in the equilibrium.

The halide ion activity in acetone – concentrated hydrochloric acid mixtures, having a final concentration of approximately 1–4 *M* for the acid, is comparable to that in chloride melts such as those used by Gruen and McBeth. For example, these workers estimate that the ratio of the concentrations of the tetrahedral and octahedral chlorocopper species in a LiCl–KCl melt at 1 000 °K is 2.2. In the present work (Fig. 4) this ratio corresponds to a solution in which the total molar concentration of hydrochloric acid is 1–1.5 *M*.

ACKNOWLEDGMENT

The author wishes to express appreciation to Dr. P. G. Manning for his sincere interest and for his valuable advice during the course of this work.

REFERENCES

1. L. Helmholz and R. F. Kruh. J. Am. Chem. Soc. **74**, 1176 (1952).
2. N. S. Gill and R. S. Nyholm. J. Chem. Soc. 3997 (1959).
3. D. M. Gruen and R. L. McBeth. Pure Appl. Chem. **6**, 23 (1963).
4. G. P. Smith and T. R. Griffiths. J. Am. Chem. Soc. **85**, 4051 (1963).
5. J. C. Barnes and D. N. Hume. Inorg. Chem. **2**, 444 (1963).
6. C. Furlani and G. Morpurgo. Theoret. Chim. Acta Berlin, **1**, 102 (1963).
7. I. I. Antipova-Karataeva and E. E. Vainshtein. Russ. J. Inorg. Chem. English Transl. **6**, 569 (1961).
8. C. J. Ballhausen. Ligand field theory. McGraw-Hill Book Co., Inc., New York and London. 1962. p. 272.
9. J. Bjerrum, C. J. Ballhausen, and C. K. Jorgenson. Acta Chem. Scand. **8**, 1275 (1954).
10. T. M. Dunn. *In* Modern coordination chemistry. *Edited by* J. Lewis and R. G. Wilkins. Interscience Publishers, Inc., New York. 1958. p. 241.
11. G. Felsenfeld. Proc. Roy. Soc. London, Ser. A, **236**, 506 (1956).
12. C. J. Ballhausen and A. D. Liehr. J. Mol. Spectry. **2**, 342 (1958).
13. J. Gažo. Chem. Zvesti, **10**, 509 (1956).
14. K. B. Yatsimirskii and T. V. Malkova. Russ. J. Inorg. Chem. English Transl. **6**, 426 (1961).
15. N. J. Friedman and R. A. Plane. Inorg. Chem. **2**, 11 (1963).
16. C. J. Ballhausen. Progress in inorganic chemistry. Vol. II. *Edited by* F. A. Cotton. Interscience Publishers, Inc., New York. 1960. p. 253.
17. P. G. Manning. Can. J. Chem. **43**, 3258 (1965).
18. J. Ferguson. J. Chem. Phys. **40**, 3406 (1964).
19. M. Mori. Bull. Chem. Soc. Japan, **34**, 454 (1961).
20. W. E. Hatfield and T. S. Piper. Inorg. Chem. **3**, 841 (1964).
21. J. J. Zuckerman. J. Chem. Educ. **42**, 315 (1965).
22. A. F. Wells. Structural inorganic chemistry. Oxford University Press, London. 1961. p. 337.

Can. J. Chem. Downloaded from www.nrcresearchpress.com by 210.87.254.6 on 09/05/12
For personal use only.

Can. J. Chem. Downloaded from www.nrcresearchpress.com by 210.87.254.42 on 09/05/12
For personal use only.

ION–MOLECULE REACTIONS IN METHYL ALCOHOL AND METHYL-d_3 ALCOHOL

J. C. J. THYNNE,[1] F. K. AMENU-KPODO, AND A. G. HARRISON
Department of Chemistry, University of Toronto, Toronto, Ontario

Received March 10, 1966

ABSTRACT

The rate constants for the hydrogen-transfer ion–molecule reactions

[*a*] $CH_3OH^+ + CH_3OH \rightarrow CH_3OH_2^+ + CH_3O$ (or CH_2OH)

[*b*] $CH_2OH^+ + CH_3OH \rightarrow CH_3OH_2^+ + CH_2O$

have been measured at thermal ion energies and found to be 12×10^{-10} cm^3 molecule^{-1} s^{-1} and 8.0×10^{-10} cm^3 molecule^{-1} s^{-1} respectively. The rate coefficients at higher ion energies (3.7 eV ion exit energy) show little change from these values. Reactions [*a*] and [*b*] have also been studied using CD_3OH and it is found that in reaction [*a*] the hydroxyl hydrogen is transferred 2.5 times more readily at low ion energies and 1.8 times more readily at high ion energies than a methyl hydrogen. This rather small specificity would appear to preclude formation of a "locked-in" collision complex even at low ion energies.

INTRODUCTION

Although the ion–molecule reaction producing $CH_3OH_2^+$ in the high-pressure mass spectrum of methyl alcohol originally was assumed (1, 2) to be

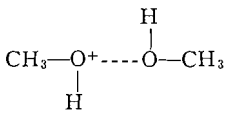
[1] $$CH_3OH^+ + CH_3OH \rightarrow CH_3OH_2^+ + CH_2OH \text{ (or } CH_3O),$$

Moran and Hamill (3) have shown that the apparent cross section decreases with decreasing electron energy, near the threshold, indicating reactions involving ions with appearance potentials higher than that of CH_3OH^+. Lindholm and Wilmenius (4, 5), using mass spectrometric selection of the reactant ions, observed both reaction [1] and reaction [2]

[2] $$CH_2OH^+ + CH_3OH \rightarrow CH_3OH_2^+ + CH_2O$$

in methyl alcohol. More recently, Ryan *et al.* (6) have re-investigated the reactions in methyl alcohol and methyl-d_3 alcohol using conventional mass spectrometric techniques and have reported cross sections for both reactions [1] and [2].

Our interest in the methyl alcohol system arose from the fact that the reactant species contain non-equivalent hydrogens and as a result one might expect to observe selectivity in the transfer reactions. In particular, the CH_3OH^+ ion is formed by removal of a non-bonding oxygen electron and ion–dipole interaction of this species with the polar CH_3OH molecule might be expected to lead to a collision complex (Structure I) in which the two hydroxyl groups are adjacent. Such a "locked-in" complex, if formed, would be



I

more probable at low ion energies, since as the ion energy increases a random orientation in the collision complex would be anticipated. In such a "locked-in" complex one would anticipate predominately hydroxyl-hydrogen transfer, whereas a random orientation of

[1]*Visiting Scientist. Permanent Address: Department of Chemistry, University of Edinburgh, Edinburgh, Scotland.*

the complex (at higher ion energies) or a stripping mechanism would probably result in a much less specific hydrogen transfer. Thus one might anticipate predominate hydroxyl-hydrogen transfer at low (or thermal) ion energies with this specificitiy decreasing to essentially a random selection of hydrogens as the ion energy increases. This argument presupposes that no other factors such as bond dissociation energies determine the detailed course of the reaction.

The hydrogen transferred in reaction [1] can be determined by suitable deuterium labelling and some experiments along these lines have been carried out. Using a preselected beam of CD_3OH^+ impinging on CD_3OH, Lindholm and Wilmenius (5) found $I_{CD_3OH_2^+}/I_{CD_3OHD^+} = 0.66$ at a reactant ion energy of 5 eV. Ryan *et al.* (6) report that reaction [1] in CD_3OH leads to $I_{CD_3OH_2^+}/I_{CD_3OHD^+} = 0.92$. This ratio represents a mean value for reaction of ions with energies ranging from zero to the final exit energy of 2.3 eV. Although the latter workers reported that no variation of the ratio with ion exit energy could be observed, a more detailed investigation, particularly at low ion energies, appeared desirable. We therefore have undertaken a detailed study of the ion–molecule reactions in CH_3OH and CD_3OH at thermal ion energies and over a range of repeller voltages corresponding to a range of final ion energies. The reactions were studied at thermal energies using the pulsing techniques previously described (7, 8), while for ions accelerated by the repeller field the ratio plot technique (9) was used to estimate the contributions of the various reactions occurring.

EXPERIMENTAL

The mass spectrometer used was an A.E.I. MS-2 instrument modified as previously described (7). The techniques for determining kinetic data for reactions of thermal energy ions have been adequately described (7, 8) as has the use of the ratio plot technique (9) for the study of concurrent reactions under conditions of constant ion acceleration.

The methyl alcohol used was a reagent grade sample. The methyl-d_3 alcohol was obtained from Merck Sharp and Dohme, Montreal, and had an isotopic purity of ~99% as determined by low-energy analysis.

RESULTS AND DISCUSSION

For the two concurrent reactions, [1] and [2], studied under conditions of constant ion acceleration, the total secondary ion current, $I_{CH_3OH_2^+}$, is given by eq. [3] where Q_X is the macroscopic cross section for reaction [X], d is the distance of reactant ion travel in the ion source, and the square brackets denote concentrations in units molecule cm^{-3}. In formulating eq. [3] we have neglected the small differences (9) in collection efficiencies.

$$[3] \qquad I_{CH_3OH_2^+} = Q_1 d[CH_3OH] I_{CH_3OH^+} + Q_2 d[CH_3OH] I_{CH_2OH^+}$$

Division of eq. [3] by $I_{CH_3OH^+}$ yields eq. [4]

$$[4] \qquad \frac{I_{CH_3OH_2^+}}{I_{CH_3OH^+}} = Q_1 d[CH_3OH] + Q_2 d[CH_3OH] \frac{I_{CH_2OH^+}}{I_{CH_3OH^+}}$$

which predicts that a plot of $I_{CH_3OH_2^+}/I_{CH_3OH^+}$ versus $I_{CH_2OH^+}/I_{CH_3OH^+}$ should yield a straight line with the relevant cross sections being obtainable from the slope and intercept. Division of eq. [3] by $I_{CH_2OH^+}$ leads to an analogous equation, and in practice the experimental data were analyzed by both equations.

Figure 1 shows typical results obtained for CH_3OH at 10.5 V cm^{-1} repeller (3.7 eV ion exit energy) plotted in the manner indicated by eq. [4]. The ion current ratios were varied by changing the ionizing electron energy and all measurements were made at energies where only CH_2OH^+ and CH_3OH^+ were significant primary ions. The non-zero intercept and slope clearly show the occurrence of both reactions [1] and [2]. The $CH_3OH_2^+$

Can. J. Chem. Downloaded from www.nrcresearchpress.com by 210.87.254.42 on 09/05/12
For personal use only.

ion current at $m/e = 33$ has not been corrected for $^{13}CH_3OH^+$ with the result that the intercept of Fig. 1 actually gives $0.011 + Q_1d[CH_3OH]$. Table I summarizes the experimental cross sections obtained by least squares analysis and the rate constants calculated by the relation (10)

$$[5] \qquad k = \frac{Qd}{\tau},$$

where τ is the primary ion residence time.

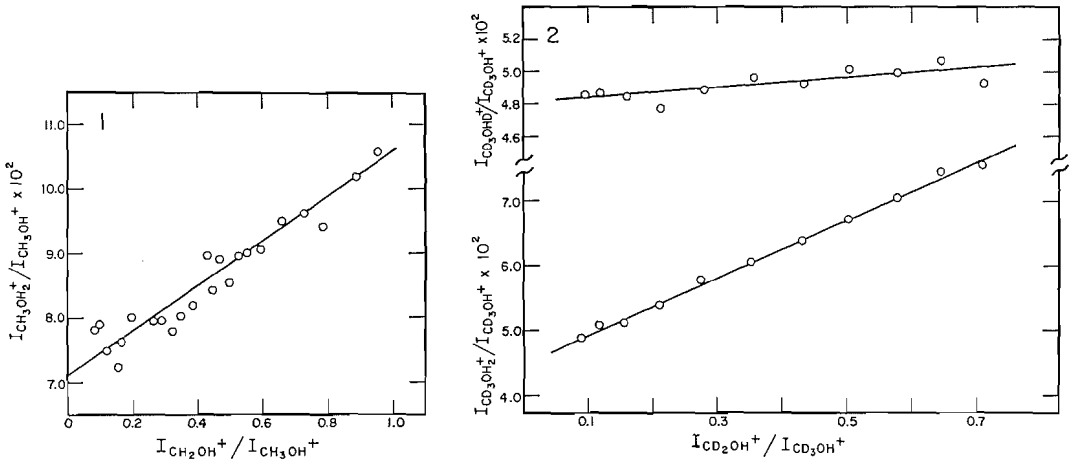


FIG. 1. Ratio plot for CH_3OH.
FIG. 2. Ratio plots for CD_3OH.

TABLE I

Cross sections and derived rate constants at 3.7 eV ion energy

	Reaction	Q (cm^2 molecule^{-1} $\times 10^{10}$)	k (cm^3 molecule^{-1} $s^{-1} \times 10^{10}$)
[1]	$CH_3OH^+ + CH_3OH \rightarrow CH_3OH_2^+ + CH_3O$ (CH_2OH)	62.3	14.6
[2]	$CH_2OH^+ + CH_3OH \rightarrow CH_3OH_2^+ CH_2O$	34.9	8.3_5
[6]	$CD_3OH^+ + CD_3OH \rightarrow CD_3OH_2^+ + CD_3O$	28.2±0.6	6.3_0
[7]	$CD_3OH^+ + CD_3OH \rightarrow CD_3OHD^+ + CD_2OH$	36.9±0.2	8.2_5
[8]	$CD_2OH^+ + CD_3OH \rightarrow CD_3OH_2^+ + CD_2O$	29.3±0.7	6.6_8
[9]	$CD_2OH^+ + CD_3OH \rightarrow CD_3OHD^+ + CDOH$	2.0±0.3	0.4_5

In CD_3OH both $CD_3OH_2^+$ and CD_3OHD^+ are observed as the products of ion–molecule reactions. Since the ion corresponding to CH_2OH^+ is predominately (>95%) CD_2OH^+ in the labelled alcohol, only the following four reactions need be considered at low electron energies.

$$[6] \qquad CH_3OH^+ + CD_3OH \rightarrow CH_3OH_2^+ + CD_3O$$

$$[7] \qquad CD_3OH^+ + CD_3OH \rightarrow CD_3OHD^+ + CD_2OH$$

$$[8] \qquad CD_2OH^+ + CD_3OH \rightarrow CD_3OH_2^+ + CD_2O$$

$$[9] \qquad CD_2OH^+ + CD_3OH \rightarrow CD_3OHD^+ + CDOH$$

Can. J. Chem. Downloaded from www.nrcresearchpress.com by 210.87.254.42 on 09/05/12
For personal use only.

A treatment similar to the above leads to the following ratio equations for $I_{CD_3OH_2^+}$ and $I_{CD_3OHD^+}$.

$$[10] \qquad \frac{I_{CD_3OH_2^+}}{I_{CD_3OH^+}} = Q_6 d[CD_3OH] + Q_8 d[CD_3OH]\frac{I_{CD_2OH^+}}{I_{CD_3OH^+}}$$

$$[11] \qquad \frac{I_{CD_3OHD^+}}{I_{CD_3OH^+}} = Q_7 d[CD_3OH] + Q_9 d[CD_3OH]\frac{I_{CD_2OH^+}}{I_{CD_3OH^+}}$$

Figure 2 shows typical results obtained for the CD_3OH system plotted in the manner of eqs. [10] and [11]. The cross sections obtained by least squares analysis are summarized in Table I, where the limits of error represent the mean deviation of three separate runs. The results show that the CD_2OH^+ ion transfers predominately the hydroxyl hydrogen, in agreement with earlier conclusions (5).

The results for the labelled and unlabelled alcohols are internally consistent and any small differences should not be attributed to isotopic effects since the results were obtained some months apart and experimental conditions may have changed slightly. The present value for k_1 is considerably lower than the value of 24.5×10^{10} cm^3 molecule^{-1} s^{-1} reported by Ryan *et al.* (6) although our ratio $k_6/k_7 = 0.767$ is in reasonable agreement with their value of 0.92. The reasons for the discrepancies in the rate coefficients are not apparent. For reaction [2] our rate constant of $8.3_5 \times 10^{-10}$ cm^3 molecule^{-1} s^{-1} is in reasonable agreement with Ryan *et al.*'s value of 6.8×10^{-10} cm^3 molecule^{-1} s^{-1}.

The rate coefficients for the reactions of thermal energy ions were obtained by the pulsing techniques described previously (7, 8), where reaction time is the experimental variable. For the unlabelled alcohol the total secondary ion current observed after a time delay, t, between the ionizing and ion withdrawal pulses can be expressed as follows (for a small extent of reaction)

$$[12] \qquad I_{CH_3OH_2^+} = (k_1[CH_3OH]I_{CH_3OH^+} + k_2[CH_3OH]I_{CH_2OH^+})t + C$$

where k_1 and k_2 are the thermal rate constants for reactions [1] and [2] and C is a constant reflecting the $CH_3OH_2^+$ formed during the ionizing and withdrawal pulses. Rearrangement of eq. [12] gives

$$[13] \qquad \frac{I_{CH_3OH_2^+}}{I_{CH_3OH^+}} = \left(k_1[CH_3OH] + k_2[CH_3OH]\frac{I_{CH_2OH^+}}{I_{CH_3OH^+}}\right)t + C'$$

which predicts that the slopes of the experimental $I_{CH_3OH_2^+}/I_{CH_3OH^+}$ versus t plots should be a linear function of the reactant ion current ratio $I_{CH_2OH^+}/I_{CH_3OH^+}$ at constant ion source concentration. Figure 3 shows typical results obtained for CH_3OH and shows the increase in slope with increasing primary ion current ratio. This ratio was varied by changing the ionizing electron energy and was independent of delay time over the time range covered. The experimental slopes are shown in Fig. 4 plotted against the ratio $I_{CH_2OH^+}/I_{CH_3OH^+}$. Although the scatter is rather large a satisfactory least squares line can be drawn. Two such determinations yielded the values of k_1(thermal) and k_2(thermal) tabulated in Table II.

For the $CD_3OH_2^+$ and CD_3OHD^+ ions formed in CD_3OH, eqs. [14] and [15] can be written expressing the time dependence of the ion current ratios.

$$[14] \qquad \frac{I_{CD_3OH_2^+}}{I_{CD_3OH^+}} = \left(k_6[CD_3OH] + k_8[CD_3OH]\frac{I_{CD_2OH^+}}{I_{CD_3OH^+}}\right)t + B$$

$$[15] \qquad \frac{I_{CD_3OHD^+}}{I_{CD_3OH^+}} = \left(k_7[CD_3OH] + k_9[CD_3OH]\frac{I_{CD_2OH^+}}{I_{CD_3OH^+}}\right)t + B'$$

Can. J. Chem. Downloaded from www.nrcresearchpress.com by 210.87.254.42 on 09/05/12
For personal use only.

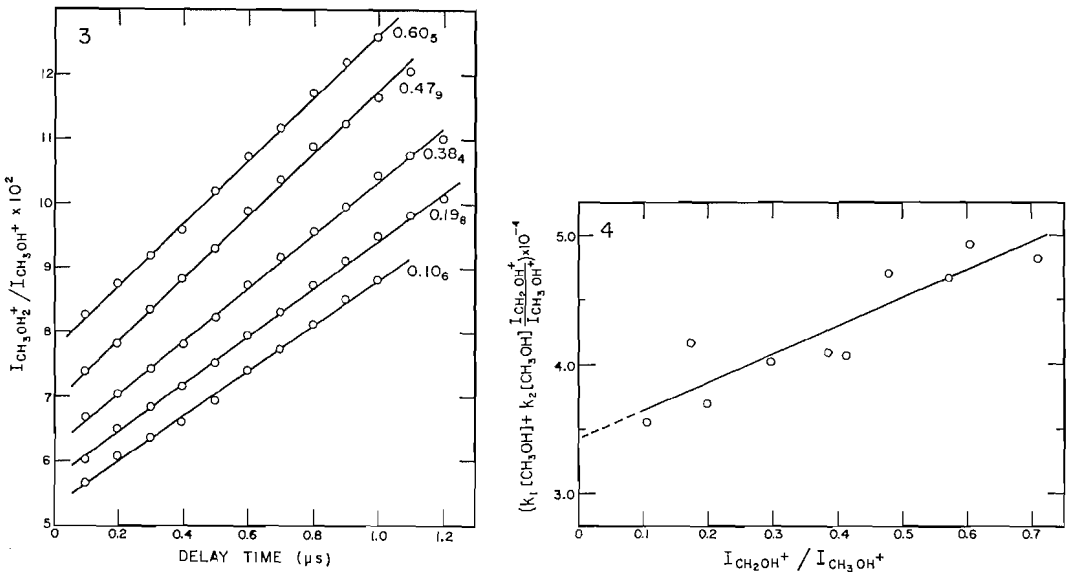


FIG. 3. $I_{CH_3OH_2^+}/I_{CH_3OH^+}$ versus delay time for CH_3OH. The successive plots are displaced upwards for clarity. The numbers give the $I_{CH_2OH^+}/I_{CH_3OH^+}$ ratio.
FIG. 4. Analysis of delay time plots for CH_3OH.

TABLE II
Rate constants at thermal ion energies

	Reaction	k(thermal) (cm^3 molecule^{-1} $s^{-1} \times 10^{10}$)	k(10.5 V/cm) (cm^3 molecule^{-1} $s^{-1} \times 10^{10}$)
[1]	$CH_3OH^+ + CH_3OH \rightarrow CH_3OH_2^+ + CH_3O$ (CH_2OH)	13.4_4, 10.9_8	14.6
[2]	$CH_2OH^+ + CH_3OH \rightarrow CH_3OH_2^+ + CH_2O$	8.5_6, 7.3_7	8.3_5
[6]	$CD_3OH^+ + CD_3OH \rightarrow CD_3OH_2^+ + CD_3O$	4.7_8, 5.1_6	6.3_0
[7]	$CD_3OH^+ + CD_3OH \rightarrow CD_3OHD^+ + CD_2OH$	6.0_7, 5.9_1	8.2_5
[8]	$CD_2OH^+ + CD_3OH \rightarrow CD_3OH_2^+ + CD_2O$	7.0_9, 7.2_9	6.6_8
[9]	$CD_2OH^+ + CD_3OH \rightarrow CD_3OHD^+ + CDOH$	0.01, 0.3	0.4_5

Typical results for $CD_3OH_2^+$ plotted in the form of eq. [14] are shown in Fig. 5 where the increase in slope with increasing $I_{CD_2OH^+}/I_{CD_3OH^+}$ is clearly evident. The slopes of such plots are shown in Fig. 6 plotted against the $I_{CD_2OH^+}/I_{CD_3OH^+}$ ratio. Also shown in Fig. 6 are the slopes of the experimental plots of eq. [15] as a function of the primary ion current ratio. The relevant rate constants obtained by least squares analyses of two sets of runs are summarized in Table II.

Again the results for the labelled and unlabelled alcohols are in reasonable agreement with each other. The thermal rate constants are compared in Table II with the rate constants derived from the data at 10.5 V/cm. On the whole the thermal rate constants are slightly lower than the 10.5 V/cm data. This result is in agreement with the results obtained previously (8) for the hydrogen transfer reactions in methane, CH_3CN, CH_3OCH_3, and some deuteriated equivalents.

The two sets of thermal data give $k_6/k_7 = 0.79$ and 0.87 while the average results at 3.7 eV ion exit energy $k_6/k_7 = 0.67$. Although these data suggest little change in the hydrogen selectivity with ion energy, a more extensive study of reactions [6], [7], and [8]

Can. J. Chem. Downloaded from www.nrcresearchpress.com by 210.87.254.42 on 09/05/12
For personal use only.

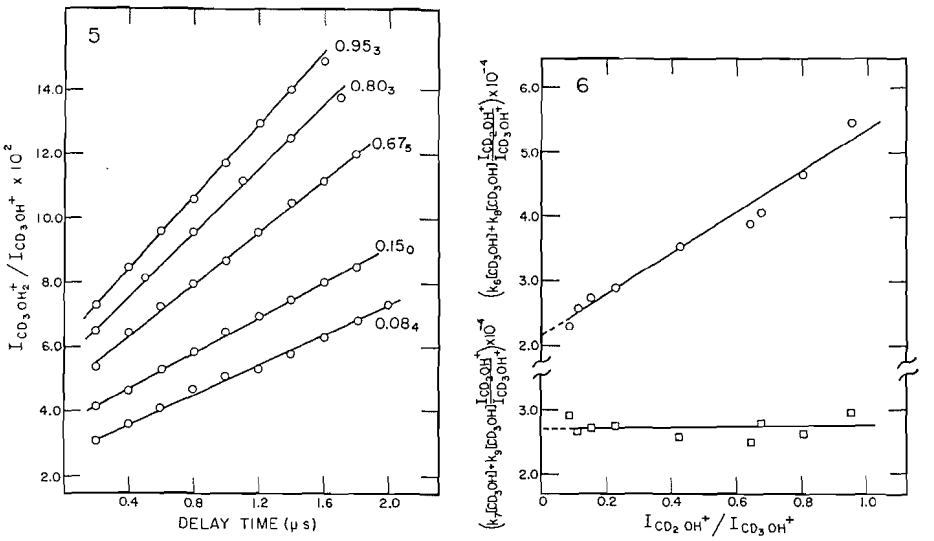


FIG. 5. $I_{CD_3OH_2^+}/I_{CD_3OH^+}$ versus delay time for CD_3OH. The successive plots are displaced upwards for clarity, and the numbers give the $I_{CD_2OH^+}/I_{CD_3OH^+}$ ratio.
FIG. 6. Analyses of delay time plots for CD_3OH.

was undertaken by the ratio plot technique over a range of repeller voltages from 4 V to 36 V. The cross sections obtained are summarized in Table III. As can be seen by the last column the ratio Q_6/Q_7 (and hence k_6/k_7) decreases from ~0.83 at the lowest ion exit energy to 0.59 at 13.3 V ion exit energy. Neglecting any isotopic effects and allowing for the 3:1 ratio of methyl to hydroxyl hydrogens, these results show that a hydroxyl hydrogen is transferred 2.5 times more readily at thermal and low ion energies and 1.8 times more readily at the highest ion exit energies than a methyl hydrogen. Although these results show a preference for hydroxyl-hydrogen transfer and also the expected trend with ion energy neither the magnitude of the rate constant ratio nor its energy dependence appear to be sufficiently large to support the suggestion of a "locked-in" collision complex. The factors which determine the hydrogen transferred would thus appear to other than the primary interaction forces. In this regard we might point out that reaction [2] (and the equivalent reactions [8] and [9]) involves exclusively the hydroxylic

TABLE III
Cross sections for reactions in CD_3OH as a function of ion exit energy

Ion exit energy (eV)	Q (cm² molecule⁻¹ × 10^{16})			
	Q_6	Q_7	Q_8	Q_6/Q_7
1.47	46.7	56.0	83.5	0.83
2.03	45.5	54.3	47.2	0.84
2.58	31.6	40.5	35.0	0.78
3.69	28.2	36.9	29.3	0.76
4.43	20.6	28.5	25.0	0.72
5.15	21.4	29.6	22.9	0.72
6.26	13.2	20.4	20.4	0.64
7.36	13.6	23.7	16.3	0.57
9.21	12.6	17.7	8.2_8	0.71
11.1	6.7	11.4	9.7_5	0.59
13.3	6.3	10.8	7.9_5	0.59

Can. J. Chem. Downloaded from www.nrcresearchpress.com by 210.87.254.42 on 09/05/12
For personal use only.

hydrogen and this is undoubtedly due to the greater stability of the $H_2C{=}O$ neutral compared to HC—OH. Further we have found (Thynne and Harrison. To be published) that the reaction analogous to reaction [1] in CH_3SH proceeds predominately by transfer of the mercaptyl hydrogen over the whole range of ion energies studied and in this case we would suggest that the specificity arises primarily from bond strength effects.

ACKNOWLEDGMENTS

The authors are indebted to the National Research Council of Canada for financial support through grant T-909 (to A. G. H.). F. K. A.-K. gratefully acknowledges financial support in the form of a Government of Ghana Scholarship and J. C. J. T. wishes to thank the Ramsay Memorial Fellowships Trust for financial aid.

REFERENCES

1. D. O. SCHISSLER and D. P. STEVENSON. J. Chem. Phys. **24**, 926 (1956).
2. D. P. STEVENSON. J. Phys. Chem. **61**, 1453 (1957).
3. T. F. MORAN and W. H. HAMILL. J. Chem. Phys. **39**, 1413 (1963).
4. P. WILMENIUS and E. LINDHOLM. Arkiv Fysik, **21**, 97 (1962).
5. E. LINDHOLM and P. WILMENIUS. Arkiv Kimi, **20**, 255 (1963).
6. K. R. RYAN, L. SIECK, and J. H. FUTRELL. J. Chem. Phys. **41**, 111 (1964).
7. T. W. SHANNON, F. MEYER, and A. G. HARRISON. Can. J. Chem. **43**, 159 (1965).
8. A. G. HARRISON, A. IVKO, and T. W. SHANNON. Can. J. Chem. **44**, 1351 (1966).
9. T. W. SHANNON and A. G. HARRISON. J. Chem. Phys. **43**, 4201 (1965).
10. G. GIOMOUSIS and D. P. STEVENSON. J. Chem. Phys. **29**, 294 (1958).

Can. J. Chem. Downloaded from www.nrcresearchpress.com by 210.87.254.42 on 09/05/12
For personal use only.

Can. J. Chem. Downloaded from www.nrcresearchpress.com by 210.87.254.105 on 09/05/12
For personal use only.

STUDIES OF THE DISSOCIATION OF OXIDE SURFACES AT THE LIQUID–SOLID INTERFACE[1]

SYED M. AHMED[2]
Mines Branch, Department of Mines and Technical Surveys, Ottawa, Canada

Received October 13, 1965

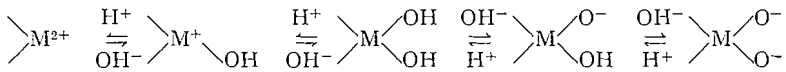
ABSTRACT

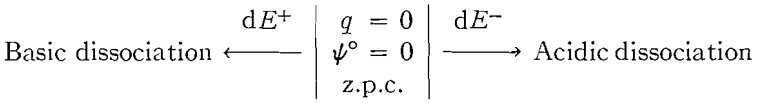
The dissociation of surface hydroxyl groups of crystalline SiO_2, ZrO_2, and ThO_2, in aqueous suspensions, has been studied as a function of pH_s at different ionic strengths of KNO_3. The surface groups of quartz dissociate as weak acids, while those of ZrO_2 and ThO_2 dissociate amphoterically. A reversible double layer is formed at the oxide–solution interface, and H^+ and OH^- function as the potential-determining ions. Quantitative data have been obtained on (*a*) surface charge densities, (*b*) zero point of charge, (*c*) differential capacities of the double layer on quartz and ZrO_2, and (*d*) the effect of surface charge density and ionic strength on the interfacial tension. The differential capacities indicate specific adsorption of NO_3^- on ZrO_2 and ThO_2 while NO_3^- has zero affinity for quartz surfaces. At low negative charge densities, solvated K^+ are adsorbed on quartz and ZrO_2 through coulombic interactions while at $pH_s > 10$ specific adsorption of K^+ predominates. ThO_2 appears to exhibit a greater tendency for the specific adsorption of K^+.

INTRODUCTION

The double layer at an oxide–solution interface can be investigated by studying the equilibrium distribution of the potential-determining ions (H^+ and OH^-) between the interface and the bulk solution, as a function of pH_s and ionic strength. The experimental and thermodynamic principles underlying this method are well established in the earlier works of others on AgI (1, 2), Ag_2S (3, 4), and Fe_2O_3 (5). The present work, using crystalline samples of quartz, ZrO_2, and ThO_2 of low and known surface areas, is based on similar principles but uses different techniques so as to minimize any secondary effects that may arise from slime formation and solubility of the material. The work is primarily aimed at deriving information on the nature of interactions at the interface from the double layer characteristics. The thermodynamic principles from this point of view are outlined below for the purpose of the discussion to follow.

The origin of charge ($\pm$) at an amphoteric oxide–solution interface may be attributed to the basic or acidic dissociation of the metal hydroxide groups on the surface. The equilibria are





The pH_s (6) at which the surface is undissociated is the zero point of charge (z.p.c.), where the charge density q is zero. It is seen from the above equilibria that addition of the oxide to a solution in the region of acidic dissociation will decrease the pH_s of the bulk solution and the surface will have a negative charge. In the region of basic dissociation, however, the pH_s of the bulk solution will increase on adding an amphoretic oxide and

[1]*Presented at the 48th C.I.C. Chemical Conference and Exhibition, Montreal, May 31 – June 2, 1965.*
Crown Copyright Reserved.
[2]*National Research Council Postdoctorate Fellow, 1963–1965.*

the surface acquires a positive charge. It is the extent of these changes in pH_s of the solution at a constant ionic strength that are measured in the present work. Applying Gibbs' adsorption equation to the system at constant temperature, pressure, and ionic strength, the latter controlled by KNO_3, it can be shown that

$$[1] \qquad d\gamma = -F[\Gamma_{H^+} - \Gamma_{OH^-}]_{\mu_{K^+,NO_3^-}} \cdot dE^{\pm},$$

where γ is the interfacial energy, Γ_{H^+} and Γ_{OH^-} are the surface excess (1, 7) of H^+ and OH^- respectively in moles/cm^2 and the rest of the terms have their usual meaning. The change dE in the electrochemical potential of H^+ and OH^- in solution is measured using a standardized glass electrode, and, when taken from the z.p.c., may also be identified with the variation of potential in the double layer. The charge density q, which is a result of surface dissociation, can be regarded as the difference in the adsorption densities of H^+ and OH^- on the surface, so that

$$[2] \qquad d\gamma = -(q^{\pm}./dE^{\pm})_{\mu_{K^+,NO_3^-}} \quad \text{or} \quad (d\gamma/dE^{\pm})_{\mu_{K^+,NO_3^-}} = -q^{\pm}.$$

The charge density q is positive, zero, or negative in sign depending on whether $\Gamma_{H^+} > = \text{or} < \Gamma_{OH^-}$. The charge density q is zero (z.p.c.) when the interfacial energy is a maximum. The differential capacity C of the entire double layer can be written from eq. [2] as

$$[3] \qquad (d^2\gamma/dE^2)_{\mu_{K^+,NO_3^-}} = -(dq/dE)_{\mu_{K^+,NO_3^-}} = C.$$

By following the variation in C, inferences can be drawn as to the nature of interactions at the interface. A good discussion on this subject is available elsewhere (7–12). Assigning a hypothetical value γ_0 (the absolute value is not known) for the interfacial energy when $q = 0$, and taking into account chemisorption of K^+ and NO_3^- on the surface at the z.p.c., the integration of the more general form of eq. [2] gives

$$[4] \qquad \gamma - \gamma_0 = \left(\int_{E_0}^{E} q^{\pm}\, dE^{\pm}\right)_{\mu_{K^+,NO_3^-}} = -\infty - \left(\int_{-\infty}^{\mu} \Gamma_{K^+,NO_3^-} \cdot d\mu_{K^+,NO_3^-}\right)_E.$$

If the chemisorption of K^+, NO_3^-, is neglegible, the last term in eq. [4] may be omitted. At a constant pH_s ($dE^{\pm} = 0$), the degree of dissociation of the surface is constant and the effect of changing the ionic strength of the indifferent electrolyte on the interfacial energy can be described according to eqs. [5] and [6], which follow from the more general form of eq. [1].

$$[5] \qquad d\gamma_{H^+/OH^-} = -\Gamma_{K^+} \cdot d\mu_{K^+} \quad \text{for } q^- \text{ and}$$

$$[6] \qquad d\gamma_{H^+/OH^-} = -\Gamma_{NO_3^-} \cdot d\mu_{NO_3^-} \quad \text{for } q^+.$$

It is assumed that ions having the same charge as that on the surface have no influence on γ.

In the present work quantitative data have been obtained on the double layer characteristics considered above, and inferences have been drawn qualitatively as to the nature of interactions at the surface. Such information would be of considerable practical value in various fields of studies such as adsorption, adhesion, flotation, etc., dealing with nonmetallic substances.

EXPERIMENTAL

Materials

Brazilian quartz and crystalline forms of fused ZrO_2 and ThO_2 were used, the two latter being supplied by The Norton Co., Chippawa, Ontario. The material in −100+150 mesh size was leached for 24 h with 20% HCl in an all-glass Soxhlet. The samples were washed free of chloride, deslimed, and stored in degassed conductivity water, which was replaced frequently. For desliming, the material was packed in a long glass

Can. J. Chem. Downloaded from www.nrcresearchpress.com by 210.87.254.105 on 09/05/12
For personal use only.

tube with a fritted-glass bottom and elutriated with a rising current of distilled water. Quartz and ThO_2 samples were found by spectrographic analysis to be >99.9% pure. ZrO_2 contained ~0.5% trace impurities mainly TiO_2, SiO_2, Fe_2O_3, and CaO. These impurities may, however, be leached out of the surface in the acid treatment. X-Ray diffraction analysis indicated that quartz was the usual α form (hexagonal) and that ZrO_2 and ThO_2 were single phase baddelyite (monoclinic) and thorianite (cubic) respectively. Analytical reagent grade KNO_3 was recrystallized from water. HNO_3 (A.R.) was purified from any dissolved oxides of nitrogen by bubbling argon through a hot 1:2 solution of the acid and stored cool in the dark.

Method

The oxide samples were given a blank stirring treatment in water under the same conditions as used in the experiment. The specific areas of the resultant material were determined by the B.E.T. krypton gas adsorption method (13). The specific areas of quartz, ZrO_2, and ThO_2 were found to be 429, 1 438, and 192 cm^2/g respectively. A Beckman Research pH meter that could be read with a relative accuracy of 0.002 pH unit was enclosed in a constant humidity (~50%) box leaving the electrodes outside. The dissociation studies were carried out in a Pyrex glas tube ($2\frac{1}{8}$ in. × $1\frac{1}{8}$ in.) provided with an outer jacket for the circulation of water at 25 ± 0.05 °C. An inert atmosphere was maintained above the solutions by passing argon through two side vents fitted to the main chamber which was also closed to the open air by a flexible covering. Argon was purified to remove traces of CO_2 and other acidic impurities. A Beckman micro glass electrode and a KCl – saturated calomel electrode were used, the latter being separated from the experimental solution by a saturated KNO_3 solution bridge through a fiber junction. A series of oxide samples (1.5 to 3 g each) were rewashed and freshly dried at room temperature in a vacuum desiccator that was subsequently opened in an atmosphere of argon. Published information (14, 15) indicates that the chemisorbed water is retained on the surface of quartz through the formation of hydroxyl bonds, and ZrO_2 and ThO_2 are assumed to behave similarly. The glass electrode was calibrated against Beckman and Coleman buffers in the pH range 2.4 to 11.0.

A 10 ml solution of KNO_3 was taken in the reaction vessel and the dissolved CO_2 was first expelled by rapid stirring under a current of argon. The pH_s was adjusted as required by means of HNO_3 or KOH and the variation in pH_s on stirring of the blank solution was followed at time intervals of 2 min. When the solution attained a steady pH_s, a sample of the prepared oxide was added and the variation in pH_s with time again followed at intervals of 2 min. Fresh samples of oxides and solution were used for each run. Smaller quantities (~1.5 g) of oxide were used near the z.p.c. than at other pH_s (~2.5–3.0 g). It was found that almost all the change in pH_s occurred within 2–6 min of the addition of oxide. This was followed by a much slower variation (<5% of the initial change) in the pH_s that was attributed to secondary effects such as slime formation and solubility of the material. Corrections for these effects and for the blank were made. Verwey (16) has also reported that equilibrium is attained almost immediately in such oxide systems. The solubility[3] of the oxides under similar experimental conditions was also studied as a function of pH_s and time, using standard colorimetric methods. No dissolved material could be detected (sensitivity 1 μmole/l) under the present conditions of experiments, whereas stirring for prolonged periods (about half an hour or longer) produced dense colloidal solutions in the case of ZrO_2 and ThO_2. Stirring was found to cause random variation in the liquid junction potentials and, hence, in the pH_s; stirring was therefore interrupted at the time of reading the meter at high sensitivity. It was also noted that any stirring method which crushed the material and produced more slimes, gave erratic results. In the present work a tiny glass stirrer was used.

The activity coefficients of H^+ and OH^- in 10^{-3} *M* and 1 *M* KNO_3 solutions were experimentally determined for each buffer over the relevant pH_s range, and the factors $1/f_{H^+}$ and $1/f_{OH^-}$ below and above pH_s 7 respectively were calculated. These factors are markedly dependent on ionic strength of the solution and to a lesser degree on pH_s.

RESULTS

In solutions of pH_s > the z.p.c. of the oxide, a decrease in pH_s occurred on adding quartz, ZrO_2, or ThO_2. In this range of pH_s, q is assigned a negative charge as per the mechanism already considered. In solutions of pH_s < the respective z.p.c. of the oxide, an increase in pH_s occurred on adding ZrO_2 and ThO_2 and their surfaces are assigned a positive charge. The decrease in pH_s on adding quartz to 1 *M* KNO_3 solutions, as stated above, occurred only above pH_s 4, but below this pH_s no change could be observed experimentally. From the initial and final pH_s (if <7) or pOH_s (if pH_s > 7), the respective values of a_{H^+} or a_{OH^-} are calculated. The necessary corrections for blank, solubility, and slime formation if any, are made. The activities are converted into concentration terms

[3]*Similar studies of the solubility of specular hematite near the z.p.c. indicate that in a period of 1 h about 10^{-5} mole of Fe/l goes into solution, whereas in the first few minutes, during which almost all the change in pH_s occurs, the solubility of iron was below detection limits (1 μmole/l).*

Can. J. Chem. Downloaded from www.nrcresearchpress.com by 210.87.254.105 on 09/05/12
For personal use only.

c_{H^+} or c_{OH^-}, by multiplying with the respective activity coefficient factors $1/f_{H^+}$ (for $pH_s < 7$) and $1/f_{OH^-}$ (for $pH_s > 7$). From the resulting data one can calculate (Δc_{H^+} or Δc_{OH^-})/10 ml cm^{-2} oxide, and hence the charge densities q.

In Figs. 1, 2, and 3 the positive and negative charge densities for the oxides (only q^- for quartz) are plotted on a linear scale against the final pH_s and the potential difference in mV relative to the z.p.c. The plotted values of q^- for quartz in 10^{-3} M KNO_3 solution (Fig. 1) have been expanded in order to show finer details. The differential capacity C ($\mu F/cm^2$) of the whole double layer on quartz and zirconia in 10^{-3} M KNO_3 solutions has been obtained by the graphical differentiation of the smoothened charge density curves of

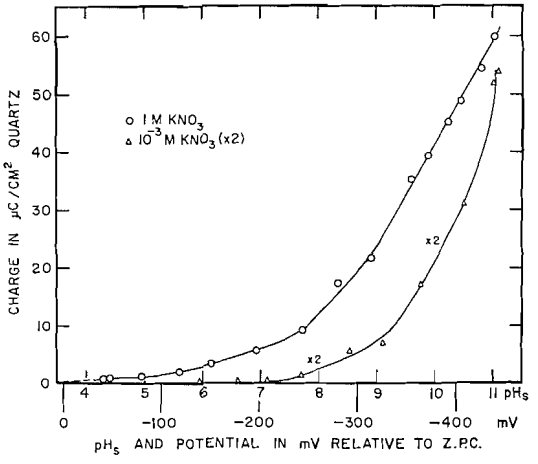


FIG. 1. Variation in charge density (−) on quartz with final pH_s and potential difference relative to the z.p.c. Indifferent electrolyte is KNO_3.

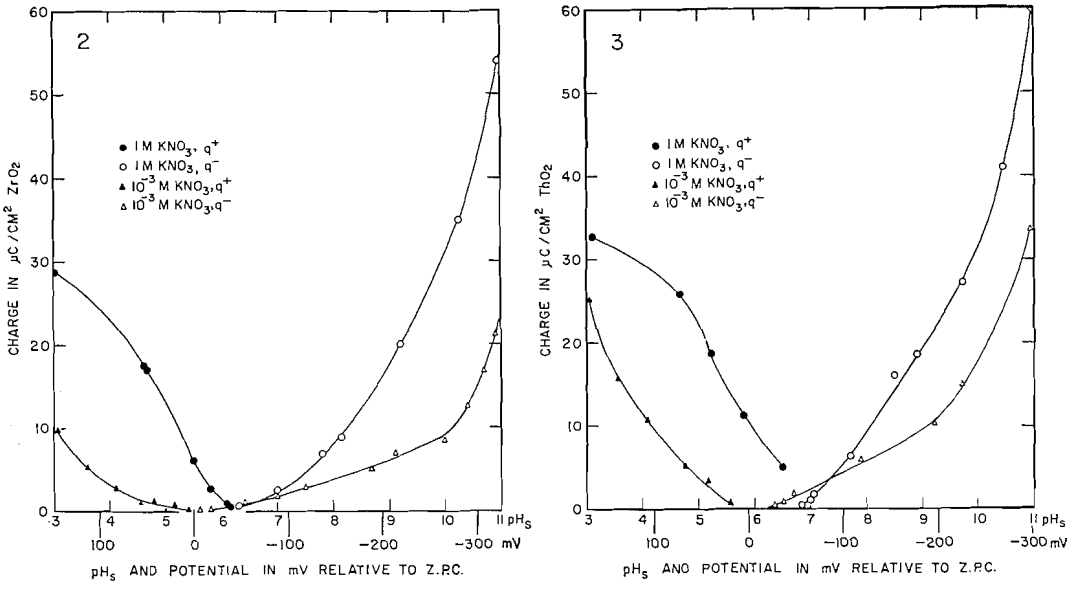


FIG. 2. Variation in charge density (±) on ZrO_2 with final pH_s and potential difference relative to the z.p.c. Indifferent electrolyte is KNO_3.

FIG. 3. Variation in charge density (±) on ThO_2 with final pH_s and potential difference relative to the z.p.c. Indifferent electrolyte is KNO_3.

Can. J. Chem. Downloaded from www.nrcresearchpress.com by 210.87.254.105 on 09/05/12
For personal use only.

Figs. 1 and 2. The results are shown plotted in Fig. 4. The q^- values for quartz below pH_s 7 in 10^{-3} M KNO_3 solutions are too low for an accurate measurement of the slopes, and, hence, the C values obtained at and above pH_s 7 are shown in Fig. 4. The C values obtained similarly for ThO_2 were comparatively higher in magnitude and this behavior will be discussed later. The changes in the interfacial energy, $(\gamma - \gamma_0)$ in ergs/cm^2, have been obtained by the graphical integration of the charge density plots of Figs. 1, 2, and 3. The results are plotted for the three oxides in Figs. 5, 6, and 7.

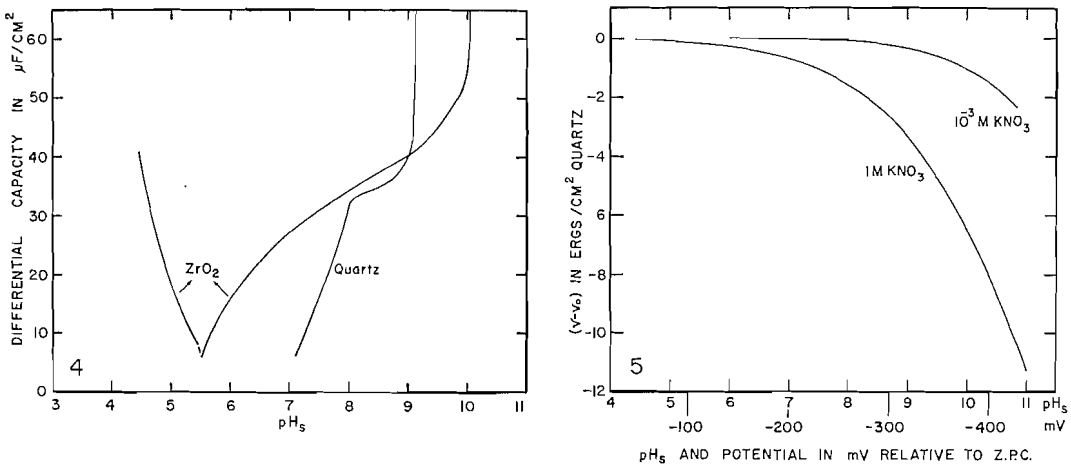


FIG. 4. Variation in the differential capacity of the double layer on quartz and ZrO_2 with pH_s. Indifferent electrolyte is 10^{-3} M KNO_3.

FIG. 5. Changes in the interfacial tension at the quartz–solution interface with pH_s and potential difference relative to the z.p.c. Indifferent electrolyte is KNO_3.

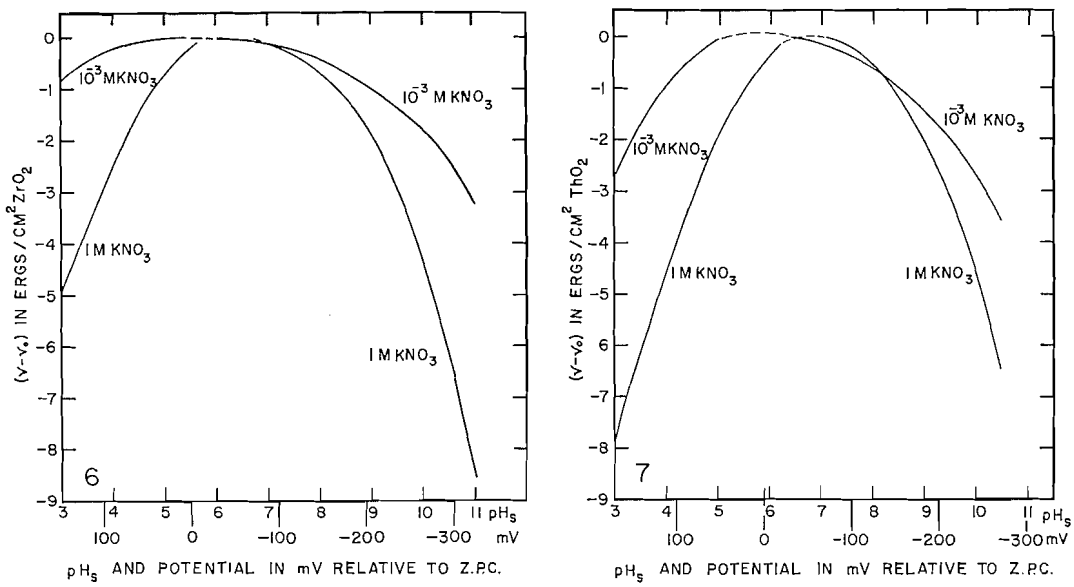


FIG. 6. Changes in the interfacial tension at the ZrO_2–solution interface with pH_s and potential difference relative to the z.p.c. Indifferent electrolyte is KNO_3.

FIG. 7. Changes in the interfacial tension at the ThO_2–solution interface with pH_s and potential difference relative to the z.p.c. Indifferent electrolyte is KNO_3.

Can. J. Chem. Downloaded from www.nrcresearchpress.com by 210.87.254.105 on 09/05/12
For personal use only.

Can. J. Chem. Downloaded from www.nrcresearchpress.com by 210.87.254.105 on 09/05/12
For personal use only.

DISCUSSION

The Charge Densities and the Zero Point of Charge

The silanol groups on quartz surfaces dissociate as acids and the surface therefore has a negative charge throughout the pH_s range shown in Fig. 1. It is also evident from the experimental results that NO_3^- has no affinity for quartz surfaces in the presence of H^+ and OH^-, and, hence, the silanol groups show no signs of basic dissociation. Although no change in pH_s of 1 *M* KNO_3 solutions could be experimentally detected below pH_s 4 on adding quartz, an extrapolation of the charge density plot (Fig. 1) to zero charge gives a $pH_s = 3.6 \pm 0.05$ as the z.p.c. of quartz. Since there is no evidence of specific adsorption of K^+ or NO_3^- on quartz at low pH_s (cf. discussion on *C*), this value for the z.p.c. of quartz is acceptable. It is in close agreement with the isoelectric point (pH 3.7) of coarse and crystalline quartz obtained by electrokinetic measurements (17). The hydroxyl groups on ZrO_2 and ThO_2 dissociate amphoterically (Figs. 2 and 3) and as a result the surface could be either positively or negatively charged. The charge density plots of quartz and ZrO_2 in 10^{-3} *M* KNO_3 solutions show a sharp change in slope at $pH_s \approx 9$ and 10 respectively. The significance of this behavior could be best discussed in light of the differential capacities. The z.p.c. of ZrO_2 and ThO_2 in 10^{-3} *M* KNO_3 solutions occur at pH_s 5.5 ± 0.05 and 5.9 ± 0.05 respectively and the corresponding values in 1 *M* KNO_3 are 6.2 ± 0.05 and 6.8 ± 0.1. The glass electrode in this range of pH_s was found to record a somewhat lower value on increasing the ionic strength of the solution from dilute to 1 *M* KNO_3. Hence the actual shift in the z.p.c. could be somewhat more than what is noted above. This shift in the z.p.c. towards a more negative potential can be attributed to the specific adsorption of NO_3^- and also of any dissolved complexes, at the z.p.c. (eq. [6]). There is clear evidence from the differential capacity curves that NO_3^- is specifically adsorbed on positively charged ZrO_2 and ThO_2, particularly at high charge densities.

A comparison of q^- values with the total number of sites available per cm^2 of quartz ($\sim$2 sites/23.4 Å^2) indicates an almost monolayer dissociation of quartz surfaces at $pH_s \approx 11.5$, whereas the fraction of the surface groups on ZrO_2 and ThO_2 dissociated at this pH_s is much less. At very high and low pH_s solubility effects may become considerable and the measurements less accurate because of small changes in pH_s. As a result of surface heterogeneity, some groups on the surface of a given oxide may dissociate as acids and others as bases giving an overall neutral reaction. It is then possible that the experimental values obtained for the z.p.c. of ZrO_2 and ThO_2 may not be accurate; they should, nevertheless, be good approximations.

The Differential Capacity Curves

The minimum values of the differential capacity, *C*, obtained for quartz and ZrO_2 in 10^{-3} *M* KNO_3 solutions at the z.p.c. are in agreement with the theoretically expected value (6 μF/cm^2) (7) in the absence of specific adsorption. As the *C* curves were obtained by the graphical differentiation of the smoothened charge density curves, no quantitative precision, either in the upper range of *C* values or in the shape of the curves can be expected. The following conclusions can, however, be drawn qualitatively. The positive branch of the *C* curve for quartz is absent for reasons already discussed. The *C* curves on positively charged ZrO_2 (and also ThO_2) indicate considerable specific adsorption of NO_3^- on the surface, even at low charge densities. Above pH_s 9 and 10 for quartz and ZrO_2 respectively, there is a relatively steep rise in *C* with increasing pH_s, indicating specific adsorption of K^+. Such behavior is not encountered on Hg except in the rare cases, such as Tl^+ and to some extent Cs^+ (18, 19). However, there is considerable evidence for a similar behavior on the

cathodic surfaces of metals, particularly those bearing an oxide film (19, 11 p. 670). It has been reported (11 p. 670) that on removing the oxide film from the metal such as Pt, the metal behaves like Hg in its differential capacity curves. Super-equivalent adsorption (18) of cations on the cathodic surface of Hg through specifically adsorbed anions is also known. In the present case of oxides, specific adsorption of cations may be said to occur on the metal through chemisorbed O^{2-}. Further evidence for the specific adsorption of cations on oxides at high pH_s is obtained from the adsorption of Ca^{2+} on quartz (20), which has been found to increase sharply at $pH_s > 9$. This effect is also indicated by a drop in the negative zeta-potential (17) (which is approximately the difference in potential between the outer Helmholtz plane and the bulk solution) of quartz at $pH_s > 10$.

Compared to the other oxides, higher values of C (cf. higher $q^{\pm}$ values) were obtained for ThO_2 in 10^{-3} M KNO_3 solutions. This effect could be due to a higher tendency for the specific adsorption of K^+ and NO_3^- on ThO_2 than on the other oxides. It may also be partly due to a greater tendency of ThO_2, as noticed experimentally, to form slimes and colloidal solutions even in short time intervals. If the formation of slimes and the solubility of the material are not checked and corrected for, abnormal values of q and C could be obtained. Also, the slimes may have a different z.p.c. from the coarse and crystalline material. The dissolved hydroxy complexes may have different degrees of hydration and dissociation and a different isoelectric point from those of the surface. The polyvalent ions could also increase the ionic strength of the solution considerably, and all these effects could be different in magnitude at different pH_s.

The Interfacial Energy Curves

The $(\gamma - \gamma_0)$ against pH_s curves shown in Figs. 5, 6, and 7 are very similar to the electrocapillary curves of Hg (7), with a maximum at the z.p.c. as predicted from theory (eq. [2]). The decrease in $(\gamma - \gamma_0)$ on the positive or negative side of the z.p.c. may be attributed to the dissociation of OH^- or H^+ and the subsequent adsorption of anions or cations respectively on the surface as counter ions. The more negative value of $(\gamma - \gamma_0)$ on the surfaces of ThO_2 is probably due to the high specific adsorption of K^+ and NO_3^-. There is also a shift in the maxima of these curves corresponding to the shift in the z.p.c. on changing the ionic strength from 10^{-3} M to 1 M KNO_3.

Applications

The information thus obtained on the double layer characteristics of non-metallic substances will be useful in practical problems such as flotation. The nature and the amount of collectors, activators, and depressants (anionic, cationic, or neutral) that are used in the flotation of minerals depend on the nature (+ or −) and the magnitude of the surface charge, the role of the potential determining ions, the indifferent electrolytes, the ionic strength and the degree of specific interactions. In a mixture of solids, whose z.p.c. are sufficiently apart, the surface of one will be positively charged and of the other negatively charged in the range between their z.p.c. In such a case, a selective or a collective flotation may be brought about by choosing collectors and activators of suitable charge. It is hoped to discuss this aspect in greater detail in a future publication.

ACKNOWLEDGMENTS

The author is grateful to the National Research Council of Canada for awarding the fellowship and to Mines Branch, Department of Mines and Technical Surveys, for providing the research facilities. The X-ray and spectrographic analyses were performed by the respective sections of the Mines Branch. Helpful discussions on the subject with

Can. J. Chem. Downloaded from www.nrcresearchpress.com by 210.87.254.105 on 09/05/12
For personal use only.

Professor B. E. Conway, University of Ottawa, and Dr. J. D. Keys, Mines Branch, are gratefully acknowledged. Sincere thanks are due to Dr. C. Lapointe for his aid in instrumentation and to Dr. P. G. Manning in the preparation of the manuscript.

REFERENCES

1. E. L. MACKOR. Rec. Trav. Chim. **70**, 663, 747, 763 (1951).
2. J. TH. G. OVERBEEK. Semicentennial Symposium, Electrochemical Constants, Nat. Bur. Std. (U.S.), Circ. No. 524, 213 (1953).
3. W. L. FREYBERGER and P. L. DE BRUYN. J. Phys. Chem. **61**, 586 (1957).
4. I. IWASAKI and P. L. DE BRUYN. J. Phys. Chem. **62**, 594 (1958).
5. G. A. PARKS and P. L. DE BRUYN. J. Phys. Chem. **66**, 967 (1962).
6. ROGER G. BATES. J. Res. Nat. Bur. Std., A, **66**, 179 (1962).
7. D. C. GRAHAME. Chem. Rev. **41**, 441 (1947).
8. D. C. GRAHAME. J. Electrochem. Soc. **98**, 343 (1951).
9. D. C. GRAHAME, M. A. POTH, and J. I. CUMMINGS. J. Am. Chem. Soc. **74**, 4422 (1952).
10. D. C. GRAHAME and B. A. SODERBERG. J. Chem. Phys. **22**, 449 (1954).
11. M. A. V. DEVANATHAN and B. V. K. S. R. A. TILAK. Chem. Rev. **65**, 635 (1965).
12. J. O'M. BOCKRIS, M. A. V. DEVANATHAN, and K. MÜLLER. Proc. Roy. Soc. London, Ser. A, **274**, 55 (1963).
13. A. J. ROSENBERG. J. Am. Chem. Soc. **78**, 2929 (1956).
14. M. M. EGOROV and V. F. KISELEV. Zh. Fiz. Khim. **36**, 318 (1962); Russ. J. Phys. Chem. **36**, 158 (1962).
15. W. H. WADE, H. D. COLE, D. E. MEYER, and N. HACKERMAN. Advan. Chem. Ser. **33**, 35 (1961).
16. E. J. W. VERWEY. Rec. Trav. Chim. **60**, 625 (1941).
17. A. M. GAUDIN and D. W. FUERSTENAU. Trans. AIME, **202**, 66 (1955).
18. D. C. GRAHAME, A. E. HIGINBOTHAM, and F. R. M. DEANE. Trans. Symp. Electrode Processes, Philadelphia, Pa., 1959. John Wiley & Sons, Inc., N.Y. p. 197.
19. A. FRUMKIN. Trans. Symp. Electrode Processes, Philadelphia, Pa., 1959. John Wiley & Sons, Inc., N.Y. p. 1.
20. S. M. AHMED and A. B. VAN CLEAVE. Can. J. Chem. Eng. **43**, 23 (1965).

Can. J. Chem. Downloaded from www.nrcresearchpress.com by 210.87.254.105 on 09/05/12
For personal use only.

Can. J. Chem. Downloaded from www.nrcresearchpress.com by 210.87.254.6 on 09/05/12
For personal use only.

THE POLYMERIZATION OF STYRENE BY ANHYDROUS PERCHLORIC ACID AND THE SPECTRA OF BENZYLIC CARBONIUM IONS[1]

S. BYWATER AND D. J. WORSFOLD
Division of Applied Chemistry, National Research Council, Ottawa, Canada

Received March 24, 1966

ABSTRACT

A spectroscopic investigation of the reaction of anhydrous perchloric acid with styrene in methylene chloride solution has been carried out, together with a study of the spectra of styrene and its derivatives dissolved in sulfuric acid. From the results it was decided that the absorbing species formed at the end of the reaction in methylene chloride are derivatives formed from the cyclized end groups of the polymer chain, and not the polystyrylcarbonium ion. It is not thought possible to determine from spectroscopic studies whether the polymerization reaction goes via a true ionic intermediate or a perchlorate ester.

The established view that the polymerization of vinyl compounds by acidic catalysts goes via an ionic intermediate has recently been challenged by Gandini and Plesch (1) who have proposed that the intermediate is an ester in some of the systems they have studied. In particular they have studied the reaction of perchloric acid with styrene in methylene chloride solution. From previous kinetic studies by Pepper and Reilly (2), confirmed by Gandini and Plesch, the simplest reaction scheme involves the rapid reaction of the acid with monomer to form the reaction centers, which then propagate and transfer, but have no effective kinetic termination step. Pepper suggested that the reaction centers were ion pairs, but Gandini and Plesch noted that no color developed during the polymerization and hence concluded that no appreciable concentration of polystyrylcarbonium ions could be present, and that the active centers must be perchlorate esters. Color does develop after the styrene has been consumed, caused by an absorption band ~ 420 mμ which was identified as that of the polystyrylcarbonium ion. The fact that the color formed only after polymerization, together with a large increase in electrical conductivity, was the major evidence for the absence of carbonium ions during polymerization.

Doubt of the validity of the assignment of this absorption band suggested that some further work on the subject was warranted.

EXPERIMENTAL

The purification of styrene has been described before (3).

Methylene chloride was stirred with concentrated sulfuric acid for 3 days, washed with water and dilute alkali, and dried with calcium hydride. Since vapor phase chromatographic analysis showed the impurity level to be very low, the solvent was then stored over fresh calcium hydride on the vacuum line.

Anhydrous perchloric acid was prepared in an all-glass apparatus (4), and in the same apparatus metered as the vapor into small fragile bulbs which were frozen and sealed off. The bulbs were stored in a freezer.

The polymerization reactions were performed under normal high vacuum conditions in an all-glass apparatus containing a quartz optical cell. The solvent was distilled in under vacuum and the apparatus sealed off. The styrene and perchloric acid were contained in fragile bulbs, broken with a glass-covered magnetic bar.

The spectra in sulphuric acid were measured in cells open to the atmosphere. Measurements were made immediately (20 s) after mixing. The acid was added to neat α-methylstyrene derivatives, but to 0.1% acetic acid solutions of the styrene derivatives to avoid polymer precipitation and to obtain more reproducible spectra.

The spectra for a duplicate experiment was measured in vacuum with degassed sulfuric acid; the result was the same. All spectra were measured on a Bausch and Lomb 505 spectrophotometer at room temperature, except for a few measured at low temperatures where the reaction vessel was immersed in a quartz dewar vessel with flat windows.

[1]*Issued as N.R.C. No. 9048.*

Can. J. Chem. Downloaded from www.nrcresearchpress.com by 210.87.254.6 on 09/05/12
For personal use only.

RESULTS AND DISCUSSION

(a) Spectra of Styrene and Its Derivatives in the Presence of Acids

Gandini and Plesch assigned to the polystyrylcarbonium ion an absorption whose major maximum was near 420 mμ from spectral measurements in $HClO_4/CH_2Cl_2$ (Fig. 1A). Molecular orbital theory suggests the position of absorption bands of corresponding carbonium ions and carbanions to be similar and this is found to be true for di- and tri-phenylmethyl ions, and also for allylic ions. The assignment of an absorption maximum at 420 mμ to the polystyrylcarbonium ion is greatly at variance with the well-established absorption of the polystyryl carbanion near 340 mμ (5).

Deno (6) has recently questioned the validity of assignments of ultraviolet spectra of benzyl-type cations except for certain α,α-alkyl-substituted benzyl ions, suggesting that the former were too unstable to measure under the conditions used. Recently, apparently reliable nuclear magnetic resonance (n.m.r.) spectra have been obtained of α,α-dimethylbenzyl and some polymethyl ring substituted benzyl carbonium ions in $SbF_5/FHSO_3$ at low temperature (7) and their ultraviolet spectra have been measured (R. Waack, private communication). All spectra showed a major maximum in the region 320–370 mμ ($\epsilon \sim 10^4$), with a much smaller absorption at longer wavelengths (ca. 400 mμ).

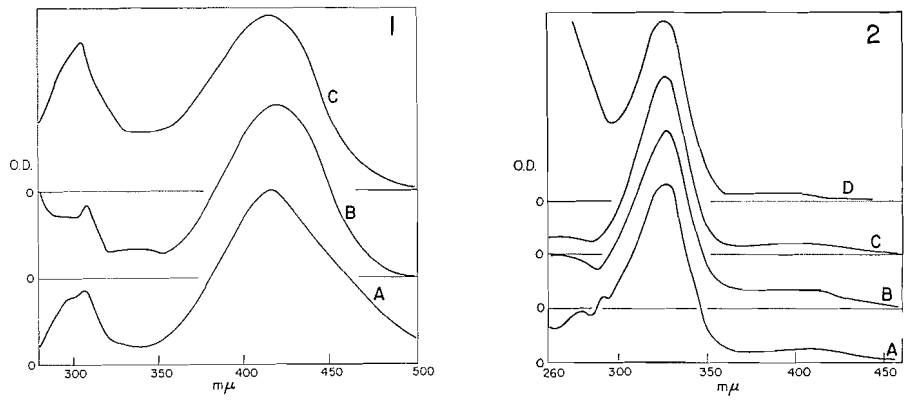
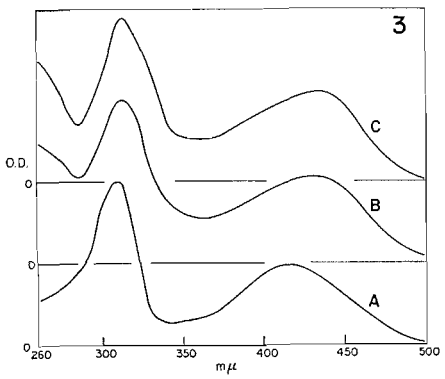


FIG. 1. (A) Spectrum obtained when 5×10^{-3} *M* $HClO_4$ was reacted with 0.2 *M* styrene in CH_2Cl_2 solution and the absorption at 420 mμ had reached its maximum. The carbonium ion was destroyed by adding methanol (in vacuum), and the polystyryl background absorption subtracted ($\epsilon_{420} = 1.3 \times 10^3$ based on $HClO_4$). (B) Spectrum immediately formed from 7×10^{-3} *M* saturated dimer of styrene and 3×10^{-3} *M* $HClO_4$ in CH_2Cl_2 solution ($\epsilon_{420} = 6.5 \times 10^2$ based on $HClO_4$). (C) Spectrum from 3×10^{-4} *M* saturated dimer of styrene in 96% H_2SO_4 ($\epsilon_{410} = 1.1 \times 10^3$).

FIG. 2. Spectra in 96% sulfuric acid. (A) 10^{-3} *M* α,α-dimethylbenzyl alcohol ($\epsilon_{327} = 8 \times 10^2$). (B) 2×10^{-4} *M* unsaturated dimer of α-methylstyrene ($\epsilon_{327} = 1.9 \times 10^3$). (C) 10^{-3} *M* α-methylstyrene ($\epsilon_{327} = 1.4 \times 10^3$). (D) 4×10^{-4} *M* α-methylstyrene in 30% fuming sulfuric acid ($\epsilon_{327} = 7 \times 10^2$).

Spectra obtained when α-methylstyrene (8), α,α-dimethylbenzyl alcohol, or the unsaturated dimer of α-methylstyrene are dissolved in concentrated H_2SO_4 (Fig. 2) have the same maxima as those found for the α,α-dimethylbenzyl carbonium ion in $SbF_5/FHSO_3$, except for a somewhat lower extinction coefficient (10^3 as compared with 10^4 (R. Waack, private communication)). When the sulfuric acid solution of α,α-dimethylbenzyl alcohol was added to iced dilute alkali, the products were a mixture of the saturated and unsaturated dimer of α-methylstyrene, and the spectrum in Fig. 2 is probably that of the 1:3 dimethyl, 1:3 diphenylbutyl carbonium ion. Its main absorption is close, as expected, to that of the corresponding poly α-methylstyryl carbanion (342 mμ in tetrahydrofuran) in poly α-methylstyryllithium.

When a large excess of sulfuric acid is added to a dilute acetic acid solution of styrene, or the corresponding alcohol or unsaturated dimer, the spectra in Fig. 3 are obtained, and are similar to those found by others (9). The spectrum in general is similar to that expected for the polystyrylcarbonium ion except the longer wavelength band is larger than expected, but since it appears variable in size and position it may well be due at least partly to a side product. The apparent extinction coefficient of the major peak at 318 mμ is low, near 3×10^3. Isolation of the products by adding to iced alkali solution gave low molecular weight polystyrene containing some unsaturation. Although there can be no certainty that this is the spectrum of the polystyrylcarbonium ion, it is greatly different from that obtained by Gandini and Plesch, or in general in $HClO_4/CH_2Cl_2$ systems, but the conditions here are likely to give a more nearly correct spectrum than those used by Gandini and Plesch. The only times that a spectrum resembling that in Fig. 3 was obtained in the $HClO_4/CH_2Cl_2$ system were in reactions at low temperatures, $< -50°$, where Gandini and Plesch report anomalous behavior. When the cell was warmed, the spectrum became similar to Fig. 1A.



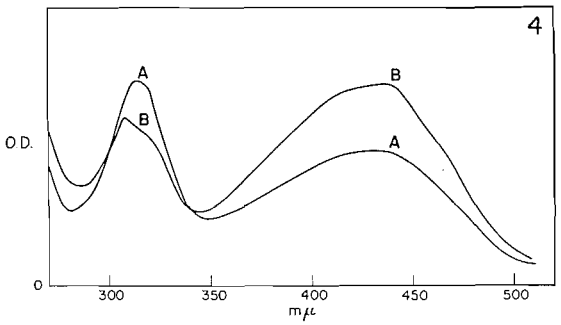


FIG. 3. Spectra in 96% sulfuric acid. (A) 3×10^{-4} *M* unsaturated dimer of styrene ($\epsilon_{314} = 10^3$). (B) 10^{-4} *M* α-methylbenzylalcohol ($\epsilon_{314} = 3 \times 10^3$). (C) 10^{-4} *M* styrene ($\epsilon_{314} = 2 \times 10^3$).

FIG. 4. Spectra of 10^{-4} *M* styrene in 10% H_2SO_4 in CF_3COOH solution. (A) After 4 min ($\epsilon_{314} = 2.8 \times 10^3$). (B) After 2 days.

If the medium in which the spectrum derived from styrene was formed is made less acidic by diluting the sulfuric acid with trifluoracetic acid, it is found at moderate dilution that the spectrum formed initially is similar to that in 96% sulfuric acid. But if the sulfuric acid content is reduced to 1%, the absorption obtained is similar to that found by Gandini and Plesch in methylene chloride (Fig. 1). In an intermediate solvent, say 10% sulfuric acid in trifluoracetic acid, the initially formed spectrum, which is similar to that in 96% sulfuric acid (Fig. 4A), slowly changes to that found in the 1% sulfuric acid solution (Fig. 4B). This suggests that the spectrum observed by Gandini and Plesch is at best caused by a secondary product.

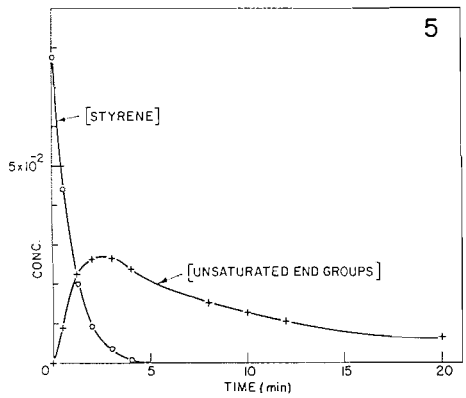
In summary, it would seem that the spectra in sulfuric acid offer the closest approach to that of the true polystyrylcarbonium ion, although some side reactions may have occurred even in this case. The spectra of α-substituted derivatives in strong acids all show the major absorption around 320 mμ and so it is unlikely that strong absorption around 420 mμ would be characteristic of the polystyrylcarbonium ion, since shifts of this magnitude on α-methyl substitution are unknown. Rapid rearrangements in media of low acidity and low dielectric constant must be held responsible for the spectra observed under these conditions.

Can. J. Chem. Downloaded from www.nrcresearchpress.com by 210.87.254.6 on 09/05/12
For personal use only.

(b) Observations on the Polymerization of Styrene by $HClO_4$

If the spectrum of the reaction mixture of styrene with anhydrous perchloric acid in methylene chloride is observed in the region of 260–300 mμ, it is seen that as the styrene is consumed the absorption of styrene decreases and is replaced by an absorption of the type associated with the unsaturated dimer of styrene. This is a small change, but readily observable as the sharp peak of styrene at 291 mμ changes to a sharp peak at 294 mμ together with other changes near 280 mμ. This is attributed to the formation of low molecular weight polystyrene with an unsaturated end group. When all the styrene has gone, it is seen that the spectrum of the unsaturated end group itself decreases and the comparatively low intensity spectrum of low molecular weight polystyrene with a saturated cyclized indane end group emerges. The disappearance of styrene and the appearance and disappearance of the unsaturated end group is illustrated in Fig. 5.

It is during the second period, as the unsaturated end group disappears and is replaced by a cyclized end group, that the absorption near 420 mμ observed by Gandini and Plesch grows. To see if there is any connection between the cyclized end groups and the appearance of this spectrum, both the saturated and unsaturated dimer of styrene were prepared, and reacted with perchloric acid in methylene chloride. The saturated dimer instantly gave the spectrum as in Fig. 1B, whereas the unsaturated dimer only gave it slowly (as it cyclized). Moreover, when the dimers were dissolved in concentrated sulfuric acid, the unsaturated dimer gave the spectrum in Fig. 3A (major abs. 320); the saturated dimer gave the spectrum in Fig. 1C (major abs. 420). From the similarity of the spectra in Fig. 1 to that of the diphenylmethyl carbonium ions in Fig. 6A, it can be suggested that the absorption at 420 mμ is due to a diphenyl-substituted carbonium ion derived from the cyclized end group, the exact nature of which is not known.



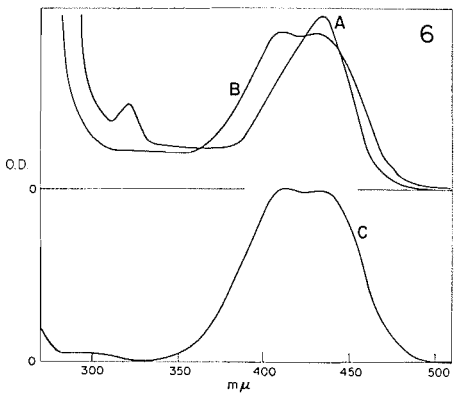


FIG. 5. Reaction curve of styrene with ca. 10^{-3} *M* $HClO_4$ showing rise and fall of the unsaturated end group concentration.

FIG. 6. (A) Spectrum formed initially when 5×10^{-2} *M* diphenylethylene is added to 10^{-3} *M* $HClO_4$. (B) The same reaction mixture after 2 days. (C) Spectrum formed from triphenylcarbinol with H_2SO_4 in CH_2Cl_2 solution.

This interpretation is strengthened by experiments carried out on diphenylethylene and α-methylstyrene. When 1,1-diphenylethylene is polymerized in methylene chloride solution with anhydrous perchloric acid, the initially formed diphenylethyl carbonium ion spectrum (Fig. 6) changes slowly, and after several days becomes identical to that of the triphenylcarbonium ion (Fig. 6C). During this time the initially formed unsaturated dimer

Can. J. Chem. Downloaded from www.nrcresearchpress.com by 210.87.254.6 on 09/05/12
For personal use only.

cyclizes to the saturated dimer. α-Methylstyrene gives a very similar reaction with perchloric acid to rapidly produce a saturated dimer. No corresponding visible spectrum is observed, probably because the extra methyl group blocks the reactive diphenyl-substituted carbon atom in the saturated dimer.

Previous interpretations of the mechanism of $HClO_4$-initiated polymerization assume that the acid is consumed rapidly. This requirement has never been confirmed directly, so three experiments were performed to check this point. In the first a methylene chloride solution of anhydrous perchloric acid was half distilled from one part of an evacuated reaction vessel to another. A styrene bulb was broken into the distillate, and the styrene polymerized normally with subsequent formation of the 420 mμ absorption. This indicated that, as expected, the perchloric acid distilled over with the solvent. The same experiment was repeated, but instead of only a solution of perchloric acid being used, a solution in which styrene had been polymerized by perchloric acid and allowed to cyclize and form the 420 mμ absorption was distilled. Again when a styrene bulb was broken into the distillate, the styrene polymerized and the 420 mμ absorption appeared. In the third experiment, the solution distilled was a polymerizing solution of styrene and the distillation stopped before absorption at 420 mμ appeared. The distillate was found to contain a little styrene. In this case no color appeared in the distillate, even on adding a further bulb of styrene, but the styrene did polymerize very slowly, at about 1% of the normal rate. It appears that during the polymerization the perchloric acid is in a combined, nonvolatile form, and is released again as the end groups cyclize. The suggestion of Gandini and Plesch that an ester is formed would be in accord with the experiments, although it might be suggested that the perchloric acid is tied up as a π-complex with styrene.

Regardless of the exact position of the polystyrylcarbonium ion absorption, it is possible to show that under the best conditions, during the polymerization of styrene with anhydrous perchloric acid in methylene chloride solution at room temperature, there is no appreciable absorption from the foot of the styrene absorption between 300 and 310 mμ and out through the visible spectrum, not merely at 420 mμ as stated by Gandini and Plesch. If an extinction coefficient of 10^4 is assumed for the polystyrylcarbonium ion, the highest concentration that could be undetected would be less than 10^{-6} mole/l. To give the propagation reaction rates suggested by the kinetics, a concentration of ions of 10^{-6} M would require a rate constant of 10^4–10^5 moles/l s. This is in the region found for the propagation rate constant for the free polystyrylcarbanion in tetrahydrofuran (11), and considerably less than the 10^6 suggested recently by Ffrancon Williams (11) for the free polystyrylcarbonium ion rate constant. Thus the absence of absorption in this region by no means excludes the possibility of an ionic mechanism. It is possible that if the rate constant of ionic propagation is at the high end of the suggested values, it may approach that of the carbonium ion with water, and account for the seeming insensitivity of the reaction to water concentrations, low compared with the styrene.

If the reaction does go through an ionic intermediate, it is likely to be the free carbonium ion because any ion pairing in the probable concentration range will be very slight in this solvent with a dielectric constant near 9. It is, in fact, possible to show that the ionic species (of comparatively high concentration) formed when the styrene has been consumed are fully dissociated, since there is a linear relationship between the increase in optical density at 420 mμ and the increase in electrical conductance of the solution.

If we assume, according to the above evidence, a covalent perchlorate is formed almost instantaneously, any equilibrium between free ions and the proposed ester would cause the order of the polymerization reaction to be half in the initial perchloric acid concentration,

Can. J. Chem. Downloaded from www.nrcresearchpress.com by 210.87.254.6 on 09/05/12
For personal use only.

instead of first order as found. But if the rate-determining step is the rate of ionization of the ester, the rate would be first order in the ester concentration.

It is possible to write such schemes, which give the appropriate kinetics, as below.

$$HClO_4 + PhCH{=}CH_2 \xrightarrow{\text{fast}} CH_3PhCHClO_4$$

$$CH_3PhCHClO_4 \xrightarrow{\text{slow}} CH_3PhCH^+ + ClO_4^-$$

$$\sim CH_2PhCH^+ + PhCH{=}CH_2 \rightarrow \sim CH_2PhCHCH_2PhCH^+$$

$$\sim CH_2PhCHCH_2PhCH^+ \xrightarrow{\text{normal propagation and transfer reaction}} \sim CH_2PhCHCH{=}CHPh + H^+$$

$$H^+ + ClO_4^- \rightarrow HClO_4$$

The major transfer process is probably monomer transfer, and gives an unsaturated end group, although it has been suggested that some cyclized end groups are formed during the polymerization (12). In this scheme the overall rate constant would be a composite of the initiation, propagation, and termination constants.

CONCLUSIONS

It has been shown that the polystyrylcarbonium ion probably shows maximum absorption around 320 mμ and not at 420 mμ. The latter absorption is associated with the reaction products from cyclic end groups in the polymer. During the polymerization of styrene with $HClO_4$ in CH_2Cl_2 there is not only no measurable absorption at $\sim$ 420 mμ, as shown by Gandini and Plesch, but none at 320 mμ, so the concentration of carbonium ions (if any) is very low. It has been confirmed that there is little free $HClO_4$ during the polymerization, which suggests that Gandini and Plesch's deduction that most of the $HClO_4$ is present as a perchlorate ester may very well be correct. The spectral and kinetic evidence cannot distinguish between chain propagation by perchlorate esters or by free carbonium ions if the latter have a very high rate constant as is suggested by recent evidence. Only the insensitivity of the polymerization rate to small concentrations of water suggests that the propagation by esters is more likely. The fact that the rate of polymerization is very sensitive to the dielectric constant of the medium (2), however, is more in accord with carbonium ion intermediates as reactive species.

REFERENCES

1. A. Gandini and P. H. Plesch. Proc. Chem. Soc. 240 (1964); J. Chem. Soc. 4765, 4826 (1965); J. Polymer Sci. Pt. B, **3**, 127 (1965).
2. D. C. Pepper and P. J. Reilly. J. Polymer Sci. **58**, 639 (1962).
3. S. Bywater and D. J. Worsfold. J. Phys. Chem. **70**, 162 (1966).
4. S. J. Tauber and A. M. Eastham. J. Am. Chem. Soc. **82**, 4888 (1960).
5. S. Bywater, A. F. Johnson, and D. J. Worsfold. Can. J. Chem. **42**, 1255 (1964).
6. N. C. Deno. Progr. Phys. Org. Chem. **2**, 129 (1964).
7. G. A. Olah. J. Am. Chem. Soc. **86**, 932 (1964). G. A. Olah, M. B. Comisarow, C. A. Cupas, and C. U. Pittman. J. Am. Chem. Soc. **87**, 2997 (1965).
8. I. Hanazaki and S. Nagakura. Tetrahedron, **21**, 2441 (1965).
9. R. Inoue and S. Mima. Kobunshi Kagaku, **14**, 402 (1957). D. O. Jordan and F. E. Treloar. J. Chem. Soc. 729 (1961).
10. D. N. Bhattacharyya, C. L. Lee, J. Smid, and M. Szwarc. J. Phys. Chem. **69**, 612 (1965).
11. Ffrancon Williams. Polymer Preprints, **7**, 47 (1966).
12. D. C. Pepper and P. J. Reilly. Proc. Roy. Soc. London, Ser. A, **263**, 63 (1961).

Can. J. Chem. Downloaded from www.nrcresearchpress.com by 210.87.254.6 on 09/05/12
For personal use only.

Can. J. Chem. Downloaded from www.nrcresearchpress.com by 210.87.254.105 on 09/05/12
For personal use only.

PHOTOLYSIS OF SOLID CARBONYL SELENIDE AND CARBON DISELENIDE

D. A. STILES, W. J. R. TYERMAN, O. P. STRAUSZ, AND H. E. GUNNING
Department of Chemistry, University of Alberta, Edmonton, Alberta

Received March 4, 1966

ABSTRACT

Samples of COSe and CSe_2 were photolyzed at 77 °K, either pure or in matrices of Xe or *trans*-2-butene. Observed electron spin resonance spectra are assigned to $Se(4^3P)$, to Se_2, and to chains of selenium atoms, $\cdot Se(Se)_nSe\cdot$. The selenium chains exhibit metallic behavior intermediate between that of sulfur and tellurium. It is suggested that polymeric chains of CSe are formed on warming photolyzed samples containing CSe_2. The ultraviolet absorption spectrum of COSe vapor is reported.

INTRODUCTION

By comparison with sulfur-containing species, radicals containing selenium atoms have received little attention by electron spin resonance (e.s.r.) spectroscopy. The presence of free radicals in elemental selenium, both pure and with added impurities, has been inferred from the observation of two e.s.r. lines at $g = 2.00$ and $g = 2.04$ (1). Windle, Wiersema, and Tappel (2) photolyzed a number of selenomercaptans at 77 °K and postulated that C—H cleavage was preferred to rupture of a bond to selenium. After several hours irradiation of the substrates ($\lambda = 2\,537$ Å), the selenide spectra were weaker than those produced from sulfides after much shorter periods of photolysis. The low intensity and the broadness of the selenide spectra handicap identification of the carriers and obscure hyperfine splitting (3) due to $^{77}Se(I = 1/2)$ which has a natural abundance of 7.5%. For this reason most authors have preferred to identify their spectra by analogy with the sulfides.

During an earlier investigation of COS photolysis in various matrices at 77 °K (4), three intense e.s.r. lines with an average g-value of 2.024 were observed. This spectrum was assigned to unbranched chains of $\sim 10^3$ sulfur atoms. These possess an unpaired electron on each terminal atom, sufficiently separated to behave independently, i.e. the radicals exist in double doublet rather than triplet electronic states. No spectra were attributed to the anticipated precursors of the S chains, the triplet species $S(^3P)$ and $S_2(^3\Sigma)$. Since Se and Se_2 are larger than S and S_2, they should migrate less readily through a matrix at 77 °K, and recombination should be slower. We have therefore extended the investigation to COSe and CSe_2, which have been previously studied in the gas phase by flash photolysis (5). Photolysis of CSe_2 vapor yields triplet atoms, $Se(4^3P)$, but there was chemical evidence for formation of excited singlet atoms, $Se(4^1D_2)$, by photolysis of COSe. The distinction is analogous to that between CS_2(6) and COS vapor (7).

To assist interpretation of our results, experiments were also performed with allotropes of selenium. Long-chain polymers exist in selenium at its melting point (8), and contain about 10^4 atoms. The e.s.r. spectrum is unlike that of sulfur samples but the line at $g = 2.00$ (1) may be the analog of that observed at the same value in metallic tellurium (9), and assigned to free holes in its valence band.

RESULTS

Ultraviolet Spectrum of COSe Vapor

To check that this compound absorbs light at wavelengths emitted by the photolysis lamps, the ultraviolet spectrum of the vapor was determined (Fig. 1). Under low dispersion the spectrum appears very similar to those of the analogous compounds CS_2 (6, 10) and

CSe_2 (5), exhibiting intense transitions in the far ultraviolet and weaker systems in the near ultraviolet regions. It is interesting to note that the 1 940 Å system of COSe is banded, although the spectrum at 2 500 Å exhibits little sign of structure. The solid phase absorption spectra of COSe and CSe_2 were not studied.

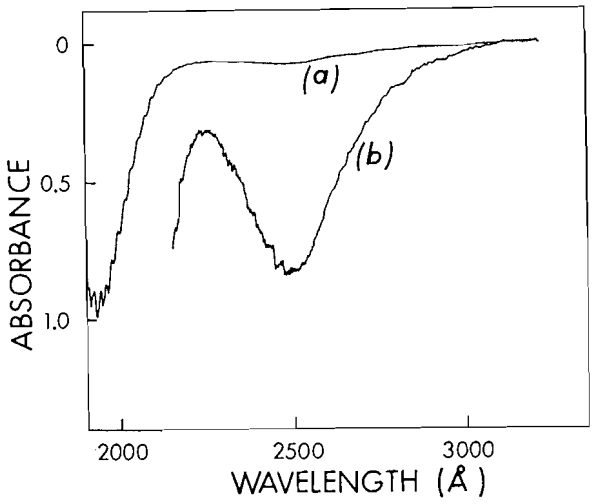


FIG. 1. Ultraviolet absorption spectrum of carbonyl selenide for a path-length of 10 cm: (*a*) 1 Torr COSe, (*b*) 15 Torr COSe.

Electron Spin Resonance Spectra

The observed e.s.r. signals will be separated into six distinct spectra. These are listed in Table I, together with assignments which will be discussed below.

TABLE I

Assignments of observed e.s.r. signals

Spectrum	Source	g	Assignment
A	Unirradiated amorphous selenium	2.0	Free electrons or conduction band
B	*In situ* photolysis of COSe	3	Se(4^3P)
C	*In situ* photolysis of COSe	2.2	Se_2
D	Photolysis of COSe or CSe_2	2.0	Selenium chains
E	Photolysis of CSe_2	2.05	$\cdot(CSe)_n\cdot$
F	Photolysis of COSe (1% in Xe)	2.3	Unassigned

Selenium

A degassed sample of amorphous selenium was melted in a sample tube, and rapidly cooled by plunging into liquid nitrogen. A comparatively narrow e.s.r. line (5 G half-line width) at $g = 2.00$ was detected at temperatures between 77 and 512 °K (Fig. 2) (A). When the sample was melted in the cavity a very broad e.s.r. absorption also appeared at lower fields. The line at $g = 2.04$ reported by Gager (1) was absent. Unlike sulfur, which in amine solutions exhibits a spectrum characteristic of sulfur chains (11), no spectra were obtained at 77 °K or at room temperature from solutions of selenium in piperidine or CS_2.

Can. J. Chem. Downloaded from www.nrcresearchpress.com by 210.87.254.105 on 09/05/12
For personal use only.

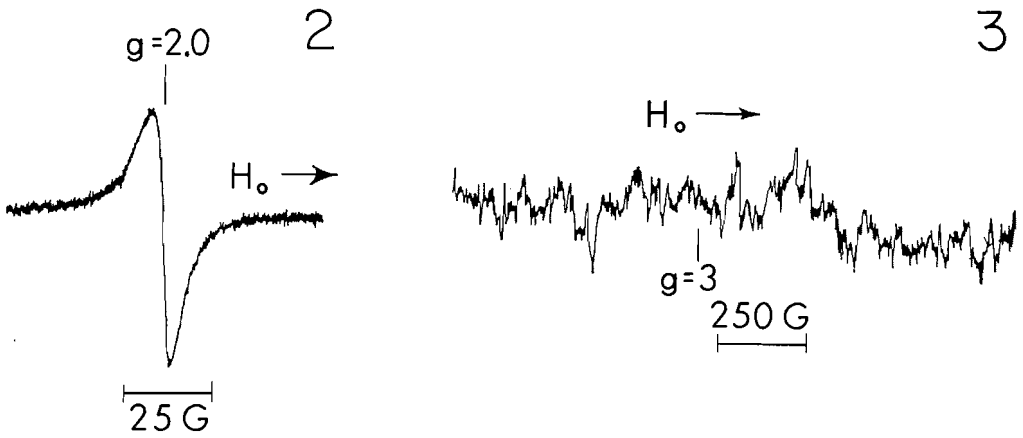


FIG. 2. Electron spin resonance spectrum of elemental selenium (A) for an integrative time constant of 0^{-4} s and an amplifier gain of 320 (arbitrary scale).

FIG. 3. Electron spin resonance absorption near $g = 3$ observed during *in situ* photolysis of COSe (1% in Xe) (B) for an integrative time constant of 0.3 s and an amplifier gain of 4 000 (arbitrary scale).

Selenides

The following mixtures were photolyzed for 24 h at 77 °K:

COSe	100%; 1% in Xe; 1% in *trans*-2-butene
CSe_2	5% in Xe; 0.1% in Xe.

During irradiation samples gradually reddened, suggesting the formation of elemental selenium. Samples containing CSe_2 became distinctly darker than those containing COSe.

In addition, a sample of COSe (1%) in Xe was photolyzed in the microwave cavity. During this *in situ* photolysis, three weak absorption signals were observed. A broad, ill-defined signal centered close to $g = 3$ (Fig. 3) (B), formed very rapidly and reached its maximum intensity after a few minutes irradiation. Meanwhile, a single line (C) at $g = 2.2$ built up, as well as a broad signal which appeared to contain spectrum A, partially obscured by a line at $g = 2.0$ due to radicals trapped in the wall of the quartz insert Dewar. When the mercury lamp was extinguished, the spectra at $g = 3.0$ and $g = 2.2$ decayed very rapidly.

The spectra obtained from COSe and CSe_2 matrices were generally very similar, particularly when the samples were warmed above 77 °K. When COSe (100%) was irradiated through a 7910 Vycor filter, which cut off light with $\lambda < 2\,300$ Å, no spectrum was observed. Since the sample remained colorless throughout the irradiation it was assumed that photolysis had been prevented (COSe vapor is decomposed by λ 2 537 Å. W. J. R. Tyerman. Unpublished results). No e.s.r. spectrum was obtained from irradiated COSe–*trans*-2-butene mixtures, although these samples became red during irradiation. In the gas phase, selenium atoms react very rapidly with *trans*-2-butene (A. B. Callear and W. J. R. Tyerman. To be published), forming an adduct which decomposes in ~1 s. Evidently *trans*-2-butene acts as a scavenger of Se during solid-phase photolysis, although elemental selenium is still ultimately produced. From the results of Windle, Wiersema, and Tappel (2), we anticipate that e.s.r. absorption of any selenide radical intermediate would be of very low intensity.

At 77 °K, both COSe and CSe_2 samples displayed the broad and narrow signals A and D (Fig. 4). A line also formed at $g = 2.2$ in some samples. In the COSe–Xe matrix a very

Can. J. Chem. Downloaded from www.nrcresearchpress.com by 210.87.254.105 on 09/05/12
For personal use only.

intense asymmetric line appeared at $g = 2.3$ (half-line width ~130 G) (Fig. 5) (F), and the signals at $g = 2.0$ were absent.

Two types of warm-up experiment were performed; first the spectrum of the sample was run at the temperature cited (internal warm-up) and then the sample was returned to 77 °K and a second spectrum was obtained (external warm-up). The significance of changes in spectra at different temperatures has been discussed by Ingram (12). At 93 °K, all samples showed some alteration in their spectra, the most striking change being the appearance of a strong line at $g = 2.3$, similar to F. This line decreased markedly in intensity when the sample was returned to 77 °K. Upon further warming between 93 and 130 °K, however, the general characteristics of this line altered little.

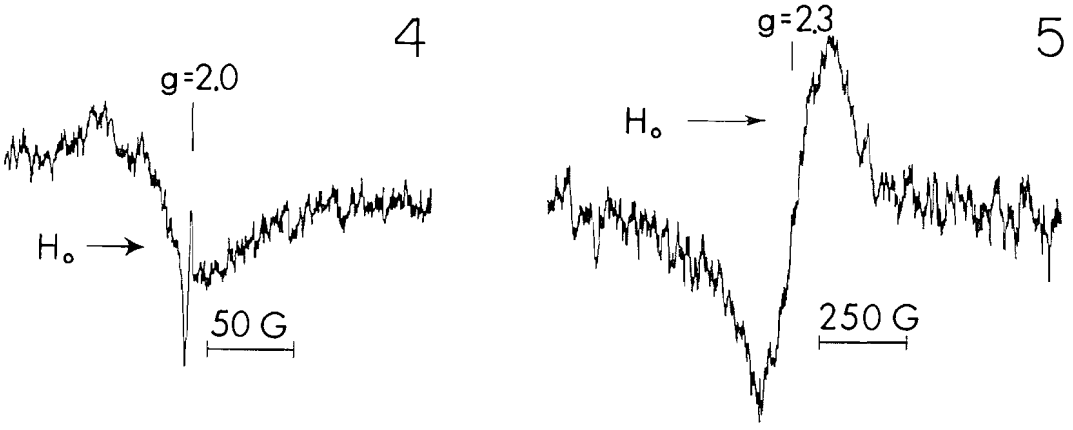


FIG. 4. Electron spin resonance spectrum observed in CSe_2 (5% in Xe) after photolysis (A, D, and E) for an integrative time constant of 0.3 s and an amplifier gain of 2 000 (arbitrary scale).
FIG. 5. Electron spin resonance line at $g = 2.3$ detected in photolyzed COSe (1% in Xe) (F) for an integrative time constant of 0.3 s and an amplifier gain of 2 000 (arbitrary scale).

Significant changes were also observed in spectrum D as the temperature was increased from 93 to 130 °K (internal and external warm-up) (Fig. 6). In addition slight differences appeared between the COSe and CSe_2 matrices. The spectrum broadened considerably, developing a structure similar to that of sulfur chains (4). Near $g = 2.05$ a broad line (E) was evident in CSe_2 samples, but absent in those of COSe.

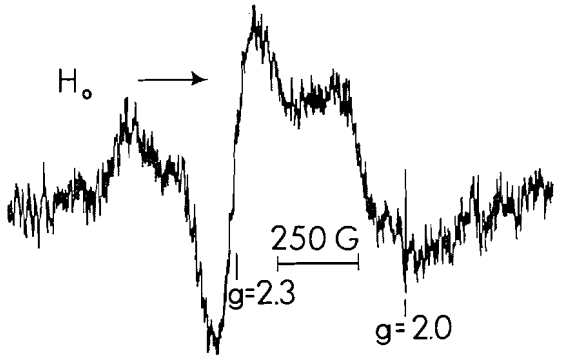


FIG. 6. Electron spin resonance spectrum of photolyzed COSe (1% in Xe) after warm-up of sample to 130 °K (A, D, and F) for an integrative time constant of 0.3 s and an amplifier gain of 4 000 (arbitrary scale).

Can. J. Chem. Downloaded from www.nrcresearchpress.com by 210.87.254.105 on 09/05/12
For personal use only.

The narrow line at $g = 2.0$ did not change appreciably up to 130 °K, which was the highest temperature at which our experiments were performed.

DISCUSSION

Most of the observed spectra are broad and lack structure; we must therefore attempt to identify their carriers from chemical and physical evidence, rather than by analysis of the line positions. However, it is useful first to predict the g-values at which we might expect to detect resonance. A ground state selenium atom (4^3P_2) contains two unpaired electrons in 4p orbitals, and the corresponding Landé g-factor is 1.5. A half-field transition (in which both electron spins are simultaneously reversed) should also appear at $g = 3.0$; this is expected to be less broad and therefore more readily detectable than the line at $g = 1.5$ (E. Wasserman. Private communication). The ground state of Se_2 approaches Hund's case c (13) in the gas phase and the Zeeman effect for such molecules has been described (14). At low rotational quantum numbers it is equivalent to that of a case b molecule such as O_2; e.s.r. transitions will therefore occur at $g = 2.0$ and $g = 4.0$, if the zero-field splitting of Se_2 is small. In the gas phase, O_2 displays paramagnetic resonance at $g = 1.9998$ (15); g-values observed in O_2 – quinol clathrates are slightly lower (16). Selenium chains, $\cdot Se(Se)_nSe\cdot$, might also be produced and, if n is sufficiently large, these behave as biradicals (double doublet states and not triplets), with e.s.r. signals near $g = 2.0$. Additionally in CSe_2 samples we might expect $(CSe)_n$ polymers to form; these will behave also as double doublet species. Interaction of the electrons with the d-orbitals or nuclei of Se act as further perturbations, tending to increase the g-value of a doublet radical by about 5% (2, 3).

During *in situ* photolysis of COSe, a signal appeared weakly at $g = 3.0$ (B), relatively more intense than the lines near $g = 2.0$, and decayed rapidly when irradiation ceased. This is therefore borne by a precursor of the carriers of the spectra, and on the basis of the g-values suggested above, we assign it to $Se(4^3P)$. Evidently, $Se(4^1D_2)$, produced by photolysis of COSe, is rapidly relaxed in the matrix to the triplet state. A similar conclusion was derived from the work on COS (4). In the gas phase, the abstraction reaction

$$Se(4^1D_2) + COSe \rightarrow CO + Se_2$$

may be important, although it is spin-forbidden if a product is $Se_2(X^3\Sigma)$. The spin rule will be somewhat relaxed for Hund's case c coupling, where the spin quantum number is no longer a 'good' quantum number.

The dissociation energy of COSe is unknown, but the gas-phase reaction

$$COSe + Se(4^3P) \rightarrow CO + Se_2$$

would probably be almost thermoneutral; abstraction from CSe_2 is ~40 kcal endothermic, and is therefore unlikely to occur under our conditions. Se_2 formed by combination of two (4^3P) atoms bears 73 kcal/mole (13) and may therefore induce local melting of the matrix, facilitating migration prior to polymerization. At 77 °K, we therefore expect atomic selenium to polymerize, either by abstraction of Se from COSe or by combination of free atoms. The first product in either case is Se_2, and it seems reasonable to assign the spectrum at $g = 2.2$, observed in *in situ* photolyses of COSe, to Se_2 in spite of there being no resonance at the half-field value, $g = 4.4$. This spectrum and B decay very rapidly, showing that polymerization of Se and Se_2 is fast, even in the solid state at 77 °K.

The spectrum at $g = 2.0$ is more interesting because it contains two distinct lines, one of which, A, was also observed in elemental selenium. This comparatively narrow line (half-line width 5 G) in the photolyzed selenides cannot correspond to the same radical as the

Can. J. Chem. Downloaded from www.nrcresearchpress.com by 210.87.254.105 on 09/05/12
For personal use only.

broader signal, since the relative intensities of the two lines varied with temperature. A very broad line (half-line width 225 G) from metallic tellurium has been reported, and is attributed to the presence of free holes in the valence band (9). We propose that this signal in selenium corresponds either to free electrons (F centers) or to free holes (V centers), which may have line-widths of the order of a few gauss (12, 17). It is surprising that no signal in elemental selenium could be assigned to selenium chains, as these are known to be present in molten Se (8). It is reasonable, however, to assign spectrum D from photolyzed selenides to selenium chains, which must ultimately form by combination of Se_2, etc., and which would account for the red coloration of the samples. When the samples were warmed to 113 °K, this spectrum developed structure which was very similar to that of sulfur chains between 77 and 298 °K (Fig. 6); this is evidence in support of our assignment. A very crude estimate of the chain-length is made by assuming that the signals correspond to at least ten times the minimum that can be detected by the spectrometer ($\sim 10^{14}$ free spins). About 2×10^{-6} moles of Se atoms were produced in the COSe matrices during 24 h irradiation (as determined from the amount of CO formed, each mole of which corresponds to one mole of Se atoms). Each chain bears two free spins, and therefore we were detecting $\sim 5 \times 10^{14}$ chains, and 12×10^{17} atoms. If no ring polymers exist, an upper limit for the average chain length is 2 400 atoms, which may be compared with the value of 10^4 atoms at 490 °K (8).

Presumably the free electrons in $(CSe)_n$ chains are localized on C, rather than Se, atoms; their g-value is therefore expected to lie closer to 2.0 than that of free electrons in a selenium chain. We therefore assign the spectrum at $g = 2.05$, (E) observed in CSe_2 samples, to $\cdot(Se)\cdot_n$.

We have been unable to assign spectrum F, at $g = 2.3$. At 77 °K, this signal and that at $g = 2.0$ are both very broad, and their overlap probably results in the appearance of the line at $g = 2.2$ in samples externally photolyzed; i.e. this signal is quite distinct from the signal at $g = 2.2$ observed during *in situ* photolysis and attributed to Se_2. The very large reversible temperature effects of the spectrum at $g = 2.3$ indicate that it is carried by a simple species rather than, for example, a long-chain polymer.

CONCLUSION

Polymeric chains of selenium build up in photolyzed samples of COSe and CSe_2 at 77 °K; $Se(4^3P)$ and Se_2 were identified as precursors, by e.s.r. spectroscopy. The e.s.r. spectrum of selenium contains a line which is attributed to free electrons or free 'holes' in its valence bands; this is an example of metallic behavior intermediate between that of sulfur and tellurium.

EXPERIMENTAL

Spectra were recorded as the first derivative of the resonance absorption using a Varian E.P.R. spectrometer (type 4502), operating at a nominal frequency of 9.5 Gc/s and using 100 kc/s magnetic field modulation. The spectrometer was fitted with a dual cavity (V4532), a variable temperature accessory, and a Fieldial (V-FR-2503) magnetic field regulator. The g-values of the spectra were measured by extrapolation from the three lines of Fremy's salt (18). It was not necessary to calibrate the spectrometer precisely at g-values far removed from 2.0 because the spectra were too broad for accurate measurements of line centers. All spectra, except those from Fremy's salt, were recorded with a modulation amplitude of about 2 G. Those from the calibrating standard were recorded using 0.2 G modulation. Other experimental parameters for each spectrum are listed with the corresponding figure.

Gas mixtures were prepared in 5 l bulbs and left for several hours to equilibrate, before being distilled into thin-walled quartz sample tubes and degassed. Despite large differences in the boiling points of the components, no difficulty was encountered due to separation of the mixtures in handling. Each sample was irradiated in a quartz Dewar cooled by liquid N_2 (77 °K), using the output of a Hanovia medium-pressure mercury arc, which emits discontinuously at $\lambda > 2\,200$ Å. The usual period of irradiation was 24 h. In one

Can. J. Chem. Downloaded from www.nrcresearchpress.com by 210.87.254.105 on 09/05/12
For personal use only.

series of experiments, the sample was photolyzed in the microwave cavity, by focussing light from a high-pressure mercury arc through a slotted plate which formed one boundary of the cavity. All samples were stored at 77 °K after irradiation.

Materials

Assayed reagent grade xenon (Airco), ethylene, and *trans*-2-butene (Phillips Petroleum Co. Research Grade) were used without further purification.

CSe_2 was prepared by the reaction of CH_2Cl_2 with molten Se at 500 °C (19). The product was separated from CH_2Cl_2 by distillation at 193 °K. COSe was obtained in low yield by passing dry CO over molten selenium (20); the product was distilled and degassed, and the infrared spectrum of the vapor showed no bands which could not be assigned to COSe (21), apart from CO_2 bands observed at low intensity. The ultraviolet absorption spectrum of COSe was obtained with a Perkin-Elmer model 202 recording spectrophotometer. Selenium was obtained from Fisher, and was >99.9% pure.

ACKNOWLEDGMENT

The authors are indebted to the National Research Council for financial assistance.

REFERENCES

1. W. B. GAGER. Private communication. Cited in ref. 2.
2. J. J. WINDLE, A. K. WIERSEMA, and A. L. TAPPEL. J. Chem. Phys. **41**, 1996 (1964).
3. E. MÜLLER, H. B. STEGMANN, and K. SCHEFFLER. Ann. **657**, 5 (1962).
4. D. A. STILES, R. KEWLEY, O. P. STRAUSZ, and H. E. GUNNING. Can. J. Chem. **43**, 2442 (1965).
5. A. B. CALLEAR and W. J. R. TYERMAN. Trans. Faraday Soc. **61**, 2395 (1965).
6. A. B. CALLEAR. Proc. Roy. Soc. Ser. A, **276**, 401 (1963). M. DESORGO, A. J. YARWOOD, O. P. STRAUSZ, and H. E. GUNNING. Can. J. Chem. **43**, 1886 (1965).
7. K. S. SIDHU, I. G. CSIZMADIA, O. P. STRAUSZ, and H. E. GUNNING. J. Am. Chem. Soc. In press. 1966.
8. A. EISENBERG and A. V. TOBOLSKY. J. Polymer Sci. **46**, 19 (1960).
9. W. R. DATARS, G. FISCHER, and P. C. EASTMAN. Can. J. Phys. **41**, 178 (1963).
10. A. E. DOUGLAS and E. R. V. MILTON. J. Chem. Phys. **41**, 357 (1964).
11. W. A. HODGSON, S. A. BUCKLER, and G. PETERS. J. Am. Chem. Soc. **85**, 543 (1963).
12. D. J. INGRAM. Free radicals as studied by e.s.r. Butterworths, London. 1958.
13. G. G. CHANDLER, R. F. BARROW, and C. B. MEYER. Phil. Trans. Roy. Soc. London, Ser. A. In press. 1966.
14. F. H. CRAWFORD. Rev. Mod. Phys. **6**, 90 (1934).
15. K. D. BOWERS, R. A. KAMPE, and C. D. LUSTIG. Proc. Roy. Soc. London, Ser. A, **251**, 565 (1959).
16. S. FONER, H. MEYER, and W. H. KLEINER. J. Phys. Chem. Solids, **18**, 273 (1961).
17. D. R. SMITH and J. J. PIERONI. Can. J. Chem. **43**, 876 (1965).
18. G. E. PAKE, J. TOWNSEND, and S. I. WEISSMAN. Phys. Rev. **85**, 682 (1952).
19. D. J. G. IVES, R. W. PITTMAN, and W. WARDLAW. J. Chem. Soc. 1080 (1947).
20. T. G. PEARSON and P. L. ROBINSON. J. Chem. Soc. 652 (1932).
21. T. WENTINK. J. Chem. Phys. **29**, 188 (1958).

Can. J. Chem. Downloaded from www.nrcresearchpress.com by 210.87.254.105 on 09/05/12
For personal use only.

Can. J. Chem. Downloaded from www.nrcresearchpress.com by 210.87.254.42 on 09/05/12
For personal use only.

THE DESCRIPTION AND USE OF A SPIN-ECHO SPECTROMETER TO STUDY CHEMICAL EXCHANGE[1]

K. H. Abramson, P. T. Inglefield, E. Krakower, and L. W. Reeves
Chemistry Department, University of British Columbia, Vancouver, British Columbia

Received February 1, 1966

ABSTRACT

A spin-echo spectrometer, suitable for studies of chemical exchange, is described. The performance of the apparatus is described and illustrated. From a Carr–Purcell sequence of pulses T_2 measurements have been made using two alternative schemes for the correction of cumulative error in the width of π pulses. Agreement is satisfactory and the standard errors in each method are $\pm 5\%$ of the average T_2. The Meiboom and Gill method of phase-shifting the r.f. in the first pulse has the advantage of more flexibility in the choice of pulse intervals.

A theory developed by Bloom, Reeves, and Wells for the dependence of T_2 measured in a Carr–Purcell experiment on pulse intervals in the presence of a suitable exchange process has been tested experimentally for two molecules. The rate constants for the hindered internal rotation about the N=N bond in *N,N*-dimethylnitrosamine agree for the following sets of data: (*a*) a previous high-resolution study by Phillips, (*b*) a repeated high-resolution study made in this work, (*c*) spin-echo studies using the complete closed expression for a two site exchange process, and (*d*) the approximate expression derived for the limit of fast pulse repetition rates.

A similar study by the spin-echo method of the rates of internal rotation about the C=N bond in *N,N*-dimethyltrifluoroacetamide does not agree with a previous high-resolution study. Since the chemical shift between the inequivalent methyl groups is so small, it is suggested that the rates of rotation in this molecule are much better evaluated by the spin-echo method.

The spin-echo method can more easily take account of variations with temperature of the natural relaxation time and the chemical shift. The non-selective nature of an experiment with such a large H_1 field remains a disadvantage at this time. The selective deuteration of sites unaffected by exchange is in general difficult enough to limit the scope of the spin-echo method when protons are observed.

INTRODUCTION

The time constant for the decay of echo amplitudes in a Carr–Purcell spin-echo experiment (2) is affected by the pulse interval, even in a homogeneous magnetic field, if there is a chemical exchange which modulates the Larmor frequencies at a rate comparable to the frequency difference (17, 3, 4). The general solution for the decay of echo amplitudes has been presented by Bloom, Reeves, and Wells (1) for the case of exchange involving two Larmor frequencies in the absence of spin-coupling. From considerations of simple probability theory for phase angle distribution in the $x'y'$ plane and the use of a matrix operator technique to generate the amplitude of alternate echoes, it can be shown that the magnetization at a time $4n\tau$ is related to the initial magnetization by an expression involving the sum of two exponentials;

$$[1] \qquad M(4n\tau) = A_1 \exp(-r_1 4n\tau) + A_2 \exp(-r_2 4n\tau)$$

where $\tau = \frac{\pi}{2}$, π pulse interval, $n = 0, 1, 2 \ldots$ etc., A_1 and A_2 are constants which depend upon the initial conditions, and r_1 and r_2 are two time constants, which are independent of the initial conditions. A similar relationship has been derived (5) by the use of the Bloch equations (6).

In this paper, experimental results will be presented for two special cases when the

[1]*Paper presented in part at International Symposium on Nuclear Magnetic Resonance, Tokyo, Japan, September 3, 1965.*

population of one site is equal to that of the other. In this event a single time constant r_1 dominates the decay of echo amplitudes and this is given by (1)

$$[2] \qquad r_1 = k - \frac{1}{2\tau}\sinh^{-1} F$$

where

$$\text{if } \omega > k,\ F = \frac{k}{(\omega^2 - k^2)^{1/2}} \sin 2\tau(\omega^2 - k^2)^{1/2}$$

$$\text{if } \omega < k,\ F = \frac{k}{(k^2 - \omega^2)^{1/2}} \sinh 2\tau(k^2 - \omega^2)^{1/2}$$

$$\text{if } \omega = k,\ F = 2k\tau$$

$$k = \frac{k_a + k_b}{2} = \text{mean rate constant for the exchange process}$$

$$\omega = \frac{\omega_a - \omega_b}{2} = \text{half chemical shift in radians } s^{-1}$$

$$\tau = \frac{\pi}{2},\ \pi \text{ pulse interval.}$$

In much of the experimentation described here a further simplification can be made if $k\tau \ll 1$ and $\omega\tau \ll 1$:

$$[3] \qquad r_1 = \tfrac{2}{3}k\omega^2\tau^2.$$

This assumption is valid for $\omega > k$ and $k > \omega$ and applies in the region of small pulse intervals (short τ limit). The time constants r result entirely from the exchange effect, and in the actual experiments account is taken of the additional natural relaxation processes expressed as the time constant $1/T_{2_0}$.

$$[4] \qquad \frac{1}{T_{2(\mathrm{CP})}} = \frac{1}{T_{2_0}} + r_1$$

where $1/T_{2(\mathrm{CP})}$ = time constant of exponential decay observed in the Carr–Purcell experiment.

The application of spin-echo methods to the study of chemical exchange have been made previously by Reeves and co-workers (3, 4) and Luz and Meiboom (7). The latter workers derived an approximate expression for a multi-site exchange process for the limit of short pulse intervals and fast exchange, $k \gg \omega$. This equation will not be used here. A considerable volume of work by Gutowsky and co-workers has appeared while this present study was in progress (8–11). Insofar as the present study applies our original equations (1) to different rate processes, there is no overlap in the two parallel investigations. This paper should serve as an independent evaluation of the advantages and limitations of the spin-echo method to the study of chemical kinetics in the simplest cases (8–11).

EXPERIMENTAL

Chemicals

N,N-dimethylnitrosamine was prepared by the reaction of dimethylamine hydrochloride and sodium nitrite in acid solution. The mixture was distilled to dryness and the distillate was treated with an excess of solid potassium carbonate. The nitrosamine appeared as a yellow oil which was further treated with potassium carbonate to remove water. The dimethylnitrosamine, b.p. 150–151 °C, was then doubly distilled.

The overall reaction is given as:

$$(CH_3)_2NH + HNO_2 \rightarrow (CH_3)_2NNO + H_2O.$$

Can. J. Chem. Downloaded from www.nrcresearchpress.com by 210.87.254.42 on 09/05/12
For personal use only.

N,N-dimethyltrifluoroacetamide was prepared by the reaction of methyl trifluoroacetate and dimethylamine gas at −7 °C. The solution was then left at room temperature for 12 h and the product *N,N*-dimethyltrifluoroacetamide (b.p. 134–136 °C) was distilled out to 81% yield:

$$CF_3CO.OMe + NMe_2H \xrightarrow[\text{saturate}]{-7\ ^\circ C} MeOH + CF_3CO.NMe_2.$$

The steady state spectrum of pure *N,N*-dimethylnitrosamine was studied at 60 Mc/s on a Varian A60 spectrometer at temperatures in the range 125–195 °C. The exchange-modified spectrum was similar to that reported by Phillips (12) and Blears (13). The equations of Piette and Anderson (14) were used to derive rate constants from the line widths in the slow exchange limit.

Spin-Echo Apparatus

The spin-echo spectrometer operated at 40 Mc/s and was constructed in our own laboratories. It has not been reported previously, hence some description will be given here. The magnetic field was provided by a Varian 12 in. magnet shimmed for high-resolution experiments and with additional homogeneity trimming provided by a Varian V-4365 field homogeneity control unit. The non-spinning samples had a T_2^* (measured from the free induction tail) of 150 ms.

Figure 1 illustrates the generation of the Carr-Purcell pulse sequence. The r.f. generator, Fig. 2, consisted of a highly stable 10 Mc/s crystal oscillator, a pulse modulator stage, two frequency doublers, a 40 Mc/s driver stage and a push-pull final amplifier stage. The 10 Mc/s crystal was thermostatically maintained at

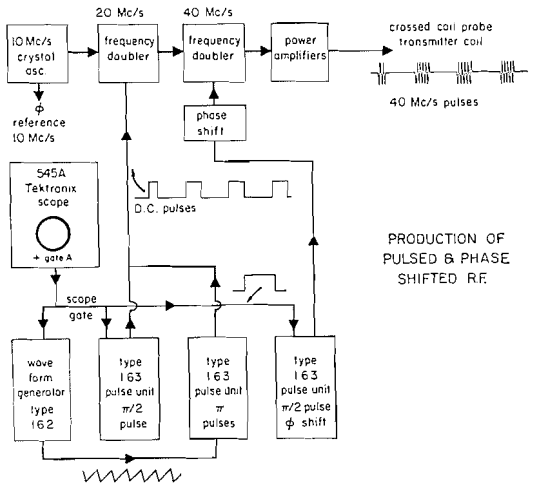


FIG. 1. Generation of the Carr–Purcell pulse sequence.

85 °C in a crystal oven. Careful interstage shielding was used to virtually eliminate 40 Mc/s leakage during the "pulse off" period. Phase coherent 40 Mc/s r.f. pulses were obtained by allowing the 10 Mc/s oscillator to run continuously while pulse-modulating the first doubler stage. A 90 degree r.f. phase shift during the $\frac{\pi}{2}$ pulse was accomplished in the second doubler grid circuit by means of the Meiboom and Gill method (15). In this method a pulse, identical to the $\frac{\pi}{2}$ modulation pulse, switches a back-biased semiconductor diode into its conductive stage; this procedure effectively places a phase-changing capacitor across the tuned circuit for the duration of the $\frac{\pi}{2}$ pulse. The 90 degree r.f. phase shift during the $\frac{\pi}{2}$ pulse served to minimize the effect of accumulative error which might occur in the width of the π pulses. The peak r.f. output power of this unit was approximately 250 W, giving a π rotation of magnetization in ~15 μs.

The modulating pulse train was synthesized by the combined use of a Tektronix 545A oscilloscope, a Tektronix Type 162 waveform generator and three Type 163 pulse generators. A positive gate voltage was fed from the +Gate A terminal of the oscilloscope to the trigger inputs of two Type 163 pulse generators (modified to give pulse amplitudes of +90 V peak). These two generators produced the single $\frac{\pi}{2}$ modulating pulse and the 90 degree r.f. phase shifting pulse. The $\frac{\pi}{2}$ and r.f. phase shift pulses were thus synchronized with

Can. J. Chem. Downloaded from www.nrcresearchpress.com by 210.87.254.42 on 09/05/12
For personal use only.

Can. J. Chem. Downloaded from www.nrcresearchpress.com by 210.87.254.42 on 09/05/12
For personal use only.

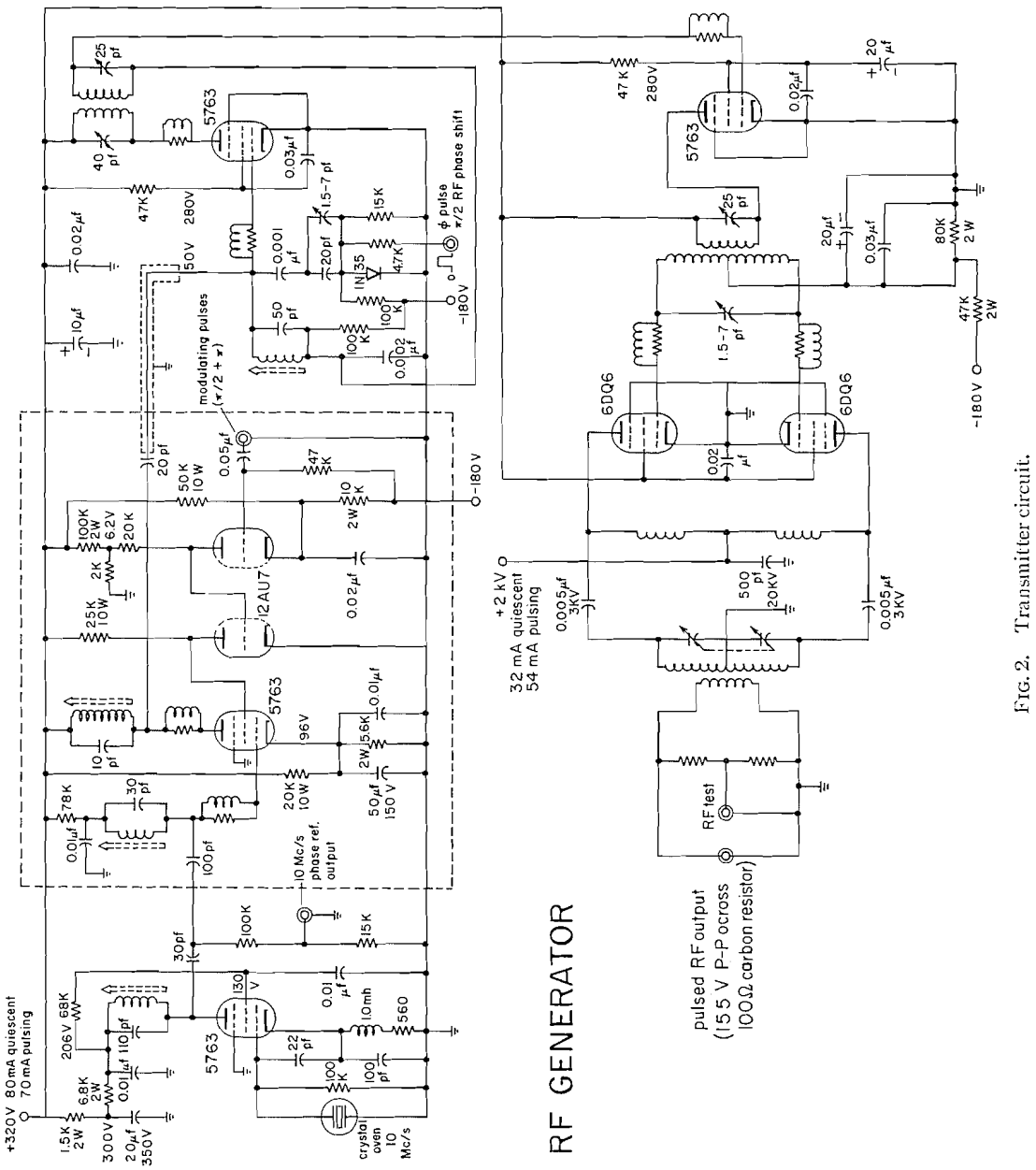


FIG. 2. Transmitter circuit.

the beginning of the oscilloscope sweep. To produce the modulating train of π pulses at times τ, 3τ, 5τ, etc., the same + Gate A from the oscilloscope was used to gate a Type 162 waveform generator, producing a negative sawtooth train of variable frequency. This negative sawtooth train was used to trigger the remaining Type 163 pulse generator ("negative trigger" mode), producing the train of π modulating pulses. The train of π pulses could be delayed from the $\frac{\pi}{2}$ pulse simply by adjusting the "output pulse delay" control. The π pulse repetition period was adjusted by means of the "pulse interval" control on the waveform generator (Type 162).

A Varian crossed coil probe was used and modified by appropriate changes of capacitors in the transmitter coil circuit to facilitate impedance matching. The probe can be used both for high-resolution and spin-echo experiments. The Varian probe, although quite inefficient in coupling r.f. energy from the transmitter coil to the sample, did give a homogeneous H_1 field as indicated by the complete disappearance of the induction tail after a π pulse in a $\frac{\pi}{2}$, π pulse sequence. Receiver coil orthogonality and the leakage paddles used normally for high-resolution studies could be adjusted to obtain excellent isolation between the transmitting and receiving coils. This adjustment was made such that the central portion of the r.f. pulse sensed by the receiver was negligible and only the high-frequency components (the leading and trailing edges) of the pulse were detected (as two small spikes). This optimal isolation condition facilitated quick receiver recovery time ($\sim$3 μs) and avoided inducing into the receiver coil large "ringing currents" which could distort the overall H_1 from the transmitter coils. Such optimal conditions were not required for all of the present work, but were maintained as a matter of routine. The experiments described here were performed in a relatively homogeneous H_0 field so that a continuous signal of detected pulses and echoes occurred.

The receiver was a modified L.E.L.-I.F. amplifier which was used as a 40 Mc/s broadband receiver (Figs. 3*a*, 3*b*). The preamplifier section used cascaded 5 842 stages. Manual control of receiver gain was provided by varying the grid bias of the third and fourth stages. Two means of signal detection were provided: ordinary diode detection and phase detection. In the phase detection mode, any attempt to draw more power from the transmitter oscillator to achieve frequency quadrupling resulted in loss of drive to the subsequent stages of the transmitter with loss of and varying power to the probe. An amplifying stage was used

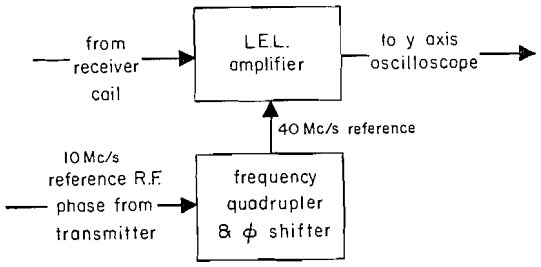


FIG. 3*a*. Block diagram of receiver circuit.

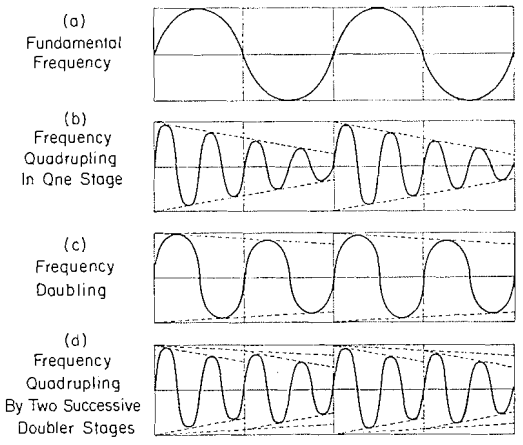


FIG. 3*d*. Waveforms resulting from frequency multiplication showing respective amplitudes.

Can. J. Chem. Downloaded from www.nrcresearchpress.com by 210.87.254.42 on 09/05/12
For personal use only.

Can. J. Chem. Downloaded from www.nrcresearchpress.com by 210.87.254.42 on 09/05/12
For personal use only.

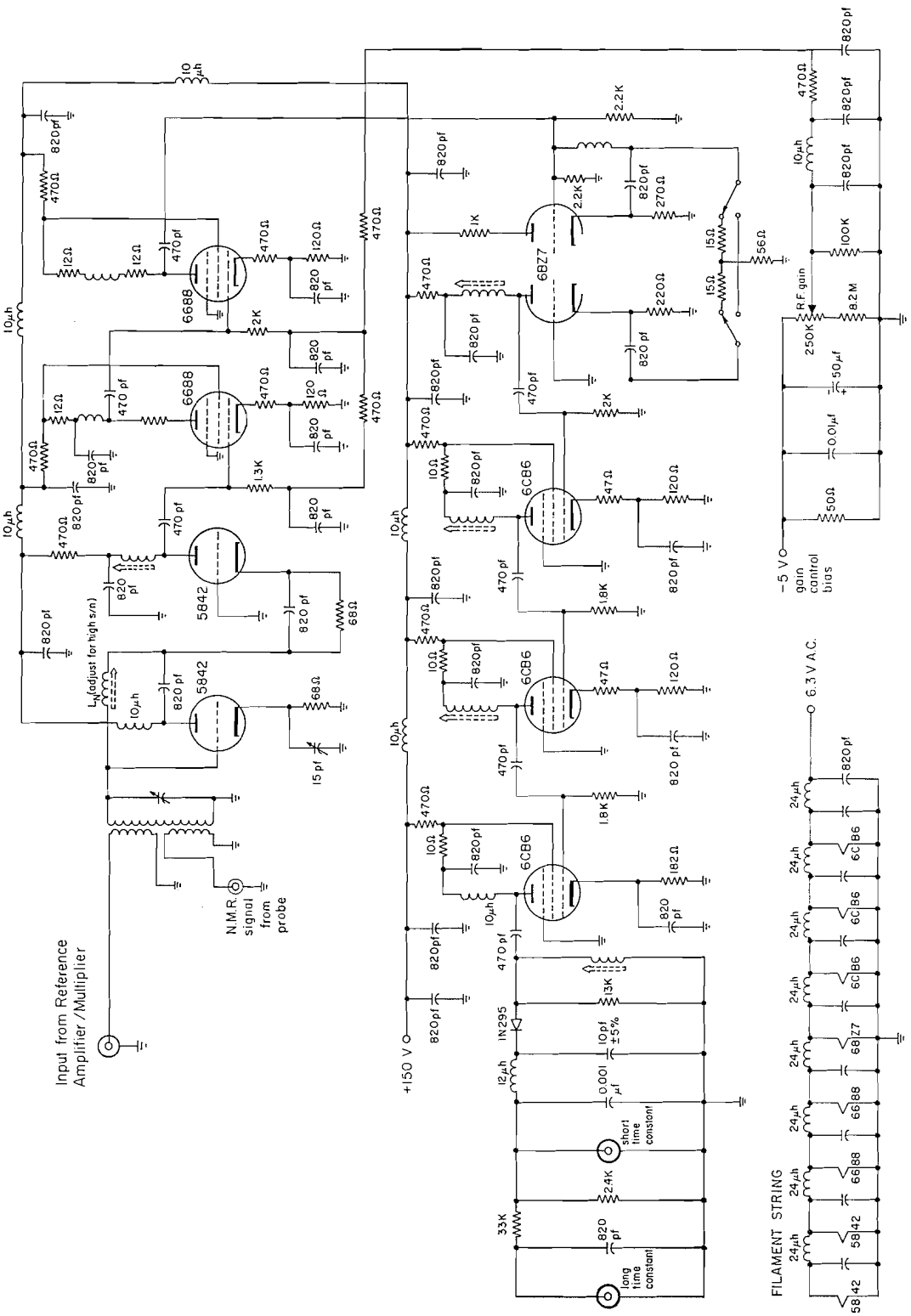


FIG. 3b. Receiver circuit.

Can. J. Chem. Downloaded from www.nrcresearchpress.com by 210.87.254.42 on 09/05/12
For personal use only.

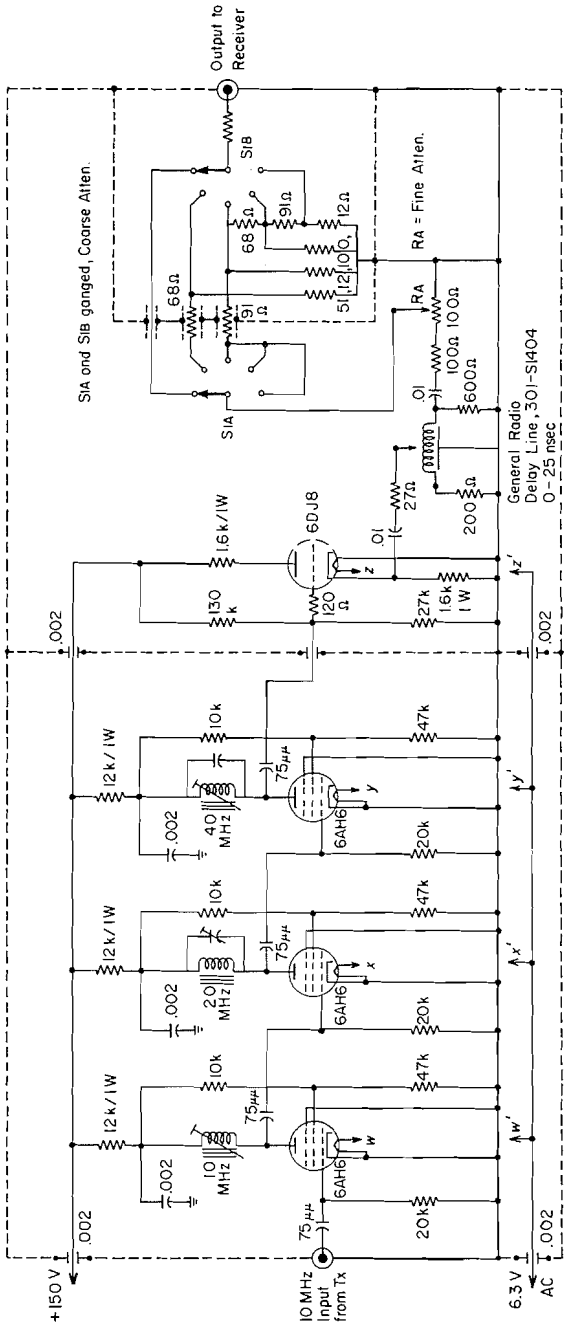


FIG. 3c. Reference signal amplifier, multiplier, phaser, and attenuator.

to raise the power available from the transmitter oscillator to that required for frequency modulating (V1 in Fig. 3*c*). To achieve efficient frequency multiplication with reasonably uniform output amplitude, two stages of frequency doubling were used (Fig. 3*d*). The original tube Type 6AH6 was used for all three stages; V1 as a 10 Mc/s amplifier, V2 doubling to 20 Mc/s, and V3 doubling to 40 Mc/s. An additional advantage of this method is the minimizing of the risk of self-oscillation present when more than one stage is tuned to the same frequency. Reference to the paper by W. Gilbert Clark (24) was made to achieve good control of the phasing and attenuation for the system (Fig. 3*c*). In most cases the experiments presented here did not require the use of the phase detector. The maximum receiver gain was 2×10^5 with a bandwidth of 3 Mc/s.

The echo amplitudes were photographed with a Polaroid oscilloscope camera on 3 000 A.S.A. film. Photographs were subsequently measured for echo amplitudes. Typical experiments are illustrated to indicate the performance of the apparatus. The π pulse interval was timed on a Hewlett Packard 522B electronic counter.

RESULTS

Some attempt has been made in this work to investigate the precision of our T_2 measurements in the Carr–Purcell experiment. The measurement is very sensitive to the resonance condition (16), the inclusion of a $\frac{\pi}{2}$ phase shift, and the homogeneity of the H_1 field.

The resonance condition in such a homogeneous field is quite difficult to maintain. The oscillator frequency was certainly stable enough but small magnetic field drifts over a period of even 5 min necessitated readjustments. These were easily achieved by observation of the free induction decay with phase sensitive detection. The field was swept to give zero beat each time. The measurements of T_2 values >5 s were appreciably shortened for slight field drifts from resonance. Satisfying the resonance condition is the most tedious part of the experimental procedure, and in future work, further precautions concerning this field drift will be taken. The magnitude of the magnetic field instability may be only 1 c.p.s. per minute but deterioration in performance can be detected after 15 min.

The accumulated error in echo amplitudes due to error in the width of the π pulse can also be corrected by working at certain off resonance conditions without a $\frac{\pi}{2}$ r.f. phase shift in the first pulse (18). In the off resonance experiment we have to observe the condition that the π–π pulse spacing is given by

$$2\tau = (2n + 1 \pm \tfrac{1}{2})T \qquad [5]$$

where $T = 2\pi/(\Delta\omega)_0$, 2τ is the 180°/180° pulse spacing, n is an integer, and $(\Delta\omega)_0$ is the angular frequency difference between the resonance condition and the applied frequency.

We found it satisfactory to work at about 4.5 Kc/s off resonance where the above condition could be satisfied for a range of 2τ between 1 and 10 ms. It must be noted that these off resonance experiments have far less flexibility in the pulse interval range and we found them much more difficult to perform when the pulse intervals were greater than 10 ms. All kinetic experiments reported here are repeated using both methods of obtaining T_2 and agreement to $\pm 5\%$ on T_2 is claimed. The performance of the apparatus, while using the Meiboom and Gill (15) phase shift is shown in Fig. 4. The column of figures on the left of this figure indicates the pulse interval 2τ. Experimental Carr–Purcell trains are given in the next column corresponding to these pulse spacings. The computed T_2 values in the third column vary, in this particular experiment performed on *N*,*N*-dimethylnitrosamine at 135 °C, from 10.1 s to 0.2 s. The time calibration for the decay can be obtained from the figures in column 4. The decays are all accurately exponential and with the large pulse spacing of 40.75 ms the individual echoes can be resolved.

A typical experiment such as that illustrated was performed at a series of temperatures

Can. J. Chem. Downloaded from www.nrcresearchpress.com by 210.87.254.42 on 09/05/12
For personal use only.

CARR-PURCELL TRAINS; N,N-DIMETHYLNITROSAMINE

Pulse Interval (2 τ), (ms)		$T_{2\,(C.P.)}$ (s)	Time Base (s/div.)
1.30		10.1	2.0
2.05		9.21	2.0
2.58		6.30	2.0
8.11		2.68	1.0
10.24		2.03	1.0
13.02		1.44	0.5
20.48		0.72	0.2
40.72		0.20	0.1

FIG. 4. Representative Carr–Purcell trains at different pulse intervals.

for each of the two molecules under study. The results in the form of log $1/T_{2(CP)}$ versus log $1/2\tau$ are plotted in Figs. 5 and 6 for *N,N*-dimethylnitrosamine and *N,N*-dimethyltrifluoroacetamide respectively. The general shape for the complete dependence of $T_{2(CP)}$ upon pulse separation 2τ is best seen in Fig. 6. When $1/2\tau$ is large the value of $1/T_2$ approaches the natural value in the absence of chemical exchange. At large pulse separations (2τ) the curve approaches the line width in the exchange-broadened steady state spectrum for the fast exchange limit. Both off-resonance and on-resonance results are plotted in Fig. 5. A considerable temperature dependence of T_{2_0}, the natural relaxation time in *N,N*-dimethylnitrosamine, can be seen in Fig. 5, which is very unusual because it indicates a shorter T_{2_0} as the temperature increases. This unusual behavior can be associated with the equilibrium

$$(CH_3)_2NNO \rightleftharpoons (CH_3)_2N\text{–}N(CH_3)_2 + 2NO,$$

which produces small but increasing amounts of paramagnetic nitric oxide as the temperature is raised. This unusual temperature dependence of T_{2_0} is not observed in *N,N*-dimethyltrifluoroacetamide. The requirement of a rather more homogeneous field is important for *N,N*-dimethylnitrosamine because it is necessary to extend measurements to the relatively high temperature of 190–195 °C where diffusion processes are rapid.

The value of the rate constant k was obtained by use of eq. [2]. The experimentally observed value of r was obtained from eq. [4]. The value of T_{2_0} was equated to T_1 measured in a separate experiment or was estimated by using the T_{2_0} indicated from Fig. 5 and 6 at infinitely fast pulse rates (a third method of estimating T_{2_0} from eq. [3] is described below.) An iterative FORTRAN program for an I.B.M. 7040 was used in which trial values of ω and k were inserted and for the experimental values of (2τ) the value of r was computed. These values of r were compared to experimental values and deviations were sensed by the computer. Changes in trial values of k were then made in order to minimize deviations from experimental values. The deviations were finally minimized by small changes in the choice of ω. The best overall values of k to fit as many as 20 experimental determinations of T_2 were found.

Can. J. Chem. Downloaded from www.nrcresearchpress.com by 210.87.254.42 on 09/05/12
For personal use only.

Can. J. Chem. Downloaded from www.nrcresearchpress.com by 210.87.254.42 on 09/05/12
For personal use only.

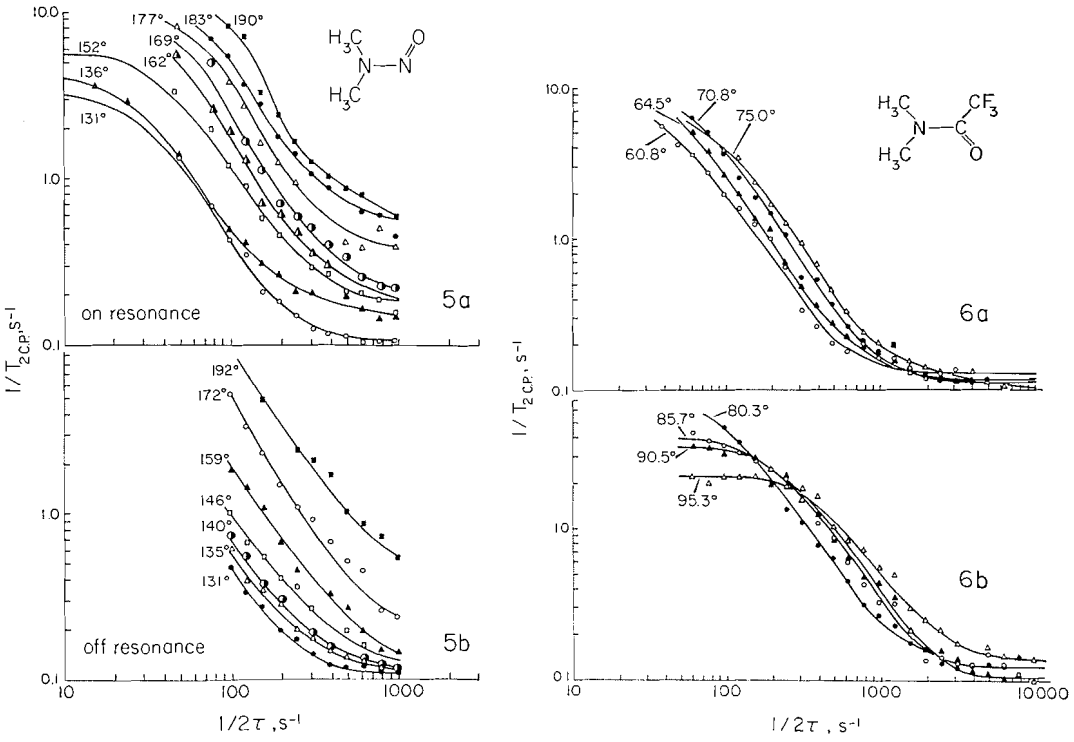


FIG. 5. Dependence of $T_{2(CP)}$ upon the pulse interval 2τ for *N,N*-dimethylnitrosamine: (*a*) on resonance, (*b*) off resonance.

FIG. 6. Dependence of $T_{2(CP)}$ upon the pulse interval 2τ for *N,N*-dimethyltrifluoroacetamide, on resonance: (*a*) 60.8 to 75.0 °C; (*b*) 80.3 to 95.3 °C.

It is of some interest to compare these values of k with those from the equation for the fast pulsing limit. Within the validity of eq. [3] the value of $1/T_{2(CP)}$ was plotted against $(\omega\tau)^2$ and a straight line was obtained for each temperature. The results for the two compounds studied are given in Figs. 7 and 8. Note that in Fig. 8, to avoid crowding, the values of $1/T_2$ are plotted without a scale and each temperature is vertically displaced on the diagram. The value of $1/T_2$ when $(\omega\tau)^2 = 0$ gives the natural relaxation time T_{2_0} which may be used also in the curve-fitting procedure for the full dependence of $1/T_{2(CP)}$ on

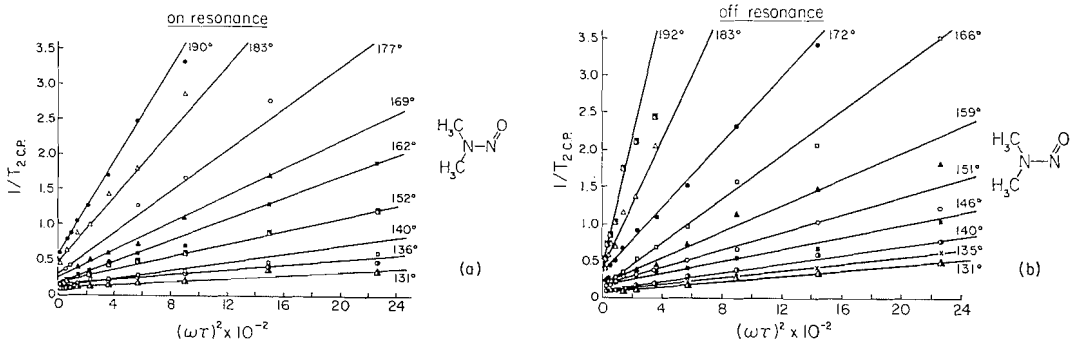


FIG. 7. "Short τ" limit plot for *N,N*-dimethylnitrosamine: (*a*) on resonance; (*b*) off resonance.

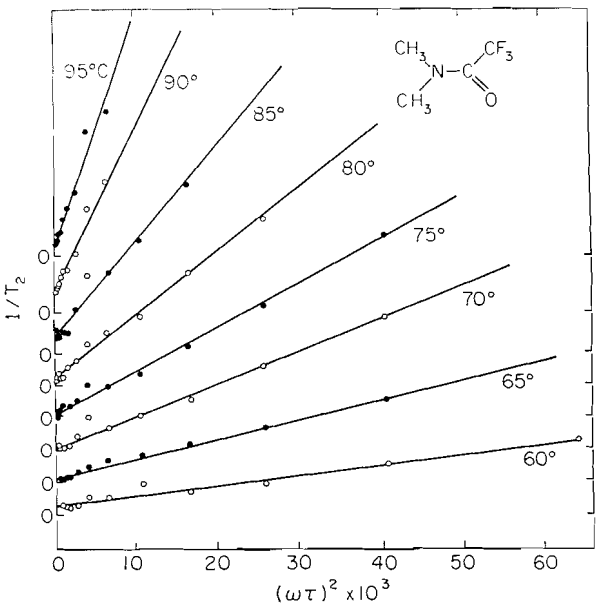


FIG. 8. "Short τ" limit plot for *N,N*-dimethyltrifluoroacetamide, on resonance.

$1/2\tau$. The values of ω chosen were those obtained in high-resolution experiments. A simple computer program was devised to obtain a least squares fit to the straight lines in Figs. 7 and 8 and the resulting slopes were converted to rate constants for each temperature. Then a least squares fit to the usual Arrhenius temperature dependence was used to evaluate the activation energy and frequency factor.

The important information derived from these experiments is the rate constant, k, and we compare the values of k for *N,N*-dimethylnitrosamine and *N,N*-dimethyltrifluoroacetamide in Tables I and II. The comparison with the high-resolution method

TABLE I

Comparison of rate constants (s^{-1}) for *N,N*-dimethylnitrosamine

T (°C)	k* off ω_0 spin-echo	k* on ω_0 spin-echo	k‡ A-60	k† off ω_0 spin-echo	k† on ω_0 spin-echo
140	2.52	1.97	2.55	3.70	3.40
151	7.56	6.44	4.90	5.80	6.30
160	11.8	8.73	10.3	10.1	8.00
172	33.0	25.5	21.9	55.4	31.9
183	48.7	27.4	44.0	74.9	47.5

*Least square analysis of $r_i \simeq k \mp k \pm 2k(\omega\tau)^2/3$.
†Computer-calculated $\sinh^{-1} F$ fit.
‡Steady state: Piette and Anderson (ref. 14).

in Table I refers to our own determination. The agreement between the various methods is remarkably good except for the comparisons in Table II with the data of Woodbury and Rogers (23). In view of the small chemical shift difference in the molecule studied we would suggest that the rates determined by the spin-echo method in the present paper are better estimations of the true rates.

Can. J. Chem. Downloaded from www.nrcresearchpress.com by 210.87.254.42 on 09/05/12
For personal use only.

TABLE II

Comparison of rate constants (s^{-1}) for *N,N*-dimethyltrifluoroacetamide

T (°C)	k* steady state	k† on ω_0 spin-echo	k‡ on ω_0 spin-echo
60.0	4.98	4.72	4.20
64.5	—	9.00	9.10
70.0	6.53	14.54	12.90
75.0	8.04	19.80	17.30
80.3	9.46	28.82	18.40
85.7	12.60	44.72	35.70
90.5	14.40	81.39	47.00
95.3	—	103.11	88.70

*Steady state: Woodbury and Rogers (ref. 23).
†Least square analysis of $r_i \simeq k \mp k \pm 2k(\omega\tau)^2/3$ ($E_a = 20.6 \pm 1.4$ kcal).
‡Computer-calculated $\sinh^{-1} F$ fit ($E_a = 18.5 \pm 2.7$ kcal).

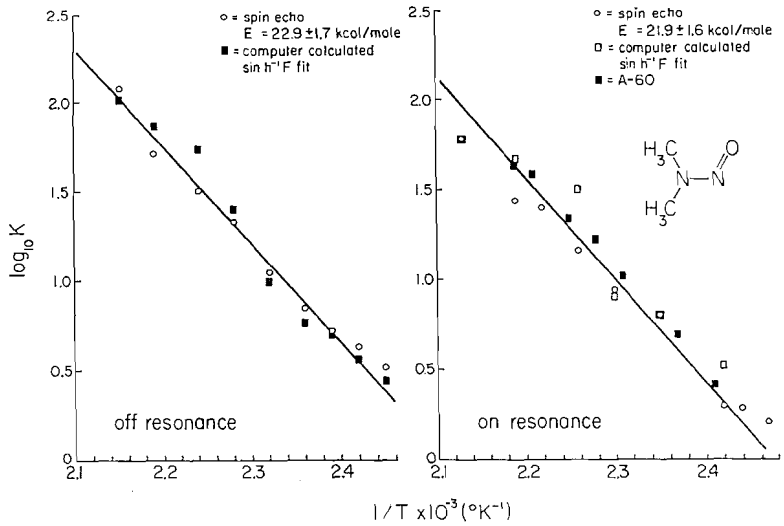


FIG. 9. Activation energy determination for *N,N*-dimethylnitrosamine.

In Figs. 9 and 10 the activation energies are determined as least squares lines to all rate constant determinations. In Fig. 9 the origin of the T_2 measurements is from both on- and off-resonance experiments for *N,N*-dimethylnitrosamine.*

In Table III the best activation parameters are quoted for the two molecules studied.

DISCUSSION

The spin-echo method for determining rate constants is now fairly well established and will serve as an independent check on high-resolution studies of rate constants. When both methods are in agreement a satisfactory set of activation parameters can be established for a given rate process. Unless this is the case, however, caution should be exercised in using the results. Abnormal frequency factors for simple hindered rotation barriers should be regarded with suspicion. In *N,N*-dimethyltrichloroacetamide, Gutowsky and Allerhand (19) were not able to obtain satisfactory agreement between steady state and spin-echo

**In Fig. 10, the on-resonance activation energy determination is illustrated for N,N-dimethyltrifluoroacetamide.*

Can. J. Chem. Downloaded from www.nrcresearchpress.com by 210.87.254.42 on 09/05/12
For personal use only.

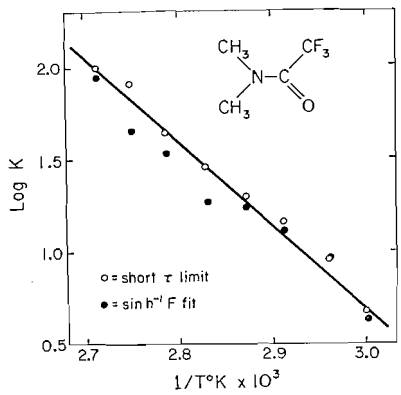


FIG. 10. Activation energy determination for *N,N*-dimethyltrifluoroacetamide, on resonance.

TABLE III
Activation parameters

	E_a (kcal/mole)	A ($10^{12} \times s^{-1}$)	S (e.u.)
N,N-Dimethylnitrosamine on resonance	21.9±1.6	1.00	−2.93
N,N-Dimethylnitrosamine off resonance	22.9±1.7	6.04	−3.92
N,N-Dimethyltrifluoroacetamine on resonance			
Short τ limit	20.6±1.4	182	+4.22
Sinh^{-1} F fit	18.5±2.7	6.90	−2.33

techniques. The case of the activation parameters for inversion in c-$C_6D_{11}H$ (8) can be considered to be solved. The rate constants have been determined over a spectacularly large range of temperature and agreement with the high-resolution studies is now complete (20, 21). A quantum mechanical theory of the spin-echo experiment on an exchanging system has now been given (22). The primary disadvantage of the spin-echo method is its lack of selectivity. Usually all nuclei of one type are in or near the resonance condition during pulses.

ACKNOWLEDGMENTS

The research was generously supported by the Petroleum Research Fund of the American Chemical Society and the National Research Council of Canada. The authors are grateful for discussions with Professor Myer Bloom and Dr. E. J. Wells and for help with computer programs from Mr. Robert Wolfe. Thanks are also accorded to Mr. E. Fisher for help in the construction of the spin-echo spectrometer.

REFERENCES

1. M. BLOOM, L. W. REEVES, and E. J. WELLS. J. Chem. Phys. **42**, 1615 (1965).
2. H. Y. CARR and E. M. PURCELL. Phys. Rev. **94**, 630 (1954).
3. E. KRAKOWER, L. W. REEVES, and E. J. WELLS. Discussions Faraday Soc. **34**, 199 (1962).
4. L. W. REEVES and E. J. WELLS. Discussions Faraday Soc. **34**, 177 (1962).
5. A. ALLERHAND and H. S. GUTOWSKY. J. Chem. Phys. **42**, 1587 (1965).
6. F. BLOCH. Phys. Rev. **70**, 460 (1946).
7. Z. LUZ and S. MEIBOOM. J. Chem. Phys. **39**, 366 (1963). S. MEIBOOM. Paper presented at Special Meeting, Physical Chemistry Division, American Chemical Society, Boulder, Colorado, 1962.
8. A. ALLERHAND, FU-MING CHEN, and H. S. GUTOWSKY. J. Chem. Phys. **42**, 3040 (1965).
9. A. ALLERHAND and H. S. GUTOWSKY. J. Chem. Phys. **42**, 4203 (1965).
10. H. S. GUTOWSKY and FU-MING CHEN. J. Phys. Chem. **69**, 3216 (1965).

Can. J. Chem. Downloaded from www.nrcresearchpress.com by 210.87.254.42 on 09/05/12
For personal use only.

11. A. ALLERHAND and H. S. GUTOWSKY. J. Am. Chem. Soc. **87**, 4092 (1965).
12. W. D. PHILLIPS. Ann. N.Y. Acad. Sci. **70**, 817 (1958).
13. D. J. BLEARS. J. Chem. Soc. Suppl. **2**, 6256 (1964).
14. L. PIETTE and W. A. ANDERSON. J. Chem. Phys. **30**, 899 (1959).
15. S. MEIBOOM and D. GILL. Rev. Sci. Instr. **29**, 688 (1958).
16. J. POWLES and K. LUSZCZYNSKI. J. Sci. Instr. **36**, 57 (1959).
17. D. E. WOESSNER. J. Chem. Phys. **35**, 41 (1961).
18. R. C. WAYNE, D. ZAMIR, and J. M. STRANGE. Rev. Sci. Instr. **35**, 1051 (1964).
19. A. ALLERHAND and H. S. GUTOWSKY. J. Chem. Phys. **41**, 2115 (1964).
20. F. A. BOVEY, F. P. HOOD, E. W. ANDERSON, and R. L. KORNEGAY. J. Chem. Phys. **41**, 2041 (1964).
21. F. A. L. ANET, M. AHMAD, and L. D. HALL. Proc. Chem. Soc. 145 (1964).
22. H. S. GUTOWSKY, R. L. VOLD, and E. J. WELLS. J. Chem. Phys. In press. 1966.
23. J. C. WOODBURY and M. T. ROGERS. J. Phys. Chem. **66**, 540 (1962).
24. W. GILBERT CLARK. Rev. Sci. Instr. **35**, 316 (1964).

Can. J. Chem. Downloaded from www.nrcresearchpress.com by 210.87.254.42 on 09/05/12
For personal use only.

INFRARED SPECTRUM AND STRUCTURE OF LIQUID WATER[1]

MICHAEL FALK[2]
Atlantic Regional Laboratory, National Research Council, Halifax, Nova Scotia
AND
T. A. FORD[3]
Chemistry Department, Dalhousie University, Halifax, Nova Scotia
Received February 18, 1966

ABSTRACT

The infrared spectrum of HDO at low concentrations in H_2O and in D_2O was studied between 0° and 130° by a double-beam technique. Each of the three fundamentals of HDO shows nearly Gaussian contours, complete absence of shoulders, and a single maximum at a frequency intermediate between those of HDO in ice and in vapor. Increase of temperature causes a gradual shift of each band in the direction of the frequency in vapor. These observations fully support the "continuum" models of the structure of liquid water and present strong evidence against the "mixture" models. It is concluded that hydrogen bonds in liquid water have a broad, smooth, single-peaked distribution of strengths which gradually shifts with temperature. The hydrogen bonds at one end of this distribution have strengths comparable to those in ice, whereas those at the other end are very weak. These extremes do not correspond to distinct molecular species. Every description of liquid water in terms of "broken" and "unbroken" bonds, or "monomers" and "clusters", is therefore arbitrary.

INTRODUCTION

"Mixture" Models and "Continuum" Models

There exists a very considerable amount of evidence that hydrogen bonds in liquid water form an extensive, though short-lived three-dimensional network (1–14). This network must differ from the corresponding network in ice by an absence of long-range order, denser overall packing, and lower average strength of hydrogen bonding. A structure which meets the above conditions may arise in a variety of ways and a number of structural models have been postulated for liquid water. Most of these models can be grouped into two general categories: "mixture" models and "continuum" models.

By *mixture models* we understand those (5, 9, 12, 13, 15–31) which describe liquid water as an equilibrium mixture of molecular species with different numbers of hydrogen bonds per molecule. Such a description implies the disruption of a well-defined proportion of hydrogen bonds at any temperature. Some estimates of the percentage of broken hydrogen bonds in water are recorded in Table I. A similar table has been compiled by Luck (10).

By *continuum models* we mean those (2–4, 6, 44) which describe liquid water as a still essentially complete hydrogen-bonded network, with a distribution of hydrogen-bond energies and geometries. These models consider the average strength of hydrogen bonds in water to be weaker than in ice as a result of irregular distortion and elongation, both of which increase with temperature.

Evidence from Spectroscopic Studies

It should be possible to choose between the two types of structural models on the basis of the vibrational spectrum, which is highly sensitive to the strength and extent of hydrogen bonding. The vibrational spectrum also represents a nearly instantaneous "picture" of water, in that it allows the detection of species having a lifetime as short as 10^{-13} s.

[1]*Issued as N.R.C. No. 9042. This paper was presented at the Symposium on Molecular Structure and Spectroscopy, Columbus, Ohio, June 14–18, 1965.*
[2]*To whom requests for reprints should be addressed.*
[3]*This work was carried out by T.A.F. at the Atlantic Regional Laboratory in partial fulfillment of the requirements for the Ph.D. degree at Dalhousie University.*

Can. J. Chem. Downloaded from www.nrcresearchpress.com by 210.87.254.6 on 09/05/12
For personal use only.

TABLE I

Estimates of the percentage of "broken hydrogen bonds" in water

Authors	% estimated	T (°C)	Experimental basis
Litovitz and Carnevale (32)	71.5	0	Ultrasonic absorption
Eucken (15)	66	0	Heat capacity
Fox and Martin (33)	60	0	Infrared spectrum
Wada (22)	57.5	0	Volume
Grjotheim and Krogh-Moe (16)	56	0	Volume
Cross, Burnham, and Leighton (34)	50	26	Raman spectrum
Némethy and Scheraga (5)	47	0	Structural model
Ewell and Eyring (35)	46	0	Viscosity
Buijs and Choppin (36)	46	0	Near infrared
Thomas, Scheraga, and Schrier (37)	38	0	Near infrared
Goldstein and Penner (38)	32	0	Near infrared
Hall (39)	30	0	Ultrasonic absorption
Pauling (20)	28.5		Structural model
Danford and Levy (31)	20	25	X-ray diffraction
Frank and Quist (21)	18	0	Volume
Davis and Litovitz (30)	18	0	Volume
Nomoto (17)	17.5	20	Ultrasonic absorption
Pauling (40)	15	0	Heat of melting
Luck (25)	9–16	0	Near infrared
Walrafen (41)	10.5	0	Raman spectrum
Haggis, Hasted, and Buchanan (42)	9	0	Dielectric constant
Marchi and Eyring (13)	2.5	0	Volume
Stevenson (43)	0.1	25	Far ultraviolet

The frequency of OH stretching vibrations is known to *decrease* in a regular manner with the strength of hydrogen bonding (45). Thus every Raman or infrared fundamental, overtone, or combination band, which involves OH stretching, may serve as a probe of hydrogen bonding. Frequencies of bending vibrations *increase* upon hydrogen bonding but the shifts are much smaller, hence somewhat less useful as a structural probe.

If liquid water consists of a mixture of molecules with broken and unbroken hydrogen bonds, then every OH stretching band would consist of two sub-bands. The sub-band corresponding to the non-hydrogen-bonded OH groups should occur at a frequency considerably higher than that of the sub-band due to the hydrogen-bonded OH groups, and ought to be detectable. Moreover, the relative intensity of this high-frequency sub-band would increase rapidly with temperature as the proportion of broken hydrogen bonds increased.

If, on the contrary, liquid water contains a continuous distribution of hydrogen-bond energies, then a single, broad band would be expected, which would shift gradually towards higher frequencies as the temperature increased and the average strength of hydrogen bonding decreased.

Thus, in principle, the changes of the band shape with temperature for any Raman or infrared vibrational band which involves OH stretching should allow a choice between the mixture and continuum models. Unfortunately, the bands in the spectra of liquid H_2O and D_2O are extremely broad, overlap considerably, and have a highly complicated temperature dependence, which makes distinction between the two predicted types of behavior extremely difficult. Some of the causes for these complications are:

1. The frequencies of the two fundamental OH stretching vibrations, ν_1 and ν_3, and of the first overtone of the bending vibration, $2\nu_2$, happen to lie very close to one another in liquid H_2O.

2. A similar, but even more complex situation holds for higher overtone and combination bands, so that the spectrum in fact consists not of single bands but of "band

Can. J. Chem. Downloaded from www.nrcresearchpress.com by 210.87.254.6 on 09/05/12
For personal use only.

clusters", which contain a rapidly increasing number of contributing vibrational transitions (Fig. 1).

3. The situation in D_2O is the same as in H_2O, all the vibrational frequencies being simply shifted down by a nearly constant factor of about 1.36.

4. Because of the asymmetry of the local field of force about a water molecule in the liquid, the effective symmetry of water molecules is lowered from C_{2v} to C_s. Therefore the vibrations ν_1 and ν_3 are no longer purely the symmetric and antisymmetric stretching vibrations, and both may enter into Fermi resonance with the overtones of ν_2 (46).

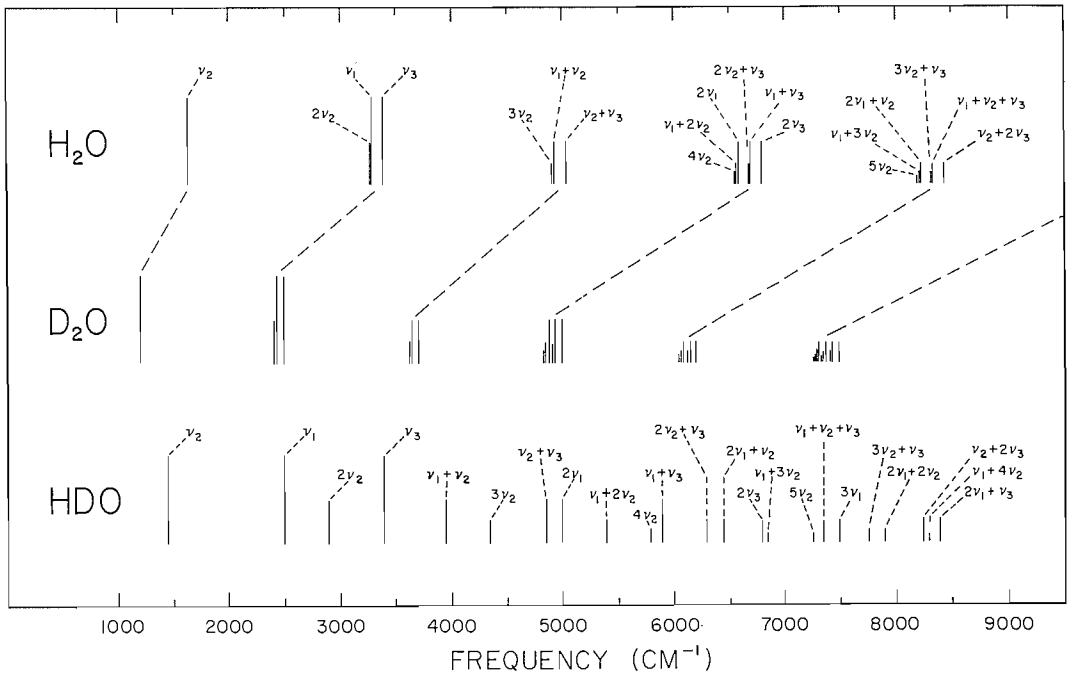


FIG. 1. Intramolecular vibrations of H_2O, D_2O, and HDO in liquid water (*highly schematic*). The frequencies of the overtone and combination bands were computed from the three fundamental frequencies, neglecting anharmonicity and Fermi resonance effects.

5. Fermi resonance within each "band cluster" may produce intensity borrowing and frequency shifts which will vary with temperature in a complex manner, since the frequencies of the three fundamentals vary differently with temperature.

6. Intermolecular coupling occurs between like vibrations of neighboring molecules, leading to a general broadening and distortion of all band shapes.

Many workers have neglected the above complications and have treated the complex changes of the shapes of some infrared or Raman "band clusters" of water as if they were due to changes in equilibria between various hydrogen-bonded and non-hydrogen-bonded water molecules (25, 27, 28, 34, 36–38, 47). Some of these studies, notably that by Cross, Burnham, and Leighton (34) and the more recent one by Buijs and Choppin (36), have been widely quoted in support of the mixture models of water (7–10). The naive interpretation of the very complex bands of H_2O and D_2O in terms of distinct species differing in hydrogen bonding must be ruled out by the far simpler spectra of HDO (48).

Some of the advantages of the study of HDO have been pointed out before (48–51). The main advantage is that in HDO the three fundamentals and many of the overtone and

Can. J. Chem. Downloaded from www.nrcresearchpress.com by 210.87.254.6 on 09/05/12
For personal use only.

combination bands are widely separated (Fig. 1) so that Fermi resonance does not occur. In addition, the spectra of *dilute* HDO in H_2O and in D_2O are free from intermolecular coupling of vibrations and thus have narrower bands of simple shapes. A further important advantage of dilute HDO solutions in H_2O and D_2O is that they make it possible to record infrared spectra in the fundamental region for films having a thickness of about 50 μ, which can be accurately measured. In contrast, the corresponding spectra of pure liquid H_2O or D_2O require the use of extremely thin films (1 to 5 μ). The thickness of such films is not usually known accurately, nor can it be kept constant when temperature is varied.

EXPERIMENTAL

The spectra were recorded on a Perkin–Elmer Model 521 grating spectrophotometer equipped with an automatic frequency indicator. The spectrometer was flushed with dry air or dry nitrogen in the regions of absorption of atmospheric water vapor and carbon dioxide. Matched liquid cells with barium fluoride windows and with an optical path of 0.050 mm were supplied by the Research and Industrial Instruments Co., London. Doubly distilled H_2O, and D_2O from the Merck, Sharp, and Dohme Company, Montreal, were used. The deuterium content of the D_2O, calculated from the HDO absorbance at 3 400 cm^{-1} was 99.85 mole %. Mixtures of H_2O and D_2O were prepared by weighing and were degassed immediately before use to prevent the formation of bubbles at higher temperatures. This incidentally allowed superheating of the samples above 100°. The sample cell, which contained a dilute solution of HDO in H_2O or in D_2O, and the reference cell, which contained pure H_2O or D_2O, were placed in an insulated aluminium chamber designed to fit the spectrometer. The chamber could be heated electrically or cooled with a mixture of dry ice and acetone. The temperature of each cell was measured with a mercury thermometer in thermal contact with the windows. The indicated temperatures were the same to within 1° for the two cells and were probably correct to within 2°, as checked by freezing the H_2O or D_2O films in the cells and observing their melting points.

The spectrometer calibration was accurate to ± 1 cm^{-1}. Centers of broad bands could be determined with an accuracy of ± 2 cm^{-1} graphically by joining the midpoints of "tie lines" drawn parallel to the base line and extrapolating the line joining these midpoints to intersect with the band.

The concentrations of HDO were chosen so as to obtain bands with absorbance of about 0.3 (50% transmittance) at a path length of 0.050 mm. The corresponding HDO concentrations were approximately 1.6 mole % for the OH stretching band (ν_3), 2.0 mole % for the OD stretching band (ν_1), and 4.0 mole % for the bending band (ν_2).[4] To calculate the concentrations of HDO the equilibrium constant for the equilibrium $H_2O + D_2O \rightleftharpoons 2HDO$ was assumed to have the value 3.96 (52).

RESULTS

The spectra of pure H_2O and D_2O at room temperature and at a thickness of 0.050 mm are shown in Fig. 2. At this thickness, the transmission of H_2O near 2 500 cm^{-1} and of D_2O near 3 400 and 1 450 cm^{-1} is high enough to observe conveniently all three fundamental bands of HDO in compensated double-beam spectra. Because of the excellent compensation of the absorption of H_2O (or D_2O), the present spectra of HDO have better band contours than those obtained previously (50–53). Moreover, the earlier spectra were recorded either at a single temperature (51–53) or over a very small temperature range (50).

Fig. 3 shows typical spectra of the three fundamental bands of HDO recorded at a high and a low temperature at a standard resolution. Figure 4 shows a typical portion of the HDO spectrum in the particularly important region of 3 550 to 3 750 cm^{-1}, recorded at a higher resolution and a higher HDO concentration.

The spectra of the three fundamental bands of HDO were recorded in several series of measurements at ascending and descending temperatures. The frequencies of the three band maxima are plotted in Fig. 5. The absorptivities and the half-widths (the band widths at half the maximum absorbance) of the three bands at 22° and 120° are recorded in Table II. Our data are in reasonable agreement with most values of frequency, absorptivity, and half-width of the bands reported in the earlier studies (Fig. 5 and Table II).

[4]*The present numbering of the three* HDO *fundamental vibrations was chosen to indicate as much as possible the correspondence with the vibrations of* H_2O *and* D_2O.

Can. J. Chem. Downloaded from www.nrcresearchpress.com by 210.87.254.6 on 09/05/12
For personal use only.

Can. J. Chem. Downloaded from www.nrcresearchpress.com by 210.87.254.6 on 09/05/12
For personal use only.

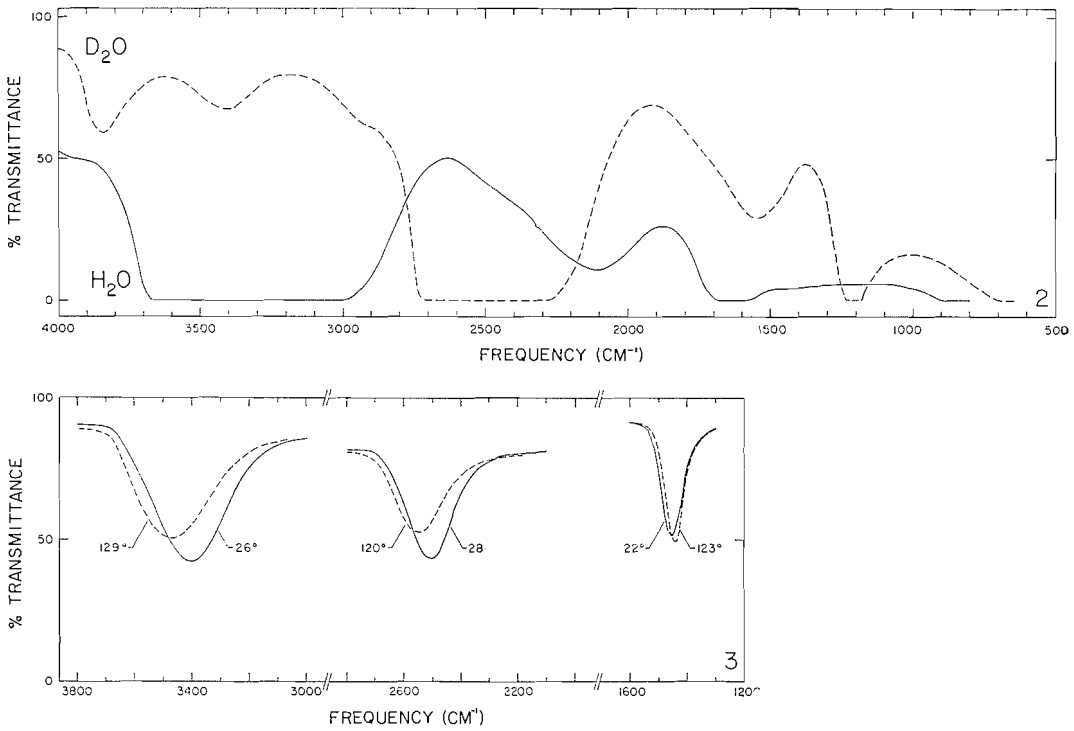


FIG. 2. Transmittance of H_2O and D_2O at a thickness of 0.050 mm. Temperature: 25°.
FIG. 3. Compensated double-beam spectra of the three fundamental bands of HDO recorded at a high and a low temperature. HDO concentration: 1.6 mole % for ν_3, 2.0 mole % for ν_1, and 4.0 mole % for ν_2. Resolution: 2 cm^{-1}.

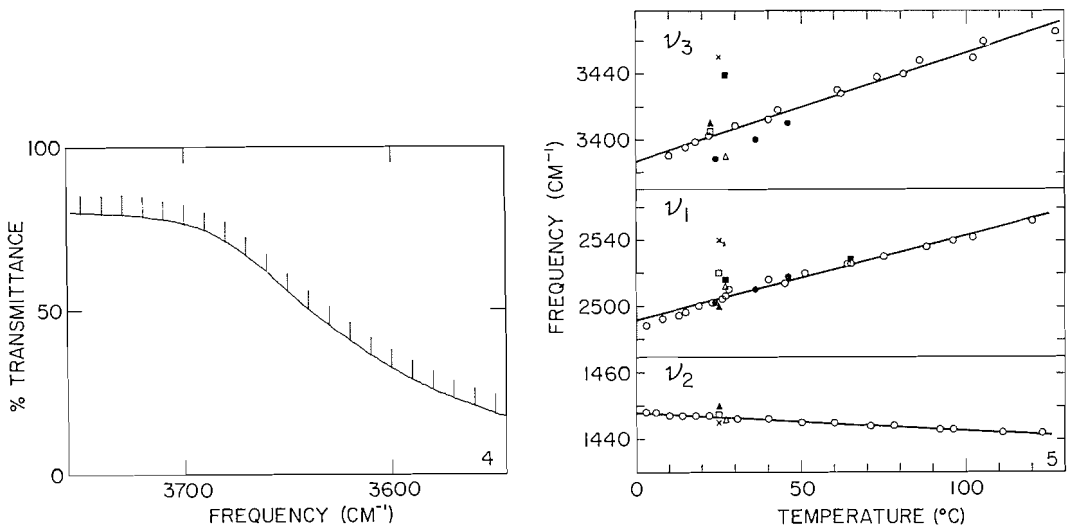


FIG. 4. A portion of the spectrum of HDO in D_2O between 3 550 and 3 750 cm^{-1}. HDO concentration: about 6.0 mole %. Resolution: 0.5 cm^{-1}. Temperature: 92°.
FIG. 5. Frequencies of the band maxima of the three HDO fundamentals: (○) this work; (●) ref. 50; (□) ref. 51; (△) ref. 52; (▲) ref. 53; (×) ref. 54; (■) ref. 55.

TABLE II
Absorptivities and half-widths of HDO fundamentals

	Absorptivities ($\times 10^{-3}$ cm^2 mole^{-1})			Half-widths (cm^{-1})			
T (°C)	ν_3	ν_1	ν_2	ν_3	ν_1	ν_2	Ref.
Infrared							
22	64±5	42±5	20±5	255±5	160±5	85±5	This work
24	—	—	—	246	160	—	50
25	—	—	—	240±5	165±5	75±5	51
25	62.5	41.4	20.7	265	185	—	53
27	—	—	—	260	175	85	52
36	—	—	—	255	165	—	50
46	—	—	—	263	170	—	50
120	44±5	26±5	26±5	270±5	180±5	70±5	This work
Raman							
25				275	185	100	54
27				278	160	—	55
65				—	166	—	55

DISCUSSION

Choice between Mixture Models and Continuum Models

Each of the three fundamental bands of HDO shows a single maximum, nearly Gaussian contour, and a complete absence of shoulders at any temperature. Increase of temperature causes a gradual shift of the whole band, to higher frequencies for the stretching vibrations, ν_3 and ν_1, and to lower frequencies for the bending vibration, ν_2. The absorbance of ν_3 and ν_1 decreases with temperature, while the absorbance of ν_2 increases. These observations are consistent with a gradual weakening of the hydrogen bonds with increasing temperature. Particularly to be noted is the absence of shoulders at 3 550 to 3 750 cm^{-1} for the ν_3 band and at 2 600 to 2 700 cm^{-1} for the ν_1 band, where the absorption of any non-hydrogen-bonded OH and OD groups would occur. These regions were investigated with special care under the most favorable conditions of high temperature, high HDO concentration, high resolution, and low noise level (Fig. 4). The infrared spectra of HDO thus fully support the continuum models and *are incompatible with the existence in water of any discrete molecular species differing in the extent of hydrogen bonding.*

This conclusion agrees with that reached by Wall and Hornig (55) on the basis of the Raman spectra of HDO. The Raman spectra have the advantage that their intensity is relatively independent of the strength of hydrogen bonding (55). On the other hand, the present infrared spectra have the advantage of much higher resolution (by a factor of 30 to 60) and of higher signal-to-noise ratios (by an estimated factor of 50), which considerably improves the detectability of small shoulders. Our study and that of Wall and Hornig thus largely complement each other, strengthening our independently derived conclusions.

Distribution of Hydrogen-Bond Strengths in Water

The profiles of the three HDO bands were studied by analytical procedures (56, 57) and were found to be very close to Gaussian form at all temperatures. The broad and nearly Gaussian band profiles must reflect a broad, smooth, single-peaked distribution of the strengths of hydrogen bonds in liquid water. The band profiles do not correspond directly to this distribution, because of distortion caused by (*a*) the variation of absorptivity of molecules with frequency across the band (55), (*b*) possible contribution of combinations involving the continuum of low-frequency intermolecular vibrations to the band intensity,

Can. J. Chem. Downloaded from www.nrcresearchpress.com by 210.87.254.6 on 09/05/12
For personal use only.

Can. J. Chem. Downloaded from www.nrcresearchpress.com by 210.87.254.6 on 09/05/12
For personal use only.

and (*c*) possible broadening due to short lifetimes of the hydrogen bonds in the liquid. The contribution of *a* is largely confined to the infrared absorption spectrum, whereas *b* and *c* tend to distort both the infrared and the Raman bands. This distortion makes it difficult to evaluate quantitatively the distribution of hydrogen-bond strengths from the profiles of the vibrational bands. Fortunately, the distortion is not very serious[5] and may be neglected in the first approximation, allowing the following *qualitative* deductions about the structure of liquid water:

The distribution of the strengths of hydrogen bonds in water is very broad. At one end of this distribution are hydrogen bonds having strengths comparable with those of hydrogen bonds in ice. These correspond to the HDO absorption at frequencies close to those of HDO in ice, which are 3 300 and 2 440 cm^{-1} at 0° (59) and 3 277 and 2 421 cm^{-1} at −170° (58). At the other end of the distribution are very weak hydrogen bonds, which correspond to the small but appreciable absorption at frequencies approaching those of non-hydrogen-bonded OH or OD groups. These frequencies are 3 705 and 2 719 cm^{-1} in the vapor (60) and 3 670 and 2 695 cm^{-1} in dilute solution in CCl_4 (59). These two extremes are simply the "wings" of a broad distribution of bond strengths and cannot be considered to correspond to distinct molecular species. Most hydrogen bonds in water fall between the two extremes. The whole distribution shifts towards lower bond strengths as temperature increases, the width of the distribution remaining essentially constant.

Quantitative estimates of the distribution of the strengths of hydrogen bonds must await a careful evaluation of the distortion inherent in the contours of the Raman and infrared bands.

Distribution of Geometries

The geometry of the hydrogen bond in water is determined by the O···O distance and by angular parameters which determine the deviation of the hydrogen bond from linearity (3). The smooth, single-peaked distribution of hydrogen-bond strengths in water appears to reflect a smooth, single-peaked distribution of geometries, with the stronger bonds corresponding to short O···O distances and small deviations from linearity, and the weaker bonds corresponding to long O···O distances and larger deviations from linearity.

Because several geometrical parameters are involved and each may be expected to have a broad distribution of values, gradually shifting with temperature, the detailed shapes of these distributions will be even more difficult to derive from the band contours than the form of the distribution of the strengths of hydrogen bonds. There is also some uncertainty as to how the distributions relating to OH···O (or OD···O) bonds of HDO dissolved in D_2O or H_2O compare with the distributions relating to pure H_2O or D_2O. Nevertheless, even when the nonlinearity of the hydrogen bonds is completely neglected and a rough correlation between O···O distances and the OH stretching frequency is used, the distribution of O···O distances in water, as derived from the contours of the Raman bands of HDO, is in surprisingly good agreement with the distribution derived from X-ray diffraction measurements (55).

"Monomers" and "Clusters"

The basic assumption underlying the mixture theories of water has been that the hydrogen bonds in water at any instant can be divided into "broken" and "unbroken" bonds. Such a division must now be rejected as completely arbitrary, in view of the broad,

[5]*That the distortion is not serious is shown by (i) the close correspondence of the band profiles in the infrared and Raman spectrum of* HDO *in water (55), (ii) the relatively narrow* HDO *bands in ice (58, 59), and (iii) the near constancy of* HDO *band-widths over a 130° range of temperature observed in this work.*

smooth, single-peaked distribution of hydrogen-bond strengths. The arbitrariness of the division into broken and unbroken bonds may have been inferred already from the scatter of the estimates by various earlier workers for the percentage of broken hydrogen bonds in water (Table I). Each such estimate is in fact based on a different "operational definition" (43) of what constitutes the rupture of a hydrogen bond, and it is not surprising that the estimates vary from 0 to 71%.

The definitions of "monomers" and "clusters" in water are of course derived from the definition of what constitutes a broken hydrogen bond and, consequently, are equally arbitrary. Depending on one's operational definition of a "broken hydrogen bond", the average size of a "cluster" may thus vary from one to an infinite number of water molecules at any temperature, while the fraction of molecules present as "clusters" may vary from 0 to 1.

Addendum

In a recent publication, K. A. Hartman, Jr. presents the infrared spectra of the OH band of HDO over a 73° range of temperature and the spectrum of the OD band of HDO at room temperature (61). Hartman's spectra are less extensive, and lack double-beam compensation above room temperature but are otherwise very similar to ours. Hartman uses his data to calculate the mole fraction of "non-hydrogen-bonded OH groups" in water. Hartman estimates that such OH groups would absorb at 3 635 cm^{-1}, and, assuming that all the absorbance at this frequency is due to such groups, derives an upper limit of 7% for HDO in D_2O at 25°. Hartman's estimate should not be taken as spectroscopic evidence for the existence of up to 7% of some *distinct molecular species* with non-hydrogen-bonded OH groups. Our approach stresses the absence of such species as shown by the lack of any shoulders in the region of 3 635 cm^{-1} in both our spectra and Hartman's.

In another recent paper (62), G. E. Walrafen obtains the value of 38% for the fraction of "unbound" water molecules at 0°. In his 1964 paper (41), Walrafen obtained the very different value of 10.5% for the same quantity. The two publications also provide vastly different estimates of the enthalpy change for the process $H_2O_{(bound)} \rightarrow H_2O_{(unbound)}$. The two sets of calculations are based on the same questionable assumption that the intensity of the Raman band of water near 175 cm^{-1} is proportional to the fraction of "bound" water molecules. Walrafen's 1966 paper makes no comment about his earlier results, and in both publications close agreement is claimed with other workers' data. This inconsistency illustrates the difficulties encountered in attempts to evaluate what is an inherently arbitrary quantity.

ACKNOWLEDGMENTS

The authors wish to thank Drs. T. T. Wall, C. R. Masson, O. Knop, and A. G. McInnes for helpful comments on the manuscript and Dr. W. R. Trost, Dean of Graduate Studies, Dalhousie University, for providing financial assistance to one of us (T. A. F.).

REFERENCES

1. J. D. Bernal and R. H. Fowler. J. Chem. Phys. **1**, 515 (1933).
2. J. Lennard-Jones and J. A. Pople. Proc. Roy. Soc. London, Ser. A, **205**, 155 (1951).
3. J. A. Pople. Proc. Roy. Soc. London, Ser. A, **205**, 163 (1951).
4. D. N. Glew. J. Phys. Chem. **66**, 605 (1962).
5. G. Némethy and H. A. Scheraga. J. Chem. Phys. **36**, 3382 (1962).
6. C. Tanford. *In* Temperature—its measurement and control in science and industry. Vol. 3. *Edited by* C. M. Herzfeld. Part 3 (*edited by* J. D. Hardy). Reinhold Publishing Corp., New York. 1963. p. 123.
7. J. L. Kavanau. Water and solute-water interactions. Holden-Day, San Francisco. 1964.
8. G. R. Choppin. Chemistry, **38**, 6 (1965).
9. H. S. Frank. Federation Proc. **24**, No. 2, Part III. Supp. No. 15, 1 (1965).

Can. J. Chem. Downloaded from www.nrcresearchpress.com by 210.87.254.6 on 09/05/12
For personal use only.

10. W. LUCK. Fortschr. Chem. Forsch. **4**, 653 (1964).
11. G. NÉMETHY. Federation Proc. **24**, No. 2, Part III. Supp. No. 15, 38 (1965).
12. O. Y. SAMOILOV. Die Struktur von Wässrigen Elektrolytlösurgen. Teubner Verlag, Leipzig. 1961.
13. R. P. MARCHI and H. EYRING. J. Phys. Chem. **68**, 221 (1964).
14. M. ABU-HAMDIYYAH. J. Phys. Chem. **69**, 2720 (1965).
15. A. EUCKEN. Z. Elektrochem. **52**, 255 (1948).
16. K. GRJOTHEIM and J. KROGH-MOE. Acta Chem. Scand. **8**, 1193 (1954).
17. O. NOMOTO. J. Phys. Soc. Japan, **11**, 1146 (1956).
18. H. S. FRANK and W. Y. WEN. Discussions Faraday Soc. **24**, 133 (1957).
19. H. S. FRANK. Proc. Roy. Soc. London, Ser. A, **247**, 481 (1958).
20. L. PAULING. *In* Hydrogen bonding. *Edited by* D. Hadži. Pergamon Press, New York. 1959. p. 1.
21. H. S. FRANK and A. S. QUIST. J. Chem. Phys. **34**, 604 (1961).
22. G. WADA. Bull. Chem. Soc. Japan, **34**, 955 (1961).
23. H. S. FRANK. Desalination Research Conference Proceedings. Washington. NAS–NRC publication no. 932, 141 (1963).
24. I. PELAH and J. IMRY. Israel Atomic Energy Commission, publication no. 1A – 875 (1963).
25. W. LUCK. Ber. Bunsenges Physik. Chem. **67**, 186 (1963).
26. G. NÉMETHY and H. A. SCHERAGA. J. Phys. Chem. **41**, 680 (1964).
27. W. LUCK. Ber. Bunsenges Physik. Chem. **69**, 626 (1965).
28. V. VAND and W. A. SENIOR. J. Chem. Phys. **43**, 1869, 1873, 1878 (1965).
29. A. BEN-NAIM. J. Phys. Chem. **69**, 1922, 3240 (1965).
30. C. M. DAVIS and T. A. LITOVITZ. J. Chem. Phys. **42**, 2563 (1965).
31. M. D. DANFORD and H. A. LEVY. J. Am. Chem. Soc. **84**, 3965 (1962).
32. T. A. LITOVITZ and E. H. CARNEVALE. J. Appl. Phys. **26**, 816 (1955).
33. J. J. FOX and A. E. MARTIN. Proc. Roy. Soc. London, Ser. A, **174**, 234 (1940).
34. P. C. CROSS, J. BURNHAM, and P. A. LEIGHTON. J. Am. Chem. Soc. **59**, 1134 (1937).
35. R. H. EWELL and H. EYRING. J. Chem. Phys. **5**, 726 (1937).
36. K. BUIJS and G. R. CHOPPIN. J. Chem. Phys. **39**, 2035 (1963).
37. M. R. THOMAS, H. A. SCHERAGA, and E. E. SCHRIER. J. Phys. Chem. **69**, 3722 (1965).
38. R. GOLDSTEIN and S. S. PENNER. J. Quant. Spectry. Radiative Transfer, **4**, 441 (1964).
39. L. HALL. Phys. Rev. **73**, 775 (1948).
40. L. PAULING. The nature of the chemical bond. 2nd. ed. Cornell University Press, Ithaca, N.Y. 1948. p. 304.
41. G. E. WALRAFEN. J. Chem. Phys. **40**, 3249 (1964).
42. G. H. HAGGIS, J. B. HASTED, and T. J. BUCHANAN. J. Chem. Phys. **20**, 1452 (1952).
43. D. P. STEVENSON. J. Phys. Chem. **69**, 2145 (1965).
44. J. A. BARKER. Ann. Rev. Phys. Chem. **14**, 229 (1963).
45. G. C. PIMENTEL and A. L. MCCLELLAN. The hydrogen bond. Freeman, San Francisco. 1960. p. 67.
46. J. SCHIFFER. Ph.D. Thesis, Princeton University, Princeton, N.J. 1963.
47. H. YAMATERA, B. FITZPATRICK, and G. GORDON. J. Mol. Spectry. **14**, 268 (1964).
48. D. F. HORNIG. J. Chem. Phys. **40**, 3119 (1964).
49. D. F. HORNIG, H. F. WHITE, and F. P. REDING. Spectrochim. Acta, **12**, 338 (1958).
50. C. L. VAN P. VAN ECK, H. MENDEL, and J. FAHRENFORT. Proc. Roy. Soc. London, Ser. A, **247**, 472 (1958).
51. R. D. WALDRON. J. Chem. Phys. **26**, 809 (1957).
52. C. A. SWENSON. Spectrochim. Acta, **21**, 987 (1965).
53. J. G. BAYLY, V. B. KARTHA, and W. H. STEVENS. Infrared Phys. **3**, 211 (1963).
54. R. E. WESTON. Spectrochim. Acta, **18**, 1257 (1962).
55. T. T. WALL and D. F. HORNIG. J. Chem. Phys. **43**, 2079 (1965).
56. R. N. JONES, K. S. SESHADRI, N. B. W. JONATHAN, and J. W. HOPKINS. Can. J. Chem. **41**, 750 (1963).
57. K. S. SESHADRI and R. N. JONES. Spectrochim. Acta, **19**, 1013 (1963).
58. J. E. BERTIE and E. WHALLEY. J. Chem. Phys. **40**, 1637 (1964).
59. T. A. FORD and M. FALK. Unpublished results.
60. G. HERZBERG. Infrared and Raman spectra of polyatomic molecules. Van Nostrand, Princeton, N.J. 1945. p. 280.
61. K. A. HARTMAN, JR. J. Phys. Chem. **70**, 270 (1966).
62. G. E. WALRAFEN. J. Chem. Phys. **44**, 1546 (1966).

Can. J. Chem. Downloaded from www.nrcresearchpress.com by 210.87.254.6 on 09/05/12
For personal use only.

HEATS OF ASSOCIATION OF AQUEOUS COPPER, NICKEL, AND COBALT IONS WITH HALIDE IONS

M. B. KENNEDY AND M. W. LISTER
Department of Chemistry, University of Toronto, Toronto, Ontario

Received September 20, 1965

ABSTRACT

Calorimetric measurements are reported for the heats of formation of $CoCl^+$, $NiCl^+$, $CuCl^+$, $CoBr^+$, $NiBr^+$, and $CuBr^+$ from simple aqueous ions. Values of ΔF, ΔH, and ΔS for these reactions at 25 and 40 °C, and an ionic strength of 2.0 were found. It was noted that ΔH and ΔS seem to be related by the equation: $\Delta H = 254\Delta S + 201$, for values at both temperatures.

Can. J. Chem. Downloaded from www.nrcresearchpress.com by 210.87.254.6 on 09/05/12
For personal use only.

In two recent papers (1, 2), one of the present writers measured the equilibrium constants for the formation of complex chlorides and bromides of divalent copper, nickel, and cobalt. The reactions were all of the type:

$$M^{++} + X^- \rightleftharpoons MX^+$$

and the equilibria were measured by means of spectrophotometry or cell voltages. The variation of the equilibrium constants with temperature in general deviated from the integrated equation:

$$\ln K = A - \Delta H/RT.$$

It was suggested that this was caused by either (i) rapid variation of ΔH with temperature, or (ii) the formation of other types of complex ions in appreciable amounts. These other complex ions would presumably have the general formula M_2X^{3+}, since in the experiments mentioned above the concentrations of metal ions were high, and those of halide ions low. It was not possible to distinguish between these two alternatives from the earlier experiments, so it was decided to attempt to measure the heats of reaction directly by calorimetry. The present paper reports the results of such measurements.

The experiments took the general form of measuring the temperature change when solutions of a metal perchlorate and a sodium halide were mixed in a differential calorimeter. However, it is not reasonable to attribute all the heat change to complex ion formation, since the surroundings of the various ions are altered on mixing two solutions even when no reaction occurs. The method used to allow for this was essentially that of Austin, Matheson, and Parton (3), who studied the heat of association for lead halide complex ions, PbX^+. They assumed that this was the difference between the heat changes when a given potassium halide solution was mixed firstly with lead perchlorate and secondly with perchloric acid solutions. In the present work we have similarly compared the heat changes when a given sodium halide solution was mixed firstly with copper (or nickel or cobalt) perchlorate and secondly with magnesium perchlorate. The ionic strengths were the same in the two compared experiments. Magnesium perchlorate was chosen because (i) the Cu^{++}, Co^{++}, Ni^{++}, and Mg^{++} ions are much the same size, and (ii) magnesium is reported to complex rather weakly with halide ions (4–6), though the evidence on this is a little uncertain. If (ii) is not correct, the results below might require some reinterpretation.

EXPERIMENTAL METHOD

Stock solutions used in the calorimetric experiments were prepared as follows. Reagent grade samples of the metal perchlorates, supplied by either the G. Frederick Smith Co. or Fisher Scientific Co., were dissolved in water, and made 0.02 *M* in perchloric acid to prevent hydrolysis. The solutions were then analyzed for

metal content. Copper perchlorate was analyzed iodometrically. Nickel and cobalt perchlorates were estimated by EDTA titration using murexide as indicator, as described by Vogel (7) or Schwarzenbach (8). In addition, the nickel was estimated with dimethylglyoxime; and cobalt by passing the solution through a cation exchange resin in its hydrogen form (Dowex 50W-X8), and titrating the perchloric acid produced with sodium hydroxide. This last method was also used for magnesium perchlorate. The stock sodium chloride and sodium bromide solutions were made from recrystallized reagent grade samples. The concentrations were checked by silver nitrate titration. These solutions were also made 0.02 M in perchloric acid.

The solutions were mixed in one half of a differential twin calorimeter of conventional design. The temperature change was measured by a 20-junction thermocouple of iron and constantan. This gave about 1 mV/deg which was measured on a Leeds and Northrup potentiometer sensitive to 0.1 μV. In a typical experiment, about 350 ml of the metal perchlorate solution was mixed with 50 ml of sodium halide solution. Both solutions were weighed to 0.01 g, and their densities were found in a separate experiment. It was assumed that the change in volume on mixing the two solutions was negligible. The heat capacity of the calorimeter plus mixed solutions was determined by electrical calibration. About 1.3 A at 4.2 V was passed for about 250 s, and the resulting temperature rise was about 0.8 °C. The voltage was measured on a potentiometer sensitive to 0.1 mV; and the current was measured by passing it through a standard 1 Ω resistance, and measuring the potential drop across the resistance, also to 0.1 mV. The time of heating was found to the nearest 0.05 s by an electrical timer operated by the same switch as the heating current. In each run, a second addition of 50 ml of sodium halide was made, and the electrical calibration was repeated. Experiments were made in which water (or some one solution) was used both in the pipette and the body of the calorimeter. The operation of the pipette was found to give a small heat change of 2.8 cal, with an average deviation of 0.2 cal (in six runs). This was not applied directly as a correction to the results, since the difference between the heat of mixing of (i) magnesium perchlorate and sodium halide solutions, and (ii) other metal perchlorate and sodium halide solutions, was taken to be the heat change due to complex formation.

The metal perchlorate solutions were about 0.67 M, and the sodium halide was about 2.0 M, so that both had an ionic strength of 2.0. This ionic strength was chosen to agree with that used in the earlier measurements of the equilibrium constants, so that these equilibrium constants could be used in the interpretation of the present results. This also permitted high enough concentrations to be used, so that considerable amounts of the complex species were formed. The number of moles of MX^+ formed varied, of course, with the particular ions being used, but was between 0.02 and 0.035 on the first addition, and between 0.015 and 0.025 on the second. If there are no other sources of error, the numbers given above would mean that the final value for ΔH was correct to 0.01 kcal/mole, allowing for the fact that four temperature measurements must be made to obtain one value of ΔH. However, the reproducibility of results was not as good as this, and suggest a possible error up to 0.05 kcal/mole. Part of this larger error is undoubtedly due to the assumption that heat changes due solely to mixing can be found from the behavior of magnesium perchlorate.

RESULTS

The primary experimental information consists of measurements of calories evolved or absorbed when two solutions are mixed. Its interpretation depends on (i) the complex species assumed to be formed; (ii) the values used for the stability constants of these complexes; and (iii) the method of correcting for the heat of mixing without chemical reaction. As mentioned above, this was done by measuring the heats of mixing of magnesium perchlorate and sodium halide solutions at the same concentrations, and subtracting them from the results with copper, nickel, or cobalt perchlorates. The results of the experiments with magnesium perchlorate are also given in Table I, and are each the mean of three experiments. The results after these subtractions are given in Tables I*a* and I*b* under the heading "Corrected heat change", and are used in the calculations reported in Tables I*a* and I*b* and later on. The different volumes of solution used in various runs were allowed for in making these subtractions. It was assumed that the correction should be proportional to the volume of the metal perchlorate solution used.

DISCUSSION OF RESULTS

Various assumptions can be made in order to interpret the data in Table I. These assumptions, and the conclusions they lead to, will now be considered. It was first assumed that only MX^+ complex ions were formed, and that the stability constants for these species are as given by Lister, Rosenblum, and Wilson (1, 2).

Can. J. Chem. Downloaded from www.nrcresearchpress.com by 210.87.254.6 on 09/05/12
For personal use only.

The values of the constants used are as follows:

25 °C: $NiCl^+$ 0.670, $NiBr^+$ 0.763, $CoCl^+$ 0.728, $CoBr^+$ 0.768, $CuCl^+$ 1.22, $CuBr^+$ 0.95;
40 °C: $NiCl^+$ 0.72, $NiBr^+$ 0.78, $CoCl^+$ 0.78, $CoBr^+$ 0.87, $CuCl^+$ 1.31, $CuBr^+$ 0.85.

From these the number of moles of complex formed in each run was calculated, and hence ΔH for the reactions

$$M^{++} + X^- \rightarrow MX^+.$$

The results of these calculations are also given in Tables I*a* and I*b*. ΔH obtained in this way may be compared with ΔH calculated from the equilibrium constants given above. In Table II the mean values of ΔH are compared with the values calculated from K at 25 and 40 °C. The average deviations are also given for the calorimetric results.

The values of ΔH obtained by the two methods agree only very moderately, though they are almost all small and positive (endothermic). ΔH for $CuBr^+$ is negative when calculated from K at 25 and 40 °C, but this equilibrium constant had an anomalous variation with temperature (1), and apparently went through a maximum between 25 and 30 °C. The calorimetric results are consistent in making the reaction endothermic, while the equilibrium constants only make it endothermic below 30 °C. While the comparison in Table II is perhaps not hopeless, it suggests that other explanations should be explored.

Firstly we may consider whether it would have been better to ascribe the total heat change to complex formation, and not make any allowance for mixing by means of measurements on magnesium perchlorate. The results are given in Table III. There is little to choose between the two, so far as agreement with ΔH calculated from K goes; however the corrected results vary much less with temperature, which is probably a point in their favor. In fact only the copper complexes show any appreciable change. The average deviations are less for the corrected results.

Secondly, it was suggested by Lister and Rosenblum (1) that ions of formula M_2X^{3+}, as well as MX^+, might be formed under their experimental conditions of a large excess of M^{++}. This explained some small drifts in K values that were observed. The best values of the equilibrium constants so found are given in Table IV. K_1 is the constant used above, and is $[MX^+]/[M^{++}].[X^-]$, while K_2 is $[M_2X^{3+}]/[M^{++}]^2.[X^-]$. The ΔH values calculated from K_1 and K_2 are listed as ΔH_1 and ΔH_2 respectively. These are ΔH for formation of the complexes from simple ions. These constants can be used to calculate amounts of MX^+ and M_2X^{3+} formed in the calorimetric experiments, and hence ΔH_1 and ΔH_2. The average values obtained are given in Table IV as ΔH_1 calorimetric and ΔH_2 calorimetric.

Agreement between the two methods of finding ΔH is appreciably worse than before and it is therefore improbable that the existence of M_2X^{3+} ions is the correct explanation for the anomalies in the equilibrium constant. All the calorimetric experiments were made at a considerable excess of metal over halide, and hence the solutions would not contain much MX_2. The possibility of this species cannot be entirely discounted as the halide concentrations could not be made too low, or the heat changes would have been too small. However, no systematic drifts that could be attributed to these species were detected.

Finally a more extensive calculation was made as follows. The possibility was considered that, in the original measurements of equilibrium constants by Lister, Rosenblum, and Wilson (1, 2), the extinction coefficients might vary slightly from one solution to another. These solutions were all at the same ionic strength, but the relative amounts of $M(ClO_4)_2$ and $NaClO_4$ varied. Accordingly the results on $CuBr^+$ were re-examined, and the % change in the extinction coefficient (ϵ) of $CuBr^+$ was found that would be necessary to keep

Can. J. Chem. Downloaded from www.nrcresearchpress.com by 210.87.254.6 on 09/05/12
For personal use only.

TABLE I*a*

Calorimetric results on mixing metal perchlorate and sodium halide solutions at 25 °C

	$M(ClO_4)_2$		NaX		Corrected heat change	Complex formed	ΔH
$M^{++}X^-$	Vol. (ml)	Conc. (*M*)	Vol. (ml)	Conc. (*M*)	(cal)	(mole)	(kcal)
$Co^{++}Cl^-$	349.8	0.634	56.63	2.002	15.7	0.0291	0.54
	349.8	0.634	54.83	2.002	10.3	0.0189	0.54
	349.6	0.634	51.98	2.002	14.05	0.0271	0.52
	349.6	0.634	50.63	2.002	10.3	0.0181	0.57
	348.5	0.634	45.61	2.002	12.1	0.0243	0.50
							0.53 mean
$Ni^{++}Cl^-$	349.8	0.632	62.12	2.002	13.3	0.0312	0.43
	349.8	0.632	54.09	2.002	7.6	0.0166	0.46
	349.7	0.632	55.84	2.002	14.6	0.0271	0.54
	349.7	0.632	56.15	2.002	10.05	0.0182	0.55
							0.50 mean
$Cu^{++}Cl^-$	349.4	0.655	52.63	2.002	58.7	0.0386	1.52
	349.4	0.655	51.84	2.002	40.2	0.0253	1.59
	349.9	0.655	57.90	2.002	59.6	0.0416	1.43
	349.9	0.655	53.72	2.002	44.8	0.0251	1.78
							1.58 mean
$Co^{++}Br^-$	349.7	0.634	53.98	1.942	5.7	0.0282	0.20
	349.7	0.634	53.64	1.942	2.65	0.0189	0.14
	350.0	0.634	51.09	1.942	5.2	0.0269	0.19
	350.0	0.634	55.73	1.942	2.8	0.0200	0.14
							0.17 mean
$Ni^{++}Br^-$	349.8	0.632	60.02	1.942	1.85	0.0305	0.06
	349.8	0.632	55.55	1.942	1.2	0.0185	0.06
	348.8	0.632	56.67	1.942	3.75	0.0292	0.13
	348.8	0.632	58.51	1.942	2.1	0.0198	0.11
							0.09 mean
$Cu^{++}Br^-$	349.7	0.655	50.72	1.942	29.7	0.0314	0.95
	349.7	0.655	60.25	1.942	23.1	0.0248	0.93
	349.7	0.655	55.26	1.942	19.2	0.0223	0.86
	336.4	0.655	45.82	1.942	19.3	0.0286	0.67
	336.4	0.655	45.69	1.942	15.2	0.0203	0.75
							0.83 mean
$Mg^{++}Cl^-$	350	0.630	45.0	2.002	1.4	—	—
$Mg^{++}Br^-$	350	0.630	45.0	1.942	2.7	—	—

the equilibrium constant the same over the range of copper concentrations used (0.126 *M* to 0.315 *M*). This % change turned out to have a minimum value at $K = 0.79$ for 25 °C, when the range of variation of ϵ was 0.81%. This is for 280 mμ, which is the absorption maximum for $CuBr^+$.

This is not an implausibly large variation of ϵ, and consequently the calculations were extended to other wavelengths and temperatures, and to other complex ions. It was assumed that ΔH varied linearly with temperature:

$$\Delta H = \alpha + \beta T$$

so that $\mathrm{d} \ln k/\mathrm{d}T = \Delta H/RT^2$ could be integrated to give

$$\ln K = A - \alpha/RT + \beta \ln T/R.$$

Can. J. Chem. Downloaded from www.nrcresearchpress.com by 210.87.254.6 on 09/05/12
For personal use only.

TABLE Ib

Calorimetric results on mixing metal perchlorate and sodium halide solutions at 40 °C

	$M(ClO_4)_2$		NaX		Corrected heat change	Complex formed	ΔH
$M^{++}X^-$	Vol. (ml)	Conc. (M)	Vol. (ml)	Conc. (M)	(cal)	(mole)	(kcal)
$Co^{++}Cl^-$	349.1	0.634	46.75	2.002	14.1	0.0260	0.54
	349.1	0.634	46.09	2.002	9.5	0.0183	0.52
	349.5	0.634	56.24	2.002	10.2	0.0303	0.34
	349.5	0.634	56.68	2.002	9.8	0.0202	0.49
	349.1	0.634	49.73	2.002	18.4	0.0275	0.67
	348.0	0.634	46.22	1.960	12.1	0.0254	0.48
	348.0	0.634	46.62	1.960	8.7	0.0183	0.48
							0.50 mean
$Ni^{++}Cl^-$	350.2	0.632	50.30	2.002	11.35	0.0262	0.43
	350.2	0.632	48.94	2.002	7.2	0.0175	0.41
	349.3	0.632	46.17	2.002	10.4	0.0244	0.43
	349.3	0.632	45.85	2.002	7.5	0.0172	0.44
							0.43 mean
$Cu^{++}Cl^-$	349.5	0.655	55.27	2.002	83.9	0.0417	2.01
	349.5	0.655	55.78	2.002	60.6	0.0273	2.22
	349.2	0.655	50.20	2.002	74.5	0.0386	1.93
	349.2	0.655	49.97	2.002	58.1	0.0262	2.22
							2.10 mean
$Co^{++}Br^-$	348.9	0.634	45.43	1.936	7.55	0.0264	0.29
	348.9	0.634	46.72	1.936	1.0	0.0195	0.05
	349.4	0.634	45.89	1.936	4.75	0.0266	0.18
	349.4	0.634	45.13	1.936	1.1	0.0188	0.06
	348.0	0.634	45.73	1.936	2.65	0.0266	0.10
	347.0	0.634	46.51	1.936	2.75	0.0274	0.10
	347.0	0.634	46.39	1.936	4.6	0.0196	0.23
							0.14 mean
$Ni^{++}Br^-$	349.4	0.632	45.43	1.936	1.0	0.0256	0.04
	349.4	0.632	46.72	1.936	0.9	0.0177	0.05
	347.0	0.646	46.01	1.936	2.4	0.0253	0.09
	347.0	0.646	45.72	1.936	1.6	0.0180	0.09
							0.07 mean
$Cu^{++}Br^-$	348.8	0.655	46.26	1.942	28.65	0.0271	1.06
	348.8	0.655	46.78	1.942	20.5	0.0196	1.05
	348.4	0.655	45.06	1.942	27.0	0.0266	1.02
	348.4	0.655	46.78	1.942	20.6	0.0197	1.05
							1.05 mean
$Mg^{++}Cl^-$	350	0.630	45.0	2.002	9.3	—	—
$Mg^{++}Br^-$	350	0.630	45.0	1.942	10.4	—	—

The value of K at 25 °C was chosen as that which gave a minimum range of ϵ values, averaged over all the wave lengths used. This, in effect, chooses A in the above equation to give a minimum variation in ϵ. Then α and β were varied until values were found which gave the same values of ΔH at 25 and 40 °C, firstly when calculated from $\Delta H = \alpha + \beta T$; and secondly, when K obtained from the above equation was applied to the calorimetric data and used to calculate the number of moles of MX^+ formed, and hence ΔH. Where cell voltages had been used to determine K, the average value at 25 °C was used in the

Can. J. Chem. Downloaded from www.nrcresearchpress.com by 210.87.254.6 on 09/05/12
For personal use only.

TABLE II

Comparison of ΔH from calorimetric measurements and equilibrium constants

Ion	ΔH (kcal) from K	ΔH calorimetric (kcal) At 25 °C	ΔH calorimetric (kcal) At 40° C
$CoCl^+$	0.85	0.53±0.02	0.50±0.06
$NiCl^+$	0.89	0.50±0.05	0.43±0.01
$CuCl^+$	1.01	1.58±0.10	2.10±0.13
$CoBr^+$	1.54	0.17±0.03	0.14±0.08
$NiBr^+$	0.27	0.09±0.03	0.07±0.02
$CuBr^+$	−0.14	0.83±0.10	1.05±0.01

TABLE III

Effect of omitting correction term to calorimetric results

Ion	At 25 °C	At 40 °C
$CoCl^+$	0.61±0.03	0.97±0.10
$NiCl^+$	0.58±0.05	0.91±0.08
$CuCl^+$	1.64±0.12	2.43±0.19
$CoBr^+$	0.31±0.00	0.61±0.08
$NiBr^+$	0.24±0.03	0.57±0.10
$CuBr^+$	0.95±0.11	1.51±0.08

calculations. The results of these calculations are given in Table V. They require the extinction coefficients to vary over a range of about 1% between a solution about 0.12 M in $M(ClO_4)_2$ and 1.60 M in $NaClO_4$, and a solution about 0.32 M in $M(ClO_4)_2$ and 1.00 M in sodium perchlorate. Otherwise the ΔH values are self-consistent.

Table V also contains the final values of K, which are not very different from those used earlier, and hence ΔF and ΔS for the reactions. The results all refer to an ionic strength of 2.0. These are probably the most reliable values for these quantities. It may be noted that a plot of ΔH against ΔS (see Fig. 1) gives a straight line, whose equation from least squares is

$$\Delta H = 254\Delta S + 201$$

if we express ΔH in calories (not kcal). All ΔH values, both at 25 and 40 °C, lie within 80 cal of this line.

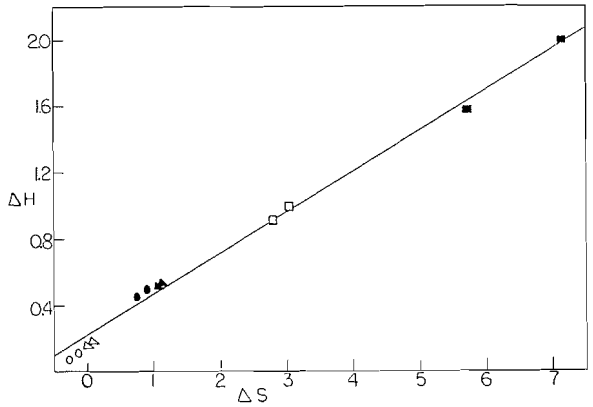


FIG. 1. H (kcal) plotted against ΔS (cal/deg) for formation of complex ions: ○, Ni (in bromide); ●, Ni (in chloride); △, Co (in bromide); ▲, Co (in chloride); □, Cu (in bromide); ■, Cu (in chloride).

Can. J. Chem. Downloaded from www.nrcresearchpress.com by 210.87.254.6 on 09/05/12
For personal use only.

Can. J. Chem. Downloaded from www.nrcresearchpress.com by 210.87.254.6 on 09/05/12
For personal use only.

TABLE IV

Calorimetric ΔH values, on the assumption that MX^+ and M_2X^{3+} ions are formed

	K_1		K_2				ΔH_1 calorimetric (kcal)		ΔH_2 calorimetric (kcal)	
$M^{++}X^-$	25 °C	40 °C	25 °C	40 °C	ΔH_1 from K_1 (kcal)	ΔH_2 from K_2 (kcal)	25 °C	40 °C	25 °C	40 °C
$Co^{++}Cl^-$	0.666	0.711	0.274	0.327	0.81	0.77	0.68	0.53	−0.35	−0.30
$Ni^{++}Cl^-$	0.569	0.620	0.407	0.409	1.06	0.06	0.64	0.52	−0.03	0.10
$Cu^{++}Cl^-$	5.47	7.35	5.21	7.79	3.65	4.97	1.01	1.25	−0.04	0.24
$Cu^{++}Br^-$	3.56	4.15	2.31	2.77	1.89	2.24	0.50	0.54	−0.02	0.18

TABLE V

Consistent values of ΔH from calorimetric data and equilibrium constants

Ion	Temp. (°C)	K (mole/l)$^{-1}$	ΔH (kcal)	ΔF (kcal)	ΔS (cal/deg)
$CoCl^+$	25	0.73	0.52	0.19	1.11
$CoCl^+$	40	0.76	0.50	0.17	1.05
$NiCl^+$	25	0.67	0.50	0.24	0.87
$NiCl^+$	40	0.70	0.44	0.23	0.61
$CuCl^+$	25	1.22	1.58	−0.11	5.67
$CuCl^+$	40	1.41	1.98	−0.21	6.99
$CoBr^+$	25	0.77	0.14	0.16	−0.07
$CoBr^+$	40	0.78	0.15	0.15	0.00
$NiBr^+$	25	0.76	0.08	0.16	−0.27
$NiBr^+$	40	0.77	0.07	0.16	−0.29
$CuBr^+$	25	0.85	0.90	0.10	2.75
$CuBr^+$	40	0.92	1.00	0.05	3.03

A possible explanation of this may be sought in terms of the strength of attachment of water molecules to the ions in solution. If the heat of hydration of the complex ion is high, ΔH for its formation will be more exothermic; but its ΔS will be lower, as the water is relatively less free. The heat of hydration presumably depends to a considerable extent on how the ionic charge is distributed between the M and X ions.

REFERENCES

1. M. W. LISTER and P. ROSENBLUM. Can. J. Chem. **38**, 1827 (1960).
2. M. W. LISTER and D. WILSON. Can. J. Chem. **39**, 2606 (1961).
3. J. M. AUSTIN, R. A. MATHESON, and H. N. PARTON. The structure of electrolyte solutions. *Edited by* W. J. Hamer. John Wiley & Sons, Inc., New York. 1959. p. 365.
4. C. W. DAVIES. Ion association. Butterworths, London. 1962. p. 170.
5. R. H. STOKES. Trans. Faraday Soc. **41**, 642 (1945).
6. J. KENTTAMAA. Suomen Kemistilehti, Sect. B, **32**, 68 (1959).
7. A. I. VOGEL. Quantitative inorganic analysis. 3rd ed. Longmans, Green & Co., Inc., New York and Toronto. 1961. p. 435.
8. G. SCHWARZENBACH. Complexometric titrations. Methuen & Co. Ltd., London. 1957. p. 78.

Can. J. Chem. Downloaded from www.nrcresearchpress.com by 210.87.254.6 on 09/05/12
For personal use only.

Can. J. Chem. Downloaded from www.nrcresearchpress.com by 210.87.254.105 on 09/05/12
For personal use only.

NOTES

KINETICS OF THE OXIDATION OF GLYCOLLIC ACID BY VANADIUM(V)

G. V. Bakore and Rama Shanker

Oxidation of glycollic acid by vanadium(V) in perchloric acid was investigated to see if the oxidation follows the scheme suggested by Jones, Waters, and Littler (1) for the oxidation of lactic, mandelic, and malic acids by vanadium(V).

An attempt was made to study the products of oxidation of glycollic acid by vanadium(V) in the presence of excess of glycollic acid. The product study was made by two independent methods.

(A) The formaldehyde produced by the oxidation of glycollic acid by vanadium(V) was estimated as its 2,4-dinitrophenylhydrazone in 2 *M* perchloric acid (2). To eliminate the possibility of low yield because of hydrolysis of the hydrazone, a control experiment was run along with the test experiment. The results are recorded in Table I.

TABLE I

Estimation of HCHO using 2,4-dinitrophenylhydrazine

Reaction mixture HCHO (g)*		Synthetic mixture, HCHO (g)†		% HCHO in the oxidized mixture
Expected	Found	Expected	Found	
0.0300	0.0024	0.0300	0.0242±0.0010	9.9±4.1
0.0375	0.0035	0.0375	0.0318±0.0013	11.0±4.0
0.0450	0.0044	0.0450	0.0412±0.0016	10.7±3.8

*Expected on the basis of the reaction $2V(V) + CH_2OHCO_2H \rightarrow HCHO + CO_2 + 2V(IV)$.
†Average of two to three runs.

(B) The oxidized mixtures were steam distilled to separate the formaldehyde produced. This was then estimated by its color reaction with chromotropic acid (3) by following the absorption at 570 mμ with a Bausch and Lomb Spectronic 20 colorimeter. A calibration curve was prepared by using standardized formaldehyde solution. From the relation between concentration and optical density, the amount of formaldehyde produced was evaluated. The results are summarized in Table II.

TABLE II

Estimation of HCHO by chromotropic acid (3)

Reaction mixture HCHO (g)*		Synthetic mixture HCHO (g)†		% HCHO in the oxidized mixture
Expected	Found	Expected	Found	
0.0500	0.0039	0.0500	0.0481±0.0018	8.1±3.7
0.0600	0.0047	0.0600	0.0550±0.0022	8.0±4.0

*Expected on the basis of the reaction: $2V(V) + CH_2(OH)CO_2H \rightarrow HCHO + CO_2 + 2V(IV)$.
†Average of three runs.

The total amount of formaldehyde and formic acid produced in the oxidized mixture was estimated both by bromometric (4) and permanganate (5) methods. From the control experiments, similar to those described in A and B, the amount of formaldehyde was estimated. This, when subtracted from the total amount of formaldehyde and formic acid, was taken to be a measure of the amount of formic acid produced in the reaction mixture.

Our results show that under these experimental conditions the amount of formaldehyde produced as a result of the oxidation of glycollic acid is about 10–15% of the yield expected on the basis of the equation and about 85% of the product is formic acid and not formaldehyde.

TABLE III

Dependence of rate on initial [V(V)] ([glycollic acid] = 0.058 M; [H^+] = 2.13 M; μ = 2.5 M; T = 38 °C)

[Vanadium(V)] (mole/l)	0.010	0.015	0.020	0.025
$k_1 \times 10^4$ (s^{-1})	1.40	2.10	2.80	3.20

TABLE IV

Dependence of rate on the concentration of glycollic acid ([vanadium(V)] = 0.02 M; [H^+] = 2.13 M; T = 38 °C)

[Glycollic acid] (mole/l)	0.060	0.083	0.165	0.250	0.350
$k_1 \times 10^4$ (s^{-1})	2.83	3.90	8.00	12.6	18.0
$k_1 \times 10^3$/[glycollic acid]	4.72	4.70	4.84	5.04	5.14

Average $k_2 (= k_1/[\text{glycollic acid}]) = 4.89 \pm 0.25 \times 10^{-3}$ l $mole^{-1}$ s^{-1}

Although the rate of disappearance of vanadium(V) follows first order kinetics for individual runs, the rate constant increases with an increase in the concentration of V(V). At higher concentrations of V(V), the rate constants tend to be independent of initial concentration of V(V) (cf. Table III). This indicates that consecutive reactions may be involved. The rate is proportional to the concentration of glycollic acid (cf. Table IV). The dependence of rate on hydrogen ion concentration in perchloric acid – sodium perchlorate mixtures of constant ionic strength follows the rate expression (1)

$$-\mathrm{d}[\mathrm{V(V)}]/\mathrm{d}t = k[\mathrm{V(V)}][\text{glycollic acid}](1 + ah_0),$$

where h_0 is the Hammett acidity function (cf. Table V).

TABLE V

Dependence of rate on acidity ([vanadium(V)] = 0.04 M; [glycollic acid] = 0.146 M; μ = 5.0 M; T = 25 °C)

[$HClO_4$] (moles/l)	h_0*	$k_1 \times 10^4$ (s^{-1})	
		Found	Calcd.†
1.0	28.2	1.25	1.30
1.5	47.9	2.00	2.07
2.0	69.2	3.00	2.90
2.5	100.0	4.00	3.92
3.0	138.0	5.87	5.58
3.5	210.0	8.42	8.39
4.0	282.0	11.1	11.2
4.5	400.0	16.0	15.8

*Values taken from ref. 13.
†Calculated using the relation $k_1 = 0.2 + 0.039h_0$.

Can. J. Chem. Downloaded from www.nrcresearchpress.com by 210.87.254.105 on 09/05/12
For personal use only.

Addition of formaldehyde has no effect on the rate of oxidation of glycollic acid by vanadium(V) (cf. Table VI).

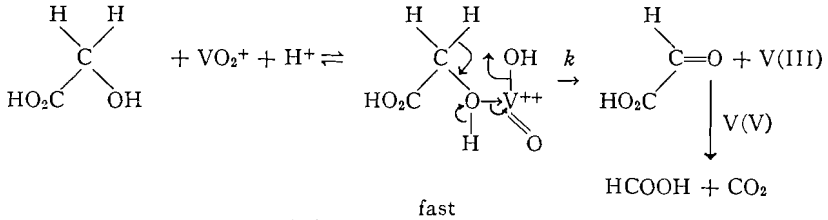
TABLE VI

Dependence of rate on initial [HCHO] ([vanadium(V)] = 0.0256 M; [glycollic acid] = 0.163 M; $[H^+]$ = 1.5 M; μ = 5.0 M; T = 38 °C)

[HCHO]$\times 10^2$ (moles/l)	0.00	2.24	4.88	11.2
$k_1 \times 10^4$ (s^{-1})	7.80	7.85	7.82	7.88

From our kinetic experiments we find that under similar conditions the rate of oxidation of glycollic acid is about 350 times the rate of oxidation of formaldehyde by vanadium(V), as observed by Kemp and Waters (6). This suggests that if the scheme suggested by Jones, Waters, and Littler (1) is correct, formaldehyde should be the main product of oxidation. The product study, however, indicates that this is not the case and that the main product of oxidation is formic acid and not formaldehyde. These facts suggest that oxidation of glycollic acid does not involve C—C fission to as great an extent as has been suggested by Jones, Waters, and Littler (1).

Shanker and Joshi (7) and Bhargava, Shanker, and Bakore (8) have suggested that vanadium(V) can act as a two-electron oxidant. Chromium(VI) also acts as a two-electron oxidant and by analogy with the oxidation of hydroxy acids by chromium(VI), the following mechanism, consistent with the facts reported here, may be suggested for the oxidation of glycollic acid by vanadium(V):



$$V(III) + V(V) \xrightarrow{\text{fast}} 2V(IV).$$

The fact that Kemp and Waters (9) have observed a kinetic isotope effect of 2.0 for the oxidation of mandelic acid and α-deuteromandelic acid by vanadium(V) indicates that C—H bond fission is appreciable in the oxidation of hydroxy acids by vanadium(V).

If the oxidation of glycollic acid and also lactic, mandelic, and malic acids involves C—H bond rupture, then a comparison of thermodynamic parameters for the oxidation of these acids with those for the oxidation of α-hydroxyisobutyric acid and pinacol, which involves C—C fission, may be expected to be different. Table VII summarizes these thermodynamic parameters.

TABLE VII

Thermodynamic parameters for the oxidation of α-hydroxy acids by vanadium(V)

Substrate	ΔE (kcal/mole)	ΔS (entropy units)	Reference
Glycollic acid	16.7	−16.0	—
Lactic acid	16.5	−20.0	(10)
Mandelic acid	14.0	−20.1	(11)
α-Hydroxyisobutyric acid	21.8	−0.4	*
Pinacol	22.8	+9.5	*
Oxalic acid	24.0	+0.6	(8)

*Data from present investigations.

Can. J. Chem. Downloaded from www.nrcresearchpress.com by 210.87.254.105 on 09/05/12
For personal use only.

The entropy of activation for the oxidation of compounds like pinacol, oxalic acid, and α-hydroxyisobutyric acid, which is known to involve C—C fission, has values from -1.0 to $+10$ e.u. (entropy units). The observed entropy of activation ($\simeq -20$ e.u.) for the oxidation of glycollic, lactic, and mandelic acids suggests that the oxidation of these hydroxy acids involves considerable C—H fission in the rate-determining step.

The relative proportions of formaldehyde and formic acid in the products of oxidation of glycollic acid also agree with the suggestion that in the oxidation of glycollic acid C—H bond rupture becomes appreciably significant.

It, therefore, appears that oxidation of glycollic acid by vanadium(V) is similar to the oxidation of α-hydroxy acids by chromium(VI) (cf. Bakore and Narain (12)).

ACKNOWLEDGMENT

The authors wish to acknowledge the helpful criticisms of one of the referees.

1. J. R. Jones, W. A. Waters, and J. S. Littler. J. Chem. Soc. 630 (1961).
2. A. I. Vogel. Elementary practical organic chemistry. Longmans, Green & Co. Ltd., London. 1958. p. 739.
3. N. D. Cheronis and T. S. Ma. Organic functional group analysis by micro and semi-micro methods. John Wiley & Sons, Inc., New York. 1964. p. 504.
4. I. M. Kolthoff and R. Belcher. Volumetric analysis. Vol. III. Interscience Publishers, Inc., New York. 1957. p. 567.
5. A. I. Vogel. A text book of quantitative inorganic analysis. Longmans, Green & Co., Ltd., London. 1955. p. 289.
6. T. J. Kemp and W. A. Waters. Proc. Roy. Soc. London, Ser. A, **274**, 480 (1963).
7. R. Shanker and S. N. Joshi. Indian J. Chem. **1**, 289 (1963).
8. N. C. Bhargava, R. Shanker, and G. V. Bakore. Z. Physik. Chem. **229**, 238 (1965).
9. T. J. Kemp and W. A. Waters. J. Chem. Soc. 1192 (1964).
10. U. S. Mahnot, R. Shanker, and S. N. Swami. Z. Physik. Chem. **222**, 240 (1963).
11. R. Shanker and S. N. Swami. J. Indian Chem. Soc. **40**, 105 (1963).
12. G. V. Bakore and S. Narain. J. Chem. Soc. 3419 (1963).
13. M. A. Paul and F. A. Long. Chem. Rev. **57**, 1 (1957).

Received April 15, 1965.
Department of Chemistry,
M. B. College,
University of Udaipur,
Udaipur, India.

LIFETIME OF THE PHOSPHORESCENCE OF HEXAFLUOROACETONE VAPOR[1]

A. Gandini[2] and K. O. Kutschke

Bowers and Porter (1) have recently shown that, contrary to previous observations by Okabe and Steacie (2), hexafluoroacetone vapor does indeed phosphoresce when excited with 3 130 Å light, and that the spectra of both fluorescence and phosphorescence of this compound can be obtained since the phosphorescence is completely quenched by small quantities of oxygen. Dr. H. W. Holden had made similar observations in these laboratories. We have undertaken a study of the mean lifetimes of these emission phenomena and the purpose of this note is to report the results obtained thus far; these pertain

[1]*Issued as N.R.C. No. 9070.*
[2]*National Research Council Postdoctorate Fellow, 1965.*

Can. J. Chem. Downloaded from www.nrcresearchpress.com by 210.87.254.105 on 09/05/12
For personal use only.

The entropy of activation for the oxidation of compounds like pinacol, oxalic acid, and α-hydroxyisobutyric acid, which is known to involve C—C fission, has values from -1.0 to $+10$ e.u. (entropy units). The observed entropy of activation ($\simeq -20$ e.u.) for the oxidation of glycollic, lactic, and mandelic acids suggests that the oxidation of these hydroxy acids involves considerable C—H fission in the rate-determining step.

The relative proportions of formaldehyde and formic acid in the products of oxidation of glycollic acid also agree with the suggestion that in the oxidation of glycollic acid C—H bond rupture becomes appreciably significant.

It, therefore, appears that oxidation of glycollic acid by vanadium(V) is similar to the oxidation of α-hydroxy acids by chromium(VI) (cf. Bakore and Narain (12)).

ACKNOWLEDGMENT

The authors wish to acknowledge the helpful criticisms of one of the referees.

1. J. R. Jones, W. A. Waters, and J. S. Littler. J. Chem. Soc. 630 (1961).
2. A. I. Vogel. Elementary practical organic chemistry. Longmans, Green & Co. Ltd., London. 1958. p. 739.
3. N. D. Cheronis and T. S. Ma. Organic functional group analysis by micro and semi-micro methods. John Wiley & Sons, Inc., New York. 1964. p. 504.
4. I. M. Kolthoff and R. Belcher. Volumetric analysis. Vol. III. Interscience Publishers, Inc., New York. 1957. p. 567.
5. A. I. Vogel. A text book of quantitative inorganic analysis. Longmans, Green & Co., Ltd., London. 1955. p. 289.
6. T. J. Kemp and W. A. Waters. Proc. Roy. Soc. London, Ser. A, **274**, 480 (1963).
7. R. Shanker and S. N. Joshi. Indian J. Chem. **1**, 289 (1963).
8. N. C. Bhargava, R. Shanker, and G. V. Bakore. Z. Physik. Chem. **229**, 238 (1965).
9. T. J. Kemp and W. A. Waters. J. Chem. Soc. 1192 (1964).
10. U. S. Mahnot, R. Shanker, and S. N. Swami. Z. Physik. Chem. **222**, 240 (1963).
11. R. Shanker and S. N. Swami. J. Indian Chem. Soc. **40**, 105 (1963).
12. G. V. Bakore and S. Narain. J. Chem. Soc. 3419 (1963).
13. M. A. Paul and F. A. Long. Chem. Rev. **57**, 1 (1957).

Received April 15, 1965.
Department of Chemistry,
M. B. College,
University of Udaipur,
Udaipur, India.

LIFETIME OF THE PHOSPHORESCENCE OF HEXAFLUOROACETONE VAPOR[1]

A. Gandini[2] and K. O. Kutschke

Bowers and Porter (1) have recently shown that, contrary to previous observations by Okabe and Steacie (2), hexafluoroacetone vapor does indeed phosphoresce when excited with 3 130 Å light, and that the spectra of both fluorescence and phosphorescence of this compound can be obtained since the phosphorescence is completely quenched by small quantities of oxygen. Dr. H. W. Holden had made similar observations in these laboratories. We have undertaken a study of the mean lifetimes of these emission phenomena and the purpose of this note is to report the results obtained thus far; these pertain

[1]*Issued as N.R.C. No. 9070.*
[2]*National Research Council Postdoctorate Fellow, 1965.*

Can. J. Chem. Downloaded from www.nrcresearchpress.com by 210.87.254.5 on 09/05/12
For personal use only.

to the mean lifetime of the phosphorescence of hexafluoroacetone and to the effect of certain gases upon it.

The apparatus used was similar to that described by Kaskan and Duncan (3). Light from an argon flash discharge lamp (kindly provided by Dr. D. A. Ramsay of these laboratories) was filtered through the "3 130 filter" described by Kasha (4) and passed as a parallel beam ($\sim$ 0.5 cm diameter) through a T-shaped cell (15 cm long, 2 cm i.d.). The emitted light was focused through a Corning filter, C.S. 0-52, onto a 6256B EMI photomultiplier tube whose output was applied to the vertical plates of a Tektronix 545 oscilloscope. The signal from the photomultiplier triggered the horizontal sweep of the oscilloscope; the decay curves thus produced were photographed. The cell was permanently connected to the vacuum line. The effect of added gases was studied by starting an experiment with the pure ketone and by adding thereafter known amounts of the second compound; mixing was achieved with a glass piston pump operated electromagnetically. Mixing for periods longer than 15 min caused no further changes in the measured lifetimes.

The intensity of the flash from the lamp rose to a maximum in 5 to 7 μs and thereafter decreased exponentially with a lifetime of 5.9 $\pm$ 0.1 μs; a tungsten wire resistor in series with the lamp eliminated oscillations which were otherwise observed in the lamp output following the main pulse (5). The scattered light arriving at the photomultiplier, when the lamp was flashed into the empty cell or into as much as 400 mm of carbon dioxide, was negligibly small.

All experiments were conducted at 25 $\pm$ 1°.

Hexafluoroacetone (Allied Chemical), acetone (B. and A.), decafluorobutane (Columbia Organic Chemicals), isobutene (Matheson), benzene, isobutane, ethylene, and propylene (all Phillips research grade) were thoroughly degassed before use; isobutane contained less than 1 part in 15 000 of isobutene as determined by gas chromatography. Oxygen (Union Carbide, 99.99% purity) was used as obtained from the supplier.

The mean phosphorescence lifetime of acetone vapor has been measured by Kaskan and Duncan (6) in the pressure region 10 to 200 mm at 25°. We repeated these determinations as a test of the present apparatus; although the effect of acetone pressure upon the mean lifetime was similar to that found by Kaskan and Duncan, the actual values of the lifetime were consistently 15% higher than those reported. Two different batches of acetone were used for these determinations and gave the same results within experimental error. It is possible that this discrepancy was caused by the presence of triplet-quenching impurities in the acetone samples used by Kaskan and Duncan. It is unlikely that systematic errors in the time scale of the oscilloscopes could cause an error of this magnitude.

Hexafluoroacetone gave decay traces which clearly indicated, as in the case of acetone (7), the occurrence of two distinct emissions; the plots of the logarithm of the emission intensity versus time produced two straight lines with markedly different slopes. The larger, which was not very well resolved because of interference from the decay of the flash, gave a mean lifetime of about 12 μs; this is attributed to the fluorescence or emission from the first excited singlet state. This lifetime is longer than the radiative lifetime expected for a spin-allowed transition (an approximate integration of the extinction coefficients in the literature (8) yielded $\tau_0 \sim 6.7$ μs) and is much longer than that expected when paths other than fluorescence are available to dissipate the energy. Instances are known in which the measured lifetimes, extrapolated to zero pressure, are greater than those calculated from integrated absorption coefficients (9, 10). Mechanisms which might

Can. J. Chem. Downloaded from www.nrcresearchpress.com by 210.87.254.5 on 09/05/12
For personal use only.

be responsible for such effects have been discussed (11). The smaller slope, always much better defined, gave a mean lifetime of 286 ± 5 μs; this is attributed to the phosphorescence, or emission from the triplet state, since additions of a few millimeters of oxygen eliminated it completely.

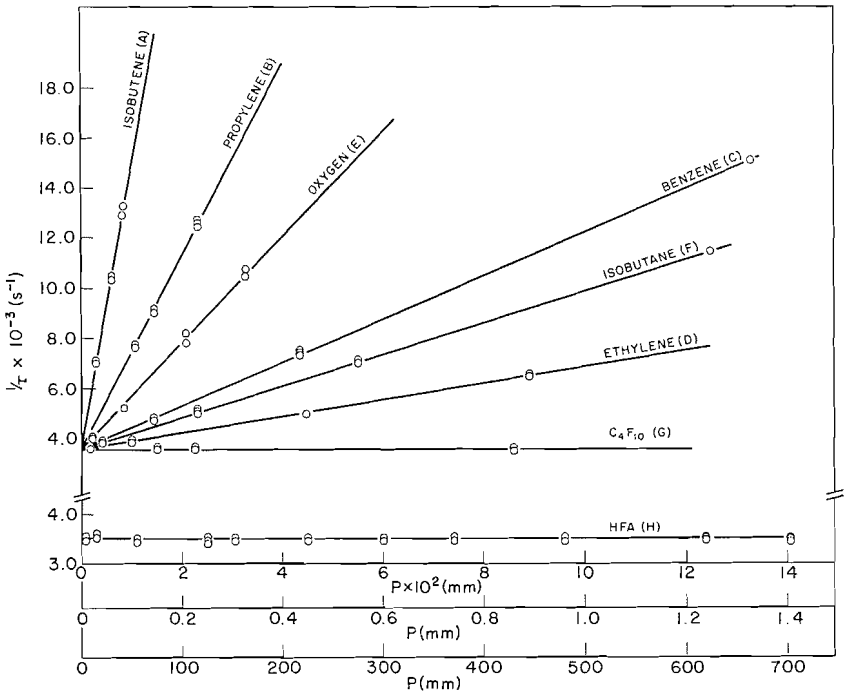


FIG. 1. The effect of various gases upon the phosphorescence lifetime of hexafluoroacetone at 25°. The top abscissa scale refers to A, B, C, and D; the middle scale to E and F; the bottom scale to G and H.

The pressure dependence of the phosphorescence lifetime was studied and the results are shown in Fig. 1. The lowest working pressure was that below which reasonable accuracy in determining lifetimes became technically unattainable. It must be pointed out that over 100 determinations were made in the pressure range shown in the graph and that they all fell within the scatter given above for the mean lifetime. It can be concluded that if there is any effect of pressure upon the phosphorescence of hexafluoroacetone between 4 and 704 mm, this must be less than the experimental scatter of ±2%. Several samples from one batch of the ketone were used; the degassing procedure varied greatly but no change in the lifetime was observed. Samples from other cylinders of the ketone gave this lifetime as a limiting value after rigorous purification which involved discarding the most volatile (at −110 °C) 80% of the sample. Similar results were obtained by Kaskan and Duncan (6) with biacetyl vapor, although the pressure range investigated by them was much more limited.

The effect of various gaseous compounds upon the mean lifetime of phosphorescence of hexafluoroacetone is also illustrated in Fig. 1 and the quenching rate constants given in Table I. The quenching effect always followed the simple relationship

$$1/\tau = k_1 + k_2[G],$$

Can. J. Chem. Downloaded from www.nrcresearchpress.com by 210.87.254.5 on 09/05/12
For personal use only.

where τ is the mean lifetime of phosphorescence of the mixture, $1/k_1$ the mean lifetime of the pure ketone, and [G] the concentration of the added gas; k_2 represents the quenching rate constant.

TABLE I

Quenching efficiency of various gases upon the phosphorescence lifetime of hexafluoroacetone (HFA) at 25°

	$k_2 \times 10^{-11}$ $((\text{mole/ml})^{-1}\ \text{s}^{-1})$	P_{HFA} (mm)
Hexafluoroacetone	0.0	4 to 704
Decafluorobutane	0.0	76 and 302
Isobutane	1.2	142 and 362
Oxygen	4.5	209
Ethylene	5.9	153
Benzene	16.1	119
Propylene	72.6	190, 271, and 478
Isobutene	214	228

The following considerations must be included in an interpretation of these results

(*a*) The quenching effect of oxygen upon the triplet state of ketone vapors has been reported by several investigators (1, 6, 7, 12), although a clear understanding of the details of the quenching action has not been attained as yet. The present results show that oxygen is about 20 times more powerful in quenching the triplet state of acetone (7) than in quenching that of hexafluoroacetone, and that it displays approximately the same quenching efficiency with biacetyl (6) and with hexafluoroacetone, at 25°.

(*b*) Decafluorobutane has no effect upon the phosphorescence lifetime of hexafluoroacetone up to a ratio [fluorocarbon]/[ketone] of 6/1. Similar observations were made when studying the total emission of mixtures of these two compounds with a static system (13).

(*c*) The effect of the three olefins studied could in principle be interpreted according to one or more of the following mechanisms:

1. The ketone molecules in the triplet state transfer their energy to the olefin molecules.

[1] $$^3\text{A} + \text{O} \rightarrow \text{A} + {}^3\text{O}$$

2. Intersystem crossing to the ground state by collision with olefin molecules is the cause of the quenching.

3. The ketone molecules in the triplet state undergo a chemical reaction with the olefin.

A mechanism based on simple energy transfer to the triplet state of the olefin (reaction [1]) encounters energetic difficulties. The location of the O—O band of the T_1–S_0 transition for hexafluoroacetone is unknown, but, from the known (2) S_1–S_0 separation and by accepting a S_1–T_1 separation near 9 kcal/mole as is known for formaldehyde (14), the T_1–S_0 separation becomes 71 kcal/mole. The only monoolefin for which this separation is known from spectroscopic data is ethylene; Evans (15) gave a value of 82 kcal/mole. Triplet state levels for higher homologs are expected to lie somewhat lower; thus values of k_2 are expected to be greater for propylene and isobutene than for ethylene, as indeed is observed. However, the magnitudes involved become quite unreasonable if only low vibrational levels of the ketone triplet state are involved. For example, if the rate constant for [1] is written as $k_2 = A_2 \exp(-E_2/RT)$ and if E_2 is taken as the endothermicity of the reaction ($\sim$ 11 kcal/mole), the experimental value of k_2 for ethylene requires that

Can. J. Chem. Downloaded from www.nrcresearchpress.com by 210.87.254.5 on 09/05/12
For personal use only.

$A_2(C_2H_4) \simeq 10^{20}$ (mole/ml)$^{-1}$ s^{-1}, which suggests a collision cross-section of $\sim 8 \times 10^6$ Å^2. More reasonable values of A_2 are obtained if smaller values of E_2 are involved; in the case of ethylene if E_2 is ~ 5 kcal/mole, the collision cross-section is reduced to about 300 Å^2. A lower E_2 implies a higher triplet state energy for the ketone, or that higher vibrational levels of the triplet state are involved. Neither suggestion is unreasonable, although the latter is not supported by the lack of effect of ketone pressure on k_2 (Table I). Because of the uncertainty in the energetics it is not possible to rule out the energy transfer mechanism, although at present it seems not to provide a completely satisfactory explanation of the experimental data. Studies of the temperature dependence of k_2, soon to be undertaken, should provide further insight into the energetics of these systems.

The second possibility seems highly improbable, since other molecules of not too different size, such as decafluorobutane and hexafluoroacetone itself, have no such effect on the lifetime even at very much higher concentrations.

The possibility of a chemical interaction seems the most plausible interpretation, although it is not possible to offer any evidence on the actual mode of attack; presumably both the double bond and the methyl groups of the higher olefins must play a role. This concept is supported by the fact that ethylene and isobutane, both of which lack one of the two structures, display a finite efficiency.

The effect of isobutene on the phosphorescence of hexafluoroacetone was confirmed by static measurements on the total emission (13).

The fact that Okabe and Steacie (2) did not observe any phosphorescence emission from hexafluoroacetone is possibly explained by the presence of small quantities of ethylene in the ketone used. These could have been generated during the dehydration of the commercial ketone hydrate; it has since been observed in these laboratories that most samples of the hydrate contained some ethanol. Less than 1 mm of ethylene would have been sufficient to quench the entire phosphorescence emission.

(*d*) The deduction of a quenching mechanism for isobutane is easier, since both collisional deactivation and energy transfer can be safely ruled out in this case. A chemical reaction seems to be the only alternative. Khanna and Kutschke (16) have recently come to a similar conclusion in considering the effect of isobutane upon the quantum yield of the decomposition of hexafluoroacetone. It should be noted that the maximum isobutene impurity in the isobutane used here could have caused less than about 1% of the quenching observed. Moreover, the total level of impurities was such that quenching constants larger than the collision number would have been required for these to interfere significantly with the effect of isobutane itself.

(*e*) The effect of benzene upon the phosphorescence lifetime of hexafluoroacetone is again explained in terms of chemical reaction. Rebbert and Ausloos (17) have found that benzene produces no observable reduction of the emission yield of acetone and explained this by showing that energy transfer was too endothermic. The same can be said in the present instance, since the O—O band of the S_0–T_1 transition for benzene corresponds to 84 kcal/mole. The ratio of the values of k_2 for benzene and isobutane differs considerably from the value of $q_{i\text{-}C_4H_{10}}/q_{C_6H_6} \simeq 1$ found by Khanna and Kutschke (16). This suggests that the same quantity is not being measured in these two sets of experiments.

It will be noticed from Table I that in some instances the effect of an added gas was studied at more than one pressure of ketone and that this did not alter the efficiency of the added compound. This confirms the observation that the mean lifetime of phosphorescence of hexafluoroacetone is independent of the pressure of the ketone.

Further work on both emissions of hexafluoroacetone is in progress.

Can. J. Chem. Downloaded from www.nrcresearchpress.com by 210.87.254.5 on 09/05/12
For personal use only.

NOTE ADDED IN PROOF: The present experiments were done in an apparatus in which mercury was present near its saturation pressure at 25 °C. Very recently we measured τ at $\sim$ 50 mm HFA under mercury-free conditions and obtained $\tau = 2.3 \pm 0.2$ ms in two experiments. Moreover when a drop of mercury was added to the cell τ returned to less than 300 μs; condensation of the mixture at −196 °C followed by reevaporation produced no significant changes in τ. These observations suggest that mercury vapor acts as a quencher. The quenching constants in Table I should not be greatly affected by the presence of this second quencher at an essentially constant concentration. Quantum yields of decomposition of HFA probably also are affected by the presence of mercury vapor, however. Under mercury-free conditions τ for acetone remained near the value found in the presence of mercury.

1. P. G. Bowers and G. B. Porter. J. Phys. Chem. **68**, 2982 (1964).
2. H. Okabe and E. W. R. Steacie. Can. J. Chem. **36**, 137 (1958).
3. W. E. Kaskan and A. B. F. Duncan. J. Chem. Phys. **16**, 223 (1948).
4. M. Kasha. J. Opt. Soc. Am. **38**, 929 (1948).
5. L. Fischer. Photochem. Photobiol. **2**, 411 (1963).
6. W. E. Kaskan and A. B. F. Duncan. J. Chem. Phys. **18**, 427 (1950).
7. H. J. Groh, G. W. Luckey, and W. A. Noyes, Jr. J. Chem. Phys. **21**, 115 (1953).
8. G. Giacometti, H. Okabe, and E. W. R. Steacie. Proc. Roy. Soc. London, Ser. A, **250**, 287 (1959).
9. D. Neuberger and A. B. F. Duncan. J. Chem. Phys. **22**, 1693 (1954).
10. K. F. Greenough and A. B. F. Duncan. J. Am. Chem. Soc. **83**, 555 (1961).
11. A. E. Douglas. J. Chem. Phys. In press. 1966.
12. G. B. Porter. J. Chem. Phys. **32**, 1587 (1960).
13. A. Gandini and K. O. Kutschke. Unpublished results.
14. D. A. Ramsay. *In* Determination of organic structure by physical methods. Vol. 2. *Edited by* F. C. Nachod and W. D. Phillips. Academic Press, New York. 1962. Chap. 4.
15. D. F. Evans. J. Chem. Soc. 1735 (1960).
16. S. N. Khanna and K. O. Kutschke. Can. J. Chem. **44**, 1465 (1966).
17. R. E. Rebbert and P. Ausloos. J. Am. Chem. Soc. **87**, 5569 (1965).

Received March 17, 1966.
Division of Pure Chemistry,
National Research Council,
Ottawa, Canada.

THE HIGH RESOLUTION NUCLEAR MAGNETIC RESONANCE SPECTRUM OF THE NONRIGID AB_2X_2 SYSTEM

R. G. Jones

The high resolution nuclear magnetic resonance (n.m.r.) spectrum of the rigid ABB′XX′ (1, 2) and AB_2X_2 (2) systems have been studied in some detail. The ABB′XX′ system provides a good example of the application of the principles of sub-spectral analysis (2) and the AB_2X_2 system illustrates the special case of effective frequency spectra (3, 4).

The nonrigid AB_2X_2 system received a mention by Diehl *et al.* (2) as a further system in which the special conditions of effective frequencies apply because of the magnetic equivalence of the two B nuclei and the two X nuclei as a result of intramolecular torsional oscillations. However, the basic symmetry wave function diagram was not derived because the appropriate point group was not determined.

It is the purpose of this paper to show the way in which it is possible to elucidate the

Can. J. Chem. Downloaded from www.nrcresearchpress.com by 210.87.254.5 on 09/05/12
For personal use only.

NOTE ADDED IN PROOF: The present experiments were done in an apparatus in which mercury was present near its saturation pressure at 25 °C. Very recently we measured τ at $\sim$ 50 mm HFA under mercury-free conditions and obtained $\tau = 2.3 \pm 0.2$ ms in two experiments. Moreover when a drop of mercury was added to the cell τ returned to less than 300 μs; condensation of the mixture at −196 °C followed by reevaporation produced no significant changes in τ. These observations suggest that mercury vapor acts as a quencher. The quenching constants in Table I should not be greatly affected by the presence of this second quencher at an essentially constant concentration. Quantum yields of decomposition of HFA probably also are affected by the presence of mercury vapor, however. Under mercury-free conditions τ for acetone remained near the value found in the presence of mercury.

1. P. G. Bowers and G. B. Porter. J. Phys. Chem. **68**, 2982 (1964).
2. H. Okabe and E. W. R. Steacie. Can. J. Chem. **36**, 137 (1958).
3. W. E. Kaskan and A. B. F. Duncan. J. Chem. Phys. **16**, 223 (1948).
4. M. Kasha. J. Opt. Soc. Am. **38**, 929 (1948).
5. L. Fischer. Photochem. Photobiol. **2**, 411 (1963).
6. W. E. Kaskan and A. B. F. Duncan. J. Chem. Phys. **18**, 427 (1950).
7. H. J. Groh, G. W. Luckey, and W. A. Noyes, Jr. J. Chem. Phys. **21**, 115 (1953).
8. G. Giacometti, H. Okabe, and E. W. R. Steacie. Proc. Roy. Soc. London, Ser. A, **250**, 287 (1959).
9. D. Neuberger and A. B. F. Duncan. J. Chem. Phys. **22**, 1693 (1954).
10. K. F. Greenough and A. B. F. Duncan. J. Am. Chem. Soc. **83**, 555 (1961).
11. A. E. Douglas. J. Chem. Phys. In press. 1966.
12. G. B. Porter. J. Chem. Phys. **32**, 1587 (1960).
13. A. Gandini and K. O. Kutschke. Unpublished results.
14. D. A. Ramsay. *In* Determination of organic structure by physical methods. Vol. 2. *Edited by* F. C. Nachod and W. D. Phillips. Academic Press, New York. 1962. Chap. 4.
15. D. F. Evans. J. Chem. Soc. 1735 (1960).
16. S. N. Khanna and K. O. Kutschke. Can. J. Chem. **44**, 1465 (1966).
17. R. E. Rebbert and P. Ausloos. J. Am. Chem. Soc. **87**, 5569 (1965).

Received March 17, 1966.
Division of Pure Chemistry,
National Research Council,
Ottawa, Canada.

THE HIGH RESOLUTION NUCLEAR MAGNETIC RESONANCE SPECTRUM OF THE NONRIGID AB_2X_2 SYSTEM

R. G. Jones

The high resolution nuclear magnetic resonance (n.m.r.) spectrum of the rigid ABB′XX′ (1, 2) and AB_2X_2 (2) systems have been studied in some detail. The ABB′XX′ system provides a good example of the application of the principles of sub-spectral analysis (2) and the AB_2X_2 system illustrates the special case of effective frequency spectra (3, 4).

The nonrigid AB_2X_2 system received a mention by Diehl *et al.* (2) as a further system in which the special conditions of effective frequencies apply because of the magnetic equivalence of the two B nuclei and the two X nuclei as a result of intramolecular torsional oscillations. However, the basic symmetry wave function diagram was not derived because the appropriate point group was not determined.

It is the purpose of this paper to show the way in which it is possible to elucidate the

Can. J. Chem. Downloaded from www.nrcresearchpress.com by 210.87.254.40 on 09/05/12
For personal use only.

symmetry point group for the nonrigid AB_2X_2 system (from first principles) with particular regard to the specific requirements of the n.m.r. problem involved.

The paper by Longuet-Higgins (5) provides the basic ideas and definitions necessary for the extrapolation of our ideas about the symmetry point groups of rigid molecules to those of nonrigid molecules. Longuet-Higgins suggests that the clearest and most useful definition of the molecular symmetry point group appears to be, all feasible permutations of the positions and spins of identical nuclei or any product of such permutations, including E, the identity, and all feasible P^* ($PE^* = E^*P$) not necessarily including E^*. E^* is defined as the inversion of all particle positions, through the center of mass.

The simple product spin functions used as a representation of an n.m.r. problem are invariant under E^* (5). They are, therefore, transformed by P^* in the same way as by P. Hence it is only necessary to use the P elements of the group to characterize the symmetry point group for the n.m.r. problem. This point group is usually a sub-group of the molecular symmetry point group.

The feasible P for the nonrigid AB_2X_2 system can be defined using the numbering notation of Fig. 1.

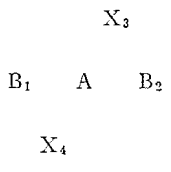


FIG. 1. Model for nonrigid AB_2X_2 systems.

The feasible P are E, (12), (34), and (12)(34). The multiplication table for the group is shown in Table I.

TABLE I

Transformations of the elements E, (12), (34), and (12)(34)

	E	12	34	12 34
E	E	12	34	12 34
12	12	E	12 34	34
34	34	12 34	E	12
12 34	12 34	34	12	E

Every element of the group is conjugate with itself but no other element and therefore each element belongs to a unique class (6). There are four classes and therefore there are four irreducible representations.

It is possible to derive the characters of these four irreducible representations on the basis of the vector properties of the representations and four important rules (6, p. 64). A basis for a representation of a group may be any set of algebraic functions or vectors. Let the vectors $\overrightarrow{12}$ and $\overrightarrow{34}$ be the basis, at least in part, for the group under consideration. These vectors transform as follows

E	(12)	(34)	(12)(34)
$\overrightarrow{12}$	$-\overrightarrow{12}$	$\overrightarrow{12}$	$-\overrightarrow{12}$
$\overrightarrow{34}$	$\overrightarrow{34}$	$-\overrightarrow{34}$	$-\overrightarrow{34}$

Can. J. Chem. Downloaded from www.nrcresearchpress.com by 210.87.254.40 on 09/05/12
For personal use only.

The matrix representations are

$$\begin{array}{cccc} E & (12) & (34) & (12)(34) \\ \begin{bmatrix} 1, & 0 \\ 0, & 1 \end{bmatrix} & \begin{bmatrix} -1 & 0 \\ 0 & 1 \end{bmatrix} & \begin{bmatrix} 1 & 0 \\ 0 & -1 \end{bmatrix} & \begin{bmatrix} -1 & 0 \\ 0 & -1 \end{bmatrix} \end{array} .$$

Hence $$(12)\begin{bmatrix} \overrightarrow{12} \\ \overrightarrow{34} \end{bmatrix} = \begin{bmatrix} -1 & 0 \\ 0 & 1 \end{bmatrix}\begin{bmatrix} \overrightarrow{12} \\ \overrightarrow{34} \end{bmatrix} = \begin{bmatrix} -\overrightarrow{12} \\ \overrightarrow{34} \end{bmatrix} .$$

The vectors 12 and 34 are not mixed by the elements E, (12), (34), (12)(34) and therefore each forms an independent representation of the group

	E	(12)	(34)	(12)(34)	
$\Gamma_{\overrightarrow{12}}$	1	−1	1	−1	$\overrightarrow{12}$
$\Gamma_{\overrightarrow{34}}$	1	1	−1	−1	$\overrightarrow{34}$

These representations are orthogonal and the sums of the squares of the characters in these representations equal the order of the group (four elements). Thus they satisfy two of the four rules. The product of their characters within each class produces a new representation,

	E	(12)	(34)	(12)(34)
$\Gamma = \Gamma_{12} \times \Gamma_{34}$	1	−1	−1	1

which is orthogonal to both of them and therefore independent. The remaining independent representation which must be orthogonal to those defined above has the dimension $\chi(E) = 1$ (third rule (6)).

E	(12)	(34)	(12)(34)
1	1	1	1

The character table for the point group of the nonrigid AB_2X_2 system is therefore

	E	(12)(34)	(34)	(12)	
Γ_1	1	1	1	1	
Γ_2	1	1	−1	−1	$\overrightarrow{34}$
Γ_3	1	−1	1	−1	$\overrightarrow{12}$
Γ_4	1	−1	−1	1	

This point group is isomorphic with C_{2v}, the point group of the rigid AB_2X_2 system. It is obvious therefore that the factorization of the secular determinant will be identical both for the rigid and nonrigid AB_2X_2 systems (2). The AB_2 part of the spectrum is composed of three superimposed ab_2 sub-spectra corresponding to $F_s(X_2) = 1, 0, -1$ with statistical weight 1:2:1 respectively, as predicted by the effective frequency method (3, 4).

Can. J. Chem. Downloaded from www.nrcresearchpress.com by 210.87.254.40 on 09/05/12
For personal use only.

1. W. G. SCHNEIDER, H. J. BERNSTEIN, and J. A. POPLE. Can. J. Chem. **35**, 1487 (1957).
2. P. DIEHL, R. G. JONES, and H. J. BERNSTEIN. Can. J. Chem. **43**, 81 (1965).
3. J. A. POPLE and T. SCHAEFER. Mol. Phys. **3**, 547 (1961).
4. P. DIEHL and J. A. POPLE. Mol. Phys. **3**, 557 (1961).
5. H. C. LONGUET-HIGGINS. Mol. Phys. **6**, 445 (1963).
6. F. A. COTTON. Chemical applications of group theory. Interscience Publishers, Inc., New York. 1964.

RECEIVED FEBRUARY 28, 1966.
DEPARTMENT OF CHEMISTRY,
UNIVERSITY OF ESSEX,
WIVENHOE PARK,
COLCHESTER,
ESSEX, ENGLAND.

Can. J. Chem. Downloaded from www.nrcresearchpress.com by 210.87.254.40 on 09/05/12
For personal use only.

THE HYDROLYSIS OF DIMETHYLSULFATE AND DIETHYLSULFATE IN WATER[1]

R. E. ROBERTSON AND S. E. SUGAMORI

In this note we supply kinetic data for the hydrolysis of dimethylsulfate and diethylsulfate in water for a range of temperatures and compare the derived parameters with similar terms from the hydrolysis of the corresponding methanesulfonates and benzenesulfonates.

At one time questions were raised as to whether solvolysis involved the cleavage of the O—S or O—C bond or most probably both in varying proportion depending on reaction conditions (1, 2). Results of research on this question by Ader (3), by Kaiser (4*, 5), and by Lauder, Wilson, and Zerner (6) show that the reaction involves C—O cleavage only. Kaiser (4) has shown that $MeSO_4^-$ ion will exchange with $H_2{}^{18}O$ and that the conflicting evidence based on ^{18}O tracer techniques is removed if the sulfate ion is precipitated as quickly as formed.

In the hydrolysis of dimethylsulfate, some degree of nucleophilic interaction with a single water molecule is indicated by the k_{OH^-}/k_{H_2O} ratio of 45–50 and the inverse secondary α-deuterium isotope effect (7) ($k_H/k_D = 0.97$). These values lie in the general range of the benzenesulfonates rather than that of the methyl halides, but it may be significant to note here that the k_{OH^-}/k_{H_2O} ratio and the k_H/k_D ratio for dimethylsulfate are both a little closer to unity than for the corresponding sulfonates. Moreover, the solvent isotope effect (k_{H_2O}/k_{D_2O}) 0.899 lies at the low end of the sulfonate range (8) a value which indicates less availability of the unshared electrons on the oxygens for hydrogen bonding. Because we shall have reason to return to this point later, we note here that a difference in hydrogen bonding ability of the sulfonates and the sulfates has been clearly indicated by the careful infrared investigation of Kartha *et al.* (9) on the relative hydrogen bonding to *p*-chlorophenol in CCl_4.

EXPERIMENTAL SECTION

Distilled water was purified by passage through an acid–base ion exchange column. A backing electrolyte (potassium methylsulfate) was added to give a 0.002 *M* solution.

Dimethylsulfate.—Matheson dimethylsulfate b.p. 75–77 °C (15 mm) was redistilled under vacuum and the distillate repeatedly purified by partial freezing to give a product with m.p. −26.9 and n_D^{25} 1.3858.

[1]*Issued as N.R.C. No. 9010.*
**We wish to acknowledge receipt of Dr. Kaiser's thesis prior to publication.*

1. W. G. SCHNEIDER, H. J. BERNSTEIN, and J. A. POPLE. Can. J. Chem. **35**, 1487 (1957).
2. P. DIEHL, R. G. JONES, and H. J. BERNSTEIN. Can. J. Chem. **43**, 81 (1965).
3. J. A. POPLE and T. SCHAEFER. Mol. Phys. **3**, 547 (1961).
4. P. DIEHL and J. A. POPLE. Mol. Phys. **3**, 557 (1961).
5. H. C. LONGUET-HIGGINS. Mol. Phys. **6**, 445 (1963).
6. F. A. COTTON. Chemical applications of group theory. Interscience Publishers, Inc., New York. 1964.

RECEIVED FEBRUARY 28, 1966.
DEPARTMENT OF CHEMISTRY,
UNIVERSITY OF ESSEX,
WIVENHOE PARK,
COLCHESTER,
ESSEX, ENGLAND.

Can. J. Chem. Downloaded from www.nrcresearchpress.com by 210.87.254.6 on 09/05/12
For personal use only.

THE HYDROLYSIS OF DIMETHYLSULFATE AND DIETHYLSULFATE IN WATER[1]

R. E. ROBERTSON AND S. E. SUGAMORI

In this note we supply kinetic data for the hydrolysis of dimethylsulfate and diethylsulfate in water for a range of temperatures and compare the derived parameters with similar terms from the hydrolysis of the corresponding methanesulfonates and benzenesulfonates.

At one time questions were raised as to whether solvolysis involved the cleavage of the O—S or O—C bond or most probably both in varying proportion depending on reaction conditions (1, 2). Results of research on this question by Ader (3), by Kaiser (4*, 5), and by Lauder, Wilson, and Zerner (6) show that the reaction involves C—O cleavage only. Kaiser (4) has shown that $MeSO_4^-$ ion will exchange with $H_2{}^{18}O$ and that the conflicting evidence based on ^{18}O tracer techniques is removed if the sulfate ion is precipitated as quickly as formed.

In the hydrolysis of dimethylsulfate, some degree of nucleophilic interaction with a single water molecule is indicated by the k_{OH^-}/k_{H_2O} ratio of 45–50 and the inverse secondary α-deuterium isotope effect (7) ($k_H/k_D = 0.97$). These values lie in the general range of the benzenesulfonates rather than that of the methyl halides, but it may be significant to note here that the k_{OH^-}/k_{H_2O} ratio and the k_H/k_D ratio for dimethylsulfate are both a little closer to unity than for the corresponding sulfonates. Moreover, the solvent isotope effect (k_{H_2O}/k_{D_2O}) 0.899 lies at the low end of the sulfonate range (8) a value which indicates less availability of the unshared electrons on the oxygens for hydrogen bonding. Because we shall have reason to return to this point later, we note here that a difference in hydrogen bonding ability of the sulfonates and the sulfates has been clearly indicated by the careful infrared investigation of Kartha *et al.* (9) on the relative hydrogen bonding to *p*-chlorophenol in CCl_4.

EXPERIMENTAL SECTION

Distilled water was purified by passage through an acid–base ion exchange column. A backing electrolyte (potassium methylsulfate) was added to give a 0.002 *M* solution.

Dimethylsulfate.—Matheson dimethylsulfate b.p. 75–77 °C (15 mm) was redistilled under vacuum and the distillate repeatedly purified by partial freezing to give a product with m.p. −26.9 and n_D^{25} 1.3858.

[1]*Issued as N.R.C. No. 9010.*
**We wish to acknowledge receipt of Dr. Kaiser's thesis prior to publication.*

Diethylsulfate.—Diethylsulfate was redistilled and subsequently fractionated by partial freezing; m.p. −24.0–24.5, D_0^{25} 1.1725. Neither compound gave kinetic evidence of the presence of significant impurity.

Rate data were obtained by a conductance method. The experimental method, calculations, and details of temperature measurement and control have been described elsewhere (10, 11). In the present instance there is the theoretical possibility that the rate data might be confused by the subsequent hydrolysis of the methyl sulfuric ion. Lewis, Mason, and Morgan (12) showed many years ago that the latter reaction is much slower than the hydrolysis of the first methyl group, and we have not been able to detect any appreciable reaction of the methyl ion at 100 °C in 10 h. Since hydrolysis occurs readily at this temperature in concentrated solutions (6), it must be concluded that in the latter case it is the un-ionized acid which is reacting. In no case were our initial concentrations of sulfuric ester higher than 0.005 M, hence the hydrolysis reaction of the methyl sulfuric ion can be safely neglected.

Individual rate determinations for a range of temperatures have been deposited with the Depository of Unpublished Data.* These rates could be fitted by least mean squares to the usual three constant equation $\log_{10} k = A/T + B \log_{10} T + C$. The corresponding values of the empirical constants are given in Table I, and provide a means of calculating the rate for any particular temperature. The constants of these empirical equations give† corresponding values of $\Delta H^{\neq}$, $\Delta S^{\neq}$, and $\Delta C_p^{\neq}$, granted transition state assumptions are accepted and $d\Delta C_p^{\neq}/dT$ is assumed to be small. Corresponding values of these terms and some comparable values of analogous compounds are given in Table II.

TABLE I

Empirical constants for the rate equation $\log_{10} k = A/T + B \log_{10} T + C$

Compound	A	B	C
Dimethylsulfate	−7609.092	−22.1323	76.5044
Diethylsulfate	−7548.588	−20.7590	72.7329

TABLE II

Kinetic parameters derived from rate–temperature relationships at 25 °C

	$k_1 \times 10^5$* (s^{-1})	$\Delta H^{\neq}$ (cal/mole)	$\Delta S^{\neq}$ (cal/mole deg)	$\Delta C_p^{\neq}$ (cal/mole deg)
Dimethylsulfate	16.60	21 110	−5.03	−46
Diethylsulfate	11.15	21 650	−4.0	−43
Methyl methane sulfonate	0.5007	21 390	−11.03	−38
Ethyl methane sulfonate	0.3094	22 010	−9.4	−35
Methyl benzene sulfonate	1.170	21 470	−9.1	−36
Ethyl benzene sulfonate	1.017	22 020	−7.5	−34

*Calculated from corresponding three constant equations for 25 °C.

A comparison of the derived parameters for the hydrolysis of the two sulfates with the corresponding terms from the sulfonates (Table II) reveals two noteworthy differences. The values of the entropy of activation ($\Delta S^{\neq}$) for the sulfates are more positive by 4–7 e.u. (entropy units) and the corresponding values of the heat capacity of activation more

**Photocopies of deposited material may be obtained upon request to: Depository of Unpublished Data, National Science Library, National Research Council, Ottawa, Canada.*

†$A = -\Delta H^{\neq}/2.3026R$; $B = \Delta C_p^{\neq}/R + 1$; $C = (\Delta S_0^{\neq} - \Delta C_p^{\neq})2.3026R + \log k/h$, hence $\Delta H_T^{\neq} = \Delta H_0^{\neq} + \Delta C_p^{\neq} T$ and $S_T^{\neq} = \Delta S_0^{\neq} + 2.3026\Delta C_p^{\neq} \log T$.

Can. J. Chem. Downloaded from www.nrcresearchpress.com by 210.87.254.6 on 09/05/12
For personal use only.

negative by about 10 cal/mole deg. Part of the difference in $\Delta S^{\neq}$ can be attributed to a statistical factor due to symmetry ($2.3R \log 2 \simeq 1.4$ e.u.) and part may be attributed to a somewhat more stable solvent shell about the sulfate than about the sulfonate group. The latter difference is probably marginal, as indicated by the similar kinetic solvent isotope effects noted above. We believe that the most important factor contributing to this difference may be the enhanced probability of nucleophilic attack due to the enhanced polarizability of the  system, but this effect is difficult to estimate by independent means.

The more negative $\Delta C_p^{\neq}$ for the two sulfates compared with the values for the sulfonates is consistent with the suggestion that the initial state solvation shell is somewhat more stable about the former solutes. The more positive entropy due to a greater degree of disruption of solvent in the transition state would be consistent with this suggested hypothesis (13). This difference is not nearly large enough to suggest a similarity to that accompanying a change of mechanism from SN2 to SN1 (14) and hence we cannot agree with the suggestion of Lauder and co-authors (6) that the hydrolysis of these compounds in water follows the latter mechanism.

1. D. N. KURSANOV and R. V. KUDRYAVTSEV. J. Gen. Chem. USSR, **22**, 3323 (1956).
2. M. ANABAR, I. DOSTROVSKY, D. SAMUEL, and A. D. YAFFE. J. Chem. Soc. 3603 (1954).
3. G. ADER. Ph.D. Thesis, University of London, London, England. 1965.
4. E. T. KAISER. Ph.D. Thesis, Harvard University, Cambridge, Mass. 1959.
5. E. T. KAISER, M. RANAR, and F. H. WESTHEIMER. J. Am. Chem. Soc. **85**, 602 (1963).
6. I. LAUDER, I. R. WILSON, and B. ZERNER. Australian J. Chem. **14**, 41 (1961).
7. J. A. LLEWELLYN, R. E. ROBERTSON, and J. M. W. SCOTT. Can. J. Chem. **38**, 222 (1960).
8. R. E. ROBERTSON and P. M. LAUGHTON. Can. J. Chem. **35**, 1319 (1957).
9. V. B. KARTHA, R. N. JONES, and R. E. ROBERTSON. Proc. Indian Acad. Sci. 216 (1963).
10. R. E. ROBERTSON. Can. J. Chem. **33**, 1536 (1955).
11. R. L. HEPPOLETTE and R. E. ROBERTSON. J. Am. Chem. Soc. **83**, 1834 (1961).
12. H. F. LEWIS, O'N. MASON, and R. MORGAN. Ind. Eng. Chem. **16**, 811 (1924).
13. R. E. ROBERTSON. Can. J. Chem. **42**, 1707 (1964).
14. E. A. MOELWYN-HUGHES, R. E. ROBERTSON, and S. E. SUGAMORI. J. Chem. Soc. 1965 (1965).

RECEIVED MARCH 8, 1966.
DIVISION OF PURE CHEMISTRY,
NATIONAL RESEARCH COUNCIL,
OTTAWA, CANADA.

ADDENDUM: STEREOCHEMISTRY AND SEVEN COORDINATION[1]

T. A. CLAXTON AND G. C. BENSON

(Ref. Can. J. Chem. 44, 157 (1966))

In our paper (1) attention was drawn to the importance of the nuclear repulsion and *net* electron attraction (2) terms in deciding molecular structure. Application of the arguments to the fluorine compounds of xenon suggests that the structure of XeF_6 is determined by the *net* electron attraction term, since XeF_7^- and XeF_8^{2-} presumably are present in the corresponding alkali metal salts (3). In this case the methods used by Gillespie (4) are applicable and the accumulating evidence for a distorted XeF_6 (5, 6) appears to provide

[1]*Issued as N.R.C. No. 8997.*

Can. J. Chem. Downloaded from www.nrcresearchpress.com by 210.87.254.6 on 09/05/12
For personal use only.

negative by about 10 cal/mole deg. Part of the difference in $\Delta S^{\neq}$ can be attributed to a statistical factor due to symmetry ($2.3R \log 2 \simeq 1.4$ e.u.) and part may be attributed to a somewhat more stable solvent shell about the sulfate than about the sulfonate group. The latter difference is probably marginal, as indicated by the similar kinetic solvent isotope effects noted above. We believe that the most important factor contributing to this difference may be the enhanced probability of nucleophilic attack due to the enhanced polarizability of the  system, but this effect is difficult to estimate by independent means.

The more negative $\Delta C_p^{\neq}$ for the two sulfates compared with the values for the sulfonates is consistent with the suggestion that the initial state solvation shell is somewhat more stable about the former solutes. The more positive entropy due to a greater degree of disruption of solvent in the transition state would be consistent with this suggested hypothesis (13). This difference is not nearly large enough to suggest a similarity to that accompanying a change of mechanism from SN2 to SN1 (14) and hence we cannot agree with the suggestion of Lauder and co-authors (6) that the hydrolysis of these compounds in water follows the latter mechanism.

1. D. N. KURSANOV and R. V. KUDRYAVTSEV. J. Gen. Chem. USSR, **22**, 3323 (1956).
2. M. ANABAR, I. DOSTROVSKY, D. SAMUEL, and A. D. YAFFE. J. Chem. Soc. 3603 (1954).
3. G. ADER. Ph.D. Thesis, University of London, London, England. 1965.
4. E. T. KAISER. Ph.D. Thesis, Harvard University, Cambridge, Mass. 1959.
5. E. T. KAISER, M. RANAR, and F. H. WESTHEIMER. J. Am. Chem. Soc. **85**, 602 (1963).
6. I. LAUDER, I. R. WILSON, and B. ZERNER. Australian J. Chem. **14**, 41 (1961).
7. J. A. LLEWELLYN, R. E. ROBERTSON, and J. M. W. SCOTT. Can. J. Chem. **38**, 222 (1960).
8. R. E. ROBERTSON and P. M. LAUGHTON. Can. J. Chem. **35**, 1319 (1957).
9. V. B. KARTHA, R. N. JONES, and R. E. ROBERTSON. Proc. Indian Acad. Sci. 216 (1963).
10. R. E. ROBERTSON. Can. J. Chem. **33**, 1536 (1955).
11. R. L. HEPPOLETTE and R. E. ROBERTSON. J. Am. Chem. Soc. **83**, 1834 (1961).
12. H. F. LEWIS, O'N. MASON, and R. MORGAN. Ind. Eng. Chem. **16**, 811 (1924).
13. R. E. ROBERTSON. Can. J. Chem. **42**, 1707 (1964).
14. E. A. MOELWYN-HUGHES, R. E. ROBERTSON, and S. E. SUGAMORI. J. Chem. Soc. 1965 (1965).

RECEIVED MARCH 8, 1966.
DIVISION OF PURE CHEMISTRY,
NATIONAL RESEARCH COUNCIL,
OTTAWA, CANADA.

ADDENDUM: STEREOCHEMISTRY AND SEVEN COORDINATION[1]

T. A. CLAXTON AND G. C. BENSON

(Ref. Can. J. Chem. 44, 157 (1966))

In our paper (1) attention was drawn to the importance of the nuclear repulsion and *net* electron attraction (2) terms in deciding molecular structure. Application of the arguments to the fluorine compounds of xenon suggests that the structure of XeF_6 is determined by the *net* electron attraction term, since XeF_7^- and XeF_8^{2-} presumably are present in the corresponding alkali metal salts (3). In this case the methods used by Gillespie (4) are applicable and the accumulating evidence for a distorted XeF_6 (5, 6) appears to provide

[1]*Issued as N.R.C. No. 8997.*

Can. J. Chem. Downloaded from www.nrcresearchpress.com by 210.87.254.5 on 09/05/12
For personal use only.

substantiation. XeF_6 is therefore different from the relatively small number of known examples of molecules of the type MX_6, except the isolectronic IF_6^- ion, with M containing seven electron pairs in the valence shell, in that the *net* electron attraction term is dominant. We should emphasize that XeF_6 is distinctive in that it is the only molecule of the type discussed that has been studied in the vapor phase. Furthermore, it should be noted that in the other cases the crystal forces may be important in determining the shape.

It is also not surprising that there are indications from the Raman spectrum of IF_6^- in solution in anhydrous hydrogen fluoride[2] that this ion too is distorted; there appeared to be more Raman bands than one would expect for an octahedral ion. This distortion is consistent with the hypothesis that the *net* electron attraction term is dominant, since IF_7 exists. The Raman spectrum in the solid state also indicated[2] that IF_6^- is distorted. Thus it seems in this case that crystal forces do not provide an alternative explanation to the one proposed (1) for the existence of octahedral complexes with the central atom having seven electron pairs in the valence shell.

1. T. A. CLAXTON and G. C. BENSON. Can. J. Chem. **44**, 157 (1966).
2. B. F. GRAY and H. O. PRITCHARD. J. Chem. Phys. **25**, 779 (1956).
3. R. D. PEACOCK, H. SELIG, and I. SHEFT. Proc. Chem. Soc. 285 (1964).
4. R. J. GILLESPIE. Can. J. Chem. **38**, 818 (1960).
5. L. S. BARTELL, R. M. GAVIN, JR., H. B. THOMPSON, and C. L. CHERNICK. J. Chem. Phys. **43**, 2547 (1965).
6. K. HEDBERG, S. H. PETERSON, R. R. RYAN, and B. WEINSTOCK. J. Chem. Phys. **44**, 1726 (1966).

RECEIVED FEBRUARY 7, 1966.
DEPARTMENT OF CHEMISTRY,
THE UNIVERSITY,
LEICESTER, ENGLAND,
AND
DIVISION OF PURE CHEMISTRY,
NATIONAL RESEARCH COUNCIL,
OTTAWA, CANADA.

[2]*D. W. A. Sharp. Private communication.*

Can. J. Chem. Downloaded from www.nrcresearchpress.com by 210.87.254.5 on 09/05/12
For personal use only.

Can. J. Chem. Downloaded from www.nrcresearchpress.com by 210.87.254.6 on 09/05/12
For personal use only.

Canadian Journal of Chemistry

Issued by THE NATIONAL RESEARCH COUNCIL OF CANADA

VOLUME 44 AUGUST 1, 1966 NUMBER 15

ORGANIC SULFUR COMPOUNDS

II. CATALYZED SODIUM BOROHYDRIDE REDUCTIONS OF SELECTED α-(*o*-NITROPHENYLTHIO) ACIDS[1]

R. T. COUTTS, D. L. BARTON, AND ELIZABETH M. SMITH

College of Pharmacy, University of Saskatchewan, Saskatoon, Saskatchewan

Received February 28, 1966

ABSTRACT

The products obtained when α-(*o*-nitrophenylthio) acids are reduced by means of sodium borohydride and palladium–charcoal depend on (*a*) the reaction temperature, (*b*) the solvent, (*c*) the length of time in which the α-(*o*-nitrophenylthio) acid is in contact with the reducing agent, and (*d*) the nature of the substituents on the α-(*o*-nitrophenylthio) acid. By varying these conditions, benzothiazine hydroxamic acids (i.e. substituted 3,4-dihydro-4-hydroxy-3-oxo-2*H*-1,4-benzothiazines), the corresponding lactams (3,4-dihydro-3-oxo-2*H*-1,4-benzothiazines), and derivatives of 2-carboxymethylthioazobenzene can be prepared.

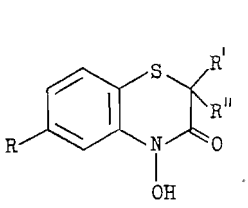
In two cases, additional products were obtained. When (*o*-nitrophenylthio)acetic acid was catalytically reduced for 30 min in dioxane, 3,4-dihydro-3-oxo-2*H*-1,4-benzothiazine-1,1-dioxide (VI*c*) was an unexpected product, and when α-(4-trifluoromethyl-2-nitrophenylthio)-isobutyric acid was left for a prolonged time in contact with sodium borohydride and palladium–charcoal, a derivative of hydrazobenzene, namely, 2-carboxy(α,α-dimethyl)methylthio-5-trifluoromethylhydrazobenzene (V), was one of the three identified products.

When reduced by means of sodium borohydride and palladium–charcoal, certain aromatic nitro compounds which possess an ester group in a position suitably orientated with respect to the *o*-nitrophenyl group are converted into cyclic hydroxamic acids (1–3); the nitro group is reduced to a hydroxylamino group which then cyclizes with the ester function. When two nitro acids were reduced by similar means, however, complete reduction to the corresponding amines occurred, and in both cases, lactamisation resulted on acidification (1).

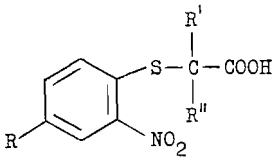
We have recently reported (3) that 2*H*-1,4-benzothiazine hydroxamic acids (I) are readily obtained by reducing suitably substituted (*o*-nitrophenylthio)acetates by means of sodium borohydride and palladium–charcoal. On the supposition that reduction of the corresponding acids would yield the related lactams (III), which could be expected to possess anthelmintic properties (4, 5), substituted (*o*-nitrophenylthio)acetic acids were reduced with sodium borohydride and palladium–charcoal. The resulting products depended on (*a*) time, (*b*) solvent, (*c*) nature of the substituents, and (*d*) temperature.

When α-(4-trifluoromethyl-2-nitrophenylthio)propionic acid (II*f*) was reduced in dioxane or methanol over a period of 30 min with excess sodium borohydride in the presence of palladium–charcoal, the corresponding amino compound was not formed (6). The isolation of 6-trifluoromethyl-3,4-dihydro-4-hydroxy-2-methyl-3-oxo-2*H*-1,4-benzothiazine (I*f*) in good yield, on acidification of the filtrate, indicated that reduction had proceeded only as far as the hydroxylamino stage. This reaction is a general one. A total

[1]*For part I in this series, see ref. 3.*



I



II

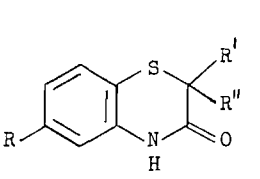
	R	R′	R″
a	Br	H	H
b	Cl	H	H
c	Cl	Me	H
d	Br	Me	H
e	CF_3	H	H
f	CF_3	Me	H

	R	R′	R″
g	CF_3	CH_2COOH	H
h	Me	Me	H
i	H	CH_2COOH	H
j	H	Me	H
k	Me	H	H
l	Br	Me	Me
m	CF_3	Me	Me

of 13 acids having the general formula II (i.e. II*a*–II*m*) were reduced by this method. In every case, the corresponding hydroxamic acid (I*a*–I*m*) was obtained, usually in good yield, regardless of whether methanol or dioxane was used as solvent (Table I).

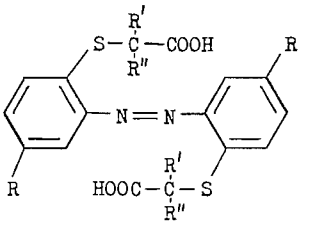
A different result was obtained, however, when simple derivatives of (*o*-nitrophenylthio)acetic acid were left in contact with sodium borohydride and palladium–charcoal for extended periods of time. Reduction of (4-trifluoromethyl-2-nitrophenylthio)acetic acid (II*e*) in aqueous dioxane by this method gave initially an almost colorless solution which slowly darkened when left to stand at room temperature. After an interval of 72 h the solution was orange-red in color; at this stage the catalyst was removed and the filtrate acidified. No hydroxamic acid was obtained. Chromatographic analysis of the product showed that it was a mixture containing 6-trifluoromethyl-3,4-dihydro-3-oxo-2*H*-1,4-benzothiazine (III*a*), 2-carboxymethylthio-5-trifluoromethylazobenzene (IV*a*), and other unidentified material. In the same way, prolonged reductions of α-(4-bromo-2-nitrophenylthio)propionic acid (II*d*), α-(4-trifluoromethyl-2-nitrophenylthio)propionic acid (II*f*), α-(4-methyl-2-nitrophenylthio)propionic acid (II*h*), α-(*o*-nitrophenylthio)propionic acid (II*j*), and α-(4-bromo-2-nitrophenylthio)isobutyric acid (II*l*) with sodium borohydride and palladium–charcoal gave derivatives of 3,4-dihydro-3-oxo-2*H*-1,4-benzothiazine (III*b*–III*f*, respectively), and azo compounds (IV*b*–IV*f*, respectively). Yields were generally poor, and other unidentified products were also obtained. A similar prolonged reduction of α-(4-trifluoromethyl-2-nitrophenylthio)isobutyric acid (II*m*) again failed to give hydroxamic acid. In this case, the solution had darkened appreciably after the reagents had been in contact for only 24 h. At this stage, the solution was filtered and acidified. Three identifiable products were isolated, two of which were the expected 2-carboxy-(α,α-dimethyl)methylthio-5-trifluoromethylazobenzene (IV*g*) and 6-trifluoromethyl-3,4-dihydro-2,2-dimethyl-3-oxo-2*H*-1,4-benzothiazine (III*g*). The third product has been deduced to be the hydrazo compound (V). Such a structure is compatible with elemental analysis and with equivalent and molecular weight determinations. Evidence from infrared studies also suggests this molecular structure. The infrared spectra of IV*g* and V are similar, except for absorption peaks attributable to the NH group, which occur only in compound V. The infrared spectra of azobenzene and hydrazobenzene were recorded for comparison purposes. As expected, they also showed many similarities, with differences mainly in the regions where NH absorption occurs.

Can. J. Chem. Downloaded from www.nrcresearchpress.com by 210.87.254.6 on 09/05/12
For personal use only.



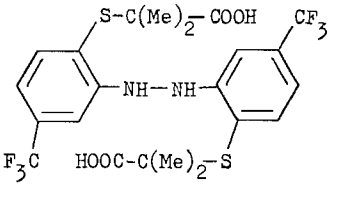
III

	R	R′	R″
a	CF_3	H	H
b	Br	Me	H
c	CF_3	Me	H



IV

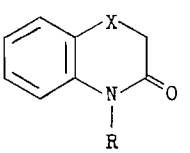
	R	R′	R″
d	Me	Me	H
e	H	Me	H
f	Br	Me	Me
g	CF_3	Me	Me



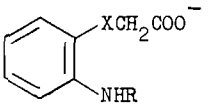
V

In addition to the expected hydroxyl and carbonyl absorption, it was noticeable that the infrared spectra of all the azo compounds (IV*a*–IV*g*) in potassium bromide had an absorption band of weak to medium intensity in the range 1 418 – 1 444 cm^{-1}. Such a band may be ascribed to the azo group (7). The mechanism involved in the formation of the azo and hydrazo compounds from the hydroxylamino intermediates is being investigated at present.

The products obtained from the reduction of (*o*-nitrophenylthio)acetic acid were also dependent on the rate of reduction and on the nature of the solvent used. A fast reduction (30 min) in dioxane gave 3,4-dihydro-4-hydroxy-3-oxo-2*H*-1,4-benzothiazine (VI*a*) as the major product, though some of the corresponding lactam 3,4-dihydro-3-oxo-2*H*-1,4-benzothiazine (VI*b*) was also formed. In addition to these products, an unexpected third product, namely, 3,4-dihydro-3-oxo-2*H*-1,4-benzothiazine-1,1-dioxide (VI*c*), was isolated from the reaction mixture. One explanation for the formation of VI*c* is a concurrent oxidation and reduction of the intermediate VII*a* to yield VII*b* and VII*c*, which cyclize on acidification. A prolonged reduction of (*o*-nitrophenylthio)acetic acid in dioxane gave the lactam in very good yield, and rather surprisingly, no azo compound was obtained. The lactam (VI*b*) was also the only product isolated when the same acid was reduced over a 15 min period in methanol. A similar result was obtained when *o*-chloro-*α*-(*o*-nitrophenylthio)cinnamic acid (VIII) was reduced with an excess of sodium borohydride and palladium–charcoal. A fast reduction in dioxane yielded the hydroxamic acid (IX*a*) as the major product; some lactam (IX*b*) was also isolated. The lactam was the only product obtained when the fast reduction was repeated with methanol as solvent or when the reduction in dioxane was prolonged.



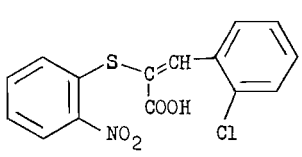
VI



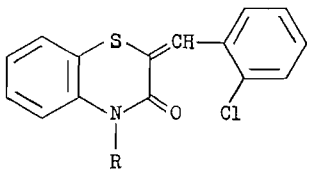
VII

a R = OH, X = S *b* R = H, X = S *c* R = H, $X = SO_2$

Can. J. Chem. Downloaded from www.nrcresearchpress.com by 210.87.254.6 on 09/05/12
For personal use only.

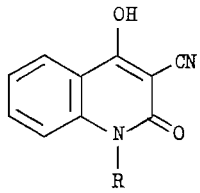


VIII



IX

a R = OH
b R = H



X

a R = OH
b R = H

This is not the first instance of solvent influencing the nature of the product obtained when sodium borohydride and palladium–charcoal are employed to reduce nitro compounds. We have previously reported (1) that the reduction of methyl (*o*-nitrobenzoyl)-cyanoacetate in sodium hydroxide solution gave 3-cyano-1,2-dihydro-1,4-dihydroxy-2-oxoquinoline (X*a*) in excellent yield. We have since found[2] that, when the solvent is changed to methanol, the hydroxamic acid does not form. The product is then the lactam (X*b*).

When α-(4-trifluoromethyl-2-nitrophenylthio)propionic acid (II*f*) was reduced in dioxane with sodium borohydride and palladium–charcoal over a period of 15 min at room temperature and left at 0° for 72 h before filtering and acidifying, the reaction mixture did not darken appreciably. On acidification, the hydroxamic acid (I*f*) was obtained as the major product, even though an excess of sodium borohydride was employed in the reaction. The corresponding lactam (III*c*) was the minor product of this reaction.

The results of this study should be compared with those of Neilson *et al.* (6), who showed that aromatic nitro compounds were smoothly reduced to amines with sodium borohydride and palladium–charcoal. These authors were unable to isolate any intermediate compounds in the reduction and they presented evidence that by-products of the azobenzene, azoxybenzene, or hydrazobenzene type were not formed and subsequently reduced to the amine.

EXPERIMENTAL

Melting points are uncorrected. Infrared spectra were recorded on a Unicam SP200 spectrophotometer. Palladium–charcoal refers to 10% palladium on charcoal.

Preparation of α-(o-Nitrophenylthio) Acids (IIa–IIm)

With the exception of compounds II*b* and II*c*, the preparations of the acids used in this study were reported in part I (3).

(4-Chloro-2-nitrophenylthio)acetic acid (II*b*) was obtained in 96% yield by the previously described (3) general method for preparing 2-(*o*-nitrophenylthio) acids. It was a yellow solid, m.p. 209°, when recrystallized from methanol (lit. (8) m.p. 209–210°).

α-(4-Chloro-2-nitrophenylthio)propionic acid (II*c*) was prepared by the method described for II*b*. The title compound was obtained as a yellow solid (95% yield), m.p. 134–135°, when recrystallized from methanol. Infrared spectrum (KBr disk): broad absorption 2 400 – 3 300 (m) (OH); 1 700 (s) (C=O); 1 525 (s), 1 340 (s), and 832 (m) (NO_2) cm^{-1}.

Anal. Calcd. for $C_9H_8ClNO_4S$: C, 41.30; H, 3.07. Found: C, 41.63; H, 3.05.

Fast Reductions of α-(o-Nitrophenylthio) Acids (IIa–IIm)

The method of reduction was similar to the one previously used for the reduction of the corresponding esters (3). Palladium–charcoal (0.2 g), suspended in water (10 ml), was added carefully to a solution of sodium borohydride (1 g) in water or 2% sodium hydroxide solution (10 ml) (see Table I). The suspension was diluted with dioxane or methanol (20 ml), and nitrogen was passed through the mixture while a solution of the acid (1 g) in dioxane or methanol (20–40 ml) was added dropwise over a period of 15 min. The reaction was

[2]*R. T. Coutts and S. J. Storey, unpublished results.*

Can. J. Chem. Downloaded from www.nrcresearchpress.com by 210.87.254.6 on 09/05/12
For personal use only.

allowed to continue for a further 15 min in an atmosphere of nitrogen; then the catalyst was removed by filtration and the hydroxamic acid was isolated from the filtrate by the methods reported earlier (3).

The yields of hydroxamic acids are recorded in Table I. Four hydroxamic acids (I*b*, I*c*, I*g*, and I*i*) have not been reported previously. Apart from these four compounds, all the hydroxamic acids listed in Table I had properties identical with those already reported (3) for these compounds.

6-Chloro-3,4-dihydro-4-hydroxy-3-oxo-2H-1,4-benzothiazine (I*b*) was a colorless compound, m.p. 179–180°, when recrystallized from ethanol. Infrared spectrum (KBr disk): 3 180 (m) (OH); 1 675 (s) and 1 628 (m) (free and hydrogen-bonded C=O) cm^{-1}.

Anal. Calcd. for $C_8H_6ClNO_2S$: C, 44.55; H, 2.80; N, 6.50. Found: C, 44.15; H, 2.78; N, 6.67.

6-Chloro-3,4-dihydro-4-hydroxy-2-methyl-3-oxo-2H-1,4-benzothiazine (I*c*) was a pale, tan-colored solid, m.p. 160–161°, when recrystallized from ethanol. Infrared spectrum (KBr disk): 3 120 (m) (OH); 1 675 (s) and 1 638 (s) (free and hydrogen-bonded C=O) cm^{-1}.

Anal. Calcd. for $C_9H_8ClNO_2S$: C, 47.06; H, 3.51; N, 6.10. Found: C, 47.27; H, 3.27; N, 6.43.

2-Carboxymethyl-6-trifluoromethyl-3,4-dihydro-4-hydroxy-3-oxo-2H-1,4-benzothiazine (I*g*) was a pale-yellow solid, m.p. 178–180°, when recrystallized from aqueous ethanol. Infrared spectrum (KBr disk): broad absorption 2 800 – 3 600 (m) with maximum at 3 300 (OH); 1 700 (s) (acid C=O); 1 642 (s) (hydroxamate C=O) cm^{-1}.

Anal. Calcd. for $C_{11}H_8F_3NO_4S$: C, 43.00; H, 2.63; N, 4.56. Found: C, 43.13; H, 2.70; N, 4.47.

2-Carboxymethyl-3,4-dihydro-4-hydroxy-3-oxo-2H-1,4-benzothiazine (I*i*) was a very pale yellow solid, m.p. 186–188°, when recrystallized from aqueous ethanol. Infrared spectrum (KBr disk): broad absorption 2 400 – 3 400 with maximum at 3 300 (s) (OH); 1 698 (s) (acid C=O); 1 645 (s) (hydroxamate C=O) cm^{-1}.

Anal. Calcd. for $C_{10}H_9NO_4S$: C, 50.20; H, 3.79; N, 5.86. Found: C, 50.56; H, 3.70; N, 5.48.

TABLE I

2*H*-1,4-Benzothiazine hydroxamic acids (I) obtained by reducing (*o*-nitrophenylthio) acids (II) with sodium borohydride and palladium–charcoal

Compound	Solvent*	Yield (%)	Compound	Solvent*	Yield (%)
I*a*	d	68	I*f*	m	79
I*b*	d	68	I*g*	d + s	95
I*c*	d	54	I*h*	d	68
I*d*	d	49	I*i*	d	59
I*e*	d	85	I*j*	d	76
I*e*	d + s	84	I*k*	d	30
I*e*	m	94	I*l*	d + s	91
I*f*	d	87	I*m*	d	89

*d = dioxane; d + s = dioxane + 2% sodium hydroxide; m = methanol.

Preparation of o-Chloro-α-(o-nitrophenylthio)cinnamic Acid (VIII)

The title compound was prepared by the reported (9) method. It was a yellow solid, m.p. 213–215°, when recrystallized from methanol (lit. (9) m.p. 215–217°).

Reduction of o-Chloro-α-(o-nitrophenylthio)cinnamic Acid

Method a

A fast reduction of the title compound (1.007 g) was carried out in dioxane by the previously described general method for the reduction of α-(*o*-nitrophenylthio) acids. The filtrate was acidified with concentrated hydrochloric acid, and 2-(*o*-chlorobenzylidene)-3,4-dihydro-4-hydroxy-3-oxo-2*H*-1,4-benzothiazine (IX*a*) was precipitated as a yellow solid (0.506 g), m.p. 140–143°, which gave a violet color when treated with ethanolic ferric chloride solution. Two recrystallizations from methanol raised the melting point to 143–144°. Infrared spectrum (KBr disk): broad absorption 2 500 – 3 400 with maximum at 3 220 (m) (OH); 1 665 (m) and 1 624 (s) (free and hydrogen-bonded hydroxamate C=O) cm^{-1}.

Anal. Calcd. for $C_{15}H_{10}ClNO_2S$: C, 59.30; H, 3.32; N, 4.67. Found: C, 59.40; H, 3.29; N, 4.76.

The aqueous acidic filtrate remaining after removal of the above hydroxamic acid was completely extracted with ether, and then the combined ether extracts were re-extracted with 10% sodium carbonate solution. Evaporation of the ether solution gave 2-(*o*-chlorobenzylidene)-3,4-dihydro-3-oxo-2*H*-1,4-benzothiazine (IX*b*) (0.27 g) as a yellow solid, m.p. 229–230°, after recrystallization from methanol (lit. (9) m.p. 225–227°).

Anal. Calcd. for $C_{15}H_{10}ClNOS$: C, 62.60; H, 3.50; N, 4.87. Found: C, 62.99; H, 3.58; N, 4.89.

The sodium carbonate extract was acidified with concentrated hydrochloric acid and extracted with ether. Removal of the ether gave a brown oil (0.1282 g) which was rejected.

Method b

The title compound (1.003 g) was reduced as described in method *a*, except that methanol was used as solvent. The filtrate was acidified with concentrated hydrochloric acid, and when the solution was cooled,

Can. J. Chem. Downloaded from www.nrcresearchpress.com by 210.87.254.6 on 09/05/12
For personal use only.

2-(*o*-chlorobenzylidene)-3,4-dihydro-3-oxo-2*H*-1,4-benzothiazine (IX*b*) (0.346 g) separated as a pale-yellow solid, m.p. 229–230° after recrystallization from methanol. A further yield of IX*b* (0.360 g) was obtained by means of ether extraction of the aqueous acidic filtrate as described in method *a*.

Method c

The title compound (3.04 g) in dioxane (150 ml) was added in small portions over a period of ½ h to a suspension of palladium–charcoal (0.5 g) in 50% aqueous dioxane (50 ml), in which was dissolved sodium borohydride (2.5 g). Nitrogen was passed through the mixture during the addition of the solution of the title compound. The mixture was left for 72 h; then the solution was filtered and the filtrate acidified with concentrated hydrochloric acid. 2-(*o*-Chlorobenzylidene)-3,4-dihydro-3-oxo-2*H*-1,4-benzothiazine (0.928 g) precipitated as a yellow solid, m.p. 214–217°, raised to 228–230° when recrystallized from methanol. The infrared spectrum was identical with that of an authentic sample. A further yield of IX*b* (0.896 g) was obtained from an ether extraction of the aqueous acidic filtrate as described in method *a*.

Reduction of (o-Nitrophenylthio)acetic Acid

This compound was reduced by methods which were essentially the same as those described under the reduction of *o*-chloro-α-(*o*-nitrophenylthio)cinnamic acid.

(*o*-Nitrophenylthio)acetic acid (1.06 g) in dioxane (50 ml) was reduced as described in method *a*, the solution filtered, and the filtrate acidified. A white solid (0.157 g), m.p. 187–189°, separated. Two recrystallizations from methanol gave 3,4-dihydro-3-oxo-2*H*-1,4-benzothiazine-1,1-dioxide as a colorless solid, m.p. 208–209° (lit. (10) m.p. 207–208°). Infrared spectrum (KBr disk): broad absorption 2 800 – 3 400 with maxima at 3 090 (m) and 3 210 (m) (lactam NH); 1 682 (s) (C=O) cm^{-1}.

Anal. Calcd. for $C_8H_7NO_3S$: C, 48.72; H, 3.58; N, 7.10; S, 16.26. Found: C, 49.02; H, 3.28; N, 6.92; S, 16.00.

The acidic filtrate remaining after removal of the above product was extracted with ether; then the ether solution was re-extracted with 10% sodium carbonate solution. Evaporation of the ether solution gave 3,4-dihydro-4-hydroxy-3-oxo-2*H*-1,4-benzothiazine (0.482 g), m.p. 179–180°, when recrystallized from methanol (lit. (11) m.p. 179°). The sodium carbonate solution was acidified and extracted with ether. Removal of the ether gave 3,4-dihydro-4-hydroxy-3-oxo-2*H*-1,4-benzothiazine (0.482 g) as colorless crystals, m.p. 149–150°, when recrystallized from methanol (lit. (1) m.p. 151–152°). The infrared spectra of both compounds were identical with those of authentic samples, and only the latter compound, m.p. 149–150°, gave a violet color when alcoholic ferric chloride solution was added.

This reduction by method *a* has been repeated a number of times. On two occasions, no product separated when the initial filtrate was acidified. The acidic solution was then extracted with ether and the ether-soluble material separated into neutral and acidic products. The neutral material was shown to contain 3,4-dihydro-3-oxo-2*H*-1,4-benzothiazine (VI*b*) and the corresponding dioxide (VI*c*) by subjecting the mixture to chromatography on Whatman No. 1 paper with methanol–water (1:4) as solvent and locating the spots by means of ultraviolet light. The R_f values for VI*b* and VI*c* are 0.61 and 0.45, respectively.

When the title compound (1.02 g) was reduced by method *b*, a total yield of 0.581 g of 3,4-dihydro-3-oxo-2*H*-1,4-benzothiazine was obtained and no hydroxamic acid was isolated.

When the title compound (3.032 g) was reduced by method *c*, a total yield of 1.990 g of 3,4-dihydro-3-oxo-2*H*-1,4-benzothiazine was isolated.

Prolonged Reductions of α-(o-Nitrophenylthio) Acids

General Method

The α-(*o*-nitrophenylthio) acid (3 g) was dissolved in dioxane (minimum volume) and the resulting solution was added in small portions over a period of 15 min to an aqueous dioxane solution of sodium borohydride (3 g) in which was suspended palladium–charcoal (0.6 g). Nitrogen was passed through the mixture while the solution of the α-(*o*-nitrophenylthio) acid was added and for a further 15 min. The reaction mixture was then left exposed to the atmosphere at room temperature for 72 h, during which time the almost colorless solution turned dark red in color. The solution was then filtered and the filtrate was acidified with concentrated hydrochloric acid. This gave a dark-colored solid. The solid and the filtrate which remained after its removal were treated as described in individual examples.

Prolonged Reduction of (4-Trifluoromethyl-2-nitrophenylthio)acetic Acid (IIe)

The title compound (2.906 g) was reduced by the general method, and a pale-brown precipitate (2.118 g), m.p. 211–218°, was obtained. A portion (0.522 g) was recrystallized from ethanol and gave 2-carboxymethylthio-5-trifluoromethylazobenzene (IV*a*) (0.155 g) as an orange solid, m.p. 252–253°. Infrared spectrum (KBr disk): broad absorption 2 400 – 3 300 with maxima at 3 050 (m) and 2 900 (m) (OH); 1 700 (s) (C=O); 1 426 (m) (azo) cm^{-1}.

Anal. Calcd. for $C_{18}H_{12}F_6N_2O_4S_2$: C, 43.37; H, 2.43; N, 5.62; S, 12.87. Found: C, 43.68; H, 2.64; N, 5.57; S, 12.83.

A second portion (0.404 g) of the product, m.p. 211–218°, was chromatographed on alumina (8 cm × 1 cm). Elution with benzene gave 6-trifluoromethyl-3,4-dihydro-3-oxo-2*H*-1,4-benzothiazine (III*a*) (0.077 g) as a white solid, m.p. 186–187°. Infrared spectrum (KBr disk): broad absorption 2 700 – 3 350 with maxima at 3 190 (m) and 3 095 (m) (lactam NH); 1 672 (s) (C=O) cm^{-1}.

Anal. Calcd. for $C_9H_6F_3NOS$: C, 46.35; H, 2.59; N, 6.01. Found: C, 46.76; H, 2.71; N, 5.57.

Can. J. Chem. Downloaded from www.nrcresearchpress.com by 210.87.254.6 on 09/05/12
For personal use only.

The solvent was then changed to methanol, which eluted unidentified material (0.105 g, m.p. 265–285°). Finally a mixture of methanol – 5% sodium hydroxide solution (19:1) was used as eluant. A dark-red solution was obtained which was concentrated to a small volume, diluted with water, acidified with hydrochloric acid, and extracted with ether. Evaporation of the ether solution gave a further quantity of 2-carboxymethylthio-5-trifluoromethylazobenzene (IV*a*) (0.134 g), m.p. 243–251°, raised to 251–253° when recrystallized from methanol–benzene. The infrared spectrum was superimposable on that of the earlier fraction of IV*a* obtained as described above.

*Prolonged Reduction of α-(4-Methyl-2-nitrophenylthio)propionic Acid (II*h*)*

The title compound (2.995 g) was reduced by the general method, and an orange-brown solid (1.092 g), m.p. 170–180°, was obtained. Three recrystallizations from methanol gave 2-carboxy(α-methyl)methylthio-5-methylazobenzene (IV*d*) as a pale-orange solid, m.p. 205–208°. Infrared spectrum (KBr disk): broad absorption 2 400 – 3 300 with maximum at 2 940 (m) (OH); 1 698 (s) (C=O); 1 442 (w) (azo) cm^{-1}.

Anal. Calcd. for $C_{20}H_{22}N_2O_4S_2$: C, 57.39; H, 5.30; N, 6.69. Found: C, 57.63; H, 5.20; N, 6.63.

The filtrate remaining after removal of the above solid, m.p. 170–180°, was extracted with ether. The product obtained on evaporation of the ether was dissolved in methanol and chromatographed on alumina (8 cm × 1 cm). Eluate (100 ml) was collected and evaporated. The resulting product was dissolved in ether (ca. 100 ml) and extracted with 10% sodium bicarbonate solution (3 × 50 ml). Evaporation of the washed and dried ether solution gave 3,4-dihydro-2,6-dimethyl-3-oxo-2*H*-1,4-benzothiazine (III*d*) as a pale-brown solid (0.541 g), m.p. 146–152°, raised to 158–159° when recrystallized from aqueous methanol. Infrared spectrum (KBr disk): broad absorption 2 800 – 3 400 with maxima at 3 225 (w) and 3 110 (w) (lactam NH); 1 660 (s) (C=O) cm^{-1}.

Anal. Calcd. for $C_{10}H_{11}NOS$: C, 62.14; H, 5.75; N, 7.25; S, 16.59. Found: C, 62.09; H, 6.28; N, 6.90; S, 16.06.

Acidification of the aqueous sodium bicarbonate extract gave an ether-soluble brown oil (0.277 g) which was rejected. A similar oil (0.179 g) was obtained when the eluant for the column was changed to methanol – 5% sodium hydroxide (19:1). It was also rejected.

*Prolonged Reduction of α-(4-Trifluoromethyl-2-nitrophenylthio)propionic Acid (II*f*)*

Method a.—After the title compound (3.018 g) was reduced by the general method, acidification of the filtrate gave no precipitate, and so the solution was concentrated and extracted with ether. The product remaining after removal of the ether was chromatographed on alumina (8 cm × 1 cm) with methanol as eluant. Eluate (100 ml) was collected and evaporated to give product A, which was treated as described below. The eluant was then changed to methanol – 5% aqueous sodium hydroxide solution (19:1), and 100 ml was collected. The solvent was removed and the resulting product (product B) was treated as described below.

Product A was dissolved in ether (100 ml) and the ether solution was extracted with 10% sodium bicarbonate solution. Evaporation of the washed and dried ether solution gave 6-trifluoromethyl-3,4-dihydro-2-methyl-3-oxo-2*H*-1,4-benzothiazine (III*c*) (0.502 g), m.p. 166–167°, as a pale-brown solid after two recrystallizations from aqueous methanol. Infrared spectrum (KBr disk): broad absorption 2 800 – 3 400 with maxima at 3 180 (w) and 3 080 (w) (lactam NH); 1 660 (s) (C=O) cm^{-1}.

Anal. Calcd. for $C_{10}H_8F_3NOS$: C, 48.58; H, 3.26; N, 5.67. Found: C, 48.20; H, 3.29; N, 5.15.

Acidification of the aqueous sodium bicarbonate extract with concentrated hydrochloric acid gave 2-carboxy(α-methyl)methylthio-5-trifluoromethylazobenzene (IV*c*) (0.980 g) as an orange solid, m.p. 243–245°, after two recrystallizations from methanol. Infrared spectrum (KBr disk): broad absorption 2 400 – 3 700 with maximum at 2 950 (m) (OH); 1 704 (s) (C=O); 1 432 (m) (azo) cm^{-1}.

Anal. Calcd. for $C_{20}H_{16}F_6N_2O_4S_2$: C, 45.62; H, 3.06; N, 5.32; S, 12.18. Found: C, 45.38; H, 3.31; N, 5.65; S, 12.19.

A solution of product B in water was acidified with concentrated hydrochloric acid, and a further 0.355 g of IV*c* was obtained, m.p. 227–230°, raised to 242–244° when recrystallized from methanol. The infrared spectra of this and the previous product were identical.

Method b.—The title compound (3.012 g) in dioxane (100 ml) was reduced by the general method, except that the reaction mixture was left at 0 °C for the 72 h period. The yellow filtrate was acidified and extracted with ether; the ether solution was re-extracted with 10% sodium carbonate solution. Evaporation of the resulting ether solution left an orange-brown oil which, on trituration with methanol, gave 6-trifluoromethyl-3,4-dihydro-2-methyl-3-oxo-2*H*-1,4-benzothiazine (0.156 g), m.p. 158–161°, raised to 165–167° when recrystallized from methanol.

The sodium carbonate solution was acidified with concentrated hydrochloric acid, and then extracted with ether. The ether solution, on evaporation, gave 6-trifluoromethyl-3,4-dihydro-4-hydroxy-2-methyl-3-oxo-2*H*-1,4-benzothiazine (I*f*) (1.438 g) as a pale-yellow solid, m.p. 105–109°. Recrystallization from methanol raised the melting point to 124–126° (lit. (3) m.p. 126–128°). The infrared spectrum was identical with that of an authentic sample of the hydroxamic acid.

*Prolonged Reduction of α-(o-Nitrophenylthio)propionic Acid (II*j*)*

The method used to reduce the title compound (3.034 g) was similar to that described for the reduction of α-(4-trifluoromethyl-2-nitrophenylthio)propionic acid (method *a*). With methanol as eluant, acidic and

Can. J. Chem. Downloaded from www.nrcresearchpress.com by 210.87.254.6 on 09/05/12
For personal use only.

neutral products were isolated. The acidic material, 2-carboxy(α-methyl)methylthioazobenzene (IV*e*) (0.902 g), was obtained initially as a red oil which solidified (m.p. 138–142°) when triturated with methanol. Recrystallization from aqueous methanol gave an orange solid, m.p. 151–152°. Infrared spectrum (KBr disk): broad absorption 2 400 – 3 300 with maximum at 2 920 (m) (OH); 1 700 (shoulder) (s) and 1 688 (s) (C=O); 1 422 (w) (azo) cm^{-1}.

Anal. Calcd. for $C_{18}H_{18}N_2O_4S_2$: C, 55.36; H, 4.65; N, 7.17. Found: C, 55.72; H, 4.37; N, 7.58.

The neutral material, 3,4-dihydro-2-methyl-3-oxo-2*H*-1,4-benzothiazine (III*e*) (0.508 g), was obtained as an orange solid, m.p. 117–120°. Recrystallization from aqueous methanol gave a pale-brown solid, m.p. 126–128°. Infrared spectrum (KBr disk): broad absorption 2 700 – 3 400 with maxima at 3 215 (w) and 3 080 (w) (lactam NH); 1 662 (s) (C=O) cm^{-1}.

Anal. Calcd. for C_9H_9NOS: N, 7.82. Found: N, 7.79.

With methanol – 5% sodium hydroxide (19:1) as eluant, a red acidic oil (0.205 g) was obtained which was not investigated further.

Prolonged Reduction of α-(4-Bromo-2-nitrophenylthio)propionic Acid (IId)

This compound (3.052 g) was reduced by the general method, and the subsequent treatment was similar to that described for the prolonged reduction of α-(4-methyl-2-nitrophenylthio)propionic acid. 5-Bromo-2-carboxy(α-methyl)methylthioazobenzene (IV*b*) (1.707 g) was obtained initially as a red-brown solid, m.p. 167–170°. Two recrystallizations gave an orange solid, m.p. 235–236°. Infrared spectrum (KBr disk): broad absorption 2 400 – 3 700 with maxima at 2 990 (m) and 3 080 (m) (OH); 1 702 (s) (C=O); 1 424 (w) (azo) cm^{-1}.

Anal. Calcd. for $C_{18}H_{16}Br_2N_2O_4S_2$: C, 39.43; H, 2.94; N, 5.11; S, 11.70. Found: C, 39.21; H, 2.86; N, 5.10; S, 11.90.

The neutral product was initially obtained as an orange oily solid which was triturated with methanol. In this way, 6-bromo-3,4-dihydro-2-methyl-3-oxo-2*H*-1,4-benzothiazine (III*b*) (0.696 g) was obtained as a colorless solid, m.p. 188–190°, raised to 192–193° when recrystallized from methanol. Infrared spectrum (KBr disk): broad absorption 2 500 – 3 400 with maxima at 2 980 (m), 3 110 (m), and 3 210 (m) (lactam NH); 1 674 (s) (C=O) cm^{-1}.

Anal. Calcd. for C_9H_8BrNOS: C, 41.87; H, 3.12; N, 5.43. Found: C, 42.18; H, 3.20; N, 5.17.

Prolonged Reduction of α-(4-Bromo-2-nitrophenylthio)isobutyric Acid (IIl)

The title compound (2.89 g) was reduced by the general method. The acidified filtrate was extracted with ether, and the combined ether extracts were re-extracted with 2% sodium hydroxide solution. The dried ether solution, on evaporation, gave 6-bromo-3,4-dihydro-2,2-dimethyl-3-oxo-2*H*-1,4-benzothiazine (III*f*) (0.564 g) as a cream-colored solid, m.p. 178–181°. Recrystallization from benzene gave a colorless solid, m.p. 188–189°. Infrared spectrum (KBr disk): broad absorption 2 700 – 3 350 with maxima at 3 000 (m), 3 130 (m), and 3 230 (m) (lactam NH); 1 670 (s) (C=O) cm^{-1}.

Anal. Calcd. for $C_{10}H_{10}BrNOS$: C, 44.13; H, 3.70; N, 5.15. Found: C, 44.34; H, 3.66; N, 5.20.

The aqueous alkaline extract was acidified and extracted with ether. The dark-red ether extract was dried and evaporated to give a purple solid (1.740 g) which was triturated with methanol, in which a portion (0.820 g) was insoluble. This insoluble portion was recrystallized from methanol to give 5-bromo-2-carboxy-(α,α-dimethyl)methylthioazobenzene (IV*f*) as purple prisms, m.p. 220–222°. Infrared spectrum (KBr disk): broad absorption 2 400 – 3 300 with maxima at 2 970 (m) and 3 075 (m) (OH); 1 688 (s) (C=O); 1 418 (w) (azo) cm^{-1}.

Anal. Calcd. for $C_{20}H_{20}Br_2N_2O_4S_2$: C, 41.68; H, 3.50; N, 4.86; S, 11.13. Found: C, 41.32; H, 3.52; N, 4.82; S, 11.43.

The portion of the purple solid which dissolved when triturated with methanol was not investigated further.

Prolonged Reduction of α-(4-Trifluoromethyl-2-nitrophenylthio)isobutyric Acid (IIm)

The title compound (3.026 g) was reduced by the general method, except that the reaction was allowed to continue for only 24 h, at which time the solution was dark orange in color. The filtrate was acidified with concentrated hydrochloric acid and extracted with ether. The combined ether extracts were dried and evaporated to give a dark-red solid (2.457 g), m.p. 110–121°. A portion (1.40 g) of this solid was chromatographed on alumina (8 cm × 1 cm) with methanol as solvent. Suitable volumes of eluate were collected and evaporated, and the following fractions were collected.

Fraction No.	Weight	Color	Melting point
1	0.089 g	Colorless	139–142°
2	0.364 g	Colorless	135–139°
3	0.376 g	Pink	158–163°
4	0.077 g	Pink	157–160°
5	0.009 g	Cream	136–139°
6	0.065 g	Pink	135–149°

Can. J. Chem. Downloaded from www.nrcresearchpress.com by 210.87.254.6 on 09/05/12
For personal use only.

The eluant was changed to methanol – 5% sodium hydroxide (19:1), and the following fractions were isolated after evaporation and acidification.

Fraction No.	Weight	Color	Melting point
7	0.252 g	Pink	151–160°
8	0.061 g	Pink	179–200°

Fractions 1 and 2 were combined and recrystallized from aqueous ethanol to give 6-trifluoromethyl-3,4-dihydro-2,2-dimethyl-3-oxo-2*H*-1,4-benzothiazine (III*g*) as a cream-colored solid, m.p. 144–145°. Infrared spectrum (KBr disk): broad absorption 2 800 – 3 400 with maxima at 3 095 (m) and 3 200 (m) (lactam NH); 1 665 (s) (C=O) cm^{-1}.

Anal. Calcd. for $C_{11}H_{10}F_3NOS$: C, 50.57; H, 3.86; N, 5.36. Found: C, 50.80; H, 3.79; N, 5.29.

Fractions 3, 4, and 6 were mixtures and not investigated further at this time. Fraction 7 was recrystallized from aqueous ethanol to give 2-carboxy(α,α-dimethyl)methylthio-5-trifluoromethylhydrazobenzene (V) as a pale-pink solid, m.p. 166–168°. To enable direct comparison with the infrared spectrum of IV*g* (see later), the infrared spectrum of V (KBr disk) is given in detail (main peaks only): broad absorption 2 350 – 3 500 with maxima at 3 340 (w), 2 980 (m), 1 686 (shoulder) (s), 1 678 (s) 1 610 (m), 1 585 (m), 1 520 (m), 1 452 (s), 1 424 (s), 1 376 (w), 1 336 (s), 1 276 (s), 1 172 (s), 1 138 (s), 1 128 (s), 1 090 (s), 936 (m), 904 (m), 892 (m), 836 (m), 830 (m), 724 (w), and 678 (w) cm^{-1}.

Anal. Calcd. for $C_{22}H_{22}F_6N_2O_4S_2$: C, 47.48; H, 3.98; N, 5.03; S, 11.52; mol. wt. 556.5; equiv. wt. 278.3. Found: C, 47.55; H, 3.97; N, 4.92; S, 11.66; mol. wt. (vapor pressure) 552; equiv. wt. (direct titration with barium hydroxide in aqueous methanol) 282 ± 12.

Fraction 8 recrystallized from aqueous methanol as a red solid, m.p. 211–213°. It was 2-carboxy(α,α-dimethyl)methylthio-5-trifluoromethylazobenzene (IV*g*). Infrared spectrum (KBr disk): broad absorption 2 300 – 3 500 with maxima at 2 950 (m), 1 692 (s), 1 600 (w), 1 470 (m), 1 444 (w), 1 416 (m), 1 406 (m), 1 376 (w), 1 332 (s), 1 294 (s), 1 186 (s), 1 136 (shoulder) (s), 1 126 (s), 1 088 (s), 954 (m), 924 (shoulder) (s), 918 (s), 850 (s), 826 (w), 736 (w), and 682 (w) cm^{-1}.

Anal. Calcd. for $C_{22}H_{20}F_6N_2O_4S_2$: C, 47.65; H, 3.64; N, 5.05; S, 11.56; mol. wt. 554.5. Found: C, 47.96; H, 3.67; N, 4.91; S, 11.98; mol. wt. (vapor pressure) 548.

ACKNOWLEDGMENT

The financial assistance of the National Research Council of Canada is greatly appreciated.

REFERENCES

1. R. T. Coutts and D. G. Wibberley. J. Chem. Soc. 4610 (1963).
2. R. T. Coutts, D. Noble, and D. G. Wibberley. J. Pharm. Pharmacol. **16**, 773 (1965).
3. R. T. Coutts, H. W. Peel, and E. M. Smith. Can. J. Chem. **43**, 3221 (1965).
4. A. Mackie and J. Raeburn. J. Chem. Soc. 787 (1952).
5. A. Mackie and A. A. Cutler. J. Chem. Soc. 3716 (1953).
6. T. Neilson, H. C. S. Wood, and A. G. Wylie. J. Chem. Soc. 371 (1962).
7. R. J. W. LeFevre and R. L. Werner. Australian J. Chem. **10**, 26 (1957).
8. A. Roe and J. W. McGeehee. J. Am. Chem. Soc. **70**, 1662 (1948).
9. V. Baliah and T. Rangarajan. J. Chem. Soc. 4703 (1960).
10. M. Claass. Chem. Ber. **45**, 747 (1912).
11. M. A. T. Rogers and W. A. Sexton. J. Chem. Soc. 1619 (1947).

Can. J. Chem. Downloaded from www.nrcresearchpress.com by 210.87.254.6 on 09/05/12
For personal use only.

Can. J. Chem. Downloaded from www.nrcresearchpress.com by 210.87.254.6 on 09/05/12
For personal use only.

REARRANGEMENT OF ALLYL 2,6-DICHLOROPHENYL ETHER ON COLUMN PACKINGS DURING GAS–LIQUID CHROMATOGRAPHIC ANALYSIS[1]

M. J. BALDWIN AND R. K. BROWN
Department of Chemistry, University of Alberta, Edmonton, Alberta

Received April 7, 1966

ABSTRACT

At temperatures above 175° and with packed columns, rearrangement of allyl 2,6-dichlorophenyl ether occurs during gas–liquid chromatographic analysis with a contact time of no more than 4 min. For example, at a temperature of 205° with Gas Chrom P as packing material, about 7% of the ether is changed, but the packing 20% Apiezon L on Gas Chrom P increases this to about 50%. Products characteristic of both thermal and acid-catalyzed rearrangements are obtained. The number of such products increases to a maximum of five as the temperature is increased to 228°.

Accordingly, the results of gas–liquid chromatographic analysis of mixtures obtained from the Claisen rearrangement of allyl phenyl ethers must be interpreted with care if unchanged ether is present.

INTRODUCTION

The products of rearrangement and halogen elimination obtained from the Claisen rearrangement of allyl 2,6-dichlorophenyl ether have been found to be stable under reaction conditions, and also remain unchanged during analysis by gas–liquid chromatography (1). However, the extent, if any, of rearrangement of allyl 2,6-dichlorophenyl ether itself during gas–liquid chromatographic analysis is not known. This paper describes the results obtained in experiments designed to discover whether such rearrangement does occur during analysis by gas–liquid chromatography.

RESULTS AND DISCUSSION

Pure allyl 2,6-dichlorophenyl ether (1) was passed through a column packed with 20% Apiezon L on Gas Chrom P (60–80 mesh) (column No. 1) at a helium flow rate of 100 ml/min. The number of peaks obtained, increasing from two to a maximum of five, was dependent upon the temperature of the column. The influence of temperature on the number of compounds formed and their relative molar amounts are shown in Table I.

TABLE I

The influence of temperature on the number of compounds formed from allyl 2,6-dichlorophenyl ether during analysis by gas–liquid chromatography*

	% of total product as:				
Column temperature (°C)	2,6-Dichlorophenol (peak A)	2-Allyl-6-chlorophenol (peak B)	Allyl 2,6-dichlorophenyl ether (peak C)	4-Allyl-2,6-dichlorophenol (peak D)	7-Chloro-2-methylcoumaran (peak E)
176	0	2.4	97.6	0	0
195	0	29.1	70.9	0	0
205	Trace	49.7	50.0	Trace	Trace
215	2.4	63.4	24.3	4.7	4.9
228†	4.3	70.0	6.3	9.7	10.1

*Peaks are arranged in order of increasing retention time at a helium flow rate of 100 ml/min. Quantitative analyses were made against the standard, nitrobenzene.
†Retention times for peaks A to E at 228° are, respectively, 45, 85, 105, 165, and 190 s.

[1]*Part of the work of M. J. Baldwin to be submitted to the Graduate School, University of Alberta, Edmonton, in partial fulfillment of the requirements for the degree of Doctor of Philosophy.*

A column temperature lower than 176° gave peaks which were too broad and had too long a retention time for convenient analysis; hence the temperature range of 176° to 228° was employed. Peaks A, B, and C were identified by collecting small amounts of the actual substances represented by these peaks. Each of the isolated materials A and B was reinjected separately, and each gave only a single peak having the same retention time as before, thus showing that these products are stable under gas–liquid chromatography conditions. Compound C gave the same pattern of five peaks found upon injection of the original ether.

The infrared and nuclear magnetic resonance spectra, refractive indices, and gas–liquid chromatography retention times showed that A, B, and C were, respectively, 2,6-dichlorophenol, 2-allyl-6-chlorophenol, and the original allyl 2,6-dichlorophenyl ether. Substances D and E were not as clearly resolved. This fact, plus their presence in only small amounts, prevented their isolation in the pure state. However, their retention times were identical with those of authentic 4-allyl-2,6-dichlorophenol and 7-chloro-2-methylcoumaran, respectively. These products can be expected, since 4-allyl-2,6-dichlorophenol is one of the major products from the *thermal* rearrangement of allyl 2,6-dichlorophenyl ether, and 7-chloro-2-methylcoumaran is obtained from the *acid-catalyzed* cyclization of 2-allyl-6-chlorophenol (peak B) (1, 2).

Rearrangement of allyl 2,6-dichlorophenyl ether was found to occur also when this ether was passed through the following columns: column No. 2, 25% silicone rubber on Gas Chrom P (60–80 mesh); column No. 3, a 1:1 mixture of 20% Apiezon M on Chromosorb W (nonacid-washed) and 20% butanediol succinate on Chromosorb W (nonacid-washed); column No. 4, 20% Carbowax 20 M on Chromosorb W (acid-washed, 60–80 mesh). Several peaks were observed when columns 2 and 4 were used, but they were too poorly resolved for isolation of products. Column No. 3, on the other hand, gave a single peak when the ether was injected under test conditions (column temperature 205°, helium flow rate 100 ml/min). This substance, when collected and analyzed, proved to be 2-allyl-6-chlorophenol. For our purposes, column No. 1 gave the best separation of products, and hence was used throughout this work.

The rearrangement on these columns is quite rapid, since the contact time is no more than 4 min. Usually, thermal rearrangement requires considerable time (2, 4).[2] Hence it is apparent that the column material has catalyzed the rearrangement as well as strongly directed the course of the reaction.[3]

To observe the effect of the packing for column No. 1 under other conditions, some allyl 2,6-dichlorophenyl ether was mixed in a round-bottomed flask with 2 g of column packing No. 1 (20% Apiezon L on Gas Chrom P (60–80 mesh)). The vessel and contents were heated rapidly to 190° with stirring, while under an atmosphere of nitrogen, and then quickly cooled. The total heating time was 15 min. The temperature of 190° was chosen since, from Table I, temperatures in this region had led to the production of only two substances, whose separation by fractional distillation would thus be much simpler. Considerable hydrogen chloride was evolved, a fact which would account for the acid-catalyzed effects noted above. Distillation under vacuum gave fractions whose analyses indicated that 94.8% of the total product was unchanged ether and 5.2% was 2-allyl-6-chlorophenol. This is about one-sixth the extent of rearrangement found at 195° during gas–liquid chromatographic analysis.

[2]*Compare with 90 min for the rearrangement of this ether to 4-allyl-2,6-dichlorophenol (2, 4).*

[3]*A column used for several weeks caused considerably less rearrangement, but even under these conditions of column aging, the major product was 2-allyl-6-chlorophenol.*

Can. J. Chem. Downloaded from www.nrcresearchpress.com by 210.87.254.6 on 09/05/12
For personal use only.

Can. J. Chem. Downloaded from www.nrcresearchpress.com by 210.87.254.6 on 09/05/12
For personal use only.

Passage of the ether through an unpacked column under otherwise identical gas–liquid chromatography conditions (temperature 205°) failed to cause rearrangement, whereas a packing of just Gas Chrom P was found to produce 7.6% rearrangement (cf. 50% rearrangement found for a column containing Apiezon L on Gas Chrom P at 205° (Table I)).

It is clear that the "inert" solid support promotes some rearrangement within the 4 min contact time, but that the coated solid support is much more effective.

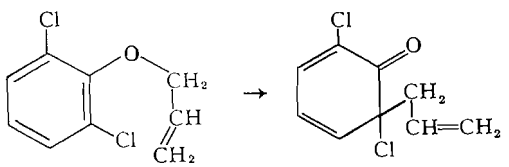
The above results are of twofold interest. They show that (*a*) allyl 2,6-dichlorophenyl ether does rearrange quite extensively on a column at a temperature above 176° during analysis by gas–liquid chromatography, and (*b*) the facility of rearrangement and the pattern of products obtained are indicative of catalysis by an acidic species.

Previous work (expt. 1 of Table II in ref. 2) has shown that the *thermal* rearrangement of allyl 2,6-dichlorophenyl ether (at 193–200°) gave most of the product (91.3%) as 4-allyl-2,6-dichlorophenol (the result of rearrangement of only the allylic group), 6.7% as 2-allyl-6-chlorophenol (from halogen elimination and allyl rearrangement), and 2.0% as 2-allyl-4,6-dichlorophenol (from both halogen and allyl rearrangement). No 2,6-dichlorophenol was found as a reaction product. On the other hand, the presence of the Lewis acid zinc chloride not only hastened the rearrangement of the ether but also changed the course of the reaction markedly, so that (at 150–155°) most of the product (88.3%) was 2-allyl-4,6-dichlorophenol (from halogen *and* allyl migration); in addition, 4.1% of the product was 2,6-dichlorophenol (the result of ether cleavage) and 7.7% was 5,7-dichloro-2-methylcoumaran. Neither 2-allyl-6-chlorophenol (the result of halogen elimination and allyl migration) nor 4-allyl-2,6-dichlorophenol (from only allyl migration) was found in the zinc chloride catalyzed reaction (expt. 3 of Table I in ref. 2).

In the present case, as the column temperature was increased from 176° to 228°, the extent of conversion of allyl 2,6-dichlorophenyl ether rose from 2.4% to 93.7%. Two of the products, 2,6-dichlorophenol (peak A) and 7-chloro-2-methylcoumaran (peak E), are those which arise characteristically from the presence of acidic substances such as zinc chloride (2). Most of the product (70% at 228°), however, is 2-allyl-6-chlorophenol, a product obtained previously from only the *thermal* rearrangement, and then merely in small amounts (see above). This compound arose from loss of halogen as well as allyl migration. Such loss of halogen has been attributed to reaction with some oxidizable material such as the solvent used for the reaction, a catalyst such as stannous chloride, or the phenolic products of rearrangement (1). What constitutes the oxidizable species during gas–liquid chromatographic analysis is not known. When nitrobenzene was used as the standard, the yield of products obtained from the injection of a known amount of ether was found to be practically quantitative, thus suggesting that the phenolic products are not lost extensively by oxidation in this case.

Reductive removal of halogen is most likely to occur at the intermediate dienone stage (eq. [1]), where the allylic halide structure is formed (1). All attempts to isolate for study the intermediate 6-allyl-2,6-dichlorocyclohexa-2,4-dienone, as had been done for the analogous 6-allyl-2,6-dimethylcyclohexa-2,4-dienone (3), have failed, and only 4-allyl-2,6-dichlorophenol was obtained.

[1]



This work shows that estimation by gas–liquid chromatography of the amount of unchanged allyl 2,6-dichlorophenyl ether and of the products obtained in experiments involving the Claisen rearrangement of this ether may lead to erroneous conclusions. Of even more significance is the pattern of products obtained from rearrangement of the ether on the column employed. The very large preponderance of 2-allyl-6-chlorophenol obtained in this case, compared with the relatively small proportion obtained during *thermal* rearrangement, and its total absence in the zinc chloride catalyzed rearrangement (2) are quite striking. Their significance with respect to the mechanism of halogen elimination during the Claisen rearrangement of allyl 2,6-dichlorophenyl ether is being examined.

EXPERIMENTAL

Rearrangement of Pure Allyl 2,6-Dichlorophenyl Ether During Analysis by Gas–Liquid Chromatography

Via a Burrell K-2 Kromo-Tog (Fitted with an Integrator and a Fraction Collector)

A 2 m glass column was packed with Gas Chrom P (60–80 mesh) previously coated with Apiezon L (20%). Ten microliter quantities of allyl 2,6-dichlorophenyl ether (2) were injected at various column temperatures (see Table I) with the helium flow rate at 100 ml/min. Reaction products representing the first three peaks (A to C), which were clearly resolved, were collected with a fraction collector cooled in a dry ice – acetone bath. These three peaks as well as the smaller and poorly resolved peaks D and E were identified as described in Results and Discussion.

Via an Aerograph Autoprep

Fifty microliter quantities of allyl 2,6-dichlorophenyl ether were injected into the Autoprep equipped with a 20 ft × $\frac{3}{8}$ inch (inside diameter) aluminium column packed with 20% Apiezon L on Gas Chrom P (60–80 mesh). The helium flow rate was 300 ml/min and the column temperature was 205°. Although three peaks (A to C) were obtained, the products represented by only the two major peaks, B and C (Table I), were collected automatically. The substances represented by peaks B and C were identified as 2-allyl-6-chlorophenol and allyl 2,6-dichlorophenyl ether by comparison of their nuclear magnetic resonance and infrared spectra, as well as gas–liquid chromatography retention times, with those of authentic samples. The refractive indices (η_D^{25} 1.5441 and 1.5393 for B and C, respectively) agreed with the literature values (4).

Via an Aerograph Autoprep Containing either an Unpacked Column or One Packed with Only Gas Chrom P

Either a clean aluminium column (20 ft × $\frac{3}{8}$ inch (inside diameter)) with no packing or one packed with only Gas Chrom P (60–80 mesh) was used, under gas–liquid chromatography conditions identical with those stated immediately above. In each case, only a single peak was observed. Analysis of the material collected was conveniently accomplished by nuclear magnetic resonance. Since the characteristic doublet for the allylic methylene group attached directly to the aromatic ring occurs at τ 6.7 (J = 7.0 c.p.s.) (tetramethylsilane as internal standard; neat) whereas that for the allylic methylene group attached directly to oxygen is found at τ 5.5 (J = 6.0 c.p.s.), it was easy to obtain the relative amounts of unchanged allyl 2,6-dichlorophenyl ether and the rearranged products from the integrated areas. The material obtained when an unpacked column was used showed a doublet at τ 5.5 (J = 6.0 c.p.s.), and none at τ 6.7. The material obtained from the column packed with only Gas Chrom P showed doublets at τ 5.5 and τ 6.7 whose integrated areas were in the ratio of 92.4 to 7.6.

The Effect of Column Packing Alone on the Rearrangement of Allyl 2,6-Dichlorophenyl Ether

To a 100 ml, three-necked, round-bottomed flask fitted with a stirrer and reflux condenser was added 20 g of pure allyl 2,6-dichlorophenyl ether along with 2 g of 20% Apiezon L on Gas Chrom P (60–80 mesh). The flask and contents were then heated rapidly, over a period of 10 min, to 190°, and this temperature was maintained for an additional 5 min. The mixture, quickly cooled to room temperature, was freed from the solid packing by filtration under suction. Fractional distillation at 3 mm pressure gave the following results.

Fraction	Boiling range	Amount (g)
I	80–85°	2.7
II	85–95°	3.4
III	95–100°	10.3
Residue		2.8

The gas–liquid chromatographic spectra of fractions I, II, and III were compared with those obtained under identical conditions from known amounts of pure allyl 2,6-dichlorophenyl ether, with nitrobenzene as the internal standard. The proportions of products obtained from definite quantities of the ether under identical conditions were repeatedly the same. Hence, by measuring the amounts of the products obtained in the analyses of fractions I–III, one can, by comparison with standard spectra, estimate the amount of ether present in the original material (fractions I–III) which would give the proportion of products found.

Can. J. Chem. Downloaded from www.nrcresearchpress.com by 210.87.254.6 on 09/05/12
For personal use only.

Only two products were obtained: allyl 2,6-dichlorophenyl ether and 2-allyl-6-chlorophenol, in the ratio of 94.8 to 5.2.

Attempted Preparation of 6-Allyl-2,6-dichlorocyclohexa-2,4-dienone

The literature procedure for the preparation of 6-allyl-2,6-dimethylcyclohexa-2,4-dienone (3) was employed in the attempted preparation of the dichloro dienone, but with some modification. When all the methanol had been removed, 30 ml of pure, dry toluene was added, and to the resulting solution, first cooled to −5°, was added cold (−5°) allyl bromide. The whole mixture was stirred at −5° for 80 h under nitrogen. Fractional distillation under vacuum gave a material boiling at 76–77° and 0.5 mm. This was the only product obtained and proved to be identical with authentic 4-allyl-2,6-dichlorophenol (4).

ACKNOWLEDGMENT

We thank the National Research Council of Canada for their financial support during the course of this work.

REFERENCES

1. E. PIERS and R. K. BROWN. Can. J. Chem. **41**, 2917 (1963).
2. E. PIERS and R. K. BROWN. Can. J. Chem. **41**, 329 (1963).
3. D. Y. CURTIN and R. J. CRAWFORD. J. Am. Chem. Soc. **79**, 3156 (1957).
4. D. S. TARBELL and J. W. WILSON. J. Am. Chem. Soc. **64**, 1066 (1942).

Can. J. Chem. Downloaded from www.nrcresearchpress.com by 210.87.254.6 on 09/05/12
For personal use only.

Can. J. Chem. Downloaded from www.nrcresearchpress.com by 210.87.254.42 on 09/05/12
For personal use only.

OXIDATION OF POLYSACCHARIDES BY LEAD TETRAACETATE IN DIMETHYL SULFOXIDE[1]

V. ZITKO[2] AND C. T. BISHOP
Division of Biosciences, National Research Council, Ottawa, Canada

Received March 25, 1966

ABSTRACT

Neutral polysaccharides can be oxidized by lead tetraacetate in dimethyl sulfoxide if 15–20% of glacial acetic acid is added to prevent oxidation of the solvent. The oxidation proceeds at a rate which is several times faster than that of periodate oxidation in aqueous solution, and the same amount of oxidant is consumed. Polysaccharides oxidized by lead tetraacetate in dimethyl sulfoxide can be recovered in excellent yield by precipitation with alcohol, and have been shown to contain free aldehyde groups. Identification of the products of reduction and hydrolysis of the oxidized polysaccharides showed that the oxidation followed the normal glycol-cleavage pattern given by lead tetraacetate in other solvents. Addition of potassium acetate to the oxidations in dimethyl sulfoxide decreased the consumption of lead tetraacetate by dextran (mainly α-(1 $\rightarrow$ 6) and α-(1 $\rightarrow$ 4)). Reduction and hydrolysis of dextrans oxidized in the presence and absence of potassium acetate yielded glycerol and erythritol in the respective ratios of 3.8:1 and 8.7:1. This result indicated that potassium acetate inhibited oxidation of the C-3, C-4 glycol groups in the dextran. Acidic polysaccharides behaved atypically in this oxidation system, and those containing a high proportion of uronic acid units were resistant to oxidation.

Oxidation of polysaccharides by lead tetraacetate has received little attention, undoubtedly because this oxidant must be used in nonaqueous solvents, in which most polysaccharides are insoluble (1, 2). Oxidations of pulps (3–5) and of a spruce-wood glucomannan (6) by lead tetraacetate under heterogeneous conditions have been studied; evidence was obtained that the D-mannose units in the polysaccharides were attacked preferentially. In cellulose acetates of various degrees of substitution it appeared that unsubstituted end groups were attacked by lead tetraacetate (7). Cellulose, starch, amylose, and amylopectin are only partially oxidized, at a very slow rate, by lead tetraacetate in aqueous acetic acid (8).

For another project we wished to obtain substantial quantities of polysaccharides which had been oxidized by a glycol-cleaving oxidant. Yields of products recovered from periodate oxidations are often low, probably because of hydrolysis of the very labile acetal linkages during deionization procedures and subsequent loss of low molecular weight material. Dimethyl sulfoxide is an excellent solvent for many polysaccharides. If lead tetraacetate could be used as an oxidant in this solvent, the oxidized polysaccharides should be recoverable directly by precipitation with alcohol, in which the other reactants would be soluble.

Solutions of lead tetraacetate in dimethyl sulfoxide have a red color, apparently because of decomposition of lead tetraacetate. Under these conditions polysaccharides were oxidized, but so was the solvent, and the amount of oxidant consumed by the polysaccharide could not be determined. Addition of 15–20% of glacial acetic acid to the dimethyl sulfoxide solution eliminated completely both of these undesirable side reactions. It was observed previously that acetic acid inhibits the hydrolysis of lead tetraacetate in other solvents (9).

[1]*Issued as N.R.C. No. 9031. Presented at the 49th annual conference of the Chemical Institute of Canada, Saskatoon, Saskatchewan, June 1966.*
[2]*N.R.C. Postdoctorate Fellow, 1964–1966.*

Can. J. Chem. Downloaded from www.nrcresearchpress.com by 210.87.254.42 on 09/05/12
For personal use only.

The results of oxidations of several polysaccharides by lead tetraacetate in dimethyl sulfoxide – acetic acid and by aqueous sodium metaperiodate are shown in Figs. 1–4. With only two exceptions there was excellent agreement between the amounts of the two oxidants consumed by these neutral polysaccharides. The levan from *L. mesenteroides* 1149 consumed substantially higher amounts of lead tetraacetate than periodate and showed significant overoxidation (Fig. 3), possibly because of the acid lability of fructofuranoside units. Potato starch was resistant to oxidation by lead tetraacetate (Fig. 4), possibly because it was insoluble in dimethyl sulfoxide. However, insolubility had no effect on the oxidation of cotton linters, and the lead tetraacetate system was slightly more active than aqueous periodate (Fig. 4).

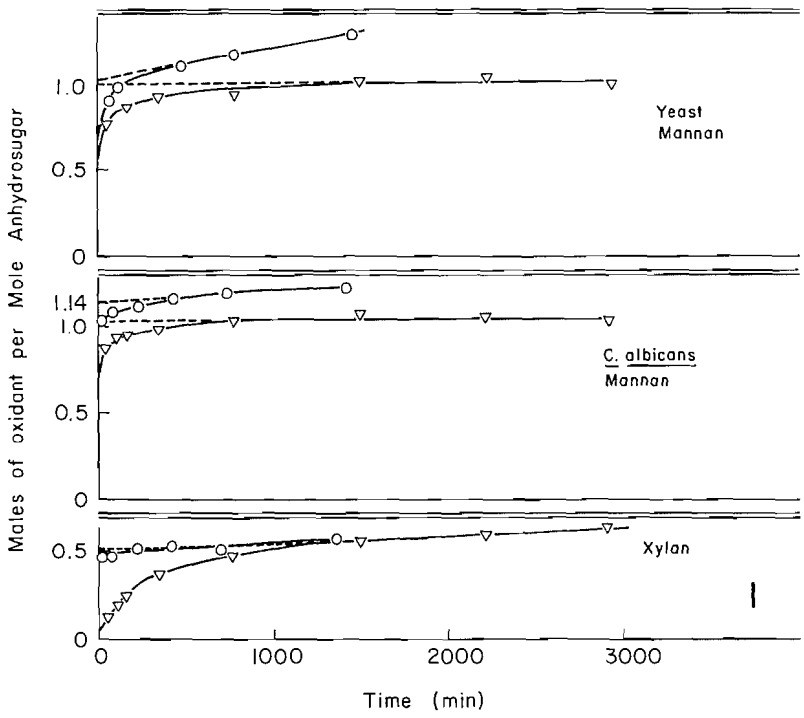
Since the consumptions of the two oxidants by the polysaccharides were the same, it was apparent that formic acid, produced by cleavage of a triol, was not oxidized by lead tetraacetate under these conditions. In separate experiments we found that formic acid added to dimethyl sulfoxide was oxidized by lead tetraacetate but that methyl formate was resistant to oxidation. It seems likely that HCO^+ species is generated by lead tetraacetate oxidation of triols and reacts immediately with dimethyl sulfoxide in a Pummerer-type reaction to give an ester which is resistant to oxidation (10–12).

The presence of potassium acetate catalyzes the oxidation of formic acid by lead tetraacetate in glacial acetic acid. However, when potassium acetate was added to oxidations by lead tetraacetate in dimethyl sulfoxide – acetic acid, it had no effect on the oxidation of amylose but caused a *decrease* in the consumption of oxidant by dextran. These results are shown in Fig. 5, and it can be seen that a 4.5-fold molar excess of potassium acetate over lead tetraacetate is as effective as a 9-fold excess in inhibiting the oxidation. The lower limits of concentration of potassium acetate required for inhibition were not investigated. Dextrans oxidized by lead tetraacetate in the presence and absence of potassium acetate were reduced and hydrolyzed to yield glycerol and erythritol in the respective molar ratios of 3.8:1 and 8.7:1. The decrease in the amount of glycerol in the product from the inhibited oxidation showed that the potassium acetate interfered in some way with the oxidation of the C-3, C-4 glycol groupings in the α-(1 $\rightarrow$ 6) linked D-glucopyranose units. This conclusion was supported by the lack of inhibition by potassium acetate in the oxidation of amylose (Fig. 5), which is an α-(1 $\rightarrow$ 4) linked glucan and therefore contains only C-2, C-3 glycol groups.

The addition of other salts (potassium chloride, lithium chloride, lithium fluoride, or mercuric chloride) catalyzed the oxidation of dimethyl sulfoxide by lead tetraacetate and promoted a fast decomposition of the oxidant.

The oxidation of acidic polysaccharides by lead tetraacetate in dimethyl sulfoxide was less straightforward than the oxidations of neutral polysaccharides. Thus, methyl or ethylene glycol esters of pectin consumed only 0.2 mole of lead tetraacetate per mole of anhydrogalacturonic acid as compared with 0.6–0.7 mole of periodate per mole of anhydrogalacturonic acid (Fig. 6). As also shown in Fig. 6, the consumption of lead tetraacetate by a series of carboxyl-reduced pectins (13) increased with decreasing D-galacturonic acid content but was always less than the consumption of periodate by the same products. Two other acidic polysaccharides, a 4-*O*-methylglucuronoxylan from beech wood (14) and the acidic capsular polysaccharide from pneumococcus type VIII (15), were both insoluble in dimethyl sulfoxide and were resistant to oxidation by lead tetraacetate in that solvent, consuming only 0.2 mole of oxidant per mole of anhydrosugar. However, esterification of these two polysaccharides with propylene oxide yielded products which were soluble in dimethyl sulfoxide. Figure 7 shows the rates of oxidation of the propylene glycol esters of these two polysaccharides by lead tetraacetate in dimethyl

Can. J. Chem. Downloaded from www.nrcresearchpress.com by 210.87.254.42 on 09/05/12
For personal use only.



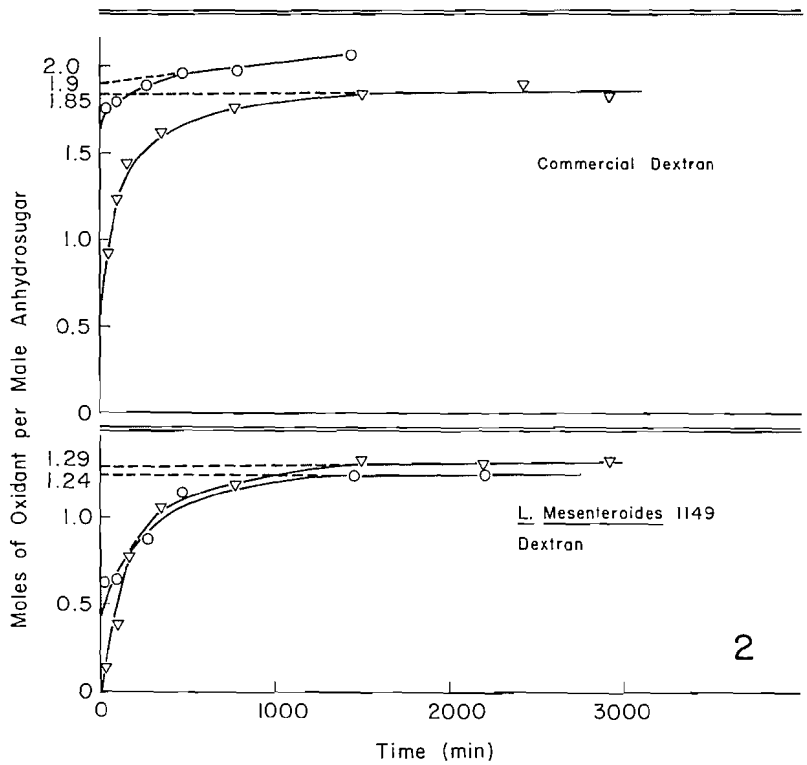


FIG. 1. Oxidations of neutral polysaccharides by lead tetraacetate and by periodate. LEGEND: ▽, periodate; ○, lead tetraacetate.

FIG. 2. Oxidations of neutral polysaccharides by lead tetraacetate and by periodate. LEGEND: ▽, periodate; ○, lead tetraacetate.

Can. J. Chem. Downloaded from www.nrcresearchpress.com by 210.87.254.42 on 09/05/12
For personal use only.

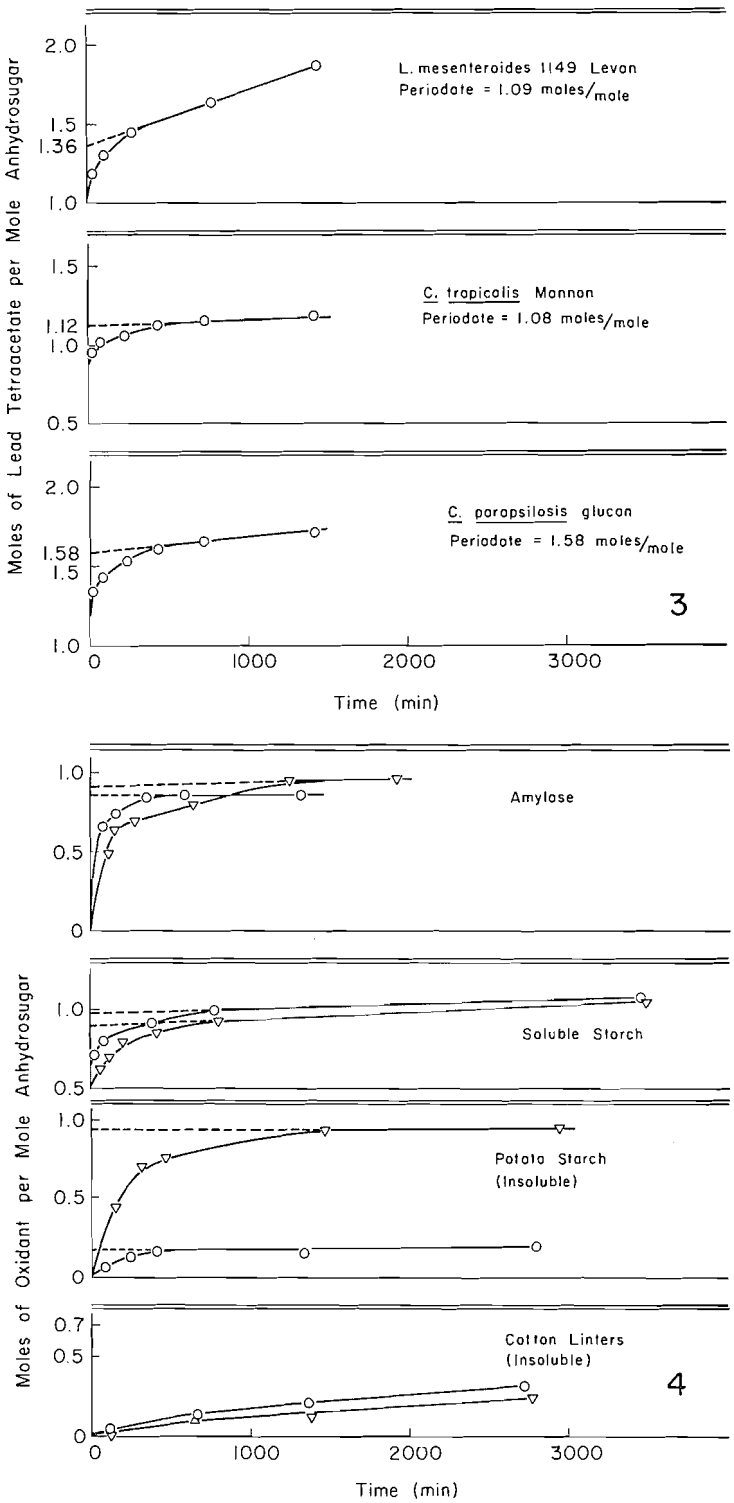


FIG. 3. Oxidations of neutral polysaccharides by lead tetraacetate.
FIG. 4. Oxidations of neutral polysaccharides by lead tetraacetate and by periodate. LEGEND: ▽, periodate; O, lead tetraacetate.

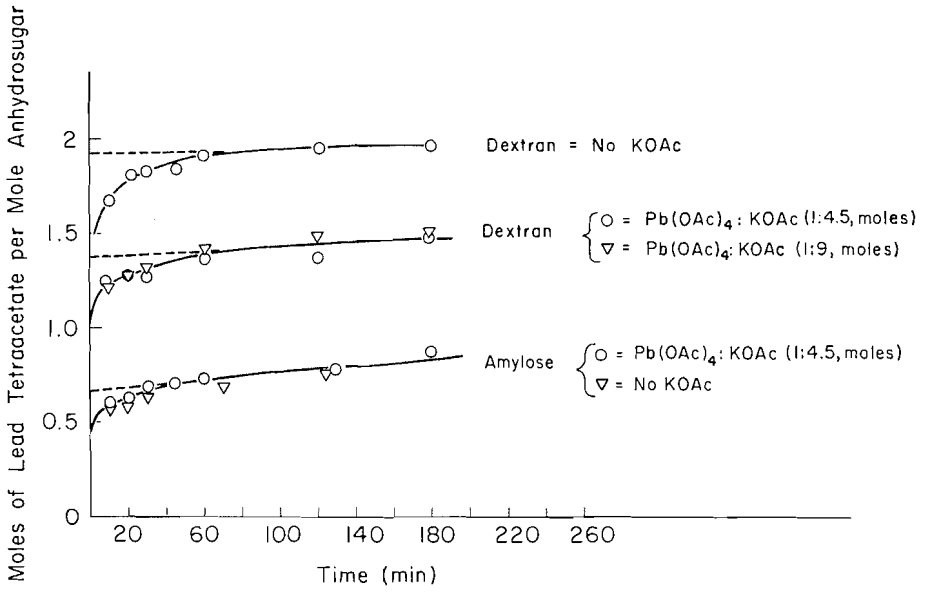


FIG. 5. Effect of potassium acetate on oxidations of dextran and amylose by lead tetraacetate.

sulfoxide – acetic acid and by aqueous periodate. The results for the 4-*O*-methylglucuronoxylan are in fair agreement; the esterified pneumococcus type VIII polysaccharide consumed more lead tetraacetate than it did periodate. It is clear that solubility is a major factor in the oxidation of acidic polysaccharides by lead tetraacetate in dimethyl sulfoxide and that insoluble products are not oxidized. Esterification of acidic polysaccharides promotes solubility in dimethyl sulfoxide, but even then the oxidations are atypical, vary with uronic acid content (Fig. 6), and apparently depend on variations in the secondary structure.

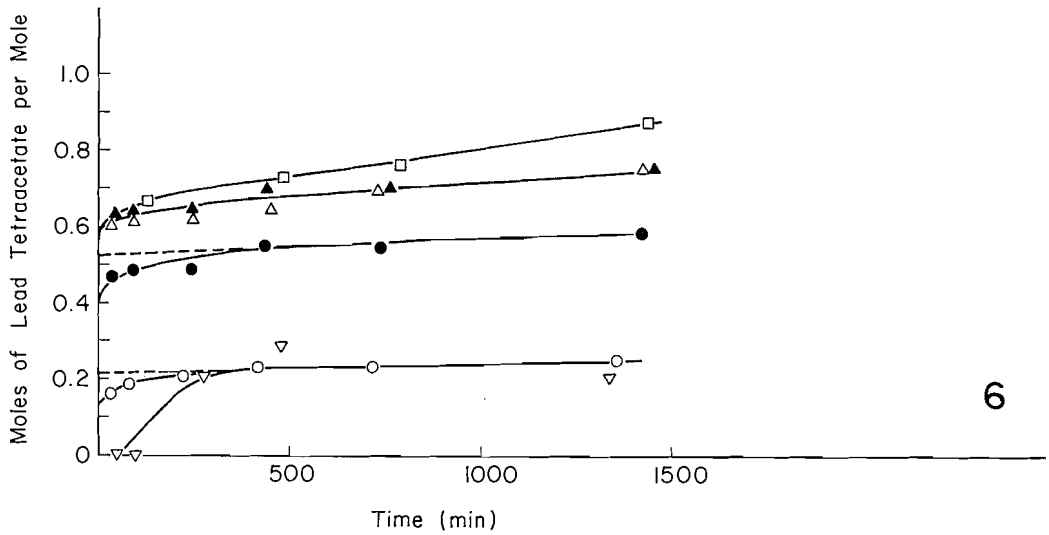
Identification of the products from the successive oxidation, reduction, and hydrolysis of the polysaccharides (16) showed that the lead tetraacetate oxidations in dimethyl sulfoxide followed the normal pattern of glycol cleavage. As described above, oxidized dextrans were reduced and hydrolyzed to yield glycerol and erythritol. A yeast mannan, oxidized by lead tetraacetate in dimethyl sulfoxide – acetic acid, was reduced and hydrolyzed to yield glycerol and a small amount of mannose. The products obtained from starch by the same procedures were erythritol (as the main component) and small amounts of glycerol. These were the products that would be expected from glycol-cleavage oxidations of these polysaccharides.

The major advantage of the oxidation of polysaccharides by lead tetraacetate in dimethyl sulfoxide – acetic acid rather than by aqueous periodate was the ease of recovery of the oxidized product. Addition of ethanol precipitated the oxidized polysaccharides in excellent yield, as shown in Table I. The low yield from the carboxyl-reduced pectin was caused by the low degree of polymerization of this material (13), which made the oxidized product partly soluble in alcohol. The oxidized polysaccharides contained only small amounts of ash and showed high contents of dialdehyde units. Some of these dialdehyde units were present as free aldehyde groups, since infrared spectroscopy of the oxidized polysaccharides showed strong absorption at 1 730 cm^{-1}. As far as we are aware, this is the first time that the presence of free aldehyde groups has been demonstrated in the

Can. J. Chem. Downloaded from www.nrcresearchpress.com by 210.87.254.42 on 09/05/12
For personal use only.

Can. J. Chem. Downloaded from www.nrcresearchpress.com by 210.87.254.42 on 09/05/12
For personal use only.

	Periodate (Mole/Mole)	Galacturonic acid (Mole %)
▽ = Ethylene glycol ester, apple pectin	0.7	92.7
○ = Methyl ester, sunflower pectin	0.6	89.7
● = Carboxyl-reduced sunflower pectin	0.9	42.7
△ = " " " "	0.8	19.9
▲ = " " " "	0.8	11.0
□ = " " " "	0.8	0.7



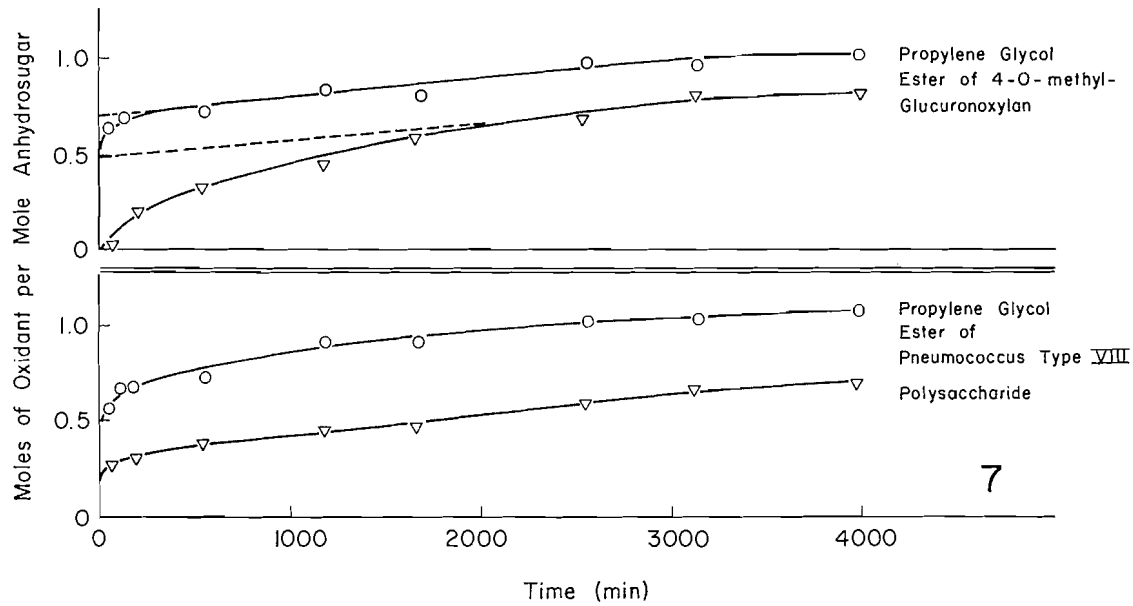


FIG. 6. Oxidations of pectins and some carboxyl-reduced pectins by lead tetraacetate.
FIG. 7. Oxidations of two acidic polysaccharides by lead tetraacetate and by periodate. LEGEND: ▽, periodate; ○, lead tetraacetate.

TABLE I

Recoveries of oxidized products from lead tetraacetate oxidations in dimethyl sulfoxide – acetic acid

Polysaccharide	Yield of oxidized product (% of theory)	Ash	Dialdehyde units (23) (%)
Dextran 500	101	2.3	84
Dextran 500 (in the presence of potassium acetate)	104	4.2	85
Yeast mannan	70	4.7	68
Soluble starch*	65	3.0	92
Carboxyl-reduced pectin	12	11.1	Not analyzed

*Oxidized for 7 h; probably extensively overoxidized.

polysaccharides oxidized by glycol-cleaving reagents. Polysaccharides oxidized by aqueous periodate show no absorption at 1 730 cm^{-1}, and the "dialdehyde" groups have been shown to be involved in a cyclic acetal structure (17).

EXPERIMENTAL

Paper chromatograms were run by the descending method in *n*-butanol–pyridine–water (6:4:3 v/v/v). A Pye argon chromatograph was used for gas–liquid chromatography (18); the column packing was 10% neopentylglycol sebacate on Gas Chrom Z, 100–120 mesh; the column temperature was 180 °C. Sugars and glycols were detected on paper chromatograms by *p*-anisidine hydrochloride (19) and alkaline silver nitrate (20), respectively. Iodometric methods were used to determine concentrations of periodate (21) and lead tetraacetate (22).

Analytical Oxidations with Lead Tetraacetate

Lead tetraacetate (2 g) was dissolved in a 1:1 (v/v) mixture (100 ml) of dimethyl sulfoxide and glacial acetic acid. The polysaccharide sample (20–30 mg) was dissolved or suspended in dimethyl sulfoxide (10 ml) in a 25 ml volumetric flask, the lead tetraacetate solution (10–13 ml) was added, and the solution was made up to 25 ml with dimethyl sulfoxide. Blanks without polysaccharides were prepared in the same way. At intervals aliquots (2 ml) were pipetted into an aqueous solution (10 ml) containing sodium acetate (250 g/l) and potassium iodide (20 g/l), and liberated iodine was titrated with 0.05 *N* sodium thiosulfate, with Thyodene as indicator.

When potassium acetate was used in the oxidations it was dissolved with the lead tetraacetate in the 1:1 mixture of dimethyl sulfoxide and glacial acetic acid.

Analytical Oxidations with Periodate

The polysaccharide sample (20–30 mg) was dissolved or dispersed in water (10 ml) in a 25 ml volumetric flask. Aqueous sodium metaperiodate (5 ml, 0.12 *M*) was added and the solution was made up to volume with water. At intervals aliquots (2 ml) were pipetted into phosphate buffer of pH 7.0 (20 ml), solid potassium iodide was added, and liberated iodine was titrated as described above.

Preparative Oxidations with Lead Tetraacetate

The polysaccharide (500 mg) was dissolved in dimethyl sulfoxide (37 ml), and glacial acetic acid (13 ml) was added dropwise followed by solid lead tetraacetate (4.4 g). The mixture was stirred until all the solid had dissolved and was then stored in the dark for 3 h. The solution was then poured into ethanol (150 ml) to precipitate the oxidized polysaccharide, which was washed three times with ethanol and once with ether, and then air-dried. The 3 h period for the preparative oxidations was the time at which most of the polysaccharides had consumed the theoretical amount of oxidant. For polysaccharides which are only partly soluble in dimethyl sulfoxide or are prone to overoxidation, the course of the reaction should be followed titrimetrically or by polarimetry. Dialdehyde units in the oxidized products were determined by the method of Hofreiter *et al.* (23). Infrared spectra of the oxidized products were obtained by the potassium bromide disk technique.

Reduction and Hydrolysis of Oxidized Polysaccharides

Samples (100 mg) of oxidized dextrans, mannan, and starch were reduced by potassium borohydride (100 mg) in aqueous solution (5 ml). Excess borohydride was destroyed by Rexyn 101 (H^+) ion-exchange resin and the solutions were evaporated to dryness. Boric acid was removed by repeated addition and evaporation of methanol. The residual syrups (average yield, 70 mg) were hydrolyzed by 0.5 *N* hydrochloric acid (2 ml) on a boiling water bath for 4 h. The hydrolysates were neutralized by Duolite A4 (OH^-) and examined by paper chromatography. Portions of the hydrolysates were evaporated to dryness and acetylated by acetic anhydride and pyridine (1:1 v/v) at 60 °C for 30 min. The acetates were examined by gas–liquid chromatography to give the quantitative estimates of glycerol and erythritol.

Can. J. Chem. Downloaded from www.nrcresearchpress.com by 210.87.254.42 on 09/05/12
For personal use only.

Polysaccharides

Dextran 500 was a commercial product obtained from Pharmacia, Uppsala; xylan and amylose were obtained from Nutritional Biochemicals Corp. Soluble starch was a Merck preparation and potato starch was a commercial sample from an unidentified source. *L. mesenteroides* 1149 dextran and levan, yeast mannan, cotton linters, *C. albicans* mannan, *C. tropicalis* mannan, and *C. parapsilosis* glucan were laboratory samples. Sunflower pectin and its carboxyl-reduced fractions were prepared previously in this laboratory (13). Beech-wood 4-*O*-methylglucuronoxylan (14) and pneumococcus type VIII polysaccharide (15) were donated by Dr. G. A. Adams and Dr. M. B. Perry, respectively. The method for esterification of acidic polysaccharides by propylene oxide has been published (24).

REFERENCES

1. A. S. PERLIN. Advan. Carbohydrate Chem. **14**, 9 (1959).
2. A. S. PERLIN and A. R. LANSDOWN. Can. J. Chem. **34**, 451 (1956).
3. H. W. STEINMANN and B. B. WHITE. Tappi, **37**, 225 (1954).
4. K. MATSUZAKI and K. WARD. Tappi, **42**, 516 (1959).
5. R. W. DETRICK. Tappi, **43**, 634 (1960).
6. J. M. VAUGHAN and E. E. DICKEY. J. Org. Chem. **29**, 715 (1964).
7. K. MATSUZAKI, K. SATO, K. ISKII, M. MORYA, and H. SOBUE. Kogyo Kagaku Zasshi, **62**, 1227 (1959); Chem. Abstr. **57**, 15392*d* (1962).
8. M. ABDEL-AKHER, A.-M. YOUSSEF, Y. GALI, and A. N. MICHALINOS. J. Chem. U.A.R. **6**, 107 (1963).
9. R. CRIEGEE, L. KRAFT, and B. RANK. Ann. **507**, 159 (1933).
10. R. PUMMERER. Ber. **43**, 1401 (1910).
11. L. HORNER and P. KAISER. Ann. **626**, 19 (1959).
12. S. OAE, T. KITAO, S. KAWAMURA, and Y. KITAOKA. Tetrahedron, **19**, 817 (1963).
13. V. ZITKO and C. T. BISHOP. Can. J. Chem. **44**, 1275 (1966).
14. G. A. ADAMS. Can. J. Chem. **35**, 556 (1957).
15. J. K. N. JONES and M. B. PERRY. J. Am. Chem. Soc. **79**, 2787 (1957).
16. G. W. HAY, B. A. LEWIS, and F. SMITH. Methods Carbohydrate Chem. **5**, 381 (1965).
17. J. E. CADOTTE, G. G. S. DUTTON, I. J. GOLDSTEIN, B. A. LEWIS, F. SMITH, and J. W. VAN CLEVE. J. Am. Chem. Soc. **79**, 691 (1957).
18. C. T. BISHOP. Advan. Carbohydrate Chem. **19**, 95 (1964).
19. L. HOUGH, J. K. N. JONES, and W. H. WADMAN. J. Chem. Soc. 1702 (1950).
20. W. E. TREVELYAN, D. P. PROCTER, and J. S. HARRISON. Nature, **166**, 444 (1950).
21. G. NEUMULLER and E. VASSEUR. Arkiv Kemi, **5**, 235 (1953).
22. A. S. PERLIN. Methods Carbohydrate Chem. **1**, 427 (1962).
23. B. T. HOFREITER, B. H. ALEXANDER, and I. A. WOLFF. Anal. Chem. **27**, 1930 (1955).
24. S. S. BHATTACHARJEE and T. E. TIMELL. Can. J. Chem. **43**, 758 (1965).

Can. J. Chem. Downloaded from www.nrcresearchpress.com by 210.87.254.42 on 09/05/12
For personal use only.

Can. J. Chem. Downloaded from www.nrcresearchpress.com by 210.87.254.40 on 09/05/12
For personal use only.

NUCLEAR MAGNETIC RESONANCE SPECTRA OF GLYCOL-CLEAVAGE OXIDATION PRODUCTS OF METHYL ALDOPENTOPYRANOSIDES[1]

A. S. PERLIN

Prairie Regional Laboratory, National Research Council of Canada, Saskatoon, Saskatchewan
Received March 24, 1966

ABSTRACT

The products obtained by the periodate oxidation of methyl α- and β-D-xylopyranosides have been examined by nuclear magnetic resonance spectroscopy. In deuterium oxide each product exists mainly in two forms, one of which is a hydrated dialdehyde and the other a hemialdal (1,4-dioxane derivative). In dimethyl sulfoxide the dialdehyde cyclizes slowly to yield the hemialdal which, at equilibrium, is found to be by far the most stable of the many isomeric forms possible. The spectrum of this hemialdal in both solvents provides an example of a degenerate ABX type of pattern. The spectra of the products prepared from 5-deuterated xylosides show that the 1-methoxyl group of each hemialdal is axial and the 4-hydroxyl group equatorial, and that the one derived from the β-anomer possesses an inverted chair conformation relative to that of the other hemialdal and of the glycoside itself. The 2-hydroxyl group of each hemialdal appears to be axially oriented. The data support the long-standing view that glycol scission of anomeric aldopentopyranosides leads to products that are mirror images.

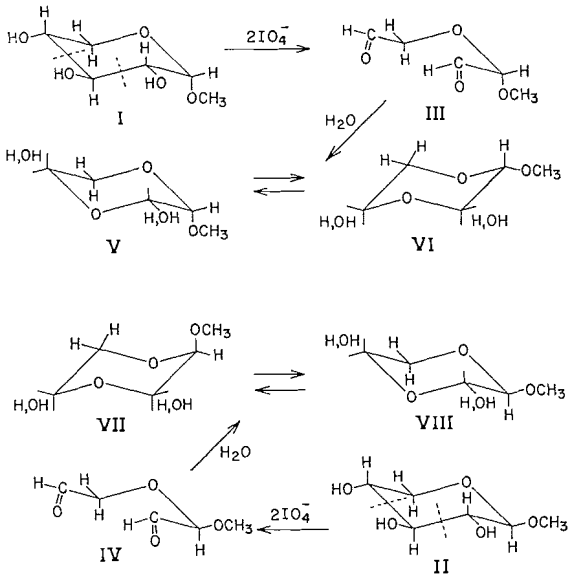
It has been found also that each product yields a mixture of several *p*-nitrobenzoates.

Glycol-cleavage oxidation of a pair of anomeric methyl aldopentopyranosides, e.g. methyl α- and β-D-xylopyranoside (I and II, Reaction Scheme 1), leads to a pair of syrupy products having numerically equal optical rotations, but of opposite sign (1). By appropriate treatment these products are converted into enantiomorphic dicarboxylic acids (1, 2), diols (3), and hydrazones (4). Although they may be regarded as enantiomorphic dialdehydes (III and IV), many of their properties are more consistent with the hemialdal (1,4-dioxane) type of structure (V or VI and VII or VIII, and stereoisomers of these) (5, 6). Guthrie (7) has discussed these properties in detail. In a recent paper, Chittenden and Guthrie (4) describe di-*p*-nitrobenzoates of hemialdal forms, but those derived from the different anomeric glycosides are not enantiomorphs, suggesting that the mirror-image relationship depicted for compounds II–VIII does not necessarily hold true. Hence, these diverse data provide only a partial, and at present conflicting, characterization of the glycol-cleavage products themselves.

In seeking additional information, especially about the structure of these oxidation products in solution, their nuclear magnetic resonance (n.m.r.) spectra have been examined. Deuterium oxide solutions of the compounds derived from the α- and β-anomers of methyl D-xylopyranoside are indistinguishable. As seen in Fig. 1B, the multiplicity of signals and their widely varied relative intensities show that a mixture of several forms is present. Since a hemialdal (e.g. V–VIII) contains two hydroxyl groups whereas a hydrated form of the acyclic dialdehyde (III or IV) has four hydroxyl groups, the hydroxyl proton signals in dimethyl sulfoxide (8) have been examined as a possible means for assessing the relative populations of these two structural types (9).[2] However, these signals are not well resolved for a freshly prepared dimethyl sulfoxide solution, and a change in composition soon becomes evident (9). At equilibrium, only two hydroxyl proton doublets of significant intensity are found (Fig. 2), and after deuterium exchange a relatively simple proton spectrum emerges (Fig. 3B). Aside from the signals for the methoxyl protons, there are a

[1]*Issued as N.R.C. No. 9029.*

[2]*The author acknowledges his indebtedness to an anonymous referee who, in reviewing this earlier paper, made comments which have proven to be very helpful to the current study.*



REACTION SCHEME 1. Schematic representation of the periodate oxidation of methyl α-D-xylopyranoside (I) and of its β-anomer (II) to yield dialdehyde and hemialdal products.

triplet and three doublets, the relative intensities of which are approximately 1:1:1:2. By spin decoupling, the triplet (spacings of 5.3 c.p.s.) is shown to be associated with the upfield two-proton doublet (spacing of 5.3 c.p.s.), and since it also reflects hydroxyl coupling before deuterium exchange (Fig. 2), these signals are ascribed to H-4 and the methylenic 5-protons, respectively (retaining the numerical order of the parent glycoside). Similarly, the two doublets (spacings of 1.8 c.p.s.) are due to spin-coupled protons and are attributed to H-1 and H-2, the pair being distinguished by the fact that the latter is coupled to a hydroxyl proton before deuterium exchange (Fig. 2). The two minor upfield singlets are ascribed to methoxyl protons of minor components; at 60–80° these signals tend to merge whereas the major signals are not noticeably altered. Signals comprising the spectrum shown in Fig. 3B have their counterpart in the spectrum shown in Fig. 1B, this relationship being emphasized by inset tracings (Fig. 1A). Hence, the data indicate that one component of the aqueous oxidation mixture becomes overwhelmingly dominant in dimethyl sulfoxide solution, and that this component has a hemialdal structure (and hence only two hydroxyl groups (Fig. 2)).

The small H-1 and H-2 spacing is consistent with a gauche interaction in 1,4-dioxane (10), as well as in related sugar derivatives (11), and shows that the methoxyl or 2-hydroxyl group (or both) is axially oriented. Since the methylene protons would not be expected to be equivalent, they, together with H-4, should comprise an ABX system (12). Although the signals appear to be those of an A_2X system, it has been shown that spectra of the ABX type sometimes become deceptively simple in form (13).[3] Thus, the X proton can give a triplet rather than a higher multiplet when, for example, $J_{AX} = J_{BX}$ or when δ_{AB} approaches zero. In terms of a hemialdal molecule, the case $J_{AX} = J_{BX}$ would be consistent with an axially oriented 4-hydroxyl group whereas the second condition could

[3]*Dr. H. J. Bernstein has pointed out (private communication) that a system of this latter type would be anticipated from the fact that the line width at half height for the H-4 signal (in Fig. 1A or 1B) is considerably larger (1.7 c.p.s.) than that (1.0 c.p.s.) for the* O—CH_3 *singlet (inset, Fig. 1A).*

Can. J. Chem. Downloaded from www.nrcresearchpress.com by 210.87.254.40 on 09/05/12
For personal use only.

Can. J. Chem. Downloaded from www.nrcresearchpress.com by 210.87.254.40 on 09/05/12
For personal use only.

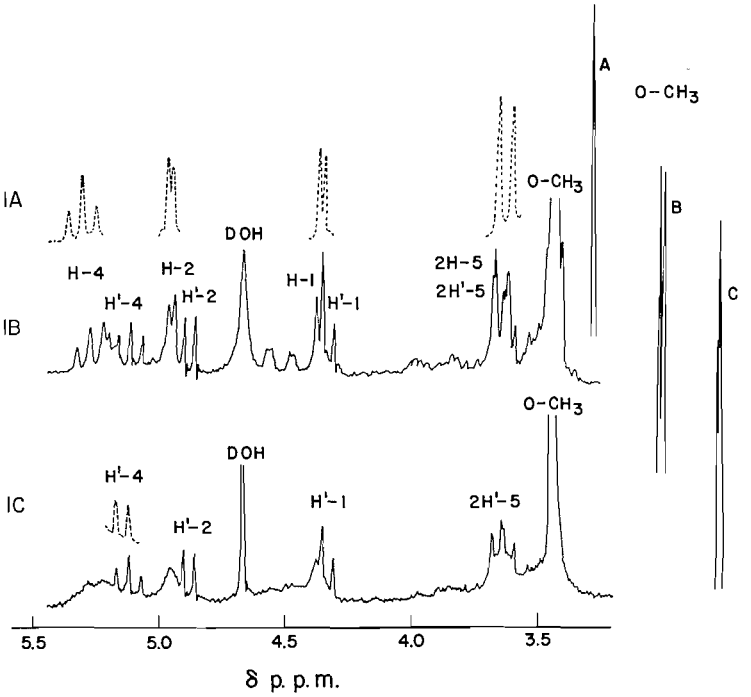


FIG. 1. Nuclear magnetic resonance spectra at 100 Mc.p.s. of the periodate oxidation products from methyl α- and β-D-xylopyranoside (B) in an equilibrated deuterium oxide solution, and (C) in a freshly prepared deuterium oxide solution. The inset signals (A) are taken from Fig. 3B for comparison. The primed numbers refer to proton signals common to spectra B and C; the inset H'-4 doublet in C is due to the 5-deuterio isomer. The other numbers refer to signals common to the spectra shown in Figs. 1B and 3B. Signals designated O—CH_3 are the upper portions of methoxyl proton signals corresponding to 1A, 1B, or 1C.

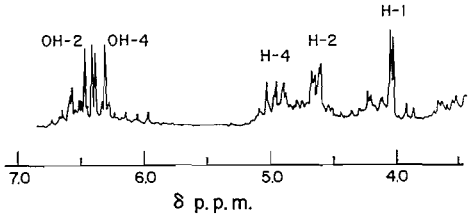


FIG. 2. Partial n.m.r. spectrum at 100 Mc.p.s. of the periodate oxidation product from methyl α- or β-D-xylopyranoside in dimethyl sulfoxide-d_6 (OH refers to hydroxyl proton signals).

arise also when the 4-hydroxyl is equatorial. With an ABX system of this kind, a change of solvent may substantially alter the spectrum (13), but such a criterion could be unreliable in the present instance since several components are in equilibrium.

A choice between these possibilities has been provided by the use of 5-deuterated methyl α- and β-D-xylopyranosides. The latter were prepared from D-xylose-5-*d* in which two-thirds of the isotope has been introduced equatorially and one-third axially (14). Oxidation products of these glycosides, after equilibration in dimethyl sulfoxide, give the spectra shown in Figs. 3A and 3C. Consistent with the assignments made above, only the H-4 and H-5 signals are modified, and particularly pertinent is the fact that they vary in appearance depending on the anomer used.

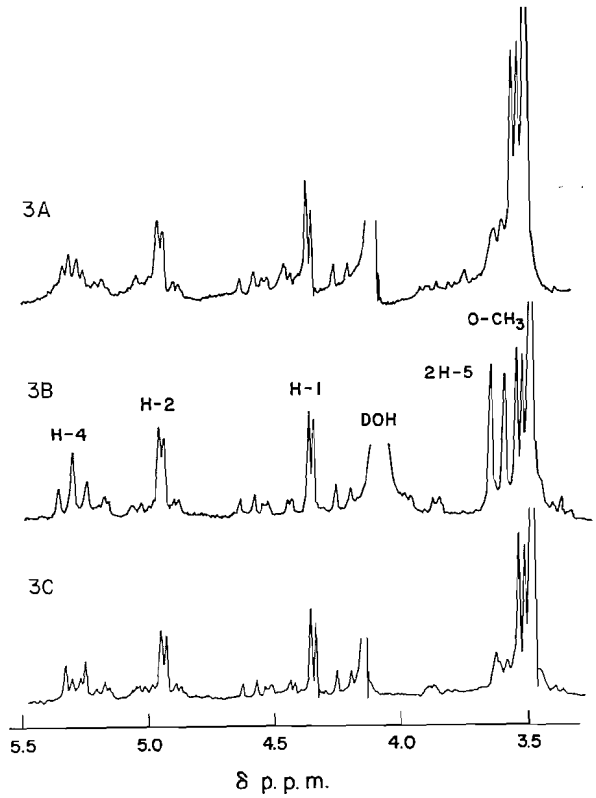
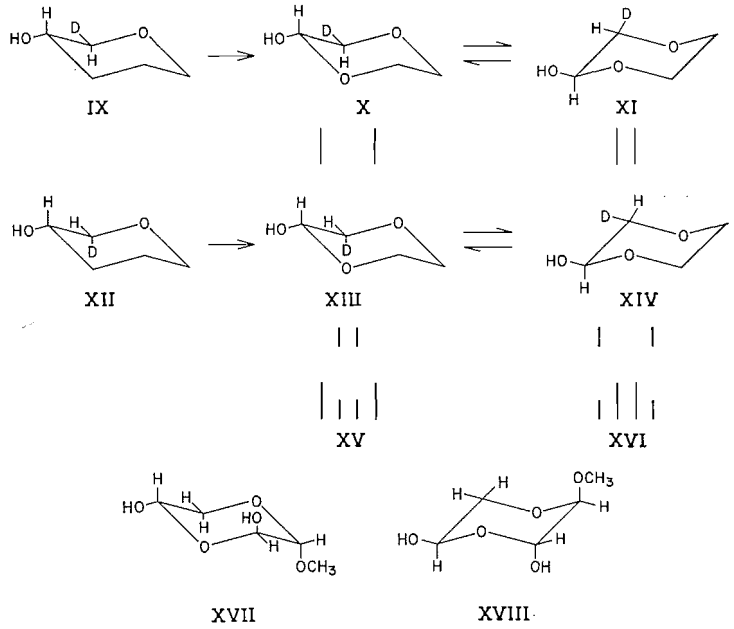


FIG. 3. Nuclear magnetic resonance spectra at 100 Mc.p.s. of dimethyl sulfoxide-d_6 solutions (at equilibrium) of the periodate oxidation products from (A) methyl α-D-xylopyranoside-5-*d*, (B) methyl α- or β-D-xylopyranoside, and (C) methyl β-D-xylopyranoside-5-*d*. Signal designations apply to all three spectra.

These results have been interpreted as follows. The multiplet structure of H-4 must be due basically to both a small (gauche) and a large (diaxial) coupling with H-5. Hence OH-4 must be equatorially oriented. Consider, for example, the oxidation of methyl D-xylopyranoside-5-*d*, in which the isotope is equatorial (IX), i.e. two-thirds of the material. Hemialdal X should give a H-4 doublet of $\frac{2}{3}$ proton intensity having a large (diaxial) spacing (10, 11), whereas XI should show a doublet with a narrow (gauche) spacing (if hydrogen–deuterium coupling is ignored for the moment). Simultaneously, the xyloside component in which the deuterium is axial (XII) (i.e. one-third of the material) yields a hemialdal (XIII) characterized by a H-4 doublet of $\frac{1}{3}$ proton intensity having a narrow spacing, or XIV, in which the spacing is broad. Therefore, the 2:1 mixture of X and XIII should give a composite H-4 signal consisting of a relatively strong ($\frac{2}{3}$ proton) broad doublet upon which a weak ($\frac{1}{3}$ proton) narrow doublet is superimposed, e.g. as in quartet XV. In contrast, the mixture of XI and XIV should show a quartet as in XVI, with the relative intensities of the two superimposed signals reversed.

According to these considerations, the spectrum in Fig. 3C shows that the hemialdal derived from methyl α-D-xyloside may be formulated, *in part*, by XVII. Its chair conformation must be the same as in the parent glycoside, since the H-4 signal is of the type represented by quartet XV, the OH-4 group is equatorial, and the axial orientation of the methoxyl group must be retained. Analogous considerations apply for the β-D-xyloside.

Can. J. Chem. Downloaded from www.nrcresearchpress.com by 210.87.254.40 on 09/05/12
For personal use only.



Since the signal observed for H-4 in Fig. 3A corresponds to quartet XVI, the oxidation product of II may be represented by XVIII, the mirror image of XVII. Its formation thus involves a ring-chair inversion.

The configuration of OH-2 has not been deduced from these data. However, its arrangement should be of considerable significance because of the remarkable stability in dimethyl sulfoxide of the one particular form that is detected, relative to the stabilities of the other seven isomers that are possible for each product. A comparison of all eight possibilities has been made in a semiquantitative way by conformational analysis along the lines formulated especially by Angyal (15) and by Lemieux (16). The main factors taken into account are the anomeric effect, the 1,3-diaxial interactions of *O*-substituents, and the gauche O—O interactions. On this basis structure XVII or XVIII, in which OH-2 is axially oriented, appears to be a most likely possibility, since it lacks both of the unfavorable factors and incorporates two stabilizing anomeric effects. Also pertinent in this connection is the observation that a 1,2-diaxial orientation (as in α-D-mannose and related compounds) is particularly favored in dimethyl sulfoxide solution (unpublished data). In addition, there is the fact that the halogen atoms of *trans*-2,3-dibromo-1,4-dioxane prefer the 1,2-diaxial orientation (17).

The hydroxyl proton signals may also yield some information about the configuration of OH-2. In Fig. 2 the OH-2 doublet has a spacing of 5.5 c.p.s., and that of OH-4 a spacing of 7.5 c.p.s. The equatorial orientation of the latter is consistent with a relatively large spacing of this magnitude for equatorial anomeric hydroxyl protons (spacings of 6.5–8 c.p.s.), whereas the OH-2 spacing is closer to that found for axial anomeric hydroxyl groups (4–5 c.p.s.) (9 and unpublished data). Hence, these values suggest that XVII and XVIII should be formulated as shown.

Outer spacings caused by the 4,5-diaxial interactions observed for the H-4 signals in Figs. 3A and 3C are 8.0 c.p.s. Since the 10.6 c.p.s. total spacing of the H-4 triplet (Fig. 3B) is $J_{AX} + J_{BX}$ (13), the gauche interaction must involve a coupling of about 2.6 c.p.s. This,

Can. J. Chem. Downloaded from www.nrcresearchpress.com by 210.87.254.40 on 09/05/12
For personal use only.

in fact, is close to the spacing (2.8 c.p.s.) observed for the inner component of the H-4 signals in Figs. 3A and 3C. However, small additional splittings caused by axial hydrogen–deuterium coupling would be expected. It is pertinent, therefore, that these signals are relatively broad doublets as compared with the outer doublet components. This becomes more obvious when the scale of the signals is expanded several fold over that shown; a multiplet structure is then discernible. Mention also should be made of the H-5 proton signals in Figs. 3A and 3B. Although these are obscured somewhat by overlapping signals for the methoxyl protons, their general characteristics parallel those of the corresponding H-4 protons, in agreement with expectation.

As noted above, the signals in Fig. 3B correspond very closely to some of those in Fig. 1B. A similar relationship holds when the spectra of the deuterated products are compared in the two solvents. In particular, despite the overlap of other signals, multiplets closely resembling those for H-4 in Figs. 3A and 3C are evident in the spectra of the deuterium oxide solutions. By relating these two groups of spectra, a second pattern of signals becomes apparent in Fig. 1B. Fortuitously, it has been possible to delineate this group even more clearly by examining the (thoroughly dried) syrupy oxidation products soon after solution in deuterium oxide, since the other signals are remarkably diffuse under these conditions (Fig. 1C). Both I and II give the same result, and on equilibration each spectrum slowly reverts to that represented by Fig. 1B. Two doublets and a triplet, each of about the same intensity, are found in Fig. 1C, together with a stronger high-field multiplet. Spin decoupling shows that the latter is associated with the triplet (spacings of 4.7 c.p.s.), these signals being ascribed to the 4- and 5-protons. Similarly, the spin-coupled doublets (spacings of 4.3 c.p.s.) are attributed to H-1 and H-2. The intermediate magnitude of the spacings indicates that this group of signals is due to the acyclic dialdehyde (hydrated III or IV), or else to a hemialdal undergoing a rapid chair interconversion (see, for example, ref. 18). Of these possibilities, the dialdehyde structure is the more likely. This follows from the fact that in the spectra of the 5-deuterio compounds each H-4 signal appears as a doublet of 4.7 c.p.s. spacing (inset, Fig. 1C), i.e. in this instance the product from each anomer gives the same type of signal. If the compound were a hemialdal, however, the product derived from each anomer should give a different result. That is, the spacings of the H-4 doublet should be either smaller or larger than that of the H-4 triplet, because the uneven isotope distribution would result in disproportionate contributions from the H-4 and H-5 gauche and diaxial interactions to the average values.

On this basis it is concluded that an almost equimolar mixture of open-chain (III or IV) and hemialdal (XVII or XVIII) forms is present in the aqueous solution after periodate oxidation of I and II, together with more minor, unidentified components. In dimethyl sulfoxide, however, the equilibrium is displaced almost entirely in favor of the hemialdal.

The foregoing data are clearly consistent with the view that the oxidation products derived from two anomeric aldopentopyranosides are enantiomorphic. Although this disagrees with the recent findings of Chittenden and Guthrie (4), the fact that the oxidation products can exist in more than one form enhances the possibility that the preparation of certain derivatives could conceivably involve mixtures of products. Preliminary results show that a situation of this kind can arise. Thus, amorphous *p*-nitrobenzoates have been prepared as described by the above workers, from the syrupy oxidation products obtained from I and II. Each of these products gives a n.m.r. spectrum consisting of a profusion of signals that undoubtedly reflects the presence of several admixed components; in particular, three singlets attributable to methoxyl groups are readily evident in each spectrum. All of the signals are common to both spectra, although their relative intensities vary

Can. J. Chem. Downloaded from www.nrcresearchpress.com by 210.87.254.40 on 09/05/12
For personal use only.

slightly from one to the other. However, these small compositional differences have little overall effect on the optical rotatory values, which, for the two products, are almost equal and of opposite sign. On balance, therefore, there appears to be little reason to doubt Jackson and Hudson's original postulate that the products derived by glycol-cleavage oxidation of anomeric aldopentopyranosides are enantiomorphic.

EXPERIMENTAL

Nuclear magnetic resonance signals were recorded on a Varian HA-100 high-resolution spectrometer, with tetramethylsilane contained in a coaxial capillary as the internal control reference signal. Chemical shift values obtained in this way are about 45 c.p.s. higher than when tetramethylsilane is present in the solution; hence the values reported herein have been corrected by −0.45 p.p.m. Spin-decoupling experiments were carried out with the frequency-sweep facility of this instrument.

Methyl α- and β-D-Xylopyranoside-5-d

D-Xylose-5-*d* was prepared essentially according to the procedure described by Lemieux and Howard (14). In the present study, 1,2-*O*-isopropylidene-α-D-glucofuranose was used as the starting material (instead of the 3-*O*-benzyl derivative) and the 5-oxoxylose intermediate was reduced with sodium borodeuteride in water (instead of with lithium aluminium deuteride in ether). The 1,2-*O*-isopropylidene-α-D-xylofuranose-5-*d* was treated directly with 1% methanolic hydrogen chloride under reflux for 6 h to prepare the anomeric xylosides according to Hudson's conditions (19). Methyl β-D-xylopyranoside, m.p. 154–156°, was obtained by crystallization from ethanol. As found for the configerationally related 1,2,3,4-tetra-*O*-acetyl-β-D-xylose (14), methyl β-D-xyloside (in deuterium oxide) gives a quartet (spacings of 4.4 and 10.3 c.p.s.) for the equatorial 5-proton well shifted (4.0 p.p.m.) from that of the axial proton (ca. 3.4 p.p.m.). Also, in the spectrum of the deuterated compound this signal appears as a broad doublet, its intensity being approximately 35% of that of the nearby H-1 doublet, in agreement with the data of Lemieux and Howard (14).

Methyl α-D-xylopyranoside-5-*d* was difficult to obtain in a crystalline form, although several solvents, including methyl ethyl ketone (19), were tested as crystallization media. However, repeated precipitation from ethyl acetate – ether solution gave the pure compound, as judged from its n.m.r. spectrum and by paper chromatography. The H-5 signals of methyl α-D-xylopyranoside and of its deuterated counterpart are not well resolved; hence, the distribution of isotope was not cross-checked in this way.

Periodate Oxidation of Glycosides

These oxidations were carried out with periodic acid as described by Jackson and Hudson (1), except that the iodate and excess of the oxidant were removed with Dowex-1 resin (bicarbonate form). In the deionization step the suspension was shaken with an excess of resin for several hours; otherwise, when the syrupy oxidation product was dissolved in dimethyl sulfoxide, iodine was slowly released.

p-Nitrobenzoates of the Oxidation Products

The syrupy product (0.2 g) obtained by oxidation of either methyl α- or β-D-xylopyranoside was dissolved in pyridine (15 ml). (A n.m.r. spectrum of a more concentrated solution, which differed somewhat from those shown in Figs. 1 and 3 but was the same for each product, indicated that a mixture of components was present, although one component greatly predominated.) *p*-Nitrobenzoyl chloride (0.6 g) was added, and after 20 h at room temperature the solution was treated with 2–3 ml of ice water and then poured onto cracked ice admixed with an excess of sodium bicarbonate. The suspension was stirred for 30 min, and filtered; then the precipitate was washed on the filter with ice water and dried *in vacuo*. The yields of cream-colored powder were 0.31 g (from the α-anomeric product) and 0.30 g (from the β-anomeric product). The derivative was dissolved in chloroform, ether was added to turbidity, a small quantity of dark precipitate was filtered off, and on removal of the chloroform a white crust was obtained; $[\alpha]_D$ +58° (α-product) and −53° (β-product) (*c*, 3 in chloroform) (these solutions gave plain optical rotary dispersion curves which were virtually mirror images).

In the n.m.r. spectrum of each product (recorded in chloroform) three sharp singlets ascribable to methoxyl protons were found at 3.45, 3.48, and 3.53 p.p.m., respectively. The relative intensities of these signals, as well as of some other signals present, differed slightly in the two spectra. The spectra were found to be unaltered after the products had been treated with *p*-nitrobenzoyl chloride (as above) to ensure complete esterification.

ACKNOWLEDGMENTS

The author expresses sincere thanks to M. Mazurek, who recorded the spectra, and to Dr. H. J. Bernstein and Dr. W. Quail for very helpful discussions.

Can. J. Chem. Downloaded from www.nrcresearchpress.com by 210.87.254.40 on 09/05/12
For personal use only.

REFERENCES

1. E. L. JACKSON and C. S. HUDSON. J. Am. Chem. Soc. **59**, 994 (1937).
2. W. S. MCCLENAHAN and R. C. HOCKETT. J. Am. Chem. Soc. **60**, 2061 (1938).
3. F. SMITH and J. W. VAN CLEVE. J. Am. Chem. Soc. **77**, 3091 (1955).
4. G. J. F. CHITTENDEN and R. D. GUTHRIE. J. Chem. Soc. 2271 (1965).
5. I. J. GOLDSTEIN, B. A. LEWIS, and F. SMITH. Chem. Ind. London, 595 (1958).
6. I. J. GOLDSTEIN and F. SMITH. J. Am. Chem. Soc. **82**, 3421 (1960).
7. R. D. GUTHRIE. Advan. Carbohydrate Chem. **16**, 105 (1961).
8. O. L. CHAPMAN and R. W. KING. J. Am. Chem. Soc. **86**, 1256 (1964).
9. A. S. PERLIN. Can. J. Chem. **44**, 539 (1966).
10. A. D. COHEN, N. SHEPPARD, and T. J. TURNER. Proc. Chem. Soc. 118 (1958).
11. R. U. LEMIEUX, R. K. KULLNIG, H. J. BERNSTEIN, and W. G. SCHNEIDER. J. Am. Chem. Soc. **80**, 6098 (1958).
12. J. A. POPLE, W. G. SCHNEIDER, and H. J. BERNSTEIN. High resolution nuclear magnetic resonance. McGraw-Hill Book Co., Inc., New York. 1959.
13. R. J. ABRAHAM and H. J. BERNSTEIN. Can. J. Chem. **39**, 216 (1961).
14. R. U. LEMIEUX and J. HOWARD. Can. J. Chem. **41**, 308 (1963).
15. S. J. ANGYAL. *In* Conformational analysis. E. L. Eliel, N. L. Allinger, S. J. Angyal, and G. A. Morrison. John Wiley & Sons, Inc., New York. 1965.
16. R. U. LEMIEUX. *In* Molecular rearrangements. P. de Mayo (*Editor*). Interscience Publishers, Inc., New York. 1964. Part 2.
17. C. ALTONA, C. ROMERS, and E. HAVINGA. Tetrahedron Letters, **10**, 16 (1959).
18. R. R. FRASER and C. REYES-ZAMORA. Can. J. Chem. **43**, 3445 (1965).
19. C. S. HUDSON. J. Am. Chem. Soc. **47**, 265 (1925).

Can. J. Chem. Downloaded from www.nrcresearchpress.com by 210.87.254.40 on 09/05/12
For personal use only.

Can. J. Chem. Downloaded from www.nrcresearchpress.com by 210.87.254.105 on 09/05/12
For personal use only.

AROMATIC SUBSTITUTION

XIV. THE HOMOLYTIC PHENYLATION OF 3- AND 4-PICOLINE. A QUANTITATIVE STUDY OF ISOMER AND TOTAL RATE RATIOS[1]

R. A. Abramovitch and Maitreyi Saha
Department of Chemistry, University of Saskatchewan, Saskatoon, Saskatchewan
Received March 15, 1966

ABSTRACT

The homolytic phenylation of 3- and 4-picoline under the conditions of the Gomberg–Hey reaction has been studied quantitatively. The methyl group in both picolines was found to activate the nucleus to the same extent. All the nuclear positions in both systems, except for C_5 in 3-picoline, were slightly activated as compared with any one position in benzene. The significance of these results is discussed.

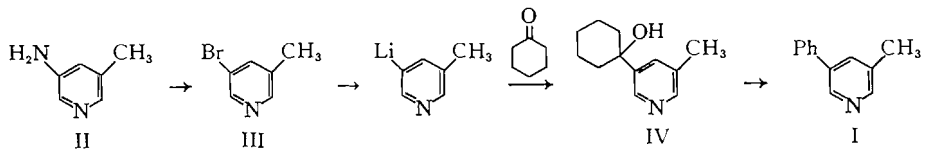
In previous parts of this series (1, 2), the effects of substituents in the aryl radical upon the isomer ratio and upon the relative reactivities of the nuclear positions in pyridine towards free-radical arylation have been studied. On the other hand, the effects of substituents present in the pyridine nucleus upon the reactivity of the various positions towards homolytic attack have received little attention. A qualitative analysis of the products formed in the substitution of 4-picoline by 3-pyridyl radicals showed that both the 2- and 3-(3′-pyridyl) isomers were formed in the ratio of 3:11 (3). Similar results were obtained with 4-ethylpyridine (3). Ethyl isonicotinate is reported to give only ethyl 2-(3′-quinolyl)isonicotinate with the 3-quinolyl radical (4). The alkylation of 3-picoline by methyl radicals (from lead tetraacetate) is said to give a mixture of 2,3- and 2,5-lutidine (5), though the other isomers are undoubtedly present as well (6). Methylation of 3-*n*-butylpyridine with lead tetraacetate in acetic acid (in which the pyridine is undoubtedly *N*-protonated to a large extent) has been examined semiquantitatively (7). The main product of monomethylation (60% of total) was 3-*n*-butyl-2-methylpyridine, and about equal amounts (slightly less than 20%) of each of the 4- and 6-methyl derivatives were obtained. About 2% of the total product was thought to consist of 3-*n*-butyl-5-methylpyridine. A small amount of the dimethylated 3-*n*-butylpyridines was obtained together with an appreciable quantity of a high-boiling residue.

The present work reports a quantitative study of the homolytic phenylation of 3- and 4-picoline under the conditions of the Gomberg–Hey reaction. Since the reactivities of the various nuclear positions of pyridine (1) and toluene (8, 9) towards attack by phenyl radicals are known, it was of interest to determine whether the effects of the nitrogen atom and of the methyl group in the picolines were additive in this reaction.

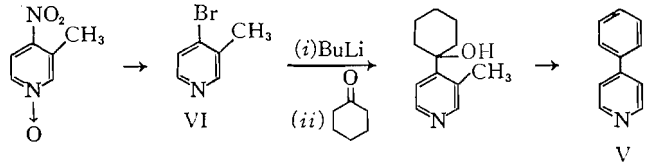
Of the possible products from the phenylation of 3-picoline, 4-phenyl-3-picoline was not known. 5-Phenyl-3-picoline (I) had previously been prepared by the condensation of phenylacetaldehyde, propionaldehyde, and ammonia, and had been obtained as a mixture with 3,5-diphenylpyridine, 3,5-diphenyl-2-ethylpyridine, and 2-ethyl-3-methyl-5-phenylpyridine (10). A more conventional approach to this compound was used here, starting with 3-methyl-5-pyridyllithium and cyclohexanone. 5-Bromo-3-picoline (III) was required and was prepared from 5-amino-3-picoline (II) by the Craig perbromide procedure. An attempt to make use of the Gattermann reaction for this purpose gave a basic product

[1]*For part XIII in this series, see ref. 2.*

whose picrate did not analyze correctly for that of III. When the bromination of 3-picoline with bromine and aluminium chloride (swamping catalyst method (11)) was carried out, a mixture of three products was obtained, more than 85% of which was 5-bromo-3-picoline. The formation of I from 1-(3′-methyl-5′-pyridyl)cyclohexanol (IV) with concentrated sulfuric acid and glacial acetic acid was unexceptional.



4-Phenyl-3-picoline (V) was prepared similarly from 3-methyl-4-pyridyllithium and cyclohexanone. A number of attempts were made at preparing pure 4-bromo-3-picoline (VI). 4-Bromo-3-picoline 1-oxide, m.p. 112–113° (reported (12) m.p. 72–73°), decomposed very readily and could not be used conveniently. Reduction of 4-nitro-3-picoline 1-oxide with iron and acetic acid gave 4-amino-3-picoline which, in turn, gave 4-bromo-3-picoline (VI) by the Craig method. The yields of VI were very poor and the compound obtained in this way underwent self-addition very readily, a process probably catalyzed by some impurity that was present. On the other hand, a reasonably good yield (47%) of VI was obtained on treatment of 4-nitro-3-picoline 1-oxide with phosphorus tribromide in ethyl acetate. The product could be distilled without decomposition.



EXPERIMENTAL

Melting points are uncorrected. Only the main peaks are reported for the infrared spectra.

5-Bromo-3-picoline

(a) From 5-Amino-3-picoline

A solution of 5-amino-3-picoline (2.0 g) (13) in constant-boiling hydrobromic acid (8.0 ml) was treated with bromine (2.4 ml) dropwise at 0°, stirring was continued for 15 min, and then a solution of sodium nitrite (4.0 g) in water (12.0 ml) was added at such a rate as to keep the temperature at 0–5°. A vigorous evolution of gas occurred at the end of the addition. When the effervescence had subsided the mixture was made alkaline and then steam-distilled. The distillate was extracted with ether, the ethereal layer was dried (Na_2SO_4) and evaporated, and the residue was distilled to give 5-bromo-3-picoline (1.38 g), b.p. 108–110° at 25 mm. Infrared spectrum (liquid film): 1 595 (m), 1 445 (s), 1 165 (m), 1 105 (s), 1 035 (s), 1 005 (w), 870 (s), 860 (s), 700 (s), and 665 (w) cm^{-1}. The picrate crystallized from ethanol and was recrystallized from the same solvent. It had m.p. 180–181°.

Anal. Found: C, 36.25; H, 2.47. $C_6H_6NBr \cdot C_6H_3N_3O_7$ requires C, 35.91; H, 2.24.

The use of the Gattermann reaction in the synthesis of this compound gave a very impure material which did not analyze correctly.

(b) By the Swamping Catalyst Method

Anhydrous 3-picoline (4 g, 0.041 mole) was added dropwise to stirred anhydrous aluminium chloride (14 g, 0.103 mole) (calcium chloride guard tube). Heat was evolved and bromine (4.0 g) was added to the mixture over a period of 1.5 h while the temperature was maintained at 95–100°. After being kept at room temperature overnight the mixture was decomposed with ice water, made alkaline, and extracted with ether. The ether layer was dried ($MgSO_4$), the solvent evaporated, and the residue distilled at 112–114° and 60 mm to give a yellow oil (1.22 g). This was analyzed by gas chromatography with a 6 ft × ¼ inch 15% asphalt on Chromosorb W column operated at 165° and a helium inlet pressure of 45 p.s.i. Three peaks were observed; the substance giving rise to the major peak (>85%) was collected and shown to be identical with 5-bromo-3-picoline by a comparison of its infrared spectrum with that of a sample prepared by method *a* above.

Can. J. Chem. Downloaded from www.nrcresearchpress.com by 210.87.254.105 on 09/05/12
For personal use only.

Can. J. Chem. Downloaded from www.nrcresearchpress.com by 210.87.254.105 on 09/05/12
For personal use only.

The attempted bromination of 3-picoline in the presence of thionyl chloride gave a complex mixture of at least four products which was not examined further.

1-(3′-Methyl-5′-pyridyl)cyclohexanol

A solution of *n*-butyllithium in hexane (3.5 ml of a 14.9% solution) and dry ether (2.0 ml) was stirred vigorously under dry, oxygen-free nitrogen and cooled to −62° to −74°. 5-Bromo-3-picoline (1.0 g) in dry ether (2.0 ml) was added dropwise over a period of 15 min, the mixture was stirred for a further 15 min, and a solution of freshly distilled cyclohexanone (3.0 ml) in dry ether (2.0 ml) was then added slowly during 30 min. After being stirred for another 3 h at −62° to −74° the reaction mixture was allowed to come to room temperature, poured onto crushed ice, and extracted with ether. The dried ($MgSO_4$) ether extract was evaporated to give 1-(3′-methyl-5′-pyridyl)cyclohexanol (0.97 g) which, after recrystallization from acetone, had m.p. 144–144.5°. Infrared spectrum (KBr disk): 3 250 (s), 1 595 (m), 1 440 (s), 1 395 (s), 1 320 (m), 1 272 (s), 1 180 (s), 1 145 (s), 1 045 (s), 995 (s), 870 (s), 815 (m), 795 (w), 715 (s), and 695 (w) cm^{-1}.

Anal. Found: C, 74.94; H, 8.97. $C_{12}H_{17}NO$ requires C, 75.35; H, 8.96.

5-Phenyl-3-picoline

1-(3′-Methyl-5′-pyridyl)cyclohexanol (0.2 g) was boiled under reflux with a mixture of concentrated sulfuric acid (1.0 ml) and glacial acetic acid (3.0 ml) for 4 h. Most of the acetic acid was then distilled off, the residue was poured into water, and the solution was made basic and extracted with ether. The dried ($MgSO_4$) ether extract was evaporated and the residue distilled to give 5-phenyl-3-picoline (0.14 g), b.p. 208–210° at 60 mm. Infrared spectrum (liquid film): 3 070 (m), 1 505 (w), 1 425 (m), 1 155 (m), 1 035 (m), 840 (m), 815 (s), 760 (s), 710 (s), 695 (s), and 660 (w) cm^{-1}. The picrate was recrystallized from ethanol and had m.p. 200–201°. Farley and Eliel (10) give m.p. 191–192° for this picrate.

Anal. Found: C, 53.80; H, 3.88. $C_{12}H_{11}N \cdot C_6H_3N_3O_7$ requires C, 54.27; H, 3.54.

3-Benzylpyridine

Because the red phosphorus and hydriodic acid method of reduction of 3-benzoylpyridine (14) proved to be unsatisfactory in our hands, a Wolff–Kishner reduction was used.

3-Benzoylpyridine (3.6 g) was dissolved in diethylene glycol (30.0 ml), and 90% hydrazine hydrate (3.0 ml) and potassium hydroxide (4.0 g) were added. The mixture was boiled under reflux for 6–7 h, cooled, and extracted with ether. The dried ($MgSO_4$) ether layer was evaporated and the residue distilled. The fraction (0.92 g), b.p. 285–288°, crystallized in the refrigerator and gave a picrate, m.p. 124–126° when crystallized from ethanol. Tschitschibabin (14) reported m.p. 34° for 3-benzylpyridine and m.p. 126–127° for its picrate.

4-Bromo-3-picoline 1-Oxide

4-Nitro-3-picoline 1-oxide (1.0 g) (15) was heated under reflux with constant-boiling hydrobromic acid (40 ml) for 24 h. The reaction mixture was poured onto crushed ice and neutralized with aqueous sodium hydroxide. The product was extracted with chloroform, the extract dried (Na_2CO_3), and the solvent evaporated to give a light-yellow solid (0.92 g) which, after recrystallization from light petroleum (b.p. 60–80°), gave fine white needles of the bromo *N*-oxide, m.p. 112–113°. Infrared spectrum (KBr disk): 3 400 (m, br), 1 450 (s), 1 400 (s), 1 390 (w), 1 290 (s), 1 245 (s), 1 205 (m), 1 155 (s), 1 005 (m), 850 (w), 845 (w), 835 (w), 745 (s), and 695 (m) cm^{-1}.

Anal. Found: C, 38.80; H, 3.51. C_6H_6NOBr requires C, 38.32; H, 3.19.

Hai and Ogura (12) reported m.p. 72–73° for this compound. The picrate was recrystallized from benzene and had m.p. 117–118°, depressed on admixture with picric acid.

4-Bromo-3-picoline

(a) By the Craig Procedure

4-Amino-3-picoline (2.0 g) (15) in constant-boiling hydrobromic acid (8 ml) was cooled to 0° and treated with bromine (2.4 ml) dropwise. Stirring at 0° was continued for 15 min, and a solution of sodium nitrite (4.0 g) in water (12 ml) was then stirred in at such a rate that the temperature of the mixture remained at 0–5°. At the end of the addition a vigorous evolution of gas occurred. The solution was made basic with 10% sodium hydroxide solution, the temperature not being allowed to rise above 25°, and then steam-distilled. The distillate was extracted with ether, the organic layer dried ($MgSO_4$), and the solvent evaporated. The residue was distilled to give 4-bromo-3-picoline (0.185 g, 5.8%), b.p. 108–110° at 60 mm. The picrate (crystallized from benzene) was recrystallized from ethanol and had m.p. 139–141°.

Anal. Found: C, 35.75; H, 2.55. $C_6H_6NBr \cdot C_6H_3N_3O_7$ requires C, 35.91; H, 2.24.

(b) From 4-Nitro-3-picoline 1-Oxide

Phosphorus tribromide (36.0 g) was added to a mixture of 4-nitro-3-picoline 1-oxide (5.0 g) and dry ethyl acetate (300 ml), and the mixture was boiled under reflux for 30 min. The reaction mixture was poured into water and the solution extracted with ether. The aqueous layer was made alkaline, care being taken to maintain the temperature at 25–30°. The solution was extracted with ether, the ether layer was dried (Na_2CO_3) and evaporated, and the residue was distilled under vacuum to give 4-bromo-3-picoline (2.06 g), b.p. 104–107° at 60 mm. The picrate had m.p. 137–138°, undepressed on admixture with a sample prepared by method *a* above. Infrared spectrum of the free base (liquid film): 3 040 (m), 1 600 (w), 1 520 (s), 1 470 (m), 1 440 (m), 1 380 (m), 1 350 (s), 1 230 (s), 1 065 (s), 840 (s), 790 (s), 750 (s), 715 (w), 690 (s), and 670 (s) cm^{-1}.

1-(3′-Methyl-4′-pyridyl)cyclohexanol

A solution of *n*-butyllithium in ether was prepared from lithium (0.07 g), *n*-butyl bromide (4 ml), and dry ether (25 ml) at −62° to −74°. A solution of 4-bromo-3-picoline (0.860 g) in dry ether (5 ml) was added dropwise, with stirring, to the butyllithium solution over a period of 30 min, the temperature being maintained at −62° to −74°. Cyclohexanone (3.0 g) in dry ether was added dropwise over a period of ½ h, and then stirring was continued for another 3 h, during which time the reaction mixture was allowed to come to room temperature. The resulting mixture was poured onto crushed ice and extracted with ether. The dried ($MgSO_4$) ethereal layer was evaporated to give the alcohol (0.418 g), which was vacuum-distilled at 205–209° and 60 mm and then recrystallized from light petroleum (b.p. 60–80°). It was obtained as colorless prisms, m.p. 95°. Infrared spectrum (KBr disk): 3 180 (s), 1 590 (s), 1 255 (m), 1 210 (m), 1 165 (s), 1 125 (s), 1 065 (s), 965 (s), 822 (s), 805 (w), 755 (w), 745 (m), and 645 (s) cm^{-1}.

Anal. Found: C, 75.64; H, 8.81. $C_{12}H_{17}NO$ requires C, 75.35; H, 8.96.

4-Phenyl-3-picoline

1-(3′-Methyl-4′-pyridyl)cyclohexanol (0.20 g) was boiled under reflux with concentrated sulfuric acid (1.0 ml) and glacial acetic acid (3.0 ml) for 4 h, and the reaction mixture worked up as described for 5-phenyl-3-picoline. The product (0.054 g) had b.p. 195–198° at 60 mm. Infrared spectrum (liquid film): 3 340 (m, br), 1 585 (s), 1 475 (m), 830 (m), 805 (w), 760 (s), 735 (m), and 695 (s) cm^{-1}. Nuclear magnetic resonance spectrum (in CCl_4): τ 7.80 (3H, singlet, CH_3—Ar), 2.67 (5H, singlet, phenyl protons), 2.1 (1H, doublet, J = 5 c/s, C_5—H), and 1.4 (2H, multiplet caused by the superimposed singlet and doublet of C_2—H and C_6—H). The picrate (crystallized from benzene) had m.p. 168–169°.

Anal. Found: C, 54.07; H, 3.70. $C_{12}H_{11}N \cdot C_6H_3N_3O_7$ requires C, 54.27; H, 3.54.

General Method Used for the Phenylation of the Picolines and the Determination of the Isomer Ratios

A mixture of aniline (0.5 g) and concentrated hydrochloric acid (1 ml) was cooled to 0–5° and diazotized below 5° with a solution of sodium nitrite (0.42 g) in water (0.75 ml). The diazonium salt solution was slowly added over a period of 15 min to the picoline (100 ml), which was being stirred vigorously in a thermostat maintained at 40 ± 1°; the solution was then stirred at that temperature for a further 6 h. Sodium carbonate (5 g) was now added, the mixture was stirred at room temperature for 15 min and, after being allowed to stand for some time, was filtered into a distillation flask, and the solids were washed thoroughly with ether until free of picoline. The combined filtrates were concentrated carefully with a fractionating column to a volume of 20–30 ml. This was transferred quantitatively to a conical flask with the help of ether, the total volume being kept below 50 ml, and this solution was used directly for the quantitative analyses of the isomer ratios by gas–liquid chromatography.

For the quantitative analyses, the internal standard method (16) was used. The introduction of a known weight of internal standard in the final reaction mixture also permitted the yield of products to be determined. The authentic samples prepared as described above were all gas chromatographically pure. The conditions for the gas–liquid chromatographic analyses are given in each individual case.

Phenylation of 3-Picoline

The diazonium salt solution, prepared as described above, was added to 3-picoline (100 ml) at 40 ± 1° and worked up as usual. The reaction mixture was best resolved on a 5 ft × ¼ inch column packed with asphalt (15% w/w) on Chromosorb W (80–100 mesh) and operated at 220° and a helium inlet pressure of 40 p.s.i. (flow rate 75 ml/min). Under these conditions, four peaks were well resolved and had retention times of 24.5, 28.5, 39.5, and 45.0 min, respectively. These correspond to 2-phenyl-3-picoline, 4-phenyl-3-picoline, 6-phenyl-3-picoline, and 5-phenyl-3-picoline, respectively, and were identified by collecting samples corresponding to the individual peaks and comparing their infrared spectra with those of authentic samples. 2-Phenyl-3-picoline and 6-phenyl-3-picoline were available from a previous study (17). No 3-benzylpyridine (retention time 12.5 min) could be detected in the reaction mixture. The thermal detector responses of the four isomeric phenylpicolines were found to be the same, so that the relative areas under the chromatographic peaks could be used directly in the determination of the isomer ratios. 2-Methylbiphenyl was used as the internal standard. The percentage composition thus obtained (average of two runs in triplicate) was: 2-phenyl-, 43.3 ± 0.5%; 4-phenyl-, 28.7 ± 0.6%; 5-phenyl-, 6.9 ± 0.8%; and 6-phenyl-3-picoline, 21.1 ± 0.5%.

Phenylation of 4-Picoline

The reaction mixture was best resolved on a 6 ft × ¼ inch column packed with precipitated asphalt (25% by weight) on Chromosorb W (60–80 mesh) and operated at 175° and a helium inlet pressure of 40 p.s.i. (flow rate 80 ml/min). Under these conditions 3-phenyl-4-picoline had a retention time of 19.3 min and 2-phenyl-4-picoline a retention time of 27.4 min. Only two peaks were observed. Coumarin (retention time 22.2 min) was used as the internal standard. The compound giving rise to the peak corresponding in retention time to 2-phenyl-4-picoline was collected and found to be identical (melting point and infrared spectrum) with a sample prepared from phenyllithium and 4-picoline (18). The compound giving rise to the peak corresponding to 3-phenyl-4-picoline was collected and gave a picrate, m.p. 145°, undepressed on admixture with an authentic sample of the picrate of this base kindly supplied by Dr. J. N. Chatterjee (19). Infrared spectrum of the free base (liquid film): 1 610 (s), 1 475 (m), 1 455 (m), 1 415 (m), 1 225 (m), 1 015 (s), 830 (s), 765 (s), 730 (w), and 700 (s) cm^{-1}.

The molar thermal responses of the two isomers were different, so that the internal standard had to be

Can. J. Chem. Downloaded from www.nrcresearchpress.com by 210.87.254.105 on 09/05/12
For personal use only.

Can. J. Chem. Downloaded from www.nrcresearchpress.com by 210.87.254.105 on 09/05/12
For personal use only.

introduced in all the samples being analyzed. The percentage composition thus obtained (two runs in triplicate) was: 2-phenyl-, 44.9 ± 1.0%; and 3-phenyl-4-picoline, 55.1 ± 0.6%.

Determination of ${}^{3\text{-Pic}}_{C_6H_6}K$ *for the Phenylation of 3-Picoline*

(i) With a Molar Ratio of 3-Picoline to Benzene of 4:1

The ratio of aniline to total solvent was 1:200.

The diazonium salt solution from aniline (0.5 g), concentrated hydrochloric acid (1.0 ml), sodium nitrite (0.42 g), and water (0.7 ml) was added over a period of 15 min, with vigorous stirring, to a mixture of 3-picoline (83.0 ml) and benzene (19.0 ml) maintained at 40 ± 1° in a thermostat. The reaction mixture was stirred for a further 6 h and then worked up as described in the determination of the isomer ratios. It was analyzed by gas–liquid chromatography on a 6 ft × ¼ inch column packed with precipitated asphalt (15% w/w) on Chromosorb W (80–100 mesh) and operated at 220° and a helium inlet pressure of 40 p.s.i. Under these conditions biphenyl had a retention time of 8.3 min. Advantage was taken here of the fact that the phenyl-3-picolines have the same thermal detector response, so that no special calibrations were necessary. 2-Bromobiphenyl was used as the internal standard. The mean of the results of three runs carried out in duplicate gave ${}^{3\text{-Pic}}_{C_6H_6}K = 1.39 \pm 0.05$.

(ii) With a Molar Ratio of 3-Picoline to Benzene of 6:1

The same proportions of amine to total solvent were used. In this way, ${}^{3\text{-Pic}}_{C_6H_6}K$ was found to be 1.40±0.06.

Determination of ${}^{4\text{-Pic}}_{C_6H_6}K$ *for the Phenylation of 4-Picoline*

The reaction was carried out as described above, but with 4- instead of 3-picoline. The mixtures were analyzed on a 6 ft × ¼ inch column packed with precipitated asphalt (25% w/w) on Chromosorb W and operated at 175° and a helium inlet pressure of 40 p.s.i. (flow rate 80 ml/min). Under these conditions biphenyl had a retention time of 8.3 min, and 2- and 3-phenyl-4-picolines retention times of 22.6 and 16.4 min, respectively. Coumarin was used as the internal standard. The average of the results of three runs carried out in duplicate gave ${}^{4\text{-Pic}}_{C_6H_6}K = 1.39 \pm 0.1$.

DISCUSSION

Since the reaction mixtures were homogeneous in all cases, the argument sometimes levelled (20) against the suitability of the Gomberg–Hey reaction for quantitative work that, with the usual aromatic solvents, the reaction is a heterogeneous one does not apply. Selective solvation was not important within the range of solvent ratios used. The validity of isomer ratios obtained in the Gomberg–Hey arylation has already been discussed (1), and the conclusion was reached that the σ-complexes formed are not selectively removed by dimerization or disproportionation. No high-boiling products could be isolated in the reactions with the picolines. In view of the work-up and analytic procedure used the errors in the quantitative estimations are small and the results are reproducible within ±2% (in most cases much better than this).

The averaged proportions of isomeric phenylpicolines are given in Table I, which also includes the data for the phenylation of pyridine (1). The values of the total rate ratios

TABLE I

Averaged percentage ratios of phenylated pyridines formed at 40 ± 1° and total rate ratios

Compound	Isomer distribution					${}^{XC_5H_4N}_{C_6H_6}K$
	2-	3-	4-	5-	6-	
Pyridine (1)	52.4	29.6	18.0	—	—	1.14
3-Picoline	43.3	—	28.7	6.9	21.1	1.39
4-Picoline	44.9	55.1	—	—	—	1.39

${}^{XC_5H_4N}_{C_6H_6}K$ relative to benzene are also given (corrected for the statistical relative amounts of benzene and XC_5H_4N used in the competitive reactions). A previous study (1) had shown that the most convenient molar ratio of pyridine to benzene to use in the competitive runs was 4:1. Under such conditions the mixtures were homogeneous and no selective solvation of the diazonium salt or covalent diazo compound was occurring. This was also found to be the case here in the competitive runs with the picolines and benzene. Increasing the molar ratio of 3-picoline to benzene to 6:1 had no effect upon the total rate ratio.

The results indicate that the 3- and 4-methyl groups activate the pyridine nucleus slightly (as expected) towards attack by phenyl radicals, and to the same extent (${}^{Plc}_{Pyr}K$ = 1.22). This is about the same degree of activation as is imparted by a methyl substituent onto a benzene ring (${}^{C_6H_5CH_3}_{C_6H_6}K$ = 1.23) (21). (See, however, the more recent results with triphenylbismuth as the source of phenyl radicals to substitute toluene, in which ${}^{CH_3}_{H}K$ was found to be 1.99 on the assumption that there is no side-chain attack (9). This value appears to be too high. Abramovitch and Saha (22), using benzenediazonium tetrafluoroborate and pyridine as the source of phenyl radicals, obtained a value of 1.20 for this total rate ratio.)

The most abundant isomers obtained in the phenylation of the picolines are those in which the phenyl group enters ortho to the methyl group, which is consistent with the orientation observed in previous homolytic substitutions of 3- and 4-alkylpyridines (3, 5, 7). The effect of the methyl group may be seen more clearly from a consideration of the partial rate factors for the phenylations. These are given in Table II together with the data for pyridine itself (1).

TABLE II

Partial rate factors for phenylation at 40 ± 1°

	Partial rate factors				
Compound	F_2	F_3	F_4	F_5	F_6
Pyridine (1)	1.83	1.00	1.18	—	—
3-Picoline	3.5	—	2.37	0.57	1.74
4-Picoline	1.87	2.29	—	—	—

If the principle of additivity (23) is presumed to hold in these substitutions, then the partial rate factors for the various positions in the picolines can be calculated from the partial rate factors for the phenylation of pyridine and of toluene. The data for toluene are, as mentioned above, not definitive. The latest values of the isomer ratios as obtained from the phenylation with triphenylbismuth (9) have been confirmed in our laboratories with benzoyl peroxide as the source of phenyl radicals, the analysis being carried out by gas–liquid chromatography, using the internal standard technique. The isomer ratio so obtained is: *o*-, 57%; *m*-, 25%; and *p*-, 18% (24). If the values for the partial rate factors originally given by Hey *et al.* (21) are used in conjunction with our data for pyridine, the values calculated for 3-picoline are: F_2 = 4.58, F_4 = 2.95, F_5 = 0.71, and F_6 = 1.83; and those for 4-picoline are: F_2 = 1.30 and F_3 = 2.50. If the partial rate factors based on ${}^{C_6H_5CH_3}_{C_6H_6}K$ = 1.99 (9) are used, then the calculated values for 3-picoline are: F_2 = 6.22, F_4 = 4.0, F_5 = 1.6, and F_6 = 3.48; and those for 4-picoline are: F_2 = 2.93 and F_3 = 3.4. These values are obviously much too high and confirm that the total rate ratio for toluene is probably close to 1.23. Using this figure and our data for the isomer ratios (24) leads to the following predicted values for 3-picoline: F_2 = 3.85, F_4 = 2.47, F_5 = 0.92, and F_6 = 2.43; and for 4-picoline: F_2 = 1.69 and F_3 = 2.10. Except for F_5 in 3-picoline (and perhaps F_6 as well), these agree reasonably well with the experimentally found values. This additivity of the substituent effects supports the assumption that formation of the σ-complexes is the rate-determining step in such substitution reactions.

The apparent deactivation of C_5 in 3-picoline towards attack by phenyl radicals is unexpected. The proportion of 5-isomer obtained in the methylation of 3-*n*-butylpyridine was similarly low (2%) (7), but partial rate factors are not available in this case. A similar, though lesser, deactivation of the meta position in toluene has been reported (F_m = 0.71 (21), F_m = 0.76 (22)) but the data from the reaction with triphenylbismuth give F_m = 1.6

Can. J. Chem. Downloaded from www.nrcresearchpress.com by 210.87.254.105 on 09/05/12
For personal use only.

(9). Again, using our data for the isomer ratio (24) and ${}^{C_6H_5CH_3}_{C_6H_6}K = 1.23$, one gets $F_m = 0.92$, which is close enough to 1 to be well within the experimental error. The still lower yield of 3-*n*-butyl-5-methylpyridine obtained in the methylation of 3-*n*-butylpyridine is readily explained on the basis that methyl radicals are more nucleophilic than phenyl radicals (20), so that a deactivation of the pyridine β-position is to be expected towards "nucleophilic" attack. The low value of F_5 found for the phenylation of 3-picoline might be due to a systematic experimental error and could be without real significance. This seems to be rather unlikely at the moment. Another possibility worth considering is that phenyl radicals have a slight nucleophilic character. All substituents activate the benzene nucleus towards attack by phenyl radicals, barring steric hindrance (25). This is probably due to the fact that substituents, whether electron attracting or donating, can delocalize a single electron in the σ-complexes obtained by attack at the ortho and para positions. When the substrate is pyridine, attack by the radical at the α- and γ-positions will eventually lead to σ-complexes in which one of the contributing structures has the odd electron on the nitrogen atom. No further delocalization is, however, possible. It has tentatively been suggested (2) that, if anything, the phenyl radical has to be slightly nucleophilic to account for the slightly greater reactivity of pyridine compared with that of benzene. Although this would explain the deactivation of C_5 in 3-picoline, it would leave other data unaccounted for, e.g. F_m for nitrobenzene is reported to be 0.86 (25). Since many of these values are very close to 1, however, the slight variations around this figure may, in some cases, be within the limits of experimental error and not be significant at all. In any event, no firm statement is warranted at this time.

The formation of the 3-phenyl derivative as the main product in the phenylation of 4-picoline is another example of a case in which the 3-isomer is the predominant one formed. Other examples are the *o*-nitrophenylation (1) and the *o*-bromophenylation (2) of pyridine.

ACKNOWLEDGMENTS

Financial support of this work by the National Research Council is gratefully acknowledged, as are the awards of a National Research Council Studentship (1963–1964) and a Shell Oil of Canada Fellowship (1964–1965) to M. S.

REFERENCES

1. R. A. ABRAMOVITCH and J. G. SAHA. J. Chem. Soc. 2175 (1964).
2. R. A. ABRAMOVITCH and M. SAHA. J. Chem. Soc. In press.
3. R. L. FRANK and J. V. CRAWFORD. Bull. Soc. Chim. France, 419 (1958).
4. D. H. HEY and J. M. WILLIAMS. J. Chem. Soc. 1678 (1950).
5. W. H. RIEGER. U.S. Patent No. 2,502,174 (March 28, 1950); Chem. Abstr. **44**, 5396 (1950).
6. R. A. ABRAMOVITCH and K. KENASCHUK. Unpublished results.
7. E. HARDEGGER and E. NIKLES. Helv. Chim. Acta, **40**, 242 (1954).
8. D. H. HEY, S. ORMAN, and G. H. WILLIAMS. J. Chem. Soc. 565 (1961).
9. D. H. HEY, D. A. SHINGLETON, and G. H. WILLIAMS. J. Chem. Soc. 5612 (1963).
10. C. P. FARLEY and E. L. ELIEL. J. Am. Chem. Soc. **78**, 3477 (1956).
11. D. E. PEARSON, W. W. HARGROVE, J. K. T. CHOW, and B. R. SUTHERS. J. Org. Chem. **26**, 789 (1961).
12. T. HAI and H. OGURA. J. Pharm. Soc. Japan, **75**, 292 (1955); Chem. Abstr. **50**, 1809 (1956).
13. G. F. HAWKIN and A. ROE. J. Org. Chem. **14**, 328 (1949).
14. A. E. TSCHITSCHIBABIN. Ber. **36**, 2711 (1903).
15. E. C. TAYLOR and H. J. CROVETTI. J. Org. Chem. **19**, 1633 (1954).
16. T. C. CHANG and C. KARR, JR. Anal. Chim. Acta, **21**, 474 (1959).
17. R. A. ABRAMOVITCH and C. S. GIAM. Can. J. Chem. **40**, 213 (1962).
18. C. OSUCH and R. LEVINE. J. Org. Chem. **22**, 939 (1957).
19. J. N. CHATTERJEE and K. PRASAD. Ber. **93**, 1744 (1960).
20. G. H. WILLIAMS. Homolytic aromatic substitution. The Pergamon Press, Ltd., London. 1960.
21. D. H. HEY, B. W. PENGILLY, and G. H. WILLIAMS. J. Chem. Soc. 1463 (1956).
22. R. A. ABRAMOVITCH and J. G. SAHA. Tetrahedron, **21**, 3297 (1965).
23. P. B. D. DE LA MARE and J. H. RIDD. Aromatic substitution: nitration and halogenation. Butterworth Scientific Publications, London. 1959. p. 88.
24. R. A. ABRAMOVITCH and F. F. GADALLAH. Unpublished results.
25. G. H. WILLIAMS. Chem. Ind. London, 1286 (1961).

Can. J. Chem. Downloaded from www.nrcresearchpress.com by 210.87.254.105 on 09/05/12
For personal use only.

Can. J. Chem. Downloaded from www.nrcresearchpress.com by 210.87.254.6 on 09/05/12
For personal use only.

SUBSTITUTION OF ACYCLIC SUGAR ACETALS

RATE OF PERCHLORIC ACID CATALYZED ACETOLYSIS OF 2,3,4,5,6-PENTA-*O*-ACETYL-D-GLUCOSE DIETHYL DITHIOACETAL AND 1,2,3,4,5,6-HEXA-*O*-ACETYL-D-GLUCOSE *S*-ETHYL MONOTHIOACETAL

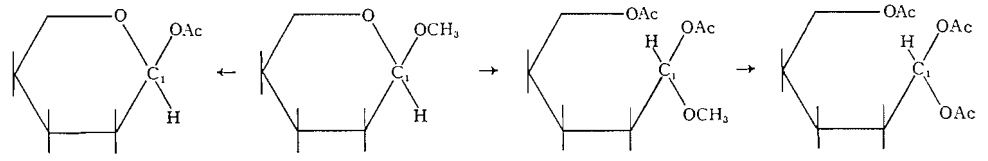
NORMAN H. KURIHARA AND EDGAR PAGE PAINTER
Department of Chemistry, University of California, Davis, California

Received February 2, 1966

ABSTRACT

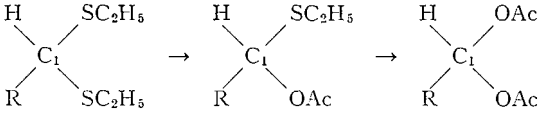
The rate constants for the perchloric acid catalyzed substitution of one ethylthio group of 2,3,4,5,6-penta-*O*-acetyl-D-glucose diethyl dithioacetal (V*a*) and the acetoxy group bonded to C_1 of 1,2,3,4,5,6-hexa-*O*-acetyl-D-glucose *S*-ethyl monothioacetal (VI*a*) have been measured when the substrates were dissolved in solutions of acetic acid and acetic anhydride. The rate-determining step is interpreted to be the dissociation of the substrate conjugate acid to give a carbonium–sulfonium cation. The rate constants indicate that acyclic sugar derivatives are substituted faster than cyclic (pyranose) derivatives, and that an acetoxy group is substituted faster than an ethylthio group.

Acetals dissolved in mixtures of acetic acid and acetic anhydride which contain a strong acid give substitution products which arise by cleaving either C—O bond of the substrate. The product has a C—OAc bond in place of the C—O bond cleaved. Thus methyl 2,3,4-tri-*O*-acetyl-β-arabinoside (I) gave both II and III when the acid was zinc chloride or 0.16% sulfuric; and gave the C_1 *gem*-diacetate (IV), a product which required cleavage of both the C_1—OCH_3 and C_1—O ring bonds of I, when the catalyst was 4% sulfuric acid (1).

[1] 

II I III IV

Poly-*O*-acetyl diethyl dithioacetals of the common monosaccharides behave in much the same way. Pirie (2) dissolved dithioacetals (V) in acetic anhydride which contained 1.8 *M* sulfuric acid, and isolated products (C_1 *gem*-diacetates (VII)) formed by substitution after cleavage of each ethylthio group. Similar to the observation of Montgomery *et al.* (1) when I was the substrate, acids at low concentration catalyze a fast substitution of one

[2] 

V VI VII

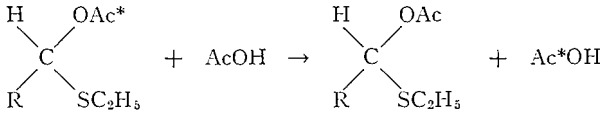
SC_2H_5 group of V to give VI (3). The products of a single substitution by an acetoxy group (II, III, and VI) are diastereomeric pairs (1, 3). Strong acids in acetic acid epimerize to give equilibrium mixtures. A C_1—OAc bond is broken in the process. *gem*-Diacetates are acetolysis products formed by cleavage of a C_1—OCH_3 bond (of III) or a C_1—SC_2H_5 bond (of VI). The rate of substitution of the monoacetals (III and VI) to give *gem*-diacetates is several powers of 10 slower than the rate of substitution of the acetals (I and

V) or the rate of epimerization of the monothioacetals. Since relative rates differ so greatly, the reaction can be quenched after the initial fast substitution of V, so that good yields of monothioacetals are obtained (3, 4). When dilute perchloric acid was the catalyst, we were unable to isolate a *gem*-diacetate which would show that the substitution VI → VII took place.

We cannot find in the literature rate constants for the substitution of dithioacetals or for the substitution (at C_1) of a single acyclic sugar derivative. We therefore measured concentration changes when 2,3,4,5,6-penta-*O*-acetyl-D-glucose diethyl dithioacetal (V*a*) was converted into 1,2,3,4,5,6-hexa-*O*-acetyl-D-glucose *S*-ethyl monothioacetal (VI*a*). To compare the rate of acetoxy substitution of an acyclic sugar with that of a pyranose,

[3] $$Va \rightarrow VIa\ (\alpha + \beta)$$

VI*a* has been prepared with ^{14}C-acetoxy at C_1 and reaction [4] followed by measuring the loss of ^{14}C from the substrate. The experimental conditions for reactions [3] and [4] were

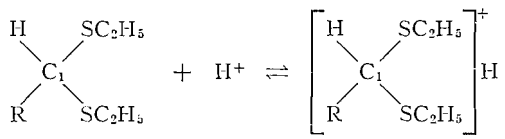
[4] 

α-VI*a* VI*a* (α + β)

those previously used to obtain data for a comparison of inversion and substitution rates of pyranose pentaacetates. Lemieux *et al.* (5) demonstrated, by measuring ^{14}C-acetoxy exchange of pentaacetates, that substitution rate constants may be much larger than inversion rate constants.

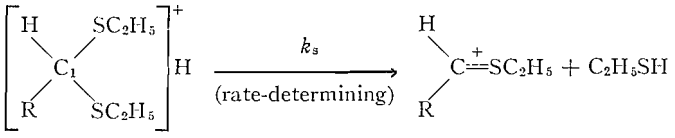
No studies comparable to those on the hydrolysis of oxygen acetals (6–9) have been reported on the hydrolysis of sulfur acetals. Hydrolysis rates of many α-halo thioethers (10–12) have, however, been measured. Bordwell *et al.* (12) gave convincing evidence that the rate-determining step for the solvolysis of α-halo thioethers is the formation of a sulfonium ion ($>C^{+}=SR$) by a unimolecular ionization analogous to the formation of the oxonium ion ($>C^{+}=OR$) which Newth and Phillips (13) proposed to explain the solvolysis of α-haloethers. Dissociation of an acetal conjugate acid to give the above oxonium ion is the rate-determining step when acetals are hydrolyzed by acids (6–9). Based on the similar behavior of the α-halo derivatives and the experimental observation that thioacetals are hydrolyzed under the same conditions as oxygen acetals, we believe that the rate-determining step for the substitution of our substrates is a first-order dissociation of the substrate conjugate acid to give a sulfonium ion.

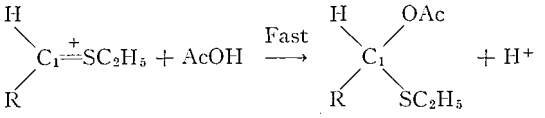
The conjugate acids of the dithioacetal (V) and monothioacetal (VI) give the same sulfonium ion by the mechanism proposed. The former will be used to illustrate the steps shown in eqs. [5] to [7] (R = $AcOCH_2$—$(CHOAc)_4$—). Both substrates have an acetoxy group in a position to give anchimeric assistance, but we will limit our example to the cationic species without neighboring acetoxy participation.

[5] 

V

Can. J. Chem. Downloaded from www.nrcresearchpress.com by 210.87.254.6 on 09/05/12
For personal use only.

[6] 

[7] 

VI ($\alpha + \beta$)

Since a new asymmetric carbon is formed by the substitution of the dithioacetal, the product is a pair of diastereomers. Both isomers (called α and β: the absolute configuration at C_1 is not known) were obtained from three sugar dithioacetals (3, 4). The diastereomer composition given by dithioacetals under conditions whereby the monothioacetal product is stable may be different from that given under conditions (such as the presence of perchloric acid) which give an equilibrium between the diastereomeric pairs. When, however, the substrate is the glucose dithiodiacetal, the product composition at epimeric equilibrium

$$\alpha\text{-VI} \underset{k_\beta}{\overset{k_\alpha}{\rightleftharpoons}} \beta\text{-VI}$$

is almost identical with the composition obtained by substitution under conditions whereby the substitution product is stable (3). The rate measurement on the glucose dithioacetal is then not complicated by consecutive reactions, so that $k_\alpha + k_\beta$ can be ignored.

RESULTS

Based on the steps given for the substitution we have described, the rate (V is now written as RSC_2H_5) is given by

$$\text{rate} = k[(RSC_2H_5)H^+]. \quad [8]$$

Substrate conjugate acid concentration is dependent upon the equilibrium

$$RSC_2H_5 + AcOH_2^+ \underset{}{\overset{K_1}{\rightleftharpoons}} (RSC_2H_5)H^+ + AcOH. \quad [9]$$

If we consider that perchloric acid is completely dissociated in acetic acid,[1] the concentration of substrate conjugate acid is given by eq. [11].

$$[HClO_4]_0 = [(RSC_2H_5)H^+] + [AcOH_2^+] \quad [10]$$

$$[(RSC_2H_5)H^+] = \frac{K_1[RSC_2H_5][HClO_4]_0}{[AcOH] + K_1[RSC_2H_5]} \quad [11]$$

By eq. [11] the rate constant will be first order with respect to perchloric acid. Provided that K_1 is small, the first-order constant will vary as 1/[AcOH]. The data in Table I show that the rate constant is first order with respect to acid, as observed when perchloric acid anomerized glucose pentaacetates (15) in mixtures of acetic acid and acetic anhydride.

[1]*Kolthoff and Bruckenstein (27) give experimental evidence that perchloric acid is half ionized (to ion pairs) in acetic acid, i.e.* $HClO_4 = AcOH_2^+ \cdots ClO_4^-$. *Including an additional term for undissociated perchloric acid and considering acetic acid as a dimer does not lead to a more useful equation than eq. [11].*

Can. J. Chem. Downloaded from www.nrcresearchpress.com by 210.87.254.6 on 09/05/12
For personal use only.

TABLE I

Rate constants for the conversion of 0.0806 *M* dithioacetal (V*a*) into monothioacetal (VI*a*) in acetic acid plus 4% acetic anhydride at 25°

$[HClO_4]$ (*M*)	$k_{obs.}$ (min^{-1})	$k_{obs.}/[HClO_4]$
4.76×10^{-2}	8.57×10^{-2}	1.80
3.26×10^{-2}	5.86×10^{-2}	1.80
1.09×10^{-2}	1.98×10^{-2}	1.81
8.30×10^{-3}	1.50×10^{-2}	1.81
4.15×10^{-3}	7.35×10^{-3}	1.77

We have no measure of the relative basic strength of the solvent acetic acid and the substrate. Unless K_1 (eq. [9]) is large, the concentration of $AcOH_2^+$ is greater than that of $(RSC_2H_5)H^+$ because the concentration of solvent molecules is in large excess. If the $K_1[RSC_2H_5]$ term in the denominator (eq. [11]) is small compared with the [AcOH] term, the rate constant should increase when the concentration of acetic acid is reduced by increasing the substrate concentration, and also when part of the acetic acid is replaced by an aprotic solvent. The solubility of the substrate (molecular weight = 496) is great enough to reduce the acetic acid concentration to one-half the concentration at dilute substrate concentrations. Concentrated solutions become so colored soon after the addition of perchloric acid that the reaction cannot be followed polarimetrically. The rate was measured at different concentrations of acetic acid by replacing part of the acetic acid with methylene chloride. Qualitatively, the rate constant (Table II) increased as required by eq. [11], provided that the $K_1[RSC_2H_5]$ term can be neglected.

TABLE II

Rate constants for the conversion of dithioacetal (V*a*) into 1-acetoxy monothioacetal (VI*a*) in mixtures of acetic acid and methylene chloride at 25°

AcOH (% by volume)	$[HClO_4]$ (*M*)	$k_{obs.}$ (min^{-1})	$k/[HClO_4]$ Observed	$k/[HClO_4]$ Calculated
100	0.037	0.036	0.97	—
82	0.037	0.043	1.17	1.18
71.5	0.037	0.049	1.33	1.36
61.8	0.037	0.061	1.64	1.56
52.3	0.037	0.072	1.94	1.85
42.8	0.037	0.102	2.75	2.26
33.4	0.0185	0.086	4.15	2.90
23.8	0.0185	0.15	8.1	4.06

NOTE: The substrate concentration was 0.31 *M*. The acetic acid contained a small amount of acetic anhydride to ensure the absence of water.

While exploring synthetic procedures for the preparation of poly-*O*-acetyl 1-acetoxy-*S*-ethyl monothioacetals of sugars from the diethyl dithioacetals, we observed that the substitution rate was faster in acetic acid – acetic anhydride (equal volume mixtures) than in acetic acid alone. To determine whether the rate was influenced by solvent composition in the same way as anomerization (15) of glucose pentaacetates (also a substitution process), we measured the rate in mixtures of the two solvents (Table III).

A plot of some of these rate constants and anomerization rate constants measured in the same solvents shows how much the relative magnitude of the rates is influenced by the ratio of acetic acid to acetic anhydride.

Can. J. Chem. Downloaded from www.nrcresearchpress.com by 210.87.254.6 on 09/05/12
For personal use only.

TABLE III

Rate constants for the conversion of 0.0806 *M* dithioacetal (V*a*) into 1-acetoxy monothioacetal (VI*a*) in acetic acid – acetic anhydride mixtures at 25°

Ac_2O (% by volume)	$[HClO_4]$ (*M*)	$k_{obs.}$ (min^{-1})	$k_{obs.}/[HClO_4]$
2	8.3×10^{-3}	8.03×10^{-3}	0.97
4	8.3×10^{-3}	1.50×10^{-2}	1.81
8	8.3×10^{-3}	3.36×10^{-2}	4.05
20	1.06×10^{-3}	1.17×10^{-2}	11.0
40	4.10×10^{-4}	2.5×10^{-2}	61.2
60	4.10×10^{-4}	9.35×10^{-2}	228
78	1.06×10^{-4}	9.9×10^{-2}	935
91	5.12×10^{-5}	6.0×10^{-2}	1 170
96	4.10×10^{-5}	2.95×10^{-2}	720
99.4	3.07×10^{-5}	5.9×10^{-3}	192
100	1.28×10^{-2}	5.2×10^{-2}	4.05

Rate constants (averages of two or more measurements) for the substitution of V*a* in acetic acid plus 4% acetic anhydride with 0.0083 *M* perchloric acid at each of three temperatures are as follows.

Temperature	15°	25°	35°
$k_{obs.}$ (min^{-1})	4.84×10^{-3}	1.50×10^{-2}	3.49×10^{-2}

These data give: $\Delta H^{+} = 16.6 \pm 1.3$ kcal/mole; $\Delta S^{\pm} = -10.5 \pm 4.4$ e.u.

First-order rate constants for the substitution of the acetoxy group of 1,2,3,4,5,6-hexa-*O*-acetyl-D-glucose 1-^{14}C-acetoxy-*S*-ethyl monothioacetal (reaction [4]) are given in Table IV.

TABLE IV

Rate constants for the acid-catalyzed acetoxy exchange of monothioacetal (α-VI*a*) in acetic acid and acetic anhydride at 25°

Ac_2O (% by volume)	[Substrate] (*M*)	$[HClO_4]$ (*M*)	$k_{obs.}$ (min^{-1})	$k_{obs.}/[HClO_4]$
4	0.093	2.04×10^{-4}	4.29×10^{-2}	210
50	0.081	2.40×10^{-4}	1.39×10^{-1}	503

DISCUSSION

Provided that the $K_1[RSC_2H_5]$ term in eq. [11] is small compared with the [AcOH] term, the calculated rate constants will be first order with respect to perchloric acid and will vary as 1/[AcOH]. The rate constant for the substitution of the dithioacetal is first order with respect to acid in all solvent mixtures tested. Replacing part of the acetic acid with the non-basic solvent methylene chloride produces an increase in the rate constant which follows eq. [11] until about one-half the solvent volume is non-basic solvent. At higher volume fractions of non-basic solvent, the rate constants become progressively larger than predicted by eq. [11]. The effect of methylene chloride on the rate constant is almost identical with that observed when the reaction is the substitution of the acetoxy group of glucose pentaacetate (15).

Replacing a given volume of acetic acid by acetic anhydride resulted in a greater rate increase than replacing the same volume by methylene chloride. This result is surprising. Even though $K_2 > K_1$, acetic anhydride must be a base in our solutions; if it is a very weak

[12] $$RSC_2H_5 + Ac_2OH^{+} \overset{K_2}{\rightleftharpoons} (RSC_2H_5)H^{+} + Ac_2O$$

Can. J. Chem. Downloaded from www.nrcresearchpress.com by 210.87.254.6 on 09/05/12
For personal use only.

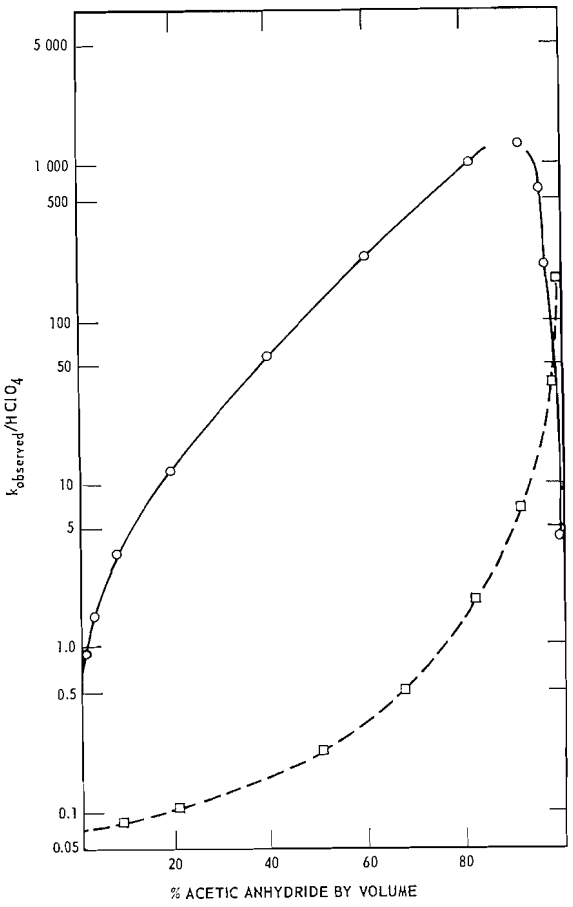


FIG. 1. Effect of solvent composition on the acetolysis rates of V*a* (○) and glucose pentaacetate (□).

base, eq. [11] should be obeyed. The rate constants calculated from the experimental data increased much faster when the solvent fraction of acetic anhydride increased than was predicted by eq. [11].

The data plotted in Fig. 1 show that the substitution of the dithioacetal increases much faster than the substitution of the pyranosyl acetoxy as the ratio of acetic anhydride to acetic acid increases. The rate constant increases faster than a measured acidity function (H_0) (16) in the solvent mixture, and the rate constant for dithioacetal substitution, unlike anomerization, reaches a maximum near 90% acetic anhydride. At this solvent composition, acetic acid (in acetic anhydride) is almost completely dissociated to monomer (16). Apparently the ratio of f substrate conjugate acid to $f^{\pm}$ becomes larger (at higher acetic anhydride concentration) when the substrate is the dithioacetal than when the substrate is glucose pentaacetate. One difference in the two reactions should be noted: acetoxy, presumably from acetic acid, is consumed when thioacetals are substituted but not when acetoxy substitutes for acetoxy in the anomerization step. With the solvent composition where the rate constant begins to decrease, acetic acid should not be limiting because the ratio of acetic acid to substrate is approximately 25.

Since the rate of acetoxy substitution of β-glucose pentaacetate is larger than the

Can. J. Chem. Downloaded from www.nrcresearchpress.com by 210.87.254.6 on 09/05/12
For personal use only.

anomerization rate (based on experimental data (5, 17) the factor is within the range 11.4 to 15.5), the differences between the rate constants for the two substrates plotted in Fig. 1 are larger than the differences between the substitution rate constants. At concentrations of acetic anhydride greater than 50%, the relative substitution rates of the two substrates are uncertain because ^{14}C-acetoxy exchange has not been measured for glucose pentaacetate in solutions which have acetic anhydride as the major component.

The available data do not permit an unqualified decision about which substrate, the one giving the oxonium ion or the one giving the sulfonium ion, will be substituted by the faster rate. Solvolysis of α-haloethers indicates that oxygen is the better electron donor: the oxonium cation is more stable than the sulfonium cation. Relative solvolysis rates (10, 11) measured in dioxane–water were: α-chloromethyl ether/α-chloro-*S*-methyl ether = 1–2 $\times$ 10^4. The difference in the methanolysis rate of α-haloethers with oxygen or sulfur in a pyranose ring (18) was much less: 2,3,4-tri-*O*-acetyl-α-xylopyranosyl bromide/2,3,4-tri-*O*-acetyl-α-xylothiopyranosyl bromide = 40.

A comparison of the rate constants for the acid-catalyzed substitution of oxygen acetals with those for acetals which have both sulfur and oxygen (—S—C(—)—O—) reveals data which places in doubt the relative donor capacity of sulfur and oxygen. Horton and Hutson (19) state that "1-thioglycosides are more resistant to acid hydrolysis than their glycoside analogs". Methyl and ethyl oxygen xylosides and glucosides were hydrolyzed only 2–3 times faster than their sulfur analogues (18, 20). When, however, sulfur was in the pyranose ring, the acetal was substituted faster than when oxygen was in the ring. Methyl β-xylothiopyranoside was hydrolyzed nearly 30 times faster (by acid catalysis) than methyl β-xylopyranoside (18). The Lewis acid aluminium chloride cleaved a C—O bond of dioxolanes but not a C—S bond of dithiolanes (21).

The data in Table V summarize the acid-catalyzed substitution rate constants of di- and mono-acetal substrates in solutions of acetic acid and acetic anhydride. The substrates are poly-*O*-acetyl derivatives of glucose (both acyclic and pyranose), and in all cases an acetoxy group from the solvent substitutes for one of the groups bonded to the anomeric carbon. To aid the comparison, some of the rate constants for substitution in the 1:1 solvent mixture have been recorded as the value estimated, had perchloric acid been the catalyst.[2]

The data in Table V show that, when measured in equal volumes of acetic acid and acetic anhydride, acetoxy bonded to C_1 was substituted 36 times faster than methoxyl when oxygen in a pyranose ring was the electron donor. Acetoxy was substituted only 4 times faster than ethylthio when sulfur bonded to C_1 in the acyclic substrate was the electron donor. When measured in acetic acid with 4% acetic anhydride, acetoxy was substituted 116 times faster than ethylthio. It is tempting to say that acetoxy is the better leaving group (as acetic acid), but the concentration of substrate conjugate acids [—Y—C(—)—X]H$^+$, where Y = O or S and X = CH_3O, C_2H_5S, or CH_3CO, is dependent upon equilibria we cannot measure.

The data (Table V) show that, when the leaving group was the same, acyclic derivatives were substituted faster (about 190 times) than pyranose derivatives. Rate differences

[2]*Both substitution and inversion rate constants have been calculated for the sulfuric acid catalyzed reactions of glucose pentaacetates when measured in the 1:1 solvent (17). Inversion rate constants for the same substrate have been calculated from measurements with both sulfuric and perchloric acids in mixtures of acetic acid and acetic anhydride (15). For the 1:1 mixture* $k_{obs.}/[HClO_4] = 3.5k_{obs.}/[H_2SO_4]$.

Can. J. Chem. Downloaded from www.nrcresearchpress.com by 210.87.254.6 on 09/05/12
For personal use only.

Can. J. Chem. Downloaded from www.nrcresearchpress.com by 210.87.254.6 on 09/05/12
For personal use only.

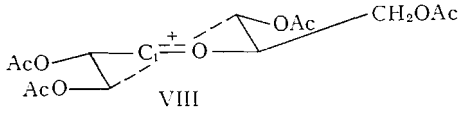
TABLE V

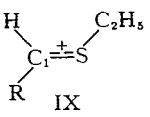
Acid-catalyzed substitution of di- and mono-acetals in acetic acid and acetic anhydride solutions

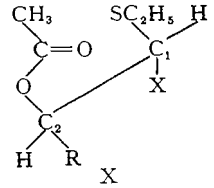
Substrate	Group substituted by acetoxy	% Ac_2O by volume	Catalyst	$k_{obs.}$ (min^{-1})/[acid] (M)		Reference
				Experimental	Calculated for $HClO_4$	
β-Glucose pentaacetate	$CH_3\overset{O}{\overset{\|}{C}}O$	0	H_2SO_4	0.109		17
2,3,4,5,6-Penta-*O*-acetyl-D-glucose diethyl dithioacetal	C_2H_5S	4	$HClO_4$	1.81	1.81	This work
1,2,3,4,5,6-hexa-*O*-acetyl-D-glucose *S*-ethyl monothioacetal	$CH_3\overset{O}{\overset{\|}{C}}O$	4	$HClO_4$	210	210	This work
β-Glucose pentaacetate	$CH_3\overset{O}{\overset{\|}{C}}O$	50	H_2SO_4	0.865	3.03*	17
β-Glucose pentaacetate	$CH_3\overset{O}{\overset{\|}{C}}O$	50	H_2SO_4	0.87	3.05*	5
β-Glucose pentaacetate	$CH_3\overset{O}{\overset{\|}{C}}O$	50	$HClO_4$	3.19	3.19†	
α-Glucose pentaacetate	$CH_3\overset{O}{\overset{\|}{C}}O$	50	H_2SO_4	0.0102	0.0353*	5
α-Glucose pentaacetate	$CH_3\overset{O}{\overset{\|}{C}}O$	50	H_2SO_4	0.0084	0.0294*	17
Methyl 2,3,4,6-tetra-*O*-acetyl-β-glucoside	CH_3O	50	H_2SO_4	0.024		22
Methyl 2,3,4,6-tetra-*O*-acetyl-α-glucoside	CH_3O	50	H_2SO_4	0.015		22
2,3,4,5,6-Penta-*O*-acetyl-D-glucose diethyl dithioacetal	C_2H_5S	50	$HClO_4$	130	130	This work
1,2,3,4,5,6-Hexa-*O*-acetal-D-glucose *S*-ethyl monothioacetal	$CH_3\overset{O}{\overset{\|}{C}}O$	50	$HClO_4$	563	563	This work

*$3.5k_{obs.}/[H_2SO_4]$.
†Anomerization rate constant for M $HClO_4$ × ^{14}C-acetoxy exchange/inversion rate in 1:1 solvent.

caused by the relative conjugate acid concentrations of these substrates seem to be unlikely. The differences are not those expected if the relative rates are solely dependent upon oxygen or sulfur as electron donors. We attribute the rate constant differences to steric factors in the step leading to the cationic intermediates VIII and IX. To attain the







planar carbonium ion VIII requires eclipsing of more bulky groups (which are staggered in the substrate conformer of lowest energy) than is required to form IX. The potential energy difference (ground state → carbonium ion) caused by steric factors must be less for our acyclic substrates than it is for pyranose substrates. The activation energy (E_a) is smaller when the reaction is the substitution of glucose dithioacetal by acetoxy than when the reaction is the substitution of glucose pentaacetate by acetoxy (23, 24). The activation energy for the hydrolysis of thioglycosides (20) is slightly larger than that for oxygen glycosides.

In case the substitution at C_1 is anchimerically assisted, a conformation with the acetoxy group at C_2 *trans* to the group substituted (X in X) is energetically favored when the substrate is an acyclic derivative (V or VI). When, however, the substrate is a 2,3,4,6-tetra-*O*-acetyl β-glucopyranose derivative, the conformer with the group at C_1 *trans*-diaxial to the acetoxy group at C_2 has all polar groups axial, so that this conformer is far less stable than the conformer (the major species) which has all polar groups equatorial.

EXPERIMENTAL

Acetic acid was purified by partial freezing, and displacing the melt with dry nitrogen. This step was repeated 3 times on the solid. Acetic anhydride (99.5% pure, as determined by the supplier) was purified in the same way to remove the small amount of acetic acid.

Perchloric acid in acetic acid or acetic anhydride was prepared by dissolving silver perchlorate (dried at 110 °C) in the solvent and by gassing the solution with dry hydrogen chloride to precipitate silver chloride. Excess hydrogen chloride was removed by a stream of dry nitrogen. The perchloric acid concentration was measured by titration with potassium acid phthalate (25).

The dithioacetal substrate was dissolved in solvents with the compositions listed in the tables, and the flasks containing the solutions were placed in a constant-temperature bath. When the bath temperature was reached, a measured volume of perchloric acid in acetic acid was added and the solution poured into jacketed polarimeter tubes held to within ±0.1° by circulating water from the constant-temperature bath. Rotation was measured until equilibrium was reached. Rate constants were calculated from the equation

$$k_{obs.} = \frac{2.3}{t} \log \frac{a_0 - a_\infty}{a_t - a_\infty}.$$

*1,2,3,4,5,6-Hexa-O-acetyl-*D*-glucose 1-*^{14}*C-Acetoxy-S-ethyl Monothioacetal*

The preparation of α-1,2,3,4,5,6-hexa-*O*-acetyl-D-glucose *S*-ethyl monothioacetal (VI*a*) from the dithioacetal (V*a*) by a modification of the method of Wolfrom *et al.* (14) has been described (3, 4).

The source of ^{14}C-acetoxy used to label VI*a* was acetic acid-1-^{14}C obtained by distilling the solvent from a solution of sodium acetate (0.41 g containing 1 mcurie of ^{14}C) in 100 cc of acetic acid plus 5% acetic anhydride.

The ^{14}C-acetoxy group was incorporated by an exchange reaction with unlabeled substrate (VI*a*). VI*a* (5 g) was dissolved in 20 cc of acetic acid-1-^{14}C which was 4% in acetic anhydride, perchloric acid was added to give a concentration of 2.44×10^{-4} *M*, and the reaction mixture was allowed to stand for 48 h at 24°. The reaction was then quenched by neutralizing the perchloric acid with anhydrous sodium acetate. The excess acetic acid was removed *in vacuo*, the resulting solid material was extracted with 100 cc of hot methylene chloride, and the solution was filtered to remove suspended sodium acetate. Removal of the solvent at reduced pressure gave a white crystalline residue. Two recrystallizations from 95% ethanol yielded 3.04 g, m.p. 103–104°, of labelled VI*a*.

Can. J. Chem. Downloaded from www.nrcresearchpress.com by 210.87.254.6 on 09/05/12
For personal use only.

Kinetics of Acetoxy Exchange

One gram of labeled VI*a* was dissolved in each of the solvents listed in Table IV. These solutions were placed in a constant-temperature bath kept at 25 ± 0.1°. Perchloric acid catalyst was added until the concentration given in Table IV was reached, and at 5 min intervals 5 cc aliquots were removed and quenched in 5 cc of acetic acid saturated with sodium acetate. The acetic acid in each sample was removed *in vacuo* and the resulting solid was extracted with 30 cc of chloroform. The chloroform extract was washed 3 times with 30 cc portions of water. Crystalline material was obtained after final removal of the chloroform at reduced pressure. This material was assayed by the technique of liquid scintillation counting in a Packard Tri-Carb liquid scintillation spectrometer.

The scintillation fluid consisted of 60 g of naphthalene, 4 g PPO (2,5-diphenyloxazole) (scintillation grade), 0.2 g POPOP (1,4-bis-2-(5-phenyloxazolyl)-benzene) (scintillation grade), 20 cc ethylene glycol, and 100 cc methanol made up to a volume of 1 l with dioxane (26). The samples assayed were each 0.1000 g and were dissolved in 20 cc of the scintillation fluid. Low-potassium vials were used. The experimental data for a run in acetic acid and first-order rate constants calculated at the time intervals listed are given in Table VI.

TABLE VI

Acid-catalyzed loss of ^{14}C activity from C_1-labeled VI in acetic acid

Time (min)	Activity (mcurie/mole)	$10^2 k_{obs.}$ (min^{-1})
0	0.1949	
5	0.1564	4.46
10	0.1274	4.31
15	0.1009	4.53
20	0.0850	4.22
∞	0.0022	

The first-order rate constants recorded in Table IV were estimated from the slope of the line obtained by plotting log $(\alpha_t - \alpha_\infty)$, where α = activity, against time.

To be confident that the exchange is specific for C_1—OAc, we dissolved glucose heptaacetate in a solution containing acetic acid-1-^{14}C and added perchloric acid (2×10^{-4} *M*). The count of the heptaacetate isolated was 64 c.p.m./0.1 g (count of blank was 41 c.p.m./0.1 g). A sample of *S*-ethyl monothioacetal treated in the same way gave 10 635 c.p.m./0.1 g.

REFERENCES

1. E. M. Montgomery, R. M. Hann, and C. S. Hudson. J. Am. Chem. Soc. **59**, 1124 (1937).
2. N. W. Pirie. Biochem. J. **30**, 374 (1936).
3. E. P. Painter. Tetrahedron, **21**, 1337 (1965).
4. E. P. Painter. Can. J. Chem. **42**, 2018 (1964).
5. R. A. Lemieux, C. Brice, and G. Huber. Can. J. Chem. **33**, 134 (1955).
6. J. M. O'Gorman and H. J. Lucas. J. Am. Chem. Soc. **72**, 5489 (1950).
7. C. K. Ingold. Structure and mechanism in organic chemistry. Cornell University Press, Ithaca, New York. 1953. p. 334.
8. M. M. Kreevoy and R. M. Taft, Jr. J. Am. Chem. Soc. **77**, 3146 (1955); **77**, 5590 (1955).
9. D. McIntyre and F. H. Long. J. Am. Chem. Soc. **76**, 3240 (1954).
10. H. Bohme. Ber. **74**, 248 (1941).
11. H. Bohme, H. Fischer, and R. Frank. Ann. **563**, 54 (1949).
12. F. H. Bordwell, G. D. Cooper, and H. Morita. J. Am. Chem. Soc. **79**, 376 (1957).
13. F. H. Newth and G. O. Phillips. J. Chem. Soc. 2896 (1953); 2904 (1953).
14. M. L. Wolfrom, D. I. Weisblat, and A. R. Hanzo. J. Am. Chem. Soc. **62**, 3246 (1940).
15. E. P. Painter. J. Am. Chem. Soc. **75**, 1137 (1953); **81**, 5696 (1959).
16. H. A. E. MacKenzie and E. R. S. Winter. Trans. Faraday Soc. **44**, 159 (1948).
17. W. A. Bonner. J. Am. Chem. Soc. **81**, 5171 (1959).
18. R. L. Whistler and T. VanEs. J. Org. Chem. **28**, 2303 (1963).
19. D. Horton and D. H. Hutson. Advan. Carbohydrate Chem. **18**, 141 (1963).
20. C. Bamford, B. Capon, and W. G. Overend. J. Chem. Soc. 5138 (1962).
21. B. E. Leggetter and R. K. Brown. Can. J. Chem. **41**, 2671 (1963).
22. R. U. Lemieux, W. P. Shyluk, and G. Huber. Can. J. Chem. **33**, 148 (1955).
23. W. A. Bonner. J. Am. Chem. Soc. **73**, 2659 (1951).
24. N. J. Chü. Ph.D. Thesis, University of Ottawa, Ottawa, Canada. 1959.
25. J. S. Fritz. G. Frederick Smith Chemical Co. Bulletin, Columbus, Ohio, 1952.
26. G. A. Bray. Anal. Biochem. **1**, 279 (1960).
27. I. M. Kolthoff and S. Bruckenstein. J. Am. Chem. Soc. **78**, 1 (1956).

Can. J. Chem. Downloaded from www.nrcresearchpress.com by 210.87.254.6 on 09/05/12
For personal use only.

Can. J. Chem. Downloaded from www.nrcresearchpress.com by 210.87.254.40 on 09/05/12
For personal use only.

ÉTUDE DE LA FLUORESCENCE DES DÉRIVÉS DE LA PHÉNOTHIAZINE

E. Adonai Martin
Faculté de Pharmacie, Université de Montréal, Montréal, Québec

Reçu le 9 mars 1966

RÉSUMÉ

Certains dérivés de la phénothiazine développent en milieu sulfurique, après dilution par le diméthylsulfoxyde, une fluorescence qui permet un dosage fluorométrique d'une très grande sensibilité variant, suivant les substances employées, de 0.01 à 0.06 μg/ml.

Les radicaux fixés sur le noyau influencent l'intensité de la fluorescence. En général, une substitution sur l'atome de carbone de ce dernier, par certains radicaux, produit un effet extinctif plus marqué que celle, par différentes chaînes, sur l'atome d'azote de la phénothiazine. Cette méthode pourrait servir à déterminer ces substances dans les liquides biologiques.

L'identification des dérivés de la phénothiazine par la fluorescence a déjà été signalée par Mellinger et Keeler (1). Ces derniers, en effet, identifient ces substances sur chromatogrammes, en utilisant de l'acide sulfurique à 40% comme révélateur. De plus, Udenfriend et ses collaborateurs soulignent que certains composés de la phénothiazine possèdent une légère fluorescence naturelle (2, 3).

Comme la spectrophotofluorométrie s'avère un procédé analytique de très grande précision dans l'étude des substances biologiques et médicamenteuses, nous avons entrepris à la lumière de ces références d'étudier la fluorescence des dérivés de la phénothiazine afin de mettre au point une méthode de dosage de ces composés, si utilisés en thérapeutique.

PARTIE EXPÉRIMENTALE

A partir d'une solution contenant 0.1 μg de substance à doser/ml, dissoute dans le dichlorométhane, on introduit respectivement dans cinq petits tubes à essai 0.3, 0.5, 1.0, 1.5 et 2.5 ml. Après avoir complété le volume à 2.5 ml avec le même solvant, on évapore à sec sous vide, on introduit 0.5 ml d'acide sulfurique concentré et on place les tubes dans un bain-marie à la température de 75 °C durant 15 min. Alors on ajoute 0.3 ml de diméthylsulfoxyde tout en refroidissant dans de l'eau glacée, et on porte de nouveau les tubes au bain-marie durant 15 min. Après refroidissement, on dilue par 0.2 ml d'eau bidistillée.

La solution de chaque spécimen présente alors, après 10 min de repos, une certaine fluorescence dont l'intensité est déterminée à l'aide du spectrophotofluoromètre Aminco. La gamme d'échantillons permet de repérer les longueurs d'onde optima et la limite du dosage, et d'élaborer une courbe de référence pour les déterminations subséquentes.

RÉSULTATS ET DISCUSSION

Tous les dérivés de la phénothiazine figurant aux Tableaux I et II, sauf la thiopropérazine (Majeptil), développent, en concentration suffisante, en présence d'acide sulfurique concentré, une réaction colorée dont l'intensité varie suivant les radicaux fixés sur le noyau. La limite de sensibilité de cette réaction colorimétrique est de l'ordre de 0.1 mg.

Toutes les substances étudiées développent, suivant les conditions énumérées plus haut, une fluorescence jaune verdâtre dont la longueur d'onde d'excitation et d'émission, pour l'obtention de l'intensité maximale de fluorescence, se situent respectivement à 350 et 500 mμ, sauf pour la trifluopérazine, la trifluopromazine et la fluphénazine, qui accusent un maximum d'intensité à 500 mμ lorsque l'excitation maximale s'effectue à 325 mμ. Le radical —CF_3 retenu en position R_2 par ces substances causerait cette variation. Une autre longueur d'onde d'excitation a été repérée, mais son intensité énergétique lumineuse semble altérer la structure chimique du dérivé obtenu, car l'intensité de la fluorescence diminue progressivement durant la lecture des déterminations. De façon

générale, les dérivés qui fournissent une coloration rouge ou violette en milieu sulfurique développent plus de fluorescence que ceux qui donnent une coloration jaune.

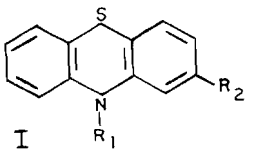
La limite de sensibilité de la fluorescence définie par Duggan et ses collaborateurs (4) s'établit à 10% de la déflection de l'échelle galvanométrique de l'appareil Aminco en utilisant une bande de $\frac{1}{16}$ de pouce; comme une bande de $\frac{1}{32}$ de pouce a été employée, nous l'avons fixée à 7%. Dans ces conditions, la limite de sensibilité varie, suivant les substances étudiées,[1] de 0.01 μg/ml à 0.06 μg/ml (Tableaux I et II, Figs. 1 et 2).

Si l'on compare les dérivés dont R_1 représente un radical aliphatique non cyclique (Tableau I et Fig. 1), on en déduit les constatations suivantes. Les deux substances de cette catégorie qui développent le maximum de fluorescence sont la promazine et la diéthazine dont R_1 désigne respectivement le radical $-CH_2CH_2CH_2N(CH_3)_2$ et $-CH_2CH_2N(C_2H_5)_2$, et R_2 désigne dans les deux cas l'atome d'hydrogène. La limite de fluorescence de ces composés s'établit à 0.02 μg/ml. Par contre, une substitution sur ces deux derniers radicaux par un groupement méthyle ou diméthylamino cause une diminution dans l'intensité de la fluorescence; en effet, la triméprazine, la prométhazine, la profénamine et l'aminopromazine illustrent bien ce fléchissement.

En outre, lorsque R_2 représente un radical ou un élément autre que l'hydrogène, l'intensité de la fluorescence diminue dans l'ordre $Cl < CF_3 < OCH_3 < SO_2N(CH_3)_2$.

TABLEAU I

Dérivés de la phénothiazine (chaîne acyclique)



I

Substances	R_1	R_2	Coloration de la solution sulfurique	Limite de sensibilité (μg/ml)*
Promazine (Sparine)	$CH_2CH_2CH_2N(CH_3)_2$	H	Rouge brun	0.02
Chlorpromazine (Largactil)	$CH_2CH_2CH_2N(CH_3)_2$	Cl	Pourpre	0.035
Trifluopromazine (Vesprin)	$CH_2CH_2CH_2N(CH_3)_2$	CF_3	Jaune rose	0.05
Triméprazine (Panectil)	$CH_2CHCH_2N(CH_3)_2$ CH_3	H	Rose foncé	0.025
Lévopromazine (Nozinan)	$CH_2CHCH_2N(CH_3)_2$ CH_3	OCH_3	Violacée	0.06
Aminopromazine (Lispamol)	$CH_2CHCH_2N(CH_3)_2$ CH_3NCH_3	H	Violacée	0.03
Diéthazine (Diparcol)	$CH_2CH_2N(C_2H_5)_2$	H	Rouge brun	0.02
Profénamine (Parsidol)	$CH_2CHN(C_2H_5)_2$ CH_3	H	Rouge brun	0.03
Prométhazine (Phénergan)	$CH_2CHN(CH_3)_2$ CH_3	H	Rouge	0.03
Le composé 8599 (R.P.)	$CH_2CHN(CH_3)_2$ CH_3	$SO_2N(CH_3)_2$	Rouge foncé	10

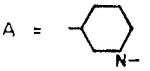
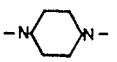
*Exprimés en chlorhydrate de la substance.

[1]*En raison de la faible fluorescence de la thiopropérazine et du composé 8599 (R.P.), nous avons cru bon de les éliminer.*

Can. J. Chem. Downloaded from www.nrcresearchpress.com by 210.87.254.40 on 09/05/12
For personal use only.

TABLEAU II

Dérivés de la phénothiazine (chaîne cyclique)

A =  B =  X = 

II III IV

Substances*	R_1	R_2	Coloration de la solution sulfurique	Limite de sensibilité (μg/ml)†
Mépazine (Pacatal)	CH_2ACH_3‡	H	Rouge brun	0.02
Thioridazine (Mellaril)	CH_2BCH_3	SCH_3	Bleue	0.03
Prochlorpérazine (Stémétil)	$CH_2CH_2CH_2XCH_3$	Cl	Rouge	0.01
Thiopropérazine (Majeptil)	$CH_2CH_2CH_2XCH_3 \cdot 2CH_3SO_3H$	$SO_2N(CH_3)_2$	Incolore	8.0
Trifluopérazine (Stélazine)	$CH_2CH_2CH_2XCH_3$	CF_3	Jaune	0.03
Perphénazine (Trilafon)	$CH_2CH_2CH_2XCH_2CH_2OH$	Cl	Rouge	0.02
Fluphénazine (Prolixin)	$CH_3CH_2CH_2XCH_2CH_2OH$	CF_3	Jaune	0.03

*Voir Tableau I, formule I.
†Exprimés en chlorhydrate de la substance.
‡A, B et X représentent des noyaux cycliques.

Les dérivés dont R_1 désigne un radical renfermant une chaîne aliphatique (Tableau II et Fig. 2) soudée à un noyau pipéridyle (II et III) ou pipérazinyle (IV) développent aussi de la fluorescence, et le noyau hétérocyclique ne semble pas influencer de façon appréciable son intensité. La prochlorpérazine produit, dans les conditions mentionnées plus haut, la substance la plus fluorescente de tous les composés étudiés. En effet, elle permet de détecter 0.01 μg/ml. Cependant, la substitution du radical $-CH_2CH_2OH$ au groupement CH_3 terminal soudé au noyau hétérocyclique de la prochlorpérazine donne un dérivé moins fluorescent, la perphénazine.

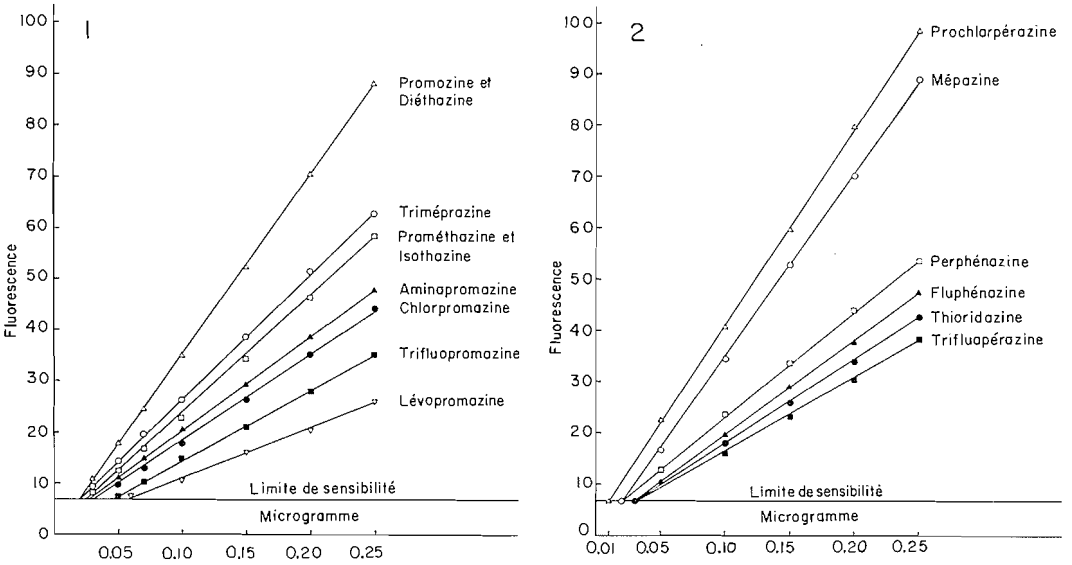


FIG. 1. Fluorescence des dérivés de la phénothiazine dont l'atome d'azote du noyau porte une chaîne aliphatique saturée.

FIG. 2. Fluorescence des dérivés de la phénothiazine dont l'atome d'azote du noyau porte une chaîne aliphatique saturée contenant un radical hétérocyclique.

Can. J. Chem. Downloaded from www.nrcresearchpress.com by 210.87.254.40 on 09/05/12
For personal use only.

L'examen du Tableau II révèle, comme précédemment, que la substitution de l'atome d'hydrogène en position R_2 (I) par un autre élément ou un radical produit un effet d'extinction beaucoup plus marqué que celle effectuée, par différentes chaînes, sur l'atome d'azote du noyau de la phénothiazine. Quant au radical $—SO_2N(CH_3)_2$, son effet extinctif sur la fluorescence s'avère tellement intense qu'il relègue au second plan, le dosage fluorométrique des composés qui le portent. De plus, le radical $—SCH_3$ confère à la thioridazine une fluorescence fugitive qui oblige à effectuer le dosage durant les quinze minutes qui suivent la dilution aqueuse.

Ces expériences ne permettent pas de discuter la structure chimique du composé fluorescent obtenu. Cependant, l'oxydation du soufre du noyau de la phénothiazine ne semble pas donner une substance fluorescente. En effet, l'oxomémazine (R.P.) (dioxo-9,9 (diméthylamino-3 méthyl-2 propyl)-10 phénothiazine), qui ne diffère de la triméprazine (Tableau I) que par deux atomes d'oxygène, fixés sur le soufre du noyau, ne développe aucune fluorescence dans les conditions énumérées plus haut, ni dans les solvants ou réactifs utilisés. Il faut donc conclure que le composé fluorescent répond à une formule chimique différente.

La dilution par l'alcool et l'addition d'une quantité d'eau ou de diméthylsulfoxyde supérieure à celle qui a été mentionnée diminuent la fluorescence. De plus, l'exposition prolongée de 2 ou 3 min de la cellule aux rayons de la source lumineuse de l'appareil peut entraîner, dans certains cas, une diminution de la fluorescence.

Pour vérifier la précision de cette méthode de dosage, cinq échantillons de 5 ml de sérum additionnés de 100 μg de chlorpromazine ont été traités suivant la technique d'extraction élaborée par la compagnie Poulenc. La méthode nous a permis de retrouver en moyenne 91% de la substance ajoutée au sérum ; ce qui prouve que ce procédé analytique pourrait servir à déterminer ces substances médicamenteuses dans les liquides biologiques.

Ces résultats démontrent avec évidence que ces composés de la phénothiazine, à l'état pur, sauf le composé 8599 (R.P.) et la thiopropérazine, peuvent être dosés par méthode fluorométrique avec une sensibilité variant, suivant les substances, de 0.01 à 0.06 μg/ml.

REMERCIEMENTS

Ce travail a été réalisé grâce à un octroi du Conseil National de Recherches du Canada, que nous remercions sincèrement.

L'auteur désire exprimer sa reconnaissance aux compagnies pharmaceutiques suivantes, qui ont fourni gracieusement les substances utilisées dans ces expériences: Sandoz, Schering, Smith Kline & French, Squibb, Warner-Chilcott, Wyeth et Poulenc.

BIBLIOGRAPHIE

1. T. J. Mellinger et C. E. Keeler. J. Pharm. Sci. **51**, 1169 (1962).
2. G. Udenfriend, D. E. Duggan, B. M. Vasta et B. B. Brodie. J. Pharmacol. Exptl. Therap. **120**, 26 (1957).
3. S. Udenfriend. Fluorescence assay in biology and medicine. Academic Press, Inc., New York. 1962. p. 437.
4. D. E. Duggan, R. L. Beromeen, B. B. Brodie et S. Udenfriend. Arch. Biochem. Biophys. **68**, 1 (1957).

Can. J. Chem. Downloaded from www.nrcresearchpress.com by 210.87.254.40 on 09/05/12
For personal use only.

Can. J. Chem. Downloaded from www.nrcresearchpress.com by 210.87.254.6 on 09/05/12
For personal use only.

PREPARATION AND STEREOCHEMISTRY OF 1,2-*O*-(2′-HYDROXYETHYLIDENE)- AND 1,2-*O*-(HYDROXYISOPROPYLIDENE)-GLYCEROLS[1]

P. A. J. GORIN AND T. ISHIKAWA[2]

Prairie Regional Laboratory, National Research Council of Canada, Saskatoon, Saskatchewan

Received February 17, 1966

ABSTRACT

The *cis*- and *trans*-isomers of 1,2-*O*-(2′-hydroxyethylidene)-glycerol (I and II) and 1,2-*O*-(hydroxyisopropylidene)-glycerol (V and VI) were prepared and their configurations assigned by stereospecific chemical synthesis. Equilibration of 1,2-*O*-(2′-*cis*-hydroxyethylidene)-L-glycerol (I) in acidified chloroform gave mainly 1,3-*O*-(2′-*cis*-hydroxyethylidene)-glycerol (III). In the 1,2-*O*-(hydroxyisopropylidene)-glycerol series, equilibration data and infrared absorption studies showed that hydrogen bonding of the *O*-(hydroxyisopropylidene) hydroxyl group was more pronounced in the *cis*-isomers.

Starch polyalcohol, prepared by oxidation of starch with sodium periodate followed by reduction of the polyaldehyde with sodium borohydride, was treated with aqueous acid at 100°. An apparently stereospecific acetal migration resulted which gave 1,2-*O*-(2′-*cis*-hydroxyethylidene)-DL-erythritol (1). This compound has been characterized by oxidation with periodic acid followed by reduction with sodium borohydride to give 1,2-*O*-(2′-*cis*-hydroxyethylidene)-DL-glycerol (I), which has a nuclear magnetic resonance (n.m.r.) spectrum identical with that of the L-isomer (2) prepared from 1,6-anhydro-D-glucopyranose (1). Since acetal isomerization may have taken place during the above reactions, it was necessary to obtain the n.m.r. spectrum of 1,2-*O*-(2′-*trans*-hydroxyethylidene)-glycerol (II) for comparison purposes. This compound was prepared, as a minor product, by treating D′-methoxyhydroxymethyldiethylene glycol (3) at 100° in an aqueous solution adjusted to pH 2. The main product was shown by thin-layer chromatography (t.l.c.) on silica gel to be faster moving 1,2-*O*-(2′-*cis*-hydroxyethylidene)-glycerol (DL-isomer of I, 4.0% yield), and the mixture was fractionated by cellulose column chromatography to obtain the required slower moving minor component. The first fraction was characterized by conversion into 1,2-*O*-(2′-*cis*-hydroxyethylidene)-DL-glycerol bis-*p*-nitrobenzoate. The second fraction (DL-isomer of II, 1.3% yield) consisted of the *trans*-isomer contaminated with an unidentified material. Methylation of a small portion followed by acid hydrolysis gave a mixture shown to consist of 1- and 2-*O*-methyl glycerol in a 4:1 ratio by gas–liquid chromatography (g.l.c.) of their acetates. The contaminant, probably 1,3-*O*-(2′-hydroxyethylidene)-glycerol, could be removed by fractional crystallization of the derived *p*-nitrobenzoates, and the resulting *trans*-bis-*p*-nitrobenzoate was clearly distinguishable from the *cis*-isomer by its n.m.r. spectrum. The 1,2-*O*-(2′-hydroxyethylidene)-DL-glycerols obtained on saponification were similarly distinguishable.

An alternative synthesis of 1,2-*O*-(2′-*trans*-hydroxyethylidene)-glycerol (II) was attempted by isomerization of 1,2-*O*-(2′-*cis*-hydroxyethylidene)-L-glycerol (I) in chloroform containing hydrogen chloride. Equilibration was readily followed by n.m.r. spectroscopy, since the C-1′ proton signals of the four isomeric *O*-(2′-hydroxyethylidene)-glycerol components in chloroform were distinguishable. At equilibrium the mixture contained, presumably in the DL-form, 1,2-*O*-(2′-*trans*-hydroxyethylidene)-glycerol (12%; triplet,

[1]*Issued as N.R.C. No. 9043.*
[2]*National Research Council Postdoctorate Fellow, 1964–1966.*

4.78 τ) and its *cis*-isomer (26%; triplet, 4.97 τ). Also formed were two 1,3-*O*-(2′-hydroxyethylidene)-glycerols, one in 55% yield (triplet, 5.68 τ) and the other in 7% yield (triplet, 6.05 τ). Cellulose column chromatography of the mixture only partially purified the major 1,3-*O*-isomer; a pure sample was obtained after fractional crystallization of its relatively insoluble bis-*p*-nitrobenzoate. Methylation followed by hydrolysis gave 2-*O*-methyl glycerol, as shown by g.l.c. of its diacetate.

No acetal migration or change in stereochemistry was observed on treatment of 1,2-*O*-(2′-*cis*-hydroxyethylidene)-L-glycerol at 100° in an aqueous solution at pH 2.

The isolated 1,3-*O*-(2′-hydroxyethylidene)-glycerol (III) should have the *cis*-configuration according to the results of Baggett and his co-workers (4), who showed that 1,3-*O*-*cis*-benzylidene glycerol was more stable than its *trans*-isomer in hot isopropanol and acetone containing aluminium isopropoxide. The stability of the *cis*-isomer was attributed to the observed hydrogen bonding, which was more general in the *cis*-isomer than in the *trans*-isomer. Similarly, the 1,3-*O*-*cis*-isomer is more stable than its *trans*-isomer in acidified chloroform. Nuclear magnetic resonance spectral evidence showed that equilibration of benzylidene glycerols gave the 1,3-*O*-*cis*-isomer (44%), the 1,3-*O*-*trans*-isomer (15%), and two 1,2-*O*-isomers in equal proportions (42% total). III produced infrared absorption (chloroform) at 3 600 cm^{-1}, which was consistent with the intramolecularly hydrogen bonded hydroxyl groups as depicted.

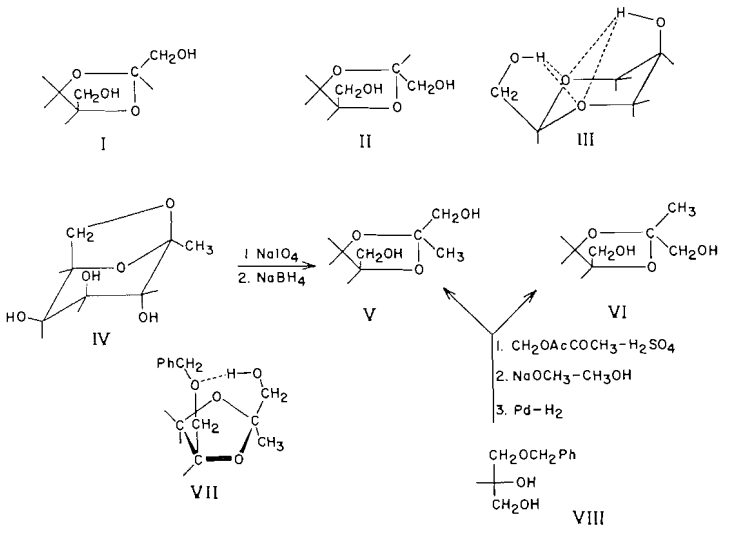
The equilibrium composition of *O*-(2′-hydroxyethylidene)-glycerols is in agreement with previous work carried out on the relative stabilities of cyclic glycerol acetals. There was no marked preference for the formation of either the five- or six-membered *O*-(2′-hydroxyethylidene) acetals, a result similar to the reaction of glycerol with trimethylacetaldehyde, which gave six- and five-membered acetals in a 2:3 ratio (5). Similarly, both five- and six-membered *O*-methylene glycerols were formed on condensation of formaldehyde with glycerol (6). In the five-membered series, Barker and his co-workers (7) have assigned configurations to isomeric 2,4-dimethyl-1,3-dioxolanes by comparing their boiling points, refractive indices, and stabilities, and by correlating these physical properties with those of known *cis*- and *trans*-1,3-dimethylcyclopentanes (8). *cis*-2,4-Dimethyl-1,3-dioxolane is more stable than the *trans*-isomer since they were formed in a ratio of 13:7, thus agreeing with the relative stabilities of 1,2-*O*-(2′-*cis*-hydroxyethylidene)-glycerol and its *trans*-isomer.

The preceding chemical proof of the stereochemistry of 1,2-*O*-(2′-hydroxyethylidene)-acetals of glycerol could be extended to the 1,2-*O*-(hydroxyisopropylidene)-ketals of glycerol (V and VI). These compounds have been obtained by saponification of the mixed 1,2-*O*-(acetoxyisopropylidene)-DL-glycerols, which Evlampiev prepared by condensation of acetoxyacetone with glycerol in the presence of acid (9). 1,2-*O*-(Hydroxyisopropylidene)-DL-glycerols were separated by cellulose chromatography and were converted into crystalline bis-*p*-nitrobenzoates.

The key compound in stereochemical assignments in the five-membered *O*-hydroxyisopropylidene series was 2,7-anhydro-1-deoxy-β-D-galactoheptulopyranose (IV), prepared by pyrolysis of 1-deoxy-D-galactoheptulose under reduced pressure. The anhydride, isolated as crystals in 0.5% yield by cellulose column chromatography, had carbon and hydrogen contents and a molecular weight which corresponded to the molecular formula $C_7H_{12}O_4$, and consumed 2 moles of sodium periodate with concomitant production of 1 mole of acid. On a preparative scale, the resulting dialdehyde was reduced with sodium borohydride to 1,2-*O*-(*cis*-hydroxyisopropylidene)-L-glycerol (V).

The two optically active, stereoisomeric 1,2-*O*-(hydroxyisopropylidene)-L-glycerols (V

Can. J. Chem. Downloaded from www.nrcresearchpress.com by 210.87.254.6 on 09/05/12
For personal use only.



and VI) were prepared by condensation of acetoxyacetone and 1-*O*-benzyl-D-glycerol (VIII) with sulfuric acid as catalyst followed by saponification of the resulting mixture with sodium methoxide in methanol. 3-*O*-Benzyl-1,2-*O*-(*cis*-hydroxyisopropylidene)-L-glycerol and its *trans*-isomer were present in equal amounts, and had R_F 0.70 and 0.49, respectively, on silica gel t.l.c. The isomers were separated by silicic acid column chromatography. Hydrogenolysis of the isomers in the presence of palladium on barium sulfate gave syrupy 1,2-*O*-(hydroxyisopropylidene)-L-glycerols, which could be converted into their crystalline bis-*p*-nitrobenzoates. The bis-*p*-nitrobenzoate arising from the 3-*O*-benzyl-1,2-*O*-(hydroxyisopropylidene)-L-glycerol, with R_F 0.70, was identical with that prepared from 2,7-anhydro-1-deoxy-β-D-galactoheptulopyranose.

The n.m.r. spectra of 1,2-*O*-(*cis*-hydroxyisopropylidene)-L-glycerol (V) and its *trans*-isomer (VI) in deuterium oxide were virtually identical in that part of the spectrum attributable to the protons on C-1, C-2, and C-3, thus indicating conformational similarity. In chloroform, however, this part of the n.m.r. spectra was readily distinguishable, thus suggesting that the *cis*- and *trans*-stereoisomers are conformationally different in this solvent, likely because of hydrogen bonding. However, infrared studies on hydrogen bonding were hindered in this series, since assignment of OH absorptions to either of the two hydroxyl groups was difficult. Instead, the OH absorptions of 3-*O*-benzyl-1,2-*O*-(hydroxyisopropylidene)-L-glycerols were measured in 0.005 *M* solutions. The spectrum of the *trans*-isomer in carbon tetrachloride showed absorption at 3 625 cm^{-1}, a frequency shift ($\Delta\nu$) of 17 cm^{-1} from the value of 3 642 cm^{-1} expected for unbonded primary hydroxyl groups (10). The spectrum of the *cis*-isomer showed, in addition to a band at 3 616 cm^{-1} ($\Delta\nu$ 26 cm^{-1}), absorption at 3 480 cm^{-1} ($\Delta\nu$ 162 cm^{-1}), thus indicating strong hydrogen bonding. Similarly, the spectrum of the *trans*-isomer in chloroform solution showed absorption at 3 620 cm^{-1}, and that of the *cis*-isomer showed bands at 3 620 cm^{-1} and 3 480 cm^{-1}. The large spectral shift of the *cis*-isomer is comparable to those of long-range hydrogen bonds which occur in 1,4-diols ($\Delta\nu$ 100–200 cm^{-1}) (11) and which are caused by bonding between the two hydroxyl groups. In the *O*-*cis*-hydroxyisopropylidene derivative the hydroxyl group can form a bond with the oxygen atom of the *O*-benzyl group (VII), an association which is not sterically allowed in the *trans*-isomer. The weaker hydrogen bonds

Can. J. Chem. Downloaded from www.nrcresearchpress.com by 210.87.254.6 on 09/05/12
For personal use only.

appear to be formed by chelation between the hydroxyl groups and the ring oxygens of the 1,3-dioxolane rings.

Hydrogen bonding appears to influence the equilibrium position of isomeric 3-*O*-benzyl-1,2-*O*-(hydroxyisopropylidene)-glycerols in chloroform containing hydrogen chloride. The ratio of *cis*- to *trans*-isomer, as determined by n.m.r. spectroscopy, was 57:43, whereas treatment of 1-*O*-benzyl-D-glycerol with acetoxyacetone in the presence of sulfuric acid gave equal amounts of 1,2-*O*-(*cis*-acetoxyisopropylidene)-3-*O*-benzyl-L-glycerol and its *trans*-isomer. Similar considerations probably govern the equilibration of 1,2-*O*-(hydroxyisopropylidene)-L-glycerols, which favors the *cis*- over the *trans*-isomer in the surprisingly high ratio of 2:1.

The n.m.r. spectra of various five-membered *O*-2′-hydroxyethylidene and *O*-hydroxyisopropylidene derivatives of glycerol have been examined. In general, protons in groups *cis* to the C-3 hydroxymethyl group gave signals at lower field than the corresponding proton(s) in the *trans*-position. This property is also true of *O*-ethylidene derivatives of glycerol and 1-*O*-benzyl-D-glycerol after assignment of signals to the *cis*- and *trans*-isomers. Brimacombe and his co-workers (12) have predicted that the reaction of acetaldehyde with 1-*O*-benzyl-D-glycerol would give mainly 3-*O*-benzyl-1,2-*O*-*cis*-ethylidene-L-glycerol and a smaller proportion of the *trans*-isomer, assignments which were later confirmed chemically by Triggle and Belleau (2). The n.m.r. spectrum of the 1,2-*O*-*cis*,*trans*-ethylidene-D-glycerols formed on hydrogenolysis contains predominant signals (63:37 ratio) at low field which should correspond to the *cis*-isomer.

EXPERIMENTAL

Specific rotations were measured at 25°. Nuclear magnetic resonance spectra were obtained on a Varian A-100 high-resolution spectrometer with tetramethylsilane as standard.

Preparation of 1,2-O-(2′-trans-Hydroxyethylidene)-DL-glycerol and its cis-Isomer from D′-Methoxyhydroxymethyldiethylene Glycol

An aqueous solution (100 ml) of D′-methoxyhydroxymethyldiethylene glycol prepared by successive treatments of methyl α-D-glucopyranoside with periodate and sodium borohydride (15 g (3)) was adjusted to pH 2 with hydrochloric acid and heated at 100° for 30 min. After neutralization (Ag_2CO_3) and filtration the solution was extracted continuously with chloroform for 3 days. The extract (2.1 g) was examined by t.l.c. on silica gel G (solvent: chloroform–methanol (9:1 v/v); spray: 50% sulfuric acid), and a spot with R_F 0.41 corresponding to 1,2-*O*-(2′-*cis*-hydroxyethylidene)-glycerol and a minor spot with R_F 0.33 were detected. The mixture was fractionated by cellulose column chromatography with benzene–ethanol–water (1000:50:1 v/v/v) as eluent. The component with R_F 0.41 (0.48 g) was eluted initially followed by a mixed fraction (0.10 g) and the component with R_F 0.33 (0.16 g). The initial fraction was converted into 1,2-*O*-(2′-*cis*-hydroxyethylidene)-DL-glycerol bis-*p*-nitrobenzoate, which had m.p. 97–98° and $[\alpha]_D$ 0° (*c*, 1.0 in $CHCl_3$) after two recrystallizations from ethyl acetate – *n*-hexane. Its n.m.r. spectrum was identical with that of an authentic specimen (1).

Anal. Calcd. for $C_{19}H_{16}O_{10}N_2$: C, 52.78; H, 3.73. Found: C, 52.7; H, 3.75.

A portion of the fraction with R_F 0.33 (10 mg) was methylated by refluxing it for 3 days in methyl iodide (5 ml) containing silver oxide. The product was hydrolyzed for 1 h in refluxing methanol (5 ml) containing water (1 ml) and *N* hydrochloric acid (0.1 ml). The solution was neutralized (Ag_2CO_3), filtered, and evaporated to a syrup which was acetylated at 100° in acetic anhydride containing sodium acetate. The reagent was destroyed in ice-cold aqueous sodium bicarbonate, and the resulting *O*-methyl glycerol diacetates were extracted with chloroform. These were examined by g.l.c., using 2% silicone nitrile gum XE-60 on Chromosorb W (80–100 mesh) in a 4 ft × ¼ inch (outside diameter) copper tube at 100°, helium (30 p.s.i.) as the carrier gas, and a g.l.c. apparatus of conventional design with thermal conductivity detectors. The product contained 1-*O*-methyl glycerol diacetate (retention time 9.7 min (80%)) and 2-*O*-methyl glycerol diacetate (retention time 12.0 min (20%)). A derivative of the major component of the fraction with R_F 0.33 (0.10 g) was obtained by conversion into 1,2-*O*-(2′-*trans*-hydroxyethylidene)-DL-glycerol bis-*p*-nitrobenzoate (96 mg), which had m.p. 116–117° and $[\alpha]_D$ 0° (*c*, 1.0 in $CHCl_3$) after two recrystallizations from ethyl acetate – *n*-hexane.

Anal. Calcd. for $C_{19}H_{16}O_{10}N_2$: C, 52.78; H, 3.73. Found: C, 52.9; H, 3.85.

Methylation of the deesterified product followed by hydrolysis gave 1-*O*-methyl glycerol, as shown by g.l.c. of its diacetate.

Can. J. Chem. Downloaded from www.nrcresearchpress.com by 210.87.254.6 on 09/05/12
For personal use only.

The bis-*p*-nitrobenzoates of 1,2-*O*-(2′-*trans*-hydroxyethylidene)-DL-glycerol and its *cis*-isomer were examined by n.m.r. spectroscopy in chloroform. Each specimen contained a C-1′ proton triplet (*cis*-isomer: 4.72 τ, J 2.0 c.p.s.; *trans*-isomer: 4.55 τ, J 1.8 c.p.s.) and a C-2′ CH_2 doublet (*cis*-isomer: 5.54 τ; *trans*-isomer: 5.58 τ). The derived 1,2-*O*-(2′-*cis*-hydroxyethylidene)-glycerol and its *trans*-isomer in D_2O gave C-1′ proton triplets (*cis*-isomer: 4.51 τ, J 1.7 c.p.s.; *trans*-isomer: 4.44 τ, J 1.7 c.p.s.) and C-2′ CH_2 doublets (*cis*-isomer: 5.86 τ; *trans*-isomer: 5.93 τ). All τ values for multiple signals refer to the average τ value.

Equilibration of O-(2′-Hydroxyethylidene)-glycerols

A solution of 1,2-*O*-(2′-*cis*-hydroxyethylidene)-L-glycerol (50 mg) in chloroform (1 ml), adjusted to 0.1 *N* with hydrogen chloride, was examined at intervals by n.m.r. spectroscopy. In addition to the triplet corresponding to starting material, three new triplets appeared, one of them corresponding to 1,2-*O*-(2′-*trans*-hydroxyethylidene)-glycerol. The equilibration was virtually complete after 4 h, and at 24 h the mixture contained the *cis*-1,2-isomer (26%; 4.97 τ, J 2.5 c.p.s.), the *trans*-1,2-isomer (12%; 4.78 τ, J 3.5 c.p.s.), and two other isomers (55%; 5.68 τ, J 3.6 c.p.s., and 7%; 6.05 τ, J 4.0 c.p.s.).

The equilibration products obtained from 0.60 g of the *cis*-1,2-*O*-isomer were chromatographed on a cellulose column with benzene–ethanol–water (1000:50:1 v/v/v) as eluent, and the separation was followed by t.l.c. on silica gel G. The first fraction contained the *cis*-1,2-*O*-isomer as the main component, and the second fraction contained every component except the *cis*-1,2-*O*-isomer. The first fraction was converted into mixed bis-*p*-nitrobenzoates which, after three recrystallizations from ethyl acetate, gave 1,3-*O*-(2′-hydroxyethylidene)-glycerol bis-*p*-nitrobenzoate, with m.p. 179–181° and $[\alpha]_D$ 0° (*c*, 1.0 in $CHCl_3$).

Anal. Calcd. for $C_{19}H_{16}O_{10}N_2$: C, 52.78; H, 3.73. Found: C, 52.7; H, 3.7.

(The infrared spectrum of a 0.005 *M* solution of the derived diol in chloroform showed absorption at 3 600 cm^{-1}. Under these conditions the infrared spectrum of cyclohexanol showed absorption at 3 630 cm^{-1}, and that of *n*-butyl alcohol showed absorption at 3 642 cm^{-1}.) Its n.m.r. spectrum in $CHCl_3$ contained a C-1′ proton triplet (4.96 τ, J 3.2 c.p.s.), a C-2′ CH_2 doublet (5.56 τ), and complex signals at 5.09 τ corresponding to the C-2 proton. The free diol in D_2O gave a triplet (4.78 τ, J 2.1 c.p.s.) coupled to a doublet (5.99 τ). Methylation of the free diol followed by hydrolysis gave 2-*O*-methyl glycerol, as shown by g.l.c. of its diacetate.

Equilibration of O-Benzylidene Glycerols

Equilibration of 1,3-*O*-*cis*-benzylidene glycerol under conditions similar to those described above gave four isomers. Nuclear magnetic resonance spectroscopic examination of the chloroform solution revealed *O*-benzylidene ring proton signals at 4.10 τ and 4.23 τ (1,2-*O*-isomers, 21% each), 4.50 τ (1,3-*O*-*cis*-isomer, 44%), and 4.66 τ (1,3-*O*-*trans*-isomer, 15%).

Condensation of Acetoxyacetone with Glycerol

Glycerol (0.50 ml) was shaken for 4 h in acetoxyacetone (13) (10 ml) containing sulfuric acid (0.1 ml). The solution was neutralized ($BaCO_3$), filtered, and evaporated to a syrup (0.89 g) which was deacetylated with 0.1 *N* sodium methoxide (3 ml). The product was fractionated on a cellulose column with benzene–ethanol–water (1000:50:1 v/v/v) as eluent. The eluate was examined by t.l.c. on silica gel (solvent: chloroform–methanol (9:1 v/v)). The first fraction contained components with R_F 0.61 and 0.63 (0.49 g); the former, which was 1,2-*O*-(*cis*-hydroxyisopropylidene)-DL-glycerol, was isolated as its bis-*p*-nitrobenzoate, which had m.p. 125–127° after crystallization from ethyl acetate – *n*-hexane.

Anal. Calcd. for $C_{20}H_{18}O_{10}N_2$: C, 53.81; H, 4.06. Found: C, 53.6; H, 4.2.

The second fraction (0.15 g), R_F 0.50, contained 1,2-*O*-(*trans*-hydroxyisopropylidene)-DL-glycerol, which was converted into its bis-*p*-nitrobenzoate, m.p. 125–127° after crystallization from ethyl acetate – *n*-hexane.

Anal. Calcd. for $C_{20}H_{18}O_{10}N_2$: C, 53.81; H, 4.06. Found: C, 54.0; H, 4.3.

The above structures were assigned since their n.m.r. spectra were respectively identical with those of 1,2-*O*-(*cis*-hydroxyisopropylidene)-L-glycerol bis-*p*-nitrobenzoate and its *trans*-isomer.

Preparation of 2,7-Anhydro-1-deoxy-β-D-galactoheptulopyranose and 1,2-O-(cis-Hydroxyisopropylidene)-L-glycerol

1-Deoxy-*keto*-D-galactoheptulose pentaacetate (14) was deacetylated in methanolic sodium methoxide, and the solution was evaporated and deionized in water containing approximately equal amounts of Amberlite IR-120 and Dowex-1. The resulting syrupy 1-deoxy-D-galactoheptulose (11.8 g) was heated in a small tube for 2–3 h at 300–350° and a pressure of <0.1 mm (15). The amber-colored distillate (0.60 g) was fractionated on a cellulose column with benzene–ethanol–water (400:50:1 v/v/v) as solvent. A crystalline fraction was obtained which, after two recrystallizations from ethyl acetate – ether, gave 2,7-anhydro-1-deoxy-β-D-galactoheptulopyranose (60 mg), m.p. 124–127°, $[\alpha]_D$ −25° (*c*, 1 in EtOH), $[\alpha]_D$ −26.5° (*c*, 1 in H_2O).

Anal. Calcd. for $C_7H_{12}O_5$: C, 47.72; H, 6.87; mol. wt. 176. Found: C, 47.7; H, 6.8; mol. wt. (in H_2O) 175.

Oxidation with sodium periodate for 24 h resulted in consumption of 2.03 moles of oxidant and formation of 0.98 mole of acid.

The anhydride (40 mg) was oxidized for 20 h in sodium periodate (200 mg) and water (5 ml), and the solution was adjusted to pH 7 with sodium carbonate and evaporated. The residue was extracted with acetone and the syrupy extract was treated with sodium borohydride (0.20 g) in a few milliliters of water for 2 h. The pH was adjusted to 8 and the solution was extracted continuously with chloroform to give a syrup

Can. J. Chem. Downloaded from www.nrcresearchpress.com by 210.87.254.6 on 09/05/12
For personal use only.

which contained a little boric acid. Repeated evaporations in methanol gave 1,2-*O*-(*cis*-hydroxyisopropylidene)-L-glycerol (31 mg). Its bis-*p*-nitrobenzoate derivative had m.p. 139–141° and $[\alpha]_D$ −42° (*c*, 2.0 in $CHCl_3$) after crystallization from ethyl acetate – *n*-hexane.

Anal. Calcd. for $C_{20}H_{18}O_{10}N_2$: C, 53.81; H, 4.06; N, 6.27. Found: C, 53.6; H, 4.1; N, 6.2.

Condensation of 1-O-Benzyl-D-glycerol with Acetoxyacetone

1-*O*-Benzyl-D-glycerol was prepared from 1,2-*O*-isopropylidene-D-glycerol by the method of Schmidt and Blank (16), who worked on the corresponding racemates. 1-*O*-Benzyl-D-glycerol (2.0 g) was treated with acetoxyacetone (20 ml) and sulfuric acid (0.1 ml) for 4 h, and the reaction mixture was added to aqueous sodium bicarbonate. Extraction with chloroform and evaporation with heat *in vacuo* gave a mixture of 1,2-*O*-(*cis*-acetoxyisopropylidene)-3-*O*-benzyl-L-glycerol and its *trans*-isomer, which was treated for 2 h in 0.1 *N* sodium methoxide in methanol (5 ml). The deacetylated mixture was examined by t.l.c. on silica gel with chloroform as solvent, and spots with R_F 0.49 and 0.70 were detected. The 3-*O*-benzyl-1,2-*O*-(hydroxyisopropylidene)-glycerols in chloroform gave a n.m.r. spectrum showing C—CH_3 proton signals at 8.66 τ and 8.72 τ in a ratio of 1:1.

The mixture was chromatographed on a silicic acid column with hexane–chloroform (3:2 v/v) as solvent, and the syrupy *cis*-isomer (0.75 g) with R_F 0.70 was isolated. It had a C—CH_3 proton signal at 8.72 τ, $[\alpha]_D$ +10° (*c*, 2.0 in EtOH), and infrared absorptions at 3 616 and 3 480 cm^{-1} (0.005 *M* in CCl_4) and at 3 620 and 3 480 cm^{-1} (0.005 *M* in $CHCl_3$). These frequencies were unchanged after hydrogen chloride was bubbled into the CCl_4 and $CHCl_3$ solutions.

Anal. Calcd. for $C_{13}H_{18}O_4$: C, 65.53; H, 7.61. Found: C, 65.3; H, 7.4.

After a mixed fraction (0.48 g) was eluted, the syrupy *trans*-isomer (0.90 g) with R_F 0.49 appeared. It had a C—CH_3 proton signal at 8.66 τ, $[\alpha]_D$ +13° (*c*, 2.0 in EtOH), and infrared absorption at 3 625 cm^{-1} (0.005 *M* in CCl_4) and at 3 620 cm^{-1} (0.005 *M* in $CHCl_3$). These frequencies were also unchanged after hydrogen chloride was bubbled into the solutions.

Anal. Calcd. for $C_{13}H_{18}O_4$: C, 65.53; H, 7.61. Found: C, 65.15; H, 7.55.

Hydrogenolysis Products of 3-O-Benzyl-1,2-O-(hydroxyisopropylidene)-L-glycerols

These were hydrogenolyzed over palladium – barium sulfate according to the method of Mozingo (17). The *cis*-isomer gave rise to syrupy 1,2-*O*-(*cis*-hydroxyisopropylidene)-L-glycerol, with $[\alpha]_D$ +9° (*c*, 1.3 in EtOH) and R_F 0.61 on t.l.c. (solvent: chloroform–methanol (9:1 v/v)). Its n.m.r. spectrum in D_2O was identical with that of an authentic specimen obtained from 2,7-anhydro-1-deoxy-β-D-galactoheptulopyranose. The derived bis-*p*-nitrobenzoate, crystallized twice from ethyl acetate – *n*-hexane, had m.p. and mixed m.p. 138–139° and $[\alpha]_D$ −36° (*c*, 1.8 in $CHCl_3$), and gave a X-ray diffraction pattern identical with that of an authentic specimen. Its n.m.r. spectrum was identical with that of authentic material, with a C—CH_3 signal in chloroform at 8.52 τ.

Anal. Calcd. for $C_{20}H_{18}O_{10}N_2$: C, 53.81; H, 4.06. Found: C, 54.0; H, 4.0.

The *trans*-isomer gave rise to syrupy 1,2-*O*-(*trans*-hydroxyisopropylidene)-L-glycerol, with $[\alpha]_D$ +17° (*c*, 1.3 in EtOH) and R_F 0.50 on t.l.c. Its bis-*p*-nitrobenzoate, after two recrystallizations from ethyl acetate – *n*-hexane, had m.p. 85–86° and $[\alpha]_D$ +15° (*c*, 2.0 in $CHCl_3$).

Anal. Calcd. for $C_{20}H_{18}O_{10}N_2$: C, 53.81; H, 4.06. Found: C, 53.6; H, 4.25.

Its n.m.r. spectrum in $CHCl_3$ contained a C—CH_3 signal at 8.47 τ. The n.m.r. spectrum of 1,2-*O*-(*cis*-hydroxyisopropylidene)-L-glycerol in D_2O contained a C—CH_3 signal at 8.22 τ and a hydroxyisopropylidene CH_2 signal at 6.02 τ. The *trans*-isomer had a C—CH_3 signal at 8.18 τ and a hydroxyisopropylidene CH_2 signal at 6.06 τ.

Equilibration of 1,2-O-(Hydroxyisopropylidene)-L-glycerol and 3-O-Benzyl-1,2-O-(hydroxyisopropylidene)-L-glycerols

A solution of 1,2-*O*-(*cis*-hydroxyisopropylidene)-L-glycerol (50 mg) in chloroform (1 ml), adjusted to 0.1 *N* with hydrogen chloride, was examined by n.m.r. spectroscopy at intervals. The C—CH_3 proton signals showed that, at equilibrium (1 day), the *cis*- and *trans*-isomers were present in a ratio of 2:1 (8.22 τ and 8.18 τ, respectively, in D_2O).

Under similar conditions equilibration of the 3-*O*-benzyl derivatives resulted in a ratio of *cis*- to *trans*-isomer of 57:43 (C—CH_3 signals at 8.72 τ and 8.66 τ, respectively).

Nuclear Magnetic Resonance Spectra of 1,2-O-cis,trans-Ethylidene-L-glycerol and its 3-O-Benzyl Derivative

In chloroform, 3-*O*-benzyl-1,2-*O*-*cis*,*trans*-ethylidene-L-glycerol gave two superimposed C-1′ proton quadruplets, the larger at higher field at approximately 5.02 τ and the minor component at approximately 4.98 τ. Doublets from C-2′ methyl protons appeared at 8.63 τ (average value; *J* 2.4 c.p.s., major signal) and at 8.68 τ (*J* 2.4 c.p.s.).

In deuterium oxide, 1,2-*O*-*cis*,*trans*-ethylidene-L-glycerol gave two C-1′ proton quadruplet signals, one at 4.33, 4.37, 4.43, and 4.47 τ (37%) and the other at 4.42, 4.47, 4.52, and 4.5 τ (63%). Doublets corresponding to the C-2′ methyl protons appeared at 8.16 τ (average value; *J* 2.2 c.p.s., major signal) and at 8.20 τ (average value; *J* 2.2 c.p.s.).

Can. J. Chem. Downloaded from www.nrcresearchpress.com by 210.87.254.6 on 09/05/12
For personal use only.

ACKNOWLEDGMENTS

The authors thank Mr. M. Mazurek for preparation of the n.m.r. spectra, and Mr. W. C. Haid for microanalytical determinations.

REFERENCES

1. P. A. J. GORIN and J. F. T. SPENCER. Can. J. Chem. **43**, 2978 (1965).
2. D. J. TRIGGLE and B. BELLEAU. Can. J. Chem. **40**, 1201 (1962).
3. F. SMITH and J. W. VAN CLEAVE. J. Am. Chem. Soc. **77**, 3091 (1955).
4. N. BAGGETT, J. S. BRIMACOMBE, A. B. FOSTER, M. STACEY, and D. H. WHIFFEN. J. Chem. Soc. 2574 (1960).
5. S. M. TRISTER and H. HIBBERT. Can. J. Res., B, **14**, 415 (1936).
6. H. HIBBERT and N. M. CARTER. J. Am. Chem. Soc. **50**, 3120 (1928).
7. S. A. BARKER, E. J. BOURNE, R. M. PINKARD, M. STACEY, and D. H. WHIFFEN. J. Chem. Soc. 3232 (1958).
8. S. F. BIRCH and R. A. DEAN. J. Chem. Soc. 2477 (1953).
9. V. V. EVLAMPIEV. J. Gen. Chem. USSR Engl. Transl. **7**, 2941 (1937).
10. A. R. H. COLE and P. R. JEFFERIES. J. Chem. Soc. 4391 (1956).
11. L. P. KUHN, P. VON R. SCHLEYER, W. F. BAITINGER, JR., and L. EBERSON. J. Am. Chem. Soc. **86**, 650 (1964).
12. J. S. BRIMACOMBE, A. B. FOSTER, and A. H. HAINES. J. Chem. Soc. 2582 (1960).
13. W. MADELING and M. E. OBERWEGNER. Chem. Ber. **65**, 931 (1932).
14. M. L. WOLFROM and R. L. BROWN. J. Am. Chem. Soc. **65**, 1516 (1943).
15. R. J. DIMLER, H. A. DAVIS, and G. H. HIBBERT. J. Am. Chem. Soc. **68**, 1377 (1946).
16. O. T. SCHMIDT and W. BLANK. Chem. Ber. **89**, 283 (1956).
17. R. MOZINGO. Org. Syn. **26**, 77 (1946).

Can. J. Chem. Downloaded from www.nrcresearchpress.com by 210.87.254.6 on 09/05/12
For personal use only.

Can. J. Chem. Downloaded from www.nrcresearchpress.com by 210.87.254.42 on 09/05/12
For personal use only.

THE SYNTHESIS OF SOME 6,7-METHYLENEDIOXY- AND 6,7-DIMETHOXY-1,4-BENZOXAZIN-2-ONES[1]

D. G. Orphanos and A. Taurins
Department of Chemistry, McGill University, Montreal, Quebec
Received February 22, 1966

ABSTRACT

3,4-Methylenedioxy-6-aminophenol (I) and 3,4-dimethoxy-6-aminophenol (IV) were condensed with various α-ketoesters to give the corresponding 6,7-methylenedioxy- and 6,7-dimethoxy-1,4-benzoxazin-2-ones.

Wislicenus and his co-workers (1, 2) discovered that *o*-aminophenols reacted with α-ketoesters to give the ring system of 1,4-benzoxazin-2-ones. Biekert *et al.* (3) investigated the scope of this reaction by varying both components. The objective of our work was the extension of this reaction to *o*-aminophenols containing either a methylenedioxy group or two ortho dimethoxy groups, to synthesize 1,4-benzoxazin-2-ones carrying these substituents on the benzenoid ring.

The synthesis was accomplished by the condensation of 3,4-methylenedioxy-6-aminophenol (I) (4) and 3,4-dimethoxy-6-aminophenol (IV) (4) with a number of α-ketoesters. A general reaction scheme illustrating the synthesis of 6,7-methylenedioxy- and 6,7-dimethoxy-1,4-benzoxazin-2-ones is given in Reaction Scheme 1. The structures of the products III*a*–III*e* and V*a*–V*e* were assigned on the basis of analogy, analytical data, and infrared spectra.

The starting materials I and IV were prepared readily by catalytic reduction of the corresponding nitrophenols (4). The 6-aminophenols I and IV, being extremely sensitive to oxidation, were filtered under a nitrogen atmosphere into a glacial acetic acid solution of the appropriate α-ketoester, and converted directly into the stable 1,4-benzoxazin-2-ones. Although the condensation of *o*-aminophenols with α-ketoesters proceeds at a slow rate in the absence of acids, in most cases it is speeded up by the presence of glacial acetic acid. However, the synthesis of 6,7-methylenedioxy- and 6,7-dimethoxy-1,4-benzoxazin-2-ones possessing methyl or phenyl substituents in the 3-position could not be accomplished without the presence of glacial acetic acid in the reacting mixture.

6,7-Methylenedioxy-1,4-benzoxazin-2-ones were obtained in high yields in an almost pure state, at temperatures ranging from room temperature to 60°, and a reaction time of 1 to 6 h. On the other hand, the preparation of all 6,7-dimethoxy-1,4-benzoxazin-2-ones required heating at 70° for a long period of time, and considerable amounts of dark decomposition products were formed, which could be removed only with difficulty. All the dialkoxybenzoxazinones that were prepared were highly colored. The nature of the substituent in the 3-position appears to be responsible for the color. Substitution of a phenyl group in the 3-position causes the substances, in acetone, to show a strong blue-green fluorescence. This effect, but with less intensity, is also observed when these compounds are dissolved in several other polar and inert solvents.

Catalytic hydrogenation of benzoxazin-2-ones to give 2-phenomorpholones has been reported to occur at a pressure of 50 atm (5). In this work, a much lower hydrogen pressure (0.2 atm) was used and the 6,7-substituted 2-phenomorpholone derivatives VI*a*, VI*b*,

[1]*This work received financial assistance from the National Research Council of Canada, Ottawa, Canada.*

Can. J. Chem. Downloaded from www.nrcresearchpress.com by 210.87.254.42 on 09/05/12
For personal use only.

TABLE II

Condensation of α-ketoesters with 3,4-dimethoxy-6-aminophenol

No.	α-Ketoester	Method of purification*	Molecular formula, melting point, etc., of benzoxazinones	Yield (%)	Analyses (%) Calculated C	H	N	Found C	H	N	ν_{max} (cm^{-1})
V*a*	Ethyl pyruvate (7)	A	$C_{11}H_{11}NO_4$, 188–189°, yellow needles	8.1	59.73	5.01	6.33	59.92	5.17	6.47	1 750 1 623
V*b*	Ethyl benzoyl-formate (8)	A	$C_{16}H_{13}NO_4$, 169°, yellow needles	64.3	67.83	4.62	4.94	67.63	4.70	5.13	1 724 1 617
V*c*	Diethyl oxalacetate (6)	A	$C_{14}H_{15}NO_6$, 157–159°, yellow needles	11.9	57.33	5.15	4.77	57.05	5.11	5.02	1 732 1 623
V*d*	Methyl acetopyruvate (9)	B	$C_{13}H_{13}NO_5$, 187–188°, orange crystals	65.0	59.31	4.98	5.32	59.03	4.90	5.22	1 742 1 627
V*e*	Methyl benzoyl-pyruvate (9)	C	$C_{18}H_{15}NO_5$, 175–176°, deep-red crystals	81.5	66.45	4.65	4.30	66.69	4.84	4.16	1 750 1 615

*A, the product was dissolved in methanol, boiled with charcoal, and filtered; the filtrate deposited yellow needles when chilled in a dry ice – acetone bath. B, recrystallization from ethanol. C, for analysis, a small sample was dissolved in diethyl ether, boiled with charcoal, and filtered; the filtrate, on partial concentration, deposited deep-red crystals.

Can. J. Chem. Downloaded from www.nrcresearchpress.com by 210.87.254.42 on 09/05/12
For personal use only.

TABLE III

Physical constants and analytical data of 2-phenomorpholones

No.	Compound	Molecular formula, melting point, etc.	Yield (%)	Analyses (%) Calculated C	Calculated H	Calculated N	Found C	Found H	Found N	ν_{max} (cm^{-1})
VI*a*	6,7-Methylenedioxy-3-methyl-2-phenomorpholone	$C_{10}H_9NO_4$, 177–179°, white needles	92	57.96	4.38	6.76	57.96	4.41	6.95	3 340 1 748
VI*b*	6,7-Methylenedioxy-3-phenyl-2-phenomorpholone	$C_{15}H_{11}NO_4$, 191–192°, white needles	94	66.91	4.12	5.20	67.16	4.08	5.11	3 350 1 757
VI*c*	6,7-Methylenedioxy-2-phenomorpholone-3-acetic acid ethyl ester	$C_{13}H_{13}NO_6$, 110.5–111°, white needles	86	55.91	4.69	5.02	55.98	4.75	5.20	3 360 1 745
VII	6,7-Dimethoxy-3-phenyl-2-phenomorpholone	$C_{16}H_{15}NO_4$, 116–117°, white needles	90	67.35	5.30	4.91	67.17	5.23	5.15	3 335 1 748

for a certain length of time (refer to Table I), with occasional shaking. Heat was not applied unless noted in the table. The crystalline product was isolated by filtration and purified as outlined in Table I. By this general procedure, the following five methylenedioxybenzoxazinones were prepared and characterized: III*a*, 6,7-methylenedioxy-3-methyl-1,4-benzoxazin-2-one; III*b*, 6,7-methylenedioxy-3-phenyl-1,4-benzoxazin-2-one; III*c*, 6,7-methylenedioxy-1,4-benzoxazin-2-one-3-acetic acid ethyl ester; III*d*, 6,7-methylenedioxy-3-acetonyl-1,4-benzoxazin-2-one; and III*e*, 6,7-methylenedioxy-3-phenacyl-1,4-benzoxazin-2-one.

Condensation of α-Ketoesters with 3,4-Dimethoxy-6-aminophenol (IV)

At room temperature and in a nitrogen atmosphere, a methoxyethylene glycol solution of IV (0.01 mole) was added to a solution of α-ketoester (10% excess) in glacial acetic acid. The reaction mixture was heated at 65–70° for 12 h, with occasional shaking. The deep-orange reaction solution was concentrated under reduced pressure to one-half its volume, and then refrigerated for 2–3 h. The solid product was collected and purified (refer to Table II). By this method, the following five dimethoxybenzoxazinones were prepared and characterized: V*a*, 6,7-dimethoxy-3-methyl-1,4-benzoxazin-2-one; V*b*, 6,7-dimethoxy-3-phenyl-1,4-benzoxazin-2-one; V*c*, 6,7-dimethoxy-1,4-benzoxazin-2-one-3-acetic acid ethyl ester; V*d*, 6,7-dimethoxy-3-acetonyl-1,4-benzoxazin-2-one; and V*e*, 6,7-dimethoxy-3-phenacyl-1,4-benzoxazin-2-one.

Preparation of 6,7-Methylenedioxy-2-phenomorpholones (VI)

A suspension of 6,7-methylenedioxy-3-R-1,4-benzoxazin-2-one (R = CH_3, $CH_2COOC_2H_5$, or C_6H_5) (0.5 g) in absolute ethanol (50 ml) was hydrogenated for 30 min at room temperature and 0.3 atm pressure with 10% palladium on charcoal (0.05 g) as a catalyst. Removal of the catalyst by filtration in a nitrogen atmosphere gave a colorless solution, which was then concentrated to one-quarter its volume under reduced pressure at room temperature. White crystalline material separated from the residual solution. The mixture was cooled in an ice-water bath and filtered in a nitrogen atmosphere. The white crystalline product was washed with 5 ml of light petroleum ether and dried *in vacuo*. The melting points of the individual compounds were not improved after recrystallization from benzene. These substances, on contact with air, slowly dehydrogenated to their parent 6,7-methylenedioxy-1,4-benzoxazinones; in glacial acetic acid solution the same reaction occurred in a few hours. The methylenedioxyphenomorpholones obtained are recorded in Table III.

6,7-Dimethoxy-3-phenyl-2-phenomorpholone (VII)

6,7-Dimethoxy-3-phenyl-1,4-benzoxazin-2-one (V*b*) (0.5 g) was hydrogenated to VII by a procedure similar to that used for the reduction of the analogous methylenedioxy compounds. The method of isolation and the physical and chemical properties of VII are comparable to those of VI (Table III).

REFERENCES

1. W. Wislicenus and W. Beckh. Liebigs Ann. Chem. **295**, 339 (1897).
2. W. Wislicenus and F. Schultz. Liebigs Ann. Chem. **436**, 57 (1924).
3. E. Biekert, D. Hoffmann, and F. J. Meyer. Chem. Ber. **94**, 1664 (1961).
4. D. G. Orphanos and A. Taurins. Can. J. Chem. This issue.
5. E. Biekert, D. Hoffmann, and F. J. Meyer. Chem. Ber. **94**, 1676 (1961).
6. W. Wislicenus. Ber. Deut. Chem. Ges. **19**, 3225 (1886); Liebigs Ann. Chem. **246**, 307 (1888).
7. R. S. Schreiber (*Editor*). Organic syntheses. Vol. 31. John Wiley & Sons, Inc., New York. 1951. p. 59.
8. H. A. Blatt (*Editor*). Organic syntheses. Collective Vol. I. John Wiley & Sons, Inc., New York. 1951. p. 241.
9. M. Freri. Gazz. Chim. Ital. **68**, 612 (1938).

Can. J. Chem. Downloaded from www.nrcresearchpress.com by 210.87.254.42 on 09/05/12
For personal use only.

Can. J. Chem. Downloaded from www.nrcresearchpress.com by 210.87.254.105 on 09/05/12
For personal use only.

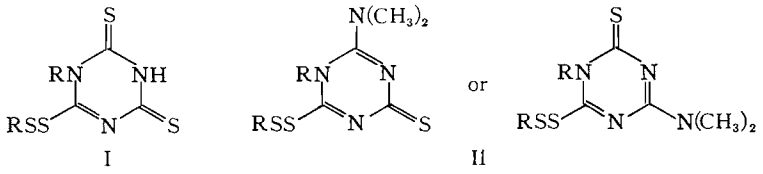
DERIVATIVES OF ISOTRITHIOCYANURIC ACID

D. L. GARMAISE
Research Department, Abbott Laboratories Limited, Montreal, Quebec
Received March 31, 1966

ABSTRACT

A by-product isolated in low yield from the reaction of *p*-chlorobenzyl chloride with potassium thiocyanate and sodium iodide in dimethylformamide was shown to be the isotrithiocyanuric acid derivative I (R = *p*-chlorobenzyl). I gave the isodithiocyanuric acid ester (III) on alkaline hydrolysis, and mono-*p*-chlorobenzyl isotrithiocyanurate (IV) on reduction with sodium hydrosulfite. Treatment of I with sodium hypochlorite in aqueous alcoholic medium resulted in the direct replacement of the sulfhydryl group by an alkoxyl group. The *N,S,S*-triester VIII rearranged, on heating, to the symmetrical *S,S,S*-triester IX; this behavior is opposite to that shown by the oxygen analogues.

During the preparation of *p*-chlorobenzyl isothiocyanate by treatment of *p*-chlorobenzyl chloride with potassium thiocyanate and sodium iodide in dimethylformamide at 150° for 30 min, a mixture of two crystalline by-products separated out in low yield. The major component, which was isolated by extracting the mixture with alcoholic sodium hydroxide and acidifying the alcoholic extract, was a pale-yellow solid with the formula $C_{17}H_{13}Cl_2N_3S_4$. Evidence obtained during this work has led to the assignment of structure I (1-(*p*-chlorobenzyl)-6-(*p*-chlorobenzyldithio)-*s*-triazine-2,4(1*H*,3*H*)-dithione) to this substance. The minor component, which was insoluble in alcoholic sodium hydroxide solution, was an orange-colored substance with the formula $C_{16}H_{12}Cl_2N_2S_4$. When the reaction temperature was maintained at 150° for 3 h instead of 30 min, apparent interaction with dimethylformamide led to the disappearance of I, and a neutral compound (II), which is presumed to have one of the isomeric structures indicated, was isolated.

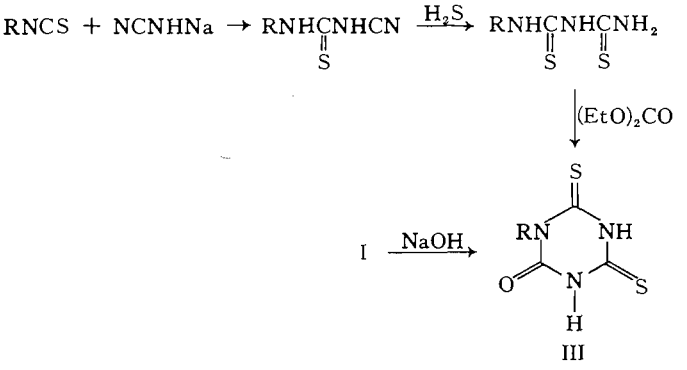


R = *p*-chlorobenzyl throughout

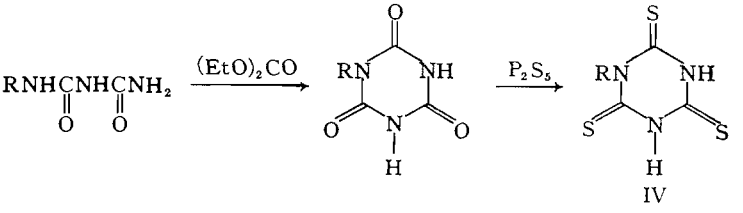
Alkaline hydrolysis of I resulted in the loss of the 4-chlorobenzyldithio group, and the formation of an acidic substance (III) with the formula $C_{10}H_8ClN_3OS_2$. III was shown to be 1-(*p*-chlorobenzyl)-2,4-dithio-*s*-triazine-2,4,6(1*H*,3*H*,5*H*)-trione by synthesis from 1-*p*-chlorobenzyldithiobiuret and diethyl carbonate. The dithiobiuret was prepared by adding *p*-chlorobenzyl isothiocyanate to sodium cyanamide followed by hydrogen sulfide (1).

Reduction of I with sodium hydrosulfite in alkaline medium yielded *p*-chloro-α-toluenethiol (isolated as the disulfide) and 1-(*p*-chlorobenzyl)-*s*-triazine-2,4,6(1*H*,3*H*,5*H*)-trithione (IV), along with some III arising from alkaline hydrolysis of I.

The structure of compound IV, which appears to be the first monoester of isotrithiocyanuric acid to have been described, was confirmed by direct synthesis. 1-*p*-Chlorobenzylbiuret was treated with diethyl carbonate (2) to give mono-*p*-chlorobenzyl isocyanurate.

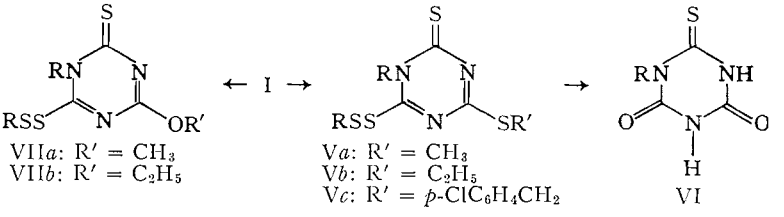


The isocyanurate was not affected by treatment with phosphorus pentasulfide in refluxing pyridine, but fusion with the reagent at 265 °C gave IV in 51% yield.



I was readily alkylated in alkaline alcoholic medium to give the neutral esters V*a*–V*c*. When the methyl ester V*a* was treated with hot concentrated sodium hydroxide solution, both the 4-thio and 6-dithio substituents were hydrolyzed, and 1-(*p*-chlorobenzyl)-2-thio-*s*-triazine-2,4,6(1*H*,3*H*,5*H*)-trione (VI) was obtained.

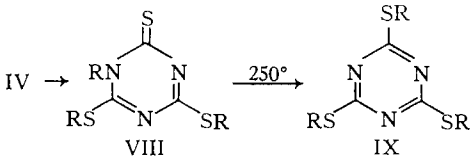
Treatment of I with sodium hypochlorite in aqueous methanol caused the direct replacement of the sulfhydryl group by methoxyl to give VII*a* in good yield; the ethoxy derivative VII*b* was obtained in lower yield by performing the reaction in aqueous ethanol. This rather unexpected replacement reaction is presumed to proceed via the chloro derivative as an intermediate, and its possible application to other thiols is being investigated.



The mixed triester VIII (m.p. 171°), which was prepared by the esterification of IV, rearranged, on heating, to the symmetrical tri-*p*-chlorobenzyl trithiocyanurate (IX), m.p. 122°. The direction of the rearrangement is in interesting contrast to the behavior of the oxygen analogues, since alkyl and aralkyl cyanurates rearrange, on heating, to the isocyanuric acid esters (3, pp. 398–421). The difference in behavior between the thioxo and oxo analogues is consistent with the relative instability of doubly bound sulfur as compared with doubly bound oxygen.

Can. J. Chem. Downloaded from www.nrcresearchpress.com by 210.87.254.105 on 09/05/12
For personal use only.

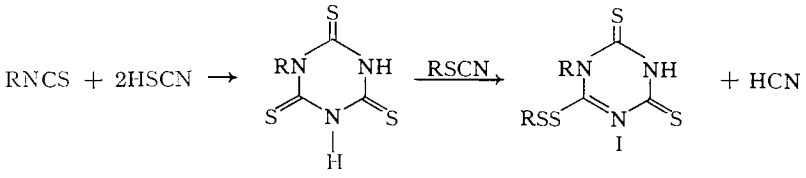
The ultraviolet spectrum of VIII (λ_{max} 288 and 330 mμ) showed peaks at higher wavelengths than that of the normal ester IX (λ_{max} 263 mμ). A similar though smaller difference was observed with mono-*p*-chlorobenzyl isotrithiocyanurate (IV) (λ_{max} 292 mμ) and mono-*p*-chlorobenzyl trithiocyanurate (XII) (λ_{max} 280 mμ).



VIII IX

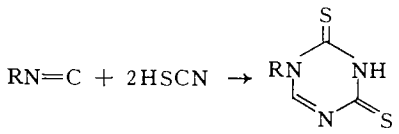
Relatively few derivatives of isotrithiocyanuric acid have been described. Alkyl and aralkyl thiocyanates have long been known to trimerize readily to the normal trithiocyanurates (3, p. 111), but little has been reported on the comparable trimerization of isothiocyanates. In a recent publication (4) it was stated that heating methyl isothiocyanate at 200° in dioxane gave 1,3,5-trimethyl dithioisocyanurate, but the corresponding isotrithiocyanurate has never been described. With respect to monoesters of isotrithiocyanuric acid, no examples could be found in the literature.

The reaction mixture from which I was isolated contains, among other components, *p*-chlorobenzyl isothiocyanate, *p*-chlorobenzyl thiocyanate, and excess thiocyanate ion. The initial reaction in the sequence leading to the formation of I may be the condensation of *p*-chlorobenzyl isothiocyanate with thiocyanic acid to give mono-*p*-chlorobenzyl isotrithiocyanurate (IV), followed by condensation with *p*-chlorobenzyl thiocyanate with the elimination of hydrogen cyanide.



IV I

The suggested cyclization reaction is similar to the recently described condensation of isonitriles with thiocyanic acid to give 1-substituted-*s*-triazine-2,4(1*H*,3*H*)-dithiones (5).



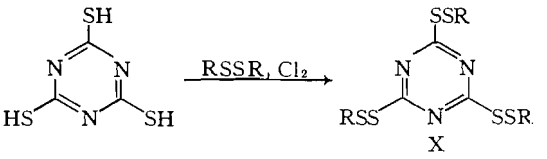
These condensations are stated to occur readily at −20 °C in ether solution, giving the triazine-2,4-dithiones in high yield.

The reaction between thiols and thiocyanates to give disulfides, with the elimination of hydrogen cyanide, has been studied by several investigators (6, 7). This reaction is distinguished from the standard preparation of disulfides by the alkaline hydrolysis of thiocyanates to thiols followed by air oxidation, since it was shown to proceed in a nitrogen atmosphere. Thus, heating *p*-chlorothiophenol and *p*-chlorophenyl thiocyanate at 100° in nitrogen gave a nearly quantitative yield of the disulfide in 8 h.

For purposes of comparison with the isotrithiocyanurate I and its derivatives, a number of derivatives of trithiocyanuric acid with *p*-chlorobenzylthio and *p*-chlorobenzyldithio

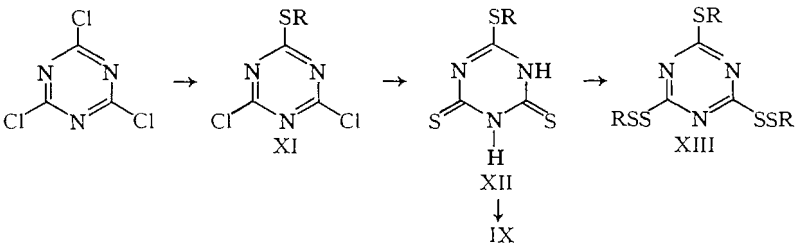
Can. J. Chem. Downloaded from www.nrcresearchpress.com by 210.87.254.105 on 09/05/12
For personal use only.

substituents were synthesized. Some tri(alkyldithio)-*s*-triazines have been prepared (8) by treating alkanethiols with excess chlorine to give the alkylsulfenyl chlorides, which were then allowed to react with trithiocyanuric acid. This procedure did not work with *p*-chloro-α-toluenethiol, but it was found that addition of the calculated amount of chlorine to bis-(*p*-chlorobenzyl) disulfide and trithiocyanuric acid gave 2,4,6-tri-(*p*-chlorobenzyldithio)-*s*-triazine (X) in fair yield.



X

Cyanuric chloride was converted into 2-(*p*-chlorobenzylthio)-4,6-dichloro-*s*-triazine (XI) by treatment with *p*-chloro-α-toluenethiol in the presence of lutidine at −40° by the method of Koopman *et al.* (9).

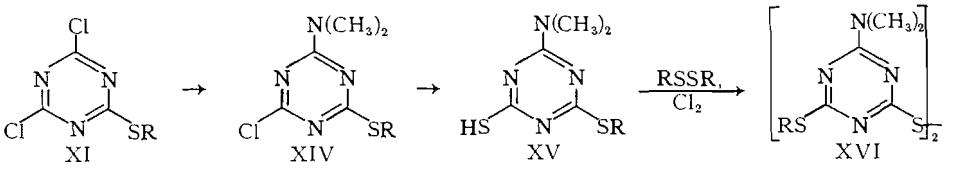


XI XII XIII

↓

IX

Reaction of XI with sodium hydrosulfide gave mono-(*p*-chlorobenzyl) trithiocyanurate (XII). This monoester melted at a higher temperature than its isomer IV, but was considerably more soluble in ether and ethanol. It was readily esterified to the symmetrical triester (IX) (which could also be prepared from cyanuric chloride and *p*-chloro-α-toluenethiol). Treatment of XII with bis-(*p*-chlorobenzyl) disulfide and chlorine gave the di-disulfide (XIII).



XI XIV XV XVI

In an attempt to prepare a compound containing both a *p*-chlorobenzyldithio and a dimethylamino substituent, as in the by-product II, the dichloro derivative (XI) was first treated with dimethylamine to give XIV, and the remaining chlorine was replaced by a sulfhydryl group to yield the monothiol XV. The reaction of XV with bis-(*p*-chlorobenzyl) disulfide and chlorine, however, yielded the bis-(triazinyl) disulfide (XVI) instead of the desired *p*-chlorobenzyldithio derivative.

EXPERIMENTAL

All melting points are uncorrected. Analytical data were supplied by Dr. C. Daessle, Montreal, Quebec, and by the Microanalytical Department, Abbott Laboratories, North Chicago, Illinois.

1-(p-Chlorobenzyl)-6-(p-chlorobenzyldithio)-s-triazine-2,4(1H,3H)-dithione (I)

p-Chlorobenzyl chloride (500 g, 3.1 moles) was added to a solution of potassium thiocyanate (330 g, 3.4 moles) and sodium iodide (23 g, 0.15 mole) in dimethylformamide (250 ml) at 130° over a period of 15 min.

Can. J. Chem. Downloaded from www.nrcresearchpress.com by 210.87.254.105 on 09/05/12
For personal use only.

Can. J. Chem. Downloaded from www.nrcresearchpress.com by 210.87.254.105 on 09/05/12
For personal use only.

The temperature was allowed to increase to 150°, and the reaction was maintained at that temperature for 30 min. The hot reaction mixture was poured onto ice, and the mixture was extracted with chloroform (250 ml). The chloroform solution was washed with water and dried. Petroleum ether (500 ml) was added and the solution was allowed to stand at 5° overnight. The precipitated solid (5.7 g, m.p. 190–204°) was extracted with sodium hydroxide (*N*, 30 ml) in ethanol (250 ml), giving an orange-colored residue, yield 0.4 g, m.p. 170–175°. Recrystallization from dimethylformamide raised the melting point to 174–175°.

Anal. Calcd. for $C_{16}H_{12}Cl_2N_2S_4$: C, 44.54; H, 2.81; Cl, 16.44; N, 6.49; S, 29.72. Found: C, 44.50; H, 2.42; Cl, 16.80; N, 6.32; S, 29.70.

Acidification of the alkaline filtrate with 5% hydrochloric acid gave crude I, m.p. 205–206°, yield 5.2 g (0.8%). Recrystallization from dimethylformamide raised the melting point to 207–208°.

Anal. Calcd. for $C_{17}H_{13}Cl_2N_3S_4$: C, 44.53; H, 2.86; Cl, 15.41; N, 9.17; S, 27.97. Found: C, 44.52; H, 2.90; Cl, 15.31; N, 9.19; S, 27.56.

1-(p-Chlorobenzyl)-4(or 2)-dimethylamino-6-(p-chlorobenzyldithio)-s-triazine-2(or 4)(1H)-thione (II)

The reaction was performed as described above, except that the period of heating at 150° was extended to 3 h. The reaction mixture was worked up in the same way, resulting in the isolation of a neutral product, m.p. 225–229°, yield 8.5 g. Recrystallization from dimethylformamide raised the melting point to 232–233°.

Anal. Calcd. for $C_{19}H_{18}Cl_2N_4S_3$: C, 48.61; H, 3.86; Cl, 15.10; N, 11.94; S, 20.49. Found: C, 48.32; H, 4.08; Cl, 15.13; N, 12.08; S, 20.25.

1-(p-Chlorobenzyl)-2,4-dithio-s-triazine-2,4,6(1H,3H,5H)-trione (III)

By Hydrolysis of I

I (1.5 g) was added to a solution of sodium hydroxide (7.5 g) in water (30 ml) and methanol (60 ml), and the mixture was heated on the steam bath for 2 h. The methanol was distilled off slowly as the hydrolysis proceeded. The solution was cooled and acidified, giving the crude product, m.p. 254–262°, yield 0.51 g (51%). Recrystallization from methanol raised the melting point to 280–282 °C.

Anal. Calcd. for $C_{10}H_8ClN_3OS_2$: C, 42.03; H, 2.82; Cl, 12.41; N, 14.70; mol. wt. 285.76. Found: C, 42.34; H, 3.31; Cl, 12.69; N, 14.16; mol. wt. 283.

Via 1-p-Chlorobenzyldithiobiuret

Cyanamide (2.1 g, 0.05 mole) was added to a solution of sodium methoxide (prepared from 1.15 g sodium) in ethanol (20 ml). *p*-Chlorobenzyl isothiocyanate (9.1 g, 0.05 mole) was added and the solution was refluxed for 30 min. The solution was evaporated to dryness and the solid residue was dissolved in 75 ml H_2O, to which was added 2.4 g ammonium chloride and 8.0 ml concentrated ammonium hydroxide. Hydrogen sulfide was bubbled through the solution at 90° for 6 h, giving the crude dithiobiuret, m.p. 160–165°, yield 8.1 g (62%). Recrystallization from methanol raised the melting point to 167–169 °C.

Anal. Calcd. for $C_9H_{10}ClN_3S_2$: C, 41.61; H, 3.88; Cl, 13.65; N, 16.18; S, 24.68. Found: C, 41.75; H, 3.96; Cl, 13.84; N, 16.14; S, 24.47.

Sodium (0.23 g) was dissolved in 10 ml ethanol, and diethyl carbonate (1.2 g, 0.1 mole) and 1-*p*-chlorobenzyldithiobiuret (1.3 g, 0.05 mole) were added. The solution was refluxed for 40 min and then evaporated to dryness. The residue was dissolved in water (100 ml) and the solution was washed with ether to remove the unreacted diethyl carbonate. Acidification of the aqueous solution gave a precipitate which was extracted with chloroform (100 ml) and recrystallized from ethanol to give the pure product, m.p. 270–272°, yield 0.25 g (18%). There was no melting point depression on admixture with the product obtained from I, and the ultraviolet and infrared spectra were identical.

1-(p-Chlorobenzyl)-s-triazine-2,4,6(1H,3H,5H)-trithione (Mono-p-chlorobenzyl Isotrithiocyanurate) (IV)

By Reduction of I

Sodium hydrosulfite (17.4 g, 0.1 mole) was added to a solution of I (2.5 g, 0.0055 mole) in 50% methanol (300 ml) containing sodium hydroxide (1.2 g, 0.03 mole). The solution was refluxed for 2 h, and *N* sodium hydroxide was added continuously to maintain a pH of 8. After being allowed to stand overnight, the solution deposited crystals of bis-(*p*-chlorobenzyl) disulfide (10), m.p. 58°. Acidification of the filtrate gave a mixture (2.1 g) of compounds I, III, and IV. The mixture was extracted with boiling absolute ethanol (100 ml), in which only the isodithiocyanurate III was soluble. The residue, consisting of I and IV, was suspended in 20 ml *N* aqueous sodium hydroxide, and the insoluble sodium salt of I was removed by filtration. Acidification of the alkaline filtrate gave pure IV, m.p. 320° (decomp.) (crystal change at 275°), yield 0.26 g (16%).

Anal. Calcd. for $C_{10}H_8ClN_3S_3$: C, 39.79; H, 2.67; Cl, 11.75; N, 13.92; S, 31.87. Found: C, 40.05; H, 2.86; Cl, 11.66; N, 13.74; S, 31.71.

From Mono-p-chlorobenzyl Isocyanurate

p-Chlorobenzylamine (24 g, 0.17 mole) and nitrobiuret (25 g, 0.17 mole) were heated in 150 ml water at 95° for 1 h. Filtration of the hot solution gave 1-(*p*-chlorobenzyl)-biuret, m.p. 190–192°.

Anal. Calcd. for $C_9H_{10}ClN_3O_2$: C, 47.48; H, 4.43; Cl, 15.58. Found: C, 47.55; H, 4.58; Cl, 15.71.

The biuret (22.8 g, 0.1 mole) and diethyl carbonate (23.6 g, 0.2 mole) were added to a solution of sodium methoxide (0.2 mole) in methanol (200 ml), and the solution was refluxed for 2 h. The precipitated solid was

filtered off and extracted with 600 ml water; acidification of the filtrate gave mono-*p*-chlorobenzyl isocyanurate, m.p. 249–251°.

Anal. Calcd. for $C_{10}H_8ClN_3O_3$: C, 47.35; H, 3.18; Cl, 13.98; N, 16.57. Found: C, 47.47; H, 3.20; Cl, 13.70; N, 16.49.

A mixture of mono-*p*-chlorobenzyl isocyanurate (8.8 g, 0.035 mole) and phosphorus pentasulfide (8.0 g, 0.036 mole) was heated at 255–265° for 20 min. Water (50 ml) was added, and the suspension was boiled for 10 min and filtered. The precipitate was extracted with 4% sodium hydroxide (300 ml) and the alkaline extract was acidified to give the product (8.8 g, 83%), m.p. 295–300°. Recrystallization from dimethylformamide–methanol raised the melting point to 320°; the ultraviolet and infrared spectra were identical with those of the product obtained by reduction of I.

1-(p-Chlorobenzyl)-4-methylthio-6-(p-chlorobenzyldithio)-s-triazine-2(1H)-thione (Va)

I (498 mg, 1.09 mmoles) was dissolved in a solution of sodium hydroxide (*N*, 1.8 ml) in methanol (40 ml), and methyl iodide (1.0 ml) was added at 0°. The product separated out immediately, giving 425 mg (82%), m.p. 163–165°. Recrystallization from dimethylformamide raised the melting point to 169–170°.

Anal. Calcd. for $C_{18}H_{15}Cl_2N_3S_4$: C, 45.75; H, 3.20; Cl, 15.01; N, 8.89; S, 27.14. Found: C, 45.73; H, 3.72; Cl, 14.88; N, 9.08; S, 26.94.

1-(*p*-Chlorobenzyl)-4-ethylthio-6-(*p*-chlorobenzyldithio)-*s*-triazine-2(1*H*)-thione (V*b*), prepared in the same way with ethyl iodide, melted at 115–116° after recrystallization from methanol.

Anal. Calcd. for $C_{19}H_{17}Cl_2N_3S_4$: C, 46.90; H, 3.52; Cl, 14.58; N, 8.64. Found: C, 47.09; H, 3.77; Cl, 14.91; N, 8.89.

1-(*p*-Chlorobenzyl)-4-(*p*-chlorobenzylthio)-6-(*p*-chlorobenzyldithio)-*s*-triazine-2(1*H*)-thione (V*c*), m.p. 120–122°, was obtained in 87% yield.

Anal. Calcd. for $C_{24}H_{18}Cl_3N_3S_4$: C, 49.44; H, 3.11; Cl, 18.24; N, 7.21; S, 22.00. Found: C, 49.82; H, 3.17; Cl, 17.79; N, 6.90; S, 21.64.

1-(p-Chlorobenzyl)-2-thio-s-triazine-2,4,6(1H,3H,5H)-trione (VI)

A suspension of the methyl derivative V*a* (730 mg) in methanol (50 ml) and 50% sodium hydroxide solution (16 g) was heated on the steam bath for 2 h, and the methanol was evaporated. The alkaline solution was diluted with water (150 ml) and filtered, and the filtrate was acidified. The crude precipitate (185 mg) was recrystallized from glacial acetic acid to a constant melting point of 279–281°, yield 132 mg (32%).

Anal. Calcd. for $C_{10}H_8ClN_3O_2S$: C, 44.53; H, 2.99; Cl, 13.15; N, 15.58; S, 11.89. Found: C, 44.54; H, 3.05; Cl, 13.19; N, 15.55; S, 11.76.

1-(p-Chlorobenzyl)-4-methoxy-6-(p-chlorobenzyldithio)-s-triazine-2(1H)-thione (VIIa)

I (0.68 g, 1.48 mmoles) was dissolved in methanol (60 ml) containing 3.4 ml of aqueous *N* sodium hydroxide, and sodium hypochlorite solution (9 ml, available chlorine 5%) was added. The suspension was stirred at room temperature for 2 days. The precipitated product (0.51 g, 75%) melted at 142–143° after recrystallization from methanol.

Anal. Calcd. for $C_{18}H_{15}Cl_2N_3OS_3$: C, 47.36; H, 3.31; Cl, 15.54; N, 9.21; S, 21.07. Found: C, 47.11; H, 3.43; Cl, 15.35; N, 9.07; S, 21.25.

1-(p-Chlorobenzyl)-4-ethoxy-6-(p-chlorobenzyldithio)-s-triazine-2(1H)-thione (VIIb)

Sodium hypochlorite (10 ml, available chlorine 5%) was added to a solution of I (458 mg, 1 mmole) and aqueous sodium hydroxide (*N*, 1.5 ml) in ethanol (50 ml). After being allowed to stand for 1 day, the reaction solution was evaporated, and the residue was extracted with chloroform (50 ml). The chloroform was washed with water, dried, and evaporated, and the residue was crystallized from ethanol to give the product, m.p. 130–131°, yield 108 mg (23%).

Anal. Calcd. for $C_{19}H_{17}Cl_2N_3OS_3$: C, 48.51; H, 3.64; Cl, 15.07; N, 8.93; S, 20.44. Found: C, 48.27; H, 3.65; Cl, 15.21; N, 9.04; S, 20.23.

1-p-Chlorobenzyl-4,6-di-(p-chlorobenzylthio)-s-triazine-2(1H)-thione (VIII)

A solution of III (91 mg, 0.3 mmole) in 0.66 ml of *N* sodium hydroxide (0.66 mmole) was added to *p*-chlorobenzyl chloride (106 mg, 0.66 mmole) in ethanol (6 ml). The product separated out after the solution had stood for 12 h, yield 166 mg (70%), m.p. 172–174° after recrystallization from methanol.

Anal. Calcd. for $C_{24}H_{18}Cl_3N_3S_3$: C, 52.32; H, 3.29; N, 7.63; S, 17.46. Found: C, 52.01; H, 3.30; N, 8.04; S, 17.89.

Rearrangement of VIII to 2,4,6-Tri-(p-chlorobenzylthio)-s-triazine (IX)

A sample of VIII (m.p. 174°) (10 mg) was heated in a tube sealed *in vacuo* at 250° for 1 h. The product was crystallized from ether–alcohol, m.p. 117 °C. The product was identical with the triester prepared by esterification of either trithiocyanuric acid or the monoester XI with *p*-chlorobenzyl chloride. The analytical sample melted at 120–122°.

Anal. Calcd. for $C_{24}H_{18}Cl_3N_3S_3$: C, 52.32; H, 3.29; Cl, 19.31; N, 7.63; S, 17.46. Found: C, 52.26; H, 3.23; Cl, 19.70; N, 7.80; S, 17.59.

Can. J. Chem. Downloaded from www.nrcresearchpress.com by 210.87.254.105 on 09/05/12
For personal use only.

2,4,6-Tri-(p-chlorobenzyldithio)-s-triazine (X)

Chlorine (0.55 ml, 0.025 mole) was added to bis-(*p*-chlorobenzyl) disulfide (7.89 g, 0.025 mole) in carbon tetrachloride (20 ml) at −8° to −10° over a period of 25 min. This solution was added to trithiocyanuric acid (0.7 g, 0.004 mole) suspended in a mixture of carbon tetrachloride (20 ml) and chloroform (10 ml) at −10° with stirring, and the stirring was continued for 1 h at 10°. The solution was evaporated at room temperature and the residue was crystallized from ethanol, giving 1.2 g (46%), m.p. 119–120°.

Anal. Calcd. for $C_{24}H_{18}Cl_3N_3S_6$: C, 44.54; H, 2.80; Cl, 16.44; N, 6.49; S, 29.73. Found: C, 44.04; H, 2.79; Cl, 16.61; N, 6.50; S, 29.79.

2-(p-Chlorobenzylthio)-4,6-dichloro-s-triazine (XI)

To a stirred solution of cyanuric chloride (29.1 g, 0.158 mole) in acetone (200 ml) was added dropwise a mixture of *p*-chloro-α-toluenethiol (25 g, 0.158 mole) and lutidine (20 ml) at −40° over a 15 min period. The stirring was continued at −25° for a further 2 h. The reaction mixture was poured into ice water (1 000 ml) and the precipitated solid was recrystallized from heptane, giving 21.0 g (38%), m.p. 72–75 °C. The analytical sample melted at 75–77 °C.

Anal. Calcd. for $C_{10}H_6Cl_3N_3S$: C, 39.17; H, 1.97; Cl, 34.69; N, 13.71; S, 10.46. Found: C, 39.08; H, 1.89; Cl, 34.83; N, 13.81; S, 10.77.

2-(p-Chlorobenzylthio)-s-triazine-4,6(3H,5H)-dithione (XII)

A solution of XI (13.0 g, 0.0424 mole) in dioxane (20 ml) was added to aqueous sodium hydrosulfide (50%, 20 ml) in methanol (40 ml). The solution was boiled briefly, cooled, and acidified, and the precipitated product was recrystallized from dimethylformamide, yield 8.4 g (65%). The purified product underwent a crystal change at 239–240°, and did not melt below 330 °C.

Anal. Calcd. for $C_{10}H_8ClN_3S_3$: C, 39.79; H, 2.67; Cl, 11.75; N, 13.92; S, 31.87. Found: C, 39.91; H, 2.75; Cl, 11.89; N, 13.77; S, 32.18.

2-(p-Chlorobenzylthio)-4,6-di-(p-chlorobenzyldithio)-s-triazine (XIII)

A solution of chlorine (0.11 ml, 5 mmoles) and bis-(*p*-chlorobenzyl) disulfide (1.58 g, 5 mmoles) in carbon tetrachloride (4 ml) was prepared at −10 °C. A suspension of XII (0.245 g, 0.81 mmole) in carbon tetrachloride (10 ml) was added at the same temperature, and the clear solution was allowed to stand at 10° for 30 min. The solution was evaporated and the residue was crystallized from petroleum ether to give the product, m.p. 93–95°, yield 85 mg (17%).

Anal. Calcd. for $C_{24}H_{18}Cl_3N_3S_5$: C, 46.86; H, 2.95; Cl, 17.29; N, 6.83; S, 26.07. Found: C, 46.88; H, 2.99; Cl, 17.64; N, 6.73; S, 26.38.

2-Chloro-4-(p-Chlorobenzylthio)-6-dimethylamino-s-triazine (XIV)

To a solution of X (3.07 g, 0.01 mole) in acetone (350 ml), aqueous dimethylamine solution (1.43 *N*, 70 ml, 0.01 mole) and 60 ml of aqueous sodium bicarbonate (1.18 g, 0.02 mole) were added at 25–35° over 1 h. The pH of the reaction mixture was kept at 8–8.5. The reaction temperature was allowed to rise to 35–40° for 10 min. Water (300 ml) was added to precipitate the product, yield 2.65 g (84%), m.p. 128–130°. The analytical sample was recrystallized from methanol, m.p. 129–130°.

Anal. Calcd. for $C_{12}H_{12}Cl_2N_4S$: C, 45.72; H, 3.83; Cl, 22.50; N, 17.77; S, 10.17. Found: C, 45.58; H, 3.77; Cl, 22.86; N, 17.55; S, 10.12.

4-(p-Chlorobenzylthio)-6-dimethylamino-s-triazine-2(1H)-thione (XV)

A solution of XIV (2.3 g) in dioxane (50 ml) was added to sodium hydrosulfide (0.84 g) in water (25 ml), and the reaction mixture was boiled for 5 min. The solution was cooled and acidified, and the product was purified by crystallization from chloroform, yield 1.5 g (66%), m.p. 250–253°.

Anal. Calcd. for $C_{13}H_{13}ClN_4S_2$: C, 46.07; H, 4.18; Cl, 11.33; N, 17.91; S, 20.50. Found: C, 45.71; H, 4.00; Cl, 11.62; N, 18.04; S, 20.61.

2,2'-Dithiobis-(4-(p-chlorobenzylthio)-6-dimethylamino-s-triazine) (XVI)

Treatment of XV with bis-(*p*-chlorobenzyl) disulfide and chlorine as described for the preparation of XII and XIII gave the ditriazinyl disulfide, yield 88%, m.p. 183–184° after crystallization from dimethylformamide.

Anal. Calcd. for $C_{24}H_{24}Cl_2N_8S_4$: C, 46.21; H, 3.88; Cl, 11.37; N, 17.97; S, 20.57. Found: C, 45.98; H, 3.98; Cl, 11.63; N, 17.76; S, 21.00.

ACKNOWLEDGMENT

The assistance of Miss Josephine Jaworska in some of the experimental work is gratefully acknowledged.

REFERENCES

1. A. E. S. Fairfull and D. A. Peak. J. Chem. Soc. 796 (1955).
2. W. J. Close. J. Am. Chem. Soc. **75**, 3617 (1953).
3. E. M. Smolin and L. Rapoport. *s*-Triazines and derivatives. Interscience Publishers, Inc., New York. 1959.

Can. J. Chem. Downloaded from www.nrcresearchpress.com by 210.87.254.105 on 09/05/12
For personal use only.

4. V. S. ETLIS, A. P. SINEOKOV, and G. A. RAZUVAEV. Izv. Akad. Nauk SSSR Ser. Khim. 737 (1964); Chem. Abstr. **61**, 3112*a* (1964).
5. I. UGI and K. ROSENDAHL. Ann. **670**, 80 (1963).
6. E. HOGGARTH and W. A. SEXTON. J. Chem. Soc. 815 (1947).
7. M. NAKAZAKI. J. Chem. Soc. Japan, Pure Chem. Sect. **75**, 338 (1954); Chem. Abstr. **49**, 10216*h* (1955).
8. C. S. SCANLEY, E. E. RICHARDSON, and E. K. FIELDS. U.S. Patent No. 2,854,411 (September 30, 1958).
9. H. KOOPMAN, J. H. UHLENBROEK, H. H. HAECK, J. DAAMS, and M. J. KOOPMANS. Rec. Trav. Chim. **78**, 967 (1959).
10. J. E. CHRISTIAN, G. L. JENKINS, L. R. C. KEAGLE, and J. A. CRUM. J. Am. Pharm. Assoc. **35**, 329 (1946).

Can. J. Chem. Downloaded from www.nrcresearchpress.com by 210.87.254.105 on 09/05/12
For personal use only.

Can. J. Chem. Downloaded from www.nrcresearchpress.com by 210.87.254.5 on 09/05/12
For personal use only.

ACID-CATALYZED REACTIONS OF VINYL COMPOUNDS

IV. MECHANISM OF FORMATION OF THE PRODUCTS OF THE REACTION OF VINYL ACETATE AND BENZENE[1]

J. M. PEPPER AND B. P. ROBINSON

Department of Chemistry and Chemical Engineering, University of Saskatchewan, Saskatoon, Saskatchewan

Received February 23, 1966

ABSTRACT

In part II of this series the isolation and identification of nine products from the reaction of vinyl acetate with benzene and aluminium chloride were described. This paper presents a discussion of the mechanism of formation of these compounds.

A comparison of the aluminium chloride catalyzed reactions of benzene with vinyl acetate and ethyl acetate is described. The reaction with ethyl acetate gave all the monocyclic products obtained from the reaction involving vinyl acetate, as well as *m*-diethylbenzene. The ratio of the ortho and para isomers of ethylacetophenone is the same in both reactions, which suggests that the same acetylating species is involved. The fact that none of the three polycyclic products is obtained from the reaction involving ethyl acetate suggests that the vinyl moiety of the ester is involved in the formation of these compounds from vinyl acetate. The use of ^{14}C-labelled vinyl acetate confirmed the fact that the synthesis of 9,10-dimethylanthracene involved only the vinyl part of the ester.

A study of the reactions of ethyl acetate and vinyl acetate with aluminium chloride showed that ethyl chloride and vinyl chloride, respectively, may be intermediates in the alkylation of benzene with these reagents. Evidence is presented that 1-phenylethyl chloride may also be an intermediate product in the reaction of vinyl acetate and benzene. 1,1-Diphenylethane is believed to be involved in the formation of 9,10-dimethylanthracene, the final step of which is thought to occur by the dehydrogenation of 9,10-dihydro-9,10-dimethylanthracene.

The isolation and characterization of nine products from the aluminium chloride catalyzed interaction of vinyl acetate and benzene have been described in an earlier communication (1). These products were ethylbenzene, acetophenone, *o*- and *p*-ethylacetophenone, 2,4- and 3,4-diethylacetophenone, 1,1-diphenylethane, 1,1-diphenylethene, and 9,10-dimethylanthracene. This communication describes experiments that were carried out in an attempt to obtain information regarding the mechanism of their formation.

There appeared to be a close similarity between the products obtained from the reaction of ethyl acetate and benzene in the presence of aluminium chloride (2–9) and those obtained from the corresponding reaction with vinyl acetate. A detailed study was therefore made, under identical conditions, of these two reactions, and the nature and relative yields of the products were compared. The ester was added slowly to a cooled mixture of benzene and aluminium chloride, and the resulting mixture was heated under reflux for 3 h before decomposition. From the ethyl acetate reaction, the liquid product was analyzed by gas–liquid chromatography. From the reaction involving vinyl acetate, 9,10-dimethylanthracene was separated by filtration from the semisolid crude product (10) and the filtrate was analyzed by gas–liquid chromatography. The identities of the products from the vinyl acetate reaction had already been established (1), and those from the ethyl acetate reaction were confirmed by isolation and infrared analysis. The identities and yields of products are given in Table I. There are significant variations in the nature of the products obtained from the two reactions. The absence of the polycyclic compounds and higher yields of all products containing the ethyl group are characteristic of the reaction

[1]*Presented at the 46th annual conference, Chemical Institute of Canada, Toronto, Ontario, June 1963. For parts I, II, and III of this series, see refs. 10, 1, and 30, respectively.*

TABLE I

Products of the reactions of vinyl acetate and ethyl acetate with benzene*

Product	Vinyl acetate			Ethyl acetate		
	Yield (g)		% yield (average)	Yield (g)		% yield (average)
	Run 1	Run 2		Run 1	Run 2	
Ethylbenzene	0.09	0.10	0.85†	0.37	0.47	3.95†
m-Diethylbenzene	—	—	—	0.19	0.14	2.45‡
Acetophenone	3.09	3.03	25.5†	0.99	1.08	8.6†
o-Ethylacetophenone	0.25	0.26	1.75†	0.32	0.37	2.35†
p-Ethylacetophenone	3.92	3.70	25.8†	4.78	5.00	33.1†
2,4-Diethylacetophenone	0.45	0.49	5.6‡	3.16	3.24	36.4‡
3,4-Diethylacetophenone	Trace	Trace		Trace	Trace	
1,1-Diphenylethane	0.18	0.12	0.85†	—	—	—
1,1-Diphenylethene	0.47	0.59	2.95†	—	—	—
9,10-Dimethylanthracene	3.24	3.08	30.7‡	—	—	—

*Ester (0.1 mole), benzene (1 mole), and aluminium chloride (0.3 mole).
†If it is assumed that 1 mole of ester is required to produce 1 mole of product.
‡If it is assumed that 2 moles of ester is required to produce 1 mole of product.

involving ethyl acetate, whereas high yields of acetophenone and the presence of the polycyclic derivatives are associated with the vinyl acetate reaction.

In an attempt to establish the nature of the alkylating and acylating species which may be responsible for these products, the reactions of ethyl acetate and vinyl acetate with aluminium chloride (in the absence of benzene) were studied. In equimolar proportions, ethyl acetate and aluminium chloride formed a complex which was stable at 80°. If the aluminium chloride were in excess, decomposition occurred with evolution of ethyl chloride and hydrogen chloride. The yield of ethyl chloride increased, reaching a maximum (0.7–0.8 mole/mole of ester) if the molar ratio of aluminium chloride to ester were 2:1. Under these conditions, the amount of hydrogen chloride evolved was about 0.2 mole/mole of ester.

An attempt to determine if, as a result of the indicated alkyl–oxygen type of fission, acetic acid would result from hydrolysis of the residue resulted in only a small amount being isolated. If, however, the residue from the reaction of ethyl acetate (1 mole) and aluminium chloride (2 or more moles) was treated with benzene, acetophenone (0.6 mole) was obtained. This molar yield compared well with the amount of ethyl chloride obtained under similar conditions. On the other hand, the reaction of vinyl acetate and aluminium chloride led to extensive polymerization. As expected, no vinyl chloride was detected, since it is known to polymerize under these conditions (11). The residue from a reaction involving 1 mole of vinyl acetate and 3 moles of aluminium chloride, on treatment with benzene, gave only 0.2 mole of acetophenone.

On the basis of this study, the reaction of ethyl acetate and aluminium chloride may be formulated as shown in eq. [1].

[1] $$MeCO_2Et + AlCl_3 \rightarrow \underset{\text{I}}{MeC(OEt)(O^+-AlCl_3)} \xrightarrow{AlCl_3} MeC(O^+-AlCl_3)(OAlCl_2) + EtCl$$

The formation of hydrogen chloride is not accounted for by this sequence of reactions, and it may result from decomposition of ethyl chloride by aluminium chloride (12, 13). The isolation of ethyl chloride suggests that it may be the alkylating agent in the reaction of

Can. J. Chem. Downloaded from www.nrcresearchpress.com by 210.87.254.5 on 09/05/12
For personal use only.

ethyl acetate with benzene. In a similar way, vinyl chloride may be the reactive intermediate in the reaction involving vinyl acetate. Such conclusions are supported by the work of Baddeley (14), who reported that alkylation with ethers and alcohols requires an excess of aluminium chloride and is probably effected by alkyl halide. Alternatively, Takegami and Shingu (15), who studied the reaction of ethyl acetate with aluminium bromide at 20°, reported that ethyl acetate is only slightly decomposed (4–9%), even in the presence of an excess of aluminium bromide, and that no ethyl bromide is produced. These authors concluded that the alkyl cation alkylates benzene and that no alkyl halide is involved.

The results reported by Illari (16), who studied the reaction of ethyl acetate with aluminium chloride, are not in accord with those obtained in this study. He reported that, even in the presence of an excess of the ester, hydrogen chloride (0.56 mole/mole of aluminium chloride) is liberated. This difference may not be real, since he added the ester slowly to the metal halide and hence, regardless of the final molar ratio of ester to halide, the metal halide was always initially in excess, and decomposition would occur. Norris and Arthur (7) also believed that ethyl chloride was the alkylating species in the aluminium chloride catalyzed reaction of ethyl acetate with benzene. They considered that the ethyl chloride arose by the decomposition of an equimolar complex of the ester and the metal halide, but since this occurs only at a temperature of 140–170°, it is more reasonable to assume, for the low-temperature reaction, that the decomposition is effected by the excess of aluminium chloride. The suggestion of Bowden (5) that the alkylation of benzene by ethyl acetate in the presence of aluminium chloride proceeds via the intermediate formation of ethylene is not supported by any experimental evidence.

The observed isomer distributions of $6.5 \pm 0.5\%$ and $93.5 \pm 0.5\%$ for the *o*- and *p*-ethylacetophenone, respectively, were the same for both the vinyl acetate and the ethyl acetate reactions, which would suggest that the same acylating species was involved. The acylating species might be formulated as shown in structure I. Alternatively, acetyl chloride may be formed *in situ* and may be responsible for the acylation reaction. Other workers have presented evidence for the intermediate formation of acyl halide in acylation reactions involving acid anhydrides and carboxylic acids (17–20).

Consideration was given to the possibility that vinyl chloride could react to give either styrene or 1-phenylethyl chloride, which could react further to give the final polycyclic products. To test the first suggestion, the reaction of styrene with aluminium chloride and benzene was investigated. None of the products of the vinyl acetate – benzene reaction was detected, except for a very small amount (0.2%) of ethylbenzene. It was therefore concluded that styrene is not an intermediate. Schramm (21) reported that 1-phenylethyl chloride reacted with benzene in the presence of aluminium chloride at 0° to give 1,1-diphenylethane, ethylbenzene, and 9,10-dihydro-9,10-dimethylanthracene.[2] In the present investigation, this reaction gave ethylbenzene, *m*-diethylbenzene, 1,1-diphenylethene, and 1,1-diphenylethane at room temperature. If, on the other hand, the reaction were carried out at reflux temperature, ethylbenzene, *m*-diethylbenzene, and 9,10-dimethylanthracene were obtained. The conversion of 1-phenylethyl chloride into ethylbenzene may occur in a manner analogous to the decomposition of other alkyl halides (12, 13) and as indicated in eqs. [2]–[4]. This sequence of reactions would also explain the formation of 1,1-diphenylethene. The almost exclusive formation of the *m*-diethylbenzene would indicate an isomerization of either the *o*- or *p*-diethyl isomer, or disproportionation of ethylbenzene (22).

[2]*This compound was actually 9,10-dimethylanthracene (see ref. 10).*

Can. J. Chem. Downloaded from www.nrcresearchpress.com by 210.87.254.5 on 09/05/12
For personal use only.

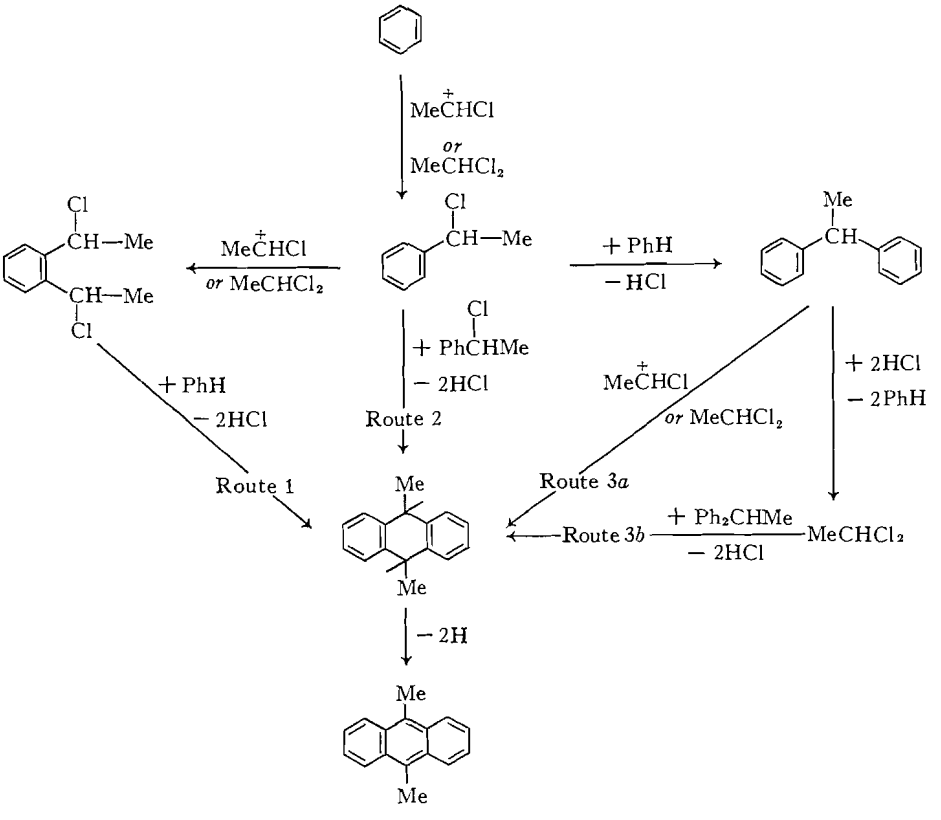
[2] $$PhCHClCH_3 + AlCl_3 \rightleftharpoons Ph\overset{+}{C}HCH_3AlCl_4^-$$

[3] $$PhCHClCH_3 + Ph\overset{+}{C}HCH_3AlCl_4^- \rightarrow Ph\overset{+}{C}ClCH_3AlCl_4^- + PhCH_2CH_3$$

[4] $$Ph\overset{+}{C}ClCH_3AlCl_4^- \rightarrow HCl + AlCl_3 + PhCCl{=}CH_2$$

The formation of the polycyclic products, 1,1-diphenylethene, 1,1-diphenylethane, and 9,10-dimethylanthracene, from the vinyl moiety of vinyl acetate and benzene was indicated by the fact that these compounds were not obtained from the reaction involving ethyl acetate. Further evidence that 9,10-dimethylanthracene and 1,1-diphenylethane are derived by a reaction involving the vinyl group is provided by the fact that these compounds may be obtained by the reaction of vinyl halides with benzene and Friedel–Crafts catalysts (23–28). The reaction of vinyl formate with benzene and aluminium chloride also gives 9,10-dimethylanthracene (10).

Experiments with ^{14}C-labelled vinyl acetate confirmed the fact that the *meso* carbon atoms in 9,10-dimethylanthracene originated from the vinyl group. When vinyl-1,2-^{14}C acetate was used the activity was incorporated into the 9,10-dimethylanthracene. The use of vinyl acetate-1-^{14}C resulted in the formation of inactive 9,10-dimethylanthracene. The formation of 9,10-dimethylanthracene could occur by one of three possible routes, as shown in Reaction Scheme 1. All of the three possible routes are consistent with the fact that the yield of 9,10-dimethylanthracene decreases if a very large excess of benzene is used (10). All three routes involve the intermediate formation of 9,10-dihydro-9,10-dimethylanthracene.



REACTION SCHEME 1. Possible routes for the formation of 9,10-dimethylanthracene.

Can. J. Chem. Downloaded from www.nrcresearchpress.com by 210.87.254.5 on 09/05/12
For personal use only.

Korshak *et al.* (27) found that the yield of 9,10-dimethylanthracene increased and of 1,1-diphenylethane decreased as the time of the vinyl acetate – benzene reaction increased. They suggested that 1,1-diphenylethane is an intermediate in the formation of 9,10-dimethylanthracene. These same authors (27) also reported the isolation of 9,10-dihydro-9,10-dimethylanthracene[2] by treatment of 1,1-diphenylethane with aluminium chloride, and suggested that the anthracene derivative was formed by disproportionation of 1,1-diphenylethane. Further, Radziewanowski (29) has reported that the treatment of 1,1-diphenylethane with aluminium chloride in the absence of benzene gives rise to the dihydroanthracene derivative.[2] The conversion of 1,1-diphenylethane into 1-phenylethyl chloride, followed by elimination of hydrogen chloride, was proposed to account for the reaction.

Experiments carried out during the present investigation did not result in the formation of 9,10-dimethylanthracene by the action of aluminium chloride on 1,1-diphenylethane, under the conditions described by Korshak *et al.* (27). However, when 1,1-diphenylethane was treated with aluminium chloride in the presence of benzene, 9,10-dimethylanthracene was obtained. This indicates that the anthracene derivative may be formed by route 3*b* (Reaction Scheme 1). 9,10-Dimethylanthracene was also obtained when 1,1-diphenylethane was treated with vinyl acetate and aluminium chloride, which indicates that the anthracene derivative may be formed by route 3*a*.

It was concluded that 1,1-diphenylethene is not an intermediate in the formation of 9,10-dimethylanthracene, because this compound, when treated with aluminium chloride either in the presence or absence of benzene, did not give rise to the anthracene derivative. Further, no 9,10-dimethylanthracene was obtained by treating 1,1-diphenylethene with vinyl acetate and aluminium chloride.

The formation of 9,10-dimethylanthracene by routes 3*a* and 3*b* is supported by studies on the reaction of toluene with vinyl acetate and aluminium chloride (30). In this case 2,7,9,10-tetramethylanthracene is formed. The final step in the formation of 9,10-dimethylanthracene involves the dehydrogenation of the dihydro compound. This dehydrogenation will be discussed in a forthcoming communication.

EXPERIMENTAL

Melting points are uncorrected. The infrared spectra were measured on a Perkin–Elmer model 21 instrument with sodium chloride optics. Gas–liquid chromatography was effected with a Beckman GC-2 chromatograph which had a thermal conductivity detector unit and which had been modified by placing the injection system as close as possible to one end of the column and by making it more comparable electronically to the GC-2A.

In all the reactions involving the use of anhydrous aluminium chloride, the ingress of moisture into the apparatus was prevented by the use of calcium chloride drying tubes.

The Reaction of Ethyl Acetate with Aluminium Chloride

The apparatus consisted of a three-necked flask fitted with a dropping funnel, a mercury-sealed stirrer, and a reflux condenser. A suitable attachment was connected to the top of the condenser for trapping the gaseous products. The exit gases were passed successively through a U-tube containing calcium chloride to prevent ingress of moisture into the flask, two scrubbers containing sodium hydroxide solution (to trap hydrogen chloride), a calcium chloride tube, an acetone – dry ice trap (to trap ethyl chloride), and finally another calcium chloride tube.

The procedure for a typical experiment was as follows. Aluminium chloride (40 g, 0.3 mole) was placed in the reaction flask. Ethyl acetate (8.8 g, 0.1 mole) was added dropwise, with stirring. During the addition heat was evolved and the evolution of gas was observed (bubbling through the scrubbers). At the end of the addition there was 0.4 ml of condensate in the acetone – dry ice trap. Five minutes after the end of the addition, bubbling of gas through the scrubbers ceased, and the mixture was heated to 80°. Gas started to bubble through the scrubbers when the temperature reached 60°. The mixture was maintained at 80° until bubbling ceased (ca. 1 h).

Can. J. Chem. Downloaded from www.nrcresearchpress.com by 210.87.254.5 on 09/05/12
For personal use only.

Can. J. Chem. Downloaded from www.nrcresearchpress.com by 210.87.254.5 on 09/05/12
For personal use only.

The reaction flask was allowed to cool and the system was flushed out with nitrogen. The condensate in the acetone – dry ice trap was allowed to warm up to about 0° and then measured. The volume of condensate was 5.3 ml at 2°. The infrared spectrum of the condensate was identical with that reported for ethyl chloride (31). Titration of the sodium hydroxide solution in the scrubbers indicated that 0.016 mole of hydrogen chloride had been produced by the reaction.

The residue in the reaction flask was treated as follows. Benzene (15.6 g, 0.2 mole) was added to the reaction flask over a period of 10 min. The mixture was stirred for 1 h at room temperature and then heated under reflux for 1 h. The reaction mixture was decomposed and worked up in the usual manner. Distillation of the crude product under reduced pressure gave acetophenone (2.75 g), b.p. 82–84° at 12 mm.

The Reaction of Vinyl Acetate with Aluminium Chloride

The apparatus and procedure were the same as for the corresponding reaction of ethyl acetate. There was evidence of polymerization in the condenser, and no vinyl chloride was isolated.

Vinyl acetate (0.1 mole) and aluminium chloride (0.3 mole) gave hydrogen chloride (0.025 mole). The residue, when heated under reflux for 3.5 h with benzene (15.6 g), gave, after the usual treatment, acetophenone (2.2 g, 18%), b.p. 80–83° at 12 mm.

The Reaction of Styrene with Benzene and Aluminium Chloride

Styrene (10.4 g, 0.1 mole) was added slowly over a period of 1 h to a stirred mixture of benzene (78 g, 1.0 mole) and aluminium chloride (40 g, 0.3 mole) in a 200 ml, three-necked flask equipped with a reflux condenser, a dropping funnel, and a mechanical stirrer. Both the condenser and dropping funnel were fitted with calcium chloride drying tubes. Throughout the addition, the flask was cooled in an ice bath, but after the addition the mixture was heated under reflux for 3 h. The reaction mixture was decomposed and worked up in the usual manner, whereby a black liquid was obtained.

The crude product was analyzed by gas–liquid chromatography on a Beckman silicone column, No. 17,449 (6 ft), at a temperature of 210° with a helium flow rate of 27 ml/min. Peaks corresponding to benzene, ethylbenzene, and styrene were observed. No peaks corresponding to diethylbenzene, diphenylethane (1,1- or 1,2-), or 1,1-diphenylethene were obtained. Analysis with a SE 30 (5%) on Chromosorb W column at a temperature of 210° with a helium flow rate of 23 ml/min showed the absence of 9,10-dimethylanthracene. Quantitative analysis by gas–liquid chromatography showed that the size of the peak corresponding to ethylbenzene indicated that 0.03 g ((0.28%) of ethylbenzene was formed. The peak corresponding to styrene was very small (comparable in size to that corresponding to ethylbenzene), which indicated that almost all the styrene had reacted.

The Reaction of Styrene with Benzene, Aluminium Chloride, and Hydrogen Chloride

The procedure was the same as for the above experiment, except that hydrogen chloride gas was bubbled through the reaction mixture throughout the reaction. As in the above experiment, gas–liquid chromatography showed the absence of diethylbenzene, diphenylethane (1,1- and 1,2-), 1,1-diphenylethene, and 9,10-dimethylanthracene. Peaks corresponding to benzene, ethylbenzene, and styrene were detected. The peaks corresponding to ethylbenzene and styrene were of comparable size. Quantitative analysis indicated that 0.015 g (0.14%) of ethylbenzene was formed.

The Reaction of 1-Phenylethyl Chloride with Benzene and Aluminium Chloride

Run 1

1-Phenylethyl chloride (7.25 g, 0.05 mole) was added slowly over a period of 1 h to a stirred, cooled mixture of benzene (39 g, 0.5 mole) and aluminium chloride (20 g, 0.15 mole) in a three-necked flask equipped with a reflux condenser, a dropping funnel, and a mechanical stirrer. Both the condenser and the dropping funnel were fitted with calcium chloride drying tubes. After the addition the mixture was heated under reflux for 3 h, and then decomposed and worked up in the usual manner. The crude product (9.65 g) consisted of a yellow solid and an orange liquid. The yellow solid was removed by filtration and washed with methanol to yield 2.35 g, m.p. 178–180°, which was readily shown to be 9,10-dimethylanthracene by a mixed melting point with an authentic sample and by determination of its infrared spectrum.

The filtrate was analyzed by gas–liquid chromatography on a Beckman silicone column, No. 17,449 (6 ft), at a temperature of 210° with a helium flow rate of 27 ml/min. Peaks corresponding to ethylbenzene and *m*-diethylbenzene were observed. The fact that these peaks were due to ethylbenzene and *m*-diethylbenzene was confirmed by collection of samples (gas–liquid chromatography). These two samples had infrared spectra which were identical with those of authentic samples of ethylbenzene and *m*-diethylbenzene, respectively. Quantitative analysis showed that the yield of ethylbenzene was 0.29 g (5.5%) and of *m*-diethylbenzene 0.215 g (6.4%). Analysis with a SE 30 (5%) on Chromosorb W column at a temperature of 210° showed that the filtrate contained a negligible amount of 9,10-dimethylanthracene.

Run 2

An experiment similar to the above was carried out in which the reaction mixture was not heated under reflux. 1-Phenylethyl chloride (7.25 g, 0.05 mole) was added, in the manner described in run 1 above, to benzene (39 g, 0.5 mole) and aluminium chloride (20 g, 0.15 mole). After the addition the mixture was stirred for 0.5 h at room temperature, and then decomposed and worked up. The crude product (9.5 g), an orange

oil, was analyzed by gas–liquid chromatography. Peaks corresponding to ethylbenzene, *m*-diethylbenzene, 1,1-diphenylethane, and 1,1-diphenylethene were observed. The presence of these four compounds was confirmed by collection of samples. The infrared spectra of these samples were identical with those of the authentic compounds. Gas–liquid chromatography showed the absence of 9,10-dimethylanthracene. Quantitative analysis showed that the yields of ethylbenzene, *m*-diethylbenzene, 1,1-diphenylethane, and 1,1-diphenylethene were 0.59 g (11.2%), 0.59 g (17.6%), 0.50 g (5.5%), and 0.82 g (9.1%), respectively.

The Reaction of ^{14}C-Labelled Vinyl Acetate with Benzene and Aluminium Chloride

Vinyl-1,2-^{14}C acetate[3] (8.6 g, 0.1 mole, ca. 0.1 mcurie) was treated with benzene (78 g, 1.0 mole) and anhydrous aluminium chloride (40 g, 0.3 mole) in the same manner as previously described (1). The 9,10-dimethylanthracene obtained after recrystallization was shown to be pure by elemental analysis.

Anal. Calcd. for $C_{16}H_{14}$: C, 93.16; H, 6.84. Found: C, 93.14; H, 6.91.

The activities of the 9,10-dimethylanthracene and its oxidation product anthraquinone (9) were determined. The activity of the vinyl-1,2-^{14}C acetate was determined by the conversion of this compound into iodoform (32). The ratio of the activities of 9,10-dimethylanthracene, anthraquinone, and vinyl acetate was 2.05:1.0:1.04.

When vinyl acetate-1-^{14}C[4] was used the 9,10-dimethylanthracene obtained was essentially inactive.

The Reaction of 1,1-Diphenylethane with Aluminium Chloride

(*i*) 1,1-Diphenylethane (1.8 g) was treated with aluminium chloride (1.3 g) according to the procedure of Korshak *et al.* (27). Distillation of the crude product gave 1,1-diphenylethane (0.2 g), b.p. 146–155° at 13 mm. No more material distilled over until the temperature reached 230–240° (at 15 mm). This indicated the absence of 9,10-dimethylanthracene, b.p. 180–182° at 15 mm (27).

(*ii*) 1,1-Diphenylethane (3.64 g) and aluminium chloride (2.7 g) were heated together at 60–70° for 3 h. The mixture was decomposed and worked up in the usual manner. Unchanged 1,1-diphenylethane (0.45 g), b.p. 148–156° at 15 mm, was recovered by distillation of the crude product (1.85 g). The residue (1.33 g) was chromatographed on alumina (50 g). Nothing was eluted from the column by light petroleum (700 ml). Since 9,10-dimethylanthracene is readily removed from alumina by this solvent, it is clear that no 9,10-dimethylanthracene was present.

(*iii*) 1,1-Diphenylethane (1.8 g), aluminium chloride (1.3 g), and benzene (10 ml) were heated together under reflux for 3 h. The mixture was decomposed and worked up in the usual manner. The crude product (0.75 g) was a brown waxy solid. Gas chromatographic analysis of the crude product, with a SE 30 (5%) on Chromosorb W column (6 ft) at 205° with a helium flow rate of 21 ml/min, indicated the presence of 9,10-dimethylanthracene. 9,10-Dimethylanthracene was obtained by chromatography of the crude product on alumina (30 g), with light petroleum as eluent. Recrystallization from benzene gave yellow needles (0.08 g, 8%), m.p. 178–180°.

The Reaction of 1,1-Diphenylethane with Vinyl Acetate and Aluminium Chloride

(*i*) Vinyl acetate (0.86 g) was added dropwise to a stirred mixture of 1,1-diphenylethane (4.0 g) and aluminium chloride (4.0 g). The mixture was heated at 80° for 3 h, and then decomposed and worked up in the usual manner. Distillation of the crude product (2.8 g) gave 9,10-dimethylanthracene (crude), b.p. ca. 180° at 15 mm. Recrystallization from benzene gave 9,10-dimethylanthracene (0.24 g, 11.5%), m.p. 178–180°.

(*ii*) Vinyl acetate (0.86 g) was added dropwise to a stirred mixture of 1,1-diphenylethane (5.0 g) and aluminium chloride (4.0 g). The mixture was heated at 70–80° for 3 h, and then decomposed and worked up in the usual manner. The crude product (3.0 g) was chromatographed on alumina (50 g). Elution of the column with light petroleum gave 9,10-dimethylanthracene, m.p. ca. 170–176°. Recrystallization from benzene gave yellow needles (0.26 g, 12.5%), m.p. 178–180°.

The Reaction of 1,1-Diphenylethene with Aluminium Chloride

(*i*) 1,1-Diphenylethene (1.8 g) and aluminium chloride were heated together at 70–80° for 3 h. The mixture was decomposed and worked up in the usual manner. Distillation of the crude product did not give 9,10-dimethylanthracene (b.p. 180–182° at 15 mm (27)).

(*ii*) 1,1-Diphenylethene (3.6 g) and aluminium chloride (2.7 g) were heated together at 70–80° for 3 h. The mixture was decomposed and worked up in the usual manner. The crude product (3.6 g) was chromatographed on alumina (50 g). The column was eluted with light petroleum. No 9,10-dimethylanthracene was obtained, but a colorless oil, which crystallized (when washed with methanol) to give a white solid (0.5 g), m.p. 143–145°, was obtained. Schoepfle and Ryan (34) reported that 1,1-diphenylethene, when treated with aluminium chloride, was converted into 1,1,3-triphenyl-3-methylhydrindene, m.p. 143°.

(*iii*) 1,1-Diphenylethene (1.8 g), aluminium chloride (1.3 g), and benzene (10 ml) were heated together under reflux for 3 h. The mixture was decomposed and worked up in the usual manner. The crude product was a dark-colored, viscous liquid (1.56 g). Gas chromatographic analysis of the crude product, with a SE 30 (5%) on Chromosorb W column (6 ft) at 205° with a helium flow rate of 21 ml/min, showed that no 9,10-dimethylanthracene was present.

[3]*Vinyl-1,2-^{14}C acetate (208 mg, 0.5 mcurie) was diluted with inactive vinyl acetate (50 ml); 8.6 g of this material was used.*

[4]*Prepared from acetic acid-1-^{14}C and acetylene (33).*

Can. J. Chem. Downloaded from www.nrcresearchpress.com by 210.87.254.5 on 09/05/12
For personal use only.

The Reaction of 1,1-Diphenylethene with Vinyl Acetate and Aluminium Chloride

Vinyl acetate (0.86 g) was added dropwise to a stirred mixture of 1,1-diphenylethene (4.8 g) and aluminium chloride (4.0 g). The mixture was heated at 70–80° for 3 h, and then decomposed and worked up in the usual manner. The crude product (4.3 g) was chromatographed on alumina (100 g). The column was eluted with light petroleum (700 ml). No eluate was obtained, which indicated that no 9,10-dimethylanthracene was present.

ACKNOWLEDGMENTS

Grateful acknowledgment is made of the financial assistance provided by Imperial Oil Limited. The authors thank both the University of Saskatchewan and Canadian Industries Limited for the award to one of them (B. P. R.) of a graduate assistantship (1961–1962) and a fellowship (1962–1963), respectively. The molecular weights and radioactivities were determined by Mr. E. Mazurek and Mr. J. Dyck, National Research Council, Saskatoon.

REFERENCES

1. J. M. PEPPER and B. P. ROBINSON. Can. J. Chem. **41**, 2103 (1963).
2. J. CRYER. Trans. Roy. Soc. Can., Sect. III, **19**[3], 29 (1925).
3. L. I. KASHTANOV. Zh. Obshch. Khim. **2**, 515 (1932); Chem. Abstr. **27**, 975 (1933).
4. I. G. FARBENINDUSTRIE A.-G. Ger. Patent No. 637,384 (October 1936).
5. E. BOWDEN. J. Am. Chem. Soc. **60**, 645 (1938).
6. J. F. NORRIS and B. M. STURGIS. J. Am. Chem. Soc. **61**, 1413 (1939).
7. J. F. NORRIS and P. ARTHUR. J. Am. Chem. Soc. **62**, 874 (1940).
8. D. N. KURSANOV and R. R. ZEL'VIN. Zh. Obshch. Khim. **9**, 2173 (1939); Chem. Abstr. **34**, 4062 (1940).
9. D. N. KURSANOV and R. R. ZEL'VIN. Compt. Rend. Acad. Sci. URSS, **36**, 17 (1942).
10. J. M. PEPPER, B. P. ROBINSON, and G. W. SCHWANBECK. Can. J. Chem. **40**, 122 (1962).
11. C. A. THOMAS. Anhydrous aluminium chloride in organic chemistry. Reinhold Publishing Corp., New York. 1941. p. 816.
12. G. BADDELEY and W. PICKLES. J. Chem. Soc. 3726 (1953).
13. P. NIELD, W. PICKLES, H. T. TAYLER, S. VARMA, R. WILLIAMSON, D. B. WOOTON, and E. WRENCH. Unpublished results.
14. G. BADDELEY. Quart. Rev. London, **8**, 355 (1954).
15. Y. TAKEGAMI and H. SHINGU. Bull. Inst. Chem. Res. Kyoto Univ. **24**, 84 (1951).
16. G. ILLARI. Gazz. Chim. Ital. **77**, 352 (1947).
17. P. H. GROGGINS and R. H. NAGEL. Ind. Eng. Chem. **26**, 1313 (1934).
18. P. H. GROGGINS, R. H. NAGEL, and A. J. STIRTON. Ind. Eng. Chem. **26**, 1317 (1934).
19. G. ILLARI. Gazz. Chim. Ital. **78**, 687 (1948).
20. N. M. CULLINANE, S. J. CHARD, and D. M. LEYSHON. J. Chem. Soc. 376 (1952).
21. J. SCHRAMM. Ber. **26**, 1706 (1893).
22. G. A. OLAH. Friedel–Crafts and related reactions. Interscience Publishers, Inc., New York. 1963.
23. R. ANSCHÜTZ. Ann. **235**, 299 (1886).
24. A. ANGEBLIS and R. ANSCHÜTZ. Ber. **17**, 167 (1884).
25. J. BOESEKEN and M. C. BASTET. Rec. Trav. Chim. **32**, 184 (1913).
26. J. M. DAVIDSON and A. LOWY. J. Am. Chem. Soc. **51**, 2978 (1929).
27. V. V. KORSHAK, K. K. SAMPLAVSKAYA, and A. I. GERSHANOVICH. Zh. Obshch. Khim. **16**, 1065 (1946); Chem. Abstr. **41**, 2715 (1947).
28. M. S. MALINOVSKII. Zh. Obshch. Khim. **17**, 2235 (1947).
29. C. RADZIEWANOWSKI. Ber. **27**, 3235 (1894).
30. J. M. PEPPER, M. HOWELL, and B. P. ROBINSON. Can. J. Chem. **42**, 1242 (1964).
31. Infrared spectral data. Am. Petrol. Inst. Res. Proj. 44. 1962. Serial No. 46.
32. M. F. SHOSTAKOVSKII, F. P. SIDEL'KOVSKAYA, and M. G. ZELENSKAYA. Izv. Akad. Nauk SSSR Otd. Khim. Nauk, 615 (1956).
33. J. D. ROBERTS, C. C. LEE, and W. H. SAUNDERS. J. Am. Chem. Soc. **76**, 4501 (1954).
34. C. S. SCHOEPFLE and J. D. RYAN. J. Am. Chem. Soc. **52**, 4021 (1930).

Can. J. Chem. Downloaded from www.nrcresearchpress.com by 210.87.254.5 on 09/05/12
For personal use only.

Can. J. Chem. Downloaded from www.nrcresearchpress.com by 210.87.254.105 on 09/05/12
For personal use only.

LIQUID-PHASE OXIDATION OF CYCLOHEXENE IN THE PRESENCE OF BENZALDEHYDE

TSUNEO IKAWA AND TOSHIYUKI FUKUSHIMA
Tokyo Institute of Technology, Ōokayama, Meguro-ku, Tokyo, Japan

AND

MINORU MUTO AND TADAHISA YANAGIHARA
Tōyō Sōda Manufacturing Co., Ltd., Nanyō-chō, Tsuno-gun, Yamaguchi-Ken, Japan

Received January 25, 1966

ABSTRACT

The kinetics, at room temperature, of the oxidation of cyclohexene in the presence of benzaldehyde have been measured, and the nature of the products when this oxidation was performed at 70 and 110 °C has been studied. The results indicate that the attack of benzoyl peroxy radical on the double bond of cyclohexene retards the rate of oxygen absorption and also causes epoxidation of cyclohexene. The epoxidation of cyclohexene by peroxybenzoic acid (produced from aldehyde) seems to proceed simultaneously with the epoxidation by peroxy radicals during the oxidation of cyclohexene in the presence of benzaldehyde.

INTRODUCTION

It is known that the autoxidation of olefin in the presence of aldehyde gives a quite sizable amount of epoxide (1–3) and ester (4, 5), and also that the olefin retards (6) the oxidation of aldehyde.

We have reported (7) that retardation of the liquid-phase oxidation of benzaldehyde caused by the addition of a small amount of non-olefinic compounds (tetralin and cumene) can be explained reasonably well by the co-oxidation scheme postulated by Walling (8), and also (9) that acetaldehyde works as the most effective reaction accelerator for the air oxidation of propylene, doubling the yield of propylene oxide.

The purpose of this paper is to clarify (*a*) the retarding effect of cyclohexene on the rate of oxidation of benzaldehyde, and (*b*) the reaction mechanism of the epoxidation of cyclohexene in the presence of benzaldehyde.

The mechanism of retardation was examined kinetically, and the mechanism of epoxidation was investigated by means of the reaction products.

EXPERIMENTAL

Materials

Cyclohexene was purified by distillation under a nitrogen stream. Benzene was washed successively with concentrated sulfuric acid, dilute alkali, and distilled water, and then dried with sodium metal. Benzaldehyde was purified just before use by fractional distillation under a nitrogen stream at 60 mm Hg pressure and 99.8–100.3 °C.

Oxygen and nitrogen, both 99.9% pure, were dried with calcium chloride. Peroxybenzoic acid was prepared from benzoyl peroxide according to Braun's procedure as modified by Kolthoff *et al.* (10). The following materials were used as reference substances for gas chromatographic analysis: cyclohexene oxide and benzoic acid were used without further purification; cyclohexane-1,2-diol was prepared (11) from cyclohexene and hydrogen peroxide; cyclohexane-1,2-diol monobenzoate was prepared from cyclohexane-1,2-diol and benzoic acid by Owens' procedure (12); cyclohexene-3-ol and cyclohexene-3-on were obtained from the autoxidation of cyclohexene.

Kinetic Measurements at Room Temperature

The rate of oxygen absorption was measured in an oxygen atmosphere with benzene as solvent without cobalt catalyst by the same method as already described in a previous paper (7). The reaction temperature and the concentration of benzaldehyde were kept constant at 19 °C and 3.5 moles/l, respectively, in each run.

Product Study at High Temperatures

The general procedure was essentially the same as described in a previous paper (9). Benzene was added to a mixture of 20 cc of cyclohexene and 6–20 cc of benzaldehyde, up to a total volume of 100 cc. This solution was placed in an autoclave having a 200 cc volume and a magnetic stirrer. Nitrogen was introduced into the autoclave up to 5 kg/cm^2, with and without cobalt acetate. To keep the partial pressure of oxygen at about 3 kg/cm^2, oxygen was occasionally added from an oxygen accumulator. Unreacted cyclohexene, unreacted benzaldehyde, cyclohexene oxide, cyclohexene-3-ol, and cyclohexene-3-on were analyzed by gas chromatography on a 3 m column of P.E.G. 1000 at 110 °C with a hydrogen flow rate of 50 cc/min. Cyclohexene-1,2-diol monobenzoate, cyclohexylbenzoate, and benzoic acid were analyzed on a 2 m column of P.E.G. 20 M at 200 °C with a hydrogen flow rate of 50 cc/min. The retention times of these compounds were 2.3, 52, 10, 43.5, 37, 53, 10.5, and 14 min, respectively. The total acid was measured by titration with alcoholic potassium hydroxide. Carbon dioxide was found to be the major gaseous product on the gas chromatogram. The amount of cyclohexane-1,2-diol dibenzoate was not measured.

Epoxidation of Cyclohexene with Peroxybenzoic Acid

A solution of 20 cc of cyclohexene and 0.165 g of cobalt acetate dissolved in 100 cc of benzene was refluxed in a 250 cc glass flask at 70 °C under a nitrogen atmosphere, a benzene solution containing 0.345 mole peroxybenzoic acid/100 cc being added at the rate of 0.05 mole peroxybenzoic acid/h during 2 h.

RESULTS

Kinetic Measurements

The reaction conditions and results of the kinetic study are summarized in Table I. Since the amount of oxygen absorbed during each measurement was not large, the concentrations of cyclohexene and benzaldehyde could be considered to be constant. Therefore, without any further reaction of peroxides affecting the oxygen absorption, the rate of oxygen absorption should be constant. Typical absorption curves are shown in Fig. 1. The initial absorption rate was different in each run under the same reaction conditions, probably because of a trace of impurity in the reactants. However, at steady state the same rate was obtained under the same reaction conditions. Absorption rates were calculated from the slopes of the straight lines. Since cyclohexene is considered to be an inhibitor during the oxidation of benzaldehyde, the antioxidation during sufficient oxygen pressure can be represented by eqs. [1]–[5] (13).

TABLE I

Reaction conditions and results of the kinetic measurements

Run No.	Initial concentration of benzaldehyde (mole/l)	Observed rate of oxygen absorption (mole/l s)	k_5 (l/mole s)	Calculated rate of oxygen absorption (mole/l s)
1	0	6.61×10^{-5}		
2	0.000395	5.28	2.51×10^{3}	5.66×10^{-5}
3	0.00158	3.67	1.63	3.51
4	0.00395	2.1	1.46	1.87
5	0.0079	1.1	1.50	1.11
6	0.0158	0.77	1.08	0.79
7	0.0790	0.108	1.57	0.095
8	0.197	0.0285	2.39	0.038

Steady-state methods lead to the rate equation shown in eq. [6].

The rate constant k_1 was calculated to be 0.48×10^{-8} l/mole s from the equation of the oxidation rate of pure benzaldehyde. By using values of k_1 and k_3 equal to 2.2×10^3 l/mole s (14) and $k_4 = 2.3 \times 10^8$ l/mole s (14) and the observed oxidation rates of the mixture at 19 °C, the values of k_5 are calculated from eq. [6] (Table I). The values of k_5 should be constant regardless of the concentration of reactant; the calculated values of k_5 appear to be roughly constant. By using the k values noted above and k_5 (mean) = 1.79

Can. J. Chem. Downloaded from www.nrcresearchpress.com by 210.87.254.105 on 09/05/12
For personal use only.

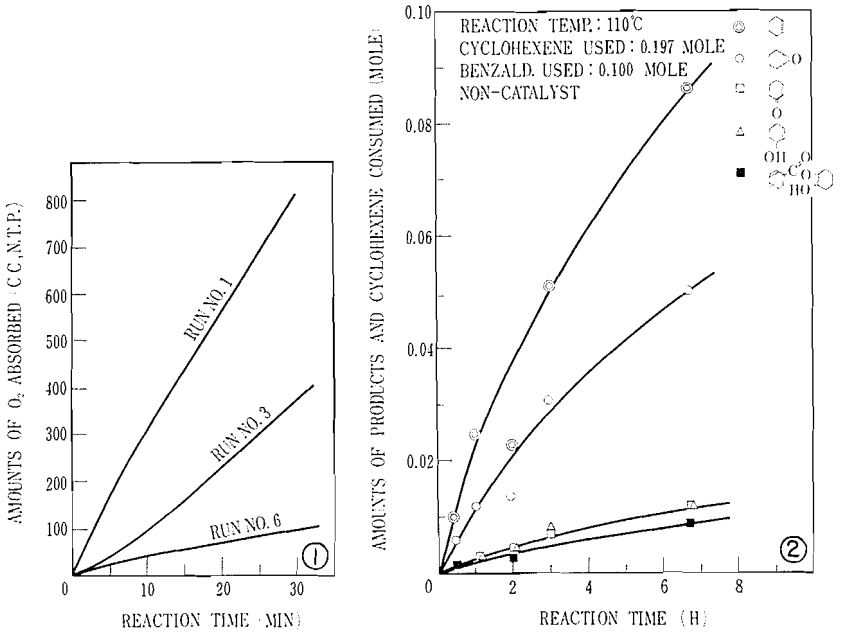
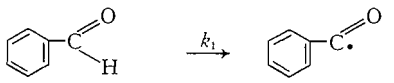
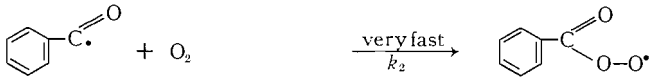


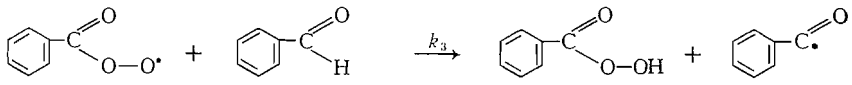
FIG. 1. Oxidation of binary system.
FIG. 2. Products versus reaction time.

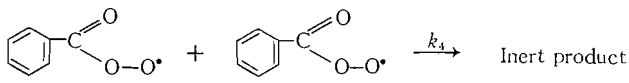
$\times 10^3$ l/mole s, the rates of oxygen absorption are calculated (Table I); the results were in good agreement with the observed values. The reaction schemes of the co-oxidation suggested by Walling (8) and by Ikawa *et al.* (7), in addition to other assumptions, have been applied to this reaction system, but the retardation of the oxidation rate could not be explained very well. It therefore seems that cyclohexene combines with benzoyl peroxy radical as shown in eq. [5], and reduces the oxidation rate.

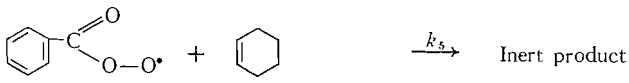
It was difficult to analyze accurately the reaction products at room temperature, because only a small amount of cyclohexene had reacted. Therefore, the products were

[1] 

[2] 

[3] 

[4] 

[5] 

[6] $$-d[O_2]/dt = -\{k_3k_5[C_7H_6O][C_6H_{10}] + k_3[C_7H_6O](k_5^2[C_6H_{10}]^2 + 4k_4k_1[C_7H_6O])^{\frac{1}{2}}\}/2k_4$$

Can. J. Chem. Downloaded from www.nrcresearchpress.com by 210.87.254.105 on 09/05/12
For personal use only.

analyzed at high temperatures. It is uncertain whether the reaction mechanism at room temperature holds at 70–100 °C, but it can serve to clarify the mechanism of epoxidation at high temperatures.

Product Study at High Temperatures

The reaction conditions and results are presented in Table II. The rate of oxidation without catalyst was so slow at 70 °C that oxidation had to be carried out at 110 °C. The variations in the yields of products and in the amounts of cyclohexene and benzaldehyde consumed are shown in Figs. 2 and 3. The effect of the concentration of benzaldehyde on the selectivities of products is shown in Fig. 4. Cyclohexene oxide was obtained in a good

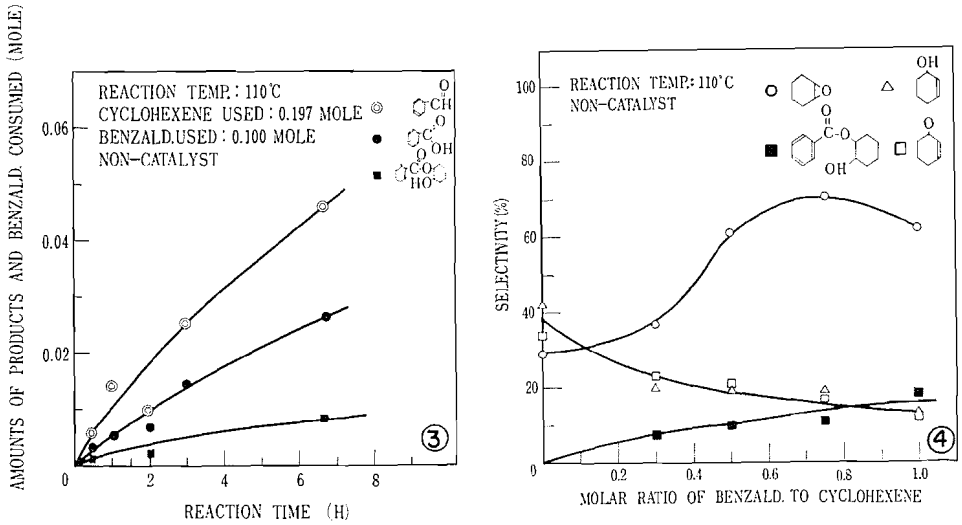


FIG. 3. Products versus reaction time.
FIG. 4. Selectivity of products.

yield. The selectivity of the epoxide was increased by adding benzaldehyde. Although the rate of oxygen absorption has not been measured exactly, during the oxidation of pure cyclohexene the rate was different in every run, but the selectivities of products remained roughly constant. Run 20 (Table II) is an example of these runs. By adding cobalt acetate or benzaldehyde the reproducibility of this procedure became satisfactory. A trace of cyclohexylbenzoate but no cyclohexane-1,2-diol was found on the gas chromatogram, and a trace of peroxide was detected by iodometry. Acid and carbon dioxide appear to have been formed from benzaldehyde, since they were detected in only small amounts in the oxidation products of pure cyclohexene. A sizable amount of polymerized product was found in the residue after distillation of the products.

Epoxidation with Peroxybenzoic Acid

The most probable reaction mechanism for epoxidation during the autoxidation of olefin in the presence of aldehyde seems to be the reaction of olefin with peracid produced by aldehyde. However, it must also be considered that benzoyl peroxy radical reacts directly with cyclohexene to form the epoxide by a mechanism similar to that postulated by Twigg (15) for the oxidation of pure olefin and confirmed by Brill (16, 17) and Roch (18). To ascertain which of these processes was of importance, epoxidation by peroxybenzoic acid was studied in the presence of cobalt acetate. No peroxide and peracid were detected

Can. J. Chem. Downloaded from www.nrcresearchpress.com by 210.87.254.105 on 09/05/12
For personal use only.

Can. J. Chem. Downloaded from www.nrcresearchpress.com by 210.87.254.105 on 09/05/12
For personal use only.

TABLE II

Reaction conditions and results of the product study at high temperatures

Run No.	Temperature (°C)	Time (h)	Oxygen absorbed (cc)	C_6H_5CHO used (mole)	% conversion		% selectivity					
					C_6H_{10}	C_6H_5CHO	$C_6H_{10}O$	$C_6H_{10}(OH)$-$O(CO)C_6H_5$	C_6H_9OH	$C_6H_8{=}O$	C_6H_5COOH†	CO_2†
9*	70	3.0	670	0.100	21.6	35.6	45.7	11.2	17.7	15.5	35.2	2.32
10*	70	6.5	230	0.060	7.3	9.0	40.8	14.7	26.8	23.9	60.3	3.98
11*	70	8.0	250	0	11.7		~0	0	50.6	28.9	0	~0
12*	110	1.0	360	0	13.0		8.6	0	49.2	24.2	0	~0
13*	110	1.5	1 400	0.100	38.3	47.4	33.3	10.3	18.3	20.9	47.9	7.81
14*	110	0.5	830	0.100	22.9	31.1	38.1	10.8	18.0	29.5	46.0	6.37
15	110	0.5	190	0.100	4.9	6.0	74.0	11.8	~0	~0	72.2	6.78
16‡	110	1.0	500	0.100	12.7	13.4	48.0		8.0	12.0	40.3	6.06
17	110	2.0	470	0.100	11.7	10.0	60.9	9.7	20.0	21.3	74.3	7.60
18	110	3.0	1 000	0.100	26.0	24.9	62.0		12.6	19.0	61.0	4.90
19	110	6.7	2 000	0.100	43.9	45.7	59.0	10.6	14.6	14.0	57.5	6.68
20	110	2.2	580	0	24.1		29.5		43.2	34.1	0	~0
21	110	2.0	500	0.060	24.2	21.7	36.7	7.1	20.4	23.0	60.2	2.60
22	110	1.6	500	0.150	17.2	17.0	70.7	10.3	19.1	17.3	56.1	4.94
23	110	1.5	500	0.200	21.6	18.9	62.0	18.3	13.6	11.8	43.7	3.19

*Cobalt acetate (0.165 g) added.
†Selectivity to benzaldehyde consumed, others to cyclohexene consumed.
‡Partial pressure of oxygen, 5 kg/cm²; cyclohexene used, 0.197 mole.

in the product by iodometry. In spite of a high rate of epoxidation, only 3% of the peracid reacted with cyclohexene to form cyclohexene oxide in the presence of cobalt acetate. This result shows that the rate of catalytic decomposition of peroxybenzoic acid is much larger than the rate of epoxidation.

DISCUSSION

The results of the kinetic study indicate that cyclohexene works as an acceptor for benzoyl peroxy radical and reduces the rate of oxygen absorption at room temperature.

If the results of the epoxidation of cyclohexene with peracid in the presence of cobalt acetate are considered, it is unlikely that epoxidation with peracid is the main epoxidation route in the actual cobalt-catalyzed oxidation. Cyclohexenyl or benzoyl peroxy radical seems to take part in epoxidation. Brill (16) reported that cyclohexenyl peroxy radical combined with a double bond of cyclohexene to form cyclohexene oxide and cyclohexenyl alkoxy radical, which were converted into cyclohexenol and cyclohexenone. We have obtained cyclohexene oxide in the products of the oxidation of pure cyclohexene, and a fair amount of cyclohexene-3-ol and cyclohexene-3-on in the products of the catalytic oxidation in the presence of benzaldehyde. These results indicate the considerable contribution of cyclohexenyl peroxy radical in epoxidation, whereas increasing the selectivity of the epoxide by the addition of benzaldehyde supports the contribution of benzoyl peroxy radical in epoxidation. It is considered that benzaldehyde reacts easily to form benzoyl peroxy radical, which then attacks the hydrogen atom of cyclohexene and causes the increase in the concentration of cyclohexenyl peroxy radical, the latter contributing to the epoxidation. This reaction scheme may be negligible at room temperature, if the results of the kinetic study are taken into account. It is usually considered (19) that most of the additions of radicals at double bonds of olefins involve very low activation energies; consequently, at low temperatures their rates exceed those of the competing abstraction of hydrogen from the olefins. This situation is reversed at high temperatures, abstraction then becoming dominant. Therefore, cyclohexenyl peroxy radical appears to contribute much to the epoxidation at high temperatures. The increase in the molar ratio of cyclohexene oxide to cyclohexenol and cyclohexenone, both of which result from cyclohexenyl peroxy radical, with the addition of benzaldehyde is shown in Fig. 5, and the decrease in the selectivities of cyclohexenol and cyclohexenone with the addition of benzaldehyde is shown in Table II. These results indicate that the attack of benzoyl peroxy radical on the hydrogen of cyclohexene is not dominant at 70–110 °C, and lead to the speculation that benzoyl peroxy radical plays a considerable role directly in the epoxidation during the cobalt-catalyzed oxidation. A probable reaction scheme for the epoxidation during the cobalt-catalyzed oxidation is the attack of benzoyl peroxy radical on a double bond of cyclohexene to form the epoxide and benzoyl alkoxy radical; this mechanism is similar to that postulated by Twigg (15).

The increase in the selectivity of the epoxide in the non-catalytic oxidation compared with that in the cobalt-catalyzed oxidation will result from the epoxidation of cyclohexene with peroxybenzoic acid, the rate of which (20) is larger than the rate (21) of the thermal decomposition of the peracid and the rate (22) of the Baeyer–Villiger reaction of benzaldehyde with the peracid.

Since the kinetic study has shown that the rate of reaction [5] is comparable with that of reaction [3] at room temperature, it may be concluded that the combination of benzoyl peroxy radical with a double bond of cyclohexene also contributes more than a little to the epoxidation during the non-catalytic oxidation at 70–110 °C.

Can. J. Chem. Downloaded from www.nrcresearchpress.com by 210.87.254.105 on 09/05/12
For personal use only.

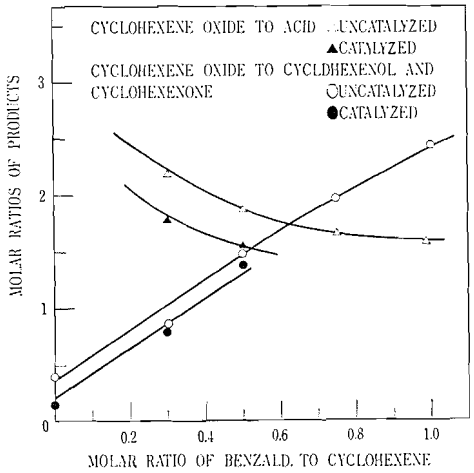


FIG. 5. Molar ratio of products.

Most of the benzoyl alkoxy radical may be converted into benzoic acid, and the rest of it seems to combine with a double bond of cyclohexene, possibly to form esters. However, the latter is unlikely because (*a*) cyclohexane-1,2-diol monobenzoate is obtained at the same selectivity in the non-catalytic and the catalytic oxidation (in the latter case there is a greater concentration of benzoyl alkoxy radical in the reaction mixture than in the former case because of a sizable amount of benzoyl alkoxy radical produced by the catalytic decomposition of peroxybenzoic acid), and (*b*) a trace of cyclohexyl benzoate is obtained.

If one considers the fact (4) that cyclohexene gives a large amount of cyclohexane-1,2-diol monobenzoate at 50 °C in the oxidation with benzaldehyde, the ester seems to be produced by reaction [5] at low temperatures. At 110 °C, the ester appears to be produced by the reaction of cyclohexene oxide with benzoic acid, because no cyclohexane-1,2-diol is found in the oxidation products and the calculated amount of the ester is of about the same order of magnitude as that obtained in the actual oxidation at 110 °C by using the observed rate of esterification of cyclohexene oxide with benzoic acid and the assumed rate of formation of the epoxide and the acid. Unbalanced benzaldehyde and cyclohexene are considered to be polymerized product and the unknown products on the gas chromatogram.

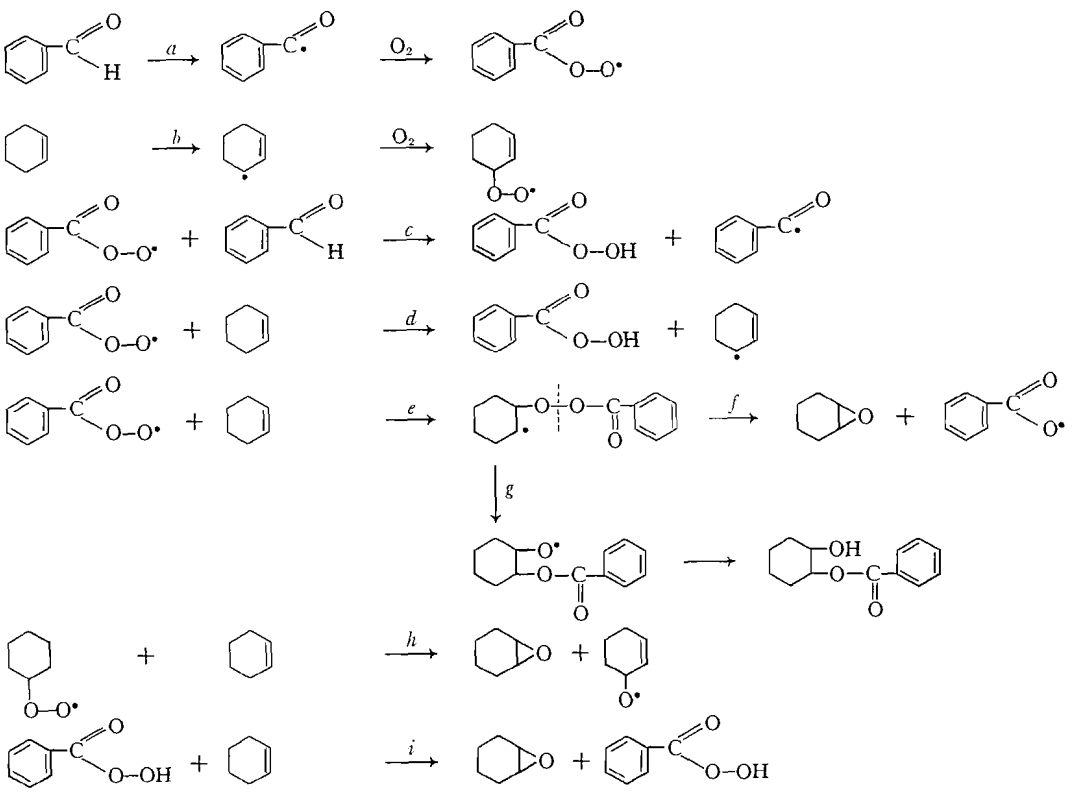
Based on the speculation described above, the probable reaction schemes for the epoxidation will be as shown in Reaction Scheme 1.

The fact that propylene gives propane-1,2-diol monoacetate (5) at low temperatures and propylene oxide (9) at high temperatures in the air oxidation with acetaldehyde, and the fact that cyclohexene gives cyclohexane-1,2-diol monobenzoate (4) at 50 °C in the oxidation with benzaldehyde, support reactions *e*, *f*, and *g*.

In the non-catalytic oxidation at room temperature, the rates of reactions *b* and *d* are so slow that they can be neglected, and the concentration of cyclohexenyl peroxy radical is low in the reaction system. Therefore, the oxidation scheme consists of reactions *a*, *c*, and *e*, and the rate equation shown in eq. [6] can be derived. The reactivity of the radical $C_6H_5CO_2OC_6H_{10}\cdot$ could be considered to be not too high.

The rate of reaction *d* is considered during the oxidation at 70–110 °C, but if it is assumed that this rate is slower than those of reactions *c* and *e*, the increase in the molar

Can. J. Chem. Downloaded from www.nrcresearchpress.com by 210.87.254.105 on 09/05/12
For personal use only.



REACTION SCHEME 1.

ratio of the epoxide to cyclohexenol and cyclohexenone and the decrease in the selectivities of cyclohexenol and cyclohexenone with the addition of benzaldehyde are consistently explained.

Finally, concerning the mechanism of the formation of the epoxide, the main reaction occurs between benzoyl peroxy radical and cyclohexene (reactions *e* and *f*) in the case of cobalt-catalyzed oxidation. It seems that the minor reaction between cyclohexenyl peroxy radical and cyclohexene (reaction *h*) could occur besides the main reaction. However, the minor reaction would not contribute very much at a high concentration of benzaldehyde. In the non-catalytic oxidation, besides the above two reactions, the reaction between peroxybenzoic acid and cyclohexene (reaction *i*) would be added to the epoxidation; thus the overall selectivity of the epoxide has been increased.

ACKNOWLEDGMENTS

The authors express their appreciation to Prof. Ikuzo Tanaka, Tokyo Institute of Technology, for his helpful discussions. The authors also thank Mr. Takashi Shintani for his technical assistance. One of the authors (T. I.) thanks the Tōyō Sōda Manufacturing Co., Ltd., for its financial support.

REFERENCES

1. E. RAYMOND. J. Chim. Phys. **28**, 480 (1931).
2. D. SWERN, T. W. FINDLEY, and J. T. SCAULAN. J. Am. Chem. Soc. **66**, 1925 (1944).
3. D. SWERN and T. W. FINDLEY. J. Am. Chem. Soc. **72**, 4315 (1950).
4. W. TREIBS and L. SCHULTZ. Ber. **80**, 214 (1947).

Can. J. Chem. Downloaded from www.nrcresearchpress.com by 210.87.254.105 on 09/05/12
For personal use only.

5. J. T. HACKMANN. U.S. Patent No. 2,600,054 (June 1952).
6. G. WITTIG. Ann. **58**, 201 (1947).
7. T. IKAWA, M. MUTO, and T. SHINTANI. Bull. Japan Petrol. Inst. **7**, 41 (1965).
8. C. WALLING and E. A. MCELHILL. J. Am. Chem. Soc. **73**, 2927 (1951).
9. T. IKAWA, M. MUTO, T. SHINTANI, M. MATSUMOTO, and N. NAGASAKO. Bull. Japan Petrol. Inst. **6**, 864 (1963).
10. I. M. KOLTHOFF, T. S. LEE, and M. ANNEMAIRS. J. Polymer Sci. **2**, 199 (1947).
11. J. ENGLISH, JR. and J. D. GREGORY. J. Am. Chem. Soc. **69**, 2120 (1947).
12. L. N. OWENS and P. A. ROBINS. J. Chem. Soc. 320 (1949).
13. W. O. LUNDBERG. Autoxidation and antioxidants. Vol. 1. John Wiley & Sons, Inc., New York. 1961. p. 133.
14. H. W. MELVILLE and T. A. INGLES. Proc. Roy. Soc. London, Ser. A, **218**, 175 (1952).
15. G. H. TWIGG. Chem. Eng. Sci. **3** (Spec. Suppl.), 5 (1954).
16. W. F. BRILL. J. Am. Chem. Soc. **85**, 141 (1963).
17. W. F. BRILL and B. J. BARONE. J. Org. Chem. **29**, 140 (1964).
18. I. S. ROCH and J. C. BALACEANU. Bull. Soc. Chim. France, 1393 (1964).
19. N. N. SEMENOV. Some problems of chemical kinetics and reactivity. Vol. 1. Pergamon Press, Princeton, New Jersey. 1958. p. 52.
20. B. M. LYNCH and K. H. PAUSACKER. J. Chem. Soc. 1525 (1955).
21. C. E. H. BAWN and J. E. JOLLEY. Proc. Roy. Soc. London, Ser. A, **237**, 297 (1956).
22. Y. OGATA, I. TABUSHI, and H. AKIMOTO. J. Org. Chem. **26**, 4803 (1961).

Can. J. Chem. Downloaded from www.nrcresearchpress.com by 210.87.254.105 on 09/05/12
For personal use only.

LIGNANS OF WESTERN RED CEDAR (THUJA PLICATA DONN)

V. HYDROXYTHUJAPLICATIN METHYL ETHER

HAROLD MACLEAN[1] AND KOJI MURAKAMI[2]

Forest Products Laboratory, Department of Forestry of Canada, Vancouver, British Columbia

Received March 3, 1966

ABSTRACT

The structure of another guaiacyl–syringyl type lignan, which was previously separated from the hot-water extractive of western red cedar (*Thuja plicata* Donn), has now been determined as 2-hydroxy-2-(4″-hydroxy-3″,5″-dimethoxybenzyl)-3-(4′-hydroxy-3′-methoxybenzyl)-butyrolactone (III). This lignan is the third member of the thujaplicatin series and has been given the name of hydroxythujaplicatin methyl ether. Analytical data and degradational and spectral studies of the parent compound and its methylated derivatives are presented as proof of structure.

Can. J. Chem. Downloaded from www.nrcresearchpress.com by 210.87.254.105 on 09/05/12
For personal use only.

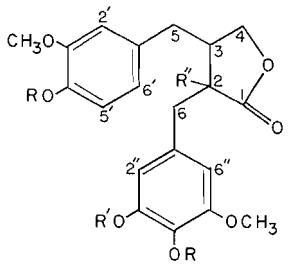
The separation of several new components from the hot-water extractive of western red cedar (*Thuja plicata* Donn) heartwood as well as the structural characterization of two of them, thujaplicatin (I) and thujaplicatin methyl ether (II), was reported in a previous paper (1). Another of the components whose separation was reported in the foregoing paper (R_f 0.25 by thin-layer chromatography) has now been determined as hydroxythujaplicatin methyl ether (III).

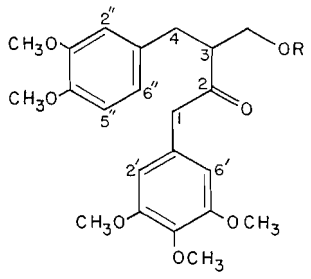
The aromatic rings of III were identified by nitrobenzene oxidation, which yielded both vanillin and syringaldehyde (2). Hydroxythujaplicatin methyl ether (III) and its dimethyl ether derivative (IV) both gave the expected infrared and ultraviolet spectra. Nuclear magnetic resonance (n.m.r.) spectra with integrals of both compounds accounted for all protons and proton species. The four (C5-C6) methylene protons and the one (C3) methine proton could not be assigned with certainty, but occurred in the expected range in both cases, 2.4–3.3 δ. The methylene protons of the lactone ring (C4) were shifted downfield as expected, and appeared as a doublet centered near 4.0 δ with unresolved splitting indicative of the AB portion of an ABX spectrum. Carbon–hydrogen, methoxyl, and equivalent and molecular weight data agreed with the theoretical calculations for both compounds III and IV. The equivalent weight titration was carried out by dissolving hydroxythujaplicatin methyl ether in sodium hydroxide solution to open the lactone ring, and then back-titrating with acid. The product reclaimed from the solution was identical with the starting material. Thus no change of configuration had taken place. A plot of this back-titration curve showed hydroxythujaplicatin methyl ether (III) to be a stronger acid than thujaplicatin methyl ether (II), and indicated that the alcoholic hydroxyl group was alpha to the carbonyl group. Since reaction with manganese dioxide failed to form a ketone group (3), a benzyl alcohol group was not present on either carbon 5 or carbon 6.

Periodate oxidation of dimethyl ether derivative IV at pH 5 was slow and yielded 1-(3′,4′,5′-trimethoxyphenyl)-4-(3″,4″-dimethoxyphenyl)-3-hydroxymethyl-2-butanone (V). Since formaldehyde was not produced in this reaction, the alcoholic hydroxyl group was not attached to carbon 3 of the di-*O*-methyl compound (IV). Slow periodate oxidation at this pH was indicative of an α-hydroxy acid (4). Infrared spectral comparison of IV

[1]*Research Officer, Forest Products Laboratory, Department of Forestry of Canada, Vancouver, British Columbia.*
[2]*National Research Council Postdoctorate Fellow, 1963–1965. Present address: Faculty of Agriculture, Shinshu University, Ina, Nagano-ken, Japan.*

and V showed the disappearance of the lactone carbonyl and appearance of a ketone carbonyl at 1 700 cm^{-1}. Acetylation of the butanone V to form the butanone acetate (VI) shifted the hydroxymethylene protons downfield from the 3.7–3.9 δ region, where they were obscured by the methoxyl protons, to form a doublet centered at 4.19 δ. This shift allowed the unambiguous assignment of all protons and proton species in both V and VI (see Experimental). The fact that V was an oxidation product proved that the





I R,R′,R″ = H

II R,R″ = H; R′ = CH_3

III R = H; R′ = CH_3; R″ = OH

IV R,R′ = CH_3; R″ = OH

V R = H

VI R = CH_3CO

alcoholic hydroxyl group and the carbonyl of the lactone ring were attached to carbon 2 of the original compound (III). Periodate oxidation of V at pH 8–9 yielded 3,4,5-trimethoxybenzaldehyde, identical with an authentic sample. The formation of this aldehyde, as a result of periodate reaction with the active methylene group (5) at carbon 1 of the butanone derivative V, proved that the syringyl group of the original compound was attached as shown in III.

Hydroxythujaplicatin methyl ether is therefore 2-hydroxy-2-(4″-hydroxy-3″,5″-dimethoxybenzyl)-3-(4′-hydroxy-3′-methoxybenzyl)-butyrolactone (4,4′,8′-trihydroxy-3,3′,5-trimethoxy-lignan-olid (9,9′) by the nomenclature of Freudenberg and Weinges (6)).

EXPERIMENTAL

The following equipment was used: melting points, Fisher–Johns heated block; infrared spectra, Baird-Atomic KM-1 spectrometer (KBr disks); ultraviolet spectra, Beckman DK-2 spectrophotometer (ethanol); n.m.r. spectra, Varian A.60 spectrophotometer with tetramethylsilane ($\delta = 0$) as internal standard in deuteriochloroform; molecular weights, Mechrolab osmometer 301A with benzil and β-conidendrin as reference compounds. Analyses were carried out by Clark Microanalytical Laboratories, Urbana, Illinois. The thin-layer chromatography values were obtained with silica gel G (Merck) as adsorbent and with benzene – ethanol – acetic acid (100:10:1 v/v/v) as solvent; the spots were detected by ultraviolet light followed by nitric acid – sulfuric acid (1:1) spray and heat. For preparative layer chromatography a mixture of silica gel G and GF 254 (Merck) (2:1) was used as adsorbent with the thin-layer chromatographic solvent, and the spots were detected by ultraviolet light.

Hydroxythujaplicatin Methyl Ether (III)

Separation of this compound (R_f 0.25) from the hot-water extractive of western red cedar heartwood has been described previously (1). The crude hydroxythujaplicatin methyl ether (430 mg) was purified by cellulose column chromatography with carbon dioxide saturated water, and crystallized from ether (110 mg). The crystals contained ether, and melted at 55–60 °C with foaming. After the crystals were dried for 2 h under vacuum at 54 °C, the melting point was raised to 128.5–129.5 °C. Nitrobenzene oxidation yielded vanillin (3.9%) and syringaldehyde (6.5%) by the modified method of Pepper and Siddequeullah (2).

Anal. Calcd. for $C_{21}H_{24}O_8$: C, 62.38; H, 5.98; OCH_3, 23.02; mol. wt. 404. Found: C, 62.42, 62.31; H, 5.98, 6.00; OCH_3, 22.74, 22.96; equiv. wt. (by back-titration) 396; mol. wt. 409.

Spectra: λ_{max} 281 mμ (log ϵ 3.58); in 0.025 *N* sodium ethoxide, 292 mμ (log ϵ 3.87); ν_{max} 3 500 (OH) and 1 768 cm^{-1} (lactone); n.m.r. 6.86 (1H-C5′, doublet, $J = 8.5$ c.p.s.), 6.67 (1H-C6′, quartet, $J = 1.7$ and

Can. J. Chem. Downloaded from www.nrcresearchpress.com by 210.87.254.105 on 09/05/12
For personal use only.

8.5 c.p.s.), 6.65 (1H-C2′, doublet, J = 1.7 c.p.s.), 6.40 (2H-C2″,6″, singlet), 5.62 and 5.55 (2H-phenols, singlets, quenched by deuterium exchange), 4.05 (2H-C4, doublet, separation of 6.0 c.p.s., with unresolved fine structure), 3.85 and 3.86 (9H-OCH_3, singlets), 2.78 (1H-hydroxyl, singlet, shifted to 2.65 by increasing the temperature to 50 °C and quenched by deuterium exchange), and 2.4–3.1 δ (5H-C3,5,6, unresolved multiplet). $[\alpha]_D^{25}$ −54.8° (c, 0.88 in chloroform).

Di-O-methyl Hydroxythujaplicatin Methyl Ether (IV)

Hydroxythujaplicatin methyl ether (III) (300 mg) in methanol (0.7 ml) was treated with excess diazomethane in ether at room temperature for 24 h. The reaction was monitored during its early stages, when it showed spots at R_f 0.25 (unreacted III), R_f 0.36 and 0.41 (the two monomethyl derivatives), and R_f 0.51 (the dimethyl product IV). At the end of the reaction, only the dimethyl product was detected. The product was reclaimed by evaporation (304 mg) and recrystallized from ether (225 mg), m.p. 113.5–114.5° C, $[\alpha]_D^{25}$ −50.0° (c, 0.92 in chloroform).

Anal. Calcd. for $C_{23}H_{28}O_8$: C, 63.89; H, 6.50; OCH_3, 35.88; mol. wt. 432. Found: C, 63.55, 63.65; H, 6.43, 6.45; OCH_3, 35.80, 35.99; mol. wt. 432.

Spectra: ν_{max} 3 500 (hydroxyl, 3 588 in $CHCl_3$) and 1 776 cm^{-1} (lactone); n.m.r. 6.6–6.9 (3H-C2′,5′,6′, unresolved multiplet), 6.44 (2H-C2″,6″, singlet), 4.07 (2H-C4, doublet, separation of 6.0 c.p.s., with unresolved fine structure), 3.85 and 3.86 (15H-OCH_3, singlets), 3.34 (1H-hydroxyl, singlet, quenched by deuterium oxide with trifluoroacetic acid), and 2.4–3.3 δ (5H-C3,5,6, unresolved multiplet).

Periodate Oxidation of Di-O-methyl Hydroxythujaplicatin Methyl Ether (IV)

Dimethyl derivative IV (600 mg) was dissolved in an equivalent amount of 0.6 N methanolic sodium hydroxide and refluxed for several minutes. Water (10 ml) and 0.1 M sodium metaperiodate (14 ml) were added and the pH was adjusted to 5 with 1 N acetic acid. The reaction mixture was maintained at 0 °C overnight, acidified with dilute hydrochloric acid to pH 2–3, and left for another hour at room temperature. It was then extracted with chloroform (5 × 30 ml), and the chloroform extracts were combined, dried over sodium sulfate, and concentrated. The products were separated by preparative layer chromatography to yield, on crystallization from carbon tetrachloride and recrystallization from ether, the butanone V (R_f 0.30) (65 mg), m.p. 101–101.5 °C, as well as unreacted crystalline starting material (430 mg). No formaldehyde was detected by dimedone precipitation (7).

Anal. Calcd. for 1-(3′,4′,5′-trimethoxyphenyl)-4-(3″,4″-dimethoxyphenyl)-3-hydroxymethyl-2-butanone (V) ($C_{22}H_{28}O_7$): C, 65.35; H, 6.95; OCH_3, 38.37. Found: C, 65.07; H, 6.91; OCH_3, 38.14.

Spectra: ν_{max} 3 450 (hydroxyl) and 1 700 cm^{-1} (carbonyl); n.m.r. 6.82 (1H-C5″, doublet, J = 8.6 c.p.s.), 6.65 (1H-C2″, doublet, J = 1.7 c.p.s.), 6.63 (1H-C6″, quartet, J = 1.7 and 8.6 c.p.s.), 6.27 (2H-C2′,6′, singlet), 3.79, 3.81, and 3.83 (15H-OCH_3, singlets), 3.7–3.9 (2H-hydroxymethylene, overlapping methoxyl), 3.52 (2H-C1, singlet), 2.95–3.30 (1H-C3, multiplet), 2.77 (2H-C4, doublet, J = 6.0 c.p.s.), and 2.41 δ (1H-OH, broad singlet). $[\alpha]_D^{22}$ −72.0° (c, 0.20 in chloroform).

1-(3′,4′,5′-Trimethoxyphenyl)-4-(3″,4″-dimethoxyphenyl)-3-acetoxymethyl-2-butanone (VI)

The butanone (V, 50 mg) from the foregoing periodate oxidation was treated with acetic anhydride in pyridine (1:2 v/v, 0.8 ml) overnight. The solvents were evaporated and the product was purified by preparative layer chromatography. The acetate (VI) was recovered from the silica gel with CCl_4 and, on solvent removal by vacuum evaporation, crystallized spontaneously (45 mg), m.p. 67–68.5 °C. Spectra: ν_{max} no hydroxyl band, 1 730 (acetoxyl) and 1 708 cm^{-1} (carbonyl); n.m.r. 6.76 (1H-C5″, doublet, J = 8.5 c.p.s.), 6.60 (1H-C2″, doublet, J = 1.7 c.p.s.), 6.59 (1H-C6″, quartet, J = 1.8 and 8.5 c.p.s.), 6.21 (2H-C2′,6′, singlet), 4.19 (2H-hydroxymethylene, doublet, J = 6.4 c.p.s.), 3.82 and 3.79 (15H-OCH_3, singlets), 3.43 (2H-C1, singlet), 3.05–3.40 (1H-C3, multiplet), 2.72 (2H-C4, doublet, J = 6.8 c.p.s.), and 1.95 δ (3H-acetyl, singlet).

Periodate Oxidation of 1-(3′,4′,5′-Trimethoxyphenyl)-4-(3″,4″-dimethoxyphenyl)-3-hydroxymethyl-2-butanone (V)

Periodate oxidation of V at pH 5 was unsuccessful. The butanone derivative V (42 mg) was dissolved in water containing 20% methanol (10 ml), and potassium metaperiodate (80 mg) was added. The reaction mixture was adjusted to pH 8–9 with sodium carbonate and left at room temperature for 2.5 h. After acidification with dilute hydrochloric acid, the reaction products were reclaimed by chloroform extraction and subsequent evaporation. These products were purified by preparative layer chromatography to yield crystalline 3,4,5-trimethoxybenzaldehyde (R_f 0.70) (2 mg), m.p. 72–73.5 °C, identical by mixed melting point and infrared spectral comparison with an authentic sample prepared from gallic acid trimethyl ether (8, 9). No other discrete spots capable of being identified, other than that of unreacted V, were found by thin-layer chromatography.

ACKNOWLEDGMENT

The authors are indebted to Dr. L. D. Hall, Chemistry Department, University of British Columbia, for helpful discussions on the interpretation of the n.m.r. spectra.

Can. J. Chem. Downloaded from www.nrcresearchpress.com by 210.87.254.105 on 09/05/12
For personal use only.

REFERENCES

1. H. MacLean and K. Murakami. Can. J. Chem. **44**, 1541 (1966).
2. J. M. Pepper and M. Siddequeullah. Can. J. Chem. **39**, 390 (1961).
3. W. J. Gensler, F. Johnson, and A. D. B. Sloan. J. Am. Chem. Soc. **82**, 6074 (1960).
4. J. R. Dyer. Methods Biochem. Analy. **3**, 111 (1956).
5. H. Felkin. Bull. Soc. Chim. France, 915 (1951).
6. K. Freudenberg and K. Weinges. Tetrahedron, **15**, 115 (1961).
7. J. L. Hartwell and A. W. Schrecker. J. Am. Chem. Soc. **73**, 2915 (1951).
8. H. C. Brown and R. F. McFarlin. J. Am. Chem. Soc. **78**, 252 (1956).
9. I. A. Pearl and S. F. Darling. J. Org. Chem. **25**, 1266 (1957).

Can. J. Chem. Downloaded from www.nrcresearchpress.com by 210.87.254.105 on 09/05/12
For personal use only.

Can. J. Chem. Downloaded from www.nrcresearchpress.com by 210.87.254.105 on 09/05/12
For personal use only.

PYRROLE CHEMISTRY

V. FRIEDEL–CRAFTS ISOPROPYLATIONS OF SOME PYRROLE DERIVATIVES

HUGH J. ANDERSON AND L. CAMERON HOPKINS
Department of Chemistry, Memorial University, St. John's, Newfoundland

Received March 4, 1966

ABSTRACT

The Friedel–Crafts isopropylations of methyl 2-pyrrolecarboxylate, 2-pyrrolecarboxaldehyde, and 2-pyrryl methyl ketone have been investigated under a variety of conditions. Products have been isolated and identified. The effects of different Lewis acid catalysts, solvents, and reaction times upon conversion and product isomer distribution have been determined. These results support the sequence of mechanistic steps suggested in an earlier publication. Further experiments have involved attempted rearrangements and disproportionations under alkylation conditions. The evidence indicates that Lewis acid complexing of the carbonyl oxygen deactivates position 4 in electrophilic substitution less than it does positions 3 and 5. The extent of deactivation of the different positions varies from 2-ester to 2-ketone to 2-aldehyde. Some proton nuclear magnetic resonance investigations of the Lewis acid complexes of these 2-carbonyl pyrroles are also reported.

INTRODUCTION

In a previous publication (1) we have discussed the Friedel–Crafts isopropylation of methyl 2-pyrrolecarboxylate catalyzed by aluminium chloride with carbon disulfide as solvent. It was suggested that electrophilic attack occurred primarily at the 4-position, leading to the formation of methyl 4-isopropyl-2-pyrrolecarboxylate as the major product, and that methyl 5-isopropyl-2-pyrrolecarboxylate arose mainly from the concurrent or consecutive intramolecular rearrangement of the isopropyl group. The third reaction product, methyl 4,5-diisopropyl-2-pyrrolecarboxylate, appeared to result principally from isopropylation of the 5-isopropyl-2-ester. In the present work we have extended the study to include 2-pyrrolecarboxaldehyde and 2-pyrryl methyl ketone (2-acetylpyrrole) as substrates, and have used a wider range of solvents and Lewis acid catalysts with all three carbonyl compounds.

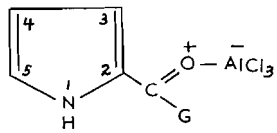
2-Pyrryl methyl ketone was prepared by the reaction of acetic anhydride with pyrrylmagnesium bromide as described by Oddo and Dainotti (2), and 2-pyrrylcarboxaldehyde by a Vilsmeier synthesis (3).

The structures of the 4-isopropyl-, 5-isopropyl-, and 4,5-diisopropyl-2-esters have already been established (1). Isopropylation of 2-pyrrolecarboxaldehyde gave only the 4-isopropyl derivative. The nuclear magnetic resonance (n.m.r.) spectra and elemental analyses were in agreement with the assigned structure, and oxidation with silver oxide produced the known 4-isopropyl-2-pyrrolecarboxylic acid (1, 4).

Gas–liquid partition chromatography of the isopropylation product from 2-acetylpyrrole indicated three products. These were isolated by column chromatography on alumina and identified by their elemental analyses and n.m.r. spectra as the 4-isopropyl-, 5-isopropyl-, and 4,5-diisopropyl-2-pyrryl methyl ketones by analogy with the corresponding esters. In addition, the reaction of acetic anhydride with the Grignard reagent from a mixture of isopropylpyrroles, of which more than 80% was the 2-isomer, gave as the major product a compound having the same retention time on the gas chromatograph as the product we presumed to be the 5-isopropyl-2-pyrryl methyl ketone.

Before the results of the isopropylation reactions are discussed, it seems useful to consider two other related studies, since they indicate possible explanations for many of the observed facts.

In the earlier publication (1) it was suggested that the predominant electronic effect in compounds of this sort should be electron withdrawal by the 2-substituent. This would be expected to be enhanced greatly by the complexing of the carbonyl oxygen with a Lewis acid (see structure I). The consequent deactivation of positions 3 and 5 should lead to predominantly 4-isopropylation, as observed.



G = H, CH_3, OCH_3

I

This simple picture was supported by Hückel molecular orbital calculations (5) of the localization energies for electrophilic substitution at the 3-, 4-, and 5-positions of 2-pyrrolecarboxaldehyde. These calculations indicated that the localization energy required at position 4 was substantially less than that required at positions 3 and 5. Further, as the carbonyl oxygen was made increasingly electronegative, the localization energies at all open aromatic carbons increased. However, the increase was proportionately far greater at the 3- and 5-positions than at the 4-position. Thus, Lewis acid complexing should lead to an even higher proportion of the 4-isomer in electrophilic substitution. However, the complexing does deactivate all aromatic positions to some extent.

It was found that Lewis acid complexing of these 2-carbonyl compounds had a marked effect on the n.m.r. chemical shift positions of the aromatic (and other) protons, as indicated in Tables I and II. The signal positions obtained from each of the parent compounds were assigned (Table I) through their coupling constants (Table II) and by other means (6), and were found to be 5, 3, and 4 in order of increasing field. When these carbonyl compounds, in the same solvent, were complexed with a Lewis acid the signal positions of aromatic protons were all moved to lower field, with the 3- and 5-signals moving nearly twice as far as the 4-signal in each system (Table III).

The chemical shift positions of the 4- and 5-protons in the complexed ester spectrum were closer together than was found with either the complexed aldehyde or the complexed ketone. It was also observed that the downfield shift of the proton signal positions caused by complexing the ester was much less than that caused by complexing the aldehyde and ketone. It is interesting that these observations, referring as they do to electron density in the ground state, parallel some of the calculations discussed above involving the transition state. The most deactivated positions show the greatest change in shift with complexing. This is possibly indicative of a similarity between ground and transition states for 4- and 5-substitution in these compounds.

The inductive withdrawal of electrons caused by complex formation was also observed in the movement to lower field of the n.m.r. signals of the ketone CH_3 and ester OCH_3 protons. However, the aldehyde proton signal was moved instead to higher field by Lewis acid complexing. Complex formation should lead to a withdrawal of electrons from the carbonyl bond, changing the bond order and decreasing the strength of the deshielding induced magnetic field, thus moving the resonance signal to higher field as observed.

Alkylation Experiments

The effects of substituent, catalyst, solvent, and time on the rate of reaction and product distribution were determined for the three 2-carbonyl pyrroles. The results of these experiments are presented in Table IV.

Can. J. Chem. Downloaded from www.nrcresearchpress.com by 210.87.254.105 on 09/05/12
For personal use only.

Can. J. Chem. Downloaded from www.nrcresearchpress.com by 210.87.254.105 on 09/05/12
For personal use only.

TABLE I

Nuclear magnetic resonance spectra*

Compound	Solvent	Aliphatic			Aromatic		
		C—CH_3†	C—H†	Other	3-Proton	4-Proton	5-Proton
Methyl 2-pyrrole-carboxylate	CCl_4	—	—	3.83 (OCH_3)	6.84	6.18	6.91
	$CDCl_3$	—	—	3.87	6.98	6.30	6.98
	CH_3NO_2	—	—	3.84	6.92	6.28	7.10
Methyl 4-isopropyl-2-pyrrolecarboxylate	CCl_4	1.20	2.83	3.83 (OCH_3)	6.73	—	6.73
Methyl 5-isopropyl-2-pyrrolecarboxylate	CCl_4	1.30	2.91	3.83 (OCH_3)	6.72	5.89	—
	$CDCl_3$	1.28	3.00	3.83	6.87	6.00	—
Methyl 4,5-diisopropyl-2-pyrrolecarboxylate	CCl_4	1.17, 1.32	2.9	3.83 (OCH_3)	6.63	—	—
	$CDCl_3$	1.16, 1.27	2.9 (approx.)	3.83	6.79	—	—
2-Pyrrolecarboxaldehyde‡	CCl_4	—	—	9.52 (CHO)	6.98	6.32	7.23
	$CDCl_3$	—	—	9.60	7.04	6.42	7.22
	CH_3NO_2	—	—	9.52	7.06	6.38	7.27
	$C_2H_4Cl_2$	—	—	9.52	7.03	6.35	7.22
4-Isopropyl-2-pyrrole-carboxaldehyde‡	CCl_4	1.23	2.86	9.38 (CHO)	6.80	—	7.02
	$CDCl_3$	1.22	2.88	9.47	6.89	—	7.02
2-Pyrryl methyl ketone	CCl_4	—	—	2.42 ($COCH_3$)	6.83	6.15	7.06
	$CDCl_3$	—	—	2.48	7.00	6.35	7.16
	CH_3NO_2	—	—	2.39	6.99	6.30	7.13
4-Isopropyl-2-pyrryl methyl ketone	CCl_4	1.23	2.83	2.38 ($COCH_3$)	6.70	—	6.88
	$CDCl_3$	1.24	2.8 (approx.)	2.43	6.79	—	6.86
5-Isopropyl-2-pyrryl methyl ketone	CCl_4	1.31	3.0 (approx.)	2.37 ($COCH_3$)	6.82	5.98	—
4,5-Diisopropyl-2-pyrryl methyl ketone	CCl_4	1.18, 1.34	3.0 (approx.)	2.33 ($COCH_3$)	6.65	—	—

*In parts per million on the δ scale from internal tetramethylsilane.
†Isopropyl protons were correctly split.
‡Aldehyde protons were coupled with the 5-proton.

TABLE II

Aromatic proton coupling constants (in cycles per second)

Compound	$J_{3,4}$	$J_{4,5}$	$J_{3,5}$
Methyl 2-pyrrole-carboxylate	3.84	2.56	1.46
Methyl 4-isopropyl-2-pyrrolecarboxylate	—	—	1.50
Methyl 5-isopropyl-2-pyrrolecarboxylate	3.85	—	—
2-Pyrrolecarboxaldehyde	3.92	2.44	1.40
4-Isopropyl-2-pyrrolecarboxaldehyde	—	—	1.5 (approx.)
2-Pyrryl methyl ketone	3.79	2.53	1.43
4-Isopropyl-2-pyrryl methyl ketone	—	—	1.55
5-Isopropyl-2-pyrryl methyl ketone	3.80	—	—

NOTE: The *N*-protons were uncoupled by D_2O exchange.

TABLE III

Complex formation and change in chemical shift position*

Complex	Solvent	3-Proton	4-Proton	5-Proton	Side chain
Methyl 2-pyrrole-carboxylate·$AlBr_3$	CH_3NO_2	−0.52	−0.23	−0.42	−0.35 (OCH_3)
2-Pyrryl methyl ketone·$AlBr_3$	CH_3NO_2	−0.92	−0.51	−0.89	−0.58 ($COCH_3$)
2-Pyrrolecarboxaldehyde·$AlBr_3$	CH_3NO_2	−0.93	−0.54	−0.92	+0.67 (CHO)
2-Pyrrolecarboxaldehyde·$AlCl_3$	CH_3NO_2	−0.93	−0.54	−0.92	+0.67 (CHO)
2-Pyrrolecarboxaldehyde·$AlBr_3$	$C_2H_4Cl_2$	−0.89	−0.52	−0.86	+0.80 (CHO)

*Values are in parts per million; positive is to higher and negative to lower field from the uncomplexed chemical shift positions given in Table I.

Most of these reactions were carried out under the standardized conditions reported earlier (1). As Table IV indicates, the aldehyde appeared to be the most reactive in all such experiments and formed only the 4-isopropyl-2-aldehyde under nearly all experimental conditions. However, the 2-ketone generally gave small amounts of both the 5-isopropyl and 4,5-diisopropyl derivatives (but far less than had been obtained with the 2-ester), along with the 4-isopropyl-2-ketone.

Under the same conditions the order of reactivity of these carbonyl compounds was aldehyde > ketone > ester. However, the physical states of the reaction mixtures were at least partly responsible for this. The reactions in carbon disulfide with aluminium chloride as a catalyst produced a heterogeneous mixture which formed a "red oil" layer below the carbon disulfide. This took place quite slowly with the ester, whereas both the aldehyde and the ketone rapidly formed the red oil.[1] In this highly polar and acidic medium with a high concentration of reactants, the reaction would be expected to occur much faster than in the less polar and more dilute carbon disulfide layer. In fact, the reactions proceeded very much more rapidly as soon as this layer formed. Separate preliminary examinations of the red oil and solvent phases by gas chromatography revealed

[1]*The actual color of the oil obtained from the 2-ester was yellow-amber, whereas the oils separating in the aldehyde and ketone experiments were red.*

Can. J. Chem. Downloaded from www.nrcresearchpress.com by 210.87.254.105 on 09/05/12
For personal use only.

TABLE IV

Isopropylation of 2-substituted pyrrole derivatives (at 50°)

2-Substituent	Catalyst (mole)	Solvent	Time (min)	Conversion (mole %)	Product distribution (mole %)		
					4-Isopropyl-	5-Isopropyl-	4,5-Diisopropyl-
—$COOCH_3$	$AlCl_3$ (0.012)	CS_2	60	24.8	11.6	10.1	3.2
,,	,,	,,	1 080	61.8	34.6	11.6	15.6
,,	$AlBr_3$ (0.012)	,,	60	64.3	47.2	7.3	9.8
,,	,,	,,	120	67.8	46.3	11.7	9.7
,,	,,	,,	1 080	77.1	51.9	17.3	7.8
,,	$GaCl_3$ (0.012)	,,	60	94.3	80.4	9.2	4.8
,,	$FeCl_3$ (0.012)	,,	1 080	<2	Trace	Trace	—
,,	$TiCl_4$ (0.012)	,,	1 080	0.0	—	—	—
,,	$AlCl_3$ (0.020)	CH_3NO_2	1 080	16.3	Trace	12.2	4.1
,,	$AlCl_3$ (0.012)	$C_2H_4Cl_2$	60	86.8	62.4	8.8	15.7
,,	$AlCl_3$ (0.024)	CS_2	1 080	78.0	8.0	70.0	Trace
—CHO	$AlCl_3$ (0.012)	,,	1	12.1	12.1	—	—
,,	,,	,,	5	51.5	51.5	—	—
,,	,,	,,	15	77.4	77.4	—	—
,,	,,	,,	30	80.3	80.3	—	—
,,	,,	,,	60	81.8	81.8	—	—
,,	,,	,,	120	83.6	83.6	—	—
,,	$AlBr_3$ (0.012)	,,	1	22.7	22.7	—	—
,,	,,	,,	5	50.7	50.7	—	—
,,	,,	,,	15	74.1	74.1	—	—
,,	,,	,,	30	77.2	77.2	—	—
,,	,,	,,	60	83.2	83.2	—	—
,,	,,	,,	120	83.8	83.8	—	—
,,	$GaCl_3$ (0.012)	,,	60	73.2	73.2	Trace	Trace
,,	$FeCl_3$ (0.012)	,,	60	46.9	46.9	—	—
,,	,,	,,	120	52.2	52.2	—	—
,,	,,	,,	1 080	59.2	59.2	—	—
,,	$TiCl_4$ (0.012)	,,	1 080	0.0	—	—	—
,,	$AlCl_3$ (0.020)	CH_3NO_2	1 080	0	Trace	—	—
,,	$AlCl_3$ (0.012)	$C_2H_4Cl_2$	60	45.6	45.6	—	—
,,	,,	,,	120	55.8	55.8	—	—
,,	$AlCl_3$ (0.024)	CS_2	120	89.1	89.1	Trace	Trace
—$COCH_3$	$AlCl_3$ (0.012)	,,	30	81.5	75.9	1.4	4.2
,,	$AlBr_3$ (0.024)	,,	60	75.5	71.1	2.7	1.6
,,	$AlCl_3$ (0.024)	,,	240	92.7	86.3	3.0	3.4
,,	,,	,,	1 080	85.5	67.0	11.2	7.3
,,	$AlCl_3$ (0.020)	CH_3NO_2	1 080	0.0	Trace	—	—
,,	$TiCl_4$ (0.012)	CS_2	1 080	0.0	—	—	—

Can. J. Chem. Downloaded from www.nrcresearchpress.com by 210.87.254.105 on 09/05/12
For personal use only.

a higher proportion of product in the oil layer than in the carbon disulfide. This was found to be qualitatively true for reactions of all three carbonyl compounds, and will be investigated further. Olah and Meyer (7) discuss previous investigations concerning the nature of the red oil. However, these studies have mainly involved aromatic hydrocarbons.

Presumably, a complex between the carbonyl oxygen and the Lewis acid has been formed when the red oil separates. If complex formation is not complete, then both free and complexed substrate are present, and the former would be expected to react very much more rapidly and to form both 4- and 5-substituted products. This would require different equilibrium constants for each substrate – Lewis acid complex. There is no real evidence to support this. Indeed, the ester in carbon disulfide forms the red oil most slowly and reacts more slowly than the aldehyde (even with $AlBr_3$), but produces the most 5-isomer.

If, however, all three carbonyl compounds are completely complexed, we are dealing with the relative localization energies for electrophilic attack at positions 4 and 5 in each complex system. The Hückel molecular orbital calculations mentioned above support the idea that Lewis acid complexing of the carbonyl group greatly increases the required energy at all positions, but most markedly at positions 3 and 5. The isopropylation results indicate that this effect is felt most in the aldehyde and least in the ester. Thus the barrier to 5-substitution, either by direct attack or by rearrangement, is lowest for the complexed ester. The fact that the observed behavior of the 4- and 5-proton signals in the n.m.r. spectra of the complexed carbonyl compounds indicates that this is the order of electron density in the ground state is interesting and supports this idea.

Both aluminium bromide and gallium chloride were soluble in carbon disulfide, and a very rapid formation of the red oil layer with the ester and a very much more rapid isopropylation took place than when aluminium chloride was used. With these last two catalysts the degree of rearrangement and diisopropylation of the ester was significantly less. However, the ketone and the aldehyde product distributions in isopropylations with these catalysts were not particularly different from those obtained with aluminium chloride.

Under the conditions used in the rearrangement (1) of the 4-isopropyl- to the 5-isopropyl-2-ester, no change took place with the 4-isopropyl-2-aldehyde. Similar attempted rearrangements of the 4-isopropyl-2-ketone were inconclusive, but gas chromatography indicated that the extent of rearrangement must be very much less than that observed for the corresponding ester. The 4,5-diisopropyl-2-ketone did not disproportionate under these conditions, in agreement with the behavior of the correspondingly substituted 2-ester (1).

The complete absence of 5-isopropylation of the 2-aldehyde and the very low percentage with the 2-ketone may be linked with the failure of the rearrangement experiments with the 4-isopropyl-2-aldehyde and 4-isopropyl-2-ketone. Complexing of these two compounds with the Lewis acid catalyst leads to electron withdrawal from the 5-position to such an extent that the π-electron localization energy for the sigma complex precludes, or nearly precludes, 5-substitution either by direct attack or by rearrangement from the 4-position. The corresponding electron withdrawal at the 4-position is apparently much less.

On the other hand, the 2-ester seems to have a lower energy sigma complex for Friedel–Crafts isopropylation at the 5-position and may undergo 5-isopropylation by both rearrangement and direct attack. As indicated in the earlier publication, rearrangement appears to be a much more important pathway.

The use of a swamping amount of catalyst in 2-ester isopropylations led to methyl 5-isopropyl-2-pyrrolecarboxylate almost exclusively. Reactions of 2-ketone and 2-aldehyde under the swamping catalyst conditions led to a much smaller increase in the percentage

Can. J. Chem. Downloaded from www.nrcresearchpress.com by 210.87.254.105 on 09/05/12
For personal use only.

of 5-isopropyl-2-ketone and none of the 5-isopropyl-2-aldehyde. These alkylation experiments with a swamping amount of catalyst appear to be analogous to the behavior of monoalkylbenzenes and phenol on alkylation. In each example it is the most basic isomer which forms the most stable sigma complex (8, 9). Thus, migration will occur unless the alternate position is too deactivated.

The use of ethylene chloride as a solvent with aluminium chloride catalyst once again produced a homogeneous solution with the ester and thus a much more rapid reaction with the usual products, although somewhat more diisopropylation than before. However, the rate of the aldehyde reaction was much slower and, as usual, only 4-isopropylation was observed. Significantly, only very small amounts of the red oil formed in this solvent. Thus, in this solvent where the catalyst and carbonyl compounds were soluble, the order of reactivity was ester > aldehyde.

The use of nitromethane as solvent produced the very mild nitromethane – aluminium chloride complex and homogeneous reaction conditions. Here, only the ester reacted, and then only to a small extent. The aldehyde and ketone were sufficiently deactivated by complexing to prevent isopropylation when this weak Friedel–Crafts catalyst was used. All aromatic positions of the ester would be the least deactivated in this basic medium at the low concentrations used. However, mainly 5-isopropyl- and 4,5-diisopropyl-2-ester were obtained. Olah *et al.* (10) have found that isopropylations in nitromethane were highly selective and that the basic conditions of reaction largely eliminated consecutive rearrangement, except where "water-promoted" aluminium chloride was used (11). Thus it might be expected that such a highly selective species would attack the 2-ester exclusively at the 4-position. The observed results, however, suggest that the first-formed 4-sigma complex rearranges rapidly to the 5-isomer, which can undergo further alkylation to form the 4,5-diisopropylated product. It would appear that rearrangement before deprotonation may be quite important.

Finally, ferric chloride was found to be ineffective as a catalyst for isopropylation of the ester, and only moderately successful for the aldehyde. Titanium tetrachloride catalysis failed for both, although it produced an intense red color with the aldehyde. The addition of aluminium chloride and isopropyl chloride to the red aldehyde – titanium tetrachloride complex produced only a minor amount of alkylation.

The results of these experiments seem to be consistent with our earlier description of the reaction path (1). That is, the carbonyl group is complexed by the Lewis acid catalyst, and then electrophilic attack takes place primarily at the least deactivated 4-position, forming a sigma complex. This complex can then lose a proton; rearrange to give, eventually, the 5-isomer; or disproportionate through attack by a molecule of the 5-isopropyl derivative to form one molecule each of diisopropyl and unsubstituted compound. The extent to which the secondary reactions take place will depend upon the degree of deactivation of the 5-position. As indicated above, solubility factors also play an important role.

EXPERIMENTAL

General

Melting points were determined on a Fisher–Johns apparatus and are uncorrected. Ultraviolet spectra were determined with a Beckman DK-2A recording spectrophotometer; samples were dissolved in ethanol (95%) at a concentration of 10 mg/l. Nuclear magnetic resonance spectra were determined at 60 Mc.p.s. in the solvents stated in Tables I and III, with a Varian A-60 instrument. The chemical shifts are in parts per million on the δ scale from tetramethylsilane as internal reference.

Analyses of reaction mixtures were carried out by means of gas–liquid partition chromatography with a Beckman GC-2A gas chromatograph, equipped with a 30 in. column (No. 70007) packed with Carbowax 4000 dioleate on fire brick, with helium as the carrier gas. Analyses were accurate to $\pm 2\%$, as shown by gas chromatographic examination of a series of known mixtures.

Can. J. Chem. Downloaded from www.nrcresearchpress.com by 210.87.254.105 on 09/05/12
For personal use only.

Can. J. Chem. Downloaded from www.nrcresearchpress.com by 210.87.254.105 on 09/05/12
For personal use only.

Elemental analyses were determined by Alfred Bernhardt, Mülheim (Ruhr), Germany.

The Lewis acids used were aluminium chloride (Fisher reagent grade), aluminium bromide (Fluka purum), gallium chloride (Fluka puriss), and ferric chloride (British Drug Houses anhydrous). These were all used without further purification and with no precautions beyond those required for ordinary handling. The solvents used were reagent grade and were not further purified.

Methyl 2-pyrrolecarboxylate, m.p. 72–73° (crystallized from methanol), was prepared as described previously (1). 2-Pyrrolecarboxaldehyde, m.p. 44–45° (crystallized from petroleum pentane), was prepared by the method of Silverstein *et al.* (3). 2-Pyrryl methyl ketone (2-acetylpyrrole), m.p. 88–89° (crystallized from methanol), was prepared by the method of Oddo and Dainotti (2).

These carbonyl compounds were all purified until they showed only a single peak on gas–liquid partition chromatography. In addition, the n.m.r. spectrum showed no impurity within the limits of its sensitivity.

General Procedure for Alkylations

The reaction vessel was a 100 ml, three-necked, round-bottomed flask equipped with a stirrer, a dropping funnel, and a condenser with a drying tube, and immersed in an oil bath maintained at 50°. The 2-carbonyl compound (0.01 mole) and the anhydrous catalyst (0.012 mole) were placed in the reaction vessel with 40 ml of carbon disulfide. Isopropyl chloride (0.01 mole) in 10 ml of carbon disulfide was added after 15 min, and the reaction mixture was refluxed and stirred for the required period. The reaction was quenched by pouring the mixture onto ice. The aqueous layer was separated, saturated with sodium chloride, and extracted with ether. The combined organic extracts were washed with sodium acetate (saturated aqueous solution) and dried over anhydrous sodium sulfate. The solvent was removed by distillation and the residue analyzed by gas chromatography. The results are tabulated in Table IV.

Isolation of Alkylation Products

After preparative-scale isopropylation of the three substrate molecules, the dried ether layer was evaporated to dryness and the products separated by column adsorption chromatography on alumina (Fisher reagent grade). Purifications were accomplished through recrystallization from methanol and occasionally sublimation.

The analyses, physical constants, and proofs of structure for the isopropylation products from methyl 2-pyrrolecarboxylate are given in an earlier paper (1).

4-Isopropyl-2-pyrrolecarboxaldehyde, m.p. 31°. Ultraviolet: λ_{max} 257.5 mμ (log ε 3.84) and 302 mμ (log ε 4.20).

Anal. Calcd. for $C_8H_{11}NO$: C, 70.04; H, 8.09; N, 10.20. Found: C, 70.42; H, 8.06; N, 10.16.

Oxime, m.p. 124° (crystallized from ethanol).

Anal. Calcd. for $C_8H_{12}N_2O$: C, 63.14; H, 7.95; N, 18.40. Found: C, 63.20; H, 7.76; N, 18.39.

Semicarbazone, m.p. 173–175° (crystallized from ethanol–water).

Anal. Calcd. for $C_9H_{14}N_4O$: C, 55.66; H, 7.26; N, 28.84. Found: C, 55.85; H, 7.82; N, 28.24.

4-Isopropyl-2-pyrryl methyl ketone, m.p. 46.5–47.5°.

Anal. Calcd. for $C_9H_{13}NO$: C, 71.52; H, 8.61; N, 9.27. Found: C, 71.51; H, 8.85; N, 9.40.

5-Isopropyl-2-pyrryl methyl ketone, m.p. 58–59°.

Anal. Calcd. for $C_9H_{13}NO$: C, 71.52; H, 8.61; N, 9.27. Found: C, 72.15; H, 8.42; N, 9.24.

4,5-Diisopropyl-2-pyrryl methyl ketone, m.p. 103–104°.

Anal. Calcd. for $C_{12}H_{19}NO$: C, 74.57; H, 9.91; N, 7.25. Found: C, 74.58; H, 9.85; N, 7.41.

The n.m.r. proton chemical shifts are given in Table I, and the aromatic proton coupling constants in Table II. The latter values are in agreement with those reported by Gronowitz *et al.* (12).

At no time was there any indication, in gas chromatography or n.m.r. spectra, of the presence of propyl products along with the isopropyl products.

Oxidation of 4-Isopropyl-2-pyrrolecarboxaldehyde

4-Isopropyl-2-pyrrolecarboxaldehyde was oxidized to the corresponding acid with alkaline silver oxide (6). This acid had a melting point of 182–184°. The mixed melting point with a sample of 4-isopropyl-2-pyrrolecarboxylic acid obtained by hydrolysis of the corresponding ester (1) was not depressed from this value. The infrared spectra showed no significant difference.

Attempted Disproportionation of 4,5-Diisopropyl-2-pyrryl Methyl Ketone

4,5-Diisopropyl-2-pyrryl methyl ketone (0.001 mole) and 2-pyrryl methyl ketone (0.001 mole) were dissolved in 10 ml carbon disulfide together with aluminium chloride (0.0024 mole). The mixture was refluxed for 4 h in the presence of a continuous stream of dry hydrogen chloride. The reaction mixture was worked up in the usual manner and the products analyzed by gas chromatography. No elimination or disproportionation of isopropyl groups was observed.

Attempted Rearrangement of 4-Isopropyl Derivatives

4-Isopropyl-2-aldehyde or 4-isopropyl-2-ketone (0.001 mole) and aluminium chloride (0.0024 mole) in 10 ml carbon disulfide were refluxed (50°) for 2 h in the presence of a continuous stream of dry hydrogen chloride. The reaction mixture was worked up in the usual manner and the products analyzed by gas chromatography. The amount of rearrangement to 5-isopropyl-2-ketone was very small, but apparently greater than the limits of experimental error. The 4-isopropyl-2-aldehyde showed only a trace of a new product, whose retention time indicated that it could have been the 5-isopropyl-2-aldehyde.

ACKNOWLEDGMENT

The authors are pleased to acknowledge the continued financial support of the National Research Council.

REFERENCES

1. H. J. ANDERSON and L. C. HOPKINS. Can. J. Chem. **42**, 1279 (1964).
2. B. ODDO and C. DAINOTTI. Gazz. Chim. Ital. **42**, 727 (1912).
3. R. M. SILVERSTEIN, E. E. RYSKIEWICZ, and C. WILLARD. Org. Syn. **36**, 74 (1956).
4. T. SUGAWA, Y. SANNO, and A. KURITA. Chem. Abstr. **50**, 4119 (1956).
5. L. C. HOPKINS. M.Sc. Thesis, Memorial University, St. John's, Newfoundland. 1965.
6. H. J. ANDERSON and S. F. LEE. Can. J. Chem. **43**, 409 (1965).
7. G. A. OLAH and M. W. MEYER. *In* Friedel–Crafts and related reactions. Vol. 1. *Edited by* G. A. Olah. Interscience Publishers, Inc., New York. 1962. p. 731.
8. G. A. OLAH. *In* Friedel–Crafts and related reactions. Vol. 1. *Edited by* G. A. Olah. Interscience Publishers, Inc., New York. 1962. p. 905.
9. L. A. FURY, JR. and D. E. PEARSON. J. Org. Chem. **30**, 2301 (1965).
10. G. A. OLAH, S. H. FLOOD, S. J. KUHN, M. E. MOFFATT, and N. A. OVERCHUCK. J. Am. Chem. Soc. **86**, 1046 (1964).
11. G. A. OLAH, M. W. MEYER, and N. A. OVERCHUCK. J. Org. Chem. **29**, 2315 (1964).
12. S. GRONOWITZ, A.-B. HORNFELDT, B. GESTBLOM, and R. A. HOFFMAN. Arkiv Kemi, **18**, 133 (1961).

Can. J. Chem. Downloaded from www.nrcresearchpress.com by 210.87.254.105 on 09/05/12
For personal use only.

Can. J. Chem. Downloaded from www.nrcresearchpress.com by 210.87.254.5 on 09/05/12
For personal use only.

LONG CARBON CHAIN CARBOHYDRATE POLYMERS

1,3-(BIS-5-ALDOXYLOSYLIDENE-1)-ACETONE AND ITS POLYMER WITH 1,3-DICARBETHOXYACETONE

PHILIPPOS E. PAPADAKIS AND S. M. PHILIP

Special Laboratory of Nuclear Medicine and Biology, Veterans Administration Hospital, and Department of Chemistry, Creighton University, Omaha, Nebraska

Received March 10, 1966

ABSTRACT

1,3-Dicarbethoxy-1,3-(bis-(4′,5′-*O*-isopropylidene-D-xylofuranosylidene))-acetone was hydrolyzed and decarboxylated to produce 1,3-(bis-D-xylofuranosylidene-5)-acetone (III) and 1,3-(bis-5-aldoxylosylidene-1)-acetone (IV). Compound IV reacted with 1,3-dicarbethoxyacetone in 75% methanol, with piperidine as catalyst, to give polymers V and VI and some intermediates. The main component of polymer V had a molecular weight between 2 000 and 4 000, and there were six to seven components with molecular weights of less than 2 000. Because the molecular weight of the repeating unit is approximately 500, a polymer with a molecular weight of 2 500 would have 80 carbons in a continuous chain, and one with a molecular weight of 3 500 would have 112 carbons. The work presented in this article may open broad areas of further research.

INTRODUCTION

It has been shown previously that 1 mole of diethylacetonedicarboxylate condenses with 2 moles of an aldose in a 75% methanol solution, with piperidine as catalyst, to give long carbon chain sugars (1). In another method (2), diethylacetonedicarboxylate was condensed with an aldose in the molar proportions of 1:2 in concentrated hydrochloric acid at 0° to form long carbon chain sugars.

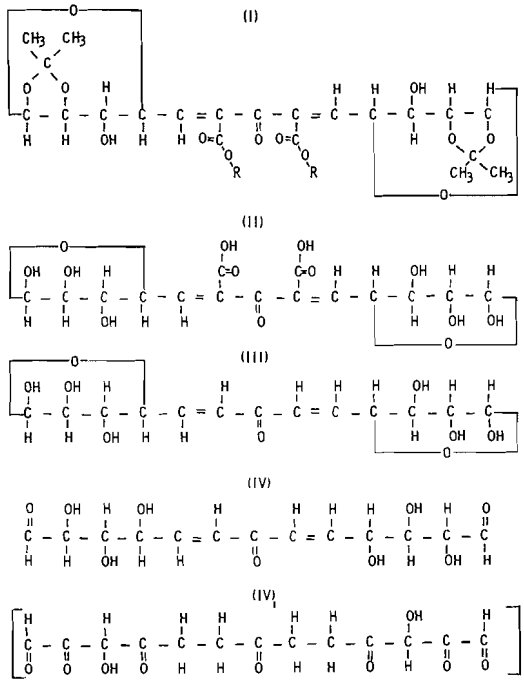
On one occasion, 2 moles of 1,2-*O*-isopropylidene-D-xylopentodialdose was condensed with 1 mole of diethylacetonedicarboxylate, with piperidine as catalyst, to give 1,3-dicarbethoxy-bis-(4′,5′-*O*-isopropylidene-D-xylofuranosylidene)-acetone, which is a dialdehydo unsaturated keto sugar with a chain of 13 carbon atoms (I) (1).

It was pointed out then that the hydrolysis of the isopropylidene groups of compound I could give rise to two free aldehyde groups in this compound, and might open the way for chain polymerization with diethylacetonedicarboxylate or other appropriate reagents.

Schaffer and Isbell (3) observed that the hydrogen on carbon 4 in 5-aldo-1,2-*O*-isopropylidene-D-xylopentodialdofuranose is alpha with respect to the aldehyde group, and helps to make the compound susceptible to aldol condensation. They observed the aldol reaction of two molecules of this compound to form a branched-chain 10-carbon sugar.

The present report deals with the hydrolysis of the isopropylidene and the carbethoxy groups of I to give compound II, the decarboxylation of the resulting β-ketonic acids to produce compound III, and the aldol condensation of the dialdehydo form of the resulting 13 carbon atom sugar (IV) with 1,3-dicarbethoxyacetone to give polymer V. An intermediate compound representing the first step of the aldol condensation was isolated and is represented by formula VI. The formulae may represent one of the possible *cis–trans* isomers.

Thus, 1,3-dicarbethoxy-1,3-(bis-(4′,5′-*O*-isopropylidene-D-xylofuranosylidene))-acetone (I) was hydrolyzed with 1% H_2SO_4. Both the isopropylidene and the carbethoxy esters were hydrolyzed. The latter gave rise to carboxylic groups (II), both of which have the keto group in the β-position. It is known that β-ketonic acids lose CO_2 when heated in an acid solution. Under such conditions, compound II was decarboxylated to give III, the alpha and beta forms of which are expected, in aqueous solution, to form an equilibrium with the dialdehydo form (IV).



In the next step, compound IV and 1,3-dicarbethoxyacetone, in the molar proportions of 1:1, were condensed in 75% methanol with piperidine as catalyst. After the product was processed, it analyzed as if polymerization had taken place. The polymer unit, taken x times, is shown within the brackets of formula V.

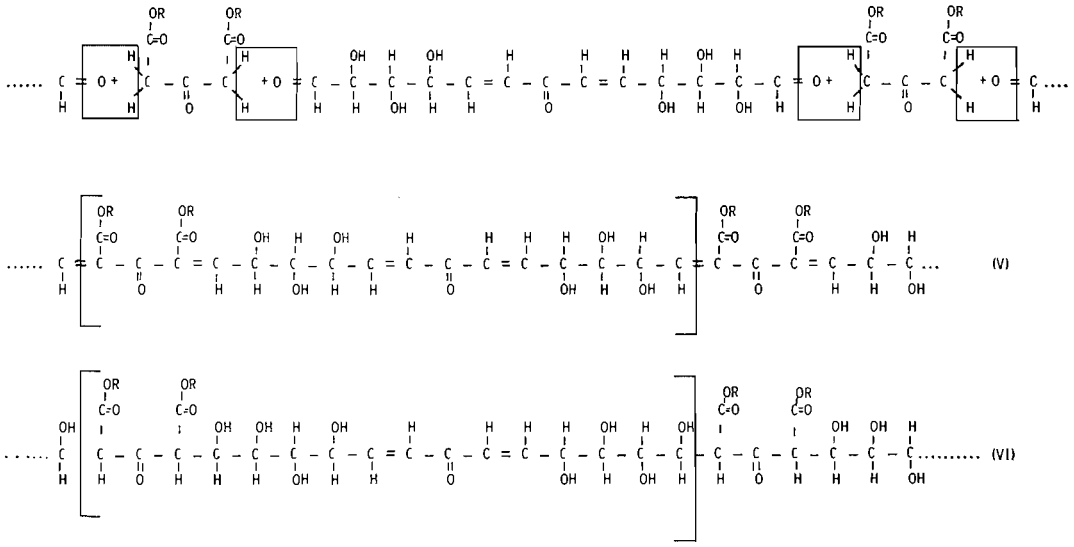
The approximate molecular weights were determined as follows by Dr. Wayne Ryan and James Dworak of the Eugene C. Eppley Institute for Research in Cancer and Allied Diseases. "The polymer was chromatographed on Bio-rad polyacrylamide gels with a 0.9 × 150 cm column and a flow rate of 20 ml/h, which was maintained with a Spinco accu-flow pump. The effluent from the column was monitored by a Spinco 135 Spectro-monitor programmed at 220 mμ and at 260 mμ. Polyacrylamide gels with exclusion limits of 2 000, 4 000, and 10 000 were used. The results of this study indicated that the polymer contained one component with a molecular weight between 2 000 and 4 000, and six to seven components with a molecular weight of less than 2 000."

The main product of the polymerization is the compound with a molecular weight between 2 000 and 4 000. On the basis of this information, the molecular weight of this component may have approximately one of the following values: 2 000, 2 500, 3 000, 3 500, or 4 000. With a molecular weight of 2 500 there would be 80 carbon atoms in the long carbon chain. A molecular weight of 3 500 would correspond to a carbohydrate with a chain of 112 carbon atoms.

The ultraviolet and infrared spectra were taken and interpreted by Dr. Curtis Leicht, Chemistry Department, Creighton University.

The ultraviolet spectral data tentatively support the structural assignments given for V and VI. These polymers, as well as compound I, exhibited absorption in a region near 240 mμ, the intensity being somewhat greater for the polymers. Unfortunately, both ethylmethyleneacetoacetate, deemed to be an approximate model for compound V, and diethylacetonedicarboxylate, a model for formula VI, also exhibit absorption very near

Can. J. Chem. Downloaded from www.nrcresearchpress.com by 210.87.254.5 on 09/05/12
For personal use only.



240 mμ, with very similar intensities (λ_{max} 239 mμ, log ε = 3.24 (4), and λ_{max} 237 mμ log ε = 3.5, respectively).

However, diethylacetonedicarboxylate dissolved in approximately 1% ethanolic KOH demonstrated a bathochromic shift of about 35 mμ, with a concomitant 12-fold increase in the absorption intensity (λ_{max} 272 mμ, log ε = 4.6). A very similar change in the wavelength and intensity of absorption was shown by compound VI with the same solvent change (λ_{max} 278 mμ, $E^{1\,cm}_{1\%}$ = 8 000). Although compounds I and V also demonstrated similar bathochromic shifts, the changes in intensity were much more modest (λ_{max} 282 mμ, log ε = 4.4, and λ_{max} 280 mμ, $E^{1\,cm}_{1\%}$ = 315, respectively). The tenuous nature of these interpretations is demonstrated by the fact that polymer VI and ethylmethyleneacetoacetate both exhibit somewhat similar longer wavelength absorptions (λ_{max} 324 mμ, $E^{1\,cm}_{1\%}$ = 17.5, and λ_{max} 307 mμ, log ε = 1.5, respectively). Furthermore, polymer VI and compound I show very similar longer wavelength absorptions in basic solution (λ_{max} 355 mμ, $E^{1\,cm}_{1\%}$ = 406, and λ_{max} 352 mμ, log ε = 3.7, respectively).

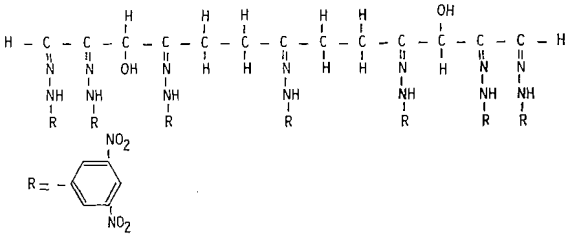
Since the infrared spectra of compounds V and VI were so similar, no further support for the structural assignments could be obtained by this means.

This work opens the way for several investigations. Further research will be carried out on the preparation of other polymers and the synthesis of derivatives analogous to those of the simpler carbohydrates which may have scientific, medicinal, or industrial importance.

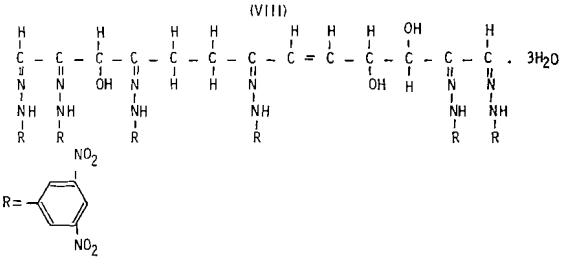
During this investigation, the following derivatives (new compounds) were made and analyzed: (*a*) a crystalline 1,2-*O*-isopropylidene-3-*O*-(3,5-dinitrobenzoate)-D-xylopentofuranose; (*b*) a 3,5-dinitrobenzoate ester of I (the product corresponds to 1,2-*O*-isopropylidene-6,8-dicarbethoxy-7-oxo-3,11-di-(*O*-benzoate-3,5-dinitro)-5,8-diene-D-tridecadialdoxyfuranose; an *O*-diisopropylidene derivative was expected; apparently in the process one isopropylidene group was hydrolyzed); and (*c*) a 2,4-dinitrophenylhydrazine derivative of IV, 3,10,11-trihydroxy-hexakis-1,2,4,7,12,13-(2,4-dinitrophenylhydrazone)-tridecaene-8 (VIII) (osazone reaction and tautomerization of the hydrogens in IV and hydrazone reaction of the resulting carbonyl groups in $(IV)_1$ should result in compound VII; because of the inadequate amount of 2,4-dinitrophenylhydrazine used, only six 2,4-dinitrophenylhydrazines reacted, thereby giving compound VIII).

Can. J. Chem. Downloaded from www.nrcresearchpress.com by 210.87.254.5 on 09/05/12
For personal use only.

(VII)



(VIII)



EXPERIMENTAL

Ultraviolet spectra were run on a Beckman DU spectrophotometer in 95% ethanol. Infrared spectra were run on a Beckman IR-8 instrument in chloroform solution.

*5-Aldo-1,2-O-isopropylidene-*D*-xylopentofuranose (5–7)*

This was prepared according to the method described by Grosheintz and Fischer.

*1,2-O-Isopropylidene-3-O-(3,5-dinitrobenzoate)-*D*-xylopentodialdose*

1,2-*O*-Isopropylidene-D-xylopentodialdose (1.88 g, 0.01 mole), 3,5-dinitrobenzoyl chloride (2.30 g, 0.01 mole), pyridine (1 ml), and dry ether (30 ml) were mixed at 0° for ½ h, and then allowed to stand at room temperature overnight. The mixture was then refluxed for 1 h, allowed to cool, and poured into ice water. A precipitate was collected and recrystallized from methyl alcohol, m.p. 150°.

Anal. Calcd. for $C_{15}H_{14}O_{10}N_2$: C, 47.12; H, 3.69. Found: C, 47.43; H, 3.32.

*1,2;12,13-O-Diisopropylidene-6,8-dicarbethoxy-7-oxo-3,11-dihydroxy-5,8-diene-*D*-tridecadialdoxylofuranose or 1,3-Dicarbethoxy-1,3-(bis-(4',5'-O-isopropylidene-*D*-xylofuranosylidene))-acetone (I)*

The title compound was prepared according to the method described by Papadakis (1). The analytical results agreed with the experimental values found previously (1) and with the theoretical values.

Anal. Calcd. for $C_{25}H_{34}O_{13}$: C, 55.35; H, 6.31. Found: C, 55.37; H, 6.34.

Specific rotation: $[\alpha]_D^{18}$ +45.62° (*c*, 3.051 in acetone); after 16 h $[\alpha]_D^{21}$ +22.9°; after 40 h $[\alpha]_D^{21}$ +22.9°. Ultraviolet spectrum: λ_{max} 234 and 247 mμ, log ε = 3.7 and 3.8, respectively. Infrared spectrum: absorption at 3 420, 3 020, 2 985, 2 940, 1 725, 1 655, 1 620, 1 370, 1 230, 1 080, and 1 020 cm^{-1}.

3,5-Dinitrobenzoyl Chloride Derivative of I

A mixture of 1.0 g (0.0018 mole) of I, 0.92 g (0.0036 mole) of 3,5-dinitrobenzoyl chloride, and 0.32 ml (0.0036 mole) of pyridine in a dry dioxane medium was kept at 0° for 1 h. After having stood at room temperature overnight, the mixture was heated at 60° under reflux for 1 h. The dioxane was removed under reduced pressure and the product poured over crushed ice. The residue was washed with 10 ml of 2% sodium bicarbonate. Recrystallization from ether – petroleum ether gave a white solid, m.p. 150–152°.

Anal. Calcd. for $C_{36}H_{36}O_{24}N_4$: C, 47.57; H, 3.99; N, 6.16. Found: C, 47.45; H, 4.26; N, 6.06. (In the process one isopropylidene was hydrolyzed.)

1,3-(Bis-5-aldoxylosylidene-1)-acetone (IV)

Hydrolysis of I was accomplished by heating with dilute acid. To a solution of 5 g of I in dioxane, 50 ml of 0.1 *N* sulfuric acid was added. The mixture was heated under reflux on a water bath at 75–80° for 2½ h. The sulfuric acid was neutralized with barium hydroxide, the $BaSO_4$ filtered off, and the filtrate evaporated to dryness. The residue was boiled with distilled water and filtered to remove any unhydrolyzed I, which is insoluble in water. The solution was evaporated again to dryness and the material was pulverized to an amorphous powder which softened at 93° and completely melted at 110°.

Anal. Calcd. for $C_{13}H_{18}O_9 \cdot 1\frac{1}{2}H_2O$: C, 45.21; H, 6.08. Found: C, 44.85; H, 6.31.

The analytical results correspond to a hydrated compound (IV).

Can. J. Chem. Downloaded from www.nrcresearchpress.com by 210.87.254.5 on 09/05/12
For personal use only.

3,10,11-Trihydroxy-hexakis-1,2,4,7,12,13-(2,4-dinitrophenylhydrazone)-tridecaene-8 (VIII)

To 1.11 g (0.0056 mole) of 2,4-dinitrophenylhydrazine, 2.5 ml of concentrated sulfuric acid was added. Water was added dropwise, with stirring, until solution was completed. To a solution of 0.3 g (0.0008 mole) of crude IV in ethanol, the 2,4-dinitrophenylhydrazine – sulfuric acid solution was added, and the mixture was allowed to stand overnight. After centrifugation the red precipitate was collected and recrystallized from 95% alcohol. It sintered at 224° and melted at 229–235°.

Anal. Calcd. for $C_{49}H_{44}O_{30}N_{24}$: C, 40.60; H, 3.04; N, 23.20. Found: C, 40.48; H, 2.71; N, 23.76.

Preparation of the Long Carbon Chain Polymers V and VI

A quantity of 1.53 ml (0.008 mole) of diethylacetonedicarboxylate was added to 2.832 g (0.008 mole) of 1,3-(bis-5-aldoxylosylidene-1)-acetone (IV) in a benzene medium. After piperidine (five drops) was added to catalyze the reaction, the mixture was left at room temperature overnight. This was followed by heating under reflux in a water bath at 80° for 1 h. After a second day of standing, it was again heated for 1 h. The solution was then filtered and the filtrate evaporated to dryness. The hardened syrup was purified in the following manner. It was divided into two portions, one soluble in water and the other in 95% ethanol. A residue was precipitated from the former by the addition of 95% ethanol, and from the latter by the addition of water. The residue was removed by filtration (analysis later proved that it was not the polymer). This purification process was repeated several times. The amber solution of the water-soluble and alcohol-soluble materials containing the polymer was treated with Darco in an unsuccessful attempt to remove the color. This was followed by evaporation to dryness. The hardened amber syrups were pulverized.

The material from the first portion (represented by VI) softened at 72° and had completely melted at 85°. The material from the second portion (represented by V) melted at 78–81°.

Compound VI

Anal. Calcd. for $C_{22}H_{32}O_{14}$: C, 50.76; H, 6.15. Found: C, 50.86; H, 6.01.

Ultraviolet spectrum: λ_{max} 238 (4) and 324 mμ, $E^{1\,cm}_{1\%}$ = 406 and 17.5, respectively. Infrared spectrum: absorption at 3 400, 3 010, 2 980, 1 720, 1 580 (broad), 1 440, 1 370, 1 220, 1 090, and 1 030 cm^{-1}.

Compound V

Anal. Calcd. for $C_{22}H_{28}O_{12}$: C, 54.54; H, 5.78. Found: C, 54.77; H, 6.07.

Ultraviolet spectrum: λ_{max} 240 mμ (4), $E^{1\,cm}_{1\%}$ = 180. Infrared spectrum: absorption at 3 400, 3 010, 2 920, 1 720, 1 615 (broad), 1 440, 1 370, 1 220, and 1 020 cm^{-1}.

REFERENCES

1. P. E. Papadakis. J. Org. Chem. **20**, 630 (1955).
2. P. E. Papadakis. J. Org. Chem. **26**, 199 (1961).
3. R. Schaffer and H. S. Isbell. J. Am. Chem. Soc. **79**, 3864 (1957); **80**, 756 (1958).
4. W. Cocker and T. B. H. McMurry. J. Chem. Soc. 4430 (1955).
5. K. Iwadare. Bull. Chem. Soc. Japan, **16**, 40 (1941); Chem. Abstr. **35**, 4740 (1941).
6. J. M. Grosheintz and H. O. L. Fischer. J. Am. Chem. Soc. **70**, 1476 (1948).
7. J. C. Sowden. J. Am. Chem. Soc. **74**, 4377 (1952).

Can. J. Chem. Downloaded from www.nrcresearchpress.com by 210.87.254.5 on 09/05/12
For personal use only.

Can. J. Chem. Downloaded from www.nrcresearchpress.com by 210.87.254.40 on 09/05/12
For personal use only.

THE PHOTOLYSIS OF 4,4-DIMETHYLANDROST-5-EN-17β-OL-3-ONE[1]

RONALD T. TAYLOR[2] AND GEORGE JUST
Department of Chemistry, McGill University, Montreal, Quebec

Received March 16, 1966

ABSTRACT

The photolysis of 4,4-dimethylandrost-5-en-17β-ol-3-one (I) in aqueous tetrahydrofuran has been shown to give products of reduction, adducts with tetrahydrofuran, and 5-isopropyl-lactones VI and VII.

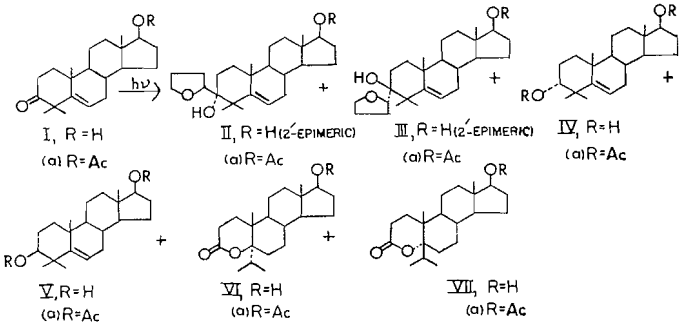
It is well known that the carbonyl chromophore of a β,γ-unsaturated ketone can overlap with the carbon–carbon double bond chromophore, giving rise to an exalted intensity of the $n \rightarrow \pi^*$ transition or to a shift towards longer wavelength of the chromophore. From this type of data, conformations of ring A of 4,4-dimethylcholest-5-en-3-one have been deduced (1, 2).

We were interested in determining whether this type of interaction would lead to products analogous to those formed in the solvolysis of cholesteryl derivatives in which the double bond of a β,γ-unsaturated tosylate interacts with the incipient carbonium ion. We therefore studied the photolysis of 4,4-dimethylandrost-5-en-17β-ol-3-one, which is readily available from testosterone (3).

RESULTS

Photolysis of a 0.033 *M* aqueous tetrahydrofuran solution of 4,4-dimethylandrost-5-en-17β-ol-3-one (I) in a helium atmosphere gave a mixture of products, which could be resolved by chromatographic means only with difficulty. When the crude reaction mixture was steam distilled, a reasonable separation of the residue was effected by a combination of chromatography on alumina and thin-layer chromatography (t.l.c.), with silica gel as the adsorbent. The purity of the components and the yields were established by gas–liquid chromatography (g.l.c.). The details of the separation procedure, as well as relevant analytical and spectral data, are described in the Experimental section.

Diols IV and V were obtained as a mixture which was not resolved. Oxidation with chromium trioxide in pyridine (4) gave in good yield 4,4-dimethylandrost-5-ene-3,17-dione (VIII), identical with the oxidation product of I. The diol mixture (IV and V) was then



[1]*This work was supported by the National Research Council of Canada. Abstracted from part of the Ph.D. thesis of R. T. T.*
[2]*Holder of a McGill University Fellowship, 1962–1963.*

Can. J. Chem. Downloaded from www.nrcresearchpress.com by 210.87.254.40 on 09/05/12
For personal use only.

acetylated. Gas–liquid chromatographic analysis of this mixture indicated the presence of two components (IV*a* and V*a*), with retention times identical with those of an authentic mixture of IV*a* and V*a*, obtained by sodium borohydride reduction of ketone I (3) followed by acetylation.

Diol III was characterized in the following manner. Acetylation with acetic anhydride in pyridine at room temperature gave a diol monoacetate III*a*. The mass spectrum of III*a* indicated it to be an adduct of ketone I*a* and tetrahydrofuran. The proton magnetic resonance (p.m.r.) spectrum[3] of III*a* showed the C_6-olefinic proton at 5.68 p.p.m. and a three-proton signal centered at 3.89 p.p.m., characteristic of the low-field protons in tetrahydrofuran. The most probable mode of attachment of the tetrahydrofuryl moiety was as depicted in III*a*. The synthesis of III*a* was therefore undertaken. Ketone I*a* was reacted with an ethereal solution of 2-furylmagnesium iodide (5). After acetylation, a low yield (high conversion) of product IX was obtained. Catalytic reduction of IX gave, after acetylation, the tetrahydrofuryl derivative III*a* in very low yield.

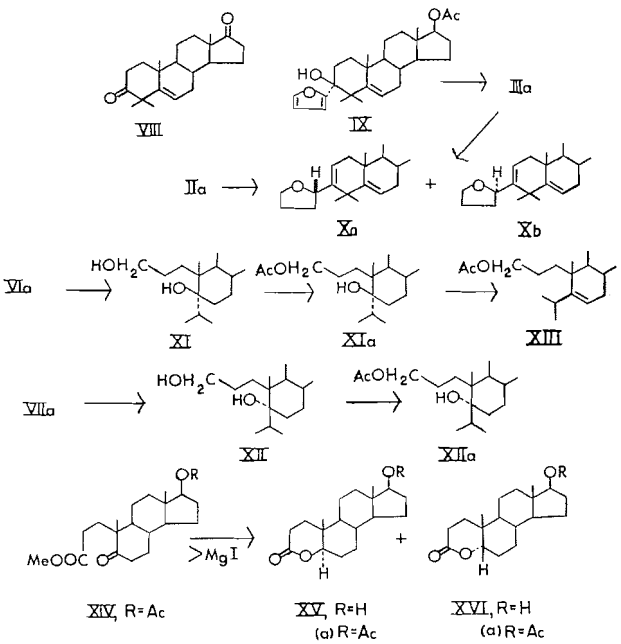
Diol II was apparently the C_3-epimer of diol III. It gave, upon acetylation, a diol monoacetate II*a*. Dehydration of this monoacetate with thionyl chloride in pyridine gave product X, identical with the product obtained by dehydration of diol monoacetate III*a*. Product X was a mixture of the 2′-epimers X*a* and X*b*. It could be resolved into its constituents[4] by t.l.c., with silver nitrate impregnated silica gel as the adsorbent and hexane–ether (6.5:3.5 v/v) as the developing solvent.

The configurational assignment at C-3 of II and III was based on the following arguments. The 3α-alcohol (axial) II had a higher chromatographic mobility on alumina (column). This criterion has often and successfully been applied for this type of assignment (6, 7). Similarly, II*a* had a larger R_f value than III*a* on t.l.c. with alumina as adsorbent (8, 9). Gas–liquid chromatography gave similar results when applied to II*a* and III*a* (10). Comparison of the mode of addition of 2-furylmagnesium iodide and ketone I*a* to that of similar Δ^5-3-ketones and Grignard reagents (11) confirmed the stereochemical assignment at C-3 of II and III.

Lactones VI and VII, which absorbed in the infrared at 1 740 cm^{-1}, were the third type of compound obtained. Both lactones gave monoacetates (VI*a* and VII*a*), which could be converted into triols (XI and XII) by lithium aluminium hydride treatment. Acetylation of XI and XII gave triol diacetates XI*a* and XII*a*, whose infrared spectra were superimposable and displayed hydroxyl bands at 3 620 cm^{-1}. The p.m.r. spectra of XI*a* and XII*a* showed a two-proton signal (triplet) at 4.09 p.p.m. (C—CH_2—OAc). Dehydration of XI*a* gave olefinic diacetate XIII (δ 5.62 p.p.m. (1H)). The mass spectrum of VII*a* showed a very small parent peak at *m/e* 376 and the base peak at *m/e* 333, corresponding to the loss of an isopropyl radical. The subsequent fragmentation pattern was essentially identical with the mass spectrum of the mixture of lactones XV*a* and XVI*a*.[5]

The stereochemical assignment at C-5 in lactones VI*a* and VII*a* was based on (*i*) differences in the molecular rotations (ΔM_D (VI*a* − VII*a*) = 308°) of these substances compared with those of the corresponding lactones (ΔM_D (XV − XVI) = 237°) described by Atwater and Ralls (12); (*ii*) the relative R_f values of triol diacetates XI*a* (0.87) and XII*a* (0.98) on t.l.c.[6] (8, 9); and (*iii*) the chemical shift of the 19-CH_3, which is more deshielded in the *trans*-lactone VI*a* (1.15 p.p.m.) than in the *cis*-lactone VII*a* (1.09 p.p.m.).

[3]*The p.m.r. spectra were taken in* $CDCl_3$ *(tetramethylsilane = 0 p.p.m.).*
[4]*A stereochemical assignment at C-2′ is discussed in the Ph.D. thesis of R. T. T.*
[5]*Lactones XV*a *and XVI*a *were obtained as a mixture from the attempted synthesis of lactones VI*a *and VII*a *outlined in the Experimental section.*
[6]*The procedure for the comparison is described in the Experimental section.*



The yields of the photoproducts in tetrahydrofuran–water (3:1 v/v) and in tetrahydrofuran were established by g.l.c. of the crude, steam distilled, and acetylated reaction mixtures, and are summarized in Table I.

TABLE I

Photoproduct	% yield: Tetrahydrofuran–water (3:1)	% yield: Tetrahydrofuran	Retention times* (min)
IV*a*	8	16	2.6
V*a*	8	4	2.2
II*a*	7	3	12.0
III*a*	6	0	15.2
VI*a*	7	0	9.3
VII*a*	6	0	4.7
A†	7	0	4.2

*Determined at 270° on a 6 ft × ¼ in. (inside diameter) glass column packed with 5% DC 710 on silanized Gas Chrom P; helium was used as the carrier gas at 30 p.s.i.
†Product A was not isolated.

DISCUSSION

Diols IV and V are products of photoreduction, a well-documented (13, 14) occurrence in ketone photochemistry. Adducts II and III find complete analogy in the photochemical addition of tetrahydrofuran to acetone observed by Shima and Tsutsumi (15). Both reduction and adduct formation arise from $n \rightarrow \pi^*$ excitation of the ketone (I) carbonyl to a biradical triplet state (16). The intermediate biradical reacts with solvent molecules to give IV, V, II, and III in yields of 8, 8, 7, and 6%, respectively. When the photolysis of I was performed in tetrahydrofuran, the yields of IV, V, and II were 16, 4, and 3%, respectively, and no III could be detected.[7] This alteration in product distribution from

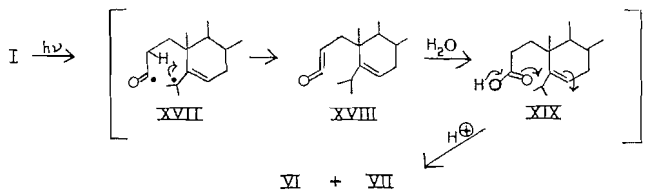
[7]*The irradiation was performed in a standard quartz water-cooled immersion apparatus.*

Can. J. Chem. Downloaded from www.nrcresearchpress.com by 210.87.254.40 on 09/05/12
For personal use only.

aqueous tetrahydrofuran to tetrahydrofuran most probably reflects the differences in solvation of the electronically excited species.

That the C_3—C_4 bond in ketone I underwent cleavage during the photolysis is evident from the presence of lactones VI (7%) and VII (6%).[7] The α-cleavage of ketones also arises from a biradical state, from which is generated an acyl and alkyl radical (17). It is to be expected that cleavage would occur between C-3 and C-4 to give the more stable biradical, e.g. lanostanone yields ca. 34% primary acid (18).

Lactones VI and VII are most likely formed by the known process outlined below. A similar transformation has recently been described (19). An olefinic acid (such as XIX) is known to give a δ-lactone under acidic conditions (20); recently, Mousseron-Canet *et al.* (21) explained their isolation of a δ-lactone from the photolysis of an olefinic acid similar to XIX on the basis of lactonization catalyzed by traces of acid.



Inspection of the g.l.c. spectrum showed that all major components but one were accounted for. This product A, present in approximately 7% yield, was not isolated. The balance of the isolated compounds indicated that no participation of the double bond has to be invoked to explain the products formed.

EXPERIMENTAL

Proton magnetic resonance spectra were recorded on a Varian A-60 (60 Mc.p.s.) spectrometer with deuteriochloroform as solvent and tetramethylsilane (0 p.p.m.) as internal standard. Infrared spectra were taken on Perkin–Elmer grating spectrophotometers, models 337 and 521, with carbon tetrachloride as solvent. Melting points were determined in open capillary tubes on a Gallenkamp apparatus, and are corrected. Optical rotations were measured on a Carl Zeiss photoelectric precision polarimeter. Ultraviolet absorption spectra were taken on a Beckman DK 1 recording spectrophotometer. Schwarzkopf Microanalytical Laboratories, Woodside 77, New York, and Dr. A. Bernhardt, Mülheim, Germany, performed the microanalyses. Mass spectra were recorded by S. Meyerson, American Oil Co., Whiting, Indiana, and by Morgan–Schaffer, Montreal, Quebec. Gas–liquid chromatographic determinations were made on a F and M model 700 gas chromatograph. All acetylations were performed with acetic anhydride in pyridine at room temperature. Silica gel 0.75 mm thick on 8 × 8 in. glass plates was used for plate chromatography, with water as the detector.

Irradiation of Ketone I (3) in Tetrahydrofuran–Water

Ketone I (6.67 g) dissolved in 500 ml of tetrahydrofuran–water (3:1 v/v) was irradiated[7] with a Hanovia 450 W lamp until no starting material remained by t.l.c. analysis (72 h). The addition of 4 g of sodium chloride to the reaction solution gave two layers, which were separated. The tetrahydrofuran layer was dried with magnesium sulfate and concentrated to give 13.03 g of viscous oil. This product was steam distilled and the residue extracted with 1% sodium hydroxide solution, which removed 0.975 g of acidic material. The remaining 7.17 g of oil was chromatographed on 300 g of alumina (activity II–III).

Elution with 120 ml of benzene–ether (9:1 v/v) gave 0.118 g of oil which was not characterized.

Further elution (320 ml) gave 0.321 g of an oil which was then acetylated. Plate chromatography with benzene–ether (4:1 v/v) as the developing solvent gave a major band with R_f 0.78. Ether elution of this band yielded 0.276 g of 17β-acetoxy-4,4-dimethyl-3β-(2-tetrahydrofuryl)androst-5-en-3α-ol (11*a*), m.p. 159.5–161°. Recrystallization from methanol raised the melting point to 160–162°; $[\alpha]_D^{25}$ −94° (*c*, 0.52 in $CHCl_3$); ν_{max} 3 592 (OH) and 1 052 cm^{-1} (C—O—C); δ 5.57 (1H, C=C$_6$—H), 3.80 (3H, poorly resolved CH_2—O—CH), and 1.21 and 1.16 p.p.m.; g.l.c. retention time 12.0 min.

Anal. Calcd. for $C_{27}H_{42}O_4$: C, 75.31; H, 9.83. Found: C, 75.73; H, 9.99.

Continued elution (360 ml) with the same solvent gave 1.25 g of oil, which crystallized overnight from

Can. J. Chem. Downloaded from www.nrcresearchpress.com by 210.87.254.40 on 09/05/12
For personal use only.

methanol, m.p. 167–180°. Four recrystallizations from methanol provided 0.205 g of 4,4-dimethyl-3α-(2-tetrahydrofuryl)androst-5-ene-3β,17β-diol (III), m.p. 183–184°; $[\alpha]_D^{25}$ −73° (*c*, 1.37 in $CHCl_3$); ν_{max} 3 562 (tertiary OH) and 1 052 cm^{-1}; δ 5.62 (1H, broad) and 3.75 p.p.m. (4H, broad, O—C_{17}H and CH_2—O—CH).

Anal. Calcd. for $C_{25}H_{40}O_3$: C, 77.27; H, 10.38. Found: C, 77.52; H, 10.38.

Further elution (160 ml) gave 0.830 g of oil. Acetylation followed by plate chromatography in benzene–ether (4:1 v/v) gave two bands at R_f 0.85 and 0.73. The band with R_f 0.85 provided 0.085 g of epimeric 3-acetoxy-4,4-dimethylandrost-5-en-17β-ol acetate (IV*a* and V*a*), m.p. 157–160°; δ 4.58 (1H, triplet, AcO—C_{17}H) and 4.42 p.p.m. (1H, triplet, AcO—C_3H); g.l.c. retention times 2.6 and 2.2 min, respectively.

Anal. Calcd. for $C_{25}H_{38}O_4$: C, 74.59; H, 9.52. Found: C, 74.77; H, 9.62.

The band at R_f 0.73 gave 0.337 g of 17β-acetoxy-4,4-dimethyl-3α-(2-tetrahydrofuryl)androst-5-en-3β-ol (III*a*), m.p. 199–201°. An analytical sample was prepared by recrystallization from methanol, m.p. 201–202°; $[\alpha]_D^{25}$ −78° (*c*, 0.87 in $CHCl_3$); ν_{max} 3 562 (OH) and 1 052 cm^{-1}; δ 4.67 (1H, triplet, AcO—C_{17}H), 3.89 (3H, approximating a triplet, CH_2—O—CH), and 2.47 p.p.m. (OH, exchanged with D_2O); g.l.c. retention time 15.2 min.

Anal. Calcd. for $C_{27}H_{42}O_4$: C, 75.31; H, 9.83. Found: C, 75.78; H, 10.08; mol. wt. 430 (mass spectrometry).

Continued elution (280 ml) provided an oil (0.563 g), from which III*a*, IV*a*, and V*a* were isolated by t.l.c. as described above.

Further elution (80 ml) gave 0.102 g of epimeric 3-hydroxy-4,4-dimethylandrost-5-en-17β-ol (IV and V), m.p. 201–204° (crystallization from ether). Three recrystallizations from acetone gave an analytical sample having m.p. 204–206°; ν_{KBr} 3 500 – 3 452 (broad) and 3 053 cm^{-1} (olefinic C—H); δ (pyridine) 3.87 (1H, triplet, O—C_{17}H), 3.48 (1H, triplet, O—C_3H), and 1.40 and 1.32 p.p.m. (3H each, two singlets, 4,4-dimethyl).

Anal. Calcd. for $C_{21}H_{34}O_2$: C, 79.19; H, 10.76. Found: C, 78.97; H, 10.82.

Elution (160 ml) with benzene–ether (8.5:1.5 v/v) gave 1.34 g of oil. Acetylation followed by hexane trituration of the recovered oil provided long fibers melting at 151–156°. Crystallization from hexane gave 0.184 g of 17β-acetoxy-5α-isopropyl-4-oxaandrostan-3-one (VI*a*), m.p. 162–163°; $[\alpha]_D^{25}$ +87° (*c*, 0.13 in $CHCl_3$); ν_{max} 1 740 (acetate carbonyl and δ-lactone), 1 425 (C—H of CH_2COO), and 1 391 and 1 382 cm^{-1} (isopropyl group); δ 2.62 (2H, AB system, CH_2—COO),[8] 1.20 and 1.12 (3H each, two doublets, J = 7 c.p.s., isopropyl Me_2), and 1.15 p.p.m. (19-Me); g.l.c. retention time 9.3 min (broad, with decomposition).

Anal. Calcd. for $C_{23}H_{36}O_4$: C, 73.36; H, 9.64. Found: C, 73.29; H, 9.77.

Elution with 250 ml of benzene–ether (1:1 v/v) gave 0.51 g of oil. Acetylation followed by plate chromatography in benzene–ether (3:1 v/v) gave a major band with R_f 0.51. Ether elution of this band provided 0.252 g of 17β-acetoxy-5β-isopropyl-4-oxaandrostan-3-one (VII*a*), m.p. 121–123.5° (crystallization from hexane); $[\alpha]_D^{25}$ +5° (*c*, 1.38 in $CHCl_3$); δ 2.48 (2H, AB system, CH_2—COO), 1.09 (19-Me), and 1.05 and 1.01 p.p.m. (3H each, two doublets, J = 7 c.p.s., isopropyl Me_2); g.l.c. retention time 4.7 min (with decomposition).

Anal. Calcd. for $C_{23}H_{36}O_4$: C, 73.36; H, 9.64. Found: C, 73.40; H, 9.57; mol. wt. 376 (mass spectrometry).

Oxidation of Epimeric 3-Hydroxy-4,4-dimethylandrost-5-en-17β-diol (IV and V) with Chromium Trioxide (4)

Chromium trioxide (61 mg) dissolved in 5 ml of pyridine was added to a solution of 140 mg of the mixture (IV and V) in 7 ml of pyridine. After having stood overnight, the reaction mixture was filtered through an asbestos pad and the inorganic residue was washed with two 10 ml portions of benzene. The usual work-up and plate chromatography of the recovered oil with benzene–ether (4:1 v/v) gave 99 mg of powder, m.p. 151–154°. One recrystallization from hexane–ether gave 83 mg of dione VIII, m.p. 161–162°; ν_{max} 1 734 and 1 705 cm^{-1} (ketones having five- and six-membered rings, respectively). No depression in the melting point was observed on admixture with the product obtained from the corresponding oxidation of I.

Anal. Calcd. for $C_{21}H_{30}O_2$: C, 80.21; H, 9.62. Found: C, 80.41; H, 9.63.

17β-Acetoxy-4,4-dimethyl-3α-(2-furyl)androst-5-en-3β-ol (IX)

A mixture of I*a* (1.1 g) in 15 ml of ether and 2-furylmagnesium iodide (prepared by reacting 0.425 g of magnesium with 2.4 g of 2-iodofuran (5) in 6 ml of ether) was heated under reflux for 7 h. Ammonium chloride (20 ml of a 5% solution) was added to the cooled reaction mixture, followed by filtration through an asbestos pad. The ether layer was dried and concentrated to give 1.3 g of oil, which was then acetylated. Plate chromatography of the recovered oil with 15% ether in benzene gave two bands at R_f 0.61 and 0.54. The band at R_f 0.61 provided 0.401 g of I*a* (identified by mixed melting point and infrared spectrum). The band with R_f 0.54 gave an oil which provided a partially crystalline material when passed through 20 g of alumina (activity I) with benzene–ether (1:1) as eluent. Crystallization from methanol yielded 0.410 g of IX as platelets, m.p. 213–215°. Five recrystallizations from methanol raised the melting point to 215–216° (yellow color persisted); $[\alpha]_D^{25}$ −37° (*c*, 0.40 in $CHCl_3$); $\lambda_{max}^{Et_2O}$ 223 mμ (ϵ 4 700); ν_{max} 3 620 (OH) and 3 045 and 1 047 cm^{-1}; δ 7.23 (1H, complex splitting, C=$C_{5'}$H—O), 6.28 (2H, complex multiplet, C=$C_{3'}$H—$C_{4'}$H=C), and 2.58 p.p.m. (OH).

Anal. Calcd. for $C_{27}H_{38}O_4$: C, 76.02; H, 8.98. Found: C, 76.51; H, 8.47.

[8]*When the p.m.r. spectrum of lactone VIa was taken in 30% deuterium oxide in pyridine, the AB system (in* $CDCl_3$*) became a two-proton triplet centered at 2.79 p.p.m.*

Can. J. Chem. Downloaded from www.nrcresearchpress.com by 210.87.254.40 on 09/05/12
For personal use only.

Can. J. Chem. Downloaded from www.nrcresearchpress.com by 210.87.254.40 on 09/05/12
For personal use only.

Hydrogenation of IX

A mixture of Raney nickel (45 mg), acetate IX (150 mg), and ethanol (50 ml) was hydrogenated (3 100 p.s.i.) at 160 ± 4° for 17 h. Filtration and concentration gave 135 mg of oil. Acetylation followed by plate chromatography, with 30% ether in benzene, gave a series of closely moving bands with R_f values ranging from 0.98 to 0.17. Collection of the bands between R_f 0.98 and 0.55 and separation by plate chromatography with benzene–ether (4:1) gave a band at R_f 0.73 which provided 8 mg of oil. The oil crystallized from methanol, m.p. 196–198°, and was identical with III*a* obtained from photolysis (mixture melting point, comparison of t.l.c. behavior and infrared spectrum).

Dehydration of IIIa (or IIa) with Thionyl Chloride

Thionyl chloride (0.8 ml) was added dropwise to a stirred solution of 184 mg of III*a* in 6 ml of dry pyridine at 0°. After addition, stirring was continued at room temperature for 1 h. Ice chips were then added cautiously and 115 mg of oil was recovered by ether extraction. The oil crystallized from ethanol after 5 days, m.p. 148–151°. Plate chromatography of the product (X) with silver nitrate impregnated silica gel[9] as the adsorbent and 35% ether in hexane as the developing solvent gave two bands, detected by ultraviolet light at R_f 0.62 and 0.57, respectively. The band at R_f 0.62 provided 23 mg of 17β-acetoxy-4,4-dimethyl-3-(2-tetrahydrofuryl)androsta-2,5-diene (X*a*), m.p. 154–156°; $[\alpha]_D^{25}$ −59° (*c*, 0.96 in $CHCl_3$); ν_{max} 3 030 and 1 048 cm^{-1}; δ 5.84 (1H, unresolved, C=C$_2$—H), 5.60 (1H, broad, C=C$_6$—H), 4.32 (1H, triplet, O—C$_{2'}$H—C=O), and 3.87 p.p.m. (2H, poorly resolved, O—C$_{5'}$H$_2$—C); g.l.c. retention time 8.0 min.

Anal. Calcd. for $C_{27}H_{40}O_3$: C, 78.59; H, 9.77. Found: C, 78.78; H, 9.77.

The band with R_f 0.57 gave 20 mg of X*b*, m.p. 171–172.5°; $[\alpha]_D^{25}$ −74° (*c*, 0.94 in $CHCl_3$). The infrared and p.m.r. spectra were essentially the same as those for X*a*.

Anal. Calcd. for $C_{27}H_{40}O_3$: C, 78.59; H, 9.77. Found: C, 78.48; H, 9.74.

3,4-Seco-4,4-dimethylandrostane-3,5β,17β-triol (XI)

A solution of 318 mg of VI*a* in 10 ml of dry ether was added slowly to 126 mg of lithium aluminium hydride in 4 ml of ether. The mixture was heated under reflux for 1 h and worked up in the usual way to give 306 mg of XI, m.p. 184–187°. Three recrystallizations from ether–acetone raised the melting point to 196–198.5°; $[\alpha]_D^{25}$ +4° (*c*, 0.98 in pyridine).

Anal. Calcd. for $C_{21}H_{38}O_3$: C, 74.51; H, 11.32. Found: C, 74.35; H, 11.25.

Acetylation of XI (100 mg) gave 104 mg of 3,17β-diacetoxy-3,4-seco-4,4-dimethylandrostan-5β-ol (XI*a*) as an oil, which was shown to be homogeneous by t.l.c.; ν_{max} 3 620 (free OH) and 1 740 cm^{-1} (intense); δ 4.69 (1H, triplet, AcO—C$_{17}$H) and 4.09 p.p.m. (2H, triplet, C—CH$_2$—OAc).

3,17β-Diacetoxy-3,4-seco-4,4-dimethylandrost-5-ene (XIII)

The dehydration of 104 mg (oil) of XI*a* was carried out as described for III*a*. The resulting oil was purified by plate chromatography with 35% ether in hexane to give XIII, R_f 0.98; m.p. 116–116.5°; ν_{max} 1 742 cm^{-1} (intense); δ 5.62 (1H, poorly resolved, C=C$_6$—H), 4.67 (1H, triplet, AcO—C$_{17}$H), and 4.03 p.p.m. (2H, triplet, C—CH$_2$—OAc).

Anal. Calcd. for $C_{25}H_{40}O_4$: C, 74.21; H, 9.97. Found: C, 74.19; H, 9.54.

3,4-Seco-4,4-dimethylandrostane-3,5α,17β-triol (XII)

Lactone VII*a* (112 mg) was treated as described for VI*a*. Triol XII (91 mg) was isolated, m.p. 143–144.5°; $[\alpha]_D^{24}$ +41° (*c*, 0.94 in pyridine).

Anal. Calcd. for $C_{21}H_{38}O_3$: C, 74.51; H, 11.32. Found: C, 74.18; H, 11.14.

Acetylation of 65 mg of XII provided 61 mg of 3,17β-diacetoxy-3,4-seco-4,4-dimethylandrostan-3α-ol (XII*a*), m.p. 141–143° after crystallization from methanol; $[\alpha]_D^{24}$ +1° (*c*, 0.6 in $CHCl_3$). The infrared spectrum was indistinguishable from that of XI*a*. The p.m.r. spectrum was also very similar to that of XI*a*.

Anal. Calcd. for $C_{25}H_{42}O_5$: C, 71.09; H, 9.95. Found: C, 70.97; H, 10.26.

Thin-Layer Chromatographic Comparison of XIa and XIIa

Both XI*a* and XII*a* were spotted on a microscope slide coated evenly (0.5 mm) with Woelm neutral alumina (for t.l.c.). With ethyl acetate – hexane (3:2 v/v) as the developing solvent, XII*a* had a R_f value of 0.98 whereas XI*a* was at R_f 0.87.

Attempted Synthesis of Lactones VIa and VIIa; Lactones XVa and XVIa

An ethereal solution of isopropylmagnesium iodide was added to 431 mg of 17β-acetoxy-5-oxo-3,5-seco-A-norandrostan-3-oic acid methyl ester (XIV)[10] in 35 ml of dry ether until t.l.c. analysis indicated that only a trace of XIV remained. Ammonium chloride (10 ml of a 3% solution) was then introduced and the ether solution dried and concentrated. Acetylation of the residual oil followed by plate chromatography with 30% ether in benzene gave two bands at R_f 0.77 and 0.54. Ether elution of the band at R_f 0.77 provided 120 mg

[9]*The plates ordinarily used for plate chromatography were sprayed with 5% silver nitrate solution until the adsorbent was saturated. The plates were then air dried overnight.*

[10]*Prepared from testosterone acetate in accordance with a procedure described by Atwater and Ralls (12), followed by treatment with diazomethane.*

of starting material (identified by infrared and p.m.r. spectra and mixed melting point), m.p. 90–91.5°. The other band (R_f 0.54) gave a mixture of 17β-acetoxy-4-oxa-5α-androstan-3-one (XV*a*) and the 5β-epimer (XVI*a*), m.p. 150–164°; ν_{max} 1 740 cm^{-1} (intense); δ 4.22 (0.6H, triplet, 5β-hydrogen of XVI*a*) and 3.70 p.p.m. (0.5H, broad, 5α-hydrogen of XV*a*).[11]

Anal. Calcd. for $C_{20}H_{30}O_4$: C, 71.85; H, 8.98. Found: C, 72.05; H, 9.01; mol. wt. 334 (mass spectrometry).

The Grignard reaction therefore resulted in only reduction and enolization.

ACKNOWLEDGMENTS

We thank Mr. K. Valentin for taking the p.m.r. spectra; Dr. G. Schilling and Mr. J. Kastner, Ayerst Laboratories, Montreal, for providing g.l.c. supports and performing the high-pressure catalytic reduction of IX; Mr. S. Meyerson, American Oil Co., for taking a mass spectrum; and G. D. Searle and Co., Syntex Corporation, and Ayerst Laboratories for generous gifts of starting material.

REFERENCES

1. M. Gorodetsky and Y. Mazur. Tetrahedron Letters, 227 (1964).
2. B. B. Dewhurst, J. E. Holker, A. Lablanche-Combier, M. G. Leeming, J. Levisalles, and J. P. Pete. Bull. Soc. Chim. France, 3259 (1964).
3. H. J. Ringold and G. Rosenkrantz. J. Org. Chem. **22**, 602 (1957).
4. G. Poos, G. Arth, R. Beyler, and L. Sarett. J. Am. Chem. Soc. **75**, 422 (1953).
5. H. Gilman, H. E. Mallory, and G. F. Wright. J. Am. Chem. Soc. **54**, 733 (1932).
6. D. H. R. Barton and R. C. Cookson. Quart. Rev. London, **10**, 44 (1956).
7. C. S. Barnes and A. Palmer. Australian J. Chem. **9**, 105 (1956).
8. L. Labler and V. Cerny. Collection Czech. Chem. Commun. **28**, 2932 (1963).
9. H. J. Petrowitz. Angew. Chem. **72**, 921 (1960).
10. R. B. Clayton. Nature, **190**, 1071 (1961).
11. G. Just and V. DiTullio. Can. J. Chem. **42**, 2695 (1964).
12. N. W. Atwater and J. W. Ralls. J. Am. Chem. Soc. **82**, 2011 (1960).
13. G. S. Hammond and N. Turro. Science, **142**, 1541 (1963).
14. C. Walling and M. J. Gibian. J. Am. Chem. Soc. **87**, 3361 (1965).
15. K. Shima and S. Tsutsumi. Bull. Chem. Soc. Japan, **36**, 121 (1963).
16. H. E. Zimmerman. *In* Advances in photochemistry. Vol. 1. Interscience Publishers, Inc., New York. 1963. p. 184.
17. N. J. Turro. Molecular photochemistry. W. A. Benjamin, Inc., New York. 1965. p. 225.
18. D. Arigoni, D. H. R. Barton, R. Bernasconi, C. Djerassi, J. S. Mills, and R. Wolf. Proc. Chem. Soc. 306 (1959).
19. G. O. Schenck and F. Schaller. Chem. Ber. **98**, 2056 (1965).
20. M. F. Ansell and M. H. Palmer. Quart. Rev. London, **18**(2), 211 (1964).
21. M. Mousseron-Canet, M. Mousseron, and P. Legendre. Bull. Soc. Chim. France, 1509 (1961).
22. H. O. House, H. Badad, R. B. Toothill, and A. W. Nottes. J. Org. Chem. **27**, 4141 (1962).

[11]*House et al. (22) found that the 5-proton (axial) in a lactone such as XV absorbed at higher field (closer to tetramethylsilane) than its equatorial epimer (such as XVI).*

Can. J. Chem. Downloaded from www.nrcresearchpress.com by 210.87.254.40 on 09/05/12
For personal use only.

Can. J. Chem. Downloaded from www.nrcresearchpress.com by 210.87.254.40 on 09/05/12
For personal use only.

REACTIONS OF 2-ACETOXY-4,6-DI-*O*-ACETYL-3-*O*-(2,6-DICHLOROBENZOYL)-D-GLUCAL, TRI-*O*-ACETYL-3-DEOXY-α-D-*erythro*-HEX-2-ENOPYRANOSYL CHLORIDE, AND RELATED COMPOUNDS

R. U. LEMIEUX AND R. J. BOSE[1]

Department of Chemistry, University of Alberta, Edmonton, Alberta

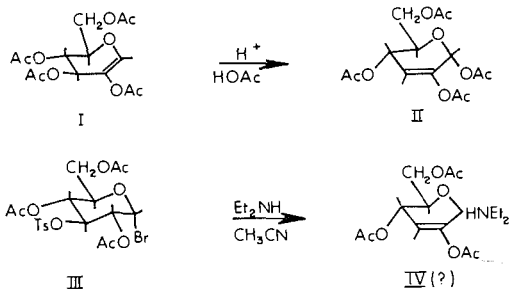
Received March 15, 1966

ABSTRACT

Attempts to dehydrobrominate tri-*O*-acetyl-3-*O*-tosyl-α-D-glucopyranosyl bromide with diethylamine led directly to products resulting from the replacement of the tosyloxy group by the diethylamine. It was readily possible to prepare 2-acetoxy-di-*O*-acetyl-3-(2,6-dichlorobenzoyl)-D-glucal (V). Acetolysis of this compound gave an equimolar mixture of the α- and β-anomers (II and VI, respectively) of 2-acetoxy-di-*O*-acetyl-pseudo-D-glucal as the first products of the reaction. Compound V reacted only reluctantly with methanol in pyridine to give a mixture of the anomeric methyl di-*O*-acetyl-3-deoxy-D-*erythro*-hex-2-enopyranosides. These glycosides were readily prepared by reaction of tri-*O*-acetyl-3-deoxy-α-D-*erythro*-hex-2-enopyranosyl chloride with methanol in the presence of pyridine. 2-Acetoxy-di-*O*-acetyl-3-*O*-mesitoyl-D-glucal was prepared from 3-*O*-mesitoyl-β-D-glucose. The anomerizations of compounds II and VI were examined with both sulfuric acid in 1:1 acetic acid – acetic anhydride and potassium acetate in acetic acid. The conformations of II and VI are discussed, as are a number of the mechanistic features of the reactions studied.

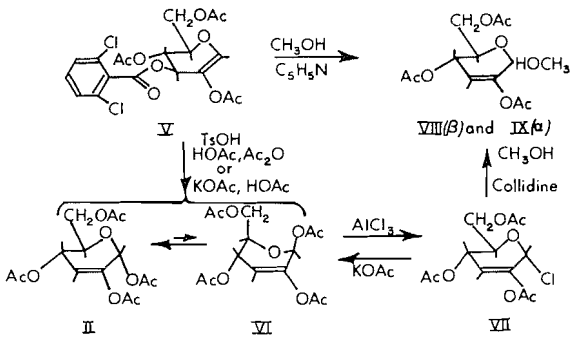
Lemieux *et al.* (1) have reported the acid-catalyzed isomerization of tetra-*O*-acetyl-1-deoxy-D-*arabino*-hex-1-enopyranose (I) (2-acetoxy-D-glucal triacetate) to tetra-*O*-acetyl-3-deoxy-α-D-*erythro*-hex-2-enopyranose (II) (2-acetoxy-pseudo-D-glucal triacetate). The main objective of this research was to prepare a 3-*O*-derivative of 4,5-di-*O*-acetyl-2-acetoxy-D-glucal wherein the substituent at the 3-position was a sufficiently good leaving group for the compound to undergo solvolysis in the absence of acid, with attack of the entering group at the anomeric center. It was anticipated that if this could be accomplished the stereochemical route of the reaction could be established and compared with the S_N2' mechanism (2). Furthermore, the compound could conceivably be useful as a reagent for the synthesis of 2,3-unsaturated glycopyranosides, which could then presumably be converted into 2-ketoglycosides and so on.

In the first attempt, the tosyloxy group was chosen for the 3-substituent. Tri-*O*-acetyl-3-*O*-tosyl-α-D-glucopyranosyl bromide (III) was readily prepared by established procedures (3) from 1,2;5,6-di-*O*-isopropylidene-α-D-glucose. By use of the optimum conditions developed by Lemieux and Lineback (4) for dehydrobromination, the tosyloxy group was



[1]*Corn Industries Research Foundation Postdoctorate Fellow, 1964–1965. Present address: Fisheries Research Board of Canada, Technological Research Laboratory, Vancouver 8, British Columbia.*

removed and derivatives of the diethylamine were obtained in about 80% yield. Evidently, the initially formed 2-acetoxy-3-*O*-tosyl-D-glucal diacetate underwent extremely facile replacement of the tosyloxy group by the amine, most probably with migration of the double bond from the 1,2- to the 2,3-position. The nuclear magnetic resonance (n.m.r.) spectrum of the crude product showed the presence of at least two main components. As judged from the relative intensities of the signals, 1 mole of diethylamine had replaced the tosyloxy group. The product was very unstable and readily consumed about 2 moles of hydrogen when hydrogenated in the presence of palladium. These properties are consistent with those expected for an unsaturated glycosylamine (IV). The actual structures were not established, since the separation and purification of the compounds were not accomplished. Also, the product from the hydrogenation was found, by gas–liquid preparative chromatographic examination, to be a complex mixture.



The use of the mesyloxy rather than the tosyloxy group in the above sequence of reactions gave comparable results. This experience is analogous to that of Stork and White (2), who were unable to prepare *trans*-4-alkyl-3-tosyloxycyclohexene. Since these authors found the 2,6-dichlorobenzoyloxy group to be a useful leaving group in their research on the S_N2' reaction, 2-acetoxy-3-*O*-(2,6-dichlorobenzoyl)-D-glucal diacetate (V) was prepared by conventional methods. That the 2,6-dichlorobenzoyl group was, in fact, at the 3-position of V was demonstrated by conversion of the compound into the equilibrium mixture of the anomeric forms of 2-acetoxy-pseudo-D-glucal diacetate (II and IV) in a nearly quantitative yield (n.m.r.) by treatment with *p*-toluenesulfonic acid in a 1:5 acetic anhydride – acetic acid mixture under the conditions reported (1) for the isomerization of 2-acetoxy-D-glucal triacetate. Also, the n.m.r. spectrum of V was in complete agreement with that of a compound having the assigned structure.

Extensive reaction of compound V with methanol in the presence of pyridine occurred after 3 h at 100°. However, much decomposition to intractable material took place and the reaction showed no promise as a synthetic approach to glycosides. Nuclear magnetic resonance examination of the crude product indicated that the α- and β-methyl glycosides (IX and VIII, respectively) described below were present along with starting material (V).

Ferrier *et al.* (5) have recently reported the β-anomer (VI) of II. As was anticipated (1), the use of *p*-toluenesulfonic acid (0.05 *M*) in 1:5 acetic anhydride – acetic acid to isomerize I to II caused the equilibration of II and VI at a rate much faster than that of the isomerization. However, the equilibration reaction was followed with 0.00037 *M* sulfuric acid in 1:1 acetic acid – acetic anhydride. The half-life of the reaction was about 14 min at 23°. It is of interest to note that the half-life for the anomerization of the tetra-*O*-acetyl-2-deoxy-D-glucopyranoses under these conditions, but with 0.001 *M* acid,

Can. J. Chem. Downloaded from www.nrcresearchpress.com by 210.87.254.40 on 09/05/12
For personal use only.

is 4 min (6). Thus the increased opportunity for charge delocalization provided by the allylic double bond effectively cancels the effect of the 2-acetoxy group (7). The solvent itself did not cause equilibration at a measurable rate. The equilibrium constant was about 4.0 in favor of the α-anomer, both by n.m.r. analysis and from the optical rotation of the mixture. As indicated by Ferrier and his co-workers, the anomeric effect (8) may be mainly responsible for the greater stability of the α-form. In this regard, it is of interest to note the n.m.r. parameters for II and VI listed in Table I. In view of the differences in both $J_{3,4}$ and $J_{4,5}$, it is evident that the pyranose ring has different conformations for these compounds. From the value of $J_{4,5}$ for the α-anomer (9 c.p.s.), it follows that the 4-acetoxy and 4-acetoxymethyl groups are in an equatorial orientation and that the compound resides in the "regular" half-chair conformation, with the 1-acetoxy group in a quasi-axial orientation. Since these compounds have two trigonal carbons and an oxygen atom in the pyranose ring, the destabilizing interactions between opposing axial groups must be much less than in a chair conformation. Thus, it is reasonable to expect that the β-anomer may closely achieve a conformation which has the 4- and 5-substituents in a quasi-axial orientation to decrease the non-bonding interaction between these substituents. In fact, the n.m.r. data require that the 4- and 5-substituents be much further apart in the β- than in the α-anomer. Evidently, for the α-form, the anomeric effect is sufficiently great to overcome the gauche interaction between the 4- and 5-substituents.

TABLE I

Nuclear magnetic resonance parameters for derivatives of 2-acetoxy-pseudo-D-glucal

Compound	Chemical shifts (τ)			Coupling constants (c.p.s.)	
	H^1	H^3	H^4	$J_{3,4}$	$J_{4,5}$
α-Tri-*O*-acetyl (II) (1)	3.69	4.13	4.47	2.2	9
β-Tri-*O*-acetyl (VI)	3.63	4.04	4.69	5.5	~1
α-Di-*O*-acetyl-1-*O*-methyl (IX)	5.07	4.28	4.58	2	~9
β-Di-*O*-acetyl-1-*O*-methyl (VIII)	4.85	4.23	4.69	4.7	4.5
α-Di-*O*-acetyl-1-chloro-1-deoxy (VII)	3.72	4.19	4.4	2	~9

The anomeric compounds II and VI could also be equilibrated by heating them in acetic acid with potassium acetate, although substantial decomposition to other products occurred. The equilibrium constant was, within experimental error, the same as that observed under the acid conditions. The half-life of the reaction with M potassium acetate in acetic acid at 100° was about 100 min.

Di-*O*-acetyl-2-acetoxy-3-*O*-(2,6-dichlorobenzoyl)-D-glucal (V) also gave the anomeric tri-*O*-acetyl-2-acetoxy-pseudo-D-glucals (II and VI) on treatment with potassium acetate in acetic acid at 100°. The half-life of the reaction was about 10 min. Thus, this reaction is about 10 times faster than the anomerization of the products, and the stereochemistry of the reaction was readily established. In fact, compound V could be converted into an almost exactly equimolar mixture of the anomeric acetates (II and VI) in 27% yield by heating it for 5 min at 100° in M potassium acetate in acetic acid, conditions which left the products virtually unchanged. Thus, unlike the S_N2' reaction (2), this transformation was devoid of stereospecificity. This is not surprising since the ring oxygen must participate in the reaction to help delocalize the developing positive charge, and thus obviates the need for an attack by the entering nucleophile in *cis*-relationship to the leaving group to maximize the stability of the transition state. The molecularity of the reaction was not

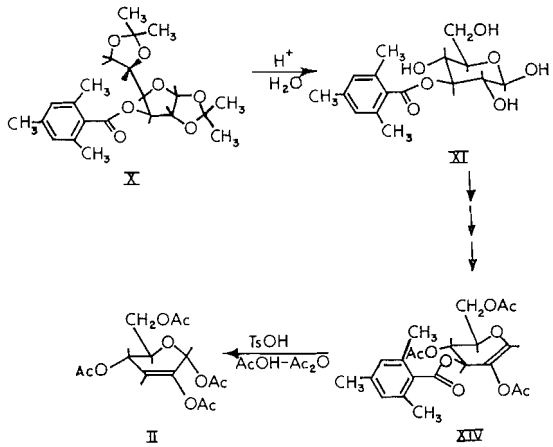
Can. J. Chem. Downloaded from www.nrcresearchpress.com by 210.87.254.40 on 09/05/12
For personal use only.

established, and it is possible that the reaction proceeds by way of an ionic intermediate (S_N1).

Reaction of 2-acetoxy-pseudo-α-D-glucal triacetate (II) with aluminium chloride in chloroform under carefully controlled conditions gave the highly reactive tri-*O*-acetyl-3-deoxy-α-D-*erythro*-hex-2-enopyranosyl chloride (VII). The syrupy product appeared (n.m.r.) to be over 80% pure. The same product was obtained from 2-acetoxy-pseudo-β-D-glucal triacetate (VI).

The structure of the chloride (VII) was substantiated by reaction with sodium acetate in acetic acid to yield a mixture of II and VI in the ratio of 1:2, respectively. Thus, it was apparent that the compounds underwent replacement of the chlorine predominantly with inversion of the reacting center, as is normally found in these reactions (9).[2] The configuration of the chloride (VII) was established by the n.m.r. parameters listed in Table I.

At one point in this research, it was thought of interest to prepare 3-*O*-mesitoyl-2-acetoxy-D-glucal diacetate (XIV) to test the leaving power of the mesitoyloxy group. This preparation was readily possible by using the recently published method for preparing esters of hindered acids, which employs the use of trifluoroacetic anhydride as the activating reagent (10). It was remarkable to find that crystalline 1,2;5,6-di-*O*-isopropylidene-3-*O*-mesitoyl-α-D-glucose (X) was readily prepared in this way in 94% yield. The compound was hydrolyzed to crystalline 3-*O*-mesitoyl-β-D-glucose (XI), which was converted in the usual manner by way of the acetobromo derivative (XIII) into compound XIV. The compound seemed to be as stable as the tetraacetate (I), and underwent conversion into the 2-acetoxy-pseudo-D-glucal triacetates (II and VI) in 5:1 acetic acid – acetic anhydride 0.05 *M* in *p*-toluenesulfonic acid (1) at 0.34 times the rate of I and 6.7 times the rate of V.



Although this research failed to yield a 3-*O*-substituted-2-acetoxy-D-glucal diacetate of sufficient reactivity to serve as a useful reagent for the synthesis of 2,3-unsaturated glycosides, the tri-*O*-acetyl-3-deoxy-α-D-*erythro*-hex-2-enopyranosyl chloride (VII) described above shows considerable promise in this regard. The compound is extremely reactive, as shown by the fact that its reactions with methanol and ethanol to form glycosides were complete within minutes at room temperature in the presence of *sym*-collidine as buffer. The α- and β-anomers were formed in about equal amounts.

[2]*R. U. Lemieux and R. J. Bose, in preparation.*

Can. J. Chem. Downloaded from www.nrcresearchpress.com by 210.87.254.40 on 09/05/12
For personal use only.

Can. J. Chem. Downloaded from www.nrcresearchpress.com by 210.87.254.40 on 09/05/12
For personal use only.

EXPERIMENTAL

Unless otherwise stated, the optical rotations were measured in 1 dm tubes at the D-line of sodium and room temperature (23–24°). The n.m.r. spectra were determined in deuterated chloroform on the spectrometers previously described (4). The melting points were determined on a microstage and are uncorrected.

Attempts to Prepare a 3-O-Sulfonyl Derivative of 4,6-Di-O-acetyl-2-acetoxy-D-glucal

The 2,4,6-tri-*O*-acetyl-3-*O*-tosyl (3) and 2,4,6-tri-*O*-acetyl-3-*O*-mesyl (11) derivatives of α-D-glucosyl bromide were prepared as previously described. The physical constants were in close agreement with those published for these compounds. Furthermore, the n.m.r. spectra were in complete agreement with those of compounds having the assigned structures.

When the compounds were treated with diethylamine in acetonitrile according to the directions reported by Lemieux and Lineback (4) for the dehydrobromination of tetra-*O*-acetyl-α-D-glucopyranosyl bromide, a syrupy product was obtained which darkened rapidly when allowed to stand. The n.m.r. spectra showed the products to be devoid of the sulfonate ester grouping and to be virtually identical. Although integration showed the presence of one diethylamino group per tri-*O*-acetyl sugar residue, it was evident that the product was a mixture of at least two compounds. Attempts to obtain a pure compound failed. Hydrogenation in ethanol in the presence of 5% palladium on charcoal led to extensive hydrogenolysis as well as hydrogenation, as indicated by the rapid consumption of 2 moles of hydrogen. The product was deacetylated and converted into the trimethylsilyl derivative for analysis by gas–liquid preparative chromatography. Although a band corresponding to 80% of the mixture appeared to provide a single component, the n.m.r. spectrum required this fraction to be a mixture of several compounds.

Reaction of the crystalline 2,4,6-tri-*O*-acetyl-3-*O*-tosyl-α-D-glucosyl bromide with 1 mole equivalent of diethylamine and 3 moles of methanol in acetonitrile led to a reaction which was complete after 10 h. The observed decrease in rotation was 0.76°. When 2 more mole equivalents of diethylamine was added, the rotation decreased 0.89° in 10 h and then remained constant. The product of this reaction was identical with that described above, obtained in the absence of methanol and with a large excess of diethylamine. Increased concentrations of methanol had no effect on the course of the reaction.

1,2;5,6-Di-O-isopropylidene-3-O-(2,6-dichlorobenzoyl)-α-D-glucose

1,2;5,6-Di-O-isopropylidene-α-D-glucose (1.0 g, 3.00 mmoles) was dissolved in 3 ml dry pyridine containing 1 ml 2,6-dichlorobenzoyl chloride (2). The reaction mixture was heated for 2.5 h on the steam bath, cooled, and poured onto ice. The mixture was extracted with chloroform. Evaporation of the chloroform extract gave a deep-red syrup which was extracted with ether. The red ethereal solution was concentrated to a syrup (2.26 g) which was subsequently fractionated on a column of 30 g silicic acid (Mallinckrodt, 100 mesh, analytical reagent) with chloroform as the eluting solvent. A pale-yellow syrup (1.06 g) was obtained from the fast-moving zone; this syrup crystallized when allowed to stand and was recrystallized from ethanol as long needles, m.p. 122–123°, $[\alpha]_D$ −14.45° (*c*, 1.4 in chloroform).

Anal. Calcd. for $C_{19}H_{22}Cl_2O_7$: C, 52.67; H, 5.12. Found: C, 52.51; H, 5.11.

4,6-Di-O-acetyl-2-acetoxy-3-O-(2,6-dichlorobenzoyl)-D-glucal (V)

1,2;5,6-Di-*O*-isopropylidene-3-*O*-(2,6-dichlorobenzoyl)-D-glucose was heated on the steam bath under reflux for 2 h in 1:1 ethanol – 2 *N* sulfuric acid. Thin-layer chromatography of the resulting hydrolysate showed only one spot. The reaction mixture was diluted with water and neutralized with barium carbonate. The filtrate was concentrated to a syrup, $[\alpha]_D^{23}$ −29.1° (*c*, 2.6 in ethanol), which was directly acetylated in the usual manner with sodium acetate and acetic anhydride.

In a typical experiment, the syrupy 1,2,4,6-tetra-*O*-acetyl-3-*O*-(2,6-dichlorobenzoyl)-D-glucose (0.41 g, $[\alpha]_D$ +24.4° (*c*, 3 in chloroform)) was dissolved in an ice-cold mixture of 5 ml 32% hydrogen bromide in glacial acetic acid containing 1 ml of acetic anhydride. The reaction mixture remained overnight at room temperature and then was poured onto 100 g ice. The amorphous precipitate was recovered by filtration, washed with ice water, and dissolved in chloroform. The solution was washed with ice-cold sodium bicarbonate solution and then water, and finally dried over sodium sulfate. Evaporation gave a syrup, 0.28 g, $[\alpha]_D$ +120° (*c*, 2.8 in acetonitrile), which resisted crystallization. The n.m.r. spectrum in deuterated chloroform required the substance to be virtually pure 2,4,6-tri-*O*-acetyl-3-*O*-(2,6-dichlorobenzoyl)-α-D-glucopyranosyl bromide. The chemical shifts for H^1, H^2, H^3, and H^4 were τ 3.27, 5.07, 4.03, and 4.66, and the spacings in the closely first-order spectrum indicated $J_{1,2} = 4.0$, $J_{2,3} = J_{3,4} = 10.0$, and $J_{4,5} = 9.5$ c.p.s. The relative intensities of the signals in the spectrum were as expected. The three protons on the benzene ring gave a sharp singlet at τ 2.63.

2,4,6-Tri-*O*-acetyl-3-*O*-(2,6-dichlorobenzoyl)-α-D-glucopyranosyl bromide (0.282 g, 0.52 mmole) was dissolved in 10 ml dry acetonitrile. Dry diethylamine (0.4 ml, 3.9 mmoles) was added and the change in rotation observed. From an initial observed rotation of +3.39°, a final rotation of 1.11° was reached in 11 h. The reaction mixture was poured into 150 ml of ice-cold chloroform and washed successively with 100 ml 0.2 *N* hydrochloric acid (ice-cold) and ice-cold sodium bicarbonate solution. When the chloroform solution was concentrated a syrup (0.21 g) was obtained, $[\alpha]_D$ −11.35° (*c*, 3.13 in chloroform), which discolored when allowed to stand. In a separate experiment 4.24 g of the syrup was applied to a 30 g silicic acid column and

eluted with chloroform. A single, sharp band appeared on the column which was recovered as a single fraction (4.02 g). The pale-yellow syrup (V), $[\alpha]_D$ −9.32° (*c*, 2 in chloroform), was dried for 12 h at 100° and 0.5 mm pressure without appreciable darkening.

Anal. Calcd. for $C_{19}H_{18}O_9Cl_2$: C, 49.47; H, 3.93. Found: C, 48.99; H, 3.96.

Although the compound resisted crystallization, the n.m.r. spectrum in deuterated chloroform indicated a high degree of purity. Only the expected signals, having the proper relative intensities, were observed. The signals for H^1 (singlet), H^3 (doublet), and H^4 (triplet) were at τ 3.28, 4.06, and 4.58, respectively, with $J_{3,4} = J_{4,5} = 5$ c.p.s. The signals for the three acetyl groups were well separated, and the three protons on the benzene ring gave a sharp singlet at τ 2.67.

*Tetra-O-acetyl-β-*D*-erythro-hex-2-enopyranose (VI)*

The α-anomer (II) was prepared from 65 g of tri-*O*-acetyl-2-acetoxy-D-glucal according to the directions of Lemieux and his co-workers (1), with *p*-toluenesulfonic acid as catalyst. The reaction mixture was poured onto 2 l of crushed ice. The crude crystalline α-anomer was isolated by filtration and recrystallized from 600 ml of 1:1 ethanol–water to give 39.5 g of pure compound. The mother liquors from the above filtrations were combined and thoroughly extracted with chloroform. The neutralized and dried extract was concentrated to a syrup (23.2 g), which was a 1.6:1 mixture of VI and II, respectively. The β-anomer (VI) crystallized readily when the mixture was seeded with an authentic sample kindly provided by Dr. R. J. Ferrier, Birkbeck College. The compound, m.p. 81.5–83.5°, $[\alpha]_D$ +146° (*c*, 2.4 in chloroform), was purified by repeated recrystallizations from 95% ethanol. Ferrier and his co-workers (5) reported m.p. 81–83°, $[\alpha]_D$ +156° (*c*, 1 in chloroform). The n.m.r. parameters measured at 100 Mc.p.s. are reported in Table I.

Anomerization Reactions of Compounds II and VI

Acid-Catalyzed

When 0.2 g of II was dissolved at 25° in 3 ml of 1:1 acetic acid – acetic anhydride 0.37 *M* in sulfuric acid, the rotation fell from an initially observed value of +4.6° to 3.28° in 5 min and eventually to a nearly constant value of −3.12°. Since these observed rotational changes were in the direction opposite to that expected for anomerization, it was evident that these strongly acid conditions had caused rapid changes other than anomerization. Solutions of compounds II and VI in 1:1 acetic acid – acetic anhydride showed no change in rotation during 24 h at 25°. It was found that reactions limited to anomerization could be achieved by using 0.00037 *M* sulfuric acid. Under these conditions, the rotation increased from 3.2° after 3 min to a constant value of +4.02° in 30 min. The rate of change in rotation followed first-order kinetics ($k_\alpha + k_\beta = 5 \pm 1 \times 10^{-2}$ min^{-1}). After 80 min, 0.1 ml of collidine was added and the product isolated in the usual manner. The n.m.r. spectrum showed the product to be a 4:1 mixture of the α- and β-anomers, respectively. Based on the rotations at zero time obtained by plotting the rotational data for both II and VI, the equilibrium rotation for the 4:1 mixture is expected to be 4.10°.

Anomerization of compound VI under the above conditions gave a change in rotation from +8.40° at zero time to a nearly constant value of +4.05° in 60 min. The velocity of the reaction was, within experimental error, the same as that when the α-anomer was used.

Base-Catalyzed

Solutions (0.1 *M*) of II and VI were made up at room temperature in acetic acid 1 *M* in potassium acetate, and placed in sealed tubes. At zero time, the tubes were immersed in a boiling water bath. After various intervals of time, the solutions were added to cold chloroform and the mixtures immediately washed with water and then sodium bicarbonate solution, dried, and evaporated to the syrupy products. The compositions of the products were determined by n.m.r. The β-anomer (VI) was anomerized to a 2:1 mixture of the α- and β-forms, respectively, in 180 min. After 5 min, only 5% anomerization had occurred. The α-anomer (II) was isomerized to a 4:1 mixture of II and VI, respectively, after 16 h. The isolated yield of the product was 40%.

*Conversions of 4,6-Di-O-acetyl-2-acetoxy-3-O-(2,6-dichlorobenzoyl)-*D*-glucal (V) into the Anomeric Tetra-O-acetyl-*D*-erythro-hex-2-enopyranoses (II and VI)*

Acid Catalysis

Compound V (a 0.1 *M* solution in 1:5 acetic anhydride – acetic acid containing 0.05 *M* *p*-toluenesulfonic acid) was treated at 25° as described by Lemieux and his co-workers (1) for the isomerization of I. The rate of rotational change indicated a velocity constant of 2×10^{-2} h^{-1}. The product of reaction was a 4:1 equilibrium mixture of II and VI. The velocity constants for the conversions of compounds I and XIV were 40×10^{-2} and 13.5×10^{-2} h^{-1}, respectively.

Base Catalysis

Compound V was allowed to react in acetic acid 1 *M* in potassium acetate at 100° as described above for compounds II and VI. Products were isolated after reaction times of 5, 15, 30, and 180 min and contained 73, 29, 11, and 0% of the starting material, respectively, as indicated by the n.m.r. spectra. Compounds II and VI were the sole products of the reaction and were present in the products in ratios (α/β) of 1.08, 1.27, 1.54, and 2.70, respectively.

Can. J. Chem. Downloaded from www.nrcresearchpress.com by 210.87.254.40 on 09/05/12
For personal use only.

Tri-O-acetyl-3-deoxy-α-D-erythro-hex-2-enopyranosyl Chloride (VII)

Compound II (5.08 g, 15.4 mmoles) was dissolved in 100 ml of alcohol-free dry chloroform. Powdered aluminium chloride (2.1 g, 15.8 mmoles) was added and the mixture was vigorously shaken for 1 h at room temperature. The mixture was poured into 300 ml of dry benzene and filtered through a cotton plug. Evaporation of the solvents under reduced pressure left 3.07 g of a colorless syrup, $[\alpha]_D$ +53.4° (*c*, 2.5 in chloroform). The n.m.r. spectrum (see Table I) left no doubt that the product was virtually one compound. Characterization as VII is based on its n.m.r. spectrum and conversion into II and VI in high yield. Virtually the same product as described above was obtained when the β-anomer (VI) was treated with aluminium chloride.

The syrupy chloride (VII) (0.25 g) was dissolved in 5 ml of acetic acid containing 0.5 g of anhydrous sodium acetate and 1 ml of acetic anhydride. After 75 min at room temperature, 0.225 g of the product was isolated in the usual manner. Examination by n.m.r. showed the presence of a 2:1 mixture of VI and II, respectively, along with some impurity, giving rise to minor signals, particularly at τ 2.75.

Methyl Di-O-acetyl-3-deoxy-β-D-erythro-hex-2-enopyranoside (VIII)

Compound VII (3.07 g) was dissolved in a mixture of 5 ml of dry *sym*-collidine and 25 ml of anhydrous methanol. The observed rotation changed from an initial value of +7.74° to a constant value of +6.30° in 1 h. The solvents were largely removed by evaporation *in vacuo*, the residue was dissolved in ether, and the ethereal solution was washed with water, decolorized with charcoal, and evaporated to dryness in a high vacuum. The residue, 2.58 g (96% yield), had a n.m.r. spectrum consistent with that expected for an equimolar mixture of VIII and its α-anomer IX. A 0.91 g sample of the product was chromatographed on a 50 g column of silicic acid with chloroform as the eluting solvent. Although a clear separation was not obtained, a 0.07 g fraction had a n.m.r. spectrum (see Table I) consistent with that of a pure compound in the β-D-configuration. The specific rotation was +104° (*c*, 4 in chloroform) and showed a strongly plain, positive rotatory dispersion curve, as found by Ferrier and his co-workers (5) for the related β-anomer (VI).

1,2;5,6-Di-O-isopropylidene-3-O-mesitoyl-α-D-glucose (X)

Mesitoic acid (1.01 g, 0.1 mmole) (I) was dissolved in 5 ml trifluoroacetic anhydride and the mixture cooled in an ice bath. 1,2;5,6-Di-*O*-isopropylidene-α-D-glucose (1.82 g, 7.0 mmoles) was added and, after 30 min, the yellowish reaction mixture was diluted with 100 ml dry benzene. The solution was washed with ice-cold 10% aqueous sodium hydroxide and then with ice water. The benzene solution was dried over anhydrous sodium sulfate, filtered, and evaporated *in vacuo* to a pale-yellow, viscous syrup, 2.66 g, $[\alpha]_D$ −28.8° (*c*, 1.8 in chloroform). The n.m.r. spectrum was in complete agreement with that of a compound having the assigned structure.

3-O-Mesitoyl-β-D-glucose (XI)

1,2;5,6-Di-*O*-isopropylidene-3-*O*-mesitoyl-α-D-glucose (X) was dissolved in 20 ml of refluxing methanol, and 20 ml of 2 *N* sulfuric acid was added dropwise during 10 min. The mixture was refluxed for a further 60 min, cooled, and diluted with 50% aqueous methanol. The solution was shaken with Dowex 3 (OH^-) until neutral, filtered, and concentrated to a syrup, 1.615 g (98% yield). The compound was crystallized from water, and after two recrystallizations from this solvent melted at 153–154°, $[\alpha]_D$ +17.1° → +49.8° after 20 h (*c*, 1.55 in 95% ethanol 0.2% in pyridine).

Anal. Calcd. for $C_{16}H_{22}O_7$: C, 58.89; H, 6.79. Found: C, 58.95; H, 6.60.

1,2,4,6-Tetra-O-acetyl-3-O-mesitoyl-β-D-glucose (XII)

3-*O*-Mesitoyl-β-D-glucose (XI) (6.54 g) was heated for 2.5 h on the steam bath with 7 g of anhydrous sodium acetate and 70 ml of acetic anhydride. The mixture was poured onto 500 g of crushed ice, and the resulting solid product was washed with cold water. Recrystallization from 95% ethanol gave 5.36 g of fine needles, m.p. 170–171°, $[\alpha]_D$ +9.4° (*c*, 2.9 in chloroform). The n.m.r. spectrum was in complete agreement with that of a compound having the assigned structure.

Anal. Calcd. for $C_{24}H_{30}O_{11}$: C, 58.29; H, 6.12. Found: C, 58.21, H, 5.86.

2,4,6-Tri-O-acetyl-3-O-mesitoyl-α-D-glucosyl Bromide (XIII)

Compound XII was treated with 32% hydrogen bromide in glacial acetic acid in the usual manner to give a colorless syrup, in a nearly quantitative yield, which failed to crystallize. The high rotation ($[\alpha]_D$ +149° (*c*, 1.5 in acetonitrile)) and the n.m.r. spectrum were in complete agreement with those of a compound having the assigned structure.

4,6-Di-O-acetyl-2-acetoxy-3-O-mesitoyl-D-glucal (XIV)

Compound XIII was reacted with diethylamine in acetonitrile according to the directions described by Lemieux and his co-workers (1) for the preparation of I. The crude product was virtually pure XIV and was obtained in a nearly quantitative yield. The compound crystallized readily on trituration with methanol. Recrystallization from methanol gave pure material, m.p. 114–116°, $[\alpha]_D$ −39.6° (*c*, 1.2 in acetonitrile). The n.m.r. spectrum was in complete agreement with that of a compound having the assigned structure.

Anal. Calcd. for $C_{22}H_{26}O_9$: C, 60.82; H, 6.03. Found: C, 61.2; H, 6.04.

Can. J. Chem. Downloaded from www.nrcresearchpress.com by 210.87.254.40 on 09/05/12
For personal use only.

ACKNOWLEDGMENTS

The authors acknowledge partial support of this research through a National Research Council grant (T-172) to R. U. L. The n.m.r. spectra and microanalyses were determined by the Department of Chemistry, University of Alberta, Edmonton.

REFERENCES

1. R. U. LEMIEUX, D. R. LINEBACK, M. L. WOLFROM, F. B. MOODY, E. G. WALLACE, and F. KOMITSKY, JR. J. Org. Chem. **30**, 1092 (1965).
2. G. STORK and W. N. WHITE. J. Am. Chem. Soc. **78**, 4609 (1956).
3. K. FREUDENBERG and O. IVERS. Ber. **55**, 929 (1922).
4. R. U. LEMIEUX and D. R. LINEBACK. Can. J. Chem. **43**, 94 (1965).
5. R. J. FERRIER, W. G. OVEREND, and G. H. SANKEY. J. Chem. Soc. 2830 (1965).
6. W. A. BONNER. J. Am. Chem. Soc. **83**, 962 (1961).
7. R. U. LEMIEUX, C. BRICE, and G. HUBER. Can. J. Chem. **33**, 134 (1955).
8. R. U. LEMIEUX. *In* Molecular rearrangements. Paul de Mayo (*Editor*). Interscience Publishers, Inc., New York. 1964. Part 2.
9. R. U. LEMIEUX and J. HAYAMI. Can. J. Chem. **43**, 2162 (1965).
10. R. C. PARISH and L. M. STOCK. Tetrahedron Letters, **20**, 1285 (1964).
11. B. HELFERICH, H. DRESSLER, and R. BRIEGEL. J. Prakt. Chem. **153**, 285 (1939).

Can. J. Chem. Downloaded from www.nrcresearchpress.com by 210.87.254.40 on 09/05/12
For personal use only.

Can. J. Chem. Downloaded from www.nrcresearchpress.com by 210.87.254.6 on 09/05/12
For personal use only.

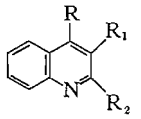
4-HYDROXYQUINALDINES IN THE MANNICH REACTION[1]

I. NABIH AND M. NASR

Many quinoline derivatives possess chemotherapeutic activity, but their usefulness may be interfered with by water insolubility. It was anticipated that introduction of a basic side chain would overcome the difficulty through hydrochloride formation. Quinaldine itself had been treated with formaldehyde and a primary or secondary amine hydrochloride to form 2-B-aminoethylquinoline derivatives (1). A German patent reported that treatment of 2-methyl-8-nitroquinoline with a primary amine hydrochloride gave a product having the basic side chain at the 2-position (2).

The same patent claims that, in the case of 4-hydroxyquinaldine, the reaction involves the methyl group at the 2-position (3). Price and Jackson carried out the reaction with 7-methoxy-4-hydroxyquinaldine, formaldehyde, and di-*n*-butylamine; they obtained the 3-dibutylaminomethyl derivative (4). Ghosh and Chandhuri treated 4-hydroxyquinaldine with diethylamine and formaldehyde and obtained 3-diethylaminomethyl-4-hydroxyquinaldine (5) (I), but they did not demonstrate its structure.

In the present work, 4-hydroxyquinaldine was treated with paraformaldehyde and diethylamine in 95% alcoholic solution at room temperature for 24 h. The product was assigned structure I, with the basic side chain attached to the 3-position. The methyl group at the 2-position remained intact, as shown by its condensation with *p*-dimethylaminobenzaldehyde in the presence of zinc chloride to give the carbostyryl derivative II. Also, hydrogenolysis of I with copper chromite catalyst gave 2,3-dimethyl-4-quinolinol (6) (III). The 4-hydroxyl group of I, in contrast to that of 4-hydroxyquinaldine, could be acetylated. When the product IV was treated with alkali, it hydrolyzed to regenerate I. Also, I, when condensed with chloroacetic acid, gave V.

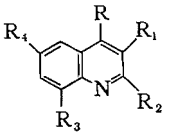


I: R = OH, R_1 = $CH_2N(C_2H_5)_2$, R_2 = CH_3
II: R = OH, R_1 = $CH_2N(C_2H_5)_2$, R_2 = $CH{=}CHC_6H_5N(CH_3)_2$
III: R = OH, R_1 = R_2 = CH_3
IV: R = $OCOCH_3$, R_1 = $CH_2N(C_2H_5)_2$, R_2 = CH_3
V: R = OCH_2COOH, R_1 = $CH_2N(C_2H_5)_2 \cdot HCl$, R_2 = CH_3

When diethylamine hydrochloride was used in place of diethylamine, the product was the hydrochloride of I. When diethylamine was used in the presence of excess concentrated hydrochloric acid, the reaction failed to occur.

The Mannich reaction was carried out with 6- and 8-methyl-4-hydroxyquinaldine to give VI and VII, respectively. Upon hydrogenolysis, the corresponding 3-methyl derivatives VIII and IX were obtained. Both were identical with authentic samples prepared by condensation of α-methyl acetoacetic ester with *p*- and *o*-toluidine, respectively, followed by cyclization of the resulting crotonate derivatives.

[1]*Taken from the M.Sc. dissertation of M. Nasr, National Research Centre, Dokki, Cairo, 1965.*



VI: R = OH, $R_1 = CH_2N(C_2H_5)_2$, $R_2 = R_4 = CH_3$, $R_3 = H$
VII: R = OH, $R_1 = CH_2N(C_2H_5)_2$, $R_2 = R_3 = CH_3$, $R_4 = H$
VIII: R = OH, $R_1 = R_2 = R_4 = CH_3$, $R_3 = H$
IX: R = OH, $R_1 = R_2 = R_3 = CH_3$, $R_4 = H$

EXPERIMENTAL

All melting points are uncorrected and were determined on a Kofler hot stage.

3-Diethylaminomethyl-4-hydroxyquinaldine (I)

A mixture of 1.6 g of paraformaldehyde (0.017 mole), 25 ml of 95% ethyl alcohol, and 20 ml (14.22 g, 0.194 mole) of diethylamine was refluxed until the paraformaldehyde had dissolved. To this solution was added 7.95 g (0.05 mole) of 4-hydroxyquinaldine (7) dissolved in the least amount of 95% ethanol; then the mixture was kept for 48 h at room temperature. White needles were formed. Recrystallization from alcohol gave 10.98 g (90% yield) of I, which decomposed at 348–350° (lit. (5) no melting until 300°).

Anal. Calcd. for $C_{15}H_{20}ON_2$: C, 73.73; H, 8.25; N, 11.47. Found: C, 73.60; H, 8.30; N, 11.36.

3-Diethylaminomethyl-4-hydroxyquinaldine Hydrochloride (Ia)

The foregoing procedure was applied, except that diethylamine was replaced by its hydrochloride. The reaction mixture was refluxed for 5 h. The solvent was then evaporated and the residue was recrystallized from aqueous alcohol to give a 95% yield of I*a*, m.p. 313–315°.

Anal. Calcd. for $C_{15}H_{21}ON_2Cl$: N, 9.98; Cl, 12.65. Found: N, 9.65; Cl, 12.14.

When I*a* was heated with 10% potassium hydroxide solution, I was recovered.

Condensation of I with p-Dimethylaminobenzaldehyde

A mixture of 2.44 g (0.01 mole) of I, 1.49 g (0.01 mole) of *p*-dimethylaminobenzaldehyde, and 0.5 g of zinc chloride was heated in an oil bath at 180 °C for 3 h. The reaction mixture was dissolved in alcohol. Upon addition of sodium hydroxide solution, a yellow substance was precipitated. Recrystallization from alcohol gave 2.6 g (70% yield) of 2-(*p*-dimethylaminostyryl)-3-diethylaminomethyl-4-quinolinol (II), m.p. 185–187°, which was soluble in alcohol but insoluble in water, ether, and petroleum ether.

Anal. Calcd. for $C_{24}H_{29}ON_3$: C, 76.59; H, 7.73; N, 11.20. Found: C, 76.44; H, 7.54; N, 11.12.

Hydrogenolysis of I

A mixture of 7.32 g (0.03 mole) of I, 150 ml of absolute ethyl alcohol, and 5 g of copper chromite was placed in a bomb, hydrogen was added, and the mixture was shaken and heated gradually to 175° at an equilibrium pressure of 3 000 lb, for 4 h, until the calculated amount of hydrogen was consumed (0.045 mole). The bomb was allowed to cool to room temperature. The reaction mixture was filtered from the catalyst, concentrated, and cooled in ice. Precipitation by addition of ether and recrystallization from water gave 1.7 g (34% yield) of III, m.p. 319–320°. Its melting point was identical with that of an authentic sample of III and showed no depression upon admixture (lit. (6) m.p. 319–320°).

Acetylation of I

A mixture of 1.55 g (0.012 mole) of I and 2 ml of acetic anhydride was heated in an oil bath at 180 °C for 3 h. The reaction mixture changed to a dark-red syrup. When this was poured into boiling water, a brown solid separated. This was filtered off, dried, and then recrystallized from absolute ethyl alcohol to give 1.5 g (85% yield) of 3-diethylaminomethyl-4-acetoxyquinaldine (IV), m.p. 314–316°, as yellow crystals insoluble in water, ether, petroleum ether, and chloroform, and soluble (with difficulty) in alcohol.

Anal. Calcd. for $C_{17}H_{22}O_2N_2$: C, 71.30; H, 7.74; N, 9.79. Found: C, 71.15; H, 7.59; N, 9.61.

Acetylation of III

The above procedure was applied to III, which was recovered unchanged (no depression in mixed melting point).

Attempt to Acetylate 4-Hydroxyquinaldine

The foregoing procedure was applied to 4-hydroxyquinaldine but the compound was recovered unchanged (no depression in melting point when mixed with starting material).

Hydrolysis of IV

A mixture of 0.15 (0.0006 mole) of IV, 0.2 g (0.0036 mole) of potassium hydroxide, and 5 ml of ethyl alcohol was refluxed on the water bath for 3 h, cooled, and poured into cold water. The precipitated solid was 3-diethylaminomethyl-4-hydroxyquinaldine (I), which decomposed at 348–350° (undepressed upon admixture with an authentic sample).

Reaction of I with Chloroacetic Acid

A mixture of 2.44 g (0.01 mole) of I and 0.945 g (0.01 mole) of chloroacetic acid was heated in an oil bath until solution was complete. The mixture was cooled and made alkaline with aqueous sodium hydroxide.

Can. J. Chem. Downloaded from www.nrcresearchpress.com by 210.87.254.6 on 09/05/12
For personal use only.

The yellow solid that separated was filtered off, dissolved in alcohol, and precipitated by a stream of hydrogen chloride to give 2.1 g (70% yield) of 3-diethylaminomethyl-4-carboxymethoxyquinaldine hydrochloride (V). It was recrystallized from absolute alcohol, and had m.p. 360–363°.

Anal. Calcd. for $C_{17}H_{23}O_3N_2Cl$: C, 60.26; H, 6.84; N, 8.27. Found: C, 60.12; H, 6.71; N, 8.41.

Attempted Reaction of Chloroacetic Acid with 4-Hydroxyquinaldine

The foregoing procedure was applied to 4-hydroxyquinaldine, but only unchanged starting material was obtained.

6-Methyl-3-diethylaminomethyl-4-hydroxyquinaldine (VI)

A mixture of 1.6 g (0.017 mole) of paraformaldehyde, 25 ml of 95% ethyl alcohol, and 20 ml (14.22 g, 0.194 mole) of diethylamine was refluxed on the water bath until the paraformaldehyde had dissolved, and then allowed to cool to room temperature. To this solution was added 8.65 g (0.05 mole) of 2,6-dimethyl-4-quinolinol dissolved in the least amount of 95% ethanol; then the mixture was refluxed for 3 h and allowed to cool to room temperature. White needles insoluble in water and alkali but soluble in 5% hydrochloric acid were formed. Recrystallization from ethyl alcohol gave 11.52 g (90% yield) of VI, which decomposed at 320°.

Anal. Calcd. for $C_{16}H_{22}ON_2$: C, 74.40; H, 8.58; N, 10.85. Found: C, 74.39; H, 8.47; N, 10.78.

Hydrogenolysis of VI

The hydrogenolysis of VI was effected in a manner similar to that used for the hydrogenolysis of I. The resulting reaction product was recrystallized from aqueous alcohol to give needles, m.p. 349–352°, easily soluble in alcohol and soluble (with difficulty) in water. The product showed no depression in the melting point upon admixture with an authentic sample of 3,6-dimethyl-4-hydroxyquinaldine (VIII) prepared by an alternative synthesis.

Anal. Calcd. for $C_{12}H_{13}ON$: C, 77.01; H, 6.95; N, 7.49. Found: C, 76.87; H, 7.37; N, 7.25.

8-Methyl-3-diethylaminomethyl-4-hydroxyquinaldine (VII)

The foregoing procedure for VI was applied to 2,8-dimethyl-4-quinolinol. The reaction product was recrystallized from alcohol to give VII (90% yield), m.p. 338–340°, soluble in 5% hydrochloric acid and insoluble in water and alkali.

Anal. Calcd. for $C_{16}H_{22}ON_2$: C, 74.40; H, 8.58; N, 10.85. Found: C, 74.39; H, 8.59; N, 10.64.

Hydrogenolysis of VII

The same procedure as described above for I was applied. The resulting reaction product was recrystallized from aqueous alcohol. The product melted at 325–327°. It showed no depression in the mixture melting point with 3,8-dimethyl-4-hydroxyquinaldine (IX).

Anal. Calcd. for $C_{12}H_{13}ON$: C, 77.01; H, 6.95; N, 7.49. Found: C, 76.94; H, 7.10; N, 7.52.

3,6-Dimethyl-4-hydroxyquinaline (VIII)

A mixture of 10.7 g (0.1 mole) of *p*-toluidine and 14.41 g (0.1 mole) of α-methylacetoacetate ester, to which was added two drops of concentrated hydrochloric acid, was kept at room temperature for 24 h. After separation of water, the residual *p*-toluidino-α-methylcrotonate was added dropwise to hot paraffin oil (150 ml) at 240°. The temperature was raised to 265°, and the mixture was then cooled. The white crystalline product was filtered off and washed with petroleum ether. It had m.p. 347°. Recrystallization from alcohol gave 12 g (64% yield) of VIII, m.p. 349–352°.

Anal. Calcd. for $C_{12}H_{13}ON$: C, 77.01; H, 6.95; N, 7.49. Found: C, 76.95; H, 6.95; N, 7.54.

3,8-Dimethyl-4-hydroxyquinaldine (IX)

A mixture of 10.7 g (0.1 mole) of *o*-toluidine and 14.41 g (0.1 mole) of α-methylacetoacetic ester was treated similarly as above, and the isolated product was recrystallized from alcohol to give 8.4 g (45% yield) of IX, m.p. 325–327°.

Anal. Calcd. for $C_{12}H_{13}ON$: C, 77.01; H, 6.95; N, 7.49. Found: C, 76.82; H, 6.54; N, 7.61.

ACKNOWLEDGMENT

The authors express their gratitude to Professor J. H. Burckhalter, University of Michigan, Ann Arbor, for his suggestions during his visit to this laboratory.

1. W. O. KERMACK and W. J. MUIR. J. Chem. Soc. 3089 (1931).
2. I. G. FARBENINDUSTRIE. Ger. Patent No. 497,907 (April 1930); Friedlander, **16**, 2669-6 (1931).
3. I. G. FARBENINDUSTRIE. Ger. Patent No. 497,907 (April 1930); Friedlander, **16**, 2669-2 (1931).
4. C. C. PRICE and W. G. JACKSON. J. Am. Chem. Soc. **68**, 1282 (1946).
5. T. N. GHOSH and A. R. CHANDHURI. J. Indian Chem. Soc. **29**, 368 (1952).
6. S. G. P. PLANT and R. J. ROSSER. J. Chem. Soc. 1861 (1929).
7. L. LIMPACH. Chem. Ber. **64**, 969 (1931).

RECEIVED NOVEMBER 1, 1965.
NATIONAL RESEARCH CENTRE,
DOKKI, CAIRO, UNITED ARAB REPUBLIC.

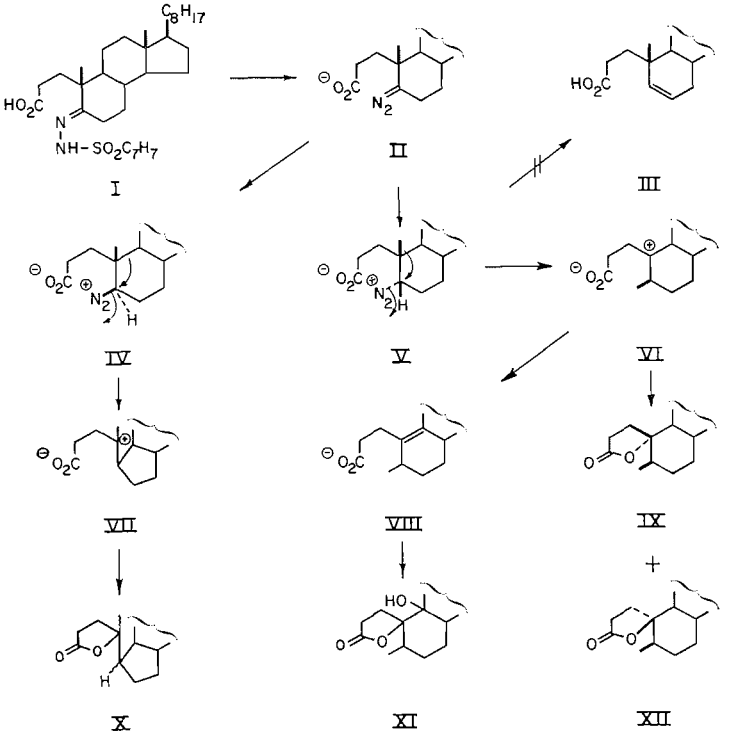
Can. J. Chem. Downloaded from www.nrcresearchpress.com by 210.87.254.6 on 09/05/12
For personal use only.

DECOMPOSITION PRODUCTS OF 5-OXO-3,5-SECO-A-NORCHOLESTAN-3-OIC ACID *p*-TOLUENESULFONYLHYDRAZONE

J. T. EDWARD,[1] DAPHNE L'ANGLAIS,[2] AND SEYMOUR MEYERSON[3]

The decomposition of 5-oxo-3,5-seco-A-norcholestan-3-oic acid *p*-toluenesulfonylhydrazone (I) was carried out in diethyl Carbitol containing sodium methoxide (the "aprotic" Bamford–Stevens reaction (1, 2)) in the hope of obtaining the unsaturated acid III. An intractable oil was obtained which appeared, from its nuclear magnetic resonance spectrum (no olefinic protons), to contain little or none of this acid. The decomposition of the *p*-toluenesulfonylhydrazone in alkaline ethylene glycol (the "protic" Bamford–Stevens reaction) also yielded a mixture that was largely intractable, but from which small amounts of several crystalline compounds were isolated. Three of these proved to be identical with compounds previously isolated from the solvolysis of 5α- or 5β-*p*-toluenesulfonyloxy-3,5-seco-A-norcholestan-3-nitrile and formulated as the lactones IX, X*a* (m.p. 114–115°), and XII (3). A fourth compound X*c*, m.p. 105–106°, is apparently a stereoisomer of X*a*.

In the earlier work, so little of the lactone XII had been obtained that it could not be analyzed. Thus, its formula was based only on the close similarity of its infrared spectrum to that of the lactone IX, the stereochemical assignments being very tentative. In the



[1]*Present address: Department of Chemistry, McGill University, Montreal, Quebec.*
[2]*Holder of N.R.C. Studentships, 1961–1963.*
[3]*Present address: Research and Development Department, American Oil Company, Whiting, Indiana.*

Can. J. Chem. Downloaded from www.nrcresearchpress.com by 210.87.254.105 on 09/05/12
For personal use only.

present study, larger amounts of the compound were obtained, and the analytical data and mass spectrum give additional support to the formulation XII, though without stereochemical implications. The mass spectrum, shown in Table I, is generally similar to that of the isomer IX (3); the most pronounced difference occurs at mass 370, corresponding to loss of H_2O, where the relative intensity of XII is far lower than that of IX. The higher intensity of the parent ion relative to that of the fragment ions suggests that XII is the more stable of the two isomers.

TABLE I

Partial mass spectra of lactones

	Relative intensity*				
Mass	XII	IX†	X*c*	X*a*†	Loss‡
388	100.0	100.0	50.6	26.0	(Parent ion)
373	6.7	13.2	6.6	7.3	CH_3
370	0.2	7.4	0.5	6.9	H_2O
331	4.4	9.2	3.9	0.4	C_3H_5O
289	0.4	0.8	29.0	34.0	$C_5H_7O_2$
287	0.3	1.3	38.0	64.6	$C_5H_9O_2$
275	11.7	25.6	12.5	15.0	C_8H_{17}
248	24.4	18.6	29.8	6.2	$C_8H_{17}CHCH_2$
234	39.8	42.0	24.4	9.8	$C_8H_{17}CHCH_2CH_2$
99	2.3	3.1	100.0	100.0	$C_{21}H_{37}$

*Scale of relative intensities defined by assigning a value of 100.0 to the most intense peak of mass greater than 90 in each spectrum.
†From ref. 3.
‡Probable composition of neutral particle(s) lost from parent ion.

The mass spectrum of X*c*, also shown in Table I, is similar enough (especially at masses 99, 287, and 289) to that of X*a*, known to be a pendant lactone, to indicate that X*c* is also a pendant lactone. The higher intensity of the parent ion relative to that of the fragment ions suggests that X*c* is the more stable isomer. Its infrared spectrum is likewise closely similar to that of X*a*, and also to that of X*b*, a stereoisomer of X*a* with m.p. 89–90° (3). Hence, X*c* is most likely another stereoisomer of these compounds. Too little of it was obtained (5 mg of crude product) to permit more detailed experimentation.

Some unsaturated acidic material was also formed, containing perhaps VIII, since oxidation of the oily fraction with osmium tetroxide gave a hydroxylactone previously formulated as XI (3). In the earlier work (3), the major unsaturated acid was believed to be III, since a large amount of a hydroxy-δ-lactone was formed when the acid fraction was oxidized with osmium tetroxide. In the present experiments, this lactone was not detected (infrared spectrum) after oxidation of the crude acidic product.

The mechanism of the "protic" Bamford–Stevens reaction is believed to involve the formation of a diazo compound (II, in the present instance) which then adds a proton from the solvent to form a diazonium ion. Possibly, addition of a proton from an equatorial direction to give the diazonium ion V proceeds more easily than addition from an axial direction to give IV. This would explain why the spiro lactones IX and XII, which probably originate from V via the stereospecifically generated carbonium ion VI (cf. ref. 3), are formed in greater amount than the pendant lactones (X), which probably originate from IV via the carbonium ion VII. The apparent failure to form any unsaturated acid III from the diazonium ion V remains puzzling, particularly since Elks *et al.* (4) obtained about a 25% yield of unrearranged olefin from the decomposition of hecogenin acetate *p*-toluenesulfonylhydrazone. This compound, like I, has a hydrazone group flanked by methylene and quaternary carbon atoms, and might be expected to display about the same propensity to rearrangement in competition with elimination.

Can. J. Chem. Downloaded from www.nrcresearchpress.com by 210.87.254.105 on 09/05/12
For personal use only.

Can. J. Chem. Downloaded from www.nrcresearchpress.com by 210.87.254.105 on 09/05/12
For personal use only.

EXPERIMENTAL

5-Oxo-3,5-seco-A-norcholestan-3-oic Acid p-Toluenesulfonylhydrazone (I)

A mixture of 5-oxo-3,5-seco-A-norcholestan-3-oic acid (9.9 g) (5) and *p*-toluenesulfonylhydrazine (8.9 g) in hexane–benzene (1:1 v/v) (500 ml) containing one drop of concentrated hydrochloric acid was refluxed for 1 h. The solution was then filtered from a small amount of unreacted *p*-toluenesulfonylhydrazine, and concentrated to 200 ml under reduced pressure. A white solid, m.p. 158–166°, was removed from the cooled solution and recrystallized twice from hexane–benzene to yield white crystals (12.1 g), m.p. 172–173°, ν_{max}^{KBr} 1 372 and 1 160 cm^{-1}.

Anal. Calcd. for $C_{33}H_{52}O_4N_2S$: C, 69.20; H, 9.15; N, 4.89. Found: C, 68.72; H, 8.88; N, 4.89.

Decomposition of 5-Oxo-3,5-seco-A-norcholestan-3-oic Acid p-Toluenesulfonylhydrazone

The *p*-toluenesulfonylhydrazone (10 g) was suspended in ethylene glycol (500 ml) to which sufficient sodium had been added to give a 1 *N* solution of alkoxide, and then heated slowly to 170°. After 30 min the solution was cooled, diluted with water (2 l), acidified with concentrated hydrochloric acid to pH 4, and extracted five times with ether. The ether solution was washed with water, dried, and evaporated to yield an oil (6.8 g). The oil was chromatographed on alumina (grade III) and yielded the following oily fractions: A (1.75 g), a clear mobile oil, $\nu_{max}^{CCl_4}$ 1 740 cm^{-1}, eluted with hexane–benzene (9:1); B (1.09 g), $\nu_{max}^{CCl_4}$ 1 770 cm^{-1}, eluted with hexane–benzene (2:1); and C (3.9 g), a series of fractions eluted with benzene–ether (1:1), ether, and ether – acetic acid – water (96:3:1), showing essentially the same infrared spectrum, with a prominent peak at 1 720 cm^{-1} and a minor peak at 1 770 cm^{-1}.

Further chromatography of fraction A on neutral alumina (grade II or grade I) effected no further purification. It did not react with 2,4-dinitrophenylhydrazine or ethanolic ammonia (cf. ref. 6). Its nature remains obscure.

Fraction B was chromatographed on alumina (grade II). Elution with hexane–benzene (14:1) removed the following fractions: 1–3 (60 mg), an oil, $\nu_{max}^{CCl_4}$ 1 740 cm^{-1}; 4–13 (90 mg), a solid, m.p. 90–95°, $\nu_{max}^{CCl_4}$ 1 770 cm^{-1}; 14–15 (200 mg), a solid, m.p. 120–126°, $\nu_{max}^{CCl_4}$ 1 770 cm^{-1}; and 16–18 (200 mg), a solid, m.p. 138–140°, $\nu_{max}^{CCl_4}$ 1 770 cm^{-1}. Elution with hexane–benzene (26:4), followed by mixtures richer in benzene and finally by pure benzene, removed fractions 19–27 (600 mg), a solid, m.p. 143–145°, $\nu_{max}^{CCl_4}$ 1 770 cm^{-1}.

The solid from fractions 4–13, after three recrystallizations from ethanol, melted at 112–113° (65 mg), and was identified by mixed melting point and infrared spectrum as the lactone X*a*, m.p. 114–115° (3).

The solid from fractions 16–27 was recrystallized four times from ethanol to give needles (530 mg), m.p. 152–153°, identical (mixed melting point and infrared spectrum) with the lactone IX (3).

The residue from the mother liquors of these crystallizations was combined with fractions 14 and 15, and fractionally crystallized from ethanol to yield further amounts of IX (81 mg, m.p. 151–152°) and X*a* (10 mg, m.p. 111–112°), and finally a small amount of the material formulated as X*c* (5 mg, m.p. 103–104°, $\nu_{max}^{CCl_4}$ 1 770 cm^{-1}). The melting point was raised to 105–106° by four recrystallizations from ethanol; it was depressed on admixture with X*a*.

Fraction C was shown by its infrared spectrum to contain aromatic sulfonyl and carboxylic ($\nu_{max}^{CCl_4}$ 1 720 cm^{-1}) compounds. It formed a gummy benzylisothiouronium salt, from which a small amount of solid was obtained by recrystallization. However, on treatment with hydrochloric acid, the latter gave only a gummy product. A portion of fraction C (1.6 g) was oxidized with osmium tetroxide (1.0 g) in anhydrous ether (40 ml) and dry pyridine (4 ml). After 6 days at room temperature, the mixture was worked up in the usual way with sodium sulfite (3) to yield an orange oil (1.3 g), which was chromatographed on neutral alumina (grade II). The following fractions were collected: D (25 mg), an oil showing no hydroxyl or carbonyl peaks in the infrared spectrum, eluted with hexane–benzene (6:4); E (103 mg), white needles, m.p. 95–98°, eluted with hexane–benzene (1:1); F (42 mg), a solid, m.p. 21–26°, eluted with hexane–benzene (28:32); G (86 mg), a solid, m.p. 105–116°, eluted with benzene–ether (2:1); and H (70 mg), an oil, $\nu_{max}^{CCl_4}$ 1 720 cm^{-1}, eluted with ether and ether – acetic acid, this could not be crystallized.

Fraction E, after two recrystallizations from ethanol, melted sharply at 97–98° (80 mg), and was identical (mixed melting point and infrared spectrum) with the compound formulated as XII (3).

Anal. Calcd. for $C_{26}H_{44}O_2$: C, 80.35; H, 11.41. Found: C, 80.54; H, 11.36.

Fraction G, after three recrystallizations from hexane–ether, melted at 201° and was identical (mixed melting point and infrared spectrum) with the hydroxylactone tentatively formulated as XI (3).

Anal. Calcd. for $C_{26}H_{44}O_3$: C, 77.17; H, 10.96. Found: C, 77.02; H, 11.07.

Mass Spectrometry

Mass spectra were measured with 70 V electrons on a modified (7) Consolidated model 21-103*c* instrument, with the sample-introduction system at 250°.

ACKNOWLEDGMENTS

We are grateful to N. E. Lawson for preparing a pure sample of 5-oxo-3,5-seco-A-norcholestan-3-oic acid *p*-toluenesulfonylhydrazone. The financial support of the National Research Council of Canada for the work performed at McGill University is gratefully acknowledged.

1. J. W. POWELL and M. C. WHITING. Tetrahedron, **7**, 305 (1959).
2. L. FRIEDMAN and H. SCHECHTER. J. Am. Chem. Soc. **81**, 5513 (1959).
3. W. H. LUNN, J. T. EDWARD, and S. MEYERSON. Can. J. Chem. **44**, 279 (1966).
4. J. ELKS, G. H. PHILLIPS, D. A. H. TAYLOR, and L. J. WYMAN. J. Chem. Soc. 1739 (1954).
5. J. T. EDWARD, D. HOLDER, W. H. LUNN, and I. PUSKAS. Can. J. Chem. **39**, 599 (1961).
6. J. T. EDWARD and P. F. MORAND. Can. J. Chem. **38**, 1325 (1960).
7. H. M. GRUBB, C. H. EHRHARDT, R. W. VANDER HAAR, and W. H. MOELLER. 7th Annual Conference of the American Society for Testing and Materials, Committee E-14, on Mass Spectrometry, Los Angeles, California, May 1959.

RECEIVED FEBRUARY 24, 1966.
DEPARTMENT OF CHEMISTRY,
MCGILL UNIVERSITY,
MONTREAL, QUEBEC,
AND
RESEARCH AND DEVELOPMENT DEPARTMENT,
AMERICAN OIL COMPANY,
WHITING, INDIANA.

ORGANIC SULFUR MECHANISMS

5. PHOTOLYSIS OF UNSATURATED SULTAMS AND THE QUESTION OF ABNORMAL ADDITION TO SULFENES

T. DURST AND J. F. KING

As would be predicted by analogy with ketenes, those products which may be derived in a simple manner from a nucleophilic reaction on sulfenes are those stemming from attack of the nucleophile on the sulfur atom of the sulfene, rather than the carbon atom (cf. refs. 1–3). However, whereas simple nucleophilic attack at the olefinic carbon of ketene would lead to a virtually unprecedented carbanion, the corresponding reaction at the carbon atom of a sulfene would give a comparatively low-energy species, a sulfinate anion. This consideration suggested that the possibility of the reaction of nucleophilic reagents at the carbon atom of a sulfene (referred to as "abnormal" attack in this note) warranted an investigation, especially since our work on the formation of the oxythiobenzoyl chlorides (4–6) led us to wonder whether a proposed precursor of these compounds might not be derived from such an abnormal attack.

One possible way of detecting the abnormal addition would be to carry out the reaction under conditions in which normal attack (i.e. at the sulfur atom) would lead only to a trivial change, such as return to the starting material, which could occur many times and still allow the sulfene to be formed anew in the reaction mixture. Under such circumstances the abnormal process might manifest itself even though it were orders of magnitude slower than the normal process.

De Mayo and his co-workers (1, 7) have shown that the irradiation of unsaturated, six membered ring sultones leads to the formation of products derivable from nucleophilic addition to a photochemically generated sulfene. In addition, Helferich *et al.* (8) have observed that pyrolysis of unsaturated, six membered ring sultams leads to the corresponding pyrroles with loss of sulfur dioxide. It occurred to us that, if the pyrrole formation were to take place via a sulfene (whether generated by heat or light), then the reaction would easily be explained on the basis of abnormal attack on the sulfene as shown in eq. [1]. Accordingly, we sought to determine whether pyrroles could be produced by photolysis of sultams and whether we could obtain evidence that sulfenes might be

Can. J. Chem. Downloaded from www.nrcresearchpress.com by 210.87.254.105 on 09/05/12
For personal use only.

1. J. W. POWELL and M. C. WHITING. Tetrahedron, **7**, 305 (1959).
2. L. FRIEDMAN and H. SCHECHTER. J. Am. Chem. Soc. **81**, 5513 (1959).
3. W. H. LUNN, J. T. EDWARD, and S. MEYERSON. Can. J. Chem. **44**, 279 (1966).
4. J. ELKS, G. H. PHILLIPS, D. A. H. TAYLOR, and L. J. WYMAN. J. Chem. Soc. 1739 (1954).
5. J. T. EDWARD, D. HOLDER, W. H. LUNN, and I. PUSKAS. Can. J. Chem. **39**, 599 (1961).
6. J. T. EDWARD and P. F. MORAND. Can. J. Chem. **38**, 1325 (1960).
7. H. M. GRUBB, C. H. EHRHARDT, R. W. VANDER HAAR, and W. H. MOELLER. 7th Annual Conference of the American Society for Testing and Materials, Committee E-14, on Mass Spectrometry, Los Angeles, California, May 1959.

RECEIVED FEBRUARY 24, 1966.
DEPARTMENT OF CHEMISTRY,
MCGILL UNIVERSITY,
MONTREAL, QUEBEC,
AND
RESEARCH AND DEVELOPMENT DEPARTMENT,
AMERICAN OIL COMPANY,
WHITING, INDIANA.

ORGANIC SULFUR MECHANISMS

5. PHOTOLYSIS OF UNSATURATED SULTAMS AND THE QUESTION OF ABNORMAL ADDITION TO SULFENES

T. DURST AND J. F. KING

As would be predicted by analogy with ketenes, those products which may be derived in a simple manner from a nucleophilic reaction on sulfenes are those stemming from attack of the nucleophile on the sulfur atom of the sulfene, rather than the carbon atom (cf. refs. 1–3). However, whereas simple nucleophilic attack at the olefinic carbon of ketene would lead to a virtually unprecedented carbanion, the corresponding reaction at the carbon atom of a sulfene would give a comparatively low-energy species, a sulfinate anion. This consideration suggested that the possibility of the reaction of nucleophilic reagents at the carbon atom of a sulfene (referred to as "abnormal" attack in this note) warranted an investigation, especially since our work on the formation of the oxythiobenzoyl chlorides (4–6) led us to wonder whether a proposed precursor of these compounds might not be derived from such an abnormal attack.

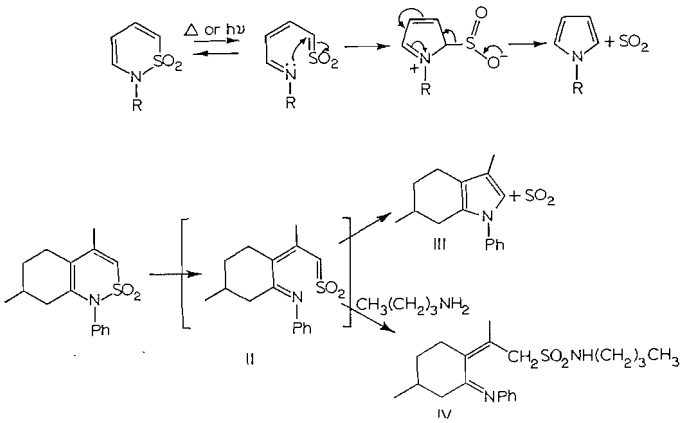
One possible way of detecting the abnormal addition would be to carry out the reaction under conditions in which normal attack (i.e. at the sulfur atom) would lead only to a trivial change, such as return to the starting material, which could occur many times and still allow the sulfene to be formed anew in the reaction mixture. Under such circumstances the abnormal process might manifest itself even though it were orders of magnitude slower than the normal process.

De Mayo and his co-workers (1, 7) have shown that the irradiation of unsaturated, six membered ring sultones leads to the formation of products derivable from nucleophilic addition to a photochemically generated sulfene. In addition, Helferich *et al.* (8) have observed that pyrolysis of unsaturated, six membered ring sultams leads to the corresponding pyrroles with loss of sulfur dioxide. It occurred to us that, if the pyrrole formation were to take place via a sulfene (whether generated by heat or light), then the reaction would easily be explained on the basis of abnormal attack on the sulfene as shown in eq. [1]. Accordingly, we sought to determine whether pyrroles could be produced by photolysis of sultams and whether we could obtain evidence that sulfenes might be

Can. J. Chem. Downloaded from www.nrcresearchpress.com by 210.87.254.42 on 09/05/12
For personal use only.

formed under these conditions. It was recognized that a sulfene formed by the photochemical opening of the unsaturated sultam ring would differ from that formed from a sultone in that the former would have a much stronger internal nucleophile (the anil nitrogen rather than the carbonyl oxygen). In the absence of external nucleophilic reagents capable of competing with it, the internal base could conceivably react with the sulfene end in two ways: (*i*) normal attack on the sulfur atom to regenerate starting material, and (*ii*) abnormal attack on the carbon atom to give the pyrrole as shown in eq. [1].

[1]



The irradiation of the sultam I (9), when carried out in dry ether, cyclohexane, or dry methanol, gave a good yield of the pyrrole III, which was identified by comparison of its infrared and nuclear magnetic resonance spectra and R_f value on thin-layer chromatography with those of an authentic sample prepared by pyrolysis of the sultam according to Helferich *et al.* (8). The reaction in methanol is noteworthy because irradiation of the unsaturated sultones in that solvent invariably led to the corresponding esters; also, in inert solvents the sultones showed little reaction on irradiation under comparable conditions (1, 7).

When the irradiation was carried out in the presence of *n*-butylamine (a strong external nucleophile), the pyrrole formation was diminished, though a 10–20% yield was obtained even when *n*-butylamine was the solvent. In addition to the pyrrole III, the reaction in *n*-butylamine gave a white crystalline compound in 60% yield. The analytical data for the crystalline material corresponded to the empirical formula $C_{20}H_{30}N_2O_2S$, thereby suggesting that the compound was the sulfonamide IV (no specification of stereochemistry is implied), derivable from 1,2 addition of *n*-butylamine to the sulfene II. This view was confirmed by the infrared and nuclear magnetic resonance spectra of the compound. The former showed bands at 1 325 and 1 138 cm^{-1} appropriate to the sulfonyl group, NH absorption at 3 360 cm^{-1}, and a band at 1 635 cm^{-1} ascribable to the conjugated carbon–nitrogen double-bond system. In addition to complex absorption between 3.3 and 0.9 p.p.m. caused by methylene and methyl protons, the nuclear magnetic resonance spectrum showed the following bands: (*i*) aromatic hydrogen absorption between 6.7 and 7.4 p.p.m., (*ii*) a broadened signal around 5.6 p.p.m. attributed to NH, (*iii*) an AB quartet, $\delta_A = 4.05$ and $\delta_B = 4.38$ p.p.m., $J_{AB} = 13$ c.p.s., assigned to a $C{=}\overset{C}{\underset{|}{C}}{-}CH_2{-}SO_2{-}$ grouping, and (*iv*) a singlet at 2.03 p.p.m. assigned to a methyl group attached to an olefinic carbon; the relative areas of the peaks agreed with these assignments.

Can. J. Chem. Downloaded from www.nrcresearchpress.com by 210.87.254.42 on 09/05/12
For personal use only.

The formation of the sulfonamide IV from the sultam[1] is exactly parallel to the production of sulfonamides and other sulfonic acid derivatives by irradiation of the sultones. There are, to be sure, differences between the reactions, but they are readily explained on the basis of the greater nucleophilicity of the anil nitrogen atom. If a sulfene is in fact formed in the sultone reaction, then one is almost certainly formed in the irradiation of the sultam, and it is reasonable to postulate that both the sulfonamide and the pyrrole arise from the proposed sulfene intermediate. In the latter case, this is most simply accounted for by abnormal attack of the nitrogen on the sulfene as shown in eq. [1].

EXPERIMENTAL

Melting points were determined on a Kofler block and are uncorrected. Infrared spectra were obtained with a Beckman IR-5 spectrophotometer equipped with sodium chloride optics. Nuclear magnetic resonance spectra were determined with a Varian A-60 instrument. The silica gel referred to is British Drug Houses "suitable for chromatography" grade.

Irradiation of N-Phenyl Pulegone Sultam (5,6,7,8-Tetrahydro-4,7-dimethyl-1-phenyl-1H-2,1-benzothiazine 2,2-Dioxide) (I)

N-Phenyl pulegone sultam (225 mg), prepared according to Helferich *et al.* (9), was dissolved in methanol (15 ml) and irradiated in a Vycor flask for 150 min in the apparatus described by de Mayo (10). During this time the solution became red. The methanol was evaporated, the residue dissolved in carbon tetrachloride, and the solution filtered through a short silica gel column. The yield of 1-phenyl-3,6-dimethyl-4,5,6,7-tetrahydroindole (III) was 105 mg (61%), identified by comparison of its infrared and nuclear magnetic resonance spectra and R_f value on thin-layer chromatography with those of a sample obtained by pyrolysis of *N*-phenyl pulegone sultam (8).

Similar irradiation of the sultam in either ether or cyclohexane solution gave a similar product.

Irradiation of N-Phenyl Pulegone Sultam in n-Butylamine Solution

N-Phenyl pulegone sultam (250 mg) was irradiated in *n*-butylamine (8 ml) for 75 min. The *n*-butylamine was evaporated under reduced pressure and the product analyzed by thin-layer chromatography. Development with 3:1 benzene–ether yielded three fractions: (*i*) 1-phenyl-3,6-dimethyl-4,5,6,7-tetrahydroindole (III) (20 mg, 11% based on utilized starting material), identified by comparison of its infrared spectrum and R_f value on thin-layer chromatography with those of a sample obtained by pyrolysis of *N*-phenyl pulegone sultam; (*ii*) starting material (22 mg); and (*iii*) sulfonamide IV (164 mg, 60% based on utilized starting material). Recrystallization of the latter compound from ether–pentane gave white crystals, m.p. 139–141°.

Anal. Calcd. for $C_{24}H_{30}N_2O_2S$: C, 66.27; H, 8.34; N, 7.73; S, 8.84. Found: C, 65.92; H, 8.53; N, 8.20; S, 9.24.

Infrared peaks ($CHCl_3$) were at 3 360, ~1 635 (broad), 1 593, 1 325, and 1 138 cm^{-1}. Nuclear magnetic resonance bands ($CDCl_3$) were at 6.7 to 7.4 p.p.m. (complex aromatic absorption, relative area 5); 5.6 p.p.m. (broad singlet, relative area 1); AB quartet, $\delta_A = 4.05$ and $\delta_B = 4.38$ p.p.m. ($J_{AB} = 13$ c.p.s., relative area 2); 2.03 p.p.m. (singlet, relative area 3); and 0.98 to 0.85 p.p.m. (complex multiplet including two similar methyl groups).

In a repeat of the experiment, *N*-phenyl pulegone sultam (285 mg) yielded pyrrole III (32 mg, 17%), starting material (45 mg), and sulfonamide IV (173 mg, 58%).

Reaction of N-Phenyl Pulegone Sultam with n-Butylamine in the Absence of Light

N-Phenyl pulegone sultam (I) (25 mg) was dissolved in dry *n*-butylamine (5 ml). The flask was wrapped in aluminium foil and heated for 2 h at 55°. The *n*-butylamine was evaporated under reduced pressure. The infrared spectrum of the product was identical with that of the starting material.

ACKNOWLEDGMENTS

Acknowledgment is made to the donors of The Petroleum Research Fund, administered by the American Chemical Society, for support of this research, and to the National Research Council of Canada for a studentship. We cordially thank Professor Paul de Mayo for his valuable discussions and for lending us equipment.

[1]*Though no attempt has been made to delineate the full scope of these reactions, the formation of the corresponding pyrrole has also been observed on irradiation of 3,5-dimethyl-2-phenylthiazine 1,1-dioxide (D. J. H. Smith and J. F. King, unpublished observations).*

Can. J. Chem. Downloaded from www.nrcresearchpress.com by 210.87.254.42 on 09/05/12
For personal use only.

1. J. F. KING, P. DE MAYO, E. MORKVED, A. B. M. A. SATTAR, and A. STOESSL. Can. J. Chem. **41**, 100 (1963).
2. W. E. TRUCE and J. R. NORELL. J. Am. Chem. Soc. **85**, 3231 (1963).
3. J. F. KING and T. DURST. J. Am. Chem. Soc. **87**, 5684 (1965).
4. J. F. KING and T. DURST. Tetrahedron Letters, 585 (1963).
5. J. F. KING and T. DURST. J. Am. Chem. Soc. **85**, 2676 (1963).
6. J. F. KING and T. DURST. Can. J. Chem. **44**, 819 (1966).
7. E. HENMO, P. DE MAYO, A. B. M. A. SATTAR, and A. STOESSL. Proc. Chem. Soc. 238 (1961).
8. B. HELFERICH, R. DHEIN, K. GEIST, H. JUNGER, and D. WHIELE. Ann. Chem. **646**, 45 (1961).
9. B. HELFERICH, R. DHEIN, K. GEIST, H. JUNGER, and D. WHIELE. Ann. Chem. **646**, 32 (1961).
10. P. DE MAYO. Advances in organic chemistry: methods and results. Vol. 2. Interscience Publishers, Inc., New York. 1960. p. 370.

RECEIVED MARCH 21, 1966.
DEPARTMENT OF CHEMISTRY,
UNIVERSITY OF WESTERN ONTARIO,
LONDON, ONTARIO.

Can. J. Chem. Downloaded from www.nrcresearchpress.com by 210.87.254.42 on 09/05/12
For personal use only.

ALKYLATION OF CYCLIC AMIDINES WITH MANNICH BASES

C. PODESVA AND K. VAGI

In a recent communication Craig and Moyle (1) reported a simple method for the preparation of Mannich bases from aromatic amines by heating an equimolecular mixture of an aromatic amine and β-diethylaminopropiophenone hydrochloride in ethanol–water. In the same paper these authors reported the isolation of β-(2-pyridylamino)-propiophenone in a 74% yield from the reaction between β-diethylaminopropiophenone hydrochloride and 2-aminopyridine; this seems to be the only reported case of an alkylation of a cyclic amidine with a Mannich base.

We now report the products obtained from a reaction of Mannich bases or their salts with 2-aminothiazoles, 2-aminobenzoxazole, and adenine. These products are summarized in Table I. (The yields indicated are pure but not optimum yields, as the optimum reaction conditions were not investigated.)

The alkylations were carried out in refluxing 50% aqeuous ethanol with equimolecular amounts of the reagents. Free Mannich bases were found to be equivalent to their salts, and β-dimethylaminopropiophenones could be used instead of β-diethylaminopropiophenones with equal success.

Alkylation of 2-aminothiazole by means of β-diethylaminopropiophenone hydrochloride yielded β-(2-thiazolylamino)-propiophenone (ν_{max} (KBr) 3 200, 1 690, 1 600, 1 575, and 1 495 cm^{-1}; λ_{max} (methanol) 245 and 206 mμ (log ε 4.18 and 4.03, respectively)), plus a yellow crystalline substance, m.p. 227–229°, analyzing for $C_{21}H_{17}NO_2S$. A corresponding product, analyzing for $C_{25}H_{19}NO_2S$, was obtained, together with the expected product, from the reaction between 2-aminobenzothiazole and β-diethylaminopropiophenone hydrochloride. Similarly, β-(2-benzoxazolylamino)-propiophenone was accompanied by a yellowish substance analyzing for $C_{25}H_{19}NO_3$. These higher molecular weight products, whose structure will be reported in a separate communication, were not formed when free Mannich bases instead of their salts were used for the alkylation. It is also noteworthy that they were not formed in reaction mixtures in which either 2-amino-5-nitrothiazole or β-diethylamino-*p*-nitropropiophenone was one of the reactants.

1. J. F. KING, P. DE MAYO, E. MORKVED, A. B. M. A. SATTAR, and A. STOESSL. Can. J. Chem. **41**, 100 (1963).
2. W. E. TRUCE and J. R. NORELL. J. Am. Chem. Soc. **85**, 3231 (1963).
3. J. F. KING and T. DURST. J. Am. Chem. Soc. **87**, 5684 (1965).
4. J. F. KING and T. DURST. Tetrahedron Letters, 585 (1963).
5. J. F. KING and T. DURST. J. Am. Chem. Soc. **85**, 2676 (1963).
6. J. F. KING and T. DURST. Can. J. Chem. **44**, 819 (1966).
7. E. HENMO, P. DE MAYO, A. B. M. A. SATTAR, and A. STOESSL. Proc. Chem. Soc. 238 (1961).
8. B. HELFERICH, R. DHEIN, K. GEIST, H. JUNGER, and D. WHIELE. Ann. Chem. **646**, 45 (1961).
9. B. HELFERICH, R. DHEIN, K. GEIST, H. JUNGER, and D. WHIELE. Ann. Chem. **646**, 32 (1961).
10. P. DE MAYO. Advances in organic chemistry: methods and results. Vol. 2. Interscience Publishers, Inc., New York. 1960. p. 370.

RECEIVED MARCH 21, 1966.
DEPARTMENT OF CHEMISTRY,
UNIVERSITY OF WESTERN ONTARIO,
LONDON, ONTARIO.

Can. J. Chem. Downloaded from www.nrcresearchpress.com by 210.87.254.42 on 09/05/12
For personal use only.

ALKYLATION OF CYCLIC AMIDINES WITH MANNICH BASES

C. PODESVA AND K. VAGI

In a recent communication Craig and Moyle (1) reported a simple method for the preparation of Mannich bases from aromatic amines by heating an equimolecular mixture of an aromatic amine and β-diethylaminopropiophenone hydrochloride in ethanol–water. In the same paper these authors reported the isolation of β-(2-pyridylamino)-propiophenone in a 74% yield from the reaction between β-diethylaminopropiophenone hydrochloride and 2-aminopyridine; this seems to be the only reported case of an alkylation of a cyclic amidine with a Mannich base.

We now report the products obtained from a reaction of Mannich bases or their salts with 2-aminothiazoles, 2-aminobenzoxazole, and adenine. These products are summarized in Table I. (The yields indicated are pure but not optimum yields, as the optimum reaction conditions were not investigated.)

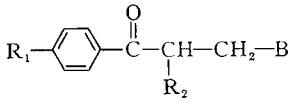
The alkylations were carried out in refluxing 50% aqeuous ethanol with equimolecular amounts of the reagents. Free Mannich bases were found to be equivalent to their salts, and β-dimethylaminopropiophenones could be used instead of β-diethylaminopropiophenones with equal success.

Alkylation of 2-aminothiazole by means of β-diethylaminopropiophenone hydrochloride yielded β-(2-thiazolylamino)-propiophenone (ν_{max} (KBr) 3 200, 1 690, 1 600, 1 575, and 1 495 cm^{-1}; λ_{max} (methanol) 245 and 206 mμ (log ε 4.18 and 4.03, respectively)), plus a yellow crystalline substance, m.p. 227–229°, analyzing for $C_{21}H_{17}NO_2S$. A corresponding product, analyzing for $C_{25}H_{19}NO_2S$, was obtained, together with the expected product, from the reaction between 2-aminobenzothiazole and β-diethylaminopropiophenone hydrochloride. Similarly, β-(2-benzoxazolylamino)-propiophenone was accompanied by a yellowish substance analyzing for $C_{25}H_{19}NO_3$. These higher molecular weight products, whose structure will be reported in a separate communication, were not formed when free Mannich bases instead of their salts were used for the alkylation. It is also noteworthy that they were not formed in reaction mixtures in which either 2-amino-5-nitrothiazole or β-diethylamino-*p*-nitropropiophenone was one of the reactants.

Can. J. Chem. Downloaded from www.nrcresearchpress.com by 210.87.254.42 on 09/05/12
For personal use only.

TABLE I

β-Amidinopropiophenones



B	R_1	R_2	Reaction time (h)	Yield (%)	Melting point (°C)	Solvent*	Formula	C (%) Calcd.	C (%) Found	H (%) Calcd.	H (%) Found	N (%) Calcd.	N (%) Found
2-Thiazolylamino	H	H	2	41	126–128	A	$C_{12}H_{12}N_2OS$†	62.04	61.81	5.21	5.19	12.06	11.85
5-Nitrothiazolyl-2-amino	H	H	1	12	195–197	B	$C_{12}H_{11}N_3O_3S$‡	51.97	51.53	4.00	4.35	15.16	15.25
2-Thiazolylamino	NO_2	H	1	91	174–176	C	$C_{12}H_{11}N_3O_3S$§	51.97	51.77	4.00	4.00	15.16	15.10
2-Benzothiazolylamino	H	H	2	52	208–210	D	$C_{22}H_{17}N_5O_8S$‖					13.70	13.43
2-Benzoxazolylamino	H	H	2	13	198–200	E	$C_{22}H_{17}N_5O_9$¶	53.33	53.27	3.46	3.73	14.14	13.90
9-Adenyl	H	H	20	43	256–257	F	$C_{14}H_{13}N_5O$	62.91	63.34	4.90	5.19	26.21	26.00
9-Adenyl	H	CH_3	20	52	189–190	G	$C_{15}H_{15}N_5O$	64.03	64.27	5.38	5.22	24.90	24.60

*Solvents: A, aqueous methanol; B, ethyl acetate; C, acetone; D, chloroform–ether; E, chloroform – ethyl acetate; F, Cellosolve; G, methanol – ethyl acetate.
†Anal. Calcd.: S, 13.80. Found: S, 14.00.
‡Anal. Calcd.: S, 11.57. Found: S, 11.78.
§Anal. Calcd.: S, 11.57. Found: S, 11.42.
‖Analyzed as the picrate. Anal. Calcd.: S, 6.27. Found: S, 6.08.
¶Analyzed as the picrate.

Can. J. Chem. Downloaded from www.nrcresearchpress.com by 210.87.254.42 on 09/05/12
For personal use only.

Surprisingly, with adenine, the alkylation was found to take place at N_9 rather than on the exocyclic nitrogen. The reaction product of β-diethylaminopropiophenone and adenine exhibited infrared absorption bands at 3 270, 3 100, 1 680 – 1 670 (a doublet), 1 600, and 1 575 cm^{-1}. The peak at 1 672 cm^{-1} in adenine has been assigned by Angell (2) to the deformation vibration of the NH_2 group. This peak obviously forms a part of the doublet at 1 680 – 1 670 cm^{-1} together with the propiophenone carbonyl, thus excluding any substitution on the 6-amino group. Further evidence for the presence of the primary amino group in β-adenylpropiophenone was obtained from the infrared spectra of the alcohol prepared by reduction of adenylpropiophenone with sodium borohydride, where the characteristic bands appeared at 3 275, 3 150, 1 707, 1 620, and 1 575 cm^{-1}. It is rather difficult to speculate about the reasons for the shift of the NH_2 deformation vibration to the higher frequency. The explanation given by Angell (2) for a similar shift in adenine hydrochloride involving protonation of N_1 cannot apply in the present case. Also, in 9-(3′-hydroxypropyl)-6-aminopurine, NH_2 deformation vibration occurs at 1 670 cm^{-1} (3), which is in good agreement with the NH_2 deformation frequency of 1 675 cm^{-1} we found for 9-(3′-phenyl-3′-hydroxy-2′-methyl)-propyladenine, obtained from the sodium borohydride reduction of the corresponding ketone.

The attachment of the propiophenone moiety to N_9 of adenine follows from the ultraviolet spectra of the ketone and the corresponding alcohol. The ketone exhibits maxima at 249 and 212 mμ (log ε 4.32 and 4.28, respectively), which are obviously composite peaks of adenine (261 mμ (log ε 4.08) and 214 mμ (log ε 3.90)) and acetophenone (243 mμ (log ε 3.99)) (4). The corresponding alcohol shows bands at 215 and 262 mμ (log ε 4.28), unaffected by pH. As the position of the ultraviolet maximum in 1-methyladenine has been shown to be dependent on pH (5), substitution on N_1 has to be excluded. Neither N_3 nor N_7 substitution can be considered seriously in view of the fact that several 3- or 7-alkyladenines exhibit a maximum in the range of 272–274 mμ (5–7). On the other hand, 9-methyladenine has been shown to possess a maximum at 260 mμ in both acidic and alkaline solutions (5), and 9-(3′-hydroxypropyl)-adenine has been reported to absorb at 259 mμ (3).

EXPERIMENTAL

The ultraviolet spectra were obtained with a Unicam SP 800 recording instrument in methanol solutions. The infrared spectra were recorded on a Perkin–Elmer 237 apparatus in Nujol, unless otherwise stated. The melting points were determined in capillaries on a Mel-Temp apparatus and are uncorrected. Microanalyses were performed by Organic Microanalysis, Dr. C. Daessle, Montreal. Starting materials were obtained from commercial sources and were used without prior purification.

General Procedures

Reactions of β-Dialkylaminopropiophenone Hydrochlorides with 2-Aminothiazoles or 2-Aminobenzoxazole

An approximately 30% solution of equimolar amounts of the reactants in 50% aqueous ethanol was refluxed for the periods of time specified in Table 1. A mixture of two products precipitated when the solution was cooled (addition of acetone was necessary in the case of 2-aminobenzoxazole), and was collected by filtration. The crystalline material was dissolved in hot acetone (in hot benzene in the case of 2-aminobenzothiazole) and allowed to cool to room temperature. The high molecular weight products were removed by filtration and the filtrates evaporated to dryness. The residues were then crystallized from the appropriate solvents. β-(2-Benzothiazolylamino)- and β-(2-benzoxazolylamino)-propiophenone melted at 137–140° and 139–140°, respectively. Because these products failed to analyze within acceptable limits even after repeated crystallizations, they were transformed into picrates by treatment with methanolic picric acid.

Reactions of β-Dialkylaminopropiophenones (Bases) with 2-Aminothiazoles or 2-Aminobenzoxazole

The same concentration of the reactants was used as described above. After the reaction mixture was cooled to room temperature, it was diluted with water and extracted with chloroform. The solvent was removed *in vacuo* and the residue purified by crystallization.

Reactions of β-Dialkylaminopropiophenone Hydrochlorides with Adenine

Because adenine is only slightly soluble in alcohol–water, the whole reaction was carried out in suspension. The crystalline reaction product was collected by filtration and recrystallized several times.

Reduction of β-(9-Adenyl)-propiophenone

A mixture of the ketone (1 g) and sodium borohydride (0.2 g) in 55 ml of isopropanol containing 5 ml of water was stirred at room temperature over the weekend. After dilution with water the reaction product was extracted with chloroform, the solvent was removed *in vacuo*, and the resin-like residue (0.9 g) was crystallized from ethyl acetate. The analytically pure product (0.66 g, 66%) had a melting point of 139–142°.

Anal. Calcd. for $C_{14}H_{15}N_5O$: C, 62.44; H, 5.62; N, 26.01. Found: C, 62.18; H, 5.86; N, 26.24.

Reduction of β-(9-Adenyl)-α-methylpropiophenone

A mixture of the ketone (4 g) and sodium borohydride (0.3 g) in methanol–isopropanol–water (1:1:0.2, 66 ml) was stirred for 17 h at room temperature. The reaction mixture was worked up as above to give 1.5 g (37%) of pure alcohol, m.p. 229–231° (crystallized from methanol – ethyl acetate).

Anal. Calcd. for $C_{15}H_{17}N_5O$: C, 63.58; H, 6.05; N, 24.72. Found: C, 63.76; H, 6.17; N, 24.56.

ACKNOWLEDGMENT

The skillful technical assistance of Mrs. C. Solomon is gratefully acknowledged.

1. J. C. Craig and M. Moyle. J. Org. Chem. **29**, 410 (1964).
2. C. L. Angell. J. Chem. Soc. 504 (1961).
3. H. J. Schaffer and P. S. Bhargava. Biochemistry, **4**, 71 (1965).
4. H. H. Jaffé and M. Orchin. Theory and applications of ultraviolet spectroscopy. John Wiley & Sons, Inc., New York. 1962.
5. N. J. Leonard and J. H. Deyrup. J. Am. Chem. Soc. **84**, 2148 (1962).
6. H. J. Schaffer and R. Vince. J. Med. Chem. **8**, 710 (1965).
7. P. Brookes and P. D. Lawley. J. Chem. Soc. 539 (1960).

Received September 17, 1965.
Delmar Chemicals Limited,
Lasalle, Quebec.

PREPARATION OF 3,4-METHYLENEDIOXY- AND 3,4-DIMETHOXY-6-AMINOPHENOL

D. G. Orphanos and A. Taurins

The work on the synthesis of 6,7-dialkoxy-1,4-benzoxazin-2-ones (1) required the preparation of 3,4-methylenedioxy- (I) and 3,4-dimethoxy-6-aminophenol (II), which had not been described in the literature. These aminophenols proved to be very sensitive to air oxidation, and could not be isolated from solutions in a pure state. Therefore, their solutions were brought directly into reactions with other components in a nitrogen atmosphere. 3,4-Methylenedioxy- and 3,4-dimethoxy-6-aminophenol were characterized as their acetanilides, which were prepared by reductive acetylation (2) of the corresponding nitro compounds. Most of the intermediates used in the preparation of I and II have been described previously; however, in the present work they were synthesized either by a modification of the known method, or by a new procedure.

3,4-Methylenedioxy-6-aminophenol (I) was prepared from piperonal (3,4-methylenedioxybenzaldehyde) (III) in five steps (Reaction Scheme 1): (*a*) oxidation of piperonal (III) with peracetic acid to give 3,4-methylenedioxyphenol (IV) (sesamol), (*b*) acetylation of sesamol, (*c*) nitration of the acetyl derivative (VI) to obtain 3,4-methylenedioxy-6-nitrophenyl acetate (VII), (*d*) hydrolysis of the latter compound to produce a free nitrophenol (VIII), and (*e*) catalytic hydrogenation of the nitro compound to obtain I. The aminophenol I was characterized as its *N*-acetyl derivative, prepared by reductive acetylation (2) of the nitro compound (VIII).

Can. J. Chem. Downloaded from www.nrcresearchpress.com by 210.87.254.42 on 09/05/12
For personal use only.

Reduction of β-(9-Adenyl)-propiophenone

A mixture of the ketone (1 g) and sodium borohydride (0.2 g) in 55 ml of isopropanol containing 5 ml of water was stirred at room temperature over the weekend. After dilution with water the reaction product was extracted with chloroform, the solvent was removed *in vacuo*, and the resin-like residue (0.9 g) was crystallized from ethyl acetate. The analytically pure product (0.66 g, 66%) had a melting point of 139–142°.

Anal. Calcd. for $C_{14}H_{15}N_5O$: C, 62.44; H, 5.62; N, 26.01. Found: C, 62.18; H, 5.86; N, 26.24.

Reduction of β-(9-Adenyl)-α-methylpropiophenone

A mixture of the ketone (4 g) and sodium borohydride (0.3 g) in methanol–isopropanol–water (1:1:0.2, 66 ml) was stirred for 17 h at room temperature. The reaction mixture was worked up as above to give 1.5 g (37%) of pure alcohol, m.p. 229–231° (crystallized from methanol – ethyl acetate).

Anal. Calcd. for $C_{15}H_{17}N_5O$: C, 63.58; H, 6.05; N, 24.72. Found: C, 63.76; H, 6.17; N, 24.56.

ACKNOWLEDGMENT

The skillful technical assistance of Mrs. C. Solomon is gratefully acknowledged.

1. J. C. Craig and M. Moyle. J. Org. Chem. **29**, 410 (1964).
2. C. L. Angell. J. Chem. Soc. 504 (1961).
3. H. J. Schaffer and P. S. Bhargava. Biochemistry, **4**, 71 (1965).
4. H. H. Jaffé and M. Orchin. Theory and applications of ultraviolet spectroscopy. John Wiley & Sons, Inc., New York. 1962.
5. N. J. Leonard and J. H. Deyrup. J. Am. Chem. Soc. **84**, 2148 (1962).
6. H. J. Schaffer and R. Vince. J. Med. Chem. **8**, 710 (1965).
7. P. Brookes and P. D. Lawley. J. Chem. Soc. 539 (1960).

Received September 17, 1965.
Delmar Chemicals Limited,
Lasalle, Quebec.

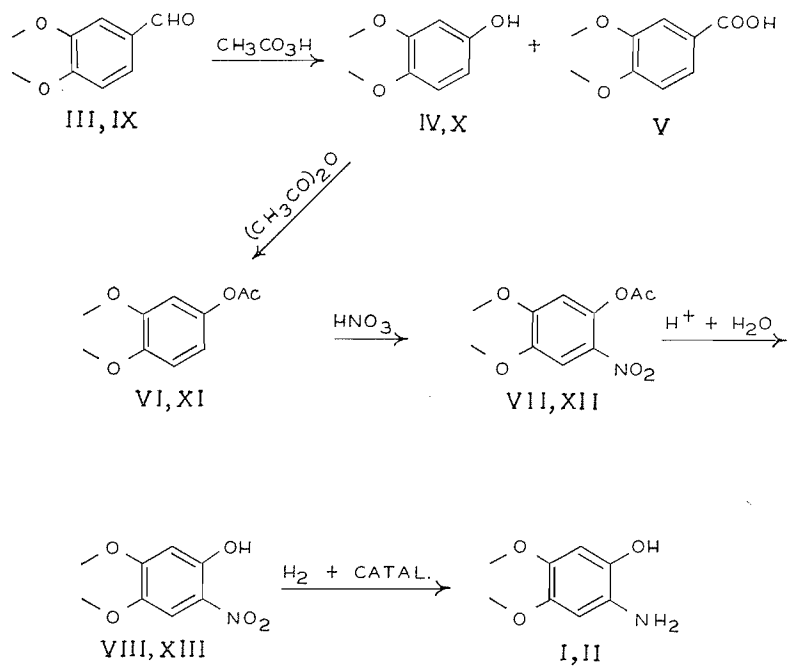
PREPARATION OF 3,4-METHYLENEDIOXY- AND 3,4-DIMETHOXY-6-AMINOPHENOL

D. G. Orphanos and A. Taurins

The work on the synthesis of 6,7-dialkoxy-1,4-benzoxazin-2-ones (1) required the preparation of 3,4-methylenedioxy- (I) and 3,4-dimethoxy-6-aminophenol (II), which had not been described in the literature. These aminophenols proved to be very sensitive to air oxidation, and could not be isolated from solutions in a pure state. Therefore, their solutions were brought directly into reactions with other components in a nitrogen atmosphere. 3,4-Methylenedioxy- and 3,4-dimethoxy-6-aminophenol were characterized as their acetanilides, which were prepared by reductive acetylation (2) of the corresponding nitro compounds. Most of the intermediates used in the preparation of I and II have been described previously; however, in the present work they were synthesized either by a modification of the known method, or by a new procedure.

3,4-Methylenedioxy-6-aminophenol (I) was prepared from piperonal (3,4-methylenedioxybenzaldehyde) (III) in five steps (Reaction Scheme 1): (*a*) oxidation of piperonal (III) with peracetic acid to give 3,4-methylenedioxyphenol (IV) (sesamol), (*b*) acetylation of sesamol, (*c*) nitration of the acetyl derivative (VI) to obtain 3,4-methylenedioxy-6-nitrophenyl acetate (VII), (*d*) hydrolysis of the latter compound to produce a free nitrophenol (VIII), and (*e*) catalytic hydrogenation of the nitro compound to obtain I. The aminophenol I was characterized as its *N*-acetyl derivative, prepared by reductive acetylation (2) of the nitro compound (VIII).

Can. J. Chem. Downloaded from www.nrcresearchpress.com by 210.87.254.40 on 09/05/12
For personal use only.



REACTION SCHEME 1.

3,4-Dimethoxy-6-aminophenol (II) (5, 6) was similarly synthesized from veratraldehyde (3,4-dimethoxybenzaldehyde).

The oxidation of piperonal with peracetic acid was reinvestigated because the experimental observations did not agree with the literature data (3, 9). According to previous views, peracetic acid oxidation of piperonal gave sesamol acetate (3), or sesamol acetate and formate (9); therefore, the oxidation product was subjected to alkaline hydrolysis to obtain a uniform substance.

In the present work, neither sesamol acetate nor formate was found to be present. Instead, the oxidation product consisted of sesamol and unreacted piperonal in a ratio of 4:1, and a small amount of piperonylic acid (3,4-methylenedioxybenzoic acid) (V). This mixture could not be separated even by fractional distillation with a spinning-band column. The oxidation of piperonal was studied under a variety of experimental conditions, and it was observed that the reaction never goes to completion. If a greater amount of peracetic acid was used than that established as an optimum, the yields of the product were noticeably lower and more resinous by-products were formed. Freshly prepared peracetic acid was decidedly most efficient, and the best yields of sesamol (45–49%) were obtained when the reaction temperature was between 32 and 38°.

3,4-Methylenedioxy- (VI) and 3,4-dimethoxy-phenyl acetate (XI) were prepared by an adaptation of a method involving the treatment of the sodium salts of phenolic substances with acetic anhydride (8). The yields of VI and XI were 92% and 88%, respectively.

Nitration of 3,4-methylenedioxyphenyl acetate (VI) was carried out by an improved method in which the mixture of nitric and acetic acids was added to the solution of VI in glacial acetic acid at 30–45°. This procedure gave a yield of 88% of pure 3,4-methylenedioxy-6-nitrophenyl acetate (VII), compared with a yield of 67% obtained by a previous

Can. J. Chem. Downloaded from www.nrcresearchpress.com by 210.87.254.40 on 09/05/12
For personal use only.

method (9). 3,4-Dimethoxy-6-nitrophenyl acetate (XII), a new compound, was prepared by a method analogous to that used for preparing VII.

Both VII and XII were hydrolyzed to give free phenols by reaction with 20% sulfuric acid for 40 min, instead of by the previous method (9) in which VII was refluxed for 20 h with ethanolic sodium hydroxide solution. Acidic hydrolysis of VII and XII produced quantitative yields of VIII and XIII as pure crystalline products.

Low-pressure catalytic hydrogenation of 3,4-methylenedioxy- (VIII) and 3,4-dimethoxy-6-nitrophenol (XIII) produced the desired products, 3,4-methylenedioxy- (I) and 3,4-dimethoxy-6-aminophenol (II), which were characterized and analyzed as their acetanilides (*N*-acetylamino derivatives). I and II were not isolated in a pure state from solutions because of their sensitivity to oxidation, but were used directly in syntheses (1).

EXPERIMENTAL

The melting points were determined in a Thiele–Dennis melting point tube containing Dow Corning silicone fluid No. D.C. 550, and are uncorrected. The analyses were carried out in the laboratory of C. Daessle, Montreal, Quebec. Infrared spectra were determined in potassium bromide, on a Perkin–Elmer model 21 double-beam instrument equipped with a sodium chloride prism.

20% Peracetic Acid Solution

This solution, containing catalytic amounts of *p*-toluenesulfonic acid, and being free of explosive Ac_2O_2, was always freshly prepared according to Böeseken *et al.* (3), and used within 24 h.

3,4-Methylenedioxyphenol (Sesamol) (IV)

To a solution of piperonal (III) (50 g, 0.333 mole) in glacial acetic acid at 32°, 20% peracetic acid solution (145 g, 0.38 mole) was added in portions of 20–30 ml, with occasional shaking. After the addition of the first portion, the temperature rose slowly to about 38°. It was allowed to fall to 32° before the next portion was added. When the addition had been completed, the reaction mixture was left at room temperature for 24 h, and then distilled under reduced pressure to free it from acetic acid. The dark-brown viscous oil was mixed with toluene (250 ml) and stirred for 15 min, during which time most of the resinous by-products separated as a viscous mass. After separation and distillation of the solvent, the residual dark-brown oil was subjected to vacuum distillation, and gave 40.5 g of a yellow oil boiling at 110–114° and 2 mm Hg. At the end of this distillation, the temperature was raised to 130–145° and piperonylic acid was distilled over. This acid, collected and crystallized from methanol, weighed 1.2 g and melted at 229°. The yellow oil obtained from the vacuum distillation was shaken with 150 ml of 10% sodium hydroxide solution and extracted three times with 50 ml portions of diethyl ether. The combined ether extracts, washed with water and dried over potassium sulfate, left 13.1 g of pure unreacted piperonal after removal of the solvent. The alkaline layer, acidified with 20% sulfuric acid solution, was then extracted with diethyl ether (200 ml). The ether extract, washed three times with 50 ml portions of 5% sodium bicarbonate solution and then with water, was dried over potassium sulfate. Removal of the ether gave a colorless to light-yellow oil which, with evolution of heat, rapidly solidified to pure sesamol (22.5 g), m.p. 64–65° (lit. (3) m.p. 65.8°). The yield of pure product, when the recovery of 13.1 g of pure unreacted piperonal was considered, amounted to 67.5%.

3,4-Dimethoxyphenol (X)

Oxidation of 55.5 g (0.333 mole) of veratraldehyde (IX) with peracetic acid was carried out under the conditions described above. Distillation of the reaction product gave 39.8 g of a yellow oil boiling at 118–127° and 2 mm Hg. Purification of the oil gave 25.8 g of crude 3,4-dimethoxyphenol, m.p. 71–76°. Crystallization from carbon tetrachloride raised the melting point to 79–80° (lit. m.p. 78–80° (6), 80–81° (7), 81.5° (5)); 11.5 g of pure unreacted veratraldehyde was isolated.

3,4-Methylenedioxyphenyl Acetate (VI)

3,4-Methylenedioxyphenol (IV) (13.8 g, 0.1 mole) was dissolved in 10% sodium hydroxide solution (60 ml), and to the cooled solution acetic anhydride (15 g, 0.15 mole) was added, with stirring, over 10 min. The reaction mixture was extracted with carbon tetrachloride. The extract was neutralized with sodium carbonate solution and dried over magnesium sulfate. The solvent was removed under reduced pressure, and the residue, 3,4-methylenedioxyphenyl acetate, was distilled at 112° and 2.5 mm Hg, yield 16.6 g (92%), n_D^{20} 1.5281 (lit. (4) n_D^{25} 1.5265).

3,4-Dimethoxyphenyl Acetate (XI)

3,4-Dimethoxyphenol (X) (15. g, 0.1 mole) was acetylated by a similar procedure. The crude acetate distilled at 128° and 2 mm, yield 17.8 g (88%). 3,4-Dimethoxyphenyl acetate forms colorless plates when crystallized from dilute ethanol, m.p. 44° (lit. (7) m.p. 44°).

Can. J. Chem. Downloaded from www.nrcresearchpress.com by 210.87.254.40 on 09/05/12
For personal use only.

3,4-Methylenedioxy-6-nitrophenyl Acetate (VII)

3,4-Methylenedioxyphenyl acetate (VI) (18 g, 0.1 mole) dissolved in glacial acetic acid (60 ml) was treated at room temperature gradually with a solution of concentrated nitric acid (11 g, 0.12 mole, specific gravity 1.42) in glacial acetic acid (20 ml). The solution was stirred for 3 h and then poured into cold water (400 ml). After 1 h the pale-yellow crystalline precipitate was separated by filtration, washed with water, and dried. 3,4-Methylenedioxy-6-nitrophenyl acetate (VII) was crystallized from ethanol, yield 19.8 g (88%), m.p. 104–105° (lit. (9) m.p. 104–105°).

3,4-Dimethoxy-6-nitrophenyl Acetate (XII)

Nitration of 3,4-dimethoxyphenyl acetate (XI) (19.6 g, 0.1 mole) was carried out by the method used for the preparation of VII. 3,4-Dimethoxy-6-nitrophenyl acetate was crystallized from ethanol as yellow prisms, m.p. 117–118°, yield 20.7 g (85.4%).

Anal. Calcd. for $C_{10}H_{11}NO_6$: C, 49.79; H, 4.59; N, 5.81. Found: C, 49.51; H, 4.47; N, 6.08.

The structure of XII was confirmed by its infrared spectrum and hydrolysis of the acetate to the known XIII.

3,4-Methylenedioxy-6-nitrophenol (VIII)

3,4-Methylenedioxy-6-nitrophenyl acetate (VII) (22.5 g, 0.1 mole), ethanol (220 ml), and 20% (by volume) sulfuric acid solution (125 ml) were heated on a water bath for 40 min. The solution deposited golden-yellow needles when cooled. The product VIII was separated by filtration, washed with cold water, and dried, yield 18.1 g (98.3%), m.p. 95–96° (crystallized from 60% ethanol) (lit. (9) m.p. 93–94°).

3,4-Dimethoxy-6-nitrophenol (XIII)

3,4-Dimethoxy-6-nitrophenyl acetate (XII) (24.1 g, 0.1 mole) was hydrolyzed under conditions similar to those employed for the preparation of VIII. The compound XIII formed yellow crystals, m.p. 145–146° (crystallized from 60% ethanol) (lit. (10) m.p. 143°).

3,4-Methylenedioxy-6-aminophenol (I) (in Ethanol Solution)

3,4-Methylenedioxy-6-nitrophenol (VIII), dissolved in 25 times its weight of 96% ethanol, was reduced at room temperature with either platinum oxide or palladium on charcoal as catalyst, and with hydrogen at 3 atm pressure, until 3 molecular equivalents had been absorbed. The time required was about 10 min. When Raney nickel was used as a catalyst, the hydrogenation was carried out at 80–90°, and the time required was 1 h. Removal of the catalyst by filtration in a nitrogen atmosphere gave a colorless solution. Many efforts to isolate the reduction product I as a solid were unsuccessful. The amino compound I was characterized as its acetanilide and hydrochloride.

3,4-Methylenedioxy-6-hydroxyacetanilide

3,4-Methylenedioxy-6-nitrophenol (VIII) (1.83 g, 0.01 mole) was mixed with glacial acetic acid (50 ml) and acetic anhydride (1.1 g, 0.011 mole). The nitro group was reduced and acetylated at room temperature and 3 atm hydrogen pressure with 10% palladium on carbon (0.015 g) as catalyst. The reaction mixture was dissolved in hot ethanol and the catalyst removed by filtration. The solution was concentrated under reduced pressure to a small volume (10 ml), and diluted with water (100 ml); the solid which precipitated was separated by filtration, washed with water, and dried. 3,4-Methylenedioxy-6-hydroxyacetanilide was crystallized from 50% ethanol as cotton-like white crystals, m.p. 209–211°, yield 1.78 g (91%); ν_{max} 3 270, 3 090, 1 648 (sh), 1 635, and 1 565 cm^{-1}.

Anal. Calcd. for $C_9H_9NO_4$: C, 55.39; H, 4.64; N, 7.18. Found: C, 55.17; H, 4.75; N, 7.33.

3,4-Methylenedioxy-6-aminophenol Hydrochloride

A mixture of VIII (0.5 g), 10% palladium on carbon (0.01 g), and anhydrous diethyl ether (250 ml) was shaken with hydrogen under 3 atm pressure at room temperature. The reduction of the nitro group was completed in about 2 h. The catalyst was filtered under a nitrogen atmosphere, and hydrogen chloride gas was introduced into the filtrate. The white crystalline hydrochloride of I was separated by filtration, washed with benzene (5 ml), and dried *in vacuo* (0.45 g yield), m.p. 195–210° (decomp.); ν_{max} 3 540 (sh), 3 450, 3 160, 2 620, 1 595, and 1 298 cm^{-1}.

Anal. Calcd. for $C_7H_7NClO_3$: N, 7.39. Found: N, 7.51.

3,4-Dimethoxy-6-aminophenol (II) (in Methoxyethylene Glycol Solution)

The procedure employed for the reduction of 3,4-dimethoxy-6-nitrophenol (XIII) was similar to that used for the preparation of I, except that methoxyethylene glycol was used as the solvent because of the low solubility of XIII in ethanol. The resulting aminophenol II was characterized as its acetanilide.

3,4-Dimethoxy-6-hydroxyacetanilide

This derivative of II was prepared by reductive acetylation of XII, in a yield of 90%. It was crystallized from benzene as colorless needles, m.p. 137–138°; ν_{max} 3 365, 3 145, 1 648, and 1 630 (sh) cm^{-1}.

Anal. Calcd. for $C_{10}H_{13}NO_4$: C, 56.86; H, 6.20; N, 6.63. Found: C, 57.08; H, 6.04; N, 6.41.

Can. J. Chem. Downloaded from www.nrcresearchpress.com by 210.87.254.40 on 09/05/12
For personal use only.

1. D. G. ORPHANOS and A. TAURINS. Can. J. Chem. This issue.
2. K. HAYES and G. GEVER. J. Org. Chem. **16**, 276 (1951).
3. J. BÖESEKEN, W. D. COHEN, and C. J. KIP. Rec. Trav. Chim. **55**, 815 (1936).
4. M. BEROZA. J. Agr. Food Chem. **4**, 49 (1956).
5. J. BÖESEKEN and J. GREUP. Rec. Trav. Chim. **58**, 528 (1939).
6. R. I. MELTZER and J. DOCZI. J. Am. Chem. Soc. **72**, 4986 (1950).
7. W. BAKER and C. EVANS. J. Chem. Soc. 372 (1938).
8. A. VOGEL. Practical organic chemistry. 3rd ed. Longmans, Green & Co., Inc., New York. 1957. p. 669.
9. S. I. GERTLER, B. H. ALEXANDER, and M. BEROZA. J. Org. Chem. **24**, 327 (1959).
10. A. OLIVERIO. Gazz. Chim. Ital. **73**, 181 (1943).

RECEIVED FEBRUARY 22, 1966.
DEPARTMENT OF CHEMISTRY,
MCGILL UNIVERSITY,
MONTREAL, QUEBEC.

Can. J. Chem. Downloaded from www.nrcresearchpress.com by 210.87.254.40 on 09/05/12
For personal use only.

Can. J. Chem. Downloaded from www.nrcresearchpress.com by 210.87.254.105 on 09/05/12
For personal use only.

Canadian Journal of Chemistry

Issued by THE NATIONAL RESEARCH COUNCIL OF CANADA

VOLUME 44 AUGUST 15, 1966 NUMBER 16

PROTON MAGNETIC RESONANCE AND INFRARED SPECTRA OF SOME COMPLEXES OF N,N-DIMETHYLACETAMIDE

A. J. CARTY

Department of Chemistry, Memorial University of Newfoundland, St. John's, Newfoundland

Received April 12, 1966

ABSTRACT

Proton magnetic resonance spectra of some complexes of In, Zn, Cd, and Sn halides and perchlorates with N,N-dimethylacetamide (DMA) have been measured in acetone-d_6. Low field shifts of the methyl resonances of DMA on complex formation are dependent on metal and anion. The similarity of the spectra of all the complexes suggests only oxygen-coordinated DMA in solution. Infrared spectra in the range 2 000 – 625 cm^{-1} are recorded. Changes in the C—O and C—N stretching frequencies of the ligand on coordination are consistent with oxygen-bonded DMA both in the solid complexes and in solution.

The new compounds $Zn(ClO_4)_2.6DMA$, $Cd(ClO_4)_2.6DMA$, $CdI_2.2DMA$, and $SnCl_4.2DMA$ are reported.

INTRODUCTION

N,N-Dimethylacetamide (DMA) is well known to form complexes with a wide range of metal salts (1–7). In general, metal perchlorates form complexes in which the metal ion exhibits its maximum coordination number; $La(ClO_4)_3.8DMA$ and $In(ClO_4)_3.6DMA$ are typical. Metal halide complexes are often unusual in that 1.0, 1.5, or 2.5 moles of amide may be coordinated per mole of salt as in $CdCl_2.DMA$, $InI_3.1.5DMA$, and $UCl_4.2.5DMA$.

The nature of the bonding in amide complexes has been the subject of some discussion. On the basis of infrared and conductivity evidence, Bull *et al.* (1) postulate that DMA is coordinated to metals via the carbonyl oxygen. Other authors interpret spectral results for complexes of related amides in terms of nitrogen bonding (8, 9). Bridging or bidentate DMA has been suggested to account for the unusual stoichiometries of some metal halide complexes (3, 10).

Proton magnetic resonance has recently been used to establish that N,N-dimethylformamide coordinates to boron trihalides (11) and to decarborane (12) via the carbonyl oxygen.

This paper describes the proton magnetic resonance (p.m.r.) spectra of some DMA complexes of non-transition metal halides and perchlorates; the results are correlated with infrared spectral measurements and discussed in terms of metal–ligand bonding and the structure of coordinated DMA.

EXPERIMENTAL

B.D.H. reagent grade DMA was dried over Linde molecular sieve type 5A and distilled under reduced pressure. Anhydrous indium trihalides were prepared as described elsewhere (13). Indium, zinc, and cadmium perchlorates were prepared from the metals and perchloric acid and were dried *in vacuo* over potassium hydroxide. Other salts were Fisher reagent grade materials.

The new compounds $CdI_2.2DMA$, $Cd(ClO_4)_2.6DMA$, $Zn(ClO_4)_2.6DMA$, and $SnCl_4.2DMA$ were prepared as follows:

(1) $CdI_2.2DMA$.—Excess DMA was added to a suspension of cadmium iodide in hot ethyl acetate and the solution filtered. On standing, colorless crystals of the complex were formed. The product was recrystallized from methanol/acetone and dried *in vacuo*.

Anal. Calcd. for $CdI_2.2(C_4H_9NO)$: C, 17.76; H, 3.40; N, 5.18; I, 47.15; Cd, 20.69. Found: C, 17.41; H, 3.52; N, 5.27; I, 46.71; Cd, 20.80.

(2) $Cd(ClO_4)_2.6DMA$.—The hydrated perchlorate was dissolved in excess DMA. Excess ligand was removed under vacuum and the viscous liquid allowed to crystallize over phosphorus pentoxide. The hygroscopic product was recrystallized from anhydrous acetone.

Anal. Calcd. for $Cd(ClO_4)_2.6(C_4H_9NO)$: C, 34.56; H, 6.48; N, 10.08; Cd, 13.49. Found: C, 34.19; H, 6.46; N, 10.01; Cd, 13.79.

(3) $Zn(ClO_4)_2.6DMA$.—An ethanolic solution of DMA was added to a solution of hydrated zinc perchlorate in the same solvent. The solution was allowed to crystallize over phosphorus pentoxide and the hygroscopic product dried *in vacuo*. Washing with ether or recrystallization led to decomposition.

Anal. Calcd. for $Zn(ClO_4)_2.6(C_4H_9NO)$: C, 36.63; H, 6.87; N, 10.69; Zn, 8.31. Found: C, 36.45; H, 6.31; N, 10.52; Zn, 8.51.

(4) $SnCl_4.2DMA$.—Addition of anhydrous tin tetrachloride in chloroform to a chloroform solution of DMA gave colorless crystals of the complex. The compound was recrystallized from acetone and dried *in vacuo*.

Anal. Calcd. for $SnCl_4.2(C_4H_9NO)$: C, 22.09; H, 4.14; N, 6.44; Cl, 32.67; Sn, 27.31. Found: C, 22.39; H, 4.13; N, 6.52; Cl, 32.54; Sn, 27.18.

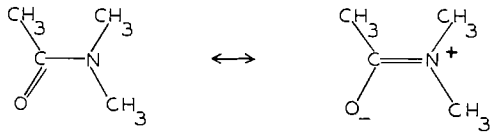
Indium complexes were prepared by literature methods (10), as were the remaining zinc and cadmium complexes (1). Microanalyses were carried out by A. Bernhardt (Mulheim).

Proton magnetic resonance spectra were measured on a Varian A60 spectrometer operating at 60 Mc/s and equipped with a Varian temperature control assembly. Tetramethylsilane (TMS) was used as an internal reference. Samples were made up in a dry box and concentrations were 0.1 *M*.

Infrared measurements were made on a Perkin–Elmer 237B spectrophotometer. Spectra were measured as Nujol mulls and as solutions in methylene chloride.

RESULTS

The structure of DMA is best described as a resonance hybrid of the primary structures.



I ⟷ II

Significant contributions from II to the ground state of the molecule result in considerable double-bond character for the C—N bond (14). Restricted rotation about the C—N bond and the planar configuration of DMA give rise to two non-equivalent N-methyl groups and a p.m.r. spectrum in acetone-d_6 at 60 Mc/s consisting of a single C-methyl resonance at δ 1.99 and two N-methyl resonances centered at δ 2.93. The N-methyl resonance to high field can be assigned to the group *cis* to the carbonyl oxygen since the high anisotropy of the carbonyl bond causes greater shielding of the *cis* than the *trans* N-methyl group. At high resolution, a slight broadening of the high field N-methyl signal can be detected which can be attributed to a small *trans* spin–spin coupling between the N-methyl and C-methyl groups. Similar couplings have been noted in ethylenic systems (15).

Data for DMA and complexes are summarized in Table I.

In a study of this type it is necessary to show that the ligand remains coordinated to the metal ion in the solvent chosen. Proton magnetic resonance spectra of the DMA complexes of Sn(IV), In(III), Zn(II), and Cd(II) in acetone-d_6, methylene chloride, or deuterochloroform show considerable low field shifts, relative to free DMA in the same solvent (Table I). Furthermore, the chemical shifts of the ligand protons are almost independent of solvent, the signals being shifted slightly to high field for solutions in the halogenated compounds. For solutions of the complexes in the strong donor solvent

Can. J. Chem. Downloaded from www.nrcresearchpress.com by 210.87.254.105 on 09/05/12
For personal use only.

TABLE I

Proton magnetic resonance data

Compound	C—Me*	N—Me*		C—Me†	N—Me†
DMA	1.99	2.85	3.01		
$In(ClO_4)_3.6DMA$	2.45	3.20	3.30	−0.46	−0.32
$InCl_3.2.5DMA$	2.30	3.06	3.19	−0.31	−0.19
$InBr_3.1.5DMA$	2.40	3.12	3.23	−0.41	−0.25
$InI_3.1.5DMA$	2.46	3.20	3.29	−0.47	−0.32
$Zn(ClO_4)_2.6DMA$	2.35	3.12	3.20	−0.36	−0.23
$ZnCl_2.2DMA$	2.30	3.01	3.18	−0.31	−0.17
$ZnBr_2.2DMA$	2.31	3.02	3.19	−0.32	−0.18
$ZnI_2.2DMA$	2.35	3.05	3.21	−0.36	−0.20
$Cd(ClO_4)_2.6DMA$	2.23	3.00	3.16	−0.24	−0.15
$CdCl_2.DMA$‡	2.22	2.97	3.12	−0.23	−0.12
$CdBr_2.DMA$	2.26	3.04	3.16	−0.27	−0.17
$CdI_2.2DMA$	2.31	3.10	3.22	−0.32	−0.22
$SnCl_4.2DMA$	2.31	3.08	3.19	−0.32	−0.20

*Chemical shifts in p.p.m. relative to TMS = 0.00 p.p.m.
†Downfield shifts measured as $\delta_{DMA} - \delta_{complex}$ p.p.m.
‡Solution in deuteromethanol.

dimethylsulfoxide-d_6, which forms complexes with the above metal ions (16, 17), both N-methyl and C-methyl resonances appear only 2 c.p.s. to low field of the corresponding signals for free DMA. It seems reasonable to assume that in this solvent, complete replacement of DMA from the coordination sphere has occurred, whereas in acetone, chloroform, and methylene chloride, DMA remains coordinated to the metal. Finally, the spectra were shown to be independent of concentration. For example, no change in relative peak position was observed for solutions of $InI_3.1.5DMA$ for the concentration range 0.01 *M* to 0.1 *M* in acetone-d_6.

The p.m.r. spectra of all the complexes studied are very similar at probe temperature (about 36°). Figure 1 illustrates the p.m.r. spectra of $In(ClO_4)_3.6DMA$ and $ZnCl_2.2DMA$ in acetone-d_6, which are typical of the perchlorate and halide complexes. A single C-methyl resonance and two N-methyl resonances occur in all cases. Perchlorates generally gave broader signals than halides and the downfield shifts of the resonances vary both with cation and anion.

For the perchlorate complexes, traces of perchloric acid remaining from the preparations caused collapse of the two N-methyl signals into a single broad resonance. Reasons for this are discussed later.

Addition of free ligand to solutions of the complexes caused high field shifts of both N-methyl and C-methyl resonances but in no case were separate signals for complexed and free DMA observed.

We have qualitatively investigated the effect of temperature on the p.m.r. spectra of these compounds. Up to the boiling point of acetone-d_6, none of the complexes prepared showed marked changes in either the N-methyl or C-methyl resonances. The barrier to internal rotation about the C—N bond in bonded DMA must be somewhat higher than in the free ligand, where broadening of the N-methyl resonances begins at $\sim 40°$ and coalescence is complete at $\sim 70°$ (18). When the complexes were cooled below −20°, whereas only slight broadening of the methyl resonances in the perchlorate complexes occurred, the indium halide complexes showed marked resolution of both N-methyl and C-methyl signals. The spectra of $InBr_3.1.5DMA$ at normal temperature (36°) and −30° are shown in Fig. 2. The indium trichloride and triiodide complexes showed similar spectral changes at low temperature but signals from the zinc and cadmium halide complexes remained unresolved.

Can. J. Chem. Downloaded from www.nrcresearchpress.com by 210.87.254.105 on 09/05/12
For personal use only.

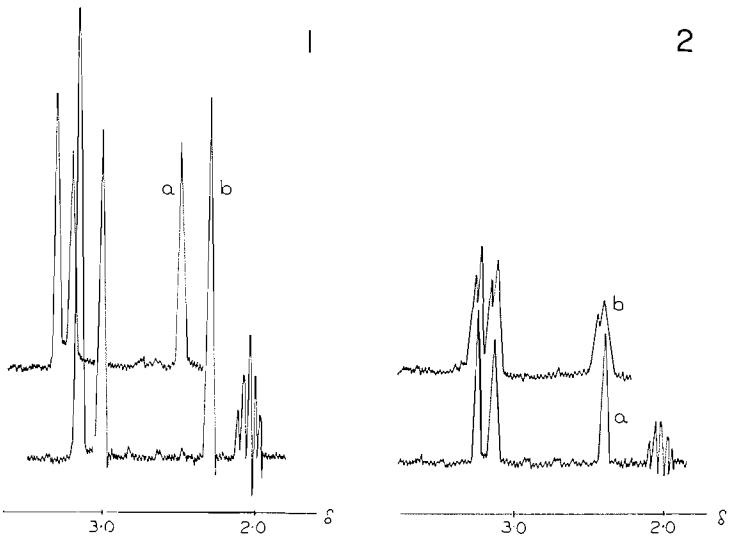


FIG. 1. Proton magnetic resonance spectra of (*a*) $In(ClO_4)_3.6DMA$ and (*b*) $ZnCl_2.2DMA$ in acetone-d_6 at 36°.

FIG. 2. Proton magnetic resonance spectra of $InBr_3.1.5DMA$ at (*a*) 36°, (*b*) −30°.

TABLE II

Infrared spectrum of N,N-Dimethylacetamide as liquid film

Frequency (cm^{-1})	Assignment
2 960 m	$\gamma C—H$
1 660 s	$\gamma C—O$*
1 500 m	$\gamma C—N$
1 422 s	$\delta_a N—CH_3$
1 400 s	$\delta_a N—CH_3$
1 400 s	$\delta_a C—CH_3$
1 368 m	$\delta_s C—CH_3$
1 275 m	$\gamma CH_3—N$
1 200 m	$\delta_{rock} CH_3—N$
1 000 m	$\delta_{rock} CH_3—C$
960	$\gamma C—C—N—C$ skeletal
730	π

NOTE: γ = stretch, δ_a = asymmetric bend, δ_s = symmetric bend, π = bending out of plane.
*$\gamma C—N$ may also contribute to this absorption.

Infrared spectra of DMA complexes have in general been measured in the solid phase and assignments have been made for only C—O stretching modes (1, 5). In this work spectra have been measured both in the solid phase and in solution in methylene chloride. Table II shows the spectrum of DMA as a liquid film. Assignments were made by comparison with the spectra of other amides (19, 20) and by analogy with assignments for N-methylacetamide based on a normal coordinate analysis (21). The frequencies of the C—N and C—O stretching modes for the complexes are shown in Table III. Considerable differences exist between solution spectra and solid phase spectra.

DISCUSSION

The p.m.r. spectrum of an oxygen-bonded DMA complex might be expected to differ radically from that of a nitrogen-bonded compound. In the latter, stabilization of resonance form (1) would reduce the C—N bond order and change the hybridization of the nitrogen

Can. J. Chem. Downloaded from www.nrcresearchpress.com by 210.87.254.105 on 09/05/12
For personal use only.

TABLE III

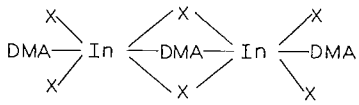
γC—O and γC—N for DMA and complexes

Compound	Frequency (cm^{-1}) in Nujol mull			Frequency (cm^{-1}) in solution		
	γC—O		γC—N	γC—O		γC—N
DMA	1 660		1 500	1 660		1 500
$In(ClO_4)_3.6DMA$	1 610		1 522	1 610	1 645 sh	1 500
$InCl_3.2.5DMA$	1 580	1 620 sh*	1 510	1 600	1 645 sh	1 510
$InBr_3.1.5DMA$	1 600	1 630 sh	1 512	1 600	1 640 sh	1 510
$InI_3.1.5DMA$	1 595	1 630 sh	1 515	1 610	1 640 sh	1 512
$Zn(ClO_4)_3.6DMA$	1 610		1 510	1 610	1 640 sh	1 510
$ZnCl_2.2DMA$	1 600	1 618 sh	1 518	1 600	1 618 sh	1 510
$ZnBr_2.2DMA$	1 600	1 622 sh	1 516	1 600	1 615 sh	1 512
$ZnI_2.2DMA$	1 590	1 610 sh	1 510	1 600	1 618 sh	1 510
$Cd(ClO_4)_2.6DMA$	1 610		1 510	1 610	1 650	1 512
$CdCl_2.DMA$	1 600		1 508		Insoluble	
$CdBr_2.DMA$	1 602		1 510	1 600	1 645 sh	1 508
$CdI_2.DMA$	1 600		1 508	1 604	1 645 sh	1 510
$SnCl_4.2DMA$	1 604		1 506	1 600 sh	1 640	1 500

*sh = shoulder.

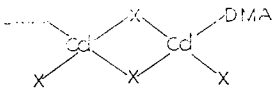
atom from sp^2 to sp^3. The N-methyl groups would then be equivalent, since free rotation about the C—N bond could occur and a single N-methyl resonance would replace the doublet observed for free DMA. The collapse of the N-methyl resonances into a single peak on protonation of N,N-dimethylformamide and N,N-dimethylacetamide has been explained in this way (23).

Analytical data suggest that the indium halide and cadmium halide adducts may contain bidentate DMA. For the indium complexes structures of type III have been envisaged in which both mono- and bi-dentate DMA are present.

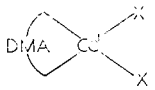


III

It should be noted, however, that many cadmium halide complexes are dimers involving halogen bridges and species such as IV may be more realistic than molecules involving bidentate DMA as in V.



IV



V

For the perchlorate complexes only monodentate DMA seems possible.

Infrared Spectra

Spectra of the solid complexes show that considerable lowering of the carbonyl frequency of DMA occurs on complexing. The frequency shift varies between 40 cm^{-1} and 80 cm^{-1} but no regular correlation between shift and cation or anion was detected. Small shifts to higher frequency were noted for the C—N stretching mode and absorptions at 730 cm^{-1} and 960 cm^{-1} in free DMA were greatly increased in intensity in the complexes. Apparently these modes which involve stretching and bending of the DMA skeleton become more infrared active on coordination.

Can. J. Chem. Downloaded from www.nrcresearchpress.com by 210.87.254.105 on 09/05/12
For personal use only.

In solution, all perchlorate complexes exhibit two C—O frequencies in the 1 600 cm^{-1} region. With halide complexes two bands were also observed; however, the $ZnX_2.2DMA$ adducts show two carbonyl absorptions in the solid phase. Bull *et al.* (1) have suggested that coupling of two C—O vibrations via the metal to which both are coordinated or the existence of nonequivalent ligands in the crystal lattice may account for the solid phase spectra. Fermi resonance is also a common cause of doubling of carbonyl absorptions (22).

Addition of excess ligand to solutions of the complexes caused an increase in intensity of the higher frequency carbonyl band relative to that at lower frequency. It is concluded that on dissolution partial dissociation of the metal complex occurs giving both bonded and free DMA in solution. An equilibrium of this type is illustrated for $In(ClO_4)_3.6DMA$.

$$In(ClO_4)_3.6DMA \rightleftarrows In(ClO_4)_3.(6 - x)DMA + xDMA$$

Further coordination of the dissociated species by solvent molecules may occur.

In summary, infrared data provide no evidence for nitrogen-bonded or bidentate DMA, since lowering of the C—O stretching frequency and raising of the C—N stretching frequency are consistent with an increased contribution of resonance form (II) to the ground state of the DMA molecule.

Proton Magnetic Resonance Spectra

The similarity in the spectra of all the complexes of In, Zn, Cd, and Sn suggests only oxygen-bonded DMA in acetone-d_6 solution at 36°. Neither the indium nor cadmium halide compounds mentioned above showed any evidence for bidentate DMA in solution.

Addition of excess DMA to solutions of the complexes produced only one set of resonance peaks, suggesting rapid exchange between bonded and unbonded DMA, the resonance positions in such a system being a weighted average of the resonances of the free and complexed DMA.

Traces of perchloric acid in the perchlorate complexes resulted in p.m.r. spectra having only one broad N-Methyl resonance. As previously stated, free rotation about the C—N bond and an sp^3-hybridized nitrogen atom are prerequisites for the equivalence of the N-methyl groups of DMA. Protonation of the nitrogen atom of the amide might be expected to produce such an effect. As pointed out by Berger *et al.* (24), a very small concentration of the nitrogen-protonated form is sufficient to bring about a collapse of the N-methyl resonances.

Complex formation results in low field shifts for all the protons in DMA. Deshielding can be attributed to a flow of electron density from the donor molecule to the acceptor and would be expected to fall off with increasing number of intervening bonds. Hence shifts for the C-methyl protons are larger than shifts for the N-methyl protons. Shifts are influenced both by cation and anion. For halide ions the order is $I^- > Br^- > Cl^-$ for each metal and for cations the larger the charge on the cation, the larger the downfield shift. Thus $Sn^{4+} > In^{3+} > Zn^{2+} \geqslant Cd^{2+}$. However, the lack of data concerning the structures of the coordinated ions in solution prevents any firm conclusions being drawn as to the relative acceptor properties of the metal halides and perchlorates. Further work is now in progress to determine the exact nature of the species in solution for each complex.

The low temperature resolution of both N-methyl and C-methyl resonances of the indium trihalide complexes is more difficult to explain. At similar temperatures the zinc, cadmium, and tin halide complexes show only signal broadening due to viscosity effects. $InI_3.1.5DMA$ and $InBr_3.1.5DMA$ at −30° show four N-methyl signals and two C-methyl resonances, the ratio of the signals at low field to those at high field being 1:2.

Can. J. Chem. Downloaded from www.nrcresearchpress.com by 210.87.254.105 on 09/05/12
For personal use only.

The frequency separation of the C-methyl resonances at this temperature was 9 c.p.s. for $InI_3.1.5DMA$ and 7 c.p.s. for $InBr_3.1.5DMA$. For $InCl_3.2.5DMA$ resolution was incomplete even at $-30°$. The lack of data concerning the species in solution prevents any firm conclusions being drawn as to the origin of these spectra but the existence of two types of coordinated DMA is not impossible. A more intensive study of low temperature spectra is now in progress.

ACKNOWLEDGMENT

The author wishes to thank Dr. Eric Bullock for many helpful discussions during this work.

REFERENCES

1. W. E. Bull, S. K. Madan, and J. E. Willis. Inorg. Chem. **2**, 303 (1963).
2. K. W. Bagnall, P. S. Robinson, and M. A. S. Stewart. J. Chem. Soc. 4061 (1961).
3. K. W. Bagnall, D. Brown, and A. M. Deane. J. Chem. Soc. 1611 (1961).
4. K. W. Bagnall, D. Brown, P. J. Jones, and P. S. Robinson. J. Chem. Soc. 2531 (1964).
5. T. Moeller and G. Vicentini. J. Inorg. Nucl. Chem. **27**, 1477 (1965).
6. R. S. Drago, P. W. Meek, M. P. Joesten, and L. Laroche. Inorg. Chem. **2**, 124 (1963).
7. T. C. Waddington (*Editor*). Non-aqueous solvent systems. Academic Press, New York. Chap. 5. p. 228.
8. M. Martinette, S. Mizushima, and J. V. Quagliano. Spectrochim. Acta, **15**, 77 (1959).
9. M. M. Fein, J. Green, J. Robinski, and M. S. Cohen. Inorg. Chem. **4**, 583 (1965).
10. A. J. Carty and D. G. Tuck. J. Chem. Soc. Suppl. **2**, 6012 (1964).
11. E. S. Gore, D. J. Blears, and S. S. Danyluk. Can. J. Chem. **43**, 2135 (1965).
12. H. R. Hertler and E. L. Muetterties. Inorg. Chem. **5**, 160 (1966).
13. A. J. Carty. Ph.D. Thesis, University of Nottingham, Nottingham, England. 1965.
14. W. D. Phillips. J. Chem. Phys. **23**, 1363 (1955).
15. R. R. Frazer and D. E. McGreer. Can. J. Chem. **39**, 505 (1961).
16. A. J. Carty and D. G. Tuck. J. Chem. Soc. In press.
17. F. A. Cotton and R. Francis. J. Am. Chem. Soc. **82**, 2986 (1960).
18. H. S. Gutowsky and C. H. Holm. J. Chem. Phys. **25**, 1228 (1956).
19. M. Davies, J. C. Evans, and R. Lumley-Jones. Trans. Faraday Soc. **51**, 761 (1955).
20. M. Davies and M. Hallam. Trans. Faraday Soc. **47**, 1170 (1951).
21. T. Miyazawa, T. Shimanouchi, and S. Mizushima. J. Chem. Phys. **24**, 408 (1956).
22. R. W. Jones, C. L. Angell, T. Ito, R. J. D. Smith. Can. J. Chem. **37**, 2007 (1959).
23. G. Fraenkel and C. Franconi. J. Am. Chem. Soc. **82**, 4478 (1960).
24. A. Berger, A. Loewenstein, and S. Meiboom. J. Am. Chem. Soc. **81**, 62 (1959).

Can. J. Chem. Downloaded from www.nrcresearchpress.com by 210.87.254.105 on 09/05/12
For personal use only.

Can. J. Chem. Downloaded from www.nrcresearchpress.com by 210.87.254.6 on 09/05/12
For personal use only.

CALCULATIONS OF KINETIC ISOTOPE EFFECTS FOR THE IODIDE EXCHANGE AND FOR THE SOLVOLYSIS OF METHYL IODIDE[1,2]

ALFRED V. WILLI[3]
Chemistry Department, Brookhaven National Laboratory, Upton, New York

Received February 11, 1966

ABSTRACT

Kinetic deuterium and carbon-13 isotope effects are calculated for the S_N2 exchange reaction of CH_3I with $*I^-$(131) and for the CH_3I solvolysis in water. The normal vibrational frequencies of CH_3I and of the transition state $I\cdots CH_3\cdots X$ (X = I or OH_2) are evaluated from force constants by solving the secular equation with an IBM 7094 computer. Values for force constants of the planar CH_3 moiety (with an sp^2 C atom) in the transition state are obtained by comparison with suitable stable molecules. For the iodide exchange reaction, there is not much dependence of the calculated D isotope effect on the particular choice of f_{CI} and f_{12} (interaction between CI stretches) if these force constants are within reasonable limits. The bending force constant $f_{HCI}(\neq)$ may then be adjusted to reproduce the experimental D isotope effect.

Based on the simple transition state model $CH_3^{\delta+}\cdots I^{\delta-}$, it is not possible to obtain agreement with the experimental D effect in the solvolysis reaction without assuming an extremely high value of f_{HCI}. If must be concluded that a water molecule is probably involved in the transition state. On the basis of the model $I\cdots CH_3\cdots OH_2$, the experimental D effect may be reproduced with a suitable choice of f_{HCI} and f_{HCO}. It is shown that, under favorable circumstances, experimental temperature dependence data may be applied for a distinction between different sets of f_{CH}, f_{HCH}, and f_{HCI} (or f_{HCO}) which reproduce the experimental isotope effect at one temperature.

INTRODUCTION AND GENERAL PROCEDURE

In recent years, refined methods have been developed for the theoretical calculation of kinetic isotope effects within the transition state theory framework (1–3). It has become possible to carry out complete calculations of vibrational frequencies of reactants and transition states by solving the secular equation with an electronic digital computer (2, 3). Some calculations have been done for particular mechanistic problems (4–6). In this work, these methods are applied to a theoretical study of some nucleophilic substitution reactions of methyl iodide in order to gain an understanding of the causes of the isotope effect and to investigate the conclusions, with respect to the transition state, which may be drawn from experimental isotope effect data. For these systems, results of some previous calculations have been reported which do not involve complete solutions of the secular equations of the 6, 7, or 8 atomic transition states (7, 8).

Experimental data are available for the kinetic isotope effects of the following four S_N reactions of methyl iodide: (*a*) $CH_3I + *I^-$, (*b*) $CH_3I + CN^-$, (*c*) $CH_3I + OH^-$, and (*d*) the solvolysis of CH_3I in water. For *b* and *c* the ^{13}C isotope effect has been measured (9), and, for *a* and *d* the D effect (rate of CH_3I divided by rate of CD_3I) is known (8, 10). Experimental data on ^{14}C isotope effects in four S_N reactions of CH_3I (11) are also available. In this paper, calculations for reactions *a* and *d* are discussed in detail. Results of calculations for reactions *b* and *c* will be reported elsewhere.

The harmonic vibrational frequencies (and isotope effects thereon) of the reactants and of the corresponding transition state were calculated with an IBM 7094 computer from

[1]*A more detailed account has been placed in the Depository of Unpublished Data. Photocopies may be obtained upon request to: The Depository of Unpublished Data, National Science Library, National Research Council, Ottawa, Canada.*

[2]*Research performed under the auspices of the U.S. Atomic Energy Commission. Presented in part at the 148th National Meeting of the American Chemical Society, Chicago, Illinois, September 1964.*

[3]*Visiting chemist, 1964. Present address: Columbia University, College of Pharmacy, 115 West 68th Street, New York, New York 10023.*

reasonable values of the force constants, with the use of programs which are modifications (2) of those of J. H. Schachtschneider (12). Effects of anharmonicity were neglected in this work.

The most important causes of the isotope effect are force constant changes which take place when the transition state is formed from the reactants (2). One possible procedure in these calculations would be as follows: usual values are introduced for the force constants of CH stretching, CI stretching, HCH bending, and HCI bending in the reactant.

With the aid of sample calculations, we may find out how some of these force constants must be changed in the transition state in order to obtain a fit with experimental isotope effect data. However, there is no set of these 4 force constants which leads to a good agreement between calculated and observed values of all six vibrational frequencies of methyl iodide. If we intend to keep the model for methyl iodide as close to reality as possible we must include interaction force constants ("off-diagonal" elements of the F matrix) in the force field. In this study, vibrational frequencies of $^{12}CH_3I$, $^{13}CH_3I$, and $^{12}CD_3I$ are calculated with a set of 13 force constants (see Table I) (including 9 interaction force constants) reported by Fenlon, Cleveland, and Meister (13) which reproduces the experimental values for $^{12}CH_3I$ within 1 wave number. The values of 4 of the interaction force constants which do not involve reacting bonds are also applied to the force field of the transition state (Table I). This must be done to compensate for an artificial isotope effect caused by the presence of these interaction force constants in the force field of the reactant. A fair comparison of force constants of the reactant and of the transition state would not be possible otherwise.

TABLE I

Bond distances, bond angles, and force constants

	CH_3I	$[I\cdots CH_3\cdots X]^*$
r_{CH} $(=d)$	1.09 Å	1.08 Å
r_{CI} $(=D)$	2.14 Å	2.35 Å
r_{CX}	—	Depending on X
$\sphericalangle$HCH $(=\alpha)$	109° 28′	120°
$\sphericalangle$HCI $(=\beta)$	109° 28′	90°
$\sphericalangle$HCX	—	90°
f_{CH} $(=f_d)$	5.0541 mdyn/Å	5.3 or 5.05 mdyn/Å
f_{CI} $(=f_D$ or $f_2)$	2.2467 mdyn/Å	*
f_{CX} $(=f_1)$	—	*
f_{12}	—	*
f_{HCH} $(=f_\alpha)$	0.52534 mdynÅ	0.36 (or 0.525) mdynÅ
f_{HCI} $(=f_\beta)$	0.55061 mdynÅ	*
f_{HCX}	—	*
g	—	0.144 mdynÅ
f_{dd}	−0.0254 mdyn/Å	−0.0254 mdyn/Å
f_{dD}	0.06351 mdyn/Å	—
$f_{d\alpha}$	0.22436 mdyn	0.2244 mdyn
$f_{d\alpha'}$	−0.09575 mdyn	−0.0958 mdyn
$f_{d\beta}$	0.40090 mdyn	—
$f_{d\beta'}$	0.18290 mdyn	—
$f_{\alpha\alpha}$	−0.01720 mdynÅ	−0.0172 mdynÅ
$f_{\alpha\beta}$	0.01526 mdynÅ	—
$f_{D\beta}$	0.12033 mdyn	—

NOTE: Designation of the force constants of CH_3I is the same as in ref. 13.

All data referring to geometry and force constants of methyl iodide and of the transition state are collected in Table I. For the general model of the transition state, $I\cdots CH_3\cdots X$, it is assumed that the CH_3 group is planar with equilibrium CH distances of 1.08 Å and equilibrium HCH angles of 120°. The positions of I and of the first atom of X are on the threefold symmetry axis with bond distances 10% greater (20% greater in the case of

Can. J. Chem. Downloaded from www.nrcresearchpress.com by 210.87.254.6 on 09/05/12
For personal use only.

OH_2) than those of stable CI or CX bonds. Now we must assign values to the force constants of the following motions: CI and CX bond stretching, the interaction (f_{12}) between these two motions, CH stretching, HCH, HCI, and HCX valence angle bending (and a few additional ones if X consists of more than one atom). In these calculations, 4 interaction force constants and a force constant for the CH_3 out-of-plane bending motion (g) are also considered (6). Thus, the situation appears unfavorable at first glance. Values of 12 force constants may be adjusted to obtain agreement with one single experimental value either for k_H/k_D or for k_{12}/k_{13} (or with two experimental data if both isotope effects have been measured). However, there is the possibility of obtaining force constants for the internal motions of the CH_3 moiety in the transition state by comparison with suitable stable molecules. We assume that the valence electrons of the central carbon atom are in an sp^2 configuration and use a CH stretching force constant and an HCH bending force constant corresponding to such bonding in stable molecules (14, 15).[4] (It may be expected that f_{CH} increases by 0.25–0.3 mdyn/Å when the central carbon atom changes from an sp^3 to an sp^2 configuration.)

There remain 5 force constants in the transition state whose values are not yet fixed (designated with asterisks in Table I). Three of these, f_{CI}, f_{CX}, and f_{12}, are directly related to stretching motions of the bonds to be broken or formed. The secular equation of the transition state will have $3n - 7$ positive solutions and one negative or zero solution. The negative (or zero) eigenvalue leads to an imaginary (or zero) frequency $\nu_L^{\ddagger}$ which means that the motion of crossing the potential barrier is aperiodic. If f_{CI}, f_{CX}, and f_{12} are assumed to be equal, $\nu_L^{\ddagger}$ will be zero, and the isotope effect on the frequency of the other stretching mode in the three particle system $I\cdots(CH_3)\cdots X$ will be negligible. (In these calculations the influence of all vibrations is fully considered, however.) The bending force constants f_{HCI} and f_{HCX} may now be adjusted to obtain agreement between the calculated and the experimental isotope effect. It should be mentioned that f_{HCI} and f_{HCX} cannot be evaluated separately from calculations for a single model. There are very many different sets of f_{HCI} and f_{HCX} (the sum of both values being nearly constant) which will reproduce the experimental data.

If f_{CI}, f_{CX}, and f_{12} are chosen in such a way that $f_{CI}f_{CX} - f_{12}^2 < 0$, then $\nu_L^{\ddagger}$ will have an imaginary value. Under these circumstances, the calculated isotope effect differs slightly from that for the case where $\nu_L^{\ddagger} = 0$, and the bending force constants must be adjusted to somewhat different values. Quite fortunately, these differences are small if $\nu_L^{\ddagger}$ remains in a reasonable order of magnitude and if the ratio f_{CI}:f_{CX} does not change much.

THE IODIDE EXCHANGE REACTION

Deuterium Isotope Effect at 298.2°

The most simple situation is the exchange reaction of methyl iodide with labeled iodide ion. In its transition state, as far as it is correct to assume that it is symmetric, f_{CX} equals f_{CI} and f_{HCX} equals f_{HCI}. There are now three free parameters only, viz. f_{CI}, f_{12}, and f_{HCI}. Results of some sample calculations are shown in Table II. Numbers 3–8 have been done to study the influence of f_{CI} and f_{12} on the isotope effect. In the calculations marked with an asterisk the bending force constant f_{HCI} is adjusted to fit the experimental isotope effect, $k_H/k_D = 1.06$.

Since there is a slight dependence of the isotope effect on the magnitude of $f_{CI}^2 - f_{12}^2$ an attempt is made to set the limits for the possible values of those two force constants: Suppose that, at the transition state, the potential energy decreases as the second power

[4]*Detailed information on the out-of-plane bending force constant g may be found in ref. 6.*

Can. J. Chem. Downloaded from www.nrcresearchpress.com by 210.87.254.6 on 09/05/12
For personal use only.

of ρ, the arithmetic mean of the increase of length (Δr_1) of one CI bond and of the decrease of length ($-\Delta r_2$) of the other CI bond.

[1] $$\rho = \tfrac{1}{2}(\Delta r_1 - \Delta r_2)$$

The potential energy, which is also taken to contain contributions of restoring forces *within* each CI bond, is then given by the equation:

[2] $$\begin{aligned} 2V &= f_{CI}'(\Delta r_1^2 + \Delta r_2^2) - f_{\mp}\rho^2 + \text{other terms (not involving } \Delta r_1 \text{ and } \Delta r_2) \\ &= f_{CI}'(\Delta r_1^2 + \Delta r_2^2) - \tfrac{1}{4}f_{\mp}(\Delta r_1 - \Delta r_2)^2 + \text{other terms.} \end{aligned}$$

This is equivalent to the expression which defines $f_{CI}(= f_{11} = f_{22})$ and f_{12} as elements of the F matrix:

[3] $$2V = f_{CI}(\Delta r_1^2 + \Delta r_2^2) + 2f_{12}\Delta r_1 \Delta r_2 + \text{other terms}$$

[4] $$f_{CI} = f_{CI}' - \tfrac{1}{4}f_{\mp}, \quad f_{12} = \tfrac{1}{4}f_{\mp}.$$

To arrive at the magnitude of $f_{\mp}$ one may proceed as follows: Let us assume that there is little energy change when the iodide ion approaches to within 2.56 Å of the C atom of the CH_3I molecule while the other CI distance is unchanged (2.14 Å). Now eq. [2] is used to describe the energy surface for the formation of the transition state with equal CI distances of 2.35 Å. With an assumed $f_{CI}' = 1.0$ mdyn/Å (in reactant $f_{CI} = 2.25$ mdyn/Å), one obtains $f_{\mp} = 8$ mdyn/Å (as an upper limit) for a barrier height of 20 kcal/mole.

If $f_{\mp}$ is increased from 2.0 to 8.0 mdyn/Å (see Nos. 3, 21, 15, 25 in Table II) while f_{HCI} is held constant at 0.250 mdynÅ, the secondary deuterium isotope effect k_H/k_D then decreases from 1.12 to 1.014 and the primary carbon isotope effect k_{12}/k_{13} increases from 1.047 to 1.061. For each of the four choices of $f_{\mp}$, the HCI bending force constant may now be adjusted to reproduce the experimental deuterium isotope effect (see Nos. 24, 21, 16, 22). The appropriate values of f_{HCI} are between 0.235 and 0.270 mdynÅ which is in the order of one half of the corresponding value for the stable molecule CH_3I, $f_{HCI} = 0.55$ mdynÅ. If the low value of $f_{CH} = 5.05$ mdyn/Å is assumed for the CH stretching force constant in the transition state, the HCI bending force constant must then be adjusted to a value 0.050–0.055 units higher than in the corresponding sample calculations with $f_{CH} = 5.3$ mdyn/Å (see Nos. 23, 18, and 20).

Fit values of f_{HCI} are also evaluated for the two sets of force constants with $f_{CH} = 5.3$ mdyn/Å, $f_{HCH} = 0.525$ mdynÅ, and with $f_{CH} = 5.05$ mdyn/Å, $f_{HCH} = 0.525$ mdynÅ (Nos. 29 and 30). The value assumed for f_{HCH} in those calculations equals that of the corresponding bending force constant in the reactant, and it may be considered as the high limit for the transition state.

Temperature Dependence of the D Isotope Effect

Table II also contains values for the different factors which contribute to the isotope effect, viz. MMI, the ratio of the isotopic ratios of the factor depending on masses and moments of inertia (isotopic ratio for the transition state divided by the isotopic ratio for the reactant); EXC, the ratio of the isotopic ratios of the excitation factor ($\prod(1 - e^{-u_i})^{-1}$); and ZPE, the zero point energy factor ($e^{-\Delta\Delta\Sigma u_i/2} \equiv e^{-\Delta\Delta E_0'/RT}$). In the analysis of experimental data, on the other hand, the isotope effect is usually expressed with the aid of an Arrhenius type equation:

[5] $$\begin{aligned} k_H/k_D &= A \times \exp(-\Delta\Delta E_0'/RT) \\ &= A \times \text{AZPE.} \end{aligned}$$

Can. J. Chem. Downloaded from www.nrcresearchpress.com by 210.87.254.6 on 09/05/12
For personal use only.

Can. J. Chem. Downloaded from www.nrcresearchpress.com by 210.87.254.6 on 09/05/12
For personal use only.

TABLE II

Calculated isotope effects for the reaction $CH_3I + {}^*I^-$ at 298.2° (values of g and of 4 interaction force constants are as in Table I)

	Transition state force constants									Factors for k_H/k_D				
No.	f_{CI}'	$f_{\neq}$	f_{CI}	f_{12}	f_{HCI}	$\nu_{L,H}^{\neq}$	$\nu_{L,H}^{\neq}/\nu_{L,D}^{\neq}$	k_H/k_D	k_{12}/k_{13}	MMI	EXC	ZPE	A	AZPE
$f_{CH}=5.3$ mdyn/Å, $f_{HCH}=0.36$ mdynÅ														
1			0.2	1.5	0.205	569.1i	1.0541	1.194		1.2657	0.8531	1.1054		
3	(1.0)	(2.0)	0.2	0.2	0.250	0	1.0899	1.121	1.0474	1.2657	0.8777	1.0090	1.050	1.068
4			0.2	0.3	0.250	154.9i	1.0867	1.114		1.2657	0.8776	1.0030		
5			0.2	0.5	0.250	269.2i	1.0806	1.101		1.2657	0.8773	0.9919		
6			0.2	1.0	0.250	442.8i	1.0674	1.075		1.2657	0.8766	0.9687		
* 7			0.2	1.5	0.250	568.2i	1.0567	1.054		1.2657	0.8761	0.9508		
8			1.0	1.5	0.250	348.6i	1.0575	1.090		1.2657	0.8770	0.9819		
*21	1.0	4.0	0	1.0	0.250	496.4i	1.0629	1.066	1.0535	1.2657	0.8764	0.9609	1.042	1.023
15	1.0	6.0	−0.5	1.5	0.250	710.3i	1.0450	1.033	1.0578	1.2657	0.8754	0.9325	1.036	0.997
25	1.0	8.0	−1.0	2.0	0.250	878.2i	1.0332	1.014	1.0609	1.2657	0.8746	0.9158	1.031	0.984
*24	(1.0)	(2.0)	0.2	0.2	0.270	0	1.0889	1.062	1.0467	1.2657	0.8860	0.9469	1.072	0.991
*16	1.0	6.0	−0.5	1.5	0.240	710.7i	1.0443	1.062	1.0582	1.2657	0.8707	0.9633	1.024	1.037
*22	1.0	8.0	−1.0	2.0	0.235	878.9i	1.0322	1.056	1.0616	1.2657	0.8674	0.9622	1.014	1.042
$f_{CH}=5.05$ mdyn/Å, $f_{HCH}=0.36$ mdynÅ														
*23	1.0	4.0	0	1.0	0.305	495.7i	1.0652	1.066	1.0530	1.2657	0.8977	0.9380	1.100	0.969
*18	1.0	6.0	−0.5	1.5	0.295	709.0i	1.0476	1.060	1.0578	1.2657	0.8934	0.9370	1.084	0.978
*20	1.0	8.0	−1.0	2.0	0.285	876.6i	1.0353	1.066	1.0614	1.2657	0.8890	0.9474	1.070	0.996
$f_{CH}=5.05$ mdyn/Å, $f_{HCH}=0.525$ mdynÅ														
26	1.0	8.0	−1.0	2.0	0.285	876.6i	1.0353	0.765		1.2657	0.8972	0.6736		
*30	1.0	8.0	−1.0	2.0	0.170	882.4i	1.0279	1.055		1.2657	0.8357	0.9977	0.971	1.087
$f_{CH}=5.3$ mdyn/Å, $f_{HCH}=0.525$ mdynÅ														
28	1.0	8.0	−1.0	2.0	0.235	878.9i	1.0322	0.758		1.2657	0.8754	0.6841		
*29	1.0	8.0	−1.0	2.0	0.120	885.8i	1.0242	1.066		1.2657	0.7912	1.0646	0.893	1.194

NOTE: Stretching force constants are in mdyn/Å and bending force constants are in mdynÅ.
*An asterisk indicates that the calculated D isotope effect agrees with the experimental value.

Can. J. Chem. Downloaded from www.nrcresearchpress.com by 210.87.254.6 on 09/05/12
For personal use only.

As suggested by Wolfsberg and Stern (2), eq. [5] is also applied here for the representation of the temperature dependence of the calculated isotope effect within a limited temperature range. For some examples (see Table II), values for the pre-exponential factor A and for the apparent zero point energy factor AZPE for 25 °C are computed from 6 calculated data for k_H/k_D in the temperature range between 293 and 333 °K by the least squares method.

The A value may now be used to draw some conclusions on the relative importance of changes of CH stretching and bending force constants (2). Therefore, it would be highly desirable to have available experimental data on the temperature dependence of the deuterium isotope effect. Though it may not be possible to draw conclusions on the best values for two force constants, f_{CH} and f_{HCH}, the temperature dependence would supply an additional piece of information. If the experimental A value were larger than 1.07 we would be able to conclude that both f_{CH} and f_{HCH} are at their low values. If A were below 0.95 we would conclude that f_{CH} and f_{HCH} are close to their high limits (see Table II). All these deductions, naturally, are valid within the limitations of the assumptions involved in these calculations (i.e., neglect of anharmonicity effects, tunneling, and of solute–solvent interactions).

Carbon-13 Isotope Effect

As can be seen from Table II, the ^{13}C isotope effect does not depend much on f_{CH} or on the bending force constants. But k_{12}/k_{13} significantly increases with increasing $f_{\neq}$. Consequently, the experimental value of the carbon isotope effect will supply information on the curvature of the potential barrier in the transition state. It is fully realized, however, that it would be difficult to obtain precise experimental data of k_{12}/k_{13} for this reaction, even if isotopically pure samples of $^{13}CH_3I$ were available.

Dependence of the Isotope Effects on the Stretching Force Constants f_{CI} and f_{12}[5]

The increase of k_{12}/k_{13} with increasing $f_{\neq}$ may easily be understood on the basis of the simple approximate equation given by Wolfsberg and Stern (2): The greater the difference $f_{CI}^{\circ} - (f_{11} + f_{22} - 2f_{12}) = f_{CI}^{\circ} - 2(f_{CI} - f_{12})$ (f_{CI}° refers to CH_3I) the higher the isotope effect. There is no force constant change at the positions of isotopic substitutions if we consider the dependence of k_H/k_D on $f_{\neq}$. On the basis of the approximate equation, the decrease of k_H/k_D can be explained partially by a decrease of the $\nu_L^{\neq}$ ratio. (For more details see the longer manuscript in the Depository.)

The changes of coupling conditions of the motions of the carbon and the hydrogen atoms can easily be observed by looking at the $\nu_L^{\neq}$ ratios. With increasing $f_{\neq}$, the $\nu_L^{\neq}$ ratio of the carbon isotope effect increases from 1.031 ($\approx \sqrt{(16/15)}$) to 1.035 while the $\nu_L^{\neq}$ ratio of the deuterium isotope effect decreases from 1.09 ($\approx \sqrt{(18/15)}$) to 1.0332. (See Nos. 3–7, 15, 25 in Table II). If in the motion of crossing the potential energy barrier the hydrogen atoms would not move at all with the central carbon atom, the $\nu_L^{\neq}$ ratios would be at the following limiting values: $\sqrt{(13/12)} \approx 1.041$ for the carbon isotope effect and 1.000 for the deuterium isotope effect.

THE SOLVOLYSIS REACTION

Isotope Effect at 343.2°

An inverse deuterium isotope effect, $k_H/k_D = 0.87$ (8), has been found in the solvolysis of methyl iodide in water at 70 °C. For this reaction, three sample calculations have been reported in a previous paper (6). It has become possible now to do much more work with the aid of the IBM 7094 computer. In the previous calculation for the model $CH_3^{\delta+} \cdots I^{\delta-}$,

[5]*The author wishes to express his thanks to Dr. Max Wolfsberg for having drawn his attention to the theoretical relations discussed in this paragraph.*

Can. J. Chem. Downloaded from www.nrcresearchpress.com by 210.87.254.6 on 09/05/12
For personal use only.

the HCI bending force constant was set equal to zero. Thus, the conclusions drawn in the previous paper are still to be supported by some additional calculations with $f_{HCI} > 0$.

In the ion pair model for the transition state, with $r_{CI} = 2.50$ Å, the $CH_3^{\delta+}$ group is also considered to be flat. Values of the force constants are the same as in Table I. The following conclusions may be drawn from the sample calculations of Table III. If among the three transition state force constants f_{CH}, f_{HCH}, and $f_{HCI} + g$, two are kept at their reactant values the third one must always be set equal to a value higher than that of the reactant (the experimental isotope effect could not be reproduced otherwise). Such a transition state must be considered as highly improbable. Presumably, the CI bond would be extended to a higher degree in the transition state of the unimolecular cleavage of CH_3I than in the transition state of the bimolecular reaction of CH_3I with $^*I^-$. In these calculations with the unimolecular model, however, f_{HCI} must always be adjusted to a value considerably larger than that of the transition state $I\cdots CH_3\cdots I$. Consequently, the ion pair model for the transition state of the solvolysis reaction cannot correspond to reality.

The calculations of Table IV are done on the basis of the model $I\cdots CH_3\cdots OH_2$ ($r_{CI} = 2.50$ Å, $r_{CO} = 1.80$ Å, planar CH_3) which had been suggested previously by Llewellyn, Robertson, and Scott (8). (This model does not necessarily represent a nucleophilic attack of H_2O with formation of a covalent bond; the water molecule may merely enter the solvation shell of the carbonium ion being formed.) In contrast to the calculations of the previous paper (6), the force field of the transition state now contains, in addition, the 4 interaction force constants of Table I. Furthermore, the H_2O moiety is formulated as a three-particle group in these calculations, with $r_{OH} = 0.958$ Å, $\sphericalangle$ HOH = 105°, $f_{OH} = 7.66$ mdyn/Å, $f_{Int} = -0.097$ mdyn/Å, $f_{HOH} = 0.703$ mdynÅ (as in water), and with $\sphericalangle$ COH = 105°, $f_{COH} = 0.01$ mdynÅ, $f_{HCOH} = 0.02$ mdynÅ (torsional force constant; 2 torsional coordinates).

There are 5 force constants in the transition state whose values are still undetermined: f_{CI}, f_{CO}, f_{12} (interaction between the CI and CO stretches), f_{HCI}, and f_{HCO}. The two bending force constants f_{HCI} and f_{HCO} cannot be evaluated separately with the aid of the H or C isotope effect. Therefore, f_{HCI} is set equal to 0.205 mdynÅ (a value about 20% smaller than the fit value for the transition state $I\cdots CH_3\cdots I$) which is identical with the value used in the previous paper. Sample calculations are carried out with four different choices of the stretching force constants f_{CI}, f_{CO}, and f_{12}, designated with I, II, III, and IV, as shown in Table IV. I and II correspond to $\nu_L^{\ddagger} = 0$, III and IV lead to an imaginary $\nu_L^{\ddagger}$. In I and II, $f_{CI}f_{CO} - f_{12}^2 = 0$, whereas in III and IV, $f_{CI}f_{CO} - f_{12}^2 = -2.0$ (mdyn/Å)^2. In I and III, $f_{CI} = f_{CO}$; in II and IV, however, $f_{CI} < f_{CO}$ ("unsymmetric" stretching force field). The latter case is considered to be more probable, since in the transition state a dipole–dipole interaction between H_2O and CH_3I goes over to a π bond (positive f_{CO}) while the CI bond is broken (zero or negative f_{CI}).

It can be seen from Table IV that there are no significant differences in the calculated deuterium isotope effect if only f_{HCO} is held constant at 0.400 mdynÅ (Nos. 19, 21, 27, 29). In the calculations for Nos. 25, 26, 31, and 33, f_{HCO} is adjusted to fit the experimental D isotope effect for each of the four sets, I–IV. Since a "symmetric" stretching force field is considered unreal, we may conclude that (with f_{HCI} at 0.205 mdynÅ) f_{HCO} must lie between 0.445 and 0.460 mdynÅ for the transition state under consideration. (It may even be lower if $f_{CI}f_{CO} - f_{12}^2$ were below -2.0(mdyn/Å)^2.) Such a value for the HCO bending force constant of the transition state $I\cdots CH_3\cdots OH_2$ appears to be reasonable. Calculations either with $f_{CH} = 5.05$ mdyn/Å or with $f_{HCH} = 0.525$ mdynÅ would lead to different f_{HCO} values, naturally.

Can. J. Chem. Downloaded from www.nrcresearchpress.com by 210.87.254.6 on 09/05/12
For personal use only.

TABLE III

Calculated isotope effects for the CH_3I solvolysis at 343.2°. Model $CH_3^{\delta+}\cdots I^{\delta-}$ (values of g and of interaction force constants are as in Table I)

	Transition state force constants							
No.	f_{CI}	f_{CH}	f_{HCH}	f_{HCI}	$\nu_{L,H}^{\ddagger}$	$\nu_{L,H}^{\ddagger}/\nu_{L,D}^{\ddagger}$	k_H/k_D	k_{12}/k_{13}
51	0	5.1	0.36	0	0	1.0844	2.301	
52	0	5.3	0.36	0	0	1.0844	2.083	1.0515
53	0	5.3	0.36	0.270	0	1.0844	1.451	1.0457
54	0	5.3	0.36	0.406	0	1.0844	1.232	
*86	0	5.3	0.36	0.730	0	1.0844	0.868	1.0393
61	−3.0	5.3	0.36	0.240	632.7i	1.0398	1.413	
62	−3.0	5.3	0.36	0.406	630.0i	1.0457	1.160	
*83	−3.0	5.3	0.36	0.670	627.1i	1.0526	0.873	1.0470
59	−6.0	5.3	0.36	0.240	909.7i	1.0216	1.381	
60	−6.0	5.3	0.36	0.406	904.5i	1.0271	1.130	
*82	−6.0	5.3	0.36	0.640	899.2i	1.0336	0.874	1.0518
87	−6.0	5.3	0.525	0.240	909.7i	1.0216	1.041	
88	−6.0	5.3	0.525	0.406	904.5i	1.0271	0.852	
*91	−6.0	5.3	0.525	0.390	905.0i	1.0266	0.868	

TABLE IV

Calculated isotope effects for the CH_3I solvolysis at 343.2°. Model $I\cdots CH_3\cdots OH_2$ (f_{CH} = 5.3 mdyn/Å, f_{HCI} = 0.205 mdynÅ. Values of g and 4 interaction force constants are as in Table I)

		Transition state force constants								Factors of k_H/k_D				
No.	Stretching force field	f_{CI}	f_{CO}	f_{12}	f_{HCH}	f_{HCO}	$\nu_{L,H}^{\ddagger}$	$\nu_{L,H}^{\ddagger}/\nu_{L,D}^{\ddagger}$	k_H/k_D	k_{12}/k_{13}	MMI	EXC	ZPE	A	AZPE
19	I	0.5	0.5	0.5	0.36	0.400	0	1.0857	0.974		1.325	0.872	0.843		
21	II	0	0.5	0	0.36	0.400	0	1.0350	0.927		1.325	0.849	0.824		
27	III	0.5	0.5	1.5	0.36	0.400	530.7i	1.0552	0.928		1.325	0.868	0.807		
29	IV	−2.0	0.5	1.0	0.36	0.400	675.9i	1.0481	0.913		1.325	0.869	0.793		
*25	I	0.5	0.5	0.5	0.36	0.510	0	1.0857	0.869	1.0379	1.325	0.887	0.739	1.152	0.755
*26	II	0	0.5	0	0.36	0.460	0	1.0350	0.871	1.0174	1.325	0.858	0.766	1.082	0.805
*31	III	0.5	0.5	1.5	0.36	0.460	530.4i	1.0563	0.872	1.0413	1.325	0.877	0.751	1.119	0.779
*33	IV	−2.0	0.5	1.0	0.36	0.445	675.4i	1.0492	0.872	1.0467	1.325	0.876	0.751	1.115	0.782
*41	IV	−2.0	0.5	1.0	0.525	0.190	678.8i	1.0421	0.868		1.325	0.834	0.786	1.023	0.848
f_{CH} = 5.05 mdyn/Å															
*42	IV	−2.0	0.5	1.0	0.36	0.575	674.1i	1.0521	0.868		1.325	0.892	0.734	1.167	0.744

ACKNOWLEDGMENT

The author wishes to express his sincere thanks to Dr. Max Wolfsberg, Brookhaven National Laboratory, for many valuable discussions and for his interest in this work, as well as making his computer programs available.

REFERENCES

1. J. BIGELEISEN and M. WOLFSBERG. Advan. Chem. Phys. **1**, 15 (1958).
2. M. WOLFSBERG and M. J. STERN. Pure Appl. Chem. **8**, 225, 325 (1964). M. J. STERN and M. WOLFSBERG. J. Chem. Phys. **39**, 2776 (1963).
3. H. S. JOHNSTON. Science, **128**, 1145 (1958). T. E. SHARP and H. S. JOHNSTON. J. Chem. Phys. **37**, 1541 (1962).
4. M. J. GOLDSTEIN and G. L. THAYER. J. Am. Chem. Soc. **87**, 1933 (1965).
5. A. V. WILLI. Z. Naturforsch. **16a**, 838 (1961); Helv. Chim. Acta, **47**, 647, 655, 837 (1964).
6. A. V. WILLI. Ber. Bunsenges Physik. Chem. **68**, 266 (1964).
7. S. I. MILLER. J. Phys. Chem. **66**, 978 (1962).
8. J. A. LLEWELLYN, R. E. ROBERTSON, and J. M. W. SCOTT. Can. J. Chem. **38**, 222 (1960).
9. K. R. LYNN and P. E. YANKWICH. J. Am. Chem. Soc. **83**, 53, 790, 3200 (1961).
10. A. A. ZAVITSAS and S. SELTZER. Brookhaven Natl. Lab. Annual Report. July 1, 1963. p. 56 (BNL 806 (As-17)).
11. M. L. BENDER and D. F. HOEG. J. Am. Chem. Soc. **79**, 5649 (1957).
12. J. H. SCHACHTSCHNEIDER and R. G. SNYDER. Spectrochim. Acta, **19**, 117 (1963).
13. P. F. FENLON, F. F. CLEVELAND, and A. G. MEISTER. J. Chem. Phys. **19**, 1561 (1951).
14. G. HERZBERG. Infrared and Raman spectra of polyatomic molecules. Van Nostrand Publishing Co., New York. 1945.
15. J. GOUBEAU. Angew. Chem. **73**, 305 (1961).

Can. J. Chem. Downloaded from www.nrcresearchpress.com by 210.87.254.6 on 09/05/12
For personal use only.

Can. J. Chem. Downloaded from www.nrcresearchpress.com by 210.87.254.40 on 09/05/12
For personal use only.

LINEAR FREE ENERGY RELATIONSHIPS CONCERNING EQUILIBRIA IN MODERATELY CONCENTRATED MINERAL ACIDS

A SIMPLE METHOD FOR ESTIMATING pK's OF WEAK BASES[1]

J. F. BUNNETT AND FREDRIC P. OLSEN
Department of Chemistry, Brown University, Providence, Rhode Island

Received March 30, 1966

ABSTRACT

Linear relationships exist between the logarithms of equilibrium quotients, $[SH^+]/[S][H^+]$, of diverse bases as they vary with acid concentration in moderately concentrated mineral acids. For purposes of formulating these linear free energy relationships in standard form, the equilibrium quotient for protonation of a hypothetical aromatic primary amine of pK_a zero has been chosen as horizontal coordinate; this is given by $(-H_0 - \log [H^+])$. Log $([SH^+]/[S]) + H_0$ is plotted against $(H_0 + \log [H^+])$. The slope, ϕ, of the linear plot is a parameter which characterizes the response of the equilibrium quotient to changing acid concentration. The intercept represents the thermodynamic pK_a of the base. This constitutes a general method for estimating the pK_a of any base which undergoes protonation in moderately concentrated mineral acid, with reference to the single acidity function, H_0. For bases of diverse type, pK's estimated by this method are in good agreement with those estimated by the acidity function method. Use of the new correlation procedure as a check on the validity of several acidity functions and its application to equilibria not involving proton gain or loss are also discussed.

Reactions which occur in moderately concentrated sulfuric, hydrochloric, or perchloric acid solution usually manifest changes in rate or state of equilibrium, on change of acid concentration, which are much greater than can be attributed merely to the change in hydrogen ion concentration. An appreciable change in mineral acid concentration constitutes an appreciable change in the medium, and these reaction rates and equilibria are subject to medium effects of considerable magnitude.

Most quantitative treatments of these effects have employed the acidity function approach. This approach, originally due to Hammett (1), has been tested, refined, and extended in recent years by several workers (2–8). The subject has been reviewed (9–12). These studies have considerably widened understanding, but the area of applicability of each acidity function, as currently applied, is rather small.

Medium effects of other kinds have been treated advantageously by means of linear free energy relationships (l.f.e.r.) (13–15), but phenomena in moderately concentrated mineral acids have not been approached within this frame of reference. In this paper, it is shown that equilibria in such systems can be dealt with profitably by the l.f.e.r. approach. The accompanying paper (16) similarly treats kinetic phenomena.

COMPOSITION OF LINEAR FREE ENERGY RELATIONSHIPS

The equilibrium protonation of a substrate (S) may be represented by

$$S + H^+ \rightleftarrows SH^+ \quad . \qquad [1]$$

Ordinarily, the concentration of mineral acid is known and the *ionization ratio*, $[SH^+]/[S]$, often symbolized I, can be measured, usually by spectrophotometry. The *equilibrium quotient*, herein symbolized as Q, is $[SH^+]/[S][H^+]$. This is the reciprocal of the concentration equilibrium constant for acid dissociation of SH^+.

[1]*Presented in part at the 150th meeting of the American Chemical Society, Atlantic City, N.J., Sept. 14, 1965. Preliminary communication: J. F. Bunnett and F. P. Olsen, Chem. Comm. 601 (1965).*

With respect to rate measurements, one normally measures the pseudo-first-order rate coefficient, k_ψ. For reactions involving acquisition of a proton in forming transition state from initial state, it is also appropriate to reckon the second-order rate coefficient, $k_\psi/[H^+]$, which we symbolize as k_2.

We have found that, in general, linear relationships exist between the logarithms of equilibrium quotients and (or) second-order rate coefficients for diverse reactions in

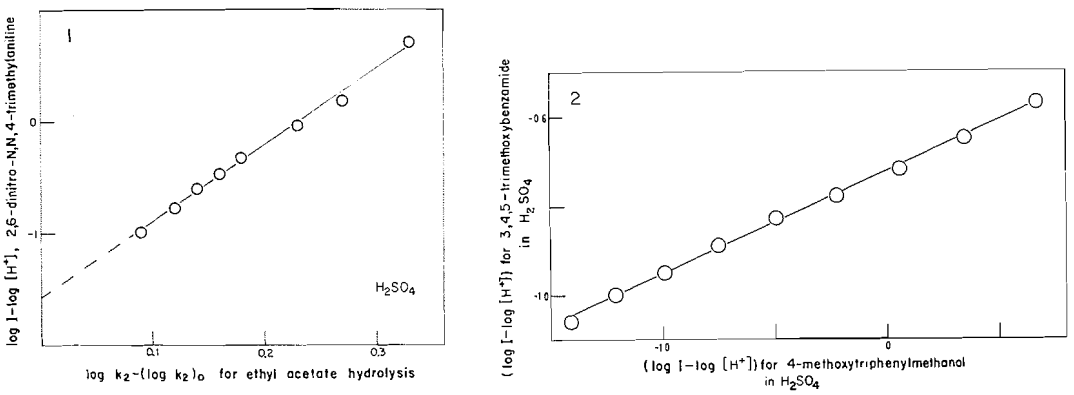


FIG. 1. Plot of log ($[SH^+]/[S][H^+]$) for equilibrium protonation of 2,6-dinitro-N,N,4-trimethylaniline against log k_2 (less log k_2 at infinite dilution) for ethyl acetate hydrolysis, both in H_2SO_4 solutions.

FIG. 2. Plot of (log $[SH^+]/[S][H^+]$) for equilibrium protonation of 3,4,5-trimethoxybenzamide against (log $[Ar_3C^+]/[Ar_3COH][H^+]$) for 4-methoxytriphenylmethanol, both in H_2SO_4 solutions.

solutions of the same mineral acid. For example (Fig. 1), log Q for protonation of 2,6-dinitro-N,N,4-trimethylaniline in sulfuric acid solutions is linearly related to log k_2 for ethyl acetate hydrolysis in sulfuric acid solutions. Each point in Fig. 1 represents log Q for a particular mineral acid concentration plotted against log k_2 at the same mineral acid concentration. Observations at lower sulfuric acid concentrations are at the left in the plot.

An example of a linear correlation between the logarithms of equilibrium quotients of two dissimilar reactions is presented as Fig. 2. One of these reactions is a simple protonation, while the other probably comprises two concurrent, consecutive equilibria.

$$Ar_3COH + H^+ \rightleftarrows Ar_3COH_2^+$$

$$Ar_3COH_2^+ \rightleftarrows Ar_3C^+ + H_2O$$

The overall equilibrium quotient for the latter case could be written as $[Ar_3C^+][H_2O]/[Ar_3COH][H^+]$, but in line with common practice (as in formulating K_W for the autoprotolysis of water) the water concentration factor will be omitted. Therefore, for triarylcarbinol – triarylcarbonium ion equilibria, Q is taken as $[Ar_3C^+]/[Ar_3COH][H^+]$. (This differs from the symbolism used by Deno *et al.* (5).)

The generality of such linear relationships warrants their organization in a standardized fashion. For this purpose, the logarithm of the rate coefficient or equilibrium constant for some standard reaction whose variation expresses the variable under study is chosen as horizontal coordinate. For example, log K for the dissociation of benzoic acids was chosen by Hammett (17) as the horizontal coordinate to represent the electronic effects of meta and para substituents, and log k for solvolysis of *tert*-butyl chloride in various solvents was chosen by Grunwald and Winstein (18) to represent solvent effects on solvolysis rates.

Can. J. Chem. Downloaded from www.nrcresearchpress.com by 210.87.254.40 on 09/05/12
For personal use only.

Can. J. Chem. Downloaded from www.nrcresearchpress.com by 210.87.254.40 on 09/05/12
For personal use only.

The standard reaction must be one for which an abundance of good data is available, covering the whole range of variation of the chemical variable of interest. A difficulty with respect to reactions in moderately concentrated acids is that the necessary data are not available, to our knowledge, for any real reaction. Data covering at least 0.5–10 M in hydrochloric, sulfuric, and perchloric acids are required. Because of the strong dependence of rates and equilibria on mineral acid concentration, only rarely can rate coefficients or equilibrium quotients be measured with precision over the specified range of acid concentrations. And when they are measurable over a broad range, as in the case of some ester hydrolyses, it is only because k_2 doesn't change much as acid concentration changes. For that very reason, log k_2 in such cases is not an optimum choice as horizontal coordinate.

There is, however, a hypothetical reaction for which an abundance of good data is available. This is the equilibrium protonation of a hypothetical aromatic primary amine (B), for which a plot of log I versus $-H_0$ is linear with slope identically 1.00, and which has pK_{BH^+} zero. The protonation of such an amine obeys the relationship (1):

$$H_0 = pK_{BH^+} + \log ([B]/[BH^+]).$$

It follows that log ($[BH^+]/[B]$) is given by $-H_0$, and log Q for protonation of the hypothetical amine by $(-H_0 - \log [H^+])$.

One may then write, for equilibria,

$$\log ([SH^+]/[S]) - \log [H^+] = (1 - \phi)(-H_0 - \log [H^+]) + \text{constant},$$

where the data on the left pertain to some real reaction and $(1 - \phi)$ is an arbitrary choice of slope parameter. It is convenient, though not necessary, to add $(H_0 + \log [H^+])$ to each side of the equation.

$$\log ([SH^+]/[S]) + H_0 = \phi(H_0 + \log [H^+]) + \text{constant}$$

To evaluate the constant, consider approach to infinite dilution in water. H_0 approaches $-\log [H^+]$; therefore the first term on the right disappears and the left side becomes log Q for the real reaction at infinite dilution in water, or pK_{SH^+}.

[2] $$\log ([SH^+]/[S]) + H_0 = \phi(H_0 + \log [H^+]) + pK_{SH^+}$$

Equation [2] is suggested as the standard formulation of this l.f.e.r., insofar as protonation equilibria are concerned. The slope of a linear plot according to eq. [2] is a parameter, ϕ, which expresses the response of the equilibrium to changing acid concentration. A negative ϕ value means that log ionization ratio for the real base increases, as the acid concentration augments, more rapidly than does $-H_0$. A positive ϕ value means that it increases less rapidly. The intercept of the plot represents pK_{SH^+} for the real base, referred to infinite dilution in water as standard state. Thus these plots offer a way of estimating pK values.

Representative plots according to eq. [2] are presented as Figs. 3 and 4. Figure 3 concerns the protonation of *m*-nitrobenzamide in sulfuric acid solutions (data of Yates, Stevens, and Katritzky (4)); the slope (ϕ) is +0.50 and the intercept (pK_{SH^+}) is −2.03. Figure 4 concerns the 4,4′,4″-trimethyltriphenylcarbinol $\rightleftarrows$ 4,4′,4″-trimethyltriphenylcarbonium ion equilibrium in sulfuric acid solutions (data of Deno, Jaruzelski, and Schriesheim (5)); ϕ is −1.21 and pK_{R^+} is −3.82.

An expression equivalent to eq. [2] is

[3] $$\log ([SH^+]/[S]) - \log [H^+] = (\phi - 1)(H_0 + \log [H^+]) + pK_{SH^+}.$$

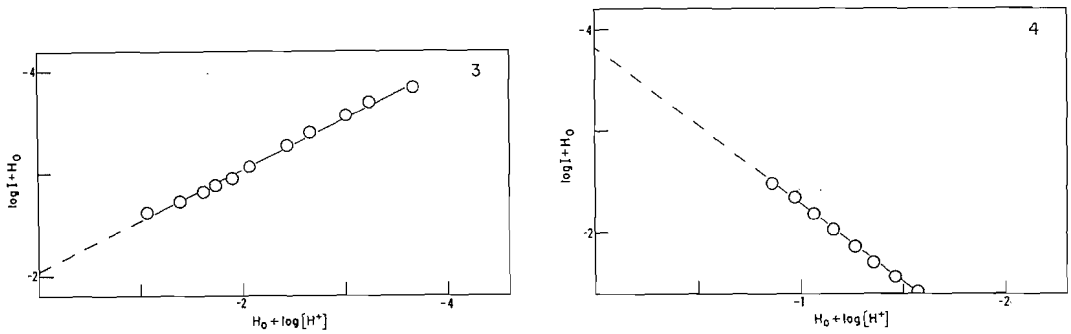


FIG. 3. Correlation of (log $I + H_0$) for *m*-nitrobenzamide in H_2SO_4 solutions with (H_0 + log [H^+]).
FIG. 4. Correlation of (log $I + H_0$) for carbonium ion formation from 4,4′,4″-trimethyltriphenylmethanol in H_2SO_4 solutions with (H_0 + log [H^+]).

If a plot according to eq. [2] is linear, a plot according to eq. [3] is necessarily also linear. Either type of plot may be used to evaluate ϕ and pK values.

Evaluation of pK's according to eq. [3] bears some similarity to an approximate method which has been widely employed (9, 19). This is to plot log Q against molar acid concentration and extrapolate to infinite dilution; the intercept is taken as pK_{SH^+}. Such plots are not linear over a broad range of acid concentrations, but they approximate linearity over short ranges. If the extrapolation is short, this method is serviceable. But the restriction to short extrapolations severely limits its applicability.

CORRELATION OF FOUR REPRESENTATIVE COLLECTIONS OF DATA

In four experimental studies of equilibrium protonation in sulfuric acid solutions, data were obtained which were used to generate four of the principal acidity functions currently available. These are the study of Deno, Jaruzelski, and Schriesheim (5) concerning triarylcarbinol – triarylcarbonium ion equilibria (the H_R function), that of Yates, Stevens, and Katritzky (4) concerning carboxamide protonation (the H_A function), that of Arnett and Mach (7) concerning protonation of aromatic tertiary amines (the H_0''' function), and that of Hinman and Lang (6) concerning protonation of indoles (the H_I function).

We have treated all the data obtained in all four studies by the l.f.e.r. method according to eq. [2], except a few which appear inappropriate for correlation. The data omitted were those in Table IV of Deno *et al.* (5) (identified by them as "less accurate"), sets of data entirely concerned with events at $< 1.1\ M$ mineral acid concentration, and all data at $> 85\%$ H_2SO_4. We have also treated the data of Arnett and Bushick (20, 21), at 30.3°, concerning some of the same triarylcarbinols studied by Deno *et al.* A total of 64 sets of data were examined. Our objective was to determine whether these data actually do give linear correlations according to eq. [2] and whether the pK's estimated from the intercepts agree with the pK's estimated in the acidity function studies. Each set of data was plotted and also subjected to standard linear regression analysis with use of a computer.

The results of the linear regression analysis are presented in Table I. Besides descriptive information, this table reports the slope (ϕ) for each correlation and the intercept, as "pK (l.f.e.r.)". Also reported are the standard deviation of individual points from the linear regression line (σ_y) and the standard deviation of the slopes of the l.f.e.r. plots (σ_{sl}). The pK's of the several substrates as evaluated in the acidity function studies are listed as "pK (a.f.)", and the slope and σ_y for plots of log I versus $-H_0$ are tabulated.

Can. J. Chem. Downloaded from www.nrcresearchpress.com by 210.87.254.40 on 09/05/12
For personal use only.

Most of the plots according to eq. [2] were linear to the eye; two are presented as Figs. 3 and 4. Scatter, probably stemming from random experimental error, was evident in many. A few plots suggested some curvature in one direction or the other, but curvature was not regular in its appearance or direction and is probably due to chance patterns of random error. The median standard deviation of points from the line (σ_y) is 0.041 log units, or 10%. This is the order of magnitude of the experimental error in the equilibrium measurements; it does not indicate any inadequacy of correlation according to eq. [2].

It is possible to compare the intercepts from 57 of the plots with pK's estimated by the acidity function (a.f.) method. In seven cases, pK's (although easily obtained by the l.f.e.r. method) could not be estimated by Hinman and Lang because of difficulties inherent in the a.f. method. The median difference in pK's estimated from the same data by the two methods is 0.25 pK unit, which is roughly the order of magnitude of the uncertainty usually imputed to pK values determined by the a.f. method. Possible sources of error in both methods are considered below.

CONCEIVABLE ALTERNATIVE FORMULATIONS OF L.F.E.R.

There are two ways in which correlations according to eq. [2] or [3] can be viewed as l.f.e.r. These differ in the standard states to which activity coefficients refer.

One way involves the unusual choice of each mineral acid solution as the standard state for measurements in that solution. f_{H^+} is defined as unity in each mineral acid solvent, and f_S and f_{SH^+} as unity at infinite dilution in that solvent, a condition closely approached in most photometric measurements of acid–base equilibria. The standard state is a hypothetical solution in that solvent in which H^+, S, and SH^+ are all present at unit concentration (1 M) with unit activity coefficient. Apart from experimental error and a very small correction due to the fact that S and SH^+ are present in finite concentrations, the measured log Q is then the thermodynamic pK_{SH^+} for that substrate in that medium. Since $-\log K_{SH^+} = \log Q = \Delta G^0/2.3RT$, a linear relationship between log Q at constant temperature amounts to a l.f.e.r. With respect to a similar definition of standard states, a linear relationship between log k_2 and log Q is by the same reasoning also a l.f.e.r.

It is evident that the value of log Q at any point on a plot of log Q versus ($H_0 + \log [H^+]$) represents the thermodynamic pK_{SH^+} of the substrate in that solution. To determine pK_{SH^+} for a substrate in a solution of any specified acid concentration, one need only look up the value of ($H_0 + \log [H^+]$) for that solution and determine (graphically or by use of eq. [3]) the value of log Q in that solution. For example, the pK's of 2,3,6-trichlorobenzamide and N,N-diethyl-2,4,6-trinitroaniline in 50% sulfuric acid are reckoned by eq. [3] from data in Table I as -1.71 and -2.13, respectively. These differ by only 0.4 pK unit although the pK's referred to infinite dilution in water differ by 2.6 units (Table I).

More commonly, infinite dilution in water is taken as the standard state for all activity coefficients.[2] One may then write

$$[4] \qquad pK_{SH^+} = \Delta G^0/2.3RT = \log [SH^+]/[S][H^+] + \log f_{SH^+}/f_S f_{H^+}$$

or, equivalently,

$$[5] \quad pK_{SH^+} = \Delta G^0/2.3RT = \log [SH^+] - \log [S] - \log [H^+] + \log f_{SH^+} - \log f_S - \log f_{H^+}.$$

[2]*Rigorously, the standard state is a hypothetical solution in which all activity coefficients are unity (as at infinite dilution) and all solutes are present at unit concentration (1 M).*

Can. J. Chem. Downloaded from www.nrcresearchpress.com by 210.87.254.40 on 09/05/12
For personal use only.

Can. J. Chem. Downloaded from www.nrcresearchpress.com by 210.87.254.40 on 09/05/12
For personal use only.

TABLE I

Equilibrium protonation in sulfuric acid solutions (correlations of (log $I + H_0$) with (H_0 + log [H^+]) according to eq. [2])

Substrate	Acid concentration range	No. of points	l.f.e.r. plots*				pK (a.f.)†	Plots of log I vs. $-H_0$		Ref.
			ϕ	σ_y	σ_{sl}	pK (l.f.e.r.)		Slope	σ_y	
2-Pyrrolecarboxamide	5–41%	9	0.31	0.021	0.01	−1.06	−1.23	0.80	0.039	4
p-Methoxybenzamide	10–50%	12	0.42	0.041	0.02	−1.17	−1.44	0.69	0.038	4
3,4,5-Trimethoxybenzamide	16–52%	10	0.43	0.018	0.01	−1.53	−1.82	0.66	0.025	4
m-Nitrobenzamide	29–62%	11	0.50	0.030	0.01	−2.03	−2.42	0.57	0.038	4
3,5-Dinitro-4-methylbenzamide	34–69%	10	0.52	0.042	0.01	−2.25	−2.69	0.54	0.037	4
2,3,6-Trichlorobenzamide	49–73%	9	0.49	0.045	0.02	−3.00	−3.30	0.55	0.047	4
2,4-Dichloro-3,5-dinitrobenzamide	56–82%	11	0.55	0.035	0.01	−3.16	−3.73	0.49	0.034	4
2,4,6-Trinitrobenzamide	62–82%	9	0.48	0.035	0.01	−3.87	−4.08	0.55	0.035	4
N,N-Dimethyl-4-nitroaniline	5–14%	5	0.83	0.020	0.13	+0.66	+0.66	1.25	0.025	7
N,N-Diethyl-2,4-dinitroaniline	5–19%	6	−0.44	0.046	0.12	+0.29	+0.21	1.19	0.040	7
N-(2,4-Dinitrophenyl)piperidine	5–23%	8	−0.62	0.058	0.10	−0.33	−0.38	1.31	0.036	7
2,6-Dinitro-N,N,4-trimethylaniline	14–35%	8	−0.58	0.036	0.04	−1.57	−1.66	1.40	0.039	7
N,N-Dimethyl-2,4-dinitro-1-naphthylamine	23–45%	10	−0.41	0.046	0.04	−2.34	−2.59	1.32	0.043	7
4-Chloro-N,N-dimethyl-2,6-dinitroaniline	27–47%	9	−0.48	0.072	0.06	−2.94	−3.12	1.38	0.068	7
N-Methyl-4-nitrodiphenylamine	30–52%	12	−0.35	0.053	0.03	−3.01	−3.42	1.30	0.048	7
4′-Bromo-N-methyl-4-nitrodiphenylamine	39–59%	10	−0.12	0.046	0.03	−3.36	−4.21	1.10	0.045	7
N,N-Diethyl-2,4,6-trinitroaniline	52–68%	9	−0.38	0.049	0.03	−5.62	−5.71	1.35	0.049	7
2,4-Dinitro-N-methyldiphenylamine	56–67%	7	−0.37	0.037	0.03	−6.08	−6.19	1.34	0.038	7
N,N-Dimethyl-2,4,6-trinitroaniline	60–71%	7	−0.33	0.032	0.03	−6.30	−6.55	1.31	0.030	7
4′-Bromo-2,4-dinitro-N-methyldiphenylamine	60–74%	9	−0.39	0.031	0.02	−6.93	−6.93	1.36	0.029	7
4′,X′-Dibromo-2,4-dinitro-N-methyldiphenylamine	68–79%	8	−0.12	0.075	0.05	−6.85	−8.17	1.11	0.074	7
4,4′-Dimethoxytriphenylmethanol	6–26%	11	−1.16	0.048	0.06	−1.15	−1.24	1.64	0.035	5
4,4′-Dimethoxytriphenylmethanol, 30.3°	7–27%	8	−1.25	0.027	0.05	−1.09	−0.89	1.67	0.052	21
4-Methoxytriphenylmethanol	24–40%	9	−1.59	0.018	0.02	−3.73	−3.40	2.16	0.038	5
4-Methoxytriphenylmethanol, 30.3°	24–40%	8	−1.54	0.078	0.10	−3.81	−3.20	2.15	0.079	21
2,2′,2″-Trimethyltriphenylmethanol	26–38%	7	−1.21	0.011	0.02	−3.22	−3.4	1.91	0.015	5
4,4′,4″-Trimethyltriphenylmethanol	24–38%	8	−1.54	0.019	0.03	−3.82	−3.56	2.15	0.017	5
4-Methyltriphenylmethanol	38–48%	6	−1.15	0.027	0.04	−4.86	−5.24	1.99	0.022	5
4-Methyltriphenylmethanol, 30.3°	38–48%	6	−1.32	0.119	0.18	−5.36	−5.25	2.15	0.117	21
4,4′-Dimethoxydiphenylmethanol	38–52%	8	−1.17	0.044	0.04	−5.36	−5.71	2.01	0.045	5
3,3′,3″-Trimethyltriphenylmethanol	44–54%	6	−1.04	0.029	0.04	−5.74	−6.35	1.92	0.029	5
4,4′-4″-Triisopropyltriphenylmethanol	44–54%	6	−1.13	0.055	0.07	−6.15	−6.54	2.00	0.052	5
Triphenylmethanol	46–54%	5	−1.02	0.057	0.10	−5.98	−6.63	1.91	0.052	5

Can. J. Chem. Downloaded from www.nrcresearchpress.com by 210.87.254.40 on 09/05/12
For personal use only.

TABLE I (*Concluded*)

Substrate	Acid concentration range	No. of points	l.f.e.r. plots*					Plots of log I vs. $-H_0$		Ref.
			ϕ	σ_y	σ_{sl}	pK (l.f.e.r.)	pK (a.f.)†	Slope	σ_y	
Triphenylmethanol, 30.3°	44–55%	7	−1.38	0.192	0.23	−6.85	−6.44	2.23	0.190	21
4,4′,4″-Trichlorotriphenylmethanol	52–59%	5	−1.20	0.018	0.03	−7.59	−7.74	2.08	0.015	5
4-Nitrotriphenylmethanol	57–64%	5	−1.47	0.023	0.04	−9.86	−9.15	2.34	0.022	5
4-Nitrotriphenylmethanol, 30.3°	59–66%	6	−1.48	0.022	0.03	−10.24	−9.44	2.36	0.035	21
3,3′,3″-Trichlorotriphenylmethanol	64–72%	5	−0.80	0.035	0.04	−9.14	−11.03	1.75	0.034	5
4,4′-Dinitrotriphenylmethanol‡	70–78%	5	−0.79	0.016	0.02	−10.95	−12.90	1.75	0.017	5
5-Methylindole	3.4–7.3 *M*	13	+0.19	0.048	0.03	−2.03		0.84	0.047	6
Unsubstituted indole	3.9–6.9 *M*	12	+0.04	0.101	0.08	−2.46		0.97	0.101	6
6-Nitroindole	7.9–10.9 *M*	10	+0.26	0.059	0.04	−4.05		0.77	0.059	6
5-Nitroindole	8.9–12.5 *M*	11	+0.20	0.086	0.04	−4.61		0.81	0.085	6
2,5-Dimethylindole	0.7–2.0 *M*	5	−0.42	0.033	0.12	+0.30	+0.26	1.19	0.036	6
2-Methylindole	1.2–2.5 *M*	5	−0.27	0.022	0.06	−0.10	−0.28	1.18	0.024	6
2-Ethylindole	1.0–2.6 *M*	6	−0.26	0.057	0.13	−0.28	−0.41	1.14	0.056	6
2,5–Dimethyl-3-propylindole	0.5–3.4 *M*	7	−0.31	0.042	0.05	−0.85	−1.03	1.17	0.046	6
2-Methyl-3-propylindole	1.0–3.4 *M*	6	−0.29	0.033	0.05	−1.19	−1.40	1.17	0.038	6
2,3-Dimethylindole	1.0–4.0 *M*	9	−0.40	0.032	0.03	−1.35	−1.49	1.25	0.040	6
2-Methyl-5-nitroindole	4.5–6.9 *M*	22	−0.42	0.046	0.03	−3.31	−3.58	1.35	0.047	6
3-*t*-Butylindole	4.8–7.5 *M*	6	−0.31	0.040	0.04	−3.35	−3.84	1.26	0.038	6
3-Ethylindole	5.9–7.9 *M*	5	−0.29	0.034	0.05	−3.71	−4.25	1.26	0.032	6
3-Methylindole	5.9–8.9 *M*	9	−0.34	0.047	0.04	−4.12	−4.55	1.30	0.046	6
3-Propylindole	5.5–7.9 *M*	6	−0.46	0.021	0.02	−4.18	−4.34	1.40	0.023	6
3-Acetic acid indole	8.2–10.2 *M*	5	−0.35	0.050	0.06	−5.76	−6.13	1.31	0.051	6
3-(β-Ammonioethyl)indole	8.5–10.9 *M*	9	−0.46	0.041	0.04	−6.39	−6.31	1.42	0.043	6
1,2-Dimethylindole	0.8–1.5 *M*	5	−0.71	0.018	0.12	+0.32	+0.30	1.31	0.015	6
1,2,3-Trimethylindole	1.5–2.5 *M*	5	−0.32	0.018	0.07	−0.48	−0.66	1.19	0.018	6
1-Methylindole	3.0–4.9 *M*	9	−0.67	0.052	0.07	−2.47	−2.32	1.51	0.051	6
1-Ethylindole	2.5–4.8 *M*	14	−0.80	0.064	0.06	−2.58	−2.30	1.60	0.064	6
1,2-Dimethyl-5-nitroindole	3.4–5.9 *M*	12	−0.70	0.060	0.06	−3.13	−2.94	1.56	0.060	6
1,3–Diethylindole	4.9–6.4 *M*	4	−0.77	0.040	0.08	−3.43		1.66	0.041	6
1,3-Dimethylindole	4.0–6.4 *M*	25	−0.85	0.049	0.04	−3.77		1.71	0.047	6
1-Methylindole-3-acetic acid	5.9–7.9 *M*	10	−0.37	0.061	0.06	−4.27		1.33	0.059	6

*ϕ is the slope of the plot, pK(l.f.e.r.) is the intercept, σ_y is the standard deviation of points from the linear regression line in the y direction, and σ_{sl} the standard deviation of the slope.
†pK(a.f.) is the pK by the acidity function method, taken from the reference cited.
‡Introduced as 4,4′-dinitrotriphenylmethyl chloride.

Can. J. Chem. Downloaded from www.nrcresearchpress.com by 210.87.254.40 on 09/05/12
For personal use only.

Each of the six logarithmic terms on the right side of eq. [5] is algebraically linear with $\Delta G^0/RT$, as is any sum of those terms. In this sense log Q (the sum of the three concentration terms) makes a linear contribution to free energy change. Consequently, linear relationships between log Q may be considered as l.f.e.r. It should be noted that ΔG^0 is now defined as constant; therefore any change in log Q with acid concentration must be offset by an equal and opposite change in log $(f_{SH^+}/f_S f_{H^+})$ (see eq. [4]).

By the same reasoning, log $([SH^+]/[S])$ or log I makes a linear contribution to free energy change, offset by an equal and opposite change in log $(f_{SH^+}/f_S a_{H^+})$. Inasmuch as $-H_0$ may be considered to represent log $([BH^+]/[B])$ for a hypothetical aromatic primary amine of pK_{BH^+} zero, the familiar plots of log I versus $-H_0$ may also be regarded as l.f.e.r.

Grunwald *et al.* (22–24) have postulated that linear relationships exist between log (f_{SH^+}/f_S) for various acid dissociation equilibria in ethanol–water mixtures. This implies (see eq. [4]) that log Q − log f_{H^+} for diverse substrates, as they vary with medium composition, should be linearly related. This postulate cannot be directly tested by experiment because values of f_{H^+} are not known, either in alcoholic solvents or in moderately concentrated mineral acids. The quantities actually related by Grunwald *et al.* were log (Q/Q'), pertaining to substrates S and S′; this allowed the inconvenient log f_{H^+} to be cancelled out. Their observation that linear relationships exist between log (Q/Q'), as they vary with solvent composition, whereas log Q's are not linearly related in ethanol–water media (cf. data in Table IV of Gutbezahl and Grunwald (23)), supports their postulate insofar as ethanol–water solutions are concerned. But when log Q's are linearly related, as in sulfuric acid media, demonstration of linear relationships between log (Q/Q') is trivial.

Let us now consider the hypotheses that linear relationships exist between log Q (or log k_2) and that they exist between log I (or log k_ψ). Let us inquire which type of linear correlation is better justified by available data.

All the data in Table I have been submitted to linear regression analysis according to both types of correlation. The qualities of fit are best judged by comparing σ_y values. Unfortunately, the σ_y values do not provide a clear distinction between the two methods. For the 64 sets of data, the σ_y's are nearly the same ($\Delta\sigma_y \leqslant 0.004$) in 48 sets and the remaining sets divide almost equally between favoring one type of correlation or the other.

The corresponding question concerning kinetic data is whether a better correlation is obtained between (log $k_\psi + H_0$) and (H_0 + log $[H^+]$) or between log k_ψ and $-H_0$. From a detailed inquiry, reported in the accompanying paper (16), a clear decision has emerged: correlations of the former type are much better. Mainly for this reason, l.f.e.r. concerning reactions in moderately concentrated mineral acids are judged to be better composed between (log $I + H_0$) or (log $k_\psi + H_0$) and (H_0 + log $[H^+]$) than between log I or log k_ψ and $-H_0$. Expressed more generally, correlations are better composed between log Q and (or) log k_2 than between log I and (or) log k_ψ.[3]

An ancillary advantage of plots of the favored type is that their intercepts are quantities of considerable interest: pK's or log k_2 values at infinite dilution. The intercepts in plots of log I or log k_ψ versus $-H_0$ represent, of course, the values of these quantities at zero H_0. Because many activity coefficient ratios differ appreciably from unity at zero H_0, an inconvenient correction of the latter intercepts would be necessary in order to evaluate the pK or log k_2 at infinite dilution. A further advantage of the favored correlations is that when a protonation equilibrium is concurrent and consecutive with one not involving proton gain or loss, the slope parameters for the two steps may be combined additively.

[3]*It should be noted that plotting (log $I + H_0$) is equivalent to plotting log Q versus (H_0 + log $[H^+]$); different slopes are obtained, but it is basically the same type of correlation either way.*

CONCERNING ACIDITY FUNCTIONS

Let us consider two bases, L and M, of a structural type other than aromatic primary amines. The condition that must be met if these are to be used in construction of an acidity function is:

$$[6] \qquad \text{d log } ([LH^+]/[L]) = \text{d log } ([MH^+]/[M]).$$

Alternatively, this may be expressed

$$[7] \qquad \text{d log } [LH^+]/[L][H^+] = \text{d log } [MH^+]/[M][H^+].$$

If log Q for L is linear with $(H_0 + \log [H^+])$,

$$[8] \qquad \text{d log } [LH^+]/[L][H^+] = (\phi - 1)\text{d}(H_0 + \log [H^+]).$$

It follows that if a set of bases are to be used to construct an acidity function, (*a*) their protonation reactions must have equal ϕ values or (*b*) $(H_0 + \log [H^+])$ must be zero. The latter special case is approximated in dilute aqueous solution, where the acidity function which prevails is pH. When $H_0 \neq -\log [H^+]$, the requirement of equal ϕ values must be met. This criterion will now be used to judge some of the published acidity functions.

The foregoing criteria for judgment of acidity functions are similar to those advanced by Gutbezahl and Grunwald (23). On the basis of the inequality of m values (which roughly correspond to the present ϕ values) for several bases in ethanol–water systems, they concluded that an acidity function cannot exist in such systems. This conclusion has been widely quoted with the implication that ethanol–water systems are inherently worse than sulfuric acid – water systems insofar as the possibility for existence of acidity functions is concerned. In 1953 it was widely believed that the protonation of all neutral bases "obeyed" the H_0 function in moderately concentrated mineral acids, but this is now known not to be the case. ϕ values for various bases in sulfuric acid solutions differ as much or more than m values in ethanol–water. The experience of Gutbezahl and Grunwald does not exclude the possibility that a set of bases of an appropriately limited structural type may define a proper acidity function in ethanol–water media. Indeed, Yeh and Jaffé (25) found the condition of eq. [6] to be satisfied for azobenzene derivatives in ethanol – water – sulfuric acid solutions. Their acidity function, unfortunately symbolized H_0, appears to be a satisfactory one for that functional class of bases.

In judging published acidity functions, one must bear in mind that errant ϕ values can be caused by random experimental error. Therefore if the bases used to construct an acidity function differ in their ϕ values, it does not necessarily follow that they are inappropriate for construction of an acidity function. On the other hand, unless the ϕ values for a set of bases are substantially equal, a necessary condition for the construction of an acidity function fails to have been satisfied.[4] Also, the manner of constructing acidity functions is such that experimental errors accumulate except as they happen to offset each other.

The H_A Function for Amides (4)

With the exception of 2-pyrrolecarboxamide, the ϕ values (Table I) for the bases used to construct the H_A function lie between +0.42 and +0.55. This is a relatively narrow range; the benzamide derivatives are thus appropriate for construction of an acidity

[4]*However, if there is persistent and regular curvature common to all bases of a functional class in plots of log Q or (log I + H_0) versus (H_0 + log [H^+]), that is, a regular violation of the linear relationships of our present concern, these conclusions do not apply. As discussed below, there are indications of such violations for some types of bases in perchloric acid solutions.*

Can. J. Chem. Downloaded from www.nrcresearchpress.com by 210.87.254.40 on 09/05/12
For personal use only.

function. However, the H_A function suffers from uncertanty at its beginning. Because no amide was available whose pK could be determined by measurements in dilute solution, the uncomfortable assumption was made that the H_A and H_0 functions coincide up to 16.1% H_2SO_4. Using a ϕ value of +0.48 (the average for the benzamide derivatives in Table I), one reckons that H_A (evaluated as $H_0 - \phi(H_0 + \log [H^+])$) should be −0.50 in 16.1% H_2SO_4 whereas Yates *et al.* (4) assumed −0.78. A further small uncertainty entered from use of 2-pyrrolecarboxamide, whose ϕ is +0.31, to carry the acidity function between 16 and 24% sulfuric acid. The H_A function as a whole appears to be too negative by about 0.3 units; appropriately, this is the direction and order of magnitude of the differences between pK(l.f.e.r.) and pK(a.f.) for the amides in Table I.

The H_0''' Function for Aromatic Tertiary Amines (7)

With a few exceptions, the ϕ values (Table I) for the bases used to construct the H_0''' function lie between −0.33 and −0.48. It is not obvious why five indicators fall outside this range. The two with unusually low negative ϕ values are both diphenylamine derivatives, but three other diphenylamines have ϕ values between −0.33 and −0.48. The generally satisfactory agreement of pK's estimated by l.f.e.r. and a.f. methods (excepting the two errant diphenylamine derivatives) suggests that the H_0''' scale as a whole is fairly accurate.

The H_R Function for Triarylcarbinol – Triarylcarbonium Ion Equilibria (5)

Despite considerable experimental attention, the set of indicators used to establish the H_R function has not been fully demonstrated to satisfy the criterion of eq. [6]; in the studies of Deno *et al.* (5) and of Arnett and Bushick (20, 21) there were gaps of little or no overlap at ca. 25%, 39%, 53%, and 71% H_2SO_4. The less rigorous but nevertheless persuasive criterion of constancy of d log I/d % H_2SO_4 between adjacent indicators was, however, rather well met. The correlations summarized in Table I, based mainly on data of Deno *et al.* but including also the 30.3° data of Arnett and Bushick, show that to a considerable extent the bases employed meet the criterion of equality of ϕ values. The ϕ values, excepting those for the last two triarylcarbinols listed, lie between −1.02 and −1.59 with an average of −1.29. It is not entirely clear whether the extremes are real or represent unusual experimental error; one of the extremes (for 4-methoxytriphenylmethanol) is confirmed by measurements in a second laboratory but another (for triphenylmethanol) is not. The agreement between pK's estimated by the l.f.e.r. and a.f. methods is nearly as good as between those estimated by the a.f. method in two different laboratories.

The ϕ values for 3,3′,3″-trichloro- and 4,4′-dinitro-triphenylmethanols (−0.8) differ sharply from the rest. This could represent unusual activity coefficient behavior in those equilibria or breakdown of the linear relationship between log Q and $(H_0 + \log [H^+])$ at very high acid concentrations. The large discrepancies between pK's estimated by the two methods are, as discussed below, a direct consequence of the deviant ϕ values in these two cases.

The H_I Function for Indoles

Of the 25 indoles investigated by Hinman and Lang (6), 23 fall neatly into categories which link structural type with ϕ value in sulfuric acid. Four indoles unsubstituted in the pyrrole ring have ϕ from +0.04 to +0.26, thirteen indoles carrying a 2- and (or) 3-substituent but no 1-substituent have ϕ from −0.26 to −0.46, and six of eight 1-substituted indoles have ϕ between −0.67 and −0.85. The two errant bases are 1,2,3-trimethylindole (ϕ −0.32) and 1-methylindole-3-acetic acid (ϕ −0.37).

Can. J. Chem. Downloaded from www.nrcresearchpress.com by 210.87.254.40 on 09/05/12
For personal use only.

Hinman and Lang also recognized three categories on the basis of d log I/d [H_2SO_4] slope values. One of their categories coincides with the first above (indoles unsubstituted in the hetero ring); properly, they eschewed those four bases in constructing a general acidity function for indoles. Their second category included all the indoles of Table I carrying a 2- and (or) 3-substituent but no 1-substituent as well as five 1-substituted indoles. Their third category included three 1,3-disubstituted indoles. Their second and third categories do not match ours.

Hinman and Lang used data for nine indole derivatives to evaluate the H_I function. These included two (1-methylindole and 1,2-dimethyl-5-nitroindole) whose ϕ values place them in our third category. The set of bases used therefore appears not to have been entirely appropriate; the H_I function of Hinman and Lang is apparently somewhat too negative above 3 M sulfuric acid.

SOURCES OF ERROR IN ESTIMATING pK VALUES

Let us consider Fig. 5, a typical l.f.e.r. plot by means of which the pK of a base (in this case, 2,4,6-trinitro-N,N-diethylaniline) can be estimated. The pK_{SH^+} is estimated as the intercept, which is -5.62 and which may be compared with pK_{SH^+} -5.71 estimated by the a.f. method. The former estimate involves the assumption that the straight line established by the experimental points (in this case at 52–67% H_2SO_4) is linear all the way to infinite dilution in water. Any fault in this assumption introduces an error into the pK estimate. Also, any experimental error which deflects the slope causes an error in the intercept which is larger the longer the extrapolation.

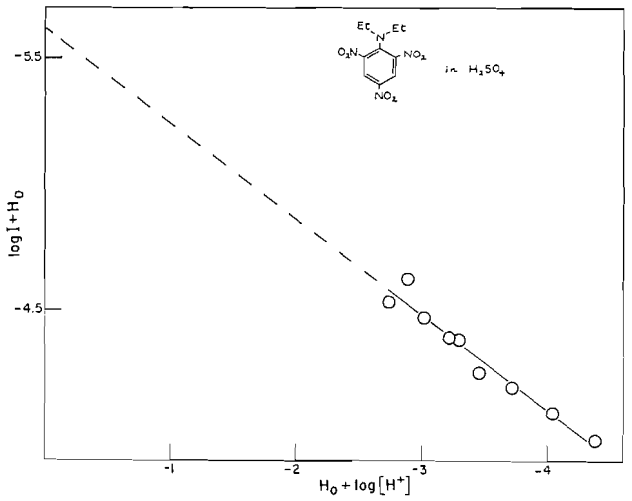


FIG. 5. Correlation of (log $I + H_0$) for N,N-diethyl-2,4,6-trinitroaniline in H_2SO_4 solutions with (H_0 + log [H^+]).

In estimating pK's by the a.f. method, one assumes that the variation of the activity coefficient ratio for a given base, through a series of acid concentrations down to infinite dilution, is the same as the variation of activity coefficient ratio by the indicator bases used to construct the acidity function. Any fault in this assumption introduces an error into the pK estimate. The pK estimate is not very sensitive to experimental error in measurements on the base under study, but errors in measurements on the bases used to

Can. J. Chem. Downloaded from www.nrcresearchpress.com by 210.87.254.40 on 09/05/12
For personal use only.

Can. J. Chem. Downloaded from www.nrcresearchpress.com by 210.87.254.40 on 09/05/12
For personal use only.

TABLE II

Equilibrium protonation in perchloric acid solutions (correlations of (log $I + H_0$) with (H_0 + log [H$^+$]) according to eq. [2])

Substrate	Acid concentration range	No. of points	ϕ^*	σ_y^*	σ_{s1}^*	Intercept	pK(l.f.e.r.) in H_2SO_4	Ref.
4,4′-Dimethoxytriphenylmethanol	7–18%	7	−2.44	0.036	0.12	−0.94	−1.12	26
4-Methoxytriphenylmethanol	20–36%	10	−1.57	0.024	0.03	−2.86	−3.77	26
Triphenylmethanol	42–51%	6	−0.89	0.026	0.03	−5.02	−6.4	26
4,4′,4″-Trichlorotriphenylmethanol	46–54%	5	−1.06	0.019	0.02	−6.57	−7.59	26
4-Nitrotriphenylmethanol	53–59%	5	−1.18	0.017	0.02	−8.75	−10.1	26
Unsubstituted indole	3.8–6.0 *M*	11	−0.10	0.034	0.03	−2.33	−2.46	6
2-Methylindole	0.8–1.8 *M*	10	−1.06	0.013	0.05	−0.14	−0.10	6
2,3-Dimethylindole	0.9–3.0 *M*	15	−1.03	0.021	0.03	−1.30	−1.35	6
2-Methyl-5-nitroindole	3.8–6.0 *M*	57	−0.49	0.036	0.02	−3.01	−3.31	6
1-Methylindole	2.2–4.3 *M*	13	−0.83	0.020	0.02	−2.04	−2.47	6
1,3-Dimethylindole	3.5–5.4 *M*	10	−1.05	0.022	0.03	−3.44	−3.77	6

*See footnotes of Table I.

TABLE III

Miscellaneous acid–base equilibria (correlations of (log $I + H_0$) with (H_0 + log [H$^+$]) according to eq. [2])

Substrate	Mineral acid and concentration range	No. of points	ϕ^*	σ_y^*	σ_{s1}^*	pK	Ref.
Benzamide	$HClO_4$ 1.1–6.1 *M*	8	+0.34	0.032	0.02	−1.53	30
4-(*p*-Sulfophenylazo)anisole	HCl 2.1–6.2 *M*	5	−0.88	0.057	0.07	−2.29	31
4-(*p*-Sulfophenylazo)anisole	H_2SO_4 15–36%	9	−0.63	0.050	0.05	−2.27	31
4-(*p*-Sulfophenylazo)-1-naphthyl methyl ether	HCl 0.5–4.1 *M*	11	−1.24	0.018	0.02	−1.20	31
1,3,5-Trihydroxybenzene	$HClO_4$ 45–56%	6	+0.16	0.030	0.02	−3.36	32
1-Methoxy-3,5-dihydroxybenzene	$HClO_4$ 44–56%	8	+0.03	0.016	0.01	−3.54	32
1,3-Dimethoxy-5-hydroxybenzene	$HClO_4$ 44–56%	6	−0.02	0.040	0.03	−3.72	32
1,3,5-Trimethoxybenzene	$HClO_4$ 45–56%	8	−0.28	0.041	0.03	−4.50	32
Azulene, 5.7°	$HClO_4$ 1.0–3.5 *M*	6	−1.54	0.036	0.06	−1.87	19
Azulene, 15.5°	$HClO_4$ 1.0–3.5 *M*	6	−1.42	0.030	0.05	−1.74	19
Azulene 25°	$HClO_4$ 1.0–3.5 *M*	6	−1.35	0.012	0.02	−1.66	19
Azulene, 38.6°	$HClO_4$ 1.0–3.5 *M*	6	−1.23	0.020	0.03	−1.47	19

*See footnotes of Table I.

construct the acidity function tend to accumulate in the function itself and to affect all pK estimates based upon it.

pK ESTIMATION WITH REFERENCE TO KINETIC DATA

We have seen that one can, by the l.f.e.r. approach, estimate the pK of any base with reference to H_0 and log [H$^+$], whether or not its protonation "obeys" H_0 in the Hammett sense. It is also possible to estimate pK's without reference to any acidity function, in the usual sense of the term. For this purpose one uses kinetic data instead of (H_0 + log [H$^+$]).

One plots log Q for protonation of the base under study against (log k_2 − log k_2^0) or (log k_ψ − log k_ψ^0) for reaction of, respectively, a weakly or strongly basic substrate. Theoretically, k_2^0 and k_ψ^0 are rate coefficients at infinite dilution in water but in practice they are measured coefficients in dilute solution, say, at pH 2. Figure 1 is such a plot. By reasoning such as employed in the derivation of eq. [2], the intercept is pK_{SH^+}. The intercept in Fig. 1 is −1.58; this agrees well with the pK of 2,6-dinitro-N,N,4-trimethylaniline as estimated by the standard l.f.e.r. (−1.57) and acidity function (−1.66) methods.

EQUILIBRIA IN PERCHLORIC ACID SOLUTIONS

Table II summarizes l.f.e.r. correlations concerning triarylcarbinol – triarylcarbonium ion equilibria (data of Berkheimer (26, 27)) and the protonation of indoles (data of Hinman and Lang (6)) in perchloric acid solutions.

The data are few, but for both types of substrates the (negative) ϕ values at low acid concentrations ($< 2\ M$) are much larger in magnitude than for substrates of similar structural type at higher acid concentrations. (At higher acid concentrations, the ϕ values are similar to those for the same substrates in sulfuric acid media.) Moreover, plots of (log I + H_0) versus (H_0 + log [H$^+$]) for 4-methyl- and 3,3′,3″-trimethyl-triphenylmethanol were smooth curves with slopes varying from ca. −1.5 at 35–38% $HClO_4$ to ca. −0.7 at 44–47% $HClO_4$. The usual pattern of uniformly linear correlations and substantially constant slopes for substrates of similar structure is apparently violated. More extensive data to substantiate or refute these indications would be desirable.

These possible violations of l.f.e.r., even if substantiated by further data, do not necessarily mean that linear relationships between (log I + H_0) and (H_0 + log [H$^+$]) are not of frequent occurrence in perchloric acid. Good linear relationships for diverse equilibria in perchloric acid are presented in Table III. Abundant kinetic data concerning reactions in perchloric acid are available; in general the plots of (log k_ψ + H_0) versus (H_0 + log [H$^+$]) are good straight lines, as reported in the accompanying paper. Among kinetic data there are, however, some reactions which do not afford linear "l.f.e.r." plots. Two examples are hydrolyses of trimethylacetic anhydride (28) and acetylimidazole (29). Such anomalies seem to be more frequent, and more serious, in perchloric than in sulfuric acid solutions.

SOME MISCELLANEOUS ACID–BASE EQUILIBRIA

Some miscellaneous correlations of protonation equilibria are summarized in Table III. These all concern equilibria for which no proper acidity function is available, except by coincidence in two cases, and for which pK's have been estimated by various methods.

For benzamide, pK's of −2.15 (30), −1.85 (33*a*), and −2.16 (33*b*) have been estimated with reference to the H_0 function which, we now realize, is not "obeyed" by amides. pK's of −1.74 and −1.68 have been estimated from different sets of data in sulfuric acid with reference to the H_A function (33*c*). The pK for benzamide in Table III, −1.53, is based on

Can. J. Chem. Downloaded from www.nrcresearchpress.com by 210.87.254.40 on 09/05/12
For personal use only.

Moodie's data in perchloric acid (30). If the whole H_A function is considered too negative by perhaps 0.3 unit, this estimate is in fairly good agreement with the (corrected) estimates based on that function.

pK's of the two azo ethers in Table III were estimated as -1.6 and -0.74, respectively, with reference to the H_0 function (31). In view of the large negative ϕ values, it is not surprising that pK's estimated by the l.f.e.r. method differ considerably from the earlier estimates. The agreement between the pK's estimated for 4-(*p*-sulfophenylazo)anisole in two mineral acids is noteworthy. The considerable difference in ϕ value for protonation of the two azo ethers in hydrochloric acid solutions also merits attention.

Schubert and Quacchia (32) noted that the protonation of 1-methoxy-3,5-dihydroxybenzene "follows" H_0 very closely. The pK estimated with reference to the H_0 function, -3.61 (average), should therefore be a good one; it agrees quite well with -3.54 as estimated by the l.f.e.r. method. The less certain ionization ratios for 1,3-dimethoxy-5-hydroxybenzene also indicated obedience to H_0, and again the pK estimated with reference to that function, -3.68 (average), agrees with the l.f.e.r. estimate (-3.72) based on the same data. Schubert and Quacchia noted that protonation of 1,3,5-trihydroxybenzene and its trimethyl ether "obeyed" H_0 less well; it is therefore reasonable that the l.f.e.r. estimates of pK differ appreciably from the (drifting) estimates based on the H_0 function.

Challis and Long (19) estimated the pK of azulene at four temperatures by the extrapolation procedure of Paul and Long (9) and at 25° by an acidity function approach via 1-methylazulene, which is more basic than azulene. Their estimates are more negative than the l.f.e.r. estimates by about 0.1 pK unit at all temperatures; the agreement is good. The consistent variation of ϕ value with temperature is noteworthy.

These diverse correlations illustrate the utility of the l.f.e.r. method for estimating pK's of bases for which no regular acidity function is available.

EQUILIBRIA NOT INVOLVING PROTONATION

A few measurements have been made on equilibria not involving acquisition or loss of a proton between initial and final states (34–36). A general symbolism for such reactions is:

$$\text{S} \overset{K_e}{\rightleftarrows} \text{V} \ (+\text{H}_2\text{O}). \qquad [9]$$

Such reactions often involve covalent addition of water, or the reverse, and we recommend writing them so that dehydration is the forward reaction. The equilibrium constant expression may be written in logarithmic form

$$\log ([\text{V}]/[\text{S}]) = \log (f_S/f_V) + \log K_e \qquad [10]$$

Equations [4] and [10] are similar in form, suggesting that linear relationships may exist between $(H_0 + \log [\text{H}^+])$ and the logarithms of equilibrium quotients such as that in eq. [10]. In the few cases known to us, $\log ([\text{V}]/[\text{S}])$ is indeed linear with $(H_0 + \log [\text{H}^+])$. The correlations are summarized in Table IV. A representative plot is presented as Fig. 6.

TABLE IV

Equilibria not involving proton gain or loss (correlations of log ([V]/[S]) with $(H_0 + \log [\text{H}^+])$)

	Mineral acid and concentration range	No. of points	ϕ	σ_y	σ_{sl}	Ref.
γ-Hydroxybutyric acid ⇌ γ-butyrolactone, 0°	HCl 0.5–3.5 *M*	9	−0.57	0.009	0.02	34
Cyclohexan-1,2-dione (hydrate) ⇌ 2-hydroxycyclohex-2-en-1-one	HCl 1.2–6.1 *M*	9	−0.34	0.072	0.06	35
	H_2SO_4 0.7–6.5 *M*	11	−0.44	0.095	0.05	35
	$HClO_4$ 0.7–5.9 *M*	24	−0.55	0.094	0.04	35

Can. J. Chem. Downloaded from www.nrcresearchpress.com by 210.87.254.40 on 09/05/12
For personal use only.

Such plots have threefold utility. The slopes (ϕ values) are useful to characterize the medium effect on the equilibrium quotient. The intercepts represent log K_c at infinite dilution in water. And for concurrent, consecutive equilibria, the ϕ values for the successive steps may be combined additively. The principle of additive combination is discussed and illustrated in the following paper.

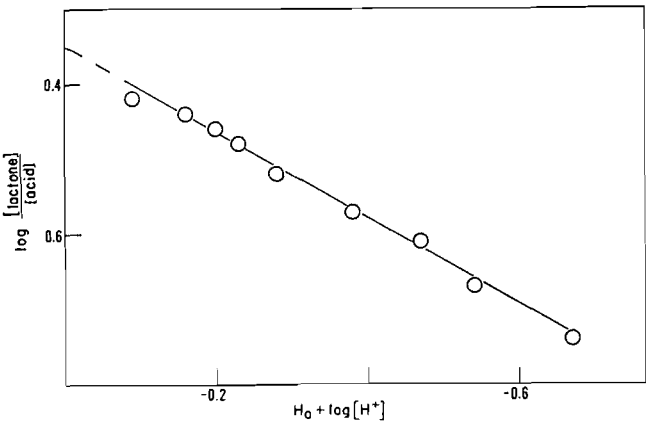


FIG. 6. Correlation of log([lactone]/[acid]) for the γ-hydroxybutyric acid – γ-butyrolactone equilibrium in HCl solutions with (H_0 + log [H^+]).

SIGNIFICANCE OF ϕ VALUES

ϕ values are useful to characterize the response of equilibrium quotients to changing acid concentration. Their utility is similar to that of Hammett *rho* values which characterize the response of reaction rates or equilibria to the polar effects of substituents.

The l.f.e.r. developed in this paper may be viewed as linear relationships between the logarithms of activity coefficient ratios. If the Hammett definition, $h_0 = a_{H^+} f_B/f_{BH^+}$, is algebraically rearranged and logarithms are taken, one obtains

$$H_0 + \log [H^+] = \log f_{BH^+}/f_B f_{H^+}. \quad [11]$$

Substituting for log [H^+] in eq. [4] its equivalent from eq. [11], one obtains

$$\log [SH^+]/[S] + H_0 = \log (f_{BH^+} f_S/f_{SH^+} f_B) + pK_{SH^+}. \quad [12]$$

Substituting from eqs. [11] and [12] into eq. [2], one obtains

$$\log f_{BH^+} f_S/f_{SH^+} f_B = \phi \log f_{BH^+}/f_B f_{H^+}.$$

ϕ is thus a proportionality constant between the logarithms of activity coefficient ratios.

Medium effects on rates and equilibria in moderately concentrated mineral acids have been interpreted in terms of hydration change by many authors (19, 33*c*, 37–42). Hydration change is recognized as a major factor affecting ratios of formal activity coefficients, but other factors probably are also significant. It being difficult to assess just how much of the medium effect is due to hydration change, we shall discuss medium effects in terms of the extreme hypothesis that hydration change is the only factor affecting the magnitude of ϕ values. We do not, however, mean to assert that hydration change is the only relevant factor.

If full account is taken of the hydration of all species, the protonation of a primary aromatic amine indicator base may be written:

$$B(H_2O)_b + H(H_2O)_n^+ \rightleftarrows BH(H_2O)_a^+ + (b + n - a)H_2O.$$

Can. J. Chem. Downloaded from www.nrcresearchpress.com by 210.87.254.40 on 09/05/12
For personal use only.

Can. J. Chem. Downloaded from www.nrcresearchpress.com by 210.87.254.40 on 09/05/12
For personal use only.

It has been shown (40) that

$$H_0 + \log [H(H_2O)_n^+] = (b + n - a) \log a_{H_2O} + \log f_{BH(H_2O)_a^+}/f_{H(H_2O)_n^+} f_{B(H_2O)_b},$$

if each species is hydrated to a constant extent in any medium. On the extreme hydration change hypothesis, the above ratio of activity coefficients for hydrated species is unity in all media, and the hydration change may be reckoned as $(H_0 + \log [H^+])/\log a_{H_2O}$. It is, however, more realistic to consider that each formal species is represented in solution by several species of differing degrees of hydration, in equilibrium with each other. In that case, the average hydration change is the slope of a plot of $(H_0 + \log [H^+])$ versus $\log a_{H_2O}$ (41). For hydrochloric, sulfuric, and perchloric acids, the slope of said plot is approximately 4.5 from about 3.5 to 7.0 M.

Similarly, the slope in a plot of $(\log ([SH^+]/[S]) + H_0)$ against $\log a_{H_2O}$ would represent the $(p - s - a + b)$, the average hydration change accompanying the hypothetical reaction:

[13] $$SH(H_2O)_p^+ + B(H_2O)_b \rightleftarrows S(H_2O)_s + BH(H_2O)_a^+ + (p - s - a + b)H_2O.$$

Accordingly,

$$\frac{d (\log ([SH^+]/[S]) + H_0)}{d (H_0 + \log [H^+])} = \phi = \frac{(p - s) - (a - b)}{b + n - a}.$$

Thus, according to the hydration change hypothesis in its extreme form, ϕ represents the ratio of average hydration change in the hypothetical reaction of eq. [13] to that in protonation of an aromatic primary amine indicator base. The larger the hydration of SH^+ relative to that of S, the more positive ϕ is. A negative ϕ suggests that $(p - s) < (a - b)$, and is expected when hydration of SH^+ is relatively low. We may estimate, on the extreme hydration change hypothesis, the average change in number of water molecules of hydration through a middle range of acid concentrations as about 4.5ϕ. In order to emphasize this feature, we have sometimes used the parameter w', defined as 4.5ϕ, in discussions (43, 44).

VALUES OF H_0 AND $[H^+]$

In our computations, the H_0 values of Paul and Long (9) were employed except at higher concentrations of sulfuric acid, where the H_0 value of Jorgenson and Hartter (2) were used.

We have taken the molar concentration of hydrogen ion to be equal to the molar concentration of the mineral acid. Vapor pressure data show that hydrochloric acid is > 99% dissociated in solutions as concentrated as 10 M (45). No Raman absorption characteristic of undissociated sulfuric acid is detectable below 14 M, although it is speculated that molecular H_2SO_4 may exist in appreciable concentrations in solutions as dilute as 12 M or even 10 M (46). Nuclear magnetic resonance measurements have been interpreted as showing as little as 80% dissociation of perchloric acid in 9 M concentration (47), but this interpretation has been challenged (48) as seriously underestimating the dissociation constant of $HClO_4$.

The thermodynamic pK_a for the second dissociation of sulfuric acid is 2.0. If the activity coefficient ratio, $f_{H^+}f_{sulfate}/f_{bisulfate}$, increases with acid concentration as such ratios for protonation equilibria usually do, or if it diminishes only slightly from unity, acid dissociation of bisulfate ion is negligible even in 1 M sulfuric acid. The apparent molal volumes of sulfuric acid solutions indicate little dissociation of bisulfate ion in 1 M sulfuric acid (49).

However, Young, Maranville, and Smith (46) have described Raman spectral measurements which they interpret as showing substantial acid dissociation of bisulfate ion at sulfuric acid concentrations as high as 11 M. Their spectra have not been published, and Raman studies on 1–10 M sulfuric acid appear not to have been made in other laboratories. The Raman interpretations of Walrafen and Young (50) in sulfuric acid solutions containing SO_3 are controversial (51, 52). Edward and Wang (53) have interpreted the ultraviolet spectra of sulfuric acid solutions at 190 mμ to indicate substantial dissociation of bisulfate ion as high as 5 M, but their estimates are in quantitative disagreement with those of Young *et al.* unless a special transparency is imputed to sulfate ion at higher acid concentrations.

It is thus not certain to what extent the bisulfate ion dissociates in moderately concentrated sulfuric acid solutions. However, if the interpretations of Young *et al.* are correct, the present l.f.e.r. correlations are not substantially affected. $H_0 + \log [H^+]$, after Young *et al.*, is uniformly higher than $H_0 + \log [H_2SO_4]$ by 0.11

$\pm$ 0.01 log unit through the concentration range 0.1 to 7.8 M sulfuric acid. Therefore ϕ values within this range would not be affected, but intercepts (pK_{SH^+} values) would be increased by 0.11ϕ. Since most ϕ values lie between -1 and $+1$ and the uncertainty in pK estimates is of the order of 0.2 pK units, changing to $(H_0 + \log [H^+])$ based on Young *et al.* would scarcely affect pK estimates.

If the interpretations of Young, Maranville, and Smith are correct, values of $(H_0 + \log [H^+])$ at $> 54\%$ sulfuric acid would differ from those we have used by varying margins. Between 55 and 70% sulfuric acid, $(H_0 + [H_2SO_4])$ changes by 1.74. The correction would tend to extend this change to about 1.82. ϕ values based on measurements within this range would be diminished about 5% in absolute magnitude, a scarcely significant change. pK estimates would also be affected by amounts less than 0.25 unit, the correction in a particular case depending on the ϕ value and the length of the extrapolation involved.

ACKNOWLEDGMENTS

We are grateful to the National Science Foundation for a large measure of financial support, to Drs. R. L. Hinman and R. B. Moodie for supplying unpublished data, and to Mr. R. P. Bell and Profs. E. Grunwald and W. M. Schubert for stimulating correspondence and conversations.

REFERENCES

1. L. P. HAMMETT. Physical organic chemistry. McGraw-Hill Book Co., New York. 1940. pp. 262–277.
2. M. J. JORGENSON and D. R. HARTTER. J. Am. Chem. Soc. **85**, 878 (1963).
3. K. YATES and H. WAI. J. Am. Chem. Soc. **86**, 5408 (1964).
4. K. YATES, J. B. STEVENS, and A. R. KATRITZKY. Can. J. Chem. **42**, 1957 (1964).
5. N. C. DENO, J. J. JARUZELSKI, and A. SCHRIESHEIM. J. Am. Chem. Soc. **77**, 3044 (1955).
6. R. L. HINMAN and J. LANG. J. Am. Chem. Soc. **86**, 3796 (1964).
7. E. M. ARNETT and G. W. MACH. J. Am. Chem. Soc. **86**, 2671 (1964).
8. R. H. BOYD. J. Phys. Chem. **67**, 737 (1963).
9. M. A. PAUL and F. A. LONG. Chem. Rev. **57**, 1 (1957).
10. E. M. ARNETT. *In* Progress in physical organic chemistry. Vol. 1. *Edited by* S. G. Cohen, A. Streitwieser, Jr., and R. W. Taft. Interscience, New York. 1963. pp. 223 ff.
11. N. C. DENO. *In* Survey of progress in chemistry. Vol. 2. *Edited by* A. F. Scott. Academic Press, New York. 1964. pp. 155 ff.
12. J. T. EDWARD. Trans. Roy. Soc. Can. [4], **2**, Sect. III, 313 (1964).
13. P. R. WELLS. Chem. Rev. **63**, 171 (1963).
14. K. B. WIBERG. Physical organic chemistry. John Wiley and Sons, Inc., New York. 1964. pp. 417 ff.
15. J. E. LEFFLER and E. GRUNWALD. Rates and equilibria of organic reactions. John Wiley and Sons, Inc., New York. 1963. p. 263.
16. J. F. BUNNETT and F. P. OLSEN. Can. J. Chem. This issue.
17. L. P. HAMMETT. Physical organic chemistry. McGraw-Hill Book Co., New York. 1940. p. 186.
18. E. GRUNWALD and S. WINSTEIN. J. Am. Chem. Soc. **70**, 846 (1948).
19. B. C. CHALLIS and F. A. LONG. J. Am. Chem. Soc. **87**, 1196 (1965).
20. E. M. ARNETT and R. D. BUSHICK. J. Am. Chem. Soc. **86**, 1564 (1964).
21. R. D. BUSHICK. Ph.D. Thesis, University of Pittsburgh, Pittsburgh, Pa. 1961.
22. E. GRUNWALD and B. J. BERKOWITZ. J. Am. Chem. Soc. **73**, 4939 (1951).
23. B. GUTBEZAHL and E. GRUNWALD. J. Am. Chem. Soc. **75**, 559 (1953).
24. B. GUTBEZAHL and E. GRUNWALD. J. Am. Chem. Soc. **75**, 565 (1953).
25. S.-J. YEH and H. H. JAFFÉ. J. Am. Chem. Soc. **81**, 3274 (1959).
26. H. E. BERKHEIMER. Ph.D. Thesis, Pennsylvania State University, University Park, Pa. 1959.
27. N. C. DENO, H. E. BERKHEIMER, W. L. EVANS, and H. J. PETERSON. J. Am. Chem. Soc. **81**, 2344 (1959).
28. C. A. BUNTON and J. H. FENDLER. J. Org. Chem. **30**, 1365 (1965).
29. S. MARBURG and W. P. JENCKS. J. Am. Chem. Soc. **84**, 232 (1962).
30. R. B. MOODIE. Personal communication. R. B. MOODIE, P. D. WALE, and T. J. WHAITE. J. Chem. Soc. 4273 (1963).
31. J. F. BUNNETT and E. BUNCEL. J. Am. Chem. Soc. **83**, 1117 (1961).
32. W. M. SCHUBERT and R. H. QUACCHIA. J. Am. Chem. Soc. **85**, 1278 (1963).
33. (*a*) J. T. EDWARD and S. C. R. MEACOCK. J. Chem. Soc. 2000 (1957). (*b*) J. T. EDWARD, H. S. CHANG, K. YATES, and R. STEWART. Can. J. Chem. **38**, 1518 (1960). (*c*) K. YATES and J. B. STEVENS. Can. J. Chem. **43**, 529 (1965).
34. F. A. LONG, W. F. MCDEVITT, and F. B. DUNKLE. J. Phys. Colloid Chem. **55**, 813 (1951).
35. R. BAKULE. Ph.D. Thesis, Cornell University, Ithaca, N.Y. 1962.
36. F. A. LONG and R. BAKULE. J. Am. Chem. Soc. **85**, 2313 (1963).
37. K. N. BASCOMBE and R. P. BELL. Discussions Faraday Soc. **24**, 158 (1957).
38. R. W. TAFT, JR. J. Am. Chem. Soc. **82**, 2965 (1960).
39. E. HÖGFELDT. Acta Chem. Scand. **14**, 1627 (1960).
40. J. F. BUNNETT. J. Am. Chem. Soc. **83**, 4973 (1961).
41. C. PERRIN. J. Am. Chem. Soc. **86**, 256 (1964).
42. E. B. ROBERTSON and H. B. DUNFORD. J. Am. Chem. Soc. **86**, 5080 (1964).

Can. J. Chem. Downloaded from www.nrcresearchpress.com by 210.87.254.40 on 09/05/12
For personal use only.

43. B. ROTH and J. F. BUNNETT. J. Am. Chem. Soc. **87**, 340 (1965).
44. J. F. BUNNETT and F. P. OLSEN. Abstracts, 145th national meeting of the American Chemical Society, New York. Sept. 1963. p. 41Q.
45. R. A. ROBINSON and R. H. STOKES. Electrolyte solutions. 2nd ed. Butterworths, London. 1959. p. 51.
46. T. F. YOUNG, L. F. MARANVILLE, and H. M. SMITH. *In* The structure of electrolytic solutions. *Edited by* W. J. Hamer. John Wiley and Sons, Inc., New York. 1959. p. 35.
47. G. C. HOOD, O. REDLICH, and C. A. REILLY. J. Chem. Phys. **22**, 2067 (1954). G. C. HOOD and C. A. REILLY. J. Chem. Phys. **32**, 127 (1960).
48. R. P. BELL. The proton in chemistry. Cornell University Press, Ithaca, N.Y. 1959. p. 84.
49. I. M. KLOTZ and C. F. ECKERT. J. Am. Chem. Soc. **64**, 1878 (1942).
50. G. E. WALRAFEN and T. F. YOUNG. Trans. Faraday Soc. **56**, 1419 (1960).
51. R. J. GILLESPIE and E. A. ROBINSON. Can. J. Chem. **40**, 658 (1962).
52. G. E. WALRAFEN. J. Chem. Phys. **40**, 2326 (1964).
53. J. T. EDWARD and I. C. WANG. Can. J. Chem. **43**, 2867 (1965).

Can. J. Chem. Downloaded from www.nrcresearchpress.com by 210.87.254.40 on 09/05/12
For personal use only.

LINEAR FREE ENERGY RELATIONSHIPS CONCERNING REACTION RATES IN MODERATELY CONCENTRATED MINERAL ACIDS[1]

J. F. BUNNETT AND FREDRIC P. OLSEN
Department of Chemistry, Brown University, Providence, Rhode Island

Received March 30, 1966

ABSTRACT

Linear relationships exist between log $k_\psi + H_0$ (for reactions of weakly basic substrates) or log k_ψ (for reactions of strongly basic substrates) and (H_0 + log [H^+]). These are linear free energy relationships. For weakly basic substrates, the correlations obtained are better than in plots of (log $k_\psi + H_0$) versus log a_{H_2O} or of log k_ψ versus $-H_0$. The slopes in plots of log k_ψ or (log $k_\psi + H_0$), as appropriate, against (H_0 + log [H^+]) are taken as parameter, ϕ, which characterizes the response of the reaction rate to changing mineral acid concentration. Values of ϕ for reactions of strongly basic substrates reflect only relationships between protonated substrate and transition state, and may be related to reaction mechanism. ϕ values for reactions of weakly basic substrates reflect both equilibrium protonation of the substrate and transformation of protonated substrate to transition state, and are therefore less directly related to mechanism. However, the ϕ values for the two steps are additive and that for the latter step can be obtained by subtraction if the overall ϕ value and that for equilibrium protonation are known.

The rates and states of equilibrium of reactions in moderately concentrated mineral acid solutions generally vary with the acid concentration. The extent and even the direction of variation differ from reaction to reaction. The description, quantification, and interpretation of these phenomena have occupied the attention of many workers, but understanding remains incomplete.

In the accompanying paper (1) it is shown that linear free energy relationships (l.f.e.r.) exist between the logarithms of equilibrium quotients, [SH^+]/[S][H^+], and (or) second-order rate coefficients for diverse reactions as these quantities vary with acid concentration. These relationships as they pertain to equilibria are considered in that paper. They are now considered as they pertain to rate phenomena.

That l.f.e.r. concerning kinetic data exist is illustrated by Fig. 1 of the accompanying paper and by Figs. 1 and 2 of this one. In the present Fig. 1, the logarithm of the second-order rate coefficient (k_ψ/[H^+], alternatively symbolized k_2) for the enolization of acetophenone (data of Zucker and Hammett (2)) in perchloric acid solutions is plotted against log k_2 for the depolymerization of trioxane (interpolated from data of Bell, Bascombe, and McCoubrey (3)) in perchloric acid solutions. Each point represents measurements at a different acid concentration, points for lower acid concentrations being toward the left of the plot. In Fig. 2, log k_2 for ethyl acetate hydrolysis (interpolated from data of Bell, Dowding, and Noble (4)) is plotted against log k_ψ for hydrolysis of N,N′-diphenylformamidine (data of DeWolfe (5)), both in hydrochloric acid solutions. The latter substrate is strongly basic, essentially fully protonated at all the acid concentrations studied, and one therefore plots log k_ψ rather than log k_2.

For purposes of formulating l.f.e.r. concerning equilibria in standard fashion, the logarithm of the equilibrium quotient for protonation of a hypothetical aromatic primary amine (B) of pK_{BH^+} zero was chosen as horizontal coordinate (1). The logarithm of the

[1]*Presented in part at the 145th national meeting of the American Chemical Society, New York, Sept. 1963. Based in part on the Ph.D. thesis of F. P. Olsen, Brown University, 1964. Preliminary communication: J. F. Bunnett and F. P. Olsen, Chem. Comm. 601 (1965).*

Can. J. Chem. Downloaded from www.nrcresearchpress.com by 210.87.254.105 on 09/05/12
For personal use only.

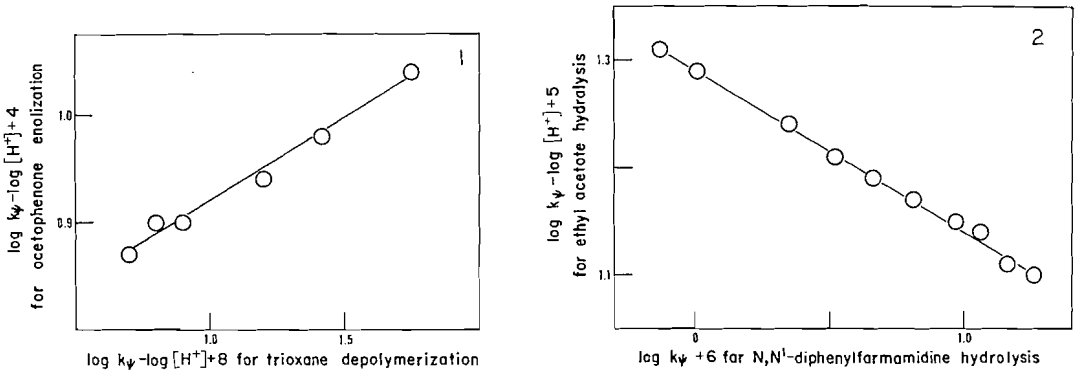


FIG. 1. Correlation of (log k_ψ − log [H⁺]) for acetophenone enolization and trioxane depolymerization in $HClO_4$ solutions.

FIG. 2. Correlation of (log k_ψ − log [H⁺]) for ethyl acetate hydrolysis with log k_ψ for N,N′-diphenylformamidine hydrolysis, in HCl solutions.

equilibrium quotient for this reaction is given by $-H_0$ − log [H⁺]. The same reference reaction will be used in the standardized correlation of kinetic data.

If log k_2 is linear with $-H_0$ − log [H⁺],

$$\log k_\psi - \log [H^+] = (1 - \phi)(-H_0 - \log [H^+]) + \text{constant},$$

where $(1 - \phi)$ is an arbitrary choice of slope parameter. It is convenient, though not necessary, to add $(H_0 + \log [H^+])$ to each side of the equation.

$$\log k_\psi + H_0 = \phi(H_0 + \log [H^+]) + \text{constant}$$

As infinite dilution in water is approached, the first term on the right disappears and the left side of the equation approaches log k_2^0, the logarithm of the second-order rate coefficient at infinite dilution in water; the constant is thus log k_2^0.

$$\log k_\psi + H_0 = \phi(H_0 + \log [H^+]) + \log k_2^0 \qquad [1]$$

Equation [1] is recommended as the standard formulation of this l.f.e.r., insofar as acid-catalyzed reactions of weakly basic substrates are concerned. If the substrate is protonated, in an equilibrium sense, to more than about 5% at the highest acid concentration studied, a different expression must be used.

It is a fact that plots of (log $k_\psi + H_0$) versus $(H_0 + \log [H^+])$ are generally linear, for reactions of weakly basic substrates. Figures 3 and 4 are illustrative.

The slope parameter, ϕ, is useful to characterize the kinetic effect of changing the reaction medium. The intercept represents log k_2 at infinite dilution in water (see eq. [1]).

COMPARISON WITH CORRELATIONS OF OTHER TYPES

An early hypothesis was that log k_ψ for all reactions of weakly basic substrates would be linear with $-H_0$ with unit slope (6). Later, such reactions were considered to fall into two categories in which slopes were unity in plots of log k_ψ against either $-H_0$ or log [H⁺] (7, 8). Since the abandonment of these hypotheses, two systems have been employed to characterize the medium effect on reaction rate. More commonly, the slope of the plot of log k_ψ versus $-H_0$ or some other acidity function has been cited. Alternatively, the slope in a plot of (log $k_\psi + H_0$) versus log a_{H_2O}, the w parameter (9), has been used for this purpose.

Can. J. Chem. Downloaded from www.nrcresearchpress.com by 210.87.254.105 on 09/05/12
For personal use only.

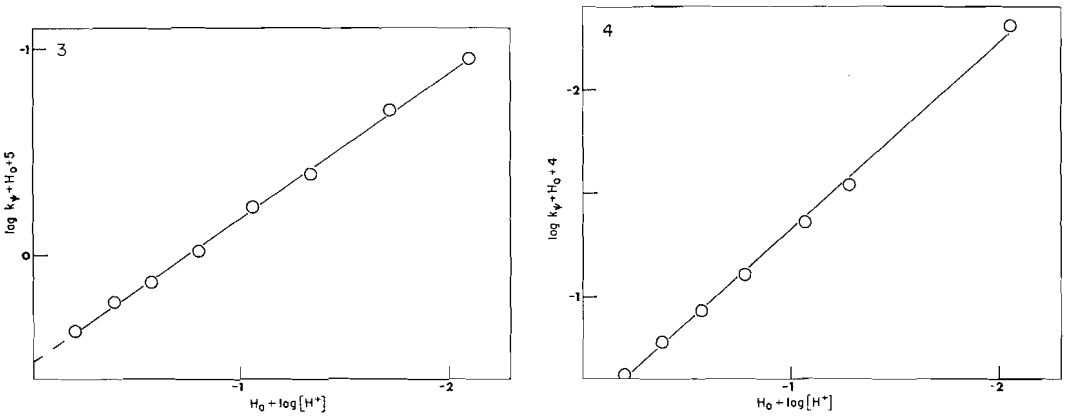


FIG. 3. Correlation of (log k_ψ + H_0) for acetone enolization in HCl solutions with (H_0 + log [H⁺]).
FIG. 4. Correlation of (log k_ψ + H_0) for isonicotinamide hydrolysis in HCl solutions with (H_0 + log [H⁺]).

A difficulty with each method is that the plots in question are not always linear. Departures from linearity appear in plots of log k_ψ versus $-H_0$ when the gradient is appreciably less than unity and in plots of (log k_ψ + H_0) versus log a_{H_2O} when a broad range of acid concentrations is concerned and w differs appreciably from zero. The linear regression "slope" of a curved plot depends on which part of it is examined; the magnitude of the slope parameter therefore depends on how broad a range of acid concentrations was covered by the kinetic experiments.

For the purpose of comparing the quality of correlation according to eq. [1] with correlations by the two foregoing methods, we have reexamined the same large body of kinetic data (nearly all the suitable kinetic data available in 1960) which was correlated by one of us to evaluate w values (9). Correlations according to eq. [1] have been made in all appropriate cases, and correlations of log k_ψ with $-H_0$ in certain test cases selected according to systematic criteria. The criteria were that the set of data comprise six or more points and that Δ log k_ψ between the first and last points be at least 1.6 or the difference in mineral acid concentration at least 5.9 M.

The results of these correlations are summarized in Table I. In addition to correlations of reactions of weakly basic substrates according to eq. [1], Table I presents some correlations of reactions of moderately basic substrates, for which the function plotted against (H_0 + log [H⁺]) is log k_ψ − log ([SH⁺]/[S]$_{st}$) (cf. ref. 10), and some for strongly basic substrates for which the function plotted is log k_ψ. The three functions plotted are designated in Table I by A, B, and C, respectively.

Table I is divided into two parts. Part I comprises reactions for which exactly the same numbers were plotted against (H_0 + log [H⁺]) as were earlier plotted against log a_{H_2O}. Reactions are numbered the same as in Table I of ref. 9, and that table should be consulted for the acid concentration ranges concerned, numbers of experimental points, and citations of original literature.

Part II of the present Table I comprises reactions reckoned on a revised basis. The principal changes are use of Jorgenson–Hartter H_0 values (11) for > 60% sulfuric acid, instead of those of Paul and Long (12), and the plotting of (log k_ψ − log ([SH⁺]/[S]$_{st}$)) instead of log k_ψ − log $h_0/(h_0 + K_{SH^+})$ against (H_0 + log [H⁺]) for most moderately basic substrates. The latter are mainly amides. From recently published amide half-protonation H_0 values and gradients[2] in plots of log ([SH⁺]/[S]) against $-H_0$ (13–17),

[2]*Where no published gradient could be found, a gradient of 0.75 was assumed.*

Can. J. Chem. Downloaded from www.nrcresearchpress.com by 210.87.254.105 on 09/05/12
For personal use only.

the fraction of amide protonated was reckoned at each acid concentration and log k_ψ − log ($[SH^+]/[S]_{st}$) was computed and plotted. Reactions 57 and 58 were handled similarly.

For each set of data in Table I, the slope of the l.f.e.r. plot is given as the ϕ value, the standard deviation in the y-direction of individual points from the linear regression as σ_y, and the standard deviation of the slope as σ_{sl}. For selected "test case" reactions of weakly basic substrates, the slope in the plot of log k_ψ versus $-H_0$ and the standard deviation of points from the linear regression line are also given. Slopes (w values) and σ_y in plots of functions A, B, and C against log a_{H_2O} for reactions in part I appear in Table I of ref. 9, and for reactions in part II in the footnotes.

For the 42 reactions selected as good test cases for correlation procedures, the quality of correlation in the present l.f.e.r. plots, w plots, and plots of log k_ψ versus $-H_0$ may be compared in terms of the standard deviations of points from the linear regression lines, this statistical parameter being directly indicative of the quality of fit.

TABLE I

Correlation of reaction rates in mineral acids with (log $[H^+] + H_0$)

Reaction No.	Reaction, mineral acid, and temperature, °C	Function plotted[a]	ϕ	σ_y[b]	σ_{sl}[c]	Plot of log k_ψ vs. $-H_0$	
						Slope	σ_y[a]
	I. Reactions reckoned on same basis as in ref. 9						
1*a*	Methylal, HCl, 25.0	*A*	−0.70	0.073	0.11	1.27	0.102
1*b*	H_2SO_4, 25.0	*A*	−0.005	0.008	0.05		
1*c*	$HClO_4$, 25.0	*A*	−0.27	0.028	0.03	1.16	0.038
2*a*	Ethylal, HCl, 0.0	*A*	−1.02	0.018	0.05	1.37	0.039
2*b*	HCl, 10.0	*A*	−0.91	0.014	0.04		
3*a*	Chloroacetal, HCl, 25.0	*A*	−0.88	0.048	0.13		
3*b*	$HClO_4$, 25.0	*A*	−0.14	0.057	0.10		
4	Methoxymethyl formate, HCl, 25.0	*A*	+0.15	0.019	0.07		
5*a*	Methoxymethyl acetate, HCl, 25.0	*A*	−0.37	0.031	0.03	1.19	0.037
5*b*	H_2SO_4, 25.0	*A*	−0.06	0.040	0.06		
6	Ethoxymethyl acetate, HCl, 25.0	*A*	−0.44	0.013	0.05		
7*a*	Trioxane depolymerization, HCl, 25.0	*A*	−0.35	0.041	0.03	1.20	0.032
7*b*	HCl, 30	*A*	−0.16	0.024	0.02		
7*c*	HCl, 40	*A*	−0.15	0.035	0.04		
7*d*	HCl, 50	*A*	−0.20	0.035	0.05		
7*e*	HCl, 60	*A*	−0.38	0.020	0.04		
7*f*	H_2SO_4, 25.0	*A*	−0.13	0.014	0.01	1.08	0.018
7*g*	$HClO_4$, 25.0	*A*	−0.30	0.034	0.02	1.19	0.037
8*a*	Paraldehyde depolymerization, HCl, 25.0	*A*	−0.58	0.061	0.15	1.23	0.062
8*b*	H_2SO_4, 25.0	*A*	−0.48	0.055	0.16		
8*c*	$HClO_4$, 25.0	*A*	−0.43	0.054	0.15		
9	Methyl α-D-glucopyranoside, $HClO_4$, 72.9	*A*	+0.22	0.020	0.03		
10	Methyl-β-D-glucopyranoside, $HClO_4$, 72.9	*A*	0.19	0.013	0.04		
11	Phenyl α-D-glucopyranoside, $HClO_4$, 57.4	*A*	0.32	0.053	0.17		
12*a*	Phenyl β-D-glucopyranoside, $HClO_4$, 72.9	*A*	0.17	0.014	0.04		
12*b*	*t*-Butyl β-D-glucopyranoside, $HClO_4$, 24.7	*A*	−0.62	0.028	0.05		
12*c*	*o*-Hydroxymethylphenyl-β-D-glucopyranoside, $HClO_4$, 72.6	*A*	+0.12	0.012	0.03		
12*d*	Methyl α-2-deoxy-D-glucopyranoside, $HClO_4$, 44.5	*A*	−0.18	0.022	0.10		

Can. J. Chem. Downloaded from www.nrcresearchpress.com by 210.87.254.105 on 09/05/12
For personal use only.

TABLE I (*Continued*)

Reaction No.	Reaction, mineral acid, and temperature, °C	Function plotted[a]	ϕ	σ_y[b]	σ_{s1}[c]	Plot of log k_ψ vs. $-H_0$ Slope	σ_y[a]
12*e*	Methyl β-2-deoxy-D-glucopyranoside, $HClO_4$, 25.0	*A*	−0.17	0.015	0.09		
12*f*	Methyl α-D-mannopyranoside, $HClO_4$, 73	*A*	+0.05	0.018	0.03		
12*g*	Maltose, $HClO_4$, 72.6	*A*	0.38	0.027	0.09		
12*h*	Lactose, $HClO_4$, 72.6	*A*	0.34	0.031	0.07		
13*a*	Sucrose, HCl, 0.0	*A*	−0.08	0.033	0.03	1.05	0.028
13*b*	HCl, 10.0	*A*	−0.06	0.019	0.03		
13*c*	HCl, 15.0	*A*	−0.10	0.002	0.02		
13*d*	HCl, 20.0	*A*	−0.10	0.004	0.01		
13*e*	HCl, 25.0	*A*	−0.04	0.008	0.03		
14	β-Hydroxy-β-phenylpropiophenone, reverse aldol, H_2SO_4, 25.1	*A*	−0.006	0.089	0.11		
15	4-(*p*-Methoxyphenyl)-4-hydroxy-2-butanone, dehydration, H_2SO_4, 25.0	*A*	−0.12	0.003	0.004		
16*a*	4-(*p*-Methoxyphenyl)-4-hydroxy-3-methyl-2-butanone, reverse aldol, H_2SO_4, 25.0	*A*	+0.22	0.057	0.03		
16*b*	dehydration, H_2SO_4, 25.0	*A*	−0.03	0.025	0.01		
18	2-Butanol, oxygen exchange, $HClO_4$, 99.8	*A*	+0.13	0.023	0.05		
19	(−)-2-Butanol, racemization, $HClO_4$, 99.8	*A*	+0.17	0.003	0.01		
20	*t*-Butyl alcohol, oxygen exchange, H_2SO_4, 25.0	*A*	−0.29	0.042	0.06		
21*a*	*t*-Amyl alcohol, dehydration, H_2SO_4, 25.0	*A*	−0.07	0.082	0.13		
21*b*	HNO_3, 30.0	*A*	+0.03	0.040	0.07		
22*a*	Pinacol, rearrangement, H_2SO_4, 72.6	*A*	0.88	0.115	0.07		
22*b*	H_2SO_4, 72.9	*A*	0.20	0.021	0.05		
22*c*	H_2SO_4, 100.0	*A*	0.47	0.019	0.06		
23	2-Methyl-1,2-propanediol, rearrangement, $HClO_4$, 72.9	*A*	−0.22	0.051	0.05	1.13	0.041
26*a*	4-Methylphenol-2-*d*, HCl, 25.0	*A*	−0.20	0.014	0.02		
26*b*	H_2SO_4, 25.0	*A*	−0.11	0.049	0.03	1.08	0.047
27	4-Chlorophenol-2-*d*, H_2SO_4, 25.0	*A*	+0.20	0.028	0.02		
29	Anisole-2-*d*, H_2SO_4, 25.0	*A*	−0.11	0.027	0.03		
30	Anisole-4-*d*, H_2SO_4, 25.0	*A*	−0.24	0.064	0.05		
31	1,3,5-Trimethoxybenzene-2-*t*, $HClO_4$, 25.0	*A*	−0.09	0.045	0.08		
38	Picolinamide, HCl, 85	*A*	+0.88	0.019	0.01	0.39	0.100
39	Nicotinamide, HCl, 76.0	*A*	0.89	0.047	0.03	0.38	0.141
40	Isonicotinamide, HCl, 68	*A*	0.90	0.027	0.02	0.39	0.113
41	Acetylglycine, HCl, 61.0	*B*	0.26	0.023	0.01		
42	Piperazine-2,5-dione, HCl, 61.0	*A*	1.07	0.031	0.01	0.21	0.133
43	Acethydrazide, HCl, 61.0	*A*	0.90	0.113	0.09	0.42	0.184
45	*d-sec*-Butyl hydrogen sulfate, racemization, H_2SO_4, 25.0	*A*	−0.006	0.026	0.02		
46	Dimethyl sulfite, $HClO_4$, 0.0	*A*	+0.48	0.082	0.04	0.60	0.101
47*a*	Diethyl sulfite, $HClO_4$, 0.0	*A*	0.43	0.051	0.02	0.66	0.038
47*b*	$HClO_4$, 24.9	*A*	0.48	0.008	0.01		
48	Ethylene sulfite, $HClO_4$, 44.6	*A*	0.68	0.019	0.01		
49	(−)-2,3-Butylene sulfite, $HClO_4$, 35.0	*A*	0.61	0.046	0.03		
50	*meso*-2,3-Butylene sulfite, $HClO_4$, 35.0	*A*	0.74	0.042	0.03		
51	Tetramethylethylene sulfite, $HClO_4$, 35.0	*A*	0.69	0.023	0.02		

Can. J. Chem. Downloaded from www.nrcresearchpress.com by 210.87.254.105 on 09/05/12
For personal use only.

TABLE I (*Continued*)

Reaction No.	Reaction, mineral acid, and temperature, °C	Function plotted[a]	ϕ	σ_ν[b]	σ_{s1}[c]	Plot of log k_ψ vs. $-H_0$	
						Slope	σ_ν[a]
52	Trimethylene sulfite, $HClO_4$, 35.0	*A*	0.53	0.017	0.02		
53	Methyl dihydrogen phosphate, $HClO_4$, 100	*A*	1.00	0.052	0.01	0.17	0.077
54	Dimethyl hydrogen phosphate, $HClO_4$, 100	*A*	0.71	0.027	0.03		
55*a*	α-D-Glucose-1-(dihydrogen phosphate), H_2SO_4, 25.0	*A*	0.32	0.044	0.14		
55*b*	$HClO_4$, 25.0	*A*	0.22	0.026	0.04		
56	Diethyl ether, $HClO_4$, 120.1, 50 atm pressure	*A*	0.46	0.023	0.02		
59	1,2-Dimethoxy-2-methyl-propane, rearrangement, $HClO_4$, 72.9	*A*	−0.50	0.010	0.01		
60	Methyl formate, HCl, 25.0	*A*	+0.74	0.014	0.02		
61	Methyl acetate, HCl, 25	*A*	0.80	0.006	0.01		
62*a*	Ethyl acetate, HCl, 25.0	*A*	0.87	0.040	0.01	0.37	0.126
62*b*	H_2SO_4, 25.0	*A*	0.84	0.047	0.02		
63	Isopropyl acetate, HCl, 25.0	*A*	0.86	0.039	0.02	0.42	0.163
64	*tert*-Butyl acetate, HCl, 25.0	*A*	−0.21	0.064	0.05	1.13	0.047
65*a*	$C_2H_5OOCCH_2SO_3K$, HCl, 25.0	*A*	+0.86	0.037	0.02	0.36	0.075
65*b*	H_2SO_4, 25.0	*A*	0.88	0.004	0.004		
66	Methyl benzoate, $HClO_4$, 90	*A*	0.98	0.010	0.02		
67*a*	Methyl mesitoate, H_2SO_4, 90	*A*	−0.25	0.150	0.19		
67*b*	$HClO_4$, 90	*A*	−0.42	0.070	0.04	1.30	0.060
68	α-Glyceryl monobenzoate, $HClO_4$, 90	*A*	+0.99	0.013	0.007		
69	α-Glyceryl monoanisoate, $HClO_4$, 90	*A*	0.96	0.012	0.009		
70	α-Glyceryl mono-3,4,5-trimethoxybenzoate, H_2SO_4, 50	*B*	0.76	0.052	0.01		
71	Methylene diacetate, HCl, 25.0	*A*	0.75	0.017	0.008	0.50	0.082
72*a*	Ethylidene diacetate, HCl, 25.0	*A*	0.74	0.016	0.008	0.51	0.080
72*b*	HCl, 25.0	*A*	0.77	0.041	0.01	0.46	0.109
73*a*	β-Propiolactone, H_2SO_4, 25.0	*A*	0.10	0.094	0.12		
73*b*	$HClO_4$, 25.0	*A*	−0.22	0.104	0.09	1.17	0.097
74*a*	γ-Butyrolactone, HCl, 0	*A*	+0.87	0.008	0.01		
74*b*	$HClO_4$, 5	*A*	1.04	0.030	0.06		
75*a*	β-Isovalerolactone, hydrolysis, $HClO_4$, 25.0	*A*	0.01	0.021	0.02		
75*b*	decarboxylation, $HClO_4$, 25.0	*A*	1.34	0.045	0.05		
76*a*	Acetone, bromination (enolization), HCl, 25.0	*A*	0.70	0.018	0.01	0.52	0.076
76*b*	Acetone, iodination (enolization), HCl, 25	*A*	0.83	0.004	0.01		
77*a*	Acetophenone, iodination (enolization), H_2SO_4, 25.0	*A*	0.62	0.030	0.01	0.59	0.081
77*b*	$HClO_4$, 25.0	*A*	0.80	0.008	0.01		
78	β-Hydroxy-β-phenylpropiophenone, dehydration (enolization), H_2SO_4, 25.1	*A*	0.58	0.026	0.02		
79*a*	4-Hydroxy-4-phenyl-2-butanone, dehydration (enolization), H_2SO_4, 25.0	*A*	0.66	0.039	0.02	0.54	0.147
79*b*	$HClO_4$, 25.0	*A*	0.64	0.262	0.11		
80	4-Hydroxy-4-(*p*-nitrophenyl)-2-butanone, dehydration (enolization), H_2SO_4, 25.0	*A*	0.70	0.029	0.02		
81*a*	*cis*-Benzalacetophenone, isomerization to *trans*, H_2SO_4, 26.0	*A*	0.44	0.035	0.03		
81*b*	H_2SO_4, 38.0	*A*	0.52	0.017	0.01		
81*c*	$HClO_4$, 26.0	*A*	0.50	0.043	0.03	0.68	0.033

Can. J. Chem. Downloaded from www.nrcresearchpress.com by 210.87.254.105 on 09/05/12
For personal use only.

TABLE I (*Continued*)

Reaction No.	Reaction, mineral acid, and temperature, °C	Function plotted[a]	ϕ	σ_y[b]	σ_{y1}[c]	Plot of log k_ψ vs. $-H_0$ Slope	σ_y[a]
82	Benzoic acid, oxygen exchange, H_2SO_4, 73.0	*A*	0.94	0.066	0.14		
83*a*	γ-Hydroxybutyric acid, lactonization, HCl, 0	*A*	0.32	0.011	0.02		
83*b*	$HClO_4$, 5	*A*	0.26	0.043	0.08		
84	N,N′-Diphenylformamidine, HCl, 25.0	*C*	1.30	0.03	0.03		
85*a*	Thioacetamide, HCl, 35.0	*B*	0.64	0.113	0.09		
85*b*	$HClO_4$, 35.0	*B*	0.80	0.034	0.03		
86*a*	Methyl benzimidate, HCl, 25.0	*C*	1.09	0.039	0.04		
86*b*	H_2SO_4, 25.0	*C*	0.99	0.109	0.10		
87*a*	Cyanamide, HNO_3, 25.0	*A*	0.19	0.009	0.02		
87*b*	HNO_3, 30.0	*A*	0.18	0.008	0.02		
87*c*	HNO_3, 25.0	*A*	0.12	0.011	0.01	0.95	0.009
88	Methyl bromide, $HClO_4$, 50[d]	*C*	0.51	0.033	0.02		
89*a*	Methylmercuric iodide, cleavage, H_2SO_4, 100	*A*	1.07	0.022	0.02		
89*b*	$HClO_4$, 100	*A*	0.74	0.171	0.06	0.41	0.105
91	3,3-Dimethyl-5-ketoheptanoic acid, cyclization to 3,3,6-trimethylcyclohexan-2,5-dione, H_2SO_4, 87.8	*A*	0.58	0.022	0.02		
94*a*	Benzeneboronic acid, reaction with H_2O_2, H_2SO_4, 25.1	*A*	0.46	0.027	0.01		
94*b*	$HClO_4$, 25.1	*A*	0.63	0.027	0.01	0.51	0.118
95	Benzhydryl azide, rearrangement, H_2SO_4, 25.0	*A*	0.07	0.116	0.10		
96	N-Isopropylnitramine, HCl, 45	*A*	0.34	0.012	0.02		
97	O,N-Dimethylnitramine, HCl, 25	*A*	−0.08	0.022	0.03		
98	Phosphoric acid, oxygen exchange, $HClO_4$, 100.1	*A*	+0.81	0.123	0.03	0.33	0.205
100	$CH_3NH_2D^+$, protodedeuteration, H_2SO_4, 25	*C*	1.31	0.009	0.006		
101	$(CH_3)_3ND^+$, protodedeuteration, H_2SO_4, 25	*C*	1.70	0.119	0.07		
	II. Reactions reckoned on a revised basis						
17*a*	2,4-Dinitrobenzyl alcohol, sulfation, H_2SO_4, 0.0[e,f]	*A*	0.11	0.053	0.02	0.90	0.053
17*b*	H_2SO_4, 25.0[e,g]	*A*	0.19	0.016	0.008	0.82	0.016
24	Benzene-*d*, H_2SO_4, 25.0[e,h]	*A*	−0.22	0.061	0.03	1.21	0.062
25	Toluene-4-*d*, H_2SO_4, 25.0[e,i]	*A*	−0.37	0.028	0.01		
28	4-Nitrophenol-2-*d*, H_2SO_4, 25.0[e,j]	*A*	+0.37	0.250	0.05	0.65	0.254
32*a*	Acetamide, HCl, 50[k,l]	*B*	0.78	0.041	0.05		
32*b*	HCl, 61.0[k,m]	*B*	0.77	0.022	0.03		
32*c*	$HClO_4$, 95[k,n]	*B*	0.48	0.0001	0.0001		
33*a*	Propionamide, HCl, 40.5[o,p]	*B*	0.57	0.040	0.02		
33*b*	HCl, 59.6[o,q]	*B*	0.53	0.036	0.02		
34*a*	Benzamide, HCl, 25.0[r,s]	*B*	0.60	0.026	0.01		
34*b*	HCl, 59.6[r,t]	*B*	0.58	0.028	0.02		
34*c*	Benzamide, H_2SO_4, 25.0[r,u]	*B*	0.74	0.025	0.01		
34*d*	$HClO_4$, 95[r,v]	*B*	0.59	0.007	0.006		
35	*p*-Methoxybenzamide, $HClO_4$, 95[w]	*B*	0.55	0.020	0.02		
36	*m*-Nitrobenzamide, $HClO_4$, 95[x]	*B*	0.55	0.008	0.006		
37	*p*-Nitrobenzamide, H_2SO_4, 25.0[y]	*B*	0.44	0.082	0.05		
44*a*	2,4-Dinitrobenzyl hydrogen sulfate, H_2SO_4, 0.0[e,z]		0.67	0.017	0.005	0.36	0.022

Can. J. Chem. Downloaded from www.nrcresearchpress.com by 210.87.254.105 on 09/05/12
For personal use only.

TABLE I (*Concluded*)

Reaction No.	Reaction, mineral acid, and temperature, °C	Function plotted[a]	ϕ	σ_y[b]	σ_{sl}[c]	Plot of log k_ψ vs. $-H_0$ Slope	Plot of log k_ψ vs. $-H_0$ σ_y[a]
44*b*	H_2SO_4, 25.0[e,aa]		0.65	0.020	0.01	0.38	0.022
57	4-(*p*-Sulfophenylazo)-anisole, HCl, 97.0[bb,cc]		0.68	0.060	0.03		
58*a*	4-(*p*-Sulfophenylazo)-1-naphthyl methyl ether, HCl, 46.0[bb,dd]		0.87	0.044	0.02		
58*b*	$HClO_4$, 46.0[bb,ee]		1.27	0.072	0.10		
90	3,3-Dimethyl-5-ketohexanoic acid, cyclization to dimedone, H_2SO_4, 130.7[e,ff]		0.62	0.027	0.02		
92	3,3-Dimethyl-5-ketooctanoic acid, cyclization to 3,3-dimethyl-6-ethylcyclohexan-2,5-dione, H_2SO_4, 85.8[e,gg]	*A*	0.62	0.154	0.04	0.43	0.168
93	3,3-Dimethyl-5-ketononanoic acid, cyclization to 3,3-dimethyl-6-propylcyclohexan-2,5-dione, H_2SO_4, 86.4[e,hh]	*A*	0.60	0.050	0.03		
99	NH_3D^+, protodedeuteration, H_2SO_4, 25[e]		1.22	0.041	0.03		

[a]The function plotted against (H_0 + log [H^+]) is: *A*, log k_ψ + H_0; *B*, log k_ψ − log (h_0/(h_0 + K_{SH^+})) (in part I) or log k_ψ − log ([SH^+]/[S]$_{st}$) (in part II); *C*, log k_ψ.
[b]Standard deviation of individual points, in the *y* direction, from the least squares line.
[c]Standard deviation of the slope, in ϕ units.
[d]Based on 3 points; two points below 0.5 *M* used in previous calculation (9) now omitted.
[e]Based on revised H_0 values of Jorgenson and Hartter (11).
[f]Revised w = +0.13, σ_y = 0.06.
[g]Revised w = +0.31, σ_y = 0.04.
[h]Revised w = −0.35, σ_y = 0.04.
[i]Revised w = −0.81, σ_y = 0.04.
[j]Revised w = +0.40, σ_y = 0.15.
[k]Based on half-protonation H_0 −1.4 (33), gradient 0.75.
[l]Revised w = +5.04, σ_y = 0.02.
[m]Revised w = +4.78, σ_y = 0.03.
[n]Revised w = +1.60, σ_y = 0.07.
[o]Based on half-protonation H_0 −1.0 (16), gradient 0.75.
[p]Revised w = +2.69, σ_y = 0.09.
[q]Revised w = +2.50, σ_y = 0.08.
[r]Based on half-protonation H_0 −2.15, gradient 0.75 (17).
[s]Revised w = +3.19, σ_y = 0.05.
[t]Revised w = +3.12, σ_y = 0.02.
[u]Revised w = +3.29, σ_y = 0.15.
[v]Revised w = +1.97, σ_y = 0.09.
[w]Based on half-protonation H_0 −1.80 (13, 14), gradient 0.75 (14); revised w = +1.83, σ_y = 0.10.
[x]Based on half-protonation H_0 −3.07 (13), gradient 0.75; revised w = +1.86, σ_y = 0.09.
[y]Based on half-protonation H_0 −3.23 (13), gradient 0.37 (14); revised w = +1.79, σ_y = 0.05; when gradient 0.75 used instead of 0.37, ϕ = +0.78.
[z]Revised w = +0.86, σ_y = 0.08.
[aa]Revised w = +1.07, σ_y = 0.07.
[bb]Based on basicity data of ref. 34.
[cc]Revised w = +3.39, σ_y = 0.10.
[dd]Revised w = +4.72, σ_y = 0.08.
[ee]Revised w = +9.11, σ_y = 0.11.
[ff]Revised w = +1.61, σ_y = 0.04.
[gg]Revised w = +1.38, σ_y = 0.04.
[hh]Revised w = +1.43, σ_y = 0.03.

Comparing l.f.e.r. with w plots, one sees that σ_y is less in l.f.e.r. plots than in w plots in 24 cases, greater in 11 cases, and equal in 7. σ_y is much less (difference of 0.05 or more) in 7 cases but much greater in only 2 cases. The superiority of l.f.e.r. over w plots is evident.

Comparing l.f.e.r. plots with plots of log k_ψ versus $-H_0$, one sees that σ_y is less in l.f.e.r. plots in 24 cases, greater in 7, and equal in 11 cases. σ_y is much less in 15 cases but much greater in only 1 case. The l.f.e.r. plots thus excel plots of log k_ψ versus $-H_0$ even more than they do w plots. Correlation by the l.f.e.r. method is clearly superior.

Among the 160 sets of data in Table I, the median standard deviation of points from the l.f.e.r. linear regression line is 0.03 log units, or 7%. This magnitude of deviation could

Can. J. Chem. Downloaded from www.nrcresearchpress.com by 210.87.254.105 on 09/05/12
For personal use only.

reasonably be ascribed to errors in the determination of rate coefficients, in the measurement of mineral acid concentration, and (for moderately basic substrates) in the reckoning of $[SH^+]/[S]_{st}$. Visual inspection of the plots does not suggest any deviation from linearity that cannot reasonably be attributed to random experimental error.

REACTIONS OF MODERATELY AND STRONGLY BASIC SUBSTRATES

It is convenient to represent an acid-catalyzed reaction in generalized fashion:

[2a] $$S + H^+ \rightleftarrows SH^+$$

[2b] $$SH^+ (+ H_2O) \rightleftarrows \ddagger \rightarrow \text{products}$$

In real reactions, additional equilibria, such as reversible addition of water to an unsaturated linkage, may intervene between protonated substrate (SH^+) and transition state. However, the above model still suffices because transition state theory assumes equilibrium between SH^+ and transition state and it does not matter whether that equilibrium comprises one or many steps.

When the substrate is strongly basic, only step [2b] need be taken into account. It is a fact that log k_ψ for reactions of such substrates is linearly related to log k_2 for reactions of weakly basic substrates (see Fig. 2) and to $(H_0 + \log [H^+])$. The latter is demonstrated by Fig. 5 and by the "C" correlations in Table I.

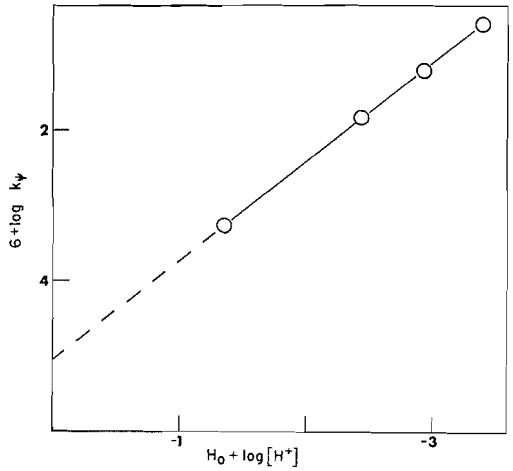


FIG. 5. Correlation of log k_ψ for protodedeuteration of $CH_3NH_2D^+$ in H_2SO_4 solutions with $(H_0 + \log [H^+])$.

With attention to eq. [2b], we may express the rate both phenomenologically and theoretically:

$$\text{rate} = k_\psi[S]_{st} = k[SH^+]f_{SH^+}/f_{\ddagger}.$$

Rearranging and taking logarithms, one obtains

[3] $$\log k_\psi - \log ([SH^+]/[S]_{st}) = \log k + \log f_{SH^+}/f_{\ddagger}.$$

When the substrate is strongly basic, the second term on the left is negligible. Thus the variation of log k_ψ expresses the variation in log $((f_{SH^+}/f_{\ddagger})$. When the substrate is moderately basic the second term on the left cannot be neglected; the variation of log k_ψ − log $([SH^+]/[S]_{st})$ is likewise expressive of variation in log $(f_{SH^+}/f_{\ddagger})$. As shown in Table I,

Can. J. Chem. Downloaded from www.nrcresearchpress.com by 210.87.254.105 on 09/05/12
For personal use only.

part II, good linear correlations of $\log k_\psi - \log([SH^+]/[S]_{st})$ versus $(H_0 + \log [H^+])$ are obtained.

In the 1961 correlations for evaluation of w values (9), the function plotted for moderately basic substrates was $\log k_\psi - \log (h_0/(h_0 + K_{SH^+}))$, this being taken to represent $\log k_\psi - \log ([SH^+]/[S]_{st})$ on the assumption that the equilibrium protonation of substrates "obeyed" H_0. We now realize that assumption to be incorrect in many cases. The original function has been retained for three reactions in Table I, part I, for lack of detailed quantitative information on the protonation equilibria involved.

SIGNIFICANCE OF ϕ VALUES

Equation [3] states that variation of $\log k_\psi - \log ([SH^+]/[S]_{st})$ represents variation in $\log (f_{SH^+}/f_{\neq})$. Equation [11] of the accompanying paper (1) states that variation of $(H_0 + \log [H^+])$ represents variation in $\log (f_{BH^+}/f_B f_{H^+})$. The linear relationship of the left side of eq. [3] to $(H_0 + \log [H^+])$ thus implies a linear relationship between the logarithms of activity coefficient ratios, the proportionality constant being ϕ.

For a weakly basic substrate, the stoichiometric substrate concentration and the unprotonated substrate concentration are virtually identical. Insertion into eq. [3] of the value of $\log ([SH^+]/[S])$ from eq. [12] of the accompanying paper gives

$$[4] \qquad \log k_\psi + H_0 = \log (f_{SH^+}/f_{\neq}) + \log (f_{BH^+} f_S / f_{SH^+} f_B) + \log k + pK_{SH^+}.$$

One could, of course, combine the two logarithms of activity coefficient ratios and cancel out f_{SH^+}. From eq. [11] of the accompanying paper and the present eq. [4], it is evident that the linearity of $(\log k_\psi + H_0)$ with $(H_0 + \log [H^+])$ also implies a linear relationship between the logarithms of activity coefficient ratios.

In terms of the extreme hypothesis that all variations in activity coefficient ratios in moderately concentrated mineral acids are due to hydration changes between initial and final or transition state, the ϕ value can be interpreted as a proportionality constant between the average hydration change in the reaction under study and the average hydration change in equilibrium protonation of a primary aromatic amine indicator base. Letting the average degrees of hydration of S, SH^+, and transition state be s, p, and t, respectively, and employing reasoning detailed elsewhere (18, 19), one infers that ϕ for reactions of moderately or strongly basic substrates represents $(t - p)/(b + n - a)$. ϕ for reactions of weakly basic substrates then represents $[(t - s) - (a - b)]/(b + n - a)$. b, n, and a are, respectively, the average degrees of hydration of primary aromatic amine indicator base, proton, and base conjugate acid.

On the extreme hydration change hypothesis, the value of $(b + n - a)$ over the range of about 3.5–7 M hydrochloric, sulfuric, or perchloric acid is about 4.5 water molecules. Within this concentration range, the average hydration change in a correlated reaction would then approximate 4.5ϕ, which we have sometimes called the w' parameter (20, 21). For reactions of weakly basic substrates, the average hydration change between reactants and transition state, $t - (s + n)$, would approximate $4.5(\phi - 1)$.

Though the hypothesis on which this reckoning is based is almost certainly an oversimplification, it does appear that hydration change is a major factor affecting activity coefficient behavior. ϕ values are useful for the purpose of roughly estimating what the average hydration change would be if the extreme hydration change hypothesis were correct.

It has long been recognized that there is some connection between reaction mechanism and medium effects on kinetic behavior. The Zucker–Hammett hypothesis (7, 8) was an

Can. J. Chem. Downloaded from www.nrcresearchpress.com by 210.87.254.105 on 09/05/12
For personal use only.

Can. J. Chem. Downloaded from www.nrcresearchpress.com by 210.87.254.105 on 09/05/12
For personal use only.

early attempt to define the relationship, but numerous exceptions to it are now known. Three categories of reaction mechanism with respect to w values were delineated by Bunnett (22) on the basis of empirical correlations between w values and the generally accepted mechanisms for certain "calibration" reactions. On the basis of the same calibration reactions, these categories are as follows in terms of ϕ values: water not involved in rate-limiting step, $\phi < 0.0$; water involved as nucleophile in rate-limiting step, ϕ +0.22 to +0.56; water involved as proton transfer agent in rate-limiting step, $\phi >$ +0.58. Carboxylic amide hydrolyses, specifically reactions 32–37, inclusive, previously used for calibration purposes, have not been heeded in stating these categories in terms of ϕ values. Although their w values as published in 1961 clustered rather closely, the ϕ values (based on better information regarding equilibrium protonation) range from +0.44 to +0.78, a broad spread which straddles the second and third mechanistic categories.

It is evident from eq. [4] that ϕ values for reactions of weakly basic substrates represent variation in both the kinetic activity coefficient ratio, $f_{SH^+}/f_{\ddagger}$, and the thermodynamic activity coefficient ratio, $f_{BH^+}f_S/f_{SH^+}f_B$. Only the former can be related to reaction mechanism. It is now clear, though it was not in 1961, that the latter ratio can change appreciably as the medium changes. For this reason, mechanistic interpretation of ϕ (or w) values *for reactions of weakly basic substrates* in the absence of quantitative information as to how the thermodynamic activity coefficient ratio varies with medium composition is fraught with uncertainty. This point was made in 1961 (23), but the reservation needs to be stated more strongly today. Mechanistic interpretation of ϕ values for reactions of moderately or strongly basic substrates is not subject to this reservation (see eq. [3]). These reactions therefore offer attractive possibilities for defining further the relationship of ϕ parameters to mechanism.

ADDITIVE COMBINATION OF ϕ VALUES

Let us symbolize the ϕ values of the separate steps [2*a*] and [2*b*] of the generalized scheme presented above as ϕ_e and ϕ_r, signifying "equilibrium" and "reaction", respectively. And let us represent the phenomenological rate coefficient for step(s) [2*b*] as k_r. We may then write for step [2*a*]

$$[5] \qquad \log ([SH^+]/[S]) + H_0 = \phi_e(H_0 + \log [H^+]) + pK_{SH^+}$$

and for step(s) [2*b*]

$$[6] \qquad \log k_r = \phi_r(H_0 + \log [H^+]) + \log k_r^0.$$

Addition gives

$$[7] \quad \log k_r + \log ([SH^+]/[S]) + H_0 = (\phi_e + \phi_r)(H_0 + \log [H^+]) + pK_{SH^+} + \log k_r^0.$$

Inasmuch as the overall rate is given alternatively by $k_\psi[S]_{st}$ or by $k_r[SH^+]$, it follows that

$$\log k_r + \log ([SH^+]/[S]_{st}) = \log k_\psi.$$

When the substrate is weakly basic, $[S] \approx [S]_{st}$; substitution into eq. [7] gives

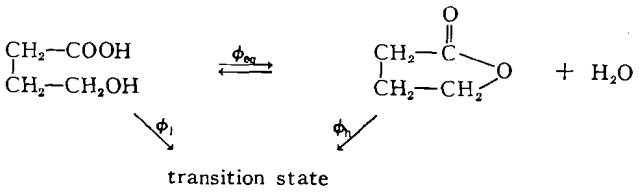
$$[8] \qquad \log k_\psi + H_0 = (\phi_e + \phi_r)(H_0 + \log [H^+]) + pK_{SH^+} + \log k_r^0.$$

Comparison with eq. [1] shows that the ϕ value as ordinarily determined is the sum of the ϕ values for the separate equilibrium and "reaction" steps.

The principle of additivity has an important bearing on the problem of relating ϕ

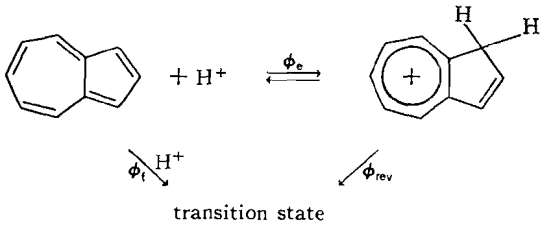
values for reactions of weakly basic substrates to reaction mechanism. Only the ϕ_r value can be related to mechanism. When the substrate is weakly basic, ϕ_r can be obtained by subtracting ϕ_e from the total ϕ value as obtained from kinetic measurements. In some cases, it should be possible to measure ϕ_e directly. In others, ϕ_e may be known for a closely related substrate and one may assume that closely related structures have similar ϕ_e values. There is evidence for the validity of this assumption in several series of bases (1).

The principle of additivity is illustrated by the measurements of Long, Dunkle, and McDevit (24) on the reversible lactonization of γ-hydroxybutyric acid in hydrochloric acid solutions. The ϕ value for the overall equilibrium (ϕ_{eq})



should be equal to the kinetic ϕ value for lactonization (ϕ_l) minus that for lactone hydrolysis (ϕ_h). ϕ_{eq} is -0.57 (Table IV, ref. 1), ϕ is 0.32 and ϕ_h is 0.87 (Table I), all in hydrochloric acid solutions. Thus the expected relationship is realized.

Another illustration concerns the protonation equilibrium and kinetics of proton addition to azulene in perchloric acid, studied by Challis and Long (25).



It is expected that ϕ_e should equal ϕ_f minus ϕ_{rev}. ϕ_e in perchloric acid at 5.7° is -1.54 (Table III, ref. 1). In the same acid at 7.3°, ϕ_f is -0.42 and ϕ_{rev} is 1.11; thus the expected relationship is satisfied. The two kinetic ϕ values are not tabulated in the present paper; the former is based on a plot of log $k_\psi + H_0$ and the latter on a plot of log k_ψ against $(H_0 + \log [H^+])$.

Recently Kresge, O'Ferrall, Hakka, and Vitullo (26) have approached this general problem in a different way. They considered hydrogen isotope exchange reactions of 1,3,5-trihydroxybenzene and its trimethyl ether, which are analogous to the azulene protonation reaction if differences between hydrogen isotopes are disregarded. A parameter α was taken to represent the degree to which the transition state resembles the σ-complex protonation product. α was related to experimentally measurable quantities by the equation

$$k_\psi/[H^+] = k_2^0 K_{SH^+}^{\alpha}([SH^+]/[S][H^+])^{\alpha}.$$

(The symbols of the present paper are employed.) If this equation is written in logarithmic form, substitutions are made from the two l.f.e.r. equations,

$$\log k_\psi - \log [H^+] = (\phi - 1)(H_0 + \log [H^+]) + \log k_2^0$$

$$\log ([SH^+]/[S]) - \log [H^+] = (\phi_e - 1)(H_0 + \log [H^+]) - \log K_{SH^+},$$

Can. J. Chem. Downloaded from www.nrcresearchpress.com by 210.87.254.105 on 09/05/12
For personal use only.

and allowable cancellations are made, there results

$$(\phi - 1) = \alpha(\phi_e - 1).$$

There α parameter therefore amounts to a *proportionality constant* between l.f.e.r. slope parameters. In contrast, we are inclined to relate the *difference* between slope parameters, $\phi - \phi_e$, to reaction mechanism. Time will tell which approach is the more profitable. Notwithstanding, the utility of the α parameter would appear to be limited to cases where the transition state lies between substrate and protonated substrate. The additivity of ϕ values is subject to no such restriction. Moreover, it will be advantageous to compare $(\phi - \phi_e)$ for reactions of weakly basic substrates with ϕ_r determined directly from studies on strongly basic substrates.

We have discussed the additivity of ϕ values for equilibrium [2*a*] and quasi-equilibrium [2*b*]. It is evident that the principle of additivity would likewise prevail if [2*b*] were a true equilibrium; that would be the case of concurrent, consecutive equilibria referred to in the accompanying paper.

SIGNIFICANCE OF NONLINEARITY IN L.F.E.R. PLOTS

The more than 200 l.f.e.r. plots considered in this and the accompanying paper (1) are linear almost without exception. This warrants the conclusion that it is normal or regular for a reaction to give a linear l.f.e.r. plot.

However, not all plots of this type are linear. Plots with severe scatter, severe curvature, and even maxima or minima are known. Most of these "misbehaved" reactions also give nonlinear w plots. Several were mentioned in a 1961 paper (9) and examples have been published by other authors (20, 27–29).

Several causes of deviations from linearity can be recognized:

(*a*) *Experimental error.*—Random errors usually cause scatter, and most of the larger deviations (σ_y) of points from the linear regression line in Table I are of this character. A severe systematic error or certain chance patterns of random error would cause an otherwise linear l.f.e.r. plot to be curved.

(*b*) *Misjudgment of substrate basicity.*—If a substrate treated as weakly basic actually becomes substantially protonated within the acid concentration range of kinetic study, a curved plot results. A probable example has been described by Roth and Bunnett (20).

(*c*) *The inception of a second reaction mechanism.*—If two mechanisms for a reaction are in competition, or if a substrate undergoes two competing reactions, the relative contributions of the two at various acid concentrations depend on their ϕ values. The reaction of lower ϕ value will go relatively faster at higher acid concentrations and the slope of the "l.f.e.r." plot based on overall rate coefficients will decrease. If an intermediate were partitioned between reversion to reactants and progression to products and the ϕ values for the two pathways were different, a curved "l.f.e.r." plot could also result. Examples of competing mechanisms which give rise to curved plots (not shown here) have been discussed by Buchholz and Powell (27) and by Noyce and Jorgenson (30).

(*d*) *Abnormal variation in activity coefficient ratios.*—This would represent departure from the usual linear relationship between the logarithms of activity coefficient ratios. An example concerning the hydrolysis of carboxylic anhydrides has been described by Bunton and Fendler (29), and it is possible that the irregular behavior of acetylimidazole hydrolysis (28) is another. Arnett (31) has cited reasons to expect irregular activity coefficient variation for benzoic acid in sulfuric acid solutions, but no kinetic or protonation equilibrium data are available to bear out his expectations.

Can. J. Chem. Downloaded from www.nrcresearchpress.com by 210.87.254.105 on 09/05/12
For personal use only.

Because l.f.e.r. plots are normally linear, the occasional appearance of a curved plot has diagnostic value. It suggests that one of the above four factors is responsible for the curvature. It alerts the investigator to reexamine his experimental procedures and his assumptions as to substrate basicity, and to consider the possibility that competition between reactions or mechanisms obtains. A curved plot may be a valuable clue.

TABLE II

Correlation of reaction rates in media containing organic solvent components

Reaction and conditions	ϕ	$\sigma^{\phi *}$	σ_y †	Reference
Sucrose, hydrolysis, 50/50 (v/v) H_2O – ethylene glycol, $HClO_4$, 0.7–2.2 *M*, 30°	+0.146‡	0.121	0.05	§
Paraldehyde, depolymerization, 50/50 (v/v) H_2O – ethylene glycol, HCl, 1.0–3.0 *M*, 30°	−0.749	0.237	0.08	§
Acetone, iodination, 50/50 (v/v) H_2O – ethylene glycol, $HClO_4$, 0.7–2.2 *M*, 30°	+1.028	0.037	0.04	§
Acetone, iodination, 10/90 (v/v) H_2O – ethylene glycol, $HClO_4$, 0.2–1.0 *M*, 30°	+0.993	0.105	0.03	§
Methyl toluene-*p*-sulfinate, 0.2 *M* $HClO_4$, 25.2°, solvent varied from 40/60 to 90/10 (v/v) dioxane–water	+0.553	0.131	0.07	‖

*Standard deviation of the slope.
†Standard deviation of individual points, in the *y* direction, from the least squares line.
‡If one widely variant point is omitted, ϕ = +0.411, σ_ϕ = 0.049, and σ_y = 0.01.
§Reference 35.
‖Reference 36.

KINETICS IN MEDIA CONTAINING ORGANIC SOLVENT COMPONENTS

H_0 values have been determined for many mixtures of mineral acid, water, and an organic solvent component such as ethanol, acetic acid, or dioxane (32). In a few cases examined, plots of (log k_ψ + H_0) versus (H_0 + log [HX]) have been found to be straight; these are summarized in Table II. How general such behavior is, we do not know.

ACKNOWLEDGMENT

We are grateful to the National Science Foundation for a large measure of financial support.

REFERENCES

1. J. F. Bunnett and F. P. Olsen. Can. J. Chem. This issue.
2. L. Zucker and L. P. Hammett. J. Am. Chem. Soc. **61**, 2791 (1939).
3. R. P. Bell, K. N. Bascombe, and J. C. McCoubrey. J. Chem. Soc. 1286 (1956).
4. R. P. Bell, A. L. Dowding, and J. A. Noble. J. Chem. Soc. 3106 (1955).
5. R. H. DeWolfe. J. Am. Chem. Soc. **82**, 1585 (1960).
6. L. P. Hammett. Chem. Rev. **16**, 67 (1935).
7. L. B. Hammett. Physical organic chemistry. McGraw-Hill Book Co., New York. 1940. pp. 262 ff.
8. F. A. Long and M. A. Paul. Chem. Rev. **57**, 935 (1957).
9. J. F. Bunnett. J. Am. Chem. Soc. **83**, 4956 (1961).
10. W. M. Schubert and H. K. Latourette. J. Am. Chem. Soc. **74**, 1829 (1952).
11. M. J. Jorgenson and D. R. Hartter. J. Am. Chem. Soc. **85**, 878 (1963).
12. M. A. Paul and F. A. Long. Chem. Rev. **57**, 1 (1957).
13. J. T. Edward, H. S. Chang, K. Yates, and R. Stewart. Can. J. Chem. **38**, 1518 (1960).
14. A. R. Katritzky, A. J. Waring, and K. Yates. Tetrahedron, **19**, 465 (1963).
15. J. T. Edward and I. C. Wang. Can. J. Chem. **40**, 966 (1962).
16. J. T. Edward, J. B. Leane, and I. C. Wang. Can. J. Chem. **40**, 1521 (1962).
17. R. B. Moodie, P. D. Wale, and T. J. Whaite. J. Chem. Soc. 4273 (1963).
18. J. F. Bunnett. J. Am. Chem. Soc. **82**, 4973 (1961).
19. C. Perrin. J. Am. Chem. Soc. **86**, 256 (1964).
20. B. Roth and J. F. Bunnett. J. Am. Chem. Soc. **87**, 340 (1965).
21. J. F. Bunnett and F. P. Olsen. Abstracts, 145th national meeting of the American Chemical Society, New York. Sept. 1963. p. 41Q.
22. J. F. Bunnett. J. Am. Chem. Soc. **83**, 4968 (1961).
23. J. F. Bunnett. J. Am. Chem. Soc. **83**, 4978 (1961).
24. F. A. Long, F. B. Dunkle, and W. F. McDevit. J. Phys. Colloid Chem. **55**, 829 (1951).
25. B. C. Challis and F. A. Long. J. Am. Chem. Soc. **87**, 1196 (1965).

Can. J. Chem. Downloaded from www.nrcresearchpress.com by 210.87.254.105 on 09/05/12
For personal use only.

26. A. J. KRESGE, R. A. MORE O'FERRALL, L. E. HAKKA, and V. P. VITULLO. Chem. Comm. **46** (1965).
27. J. R. BUCHHOLZ and R. E. POWELL. J. Am. Chem. Soc. **85**, 509 (1963).
28. S. MARBURG and W. P. JENCKS. J. Am. Chem. Soc. **84**, 232 (1962).
29. C. A. BUNTON and J. H. FENDLER. J. Org. Chem. **30**, 1365 (1965).
30. D. S. NOYCE and M. J. JORGENSON. J. Am. Chem. Soc. **85**, 2427 (1963).
31. E. M. ARNETT. *In* Progress in physical organic chemistry. Vol. 1. *Edited by* S. G. Cohen, A. Streitwieser, Jr., and R. W. Taft. Interscience, New York. 1963. p. 238.
32. N. C. DENO. *In* Survey of progress in chemistry. Vol. 2. *Edited by* A. F. Scott. Academic Press, New York. 1964. pp. 176–177.
33. N. C. DENO and M. J. WISOTSKY. J. Am. Chem. Soc. **85**, 1735 (1963).
34. J. F. BUNNETT and E. BUNCEL. J. Am. Chem. Soc. **83**, 1117 (1961).
35. C. KALIDAS and S. R. PALIT. J. Chem. Soc. 3998 (1961).
36. C. A. BUNTON and B. N. HENDY. J. Chem. Soc. 2562 (1962).

Can. J. Chem. Downloaded from www.nrcresearchpress.com by 210.87.254.105 on 09/05/12
For personal use only.

COULOMB PARAMETERS IN SIMPLE HUCKEL AND OMEGA TECHNIQUE MOLECULAR ORBITAL METHODS[1]

N. C. BAIRD[2] AND M. A. WHITEHEAD

Theoretical Chemistry Laboratory, Chemistry Department, McGill University, Montreal, Quebec

Received May 2, 1966

ABSTRACT

The well-known similarities of the simple Huckel and omega technique molecular orbital procedures for pi electrons to Pople's self-consistent field method are extended by considering systematic approximations to the latter. From the relationships found, Huckel-method Coulomb integrals and omega values for a variety of atoms (Be, B, C, N, O, F, Mg, Al, Si, P, S, Cl, Ge, As, Se, Sn, Sb, Te) are derived. The Huckel and omega Coulomb integrals are shown to be directly related to a recent definition of orbital electronegativity. The ability of the omega techniques to improve upon the Huckel-method charge distributions is discussed by use of an arbitrary but typical example.

INTRODUCTION

Semi-empirical pi-electron molecular orbital methods, using atomic orbitals as a basis set, continue to be extensively employed in discussions of the structure, stability, reactivity, and spectra of conjugated organic molecules. Three such procedures, the Pariser–Parr–Pople method (1–3), the simple Huckel method (4, 5), and the "omega" technique (5, 6), have been widely applied to such problems (3, 5). The evaluation of the necessary secular determinant matrix elements for the latter two methods is usually empirical, although attempts have been made to estimate the Coulomb integrals from electronegativities, atomic spectral data, and the parameters or results of the Pariser–Parr–Pople technique (7).

In the present study, the well-known similarities among the Huckel, omega, and Pariser–Parr–Pople methods will be considered in some detail, and extended. In particular, quantitative relations between the Coulomb parameters of the three techniques will be derived, and these relationships exploited to provide theoretical estimates of the Coulomb integrals for a wide variety of atoms.

THEORY AND DISCUSSION

All the molecular orbital procedures to be discussed consider only the "pi" electrons of conjugated molecules. The one-electron molecular orbitals (MOs) ψ_i for such electrons are approximated as linear combinations of atomic orbitals (AOs) ϕ_u, with coefficients c_{iu} determined by an energy minimization process; thus

$$\psi_i = \sum_u c_{iu}\phi_u. \qquad [1]$$

The total electronic wave function representing the ground state of a closed shell of pi electrons in a conjugated molecule can normally be accurately expressed as a single Slater determinant of the occupied MOs ψ_i. Pople (2, 8) introduced a simplified self-consistent field procedure to deal with such systems. Various systematic approximations were introduced by Pople (neglect of differential overlap, treatment of the sigma electrons

[1]*Financial support of this work is by the National Research Council of Canada.*
[2]*Holder of N.R.C. Postgraduate Scholarships 1963–1966.*

Can. J. Chem. Downloaded from www.nrcresearchpress.com by 210.87.254.5 on 09/05/12
For personal use only.

as a non-polarizable core, approximation of certain integrals, etc. (2, 3, 8)) which reduce the elements of the F matrix of the secular determinant.

[2] $$\det |F_{uv} - ES_{uv}| = 0$$

to the form

[3] $$F_{uu} = U_{uu} + \tfrac{1}{2}P_{uu}\gamma_{uu} + \sum_{w \neq u} (P_{ww} - Z_w)\gamma_{uw}$$

and

[4] $$F_{uv} = H_{uv} - \tfrac{1}{2}P_{uv}\gamma_{uv} \qquad (u \neq v),$$

where the bond-order matrix elements P_{uv} are defined as

[5] $$P_{uv} = 2\sum_{i} c_{iu}c_{iv},$$

the summation i being over the occupied MOs only. With the approximation for the overlap integrals S_{uv} that

[6] $$S_{uv} = \delta_{uv} = 1 \quad \text{if } u = v,$$
$$= 0 \quad \text{if } u \neq v$$

the diagonal elements P_{uu} of the bond-order matrix P may be identified with q_u, the total pi-electron charge density in AO u,

[7] $$q_u = P_{uu}.$$

In [3] and [4], the Z_w represent the pi-electron core charge of the atom associated with AO w, and in neutral molecules this is equal to the number of pi electrons (0, 1, or 2) contributed by AO w to the pi system. The γ_{uv} (and γ_{uu}) are the two-electron repulsion integrals

[8] $$\gamma_{uv} = \int\int \phi_u^*(1)\,\phi_v^*(2)\,(1/r_{12})\,\phi_u(1)\,\phi_v(2)\,d\tau(1)\,d\tau(2).$$

The one-center repulsion integrals of [8], γ_{uu}, are normally approximated as (1, 3, 8)

[9] $$\gamma_{uu} = I_u - A_u,$$

where I_u, A_u are the valence-state ionization potential and electron affinity of AO u.

The core integral U_{uu} is associated with the ionization potential I_u by (3, 9, 10)

[10] $$U_{uu} = -I_u.$$

The core resonance integral H_{uv} is normally obtained empirically.

Substitution of the relations [7], [9], [10] into eq. [3] for F_{uu} gives

[11] $$F_{uu} = -I_u + \tfrac{1}{2}q_u(I_u - A_u) + \sum_{w \neq u} (q_w - Z_w)\gamma_{uw},$$

which may be rearranged, by use of the core charge Z_u of AO u, to give

[12] $$F_{uu} = [-I_u + \tfrac{1}{2}Z_u(I_u - A_u)] + [\tfrac{1}{2}(q_u - Z_u)(I_u - A_u)] + \left[\sum_{w \neq u} (q_w - Z_w)\gamma_{uw}\right].$$

This can be shortened to

[13] $$F_{uu} = J(u) + K(u, q_u) + L(u, q_w),$$

Can. J. Chem. Downloaded from www.nrcresearchpress.com by 210.87.254.5 on 09/05/12
For personal use only.

in which J, K, L represent the first, second, and third square brackets on the right-hand side of [12].

The term $J(u)$ represents the F_{uu} of AO u for a molecular charge distribution in which all the AO u charge densities q are exactly equal to the corresponding core charges Z ("neutral" AOs).

The term $K(u, q_u)$ represents the correction to $J(u)$ for a non-neutral charge density in AO u.

The term $L(u,q_w)$ is the correction to $J(u)$ for non-neutral charge densities in all the other atomic orbitals.

In the simple (non-overlap) Huckel and omega technique methods, the same secular determinant [2] is solved with the overlap assumption [6] for the conjugated system. In these methods, the F matrix elements are not defined explicitly as in [3] and [4], but are left as empirical quantities α_u and β_{uv}, the Coulomb and resonance integrals:

$$F_{uu} = \alpha_u = \int \phi_u^* H_{\text{eff}}^0 \, \phi_u \, d\tau, \tag{14}$$

$$F_{uv} = \beta_{uv} = \int \phi_u^* H_{\text{eff}}^0 \, \phi_v \, d\tau. \tag{15}$$

Here H_{eff}^0 is an "effective" Hamiltonian operator for the pi system. For computational purposes, α_u and β_{uv} are normally expressed in terms of a "standard" α^0 and β^0 (5), such that

$$\alpha_u = \alpha^0 + h_u\beta^0, \tag{16}$$

$$\beta_{uv} = k_{uv}\beta^0. \tag{17}$$

The quantitative relationships between Pople's method and the simpler MO techniques (Huckel, omega) will now be investigated by considering a set of systematic approximations to the former, and numerically evaluating the simplified F matrix elements for a variety of atoms.

Approximation Method A

The "Pople" expressions for F_{uu}, [11], [12], and [13], may be rewritten for convenience by introducing ϵ terms defined as

$$\epsilon_{uu} = \tfrac{1}{2}\gamma_{uu} = \tfrac{1}{2}(I_u - A_u), \tag{18}$$

$$\epsilon_{uw} = \gamma_{uw} \qquad (w \neq u) \tag{19}$$

to give

$$F_{uu} = J(u) + \sum_w (q_w - Z_w)\epsilon_{uw}, \tag{20}$$

where the sum over w *includes* u.

In method A, the following approximations will be made:

(*a*)

$$\sum_w (q_w - Z_w)\epsilon_{uw} = 0. \tag{21}$$

(*b*) For $u \neq v$,

$$F_{uv} = 0, \tag{22}$$

unless u, v are "nearest neighbors" in the pi system.

Can. J. Chem. Downloaded from www.nrcresearchpress.com by 210.87.254.5 on 09/05/12
For personal use only.

(*c*) For nearest neighbors u and v, F_{uv} can be expressed in terms of $F_{CC'}$, the nearest neighbor F_{uv} for the ground state of benzene, thus

$$F_{uv} = k_{uv}F_{CC'}, \qquad [23]$$

where k_{uv} is an empirical constant for the pair u, v.

Since for neutral molecules

$$\sum_w (q_w - Z_w) = 0, \qquad [24]$$

approximation *a* would be exact if all the ϵ_{uw} were identical, i.e.

$$\epsilon_{u1} = \epsilon_{u2} = \quad = \epsilon_{uu} = \epsilon. \qquad [25]$$

In this case the equation reduces to

$$\sum_w (q_w - Z_w)\epsilon_{uw} = \epsilon \sum_w (q_w - Z_w) = 0. \qquad [26]$$

The equalities [25] are usually incorrect for real systems; however, the ϵ_{uw} for small ring systems are all of the same order of magnitude. In benzene, for example, Pariser and Parr's (1) empirical γ_{uu}, γ_{uv} integrals give ϵ_{uw} for $u = 1$ of

$$\epsilon_{11} = 5.3 \text{ eV}$$

$$\epsilon_{12} = \epsilon_{16} = 7.3 \text{ eV}$$

$$\epsilon_{13} = \epsilon_{15} = 5.5 \text{ eV}$$

$$\epsilon_{14} = 4.9 \text{ eV}$$

$$\text{i.e. all } \epsilon_{uw} = 6.1 \pm 1.2 \text{ eV}.$$

Approximation *b* is not a drastic one since in the Pariser–Parr–Pople method, the off-diagonal F_{uv} for non-nearest neighbors are assumed to have $H_{uv} = 0$ (1, 2, 3). The remaining term $-P_{uv}\epsilon_{uv}$, of F_{uv} would be expected to be small in most cases.

The F_{uu} for method A is then simply $J(u)$ of [13], or

$$F_{uu} = -\left[I_u + Z_u \frac{(A_u - I_u)}{2} \right]. \qquad [27]$$

The term in square brackets of [27] corresponds exactly to the orbital electronegativity χ_u of the "neutral" AO u using the "molecular orbital" definition of bond electronegativity (11). Three neutral orbital cases are possible, corresponding to vacant, singly occupied, and lone-pair atomic orbitals,

$$F_{uu}\,(Z_u = 0) = -I_u = -\chi_u\,(Z_u = 0), \qquad [28]$$

$$F_{uu}\,(Z_u = 1) = -(I_u + A_u)/2 = -\chi_u\,(Z_u = 1), \qquad [29]$$

$$F_{uu}\,(Z_u = 2) = -A_u = -\chi_u\,(Z_u = 2). \qquad [30]$$

Coulomb integrals have been previously associated with orbital electronegativities for singly occupied ($Z_u = 1$) AOs (3, 12, 13) and the above relations show the association to be a general one.

Numerical values of the terms $J(u)$, evaluated from the valence-state energy data of Hinze and Jaffe (14) for a variety of atoms which could use p_π AOs in a conjugated network are listed in Table I. The $J(u)$ are in electron volts, whereas in simple Huckel

Can. J. Chem. Downloaded from www.nrcresearchpress.com by 210.87.254.5 on 09/05/12
For personal use only.

TABLE I

Coulomb integral parameters* for methods "A" and "B"

Atom	Valence state of core	Z_u	I_u (eV)†	A_u (eV)†	$I_u - A_u$ (eV)	$J(u)$ (eV)	$J(u) - J(C)$ (eV)	Empirical‡ h_u	h_u	ω_u
Be	di^1di^1	0	0.17	−0.85	1.02	−0.17	+5.42	−1.28		0.1_2
B	$tr^1tr^1tr^1$	0	1.06	−5.32	6.38	−1.06	+4.53	−1.07	−1.0	0.7_5
C	$tr^1tr^1tr^1$	1	11.16	0.03	11.13	−5.59	0.00	0.00	0.0	1.3_2
N	$tr^2tr^1tr^1$	1	14.12	1.78	12.34	−7.95	−2.36	0.56	0.5	1.4_6
N	$tr^1tr^1tr^1$	2	28.71	11.95	16.76	−11.95	−6.36	1.50	1.5	1.9_8
O	$s^2p^2p^1$	1	17.28	2.01	15.27	−9.65	−4.06	0.96	1.0	1.8_0
O	$s^2p^1p^1$	2	34.15	14.61	19.54	−14.61	−9.02	2.13	2.0	2.3_1
F	$s^2p^2p^1$	2	39.67	18.11	21.56	−18.11	−12.52	2.96	3.0	2.5_5
Mg	di^1di^1	0	0.16	−1.94	2.10	−0.16	+5.43	−1.28		0.2_5
Al	$tr^1tr^1tr^1$	0	1.62	−2.51	4.13	−1.62	+3.97	−0.94		0.4_9
Si	$tr^1tr^1tr^1$	1	9.17	2.00	7.17	−5.59	0.00	0.00		0.8_5
P	$tr^2tr^1tr^1$	1	11.14	1.80	9.34	−6.47	−0.88	0.21		1.1_0
P	$tr^1tr^1tr^1$	2	20.68	10.26	10.42	−10.26	−4.67	1.10		1.2_3
S	$s^2p^2p^1$	1	12.39	2.38	10.01	−7.39	−1.80	0.43		1.1_8
S	$s^2p^1p^1$	2	22.97	11.05	11.92	−11.05	−5.46	1.29		1.4_1
Cl	$s^2p^2p^1$	2	26.36	13.38	12.98	−13.38	−7.79	1.84	2.0	1.5_3
Ge	$tr^1tr^1tr^1$	1	8.72	4.11	4.61	−6.41	−0.82	0.19		0.5_5
As	$tr^2tr^1tr^1$	1	11.24	2.64	8.60	−6.94	−1.35	0.32		1.0_2
Se	$s^2p^2p^1$	1	11.68	2.52	9.16	−7.10	−1.51	0.36		1.0_8
Sn	$tr^1tr^1tr^1$	1	8.02	4.89	3.13	−6.46	−0.87	0.21		0.3_7
Sb	$tr^2tr^1tr^1$	1	10.51	2.77	7.74	−6.64	−1.05	0.25		0.9_1
Te	$s^2p^2p^1$	1	11.04	2.58	8.46	−6.81	−1.22	0.29		1.0_0

*All energy data and parameters are listed for pure, unhybridized p_π atomic orbitals.
†All valence state energy data is from ref. 14*c*.
‡Arbitrarily chosen (see text) as the "best" values listed on page 135 of ref. 5.

methods it is conventional to express the Coulomb integrals in terms of the standard Coulomb and resonance integrals, α^0 and β^0 for benzene. If one adopts this form of expression,

$$J(u) = J(\mathrm{C}) + h_u F_{\mathrm{CC}'}, \qquad [31]$$

where $J(\mathrm{C})$ and $F_{\mathrm{CC}'}$ represent the $J(u)$ and nearest-neighbor F_{uv} terms for benzene. From [31]

$$h_u = \frac{J(u) - J(\mathrm{C})}{F_{\mathrm{CC}'}}, \qquad [32]$$

which requires the numerical value of $F_{\mathrm{CC}'}$ before the h_u can be evaluated. Now from [4], for the nearest neighbors in benzene,

$$F_{\mathrm{CC}'} = H_{\mathrm{CC}'} - \tfrac{1}{2} P_{\mathrm{CC}'} \gamma_{\mathrm{CC}'}. \qquad [33]$$

For this case, $P_{\mathrm{CC}'}$ is 2/3, and using the Pariser–Parr (1) value of $\gamma_{\mathrm{CC}'}$, 7.30 eV, [33] becomes

$$F_{\mathrm{CC}'} = H_{\mathrm{CC}'} - 2.43 \text{ eV}. \qquad [34]$$

The core resonance integral $H_{\mathrm{CC}'}$ is normally determined empirically from some property of benzene. From the ultraviolet spectrum of benzene, Pariser and Parr (1) derived $H_{\mathrm{CC}'} = -2.39$ eV; from a bond-length correlation function, Chung and Dewar (15) obtain −1.75 eV, and from the resonance energy of benzene these authors obtain −1.92 eV. The observed electron-impact ionization potential of 9.52 eV for benzene (6) can be used to derive $H_{\mathrm{CC}'}$ of −1.50 eV. The magnitude of $F_{\mathrm{CC}'}$ in the cases mentioned above is then −4.82, −4.18, −4.35, and −3.93 eV respectively.

Can. J. Chem. Downloaded from www.nrcresearchpress.com by 210.87.254.5 on 09/05/12
For personal use only.

The correspondence between method A and the simple Huckel method can now be demonstrated by showing the one-to-one relation between Huckel h_u values obtained empirically and the h_u calculated by [32] from the valence-state energy data. The only difficulty in such an analysis is the choice of appropriate Huckel h_u to be used. For the purposes of this study, the consistent and widely used "best" values listed by Streitwieser (*7a*) have been adopted. The correlation of these h_u with the term $(J(u) - J(\mathrm{C}))$ is given in Fig. 1. The correlation line is excellent, considering that the "best" h_u are only estimated to within ± 0.25.* The slope of the line, -4.2_3 eV, is within the range of the estimates of $F_{CC'}$ given above.

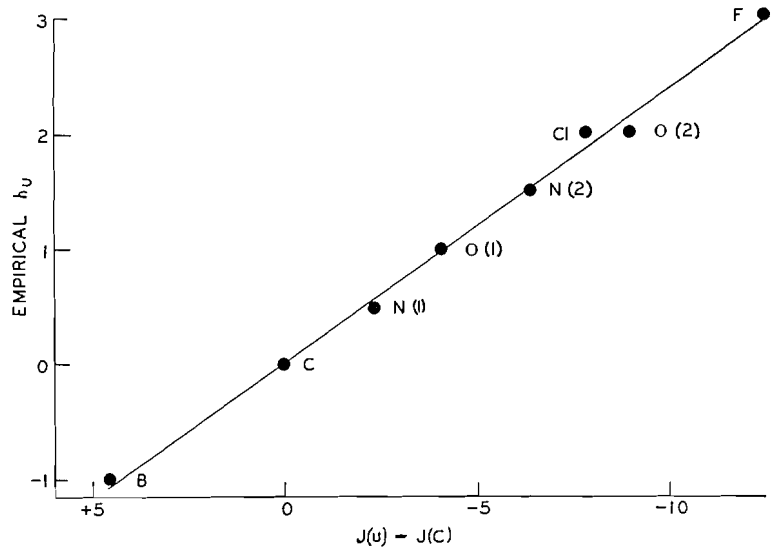


FIG. 1. Plot of $J(u) - J(\mathrm{C})$ against the empirical Huckel h_u. NOTE: The integer in brackets following the atomic symbol represents the core charge Z_u for atoms having more than one value of Z_u listed in Table I.

The quantitative correspondence between the theoretical and empirical h_u gives some insight into the nature of the effective hamiltonian H_{eff}^0 of [14]. The H_{eff}^0 corresponds to the Pople-method hamiltonian for a molecular charge distribution in which all the pi atomic orbitals are neutral (i.e. all $q_u = Z_u$). From this elucidation, the Huckel h_u for a variety of atoms not considered by Streitwieser may be calculated. These h_u, evaluated using $F_{CC'} = -4.23$ eV, are listed in Table I.

Certain trends in the h_u are evident:

(I) Atoms of Groups 2 and 3, the p_π AOs of which are normally vacant, have very low h_u, of the order of -1.

(II) Group 4 atoms have h_u close to zero.

(III) Group 5, 6, and 7 atoms display a wide range of h_u depending upon Group, Period, and pi core charge of the atoms, although in general all the h_u are quite high, and for a given atom $h_u\,(Z_u = 2) > h_u\,(Z_u = 1)$. The term for sulfur $(Z_u = 2)$ is close to that of nitrogen $(Z_u = 2)$ as anticipated (*7a*).

All the atomic energy terms used in the derivation of the $J(u)$ values in Table I were obtained by assuming that the sigma-bonded AOs of the valence shell were "neutral" (that

**The excellent correlation obtained may be due in part to the use of atomic and molecular ionization potential data in deriving some Huckel h_u which would have been considered in arriving at the "best" values.*

Can. J. Chem. Downloaded from www.nrcresearchpress.com by 210.87.254.5 on 09/05/12
For personal use only.

is, the sigma bonds are completely nonpolar). The close agreement between theoretical and empirical Coulomb integrals in Table I indicates that this "assumption" must be an additional feature of the simple Huckel-method H_{eff}^0.

The explicit dependence of h_u on the net *excess* charge Q_σ of the sigma core, the deviation from neutrality, may be evaluated by using the approximate dependence of I_u and A_u upon Q_σ as previously outlined (16). By use of this dependence, and the energy data of Hinze (14*c*), then the h_u dependence upon Q_σ is

$$h_{\text{C}} = 0.00 + 2.28Q_\sigma + 0.43Q_\sigma^2, \quad [35]$$

$$h_{\text{N}} = 0.56 + 2.43Q_\sigma + 0.49Q_\sigma^2, \quad [36]$$

$$h_{\text{O}} = 0.96 + 3.17Q_\sigma + 0.32Q_\sigma^2 \quad [37]$$

for the $Z_u = 1$ cases of carbon, nitrogen, and oxygen respectively. The dependence of h_u upon the sigma net charge, excess or deficit, is about 2 to 3 units per electron. This dependence will be important for protonated nitrogen and oxygen atoms, for which Streitwieser lists $h_{\text{N}^+} = 2.0$, and $h_{\text{O}^+} = 2.5$. These h_u correspond to Q_σ of about $+0.5$ electron in each case. Such a deficit of less than $+1.0$ electron is acceptable, since the sigma bonds from nitrogen and oxygen will be quite polar in such cases, effectively spreading the positive charge throughout the sigma system.

Approximation Method B

Several attempts have been made to explicitly incorporate a certain amount of electron repulsion as a function of molecular charge distribution into the simple Huckel method (6, 17–20). Streitwieser (6) systematized these attempts into a scheme now known as the omega (ω) technique, in which the Coulomb integral α_u is dependent upon the charge density q_u of the AO u, hence

$$\alpha_u = \alpha^0 + h\beta^0 + (Z_u - q_u)\omega\beta^0. \quad [38]$$

where ω is an empirical constant.

By analogy with the ω technique, the first two terms $J(u)$ and $K(u,q_u)$ of the Pople expression [13] will be considered to yield an appropriate F_{uu} expression in method "B". Approximations *b* and *c* of method A will remain unchanged in this technique.

The approximation to the Pople F_{uu} expression in method B is, therefore, that the term $L(u,q_w)$ of [13] is zero;

$$L(u,q_w) = \sum_{w \neq u} (q_w - Z_w)\gamma_{uw} = 0. \quad [39]$$

By retaining the definition of h_u in [32], the approximate diagonal matrix term F_{uu} then becomes

$$F_{uu} = J(\text{C}) + h_u F_{\text{CC}'} + \omega_u F_{\text{CC}'}(Z_u - q_u), \quad [40]$$

where

$$\omega_u = \frac{\frac{1}{2}(A_u - I_u)}{F_{\text{CC}'}}. \quad [41]$$

Equation [40] may be written directly in terms of I_u and A_u; dropping the last term (see [39]) of eq. [11] gives

$$F_{uu} = -[I_u + \tfrac{1}{2}q_u(A_u - I_u)]. \quad [42]$$

Can. J. Chem. Downloaded from www.nrcresearchpress.com by 210.87.254.5 on 09/05/12
For personal use only.

The term of [42] in square brackets represents the molecular-orbital definition of the bond electronegativity function for AO u (11) with charge density q_u. The method B Coulomb integrals are then directly associated with the bond electronegativities of the pi AOs; in method A this association held only for the "neutral" orbital electronegativities. Klopman (13) has previously noted the correspondence between electronegativity and Coulomb integrals in omega-type methods.

By use of the value of $F_{CC'}$ from method A of -4.23 eV, the terms ω_u for various atomic p_π orbitals u may be evaluated (eq. [41]). These parameters are listed in Table I. Empirical values of ω for carbon have ranged from 0.33 to 1.8 (7*a*), but the widely used and "best" value is $\omega_C = 1.4$ (6, 7*a*, 20). The theoretical value of ω_C in Table I is 1.32, in excellent agreement with the empirical result. Although Pritchard and Sumner (19) derived quite different ω_u for different atoms, the ω value for *all* atoms is normally taken to be the same as that for carbon (6). The widely different ω_u's for different atoms (and different Z_u) listed in Table I indicate that this extension is not justified.

Within each Period, there appears to be a good correlation of ω_u with h_u, ω_u generally increasing with atomic number. Within each Group of the Periodic Table, ω_u decreases as the atomic number increases. For atoms with different possible pi core charges Z_u, ω_u for $Z_u = 2$ is greater than that for $Z_u = 1$.

The relation between ω_u and h_u for the first Period atoms (except Be†) is illustrated in Fig. 2. This relation may be expressed as

[43] $$\omega_u = 0.45h_u + 1.3_0.$$

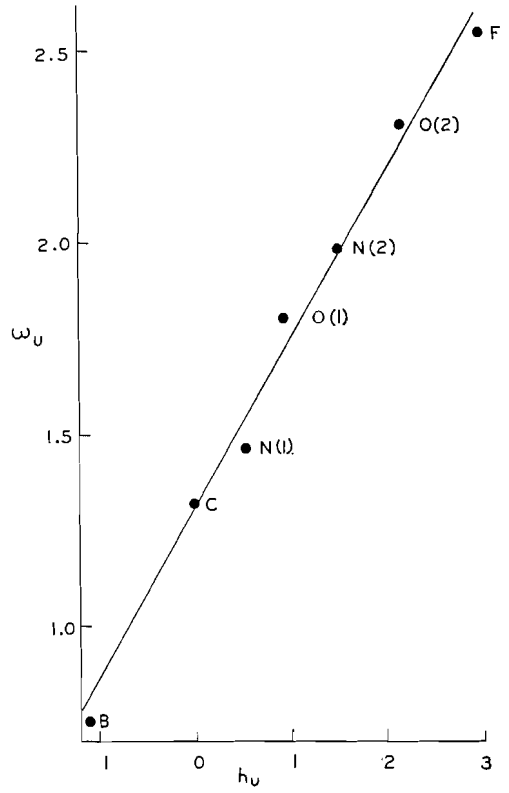


FIG. 2. Plot of ω_u against h_u for atoms of the first Period.

†*The Group 2 elements for the first and second Periods fall significantly off the correlation lines.*

Can. J. Chem. Downloaded from www.nrcresearchpress.com by 210.87.254.5 on 09/05/12
For personal use only.

The corresponding relation for the second Period atoms may be approximately expressed as

[44] $$\omega_u = 0.42h_u + 0.8_6$$

for the elements Al to Cl. The two correlation lines are almost parallel to each other.

Equations [40], [43], and [44] may be combined to give

[45] $$F_{uu} = J(\mathrm{C}) + h_u{}^* F_{\mathrm{CC}'}$$

with

[46] $$h_u{}^* = h_u + (Z_u - q_u)(0.45h_u + 1.3)$$

for the atoms B, C, N, O, and F, and

[47] $$h_u{}^* = h_u + (Z_u - q_u)(0.42h_u + 0.86)$$

for the atoms Al, Si, P, S, and Cl. In [46] and [47], the h_u are those for the simple Huckel method listed in Table I.

Streitwieser attempted to compare the omega technique with Pople's method by noting that the term $\frac{1}{2}\gamma_{uu}$ of [3] should be numerically identical with $-\omega\beta^0$ of [38] if the omega technique did include only the terms $J(u)$ and $K(u,q_u)$ of [13], and completely neglected the remaining term $L(u,q_w)$ (6). By using $\beta^0 = -2.11$ eV and the $\frac{1}{2}\gamma_{uu}$ (for carbon) of 5.3 eV, he showed that $-\omega\beta^0$ was about 2.9 eV, little more than half the value of the $\frac{1}{2}\gamma_{uu}$ (6). This low value of $-\omega\beta^0$ was taken as evidence that the omega technique in fact allowed for the term $L(u,q_w)$ of [13] in some average way. The value of β^0 used in this analysis (by Streitwieser) was computed by a correlation of experimental molecular ionization potentials with the calculated difference in pi energy between the neutral molecules and their positive ions. The energies were computed by adding the one-electron energies of the occupied MOs. This method of obtaining the total pi energy by adding the one-electron levels is actually inconsistent with the effective inclusion of electron repulsions in the F_{uu} terms, since in self-consistent field MO methods, this simple addition process includes electron repulsions twice (3). The use of a self-consistent field $H_{\mathrm{CC}'}$ value of about -2 eV, giving an $F_{\mathrm{CC}'}$ of about -4.2 eV, leads to a ω_{C} value very close to the empirical estimate when the $L(u,q_w)$ term is completely neglected. There is no averaged correction for this term in empirical omega techniques for this reason. Method B is then computationally equivalent to the omega technique for hydrocarbons.

Comparison of the Methods

Now that methods A and B, corresponding in fact to the simple Huckel and omega procedures, have been outlined, it is instructive to try to compare the actual validities of each method to Pople's scheme. For purposes of the comparison, a typical molecular

TABLE II

Calculated ΔF_{uu} and Huckel charges for pyridine-like molecule (Fig. 3)

Atom number*	Huckel charge $(Z_u - q_u)$	ΔF_{uu} Simple Huckel	ω-type technique	ω + nearest neighbors	ω + 1st + 2nd neighbors	Pople† method
1	−0.3697	0.00	+1.95	−0.17	−0.08	−0.55
2	+0.1452	0.00	−0.76	+1.99	+0.68	+0.72
3	−0.0082	0.00	+0.04	−1.72	+0.35	−0.36
4	+0.0957	0.00	−0.50	−0.38	−1.97	−0.16

*Numbering scheme as in Fig. 3.
†Equivalent to ω + *all* neighbors.

Can. J. Chem. Downloaded from www.nrcresearchpress.com by 210.87.254.5 on 09/05/12
For personal use only.

system was chosen and calculations were performed to establish the extent to which the omega technique improved the Huckel F_{uu} parameters, during the self-consistent field calculations, towards those required by Pople's method.

The example used is a six-membered ring system containing five carbon atoms, each having a p_π AO (with $h_u = 0$), and one conjugating heteroatom, X, with $h_X = 1.0$. The pi system of the molecule is assumed to contain 6 electrons, and all nearest neighbors are assumed to have F_{uv} equal to that of benzene. For simplicity, the geometry of the ring is taken to be identical to that of benzene, and the heteroatom X is assumed to have all γ_{uX} equal to those of the carbon atoms. The values of the latter integrals were taken from Pariser and Parr's paper (1).

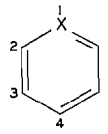


FIG. 3.

The simple Huckel charge distribution based on these assumptions is given in Table II. The ΔF_{uu} listed in the remaining columns of Table II corresponds to the differences between $J(u)$, the simple Huckel F_{uu}, and the F_{uu} for the various methods calculated on the basis of the Huckel charge distribution;

$$\Delta F_{uu} = F_{uu} - J(\mathrm{C}). \qquad [48]$$

The ΔF_{uu}'s corresponding to the omega technique (column 4 of Table II) bear little resemblance in sign, magnitude, or relative order for the different atoms to those required by the Pople method (column 7) for the same charge distribution. The correspondence between the omega ΔF_{uu} and the Pople ΔF_{uu} is not substantially improved by adding nearest-neighbor terms (column 5) and first and second nearest-neighbor terms (column 6) to the ΔF_{uu} of the omega technique. The inclusion of the first, or first and second nearest-neighbor terms has been previously suggested (21, 22) as a means of improving the omega technique. The simple Huckel ΔF_{uu}, all zero of course, are actually closer to those of Pople's method than are the ΔF_{uu} of any other of the techniques.

Since the second iteration F_{uu}'s of the omega techniques are not altered from the Huckel F_{uu}'s in even qualitatively the same manner as those in the Pople method, it is difficult to see why the self-consistent field charges of the ω methods represent an improvement over those of the Huckel method. The ω technique will have the effect of "smoothing out" the net excess charges calculated by the Huckel method, but will not necessarily lead to any improvement in the relative *order* of charge densities among the atoms.

REFERENCES

1. R. PARISER and R. G. PARR. J. Chem. Phys. **21**, 466, 767 (1953).
2. J. A. POPLE. Trans. Faraday Soc. **49**, 1375 (1953).
3. R. G. PARR. Quantum theory of molecular electronic structure. Benjamin, New York. 1964. Chap. 3.
4. C. A. COULSON and H. C. LONGUET-HIGGINS. Proc. Roy. Soc. London, Ser. A, **191**, 39 (1947).
5. A. STREITWIESER. Molecular orbital theory for organic chemists. Wiley, New York. 1961.
6. A. STREITWIESER. J. Am. Chem. Soc. **82**, 4123 (1960).
7. (*a*) A. STREITWIESER. Molecular orbital theory for organic chemists. Wiley, New York. 1961. Chap. 5. (*b*) F. PERADEJORDI. Cahiers Phys. **17**, 393 (1963).
8. N. S. HUSH and J. A. POPLE. Trans. Faraday Soc. **51**, 600 (1955).
9. H. KON. Bull. Chem. Soc. Japan, **28**, 275 (1955).
10. M. J. S. DEWAR. Rev. Mod. Phys. **35**, 586 (1963).
11. N. C. BAIRD, J. M. SICHEL, and M. A. WHITEHEAD. To be published.

Can. J. Chem. Downloaded from www.nrcresearchpress.com by 210.87.254.5 on 09/05/12
For personal use only.

12. R. S. MULLIKEN. J. Chem. Phys. **2**, 782 (1934).
13. G. KLOPMAN. J. Am. Chem. Soc. **86**, 1463 (1964).
14. (*a*) J. HINZE and H. H. JAFFE. J. Am. Chem. Soc. **84**, 540 (1962). (*b*) J. HINZE and H. H. JAFFE. J. Phys. Chem. **67**, 1501 (1963). (*c*) J. HINZE. Ph.D. Thesis, University of Cincinnati, Cincinnati, Ohio. 1962.
15. A. L. H. CHUNG and M. J. S. DEWAR. J. Chem. Phys. **42**, 756 (1965).
16. M. A. WHITEHEAD, N. C. BAIRD, and M. KAPLANSKY. Theoret. Chim. Acta, **3**, 135 (1965).
17. G. W. WHELAND and D. E. MANN. J. Chem. Phys. **17**, 264 (1949).
18. N. MULLER, L. W. PICKETT, and R. S. MULLIKEN. J. Am. Chem. Soc. **76**, 4770 (1954).
19. H. O. PRITCHARD and F. H. SUMNER. Proc. Roy. Soc. London, Ser. A, **235**, 136 (1956).
20. A. STREITWIESER and P. M. NAIR. Tetrahedron, **5**, 149 (1959).
21. W. KUHN. Tetrahedron, **19**, Suppl. **2**, 88, 389, 437 (1963).
22. A. STREITWIESER, A. HELLER, and M. FELDMAN. J. Phys. Chem. **68**, 1224 (1964).

Can. J. Chem. Downloaded from www.nrcresearchpress.com by 210.87.254.5 on 09/05/12
For personal use only.

SIMULTANEOUS ANALYSIS OF TWO-COMPONENT SYSTEMS BY DIFFUSE REFLECTANCE SPECTROSCOPY[1]

R. W. Frei and D. E. Ryan
Department of Chemistry, Dalhousie University, Halifax, Nova Scotia

AND

V. T. Lieu
Department of Chemistry, University of Hawaii, Honolulu, Hawaii

Received February 3, 1966

ABSTRACT

Diffuse reflectance spectroscopy can be used for the analysis of multicomponent systems in the adsorbed state. The Kubelka–Munk theory for diffuse reflection and transmission on light-scattering layers has been applied for this analysis. Simple dye mixtures adsorbed on thin-layer chromatography-grade adsorbents were employed. The method can be adapted directly to the analysis of incompletely separated components on chromatographic adsorbents.

INTRODUCTION

Analytical applications of diffuse reflectance spectroscopy to chromatographic separation procedures (1–4) have stimulated development, by the same techniques, of a method for simultaneous analysis of multicomponent systems. Such a method is analogous to procedures for absorptiometric analysis of multicomponent mixtures in solution and would find application for systems in which incomplete chromatographic separation would ordinarily prevent quantitative evaluation by reflectance spectroscopy. The requirements, of course, are similar to those necessary for successful analysis of mixtures of absorbing substances in solution; no interaction between components should occur and one species should absorb at a wavelength where the others absorb weakly. In addition, the reflectance spectra, or some suitable function of the reflectance, should be additive. For a solid powder system, where the chromophoric species are adsorbed on the surface of a chromatographic adsorbent, it is necessary to adopt a theory which deals with the diffuse reflection and the transmission of light-scattering layers.

The widely accepted theory of Kubelka and Munk (5, 6) proves most appropriate. For an infinitely thick, opaque layer the Kubelka–Munk equation may be written

$$[1] \qquad \frac{(1 - R_\infty')^2}{2R_\infty'} = \frac{k}{s}$$

where R_∞' is the absolute reflectance of the layer, k is the absorption coefficient, and s is the scattering coefficient.

The relative reflectance R_∞, which is measured against a reference standard such as MgO, $CaSO_4$, or $MgCO_3$, is usually used rather than the absolute reflectance R_∞'. The equation then becomes

$$[2] \qquad F(R_\infty) = \frac{(1 - R_\infty)^2}{2R_\infty} = \frac{k}{s}$$

and a linear relationship should be observed between $F(R_\infty)$ and the absorption coefficient k if s is constant. This is achieved by using powders with large particle size in comparison

[1]*Paper presented at the Fifth National Meeting, Society for Applied Spectroscopy, Chicago, June 16, 1966.*

Can. J. Chem. Downloaded from www.nrcresearchpress.com by 210.87.254.6 on 09/05/12
For personal use only.

with the wavelength used for measurement; since adsorbents for thin-layer and column chromatography usually have particle sizes larger than 5 μ, s will be independent of wavelength.

To obtain a straight-line calibration curve from reflectance measurements it is also essential that concentrations of adsorbed components be such that absorption of light is not greater than 50% (11); this can be achieved by dilution of the sample, when necessary, with the adsorbent powder. To exclude specular reflectance, which results in deviations from the Kubelka–Munk law, powder particle size should not be too large (7–9).

For a powder mixture containing n light-absorbing components whose reflectance functions are additive, the Kubelka–Munk function $F(R_\infty)$ can be adapted for simultaneous analysis. The function of the total reflectance R_{∞_T} of the mixture at some wavelength i may be represented as the sum of all individual reflectance functions.

$$[3] \qquad F(R_{\infty_T})_i = \sum_{j=i}^{n} \tau_{ij} C_j$$

where j refers to components and τ is the slope of the Kubelka–Munk plot of $F(R_\infty)$ versus C.

Equation [3] can be written in a more explicit manner by writing as many equations as there are components in the mixture.

$$[4] \qquad F(R_{\infty_T})_1 = \tau_{11} C_1 + \tau_{12} C_2 + \ldots \tau_{1n} C_n$$

$$[5] \qquad F(R_{\infty_T})_2 = \tau_{21} C_1 + \tau_{22} C_2 + \ldots \tau_{2n} C_n$$

These equations are, of course, only valid for a concentration range within that prescribed by the Kubelka–Munk law. At higher concentrations interference due to saturation of the first monomolecular adsorption layer (10) results in marked deviations from linearity and, in extreme cases, gives a calibration curve asymptotic to the horizontal axis. The useful concentration range can, however, be extended by use of the semi-empirical relationship

$$[6] \qquad \frac{(1 - R_\infty)^2}{2R_\infty} = k \log C$$

suggested in an earlier paper (11) which resulted in an almost fivefold extension of the range. Other functions which tend to give linear calibration curves under suitable conditions, $\log R_\infty$ versus C^2, R_∞ versus $\sqrt[3]{C}$ or $\sqrt{(C/(1 - C))}$, have been proposed by Lermond and Rogers (12) and could be applied as well for simultaneous analysis.

EXPERIMENTAL

Reagents

All reagents were of analytical grade and the dye solutions of Orange G, Crystal Violet, Fuchsin, and Brilliant Green were prepared by dissolving weighed amounts in 1:1 ethanol–water. The absorbent was Silicagel G from "Merck Darmstadt", of a grade suitable for thin-layer chromatography, with a particle size ~5 μ.

Apparatus

The diffuse reflectance spectra (400–700 mμ) were measured with an automatic recording Spectronic 505 spectrophotometer equipped with the standard reflectance attachment; barium sulfate was used as the reference standard. Quantitative photometric studies were done with a Beckman DU spectrophotometer, equipped with a reflectance attachment, at wavelengths determined from the reflectance spectra; the reference standard was magnesium carbonate. A "Desaga" variable thickness thin-layer-chromatography applicator was used to prepare the 5 × 20 cm chromatoplates.

Procedure

Stock solutions containing 0.380 mg/ml for Orange G and 0.300 mg/ml for Crystal Violet, Fuchsin, and Brilliant Green were prepared. Dilution series of eight different concentrations (from 0.100 to 0.300 mg/ml)

Can. J. Chem. Downloaded from www.nrcresearchpress.com by 210.87.254.6 on 09/05/12
For personal use only.

were made up for each dye. The solutions were applied to chromatoplates by means of a 10 μl graduated "Hamilton" microsyringe. The plates were dried for 5 min at 110 °C; each spot was removed from the plate and diluted with silica gel from the same plate until the aggregate totalled 40.0 ± 0.2 mg. The sample was then ground in an agate mortar for two periods of 15 s each to ensure homogeneity and uniform particle size. The sample was packed in a semimicro cell (11) and its reflectance was measured.

RESULTS AND DISCUSSION

The dye pairs Orange G – Crystal Violet and Fuchsin – Brilliant Green were chosen for study. Figures 1 and 2 show the individual spectra of the dyes and the spectra of the

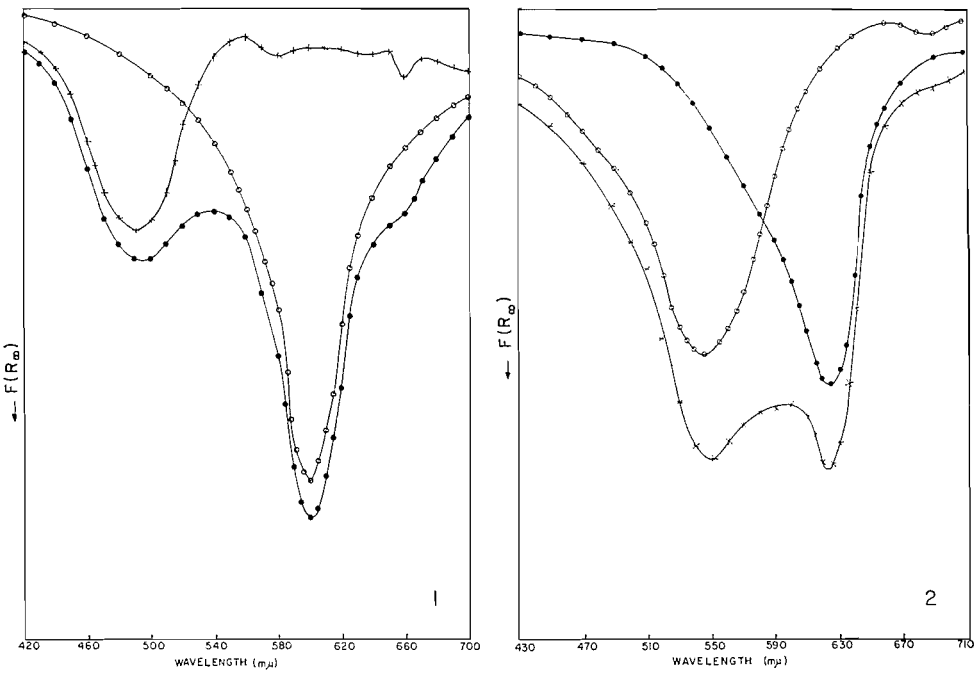


FIG. 1. Reflectance spectra of +, Orange G; ○, Crystal Violet; ●, a mixture of the two.
FIG. 2. Reflectance spectra of ○, Fuchsin; ●, Brilliant Green; ×, a mixture of the two.

mixtures of the two pairs; the theoretically computed total spectra of the pairs (by addition of the individual reflectance functions) are essentially identical with the measured spectra. The absorption maxima for all four dyes did not vary significantly throughout the entire concentration range studied. Figures 3 and 4 show adsorption characteristics and interferences of Fuchsin and Brilliant Green and mixtures of the two dyes; these results show the absence of interferences due to molecular dissociation, association, and abnormal adsorbent–adsorbate interactions and show that the dye systems were satisfactory for further investigation. The absorption maxima determined from Figs. 1–4 (626 mμ for Brilliant Green, 600 mμ for Crystal Violet, 545 mμ for Fuchsin, and 490 mμ for Orange G) were used for quantitative analysis. Calibration plots for the Fuchsin – Brilliant Green pair are shown in Fig. 5. Within the concentration ranges studied, the Kubelka–Munk relationship was valid for all four dyes, and the τ values for the slopes of the Kubelka–Munk curves required for eqs. [4] and [5] were readily obtained.

Sample mixtures were prepared and, to test the reliability of the method, were analyzed as unknowns by students of the junior and senior level. To avoid fluctuations due to temperature, humidity changes, and bleaching effects the dilution series were processed

Can. J. Chem. Downloaded from www.nrcresearchpress.com by 210.87.254.6 on 09/05/12
For personal use only.

Can. J. Chem. Downloaded from www.nrcresearchpress.com by 210.87.254.6 on 09/05/12
For personal use only.

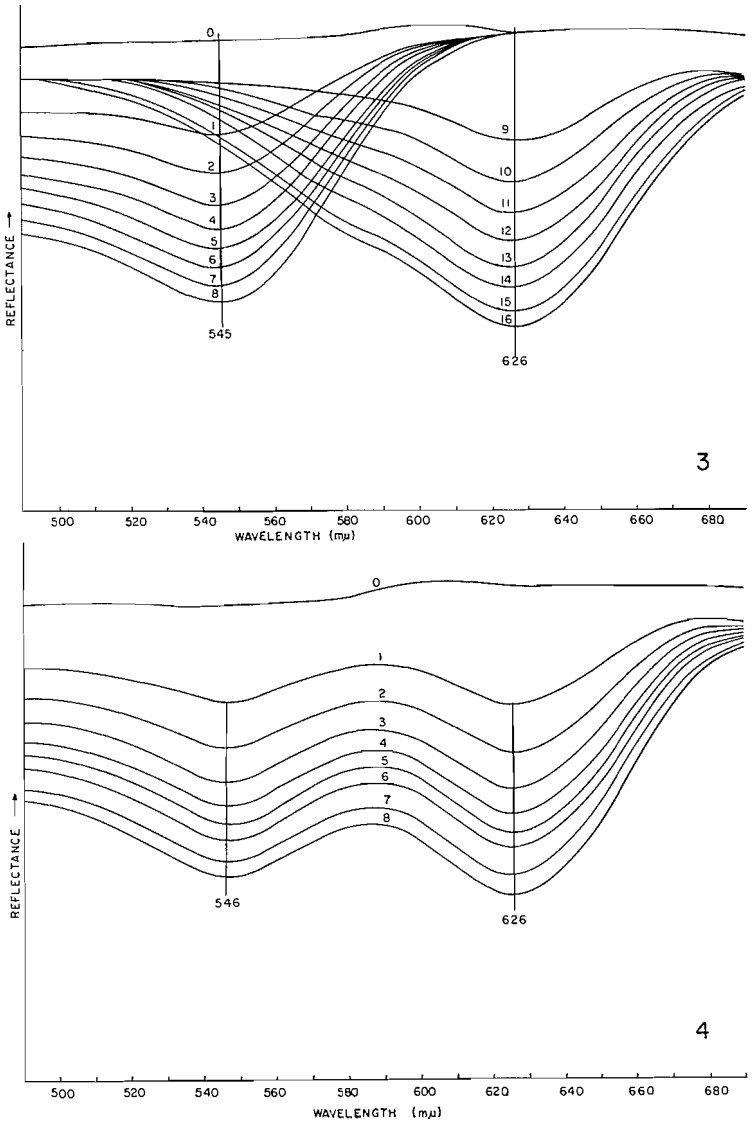


FIG. 3. Reflectance spectra of dilution series of Fuchsin (1–8) and Brilliant Green (9–16) adsorbed on Silicagel G, recorded against a barium sulfate reflectance standard. The zero line is for pure Silicagel G. The concentration of dye in μg per sample is as follows. Fuchsin: (1) 0.3, (2) 0.6, (3) 0.9, (4) 1.2, (5) 1.5, (6) 1.8, (7) 2.4, (8) 3.0. Brilliant Green: (9) 0.3, (10) 0.6, (11) 0.9, (12) 1.2, (13) 1.5, (14) 1.8, (15) 2.4, (16) 3.0.

FIG. 4. Reflectance spectra of dilution series of a mixture of Fuchsin and Brilliant Green adsorbed on Silicagel G, recorded by diffuse reflectance spectroscopy against a barium sulfate reflectance standard. The zero line is for pure Silicagel G. Concentration of each dye in μg per sample: (1) 0.3, (2) 0.6, (3) 0.9, (4) 1.2, (5) 1.5, (6) 1.8, (7) 2.4, (8) 3.0.

simultaneously with the unknowns. Six readings were taken for each calibration curve and four samples of each dye pair were prepared. The students' results are shown below.

Precision (average standard deviation for four sets of four samples) = ±2.4%

Accuracy (average deviation of four samples from true value)

Dye pair 1		Dye pair 2	
Orange G	Crystal Violet	Fuchsin	Brilliant Green
1.9%	3.3%	2.1%	3.1%

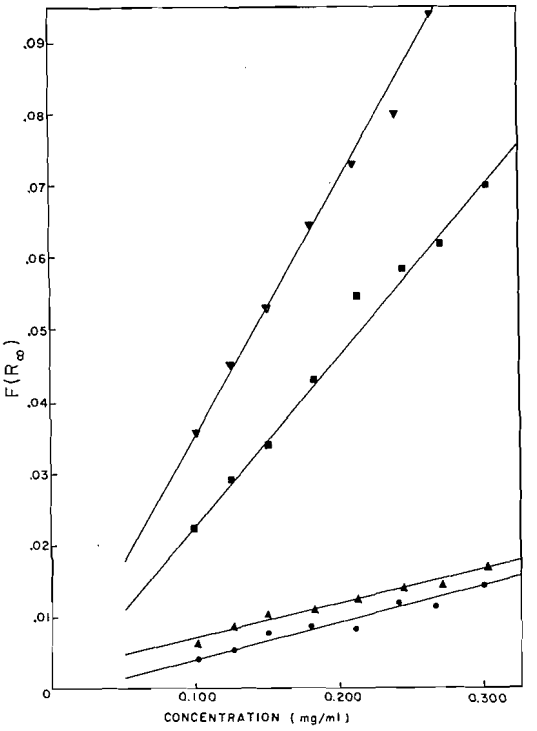


FIG. 5. Kubelka–Munk plots for ▼, Brilliant Green at 626 mμ; ▲, Fuchsin at 626 mμ; ●, Brilliant Green at 545 mμ; ■, Fuchsin at 545 mμ.

The precision is, as expected, somewhat lower than for single component analysis; the factors limiting precision for such simple systems were found to be the packing reproducibility and the homogeneity of the samples, which is in agreement with earlier findings (1). The accuracy is competitive with that obtained from transmission spectroscopy techniques.

CONCLUSIONS

Diffuse reflectance spectroscopy can be applied to the quantitative analysis of mixtures of chromogenic compounds adsorbed on powders. The samples can be analyzed directly on the powder without elution of the adsorbed compounds. The method is relatively simple and inexpensive and can be used in the hands of inexperienced analysts with satisfactory accuracy.[2]

Its major value will be in analysis of mixed zones in chromatography where incomplete separation is encountered. The technique should be useful in thin-layer chromatography, in column chromatography, and in powder electrophoresis. Although this study has been done on simple two-component systems, there is little doubt that the method could be extended successfully to multicomponent systems and to compounds which have to be rendered visible by chromogenic agents or which absorb in the ultraviolet region of the spectrum.

ACKNOWLEDGMENTS

This work was supported, in part, by grants from the Defence Research Board and the National Research Council. R. W. F. gratefully acknowledges support provided by Dalhousie University through a Dalhousie Postdoctoral Fellowship.

[2] *M. M. Frodyma and R. W. Frei. Unpublished data on student experiment, 1965.*

Can. J. Chem. Downloaded from www.nrcresearchpress.com by 210.87.254.6 on 09/05/12
For personal use only.

REFERENCES

1. M. M. FRODYMA, R. W. FREI, and D. J. WILLIAMS. J. Chromatog. **13**, 61 (1964).
2. M. M. FRODYMA and R. W. FREI. J. Chromatog. **15**, 501 (1964).
3. M. M. FRODYMA and R. W. FREI. J. Chromatog. **17**, 131 (1965).
4. M. M. FRODYMA, V. T. LIEU, and R. W. FREI. J. Chromatog. **18**, 520 (1965).
5. P. KUBELKA and F. MUNK. Z. Techn. Phys. **12**, 593 (1931).
6. P. KUBELKA. J. Opt. Soc. Am. **38**, 448 (1948).
7. G. KORTÜM. Spectrochim. Acta Suppl. 448 (1957).
8. G. KORTÜM and S. VOGEL. Z. Phys. Chem. Frankfurt, **18**, 110, 230 (1958).
9. G. KORTÜM. Trans. Faraday Soc. **58**, 1624 (1962).
10. G. KORTÜM, S. VOGEL, and W. BRAUN. Angew. Chem. **70**, 651 (1958).
11. R. W. FREI and M. M. FRODYMA. Anal. Chim. Acta, **32**, 501 (1965).
12. C. A. LERMOND and L. B. ROGERS. Anal. Chem. **27**, 340 (1955).

Can. J. Chem. Downloaded from www.nrcresearchpress.com by 210.87.254.6 on 09/05/12
For personal use only.

Can. J. Chem. Downloaded from www.nrcresearchpress.com by 210.87.254.40 on 09/05/12
For personal use only.

ELECTRON SPIN RESONANCE SPECTRA OF ^{15}N-CENTERED RADICALS AT LOW TEMPERATURES

II. THE RADIOLYSIS OF POTASSIUM SULFAMATE[1]

J. R. MORTON[2] AND D. R. SMITH

Research Chemistry Branch, Atomic Energy of Canada Limited, Chalk River, Ontario

Received April 14, 1966

ABSTRACT

Single crystals of potassium sulfamate, KNH_2SO_3, enriched in the isotope ^{15}N, were irradiated, and examined at 77° K by electron spin resonance. Two intermediates, neither of which are present on examination at 300 °K, have been identified as NH_2 and NH_2SO_3. A possible radiolysis mechanism is discussed.

INTRODUCTION

Electron spin resonance (e.s.r.) spectra of single crystals of potassium sulfamate (KNH_2SO_3) γ-irradiated at room temperature reveal the presence of the radicals SO_3^- (1) and $NHSO_3^-$ (2). Two mechanisms may be envisaged as contributing to the radiation damage process in potassium sulfamate. The "cage" effect (3) would favor the formation of $NHSO_3^-$ over the formation of NH_2 and SO_3^-.

[1] $$NH_2SO_3^- \longrightarrow\!\!\!\!\!\sim\!\!\!\!\!\rightarrow NHSO_3^- + H$$

However, the presence of SO_3^- suggests an alternative mechanism involving the intermediate NH_2:

[2a] $$NH_2SO_3^- \longrightarrow\!\!\!\!\!\sim\!\!\!\!\!\rightarrow NH_2 + SO_3^-$$

[2b] $$NH_2 + NH_2SO_3^- \rightarrow NH_3 + NHSO_3^-$$

The purpose of the present study was to determine, if possible, the mechanism of the radiolysis of potassium sulfamate, by carrying out the process at low temperatures with the hope of identifying any intermediates by means of electron spin resonance.

EXPERIMENTAL

To obtain improved resolution of the e.s.r. spectra, potassium sulfamate enriched in the isotope ^{15}N was prepared. Sulfamic acid containing 95% $^{15}NH_3SO_3$, purchased from Merck Sharp and Dohme Ltd., Montreal, was neutralized with aqueous potassium hydroxide solution. Single crystals of potassium sulfamate were grown by slow evaporation of this solution. The crystals are orthorhombic (4), and the unit cell, which contains four molecules of KNH_2SO_3, has dimensions $a = 8.32$ Å, $b = 8.28$ Å, $c = 5.90$ Å, in the space group *Pbma*. The crystals usually formed hexagonal tablets on (001), elongated along [010].

The samples were γ-irradiated at 77 °K in an 18 000 curie ^{60}Co source (Gammacell 220), at a dose rate of 1 Mrad/h. Irradiation at 77 °K was carried out after positioning the crystals in thin-walled quartz (Spectrosil) tubes. The γ-ray induced e.s.r. signal from the quartz was subsequently removed by illumination with a low-pressure Hg lamp. This was found to have no effect on the e.s.r. spectrum of the sample. Dosimetry measurements were made using the ferrous sulfate method (5). The electron spin resonance spectrometer has already been described (6). Conventional methods (7) were used to determine the elements of the hyperfine interaction tensors, an isotropic g-factor of 2.004 being assumed. The total radical concentration was measured in a powdered sample of $K^{14}NH_2SO_3$, using a previously described e.s.r. technique (8). The relative radical concentrations were estimated using a single crystal of $K^{15}NH_2SO_3$. The spectral line-widths of the different radicals were almost equal, and no line-width corrections were applied.

RESULTS

The electron spin resonance spectrum of a crystal of $K^{15}NH_2SO_3$ freshly irradiated at 77 °K is shown in Fig. 1(*a*), for the orientation H_0 parallel to the c-axis. It will be seen that, in addition to $NHSO_3^-$ (C), two other radicals are present (A and B).

[1] *A.E.C.L. No. 2465.*

[2] *Visiting Scientist. Permanent address: Division of Applied Chemistry, National Research Council, Ottawa.*

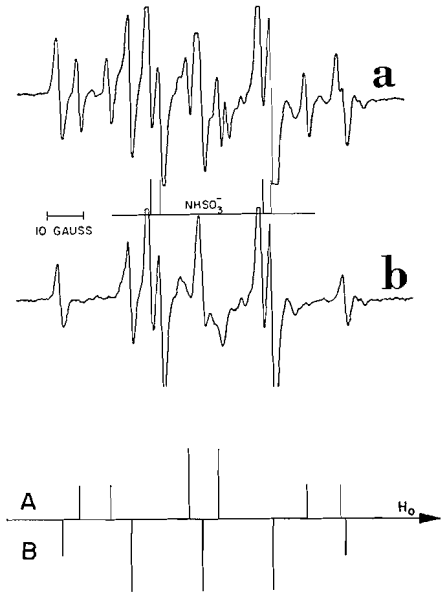


FIG. 1. Electron spin resonance spectra of a crystal of $K^{15}NH_2SO_3$ for the orientation H_0 parallel to c-axis: (a) freshly irradiated at 77 °K; (b) after annealing to 195 °K for 1 min.

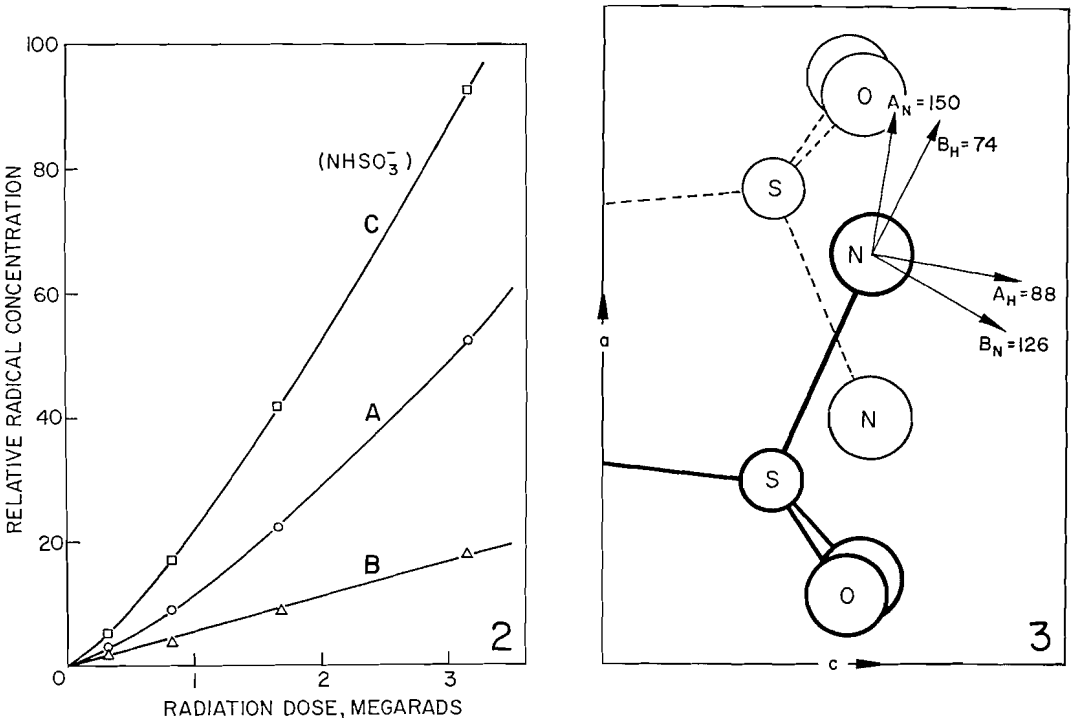


FIG. 2. Relative concentration of radicals A, B, and C in crystals of $K^{15}NH_2SO_3$ as a function of radiation dose.

FIG. 3. Projection on to (010) of part of the unit cell of potassium sulfamate, showing also the directions of certain principal values of the hyperfine tensors of radicals A (NH_2) and B (NH_2SO_3).

Can. J. Chem. Downloaded from www.nrcresearchpress.com by 210.87.254.40 on 09/05/12
For personal use only.

The spectra of radicals A and B were both analyzed in terms of hyperfine interaction with three spin $\frac{1}{2}$ nuclei, two of which were equivalent for all crystal orientations. Since the spin of ^{15}N is $\frac{1}{2}$ it seemed a reasonable assumption that both A and B were radicals of the type R—NH_2; in the next section, evidence will be offered suggesting that A and B were NH_2 and NH_2SO_3 respectively.

The estimated buildup of these three radicals as a function of radiation dose in the freshly irradiated crystals is shown in Fig. 2. On annealing the crystal at 195 °K for 1 min the spectrum of radical A had disappeared, as will be apparent from Fig. 1(*b*). On warming to room temperature only the spectra of SO_3^- and $NHSO_3^-$ remained. The total radical concentration after a 1 Mrad irradiation at 77 °K was $(1.0 \pm 0.1) \times 10^{17}$ radicals/g, and $(1.4 \pm 0.1) \times 10^{17}$ radicals/g after warming to room temperature. These figures correspond to a radiation-chemical yield[3] G(total) of 0.16 at 77 °K and 0.22 at room temperature, and estimated yields of 0.03, 0.03, 0.03, and 0.07 for the radicals NH_2, SO_3^-, NH_2SO_3, and $NHSO_3^-$ respectively at 77 °K.

In Table I the ^{15}N and proton hyperfine tensors of radicals A, B, and C ($NHSO_3^-$) determined at 77 °K are listed; the data for radical C ($NHSO_3^-$) are included for the sake of completeness although little is added to those of Rowlands (2).

TABLE I

Proton and ^{15}N hyperfine tensors (Mc/s) of radicals trapped in irradiated $K^{15}NH_2SO_3$ at 77 °K

Radical	Tensor in *abc* axis-system			Principal values	Principal directions in *abc* axis-system
A(^1H)	70.7	0	∓3.2	88.0	(0.176, 0.000, ∓0.984)
	0	71.5	0	71.5	*
	∓3.2	0	87.4	70.1	*
A(^{15}N)	146.6	0	±21.9	149.9	(0.989, 0.000, ±0.149)
	0	5.5	0	5.5	(0.000, 1.000, 0.000)
	±21.9	0	4.3	1.0	(0.149, 0.000, ∓0.989)
B(^1H)	69.6	0	±9.2	74.1	(0.899, 0.000, ±0.437)
	0	27.5	0	50.8	(0.437, 0.000, ∓0.899)
	±9.2	0	55.3	27.5	(0.000, 1.000, 0.000)
B(^{15}N)	38.3	0	∓51.4	125.9	(0.507, 0.000, ∓0.862)
	0	19.2	0	19.2	(0.000, 1.000, 0.000)
	∓51.4	0	95.7	8.1	(0.862, 0.000, ±0.507)
C(^1H)	55.0	0	±39.9	105.4	(0.621, 0.000, ±0.784)
	0	60.0	0	60.0	(0.000, 1.000, 0.000)
	±39.9	0	73.8	23.4	(0.784, 0.000, ∓0.621)
C(^{15}N)	7.9	0	±3.1	143.3	(0.000, 1.000, 0.000)
	0	143.3	0	9.4	(0.896, 0.000, ±0.445)
	±3.1	0	3.2	1.7	(0.445, 0.000, ∓0.896)

*These directions have no significance since the tensor has axial symmetry.

DISCUSSION

A. Identification of the Radicals

The species A and B are both nitrogen-centered π-radicals, in which the unpaired electron occupies an orbital to which the dominant contribution is that of the nitrogen $2p_\pi$ atomic orbital. Both radicals exhibit the characteristically (7) large ^{15}N hyperfine interaction when H_0 is perpendicular to the nodal plane of the radical, and very much smaller ^{15}N interactions when H_0 explores this plane. It is reasonable to suppose that one of these radicals be NH_2 and the other NH_2SO_3. Since A is the more labile species, it is tempting to identify it provisionally with NH_2. In the potassium sulfamate crystal

[3]*G = number of radicals formed per 100 eV deposited in the sample.*

Can. J. Chem. Downloaded from www.nrcresearchpress.com by 210.87.254.40 on 09/05/12
For personal use only.

(4) the S—N bonds have direction cosines (0.920, 0.000, ±0.392) in the *abc* axis-system. The angle between this direction and that of the 150 Mc/s principal value of the ^{15}N tensor of radical A is $\cos^{-1}$ 0.968 or 14°, and the unique direction of the proton tensor in radical A is inclined $\cos^{-1}$ 0.224 or 77° to the S—N bonds in the crystal. These observations are not unreasonable if A is the radical NH_2 formed by scission of the N—S bond, but are difficult to explain on the postulate that A is NH_2SO_3. The latter radical would be expected to lie in an orientation similar to that of the ion from which it had been formed. It would therefore be anticipated that in the case of NH_2SO_3 the largest principal value of the ^{15}N and proton tensors would be respectively perpendicular and parallel to the S—N bonds in the crystal. The data for radical B fit these criteria: the angle between the S—N bond and the direction of the 126 Mc/s principal value of the ^{15}N tensor being $\cos^{-1}$ 0.129 or 83°, and between the S—N bond and the direction of the 74 Mc/s principal value of the proton tensor being $\cos^{-1}$ 0.998 or 4°. These observations are illustrated in Fig. 3, where arrows representing the directions of the above principal values are superimposed on a projection of part of the unit cell of potassium sulfamate.

The above discussion provides confirmatory evidence that A and B may be identified with NH_2 and NH_2SO_3, respectively. Since both these radicals have bene detected previously by e.s.r. (9–11) a comparison with the earlier data is of interest. In the case of NH_2 in an argon matrix (9) the isotropic proton and ^{14}N interactions were 67.0 and 28.9 Mc/s respectively, the latter corresponding to a ^{15}N interaction of 40.5 Mc/s. These figures are to be compared with those for radical A: 76.5 ± 5 and 52.1 ± 5 Mc/s for the isotropic proton and ^{15}N interactions respectively. The discrepancy between the isotropic nitrogen interactions is not too serious when it is recalled that for ND_2 in an argon matrix the ^{14}N interaction was 33.3 Mc/s, equivalent to 46.6 Mc/s for a ^{15}N nucleus. The isotropic nitrogen interaction in NH_2 is clearly somewhat dependent upon environment. It appears (Table I) that the re-orientation of the NH_2 radical between the two equivalent positions is so rapid that the proton tensor exhibits axial symmetry about the rotation axis which is the two-fold axis of the molecule. The unique direction of the proton tensor (principal value 88 Mc/s) lies in the radical plane, being approximately perpendicular ($\cos^{-1}$ 0.027 or 88°) to the direction of the largest (150 Mc/s) ^{15}N principal value, and approximately parallel ($\cos^{-1}$ 0.999 or 2°) to the direction of the smallest (1 Mc/s) ^{15}N principal value. A similar relationship between the principal values of the proton and ^{13}C tensors was noted in the case of the radical $^{13}CH_2CO_2^-$ (12), in which the CH_2 group was also re-orienting about the two-fold axis.

Within the experimental error (5°) the proton and ^{15}N hyperfine tensors of radical B (NH_2SO_3) are diagonal in a common axis-system: parallel to the nitrogen $2p_\pi$ orbital (B_N = 126 Mc/s, B_H = 51 Mc/s); bisecting the HNH angle and parallel to the S—N bonds in the crystal (B_N = 8 Mc/s, B_H = 74 Mc/s); and the mutually perpendicular direction (B_N = 19 Mc/s, B_H = 27 Mc/s). In this case the re-orientation of the NH_2 group is not rapid enough to eliminate the anisotropy in the proton tensor, although it is rapid enough to render the protons equivalent as far as the resonance is concerned. It will be noted, however, that the *largest* proton hyperfine interaction and the *smallest* ^{15}N interaction are obtained when H_0 is parallel to the bisector of the HNH angle, just as in the case of NH_2 discussed above. Exactly analogous relationships were observed for the radical NH_2SO_3 trapped in sulfamic acid (11), although the principal values of the respective tensors differ somewhat.

B. The Radiolysis Mechanism

The results suggest that the radiolysis mechanism of potassium sulfamate is more complex than the alternatives represented by reactions [1] and [2]. A reaction scheme

Can. J. Chem. Downloaded from www.nrcresearchpress.com by 210.87.254.40 on 09/05/12
For personal use only.

which accounts for many of the present observations is outlined and discussed below. Untrapped electrons and trapped electrons are represented by e^- and e_t^- respectively.

(i) Irradiation at 77 °K.—The following reactions are thought to occur:

[3] $$NH_2SO_3^- \longrightarrow\!\!\!\!\!\sim\!\!\!\!\!\rightarrow NH_2SO_3 + e^-$$

[4] $$NH_2SO_3 + e^- \rightarrow NHSO_3^- + H$$

[5] $$H + NH_2SO_3^- \rightarrow NHSO_3^- + H_2$$

[6] $$NH_2SO_3 + e^- \rightarrow NH_2 + SO_3^-$$

[7] $$e^- \rightarrow e_t^-$$

The primary reaction is thought to be ionization of $NH_2SO_3^-$ [3], and some recombination must occur [4, 6] since NH_2 and $NHSO_3^-$ are detected. It is estimated that reactions [4] and [6] are approximately of equal importance in the recombination of NH_2SO_3 and e^-. Reaction [5] accounts for the absence of trapped hydrogen atoms and gives rise to further $NHSO_3^-$.

(ii) Annealing at 195 °K for 1 min.—

[8] $$NH_2 + NH_2SO_3^- \rightarrow NHSO_3^- + NH_3$$

Since no NH_2SO_3 disappeared, the electrons must remain trapped at this temperature.

(iii) Warming to room temperature.—The untrapping of the electrons

[9] $$e_t^- \rightarrow e^-$$

must be followed by reactions [4], [5], [6], and [8], since only $NHSO_3^-$ and SO_3^- are detected at room temperature. Since the total radical yield at 77 °K did not include $G(e_t^-)$, the total radical yield after warming to room temperature (~298 °K) should increase by this amount. If $G(e_t^-) = G(NH_2SO_3)$, then

$$[G(NHSO_3^-) + G(SO_3^-)]_{298°K} = [G(NH_2SO_3) + G(\text{total})]_{77°K} = 0.19.$$

The increase in total yield from 0.16 at 77 °K to 0.22 at room temperature provides qualitative support for the above mechanism.

ACKNOWLEDGMENTS

The authors are grateful to Dr. L. D. Calvert for determining the unit-cell directions of the crystals by means of X-ray diffraction photographs.

REFERENCES

1. G. W. Chantry, A. Horsfield, J. R. Morton, J. R. Rowlands, and D. H. Whiffen. Mol. Phys. **5**, 233 (1962).
2. J. R. Rowlands. Mol. Phys. **5**, 565 (1962).
3. V. V. Voevodskii and Y. N. Molin. Radiation Res. **17**, 366 (1962).
4. C. J. Brown and E. G. Cox. J. Chem. Soc. 1 (1940).
5. J. Weiss, A. O. Allen, and H. A. Schwarz. Proc. Intern. Conf. Peaceful Uses At. Energy, United Nations, N.Y. **14**, 179 (1956).
6. D. R. Smith and J. J. Pieroni. Can. J. Chem. **42**, 2209 (1964).
7. J. R. Morton. Chem. Rev. **64**, 453 (1964).
8. D. R. Smith and J. J. Pieroni. Can. J. Chem. **43**, 2141 (1965).
9. S. N. Foner, E. L. Cochran, V. A. Bowers, and C. K. Jen. Phys. Rev. Letters, **1**, 91 (1958).
10. J. R. Rowlands and D. H. Whiffen. Nature, **193**, 61 (1962).
11. N. M. Atherton and J. R. Morton. Nature, **209**, 294 (1966).
12. J. R. Morton. J. Am. Chem. Soc. **86**, 2325 (1964).

Can. J. Chem. Downloaded from www.nrcresearchpress.com by 210.87.254.40 on 09/05/12
For personal use only.

Can. J. Chem. Downloaded from www.nrcresearchpress.com by 210.87.254.105 on 09/05/12
For personal use only.

ELECTRON SPIN RESONANCE SPECTRA OF $N_2H_4^+$ AND PF_2[1]

J. K. S. WAN,[2] J. R. MORTON, AND H. J. BERNSTEIN
Divisions of Pure and Applied Chemistry, National Research Council, Ottawa, Canada

Received April 18, 1966

ABSTRACT

The radicals $N_2H_4^+$ and PF_2 have been detected by electron spin resonance in γ-irradiated NH_4PF_6. The radical $N_2H_4^+$ was shown to be formed from NH_3^+ radicals detectable after low-temperature irradiation.

INTRODUCTION

It has recently been shown that the radicals PF_4 and $PF^{\pm}$ can be trapped in irradiated NH_4PF_6 (1). In addition to these fragments, there was evidence of a nitrogen- and hydrogen-containing specie the nature of which was not discussed. The present re-examination of the e.s.r. spectra of irradiated powdered NH_4PF_6 was undertaken in the hope that the nitrogen- and hydrogen-containing specie might prove to be NH_4. This radical has been predicted to be stable (2, 3), but has never been detected experimentally.

It will be shown that the nitrogen- and hydrogen-containing specie is $N_2H_4^+$. In addition, the previously unknown radical PF_2 was discovered during this investigation.

RESULTS

Part of the spectrum of NH_4PF_6 irradiated at 300 °K is shown in Fig. 1. Not shown in this figure are the spectra of PF_4 and $PF^{\pm}$ which extend from 2 000 to 4 500 G (1), but which do not obscure the region 3 300 – 3 500 G. The spectrum of the nitrogen- and hydrogen-containing specie shown in Fig. 1 is seen to consist of nine lines centered at $g = 2.0030$ and separated by equal intervals of 12.0 G. The estimated intensity ratios of the nine lines were approximately 1:6:17:29:36:29:17:6:1.

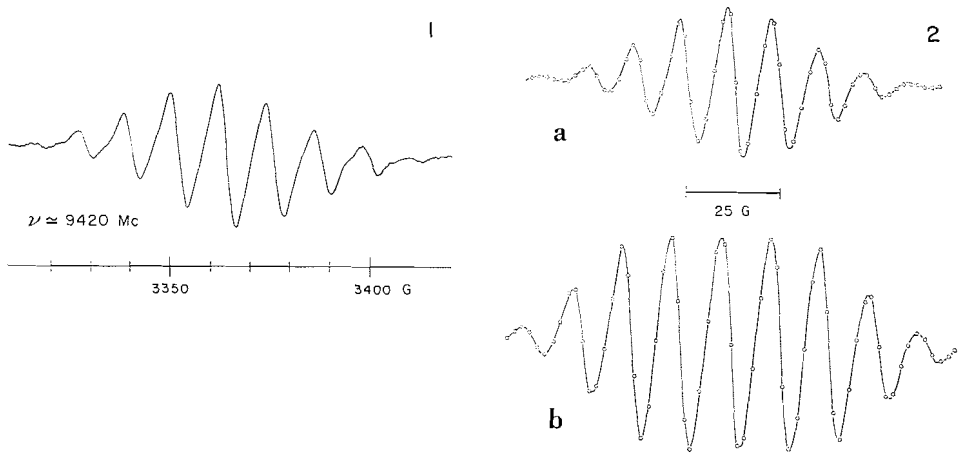


FIG. 1. The e.s.r. spectrum of NH_4PF_6 irradiated at 300 °K, between 3 300 and 3 400 G.
FIG. 2. Calculated e.s.r. spectra of (*a*) $N_2H_4^+$ and (*b*) NH_4 using the parameters quoted in the text.

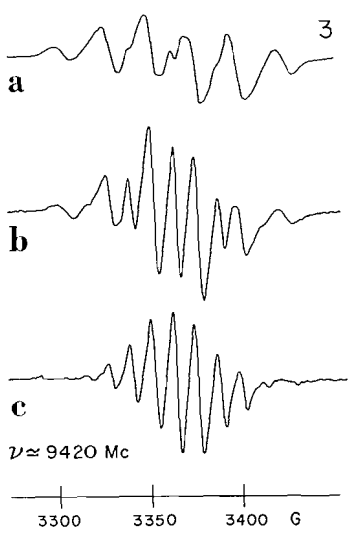
[1]*Issued as N.R.C. No. 9057.*
[2]*National Research Council Postdoctorate Fellow 1965–1966; present address: Department of Chemistry, Queen's University, Kingston, Ontario.*

In attempting to identify the species responsible for this spectrum, several possibilities were considered: NH_2, NH_3^+, NH_4, and $N_2H_4^+$. Of these, only NH_4 has not been identified previously by e.s.r. The available parameters for NH_2 (4) and NH_3^+ (5, 6) eliminate them as possibilities. However, $N_2H_4^+$ in solution has spectral parameters (7) $a_N = 11.5$ G, $a_H = 11.0$ G, and $g = 2.0034$. From these data and a maximum-slope half-width of 4.5 G the calculated spectrum of $N_2H_4^+$ shown in Fig. 2(*a*) was prepared.[3] An analysis of Fig. 1 in terms of NH_4 was also attempted, using $a_N = 24$ G and $a_H = 12$ G. The calculated spectrum in Fig. 2(*b*) was obtained. It is apparent that the evidence favors identification of the radical as $N_2H_4^+$. Experiments with irradiated ND_4PF_6 supported this assignment: the observed spectrum consisted of a broad, almost featureless, absorption due to $N_2D_4^+$ (upon which was superimposed the six-line spectrum of PF_2 discussed later), very similar to the spectrum calculated for $N_2D_4^+$. The spectrum calculated for ND_4 was a well-resolved triplet.

Experiments were carried out also at 77 °K, in the hope of detecting NH_4 at this temperature. Samples of NH_4PF_6 irradiated at 77 °K and examined at either 77 °K or 300 °K revealed a six-line spectrum which was attributed to NH_3^+, by comparison with existing data (5, 6). The reaction

$$2NH_3^+ \rightarrow N_2H_4^+$$

took several days to complete at room temperature, but only 40 min at 120 °C, as illustrated in Fig. 3. By observation of the relative rates of disappearance of NH_3^+ at various temperatures the activation energy for the process (probably diffusion-controlled) was estimated to be 15 ± 2 kcal/mole.



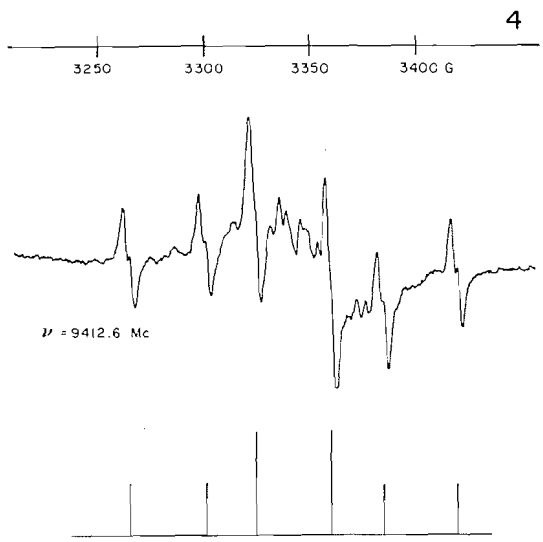


FIG. 3. The e.s.r. spectra at 393 °K of NH_4PF_6 irradiated at 77 °K showing the conversion of NH_3^+ into $N_2H_4^+$: (*a*) 0 min, (*b*) 20 min, (*c*) 40 min at 393 °K.

FIG. 4. The e.s.r. spectrum of PF_2 superimposed on the broad absorption due to $N_2D_4^+$ in irradiated ND_4PF_6.

The spectrum of irradiated ND_4PF_6 (Fig. 4) revealed, in addition to the absorption due to $N_2D_4^+$, a six-line spectrum consisting of a pair of 1:2:1 triplets. This hyperfine structure must be due to interaction with three nuclei of spin $\frac{1}{2}$, two of which are equivalent. In the deuterated material the only nuclei of spin $\frac{1}{2}$ are ^{31}P and ^{19}F, so that the six-line

[3]*A computer program made available by Atomic Energy of Canada Limited was used.*

Can. J. Chem. Downloaded from www.nrcresearchpress.com by 210.87.254.105 on 09/05/12
For personal use only.

spectrum must be due to PF_2, FP_2, F_3, P_3, or a doubly charged analogue of one of these. The most reasonable choice was thought to be PF_2, the spectral parameters being:

$$a_P = 36.0 \pm 0.5 \text{ G}, a_F = 60.5 \pm 0.5 \text{ G}, g = 2.0108 \pm 0.0002.$$

This identification was confirmed by comparing these data with those for NF_2 (8). These 19-electron radicals are expected to be bent (9), and to possess $^2B_1$ ground states.

Several attempts were made to detect PF_2 in irradiated NH_4PF_6. Because of the different g-factors of PF_2 and $N_2H_4^+$ the PF_2 line at lowest field should have been resolved from the $N_2H_4^+$ absorption. In the radiation dose range 1–5 Mrad PF_2 could be detected in ND_4PF_6, but not in similarly processed NH_4PF_6. No explanation can be offered for this strange isotope effect.

EXPERIMENTAL

Ammonium hexafluorophosphate (Ozark-Mahoning Co.) was recrystallized three times from distilled water or 99.95% D_2O. The recrystallized compounds were checked by infrared, n.m.r., and microanalysis for purity. The powder samples were irradiated in a 20 000 Curie source of 1.3 MeV ^{60}Co γ-rays. The dose rate was approximately 2 Mrad/h and the total dose was 1–5 Mrad. Electron spin resonance spectra were obtained with a Varian V-4502-14 spectrometer and auxiliary equipment.

ACKNOWLEDGMENTS

The authors are grateful to Atomic Energy of Canada Limited for use of irradiation facilities and for the computation of e.s.r. spectra.

REFERENCES

1. J. R. Morton. Can. J. Phys. **41**, 706 (1963).
2. H. J. Bernstein. J. Am. Chem. Soc. **85**, 484 (1963).
3. D. M. Bishop. J. Chem. Phys. **40**, 432 (1964).
4. S. N. Foner, E. L. Cochran, V. A. Bowers, and C. K. Jen. Phys. Rev. Letters, **1**, 91 (1958).
5. T. Cole. J. Chem. Phys. **35**, 1169 (1961).
6. J. S. Hyde and E. S. Freeman. J. Phys. Chem. **65**, 1636 (1961).
7. J. Q. Adams and J. R. Thomas. J. Chem. Phys. **39**, 1904 (1963).
8. C. B. Colburn, R. Ettinger, and F. A. Johnson. Inorg. Chem. **3**, 455 (1964).
9. M. D. Harmony, R. J. Myers, L. J. Schoen, D. R. Lide, and D. E. Mann. J. Chem. Phys. **35**, 1129 (1961).

Can. J. Chem. Downloaded from www.nrcresearchpress.com by 210.87.254.105 on 09/05/12
For personal use only.

ULTRAVIOLET, INFRARED, AND RAMAN SPECTRA OF PROTONATED CARBOXYLIC ACIDS

SUMIE HOSHINO, HARUO HOSOYA,[1] AND SABURO NAGAKURA
The Institute for Solid State Physics, The University of Tokyo, Tokyo, Japan
Received January 5, 1966

ABSTRACT

Ultraviolet, infrared, and Raman spectra were measured for acetic acid and propionic acid in sulfuric acid solutions of various acidities. Infrared spectra of acetic acid and benzoic acid were measured in deuterosulfuric acid and aqueous deuterated sodium hydroxide solutions. From the detailed analyses of the ultraviolet absorption change the pK_{BH^+} values of acetic and propionic acids were found to be -6.12 and -6.33, respectively. In the infrared and Raman spectra of the protonated acids, the C=O stretching band at about 1 700 cm^{-1} disappeared and a new strong infrared absorption band appeared at about 1 600 cm^{-1}. The frequency of the latter band, which can be assigned to antisymmetric C—O stretching band, is very similar to that of the carboxylate group. The acidity dependence of these infrared spectra was parallel with that of the ultraviolet absorption. These facts confirm that the protonated carboxyl group has a skeleton $[-C(OH)_2]^+$ similar to the carboxylate group $[-CO_2]^-$.

INTRODUCTION

Aromatic and aliphatic carboxylic acids have been found, from cryoscopic (1) and other chemical studies (2), to be protonated in concentrated sulfuric acid solution:

$$R—COOH + H^+ \rightleftharpoons R—COOH_2^+.$$

The structure of protonated species $R—COOH_2^+$ is important because it is known to be one of the reactive intermediates for the acid-catalyzed esterification of carboxylic acids (3). The basic strengths of the carboxylic acids have been extensively studied by observing the change in ultraviolet absorption spectrum with changing acidity of the medium. The observed basicities, pK_{BH^+}, are of the same order of magnitude as those of analogous aldehydes and ketones (4). Raman spectral measurements showed that protonation occurs at the carbonyl oxygen atom in accordance with the predicted electronic structures (5), while the results of n.m.r. studies show the spectra to be influenced by medium effects as well as by protonation (6). On the other hand, infrared spectra of protonated species in strong acid solutions have never been observed. The purpose of the present series of experiments is to investigate the extent to which the results of these various kinds of spectroscopic measurements, when applied to the same system, accord with and make up for each other.

EXPERIMENTAL

Materials

Acetic acid and propionic acid of G.R. grades were refluxed over potassium permanganate followed by careful distillation. Benzoic acid for analytical purpose specially supplied by the Osaka Industrial Research Institute was used without further purification. Sulfuric acid of G.R. grade (Wako Pure Chemical Industries, Ltd.) and deuterosulfuric acid (Showa Denko K.K., 99% deuterium concentration and 97% acid concentration) were used without further purification. Deuterated sodium hydroxide solution (~6 *N*) was prepared by dissolving carefully the freshly cut sodium metal into deuterated water purchased from Showa Denko K.K.

Measurements

A Cary model 14M recording spectrophotometer was used to measure the ultraviolet absorption spectra of acetic acid and propionic acid in sulfuric acid solutions of various acidities, and the solute concentrations were adjusted as high as $10^{-2}M$. The values of Hammett's acidity functions were taken from the table by Paul and Long (7).

[1]*Present address: The Institute of Physical and Chemical Research, Komagome, Bunkyo-ku, Tokyo.*

Can. J. Chem. Downloaded from www.nrcresearchpress.com by 210.87.254.6 on 09/05/12
For personal use only.

The Raman spectra of acetic and propionic acids were measured in sulfuric acid solutions with a Cary model 81 recording Raman spectrophotometer located at the Government Chemical Industrial Research Institute, Tokyo.[2]

The infrared spectra of acetic and benzoic acids in deuterosulfuric acid and deuterated sodium hydroxide solutions were measured with a Hitachi EPI-2 recording spectrophotometer. Envelope cells were made from two sheets of polyethylene films (8). The cells containing a few drops of the sample solution were pressed by fingers from the bottom to the top in order to get them as thin as possible. Thereafter they were held by commercial cell holders. They were transparent enough for the measurements in the carbonyl-stretching region. Deuterium–hydrogen exchange was observed but was found to be slow enough for accurate infrared absorption measurements.

All the measurements were carried out at a constant temperature, 20 °C.

RESULTS AND DISCUSSION

pK_{BH^+} *Determination of Acetic Acid in Concentrated Sulfuric Acid*

The ultraviolet absorption spectra of acetic acid in water and in 10% sulfuric acid showed an absorption peak at 203 mμ (ϵ = 38, see Fig. 1). This is undoubtedly due to the unprotonated molecule. With the increase of the sulfuric acid concentration, the peak shifted to shorter wavelengths and finally disappeared. For a given wavelength, the plot of the molar extinction coefficient ϵ against the H_0 value of the solvent gave a sigmoid curve (Fig. 2). The pK_{BH^+}, ϵ_B, and ϵ_{BH^+} were found to be −6.12, 36.38, and 3.57, respectively, by applying the least squares method to the observed apparent molar extinction coefficients at 200 mμ:

$$[1] \qquad pK_{BH^+} = H_0 - \log [(\epsilon_{BH^+} - \epsilon)/(\epsilon - \epsilon_B)].$$

This means that acetic acid is half-protonated in 74% sulfuric acid. Details of the method were described elsewhere (3).

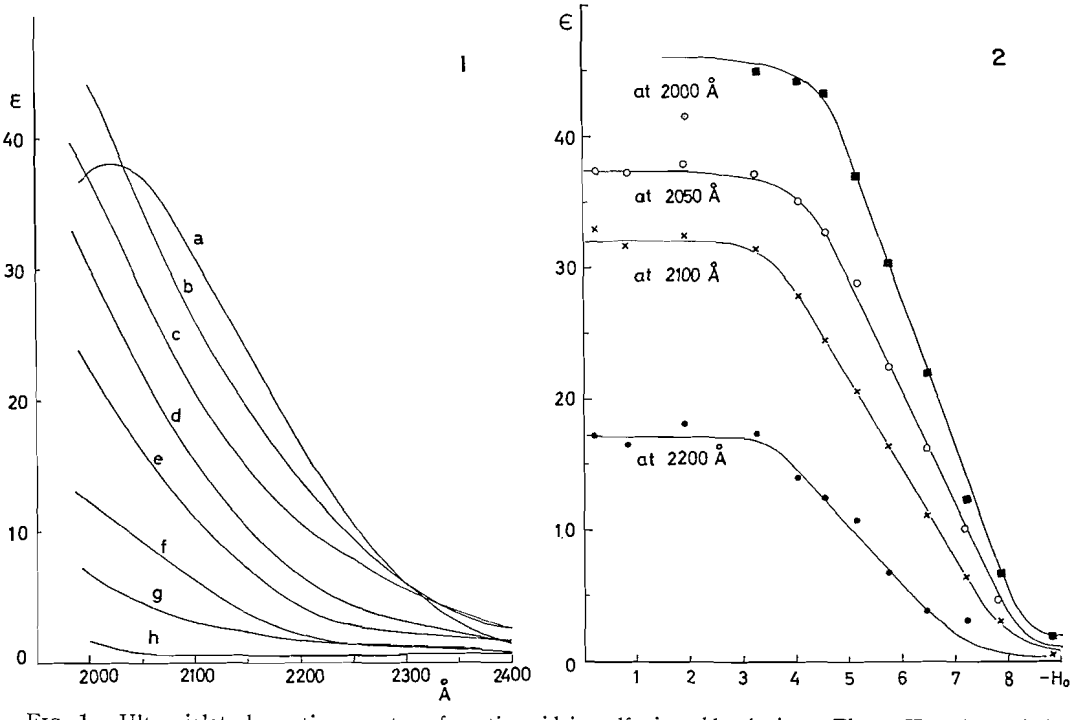


FIG. 1. Ultraviolet absorption spectra of acetic acid in sulfuric acid solutions. The $-H_0$ values of the solvent acid are, respectively: (*a*) 0.84; (*b*) 4.07; (*c*) 5.16; (*d*) 5.78; (*e*) 6.50; (*f*) 7.23; (*g*) 7.86; (*h*) 8.86.

FIG. 2. The change of the apparent molar extinction coefficient of acetic acid in sulfuric acid solutions of various acidities.

[2]*The authors wish to thank Mrs. Michiko Fukuyama for the measurements of Raman spectra.*

Can. J. Chem. Downloaded from www.nrcresearchpress.com by 210.87.254.6 on 09/05/12
For personal use only.

The following facts lead to the conclusion that acetic acid is really a Hammett base: (i) The plot of $\log [(\epsilon - \epsilon_{BH^+})/(\epsilon_B - \epsilon)]$ against H_0 gave a straight line with a slope of near unity (Fig. 3), and (ii) almost the same pK_{BH^+} values were obtained for several different wavelength plots (3).

The pK_{BH^+} value (−6.33 at 210 mμ) of propionic acid was also determined by the same method (half-protonated in 75% sulfuric acid). The pK_{BH^+} values determined by the present authors for both acids coincide well with those obtained by other authors:[3] −6.10 (9) and −6.20 (7) for acetic acid and −6.8 (10) for propionic acid.

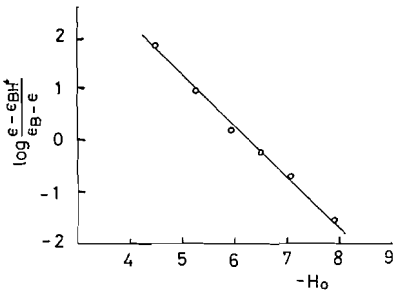
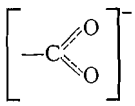


FIG. 3. The plots showing that acetic acid is one of the typical Hammett bases. The ϵ values were taken at 200 mμ.

Structure Determination of the Protonated Carboxylic Group

Raman spectra of the 6 μ region were measured with acetic acid in sulfuric acid solutions of various acidities. The results are shown in Fig. 4. The 1 700 cm^{-1} band due to C=O stretching vibration decreases in intensity with increasing concentration of sulfuric acid and disappears for the 98% sulfuric acid solution. The same tendency was also observed with benzoic acid.[4] The disappearance of the 1 700 cm^{-1} band means that the protonation of acetic acid occurs on the oxygen atom of the carbonyl group, as in the case of the protonation of benzoic acid.

The Raman spectra of the simple carboxylic acids show that the carbonyl-stretching band disappears in the aqueous sodium hydroxide solutions, in which the carboxylate anion is produced (11).

[2] 

The infrared carbonyl-stretching band at 1 715 cm^{-1} in water (1 717 cm^{-1} in methanol) gradually diminishes in intensity and a new band appears at lower frequencies (1 600 cm^{-1}) with the increase of the solvent sulfuric acid concentration. The infrared spectrum of acetic acid in deuterated sodium hydroxide solution has an absorption peak at 1 560 cm^{-1}. This corresponds to the known antisymmetric C—O stretching band at 1 584 cm^{-1} for solid sodium acetate (1 425 cm^{-1} for the symmetric one) (Fig. 5).

For the infrared spectra of benzoic acid, a band appears at 1 603 cm^{-1} in concentrated deuterosulfuric acids (Fig. 6). Although a large number of simple benzene derivatives show weak ring-stretching bands near 1 600 cm^{-1}, the new band must have another origin

[3]*The previous results of the pK_{BH^+} values of acetic acid obtained from the change of the ultraviolet spectrum were not as accurate as the present one. For example, whether or not acetic acid may be regarded as a Hammett base was not checked by the previous authors (7, 9).*

[4]*Although the acidity dependence of the Raman spectrum could not give the accurate pK_{BH^+} value of acetic acid because of its inaccuracy in the absolute intensities, the results given in Fig. 4 show that the pK_{BH^+} value lies in between −5 and −9.*

Can. J. Chem. Downloaded from www.nrcresearchpress.com by 210.87.254.6 on 09/05/12
For personal use only.

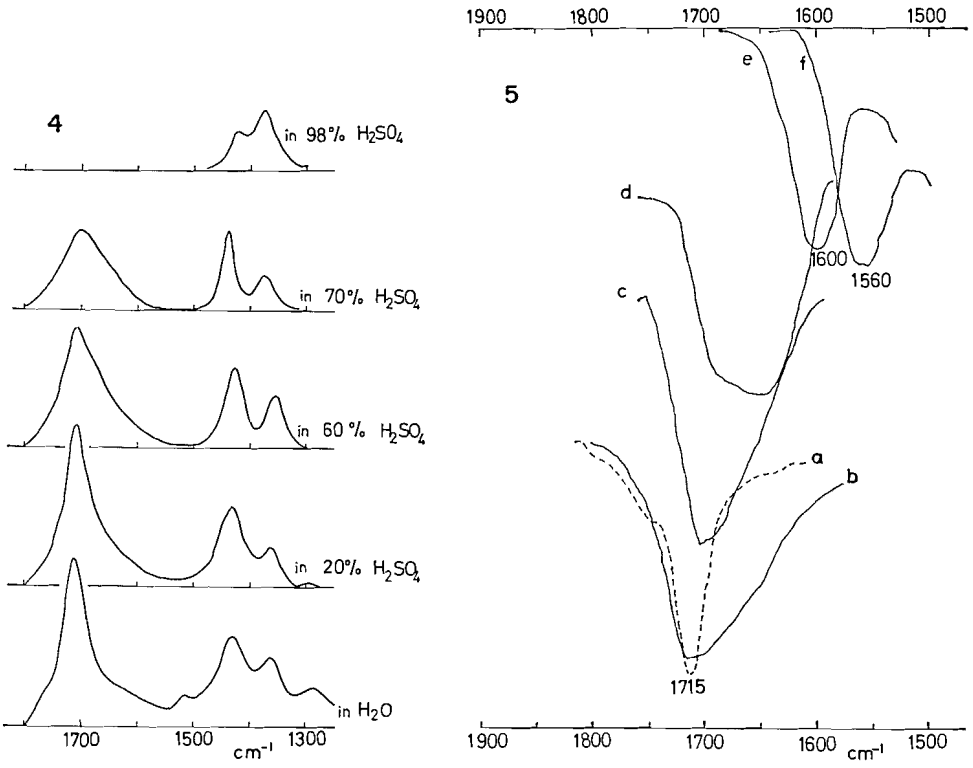


FIG. 4. The Raman spectra of acetic acid in sulfuric acid solutions.
FIG. 5. The infrared absorption spectra of acetic acid in various states: (*a*) pure liquid; (*b*) in D_2O; (*c*) in 50% D_2SO_4; (*d*) in 70% D_2SO_4; (*e*) in 95% D_2SO_4; (*f*) in aqueous NaOD.

in view of its strong intensity. By an analogy with the case of the protonated acetic acid, the new band may be assigned to the antisymmetric C—O stretching band. The observed band positions of the 6 μ region of the infrared and Raman spectra of acetic acid and

TABLE I

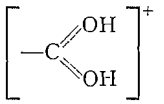
The infrared and Raman spectral peaks (in cm^{-1}) of acetic acid and benzoic acid in the 6 μ region

	CH_3COOH		C_6H_5COOH	
State	Infrared	Raman	Infrared	Raman
In NaOD aq.	1 570	—	1 599	—
In D_2SO_4	1 600	—	1 603	—
In D_2O	1 715	1 700	Insoluble	1 650 (ref. 3)
Liquid	1 715		1 705*	

*In methanol.

benzoic acid are summarized in Table I. It can safely be concluded again that in concentrated sulfuric acid solutions the carbonyl groups exist as the structure [3],

[3]



Can. J. Chem. Downloaded from www.nrcresearchpress.com by 210.87.254.6 on 09/05/12
For personal use only.

but not as [—C(=O)OH_2^+]. The similarity between the structures [2] and [3] gave the similar spectra pertinent to the C—O bonds. It is acceptable that the presence of the two protons is felt by these bonds as a minor perturbation (the mass ratio of O and OH being 0.94). The absence of the 1 600 cm^{-1} bands of the Raman spectra in the acidic and alkaline media can be explained as due to the antisymmetric vibrational mode of their similar skeletons. The symmetric ones are expected to be located at lower frequencies, but they were masked by the strong absorption of the solvent and polyethylene cells.

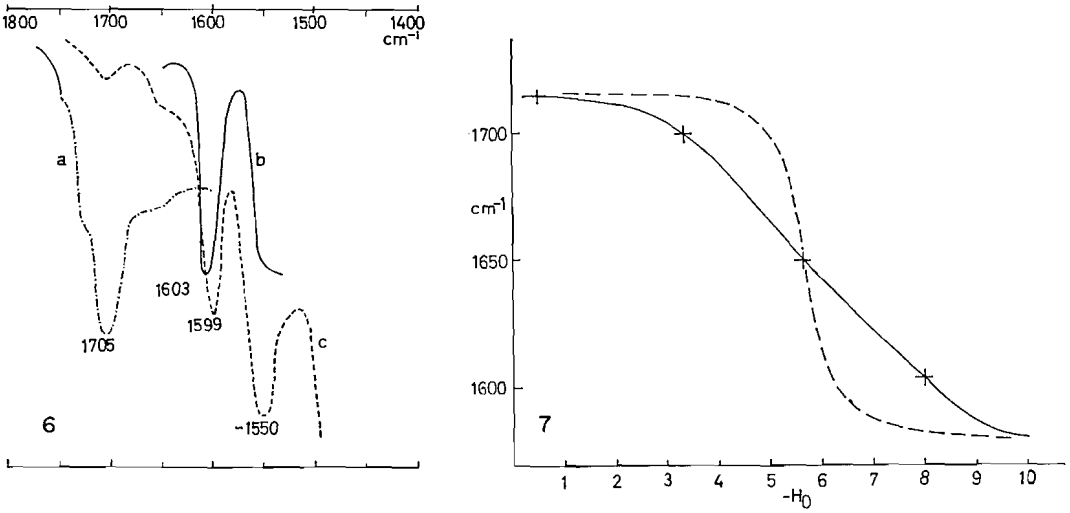


FIG. 6. Infrared absorption spectra of benzoic acid in various solutions. The solvents are: (*a*) methanol; (*b*) concentrated D_2SO_4; (*c*) aqueous NaOD.

FIG. 7. The change of the peak wave number of the infrared absorption spectra of acetic acid in deuterosulfuric acid solutions. The broken line represents a theoretical curve,

$$-5.80 = H_0 - \log [(\nu_{max} - 1\,562)/(1\,728 - \nu_{max})].$$

Since the accurate intensities of the infrared absorption were not obtained, we tried to estimate the pK_{BH^+} value of this compound from the change in the wave number of the absorption peak. The plot of the wave number against the H_0 values of the solvent gave the curve shown in Fig. 7. The general shape of this curve indicates a pK_{BH^+} of about −6 in agreement with the results of ultraviolet spectra.[5]

REFERENCES

1. H. P. TREFFERS and L. P. HAMMETT. J. Am. Chem. Soc. **59**, 1708 (1937).
2. M. S. NEWMAN, H. G. KUIVILA, and A. B. GARRETT. J. Am. Chem. Soc. **67**, 704 (1945). L. P. KUHN and A. H. CORWIN. J. Am. Chem. Soc. **70**, 3370 (1948). M. S. NEWMAN, R. A. CRAIG, and A. B. GARRETT. J. Am. Chem. Soc. **71**, 869 (1949).
3. H. HOSOYA and S. NAGAKURA. Spectrochim. Acta, **17**, 324 (1961).
4. R. STEWART and K. YATES. J. Am. Chem. Soc. **82**, 4059 (1960).
5. H. HOSOYA and S. NAGAKURA. Bull. Chem. Soc. Japan, **37**, 1500 (1964).
6. J. T. EDWARD, J. B. LEANE, and I. C. WANG. Can. J. Chem. **40**, 1521 (1962). E. M. ARNETT. *In* Progress in physical organic chemistry. Vol. 1. *Edited by* S. G. COHEN, A. STREITWIESER, and R. W. TAFT. Interscience Publishers, Inc., New York. 1963. p. 223.
7. M. A. PAUL and F. A. LONG. Chem. Rev. **57**, 1 (1957).
8. H. HOSOYA and S. NAGAKURA. Bull. Chem. Soc. Japan, **37**, 249 (1964).
9. A. R. GOLDFARB, A. MELE, and N. GUTSTEIN. J. Am. Chem. Soc. **77**, 6194 (1955).
10. J. T. EDWARD and I. C. WANG. Can. J. Chem. **40**, 966 (1962).
11. J. E. HIBBEN. *In* The Raman effect and its chemical applications. Reinhold Publishing Corp., New York. 1939. p. 178.

[5]*However, if we plot a theoretical* ν_{max} *vs.* H_0 *curve calculated from eq. [1] (*ν_{max} *for* ϵ*) by assuming appropriate values for the constants, it deviates appreciably from the observed one. This seems to indicate large solvent effects to the infrared absorption peaks. Detailed analyses for this proposed method will be given in a forthcoming paper (S. Hoshino, H. Hosoya, and S. Nagakura. To be published).*

Can. J. Chem. Downloaded from www.nrcresearchpress.com by 210.87.254.6 on 09/05/12
For personal use only.

TOTAL CROSS SECTIONS FOR IONIZATION BY ELECTRON IMPACT

A. G. HARRISON,[1] E. G. JONES, S. K. GUPTA, AND G. P. NAGY
Department of Chemistry, University of Toronto, Toronto, Ontario
Received March 17, 1966

ABSTRACT

Total cross sections for ionization by 75 V electrons have been measured for a wide range of molecules. On the whole the results are in agreement with the cross sections reported by Lampe *et al.* rather than those reported by Otvos and Stevenson. The results fit neither a single linear correlation with molecular polarizability nor a simple postulate of additivity of atomic ionization cross sections.

INTRODUCTION

Otvos and Stevenson (1) have reported the cross sections for ionization by electron impact for a number of gaseous molecules and have concluded from their data that the ionization cross section is a constitutive molecular property which can be estimated from suitable atomic ionization cross sections. More recently, Lampe, Franklin, and Field (2) have reported cross sections, determined in a similar manner, which are, in many cases, in disagreement with the values reported by Otvos and Stevenson. Further, Lampe *et al.* (2) showed that the postulate of additivity did not fit their data but rather suggested that the cross sections were linearly related to the polarizability of the neutral molecule.

In the hope of resolving this conflict in experimental results and to provide more extensive tests of the additivity concept and of the correlation with polarizability, we have measured the ionization cross sections for a wide variety of molecules. Our results are, on the whole, in agreement with those of Lampe *et al.* (2), but they fit neither a simple additivity postulate nor a simple correlation with molecular polarizability.

EXPERIMENTAL

As in previous studies (1, 2) the method consisted of measuring as a function of the sample reservoir pressure the total positive ion current to the negatively biased repeller of a mass spectrometer ion source. This total ion current, I_+, is given by the relation

$$I_+ = Q_i I_e d N \qquad [1]$$

where Q_i is the ionization cross-section, I_e is the ionizing electron current, d is the ionizing path length, and N is the concentration of molecules in the ion source. For molecular or effusive flow into and out of the ionization region the concentration of all gases in the ion source will be the same for a given reservoir pressure. Consequently a plot of I_+ versus reservoir pressure should be linear with a slope proportional to the total ionization cross section, and relative cross sections may be obtained by comparison of these slopes.

The present results were obtained using the ion source of a 2 in., 180° magnetic deflection instrument (A.E.I. MS-10). The total ion current to the repeller rose sharply to 4 V repeller bias after which it remained constant; measurements were taken on this plateau region. The current was measured with a General Radio model 1230A electrometer and recorded on a strip chart recorder. Typically, currents were in the range 10^{-10} to 10^{-8} A. The electron accelerating voltage was 75 V and the ionizing current 20 μA.

The reservoir pressure was read by a C.E.C. micromanometer and typically was varied from 5 to 150 μ. The gas admission leak was a porous plug (Metrosil) which tests showed to exhibit effusive flow to pressures of at least 20 mm. Initially some problems were encountered in the gas flow out of the ionization region. Preliminary experiments showed that for condensible gases the measured ion current at constant reservoir pressure was strongly dependent on the temperature of the cold trap, which indicated changes in the effective pumping speed. Therefore a number of baffle plates were placed in the pumping lead directly below the ion source. After this change the ion current was found to change by $<1\%$ for all compounds when the cold trap was cooled from dry ice temperature to liquid N_2 temperature.

[1]*Alfred P. Sloan Fellow 1962–1964. All correspondence should be addressed to this author.*

Can. J. Chem. Downloaded from www.nrcresearchpress.com by 210.87.254.105 on 09/05/12
For personal use only.

Typical ion current versus pressure plots are shown in Fig. 1. The cross sections were measured relative to that of krypton which was run periodically during each day's work. The slope of the krypton plot changed by <1% during the course of a day while cross sections relative to that for krypton were reproducible to ~3%.

All chemicals used were commercially available. The mass spectra were checked for impurities before use and the samples were carefully degassed before admission to the reservoir system.

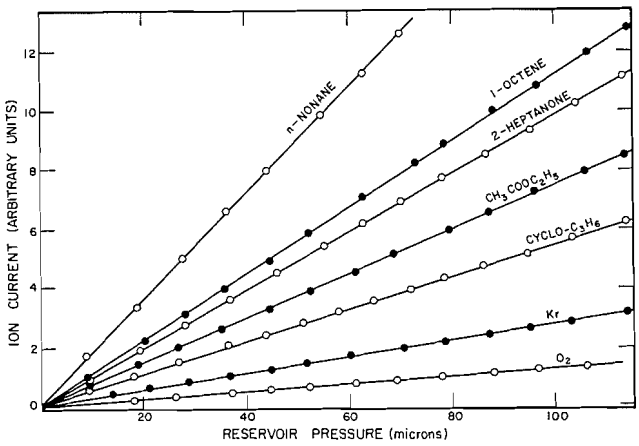


FIG. 1. Typical ion current versus pressure plots.

RESULTS AND DISCUSSION

The ionization cross sections obtained in the present work are compared with previous measurements in Table I. On the whole our results are in satisfactory agreement with the results of Lampe *et al.* (2) although we find significantly lower values for a number of cyclic and unsaturated hydrocarbons. The present results are also in reasonable agreement with the cross sections quoted by Massey and Burhop (3) and the values reported recently by Rapp and Englander-Golden (4). Indeed if we normalized our results to the Q_1(Kr) reported by the latter workers the only significant differences would occur for Ne and Xe. On the other hand, our cross sections, and those of Lampe *et al.* (2) are considerably higher than the values reported by Otvos and Stevenson (1) and the few cross sections reported by De Maria *et al.* (5). This is particularly true for organic molecules.

More extensive results were obtained for homologous series of alkanes, alkenes, alkynes, alkylbenzenes, ethers, aldehydes, ketones, and carboxylic esters. The cross sections are tabulated in Tables II and III. With the exception of those values reproduced from Table I these cross sections have not been previously measured. The upper limit to each series was determined by volatility since the sample reservoir was operated at room temperature.

The results in Tables II and III give numerous examples of structural isomers and show that, within experimental error, the cross sections are independent of structure within a given class of compound. This is particularly evident for the alkylbenzenes and carboxylic esters (Table III) and is shown further by the cross sections for isomeric C_6 alkanes recorded in Table IV. On the other hand isomers belonging to different functional classes in many cases show significantly differing cross sections. This is indicated by the data for a number of isomer pairs collected in Table IV.

The cross sections in Tables I to IV cannot be reproduced by assuming additivity of atomic ionization cross sections and assigning atomic cross sections to C, H, and O. If a

Can. J. Chem. Downloaded from www.nrcresearchpress.com by 210.87.254.105 on 09/05/12
For personal use only.

TABLE I

Comparison of total cross sections with previous measurements

Molecule	Cross section (cm^2 $molecule^{-1}$) × 10^{16}			
	This work	Lampe *et al.*	Otvos and Stevenson	Others
Ar	3.53	(3.52)	(3.52)	3.52 (3), 3.20 (4), 3.5 (5)
Ne	0.56_9	0.61_5	0.56_2	0.62_2 (3), 0.62_2 (4)
Kr	(5.18)	5.18	5.39	4.83 (4)
Xe	7.49	7.31		5.84 (4)
H_2	1.29	1.21	0.87_2	1.01 (3), 1.10 (4)
N_2	2.81	2.88	2.64	2.74 (3)
O_2	3.04	2.51	2.28	2.70 (3), 2.80 (4)
CO	3.03	2.99	2.66	2.99 (3), 2.88 (4), 2.9 (5)
CO_2	4.05	4.31	3.46	
H_2S	6.92	6.42	4.23	
CH_4	4.67	4.65	2.84	
C_2H_2	4.61	5.92		4.98 (3), 3.2 (5)
C_2H_4	6.12	6.66	4.17	
C_2H_6	8.39	8.35	4.91	
C_3H_6	8.97	9.73	6.20	
cyclo-C_3H_6	10.4	10.8		
C_3H_8	11.6	11.1	6.85	
n-C_4H_{10}	14.4	14.1	8.91	
cyclo-C_5H_{10}	16.9	17.3		
n-C_5H_{12}	17.7	18.6	11.1	
neo-C_5H_{12}	17.0	16.9		
C_6H_6	13.4	16.9	10.8	
cyclo-C_6H_{10}	15.5		11.6	
cyclo-C_6H_{12}	17.9	23.6	11.5	
n-C_6H_{14}	20.8	22.3	12.8	
n-C_7H_{16}	22.5		15.7	
C_2H_5Cl	10.8	12.1		
CH_3CHO	6.93		4.42	
$(CH_3)_2O$	9.33		5.36	
$(CH_3)_2CO$	10.2		6.71	
$(C_2H_5)_2O$	15.5			8.0 (5)

TABLE II

Total ionization cross sections for normal alkanes, alkenes, and alkynes

Number of Carbons	Cross section × 10^{16} (cm^2 $molecule^{-1}$)		
	Q_i(alkane)	Q_i(alkene)*	Q_i(alkyne)*
1	4.67		
2	8.39	6.12	4.61
3	11.6	8.97	7.65
4	14.4	11.5	9.43
5	17.7	14.1	12.4
6	20.0	16.4	15.0
7	22.5	19.6	17.9
8	25.0	21.5	19.1
9	27.0		22.3
10	30.0		24.8

*Alkenes and alkynes with terminal unsaturation.

simple additivity postulate held, one would expect $Q_i(O)$, given by the following differences, to be constant.

$$Q_i(O) = Q_i(C_nH_{2n+2}O) - Q_i(C_nH_{2n+2}) = Q_i(\text{ether}) - Q_i(\text{alkane}) = 0.60 \times 10^{-16}$$
$$Q_i(O) = Q_i(C_nH_{2n}O) - Q_i(C_nH_{2n}) = Q_i(\text{ketone}) - Q_i(\text{alkene}) = 1.30 \times 10^{-16}$$
$$Q_i(O) = Q_i(C_nH_{2n}O_2) - Q_i(C_nH_{2n}O) = Q_i(\text{ester}) - Q_i(\text{ketone}) = 0.90 \times 10^{-16}$$

Can. J. Chem. Downloaded from www.nrcresearchpress.com by 210.87.254.105 on 09/05/12
For personal use only.

Can. J. Chem. Downloaded from www.nrcresearchpress.com by 210.87.254.105 on 09/05/12
For personal use only.

TABLE III

Total ionization cross sections

	Molecule	$Q_i \times 10^{16}$ (cm^2 molecule^{-1})
Alkylbenzenes	Benzene	13.4
	Toluene	16.1
	o-Xylene	18.7
	Ethylbenzene	19.0
	n-Propylbenzene	22.2
	Cumene	22.2
	p-Ethyltoluene	22.1
	1,2,3-Trimethylbenzene	21.6
	1,2,4-Trimethylbenzene	21.8
	n-Butylbenzene	24.1
	t-Butylbenzene	24.1
	1,2,3,5-Tetramethylbenzene	23.6
Ethers, aldehydes, ketones	CH_3OCH_3	9.33
	$CH_3OC_2H_5$	12.8
	$C_2H_5OC_2H_5$	15.5
	n-$C_4H_9OCH_3$	18.0
	t-$C_4H_9OCH_3$	18.2
	$(n$-$C_3H_7)_2O$	19.8
	CH_3CHO	6.93
	C_2H_5CHO	9.38
	i-C_3H_7CHO	12.4
	CH_3COCH_3	10.2
	$C_2H_5COCH_3$	12.9
	n-$C_3H_7COCH_3$	15.2
	$C_2H_5COC_2H_5$	15.8
	n-$C_5H_{11}COCH_3$	19.4
	n-$C_6H_{13}COCH_3$	23.9
Carboxylic esters	$HCOOCH_3$	8.22
	$HCOOC_2H_5$	10.8
	$HCOOC_3H_7$	13.6
	$HCOOCH(CH_3)_2$	13.4
	$HCOOC_4H_9$	16.2
	$HCOOCH_2CH(CH_3)_2$	16.3
	CH_3COOCH_3	11.2
	$CH_3COOC_2H_5$	14.3
	$C_2H_5COOCH_3$	14.0
	$C_3H_7COOCH_3$	16.4
	$C_4H_9COOCH_3$	18.5

TABLE IV

Effect of structural isomerism on ionization cross sections

Molecule	$Q_i \times 10^{16}$ (cm^2 molecule^{-1})	Molecule	$Q_i \times 10^{16}$ (cm^2 molecule^{-1})
n-C_6H_{14}	20.0	C_3H_6	8.97
2-Methylpentane	19.6	cyclo-C_3H_6	10.4
3-Methylpentane	19.7		
2,2-Dimethylbutane	20.0	C_5H_{10}	14.1
2,3-Dimethylbutane	19.7	cyclo-C_5H_{10}	16.9
C_2H_5OH	8.66	C_6H_{10}	15.0
CH_3OCH_3	9.33	cyclo-C_6H_{10}	15.5
C_2H_5CHO	9.38	C_6H_{12}	16.4
CH_3COCH_3	10.2	cyclo-C_6H_{12}	17.9

The variation in these differences and comparison with $Q_i(O_2) = 3.04 \times 10^{-16}$ cm^2 molecule^{-1} indicates a breakdown of the additivity postulate. By similar reasoning the additivity concept implies that $Q_i(H_2)$ can be evaluated as follows.

$$Q_i(H_2) = Q_i(C_nH_{2n+2}) - Q_i(C_nH_{2n}) = Q_i(\text{alkane}) - Q_i(\text{alkene})$$
$$Q_i(H_2) = Q_i(C_nH_{2n}) - Q_i(C_nH_{2n-2}) = Q_i(\text{alkene}) - Q_i(\text{alkyne})$$

From Table I, $Q_i(H_2) = 1.2_9 \times 10^{-16}$ cm^2 molecule while from Table II the average difference $Q_i(\text{alkane}) - Q_i(\text{alkene}) = 3.1 \times 10^{-16}$ and the average $Q_i(\text{alkene}) - Q_i(\text{alkyne}) = 1.5 \times 10^{-16}$. A further indication of the failure of the additivity concept is, of course, supplied by the differences for the isomer pairs recorded in Table IV.

On the other hand, the cross-sections within an homologous series do fit a modified additivity rule. This is shown graphically in Fig. 2 where for each homologous series the total cross sections are plotted as a function of the number of carbon atoms in the molecule. With the exception of the lower alkanes a satisfactory straight line is obtained for each series, which indicates that increasing the chain length by successive introductions of CH_2 brings about a regular increase in the cross sections. Further, it should be noted that, within experimental error, the slopes of the straight lines are identical; this indicates that for each series the effect of CH_2 introduction is identical. For the alkanes those above C_3 fit a straight line relation while methane, ethane, and possibly propane lie below the straight line. A similar linear correlation with a number of carbon atoms has been noted recently by Schram *et al.* (6) for the ionization cross sections of a limited number of alkanes and alkenes in the electron energy region 1 keV to 12 keV.

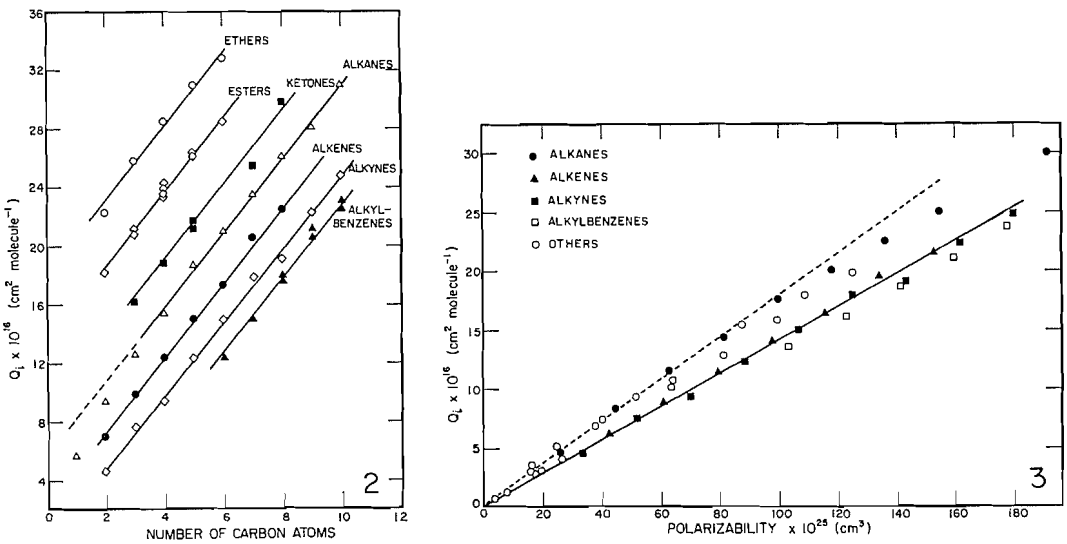


FIG. 2. Total ionization cross sections as a function of the number of carbon atoms. The scales for some series have been shifted for clarity. See Tables for absolute values.
FIG. 3. Total ionization cross sections plotted against polarizability.

The straight line relationships of Fig. 2 permit an estimation of the cross sections of higher members of each series by simple extrapolation. The best fits for the straight lines are given below, where N_C is the number of carbon atoms in the molecule, and the equation for the alkanes applies only for C_4 and higher.

Can. J. Chem. Downloaded from www.nrcresearchpress.com by 210.87.254.105 on 09/05/12
For personal use only.

Alkanes	$Q_i \times 10^{16} =$	$4.4_0 + 2.5_4 N_C$
Alkenes	$Q_i \times 10^{16} =$	$1.3_0 + 2.5_4 N_C$
Alkynes	$Q_i \times 10^{16} =$	$-0.2_5 + 2.5_4 N_C$
Alkylbenzenes	$Q_i \times 10^{16} =$	$-1.4 + 2.5_4 N_C$
Alkyethers	$Q_i \times 10^{16} =$	$5.0_0 + 2.5_4 N_C$
Carboxylic esters	$Q_i \times 10^{16} =$	$3.5_0 + 2.5_4 N_C$
Ketones	$Q_i \times 10^{16} =$	$2.6_0 + 2.5_4 N_C$

Lampe *et al.* (2) have suggested on the basis of their results that the ionization cross sections are a linear function of the polarizability of the neutral molecule. With the extensive data now available a more rigorous test of this correlation can now be made. The plot of cross section versus polarizability is shown in Fig. 3. The closed circles represent the data for the alkanes and the open circles the data for other molecules whose polarizabilities are tabulated in Landolt-Bornstein (7). The polarizabilities of the higher alkenes, alkynes, and alkylbenzenes were estimated from the reported values for the first members by assuming the same increment per CH_2 (18.3×10^{-25}) as found for the alkanes; this procedure gives slightly lower polarizabilities than would be obtained by using bond polarizabilities (8).

The data obviously do not fit a single linear relationship. The broken line is the straight line of slope equal to that given by Lampe *et al.* (2) from their correlation. As can be seen it fits the data for the lower alkanes and a number of other molecules. However, the higher alkanes, alkenes, alkynes, and alkylbenzenes fall below this straight line. The alkene and alkyne cross sections fit a single linear correlation with polarizability, but the slope of the line is about 20% lower than the line which fits the lower alkanes. We conclude from Fig. 3 that no single, simple correlation of total ionization cross section with polarizability holds. It might be noted that Lampe *et al.* (2) did not measure cross sections for the higher alkanes, alkenes, and alkynes where the most significant deviations are found.

In summary, it is apparent that molecular ionization cross sections fit neither a simple additivity postulate nor a single linear correlation with polarizability. Stevenson and Schissler (9) reviewing the data available in 1961 reached a similar conclusion concerning the additivity concept and suggested that the correlation with polarizability should be viewed with caution. The present results do show that within any homologous series the data can be correlated with polarizabilities or accommodated by a modified additivity rule. Difficulties arise only when comparing one homologous series with another, indicating that the cross section is determined, in part, by the nature of the functional group.

Stevenson and Schissler (9) have presented arguments suggesting that the additivity rule breaks down for the cases where an appreciable number of collisions lead to excitation rather than ionization. A rather similar explanation has been advanced (10) to explain the isotope effects observed in total ionization experiments. It has been found consistently that total cross sections for ionization of deuterated molecules are greater than for the undeuterated form, regardless of whether this ionization is brought about by collision with metastable atoms (11), beta rays (12), or electrons (13). This has been explained on the assumption that the initial impact process leads, in part, to formation of highly excited (super-excited) neutral molecules which may either undergo neutral dissociation or autoionization and subsequent fragmentation. The replacement of hydrogen by deuterium is considered to retard the neutral fragmentation reactions preferentially and thus lead to a higher ionization cross section.

Such a postulate can explain the present results if we assume that either the number of

Can. J. Chem. Downloaded from www.nrcresearchpress.com by 210.87.254.105 on 09/05/12
For personal use only.

"super-excited" molecules or the fraction of these which undergo neutral dissociation reactions is dependent on the functional group present. Thus we would suggest, for example, that for the alkenes and alkynes the fraction of electron impact events leading to neutral fragmentation is considerably greater than for the lower alkanes, resulting in deviations from a single correlation with polarizability. In this regard we would note that our measurements give $Q_1(C_2D_6)/Q_1(C_2H_6) = 1.01_3$ compared to $Q_1(C_2D_2)/Q_1(C_2H_2) = 1.04_1$, $Q_1(C_2D_4)/Q_1(C_2H_4) = 1.03_8$, and $Q_1(C_7D_8)/Q_1(C_7H_8) = 1.04_2$. This latter value is identical with the ratio 1.04 reported by Meyerson *et al.* (13). The lower isotope effect for ethane could be taken to indicate that neutral fragmentation events are less important in this case. More extensive investigations of isotope effects particularly among higher members of the series would be of considerable interest.

ACKNOWLEDGMENTS

The authors are indebted to the National Research Council of Canada for financial support of this work.

REFERENCES

1. J. W. Otvos and D. P. Stevenson. J. Am. Chem. Soc. **78**, 546 (1956).
2. F. W. Lampe, J. L. Franklin, and F. H. Field. J. Am. Chem. Soc. **79**, 6129 (1957).
3. H. S. W. Massey and E. H. S. Burhop. Electronic and ionic impact phenomena. Oxford University Press, London. 1952.
4. D. Rapp and P. Englander-Golden. J. Chem. Phys. **43**, 1464 (1965).
5. G. De Maria, G. Balducci, and L. Malaspina. Ann. Chim. Rome, **53**, 1039 (1963).
6. B. L. Schram, M. J. van der Weil, F. J. de Heer, and R. H. Moustafa. J. Chem. Phys. **44**, 49 (1966).
7. Landolt-Bornstein. Zahlenwerte und functionen. 6 Auflage. Atom und molecular physik. 3 Teil. Springer-Verlag, Berlin. 1950.
8. J. O. Hirschfelder, C. F. Curtiss, and R. B. Bird. Molecular theory of liquids and gases. J. Wiley and Sons, Inc., New York. 1954.
9. D. P. Stevenson and D. O. Schissler. The chemical and biological actions of radiation. Vol. 5. *Edited by* M. Haissinsky. Academic Bks., Ltd., London. 1961. 181–192.
10. R. L. Platzman. J. Phys. Radium, **31**, 853 (1960); Vortex, **23**, No. 8 (1962).
11. W. P. Jesse. J. Chem. Phys. **41**, 2060 (1964).
12. W. P. Jesse. J. Chem. Phys. **38**, 2774 (1963).
13. S. Meyerson, H. M. Grubb, and R. W. Van der Haar. J. Chem. Phys. **39**, 1445 (1963).

Can. J. Chem. Downloaded from www.nrcresearchpress.com by 210.87.254.105 on 09/05/12
For personal use only.

Can. J. Chem. Downloaded from www.nrcresearchpress.com by 210.87.254.105 on 09/05/12
For personal use only.

A CORRELATION OF STEPWISE STABILITY CONSTANT RATIOS AND SOME BONDING PROPERTIES OF TRANSITION METAL AND ZINC COMPLEXES[1]

P. G. MANNING
Mines Branch, Department of Mines and Technical Surveys, Ottawa, Canada

Received January 20, 1966

ABSTRACT

Stepwise stability constant ratios for some transition metal and zinc amino acid complexes are analyzed. It is shown that the observed ratios for Cu and Ni amino acid complexes are larger than the calculated ratios by a factor R, the Bjerrum rest effect. It is suggested that the rest effect is due to metal–nitrogen covalency, there being sufficient transfer of charge from ligand to metal in the first association stage to reduce markedly the electrostatic attraction between ligand and metal in the second.

For Zn complexes, the observed and calculated ratios are in excellent agreement. A small rest effect would seem to be present in the Co system, but experimental errors render any conclusions uncertain.

INTRODUCTION

The absolute magnitudes of stepwise stability constants for metal–ligand ion association reactions are useful in choosing the ligands that might be of application in, e.g. the ion-exchange separation of rare earths. However, the stability constants often do not tell us the nature of the species formed. In an earlier publication in this series (1), the ratios of stepwise stability constants for some simple rare earth and cupric ion association systems were analyzed using the Bjerrum relationship (2)

$$P = K_1{:}K_2 = S \times T \times R,$$

where K_1 and K_2 are stepwise stability constants defined by

$$K_n = [\mathrm{ML}_n]/[\mathrm{ML}_{n-1}][\mathrm{L}]$$

where M = metal ion and L = ligand. The S, T, and R factors are as follows.

S factor.—S is purely statistical and can be evaluated from a knowledge of the number of available cation sites and ligand groups. For a bidentate ligand binding to a hexahydrated cation (octahedral), $S = 2 \times 12/5 = 4.8$. The factor 2 arises because the probability of a ligand's leaving the 1:2 associate is twice that of the ligand's leaving the 1:1.

T factor.—This factor is a measure of the work done in bringing a second ligand from infinity to its equilibrium position in the 1:2 (metal:ligand) associate against the repulsive force exerted by the already bound ligand. Therefore, T, being electrostatic in nature, should be independent of the nature of cation and ligand. Table I lists T values derived from experimental P values for rare earth, cupric, and zinc ion association systems. The characterization of certain metal–ligand systems by a given T value would aid considerably in the interpretation of the vast compilations of stability constants, e.g. the Chemical Society publications (3). One of the aims of this work is the analysis of stepwise stability constant ratios for transition metal amino acid complexes in order to determine whether a T value = 1.6 holds for these singly charged ligand systems. The simpler ligands have been studied so as to minimize steric hindrance effects and long-chain hydrocarbon

[1]*Crown Copyright Reserved.*

TABLE I

Values of T for metal–ligand complexes

Metal	Ligand	Bonding	T
Rare earth	R′·CH(OH)·COOH*	Monodentate	1.5±0.25
Cu^{2+}	Glycolate	Bidentate	1.5±0.3
Cu^{2+}	Acetate	Monodentate	1.75±0.1
Zn^{2+}	Mandelate	Monodentate	1.5

*R' = organic group.

interactions with the water structure. The latter effect could introduce important entropy changes.

R factor.—R, the rest effect, covers those effects that are neither electrostatic nor statistical. Bjerrum (2) defined R as "the influence of bound ligands on the binding power of the metal ion." In this paper, it is demonstrated that rest effects are present in transition metal amino acid complexes, and the significance of the R term is discussed.

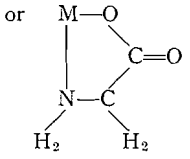
DISCUSSION

The possible reactions between a cation and a simple (primary amino) amino acid (e.g. glycine) may be formulated as follows (4),

[1] $$M + NH_2CH_2COO = M—O·CO·CH_2·NH_2$$

[2] $$\text{or } M—NH_2·CH_2·COO$$

[3] or



The (primary amino) amino acids are generally regarded as being bidentate ligands (4), and this may be readily confirmed from the magnitudes of P_{obs}. The above reactions are analagous to monodentate and bidentate glycolate interaction with Cu, Zn, and the rare earths, so that a value of $T = 1.6$ (Table I) may be postulated for reactions [1], [2], and [3]. The S factors for reactions [1], [2], and [3] are 2.4 ($= 2 \times 6/5$), 2.4, and 4.8 respectively for a cation with six equivalent binding sites. The corresponding P_{calc} values are, therefore, 3.8, 3.8, and 7.7. Table II presents P_{obs} for some (primary amino) amino acid complexes of Cu, Ni, Co, Fe, Mn, and Zn. The P_{calc} and P_{obs} values for Zn are in excellent agreement, indicating that a value of $T = 1.6$ holds for this system and that the ligands are bidentate. The data for Mn and Fe glycine complexes are too few for any unequivocal conclusions to be drawn, but the P_{obs} values would tend to favour bidentate ligandcy. For the leucine and valine complexes of Mn, $P_{obs} < S$. Consequently, the latter systems would seem to warrant reinvestigation.

It was shown in an earlier publication (30) that $T = 1.1$ for singly charged ligands (e.g. chloride) ion pairing with the rare earth hydration sheath. When this T value was corrected for the smaller separation of ligands in a complex, then T (monovalent ligand complexing) $\sim$1.4, a value in good agreement with the directly derived T values listed in Table I. It would seem, therefore, that the metal–oxygen bonding in the complexes listed in Table I is of low covalent character, i.e. mainly ionic. A T value of 1.6 also holds for ferric chloride complexes (31), which are generally regarded as being mainly ionic (32).

Can. J. Chem. Downloaded from www.nrcresearchpress.com by 210.87.254.105 on 09/05/12
For personal use only.

TABLE II

Values of log P for metal–ligand complexes*

Ligand	Cu	Ni	Co	Fe	Mn	Zn
Glycine	1.65	1.22 1.02	1.21	0.8	0.9	1.08
	1.25	0.97 1.02	0.86		0.69	0.66
	1.60	1.2 1.02	0.87			0.94
	1.51 1.28	1.09	0.96			
	1.21 1.2	0.97	1.05			0.82
	1.6 1.65	1.08	0.86			0.90
	1.29 1.66		1.3			0.76
Alanine	1.04 1.65 1.53	1.26	1.16 0.82 0.88		0.43	0.82 0.88
Leucine	1.45	1.02	0.84		0.11	0.91 0.61
β-Alanine	1.66	1.23				
α-Aminobutyric acid			0.96			0.84
Norvaline	1.58	1.26	1.22			0.99
Valine	1.22	1.21 1.18	1.00		0.12	0.90
	1.40	1.21 1.20 1.18 1.18	0.90			
Average P	29±10	14±3	10±3	~6.5	6.5	7.4±1.5

*Source of P values, refs. 5–29.

In a recent review article (33), Moeller and co-workers concluded that rare earth – oxygen bonds were mainly ionic. Later in this publication, it is shown that M—L covalency (transfer of charge from M → L) increases the magnitude of P. It would seem, therefore, that the Zn—O and Zn—N bonds in the amino acid systems are of low covalent character.

The observed P values for the Cu and Ni complexes indicate that the value of R is appreciable (Table III). These cations form much stronger complexes with the (primary amino) amino acids than does Zn, showing that the ligands are probably bidentate. The S values for Cu have been computed on the basis of four available cation sites. The Jahn–Teller effect was shown to be operative in the cupric glycolate and acetate systems (1), and the effect has also been observed in the Cu ethylenediamine system (34). Furthermore,

TABLE III

R factors for metal – amino acid complexes

Factor	Cu	Ni	Co	Fe	Mn	Zn
P_{obs}	29	14	10	~6.5	6.5	7.4
S	8.0	4.8	4.8	4.8	4.8	4.8
T	1.6	1.6	1.6	1.6	1.6	1.6
P_{calc}	12.8	7.7	7.7	7.7	7.7	7.7
R	2.3	1.8	1.3±0.4	~1	1	1.0

Can. J. Chem. Downloaded from www.nrcresearchpress.com by 210.87.254.105 on 09/05/12
For personal use only.

the log K values for the three stages of Cu glycine association (6) are 8.33, 6.97, and <1, while the corresponding figures for Co (6) are 4.61, 3.75, and 2.56. For Co, however, the average P_{obs} value of 10 ± 3 overlaps the P_{calc} value of 7.7 calculated on the basis of $S = 4.8$ and $T = 1.6$.

The value $T = 1.6$ for singly-charged ligand systems covers contributions to the magnitude of P from, e.g. preferential disruption of the hydration sheath in a given stage of ion association and also any solvent structure and dielectric effects. The rest effect may therefore be associated with metal–ligand interaction, notably the bonding properties. Possible reasons for a large R factor are:

(i) The M—L bond length increases as the number of bound ligands increases. Such an effect was not noted in the α-hydroxymonocarboxylate systems listed in Table I, and it is unlikely to be present here. Bjerrum (2) has shown that the M—L bond length does not change upon higher association for simple nitrogen-bonding ligands.

(ii) The ligand is bidentate in the first association stage and monodentate in the second. This possibility has been eliminated earlier in this work.

(iii) The metal–ligand bond is sufficiently covalent that considerable charge is transferred from ligand to metal. The electrostatic attractive force between metal and ligand in the second association stage is then reduced. The greater the covalency of the metal–ligand bond the greater will be R. Copper–oxygen bonds would seem to be mainly ionic, however, as the Cu glycolate data in Table I show ($T = 1.6$). Covalent bonding can therefore be attributed to Cu–N bonds. The magnitude of R shows that the order of metal–ligand covalency for (primary amino) amino acid systems is Cu > Ni > Co $\geqslant$ Fe = Mn = Zn $\sim$ O. This series is in accord with the deductions of Martell and Calvin (4) from the slopes of plots of the second ionization potential of the metal against complex stability, for different oxygen- and nitrogen-bonding ligands. It is of interest to note that the above ordering of metals according to the magnitudes of their R values follows closely the Irving–Williams order (35), which compares the absolute stabilities of complexes. Thus the R factor could be put in the order Mn = Fe $\leqslant$ Co < Ni < Cu > Zn. The Irving–Williams order can be interpreted on the basis of the ability of the cation to accept charge from a ligand, and the sequence can be correlated with the standard electrode potential of the metal (36). The correlation between the magnitude of R and the ability of a metal to accept charge is good. The R sequence also suggests that the R value for Co is significantly greater than 1.0. While the R values could tell us, in principle, the amount of charge transferred to the metal (metal–ligand covalency), the calculation becomes impractical because of the unknowns associated with the M—L distance over which the continuous transfer of charge takes place.

Values of P for the (secondary amino) amino acids (Table IV) suggest that Cu—N

TABLE IV

Values of log P, P_{obs}, and P_{calc} for Cu and Ni complexes

	Cu	Ni
Log P for iso-$C_3H_7 \cdot NH \cdot CH_2 \cdot COOH$	0.95	
Log P for $C_4H_9 \cdot NH \cdot CH_2 \cdot COOH$	1.12	1.14
Log P for n-$C_3H_7 \cdot NH \cdot CH_2 \cdot COOH$	1.19	1.12
Log P for $CH_3 \cdot NH \cdot CH_2 \cdot COOH$	1.29	1.12
Log P for $C_2H_5 \cdot NH \cdot CH_2 \cdot COOH$	1.13	1.08
Average P_{obs} (ref. 12)	14±3	13.0±0.5
P_{calc}	12.8*	7.7

*Calculated for four available cation sites.

Can. J. Chem. Downloaded from www.nrcresearchpress.com by 210.87.254.105 on 09/05/12
For personal use only.

covalency is small and $R = 1.1$. For Ni, however, the Ni—N bond would seem to be of similar covalency to the primary amino system ($R = 1.7$). It is possible that the coordinating acid oxygen atom of the (secondary amino) amino acid has similar bonding properties to the oxygen atom of water. The (secondary amino) amino acids are therefore capable of displacing all six waters of the Cu^{2+} primary hydration sheath with equal facility. The N atom would bind in the square plane and the O atom either in the square plane or perpendicular to the square plane. For this model, $S = 4.8$, $S \times T = 7.7$ and $R = 1.8$, corresponding to $P_{obs} = 14$. This R value is more consistent with that for Ni. Furthermore, for the Cu—$OOC \cdot CH_2 \cdot N(CH_3)_2$ system (12), $P_{obs} = 9$, whereas for square planar bonding only, $S = 8.0$. For six available Cu sites, $S \times T = 7.7$, giving an R value = 1.2. The R value for the Ni system is 1.4, since $P_{obs} = 11$. It would seem, therefore, that the secondary amino and tertiary amino amino acids can displace all six waters of the Cu^{2+} sheath.

CONCLUSION

Interpretations of the magnitudes of stepwise stability constant ratios for transition metal and zinc amino acid complexes have led us to the following conclusions:

(*a*) The method is capable of giving reliable information on the nature of metal–ligand bonding.

(*b*) Electrostatic repulsion between a bound ligand (in a M—L complex) and a potentially binding ligand contributes a factor of 1.6 to the magnitude of the stepwise stability constant ratio, where L = singly charged ligand and M = transition metal, Zn, or rare earth ion.

(*c*) M—N bond covalency follows the order Cu > Ni > Co $\gg$ Mn = Fe = Zn $\sim$ O.

(*d*) In the Cu^{2+} systems, the (primary amino) amino acids bind in the square plane. The (secondary and tertiary amino) amino acids displace all six waters of hydration.

REFERENCES

1. P. G. Manning. Can. J. Chem. **43**, 3258 (1965).
2. J. Bjerrum. Metal ammine formation in aqueous solution. P. Haase and Son, Copenhagen. 1941.
3. The Chemical Society, London. Stability constants. Parts I and II. 1957. *Also* Chemical Society, London. 1964.
4. A. E. Martell and M. Calvin. Chemistry of the metal chelate compounds. Prentice-Hall, Englewood Cliffs, N.J. 1952.
5. C. B. Monk. Trans. Faraday Soc. **47**, 292, 297 (1951).
6. H. V. Flood and V. Loras. Tidsskr. Kjemi Bergvesen, **5**, 83 (1945).
7. C. Tanford and W. S. Shore. J. Am. Chem. Soc. **75**, 816 (1953).
8. L. E. Maley and D. P. Mellor. Nature, **165**, 453 (1950).
9. J. I. Evans and C. B. Monk. Trans. Faraday Soc. **51**, 1244 (1955).
10. J. B. Gilbert, M. C. Otey, and J. Z. Hearon. J. Am. Chem. Soc. **77**, 2599 (1955).
11. A. Albert. Biochem. J. **47**, 531 (1950).
12. F. Basolo and Y. T. Chen. J. Am. Chem. Soc. **76**, 953 (1954).
13. H. Irving, R. J. P. Williams, D. J. Ferrett, and A. E. Williams. J. Chem. Soc. 3493 (1954).
14. A. Albert. Biochem. J. **54**, 646 (1953).
15. L. E. Maley and D. P. Mellor. Australian J. Sci. Res. **2**, 579 (1955).
16. N. C. Li and R. A. Manning. J. Am. Chem. Soc. **77**, 5225 (1955).
17. R. M. Keefer. J. Am. Chem. Soc. **68**, 2329 (1946).
18. J. A. Martus. Rept. to the Office of Naval Research N. Da-19-020-ORD 1614.
19. R. L. Rebertus. Dissertation, Urbana Junior College, Urbana, Ohio. 1952.
20. A. Albert and E. P. Sargeant. Biochem. J. **76**, 621 (1960).
21. A. Weiss and S. Fallab. Helv. Chim. Acta, **40**, 576 (1957).
22. C. B. Murphy and A. E. Martell. J. Biol. Chem. **226**, 37 (1957).
23. V. Cieleszky, A. Dines, and E. Sandi. Acta Chim. Acad. Sci. Hung. **9**, 381 (1956).
24. B. Dos Sarma and P. Ray. J. Indian Chem. Soc. **33**, 841 (1956).
25. N. C. Li, J. M. White, and R. L. Yoest. J. Am. Chem. Soc. **78**, 5218 (1956).
26. H. A. Mackenzie and D. P. Mellor. Thesis of H. A. Mackenzie, Sydney, Australia. 1955.
27. S. P. Dalta, R. Lebermann, and B. R. Rabin. Trans. Faraday Soc. **55**, 1982, 2141 (1959).
28. S. Pelletier, J. Curchod, and M. Quintin. Compt. Rend. **243**, 1868 (1956).
29. S. Pelletier. Dissertation, Univ. of Paris, France, 1960.

Can. J. Chem. Downloaded from www.nrcresearchpress.com by 210.87.254.105 on 09/05/12
For personal use only.

30. P. G. MANNING. Can. J. Chem. **43**, 2911 (1965).
31. P. G. MANNING. Complexes present in aqueous ferric chloride solutions. Can. J. Chem. This issue.
32. D. P. CRAIG and R. S. NYHOLM. The nature of the metal–ligand bond. *In* Chelating agents and metal chelates. Chap. 2. *Edited by* F. P. Dwyer and D. P. Mellor. Academic Press, New York and London. 1964.
33. T. MOELLER, D. F. MARTIN, L. C. THOMPSON, R. FERRUS, G. FIESTAL, and W. J. RANDALL. Chem. Rev. **65**, 1 (1965).
34. F. A. COTTON and G. WILKINSON. Advanced inorganic chemistry. Interscience Publishers, Inc., New York. 1962.
35. H. IRVING and R. J. P. WILLIAMS. Nature, **162**, 746 (1948).
36. D. P. GRADDON. An introduction to coordination chemistry. The Pergamon Press, Ltd., London. 1961.

Can. J. Chem. Downloaded from www.nrcresearchpress.com by 210.87.254.105 on 09/05/12
For personal use only.

Can. J. Chem. Downloaded from www.nrcresearchpress.com by 210.87.254.5 on 09/05/12
For personal use only.

THE PHOTOLYSIS OF CO_2 AT 1 470 Å[1]

A.-Y. UNG[2] AND H. I. SCHIFF[3]
Upper Atmosphere Chemistry Group, McGill University, Montreal, Quebec

Received March 16, 1966

ABSTRACT

The apparatus used to study the photolysis contained a collimating region which minimized the effect of divergent light, and permitted the temperature of the cell and lamp to be controlled separately. Analytical sensitivity was such that conversions less than 0.2% were possible.

Although CO and O_2 were the only stable products, the CO/O_2 ratios were higher than those required by mass balance. The product yields were found to be independent of CO_2 pressure and to be linear with irradiation time at 25 °C. At higher temperatures the quantum yields decreased and at 200 °C were no longer linear functions of irradiation time. The O_2 yields decreased when CO was added, the effect increasing with temperature. The overall quantum yield was less than unity. Reactions were observed with CH_4, H_2, and N_2O when these were added in small amount. These results indicated the presence of a reactive species, capable of promoting back reactions and of being adsorbed on the walls. A mechanism is suggested which best fits the results and which postulates CO_3 as the reactive species.

The ultraviolet photolysis of CO_2 is of interest for a number of reasons. It has been widely used as an actinometer for determining the quantum yields of other photolyses at short wavelengths. Although it has generally been assumed that the CO quantum yield is unity, this has never been convincingly demonstrated. The photolysis also provides a potential source of metastable $O(^1D)$ atoms, which possesses advantages over alternate sources. Reactions of these metastable atoms play an important role in the chemistry of the earth's atmosphere but have received little study in the laboratory. The photolysis of CO_2 is also of interest in understanding the photochemistry of the atmospheres of Mars and Venus. However, the results obtained by previous investigators have not been satisfactorily interpreted by any mechanism thus far proposed.

A number of investigators (1–3) have found that, although CO and O_2 are the only products detected, oxygen is not recovered in the amounts required for mass balance. Formation of ozone has been postulated by Mahan (1) and by Warneck (3), although Warneck (4) recently claimed to have found evidence for incipient CO_3 formation.

Although Jucker and Rideal (5) concluded that the primary photolytic product is electronically excited CO_2, the consensus now seems to favor the initial production of CO and $O(^1D)$ atoms, in agreement with spectroscopic evidence (6, 7). Yamazaki and Cvetanovic (8–10), however, found that $O(^1D)$ atoms are rapidly quenched by CO_2 and should therefore have negligible lifetimes in systems in which they are generated by CO_2 photolysis.

Finally, no systematic study has yet been reported on the effect of temperature on the photolysis. The present work was undertaken as an attempt to clarify some of these problems. In particular, the results indicated the necessity for considering a back reaction.

EXPERIMENTAL

The essential features of all the glass and quartz apparatus are shown in Fig. 1. The light source was a microwave discharge through Xe operating at the vapor pressure of Xe at 83 °K. To minimize self-absorption the discharge was excited close to the sapphire window by suitable choice of pressure and by tuning of the

[1]*Work supported by the U.S. Army Research Office, Durham, and by the Defence Research Board of Canada.*
[2]*Present address: Stanford Research Laboratories, Palo Alto, California.*
[3]*Present address: York University, Toronto 12, Ontario.*

microwave cavity. The lamp was connected to a 1 l ballast volume to reduce pressure fluctuations. The sapphire window, 1 mm thick and 38 mm in diameter, was 40% transparent to 1 407 Å radiation and showed a sharp cut-off below 1 420 Å. This arrangement provided essentially monochromatic light at 1 470 Å.

The photolysis cell was separated from the lamp by a thermostatted chamber 28 cm in length and another sapphire window, 1 mm thick and 30% transparent at 1 470 Å. This chamber acted as a collimating region to reduce the divergence of the light beam. Experiments showed that light lost by divergence through the outer walls was 40 times the intensity reaching the cell. The need for collimation has not been fully appreciated by previous investigators and is particularly important when comparisons are made of quantum yields of systems with widely differing absorption.

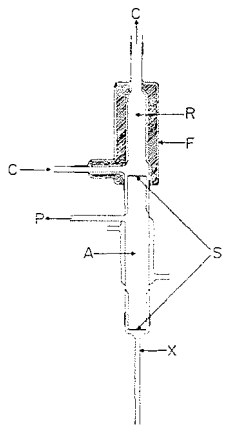


FIG. 1. Schematic diagram of photolysis apparatus: X, the xenon lamp; A, central, thermostatted collimating region; S, sapphire windows; P, to vacuum pump; C, circulating system; F, furnace; R, the photolysis cell.

The chamber also permitted alteration of the cell temperature without affecting the lamp outlet. Conversely, it prevented the lamp from heating the cell window. Finally, the chamber served as an optical shutter when filled with air, which permitted the lamp to be stabilized before the photolysis was initiated.

The cell was 10 cm in length and 34 mm i.d. Circulation of gas through the cell and connecting trap (total volume = 285 ml) to prevent accumulation of products near the entrance window, was effected by a glass-enclosed paddle wheel actuated by an external magnetic field. This reduced the "inner-filter" effect and the complications of secondary reactions at the window. Conversions never exceeded 0.2%.

The experimental procedure consisted of allowing the lamp to operate for at least 15 min with air at 1 atm pressure in the middle chamber. After the lamp had become stabilized the photolysis was begun by rapid evacuation of the middle chamber. Since the photolysis time τ was from 5 to 120 min, the 2 s evacuation time introduced little error. Condensable gases were removed from the products at 83 °K. Non-condensable products were analyzed by means of a gas burette and a gas chromatograph containing a 7 ft column of 5A molecular seive. Analysis of as little as 10^{-10} moles of H_2, O_2, N_2, CH_4, CO, and CO_2 could be effected. The photolysis apparatus was protected from intrusion of Hg vapor from the analytical section by refrigerated traps. Pressures were measured with Bourdon and ionization gauges.

Matheson 'Research' grade CO_2 was used after rigorous degassing and numerous trap-to-trap distillations. All other gases were Matheson 'Research' grade assayed reagents.

RESULTS

CO and O_2 were the only stable products detected. Figure 2 shows the yields of these products as a function of the CO_2 pressure at 25 °C for two different light intensities, and Fig. 3 shows similar results at 200 °C at a still lower light intensity. The plateau behavior at higher pressures indicates complete absorption in this region. The ratios of the CO/O_2 yields, however, are approximately 5.5 instead of 2 as required by mass balance.

Figure 4 shows the product yields as a function of irradiation time at 25 °C for two different light intensities and at a sufficiently high pressure to correspond to complete absorption. The slopes of the CO and O_2 curves are also in the ratio of about 5.5. Figure

Can. J. Chem. Downloaded from www.nrcresearchpress.com by 210.87.254.5 on 09/05/12
For personal use only.

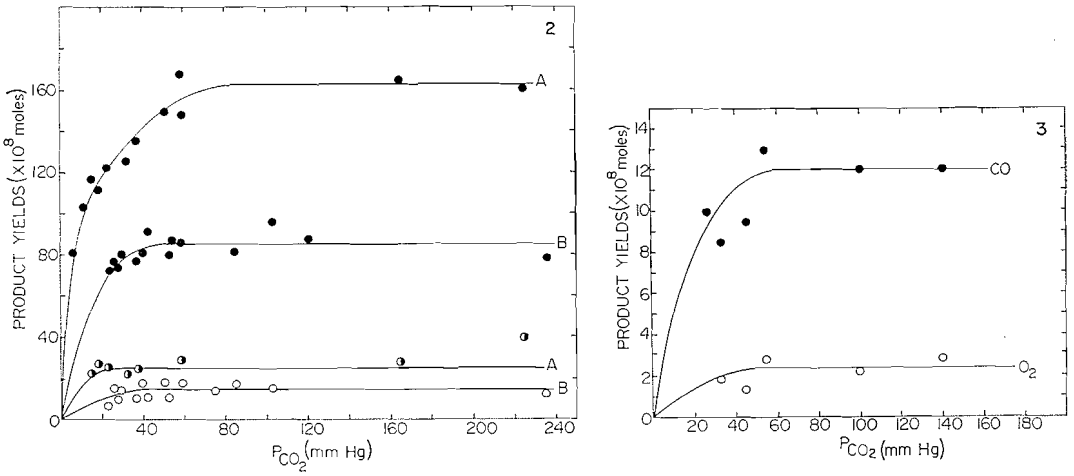


FIG. 2. Product yields as a function of CO_2 pressure at 25 °C for an irradiation time of 30 min: ●, CO; ○ and ◑, O_2; A, high light intensity; B, low light intensity.

FIG. 3. Product yields as function of CO_2 pressure at 200 °C for an irradiation time of 20 min and low light intensity.

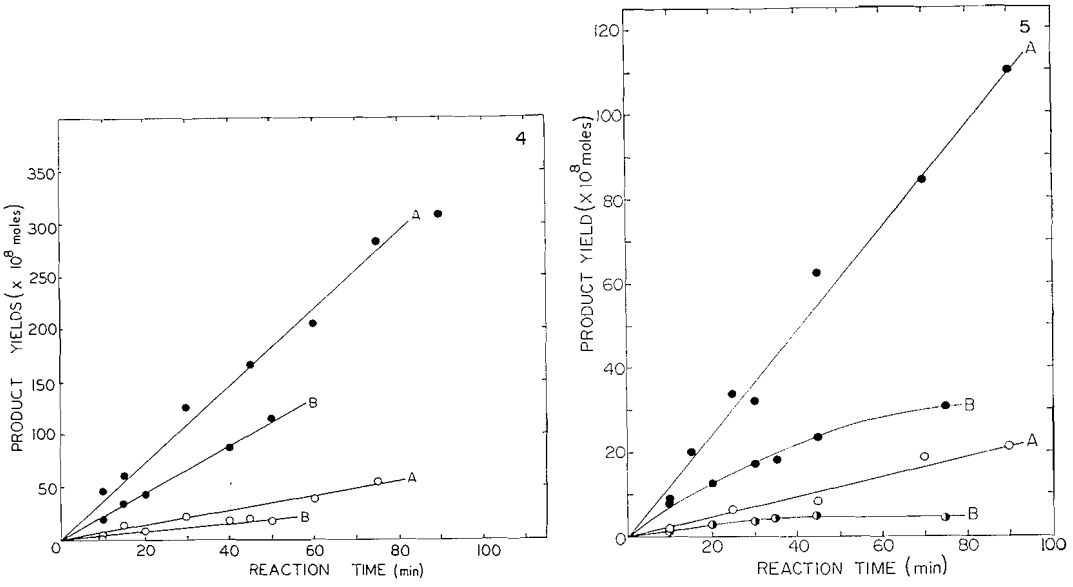


FIG. 4. Product yields as a function of irradiation time at 25 °C for two different light intensities: ●, CO; ○, O_2; A, higher light intensity and P_{CO_2} = 50 Torr; B, lower light intensity, and P_{CO_2} = 54 Torr.

FIG. 5. Product yields as function of irradiation time at two different temperatures for the same light intensity: ●, CO; ○ and ◑, O_2; A, 25 °C and P_{CO_2} = 45 Torr; B, 200 °C and P_{CO_2} = 51 Torr.

5 shows similar plots at constant light intensity but at 25 °C and at 200 °C. The results in Figs. 4 and 5 were obtained in a random order both in reaction time and in temperature which attests to the reproducibility and to the unchanged transparency of the windows. At 200 °C the linear relationship between the product yield and irradiation time no longer applies, while these and other experiments at 25, 110, and 200 °C show that the product yields decrease with increasing temperature.

Can. J. Chem. Downloaded from www.nrcresearchpress.com by 210.87.254.5 on 09/05/12
For personal use only.

Table I shows the results of a number of experiments designed to discover the fate of the missing O_2. In series A, clean Pyrex wool was placed alternately in the photolysis cell and just beyond it. Blank experiments showed that there was no detectable adsorption of O_2 by packing. Inclusion of the packing in the cell results in a marked decrease in the O_2 quantum yield.

TABLE I*a*

Experimental Series A—Photolysis of CO_2 in reaction cell packed with Pyrex glass wool; reaction time 120 min

Expt. No.	Reaction temp. (°C)	P_{CO_2} (Torr)	Position of glass wool	O_2 (moles $\times 10^8$)	CO (moles $\times 10^8$)	O_2/CO
1	25	42.0	In the cell	Nil	12	0
2	200	45.5	In the cell	Nil	11	0
3	25	300	In the cell	0.5	11	0.045
4	200	300	In the cell	<0.5	10	<0.045
5	25	300	Beyond the cell	2.7	9	0.30
6	200	300	Beyond the cell	1.0	4.0	0.25

TABLE I*b*

Experimental Series B—Photolysis of CO_2 in reaction cell which was previously saturated with O atoms produced by microwave discharge of O_2 in the system; reaction time 120 min

Exposure time (min)	Reaction temp. (°C)	P_{CO_2} (Torr)	O_2/CO
120	25	37.9	0.60
120	25	38.7	0.76
120	200	40.5	0.68
60	200	37.7	0.15
0	200	37.7	0.10

TABLE I*c*

Experimental Series C—Photolysis of CO_2 with a cylinder of thin gold foil inserted in the center of the reaction cell; reaction temperature 25 °C

Photolysis time (min)	P_{CO_2} (Torr)	CO (moles$\times 10^8$)	O_2 (moles$\times 10^8$)	O_2/CO
120	31.8	6.2	2.6	0.42
120	31.5	6.2	2.6	0.42

In series B the walls of the cell were first conditioned by filling the cell with O_2 at a pressure of 2 Torr, subjecting it to a microwave discharge for the times shown, and then evacuating the cell to a pressure at least as low as 10^{-6} Torr. CO_2 was then put in the cell and photolyzed in the normal way. The O_2/CO quantum yield ratios were observed to increase markedly and even to exceed the theoretical value of 0.5.

In series C a cylinder of thin gold foil, 2 cm in diameter was inserted in the center of the cell. This also produced an increase in the O_2/CO ratio to a value close to 0.5.

Figure 6 shows the effect of adding CO at three different temperatures. The ordinate represents O_2 yields relative to the value obtained in the absence of added CO. These results indicate a decrease in O_2 yield, the effect increasing with temperature.

Can. J. Chem. Downloaded from www.nrcresearchpress.com by 210.87.254.5 on 09/05/12
For personal use only.

Figure 7 shows the effect of added H_2 and CH_4 on the yields of CO and O_2 when CO_2 was photloyzed at 25 °C. In both cases the O_2 quantum yield dropped rapidly to zero. The CO quantum yield was increased by addition of CH_4 but not by addition of H_2. No H_2 was observed among the products when CH_4 was added. Reaction was also observed with N_2O when this substance was added in small amounts.

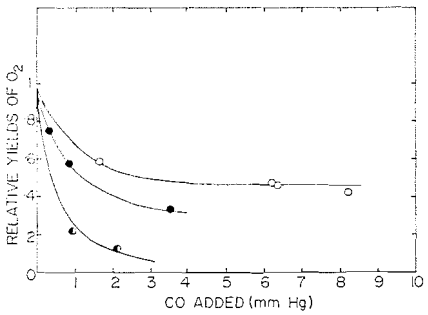


FIG. 6. Effect of added CO on the relative quantum yield of O_2: ○, 25 °C; ●, 110 °C; ◑, 200 °C.

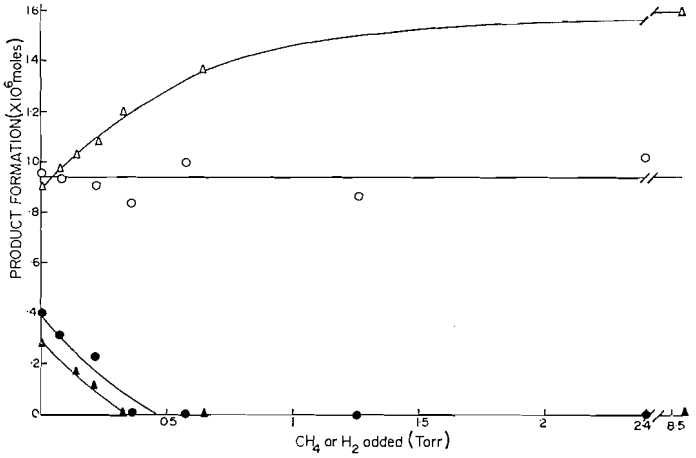


FIG. 7. Effect of added H_2 and CH_4 on product yields for an irradiation time of 15 min and $P_{CO_2} = 35$ Torr: △, yield of CO when methane added; ▲, yield of O_2 when methane added; ○, yield of CO when hydrogen added; ●, yield of O_2 when hydrogen added.

Comparisons were made between the CO and O_2 quantum yields in the photolysis of CO_2 and the quantum yields of CO_2 formed in the photolysis of mixtures of CO and O_2 containing <0.5 mole % O_2 for which the light incident on the cell was absorbed to the extent of 70%. The results are shown in Table II. This table also shows comparisons with the N_2 yields formed in the photolysis of N_2O. Light intensities and other parameters were kept constant throughout these experiments, which were performed in a random order. It is worth noting that the CO_2 quantum yields from the CO–O_2 actinometer did not change with temperature over the range 25–200 °C. This indicates that the temperature effects reported were not the result of a decrease in transparency of the sapphire windows with increasing temperature. Assuming a value of $\varphi_{CO_2} = 2$ for the CO–O_2 actinometer (1), gives $\varphi_{CO} = 0.25$ for the CO_2 photolysis at 25 °C, while a value of $\varphi_{N_2} = 1.4$ for the N_2O photolysis (11, 12) gives $\varphi_{CO} = 0.27$.

Can. J. Chem. Downloaded from www.nrcresearchpress.com by 210.87.254.5 on 09/05/12
For personal use only.

TABLE II*a*

Quantum yield measurements for the photolysis of a mixture of O_2 + CO

Temp. (°C)	Reaction time (min)	P_{O_2} (Torr)	P_{CO} (Torr)	CO_2 (moles × 10^6)	R_{CO_2} (moles $s^{-1} \times 10^{10}$)
25	30	0.143	62.0	0.186	1.03
25	30	0.179	100.0	0.197	1.095
25	30	0.179	75	0.204	1.13
200	30	0.215	75	0.197	1.095
200	30	0.215	70	0.208	1.16
					av. 1.1

TABLE II*b*

Quantum yield measurements for the photolysis of CO_2

Temp. (°C)	Reaction time (min)	P_{CO_2} (Torr)	CO (moles × 10^8)	R_{CO} (moles $s^{-1} \times 10^{10}$)
25	60	42.7	7.0	0.195
25	120	47.6	14.0	0.195
25	60	41.9	7.0	0.195
				av. 0.195

TABLE II*c*

Quantum yield measurements for the photolysis of N_2O

Temp. (°C)	Reaction time (min)	P_{N_2O} (Torr)	N_2 (moles × 10^8)	R_{N_2} (moles $s^{-1} \times 10^{10}$)
25	60	45.5	37.8	1.05
25	60	30.5	36.5	1.01
25	30	50.2	17.5	0.97
25	30	16.7	17.5	0.97
				av. 1.0

Warneck (3) has recently reported that the ratio of the O_2/CO yields increases with elapsed time (up to 60 min) between CO_2 photolysis and product analysis, which was taken as evidence for incipient CO_3 formation. However, in the present work no change in this ratio was ever observed for periods up to 75 min after photolysis.

DISCUSSION

The salient results which require explanation are: (i) the oxygen deficiency in the product yields; (ii) the independence of the product yields on CO_2 pressure; (iii) the linear dependence of the yields on irradiation time at the lower temperatures and the non-linearity at higher temperatures; (iv) the decrease in O_2 yield with added CO, and the increase of this effect with temperature; (v) an overall quantum yield less than unity; and (vi) the reaction with H_2, CH_4, and N_2O when these gases are present in the system in small amount.

The primary photolytic process could be either

[1] $$CO_2 + h\nu \rightarrow CO + O(^1D)$$

or

[1′] $$CO_2 + h\nu \rightarrow CO_2^*$$

Can. J. Chem. Downloaded from www.nrcresearchpress.com by 210.87.254.5 on 09/05/12
For personal use only.

If [1] is the predominant process then it could be followed by

[2] $$O + O + M \rightarrow O_2 + M$$

[3] $$O \xrightarrow{\text{wall}} \tfrac{1}{2}O_2$$

The ratio of the CO/O_2 quantum yields should then equal 2 while the present results show values of ~5.5 over a considerable range of pressure and light intensity. Other investigators (1–3) also find high ratios ranging from 3 to 110, although Groth (13) obtained a value close to 2 using a flow system and a gold-plated cell. Mahan (1) and Warneck (3) attributed the missing oxygen to O_3 formation; both detected O_3 in their systems by ultraviolet absorption, but in amounts too small for quantitative estimates.

However, it can readily be shown that O_3 formation cannot account for the magnitude of the missing O_2. If O_3 is formed by the process

[4] $$O + O_2 + CO_2 \rightarrow O_3 + CO_2$$

and destroyed by

[5] $$O + O_3 \rightarrow 2O_2$$

then the maximum amount of O_3 which could be formed is given by the steady state expression

[6] $$[O_3] = \frac{k_4}{k_5}[O_2][CO_2] = \gamma[O_2].$$

For mass balance we must have

[7] $$[CO] = 3[O_3] + 2[O_2]$$

so that

[8] $$\frac{[O_2]}{[CO]} = \frac{1}{3\gamma + 2}.$$

This would be consistent with the O_2 yield being linear with irradiation time if the CO curves were linear, as shown in Fig. 4. However, the expression is not consistent with our observation that the ratio is independent of CO_2 pressure since γ is proportional to $[CO_2]$.

But, most important, the expression is quantitatively incorrect. The most reliable values for k_4 and k_5 reported for these reactions (14) when the O atoms are in the ^3P ground state give a value of $\gamma = 0.12$ at 50 Torr which would result in $CO/O_2 = 2.4$. Values of 5.5 for this ratio would require γ to be an order of magnitude greater than has ever been reported for these reactions, when $O(^3P)$ atoms were involved. For $O(^1D)$ atoms, γ should be even lower since the reaction

[9] $$O(^1D) + O_2(^3\Sigma) \rightarrow O_3(^1A)$$

is spin forbidden, while there is evidence that [5] is faster with $O(^1D)$ than with $O(^3P)$ atoms and can even produce chain decomposition of O_3.

If [1′] is the predominant primary process, as favored by Jucker and Rideal (5), and if the reaction leading to product formation is

[10] $$CO_2^* + CO_2 \rightarrow 2CO + O_2$$

then again the CO/O_2 ratio should be 2.

Recently, Warneck (4) has suggested that the missing O_2 is due to the formation of unstable CO_3 molecules which releases O_2 slowly, based on the observation that the

Can. J. Chem. Downloaded from www.nrcresearchpress.com by 210.87.254.5 on 09/05/12
For personal use only.

O_2/CO ratio increases slowly after irradiation. However, no such increase was ever observed in the present work.

A possible explanation for the missing O_2 is adsorption of O atoms on the walls of the reaction cell. This explanation would be consistent with the observation that the O_2/CO ratio approached zero when the cell was packed with glass wool and 0.5 when gold foil was inserted in the cell, similar to the results reported by Groth (13). The results obtained when the cell was previously exposed to relatively large concentrations of O atoms also support this explanation; O_2/CO ratios greater than 0.5 could result from the reaction of O atoms produced by photolysis with atoms adsorbed on the walls.

The linearity of the product yields with irradiation time at 25 °C agrees with the findings of Warneck (3). Mahan (1) also reported a linear relation for CO production but a decrease in the rate of O_2 production with τ. If the fraction of O atoms that recombine on the wall is α (with $1 - \alpha$ the fraction that is adsorbed) then the relationship between the CO and O_2 yields is given by

$$[11] \qquad [CO] = \left(2 + \alpha + 3\frac{k_4}{k_5}[M]\right)[O_2],$$

so that for a given pressure the curves for the CO and O_2 yields should be proportional.

The decrease in quantum yield with added CO could be explained by the back reaction

$$[12] \qquad O(^1D) + CO\ (+M) \rightarrow CO_2\ (+M).$$

Although Groth (13) believed that this reaction was unimportant, he offered no evidence to support this view. DeMore and Raper (15) studied this reaction in liquid CO and concluded that it would be slow in the gas phase. Popov (16), on the other hand, claimed that it occurs readily.

There are, however, a number of difficulties with this mechanism: the temperature dependence of the effect of added CO (Fig. 6), on the yields as functions of irradiation time (Fig. 5), and on the overall quantum yield would require reaction [12] to have an appreciable activation energy. This would seem unlikely if it were a three-body reaction. However, if [12] is bimolecular, difficulties are encountered in trying to explain the independence of the product yields as a function of pressure and simultaneously the linearity of these yields with irradiation time at the lower temperatures. Finally, Cvetanovic (17) has presented rather convincing evidence that $O(^1D)$ atoms have very short lifetimes in the presence of CO_2.

These objections can be overcome if we postulate the conversion of $O(^1D)$ to CO_3 by a rapid reaction

$$[13] \qquad CO_2 + O\ (+M) \rightarrow CO_3\ (+M).$$

The missing oxygen could then be equally well explained by adsorption of CO_3 on the walls. The results of the experiments shown in Table I could be understood simply by substituting CO_3 for O atoms in the explanations offered above. Indeed a strong adsorption might appear more likely for CO_3 than for O because of the possibility of a type of carbonate formation.

The back reaction can take the form

$$[14] \qquad CO_3 + CO \rightarrow 2CO_2.$$

If the other destructive processes for CO_3 are mainly

$$[15] \qquad CO_3 \rightarrow CO + O_2$$

$$[16] \qquad CO_3 \xrightarrow{\text{wall}} CO_3(\text{adsorbed}),$$

Can. J. Chem. Downloaded from www.nrcresearchpress.com by 210.87.254.5 on 09/05/12
For personal use only.

then steady state treatments for CO_3 and for O atoms leads to the expression

$$[17] \qquad \frac{d[CO]}{dt} = \varphi_1 I_a \left(1 + \frac{k_{15} - k_{14}[CO]}{k_{15} + k_{16} + k_{14}[CO]}\right).$$

It should be noted that the same result is obtained whether [13] is a bimolecular or a three-body reaction. A similar expression can be derived for the rate of O_2 formation in agreement with the findings that the O_2/CO ratios are independent of light intensity and temperature. These expressions are consistent with the observations that the yields are independent of total pressure. At the lower temperatures the linearity of the yields with irradiation time follows if $k_8[CO] < k_{10}$. The effect of temperature on the yields, on the results of addition of CO, and on the drop-off from linearity with τ can be attributed to the activation energy of [14] which would then become increasingly important at the higher temperatures. It appears more plausible to attribute a significant activation energy to a reaction such as [14] rather than to one such as [12].

The only previous measurements on the effect of temperature on CO_2 photolysis was made by Wijnen (18). Four experiments were reported, two at 25 °C and two at 270 °C which indicated a CO quantum yield 1.4 times greater at the higher temperature. These results are, however, in disagreement with our results at 25, 110, and 200 °C in which the quantum yields were found to decrease with temperature.

The importance of wall adsorption can be seen by comparing experiments 1 and 3 in Table I. At the higher pressure diffusion and therefore k_{10} are lower. Similarly, comparison of experiments 1 and 2 shows that the same CO yield is obtained at 25 ° and at 200 °C when the cell is packed with glass wool. Under these conditions all the CO_3 (or O atoms) are adsorbed and no back reaction is possible.

It is interesting to note that a similar expression for the rate of CO production is obtained if one assumes reaction [1′] for the initial process and the main destructive steps for CO_2^* to be

$$[18] \qquad CO_2^* + CO_2 \rightarrow CO_3 + CO$$

$$[19] \qquad CO_2^* + CO_2 \rightarrow 2CO_2.$$

The bracket on the right hand side of the rate equation [17] is then simply multiplied by the factor

$$\varphi_1' I_a \frac{k_{18}}{k_{18} + k_{19}}.$$

However, [1′] is not likely to be the sole primary step since Young[4] has recently found emission when NO is added in small amount, in contrast to the previous results of Mahan (19). This implies the presence of O atoms in the system, and consequently the occurrence of reaction [1].

On the other hand the value of φ_1 cannot be unity, since if it were, the rate expression would lead to a quantum yield greater than unity. The present results show that at 25 °C, $\varphi_{CO} = 0.25$ based on O_2–CO mixtures as the actinometer standard, and $\varphi_{CO} = 0.27$ based on N_2O as a standard. Any errors introduced by the use of these standards are such as to give φ_{CO} upper limits.

This result appears to be in conflict with previous investigations which, with the exception of a value of $\varphi_{CO} = 2$ reported by Jucker and Rideal (5) seem to favor a value of unity. Verhock (20), however, finds that a value of unity is only obtained in a flow system, but is much smaller in static systems.

[4]*R. A. Young. Private communication.*

Can. J. Chem. Downloaded from www.nrcresearchpress.com by 210.87.254.5 on 09/05/12
For personal use only.

In their study of the photolysis of N_2O at 1 470 Å Doering and Mahan (21) obtained values for φ_{N_2} greater than 2 if CO_2 was used as an actinometer and φ_{CO} was assumed to be unity. This result is greater than the theoretical upper limit and considerably above the value of 1.4 found by other workers. They explained their results by postulating a reaction between electronically excited and ground state N_2O molecules. A lower value for φ_{CO} would also have been consistent with their result.

More disturbing is the finding by Mahan (1) that $\varphi_{CO} = 1.1$ based on the same reference O_2–CO standard as used in the present work. However, consideration of his experimental conditions reveals that the absorption path lengths were very much larger in the O_2–CO system than in the CO_2 photolysis. With uncollimated light many more quanta would be absorbed by the CO_2 system and result in an overestimation of φ_{CO}. This is felt to be a major source of error in much of the previous work and was the main reason why the central collimating chamber was used in the present work.

More recently, Groth (22) reinvestigated the photolysis of ammonia. He found consistent values for φ_{NH_3} when he used $\varphi_{CO} = 1.1$ from a CO_2 actinometer and $\varphi_{O_3} = 1.9$ from an O_2 actinometer. The pressures used were sufficiently high that collimation should not have been a serious problem.

Nevertheless, quantum yields of unity for CO_2 photolysis would be extremely unlikely if adsorption and back reactions play significant roles, as indicated in the present work. The strongest evidence for the presence of energetic species capable of promoting back reactions is provided by the experiments in which reaction occurred when small amounts of CO, H_2, CH_4, and N_2O were added. None of these gases react at an appreciable rate with ground state $O(^3P)$ atoms.

Although Warneck (23) postulated CO_3 formation to explain the oxygen loss in the system, he maintained that $O(^1D)$ is the reactive species. However, the results of Cvetanovic (17) and of Young[4] strongly suggest a rapid disappearance of $O(^1D)$ in the presence of CO_2. The present results do appear to show a better kinetic fit when CO_3 is assumed to be the reactive species present.

The detailed mechanism for the ultraviolet photolysis of CO_2 cannot, however, be considered to be firmly established. Further work in this direction is in progress in our laboratories. Nevertheless the results do give clear evidence for the existence of reactions which would make the use of this photolysis as an actinometer, with a quantum yield of unity, at best rather questionable. The back reaction is also of considerable aeronomic significance. It could, for example, explain the failure to observe any CO in the atmosphere of Venus (24).

ACKNOWLEDGMENT

The authors would like to thank Dr. Cvetanovic for helpful discussions on this problem.

REFERENCES

1. B. H. Mahan. J. Chem. Phys. **33**, 959 (1960).
2. M. H. J. Wijnen. J. Chem. Phys. **24**, 851 (1956).
3. P. Warneck. Discussions Faraday Soc. **37**, 57 (1964).
4. P. Warneck. J. Chem. Phys. **41**, 3435 (1964).
5. H. Jucker and E. K. Rideal. J. Chem. Soc. 1058 (1957).
6. A. D. Walsh. J. Chem. Soc. 2260 (1953).
7. R. S. Mulliken. Can. J. Chem. **36**, 10 (1958).
8. H. Yamazaki and R. J. Cvetanovic. J. Chem. Phys. **39**, 1902 (1963).
9. H. Yamazaki and R. J. Cvetanovic. J. Chem. Phys. **40**, 582 (1964).
10. H. Yamazaki and R. J. Cvetanovic. J. Chem. Phys. **41**, 3703 (1964).
11. M. Zelikoff and L. M. Aschenbrand. J. Chem. Phys. **22**, 1680 (1954).
12. W. E. Groth and H. Schierholz. Planet. Space Science, **1**, 333 (1959).
13. W. E. Groth. Z. Physik. Chem. Leipzig, B, **37**, 307 (1937).

Can. J. Chem. Downloaded from www.nrcresearchpress.com by 210.87.254.5 on 09/05/12
For personal use only.

14. A. MATHIAS and H. I. SCHIFF. Discussions Faraday Soc. **37**, 38 (1964).
15. O. F. RAPER and W. B. DEMORE. J. Chem. Phys. **40**, 1047 (1964).
16. B. POPOV. Acta Physicochim. URSS, **3**, 223 (1935).
17. R. J. CVETANOVIC. J. Chem. Phys. **43**, 1850 (1965).
18. M. H. J. WIJNEN and H. A. TAYLOR. J. Chem. Phys. **21**, 233 (1953).
19. B. H. MAHAN and R. B. SOLO. J. Chem. Phys. **37**, 2669 (1962).
20. W. A. NOYES and P. A. LEIGHTON. The photochemistry of gases. Reinhold Publishing Corp., New York. 1941. p. 397.
21. J. P. DOERING and B. H. MAHAN. J. Chem. Phys. **36**, 1682 (1962).
22. W. E. GROTH. Z. Physik. Chem. **45**, 6 (1965).
23. P. WARNECK. J. Chem. Phys. **43**, 1849 (1965).
24. G. P. KUIPER. The atmospheres of the earth and the planets. University of Chicago Press, Chicago. 1957.

Can. J. Chem. Downloaded from www.nrcresearchpress.com by 210.87.254.5 on 09/05/12
For personal use only.

Can. J. Chem. Downloaded from www.nrcresearchpress.com by 210.87.254.42 on 09/05/12
For personal use only.

NOTES

SOME COMPLEXES PRESENT IN AQUEOUS FERRIC CHLORIDE SOLUTIONS

P. G. MANNING

Friedman (1) has shown that $FeCl_4^-$ complexes exist in solutions of ferric ion in 12 *M* HCl, and that the four-coordinate (tetrahedral) species was in equilibrium with a six-coordinate hydrated $FeCl_n$ complex. Friedman (1) concluded his paper by posing the problem as to where in the series of complexes, $FeCl^{2+}$, $FeCl_2^+$, $FeCl_3$, etc., the cation coordination number changed from 6 to 4. Such a structural change would lead to anomalous stepwise stability constant ratios (P), e.g. the Ag—NH_3 system (2). In this work, we have analyzed Lister and Rivington's (3) stability constants for Fe^{3+} complexes with Cl^- and other simple ligands. Since Fe^{3+}—Cl^- bonds are considered to be mainly ionic, then for simple complexes the ratio of stepwise stability constants may be given by (4)

$$P = S \times T, \qquad [1]$$

where S is a statistical factor and T is a measure of the work being done in bringing a second charged ligand from infinity to its equilibrium position in the 1:2 metal:ligand complex. For monovalent ligands associating with a number of different cations, $T = 1.6$ (4).

A stability constant is defined as

$$b_n = [ML_n]/[ML_{n-1}][L], \qquad [2]$$

where M = metal and L = ligand. According to Lister and Rivington (3), the b_1 and b_2 values for the reactions $Fe^{3+} + Cl^- = FeCl^{2+}$ and $FeCl^{2+} + Cl^- = FeCl_2^+$ are 4.1 and 1.5 respectively, so that P(obs.) = 2.7. From eq. [1], P(calcd.) = $2 \times 6/5 \times 1.6 = 3.85$. The agreement between P(obs.) and P(calcd.) is reasonably good, considering the low stability of the complexes.

Lister and Rivington (3) have also reported data for the addition of Cl^- to $FeSCN^{2+}$ complexes, the stability constants being

$$Fe^{3+} + SCN^- = FeSCN^{2+}, \quad b_x = 130 \qquad [3]$$

$$FeSCN^{2+} + Cl^- = FeSCNCl^+, \quad b_y = 2.0 \qquad [4]$$

$$FeSCNCl^+ + Cl^- = FeSCNCl_2, \quad b_z = 0.45 \qquad [5]$$

$$Fe^{3+} + Cl^- = FeCl^{2+}, \quad b_1 = 4.1. \qquad [6]$$

Now P_{yz}(calcd.) = $2 \times 5/4 \times 1.6 = 4.0$, in excellent agreement with P_{yz}(obs.). Furthermore, $b_1{:}b_y$(calcd.) = $6/5 \times 1.6 = 1.9$, a value that compares favorably with $b_1{:}b_y$(obs.). These calculations are based on the premise that $T_{12} = T_{23}$, but it has been shown in an earlier publication (4) that this is the case for some Cu-monodentate ligand complexes.

The corresponding ferric bromide complexes are much weaker, and it would seem that the P(obs.) values are too inaccurate for any clear conclusions to be reached. However, some of the SO_4 and HSO_4 data are of interest. Thus for the reactions

$$Fe^{3+} + SO_4^{2-} = FeSO_4^+, \quad b_s = 170 \qquad [7]$$

$$FeSO_4^+ + HSO_4^- = FeSO_4.HSO_4, \quad b_t = 2.2 \qquad [8]$$

$$Fe^{3+} + HSO_4^- = FeHSO_4^{2+}, \quad b_u = 6. \qquad [9]$$

According to Bjerrum (5), log T is proportional to e_1e_2, where e_1 and e_2 are the ionic charges on the ligands. Hence, $P_{ut} = b_u:b_t(\text{calcd.}) = 6/5 \times 1.6^2 = 3.1$, whereas the observed ratio is 2.7.

Stepwise stability constants for three stages of Fe^{3+}—Cl^- association have been reported by Rabinowitch and Stockmayer (6) and Olerup (7). The $b_1:b_2$ values (3.2 and 2.9) are in agreement with Lister and Rivington's (3). The P_{23}(obs.) values of the two investigations differ, however. Rabinowitch and Stockmayer (6) report a P_{23} value = 32 and Olerup (7) reports a value of 2.3. If the 1:3 chloride complex is octahedral, P_{23}(calcd.) $= 3/2 \times 5/4 \times 1.6 = 2.8$, a value in agreement with Olerup's determination. If Rabinowitch and Stockmayer's (6) P_{23}(obs.) value is indicative of a change in coordination from 6 to 4 in the second association stage, then P_{12}(obs.) would be considerably smaller than calculated; and yet the observed and calculated P_{12} values are in good agreement. Olerup's P_{23}(obs.) value would therefore seem to be the better.

It would appear from our treatment that the complexes $FeCl_2^+$, $FeSCNCl_2$, and $FeSO_4.HSO_4$ are octahedral. Olerup's (7) P_{23}(obs.) value suggests that $FeCl_3$ is also octahedral. It is likely that the transition from six- to four-coordination occurs in either the third or fourth association stage, probably the fourth.

It is of interest to note that Gamlen and Jordan (8) concluded from a comparison of P_{12}, P_{23}, and P_{34} values that the structural change occurred in the fourth chloride association stage. These workers used Rabinowitch and Stockmayer's (6) b_1 and b_2 values together with their own b_3 and b_4 figures. The T_{12} and T_{23} correlated reasonably well, but the T_{34} was extremely high.

1. H. L. Friedman. J. Am. Chem. Soc. **74**, 5 (1952).
2. Stability constants of metal-ion complexes. The Chemical Society, London. 1964.
3. M. W. Lister and D. E. Rivington. Can. J. Chem. **33**, 1603 (1955).
4. P. G. Manning. Can. J. Chem. **43**, 3258 (1965).
5. N. Bjerrum. Z. Physik. Chem. Leipzig, **106**, 238 (1923).
6. E. Rabinowitch and W. H. Stockmayer. J. Am. Chem. Soc. **64**, 335 (1942).
7. H. Olerup. Svensk Kem. Tidskr. **55**, 324 (1943).
8. G. A. Gamlen and D. O. Jordan. J. Chem. Soc. 1435 (1953).

Received March 4, 1966.
Mineral Physics Section,
Mineral Sciences Division,
Mines Branch,
Department of Mines and Technical Surveys,
Ottawa, Canada.

PREPARATION OF FREMY'S SALT, POTASSIUM NITROSODISULFONATE

R. P. Singh

This note describes an improved method for the preparation of a stable Fremy's salt, $K_2[ON(SO_3)_2]$, which has been used as an analytical tool for estimating free phenolic hydroxyl groups in isolated lignin (1) and also in lignins present in groundwood pulp (2, 3). The usual methods (4–10) for its preparation consisted essentially in preparing the sodium or potassium salts of hydroxylamine disulfonic acid followed by oxidation with either lead oxide, silver oxide, or potassium permanganate. Fremy's salt prepared from this material is known to be unstable, and the degree of instability has often been

Can. J. Chem. Downloaded from www.nrcresearchpress.com by 210.87.254.42 on 09/05/12
For personal use only.

According to Bjerrum (5), log T is proportional to e_1e_2, where e_1 and e_2 are the ionic charges on the ligands. Hence, $P_{ut} = b_u:b_t(\text{calcd.}) = 6/5 \times 1.6^2 = 3.1$, whereas the observed ratio is 2.7.

Stepwise stability constants for three stages of Fe^{3+}—Cl^- association have been reported by Rabinowitch and Stockmayer (6) and Olerup (7). The $b_1:b_2$ values (3.2 and 2.9) are in agreement with Lister and Rivington's (3). The P_{23}(obs.) values of the two investigations differ, however. Rabinowitch and Stockmayer (6) report a P_{23} value = 32 and Olerup (7) reports a value of 2.3. If the 1:3 chloride complex is octahedral, $P_{23}(\text{calcd.}) = 3/2 \times 5/4 \times 1.6 = 2.8$, a value in agreement with Olerup's determination. If Rabinowitch and Stockmayer's (6) P_{23}(obs.) value is indicative of a change in coordination from 6 to 4 in the second association stage, then P_{12}(obs.) would be considerably smaller than calculated; and yet the observed and calculated P_{12} values are in good agreement. Olerup's P_{23}(obs.) value would therefore seem to be the better.

It would appear from our treatment that the complexes $FeCl_2^+$, $FeSCNCl_2$, and $FeSO_4.HSO_4$ are octahedral. Olerup's (7) P_{23}(obs.) value suggests that $FeCl_3$ is also octahedral. It is likely that the transition from six- to four-coordination occurs in either the third or fourth association stage, probably the fourth.

It is of interest to note that Gamlen and Jordan (8) concluded from a comparison of P_{12}, P_{23}, and P_{34} values that the structural change occurred in the fourth chloride association stage. These workers used Rabinowitch and Stockmayer's (6) b_1 and b_2 values together with their own b_3 and b_4 figures. The T_{12} and T_{23} correlated reasonably well, but the T_{34} was extremely high.

1. H. L. Friedman. J. Am. Chem. Soc. **74**, 5 (1952).
2. Stability constants of metal-ion complexes. The Chemical Society, London. 1964.
3. M. W. Lister and D. E. Rivington. Can. J. Chem. **33**, 1603 (1955).
4. P. G. Manning. Can. J. Chem. **43**, 3258 (1965).
5. N. Bjerrum. Z. Physik. Chem. Leipzig, **106**, 238 (1923).
6. E. Rabinowitch and W. H. Stockmayer. J. Am. Chem. Soc. **64**, 335 (1942).
7. H. Olerup. Svensk Kem. Tidskr. **55**, 324 (1943).
8. G. A. Gamlen and D. O. Jordan. J. Chem. Soc. 1435 (1953).

Received March 4, 1966.
Mineral Physics Section,
Mineral Sciences Division,
Mines Branch,
Department of Mines and Technical Surveys,
Ottawa, Canada.

PREPARATION OF FREMY'S SALT, POTASSIUM NITROSODISULFONATE

R. P. Singh

This note describes an improved method for the preparation of a stable Fremy's salt, $K_2[ON(SO_3)_2]$, which has been used as an analytical tool for estimating free phenolic hydroxyl groups in isolated lignin (1) and also in lignins present in groundwood pulp (2, 3). The usual methods (4–10) for its preparation consisted essentially in preparing the sodium or potassium salts of hydroxylamine disulfonic acid followed by oxidation with either lead oxide, silver oxide, or potassium permanganate. Fremy's salt prepared from this material is known to be unstable, and the degree of instability has often been

Can. J. Chem. Downloaded from www.nrcresearchpress.com by 210.87.254.40 on 09/05/12
For personal use only.

attributed to the method of preparation, to the pH of solution, and also to the presence of other ions, particularly manganese and chloride, in solution (6).

A method claiming a pure product in high yield was patented by Teuber (8) and we have found in our laboratory that certain modifications of Teuber's process produce a more stable product. Teuber's process involves

(*a*) reaction of sodium nitrite, acetic acid, and sodium bisulfite to form hydroxylamine disulfonate, $HON(SO_3Na)_2$,

(*b*) oxidative dehydrogenation of the product in *a* with potassium permanganate in the presence of ammonia,

(*c*) separation of the reduction product, manganese dioxide, from the salt solution by repeated filtration, and

(*d*) crystallization of potassium nitrosodisulfonate, $ON(SO_3K)_2$, by addition of the filtrate to a saturated solution of potassium chloride, and separation of the crystals by filtration.

Laboratory experiments showed that severe decomposition can occur during steps $a \rightarrow d$. The following modifications were introduced which resulted in marked improvement in yields and reproducibility; (i) hydroxylamine disulfonate in step *a* was prepared from sodium nitrite, sodium bicarbonate, and sulfur dioxide; (ii) the decomposition in step *b* was minimized by maintaining better pH control; (iii) separation of manganese dioxide by centrifugation before filtration in step *c* largely prevented decomposition and resulted in higher yield of the product; (iv) the final product in step *d* was collected by centrifugation and rapidly treated with potassium hydroxide. This again prevented decomposition in the final stage of preparation and resulted in simplicity of operation.

The solid salt has a yellow-orange color and gives purple solutions, which can easily be analyzed colorimetrically, since their absorptions in the 545 mμ region are directly proportional to their concentrations as measured both by weighing of the orange dimeric solid and by iodine–thiosulfate titration. Solutions in which some decomposition has occurred can still be estimated colorimetrically, though not titrimetrically, since hydrolysis products then interfere. Spectrometric analysis of the salt, obtained by the above method, showed the following traces of impurities.

Element	Percentage Limit
Mn	0.0005
Ba	0.0005
Fe	0.002
Pb	0.001
Si	0.001
Al	0.001
Ca	0.01
Mg	0.0005
Cu	0.001

The product thus obtained could be stored in the cold for several months without decomposition.

EXPERIMENTAL*

Potassium Nitrosodisulfonate

In a 2 l beaker containing distilled water (250 ml) and crushed ice (500 g) were placed 39.6 g of sodium bicarbonate and 33.0 g of sodium nitrite. The mixture was thoroughly mixed with a mechanical stirrer and was externally cooled to −5° by a freezing mixture of salt and ice. Sulfur dioxide was then passed in rapidly, and the temperature of the solution was controlled at −5° to −2°. When the pH of the mixture fell to 2 (approx. 30 min) and the color changed to orange brown, the passage of sulfur dioxide was immediately stopped. The mixture was stirred for an additional 10 min, during which time it became colorless.

**Reagent grade chemicals were used in the entire experiment.*

Can. J. Chem. Downloaded from www.nrcresearchpress.com by 210.87.254.40 on 09/05/12
For personal use only.

Clean filtered air was then bubbled though the solution for 5 min and the pH of the solution was adjusted to 10.1 with 18% ammonium hydroxide (approx. 10 ml). The solution was stirred at −2° for 30 min and 380 ml of 1 *N* potassium permanganate cooled at −3° was then added to it portion-wise at a rate which did not allow the temperature to rise above 5°. The contents were stirred for 1 h and then allowed to stand at the same temperature. The dark-brown slurry was centrifuged at 1 950 rpm for 5 min and the supernatant violet liquid was passed through a filter paper into a saturated solution of potassium chloride (250 g in 700 ml water at 30°). On cooling, the solution yielded an orange crystalline precipitate which was collected by centrifugation. The material was recrystallized from 1 *N* potassium hydroxide, washed with pure methanol until free from alkali, and stored in vacuum over P_2O_5 in a cold room. The yield of the product was 77.6%, based on sodium bicarbonate.

Anal. Calcd. for $K_2NS_2O_7$: S, 23.90; K, 29.14. Found: S, 23.90; K, 29.38.

ACKNOWLEDGMENTS

The author wishes to acknowledge the assistance of Mr. P. J. DesRosiers in the experimental work, and Dr. R. R. Barefoot for conducting the trace metal analysis.

1. E. Adler and K. Rundquist. Acta Chem. Scand. **15**, 233 (1961).
2. D. H. Andrews and P. J. DesRosiers. Pulp Paper Mag. Can. **67**, T-119 (1966).
3. R. P. Singh. Tappi. In press.
4. R. Asmussen. Z. Anorg. Chem. **212**, 317 (1933).
5. J. W. Mellor. Inorganic chemistry. Vol. VIII. p. 672 ff.
6. J. H. Murib and D. M. Ritter. J. Am. Chem. Soc. **74**, 3394 (1952).
7. G. Harvey and R. G. W. Hollingshed. Chem. Ind. London, 244 (1953).
8. H. J. Teuber. Ger. Patent No. 942,562 (May 3, 1956); U.S. Patent No. 2,782,210 (February 19, 1957); U.S. Patent No. 2,897,052 (July 28, 1959).
9. W. G. Palmer. Experimental inorganic chemistry. Cambridge University Press, London. 1954. p. 281.
10. C. Salt and M. Tomlinson. Chem. Ind. London, 549 (1961).

Received March 1, 1966.
Canadian Industries Limited,
Central Research Laboratory,
McMasterville, Que.

Can. J. Chem. Downloaded from www.nrcresearchpress.com by 210.87.254.40 on 09/05/12
For personal use only.

Can. J. Chem. Downloaded from www.nrcresearchpress.com by 210.87.254.5 on 09/05/12
For personal use only.

Canadian Journal of Chemistry

Issued by THE NATIONAL RESEARCH COUNCIL OF CANADA

VOLUME 44 SEPTEMBER 1, 1966 NUMBER 17

THE ROLE OF β-ALANINE AND OF GLYCERATE IN THE BIOSYNTHESIS OF RICININE[1]

P. R. THOMAS,[2] M. F. BARNES,[2] AND LÉO MARION[3]

Division of Pure Chemistry, National Research Council, Ottawa, Canada

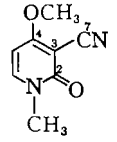
Received September 17, 1965

ABSTRACT

β-Alanine-2-^{14}C has been fed to young *Ricinus communis* L. plants and the radioactive ricinine isolated. The activity of each carbon in the alkaloid molecule was determined. Propionate-2-^{14}C was also fed to young *Ricinus* plants and the radioactivity on carbons 2 and 3 of the isolated ricinine was determined. The pattern of labelling produced by β-alanine-2-^{14}C was very similar to that produced by propionate-2-^{14}C, but was quite distinct from that produced when succinate-2,3-^{14}C or acetate-2-^{14}C was fed to the plant. Whereas with the latter, carbons 2 and 3 of the pyridone ring of ricinine are approximately equally labelled, the ricinine obtained after propionate-2-^{14}C or β-alanine-2-^{14}C was fed contains on carbon 3 almost twice the activity contained on carbon 2.

It has been found that acetate-2-^{14}C is not incorporated into carbon 6 of ricinine. It has also been established that (±)-glycerate-1-^{14}C is incorporated into ricinine only negligibly (0.12%), whereas labelled glycerol is incorporated to the extent of 2.7–3.9%. Glycerate-3-^{14}C, however, is known to be incorporated into the pyridine ring of nicotine; therefore, glyceric acid must undergo decarboxylation before incorporation.

It has been established (1) by feeding experiments with succinate-2,3-^{14}C and acetate-2-^{14}C that these two acids are precursors of carbons 2, 3, and 7 of the alkaloid ricinine (I).



I

More recently it has been found that aspartate is also a precursor of the same three carbons of ricinine, but that it is deaminated and, like succinate and acetate, goes through the Krebs cycle before incorporation (2). Feeding experiments with aspartic acid-^{15}N have shown that the ring nitrogen and the cyano group both carry the same ^{15}N abundance, and consequently that the nitrogen of the aspartic acid must have been split off and become equilibrated with the nitrogen pool before incorporation (2).[4]

[1]*Issued as N.R.C. No. 9068.*

[2]*National Research Council of Canada Postdoctorate Fellow.*

[3]*Present address: Faculty of Pure and Applied Science, University of Ottawa, Ottawa, Canada.*

[4]*Yang and Waller (Phytochemistry, 4, 881 (1965)) have fed aspartate-4-^{14}C,^{15}N to Ricinus plants and observed that the incorporation of ^{14}C into the nitrile group and that of ^{15}N into the pyridone ring were approximately in the ratio of 1:1. From this result they concluded that the ^{14}C and ^{15}N of aspartate were directly incorporated into ricinine. Johns and Marion (2) have found the very same excess of ^{15}N in both the pyridone nitrogen and the nitrile. Were the aspartate incorporated as a unit, it is highly improbable that the nitrile nitrogen could have shown the same ^{15}N abundance as the pyridone nitrogen.*

Can. J. Chem. Downloaded from www.nrcresearchpress.com by 210.87.254.5 on 09/05/12
For personal use only.

It was of interest to find out whether the simpler amino acids could also act as precursors of ricinine, and if so, which carbons did they contribute. According to Anwar *et al.* (3) propionate-2-^{14}C was incorporated into ricinine to a larger extent than acetate-2-^{14}C and 25% of the activity of the ricinine was located in the nitrile group, but they did not determine the distribution of the remaining 75% of the activity. The incorporation of activity into the nitrile group, however, is of the same order of magnitude as that observed after acetate-2-^{14}C was fed. It appeared probable, therefore, that β-alanine, which is present in some naturally occurring peptides, could also be a precursor of the alkaloid.

β-Alanine-2-^{14}C was fed by the usual procedure (1) to *Ricinus communis* L. seedlings, and the ricinine was isolated from the plant 3 days after the feeding. The radioactivity of the isolated alkaloid showed an incorporation of 1.4% of the β-alanine-2-^{14}C fed to the plants. The ricinine was degraded by the procedures described previously (1, 4) to isolate each carbon in the molecule and determine the location of the activity in the alkaloid. The results are given in Table I.

TABLE I

Distribution of activity in ricinine

Identity of carbon atom	Isolated as	Activity of $BaCO_3$ from isolated compound (d.p.m./mg)	Percentage of activity of ricinine
2	$C_6H_5{}^{14}CO_2H$	37.2	25.6
3	$Br_3{}^{14}CNO_2$	394	39.5
4	$C_6H_5{}^{14}CO_2H$	3.3	2.1
5	$Br_3{}^{14}CNO_2$	9.6	1.0
6	$C_8H_{11}O_2{}^{14}CH_2C_8H_{11}O_2$	0.9	2.2
7	See text	398*	20.9
N—CH_3	$^{14}CH_3Me_3N^{\oplus}I^{\ominus}$	3.5	1.4
O—CH_3	$^{14}CH_3Me_3N^{\oplus}I^{\ominus}$	3.4	1.4
			Total 94.1

*Activity of decyanoricinine.

For purposes of comparison, propionate-2-^{14}C was also fed to *Ricinus communis* L. seedlings, and the ricinine isolated 3 days after the feeding. The radioactivity of the alkaloid corresponded to an incorporation of 1.3% of the propionate fed, and the activity on carbon 2 was found to be 21.0% of the total activity of the ricinine, whereas that on carbon 3 was 39.8%. As shown in Table I, the feeding of β-alanine-2-^{14}C produces ricinine that contains 25.6% of its activity on carbon 2 and 39.5% on carbon 3. Both propionate and β-alanine therefore produce about the same labelling pattern, which is also in agreement with the pattern of incorporation of β-alanine-2-^{14}C into nicotine, in which approximately 25% of the total activity is found on carbon 2 and approximately 50% on carbon 3 (5).

It is known that acetate-2-^{14}C and succinate-2,3-^{14}C, when fed to *Ricinus* plants, both go through the Krebs cycle before incorporation into the alkaloid, and give rise to a four-carbon dicarboxylic acid in which the radioactivity on carbons 2 and 3 is equilibrated. Hence, the pyridone ring of the ricinine produced in these feeding experiments is always labelled essentially equally on carbons 2 and 3 (1, 4). The same holds true when acetate-2-^{14}C and succinate-2,3-^{14}C act as precursors of nicotine (6) and anabasine (7), and carbons 2 and 3 of the pyridine nucleus of both these alkaloids are also equally labelled.

The labelling pattern produced by both propionate and β-alanine is therefore quite different from that obtained with either acetate or succinate feeding, and it seems that

435706

neither propionate nor β-alanine can be converted into a four-carbon dicarboxylic acid before incorporation.

Within experimental error (eight different determinations are involved), the activities reported in Table I account for all the activity (94.1%) of the ricinine molecule. The percentages of activity located on carbons 4, 5, and 6 and on the two methyl groups are low, and the significant labelling involved carbons 2 and 3 together with the nitrile carbon.

Whether β-alanine is present in the normal *Ricinus* plant does not seem to be known. There is, however, no doubt that β-alanine, when fed to the plant, acts as a precursor of ricinine. The fact that the labelling pattern it produces is so different from that produced by acetate indicates that the biosynthetic pathway through which it is incorporated into ricinine must be very distinct from that involving acetate.

That more than one amino acid present in the normal plant can contribute to the biosynthesis of the same fragment of an alkaloid molecule may account, at least in part, for the fact that the observed incorporation into the alkaloid of a radioactive precursor fed to the plant is always rather low. It seems to suggest that there may be no single synthetic pathway to an alkaloid, but rather several simultaneous pathways from different precursors.

The feeding of acetate-2-^{14}C to *Ricinus* plants has been studied previously (1, 4) and the distribution of radioactivity in the ricinine molecule was determined for all carbons except carbon 6. Although the sums of the activities on carbons 2, 3, 4, 5, and 7 and on the two methyl groups accounted for 99.6% of the total activity, the experimental error inherent in the methods of determination made it possible for some small percentage of activity to be present at carbon 6. A sample of ricinine isolated from *Ricinus* plants fed acetate-2-^{14}C was therefore degraded so as to isolate carbon 6 (2, 4). The results showed that no measurable activity was present at carbon 6, whereas the feeding of β-alanine-2-^{14}C to the plant resulted in the incorporation of 2.4% of the total activity of the isolated ricinine at carbon 6. Hence it can be stated that acetate is a precursor of carbons 2, 3, and 7 of ricinine, but not of the remaining carbons.

Experiments involving the feeding of labelled glycerol to *Ricinus* plants have been reported previously (4). It was observed that glycerol-1-^{14}C gave rise to ricinine labelled at both carbon 4 and carbon 6, whereas glycerol-2-^{14}C produced radioactive ricinine (2.7% incorporation) labelled at carbon 5 (38.8% of the total activity) but not at carbon 4 or carbon 6. The total incorporation of radioactivity into ricinine, however, was appreciably lower than had been obtained with succinate or acetate, and it was assumed that glycerol may not be a direct precursor of carbons 4, 5, and 6, but is likely converted into an intermediate before incorporation. This assumption is supported by the fact that, with both glycerol-1-^{14}C and glycerol-2-^{14}C, labelling of the methyl groups occurs to the extent of 26–35% of the total activity of the ricinine (8) and therefore indicates appreciable breakdown of the molecule.

Leete and Friedman (9), who fed glycerol-2-^{14}C to *Nicotiana glauca*, observed that the anabasine produced by the plant was radioactive (0.36% incorporation) and that 38% of the radioactivity was present in the pyridine ring. The activity on carbon 5 of the pyridine ring, however, was 31.6% of the activity in that ring, and was therefore comparable with that observed with ricinine (38.8%) at the analogous position (4).

In the hope of obtaining a more selective labelling pattern, or an incorporation involving less preliminary breakdown of the precursor, glyceric acid-1-^{14}C, which is related to glycerol but is unsymmetrical, was fed to *Ricinus* plants. The incorporation of radioactivity, however, was only 0.12%. This low incorporation indicates that the carboxylic group

Can. J. Chem. Downloaded from www.nrcresearchpress.com by 210.87.254.5 on 09/05/12
For personal use only.

containing the radioactive carbon was mostly lost as carbon dioxide, probably through pyruvate as an intermediate stage. Griffith and Byerrum (10), who fed glycerate-3-^{14}C to tobacco plants, found a greater incorporation of ^{14}C than when acetate-2-^{14}C was fed, and that 48% of the activity of the isolated nicotine was located in the pyridine ring. They assumed that glycerate was first converted into acetate before incorporation. The low incorporation of glycerate-1-^{14}C into ricinine would tend to support this assumption, although Griffith and Byerrum (10) did not report as supporting evidence the location of the activity around the pyridine ring of nicotine. At any rate, glycerate does not act like glycerol in the biosynthesis of ricinine.

EXPERIMENTAL

All samples were ignited and the carbon dioxide evolved was converted into barium carbonate. The radioactivity was counted on thin layers of barium carbonate on aluminium planchets in a Baird-Atomic end-window proportional counter, and corrections were made for efficiency, background count, and sample self-absorption. β-Alanine-2-^{14}C was supplied by Volk Radiochemical Co., and glyceric acid-1-^{14}C and acetate-2-^{14}C by Merck Sharp & Dohme of Canada Limited.

Growth of Ricinus Plants and Administration of Tracers

Seeds of *Ricinus communis* L. were planted at a depth of ca. 1.3 cm in vermiculite which was kept moist by daily watering. The germinating plants were kept at a temperature of 25° in daytime and 21° during the night. They were fed at the same stage of growth and in the same manner as reported previously (1). β-Alanine-2-^{14}C (9.9 mg, total activity 2.22×10^8 d.p.m.) was fed to 67 plants. Glyceric acid-1-^{14}C (supplied in aqueous solution, about 1 ml, by Merck Sharp & Dohme of Canada Limited; total activity 2.22×10^8 d.p.m.) was fed to 39 plants. Acetate-2-^{14}C (5.8 mg, total activity 2.22×10^8 d.p.m.) was fed to 37 plants. Sodium propionate-2-^{14}C (total activity 2.22×10^8 d.p.m.) was also fed to a number of germinating plants.

Isolation of Ricinine

The isolation of ricinine from the plant and its purification were carried out as described previously (1, 2). From the plants that had been fed β-alanine-2-^{14}C, ricinine (731 mg) was isolated. A sample of this ricinine was ignited and the resulting carbon dioxide was converted into barium carbonate. This salt had an activity of 432 d.p.m./mg, which represents an incorporation of 1.37%. The ricinine (275 mg) isolated from the plants that had been fed glyceric acid-1-^{14}C had an activity of 104 d.p.m./mg of barium carbonate derived from it, corresponding to an incorporation of 0.124%. In accordance with previous results (1), acetate-2-^{14}C was incorporated to the extent of 6%. The ricinine (146 mg) isolated from the plants that had been fed propionate-2-^{14}C had a specific activity of 3.41×10^3 d.p.m./mg, which corresponds to an incorporation of 1.3%.

Ricinine Degradation

All degradations were carried out as reported previously (1, 2), except that tribromonitromethane (bromopicrin), corresponding to carbons 3 and 5, was extracted with ether from its aqueous mixture rather than separating it by centrifugation.

In the degradation of ricinine obtained in the acetate-2-^{14}C feeding experiment, the active ricinine was diluted with inactive ricinine by a factor of approximately 13, thus producing a base with an activity of 151 d.p.m./mg of barium carbonate. Carbon 6 of the alkaloid was isolated as formaldehyde dimedone (4), which gave inactive barium carbonate.

The results of the degradations of ricinine obtained from the plants fed β-alanine-2-^{14}C are given in Table I. For the degradations leading to the isolation of each carbon atom except carbons 6 and 7, diluted ricinine producing barium carbonate with an activity of 124 d.p.m./mg was used. For carbon 6, diluted ricinine producing barium carbonate with an activity of 86.5 d.p.m./mg was used. For the determination of carbon 7, a small sample of undiluted ricinine was hydrolyzed and decarboxylated to decyanoricinine (4-methoxy-*N*-methyl-2-pyridone), which produced barium carbonate with an activity of 398 d.p.m./mg. The percentage of activity at carbon 7 was then obtained by difference.

The ricinine isolated from plants that had been fed propionate-2-^{14}C was divided into two portions. One of the portions, after dilution with inactive ricinine, had a specific activity of 8.21 d.p.m./mg of barium carbonate. Its degradation for the isolation of carbon 2 yielded benzoic acid with a specific activity of 1.97 d.p.m./mg of barium carbonate, equivalent to 21% of the total activity.

The second portion of the ricinine obtained from the propionate experiments, after dilution with inactive alkaloid, had a specific activity of 161 d.p.m./mg of barium carbonate. Its degradation for the isolation of carbon 3 produced bromopicrin having a specific activity of 512 d.p.m./mg of barium carbonate, equivalent to 39.8% of the activity of the alkaloid.

Can. J. Chem. Downloaded from www.nrcresearchpress.com by 210.87.254.5 on 09/05/12
For personal use only.

ACKNOWLEDGMENT

Thanks are due to Mr. H. Séguin for the sample combustions.

REFERENCES

1. P. F. JUBY and L. MARION. Can. J. Chem. **41**, 117 (1963).
2. S. R. JOHNS and L. MARION. Can. J. Chem. **44**, 23 (1966).
3. R. A. ANWAR, T. GRIFFITH, and R. U. BYERRUM. Federation Proc. **20**, 374 (1961).
4. J. M. ESSERY, P. F. JUBY, L. MARION, and E. TRUMBULL. Can. J. Chem. **41**, 1142 (1963).
5. D. R. CHRISTMAN and R. F. DAWSON. Biochemistry, **2**, 182 (1963).
6. T. GRIFFITH and R. U. BYERRUM. Biochem. Biophys. Res. Commun. **10**, 293 (1963).
7. A. R. FRIEDMAN and E. LEETE. J. Am. Chem. Soc. **85**, 2141 (1963).
8. P. F. JUBY and L. MARION. Biochem. Biophys. Res. Commun. **5**, 461 (1961).
9. E. LEETE and A. R. FRIEDMAN. J. Am. Chem. Soc. **86**, 1224 (1964).
10. T. GRIFFITH and R. U. BYERRUM. Federation Proc. **21**, 398 (1962).

Can. J. Chem. Downloaded from www.nrcresearchpress.com by 210.87.254.5 on 09/05/12
For personal use only.

Can. J. Chem. Downloaded from www.nrcresearchpress.com by 210.87.254.105 on 09/05/12
For personal use only.

ÉTUDES SUR LA TRIMÉTHYL-2,4,4 CYCLOHEXANONE ET SES PRODUITS DE RÉDUCTION[1]

JEAN-CLAUDE RICHER ET DAVID PERELMAN
Département de Chimie, Université de Montréal, Montréal, Québec

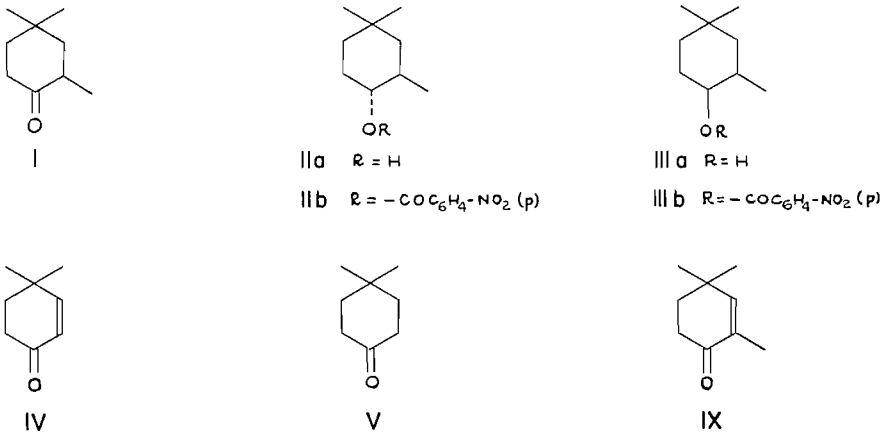
Reçu le 15 mars 1966

RÉSUMÉ

De nouvelles synthèses de la triméthyl-2,4,4 cyclohexanone sont rapportées. La configuration de chacun des produits de réduction de cette cétone est attribuée grâce à leur mode de formation, leur spectre infra-rouge et de résonance magnétique nucléaire et leur vitesse relative d'oxydation chromique.

INTRODUCTION

Dans les cadres d'une étude connexe, il était important pour nous d'avoir une méthode simple de préparer la triméthyl-2,4,4 cyclohexanone (I) et de connaître d'une façon bien définie la stéréochimie des alcools II*a* et III*a* dérivant de cette cétone. Au moment où le présent travail a été entrepris, plusieurs synthèses de la cétone I étaient connues (1–7);



il nous semblait toutefois intéressant d'appliquer d'une part à la diméthyl-4,4 cyclohexen-2 one (IV), et d'autre part à la diméthyl-4,4 cyclohexanone (V), les méthodes, mises au point respectivement par Burn et Petrow (8) et par Ireland et Marshll (9), pour la synthèse des méthyl-2 cyclanones. Ces méthodes sont schématisées dans le Schéma Réactionnel 1. Les résultats obtenus sont rapportés dans la présente publication. De plus, la configuration relative de chacun des alcools II*a* et III*a* est établie d'une manière définitive.

RÉSULTATS

1. Synthèses de la triméthyl-2,4,4 cyclohexanone

1.1. Synthèse par l'intermédiaire des éthers VII a et VII b

La condensation du *p*-thiocrésol (VI*a*) et de la formaldehyde sur la diméthyl-4,4 cyclohexen-2 one (IV) en présence de triéthylamine, suivant les indications de Burn et Petrow (8), conduit au dérivé attendu (VII*a*) avec un rendement de 72%. Les spectres

[1]*Extrait du mémoire présenté par D. Perelman en vue de l'obtention du grade de Maître ès Sciences, Faculté des Sciences, Université de Montréal, Montréal, février 1965.*

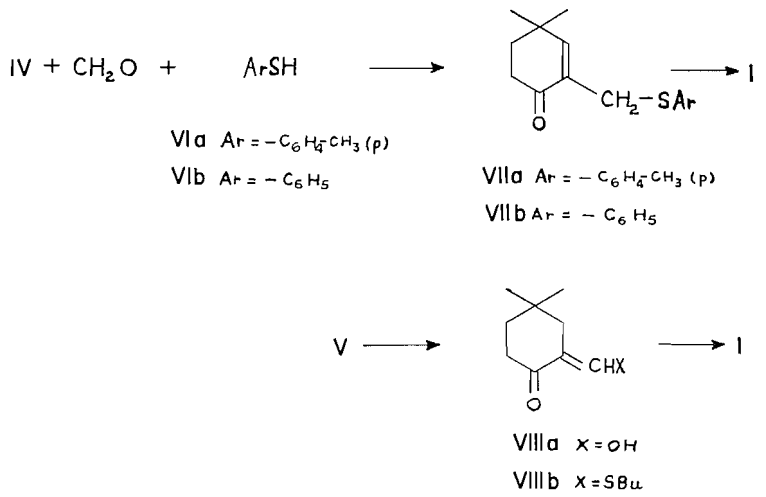


SCHÉMA RÉACTIONNEL 1.

infra-rouges et ultraviolets de ce produit sont conformes à la structure désignée et s'accordent avec les données des auteurs. La dinitro-2,4 phénylhydrazone dérivée de VII*a* fond à 139 °C. Le spectre de résonance magnétique nucléaire de ce dérivé confirme la structure proposée.

Utilisant les conditions expérimentales de Burn et Petrow (8), l'éther VII*a* a été désulfurisé en présence de nickel de Raney modifié par l'acétone. L'analyse par chromatographie en phase gazeuse, sur le produit distillé, révèle la présence de la triméthyl-2,4,4 cyclohexanone (I) (7.6%), de la triméthyl-2,4,4 cyclohexen-2 one (IX) (83.6%), et des triméthyl-2,4,4 cyclohexanols (II*a* et III*a*) (3.4%). Il s'avérait intéressant d'examiner la possibilité de poursuivre cette réaction au-delà de la désulfurisation initiale; à cette fin une série de réaction fut entreprise dans laquelle la proportion de nickel de Raney par rapport à l'éther VII*a* a été successivement augmentée. Les résultats de ces réactions, rapportés dans le Tableau I, montrent que la désulfurisation peut être amenée à produire en prépondérance soit les triméthyl-2 4,4 cyclohexanols (II*a* et III*a*) soit la triméthyl-2,4,4 cyclohexen-2 one (IX). Les cétones I et IX présentes dans les produits de désulfurisation peuvent être séparées de leurs contaminants par l'intermédiaire de leur semicarbazone; l'hydrogénation, en présence du palladium sur carbonate de calcium, du mélange des cétones récupérées conduit à la triméthyl-2,4,4 cyclohexanone (I) pure.

TABLEAU I

Désulfurisations de l'éther VII*a*

Poids de VII*a* (g)	Poids de catalyseur (g)	Produits obtenus* (%)					
		Non-identifié	I	Non-identifié	IX	III*a*	II*a*
3	26	7.2	1.8	—	—	37.3	53.7
3	17.5	8.5	33.7	—	—	24.6	33.1
3	12	3.4	39.7	11.3	42.8	—	2.8
3	6.6	0.4	12.8	6.8	75.9	2.6	1.7
49.4 (3)	108 (6.5)	1.0	20.0	7.7	65.8	3.8	1.7

*Les résultats rapportés ici ont été déterminés par chromatographie en phase gazeuse, en mesurant les surfaces sous les pics à l'aide d'un planimètre.

Can. J. Chem. Downloaded from www.nrcresearchpress.com by 210.87.254.105 on 09/05/12
For personal use only.

Can. J. Chem. Downloaded from www.nrcresearchpress.com by 210.87.254.105 on 09/05/12
For personal use only.

De la même manière, la condensation de la diméthyl-4,4 cyclohexen-2 one (IV) avec la formaldéhyde et le thiophénol en présence de triéthylamine fournit l'éther VII*b* avec un rendement de 70%. Le spectre infra-rouge du produit distillé montre les bandes attendues; la dinitro-2,4 phénylhydrazone de cet éther fond à 143.5 °C et le spectre de résonance magnétique nucléaire de ce dernier dérivé est conforme à la structure proposée. La désulfurisation de l'éther en présence d'un excès de nickel de Raney non-modifié conduit à un mélange où l'on retrouve la cétone saturée I (7.5%) et les triméthyl-2,4,4 cyclohexanols *cis* (III*a*) (24.2%) et *trans* (II*a*) (68.3%).

Afin de vérifier si une polysubstitution se produit au cours de la réaction de Burn et Petrow, une désulfurisation a été effectuée sur l'éther VII*b* brut non-distillé; la chromatographie en phase gazeuse des produits obtenus n'indique la présence que des alcools II*a* et III*a*, qui ne sont pas contaminés par des alcools polyméthylés. L'absence de composés tétra- et penta-méthylés montre clairement que la phénylthiométhylation procède seulement sur le carbone éthylénique en position 2 de la diméthyl-4,4 cyclohexen-2 one (IV).

1.2. Synthèse par l'intermédiaire de la butylthiométhylène-2 diméthyl-4,4 cyclohexanone (VIIIb)

L'action du butanethiol sur la formyl-2 diméthyl-4,4 cyclohexanone (VIII*a*) fournit l'éther énolique VIII*b*; les données spectrales (infra-rouge, ultraviolet et résonance magnétique nucléaire) de cet éther sont conformes à la structure proposée. La désulfurisation effectuée selon les indications d'Ireland et Marshall (9) conduit à un produit qui, après distillation, montre par chromatographie en phase gazeuse la présence de trois composés, à savoir la cétone saturée I (8.2%) et les triméthyl-2,4,4 cyclohexanols *cis* (III*a*) (40.7%) et *trans* (II*a*) (51.1%). Ce résultat est inattendu car les auteurs (9) ne signalent aucune formation d'alcool lors de la désulfurisation. Le mélange obtenu est oxydé par la méthode de Brown (10) et conduit à la triméthyl-2,4,4 cyclohexanone (I) pure.

Pour fins de comparaison les cétones saturée (I) et non-saturée (IX) ont été préparées à partir de l'isobutyraldéhyde et de la pentènone-3 en suivant les indications de Yanagita (4). Nous avions ainsi à l'aide des méthodes énumérées plus haut des sources d'accès simples pour obtenir la triméthyl-2,4,4 cyclohexanone (I) et ses alcools (II*a* et III*a*).

2. Propriétés des alcools épimères

La réduction des cétones cyclohexaniques par le sodium dans l'éthanol est la méthode généralement utilisée pour la synthèse des alcools équatoriaux (11). Ce procédé a été appliqué pour la préparation du triméthyl-2,4,4 cyclohexanol *trans* (II*a*). L'analyse chromatographique du produit de la réduction indique la présence de la cétone saturée I (7%) qui n'a pas réagi et des triméthyl-2,4,4 cyclohexanols *cis* (III*a*) (1%) et *trans* (II*a*) (92%). L'alcool *trans* (II*a*) est purifié par l'intermédiaire de son *p*-nitrobenzoate (II*b*), recristallisé jusqu'à point de fusion constant de 66–67 °C. Le composé isolé après saponification de ce dérivé est chromatrographiquement pur.

L'hydrogénation en milieu acide en présence d'oxyde de platine (12) a été utilisée pour la préparation du triméthyl-2,4,4 cyclohexanol *cis* (III*a*). L'alcool obtenu après saponification des acétates est contaminé par 2% de son épimère (II*a*). Ces résultats confirment la proposition de Barton (11), selon laquelle l'hydrogénation en milieu acide fournit principalement un alcool axial. Le triméthyl-2,4,4 cyclohexanol *cis* (III*a*) est isolé à l'état pur après saponification de son *p*-nitrobenzoate, recristallisé jusqu'à point de fusion constant de 82.5–83.5 °C.

Les propriétés des alcools épimères ainsi obtenus sont résumées dans le Tableau II.

Ces résultats présentent plusieurs particularités intéressantes. Selon la règle d'Auwers–Skita, les constantes physiques seraient plus élevées pour l'alcool *cis* que pour l'alcool *trans*. Les indices de réfraction suivent cette règle mais les points d'ébullition montrent la tendance inverse. Cette exception n'est pas unique; en effet, Eliel (13) a rapporté que la règle ne s'applique pas aux alkylcyclohexanols. Deuxièmement, les alcools équatoriaux montrent l'absorption typique dans l'infra-rouge à des fréquences plus élevées que celles des alcools axiaux (14). De plus, les spectres de résonance magnétique nucléaire des alcools II*a* et III*a* sont typiques (15) tant par la forme que par la position des bandes pour des cyclohexanols équatoriaux et axiaux. Les vitesses relatives d'oxydation chromique sont conformes à la théorie de la décompression stérique proposée par Schreiber et Eschenmoser (16), selon laquelle un alcool axial est oxydé plus rapidement que son isomère équatorial. La différence d'énergie libre entre les alcools II*a* et III*a*, telle qu'évaluée à l'aide de leur vitesse d'oxydation et de l'équation proposée par Sipos *et al.* (17), serait de 0.83 kcal/mole.

TABLEAU II

Propriétés physiques des triméthyl-2,4,4 cyclohexanols

Propriétés	*trans* (II*a*)	*cis* (III*a*)
η_D^{22}	1.4567	1.4600
Point d'ébullition	88–89 °C à 20 mm Hg	81–82 °C à 20 mm Hg
Spectres infra-rouges (C—O)	1 050 cm^{-1}	1 018 cm^{-1}
Déplacements chimiques (δ) des hydrogènes carbinoliques	2.98 (bande large)	3.70 (bande étroite)
Vitesses d'oxydation chromiques* ($10^3\ k_2$)	87.2 l $mole^{-1}\ s^{-1}$	384 l $mole^{-1}\ s^{-1}$

*Mesures effectuées par C. Gilardeau.

A l'aide de ces considérations, il est maintenant possible d'attribuer d'une façon définitive les configurations II*a* et III*a* aux alcools dérivant de la triméthyl-2,4,4 cyclohexanone. Ces conclusions permettent de lever l'ambiguité causée par la communication de Yanagita (4), dans laquelle est rapportée la préparation d'un triméthyl-2,4,4 cyclohexanol donnant un *p*-nitrobenzoate de p.f. 61–63 °C. Les auteurs proposaient dans la partie théorique (réf. 4, p. 1724) une configuration *trans* alors que dans la partie expérimentale (réf. 4, p. 1729) ils décrivaient le triméthyl-2,4,4 cyclohexanol *cis*.

PARTIE EXPÉRIMENTALE

Les spectres infra-rouges ont été déterminés sur un spectrophotomètre Beckman modèle IR-8 à double réseau. Les analyses par chromatographie en phase gazeuse ont été effectuées à 125 °C sur un appareil Kromo-Tog modèle K-2 de la compagnie Burrell à l'aide d'une colonne contenant 10% d'Hyprose adsorbé sur Chromosorb P. Les spectres de résonance magnétique nucléaire ont été pris sur un spectromètre modèle A-60 de la compagnie Varian. Le tetraméthylsilane est utilisé comme référence interne. Les points de fusion ont été pris sur un "Hot Stage Apparatus" de la compagnie Reichert (Autriche). Les analyses élémentaires ont été effectuées par le Docteur Claude Daesslé à Montréal.

*1. Dérivé p-tolylthiométhyl-2 diméthyl-4,4 cyclohexanone (VII*a*)*

Selon la méthode de Burn et Petrow (8), un mélange de 50.6 g (0.40 mole) de diméthyl-4,4 cyclohexen-2 one (IV), 74.2 g (0.60 mole) de *p*-thiocrésol, 50 g (0.65 mole) de formaldéhyde 37%, 60 g (0.57 mole) de triéthylamine et 125 ml d'éthanol 95% est chauffé à reflux à 60 °C pendant 48 h. Après les extractions à la façon habituelle, 76.4 g (72% du rendement théorique) du dérivé attendu sont isolés, présentant les caractéristiques suivantes: p.é. 145 °C à 0.7 mm Hg; η_D^{22} 1.5769; infra-rouge: bande à 1 675 cm^{-1} (carbonyle cétonique α,β non-saturé); ultraviolet: λ_{max} dans l'éthanol à 228 (ϵ de 16 820) et 242 mμ (ϵ de 14 920) (litt. (8) λ_{max} à 225 (ϵ de 11 390) et 254.5 mμ (ϵ de 14 300)); la dinitro-2,4 phénylhydrazone de cet éther fond à 139 °C après cristallisation d'un mélange éthanol–chloroforme.

Anal. Calc. pour $C_{23}H_{24}N_4O_4S$: C, 59.98; H, 5.49; N, 12.72; S, 7.25. Trouvé: C, 59.92; H, 5.71; N, 12.87; S, 7.47.

Can. J. Chem. Downloaded from www.nrcresearchpress.com by 210.87.254.105 on 09/05/12
For personal use only.

Le spectre de résonance magnétique nucléaire de ce dérivé montre des bandes à 1.03 (singulet, six hydrogènes des groupes méthyles), 1.71 (triplet, deux hydrogènes en position 5), 2.33 (singulet, trois hydrogènes du groupe méthyle du *p*-thiocrésol), 2.65 (triplet, deux hydrogènes en position 6), 3. 81 (singulet, deux hydrogènes du groupe CH_2S), 5.88 (singulet, hydrogène vinylique) et 7.16 p.p.m. (quatre hyrogènes aromatiques).

2. Dérivé phénylthiométhyl-2 diméthyl-4,4 cyclohexanone (VIIb)

Ce dérivé a été préparé à partir de 7.5 g (0.06 mole) de diméthyl-4,4 cyclohexen-2 one (IV), 6.5 g (0.06 mole) de thiophénol, 7.5 g de formaldéhyde 37% et 10 g de triéthylamine dissous dans 50 ml d'éthanol 95%. Après un chauffage à 56 °C pendant 26 h, 10.3 g (70% du rendement théorique) de produit ont été isolés. Le produit obtenu après distillation présente les caractéristiques suivantes: η_D^{22} 1.5802; p.é. 140 °C à 0.9 mm Hg; la dinitro-2,4 phénylhydrazone, plaques oranges fondant à 143.5 °C.

Anal. Calc. pour $C_{21}H_{22}N_4O_4S$: C, 59.14; H, 5.20; N, 13.14; S, 7.48. Trouvé: C, 58.71; H, 5.30; N, 13.36; S, 7.39.

Le spectre de résonance magnétique nucléaire de ce dérivé montre une bande à 1.03 (singulet, six hydrogènes des groupes méthyles), 1.70 (triplet, deux hydrogènes en position 5), 2.61 (triplet, deux hydrogènes en position 6), 3.85 (singulet, deux hydrogènes du groupe CH_2S), 5.93 (singulet, hydrogène vinylique) et 7.30 p.p.m. (cinq hydrogènes aromatiques).

3. Dérivé butylthiométhylène-2 diméthyl-4,4 cyclohexanone (VIIIb)

Un mélange de formyl-2 diméthyl-4,4 cyclohexanone (VIII*a*) (11.1 g), de butanethiol (12.3 g) et de benzène anhydre (80 ml) est chauffé à reflux sous atmosphère d'azote en présence d'acide *p*-toluène sulfonique (100 mg); l'eau formée est séparée par distillation azéotrope et recueillie dans un séparateur Dean–Stark. Le produit désiré (10.9 g, 68.1% du rendement théorique) est isolé selon les indications d'Ireland et Marshall (9). Un échantillon analytique présente les caractéristiques suivantes: η_D^{23} 1.5339; p.é. 122–124 °C à 1.5 mm Hg; infra-rouge: bande carbonyle α,β non-saturée à 1 660 cm^{-1}; ultraviolet: λ_{max} à 315 mμ (ϵ de 15 150) (litt. (9) λ_{max} à 313 mμ (ϵ de 18 000)); le spectre de résonance magnétique nucléaire montre des bandes à 2.93 (triplet, deux hydrogènes du groupe —SCH_2—) et à 7.60 p.p.m. (triplet, hydrogène vinylique).

Anal. Calc. pour $C_{13}H_{22}OS$: C, 68.99; H, 9.79; S, 14.14. Trouvé: C, 69.23; H, 9.75; S, 14.15.

REMERCIEMENTS

Les auteurs remercient le Conseil National de Recherches du Canada et le Ministère de l'Education du Québec pour l'aide financière apportée sous forme d'octroi de recherches (A-1295) et de bourse de perfectionnement (D. P.); la compagnie Pitt-Consol Chemical Library, Pennsylvania, pour le généreux échantillon de *p*-thiocrésol; et le Docteur Claude Gilardeau pour la détermination des vitesses d'oxydation chromique des triméthyl-2,4,4 cyclohexanols.

BIBLIOGRAPHIE

1. O. WALLACH. Ann. **324**, 107 (1902).
2. I. ALKONYI. Ber. **94**, 2486 (1961).
3. I. ALKONYI. Ber. **95**, 279 (1962).
4. M. YANAGITA et S. INAYAMA. J. Org. Chem. **19**, 1724 (1954).
5. S. JULIA, M. JULIA, H. LINARÈS et J. C. BLONDEL. Bull. Soc. Chim. France, 1952 (1962).
6. W. REUSCH et R. LE MAHIEU. J. Am. Chem. Soc. **86**, 3068 (1964).
7. F. BRUDERLEIN. Thèse de Doctorat, Université de Montréal, Montréal, Québec. 1960.
8. D. BURN et V. PETROW. J. Chem. Soc. 1223 (1962).
9. R. E. IRELAND et J. A. MARSHALL. J. Org. Chem. **27**, 1615 (1962).
10. H. C. BROWN et C. P. CARG. J. Am. Chem. Soc. **83**, 2952 (1961).
11. D. H. R. BARTON et R. COOKSON. Quart. Rev. London, **10**, 44 (1956).
12. E. L. ELIEL et R. S. RO. J. Am. Chem. Soc. **79**, 5992 (1957).
13. E. L. ELIEL. *Dans* Stereochemistry of organic compounds. McGraw-Hill Book Co., Inc., New York. 1962.
14. A. R. H. COLE, R. N. JONES et K. DOBRINER. J. Am. Chem. Soc. **74**, 5771 (1952).
15. E. L. ELIEL et M. H. GIANNI. Tetrahedron Letters, 97 (1962).
16. J. SCHREIBER et A. ESCHENMOSER. Helv. Chim. Acta, **38**, 1529 (1955).
17. J. SIPOS, J. KRUPICKA, M. TICHY et J. SICHER. Collection Czech. Chem. Commun. **27**, 2079 (1962).

Can. J. Chem. Downloaded from www.nrcresearchpress.com by 210.87.254.105 on 09/05/12
For personal use only.

Can. J. Chem. Downloaded from www.nrcresearchpress.com by 210.87.254.40 on 09/05/12
For personal use only.

THE PREPARATION OF 9-HYDROXYPYRAZOLO[3,4-*b*]QUINOLINES

R. T. COUTTS AND J. B. EDWARDS
College of Pharmacy, University of Saskatchewan, Saskatoon, Saskatchewan

Received March 28, 1966

ABSTRACT

4-(2-Nitrobenzylidene)-2-pyrazolin-5-ones (I) were best prepared by heating *o*-nitrobenzaldehyde and 2-pyrazolin-5-ones in acetic anhydride containing fused sodium acetate (cf. Erlenmeyer azlactone synthesis). Pyrazolones of type I were reductively cyclized with cyclohexene and palladium–charcoal, and gave 3*a*,4,9,9*a*-tetrahydro-9-hydroxy-1*H*-pyrazolo-[3,4-*b*]quinolines (II) which, as expected, were amphoteric compounds. Of the three other methods of reduction used in this study, two (zinc and acetic acid; sodium borohydride and palladium–charcoal) were capable of producing pyrazoloquinolines, but were less reliable. The other method employed (hydrazine hydrate and palladium–charcoal) caused degradation of the pyrazolone molecule in the two cases examined, and in both, bis(2-aminobenzylidene) hydrazine (V) was the reduction product isolated.

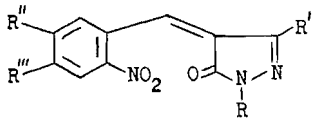
In our earlier studies (1–3) we investigated the reduction of aromatic nitro compounds which possessed an ester or an acid group in a position capable of undergoing cyclization, with a view to finding a system of reduction which would give cyclic compounds containing a *N*-hydroxy group. Such compounds were required for pharmacological evaluation.

We have now extended our studies to the reduction of aromatic systems which possess both a nitro group and a lactam carbonyl group in a position capable of undergoing cyclization, to see whether cyclic *N*-oxy or *N*-hydroxy compounds could conveniently be prepared in this way.

o-Nitrobenzaldehyde and its simple derivatives are known (4) to condense with 3-methyl-1-phenyl-2-pyrazolin-5-one to give 4-(*o*-nitrobenzylidene) derivatives. Preparations of 3-methyl-4-(*o*-nitrobenzylidene)-1-phenyl-2-pyrazolin-5-one (I*a*) and its dimethoxy (I*b*) and methylenedioxy (I*c*) derivatives have been reported (4), and of these three compounds, only one (I*a*) yielded a reduced product (II*a*) which was the result of cyclization at the hydroxylamino stage of reduction.

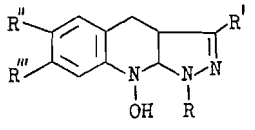
Compounds having the general formula I were selected, therefore, for our initial investigation of reductive cyclizations involving an amide carbonyl group. Four methods of reduction were chosen, all of which were known to yield *N*-oxy or *N*-hydroxy compounds in certain instances. The four methods were as follows: sodium borohydride in the presence of palladium–charcoal (1–3); zinc and acetic acid (4); hydrazine hydrate and palladium–charcoal (5); and cyclohexene and palladium–charcoal (6).

Attempts by us to prepare I*a* and I*b* by the reported method (4) gave poor yields of products. Heating *o*-nitrobenzaldehyde and 3-methyl-1-phenyl-2-pyrazolin-5-one in ethanol containing a catalytic quantity of piperidine gave a slightly better yield of the



I

	R	R′	R″	R‴
a	Ph	Me	H	H
b	Ph	Me	OMe	OMe
c	Ph	Me	O—CH_2—O	
d	Ph	Me	Cl	H



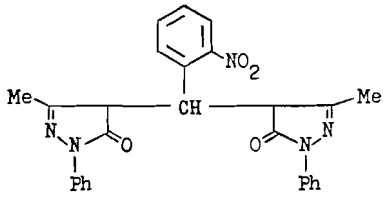
II

	R	R′	R″	R‴
e	Ph	Ph	H	H
f	H	Me	H	H
g	Ac	Me	H	H

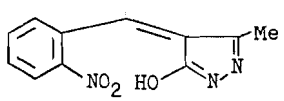
Can. J. Chem. Downloaded from www.nrcresearchpress.com by 210.87.254.40 on 09/05/12
For personal use only.

desired product (I*a*), though an appreciable yield of the bis compound, 4,4′-(*o*-nitrobenzylidene)bis(3-methyl-1-phenyl-2-pyrazolin-5-one) (III), was also isolated. 3-Methyl-4-(*o*-nitrobenzylidene)-1-phenyl-2-pyrazolin-5-one (I*a*) was best prepared by heating *o*-nitrobenzaldehyde and the pyrazolone in acetic anhydride containing anhydrous sodium acetate. By the same method, the related *o*-nitrobenzylidene-pyrazolones (I*b*, I*d*, and I*e*) were also obtained. An attempt to prepare 3-methyl-4-(*o*-nitrobenzylidene)-2-pyrazolin-5-one (I*f*) by this method gave what appeared to be the *N*-acetyl derivative (I*g*). Compound I*f* was obtained by the alternative method of reacting the aldehyde with the pyrazolone in ethanol containing piperidine. An infrared spectrum of the product (I*f*) indicated the presence of hydroxyl and nitro groups and the absence of carbonyl absorption, which suggested that the compound existed in the lactim form (IV) in the solid state.

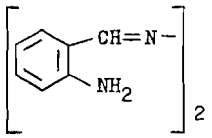
It has been reported (4) that the reduction of I*a* with zinc and acetic or hydrochloric acid, or with aluminium amalgam, gave 3*a*,4,9,9*a*-tetrahydro-9-hydroxy-3-methyl-1-



III



IV



V

phenyl-1*H*-pyrazolo[3,4-*b*]quinoline (II*a*), which was isolated as its yellow hydrochloride, m.p. 251–252°. Treatment of this hydrochloride with ammonia is said (4) to yield the base (II*a*), m.p. 142°, in excellent yield. The product obtained when we reduced I*a* with sodium borohydride and palladium–charcoal depended on the nature of the solvent used. When a mixture of methanol and ethanol was employed, a pale-yellow solid, m.p. 252–254°, slowly precipitated from the acidified filtrate. It analyzed correctly for $C_{17}H_{17}N_3O \cdot HCl$ and was identical with the compound prepared as described by the Indian workers (4). Using their method, we failed to liberate the base (II*a*), but found that it was more conveniently prepared from its hydrochloride by making use of the fact that II*a* is also an acid as well as a base. In agreement with its structure, it was readily soluble in aqueous sodium hydroxide or sodium carbonate. Addition of acetic acid to either solution precipitated II*a*; addition of hydrochloric acid, however, resulted in the precipitation of the sparingly soluble hydrochloride.

Reduction of I*a* with sodium borohydride and palladium–charcoal in dioxane gave only a small amount of II*a* hydrochloride. The main product was a colorless solid which was insoluble in both acidic and basic solutions. Reduction of the related chloro compound (I*d*) in dioxane with the same reducing system gave a similar neutral compound. Evidence from infrared studies indicates that the nitro group was reduced and the carbonyl group retained in both cases. As yet, these products remain unidentified.

The pyrazolone (I*a*) was then reduced with cyclohexene and palladium–charcoal, and the *N*-hydroxypyrazoloquinoline (II*a*) was the major product isolated. A colorless hydrochloride was formed on recrystallization of this product from methanol to which a few drops of hydrochloric acid had been added. Despite the difference in color, this hydrochloride was the same compound as that isolated by the Indian workers.

Reduction of I*a* with zinc and acetic acid containing acetic anhydride yielded the

O-acetyl derivative of II*a*. Such a structure was suggested by elemental analysis and by the insolubility of the product in sodium carbonate solution. Confirmation was obtained when the same compound was produced by acetylating II*a*.

When I*a* was reduced by means of hydrazine hydrate and palladium–charcoal, a pyrazoloquinoline was not obtained. Instead, bis(2-aminobenzylidene) hydrazine (V) was the product isolated. The same compound resulted when both 3-methyl-4-(*o*-nitrobenzylidene)-2-pyrazolin-5-one (I*f*) and *o*-nitrobenzaldehyde were similarly reduced, which indicated that cleavage of the molecule occurred with this treatment. This method of reduction, therefore, was not suitable for the preparation of *N*-hydroxy compounds.

Reduction of 4-(4,5-dimethoxy-2-nitrobenzylidene)-3-methyl-1-phenyl-2-pyrazolin-5-one (I*b*) by means of zinc and acetic acid is reported (4) to yield 4-(2-amino-4,5-dimethoxybenzylidene)-3-methyl-1-phenyl-2-pyrazolin-5-one (I*b*, NH_2 replacing NO_2). When I*b* was reduced with sodium borohydride and palladium–charcoal in methanol, or by means of cyclohexene and palladium–charcoal, the amino compound was not obtained. As in the case of the reduction of I*a*, a *N*-hydroxypyrazoloquinoline, namely, 3*a*,4,9,9*a*-tetrahydro-9-hydroxy-6,7-dimethoxy-3-methyl-1-phenyl-1*H*-pyrazolo[3,4-*b*]quinoline (II*b*), was isolated as its hydrochloride. Once again, it was converted into the free base by making use of the acidic properties of the *N*-hydroxy group.

It was found that the hydrochloride of II*b* had a variable melting point. Some samples melted at 211–212° whereas others melted as low as 195–197°. Except for very minor differences, the infrared spectra were identical and both samples analyzed correctly for $C_{19}H_{19}N_3O_3 \cdot HCl$.

The reduction of 4-(5-chloro-2-nitrobenzylidene)-3-methyl-1-phenyl-2-pyrazolin-5-one (I*d*) followed the same pattern. Reduction by means of zinc and acetic acid, or by means of cyclohexene and palladium–charcoal, gave 6-chloro-3*a*,4,9,9*a*-tetrahydro-9-hydroxy-3-methyl-1-phenyl-1*H*-pyrazolo[3,4-*b*]quinoline (II*d*), which had the same solubility characteristics as II*a*. The reduction of 4-(*o*-nitrobenzylidene)-1,3-diphenyl-2-pyrazolin-5-one (I*e*) by means of cyclohexene and palladium–charcoal gave rise, on acidification, to the hydrochloride of 3*a*,4,9,9*a*-tetrahydro-9-hydroxy-1,3-diphenyl-1*H*-pyrazolo[3,4-*b*]-quinoline (II*e*) which, on the basis of its elemental analysis, was isolated as the monohydrate. The base was readily obtained from the hydrochloride by the method described for the other pyrazoloquinolines. As expected, it was an amphoteric substance which was difficult to purify, and even after repeated reprecipitations and crystallizations it analyzed only indifferently for $C_{22}H_{19}N_3O$.

The insolubility of 4-(*o*-nitrobenzylidene)-3-methyl-2-pyrazolin-5-one (I*f*) in common solvents precluded its reduction.

The results of this investigation contrast with the findings of Narang *et al.* (4). All four pyrazolones (I*a*, I*b*, I*d*, and I*e*) reduced in this study gave cyclic *N*-hydroxy compounds, and in each case, the benzylidene double bond was also reduced. This study has also shown that only reduction with cyclohexene and palladium–charcoal consistently yielded 3*a*,4,9,9*a*-tetrahydro-9-hydroxy-1*H*-pyrazolo[3,4-*b*]quinolines.

EXPERIMENTAL

Melting points are uncorrected. Infrared spectra (KBr disks) were recorded on a Beckmann IR.8 spectrophotometer except where stated otherwise. Palladium–charcoal refers to 10% palladium on charcoal.

Preparation of 3-Methyl-4-(o-nitrobenzylidene)-1-phenyl-2-pyrazolin-5-one (Ia)

Method a

o-Nitrobenzaldehyde (6.0 g) and 3-methyl-1-phenyl-2-pyrazolin-5-one (7.0 g) were reacted by the reported (4) method. The title compound (3.82 g, 31%), m.p. 159–161°, was obtained as a red solid (lit. (4) m.p. 162°).

Can. J. Chem. Downloaded from www.nrcresearchpress.com by 210.87.254.40 on 09/05/12
For personal use only.

Method b

o-Nitrobenzaldehyde (4.1 g) and 3-methyl-1-phenyl-2-pyrazolin-5-one (4.35 g) were dissolved in ethanol (50 ml) containing piperidine (0.5 ml), and the resulting solution was heated under reflux for ½ h. The title compound (1.44 g) separated as orange-red crystals, m.p. 162°. A further crop (1.08 g), m.p. 259–261°, was obtained by concentrating the mother liquors (total yield 34%). When the concentrate was allowed to stand, a pale-yellow second product (2.65 g), m.p. 203° (decomp.), separated. This was 4,4′-(*o*-nitrobenzylidene)-bis(3-methyl-1-phenyl-2-pyrazolin-5-one) (lit. (7) m.p. 203–205°).

Anal. Calcd. for $C_{27}H_{23}N_5O_4$: N, 14.55. Found: N, 14.48.

Method c

A mixture of *o*-nitrobenzaldehyde (6.7 g), 3-methyl-1-phenyl-2-pyrazolin-5-one (7.0 g), fused sodium acetate (3.8 g), and acetic anhydride (12 ml) was heated on a hot plate until a homogeneous red solution formed (15 min). When cooled, a dark-red solid formed. It was washed with water and cold ethanol, and then recrystallized from ethanol to give the title compound (8.31 g, 61%) as orange-red crystals, m.p. 160–162°.

Preparations of Pyrazolones Ib, Id, and Ie

Under the conditions described for the preparation of I*a* (method *c*), the following compounds were obtained in the yields stated.

4-(4,5-Dimethoxy-2-nitrobenzylidene)-3-methyl-1-phenyl-2-pyrazolin-5-one (I*b*) (4.6 g, 40%), m.p. 183–185°, was obtained as a light-brown solid from 4,5-dimethoxy-2-nitrobenzaldehyde (6.6 g) and 3-methyl-1-phenyl-2-pyrazolin-5-one (6.9 g) (lit. (4) m.p. 183°).

4-(5-Chloro-2-nitrobenzylidene)-3-methyl-1-phenyl-2-pyrazolin-5-one (I*d*) (4.2 g, 62%), m.p. 140–142°, was obtained as orange-red needles from 3-chloro-6-nitrobenzaldehyde (7.4 g) and 3-methyl-1-phenyl-2-pyrazolin-5-one (7.0 g). The infrared spectrum had absorption peaks at 1 690 (s) (C=O) and at 1 520 (s) and 1 330 (s) (NO_2) cm^{-1}.

Anal. Calcd. for $C_{17}H_{12}ClN_3O_3$: C, 59.75; H, 3.42; Cl, 10.38; N, 12.30. Found: C, 59.50; H, 3.54; Cl, 10.49; N, 12.57.

4-(*o*-Nitrobenzylidene)-1,3-diphenyl-2-pyrazolin-5-one (I*e*) (4.9 g, 74%), m.p. 181–182°, was obtained as red needles from *o*-nitrobenzaldehyde (3.0 g) and 1,3-diphenyl-2-pyrazolin-5-one (5.0 g). The infrared spectrum had absorption peaks at 1 695 (s) (C=O) and at 1 540 (s) and 1 330 (s) (NO_2) cm^{-1}.

Anal. Calcd. for $C_{22}H_{15}N_3O_3$: C, 71.53; H, 4.09; N, 11.38. Found: C, 71.48; H, 4.26; N, 11.31.

Preparation of 3-Methyl-4-(o-nitrobenzylidene)-2-pyrazolin-5-one (If)

Method a

An attempted preparation of the title compound from *o*-nitrobenzaldehyde (4.53 g) and 3-methyl-2-pyrazolin-5-one (3.24 g) as described for the preparation of I*a* (method *c*) gave a dark-brown solid (7.6 g), m.p. 172–175°. The infrared spectrum showed broad absorption at 1 700 (s) (C=O) and at 1 520 (s) and 1 345 (s) (NO_2) cm^{-1}. This product was assumed to be 1-acetyl-3-methyl-4-(*o*-nitrobenzylidene)-2-pyrazolin-5-one (I*g*).

Anal. Calcd. for $C_{13}H_{11}N_3O_4$: C, 57.14; H, 4.06; N, 15.37. Found: C, 57.18; H, 4.18; N, 15.47.

Method b

By using the method described for the preparation of I*a* (method *b*), the title compound (3.1 g), m.p. 243–246° (decomp.), was obtained as a pale-brown solid. The product was insoluble in common organic solvents. It was boiled with alcohol and then acetone before analysis. The infrared spectrum (Unicam SP 200 spectrophotometer) showed broad absorption between 2 400 and 3 300 with a maximum at 2 900 (m) (OH), and peaks at 1 530 (s) and 1 360 (s) (NO_2) cm^{-1}.

Anal. Calcd. for $C_{11}H_9N_3O_3$: C, 57.14; H, 3.92; N, 18.18. Found: C, 56.60; H, 4.15; N, 18.30.

Reduction of 3-Methyl-4-(o-nitrobenzylidene)-1-phenyl-2-pyrazolin-5-one (Ia)

Method a

A solution of the title compound (1 g) in a mixture of ethanol (80 ml) and methanol (10 ml) was added dropwise over a 15 min period to a solution of sodium borohydride (0.5 g) in water (5 ml) and methanol (10 ml) to which had been added, previously, palladium–charcoal (0.05 g) suspended in water (5 ml). Nitrogen was bubbled through the reaction mixture during the addition of the title compound and for a further 15 min. The solution was filtered and acidified with hydrochloric acid, and a small amount (ca. 50 mg) of a pale-yellow solid, m.p. 107–115°, which was not further investigated, was deposited. The filtrate from this was concentrated and an orange product slowly deposited. It was removed and washed with cold ethanol to yield 3*a*,4,9,9*a*-tetrahydro-9-hydroxy-3-methyl-1-pheny-1*H*-pyrazolo[3,4-*b*]quinoline (II*a*) hydrochloride as a yellow solid (0.336 g), m.p. 252–254° (lit. (4) m.p. 251–252°).

Anal. Calcd. for $C_{17}H_{18}ClN_3O$: C, 64.65; H, 5.74; Cl, 11.23; N, 13.31. Found: C, 64.30, 64.64; H, 5.58, 5.71; Cl, 11.19; N, 13.26.

Method b

The reduction described under method *a* was repeated on a threefold scale with dioxane (60 ml) as solvent. A slight excess of hydrochloric acid was added to the filtrate, which, on dilution with water, gave an off-white

Can. J. Chem. Downloaded from www.nrcresearchpress.com by 210.87.254.40 on 09/05/12
For personal use only.

solid (2.1 g), m.p. 140–146° with preliminary softening. This was crystallized from aqueous ethanol to give a colorless solid, m.p. 174–176°, the infrared spectrum of which showed absorption peaks at 1 685 (s) (C=O) and at 3 280 (m) and 1 595 (s) (NH?) cm^{-1}.

Anal. Found: C, 71.25; H, 5.68; N, 13.30.

The mother liquors remaining after the removal of the above product slowly deposited II*a* hydrochloride (0.18 g) as pale-orange prisms, m.p. 241–245°.

Method c

The title compound (1 g) was heated under reflux for 24 h in ethanol (10 ml) containing cyclohexene (3 ml) in which was suspended palladium–charcoal (0.1 g). The catalyst was removed by filtration, and the filtrate was evaporated to give a dark-red oil which, on trituration with benzene, solidified. The solid was crystallized from ethanol to yield 3*a*,4,9,9*a*-tetrahydro-9-hydroxy-3-methyl-1-phenyl-1*H*-pyrazolo[3,4-*b*]-quinoline (II*a*) (0.380 g), m.p. 141–142° (lit. (4) m.p. 142°).

Anal. Calcd. for $C_{17}H_{17}N_3O$: C, 73.09; H, 6.13; N, 15.04. Found: C, 73.00; H, 6.10; N, 15.16.

The above pyrazoloquinoline dissolved readily in aqueous sodium hydroxide. When this solution was acidified with acetic acid, the pyrazoloquinoline, m.p. 142°, was regenerated. When the alkaline solution was acidified with hydrochloric acid, 3*a*,4,9,9*a*-tetrahydro-9-hydroxy-3-methyl-1-phenyl-1*H*-pyrazolo[3,4-*b*]-quinoline (II*a*) hydrochloride was precipitated quantitatively as a colorless solid, m.p. 254–256°. The infrared spectrum of the hydrochloride was identical with that of the hydrochloride obtained by method *a*.

Method d

Zinc dust (1 g) was added in small quantities to a stirred solution of the title compound (2.0 g) in boiling glacial acetic acid (20 ml) until the initially red-colored solution became pale yellow. The solution was filtered and the filtrate was diluted with water (100 ml) to which had been added concentrated hydrochloric acid (2 ml). When the solution was allowed to stand, a pale-yellow flocculant precipitate formed. Recrystallization from methanol to which had been added a few drops of concentrated hydrochloric acid gave 3*a*,4,9,9*a*-tetrahydro-9-hydroxy-3-methyl-1-phenyl-1*H*-pyrazolo[3,4-*b*]quinoline (II*a*) hydrochloride (0.43 g) as a yellow solid, m.p. 255–256°. The infrared spectrum was identical with that of the hydrochloride obtained as described under methods *a* and *c*.

Method e

The reduction described under method *d* was repeated with acetic acid containing acetic anhydride (32% v/v). The filtrate was diluted with water to yield 9-acetoxy-3*a*,4,9,9*a*-tetrahydro-3-methyl-1-phenyl-1*H*-pyrazolo[3,4-*b*]quinoline (II*a*, Ac replaced H) as a flocculant precipitate, which was crystallized from methanol as a white solid (0.115 g), m.p. 207–208°. This solid was insoluble in aqueous sodium hydroxide. The infrared spectrum showed strong absorption at 1 670 (C=O) cm^{-1}.

Anal. Calcd. for $C_{19}H_{19}N_3O_2$: C, 71.01; H, 5.96; N, 13.08. Found: C, 70.46; H, 5.90; N, 13.00.

The same compound was obtained by heating under reflux a solution of II*a* (0.5 g) in acetic anhydride (5 ml) for 1 h. The cooled solution was poured into 5% aqueous sodium hydroxide and stirred until homogeneous; then the alkaline solution was extracted with ether. When evaporated, the dried ether solution gave a brown oil, which was triturated with ethanol to yield the acetyl derivative (0.26 g), m.p. 207–208° when crystallized from ethanol.

Reduction of 4-(4,5-Dimethoxy-2-nitrobenzylidene)-3-methyl-1-phenyl-2-pyrazolin-5-one (Ib)

Method a

The title compound (3 g) was reduced with cyclohexene and palladium–charcoal as described for the reduction of I*a* (method *c*). The filtrate, on evaporation, yielded a dark-brown oil (2.85 g) which was dissolved in chloroform. Addition of hydrochloric acid to the chloroform solution (in an attempt to extract basic material) resulted in the formation of an orange solid at the interface. Crystallization from ethanol gave 3*a*,4,9,9*a*-tetrahydro-9-hydroxy-6,7-dimethoxy-3-methyl-1-phenyl-1*H*-pyrazolo[3,4-*b*]quinoline (II*b*) hydrochloride (1.12 g) as a pale-brown solid, m.p. 211–212°. The infrared spectrum showed broad absorption from 2 200 to 3 300 (m) (OH) cm^{-1}.

Anal. Calcd. for $C_{17}H_{22}ClN_3O_3$: C, 60.71; H, 5.89; N, 11.18. Found: C, 60.37; H, 5.64; N, 10.86.

Method b

The title compound (3 g) was reduced with sodium borohydride and palladium–charcoal as described for the reduction of I*a* (method *b*). The resulting reddish-brown solid (1.2 g) was crystallized from ethanol as a pale-brown solid, m.p. 195–197°. Except for very minor differences, the infrared spectrum of this compound was identical with that of II*b* hydrochloride prepared as described above.

Anal. Calcd. for $C_{17}H_{22}ClN_3O_3$: C, 60.71; H, 5.89; N, 11.18. Found: C, 61.20; H, 5.92; N, 11.32.

Reduction of 4-(5-Chloro-2-nitrobenzylidene)-3-methyl-1-phenyl-2-pyrazolin-5-one (Id)

Method a

The title compound (2 g) was reduced with zinc and acetic acid as described for the reduction of I*a* (method *d*) to give 6-chloro-3*a*,4,9,9*a*-tetrahydro-5-hydroxy-3-methyl-1-phenyl-1*H*-pyrazolo[3,4-*b*]quinoline (II*d*) hydrochloride (1.22 g) as a pale-yellow solid, m.p. 224–225°. The infrared spectrum showed broad absorption from 2 300 to 3 280 with a broad maximum centered at 2 900 (s) (OH) cm^{-1}.

Anal. Calcd. for $C_{17}H_{17}Cl_2N_3O$: C, 58.30; H, 4.89. Found: C, 58.78; H, 5.10.

Can. J. Chem. Downloaded from www.nrcresearchpress.com by 210.87.254.40 on 09/05/12
For personal use only.

Method b

The title compound (2 g) was reduced with cyclohexene and palladium–charcoal as described for the reduction of I*a* (method *c*). The resulting red oil (1.7 g) was dissolved in ether, and the ether solution was extracted with 5% aqueous sodium hydroxide. When the aqueous extract was acidified with acetic acid, the pyrazoloquinoline (II*d*) was isolated as a pale-yellow solid (0.48 g), m.p. 108–110° after crystallization from ethanol. This product was identical with II*d* obtained from its hydrochloride as described later.

Method c

The title compound (3 g) was reduced with sodium borohydride and palladium–charcoal as described for the reduction of I*a* (method *b*). The resulting orange-brown solid (1.92 g) was crystallized from dilute acetic acid as a light-brown solid, m.p. 140–142°. The infrared spectrum (Unicam SP 200 spectrophotometer) showed absorption peaks at 1 695 (s) (C=O) and at 1 605 (m) and 3 290 (m) (NH?) cm^{-1}.

Anal. Found: C, 63.51; H, 4.58; N, 13.10.

Reduction of 4-(o-Nitrobenzylidene)-1,3-diphenyl-2-pyrazolin-5-one (Ie)

The title compound (3 g) was reduced by means of cyclohexene and palladium–charcoal as described for the reduction of I*a* (method *c*). An ether solution of the resulting dark-red oil (2.90 g) was extracted with 5% aqueous sodium hydroxide; when this extract was acidified with hydrochloric acid, a pale-brown solid was obtained. Crystallization from ethanol gave 3*a*,4,9,9*a*-tetrahydro-9-hydroxy-1,3-diphenyl-1*H*-pyrazolo-[3,4-*b*]quinoline (II*e*) hydrochloride monohydrate (2.11 g) as an off-white solid, m.p. 182–183°. The infrared spectrum showed broad absorption from 2 200 to 3 200 with a broad maximum centered at 2 860 (s) (OH) cm^{-1}.

Anal. Calcd. for $C_{22}H_{22}ClN_3O_2$: C, 66.74; H, 5.60; N, 10.50. Found: C, 66.83; H, 5.64; N, 10.13.

Isolation of Free Bases (II) from their Hydrochlorides

The hydrochloride was dissolved in aqueous sodium hydroxide; when acetic acid was added, the base precipitated. These amphoteric products were crystallized from methanol or ethanol. When the aqueous solution was acidified with hydrochloric acid, the hydrochloride precipitated. The infrared spectra of the free bases all showed broad absorption in the 2 100 – 3 500 range with maxima (m,s) between 2 850 and 3 090 (OH) cm^{-1}.

The pyrazoloquinoline (II*b*) was a light-brown solid, m.p. 88–90°.

Anal. Calcd. for $C_{19}H_{21}N_3O_3$: N, 12.38. Found: N, 12.01.

The base (II*d*) was a yellow solid, m.p. 109–111°.

Anal. Calcd. for $C_{17}H_{16}ClN_3O$: C, 65.06; H, 5.14; Cl, 11.30; N, 13.39. Found: C, 65.14; H, 5.11; Cl, 11.53; N, 13.49.

The base (II*e*) was a brown solid, m.p. 109–110° after repeated crystallization from ethanol.

Anal. Calcd. for $C_{22}H_{19}N_3O$: C, 77.39; H, 5.61; N, 12.31. Found: C, 76.63; H, 5.36; N, 11.80.

Reductions with Hydrazine Hydrate and Palladium–Charcoal

Reduction of 3-Methyl-4-(o-nitrobenzylidene)-1-phenyl-2-pyrazolin-5-one (Ia)

The title compound (1 g) was heated under reflux for 30 min in ethanol (40 ml) containing hydrazine hydrate (1.5 ml) and palladium–charcoal (0.1 g). The catalyst was removed, and the filtrate was diluted with water and left to stand overnight. Bis(2-aminobenzylidene) hydrazine (V) (0.41 g) separated as bright-yellow crystals, m.p. 251–252° when crystallized from ethanol (lit. (8) m.p. 248°).

Anal. Calcd. for $C_{14}H_{14}N_4$: C, 70.56; H, 5.92; N, 23.51; mol. wt. 238.3. Found: C, 70.52; H, 5.94; N, 23.39; mol. wt. (vapor pressure) 231.

Reduction of 3-Methyl-4-(o-nitrobenzylidene)-2-pyrazolin-5-one (If)

Reduction of the title compound (1 g) with hydrazine hydrate and palladium–charcoal as described above also gave bis(2-aminobenzylidene) hydrazine (0.48 g), m.p. 251–252°.

Reduction of o-Nitrobenzaldehyde

Reduction of the title compound (1 g) with hydrazine hydrate and palladium–charcoal by the method described above also gave bis(2-aminobenzylidene) hydrazine (0.71 g), m.p. 251–252°.

ACKNOWLEDGMENTS

One of us (J. B. E.) was the recipient of a National Research Council of Canada bursary, which is gratefully acknowledged. Miss S. J. Storey's assistance in this project is appreciated.

REFERENCES

1. R. T. COUTTS, H. W. PEEL, and E. M. SMITH. Can. J. Chem. **43**, 3221 (1965), and references therein.
2. R. T. COUTTS and K. W. HINDMARSH. Can. J. Pharm. Sci. **1**, 11 (1966).
3. R. T. COUTTS, D. L. BARTON, and E. M. SMITH. Can. J. Chem. **44**, 1733 (1966).
4. K. S. NARANG, J. N. RAY, and A. SINGH. J. Indian Chem. Soc. **11**, 427 (1934).
5. R. T. COUTTS, M. HOOPER, and D. G. WIBBERLEY. J. Chem. Soc. 5058 (1961).
6. R. T. COUTTS and D. G. WIBBERLEY. J. Chem. Soc. 2518 (1962).
7. A. E. PORAI-KOSHITS, B. A. PORAI-KOSHITS, and N. G. LIPINA. Zh. Obshch. Khim. **26**, 872 (1956); Chem. Abstr. **50**, 14720*f* (1956).
8. P. COHN and A. BLAU. Monatsh. **25**, 365 (1904).

Can. J. Chem. Downloaded from www.nrcresearchpress.com by 210.87.254.40 on 09/05/12
For personal use only.

Can. J. Chem. Downloaded from www.nrcresearchpress.com by 210.87.254.6 on 09/05/12
For personal use only.

GAS–LIQUID CHROMATOGRAPHY OF TERPENES

XV. THE VOLATILE OIL OF MENTHA ARVENSIS VAR. GLABRATA RAY[1]

E. VON RUDLOFF AND F. W. HEFENDEHL[2]

Prairie Regional Laboratory, National Research Council of Canada, Saskatoon, Saskatchewan

Received April 28, 1966

ABSTRACT

The volatile oil of the North American wild mint (*Mentha arvensis* L. var. *glabrata*) was found to consist mainly of *d*-pulegone (80–90%) and smaller amounts of α-pinene, β-pinene, sabinene, limonene, 1,8-cineole, 1-octen-3-ol, menthone, isomenthone, piperitone, *cis*- and *trans*-pulegone oxide, and piperitenone. Trace amounts of γ-terpinene, menthofuran, β-caryophyllene, and ε-, δ-, and γ-cadinene were also isolated, and camphene, *p*-cymene, terpinolene, sabinene hydrate, isopulegone or its stereoisomer, β-elemene, and α-terpineol were tentatively identified. A labile autoxidation product of pulegone was also detected.

A study of the seasonal variations in the oil composition showed that significant changes in the quantitative composition occurred only in very young plants. The maximum yield of oil was obtained at the start of flowering. Practically no variation in the composition of the oil was recorded for plants from different localities.

INTRODUCTION

For a biosynthetic study of some of the terpenes found in mint plants, a knowledge of the chemical composition of the oil of local wild mint, *Mentha arvensis* L. var. *glabrata* Ray (syn. *M. arvensis* var. *villosa* (1) and *M. canadensis* L. (2)), was required. This plant differs morphologically from the European *M. arvensis* varieties (1). Gildemeister (2, 3) lists a number of older investigations which indicate that pulegone is a major constituent and that the presence of menthol and isomenthol was suspected. Gage (4) and Kremers (5) report that the main constituent of the oil of *M. canadensis* L. is *d*-pulegone, and *l*-limonene was identified (5). However, Braun (6) could not confirm these findings. In view of these uncertainties and the lack of more modern data, a detailed analysis by means of gas–liquid chromatography (g.l.c.) was undertaken.

The present study was carried out in two parts. Since it is known that the composition of the oil of *Mentha piperita* L. changes during flowering (7), a study of any such variation in *M. arvensis* var. *glabrata* was made first. When the optimum yield and best harvest time for a representative composition of the oil had been determined, a larger amount of the oil was isolated and analyzed in detail. The composition of the oil from local plants was also compared with that of plants from the Cypress Hills and Peace River districts in Alberta to establish whether variation in the composition of the oil exists in plants from different locations.

The g.l.c. techniques used were essentially those described earlier (8–10). However, a number of new liquid phases and experimental parameters were studied in more detail to improve the resolution and to obtain data which could be compared directly with those found in the literature. Thus, Levi *et al.* (11–13) and Hefendehl (14) have reported good resolution of the mint terpenes on sucrose diacetate hexaisobutyrate (SAIB) columns. Previously a sample of this liquid phase had given a poorer separation, especially of some oxygenated monoterpenes (sabinene hydrate, menthofuran, and menthones), in this laboratory. However, when a sample of SAIB from another source was tried, results similar to those reported by Levi *et al.* and Hefendehl were obtained.

[1]*Issued as N.R.C. No. 9078.*

[2]*NATO Fellow, 1965–1966. Present address: Pharmacognostic Institute, University of Freiburg, i.B., Germany.*

Can. J. Chem. Downloaded from www.nrcresearchpress.com by 210.87.254.6 on 09/05/12
For personal use only.

EXPERIMENTAL

The g.l.c. analyses were carried out with a F & M model 500 (linear temperature programming; F & M Scientific Instrument Inc.) instrument and with one of conventional design for isothermal operation (15). Preparative g.l.c. was carried out with an Aerograph Autoprep A-700 instrument (Wilkens Instrument and Research Inc.). The carrier gas was helium, and thermal conductivity detectors were employed. For very small samples a model 600-D Aerograph instrument equipped with a flame-ionization detector was used. Retention times were measured from the time of injection to the initial emergence of the peaks (16, 17). The percentage composition of the oil was calculated by summation of the areas under the peaks (triangulation method); the errors were similar to those reported by Janak (18). Infrared spectra were recorded as films between sodium chloride plates on a Perkin–Elmer model 21 (double-beam) spectrophotometer. Ultraviolet spectra were obtained in isooctane on a Bausch and Lomb model 505 spectrophotometer. Nuclear magnetic resonance spectra were determined with a Varian HA-100 instrument, tetramethylsilane being used as the internal standard.

Plant Material

Wild mint plants were collected from the Beaver Creek area (approximately 10 miles south of Saskatoon) and transplanted to experimental plots. The plants were identified as *Mentha arvensis* L. var. *glabrata* by Dr. G. W. Argus, Curator, W.P. Fraser Herbarium, University of Saskatchewan, and an herbarium specimen has been retained by us.

The seasonal variation in the composition of the oil was studied during the main growing season (July to September) of 1964. All other data were obtained from subsequent growth of the same plants. A number of wild plants from the Cypress Hills area just west of the Alberta border and from the Peace River district, Alberta, were collected during August 1965.

Recovery of Oil

The freshly harvested plants were steam-distilled for 3 to 5 h in a glass apparatus. The volatile oil was extracted with ether, washed with a little bicarbonate solution and water, and dried over anhydrous sodium sulfate. When less than 200 g plant material was available, the circulatory distillation apparatus of Kaiser and Lang (19), as modified by Hefendehl (20), was used. The latter apparatus gave a better recovery of monoterpene hydrocarbons.

Gas–Liquid Chromatographic Analyses

Column packings were prepared by the tray method, with nonacid-washed solid supports, including Chromosorb W, Gas Chrom P, and Anakrom ABS (60–80 mesh). Columns were packed by hand with gentle tapping or by applying a vibrator and vacuum. Both methods gave g.l.c. columns with the same resolving power (for the same packing), provided that only moderate vibration was used. Copper tubing was preferred over stainless-steel tubing, since the latter was found to contain an internal coating which was detrimental to the resolution of terpenes (on polar column packings) and which could not be removed easily. Comparison with a glass column of similar dimensions showed the copper column to perform equally well when the common terpenes were analyzed.

Aliquots (1 to 5 μl) of each oil sample were injected (injector at 125–140°) onto a 180 × 0.4 cm inside diameter column containing 15% polyethylene glycol (Carbowax 20M, PEG) on Chromosorb W. Linear temperature programming from 55 to 200° at 4°/min gave a satisfactory resolution of the major and most of the minor components. The percentage compositions of the oil at different stages of plant growth (as calculated from these chromatograms) are shown in Table I. The oils from the plants from both the Cypress Hills and Peace River districts had a composition similar to that of the local plants from August 5 to 13. More detailed analytical data were obtained by use of 300 × 0.3 cm PEG, SAIB (obtained from Wilkens Instrument and Research Inc.), SPEG (10% succinate polyethylene glycol polyester), and QF-1 (15% fluorinated silicone polymer on Anakrom ABS) columns, as well as a 180 × 0.4 cm EGPN (15% ethylene glycol bis-propionitrile on Chromosorb W) column. A typical chromatogram on the PEG column is shown in Fig. 1. Apiezon N, adipate, or succinate polyesters (NGA, APEG, SEG, BDS) and quadrol–SAIB mixtures did not give improved separation.

Prefractionation

The oil (10 g) was chromatographed on silicic acid (100 g, polyethylene glycol modified (9, 21)). Elution with petrol (b.p. 40–60°) gave a hydrocarbon fraction which still contained some of the less-polar oxygenated terpenes. Rechromatography gave an almost pure hydrocarbon fraction (0.8 g). Elution with methanol gave the oxygenated terpenes (9.2 g, by difference). Gas–liquid chromatographic analysis of the latter fraction showed that over three-quarters of peak 35 (see Fig. 1 and Table II) was lost in this procedure. New peaks, corresponding to the products of decomposition, could not be found. Some minor peaks also appeared to decompose.

Individual Components

Aliquots (10 to 50 μl) of the prefractionated terpenes were injected repeatedly onto a 180 or 300 × 0.4 cm PEG column. To facilitate recovery the detector current was reduced from 200 to 100 mA and the helium

flow from 110 to about 50 ml/min. Each peak was collected in a 15 × 0.2 cm inside diameter glass tube at the instrument exit, dry ice being applied at the middle of the tube. The infrared and ultraviolet spectra and physical constants were determined (see Table II), and these were compared with those of known terpenes to identify the individual components of the oil. Each fraction was analyzed on g.l.c. columns to determine the purity and relative retention times. Peaks were designated *a* and *b* if a contaminant was present (see Table II).

β-Pinene and sabinene could not be isolated separately, and their identity was confirmed by permanganate–periodate oxidation (22–24) to nopinone and sabina ketone. The terpene mixture (ca. 10 mg) was shaken vigorously with excess aqueous oxidant (100 mmoles/l, 5 ml) for 1 h. The product was extracted directly with ether (2 ml) and the ethereal solution was dried over anhydrous sodium sulfate. The ether was evaporated in a small vial (at 60–70°) and an aliquot of the residue (ca. 8 mg) was injected onto the PEG column. Two peaks with the same retention times as nopinone and sabina ketone were recorded.

Several sesquiterpene hydrocarbons were present in the oil (Fig. 1, solid black peaks in the peak 20 to peak 30 range). Of these, β-caryophyllene (peak 22), ε-cadinene (peak 26*a*), and γ- and δ-cadinene (peak 29, mixture (8, 10)) were identified by their spectral and retention characteristics. Peak 21*b* had the same retention time as β-elemene; peak 24 could not be correlated with a known sesquiterpene.

Analysis on the SAIB column showed that the menthone fraction (peak 15) contained a small amount of a contaminant with the same retention time as menthofuran. This was collected and had an ultraviolet spectrum similar to that of menthofuran. When the pulegone fraction (peak 23) was analyzed on the QF-1 column, a trace peak with the same retention time as α-terpineol was recorded.

Peaks 14, 18, 20, 30, 31, 35, 39, 40, and 41 appeared to decompose extensively during prefractionation. Attempts to isolate some of these components by g.l.c. directly from the oil met with similar difficulties, indicating that extensive decomposition of these components also takes place during g.l.c. However, enough of fractions 31 and 35 could be collected to record their spectra. The ultraviolet spectra were devoid of characteristic absorption, except for that of carbonyl groups. The infrared spectra showed the isolated fractions to consist mainly of ketones (1 715, 1 675, and 1 707 cm^{-1}, respectively). Weak to medium bands at 3 480 cm^{-1} indicated that contaminants containing hydroxyl groups were present. Absorption bands of variable (weak to medium) intensity near 3 040, 1 245, and 925 cm^{-1} could arise from epoxide groups, but such assignments are only tentative. The broad singlet near 1 375 cm^{-1} indicated that isopropyl or *gem*-dimethyl groups were absent. This suggested that these two components could be the isomeric pulegone oxides (25). The latter were synthesized by oxidation of *d,l*-pulegone with alkaline hydrogen peroxide solution (26) and separated by preparative g.l.c. The identity of the *cis*- and *trans*-isomers was established by their nuclear magnetic resonance spectra (25). If the presence of decomposition products is taken into account, there was good agreement between the spectra of components 31 and 35 and those of the synthetic oxides. Co-injection of the synthetic oxides confirmed the retention data.

In addition to *trans*-pulegone oxide, peak 35 was found to contain an autoxidation product of pulegone. These two components were partially separated on a 10% SPEG column. When the mint oil was allowed to stand in the light (daylight and fluorescent) for 24 h, peak 35*a* increased, with a concomitant decrease in the pulegone peak. When pulegone itself was allowed to autoxidize in the same manner, a second peak with the same retention time as peak 35*a* was recorded. Since polymeric autoxidation products (e.g. dimers) would not be eluted from the g.l.c. columns under the conditions used, the product must be a peroxide of pulegone. Whether this peroxide is formed in the plant or during isolation could not be established. However, the data in Table I suggest that only very small amounts can be present in the freshly distilled oil.

RESULTS AND DISCUSSION

The seasonal variation in the chemical composition of the volatile oil from *M. arvensis* var. *glabrata* is shown in Table I. From the data obtained in the main growing season of 1964, it follows that no significant variation in the chemical composition of the oil occurs just before, during, or after flowering. This is similar to our findings for the oil from *Tanacetum vulgare* L. (10), but contrasts with those reported for the oil from *M. piperita* L. (7, and the literature cited in ref. 20). Battaile and Loomis (27) have reported that the *de novo* synthesis of terpenes occurs only in very young tissues of mint plants and that interconversion (e.g. menthone → menthol → menthyl acetate) takes place only in older ones. Hence, the oil from very young (5–10 cm high) wild mint plants was also investigated. The yield of oil was much lower than that of mature plants, and a markedly different percentage composition was recorded (cf. last column, Table I). Aside from a considerably higher content of monoterpene hydrocarbons (12.5% vs. 1.5 to 2%), the oil from the young plants contained much more menthone and isomenthone. This is surprising, because the

Can. J. Chem. Downloaded from www.nrcresearchpress.com by 210.87.254.6 on 09/05/12
For personal use only.

Can. J. Chem. Downloaded from www.nrcresearchpress.com by 210.87.254.6 on 09/05/12
For personal use only.

TABLE I

Seasonal variations in the percentage composition of the volatile oil of *Mentha arvensis* var. *glabrata* Ray

	Date of harvest								
	1964								
	July 17	July 24	August 5*	August 10†	August 13	August 20	August 27	September 4	July 6, 1965
Yield of oil (g)	0.78	0.89	1.24	1.18	1.13	0.84	0.62	0.53	0.29
n_D^{23}	1.481	1.483	1.483	1.482	1.482	1.483	1.481	1.481	—
$[\alpha]_D^{23}$	+17.9°	+19.0°	+18.2°	+17.2°	+18.3°	+18.1°	+19.2°	+18.5°	—
Component (%)									
α-Pinene	Trace	0.1	0.4	0.2	0.3	0.2	0.1	0.1	1.5
β-Pinene + sabinene	Trace	0.4	0.8	0.4	0.5	0.3	0.2	0.2	2.7
Myrcene	0.1	0.2	0.4	0.3	0.3	0.2	0.1	0.2	1.0
Limonene	0.7	1.9	1.6	1.0	1.4	0.5	0.6	1.0	7.3
Cineole	0.2	0.2	0.1	Trace	0.1	Trace	0.1	Trace	
1-Octen-3-ol	0.1	0.2	0.3	0.4	0.4	0.1	0.1	0.1	
(Sabinene hydrate)	0.8	0.6	1.0	1.0	0.9	0.5	0.4	0.4	
Menthone	1.1	1.4	0.9	0.9	1.2	0.6	1.6	1.2	3.7
Isomenthone	3.0	3.1	1.9	2.0	2.4	1.5	4.2	2.7	7.4
Unidentified (peak 18)	0.9	0.4	0.6	0.5	0.6	0.4	0.3	0.3	0.8
Unidentified (peak 19)	0.6	0.4	0.3	0.3	0.3	0.2	0.3	0.2	0.7
(Isopulegone) (peak 20)	3.2	1.5	1.6	1.6	1.8	1.2	1.1	0.9	2.0
Pulegone	86	88	88	89	88	92	90	91	79
ϵ-Cadine + piperitone	0.9	0.5	0.5	0.5	0.6	0.5	0.4	0.3	1.0
γ-Cadinene + δ-cadinene	0.6	0.3	0.3	0.3	0.3	0.4	0.2	0.2	0.7
cis-Pulegone oxide	0.5	0.2	0.2	0.2	0.2	0.3	0.2	0.2	0.6
trans-Pulegone oxide‡	0.6	0.2	0.2	0.2	0.3	0.3	0.3	0.2	0.2
Piperitenone	0.8	0.5	0.4	0.4	0.5	0.4	0.4	0.4	

*Plants started to flower.
†Main flowering season.
‡Plus a peroxide of pulegone.

biogenetic sequence advanced by Reitsema (28) and extended by Bataille and Loomis (27) predicts a higher content of the unsaturated ketones (piperitenone, piperitone, and pulegone) in young plants. This is of considerable interest for biogenetic studies, and is being investigated further by us.

It is noteworthy that the oil from mature wild mint plants from the Cypress Hills area (southeastern Alberta, August 1965) and the Peace River district (northwestern Alberta, August 1965) had virtually the same composition as that of the mature plants found locally. This indicates that the composition of the oil from *M. arvensis* var. *glabrata* is relatively stable over a wide geographical area. The yield of oil from the local plants was a maximum at the beginning of flowering (cf. Table I, August 5, 1964), and dropped slowly during and after flowering. Since the chemical composition of the oil did not change to any significant degree during the flowering period, a large amount of plant material was harvested in August 1965, and the oil obtained was analyzed in detail. A typical gas–liquid chromatogram on the PEG column (as shown in Fig. 1 and Table II) lists the percentage composition and the components identified. The composition is very similar to that recorded the previous year, except that the content of component 35 is somewhat higher (1.5 to 2.0% vs. 0.2 to 0.6%). Apparently the content of the pulegone autoxidation product (peak 35*a*; cf. Experimental) was higher in the large batch.

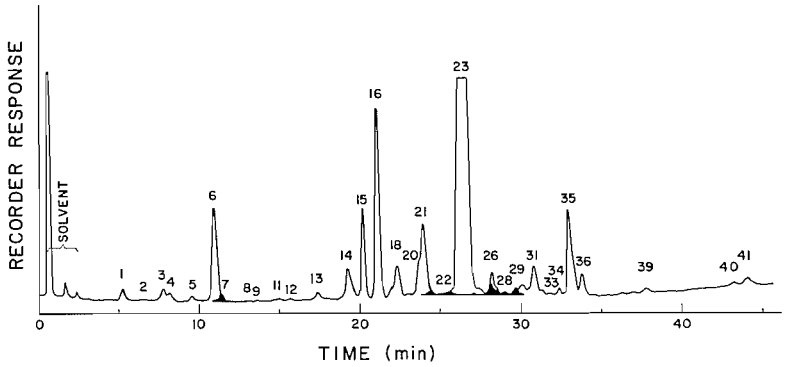


FIG. 1. Gas–liquid chromatogram of the volatile oil of *Menthaa rvensis* L. var. *glabrata* Ray (300 × 0.4 cm polyethylene glycol column, temperature programmed from 55° to 210° at 4°/min). The peaks in solid black were separated by silicic acid column chromatography; the peak identifications are shown in Table II.

Practically all of the components in the monoterpene hydrocarbon range (peaks 1–10) were identified, and α-pinene (peak 1), myrcene (peak 5), limonene (peak 6), and 1,8-cineole (peak 7) were isolated in a fairly pure state. The identity of β-pinene and sabinene (peaks 3 and 4) was confirmed by permanganate–periodate oxidation (22–24) to nopinone and sabina ketone, respectively. The infrared spectrum of peak 8 corresponded closely to that of γ-terpinene, but the optical rotation (+10°) requires the presence of an optically active contaminant. Components 9 and 10 were not obtained in sufficient amounts to record satisfactory spectra, but the retention data indicated these to be *p*-cymene and terpinolene, respectively. Ocimene isomers or phellandrenes were not detected.

The sesquiterpene hydrocarbon fraction makes up less than 0.5% of the oil, and isolation of the individual components was difficult. Peak 21*b* was only tentatively identified as β-elemene (by relative retention times), but β-caryophyllene (peak 22) and ϵ-cadinene (peak 26*a*) were sufficiently pure to permit identification by comparison of their infrared spectra. Component 29 showed an infrared spectrum typical of the mixture of δ- and

Can. J. Chem. Downloaded from www.nrcresearchpress.com by 210.87.254.6 on 09/05/12
For personal use only.

TABLE II

Percentage composition of the volatile oil of *Mentha arvensis* var. *glabrata* Ray

Peak No.	Compound*	%	$[\alpha]_D^{25}$	Relative retention times† PEG‡	EGPN§	QF-1‖
1	α-Pinene	0.25	−2.0°	0.29	0.28	0.51
2	(Camphene)	Trace		0.42	0.44	0.64
3	β-Pinene	0.25	+8.7°	0.55	0.545	0.85
4	Sabinene	0.1		0.57	0.70	0.85
5	Myrcene	0.1	+2.0°	0.82	0.88	0.85
6	Limonene	1.8	−80.8°	1.00	1.00	1.00
7	1,8-Cineole	0.15	−1°	1.07	1.65	1.45
8	γ-Terpinene	Trace	+10°	1.40	1.42	1.24
9	(p-Cymene)	Trace	Negative	1.63	2.35	1.27
10	(Terpinolene)	Trace		1.79	1.73	1.25
				PEG¶	SAIB**	QF-1††
11	Unidentified	Trace	Negative	0.43	0.12	0.12
12	Alcohol + C=O	Trace	−1.9°	0.46		
13a	Ketone	Trace				
13b	1-Octen-3-ol	0.2		0.60	0.13	0.13
14	(Sabinene hydrate)	0.55		0.67‡‡	0.65‡‡	0.54‡‡
15a	Menthone	1.5	+2.3°	0.77	0.93	0.93
15b	Menthofuran	0.1	+66.8°	0.87	0.87	—
16	Isomenthone	3.9			0.99	1.00
17	Unidentified	0.1		(0.95)		
18	Unidentified	0.55	−6°	0.98	1.09	1.10
19	Unidentified	Trace				
20	Unidentified	(0.5)‡‡		1.25‡‡	1.15‡‡	
21a	(Isopulegone)	1.35	+33.9°	1.30	1.18	1.10
21b	(β-Elemene)	Trace				
22	β-Caryophyllene	0.1	−18.7°	1.65		
23a	Pulegone	81.5	+3.8°	1.71	1.39	1.32
23b	(α-Terpineol)	Trace		2.02		0.54
24	Unidentified	Trace	+15.3°	2.05		
25	Unidentified	0.1	−49.0°	2.10		
26a	ε-Cadinene	0.2	+5.6°	2.34		
26b	Piperitone	0.2	−2.2°	2.34	1.88	1.93
27	Unidentified	0.1				
28	Unidentified	Trace		2.51		
29	γ-Cadinene + δ-cadinene	0.15		2.66		
30	Unidentified	(0.2)‡‡				
31	*cis*-Pulegone oxide	0.6	−18.3°	3.48	2.43	
32	Unidentified	Trace				
33	Isopiperitone	Trace				
34	Unidentified C=O	0.2		4.47		
35a	A Pulegone peroxide	(1.5–2.0)‡‡	Negative	4.93	2.76	2.60
35b	*trans*-Pulegone oxide	0.5				
36	Piperitenone	0.3	−5.4°	5.48	3.28	3.18
37	Unidentified	Trace				
38	Unidentified	Trace				
39	Unidentified	0.15				
40	Unidentified	0.15				
41	Unidentified	0.35				

*Names in parentheses refer to compounds which were only tentatively identified; *a* and *b* peaks were resolved on columns other than PEG.
†Monoterpene hydrocarbons relative to limonene; others relative to camphor.
‡300 × 0.3 cm polyethylene glycol column at 65 °C.
§180 × 0.4 cm ethylene glycol bis-propionitrile column at 65 °C.
‖300 × 0.3 cm QF-1 fluorinated silicone column at 65 °C.
¶PEG column at 120°.
**300 × 0.3 cm sucrose acetate isobutyrate column at 170 °C.
††QF-1 column at 130 °C.
‡‡Decomposing; approximate values only.

Can. J. Chem. Downloaded from www.nrcresearchpress.com by 210.87.254.6 on 09/05/12
For personal use only.

Can. J. Chem. Downloaded from www.nrcresearchpress.com by 210.87.254.6 on 09/05/12
For personal use only.

γ-cadinene encountered previously (8, 10). Katsuhara *et al.* (29) found in the sesquiterpene fraction of various mint oils β-elemene, β-caryophyllene, and δ- and γ-cadinene (as well as six unidentified trace components), which is in good agreement with the present findings.

All of the major oxygenated terpenes, except for the double peak 20–21, were identified, as were also some of the minor constituents. The trace peak 12 could contain octan-3-ol (relative retention times), but its infrared spectrum showed the presence of major amounts of a ketone (1 710 cm^{-1}). Peak 13*a* was not identified, but peak 13*b* had an infrared spectrum closely resembling that of 1-octen-3-ol. Levi *et al.* (13) reported the presence of 3-octanol and its acetate in mint oils, and 1-octen-3-ol was identified in *M. pulegium* by Naves (30). The menthone fraction (peak 15) was found to contain a small amount of menthofuran (peak 15*b*) by rechromatography on the SAIB column. Isomenthone (peak 16) and pulegone (peak 23), the main constituent of the oil, were readily identified. Rechromatography of the latter indicated that a trace amount of α-terpineol could be present in the oil. Piperitone (peak 26*b*) and piperitenone (peak 36) were also obtained in a fairly pure state. Considerable difficulty was encountered with components 14, 18, 20–21, 31, 35, and 40, since these appeared to decompose or rearrange during isolation. Component 14 appears to be sabinene hydrate, which dehydrates easily to form sabinene. It cannot be ruled out that the oil in the plants contains only sabinene hydrate and that sabinene is an artifact. However, sabinene is frequently found in essential oils and may thus also be a true constituent of the wild mint. Levi *et al.* (13) have shown that sabinyl acetate may be a component of mint oils, but this thujane derivative could not be detected in the oil of our local wild mint. Sabinyl acetate was isolated from *Juniperus sabina* L. by our technique (31); hence, decomposition to sabinene may be ruled out. It is noteworthy that this oil does not contain any acetates in detectable amounts. Peaks 18 and 40, although present in 0.3 to 0.5% amounts, could not be isolated. Difficulties were also encountered with the double peak 20–21. Only the main portion of peak 21 was isolated with any degree of purity. Its infrared spectrum showed strong absorption bands at 1 707, 878, and 1 370 (broad) cm^{-1} and a weak band at 3 080 cm^{-1}. These absorption bands are similar to those expected for isopulegone, but no data for comparison could be found. The presence of isopulegone or its stereoisomer may be expected on biogenetic grounds.

Components 31 and 35 appear to be most interesting from a chemical point of view. Their infrared spectra suggest that these could be epoxides, but the isolated products also showed absorption in the hydroxyl region. It is possible that the epoxide ring is opened during passage through the detector (thermal conductivity type, at 220–250°) and that only part of the isolated fractions is the original oxides. The spectra and retention data suggested that these two components could be *cis*- and *trans*-pulegone oxide, respectively. This was confirmed by preparing the isomeric pulegone oxides (25, 26) and by comparing their properties with those of components 31 and 35. However, evidence was obtained (cf. Experimental) which shows that the *trans*-pulegone oxide (peak 35*b*) was accompanied by an autoxidation product (a pulegone peroxide, peak 35*a*) of pulegone. Since the latter is labile, it was not isolated. Peak 35 was partially resolved into these two components on the SPEG column. This appears to be the first time that these pulegone oxides were found in mint oils.

Shimizu (32) has isolated piperitone oxides from mint oils. These were prepared (26) and their retention data compared with the components of *M. arvensis* var. *glabrata*. The retention times were the same as those of peaks 26 and 27. However, since component 26 was found to consist mainly of ε-cadinene and piperitone, and peak 27 mainly of an unidentified sesquiterpene hydrocarbon, only traces, if any, of the piperitone oxides can be present.

Can. J. Chem. Downloaded from www.nrcresearchpress.com by 210.87.254.6 on 09/05/12
For personal use only.

CONCLUSIONS

The chemical composition of the oil of *M. arvensis* var. *glabrata* resembles closely that of the oil of *M. pulegium* and *Hedeoma pulegioides* (American pennyroyal) (13), pulegone being the major constituent and smaller amounts of α-pinene, β-pinene, limonene, 1,8-cineole, menthofuran, menthone, isomenthone, piperitone, and piperitenone being present. However, the latter two oils are reported to contain also 3-octylacetate, linalyl acetate, and menthol (13), which were not found in the local mint oil. Another distinguishing feature appears to be the presence of the two pulegone oxides, the tentatively identified isopulegone, and possibly sabinene and its hydrate (in the oil of the local wild mint). The oils from other *M. arvensis* varieties differ markedly (13, 2, 7) from the local variety.

From the biosynthetic point of view it is noteworthy that ketones are the predominant components and that only traces of alcohols and no acetates were detected. On the basis of the scheme proposed by Reitsema (28) and extended by Bataille and Loomis (27), the hydrogenation step from pulegone to the menthones appears to be somewhat arrested and the reduction of the latter to the menthols may be blocked. This indicates a marked difference in the secondary changes as compared with *M. piperita* L., and may account for the remarkably consistent composition of the oil before, during, and after flowering of the plants.

ACKNOWLEDGMENTS

The authors thank Dr. G. Argus for confirming the identity of the plants, and Mr. M. Granat for technical assistance. The spectra were recorded by Mr. M. Mazurek and Mr. W. C. Haid.

REFERENCES

1. G. W. ARGUS. Personal communication.
2. E. GILDEMEISTER. *In* Die aetherischen Oele. Vol. VII. Akademie Verlag, Berlin. 1961. p. 390.
3. E. GILDEMEISTER. *In* Die aetherischen Oele. Vol. VII. Akademie Verlag, Berlin. 1961. p. 383.
4. F. M. GAGE. Pharmacol. Rev. **16**, 412 (1898).
5. R. E. KREMERS. J. Am. Pharm. Assoc. **14**, 32 (1925).
6. H. A. BRAUN. J. Am. Pharm. Assoc. **15**, 337 (1926).
7. E. GUENTHER. *In* The essential oils. Vol. III. D. Van Nostrand Company, Inc., New York. 1949. pp. 595–596.
8. E. VON RUDLOFF. Phytochemistry, **5**, 331 (1966).
9. F. M. COUCHMAN and E. VON RUDLOFF. Can. J. Chem. **43**, 1017 (1965).
10. E. VON RUDLOFF and E. W. UNDERHILL. Phytochemistry, 4, 11 (1965).
11. D. M. SMITH, J. C. BARTLET, and L. LEVI. Anal. Chem. **32**, 568 (1960).
12. I. C. NIGAM and L. LEVI. J. Pharm. Sci. **53**, 1008 (1964).
13. K. L. HANDA, D. M. SMITH, I. C. NIGAM, and L. LEVI. J. Pharm. Sci. **53**, 1407 (1964).
14. F. W. HEFENDEHL. Pharmazie, **18**, 777 (1963).
15. B. M. CRAIG and N. L. MURTY. J. Am. Oil Chemists' Soc. **36**, 549 (1959).
16. E. VON RUDLOFF. Can. J. Chem. **38**, 631 (1960).
17. E. VON RUDLOFF. Can. J. Chem. **39**, 1190 (1961).
18. J. JANAK. J. Chromatog. **3**, 308 (1960).
19. H. KAISER and W. LANG. Deut. Apotheker-Ztg. **91**, 163 (1951).
20. F. W. HEFENDEHL. Planta Med. **10**, 241 (1962).
21. E. KUGLER and E. SZ. KOVATS. Helv. Chim. Acta, **46**, 1480 (1963).
22. E. VON RUDLOFF. Can. J. Chem. **43**, 2660 (1965).
23. R. U. LEMIEUX and E. VON RUDLOFF. Can. J. Chem. **33**, 1701 (1955).
24. E. VON RUDLOFF. 47th Annual Meeting, Chemical Institute of Canada, Kingston, Ontario, June 1-3, 1964.
25. W. REUSCH and C. K. JOHNSON. J. Org. Chem. **28**, 2557 (1963).
26. W. TREIBS. Ber. **66**, 1492 (1933).
27. J. BATAILLE and W. D. LOOMIS. Biochim. Biophys. Acta, **51**, 545 (1961).
28. R. H. REITSEMA. J. Pharm. Sci. **47**, 267 (1958); **51**, 545 (1961).
29. J. KATSUHARA, K. HASHIMOTO, and M. KOBAYASHI. Kogyo Kagaku Zasshi, **67**, 821 (1964); Chem. Abstr. **61**, 9349*h* (1964).
30. Y. R. NAVES. Helv. Chim. Acta, **26**, 1034 (1943); **26**, 1992 (1943).
31. E. VON RUDLOFF. Can. J. Chem. **41**, 2876 (1963).
32. S. SHIMIZU. Perfumery Essent. Oil Record, **52**, 708 (1961); Proc. Symp. Perfumery Terpene Essential Oil Chem. 6th, Japan, August 1962.

Can. J. Chem. Downloaded from www.nrcresearchpress.com by 210.87.254.42 on 09/05/12
For personal use only.

STRUCTURAL BIOCHEMISTRY

II. SYNTHESIS OF 3β-HYDROXY-17β-(L-PROLYL-L-PROLYL)AMINO-5α-ANDROSTANE[1-3]

GEORGE R. PETTIT,[4] ARUN K. DAS GUPTA,[5] AND ROBERT L. SMITH

Department of Chemistry, University of Maine, Orono, Maine, and Department of Chemistry, Arizona State University, Tempe, Arizona

Received April 22, 1966

ABSTRACT

A practical synthetic route to 3β-hydroxy-17β-amino-5α-androstane (III) was developed and the configuration of the amine substituent established by proton magnetic resonance studies. Condensing amine III with carbobenzoxy-L-proline by means of Woodward's reagent K led to proline derivative IV*a*. Steroidal peptide V*b* was readily prepared by first removing the protecting group from amide IV*a* by palladium-catalyzed hydrogenolysis and then repeating the peptide-forming and hydrogenation steps. Protection of the 3β-hydroxy group proved to be unnecessary, and the presently reported approach to steroidal peptides proved to be reliable and useful.

Presently, the only fully characterized and naturally occurring amino acid linked steroids are the bile acid conjugates. These amides consist of a bile acid, for example, cholic acid, combined with either glycine or taurine (3). Evidence (4) has been accumulating, however, to indicate that steroids interact with human plasma proteins. Considering the binding of steroid proteins and the possibility that steroids linked to peptides might be involved in steroid transport, we began (in 1959) a study of synthetic approaches to steroidal peptides. The possibility that synthetic steroidal peptides might alter, or otherwise interfere with, established hormone production enhanced our interest. At first we also intended to employ certain steroids as platforms for the synthesis of peptides. The hydrocarbon segment would be expected to render peptide intermediates more soluble in nonpolar media and provide more easily purified (e.g. by column chromatography) and crystalline peptide derivatives. The latter objective was discarded in 1963 when Merrifield (5) reported the obviously superior solid-phase peptide technique employing a polymer platform. Thus, to provide steroidal peptides of possible use in advancing knowledge of steroid transport and alteration of hormone properties,[6] we proceeded initially with the synthetic approaches described in the sequel.

For practical purposes, the history of steroidal peptide syntheses begins with the Bondi and Müller (7) preparations (in 1906) of glycocholic and taurocholic acids from cholic acid azide. Later (8) an alternate synthetic route based on the triformyl derivative of cholic acid chloride was employed. More recently, efficient syntheses of bile conjugates by the mixed anhydride technique (9) has provided, for example, glycocholic acid (10) in approximately 80% yield.

[1]*A preceding paper titled "Steroidal Peptides" (1) may be considered as part I in this series. The new serial title "Structural Biochemistry" is intended for our nucleotide and peptide studies and to include overlapping aspects with our steroid program. The present manuscript may thus be considered as part XXXIV of the steroid investigations; for part XXXIII, see ref. 2.*

[2]*This investigation was aided in part by National Science Foundation research grant GB-249, and grants Nos. T-79C to T-79F from the American Cancer Society.*

[3]*Based on part of the Ph.D. dissertation submitted by R. L. Smith to the Graduate School, University of Maine, Orono, Maine, August 1965.*

[4]*Present address: Department of Chemistry, Arizona State University, Tempe, Arizona 85281.*

[5]*Present address: Research Division, East India Pharmaceutical Works, Calcutta-34, India.*

[6]*Recently the biological activity of nitrogen-containing steroids has been reviewed (6).*

Can. J. Chem. Downloaded from www.nrcresearchpress.com by 210.87.254.42 on 09/05/12
For personal use only.

In the last 5 years, several amino acid ester derivatives (e.g. 14–20 unit α-polyglycine mixtures (11*d*)) of hydroxy steroids have been described (11). Part of the present study, concerned with first syntheses of steroidal peptides derived from amino steroids, has been reported in a preliminary communication (1). Meanwhile, the preparation of, for example, the glycyl–glycyl dipeptide derivative of 3α-amino-20-oxo-5α-pregnane has been described (12).

The frequent occurrence of proline in natural peptide hormones (13) such as the hypotensive peptides bradykinin and kallidin (14), both of which contain a diprolyl unit, suggested selection of 3β-hydroxy-17β-(L-prolyl-L-prolyl)amino-5α-androstane (V*b*) as an initial synthetic objective. As noted, prolyl peptide V*b* was of biological interest, and useful synthetic techniques arising from construction of this small peptide could later be extended to yield larger steroidal polypeptides.

Dehydroepiandosterone (I*a*) served as starting material and was hydrogenated in ethanol solution containing 10% palladium on charcoal and perchloric acid to 3β-hydroxy-17-oxo-5α-androstane (II*a*). Hydrogenation of Δ^5-olefins is a routine operation in steroid chemistry, and a large number of such reactions have been conducted in our laboratory. Generally we have found (15) the product (cf. II*b*) of C-3 oxygen–carbon hydrogenolysis to accompany (ca. 5% yields) the principal product expected from 3-hydroxy- or 3-acetoxy-5-ene systems. Chromatographic separation of the dehydroepiandosterone hydrogenation product gave alcohol II*a* and 2–5% yields of ketone II*b*. Next, previously described methods for conversion of alcohol II*a* via oxime II*c* (98% yield) into amine III were also improved. The oxime → amine reduction step (90% yield) was conducted with sodium–ethanol.[7] The synthesis of amine III from 3β-acetoxy-17-oxo-androst-5-ene (I*b*) was also explored. No advantage was offered by the latter route, and amine III was routinely prepared from alcohol I*a*. Reduction of the 17-oxime proceeded in a highly stereoselective manner to give equatorial amine III.[8] Careful chromatographic purification of the reduction product failed to reveal the presence of the 17α-epimer. The appearance of a sharp singlet at 0.60 δ (C-18 angular methyl group) and a broad complex response at 2.53 δ (17α-proton) in the proton magnetic resonance spectrum of amine III verified the 17β-assignment.[9]

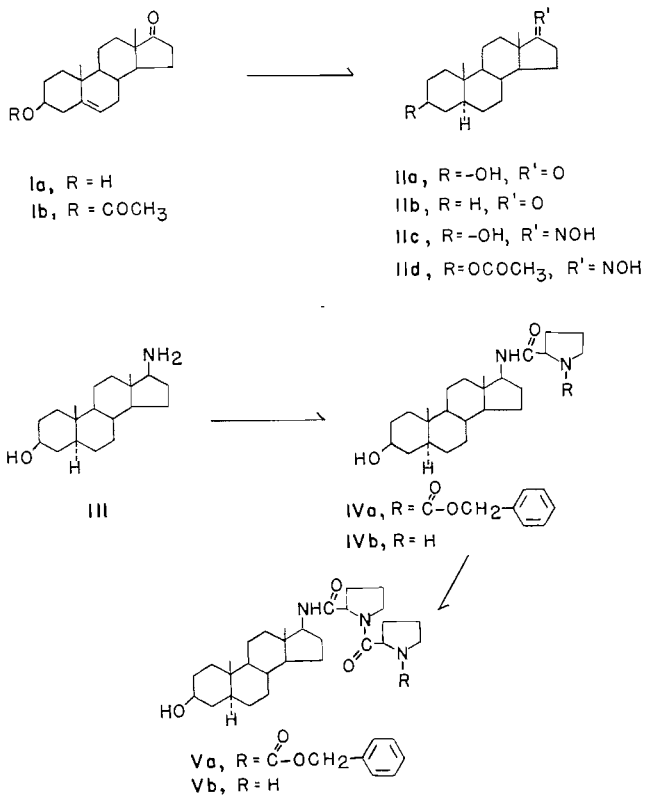
To obtain dipeptide V*b* of high optical purity, racemization during the remaining sequence had to be prevented. From a number of possible peptide-forming methods, the azide (20) and Woodward's reagent K (21) procedures were considered the most attractive. Both, particularly the azide technique, generally cause little or no detectable racemization (22). The apparent experimental simplicity with *N*-ethyl-5-phenylisoxazolium 3′-sulfonate (Woodward's reagent K) combined with the prospect that (as with the azide method) protection would probably not be necessary for the 3β-hydroxy group allowed selection of Woodward's reagent K as the condensing agent.[10] Stepwise formation of dipeptide V*b* was considered desirable to reduce racemization and for evaluating biological properties. Hence, the following route to dipeptide V*b* was employed.

[7]*In addition to ethanol (16a–16d), propanol (16e–16g), butanol (16f), pentanol (16h–16j), and isopentanol (16f) have been used as solvent for similar transformations.*

[8]*Beckmann rearrangement (17) of 20-oximino steroids or treatment of 20-oxo-pregnanes with hydrazoic acid – sulfuric acid mixtures (18) also yields 17β-acetamides in good yield (71–95% via Beckmann rearrangement and 80–82% via Schmidt transformation).*

[9]*A proton magnetic resonance study of authentic 3β-hydroxy-17α-aminoandrost-5-ene and the isomeric 17β-derivative provided the basis for this conclusion (19a). We are indebted to Prof. C. H. Robinson for providing the 17α-amino isomer and for informing us of his proton magnetic resonance study before publication (19b).*

[10]*Summaries of more recently devised peptide methods and reviews of now classical approaches are cited in ref. 23. Because proline is generally less sensitive to racemization than primary-type α-amino acids, the procedures selected here were expected to be of greater value in subsequent studies involving arginine steroidal peptides (24).*



Condensing amine III with the active ester formed by reacting Woodward's reagent K with *N*-carbobenzoxy-L-proline gave (70%) proline derivative IV*a*. The reaction was conducted at ice-bath temperature in acetonitrile solution containing triethylamine. Concomitant acylation of the alcohol group was not observed, and the crystalline amide was readily purified. Hydrogenation (with palladium black and with provision for removing carbon dioxide) of carbamate IV*a* was conducted in methanol solution. In this early series of experiments the palladium catalyst was prepared from palladium(II) chloride, but later palladium from Englehard Industries was found to be equally (and routinely) effective. Amine IV*b* was formed in excellent yield (96%). The crystalline amine (IV*b*) easily formed a hydrochloride derivative. Thin-layer or column chromatography of amines III or IV*b* with chloroform generally gave salts unless appropriate precautions (use of ammonia) were taken. Solvate and (or) hydrate formation was encountered with intermediates beginning with oxime II*c*. Analytical specimens generally required prolonged drying (48–72 h at 60–100° over phosphorus pentoxide) to attain constant weight.

Repetition of the peptide-forming sequence and subsequent hydrogenolysis of the protecting group provided, respectively, peptides IV*a* and V*b*. Peptides IV*a* to V*a* were readily purified by column chromatography, neutral alumina or silica gel being used as the solid phase. A pure specimen of dipeptide V*b* was easily prepared by recrystallization from methanol to yield crystals melting, with decomposition, at 213–217°. As with other androstane-containing peptides later prepared in our laboratories, dipeptide V*b* displayed a substantial negative rotation (−142° in methanol) at the sodium D-line.

In summary, the preceding synthetic route to peptide V*b* proved to be a practical one, and has been used to prepare a number of related steroidal peptides (19*a*, 24).

Can. J. Chem. Downloaded from www.nrcresearchpress.com by 210.87.254.42 on 09/05/12
For personal use only.

Can. J. Chem. Downloaded from www.nrcresearchpress.com by 210.87.254.42 on 09/05/12
For personal use only.

EXPERIMENTAL

Acetonitrile, dimethylformamide (from phosphorus pentoxide), and triethylamine (from potassium hydroxide) were redistilled and stored over Molecular Sieve type 4-A. The methanol used as the hydrogenation solvent was redistilled from potassium hydroxide. All chromatography solvents were also redistilled. Palladium black was either freshly prepared from palladium(II) chloride (Amend Chemical and Drug Co., New York) or used as purchased from Englehard Industries, Inc., Newark, New Jersey. Woodward's reagent K (*N*-ethyl-5-phenylisoxazolium 3′-sulfonate) was obtained from Pilot and later from Aldrich Chemical Co. The commercial product was dried (*in vacuo*) at 20° for 24 h, and employed without further purification. Carbobenzoxy-L-proline was used as received from Nutritional Biochemicals Corp. Solvent extracts of aqueous solutions were dried over magnesium sulfate.

Neutral alumina (E. Merck, A.G. Darmstadt) and silica gel (E. Merck, 0.05–0.20 mm) were used for column chromatography. Thin-layer chromatograms were prepared with silica gel G (E. Merck). Where R_f values are given, the thin-layer chromatography was performed as follows. Silica gel was uniformly spread on microscope slides and activated by heating the slides at 110° for 0.25 h. The plate was then stored over calcium chloride in a desiccator. Thin-layer plates were eluted in a closed cylindrical container (5 cm in diameter × 9 cm in height) containing a vertical paper strip (Whatman filter paper, 2 × 9 cm). All thin-layer plates were developed by either saturation with iodine vapor, or spraying them with concentrated sulfuric acid or phosphomolybdic acid (saturated solution in methanol). With the acid sprays, the plate was heated at 125° for 0.25 to 1 h. All analytical samples exhibited a single spot on a thin-layer chromatogram.

All melting points were recorded on a Kofler apparatus. Mixture melting points were determined in open Kimble glass capillary tubes in a silicone oil bath. Each new compound was colorless, and elemental microanalytical data was provided by Dr. A. Bernhardt, Max-Planck Institute, Mülheim, Germany. Optical rotation values were determined (at 20° in chloroform unless otherwise noted) in the laboratory of Dr. C. Janssen, Beerse, Belgium. R. A. Hill, Department of Chemistry, University of Maine, and P. A. Whitehouse, Arizona State University, recorded the infrared (in potassium bromide) and proton magnetic resonance spectra. The latter were determined in deuteriochloroform solution with a Varian model A-60 spectrometer. Chemical shifts are reported as frequency-independent δ values with respect to tetramethylsilane as internal standard.

3β-Hydroxy-17-oxo-5α-androstane (IIa)

A solution of 3β-hydroxy-17-oxo-androst-5-ene (I*a*, 25.0 g) and 70% perchloric acid (0.25 ml) in absolute ethanol containing 10% palladium on carbon (3.0 g) was shaken in a hydrogen atmosphere (slightly positive pressure) for 3.5 h. When the reaction was terminated, approximately the calculated amount of hydrogen had been consumed. The solution was filtered through a Celite layer, and the filtrate was concentrated *in vacuo* to a crystalline solid. A solution of the residue in chloroform was washed successively with water, 5% aqueous sodium bicarbonate, and water. Removal (*in vacuo*) of solvent gave a solid composed of four components (as indicated by thin-layer chromatography). A solution of the product in chloroform was chromatographed on neutral alumina (400 g). Elution with the same solvent (500 ml) gave impure material (12.0 g). Fractions obtained by continued elution with the same solvent and rechromatography (beginning with 4:1 benzene–chloroform) of the first fraction led to 13.8 g (55%) of alcohol II*a* (fractions melting from 173–174° to 176–177.5° after recrystallization from chloroform–hexane) and 0.43 g (2%) of ketone II*b* melting at 114–116°.

Two recrystallizations from chloroform–hexane (1:2) provided a pure specimen of *3β-hydroxy-17-oxo-5α-androstane* (II*a*) as fine needles: R_f 0.29 in ether–benzene (3:1); m.p. 176–177.5° (sintering from 172°); $[\alpha]_D$ +44.4° (*c*, 0.27); ν_{max} 3 440, 2 920, 1 730, 1 374, 1 308, 1 082, and 1 046 cm^{-1}. Melting points of 174–174.5° and 176–177° have been reported (25) for alcohol II*a*.

Anal. Calcd. for $C_{19}H_{30}O_2$: C, 78.59; H, 10.40; O, 11.01. Found: C, 78.68; H, 10.34; O, 10.93.

After three recrystallizations from hexane an analytical sample of *17-oxo-5α-androstane* (II*b*) was obtained as needles melting at 117–119° (sintering from 108°): R_f 0.77 in ether–benzene (3:1); $[\alpha]_D$ +93.7° (*c*, 1.55); ν_{max} 2 920, 1 745, 1 448, 1 376, 1 060, and 1 012 cm^{-1}. An optical rotation (26) value of $[\alpha]_D^{16}$ +87.8° and melting points of 119–120.5° and 122° have been reported (26) for ketone II*b*.

Anal. Calcd. for $C_{19}H_{30}O$: C, 83.15; H, 11.02; O, 5.83. Found: C, 83.20; H, 11.17; O, 6.00.

The preceding hydrogenation experiment was repeated several times, and yields of ketones II*a* and II*b* of up to 76 and 6%, respectively, were obtained.

3β-Hydroxy-17-oximino-5α-androstane (IIc)

A warm solution of hydroxylamine hydrochloride (8.8 g) in 10:1 ethanol–water (110 ml) was added to a solution of ketone II*a* in pyridine (100 ml). The resulting solution was heated at reflux for 5 h. The hot solution was diluted with warm (60°) water (1 l), and the product which separated was collected and washed successively with water, 5% hydrochloric acid, and water. The crude solid (10.4 g) recrystallized from methanol as needles; yield 9.0 g (85%), m.p. 191–193°. Concentrating the mother liquors led to an additional 1.4 g (13%) of oxime melting from 187–191° to 190–192°. Two recrystallizations from methanol gave a pure sample as sparkling plates: R_f 0.55 in chloroform–methanol (9:1); m.p. 194° (sintering from

140°); $[\alpha]_D$ +17.5° (*c*, 6.18); ν_{max} 3 300 (broad), 2 920, 1 450 (broad with shoulder at 1 468), 1 372, 1 138, 1 046 (shoulder at 1 038), and 930 cm^{-1}. A melting point of 185–186° has been reported (27) for oxime II*c*.

3β-Hydroxy-17β-amino-5α-androstane (III)

Method a

Freshly cut sodium (54.0 g) was added in small increments over a 2 h period to a refluxing solution of oxime II*c* (9.0 g) in absolute ethanol (450 ml). Heating was continued for 1.5 h, and the hot mixture was diluted with warm (50°) water. After 16 h at room temperature, product was collected, washed with water, and dried; yield 7.8 g (90%), m.p. 153–157°. A solution of the straw-colored product in ethanol was treated with Norit A, filtered, and concentrated (*in vacuo*) to a pale-yellow solid. Amine III crystallized from 1:2 benzene–hexane as crystal clusters weighing 4.9 g and melting at 157°. An additional 1.8 g (m.p. 156°) was isolated by concentrating the mother liquors. Recrystallization (Norit A) from benzene–hexane followed by two recrystallizations from ethanol–water yielded a pure specimen as microcrystalline platelets: R_f 0.29 in chloroform (saturated with concentrated ammonium hydroxide);[11] m.p. 158–160° (softens at 150°); $[\alpha]_D$ +10.7° (*c*, 1.41); ν_{max} 3 200, 2 930 (shoulder at 2 860), 1 590 (weak and broad), 1 446, 1 376 – 1 368 (doublet), 1 076, 1 052, and 1 034 cm^{-1}; proton magnetic resonance response at 0.60 (singlet, three protons), 0.78 (singlet, three protons), 2.53 (complex, one proton), and 3.40 (broad, one proton) δ.

Anal. Calcd. for $C_{19}H_{33}NO$: C, 78.30; H, 11.41; N, 4.80. Found: C, 78.45; H, 11.35; N, 4.87.

Amine III has been prepared (29) in 60% yield by using a sodium–propanol reduction sequence.

Method b

The series of experiments beginning above with alcohol II*a* were repeated with 3β-acetoxy-17-oxo-androst-5-ene (I*b*) as starting material. The hydrogenation step (performed by Dr. H. Klinger) gave comparable results, that is, approximately 5% of the product was one (II*b*) resulting from hydrogenolysis at C-3. The major product, 3β-acetoxy-17-oxo-5α-androstane, was converted as described in the case of oxime II*c* into acetate II*d*. Reduction of oxime II*d* (10.0 g) was conducted essentially as described in the preceding experiment (method *a*). One recrystallization from ethyl acetate – methanol gave 8.2 g melting at 153–157°. Two additional recrystallizations from the same solvent gave a pure sample (crystalline rosettes) melting at 164–165°; $[\alpha]_D$ +17.0° (*c*, 0.79 in methanol).

Anal. Found: C, 78.02; H, 11.36; N, 4.74.

Method *b* held no advantage over method *a*. In the reduction step, the use of super dry[12] ethanol or larger molar ratios of sodium or oxime was unnecessary.

3β-Hydroxy-17β-(N^{α}-carbobenzoxy-L-prolyl)amino-5α-androstane (IVa)

Woodward's reagent K (5.1 g) and triethylamine (2.0 g) were added to a cold (ice bath), rapidly stirred solution of *N*-carbobenzoxy-L-proline (4.6 g) in dry acetonitrile (250 ml). The reaction was conducted in a flask equipped with a magnetic stirrer and a calcium chloride drying tube. After the solution was stirred for 2 h at ice-bath temperature, dissolution of reactants was complete. The cold reaction mixture was next treated with amine III (5.8 g) and allowed to warm to room temperature. Before the solvent was removed (at 50°) *in vacuo*, stirring at room temperature was continued for 22 h. The residue was dissolved in chloroform and washed successively with water (100 ml), 5% hydrochloric acid (2 × 50 ml), water (100 ml), 5% sodium bicarbonate (2 × 50 ml), and water (100 ml). The chloroform solution was concentrated to approximately 30 ml and chromatographed on neutral alumina (100 g). Elution with the same solvent (300 ml) gave a colorless foam which separated from chloroform–hexane (1:2) as an amorphous powder; yield 7.3 g (70%), m.p. 187–190°. Crystallization and recrystallizations from chloroform – ethyl acetate (1:4) led to a pure sample as microcrystalline needles: R_f 0.61 in chloroform–methanol (9:1); m.p. 196.5–198° (sintering from 191°); $[\alpha]_D$ −76.9° (*c*, 1.01); ν_{max} 3 320, 2 930, 1 693 – 1 668 (broad shoulder at 1 715), 1 540 (broad), 1 420, and 1 359 cm^{-1}; proton magnetic resonance response at 0.51 (singlet, three protons), 0.76 (singlet, three protons), 4.15 (complex, one proton), 4.91 (singlet, two protons), and 7.01 (singlet, five protons) δ.

Anal. Calcd. for $C_{32}H_{46}H_2O_4$: C, 73.52; H, 8.87; N, 5.36; O, 12.25. Found: C, 73.45, 73.46; H, 8.84, 8.64; N, 5.50, 5.51; O, 12.23.

3β-Hydroxy-17β-L-prolylamino-5α-androstane (IVb)

Method a

Hydrogen was passed (at room temperature for 3 h) through a gas dispersion tube into an Erlenmeyer flask containing a solution of carbamate IV*a* (5.2 g) in methanol (250 ml) and palladium black (0.52 g). The mixture was rapidly stirred with a magnetic stirrer, and generated carbon dioxide was swept (with hydrogen) from the reaction vessel into aqueous barium hydroxide. Additional catalyst (0.5 g) was added and hydrogenation continued for 4 h. The solution was filtered through a Celite layer and the filtrate was evaporated *in vacuo* to a colorless solid. A methanol–chloroform (1:3) extract of the residue was diluted with 5% aqueous sodium bicarbonate, and the resulting chloroform phase was washed with water and concentrated (*in vacuo*) to dryness; yield 3.7 g (96%), decomposition point 226–228° (softening at 216°).

[11]*This general technique has been described by Lábler and Černý (28).*

[12]*Prepared as described by Vogel (30).*

Can. J. Chem. Downloaded from www.nrcresearchpress.com by 210.87.254.42 on 09/05/12
For personal use only.

Because a thin-layer chromatogram indicated the presence of impurities, a solution of the product in chloroform–methanol (19:1) was chromatographed on neutral alumina (100 g). Unreacted carbamate IV*a* accompanied by two unidentified by-products was eluted by the same solvent (150 ml). Continued elution with 19:1 to 4:1 chloroform–methanol led to a crystalline residue exhibiting a positive Beilstein test. The latter fraction was dissolved in chloroform and washed successively with 5% aqueous sodium bicarbonate (25 ml) and water (2 × 100 ml). Removal of solvent and recrystallization of the residue from chloroform–hexane (1:1) gave needles weighing 1.6 g and melting to 238° with decomposition. Further recrystallization from the same solvent gave a pure specimen as sparkling needles: R_f 0.24 in chloroform–methanol (4:1); decomposition point 230–238° (sintering from 223°); $[\alpha]_D$ −52.7° (*c*, 1.99); ν_{max} 3 380 – 3 250 (doublet), 2 920 (shoulder at 2 830), 1 663, 1 560, 1 524, 1 446, 1 078, and 1 038 (shoulder at 1 027) cm^{-1}; proton magnetic resonance response at 0.63 (singlet, three protons), 0.77 (singlet, three protons), and 2.79 (complex, one proton) δ.

Anal. Calcd. for $C_{24}H_{40}N_2O_2$: C, 74.20; H, 10.38; N, 7.20; O, 8.22. Found: C, 74.30, 74.03; H, 10.22, 10.33; N, 7.20; O, 8.44.

Method b

In another experiment 1.6 g of carbamate IV*a* was subjected to hydrogenolysis. The crude product weighed 1.1 g and decomposed at 222–225°. Three recrystallizations from methanol yielded an analytical sample as shiny needles decomposing at 226–228°; $[\alpha]_D$ −55.9° (*c*, 0.41).

Anal. Found: C, 74.03; H, 10.45; O, 8.44 (Calcd.: O, 8.24).

A methanol solution of amine IV*b* (0.18 g) was treated with ethereal hydrogen chloride, and the solid (0.16 g) which separated was recrystallized 3 times from methanol – diethyl ether. By this means, an analytical specimen of *amine IVb hydrochloride* was obtained as needles decomposing at 256° with sintering from 235°: R_f 0.22 in chloroform–methanol (4:1); ν_{max} 3 350, 3 200, 2 900 (shoulders at 2 820, 2 740, and 2 560), 1 672, 1 550, and 1 034 cm^{-1}.

Anal. Calcd. for $C_{24}H_{41}ClN_2O_2$: C, 67.83; H, 9.72; Cl, 8.34. Found: C, 67.91; H, 9.78; Cl, 8.26.

3β-Hydroxy-17β-(N$^{\alpha}$-carbobenzoxy-L-prolyl-L-prolyl)amino-5α-androstane (Va)

Proline derivative IV*b* (1.9 g) was allowed to react with the active ester prepared from *N*-carbobenzoxy-L-proline (1.3 g) and Woodward's reagent K (1.3 g) in the presence of triethylamine (0.5 g) as summarized above for the preparation of carbamate IV*a*. A thin-layer chromatogram (7:3 chloroform–methanol being used as the mobile phase) indicated that dipetitde V*a* was the major product accompanied by two minor by-products. Accordingly, a solution of the crude product in chloroform was chromatographed on a column of silica gel (75 g). Elution with the same solvent gave 1.2 g of peptide V*a*. An analytical sample was prepared by recrystallizing the peptide from methanol – diethyl ether – pentane: yield 0.6 g of crystals melting at 120–123°; $[\alpha]_D$ −142.9° (*c*, 0.35 in methanol).

Anal. Calcd. for $C_{37}H_{53}O_5N_3$: C, 71.69; H, 8.62; N, 6.70. Found: C, 71.66; H, 8.44; N, 6.12.

3β-Hydroxy-17β-(L-prolyl-L-prolyl)amino-5α-androstane (Vb)

Cleavage of the carbobenzoxy protecting group from peptide V*a* (0.70 g) was conducted essentially as described above (see amide IV*b*) with methanol (25 ml) as solvent and palladium black (0.20 g) as catalyst. After 6 h, the evolution of carbon dioxide appeared to be complete and hydrogenation was terminated. A thin-layer chromatogram (7:1 chloroform–methanol being used as the mobile phase) indicated that amine V*b* (0.55 g) was accompanied by a trace of starting material. Three recrystallizations from methanol (with a few drops of diethyl ether) gave pure crystals of peptide IV*b* decomposing at 213–217°; $[\alpha]_D$ −134.1° (*c*, 1.0 in methanol).

Anal. Calcd. for $C_{29}H_{47}N_3O_3$: C, 71.71; H, 9.75. Found: C, 71.29, 71.19; H, 9.51, 9.53.

REFERENCES

1. G. R. Pettit, A. K. Das Gupta, H. Klinger, and J. Occolowitz. Experientia, **20**, 545 (1964).
2. G. R. Pettit and J. Yardley. Chem. Ind. London, 553 (1966).
3. L. F. Fieser and M. Fieser. Steroids. Reinhold Publishing Corp., New York. 1959. p. 53.
4. G. W. Oertel, K. Groot, and P. Brühl. Z. Physiol. Chem. **341**, 10 (1965). H. Struck. Z. Physiol. Chem. **333**, 89 (1963). W. R. Slaunwhite, Jr., H. Rosenthal, and A. A. Sandberg. Arch. Biochem. Biophys. **100**, 486 (1963). G. Pincus and E. P. Vollmer (*Editors*). Biological activities of steroids in relation to cancer. Academic Press, Inc., New York. 1960.
5. R. B. Merrifield. Nature, **207**, 522 (1965); J. Am. Chem. Soc. **85**, 2149 (1963). M. Fridkin, A. Patchornik, and E. Katchalski. J. Am. Chem. Soc. **87**, 4646 (1965).
6. M. Martin-Smith. J. Pharm. Pharmacol. **16**, 569 (1964).
7. S. Bondi and E. Müller. Z. Physiol. Chem. **47**, 499 (1906). F. Cortese. J. Am. Chem. Soc. **59**, 2532 (1937).
8. F. Cortese and L. Bauman. J. Am. Chem. Soc. **57**, 1393 (1935).
9. R. A. Boissonnas. Helv. Chim. Acta, **34**, 874 (1951).
10. S. Borgström and A. Norman. Acta Chem. Scand. **7**, 1126 (1953). A. Norman. Arkiv Kemi, **8**, 331 (1955); Chem. Abstr. **49**, 12578 (1955). A. F. Hofmann. Acta Chem. Scand. **17**, 173 (1963).

Can. J. Chem. Downloaded from www.nrcresearchpress.com by 210.87.254.42 on 09/05/12
For personal use only.

11. (*a*) N. V. ORGANON. Dutch Patent No. 89,140 (September 15, 1958); Chem. Abstr. **54**, 1614 (1960).
(*b*) W. E. LANGE and M. E. STEIN. J. Pharm. Sci. **53**, 435 (1964).
(*c*) G. G. NATHANSOHN, G. F. ODASSO, C. R. PASQUALUCCI, and E. TESTA. Steroids, **5**, 263 (1965).
(*d*) K. L. AGARWAL and M. M. DHAR. Steroids, **4**, 495 (1964); **6**, 105 (1965).
12. N. D. TÂM. Compt. Rend. **260**, 717 (1965).
13. R. SCHWYZER. Pure Appl. Chem. **6**, 265 (1963).
14. E. SCHRÖDER. Experientia, **20**, 39 (1964); Ann. **673**, 186 (1964); **673**, 220 (1964). E. SCHRÖDER and H. GIBIAN. Ann. **673**, 176 (1964). E. SCHRÖDER and R. P. HEMPEL. Experientia, **20**, 529 (1964).
15. G. R. PETTIT, B. GREEN, and H. KLINGER. Unpublished experiments.
16. (*a*) L. RUZICKA and M. W. GOLDBERG. Helv. Chim. Acta, **19**, 107 (1936).
(*b*) H. J. ECKHARDT. Chem. Ber. **71**, 461 (1938).
(*c*) J. BARNETT, B. E. RYMAND, and F. SMITH. J. Chem. Soc. 524 (1946).
(*d*) C. W. SHOPPEE and J. C. P. SLY. J. Chem. Soc. 345 (1959).
(*e*) P. CRABBÉ, M. J. SALOMA, and P. G. HOLTON. Bull. Soc. Chim. Belges, **71**, 203 (1962); Chem. Abstr. **58**, 1512 (1963).
(*f*) T. H. WAID and A. TAURINS. Can. J. Chem. **38**, 987 (1960).
(*g*) B. G. KETCHESON and A. TAURINS. Can. J. Chem. **38**, 981 (1960).
(*h*) R. E. MARKER. J. Am. Chem. Soc. **58**, 481 (1936).
(*i*) A. S. JONES, M. WEBB, and F. SMITH. J. Chem. Soc. 2164 (1949).
(*j*) D. P. DODGSON and R. D. HAWORTH. J. Chem. Soc. 67 (1952).
17. P. L. JULIAN, J. W. COLE, E. W. MEYER, and A. MAGNANI. U.S. Patent No. 2,531,441 (November 28, 1950); Chem. Abstr. **45**, 2988 (1951). J. SCHMIDT-THOMÉ. Chem. Ber. **88**, 895 (1955).
18. P. DE RUGGIERI, C. FERRARI, and C. GAUDOLFI. Gazz. Chim. Ital. **91**, 655 (1961); Chem. Abstr. **56**, 14354 (1962).
19. (*a*) G. R. PETTIT, R. L. SMITH, and A. K. DAS GUPTA. Tetrahedron. In press.
(*b*) C. H. ROBINSON, C. ERMANN, and D. P. HOLLIS. Steroids, **6**, 509 (1965).
20. G. W. ANDERSON, J. E. ZIMMERMAN, and F. M. CALLAHAN. J. Am. Chem. Soc. **88**, 1338 (1966). D. S. JONES, G. W. KENNER, and R. C. SHEPPARD. J. Chem. Soc. 4393 (1965).
21. J. E. SHIELDS. Biochemistry, **5**, 1041 (1966). K. BLÁHA and J. RUDINGER. Collection Czech. Chem. Commun. **30**, 3325 (1965). D. S. KEMP and R. B. WOODWARD. Tetrahedron, **21**, 3019 (1965). R. B. WOODWARD, R. A. OLOFSON, and H. MAYER. J. Am. Chem. Soc. **83**, 1010 (1961).
22. S. GOLDSCHMIDT and K. K. GUPTA. Chem. Ber. **98**, 2831 (1965). I. ANTONOVICS and G. T. YOUNG. Chem. Commun. 398 (1965). H. C. BEYERMAN, W. M. VAN DEN BRINK, F. WEYGAND, A. PROX, W. KÖNIG, L. SCHMIDHAMMER, and E. NINTZ. Rec. Trav. Chim. **84**, 213 (1965). E. SCHNABEL. Ann. **688**, 238 (1965). M. W. WILLIAMS and G. T. YOUNG. J. Chem. Soc. 881 (1963).
23. T. WIELAND and C. BIRR. Angew. Chem. **5**, 310 (1966). M. BODANSZKY and M. A. ONDETTI. Chem. Ind. London, 26 (1966). E. TASCHNER, B. RZESZOTARSZKA, and L. LUBIEWSKA. Ann. **690**, 177 (1965). J. C. SHEEHAN, J. PRESTON, and P. A. CRUICKSHANK. J. Am. Chem. Soc. **87**, 2492 (1965). D. G. KNORRE and T. N. SHUBINA. Izv. Sibirsk. Otd. Akad. Nauk SSSR Ser. Khim. Nauk, 126 (1964); Chem. Abstr. **63**, 13407 (1965). E. SCHRÖDER and K. LÜBKE. The peptides. Vol. 1. Academic Press, Inc., New York. 1965.
24. G. R. PETTIT, R. L. SMITH, and H. KLINGER. J. Am. Chem. Soc. In press.
25. L. RUZICKA, M. W. GOLDBERG, and H. BRÜNGGER. Helv. Chim. Acta, **17**, 1389 (1934). A. LARDON and T. REICHSTEIN. Helv. Chim. Acta, **34**, 756 (1951).
26. A. BUTENANDT and K. TSCHERNING. Z. Physiol. Chem. **229**, 192 (1934); Chem. Abstr. **29**, 500 (1935). L. RUZICKA and A. C. MUHR. Helv. Chim. Acta, **27**, 503 (1944).
27. L. RUZICKA, M. W. GOLDBERG, H. BRÜNGGER, and E. EICHENBERGER. Helv. Chim. Acta, **17**, 1395 (1934).
28. L. LÁBLER and V. ČERNÝ. Collection Czech. Chem. Commun. **28**, 2932 (1963).
29. M. E. KEUHNE. U.S. Patent No. 3,063,990 (November 13, 1962); Chem. Abstr. **58**, 9210 (1963).
30. A. I. VOGEL. Practical organic chemistry. 3rd ed. John Wiley & Sons, Inc., New York. 1962. p. 167.

Can. J. Chem. Downloaded from www.nrcresearchpress.com by 210.87.254.42 on 09/05/12
For personal use only.

Can. J. Chem. Downloaded from www.nrcresearchpress.com by 210.87.254.40 on 09/05/12
For personal use only.

ÉTUDE CINÉTIQUE DE L'OXYDATION DE LA TRIBENZYLAMINE PAR LA *N*-BROMOSUCCINIMIDE[1]

MIKLOS ZADOR
Département de Chimie, Université de Montréal, Montréal, Québec

Reçu le 23 mars 1966

RÉSUMÉ

L'oxydation de la tribenzylamine par la *N*-bromosuccinimide a été étudiée dans un solvant méthanol–eau. La réaction procède selon deux étapes. La première, celle d'oxydation proprement dite, s'accompagne de la formation d'acide bromhydrique. Elle est suivie par la solvolyse du produit intermédiaire formé et donne lieu au benzaldéhyde.

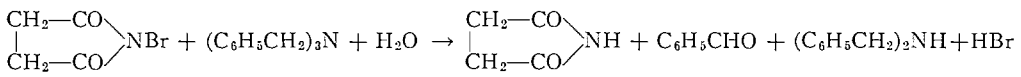
La catalyse par l'acide bromhydrique et l'inhibition par la succinimide sont interprétées en termes de mécanisme réactionnel faisant intervenir des dérivés hypobromeux.

INTRODUCTION

Les dérivés *N*-bromés des amides, tels que la *N*-bromosuccinimide, agents de bromuration allylique par excellence, se sont récemment avérés efficaces dans l'oxydation de dérivés tels que les alcools et les amines. Ils permettent également l'oxydation sélective d'une de ces fonctions dans une molécule polyfonctionnelle ainsi que la dégradation de molécules complexes.

L'ensemble de ces résultats a fait l'objet de trois articles de revue (1–3). Il en ressort qu'en milieu apolaire les réactions sont de type radicalaire, initiées par les peroxydes et les radiations ultraviolettes. En milieu polaire les initiateurs n'ont pas d'effet et la réaction procède dans ce cas "via brome positif". Bien qu'un très grand nombre de travaux aient été publiés sur l'aspect préparatif de ces réactions, on connaît peu de résultats quantitatifs concernant leur cinétique et leur mécanisme.

L'oxydation de la tribenzylamine par la *N*-bromosuccinimide a été étudiée par Dunstan et Henbest (4) et par Horner *et al.* (5). On peut écrire



ou, pour abréger,[2]

$$SNBr + B_3N + H_2O \rightarrow SNH + C_6H_5CHO + B_2NH + HBr.$$

Dunstan et Henbest (4) ont observé que dans le benzène il y a tout d'abord formation d'un intermédiaire de couleur orange, dont le spectre infrarouge est presque identique à celui d'un mélange des deux réactifs. En présence d'eau celui-ci se décompose pour donner les produits de la réaction.

Les autres auteurs (5) admettent qu'un dérivé bromé de la tribenzylamine, $C_6H_5CHBrN(CH_2C_6H_5)_2$, se forme comme intermédiaire dans la réaction. Cependant, ils ne fournissent pas de preuves expérimentales pour soutenir leur hypothèse.

Dans le présent travail nous nous sommes proposés d'élucider la cinétique et le mécanisme de cette réaction, que nous avons effectué toutefois dans un solvent méthanol–eau pour éviter les complications dues à l'hétérogénéité du mileu benzène–eau utilisé par les auteurs cités.

[1]*Présenté au 33ème congrès annuel de l'Association Canadienne-Française pour l'Avancement des Sciences, Montréal, Québec, novembre 1965.*

[2]*Nous avons préféré d'utiliser le symbole SNBr au lieu de NBS pour la N-bromosuccinimide. Ceci nous permet de symboliser la succinimide par SNH et, de plus, d'écrire une équation stoïchiométrique.*

Can. J. Chem. Downloaded from www.nrcresearchpress.com by 210.87.254.40 on 09/05/12
For personal use only.

MÉTHODES EXPÉRIMENTALES

Réactifs

Les solvants utilisés sont le méthanol de pureté analytique et l'eau distillée. La tribenzylamine est recristallisée d'un mélange éthanol–eau, et la succinimide est recristallisée d'un mélange éthanol–benzène. La *N*-bromosuccinimide utilisée est rapidement recristallisée de l'eau distillée bouillante, et on la conserve à l'abri de la luminère. L'analyse iodométrique indique une pureté supérieure à 99%. L'acide bromhydrique est de pureté analytique de composition azéotropique.

Méthodes d'analyse

Les réactions sont suivies par spectrophotométrie et par conductimétrie.

Spectrophotométrie

Le dosage du benzaldéhyde s'effectue à longueur d'onde de 281 mμ, où se situe un maximum d'absorption pour ce composé. La loi de Lambert–Beer est respectée dans les conditions expérimentales, et la valeur du coefficient d'absorption moléculaire est de 1 240 dans le méthanol contenant 5% (v/v) d'eau.

Seul le brome susceptible de se former peut interférer dans ce dosage. Cependant, dans les conditions expérimentales, c'est à dire en présence d'un excès de tribenzylamine, le brome moléculaire se transforme instantanément en dérivés hypobromeux qui n'absorbent pas à cette longueur d'onde.

Conductimétrie

La variation de conductivité, due à la formation d'acide bromhydrique, permet également de suivre la réaction. Un calibrage est effectué dans les conditions expérimentales, pour lesquelles l'acide bromhydrique se trouve sous forme de bromure de tribenzylammonium.

Appareillages

Le spectrophotomètre utilisé est un "Hitachi–Perkin–Elmer model 139", et le conductimètre est un modèle "Radiometer CDM2*d*". Le compartiment à cellules du spectrophotomètre et la cellule conductimétrique sont thermostatés à 25 ± 0.2 °C. Les résultats sont enregistrés sur un "Photovolt model Microcord 44".

Méthode cinétique

La réaction est réalisée dans des solvants mixtes méthanol–eau, pour lesquels on a vérifié que l'oxydation du méthanol est négligeable dans les conditions expérimentales; la formation du benzaldéhyde est par ailleurs quantitative.

A la solution contenant les réactifs (la *N*-bromosuccinimide exceptée), on ajoute au temps initial la quantité appropriée de solution de *N*-bromosuccinimide fraîchement préparée par dissolution du réactif solide. L'homogénéisation du mélange est réalisée par agitation magnétique. Cependant, dans le cas où l'addition des réactifs est faite directement dans les cellules, le mélange est effectué par barbotage d'air pendant quelques secondes. L'oxygène de l'air n'a pas d'influence détectable sur la vitesse des réactions.

La force ionique des solutions n'est pas maintenue constante, étant donné que l'influence de cette dernière est expérimentalement non-significative dans l'étendue de concentration étudiée (jusqu'à $\mu = 0.002$).

La reproductibilité des vitesses initiales est supérieure à 20%, ce qui est relativement médiocre mais permet néanmoins de tirer des conclusions quantitatives. En effet, dans le domaine de concentration considéré la vitesse varie d'un facteur supérieur à 100.

RÉSULTATS ET DISCUSSION

Formation de benzaldéhyde

La formation du benzaldéhyde est illustrée par la Fig. 1, où l'on porte la variation de la densité optique en fonction du temps pour trois expériences caractéristiques. Dans le cas général (courbe *a*) une période d'induction précède l'augmentation de la vitesse de la réaction. Un des produits, l'acide bromhydride, exerce une action catalytique (courbe *b*), tandis que la succinimide a une influence inhibitrice (courbe *c*).

L'ensemble des résultats obtenus par spectrophotométrie ne peut être interprété par un mécanisme simple. Nous avons donc cherché à obtenir des informations supplémentaires en étudiant la variation de conductivité due à la formation d'acide bromhydrique.

Formation d'acide bromhydrique

L'emploi simultané des deux méthodes analytiques nous permet de montrer que la réaction procède par plusieurs étapes. Une expérience caractéristique est présentée dans la Fig. 2. La formation de l'acide bromhydrique (forme réduite) est représentée par la

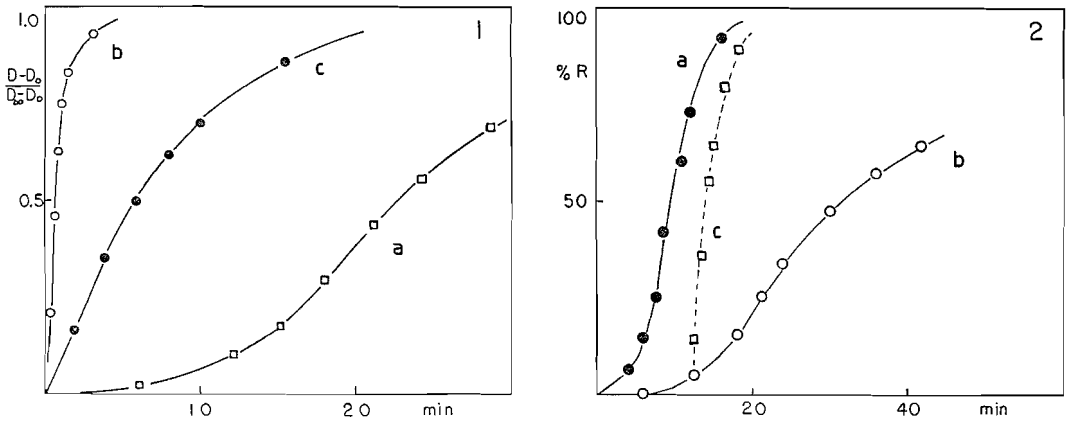


FIG. 1. Formation de benzaldéhyde. Solvant, méthanol contenant 5% (v/v) d'eau; température, 25 °C; $[B_3N] = 1.0 \times 10^{-2}$ mole l^{-1}; $[SNBr] = 5.0 \times 10^{-4}$ mole l^{-1}; courbe *a*, $[SNH] = 5.0 \times 10^{-3}$ mole l^{-1} et $[HBr] = 0$; courbe *b*, $[SNH] = 5.0 \times 10^{-3}$ mole l^{-1} et $[HBr] = 5.0 \times 10^{-4}$ mole l^{-1}; courbe *c*, $[SNH] = 1.0 \times 10^{-1}$ mole l^{-1} et $[HBr] = 5.0 \times 10^{-4}$ mole l^{-1}.

FIG. 2. Formation d'acide bromhydrique et de benzaldéhyde. Solvant, méthanol; température, 25 °C; $[B_3N] = 1.0 \times 10^{-2}$ mole l^{-1}; $[SNBr] = 5.0 \times 10^{-4}$ mole l^{-1}; $[SNH] = 5.0 \times 10^{-3}$ mole l^{-1}; courbe *a*, % HBr formé; courbe *b*, % benzaldéhyde formé; courbe *c*, % benzaldéhyde formé après l'addition de 5% (v/v) d'eau.

courbe *a*; c'est une étape d'oxydation. L'absence de réaction avec l'iodure de potassium montre que le brome oxydant est consommé à la fin de cette étape.

La courbe *b* évoque la formation du benzaldéhyde au cours de la même expérience. Ces résultats montrent clairement que le benzaldéhyde ne se forme que dans une étape postérieure à l'oxydation. L'addition de 5% (v/v) d'eau au mélange réactionnel à un stade où l'oxydation est quasi complète augmente d'une manière très importante la vitesse de formation du benzaldéhyde (courbe *c*); on peut en conclure que cette étape est la solvolyse du produit intermédiaire formé au cours du processus; cela permet en outre de déterminer la constante de vitesse de cette seconde étape.

Etant donné la difficulté d'obtenir du méthanol contenant moins de 10^{-3} mole d'eau/l, il ne nous a pas été possible de montrer qu'il s'agissait d'une hydrolyse plutôt qu'une solvolyse par les deux solvants.

Étude en cinétique initiale

La formation de l'acide bromhydrique a été beaucoup plus facile à étudier de façon significative; en effet cette étape peut être étudiée en cinétique initiale, ce qui évite l'influence de l'acide bromhydrique formé au cours de la réaction. Un certain nombre de résultats sont présentés dans le Tableau I et dans la Fig. 3. Dans cette dernière, les courbes représentent la variation de la vitesse initiale de la réaction en fonction de la concentration initiale en acide bromhydrique pour diverses concentrations en succinimide. Pour une concentration donnée de cette dernière, la vitesse initiale peut être exprimée en fonction de la concentration en acide bromhydrique par éq. [1].

$$[1] \qquad V = [SNBr](k_0 + k_{H^+}[HBr] + k_{HBr}[HBr]^2)$$

La courbe *b* de la Fig. 3 correspond aux valeurs suivantes des constantes: $k_0 = 1.8 \times 10^{-2}$ min^{-1}; $k_{H^+} = 300$ $mole^{-1}$ l min^{-1}; $k_{HBr} = 7 \times 10^5$ $mole^{-2}$ l^2 min^{-1}. Notons que dans les conditions expérimentales l'acide bromhydrique se trouve sous forme de bromure de tribenzylammonium (B_3NH^+). De plus la concentration en protons solvatés

Can. J. Chem. Downloaded from www.nrcresearchpress.com by 210.87.254.40 on 09/05/12
For personal use only.

Can. J. Chem. Downloaded from www.nrcresearchpress.com by 210.87.254.40 on 09/05/12
For personal use only.

TABLEAU I

Vitesse initiale de formation de HBr

[SNBr] (mole l^{-1})	[SNH] (mole l^{-1})	[HBr] (mole l^{-1})	$V_i = \frac{d[HBr]}{dt}$ (mole l^{-1} min^{-1})	V_i/[SNBr] (min^{-1})
5.0×10^{-4}	0.0	0.0	1.0×10^{-5}	2.0×10^{-2}
"	"	5.0×10^{-4}	$>3\times10^{-3}$	>6
"	5.0×10^{-3}	0.0	0.95×10^{-5}	1.9×10^{-2}
"	"	1.0×10^{-4}	1.1×10^{-4}	2.2×10^{-1}
"	"	2.0×10^{-4}	2.5×10^{-4}	5.0×10^{-1}
"	"	5.0×10^{-4}	$>1.5\times10^{-3}$	>1.5
"	2.0×10^{-2}	0.0	0.9×10^{-5}	1.8×10^{-2}
"	"	1.0×10^{-4}	2.9×10^{-5}	5.8×10^{-2}
"	"	2.0×10^{-4}	5.2×10^{-5}	1.04×10^{-1}
"	"	5.0×10^{-4}	1.8×10^{-4}	3.6×10^{-1}
"	"	1.0×10^{-3}	5.0×10^{-4}	1.0
"	1.0×10^{-1}	0.0	0.85×10^{-5}	1.7×10^{-2}
"	"	1.0×10^{-4}	1.2×10^{-5}	2.4×10^{-2}
"	"	2.0×10^{-4}	2.0×10^{-5}	4.0×10^{-2}
"	"	5.0×10^{-4}	5.0×10^{-5}	1.0×10^{-1}
"	"	1.0×10^{-3}	1.3×10^{-4}	2.6×10^{-1}
"	2.0×10^{-1}	0.0	0.9×10^{-5}	1.8×10^{-2}
"	"	1.0×10^{-4}	1.1×10^{-5}	2.2×10^{-2}
"	"	2.0×10^{-4}	1.5×10^{-5}	3.0×10^{-2}
"	"	5.0×10^{-4}	3.0×10^{-5}	6.0×10^{-2}
"	"	1.0×10^{-3}	8.5×10^{-5}	1.7×10^{-1}
"	5.0×10^{-1}	0.0	0.85×10^{-5}	1.7×10^{-2}
"	"	1.0×10^{-4}	0.9×10^{-5}	1.8×10^{-2}
"	"	2.0×10^{-4}	1.0×10^{-5}	2.0×10^{-2}
"	"	5.0×10^{-4}	1.7×10^{-5}	3.4×10^{-2}
"	"	1.0×10^{-3}	4.0×10^{-5}	8.0×10^{-2}
2.5×10^{-4}	2.0×10^{-2}	5.0×10^{-4}	8.0×10^{-5}	3.2×10^{-1}
"	5.0×10^{-1}	5.0×10^{-4}	0.9×10^{-5}	3.6×10^{-2}
1.0×10^{-3}	2.0×10^{-2}	5.0×10^{-4}	3.8×10^{-4}	3.8×10^{-1}
"	5.0×10^{-1}	5.0×10^{-4}	3.8×10^{-5}	3.8×10^{-2}

NOTONS: Solvant, méthanol contenant 5% (v/v) d'eau; température, 25 °C; [B_3N] = 1.0×10^{-2} mole l^{-1}.

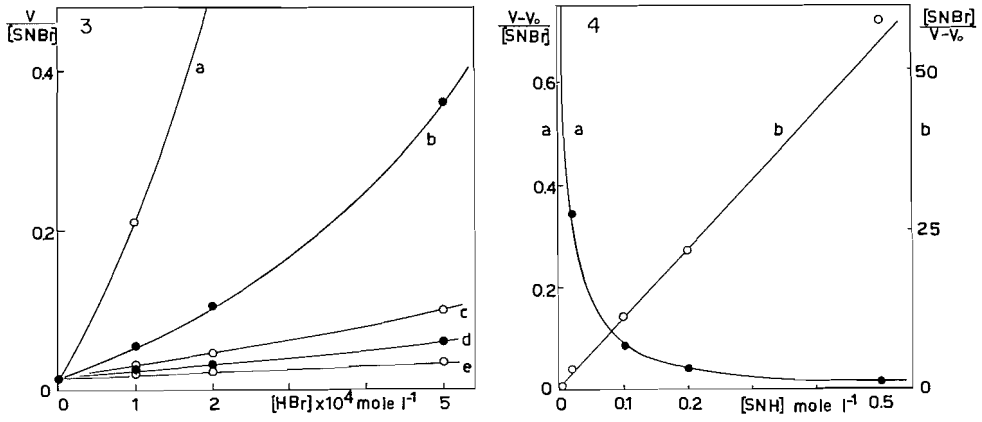


FIG. 3. Effet catalytique de l'acide bromhydrique sur la vitesse d'oxydation. Solvant, méthanol contenant 5% (v/v) d'eau; température, 25 °C; [B_3N] = 1.0×10^{-2} mole l^{-1}; [SNBr] = 5.0×10^{-4} mole l^{-1}; courbe *a*, [SNH] = 5.0×10^{-3} mole l^{-1}; courbe *b*, [SNH] = 2.0×10^{-2} mole l^{-1}; courbe *c*, [SNH] = 1.0×10^{-1} mole l^{-1}; courbe *d*, [SNH] = 2.0×10^{-1} mole l^{-1}; courbe *e*, [SNH] = 5.0×10^{-1} mole l^{-1}. Unité de vitesse, mole l^{-1} min^{-1}.

FIG. 4. Effet inhibiteur de la succinimide sur la vitesse d'oxydation. Solvant, méthanol contenant 5% (v/v) d'eau; température, 25 °C; [B_3N] = 1.0×10^{-2} mole l^{-1}; [SNBr] = 5.0×10^{-4} mole l^{-1}; [HBr] = 5.0×10^{-4} mole l^{-1}. Unité de vitesse, mole l^{-1} min^{-1}.

est, pour ce milieu tamponné B_3NH^+/B_3N, proportionnelle à la concentration en ion B_3NH^+ car la tribenzylamine est prise en grand excès. Dans ces conditions, k_{H^+} et k_{HBr} sont des constantes apparentes.

L'effet catalytique de l'acide bromhydrique varie avec la concentration en succinimide (Fig. 3, courbes *a*–*e*). Pour une concentration donnée en acide bromhydrique l'expression suivante (éq. [2]) permet de rendre compte de manière quantitative des résultats observés.

$$V = V_0 + \frac{k[\mathrm{SNBr}]}{1 + k'[\mathrm{SNH}]} \qquad [2]$$

Dans cette expression le terme V_0 représente la vitesse d'oxydation non-catalysée, qui d'ailleurs n'est pas affectée par la succinimide (ordonnée à l'origine dans la Fig. 3). Le terme suivant représente la vitesse de la réaction catalysée.

L'équation [2] peut être transformée en une relation linéaire (éq. [3]).

$$\frac{[\mathrm{SNBr}]}{V - V_0} = \frac{1}{k} + \frac{k'}{k}[\mathrm{SNH}] \qquad [3]$$

L'accord avec l'expérience est satisfaisant, comme le montre la droite de la Fig. 4, dont la pente donne la valeur de k'/k. Il n'est pas possible de calculer séparément la valeur des deux constantes, étant donné la grande incertitude sur l'ordonnée à l'origine, $1/k$.

Interprétation des résultats

Pour interpréter les résultats nous admettons le mécanisme suivant (éqs. [4]–[7]) pour l'oxydation de la tribenzylamine par la *N*-bromosuccinimide (Y = —OR, HOR ou Br^-; R = $—CH_3$ ou —H).

$$\mathrm{SNBr} + \mathrm{B_3N} + \mathrm{YH} \xrightarrow{k_0} \mathrm{SNH} + \text{Intermédiaire} + \mathrm{HBr} \qquad [4]$$

$$\mathrm{SNBr} + \mathrm{H^+} + \mathrm{Y} \underset{k_{-1}}{\overset{k_1}{\rightleftharpoons}} \mathrm{SNH} + \mathrm{YBr^+} \qquad [5]$$

$$\mathrm{YBr^+} + \mathrm{B_3N} \xrightarrow{k_2} \text{Intermédiaire} + \mathrm{HBr} \qquad [6]$$

$$\text{Intermédiaire} + \mathrm{ROH} \xrightarrow{k_3} \mathrm{C_6H_5CHO} + \mathrm{HN}\diagup\!\diagdown + \mathrm{YR} \qquad [7]$$

La *N*-bromosuccinimide peut oxyder directement la tribenzylamine pour donner un produit intermédiaire et de l'acide bromhydrique (éq. [4]). Elle peut, dans une étape parallèle, réagir selon des vitesse différentes avec les diverses espèces Y pour donner des produits contenant le brome au degré d'oxydation +1 (éq. [5]).

Les diverses espèces YBr^+ échangent le brome entre elles d'après le schéma montré dans éq. [8].

$$\begin{array}{ccc} & \mathrm{CH_3OBr} & \\ \nearrow\!\!\!

Nous négligeons de plus les formes protonées telles que $BrOH_2^+$ et CH_3OHBr^+, dont la concentration devrait être infime (7), mais qui pourront néanmoins intervenir comme agents d'oxydation (8).

Dans l'étape suivante (éq. [6]) les dérivés YBr^+ oxydent, avec des vitesses différentes, la tribenzylamine mais les concentrations relatives des formes intervenant dans l'équilibre montré dans éq. [8] restent inchangées pour les raisons mentionnées auparavant.

Le mécanisme proposé est cohérent avec éq. [1]. En effet, k_0 y représente l'oxydation "spontanée", le terme $k_{H^+}[HBr]$ correspond à la solvolyse, catalysée par H^+, de la *N*-bromosuccinimide et $k_{HBr}[HBr]^2$ est dû à la réaction de cette dernière avec l'ion bromure catalysée par H^+; ces deux dernières réactions, après l'établissement de l'équilibre montré dans éq. [8], sont suivies par l'oxydation de la tribenzylamine par YBr^+.

L'équation [5] explique bien l'influence inhibitrice de la succinimide. Elle réagit avec YBr^+ et diminue ainsi la concentration de cette forme active.

L'application formelle d'un traitement d'état stationnaire pour YBr^+ donne éq. [9],

$$[9] \qquad k_1([SNBr] - [YBr^+]) - k_{-1}[SNH][YBr^+] - k_2[YBr^+] = 0$$

où k_1 et k_{-1} sont les constantes de vitesse apparentes de éq. [5]; de même, k_2 est la constante de éq. [6] qui inclue la concentration en tribenzylamine.

A partir de éq. [9] on obtient la relation suivante (éq. [10]) pour la vitesse d'oxydation via les éqs. [5] et [6].

$$[10] \qquad V = \frac{k_1k_2[SNBr]}{k_1 + k_2 + k_{-1}[SNH]}$$

Pour la vitesse totale d'oxydation on a

$$[11] \qquad V = V_0 + \frac{k_1k_2[SNBr]}{k_1 + k_2 + k_{-1}[SNH]},$$

où V_0 représente la vitesse d'oxydation "spontanée".

Cette expression est la même que éq. [2] en posant $k = k_1k_2/(k_1 + k_2)$, $k' = k_{-1}/(k_1+k_2)$ et $k'/k = k_{-1}/k_1k_2 = 108$ mole^{-1} l min.

Enfin, éq. [7] est l'étape de solvolyse et donne lieu aux produits finals (le benzaldéhyde et la dibenzylamine). Sa constante de vitesse (k_3) a été déterminée par la méthode mentionnée plus haut, et sa valeur est 0.6 min^{-1} dans les conditions expérimentales.

La confirmation directe de ce mécanisme par l'identification des intermédiaires d'oxydation n'est pas possible. Les méthodes d'isolement sont en effet trop lentes par rapport à la solvolyse, tandis que la spectroscopie est inefficace à cause de l'excès de tribenzylamine et la nature du milieu. Comme hypothèse on peut admettre qu'il s'agit des dérivés α-bromés (5) ou α-hydroxylés de la tribenzylamine. Ces derniers peuvent d'ailleurs se former aux dépens des premiers et donneraient, par décomposition, le benzaldéhyde et la dibenzylamine. Cependant, faute de preuve éxperimentale, il n'est pas possible de formuler un mécanisme détaillé pour leur formation.

Il est à noter que le mécanisme proposé s'apparente en partie à celui de Orton *et al.* pour la transposition des *N*-halogéno-acétanilides (9–11).

$$[12] \qquad C_6H_5NXCOCH_3 + HX \overset{\text{Lent}}{\rightleftharpoons} C_6H_5NHCOCH_3 + X_2$$

$$[13] \qquad C_6H_5NHCOCH_3 + X_2 \xrightarrow{\text{Rapide}} XC_6H_4NHCOCH_3 + HX$$

L'équation de vitesse est donnée par éq. [14].

$$[14] \qquad V = k[C_6H_5NXCOCH_3][HX]^2$$

Can. J. Chem. Downloaded from www.nrcresearchpress.com by 210.87.254.40 on 09/05/12
For personal use only.

En effet, la catalyse par l'acide bromhydrique (en particulier par l'ion bromure) ne s'explique que par la formation du brome (qui est en équilibre avec les dérivés hypobromeux) comme intermédiaire réactionnel. Les différences entre les équations de vitesse obtenues sont dues à l'importance plus grande de la solvolyse du dérivé *N*-bromé ainsi qu'à l'influence inhibitrice marquée de l'amide formée (succinimide) (éqs. [1], [11] et [14]).

Il est difficile de faire une comparaison avec les études antérieures consacrées à l'oxydation de la tribenzylamine par la *N*-bromosuccinimide (4, 5), étant donné que les conditions expérimentales sont très différentes. Le fait que les vitesses de réaction soient élevées même à basse concentration permet néanmoins de mettre en doute l'intervention du complexe formé entre la tribenzylamine et la *N*-bromosuccinimide dans le benzène comme intermédiaire de réaction (4). En effet, l'acide bromhydrique et le benzaldéhyde ne se forment qu'après l'addition d'eau au mélange réactionnel, et la réaction peut très bien avoir lieu, avec une vitesse très élevée, à ce moment là.

A la lumière de ce travail l'on peut conclure que l'oxydation globale ou sélective d'une fonction particulière dans une molécule polyfonctionnelle serait principalement due au brome et aux dérivés hypobromeux qui se forment, et non pas à la *N*-bromosuccinimide, du moins en milieu organo–aqueux. L'interprétation éventuelle des résultats devrait donc être faite sur cette base.

REMERCIEMENTS

L'auteur remercie M. D. Paquette pour son assistance technique, ainsi que le Conseil National de Recherches pour l'aide financière accordée.

BIBLIOGRAPHIE

1. C. DJERASSI. Chem. Rev. **43**, 271 (1948).
2. L. HORNER et E. H. WINKELMANN. Angew. Chem. **71**, 349 (1959).
3. R. FILLER. Chem. Rev. **63**, 21 (1963).
4. S. DUNSTAN et H. B. HENBEST. J. Chem. Soc. 4905 (1957).
5. L. HORNER, E. H. WINKELMANN, K. H. KNAPP et W. LUDWIG. Chem. Ber. **92**, 288 (1959).
6. M. EIGEN et K. KUSTIN. J. Am. Chem. Soc. **84**, 1355 (1962).
7. R. P. BELL et E. GELLES. J. Chem. Soc. 2734 (1951).
8. M. ANBAR et D. GINSBERG. Chem. Rev. **54**, 925 (1954).
9. K. J. P. ORTON et W. J. JONES. J. Chem. Soc. 1456 (1909).
10. F. G. SOPER et D. R. PRYDE. J. Chem. Soc. 2761 (1927).
11. K. J. P. ORTON, F. G. SOPER et G. WILLIAMS. J. Chem. Soc. 998 (1928).

Can. J. Chem. Downloaded from www.nrcresearchpress.com by 210.87.254.40 on 09/05/12
For personal use only.

Can. J. Chem. Downloaded from www.nrcresearchpress.com by 210.87.254.6 on 09/05/12
For personal use only.

PYRANOSE–FURANOSE AND ANOMERIC EQUILIBRIA

INFLUENCE OF SOLVENT AND OF PARTIAL METHYLATION[1]

W. MACKIE[2] AND A. S. PERLIN

Prairie Regional Laboratory, National Research Council of Canada, Saskatoon, Saskatchewan

Received April 25, 1966

ABSTRACT

Sugars possessing the *arabino* (2,3,4-*trans*,*cis*) configuration exist as furanoses to a greater extent in dimethyl sulfoxide than in water. Their 2,3-di-*O*-methyl derivatives show an even stronger preference for a five membered ring structure in both solvents. This is most marked for 2,3-di-*O*-methyl-D-arabinose and 2,3-di-*O*-methyl-D-altrose, which are 65% and 80% furanose, respectively, in dimethyl sulfoxide. Compounds in the *xylo* (2,3,4-*trans*,*trans*) or *lyxo* (2,3,4-*cis*,*trans*) series show little tendency to be furanoses in either solvent. However, α-pyranoses in the *lyxo* series are relatively more stable in dimethyl sulfoxide than in water, whereas the anomeric composition for members of the *xylo* series is the same in both solvents. Some of these variations in the equilibria are attributed to the preferential stabilization of pyranose forms in water. D-Lyxose and D-ribose show nuclear magnetic resonance spectral differences in the two solvents that appear to be due to conformational, as well as tautomeric, equilibrium changes.

An equatorial anomeric hydroxyl proton of a given pair in dimethyl sulfoxide shows a larger spacing (6.5–8.0 c.p.s.) than an axial anomeric hydroxyl proton (4–5 c.p.s.). The signal for the latter proton occurs at higher field than an equatorial OH-1, except when OH-2 is axial.

In a recent study of hydroxyl proton magnetic resonance spectra it was found that certain sugars tend to exist as furanoses to a greater extent in dimethyl sulfoxide than in water (1). D-Arabinose shows this difference very markedly. At equilibrium, virtually no furanose is detected in the aqueous solution, whereas in dimethyl sulfoxide its proportion is one-third of the total (Table I). Galactose behaves similarly, although the final percentage of furanose is not as high. D-Altrose and D-fructose, both of which are configurationally related to these sugars, exist as furanoses to a very considerable extent in water. However, the tautomeric composition of the former (2) is altered significantly in dimethyl sulfoxide, in which it shows an even stronger preference for the five membered ring structure (Table I). The presence of mixed furanose and pyranose forms of D-fructose in water is shown by the fact that, when an aqueous solution of the sugar is concentrated, the resulting syrupy material shows several strong singlets ascribable to OH-2 when freshly dissolved in dimethyl sulfoxide. As equilibration proceeds in this solvent, the main change observed is a decrease in the relative intensity of the signal attributable to OH-2 of the β-pyranose form.

One possible explanation (1) of these compositional differences in the two solvents is that water may preferentially stabilize the pyranoses through hydrogen bonding. This is based on evidence (3) that, when water solvates a sugar molecule possessing a pyranose chair form, the structure of water itself suffers very little disorientation, and intermolecular association can take place readily. Although dimethyl sulfoxide also is strongly hydrogen bonding, there is no apparent relationship of this kind between its linear structure (4) and one specific type of cyclic sugar conformation.

To examine the possibility that water may stabilize pyranoses preferentially, the equilibrium compositions of some 2,3-di-*O*-methyl derivatives of sugars in water and dimethyl sulfoxide were measured. According to Kabayama and Patterson (3), the most

[1]*Issued as N.R.C. No. 9094.*

[2]*National Research Council Postdoctorate Fellow, 1964–1965.*

TABLE I

Percentage of furanose in solution at equilibrium*

	In deuterium oxide†	In dimethyl sulfoxide‡
D-Arabinose	Trace	33
2,3-Di-*O*-methyl-D-arabinose	17	65
D-Galactose	Trace	ca. 15§
2,3-Di-*O*-methyl-D-galactose	10	38
D-Altrose	34‖	44¶
2,3-Di-*O*-methyl-D-altrose	>45	ca. 80

*The measurements were made over prolonged periods (several weeks) until no further change was evident.

†Based on the intensity of the signal ascribed to H-1 of furanose components (α plus β).

‡Based on the intensity of the signal ascribed to OH-1 of furanose components (α plus β).

§The overlap of the doublet ascribed to furanose OH-1 with that of α-pyranose permits only a rough estimate.

‖Based on the combined intensities of the two weakest of four H-1 signals in deuterium oxide (2).

¶Four low-field (OH-1) doublets, all of substantial intensity but of similar chemical shift, are clearly detected when an equilibrated aqueous solution is concentrated and the syrup examined in dimethyl sulfoxide. Since these signals are closely grouped, deuterium oxide was added to the solution and the percentage of furanose estimated from the appropriate H-1 signals (preceding footnote).

effective arrangement for hydrogen bonding in aqueous solutions is that involving the oxygen of water and the hydrogen of a pyranose hydroxyl group, particularly when the latter group is equatorially oriented. Since the ether derivatives contain fewer hydroxyl groups that can bond in this way, solvent stabilization of them should be minimized accordingly. The resulting data are not inconsistent with this rationalization. Thus, 2,3-di-*O*-methyl-D-arabinose (I) shows a considerably higher content of furanose in solution than does D-arabinose itself. In deuterium oxide, I produces at least three H-1 signals, whereas only two significant ones are found for arabinose (1, 2). Although unequivocal assignments have not been made, the intensity of the weakest signal shows that a minimum of 17% of furanose is present in the solution of I. A similar value (20%) is given by the OH-1 signals observed immediately after the mixture is transferred from water to dimethyl sulfoxide (compare Fig. 1A below with Fig. 5B in ref. 2). In this instance, the assignment of a furanose OH-1 signal is more straightforward since there is a corresponding upfield multiplet signal caused by a primary carbinol group (i.e. OH-5) (1, 5), the identity of which is confirmed by the use of 2,3-di-*O*-methyl-D-arabinose-5,5′-d_2 (II), which gives a singlet signal for OH-5 (Fig. 1C).

As with D-arabinose itself (1), the equilibrium composition of I or II changes in dimethyl sulfoxide strongly in favor of a furanose component. Figures 1C and 1D illustrate this change for I and the 5,5′-dideuterated compound (II), respectively, and the equilibrium compositions of the dimethyl ether and D-arabinose are compared in Table I. Corresponding data for 2,3-di-*O*-methyl-D-galactose included in the table show that this configurationally related sugar also tends to exist as a furanose more readily than does D-galactose itself both in water and in dimethyl sulfoxide.

An additional point about the equilibrium composition of 2,3-di-*O*-methyl-D-arabinose may be noted. This compound is an oil and, based on its nuclear magnetic resonance (n.m.r.) spectrum when freshly dissolved in dimethyl sulfoxide, has approximately the same composition as found (Fig. 1C) after it has been transferred from an aqueous solution to dimethyl sulfoxide and then equilibrated. Similarly, the H-1 signal attributed above to a furanose in deuterium oxide solution is much stronger when the spectrum is recorded

Can. J. Chem. Downloaded from www.nrcresearchpress.com by 210.87.254.6 on 09/05/12
For personal use only.

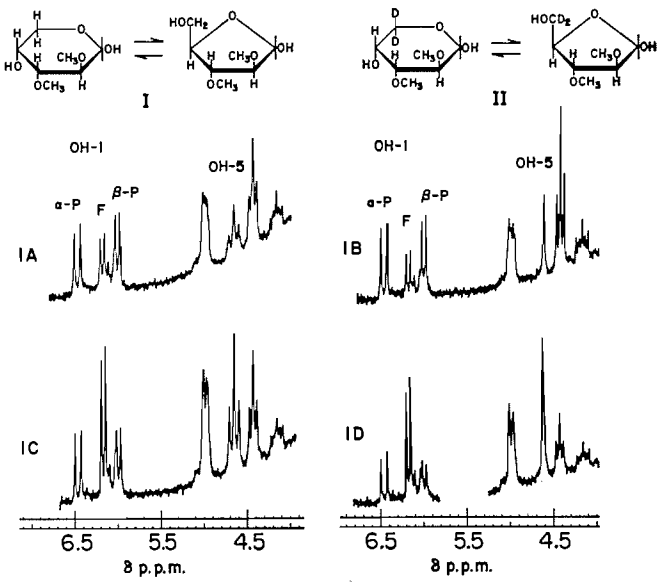


FIG. 1. Partial n.m.r. spectra at 100 Mc.p.s. of 2,3-di-*O*-methyl-D-arabinose (I) and 2,3-di-*O*-methyl-D-arabinose-5,5′-d_2 (II) in dimethyl sulfoxide. A and B are from the spectra of syrupy I and II directly after transfer from an aqueous solution; C and D are from the spectra recorded 2 weeks later. α-P and β-P = α- and β-pyranose; F = furanose.

immediately after the oil has been dissolved.[3] Hence, these observations also show that 2,3-di-*O*-methyl-D-arabinofuranose (most probably the α-anomer) is more stable than either pyranose anomer of I when water is absent.

Since only half of the hydroxyl hydrogens of I are masked, it is not unreasonable that its equilibrium composition in water does not attain the same value as does arabinose itself in dimethyl sulfoxide, i.e. that methylation has only a partial effect in reducing the stability that could be attributed to solvation by water. However, the methyl groups also may exert a different kind of influence. Bishop and Cooper (7) have shown that some partially methylated sugars yield higher proportions of methyl furanosides than do the parent sugars under equilibrating conditions. Particularly pertinent to the present study is their finding that 2,3-di-*O*-methyl-L-arabinose yields 75% of the α,β-furanosides whereas L-arabinose yields only 28%, values close to those for the free sugar equilibria in dimethyl sulfoxide. These authors suggest (7) that methylation promotes relatively stronger repulsive interactions in the pyranosides than in the furanosides by increasing the effective size of the substituents on C-2 and C-3. This idea also helps to explain the current results, although it does not account for the low proportions of furanose found in aqueous solutions. However, changes in the solvation pattern could be a complementary factor. The hydroxyl group of a sugar can form a hydrogen bond with water or dimethyl sulfoxide molecules through either its oxygen or its hydrogen atom, whereas the methoxyl group can form a hydrogen bond through only its oxygen atom. Hence, solvation should

[3]*At 1 min the estimated concentration of furanose is 34%; in 30–40 min the intensity of the signal drops to half this value (i.e. its equilibrium level), although not at a strictly exponential rate. This change provides a measure of the rate of interconversion of furanose into pyranose in water, a type of reaction that rarely has been observed in the absence of a mutarotation catalyst. The mutarotation of* D-*fructofuranose liberated by invertase is the one well-known example of this kind (6).*

Can. J. Chem. Downloaded from www.nrcresearchpress.com by 210.87.254.6 on 09/05/12
For personal use only.

increase the effective size of the methoxyl group more than that of the hydroxyl group, thereby destabilizing pyranose forms even more strongly. Similarly, dimethyl sulfoxide can form a hydrogen bond with the hydroxyl group, whereas in solvating the methoxyl group it probably interacts through its sulfur atom with the alkoxyl oxygen atom (8).

Sugars having the *xylo* or *lyxo* configuration appear to exist almost exclusively as pyranoses both in water (2, 9) and in dimethyl sulfoxide (1); accordingly, each exhibits only two anomeric proton or hydroxyl proton signals (see below, however, for an additional comment on D-lyxose). This overwhelmingly greater preference for the pyranose form is also apparent with 2,3-di-*O*-methyl-D-xylose, 2,3-di-*O*-methyl-D-glucose, and 2,3-di-*O*-methyl-D-mannose, each of which shows only two OH-1 signals[4] when equilibrated in dimethyl sulfoxide.

The relatively high stability of the altrofuranose structure is even more marked with 2,3-di-*O*-methyl-D-altrose (III), which is almost entirely in the furanose form in dimethyl sulfoxide (Table I). As seen in Fig. 2, the general characteristics of its n.m.r. spectrum show that one form greatly predominates in the solution. Although several of the signals are closely grouped together, spin decoupling permitted the chemical shifts of H-4 and H-5 to be estimated. The 6-*O*-trityl derivative of III gives a spectrum similar to that shown in Fig. 2, and permitted the H-5 signal to be located even more readily. With both compounds, irradiation at the respective frequencies of H-4 and H-5, with frequency-swept double resonance, showed that the secondary hydroxyl group proton (at 5.1 p.p.m. in Fig. 2) is coupled with H-5 but not with H-4. Hence, the 5-position of III is not engaged in ring formation, and accordingly the compound can be assigned a furanose structure. The identity of a minor component, detected from Fig. 2, is not known.

One form of 2,3-di-*O*-methyl-D-altrose is also dominant in deuterium oxide, although substantial proportions of two other components are present as well; the relative intensities

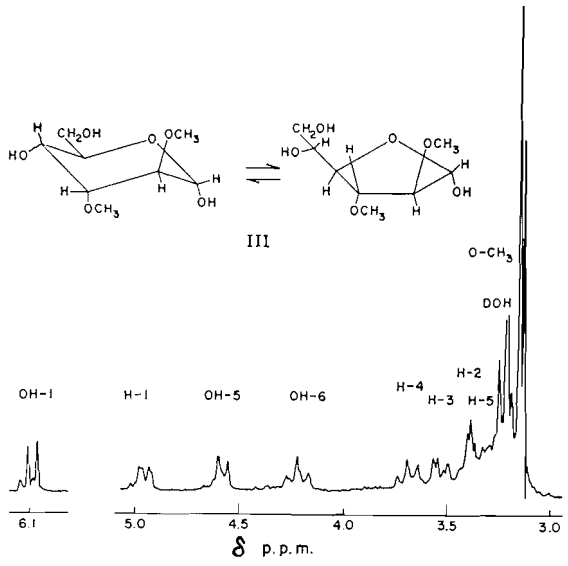


FIG. 2. The n.m.r. spectrum at 100 Mc.p.s. of 2,3-di-*O*-methyl-D-altrose in dimethyl sulfoxide-d_6.

[4]*The data for these signals are presented in Table IV.*

Can. J. Chem. Downloaded from www.nrcresearchpress.com by 210.87.254.6 on 09/05/12
For personal use only.

of the three anomeric proton signals detected are 1.0:2.5:2.0. The major component is likely the α-furanose (IV) since it shows a spacing of less than 0.5 c.p.s., which is characteristic of many 1,2-*trans*-furanoses and 1,2-*trans*-furanosides. Possibly one of the other species detected is the β-furanose, and the total percentage of furanose may be higher than indicated in Table I. This is suggested by the fact that the compound consumes periodate at a rate close to that of known aldohexofuranoses and aldohexofuranosides (Table II). Although cleavage of the C-5,C-6 bond in a compound of this type could be facilitated by rapid displacement of the pyranose–furanose equilibrium, the comparatively slower rate of 2,3-di-*O*-methyl-D-galactose and the relative inertness of 2,3-di-*O*-methyl-D-glucose and 2,3-di-*O*-methyl-D-mannose are in accord with the above information about the furanose concentration of their aqueous solutions. Thus the rate for dimethyl galactose is $\frac{1}{5}$th of that of the known galactofuranoside, whereas the rate for dimethyl glucose is $\frac{1}{36}$th of that of the glucofuranose derivative (Table II). These data also show the marked contrast between the two derivatives of D-mannose substituted at positions 2 and 3, emphasizing the striking influence of the fused five-membered ring in stabilizing the D-mannofuranose structures (1, 10).

TABLE II

Periodate oxidation rates*

Compound	$t_{\frac{1}{2}}$
1,2-*O*-Isopropylidene-D-glucofuranose	40 min
Methyl β-D-galactofuranoside	100 min
D-Mannofuranose 2,3-carbonate	35 min
2,3-Di-*O*-methyl-D-altrose	55 min
2,3-Di-*O*-methyl-D-galactose	8 h
2,3-Di-*O*-methyl-D-glucose	24 h
2,3-Di-*O*-methyl-D-mannose	24 h

*Measured spectroscopically at 223 mμ for highly dilute solutions (see Experimental).
These reactions were also examined directly in the n.m.r. sample tube by noting the rate of liberation of formaldehyde (10). However, at this relatively high concentration, oxidation was frequently too rapid for satisfactory measurement.

The wide differences observed between sugars having the *arabino* configuration on the one hand, and those having the *xylo* or *lyxo* configuration on the other, can be rationalized in a general way on conformational grounds (7, 11–13). Furanose forms of *arabino*-type compounds would be expected to be the more stable since their two-, three-, and four-ring substituents have a *trans,trans* arrangement, whereas one or two vicinal *cis* interactions are found in compounds of the latter two types. In the pyranose series, the relative order of stabilities is probably reversed. This additivity of effects appears to be particularly evident with D-altrose. In either pyranose chair conformation the *altro* configuration should result in substantial instability (11), whereas non-bonded interactions in the furanose forms should be comparatively slight, especially in the all-*trans* α-anomer (IV). According to the current findings, the relative stability of furanose forms of compounds having the *arabino* configuration is enhanced by methylation and also by changing the solvent from water to dimethyl sulfoxide.

Neither of these treatments has a pronounced influence on the energy barrier separating the pyranose and furanose forms in the *xylo* and *lyxo* series. However, the effect of dimethyl sulfoxide on the two classes of compounds is quite different from that of water. In the former solvent there is a marked increase in the ratio of α-pyranose to β-pyranose for

Can. J. Chem. Downloaded from www.nrcresearchpress.com by 210.87.254.6 on 09/05/12
For personal use only.

sugars and derivatives having the *lyxo* configuration,[5] whereas those of the *xylo* series attain nearly the same equilibrium composition in both solvents (Table III).

The overall data thus show that a change in solvent from water to dimethyl sulfoxide affects sugar equilibria in two ways. It promotes a displacement in favor of the furanose forms for compounds that would be expected to have relatively stable five membered ring structures (e.g. arabinose and galactose). With certain other sugars (e.g. mannose and lyxose) that would suffer especially unfavorable vicinal interactions as furanoses, there is a shift towards a higher proportion of α-pyranose (axial OH-1).[6] Xylose and glucose, long

TABLE III

Equilibrium anomeric composition of aldopyranoses

	% β-anomer	
	In water*	In dimethyl sulfoxide†
D-Glucose	60 (64)	62
4,6-*O*-Ethylidene-D-glucose	60	63
3-*O*-Methyl-D-glucose	58	57
6-Deoxy-6-fluoro-D-glucose (15)	60	59
D-Xylose	62 (65)	61
D-Mannose	36 (31)	14
4,6-*O*-Ethylidene-D-mannose	30	10
D-Lyxose	27 (24)	12
L-Rhamnose	33	13

*Based on the relative intensity of the OH-1 signals shown by the compound in dimethyl sulfoxide. These solutions were prepared by rapidly concentrating *in vacuo* an equilibrated aqueous solution of the compound, after which the superficially dry syrup that remained was dissolved immediately in dimethyl sulfoxide. The figures in parentheses in this column are the averages of several literature values determined for aqueous solutions of these sugars by a variety of methods, including n.m.r. spectroscopy (see refs. 12 and 13).

The anomeric designation was deduced by comparison with the spectrum recorded shortly after a known crystalline anomer of the sugar was dissolved in dimethyl sulfoxide (see refs. 1 and 16).

†After the solution described above (preceding footnote) was stored for 8 weeks at room temperature. Some of the solutions were heated at 100 °C for 1–2 h, without any noticeable effect on the anomeric composition. The changes observed in the composition of the *lyxo* compounds were essentially complete within 1 week.

regarded as the most conformationally stable of the pyranoses (11), are not influenced by the solvent change. It was surmised initially that water might selectively stabilize pyranose forms of some of the sugars by hydrogen bonding, and thereby mask the relatively high stability of their furanose forms. More effective hydrogen bonding with water is also regarded as a factor that should stabilize β-pyranoses (equatorial OH-1) more than the α-anomers (3, 12). In attempting to relate the observed changes in equilibrium in the two solvents with such hydrogen-bonding possibilities and with structural features that might be common to, for example, arabinose and mannose, one or two possibilities suggest themselves.

If, as has been suggested (3), axial groups of pyranose chair forms are not effectively solvated by water, then groups such as OH-2 of mannopyranose and OH-4 of arabinopyranose may alternatively form an intramolecular hydrogen bond with the ring oxygen

[5]*In contrast to these observations, it has been suggested recently (14) that* β-D-*mannose is stabilized by complexing with dimethyl sulfoxide. The authors have since found that this suggestion was based on incorrect information (B. Casu, private communication).*

[6]*Somewhat analogous to the effect observed with the arabino-type compounds, the ratio of* α*-anomer to* β*-anomer also increases, even with water as the solvent, when* D-*mannose is partially methylated. Thus, deuterium oxide solutions of 2,3-di- and 2,3,4,6-tetra-O-methyl-*D-*mannose contain only 20% and 14%, respectively, of the* β*-anomer, in contrast to the value of over 30% for* D-*mannose itself (Table III). These figures are based on the relative intensity of two low-field resonance signals in each spectrum that correspond closely, both in chemical shift and spacing, to the H-1 signals of* D-*mannose.*

Can. J. Chem. Downloaded from www.nrcresearchpress.com by 210.87.254.6 on 09/05/12
For personal use only.

Can. J. Chem. Downloaded from www.nrcresearchpress.com by 210.87.254.6 on 09/05/12
For personal use only.

atoms, for which they appear to be suitably oriented. In dimethyl sulfoxide, the hydrogen-bonding pattern should be different; based on the chemical shifts of hydroxyl protons, both axial and equatorial groups are strongly bonded by this solvent (1, 5, 16, 17). Hence, if the OH-2 group of mannose (or OH-4 of arabinose) were now to be reoriented away from the molecule by association with the solvent, the oxygen orbitals should become directed inwards (3). Molecular models suggest that this arrangement would increase repulsive interactions between these orbitals and the erected para orbital of the ring oxygen (see ref. 3) (and in β-mannose, also with the O-1 orbitals). The less-favorable interaction patterns introduced by these changes presumably are relieved by a shift towards a furanose form, in one instance, or in favor of the α-pyranose form, in another. None of these considerations apply to xylose or glucose, and their equilibrium compositions accordingly are about the same in water and dimethyl sulfoxide.[7]

Some other, relatively minor differences are observed when the n.m.r. spectral properties of certain sugars in water and dimethyl sulfoxide are compared. Thus, although D-lyxose appears to exist exclusively in pyranose forms in water (2, 9), an equilibrated solution of it in dimethyl sulfoxide possibly contains a small percentage of furanose forms. This is suggested by the presence of a minor low-field signal and a shoulder on the α-H-1 signal (Fig. 3A). More striking, however, is the 3.2 c.p.s. spacing of the α-pyranose signal as compared with the 4.2 c.p.s. spacing in water. In contrast, the H-1 spacings for most of the other sugars examined are influenced little by the solvent change (Table IV). If it is accepted that the intermediate size of the 4.2 c.p.s. value reflects a chair–chair interconversion for α-D-lyxopyranose (2, 9), then the position of this equilibrium in dimethyl sulfoxide appears to be shifted strongly in favor of the C1 conformation. Although the 3.3 c.p.s. spacing is much larger than that of the configurationally related α-D-mannose, it differs little from the H-1 spacings for various other α-pyranoses in dimethyl sulfoxide (Table IV). In addition, the OH-1 spacing and chemical shift are close to those of axially oriented OH-1 groups of several other sugars, including α-D-mannose (Table IV). Therefore, the properties of D-lyxose in dimethyl sulfoxide suggest that the compound exists almost entirely as the α-pyranose and in the C1 conformation in this solvent.

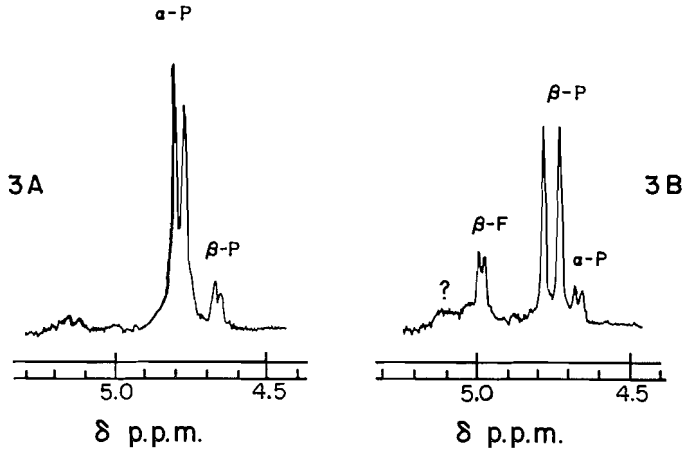


FIG. 3. Partial n.m.r. spectra at 100 Mc.p.s. of D-lyxose (A) and D-ribose (B) equilibrated in dimethyl sulfoxide-d_6 containing a small amount of deuterium oxide. α-P and β-P = α- and β-pyranose; β-F = β-furanose.

[7]*However, in less-polar solvents the composition of glucose shifts in favor of the α-anomer, which is thought to be due to an enhancement of the anomeric effect in such media (13). Since dimethyl sulfoxide possesses a relatively high dielectric constant, the current findings are not at variance with this view.*

Can. J. Chem. Downloaded from www.nrcresearchpress.com by 210.87.254.6 on 09/05/12
For personal use only.

TABLE IV

Nuclear magnetic resonance parameters for the anomeric protons (H-1) and hydroxyl protons (OH-1) of some aldopyranoses in dimethyl sulfoxide

	Spacing (c.p.s.)						
	H-1*		OH-1		Chemical shift (δ, p.p.m.)		
	α	β	α	β	α	β	$\delta_\beta - \delta_\alpha$
D-Xylose	3.2 (3.1)	7.2 (7.4)	4.5	6.6	6.00	6.40	0.40
D-Lyxose	3.2 (4.2)	1.7 (1.4)	4.9	7.9	6.04	5.92	−0.12
D-Ribose	2.2 (2.1)	5.3 (6.4)	8.0	5.5	5.92	6.18	0.26
D-Arabinose	2.5 (2.8)	6.8† (7.1)	4.4 (β)	6.6 (α)	5.88 (β)	6.28 (α)	0.40
D-Glucose	3.3 (3.5)	7.3 (7.5)	4.5	6.6	6.06	6.41	0.35
D-Galactose	2.5 (2.8)	7.2† (7.1)	4.4	6.4	5.94	6.32	0.38
D-Mannose	1.5 (1.7)	0.9 (1.0)	4.2	8.0	6.10	6.00	−0.10
D-Allose	—	7.8 (8.2)	7.4, 5.4‡	6.6	5.88, 6.08‡	6.22	0.34, 0.14
D-Altrose	ca. 1.1 (1.3)	ca. 3.0 (3.0)	—	7.6		5.92	
Miscellaneous derivatives							
2,3-Di-*O*-methyl-D-xylose			4.5	6.4	6.15	6.60	0.45
2,3-Di-*O*-methyl-D-arabinose			4.5 (β)§	6.8 (α)§	5.98 (β)§	6.43 (α)§	0.45
2,3-Di-*O*-methyl-D-galactose			4.5	6.6	6.03	6.50	0.47
2,3-Di-*O*-methyl-D-glucose			4.5	6.6	6.20	6.60	0.40
2,3-Di-*O*-methyl-D-mannose			4.0	8.0	6.30	6.28	−0.02
L-Rhamnose			4.1	8.2	6.02	5.93	−0.11
L-Fucose			4.3	6.4	5.86	6.24	0.38
3-*O*-Methyl-D-glucose			4.4	6.3	6.13	6.47	0.34
3,4-*O*-Isopropylidene-2-*O*-methyl-D-arabinose			4.4 (β)§	6.4 (α)§	6.32 (β)§	6.68 (β)§	0.36
4,6-*O*-Ethylidene-D-galactose			4.3	6.8	6.05	6.38	0.33
4,6-*O*-Ethylidene-D-glucose			4.7	6.6	6.31	6.63	0.32
4,6-*O*-Ethylidene-D-mannose			4.3	8.4	6.33	6.15	−0.18

*The values in parentheses are spacings for the corresponding signals in deuterium oxide; these agree closely with the values already reported by Lemieux and Stevens (2).
†Outer spacings; secondary splitting is evident.
‡Minor signals, probably caused by α-pyranose and β-furanose.
§Anomeric designations based on analogy with D-arabinose itself.

Can. J. Chem. Downloaded from www.nrcresearchpress.com by 210.87.254.6 on 09/05/12
For personal use only.

The n.m.r. spectrum of D-ribose in dimethyl sulfoxide differs in several respects from that in deuterium oxide. A weak low-field multiplet ascribed by Lemieux and Stevens (2) to H-1 of either the α-furanose or *aldehydo* form is replaced in the spectrum of the dimethyl sulfoxide solution by a broad, ill-defined signal comprising about 18% of the overall integral of the absorption signals in this region (Fig. 3B). The percentage contribution of the α-pyranose signal drops from 20% (2) to 10%, whereas the relative intensities of the β-furanose (21%) and β-pyranose (51%) H-1 signals are altered little. Perhaps most notable are the characteristics of the β-pyranose. There is a decrease in the H-1 spacing from 6.4 c.p.s. in deuterium oxide (2) to 5.3 c.p.s. in dimethyl sulfoxide, and the OH-1 spacing is considerably smaller than those for equatorial anomeric hydroxyl groups of other sugars (Table IV, and see the next paragraph). Hence, it appears to be unlikely that β-D-ribopyranose exists entirely in the C1 conformation in dimethyl sulfoxide, in contrast to its behavior in water (2, 9). Both the H-1 and OH-1 signals for α-D-ribopyranose are consistent with the 1C conformation attributed to this isomer in deuterium oxide (2, 9), although, as shown above by the low percentage detected, its structure is also relatively unstable in dimethyl sulfoxide. Therefore, the overall data suggest that D-ribose equilibrates in dimethyl sulfoxide to a number of forms, each of which incorporates relatively strong destabilizing interactions.

The data in Table IV permit the generalization, which has been proposed also by Casu *et al.* (17), that anomeric pyranose pairs show characteristically different OH-1 spacings. Thus, equatorial group proton signals have relatively large spacings of 6.5–8 c.p.s., whereas the axial group protons show spacings of 4.5–5 c.p.s. Although this is analogous to the fact that the axial OH signal for *cis*-4-hydroxy-*t*-butylcyclohexane has a smaller spacing than that for the equatorial *trans*-isomer (5), secondary axial and equatorial hydroxyl groups of sugars and derivatives are not as readily differentiated (ref. 17 and unpublished observations). However, the size of the hydroxyl proton spacings appears to be indicative of the orientation of the hydroxyl group of 1,4-dioxane type hemialdals (18).

Chemical shift values for anomeric hydroxyl protons also show some consistent trends. When there is an equatorial 2-*O*-substituent, the equatorial OH-1 signal occurs at lower field than that of the axial OH-1 by about 0.4 p.p.m., whereas their relative positions are reversed (by about 0.1 p.p.m.) when the substituent is axial. (Several derivatives of D-mannose, in addition to those listed, containing an *O*-acetyl, *O*-methyl, or *O*-benzyl group at C-2 give results closely similar to that for D-mannose itself.) Since 2-deoxy-D-xylohexose shows $\delta_e - \delta_a$ of 0.4 p.p.m. (17), it may be inferred that an axial oxygen at C-2 promotes increased shielding of an equatorial 1-hydroxyl proton, perhaps by weakening its ability to form a bond with dimethyl sulfoxide.

EXPERIMENTAL

Nuclear magnetic resonance spectra were recorded on a Varian HA-100 high-resolution spectrometer with tetramethylsilane contained in a coaxial capillary as the internal control reference signal. Spin-decoupling operations were carried out with the frequency-sweep mode facility of this instrument.

Except for 2,3-di-*O*-methyl-D-xylose (kindly provided by Dr. E. E. Percival), none of the di-*O*-methyl aldoses used in this study are crystalline. However, each of the syrupy compounds was shown to be pure, as judged by paper chromatography with four different solvent systems. Where possible, the sugar was obtained by acid hydrolysis or acetolysis of a crystalline glycoside.

Methyl 4,6-O-Ethylidene-2,3-di-O-methyl β-D-Mannopyranoside

4,6-*O*-Ethylidene-D-mannose (300 mg) (a gift from Dr. D. H. Ball) was dissolved in warm methanol (1.0 ml), and methyl iodide (10 ml) was added, followed by anhydrous calcium sulfate (2 g) and silver oxide (5 g). The suspension was shaken for 24 h, diluted with chloroform, and filtered; then the filtrate was concentrated. Methyl iodide (10 ml), anhydrous calcium sulfate (2 g), and silver oxide (4 g) were added to the

residue and the mixture was heated under reflux for 48 h. Chloroform-extractable material was recovered, and the second methylation procedure repeated. The chloroform-soluble product (0.37 g) crystallized and, after recrystallization from petroleum ether, melted at 70–71 °C; $[\alpha]$ −95° (*c*, 1.2 in chloroform).

Anal. Calcd. for $C_{11}H_{20}O_6$: C, 53.21; H, 8.06. Found: C, 52.9; H, 8.1.

*2,3-Di-O-methyl-*D*-mannose (19), 2,3-Di-O-methyl-*D*-glucose (20), and 2,3-Di-O-methyl-*D*-galactose (21)*

These were prepared by acid hydrolysis of the appropriate crystalline 4,6-*O*-ethylidene or 4,6-*O*-benzylidene methyl glycoside. For example, methyl 4,6-*O*-ethylidene-2,3-di-*O*-methyl β-D-glucoside (22) (m.p. 107–108°C) (150 mg) was hydrolyzed with 1 *N* sulfuric acid (10 ml) on the steam bath for 7 h. The hydrolysate was neutralized with barium carbonate, and filtered; then the solution was treated with Amberlite IR-120 (H^+) and charcoal, and concentrated *in vacuo* at 50 °C.

*2,3-Di-O-methyl-*D*-arabinose (23) and 2,3-Di-O-methyl-*D*-arabinose-5,5′-d_2*

These were prepared by hydrolysis, for 2 h with hot 0.5 *N* sulfuric acid, of methyl 2,3-di-*O*-methyl-α,β-D-arabinofuranoside and the 5,5′-dideuterated compound, respectively, which were synthesized according to the procedure described recently by Heyns and Muller (24).

*2,3-Di-O-methyl-*D*-altrose*

4,6-*O*-Benzylidene-2,3-di-*O*-methyl α-D-altropyranoside (25) (m.p. 85–86 °C) (160 mg) was dissolved in a 200:1 mixture of acetic anhydride and concentrated sulfuric acid (2 ml), and stored at 3 °C for 72 h (26). After an additional 48 h at room temperature, the solution was added to crushed ice, and carefully neutralized with sodium bicarbonate; then the aqueous suspension was extracted several times with chloroform. The combined extracts were dried and concentrated to yield a syrup (212 mg), which was dissolved in cold sodium methoxide (0.1 *N*, 2 ml). After 18 h at 3 °C the deacetylation mixture was neutralized with carbon dioxide, water was added, and the solution was treated with mixed-bed ion-exchange resins and concentrated. The chromatographically pure syrup (100 mg) had $[\alpha]$ +31° (*c*, 1.4 in water). The n.m.r. spectrum in dimethyl sulfoxide-d_6 (Fig. 2) showed that the product contained three hydroxyl groups: anomeric, secondary, and primary.

Attempts to prepare an anilide and a diphenylhydrazone failed to yield solid derivatives.

The di-*O*-methyl derivative (30 mg) was treated with triphenylchloromethane (70 mg) in dry pyridine (2 ml) for 24 h. Ice water was added, the tacky precipitate was recovered with thorough washing and dissolved in ethanol, and triphenylcarbinol was removed by repeated crystallization. The syrupy residue (52 mg) was shown by thin-layer chromatography (benzene–methanol (9:1)) to consist of one component contaminated with a trace of triphenylcarbinol. The n.m.r. spectrum of this compound, recorded in dimethyl sulfoxide, showed the presence of approximately 15 phenyl protons per 2 hydroxyl protons, consistent with the formulation of this product as 2,3-di-*O*-methyl-6-*O*-trityl-D-altrose.

Periodate Oxidations

An aqueous solution (2 ml) containing about 0.2 μmole of the sugar derivative was diluted with aqueous sodium metaperiodate (2 ml, containing 0.24 μmole of oxidant). Blank periodate and iodate solutions were also prepared by diluting the standard periodate solution (2 ml aliquots) with equal volumes of water or ethylene glycol solutions, according to the modification of Aspinall and Ferrier (27). Each reaction mixture was stored at 22 °C, and its optical density at 223 mμ was measured at chosen intervals.

Some typical periodate uptake data (mole/mole), from which the $t_{\frac{1}{2}}$ values listed in Table II are taken, are as follows.

	Time (min)						
Compound	10	30	60	80	120	240	1440
1,2-*O*-Isopropylidene-D-glucofuranose	0.18	0.41	0.62	0.72			
D-Mannose 2,3-carbonate	0.22	0.46	0.67	0.77			
Methyl α-D-galacto-furanoside	0.10	0.23	0.36	0.44	0.56		
2,3-Di-*O*-methyl-D-altrose	0.14	0.37	0.52	0.62	0.75		
2,3-Di-*O*-methyl-D-galactose					0.12	0.37	0.91
2,3-Di-*O*-methyl-D-glucose						0.11	0.49
2,3-Di-*O*-methyl-D-mannose						0.14	0.51

ACKNOWLEDGMENTS

The authors thank M. Mazurek, who recorded the n.m.r. spectra, and W. Haid, who carried out the microanalyses.

Can. J. Chem. Downloaded from www.nrcresearchpress.com by 210.87.254.6 on 09/05/12
For personal use only.

REFERENCES

1. A. S. PERLIN. Can. J. Chem. **44**, 539 (1966).
2. R. U. LEMIEUX and J. D. STEVENS. Can. J. Chem. **44**, 249 (1966).
3. M. A. KABAYAMA and D. PATTERSON. Can. J. Chem. **36**, 563 (1958).
4. H. L. SCHLAFER and W. SCHAFFERNICHT. Angew. Chem. **72**, 618 (1960).
5. O. L. CHAPMAN and R. W. KING. J. Am. Chem. Soc. **86**, 1256 (1964).
6. C. B. PURVES and C. S. HUDSON. J. Am. Chem. Soc. **56**, 702 (1934).
7. C. T. BISHOP and F. P. COOPER. Can. J. Chem. **41**, 2743 (1963).
8. A. J. PARKER. Quart. Rev. London, **16**, 163 (1962).
9. M. RUDRUM and D. F. SHAW. J. Chem. Soc. 52 (1965).
10. A. S. PERLIN. Can. J. Chem. **42**, 1365 (1964).
11. R. E. REEVES. Advan. Carbohydrate Chem. **6**, 107 (1951).
12. R. U. LEMIEUX. *In* Molecular rearrangements. Paul de Mayo (*Editor*). Interscience Publishers, Inc., New York. 1964. Part 2.
13. E. L. ELIEL, N. L. ALLINGER, S. J. ANGYAL, and G. A. MORRISON. Conformational analysis. Interscience Publishers, Inc., New York. 1965.
14. V. S. R. RAO and J. F. FOSTER. J. Phys. Chem. **69**, 656 (1965).
15. B. HELFERICH and A. GNÜCHTEL. Ber. **74**, 1035 (1941).
16. B. CASU, M. REGGIANI, G. G. GALLO, and A. VIGEVANI. Tetrahedron Letters, 2839 (1964); 2253 (1965).
17. B. CASU, M. REGGIANI, G. G. GALLO, and A. VIGEVANI. Tetrahedron. In press.
18. A. S. PERLIN. Can. J. Chem. **44**, 1757 (1966).
19. G. J. ROBERTSON. J. Chem. Soc. 330 (1934).
20. J. C. IRVINE and J. P. SCOTT. J. Chem. Soc. **103**, 575 (1913).
21. G. J. ROBERTSON and R. A. LAMB. J. Chem. Soc. 1321 (1934).
22. B. HELFERICH and H. APPEL. Ber. **64B**, 1841 (1931).
23. E. L. HIRST and J. K. N. JONES. J. Chem. Soc. 506 (1946).
24. K. HEYNS and D. MÜLLER. Tetrahedron, **21**, 55 (1965).
25. G. J. ROBERTSON and C. F. GRIFFITH. J. Chem. Soc. 1193 (1935).
26. N. K. RICHTMYER and C. S. HUDSON. J. Am. Chem. Soc. **65**, 740 (1953).
27. G. O. ASPINALL and R. J. FERRIER. Chem. Ind. London, 1216 (1956).

Can. J. Chem. Downloaded from www.nrcresearchpress.com by 210.87.254.6 on 09/05/12
For personal use only.

Can. J. Chem. Downloaded from www.nrcresearchpress.com by 210.87.254.42 on 09/05/12
For personal use only.

CYCLOADDITIONS

X. KINETICS OF THE THERMAL DECARBONYLATION OF DICYCLOPENTADIENE-1,8-DIONE[1]

JOHN E. BALDWIN
Noyes Chemical Laboratory, University of Illinois, Urbana, Illinois

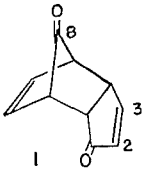
Received May 16, 1966

ABSTRACT

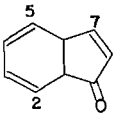
The thermal cycloelimination of carbon monoxide from dicyclopentadiene-1,8-dione is a kinetically well-behaved first-order reaction. At 380 °K the activation parameters for the process are $\Delta H^{\ddagger} = 34.5 \pm 0.8$ kcal mole^{-1} and $\Delta S^{\ddagger} = +9.8 \pm 2.3$ e.u. mole^{-1}. Application of the theoretical proposals of Woodward and Hoffmann indicates that this necessarily disrotatory decarbonylation may be concerted.

INTRODUCTION

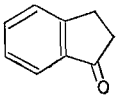
The thermal decomposition of dicyclopentadiene-1,8-dione (I) has been observed at 350° and at 240° to give carbon monoxide and *cis*-bicyclo[4.3.0]nona-2,4,7-trien-9-one (II) or 1-indanone (III) (1, 2). An analogous decarbonylation of a monochloro derivative of the dione I has been clarified (3).



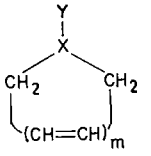
I



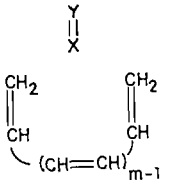
II



III



IV



V

The thermal decarbonylation of dicyclopentadiene-1,8-dione is a special case of a general reaction: cycloelimination of carbon monoxide from Δ^3-cyclopentenones (4). Indeed, the later category may be viewed as a special case of a still more general type of reaction: cycloelimination of a small molecule joined to an organic moiety through only one of its atoms, as in IV → V. Examples of this type of reaction with nitrogen, sulfur monoxide, sulfur dioxide, and nitrous oxide have been reported recently (5–8). Such reactions in the opposite direction are known, as in the cycloaddition of sulfur dioxide to 1,3-cycloheptadiene (9).

In common with other cycloaddition and cycloelimination reactions, these "end-on" reactions might proceed by a variety of mechanistic pathways (10, 11). At one extreme, the bonds to be broken (or made) between the reaction partners might be broken (or made) simultaneously or nearly simultaneously in a concerted fashion. At the other extreme, a stepwise process might give, through cleavage (or formation) of only one bond between the reaction partners, a bifunctional intermediate during the reaction.

[1]*For part IX in this series, see J. E. Baldwin, J. Org. Chem., in press.*

Can. J. Chem. Downloaded from www.nrcresearchpress.com by 210.87.254.42 on 09/05/12
For personal use only.

KINETIC RESULTS

The rate of cycloelimination of carbon monoxide from dicyclopentadiene-1,8-dione (I) could be followed conveniently at 104–125° by nuclear magnetic resonance (n.m.r.) spectroscopy.

In the olefinic proton region of the n.m.r. spectrum, dicyclopentadiene-1,8-dione exhibits a doublet of doublets at τ 2.75 which may be assigned (3) to H-3, and absorption from the other olefinic protons near τ 3.8. As the decarbonylation reaction proceeds, new doublets of doublets centered at τ 2.5 and 3.8 and a complex multiplet at 4.4 become evident. The olefinic n.m.r. absorptions in the product *cis*-bicyclo[4.3.0]-nona-2,4,7-trien-9-one (II) may be assigned as follows: τ 2.5 (1H) to H-7; τ 3.8 (1H) to H-8; and τ 4.4 (4H) to H-2, H-3, H-4, and H-5 (12).

To analyze mixtures of starting dione I and product II, one can compare the integrated absorptions caused by the single protons beta to the intact carbonyl function in both compounds, or convert the ratio (r) of areas from the τ 4.0–4.5 absorptions to those from the τ 3.4–4.0 signals to percentage of dione in the mixture by using the formula: percentage of dione $= 50(4 - r)/(2 + r)$, which takes into account the number of protons from each compound contributing to each area. The kinetic data were processed by a least-squares program for first-order reactions made available to us by Professor S. Smith and Dr. J. Petrovich. Sample kinetic data are given in Table I, and Table II summarizes all the rate constants measured with dioxane as the reaction solvent.

TABLE I

Kinetic data for the decarbonylation of dicyclopentadiene-1,8-dione in dioxane at 118.2°

Time (min)	Dione I (%)	$k_1 \times 10^4$ (s^{-1})
0	100	
61	78.4	0.6649
149	57.8	0.6132
232	42.3	0.6181
293	34.0	0.6137
364	24.0	0.6534
401	24.8	0.5795
		Average 0.6095

TABLE II

Rate constants for the decarbonylation of dicyclopentadiene-1,8-dione

Temperature (°C)	Concentration* (M)	No. points	$k_1 \times 10^4$ (s^{-1})	Deviation of $k_1 \times 10^4$ (s^{-1})	Deviation of k_1 (%)
125.2	0.27	5	1.238	0.02369	
125.2	0.53	5	1.405	0.03251	
125.2	0.99	5	1.316	0.02885	
125.2	†	15	1.294	0.02627	2.0
118.2	1.0	7	0.6095	0.01767	2.9
103.8	0.90	6	0.1069	0.002916	2.7

*Initial concentration of dione I in dioxane at room temperature.
†Points taken from the first three runs, having three different initial concentrations.

From the data in Table II, a least-squares fit to the Arrhenius equation gave $E_a = 35.24 \pm 0.43$ kcal $mole^{-1}$ and $\log_{10} A = 15.47 \pm 0.24$, where the indicated ranges are defined by the calculated probable errors.

Different results were obtained when attempts were made to follow the reaction with deuteriochloroform as solvent. During the initial phase of the reaction, n.m.r. peaks corresponding to product II and undecomposed dione were observed, but at later times the n.m.r. spectra showed that the reaction mixture contained dione I and 1-indanone (III) (13). Mixtures of the dione and indanone could be readily analyzed by n.m.r., for in a mixture of the two the absorptions below τ 3.0 are caused by the four aromatic protons of indanone and one proton of the dione, and the absorptions at τ 3.4–4.0 are caused by the other three olefinic protons of the dione I.

The shift from n.m.r. spectra indicating formation of one product (II) to those indicating formation of another (III) occurred at different points in different samples, from 10 to 30% reaction. This behavior is suggestive of the initial formation of II and carbon monoxide from I, and the subsequent acid-catalyzed rearrangement of II to the more stable 1-indanone. Once decomposition of the solvent yields some acid, the rearrangement of the initially formed product to 1-indanone becomes fast relative to the rate of decarbonylation. The kinetic data obtained in deuteriochloroform at 124.5° (10 points) gave a good first-order plot, with $k = 1.34 \pm 0.04 \times 10^{-4}$ s^{-1}.

DISCUSSION

The decarbonylation of dicyclopentadiene-1,8-dione occurs by a well-behaved first-order process at 104–125°. No significant difference in the rate is effected by changing the reaction solvent from dioxane to deuteriochloroform.

From the Arrhenius parameters for the decarbonylation, one may calculate an activation enthalpy and entropy: $\Delta H^{\ddagger} = 34.5 \pm 0.8$ kcal mole^{-1} and $\Delta S^{\ddagger} = +9.8 \pm 2.3$ e.u. mole^{-1} at 380 °K. Here, the estimated errors in $\Delta H^{\ddagger}$ and $\Delta S^{\ddagger}$ have been calculated from the equations developed by Petersen *et al.* (14), with the maximum error in rate constants being taken as 3%.

The large positive entropy of activation for the decarbonylation is suggestive of a transition-state configuration in which both bonds to the carbon of the carbon monoxide unit have been broken, thus permitting the carbon monoxide moiety to rotate about the axes perpendicular to the C—O bond. (Free carbon monoxide has a rotational entropy at 380 °K of +11.74 e.u. mole^{-1} (15, 16).) This conception of the activated complex is equally compatible with either a concerted decarbonylation or a two-step, nonconcerted decarbonylation in which one bond is cleaved first before attainment of the transition state. It views a rate-determining formation of a bifunctional intermediate as incompatible with the observed $\Delta S^{\ddagger}$.

For the generalized decarbonylation reaction of the type being considered (IV → V, where X=Y is C=O), construction of molecular orbital correlation diagrams (17, 18) and application of the theoretical proposals of Hoffmann and Woodward (11) and of Longuet-Higgens and Abrahamson (19) lead to the following conclusions: when m is zero and the reaction products are carbon monoxide and ethane, ethylene, or acetylene, the thermal decarbonylation is nonconcerted; when m is an odd integer, the disrotatory thermal decarbonylation may be concerted; when m is an even integer, the conrotatory thermal decarbonylation may be concerted.

Similar conclusions have been reached independently by Hoffmann (20)[2] and by Lemal and McGregor (5) for decarbonylations and some other "end-on" cycloeliminations.

It should be noted that the conclusions based on molecular orbital correlation diagrams are insensitive to the ordering of the energy levels in carbon monoxide with respect to

[2]*R. Hoffmann, private communication.*

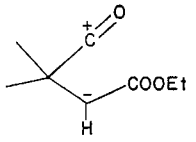
Can. J. Chem. Downloaded from www.nrcresearchpress.com by 210.87.254.42 on 09/05/12
For personal use only.

those of the olefinic cycloelimination product. They may be extended to those photochemical decarbonylations in which the $\pi \rightarrow \pi^*$ excitation of the olefinic moiety is responsible for the reaction; when m is an odd integer, the conrotatory $\pi \rightarrow \pi^*$ photochemical decarbonylation may be concerted; when m is an even integer, the disrotatory $\pi \rightarrow \pi^*$ photochemical decarbonylation may be concerted.

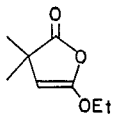
The simple molecular orbital correlation diagrams do not give any direct prediction of nonconcertedness or allowed concertedness for decarbonylations of IV (X=Y is C=O) when the $n \rightarrow \pi^*$ transition leads to reaction, for the π^* orbital of the carbonyl unit correlates with a π^* orbital in carbon monoxide and hence is not involved in the reaction.[3]

The implications of the conclusions based on molecular orbital theory[4] for "end-on" cycloeliminations of carbon monoxide from IV are interestingly reflected in chemical experience.

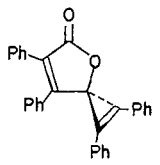
Thermal decarbonylations of saturated ketones, cyclopropanones, and cyclopropenones are predicted to occur in a stepwise, nonconcerted fashion. Thermolytic decarbonylations of ketones to ethanes are not commonly observed. The products from the reaction of ethyl diazoacetate with dimethylketene, ethyl β,β-dimethylacrylate, carbon monoxide, and the γ-lactone VII have been interpreted in terms of the intermediate formation of a cyclopropanone followed by unimolecular fission of one C—O bond to produce the bifunctional species VI, which either loses carbon monoxide or collapses to form the lactone (23). (Carbon monoxide might also stem from the Δ^3-oxacyclopentenone VII in a thermally allowed process.) More definitive evidence of the thermal decarbonylations of cyclopropanones may become available in the near future (24).



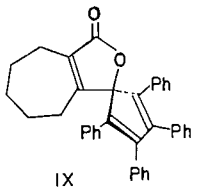
VI



VII



VIII



IX

Breslow and his co-workers have demonstrated (25, 26) that pyrolysis of diphenylcyclopropenone leads to carbon monoxide and diphenylacetylene. Concurrently, a product (VIII) is obtained in which, presumably, a bond adjacent to the carbonyl function has been cleaved and the resultant intermediate has added to the carbonyl of another ketone molecule. The decarbonylation does not follow good first-order kinetics. Cycloheptenocyclopropenone and tetracyclone at 250° give a 1:1 adduct (IX). These observations, of course, require no unique mechanistic interpretation; a precise mechanistic

[3]*Lemal and McGregor hold another opinion; cf. ref. 5, footnote 11.*

[4]*The thermal elimination of sulfur dioxide from 3-sulfolenes has just been shown to be stereospecific, in accord with theory (21, 22).*

Can. J. Chem. Downloaded from www.nrcresearchpress.com by 210.87.254.42 on 09/05/12
For personal use only.

description for the reactions leading to VIII and IX is not the issue here. That the two thermal decarbonylations occur with the concomitant formation of VIII and IX, whereas the decarbonylation of I is a smooth first-order process uncomplicated by a similar side-reaction, demonstrates a basic dissimilarity between the two cycloeliminations.

The decarbonylations of Δ^3-cyclopentenones and Δ^3-2-oxacyclopentenones are facile, common, and synthetically useful (4, 27). The kinetic data for the cycloelimination of carbon monoxide from dicyclopentadiene-1,8-dione are consistent with, but do not require, a concerted mechanism for the reaction. Here, geometric constraints demand a disrotatory stereochemical course in the process.

What information is available dovetails with the theoretical predictions based on molecular orbital correlation diagrams, but conclusive evidence of the concerted character of decarbonylations that are allowed to be concerted, and many details of the chemical behavior of ketones whose decarbonylations are predicted to be nonconcerted, remain obvious goals for further experimentation.

EXPERIMENTAL

Analyses were carried out by J. Nemeth and his associates, Urbana. Melting points are uncorrected. A Varian A-60 spectrometer was used for the n.m.r. analyses.

Dicyclopentadiene-1,8-dione (I)

The preparation of dicyclopentadiene-1,8-dione from cyclopentenone by the method of Hafner and Goliash (2) gave material having m.p. 98–101° (decomp.) (lit. (2) m.p. 103–104°) after recrystallization from ethanol. The infrared and n.m.r. spectra of the dione were consistent with published data (2, 3).

When 642 mg of dicyclopentadiene-1,8-dione, 811 mg of 2,4-dinitrophenylhydrazine, 5 ml of diglyme, 1 ml of 95% ethanol, and 3 drops of concentrated hydrochloric acid were mixed at room temperature, a precipitate formed; this 8-2,4-dinitrophenylhydrazone derivative was collected after 5 min to give 1.17 g (85.5% of theory), m.p. 197–198° (decomp.) (strong carbonyl band in the infrared at 1 710 cm^{-1}).

Anal. Calcd. for $C_{16}H_{12}N_4O_5$: C, 56.47; H, 3.55; N, 16.47. Found: C, 54.71, 54.69, 55.84; H, 3.56, 3.36, 3.70; N, 16.67.

This orange 8-2,4-dinitrophenylhydrazone was partially and smoothly rearranged to the red 1-2,4-dinitrophenylhydrazone, m.p. 200–201° (strong carbonyl in the infrared at 1 790 cm^{-1}), by attempted recrystallization from chloroform, nitromethane, or chlorobenzene, or by allowing it to remain in the acidic reaction mixture.

Anal. Found: C, 56.39, 56.35; H, 3.53, 3.49; N, 16.27, 16.55.

Mixtures of the two derivatives were separated by thin-layer chromatography on alumina, with benzene–chloroform (5:1 v/v) as developer (R_f of red 1-derivative, 0.6; of orange 8-derivative, 0.3). Quantitative estimates of the two compounds were conveniently made by infrared spectroscopy in the carbonyl region (28).

Kinetic Methods

Solutions of dicyclopentadiene-1,8-dione in dioxane or deuteriochloroform containing a small percentage of tetramethylsilane were sealed in n.m.r. tubes and heated for appropriate periods in a 40 cm diameter insulated kinetic bath, controlled to ±0.1° with a thermoregulator relay – mercury contactor and stirred by a Lightnin model L mixer. All temperatures were determined with the thermometers calibrated against National Bureau of Standards certified thermometers. The kinetic samples were analyzed by n.m.r. spectroscopy as described above. After a sample was analyzed, it was returned to the kinetic bath for further reaction. Crude kinetic data were processed by a least-squares program for computing first-order rate constants. The kinetic results are summarized in Tables I and II.

cis-Bicyclo[4.3.0]nona-2,4,7-trien-9-one (II)

Three n.m.r. tubes containing approximately 200 mg of *cis*-bicyclo[4.3.0]nona-2,4,7-trien-9-one (as judged by n.m.r. spectroscopy) and undecomposed dione I in dioxane were opened and concentrated by evaporation. Two flash distillations from a bath at 120–125° and 1 mm gave the trienone as a colorless liquid.

Anal. Calcd. for C_9H_8O: C, 81.79; H, 6.10. Found: C, 80.10, 81.43; H, 5.92, 6.27.

The infrared spectrum of the neat liquid showed ν_{max} 1 710 (vs) and 1 790, 1 650, 1 610, 1 595, and 1 585 cm^{-1} (all m). The adduct of the trienone with maleic anhydride had m.p. 239–241° (lit. (29) m.p. 240°).

Can. J. Chem. Downloaded from www.nrcresearchpress.com by 210.87.254.42 on 09/05/12
For personal use only.

ACKNOWLEDGMENTS

This work was supported in part by the Petroleum Research Fund (administered by the American Chemical Society), the National Science Foundation (grant No. GP-5226), and a DuPont grant-in-aid to the Department of Chemistry and Chemical Engineering of the University of Illinois.

I thank Professors R. Hoffmann, R. Marcus, and S. Smith for very helpful discussions.

REFERENCES

1. C. H. DePuy and C. E. Lyons. J. Am. Chem. Soc. **82**, 631 (1960).
2. K. Hafner and K. Goliasch. Chem. Ber. **94**, 2909 (1961).
3. K. V. Scherer, Jr. and L. Scerbo. Tetrahedron Letters, **30**, 2127 (1963).
4. C. F. H. Allen. Chem. Rev. **62**, 653 (1962); **37**, 209 (1945).
5. D. M. Lemal and S. D. McGregor. J. Am. Chem. Soc. **88**, 1335 (1966).
6. Y. Okumura and S. Masui. J. Org. Chem. **30**, 2060 (1965).
7. L. A. Carpino and L. V. McAdams III. J. Am. Chem. Soc. **87**, 5804 (1965).
8. L. A. Carpino and D. E. Barr. J. Org. Chem. **31**, 764 (1966).
9. S. F. Birch, R. A. Dean, N. J. Hunter, and E. V. Whitehead. J. Org. Chem. **22**, 1590 (1957).
10. R. B. Woodward and T. J. Katz. Tetrahedron, **5**, 70 (1959).
11. R. Hoffmann and R. B. Woodward. J. Am. Chem. Soc. **87**, 2047 (1965).
12. E. Vogel and E.-G. Wyes. Chem. Ber. **98**, 3680 (1965).
13. Nuclear magnetic resonance spectra catalog. Varian Associates, Palo Alto, California. 1962. Spectrum No. 229.
14. R. C. Petersen, J. H. Markgraf, and S. D. Ross. J. Am. Chem. Soc. **83**, 3819 (1961).
15. M. A. Paul. Principles of chemical thermodynamics. McGraw-Hill Book Co., Inc., New York. 1951. p. 665.
16. O. R. Gilliam, C. M. Johnson, and W. Gordy. Phys. Rev. **78**, 140 (1950).
17. C. J. Ballhausen and H. B. Gray. Molecular orbital theory. W. A. Benjamin, Inc., New York. 1964. p. 40.
18. C. A. Coulson. Valence. 2nd ed. Oxford University Press, London. 1961. p. 223.
19. H. C. Longuet-Higgens and E. W. Abrahamson. J. Am. Chem. Soc. **87**, 2045 (1965).
20. R. Hoffmann and R. B. Woodward. 150th Meeting, American Chemical Society, Atlantic City, New Jersey, September 1965. Abstr. p. 8S.
21. S. D. McGregor and D. M. Lemal. J. Am. Chem. Soc. **88**, 2858 (1966).
22. W. L. Mock. J. Am. Chem. Soc. **88**, 2857 (1966).
23. A. S. Kende. Chem. Ind. London, 1053 (1956).
24. N. J. Turro, W. B. Hammond, and P. A. Leermakers. J. Am. Chem. Soc. **87**, 2774 (1965).
25. R. Breslow, T. Eicher, A. Krebs, R. A. Paterson, and J. Posner. J. Am. Chem. Soc. **87**, 1320 (1965).
26. R. Breslow, L. J. Altman, A. Krebs, E. Mohacsi, I. Murata, R. A. Peterson, and J. Posner. J. Am. Chem. Soc. **87**, 1326 (1965). R. Breslow and L. J. Altman. J. Am. Chem. Soc. **88**, 504 (1966).
27. M. A. Ogliaruso, M. G. Romanelli, and E. I. Becker. Chem. Rev. **65**, 261 (1965).
28. J. E. Baldwin. Tetrahedron Letters, **30**, 2029 (1964).
29. K. Alder and F. H. Flock. Chem. Ber. **87**, 1916 (1954).

Can. J. Chem. Downloaded from www.nrcresearchpress.com by 210.87.254.42 on 09/05/12
For personal use only.

Can. J. Chem. Downloaded from www.nrcresearchpress.com by 210.87.254.6 on 09/05/12
For personal use only.

ÉTUDES CONFORMATIONNELLES EN SÉRIE CYCLOPENTANIQUE

II. SUR LA STÉRÉOCHIMIE DES ALCOOLS TERTIAIRES DÉRIVÉS DE LA *t*-BUTYL-3 CYCLOPENTANONE[1]

JEAN-CLAUDE RICHER ET PATRICE BÉLANGER
Département de Chimie, Université de Montréal, Montréal, Québec

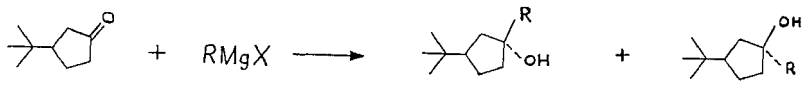
Reçu le 31 mars 1966

RÉSUMÉ

La stéréochimie des *t*-butyl-3 alkyl-1 cyclopentanols obtenus par addition d'organomagnésiens sur la *t*-butyl-3 cyclopentanone a été établie grâce à des synthèses stéréospécifiques et aussi en se basant sur les résultats d'oxydation de ces alcools par le permanganate de potassium.

INTRODUCTION

A l'occasion d'un travail précédent (1), la déshydratation d'un mélange de *t*-butyl-3 isopropyl-1 cyclopentanols (III*c* et IV*c*) obtenus par addition du bromure d'isopropylmagnésium (II*c*) sur la *t*-butyl-3 cyclopentanone (I) a été rapportée; la stéréochimie de l'addition du réactif de Grignard n'avait toutefois pas été déterminée. Le présent travail a donc été entrepris dans le but de spécifier la configuration relative des alcools tertiaires qui sont formés.



I II III IV

SCHÉMA RÉACTIONNEL 1. *a*, R = Me; *b*, R = Et; *c*, R = *i*-Pr.

RÉSULTATS

1. t-Butyl-3 cyclopentanone (I)

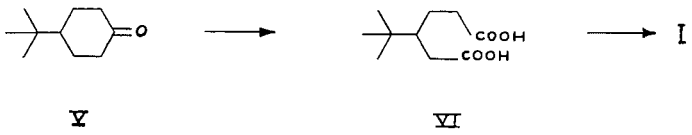
Au cours d'une étude précédente (1), une synthèse utilisant la *t*-butyl-4 cyclohexanone (V) comme produit de départ a été proposée pour la préparation de I; la série de réactions impliquées est résumée dans le Schéma Réactionnel 2. Dans les cadres du présent travail, une autre synthèse de I a été mise au point, utilisant la cyclopentanone (VII) comme produit de départ; cette méthode, basée sur la transformation de VII en cyclopentène-2 one (IX) suivant le processus expérimental de Garbisch (2) et suivi d'une addition-1,4 du chlorure de *t*-butylmagnésium, est résumée dans le Schéma Réactionnel 3. La cétone ainsi obtenue est en tous points identique à celle décrite précédemment.

2. Addition de réactifs de Grignard sur la t-butyl-3 cyclopentanone (I)

L'addition de réactifs de Grignard sur le groupement carbonyle de I conduit à deux produits principaux: les *t*-butyl-3 alkyl-1 cyclopentanols *cis* (III) et *trans* (IV). Par définition, l'isomère *cis* est celui où les deux groupes alkyles sont du même côté du cycle.

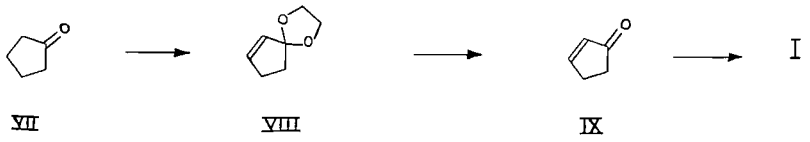
L'addition de l'iodure de méthylmagnésium (II*a*) sur I conduit au mélange des alcools tertiaires attendus (III*a* et IV*a*). Une analyse chromatographique en phase gazeuse montre que l'isomère *trans* IV*a* prédomine légèrement avec un pourcentage de 50.5%. Les alcools tertiaires peuvent être séparés par chromatographie en phase gazeuse préparative. Le

[1]*Extrait de la thèse de doctorat soumise par Monsieur Bélanger en vue de l'obtention du grade de Ph.D. en chimie, Faculté des Sciences, Université de Montréal, Montréal, février 1966.*



V VI

SCHÉMA RÉACTIONNEL 2.



VII VIII IX

SCHÉMA RÉACTIONNEL 3.

t-butyl-3 méthyl-1 cyclopentanol *cis* (III*a*) est un produit facilement sublimable fondant à 51 °C. Son épimère *trans* IV*a* est aussi un solide facilement sublimable de p.f. 56 °C.

Les *t*-butyl-3 éthyl-1 cyclopentanols *cis* (III*b*) et *trans* (IV*b*) sont préparés par l'addition du bromure d'éthylmagnésium (II*b*) sur la *t*-butyl-3 cyclopentanone (I). Une analyse par chromatographie en phase gazeuse montre la présence des deux alcools attendus; le produit *trans* IV*b* prédomine avec un pourcentage de 56.1%. Séparés l'un de l'autre par chromatographie en phase gazeuse préparative, le *t*-butyl-3 éthyl-1 cyclopentanol *cis* (III*b*) est un liquide distillant à 95 °C sous 45 mm de Hg et possédant un indice de réfraction de 1.4564 à 25 °C; son isomère *trans* IV*b* distille à 95 °C sous 45 mm de Hg et possède un indice de réfraction de 1.4510 à 25 °C.

TABLEAU I

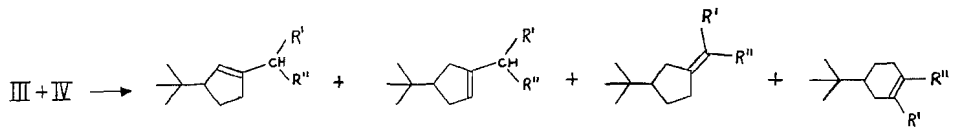
t-Butyl-3 cyclopentanols	Point de fusion (°C)	Point d'ébullition (°C)	n_D^{25}
Méthyl-1 *cis* (III*a*)	51		
Méthyl-1 *trans* (IV*a*)	56		
Éthyl-1 *cis* (III*b*)		95 sous 45 mm Hg	1.4510
Éthyl-1 *trans* (IV*b*)		95 sous 45 mm Hg	1.4564
Isopropyl-1 *cis* (III*b*)		75 sous 28 mm Hg	1.4558
Isopropyl-1 *trans* (IV*b*)		74 sous 28 mm Hg	1.4524

Les *t*-butyl-3 isopropyl-1 cyclopentanols *cis* (III*c*) et *trans* (IV*c*) sont préparés par l'addition du bromure d'isopropylmagnésium (II*c*) sur la *t*-butyl-3 cyclopentanone (I); il est à noter que les alcools tertiaires attendus ne représentent qu'environ 10% des produits de la réaction, qui sont constitués principalement de produits d'aldolisation et de réduction. Les deux alcools désirés peuvent toutefois être obtenus à l'état pur par chromatographie en phase gazeuse préparative; le *t*-butyl-3 isopropyl-1 cyclopentanol *trans* (IV*c*), qui représente 61% des alcools tertiaires attendus, distille à 74 °C sous 28 mm de Hg et possède un indice de réfraction de 1.4524 à 25 °C, alors que l'isomère *cis* III*c* (39%) distille à 74 °C sous 28 mm de Hg et possède un indice de réfraction de 1.4558 à 25 °C.

3. Préparation des t-butyl-3 alkyl-1 cyclopentènes (X) et des t-butyl-4 alkyl-1 cyclopentènes (XI)

La déshydratation du mélange des *t*-butyl-3 alkyl-1 cyclopentanols III et IV par l'acide sulfurique conduit principalement aux hydrocarbures X et XI attendus (Schéma Réactionnel 4). Dans le cas des alcools de la série éthyle (III*b* et IV*b*) et de la série isopropyle (III*c* et IV*c*) les *t*-butyl-3 alkylidène cyclopentanes (XII) et les *t*-butyl méthyl cyclohexènes

Can. J. Chem. Downloaded from www.nrcresearchpress.com by 210.87.254.6 on 09/05/12
For personal use only.



X XI XII XIII

SCHÉMA RÉACTIONNEL 4. *a*, R′ = R″ = H; *b*, R′ = H, R″ = CH_3; *c*, R′ = R″ = CH_3.

(XIII) sont aussi obtenus. Le Tableau II résume la composition des produits de déshydratation des *t*-butyl-3 alkyl-1 cyclopentanols III et IV par l'acide sulfurique. L'examen de ce tableau confirme une fois de plus que le mécanisme de déshydratation se fait par l'intermédiaire d'un carbocation et qu'il y a possibilité de réarrangement, lorsque le carbocation tertiaire peut se réarranger en un deuxième carbocation tertiaire. Les hydrocarbures du type XI et XII ont pu être isolés par chromatographie en phase gazeuse et leur identification s'est faite principalement par les spectres de résonance magnétique nucléaire. Les différentes propriétés physiques de ces hydrocarbures sont rapportées dans le Tableau III.

TABLEAU II

Deshydratation des *t*-butyl-3 alkyl-1 cyclopentanols III et IV par l'acide sulfurique

	Produit (%)			
Cyclopentanols	X	XI	XII	XIII
t-Butyl-3 méthyl-1 (III*a* et IV*a*)	61.6	38.4	—	—
t-Butyl-3 éthyl-1 (III*b* et IV*b*)	51.6	40.1	3.6	4.7
t-Butyl-3 isopropyl-1 (III*c* et IV*c*)	25.0	9.0	41.0	25.0

TABLEAU III

Propriétés physiques des hydrocarbures

Hydrocarbure	Point d'ébullition (°C)	n_D^{25}	Résonance magnétique nucléaire* (p.p.m.) A	B
t-Butyl-3 méthyl-1 cyclopentène (X*a*)	60 sous 95 mm Hg	1.4390	0.83	5.32
t-Butyl-4 méthyl-1 cyclopentène (XI*a*)	60 sous 95 mm Hg	1.4410	0.83	5.25
t-Butyl-3 éthyl-1 cyclopentène (X*b*)	74 sous 109 mm Hg	1.4428	0.87	5.33
t-Butyl-4 éthyl-1 cyclopentène (XI*b*)	74 sous 109 mm Hg	1.4450	0.87	5.25
t-Butyl-3 isopropyl-1 cyclopentène (X*c*)	67 sous 32 mm Hg	1.4478	0.85	5.28
t-Butyl-4 isopropyl-1 cyclopentène (XI*c*)	67 sous 32 mm Hg	1.4522	0.85	5.20
t-Butyl-3 isopropylidène cyclopentane (XII*c*)	67 sous 32 mm Hg	1.4640	0.88	—

*Les spectres de résonance magnétique nucléaire ont été déterminés en solution dans le chloroforme deutérié avec le tétraméthylsilane comme standard interne. A, protons du *t*-butyle; B, proton éthylénique.

4. Préparation des alcools tertiaires III et IV par l'intermédiaire d'époxydes

Une méthode simple et rapide pour passer d'un hydrocarbure non-saturé à un alcool consiste à préparer l'époxyde, qu'il ne reste qu'à réduire à l'aide d'un hydrure complexe (Schéme Réactionnel 5); une telle méthode a été utilisée très souvent (3). De plus, la réduction d'un époxyde conduit toujours à l'alcool le plus substitué. Ainsi, l'époxydation d'un *t*-butyl-3 alkyl-1 cyclopentène (X) conduira à la formation des *t*-butyl-3 alkyl-1 cyclopentanols *cis* et *trans* (III et IV). Concernant la stéréochimie de la réaction d'époxydation, Henbest (4) a trouvé lors d'une étude sur le méthyl-4 cyclopentène (XXI*a*) que, par

Can. J. Chem. Downloaded from www.nrcresearchpress.com by 210.87.254.6 on 09/05/12
For personal use only.

réaction avec un peracide, cet hydrocarbure conduit à un mélange de deux époxydes (XXII*a* et XXIII*a*) où l'isomère *trans* XXII*a* est prédominant. Dans un travail récent (5), une extension de ces résultats a été faite au *t*-butyl-4 cyclopentène (XXI*c*).

Cette méthode a été appliquée aux alcènes du type X, XI et XII. Les époxydations sont effectuées dans le chlorure de méthylène à l'aide d'acide *m*-chloroperbenzoique (XIV) d'après les indications de Rickborn (6). Par chromatographie en phase gazeuse, les

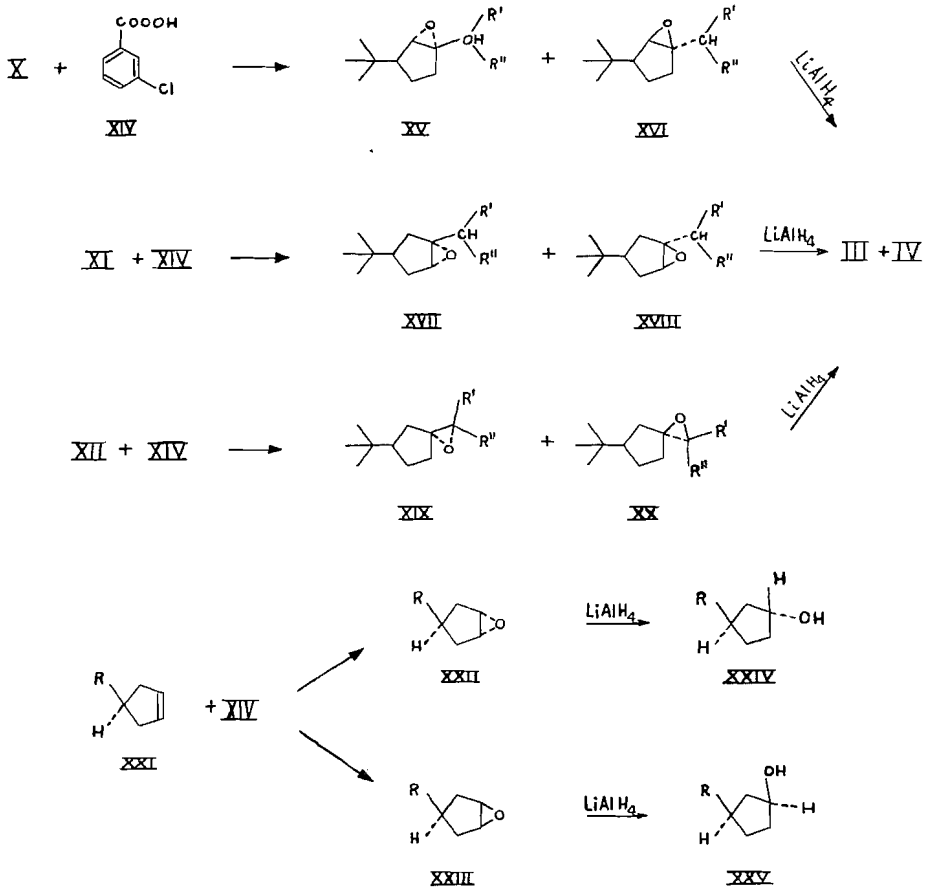


SCHÉMA RÉACTIONNEL 5. *a*, R′ = R″ = H; *b*, R′ = H, R″ = CH_3; *c*, R′ = R″ = CH_3 (se referent aux produits XV à XX). *a*, R = Me; *b*, R = *i*-Pr; *c*, R = *t*-Bu (se referent aux produits XXI à XXV).

pourcentages relatifs des époxydes *cis* et *trans* ont été déterminés; ces résultats sont résumés dans le Tableau IV. La réduction de ces époxydes par l'hydrure double de lithium et d'aluminium dans le tétrahydrofuranne conduit à un mélange de *t*-butyl-3 alkyl-1 cyclopentanols III et IV où l'isomère *cis* (provenant d'une attaque *trans* par rapport au groupe *t*-butyl durant la réaction d'époxydation) est en majorité. Les pourcentages relatifs d'alcools III et IV présents dans les milieux réactionnels sont rapportés dans le Tableau IV.

A l'aide de ces résultats et se basant sur les expériences précédentes de Henbest (4), la configuration relative de chaque alcool tertiaire obtenu par réaction de Grignard sur la *t*-butyl-3 cyclopentanone (I) peut donc être considérée comme établie.

Can. J. Chem. Downloaded from www.nrcresearchpress.com by 210.87.254.6 on 09/05/12
For personal use only.

TABLEAU IV

Époxydation et réduction

Hydrocarbure	Époxyde *trans*		*t*-Butyl-3 alkyl-1 cyclopentanol *cis*	
	No.	%	No.	%
t-Butyl-3 méthyl-1 cyclopentène (X*a*)	XV*a*	94*	III*a*	94
t-Butyl-4 méthyl-1 cyclopentène (XI*a*)	XVII*a*	93	III*a*	93
t-Butyl-3 éthyl-1 cyclopentène (X*b*)	XV*b*	95	III*b*	94
t-Butyl-4 éthyl-1 cyclopentène (XI*b*)	XVII*b*	93	III*b*	93
t-Butyl-3 isopropyl-1 cyclopentène (X*c*)	XV*c*	95	III*c*	95
t-Butyl-4 isopropyl-1 cyclopentène (XI*c*)	XVII*c*	91	III*c*	92
t-Butyl-3 isopropylidène cyclopentane (XII*c*)	XIX*c*	59	III*c*	61

*Les valeurs de ce tableau ont été déterminées par chromatographie en phase gazeuse, en calculant la surface sous les pics à l'aide d'un planimètre.

5. Oxydation permanganique des alcools III et IV

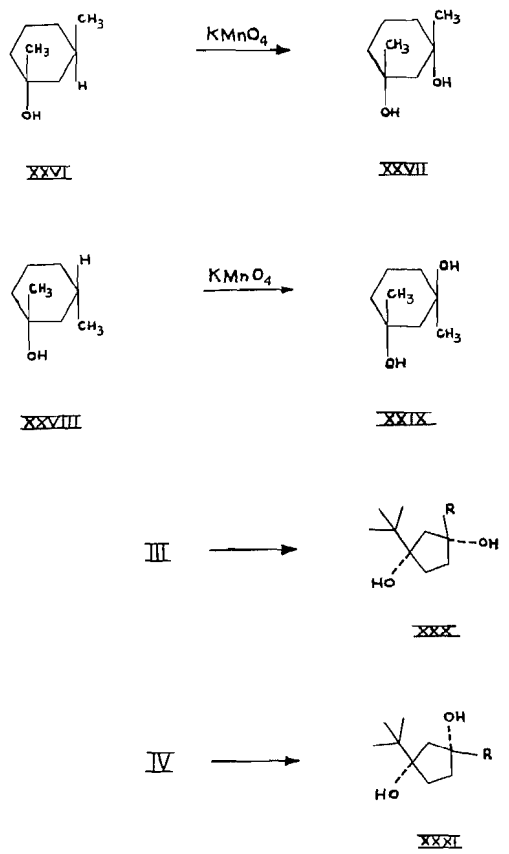
Plusieurs auteurs (7–11) ont montré que les hydrogènes tertiaires peuvent être facilement oxydés par les agents puissants. En particulier, Eastman et Quinn (10) ont noté que l'oxydation du diméthyl-1,3 cyclohexanol *cis* (XXVI) par le permanganate de potassium conduit au diméthyl-1,3 cyclohexanediol-1,3 *cis* (XXVII), lequel réagit avec l'anhydride borique pour former un borate cyclique. De même, l'oxydation du diméthyl-1,3 cyclohexanol *trans* (XXVIII) conduit au diméthyl-1,3 cyclohexanediol-1,3 *trans* (XXIX), lequel ne forme pas de borate cyclique. Les auteurs terminent leur article par la conclusion suivante: "Il existe une similitude formelle entre l'attaque, par le permanganate, d'une liaison π pour donner un glycol *cis*, et l'attaque d'un lien σ d'une liaison C—H pour mener à l'obtention d'un alcool tertiaire avec rétention de configuration du carbone." Il faut remarquer que lors de ces oxydations l'hydrogène tertiaire conduit à un hydroxyle tertiaire de même configuration.

L'application de cette méthode aux alcools tertiaires III et IV a été effectuée (Schéma Réactionnel 6);[2] les propriétés des diols obtenus (XXX et XXXI) sont résumées dans le Tableau V.

Il est maintenant bien établi (12–14) que des ponts hydrogène intramoléculaires peuvent se former lorsque les groupes hydroxyles d'un diol sont placés dans un environnement géométrique favorable. Ainsi, le diméthyl-1,3 cyclohexanediol-1,3 *cis* (XXVII) peut former ce pont hydrogène, qui est facilement détectable dans le spectre infra-rouge. Les *t*-butyl-3 alkyl-1 cyclopentanediols-1,3 *cis* (XXX) peuvent aussi former des ponts hydrogènes, ce qui n'est pas possible avec les isomères *trans* XXXI. Sachant que l'hydrogène tertiaire est oxydé en hydroxyle sans que la configuration du carbone ne soit touchée, il en résulte que les diols III*a* et III*b*, qui montrent la présence de ponts hydrogène intramoléculaires, sont dérivés des alcools tertiaires III*a* et III*b* où les groupes *t*-butyl et R étaient *cis*, l'un par rapport à l'autre. Il est à noter que les conclusions obtenues grâce à cette méthode sont identiques à celles dérivées à l'aide des concepts présentés dans la section précédente.

[2]*Cette méthode n'a pas été appliquée aux alcools tertiaires IIIc et IVc à cause des complications qui auraient pu résulter de la présence de deux types différents d'hydrogènes attachés à des carbones tertiaires.*

Can. J. Chem. Downloaded from www.nrcresearchpress.com by 210.87.254.6 on 09/05/12
For personal use only.



XXVI XXVII XXVIII XXIX XXX XXXI

SCHÉMA RÉACTIONNEL 6. *a*, R = Me; *b*, R = Et.

TABLEAU V

Oxydations permanganiques des *t*-butyl-3 alkyl-1 cyclopentanols *cis* (III) et *trans* (IV)

Alcool de départ	Diol obtenu	Point de fusion (°C)	Rendement* (%)	Pont hydrogène (cm^{-1})
t-Butyl-3 méthyl-1 cyclopentanol *cis* (III*a*)	*t*-Butyl-3 méthyl-1 cyclopentanediol-1,3 *cis* (XXX*a*)	125	10	70
t-Butyl-3 méthyl-1 cyclopentanol *trans* (IV*a*)	*t*-Butyl-3 méthyl-1 cyclopentanediol-1,3 *trans* (XXXI*a*)	107	6	0
t-Butyl-3 éthyl-1 cyclopentanol *cis* (III*b*)	*t*-Butyl-3 éthyl-1 cyclopentanediol-1,3 *cis* (XXX*b*)	104	9	90
t-Butyl-3 éthyl-1 cyclopentanol *trans* (IV*b*)	*t*-Butyl-3 éthyl-1 cyclopentanediol-1,3 *trans* (XXXI*b*)	85	7	0

*Les rendements indiqués sont des rendements, tenant compte des alcools de départ, qui ont été récupérés.

DISCUSSION

La stéréochimie relative des alcools III et IV a maintenant été établie grâce à des synthèses et des oxydations stéréospécifiques. Ces résultats indiqueraient que l'addition de réactifs de Grignard sur la *t*-butyl-3 cyclopentanone s'effectuerait avec une sélectivité minime mais définie par le côté opposé au groupe *t*-butyle. Cette légère préférence est conforme aux concepts complètement stériques proposés récemment (15) pour l'addition d'agents nucléophiles sur les groupements carbonyles cycliques.

Can. J. Chem. Downloaded from www.nrcresearchpress.com by 210.87.254.6 on 09/05/12
For personal use only.

Les configurations relatives attribuées aux alcools tertiaires III et IV sont en accord avec le temps relatif de rétention de ces alcools lors de la chromatographie en phase gazeuse. En effet, il est maintenant bien établi (16–18) que lors de chromatographie, tant sur colonne qu'en phase gazeuse, les alcools les plus empêchés sont élués les plus rapidement. Dans le cas présent, les alcools du type IV, qui ont leur groupe OH *cis* par rapport au groupement *t*-butyle et qui par conséquent sont les plus empêchés, sont toujours élués plus rapidement que leurs isomères III, dans lesquels le groupe OH est *trans* par rapport au groupement *t*-butyle.

La spectroscopie infra-rouge confirme de plus la configuration relative attribuée aux alcools tertiaires III et IV. L'utilité de cette méthode physique dans le cas des alcools secondaires est connue depuis les travaux de Jones et ses collaborateurs (19). En série cyclopentanique, Hückel (20) a montré que le cyclopentanol possède des bandes vers 1 070 et 995 cm^{-1}, attribuables à des vibrations C—O. Dans son travail sur les isopropyl-3 cyclopentanols *cis* et *trans* (XXIV*b* et XXV*b*), Hückel (21) obtint pour chacun des isomères des spectres infra-rouges différents; dans le cas du produit *cis* XXV*b* il nota la présence de bande à 1 071 et 994 cm^{-1}, alors que pour l'isopropyl-3 cyclopentanol *trans* (XXIV*b*) la bande à 1 071 cm^{-1} demeure constante mais la bande à 994 cm^{-1} se dédouble en deux bandes à 1 014 et 996 cm^{-1}. Dans le cas des *t*-butyl-3 cyclopentanols XXIV*c* et XXV*c* et des méthyl-3 cyclopentanols XXIV*a* et XXV*a*, des résultats semblables ont été rapportés récemment (5). En faisant la comparaison des spectres infra-rouges des *t*-butyl alkyl-1 cyclopentanols *cis* (III) et *trans* (IV) un dédoublement des bandes dans la région des vibrations C—O a pu être observé. Le Tableau VI résume ces observations, et les résultats confirment une fois de plus les attributions de configurations faites précédemment pour les alcools tertiaires III et IV, obtenus par l'addition de réactifs de Grignard sur la *t*-butyl-3 cyclopentanone (I).

TABLEAU VI

Spectres infra-rouges de quelques cyclopentanols substitués

Alcool	cm^{-1}	cm^{-1}
Méthyl-3 cyclopentanol *cis* (XXV*a*)*	1 068	995
Méthyl-3 cyclopentanol *trans* (XXIV*a*)*	1 065	1 010 et 995
Isopropyl-3 cyclopentanol *cis* (XXV*b*)*	1 070	997
Isopropyl-3 cyclopentanol *trans* (XXIV*b*)*	1 070	1 014 et 996
t-Butyl-3 cyclopentanol *cis* (XXV*c*)*	1 090	985
t-Butyl-3 cyclopentanol *trans* (XXIV*c*)*	1 090	1 005 et 985
t-Butyl-3 méthyl-1 cyclopentanol *cis* (III*a*)	1 075	1 047 et 1035
t-Butyl-3 méthyl-1 cyclopentanol *trans* (IV*a*)	1 080	1 035
t-Butyl-3 éthyl-1 cyclopentanol *cis* (III*b*)	1 080	1 055 et 1 047
t-Butyl-3 éthyl-1 cyclopentanol *trans* (IV*b*)	1 075	1 045
t-Butyl-3 isopropyl-1 cyclopentanol *cis* (III*c*)	1 090	1 035 et 1 020
t-Butyl-3 isopropyl-1 cyclopentanol *trans* (IV*c*)	1 087	1 040

*Les valeurs sont tirées de la réf. 5.

PARTIE EXPÉRIMENTALE

Les spectres infra-rouges ont été pris sur un spectrophotomètre Beckman modèle IR-8 à double réseau; les spectres infra-rouges des *t*-butyl-3 alkyl-1 cyclopentanols *cis* (III) et *trans* (IV) ont été déterminés sur un appareil Perkin–Elmer modèle 21; les mesures de ponts hydrogène ont été faites en solution saturée du diol dans le tétrachlorure de carbone sur un appareil Perkin-Elmer modèle 112 avec prisme de fluorure de lithium. La cellule utilisée mesurait 3 cm de longueur. Les analyses par chromatographie en phase gazeuse ont été effectuées sur un appareil Kromo-Tog modèle K-2 de la compagnie Burrell. Les séparations par chromatographie en phase gazeuse préparative ont été faites sur un appareil Prep-Partitioner modèle 24 de la compagnie Fisher Scientific. Les spectres de résonance magnétique nucléaire ont été pris à l'aide d'un spectromètre modèle A-60 de la compagnie Varian. Les déplacements chimiques (δ) sont exprimés en parties

Can. J. Chem. Downloaded from www.nrcresearchpress.com by 210.87.254.6 on 09/05/12
For personal use only.

par million. A moins d'indication contraire, le solvant utilisé est le chloroforme deutérié, et le tétraméthylsilanne est utilisé comme référence interne. Les points de fusion ont été déterminés sur un appareil Hot Stage de la compagnie Reichert (Autriche), et ne sont pas corrigés. Les indices de réfraction ont été déterminés à l'aide d'un réfractomètre de type Abbé. Les analyses élémentaires ont été faites par Claude Daesslé, Organic Microanalysis, Montréal.

1. t-Butyl-3 cyclopentanone (I)

1.1. Cyclopentène-2 one (IX)

Utilisant la procédure générale de bromuration décrite par Garbisch (2), 67.2 g (0.8 mole) de cyclopentanone (VII) ont conduits à 18.1 g de cyclopentène-2 one (IX): p.é. 78 °C sous 59 mm Hg et n_D^{25} 1.4754 (litt. (2) p.é. 68–69 °C sous 23 mm Hg et n_D^{29} 1.4739).

1.2. Addition de Grignard sur IX

A une solution de chlorure de *t*-butylmagnésium préparée à partir de 46 g de chlorure de *t*-butyl et 11.5 g de magnésium dans 300 ml d'éther, 18 g de cyclopentène-2 one (IX) sont ajoutés à 0 °C; le mélange est ensuite porté à reflux pour une durée de 6 h. Après hydrolyse du complexe par addition d'une solution d'acide acétique 10%, le produit est extrait à la manière habituelle et conduit à 18.4 g (59% du rendement théorique) de *t*-butyl-3 cyclopentanone (I): p.é. 84 °C sous 35 mm Hg et n_D^{25} 1.4512 (litt. (22) n_D^{20} 1.4505). La chromatographie en phase gazeuse de cette cétone à 180 °C à l'aide d'une colonne de 4 m contenant 10% d'Hyprose adsorbé sur du Chromosorb P révèle la présence de 2% de la cétone non-saturée IX à l'état d'impureté.

2. Addition des réactifs de Grignard sur la t-butyl-3 cyclopentanone (I)

2.1. Les t-butyl-3 méthyl-1 cyclopentanols cis (IIIa) et trans (IVa)

A une solution d'iodure de méthylmagnésium (II*a*) préparée à partir de 4.4 g de magnésium et de 22 g d'iodure de méthyle, 14 g (0.1 mole) de *t*-butyl-3 cyclopentanone sont ajoutés à 0 °C; après un reflux de 1 h, le complexe est détruit par addition de 100 ml d'une solution 1 *M* d'acide tartrique, et le produit, extrait à la manière habituelle, fournit 14 g (90% du rendement théorique) d'un solide blanc fondant à 38 °C et distillant à 22 °C sous 68 mm Hg.

Anal. Calc. pour $C_{10}H_{20}O$: C, 76.86; H, 12.90. Trouvé: C, 77.01; H, 13.09.

Une chromatographie en phase gazeuse à 110 °C à l'aide d'une colonne de 4 m contenant 10% d'Hyprose adsorbé sur du Chromosorb P montre la présence de 50.5% de l'alcool *trans* IV*a* de temps de rétention 55 min, et de 49.5% d'alcool *cis* III*a* de temps de rétention 59 min. Une chromatographie en phase gazeuse préparative à 120 °C à l'aide de huit colonnes contenant 10% d'Hyprose adsorbé sur du Chromosorb P permet d'isoler chacun des alcools, dont les propriétés sont résumées dans le Tableau I.

2.2. Les t-butyl-3 éthyl-1 cyclopentanols cis (IIIb) et trans (IV)

A une solution de bromure d'éthylmagnésium (II*b*) préparée à partir de 5 g de magnésium et de 35 g de bromure d'éthyle, 20 g (0.14 mole) de *t*-butyl-3 cyclopentanone (I) sont ajoutés à 0 °C; après un reflux de 1 h, le produit est isolé à la manière habituelle et fournit 21 g (87% du rendement théorique) d'un liquide jaunâtre distillant à 155 °C sous 185 mm Hg et ayant l'indice de réfraction de 1.4532 à 27 °C.

Anal. Calc. pour $C_{11}H_{22}O$: C, 77.58; H, 13.02. Trouvé: C, 77.52; H, 12.7.

Le spectre infra-rouge de ce produit montre la disparition totale de la bande carbonyle à 1 740 cm^{-1} et l'apparition d'une large bande hydroxyle à 3 400 cm^{-1}. La chromatographie en phase gazeuse à 135 °C montre la présence de 56.1% de l'alcool *trans* IV*b* de temps de rétention 48 min, et de 43.9% de l'alcool *cis* III*b* de temps de rétention 55 min. Une chromatographie en phase gazeuse préparative d'après les conditions déjà décrites dans la section précédente permet d'isoler chacun des constituants, dont les propriétés sont résumées dans le Tableau I.

2.3. Les t-butyl-3 isopropyl-1 cyclopentanols cis (IIIc) et trans (IVc)

A une solution de bromure d'isopropylmagnésium (II*c*) préparée à partir de 3.10 g de magnésium et de 18.6 g de bromure d'isopropyl sont ajoutés 14 g (0.1 mole) de *t*-butyl-3 cyclopentanone (I). Après un reflux de 15 h, le produit est isolé à la manière habituelle et fournit 15.4 g (76% du rendement théorique) d'un résidu jaune qui, lorsque distillé sous vide, se sépare en deux fractions: (*a*) 4.01 g (26% du total), p.é. 87 °C sous 25 mm Hg et n_D^{23} 1.4542; (*b*) 11.3 g (74% du total), p.é. 152 °C sous 2 mm Hg (il s'agit d'un produit jaune foncé très visqueux se solidifiant après quelques semaines).

Une chromatographie en phase gazeuse de la première fraction à 160 °C à l'aide d'une colonne de 4 m contenant 10% d'Hyprose adsorbé sur du Chromosorb P montre la présence de trois pics et d'un épaulement. A 35 min 37.6% du produit est élué, et par superposition de pics on peut démontrer que ce produit est la *t*-butyl-3 cyclopentanone (I) qui n'a pas réagi; 26.6% du total est élué à 41 min, et ce produit est le *t*-butyl-3 isopropyl-1 cyclopentanol *trans* (IV*c*). Le *t*-butyl-3 isopropyl-1 cyclopentanol *cis* (III*c*) et les produits de réduction (*t*-butyl-3 cyclopentanols *cis* et *trans*) sont élués à 47 min et forment 35.8% du total.

Un mélange formé de 1.5 g de la fraction volatile, 5 ml de pyridine et 5 ml d'anhydride acétique est laissé à la température de la pièce pour la nuit. Le mélange réactionnel est alors versé dans l'eau et extrait avec l'éther de pétrole. Le résidu analysé par chromatographie en phase gazeuse dans des conditions décrites plus haut montre la présence des acétates des *t*-butyl-3 cyclopentanols *cis* et *trans* (XXIV et XXV) à 33 min, qui ne sont pas séparés dans les conditions utilisées et qui représentent 15.2% du total; le pic de la

Can. J. Chem. Downloaded from www.nrcresearchpress.com by 210.87.254.6 on 09/05/12
For personal use only.

t-butyl-3 cyclopentanone (I, 36.4% du total) apparaît à 35 min; les *t*-butyl-3 isopropyl-1 cyclopentanols *trans* (IV*c*) et *cis* (III*c*), représentant respectivement 28.6 et 19.7% du total, sont élués après 41 et 47 min. Une chromatographie en phase gazeuse préparative à 125 °C à l'aide de huit colonnes contenant 10% d'Hyprose adsorbé sur du Chromosorb P permet la séparation des deux alcools tertiaires, dont les propriétés sont résumées dans le Tableau I.

Anal. Calc. pour $C_{12}H_{24}O$: C, 78.18; H, 13.13. Trouvé: C, 78.42; H, 13.01.

3. Préparation des t-butyl-3 alkyl-1 cyclopentènes (X) et des t-butyl-4 alkyl-1 cyclopentènes (XI)

3.1. t-Butyl-3 méthyl-1 cyclopentène (Xa) et t-butyl-4 méthyl-1 cyclopentène (XIa)

A 15 g (0.1 mole) d'alcools III*a* et IV*a*, 3 gouttes d'acide sulfurique concentré sont ajoutées et le tout porté à ébullition; l'eau formée est distillée au fur et à mesure de sa formation. En continuant le chauffage, le mélange d'hydrocarbures distille à 154 °C sous la pression atmosphérique. L'extraction du produit à la manière habituelle conduit à 10.7 g (77% du rendement théorique) d'un mélange d'hydrocarbures: p.é. 64 °C sous 95 mm Hg et n_D^{26} 1.4388. Le spectre infra-rouge du mélange d'hydrocarbures montre des bandes à 3 050, 1 650, 815 et 790 cm^{-1} toutes caractéristiques de produits non-saturés. Une chromatographie en phase gazeuse à 110 °C sur une colonne de 2 m contenant 20% de Ucon Polar adsorbé sur du Chromosorb P montre la présence de deux pics à 6.5 et 7.2 min dans la proportion de 61 à 39. Le premier pic correspond au *t*-butyl-3 méthyl-1 cyclopentène (X*a*) et le second correspond au *t*-butyl-4 méthyl-1 cyclopentène (XI*a*). Une chromatographie en phase gazeuse préparative à 42 °C à l'aide de huit colonnes contenant 15% de β,β'-oxydipropionitrile adsorbé sur du Chromosorb P permet la séparation de chacun de ces hydrocarbures, dont les propriétés sont résumées dans le Tableau III.

3.2. t-Butyl-3 éthyl-1 cyclopentène (Xb) et t-butyl-4 éthyl-1 cyclopentène (XIb)

A 15 g (0.088 mole) d'une mélange des alcools III*b* et IV*b*, 4 gouttes d'acide sulfurique concentré sont ajoutées, et l'eau qui se forme est éliminée au fur et à mesure par distillation. Les hydrocarbures formés sont extraits à la manière habituelle, et la distillation du produit à 74 °C sous 109 mm Hg conduit à un mélange d'hydrocarbures, dont l'indice de réfraction est de 1.4438 à 25 °C; le spectre infra-rouge de ce mélange indique la disparition complète de la bande hydroxyle à 3 400 et l'apparition de bandes à 3 050 et 1 640 cm^{-1}. Une analyse par chromatographie en phase gazeuse dans les conditions décrites à la section 3.1 montre la présence de 52% de *t*-butyl-3 éthyl-1 cyclopentène (X*b*) à 10.5 min, alors que le pic de *t*-butyl-4 éthyl-1 cyclopentène (XI*b*) apparaît à 12 min et représente 40% du total. A 16 min un pic d'un produit non-identifié avec certitude mais qui pourrait être le *t*-butyl-3 éthylidène cyclopentane (XII*b*) est élué et représente 3% du total. Finalement, le pic du *t*-butyl-4 méthyl-1 cyclohexène (XIII*b*) apparaît à 17.5 min et représente 5% du total. Une chromatographie en phase gazeuse préparative dans les conditions décrites à la section 3.1 permet d'isoler facilement les *t*-butyl-3 éthyl-1 cyclopentène (X*b*) et *t*-butyl-4 éthyl-1 cyclopentène (XI*b*), dont les propriétés sont résumées dans le Tableau III.

3.3. t-Butyl-3 isopropyl-1 cyclopentène (Xc) et ses isomères

A 1 g (5.4 mmoles) d'un mélange d'alcools tertiaires III*c* et IV*c*, 1 goutte d'acide sulfurique concentré est ajoutée, et l'eau qui se forme est éliminée par distillation. Après extraction du produit à la manière habituelle, le mélange d'hydrocarbures obtenu distille à 67 °C sous 32 mm Hg. Une chromatographie en phase gazeuse à 130 °C sur une colonne de 2.5 m contenant 20% de Carbowax 20M adsorbé sur du Chromosorb P indique la présence de 25% de *t*-butyl-3 isopropyl-1 cyclopentène (X*c*) à 10 min, alors que le pic du *t*-butyl-4 isopropyl-1 cyclopentène (XI*c*), représentant 9% du total, apparaît à 11.5 min. Les pics de *t*-butyl-3 isopropylidène cyclopentane (XII*c*) et *t*-butyl-4 diméthyl-1,2 cyclohexène (XIII*c*) apparaissent à 16 et 18 min et représentent, respectivement, 41 et 25% du total. Les hydrocarbures préparés dans la présente section étaient disponibles dans notre laboratoire, provenant d'un travail précédent (1). Il ne fut pas nécessaire de les séparer par chromatographie en phase gazeuse préparative.

4. Préparation des alcools tertiaires III et IV par l'intermédiaire d'époxydes

4.1. Procédé général; application au t-butyl-4 méthyl-1 cyclopentène (XIa)

La réaction de 138 mg (1 mmole) de *t*-butyl-4 méthyl-1 cyclopentène (XI*a*) avec 410 mg d'acide *m*-chloroperbenzoique (XIV) dans 15 ml de chlorure de méthylène pendant 1 h conduit, après extraction à la manière habituelle, à 127 mg (82% du rendement théorique) d'un mélange d'époxydes XVII*a* et XVIII*a*; par analyse par chromatographie en phase gazeuse à 55 °C à l'aide d'une colonne de 2.5 m contenant 15% de β,β'-oxydipropionitrile adsorbé sur du Chromosorb P, ces deux époxydes seraient respectivement présents dans la proportion de 94 à 6. Leur temps de rétention respectif serait de 10 et 6.5 min. La réduction de ce produit (127 mg, 0.82 mmole) par 100 mg d'hydrure double de lithium et d'aluminium dans le tétrahydrofuranne à reflux pendant 18 h conduit, après traitement habituel, à 118 mg (93% du rendement théorique) d'un mélange des alcools III*a* et IV*a* qui, par chromatographie en phase gazeuse dans les conditions décrites à la section 2.1, seraient présents dans le rapport de 95% du produit III*a* et 5% du produit IV*a*.

4.2. Epoxydations des autres hydrocarbures

De la même manière les hydrocarbures X*a*, X*b*, X*c*, XI*b*, XI*c* et XII*c* ont été traités par l'acide *m*-chloroperbenzoique (XIV) et ont fourni, après réduction des époxydes intermédiaires, les alcools tertiaires III et IV dans des proportions rapportées au Tableau IV.

Can. J. Chem. Downloaded from www.nrcresearchpress.com by 210.87.254.6 on 09/05/12
For personal use only.

5. Oxydation permanganique des alcools III et IV

5.1. Procédé général; application au t-butyl-3 méthyl-1 cyclopentanol trans (IVa)

Un gramme de *t*-butyl-3 méthyl-1 cyclopentanol *trans* (IV*a*) est mis en présence de 4 g de permanganate de potassium dans 50 ml d'eau sous agitation constante à la température de la pièce pendant 3 jours. Le mélange réactionnel est alors extrait trois fois avec l'éther. La phase éthérée, séchée sur du sulfate de sodium, est concentrée au travers d'une colonne de Widmer, et 320 mg (32%) de l'alcool IV*a* de départ sont récupérés. La couche aqueuse est filtrée et extraite d'une façon continue avec l'éther pendant 4 jours; l'évaporation de l'éther conduit à une huile qui est dissoute dans de l'hexane; de cette solution se dépose 48 mg (6.4% du rendement théorique)[3] de *t*-butyl-3 méthyl-1 cyclopentanediol-1,3 *trans* (XXXI*a*) fondant à 107 °C.

Anal. Calc. pour $C_{10}H_{20}O_2$: C, 69.72; H, 11.70. Trouvé: C, 69.42; H, 11.40.

Un spectre infra-rouge en solution diluée dans le tétrachlorure de carbone montre une seule bande à 3 610 cm^{-1}.

5.2. t-Butyl-3 méthyl-1 cyclopentanediol-1,3 cis (XXXa)

De la même manière, 1 g de *t*-butyl-3 méthyl-1 cyclopentanol *cis* (III*a*) est oxydé et conduit à 63 mg (10% du rendement théorique)[3] de *t*-butyl-1 cyclopentanediol-1,3 *cis* (XXX*a*) fondant à 124 °C.

Anal. Calc. pour $C_{10}H_{20}O_2$: C, 69.72; H, 11.70. Trouvé: C, 69.37; H, 11.55.

Un spectre infra-rouge en solution diluée dans le tétrachlorure de carbone montre une bande hydroxyle libre à 3 610 cm^{-1} et d'une bande hydroxyle liée à 3 540 cm^{-1}.

5.3. t-Butyl-3 éthyl-1 cyclopentanediols-1,3 cis et trans (XXXb et XXXIb)

De la même manière, les alcools III*b* et IV*b* ont été transformés dans les diols XXX*b* et XXXI*b* correspondants, avec des rendements variant entre 5 et 10%. Les conditions réactionnelles étant les mêmes, les rendements et les caractéristiques de ces produits sont rapportés dans le Tableau V en regard des analyses obtenues pour les produits nouveaux.

REMERCIEMENTS

Les auteurs remercient le Conseil National de Recherches du Canada et la Province de Québec pour l'aide financière apportée sous forme d'octroi de recherche (C.N.R. A-1295) et de bourse de perfectionnement (P. B.); les auteurs remercient également la compagnie Dow Chemical du Canada pour avoir fourni un généreux échantillon de *t*-butyl-4 cyclohexanone, et la compagnie Fisher Scientific du Canada, qui a gracieusement mis à leur disposition un appareil Fisher Prep-Partitioner modèle 24.

BIBLIOGRAPHIE

1. J.-C. Richer et P. Bélanger. Can. J. Chem. **42**, 2398 (1964).
2. E. W. Garbisch, Jr. J. Org. Chem. **30**, 2109 (1965).
3. B. Cross et G. H. Whitham. J. Chem. Soc. 3892 (1960).
4. H. B. Henbest. Proc. Chem. Soc. 159 (1963).
5. J.-C. Richer et C. Gilardeau. Can. J. Chem. **43**, 3419 (1965).
6. B. Rickborn et S. Y. Lwo. J. Org. Chem. **30**, 2212 (1965).
7. A. Lipp. Ber. **56**, 2098 (1923).
8. J. R. Durland et H. Adkins. J. Am. Chem. Soc. **61**, 429 (1939).
9. A. F. St. André, H. B. MacPhillamy, J. A. Nelson, A. C. Shabica et C. R. Scholz. J. Am. Chem. Soc. **74**, 5506 (1952).
10. R. H. Eastman et R. A. Quinn. J. Am. Chem. Soc. **82**, 4249 (1960).
11. H. Kwart et G. D. Null. J. Am. Chem. Soc. **82**, 2348 (1960).
12. L. P. Kuhn. J. Am. Chem. Soc. **74**, 2492 (1952).
13. L. P. Kuhn, P. von R. Schleyer, W. F. Baitinger et L. Eberson. J. Am. Chem. Soc. **86**, 650 (1964).
14. W. F. Baitinger et P. von R. Schleyer. J. Org. Chem. **29**, 989 (1964).
15. J.-C. Richer. J Org. Chem. **30**, 324 (1965).
16. D. Gravel. Thèse de Doctorat, Université de Montréal, Montréal, Québec. 1962.
17. R. Komers et K. Kochloefi. Collection Czech. Chem. Commun. **29**, 1803 (1964).
18. S. Winstein et N. J. Holness. J. Am. Chem. Soc. **77**, 5562 (1955).
19. A. R. H. Cole, R. N. Jones et K. Dobriner. J. Am. Chem. Soc. **74**, 5571 (1952).
20. W. Hückel. Bull. Soc. Chim. France, 1 (1963).
21. W. Hückel et R. Bross. Ann. **664**, 1 (1963).
22. H. Pines et V. N. Ipatieff. J. Am. Chem. Soc. **61**, 2728 (1939).

[3]*Calculé à l'aide de la quantité d'alcool tertiaire qui aurait réagi.*

Can. J. Chem. Downloaded from www.nrcresearchpress.com by 210.87.254.6 on 09/05/12
For personal use only.

Can. J. Chem. Downloaded from www.nrcresearchpress.com by 210.87.254.105 on 09/05/12
For personal use only.

ÉTUDES CONFORMATIONNELLES EN SÉRIE CYCLOPENTANIQUE

III. L'ADDITION DE DÉRIVÉS ORGANOMAGNÉSIENS SUR LA *t*-BUTYL-3 CYCLOPENTANONE[1]

JEAN-CLAUDE RICHER ET PATRICE BÉLANGER
Département de Chimie, Université de Montréal, Montréal, Québec

Reçu le 31 mars 1966

RÉSUMÉ

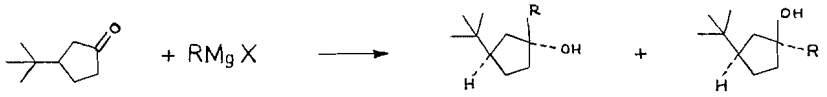
L'addition de dérivés organomagnésiens sur la *t*-butyl-3 cyclopentanone a été effectuée sous différentes conditions. L'influence sur la stéréochimie des produits obtenus de divers facteurs, tels que la nature du dérivé organomagnésien et du solvant, a été examinée. Les résultats obtenus sont discutés en fonction de facteurs stériques et électroniques.

INTRODUCTION

Dans le travail précédent (1), la stéréochimie relative des alcools tertiaires III et IV obtenus lors de l'addition de réactifs de Grignard (II) sur la *t*-butyl-3 cyclopentanone (I) a été établie; le but du présent travail était d'examiner l'influence de divers facteurs, tels que la nature du dérivé organomagnésien et du solvant, sur la stéréochimie et la nature des produits obtenus au cours de ces réactions. Le présent travail rapporte les résultats obtenus.

RÉSULTATS

L'addition de dérivés organomagnésiens (II) sur la *t*-butyl-3 cyclopentanone (I) conduit à des mélanges de *t*-butyl-3 alkyl-1 cyclopentanols *cis* (III) et *trans* (IV) (Schéma Réactionnel 1). Par définition, l'isomère *cis* est celui où les deux groupes alkyles sont du même côté du cycle.



I II III IV

SCHÉMA RÉACTIONNEL 1. *a*, R = Me; *b*, R = Et; *c*, R = *i*-Pr; *d*, R = H.

L'addition de méthylmagnésiens (II*a*) conduit à des mélanges d'alcools tertiaires où l'isomère *trans* IV*a* est en légère prédominance. Les résultats obtenus en faisant varier la nature du dérivé magnésien d'une part, et la nature du solvant d'autre part, sont résumés dans le Tableau I.

Les résultats obtenus lors de l'addition d'éthylmagnésiens (II*b*) sur la *t*-butyl-3 cyclopentanone (I) sont résumés dans le Tableau II. Il est à noter qu'avec ces magnésiens possédant un hydrogène en position β de l'atome de magnésium il y a possibilité de réduction (2) de la cétone I, qui donnerait lieu à la formation de *t*-butyl-3 cyclopentanols *cis* et *trans* (IV*d* et III*d*) d'après la mécanisme proposée dans le Schéma Réactionnel 2; la présence des alcools secondaires III*d* et IV*d* n'a toutefois été observée que dans le cas de l'addition du diéthylmagnésium (II*b* où X = CH_2CH_3) sur la cétone I. L'évaluation du degré de réduction est compilée dans le Tableau III.

[1]*Extrait de la thèse de doctorat soumise par M. Bélanger en vue de l'obtention du grade de Ph.D. en chimie Faculté des Sciences, Université de Montréal, Montréal, février 1966.*

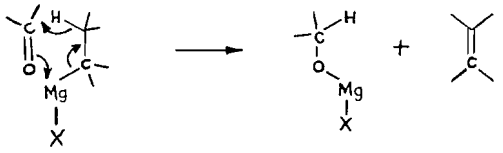


Schéma Réactionnel 2.

TABLEAU I

Pourcentage* de *t*-butyl-3 méthyl-1 cyclopentanol *trans* (IV*a*) formé par l'addition de méthylmagnésiens (II*a*)

	Solvant			
Magnésien	Éther	Tétrahydro-furanne	Anisole	Éther – méthyl-3 pentanol
CH_3MgBr	53.6	53.2	53.8	53.0
CH_3MgI	51.0	60.8	52.5	51.3
$(CH_3)_2Mg$	52.9	52.4	53.5	55.1

*Le pourcentage indiqué est le pourcentage de *t*-butyl-3 méthyl-1 cyclopentanol *trans* (IV*a*) et est relatif à la quantité totale d'isomère *cis* et *trans*. La valeur est la moyenne de trois mesures. Ces mesures ont été déterminées par chromatographie en phase gazeuse, en mesurant les surfaces sous les pics à l'aide d'un planimètre. En se basant sur les travaux de Powell et Whitting (21) et d'Eliel (22), il est permis de supposer que les deux épimères possèdent une conductivité thermique identique et que la surface sous les pics est une mesure directe du pourcentage relatif de ces deux épimères.

TABLEAU II

Pourcentage* de *t*-butyl-3 éthyl-1 cyclopentanol *trans* (IV*b*) formé par l'addition d'éthylmagnésiens (II*b*)

	Solvant			
Magnésien	Éther	Tétrahydro-furanne	Anisole	Éther – méthyl-3 pentanol
C_2H_5MgCl	55.2	55.9	55.1	56.0
C_2H_5MgBr	56.0	56.8	56.5	56.6
C_2H_5MgI	59.0	59.5	59.1	59.9
$(C_2H_5)_2Mg$	56.5	56.2	55.2	66.4

*Les remarques sous le Tableau I s'appliquent aussi au présent tableau. Il s'agit d'une mesure de l'isomère *trans* vis-à-vis de l'isomère *cis* sans tenir compte des autres produits pouvant être présents.

TABLEAU III

Réduction* de la *t*-butyl-3 cyclopentanone (XII) par le diéthylmagnésium

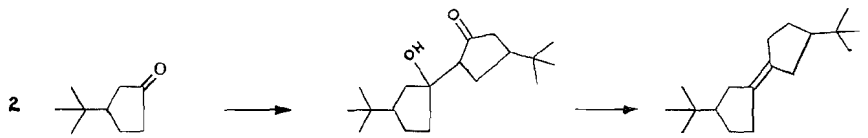
Conditions	% réduction	% *t*-butyl-3 cyclo-pentanol *cis* (IV*d*)
Éther	3	58
Tétrahydrofuranne	25	60
Anisole	17	61
Éther – $(C_2H_5)_2CH_3COMgX$	4	59
Éther – $(C_2H_5)_2CH_3COMgC_2H_5$	50	58

*Le pourcentage de réduction est le rapport des surfaces des pics de *t*-butyl-3 cyclo-pentanols *cis* (IV*d*) et *trans* (III*d*) sur la surface totale des pics des alcools secondaires et tertiaires. Il est impossible d'admettre que les conductivités thermiques des alcools secondaires et tertiaires soient identiques; cependant, si on suppose que ces conductivités thermiques sont du même ordre de grandeur, le pourcentage indiqué dans le Tableau III est une valeur donnant un ordre de grandeur de la réduction.

Le pourcentage de *t*-butyl-3 cyclopentanol *cis* (IV*d*) est une valeur déterminée en ne tenant compte que des deux alcools secondaires.

Can. J. Chem. Downloaded from www.nrcresearchpress.com by 210.87.254.105 on 09/05/12
For personal use only.

Comme il a été montré dans le travail précédent (1), l'addition de dérivés magnésiens portant un groupe isopropyle conduit à de faibles quantités d'alcools tertiaires III*c* et IV*c*. Ces produits sont accompagnés par des quantités variables d'une part d'alcools secondaires III*d* et IV*d*, provenant de la réduction de la cétone I, et d'autre part de produits qui ont des points d'ébullition très élevés et qui proviendraient selon toute probabilité d'une aldolisation (3–6) de la cétone de départ I suivant le Schéma Réactionnel 3. Dans le Tableau IV, les pourcentages de *t*-butyl-3 isopropyl-1 cyclopentanol *trans* formé par l'addition de différents organomagnésiens sur la cétone I sont rapportés; ces résultats ne tiennent compte que des alcools tertiaires III*c* et IV*c* présents dans le milieu réactionnel. Le Tableau V rapporte les résultats de réduction observés au cours de ces réactions, alors que le Tableau IV indique les pourcentages relatifs des divers produits formés au cours de ces réactions.



V VI VII

SCHÉMA RÉACTIONNEL 3.

TABLEAU IV

Pourcentage* du *t*-butyl-3 isopropyl-1 cyclopentanol *trans* (IV*c*) formé par l'addition d'isopropylmagnésiens (III*c*)

	Solvant			
Magnésien	Éther	Tétrahydro-furanne	Anisole	Éther – méthyl-3 pentanol
i-C_3H_7MgCl	62.3	64.8	64.5	69.7
i-C_3H_7MgBr	61.1	—	60.8	70.1
i-C_3H_7MgI	66.5	—	67.8	68.7
$(i\text{-}C_3H_7)_2Mg$	61.8	—	62.1	75.2

*Les remarques du Tableau I s'appliquent aussi pour ces résultats, qui ont été obtenus après les manipulations décrites dans les sections 3.1 et 3.2 de la Partie Expérimentale.

TABLEAU V

Réduction* lors de l'addition de dérivés isopropylmagnésiens (II*c*) sur la *t*-butyl-3 cyclopentanone (I)

	Solvant			
Magnésien	Éther	Tétrahydro-furanne	Anisole	Éther – méthyl-3 pentanol
i-C_3H_7MgCl	25, 60	35, 61	30, 57	30, 58
i-C_3H_7MgBr	24, 57	100, 59	37, 61	39, 63
i-C_3H_7MgI	27, 60	100, 59	52, 61	63, 63
$(i\text{-}C_3H_7)_2Mg$	41, 57	100, 57	78, 62	100, 63

*Le premier chiffre inscrit dans le Tableau V est le pourcentage des produits de réduction dans la fraction volatile tel que déterminé sous forme d'acétates après les manipulations décrites dans les sections 3.1 et 3.2 de la Partie Expérimentale.

Le second chiffre est le pourcentage de *t*-butyl-3 cyclopentanol *cis* (IV*d*) vis-à-vis son isomère *trans* (III*d*). Cette valeur est obtenue après avoir effectué les manipulations décrites dans les sections 3.1, 3.2 et 3.3 de la Partie Expérimentale.

Les remarques faites au Tableau I s'appliquent aussi ici.

Can. J. Chem. Downloaded from www.nrcresearchpress.com by 210.87.254.105 on 09/05/12
For personal use only.

TABLEAU VI

Produits* formés par l'addition d'isopropylmagnésiens (II*c*) sur la *t*-butyl-3 cyclopentanone (I)

Produits	Magnésiens		
	i-C_3H_7MgCl	*i*-C_3H_7MgBr	*i*-C_3H_7MgI
A	20.7	29.1	26.6
B	27.8	17.5	31.8
C	30.8	22.1	16.2
D	10.9	18.0	12.7
E	9.8	13.3	15.7

*A, (*t*-butyl-3 cyclopentylidène)-2 *t*-butyl-4 cyclopentanone (VII); B, mélange de *t*-butyl-3 cyclopentanone (I), de *t*-butyl-3 isopropyl-1 cyclopentanols *cis* (III*c*) et *trans* (IV*c*) et de *t*-butyl-3 cyclopentanols *cis* (IV*d*) et *trans* (III*d*); C, solide fondant à 90 °C; D, huile; E, solide fondant à 182 °C.

Les résultats obtenus ici ont été déterminés en suivant la technique décrite dans la section 3.4 de la Partie Expérimentale.

DISCUSSION

Jacques (7) a montré que l'augmentation de la grosseur d'un substituant alkyle en position 3 d'une cyclopentanone cause l'augmentation de l'effet Cotton. Cette augmentation est expliquée par l'accroissement de la taille du substituant, qui augmente la rigidé conformationnelle du cycle; cependant, contrairement à la *t*-butyl-4 cyclohexanone, la *t*-butyl-3 cyclopentanone n'existe pas dans une conformation hautement priviligiée à la température de la pièce. L'examen du modèle moléculaire de la *t*-butyl-3 cyclopentanone montre que dans la forme demi-chaise le groupe *t*-butyle doit se placer dans une position pseudo-équatoriale. Dans une telle conformation, les hydrogènes en α du carbonyle sont placés symétriquement de part et d'autre du plan formé par les carbones (1, 2, 5). Si la cétone I existe dans cette conformation, alors seule l'influence légère d'un groupe *t*-butyle en position 3 donnera une préférence à l'attaque du magnésien du côté opposé pour conduire à une majorité de l'alcool tertiaire *trans* IV. L'examen des résultats rapportés dans les Tableaux I, II et IV indique d'une façon non-ambiguë que l'attaque *trans* au groupe *t*-butyle est d'autant plus favorisée que le groupe alkyle est volumineux. Dans tous les cas sauf celui de l'addition de l'iodure de méthylmagnésium (II*a* où X = I) et de l'iodure d'éthylmagnésium (II*b* où X = I) dans le tétrahydrofuranne, il y a augmentation de l'attaque *trans* par rapport au groupe *t*-butyle lorsqu'on passe du groupe méthyle au groupe éthyle et finalement au groupe isopropyle.

Le dialkylmagnésium (II où X = R) s'additionne à une cétone comme le font les dérivés magnésiens ordinaires (II où X = halogènes). Houlihan (8) a trouvé que le comportement du diméthylmagnésium (II*a* où X = CH_3) est identique à celui du chlorure (II*a* où X = Cl) ou du bromure (II*a* où X = Br) de méthylmagnésium quant à la stéréochimie d'addition sur la *t*-butyl-4 cyclohexanone. Dans les Tableaux I, II et IV il est possible de se rendre compte que les résultats obtenus indiquent un comportement semblable à celui des chlorure et bromure d'alkylmagnésium si les pourcentages de *t*-butyl-3 alkyl-1 cyclopentanols *trans* sont considérés. Cependant, lorsque l'addition du dialkylmagnésium se fait en présence de méthyl-3 pentanol-3, House (9) a montré que la stéréochimie de l'addition peut être changée, et il en a été conclu que les résultats suggèrent que l'espèce réactionnelle obtenue par l'action du dialkylmagnésium sur le méthyl-3 pentanol-3 possède un plus grand volume stérique. L'examen des résultats rapportés dans les Tableaux I, II et IV nous permet de confirmer ces remarques pour l'addition du dialkylmagnésium sur la cétone I.

Can. J. Chem. Downloaded from www.nrcresearchpress.com by 210.87.254.105 on 09/05/12
For personal use only.

Can. J. Chem. Downloaded from www.nrcresearchpress.com by 210.87.254.105 on 09/05/12
For personal use only.

Des facteurs de même nature devraient influencer la stéréochimie de la réduction de la *t*-butyl-3 cyclopentanone (I) par les organomagnésiens; en effet, lors de la réduction, un groupe alkyl doit s'approcher du groupement carbonyle pour effectuer la réduction, et l'effet stérique faible mais décisif du groupe *t*-butyle en position 3 devrait influencer la réduction de la même manière qu'il influence la réaction d'addition conduisant aux alcools tertiaires. L'examen des résultats rapportés dans les Tableaux III et V indique clairement que les groupes alkyles provoquant la réduction s'approchent par la face *trans* (par rapport au groupe *t*-butyle) de la molécule et conduisent en légère prépondérance à la formation du *t*-butyl-3 cyclopentanol *cis* (IV*d*). Ces résultats sont comparables à ceux obtenus précédemment (10) lors de la réduction de la cétone I par l'isopropylate d'aluminium; il existe une analogie très marquée entre les deux intermédiaires qui se forment au cours de ces réactions de réduction. Dans les deux cas, il s'agit de mécanisme cyclique où se fait un déplacement d'hydrure.

L'examen des résultats rapportés dans les Tableaux I, II et IV rend visible l'effet stérique des halogènes; les résultats obtenus lors de l'addition du chlorure (II*b* où X = Cl), du bromure (II*b* où X = Br) et de l'iodure (II*b* où X = I) d'éthylmagnésium sur la *t*-butyl-3 cyclopentanone (I) sont 55.2, 56 et 59% de *t*-butyl-3 éthyl-1 cyclopentanol *trans* (IV). Il faut donc en conclure que plus l'halogène est volumineux, plus le dérivé magnésien est volumineux et plus l'attaque du côté le plus dégagé sera favorisée. D'ailleurs, un tel effet stérique des halogènes a déjà été remarqué par plusieurs chercheurs (11, 12). Dans le cas du chlorure (II*c* où X = Cl), du bromure (II*c* où X = Br) et de l'iodure (II*c* où X = I) d'isopropylmagnésium, il est fort probable que des résultats semblables auraient été obtenus si les *t*-butyl-3 cyclopentanols *cis* et *trans* (IV*d* et III*d*) n'avaient pas interféré au cours de l'analyse des produits normaux d'addition. En effet, il a fallu effectuer une réaction d'acétylation sur le mélange isolé, ce qui a pour effet de diminuer la précision des résultats; l'erreur devient alors plus importante et un effet ayant le même ordre de grandeur que l'erreur rend les résultats moins sûrs. Néanmoins, il est possible de constater l'effet stérique des halogènes si l'attaque du chlorure ou du bromure d'isopropylmagnésium est comparé à celle de l'iodure d'isopropylmagnésium. L'iode étant beaucoup plus volumineux que le chlore ou le brome, le dérivé magnésien de l'iode fournit un pourcentage de *t*-butyl-3 isopropyl-1 cyclopentanol *trans* (IV*c*) plus important que les dérivés magnésiens du chlore ou du brome. Le cas des halogénures de méthylmagnésium (I*a*) montre un accroissement inversé, ce qui semble indiquer que le bromure de méthylmagnésium (I*a* où X = Br) est plus volumineux que l'iodure de méthylmagnésium (I*a* où X = I). Cet accroissement va à l'inverse de l'ordre de grandeur. Cependant, il ne faut pas s'étonner d'un tel résultat puisque Houlihan (8), dans son étude des additions de dérivés organomagnésiens sur la *t*-butyl-4 cyclohexanone, a observé un phénomène semblable. L'explication d'un tel phénomène a été suggéré à la suite du travail de Kirrmann et ses collaborateurs (13), qui ont déterminé le nombre de molécules de solvant autour du bromure d'éthylmagnésium. En se servant de solvants de différentes basicités, ils ont noté que le nombre de molécules de solvant autour d'un dérivé magnésien varie en fonction de la basicité du solvant. Lorsque le solvant est fortement basique, il y a autour du magnésien une plus forte quantité de solvant, ce qui rend le dérivé magnésien plus volumineux. Dans un solvant faiblement basique, le nombre de molécules de solvant entourant le magnésium sera plus petit. Dans notre cas, ce n'est pas la basicité du solvant qui change mais celle du dérivé magnésien. L'iodure de méthylmagnésium étant moins acide que le bromure de méthylmagnésium, un effet semblable à celui observé par Kirrmann (13) doit se produire. Le bromure de méthylmagnésium, étant plus acide, sera

entouré d'une plus grande quantité de molécules de solvant, ce qui augmentera le volume effectif du bromure de méthylmagnésium et conduira aux résultats obtenus.

Outre l'effet stérique faible mais existant des halogènes, il y a un second effet qui est responsable des réactions secondaires de réduction ou d'énolisation. Cet effet électronique peut aussi jouer un rôle en ralentissant la vitesse d'addition d'un magnésien sur une cétone. L'acidité d'un dérivé magnésien dépend de l'électronégativité de l'halogène. Le chlore est plus électroaffinitaire que le brome, et aura tendance à faire paraître une charge positive sur le magnésium beaucoup plus facilement que le brome. Cette propriété de donner au magnésium des propriétés plus acides expliquerait pourquoi le chlorure d'alkylmagnésium n'existe que sous forme dimérique. Le magnésium est très acide et accepte facilement le doublet d'électrons du chlore, formant un dimère. Cette acidité le rend aussi plus apte à former un complexe avec le solvant, qui est une base. Ainsi, le chlorure de méthylmagnésium est un acide beaucoup plus fort que le bromure de méthylmagnésium, car le chlore est plus électroaffinitaire que le brome. Un tel effet serait la raison du ralentissement de la vitesse d'addition, car il est admis que la première étape pour une telle réaction consiste en une formation de complexes magnésiens–cétones. La stabilité d'un complexe magnésien–éther rend difficile la formation de l'important complexe magnésien–cétone, ce qui est l'étape déterminante de la réaction. Cet effet électronégatif causera un ralentissement de la vitesse de réaction dans le même ordre que l'acidité du magnésien ou de l'électronégativité de l'halogène. C'est ce que Anteunis (14) a observé lors de l'addition du bromure de méthylmagnésium, de l'iodure de méthylmagnésium ou du méthylmagnésium sur le benzophénone. La deuxième façon pour cet effet de se manifester est la variation du pourcentage des produits secondaires de la réaction d'addition de magnésiens sur une cétone. La nature des halogènes cause un changement dans le pourcentage de la réaction dite anormale, et Grignard (15) a noté que durant l'addition de dérivés magnésiens sur la pulégone le degré d'énolisation diminue avec augmentation du poids atomique de l'halogène. Kharasch (16) a aussi noté un tel effet. Il est à remarquer que l'augmentation du poids atomique va de pair avec la diminution de l'électronégativité, ce qui revient à dire que plus l'électronégativité est faible plus l'énolisation sera diminuée. L'énolisation est donc une mesure de l'électronégativité de l'halogène et, tel que montré précédemment, l'halogène a une grande influence sur l'acidité du magnésien. On sait que l'énolisation d'une cétone est d'autant plus favorisée que l'acidité du milieu est grande. Il en résulte que plus le magnésien est acide plus l'énolisation sera poussée. D'autre part, l'étude de Shine (17) montre que la réduction est faible lorsque l'énolisation est forte. Ce fait est aussi observé dans le cas de l'addition de magnésiens sur la cétone I. Cette augmentation dépend indirectement de l'électronégativité des halogènes. Ainsi, pour les dérivés de l'iodure d'alkylmagnésium, l'énolisation est très favorisée par la faible acidité du magnésien. La réduction devient prédominente, étant donné que la réaction normale est de beaucoup empêchée par des effets stériques importants.

Les changements de solvant dans la réaction d'addition de dérivés organomagnésiens ont généralement un effet marqué sur le cours de la réaction de Grignard. Ainsi, Lewis (18) avait remarqué que l'anisole favorise les réactions normales d'addition au dépens de réactions anormales de réduction, d'énolisation ou d'aldolisation. De plus, Bromberg (19) a pu effectuer des synthèse asymétriques en utilisant des solvants optiquement actifs, alors que Houlihan (8) a montré que le solvant possède une influence dans la répartition des pourcentages de *t*-butyl-4 méthyl-1 cyclohexanols *cis* et *trans*. L'examen des Tableaux I, II et IV montre que le solvant ne possède que peu ou pas d'influence

Can. J. Chem. Downloaded from www.nrcresearchpress.com by 210.87.254.105 on 09/05/12
For personal use only.

sur la stéréochimie de l'addition des magnésiens sur la cétone I. Ce résultat n'est pas surprenant, puisque les effets stériques du *t*-butyle sont relativement faibles et puisque l'addition de molécules de solvant ne semble pas provoquer des changements majeurs dans la grosseur des entitées réactives au cours des réactions d'addition de magnésiens sur la *t*-butyl-3 cyclopentanone (I). Il est à noter toutefois que les observations de Lewis (18), à savoir qu'une réaction de Grignard faite dans l'anisole conduit à une plus grande proportion de produits normaux, ne sont pas observés dans nos travaux; les résultats obtenus semblent même indiquer une tendance contraire. Il pourrait donc être suggérer que les observations de Lewis (18) ne sont pas générale et que la basicité d'un solvant ne joue un rôle vraiment important qu'au point de vue cinétique.

Les résultats obtenus au cours du présent travail montreraient donc d'une façon définitive que l'addition sur I de réactifs nucléophiles se fait généralement par le côté opposé au groupe *t*-butyle. Les facteurs qui auraient comme influence d'augmenter la grosseur effective des réactifs tendraient à favoriser encore plus cette stéréochimie. Ces résultats sont conformes au concept complètement stérique proposé récemment (20) pour expliquer les résultats d'addition sur des carbones du type sp^2 en série cyclique.

PARTIE EXPÉRIMENTALE[2]

1. Additions de dérivés méthylmagnésiens (IIa) sur la t-butyl-3 cyclopentanone (I)

1.1. Préparation du bromure de méthylmagnésium (IIa où X = Br) et détermination de sa concentration

Le bromure de méthylmagnésium (II*a* où X = Br) est préparé en chauffant à reflux pendant 1 h un mélange de 9.5 g de bromure de méthyle et 2.3 g de magnésium dans 150 ml d'éther. La solution éthérée est alors décantée, permettant l'obtention d'une solution claire de magnésien. La concentration de cette solution est alors déterminée en titrant la quantité de base formée lorsque le dérivé est hydrolysé par l'eau. Ainsi, 2 ml de la solution éthérée du dérivé magnésien sont hydrolysés par de l'eau, et il faut 10.6 ml d'acide chlorhydrique 0.1 *N* pour effectuer la neutralisation; la solution éthérée est donc 0.53 *M* en bromure de méthylmagnésium.

1.2. Addition du bromure de méthylmagnésium sur la t-butyl-3 cyclopentanone

Le dérivé magnésien (II*a* où X = Br) (1.8 ml, 1 mmole) est placé dans une éprouvette plongée dans de la glace, et 70 mg (0.5 mmole) de la cétone I dans 1.8 ml d'éther sont ajoutés lentement. L'éprouvette est placée dans un bain d'huile maintenu à 36 °C. Après 1 h, le mélange réactionnel est hydrolysé, et le résidu obtenu après le traitement habituel est analysé par chromatographie en phase gazeuse à 110 °C à l'aide d'une colonne de 4 m contenant 10% d'Hyprose adsorbé sur du Chromosorb P. Le résultat de cette chromatographie est décrit dans le Tableau I.

1.3. Addition du bromure de méthylmagnésium sur la t-butyl-3 cyclopentanone dans le tétrahydrofuranne

Le dérivé magnésien (II*a* où X = Br) (1.8 ml, 1 mmole) est placé dans une éprouvette et l'éther est évaporé sur le bain-marie. Le magnésien cristallise sur les parois de l'éprouvette, et 2 ml de tétrahydrofuranne sont alors ajoutés; la solution est placée sur le bain-marie pour permettre le dégagement des dernières traces d'éther. La solution est refroidie dans un bain de glace, et 70 mg (0.5 mmole) de I dans 2 ml de tétrahydrofuranne sont alors ajoutés. L'éprouvette est bouchée et placée dans un bain d'huile maintenu à 36 °C. Après 1 h, le mélange réactionnel est hydrolysé, et le résidu recueilli est analysé par chromatographie en phase gazeuse dans les conditions décrites dans la section 1.2. Les résultats obtenus sont rapportés dans le Tableau I.

1.4. Addition du bromure de méthylmagnésium sur la t-butyl-3 cyclopentanone dans l'anisole

Le dérivé magnésien (II*a* où X = Br) (1.8 ml, 1 mmole) est placé dans une éprouvette et l'éther est évaporé sur le bain-marie. Le magnésien cristallise sur les parois de l'éprouvette, et 2 ml d'anisole sont ajoutés. La solution est chauffée sur le bain-marie pour chasser les dernières traces d'éther, et puis est refroidie dans un bain de glace. La cétone I (70 mg, 0.5 mmole) dans 2 ml d'anisole est alors ajoutée. L'éprouvette est bouchée et placée sur un bain d'huile maintenu à 36 °C. Après 1 h, le mélange réactionnel est traité à la façon habituelle, et le résidu obtenu est analysé par chromatographie en phase gazeuse dans les conditions décrites dans la section 1.2. Les résultats obtenus sont rapportés dans le Tableau I.

1.5. Addition du bromure de méthylmagnésium sur la t-butyl-3 cyclopentanone dans l'éther contenant du méthyl-3 pentanol

Le dérivé magnésien (II*a* où X = Br) (1.8 ml, 1 mmole) est ajouté à un solution de méthyl-3 pentanol (115 mg, 1 mmole) dans 2 ml d'éther. A ce mélange, 1.8 ml (1 mmole) de bromure de méthylmagnésium

[2]*Les techniques expérimentales utilisées pour la réalisation du présent travail ont été décrites dans le travail précédent (1).*

Can. J. Chem. Downloaded from www.nrcresearchpress.com by 210.87.254.105 on 09/05/12
For personal use only.

sont ajoutés. Finalement, 70 mg (1 mmole) de la cétone I dans 2 ml d'éther sont introduits dans le mélange refroidi dans un bain de glace. La solution est maintenue à 36 °C pendant 1 h, et puis hydrolysée. Après le traitement habituel le résidu obtenu est analysé par chromatographie en phase gazeuse dans les conditions décrites dans la section 1.2. Les résultats obtenus sont rapportés dans le Tableau I.

1.6. Préparation du diméthylmagnésium (IIa où X = CH_3) à partir de bromure de méthylmagnésium

Le diméthylmagnésium est préparé d'après les indications de Kirrmann (13) à partir de 100 ml de bromure de méthylmagnésium (53 mmoles) auxquels sont ajoutés 4.5 g (55 mmoles) de dioxanne et 100 ml d'éther. Le mélange réactionnel est laissé à la température de la pièce pour la nuit, et 80 ml d'une solution de magnésien dans l'éther peuvent alors être décantés et analysés. Un titrage acide du magnésien hydrolysé indique une concentration de 0.107 *M* en dérivé magnésien hydrolysable. Un titrage du bromure par la méthode standard indique la présence de 0.001 *M* de bromure. La solution éthérée contient donc 0.106 mole de diméthylmagnésium, ce qui fait un ordre de pureté de plus de 99%.

1.7. Addition du diméthylmagnésium sur la t-butyl-3 cyclopentanone

La technique expérimentale est la même que celle qui a été décrite auparavant, sauf qu'il faut utiliser 9.5 ml de magnésien (1 mmole) sur 70 mg (1 mmole) de cétone I.

2. Additions de dérivés éthylmagnésiens (IIb) sur la cétone I

Les techniques expérimentales utilisées dans ces cas sont les mêmes que celles décrites dans la section 1. Les produits obtenus ont été analysés par chromatographie en phase gazeuse à 135 °C sur une colonne de 4 m contenant 10% d'Hyprose adsorbé sur du Chromosorb P. Dans ces conditions, les temps relatifs de rétention des *t*-butyl-3 éthyl-1 cyclopentanols *trans* (IV*b*) et *cis* (III*b*) et des *t*-butyl-3 cyclopentanols *cis* (IV*d*) et *trans* (III*d*) sont, respectivement, de 48, 55, 58 et 60 min. La stéréochimie des produits d'addition est rapportée dans le Tableau II, alors que les pourcentages relatifs de *t*-butyl-3 cyclopentanols (III*d* et IV*d*), provenant de la réduction de I, sont rapportés dans le Tableau III.

3. Additions d'isopropylmagnésiens (IIc) sur la cétone I

3.1. Addition du chlorure d'isopropylmagnésium (IIc où X = Cl) sur la cétone I

A une solution de chlorure d'isopropylmagnésium préparé à partir de 0.9 g de magnésium et de 3 g de chlorure d'isopropyl, 2.8 g (0.02 mole) de I sont ajoutés lentement à 0 °C. Le mélange réactionnel est porté à reflux durant 15 h, et le complexe intermédiaire est alors détruit par addition de 50 ml d'une solution d'acide acétique à 10%. La couche éthérée est décantée et la phase aqueuse extraite avec de l'éther. Après extraction à la manière habituelle, 3.05 g (87% du rendement théorique) de produit sont obtenus. Une chromatographie en phase gazeuse de ce résidu à 160 °C à l'aide d'une colonne de 4 m contenant 10% d'Hyprose adsorbé sur du Chromosorb P montre la présence de trois pics et d'un épaulement: à 35 min la *t*-butyl-3 cyclopentanone (I) qui n'a pas réagi (27.6% du produit) est éluée; la *t*-butyl-3 isopropyl-1 cyclopentanol *trans* (IV*c*, 28.9% du produit) apparaît à 41 min; à 47 min un mélange formé de *t*-butyl-3 isopropyl-1 cyclopentanol *cis* (III*c*) et de *t*-butyl-3 cyclopentanols *cis* et *trans* (IV*d* et III*d*), formant au total 43.5% du produit, apparaissent sous forme de pic et d'un épaulement sur le chromatogramme.

3.2. Acétylation du mélange préparé dans la section 3.1

Un mélange formé de 100 mg du produit préparé à la section 3.1, de 1 ml de pyridine et de 1 ml d'anhydride acétique est laissé à la température de la pièce pour la nuit. Après traitement à la manière habituelle, un résidu est obtenu et analysé par chromatographie en phase gazeuse d'après les conditions décrites à la section 3.1. Les acétates de *t*-butyl-3 cyclopentanols *cis* et *trans*, qui interféraient dans le chromatogramme précédent, apparaissent maintenant ensemble à 33 min et forment 25.5% du total. A 35 min le pic de la *t*-butyl-3 cyclopentanone (I) qui n'a pas réagi apparaît; il représente 27.6% du total. Les *t*-butyl-3 isopropyl-1 cyclopentanols *trans* (IV*c*) et *cis* (III*c*) apparaissent alors, respectivement, à 41 et 47 min; ils représentent 27.9 et 19% du total. Il est à noter que l'acétylation ne semble pas provoquer de changements dans les pourcentages relatifs des divers constituants, puisque dans le mélange brut la cétone I qui n'a pas réagi représentait 27.6% du total et puisqu'après acétylation la quantité présente est encore de 27.6%; d'autre part, le *t*-butyl-3 isopropyl-1 cyclopentanol *trans* (IV*c*), qui formait 28.9% du total dans le produit brut, représente 27.9% du total dans le produit acétylé.

3.3 Déshydratation du mélange de la section 3.2 et saponification du produit

Afin de déterminer la quantité relative des *t*-butyl-3 cyclopentanols *cis* et *trans* (IV*d* et III*d*) présents dans les produits volatils, 150 mg du produit obtenu à la section 3.2 ont été traités par quelques cristaux d'iode sur un bain-marie pendant 15 min. Le mélange réactionnel est alors extrait à la manière habituelle et fournit un produit qui est traité par 1 ml d'une solution de méthanol–eau contenant une pastille d'hydroxyde de sodium. Le mélange réactionnel est laissé pendant 1 h sur le bain-marie et est ensuite extrait à l'éther. Le produit obtenu est alors chromatographié en phase gazeuse dans les conditions décrites à la section 3.1. Les *t*-butyl-3 cyclopentanols *cis* (IV*d*) et *trans* (III*d*) sont élués à 47 et 48.5 min; l'isomère *cis* prédomine dans le mélange avec un pourcentage de 60. La série de tests décrite dans les sections 3.1, 3.2 et 3.3 nous permet donc de déterminer la composition des produits volatiles obtenus par réaction entre la *t*-butyl-3 cyclopentanone (I) et les isopropylmagnésiens (II*c*). Les pourcentages relatifs de *t*-butyl-3 isopropyl-1 cyclopentanols *cis* (III*c*) et *trans* (IV*c*), tels que mesurés dans la section 3.2, sont rapportés dans le Tableau IV, alors que les pourcentages relatifs de *t*-butyl-3 cyclopentanols *cis* (IV*d*) et *trans* (III*d*), tels que mesurés dans la section 3.3, sont rapportés dans le Tableau V.

Can. J. Chem. Downloaded from www.nrcresearchpress.com by 210.87.254.105 on 09/05/12
For personal use only.

3.4. Chromatographie sur colonne

Le mélange brut (850 mg) obtenu à la section 3.1 est placé sur 100 g de silica gel. En éluant avec de l'éther de pétrole, 16 mg d'une huile jaune, qui n'a pas été étudiée, sont recueillis. Continuant l'élution à l'aide d'éther de pétrole, 134 mg de (*t*-butyl-3 cyclopentylidène)-2 *t*-butyl-4 cyclopentanone (VII) fondant à 124 °C après recristallisation de l'éther de pétrole sont recueillis. Son spectre infra-rouge montre la présence de bandes à 1 680 et 1 640 cm^{-1}, alors que le spectre ultraviolet montre une absorption à 258 mμ avec un ϵ de 11 500.

Anal. Calc. pour $C_{18}H_{30}O$: C, 82.38; H, 11.52. Trouvè: C, 82.74; H, 11.38.

La dinitro-2,4 phénylhydrazone de cette cétone, préparée à la manière habituelle, fond à 235 °C.

Anal. Calc. pour $C_{24}H_{34}O_4N_4$: C, 65.14; H, 7.74; N, 12.66. Trouvé: C, 65.42; H, 7.83; N, 12.36.

Continuant l'élution avec de l'éther de pétrole contenant 5% d'éther, 207 mg d'un mélange de plusieurs produits sont obtenus. Le spectre infra-rouge montre une bande à 3 400 cm^{-1} et une autre à 1 740 cm^{-1}. Une analyse par chromatographie en phase gazeuse dans les conditions décrites à la section 3.1 montre la présence de trois pics et d'un épaulement. Cette fraction représente les produits volatiles déjà étudiés dans les sections 3.1, 3.2 et 3.3.

En éluant avec de l'éther de pétrole contenant 10% d'éther, 251 mg d'un solide qui, après sublimation à 80 °C sous 1 mm Hg, fond à 90 °C sont recueillis. Son spectre infra-rouge montre une bande à 1 730 cm^{-1}, alors que le spectre de résonance magnétique nucléaire montre des pics à 0.85 et 0.92 p.p.m., fournissant une intégration dans le rapport de 1 à 3. Le produit ne fut pas examiné de plus près.

L'élution par de l'éther de pétrole contenant 15% d'éther conduit à l'obtention d'une huile (113 mg) qui ne fut pas examinée plus attentivement. Finalement, l'élution avec de l'éther anhydre fournit 102 mg d'un solide qui, après sublimation à 150 °C sous 1 mm Hg, fond à 182 °C. La structure de ce produit ne fut pas déterminée.

Utilisant la technique décrite dans cette section, les quantités relatives des divers produits obtenus par réaction d'isorpopylmagnésiens (IIc) sur la *t*-butyl-3 cyclopentanone (I) peuvent être déterminées; les résultats obtenus sont résumés dans le Tableau VI.

REMERCIEMENTS

Les auteurs remercient le Conseil National de Recherches du Canada et la Province de Québec pour l'aide financière apportée sous forme d'octroi de recherche (C.N.R. A-1295) et de bourse de perfectionnement (P. B.); les auteurs remercient également la compagnie Dow Chemical du Canada, qui a fourni le généreux échantillon de *t*-butyl-4 cyclohexanone utilisée pour la synthèse de la *t*-butyl-3 cyclopentanone.

BIBLIOGRAPHIE

1. J.-C. RICHER et P. BÉLANGER. Can. J. Chem. Ce numero.
2. R. HAMELIN. Bull. Soc. Chim. France, 1411 (1963).
3. D. IVANOFF et A. SPASSOFF. Bull. Soc. Chim. France, **2**[5], 1435 (1935).
4. H. MEERWEIN. Ann. **405**, 129 (1914).
5. H. PINES et V. N. IPATIEFF. J. Am. Chem. Soc. **61**, 1076 (1939).
6. G. CRANE, C. E. BOORD et A. L. HENNE. J. Am. Chem. Soc. **67**, 1237 (1945).
7. C. OUANNES et J. JACQUES. Bull. Soc. Chim. France, 3601 (1965); 3611 (1965).
8. W. J. HOULIHAN. J. Org. Chem. **27**, 3860 (1962).
9. H. O. HOUSE et W. L. RESPESS. J. Org. Chem. **30**, 301 (1965).
10. J.-C. RICHER et C. GILARDEAU. Can. J. Chem. **43**, 3419 (1965).
11. J. MILLER, G. GRÉGORIOU et H. S. MOSHER. J. Am. Chem. Soc. **83**, 3966 (1961).
12. J. H. STOCKER, P. SIDISUNTHORN, B. M. BENJAMIN et C. J. COLLINS. J. Am. Chem. Soc. **82**, 3913 (1960).
13. A. KIRRMANN, R. HAMELIN et S. HAYES. Bull. Soc. Chim. France, 1395 (1963).
14. M. ANTEUNIS. J. Org. Chem. **27**, 596 (1962).
15. V. GRIGNARD et J. SAVARD. Bull. Soc. Chim. Belges, **36**, 97 (1927).
16. M. S. KHARASCH et S. WEINHOUSE. J. Org. Chem. **1**, 209 (1936).
17. H. J. SHINE. J. Chem. Soc. 8 (1951).
18. R. N. LEWIS et J. R. WRIGHT. J. Am. Chem. Soc. **74**, 1253 (1952).
19. C. BROMBERG et J. COOPS. Rec. Trav. Chim. **83**, 1083 (1964).
20. J.-C. RICHER. J. Org. Chem. **30**, 324 (1965).
21. J. W. POWELL et M. C. WHITTING. Tetrahedron, **12**, 163 (1961).
22. E. L. ELIEL et S. H. SCHROETER. J. Am. Chem. Soc. Sous presse.

Can. J. Chem. Downloaded from www.nrcresearchpress.com by 210.87.254.105 on 09/05/12
For personal use only.

Can. J. Chem. Downloaded from www.nrcresearchpress.com by 210.87.254.42 on 09/05/12
For personal use only.

THE BIOSYNTHESIS OF FUSARIC ACID FROM ^{14}C-LABELLED ACETATE IN GIBBERELLA FUJIKUROI

R. D. HILL,[1] A. M. UNRAU,[2] AND D. T. CANVIN[3]
Department of Plant Science, University of Manitoba, Winnipeg, Manitoba
Received April 21, 1966

ABSTRACT

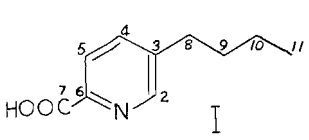
Acetate-1-^{14}C and acetate-2-^{14}C were supplied to cultures of *Gibberella fujikuroi* (Saw.) Wr., and the radioactive fusaric acid consequently formed was isolated. Acetate-1-^{14}C contributed activity mainly to C-4, C-6, C-7, C-8, and C-10 of fusaric acid, whereas acetate-2-^{14}C contributed activity to C-2, C-3, C-5, C-9, and C-11 of fusaric acid. These results are consistent with the hypothesis that fusaric acid is formed from a polyacetate unit and aspartic acid or closely related metabolites.

It is well established that more than one route exists for the biological formation of the pyridine ring. Nicotinic acid is formed from tryptophan in mammals and in the fungus *Neurospora crassa* (1). In higher plants (2) and certain bacteria (3), however, experiments with isotopically labelled tryptophan have failed to show any transformation to nicotinic acid. Glycerol and succinate have been shown to be precursors of nicotinic acid in *Escherichia coli* (4, 5). Aspartate and glycerol are incorporated into nicotinic acid in *Mycobacterium tuberculosis* (6).

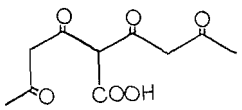
Nicotinic acid is a precursor of the pyridine ring of nicotine (7) and anabasine (8) and of the pyridone-ring compound ricinine (9, 10). Nicotine derived from acetate-2-^{14}C (11) or aspartate-3-^{14}C (12) was shown to have one-half of the activity of the pyridine ring at C-3. Acetate-2-^{14}C (13) labelled C-2 and C-3 of the pyridine ring of anabasine equally, with little activity on C-4 and C-6. Administration of acetate-2-^{14}C or succinate-2,3-^{14}C to *Ricinus communis* plants yielded ricinine labelled equally at C-2 and C-3 (15); succinate-1,4-^{14}C gave radioactive ricinine in which most of the activity was located on the nitrile carbon (16). Glycerol-1,3-^{14}C and glycerol-2-^{14}C were also incorporated into the pyridone ring (17, 18), the pattern of labelling strongly suggesting that the three-carbon chain of glycerol formed C-4, C-5, and C-6 of ricinine. The accumulated evidence thus suggests that, in higher plants, nicotinic acid is formed from a condensation of glycerol and succinate or closely related metabolites.

The structure of the wilt toxin, fusaric acid (I), suggests that the pyridine ring of this compound may not be derived from glycerol and succinate. Leete (19) has suggested that the molecule may be formed biologically from a branched chain derived from five acetate units (structure I*a*). Vining[4] has proposed a slightly different condensation involving a polyacetate unit and aspartic acid (structure I*b*). The two hypotheses differ only in the origin of C-2, C-3, C-4, and C-7 of fusaric acid. In Leete's scheme, C-7 and C-3 would be derived from the methyl group of acetate, with C-2 and C-4 originating from the carboxyl group. Vining's suggestion requires C-2 and C-3 to be formed from the methyl group of acetate, with C-7 and C-4 being formed primarily from the carboxyl group.

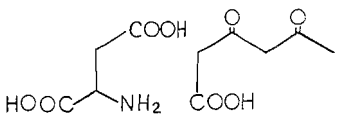
[1]*Holder of a National Research Council Studentship, 1964–1965. Present address: Molecular Biology Institute, Department of Chemistry, University of California, Los Angeles, California 90024.*
[2]*Present address: Department of Chemistry, Simon Fraser University, Burnaby 2, British Columbia.*
[3]*Present address: Department of Biology, Queen's University, Kingston, Ontario.*
[4]*L. C. Vining, private communication.*



I



Ia



Ib

The incorporation of acetate-1-^{14}C, acetate-2-^{14}C, aspartate-1-^{14}C, and aspartate-4-^{14}C into fusaric acid by *Fusarium orthoceras* cultures has been demonstrated.[5] Aspartate contributed activity only to C-7 and the pyridine ring. Partial degradation of the labelled fusaric acid derived from acetate feedings suggested that the activity was probably distributed in a manner consistent with Vining's hypothesis.

The purpose of this investigation was to determine the complete distribution of label in fusaric acid derived from acetate-^{14}C in *G. fujikuroi* (Saw.) Wr. cultures. The incorporation data for acetate-1-^{14}C and acetate-2-^{14}C presented in Table I demonstrate that the methyl carbon and carboxyl carbon of acetate are equally efficient precursors of the carbon skeleton.

TABLE I

Incorporation of acetate-^{14}C into fusaric acid by *G. fujikuroi*

Compound supplied	Fusaric acid		Dilution of specific activity	Incorporation (%)
	Yield (g)	Specific activity (d.p.m.$\times 10^{-6}$/mmole)		
Acetate-1-^{14}C*	1.084	1.07	810	12.9
Acetate-2-^{14}C†	1.427	2.0	275	15.1

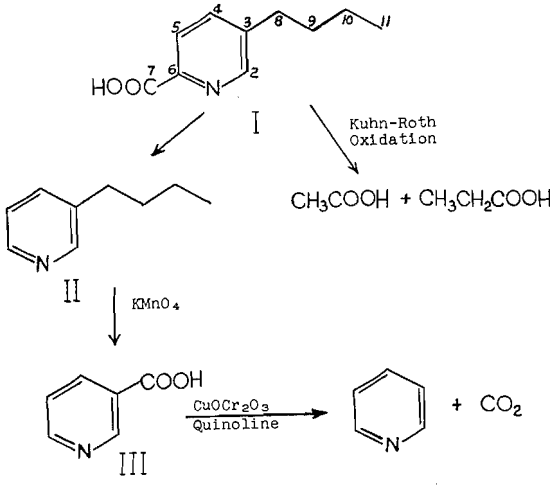
*5×10^7 d.p.m.; 8.5×10^8 d.p.m./mmole.
†1.06×10^8 d.p.m.; 5.5×10^8 d.p.m./mmole.

The radioactive fusaric acid was degraded as illustrated in Reaction Scheme 1. Chromic acid oxidation of fusaric acid (I) yielded a mixture of acetic and propionic acids which was separated by gas–liquid chromatography. A Schmidt reaction on the sodium salt of acetic acid gave carbon dioxide (C-10) and methylamine. The activity at C-11 was determined either by difference or by oxidation of the methylamine to yield carbon dioxide. The propionic acid was degraded by the Schmidt reaction to yield carbon dioxide (C-9). Decarboxylation of fusaric acid gave carbon dioxide (C-7) and 3-butylpyridine (II), which was oxidized with potassium permanganate to nicotinic acid (III). Decarboxylation of nicotinic acid with copper chromite in quinoline yielded carbon dioxide (C-7). Sequential degradation of the pyridine ring of nicotinic acid was accomplished by the method described by Friedman and Leete (13 14), with the exception that, in one case, the activity at C-4 was determined directly by a Schmidt reaction of the 2-methyl-3-phenylpropanoic acid obtained by permanganate oxidation of 2-methyl-3-phenylpropylamine.

The distribution of activity in fusaric acid from acetate-1-^{14}C is presented in Table II. The specific activity values reported are for undiluted material. It is apparent that the activity from acetate-1-^{14}C is concentrated on C-4, C-6, C-7, C-8, and C-10 of the molecule. The distribution of activity at three of the positions approaches the value expected if one-half of the carbon atoms of fusaric acid were derived from the carboxyl group of acetate. The low activity at C-10 may have resulted from contamination of the acetic

[5]*T. A. Dobson and L. C. Vining, unpublished results.*

Can. J. Chem. Downloaded from www.nrcresearchpress.com by 210.87.254.42 on 09/05/12
For personal use only.



REACTION SCHEME 1.

acid by propionic acid in the gas chromatographic separation. This would also account for the presence of activity at C-11 in this degradation.

The distribution of activity in fusaric acid from acetate-2-^{14}C (Table III) is compatible with the data obtained for the acetate-1-^{14}C feeding experiment. The activity is found mainly in positions 2, 3, 5, 9, and 11 of the fusaric acid. The low activity at C-2 and C-3 of the pyridine ring and the presence of activity at C-4 and C-7 are consistent with the participation of a four-carbon Krebs cycle acid or its equivalent.[6]

TABLE II

Distribution of activity in the degradation products of fusaric acid synthesized from acetate-1-^{14}C by *G. fujikuroi*

Compound	Carbon No.	Specific activity (d.p.m. × 10^{-5}/mmole)	Distribution of activity (%)
Fusaric acid	All	10.7	100
Barium carbonate*	7	1.52	14.2
Sodium propionate†	9, 10, 11	2.22	20.7
Sodium acetate†	10, 11	2.15	20.1
Barium carbonate‡	9	0.0	0.0
Barium carbonate§	10	1.4	13.1
Barium carbonate‖	11	0.78	7.3
Barium carbonate¶	8	2.08	19.4
Nicotinic acid	2, 3, 4, 5, 6, 8	6.49	60.4
Benzoic acid**	6	2.06	19.3
Barium carbonate††	5	0.0	0.0
Formaldehyde dimedone	2	0.37	0.35
Barium carbonate‡‡	3	2.90	2.71
By difference	4	—	18.6

*Obtained from the decarboxylation of fusaric acid.
†Obtained from the Kuhn–Roth oxidation of fusaric acid.
‡Obtained from a Schmidt reaction on sodium propionate.
§Obtained from a Schmidt reaction on sodium acetate.
‖Obtained by alkaline premanganate oxidation of the residue from the Schmidt reaction on sodium acetate.
¶Obtained from the decarboxylation of nicotinic acid.
**Obtained from the Kuhn–Roth oxidation of 1,3-dimethyl-2-phenylpiperidine.
††Obtained from a Schmidt reaction on sodium acetate derived from a Kuhn–Roth oxidation of 1,3-dimethyl-2-phenylpiperidine.
‡‡Obtained from a Schmidt reaction on the sodium salt of 3-methyl-4-phenylbutanoic acid.

[6]*For example, the equilibrium distribution of label in oxalacetate derived from acetate-2-^{14}C via the Krebs cycle is: C-1, 16.7%; C-2, 33.3%; C-3, 33.3%; and C-4, 16,7%. If C-7, C-2, C-3, and C-4 of fusaric acid are formed from a four-carbon dicarboxylic acid and contain 40% of the activity derived from acetate-2-^{14}C, then the percentage contribution of each carbon would be 6.65, 13.3, 13.3, and 6.65, respectively.*

Can. J. Chem. Downloaded from www.nrcresearchpress.com by 210.87.254.42 on 09/05/12
For personal use only.

TABLE III

Distribution of activity in the degradation products of fusaric acid synthesized from acetate-2-^{14}C by *G. fujikuroi*

Compound	Carbon No.	Specific activity (d.p.m. × 10^{-5}/mmole)	Distribution of activity (%)
Fusaric acid	All	20.0	100
Barium carbonate*	7	0.89	4.46
Sodium acetate†	10, 11	3.6	18.0
Barium carbonate‡	9	3.94	19.7
Barium carbonate§	10	0.12	0.6
By difference	11	—	17.4
Barium carbonate‖	8	0.0	0.0
3-Methylpyridine	2, 3, 4, 5, 6, 8	10.0	50.2
Benzoic acid¶	6	0.08	0.44
Barium carbonate**	5	3.34	16.7
Formaldehyde dimedone	2	2.1	10.5
Barium carbonate††	3	2.0	10.0
Barium carbonate‡‡	4	0.44	2.21

*Obtained from the decarboxylation of fusaric acid.
†Obtained from the Kuhn–Roth oxidation of fusaric acid.
‡Obtained from a Schmidt reaction on sodium propionate.
§Obtained from a Schmidt reaction on sodium acetate.
‖Obtained from the decarboxylation of nicotinic acid.
¶Obtained from the Kuhn–Roth oxidation of 1,3-dimethyl-2-phenylpiperidine.
**Obtained from a Schmidt reaction on sodium acetate derived from the Kuhn–Roth oxidation of 1,3-dimethyl-2-phenylpiperidine.
††Obtained from a Schmidt reaction on the sodium salt of 3-methyl-4-phenylbutanoic acid.
‡‡Obtained from a Schmidt reaction on the sodium salt of 2-methyl-3-phenylpropanoic acid.

The evidence presented in this communication thus indicates that all the carbons of fusaric acid are derived from acetate or closely related metabolites. The pattern of labelling is consistent with the aspartate–polyacetate hypothesis[4] for fusaric acid formation, and is not consistent with the polyacetate hypothesis (19). The incorporation of ^{14}C-labelled aspartate into fusaric acid[5] and the incorporation of aspartate-1,4-^{14}C,^{15}N into nicotinic acid in *M. tuberculosis* (6) suggest that aspartate may be incorporated intact into fusaric acid.

EXPERIMENTAL

Conditions of Culture

Gibberella fujikuroi (Saw.) Wr., strain ETH M 82, was obtained from the Department of Special Botany, Swiss Federal Institute of Technology, Zurich, Switzerland. The fungus was maintained on malt agar or Difco potato-dextrose agar slants at 4 °C, with regular subculturing every 2 months.

Inoculum was prepared by transferring a suspension of the mycelium to 125 ml Erlenmeyer flasks containing sterile, water-saturated rice. After 5 days in the dark, the conidia were harvested by shaking the mixture with sterile, distilled water (60 ml). This spore suspension was transferred to a 250 ml Erlenmeyer flask and incubated on a shaker in the dark for 24 h. Ten milliliters of this inoculum was added to 250 ml of Czapek's medium in 1 l Erlenmeyer flasks, and the fungus was grown in the dark in shake culture.

Czapek's medium has the following composition: sucrose, 4%; sodium nitrate, 0.3%; monopotassium phosphate, 0.1%; magnesium sulfate, 0.05%; potassium chloride, 0.05%; ferrous sulfate, 0.001%; all in distilled water. The pH of the medium was adjusted to 5.5 before autoclaving.

Administration of Labelled Compounds

The fungus from shake cultures that were 3 days old was collected by low-speed centrifugation. The harvest from two culture flasks was resuspended in Czapek's medium (50 ml) and used to inoculate fresh medium (200 ml). Six flasks were normally used for each tracer experiment.

Aqueous solutions of sodium acetate-1-^{14}C or sodium acetate-2-^{14}C (Atomic Energy of Canada, Ltd.) were prepared and divided equally between the six flasks. After the flasks were shaken for 24 h in the dark, they were removed and the fusaric acid was extracted from the culture filtrate.

Assay of Radioactivity

Samples were counted in a Nuclear-Chicago model 725 liquid scintillation counter using, as solvents, either (*a*) toluene containing 0.4% 2,5-diphenyloxazole (PPO) and 0.005% 1,4-bis-2-(5-phenyloxazolyl)-benzene (POPOP); or (*b*) dioxane – ethyl cellosolve (5:1) containing 5% naphthalene, 0.4% PPO, and 0.01% POPOP. Sample activities were determined in duplicate, with a counting error of 5% or less in each determination.

Can. J. Chem. Downloaded from www.nrcresearchpress.com by 210.87.254.42 on 09/05/12
For personal use only.

Can. J. Chem. Downloaded from www.nrcresearchpress.com by 210.87.254.42 on 09/05/12
For personal use only.

Extraction and Isolation of the Fusaric Acid

Celite was added to the culture flasks and the slurry filtered. The filtrate was reduced to one-quarter of its volume on a rotary evaporator and filtered. The filtrate (ca. 400 ml) was adjusted to pH 4.0 and extracted with ethyl acetate (3 × 300 ml). The ethyl acetate fraction was evaporated to dryness, the residue dissolved in water (50 ml), and the pH adjusted to 8.0 with 2 *N* sodium hydroxide. After extraction with ether (25 ml), the aqueous phase was adjusted to pH 4.0 with dilute hydrochloric acid and extracted with ether for 36 h in a continuous liquid–liquid extractor. The ether extract was dried with anhydrous magnesium sulfate, filtered, and evaporated to dryness on a rotary evaporator. The residue was extracted with petroleum ether (5 × 100 ml) and the extract evaporated to dryness. The residue was crystallized three times from petroleum ether to give colorless needles of fusaric acid, m.p. 101–102 °C.

Degradation of the Fusaric Acid

Dilutions with non-radioactive intermediates were made whenever the amounts available were too small for subsequent degradation steps.

Kuhn–Roth Oxidation of Fusaric Acid

Fusaric acid (123 mg) in water (2 ml) was added to a refluxing solution of chromium trioxide (0.8 g) in 10% sulfuric acid (14 ml). Distillation was started immediately. The volume of the reaction mixture was maintained by addition of distilled water through a dropping funnel. The distillate (130 ml) was titrated to pH 8.0 with 0.03227 *N* sodium hydroxide solution (20.1 ml) and evaporated to dryness. The residue was dissolved in water (5 ml), acidified (pH < 1) with sulfuric acid, and extracted with ether (4 × 5 ml). The ether extract, containing acetic and propionic acids, was dried, filtered, and evaporated to ca. 0.5 ml in an air stream at room temperature.

The mixture of acetic and propionic acids was separated by gas chromatography, with a copper column (6 ft × 0.25 in. outside diameter) packed with 20% neopentyl glycol succinate on 60–80 mesh firebrick treated with 2% phosphoric acid. The column temperature was 128 °C and the helium flow rate was 50 ml/min. The pure acids were collected by bubbling the exit gas through distilled water, and the solutions were then titrated to pH 8.0 with 0.03227 *N* sodium hydroxide solution (4.56 ml for propionic acid; 3.32 ml for acetic acid). The solutions were each evaporated to dryness *in vacuo*, the residues dissolved in absolute ethanol (10 ml), and the solutions evaporated to dryness again. Treatment with absolute ethanol was repeated twice, followed by final treatment with absolute ether (10 ml) and evaporation to dryness to yield the dry sodium salts of acetic and propionic acids.

Schmidt Reaction on Sodium Acetate or Sodium Propionate

The flask containing the dry sodium salt of the acid (0.1–0.15 mmole) was cooled in an ice bath, 100% sulfuric acid (0.1 ml) was added, and the contents were dissolved by rotating the flask. Sodium azide (15 mg) was added and the flask was connected to a gas train containing a 5% potassium permanganate in 5% sulfuric acid scrubber (to remove sulfur dioxide). The flask was flushed for 2 min with carbon dioxide free nitrogen, and a carbon dioxide trap of ethanolamine or barium hydroxide was attached after the permanganate scrubber. The nitrogen flow was stopped and the reaction flask was heated on a water bath at 75–80 °C for 1 h. The system was flushed with nitrogen for 15 min, after which the carbon dioxide trap was removed and analyzed for carbon dioxide and radioactivity.

Degradation of Methylamine from Schmidt Reaction on Sodium Acetate

A solution of 3% potassium permanganate (5ml) was added to the residue from the Schmidt reaction, followed by the addition of a 40% sodium hydroxide solution (0.2 ml). The flask was connected to the gas train, containing a fresh carbon dioxide trap, and was heated for 15 min on a boiling water bath. The system was flushed with nitrogen, the water bath removed, and the reaction mixture acidified with sulfuric acid to release carbon dioxide. After the system was flushed with nitrogen for 15 min, the carbon dioxide trap was removed and the contents were analyzed for radioactivity and carbon dioxide.

3-n-Butylpyridine

A flask containing fusaric acid (2.95 g) was connected to a reflux condenser and flushed with carbon dioxide free nitrogen. A gas train containing a dilute sulfuric acid scrubber and a carbon dioxide trap was connected after the condenser. The nitrogen flow was stopped, and the reaction flask heated at 200 °C on an oil bath. After 5 h the oil bath was removed and the system flushed with nitrogen for 10 min. The carbon dioxide trap was removed and the contents were analyzed for carbon dioxide and radioactivity. The condenser was set for distillation and the flask contents were distilled under reduced pressure to give 3-*n*-butylpyridine (2.04 g, 94%).

Nicotinic Acid

3-*n*-Butylpyridine (2.04 g), mixed with water (50 ml), was reacted with potassium permanganate (4 g). The potassium permanganate was added in 0.5 g portions over a 4 h period to the stirred solution. The temperature of the reaction mixture was raised to 40 °C, and additional portions of permanganate (4 g) were added after 12 and 24 h. After 48 h the excess permanganate was decomposed by the addition of methanol. The manganese dioxide was filtered off and thoroughly washed with hot water. The combined filtrates were evaporated to dryness, the residue was redissolved in water (25 ml), and the pH of the solution was adjusted to 8.0 with dilute hydrochloric acid. A saturated aqueous solution of cupric acetate (50 ml)

was added, and the resultant precipitate of cupric nicotinate was filtered off and washed with water. The copper salt was suspended in water and decomposed with hydrogen sulfide. The mixture was filtered and the filtrate evaporated to dryness. The residue was crystallized from ethanol to yield nicotinic acid (862 mg, 47%).

Decarboxylation of Nicotinic Acid

Nicotinic acid (35 mg) was refluxed with quinoline (1 ml) and copper chromite (40 mg) for 20 min in a stream of nitrogen. The liberated carbon dioxide was passed through a solution of 2 *N* sulfuric acid (to remove pyridine vapors), and then trapped in ethanolamine – methyl cellosolve or barium hydroxide solution. The yield of carbon dioxide in the reaction was 91% of the theoretical yield.

Degradation of the Pyridine Ring

Sequential degradation of the pyridine ring was accomplished by previously described methods (36, 37).

ACKNOWLEDGMENTS

The authors are indebted, and express their appreciation, to Dr. L. C. Vining for access to some unpublished work concerned with the biosynthesis of fusaric acid by *Fusarium orthoceras* App. and Wr. Financial assistance from the National Research Council is also gratefully acknowledged.

REFERENCES

1. G. M. Brown. Physiol. Rev. **40**, 331 (1960).
2. E. Leete. Science, **147**, 1000 (1965).
3. C. Yanofsky. J. Bacteriol. **68**, 577 (1954).
4. M. V. Ortega and G. M. Brown. J. Am. Chem. Soc. **81**, 4437 (1959).
5. M. V. Ortega and G. M. Brown. J. Biol. Chem. **235**, 2939 (1960).
6. D. Gross, H. R. Schutte, G. Hubner, and K. Mothes. Tetrahedron Letters, 541 (1963).
7. R. F. Dawson, D. R. Christman, A. D'Adamo, M. L. Solt, and A. P. Wolf. J. Am. Chem. Soc. **82**, 2628 (1960).
8. M. L. Solt, R. F. Dawson, and D. R. Christman. Plant Physiol. **35**, 887 (1960).
9. E. Leete and F. H. B. Leitz. Chem. Ind. London, 1572 (1957).
10. G. R. Waller and L. M. Henderson. J. Biol. Chem. **236**, 1186 (1961).
11. T. Griffith, K. P. Hellman, and T. Byerrum. J. Biol. Chem. **235**, 800 (1960).
12. T. Griffith, K. P. Hellman, and T. Byerrum. Biochemistry, **1**, 336 (1962).
13. A. R. Friedman and E. Leete. J. Am. Chem. Soc. **85**, 2141 (1963).
14. A. R. Friedman and E. Leete. J. Am. Chem. Soc. **86**, 1224 (1964).
15. P. F. Juby and L. Marion. Can. J. Chem. **41**, 117 (1963).
16. G. R. Waller and L. M. Henderson. Biochem. Biophys. Res. Commun. **6**, 398 (1961).
17. J. Essery, P. F. Juby, L. Marion, and E. Trumbull. J. Am. Chem. Soc. **84**, 4597 (1962).
18. J. Essery, P. F. Juby, L. Marion, and E. Trumbull. Can. J. Chem. **41**, 1142 (1963).
19. E. Leete. Biogenesis of natural products. *Edited by* P. Bernfeld. The MacMillan Co., New York. 1963. p. 754.

Can. J. Chem. Downloaded from www.nrcresearchpress.com by 210.87.254.42 on 09/05/12
For personal use only.

Can. J. Chem. Downloaded from www.nrcresearchpress.com by 210.87.254.105 on 09/05/12
For personal use only.

NOTES

A NEW GALACTOBIOSYL GLUCOSE FORMED FROM LACTOSE BY CHAETOMIUM GLOBOSUM[1]

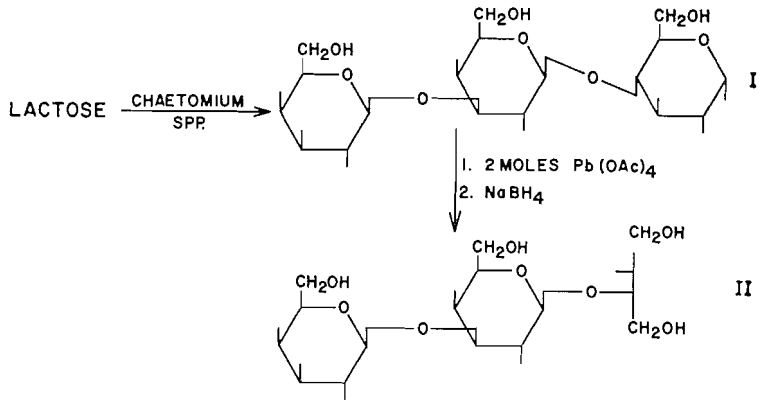
P. A. J. Gorin, R. H. Haskins, and D. W. S. Westlake[2]

During the production of lactose from cheese whey, the crystal habit of lactose sometimes becomes adversely modified so that crystal recovery by centrifugation is affected. It appears that this occurrence is due to the presence of very small amounts of a galactobiosyl glucose arising from lactose.[3] It was therefore of interest to prepare new galactobiosyl glucoses of this type for comparison and for crystal habit modification studies. So far, *O*-β-D-galactopyranosyl-(1 → 6)-*O*-β-D-galactopyranosyl-(1 → 4)-D-glucose (1–3) and *O*-β-D-galactopyranosyl-(1 → 4)-*O*-β-D-galactopyranosyl-(1 → 4)-D-glucose (4) have been prepared. The present publication describes the synthesis of *O*-β-D-galactopyranosyl-(1 → 3)-*O*-β-D-galactopyranosyl-(1 → 4)-D-glucose by *Chaetomium globosum* PRL 2200, *Chaetomium cochlioides* PRL 1907, and *Chaetomium funicola* PRL 2184.

These isolates were grown under rotary shake-culture conditions on a medium containing 5% lactose and 0.75% yeast extract. The culture filtrates were examined on paper chromatograms at intervals for the production of tri- and tetra-saccharides. Under these cultural conditions *C. globosum* produced two trisaccharide spots[4] (R_L 0.49 and 0.66), and *C. funicola* and *C. cochlioides* produced one trisaccharide spot (R_L 0.49). Small amounts of tetrasaccharide were also detected on some chromatograms.

The culture filtrate from *C. globosum* was fractionated by charcoal column chromatography to give *O*-β-D-galactopyranosyl-(1 → 4)-*O*-β-D-galactopyranosyl-(1 → 4)-D-glucose in 1% yield based on lactose. The other component crystallized in 3% yield as a hydrate of *O*-β-D-galactopyranosyl-(1 → 3)-*O*-β-D-galactopyranosyl-(1 → 4)-α-D-glucose (I), which could be converted by sodium borohydride reduction into crystalline *O*-β-D-galactopyranosyl-(1 → 3)-*O*-β-D-galactopyranosyl-(1 → 4)-D-sorbitol. Hydrolysis of the product gave galactose and a hexitol (paper chromatogram), thus indicating a glucose reducing end, which lead tetraacetate oxidation kinetics (5) showed was 1,4-linked. Oxidation with 2 moles of lead tetraacetate on a larger scale followed by sodium borohydride reduction gave *O*-β-D-galactopyranosyl-(1 → 3)-*O*-β-D-galactopyranosyl-(1 → 2)-D-erythritol (II), which consumed 3 moles of sodium periodate with release of 1 mole of acid, in accord with the structure formulated. The β-configurations of the glycosidic linkages in trisaccharide I were demonstrated by partial hydrolysis to two disaccharides. Since these were not readily separable by cellulose chromatography, they were converted into a mixture of *O*-β-galactosyl glycitols by successive lead tetraacetate oxidation and sodium borohydride reduction. The two products were separated and identified as 2-*O*-β-D-galactopyranosyl-D-lyxitol, arising from 3-*O*-β-D-galactopyranosyl-D-galactose, and 2-*O*-β-D-galactopyranosyl-D-erythritol, arising from lactose.

[1]*Issued as N.R.C. No. 9067.*
[2]*Present address: Department of Microbiology, Faculty of Science, University of Alberta, Edmonton, Alberta.*
[3]*J. M. Wood, personal communication.*
[4]*Rate on a paper chromatogram compared with lactose.*



The low yield of galactobiosyl glucoses from lactose did not promise effective β-galactopyranosyl disaccharide synthesis in a medium containing lactose and a sugar acceptor (6). In addition, *Chaetomium globosum* rapidly utilized as carbon sources such possible acceptors as xylose and arabitol. However, the system had some interest as a method of producing new disaccharides as reference compounds. 3-*O*-β-D-Galactopyranosyl-L-arabinose and 3-*O*-β-D-galactopyranosyl-D-ribose could be prepared, although these disaccharides were synthesized much better by *Sporobolomyces singularis* (6). Transfer of galactose to L-rhamnose gave rise to a mixture of two disaccharides, from which 3-*O*-β-D-galactopyranosyl-L-rhamnose was crystallized. The position of the glycosidic linkage was shown by lead tetraacetate oxidation kinetics. The other component, 2-*O*-β-D-galactopyranosyl-L-rhamnose, could be isolated in an unchanged form by oxidation of the mother liquor components with lead tetraacetate. Although syrupy, it could be reduced with sodium borohydride to give crystalline 2-*O*-β-D-galactopyranosyl-L-rhamnitol.

O-β-D-Galactopyranosyl-(1 → 3)-*O*-β-D-galactopyranosyl-(1 → 4)-α-D-glucose (I) was formed from lactose by *C. cochlioides* and isolated by charcoal column chromatography in a somewhat lower yield than from *C. globosum*. However, contamination of the product with *O*-β-D-galactopyranosyl-(1 → 4)-*O*-β-D-galactopyranosyl-(1 → 4)-D-glucose was less pronounced.

The trisaccharide produced by *C. funicola* was isolated by charcoal column chromatography but could not be induced to crystallize. Lead tetraacetate oxidation kinetics indicated a 1,4-*O*-linked reducing end. Two galactobiosyl glucoses appeared to be present, since methylation of the derived galactobiosyl sorbitols followed by methanolysis gave methyl 2,3,4,6-tetra-*O*-methyl-α,β-galactoside, 1,2,3,5,6-penta-*O*-methyl sorbitol, and two methyl tri-*O*-methyl-α,β-galactosides (gas–liquid chromatography). The tri-*O*-methyl components appeared to correspond to the 2,4,6-isomer (62%) and the 2,3,4-isomer (38%) arising from trisaccharide I and *O*-β-D-galactopyranosyl-(1 → 6)-*O*-β-D-galactopyranosyl-(1 → 4)-D-glucose, respectively.

EXPERIMENTAL

Production of Galactobiosyl Glucoses with Chaetomium spp.

Stock cultures of the isolates used in these studies were maintained on potato-dextrose agar (Difco) slants at 5°. The inoculum used for the production studies was grown in 250 ml Erlenmeyer flasks containing distilled water (50 ml), glucose (1 g), and yeast extract (0.375 g (Difco)). The production medium that was used

Can. J. Chem. Downloaded from www.nrcresearchpress.com by 210.87.254.105 on 09/05/12
For personal use only.

contained distilled water (100 ml), lactose (5 g), and yeast extract (0.75 g (Difco)) per 500 ml Erlenmeyer flask. All cultures were incubated at 25° on a Gump rotary shaker ($1\frac{1}{4}$ inch eccentricity, 110 r.p.m.). Cells were removed from cultures by filtration, under vacuum, with Whatman No. 5 filter paper.

Isolation of Galactobiosyl Glucose from C. globosum Culture Filtrate

The culture filtrate (500 ml) was fractionated on a charcoal G60 – Celite 545 column; 10% aqueous ethanol eluted lactose and 20% ethanol eluted the trisaccharide having R_L 0.66 (0.80 g) and the trisaccharide having R_L 0.49 (2.70 g) (paper chromatography in ethyl acetate – acetic acid – water (9:2:2 v/v/v) (solvent A)). The faster moving trisaccharide was recrystallized from aqueous methanol to give *O*-β-D-galactopyranosyl-(1 → 4)-*O*-β-D-galactopyranosyl-(1 → 4)-D-glucose, m.p. 227–229°, $[\alpha]_D$ +59 → +39° (constant value; *c*, 1.1 in H_2O). It gave a X-ray diffraction pattern identical with that of an authentic specimen (4).

The slower moving trisaccharide was recrystallized from aqueous methanol. The product (1.4 g) was recrystallized from aqueous dioxane to give hydrated *O*-β-D-galactopyranosyl-(1 → 3)-*O*-β-D-galactopyranosyl-(1 → 4)-α-D-glucose (I), m.p. 197–200°, $[\alpha]_D$ +56 → +43° (constant value; *c*, 1.0 in H_2O).

Anal. Calcd. for $2C_{18}H_{32}O_{16}\cdot 3H_2O$: C, 40.68; H, 6.64; mol. wt. 531. Found: C, 40.9; H, 6.6; mol. wt. (in H_2O) 530.

Based on this formula the trisaccharide consumed 0.28, 0.65, and 1.44 moles of lead tetraacetate after 2, 5, and 15 min, respectively. These figures are consistent with a 1,4-*O*-linked reducing end (5).

Derivatives from O-β-D-Galactopyranosyl-(1 → 3)-O-β-D-galactopyranosyl-(1 → 4)-D-glucose (I)

The trisaccharide was reduced with sodium borohydride to give *O*-β-D-galactopyranosyl-(1 → 3)-*O*-β-D-galactopyranosyl-(1 → 4)-D-sorbitol, which, after two recrystallizations from aqueous methanol, had m.p 202–203° and $[\alpha]_D$ +20° (*c*, 0.9 in H_2O).

Anal. Calcd. for $C_{18}H_{34}O_{16}$: C, 42.68; H, 6.76. Found: C, 42.5; H, 6.9.

This material gave galactose and a hexitol (paper chromatogram) on hydrolysis with *N* HCl at 100° for 18 h.

The trisaccharide (0.26 g) in water (2 ml) was oxidized by addition of 1% lead tetraacetate (2 moles) in acetic acid. After 18 h, oxalic acid (2 moles) in acetic acid was added, the precipitate filtered off, and the filtrate evaporated to dryness. The oxidized trisaccharide was reduced with sodium borohydride to give *O*-β-D-galactopyranosyl-(1 → 3)-*O*-β-D-galactopyranosyl-(1 → 2)-D-erythritol (II), which, after two recrystallizations from aqueous methanol, had m.p. 210–213° and $[\alpha]_D$ +18° (*c*, 1.0 in H_2O); yield 73 mg.

Anal. Calcd. for $C_{16}H_{30}O_{14}$: C, 43.04; H, 6.77. Found: C, 42.7; H, 6.9.

Oxidation with aqueous sodium periodate for 18 h resulted in the consumption of 3.0 moles of oxidant and the formation of 1.0 mole of acid. The oxidation product was reduced with sodium borohydride and the product hydrolyzed with *N* HCl at 100° for 24 h. Galactose and glycerol were detected on a paper chromatogram (sprays: *p*-anisidine hydrochloride and ammoniacal silver nitrate; solvent: *n*-butanol–ethanol–water (40:11:19 v/v/v)).

Partial Hydrolysis of O-β-D-Galactopyranosyl-(1 → 3)-O-β-D-galactopyranosyl-(1 → 4)-D-glucose (I)

Trisaccharide I (0.50 g) was partially hydrolyzed by treatment in *N* HCl (5 ml) at 80° for 45 min. The solution was neutralized (Ag_2CO_3), filtered, and evaporated to a syrup which contained some disaccharide in addition to unchanged trisaccharide, glucose, and galactose. The mixture was oxidized with 1.5 moles of lead tetraacetate (based on hexose) as described previously. The product was reduced with sodium borohydride and the mixture fractionated on a cellulose column with *n*-butanol saturated with water as eluent. 2-*O*-β-D-Galactopyranosyl-D-erythritol (56 mg) was eluted and had m.p. and mixed m.p. 182–184° (after crystallization from ethanol). The next fraction contained 2-*O*-β-D-galactopyranosyl-D-lyxitol (38 mg), which, after crystallization from ethanol, had m.p. and mixed m.p. 175–177°. The X-ray diffraction patterns of the above galactosyl polyols were identical with those of authentic specimens.

3-O-β-D-Galactopyranosyl-L-arabinose and 3-O-β-D-Galactopyranosyl-D-ribose

C. globosum, after 7 days growth on a medium (1 l) containing 5% lactose and 2.5% L-arabinose, gave a mixture of compounds which was fractionated on a charcoal column. Elution with 10% ethanol gave lactose and another disaccharide. The mixture was then fractionated on a cellulose column with *n*-butanol saturated with water as solvent. 3-*O*-β-D-Galactopyranosyl-L-arabinose (0.18 g) was isolated and, after recrystallization from methanol–ethanol, had m.p. 192–194° and $[\alpha]_D$ +80 → +65° (constant value; *c*, 1.0 in H_2O). It gave a X-ray diffraction pattern identical with that of an authentic specimen.

From a medium containing 5% lactose and 2.5% D-ribose, a disaccharide having R_{Gal} 0.92 in solvent A (0.57 g) was isolated by a similar procedure. This material consumed 0.63, 0.67, and 0.76 mole of lead tetraacetate after 2, 5, and 15 min, respectively. Reduction of the product with sodium borohydride followed by hydrolysis gave galactose and erythritol (paper chromatogram), consistent with a 3-*O*-β-D-galactopyranosyl-D-ribose structure.

2-O- and 3-O-β-D-Galactopyranosyl-L-rhamnose

C. globosum was grown for 7 days on a medium (1 l) containing 5% lactose and 2.5% L-rhamnose, and the resulting mixture was fractionated on a charcoal column. Elution with 10% ethanol gave lactose and then a

Can. J. Chem. Downloaded from www.nrcresearchpress.com by 210.87.254.105 on 09/05/12
For personal use only.

mixture of disaccharides (1.0 g) having R_{Gal} 1.09 (solvent A). Crystallization from ethanol gave 3-*O*-β-D-galactopyranosyl-α-L-rhamnose (0.40 g), m.p. 200–202°, $[\alpha]_D$ +2 → +15° (constant value; *c*, 1.2 in H_2O).

Anal. Calcd. for $C_{12}H_{22}O_{10}$: C, 44.17; H, 6.80. Found: C, 44.1; H, 6.8.

The disaccharide consumed 0.91, 0.94, and 0.98 mole of lead tetraacetate after 2, 5, and 15 min, respectively, consistent with a 3-*O*-link.

The mother liquor appeared to contain equal amounts of 2-*O*- and 3-*O*-β-D-galactopyranosyl-L-rhamnose, as shown by lead tetraacetate oxidation kinetics. A portion (0.24 g) was oxidized with 0.6 mole of lead tetraacetate for 30 min and the product fractionated on a cellulose column with *n*-butanol one-half saturated with water as solvent. The resulting 2-*O*-β-D-galactopyranosyl-L-rhamnose was syrupy, but 2-*O*-β-D-galactopyranosyl-L-rhamnitol, obtained on sodium borohydride reduction, was crystalline and had m.p. 101–103° (after crystallization from ethanol) and $[\alpha]_D$ +9° (*c*, 0.8 in H_2O).

Anal. Calcd. for $C_{12}H_{24}O_{10}$: C, 43.90; H, 7.37. Found: C, 43.8; H, 7.8.

Isolation of O-β-D-Galactopyranosyl-(1 → 3)-O-β-D-galactopyranosyl-(1 → 4)-D-glucose (I) from C. cochlioides Culture Filtrate

Isolation of I from the culture filtrate (2 l) was effected as described for the experiment with *C. globosum*. The product (1.82 g), on crystallization from aqueous methanol, had m.p. 195–199° and $[\alpha]_D$ +57 → +45° (constant value; *c*, 1.0 in H_2O). It gave a X-ray diffraction pattern different from that of the authentic specimen of I crystallized from aqueous dioxane. However, the product proved to be only a different crystalline form of I, since sodium borohydride reduction gave *O*-β-D-galactopyranosyl-(1 → 3)-*O*-β-D-galactopyranosyl-(1 → 4)-D-sorbitol. It had m.p. 201–203° and $[\alpha]_D$ +20° (*c*, 1.1 in H_2O), and gave a X-ray diffraction pattern identical with that of an authentic specimen.

Isolation and Identification of Galactobiosyl Glucoses from C. funicola Culture Filtrate

The culture filtrate (1 l) was fractionated on a charcoal column; 10% aqueous ethanol eluted lactose and 20% ethanol eluted galactobiosyl glucoses (1.1 g) having R_L 0.49. The trisaccharide mixture gave galactose and glucose on acid hydrolysis, and consumed 0.41, 0.80, and 1.24 moles of lead tetraacetate after 2, 5, and 15 min, respectively.

The trisaccharide mixture was reduced to give galactobiosyl sorbitols, which gave galactose and hexitol on hydrolysis (paper chromatograms). A sample (100 mg) of the galactobiosyl sorbitols was methylated by the sodium hydroxide – dimethyl sulfate method (7). Excess reagent was destroyed with heat, the solution neutralized and continuously extracted with chloroform, and the extracted material (120 mg) further methylated with silver oxide and methyl iodide under reflux (8). The fully methylated material, on hydrolysis with *N* H_2SO_4 at 100° for 18 h, gave tetra-*O*-methyl- and tri-*O*-methyl-galactoses on paper chromatograms (*p*-anisidine hydrochloride spray). Treatment with 3% methanolic hydrogen chloride under reflux for 4 h gave a mixture of 1,2,3,5,6-penta-*O*-methyl sorbitol and methyl 2,3,4,6-tetra-*O*-methyl- and methyl tri-*O*-methyl-α,β-galactosides. It was examined by gas–liquid chromatography with 2% neopentyl glycol succinate (9) on hexamethyldisilazane-treated Chromosorb W (80–100 mesh) in 8 ft × ¼ inch outside diameter copper tubing at 143°, with helium (30 p.s.i.) as carrier gas. The gas–liquid chromatographic unit was of conventional design and had thermal conductivity detectors. The following peaks were detected (retention times in parentheses): methyl 2,3,4,6-tetra-*O*-methyl-α,β-galactoside (10.0 and 10.5 min), 1,2,3,5,6-penta-*O*-methyl sorbitol (15.5 min), methyl 2,4,6-tri-*O*-methyl-α,β-galactoside (21.0 and 24.5 min), and methyl 2,3,4-tri-*O*-methyl-α,β-galactoside (40.5 min). The 2,3,4-*O*- and 2,4,6-*O*-isomers were present in a 19:31 ratio.

ACKNOWLEDGMENTS

The authors thank Mrs. C. Knapp for technical assistance and Mr. W. C. Haid for microanalytical determinations.

1. J. H. PAZUR. Science, **117**, 335 (1953).
2. J. H. PAZUR. J. Biol. Chem. **208**, 439 (1954).
3. A. BALLIO and S. RUSSI. Tetrahedron, **9**, 125 (1960).
4. P. A. J. GORIN, J. F. T. SPENCER, and H. J. PHAFF. Can. J. Chem. **42**, 1341 (1964).
5. A. J. CHARLSON and A. S. PERLIN. Can. J. Chem. **34**, 1200 (1956).
6. P. A. J. GORIN, J. F. T. SPENCER, and H. J. PHAFF. Can. J. Chem. **42**, 2307 (1964).
7. W. N. HAWORTH. J. Chem. Soc. 8 (1915).
8. T. PURDIE and J. C. IRVINE. J. Chem. Soc. 1021 (1903).
9. P. A. J. GORIN. Can. J. Chem. **43**, 2078 (1965).

RECEIVED MARCH 7, 1966.
PRAIRIE REGIONAL LABORATORY,
NATIONAL RESEARCH COUNCIL OF CANADA,
SASKATOON, SASKATCHEWAN.

Can. J. Chem. Downloaded from www.nrcresearchpress.com by 210.87.254.105 on 09/05/12
For personal use only.

ESTIMATED MOLECULAR WEIGHT OF AMYLOSE FROM THE YEAST RHODOTORULA PENEAUS[1]

P. A. J. GORIN, J. F. T. SPENCER, AND S. L. MACKENZIE[2]

Starch and starch-like substances are produced by a number of bacteria and fungi. Members of the genus *Cryptococcus* are known to excrete polysaccharides which give a blue color with iodine – potassium iodide solution (1); this characteristic has been used in yeast taxonomy (2). In addition to starch-like material, a pentose-containing polysaccharide has been detected (3), its production being favored at pH values higher than 5. Abercrombie *et al.* (4) investigated the exocellular polysaccharide of *Cr. laurentii* grown at pH 7, and isolated a heteropolymer containing mannose, xylose, and glucuronic acid. A glucan containing 1,3-, 1,4-, 1,2-, and (or) 1,6-links was also isolated. Miyazaki (5) investigated in detail the structure of a capsular polysaccharide from *Cr. neoformans* which also contained mannose, xylose, and glucuronic acid.

Kooiman has found that cultures of *Cr. albidus* and *Cr. laurentii* contain a mixture of starch and heteropolymer (6). The starch from *Cr. albidus* was isolated by fractionation and assigned a molecular weight of 7 000 by the hypoiodite oxidation method. The reliability of this method for molecular weight determination, however, is questionable; in addition, the author pointed out that the polymer may have suffered degradation during the fractionation processes. These involved the use of aqueous alkali, which would degrade amylose unless care was taken to exclude oxygen (7).

Exocellular polysaccharides from *Rhodotorula macerans*, *R. peneaus*, and *R. infirmo-miniata* have now been found to contain starch-like material, as indicated by the iodine blue test. The neutral exocellular polysaccharide from *R. peneaus* was investigated in more detail and was found to be indistinguishable from amylose. The organism was grown on a defined medium (8), and after removal of cells by centrifugation the supernatant liquid was allowed to stand at 3° for a few days. Amylose settled out as a slime and was readily separable from the supernatant. This contained some amylose and an acidic heteropolymer which gave an aldobiouronic acid, mannose, and xylose on hydrolysis. The heteropolymer could readily be purified through an insoluble Cetavlon complex (4).

The isolated amylose gave only glucose on acid hydrolysis, and was hydrolyzed to maltose with β-amylase. The polymer consumed 1 mole of oxidant when treated with sodium periodate; reduction of the oxidized polysaccharide followed by hydrolysis gave erythritol, thus indicating 1,4-*O*-links. The polysaccharide further resembled amylose in that its acetate had a specific rotation close to that of amylose acetate.

Methylation of the yeast amylose followed by hydrolysis showed it was a straight-chain polymer. The *O*-methyl hexose product, from which 2,3,6-tri-*O*-methyl-D-glucose was isolated, was treated with methanolic hydrogen chloride and the resulting methyl glucosides were examined by gas–liquid chromatography. Methyl 2,3,6-tri-*O*-methyl-α,β-glucoside and a trace of methyl-di-*O*-methyl-glucosides resulting from demethylation or undermethylation were detected. The absence of methyl 2,3,4,6-tetra-*O*-methyl-α,β-glucoside (<0.2%) indicated, barring cyclic structures, a straight-chain amylose of more than 500 anhydroglucose units and the absence of amylopectin.

[1]*Issued as N.R.C. No. 9062.*

[2]*Postdoctorate Fellow, 1964–1966, Division of Biosciences, National Research Council of Canada, Ottawa, Canada.*

An estimate of the molecular weight was provided by ultracentrifugal and viscosity measurements. The weight-average molecular weight of the amylose in 0.15 *M* KOH was approximately 2×10^6, as determined by substitution of the observed viscosity and sedimentation coefficient into the Scheraga–Mandelkern equation (9, 10). The limiting viscosity of an amylose sample in aqueous potassium hydroxide is related linearly to the degree of polymerization (as determined by osmotic pressure measurements) of the derived acetate (11). If the observed viscosity of yeast amylose in 0.15 *M* KOH is adjusted to the expected value in *M* KOH, the degree of polymerization should be about 3 700, corresponding to a number-average molecular weight of about 7×10^5. The difference between the number- and weight-average molecular weights reflects the polydispersity of the amylose.

The molecular weight of isolated yeast amylose, which could have undergone fractionation during the 'retrogradation' process, is only accurate to 10–15%. On the other hand, it is evident that the yeast amylose molecule is of the same order of size as 'large' amyloses from plant sources. One example is potato amylose, which has a minimum number-average molecular weight of 1.1×10^6 (11).

EXPERIMENTAL

Cultural Conditions for Amylose Production

Rhodotorula peneaus, strain 48-206, was obtained from Dr. H. J. Phaff of the University of California, Davis, California. It was maintained on slants of malt extract agar.

For production of polysaccharides it was grown in shaken cultures in 500 ml Erlenmeyer flasks containing 100 ml of media. The medium contained a yeast–nitrogen base (Difco), 5% glucose, 0.2% Casamino acids, and 0.02% of a vitamin mixture (8). The liquid medium was inoculated from the slants, and incubated at 25° on a rotary shaker operated at 230 r.p.m. and having an eccentricity of 1 inch. After 3 or 4 days the pH of the solution was 2.0; then cells were removed by centrifugation and the supernatant liquid was allowed to stand at 3°. In 24–48 h the starch settled to the bottom of the container as a viscous slime, and the supernatant solution containing the acidic heteropolysaccharide could be decanted. Alternatively, under certain conditions the starch could be separated by centrifugation, appearing as a layer of slime immediately above the layer of packed cells. The acidic heteropolysaccharide could then be removed by decantation as before. From 3 l of medium was obtained 3.27 g of amylose. Increasing the concentration of glucose to 7.5% and 10% resulted in the production of 3.55 g and 0.71 g of starch, respectively. Hydrolysis with *N* H_2SO_4 at 100° gave only glucose, as shown by paper chromatography (solvent: *n*-butanol–ethanol–water (40:11:19 v/v/v); spray: *p*-anisidine hydrochloride).

Treatment of amylose with *N*,*N*-dimethylformamide containing acetic anhydride and pyridine gave an acetate having $[\alpha]_D^{25}$ $+159 \pm 3°$ (*c*, 0.2 in $CHCl_3$), which compares with $[\alpha]_D^{19}$ $+170°$ (*c*, 0.7 in $CHCl_3$) for the acetate of potato amylose (12).

Using the method of Bernfeld and Gürther (13), we dissolved amylose in 2 *N* NaOH and then added the alkaline solution to a β-amylase (Nutritional Biochemicals Corp.; 0.2 times the weight of amylose) solution buffered to pH 4.8. After 18 h the solution was deionized with Amberlite IR 120 and Dowex 1 (bicarbonate form) and evaporated to a syrup which was examined by paper chromatography (solvent: ethyl acetate – acetic acid – water (9:2:2 v/v/v); spray: *p*-anisidine hydrochloride). Spots corresponding to maltose and a trace of glucose were detected.

The soluble portion from the fermentation was concentrated to 500 ml and polysaccharide was precipitated by addition of methanol (2 l). Using 5%, 7.5%, and 10% glucose in the medium gave polysaccharide yields of 6.75 g, 6.73 g, and 5.73 g, respectively. These polysaccharides contained some amylose, since a blue color with iodine was obtained. Acid hydrolysis gave galactose, glucose, mannose, xylose, and an aldobiouronic acid having R_{lactose} 1.2 on paper chromatography in the ethyl acetate – acetic acid – water (9:2:2 v/v/v) solvent.

The water-soluble polysaccharide (1 g) obtained with a 5% glucose medium was dissolved in water (100 ml), and 1% Cetavlon in water (200 ml) was added. The precipitated complex (0.21 g) which separated on centrifugation was hydrolyzed to give mannose, xylose, and an aldobiouronic acid.

Periodate Oxidation of Amylose

After 3.5, 7, 24, 48, and 96 h the polymer respectively consumed 0.77, 0.92, 1.00, 1.08, and 1.15 moles of oxidant per anhydroglucose unit with the concomitant formation of 0.02, 0.05, 0.09, 0.12, and 0.19 mole of acid. The final product was precipitated by addition of 5 volumes of acetic acid, isolated, and reduced with sodium borohydride. Hydrolysis of the resulting polyalcohol with *N* H_2SO_4 at 100° gave erythritol, as shown by paper chromatography (spray: ammoniacal silver nitrate).

Methylation of Amylose

Amylose (0.10 g) was methylated by the Haworth procedure at room temperature (14), and after destruction of dimethyl sulfate and neutralization the solution was extracted continuously with chloroform; yield 0.12 g. The partly methylated amylose was further methylated during 7 days by the method of Kuhn (15). The product was methanolyzed for 18 h in 3% methanolic hydrogen chloride (10 ml); the solution was neutralized (Ag_2CO_3), filtered, and evaporated, and the partly degraded material was hydrolyzed for 18 h in 2 *N* sulfuric acid (5 ml) at 100°. The solution was neutralized ($BaCO_3$), filtered, and evaporated; examination by paper chromatography (solvent: *n*-butanol–ethanol–water (40:11:19 v/v/v); spray: *p*-anisidine hydrochloride) showed the presence of tri-*O*-methyl glucose and a barely detectable amount of di-*O*-methyl glucose. No tetra-*O*-methyl glucose was detected. A portion of the mixture was treated with 3% methanolic hydrogen chloride for 4 h and the resulting methyl glucosidic mixture was analyzed by gas–liquid chromatography.

The product was examined by gas–liquid chromatography with 2% neopentyl glycol succinate (16) on hexamethyldisilazane-treated Chromosorb W (80–100 mesh) in a 4 ft × $\frac{1}{4}$ inch outside diameter copper tube at 143°, with helium at 30 p.s.i. as the carrier gas. The gas–liquid chromatographic unit was of conventional design, with thermal conductivity detectors. Methyl 2,3,6-tri-*O*-methyl-α,β-glucoside was shown to be present, but even with heavy applications of the mixture no methyl 2,3,4,6-tetra-*O*-methyl-α,β-glucoside was detected.

The above aqueous hydrolysate of methylated starch crystallized from ether, and 2,3,6-tri-*O*-methyl-α-D-glucose, m.p. 117–119° and $[\alpha]_D$ +90 → +66° (constant value; *c*, 1.3 in H_2O), was isolated. It gave a X-ray diffraction pattern identical with that of an authentic specimen.

Molecular Weight of Amylose from Rhodotorula peneaus

Ultracentrifugal and viscosity measurements were combined in the Scheraga–Mandelkern equation (9, 10) to provide an estimate of the molecular weight.

The limiting viscosity number $\left(\lim_{c\to 0} \frac{\eta_{sp}}{c}\right)$ was determined as a 0.15 *M* KOH solution in oxygen-free water at 20° with a Cannon–Ubbelohde viscometer, and found to be 590 ml/g. This value alone indicates that the amylose chain is long (cf. ref. 17); a $[\eta]$ of 590 ml/g in 0.15 *M* KOH would correspond[3] to a $[\eta]$ of approximately 495 ml/g in *M* KOH and, hence (11), to a number-average degree of polymerization of approximately 3 700. This observation, however, is based on the assumption that amylose from *R. peneaus* behaves, in solution, in a manner similar to that of potato amylose.

A Spinco model E analytical ultracentrifuge was used to determine the sedimentation coefficient in 0.15 *M* KOH at 20°. Precautions were taken to exclude oxygen from the solution throughout the determination. The schlieren patterns that were obtained consisted of one peak in each case, indicating the absence of any amylopectin. However, the homogeneity of the amylose may only be apparent (18). Because of the concentration dependence of the sedimentation coefficient of most long polymers, S_{20} was determined at several concentrations and a graph of $1/S_{20}$ versus concentration was extrapolated to zero concentration. The resultant value of S_{20} (13.5×10^{-13} s) is somewhat higher than might be expected for even a large amylose molecule; this is due to the extreme concentration dependence of the sedimentation coefficient. However, the extrapolation based on S_{20} values at lower concentrations does appear to be valid.

The equation of Scheraga and Mandelkern as outlined by Greenwood and Thomson gave

$$M = \left(\frac{N\eta_0}{\beta(1 - \bar{v}\rho)}\right)^{\frac{3}{2}} (S^0)^{\frac{3}{2}} \left(\frac{[\eta]}{100}\right)^{\frac{1}{2}},$$

where η_0 is the solvent viscosity (0.010256 dyne s/cm²), *N* is Avogadro's No. (6.02×10^{23}), $\bar{v}$ is the partial specific volume of the solute (0.62 (10)), ρ is the solvent density (1.00589 g/cm³), S^0 is the sedimentation coefficient at infinite dilution (13.5×10^{-13} s), $[\eta]$ is the limiting viscosity number (590 ml/g), β is a constant (2.5×10^6 for a random-coil configuration), and *M* is the molecular weight.

It must be emphasized that this molecular weight is an estimate based on the assumption that the partial specific volume of amylose from *R. peneaus* is close to that of potato amylose. The molecular weight is therefore only accurate to 10–15%.

1. M. Aschner, J. Mager, and J. Lubowitz. Nature, **156**, 295 (1945).
2. J. Lodder and N. J. W. Kreger-van Rij. The yeasts of a taxonomic study. North-Holland Pub. Co., Amsterdam. 1952.
3. J. Mager and M. Aschner. J. Bacteriol. **53**, 283 (1947).
4. M. J. Abercrombie, J. K. N. Jones, M. V. Lock, M. B. Perry, and R. J. Stoodley. Can. J. Chem. **38**, 1617 (1960).
5. T. Miyazaki. Chem. Pharm. Bull. Tokyo, **9**, 715 (1961).
6. P. Kooiman. A. van Leeuwenhoek, **29**, 169 (1963).
7. C. T. Greenwood. Advan. Carbohydrate Chem. **11**, 360 (1956).

[3]*This observation is based on the determination by one of us (S. M.) of the viscosity of amylose samples in both solvents, e.g. two amylose samples with limiting viscosity numbers of 630 and 600 ml/g in 0.15 M* KOH *had* $[\eta]$ *values of 530 and 505 ml/g, respectively, in M* KOH.

8. D. W. S. WESTLAKE and F. J. SIMPSON. Can. J. Microbiol. **7**, 34 (1961).
9. H. A. SCHERAGA and L. MANDELKERN. J. Am. Chem. Soc. **45**, 179 (1953).
10. C. T. GREENWOOD and J. THOMSON. Biochem. J. **82**, 156 (1962).
11. J. M. G. COWIE and C. T. GREENWOOD. J. Chem. Soc. 2862 (1957).
12. E. L. HIRST, M. M. T. PLANT, and M. D. WILKINSON. J. Chem. Soc. 2375 (1932).
13. P. BERNFELD and P. GÜRTHER. Helv. Chim. Acta, **31**, 106 (1948).
14. W. N. HAWORTH. J. Chem. Soc. 8 (1915).
15. R. KUHN, H. TRISCHMANN, and I. LÖW. Angew. Chem. **67**, 32 (1955).
16. C. E. BALLOU and Y. C. LEE. Biochemistry, **3**, 682 (1964).
17. R. GEDDES, C. T. GREENWOOD, and S. L. MACKENZIE. Carbohydrate Res. **1**, 71 (1965).
18. W. BANKS and C. T. GREENWOOD. Advan. Carbohydrate Chem. **18**, 357 (1963).

RECEIVED MARCH 24, 1966.
PRAIRIE REGIONAL LABORATORY,
NATIONAL RESEARCH COUNCIL OF CANADA,
SASKATOON, SASKATCHEWAN,
AND
DIVISION OF BIOSCIENCES,
NATIONAL RESEARCH COUNCIL OF CANADA,
OTTAWA, CANADA.

ALKALINE PERMANGANATE DECARBOXYLATION OF β-AMINO- AND β-HYDROXY-PROPIONIC ACID

A. M. UNRAU[1] AND MAY-LAY FAN[2]

In a previous communication (1), it was reported that the alkaline permanganate oxidation of β-hydroxypropionic acid gave a quantitative yield of carbon dioxide upon acidification. Furthermore, the remaining two-carbon fragment was acetate, and the correct analytical values were obtained in a Schmidt degradation (2); also, 2 equivalents of carbon dioxide was obtained by oxidation with persulfate. The possible oxidation of β-hydroxypropionic acid to malonic acid had, however, not been considered.[3] If malonate was indeed formed, then the degradative procedure developed for the sequential degradation of 2-deoxy-D-ribose (1) would obviously be of much reduced value in biosynthesis experiments involving ^{14}C-labelled metabolic intermediates. It was necessary, therefore, to establish the reaction sequence involved in the alkaline permanganate decarboxylation of β-hydroxypropionic acid. A simple approach to a solution of this problem entailed the decarboxylation of compounds appropriately labelled with ^{14}C.

β-Alanine-1-^{14}C was commercially available and was subsequently used in the preparation of β-hydroxypropionic acid-1-^{14}C. Decarboxylation of unlabelled β-alanine gave a fully quantitative yield of carbon dioxide (Table I). Since it was possible that this compound might also be oxidized to malonic acid before decarboxylation, it was necessary to degrade the appropriate ^{14}C-labelled compound.

Decarboxylation of carboxyl-labelled β-alanine (Table II) gave 85 to 90% $^{14}CO_2$ in four different experiments, thus indicating that a concerted elimination of the carboxyl carbon occurred by a mechanism probably involving a β-elimination in the semialdehyde intermediate.

[1]*Present address: Department of Chemistry, Simon Fraser University, Burnaby, British Columbia.*
[2]*Present address: Department of Plant Science, University of Manitoba, Winnipeg, Manitoba.*
[3]*R. Stewart, private discussions.*

8. D. W. S. WESTLAKE and F. J. SIMPSON. Can. J. Microbiol. **7**, 34 (1961).
9. H. A. SCHERAGA and L. MANDELKERN. J. Am. Chem. Soc. **45**, 179 (1953).
10. C. T. GREENWOOD and J. THOMSON. Biochem. J. **82**, 156 (1962).
11. J. M. G. COWIE and C. T. GREENWOOD. J. Chem. Soc. 2862 (1957).
12. E. L. HIRST, M. M. T. PLANT, and M. D. WILKINSON. J. Chem. Soc. 2375 (1932).
13. P. BERNFELD and P. GÜRTHER. Helv. Chim. Acta, **31**, 106 (1948).
14. W. N. HAWORTH. J. Chem. Soc. 8 (1915).
15. R. KUHN, H. TRISCHMANN, and I. LÖW. Angew. Chem. **67**, 32 (1955).
16. C. E. BALLOU and Y. C. LEE. Biochemistry, **3**, 682 (1964).
17. R. GEDDES, C. T. GREENWOOD, and S. L. MACKENZIE. Carbohydrate Res. **1**, 71 (1965).
18. W. BANKS and C. T. GREENWOOD. Advan. Carbohydrate Chem. **18**, 357 (1963).

RECEIVED MARCH 24, 1966.
PRAIRIE REGIONAL LABORATORY,
NATIONAL RESEARCH COUNCIL OF CANADA,
SASKATOON, SASKATCHEWAN,
AND
DIVISION OF BIOSCIENCES,
NATIONAL RESEARCH COUNCIL OF CANADA,
OTTAWA, CANADA.

Can. J. Chem. Downloaded from www.nrcresearchpress.com by 210.87.254.5 on 09/05/12
For personal use only.

ALKALINE PERMANGANATE DECARBOXYLATION OF β-AMINO- AND β-HYDROXY-PROPIONIC ACID

A. M. UNRAU[1] AND MAY-LAY FAN[2]

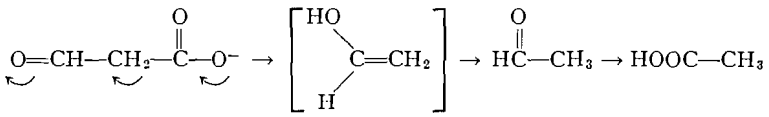
In a previous communication (1), it was reported that the alkaline permanganate oxidation of β-hydroxypropionic acid gave a quantitative yield of carbon dioxide upon acidification. Furthermore, the remaining two-carbon fragment was acetate, and the correct analytical values were obtained in a Schmidt degradation (2); also, 2 equivalents of carbon dioxide was obtained by oxidation with persulfate. The possible oxidation of β-hydroxypropionic acid to malonic acid had, however, not been considered.[3] If malonate was indeed formed, then the degradative procedure developed for the sequential degradation of 2-deoxy-D-ribose (1) would obviously be of much reduced value in biosynthesis experiments involving ^{14}C-labelled metabolic intermediates. It was necessary, therefore, to establish the reaction sequence involved in the alkaline permanganate decarboxylation of β-hydroxypropionic acid. A simple approach to a solution of this problem entailed the decarboxylation of compounds appropriately labelled with ^{14}C.

β-Alanine-1-^{14}C was commercially available and was subsequently used in the preparation of β-hydroxypropionic acid-1-^{14}C. Decarboxylation of unlabelled β-alanine gave a fully quantitative yield of carbon dioxide (Table I). Since it was possible that this compound might also be oxidized to malonic acid before decarboxylation, it was necessary to degrade the appropriate ^{14}C-labelled compound.

Decarboxylation of carboxyl-labelled β-alanine (Table II) gave 85 to 90% $^{14}CO_2$ in four different experiments, thus indicating that a concerted elimination of the carboxyl carbon occurred by a mechanism probably involving a β-elimination in the semialdehyde intermediate.

[1]*Present address: Department of Chemistry, Simon Fraser University, Burnaby, British Columbia.*
[2]*Present address: Department of Plant Science, University of Manitoba, Winnipeg, Manitoba.*
[3]*R. Stewart, private discussions.*

Decarboxylation of β-hydroxypropionic acid-1-^{14}C gave similar results, in that, in four experiments, the ^{14}C-labelled carboxyl carbon was essentially eliminated quantitatively. This observation thus shows that the alkaline permanganate decarboxylation likely proceeds via a β-elimination mechanism at the intermediate semialdehyde stage, as illustrated below. The first reaction product, apart from carbon dioxide, would be acetaldehyde, which is then further oxidized to acetate. In previous experiments (1) involving



unlabelled starting compound, a Schmidt degradation of the residue from the permanganate decarboxylation gave the expected analytical values. When these experimental results are considered, the methods and reactions described earlier (1) for the sequential degradation of 2-deoxy-D-ribose are further established and verified.

EXPERIMENTAL

Synthesis of β-Hydroxypropionic Acid-1-^{14}C from β-Alanine-1-^{14}C

A concentrated aqueous solution of sodium nitrite (2 moles of $NaNO_2$ per mole of amino acid) was added slowly to an ice-chilled solution of β-alanine (117 mg unlabelled β-alanine and 6×10^5 d.p.m. β-alanine-1-^{14}C) in 50% aqueous acetic acid under a nitrogen atmosphere. The chilled mixture was stirred for 40–48 h, the solution concentrated under reduced pressure to a small volume, and the concentrate applied as a narrow band on sheets of Whatman No. 1 paper. Standard β-hydroxypropionic acid was used as a marginal marker. Chromatography was carried out with ethyl acetate – acetic acid – water (8:2:2 v/v/v) as the eluent and with a developing time of 16 h. The paper was dried in a stream of warm air until free of acetic acid. Two marginal guide strips were cut and sprayed with bromocresol green reagent. The β-hydroxypropionic acid in the remaining unsprayed central portion of the paper was eluted with water. The percentage yield of β-hydroxypropionic acid synthesized from β-alanine was found to be 34.4. This was determined by comparing the disintegrations per minute of the mixture before chromatography (8 825 d.p.m.) and the disintegrations per minute of the β-hydroxypropionic acid eluted from the paper chromatograms (3 040 d.p.m.).

Decarboxylation with Potassium Permanganate

Unlabelled β-Alanine

β-Alanine (10.25 mg) was dissolved in distilled water (5 ml) in a 50 ml distillation flask. The solution was made neutral, and then 3 ml alkaline permanganate solution (consisting of 0.1 *M* NaOH, 0.2 *M* $KMnO_4$, and 0.02 *M* $MnSO_4$) was added. The flask was fitted to an aeration train and the contents held at room temperature for about 45 min. Before the solution was acidified, the train was flushed with nitrogen for 10 to 15 min. The solution was then acidified (2 *N* H_2SO_4, 2 ml), and the CO_2 that was evolved was swept into a $Ba(OH)_2$ trap. The precipitate that formed ($BaCO_3$) was collected on tared porcelain planchets, dried, and weighed. The results are given in Table I.

TABLE I

Permanganate decarboxylation of β-alanine

Weight of β-alanine (mg)	Weight of $BaCO_3$ expected (mg)	Weight of $BaCO_3$ obtained (mg)
21.4	44	43.6
25.1	52	51.8
19.6	39	34.2

β-Alanine-1-^{14}C

The procedure used was the same as described above, except that the CO_2 was swept into an ethanolamine trap (ethanolamine – methyl cellosolve (1:2 v/v)). The radioactivity was determined on a liquid scintillation counter. The results are given in Table II.

β-Hydroxypropionic Acid-1-^{14}C

The procedures employed were the same as described for the decarboxylation of β-alanine-1-^{14}C. The results are given in Table III.

Can. J. Chem. Downloaded from www.nrcresearchpress.com by 210.87.254.5 on 09/05/12
For personal use only.

TABLE II

Percentage recovery of $^{14}CO_2$ from permanganate decarboxylation of β-alanine-1-^{14}C

Disintegrations per minute expected	Disintegrations per minute obtained	$^{14}CO_2$ recovered (%)
4 974	4 266	87
4 974	4 225	85
4 974	4 450	89.7
4 974	4 320	87.5

TABLE III

Percentage recovery of $^{14}CO_2$ from permanganate decarboxylation of β-hydroxypropionic acid-1-^{14}C

Disintegrations per minute expected	Disintegrations per minute obtained	$^{14}CO_2$ recovered (%)
6 080	5 050	83
6 080	6 324	107
6 080	6 650	110
6 080	6 240	102

ACKNOWLEDGMENT

Helpful discussions with Dr. Ross Stewart, Department of Chemistry, University of British Columbia, are gratefully acknowledged.

1. A. M. Unrau and D. T. Canvin. Can. J. Chem. **41**, 607 (1963).
2. S. Aronoff. Techniques of radiobiochemistry. Iowa State College Press, Ames, Iowa. 1956.

Received April 21, 1966.
Department of Chemistry,
Simon Fraser University,
Burnaby, British Columbia,
and
Department of Plant Science,
University of Manitoba,
Winnipeg, Manitoba.

REACTION OF SODIUM *o*-NITROPHENOLATES WITH ETHYL 2-BROMO-2-CYANOACETATE

R. T. Coutts and K. W. Hindmarsh

We have reported earlier that the 2-(*o*-nitrophenoxy) esters required for the synthesis of benzoxazine hydroxamic acids were prepared by the interaction of ethyl 2-bromoesters and the sodium salts of various *o*-nitrophenols (1). We now report that, when ethyl 2-bromo-2-cyanoacetate is the ester employed, a different reaction occurs.

An attempt to prepare ethyl 2-(4,6-dibromo-2-nitrophenoxy)-2-cyanoacetate (I) from 2-bromo-2-cyanoacetate and the sodium salt of 4,6-dibromo-2-nitrophenol yielded a yellow product (product A) which, because of its infrared spectrum and its elemental analysis, was thought to be a solvated form (i.e. $C_{11}H_8Br_2N_2O_5 \cdot \frac{1}{2}EtOH$) of the required compound. An effort to remove the suspected ethanol of crystallization by heating the

Can. J. Chem. Downloaded from www.nrcresearchpress.com by 210.87.254.5 on 09/05/12
For personal use only.

TABLE II

Percentage recovery of $^{14}CO_2$ from permanganate decarboxylation of β-alanine-1-^{14}C

Disintegrations per minute expected	Disintegrations per minute obtained	$^{14}CO_2$ recovered (%)
4 974	4 266	87
4 974	4 225	85
4 974	4 450	89.7
4 974	4 320	87.5

TABLE III

Percentage recovery of $^{14}CO_2$ from permanganate decarboxylation of β-hydroxypropionic acid-1-^{14}C

Disintegrations per minute expected	Disintegrations per minute obtained	$^{14}CO_2$ recovered (%)
6 080	5 050	83
6 080	6 324	107
6 080	6 650	110
6 080	6 240	102

ACKNOWLEDGMENT

Helpful discussions with Dr. Ross Stewart, Department of Chemistry, University of British Columbia, are gratefully acknowledged.

1. A. M. UNRAU and D. T. CANVIN. Can. J. Chem. **41**, 607 (1963).
2. S. ARONOFF. Techniques of radiobiochemistry. Iowa State College Press, Ames, Iowa. 1956.

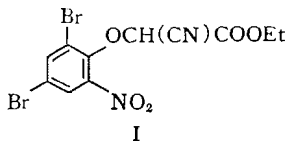
RECEIVED APRIL 21, 1966.
DEPARTMENT OF CHEMISTRY,
SIMON FRASER UNIVERSITY,
BURNABY, BRITISH COLUMBIA,
AND
DEPARTMENT OF PLANT SCIENCE,
UNIVERSITY OF MANITOBA,
WINNIPEG, MANITOBA.

REACTION OF SODIUM *o*-NITROPHENOLATES WITH ETHYL 2-BROMO-2-CYANOACETATE

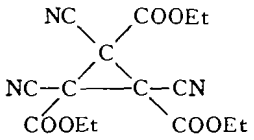
R. T. COUTTS AND K. W. HINDMARSH

We have reported earlier that the 2-(*o*-nitrophenoxy) esters required for the synthesis of benzoxazine hydroxamic acids were prepared by the interaction of ethyl 2-bromoesters and the sodium salts of various *o*-nitrophenols (1). We now report that, when ethyl 2-bromo-2-cyanoacetate is the ester employed, a different reaction occurs.

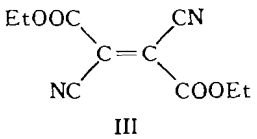
An attempt to prepare ethyl 2-(4,6-dibromo-2-nitrophenoxy)-2-cyanoacetate (I) from 2-bromo-2-cyanoacetate and the sodium salt of 4,6-dibromo-2-nitrophenol yielded a yellow product (product A) which, because of its infrared spectrum and its elemental analysis, was thought to be a solvated form (i.e. $C_{11}H_8Br_2N_2O_5 \cdot \frac{1}{2}EtOH$) of the required compound. An effort to remove the suspected ethanol of crystallization by heating the



I



II



III

product under vacuum, however, resulted in partial sublimation, and a nonvolatile, non-aromatic residue was obtained. Furthermore, reduction of product A with sodium borohydride and palladium–charcoal gave 2-amino-4,6-dibromophenol. Both of these results indicated that product A did not possess the anticipated structure, but rather appeared to be a mixture of 4,6-dibromo-2-nitrophenol and a nonvolatile second product.

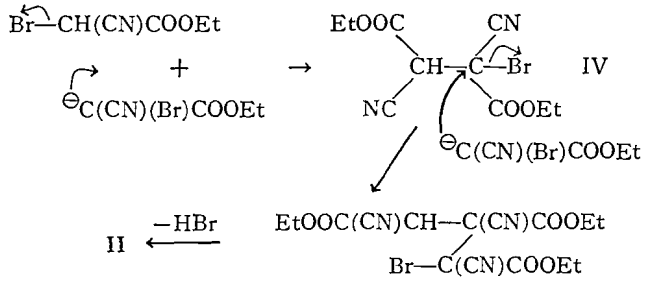
Identification of the products obtained from the interaction of sodium *o*-nitrophenolate and ethyl 2-bromo-2-cyanoacetate established the structure of the nonvolatile portion. In this case, an instantaneous reaction occurred and a colorless solid (product B), m.p. 122–124°, separated initially from the concentrated filtrate, followed by precipitation of *o*-nitrophenol. A similar condensation involving the sodium salt of 4-methyl-2-nitrophenol also gave the same product, m.p. 122–124°. An infrared study showed that these two products and the nonvolatile, non-aromatic residue previously described were all identical.

Elemental analysis of product B indicated the empirical formula to be $C_5H_5NO_2$. It was therefore thought to be either triethyl 1,2,3-tricyanocyclopropane-1,2,3-tricarboxylate ($C_{15}H_{15}N_3O_6$) (II) or diethyl 1,2-dicyanoethylene-1,2-dicarboxylate ($C_{10}H_{10}N_2O_4$) (III), because both compounds can be prepared from ethyl 2-bromo-2-cyanoacetate under conditions which differ from those described in this note. The melting point of the former is reported as 122–123° (2); the latter has a melting point of 117–117.5° (3). On the basis of its melting point and because product B did not decolorize bromine water and did not have an infrared spectrum characteristic of a tetra-substituted alkene, it was concluded that product B was triethyl 1,2,3-tricyanocyclopropane-1,2,3-tricarboxylate. A molecular weight determination agreed with this conclusion.

Product A, therefore, was a mixture of 4,6-dibromo-2-nitrophenol and II. An infrared spectrum of a known mixture of both components was identical with that of product A.

The formation of triethyl 1,2,3-tricyanocyclopropane-1,2,3-tricarboxylate in these reactions is due presumably to the fact that ethyl 2-bromo-2-cyanoacetate is sufficiently acidic to permit the equilibrium shown in eq. [1]. The reaction sequence shown in eq. [2], therefore, is plausible. Alternatively,[1] dehydrobromination of the diethyl monobromodicyanosuccinate (IV) could occur, and II could then be formed from the resulting

[1] $$ArO^{\ominus}Na^{\oplus} + HC(CN)(Br)COOEt \leftrightharpoons ArOH + {}^{\ominus}C(CN)(Br)COOEt + Na^{\oplus}$$

[2] 

[1]*The authors thank Dr. R. A. Abramovitch for suggesting that another explanation of the formation of II could involve the intervention of a carbene intermediate.*

diethyl 1,2-dicyanoethylene-1,2-dicarboxylate by a mechanism similar to that described by Krapcho and Huyffer (2).

These results should be contrasted with the findings of Griffin and Peterson (4), who obtained a *cis* and *trans* mixture of 1,2,3-tricyanocyclopropane by reacting ethyl 2-bromo-2-cyanoacetate with potassium acetate in ethanol at room temperature. Triethyl 1,2,3-tricyanocyclopropane-1,2,3-tricarboxylate (II) was postulated as an intermediate in their reaction, but was not isolable. It hydrolyzed and decarboxylated spontaneously to give the previously mentioned products. In contrast, the present study has shown that, by replacing potassium acetate with sodium *o*-nitrophenolates, the tri-ester II is formed and the reaction proceeds no further.

EXPERIMENTAL

Reaction of Ethyl 2-Bromo-2-cyanoacetate with Sodium o-Nitrophenolates

Reaction with 4,6-Dibromo-2-nitrophenol

The sodium salt of 4,6-dibromo-2-nitrophenol (15.94 g) was suspended in acetone (100 ml). Ethyl 2-bromo-2-cyanoacetate (9.6 g) was added and the mixture was heated to boiling, allowed to stand for 45 min, and then filtered. The filtrate, when cooled to 0°, deposited a green-colored solid which was recrystallized from aqueous ethanol to give a greenish-yellow product (product A) (11.4 g), m.p. 101–104°. A further recrystallization did not alter this melting point. The infrared spectrum (KBr disk), recorded on a Unicam SP 200 spectrophotometer, showed absorption peaks at 1 760 (s) (ester carbonyl); 1 540 (m), 1 335 (m) (shoulder), or 1 280 (s) (NO_2) cm^{-1}.

Anal. Found: C, 33.43; H, 2.46; N, 6.92; Br, 37.27, 37.41. This analysis apparently indicated a formula of $C_{11}H_8Br_2N_2O_5 \cdot \frac{1}{2}EtOH$ (Calcd.: C, 33.42; H, 2.56; N, 6.50; Br, 37.15).

When product A was heated at 78° and 0.5 mm for 1 week, a bromine-free solid, m.p. 110–114°, remained. Recrystallization from aqueous alcohol raised the melting point to 122–124°. This melting point, a mixed melting point, and the infrared spectrum confirmed that this product was identical with the sample of triethyl 1,2,3-tricyanocyclopropane-1,2,3-tricarboxylate obtained as described below.

When product A (2 g) was reduced by means of sodium borohydride and palladium–charcoal, by the reported (5) method, 2-amino-4,6-dibromophenol (0.65 g), m.p. 97–98°, was isolated.

Reaction with o-Nitrophenol

To a solution of ethyl 2-bromo-2-cyanoacetate (9.6 g) in acetone (100 ml) was added the sodium salt of *o*-nitrophenol (8.1 g). An immediate reaction occurred. After 10 min, unreacted salt and sodium bromide were removed by filtration; when the filtrate was concentrated, an almost colorless solid, m.p. 102–106°, separated. After the filtrate had stood for 24 h, a second product was obtained.

The first product was recrystallized three times from ethanol to give triethyl 1,2,3-tricyanocyclopropane-1,2,3-tricarboxylate (II) (2.59 g), m.p. 122–124° (lit. (2) m.p. 122–123°). The infrared spectrum in KBr showed strong ester absorption at 1 762 cm^{-1}.

Anal. Calcd. for $C_{15}H_{15}N_3O_6$: C, 54.05; H, 4.54; N, 12.61; mol. wt. 333.5. Found: C, 53.83; H, 4.43; N, 12.52; mol. wt. (vapor pressure) 309.

The second product was recrystallized from aqueous ethanol to give a yellow solid (2.63 g), m.p. 46–47°, which was shown by means of melting point, mixed melting point, and infrared spectrum to be *o*-nitrophenol.

Reaction with 4-Methyl-2-nitrophenol

Ethyl 2-bromo-2-cyanoacetate (9.6 g) and the sodium salt of 4-methyl-2-nitrophenol (8.75 g), when treated as described in the reaction immediately above, gave triethyl 1,2,3-tricyanocyclopropane-1,2,3-tricarboxylate (1.82 g), m.p. 122–124°.

1. R. T. Coutts and K. W. Hindmarsh. Can. J. Pharm. Sci. **1**, 11 (1966).
2. A. P. Krapcho and P. S. Huyffer. J. Org. Chem. **28**, 2904 (1963).
3. D. G. I. Felton. J. Chem. Soc. 515 (1955).
4. G. W. Griffin and L. I. Peterson. J. Org. Chem. **28**, 3219 (1963).
5. T. Neilson, H. C. S. Wood, and A. G. Wylie. J. Chem. Soc. 371 (1962).

Received February 16, 1966.
College of Pharmacy,
University of Saskatchewan,
Saskatoon, Saskatchewan.

LA SYNTHÈSE DE QUELQUES NOUVELLES PYRIDAZINES BICYCLIQUES

L. ERICHOMOVITCH ET FRANCIS L. CHUBB

Depuis la découverte par Druey des propriétés pharmacologiques des phtalazines (1, 2), de nombreux chercheurs ont orienté leurs travaux vers des composés bicycliques similaires, l'un des cycles étant une pyridazine plus ou moins substituée, l'autre étant un hétérocycle (3–5). D'autre part, la généralisation par Huisgen des réactions de cycloaddition 1,3 dipolaire a permis une synthèse facile de certains esters de diacides carboxyliques hétérocycliques, lesquels sont de très utiles produits de départ dans la synthèse de pyridazines bicycliques. Jones (3) et d'autres chercheurs (4,5) ont déja rapporté la synthèse de pyridazines bicycliques par réaction de l'hydrazine sur des esters ou des anhydrides d'acides dicarboxyliques. Dans cette communication, nous nous proposons de décrire la synthèse de quelques nouveaux dérivés de pyridazine en partant de la réaction de l'hydrazine, soit avec le phényl-1 triazole-1,2,3 dicarboxylate de diméthyle (I), soit avec le phényl-3 isoxazole dicarboxylate de diméthyle (XII).

Le phényl-1 triazole-1,2,3 dicarboxylate de diméthyle préparé selon Michael (6) a été converti en dihydrazide II par action de l'hydrazine en milieu alcoolique. La cyclisation de II conduit à la dihydroxy-4,7 phényl-1 triazolo (4,5-*d*) pyridazine (III). Néanmoins, selon la méthode de préparation utilisée, deux modifications solides différentes mais interconvertibles ont été obtenues, lesquelles différent seulement par leur spectre infrarouge (pastilles de KBr).

La pyrolyse de II donne un solide A dont le spectre infrarouge montre des pics à 1 720 et 1 650 cm^{-1}. Le même composé A a été obtenu par acidification de la solution résultant du traitement de II par un large excès d'hydrazine à reflux. En chauffant le dihydrazide II avec une solution d'acide chlorhydrique 2 *N* pendant 4 h au bain-marie, on a obtenu un composé B montrant deux pics à 1 690 et 1 575 cm^{-1} à l'infrarouge. On peut convertir A en B par recristallisation dans eau–dioxane. Une solution de B dans NaOH, acidifiée par HCl, donne naissance au produit A. En solution, A et B montrent des spectres ultraviolets identiques (il est possible que A et B soient deux des formes tautomériques de III). (Voir le Schéma 1.)

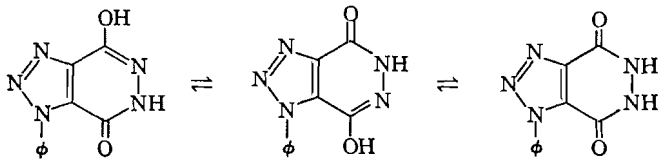


SCHÉMA 1.

La dihydroxypyridazine III, traitée par $POCl_3$, donne le composé dichloré IV ainsi que le composé monochloré V. Le spectre infrarouge de V montre un pic à 1 700 cm^{-1}, indiquant qu'il existe sous la forme cétonique. Aucune absorption dans la région OH n'a été observée. Pour ce dernier composé V nous n'avons pas encore déterminé la position exacte du chlore et du carbonyle. Il convient de noter que le même problème s'est presenté dans le cas des composés VIII, XI, XIII et XVII. En traitant le composé dichloré IV par deux molécules de méthoxide de sodium, on obtient le dérivé VI correspondant. L'action de deux molécules de diméthylaminoéthanolate de sodium sur le composé dichloré IV nous a conduit au

Can. J. Chem. Downloaded from www.nrcresearchpress.com by 210.87.254.6 on 09/05/12
For personal use only.

dérivé disubstitué VII. Ce dernier, traité par HCl alcoolique, s'hydrolyse partiellement pour conduire au chlorhydrate du dérivé monosubstitué VIII.

Des tentatives de conversion du composé dichloré IV en composé diaminé ou dihydraziné correspondant, par action d'ammoniac ou d'hydrazine en autoclave, ont échoué. Cependant, IV a été converti en dimercaptan IX, qui à son tour a été méthylé en diméthylmercaptan X. Ce dernier traité par de l'hydrazine en excès a donné naissance au dérivé monohydrazino monométhylmercapto XI.

Toutes ces réactions sont résumées dans le Schéma 2.

Dans le cas des composés dérivés du phényl-3 isoxazole, nous avons suivi une procédure analogue à celle du phényl-1 triazole-1,2,3. Nous avons ainsi préparé les dérivés suivants (voir le Schéma 3): dihydroxy-4,7 phényl-3 isoxazolo (4,5-*d*) pyridazine (XIV), diméthoxy-4,7 phényl-3 isoxazolo (4,5-*d*) pyridazine (XVIII), dichloro-4,7 phényl-3 isoxazolo (4,5-*d*) pyridazine (XVI), chloro-7(4) oxo-4(7) phényl-3 isoxazolo (4,5-*d*) pyridazine (XVII), diméthylmercapto-4,7 phényl-3 isoxazolo (4,5-*d*) pyridazine (XX) et diméthylamino-éthoxy-4,7 phényl-3 isoxazolo (4,5-*d*) pyridazine (XIX).

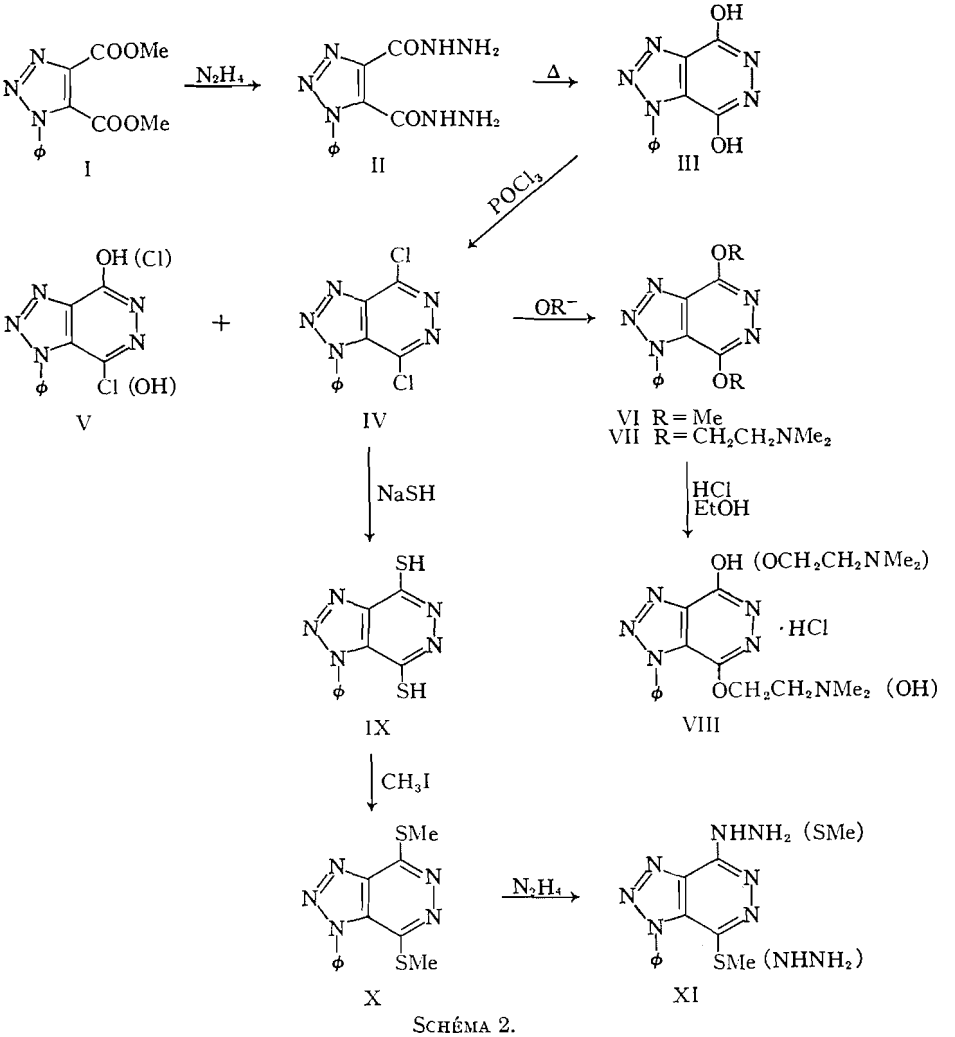


Schéma 2.

Can. J. Chem. Downloaded from www.nrcresearchpress.com by 210.87.254.6 on 09/05/12
For personal use only.

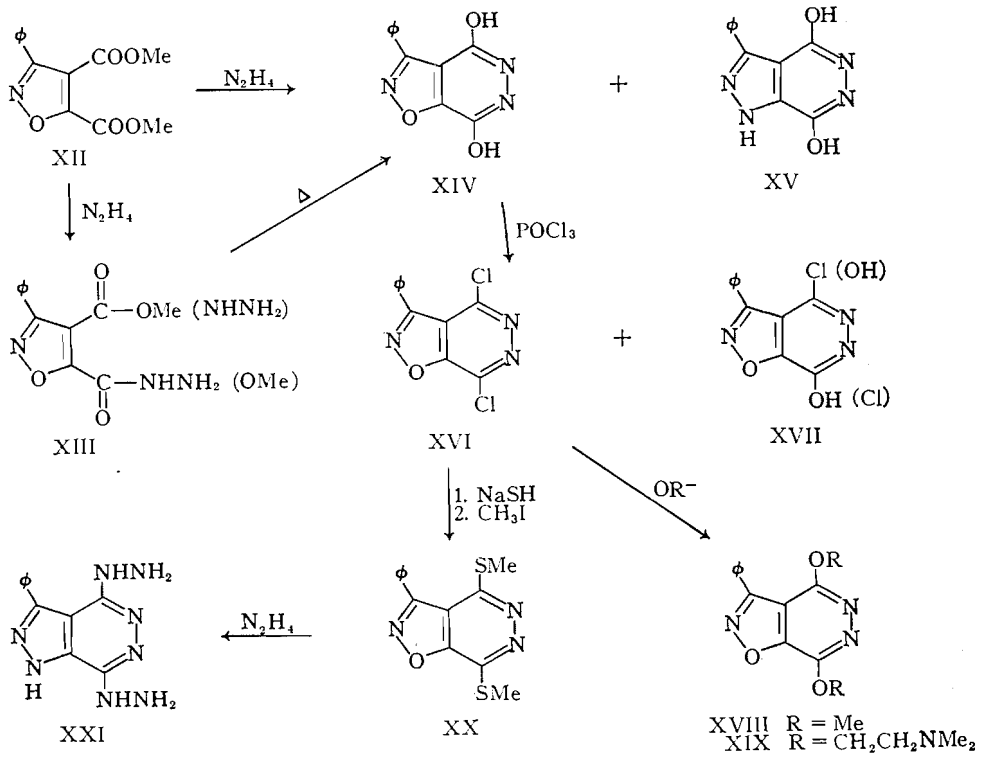


SCHÉMA 3.

Il faut, néanmoins, noter quelques différences. Lors de l'action de l'hydrazine sur l'ester méthylique du dicarboxy-4,5 phényl-3 isoxazole (XII), nous avons pu obtenir trois produits différents selon les conditions employées. L'action d'une molécule d'hydrazine sur 1 mole de diester XII conduit, avec un rendement de 40%, au monohydrazide XIII. L'action de deux molécules d'hydrazine sur le diester conduit au dérivé cyclique XIV (40%) plus un dérivé pyrazolique, la dihydroxy-4,7 phényl-3 pyrazolo (4,5-*d*) pyridazine (XV) (40%). La formation de ce dernier est facilement explicable par hydrazinolyse du dérivé XIV (7). Ici aussi, la pyrolyse du monohydrazide XIII conduit au produit cyclique XIV. Il est à noter que nous n'avons pu obtenir un dihydrazide comme dans le cas des dérivés du phényl-1 triazole-1,2,3 (II).

Autre différence qu'il convient de noter, au cours de la réaction de l'hydrazine sur le diméthylmercaptan XX, nous avons obtenu la dihydrazino-4,7 pyrazolo (4,5-*d*) pyridazine (XXI), un autre exemple de l'hydrazinolyse du cycle isoxazole.

PARTIE EXPÉRIMENTALE

Les microanalyses ont été faites par le Dr. Claude Daesslé, 5757 Decelles, Montréal. Les points de fusion ne sont pas corrigés. Les spectres infrarouges sont mesurés avec un appareil Perkin–Elmer modèle 237 dans du Nujol.

Dicarboxyhydrazide-4,5 phényl-1 triazole-1,2,3 (II)

L'ester diméthylique du dicarboxy-4,5 phényl-1 triazole-1,2,3 (6) (50 g) est mis en suspension dans 200 ml de méthanol et on y ajoute, en agitant, 32 g d'hydrate d'hydrazine à 85%. La réaction est exothermique. On chauffe ensuite la masse pendant 40 min au bain-marie, puis filtre et obtient 46 g (90%) de produit, p.f. 160°.

Anal. Calc. pour $C_{10}H_{22}N_7O_2$: C, 45.96; H, 4.24; N, 37.53. Trouvé: C, 45.77; H, 3.83; N, 38.15.

Can. J. Chem. Downloaded from www.nrcresearchpress.com by 210.87.254.6 on 09/05/12
For personal use only.

Dihydroxy-4,7 phényl-1 triazolo (4,5-d) pyridazine (III)

(*a*) Le dihydrazide II (10 g) est chauffé pendant 6 h à 240°. On obtient ainsi 8.7 g de produit brut qui, recristallisé dans eau–dioxane plus charbon, donne 6.8 g (75%) de solide, p.f. 310–312°. Infrarouge: 1 720 et 1 650 cm^{-1}.

Le dihydrazide II (5 g) est chauffé à reflux pendant 4 h avec 10 ml d'hydrazine. On laisse refroidir et dilue avec 100 ml d'eau. On acidifie ensuite avec HCl. On obtient ainsi 3.6 g (80%) de solide, p.f. 310–312° (recristallisé dans eau–dioxane). Infrarouge: 1 720 et 1 650 cm^{-1}.

(*b*) Le dihydrazide II (3 g) est chauffé pendant 4 h avec 25 ml d'HCl 2 *N*. On obtient ainsi 2.4 g (88%) de solide, p.f. 306–308°. Infrarouge: 1 690 et 1 575 cm^{-1}. Ce dernier produit, recristallisé dans eau–dioxane, donne un point de fusion de 310–312°. Infrarouge: 1 720 et 1 650 cm^{-1}.

Anal. Calc. pour $C_{10}H_7N_5O_2$: C, 52.40; H, 3.08; N, 30.56. Trouvé: C, 52.48; H, 3.39; N, 30.77.

Dichloro-4,7 phényl-1 triazolo (4,5-d) pyridazine (IV)

La dihydroxy-4,7 phényl-1 triazolo (4,5-*d*) pyridazine (III) (5 g) est chauffée pendant 6 h à reflux dans 50 ml de $POCl_3$. Le tout se dissout. On chasse ensuite $POCl_3$ sous vide et verse le résidu sur de la glace pilée. On neutralise avec NH_4OH 28%, filtre et recristallise le solide dans l'éthanol. On obtient 2.7 g (50%), p.f. 168–170°.

Anal. Calc. pour $C_{10}H_5N_5Cl_2$: C, 45.13; H, 1.89; N, 26.32; Cl, 26.64. Trouvé: C, 45.26; H, 2.03; N, 26.04; Cl, 26.86.

Chloro-4(7) oxo-7(4) phényl-1 dihydro-4,5(6,7) triazolo (4,5-d) pyridazine (V)

En évaporant à sec les eaux-mères alcooliques de recristallisation du composé dichloré IV, on a pu isoler 0.5 g (9%) de V.

Anal. Calc. pour $C_{10}H_6N_5OCl$: C, 48.49; H, 2.44; N, 28.28; Cl, 14.31. Trouvé: C, 48.29; H, 2.71; N, 28.57; Cl, 14.16.

Diméthoxy-4,7 phényl-1 triazolo (4,5-d) pyridazine (VI)

Le composé IV (2.65 g) est traité par du méthoxide de sodium (0.5 g de sodium dissout dans 50 ml méthanol) dans la bombe Parr à 120° pendant 6 h. On obtient 2.15 g (68%) de solide après lavage à l'eau bouillante pour éliminer NaCl. Le produit, recristallisé dans eau–dioxane, fond à 195–197°.

Anal. Calc. pour $C_{12}H_{11}N_5O_2$: C, 56.02; H, 4.31; N, 27.22. Trouvé: C, 55.77; H, 4.12; N, 27.17.

Bis diméthylaminoéthoxy-4,7 phényl-1 triazolo (4,5-d) pyridazine (VII)

A une solution de 1.80 g de diméthylaminoéthanol, 0.5 g de sodium et 20 ml de xylène, on ajoute 2.65 g de composé dichloré IV. La réaction est exothermique. On reflue pendant 4 h, filtre à chaud le NaCl formé puis chasse le xylène sous vide. Il reste 2.4 g de résine. On chromatographie ces 2.4 g sur une colonne d'alumine et on obtient 1 g d'huile (30%) en éluant avec une solution benzene–éther. Cette huile peu à peu cristallise et fond à 58–61°.

Anal. Calc. pour $C_{18}H_{25}N_7O_2$: C, 58.20; H, 6.78; N, 26.39. Trouvé: C, 57.73; H, 6.50; N, 26.36.

Une tentative de préparer le chlorhydrate de ce dernier produit nous a amené à un rendement quantitatif de chlorhydrate de diméthylaminoéthoxy-7(4) oxo-4(7) phényl-1 dihydro-4,5(6,7) triazolo (4,5-*d*) pyridazine (VIII), fondant à 257–258° (recristallisé dans alcool).

Anal. Calc. pour $C_{14}H_{17}N_6O_2Cl$: C, 49.92; H, 5.09; N, 24.95; Cl, 10.52. Trouvé: C, 49.91; H, 5.19; N, 24.90; Cl, 10.32.

Dimercapto-4,7 phényl-1 triazolo (4,5-d) pyridazine (IX)

Le composé dichloré IV (5 g) est agité avec 4 g de NaSH et 40 ml d'éthanol absolu pendant 4 h à température ordinaire. La réaction est exothermique. On étend d'eau, puis acidifie par 4 ml d'HCl concentré. Il se forme un précipité que l'on filtre. On obtient 3.5 g (70%) de composé IX, p.f. 195–198° (recristallisé dans alcool).

Anal. Calc. pour $C_{10}H_7N_5S_2$: C, 45.96; H, 2.70; N, 26.80. Trouvé: C, 46.32; H, 2.99; N, 26.86.

Diméthylmercapto-4,7 phényl-1 triazolo (4,5-d) pyridazine (X)

Les 3.5 g précédents (IX) sont dissouts dans 50 ml de NaOH 15%. On ajoute 5 ml de CH_3I et agite pendant 2 h à température ordinaire. On chasse le CH_3I sous vide et extrait au chloroforme. On chasse ce dernier et cristallise le solide dans du méthanol. On obtient 2.6 g (70%), p.f. 167–168°.

Anal. Calc. pour $C_{12}H_{11}N_5S_2$: C, 49.80; H, 3.83; N, 24.20; S, 22.16. Trouvé: C, 50.07; H, 3.88; N, 24.22; S, 22.38.

Hydrazino-4(7) méthylmercapto-7(4) phényl-1 triazolo (4,5-d) pyridazine (XI)

Le dérivé précédent (X) (1 g) est dissout dans 40 ml d'isopropanol auquel on ajoute 3 ml d'hydrazine 95%. On chauffe pendant 14 h à reflux. Au refroidissement un précipité volumineux se forme. On filtre et on obtient 6 g (66%) de solide, p.f. 210–211° (recristallisé dans isopropanol).

Anal. Calc. pour $C_{11}H_{11}N_2S$: C, 48.30; H, 4.05; N, 35.87; S, 11.73. Trouvé: C, 48.41; H, 3.89; N, 36.07; S, 11.87.

Can. J. Chem. Downloaded from www.nrcresearchpress.com by 210.87.254.6 on 09/05/12
For personal use only.

Ester méthylique du dicarboxy-4,5 phényl-3 isoxazole (XII)

A une solution éthérée comprenant un mélange de 40 g d'ester méthylique du dicarboxy-1,2 acétyléne et de 40 g de chlorure de l'acide benzhydroxamique, on ajoute, après avoir refroidi à −5°, 40 g de triéthylamine goutte à goutte en agitant fortement. On filtre le chlorhydrate de triéthylamine et lave ce dernier à l'éther. On sèche le filtrat éthéré sur sulfate de sodium et chasse l'éther. On obtient 53 g (72%) d'une huile qui cristallise, p.f. 62–63°.

Anal. Calc. pour $C_{13}H_{11}NO_5$: C, 59.76; H, 4.24; N, 5.36. Trouvé: C, 59.64; H, 4.24; N, 5.31.

Carboxyhydrazide-4(5) carbométhoxy-5(4) phényl-3 isoxazole (XIII)

Le diester XII (5 g) dissout dans 30 ml d'alcool absolu est chauffé pendant 2 h à reflux avec une solution de 1.2 g d'hydrate d'hydrazine 85% dans 10 ml d'alcool. La solution évaporée à sec, donne 2 g (40%) d'une huile qui cristallise, p.f. 100–101°.

Anal. Calc. pour $C_{12}H_{11}N_3O_4$: C, 55.36; H, 4.74; N, 15.75. Trouvé: C, 55.16; H, 4.24; N, 16.08.

Dihydroxy-4,7 phényl-3 isoxazolo (4,5-d) pyridazine (XIV)

Le diester XII (5 g) dissout dans 30 ml d'alcool absolu est chauffé pendant 45 min avec 3.6 g d'hydrate d'hydrazine 85%. On concentre la solution à moitié, puis refroidit et filtre. On traite le solide par de l'acide chlorhydrique 2 *N* pendant 1 h au bain-marie. On filtre à froid le solide et on obtient 2.5 g (50%), p.f. 280° (recristallisé dans eau–dioxane).

Anal. Calc. pour $C_{11}H_7N_3O_3$: C, 57.63; H, 3.07; N, 18.34. Trouvé: C, 57.73; H, 3.04; N, 18.19.

Dihydroxy-4,7 phényl-3 pyrazolo (4,5-d) pyridazine (XV)

Le filtrat éthanolique obtenu au cours de la préparation précédente du composé XIV est évaporé à sec. On obtient 2 g (40%) de solide, p.f. >300° (recristallisé dans eau–dioxane).

Anal. Calc. pour $C_{11}H_8N_4O_2$: C, 57.89; H, 3.53; N, 24.55. Trouvé: C, 57.53; H, 3.70; N, 24.88.

Dichloro-4,7 phényl-3 isoxazolo (4,5-d) pyridazine (XVI)

On chauffe à reflux 10 g de dérivé XIV dans 100 ml $POCl_3$ pendant 5 h. Puis on chasse le $POCl_3$ sous vide et traite le résidu par de la glace pilée. On neutralise la suspension aqueuse par de l'ammoniaque 28%. On filtre et recristallise dans l'alcool absolu, et on obtient 5 g (45%), p.f. 158–160°.

Anal. Calc. pour $C_{11}H_5N_3OCl_2$: C, 49.65; H, 1.89; N, 15.78; Cl, 26.64. Trouvé: C, 49.58; H, 1.88; N, 16.11; Cl, 27.07.

Chloro-4(7) oxo-7(4) phényl-3 dihydro-6,7(4,5) isoxazolo (4,5-d) pyridazine (XVII)

Des eaux-mères alcooliques du produit précédent (XVI) on a obtenu 2 g (20%) d'un produit fondant à 235°.

Anal. Calc. pour $C_{11}H_6O_2N_3Cl$: C, 53.34; H, 2.44; N, 16.96; Cl, 14.31. Trouvé: C, 53.29; H, 3.02; N, 16.37; Cl, 14.81.

Diméthoxy-4,7 phényl-3 isoxazolo (4,5-d) pyridazine (XVIII)

On chauffe pendant 6 h à 120° dans la bombe Parr un mélange de 2.65 g de produit dichloré XVI et de 0.5 g de sodium dissout dans 50 ml de méthanol. On obtient, après filtration, 2.5 g (90%) de fines aiguilles, p.f. 114–115° (recristallisé dans eau–dioxane).

Anal. Calc. pour $C_{13}H_{11}O_3N_3$: C, 60.69; H, 4.31; N, 16.33. Trouvé: C, 61.14; H, 4.65; N, 16.12.

Bis diméthylaminoéthoxy-4,7 phényl-3 isoxazolo (4,5-d) pyridazine (XIX)

On dissout 1.5 g de sodium dans un mélange de 5.4 g de diméthylaminoéthanol et de 60 ml de xylène. On y ajoute 7.95 g de composé dichloré XVI et on chauffe le tout à reflux pendant 4 h. On filtre le chlorure de sodium et chasse le xylène sous vide. On obtient 7 g (70%) d'huile qui se solidifie peu à peu, p.f. 52–56°. On a identifié ce produit par son dipicrate, p.f. 157–160° (recristallisé dans eau–dioxane).

Anal. Calc. pour $C_{31}H_{31}N_{11}O_{17}$: C, 44.86; H, 3.78; N, 18,57. Trouvé: C, 44.70; H, 3.89; N, 18.52.

Diméthylmercapto-4,7 phényl-3 isoxazolo (4,5-d) pyridazine (XX)

On agite à température ordinaire pendant 4 h un mélange de 5 g de produit dichloré XVI, 4 g de sulfhydrate de sodium et 40 ml d'alcool absolu. La réaction est exothermique. On dissout le tout dans une solution d'hydroxyde de sodium 10%, filtre et acidifie la solution. Il se forme un précipité que l'on filtre, dissout dans de l'hydroxyde de sodium 15% et agite pendant 2 h avec 5 ml d'iodure de méthyle. On chasse l'iodure de méthyle sous vide et extrait au chloroforme. On chasse le solvant et recristallise le solide obtenu dans du méthanol. On obtient ainsi 4.4 g (85%), p.f. 134–136°.

Anal. Calc. pour $C_{13}H_{11}N_3OS_2$: C, 53.95; H, 3.83; N, 14.52. Trouvé: C, 53.69; H, 4.14; N, 14.34.

Dihydrazino-4,7 phényl-3 pyrazolo (4,5-d) pyridazine (XXI)

La diméthylmercapto-4,7 phényl-3 isoxazolo (4,5-*d*) pyridazine (1 g) est chauffée à reflux pendant 12 h avec 6 ml d'hydrazine (95%) et 15 ml d'isopropanol. Le tout se dissout, puis reprécipite peu à peu. On obtient ainsi 0.6 g (70%), p.f. 265°.

Anal. Calc. pour $C_{11}H_{12}N_8$: C, 51.55; H, 4.71; N, 43.72. Trouvé: C, 51.33; H, 4.98; N, 43.02.

Can. J. Chem. Downloaded from www.nrcresearchpress.com by 210.87.254.6 on 09/05/12
For personal use only.

1. F. GROSS, J. DRUEY et R. MEIER. Experientia, **6**, 19 (1950).
2. B. N. GRAVES et F. F. YONKMAN. Federation Proc. **9**, 265 (1950). J. DRUEY et B. H. RINGIER. Helv. Chim. Acta, **34**, 195 (1951).
3. R. G. JONES. J. Am. Chem. Soc. **78**, 159 (1956).
4. R. SEKA et H. PREISSEKER. Monatsh. **57**, 71 (1931).
5. M. MALM et R. CASTLE. J. Heterocyclic Chem. **1**, 182 (1965).
6. A. MICHAEL. J. Prakt. Chem. **2**, 48 (1893).
7. C. MUSANTE et S. FATTUTA. Gazz. Chim. Ital. **88**, 879 (1958).

REÇU LE 15 MARS 1966.
RESEARCH LABORATORIES,
FRANK W. HORNER LIMITED,
MONTRÉAL, QUÉBEC.

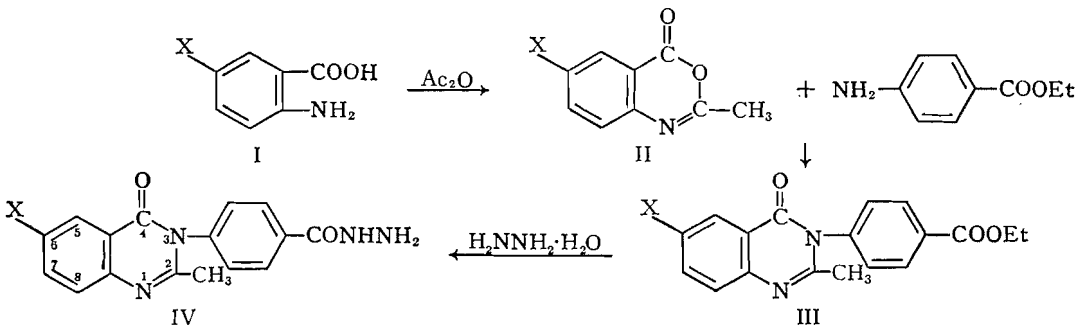
Can. J. Chem. Downloaded from www.nrcresearchpress.com by 210.87.254.6 on 09/05/12
For personal use only.

SYNTHESIS OF QUINAZOLONE HYDRAZIDES AS MONOAMINE OXIDASE INHIBITORS[1]

SURENDRA S. PARMAR AND R. C. ARORA

The specific inhibition of monoamine oxidase by the hydrazine derivative iproniazid, 1-isonicotinic acid-2-isopropyl hydrazine, was reported by Zeller *et al.* (1). Monoamine oxidase, an enzyme responsible for oxidative deamination of biologically active amines, is considered to play a role in the activity of the central nervous system, and the inhibitors of this enzyme have been shown to possess pronounced anticonvulsant properties (2). Furthermore, when 2,3-disubstituted quinazolones were investigated (3), 2-methyl-3-*o*-tolyl-4-quinazolone was found to be a potent anticonvulsant, and was superior to sodium phenobarbitone when used against pentylenetetrazole-induced seizures (4). In a continuation of our work on the synthesis of 2,3-disubstituted quinazolones (5), we have synthesized some hydrazides having a quinazolone moiety, with a view to obtaining compounds affecting the activity of the central nervous system. The present study describes the synthesis and the inhibition of the rat liver mitochondrial monoamine oxidase by such hydrazide derivatives. Structure–activity relationships have been examined briefly.

The quinazolone hydrazides have been synthesized according to the following scheme (X = H, Cl, Br, I, or NO_2).



EXPERIMENTAL[2]

Synthesis of Anthranilic Acids (I)

The various substituted anthranilic acids (I) were synthesized according to the methods reported earlier in the literature. The anthranilic acids used were 5-chloroanthranilic acid (6), 5-bromoanthranilic acid (7), 5-iodoanthranilic acid (8), and 5-nitroanthranilic acid (9); their melting points were found to be identical with those reported earlier.

[1]*This investigation was supported in part by the State Medical Research Council, Lucknow (U.P.), and the Council of Scientific and Industrial Research, New Delhi, India. A summary of this work was presented at the 23rd International Congress of Physiological Sciences, Tokyo, Japan, September 1965.*

[2]*Melting points were determined in a capillary tube and are corrected.*

1. F. GROSS, J. DRUEY et R. MEIER. Experientia, **6**, 19 (1950).
2. B. N. GRAVES et F. F. YONKMAN. Federation Proc. **9**, 265 (1950). J. DRUEY et B. H. RINGIER. Helv. Chim. Acta, **34**, 195 (1951).
3. R. G. JONES. J. Am. Chem. Soc. **78**, 159 (1956).
4. R. SEKA et H. PREISSEKER. Monatsh. **57**, 71 (1931).
5. M. MALM et R. CASTLE. J. Heterocyclic Chem. **1**, 182 (1965).
6. A. MICHAEL. J. Prakt. Chem. **2**, 48 (1893).
7. C. MUSANTE et S. FATTUTA. Gazz. Chim. Ital. **88**, 879 (1958).

REÇU LE 15 MARS 1966.
RESEARCH LABORATORIES,
FRANK W. HORNER LIMITED,
MONTRÉAL, QUÉBEC.

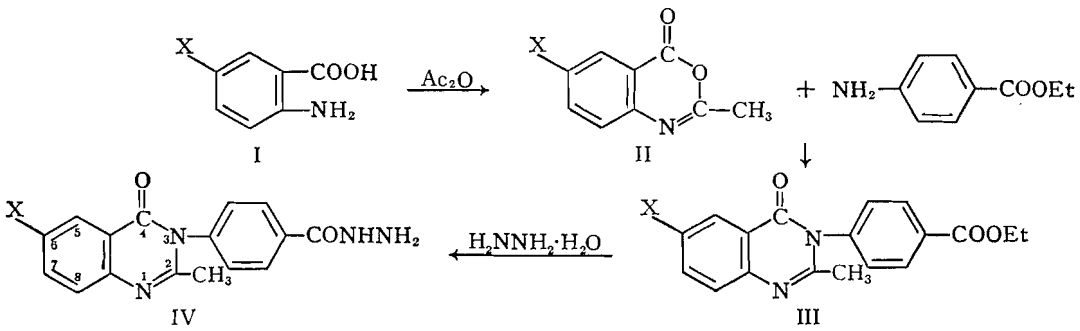
Can. J. Chem. Downloaded from www.nrcresearchpress.com by 210.87.254.42 on 09/05/12
For personal use only.

SYNTHESIS OF QUINAZOLONE HYDRAZIDES AS MONOAMINE OXIDASE INHIBITORS[1]

SURENDRA S. PARMAR AND R. C. ARORA

The specific inhibition of monoamine oxidase by the hydrazine derivative iproniazid, 1-isonicotinic acid-2-isopropyl hydrazine, was reported by Zeller *et al.* (1). Monoamine oxidase, an enzyme responsible for oxidative deamination of biologically active amines, is considered to play a role in the activity of the central nervous system, and the inhibitors of this enzyme have been shown to possess pronounced anticonvulsant properties (2). Furthermore, when 2,3-disubstituted quinazolones were investigated (3), 2-methyl-3-*o*-tolyl-4-quinazolone was found to be a potent anticonvulsant, and was superior to sodium phenobarbitone when used against pentylenetetrazole-induced seizures (4). In a continuation of our work on the synthesis of 2,3-disubstituted quinazolones (5), we have synthesized some hydrazides having a quinazolone moiety, with a view to obtaining compounds affecting the activity of the central nervous system. The present study describes the synthesis and the inhibition of the rat liver mitochondrial monoamine oxidase by such hydrazide derivatives. Structure–activity relationships have been examined briefly.

The quinazolone hydrazides have been synthesized according to the following scheme (X = H, Cl, Br, I, or NO_2).



EXPERIMENTAL[2]

Synthesis of Anthranilic Acids (I)

The various substituted anthranilic acids (I) were synthesized according to the methods reported earlier in the literature. The anthranilic acids used were 5-chloroanthranilic acid (6), 5-bromoanthranilic acid (7), 5-iodoanthranilic acid (8), and 5-nitroanthranilic acid (9); their melting points were found to be identical with those reported earlier.

[1]*This investigation was supported in part by the State Medical Research Council, Lucknow (U.P.), and the Council of Scientific and Industrial Research, New Delhi, India. A summary of this work was presented at the 23rd International Congress of Physiological Sciences, Tokyo, Japan, September 1965.*

[2]*Melting points were determined in a capillary tube and are corrected.*

Synthesis of Acetanthranils (II)

The acetanthranils (II) were synthesized by refluxing 1 mole of the appropriate anthranilic acid with 2 moles of acetic anhydride for 1 h. After the excess of acetic anhydride was distilled off, the acetanthranils, which separated out as a solid mass, were used without further purification. These acetanthranils have been reported earlier, except for that prepared from 5-nitroanthranilic acid (6-nitroacetanthranil, m.p. 217–219 °C, yield 40%).

Anal. Calcd. for $C_9H_6N_2O_4$: C, 52.42; H, 2.9; N, 13.59. Found: C, 52.0; H, 2.4; N, 13.9.

Synthesis of Quinazolones (III)

The quinazolones (III) were synthesized by heating equimolar proportions of the substituted acetanthranils and *p*-aminoethyl benzoate (benzocaine) as reported earlier (10). The quinazolones shown in Table I were characterized by their melting points and empirical compositions.

TABLE I

Substituted quinazolones (III)

X	Melting point (°C)	Yield (%)	Formula	Nitrogen (%) Calculated	Nitrogen (%) Found
H	174–175	60	$C_{18}H_{16}N_2O_3$	9.09	8.8
Cl	186–187	55	$C_{18}H_{15}ClN_2O_3$	8.1	8.6
Br	170	58	$C_{18}H_{15}BrN_2O_3$	7.25	7.18
I	196–197	58	$C_{18}H_{15}IN_2O_3$	6.45	6.9
NO_2	222	50	$C_{18}H_{15}N_3O_5$	11.19	11.15

Synthesis of Quinazolone Hydrazides (IV)

Quinazolone hydrazides (IV) were synthesized as described earlier (11) by refluxing 1 mole of quinazolone with 2 moles of hydrazine hydrate (99–100%) in absolute ethanol for 6 to 8 h. When the excess of alcohol was distilled off, the quinazolone hydrazides separated out as solid masses. These hydrazides were recrystallized from ethanol. The physical constants are given in Table II.

Determination of Monoamine Oxidase Activity

The monoamine oxidase activity of rat liver mitochondria was determined by the conventional Warburg manometric method (12) as described earlier (13). Mitochondria were isolated by differential centrifugation of rat liver homogenate in ice-cold 0.25 *M* sucrose (10% w/v) by the method (14) of Hogeboom *et al.* (15). The enzyme was assayed by measuring the oxygen consumption after the addition of tyramine.

TABLE II

Quinazolone hydrazides (IV) and their monoamine oxidase inhibition

X	Melting point (°C)	Yield (%)	Formula	Nitrogen (%) Calculated	Nitrogen (%) Found	% inhibition
H	114–116	60	$C_{16}H_{14}N_4O_2$	19.04	18.8	9.5 9.5 (11.33) 15.0
Cl	167–170	55	$C_{16}H_{13}ClN_4O_2$	17.04	17.27	59.3 61.5 (60.27) 60.0
Br	155–157	58	$C_{16}H_{13}BrN_4O_2$	15.37	15.7	52.5 52.8 (52.6) 52.5
I	179	50	$C_{16}H_{13}IN_4O_2$	13.4	13.54	73.7 76.3 (75.03) 75.1
NO_2	204–206	45	$C_{16}H_{13}N_5O_4$	20.6	20.1	52.0 48.0 (50.66) 52.0

NOTE: The percentage inhibition was calculated from the decrease in the oxygen uptake during 1 h. Washed rat liver mitochondria equivalent to 250 mg of fresh tissue were used in each Warburg vessel in a total volume of 3 ml containing 66 m*M* phosphate buffer (pH 7.4) and 10 m*M* tyramine (substrate). The inhibitors present in the side arm at a final concentration of 1×10^{-4} *M* were incubated with the enzyme preparation for 10 min before tyramine was added. The enzyme system was further incubated at 37 °C for 1 h in an atmosphere of oxygen. The figures in parentheses are averages.

Can. J. Chem. Downloaded from www.nrcresearchpress.com by 210.87.254.42 on 09/05/12
For personal use only.

Can. J. Chem. Downloaded from www.nrcresearchpress.com by 210.87.254.42 on 09/05/12
For personal use only.

RESULTS AND DISCUSSION

Oxygen uptake has been shown to reflect the true monoamine oxidase activity in washed mitochondrial preparations during oxidation of tyramine (16). The use of cyanide and semicarbazide, as suggested earlier (12), was therefore not necessary in the present investigation. The relative percentage of enzyme inhibition by the new hydrazides was estimated (see Table II) at a fixed concentration of 10^{-4} M of inhibitors.

It was found that a substituent at position 6 of the quinazolone ring markedly enhanced inhibition, a maximum effect being obtained with iodine as a substituent. However, 6-iodo-substituted quinazolone hydrazide, the most potent compound in the present series, was found to be a rather weak inhibitor as compared with other classical inhibitors. The relative electronegativity of the 6-substituents does not appear to be the factor affecting the inhibitory power of the various analogues. The parameter(s) controlling the structure–activity relationship is (are) not discernible. The active surface of the enzyme and the uptake sites of the mitochondria appear to require structural features other than the basic hydrazine moiety for optimum binding. It has already been shown that the presence of an iodine substituent on the ring of benzylamine substrates markedly enhances their affinity for the enzyme (17). Further studies on the determination of the nature of the inhibition produced by these compounds and the synthesis of other related structures carrying different substituents[3] may contribute to a better understanding of the chemical requirements of the active sites of the enzyme.

ACKNOWLEDGMENTS

The authors express their thanks to Dr. Sabit Gabay and Mr. K. Kishor for their advice and encouragement. Grateful acknowledgment is made to Dr. M. L. Dhar, Director, Central Drug Research Institute, Lucknow, for providing microanalysis facilities.

1. E. A. Zeller, J. Barsky, J. R. Fouts, W. F. Kirchheimer, and L. S. Van Orden. Experientia, **8**, 349 (1952).
2. J. P. Darwin, P. A. Shore, and B. B. Brodie. Ann. N.Y. Acad. Sci. **83**, 643 (1959).
3. I. K. Kacker and S. H. Zaheer. J. Indian Chem. Soc. **28**, 344 (1951).
4. M. L. Gujral, P. N. Saxena, and R. P. Kohli. Indian J. Med. Res. **45**, 207 (1957).
5. K. Kishor, R. C. Arora, and S. S. Parmar. J. Med. Chem. **8**, 550 (1965).
6. M. M. Endicott, B. B. Alden, and M. L. Sherrill. J. Am. Chem. Soc. **68**, 1303 (1946).
7. A. S. Wheeler and W. M. Oats. J. Am. Chem. Soc. **32**, 770 (1910).
8. C. J. Klemme and J. H. Hunter. J. Org. Chem. **5**, 227 (1940).
9. O. Yu. Magidson and E. S. Golovechinskaya. J. Gen. Chem. USSR Engl. Transl. **8**, 1797 (1938).
10. K. Kishor, R. Kumar, and S. S. Parmar. J. Med. Chem. **7**, 831 (1964).
11. Ng. Ph. Buu Hoi, Ng. D. Xuong, Ng. H. Nam, E. Binnon, and R. Royer. J. Chem. Soc. 1358 (1953).
12. N. H. Creasey. Biochem. J. **64**, 178 (1956).
13. M. C. Pant, S. S. Parmar, and K. P. Bhargava. Can. J. Biochem. **42**, 1114 (1964).
14. J. Hawkins. Biochem. J. **50**, 577 (1952).
15. G. H. Hogeboom, W. C. Schneider, and G. E. Palade. J. Biol. Chem. **172**, 619 (1948).
16. S. S. Parmar and M. Nickerson. Biochem. Pharmacol. **8**, 10 (1961).
17. E. A. Zeller. Ann. N.Y. Acad. Sci. **107**, 811 (1963).

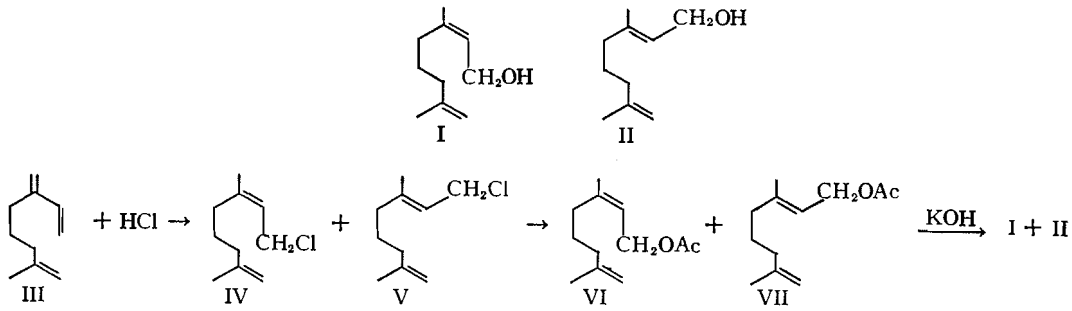
Received March 9, 1966.
Department of Pharmacology and Therapeutics,
King George's Medical College,
Lucknow University,
Lucknow, India,
and
Biochemical Research Laboratory,
Boston University, Veterans Administration Hospital,
Brockton, Massachusetts.

[3]*S. S. Parmar, R. C. Arora, and S. Gabay, in preparation.*

α-NEROL AND α-GERANIOL

BERNARD M. MITZNER, VITO J. MANCINI, AND SEYMOUR LEMBERG

Neither α-nerol nor α-geraniol has been reported as occurring in nature. The two isomeric materials have not previously been prepared in a pure form synthetically, and their spectra have not been characterized.[1] In this note we report the preparation of pure α-nerol (I) (*cis*-2,6-dimethyl-1,6-octadiene-8-ol) and pure α-geraniol (II) (*trans*-2,6-dimethyl-1,6-octadiene-8-ol). (Their purity was ascertained by gas chromatography, with a nonpolar and a polar column.)



α-Myrcene (III) was hydrochlorinated to give α-neryl chloride (IV) and α-geranyl chloride (V) which, when treated with sodium acetate, gave the α-acetates VI and VII; hydrolysis with potassium hydroxide gave the alcohols I and II.

Proof of Structure

The infrared spectra of α-nerol and α-geraniol are shown in Fig. 1. The isopropenyl moiety is clearly visible at 11.25 μ (CH_2 out-of-plane deformation) and at 6.05 μ (C—C stretching). The allylic hydroxyl exhibits very strong absorption at 10 μ (C—O stretching); the trisubstituted double bond allylic to the hydroxyl exhibits very strong absorption at 5.95 μ (C—C stretching). The nuclear magnetic resonance spectra of the two isomeric alcohols are shown in Fig. 2. The terminal groups have a τ value of 5.33 (α-nerol) and 5.37 (α-geraniol). The significant allylic methylene groups have a τ value of about 8.31. The pertinent assignments are illustrated in Fig. 2.

A small sample of pure α-nerol was subjected to hydrogenation with 10% palladium on carbon at atmospheric pressure. The isopropenyl double bond was completely hydrogenated and dihydro-nerol (*cis*-2,6-dimethyl-6-octen-8-ol) was obtained. The same process was carried out with pure α-geraniol to give dihydro-geraniol (*trans*-2,6-dimethyl-6-octen-8-ol). The structures of the last two compounds are well characterized in the literature (3–5). When a mixture of nerol and geraniol along with their alpha isomers was subjected to gas chromatography on a Carbowax column, the order of elution was nerol, α-nerol, geraniol, and α-geraniol. It should be noted that, in systems where *cis* and *trans* double bonds are in position 6 (in the C-10 terpene series), the *cis* isomer is always eluted first. The molecular weight of the two alcohols is 154 ($C_{10}H_{18}O$). The cracking pattern of the molecular weight determination was carried out with a C.E.C. model 103 mass spectrometer. The pattern of α-nerol closely resembled that of nerol; those of the two geraniols were likewise similar.

[1]*The existence of α-nerol and (or) α-geraniol is suggested, or their presence in a mixture is postulated, in the papers listed in ref. 1.*

Can. J. Chem. Downloaded from www.nrcresearchpress.com by 210.87.254.105 on 09/05/12
For personal use only.

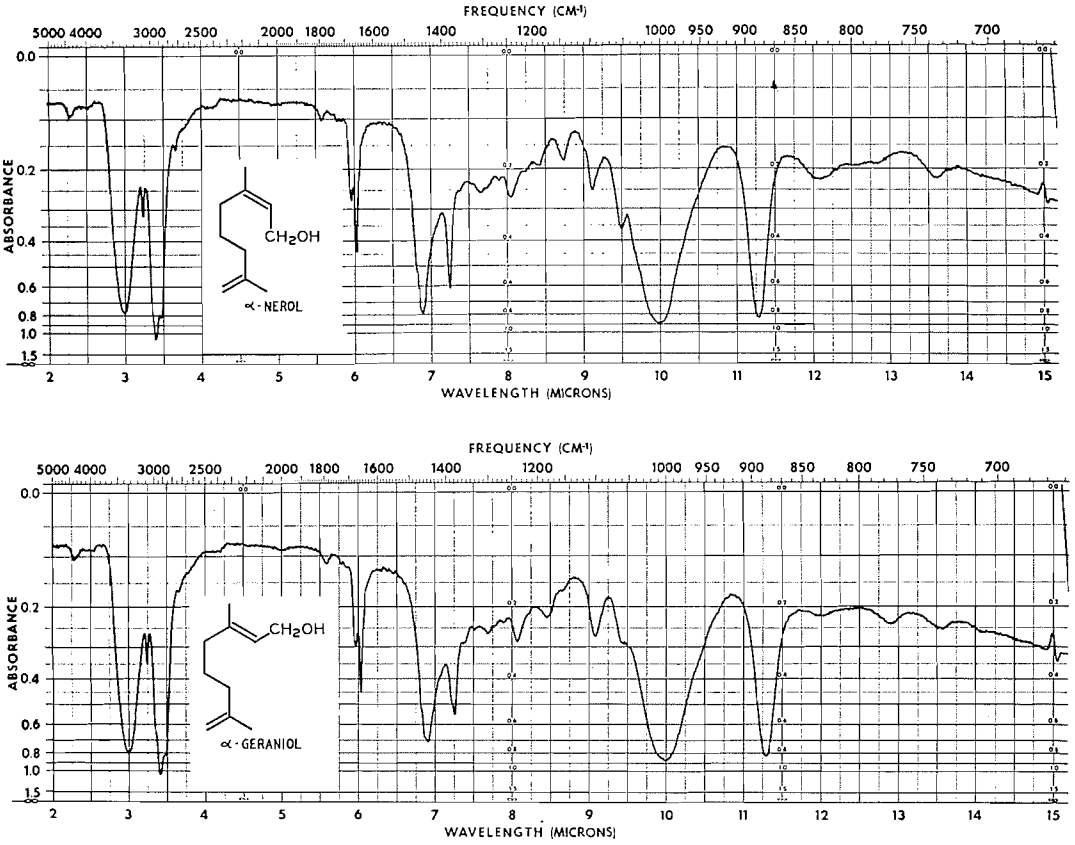


FIG. 1.

EXPERIMENTAL

α-Myrcene (50 g, 0.37 mole), prepared via the pyrolysis of myrcenyl acetate (2), was hydrochlorinated at ambient temperature and pressure with 2 mole % copper bronze as catalyst. Anhydrous hydrogen chloride (0.33 *M*) was added, and the resultant hydrochloride was washed with water until neutral, dried with magnesium sulfate, and reacted with 1 mole of sodium acetate and 0.5 mole of acetic anhydride at 75 °C for 6 h to yield 45 g of the ester mixture; this was washed with water until neutral. An aliquot of the mixture (35 g) was hydrolyzed by refluxing it in 20% ethanolic KOH; the resulting alcohols were washed until neutral. Approximately 20 g of a mixture consisting of α-nerol and α-geraniol was obtained. Preparative gas chromatography led to the isolation of pure α-nerol and pure α-geraniol. The following gas–liquid chromatographic parameters were employed: a 10 ft ($\frac{3}{8}$ inch outside diameter) × $\frac{5}{16}$ inch inside diameter copper column filled with 20% Carbowax 20M adsorbed on silane-treated Celite of 60–80 mesh, maintained at a temperature of 150 °C with a flow rate of 250 ml of helium/min; repeated injections of 0.1 ml of the alcohol mixture were employed.

DISCUSSION

There has been a great deal of controversy regarding the actual structure of nerol and geraniol for many years. Many workers, especially in the past, have ascribed the previously described alpha structure to nerol and geraniol. This present work has served to synthesize, isolate, and characterize the alpha compounds, thus aiding in definitively establishing the structure of nerol and geraniol as having an isopropylidene group.

Experimental work carried out in our laboratories over the last 7 years on the examination of various natural oils containing geraniol has failed to reveal a compound having the alpha structure reported in this paper.

Can. J. Chem. Downloaded from www.nrcresearchpress.com by 210.87.254.105 on 09/05/12
For personal use only.

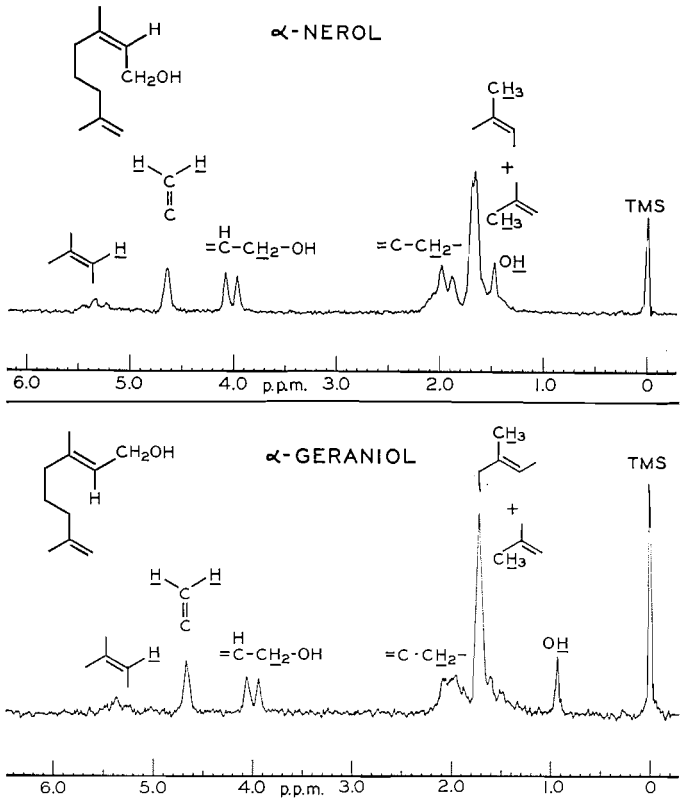


FIG. 2. TMS = tetramethylsilane.

1. H. KAPPELER, D. STAUFFACHER, A. ESCHENMOSHER, and H. SCHINTZ. Helv. Chim. Acta, **37**, 957 (1954). Ger. Patent No. 960,278 (1957). H. FARNOW and F. PORSCH. Dragoco Rept. **1**, 1 (1960). Y. NAVES. P.E.O.R. **48**, 118 (1952).
2. B. MITZNER, E. T. THEIMER, L. STEINBACH, and J. WOLT. J. Org. Chem. **30**, 646 (1965).
3. R. HEILMANN and R. GLENAT. Bull. Soc. Chim. France, 1586 (1955).
4. U.S. Patent No. 2,833,811 (1958).
5. B. N. JOSHI *et al.* Tetrahedron, **20**, 2911 (1964).

RECEIVED FEBRUARY 21, 1966.
INTERNATIONAL FLAVORS & FRAGRANCES (U.S.),
NEW YORK, NEW YORK.

ORGANIC SULFUR COMPOUNDS
III. CONDENSATIONS INVOLVING *o*-NITROBENZENESULFENYL CHLORIDE[1]

R. T. COUTTS, K. W. HINDMARSH, AND N. J. POUND

o-Nitrobenzenesulfenyl chloride, 2,4-dinitrobenzenesulfenyl chloride, and 4-chloro-2-nitrobenzenesulfenyl chloride are known to react with ketones possessing an active methylene group to yield α-(*o*-nitrophenylthio), α-(2,4-dinitrophenylthio), and α-(4-chloro-2-nitrophenylthio) ketones, respectively (1–3). Typical of this reaction is the condensation of *o*-nitrobenzenesulfenyl chloride with ethyl acetoacetate, which gives rise

[1]*For part II in this series, see R. T. Coutts, D. L. Barton, and E. M. Smith, Can. J. Chem., 44, 1733 (1966).*

Can. J. Chem. Downloaded from www.nrcresearchpress.com by 210.87.254.105 on 09/05/12
For personal use only.

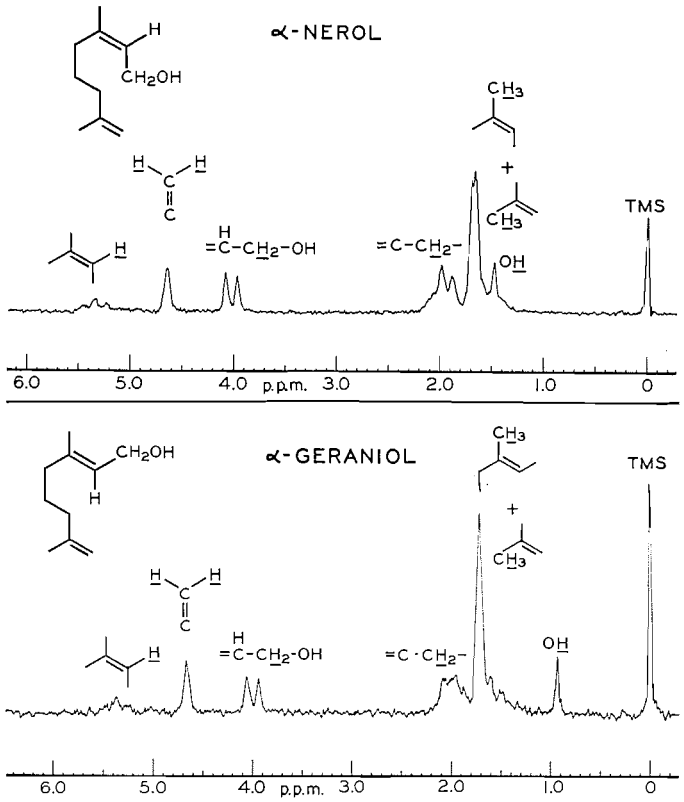


FIG. 2. TMS = tetramethylsilane.

1. H. KAPPELER, D. STAUFFACHER, A. ESCHENMOSHER, and H. SCHINTZ. Helv. Chim. Acta, **37**, 957 (1954). Ger. Patent No. 960,278 (1957). H. FARNOW and F. PORSCH. Dragoco Rept. **1**, 1 (1960). Y. NAVES. P.E.O.R. **48**, 118 (1952).
2. B. MITZNER, E. T. THEIMER, L. STEINBACH, and J. WOLT. J. Org. Chem. **30**, 646 (1965).
3. R. HEILMANN and R. GLENAT. Bull. Soc. Chim. France, 1586 (1955).
4. U.S. Patent No. 2,833,811 (1958).
5. B. N. JOSHI *et al.* Tetrahedron, **20**, 2911 (1964).

RECEIVED FEBRUARY 21, 1966.
INTERNATIONAL FLAVORS & FRAGRANCES (U.S.),
NEW YORK, NEW YORK.

ORGANIC SULFUR COMPOUNDS
III. CONDENSATIONS INVOLVING *o*-NITROBENZENESULFENYL CHLORIDE[1]

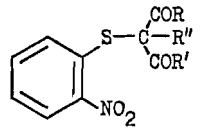
R. T. COUTTS, K. W. HINDMARSH, AND N. J. POUND

o-Nitrobenzenesulfenyl chloride, 2,4-dinitrobenzenesulfenyl chloride, and 4-chloro-2-nitrobenzenesulfenyl chloride are known to react with ketones possessing an active methylene group to yield α-(*o*-nitrophenylthio), α-(2,4-dinitrophenylthio), and α-(4-chloro-2-nitrophenylthio) ketones, respectively (1–3). Typical of this reaction is the condensation of *o*-nitrobenzenesulfenyl chloride with ethyl acetoacetate, which gives rise

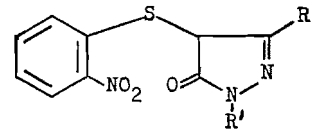
[1]*For part II in this series, see R. T. Coutts, D. L. Barton, and E. M. Smith, Can. J. Chem., 44, 1733 (1966).*

Can. J. Chem. Downloaded from www.nrcresearchpress.com by 210.87.254.105 on 09/05/12
For personal use only.

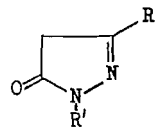
to ethyl α-(*o*-nitrophenylthio)acetoacetate (I*a*). When, however, 4-chloro-2-nitrobenzenesulfenyl chloride was reacted with diethyl malonate, the expected product, diethyl α-(4-chloro-2-nitrophenylthio)malonate, was not produced (3). The major product in this case was bis(4-chloro-2-nitrophenyl) disulfide. *o*-Nitrobenzenesulfenyl chloride also reacts atypically with diethyl malonate, with malonic acid, and with ethylmalonic acid. The products identified by us were bis(*o*-nitrophenyl) disulfide and the *S*-*o*-nitrophenyl ester of *o*-nitrothiobenzenesulfonic acid; α-(*o*-nitrophenylthio)butyric acid was an additional product in the reaction with ethylmalonic acid which yielded none of the desired compound (I*e*).



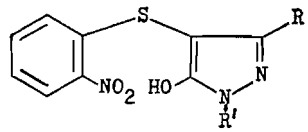
	R	R'	R''
Ia	Me	OEt	H
Ib	OH	OH	H
Ic	NH_2	NH_2	H
Id	NH-CO-NH		H
Ie	OH	OH	Et



	R	R'
IIa	Me	H
IIb	Me	Ph
IIc	Ph	Ph



III



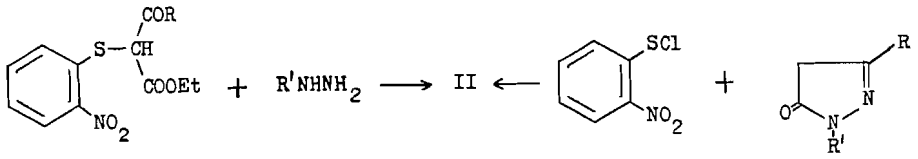
IV

In contrast with these results, when malonamide was reacted at room temperature with *o*-nitrobenzenesulfenyl chloride in acetonitrile, an almost quantitative yield of α-(*o*-nitrophenylthio)malonamide (I*c*) was obtained. As expected, this compound is a weak acid and is insoluble in sodium bicarbonate solution but readily soluble in aqueous sodium hydroxide, giving an orange solution from which I*c* is reprecipitated when acid is added. When the aqueous sodium hydroxide solution was heated, ammonia was rapidly evolved, but no α-(*o*-nitrophenylthio)malonic acid (I*b*) was isolable. An obvious extension of the above successful condensation was the interaction of *o*-nitrobenzenesulfenyl chloride with barbituric acid. This reaction occurred readily, and 5-(*o*-nitrophenylthio)barbituric acid (I*d*) was isolated in excellent yield. It is a relatively strong acid which dissolves in sodium bicarbonate solution. Also, it is stable in hot concentrated sulfuric acid. After such a solution was heated at 80–100° for 6 h, the addition of water precipitated the unchanged acid, almost quantitatively.

Our attention was then directed towards the preparation of 4-(*o*-nitrophenylthio)-2-pyrazolin-5-ones (II), which were required for our reductive cyclization studies (4). The initial method chosen to prepare the 4-(*o*-nitrophenylthio)-2-pyrazolin-5-ones was by the interaction of hydrazine or phenylhydrazine with ethyl α-(*o*-nitrophenylthio)acetoacetate or ethyl α-(*o*-nitrophenylthio)benzoylacetate. The action of phenylhydrazine on ethyl

Can. J. Chem. Downloaded from www.nrcresearchpress.com by 210.87.254.105 on 09/05/12
For personal use only.

α-(*o*-nitrophenylthio)acetoacetate gave the expected product (II*b*) in poor yield; however, when ethyl α-(*o*-nitrophenylthio)acetoacetate was treated with hydrazine hydrate, hydrolysis occurred and the only product isolated was the hydrazide of (*o*-nitrophenylthio)acetic acid. The action of phenylhydrazine on ethyl α-(*o*-nitrophenylthio)benzoylacetate was more complex; once again, the expected product (II*c*) was not obtained.



Instead, two red products were isolated in poor yields. The first contained sulfur and melted at 158°; the second product, m.p. 173°, was sulfur-free. Because neither product was the desired one, these compounds were not identified at this time. In view of these results, this synthetic approach was abandoned.

The fact that *o*-nitrobenzenesulfenyl chloride readily reacts with malonamide suggested that it might also condense with the active methylene group of the structurally related 2-pyrazolin-5-ones (III). Thus, *o*-nitrobenzenesulfenyl chloride was reacted in acetonitrile with 3-methyl-2-pyrazolin-5-one, with 3-methyl-1-phenyl-2-pyrazolin-5-one, and with 1,3-diphenyl-2-pyrazolin-5-one; in each case the reaction proceeded as expected, yielding the corresponding 4-(*o*-nitrophenylthio) derivatives (II*a*, II*b*, and II*c*, respectively).

The infrared spectra of the pyrazolones (II*a*–II*c*) in potassium bromide were of interest. They showed no carbonyl absorption, whereas absorption attributable to the hydroxyl group was present, which indicated that, in the solid state, the pyrazolones are better represented in the tautomeric form (IV). This conclusion is in agreement with the findings of Katritzky and Maine (5), who have studied in detail the tautomerism of pyrazolin-5-ones.

EXPERIMENTAL

Melting points are uncorrected. Infrared spectra (KBr disks) were recorded on a Unicam SP 200 spectrophotometer. Palladium–charcoal refers to 10% palladium on charcoal.

Ethyl 2-(*o*-nitrophenylthio)acetoacetate (1) and *o*-nitrobenzenesulfenyl chloride (6), which was obtained by the action of chlorine on bis(*o*-nitrophenyl) disulfide (7), were prepared by previously reported methods.

Reaction of o-Nitrobenzenesulfenyl Chloride with Ethylmalonic Acid

A solution of *o*-nitrobenzenesulfenyl chloride (3.0 g) and ethylmalonic acid (2.5 g) in acetonitrile (60 ml) was heated under reflux for 6 h; then the solution was concentrated to ca. 30 ml, from which, when it was allowed to stand, bis(*o*-nitrophenyl) disulfide (0.72 g), m.p. 195–200° (decomp.), precipitated and was filtered off. A yellow solid (0.82 g), m.p. 125–130°, slowly precipitated from the mother liquors over a period of 48 h. Crystallization of this solid from methanol gave the *S*-*o*-nitrophenyl ester of *o*-nitrothiobenzenesulfonic acid (0.54 g), m.p. 140–142° (lit. (8) m.p. 142–143°), the infrared spectrum of which was superimposable on that of an authentic sample. The mother liquors remaining were evaporated to dryness, and the resulting waxy solid was treated with 5% aqueous sodium hydroxide (50 ml). The solution was filtered and the filtrate, on acidification, gave α-(*o*-nitrophenylthio)butyric acid (0.39 g), m.p. 105–108°, as a yellow solid, the melting point of which was raised to 112–114° on crystallization from aqueous ethanol. Infrared spectrum: broad absorption from 2 100 to 3 400 with maxima at 2 970 (m) and 2 910 (m) (OH); 1 702 (s) (C=O); 1 520 (s), 1 338 (s), and 868 (m) (NO_2) cm^{-1}.

Anal. Calcd. for $C_{10}H_{11}NO_4S$: C, 49.78; H, 4.59; S, 13.29. Found: C, 49.75; H, 4.40; S, 12.66.

(o-Nitrophenylthio)malonamide (Ic)

Malonamide (1.0 g) was added to a solution of *o*-nitrobenzenesulfenyl chloride (1.9 g) in acetonitrile (60 ml), and the resulting suspension was stirred at room temperature for 24 h. The yellow solid which formed (2.48 g), m.p. 222–225° (decomp.), dissolved completely in aqueous sodium hydroxide or sodium carbonate to give an orange solution. The title compound was reprecipitated when hydrochloric acid was

Can. J. Chem. Downloaded from www.nrcresearchpress.com by 210.87.254.105 on 09/05/12
For personal use only.

added. Infrared spectrum: broad absorption from 2 900 to 3 500 (s) with maxima at 3 400, 3 280, and 3 200 (amide NH_2); 1 665 (s) (C=O); 1 515 (s), 1 345 (s), and 865 (w) (NO_2) cm^{-1}.

Anal. Calcd. for $C_9H_9N_3O_4S$: C, 42.35; H, 3.55; N, 16.47; S, 12.56. Found: C, 42.16; H, 3.58; N, 16.08; S, 12.41.

Hydrolysis of (o-Nitrophenylthio)malonamide

The title compound (8 g) was dissolved in 10% aqueous sodium hydroxide (200 ml), and this solution was gently boiled until the evolution of ammonia ceased (90 min). The solution was cooled, acidified with hydrochloric acid, and extracted with ether. The dried ether solution, on evaporation, gave a brown oil (1.2 g) which was only partially soluble in sodium bicarbonate solution and was therefore not further investigated.

5-(o-Nitrophenylthio)barbituric Acid (Id)

Barbituric acid (2.56 g) was added to a solution of *o*-nitrobenzenesulfenyl chloride (3.8 g) in acetonitrile (100 ml), and the resulting suspension was stirred at room temperature for 30 h. The yellow solid (5.23 g), m.p. 243° (decomp.), was removed. This was the title compound. Crystallization from acetonitrile did not raise the melting point. Infrared spectrum: broad absorption from 2 100 to 3 350 (m) with maxima at 2 600, 2 680, 3 120, and 3 280 (cyclic ureide); 1 728 (s) (C=O); 1 525 (s), 1 375 or 1 345 (s), and 865 (w) (NO_2) cm^{-1}.

Anal. Calcd. for $C_{10}H_7N_3O_5S$: C, 42.70; H, 2.51; N, 14.95; S, 11.40. Found: C, 42.47; H, 2.58; N, 14.54; S, 11.06.

Crystallization from water gave the monohydrate as a yellow solid, m.p. 244–246° (decomp.).

Anal. Calcd. for $C_{10}H_7N_3O_5S \cdot H_2O$: C, 40.13; H, 3.03. Found: C, 40.38, 40.21; H, 3.14, 3.12.

The acid (I*d*) was soluble, with vigorous effervescence, in aqueous sodium bicarbonate, giving an orange solution, from which the acid was reprecipitated when hydrochloric acid was added. A suspension of the acid (I*d*) (2.2 g) in 80% sulfuric acid (250 ml) was heated on a boiling water bath for 6 h, during which time the acid dissolved completely. The orange solution was poured into water (500 ml); the resulting yellow crystalline precipitate (1.7 g) melted at 248° (decomp.). An infrared spectrum confirmed that I*d* had been recovered.

3-Methyl-4-(o-nitrophenylthio)-1-phenyl-2-pyrazolin-5-one (IIb)

Method a

When a solution of *o*-nitrobenzenesulfenyl chloride (3.0 g) in acetonitrile (20 ml) was added to a suspension of 3-methyl-1-phenyl-2-pyrazolin-5-one (3.0 g) in acetonitrile (20 ml), the latter dissolved and a yellow precipitate formed almost immediately. The mixture was heated under reflux for 4 h (during which time hydrochloric acid was evolved), cooled, and filtered to give the title compound (4.6 g) as a bright-yellow solid, m.p. 209–211° (decomp.) when crystallized from aqueous ethanol (lit. (9) m.p. 207°). Infrared spectrum: broad absorption from 2 000 to 3 200 with a broad maximum centered at 2 600 (m) (OH); 1 520 (s), 1 340 (s), and 855 (w) (NO_2) cm^{-1}; carbonyl absorption absent.

Anal. Calcd. for $C_{16}H_{13}N_3O_3S$: C, 58.70; H, 4.00; N, 12.84; S, 9.80. Found: C, 58.68; H, 4.20; N, 12.10; S, 10.21.

Method b

A solution of phenylhydrazine (2.1 g) and ethyl 2-(*o*-nitrophenylthio)acetoacetate (3.0 g) in acetonitrile (30 ml) was heated under reflux for 5 h. When the red solution was allowed to cool and stand, the title compound (1.35 g) precipitated out, m.p. 200–202°, raised to 208–210° (decomp.) when crystallized from ethanol. The infrared spectrum was identical with that of the product obtained by method *a*.

3-Methyl-4-(o-nitrophenylthio)-2-pyrazolin-5-one (IIa)

Method a

This pyrazolone was obtained by the method used in the preparation of II*b* (method *a*). The bright-yellow solid (91% yield) was dissolved in 10% sodium hydroxide solution, this solution was extracted with ether, and the ether extract was rejected. The aqueous layer was acidified with hydrochloric acid; the resulting yellow solid had m.p. 273–274° (decomp.) when crystallized from ethanol. Infrared spectrum: 3 390 (m) (NH); broad absorption from 3 300 to 2 000 with a maximum at 2 600 (w) (OH); 1 525 (s), 1 345 (s), and 855 (w) (NO_2) cm^{-1}; carbonyl absorption absent.

Anal. Calcd. for $C_{10}H_9N_3O_3S$: C, 47.81; H, 3.61; N, 16.72; S, 12.76. Found: C, 47.40; H, 3.60; N, 16.89; S, 13.09.

Method b

Hydrazine hydrate (2.1 g) was added to a solution of ethyl (*o*-nitrophenylthio)acetoacetate (4.0 g) in acetonitrile (25 ml), and the resulting deep-red solution was stirred for 2 h. The crystalline yellow precipitate (2.7 g), m.p. 163–165°, which formed was the hydrazine of (*o*-nitrophenylthio)acetic acid (lit. (10) m.p. 164°). The infrared spectrum was identical with that of an authentic sample.

Anal. Calcd. for $C_8H_9N_3O_3S$: C, 42.28; H, 3.99; N, 18.50. Found: C, 42.59; H, 3.76; N, 18.25.

Can. J. Chem. Downloaded from www.nrcresearchpress.com by 210.87.254.105 on 09/05/12
For personal use only.

4-(o-Nitrophenylthio)-1,3-diphenyl-2-pyrazolin-5-one (IIc)

Using essentially the conditions described for the preparation of II*b* (method *a*), we obtained the title compound (8.9 g), initially as a brown oil which quickly solidified, from *o*-nitrobenzenesulfenyl chloride (4.6 g) and 1,3-diphenyl-2-pyrazolin-5-one (5.8 g). Crystallization from anhydrous benzene gave a yellow solid, m.p. 182–183° (decomp.) after preliminary softening around 110°. Infrared spectrum: broad absorption from 2 100 to 3 200 with maxima at 3 080 (w) and 2 260 (w) (OH); 1 525 (s), 1 340 (m), and 860 (w) (NO_2) cm^{-1}; carbonyl absorption absent.

Anal. Calcd. for $C_{21}H_{15}N_3O_3S$: C, 64.76; H, 3.88; N, 10.79; S, 8.23. Found: C, 64.46; H, 3.84; N, 10.64; S, 8.27.

ACKNOWLEDGMENTS

The financial support of the National Research Council of Canada is gratefully acknowledged. The authors also thank H. W. Peel, M.Sc., for his assistance in this project.

1. J. A. Baltrop and K. J. Morgan. J. Chem. Soc. 4486 (1960).
2. N. Kharasch. J. Chem. Educ. **33**, 585 (1956).
3. T. Zinke and J. Baeumer. Ann. Chem. **416**, 86 (1918), and references therein.
4. R. T. Coutts and J. B. Edwards. Can. J. Chem. This issue.
5. A. R. Katritzky and F. W. Maine. Tetrahedron, **20**, 299 (1964).
6. M. H. Hubacher. *In* Organic syntheses. Vol. XV. *Edited by* C. R. Noller. John Wiley & Sons, Inc., New York. 1935. p. 45.
7. M. T. Bogert and A. Stull. *In* Organic syntheses. Collective Vol. I. *Edited by* H. Gilman. John Wiley & Sons, Inc., New York. 1947. p. 220.
8. T. Zinke and F. Farr. Ann. Chem. **391**, 55 (1912).
9. C. Angelini and A. Martani. Ann. Chim. Rome, **45**, 156 (1955); Chem. Abstr. **50**, 3146*b* (1956).
10. R. T. Coutts, H. W. Peel, and E. M. Smith. Can. J. Chem. **43**, 3221 (1965).

Received April 13, 1966.
College of Pharmacy,
University of Saskatchewan,
Saskatoon, Saskatchewan.

ON THE FORMATION OF A PEROXY PHTHALAZINE COMPOUND BY THE AUTOXIDATION OF 1-METHYL-1,2-DIHYDROPHTHALAZINE

Arthur Hirsch and Demetrius G. Orphanos

It was recently shown (1) that autoxidation of 1-methyl-1,2-dihydrophthalazine (I), prepared by the reaction of phthalazine with methyllithium, yields a mixture of 1-methylphthalazine (III) and an organic peroxide. The isolation of III has been successful. However, the peroxy compound, although it was the main reaction product, could not be obtained in a pure state. Formation of an organic peroxide in the phthalazine series, as far as we are aware, has not been reported previously.

However, it has now been possible, by applying the chromatographic technique of Milas *et al.* (2), to isolate such a substance and to determine its structure.

The elemental analysis, molecular weight and active oxygen determinations, and infrared and nuclear magnetic resonance spectra of this compound were compatible with a structure such as II. Additional support for II was obtained by the fact that the organic peroxide, on reduction with Na_2SO_3, was quantitatively converted into the known 1-methylphthalazine (III) (1). The conversion of II into III could proceed by a mechanism involving the unstable intermediate IV (Reaction Scheme 1).

Can. J. Chem. Downloaded from www.nrcresearchpress.com by 210.87.254.105 on 09/05/12
For personal use only.

4-(o-Nitrophenylthio)-1,3-diphenyl-2-pyrazolin-5-one (IIc)

Using essentially the conditions described for the preparation of II*b* (method *a*), we obtained the title compound (8.9 g), initially as a brown oil which quickly solidified, from *o*-nitrobenzenesulfenyl chloride (4.6 g) and 1,3-diphenyl-2-pyrazolin-5-one (5.8 g). Crystallization from anhydrous benzene gave a yellow solid, m.p. 182–183° (decomp.) after preliminary softening around 110°. Infrared spectrum: broad absorption from 2 100 to 3 200 with maxima at 3 080 (w) and 2 260 (w) (OH); 1 525 (s), 1 340 (m), and 860 (w) (NO_2) cm^{-1}; carbonyl absorption absent.

Anal. Calcd. for $C_{21}H_{15}N_3O_3S$: C, 64.76; H, 3.88; N, 10.79; S, 8.23. Found: C, 64.46; H, 3.84; N, 10.64; S, 8.27.

ACKNOWLEDGMENTS

The financial support of the National Research Council of Canada is gratefully acknowledged. The authors also thank H. W. Peel, M.Sc., for his assistance in this project.

1. J. A. Baltrop and K. J. Morgan. J. Chem. Soc. 4486 (1960).
2. N. Kharasch. J. Chem. Educ. **33**, 585 (1956).
3. T. Zinke and J. Baeumer. Ann. Chem. **416**, 86 (1918), and references therein.
4. R. T. Coutts and J. B. Edwards. Can. J. Chem. This issue.
5. A. R. Katritzky and F. W. Maine. Tetrahedron, **20**, 299 (1964).
6. M. H. Hubacher. *In* Organic syntheses. Vol. XV. *Edited by* C. R. Noller. John Wiley & Sons, Inc., New York. 1935. p. 45.
7. M. T. Bogert and A. Stull. *In* Organic syntheses. Collective Vol. I. *Edited by* H. Gilman. John Wiley & Sons, Inc., New York. 1947. p. 220.
8. T. Zinke and F. Farr. Ann. Chem. **391**, 55 (1912).
9. C. Angelini and A. Martani. Ann. Chim. Rome, **45**, 156 (1955); Chem. Abstr. **50**, 3146*b* (1956).
10. R. T. Coutts, H. W. Peel, and E. M. Smith. Can. J. Chem. **43**, 3221 (1965).

Received April 13, 1966.
College of Pharmacy,
University of Saskatchewan,
Saskatoon, Saskatchewan.

ON THE FORMATION OF A PEROXY PHTHALAZINE COMPOUND BY THE AUTOXIDATION OF 1-METHYL-1,2-DIHYDROPHTHALAZINE

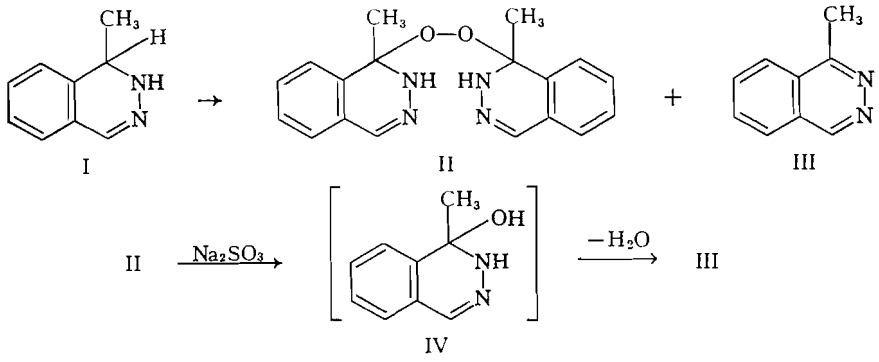
Arthur Hirsch and Demetrius G. Orphanos

It was recently shown (1) that autoxidation of 1-methyl-1,2-dihydrophthalazine (I), prepared by the reaction of phthalazine with methyllithium, yields a mixture of 1-methylphthalazine (III) and an organic peroxide. The isolation of III has been successful. However, the peroxy compound, although it was the main reaction product, could not be obtained in a pure state. Formation of an organic peroxide in the phthalazine series, as far as we are aware, has not been reported previously.

However, it has now been possible, by applying the chromatographic technique of Milas *et al.* (2), to isolate such a substance and to determine its structure.

The elemental analysis, molecular weight and active oxygen determinations, and infrared and nuclear magnetic resonance spectra of this compound were compatible with a structure such as II. Additional support for II was obtained by the fact that the organic peroxide, on reduction with Na_2SO_3, was quantitatively converted into the known 1-methylphthalazine (III) (1). The conversion of II into III could proceed by a mechanism involving the unstable intermediate IV (Reaction Scheme 1).

Can. J. Chem. Downloaded from www.nrcresearchpress.com by 210.87.254.5 on 09/05/12
For personal use only.



REACTION SCHEME 1.

EXPERIMENTAL[1]

Preparation of Peroxide II

A solution of phthalazine (2 g) (3) in dry diethyl ether (150 ml) was cooled to 0°. Into it, under a blanket of nitrogen and with vigorous stirring, 12 ml of 6% methyllithium solution[2] was added dropwise during 15 min. Stirring was continued for an additional 15 min. The light orange colored reaction solution was poured onto crushed ice and stirred for a few minutes. The organic layer was separated, washed once with 15 ml of water, and dried over K_2CO_3. The ether was removed under reduced pressure and the oily residue subjected to a high vacuum for half an hour. The yellow oil thus obtained, being crude 1-methyl-1,2-dihydrophthalazine (I) (1), was dissolved in diethyl ether (50 ml) and stirred for 8 h at about 10°. The separated white solid was collected and dried. It melted at 96–98° and weighed 1.2 g. This crude peroxidic product was chromatographed on a column maintained at 0° and packed with cellulose powder impregnated with dimethylformamide. The peroxide was eluted with diethyl ether. In this manner a pure organic peroxide melting at 100–101° and weighing 0.98 g was obtained. When the column was washed out with methanol, a small amount of impure 1-methylphthalazine (III) was isolated.

Anal. Calcd. for $C_{18}H_{18}N_4O_2$: C, 67.06; H, 5.63; N, 17.38; active oxygen, 4.96; mol. wt. 322.37. Found: C, 67.23; H, 5.66; N, 17.54; active oxygen, 4.94; mol. wt. 328.

The active oxygen was determined iodometrically with potassium iodide in glacial acetic acid. The infrared spectrum showed a strong absorption at 3 125 cm^{-1} caused by NH, and a weak band at 828 cm^{-1} which may be attributed to the peroxy group. The integrated nuclear magnetic resonance spectrum, in deuteriochloroform with tetramethylsilane = 0 p.p.m., showed a multiplet centered at 7.96 (8H) p.p.m., and singlets at 9.43 (2H), 9.16 (2H), and 3.03 (6H) p.p.m. The spectrum, after addition of deuterium oxide, showed no signal at 9.16 p.p.m.

1-Methylphthalazine (III) from Peroxide II

A mixture of 1 g of peroxide II and 25 ml of a saturated solution of Na_2SO_3, maintained at 0° under a blanket of nitrogen, was stirred for 4 h. The resulting solution was extracted with diethyl ether (25 ml) to remove some yellow impurities, and then extracted with methylene chloride (100 ml). The latter extract was washed with water and dried over K_2CO_3. Removal of the solvent under reduced pressure, followed by a high vacuum, led to a yellowish oily material which, when scratched with a spatula, rapidly solidified. It melted at 68–70° and weighed 0.8 g. This slightly impure material was dissolved in methanol and passed through a short silica gel column packed on the top with a small amount of charcoal. The colorless solution, after removal of the methanol, gave pure 1-methylphthalazine, m.p. 71–72°, which had an infrared spectrum identical with that of an authentic sample (1).

ACKNOWLEDGMENT

We thank the National Research Council of Canada for financial support of this work, under the Industrial Research Grant Program.

1. A. HIRSCH and D. G. ORPHANOS. J. Heterocyclic Chem. **3**, 38 (1966).
2. N. MILAS, R. HARRIS, and A. GOLUBOVIC. Radiation Res. Suppl. **3**, 71 (1963). N. MILAS and A. GOLUBOVIC. J. Am. Chem. Soc. **81**, 3361 (1959); **81**, 5824 (1959); **81**, 6461 (1959).
3. A. HIRSCH and D. G. ORPHANOS. J. Heterocyclic Chem. **2**, 206 (1965).

RECEIVED APRIL 21, 1966.
CANADIAN TECHNICAL TAPE, LTD.,
MONTREAL, QUEBEC.

[1]*The melting points are uncorrected. The analyses were carried out by Dr. C. Daessle, Montreal, Quebec. The infrared absorption spectra were obtained with Nujol mulls. The molecular weights were determined in Exaltone.*
[2]*Purchased from Alfa Inorganic Chemicals, Beverly, Massachusetts.*

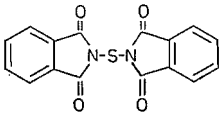
Can. J. Chem. Downloaded from www.nrcresearchpress.com by 210.87.254.5 on 09/05/12
For personal use only.

REACTIONS OF PHTHALIMIDE AND POTASSIUM PHTHALIMIDE WITH SULFUR MONOCHLORIDE

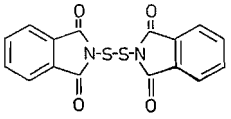
MALDA V. KALNINS

The reaction of amines and amides with sulfur monochloride (S_2Cl_2) in a variety of nonpolar solvents and in absolute ethanol has been reported to yield mixtures of *N,N'*-dithio and *N,N'*-polythio compounds (1–11). In a few instances, substances identified as *N,N'*-monothio derivatives of amines and amides have been isolated (2, 3, 12, 13). The unreactivity of imides, such as phthalimide, toward sulfur monochloride has been attributed to the decreased basicity of the nitrogen atom (2). However, potassium phthalimide has been reported to react with sulfur monochloride in light petroleum to give a compound which melted at 190° and decomposed when allowed to stand. On the basis of nitrogen and sulfur analyses, Naik assigned structure I to this product (2).

In our hands, reinvestigation of the reaction between potassium phthalimide and sulfur monochloride in petroleum ether did not provide a product, m.p. 190°, which Naik (2) described as *N,N'*-thiobisphthalimide (I). Instead, a higher melting compound (m.p. 228–230°) was formed, the elemental analyses of which suggested the empirical formula $C_{16}H_8N_2S_2O_4$. The infrared and nuclear magnetic resonance spectra[1] of the product (m.p. 228–230°) were consistent with structure II. Therefore, the compound reported by Naik (2) is not I but probably a mixture of II and phthalimide.



I



II

In addition, we have found that phthalimide itself reacts very readily with sulfur monochloride in *N,N*-dimethylformamide (DMF) at room temperature to give a colorless crystalline solid, m.p. 315–317°. The elemental analysis, molecular weight determination, infrared absorption spectrum, and nuclear magnetic resonance spectrum[1] of the compound were consistent with structure I. The structural assignment was supported by the fact that desulfurization of the reaction product with Raney nickel under anhydrous conditions provided phthalimide. The synthesis of I from potassium phthalimide and sulfur dichloride (SCl_2) in petroleum ether afforded additional support for the assigned structure. Compound I was also obtained from the reaction of sulfur monochloride and potassium phthalimide in DMF.

The reactions of phthalimide and its potassium salt with sulfur monochloride were explored in a variety of solvents. The results showed that sulfur monochloride converted phthalimide or its potassium salt into I only in DMF. Treatment of phthalimide with sulfur monochloride in as similar a solvent as *N,N*-dimethylacetamide, as well as in more basic solvents such as pyridine or trimethylamine, gave only II. The reaction of sulfur monochloride with potassium phthalimide in acetone or nitrobenzene also provided II. In view of these experimental observations, it appears that I is probably formed by the reaction of phthalimide with an adduct of sulfur monochloride and DMF.[2] It

[1]*The nuclear magnetic resonance spectrum was obtained in deuterated chloroform on a Varian model A-60 spectrometer by Dr. J. E. Lancaster at the American Cyanamid Company, Stamford, Connecticut.*

[2]*The existence of adducts of DMF with thionyl chloride, phosphorus oxychloride, and phosgene has been well established. For example, consult refs. 14–17.*

Can. J. Chem. Downloaded from www.nrcresearchpress.com by 210.87.254.5 on 09/05/12
For personal use only.

may be of interest to note that a quantitative study demonstrated that the conversion of 2 moles of phthalimide into 1 mole of I requires 2 moles of sulfur monochloride.

Thus, reinvestigation of the reaction between phthalimide (or potassium phthalimide) and sulfur monochloride in various solvents led to a convenient synthesis of either *N,N'*-thiobisphthalimide (I) or *N,N'*-dithiobisphthalimide (II). The type of product depends upon the choice of solvent.

EXPERIMENTAL

Melting points were determined using open-glass capillaries either in a Thomas–Hoover melting point apparatus or in an aluminium block, and are uncorrected. Microanalyses were provided by Galbraith Microanalytical Laboratory, Knoxville, Tennessee. Infrared spectra were recorded on a Perkin–Elmer Infracord spectrophotometer.

N,N'-Thiobisphthalimide (I)

(a) From Phthalimide and Sulfur Monochloride

Phthalimide (7.36 g, 0.05 mole) was dissolved in anhydrous DMF (40 ml, dried over Molecular Sieve type 4A), and to the resulting solution sulfur monochloride[3] (6.75 g, 0.05 mole) was added in several portions at 28° (anhydrous conditions). After 20 min a precipitate appeared. The yellow mixture was stirred for 20 h at 28° before collection of the colorless, crystalline solid by filtration. The dry product (7.46 g, 92% yield) melted at 280–288°. The infrared spectrum of the solid exhibited no $-NH_2$, $=NH$, —OH, or —COOH bands.

Recrystallization of the product from dry chloroform gave a sample of I, m.p. 315–317°; λ_{max}^{Nujol} 5.66, 8.07, 9.71, 11.50, and 14.00 μ.

Anal. Calcd. for $C_{16}H_8N_2SO_4$: C, 59.26; H, 2.49; N, 8.64; S, 9.89; mol. wt. 324. Found: C, 59.06; H, 2.46; N, 8.79; S, 10.03; mol. wt. 320.

The approximate solubility of I in DMF was found to be 1.87 g/100 ml at 28°. Product I exhibited no signs of decomposition in water or 6 *N* HCl at room temperature; however, I hydrolyzed readily in 5% sodium hydroxide at 28°.

Reactions performed at 50° resulted in a considerable decrease in the yield of I, but at temperatures above 90° no product (I) was isolated. The use of purified sulfur monochloride (18) in the reaction proved of no particular advantage.

(b) From Potassium Phthalimide and Sulfur Monochloride

To a mixture of potassium phthalimide (9.26 g, 0.05 mole) and dry DMF (40 ml), sulfur monochloride (6.75 g, 0.05 mole) was added dropwise at 28–32° (anhydrous conditions), with cooling. After the addition was completed, the reaction mixture was allowed to remain at 28° for 20 h (continuous stirring) before collection of the solid by filtration. Extraction of the crude, dry solid with hot chloroform and removal of the solvent gave a colorless product (7.0 g, 86% yield) which melted at 315°. The infrared spectrum of this solid was identical with that of the product obtained by method *a*.

(c) From Potassium Phthalimide and Sulfur Dichloride

To a suspension of potassium phthalimide (9.26 g, 0.05 mole) in dry petroleum ether (25 ml, b.p. 36–54°), sulfur dichloride (2.58 g, 0.025 mole) was added, and the mixture heated at reflux for 1 h. The solid was collected by filtration, washed with dry petroleum ether, and extracted with hot chloroform. Concentration of the extracts gave a colorless solid (6.5 g, 80% yield), which was shown by melting point and infrared spectral comparison to be identical with the product obtained by method *a*.

Similarly, I can be obtained in about 80% yield from the reaction of phthalimide with the calculated amount of sulfur dichloride in DMF.

N,N'-Dithiobisphthalimide (II)[4]

A stirred suspension of potassium phthalimide (9.26 g, 0.05 mole) and dry petroleum ether (25 ml, b.p. 36–60°) was treated with sulfur monochloride (6.75 g, 0.05 mole; dropwise addition), and the resulting mixture was refluxed for 1 h. The liquid was then decanted, and the residue washed thoroughly with fresh petroleum ether and filtered. Extraction of the solid with hot dry chloroform and subsequent removal of the solvent gave 4.6 g (51%) of large colorless needles, m.p. 190–210°. The infrared spectrum of this material indicated a weak —NH— absorption band, which disappeared upon recrystallization from chloroform. Two additional recrystallizations from the same solvent raised the melting point to 228–230°; λ_{max}^{Nujol} 5.73, 7.86, 8.01, 9.61, 11.50, and 13.95 μ.

Anal. Calcd. for $C_{16}H_8N_2S_2O_4$: C, 53.92; H, 2.26; N, 7.86; S, 17.99; mol. wt. 356. Found: C, 54.01; H, 2.22; N, 7.93; S, 18.05; mol. wt. 360.

[3]*Sulfur monochloride (Baker Chemical Co.) was assayed by gas–liquid chromatography. The analysis, performed by Mr. H. V. Lewry on a F & M Scientific Corporation model 500 instrument and a diethylene glycol succinate column at 50°, showed that the sample contained 98%* S_2Cl_2.

[4]*For comparison of the experimental conditions, consult ref. 2.*

Can. J. Chem. Downloaded from www.nrcresearchpress.com by 210.87.254.5 on 09/05/12
For personal use only.

Desulfurization of N,N-'Thiobisphthalimide (I)

A solution of I (0.5 g) in anhydrous DMF (90 ml) was treated with W-4 Raney nickel (19) (1.1 ml, 18 days old). The continuously stirred mixture was heated at 60–70° for 25 h (anhydrous conditions). At the end of the reaction period, the hot mixture was filtered through a sintered-glass funnel, the residue was washed once with a small amount of dry DMF, and the combined filtrate was concentrated *in vacuo* at 60–70°. The residual crystalline solid (0.4 g) was identified by melting point and infrared spectrum as phthalimide. A mixture melting point of the product with authentic phthalimide exhibited no depression.

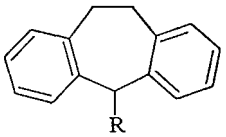
1. A. Michaelis and K. Luxembourg. Ber. **28**, 165 (1895).
2. K. G. Naik. J. Chem. Soc. **119**, 1166 (1921).
3. K. G. Naik and C. S. Patel. J. Indian Chem. Soc. **1**, 27 (1924).
4. K. G. Naik and Y. N. Bhat. J. Indian Chem. Soc. **4**, 525 (1927).
5. E. I. Orlov. Z. Farben-Ind. **20**, 121 (1928).
6. M. C. Throdahl and M. W. Harman. Ind. Eng. Chem. **43**, 421 (1951).
7. M. W. Harman. U.S. Patent No. 2,649,470 (August 18, 1953).
8. E. Kuhle, R. Wegler, and P. Schneider. Ger. Patent No. 951,719 (October 31, 1956).
9. M. Becke-Goehring and H. Jenne. Angew. Chem. **70**, 399 (1958).
10. A. Guillemonat and J. L. Chevalier. Compt. Rend. **252**, 4007 (1961).
11. P. Hope and L. A. Wiles. J. Chem. Soc. 5679 (1964).
12. J. A. Roorda Smit. Ber. **8**, 1445 (1875).
13. P. Hope and L. A. Wiles. J. Chem. Soc. 4583 (1965).
14. Z. Arnold and A. Holy. Collection Czech. Chem. Commun. **27**, 2886 (1962).
15. H. H. Bosshard and Hch. Zollinger. Helv. Chim. Acta, **42**, 1659 (1959).
16. H. Bredereck, P. Gompper, K. Klemm, and H. Rempfer. Ber. **92**, 837 (1959).
17. G. Martin and M. Martin. Bull. Soc. Chim. France, 1637 (1963).
18. Z. S. Ariyan and L. A. Wiles. J. Chem. Soc. 4510 (1961).
19. A. A. Pavlic and H. Adkins. J. Am. Chem. Soc. **68**, 1471 (1946).

Received April 22, 1966.
Chemical Research and Development Laboratories,
Agricultural Division,
American Cyanamid Company.
Princeton, New Jersey.

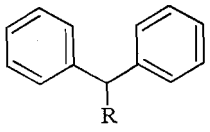
THE DEHYDRATION OF AMIDES TO NITRILES WITH LITHIUM ALUMINIUM HYDRIDE

L. G. Humber and M. A. Davis

In connection with the synthesis of the benzo[1,2]cyclohepta[3,4,5-*d*,*e*]isoquinoline ring system (1), we required 10,11-dihydro-5*H*-dibenzo[*a*,*d*]cycloheptene-5-methylamine (I) as an intermediate. Our initial attempts were directed to the lithium aluminium hydride reduction of the carbonitrile II, and to the lithium aluminium hydride – mercuric chloride reduction of the carboxamide III.



I R = CH_2NH_2
II R = C≡N
III R = $CONH_2$



IV R = CH_2NH_2
V R = C≡N
VI R = $CONH_2$

In the former case the carbonitrile was recovered essentially unchanged, and in the latter the product obtained from the reaction consisted of a mixture of carbonitrile II (67%) and amine I (19.8%). Reduction of carboxamide III with lithium aluminium hydride alone gave the carbonitrile II, in 92% yield, as the only isolable product. The

Can. J. Chem. Downloaded from www.nrcresearchpress.com by 210.87.254.5 on 09/05/12
For personal use only.

Desulfurization of N,N-'Thiobisphthalimide (I)

A solution of I (0.5 g) in anhydrous DMF (90 ml) was treated with W-4 Raney nickel (19) (1.1 ml, 18 days old). The continuously stirred mixture was heated at 60–70° for 25 h (anhydrous conditions). At the end of the reaction period, the hot mixture was filtered through a sintered-glass funnel, the residue was washed once with a small amount of dry DMF, and the combined filtrate was concentrated *in vacuo* at 60–70°. The residual crystalline solid (0.4 g) was identified by melting point and infrared spectrum as phthalimide. A mixture melting point of the product with authentic phthalimide exhibited no depression.

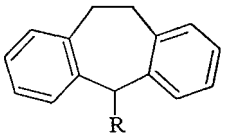
1. A. MICHAELIS and K. LUXEMBOURG. Ber. **28**, 165 (1895).
2. K. G. NAIK. J. Chem. Soc. **119**, 1166 (1921).
3. K. G. NAIK and C. S. PATEL. J. Indian Chem. Soc. **1**, 27 (1924).
4. K. G. NAIK and Y. N. BHAT. J. Indian Chem. Soc. **4**, 525 (1927).
5. E. I. ORLOV. Z. Farben-Ind. **20**, 121 (1928).
6. M. C. THRODAHL and M. W. HARMAN. Ind. Eng. Chem. **43**, 421 (1951).
7. M. W. HARMAN. U.S. Patent No. 2,649,470 (August 18, 1953).
8. E. KUHLE, R. WEGLER, and P. SCHNEIDER. Ger. Patent No. 951,719 (October 31, 1956).
9. M. BECKE-GOEHRING and H. JENNE. Angew. Chem. **70**, 399 (1958).
10. A. GUILLEMONAT and J. L. CHEVALIER. Compt. Rend. **252**, 4007 (1961).
11. P. HOPE and L. A. WILES. J. Chem. Soc. 5679 (1964).
12. J. A. ROORDA SMIT. Ber. **8**, 1445 (1875).
13. P. HOPE and L. A. WILES. J. Chem. Soc. 4583 (1965).
14. Z. ARNOLD and A. HOLY. Collection Czech. Chem. Commun. **27**, 2886 (1962).
15. H. H. BOSSHARD and HCH. ZOLLINGER. Helv. Chim. Acta, **42**, 1659 (1959).
16. H. BREDERECK, P. GOMPPER, K. KLEMM, and H. REMPFER. Ber. **92**, 837 (1959).
17. G. MARTIN and M. MARTIN. Bull. Soc. Chim. France, 1637 (1963).
18. Z. S. ARIYAN and L. A. WILES. J. Chem. Soc. 4510 (1961).
19. A. A. PAVLIC and H. ADKINS. J. Am. Chem. Soc. **68**, 1471 (1946).

RECEIVED APRIL 22, 1966.
CHEMICAL RESEARCH AND DEVELOPMENT LABORATORIES,
AGRICULTURAL DIVISION,
AMERICAN CYANAMID COMPANY.
PRINCETON, NEW JERSEY.

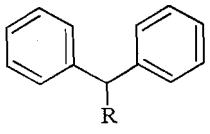
THE DEHYDRATION OF AMIDES TO NITRILES WITH LITHIUM ALUMINIUM HYDRIDE

L. G. HUMBER AND M. A. DAVIS

In connection with the synthesis of the benzo[1,2]cyclohepta[3,4,5-*d*,*e*]isoquinoline ring system (1), we required 10,11-dihydro-5*H*-dibenzo[*a*,*d*]cycloheptene-5-methylamine (I) as an intermediate. Our initial attempts were directed to the lithium aluminium hydride reduction of the carbonitrile II, and to the lithium aluminium hydride – mercuric chloride reduction of the carboxamide III.



I R = CH_2NH_2
II R = C≡N
III R = $CONH_2$



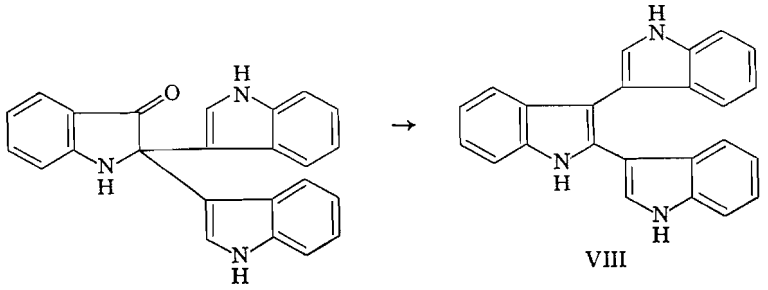
IV R = CH_2NH_2
V R = C≡N
VI R = $CONH_2$

In the former case the carbonitrile was recovered essentially unchanged, and in the latter the product obtained from the reaction consisted of a mixture of carbonitrile II (67%) and amine I (19.8%). Reduction of carboxamide III with lithium aluminium hydride alone gave the carbonitrile II, in 92% yield, as the only isolable product. The

desired amine I has subsequently been obtained in high yields (1) either by the lithium aluminium hydride – aluminium chloride reduction, or by the Raney nickel catalyzed hydrogenation, of the carbonitrile II.

We have also treated 2,2-diphenylacetamide (VI) with lithium aluminium hydride – mercuric chloride, and the product consisted of 81% of carbonitrile V and 13% of amine IV.

The use of lithium aluminium hydride alone or in combination with mercuric chloride has not previously been observed to effect the dehydration of carboxamides to carbonitriles; however, in at least one instance, lithium aluminium hydride behaves as a Lewis acid, causing the skeletal rearrangement VII → VIII (2). The present observations may constitute another example of such behavior by lithium aluminium hydride; this suggests that, in some limited situations, this reagent may be of use in the preparation of nitriles.



VII VIII

EXPERIMENTAL

Treatment of 10,11-Dihydro-5H-dibenzo[a,d]-cycloheptene-5-carboxamide with Lithium Aluminium Hydride – Mercuric Chloride

10,11-Dihydro-5*H*-dibenzo[*a,d*]cycloheptene-5-carboxamide (III) (3) (10.0 g), lithium aluminium hydride (5.0 g), and mercuric chloride (500 mg) were mixed in tetrahydrofuran (250 ml) and refluxed for 16 h. Water (22.5 ml) was added and the mixture filtered. Treatment of the dried filtrate with ethereal hydrogen chloride yielded the hydrochloride of I, m.p. >295° (2.1 g, 19.8%). The analytical sample was crystallized from a methanol – ethyl acetate mixture.

Anal. Calcd. for $C_{16}H_{18}ClN$: C, 73.97; H, 6.98; Cl, 13.65; N, 5.39. Found: C, 73.81; H, 6.92; Cl, 13.66; N, 5.71.

The free base I had b.p. 127° at 0.15 mm, n_D^{23} 1.6122.

Anal. Calcd. for $C_{16}N_{17}N$: C, 86.05; H, 7.67; N, 6.27. Found: C, 86.08; H, 7.51; N, 6.16.

The filtrate from the preparation of the hydrochloride of I was evaporated and the residue crystallized from methanol to yield the carbonitrile II (6.2 g, 67%), $\nu_{max}^{CHCl_3}$ 2 245 cm^{-1}, m.p. 91–93° (lit. (4) m.p. 91–92°). When the carboxamide III (1.0 g) was refluxed with lithium aluminium hydride (1.0 g) alone in tetrahydrofuran (50 ml) for 16 h, the carbonitrile II (850 mg, 92%) was obtained along with traces of basic material.

Treatment of 2,2-Diphenylacetamide with Lithium Aluminium Hydride – Mercuric Chloride

2,2-Diphenylacetamide (1.0 g), lithium aluminium hydride (500 mg), and mercuric chloride (50 mg) were mixed in tetrahydrofuran (100 ml) and refluxed for 16 h. Water (4.5 ml) was added and the mixture filtered to yield, after drying (Na_2SO_4) and evaporation, a light-yellow oil that solidified when allowed to stand. It was dissolved in ether and treated with ethereal hydrogen chloride to yield the hydrochloride of IV (145 mg, 13%), m.p. 263–265° (lit. (5) m.p. 263°).

The filtrate from above was evaporated to yield an oil (750 mg, 81%), which was shown to be homogeneous by thin-layer chromatography. It was crystallized from acetonitrile to give V (500 mg), $\nu_{max}^{CHCl_3}$ 2 250 cm^{-1}, m.p. 74–75° (lit. (6) m.p. 72–73.5°) (undepressed when mixed with an authentic sample of V).

1. L. G. Humber, M. A. Davis, R. A. Thomas, R. Otson, and J. R. Watson. J. Heterocyclic Chem. In press.
2. B. Witkop and J. B. Patrick. J. Am. Chem. Soc. **73**, 713 (1951).
3. M. A. Davis, S. O. Winthrop, R. A. Thomas, F. Herr, M. P. Charest, and R. Gaudry. J. Med Chem. **7**, 88 (1964).

4. M. A. DAVIS, S. O. WINTHROP, J. STEWART, F. A. SUNAHARA, and F. HERR. J. Med. Chem. **6**, 251 (1963).
5. A. RAHMAN and M. O. FAROOQ. Rec. Trav. Chim. **73**, 423 (1954).
6. S. K. FREEMAN, W. F. RINGK, and P. E. SPOERRI. J. Am. Chem. Soc. **69**, 858 (1947).

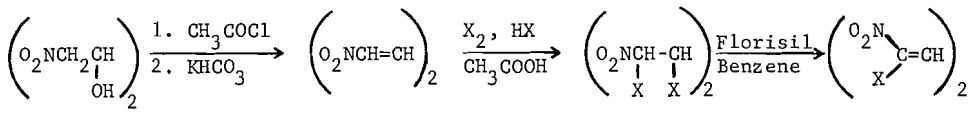
RECEIVED MAY 3, 1966.
AYERST RESEARCH LABORATORIES,
MONTREAL, QUEBEC.

THE SYNTHESIS OF 1,4-DICHLORO-1,4-DINITRO-1,3-BUTADIENE

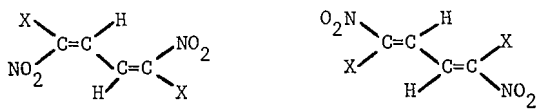
F. I. CARROLL, SANDRA C. KERBOW, AND MONROE E. WALL

1,4-Dichloro-1,4-dinitro-1,3-butadiene (IV, X = Cl) was first prepared by Reppe and his co-workers (1) in 1948 by the nitration of 1,4-dichloro-1,3-butadiene. The synthesis was improved by Braye (2), but under optimum conditions only a 7.7% yield of the dichlorodinitrodiene was obtained.

This note reports an entirely different synthesis of IV (X = Cl). 1,4-Dinitro-1,3-butadiene (II), prepared from DL- or *meso*-1,4-dinitro-2,3-butanediol (I) (3, 4), was chlorinated in acetic acid saturated with hydrogen chloride, to give a 98.5% yield of 1,2,3,4-tetrachloro-1,4-dinitrobutane (III, X = Cl). When the tetrachlorodinitrobutane was stirred with a suspension of Florisil in benzene for 4 h, a 99% yield of IV (X = Cl) was obtained. Attempts to dehydrochlorinate III (X = Cl) with pyridine or triethylamine yielded a dark mass from which only very small yields of IV (X = Cl) could be obtained. Lipina and Perekalin (5) have reported a similar synthesis of 1,4-dibromo-1,4-dinitro-1,3-butadiene (IV, X = Br), in which III (X = Br) was dehydrobrominated by heating it in alcohol. We found that IV (X = Br) was more conveniently prepared by bromination of II in chloroform or dioxane followed by dehydrobromination of the intermediate 1,2,3,4-tetrabromo-1,4-dinitrobutane (III, X = Br) with Florisil. When II was treated with iodine in chloroform a quantitative recovery of II was obtained.



I II III IV



IVa IVb

The structure of the 1,4-dichloro- and 1,4-dibromo-1,4-dinitro-1,3-butadienes is not known. However, the nuclear magnetic resonance spectra of both compounds show only one peak, indicating that they have the symmetrical structure IV*a* or IV*b*.

4. M. A. DAVIS, S. O. WINTHROP, J. STEWART, F. A. SUNAHARA, and F. HERR. J. Med. Chem. **6**, 251 (1963).
5. A. RAHMAN and M. O. FAROOQ. Rec. Trav. Chim. **73**, 423 (1954).
6. S. K. FREEMAN, W. F. RINGK, and P. E. SPOERRI. J. Am. Chem. Soc. **69**, 858 (1947).

RECEIVED MAY 3, 1966.
AYERST RESEARCH LABORATORIES,
MONTREAL, QUEBEC.

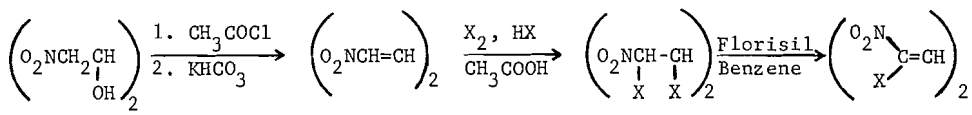
Can. J. Chem. Downloaded from www.nrcresearchpress.com by 210.87.254.105 on 09/05/12
For personal use only.

THE SYNTHESIS OF 1,4-DICHLORO-1,4-DINITRO-1,3-BUTADIENE

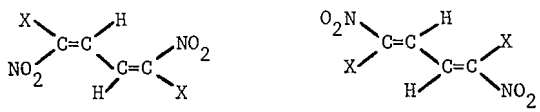
F. I. CARROLL, SANDRA C. KERBOW, AND MONROE E. WALL

1,4-Dichloro-1,4-dinitro-1,3-butadiene (IV, X = Cl) was first prepared by Reppe and his co-workers (1) in 1948 by the nitration of 1,4-dichloro-1,3-butadiene. The synthesis was improved by Braye (2), but under optimum conditions only a 7.7% yield of the dichlorodinitrodiene was obtained.

This note reports an entirely different synthesis of IV (X = Cl). 1,4-Dinitro-1,3-butadiene (II), prepared from DL- or *meso*-1,4-dinitro-2,3-butanediol (I) (3, 4), was chlorinated in acetic acid saturated with hydrogen chloride, to give a 98.5% yield of 1,2,3,4-tetrachloro-1,4-dinitrobutane (III, X = Cl). When the tetrachlorodinitrobutane was stirred with a suspension of Florisil in benzene for 4 h, a 99% yield of IV (X = Cl) was obtained. Attempts to dehydrochlorinate III (X = Cl) with pyridine or triethylamine yielded a dark mass from which only very small yields of IV (X = Cl) could be obtained. Lipina and Perekalin (5) have reported a similar synthesis of 1,4-dibromo-1,4-dinitro-1,3-butadiene (IV, X = Br), in which III (X = Br) was dehydrobrominated by heating it in alcohol. We found that IV (X = Br) was more conveniently prepared by bromination of II in chloroform or dioxane followed by dehydrobromination of the intermediate 1,2,3,4-tetrabromo-1,4-dinitrobutane (III, X = Br) with Florisil. When II was treated with iodine in chloroform a quantitative recovery of II was obtained.



I II III IV



IVa IVb

The structure of the 1,4-dichloro- and 1,4-dibromo-1,4-dinitro-1,3-butadienes is not known. However, the nuclear magnetic resonance spectra of both compounds show only one peak, indicating that they have the symmetrical structure IV*a* or IV*b*.

Can. J. Chem. Downloaded from www.nrcresearchpress.com by 210.87.254.105 on 09/05/12
For personal use only.

EXPERIMENTAL

The melting points were obtained on a Kofler hot stage and are corrected. The infrared spectra were obtained with a Perkin–Elmer model 221 spectrophotometer. The nuclear magnetic resonance spectra were obtained on a Varian A-60 spectrometer with samples dissolved in deuteriochloroform (the internal standard was tetramethylsilane). The ultraviolet spectra were obtained with a Bausch and Lomb model 505 spectrophotometer. The thin-layer chromatograms were obtained on columns of silica gel HF. The microanalyses were carried out by Micro-Tech Laboratories, Inc., Skokie, Illinois.

Preparation of meso-1,4-Dinitro-2,3-diacetoxybutane

A mixture of 36 g (0.2 mole) of *meso*-1,4-dinitro-2,3-butanediol (3), 44 g (0.56 mole) of acetyl chloride, and 70 ml of acetic acid was warmed gently until hydrogen chloride evolution ceased. The mixture was cooled and diluted with water until crystallization started. The crystals were collected, washed with water, and dried. Recrystallization from ethanol gave 43.4 g (82.4%) of *meso*-1,4-dinitro-2,3-diacetoxybutane, m.p. 94.5–96.5° (reported (4) m.p. 91.5–92°).

Anal. Calcd. for $C_8H_{12}N_2O_8$: C, 36.37; H, 4.58; N, 10.61. Found: C, 36.57; H, 4.48; N, 10.44.

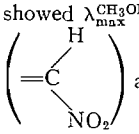
Preparation of DL-*1,4-Dinitro-2,3-diacetoxybutane*

Acetylation of DL-1,4-dinitro-2,3-butanediol (3) in the same manner as described for the preparation of *meso*-1,4-dinitro-2,3-diacetoxybutane gave a 72.6% yield of DL-1,4-dinitro-2,3-diacetoxybutane, m.p. 94–95° (reported (4) m.p. 89.5–90°). A mixture of this acetate and *meso*-1,4-dinitro-2,3-diacetoxybutane melted at 79–95°.

Anal. Calcd. for $C_8H_{12}N_2O_8$: C, 36.37; H, 4.58; N, 10.61. Found: C, 36.58; H, 4.62; N, 10.78.

Preparation of 1,4-Dinitro-1,3-butadiene (II)[1]

According to the procedure reported by Noviko *et al.* (4), *meso*- or DL-1,4-dinitro-2,3-diacetoxybutane was refluxed with a catalytic amount of anhydrous potassium hydrogen carbonate in chloroform to give 70–85% of 1,4-dinitro-1,3-butadiene, m.p. 150–150.5° (reported (4) m.p. 146.5–147°). The ultraviolet spectrum showed $\lambda_{max}^{CH_3OH}$ 281 mμ (ϵ = 18 487). The nuclear magnetic resonance spectrum showed a singlet at δ 7.52



and a singlet at δ 7.55 p.p.m. (=CH—).[2]

Anal. Calcd. for $C_4H_4N_2O_4$: C, 33.33; H, 2.78. Found: C, 33.27; H, 2.70.

Preparation of 1,4-Dichloro-1,4-dinitro-1,3-butadiene (IV, X = Cl)

A stream of chlorine and hydrogen chloride was passed simultaneously through a solution of 9.98 g (0.0693 mole) of 1,4-dinitro-1,3-butadiene in 645 ml of acetic acid (distilled from potassium permanganate) heated to 56°. A thin-layer chromatogram (benzene) after $3\frac{3}{4}$ h indicated that all of the diene had reacted. After concentration by freeze-drying, 19.4 g (98.5%) of a white solid was obtained. The infrared spectrum (methylene chloride) showed peaks at 3 022, 2 970, and 2 915 (C—H), and at 1 580 and 1 348 cm^{-1} (NO_2). The crude 1,2,3,4-tetrachloro-1,4-dinitrobutane (III, X = Cl) was used, without further purification, for the preparation of 1,4-dichloro-1,4-dinitro-1,3-butadiene. When the chlorination was conducted at a higher temperature or higher concentration an oil was obtained. The infrared spectrum (methylene chloride) showed, in addition to the absorption mentioned above, weak peaks in the carbonyl region and a sharp peak at 1 600 cm^{-1}.

A mixture of 1,2,3,4-tetrachloro-1,4-dinitrobutane (19.4 g, 0.0680 mole), 1 500 ml of benzene, and 500 g of Florisil was stirred at room temperature for 4 h. The mixture was then placed on a chromatography column and eluted with benzene until a thin-layer chromatogram (benzene) indicated that all of the product had been eluted (3 l of benzene). Concentration of the benzene gave 15 g of a yellow solid. Recrystallization from carbon tetrachloride yielded 14.20 g (99%) of 1,4-dichloro-1,4-dinitro-1,3-butadiene, m.p. 124–125° (reported (2) m.p. 124–125°). The infrared spectrum (potassium bromide) showed absorption at 3 110 and 3 080 (=C—H), at 1 568 (C=C), and at 1 532 and 1 322 cm^{-1} (NO_2). The ultraviolet spectrum showed $\lambda_{max}^{CH_3OH}$ 330 mμ (ϵ = 12 928). The nuclear magnetic resonance spectrum showed only one resonance, a singlet at δ 8.03 p.p.m.

Anal. Calcd. for $C_4H_2N_2Cl_2O_4$: C, 22.54; H, 0.95; N, 13.16; Cl, 33.29. Found: C, 22.75; H, 0.87; N, 12.88; Cl, 33.25.

[1]*Subsequent work has shown that 1,4-dinitro-1,3-butadiene can be caused to explode forcefully when heated in a closed container or when detonated by a blasting cap; accordingly, due precaution should be taken when this and related compounds are handled.*

[2]NOTE ADDED IN PROOF: *A 100 Mc.p.s. nuclear magnetic resonance spectrum of II obtained in dimethyl sulfoxide showed 12 peaks. We thank Dr. Charles G. Moreland, North Carolina State University, for determining this spectrum.*

Preparation of 1,4-Dibromo-1,4-dinitro-1,3-butadiene (IV, X = Br)

A solution of 1.44 g (0.01 mole) of 1,4-dinitro-1,4-butadiene and 3.19 g (0.02 mole) of bromine in 150 ml of chloroform was refluxed for 2 h. A thin-layer chromatogram (benzene) indicated that all of the diene had reacted. The reaction mixture was concentrated to give 4.6 g (99.2%) of crude 1,2,3,4-tetrabromo-1,4-dinitrobutane (III, X = Br). The infrared spectrum (CH_2Cl_2) showed absorption at 3 025 and 2 968 (C—H) and at 1 577 and 1 347 cm^{-1} (NO_2). The crude product was used, without further purification, for the preparation of 1,4-dibromo-1,4-dinitro-1,3-butadiene. Similar results were obtained when the bromination was carried out in dioxane.

A mixture of 4.6 g (0.00992 mole) of 1,4-dinitro-1,2,3,4-tetrabromobutane, 160 ml of benzene, and 60 g of Florisil was stirred at room temperature overnight. The mixture was transferred to a chromatography column and eluted with benzene. Concentration of the benzene solution gave 2.91 g of a solid that showed only one spot on a thin-layer chromatogram (benzene–cyclohexane (1:1)). Recrystallization from carbon tetrachloride gave 2.5 g (84.6%) of 1,4-dibromo-1,4-dinitro-1,3-butadiene, m.p. 123.5–125.5° (reported (5) m.p. 125–126°). The infrared spectrum (potassium bromide) showed absorption at 3 068 (=CH), at 1 610 (C=C), and at 1 525 and 1 310 cm^{-1} (NO_2). The ultraviolet spectrum (CH_3OH) showed λ_{max} 339 mμ (ϵ = 10 023). The nuclear magnetic resonance spectrum showed only one resonance, that at δ 8.22.

Anal. Calcd. for $C_4H_2N_2O_4Br_2$: C, 15.90; H, 0.66; N, 9.27; Br, 52.98. Found: C, 16.17; H, 0.62; N, 9.07; Br, 52.77.

ACKNOWLEDGMENTS

We gratefully acknowledge support of this work by the Union Carbide Chemicals Corp., South Charleston, West Virginia, and thank Dr. Donald L. Heywood and Dr. John Durden, Union Carbide Chemicals Corp., South Charleston, West Virginia, for helpful discussions.

1. W. Reppe, O. Schlichting, K. Klager, and T. Toepel. Ann. **560**, 1 (1948).
2. E. H. Braye. Bull. Soc. Chim. Belges, **72**, 699 (1963).
3. F. I. Carroll. J. Org. Chem. **31**, 366 (1966).
4. S. S. Novikov, I. S. Korsakova, and K. K. Babievskii. Bull. Acad. Sci. USSR Div. Chem. Sci. Engl. Transl. 882 (1960).
5. E. S. Lipina and V. V. Perekalin. Zh. Obshch. Khim. **34**, 3644 (1964).

Received April 19, 1966.
Natural Products Laboratory,
Research Triangle Institute,
Durham, North Carolina.

Can. J. Chem. Downloaded from www.nrcresearchpress.com by 210.87.254.105 on 09/05/12
For personal use only.

Can. J. Chem. Downloaded from www.nrcresearchpress.com by 210.87.254.42 on 09/05/12
For personal use only.

Canadian Journal of Chemistry

Issued by THE NATIONAL RESEARCH COUNCIL OF CANADA

VOLUME 44 SEPTEMBER 15, 1966 NUMBER 18

ELECTROLYTIC REDUCTION AND ELLINGHAM DIAGRAMS FOR OXY-ANION SYSTEMS

H. E. BARTLETT AND K. E. JOHNSON[1]

Department of Chemistry, Sir John Cass College, Jewry Street, London, England

Received April 28, 1966

ABSTRACT

Standard reversible decomposition voltages, E^0, for various decomposition reactions of K_2CO_3, Na_2CO_3, Li_2CO_3, $BaCO_3$, $CaCO_3$, $MgCO_3$, Na_2SO_4, $NaNO_3$, and KNO_3 are calculated from thermal data and the values obtained plotted against temperature. That reaction which has the lowest values of E^0 is considered to be the most likely to occur when the particular salt is electrolyzed. The results obtained indicate that in the case of the carbonates metal deposition is possible only for K_2CO_3 and Na_2CO_3 above 870 °K. In all other cases metal oxide and carbon (or CO at higher temperatures) are the favored cathode products. For Na_2SO_4, Na_2S and Na_2O are the favored cathode products and for the nitrates, nitrite and oxide or nitrogen evolution and oxide formation appear equally feasible thermodynamically.

Once the likely electrolytic decomposition products are known, a method is presented whereby the products formed by reduction of the oxy-anions by metals (and in the case of the carbonates, by carbon) may be predicted. This method involves drawing an appropriate redox line on an Ellingham diagram. Finally, a comparison is made between the thermodynamic predictions and the few experimental results available.

INTRODUCTION

Hamer and co-workers have published theoretical electromotive force (e.m.f.) series for chlorides, fluorides, and oxides at various temperatures (1–3). These series were obtained by calculating the reversible decomposition potentials of cells such as

$$M|MX|\tfrac{1}{2}X_2 \quad \text{or} \quad M|MO|\tfrac{1}{2}O_2 \quad (X = \text{halogen}).$$

This present work applies the same type of treatment to Na_2CO_3, K_2CO_3, Li_2CO_3, $CaCO_3$, $BaCO_3$, $MgCO_3$, Na_2SO_4, KNO_3, and $NaNO_3$ in an attempt to predict (*a*) their electrolytic reduction products at various temperatures, (*b*) their reversible decomposition potentials, and (*c*) which metals will reduce them.

A complementary approach to this work has been provided in the form of potential vs. pO^{2-} diagrams (analogous to potential vs. pH diagrams (4)) by Littlewood (5) and others (6, 7).

CARBONATES

Electrolytic Reduction of Carbonates

When a solid or liquid carbonate is electrolyzed, CO_2 and O_2 are evolved at the anode according to the equation

$$CO_3^{2-} = CO_2 + \tfrac{1}{2}O_2 + 2e,$$

[1]*To whom all communications should be sent. Present address: University of Saskatchewan, Regina, Sask.*

whereas at the cathode there are at least four possible processes:

(*a*) the formation of carbon and oxide

$$CO_3^{2-} + 4e = C\downarrow + 3O^{2-},$$

(*b*) the formation of carbon monoxide and oxide

$$CO_3^{2-} + 2e = CO + 2O^{2-},$$

(*c*) the deposition of metal

$$M^{n+} + ne = M\downarrow,$$

(*d*) the formation of carbide and oxide

$$2CO_3^{2-} + 10e = C_2^{2-} + 6O^{2-},$$

Combination of the anodic reaction with the various cathodic reductions gives eqs. [1] to [4].

[1] $$3M_2CO_3 = 3M_2O + C + 2CO_2 + O_2$$

[2] $$2M_2CO_3 = 2M_2O + CO + CO_2 + \tfrac{1}{2}O_2$$

[3] $$M_2CO_3 = 2M + CO_2 + \tfrac{1}{2}O_2$$

[4] $$7M_2CO_3 = M_2C_2 + 6M_2O + 5CO_2 + \tfrac{5}{2}O_2$$

Each equation may be represented by one of the cells 1*a* to 4*a*. The double vertical lines represent salt bridges with assumed liquid junction potentials equal to 0.

$$C|M_2O, M_2CO_3||M_2CO_3|CO_2, O_2, Pt \qquad (1a)$$

$$Pt, CO|M_2O, M_2CO_3||M_2CO_3|CO_2, O_2, Pt \qquad (2a)$$

$$M|M_2CO_3|CO_2, O_2, Pt \qquad (3a)$$

$$Pt|M_2O, M_2C_2, M_2CO_3||M_2CO_3|CO_2, O_2, Pt \qquad (4a)$$

The standard free energy of reaction, ΔG^0, was calculated for reactions [1] to [4] at various temperatures using the low temperature data of the National Bureau of Standards (8) and, where available, the high temperature data listed by Kelley (9). Where Kelley has no data, the estimates given in the JANAF tables (10) were used. The free energies of formation of Li_2CO_3 at high temperatures were calculated from enthalpy data given by Janz (11) and the free energies of formation of Li_2C_2 at various temperatures were estimated using methods suggested by Kubaschewski and Evans (12).

ΔG^0 was then converted to E^0, the standard reversible decomposition potential, by means of the relationship

$$\Delta G^0 = -nFE^0.$$

For the purposes of the calculations it was assumed that (i) all electrode processes were reversible; (ii) all components were in their standard states, i.e., all gases were ideal and at 1 atm partial pressure, any deposited metal was neither alloyed with the indicator electrode nor dissolved in the carbonate, and the carbonates, oxides, and carbides were all in the form of pure crystals or melts; (iii) the carbonates were thermally stable.

The thermal decomposition of the carbonates can be inhibited by keeping them under CO_2. However, this introduces the complication that the CO_2 itself can be reduced, either to carbon or to carbon monoxide as in eqs. [5] and [6].

(*e*) Reduction to carbon.

$$3CO_2 + 4e = 2CO_3^{2-} + C \qquad \text{at the cathode,}$$

$$CO_3^{2-} = CO_2 + \tfrac{1}{2}O_2 + 2e \qquad \text{at the anode.}$$

Can. J. Chem. Downloaded from www.nrcresearchpress.com by 210.87.254.42 on 09/05/12
For personal use only.

Overall process

[5] $$CO_2 = C + O_2.$$

(*f*) Reduction to carbon monoxide.

$$2CO_2 + 2e = CO_3^{2-} + CO \qquad \text{at the cathode,}$$

$$CO_3^{2-} = CO_2 + \tfrac{1}{2}O_2 + 2e \qquad \text{at the anode.}$$

Overall process

[6] $$CO_2 = CO + \tfrac{1}{2}O_2.$$

Figures 1 to 6 show the variation of E^0 with temperature for the decomposition of potassium, sodium, lithium, barium, calcium, and magnesium carbonates according to eqs. [1] to [4]. On Fig. 2 the decomposition of CO_2 is also plotted.

From these graphs it is evident that in the case of K_2CO_3 (Fig. 1), the deposition of alkali metal is the favored electrode process at all temperatures, whereas with Na_2CO_3 (Fig. 2) carbon production is favored up to a temperature of about 870 °K after which alkali metal deposition is again preferred. With the other carbonates the favored processes are, at low temperatures, carbon, production and, at high temperatures, CO evolution. In all cases, however, direct reduction of CO_2 (eqs. [5] and [6]) would be favored but the low activity of CO_2 in carbonates should prevent significant contributions from this reaction.

Reduction of Carbonates with Metals and Carbon

Carbonates can be reduced with reactive metals or with carbon and, as in the case of electrolytic reduction, the products depend on both the carbonate cation and on the temperature at which the reduction takes place.

The easiest way to present the data is on an Ellingham diagram (13) as shown in Fig. 7. On the conventional Ellingham diagram the standard free energy of formation, ΔG^0, is plotted against temperature T, for oxidations such as

[7] $$2Fe + O_2 = 2FeO.$$

In the case of the carbonates there are several ways in which the carbonate can be reduced and each of these ways can be represented as a line on the Ellingham diagram. For instance the carbonate can be reduced to metal oxide and carbon. This redox process may be represented as

[8] $$M_2O + C + O_2 = M_2CO_3.$$

At higher temperatures carbon monoxide rather than carbon will be produced and the corresponding redox process would be

[9] $$2M_2O + 2CO + O_2 = 2M_2CO_3.$$

The temperature at which ΔG^0 for reaction [9] becomes numerically lower than ΔG^0 for reaction [8] will be given by the point at which line [8] intersects the $2C + O_2 = 2CO$ line on the Ellingham diagram. For K_2CO_3 and Na_2CO_3 above about 870 °K alkali metal is produced on reduction of the carbonate. Before the $2C + O_2 = 2CO$ line is crossed, alkali metal production may be represented as

[10] $$\tfrac{4}{3}M + \tfrac{2}{3}C + O_2 = \tfrac{2}{3}M_2CO_3,$$

and after crossing as

[11] $$2M + CO + O_2 = M_2CO_3.$$

Can. J. Chem. Downloaded from www.nrcresearchpress.com by 210.87.254.42 on 09/05/12
For personal use only.

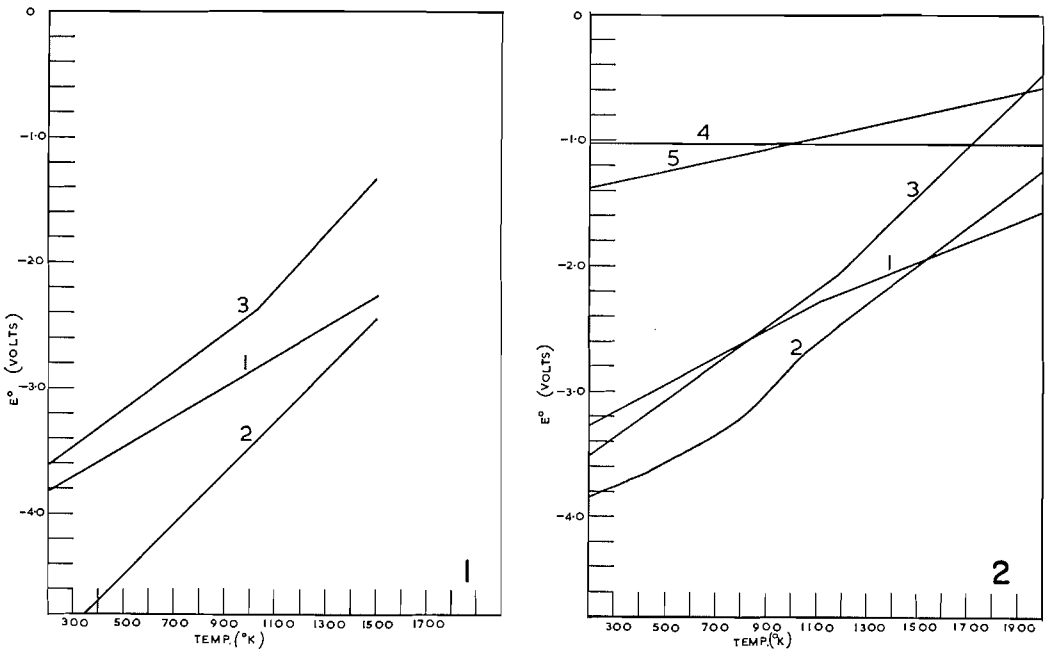


FIG. 1. Variation with temperature of the standard reversible decomposition voltage, E^0, of potassium carbonate. Line 1, K_2O and C formed. Line 2, K_2O and CO formed. Line 3, K deposited.

FIG. 2. Variation with temperature of the standard reversible decomposition voltage, E^0, of sodium carbonate. Line 1, Na_2O and C formed. Line 2, Na_2O and CO formed. Line 3, Na deposited. Line 4, CO_2 decomposed to C and O_2. Line 5, CO_2 decomposed to CO and O_2.

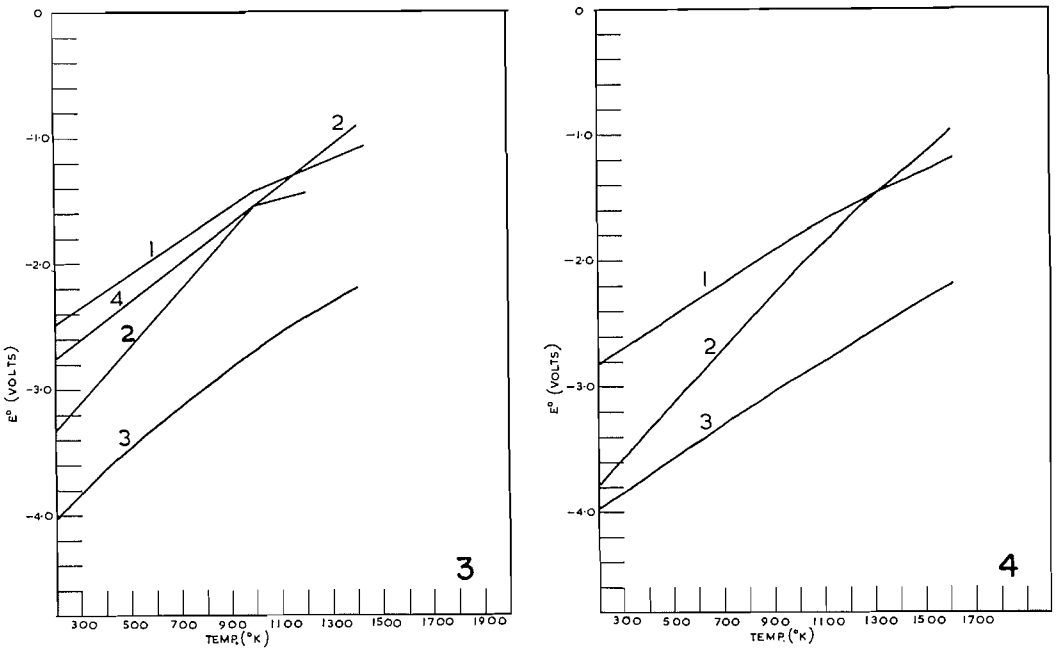


FIG. 3. Variation with temperature of the standard reversible decomposition voltage, E^0, of lithium carbonate. Line 1, Li_2O and C formed. Line 2, Li_2O and CO formed. Line 3, Li deposited. Line 4, Li_2O and Li_2C_2 formed.

FIG. 4. Variation with temperature of the standard reversible decomposition voltage, E^0, of barium carbonate. Line 1, BaO and C formed. Line 2, BaO and CO formed. Line 3, Ba deposited.

Can. J. Chem. Downloaded from www.nrcresearchpress.com by 210.87.254.42 on 09/05/12
For personal use only.

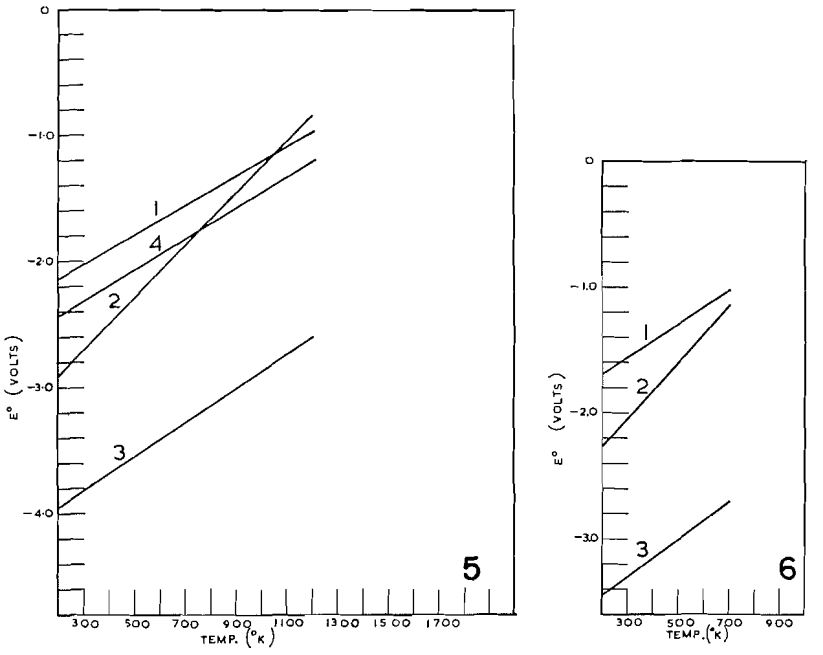


FIG. 5. Variation with temperature of the standard reversible decomposition voltage, E^0, of calcium carbonate. Line 1, CaO and C formed. Line 2, CaO and CO formed. Line 3, Ca deposited. Line 4, CaO and CaC_2 formed.

FIG. 6. Variation with temperature of the standard reversible decomposition voltage, E^0, of magnesium carbonate. Line 1, MgO and C formed. Line 2, MgO and CO formed. Line 3, Mg deposited.

In Fig. 7, of the reactions [8] to [11], the reaction which has the lowest value of ΔG^0 is plotted for each of the carbonates. The plain carbonate lines below the $2C + O_2 = 2CO$ line refer to the production of the metal oxide and carbon (reaction [8]), those above refer to the production of CO and oxide (reaction [9]). The dashed line below the $2C + O_2 = 2CO$ line refers to the metal and carbon deposition reactions (reaction [10]) and the dashed line above to the deposition of metal and evolution of CO (reaction [11]). Also on the diagram are the lines corresponding to the various carbon oxidations viz.

[12] $$C + O_2 = CO_2$$

[13] $$2CO + O_2 = 2CO_2$$

[14] $$2C + O_2 = 2CO$$

For the sake of clarity only a few of the metal oxidation lines are plotted. Data for plotting any others may be obtained either from Hamer (3) or from Richardson and Jeffes (14).

If a metal oxidation line lies below a carbonate redox line, that metal will reduce the carbonate. At a temperature of 700 °K, for instance, the sodium oxidation line lies below all the carbonate lines. Hence at this temperature sodium will reduce all the carbonates. For example sodium carbonate will be reduced thus:

	ΔG^0 at 700 °K (kcal mole^{-1} O_2)
$4Na + O_2 = 2Na_2O$	−153.1
$Na_2O + C + O_2 = Na_2CO_3$	−147.6

Subtracting

[15] $$4Na + Na_2CO_3 = 3Na_2O + C \qquad -5.5$$

Can. J. Chem. Downloaded from www.nrcresearchpress.com by 210.87.254.42 on 09/05/12
For personal use only.

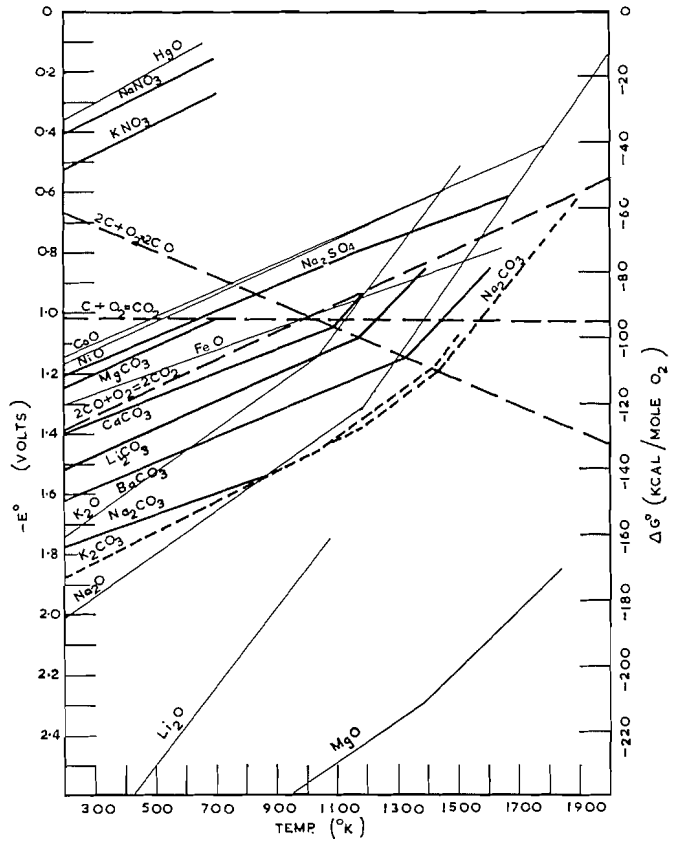


FIG. 7. Variation with temperature of the standard free energy of reaction (ΔG^0) and of the standard reversible decomposition voltage, E^0, for various oxy-anion systems and oxides (see text).

This gives the value for ΔG^0 for reaction [15] as -5.5 kcals mole^{-1} at 700 °K.

It is also possible to estimate the standard reversible decomposition potential of a carbonate by means of this diagram. As an example the overall decomposition reaction for K_2CO_3 is

$$K_2CO_3 = 2K + CO_2 + \tfrac{1}{2}O_2.$$

This can be split up as follows (where m is the number of moles of oxygen involved in a process):

	m	mE^0 (1 000 °K), V
$3 \times (\frac{2}{3}K_2CO_3 = \frac{4}{3}K + \frac{2}{3}C + O_2)$	3	$-3 \times 1.48 = -4.44$
$2 \times (C + O_2 = CO_2)$	2	$-2 \times 1.02 = -2.04$

Subtracting

$2 \times (K_2CO_3 = 2K + CO_2 + \frac{1}{2}O_2)$	1	-2.40

This value of -2.40 V is precisely that obtained from Fig. 1.

Comparison with Experiment

Most of the experimental work on the electrolysis of carbonates has been conducted on eutectics, one component of which is usually Li_2CO_3. With such eutectics several

Can. J. Chem. Downloaded from www.nrcresearchpress.com by 210.87.254.42 on 09/05/12
For personal use only.

workers (15–17) have identified carbon as one of the cathode products at temperatures between 500 °C and 600 °C. At a temperature of 700 °C there is apparently no deposit of carbon (18) but at such temperatures any carbon produced would react with CO_2 to produce CO.

There is only one report of the electrolytic production of sodium from molten sodium carbonate (19) but the now obsolete Deville process for the production of sodium relied upon the reduction of Na_2CO_3 with carbon at a temperature of 1 200 °C. Very similar to the Deville process is Curaudaus' process (20) for the reduction of K_2CO_3 to potassium with carbon. This process works for all alkali metals except lithium, in which case carbon monoxide and lithium oxide are the products. There are also reports of the production of sodium from sodium carbonate by reduction with aluminium and magnesium (19).

Although the thermodynamic treatment so far presented enables one to predict the products of reduction, it is difficult to relate the standard reversible decomposition voltage, E^0, to the actual decomposition voltage as measured experimentally. There are several reasons for this. Firstly all the electrode processes envisaged may not be reversible, secondly polarization effects are not considered, and thirdly the activities of the reduction products produced in the carbonate are unknown. However, the decomposition voltage of a ternary carbonate eutectic has been reported by Dubois (16) to be of the order of -1.8 to -2.5 V at 560 °C. Work in this laboratory (17) on the current–voltage behavior of $LiNaCO_3$ at 550 °C supports Dubois' results but a wave was observed at a potential of about -1.2 V versus a $Ag|Ag^+$ reference electrode. The standard reversible decomposition voltage of lithium carbonate at 550 °C is -1.65 V (Fig. 3), whereas that for CO_2 is -1.01 V (Fig. 2). The wave occurring at -1.2 V probably corresponds to the reduction of CO_2, whereas the lithium carbonate is not decomposed until a potential of about 2.0 V is applied across the cell.

Examination of Fig. 7 shows that the CoO and NiO lines are above those for all the carbonates and hence it is to be expected that cobalt and nickel would not reduce a $LiNaCO_3$ eutectic. This is in fact the case since it is possible to measure reversible $Co|Co^{2+}$ and $Ni|Ni^{2+}$ potentials in such a eutectic at 550 °C provided water is rigorously excluded from the system (17). However, an $Fe|Fe^{2+}$ potential is unstable and indeed the FeO line lies below the CO_2 lines in accord with iron being oxidized by CO_2 dissolved in the melt. For the same reason it would not be possible to measure a $Na|Na^+$ potential in molten sodium carbonate at any temperature below about 1 570 °K where the Na_2O line crosses the CO_2 line because the sodium would be oxidized. This is presumably one of the reasons for the low yields obtained from the Deville process (19). However, the K_2O line crosses the CO_2 line at a far lower temperature (1 200 °K) and hence it is to be expected that the reduction of K_2CO_3 would give higher yields.

SULFATES

Electrolytic Reduction of Sulfates

When a solid or liquid sulfate is electrolyzed, it is assumed that SO_3 and O_2 are evolved at the anode at temperatures below 1 200 °K. Above this temperature SO_2 and O_2 evolution is thermodynamically more favored. Hence all potentials below 1 000 °K are referred to a SO_3, $O_2|SO_4^{2-}$ electrode and those above to a SO_2, $O_2|SO_4^{2-}$ electrode. As with the carbonates it is assumed that all components are in their standard states.

Again there are a number of feasible cathode processes:

(*g*) the formation of sulfur and oxide

$$SO_4^{2-} + 6e = \tfrac{1}{2}S_2 + 4O^{2-},$$

Can. J. Chem. Downloaded from www.nrcresearchpress.com by 210.87.254.42 on 09/05/12
For personal use only.

(*h*) the formation of sulfide and oxide

$$SO_4^{2-} + 8e = S^{2-} + 4O^{2-},$$

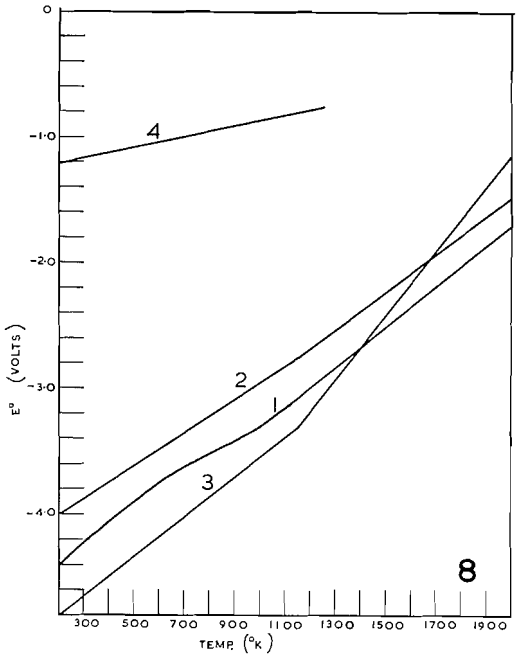
(*j*) the deposition of alkali metal.

It is also possible that sulfite is formed as an unstable intermediate which decomposes to sulfate and sulfide.

Each of the three cathode processes may be combined with the anode processes giving as overall cell reductions:

[16]	$4Na_2SO_4 = \frac{1}{2}S_2 + 4Na_2O + 3SO_3 + \frac{3}{2}O_2$	below 1 200 °K
and	$4Na_2SO_4 = \frac{1}{2}S_2 + 4Na_2O + 3SO_2 + 3O_2$	above 1 200 °K
[17]	$5Na_2SO_4 = Na_2S + 4Na_2O + 4SO_3 + 2O_2$	below 1 200 °K
and	$5Na_2SO_4 = Na_2S + 4Na_2O + 4SO_2 + 4O_2$	above 1 200 °K
[18]	$Na_2SO_4 = 2Na + SO_3 + \frac{1}{2}O_2$	below 1 200 °K
and	$Na_2SO_4 = 2Na + SO_2 + O_2$	above 1 200 °K.

ΔG^0 and E^0 are plotted against T for each of these reactions in Fig. 8. From this it can be seen that sulfide formation is favored up to a temperature of about 1 700 °K after which alkali metal evolution is favored.



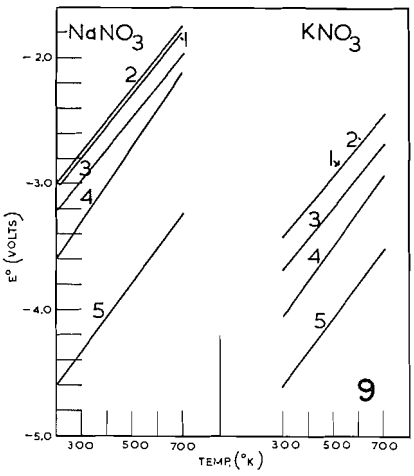


FIG. 8. Variation with temperature of the standard reversible decomposition voltage, E^0, of sodium sulfate. Line 1, Na_2O and sulfur produced. Line 2, Na_2S and Na_2O produced. Line 3, Na deposited. Line 4, SO_3 reduction.

FIG. 9. Variation with temperature of the standard reversible decomposition voltage, E^0, of sodium nitrate and potassium nitrate. Line 1, nitrite and oxide production. Line 2, nitrogen evolution and oxide production. Line 3, N_2O evolution and oxide production. Line 4, NO evolution and oxide production. Line 5, alkali metal deposition.

Can. J. Chem. Downloaded from www.nrcresearchpress.com by 210.87.254.42 on 09/05/12
For personal use only.

It is also possible that any SO_3 that is formed by thermal decomposition of the sulfate may be reduced. This may first be reduced to sulfite which decomposes to sulfide and sulfate.

$$4SO_3 + 8e = 4SO_3^{2-}$$

$$4SO_3^{2-} = S^{2-} + 3SO_4^{2-}$$

Combination of these reactions with the anodic reaction yields as the overall cell reaction

[19] $$Na_2SO_4 = Na_2S + 2O_2.$$

This, too, is plotted on Fig. 8.

Reduction of Sodium Sulfate with Metals

At temperatures below 1 700 °K the favored electrolytic reduction products of sodium sulfate are sodium sulfide and sodium oxide (Fig. 8). Hence should a reactive metal M be added to sodium sulfate it would be reasonable to assume that sulfide and oxide would be formed. However, for the purposes of the thermodynamic calculations the sulfide may combine with the metal M or with the sodium in the melt. Hence there are two possible equations

[20] $$4M + Na_2SO_4 = 4MO + Na_2S$$

or

[21] $$4M + Na_2SO_4 = 3MO + MS + Na_2O.$$

Each of these reactions may be split up for plotting on an Ellingham diagram

$$4M + 2O_2 = 4MO$$

[22] $$Na_2S + 2O_2 = Na_2SO_4.$$

Subtracting

$$4M + Na_2SO_4 = Na_2S + 4MO$$

or

$$4M + \tfrac{1}{2}S_2 + \tfrac{3}{2}O_2 = 3MO + MS$$

[23] $$Na_2O + \tfrac{1}{2}S_2 + \tfrac{3}{2}O_2 = Na_2SO_4$$

Subtracting

$$4M + Na_2SO_4 = Na_2O + 3MO + MS.$$

In the first case the sulfate redox line (eq. [22]) may be plotted directly on an oxide Ellingham diagram (Fig. 7), but in the second (eq. [23]) a composite diagram has to be drawn incorporating both the sulfides and oxides. It has been found that reaction [20] is in general the thermodynamically more favored and hence the composite sulfide, oxide diagram is not presented.

Comparison with Experiment

The products of electrolytic reduction of a lithium sodium potassium sulfate eutectic at temperatures between 550 °C and 580 °C have been identified by Johnson and Laitinen (21) as sulfur, oxide, and sulfite, whereas Liu (22) reported the production of oxide and sulfide from a lithium potassium sulfate eutectic at 625 °C. The decomposition potential of these eutectics is of the order of −3 V compared with the standard reversible decomposition voltage of sodium sulfate which is about −3.1 V at 900 °K (Fig. 8). This indicates that it is the sulfate anion which is being reduced and not the SO_3 evolved thermally. However, the current–voltage curve of a sulfate eutectic exhibits a high residual current which may be caused by this SO_3 reduction.

Can. J. Chem. Downloaded from www.nrcresearchpress.com by 210.87.254.42 on 09/05/12
For personal use only.

From Fig. 7 it can be seen that iron reduces sodium sulfate melts but cobalt and nickel apparently do not. It has been shown experimentally that iron is in fact attacked in sulfate media and that cobalt is sufficiently noble for its standard electrode potential to be measured (21). On the other hand, nickel is slowly attacked in sulfate media. The thermodynamic treatment presented here offers no explanation for the different behavior of cobalt and nickel. It has been suggested that SO_3 corrodes the nickel (7) but should this be the case the cobalt would also be attacked. The explanation may lie in the different solubilities of the cobalt and nickel oxides and sulfides in the melt.

NITRATES

Electrolytic Reduction of Nitrates

When a solid or liquid alkali nitrate is electrolyzed it is assumed that NO_2 and O_2 are evolved at the anode. The feasible cathode processes are:

(*k*) formation of nitrite and oxide

$$NO_3^- + 2e = NO_2^- + O^{2-},$$

(*l*) evolution of nitrogen and formation of oxide

$$NO_3^- + 5e = \tfrac{1}{2}N_2 + 3O^{2-},$$

(*m*) evolution of N_2O and formation of oxide

$$2NO_3^- + 8e = N_2O + 5O^{2-},$$

(*n*) evolution of NO and formation of oxide

$$NO_3^- + 3e = NO + 2O^{2-},$$

(*o*) deposition of alkali metal

$$M^+ + e = M\downarrow.$$

Combination of each of these cathode reactions with the anode reaction gives equations

[24] $$3MNO_3 = MNO_2 + M_2O + 2NO_2 + O_2$$

[25] $$6MNO_3 = \tfrac{1}{2}N_2 + 3M_2O + 5NO_2 + \tfrac{5}{2}O_2$$

[26] $$10MNO_3 = N_2O + 5M_2O + 8NO_2 + 4O_2$$

[27] $$4MNO_3 = NO + 2M_2O + 3NO_2 + \tfrac{3}{2}O_2$$

[28] $$MNO_3 = M + NO_2 + \tfrac{1}{2}O_2.$$

The data for the calculation of E^0 were obtained from refs. 8–10. The data for the nitrites were estimated. ΔG^0 and E^0 are plotted against T for sodium and potassium nitrates (Fig. 9). From the diagram it can be seen that nitrite production (reaction [24]) and nitrogen evolution (reaction [25]) are almost equally thermodynamically favored with N_2O and NO production following fairly closely behind. Alkali metal production, however, appears to be out of the question.

Reduction of Nitrates with Metals

Either the nitrate to nitrite process (reaction [24]) or the nitrogen evolution reaction (reaction [25]) can be chosen as the redox line on the oxide Ellingham diagram. However, since the data for the nitrogen evolution is the more readily available, this line has been plotted on Fig. 7. This line may be represented as

$$\tfrac{1}{5}(2M_2O + 2N_2 + 5O_2 = 4MNO_3).$$

Can. J. Chem. Downloaded from www.nrcresearchpress.com by 210.87.254.42 on 09/05/12
For personal use only.

Comparison with Experiment

An analysis of the cathodic reduction products of potassium and sodium nitrates is presented elsewhere (23).

From the position of the sodium and potassium nitrate redox lines on Fig. 7 it can be seen that these two melts are strongly oxidizing and hence most of the common structural metals will reduce these melts. However, the HgO line is above the nitrate redox lines and hence it is to be expected that mercury would not be oxidized in the melt. This is the case at comparatively low temperatures, since a dropping mercury electrode can be used in nitrate media at 250 °C (24). At higher temperatures the mercury is oxidized but this is probably by the oxygen evolved in the thermal dissociation of the nitrate ion.

ACKNOWLEDGMENTS

We are grateful to Texas Instruments Inc. for a maintenance grant (to H. E. B.).

REFERENCES

1. W. J. HAMER, M. S. MALMBERG, and B. RUBIN. J. Electrochem. Soc. **103**, 8 (1956).
2. W. J. HAMER, M. S. MALMBERG, and B. RUBIN. J. Electrochem. Soc. **112**, 750 (1965).
3. W. J. HAMER. J. Electroanal. Chem. **10**, 140 (1965).
4. M. POURBAIX. Thermodynamics of dilute aqueous solutions. Arnold, London. 1949.
5. R. LITTLEWOOD. J. Electrochem. Soc. **109**, 525 (1962).
6. M. D. INGRAM and G. J. JANZ. Electrochim. Acta, **10**, 783 (1965).
7. G. J. HILLS. J. Inst. Fuel. 1966. In press.
8. NATL. BUR. STDS. (U.S.) Circ. 500 (1952).
9. K. K. KELLEY. U.S. Bur. Mines, Bull. 584.
10. JANAF THERMOCHEMICAL TABLES. Advanced Research Agency Program, U.S. Air Force Contract No. AF33 (616)-6149.
11. G. J. JANZ, E. NEUENSCHWANDER, and F. J. KELLY. Trans. Faraday Soc. **59**, 841 (1963).
12. O. KUBASCHEWSKI and E. L. EVANS. Metallurgical thermochemistry. Pergamon, London. 1958.
13. C. W. DANNATT and H. J. T. ELLINGHAM. Discussions Faraday Soc. **4**, 126 (1948).
14. F. D. RICHARDSON and J. H. E. JEFFES. J. Iron Steel Inst. London, **160**, 261 (1948).
15. P. DEGOBERT and O. BLOCH. Bull. Soc. Chim. France, 1887 (1962).
16. J. DUBOIS. Ann. Chim. Paris, **10**, 145 (1965).
17. H. E. BARTLETT and K. E. JOHNSON. J. Electrochem. Soc. Submitted for publication.
18. G. J. JANZ and A. CONTE. Electrochim. Acta. **9**, 1269 (1964).
19. M. SITTIG. Sodium. Its manufacture and uses. Reinhold, New York. 1956.
20. J. W. MELLOR. A comprehensive treatise on inorganic and theoretical chemistry. Vol. II (1923) and Vol. II, Suppl. II (1961). Longmans, New York and Toronto.
21. K. E. JOHNSON and H. A. LAITINEN. J. Electrochem. Soc. **110**, 314 (1963).
22. C. H. LIU. J. Phys. Chem. **66**, 164 (1962).
23. H. E. BARTLETT and K. E. JOHNSON. J. Electrochem. Soc. In press.
24. H. S. SWOFFORD and H. A. LAITINEN. J. Electrochem. Soc. **110**, 814 (1963).

Can. J. Chem. Downloaded from www.nrcresearchpress.com by 210.87.254.42 on 09/05/12
For personal use only.

Can. J. Chem. Downloaded from www.nrcresearchpress.com by 210.87.254.105 on 09/05/12
For personal use only.

HALIDE ALKOXIDES OF SAMARIUM

III. REACTIONS OF SAMARIUM ALKOXIDES WITH ACETYL CHLORIDE AND ACETYL BROMIDE

B. S. SANKHLA AND R. N. KAPOOR
Chemical Laboratories, University of Jodhpur, Jodhpur, India

Received February 8, 1966

ABSTRACT

The reactions of samarium *n*-butoxide, isopropoxide, and *tert*-butoxide with acyl halides in different stoichiometric ratios have been studied and products of the type $Sm(OR)_2X$, $Sm(OR)X_2.0.5CH_3COOR$ and $SmX_3.CH_3COOR$ (where R = $C_4H_9^n$, $C_3H_7^i$, or $C_4H_9^t$ and X = Cl or Br) have been isolated in quantitative yields. All these reactions are exothermic and the amount of heat liberated also increases with the increase in the concentration of acyl halide. These reactions have been further confirmed by the reactions with anhydrous samarium trichloride and the corresponding esters, which are also exothermic reactions. Attempts to sublime the dialkoxy monohalide derivatives of samarium were unsuccessful. The reaction of a dry current of hydrogen chloride gas on samarium isopropoxide has also been investigated.

INTRODUCTION

Considerable work has been carried out on the reactions of alkoxides of aluminium (1–2), titanium (3), zirconium (4), germanium (5), tin (6), vanadium (7), and niobium (8) with acyl halides (chloride and bromide). Mehrotra *et al.* (2) have studied the reactions of aluminium isopropoxide with acetyl chloride, which have been represented by the general equation:

$$Al(OPr^i)_3 + xCH_3COCl \rightarrow Al(OPr^i)_{3-x}Cl_x + xCH_3COOPr^i.$$

The reaction between aluminium *tert*-butoxide and acetyl chloride is complicated and leads to the formation of acetoxy derivatives of the type $AlCl_x(OAc)_y(OBu^t)_{3-x-y}$. They have also reported a novel method for the preparation of tetraacetate derivatives of silicon, titanium, and zirconium by the reaction of the corresponding chlorides with *tert*-butyl acetate (9):

$$MCl_4 + 4Bu^tOAc \rightarrow M(OAc)_4 + 4Bu^tCl.$$

In view of the interesting results obtained in the above experiments, it was considered worthwhile to carry out the reactions of samarium alkoxides (*n*-butoxide, isopropoxide, and *tert*-butoxide) with acyl halides (chloride and bromide) and also the reactions of samarium trichloride and corresponding esters.

The technique for these reactions consists of adding the requisite amount of acyl halide to a solution of alkoxide in benzene whereupon an exothermic reaction takes place. The products precipitate quickly, suggesting apparent completion of the reaction; however, the mixture was heated under reflux for 1 h to ensure completion. The reactions of samarium alkoxides with acyl halides (chloride and bromide) have been carried out in different molar ratios and can be represented by the following general equations:

$$Sm(OR)_3 + 1CH_3COX \rightarrow Sm(OR)_2X + CH_3COOR.$$

$$Sm(OR)_3 + 2CH_3COX \rightarrow Sm(OR)X_2.0.5CH_3COOR + 1.5CH_3COOR.$$

$$Sm(OR)_3 + 3CH_3COX \text{ or excess} \rightarrow SmX_3.CH_3COOR + 2CH_3COOR.$$

(Where R = $C_4H_9^n$, $C_3H_7^i$, or $C_4H_9^t$ and X = Cl or Br.)

Can. J. Chem. Downloaded from www.nrcresearchpress.com by 210.87.254.105 on 09/05/12
For personal use only.

It was noteworthy that the halide alkoxides so formed exhibit an increasing tendency to add on the molecule of ester formed in the reaction itself. It may be that the replacement of the alkoxy group by a more electronegative halide radical would tend to decrease electron density around the samarium atom thereby increasing the tendency to accept donor bonds from organic ester molecules.

All these halide alkoxides are sparingly soluble in the alcohol of the parent alkoxide and are insoluble in benzene. Thus the molecular weight could not be determined.

To give support to the above reactions, the reactions of anhydrous samarium trichloride with excess of the corresponding ester were carried out. Products of the type $SmCl_3.CH_3COOR$ (where R = $C_4H_9^n$, $C_3H_7^i$, $C_4H_9^t$, $C_3H_7^n$, $C_4H_9^s$, $C_4H_9^i$, CH_3, and $C_5H_{11}^n$) were obtained.

For a complete comparative study, the reaction of samarium isopropoxide with anhydrous hydrogen chloride gas was also studied. The reaction was exothermic and the product (chlorine to samarium ratio 3:1) insoluble in benzene was obtained. When the mixture was cooled, the triisopropanol derivative crystallized from the solution. This shows that the product obtained as above is the same as that obtained by a reaction between anhydrous samarium trichloride and isopropanol.

$$Sm(OPr^i)_3 + 3HCl \rightarrow SmCl_3.3Pr^iOH$$

$$SmCl_3 + 3Pr^iOH \rightarrow SmCl_3.3Pr^iOH$$

EXPERIMENTAL

Apparatus

An all-glass apparatus fitted with interchangeable standard joints was employed and adequate precautions were taken to exclude moisture. Fractionations were carried out in a column packed with Raschig rings and fitted to a stillhead.

Materials

Samarium isopropoxide and normal butoxide were prepared by the sodium alkoxide method (10) and were analyzed before use. Samarium *tert*-butoxide was prepared from isopropoxide by alcohol interchange technique. Benzene (B.D.H.) was dried over sodium wire followed by a careful fractionation over a long column. Acetyl chloride (B.D.H./A.R) and acetyl bromide (B.D.H./A.R.) were distilled at 51–52 °C and 76 °C respectively before use. The organic esters were prepared (11), dried over anhydrous sodium sulfate, and purified by careful fractionation, and a middle fraction was taken.

Analytical Methods

Samarium was estimated gravimetrically as its sesquioxide (Sm_2O_3) by igniting the oxalate. Halogens were estimated as silver halide by gravimetry. The isopropoxy group was estimated by oxidation with normal potassium dichromate in 12.5% sulfuric acid (12).

Reactions

Reaction of Samarium Isopropoxide with Acetyl Chloride in Molar Ratio 1:1

When samarium isopropoxide (1.15 g) was allowed to react with acetyl chloride (0.280 g) in benzene, an exothermic reaction occurred. The contents were shaken well and then refluxed at low temperature for 1 h. The compound settled from the reaction mixture as soon as the acetyl chloride was added to the alkoxide solution. The excess of the solvent was then removed at room temperature and under reduced pressure. On drying, a white powdered compound was obtained. Yield 1.02 g.

Anal. Calcd. for $SmCl(OPr^i)_2$: Sm, 49.5; Cl, 11.7. Found: Sm, 49.1; Cl, 11.9.

Reaction of Samarium tert-Butoxide with Acetyl Bromide in Molar Ratio 1:Excess

When acetyl bromide (2.67 g) was admitted to a benzene solution of samarium *tert*-butoxide (1.23 g), an exothermic reaction occurred with the precipitation of a yellow solid. The reaction mixture was refluxed for 1 h. The excess solvent was then removed under reduced pressure at room temperature and finally a yellow powdered solid was obtained. Yield 1.24 g.

Anal. Calcd. for $SmBr_3.CH_3COOBu^t$: Sm, 29.7; Br, 47.4. Found: Sm, 30.2; Br, 47.0.

Other reactions of samarium alkoxides with acyl halides are summarized in Tables I, II, and III.

Reaction of Samarium Trichloride with tert-Butyl Acetate (Excess)

When samarium trichloride (1.23 g) was allowed to react with *tert*-butyl acetate (39.7 g), an exothermic reaction occurred. After the mixture was shaken for 15 min, a curdy precipitate appeared. The reactants

Can. J. Chem. Downloaded from www.nrcresearchpress.com by 210.87.254.105 on 09/05/12
For personal use only.

TABLE I

Reactions of samarium *n*-butoxide with acyl halides

(*a*) Alkoxide (g)	(*b*) Acetyl chloride (g)	(*b*) Acetyl bromide (g)	Molar ratio (*a*/*b*)	Product, its state and amount	Analysis					
					Found (%)			Calcd. (%)		
					Sm	Cl	Br	Sm	Cl	Br
1.36	0.29	—	1:1	$SmCl(OBu^n)_2$ faint-yellow solid (1.27 g)	44.8	11.2	—	45.3	10.7	—
1.48	0.63	—	1:2	$SmCl_2(OBu^n).0.5CH_3COOBu^n$ faint-yellow solid (1.32 g)	42.4	21.0	—	42.7	20.2	—
1.37	2.45	—	1:excess	$SmCl_3.CH_3COOBu^n$ yellow crystalline solid (1.22 g)	40.7	28.0	—	40.3	28.6	—
1.072	—	0.358	1:1	$SmBr(OBu^n)_2$ light-brown solid (1.01 g)	40.1	—	21.7	39.9	—	21.2
1.401	—	0.934	1:2	$SmBr_2(OBu^n).0.5CH_3COOBu^n$ brown solid (1.35 g)	33.7	—	36.2	34.1	—	36.2
1.462	—	2.61	1:excess	$SmBr_3.CH_3COOBu^n$ brown solid (1.51 g)	29.9	—	46.8	29.7	—	47.3

Can. J. Chem. Downloaded from www.nrcresearchpress.com by 210.87.254.105 on 09/05/12
For personal use only.

TABLE II

Reactions of samarium isopropoxide with acyl halides

(*a*) Alkoxide (g)	(*b*) Acetyl chloride (g)	(*b*) Acetyl bromide (g)	Molar ratio (*a*/*b*)	Product, its state and amount	Analysis					
					Found (%)			Calcd. (%)		
					Sm	Cl	Br	Sm	Cl	Br
1.15	0.28	—	1:1	$SmCl(OPr^i)_2$ white powder (1.02 g)	49.1	11.9	—	49.5	11.7	—
1.096	0.526	—	1:2	$SmCl_2(OPr^i).0.5CH_3COOPr^i$ white powder (1.0 g)	45.1	21.1	—	45.4	21.4	—
1.222	0.879	—	1:3	$SmCl_3.CH_3COOPr^i$ white powder (1.26 g)	41.4	29.8	—	41.9	29.7	—
1.426	4.52	—	1:excess	$SmCl_3.CH_3COOPr^i$ white powder (1.49 g)	41.7	29.4	—	41.9	29.7	—
1.526	—	0.579	1:1	$SmBr(OPr^i)_2$ faint-yellow solid (1.49 g)	43.9	—	23.1	43.2	—	22.95
1.026	—	0.772	1:2	$SmBr_2(OPr^i).0.5CH_3COOPr^i$ faint-yellow solid (1.0 g)	35.3	—	38.7	35.8	—	38.0
1.144	—	2.52	1:excess	$SmBr_3.CH_3COOPr^i$ faint-yellow solid (1.22 g)	30.7	—	47.9	30.6	—	48.7

Can. J. Chem. Downloaded from www.nrcresearchpress.com by 210.87.254.105 on 09/05/12
For personal use only.

TABLE III

Reactions of samarium *tert*-butoxide with acyl halides

(*a*) Alkoxide (g)	(*b*) Acetyl chloride (g)	(*b*) Acetyl bromide (g)	Molar ratio (*a*/*b*)	Product, its state and amount	Analysis					
					Found (%)			Calcd. (%)		
					Sm	Cl	Br	Sm	Cl	Br
1.088	0.238	—	1:1	$Sm(OBu^t)_2Cl$ white powder (1.0 g)	45.1	10.8	—	45.3	10.7	—
1.783	0.759	—	1:2	$Sm(OBu^t)Cl_20.5CH_3COOBu^t$ white powder (1.59 g)	43.0	20.7	—	42.7	20.16	—
1.121	3.42	—	1:excess	$SmCl_3.CH_3COOBu^t$ yellow powder (1.22 g)	40.8	28.8	—	40.3	28.57	—
0.970	—	0.325	1:1	$Sm(OBu^t)_2Br$ faint-yellow powder (0.99 g)	40.2	—	21.9	39.97	—	21.25
1.464	—	0.979	1:2	$Sm(OBu^t)Br_20.5CH_3COOBu^t$ yellow powder (1.47 g)	33.7	—	35.8	34.1	—	36.23
1.226	—	2.67	1:excess	$SmBr_3.CH_3COOBu^t$ yellow powder (1.24 g)	30.2	—	47.0	29.7	—	47.4

Can. J. Chem. Downloaded from www.nrcresearchpress.com by 210.87.254.105 on 09/05/12
For personal use only.

TABLE IV

Reactions of samarium trichloride with esters

Samarium trichloride (g)	Esters (g)	Product, its state and amount	Analysis				Remarks
			Found (%)		Calcd. (%)		
			Sm	Cl	Sm	Cl	
1.426	CH_3COOPr^i (39.7)	$SmCl_3.CH_3COOPr^i$ white powdered solid (1.48 g)	41.9	29.2	41.9	29.67	All these derivatives have a fruity odor. They are solids, insoluble in benzene and readily soluble in water
1.366	CH_3COOBu^n (46.2)	$SmCl_3.CH_3COOBu^n$ yellow crystalline solid (1.41 g)	40.1	28.7	40.3	28.57	
1.227	CH_3COOBu^t (39.7)	$SmCl_3.CH_3COOBu^t$ faint-yellow solid (1.26 g)	40.7	28.9	40.3	28.57	
1.337	CH_3COOPr^n (45.3)	$SmCl_3.CH_3COOPr^n$ faint-yellow solid (1.40 g)	43.0	29.0	41.9	29.67	
1.126	CH_3COOBu^s (41.2)	$SmCl_3.CH_3COOBu^s$ yellow crystalline solid (1.21 g)	40.9	28.7	40.3	28.57	
1.219	CH_3COOBu^i (35.6)	$SmCl_3.CH_3COOBu^i$ faint-yellow solid (1.25 g)	40.0	28.9	40.3	28.57	
1.429	CH_3COOMe (38.7)	$SmCl_3.CH_3COOMe$ faint-yellow solid (1.45 g)	43.7	33.1	44.1	33.1	
1.221	CH_3COOAm^n (38.4)	$SmCl_3.CH_3COOAm^n$ deep-yellow solid (1.25 g)	39.1	27.9	38.9	27.5	

were then refluxed and the excess ester removed under reduced pressure at room temperature; on drying, a white compound was obtained.

Anal. Calcd. for $SmCl_3.CH_3COOBu^t$: Sm, 40.3; Cl, 28.57. Found: Sm, 40.7; Cl, 28.9.

Other reactions of samarium trichloride with esters are given in Table IV.

Reaction of Samarium Isopropoxide and Anhydrous Hydrogen Chloride Gas in Benzene

Samarium isopropoxide (1.23 g) was dissolved in benzene (60.2 g) and a controlled current of dry hydrogen chloride gas was passed through the solution. The reaction was exothermic and immediately a faint-yellow solid separated from the solution. After completion of the reaction, indicated by the cooling of the reaction flask, the solution was filtered and the precipitate was dried under reduced pressure.

Anal. Calcd. for $SmCl_3.3Pr^iOH$: Sm, 34.4; Cl, 24.34; Pr^iOH, 41.2. Found: Sm, 34.7; Cl, 24.8; Pr^iOH, 41.9.

ACKNOWLEDGMENTS

The authors are thankful to Prof. R. C. Mehrotra, Head of Chemistry Department, and Dean, Faculty of Science, Rajasthan University, Jaipur, for his valuable suggestions and to Dr. S. N. Misra for his interest in the work. Thanks are also due to Prof. R. C. Kapoor, Head of Chemistry Department, and Dean, Faculty of Science, Jodhpur University, for laboratory facilities. One of us (B. S. S.) is thankful to Ministry of Education, Govt. of India, for a research fellowship, during the tenure of which this work was carried out.

REFERENCES

1. R. C. Mehrotra and R. K. Mehrotra. J. Indian Chem. Soc. **39**, 23 (1962).
2. R. C. Mehrotra and R. A. Misra. Can. J. Chem. **42**, 717 (1964).
3. D. C. Bradley, D. C. Hancock, and W. Wardlaw. J. Chem. Soc. 2773 (1952).
4. D. C. Bradley, F. M. A. Halim, R. C. Mehrotra, and W. Wardlaw. J. Chem. Soc. 4609 (1952).
5. R. C. Mehrotra and G. Chandra. Rec. Trav. Chim. **82**, 683 (1963).
6. R. C. Mehrotra and V. D. Gupta. J. Chem. Soc. In press. 1966.
7. R. K. Mittal and R. C. Mehrotra. Z. Anorg. Allgem. Chem. **332**, 189 (1964).
8. R. C. Mehrotra and P. N. Kapoor. J. Less-Common Metals. In press. 1966.
9. R. C. Mehrotra and B. C. Pant. Tetrahedron Letters, No. 5, 321 (1963).
10. B. S. Sankhla, S. N. Misra, and R. N. Kapoor. Chem. Ind. London, 382 (1965).
11. A. I. Vogel. A textbook of practical organic chemistry. Longmans, Green & Co. Ltd., London. 1956.
12. D. C. Bradley and W. Wardlaw. J. Chem. Soc. 3450 (1950).

Can. J. Chem. Downloaded from www.nrcresearchpress.com by 210.87.254.105 on 09/05/12
For personal use only.

Can. J. Chem. Downloaded from www.nrcresearchpress.com by 210.87.254.105 on 09/05/12
For personal use only.

HEATS OF POTASSIUM–LITHIUM ION EXCHANGE ON SULFONATED POLYSTYRENE RESINS

W. R. HEUMANN AND D. PATTERSON
Département de chimie, Université de Montréal, Montreal, Quebec

Received March 11, 1966

ABSTRACT

A Tian–Calvet microcalorimeter has been used at 25 °C to measure the heats of the exchange between K^+ and Li^+ as a function of the ionic composition of commercial Dowex 50W exchange resins of the following divinylbenzene contents: 1, 4, 8, and 16%. The heats, which are exothermic for the forward reaction, where K^+ replaces Li^+ on the resin, and endothermic for the reverse direction, increase with the degree of cross-linking. A sharp variation in the heat with ionic composition of the resin is observed for the forward exchange at low K^+, and for the reverse exchange at low Li^+ content. These results are consistent with a non-uniformity of the resin.

INTRODUCTION

Only few calorimetric determinations have been made of heats of cation exchange (1–4) on sulfonated resins, or of their variation as a function of the ionic composition of the resin. In particular, results are lacking for the extreme ends of the composition range where the heat effects to be measured are relatively small. We have attempted to obtain data using a highly sensitive microcalorimetric method. The exchange between K^+ and Li^+ was studied since comparatively large heats could be expected, there being a considerable difference in selectivity of the ion exchanger toward the two cations.

EXPERIMENTAL

Materials

The ion exchangers were the commercial Dowex 50W resins of 30–50 mesh/in. size in the swollen state, and having degrees of cross-linking corresponding to 1, 4, 8, and 16% divinylbenzene content. They were purified by removing traces of heavy metals as described by Edge (5), then converted into either the potassium or the lithium form and washed with deionized distilled water. The resins are labelled according to their degree of cross-linking and the cationic form X1 K, X1 Li, X4 K, etc. Exchange capacities were determined as described by Kunin (6) by alkalimetric titrations of the hydrogen form after drying for 48 h at 120 °C.

Solutions of KCl and LiCl were prepared with reagent grade material and deionized water. Their concentrations were determined by titrating with standard $AgNO_3$ solution.

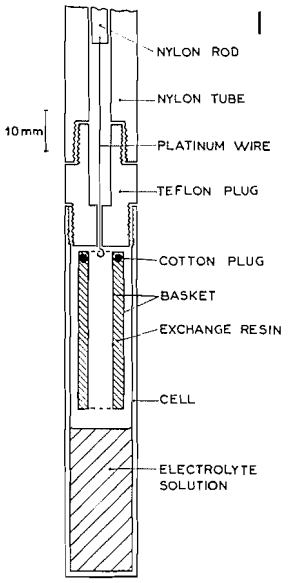
Apparatus

The calorimetric measurements were carried out using a Tian–Calvet microcalorimeter of the differential isothermal type which has been described elsewhere (7, 8). In our installation, a photo-pen recorder followed the light beam reflected from the galvanometer mirror. The instrument was calibrated electrically, and the heat absorbed or liberated by the reaction was found by measuring the area under the curve. This microcalorimeter is sensitive to a thermal effect of about 0.001 cal/h and is designed to follow thermal phenomena over extended periods of time.

The calorimetric cell is shown in Fig. 1. The cylindrical vessel containing the solution of the exchanging electrolyte was of stainless steel. The basket containing the ion exchanger consisted of two concentric cylinders of 100 mesh/in. platinum gauze, welded onto a supporting frame of platinum. The whole basket including the welding was of pure platinum to avoid any thermal effect by electrolytic corrosion. For the same reason, the inner wall of the stainless steel vessel was lined with a thin film of plastic, which was applied by vaporizing a solution in a volatile solvent. The basket was suspended by a platinum wire connected to a nylon rod. This rod, together with the surrounding nylon tube protruded through the top of the calorimeter and could be moved up and down. The opening in the Teflon plug leading the platinum wire was filled with silicone grease to avoid any thermal effect by either evaporation of water or friction due to movement of the wire.

Method

The ion exchanger sample was placed in the space between the two cylinders in the basket, dried 48 h at 120 °C to determine its anhydrous weight, then soaked in a chloride solution of its own cation having the same mean ion activity as the solution of the exchange electrolyte with which the ion exchanger was to react.



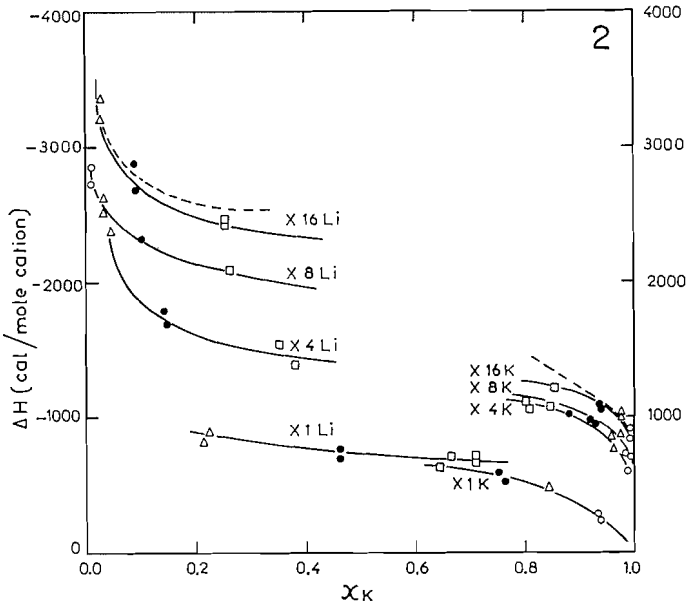


FIG. 1. Calorimetric cell assembly.

FIG. 2. Integral heats of exchange (ΔH) for Dowex 50W resins as a function of potassium mole fraction of resin cation at equilibrium, % divinylbenzene contents and original cationic forms of the resins as indicated. Left-hand scale for reaction on the resin for replacement of Li by K and the right-hand scale for replacement of K by Li. External solution molarities indicated by: ○, 0.01 M; △, 0.032 M; ●, 0.10 M; □, 0.32 M. The broken curves ($\Delta H'$) for the X16 Li and X16 K resins were obtained using the correction procedure of eq. [1].

This minimized heat effects by changes of concentration in the liquid phase during the reaction and by swelling or shrinking of the resin. The soaked sample was weighed again to determine the amount of solution retained. The basket was then suspended in the upper part of the cell as shown in Fig. 1, i.e. above 5 ml of the exchange electrolyte solution which had been placed into the cell in advance. The whole cell assembly was introduced into the calorimeter and allowed to reach thermal equilibrium overnight. All experiments were carried out at 25 ± 0.05 °C. To start the reaction, the basket was lowered until it reached the bottom to stay thus immersed during the experiment. Between 2 and 4 h were required to record the total heat effect. The larger effects obtained with the more highly cross-linked resins required more time, because the exchange reaction is slower in these resins. Stirring by moving the basket up and down then produced no further heat effect due to exchange, showing that equilibrium was attained. The basket with the exchanger was then transferred to a small column resembling the lower part of a buret, and the solution electrolyte was removed quantitatively by washing with water. The effluent was combined with the reacted solution from the cell to determine both the potassium and lithium content by flame photometry using a Zeiss PMQII spectrophotometer. From this analysis, the weight of the anhydrous exchanger and its exchange capacity, the amount of exchanged ions and the equilibrium ionic composition of the ion exchanger could be computed.

The washed exchanger in the basket was prepared for the next experiment by converting it into the desired pure cation form with the corresponding 2M chloride solution. The same sample could thus be used for a series of measurements.

Integral heats of exchange were obtained by starting each experiment with the resin in either the pure K^+ or pure Li^+ form. The extent of exchange in attaining equilibrium was varied by changing the molarity of the LiCl or KCl solutions used to effect the exchange. The effect of changing the ionic strength of the solutions on the heats of exchange will be shown below to be negligible to small.

RESULTS AND DISCUSSION

The experimental integral heats of exchange (ΔH), expressed per mole of exchanged cation, are shown in Fig. 2 as a function of the ionic composition of the resin at equilibrium, i.e. of the potassium fraction, x_K, of the resin phase ions. On the left of the figure are the negative ΔH values for reactions starting with the resin in the pure Li^+ form, and on the

Can. J. Chem. Downloaded from www.nrcresearchpress.com by 210.87.254.105 on 09/05/12
For personal use only.

right the positive ΔH values observed for the resin initially in the K^+ form. The ionic strengths of the exchange solutions are also indicated. The precision of the calorimetric results ranges from $\pm 2\%$ for the highest measured values to $\pm 10\%$ for the smallest. The accuracy is estimated to be also of this order.

Corrected values of the heat of exchange ($\Delta H'$) may be calculated bringing the pure or mixed resins and the solutions to standard states chosen to be equilibrium with pure water for the resins and infinite dilution for the solutions. Thus, for a reaction starting with the pure Li^+ resin (LiR) and KCl solution of molarity M and proceeding towards the mixed resin of composition x_K, we find

$$[1] \qquad \Delta H' = \Delta H - \{\varphi_{LiCl} M - \varphi_{KCl} M\} - \frac{}{x_K}\{\Delta H_{res}(LiR) - \Delta H_{res}(LiKR)\}.$$

Here the φ are the relative apparent molar heat contents of the indicated electrolyte solutions, values of which have been tabulated (9). The heat of mixing equal quantities of 1 M LiCl and KCl solutions is <20 cal/mole of salt (10); in the present calculation concerning much less concentrated solutions, the heat content of the mixed electrolyte has therefore been replaced with negligible error by the appropriate average of heat contents for the pure electrolytes. The ΔH_{res} are the heats, expressed per mole of resin cation, associated with swelling the pure LiR and the mixed resin as they pass to the standard state. A different, but sensitive, calorimeter was used to investigate these heats; in going from equilibrium with 1 M solutions to equilibrium with pure water no heats beyond experimental error could be found using the resins of different cross-linking in the pure forms (i.e. <20 cal/mole of cation). The concentrations of concern here are much less than 1 M, and hence the second correction term of eq. [1] can be omitted. $\Delta H'$ values are then found and are almost negligibly different from the ΔH values; they are shown in Fig. 2 for the two resins X16.

The main qualitative feature of the results is the rapid variation of the integral heats of exchange at the extremes of the range of ionic composition. (The differential heats would present a similar behavior.) Further points toward the middle of the composition range were obtained by using solutions at 1 M. They are not reproduced here because the corrections given by eq. [1] become rather large and may be uncertain. However, it seems clear that there is a relatively slow variation of the heats in the middle region. A decrease of the absolute value of the heat of exchange, $|\Delta H|$, with increasing uptake of the preferred K^+ ion, is in accord with (*a*) a non-uniformity of the resin arising from either local variations of cross-linking density (11) or of the nature of the exchange sites (12), or (*b*) ion-binding as in the Rice–Harris theory (13). In this theory, the decrease of selectivity, or of $|\Delta H|$ is due to the resin being able to hold cations in two states—an unbound state having no selectivity, and a bound state which accounts for the overall selectivity of the resin. Thus even for the uniform resin this model corresponds to two types of "sites" in the resin, leading to a decrease of $|\Delta H|$ with x_K as relatively more of the K^+ ions are found in the unbound state. Furthermore, the higher the degree of cross-linking the greater the fraction of ions in the bound state and the greater $|\Delta H|$ and its variation.

ΔH also changes owing to electrostatic effects and an increase of total ion-binding as x_K increases. These effects, however, have been shown in a number of examples (13) to be of lesser importance as far as selectivity is concerned. Neglecting them, simple calculations show that the ion-binding theory alone cannot give the S-shaped curves of Fig. 2 but only a "smooth" decrease of $|\Delta H|$. The shape of the curves suggests that the resin itself must be non-uniform as indicated by refs. 11 and 12.

Can. J. Chem. Downloaded from www.nrcresearchpress.com by 210.87.254.105 on 09/05/12
For personal use only.

ACKNOWLEDGMENTS

The authors are indebted to the National Research Council of Canada for financial support. We also thank Jacques-Louis Pingris and Branko Belovic, Ecole Polytechnique, Montreal, Quebec, for their contribution to the development of the experimental techniques and for numerous preliminary measurements which, however, were not used here.

REFERENCES

1. N. T. COLEMAN. Soil Sci. **74**, 115 (1952).
2. E. H. CRUICKSHANK and P. MEARES. Trans. Faraday Soc. **53**, 1289 (1957); **53**, 1299 (1957); **54**, 174 (1958).
3. G. E. BOYD, F. VASLOW, and S. LINDENBAUM. J. Phys. Chem. **68**, 590 (1964).
4. J. S. REDINHA and J. A. KITCHENER. Trans. Faraday Soc. **59**, 515 (1963).
5. R. A. EDGE. Chemist-Analyst, **47**, 72 (1958).
6. R. KUNIN. Ion exchange resins. 2nd ed. John Wiley & Sons, Inc., New York. 1958. p. 341.
7. E. CALVET. *In* Experimental thermochemistry. *Edited by* F. D. Rossini. Interscience Publishers, Inc., New York. 1956. Chap. 12.
8. E. CALVET et H. PRAT. Microcalorimétrie: applications physico-chimiques et biologiques. Masson et Cie, Paris. 1956.
9. H. S. HARNED and B. B. OWEN. The physical chemistry of electrolytic solutions. 2nd ed. Reinhold Publishing Corp., New York. 1950. p. 582.
10. T. F. YOUNG and M. B. SMITH. J. Phys. Chem. **58**, 716 (1954).
11. D. REICHENBERG and D. J. MCCAULEY. J. Chem. Soc. 2741 (1955).
12. G. E. MYERS and G. E. BOYD. J. Phys. Chem. **60**, 521 (1955).
13. S. A. RICE and F. E. HARRIS. Z. Physik. Chem. Frankfurt, **8**, 217 (1956).

Can. J. Chem. Downloaded from www.nrcresearchpress.com by 210.87.254.105 on 09/05/12
For personal use only.

Can. J. Chem. Downloaded from www.nrcresearchpress.com by 210.87.254.5 on 09/05/12
For personal use only.

THE THERMAL UNIMOLECULAR ISOMERIZATION OF 1,2-DICHLOROETHYLENE[1]

L. D. HAWTON AND G. P. SEMELUK
Chemistry Department, University of New Brunswick, Fredericton, New Brunswick

Received April 6, 1966

ABSTRACT

The thermal *cis–trans* isomerization of 1,2-dichloroethylene in a toluene carrier was found to follow first order kinetics at temperatures below 846 °K. Within the limits of detection, no decomposition was observed, but there was evidence of a surface contribution to the isomerization. The results, extrapolated to a surface to volume ratio of zero, give for the *cis* to *trans* conversion

$$k_1 = 5.7 \times 10^{12} \exp(-56\,000 \text{ cal}/RT)$$

and for the reverse action

$$k_{-1} = 4.8 \times 10^{12} \exp(-55\,300 \text{ cal}/RT).$$

It is concluded that previous investigations which did not use a radical scavenger most probably were observations of a mixture of radical chain, heterogeneous, and unimolecular contributions to the isomerization.

It has become increasingly evident in recent years that many of the *cis–trans* isomerizations originally classified as homogeneous unimolecular reactions were in fact radical-induced or heterogeneous processes. In particular, the low frequency factor – low activation energy isomerizations for which the (non adiabatic) singlet–triplet–singlet theory (1, 2) of the reaction path has been developed have become suspect. Implicit in many of the early studies is the assumption that "conditioning" the reaction vessel to obtain a reproducible reaction finally yields a homogeneous unimolecular reaction. A representative example is that of the isomerization of 1,2-dichloroethylene (3), in which it has been shown that the reproducibility achieved is very seldom better than 50% in the rate constants (4). Steel (5) has demonstrated that under these conditions the isomerization is a radical chain reaction, and that the best reproducibility in a static system is obtained by starting with a fresh "clean" surface for each reaction. A differential calorimetry study by Kapralova and Semenov (6) on the pyrolysis of 1,2-dichloroethane is probably pertinent in the understanding of these reactions. This investigation indicated that carbonizing the walls of the reactor did not completely eliminate radicals from the system, but only decreased their rate of production. At the same time, the heterogeneous contribution reached a limiting low value on a thoroughly conditioned surface.

Molera and Ariza (7) have reinvestigated the isomerization of dichloroethylene using essentially the same approach of conditioning the reactor through repeated runs in a painstaking attempt to achieve reproducibility. However, even for the "reproducible" reaction there was in the first five minutes of each experiment a significant deviation from a first order reaction. The reported rate constants are derived from the latter part of the reaction where first order behavior is observed. By choosing the lowest measured rate values at a number of temperatures they obtained an activation energy of 52.1 kcal/mole for the *cis* to *trans* conversion, and 51.6 kcal/mole for the reverse reaction. It would appear therefore that the mechanism in the early stages of the reaction differs in some way from that in the latter stages.

In view of the difficulties associated with the interpretation of data obtained under experimental conditions which allow a mixed mechanism to operate, we felt it would be

[1]*Abstracted from Part I of the Ph.D. thesis of L. D. Hawton, 1965.*

worthwhile to study the isomerization in a toluene carrier. The system we adopted differed from the conventional only in that the toluene pressure in the reactor was considerably higher than customary. These conditions should be unfavorable to the initiation of a radical chain conversion, and the higher pressure should decrease the proportion of the heterogeneous component. This approach has proven quite successful.

EXPERIMENTAL

The reduced pressure flow apparatus, attached at convenient points to a conventional high vacuum system, was similar to that employed by Szwarc (8) except that all sections carrying feed or effluent gases were wound with resistance wire and heated electrically to about 90 °C. The reservoir pressures of toluene and dichloroethylene were controlled by thermostating the reservoirs at the appropriate temperatures, and the flow of these gases and their ratio was controlled by means of capillary flow meters. The residence time within the reactors was determined by a capillary at the exit of the reactor, with the effluent being condensed and trapped just beyond the capillary in a modified Le Roy still so that the pressure in this section never exceeded 10^{-4} mm.

Two Vycor reactors were used in the study, one with an internal diameter of 5.15 cm and a volume of 201 ml for which $S/V = 0.88$ cm^{-1}, and one with an internal diameter of 1.08 cm and a volume of 199 ml for which $S/V = 3.7$ cm^{-1}. With these reactors it was possible to vary the surface to volume ratio by a factor of 4.2 but to have a nearly constant volume. The electrical resistance furnace which housed the reactors had two end "maintenance" heating coils and one control winding which extended the complete length of the furnace core. The current to the control winding was regulated by a phase-shift temperature control unit based on a design by Sturtevant (8). The control unit was actuated by a platinum resistance thermometer which constituted one arm of an electronic bridge circuit. The longitudinal temperature differences in the furnace were of the order of a few degrees, while during a run the variation at any one point within the furnace was $<0.5°$.

The duration of a "run" was typically 30 min. In this period all the effluent was collected at liquid air temperatures in the modified Le Roy still. After the completion of the run the contents of the Le Roy still were warmed and cooled repeatedly in the usual manner so that any HCl produced in the reaction would be released. This "HCl fraction" was then distilled onto a small amount of NaOH contained in a second detachable trap. The contents of this trap were subsequently dissolved in HNO_3 and the chloride concentration determined by the method of amperometric titration (9) with $AgNO_3$, which has a sensitivity of about 10^{-5} g ion.

The material remaining in the still after the "removal of HCl" was then subjected to the usual type of distillation from a Le Roy still to separate the dichloroethylene–toluene solution into a dichloroethylene-rich fraction and a toluene-rich fraction, the progress of the fractionation being followed with the help of a Consolidated Vacuum Corporation Pirani gauge. The dichloroethylene-rich portion was collected in a short narrow ampoule, sealed *in vacuo*, and set aside to await injection into the chromatograph. Although time consuming, this enrichment procedure was reliable and essentially quantitative, as indicated by control distillations of prepared mixtures of the isomers with toluene.

Baker Analyzed reagent grade toluene was fractionated, the middle third being retained. Gas chromatographic analysis showed it to contain <0.01 mole % impurities.

Eastman *cis*-1,2-dichloroethylene was subjected to two successive fractionations, the middle third portion of the first being used in the second fractionation. The middle third portion of the latter was then purified by preparative gas chromatography in a Perkin Elmer model 222 chromatograph equipped with a 10 ft long, 1 in. diameter, stainless steel column packed with 25% by weight of DC 710 silicone oil on 80–100 mesh Chromosorb W. This procedure lowered the *trans* isomer concentration from 4 mole % to less than 0.1 mole %, and reduced to a negligible concentration all other impurities. After purification, the *cis* isomer was stored over purified pyro-catechol, under a purified nitrogen atmosphere in hermetically sealed containers. When needed, the dichloroethylene was distilled from the catechol at low pressures.

Analyses were carried out on an F and M model 500 Linear Temperature Programmed gas chromatograph with the ampoules injected by an F and M model SI-4 injector, into a 10 ft column containing 25% by weight of tricresyl phosphate and 2% by weight of polyethylene glycol on 80–100 mesh Chromosorb W. When a hydrogen carrier inlet pressure of 30 p.s.i.g., a flow rate of 1.2 cc/s, and a column temperature of 115 °C were used, the *trans* isomer had a retention time of 3 min and the *cis* isomer 5 min 10s. Peak areas, which were used for quantitative analysis, were measured with a Keuffel and Esser model 4242 planimeter.

RESULTS AND DISCUSSION

A summary of experimental results appears in Tables I and II, with Arrhenius plots shown in Figs. 1 and 2. The data presented refer to a residence time of 4.8 s and a molar ratio of dichloroethylene to toluene of 3×10^{-2}, except for one experiment in which the

Can. J. Chem. Downloaded from www.nrcresearchpress.com by 210.87.254.5 on 09/05/12
For personal use only.

ratio was increased to 10^{-1} as a check on the reaction order with respect to dichloroethylene. The rate constants were calculated from the integrated form of the rate law for reversible first order reactions (9)

$$[1] \qquad k_1 + k_{-1} = \frac{1}{t} \ln \frac{x'_e}{x'_e + x},$$

where k_1 is the rate constant for the forward reaction (*cis* to *trans*), k_{-1} is the rate constant for the reverse reaction and x is the amount (in terms of partial pressure) of *cis* isomer converted to *trans* during the residence time t. The quantity x'_e is given by

$$[2] \qquad x'_e = \frac{K\alpha - \beta}{K + 1},$$

where $K = k_1/k_{-1}$ is the equilibrium constant for the isomerization, α is the initial pressure of *cis* isomer, and β is the initial pressure of the *trans* isomer. The equilibrium constant K was calculated from the appropriate thermodynamic functions which Pitzer and Hollenberg have derived from spectroscopic and other data (10). Since the *cis* isomer was almost exclusively used, the reverse rate constant k_{-1} reported here is actually the

TABLE I

Rate constants for the *cis–trans* isomerizations of 1,2-dichloroethylene for pressure = 3.9 ± 0.1 cm, reactor volume = 200 ± 2 ml, [*cis*]/[toluene] = 3×10^{-2}

	S/V = 3.7 cm^{-1}		S/V = 0.88 cm^{-1}		S/V = 0 (extrapolated)	
Temp. (°K)	$k_1 \times 10^3$ (s^{-1})	$k_{-1} \times 10^3$ (s^{-1})	$k_1 \times 10^3$ (s^{-1})	$k_{-1} \times 10^3$ (s^{-1})	$k_1 \times 10^3$ (s^{-1})	$k_{-1} \times 10^3$ (s^{-1})
806	4.24	5.45	3.78	4.86		
	4.42	5.68	3.78	4.86	3.65	4.70
			3.84	4.94		
826	10.02	12.76	8.96	11.41		
	10.22	13.01	8.96	11.41	8.62	10.98
846	21.18	26.71	18.73	23.61		
	20.68	26.08	19.85	25.03	18.67	23.54
			18.87	23.80		
			19.31*	24.35*		

*Result obtained when mole ratio of dichloroethylene to toluene was increased to 10^{-1}.

TABLE II

Parameters in the Arrhenius equation $k = A\ e^{-E/RT}$ s^{-1}.

	S/V = 3.7 cm^{-1}		S/V = 0.88 cm^{-1}		S/V = 0 (extrapolated)	
	$A \times 10^{12}$ (s^{-1})	E (kcal/mole)	$A \times 10^{12}$ (s^{-1})	E (kcal/mole)	$A \times 10^{12}$ (s^{-1})	E (kcal/mole)
k_1	2.0	54.1	4.2	55.4	5.7	56.0
k_{-1}	1.7	53.4	3.5	54.8	4.8	55.3

"reflection" of the forward constant through this equilibrium constant, and therefore, contains the errors of both k_1 and K. However, a few check runs carried out by using 99.5 mole % *trans* isomer and the same method of calculation gave values of k_1 and k_{-1} not significantly different from those listed. The rate constants for the two reactors having different S/V values are listed in Table I along with the values extrapolated to $S/V = 0$, according to the procedure outlined below. Table II give the Arrhenius parameters for the

Can. J. Chem. Downloaded from www.nrcresearchpress.com by 210.87.254.5 on 09/05/12
For personal use only.

forward and reverse reactions obtained by the method of least squares. The Arrhenius plots of these data are shown in Figs. 1 and 2 in order to illustrate the remarkable reproducibility which can be achieved with this experimental approach. The results obtained were independent of the order with respect to temperature in which the runs were made, but the reactors may be considered "conditioned" since a toluene–dichloroethylene feed mixture had been previously passed through for a short time. Many of the runs listed in Table I are consecutive ones, and do not represent "best" values selected from different experimental sequences, which has been the questionable practice of some previous investigators.

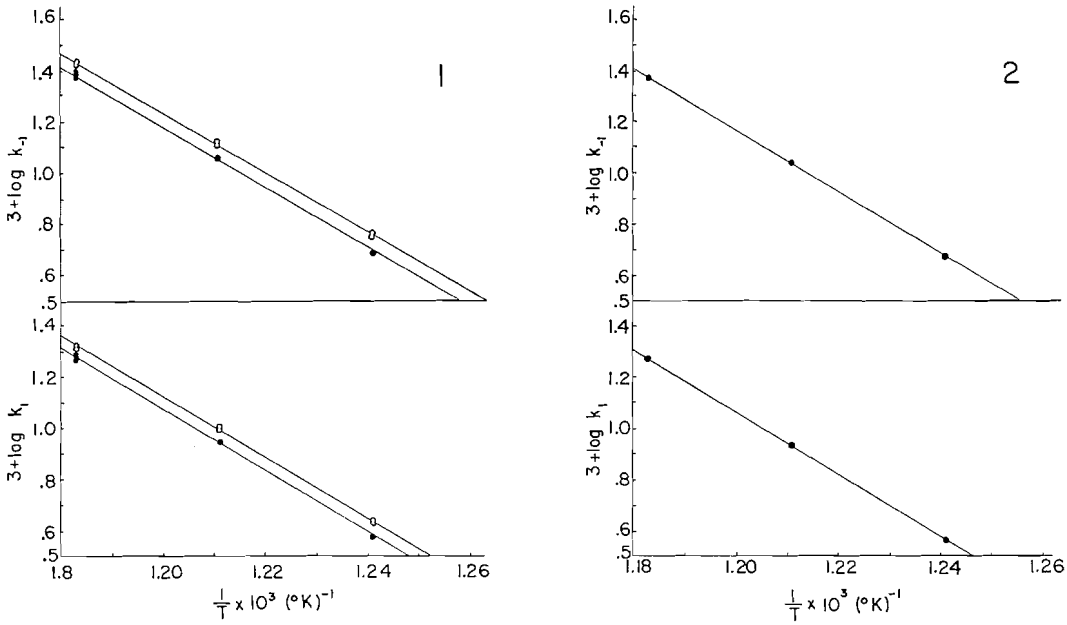


FIG. 1. Arrhenius plots of the data given in Table I: ○, $S/V = 3.7$ cm^{-1}; ●, $S/V = 0.88$ cm^{-1}.
FIG. 2. Arrhenius plots of the data given in Table I for $S/V = 0$ cm^{-1}.

Since it was obvious from the results obtained in the two reactors of different S/V values that there was a heterogeneous isomerization, the results were extrapolated to $S/V = 0$, according to the following considerations:

At the temperature and pressures used in this study, it is reasonable to assume that only a monolayer adsorption would be important, and that the extent of surface coverage would be very small. On this basis one would expect the total material adsorbed at a constant pressure to be proportional to the surface area. Since there are two unimolecular components in this reaction, the completely homogeneous and the purely heterogeneous, the rate equation can be expressed

$$[3] \qquad \text{Rate} = k_{obs}[cis]_g = k_{het}(cis)_s + k_{homo}[cis]_g,$$

where k_{obs} is the rate constant obtained directly from the experimental data, k_{het} and k_{homo} are the rate constants for the heterogeneous and homogeneous components respectively, $[cis]_g$ is the concentration or partial pressure of the *cis* isomer in the gas phase,

Can. J. Chem. Downloaded from www.nrcresearchpress.com by 210.87.254.5 on 09/05/12
For personal use only.

and $(cis)_s$ the quantity adsorbed on the surface. Further, because of monolayer adsorption, we may assume that the following relationship holds

[4] $$(cis)_s = b[cis]_g$$

where b is a proportionality factor. Putting this into [3] gives

[5] $$k_{obs} = bk_{het} + k_{homo}$$

and taking logarithms

[6] $$\ln k_{obs} = \ln \{k_{homo} + bk_{het}\}$$
$$= \ln k_{homo} + \ln \left\{1 + b\frac{k_{het}}{k_{homo}}\right\}.$$

Since the contribution from the heterogeneous reaction is small and decreases as S/V becomes smaller, this equation becomes

[7] $$\ln k_{obs} = \ln k_{homo} + b\frac{k_{het}}{k_{homo}}$$
$$= \ln k_{homo} + \frac{k_{het}}{k_{homo}} \cdot \frac{(cis)_s}{[cis]_g}.$$

Then, in any experiments which differ only in S/V values, but which have the same constant volume, the concentration of *cis* isomer in the gas phase is constant, and therefore the amount of *cis* isomer on the surface is proportional to the surface area of the reactor. Therefore a plot of $\ln k_{obs}$ versus surface area, or S/V (for reactors having equal volumes) will give a straight line as $S/V \rightarrow 0$. This extrapolation to $S/V = 0$ is readily recognized as being equivalent to an extrapolation to $(cis)_s = 0$. The value of k obtained from this extrapolation will be that for the purely homogeneous component.

The present study indicates that the effect of the heterogeneous component is to decrease both the observed activation energy and the pre-exponential factor of the rate constant. As a consequence of these observations, it is not surprising that the activation energies reported by Molera and Ariza are somewhat lower than those observed in this investigation. In fact, the activation energies which are noted in Table II are, to the best of our knowledge, the highest ever reported for this isomerization. It seems possible that the reaction observed by Molera and Ariza contained not only a homogeneous and heterogeneous component, but quite probably a radical-induced isomerization as well. This latter is indicated by the presence of both HCl and heavy products in their experiments. HCl was determined by the Volhard method, which is somewhat less sensitive than the amperometric titration method used in the present study. We estimate the extent of decomposition in our study to be <0.6 mole %. Neither HCl nor any other decomposition product was detected in any experiment.

Although the lower activation energies for the isomerizations reported by Molera and Ariza are readily explained as being due to contributions from heterogeneous and radical chain mechanisms, it is not entirely clear why their pre-exponential factors should be so high (10^{15} s^{-1}). Indeed, it is uncertain whether or not any significance should be attributed to them. If an explanation is sought, the clue may lie in the differences in pressure used in the two studies. Thus, our experiments were performed at pressures no greater than 4 cm Hg, while the static system studies used pressures as great as 35 cm. A classical explanation of high pre-exponented factors at such pressures has been advanced (11), which would imply that our investigations were carried out in the region of the transition

Can. J. Chem. Downloaded from www.nrcresearchpress.com by 210.87.254.5 on 09/05/12
For personal use only.

pressure where the rate of isomerization would be limited by the frequency of bimolecular collision. However, the evidence from other isomerization studies on similar molecules indicates that this is unlikely. Thus, the pre-exponential factor for the isomerization of *trans*-dideuteroethylene has been reported (12) as 3.3×10^{12} s^{-1} in substantially the same pressure region. Similarly, the isomerization of *cis*-butene-2 which has many more degrees of freedom, gives a "high pressure" pre-exponential factor in the range 6.1×10^{13} s^{-1} (13) to 10^{14} s^{-1} (14).

The results of our study suggest it may be possible to use the toluene carrier technique in isomerization investigations of other ethylenic derivatives in which radical chain contributions are suspected, especially those in which relatively reactive radicals may be formed. Although it is possible to isolate the homogeneous unimolecular isomerization reaction with this technique, it may not be readily adaptable to the testing of theories of unimolecular reactions. However, it could give a reliable estimate of the potential barrier to isomerization in the ground electronic state.

ACKNOWLEDGMENT

The authors gratefully acknowledge financial assistance from the National Research Council of Canada.

REFERENCES

1. J. L. MAGEE, W. SHAND, and H. EYRING. J. Am. Chem. Soc. **63**, 677 (1941).
2. R. B. CUNDALL. The kinetics of cis–trans isomerizations. *In* Progress in reaction kinetics. Vol. 2. *Edited by* G. Porter. The Pergamon Press, Ltd., London. 1964.
3. J. L. JONES and R. L. TAYLOR. J. Am. Chem. Soc. **62**, 3480 (1940).
4. B. S. RABINOVITCH and M. J. HULATT. J. Chem. Phys. **27**, 592 (1957).
5. C. STEEL. J. Phys. Chem. **64**, 1588 (1960).
6. G. A. KAPRALOVA and N. N. SEMENOV. Zh. Fiz. Khim. **37**, 35 (1963).
7. M. J. MOLERA and E. ARIZA. Anales Real Soc. Espan. Fis. Quim. Madrid, Ser. B, **54**, 247 (1958).
8. M. SZWARC. J. Chem. Phys. **16**, 128 (1948).
9. K. J. LAIDLER. Chemical kinetics. 1st ed. McGraw-Hill Book Co. of Canada, Ltd., Toronto. 1950.
10. K. S. PITZER and J. L. HOLLENBERG. J. Am. Chem. Soc. **76**, 1493 (1954).
11. C. STEEL and K. J. LAIDLER. J. Chem. Phys. **34**, 1827 (1961).
12. J. E. DOUGLAS, B. S. RABINOVITCH, and F. S. LOONEY. J. Chem. Phys. **23**, 315 (1955).
13. B. S. RABINOVITCH and K. W. MICHEL. J. Am. Chem. Soc. **81**, 5065 (1959).
14. R. B. CUNDALL and T. F. PALMER. Trans. Faraday Soc. **57**. 1936 (1961).

Can. J. Chem. Downloaded from www.nrcresearchpress.com by 210.87.254.5 on 09/05/12
For personal use only.

Can. J. Chem. Downloaded from www.nrcresearchpress.com by 210.87.254.40 on 09/05/12
For personal use only.

PHOTOLYSIS OF GROUP VI HYDRIDES

I. SOLID H_2S, H_2S_2, AND D_2S

D. A. STILES, W. J. R. TYERMAN, O. P. STRAUSZ, AND H. E. GUNNING
Department of Chemistry, University of Alberta, Edmonton, Alberta

Received May 2, 1966

ABSTRACT

The primary photochemical step occurring in solid H_2S, D_2S, or H_2S_2 was shown to be loss of a hydrogen or deuterium atom. Electron spin resonance spectra are assigned to HS, DS, and HS_2, which have not previously been detected in the solid phase, and behavior of these radicals on warming the samples is described. When H_2S and D_2S matrices were warmed from 77 to 125 °K, the HS and DS spectra collapsed into a doublet and singlet respectively. The hyperfine splitting in HS increased and both signals appeared at lower average g-values than when anisotropically broadened at 77 °K.

INTRODUCTION

Much attention has been devoted to the gas phase photochemistry of the Group VI hydrides as these compounds may readily be prepared and handled and, further, show simple effects of changing atomic number and size of the heavy atom. Photolysis of H_2S vapor ($\lambda > 2\,000$ Å) has been monitored by kinetic spectroscopy (1, 2) and undoubtedly the primary process is

[1] $$H_2S \rightarrow H + HS$$

Abstraction from the substrate and disproportionation of HS subsequently form H_2

[2] $$H + H_2S \rightarrow H_2 + HS$$

[3] $$HS + HS \rightarrow H_2 + S_2$$

The activation energy of reaction [2] is unknown. However, by comparison with results for mercaptans (3) the value is likely to be >5 kcal/mole, which would almost certainly preclude its occurrence at 77 °K. In addition to the intense absorption spectrum of ground state S_2, a weak band system at longer wavelengths was noted in the flash photolysis experiments. This persists for $\sim$100 μs and may be assigned to HS_2, since it is present strongly in flashed H_2S_2 (4). However, the exact course of processes forming HS_2 in flashed H_2S has not yet been determined.

Reaction [2] has been exploited in gas phase electron spin resonance (e.s.r.) studies of the radicals HS or DS, in which products of an electric discharge through H_2 or water vapor were mixed with H_2S or D_2S in specially designed spectrometer cavities. Electron spin resonance absorption was detected and assigned to HS (5, 6) and DS (5), each in the lowest rotational state, $^2\Pi_{3/2}(J = 3/2)$; e.s.r spectroscopy of molecules with smaller moments of inertia is complicated by the large array of rotational states and sub-levels populated in the gas phase. It is therefore convenient to study such species in the solid state, where rotation is restricted, although less information about the molecular parameters is obtained since the energy levels are 'broadened' by anisotropy. It is a further advantage that many radicals persist for long periods when trapped in solid matrices, particularly at low temperatures.

We have irradiated H_2S ($\lambda > 2\,200$ Å), both pure and in various matrices, in order to characterize the primary photolytic steps at 77 °K and to identify e.s.r. spectra of the radicals so formed. Earlier results from this laboratory (7) showed that sulfur atoms

and S_2, produced by photolysis of COS, polymerized rapidly to long chains of about 10^3 atoms. Emphasis in this investigation was therefore placed on the effects of different matrix materials on migration and subsequent reactions of the radicals. Acetylene, ethylene, and *trans*-2-butene were employed as reactive matrices, in an attempt to study some simple organic sulfide radicals. Additional experiments were performed with samples of H_2S_2 and D_2S, in order to accumulate further evidence concerning the photolytic steps of sulfur hydrides.

RESULTS

A pale yellow coloration formed during photolysis ($\lambda > 2\,200$ Å) in pure samples of H_2S, D_2S, and H_2S_2. No coloration or e.s.r. signals were observed in samples exposed to light filtered through Corex glass which transmits $\lambda > 2\,800$ Å. With the filter removed from the light path, all samples developed e.s.r. spectra (A, B, C, or D) during irradiation at 77 °K (Figs. 1–3), of which the principal features are listed in Table I. Substantially the same signals were present in irradiated H_2S (100%) and H_2S in inert matrices (20% in Xe or 1%, 20% in C_3F_8). In a sample of H_2S (1% in Xe) the spectrum B was enhanced slightly relative to spectrum A. Additional diffuse signals in the region of $g = 2.04$ appeared in samples of H_2S in 'reactive' matrices (1% in C_2H_2, C_2H_4, or *trans*-2-butene) but the spectra were very weak, even after prolonged periods of irradiation.

In an attempt to detect short-lived precursors of the observed radicals, some samples were irradiated in the microwave cavity. However, no differences were apparent in the relative intensities of spectral lines, and no new signals were detected. The spectra in irradiated samples persisted for several weeks on storing at 77 °K.

Significant changes occurred in the observed e.s.r. spectra of all samples, when the temperature was raised above 77 °K and the effect of different matrix materials on the fragments from H_2S was studied in detail. Interpretation in some experiments was handicapped by overlapping of lines when two or more radicals were present. When samples of irradiated H_2S (100%) were warmed to 125 °K, the spectrum illustrated in Fig. 4 was observed. Quite different behavior was noted in a sample of H_2S (20%) in a xenon matrix. On warming this sample to 100 °K, the outer lines of spectrum A decayed markedly, while the central line and spectrum B increased in relative intensity. A three-line spectrum without hyperfine structure remained at 110 °K, which degenerated

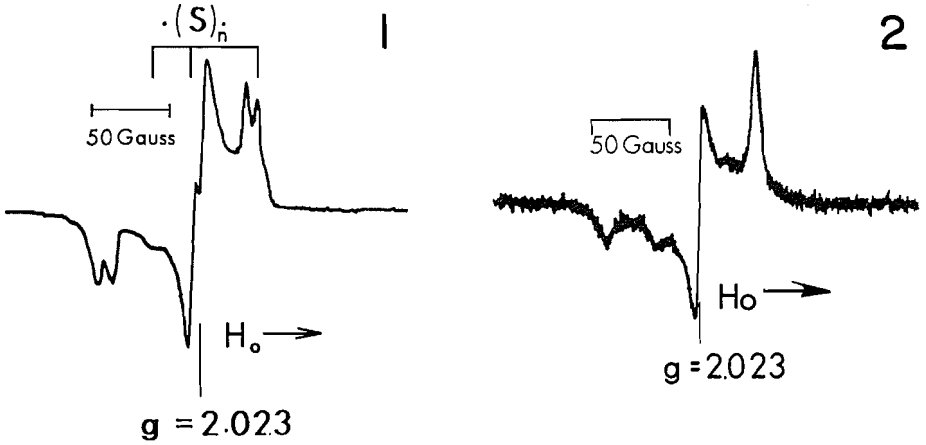


FIG. 1. Spectrum (e.s.r.) obtained from H_2S (100%) after 24 h irradiation.
FIG. 2. Spectrum (e.s.r.) obtained from D_2S (100%) after 24 h irradiation.

Can. J. Chem. Downloaded from www.nrcresearchpress.com by 210.87.254.40 on 09/05/12
For personal use only.

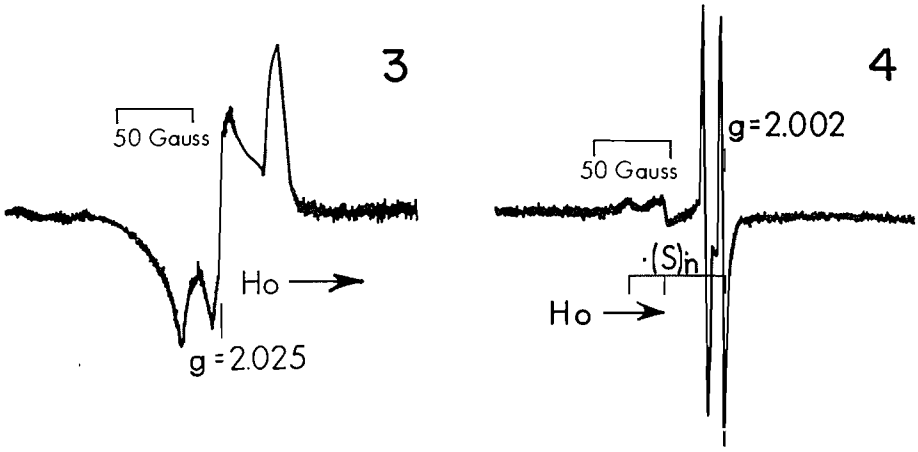


FIG. 3. Spectrum (e.s.r.) obtained by photolysis of H_2S_2 (100%) at 77 °K.
FIG. 4. Spectrum (e.s.r.) of irradiated H_2S (100%) after warming the sample to 125 °K.

TABLE I

Spectra (e.s.r.) from sulfides irradiated at 77 °K

Substrate	Matrix	Description	Experimental g-values	Assignment	
H_2S	100%	Three strong lines with hyperfine splitting	2.002, 2.004 2.019, 2.023, 2.024, 2.027 2.057, 2.064	HS	(A)
	Xe (20%) C_3F_8	Weak underlying signals	2.043	·(S)$_n$·	(B)
D_2S	100%	Three strong lines	2.003 2.022, 2.027 2.062	DS	(C)
		Weak underlying signals	2.043	·(S)$_n$·	(B)
H_2S_2	100%	Three strong lines	2.003 2.022, 2.027 2.043	HS_2	(D)
H_2S	100% (125 °K)	Single intense lines Weak structure	2.002, 2.008	HS ·(S)$_n$·	
D_2S	100% (125 °K)	Single intense line Weak structure	2.002	DS ·(S)$_n$·	

into a single line at 120 °K, but reverted to the three lines on recooling to 77 °K. At ~140 °K, a broad weak signal appeared at lower fields, and the central spectrum decayed, suggesting that the temperature was near the melting point of the matrix (m.p. of Xe, 153 °K).

There was little alteration of the spectra on warming the D_2S sample to 110 °K. At 125 °K, however, we observed rather similar changes to those detected in H_2S. Spectrum B increased in relative intensity, while spectrum C apparently had collapsed into a single line at $g = 2.00$. On recooling to 77 °K, the original three-line spectrum (C) reappeared in place of the single line, while spectrum B was altered little. By 140 °K, the spectra had decayed almost completely. The spectrum from H_2S_2 gradually decayed as the temperature was raised, without significant changes in relative intensities of the lines.

Can. J. Chem. Downloaded from www.nrcresearchpress.com by 210.87.254.40 on 09/05/12
For personal use only.

Can. J. Chem. Downloaded from www.nrcresearchpress.com by 210.87.254.40 on 09/05/12
For personal use only.

DISCUSSION

Assignment of Electron Spin Resonance Spectra

The intense three-line spectra from H_2S (A) and D_2S (C) appear at the same average g-values, within uncertainty of measurement (Table I). A three-line spectrum is characteristic of randomly orientated molecules possessing anisotropic g-tensors. (8) The hyperfine structure (h.f.s.) of A is consistent with that of a radical containing a single proton, and therefore spectra A and C are assigned, respectively, to HS and DS. The magnetic moment of a deuteron is 31% of that of a proton, and therefore the three line h.f.s. due to D($I = 1$) in DS is much smaller than that due to H in HS, and was not resolved in these experiments, or in the gas-phase work (5). The average h.f.s. in HS is 7 G, which is comparable with the gas-phase value of 5.4 G (5). To a first approximation, the h.f.s. is in direct proportion to the spin carried in the 1s orbital of the proton (9). Since the nuclear splitting of free H is 505 G, we estimate that 1.5% of the spin in HS resides in the 1s orbital of H. The Λ splitting in the spectrum (190 G for HS in the gas phase) was not detected, and its absence is attributed to decoupling of orbital and spin angular momenta of HS in the field of neighboring molecules.

The e.s.r. spectrum observed after photolysis of H_2S_2 has a rather similar appearance to the spectrum assigned to sulfur chains (7), which has principal g-values of 2.002, 2.028, and 2.042. However, the central line of the spectrum reported here lies at $g = 2.025$, differing from the position of the $\cdot(S)_n\cdot$ line by an amount greater than experimental errors. Although h.f.s. was not observed, this spectrum is assigned to HS_2, which is known to form, together with HS, in flashed H_2S_2 vapor (3). Absence of h.f.s. is consistent with a crude model of HS_2 built from S_2 by adding H$\cdot$ to one of the two equivalent orthogonal non-bonding orbitals. The single electron in the other non-bonding orbital of such a model then has zero interaction with the proton. However, a similar model predicts zero h.f.s. in HS; the observed h.f.s. is presumably due to configurational interaction of a type similar to that responsible for the h.f.s. in hydrocarbon radicals. An additional weak signal (B) was present in irradiated H_2S and D_2S, which could correspond to the low-field component of either HS_2 or $\cdot(S)_n\cdot$, the other lines being obscured by the more intense HS or DS spectra. Unequivocal distinction between these carriers is impossible here, since the spectra are very weak. Sulfur polymers form in much greater yield than HS_2 when H_2S is photolyzed in the gas phase, supporting our assignment of this spectrum to $\cdot(S)_n\cdot$. During warm-up experiments, the overall intensity of the spectra decreased greatly, with a corresponding decrease in the precision with which line positions could be measured. However, there is little doubt that sulfur chains are responsible for the three-line spectrum that appeared, although the warm-up behavior was rather different from that of $\cdot(S)_n\cdot$ formed in photolyzed COS (7). The warm-up characteristics of HS, DS, and $\cdot(S)_n\cdot$ will be discussed as matrix effects.

Primary Photochemical Processes

Evidence presented thus far characterizes photolysis of H_2S or D_2S as loss of H or D, which must dimerize rapidly at 77 °K, since no resonance of the free atoms was detected. Although the HS and DS spectra did not decay during several weeks storage at 77 °K, sulfur polymers were present after very short periods of irradiation, which suggests that HS and DS are generated in at least two types of lattice size, from one of which rapid chemical or physical migration is possible, prior to disproportionation (reaction [3]). The products of this reaction bear ~42 kcal/mole of excess energy (10) which may induce local melting of the matrices facilitating polymerization of S_2.

It is not possible to distinguish directly between two types of scission that might occur in H_2S_2

[4] $$H_2S_2 \xrightarrow{h\nu} HS + HS$$

[5] $$H_2S_2 \xrightarrow{h\nu} HS_2 + H$$

since HS formed in [4] might rapidly be consumed in the reaction

[6] $$HS + H_2S_2 \rightarrow H_2S + HS_2$$

Experiments with H_2S showed that the disproportionation of HS radicals (reaction [3]) is rapid; therefore, if [4] is important, sulfur chains should be detected in photolyzed H_2S_2, together with HS_2. In the gas phase photolysis, HS was observed strongly, as well as HS_2, indicating that reaction [5] is, at best, moderately fast at room temperature. It appears that the primary step in the solid-phase photolysis of H_2S_2 is S—H cleavage, even though dissociation to 2HS is ~30 kcal/mole less endothermic (10).

Matrix Effects

Surrounding molecules interact with radicals in what may broadly be described as physical or chemical processes. Physical effects of warming matrices have been discussed by Ingram (11) and are divided into transport phenomena (alterations in the freedom of motion and rotation of the radicals) and changes in the intermolecular interaction parameters with temperature. An interesting example of these effects is presented by the HS and DS radicals. On warming the H_2S or D_2S matrices to 125 °K, the spectra degenerated respectively into a doublet and a single line at *g*-values much lower than the average values measured at 77 °K (Table I). When the samples were recooled to 77 °K, the original three-line spectra reappeared, showing that this was indeed a physical effect, and not a chemical one. The collapse of a three-line spectrum into a single line is typical of a radical starting to rotate in a lattice as the temperature is raised. In addition to the change in the average *g*-value, the h.f.s. in HS increased to 10 G at 125 °K, suggesting that the spin of the unpaired electron was increasingly resident in the 1s orbital of the H atom. Both these effects indicate that changes occur in the coupling of the angular momenta associated with the spin and orbitals of the HS, caused by alterations of the interactions with neighboring molecules. However, no differences in the h.f.s. were detected in different matrices at 77 °K. As intermolecular forces become less important, the molecular *g*-value of HS changes to a value of 0.8739, observed in the gas phase (6), i.e. the changes shown in Table I are much smaller than those on changing from the gas to the solid phase.

Further changes in e.s.r. spectra of the samples in inert lattices (H_2S, Xe, or C_3F_8) are classified as chemical, and seem to be associated with increased ease of radical migration through the matrix at temperatures above 77 °K. Thus HS and DS decay forming sulfur chains, presumably via reaction [3], and subsequent polymerization of S_2. Sulfur chains in these matrices decayed at lower temperatures than those reported for decay of $\cdot(S)_n\cdot$ in photolyzed COS (7), and this may be due to processes such as

[7] $$\cdot(S)\cdot_n + HS \rightarrow \cdot(S)_nSH$$

No attempt was made to analyze photolyzed mixtures for polysulfides.

The excess energy with which S_2 or Se_2 are formed in matrices apparently determines their rates of polymerization. We have studied several systems in which sulfur (7) or

Can. J. Chem. Downloaded from www.nrcresearchpress.com by 210.87.254.40 on 09/05/12
For personal use only.

selenium (12) chain polymers were produced via these species and the intermediate was detected only in photolyzed COSe (12). The reaction

[8] $$COSe + Se(4^3P) \rightarrow CO + Se_2$$

is probably almost thermoneutral, and the Se_2 apparently remains trapped in the matrix. When S_2 or Se_2 were formed by exothermic processes, only chain polymers were detected by e.s.r. spectroscopy. It will be interesting to determine whether disproportionation of HSe or HTe leads to stable or labile Se_2 or Te_2.

Limited information can be derived from the experiments in which H_2S was irradiated in chemically reactive matrices (C_2H_2, C_2H_4, or *trans*-2-butene), since the new spectra are very weak. Each sample displayed the HS spectrum quite strongly, with diffuse underlying structure at *g*-values above 2.00. No spectra could be assigned to hydrocarbon radicals, which are known to react rapidly with H_2S at 195 °K (13). The high *g*-values of the observed weak lines indicate that the carriers had their spins largely associated with a sulfur atom, and not a carbon atom. However, the spectra detected in irradiated sulfides are quite different (14, 15). At 77 °K, HS reacts much more slowly with the hydrocarbons than at 195 °K, which is consistent with trapping of the radicals at lattice sites in the solid phase.

EXPERIMENTAL

The main features of our experimental techniques have been reported (7, 12). Electron spin resonance spectra were obtained as the first derivative of the resonance absorption using a Varian V4502 spectrometer, operating at a nominal frequency of 9.5 Gc/s and fitted with a dual cavity (V4532) and other Varian accessories, previously described (12). Spectra were calibrated with respect to the three lines of Fremy's salt (16).

Samples were prepared in conventional high-vacuum systems, care being taken to avoid interaction of H_2S_2 with mercury or metal surfaces. Pure compounds and mixtures were distilled into quartz sample tubes at 77 °K, degassed and sealed off under vacuum, before irradiation at 77 °K in a quartz Dewar. Most samples were photolyzed externally by a Hanovia medium-pressure mercury lamp, emitting discontinuous light ($\lambda > 2\,200$ E). Other samples were irradiated in the cavity of the spectrometer by the output of an Osram high-pressure mercury arc.

Spectra of photolyzed mixtures were first obtained at 77 °K, after which warm-up experiments were performed, in which the temperature of a sample in one cavity was raised above 77 °K, using a Varian (V4547), variable temperature device.

Materials

Hydrogen sulfide was prepared by the reaction of dilute sulfuric acid with 'Analar' sodium sulfide and distillation of the product at 140 °K. Mass spectral analysis showed that the H_2S obtained in this way contained less than 0.25% H_2O. H_2S_2 was prepared by the method described by Féher (17), and distilled carefully in a metal-free vacuum apparatus.

The Xe was Airco assayed reagent grade. Acetylene and perfluoropropane (Matheson) were purified by distillation on the vacuum line and exhibited satisfactory mass spectra. Ethylene and *trans*-2-butene (Phillips research grade) were used without further purification. D_2S was obtained from Merck, Sharp and Dohme of Canada Ltd. Care was taken to deal always with a large quantity of D_2S in order to minimize effects of equilibration with water absorbed on Pyrex surfaces.

CONCLUSION

The primary photolytic step in H_2S, D_2S, and H_2S_2 ($2\,800 > \lambda > 2\,200$ Å) is loss of a hydrogen atom. Electron spin resonance spectra were assigned to HS, DS, and HS_2. Sulfur chains are formed on warming mixtures containing HS or DS; these decay rapidly, possibly by reaction with HS or DS.

New spectra were observed weakly when H_2S was photolyzed in unsaturated hydrocarbon matrices, although reaction of HS with these compounds was slow at 77 °K. The radicals apparently have free spins associated with S rather than C atoms, and are different from those detected in irradiated sulfides.

Can. J. Chem. Downloaded from www.nrcresearchpress.com by 210.87.254.40 on 09/05/12
For personal use only.

ACKNOWLEDGMENTS

We thank the National Research Council of Canada for financial support, and Mr. M. deSorgo for the preparation of H_2S_2.

REFERENCES

1. G. PORTER. Discussions Faraday Soc. **9**, 60 (1950).
2. P. FOWLES, M. DESORGO, O. P. STRAUSZ, and H. E. GUNNING. To be published.
3. G. GREIG and J. C. J. THYNNE. Trans. Faraday Soc. **62**, 379 (1966).
4. M. DESORGO, O. P. STRAUSZ, and H. E. GUNNING. To be published.
5. C. C. MCDONALD. J. Chem. Phys. **39**, 2587 (1963).
6. H. E. RADFORD and M. LINZER. Phys. Rev. Letters, **10**, 443 (1963).
7. D. A. STILES, R. KEWLEY, O. P. STRAUSZ, and H. E. GUNNING. Can. J. Chem. **43**, 2442 (1965).
8. J. R. MORTON, J. R. ROWLANDS, and D. H. WHIFFEN. Atomic properties for interpreting e.s.r. data. National Physical Laboratory Publication. August 1962.
9. K. F. KNEUBÜHL. J. Chem. Phys. **33**, 1074 (1960).
10. H. MACKLE. Tetrahedron, **19**, 1159 (1963).
11. D. J. INGRAM. Free radicals as studied by e.s.r. Butterworths, London, 1958.
12. D. A. STILES, W. J. R. TYERMAN, O. P. STRAUSZ, and H. E. GUNNING. Can. J. Chem. **44**, 1677 (1966).
13. O. P. STRAUSZ, T. HIKIDA, and H. E. GUNNING. Can. J. Chem. **43**, 717 (1965).
14. J. J. WINDLE, A. K. WIERSEMA, and A. L. TAPPEL. J. Chem. Phys. **41**, 1996 (1964).
15. D. A. STILES, O. P. STRAUSZ, and H. E. GUNNING. To be published.
16. G. E. PAKE, J. TOWNSEND, and S. I. WEISSMAN. Phys. Rev. **85**, 682 (1952).
17. F. FÉHER. Handbook of preparative inorganic chemistry. Vol. I. 2nd ed. *Edited by* G. Brauer. Academic Press, Inc., New York. 1963.

Can. J. Chem. Downloaded from www.nrcresearchpress.com by 210.87.254.40 on 09/05/12
For personal use only.

Can. J. Chem. Downloaded from www.nrcresearchpress.com by 210.87.254.40 on 09/05/12
For personal use only.

EQUILIBRIUM CONSTANTS OF ZINC(II) AND COPPER(II) WITH HEMATOPORPHYRIN IX

D. A. Brisbin and R. J. Balahura
Department of Chemistry, University of Waterloo, Waterloo, Ontario
Received October 14, 1965

ABSTRACT

Equilibrium constants have been measured for the following displacement reactions between copper(II) and zinc(II) with hematoporphyrin IX.

$Zn^{++} + PH_2 \leftrightarrows ZnP + 2H^+$ in aqueous solution at pH 7

$Cu^{++} + PH_4^{++} \leftrightarrows CuP + 4H^+$ in glacial acetic acid solution.

Preliminary measurements have also been made for the reactions of Mn(II) and Co(II) with hematoporphyrin IX in glacial acetic acid solutions.

INTRODUCTION

Metalloporphyrins play an important role as iron complexes in the hemoproteins, as magnesium complexes in chlorophylls and as a cobalt complex in vitamin B_{12}.

The porphyrin nucleus is a tetradentate ligand which in coordination with metallic cations loses the two protons from the pyrrole nitrogen atoms, leaving two negative charges distributed about the inner ring.

Monovalent metallic complexes (Na_2P, Li_2P, etc.) are known to be of low thermodynamic stability, with the cations probably sitting one above and one below the plane of the nucleus. Divalent metallic ions such as Co(II), Ni(II), and Cu(II) form neutral square planar chelates. Mg(II), Cd(II), and Zn(II) are able to add on another ligand and form a pentacoordinate complex of a square pyramidal structure, whereas Fe(II), Co(II), and Mn(II) are able to add two extra ligand molecules and form distorted octahedral complexes.

Note is made of some of the excellent review articles which discuss the structure and properties of the porphyrin complexes (1–5) and of several pertinent books (6–9).

Since the pyrrole pigments occur in essentially aqueous environments in living cells, it would be preferable to obtain data on their formation and stability constants in this medium. Their low solubility in water has prevented much quantitative measurements in this medium, and what information is available is in essentially nonaqueous or aqueous detergent solutions.

Porphyrins, unlike many ligands, require a sizeable activation energy to incorporate metal ion, and the rate of incorporation depends on the type of solvent, the particular metal, and the porphyrin being used.

Studies of replacement and dissociation reactions of metalloporphyrins have provided many qualitative estimates of relative stabilities (10–13). However, for the stability constant,

$$K_s = \frac{[MP]}{[M^{++}][P^{=}]},$$

where [MP], [M^{++}], and [$P^{=}$] are the concentrations of the complex, metal ion, and dianionic porphyrin species respectively, the only published figure is $\log K_s = +29$,

estimated for the zinc chelate of mesoporphyrin dimethyl ester in 0.25% cetyltrimethylammonium bromide solution at room temperature (14). In the absence of acid pK data for mesoporphyrin the value of 32 for the pK_1 plus pK_2 of aetioporphyrin was used in the above estimation (15).

Our present work has been concerned with obtaining quantitative measurements for the equilibrium constants of Zn(II) and Cu(II) with hematoporphyrin IX by a spectrophotometric method. These constants can then be translated into semiquantitative stability constants.

The convention of Phillips (16) of expressing both acidity and basicity of the porphyrin nucleus in terms of the negative logarithm of the acid dissociation constant has been used here.

pK values are defined as

$$pK_1 = pH - \log [P^{=}]/[PH^{-}] \qquad pK_2 = pH - \log [PH^{-}]/[PH_2]$$

$$pK_3 = pH - \log [PH_2]/[PH_3^{+}] \qquad pK_4 = pH - \log [PH_3^{+}]/[PH_4^{++}]$$

where pK_1 and pK_2 refer to the acidic equilibria involved in dissociation of protons from the pyrrole nitrogen (—NH—) and pK_3 and pK_4 to the basic equilibria associated with the addition and loss of protons to the pyrrolenine nitrogens (=N—). The structure of hematoporphyrin IX is shown in Fig. 1.

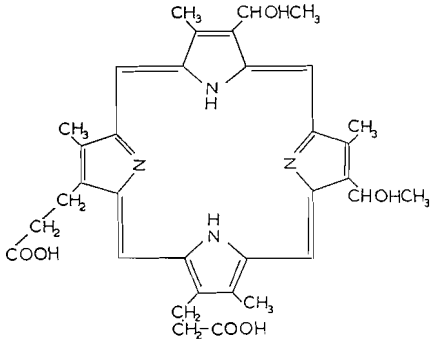


FIG. 1. Structure of hematoporphyrin IX.

Porphyrins behave as extremely weak acids. They are generally soluble in dilute acid ~ 0.1 N, and form the dication species PH_4^{++}. In general pK_3 and pK_4 differ by only 2–3 pK units, and the detection of the species PH_3^{+} is difficult, except in anionic detergent solutions.

The neutral species PH_2 is stable even in concentrated sodium hydroxide. A more alkaline medium such as sodium alkoxide is required to observe the dianion $P^{=}$ spectroscopically.

Where the porphyrin has β-substituted carboxylic acid side chains as in hematoporphyrin, there are additional pK values due to these. According to Phillips (8), the pK values of analogous pyrrole carboxylic acids are of the order of +4.8, and likely to correspond to the intrinsic pK values of similarly substituted porphyrin monocarboxylic acids. The intrinsic pK values of polycarboxylic acid porphyrins, however, would be altered by the electrostatic effect of other ionized carboxylate groups and the ionized ring nitrogens, and therefore the effective pK value will be pH dependent. The mean pK value should approach a limiting value in alkaline solutions where all carboxylic groups

Can. J. Chem. Downloaded from www.nrcresearchpress.com by 210.87.254.40 on 09/05/12
For personal use only.

are ionized. For a dicarboxylic acid porphyrin such as hematoporphyrin this value would be approximately +5.7.

METHOD

Spectrophotometric analysis in the 500–600 mμ region has been used to obtain the equilibrium constants for the following two displacement reactions

$$M^{++} + PH_2 \leftrightarrows MP + 2H^+$$

for Zn(II) and hematoporphyrin in aqueous solution at a pH of 7, and

$$M^{++} + PH_4^{++} \leftrightarrows MP + 4H^+$$

for Cu(II) and hematoporphyrin with glacial acetic acid as solvent.

Neutral hematoporphyrin PH_2 has a typical visible porphyrin spectrum of four bands in the region of 450–700 mμ (Fig. 2) where the intensity of band IV is > III is > II is > I, numbering from the red end of the spectrum.

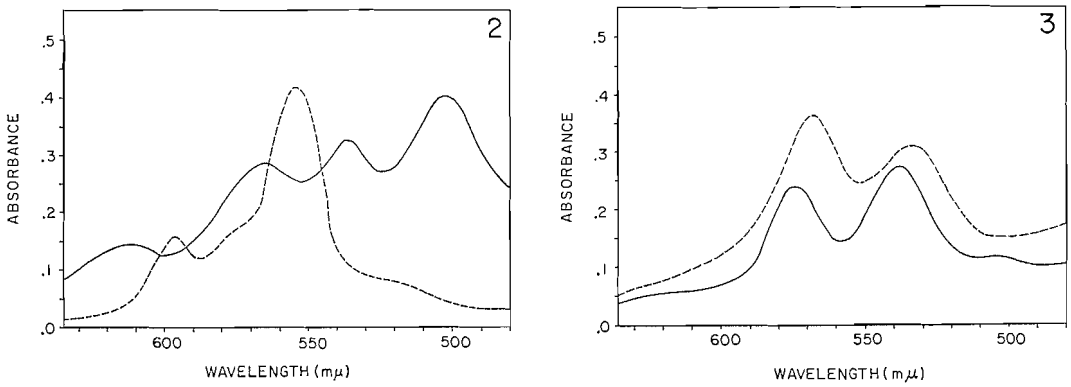


FIG. 2. Absorption spectra of hematoporphyrin IX, neutral species (PH_2), in aqueous solution, pH 7 (—) and hematoporphyrin IX, dication species (PH_4^{++}), in glacial acetic acid solution (--).

FIG. 3. Absorption spectra of Zn(II) hematoporphyrin in aqueous solution, pH 7 (—) and Cu(II) hematoporphyrin in glacial acetic acid solution (--).

The dication PH_4^{++} has a two-band spectrum (Fig. 2). When complexing occurred, the porphyrin spectrum (PH_2 or PH_4^{++}) was replaced by that of the metalloporphyrin 1:1 complex, showing two absorption peaks in the visible region known as the α and β peaks (Fig. 3). The α/β ratio of band intensities vary with the complexes. It is < 1 in ZnP and > 1 in CuP.

Since the average pK value of a porphyrin with two carboxyl side chains is considered to be about 5.7, it is probable that one if not both carboxyl groups are ionized at pH 7 and both are un-ionized in the glacial acetic acids solutions.

A series of solutions was prepared in which metal ion was complexed with porphyrin in 0.1 M sodium perchlorate at a fixed pH. The porphyrin concentrations were varied throughout the series while the metal ion concentration remained constant at a concentration in excess of any of the porphyrin concentrations used. The absorbance of each of the solutions was measured at 25 °C, at two wavelengths (one in the region of the α peak of the metalloporphyrin and one in the region of the β peak). Neither the metal ion or the background salt absorbs in the spectral region 500–600 mμ.

The extinction coefficients for the free porphyrin and the metalloporphyrins were found at the two wavelengths chosen. To obtain the extinction coefficients for the metalloporphyrins, porphyrin of a known concentration was complexed with metal ion of varying

Can. J. Chem. Downloaded from www.nrcresearchpress.com by 210.87.254.40 on 09/05/12
For personal use only.

but increasing concentrations. The absorbance of the solutions was seen to increase as the metal ion concentration increased until a maximum absorbance was reached when the metal ion concentration was 10^2 or more greater than the porphyrin. The extinction coefficient calculated for several initial concentrations of porphyrin gave the same results.

Beers-law plots of optical density versus concentration at the wavelengths used were linear.

K equilibrium constants at 25 °C could be calculated where

$$K_e(\mathrm{ZnP}) = \frac{[\mathrm{MP}][\mathrm{H}^+]^2}{[\mathrm{M}^{++}][\mathrm{PH}_2]} \quad \text{for zinc porphyrin}$$

and

$$K_e(\mathrm{CuP}) = \frac{[\mathrm{MP}][\mathrm{H}^+]^4}{[\mathrm{M}^{++}][\mathrm{PH}_4^{++}]} \quad \text{for copper porphyrin.}$$

The equations for the zinc system are developed as follows and those for the copper system are comparable.

$$[\mathrm{P}]_t = [\mathrm{PH}_2] + [\mathrm{MP}]$$

$$[\mathrm{M}]_t = [\mathrm{M}^{++}] + [\mathrm{MP}]$$

where $[\ ]_t$ represents total concentration.

$$A = A_{obs} = A_0' + A_0''$$

where $A_0' = \epsilon[\mathrm{PH}_2]$, $A_0'' = \epsilon_q[\mathrm{MP}]$, ϵ = extinction coefficient of PH_2 at the wavelength chosen, ϵ_q = extinction coefficient of metalloporphyrin (MP_q) where $q = 1$.

Since $[\mathrm{PH}_2] = A_0'/\epsilon$,

$$[1] \qquad K_e = \frac{\dfrac{A_0''}{\epsilon_q}[\mathrm{H}^+]^2}{[\mathrm{M}^{++}]\dfrac{A - A_0''}{\epsilon}} \quad \text{or} \quad K_e[\mathrm{M}^{++}]\frac{A - A_0''}{\epsilon} = \frac{A_0''}{\epsilon_q}[\mathrm{H}^+]^2.$$

$$[2] \qquad \mathrm{Log}\, K_e + \log\left([\mathrm{M}^{++}]\frac{A - A_0''}{\epsilon}\right) = \log\frac{A_0''}{\epsilon_q} + \log[\mathrm{H}^+]^2$$

When $[\mathrm{M}]_t$ is $\gg [\mathrm{PH}_2]$ then $[\mathrm{M}]_t \sim [\mathrm{M}^{++}]$. $[\mathrm{H}^+]$ is a constant.

$$[3] \qquad \mathrm{Log}\frac{K_e}{[\mathrm{H}^+]^2} + \log\left(\frac{[\mathrm{M}]_t A}{\epsilon} - \frac{[\mathrm{M}]_t A_0''}{\epsilon}\right) = \log\frac{A_0''}{\epsilon_q}$$

A_0'' is not known, but since $[\mathrm{P}]_t = [\mathrm{PH}_2] + [\mathrm{MP}]$ then

$$[\mathrm{P}]_t = \frac{A_0'}{\epsilon} + \frac{A_0''}{\epsilon_q}$$

and

$$[\mathrm{P}]_t = \frac{A - A_0''}{\epsilon} + \frac{A_0''}{\epsilon_q}.$$

A_0'' can be calculated for each value of porphyrin concentration and substituted back in [3].

A plot of $\log A_0''/\epsilon_q$ versus $\log(([\mathrm{M}]_t A/\epsilon) - ([\mathrm{M}]_t A_0''/\epsilon))$ should give a straight line of slope 1, the intercept of which is $\log K_e/[\mathrm{H}^+]^2$. K_e can then be calculated.

Where $[\mathrm{M}]_t$ is not $\gg [\mathrm{P}]_t$, $[\mathrm{M}^{++}]$ must be retained in eq. [1] and $[\mathrm{M}]_t - [\mathrm{MP}]$ substituted for it.

Can. J. Chem. Downloaded from www.nrcresearchpress.com by 210.87.254.40 on 09/05/12
For personal use only.

Equation [2] than becomes

$$\log K_e + \log \left(\left([M]_t - \frac{A_0''}{\epsilon_q} \right) \left(\frac{A - A_0''}{\epsilon} \right) \right) = \log \frac{A_0''}{\epsilon_q} + \log [H^+]^2 .$$

For purposes of comparison it is convenient to express K_e in terms of the familiar stability constant K_s, where $K_s = [MP]/([M^{++}][P^=])$. Since $K_1K_2 = ([P^=][H^+]^2)/[PH_2]$, then $K_e(ZnP) = K_sK_1K_2$ and $K_s = K_e/K_1K_2$.

For the copper porphyrin complex

$$[P]_t = [PH_4^{++}] + [MP]$$

and

$$[M]_t = [M^{++}] \text{ unbound} + [MP].$$

The copper ion not complexed with porphyrin may exist in more than one form in glacial acetic acid but this would in no way alter the calculations. It is simply referred to as $[M^{++}]$ unbound.

The intercept from the log plot would be $K_e/[H^+]^4$, and since

$$K_1 \cdot K_2 \cdot K_3 \cdot K_4 = \frac{[P^=][H^+]^4}{[PH_4^{++}]},$$

then

$$K_e(CuP) = K_s \cdot K_1 \cdot K_2 \cdot K_3 \cdot K_4 \text{ and } K_s = \frac{K_e}{K_1K_2K_3K_4}.$$

EXPERIMENTAL

All chemicals used were reagent grade. Spectrophotometric measurements were made on a Cary model 14 recording spectrophotometer, using 1 cm cells.

Recrystallized hematoporphyrin from Mann Research Laboratories (98% spectro assay) was used and standards were prepared by dissolving the reagent in a small amount of alcohol and making up to volume with doubly distilled water. When the standards were allowed to stand for periods of several weeks, there appeared to be no diminution in the absorption bands of the hematoporphyrin, nor increase in absorption in the regions where a monovinyl or divinyl group would absorb if dehydration of hematoporphyrin to protoporphyrin were occurring.

Complexing with zinc was done in aqueous solution using zinc acetate, and 0.1 *M* sodium perchlorate background. The pH was then adjusted to 7 with NaOH.

Because of the difficulty in complexing copper in aqueous medium, the method of Dorough *et al.* (17) was used. An aliquot of porphyrin, to which glacial acetic acid had been added, was boiled gently with copper(II) acetate until the spectrum of the copper porphyrin complex showed the absence of the free porphyrin absorption bands (about 5 min). The aliquot was then made up to a known volume with glacial acetic acid; the resulting solution was 75:1 (by volume) glacial acetic acid to water. The absorbances were measured at 25 °C. This method proved successful although it appears to contradict the statement of Fleischer *et al.* (18) that the diacid species is known to be unreactive to metalloporphyrin formation.

It was noted that an intermediary color of green appeared in the copper solutions. The green color disappeared on further heating, and the solutions became orange brown. The spectrum was not that of the metal complex, and could be the sitting-atop type of complex discussed by Fleischer and Wang (19). Preliminary experiments with Mn(II), Co(II), Ni(II), and Cd(II) as their acetates showed complexing in glacial acetic acid.

RESULTS

Extinction coefficients at 25 °C. (Deviation $\pm 0.05 \times 10^3$.)

At pH 7:

$\epsilon(PH_2) = 4.4 \times 10^3$ at 540 mμ.
$= 3.6 \times 10^3$ at 574 mμ.
$\epsilon_q(ZnP) = 7.6 \times 10^3$ at 540 mμ.
$= 6.5 \times 10^3$ at 574 mμ.

In glacial acetic acid:

$\epsilon(PH_4^{++}) = 6.4 \times 10^3$ at 568 mμ.
$= 3.2 \times 10^3$ at 534 mμ.
$\epsilon_q(CuP) = 11.1 \times 10^3$ at 568 mμ.
$= 9.7 \times 10^3$ at 534 mμ.

Can. J. Chem. Downloaded from www.nrcresearchpress.com by 210.87.254.40 on 09/05/12
For personal use only.

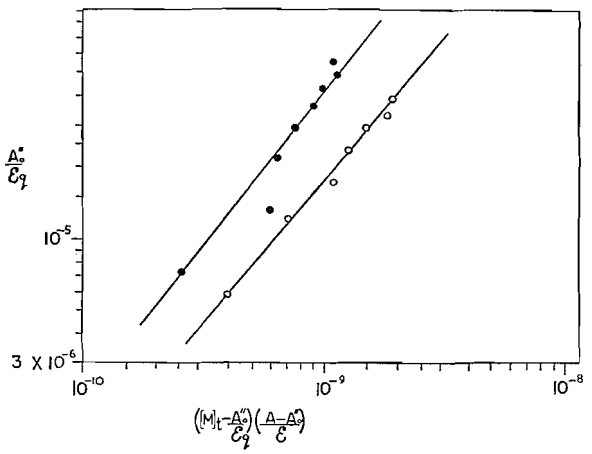


FIG. 4. Typical plots of $\log \frac{A_0''}{\epsilon_q}$ against $\log \left(([M]_t - \frac{A_0''}{\epsilon_q}) (\frac{A - A_0''}{\epsilon}) \right)$ for Zn(II) with hematoporphyrin (●) and Cu(II) with hematoporphyrin (○).

Tables I and II show typical absorbance data. Plots from such data are shown in Fig. 4.

NOTE: Slopes of the straight lines varied from 1.0 to 1.2. The lower slopes seemed to occur when the approximation $[M] \sim [M^{++}]$ was used. The more rigorous treatment of data produced slopes slightly greater than 1.

The average value obtained for $K_e/[H^+]^2$ for zinc hematoporphyrin was 1.3×10^7. Since $[H^+]$ was 10^{-7} moles/l, K_e is of the order of 1.3×10^{-7} at 25 °C.

If K_1 and K_2 were of the order of those for aetioporphyrin (i.e. 10^{-16} each), the K_s value will be large (of the order of 10^{+25}), since

$$K_s = \frac{K_e}{K_1 K_2}.$$

The average value obtained for $K_e/[H^+]^4$ for copper hematoporphyrin was 1.8×10^5. The H^+ concentration in the glacial acetic acid solution could not be determined with any meaning, but the over all acidity of the solution could be considered a constant, since the release of H^+ ions from the dication would be a negligible amount.

$$K_e = 1.8 \times 10^5 [H^+]^4 \text{ at } 25 \text{ °C}.$$

Since K_1, K_2, K_3, and K_4 are not known in glacial acetic acid, K_s cannot be estimated. It would no doubt be exceptionally large, however, since

$$K_s = \frac{K_e}{K_1 K_2 K_3 K_4}.$$

Until further work has been done with other metals in glacial acetic acid, it is too early to speculate on the orders of stability as compared with those deduced from replacement and dissociation reactions (9), where Pt(II) > Pd(II) > Ni(II) > Co(II) > Ag(II) > Cu(II) > Fe(II) > Zn(II) > Mg(II) > Cd(II) > Sn(II) > Li > Na > Ba > K > Ag.

Although the measurements in glacial acetic acid solution are only semiquantitative, they provide a means of comparison within a given medium.

Can. J. Chem. Downloaded from www.nrcresearchpress.com by 210.87.254.40 on 09/05/12
For personal use only.

Can. J. Chem. Downloaded from www.nrcresearchpress.com by 210.87.254.40 on 09/05/12
For personal use only.

TABLE I

A set of absorption data for the complexing of zinc(II) with hematoporphyrin IX ([Zn] = 1×10^{-4} mole/l at 540 mμ)

[Porphyrin] $\times 10^{-5}$ (mole/l)	A	A_0''	$\frac{A_0''}{\epsilon_q}$	$([M]_t - \frac{A_0''}{\epsilon_q})$	$(\frac{A - A_0''}{\epsilon})$	$([M]_t - \frac{A_0''}{\epsilon_q})(\frac{A - A_0''}{\epsilon})$
1	0.067	0.055	7.237×10^{-6}	0.928×10^{-4}	2.725×10^{-6}	2.529×10^{-10}
2	0.130	0.100	13.158×10^{-6}	0.868×10^{-4}	6.814×10^{-6}	5.915×10^{-10}
3	0.202	0.166	21.842×10^{-6}	0.782×10^{-4}	0.176×10^{-6}	6.394×10^{-10}
4	0.270	0.223	29.342×10^{-6}	0.707×10^{-4}	10.675×10^{-6}	7.547×10^{-10}
5	0.335	0.273	35.921×10^{-6}	0.641×10^{-4}	14.081×10^{-6}	9.026×10^{-10}
6	0.401	0.325	42.763×10^{-6}	0.572×10^{-4}	17.261×10^{-6}	9.873×10^{-10}
7	0.462	0.366	48.158×10^{-6}	0.518×10^{-4}	21.803×10^{-6}	11.294×10^{-10}
8	0.529	0.420	55.263×10^{-6}	0.447×10^{-4}	24.756×10^{-6}	11.066×10^{-10}

TABLE II

A set of absorption data for the complexing of copper(II) with hematoporphyrin IX ([Cu^{++}] = 1×10^{-4} mole/l at 568 mμ)

[Porphyrin] $\times 10^{-5}$ (mole/l)	A	A_0''	$\frac{A_0''}{\epsilon_q}$	$([M]_t - \frac{A_0''}{\epsilon_q})$	$(\frac{A - A_0''}{\epsilon})$	$([M]_t - \frac{A_0''}{\epsilon_q})(\frac{A - A_0''}{\epsilon})$
1	0.091	0.064	5.776×10^{-6}	0.942×10^{-4}	4.220×10^{-6}	3.975×10^{-10}
2	0.184	0.133	12.004×10^{-6}	0.880×10^{-4}	7.971×10^{-6}	7.014×10^{-10}
3	0.272	0.189	17.058×10^{-6}	0.829×10^{-4}	12.973×10^{-6}	10.755×10^{-10}
4	0.366	0.261	23.556×10^{-6}	0.764×10^{-4}	16.411×10^{-6}	12.538×10^{-10}
5	0.456	0.322	29.061×10^{-6}	0.709×10^{-4}	20.944×10^{-6}	14.849×10^{-10}
6	0.537	0.362	32.671×10^{-6}	0.673×10^{-4}	27.352×10^{-6}	18.408×10^{-10}
7	0.628	0.426	38.448×10^{-6}	0.616×10^{-4}	31.572×10^{-6}	19.448×10^{-10}

Can. J. Chem. Downloaded from www.nrcresearchpress.com by 210.87.254.40 on 09/05/12
For personal use only.

REFERENCES

1. S. ARONOFF. Chem. Rev. **47**, 175 (1950).
2. R. J. P. WILLIAMS. Biol. Rev. **56**, 299 (1956).
3. S. F. MASON. J. Chem. Soc. 976 (1958).
4. M. B. LOWE and J. N. PHILLIPS. Nature, **194**, 1058 (1962).
5. R. J. WALTER. J. Am. Chem. Soc. **75**, 3860 (1953).
6. R. LEMBERG and J. W. LEGGE. Hematin compounds and bile pigments. Interscience, New York. 1949.
7. R. J. P. WILLIAMS. *In* Haematin enzymes. *Edited by* J. E. Falk, R. Lemberg, and R. K. Morton. Pergamon, London. 1961.
8. J. N. PHILLIPS. *In* Comprehensive biochemistry. Vol. 9. *Edited by* Marcel Florkin and Elmer H. Stotz. Elsevier, New York. 1963. Chap. 11.
9. J. E. FALK. Porphyrins and metalloporphyrins. Vol. 2. Elsevier, New York. 1964. Chap. 2.
10. J. W. BARNES and G. D. DOROUGH. J. Am. Chem. Soc. **72**, 4045 (1950).
11. A. H. CORWIN and M. H. MELVILLE. J. Am. Chem. Soc. **77**, 2755 (1955).
12. W. S. CAUGHEY and A. H. CORWIN. J. Am. Chem. Soc. **77**, 1509 (1955).
13. J. E. FALK and R. S. NYHOLM. Current trends in heterocyclic chemistry. Butterworths, London. 1958. p. 130.
14. B. DEMPSEY, M. B. LOWE, and J. N. PHILLIPS. *In* Haematin enzymes. *Edited by* J. E. Falk, R. Lemberg, and R. K. Morton. Pergamon, London. 1961. p. 29.
15. W. K. MCEWEN. J. Am. Chem. Soc. **58**, 1124 (1936).
16. J. N. PHILLIPS. Rev. Pure App. Chem. **10**, 35 (1960).
17. G. D. DOROUGH, J. R. MILLER, and F. M. HUENNEKENS. J. Am. Chem. Soc. **73**, 4315 (1951).
18. E. B. FLEISCHER, E. I. CHOI, PETER HAMBRIGHT, and ALLEN STONE. Inorg. Chem. **3**, 1284 (1964).
19. E. B. FLEISCHER and J. W. WANG. J. Am. Chem. Soc. **82**, 3498 (1960).

Can. J. Chem. Downloaded from www.nrcresearchpress.com by 210.87.254.42 on 09/05/12
For personal use only.

THE CORRELATION OF ABSORPTION SPECTRA AND STRUCTURE OF PSEUDO-OCTAHEDRAL AND TRIGONAL BIPYRAMIDAL COPPER(II)–1,10-PHENANTHROLINE COMPLEXES IN ACETONE SOLUTIONS

G. H. FAYE

Mineral Sciences Division, Mines Branch, Department of Mines and Technical Surveys, Ottawa, Canada

Received March 17, 1966

ABSTRACT

By the use of elementary ligand field theory to interpret the absorption spectra of complexes formed in the copper(II)–1,10-phenanthrolene (Phen) system in an acetone medium, it has been shown that the mono-Phen complex is of approximately octahedral symmetry and the bis-Phen complex probably has a trigonal bipyramidal structure. At high Phen concentration, a tris-complex is formed that is probably trigonally distorted from octahedral symmetry. The results of the present work suggest that the "pentammine effect" observed in spectra of the copper(II)–ammonia complex is due to the formation of a trigonal bipyramidal complex.

INTRODUCTION

Copper(II) complexes of 1,10-phenanthroline, 2,2′-bipyridine, and their derivatives have been the subject of numerous investigations. However, the literature reveals that the structures of the species formed in solution have not been firmly established even though several studies (1–4, 7, 8) (mainly spectrophotometric) have been concerned, at least in part, with this matter; the difficulty seems to have been due to a lack of recognition of the existence of five-coordinate copper(II) species by some workers and (or) to the structural interpretations of incomplete d–d band absorption spectra by others.

Using crystal field considerations in a spectral study, Jorgensen (1) concluded that bis- and tris-phenanthroline (Phen) and bipyridine (Bip) copper(II) complexes are of approximately octahedral symmetry. Banks and Bystroff (2) measured the stability constants of the mono-, bis-, and tris-Phen complexes and assumed that all three have octahedral structures. These workers arrived at the conclusion, as did Jorgensen, that the bis-complex is of the *cis* configuration because the *trans* isomer is sterically unstable.

Using electrochemical techniques, James and Williams (3) studied the copper complexes formed with variously substituted Phens and Bips and implied that bis-complexes formed by the 3,4,5-substituted bases are planar and the tris-complexes are octahedral. With Phen substituted in the 2,9-positions, James and Williams found no evidence for a tris-complex and attributed this to steric hindrance.

From a spectrophotometric study, James, Parris, and Williams (4) concluded that unsubstituted Phens and Bips form distorted octahedral bis-complexes with copper(II), whereas Phen substituted in the 2,9-positions forms tetrahedral mono- and bis-complexes. James *et al.* made the unlikely supposition that the spectra of the octahedral and tetrahedral species were much alike.

Harris, Lockyer, and Waterman (5) and Barclay and Kennard (6) have shown that copper(II) forms a number of crystalline trigonal bipyramidal species with Phen and Bip under conditions that were apparently similar to those prevailing in certain of the studies cited above. However, these workers did not study the absorption spectra, thus a direct correlation of structure in solution with that of the solids containing five-coordinate copper has not been made.

From the foregoing it is apparent that further experimental work is required to elucidate the structure of the complexes formed by copper and relatively bulky bidentate nitrogenous bases of the Phen and Bip type.

Although ligand field theory in conjunction with a detailed examination of the absorption spectra in the near ultraviolet to near infrared region of the energy spectrum is capable of yielding a wealth of structural information about transition metal complexes, this approach seems not to have been used to full advantage in the studies discussed above. Therefore, the author has undertaken the present spectrophotometric investigation of the copper(II)–Phen system with the object of correlating the d–d absorption bands with the structure of the complexes formed in solution.

It will be shown that with unsubstituted Phen, copper(II) probably forms a pseudo-octahedral mono-complex, a trigonal bipyramidal bis-complex, and, at high ligand concentration, a tris-species, which based on a comparison with its bis-Bip analog probably has trigonal symmetry. Some speculations are made on the reason why an octahedral bis-complex does not form in detectable amounts. Also, arguments are presented which suggest that the so-called "pentammine effect" (9) observed in the spectra of the copper–ammonia system can be attributed to the formation of a trigonal bipyramidal complex.

EXPERIMENTAL

With the exception of acetonic solutions of Phen, the materials, apparatus, and experimental procedure were similar to those described previously in a spectrophotometric study (10) of halogenocopper(II) complexes in acetone media.

Extinction coefficients (ϵ) were calculated using total copper concentrations.

Preparation of $[Cu(Phen)_2ClO_4]ClO_4$ (I)

This compound was prepared at room temperature by mixing 10 ml of a 4×10^{-2} *M* solution of $Cu(ClO_4)_2$ in acetone with 16 ml of a 5×10^{-2} *M* solution of Phen in acetone. The finely divided turquoise solid (I), so produced, was allowed to settle for approximately 15 min and was then recovered by filtration, washed with acetone, and dried at approximately 100 °C. Approximately 95% of the copper was recovered as compound I.

TABLE I
Analyses of solids

	$[Cu(Phen)_2ClO_4]ClO_4$ (I)	$[Cu(Phen)_2Cl]ClO_4$ (II)	$CuPhenCl_2$ (III)
Molecular weight	623	559	315
% Cu			
Found	10.1	11.8	19.4
Calcd.	10.2	11.4	20.2
% Cl			
Found	12	13	21
Calcd.	11.4	12.7	22.5
% C			
Found	46.3	51.2	46.5
Calcd.	46.2	51.6	45.8
% H			
Found	2.7	3.4	3.0
Calcd.	2.6	2.9	2.5
% N			
Found	8.8	9.8	8.8
Calcd.	9.0	10.0	8.9

Preparation of $[Cu(Phen)_2Cl]ClO_4$ (II) and $CuPhenCl_2$ (III)

Compounds II (dark green) and III (pale green) were prepared in the same manner as I, except that Phen was added to copper solutions containing 4×10^{-4} and 8×10^{-4} mole of HCl respectively (added as a mixture of 12 *M* hydrochloric acid and acetone). Compounds II and III accounted for 90–95% of the copper used for their preparation.

Table I gives the analytical data for the three solid compounds and the formula assigned to each on the basis of the analyses and the structural implications of their absorption spectra which are discussed later in the paper.

The absorption spectra of nitromethane solutions of compounds I, II, and III are shown in Fig. 2.

Can. J. Chem. Downloaded from www.nrcresearchpress.com by 210.87.254.42 on 09/05/12
For personal use only.

Can. J. Chem. Downloaded from www.nrcresearchpress.com by 210.87.254.42 on 09/05/12
For personal use only.

RESULTS AND DISCUSSION

The spectra in Fig. 1 indicate that as the ratio of the total concentration of Phen to Cu^{2+} is increased from 0 to 3, profound changes occur in the nature of the absorbing species in the acetone medium. Associated with these changes is the appearance of turquoise crystals (compound I) when the ratio is between 1 and 3. The spectrum and structure of I is discussed under "Crystalline Compounds".

Spectrum A, with band maximum at 12 500 cm^{-1}, is considered to be due to a mixture of the distorted octahedral species $[Cu(OH_2)_5ac]^{2+}$ and $[Cu(OH_2)_4(ac)_2]^{2+}$ (10). Friedman and Plane (11) have shown that such complexes are present in acetone solutions of copper perchlorate containing small amounts of water. Because the acetone used in the present work was not dried and because the extinction coefficient, ϵ, = 17 l/mole cm is similar to that for $[Cu(OH_2)_5ac]^{2+}$ (11), it is reasonable to assume that this is the predominant species in the solution and the one reacting with Phen.

Pseudo-Octahedral Mono-Phen Complex

Spectrum C with band maximum at 14 300 cm^{-1} is that of a solution in which $[Phen]/[Cu^{2+}] = 1$. At ratios between 1 and 2 the band maximum shifts to lower energy and the spectrum changes greatly, indicating formation of a new complex. It is highly probable that spectrum C is that of a pseudo-octahedral mono-complex, $[Cu(Phen)(OH_2)_{4-x}(ac)_x]^{2+}$, formed by the replacement of two solvent molecules in $[Cu(OH_2)_5ac]^{2+}$ by a Phen molecule. An increase of 1 800 cm^{-1} in $\Delta_{\sim oct}$ (where $\Delta_{\sim oct}$ symbolizes d-orbital splitting in an approximately octahedral field) on the replacement of two Cu—O bonds by two Cu—N bonds is to be expected from the known greater perturbing effect of N-bonding ligands and also possibly to increased distortion caused by the complexing of Phen. For example, $\Delta_{\sim oct}$ for $[Cu(NH_3)_2(OH_2)_4]^{2+}$ is approximately 14 800 cm^{-1}, whereas that for $[Cu(OH_2)_6]^{2+}$ is 12 500 (9). That the field produced by a Phen molecule is less than that produced by two ammonias may be due to its poorer donor properties and (or) to longer Cu—N bond lengths in the chelate complex.

The "smearing" of the broad absorption band into the lower energy region is indicative of considerable Jahn–Teller distortion and is also consistent with the mixed-ligand coordination sphere indicated above (12).

Trigonal Bipyramidal Bis-Phen Complex

When acetonic solutions of copper perchlorate and Phen are mixed so that the final total copper concentration is greater than approximately 10^{-4} *M* and the $[Phen]/[Cu^{2+}]$ is in the range 1.5 to 2.5, the resulting solution turns pale blue and after a few minutes finely divided turquoise crystals (compound I) are formed.

Spectrum D in Fig. 1 is that of a freshly prepared solution in which $[Phen]/[Cu^{2+}] = 2$ and in which a detectable amount of crystalline material had not formed at the completion of the scan. Two prominent bands with maxima at 13 900 and 11 000 cm^{-1} are evident; these can be accounted for by the presence of a single complex in which two well-separated d-orbital transitions are possible, or by two absorbing species each exhibiting a single band as expected for copper(II) in an approximately octahedral or tetrahedral field.

Jorgensen (1) observed two bands in the spectra of aqueous solutions of the copper(II) bis-complexes of bipyridine at 13 900 and 10 500 cm^{-1} and of Phen at 13 300 and 10 200 cm^{-1} and ascribed these bands to a tetragonally distorted octahedral complex with a *cis* arrangement of the bound aromatic diimines. To account for the large separation of the bands ($> 3\,000$ cm^{-1}) such a six-coordinate complex would have to be highly distorted. If the distortion tended toward a planar configuration, the band at highest

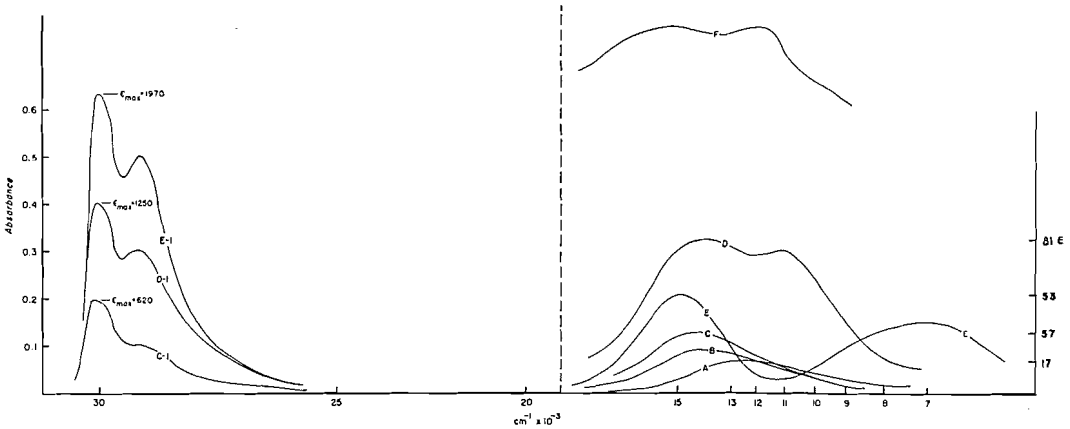


FIG. 1. Spectra of pseudo-octahedral and trigonal bipyramidal copper(II)–Phen complexes in acetone.

	$[Cu^{2+}]_{total}$	[Phen]/$[Cu^{2+}]$	Absorbing species and structure	Band max. (cm^{-1})
A	4×10^{-3} *M*	0	~Octahedral $[Cu(OH_2)_5ac]^{2+}$	12 500
B	"	0.6	Mixture of A and C	
C	"	1.0	~Octahedral $[CuPhen(OH_2)_{(4-x)}(ac)_x]^{2+}$	14 300
D	"	2.0	Trigonal bipyramidal $[Cu(Phen)_2solv]^{2+}$ or $[Cu(Phen)_2ClO_4]^+$	13 900 and 11 000
E	"	3.0 and over	Trigonal $[Cu(Phen)_3]^{2+}$	14 800 and 7 000
F	"		Crystalline $[Cu(Phen)_2ClO_4]ClO_4$ in Nujol	15 100 and 11 900
C-1 to E-1	3.2×10^{-4} *M*	1 to 3	Charge-transfer bands of mono, bis-, and tris-Phen complexes	30 000 and 29 000

energy would certainly be found at a frequency greater than that of the pseudo-octahedral mono-Phen complex, for it is well known that the ligand field splitting parameter for planar symmetry (17.4*D*q) is much larger than that for octahedral symmetry (10*D*q).

James, Parris, and Williams (4) also studied the spectra of aqueous solutions of the copper(II) bis-complexes of variously substituted Phens and Bips and concluded that the two bands observed at approximately 13 500 and 11 000 cm^{-1} were due to a distorted octahedral species in the unsubstituted aromatic diimines, and to a distorted tetrahedral complex, at least in Phen substituted in the 2- and 9-positions.

The occurrence of two widely separated bands at unlikely energies for the distorted "tetrahedral" complex was reconciled with theory by James *et al.* by assuming that for steric reasons the Cu—N distance is less than in the octahedral complex; this gives rise to a ligand field of exceptionally high strength.

It has been shown above that the pseudo-octahedral mono-Phen complex has its band maximum at 14 300 cm^{-1}. Therefore it is reasonable to assume that a pseudo-octahedral bis-complex would exhibit a maximum at significantly higher energy because of the greater field produced by the second Phen molecule. However, spectrum D in Fig. 1 shows instead that the higher energy transition of the bis-complexes lies 400–700 cm^{-1} lower than in the spectrum of the mono-complex, and this strongly suggests that the band is not due to an octahedral complex, distorted or otherwise.

Consideration of a d-orbital energy level splitting scheme for a ligand field of trigonal bipyramidal symmetry (13) indicates that a d^9 ion should give rise to two absorption bands due to the transitions $d_{x^2-y^2}$, $d_{xy} \rightarrow d_{z^2}$ and d_{xz}, $d_{yz} \rightarrow d_{z^2}$; the former accounting for 7.89*D*q or $0.806\Delta_{trl\ bp}$ and the latter 9.70*D*q. Furthermore, the high energy transition should lie somewhat below that in a corresponding octahedral complex with similar ligands.

Can. J. Chem. Downloaded from www.nrcresearchpress.com by 210.87.254.42 on 09/05/12
For personal use only.

Can. J. Chem. Downloaded from www.nrcresearchpress.com by 210.87.254.42 on 09/05/12
For personal use only.

Spectrum D in Fig. 1 can be interpreted in terms of a d-orbital splitting scheme for a trigonal bipyramidal structure, considering electrostatic effects only. Thus, if the band maximum at 13 900 cm^{-1} is taken to be due to the d_{xz}, $d_{yz} \rightarrow d_{z^2}$ transition, then, theoretically, the $d_{x^2-y^2}$, $d_{xy} \rightarrow d_{z^2}$ transition should lie at $(7.89Dq/9.79Dq) \times 13\ 900 = 11\ 200$ cm^{-1}, a value with which the observed band maximum at 11 000 cm^{-1} is in excellent agreement. Therefore, it is concluded that the complex giving rise to spectrum D is essentially trigonal bipyramidal, and, as we will show later, may be formulated $[Cu(Phen)_2solv]^{2+}$, or $[Cu(Phen)ClO_4]^+$.

Spectrum D is qualitatively very similar to that found recently by Ciampolini and Nardi (14) for trigonal bipyramidal complexes formed by copper(II) and tris(2-diethylaminoethyl)amine. Thus it would seem that five-coordinate copper(II) complexes with nitrogen-bonding ligands are relatively common (15) and this suggests that the appropriate absorption spectra should be examined routinely for the presence of such species.

Tris-Phen Complex

Spectrum E in Fig. 1 is obtained from solutions in which $[Phen]/[Cu^{2+}] = 3$ or higher. The appearance of the widely separated bands with maxima at 14 800 and 7 000 cm^{-1} with each having ϵ_{max} values significantly lower than the bands in spectrum D indicates that major structural changes occur in the dissolved species as $[Phen]/[Cu^{2+}]$ is increased from 2 to 3 and over.

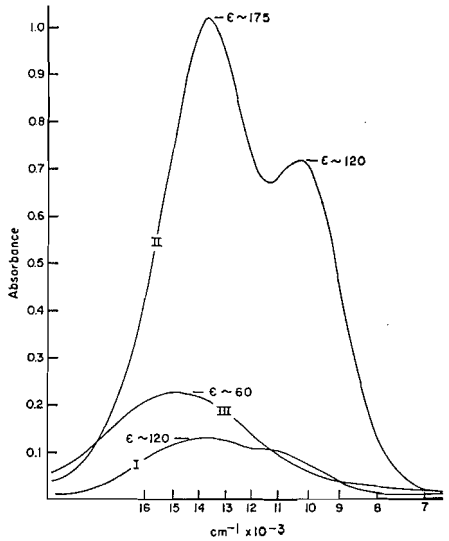


FIG. 2. Spectra of nitromethane solutions of compounds I, II, and III. Nature of absorbing solution (scanned in 5-cm cell): (I) 1.1×10^{-3} *M* solution of $[Cu(Phen)_2ClO_4]ClO_4$ in nitromethane; (II) 5.7×10^{-3} *M* solution of $[Cu(Phen)_2Cl]ClO_4$ in nitromethane; (III) $\sim 8 \times 10^{-4}$ *M* solution of $CuPhenCl_2$ in nitromethane.

Spectrum E in Fig. 2 is very similar to both the solid and solution spectrum of the tris-Bip copper(II) complex recently studied by Palmer and Piper (16). These workers concluded that their spectrum was due to a complex having trigonal symmetry. By analogy, it is probable that the copper-Phen complex giving rise to spectrum E is also of the same symmetry.

The unusually large splitting of the bands of the tris-complex earlier led this worker to consider the possibility of the coexistence of both an octahedral and a tetrahedral copper-Phen complex. If it is taken that the 14 800 cm^{-1} band in spectrum E is that of an octahedral tris-Phen complex, and the low energy band is that of a tetrahedral

bis-complex, then the band maximum of the latter can be predicted from ligand field theory ($\Delta_{tetr} \simeq 4\Delta_{oct}$) to lie at approximately 6 600 cm^{-1}, a value with which the observed frequency of approximately 7 000 cm^{-1} is in good agreement. Such agreement with theory would suggest that neither the hypothetical octahedral or tetrahedral complex is highly distorted.

It is of interest to note here that Jorgensen (1) found that the weak bands below 9 000 cm^{-1} in the spectra of the "tris-complexes" formed by copper(II) with Phen or Bip were not easily explained by ligand field theory.

When an acetone solution containing the tris-Phen complex and excess Phen is treated with Cl^-, compound II crystallizes (the nature of II is described below). The formation of the five-coordinate complex is indicative of the relatively low stability of the tris-species, a factor probably related to steric effects.

That a pseudo-octahedral bis-Phen copper(II) complex is not detected in the absence of excess Phen is considered to be due, at least in part, to the higher crystal field stabilization energy available in a d^9 ion in a trigonal bipyramidal environment than in a corresponding octahedral one, i.e. 7.07*D*q and 6*D*q respectively. Thus it is not difficult to imagine a transient *cis*-octahedral complex losing a solvent molecule and undergoing an energetically favorable rearrangement to the five-coordinate configuration.

Charge-Transfer Bands

Because of their intensity and energy, the bands at approximately 30 000 and 29 000 cm^{-1} in spectra C-1 to E-1 in Fig. 1 are considered to be of the charge-transfer type. That the intensity of the high energy band increases approximately linearly as $[Phen]/[Cu^{2+}]$ goes from 1 to 2 and the energy of the transitions remain essentially constant as the structure of the copper complexes changes radically strongly suggest that the charge-transfer processes take place within the ligand molecules.

Crystalline Compounds

Trigonal Bipyramidal Bis-Phen Complexes (I and II)

The spectra of nitromethane solutions of compounds I and II are shown in Fig. 2. It is evident that each contains two bands at energies similar to those of spectrum D in Fig. 1, and, therefore, it can be concluded that the dissolved species both have an approximately trigonal bipyramidal structure. This conclusion together with the analytical data indicates that the soluble complexes may be formulated as $[Cu(Phen)_2solv]^{2+}$ or $[Cu(Phen)_2ClO_4]^+$ and $[Cu(Phen)_2Cl]^+$.

Copper is probably also five coordinate in the corresponding solids $[Cu(Phen)_2ClO_4]ClO_4$ (I) and $[Cu(Phen)_2Cl]ClO_4$ (II); this is supported by the simliarity of the spectrum of a Nujol mull of compound I (see F in Fig. 1) to that of spectrum D in Fig. 1.

That a perchlorate is apparently coordinated directly to copper, at least in compound I, is of considerable interest because it is commonly held that there is little or no tendency for such coordination to metal cations to take place, especially in solution. Recently, however, evidence for the binding of perchlorate to transition metals has been presented (17–19).

Pseudo-Octahedral Mono-Phen Complex (III)

Spectrum III in Fig. 2 is that of a nitromethane solution of compound III. It is clear that there is only a single band with maximum at 14 500 cm^{-1} and this is indicative of a pseudo-octahedral environment for copper, as in the mono-Phen complex giving rise to spectrum C in Fig. 1. It is obvious from the analytical data that compound III may be

Can. J. Chem. Downloaded from www.nrcresearchpress.com by 210.87.254.42 on 09/05/12
For personal use only.

formulated as $CuPhenCl_2$. In the solid, copper is probably six coordinate with a Phen and two chlorines in a plane and with two chlorines perpendicular to the plane and shared by other coppers.

Some Speculations on the "Pentammine Effect"

Bjerrum, Ballhausen, and Jorgensen (9) studied the absorption spectra of copper(II)–ammonia complexes and observed what is known as the "pentammine effect". This effect refers to an "anomalous" change in the spectrum of aqueous solutions in which the $[NH_3]/[Cu^{2+}]$ ratio increases from 4 to 5. The octahedral tetrammine complex, $[Cu(NH_3)_4(OH_2)]^{2+}$, exhibits a symmetrical band with a maximum at approximately 17 000 cm^{-1}, whereas the pentammine complex (presumed to be $[Cu(NH_3)_5OH_2]^{2+}$) exhibits an absorption envelope of considerably greater intensity that contains two major components at approximately 15 400 and 11 800 cm^{-1} respectively.

The spectrum of the pentammine complex is thus very similar to that of the five-coordinate bis-Phen complex (D, in Fig. 1). Therefore, it is suggested that the pentammine complex has a trigonal bipyramidal structure and the pentammine spectral effect is a logical consequence of such geometry.

It is reported (9) that the spectrum of cupric nitrate in liquid ammonia is much like that of the pentammine complex, therefore it is probable that this system too contains the trigonal bipyramidal complex $[Cu(NH_3)_5]^{2+}$.

ACKNOWLEDGMENTS

The author wishes to express appreciation to Dr. P. G. Manning for helpful discussions during the course of this work.

Special thanks are due to George F. Morris, Analytical Chemistry Research Branch, Department of Agriculture, for the analysis of compounds I, II, and III.

REFERENCES

1. C. K. JORGENSEN. Acta. Chem. Scand. **9**, 1362 (1955).
2. C. V. BANKS and R. I. BYSTROFF. J. Am. Chem. Soc. **81**, 6153 (1959).
3. B. R. JAMES and R. J. P. WILLIAMS. J. Chem. Soc. 2007 (1961).
4. B. R. JAMES, M. PARRIS, and R. J. P. WILLIAMS. J. Chem. Soc. 4630 (1961).
5. C. M. HARRIS, T. N. LOCKYER, and H. WATERMAN. Nature, **192**, 424 (1961).
6. G. A. BARCLAY and C. H. L. KENNARD. Nature, 425 (1961).
7. W. BRACKMAN and C. J. GAASBEEK. J. Inorg. Nucl. Chem. **27**, 1793 (1965).
8. J. R. HALL, M. R. LITZOW, and R. A. PLOWMAN. Australian J. Chem. **18**, 1331 (1965).
9. J. BJERRUM, C. J. BALLHAUSEN, and C. K. JORGENSEN. Acta Chem. Scand. **8**, 1275 (1954).
10. G. H. FAYE. Can. J. Chem. **44**, 1643 (1966).
11. N. J. FRIEDMAN and R. A. PLANE. Inorg. Chem. **2**, 11 (1963).
12. T. M. DUNN. *In* Modern coordination chemistry. *Edited by* J. Lewis and R. G. Wilkins. Interscience, New York. 1958. p. 253.
13. J. J. ZUCKERMAN. J. Chem. Educ. **42**, 315 (1965).
14. M. CIAMPOLINI and N. NARDI. Inorg. Chem. **5**, 41 (1966).
15. W. R. WALKER. Australian J. Chem. **14**, 161 (1961).
16. R. A. PALMER and T. S. PIPER. Inorg. Chem. **5**, 864 (1966).
17. J. LEWIS, R. S. NYHOLM, and G. A. RADLEY. Nature, **207**, 72 (1965).
18. P. PAULING, G. B. ROBERTSON, and G. A. RADLEY. Nature, **207**, 74 (1965).
19. J. PLUŠČEC and A. D. WESTLAND. Chem. Comm. **4**, 69 (1965).

Can. J. Chem. Downloaded from www.nrcresearchpress.com by 210.87.254.42 on 09/05/12
For personal use only.

Can. J. Chem. Downloaded from www.nrcresearchpress.com by 210.87.254.6 on 09/05/12
For personal use only.

INTERSYSTEM CROSSING OF THE ELECTRONICALLY EXCITED DIDEUTEROETHYLENE MOLECULES FORMED IN BENZENE PHOTOSENSITIZATION[1]

TERUMI TERAO[2] AND SHUN-ICHI HIROKAMI[2]
Tokyo Institute of Technology, Tokyo, Japan

AND

SHIN SATO[2,3] AND R. J. CVETANOVIĆ
Division of Applied Chemistry, National Research Council of Canada, Ottawa, Canada

Received January 19, 1966

ABSTRACT

Experimental evidence is presented for a rapidly occurring intersystem crossing of the electronically excited dideuteroethylene molecules initially formed in the benzene-photosensitized reaction at 2 537 Å and 25 °C to another excited state which is responsible for the internal H-atom scrambling. The mechanism is entirely analogous to that previously postulated for the photoexcited states sensitized by $Hg(^3P_1)$ atoms but the rate constants for intersystem crossing and molecular decomposition are drastically decreased as a result of the smaller amount of energy available for the excitation.

INTRODUCTION

Electronically excited states of olefins are formed when olefin molecules absorb ultraviolet light either directly or indirectly from photosensitizers. The chemical behavior of the photoexcited states depends both on the amount of energy transferred and on the nature of the sensitizer employed. With ethylene the following reactions are observed: (i) *cis–trans* isomerization (in the reaction of *cis-* and *trans*-1,2-dideuteroethylene), (ii) internal H-atom scrambling (formation of 1,1- from 1,2-dideuteroethylene), (iii) molecular decomposition into H_2 and acetylene, and (iv) decomposition into H-atoms and vinyl radicals.

Studies of these chemical processes present an interesting opportunity to gain insight into the nature and behavior of the excited states involved. Direct photolysis and mercury-photosensitized reactions of ethylene have been investigated in considerable detail (1). In the present article we report the results of a study of the benzene-photosensitized isomerization of dideuteroethylene at room temperature.

LOW-LYING ENERGY LEVELS OF ETHYLENE

Benzene photosensitization of olefins is believed to occur through a triplet–triplet energy transfer (2, 3). Inasmuch as the transfer occurs from the lowest triplet state of benzene, the available energy is around 3.6 eV (4–6). The chemical processes likely to be energetically favorable will depend on the energy levels of the species involved. Unfortunately, there are still large uncertainties about the energy levels of ethylene, especially of the most stable configuration of the first triplet state. A very tentative energy diagram is given in Fig. 1. This is based on the low-lying electronic states according to Mulliken (7): N (ground state), T (the first triplet state, at 4.6 eV), T_R (the Rydberg triplet state, at 6.4 eV), R (The Rydberg singlet state, at 7.1 eV), and V (singlet excited

[1]*Issued as N.R.C. No. 9099.*
[2]*Department of Applied Physics, Tokyo Institute of Technology, Tokyo, Japan.*
[3]*Visiting Scientist, Applied Chemistry Division, National Research Council, Ottawa.*

state, at 7.6 eV). The excitation energies correspond to the spectroscopically observed vertical transitions (8–11). The T and V, and T_R and R states have the same electronic configurations (....$(\pi_x + \pi_x)$ $(\pi_x - \pi_x)$ and .... $(\pi_x + \pi_x)$ (3s), respectively) but different spin interactions.

From the point of view of the occurrence of the *cis–trans* isomerization it is important to know how the potential energy depends on the angle of twist (θ) around the CC bond. The stability of the Rydberg states appears to depend little on θ (11, 12). There is still a considerable divergence of views regarding the behavior of the first triplet state in this respect (13–16). The curve for the T state in Fig. 1 has been traced approximately in the following manner. The location of an imaginary averaged "center-of-gravity" state (17) between T and V is placed at 5.4 eV, i.e. $(3 \times 4.6 + 1 \times 7.6)/4$. At a 90° angle of twist, the electronic configurations (and the energy level) of this imaginary state and of the ground state would be the same. The common energy level is not known but it can be approximately assumed to be a half of the vertical level of the imaginary state, i.e. 2.7 eV. It is also assumed that the imaginary state, the T state, and the V state all show parallel dependence on the angle of twist.

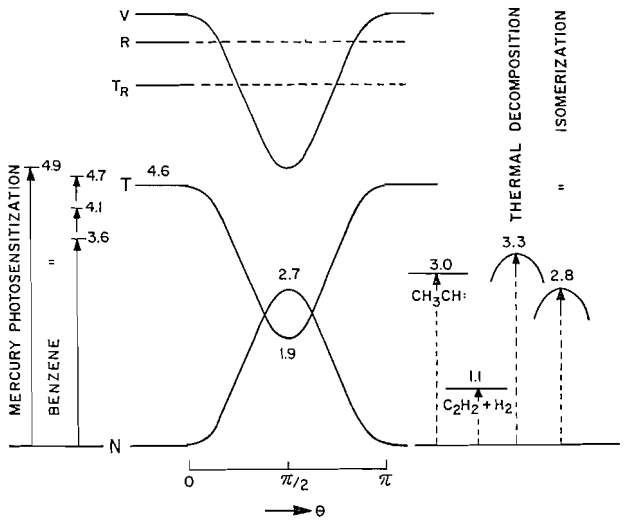


FIG. 1. Schematic diagram of the energy levels (in eV) of the low-lying electronic states of ethylene.

The lowest value of the T state is approximately placed in this manner at 1.9 eV, i.e. 2.7 − (5.4 − 4.6). This is not necessarily too low a value in view of the lack of *cis–trans* isomerization in Na photosensitization (18) (available energy 2.1 eV), since energy transfer in this process is most probably to the planar form of the triplet, although there could be some deviation from the rigorously vertical transition if an intermediate complex of finite lifetime is formed. The value of 2.7 eV for the 90°-twisted ("perpendicular") ground state should equal the activation energy of the thermal *cis–trans* isomerization if a spin multiplicity change is not involved. It agrees with the experimental value of 2.8 eV obtained by Douglas *et al.* (19), which these authors identify with the energy of the perpendicular form of the ground state of ethylene. They have also estimated the energy level of the perpendicular form of the T state and their value of 2.2 eV is only slightly higher than the value of 1.9 eV in Fig 1.

Can. J. Chem. Downloaded from www.nrcresearchpress.com by 210.87.254.6 on 09/05/12
For personal use only.

Ethylidene biradical has been postulated as an intermediate in the mercury-photosensitized reaction of ethylene (20). Its energy level above the ground state of ethylene has been estimated from the bond dissociation energies and the heat of hydrogenation at around 3.0 eV (21). The thermal decomposition of ethylene, with the activation energy of at least 3.3 eV (22), might therefore occur via an intermediate formation of ethylidene.

RESULTS AND DISCUSSION

Inspection of the diagram in Fig. 1 shows that in the benzene photosensitization of ethylene *cis–trans* isomerization, internal H-atom scrambling, and molecular decomposition into H_2 and acetylene should be energetically possible. Decomposition into H and vinyl would be quite endothermic and therefore unlikely. All the four processes occur in mercury photosensitization (20), although the fourth is of very minor importance at room temperature.

Several experiments were carried out at 25° in a mercury-free system using the 2 537 Å radiation from a low-pressure mercury arc. Figure 2 shows, as an example, the infrared spectra of 5 cm of *cis*-dideuteroethylene after irradiation for various periods of time in the absence and presence of 2.7 cm of benzene. The absorption peak at 842 cm^{-1} is assigned to *cis*, at 725 and 987 cm^{-1} to *trans*, and at 750 and 943 cm^{-1} to *asym*-dideuteroethylene (24). It is seen that *cis–trans* isomerization occurs readily but H-atom scrambling (formation of the *asym* isomer) is at best only a very minor process. Analogous behavior is shown by the corresponding infrared spectra of *trans*- and of *asym*-dideuteroethylene, which are not reproduced here for lack of space. The former readily isomerizes to the *cis* isomer but very little if at all to the *asym* isomer; the latter shows no or a very small tendency to isomerize. The lack of scrambling in the three isomers is in sharp contrast to the mercury-photosensitized reactions where, at these pressures, the scrambling and decomposition are almost the same (23). Furthermore, again in contrast to the mercury photosensitization, no evidence was found (by gas chromatography) for any decomposition of ethylene.

The lack of H-atom scrambling in ethylene in the benzene photosensitization may appear surprising. However, the corresponding process in mercury photosensitization is pressure dependent (23) with the maximum yield at about 65 mm, in agreement with the postulated (20) rapid intersystem crossing (reaction [2]) of the originally formed excited state (E*) to another excited state (E**) which is capable of decomposing:

[1] $$E + Hg^* \rightarrow E^* + Hg$$

[2] $$E^* \rightarrow E^{**}$$

[3] $$E^* + M \rightarrow E + M$$

[4] $$E^{**} \rightarrow C_2H_2 + H_2$$

[5] $$E^{**} + M \rightarrow E + M.$$

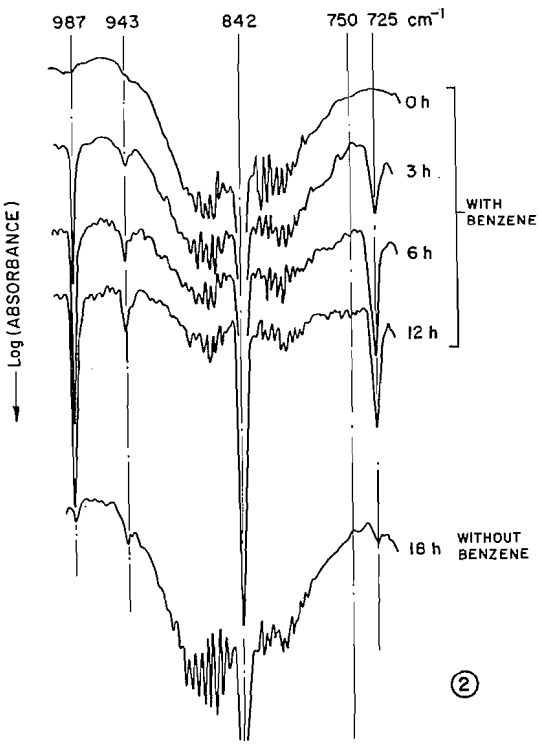
The observed kinetics require the internal scrambling of H atoms to occur in reaction [5]. At small conversions the quantum yield of the *asym*-dideuteroethylene (ϕ_{asym}), formed, for example, from the *cis* isomer, is given by

[6] $$\phi_{asym} = \frac{\alpha[M]}{\left(1 + \frac{k_3}{k_2}[M]\right)\left(\frac{k_4}{k_5} + [M]\right)}$$

with α representing the fraction of E** molecules (presumably ethylidene (20)) which are stabilized into the *asym*-dideuteroethylene. Inasmuch as the above two-state mechanism is also applicable to the benzene photosensitization, it can be seen that the ϕ_{asym}

Can. J. Chem. Downloaded from www.nrcresearchpress.com by 210.87.254.6 on 09/05/12
For personal use only.

maximum would be observed at a lower pressure if k_4 is smaller. If decomposition does not occur at all ($k_4 = 0$), eq. [6] reduces to a very simple form and the maximum value of ϕ_{asym} will be equal to α and will be reached at a negligibly small pressure. Under such conditions, therefore, at a pressure approaching zero, ϕ_{asym} may be expected to be close to the statistical factor of 1/3 and to approach ϕ_{trans} (if the original reactant is the *cis* isomer). As the pressure is increased ϕ_{asym} would continuously decrease.



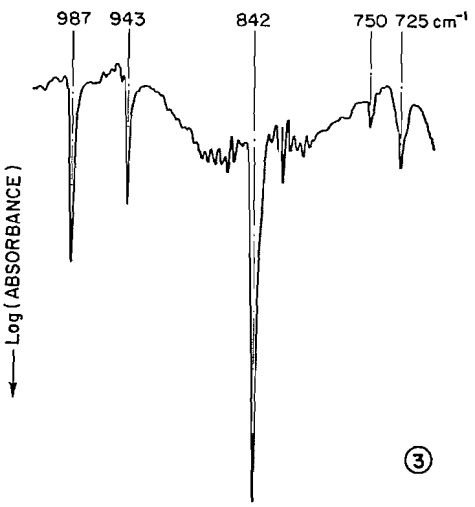


FIG. 2. Benzene-photosensitized isomerization of *cis*-dideuteroethylene. Infrared spectra of the product ethylene after various irradiation times. Initial pressures: 5 cm *cis*-dideuteroethylene, 2.7 cm benzene.
FIG. 3. Benzene-photosensitized isomerization of *cis*-dideuteroethylene at low pressure. Infrared spectrum after 12 h irradiation. Initial pressures: 2 mm *cis*-dideuteroethylene, 1.1 mm benzene.

In agreement with these predictions we find that at lower pressures H-atom scrambling does indeed become important. As shown in Fig. 3, after 12 h irradiation of 1.1 mm benzene and 2 mm *cis*-dideuteroethylene considerable isomerization is observed, with ϕ_{asym} beginning to approach ϕ_{trans}. In this experiment a longer absorption path (larger reaction vessel) was used so that both the ratio of the reactants and the light absorption were approximately the same as in the comparable experiment in Fig. 2.

These results show that more than one excited state must be involved in the process and that the initially formed excited molecules undergo intersystem crossing to another excited state in which internal H-atom scrambling occurs. If only one excited state were involved, either H-atom scrambling would not occur at all or the ratio ϕ_{asym}/ϕ_{trans} would remain the same at all pressures.

Scrambling of hydrogen atoms and ethylene decomposition have also been observed without the sensitizer (benzene) but to a very minor extent, as shown in Fig. 2 and similarly in the analogous experiments with the *trans*- and *asym*-dideuteroethylene. Since a low-pressure mercury arc was used in these experiments, the small amount of reaction

Can. J. Chem. Downloaded from www.nrcresearchpress.com by 210.87.254.6 on 09/05/12
For personal use only.

observed may be due to one of the following two possibilities: (*a*) contamination by a trace of mercury in the reagents, in spite of the precautions taken, or (*b*) direct light absorption by ethylene at 2 537 Å, which is well known to be very small (25). Two experiments were carried out in the absence of benzene with a Cd resonance lamp and with a medium-pressure mercury lamp through a mercury filter (2 cm thick, containing a drop of mercury and 70 mm hydrogen). With these light sources essentially no *cis–trans* isomerization and no decomposition were observed. These results support the first of the two possibilities mentioned above.

To determine the unimolecular rate constant (k_2) for the intersystem crossing reaction [2] we have carried out a number of experiments at two lower pressures, close to 3 mm and 0.3 mm, respectively, in a 1 100 ml reaction flask. In these experiments a medium-pressure mercury lamp (Hanovia 637A) was used to avoid any mercury photosensitization. The incident light was passed through a Corning 9–54 filter and a chlorine filter. Because of the emission characteristics of the lamp and the absorption properties of benzene vapor (26), most light absorption occurred at 2 537 Å and probably only to a considerably smaller extent at 2 482 Å. The initial excitation of benzene is therefore closely analogous to that in the earlier experiments with the use of the low-pressure mercury lamp. The results are summarized in Table I. It is seen that irradiation of *cis*-1,2-dideuteroethylene alone (run 2) does not lead to isomerization. In the presence of benzene, on the other hand, isomerization occurs and after prolonged irradiation (run 10) the statistical composition of about one third of each of the three isomers is obtained.

TABLE I

Benzene-photosensitized isomerization of *cis*-1,2-dideuteroethylene and of 1,1-dideuteroethylene at 25 °C

Run	Pressure (mm)			Exposure (h)	Product ethylene (%)			k_2 (s^{-1})
	Benzene	Ethylene	Total		*cis*	*trans*	*asym*	
I. *cis*-1,2-Dideuteroethylene as the reactant								
A. Total pressure about 3 mm								
1	1.03	1.75	2.78	16	59.8	24.6	15.6	5.9×10^7
3	1.40	1.90	3.30	4	76.2	14.2	9.6	9.3×10^7
8	1.01	1.44	2.45	4	86.6	7.6	5.8	7.8×10^7
9	0.51	2.25	2.76	4	87.0	7.4	5.6	8.4×10^7
11	1.83	1.11	2.94	4	75.3	15.2	9.5	6.7×10^7
10	1.67	0.84	2.51	65.5	32.9	33.9	33.2	
2	0	1.37	1.37	15.68	97.1	0.7	2.2	
		Initial reactant			96.7	1.2	2.1	
B. Total pressure about 0.3 mm								
5	0.13	0.23	0.36	16	74.9	12.7	12.4	
6	0.12	0.20	0.32	65.5	46.3	27.6	26.0	
II. 1,1-Dideuteroethylene as the reactant								
12	0.95	2.00	2.95	4.5	4.1	4.4	91.5	
		Initial reactant			—	—	100	

At negligibly small conversions, an expression for the intersystem crossing rate constant (k_2) based on the two-state mechanism (reactions [1]–[5]) can be readily obtained. At finite conversions the relationship is more complex, but it does simplify considerably when decomposition (reaction [4]) is negligible. It was found that even at these lower pressures extremely little or no decomposition occurs, so that the following simplified expression holds

$$[7] \qquad k_2 = k_3[\mathrm{M}] \log_{10}\left(\frac{3x-1}{3x_1-1}\right) \Big/ \log_{10}\left(\frac{0.5+(3y-1)/(3x-1)}{0.5+(3y_1-1)/(3x_1-1)}\right).$$

Can. J. Chem. Downloaded from www.nrcresearchpress.com by 210.87.254.6 on 09/05/12
For personal use only.

The quantities x and y represent, respectively, the fractions of the *asymmetric* and the *trans* isomer in the ethylene after the reaction and the subscript i indicates the corresponding fractions initially present in the reactant *cis* isomer. It is assumed that k_3 is equal to the collision frequency in reaction [3] and this is calculated using a collision diameter of 4.95×10^{-8} cm, as was done previously by Setser *et al.* (23). The values of k_2 obtained from eq. [7] are given in the last column of Table I for the experiments at 3 mm. In spite of the low precision of the infrared analyses, the values are mutually consistent. The results at 0.3 mm show the expected behavior. However, it can be readily seen that the values of k_2, although of right magnitude, are strongly affected by small analytical inaccuracies since ϕ_{asym} is very close to ϕ_{trans}. These values are therefore not included in the table. It can be seen further (Table I, run 12) that 1,1-dideuteroethylene also isomerizes readily in the benzene-photosensitized reaction, giving equal amounts of the *cis* and *trans* isomer within the analytical accuracy. Equation [7] is not applicable in this case and k_2 could not be evaluated.

The mean value of k_2 obtained in the present work is 7.6×10^7 s^{-1}. The corresponding value obtained by Setser *et al.* (23) in the mercury-photosensitized isomerization is $(k_2)_{Hg} = 3.1 \times 10^9$ s^{-1}, which is about 41 times larger than the present value, $(k_2)_B$.This difference must be ascribed to a smaller amount of energy available in the benzene photosensitization. The ratio (ρ) of the two values of k_2 based on the classical theory of Kassell is

$$[8] \qquad \rho = \frac{(k_2)_{Hg}}{(k_2)_B} = \left(\frac{(1 - \epsilon_0/\epsilon)_{Hg}}{(1 - \epsilon_0/\epsilon)_B}\right)^{s-1},$$

where ϵ represents the actual vibrational excitation energy of the electronically excited ethylene molecules E* and ϵ_0 the minimum vibrational excitation energy required for the intersystem crossing step (reaction [2]). With 12 normal vibrational modes in ethylene, the number of "effective" oscillators (s) is likely to be between 6 and 8. The values of ϵ and ϵ_0 are not known but, for a tentative evaluation of ρ, certain values can be assumed on the basis of the energy level diagram in Fig. 1. Assuming that the zero vibrational level of E* is 1.9 eV (44 kcal) and the minimum energy required for reaction [2] to correspond to the level of ethylidene (69 kcal), then ϵ_0 = 25 kcal. In the case of mercury photosensitization ϵ is then 68 kcal (112 − 44), whereas in the benzene photosensitization ϵ is 39 kcal if the transfer occurs from the lowest triplet. Transfer from the lowest triplet cannot be vertical, but some deviation from a vertical transition cannot be ruled out since it is possible that a transient complex of finite lifetime is formed between ethylene and the benzene triplet. With these assumptions $\rho = (1.76)^{s-1}$, which for $s = 8$ gives $\rho = 52$. With Kassell's expression for k_2 ($k_2 = A[1 - \epsilon_0/\epsilon]^{s-1}$) a value of about 1×10^{11} s^{-1} is obtained for A. This is probably rather low, although there may be an appreciable loss of entropy in the transition state if the intersystem crossing indeed represents the formation of a triplet ethylidene from the ethylene triplet, as tentatively postulated (20). However, it is clear that any calculations of this type can have little quantitative significance at the present time. Not only is the position of the energy levels in doubt, but it is also not certain whether energy transfer to ethylene does occur from the first triplet of benzene as is usually assumed. Such an energy transfer would have to depart considerably from a vertical transition. Alternatively, the second or third triplet of benzene (placed tentatively by Parisier (27) on theoretical grounds at 4.1 and 4.7 eV, respectively, as shown in Fig. 1) may be the energy donors or even an isomeric form of benzene. This aspect of the process will require separate studies.

Can. J. Chem. Downloaded from www.nrcresearchpress.com by 210.87.254.6 on 09/05/12
For personal use only.

Investigations of the photosensitized isomerization of dideuteroethylene with other sensitizers of known lower triplet energies would be of interest from this point of view and also from the point of view of the chemical behavior of the excited triplet of ethylene. The latter has been of primary interest in present work.

In conclusion it may be mentioned briefly that a very small amount of hydrogen and of some other products appears to be formed at prolonged irradiations, especially at very low pressures. It was difficult to carry out reliable analysis, but hydrogen appeared to contain only very little deuterium and probably results mainly from some decomposition of benzene. A trace of acetylene found in the experiments at 0.3 mm pressure could come from reaction [4], but its yield is extremely small. A conservative estimate of k_4 from the equation

$$k_4 = \tfrac{1}{3}k_5[\mathrm{M}] \Big/ \left(\frac{\phi_{asym}}{\phi_{\mathrm{decomp}}}\right)_1$$

gives a value which is at least three orders of magnitude smaller than the corresponding value of 3.5×10^8 s^{-1} found by Setser *et al.* (23) in mercury photosensitization. Evidently, the molecular detachment of hydrogen (reaction [4]) is strongly dependent on the amount of vibrational energy in E**.

EXPERIMENTAL

This investigation has been carried out at two places, at the Tokyo Institute of Technology in Tokyo (TIT) and at the National Research Council in Ottawa (NRC).

Materials

At TIT, *trans*-dideuteroethylene was synthesized (28). Special care was taken to prevent contamination by mercury.

At NRC, the three dideuteroethylenes were purchased from the Merck, Sharp and Dohme of Canada, Ltd., and were used as supplied.

Apparatus

The apparatus used was practically the same as described previously (19). At NRC, the glass system was treated with NO_2 gas before use and the storage vessel for ethylene was packed with silver foil to eliminate any traces of mercury which might be present. Experiments with the medium-pressure lamp at NRC were carried out in the presence of mercury vapor.

The 2 537 Å radiation was obtained from a low-pressure mercury lamp and was passed through a 7–54 Corning glass filter at NRC and through a UV-25 Toshiba Denki glass filter at TIT. The Cd lamp used at NRC was supplied by Phillips Electronic Co. Ltd. The medium-pressure mercury lamp used at TIT was supplied by Wako Denki Co. Ltd. and at NRC, by the Engelhard Hanovia, Inc. Infrared spectra shown in the figures were obtained on a Perkin–Elmer model 21 double-beam spectrometer.

ACKNOWLEDGMENTS

The authors are grateful to L. C. Doyle for assistance with several of the experiments and to the Analytical Section of the Division of Applied Chemistry at NRC, especially to R. Ironside, for the infrared analyses.

We also thank Professor K. Kozima for the infrared analyses and Dr. S. Ikeda for his helpful advice in the preparation of dideuteroethylene.

REFERENCES

1. R. J. Cvetanović. *In* Progress in reaction kinetics. Vol. 2. *Edited by* G. Porter. Pergamon, London. 1964. p. 40.
2. R. B. Cundall and T. F. Palmer. Trans. Faraday Soc. **56**, 1211 (1960).
3. R. B. Cundall. *In* Progress in reaction kinetics. Vol. 2. *Edited by* G. Porter. Pergamon, London. 1965. p. 165.
4. D. F. Evans. J. Chem. Soc. 1351 (1957).
5. H. Ishikawa and W. A. Noyes, Jr. J. Chem. Phys. **37**, 583 (1962).
6. S. D. Colson and E. R. Bernstein. J. Chem. Phys. **43**, 2661 (1965).

Can. J. Chem. Downloaded from www.nrcresearchpress.com by 210.87.254.6 on 09/05/12
For personal use only.

7. R. S. MULLIKEN. J. Chem. Phys. **33**, 1596 (1960).
8. D. F. EVANS. J. Chem. Soc. 1735 (1960).
9. A. KUPPERMANN and L. M. RAFF. Discussions Faraday Soc. **35**, 30 (1963).
10. C. R. BOWMAN and W. D. MILLER. J. Chem. Phys. **42**, 681 (1965).
11. P. G. WILKINSON and R. S. MULLIKEN. J. Chem. Phys. **23**, 1895 (1955).
12. R. S. MULLIKEN and C. C. J. ROOTHAAN. Chem. Rev. **41**, 219 (1947).
13. W. MOFFITT and J. SCANLAN. Proc. Roy. Soc. London, Ser. A, **218**, 483 (1953).
14. S. F. MASON. Quart. Rev. London, **15**, 287 (1961).
15. L. BURNELLE. Tetrahedron, **21**, 49 (1965).
16. J. C. BRAND and D. G. WILLIAMSON. *In* Advances in physical organic chemistry. Vol. I. *Edited by* V. Gold. Academic Press, Inc., New York. 1963. p. 401.
17. J. R. PLATT. J. Chem. Phys. **18**, 1168 (1950).
18. W. MACF. SMITH. J. Chem. Phys. **20**, 1808 (1952).
19. J. E. DOUGLAS, B. S. RABINOVITCH, and F. S. LOONEY. J. Chem. Phys. **23**, 315 (1955).
20. A. B. CALLEAR and R. J. CVETANOVIĆ. J. Chem. Phys. **24**, 873 (1956).
21. D. P. CHONG and G. B. KISTIAKOWSKY. J. Phys. Chem. **68**, 1793 (1964).
22. M. J. MOLERA and F. J. STUBBS. J. Chem. Soc. 381 (1952).
23. D. W. SETSER, B. S. RABINOVITCH, and D. W. PLACZEK. J. Am. Chem. Soc. **85**, 862 (1963).
24. R. L. ARNETT and B. L. CRAWFORD, JR. J. Chem. Phys. **18**, 118 (1950).
25. C. REID. J. Chem. Phys. **18**, 1299 (1950).
26. AMERICAN PETROLEUM INSTITUTE RESEARCH PROJECT 44: Ultraviolet spectral data (Carnegie Institute of Technology, Pittsburgh, Pa.), Serial No. 637.
27. R. PARISIER. J. Chem. Phys. **24**, 250 (1956).
28. B. S. RABINOVITCH and F. S. LOONEY. J. Am. Chem. Soc. **75**, 2652 (1953).
29. M. TANAKA, T. TERAO, and S. SATO. Bull. Chem. Soc. Japan, **38**, 1645 (1965).

Can. J. Chem. Downloaded from www.nrcresearchpress.com by 210.87.254.6 on 09/05/12
For personal use only.

Can. J. Chem. Downloaded from www.nrcresearchpress.com by 210.87.254.42 on 09/05/12
For personal use only.

MEAN MOLAL ACTIVITY COEFFICIENT RATIOS OF MIXED Na^+–K^+ SOLUTIONS OF *p*-TOLUENE AND POLYSTYRENE SULFONATES

DONALD S. GAMBLE,[1] JACOB A. MARINSKY,[2] AND JOEL P. GUPTILL
Department of Chemistry, State University of New York at Buffalo, New York

Received March 15, 1966

ABSTRACT

A zeolite ion exchange technique for measuring mean molal activity coefficient ratios of mixed electrolytes has been further developed. The work was confined to systems of the type

(Zeolite Type 4A – Na^+ – K^+)

The 4A Zeolite has been calibrated for this kind of system by fitting the function

$$Q(X_{Na}) = \ln(\gamma_{Na}/\gamma_K) - (2.303 \log a_w \Delta \bar{V})/18.016$$

to a fifth degree polynomial, in the range $0.1 \leqslant X_{Na} \leqslant 0.7$.

Selectivity coefficient measurements with calibrated zeolite have been used to calculate ratios of mean molal activity coefficients for mixed Na^+–K^+ salts of model compounds. The model compounds were: *p*-toluene sulfonate, polystyrene sulfonate (mean molecular weight 400 000), and polystyrene sulfonate (mean molecular weight 30 000 to 40 000). The agreement between these measurements of activity coefficient ratios, and those calculated by Myers and Boyd for Dowex resins, ranges from excellent to fair.

INTRODUCTION

Numerous attempts have been made to interpret the ion-exchange phenomenon by employing for the exchanger phase activity coefficients of model compounds, selected for this purpose on the basis of their close resemblance to the repeating monomer unit of the cross-linked ion-exchange resin under consideration. For example, Gregor and Bregman (1) in 1951 attempted to predict ion-exchange selectivity coefficients of copolymers of divinylbenzene and sulfonated polystyrene by substituting the solution activity coefficients of the appropriate toluene sulfonates. Bregman (2) later predicted, with some success, equilibria for K^+–Li^+ and K^+–Na^+ systems by this approach. Bonner, Holland, and Smith (3) in their attempt to interpret selectivity reversal in the H^+–Na^+ ion-exchange reaction, made isopiestic measurements of solutions containing 80% *p*-toluene sulfonate and 20% 2,5-dimethylbenzene sulfonate with the counterions, Na^+ and H^+, present in varying proportions. They computed the activity coefficient ratio of these ions as a function of ion composition and total molality and on the basis of their results concluded that polystyrene divinylbenzene sulfonate ion-exchange resins are composed of at least two kinds of sulfonate groups. Recently available for application of this manner of approach to the elucidation of ion-exchange selectivity, are the mean molal activity coefficients that have been computed for various methane and ethane sulfonates from isopiestic measurements of the pure electrolytes (4).

The above technique for the analysis of the ion-exchange phenomenon suffers from the fact that the contribution of the polyelectrolyte environment of the resin to the thermodynamic characteristics of the counterions in the exchanger phase cannot be analyzed. A first approach to overcome this deficiency has been made by Bonner and Overton, who have reported isopiestic measurements on a wide molecular weight range of polystyrene

[1]*Union Carbide Fellow, 1963–1964. This paper is based on a dissertation submitted by D. S. Gamble in partial fulfillment of the requirements of the degree of Doctor of Philosophy. Present address: Analytical Chemistry Research Service, Research Branch, Canada Agriculture, Central Experimental Farm, Ottawa, Canada.*

[2]*Requests for reprints to be addressed to this author.*

sulfonates (5). Although no attempt was made by them to apply these measurements to selectivity coefficient predictions, we believe that such use of their measurements is desirable. In earlier studies by Marinsky *et al.* (6–8), a polyelectrolyte model was employed with some success to analyze ion-exchange behavior, and justifies this prognosis. In fact, because of this estimate, the ultimate objective of the present research program was to compare directly the thermodynamic parameters of the linear sulfonated polystyrene polyelectrolyte and the cross-linked sulfonated polystyrene cation-exchange resin at similar counterion concentrations.

For this purpose, an ion-exchange method for measuring activity coefficient ratios of mixed electrolytes was employed. The synthetic A-type zeolite, (9, 10) because of its special properties of rigidity and high resistance to electrolyte incursion, maintains essentially invariant its composition-based free energy. As a consequence, once these free energy parameters have been determined experimentally for a pair of counterions over a complete composition range in the zeolite, they may be employed to probe the mixed electrolyte behavior of systems containing these counterions. The effect of variables such as the nature of the by-ion, the relative composition of counterions, and the total ionic strength on mixed electrolyte properties are thus susceptible to study by this technique.

We have, in this investigation, employed the zeolite calibration that was obtained in a separate study of the K^+–Na^+ ion pair (11) to elucidate the thermodynamic behavior of Na–K polystyrene sulfonate and Na–K paratoluene sulfonate mixtures, respectively. This calibration was based on selectivity measurements at one ionic strength for the exchange reaction

$$\bar{K}_z^+ + Na_{(aq)}^+ \rightleftarrows \bar{Na}_z^+ + K_{(aq)}^+$$

in the mixed NaCl–KCl system. The thermodynamic properties of this mixed electrolyte system have been carefully evaluated by Robinson (12, 13) and could be used with complete confidence for characterization of the zeolite. The utility of the calibration over an extensive composition range of K^+ and Na^+ in the zeolite was then demonstrated by the ability to predict within the limits of experimental error the selectivity behavior of this system at other ionic strengths and at various composition ratios of the counterions (11).

THEORETICAL BASIS OF EXPERIMENTAL METHOD

The 4-A Zeolite has been rather extensively studied and the following characteristic properties have been demonstrated for this material. (*a*) The structure is well defined (14, 15) and no perceptible contraction, swelling, or structural changes occur when it is equilibrated at 25 °C with electrolyte at any concentration. (*b*) Electrolyte sorption at 25 °C, under controlled conditions, is either absent or can be limited to insignificant proportions. Barrer and Walker (16) have shown that the rate of sorption is extremely slow at 25 °C. In our laboratory we have observed, over the period of equilibration used in our studies of the KCl – NaCl – 4-A Zeolite system (11), that the sorption of Cl^- ion at 25 °C is measurable only at external concentrations exceeding 0.5 *m* and then only when the Na^+ ion content of the zeolite is at least 2.5-fold greater than its K^+ ion content. (*c*) The H_2O content of the zeolite is an insensitive function of the water activity (a_w) of the external solution. Water sorption measurements by Breck *et al.* (10) show that above an a_w value of 0.16 additional entry of water is essentially excluded because of the rigid structure.

Bukata and Marinsky (17) concluded from these facts that the properties of the zeolite

Can. J. Chem. Downloaded from www.nrcresearchpress.com by 210.87.254.42 on 09/05/12
For personal use only.

interior should depend only on the two cations used and the ion composition and were able to verify this assumption experimentally. In the equation

$$[1] \qquad \log K_K^{Na} = \log (\bar{\gamma}_K/\gamma_{Na}) + \pi(V_K - V_{Na})/2.303RT + 2 \log (\gamma^{\pm}_{NaCl}/\gamma^{\pm}_{KCl})$$

for the Na^+–K^+ system, K_K^{Na} is the experimentally determined selectivity coefficient, $\bar{\gamma}$ is the activity coefficient of the ion in the zeolite phase, $\gamma^{\pm}$ is the mean molal activity coefficient of the electrolyte in the external solution phase, π is the difference in osmotic pressure between the interior of the zeolite and the external solution, V represents the partial molar volume of the ions at infinite dilution and the bar placed above a symbol is used to differentiate the zeolite phase from the aqueous phase. The function

$$\log (\bar{\gamma}_K/\bar{\gamma}_{Na}) = g(X_{Na})$$

is assumed to be independent of the anion composition and water activity of the external solution. Bukata and Marinsky also assumed a zeolite water activity constant at $\bar{a}_w = 0.16$, so that with $(\bar{V}_K - \bar{V}_{Na}) = 10.2\ cm^3/mole$ from the literature (18),

$$[2] \qquad \begin{aligned} \pi(\bar{V}_K - \bar{V}_{Na})/2.303RT &= (\log a_w - \log \bar{a}_w)(\bar{V}_K - \bar{V}_{Na})/18.016 \\ &\approx 0.566 \log a_w + 0.450. \end{aligned}$$

With conversion to natural logarithms, this gives

$$\ln K_K^{Na} = \ln (\gamma_K/\gamma_{Na}) + 1.04 + 0.566 \ln a_w + 2 \ln (\gamma^{\pm}_{Na}/\gamma^{\pm}_K)$$

where the terms outside the square brackets on the right hand side characterize the external solution. It is not necessary to calculate

$$- \log \bar{a}_w(\bar{V}_K - \bar{V}_{Na})/18.016$$

as was the practice in earlier work. Any error arising from small deviations from constancy of this term can be avoided by defining the function

$$[3] \qquad \begin{aligned} Q(\bar{X}_{Na}) &= \ln (\gamma_K/\gamma_{Na}) - (2.303 \log \bar{a}_w(\bar{V}_K - \bar{V}_{Na})/18.016 \\ &= \ln K_K^{Na} - 0.566 \ln a_w - 2 \ln (\gamma^{\pm}_{Na}/\gamma^{\pm}_K). \end{aligned}$$

This calibration function is calculated only from experimental selectivity coefficients and from external solution properties. It is only necessary that

$$- \log \bar{a}_w(\bar{V}_K - \bar{V}_{Na})/18.016$$

be approximately constant. The quantity $RT(Q - 1.04)$ may therefore be regarded as the excess free energy of the Na^+–K^+ ion-exchange reaction, and according to the above is a function only of $\bar{X}_{Na}$. The calibration of the zeolite therefore consists of experimentally determining the function $Q = Q(\bar{X}_{Na})$. The calibrated zeolite may then be used to measure

$$2 \ln (\gamma^{\pm}_{Na}/\gamma^{\pm}_K)$$

for any Na^+–K^+ solution for which the assumptions of Bukata and Marinsky are valid. The ratio of mean molal activity coefficients in the external solution is thus calculated from the equation

$$[4] \qquad \log (\gamma^{\pm}_{Na}/\gamma^{\pm}_K) = (1/4.606)\ (\ln K^{Na}_K - Q - 1.304 \log a_w) = f(m, X_{Na}).$$

Can. J. Chem. Downloaded from www.nrcresearchpress.com by 210.87.254.42 on 09/05/12
For personal use only.

Can. J. Chem. Downloaded from www.nrcresearchpress.com by 210.87.254.42 on 09/05/12
For personal use only.

EXPERIMENTAL

Chemicals

Baker Analyzed and Fisher Certified Reagent grade acetic acid, sodium hydroxide, potassium hydroxide, potassium acetate, potassium chloride, and sodium chloride were used as received.

The zeolite (Linde Molecular Sieve, type 4-A), supplied by the Linde Corporation of Tonawanda, New York, was prepared for use in 100 g portions. Each portion was hydrated and sieved, the residue retained by a 100 mesh screen being discarded. The screened zeolite product was then equilibrated 2 or 3 times for as long as 12 h with 1.85 *M* sodium acetate adjusted to a pH of 6.5 with acetic acid, thereby assuring the conversion of any hydrolyzed material to the sodium form. Fines were then removed by decantation after sedimentation several times in 0.2 *M* NaCl. The zeolite product was then washed with deionized water until the complete removal of Cl^- ion. An alternate final treatment of the zeolite consisted of washing with 0.2 *M* NaCl to assure removal of traces of acetate ion. Analysis of the sodium content of zeolite samples prepared by both methods were identical within experimental error limits and demonstrated conclusively that zeolite hydrolysis during the final wash with water was insignificant. In addition, selectivity measurements were reproducible from one batch to the other.

Fisher Certified Reagent *p*-toluene sulfonic acid (m.p. 104.1° to 105.1° C) was converted to the potassium salt with 1 *M* KOH. Insoluble material was removed by filtration. After concentration of the filtrate two crystallizations were effected by cooling the approximately 4 *m* solutions to 1 °C. A third set of crystals, recovered in the same way, was dissolved and decolorized with activated charcoal; it was then filtered and recrystallized before being combined with the earlier crystal product. The total sample was dissolved, decolorized, and recrystallized by evaporation at room temperature. Separate samples of sodium polystyrene sulfonate, mean molecular weight 400 000 and 30 000 – 40 000, respectively, were supplied by Dow Chemical Company, Midland, Michigan, in powder form.

Conversion of the low molecular weight polymer to the K^+ salt form was accomplished by passing a solution of the Na^+ salt (100 g dissolved in 600 g of H_2O) through an ion-exchange (Dowex 50-X8) column. A small fraction separated during the conversion to the K^+ salt was discarded. A flame test detected no Na^+ in the final polymer solution. Solutions of the higher molecular weight polymer were too viscous for the ion-exchange column operation. However, the polymer is insoluble in concentrated potassium acetate and in ethanol. The K^+ salt of the polymer was therefore prepared by repeated salting out from aqueous solution with concentrated potassium acetate. Excess potassium acetate was finally washed out of the solid polymer with ethanol.

Carrier free 2.6 y ^{22}Na was purchased from the Nuclear Science and Engineering Corporation, Pittsburgh, Pennsylvania, in half mCi amounts and was diluted to 1 ml prior to use.

Analytical Procedures

Paratoluene sulfonate solutions were quantitatively converted by ion exchange to the free acid, which was then titrated with standard NaOH. Solid samples of polystyrene sulfonate were analyzed the same way, after being dried to constant weight over P_2O_5.

The zeolite was analyzed for H_2O content by ignition at 800 °C until constant weight was attained. The precision of the dry weights after 48 h was $\pm 0.05\%$ or better. The ion exchange capacity of the zeolite was measured by an isotope dilution technique involving ^{22}Na and γ-ray counting. Typical results for 3 samples are given in Table I. Breck *et al.* (10) have reported that $96\% \pm 4\%$ of the theoretical amount of Na^+ is found in this zeolite. This corresponds to an ion-exchange capacity of $6.758 \pm 4\%$ meq/g of dry Na^+-form zeolite, a value approximately 0.7% higher than is measured. This deviation is almost within the experimental error of the tracer method. All calculations were made using the average capacity value given in Table I.

Selectivity Coefficient Measurements

Portions of zeolite, and of K^+ salt solutions containing ^{22}Na radiotracer, were weighed into polyethylene bottles. Equilibrium was established by shaking and thermostatting at 25.0 °C during two to four weeks, depending on viscosity. Solutions from the equilibrated mixtures were centrifuged free of zeolite, and weighed into cellulose nitrate test tubes for γ-ray counting. The counting was done with a NaI crystal well detector. Three aliquots of each stock solution were counted, to serve as standards.

Counting Procedure

Four 10 min counts were made on each experimental sample, and a total of twelve 10 min counts were made on each standard. The precision attained was usually within the statistical error of counting.

Isopiestic Measurements

A few isopiestic measurements were made with K^+ polystyrene sulfonate solutions at high water activities. The solutions and isopiestic standards were put into jars which were sealed with rubber gaskets and placed in the constant temperature chamber at 25.0 ± 0.02 °C. Two samples approached equilibrium from opposite directions in the same jar. No special provisions were made to promote heat and mass transfer. Instead, the isopiestic jars were simply left undisturbed for about eight weeks.

TABLE I

Ion-exchange capacity of zeolite

Sample	Capacity (meq per dry gram)
A	6.706
	6.719
	6.698
	6.697
	6.660
B	6.727
	6.726
	6.739
	6.709
	6.742
C	6.693
	6.681
	6.656*
	6.654*
	6.645*
	6.608*
	6.646*
	Av. = 6.708 ± 0.7%

*Rejected because of erratic behavior of the counting equipment.

RESULTS

(1) Selectivity Coefficients

The total radioactivity of an exchange sample (solution + zeolite) is given by

$$A_T = (C_0/t_0 - C_B/t_B)W_s/W_0 \text{ counts/min}$$

while that taken up by the zeolite is

$$A_z = [(C_0/t_0 - C_B/t_B)1/W_0 - (C_A/t_A - C_B/t_B)1/W_{AK}]W_s \text{ counts/min.}$$

The mole fraction of Na^+ in the zeolite is calculated from

[5] $$\bar{X}_{Na} = 1 - (C_A/t_A - C_B/t_B)W_0/(C_0/t_0 - C_B/t_B)W_{AK}.$$

The Na^+ ion concentration of the external solution is then

[6] $$m_{Na} = Z(W_z/W_w)(1 - \bar{X}_{Na})$$

[7] $$X_{Na} = (ZW_z/mW_w)(1 - \bar{X}_{Na}).$$

The aliquots of stock solution that are weighed out as standards contain only the pure K^+ salt, apart from the trace ^{22}Na. After equilibration of these solutions there is significant substitution of Na^+ for K^+ ion. Consequently at a given total molality, the value of W_{AK} must be modified to correct for the loss in solution weight that results from the ion exchange reaction since the selectivity coefficient is so sensitive to error. The following equation has been employed for this purpose:

[8] $$W_{AK} = (1 + mM_K/10^3)W_A^1/\{1 + m[X_{Na}(M_{Na} - M_K) + M_K]/10^3\}$$

The zeolite phase concentrations are given by

$$\bar{c}_{Na} = Z\bar{X}_{Na}$$

$$\bar{c}_K = Z(1 - \bar{X}_{Na}).$$

Can. J. Chem. Downloaded from www.nrcresearchpress.com by 210.87.254.42 on 09/05/12
For personal use only.

By using these and $m_K = m - m_{Na}$, the equation with which the selectivity coefficient is related to the experimental measurements is obtained:

$$[9] \qquad K_K^{Na} = \bar{X}_{Na}[mW_w/ZW_z - (1 - X_{Na})]/(1 - X_{Na})^2$$

In these equations C/t represents the observed counts per minute, W the weight in grams of the various samples, M the atomic weight of K^+ or Na^+ and Z the ion-exchange capacity in meq per dry gram of zeolite. The subscripts 0, s, B, A, AK, z, and w identify the operation or the sample subjected to the specified measurement, as follows:

0 = aliquot of initial equilibrating sample (standard)
s = total initial equilibrating sample
B = background measurement
A, AK = aliquot of equilibrated sample
z = zeolite
w = water.

An iterative calculation, employing eqs. [5], [7], [8], is necessary before the calculation of K_K^{Na} from eq. [9] is begun. The iteration is started by using $W_{AK} \simeq W_A$[1] to get the zeroth order approximation of X_{Na}. The calculation converges very rapidly so that very little if any change occurs within four significant figures after the first iteration.

An error in C_0 can seriously affect the shape of a K_K^{Na} vs. $\bar{X}_{Na}$ plot. Since a plot of $(C_A - C_B)$ per unit mass against (W_z/W_w) should extrapolate to $(C_0 - C_B)$ per unit mass at $(W_z/W_w) = 0$, such errors were easily found and corrected. The only requirement for this test was the increased precision which derived from the greater number of measurements. This test was made for all of the K_K^{Na} vs. $\bar{X}_{Na}$ data and is illustrated in Fig. 1 for several sets of experiments. The sample plot for 0.4960 m polystyrene sulfonate does not extrapolate to the measure value of the $(C_0 - C_B)/2.000$ g. The extrapolation value gives better agreement with another series of 0.4960 m experiments. Such correction of

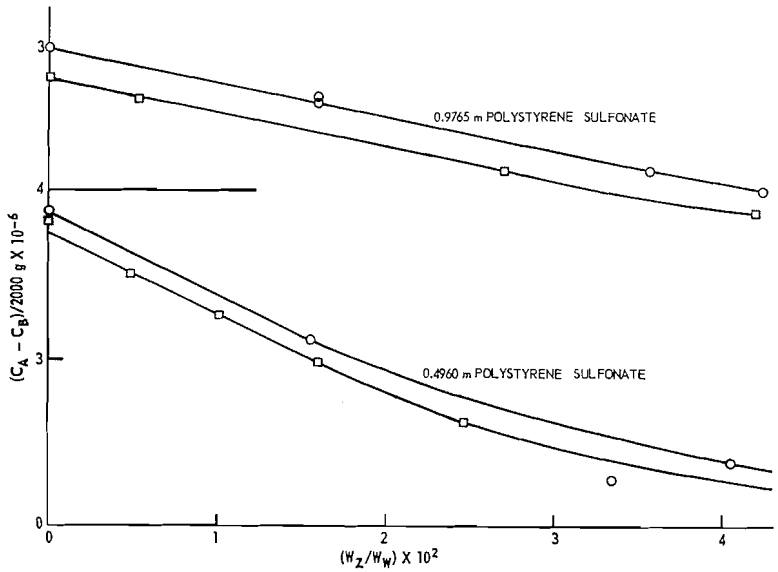


FIG. 1. Measurement calibration for 0.9765 and 0.4960 m polystyrene sulfonate.

Can. J. Chem. Downloaded from www.nrcresearchpress.com by 210.87.254.42 on 09/05/12
For personal use only.

C_0 was needed only in some of the *p*-toluene sulfonate results since repeated measurements of the standards were not made in this earlier phase of the program.

The selectivity coefficient calculations were duly programmed in Fortran II for the I.B.M. 1620 computer. This program used eqs. [5–8] and eq. [9] to calculate $\bar{X}_{Na}$, m_{Na}, and K_K^{Na}. Four iterations were used. The data are summarized in Tables II and III.

TABLE II[3]

Selectivity coefficients for *p*-toluene sulfonate solutions (total molality = 1.102)

$\bar{X}_{Na}$	m_{Na}	K_K^{Na}
0.0977	0.0947	1.15
0.204	0.178	1.33
0.265	0.226	1.40
0.351	0.302	1.43
0.405	0.360	1.40
0.452	0.417	1.35
0.667	0.742	0.975
0.707	0.815	0.846
0.747	0.881	0.743
0.783	0.944	0.603
0.841	1.03	0.374
0.243	0.208	1.38
0.554	0.544	1.27
0.624	0.671	1.06

TABLE III[3]

Selectivity coefficients for polystyrene sulfonate solutions (400 000 mean molecular weight, total molality = 0.9765)

$\bar{X}_{Na}$	m_{Na}	K_K^{Na}
0.105	0.0969	1.06
0.239	0.181	1.38
0.274	0.206	1.42
0.289	0.225	1.36
0.373	0.284	1.45
0.443	0.354	1.40
0.495	0.408	1.37
0.594	0.539	1.19
0.676	0.661	0.996
0.722	0.731	0.875
0.763	0.784	0.791
0.795	0.840	0.630
0.0390	0.0332	1.15
0.188	0.146	1.32
0.274	0.203	1.43

Figures 2 and 3 illustrate the typical shapes of the K_K^{Na} vs. $\bar{X}_{Na}$ curves. All show maxima for $0.3 < \bar{X}_{Na} < 0.4$, at $X_{Na} \approx 0.35$. For the polystyrene sulfonate solutions the value of the maximum increases with total concentration. In the *p*-toluene sulfonate system, the 2.168 *m*, 3.179 *m*, and 3.766 *m* curves are within experimental error of each other, somewhat above the 1 *m* curves. Below $\bar{X}_{Na} = 0.1$, the curves are generally ill defined. Mixing and separation problems caused by high viscosity may have contributed to the scatter in

[3]*More extensive tables of selectivity coefficients have been placed in The Depository of Unpublished Data, National Science Library, National Research Council, Ottawa, Canada, and photocopies may be obtained upon request to the Depository.*

Can. J. Chem. Downloaded from www.nrcresearchpress.com by 210.87.254.42 on 09/05/12
For personal use only.

Fig. 3. Solid circles indicate points calculated from plots similar to those presented in Fig. 2.

(2) Calibration of the Zeolite

Robinson and Stokes (19) have published the mean molal activity coefficients and H_2O activities of mixed NaCl–KCl solutions, over a complete range of X_{Na} and over a considerable range of concentration. These data are ideally suited for calibration of the zeolite.

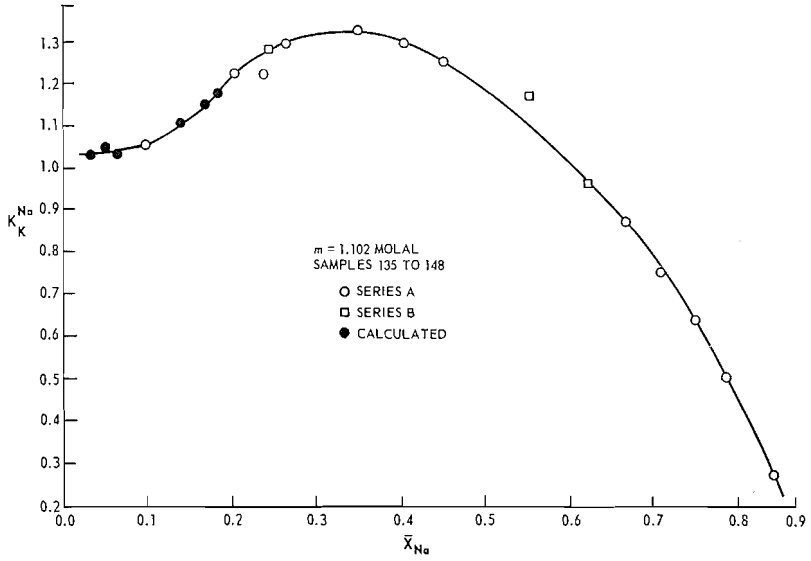


FIG. 2. Selectivity behavior of *p*-toluene sulfonate.

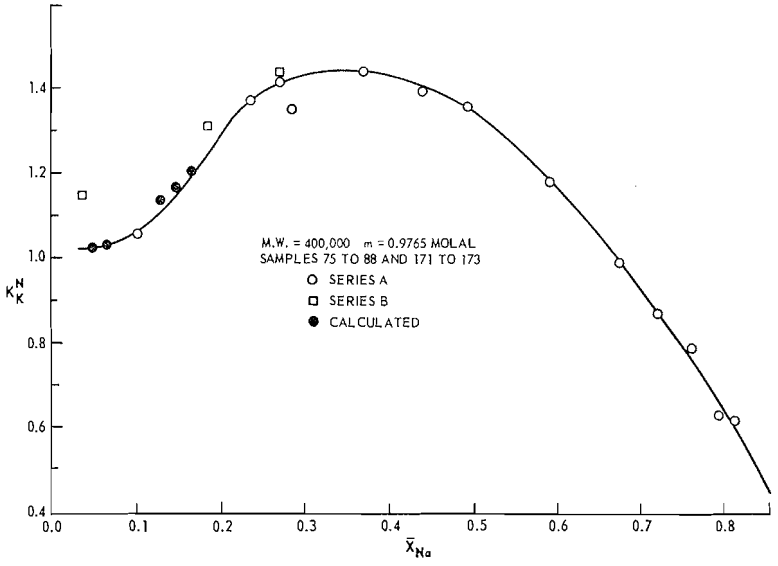


FIG. 3. Selectivity behavior of polystyrene sulfonate.

Can. J. Chem. Downloaded from www.nrcresearchpress.com by 210.87.254.42 on 09/05/12
For personal use only.

By using eq. [3], $Q = Q(X_{Na})$ has been calculated for 99 sets of K_K^{Na} measurements with NaCl–KCl solutions. These have been fitted by least squares to the polynomial,

$$[10] \qquad Q = \sum_{n=0}^{5} C_n \bar{X}_{Na}{}^n$$

within the range $0.1 \leqslant \bar{X}_{Na} \leqslant 0.7$. Both the calculation of Q and the least squares fit were accomplished with the I.B.M. 1620. The pertinent polynomial coefficients for the equation representing the zeolite calibration curve are:

$$\begin{aligned} \sigma &= 0.0225 \\ C_0 &= -0.4360 \\ C_1 &= +5.075 \\ C_2 &= -10.21 \\ C_3 &= +3.314 \\ C_4 &= +7.694 \\ C_5 &= -7.071 \end{aligned}$$

The calibration curve in Fig. 4 has the same general shape as the selectivity coefficient curves, with a maximum at $\bar{X}_{Na} = 0.34$. The fourth degree polynomial had a standard deviation almost as small, but did not give quite as good a fit at the extreme ends of the curve.

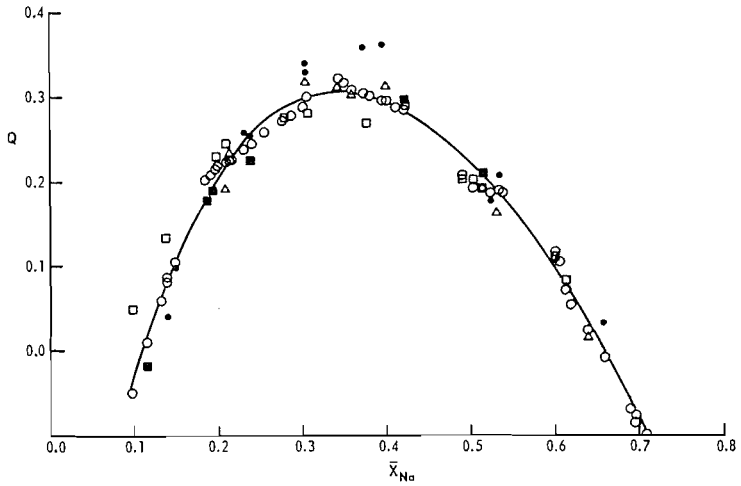


FIG. 4. Calibration of Zeolite 4-A.

(3) Solution Activity Coefficient Ratios

Equations [4], [10], and [7] were used to calculate log $(\gamma^{\pm}_{Na}/\gamma^{\pm}_{K})$ as a function of X_{Na} for each of the ten solutions studied. Water activities were taken from data published by Robinson and Stokes (19). The water activity values used for the polystyrene sulfonate solutions were taken from Fig. 5 which contains our data for the K^+ polystyrene sulfonate and the data published for the Na^+ salt by Bonner and Overton (5). In all cases a_w was assumed to be a linear function of X_{Na}. This is justified, since neglecting the a_w term completely in eq. [4] causes an error of only 1% to 3% in log $(\gamma^{\pm}_{Na}/\gamma^{\pm}_{K})$. In addition, this linear approximation causes negligible error in the NaCl–KCl computations. The solutions were fitted to straight lines by least squares.

Can. J. Chem. Downloaded from www.nrcresearchpress.com by 210.87.254.42 on 09/05/12
For personal use only.

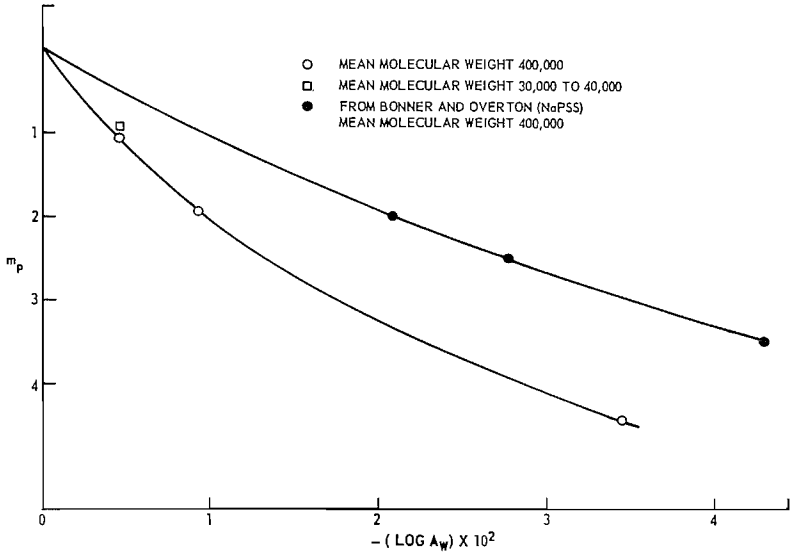


FIG. 5. Water activities of potassium polystyrene sulfonate.

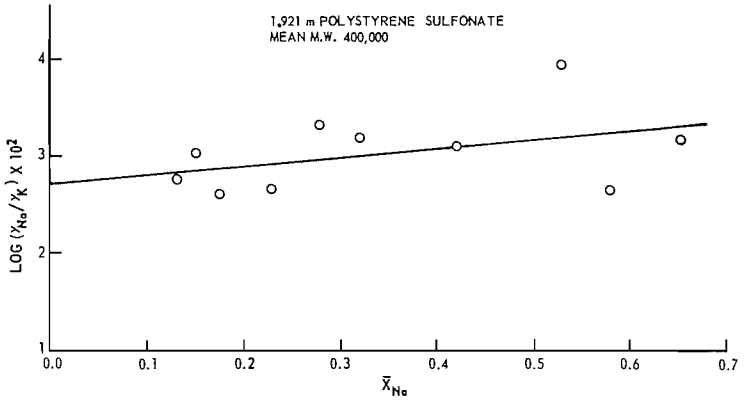


FIG. 6. Activity coefficient ratio.

A sample plot of log $(\gamma^{\pm}_{Na}/\gamma^{\pm}_{K})$ versus X_{Na} for the 1.921 *m* polystyrene sulfonate system is presented in Fig. 6. The variation of $(\gamma^{\pm}_{Na}/\gamma^{\pm}_{K})$ with mole fraction of Na in the zeolite is summarized briefly in Table IV.

(4) Experimental Errors

The experimental errors are classified according to their effects on the calculation of K_K^{Na}. In eq. [9], let

$$y = (C_A/t_A - C_B/t_B)W_0(C_0/t_0/ - C_B/t_B)W_A$$

$$u = mW_w/ZW_z$$

This gives

$$\bar{X}_{Na} = 1 - y$$
$$K_K^{Na} = (1 - y)(u - y)/y^2.$$

Can. J. Chem. Downloaded from www.nrcresearchpress.com by 210.87.254.42 on 09/05/12
For personal use only.

TABLE IV

Mean molal activity coefficient ratios
$\log (\gamma^{\pm}_{Na}/\gamma_{K}^{\pm}) = A_0 + A_1 X_{Na}$

m	A_0	A_1	σ	X_{Na}	$(\gamma^{\pm}_{Na}/\gamma^{\pm}_{K})^2$
p-Toluene sulfonate					
1.030	0.0105	+0.0104	0.005	0.116	1.06
				0.311	1.06
				0.672	1.08
1.102	0.0250	−0.0347	0.006	0.162	1.10
				0.327	1.06
				0.673	1.00
2.168	0.0363	+0.0447	0.003	0.140	1.21
				0.358	1.28
				0.674	1.34
3.179	0.0310	+0.0510	0.004	0.109	1.19
				0.341	1.25
				0.680	1.34
3.766	0.0348	+0.0507	0.002	0.107	1.21
				0.330	1.28
				0.607	1.35
Polystyrene sulfonate, mean molecular weight 400 000					
0.4960	0.0168	−0.0470	0.007	0.122	1.06
				0.329	1.00
				0.600	0.919
0.9765	0.160	−0.00816	0.005	0.186	1.06
				0.362	1.06
				0.677	1.04
1.921	0.0320	+0.028	0.007	0.131	1.14
				0.321	1.14
				0.654	1.16
2.379	0.0563	+0.052	0.007	0.122	1.23
				0.293	1.25
				0.446	1.26
Polystyrene sulfonate, mean molecular weight 30 000 – 40 000					
0.9843	0.180	−0.0368	0.009	0.151	1.06
				0.351	1.02
				0.656	0.972

Therefore, a positive error in y gives a negative error both in $\bar{X}_{Na}$ and in K_K^{Na}, with the error in K_K^{Na} being magnified. A positive error in u makes a positive error in K_K^{Na} of similar magnitude.

The error in y is less than $\pm 0.5\%$. The measurements of m and Z are the most important sources of error in u. Together they give u an error of at least $\pm 1\%$. The selectivity coefficient computer program was used to examine the effects of the errors in y and u on K_K^{Na}. These indicate that the error in K_K^{Na} is $\pm 3\%$, and that the shape of the K_K^{Na} vs. $\bar{X}_{Na}$ curve is quite uncertain for $\bar{X}_{Na} \leqslant 0.1$. From this and from the σ of the Q curve, $(\gamma^{\pm}_{Na}/\gamma^{\pm}_{K})$ is estimated to have $\sigma = \pm 8\%$, or $\rho = \pm 5.4\%$.

DISCUSSION

The objective of this program was blunted by propagation of errors. The intended calculation of Harned–Cook constants to describe the functional dependence of $(\gamma^{\pm}_{Na}/\gamma^{\pm}_{K})$ on X_{Na} in the monomer and the polyelectrolyte is not possible because of the scatter of the data points. As a result a quantitative comparison of the thermodynamic parameters for the monomer, the linear polyelectrolyte and the cross-linked ion-exchange resin (16) cannot be made. In fact, the behavior of the three systems is so similar that a qualitative comparison is difficult as well.

Resin phase single ion activity coefficient ratios calculated by Myers and Boyd (20) for Dowex 50 are given in Table V for this purpose. These authors reported a possible

Can. J. Chem. Downloaded from www.nrcresearchpress.com by 210.87.254.42 on 09/05/12
For personal use only.

TABLE V

Resin phase activity coefficient ratios calculated by Myers and Boyd (20) for Dowex 50

% DVB*	$\bar{X}_{Na}$	$(\gamma^{\pm}_{Na}/\gamma^{\pm}_{K})$ ±8 to ±14%	Resin phase total molality
2	1.0	1.34	1.95
2	0.5	1.26	1.97
2	0.0	1.19	2.00
4	1.0	1.48	3.30
4	0.5	1.38	3.36
4	0.0	1.30	3.40
8	1.0	1.71	5.81
8	0.5	1.57	5.90
8	0.0	1.44	5.99

*%DVB here means "nominal mole % divinylbenzene".

experimental error of 8% to 14% in their measurements. The error in $(\gamma^{\pm}_{Na}/\gamma^{\pm}_{K})$ was assumed to be similar since other terms made small contributions to the total error, and much better agreement than this between calculated and measured selectivity coefficients was obtained by them.

There is excellent agreement between the calculations of Myers and Boyd for 2% crosslinked Dowex 50, which has a resin phase molality of 2, and the present measurements for 2.168 *m* *p*-toluene sulfonate solution. The agreement with the 1.921 *m* and 2.379 *m* polystyrene sulfonate is not as good, but is within experimental error.

The results with the polymer appear to be consistently low. There is fair agreement between the 3.179 *m* and 3.766 *m* *p*-toluene sulfonate measurements and the calculations of Myers and Boyd for 4% crosslinked resin, in which the total exchanger phase molalities are 3.3 to 3.4.

Although the experimental program failed in its primary objective in this investigation the selectivity method for quantitative analysis of the type attempted herein is undoubtedly useful for other systems such as the Ag–Na polystyrene sulfonate where interaction effects are considerable. A recent investigation by this method of the nitrates and acetates of K and Na has proved fruitful and a report of this study is being prepared for publication (11).

REFERENCES

1. H. P. Gregor and J. I. Bregman. J. Colloid Sci. **6**, 323 (1951).
2. J. I. Bregman. Ann. N.Y. Acad. Sci. **57**, 125 (1953).
3. O. D. Bonner, V. F. Holland, and L. L. Smith. J. Phys. Chem. **60**, 1102 (1956).
4. H. P. Gregor, M. Rothenberg, and N. Fine. J. Phys. Chem. **67**, 1110 (1963).
5. O. D. Bonner and J. R. Overton. J. Phys. Chem. **67**, 1035 (1963).
6. A. Chatterjee and J. A. Marinsky. J. Phys. Chem. **67**, 41 (1963).
7. J. A. Marinsky and A. Chatterjee. J. Phys. Chem. **67**, 47 (1963).
8. J. Krasner and J. A. Marinsky. J. Phys. Chem. **67**, 2559 (1963).
9. R. M. Barrer and E. A. D. White. J. Chem. Soc. 1561 (1952).
10. D. W. Breck *et al.* J. Am. Chem. Soc. **78**, 5963, 5972 (1956).
11. J. Guptill and J. A. Marinsky. In preparation. 1966.
12. R. A. Robinson. J. Am. Chem. Soc. **74**, 6035 (1952).
13. R. A. Robinson. Trans. Faraday Soc. **49**, 1147 (1953).
14. T. B. Reed and D. W. Breck. J. Am. Chem. Soc. **78**, 5972 (1956).
15. P. A. Howell. Acta Cryst. **13**, 737 (1960).
16. R. M. Barrer and A. J. Walker. Trans. Faraday Soc. **60**, 171 (1964).
17. S. Bukata and J. A. Marinsky. J. Phys. Chem. **68**, 994 (1964).
18. P. Mukerjee. J. Phys. Chem. **65**, 740 (1961).
19. R. A. Robinson and R. H. Stokes. Electrolyte solutions. 2nd ed. Butterworth Scientific Publications, London. 1959.
20. G. E. Myers and G. E. Boyd. J. Phys. Chem. **60**, 521 (1956).

Can. J. Chem. Downloaded from www.nrcresearchpress.com by 210.87.254.42 on 09/05/12
For personal use only.

Can. J. Chem. Downloaded from www.nrcresearchpress.com by 210.87.254.40 on 09/05/12
For personal use only.

ON THE PRESSURE DEPENDENCE OF REACTION RATES

H. S. GOLINKIN, W. G. LAIDLAW, AND J. B. HYNE
Department of Chemistry, University of Calgary, Calgary, Alberta
Received March 8, 1966

ABSTRACT

The functional dependence of the rate constant for benzyl chloride solvolysis on pressure is investigated with a view to obtaining reliable values of the activation parameters. It is concluded that a second order polynomial is the best description of this system, reproducing the experimental data with a greater degree of precision than the other published functions. A method for determining the precision of the derivatives of the logarithmic rate is presented, and the pressure dependence of the activation volume is demonstrated. Various systems from the literature are analyzed to demonstrate the general applicability of the quadratic function.

INTRODUCTION

The pressure dependence of reaction rate has long been used to obtain the pseudo-thermodynamic parameter of activation, ΔV^*, the volume change on activation. The sign and numerical value of this parameter are clearly related to such important mechanistic phenomena as bond extension and solvent electrostriction during the activation process. Accordingly, considerable attention has been directed toward obtaining meaningful ΔV^* values for a number of solvolytic and displacement reactions in an attempt to further elucidate the mechanisms of these processes. The major problems faced in such determinations are twofold: firstly the determination of rate constants (k) as a function of pressure of sufficient precision to permit extraction of ΔV^* values with associated error limits that are small compared with the numerical magnitude of ΔV^* itself; and secondly the establishment of the *functional dependence* of the rate constant on pressure.

These problems are similar to those that for many years characterized the difficulties attendant upon the determination of activation enthalpy, ΔH^*. Here, the corresponding problems were those of accurate rate determinations as a function of temperature and the establishment of the functional dependence of rate constant on temperature. It was not until the postwar period that rate data of sufficient accuracy became available to permit detailed testing of various functional dependencies of rate on temperature. Such work led to the recognition of the reality of the ΔCp^* activation parameter, implying the nonlinear dependence of $\ln k$ on $1/T$, or alternatively, the temperature dependence of ΔH^* (1). Many of the analytical problems associated with the rate/pressure dependency are remarkably similar to those previously encountered in the rate/temperature relationship, as will be seen in subsequent sections of this paper.

Crucial to the whole problem of both rate/temperature and rate/pressure dependency is the determination of sufficiently accurate rate data. Although there inevitably will be continued scepticism as to whether the rate data obtained are, in fact, of sufficient accuracy to permit the refined analysis necessary to test various functional dependencies, it seems to us that at some stage a start must be made to obtain an objective technique for comparing the various functional forms. We believe that the rate data on the solvolysis of benzyl chloride in ethanol–water mixtures as a function of pressure analyzed in this paper are of sufficient accuracy. The *in situ* conductimetric technique used to follow the rate of the reaction as a function of pressure is very similar to the methods used to

obtain highly accurate rate/temperature data. We have also applied our analytical methods to a number of other sets of rate/pressure data available in the literature. Although the precision of these data may well not be sufficient to justify the refined level of analysis applied, the form of analysis used in a number of the cases cited has been the basis of protracted argument in the literature (2, pp. 98–99; 3; 4). The application of our analytical comparison to these cases therefore serves to highlight the crucial factors involved in the formulation of the rate/pressure dependency.

BENZYL CHLORIDE SOLVOLYSIS (RATE DATA)

The rate of solvolysis of benzyl chloride in various water–ethanol mixtures has been studied as a function of pressure up to 4 000 atm at 50.25 °C (5). The rate data as a function of pressure and solvent composition is reproduced in Table I. The most crucial aspect of this data as far as the purpose of this paper is concerned is the confidence that can be placed in the error limits claimed for each rate constant. The *in situ* conductimetric technique used eliminates many of the sampling and timing errors that are characteristic of aliquot sampling techniques.

TABLE I

Rate constants and activation parameters for the solvolysis of benzyl chloride in aqueous ethanol at 50.25 °C

Pressure (atm)	$10^5 \times k$ (s^{-1}) for mole fraction ethanol				
	0.000	0.100	0.200	0.300	0.400
1	23.1 ±0.4	6.690±0.007	1.93±0.01	0.80±0.01	0.459±0.007
341	24.42±0.02	8.47 ±0.01	2.46±0.01	1.06±0.01	
681	30.0 ±0.2	10.25 ±0.02	3.02±0.07	1.29±0.01	0.68 ±0.03
1 362	39.3 ±0.3	13.68 ±0.01	4.64±0.01	2.04±0.03	1.041±0.002
2 723		21. ±2.	7.7 ±0.2	3.00±0.02	1.81 ±0.02
4 084					2.6 ±0.2
ΔV_0^* (ml/mole)	−8. ±1.	−17. ±1.	−20.3±0.2	−22.9±0.2	−17.9±0.9
$10^3 \times (\partial \Delta V^*/\partial p)_T$ (ml/atm mole)	−4. ±1.	+4. ±1.	+4.9±0.3	+7.3±0.1	+3.2±0.6

The considerable variation in the percentage size of the uncertainty claimed for each rate results from the concommitant variation in the experimental difficulties encountered as solvent and pressure are varied. The uncertainty tends to be larger at higher pressures where rates are faster and pressure control more difficult.[1] Similarly in more aqueous media the rates are also faster, resulting in a shorter reaction period available for study after pressure and temperature equilibration in the pressure vessel has been attained. The combination of all of these factors results in considerable variation of the uncertainty limits associated with each rate reported. Because of the crucial nature of the rate accuracy factor in such a study, however, it would be completely unjustifiable to report a single averaged uncertainty for all of the rate values.

The actual uncertainties reported in Table I are obtained from a minimum of two independent rate determinations and in many cases from three or four independent determinations.

[1]*The automatic pressure-regulating device used in this study (5) enabled the pressure to be controlled to ±14 atm (200 psig).*

Can. J. Chem. Downloaded from www.nrcresearchpress.com by 210.87.254.40 on 09/05/12
For personal use only.

ANALYTICAL FUNCTIONS AND THEIR SIGNIFICANCE

Theoretical Considerations

No strictly theoretical, analytical function describing the pressure dependence of reaction rate is available. The usual differential form of the dependence used is that given by Evans and Polanyi (6),

$$[1] \qquad \Delta V^* = -RT(\partial \ln k/\partial p)_T,$$

but the question immediately arises as to whether ΔV^* is pressure independent or not. Precisely the same question arises for the temperature dependence of rate where ΔH^* can be written

$$[2] \qquad \Delta H^* = -RT(\partial \ln k/\partial \left(\frac{1}{T}\right)_p).$$

If the pseudo-thermodynamic ΔH^* parameter has the same form as the real thermodynamic ΔH, then it is not temperature independent, since there is a non-zero value of ΔC_p^*. In an exactly similar manner ΔV^* may be expected to be pressure dependent according to eq. [3]

$$[3] \qquad (\partial \Delta V^*/\partial p)_T = -V_0^* \kappa^* \exp(-\kappa^* p) + V_0^g \kappa^g \exp(-\kappa^g p),$$

where the first term on the right-hand side refers to the transition state with V_0^* being the partial molal volume of the transition state at some reference pressure and κ the compressibility; the second term on the right-hand side applies similarly to the initial state. Equation [3] is unusable as an anlytical function for treating experimental rate data, since the partial molal isothermal compressibilities (κ's) cannot be determined in reacting systems.

While, therefore, there is good reason to believe that the functional dependence of rate on pressure is at least of second order with respect to pressure (just as the dependence of rate on temperature is second order in temperature), there is no theoretically derive-able form of the functional dependence which has practical utility.

Two further factors must be considered as possible contributors to the pressure dependence of rate: concentration effects and viscosity effects. In solvolytic reactions of the benzyl chloride type considered here the reaction is between the molecular species of the solvent environment and the dissolved substrate. Accordingly, if the volume of the initial and transition states is considered to be the volume of the substrate *plus* its immediate solvation shell in both states the effect of pressure on "concentration" is included in the volume of the two states as so defined. The viscosity effect would not be expected to become a major contributor until the viscosity of the system increased to a point where the diffusion rate of the reacting species was significantly reduced. This requires very high pressures as has been shown by Hamann (7) where for bimolecular reactions the rate dependence on pressure actually changes sign from positive to negative at very high pressures. Again, however, in solvolyses reactions, diffusion together of the reacting species is not an important factor, since the reacting substrate is always in immediate contact with the reactant solvent.

The Functions

In the absence of a strictly based theoretical functional form of practical utility for expressing the dependence of rate on pressure, four basic semiempirical functions have been employed. It is the purpose of this paper to examine these relations between rate

Can. J. Chem. Downloaded from www.nrcresearchpress.com by 210.87.254.40 on 09/05/12
For personal use only.

Can. J. Chem. Downloaded from www.nrcresearchpress.com by 210.87.254.40 on 09/05/12
For personal use only.

and pressure from the standpoint of their utility and ability to reproduce the experimentally observed dependencies and not from the theoretical viewpoint. However, comments will be made when appropriate about the physical significance of the relationships. The first of these relationships assumes that the dependence of the logarithm of the rate constant on pressure is linear (8) (eqs. [4] and [5]). This treatment regards the activation volume as being pressure independent, and consequently neglects a possible additional activation parameter $-(\partial \Delta V^*/\partial p)_T$. The second type of function is a power series in p, usually of second order (9), which allows for the pressure dependence of the activation volume (eqs. [6] and [7]). Benson and Berson (4) have used a modified form of the Tait equation (10) to calculate both the volume of activation and the change in compressibility (eq. [8]).

Whalley has plotted the average slope of any increment of the ln k vs. p curve against the average pressure of that increment[2] (11; 2, p. 100). Extrapolation to an average pressure of zero gives an intercept which can be taken as equalling $(\partial \ln k/\partial p)_{T,p} = 0$. Such a function is given in eq. [9] in which linearity of the incremental function is assumed.

In this study we considered each of these functions in turn, using the forms shown in eqs. [4] through [9]. Here k_0 is the rate constant at atmospheric pressure, and k_{n+1} and k_n are rate constants at adjacent pressures. Equation [5] is identical to eq. [4] except that, in the former, the curve is forced to pass through the experimental ln k_0. Equations [6] and [7] also differ only in the forced intercept treatment.

$$\ln k = A + Bp \qquad [4]$$

$$\ln k = \ln k_0 + Bp \qquad [5]$$

$$\ln k = A + Bp + Cp^2 \qquad [6]$$

$$\ln k = \ln k_0 + Bp + Cp^2 \qquad [7]$$

$$\ln(k/k_0)/p = A + Bp^{0.523} \qquad [8]$$

$$\ln(k_{n+1}/k_n)/(p_{n+1} - p_n) = A + B(p_{n+1} + p_n)/2 \qquad [9]$$

TEST OF BENZYL CHLORIDE SYSTEM

Using our experimental data (5) for the solvolysis of benzyl chloride in water and in mixtures of ethanol and water (Table I), we calculated the various constants of eqs. [4] through [9] by the method of least squares using an IBM 1620 computer. A representative set of these constants is presented in Table II. From these we obtained the values of the activation volume which are presented in Table III. The value at atmospheric pressure is reported for those functions which take account of the pressure dependence of ΔV^*.

Our interest lies in the variation of ΔV^* with solvent composition. This dependence is shown in Fig. 1. The values of ΔV^* obtained from functions [6] and [7] are identical for all solvents except pure water, and the difference at this one point is probably within the experimental error. It appears that utilization of the experimental intercept introduces no significant error. The values from functions [4] and [5], which also differ only with regard to the forced intercept treatment, do not agree so well. However, the differences are less than 2 ml/mole. It may be noted that the ΔV^*'s from function [9] agree

[2]*Note that refs. 11 and 2, p. 100 contain an error in the statement of the method of extracting the pressure dependence of ln k. The corrected version, as used here, is given in ref. 12.*

TABLE II

The functional constants for 0.3 mole fraction ethanol

Function	Constants		
	A	B	C
[4]	-11.620	4.779×10^{-4} atm^{-1}	
[5]		5.379×10^{-4} atm^{-1}	
[6]	-11.743	8.615×10^{-4} atm^{-1}	-1.366×10^{-7} atm^{-2}
[7]		8.503×10^{-4} atm^{-1}	-1.334×10^{-7} atm^{-2}
[8]	9.742×10^{-4} atm^{-1}	-5.155×10^{-7} atm$^{-1.523}$	
[9]	8.284×10^{-4} atm^{-1}	-2.544×10^{-7} atm^{-2}	

TABLE III

Volumes of activation for benzyl chloride solvolysis at 50.25 °C in aqueous ethanol†

Mole fraction ethanol	ΔV^* (ml/mole) for function					
	[4]	[5]	[6]	[7]	[8]	[9]
0.000	−10.9	−10.0	−8.3	−7.2	−0.4	−7.0
0.100	−10.8	−12.0	−17.0	−17.6	−21.9	−18.0
0.200	−13.4	−14.4	−20.3	−20.0	−21.6	−19.6
0.300	−12.7	−14.3	−22.9	−22.6	−25.9	−22.0
0.400	−11.3	−12.3	−17.6	−17.7	−19.0	−17.7

†The values reported for functions [6], [7], [8], and [9] are those evaluated at atmospheric pressure.

well with those from [6] and [7]. This is not surprising since all three allow for the pressure dependence of ΔV^*, i.e. $(\partial \Delta V^*/\partial p)_T \neq 0$. For this study we consequently can restrict further consideration to eqs. [4], [6], [8], and [9].

It is readily apparent that the general shapes of the curves in Fig. 1 are similar (viz. they all show a minimum in the region between 0.2 and 0.3 mole fraction alcohol). It can therefore be concluded, from a qualitative viewpoint, that the different functions give similar results. However, from a quantitative viewpoint, there are striking differences. The depth of the minimum, as measured with respect to pure water, ranges from 2 ml/mole for the linear analysis to 26 ml/mole for the Benson–Berson equation (4). Evidently for our interest, namely the effect of solvent composition on ΔV^*, it is necessary to ascertain which analysis is the most reliable. As the measure of reliability we chose to use the ability of the functions to reproduce the experimental data.

After the constants of eqs. [4], [6], and [8] were obtained, the value of $\ln k$ at each of the experimental pressures was calculated, giving $\ln k_{\text{calcd}}$. We then used the deviation, Δ (eq. [10])

$$\Delta = \ln k_{\text{obs}} - \ln k_{\text{calcd}}, \qquad [10]$$

as a measure of the functional reproducibility (the subscript "obs" refers to the experimental value). For the Benson–Berson equation (eq. [8]) the experimental value of $\ln k_0$ was used in these calculations.

Equation [9] has two unknowns, k_{n+1} and k_n, prohibiting the determination of $\ln k_{\text{calcd}}$. Therefore only the values of $\ln(k_{n+1}/k_n)_{\text{calcd}}$ can be calculated and compared with the observed value. In this case the deviation is given by eq. [11].

$$\Delta = \ln (k_{n+1}/k_n)_{\text{obs}} - \ln (k_{n+1}/k_n)_{\text{calcd}} \qquad [11]$$

The Δ values for the four equations are shown in Fig. 2 as a function of pressure for each of the solvents.

Can. J. Chem. Downloaded from www.nrcresearchpress.com by 210.87.254.40 on 09/05/12
For personal use only.

Can. J. Chem. Downloaded from www.nrcresearchpress.com by 210.87.254.40 on 09/05/12
For personal use only.

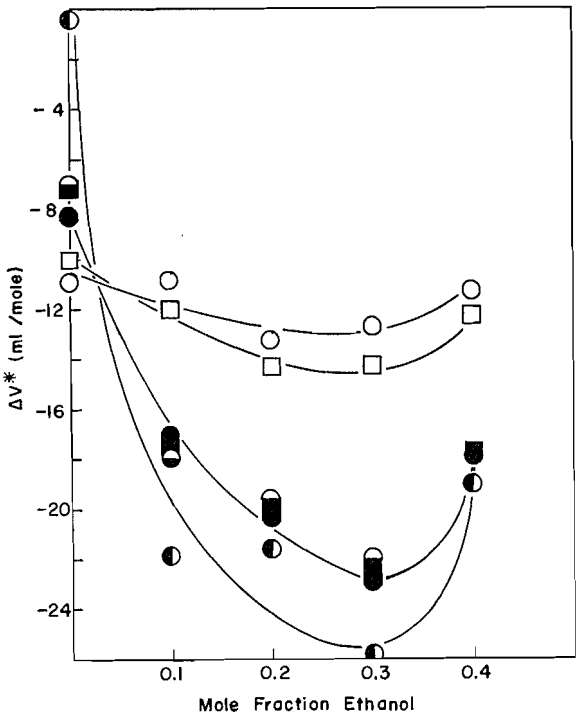


FIG. 1. The variation of ΔV^* with solvent composition: (○) eq. [2]; (□) eq. [3]; (●) eq. [4]; (■) eq. [5]; (◐) eq. [6]; (◒) eq. [7].

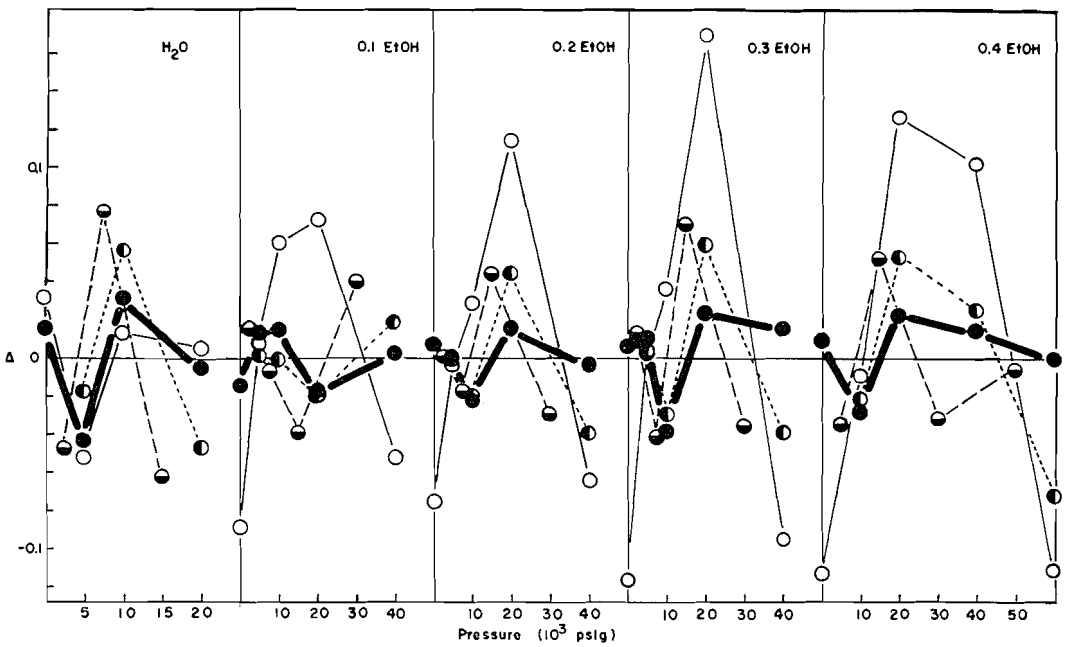


FIG. 2. Variation of the deviation of ln k with pressure for each solvent: (○) linear analysis (eq. [2]); (●) quadratic analysis (eq. [4]); (◐) Benson–Berson analysis (eq. [6]); (◒) incremental slope analysis (eq. [7]).

The most noticeable feature in Fig. 2 is the systematic error present in the linear analysis (eq. [4]). Only for pure water does the linear relationship appear to give a random error. The fact that systematic errors appear in this function suggests that it is not a reliable representative function of the present data. The second order polynomial. the Benson–Berson equation, and the incremental slope analysis (eqs. [6], [8], and [9]) all appear to give random scatter about zero. The only exception is in the Benson–Berson equation for 0.4 mole fraction ethanol. A further comparison of the four functions is shown in Table IV where the standard deviations are reported.

In accord with the above suggestion, function [4] gives a relatively large standard deviation, whereas eqs. [8] and [9] have values about twice that of eq. [6]. From the data presented in Fig. 2 and Table IV, it is evident that the quadratic function (eq. [6]) best represents our data. It must be emphasized that although we conclude the most reliable function for our data to be a second order polynomial, it need not be generally applicable to all reactions. However, by analogy, we would consider it to be generally applicable to ionic unimolecular decompositions.

TABLE IV

Standard deviation of each function

Function	Number of points	Standard deviation	Relative values
[4]	24	0.0814	4.24
[6]	24	0.0192	1.00
[8]	19	0.0374	1.94
[9]	19	0.0420	2.19

Physical Significance

We have, so far, indicated the empirical merits of various methods of handling kinetic pressure data. An analysis of the physical significance of each would be useful.

The first order polynomial (eq. [4]) ignores the fact that the transition state and substrate may have different isothermal compressibilities. Consequently, the inadequacy of this function in giving a good fit for our data is not unexpected (although Burris and Laidler (8) have found that a linear plot is satisfactory for some S_N2 reactions of ionic species). The use of a second order polynomial recognizes that $(\partial \Delta V^*/\partial p)_T \neq 0$, but requires that $(\partial^2 \Delta V^*/\partial p^2)_T = 0$.[3]

The question arises as to whether our data are precise enough to allow a meaningful calculation of $(\partial \Delta V^*/\partial p)_T$. It is readily seen that (see eqs. [6] and [1])

$$[12] \qquad (\partial \Delta V^*/\partial p)_T = -2RTC.$$

For the systems considered in this paper the percent deviation of this derivative (see *Precision Analysis*) lies between 2 and 41%. The actual values of the derivatives and their deviations are presented in Table I.

A good fit of the Benson–Berson equation (eq. [8]) is perhaps not to be expected. Benson and Berson point out that the exact pressure dependence of the rate constant reflects the change in activity coefficient as well as the change in volume during the

[3] *It is true, of course, that $(\partial^2 \Delta V^*/\partial p^2)_T$ is not generally zero. The compressibility of a real substance is known to be pressure dependent (13) so that $(\partial^2 V/\partial p^2)_T \neq 0$. It would be fortuitous indeed if two states had the same value for this derivative, especially when the polarities of the two differed markedly. Since the polarity of the initial state in the present reaction is practically negligible when compared with that of the transition state, it is not to be expected that the two states have the same value for $(\partial^2 V/\partial p^2)_T$. Hence the difference in the values of this derivative cannot be zero, i.e. $(\partial^2 \Delta V^*/\partial p^2)_T \neq 0$.*

Can. J. Chem. Downloaded from www.nrcresearchpress.com by 210.87.254.40 on 09/05/12
For personal use only.

activation process (4). For ionic reactions in water the authors demonstrated that the term due to the activity coefficients is negligibly small, but may become important in solvents of lower dielectric constant. For nonionic reactions, for which this term is zero, these authors used the Tait equation (10) to represent the compressibilities of both the initial and transition states of the reaction (4). This led to the development of eq. [8]. Since this function was developed for nonionic reactions, it appears fortuitous that it gives reasonable results when applied to the analysis of our data for an ionogenic reaction. However, the activity coefficient contribution to $(\partial \ln k/\partial p)_T$ can be shown to be negligible for the systems considered here.

The incremental slope analysis (eq. [9]) was seen to give ΔV_0^* values which coincide with the second order polynomial (Fig. 1). As stated previously, this is because they both allow for the same pressure dependence of ΔV^*. That this is true can be shown by taking the limit of infinitesimal increments and integrating eq. [9] at constant temperature. Thus there is no "a priori" advantage to using one of these methods over the other. However, eq. [6] reproduces the experimental data better than eq. [9] within a factor of two (Table IV). It may be noted that eq. [6] is a strictly analytical function, whereas eq. [9] becomes an analytical function only when the increments become infinitesimal. Therefore, it is not surprising that the two functions do not give identical results. It should also be noted that the incremental slope analysis may suffer from excessive amplification of the effect of the experimental uncertainties in the rate determinations when rate and pressure intervals used become small. Each k and p in the $\ln (k_{n+1}/k_n)$ and $(p_{n+1} - p_n)$ terms has an experimental error associated with it which is independent of the value of the difference between the logarithmic rates and pressures used in each term. Accordingly, as the rate and pressure intervals used become smaller the value of the experimental uncertainties in k and p approach the value of the differences, and increasing scatter of points in the plot of $\ln (k_{n+1}/k_n)/(p_{n+1} - p_n)$ versus $(p_{n+1} + p_n)/2$ is to be expected. This situation is analogous to that which results if one attempts to evaluate enthalpies of activation from two rate determinations at temperatures that are relatively close together. A similar argument was used by Benson and Berson (4) when they neglected the low pressure rates in their study of Walling and Peisach's data for isoprene dimerization (3) because of large scatter. For these reasons, and because eq. [6] is more convenient in that it lends itself to a precision analysis of the type described below, we prefer the quadratic function to the incremental slope analysis.

Precision Analysis

The functional dependence of the rate of benzyl chloride solvolysis on pressure having been established, the next step is to establish the precision of the derivatives. Since we have shown that eq. [6] is the desirable function it is necessary to determine the maximum deviations of the constants. It is convenient to determine these deviations by differentiation (14). By use of the least square functional forms of A, B, and C (eq. [6]), the deviations are given by [13] where f, g, and h are the least square functions for A, B, and C respectively.

$$\begin{aligned} dA &= \sum_i \left(\frac{\partial f}{\partial k_i}\right)_{p_j} dk_i + \sum_j \left(\frac{\partial f}{\partial p_j}\right)_{k_i} dp_j \\ dB &= \sum_i \left(\frac{\partial g}{\partial k_i}\right)_{p_j} dk_i + \sum_j \left(\frac{\partial g}{\partial p_j}\right)_{k_i} dp_j \\ dC &= \sum_i \left(\frac{\partial h}{\partial k_i}\right)_{p_j} dk_i + \sum_j \left(\frac{\partial h}{\partial p_j}\right)_{k_i} dp_j \end{aligned} \qquad [13]$$

Can. J. Chem. Downloaded from www.nrcresearchpress.com by 210.87.254.40 on 09/05/12
For personal use only.

These equations were solved for dA, dB, and dC on an IBM 1620 computer using the average deviation of the rate constants for the dk_i's and the pressure fluctuation limits for the dp_j's. The signs of the dp_j and dk_i were taken to be positive in all cases.

The percent deviation in ΔV_0^* is given by $100\,dB/B$, whereas that for $(\partial \Delta V^*/\partial p)_T = 100\,dC/C$. For the experimental data under consideration in this paper the former has values between 0.9 and 15%, whereas the values for the latter are between 2 and 41%. The actual values for each solvent can be found in Table I.

APPLICATION TO OTHER SYSTEMS

The relative reliability of various functional representations of the data for the pressure dependence of a unimolecular ionogenic reaction having been determined, the applicability of these functions to other reaction types is of interest.[4]

The six reactions studied were (A) bromoacetate with thiosulfate in water (8), (B) methoxide with ethyl bromide in methanol (7), (C) *t*-butyldimethyl sulfonium iodide hydrolysis (15), (D) hydroxide with bromopentammine cobaltic ion in water (8), (E) urea formation in water (16), and (F) isoprene dimerization (3). The ability of each function to reproduce the experimental rate data as a function of pressure for each reaction, together with the values of the activation volumes and the standard deviations, are shown in Fig. 3.

It can be seen that of the six reactions considered, only two (A and C) do not show a systematic error in the linear analysis. Such a situation would be expected for truly linear pressure dependencies. In reaction A all of the analyses give approximately the same value for ΔV^* as well as consistently small values for the standard deviation. In reaction C the Benson–Berson and Whalley analyses give systematic errors.

Reactions B, D, and E are much better represented by the quadratic than the linear analysis (Fig. 3). Since B was designed to demonstrate a viscosity inhibition of a bimolecular reaction in solution (7), it is not surprising that the pressure dependence is nonlinear. The fact that the Benson–Berson and Whalley treatments give rather large standard deviations is somewhat surprising, as is the fact that the Benson–Berson analysis gives a standard deviation only half as large as the quadratic analysis for reaction D. It would seem that this analysis is suited to a wider variety of systems than suggested by the original authors (4). Reaction E has identical values of the standard deviation for the quadratic and Benson–Berson analyses, but a large difference in the ΔV^* values from the two methods. Unfortunately there is no way of distinguishing between their reliability.

A great deal of attention has been given to the pressure dependence of reaction F as evidence by the papers of Walling and Peisach (3), Benson and Berson (4), and rebuttals by both groups of workers (9, 17). Benson and Berson disregarded the low pressure rate constants in analyzing the data for this reaction because of much scatter of the points (*vide supra*) (4), and obtained an activation volume some 50% more negative than the original authors (3). In this study, all of the rate constants were used, and it can be seen that, execpt for the linear analysis, the activation volumes are all very similar (Fig. 3F). A glance at Fig. 3F indicates that if any of the points were to be omitted, those between 3 500 and 5 500 kg/cm^2 should be the likely candidates. The value of -30.4 ml/mole obtained from the quadratic analysis lies midway between those calculated by the two sets of authors (-24.3 (3) and -36.5 (4) ml/mole).

[4]*This suggestion was originally made by E. M. Arnett to J. B. Hyne.*

Can. J. Chem. Downloaded from www.nrcresearchpress.com by 210.87.254.40 on 09/05/12
For personal use only.

Can. J. Chem. Downloaded from www.nrcresearchpress.com by 210.87.254.40 on 09/05/12
For personal use only.

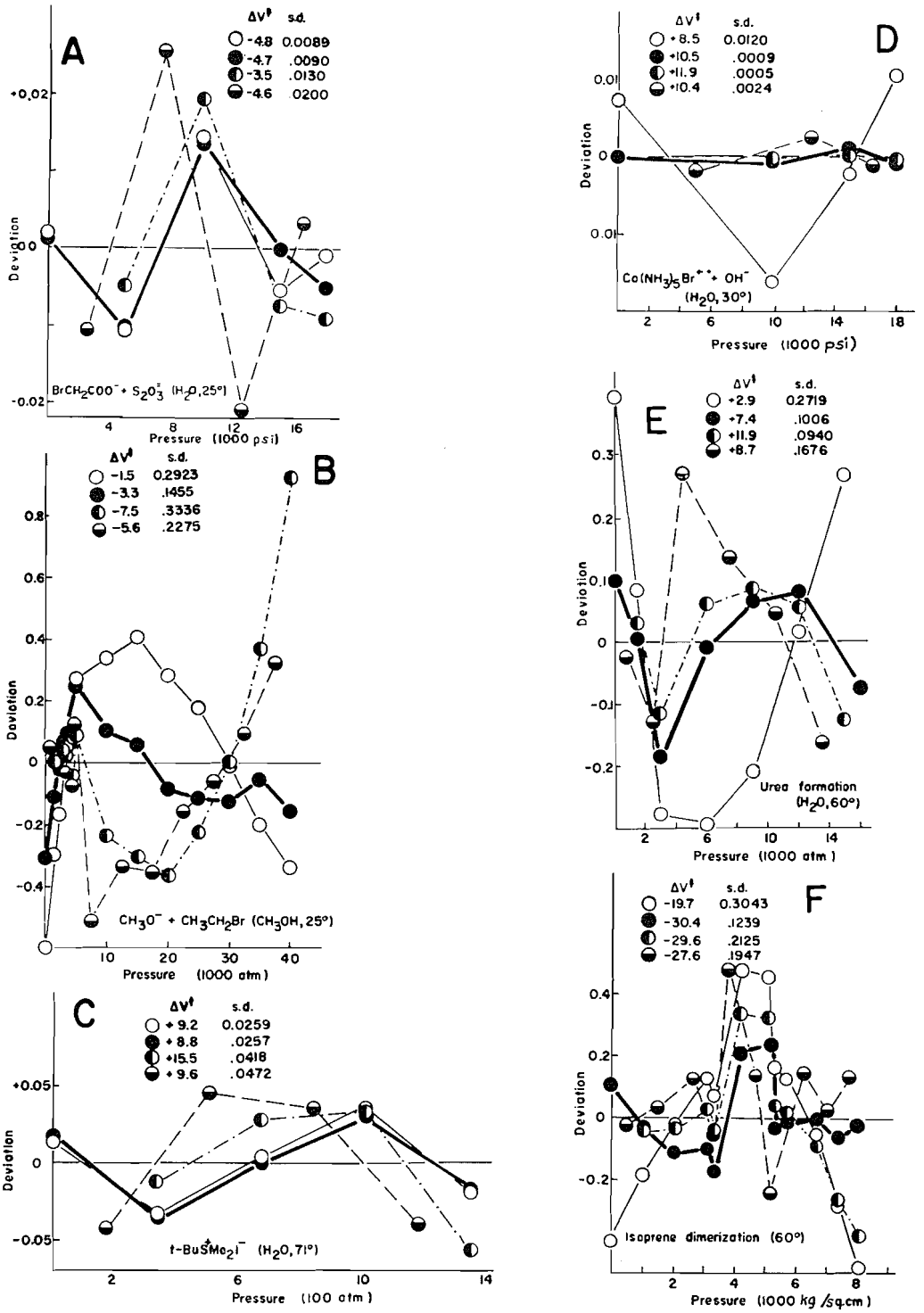


FIG. 3. Variation of the deviation of ln k with pressure for six reactions. (○) linear function; (●) quadratic function; (◐) Benson–Berson function; (◒) incremental function.

CONCLUSION

In summary it can be concluded that: (1) A quadratic polynomial is generally the best representation of the pressure dependence of a logarithmic rate constant regardless of the reaction type; (2) it appears *necessary* and *sufficient* to allow for the non-zero pressure dependence of activation volumes, and *this dependence is measurable*; and (3) differentiation of the appropriate function gives rise to a precise measurement of activation parameters.

ACKNOWLEDGMENTS

General financial assistance by the National Research Council and in particular a studentship to H. S. G. is gratefully acknowledged. The authors wish to thank the staff of the University of Calgary Computing Centre for writing the FORTRAN programs used in this study.

REFERENCES

1. J. B. HYNE and R. E. ROBERTSON. Can. J. Chem. **33**, 1544 (1955).
2. E. WHALLEY. *In* Advances in physical organic chemistry. Vol. 2. *Edited by* V. Gold. Academic Press, New York, N.Y. 1964.
3. C. WALLING and J. PEISACH. J. Am. Chem. Soc. **80**, 5819 (1958).
4. S. W. BENSON and J. A. BERSON. J. Am. Chem. Soc. **84**, 152 (1962).
5. J. B. HYNE, H. S. GOLINKIN, and W. G. LAIDLAW. J. Am. Chem. Soc. **88**, 2104 (1966).
6. M. G. EVANS and M. POLANYI. Trans. Faraday Soc. **31**, 875 (1935).
7. S. D. HAMMAN. Trans. Faraday Soc. **54**, 507 (1958).
8. C. T. BURRIS and K. J. LAIDLER. Trans. Faraday Soc. **51**, 1497 (1955).
9. C. WALLING and D. D. TANNER. J. Am. Chem. Soc. **85**, 612 (1963).
10. H. S. HARNED and B. B. OWEN. The physical chemistry of electrolytic solutions. 3rd ed. Reinhold Publishing Corp., New York, N.Y. 1958. p. 379.
11. B. T. BALIGA, R. J. WITHEY, D. POULTON, and E. WHALLEY. Trans. Faraday Soc. **61**, 517 (1965).
12. B. T. BALIGA and E. WHALLEY. Can. J. Chem. **43**, 2453 (1965).
13. P. W. BRIDGMAN. The physics of high pressure. G. Bell and Sons, Ltd., London, England. 1958. Chaps. V and VI.
14. F. DANIELS *et al.* Experimental physical chemistry. 5th ed. McGraw-Hill Book Co., New York, N.Y. 1956. p. 326.
15. K. R. BROWER. J. Am. Chem. Soc. **85**, 1401 (1963).
16. H. G. DAVID and S. D. HAMMAN. Trans. Faraday Soc. **50**, 1188 (1954).
17. S. W. BENSON and J. A. BERSON. J. Am. Chem. Soc. **86**, 259 (1964).

Can. J. Chem. Downloaded from www.nrcresearchpress.com by 210.87.254.40 on 09/05/12
For personal use only.

Can. J. Chem. Downloaded from www.nrcresearchpress.com by 210.87.254.6 on 09/05/12
For personal use only.

FREE RADICALS BY MASS SPECTROMETRY

XXXIV. A FLOW REACTOR FOR MEASUREMENT OF FAST THERMAL REACTIONS[1]

I. P. FISHER,[2] J. B. HOMER,[3] B. ROBERTS,[4] AND F. P. LOSSING
Division of Pure Chemistry, National Research Council of Canada, Ottawa, Canada

Received April 21, 1966

ABSTRACT

A new type of flow reactor for use with a mass spectrometer has been constructed, in which many of the disadvantages of flow systems for rate measurements have been overcome. Rate constants for unimolecular decompositions can be measured in the range 50 – 5 000 s^{-1}, with helium carrier gas pressures of 10–50 mm and residence times of 10^{-3} to 10^{-1} s. Measurements of the rate of thermal decomposition of trioxane are in good agreement with the rates predicted from literature data obtained at much lower temperatures.

INTRODUCTION

The ability of a mass spectrometer to follow partial pressure changes in gaseous mixtures provides in principle a means for measuring rate constants of gas-phase reactions, as well as for identifying and measuring the concentrations of free radical and other transient species. Earlier work in this field has recently been reviewed in some detail (1, 2). For measurements on fast homogeneous reactions, the reactors have usually taken the form of a heated tubular furnace, through which a gas stream consisting of the reactant, or the reactant diluted with an inert carrier gas, is passed at considerable velocity. The effluent gas is sampled through a pinhole leak leading directly to the ionization chamber of a mass spectrometer. Fast pumping must be provided at the ionization chamber to maintain it at a reasonably low pressure, and to reduce interference by secondary processes.

Attempts to make precise measurements of the rate constants of thermal decomposition reactions at elevated temperatures by means of such reactors, however, have had only limited success. One important difficulty lies in the uncertainty in the residence time – temperature relationship. Before reaching a steady temperature, the gas stream entering the reactor passes through a region of rising temperature, the length of which is not negligible compared with the total reactor length. The extent of reaction occurring in this part of the reactor is dependent on the flow rate and gas temperature and cannot be evaluated precisely. Although earlier measurements of the thermal decomposition of di-*t*-butyl peroxide using such a reactor (3) appeared to be consistent with experiments at lower temperatures, the activation energy for the thermal decomposition of dimethyl mercury at higher temperatures was in poor agreement with the literature data, probably as a result of uncertainties in the temperature profile at elevated temperatures. A further difficulty arose when the temperature in this reactor was varied, for the flow of gas through the leak was strongly dependent on the gas temperature. A correction to the observed peak heights to allow for this effect was required. This correction was large and difficult to assess accurately.

[1]*National Research Council Contribution No. 9116.*
[2]*National Research Council Postdoctorate Fellow, 1962–1964. Present address: Westcott Rocket Propulsion Laboratory, Westcott, England.*
[3]*National Research Council Postdoctorate Fellow, 1963–1965. Present address: Department of Chemistry, Harvard University, Cambridge, Massachusetts.*
[4]*National Research Council Postdoctorate Fellow, 1961–1962. Present address: Department of Chemistry, University of Saskatchewan, Saskatoon, Saskatchewan.*

An improved reactor has now been constructed which obviates many of the difficulties previously encountered. Its function is to duplicate exactly the region of temperature rise and the temperature of the gas at the leak, while the length of the intermediate region of constant temperature is extended by known amounts. The effects of the indeterminate regions can thereby be cancelled out.

EXPERIMENTAL METHODS AND RESULTS

Construction of the Reactor

A cross-sectional view of the reactor assembly is shown in Fig. 1. The reactor itself is a fused-silica tube of internal diameter 7.1 mm, on whose outer surface has been ground a spiral groove of 100 turns, forming a seat for the furnace winding. The winding is of tantalum wire (0.015 in. diameter) which is tapped at equal intervals so as to give 15 identical sections each occupying 5.05 turns. At the upstream end are two preheating sections each consisting of 10.05 turns. The overall length of the furnace winding is 6.1 cm. Leads to the 17 sections are taken out through a pinwheel kovar seal. The current to the 17 sections is controlled by 17 autotransformers each capable of supplying a maximum of 6 V.

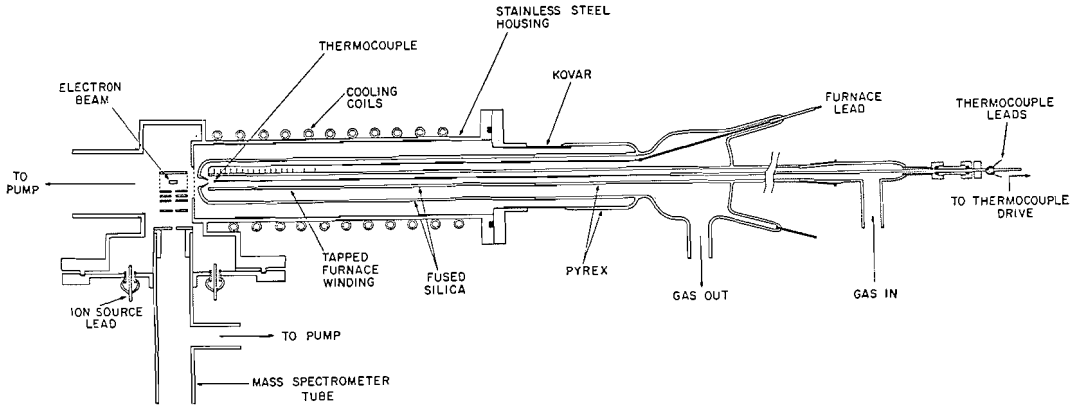


FIG. 1. Reactor assembly.

The temperature of the gas stream is measured by a 0.001 in. diameter platinum – platinum–rhodium thermocouple supported axially by a thin-walled fused-silica capillary probe. The bare junction projects 2 mm from the end of the probe. The probe is joined to a thin-walled metal tube which passes through a double O-ring seal to a rack and pinion driven by a synchronous motor. The temperature profile in the reactor can be traced on a strip-chart recorder from the preheating zone to within 1 mm of the leak.

The gas pressure in the reactor is measured by two mercury manometers, one at the inlet to the reactor and one at the outlet. At the highest pressures and flow rates the pressure drop through the reactor becomes as large as 8% of the pressure. The residence times are calculated using the mean pressure.

The reactor tube is enclosed by an outer fused-silica sheath into which is sealed a thin-walled cone which projects 2 mm into the end of the reactor tube. At the tip of the cone, which is blown out to a wall thickness of about 0.015 mm, is a hole 0.026 mm in diameter formed by an electric spark. This leak admits a small fraction of the gas stream to the ionization chamber. The reactor is surrounded by a stainless-steel vacuum housing provided with copper coils for cooling by water circulation.

Can. J. Chem. Downloaded from www.nrcresearchpress.com by 210.87.254.6 on 09/05/12
For personal use only.

By calibration with mixtures of known composition it has been established that the peak height for a component gas is proportional to its partial pressure in the helium mixture, provided that the total pressure and the gas temperature at the leak is constant. The proportionality constant (sensitivity coefficient) decreases with increasing temperature, and increases slightly with increasing helium pressure.

For greater speed of pumping in the ionization chamber, the side walls of the chamber are made of fine tungsten screen.

Operation of the Reactor

The desired gas temperature profiles and the transformer settings for these profiles are shown in Fig. 2. These are four superimposed profiles whose "temperature rise" zones are activated by sections 4, 5, 7, and 10 of the furnace winding. Each profile consists of three distinct parts: a preheating zone A maintained at a constant temperature at which thermal decomposition of the reactant is negligibly slow, a zone B of rapid temperature rise, and a zone C held at the constant temperature at which the rate of decomposition is to be measured. The length of zone C can be varied by moving zone B along the reactor. Since the tapped sections of the furnace are identical, it is possible to duplicate the profile of zone B at several positions along the reactor. The exactness of duplication can be tested by comparing plots such as those in Fig. 2. It follows that the amount of reaction occurring in zone B is the same for any position of the zone, so that the amount of reactant remaining at the onset of zone C is constant. The amount of reaction in zone C, as a function of its length, can be measured from the change in partial pressure of the reactant (or products) at the leak. It may be noted that whereas the sharpness of zone B is affected by the pressure and flow rate, the distance between corresponding positions of the profiles was found to be invariant.

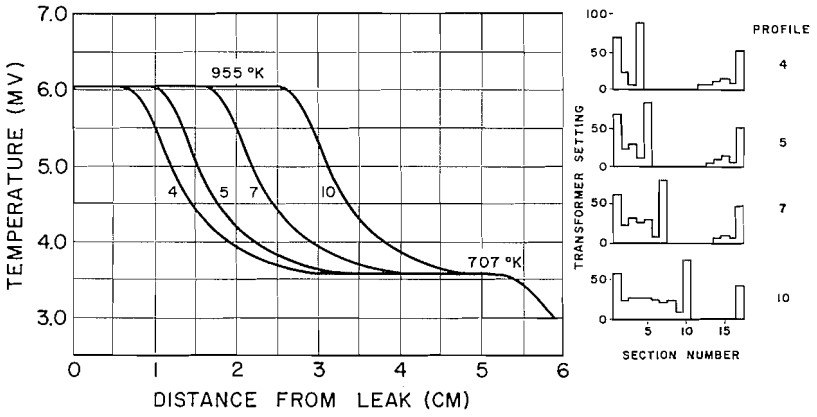


FIG. 2. Temperature profiles. The small figures at the right show the autotransformer settings required to produce the four temperature profiles. A large power input is required in the section which produces the temperature rise. A much lower setting is sufficient to maintain the temperature at a constant level. For example, in profile 10 the center of section 10 of the heater corresponds to a distance from the leak of 2.9 cm.

The transformer settings for the desired profiles are set up prior to the main experiment with a helium stream of the required pressure and velocity. Since the settings are found to be slightly dependent on the prior conditioning of the reactor, presumably as a result of reaction between the furnace winding and the reactant gas on the downstream side of the leak, it is preferable to determine the settings with the reactant present in the

Can. J. Chem. Downloaded from www.nrcresearchpress.com by 210.87.254.6 on 09/05/12
For personal use only.

stream. The profile is scanned repeatedly with the thermocouple probe and the transformer settings are adjusted until the deviations from the required profile are within $\pm 1°$. These settings are noted, and the next profile is set up. Although 2–3 h are required initially to obtain settings for four profiles at new temperature and flow conditions, a profile can be reproduced at a later time to within a few degrees from the same transformer settings. Only minor adjustments are then required to bring the profile within the $\pm 1°$ tolerance.

Measurement of First-Order Kinetic Rates

The first-order rate constant is defined by the equation $k = (2.303/t)(\log c_0 - \log c)$, where t is the time for reaction, and c_0 and c are the initial and final concentrations of the reactant. In the present apparatus, t is the average residence time, and is directly proportional to the length of zone C. The proportionality constant is the linear flow rate v calculated on the basis of plug flow through the reactor. (The assumption of plug flow will introduce an error into the absolute time scale which may be as great as a factor of 2, but which is nearly temperature independent.) If c_0 is allotted to the peak height measured with profile 4, a plot of log (peak height) against the length of zone C (taking profile 4 as a starting point) should be a straight line of slope $-k/2.303v$. Such a linearity is obtained (examples are shown in Fig. 3). For first-order reactions the sensitivity coefficient relating c to the peak height does not enter into the calculation of the rate, since it is a constant at a given temperature.

Measurement of the Gas Temperature

There is some question as to whether a thermocouple gives an accurate measurement of the temperature of a flowing gas. There is reason to believe, however, that in the present apparatus the true temperature of the gas is not significantly different from that registered by the thermocouple.

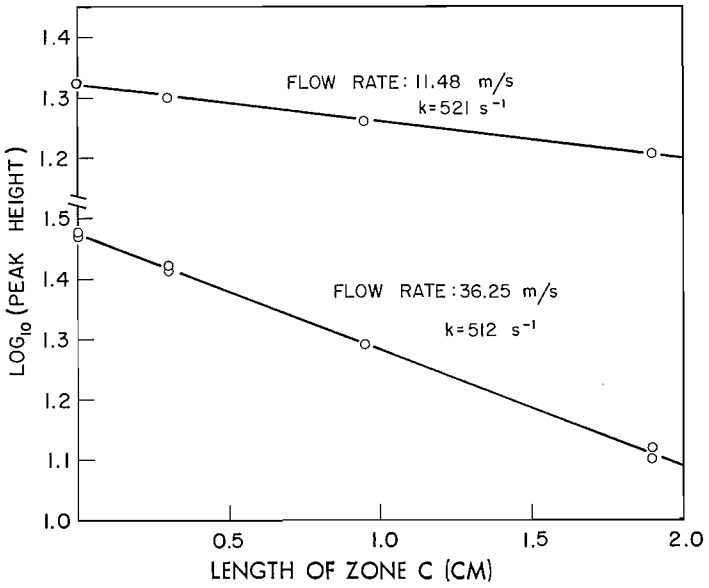


FIG. 3. Plots of $\log_{10}$ (peak height) against length of zone C, showing that the experimental rate constant is independent of the flow rate.

Can. J. Chem. Downloaded from www.nrcresearchpress.com by 210.87.254.6 on 09/05/12
For personal use only.

Can. J. Chem. Downloaded from www.nrcresearchpress.com by 210.87.254.6 on 09/05/12
For personal use only.

The bulk flow of gas down this reactor is not very large; a calculation shows Reynold's number to have a maximum of about 30. This is at least 50 times lower than that corresponding to the onset of turbulence. This is not to say that the flow is strictly laminar, since cross diffusion and disturbances from geometrical factors must surely take place. Calculations show that helium can indeed be heated as quickly as the thermocouple indicates. Calculations also show that the thermocouple leads are small enough to reduce the effect of conduction down them to negligible proportions after immersion of less than 1 cm into the hot zone. Experimentally, the presence of the thermocouple does not materially affect the gas temperature, for it can be moved in and out of the hot zone without producing a change in the partial pressure of the decomposing compound at the leak.

An experiment was performed in which benzene, which did not decompose at the temperature employed, was added to the helium stream passing through the hot reactor. The peak height was found to be independent of the length of zone C. Since the sensitivity coefficient changes detectably for a gas temperature change of $\pm 2°$ (as a result of the change in the viscosity of helium) the constant peak height for benzene provided an independent measurement of the constancy of the real temperature of the gas as a function of the length of zone C. This experiment shows that the correspondence between the temperature indicated by the thermocouple and the real temperature of the gas is not significantly affected by the temperature of the wall. Moreover, the linearity of the plot of log (peak height) against distance (Fig. 3) gives further evidence that the gas and thermocouple temperatures correspond. Let us consider the various temperatures in a cross-sectional plane containing the thermocouple as it moves into the hot zone. As it passes from zone A to zone B, the wall temperature is higher than the gas temperature, and the thermocouple indicates a temperature somewhere between. Further into the hot zone these three temperatures begin to converge, and after a certain distance will reach a common value. If this distance were longer than the combined lengths of zone B and zone C in profile 4, then the main gas temperature of zone C would increase (even though the thermocouple temperature remained constant) as it was stretched to profiles 5, 7, and 10. The plot of log (peak height) against distance would therefore be concave downwards. This trend has never been observed despite greatly varied conditions. It must be concluded that not only is the temperature in the extension of zone C uniform, but it is effectively equal to the temperature of the thermocouple.

Further evidence for the absence of serious systematic errors is provided by measurement of rate constants at the same temperature and helium pressure, but at flow rates differing by a factor greater than 3. The resultant slopes, corresponding to the first-order rates of decomposition, are given in Fig. 3. For these experiments the transformer settings required for the temperature profiles were quite different. The agreement of the rate constants is satisfactory, indicating that despite differences in wall temperature in the two experiments the measured temperatures were those of the gas.

Experimental Tests

As a test for the operation of the reactor, the thermal decomposition of *sym*-trioxane was investigated over the temperature range 748–977 °K, at helium carrier gas pressures from 5–50 Torr. In this temperature range the values of k ranged from $10 - 3\,600$ s^{-1}, and were dependent on the total pressure. These results have been described elsewhere (4). Extrapolation of the data to infinite pressure gave values for k_∞ in good agreement

with the accepted Arrhenius parameters for this reaction, derived from data at lower temperatures where k was of the order of 10^{-2}–10^{-4} s^{-1}. This result appears to confirm the main assumptions in the operation of this reactor. The magnitude of the absolute error in the rate measurements is difficult to estimate, however. Extrapolation of rate data over such a large temperature interval is almost certain to involve an appreciable error. Moreover, the extrapolation of rate constants from 50 Torr to infinite pressure introduces an additional uncertainty. Further confirmation of the performance using a unimolecular decomposition reaction which is not in the fall-off region at helium pressures of 50 Torr, and whose rate parameters are accurately known, would be desirable. Reactions which meet these specifications and which have a suitable activation energy, 35–55 kcal/mole, are extremely limited in number.

REFERENCES

1. F. P. Lossing. *In* Mass spectrometry. *Edited by* C. A. McDowell. McGraw-Hill Book Co., Inc., New York. 1963. Chap. 11.
2. A. G. Harrison. *In* Mass Spectrometry of organic ions. *Edited by* F. W. McLafferty. Academic Press, New York. 1963. Chap. 5.
3. F. P. Lossing and A. W. Tickner. J. Chem. Phys. **20**, 907 (1952).
4. I. P. Fisher, J. B. Homer, B. Roberts, and F. P. Lossing. Advances in mass spectrometry. Vol. 3. The Institute of Petroleum, London. 1966. p. 973.

Can. J. Chem. Downloaded from www.nrcresearchpress.com by 210.87.254.6 on 09/05/12
For personal use only.

Can. J. Chem. Downloaded from www.nrcresearchpress.com by 210.87.254.105 on 09/05/12
For personal use only.

FREE RADICALS BY MASS SPECTROMETRY

XXXV. THE HEAT OF FORMATION OF ALLYL RADICAL FROM BIALLYL PYROLYSIS[1]

J. B. HOMER[2] AND F. P. LOSSING

Division of Pure Chemistry, National Research Council, Ottawa, Canada

Received April 14, 1966

ABSTRACT

The thermal decomposition of biallyl has been investigated from 977 – 1 070 °K at helium carrier gas pressures of 10–50 Torr. Under these conditions the rate of central C—C bond fission to give two allyl radicals can be measured without interference from secondary reactions. The reaction at the pressures employed is first order with respect to biallyl, but between first and second order in the total pressure. The temperature dependence of the rate constants, extrapolated to infinite pressure, and corrected to 298 °K, gives an activation energy of 45.7 kcal/mole for the reaction, corresponding to ΔH_f(allyl) = 33.0 kcal/mole.

INTRODUCTION

The resonance energy of methyl-substituted allyl radical has recently been determined by Benson *et al.* (1) from the difference in the activation energies for the abstraction by I atoms of H atoms from 1-butene (E) and from propane (E'). The allylic resonance energy, defined as the difference in dissociation energy between a C—H bond conjugated with a double bond and the corresponding bond in a saturated paraffin, was obtained from the relationship $(E' - E) + (E_b - E_b')$. $(E_b - E_b')$ is the difference in activation energy for the back reactions, that is, the attack of HI on methyl allyl radicals and on isopropyl radicals. This term was assumed to be zero within ± 0.5 kcal/mole, and the possible error from all causes, including the assumption that D(*sec*-C—H) in *n*-butane was the same as that in propane, was estimated to be ± 1 kcal/mole. The value they obtained for the allylic resonance energy, 12.6 kcal/mole, is quite significantly lower than earlier experimental values for the allyl radical of around 21 kcal/mole from pyrolytic studies (2) and calculated values of 17–18 kcal/mole (3). This difference, and a comparison of their value with recent kinetic measurements (4), has been discussed by Benson *et al.* (1), who conclude that the current evidence favors a value of about 13 kcal/mole rather than the higher value. On this basis, and assuming the allylic resonance energy to be the same in allyl as in methyl allyl radical, then D(allyl—H) in propylene = $D(n\text{-}C_3H_7\text{—H}) - 13$. Since $D(n\text{-}C_3H_7\text{—H})$ is probably 98 kcal/mole with an uncertainty of about ± 2 kcal/mole, one obtains D(allyl—H) = $(98 \pm 2) - (13 \pm 1) = 85 \pm 3$ kcal/mole. From standard thermochemical data, this leads to ΔH_f(allyl) = 37.8 ± 3 kcal/mole.

Although the assumptions made in arriving at this value appear to be inherently reasonable, it would appear advantageous to try to obtain ΔH_f(allyl) by a more direct route. A measurement of the activation energy for the primary rupture of the allylic C—C bond in 1,5-hexadiene, or the C—X bond in allyl halides, would appear to be the method involving the minimum of assumptions. The thermal decomposition of 1,5-hexadiene is to be preferred for two reasons; the heat of formation of 1,5-hexadiene is known with greater accuracy than that of allyl halides (5), and secondly, since two allyl radicals are formed in the decomposition,

[1] $$CH_2{=}CHCH_2{-}CH_2CH{=}CH_2 \rightarrow 2CH_2{-}CH{=}CH_2,$$

[1] *National Research Council Contribution No. 9177.*
[2] *National Research Council Postdoctorate Fellow, 1963-1965.*

the errors in the measurement of the activation energy and in ΔH_f(1,5-hexadiene) are halved in the subsequent calculation of ΔH_f(allyl). This reaction was investigated by Ruzicka and Bryce (6) at a pressure of 70 Torr. Under these conditions interference by recombination, abstraction, and other secondary reactions made the overall reaction extremely complicated. For instance, Ruzicka and Bryce found an apparent activation energy of 31.3 ± 1 kcal/mole. This is evidently much too low to be allotted to the primary step. At low partial pressures, in a stream of helium, however, the decomposition of 1,5-hexadiene is a simple C—C bond fission with production of two allyl radicals (7), and secondary reactions become unimportant.

In the present work, the thermal decomposition of 1,5-hexadiene has been investigated in the temperature range 977 – 1 070 °K with a new type of flow reactor coupled to a mass spectrometer. Under the reaction conditions employed the rate of the primary C—C fission can be measured without interference from secondary reactions, and consequently with no assumptions as to the mechanism.

EXPERIMENTAL

A description of the flow reactor and a check of its performance using the thermal decomposition of trioxane has been published (8, 9). The extent of reaction could be monitored either by following the decrease in height of a 1,5-hexadiene peak or by the increase of the mass-41 peak of allyl radical using low energy electrons. For greatest accuracy the mass-67 peak of 1,5-hexadiene was employed, since it has a much greater intensity than the parent ion at mass 82. To confirm that the mass-67 peak was truly representative of the 1,5-hexadiene concentration. the mass spectrum of the compound was measured as a function of the length of the hot zone of the reaction (i.e. as a function of the extent of decomposition). The ratio of the peaks at masses 82 and 67 remained unaltered. No interfering reactions could be detected provided that the partial pressure of hexadiene was low enough. At the higher partial pressures (5×10^{-3} Torr) recombination of allyl radicals was observed, and manifested itself in nonlinear first-order plots of log (peak height) against distance. This effect is shown in Fig. 1. Partial pressures of the order of 5×10^{-4} Torr were therefore used in the determination of the rate of decomposition.

The rates were measured at four pressures of helium carrier gas: 10, 15, 25, and 50 Torr. Higher helium pressures, although most desirable for kinetic reasons, could not be employed since not enough power

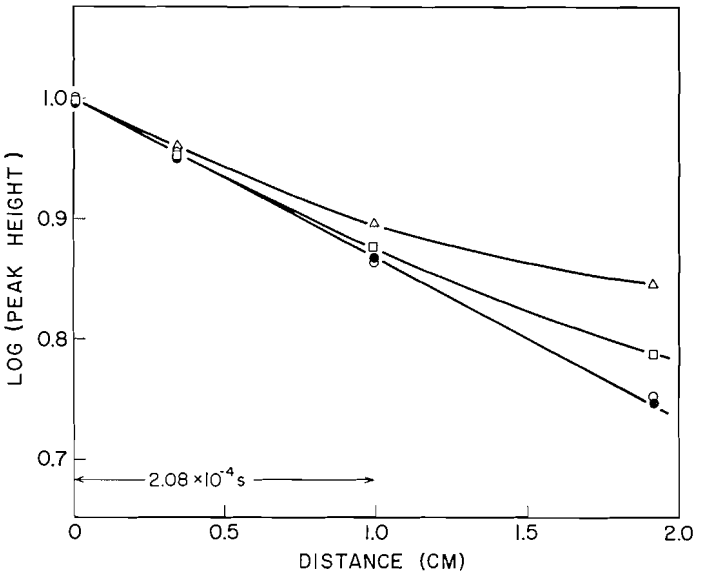


FIG. 1. Plots showing the divergence of biallyl decomposition from first-order dependence with increasing partial pressure of biallyl, and the consequent increase in the concentration of allyl radicals. The re-formation of biallyl by allyl recombination at the residence time employed becomes significant at biallyl pressures above 2×10^{-3} Torr. (△) 17.1; (□) 6.05; (○) 1.63; (●) 0.32×10^{-3} Torr.

Can. J. Chem. Downloaded from www.nrcresearchpress.com by 210.87.254.105 on 09/05/12
For personal use only.

could be applied to raise the gas temperature sufficiently rapidly to permit proper matching of the temperature profiles.

RESULTS

Table I gives the first-order rate constants that were determined, and the ranges of pressure, gas flow rates, and temperatures studied.

TABLE I

First-order rate constants

Temperature (°K)	Helium pressure (Torr)	Flow rate (m/s)	k (s^{-1})
1 070	50.7	48.58	2 226
	25.8	45.15	1 690
	15.8	41.24	1 322
	10.7	37.61	1 048
	7.5	33.28	855
1 047	50.7	48.11	1 451
	24.9	44.10	1 031
	15.7	40.90	871
	10.1	38.69	668
	7.1	34.21	570
1 033	50.8	46.92	1 130
	24.6	43.69	815
	21.1	43.15	745
	14.8	40.23	639
	10.6	36.78	521
	7.4	33.26	456
1 000	50.5	14.55	561
	25.4	13.31	424
	15.1	11.64	319
	10.0	11.70	270
977	50.7	13.97	362
	25.1	13.02	271
	15.3	12.67	219
	10.5	11.55	178

The Evaluation of the Activation Energy

For each temperature examined the rate constants are seen to decrease with decreasing pressure of helium. This indicates that while the rate of decomposition is first order with respect to 1,5-hexadiene, it is in an intermediate region between zero and first order with respect to the helium pressure. In this fall-off region the activation energy will also be a function of the helium pressure. It is therefore necessary to extrapolate the experimental rate constants as a function of helium pressure, and to evaluate the rate constants at infinite pressure (k_∞) for each temperature. An Arrhenius plot using these k_∞ values can then be used to determine the activation energy. For these results, extrapolations of $1/k$ against $1/P$ plots to infinite pressure can introduce a large source of error in evaluating k_∞, since the degree of curvature is not known above 50 Torr. Previous experience with Kassel integrals would suggest that the curve dips rather strongly as it approaches the $1/P = 0$ axis. The exact curvature cannot be predicted theoretically without assigning a number of parameters, and the pressure range experimentally examined is not wide enough to evaluate these. For the present work, in which a correct evaluation of E is more important than a correct evaluation of the pre-exponential factor, it is sufficient to provide a *consistent* method of extrapolation at the different temperatures. An examination of experimental curves determined by other workers and of theoretical curves predicted by unimolecular rate theory reveals that the shape of

Can. J. Chem. Downloaded from www.nrcresearchpress.com by 210.87.254.105 on 09/05/12
For personal use only.

these curves is virtually independent of temperature over a small temperature range. On this basis the rate data in Table I were superimposed on the same plot by varying the attenuation and origin of the $1/k$ axis. This provides the closest possible fit to an identical extrapolating curve for the results at the various temperatures. This plot is shown in Fig. 2. The fit of the experimental points for different temperatures is extremely good, indicating that extrapolation will give a nearly consistent set of k_∞ values.

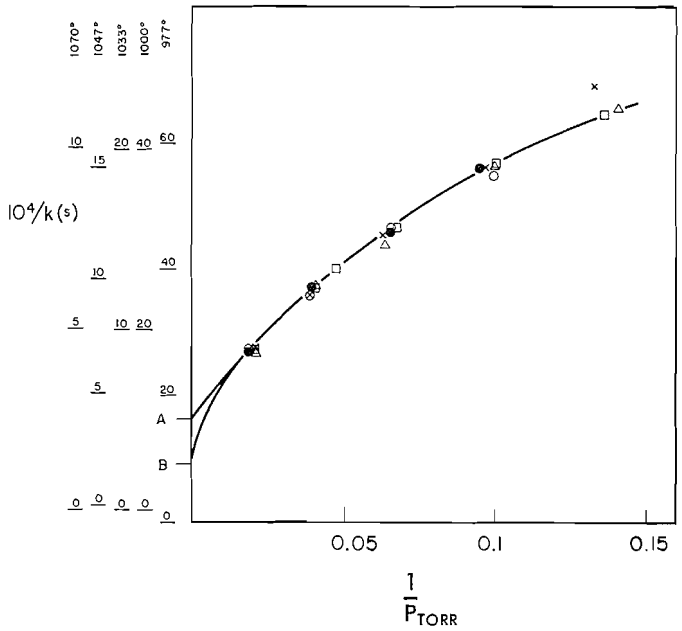


FIG. 2. Composite plot for extrapolation of rate data to infinite pressure. By varying the attenuation and origin of the $1/k$ axis, all the data can be fitted to a single curve. (×) 1 070°; (△) 1 047°; (□) 1 033°; (○) 1 000°; (●) 977°.

With reference to other theoretical and experimental curves, and taking into account the low efficiency of helium as a third body, two limits have been set on the extrapolation. The two limits are marked A and B in Fig. 2. The resultant double set of k_∞ values derived from these limits are shown as two Arrhenius plots in Fig. 3. The rate equations for these two lines are:

$$\text{(A)} \quad \log k_\infty = 12.31 - 42600/2.303RT$$
$$\text{(B)} \quad \log k_\infty = 13.26 - 45600/2.303RT.$$

Taking an average of these limiting cases, we can evaluate the activation energy for 1,5-hexadiene dissociation at 1 000 °K as $E_{1000} = 44.1$ kcal/mole. The experimental limits indicate an error of ± 1.5 kcal/mole in this result. In view of experimental uncertainties and the long extrapolation to k_∞, however, the true limit of error, although significantly larger, cannot be realistically estimated. The results are therefore given without an error limit.

Determination of ΔH_f Allyl

The heat of formation of allyl radical is given by the expression

$$\Delta H_f(\text{allyl}) = \tfrac{1}{2}(D(\text{allyl—allyl}) + \Delta H_f(\text{1,5-hexadiene})).$$

Can. J. Chem. Downloaded from www.nrcresearchpress.com by 210.87.254.105 on 09/05/12
For personal use only.

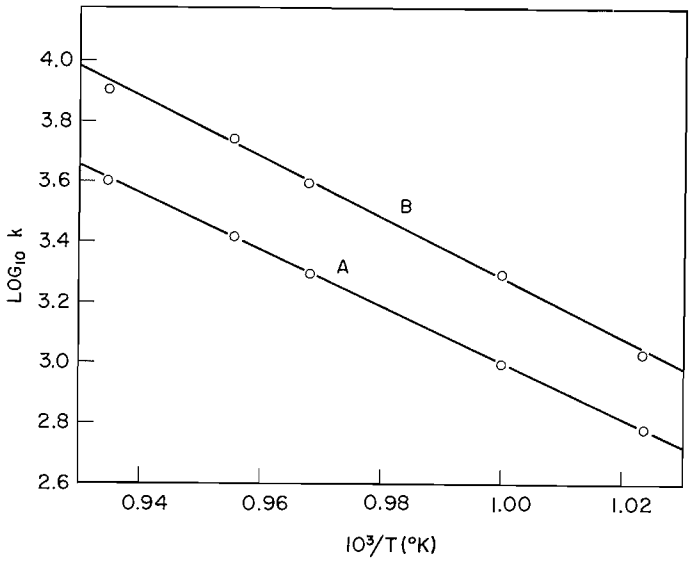


FIG. 3. Arrhenius plots obtained from the limiting values A and B of the extrapolation in Fig. 2.

To obtain ΔH_f(allyl) at 298° it is, of course, necessary to use values of D(allyl—allyl) and ΔH_f(1,5-hexadiene) corresponding to this temperature. The latter quantity is known to be 20.25 kcal/mole, calculated from its heat of hydrogenation at 298° (5). This value is in good agreement with 20.42 kcal/mole calculated from additivity rules (10). On the assumption that the recombination of allyl radicals requires zero activation energy, D_{1000}(allyl—allyl) can be taken as 44.1 kcal/mole, the experimental activation energy found for 1,5-hexadiene dissociation. It is then necessary to compute the difference $(D_{298} - D_{1000})$. This cannot be done directly since the necessary data for allyl radical are not known, but an approximate value can be obtained by considering the changes in enthalpy with temperature in the closely related hypothetical reactions:

[2] 1,5-hexadiene → propylene + allene

[3] 1-hexene → propylene + propylene.

For these reactions, a calculation (see Appendix) from standard thermochemical data (11) gives $\Delta H_{298} - \Delta H_{1000} = +1.64$ and $+1.65$ kcal/mole, respectively. There seems no reason why the change in enthalpy with temperature of reaction [1] should be appreciably different from that of reactions [2] and [3]. On this assumption, D_{298}(allyl—allyl) is 44.1 + 1.6 = 45.7 kcal/mole. From this value and ΔH_f(1,5-hexadiene) one obtains ΔH_f(allyl) = 33.0 kcal/mole at 298 °K. From ΔH_f(propylene) = 4.88 kcal/mole and $\Delta H_f°$(H) = 52.1 kcal/mole this leads to D(allyl—H) in propylene = 80.2 kcal/mole. If $D(n\text{-}C_3H_7\text{—H})$ is taken to be 98 kcal/mole, the resonance energy of allyl radical as defined above is given as 17.8 kcal/mole.

DISCUSSION

The value of ΔH_f(allyl) = 33 kcal/mole derived from the present results lies between the "low" value of 30 kcal/mole from pyrolytic studies (2, 12) and the recent "high" value of 38 kcal/mole derived from the iodine-catalyzed isomerization of 1-butene (1). It is close to a value of 34.0 ± 2.8 kcal/mole obtained recently from the thermal decomposition of sulfones (13). Although our value appears to differ from that of Benson *et al.*

Can. J. Chem. Downloaded from www.nrcresearchpress.com by 210.87.254.105 on 09/05/12
For personal use only.

by 5 kcal/mole, part of the difference may arise from the fact that the two results cannot be compared directly without making certain assumptions. The results of Benson *et al.* give a direct[3] measurement of the difference

$$D(CH_3CH_2\underset{\displaystyle CH_3}{\underset{|}{C}}H\text{—}H) - D(CH_2{=}\underset{\displaystyle CH_3}{\underset{|}{C}}HCH\text{—}H) = 13 \pm 1 \text{ kcal/mole.}$$

It is possible that this difference is less than the difference

$$D(CH_3CH_2CH_2\text{—}H) - D(CH_2{=}CHCH_2\text{—}H).$$

That is, the stabilization brought about by CH_3 substitution in the *n*-propyl radical could be greater than the stabilization brought about by substitution in the allyl radical, in which the unpaired electron is already extensively delocalized. Since $D(n\text{-}C_3H_7\text{—}H) - D(sec\text{-}C_4H_9\text{—}H)$ is probably 3–4 kcal/mole, one could perhaps allow for an extra 2 kcal/mole for the resonance energy of allyl itself over that of methyl allyl, giving 15 kcal/mole as an upper limit. To convert this to a value for ΔH_f(allyl) brings in the further uncertainty in $D(n\text{-}C_3H_7\text{—}H) = 98$ kcal/mole, which is probably ± 2 kcal/mole. On this basis one could arrive at D(allyl—H) $= 83 \pm 2$ kcal/mole and ΔH_f(allyl) $= 36 \pm 2$ kcal/mole as the lower limits consistent with the results of Benson *et al.*

It should be pointed out that there is no experimental evidence for or against a slight dependence of allylic resonance energy on substitutional effects. This question cannot be settled at present by reference to the analogous benzyl radical, since its resonance energy is similarly subject to an uncertainty of about 5 kcal/mole. As summarized by Skinner (14), there has been recent kinetic support for a low value, $D(PhCH_2\text{—}H) = 80 \pm 2$ kcal/mole, and a high value, 84.6 ± 2 kcal/mole.

The magnitude of systematic error in the present result is difficult to evaluate. The susceptibility of kinetic measurements in flow systems to large errors is well known (15). On the other hand the present reactor has been designed to eliminate the main sources of these errors. Calibration experiments on the thermal decomposition of trioxane at slightly lower temperatures, for example, gave A and E values in good agreement with those obtained by conventional experiments (8). The pre-exponential factor found here for biallyl decomposition is probably less accurate than the measurement of E as a result of the method of extrapolation described above. Nevertheless it appears that if these data are correct, A must be not much greater than 10^{13} s^{-1}. From a consideration of the high recombination efficiencies of alkyl radicals like CH_3 and C_2H_5, and the estimated entropy changes for central bond fissions in radical dimers, it has been calculated that $\log (A_{forward}/A_{reverse})$ for such reactions should be about 4, and that A_f is therefore about 10^{17} (15–17). This is interpreted in terms of an extremely loose transition state, without strong orientational effects. Owing to the configurational requirements for attainment of the electron delocalization energy in allyl radical, formation of the transition state in 1,5-hexadiene decomposition may involve a smaller change in entropy than that involved in the formation of the transition state in ethane decomposition. The combination rate and A_f for allyl may therefore be correspondingly smaller. The total entropy change for reaction [1] cannot be calculated with certainty, since it depends strongly on the assumed properties of allyl radical. On the assumption that the entropy of allyl is nearly the same as that of propylene, ΔS for reaction [1] would be about

[3]*The necessary assumptions are outlined above in the introductory paragraph.*

Can. J. Chem. Downloaded from www.nrcresearchpress.com by 210.87.254.105 on 09/05/12
For personal use only.

the same as that for the dissociation of ethane, and $\log A_f/A_r = 4.1$ (at 298 °K). If, on the other hand, the structural properties of allyl are nearly the same as those of allene, ΔS is much smaller, and $\log A_f/A_r = 1.7$. Both these numbers would imply that the efficiency of allyl recombination is very much lower than that of methyl recombination. There appears to be no experimental evidence on this point. It would seem therefore that one cannot decide a priori whether or not $A \sim 10^{13}$ for reaction [1] is smaller than might reasonably be expected for this reaction.

APPENDIX

From values given in ref. 11, ΔH_f(1,4-pentadiene) decreases from 25.20 at 298° to 20.40 kcal/mole at 1 000°. The incremental change of —CH_2— from pentane to hexane changes from −4.96 to −6.06 kcal/mole, so that ΔH_f(1,5-hexadiene) changes from 20.24 (comparing well with the experimental value of 20.25) to 14.34 kcal/mole. Also $\Delta H_{f298} - \Delta H_{f1000}$ for propylene is +4.85 and for allene is +2.69 kcal/mole. $\Delta H_{298} - \Delta H_{1000}$ for 1,5-hexadiene → propylene + allene is $(4.85 + 2.69 - (20.24 - 14.39)) = +1.64$ kcal/mole. $\Delta H_{f298} - \Delta H_{f1000}$ for 1-hexene is 8.05 kcal/mole, so that $\Delta H_{298} - \Delta H_{1000}$ for the reaction 1-hexene → propylene + propylene is $[(2 \times 4.85) - 8.05] = +1.65$ kcal/mole.

REFERENCES

1. K. W. Egger, D. M. Golden, and S. W. Benson. J. Am. Chem. Soc. **86**, 5420 (1964).
2. M. Szwarc and A. H. Sehon. J. Chem. Phys. **18**, 237 (1950).
3. J. L. Franklin and F. H. Field. J. Am. Chem. Soc. **75**, 2819 (1953).
4. R. J. Ellis and H. M. Frey. J. Chem. Soc. 959 (1964). G. S. Hammond and C. H. De Boer. J. Am. Chem. Soc. **86**, 899 (1964). D. J. Trecker and J. P. Henry. J. Am. Chem. Soc. **86**, 902 (1964).
5. H. A. Skinner. Modern aspects of thermochemistry. Lectures, Monographs and Reports No. 3. The Royal Institute of Chemistry, London. 1958.
6. D. J. Ruzicka and W. A. Bryce. Can. J. Chem. **38**, 827 (1960).
7. F. P. Lossing, K. U. Ingold, and I. H. S. Henderson. J. Chem. Phys. **22**, 621 (1954).
8. I. P. Fisher, J. B. Homer, B. Roberts, and F. P. Lossing. Advances in mass spectrometry. Vol. 3. The Institute of Petroleum, London. 1966. p. 973.
9. I. P. Fisher, J. B. Homer, B. Roberts, and F. P. Lossing. Can. J. Chem. This issue.
10. H. J. Bernstein. Trans. Faraday Soc. **58**. 2285 (1962).
11. F. D. Rossini *et al.* Selected values of physical and thermodynamic properties of hydrocarbons and related compounds. Carnegie Press, Pittsburgh. 1953
12. M. Szwarc. Chem. Rev. **47**, 75 (1950).
13. W. K. Busfield, K. J. Ivin, H. Mackle, and P. A. G. O'Hare. Trans. Faraday Soc. **57**, 1064 (1961).
14. H. A. Skinner Ann. Rev. Phys. Chem. **15**, 449 (1964).
15. S. W. Benson. The foundations of chemical kinetics. McGraw-Hill Book Company, Inc., New York. 1960.
16. A. F. Trotman-Dickenson. J. Chem. Phys. **21**, 211 (1953).
17. S. W. Benson. Advan. Photochem. **2**, 1 (1964).

Can. J. Chem. Downloaded from www.nrcresearchpress.com by 210.87.254.105 on 09/05/12
For personal use only.

Can. J. Chem. Downloaded from www.nrcresearchpress.com by 210.87.254.6 on 09/05/12
For personal use only.

NOTES

THE RADIATION-INDUCED ADDITION OF HBr TO OLEFINS IN THE LIQUID PHASE

R. C. RUMFELDT[1] AND D. A. ARMSTRONG

The occurrence of a free-radical-catalyzed chain addition reaction between HBr and the lower molecular weight olefins, ethylene and propylene, is well established. In 1942 Vaughan, Rust, and Evans (1) produced initiating radicals by the direct photolysis of HBr, and also by the photolysis of sensitizers which had been incorporated in HBr–olefin reaction mixtures. In all instances the chain length of the resulting reaction was shown to be several thousand. More recently (2, 3) it has been found that an addition reaction of similar chain length can be initiated by the action of ionizing radiation on HBr–ethylene mixtures, and this has led to the development of an industrial process for the ^{60}Co-catalyzed production of ethyl bromide (3). The purpose of the present communication is to report the results of a kinetic study of this radiation-induced reaction in the liquid phase at -79 °C. A number of experiments have also been conducted with propylene.

EXPERIMENTAL

Propylene, ethylene, and HBr were purified and stored in a suitable vacuum line (2). Mixtures of HBr and olefin in the required proportions were synthesized in this vacuum line and condensed directly into the irradiation cells. The latter consisted of round-bottomed tubes 24 cm long and of 8 mm bore. They were closed at the top end by a stopcock or break-seal. Samples were kept frozen at liquid nitrogen temperature until a few minutes before irradiation. They were then liquefied, rendered homogeneous, and placed in position in a small dewar filled with a dry ice – ethanol slurry. The liquefied samples normally had a volume of about 1 ml. After the sample had stood for a period long enough to ensure temperature equilibration the dewar was positioned in the ^{60}Co source compartment and the irradiation was started. Dose rates were determined by ferrous sulfate dosimetry with corrections for differences in the electron density of the samples and the dosimetry solution. By the use of two sources of different strength and by alteration of the source to sample distances several different dose rates were obtained.

The rate of the HBr–C_2H_4 addition reaction was followed as in the earlier study (2*a*). It has already been established that ethyl bromide is by far the major product of this reaction (2, 3), and no further gas chromatographic analyses were conducted in the present work. The rate of the γ-ray-induced addition of HBr to propylene was followed by absorbing the residual HBr in water and titrating it with a standard solution of silver nitrate. In a number of the propylene experiments the liquid irradiation product was extracted in ether solution and analyzed on a gas chromatographic column with tri-*m*-cresyl phosphate as stationary phase.

RESULTS AND DISCUSSION

Liquid mixtures of propylene and HBr undergo a spontaneous thermal addition reaction (4), the major product of which is isopropyl bromide with traces of hexyl and other higher molecular weight bromides. This type of reaction is catalyzed by Friedel–Crafts catalysts (5) and in ionizing solvents it has been postulated (6) to involve carbonium ion intermediates. In the present work the γ-ray-induced addition reaction was studied in solutions containing only HBr and propylene in a mole ratio of 1:2.66. In the absence of radiation the rate of the thermal reaction in these mixtures was found to be 0.1% of the HBr per minute (cf. the earlier work of ref. 4). The radiation-induced addition was much faster than this. In fact essentially complete addition was observed after ~ 100 s of irradiation at a dose rate of 2×10^{19} eV/l s. An average G value of about

[1]*Department of Chemistry, University of Windsor, Windsor, Ontario.*

10^5 over the period of irradiation is thus required, and the chain character of the radiation-induced addition to propylene is established. As in the photo-initiated reactions (1) *n*-propyl bromide was by far the major product. The yield of isopropyl bromide was of the order of 1% (or less) of the *n*-propyl bromide. These observations are consistent with a free-radical mechanism for this liquid phase radiation-induced reaction. The small yield of isopropyl bromide indicates that, if it occurs at all, the ionic chain reaction sequence[2]

$$i\text{-}C_3H_7^+ + HBr \rightarrow i\text{-}C_3H_7BrH^+$$
$$i\text{-}C_3H_7BrH^+ + C_3H_6 \rightarrow i\text{-}C_3H_7Br + C_3H_7^+$$

is relatively slow under the present conditions.

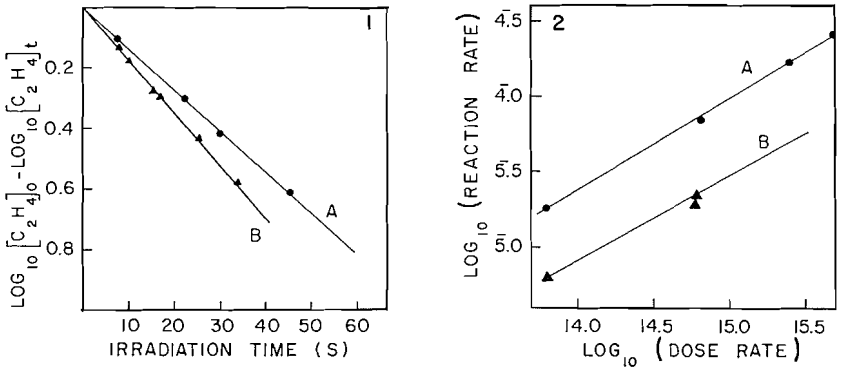


FIG. 1. First-order log plots for the consumption of ethylene in the radiation-induced addition of HBr. Line A: $[C_2H_4]_0 = 1.8$ moles/l. Line B: $[C_2H_4]_0 = 6.0$ moles/l.

FIG. 2. Logarithmic plots of reaction rate versus dose rate for the radiation-induced addition of HBr to C_2H_4. The units are: reaction rate in mole/ml s and dose rate in eV/ml s. Line A: $[C_2H_4]_0 \simeq 6 \times 10^{-3}$ mole/ml. Line B: $[C_2H_4]_0 \simeq 1.8 \times 10^{-3}$ mole/ml.

At dose rates lower than 2×10^{19} eV/l s the addition to propylene was complicated by an induction period. For this reason kinetic studies were confined to the ethylene–HBr reaction, which showed no evidence of any such behavior. The major product of this reaction is ethyl bromide (2, 3) and the thermal rate at −79 °C quite negligible (0.01%/min for a HBr:ethylene mole ratio of 5:1; see also ref. 4). The results of the kinetic studies for HBr–ethylene mixtures of mole ratios in the range 5:1 to 20:1 are presented in Table I. As shown in Fig. 1 the reaction is first order in ethylene. The slopes of the log–log plots of reaction rate versus dose rate in Fig. 2 indicate a dose rate exponent lying between 0.5 and 0.6 for dose rates in the range 6.4×10^{16} to 5.7×10^{18}. These observations can be satisfactorily accommodated by a free-radical mechanism involving the reactions (all reactions are numbered as in ref. 2*b*)

[1] $\quad HBr \overset{R}{\rightsquigarrow} H + Br$

[3*a*] $\quad H + HBr \rightarrow H_2 + Br$

[13], [16] $\quad Br + C_2H_4 \underset{k_{16}}{\overset{k_{13}}{\rightleftharpoons}} C_2H_4Br$

[14*a*] $\quad C_2H_4Br + HBr \xrightarrow{k_{14a}} C_2H_5Br + Br$

[18] $\quad Br + Br(+ M) \xrightarrow{k_{18}} Br_2(+ M).$

[2]*Because of its large relative stability, the isopropyl carbonium ion should be formed in this system by proton transfer to propylene from the* $C_3H_6^+$ *or* H_2Br^+ *ions produced by the ionizing radiation (see ref. 8). Ionic intermediates of this type have been postulated as leading to cationic polymerization reactions in irradiated liquid olefins (see refs. 9, 10). In some systems large chain lengths are observed.*

Can. J. Chem. Downloaded from www.nrcresearchpress.com by 210.87.254.6 on 09/05/12
For personal use only.

where the concentration of third body M is such that reaction [18] will be second order and its rate constant of the order of 10^{10} l/mole s (7). If reaction [16] is neglected as seems reasonable at −79 °C and with the high concentrations of HBr being employed, the rate expression takes the form required by the present data, viz.

$$d[C_2H_5Br]/dt = k_{13}[C_2H_4]\sqrt{(R/k_{18})}.$$

The quantity R is equal to the rate of formation of initiating radicals. Assuming a radical yield of 12 per 100 eV in liquid HBr[3] one arrives at the values of $k_{13}/\sqrt{k_{18}}$ given in Table I. Taking k_{18} as $\simeq 10^{10}$ l/mole s, one can show that k_{13} must be 10^6–10^7 l/mole s under the conditions stated above.

TABLE I

Kinetic data for the C_2H_4–HBr addition reaction

$[C_2H_4]$ (moles/l)	Dose rate (eV/l s)	Initial reaction rate (moles/l s)	$k_{13}/\sqrt{k_{18}}$ (l/mole s)$^{1/2}$
1.80	5.80×10^{17}	2.29×10^{-2}	37.4
1.80	5.80×10^{17}	1.94×10^{-2}	31.6
1.80	6.41×10^{16}	6.44×10^{-3}	31.7
6.13	5.70×10^{18}	2.69×10^{-1}	41.0
6.32	2.27×10^{18}	1.94×10^{-1}	45.5
6.46	5.80×10^{17}	6.48×10^{-2}	29.4
6.46	5.80×10^{17}	6.19×10^{-2}	28.2
5.62	6.41×10^{16}	2.41×10^{-2}	38.0
		Mean value	35±6

In further experiments the ethylene reaction was found to be completely inhibited by the addition of 0.1 mole % nitric oxide. The same concentration of nitric oxide reduced the rate of the propylene addition reaction to a level which was, within experimental error, the same as the rate of the thermal reaction. From experiments in the absence of radiation the latter reaction was shown to be insensitive to the presence of nitric oxide. If the free-radical mechanism is correct an inhibitory effect by nitric oxide is certainly to be expected in view of the small activation energy which would be anticipated for reaction [20]:

[20] $$NO + Br(+ M) \rightarrow NOBr(+ M) \quad .$$

Thus the results of the present study are all consistent with a free-radical mechanism for the radiation-induced addition of HBr to ethylene and propylene in the liquid phase.

ACKNOWLEDGMENT

The authors wish to acknowledge the generous support of Atomic Energy of Canada Ltd., in whose laboratories much of this investigation was conducted.

1. W. VAUGHAN, F. RUST, and T. EVANS. J. Org. Chem. **7**, 477 (1942); **7**, 491 (1942).
2. (*a*) D. A. ARMSTRONG and J. W. T. SPINKS. Can. J. Chem. **37**, 1002 (1959). (*b*) D. A. ARMSTRONG and J. W. T. SPINKS. Can. J. Chem. **37**, 1210 (1959).
3. D. E. HARMER, J. S. BEALE, C. T. PUMPELLY, and B. W. WILKINSON. *In* Industrial uses of large radiation sources. Vol. II. International Atomic Energy Agency, Vienna. 1963
4. O. MAASS and C. H. WRIGHT. J. Am. Chem. Soc. **46**, 2664 (1924).
5. F. R. MAYO and C. WALLING. Chem. Rev. **27**, 351 (1940). G. A. OLAH. Friedel Crafts and related reactions. Interscience Publishers, London. 1963. p. 148.

[3]*Calculated from* $G(H_2)$ *for liquid* HBr *(see ref. 11).*

Can. J. Chem. Downloaded from www.nrcresearchpress.com by 210.87.254.6 on 09/05/12
For personal use only.

6. Y. POCKER. J. Chem. Soc. 1292 (1960).
7. R. L. STRONG. J. Am. Chem. Soc. **87**, 3563 (1965).
8. D. P. STEVENSON and D. O. SCHISSLER. *In* The chemical and biological action of radiations. Vol. V. *Edited by* M. Haissinsky. Academic Press, London. 1961. p. 258.
9. FFRANCON WILLIAMS. Quart. Rev. **17**, 101 (1963).
10. F. W. LAMPE. J. Phys. Chem. **63**, 1986 (1959).
11. R. C. RUMFELDT and D. A. ARMSTRONG. Can. J. Chem. **41**, 1104 (1963).

RECEIVED MAY 6, 1966.
DEPARTMENT OF CHEMISTRY,
UNIVERSITY OF CALGARY,
CALGARY, ALBERTA.

Can. J. Chem. Downloaded from www.nrcresearchpress.com by 210.87.254.6 on 09/05/12
For personal use only.

MULTICOMPONENT DIFFUSION IN THE ^{85}Kr–SO_2–Kr SYSTEM

ANIL SARAN AND YASHWANT SINGH

Curtiss and Hirschfelder (1) have shown that the multicomponent diffusion coefficient D_{ij} can be written to a first approximation as

$$[1] \qquad D_{ij} = \frac{1}{M_j}\left(\sum_k x_k M_k\right)\frac{K^{ji} - K^{ii}}{|K|},$$

where $K_{ii} = 0$ and

$$K_{ij} = \frac{x_i}{(\mathfrak{D}_{ij})_1} + \frac{M_j}{M_i}\sum_{k\neq i}\frac{x_k}{(\mathfrak{D}_{ik})_1}, \quad i \neq j.$$

$|K|$ is the determinant of K_{ij} and K^{ji} are the minors. If, however, one component 'i' is present in trace quantity, then its diffusion coefficient $D_{i\to\text{mix}}$ is given by (2)

$$[2] \qquad \frac{1}{(D_{i\to\text{mix}})_1} = \sum_{j\neq i}\frac{x_j}{(\mathfrak{D}_{ij})_1},$$

where x_j is the mole fraction of the jth component and $\mathfrak{D}_{ij}$ is the usual binary diffusion coefficient. For a three-component system eq. [2] becomes

$$[3] \qquad \frac{1}{(D_{1\to 23})_1} = \frac{x_2}{(\mathfrak{D}_{12})_1} + \frac{x_3}{(\mathfrak{D}_{13})_1},$$

and hence to a first approximation:

$$[4] \qquad \frac{1}{D_{\text{expt}}} = x_3\left(\frac{1}{\mathfrak{D}_{13}} - \frac{1}{\mathfrak{D}_{12}}\right) + \frac{1}{\mathfrak{D}_{12}}, \quad (\text{since } x_1 \simeq 0).$$

The plot of $1/D_{\text{expt}}$ vs. x_3 will be a straight line whose intercepts on the ordinate at $x_3 = 0$ and $x_3 = 1$ give the values of $\mathfrak{D}_{12}$ and $\mathfrak{D}_{13}$. Applying the mass correction, we get the usual $\mathfrak{D}_{22}$ and $\mathfrak{D}_{23}$ values.

Several experiments (3–6) confirm that eq. [4] holds quite accurately. However, Watts (7) in a recent paper on the multicomponent diffusion of ^{133}Xe in binary mixtures of Xe with other inert gases has observed a departure from eq. [4]. In the present investigation we have measured the diffusion coefficient of radioactive ^{85}Kr in binary mixtures of normal krypton and SO_2 to test further the validity of eq. [4].

EXPERIMENTAL RESULTS

The apparatus employed in the present investigation is a two-chamber apparatus of the Ney and Armistead (8) type. The apparatus and the experimental procedures have been fully described by Srivastava and Paul (3). Pure dry SO_2 gas was prepared by a method

6. Y. POCKER. J. Chem. Soc. 1292 (1960).
7. R. L. STRONG. J. Am. Chem. Soc. **87**, 3563 (1965).
8. D. P. STEVENSON and D. O. SCHISSLER. *In* The chemical and biological action of radiations. Vol. V. *Edited by* M. Haissinsky. Academic Press, London. 1961. p. 258.
9. FFRANCON WILLIAMS. Quart. Rev. **17**, 101 (1963).
10. F. W. LAMPE. J. Phys. Chem. **63**, 1986 (1959).
11. R. C. RUMFELDT and D. A. ARMSTRONG. Can. J. Chem. **41**, 1104 (1963).

RECEIVED MAY 6, 1966.
DEPARTMENT OF CHEMISTRY,
UNIVERSITY OF CALGARY,
CALGARY, ALBERTA.

Can. J. Chem. Downloaded from www.nrcresearchpress.com by 210.87.254.105 on 09/05/12
For personal use only.

MULTICOMPONENT DIFFUSION IN THE ^{85}Kr–SO_2–Kr SYSTEM

ANIL SARAN AND YASHWANT SINGH

Curtiss and Hirschfelder (1) have shown that the multicomponent diffusion coefficient D_{ij} can be written to a first approximation as

$$[1] \qquad D_{ij} = \frac{1}{M_j}\left(\sum_k x_k M_k\right)\frac{K^{ji} - K^{ii}}{|K|},$$

where $K_{ii} = 0$ and

$$K_{ij} = \frac{x_i}{(\mathfrak{D}_{ij})_1} + \frac{M_j}{M_i}\sum_{k\neq i}\frac{x_k}{(\mathfrak{D}_{ik})_1}, \quad i \neq j.$$

$|K|$ is the determinant of K_{ij} and K^{ji} are the minors. If, however, one component 'i' is present in trace quantity, then its diffusion coefficient $D_{i\to\text{mix}}$ is given by (2)

$$[2] \qquad \frac{1}{(D_{i\to\text{mix}})_1} = \sum_{j\neq i}\frac{x_j}{(\mathfrak{D}_{ij})_1},$$

where x_j is the mole fraction of the jth component and $\mathfrak{D}_{ij}$ is the usual binary diffusion coefficient. For a three-component system eq. [2] becomes

$$[3] \qquad \frac{1}{(D_{1\to 23})_1} = \frac{x_2}{(\mathfrak{D}_{12})_1} + \frac{x_3}{(\mathfrak{D}_{13})_1},$$

and hence to a first approximation:

$$[4] \qquad \frac{1}{D_{\text{expt}}} = x_3\left(\frac{1}{\mathfrak{D}_{13}} - \frac{1}{\mathfrak{D}_{12}}\right) + \frac{1}{\mathfrak{D}_{12}}, \quad (\text{since } x_1 \simeq 0).$$

The plot of $1/D_{\text{expt}}$ vs. x_3 will be a straight line whose intercepts on the ordinate at $x_3 = 0$ and $x_3 = 1$ give the values of $\mathfrak{D}_{12}$ and $\mathfrak{D}_{13}$. Applying the mass correction, we get the usual $\mathfrak{D}_{22}$ and $\mathfrak{D}_{23}$ values.

Several experiments (3–6) confirm that eq. [4] holds quite accurately. However, Watts (7) in a recent paper on the multicomponent diffusion of ^{133}Xe in binary mixtures of Xe with other inert gases has observed a departure from eq. [4]. In the present investigation we have measured the diffusion coefficient of radioactive ^{85}Kr in binary mixtures of normal krypton and SO_2 to test further the validity of eq. [4].

EXPERIMENTAL RESULTS

The apparatus employed in the present investigation is a two-chamber apparatus of the Ney and Armistead (8) type. The apparatus and the experimental procedures have been fully described by Srivastava and Paul (3). Pure dry SO_2 gas was prepared by a method

described in detail by Srivastava and Saran (9). The thermostatic bath temperature was maintained constant at 30 °C within ±0.05 °C by a Sunvic electronic relay. The analysis was done by a scintillation counter.

TABLE I

Composition of SO_2	Pressure in mm Hg	D_{expt} (cm^2/s)	D_{calcd} (cm^2/s)		
			a^*	b^*	c^*
0.0000	30.70	0.1018	0.1018	0.1008	0.1008
0.2556	32.88	0.0970	0.0972	0.0966	0.0955
0.4959	25.53	0.0932	0.0932	0.0929	0.0909
0.7343	22.19	0.0894	0.0896	0.0896	0.0868
1.0000	30.54	0.0859	0.0859	0.0861	0.0827

*(*a*) Utilizing the experimental values of D_{expt} at $x = 0$ and $x = 1$ and using eq. [4]; (*b*) utilizing the unlike force parameters for the Kr–SO_2 system from observed binary diffusion coefficients (9) and eq. [4]; (*c*) utilizing the force parameters for SO_2 from viscosity (10) and the combination rules for polar–nonpolar interaction and eq. [4].

The experimental values of the diffusion coefficient for various concentrations of SO_2 are given in Table I. The D_{expt} values recorded in column 3 were obtained by reduction to atmospheric pressure. We believe that our data are correct within ±1%.

DISCUSSION

The values of D_{calcd} in column 4 have been obtained by using the D_{expt} values for 0 and 100% SO_2 and eq. [4] to calculate the composition dependence of D_{expt}. It can be seen that the agreement between the two sets is quite satisfactory. The values of D_{calcd} in column 5 have been obtained by utilizing the unlike interaction parameters for the Kr–SO_2 system from observed binary diffusion coefficients (9) and applying the mass correction. The agreement with the observed values is quite satisfactory. Column 6 gives the values of D_{calcd} obtained by utilizing the force constants of SO_2 from viscosity (10) in the combining rules for unlike force parameters and applying the mass correction. The calculated values of diffusion coefficients are somewhat smaller than the observed values. This is due to the smaller values of the binary diffusion coefficient obtained from the force constants of SO_2 from viscosity. The possible sources of discrepancy between the values of binary diffusion coefficients obtained from viscosity and those observed have been discussed elsewhere (9). After application of the mass correction, the values of $\mathfrak{D}_{13}$ and $\mathfrak{D}_{12}$ from Table I become 0.0862 and 0.102 respectively. These values compare quite well with the values $\mathfrak{D}_{23} = 0.0864$ at 30 °C (9) and $\mathfrak{D}_{22} = 0.1035$ at 31.5 °C (3).

ACKNOWLEDGMENT

The authors are grateful to Prof. B. N. Srivastava for his keen interest and valuable guidance.

1. C. F. Curtiss and J. O. Hirschfelder. J. Chem. Phys. **17**, 550 (1949).
2. J. O. Hirschfelder and C. F. Curtiss. Symposium on Combustion, 3rd, Madison, Wis., 1948. 1949. p. 124.
3. B. N. Srivastava and R. Paul. Physica, **28**, 646 (1962).
4. R. Paul. Indian J. Phys. **36**, 464 (1962).
5. L. Miller and P. C. Carman. Trans. Faraday Soc. **57**, 2143 (1961); **60**, 33 (1964).
6. H. Watts. Trans. Faraday Soc. **60**, 1745 (1964).
7. H. Watts. Can. J. Chem. **43**, 431 (1965).
8. E. P. Ney and F. C. Armistead. Phys. Rev. **71**, 14 (1947).
9. B. N. Srivastava and A. Saran. Can. J. Phys. To be published.
10. L. Monchick and E. A. Mason. J. Chem. Phys. **35**, 1676 (1961).

Received April 26, 1966.
Indian Association for the Cultivation of Science,
Calcutta, India.

Can. J. Chem. Downloaded from www.nrcresearchpress.com by 210.87.254.105 on 09/05/12
For personal use only.

SOLVENT EFFECTS ON THE ULTRAVIOLET SPECTRA OF N,N-DIMETHYLFORMAMIDE

MAHMOOD F. MAYAHI, A. H. AL-TAIAR, S. A. AL-BALDAWI, AND H. A. HUSSAIN

Can. J. Chem. Downloaded from www.nrcresearchpress.com by 210.87.254.105 on 09/05/12
For personal use only.

In recent years, many papers have appeared dealing with the chemical reaction and structures of amides. The structure of N,N-dimethylformamide (DMF) has been established by infrared and nuclear magnetic resonance spectroscopy (1–4). The infrared and nuclear magnetic resonance spectra of adducts of N,N-dialkylamides strongly support coordination at the oxygen atom (1, 5–7).

Our interest in the DMF structure was initiated by the interesting conductivity curves we obtained in work on hydrogen-bonded organic compounds in benzene (8, 9) and DMF. These curves could not be understood without a knowledge of the structure and reaction sites of DMF with the organic compounds. We report here the study of the ultraviolet spectra of DMF in hydrogen bonding and in non-H-bonding solvents. Table I shows the characteristics of the ultraviolet absorption peaks in *n*-hexane, cyclohexane, dioxane, acetonitrile, chloroform, ethyl alcohol, and water, at various concentrations of DMF. The ultraviolet absorption band in DMF is that of the carbonyl group, the $n-\pi^*$ transition. Normally, amides absorb around 214 mμ in water (10). However, Table I shows that the absorption peak shifts to shorter wavelengths as the concentration is decreased. This result might have been expected, since in our work on the absorption of the non-bonding electrons in triethylamine, ethyl acetate, and in polyvinyl acetate (11, 12), the same effect was observed and explained.

TABLE I

Ultraviolet spectra of DMF in various solvents

Solvent	Concentration (mole/l) $\times 10^2$	λ_{max} (mμ)	Optical density
n-Hexane	11.04	225	3.0
	0.088	212	2.03
	0.0071	205	0.426
Cyclohexane	12.38	227	3.0
	0.099	214	1.835
	0.008	206	0.354
Dioxane	0.740	225	2.95
	0.059	215	1.227
	0.0095	213	0.278
	0.0047	213	0.140
CH_3CN	5.93	240	1.423
$CHCl_3$	7.00	242	1.096
	1.93	240	0.632
	0.71	240	0.219
	0.385	240	0.193
Ethyl alcohol	1.14	227	3.0
	0.091	213	1.92
	0.0073	207	0.321
Water	1.118	225	3.0
	0.089	212	2.150
	0.0450	208	1.741
	0.0224	203	1.293

The n–π^* absorption band of the C=O group of acetone is at 279 mμ in hexane (10), and because of the strong electron-withdrawing inductive effect of the N atom in DMF, this band is shifted to 205 mμ in hexane (Table I). In addition the inductive effect of nitrogen makes the non-bonding electrons on the oxygen less prone to excitation and therefore less sensitive to solvent changes. This point can be appreciated if a comparison is made between the effect of solvents on the ultraviolet spectra of acetone and DMF. The n–π^* absorption bands of acetone in various solvents are at the following positions: hexane 279 mμ, chloroform 277 mμ, ethanol 272 mμ, water 264.5 mμ (10). This shows a blue shift depending on the hydrogen-bonding ability of the solvent, and the shift is 14.5 mμ (1 900 cm^{-1}) in changing from hexane to water, whereas for DMF the shift is only 5 mμ (1 200 cm^{-1}) in changing from hexane to water. Another striking difference between the n–π^* absorption band of acetone and of DMF is that $\nu_{C=O}$ of acetone is progressively shifted to higher frequencies in the solvents mentioned above, whereas $\nu_{C=O}$ of DMF is shifted to lower frequencies in $CHCl_3$ and in ethanol relative to hexane. This is similar to our results on triethylamine and ethyl acetate (11, 12).

The solvent effect on the ultraviolet absorption spectra has been treated theoretically by Bayliss (13) and McRae (14). Rao and Balazveramanien used the McRae equation for the n–π^* transition of C=O, N=N, NO_2, and C=S groups and found in nonpolar solvents and in polar non-H-bonding solvents that plots of ν_{max} vs. $(D-1)/(D+2)$ were "fairly linear" (15). Similar plots were made for triethylamine in a number of nonpolar and H-bonding solvents, but, in those cases, ν_{max} values were obtained for infinitely dilute solutions. Good straight lines were found for triethylamine, one line for the nonpolar solvents with a negative slope and another line for the H-bonding solvents with a positive slope (11). That the solvents are separated into two distinct series according to their H-bonding capabilities to the solute is in accord with the predictions made by McRae (14).

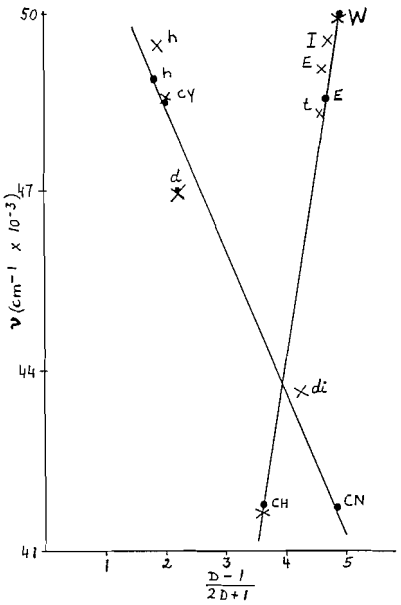


FIG. 1. ν (cm^{-1} × 10^{-3}) vs. $(D-1)/(2D+1)$ for DMF (●) and triethylamine (×), in the solvents: *n*-hexane (h), cyclohexane (cy), dioxane (d), acetonitrile (CN), chloroform (CH), dichloromethane (di), *t*-butyl alcohol (t), ethyl alcohol (E), isopropyl alcohol (I), and water (W) at 20 °C.

Can. J. Chem. Downloaded from www.nrcresearchpress.com by 210.87.254.105 on 09/05/12
For personal use only.

For DMF, ν_{max} vs. $(D-1)/(2D+1)$ is used (Fig. 1) (10, 13), where ν_{max} is that of infinitely dilute solutions obtained by graphical extrapolation of the values given in Table I. The use of $(D-1)/(2D+1)$ instead of $(D-1)/(D+2)$ gives less scatter of points, especially for the line involving the nonpolar solvents and CH_3CN. The data for triethylamine from ref. 11 are recalculated and included in Fig. 1. The point representing DMF in dioxane does not fall on the line for non-H-bonding solvents; this was also found by Rao and Balazveramanien (15) and McRae (14). The deviation was explained by McRae, who argued that the dioxane molecule has two nonadjacent dipolar groups whose moments cancel, so that the effective reaction field is probably greater than is indicated by the macroscopic properties.

1. R. A. Y. Jones and A. R. Katritzky. Chem. Ind. London, 722 (1961).
2. H. S. Gutowsky and C. H. Holm. J. Chem. Phys. **32**, 1272 (1960).
3. W. D. Phillips. J. Chem. Phys. **23**, 1363 (1955).
4. J. Archambault and R. Rivest. Can. J. Chem. **38**, 1335 (1960).
5. W. Gerhard *et al.* J. Chem. Soc. 2144 (1960).
6. S. J. Kuhn and J. S. McIntyre. Can. J. Chem. **43**, 375 (1965).
7. E. S. Gore, D. J. Belears, and S. S. Danyluk. Can. J. Chem. **43**, 2135 (1965).
8. M. F. Mayahi and A. E. Habboush. J. Electrochem. Soc. **112**, 222 (1965).
9. M. F. Mayahi and A. E. Habboush. J. Electrochem. Soc. **112**, 224 (1965).
10. H. H. Jaffe and Milton Orchin. Theory and applications of ultraviolet spectroscopy. John Wiley and Sons, Inc., New York. 1962. pp. 180–187.
11. M. F. Mayahi and A. L. K. Al-Juburry. Bull. Coll. Sci. Baghdad, Iraq, **8**, 79 (1965).
12. M. F. Mayahi and A. H. Al-Taiar. J. Polymer Sci. Pt. B, **3**, 331 (1965).
13. N. B. Bayliss. J. Chem. Phys. **18**, 292 (1950).
14. E. G. McRae. J. Phys. Chem. **61**, 562 (1957).
15. A. Balazveramanien and C. N. R. Rao. Spectrochim. Acta, **81**, 1337 (1962).

Received February 1, 1966.
Chemistry Department,
College of Science,
University of Baghdad,
Baghdad, Iraq.

PRODUCTION OF HYDRATED ELECTRONS

David C. Walker

Recent radiation chemical studies[1] have shown that ionization of liquid water leads to the formation of hydrated electrons (e_{aq}^-), rather than hydrogen atoms, as the principal reactive chemical species. In certain photochemical electron-transfer processes, in which the reducing species was formerly identified, but mistakenly, as a hydrogen atom, the characteristic absorption spectrum of e_{aq}^- has now been observed (2). A hydrated electron is barely distinguishable chemically from a hydrogen atom, its conjugate acid, but is converted to it by reaction [1] only very slowly, if at all (3).

[1] $$e_{aq}^- + H_2O \rightarrow H + OH_{aq}^-;\ k_1 \leqslant 16\ \text{mole}^{-1}\ \text{s}^{-1}$$

We have investigated three types of reaction in which e_{aq}^- could have been mistaken for H atoms as the precursors of molecular H_2. These are (i) the reaction between an alkali metal and water, (ii) the cathode reaction in the electrolytic decomposition of water, and (iii) the reduction of water by a cation having an oxidation potential > 0.413 V, such as U^{3+}.

[1]*For review of evidence, see Hart (1).*

Can. J. Chem. Downloaded from www.nrcresearchpress.com by 210.87.254.105 on 09/05/12
For personal use only.

For DMF, ν_{max} vs. $(D-1)/(2D+1)$ is used (Fig. 1) (10, 13), where ν_{max} is that of infinitely dilute solutions obtained by graphical extrapolation of the values given in Table I. The use of $(D-1)/(2D+1)$ instead of $(D-1)/(D+2)$ gives less scatter of points, especially for the line involving the nonpolar solvents and CH_3CN. The data for triethylamine from ref. 11 are recalculated and included in Fig. 1. The point representing DMF in dioxane does not fall on the line for non-H-bonding solvents; this was also found by Rao and Balazveramanien (15) and McRae (14). The deviation was explained by McRae, who argued that the dioxane molecule has two nonadjacent dipolar groups whose moments cancel, so that the effective reaction field is probably greater than is indicated by the macroscopic properties.

1. R. A. Y. Jones and A. R. Katritzky. Chem. Ind. London, 722 (1961).
2. H. S. Gutowsky and C. H. Holm. J. Chem. Phys. **32**, 1272 (1960).
3. W. D. Phillips. J. Chem. Phys. **23**, 1363 (1955).
4. J. Archambault and R. Rivest. Can. J. Chem. **38**, 1335 (1960).
5. W. Gerhard *et al.* J. Chem. Soc. 2144 (1960).
6. S. J. Kuhn and J. S. McIntyre. Can. J. Chem. **43**, 375 (1965).
7. E. S. Gore, D. J. Belears, and S. S. Danyluk. Can. J. Chem. **43**, 2135 (1965).
8. M. F. Mayahi and A. E. Habboush. J. Electrochem. Soc. **112**, 222 (1965).
9. M. F. Mayahi and A. E. Habboush. J. Electrochem. Soc. **112**, 224 (1965).
10. H. H. Jaffe and Milton Orchin. Theory and applications of ultraviolet spectroscopy. John Wiley and Sons, Inc., New York. 1962. pp. 180–187.
11. M. F. Mayahi and A. L. K. Al-Juburry. Bull. Coll. Sci. Baghdad, Iraq, **8**, 79 (1965).
12. M. F. Mayahi and A. H. Al-Taiar. J. Polymer Sci. Pt. B, **3**, 331 (1965).
13. N. B. Bayliss. J. Chem. Phys. **18**, 292 (1950).
14. E. G. McRae. J. Phys. Chem. **61**, 562 (1957).
15. A. Balazveramanien and C. N. R. Rao. Spectrochim. Acta, **81**, 1337 (1962).

Received February 1, 1966.
Chemistry Department,
College of Science,
University of Baghdad,
Baghdad, Iraq.

PRODUCTION OF HYDRATED ELECTRONS

David C. Walker

Recent radiation chemical studies[1] have shown that ionization of liquid water leads to the formation of hydrated electrons (e_{aq}^-), rather than hydrogen atoms, as the principal reactive chemical species. In certain photochemical electron-transfer processes, in which the reducing species was formerly identified, but mistakenly, as a hydrogen atom, the characteristic absorption spectrum of e_{aq}^- has now been observed (2). A hydrated electron is barely distinguishable chemically from a hydrogen atom, its conjugate acid, but is converted to it by reaction [1] only very slowly, if at all (3).

[1] $$e_{aq}^- + H_2O \rightarrow H + OH_{aq}^-;\ k_1 \leqslant 16\ \text{mole}^{-1}\ \text{s}^{-1}$$

We have investigated three types of reaction in which e_{aq}^- could have been mistaken for H atoms as the precursors of molecular H_2. These are (i) the reaction between an alkali metal and water, (ii) the cathode reaction in the electrolytic decomposition of water, and (iii) the reduction of water by a cation having an oxidation potential > 0.413 V, such as U^{3+}.

[1]*For review of evidence, see Hart (1).*

Can. J. Chem. Downloaded from www.nrcresearchpress.com by 210.87.254.105 on 09/05/12
For personal use only.

A distinction between e_{aq}^- and H atoms was made by kinetic competition studies based on the known rates of reactions [2] to [5].[2]

[2] $e_{aq}^- + N_2O \rightarrow N_2 + O^-(\rightarrow OH)$; $k_2 = 9 \times 10^9$ mole^{-1} s^{-1}

[3] $H + N_2O \rightarrow N_2 + OH$; $k_3 < 3 \times 10^5$ mole^{-1} s^{-1}

[4] $e_{aq}^- + CH_3OH \rightarrow ?$; $k_4 < 10^4$ mole^{-1} s^{-1}

[5] $H + CH_3OH \rightarrow H_2 + CH_2OH$; $k_5 = 2 \times 10^6$ mole^{-1} s^{-1}

It is evident from these rate constants that if both methanol and N_2O are present as scavengers for the precursors of molecular H_2 and if $[CH_3OH]/[N_2O] \approx 10$, that N_2 will be formed only if e_{aq}^- is a reactive intermediate. The technique employed was to add N_2O to the water in sufficient concentration to reduce the yield of H_2 significantly, with a concomitant production of N_2, for each of the reactions (i), (ii), and (iii); then to repeat this experiment with an excess of CH_3OH and note whether the yields of N_2 and H_2 were affected.

[6] $e_{aq}^- + e_{aq}^- \rightarrow H_2 + 2OH_{aq}^-$; $2k_6 = 4.5 \times 10^9$ mole^{-1} s^{-1}

[7] $H + H \rightarrow H_2$; $2k_7 = 6 \times 10^9$ mole^{-1} s^{-1}

Since in all three systems H_2 was shown to be formed in a bimolecular reaction ([6] or [7]) at the metal–water interface, it was necessary to control the rate of generation of reactive intermediates so that the N_2O could compete successfully by reaction [2] or [3]. In (i) we used very dilute sodium amalgams so that the reaction time was several hours, and N_2O at atmospheric pressure reduced the H_2 yield to $\sim 10\%$ of its value without scavenger (5). For (ii) it was necessary to use very low current densities in an electrolysis cell having a large and smooth platinum cathode. At ~ 50 μA cm^{-2} the H_2 yield was reduced to $\sim 35\%$ of its value in the absence of N_2O. Unfortunately there was no control of the rate of H_2 generation when solid lumps of uranium trichloride were added to the solution, and since the H_2 yield was reduced to only $\sim 80\%$ of its former value, this is less sensitive than (i) and (ii) but qualitatively equally valid. (We are currently repeating (iii), and are using dipositive europium salts since the oxidation potential of the Eu^{2+}/Eu^{3+} couple is much less than that of U^{3+}/U^{4+}.) Highly purified water was used, and it was thoroughly deaerated before the other reagents were added. Samples of the results are given in Tables I, II, and III.

TABLE I

Effect of [Na], [N_2O], pH, and [CH_3OH] on N_2 and H_2 yields (reaction (i))

[Na] in Hg (M)	Weight of amalgam (g)	pH	[N_2O] (M)	[CH_3OH] (M)	N_2 (μmoles)	H_2 (μmoles)
2.5×10^{-4}	~190	~7	0	0	0	1.7
2.5×10^{-2}	~190	~7	7.1×10^{-3}	0	1.4	0.3
1.4×10^{-2}	~30	~7	7.6×10^{-3}	0	6.6	8.2
1.4×10^{-2}	~30	~7	1.5×10^{-2}	0	11.7	3.3
1.4×10^{-2}	~30	2	8.5×10^{-3}	0	0.3	14.6
1.6×10^{-3}	~40	~7	2.1×10^{-2}	0	2.0	0.2
1.6×10^{-3}	~40	~7	2.1×10^{-2}	0.1	2.1	0.1
1.6×10^{-3}	~40	~13	2.1×10^{-2}	0.1	2.3	0.1

Since the addition of methanol does not affect the N_2 and H_2 yields, it is evident that in all three reactions H atoms are not reaction intermediates. Furthermore, the results are entirely consistent with the postulate that hydrated electrons are the precursors of H_2.

[2] *All rate constants quoted in this paper are taken from Anbar and Neta (4).*

Can. J. Chem. Downloaded from www.nrcresearchpress.com by 210.87.254.105 on 09/05/12
For personal use only.

TABLE II

Ratio of N_2/H_2 yields at the cathode in the electrolytic decomposition of 0.25 M Na_2SO_4 solution (reaction (ii))

Current density (μA cm^{-2})	[N_2O] (M)	CH_3OH (M)	pH	N_2/H_2 ratio*
64	0	0	~7	<0.004
80	1.9×10^{-2}	0	~7	0.40
47	1.9×10^{-2}	0	~7	1.67
47	1.9×10^{-2}	0.1	~7	1.75
47	1.9×10^{-2}	0	1.3	<0.008
47	1.9×10^{-2}	0.1	1.3	<0.001

*To minimize polarization effects, a sample of gas was extracted during steady electrolysis; hence only gas ratios are reported.

TABLE III

Effect of [N_2O] and [CH_3OH] on the yields of N_2 and H_2 by reaction of UCl_3 with 25 ml water (reaction (iii))

[U^{4+}] formed (mM)	[N_2O] (M)	CH_3OH (M)	N_2 (μmoles)	H_2 (μmoles)	N_2/H_2
1.4	0	0	<0.05	17.2	~0
0.52	1.8×10^{-2}	0	1.25	5.2	0.24
0.80	1.8×10^{-2}	0.1	2.08	8.0	0.26

This is corroborated by the effect of pH on the gas yields. Since e_{aq}^- and H can be interconverted, it follows that the species reacting in neutral water is the same as that expected at high pH values whereas, in acidic solution, e_{aq}^- would be converted to H atoms, and reaction [3] cannot compete with the formation of H_2 by reaction [7] because $k_7 > 10^4 k_3$ (contrast $k_6 \approx k_2$).

[8] $$H + OH_{aq}^- \rightarrow e_{aq}^-; \quad k_8 = 2 \times 10^7 \text{ mole}^{-1} \text{ s}^{-1}$$

[9] $$e_{aq}^- + H_{aq}^+ \rightarrow H \quad ; \quad k_9 = 2.3 \times 10^{10} \text{ mole}^{-1} \text{ s}^{-1}$$

Our results on process (i) are endorsed by the findings of Hughes and Roach (6) and since we failed to find a polarographic half-wave potential corresponding to the reduction of N_2O at a dropping-Hg electrode, the possibility that electrons at the metal surface were reacting with N_2O before they became solvated can probably be discounted. The absence of O_2 in the products and the correspondence between the diminution of H_2 and formation of N_2 are explained by the consumption of an additional e_{aq}^- at the metal–water interface by the OH radical produced in reaction [2] (5).

It is proposed that reactions [10], [11], and [12] represent the relevant primary steps.

[10] $$Na \xrightarrow{H_2O} Na_{aq}^+ + e_{aq}^-$$
(rather than $Na + H_2O \rightarrow Na_{aq}^+ + OH_{aq}^- + H$)

[11] $$e_{(cathode)}^- \xrightarrow{H_2O} e_{aq}^-$$
(rather than $e_{(cathode)}^- + H_{aq}^+ \rightarrow H$)

[12] $$U^{3+} \xrightarrow{H_2O} U_{aq}^{4+} + e_{aq}^-$$
(rather than $U^{3+} + H_2O \rightarrow U_{aq}^{4+} + OH_{aq}^- + H$)

Perhaps, in general, hydrated electrons are the reaction intermediates when water at natural pH is reduced to H_2 in reactions involving electron transfer processes.

Can. J. Chem. Downloaded from www.nrcresearchpress.com by 210.87.254.105 on 09/05/12
For personal use only.

ACKNOWLEDGMENTS

The assistance of Mr. E. A. Shaede, who performed the experimental work of reaction (i), is gratefully acknowledged. The National Research Council of Canada provided the financial support.

1. E. J. HART. Science, **146**, 19 (1964).
2. L. I. GROSSWEINER, G. W. SWENSON, and E. F. ZWICKER. Science, **141**, 805 (1963). M. S. MATHESON, W. A. MULAC, and J. RABANI. J. Phys. Chem. **67**, 2613 (1963).
3. D. C. WALKER. Quart. Rev. London. In press.
4. M. ANBAR and P. NETA. Intern. J. Appl. Radiation Isotopes, **16**, 227 (1965).
5. E. A. SHAEDE and D. C. WALKER. Intern. Symp. Alkali Metals, Nottingham, England. 1966.
6. G. HUGHES and R. J. ROACH. Chem. Commun. 600 (1965).

RECEIVED JULY 12, 1966.
CHEMISTRY DEPARTMENT,
UNIVERSITY OF BRITISH COLUMBIA,
VANCOUVER, B.C.

THE IMPORTANCE OF INDUCTIVE EFFECTS IN α-SILYL AND α-GERMYL KETONES

KEITH YATES AND FRANCO AGOLINI

The unusual spectroscopic properties of α-silyl ketones (1) have been attributed to p–π–d–π interactions involving the vacant 3d orbitals of silicon (1, 2). The α-triphenylgermyl ketones which have been previously prepared (1, 3) have spectral characteristics similar to those of the α-silyl ketones, i.e. abnormally low carbonyl stretching frequency and unusually long wavelength ultraviolet absorption resulting in yellow color. We have now prepared the first α-trimethylgermyl ketone to be reported, trimethylbenzoylgermane, by the following route using standard procedures (1).

$$Ph_4Ge + 3GeCl_4 \xrightarrow[350°]{\text{sealed tube}} 4Cl_3GePh \xrightarrow{MeMgI} Me_3GePh \xrightarrow[EtBr]{Br_2} Me_3GeBr \xrightarrow{PhCH_2MgCl}$$

$$Me_3GeCH_2Ph \xrightarrow{NBS} Me_3GeCBr_2Ph \xrightarrow{MeCOOAg} Me_3GeCOPh$$

The product (b.p. 53.5–54° (0.28 mm), $n_D^{24.5} = 1.5364$) is also yellow, with λ_{max} at 252 mμ ($\epsilon = 10\,700$) and 412 mμ ($\epsilon = 120$) in ethanol, and has an unusually low carbonyl frequency at 1 629 cm^{-1} in CCl_4. These properties are very similar to those of the previously reported triphenylbenzoylgermanes, and p–π–d–π interactions involving germanium 4d orbitals could also be responsible for the shifted $n \rightarrow \pi^*$ and carbonyl stretching bands (1). However, it has been pointed out (3; Orgel, quoted in ref. 4; 5) that inductive effects could be responsible for the spectral shifts observed when an α carbon is replaced by either silicon or germanium. Until now there has been neither experimental evidence nor theoretical calculations to indicate which effect, if either, predominates. We now present evidence to show that insofar as the electronic ground states are concerned the inductive effect of silicon or germanium predominates over any possible d-orbital interaction. We have measured the base strengths of the ketones R_3XCOPh (X = C, Si, Ge; R = Me, Ph) by two different methods and find that in each series the α-silyl or α-germyl ketone is more strongly basic than its carbon analogue. The pK values were determined in aqueous sulfuric acids by the standard spectrophotometric technique (6), except that in some cases

Can. J. Chem. Downloaded from www.nrcresearchpress.com by 210.87.254.105 on 09/05/12
For personal use only.

ACKNOWLEDGMENTS

The assistance of Mr. E. A. Shaede, who performed the experimental work of reaction (i), is gratefully acknowledged. The National Research Council of Canada provided the financial support.

1. E. J. HART. Science, **146**, 19 (1964).
2. L. I. GROSSWEINER, G. W. SWENSON, and E. F. ZWICKER. Science, **141**, 805 (1963). M. S. MATHESON, W. A. MULAC, and J. RABANI. J. Phys. Chem. **67**, 2613 (1963).
3. D. C. WALKER. Quart. Rev. London. In press.
4. M. ANBAR and P. NETA. Intern. J. Appl. Radiation Isotopes, **16**, 227 (1965).
5. E. A. SHAEDE and D. C. WALKER. Intern. Symp. Alkali Metals, Nottingham, England. 1966.
6. G. HUGHES and R. J. ROACH. Chem. Commun. 600 (1965).

RECEIVED JULY 12, 1966.
CHEMISTRY DEPARTMENT,
UNIVERSITY OF BRITISH COLUMBIA,
VANCOUVER, B.C.

THE IMPORTANCE OF INDUCTIVE EFFECTS IN α-SILYL AND α-GERMYL KETONES

KEITH YATES AND FRANCO AGOLINI

The unusual spectroscopic properties of α-silyl ketones (1) have been attributed to p–π–d–π interactions involving the vacant 3d orbitals of silicon (1, 2). The α-triphenylgermyl ketones which have been previously prepared (1, 3) have spectral characteristics similar to those of the α-silyl ketones, i.e. abnormally low carbonyl stretching frequency and unusually long wavelength ultraviolet absorption resulting in yellow color. We have now prepared the first α-trimethylgermyl ketone to be reported, trimethylbenzoylgermane, by the following route using standard procedures (1).

$$Ph_4Ge + 3GeCl_4 \xrightarrow[350°]{\text{sealed tube}} 4Cl_3GePh \xrightarrow{MeMgI} Me_3GePh \xrightarrow[EtBr]{Br_2} Me_3GeBr \xrightarrow{PhCH_2MgCl}$$

$$Me_3GeCH_2Ph \xrightarrow{NBS} Me_3GeCBr_2Ph \xrightarrow{MeCOOAg} Me_3GeCOPh$$

The product (b.p. 53.5–54° (0.28 mm), $n_D^{24.5} = 1.5364$) is also yellow, with λ_{max} at 252 mμ ($\epsilon = 10\,700$) and 412 mμ ($\epsilon = 120$) in ethanol, and has an unusually low carbonyl frequency at 1 629 cm^{-1} in CCl_4. These properties are very similar to those of the previously reported triphenylbenzoylgermanes, and p–π–d–π interactions involving germanium 4d orbitals could also be responsible for the shifted $n \rightarrow \pi^*$ and carbonyl stretching bands (1). However, it has been pointed out (3; Orgel, quoted in ref. 4; 5) that inductive effects could be responsible for the spectral shifts observed when an α carbon is replaced by either silicon or germanium. Until now there has been neither experimental evidence nor theoretical calculations to indicate which effect, if either, predominates. We now present evidence to show that insofar as the electronic ground states are concerned the inductive effect of silicon or germanium predominates over any possible d-orbital interaction. We have measured the base strengths of the ketones R_3XCOPh (X = C, Si, Ge; R = Me, Ph) by two different methods and find that in each series the α-silyl or α-germyl ketone is more strongly basic than its carbon analogue. The pK values were determined in aqueous sulfuric acids by the standard spectrophotometric technique (6), except that in some cases

Can. J. Chem. Downloaded from www.nrcresearchpress.com by 210.87.254.40 on 09/05/12
For personal use only.

Can. J. Chem. Downloaded from www.nrcresearchpress.com by 210.87.254.40 on 09/05/12
For personal use only.

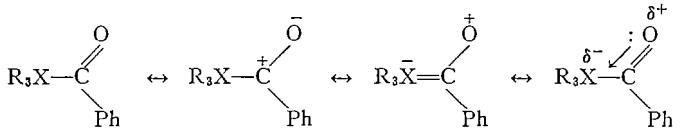
decomposition of the ketone in the highest acid concentrations made zero-time extrapolation procedures necessary. Relative base strengths were determined by measuring the effect of the ketone on the ν_{OH} bands of hydrogen bond donors such as phenol or methanol in dilute solution (0.005 M) in CCl_4, the shift $\Delta\nu$ produced being taken as a measure of the base strength of the ketone. The results given in Table I show that the order of base strength in each series is $R_3SiCOPh \geqslant R_3GeCOPh > R_3CCOPh$. Thus replacement of an α carbon by silicon or germanium increases the availability of electrons on the carbonyl oxygen. This is consistent with an increased contribution of II arising

TABLE I
Base strengths of phenyl ketones

Compound	pK_{BH^+}*	$\Delta\nu$ of 3 611 cm^{-1} band of phenol	Relative basicity	$\Delta\nu$ of 3 643 cm^{-1} band of methanol	Relative basicity
$Ph_3SiCOPh$	−7.78	139±1	1.00	58	1.00
$Ph_3GeCOPh$	†	131±1	0.94	50	0.86
Ph_3CCOPh	−8.37	117±1	0.84	45	0.78
$Me_3SiCOPh$	−6.49	180±3	1.00		
$Me_3GeCOPh$	−6.51	175±5	0.97		
Me_3CCOPh	−7.74	162±3	0.90		

*Dissociation constant of ketone conjugate acid. Since these ketones are not true Hammett bases the values given are not thermodynamic pK's.
†Spectral changes on protonation are not sufficiently pronounced to give reliable pK measurement.

from a strong inductive effect[1] of silicon or germanium on the X—C bond and explains why α-silyl and α-germyl ketones have carbonyl absorption at some 50–70 cm^{-1} lower frequency than the corresponding carbon compounds. Any important contributions from III or IV, involving d-orbital interaction, would reduce the availability of electrons on



I II III IV

oxygen in lowering the CO bond order. It should be emphasized that these considerations do not necessarily extend to the electronically excited states of these molecules. The above conclusions are supported by the results of molecular orbital calculations on the model compounds H_3XCOPh (X = C, Si, Ge). Simple Hückel molecular orbital calculations using the recently obtained heteroatom parameters of Curtis and Allred (7) for Si and Ge result in very small π-bond orders for the X–C bond, 0.097 for C—Si and 0.067 for C—Ge, and π-bond orders for the carbonyl group which are practically identical for X = C (0.781), X = Si (0.783), X = Ge (0.782). We find that only by including *both* σ- and π-type orbitals in an extended Hückel treatment (8) can we arrive at electron densities and bond orders (F. Agolini, I. G. Csizmadia, S. Klemenko, and K. Yates, unpublished results) consistent with the experimentally observed decrease in carbonyl stretching frequency and increase in basicity when α-carbon is replaced by silicon or germanium. The results of these calculations will be presented in a future paper dealing with the unusual electronic transitions of these ketones.

[1]*It is worth noting that the electronegativity differences* $(X_C - X_{Si})$ *and* $(X_C - X_{Ge})$ *are greater than the* $(X_{Cl} - X_C)$ *differences on either the Pauling or Mulliken scale.*

ACKNOWLEDGMENTS

We wish to thank Professor A. G. Brook for generous samples of α-silyl ketones and the Institute of Computer Science, University of Toronto, for use of their facilities. This work was supported by a grant from the National Research Council of Canada.

1. A. G. BROOK, M. A. QUIGLEY, G. J. D. PEDDLE, N. V. SCHWARTZ, and C. M. WARNER. J. Am. Chem. Soc. **82**, 5102 (1957).
2. D. F. HARNISH and R. WEST. Inorg. Chem. **2**, 1082 (1963).
3. D. A. NICHOLSON and A. L. ALLRED. Inorg. Chem. **4**, 1747 (1965).
4. E. B. EBSWORTH. Volatile silicon compounds. Pergamon Press Ltd., Oxford. 1963. p. 81.
5. A. G. BROOK and J. B. PIERCE. Can. J. Chem. **42**, 298 (1964).
6. E. M. ARNETT. *In* Progress in physical organic chemistry. Vol. 1. *Edited by* S. G. Cohen, A. Streitwieser, Jr., and R. W. Taft. Interscience, New York. 1963. pp. 244–246.
7. M. D. CURTIS and A. L. ALLRED. J. Am. Chem. Soc. **87**, 2554 (1965).
8. R. HOFFMAN. J. Chem. Phys. **39**, 1397 (1963).

RECEIVED APRIL 21, 1966.
DEPARTMENT OF CHEMISTRY,
UNIVERSITY OF TORONTO,
TORONTO, ONTARIO.

Can. J. Chem. Downloaded from www.nrcresearchpress.com by 210.87.254.40 on 09/05/12
For personal use only.

Can. J. Chem. Downloaded from www.nrcresearchpress.com by 210.87.254.40 on 09/05/12
For personal use only.

Canadian Journal of Chemistry

Issued by THE NATIONAL RESEARCH COUNCIL OF CANADA

VOLUME 44 OCTOBER 1, 1966 NUMBER 19

ELECTROPHILIC REACTIONS OF STEROIDAL AND OTHER α-PHENYL DIENES[1]

MAURICE DOUEK[2] AND GEORGE JUST
Department of Chemistry, McGill University, Montreal, Quebec

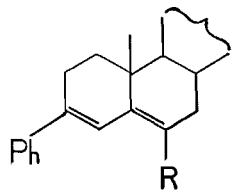
Received May 17, 1966

ABSTRACT

3-Phenylcholesta-3,5-diene (I) is shown to undergo electrophilic substitution reactions exclusively at the 6 position with formaldehyde – perchloric acid, acetic anhydride – aluminium chloride, and the Vilsmeier reagent.

In the case of formaldehyde, the final product is "dimer" II. The reaction is specific for formaldehyde and can be used to detect trace amounts of formaldehyde in, for example, commercial acetic acid and acetic anhydride.

In connection with an extension of the work on the photolysis of conjugated diene systems in various solvents (1–4), we investigated the photolysis of conjugated α-phenyl dienes in ethyl acetate – acetic acid containing 1% perchloric acid. Upon addition of perchloric acid to an ethyl acetate – acetic acid solution of 3-phenylcholesta-3,4-diene (I) at 45°, the colorless solution turned, in rapid succession, yellow, pink, red, and deep purple and a flocculent precipitate appeared. It was shown by thin-layer chromatography (t.l.c.) that a product (II) with an R_f value close to that of the starting material was formed.



I R=H
Ia R=D
Ib R=$COCH_3$
Ic R=CHO
Id R=CH_2OH

This product could be separated from the starting material I (I being the only other important fraction) either by column chromatography on alumina or simply by two careful crystallizations from hexane. Variations of the reaction conditions showed that the yield of product II was directly proportional to the amount of acetic acid used and was not increased by a prolonged reaction time. Since attempts to drive the reaction to completion by filtering the flocculent precipitate failed, it was concluded that this reaction did not produce an equilibrium mixture. Products of a similar nature were shown to be formed when 3-*p*-ethoxyphenylcholesta-3,5-diene (III), 3-phenylandrosta-3,5-diene-17β-ol acetate

[1]*Abstracted from part of the Ph.D. thesis of M. Douek.*

[2]*Holder of a National Research Council of Canada bursary, 1963–1964, and National Research Council of Canada studentships, 1964–1966.*

Can. J. Chem. Downloaded from www.nrcresearchpress.com by 210.87.254.40 on 09/05/12
For personal use only.

(IV), 3-phenylandrosta-3,5-diene-17-one (V), and 3-phenylandrosta-3,5-diene (VI) were used, thus proving that the reaction was general for conjugated α-phenyl dienes of this type.

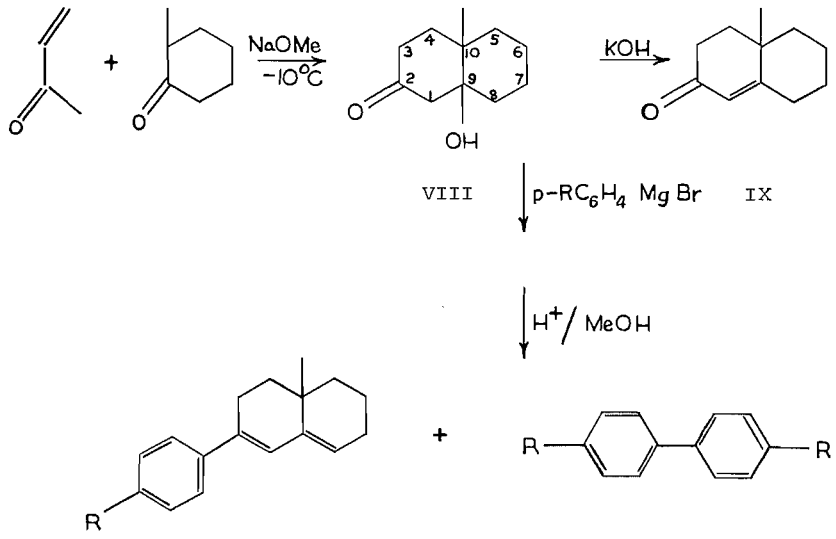
Product II, m.p. 228–229°, was shown by analysis to be a hydrocarbon. An osmometric molecular weight determination gave a molecular weight of 860 (the molecular weight of the starting material was 445). The strong ultraviolet absorption of I at 282 mμ was shifted in product II to 292 mμ, and its intensity was increased by 25%. This fact was interpreted as evidence for the retention of the unsaturated system present in I. This was confirmed by a quantitative hydrogenation in the presence of 10% palladium on charcoal, since 4 moles of hydrogen were absorbed to yield compound VII. Absorption in the 6.8–7.3 p.p.m. region in the nuclear magnetic resonance (n.m.r.) spectrum of VII proved that the phenyl rings were not affected by the hydrogenation. The n.m.r. spectrum of II showed a complex multiplet in the 7–7.4 p.p.m. region and a singlet at 6.93 p.p.m. These were respectively assigned to the five hydrogens on the benzene ring and to the two hydrogens in the 4 and 4′ positions; in addition, a singlet at 3.15 p.p.m. was interpreted as belonging to two doubly allylic protons. Since no other peaks were found in the olefinic region, it was concluded that the 6 and 6′ positions were substituted. The lowest whole number ratio of the integrated areas of the complex multiplet at 7–7.5 p.p.m., the singlet at 6.93 p.p.m., and the singlet at 3.15 p.p.m. was 5:1:1. This ratio was taken as strong evidence for a symmetrical dimer. Finally, a broad absorption centered at 2.45 p.p.m. was assigned to protons allylic to the double bonds. It was impossible to integrate this area since it overlapped with the steroid envelope. The infrared spectrum was quite similar to that of 3-phenylcholesta-3,5-diene (I). All attempts to obtain a mass spectrum of "dimer" II failed, extensive pyrolysis occurring at the high temperatures necessary to produce an appreciable vapor pressure.

Since the evidence obtained by spectral data in the steroidal models was insufficient to deduce the structure of product II, a more suitable model compound had to be found. Conjugated α-phenyl dienes in the decalin series were chosen, since it was felt that the change in the geometry of the compound would not be too large, that the vapor pressure of the resulting dimer would be high enough to take a mass spectrum, and that a fairly exact integration of the n.m.r. signals caused by all protons of the dimer would be possible.

Condensation of methyl vinyl ketone with 2-methylcyclohexanone, as described by Marshall and Fanta (5), gave a good yield of *cis*-10-methyl-2-decalon-9-ol (VIII). Dehydration of VIII with potassium hydroxide gave 10-methyl-1(9)-octalone-2 (IX). Grignard reaction of VIII or IX with phenylmagnesium bromide, followed by dehydration with 10% methanolic hydrochloric acid, gave a mixture of two compounds. All attempts to separate this mixture by column chromatography, by t.l.c., or by crystallization failed. However, vapor-phase chromatography showed that one component of the mixture was biphenyl, and comparison of the n.m.r. spectrum of the crude mixture with that of 3-phenylcholesta-3,5-diene (I) indicated that the other compound was 10-methyl-2-phenyl-$\Delta^{2,9}$-hexalin.

Since it was felt that ether X*b* would be easier to separate from bi-*p*-ethoxyphenyl (XI*b*), *p*-ethoxyphenylmagnesium bromide was added to VIII. After dehydration, a mixture containing X*b* and XI*b* was obtained. Chromatography gave 52% of α-phenyl diene X*b*.

Reaction of X*b* in acetic acid–ethyl acetate containing 1.5% perchloric acid at 50° gave a compound XII analogous to those obtained from the steroidal dienes. The infrared spectra of XII and the starting material X*b* were again quite similar. It absorbed in the ultraviolet at 296 mμ (ϵ 63 500), and its n.m.r. spectrum showed an A_2B_2 quartet at

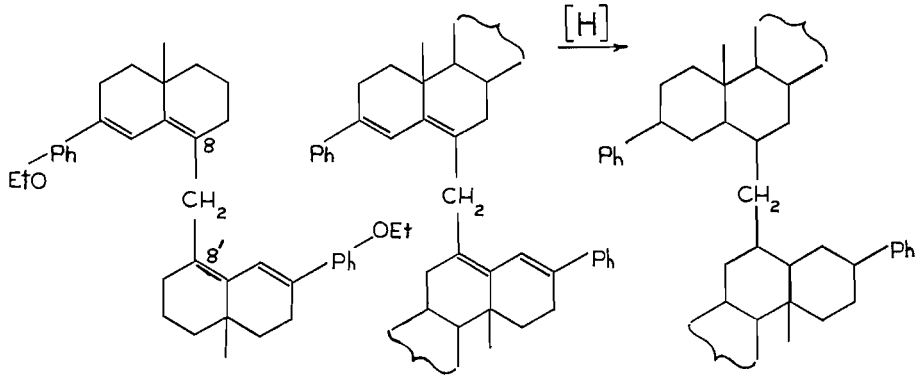


Xa R=H
Xb R=OEt

XIa R=H
XIb R=OEt

6.99 p.p.m. characteristic of the aromatic protons, a singlet at 6.87 p.p.m. caused by the 1 and 1′ protons, a quartet centered at 3.94 p.p.m. for the CH_3—CH_2—O protons, and a singlet at 3.12 p.p.m. assigned to the doubly allylic protons.

In the mass spectrum, the molecular ion peak had a mass of 548, and the elemental analysis derived for it gave an empirical formula of $C_{39}H_{48}O_2$. The elemental analysis and the molecular weight of the product were interpreted as evidence for the inclusion of a methylene group in addition to "dimerization" of the starting material.

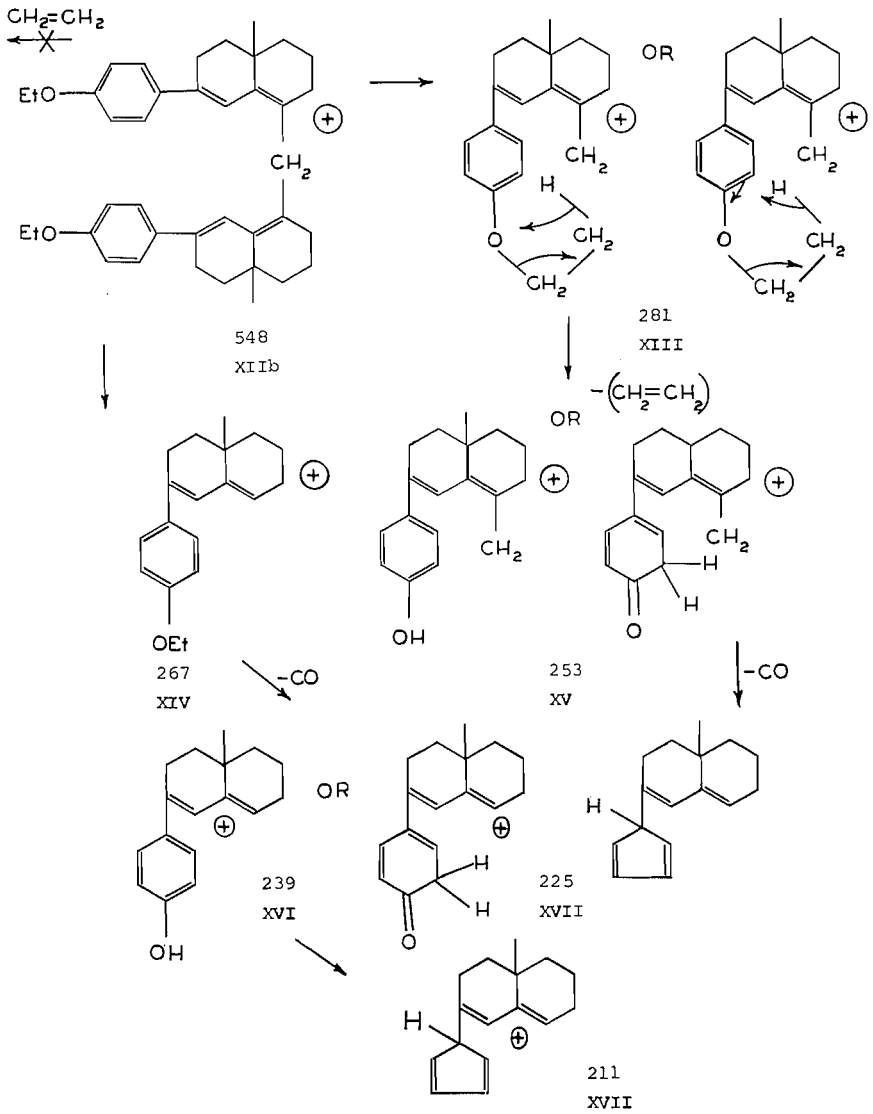


XII II VII

On the basis of structure XII, the signal at 3.12 p.p.m. in the n.m.r. spectrum can be attributed to the doubly allylic protons on the carbon between the 8 and 8′ positions. Substitution in these positions would be expected to cause a bathochromic shift in the ultraviolet spectrum. Finally, a fragmentation pattern based on structure XII may be used to explain a number of the peaks in the mass spectrum (Scheme 1).

Since the yield of "dimer" was directly proportional to the amount of acetic acid, it was felt that the source of the included methylene was probably an impurity in the acetic

Can. J. Chem. Downloaded from www.nrcresearchpress.com by 210.87.254.40 on 09/05/12
For personal use only.



SCHEME 1. Probable fragmentation pattern of product XII.

acid. Indeed, it soon was discovered that upon addition of a drop of aqueous formaldehyde the reaction went to completion, giving an almost quantitative yield of "dimer". Moreover, "dimer" formation, which previously had been impossible in solvents other than acetic acid, became possible when a small amount of formaldehyde and perchloric acid was added. Thus, the reaction was found to proceed in chloroform, ethyl acetate, benzene, and acetone. The reaction, however, seemed to be specific for formaldehyde, since attempts to use other aldehydes, such as benzaldehyde, *p*-nitrobenzaldehyde, and chloroacetaldehyde, were unsuccessful.

The specificity of this reaction provides a convenient method of estimating trace amounts of formaldehyde in the presence of other aldehydes. If one uses a steroidal compound, such as 3-phenylcholesta-3,5-diene (I), the determination[3] can become quite accurate, since the

[3]*This method is closely analogous to the chromotropic test (6).*

Can. J. Chem. Downloaded from www.nrcresearchpress.com by 210.87.254.40 on 09/05/12
For personal use only.

Can. J. Chem. Downloaded from www.nrcresearchpress.com by 210.87.254.40 on 09/05/12
For personal use only.

formaldehyde is trapped in a molecule of high molecular weight which absorbs strongly in the ultraviolet. From the average yield of "dimer", it can be concluded that the commerical acetic acid used in these experiments contains about 15 p.p.m. of formaldehyde.[4] It is interesting to note that approximately the same amount of formaldehyde was found in acetic anhydride decomposed with water. Propionic acid was also found to contain a small amount of formaldehyde. Even acetic acid which had been purified by refluxing with 5% potassium permanganate and distilled at reduced pressure still contained some formaldehyde. Formaldehyde-free acetic acid could be obtained by refluxing the acetic acid with 5% potassium permanganate, 10% water, and 1% sulfuric acid. This suggests that the aldehyde exists in acetic acid mainly in the form of diacetoxymethane.

We next studied the reactivity of α-phenyl dienes with other electrophilic reagents. The "dimerization" reaction was carried out in deuterated acetic acid with 3-phenylcholesta-3,5-diene (I) as starting material. The n.m.r. spectrum of the unreacted I showed that the C-6 proton was completely replaced by deuterium, to give 3-phenylcholesta-3,5-diene-6*d* (I*a*). In contrast, no incorporation of deuterium in the 4 position or in the aromatic ring had occurred. The signal caused by the C-4 hydrogen in the deuterated starting material was found to be much sharper than in the undeuterated starting material, thus showing that there was long-range coupling between the C-4 and C-6 protons in I. In the infrared spectrum, in addition to a band at 2 235 cm^{-1} assigned to the olefinic C—D stretching, a broad band between 2 085 cm^{-1} and 2 190 cm^{-1} suggested that some replacement of the protons by deuterium in the allylic positions had occurred. The n.m.r. spectrum of the "dimer ' showed practically no change. In the infrared spectrum, a broad band at 2 100 cm^{-1} was interpreted as being caused by allylic deuteration.

The Friedel–Crafts acylation was then investigated. Addition of 3-phenylcholesta-3,5-diene (I) to carbon tetrachloride containing acetic anhydride in the presence of anhydrous aluminium chloride gave, after chromatography on alumina, a product which was identified as 6-acetyl-3-phenylcholesta-3,5-diene (I*b*).

The Vilsmeier reaction was also studied. Formylation of 3-phenylcholesta-3,5-diene (I) with the complex prepared from phosphorus oxychloride and *N*-methylformanilide gave a high yield of a product identified as 6-formyl-3-phenylcholesta-3,5-diene (I*c*). Lithium aluminium hydride reduction of I*c* gave, in a quantitative yield, 6-hydroxymethyl-3-phenylcholesta-3,5-diene-6-yl methane (I*d*). Addition of a drop of perchloric acid to an equimolar chloroform solution of I and I*d* gave a product which was identical with II.

EXPERIMENTAL

The melting points were determined on a Gallenkamp melting point apparatus in open capillaries, and are corrected. The analyses were carried out by Dr. C. Daesslé, Montreal, and by Schwarzkopf Microanalytical Laboratory, New York. The infrared spectra were determined on a Perkin–Elmer 337 grating spectrophotometer, with 1 mm sodium chloride cells. The ultraviolet absorption spectra were measured by means of a Beckman recording spectrophotometer, model DK1. The nuclear magnetic resonance spectra were recorded on a Varian A60 instrument at 60 Mc.p.s., and carbon tetrachloride was used as solvent (tetramethylsilane = 0 p.p.m.). The optical rotations were measured on a Carl Zeiss automatic polarimeter at 25°, in an 0.5 dm tube and with chloroform as solvent. The mass spectra were taken by Morgan and Schaffer Corp., Montreal, on a Hitachi Perkin–Elmer RMU60 mass spectrometer. Woelm alumina was used for column chromatography, and silica gel for t.l.c. The glacial acetic acid used was Anachemia A.C.S. reagent grade.

Preparation of Phenyl Dienes

Bromobenzene (0.030 mole) in 30 ml of anhydrous ether was added slowly (1 h) to 0.041 mole of magnesium turnings, activated by a crystal of iodine and under a nitrogen atmosphere. The mixture was then stirred for 1 h.

To this Grignard solution, the corresponding Δ^4-3-ketone (0.020 mole) was added as a solid, followed by 50 ml of anhydrous ether. The reaction mixture was stirred under reflux for 1.5 h. Excess Grignard reagent

[4] *This value is to be compared with that of Peterson and Joslyn (7), who have estimated the amount of formaldehyde in a sample of Baker and Adamson reagent-grade glacial acetic acid to be 1–3 p.p.m.*

was destroyed by the careful addition of 50 ml of methanol. A solution of 10 ml of concentrated HCl, diluted with water in a 1:1 ratio, was then added and the mixture was refluxed for 1 h to ensure complete dehydration of the reaction product.

In the case of the steroidal 3-phenyl dienes, a large excess of water was added and the product was isolated by filtration, washed with water, and crystallized from methanol – methylene chloride.

In the case of 10-methyl-2-phenyl-$\Delta^{2,9}$-hexalin (X*a*), all attempts to isolate, on a preparative scale, this phenyl diene from biphenyl failed.

Preparation of p-Ethoxyphenyl Dienes

Exactly the same procedure as that described for the phenyl dienes was used, except that bromobenzene was replaced by *p*-bromophenetole. In the case of 10-methyl-2-*p*-ethoxyphenyl-$\Delta^{2,9}$-hexalin (X*b*), after dehydration of the reaction product, water was added and the mixture was extracted several times with ether. The combined ether extracts were washed with a saturated solution of sodium bicarbonate until acid free, and once with brine. The ether solution was dried with magnesium sulfate and the solvent evaporated. The residue was chromatographed on alumina (activity I). Elution with hexane–benzene (3:1) gave 1.5 g of X*b* which could be purified further by crystallization from methanol.

TABLE I

Compound	Melting point (°C)	$[\alpha]_D^{25}$	λ_{max} (ϵ)	Formula	Analysis (%) Found C	Found H	Calculated C	Calculated H
IV	154–156	−150°	284 mμ (20 000)	$C_{25}H_{32}O$	86.21	9.45	86.15	9.26
V	206–207	−133°	284 mμ (21 000)	$C_{25}H_{30}O$	86.46	9.03	86.65	8.73
VI	139–140	−152°	285 mμ (21 700)	$C_{25}H_{32}$	89.94	9.51	90.30	9.70
X*b*	92–92.5	—	288 mμ (30 800)	$C_{19}H_{24}O$	84.33	8.80	85.02	9.02

Bi-(3-phenylcholesta-3,5-diene-6-yl) methane (II) (General Procedure for the Preparation of the Steroidal "Dimers")

3-Phenylcholesta-3,5-diene (I) (500 mg) was dissolved in 100 ml of hot ethyl acetate, and 400 ml of glacial acetic acid was added. The temperature of the stirred solution was then adjusted to 45 °C, and 7.5 ml of 70% perchloric acid was added dropwise. A flocculent precipitate appeared after approximately 12 min. The solution was kept at 45 °C for 0.5 h, and then 500 ml of water was added. The precipitate formed by the addition of water was filtered off and washed 3 times with 50 ml of water and then once with 5 ml of methanol. Column chromatography of the precipitate on alumina (activity I) and elution with hexane gave first I and then II. Alternatively, two careful crystallizations from hexane yielded 180–200 mg of colorless beads of "dimer" II, m.p. 224–225°. Recrystallization raised the melting point to 228–229°; λ_{max}^{hexane} 296 mμ (ϵ 52 300), $[\alpha]_D^{25}$ −110°.

Anal. Calcd. for $C_{67}H_{96}$: C, 89.26; H, 10.73; mol. wt. 901.5. Found: C, 89.04; H, 11.09; mol. wt. (osmometry) 860.

The above procedure was used to prepare all the "dimers" in the steroid series.

Effect of Formaldehyde and Solvent on "Dimer" Formation

To 10 mg samples of I dissolved in 10 ml of the solvents hexane, carbon tetrachloride, ethyl acetate, chloroform, and acetone, 0.1 ml of 70% perchloric acid and 0.1 ml of an aqueous solution of formaldehyde (40%) were added. The solutions were stirred at 45° for 1.5 h. In ethyl acetate, chloroform, and acetone "dimer" formation was complete (as shown by t.l.c.), whereas in hexane and carbon tetrachloride starting material was recovered unchanged.

Catalytic Hydrogenation of II

To 75 mg of 10% palladium on charcoal in 75 ml of benzene, 65 mg of "dimer" II was added at 24 °C. The mixture was stirred until the uptake of hydrogen had stopped (about 3 h). The benzene solution was then filtered and the catalyst washed 3 times with 20 ml of benzene. The combined filtrates were then evaporated to give a crystalline material. Recrystallization from hexane gave bi-(3-phenylcholestane-6-yl) methane (VII), m.p. 251–252°, $[\alpha]_D$ +13.8°. A signal at 6.8–7.3 p.p.m. in the n.m.r. spectrum proved that the aromatic system was not affected by the hydrogenation.

Anal. Calcd. for $C_{67}H_{104}$: C, 88.48; H, 11.52. Found: C, 87.77; H, 12.24.

A duplicate hydrogenation was carried out. The hydrogen uptake corresponded to 110% and 91.2% of the value required for complete saturation of the four double bonds of II.

6-Acetylcholesta-3,5-diene (Ib)

A carbon tetrachloride solution (5 ml) of cholesta-3,5-diene (I) (500 mg) was added dropwise to a mixture of 25 ml of carbon tetrachloride, 1.5 g of finely powdered anhydrous aluminium chloride, and 1 ml of acetic anhydride. The resulting dark-brown reaction mixture was left at room temperature for 15–20 min, and 200 ml of water was then added. The carbon tetrachloride layer, which was now straw yellow, was diluted with

Can. J. Chem. Downloaded from www.nrcresearchpress.com by 210.87.254.40 on 09/05/12
For personal use only.

500 ml of ether. The organic layer was separated from the aqueous phase, and washed with bicarbonate solution until neutral and then with water. The solution was dried over magnesium sulfate, evaporated, and chromatographed on alumina (activity II–III). Elution with hexane gave 83 mg of I. Further elution with hexane–ether (19:1) gave 218 mg of 6-acetylcholesta-3,5-diene (I*b*). Two crystallizations from methanol gave light-yellow crystals, $[\alpha]_D$ −123°, m.p. 108–109°, λ_{max}^{hexane} 303 mμ (ε 18 400), ν_{CCl_4} 1 680 cm^{-1}; δ_{CCl_4} complex multiplet between 7.1 and 7.6 p.p.m. for the five aromatic protons, a singlet at 6.99 p.p.m. for the C-4 proton, and a sharp singlet at 2.18 p.p.m. for the CH_3—C protons.

Anal. Calcd. for $C_{35}H_{50}O$: C, 86.36; H, 10.35; O, 3.29. Found: C, 86.33; H, 10.33; O, 3.52.

Di(10-methyl-2-p-ethoxyphenyl-Δ^{2,9}-hexalin-8-yl) methane (XII)

10-Methyl-2-*p*-ethoxyphenyl-Δ^{2,9}-hexalin (X*b*) (700 mg) was dissolved in 100 ml of ethyl acetate, and 400 ml of acetic acid was added, followed by 7.5 ml of 70% perchloric acid. The solution was stirred for 1 h at 50°, and then 500 ml of water was added. The mixture was extracted with four 250 ml portions of ether; the ether extracts were washed with saturated sodium bicarbonate until acid free and then with brine. After the combined extracts were dried and the solvent evaporated, the residue was chromatographed on alumina (activity I). Elution with hexane–benzene (3:1) gave 200 mg of X*b*. Further elution with pure benzene gave 130 mg of XII. Crystallization from hexane gave pure XII, m.p. 163–163.5°, $\lambda_{max}^{cyclohexane}$ 295 mμ (ε 63 500).

6-Formyl-3-phenylcholesta-3,5-diene (Ic)

To 1.5 g of 3-phenylcholesta-3,5-diene dissolved in 5 ml of *o*-dichlorobenzene, 1 ml of *N*-methylformanilide mixed with 0.5 ml of $POCl_3$ was added and the reaction mixture was stirred at 90–95 °C for 2 h (8). To the cooled mixture, 20 g of sodium acetate in 25 ml of water was added, and the solution evaporated to dryness. The residue was washed with one portion of water (10 ml), one portion of 6 *N* HCl, and then water again (200 ml). The residue was crystallized once from methanol – methylene chloride. The resulting brown crystals were chromatographed on 30 g alumina (activity II–III). Elution with 300 ml of hexane gave 200 mg of starting material I. Further elution with 100 ml of hexane–ether (1:3) gave 953 mg of I*c*. Crystallization from methanol–ether gave pure light-yellow crystals of 6-formyl-3-phenylcholesta-3,5-diene (I*c*), $[\alpha]_D$ −115°, m.p. 125–126°, λ_{max}^{hexane} 315 mμ (ε 27 000), ν_{CCl_4} 1 660 cm^{-1}. In the n.m.r., a singlet at 10.62 p.p.m. was assigned to the aldehydic proton; a broad signal between 7.18 and 7.66 p.p.m. could clearly be resolved into two signals: a signal at 7.56 p.p.m. for the C-4 proton and an overlapping complex multiplet arising from the five aromatic protons.

Anal. Calcd. for $C_{34}H_{48}O$: C, 86.38; H, 10.24; O, 3.38. Found: C, 86.40; H, 10.20; O, 3.54.

6-Hydroxymethyl-3-phenylcholesta-3,5-diene (Id)

Lithium aluminium hydride (500 mg) was added to 6-formyl-3-phenylcholesta-3,5-diene (I*c*) (650 mg) dissolved in 50 ml of anhydrous ether. The light-yellow solution became colorless immediately. The reaction mixture was stirred for 0.5 h at room temperature, the excess hydride was carefully decomposed with methanol, and a small amount of 10% aqueous sodium hydroxide was added. The resulting gelatinous precipitate was filtered off and washed thoroughly with ether. The combined filtrates were then dried over magnesium sulfate and evaporated. Crystallization of the resulting oil from hexane gave 6-hydroxymethyl-3-phenylcholesta-3,5-diene (I*d*), $[\alpha]_D$ −162°, m.p. 120.5–121°, $\lambda_{max}^{methanol}$ 288 mμ (ε 26 400); δ_{CCl_4} a complex multiplet between 7 and 7.5 p.p.m. for the five aromatic protons, a singlet at 6.78 p.p.m. for the C-4 proton, and a broad band at 4.12 p.p.m. for the —CH_2—O protons. The hydroxy proton signal was hidden under the steroid envelope.

Anal. Calcd. for $C_{34}H_{50}$: C, 86.01; H, 10.62. Found: C, 86.10; H, 10.21.

Synthesis of "Dimer" II from Alcohol Id

6-Hydroxymethyl-3-phenylcholesta-3,5-diene (I*d*) (10 mg) and 3-phenylcholesta-3,5-diene (I) (10 mg) were dissolved in 10 ml of chloroform, and 1 drop of perchloric acid was added. The mixture was swirled on a warm steam bath for a few minutes, and then 50 ml of 10% aqueous sodium bicarbonate was added, followed by 50 ml of ether. The organic layer was separated, washed with water, dried, and evaporated. Crystallization of the residue from hexane gave a compound whose melting point was not depressed on admixture with "dimer" II and which was further identified by t.l.c. and its ultraviolet spectrum.

ACKNOWLEDGMENTS

We thank Mr. K. Valentin for taking the n.m.r. spectra, and Mr. Kastner of Ayerst Laboratories, Montreal, for the quantitative hydrogenation.

REFERENCES

1. W. G. DAUBEN and F. G. WILLEY. Tetrahedron Letters, 893 (1962).
2. G. JUST and C. PACE-ASCIAK. Tetrahedron, **22**, 1063 (1966); **22**, 1069 (1966).
3. G. JUST and V. DITULLIO. Can. J. Chem. **42**, 2153 (1964).
4. C. C. LEZNOFF and G. JUST. Can. J. Chem. **42**, 2801 (1964); **42**, 2919 (1964).
5. J. A. MARSHALL and W. I. FANTA. J. Org. Chem. **29**, 2501 (1964).
6. F. FEIGL. Spot test in organic analysis. Elsevier Pub. Co., Inc. ,Armsterdam. 1960. p. 349.
7. R. G. PETERSON and M. A. JOSLYN. J. Org. Chem. **24**, 1359 (1959).
8. M. R. DE MAHEAS. Bull. Soc. Chim. France, 1989 (1962).

Can. J. Chem. Downloaded from www.nrcresearchpress.com by 210.87.254.40 on 09/05/12
For personal use only.

THE ADDITION OF CARBOXYLIC ACIDS TO ACETYLENIC COMPOUNDS

J. DiPietro and W. J. Roberts
Summit Research Laboratories, Celanese Corporation of America, Summit, New Jersey
Received April 4, 1966

ABSTRACT

The free radical induced addition of acetic acid and its derivatives to olefins has been reported recently. As an extension of this reaction, the addition of acetic acid to acetylenic compounds was investigated.

Adipic acid was found to be the major product of the reaction of excess acetic acid and acetylene at 110–120 °C under pressure in the presence of organic peroxides. A second oily acidic product with a molecular weight of about 300, not yet identified, was found to the extent of about 2 parts by weight to every 3 parts of adipic acid.

Octen-3-oic acid and its anhydride were synthesized from hexyne-1 and excess acetic acid in the presence of organic peroxides. Acetic anhydride was substituted for acetic acid, with the net advantage that acetylene was more soluble in the solvent. The general scope of the reaction was expanded to include other transfer agents, such as acetone, formic acid, and propionic acid.

INTRODUCTION

Free-radical addition reactions to compounds containing a double bond have been known for some time (1, 2). Recently (3), it was reported that malonic esters, acetoacetic esters, and related compounds can be added by a free radical induced reaction to α-olefins.

$$RCH{=}CH_2 + CH_2(CO_2C_2H_5)_2 \xrightarrow[\Delta]{\text{Peroxide}} RCH_2CH_2CH(CO_2C_2H_5)_2$$

The first example of the addition of acetic acid to an olefin was the peroxide-induced reaction with ethylene, which gives a mixture of homologous acids ($CH_3(CH_2)_{2n}\cdot COOH$) (4). In 1962 Allen *et al.* reported the radical-induced addition of acetic acid and its derivatives to olefins (5). Apart from these examples, few radical addition reactions of carboxylic acids or their derivatives have been reported.

Our interest in this general type of reaction was to extend its scope to acetylenic compounds, and to suggest new synthetic routes for dicarboxylic acids in general.

EXPERIMENTAL

Addition of Acetic Acid to Hexyne-1

A 5 l, three-necked flask was charged with 3 kg of glacial acetic acid and 5.0 cc of di-*t*-butyl peroxide. The solution was heated to reflux (118 °C), and 50 g (0.70 mole) of hexyne-1, 120 cc of glacial acetic acid, and 2.0 cc of di-*t*-butyl peroxide were added. The reaction was refluxed for 24 h, and then was fractionally distilled in a 12 inch helix-packed column to yield 24% of octen-3-oic acid, b.p. 84–87 °C at 0.7–1.0 mm.

Anal. Calcd. for $C_8H_{14}O_2$: C, 67.60; H, 9.86. Found: C, 67.00; H, 9.87.

The infrared spectrum was consistent with the suggested structure. The sample shows carbonyl absorption at 5.83 μ, broad OH absorption at 3.0–3.8 μ, CH stretching at 7.75 μ, and *trans* unsaturation at 10.34 μ. The first three absorptions are characteristic of monocarboxylic acids, and the latter one is typical of double bond unsaturation. The material was quantitatively hydrogenated to yield *N*-octanoic acid, thus suggesting the absence of 3-ethynylhexanoic acid from the reaction products.

In addition to octen-3-oic acid, a 15% yield of octen-3-oic anhydride was obtained, b.p. 135–140 °C at 0.4–0.5 mm, with normal anhydride infrared absorptions at 5.51 μ and 5.66 μ.

Addition of Acetic Acid to Acetylene

The apparatus used for the free-radical addition of acetic acid to acetylene is diagrammatically shown in Fig. 1. The procedure by which adipic acid was ultimately synthesized was as follows. A 36 inch × 4 inch Aminco rocking bomb was charged with 1.8 kg of glacial acetic acid and 3.3 g (0.02 mole) of di-*t*-butyl peroxide. The bomb was then closed and purged with nitrogen, the pressure was checked, and the system was vented to atmospheric pressure. With the rocker on, the bomb was heated to 110 °C. Acetylene (4.5–5.5 g) was then added, the time of addition ranging from 1 to 1½ h. The pressure in the bomb at the end of the

Can. J. Chem. Downloaded from www.nrcresearchpress.com by 210.87.254.5 on 09/05/12
For personal use only.

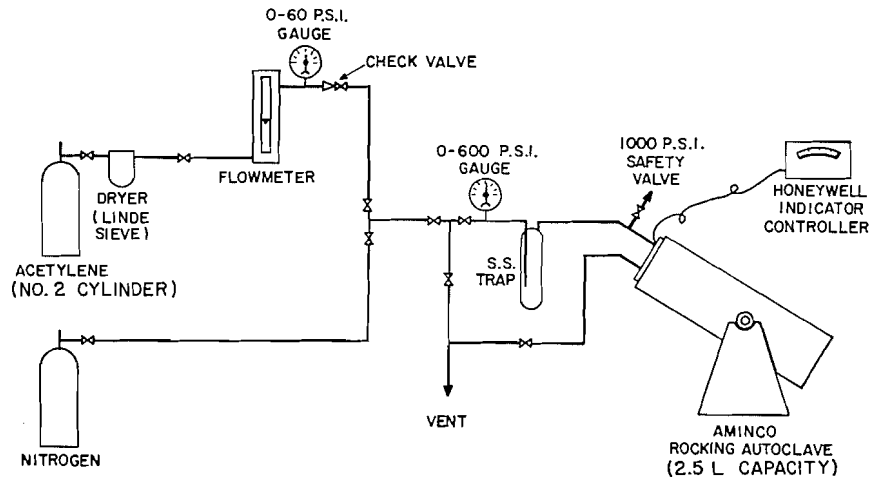


FIG. 1. Apparatus used when acetic acid was added to acetylene. All lines are $\frac{1}{4}$ inch 316 S.S. tubing. The flowmeter is a Matheson, model 620 BBV, instrument.

addition was 27–30 p.s.i.g., and the gauge reading of the rotameter through which the acetylene tank was connected was 16–18 p.s.i.g. The reaction mixture was rocked and allowed to heat up to 120 ± 5 °C for a period of 18 h, after which it was cooled down to room temperature and the gases were passed through a series of silver nitrate traps to obtain a quantitative estimate of the amount of unreacted acetylene. The liquid portion of the reaction was heated under a nitrogen atmosphere until most of the acetic acid was distilled off. The concentrated liquid was then heated until crystals appeared to form. Cold water was added to separate the water-white adipic acid from an oily product. The latter possessed a molecular weight of about 300, with a carboxyl content of 36% (by weight); an infrared spectrum did not show any unsaturation. Several runs were made to justify the validity of the reaction in question (Table I). Proof for the presence of adipic acid was obtained from the infrared spectrum, melting point determination, vapor-phase gas chromatography of the dimethyl ester, elemental analysis, determination of the neutralization equivalent, and condensation with hexamethylenediamine to m.p. 260 °C. The data given in Table I indicate a high degree of reproducibility among the various runs (e.g. runs 1, 3, and 4), and also that not all the acetylene charged is converted into products at the first pass.

TABLE I

Run	Acetylene (g) Charged	Acetylene (g) Recovered	Adipic acid recovered (g)	Oil (g)
1	4.34	2.02	3.0	2.1
2	2.87	1.34	1.9	1.4
3	4.34	2.11	3.1	2.0
4	4.34	2.16	3.1	1.9

Addition of Acetic Anhydride to Acetylene

Gaseous acetylene was slowly metered into 500 cc of anhydrous acetic anhydride kept at −50 °C. The rate of addition was 100 cc/min (0.232 g/min). The solubility of acetylene in cold acetic anhydride is much higher than it is in cold acetic acid. To a 5 l, three-necked flask containing 1.9 kg of acetic anhydride and 7.0 cc of di-*t*-butyl peroxide kept at 120 °C was added, by means of a funnel, the acetic anhydride – acetylene solution over a period of 1 h. The reaction was heated for 18 h at 120 °C; then the excess acetic anhydride was stripped off by distillation and the residue was allowed to crystallize. The analysis of the sample indicates that the product is adipic acid. The percentage conversion of acetylene into adipic acid was of the order of 25–30.

DISCUSSION

The initial study was made with acetic acid because it is an excellent transfer agent and has a high degree of purity. The relatively low explosive hazards of di-*t*-butyl peroxide made it possible to use it as a free-radical initiator at atmospheric pressure. Hexyne-1,

Can. J. Chem. Downloaded from www.nrcresearchpress.com by 210.87.254.5 on 09/05/12
For personal use only.

which contains a triple bond, was the first such compound used in this free-radical type of addition.

The major products of the reaction of *t*-butoxy radicals in the presence of two potential hydrogen donors (acetic acid and hexyne-1) are determined by the competition shown in eqs. [1]–[3].

[1] $$(CH_3)_3CO\cdot \xrightarrow{K_d} CH_3COCH_3 + CH_3\cdot$$

[2] $$(CH_3)_3CO\cdot + CH_3COOH \xrightarrow{K_{a_1}} (CH_3)_3COH + \cdot CH_2COOH$$

[3] $$(CH_3)_3CO\cdot + CH_3(CH_2)_3C{\equiv}CH \xrightarrow{K_{a_2}} (CH_3)_3COH + CH_3(CH_2)_3C{\equiv}C\cdot$$

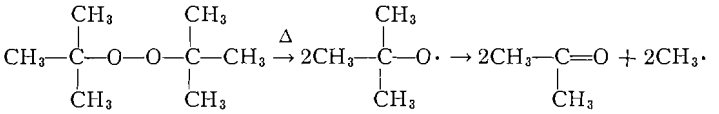
The rate constant K_{a_1}/K_{a_2} may be measured directly from the relative rates of disappearance of acetic acid and hexyne-1, or indirectly by determining K_{a_1}/K_d and K_{a_2}/K_d from the ratios of *t*-butyl alcohol to acetone obtained in separate experiments in the presence of acetic acid and hexyne-1 alone. It was found by gas chromatographic techniques that reaction [1] is the predominant one, and that reaction [3] does not occur to an appreciable extent because of the low concentration of the acetylenic compound in the reaction. It is indeed a necessary requirement that the reactants be highly diluted, to obtain the products herein described. Had reactions [2] and [3] occurred to any significant extent, the gas chromatographic analysis of the reaction product should have indicated the presence of *t*-butyl alcohol, which was proven to be absent in all cases.

These data seem to indicate that the addition of acetic acid to a compound containing a triple bond can occur in a manner analogous to that observed for compounds having a double bond.

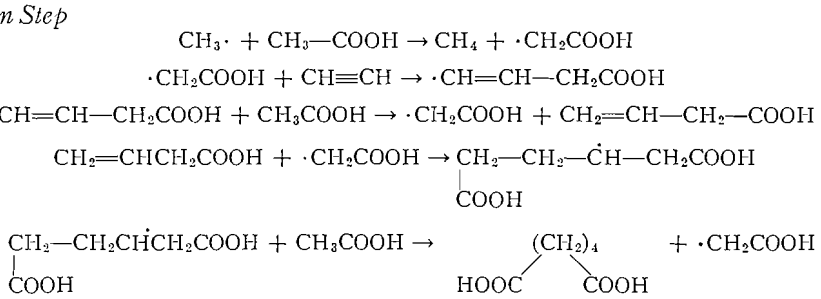
A typical reaction run for the free-radical addition of acetic acid to acetylene gave the following results. From 4.34 g of gaseous acetylene charged to the reactor, 3.0 g of adipic acid and 2.1 g of an oily, gummy material were isolated. Unreacted acetylene has been shown to be present by passage of the gaseous material remaining after the reaction into aqueous silver nitrate and by gas chromatography.

A mechanistic path for the reaction under study suggests a chain reaction with a requirement for a low level of initiator.

Initiation Step



Propagation Step



Possible Termination Step

$$\cdot CH_2COOH + CH_3\cdot \rightarrow CH_3CH_2COOH$$

Can. J. Chem. Downloaded from www.nrcresearchpress.com by 210.87.254.5 on 09/05/12
For personal use only.

A close look at the proposed mechanism shows that the methyl free-radical appears to be the crucial species for initiating the propagation step. It also appears that other peroxide initiators could be employed in producing the necessary methyl free-radical; even saturated hydrocarbons, when subjected to pyrolysis, could yield the desired methyl free-radicals.

This proposed mechanism requires a high dilution of reactants, to minimize the dimerization of the methyl free-radical with itself. It is indeed a necessary prerequisite, for the synthesis of adipic acid by this route, that the molar ratio of the solvent (acetic acid) to acetylene be kept at 50 or higher.

Whether the reaction proceeds in a stepwise manner through the formation of vinyl acetic acid, or by a simultaneous free-radical addition of 2 moles of acetic acid to acetylene still has to be determined. It is of interest to point out that vinyl acetic acid, when added to a large excess of boiling acetic acid in the presence of di-*t*-butyl peroxide, yields adipic acid, presumably because the molecule has a terminal vinyl group and thus is more reactive towards radical addition.

The catalytic effect of copper salts on the reactions of peroxides with a variety of hydrogen-donor substrates has been described by Kharasch and Fono (6). In view of this, we carried out several experiments with selected metal salts (e.g. nickel oxide and zinc carbonate) and di-*t*-butyl peroxide, to ascertain whether the half-life of the initiator, as well as its thermal stability, could be affected advantageously. We were unable to observe any change in the yield or rate of reaction.

ACKNOWLEDGMENT

The authors express their gratitude to Dr. C. L. Smart for his interest in this work.

REFERENCES

1. M. S. KHARASCH, J. SKELL, and W. FISCHER. J. Am. Chem. Soc. **70**, 1055 (1945).
2. M. S. KHARASCH, C. KUDERNA, and J. NUDENBERG. J. Org. Chem. **18**, 1225 (1953).
3. J. C. ALLEN, J. I. G. CADOGAN, J. HARRIS, and D. H. HEY. Chem. Ind. London, 830 (1961).
4. W. BANES, F. J. FITZGERALD, and M. C. NELSON. U.S. Patent No. 2,585,723 (February 1952).
5. J. C. ALLEN, J. I. G. CADOGAN, and D. H. HEY. Chem. Ind. London, 1621 (1962).
6. M. S. KHARASCH and A. FONO. J. Org. Chem. **23**, 324 (1958).

Can. J. Chem. Downloaded from www.nrcresearchpress.com by 210.87.254.5 on 09/05/12
For personal use only.

Can. J. Chem. Downloaded from www.nrcresearchpress.com by 210.87.254.6 on 09/05/12
For personal use only.

THE REACTIONS OF THE DISODIUM ADDUCT OF BENZOPHENONE ANIL[1]

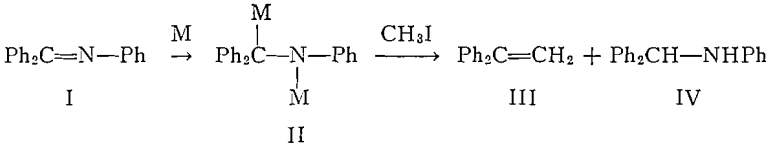
JAMES G. SMITH AND C. DOREEN VEACH
Exploratory Research Laboratory, Dow Chemical of Canada, Limited, Sarnia, Ontario
Received May 11, 1966

ABSTRACT

The disodium adduct of benzophenone anil has been treated with a variety of reagents, and the products have been isolated and identified. With alkyl halides, ethylene oxide, and diethyl sulfate, alkylation occurs at the carbon atom. With tri- and tetra-methylene dibromide, nitrogen alkylation also occurs, thereby producing substituted pyrrolidine and piperidine derivatives. Benzaldehyde abstracts the alkali metal from the adduct whereas esters react to form the *N*-acyl derivatives.

INTRODUCTION

Solutions of benzophenone anil (I) in ether solvents react with alkali metals to form a complex (II) containing two atoms of alkali metal per mole of anil (1, 2). The chemical behavior of this adduct has been examined in the past (2–4), but conflicting results have been reported. In the original study by Schlenk and Bergmann (2), benzophenone anil was the only product formed when the adduct was treated with methyl iodide or with several other reagents. On the other hand, Mikhailov (3) reported the formation of 1,1-diphenylethylene (III) and *N*-benzhydrylaniline (IV) upon treatment of II with methyl iodide.



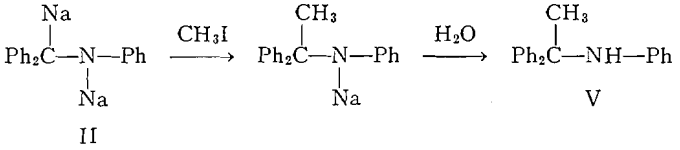
In our hands, the adduct II behaved in a manner quite different from that reported in these earlier studies. Generally speaking, the chemical behavior of the benzophenone anil adduct resembles that recently reported for the benzophenone ketyls (5–8).

Adduct Preparation

The reaction of benzophenone anil and sodium proceeds very rapidly in tetrahydrofuran. This is not surprising in view of the well-known efficacy of such solvents in the preparation of organometallic compounds. However, it is surprising that the adduct forms in diethyl ether with equal ease, especially since much longer reaction times have been employed elsewhere (2).

Reaction with Alkyl Halides

The disodium adduct II in tetrahydrofuran reacts smoothly with 1 equivalent of methyl iodide to produce the *C*-methyl derivative, *N*,1,1-triphenylethylamine (V). This behavior of the adduct was initially thought to be due to the use of tetrahydrofuran as solvent



[1]*Contribution No. 142 from the Exploratory Research Laboratory.*

rather than the diethyl ether used in the earlier investigations (2, 3). However, a repetition of the experiment with diethyl ether produced the same product accompanied by *N*-benzhydrylaniline, thus establishing that the same reaction is occurring but to a lesser extent.

The structure V of the reaction product is consistent with its nuclear magnetic resonance (n.m.r.) spectrum, and additional proof has been obtained by decomposition in 20% hydrochloric acid to 1,1-diphenylethylene and aniline.

$$\underset{\text{V}}{Ph_2C(CH_3)-NHPh} \xrightarrow[20\%\ HCl]{\text{Reflux}} Ph_2C{=}CH_2 + PhNH_2\cdot HCl$$

A similar decomposition of *N*,1,1,2-tetraphenylethylamine to *N*,1,1-triphenylethylene has been reported (9).

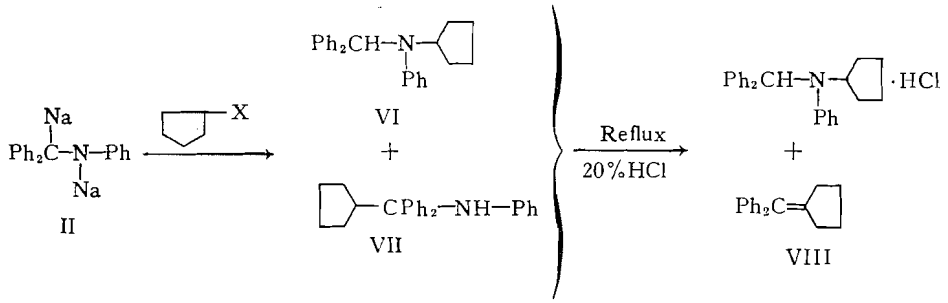
$$PhCH_2{-}CPh_2{-}NH{-}Ph \rightarrow Ph_2C{=}CHPh + PhNH_2\cdot HCl$$

This decomposition provides an explanation for Mikhailov's earlier observation (3) of the formation of 1,1-diphenylethylene from methyl halides and the alkali metal adducts of benzophenone anil. During his separation of the individual constituents of the crude reaction mixture, Mikhailov employed refluxing 20% hydrochloric acid. This undoubtedly resulted in decomposition of the initial reaction product to the observed unsaturated hydrocarbon. In the present experiments, the crude reaction product has also been examined by precipitating with hydrogen chloride the amines from the ether solution as their hydrochloride salts and examining the ether-soluble portion. Only small yields of 1,1-diphenylethylene have been observed.

The scope of this reaction has been investigated with a number of alkyl halides, and the results are summarized in Table I. Certain obvious trends are evident. The reaction is slow with bulky halides, such as *t*-butyl chloride, with a consequently reduced yield and the formation of *N*-benzhydrylaniline on hydrolysis. Inert halides, such as vinyl chloride, do not react whereas reactive halides, such as allyl or benzyl chloride, react rapidly, even at −60°.

The yield of product is lower with alkyl iodides than with alkyl bromides or chlorides. An investigation of the reaction products by thin-layer chromatography reveals the presence of unidentified by-products which increase in quantity when an alkyl iodide is used.

In the case of the simple alkyl halides, the products formed by nitrogen alkylation of the benzophenone anil adduct have not been isolated. However, with cyclopentyl halides, the amount of nitrogen alkylation is quite large and comparable to the carbon-alkylated product. The nitrogen-alkylated derivative VI may be isolated by decomposing the carbon-alkylated compound VII to cyclopentylidene diphenylmethane (VIII) with hydrochloric acid, leaving the nitrogen-alkylated product as the hydrochloride salt.



Can. J. Chem. Downloaded from www.nrcresearchpress.com by 210.87.254.6 on 09/05/12
For personal use only.

Can. J. Chem. Downloaded from www.nrcresearchpress.com by 210.87.254.6 on 09/05/12
For personal use only.

TABLE I

Reaction products with alkyl halides

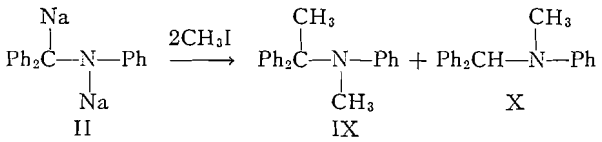
$Ph_2C(R)—NH—Ph$

Alkyl halide	R	Yield (%)	Melting point (°C)	Analysis (%) Theoretical C	H	N	Found C	H	N
CH_3I	CH_3	46	53–54*	87.9	7.02	5.12	87.9	7.00	5.20
C_2H_5I	C_2H_5	46	67–71†	87.8	7.38	4.87	87.5	7.50	4.97
C_3H_7Cl	C_3H_7	66	81–84	87.6	7.70	4.65	87.6	7.44	4.63
C_3H_7Br	C_3H_7	78							
C_3H_7I	C_3H_7	40							
i-C_3H_7Cl	$(CH_3)_2CH$	50	113–115	87.6	7.70	4.65	87.8	7.64	4.59
t-C_4H_9Cl	$(CH_3)_3C$	22	116–117	87.5	8.00	4.44	87.6	7.89	4.29
CH_2=CH—CH_2Cl	CH_2=CH—CH_2	81	75–77	88.2	7.08	4.68	88.5	7.02	4.70
$C_6H_5CH_2Cl$	$C_6H_5CH_2$	67, 64§	144–147‡	89.4	6.65	4.01	89.8	6.58	4.07
CH_2=CH—Cl	CH_2=CH	0	—						

*Literature (3) m.p. 50–53°.
†Literature (11) m.p. 72–73°.
‡Literature (9) m.p. 143.5–144.5° and (19) 152–153°.
§Diethyl ether as reaction solvent.

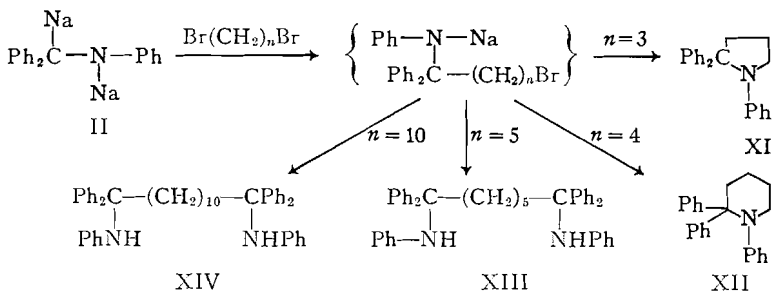
Attempts to synthesize an authentic sample of the tertiary amine VI from *N*-cyclopentylaniline and benzhydryl chloride were unsuccessful.

The reaction of the disodium adduct of benzophenone anil with 2 equivalents of methyl iodide produces a product whose n.m.r. spectrum is compatable with that expected for the dialkylated derivative, *N*-methyl-*N*,1,1-triphenylethylamine (IX). In addition to IX, a small amount of the nitrogen-alkylated derivative, *N*-methyl-*N*-benzhydrylaniline (X), can be isolated.

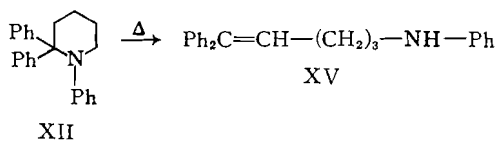


The dialkylated product IX is sufficiently stable that it can be distilled. However, attempts to purify it further by means of its hydrochloride, or by chromatography, result in it being decomposed to *N*-methylaniline and 1,1-diphenylethylene. Indeed, so facile is this decomposition that it can be effected by an equivalent amount of formic acid and the reaction followed by observation of the n.m.r. spectrum.

With polymethylene dibromides the sodium adduct of benzophenone anil reacts in two ways. Carbon alkylation presumably occurs first, and then, if the chain length of the pendant bromoalkyl group is of the proper length to bring the remaining bromo group into close proximity with the nitrogen atom, nitrogen alkylation occurs to form the heterocyclic derivative (XI or XII). However, if the chain length is too long, nitrogen alkylation is not favored and dimeric products result from the carbon alkylation of a second molecule of adduct to form the diamines (XIII or XIV).



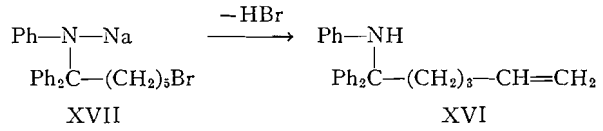
Distillation of 1,2,2-triphenylpiperidine (XII) effected its decomposition to an isomer which, on the basis of its n.m.r. spectrum, is believed to be *N*,1,1-triphenyl-5-aminopentene-1 (XV).



An additional product has also been isolated from the reaction leading to XIII. In this case, the material has been assigned the structure *N*,1,1-triphenyl-1-aminohexene-5

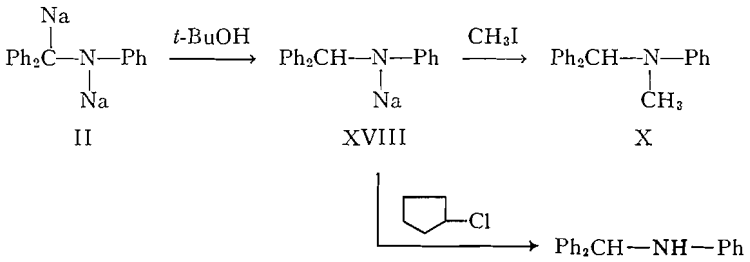
Can. J. Chem. Downloaded from www.nrcresearchpress.com by 210.87.254.6 on 09/05/12
For personal use only.

(XVI) on the basis of its n.m.r. spectrum. Its formation probably occurs by dehydrohalogenation of the intermediate XVII in a competitive side reaction.



XVII XVI

A successful attempt has been made to take advantage of the selective reactivity of the two anionic sites in the disodium adduct of benzophenone anil by treating it first with 1 equivalent of an acid to form the amide ion XVIII, and then alkylating it with methyl iodide to produce *N*-methyl-*N*-benzhydrylaniline (X).



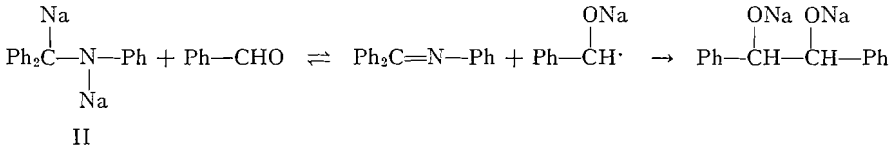
II XVIII X

An attempt to apply this to the synthesis of *N*-cyclopentyl-*N*-benzhydrylaniline by treating XVIII with cyclopentyl chloride failed; only *N*-benzhydrylaniline was produced. It is not clear why the dianion of the disodium adduct of benzophenone anil is capable of nitrogen alkylation with cyclopentyl chloride whereas the monoanion XVIII is not.

Reaction with Benzaldehyde

The reaction of the sodium adduct with aldehydes has been studied with benzaldehyde, an aldehyde free of enolizable (acidic) protons. The products which have been isolated are benzophenone anil and *dd,ll*-hydrobenzoin. In addition, the presence of *meso*-hydrobenzoin has been demonstrated spectroscopically.

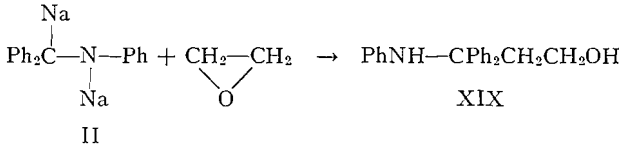
Evidently, a transfer of the sodium from the benzophenone anil to the carbonyl group of the aldehyde occurs with regeneration of the starting material. Dimerization of the radical ion formed from the benzaldehyde produces the two diastereomeric hydrobenzoins. Similar transfers of alkali metal to carbonyl groups have been reported (6, 10).



II

Reactions with Ethylene Oxide

Treatment of the sodium adduct with 1 equivalent of ethylene oxide effected alkylation at the carbon atom to produce *N*,1,1-triphenyl-3-hydroxypropylamine (XIX).



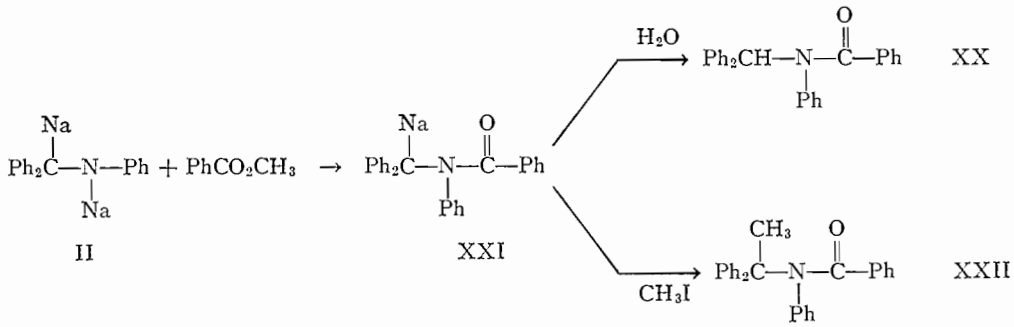
II XIX

Can. J. Chem. Downloaded from www.nrcresearchpress.com by 210.87.254.6 on 09/05/12
For personal use only.

Alkylation at the carbon atom is not surprising, since the anionic carbon should be more basic than the anionic nitrogen and should react faster.

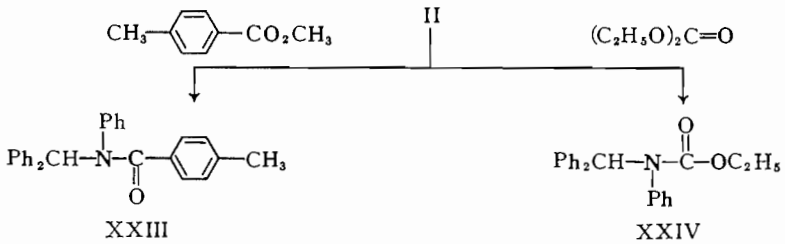
Reaction with Esters

Treatment of the disodium adduct of benzophenone anil with methyl benzoate produces *N*-benzhydrylbenzamide (XX) on hydrolysis of the initially formed reaction product XXI. That XXI is initially formed is shown by treating the intermediate with methyl iodide to produce *N*-phenyl-*N*-(1,1-diphenylethyl)benzamide (XXII).



The structure XX has been established by comparison with an authentic sample. In the infrared spectra, the amide carbonyl band appears at 1 625 cm^{-1} for XX and at 1 640 cm^{-1} for XXII. In the n.m.r. spectrum of XX, the benzylic proton is shifted downfield and becomes obscured by the aromatic proton band.

Similarly, methyl *p*-toluate and diethyl carbonate react with the disodium adduct II to produce the corresponding *N*-acyl derivatives XXIII and XXIV. In the latter case, the carbamate structure is indicated by the position of the carbonyl band in the infrared spectrum (1 690 cm^{-1}) and by the presence of an ethyl group (from the diethyl carbonate) in the n.m.r. spectrum.



EXPERIMENTAL

Melting points are uncorrected and were determined in an open capillary with a Gallenkamp melting point apparatus. Infrared spectra were recorded on a Perkin–Elmer 221 with prism-grating interchange, using Nujol mulls of the compounds. Nuclear magnetic resonance spectra were recorded on a Varian A-60 spectrometer, using deuterated chloroform solutions, with tetramethylsilane as an internal reference. The chemical shifts reported are in parts per million downfield from the tetramethylsilane.

Benzophenone anil was prepared from benzophenone and aniline, with aniline hydrochloride as catalyst (12). The product, after two recrystallizations from 95% ethanol, melted at 113.5–115°. It was dried under vacuum at 45° and stored in a dry box. All operations connected with the preparation and reaction of the alkali metal complexes were performed in an atmosphere of purified and dried nitrogen.

Tetrahydrofuran and diethyl ether were purified by refluxing for at least 8 h over lithium aluminium hydride and distilling onto a fresh batch of hydride for storage. When needed, the solvent was refluxed for 2 h and the required amount permitted to distill into the reaction vessel, a modified Schlenk tube (13). The tube was transferred to a dry box, where the benzophenone anil and the sodium metal (freshly cut) were weighed and added. After the tube was sealed, it was removed from the dry box and agitated in a horizontal shaker until the reaction was complete.

Can. J. Chem. Downloaded from www.nrcresearchpress.com by 210.87.254.6 on 09/05/12
For personal use only.

To study the rate of adduct formation, aliquot samples of the deep reddish purple solution were withdrawn periodically and quenched in 1:1 ethanol–water, and the alkaline mixture was titrated with 0.1 *N* standard hydrochloric acid to determine the extent of reaction. Preparative conditions were standardized at 50 ± 5 g of solvent/0.01 mole of benzophenone anil, a 100% excess of sodium, and a reaction time of 4 h, which was sufficient to ensure completion of the reaction in both tetrahydrofuran and diethyl ether.

Thin-layer chromatography was carried out using silica gel G adsorbent 0.25 mm thick, with a 10 cm rise of the solvent front. Developing solvents varied and are specified in the experimental details. The detecting spray was a 1% solution of *p*-nitrobenzenediazonium tetrafluoroborate (14) in water.

Reaction with Alkyl Halides

The solution of the adduct was transferred from the excess sodium to an oven-dried, nitrogen-filled flask equipped with a Teflon-coated magnetic stirrer bar. The solution was then cooled with a dry ice and methanol mixture and stirred, and an equivalent amount of alkyl halide was introduced by a pipette or syringe. Stirring was continued for an hour at dry-ice temperatures and then the reaction was permitted to warm to room temperature spontaneously. The final solution, generally a deep reddish brown color, was treated with 15 ml of water to destroy any remaining adduct. Extraction with ether, followed by washing, drying, and evaporating the ether extract, served to isolate the crude reaction product as an oil or gummy solid.

From this point on, the procedures differed depending on the nature of the product or the information desired. The purification procedures and additional comments together with the analytical and n.m.r. data are given below. Unless otherwise specified, each experiment was carried out with the disodium adduct prepared from 0.01 mole of benzophenone anil.

Reaction with Methyl Iodide

The reaction with methyl iodide was repeated several times because of the conflicting literature reports on the nature of the products. The roughly quantitative evaluation of the reaction products that was employed resembled that used by Mikhailov (3) but under milder conditions. The crude reaction product was dissolved in 50 ml of diethyl ether and treated with hydrogen chloride. The amine salt which precipitated out was filtered off, dried, and weighed, and the ether filtrate was evaporated and the residue weighed (1,1-diphenylethylene). The amine salt was then suspended in a mixture of 25 ml of water and 25 ml of benzene. Any aniline hydrochloride that was present dissolved in the water layer, from which it was subsequently isolated by the addition of base and ether extraction. The hydrochloride of *N*,1,1-triphenylethylamine dissociated and the free amine dissolved in the benzene layer, from which it was isolated by evaporation. The yields so obtained were 2–13% aniline, 7–19% 1,1-diphenylethylene, and 71–90% *N*,1,1-triphenylethylamine.

The identity of the isolated 1,1-diphenylethylene was confirmed by distillation and by comparison of the infrared spectrum with that of an authentic sample. The identity of the aniline was confirmed by preparing the benzenesulfonamide derivative.

The crude *N*,1,1-triphenylethylamine was obtained as a gum, and the presence of *N*-benzhydrylaniline was suspected. Small amounts could be detected by thin-layer chromatography with cyclohexane containing 17% acetic acid as developing solvent: *N*-benzhydrylaniline, R_f 0.60; *N*,1,1-triphenylethylamine, R_f 0.43. However, the amount was too small to show a benzylic proton peak in the n.m.r. spectrum of the crude amine.

The crude reaction product was purified by recrystallization from methanol (10 ml/g). The hydrochloride decomposes above 170°, forming two layers in the melting point capillary. Nuclear magnetic resonance: CH_3 singlet at 2.0 (3.0 H), NH singlet at 4.2 (1.0 H), aromatic H's complex band at 6.2–7.6 (15.8 H).

A repetition of the above experiment with diethyl ether as the solvent for adduct formation and for reaction with methyl iodide led to the formation of substantial amounts of *N*-benzhydrylaniline. The crude reaction product, isolated as previously described, contained 32% of *N*-benzhydrylaniline,[2] as determined by the relative areas of the appropriate n.m.r. peaks: the benzyl proton at 5.4 caused by *N*-benzhydrylaniline and the methyl protons at 2.0 caused by *N*,1,1-triphenylethylamine.

Reaction with Ethyl Iodide

The crude reaction product was dissolved in 50 ml of diethyl ether and precipitated as the hydrochloride with hydrogen chloride. The dry salt (2.535 g, 81% yield) was neutralized with aqueous sodium hydroxide, extracted with ether, concentrated, and distilled, b.p. 165–172° at 2 mm, 1.745 g (61% yield). This material crystallized and was purified for analysis by recrystallization from methanol (6 ml/g). Nuclear magnetic resonance: CH_3 triplet at 0.74 (3.0 H), CH_2 quartet at 2.53 (1.9 H), NH singlet at 4.24 (1.0 H), aromatic H's complex band at 6.2–7.6 (14.7 H).

Reaction with Propyl Halides

The crude reaction product was purified by recrystallization from methanol (6 ml/g). Nuclear magnetic resonance: CH_3CH_2 broad band at 0.7–1.5 (4.9 H) with the methyl appearing as a distorted triplet at 0.8, CH_2 triplet at 2.51 (2.0 H), NH singlet at 4.4 (1.0 H), aromatic H's complex band at 6.2–7.8 (15.0 H).

[2]*Reference 3 reports 25–33% N-benzhydrylaniline formed under similar reaction conditions.*

Can. J. Chem. Downloaded from www.nrcresearchpress.com by 210.87.254.6 on 09/05/12
For personal use only.

Identical experiments were carried out with propyl chloride, propyl bromide, and propyl iodide. The yield was obtained by dissolving the crude product in 10 ml of hot methanol, cooling, seeding, and allowing to crystallize for 2 days (see Table I).

The crude reaction product was also examined by thin-layer chromatography with cyclohexane containing 17% acetic acid as developing solvent. Besides the spot caused by the product (R_f 0.59), two additional spots appeared: R_f 0.63 and 0.72. These were readily seen in the product derived from propyl iodide, but not in that derived from propyl chloride. The product from propyl bromide showed an intermediate amount.

Reaction with Isopropyl Chloride

The crude product was purified by recrystallization from methanol (10 ml/g). Nuclear magnetic resonance: CH_3 doublet at 0.82 (6.0 H), CH multiplet at 2.8 (1.0 H), NH singlet at 4.3 (0.8 H), aromatic H's complex band at 6.2–7.7 (14.4 H).

Reaction with t-Butyl Chloride

The crude reaction product was chromatographed on 70 g of Woelm grade I acidic alumina using, as eluting solvents, 350 ml of hexane and then four 150 ml portions of hexane containing methylene chloride in concentrations of 5%, 10%, 25%, and 50% (v/v), respectively. Fifty milliliters of eluent was collected per fraction, and the fractions were examined by thin-layer chromatography with cyclohexane containing 17% acetic acid as developing solvent. The first two fractions contained 0.111 g of unidentified material, the next three fractions contained 0.683 g (22%) of the product *N*,1,1-triphenyl-2,2-dimethylpropylamine (R_f 0.68), and the remaining fractions (total weight 1.58 g) were mixtures of benzophenone anil (R_f 0.42), *N*-benzhydrylaniline (R_f 0.57), and product.

The product was purified by recrystallization from methanol (40 ml/g). Nuclear magnetic resonance: CH_3 singlet at 1.0 (9.0 H), NH singlet at 4.8 (0.9 H), aromatic H's complex band at 5.9–7.9 (15.2 H).

Reaction with Allyl Chloride

The crude product, *N*,1,1-triphenyl-1-aminobutene-3, was purified by recrystallization from methanol (6 ml/g). Nuclear magnetic resonance: CH_2 doublet at 3.2 (2.0 H), $-CH=CH_2$ multiplet at 4.7–5.5 (3.2 H), NH singlet at 4.4 (0.8 H), aromatic H's complex band at 6.1–7.7 (15.3 H).

Reaction with Benzyl Chloride

The crude product, *N*,1,1,2-tetraphenylethylamine, was purified by recrystallization from *n*-butanol (5 ml/g). Nuclear magnetic resonance: CH_2 singlet at 3.75 (2.1 H), NH singlet at 4.48 (0.91 H), aromatic H's complex band at 6.1–7.6 (20.0 H).

Reaction with Vinyl Chloride

No color change of the sodium adduct was noted over an 18 h period. The crude product was a viscous oil whose infrared spectrum was identical with that of *N*-benzhydrylaniline.

Reaction with Cyclopentyl Chloride

The crude reaction product was examined by thin-layer chromatography with cyclohexane containing 17% acetic acid as developing solvent. Two products were detected: R_f 0.57–0.59 and 0.67–0.68.

The crude product (5.24 g) from 0.02 mole of adduct was boiled with 30 ml of 20% hydrochloric acid for 2 h. The final mixture was treated with 30 ml of ether and filtered. The insoluble solid, which amounted to 3.21 g (44% yield), was the hydrochloride of *N*-cyclopentyl-*N*-benzhydrylaniline, m.p. 180–184°. Purification was effected by dissolving in 15 ml of warm methanol and adding 70 ml of ether to precipitate the salt. Two such treatments raised the melting point to 190–193°. Nuclear magnetic resonance: cyclopentyl protons broad band at 1.65 (8.9 H), benzyl proton at 5.8 (0.87 H), aromatic H's complex band at 6.4–7.5 (15.0 H).

Anal. Calcd. for $C_{24}H_{26}NCl$: C, 79.2; H, 7.22; N, 3.85. Found: C, 78.7; H, 6.95; N, 3.78.

The ether layer in the filtrate from the amine hydrochloride was separated, washed, and evaporated, and the residue was distilled, b.p. 155–170° at 3 mm, to give 1.421 g of a partially crystalline liquid. A 0.50 g sample of this was recrystallized from 2 ml of methanol to give 0.20 g of cyclopentylidene diphenylmethane, m.p. 61–63°; the mixed melting point with an authentic sample was undepressed. The crude distillate was analyzed by vapor-phase chromatography, using a 7 ft long $\frac{1}{4}$ inch outside diameter column packed with 30% Apiezon on Chromosorb W heated at 248°, and using helium as carrier gas. The material was found to consist of 70% of cyclopentylidene diphenylmethane (representing a 21% yield) and 28% of an unknown material (relative retention time 1.53).

The authentic sample of cyclopentylidene diphenylmethane, m.p. 61–63°, was prepared from methyl cyclopentanecarboxylate and excess phenylmagnesium bromide followed by dehydration of the alcohol (without isolation) in refluxing acetic anhydride (15, 16). Nuclear magnetic resonance: CH_2 multiplet at 1.6 (4.0 H), CH_2 multiplet at 2.4 (4.0 H), aromatic H's singlet at 7.2 (9.8 H).

Decomposition of N,1,1-Triphenylethylamine

N,1,1-Triphenylethylamine (2.06 g, 0.076 mole) was refluxed with 10 ml of 20% hydrochloric acid for 1 h. The acid solution was extracted with 10 ml of benzene, washed twice with 5 ml of water, and dried over sodium sulfate. The dried solution was filtered and evaporated to give 1.075 g of a liquid residue. This was

Can. J. Chem. Downloaded from www.nrcresearchpress.com by 210.87.254.6 on 09/05/12
For personal use only.

distilled under vacuum, b.p. 76–82° at 2 mm, to yield 0.965 g (71%) of 1,1-diphenylethylene, whose infrared spectrum was identical with that of an authentic sample.

The aqueous acid phase and washings were combined, made alkaline, and extracted with ether. After the ether layer was washed, dried over sodium sulfate, and evaporated, a residue of 0.441 g of aniline (62%) was obtained. Its identity was established by preparing the benzenesulfonamide, m.p. 109–110°, undepressed on admixture with an authentic sample.

Reaction with 2 Equivalents of Methyl Iodide

The disodium adduct was treated with 0.02 mole of methyl iodide at −60°. Within 2 h the solution had decolorized, and thin-layer chromatography with 7:2:2 benzene – tetrahydrofuran – 98% formic acid as solvent showed the presence of four products: R_f 0.13, 0.26, 0.45, and 0.85. The first (R_f 0.13) and last (R_f 0.85), *N*-methylaniline and 1,1-diphenylethylene, respectively, were by far the largest; the other two were relatively small. One of these (R_f 0.39) is *N*-methyl-*N*-benzhydrylaniline (see below), and the other (R_f 0.26) is unknown.

The product was isolated by an ether extraction; after evaporation of the solvent, the residue (2.43 g) was distilled. Two fractions were collected: 0.746 g, b.p. 50–140° at 2 mm, and 1.225 g, b.p. 175–180° at 2 mm; 0.121 g was left as a residue. Thin-layer chromatography showed the first fraction to contain only *N*-methylaniline and 1,1-diphenylethylene, whereas the second contained these as the major components as well as the by-products, R_f 0.26 and 0.39.

The n.m.r. spectrum of this second fraction (CH_3 singlet at 1.79 (2.7 H), CH_3 singlet at 2.71 (3.0 H), aromatic H's complex band at 6.6–7.6 (16.8 H)) strongly indicated that the material was primarily *N*-methyl-*N*,1,1-triphenylethylamine. A small peak in the n.m.r. spectrum at 5.4 (equivalent to 0.2 H) was caused by an impurity, 1,1-diphenylethylene; this, in turn, affected the integration of the aromatic protons, giving too high a value. The addition of formic acid to the solution of the amine in the n.m.r. sample tube caused a marked change in the spectrum over a 24 h period. The peaks caused by the methyl groups decreased in intensity, the peak caused by the 1,1-diphenylethylene impurity grew larger, and a new peak appeared at 3.2 caused by *N*-methylaniline (in formic acid – deuterated chloroform).

N-Methyl-*N*,1,1-triphenylethylamine (0.547 g, 0.0019 mole) was dissolved in 25 ml of ether and treated with hydrogen chloride. A gum separated which crystallized when allowed to stand for 16 h. This was filtered off and weighed (0.275 g). The ether layer was evaporated to give 0.321 g (94% yield) of 1,1-diphenylethylene, whose identity was established by its infrared spectrum. The solid which was filtered off was treated with 5 ml of water containing 1 drop of concentrated hydrochloric acid and 5 ml of ether. The ether layer was separated, washed once with water, evaporated, and dried at 40° under vacuum.

The residue from the evaporation was dissolved in 5 ml of ether and treated with hydrogen chloride. A gummy solid (0.037 g) separated out and was dissolved in 1 ml of methanol; the solution was treated with 10 ml of ether, and a solid (0.020 g, m.p. 150–152.5°) precipitated out. The mixed melting point of the solid with *N*-methyl-*N*-benzhydrylaniline hydrochloride was 153–155° and its infrared spectrum was identical with that of an authentic sample.

The aqueous acid layer was made basic, extracted with ether, and evaporated to give 0.156 g (88% yield) of *N*-methylaniline, identified by comparison of its infrared spectrum with that of an authentic sample.

Reaction with 1,4-Dibromobutane

The adduct from 0.02 mole of benzophenone anil was treated with 2.38 ml (0.02 mole) of 1,4-dibromobutane at −60°. The crude orange product, isolated as previously described, amounted to 6.25 g. This was dissolved in 40 ml of *n*-hexane, and chromatographed on 60 g of Woelm grade I basic alumina packed in a 16 × 430 mm column, with 100 ml of *n*-hexane and then 100 ml of hexane – 10% benzene as eluting solvent. The color remained on the column and was not further investigated, and 5.22 g of a semisolid was recovered. This was dissolved in 60 ml of hot methanol and cooled to approximately 30 °C, and the warm solution was decanted from the gums which separated. Cooling the decantate to 10° overnight gave 2.77 g (44% yield), m.p. 74.5–77°, of 1,2,2-triphenylpiperidine.

The gum (1.35 g) crystallized when allowed to stand, and melted at 74–76.5°; the mixed melting point with the above product was 74–76.5°. The combined yield was 65%. Nuclear magnetic resonance: CH_2 broad band at 1.6 (3.95 H), CH_2 complex triplet at 2.5 (1.9 H), CH_2 complex triplet at 3.75 (1.9 H), aromatic H's complex band at 6.5–7.6 (15.0 H). The spectrum was unchanged after the solution was shaken with D_2O, indicating the absence of an amine proton.

Anal. Calcd. for $C_{23}H_{23}N$: C, 88.1; H, 7.41; N, 4.47. Found: C, 88.1; H, 7.16; N, 4.52.

At one point, an attempt was made to purify the crude product by vacuum distillation. The main fraction, b.p. 210–220° at 1 mm, was a yellow mobile liquid (the original crude material was a gum) and had an R_f (1:1 cyclohexane–chloroform) of 0.45, whereas the original material had an R_f of 0.70. Evidently some change had occurred, perhaps caused by trace amounts of acid remaining in the crude product.

This material (1.501 g) was dissolved in 25 ml of diethyl ether and treated with hydrogen chloride. The solid which precipitated (1.326 g, m.p. 175–180°) was dissolved in 10 ml of methanol; 35 ml of diethyl ether was added to give 1.115 g, m.p. 180–183°. An analytical sample was recrystallized from methanol, m.p. 182–184°. Nuclear magnetic resonance of the free amine: CH_2 quartet at 1.65, CH_2 quintet at 2.06 (combined

Can. J. Chem. Downloaded from www.nrcresearchpress.com by 210.87.254.6 on 09/05/12
For personal use only.

areas 4.0 H), CH_2 triplet at 2.96 (1.95 H), NH singlet at 3.34 (1.0 H), CH triplet at 6.00 (0.85 H), aromatic H's complex band at 6.4–7.4 (15.5 H).

Anal. Calcd. for $C_{23}H_{24}ClN$: C, 78.9; H, 6.92; N, 4.00. Found: C, 78.8; H, 6.71; N, 3.96.

The structure appears to be *N*,1,1-triphenyl-5-aminopentene-1.

Reaction with 1,3-Dibromopropane

The reaction of the sodium adduct and 1,3-dibromopropane was quite rapid at −60 °C. The crude product (3.265 g) was crystalline and was readily purified by recrystallization from methanol (20 ml) to give 2.24 g (75% yield) of 1,2,2-triphenylpyrrolidine, m.p. 112–114°. The analytical sample, after two additional crystallizations, had m.p. 115–116.5°. Nuclear magnetic resonance: CH_2 quintet at 1.74 (1.8 H), CH_2 triplet at 2.60 (1.85 H), CH_2 triplet at 3.70 (1.85 H), aromatic H's complex band at 6.0–7.6 (15.0 H).

Anal. Calcd. for $C_{22}H_{21}N$: C, 88.2; H, 7.08; N, 4.68. Found: C, 88.6; H, 7.06; N, 4.66.

Reaction with 1,5-Dibromopentane

The crude reaction product (3.35 g) was dissolved in 15 ml of hot *n*-propanol and allowed to stand for 24 h at room temperature. The product, *N,N'*,1,1,7,7-hexaphenylheptanediamine-1,7, separated slowly, 1.513 g (51% yield), m.p. 141–145°. Two recrystallizations from *n*-propanol gave an analytical sample, m.p. 154–156°. Nuclear magnetic resonance: CH_2 broad band at 1.1 (6.0 H), CH_2 broad band at 2.4 (3.8 H), NH very broad band at 4.2 (1.7 H), aromatic H's complex band at 6.2–7.7 (30.0 H).

Anal. Calcd. for $C_{43}H_{42}N_2$: C, 88.0; H, 7.23; N, 4.78; mol. wt. 589. Found: C, 88.3; H, 6.95; N, 4.87; mol. wt. 590.

The filtrate from the crude product was concentrated under vacuum, and the residue (1.53 g) was dissolved in 20 ml of hexane and placed on a 16 × 430 mm column of Woelm grade I basic alumina. Elution was carried out with 150 ml of hexane, 100 ml of hexane – 10% benzene, 100 ml of hexane – 25% benzene, 100 ml of hexane – 50% benzene, and finally 100 ml of benzene – 50% methylene chloride. The eluate was collected in 50 ml fractions. Fractions 1, 2, and 3 contained no material, and the remaining fractions contained 1.24 g. Examination of these by thin-layer chromatography with benzene – tetrahydrofuran – 98% formic acid (70:15:15) as developing solvent showed that fractions 4–7 (1.01 g) contained an unknown material and that fraction 9 (0.131 g) was the hexaphenylheptanediamine. The unknown material was combined and recrystallized from 25 ml of methanol, with cooling to 10°, to give 0.637 g of a solid, m.p. 55–58°. This was recrystallized again for an analytical sample, m.p. 58–59°.

Anal. Calcd. for $C_{24}H_{25}N$: C, 88.0; H, 7.71; N, 4.28. Found: C, 87.8; H, 7.72; N, 4.41.

On the basis of its n.m.r. spectrum, the structure was considered to be *N*,1,1-triphenyl-1-aminohexene-5. The spectra showed a broad CH_2 band at 1.3 (2.0 H), a CH_2 quartet at 1.9 (2.2 H), a complex triplet at 2.5 (2.0 H), an NH band at 4.35 (0.85 H), two major peaks with complex fine structure at 4.7 and 4.9 caused by the vinyl group, a complex multiplet at 5.5 (total area 2.8 H), and a complex series of peaks at 6.1–7.4 (15.5 H) caused by the aromatic protons.

Reaction with 1,10-Dibromodecane

The crude reaction product from 0.01 mole of the sodium adduct in tetrahydrofuran and 1.5 g (0.005 mole) of 1,10-dibromodecane (3.751 g) was recrystallized from 25 ml of methanol and 13 ml of benzene. The recrystallized product amounted to 3.114 g (94% yield), m.p. 152–155°, of *N,N'*,1,1,12,12-hexaphenyldodecanediamine-1,12 having an orange color. Attempts to remove this color by recrystallization from *n*-butanol in the presence of Norit failed. Purification was finally effected by placing a solution of 1.65 g of the product in 30 ml of 1:1 hexane–benzene on a 16 × 450 mm column of 60 g of Woelm grade I basic alumina. Elution with 300 ml of the solvent removed 1.47 g of an almost colorless material, m.p. 147–152°; the color remained on the column. Two recrystallizations from *n*-butanol (20 ml/g) raised the melting point to 155–156.5°. Nuclear magnetic resonance: CH_2 broad band at 1.07 (8.0 H), CH_2 broad band at 2.48 (1.9 H), NH broad band at 4.26 (0.8 H), aromatic H's complex band at 6.2–7.7 (15.0 H).

Anal. Calcd. for $C_{48}H_{52}N_2$: C, 87.7; H, 7.99; N, 4.26; mol. wt. 657. Found: C, 88.0; H, 8.09; N, 4.15; mol. wt. 660.

Reaction with Benzaldehyde

The crude reaction product (3.41 g) was recrystallized from 20 ml of ethanol to give 0.987 g of benzophenone anil, m.p. 107–110°. A recrystallized sample of this, m.p. 110–113°, showed no depression on admixture with an authentic sample.

The filtrate from the recovered benzophenone anil was evaporated and the residue chromatographed on 70 g of Woelm grade I basic alumina packed into a 16 × 430 mm column. Elution with 250 ml of 1:1 benzene–hexane removed 1.36 g of a solid which, on recrystallization from 10 ml of hexane, gave 0.967 g, m.p. 77–80°. Investigation of this material by thin-layer chromatography with benzene as developer showed that it consisted of benzophenone anil (R_f 0.60) and *N*-benzhydrylaniline (R_f 0.73); n.m.r. analysis established that it was a mixture of 1 part of the former and 2 parts of the latter.

It was necessary to use methylene chloride plus 5% methanol and finally acetone plus 5% methanol to remove anything more from the alumina column. These eluents gave 0.701 g of a solid which, on recrystallization from 10 ml of benzene, gave 0.395 g of *dd,ll*-hydrobenzoin, m.p. 113–120°, undepressed on admixture

Can. J. Chem. Downloaded from www.nrcresearchpress.com by 210.87.254.6 on 09/05/12
For personal use only.

with an authentic sample. Comparison of the infrared spectrum of the isolated material with that of an authentic sample confirmed its identity.

The solvent in the benzene filtrate from the recrystallization was evaporated and the residue was recrystallized from water to give 0.176 g of a solid, m.p. 80–85°. An examination of the infrared spectrum of this material showed it to be a mixture of *dd,ll*-hydrobenzoin and *meso*-hydrobenzoin.

The authentic sample of *meso*-hydrobenzoin was prepared by sodium borohydride reduction of benzoin in 80% dioxane. It was recrystallized from water and had m.p. 134–136.5°.

dd,ll-Hydrobenzoin was prepared by acetolysis of α-stilbene dibromide by the procedure of Breuer and Zincke (17). Two recrystallizations from 80% water – 20% ethanol gave material having m.p. 117–120°.

The total yields of isolated compounds were 50% benzophenone anil and 25% *N*-benzhydrylaniline (based on the original benzophenone anil), and 65% of the diastereomeric hydrobenzoins (based on the benzaldehyde used).

Reaction with Ethylene Oxide

The crude reaction product from 0.01 mole of adduct and 0.01 mole of ethylene oxide amounted to 3.12 g. This was crystallized from 15 ml of petroleum ether (b.p. 30–60°) to give 2.17 g (72% yield) of an orange solid, m.p. 118–122°. Recrystallization from 25 ml of hexane and 10 ml of benzene with 2 g Norit and a hot filtration sufficed to remove the color and give an analytical sample, m.p. 122–125°. Nuclear magnetic resonance: CH_2 triplet at 2.67 (1.85 H), CH_2 triplet at 3.51 (2.0 H) superimposed on a broad NHOH band at 3.3–3.7, aromatic H's complex band at 6.2–7.6 (14.5 H). The peak areas were determined after the NHOH band was eliminated with D_2O. The difference between the peak areas of the 3.5 triplet plus the NHOH band before and after D_2O treatment established that the broad NHOH band corresponded to 1.9 H.

Anal. Calcd. for $C_{21}H_{21}NO$: C, 83.1; H, 6.99; N, 4.62. Found: C, 83.6; H, 6.96; N, 4.57.

Reaction with Methyl Benzoate

The crude reaction product from 0.01 mole of sodium adduct and 0.01 mole of methyl benzoate was recrystallized from 10 ml of methanol to give 2.50 g (69% yield) of *N*-benzhydrylbenzanilide, m.p. 108–110°; the mixed melting point with an authentic sample was undepressed, and the infrared spectra of the material and of an authentic sample were identical.

The authentic sample was prepared by refluxing *N*-benzhydrylaniline and an equivalent amount of benzoyl chloride in pyridine for 16 h. The crude product was crystallized from hexane, and recrystallized once from hexane and once from methanol, m.p. 108–109°. Nuclear magnetic resonance: aromatic H's only in a complex band at 6.5–7.5 (the benzylic proton is shifted into the aromatic region).

Anal. Calcd. for $C_{26}H_{21}NO$: C, 85.9; H, 5.83; N, 3.85. Found: C, 85.7; H, 5.70; N, 3.80.

Reaction with Methyl p-Toluate

The crude product was purified by one crystallization from methanol and two recrystallizations from hexane to give 1.562 g of *N*-phenyl-*N*-benzhydryl-*p*-toluamide, m.p. 112.5–114° (41% yield). Nuclear magnetic resonance: CH_3 singlet at 2.15 (3.0 H), aromatic H's complex band at 6.5–7.5 (20.0 H), indicating that the 19 aromatic protons and the 1 benzyl proton are in the same region.

Anal. Calcd. for $C_{27}H_{23}NO$: C, 85.9; H, 6.15; N, 3.71. Found: C, 85.6; H, 5.98; N, 3.58.

Reaction with Diethyl Carbonate

Diethyl carbonate (0.01 mole) produced 3.15 g of a crude product which was chromatographed on 60 g of Woelm basic alumina grade I. Fifty milliliter fractions were collected and the solvents used were 100 ml of hexane, 100 ml of hexane – 10% benzene, 50 ml of hexane – 25% benzene, and 100 ml of hexane – 50% benzene.

This treatment removed 1.82 g of material from the column. Additional eluting solvent containing methylene chloride removed the remaining material, but no products could be isolated from it.

The 1.82 g was covered with petroleum ether (b.p. 30–60°). After the mixture had stood overnight at 10°, the solution was decanted from the ethyl *N*-benzhydrylphenylcarbamate, which amounted to 1.53 g (46% yield), m.p. 54–58°. Two recrystallizations from 20 ml of petroleum ether (b.p. 30–60°), with cooling to 10°, gave 1.03 g of the carbamate, m.p. 60–62°. Nuclear magnetic resonance: CH_3 triplet at 1.1 (3.3 H), CH_2 quartet at 4.1 (2.0 H), CH singlet at 6.7 (1.0 H), aromatic H's complex band at 6.8–7.4 (15.0 H).

Anal. Calcd. for $C_{22}H_{21}NO_2$: C, 79.7; H, 6.35; N, 4.23. Found: C, 80.0; H, 6.01; N, 4.24.

Reaction with Diethyl Sulfate

The crude product obtained when the sodium adduct was treated with 0.01 mole of freshly distilled diethyl sulfate amounted to 2.98 g. One recrystallization from 10 ml of petroleum ether (b.p. 30–60°) gave 1.78 g (62% yield) of *N*,1,1-triphenylpropylamine, m.p. 67–70.5°.

Stepwise Reaction with Methyl Benzoate and Methyl Iodide

The sodium adduct (0.01 mole) was allowed to react with 0.01 mole of methyl benzoate for 1 h at −60° and for 4 h at room temperature. The solution was then cooled again to −60° and 0.01 mole of methyl iodide added; after the solution had warmed to room temperature, it was allowed to stand overnight.

Can. J. Chem. Downloaded from www.nrcresearchpress.com by 210.87.254.6 on 09/05/12
For personal use only.

The crude product, isolated by ether extraction, amounted to 3.47 g and was crystallized from 30 ml of *n*-hexane to give 2.39 g (63% yield) of the benzamide of *N*,1,1-triphenylethylamine, m.p. 142–144°. One recrystallization from *n*-butanol and one from isopropanol raised the melting point to 146.5–149°. Nuclear magnetic resonance: CH_3 singlet at 2.0 (2.9 H), aromatic H's complex band at 6.7–7.6 (20.0 H), very similar in structure to that of *N*-benzhydrylbenzanilide.

Anal. Calcd. for $C_{27}H_{23}NO$: C, 85.9; H, 6.15; N, 3.71. Found: C, 85.9; H, 6.13; N, 3.70.

Preparation of N-Methyl-N-benzhydrylaniline[3]

A solution of 15.0 g (0.074 mole) of benzhydryl chloride and 17.4 g (0.162 mole) of *N*-methylaniline in 50 ml of benzene was stirred at room temperature for 16 h, during which time a precipitate formed. The solution was examined by thin-layer chromatography with 7:2:2 benzene – tetrahydrofuran – 98% formic acid as solvent to follow the progress of the reaction: *N*-methylaniline, R_f 0.12; product, R_f 0.59; by-products of unknown constitution, R_f 0.30, 0.42, and 0.74.

The solution was washed with 10% potassium hydroxide, the benzene stripped off, and the residue distilled, collecting the main fraction, b.p. 185–205° at 4 mm, 8.50 g. This was dissolved in 100 ml of diethyl ether, and hydrogen chloride was passed briefly through the solution. The resulting precipitate amounted to 2.4 g, m.p. 152–203° (decomp.).

The filtrate from this first salt was again treated with hydrogen chloride to give 4.63 g of a second crop, m.p. 159–160°. This was dissolved in 15 ml of chloroform, the solution was filtered to remove a small amount of insoluble material, and 25 ml of ether was added. The product amounted to 4.40 g, m.p. 160–161°. Nuclear magnetic resonance: CH_3 singlet at 3.33 (2.90 H), CH singlet at 6.44 (1.02 H), aromatic H's in two broad bands at 6.9–8.7 (15.0 H); for the free amine: CH_3 singlet at 2.73 (2.95 H), CH singlet at 6.15 (0.92 H), aromatic H's complex band at 6.5–7.5 (15.0 H).

Anal. Calcd. for $C_{20}H_{20}NCl$: C, 77.5; H, 6.52; N, 4.52. Found: C, 77.1; H, 6.59; N, 4.35.

Stepwise Reaction with t-Butyl Alcohol and Methyl Iodide

The disodium adduct was treated at −60° with 0.94 ml (0.01 mole) of *t*-butyl alcohol. After the dark-green solution was allowed to warm to room temperature for 2 h, the solution was recooled and 0.62 ml (0.01 mole) of methyl iodide added. When warmed to room temperature, the solution changed from a dark-green color through a royal blue to a clear pale yellow. After 16 h, the solution was treated with water, and the reaction product isolated by ether extraction.

The gummy residue remaining after evaporation of the ether was dissolved in 50 ml of diethyl ether, and hydrogen chloride was bubbled through to precipitate the hydrochloride of *N*-methyl-*N*-benzhydrylaniline, 2.80 g, m.p. 146–149°. This salt was dissolved in 10 ml of methanol and the solution treated with 25 ml of ether. The solid which precipitated amounted to 2.0 g (65% yield), m.p. 160–161°, undepressed on admixture with an authentic sample. Its infrared spectrum was identical with that of the authentic sample.

Stepwise Reaction with t-Butyl Alcohol and Cyclopentyl Chloride

The above experiment was repeated with 0.01 mole of cyclopentyl chloride instead of the methyl iodide. The crude reaction product gave 2.77 g (92% yield) of the hydrochloride of *N*-benzhydrylaniline, m.p. 196–198°. Dissolution in 40 ml of methanol followed by crystallization from 60 ml of ether gave 2.17 g (72% yield) of the salt, m.p. 198–200°, undepressed on admixture with an authentic sample. Its infrared spectrum was identical with that of the authentic sample.

ACKNOWLEDGMENTS

The authors are indebted to Mr. H. Mak (Dow Chemical of Canada, Limited) for his assistance in recording and interpreting the n.m.r. spectra, and to Mr. L. E. Swim (The Dow Chemical Company, Midland, Michigan) for the microanalyses.

REFERENCES

1. W. Schlenk, J. Appenrodt, A. Michael, and A. Thal. Ber. **47**, 473 (1914).
2. W. Schlenk and E. Bergmann. Ann. **463**, 281 (1928).
3. B. M. Mikhailov and K. N. Kurdyumova. J. Gen. Chem. USSR Engl. Transl. **26**, 899 (1956); Zh. Obshch. Khim. **26**, 786 (1956).
4. A. Mathias and E. Warhurst. Trans. Faraday Soc. **58**, 942 (1962).
5. E. L. Anderson and J. E. Casey, Jr. J. Org. Chem. **30**, 3959 (1965).
6. S. Selman and J. F. Eastham. J. Org. Chem. **30**, 3804 (1965).
7. D. V. Ioffe. Chem. Abstr. **63**, 17953*g* (1965); Biol. Aktivn. Soedin. Akad. Nauk SSSR, 147 (1965).
8. P. J. Hamrick, Jr. and C. R. Hauser. J. Am. Chem. Soc. **81**, 493 (1959).
9. R. C. Fuson, R. J. Lokken, and R. L. Pedrotti. J. Am. Chem. Soc. **78**, 6064 (1956).
10. A. G. Brook, H. L. Cohen, and G. F. Wright. J. Org. Chem. **18**, 447 (1953).
11. H. Gilman, A. H. Haubein, G. O'Donnell, and L. A. Woods. J. Am. Chem. Soc. **67**, 922 (1945).

[3]*This procedure follows that used by Cromwell and Fitzgibbon (18) for similar compounds.*

Can. J. Chem. Downloaded from www.nrcresearchpress.com by 210.87.254.6 on 09/05/12
For personal use only.

12. G. REDDELIEN. Ber. **46**, 2718 (1913).
13. J. W. B. REESOR, J. G. SMITH, and G. F. WRIGHT. J. Org. Chem. **19**, 940 (1954).
14. N. D. CHERONIS and J. B. ENTRIKIN. Semimicro qualitative organic analysis. 2nd ed. Interscience Publishers, Inc., New York. 1957. pp. 237 and 730.
15. S. S. NAMETKIN and M. A. VOLODINA. J. Gen. Chem. USSR Engl. Transl. **18**, 2033 (1948); Chem. Abstr. **43**, 3797*a* (1949).
16. G. EGLOFF. Physical constants of hydrocarbons. Vol. III. Reinhold Publishing Corp., New York. 1946. p. 456.
17. A. BREUER and T. ZINCKE. Ann. **198**, 154 (1879).
18. N. H. CROMWELL and W. E. FITZGIBBON. J. Am. Chem. Soc. **70**, 387 (1948).
19. T. W. J. TAYLOR, J. S. OWEN, and D. WHITTAKER. J. Chem. Soc. 206 (1938).

Can. J. Chem. Downloaded from www.nrcresearchpress.com by 210.87.254.6 on 09/05/12
For personal use only.

Can. J. Chem. Downloaded from www.nrcresearchpress.com by 210.87.254.6 on 09/05/12
For personal use only.

TREIBS' 119° GLYCOL; TRANSANNULAR ATTACK AT THE TERTIARY CARBON OF A SECONDARY–TERTIARY EPOXIDE[1]

E. W. WARNHOFF AND V. SRINIVASAN
Department of Chemistry, University of Western Ontario, London, Ontario
Received May 10, 1966

ABSTRACT

The glycol, $C_{15}H_{26}O_3$, of m.p. 119° formed in the oxidation of caryophyllene oxide (I) has been found to have the structure and stereochemistry IV*a* formed by intramolecular transannular displacement at the tertiary carbon of the secondary–tertiary oxide in III. A rationalization of this mode of attack is offered. The glycol IV*a* has been transformed into the known keto epoxide XII*b* obtained from isocaryophyllene.

From the oxidation of caryophyllene oxide (I) with permanganate in acetone, Treibs (1) isolated three compounds: the keto oxide II (69%); a glycol, $C_{15}H_{26}O_3$, m.p. 141°, $[\alpha]_D$ −72° (7%); and a second glycol, $C_{15}H_{26}O_3$, m.p. 119°, $[\alpha]_D$ −1° (1.7%). Šorm *et al.* later repeated the reaction and isolated the same three substances (2).[2] These authors found that the glycol of m.p. 141–142° was cleaved by lead tetraacetate to the keto oxide II, but that the glycol of m.p. 119° was recovered unchanged from this reagent in benzene solution at 40°. From these observations it was concluded that the two glycols were "*cis* and *trans* isomerides" of the expected 1,2-diol. However, there seem to be no known examples of 1,2-diols not oxidized by lead tetraacetate (4), and therefore the 119° glycol was reexamined.

In our hands, the permanganate oxidation of I gave the same result reported earlier, but the poor yield of 119° glycol made it desirable to explore other methods of preparation. Hydroxylation of caryophyllene oxide with osmium tetroxide gave a crude product from which the 119° glycol could be crystallized in the much improved yield of 41%. The presence of the 142° glycol in the mother liquors from the crystallization could not be detected by nuclear magnetic resonance (n.m.r.) spectroscopy or optical rotation. Although this reaction was a suitable preparation of the 119° glycol, the cost of osmium tetroxide encouraged investigation of its use as a catalyst rather than a stoichiometric reactant. Oxidation of I with the hydrogen peroxide – osmium tetroxide – *t*-butyl alcohol reagent of Milas and Sussman (5) gave 25% of a diol fraction containing mainly the 119° glycol, and, surprisingly, 59% of the keto oxide II. This example of carbon–carbon bond cleavage by an oxide of osmium[3] provides, in our experience, a more convenient synthesis of the keto oxide than the permanganate oxidation of I. The glycol yield based on osmium tetroxide was much better in the catalytic than in the stoichiometric reaction, and therefore the catalytic method was adopted for larger scale reactions. It was fortunate that the 119° compound, the major constituent of the glycol fraction, could be separated by crystallization, because its chromatographic behavior was identical with that of hydroxylic

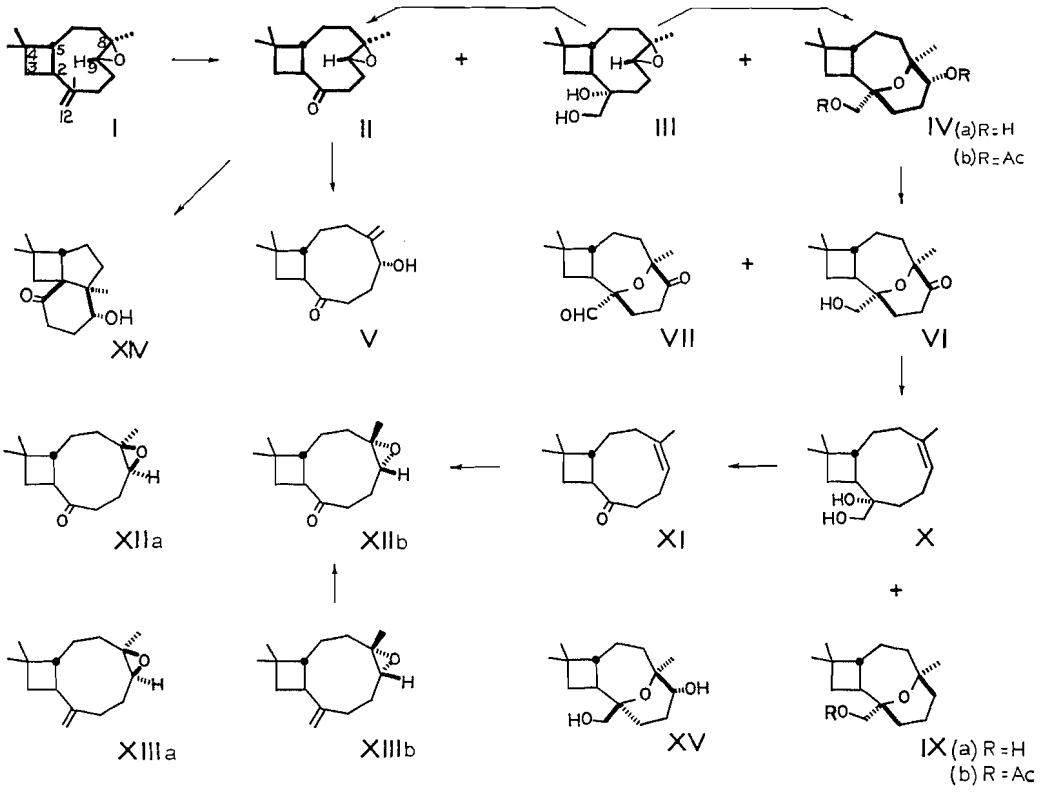
[1]*Presented in part at the 49th annual conference of the Chemical Institute of Canada, Saskatoon, Saskatchewan, June 1966.*

[2]*A fourth compound isolated, V, $C_{14}H_{22}O_2$, m.p. 110°, has since been shown (3, p. 1669) to arise by isomerization of the keto oxide II on alumina, as suspected by the Czech workers.*

[3]*Although Milas and Sussman (5) found that the hydrogen peroxide – osmium tetroxide – t-butyl alcohol reagent at low temperature gave only 1,2-diols, Criegee (6) has reported carbon–carbon bond rupture to be the normal reaction of the hydrogen peroxide – osmium tetroxide – ether reagent. As he suggested, the carbon–carbon bond scission is probably a consequence of reoxidation of the osmium(VI) in the initially formed cyclic ester to osmium(VIII) before solvolysis of the ester takes place.*

contaminants. The 142° glycol, although it also exhibits the same chromatographic behavior as the 119° glycol, could not be detected in the n.m.r. spectrum of the residue from the crystallization mother liquors.

The infrared spectrum of the 119° compound showed the presence of hydroxyl absorption and the absence of carbonyl absorption. The n.m.r. spectrum contained peaks from three unsplit methyl groups: a singlet at 1.02 p.p.m. from the *gem*-dimethyl group and a



singlet at 1.20 p.p.m. from a methyl group on a carbon atom bearing oxygen; there were no vinyl protons. The appearance of the spectrum in the 2.4–4 p.p.m. region (five protons) was concentration dependent, and in the more dilute solutions coupling of the hydroxyl protons could be observed (Fig. 1). Addition of deuterium oxide removed the peaks from two hydroxyl protons, and thereby simplified the pattern from the remaining three protons. These spectral changes could be interpreted as manifestations of a primary and a secondary alcohol function. The doublet (two protons, J = 6.5 c.p.s.) at 3.20 p.p.m., which collapses to a singlet on deuteration, would be the methylene group of the primary alcohol; the triplet from the hydroxyl proton coupled to the adjacent methylene group can be seen at 2.67 p.p.m. (J = 6.5 c.p.s.). The doublet of the secondary hydroxyl group coupled to the adjacent methine hydrogen appears at 2.47 p.p.m. (one proton, J = 8 c.p.s.), where it overlaps one peak of the hydroxyl triplet; the methine hydrogen is a broad lump at 3.55 p.p.m. Since there are no other protons at low field, the third (ethereal) oxygen atom must be bonded to two tertiary carbon atoms. Acetylation of the 119° glycol produced the expected shifts of the α-protons (7). In the liquid diacetate the methylene group of the primary alcohol was shifted downfield by 0.65 p.p.m. to 3.85 p.p.m., and

Can. J. Chem. Downloaded from www.nrcresearchpress.com by 210.87.254.6 on 09/05/12
For personal use only.

the methine proton of the secondary alcohol was moved downfield by 1.41 p.p.m. to 4.96 p.p.m. At this point, the logical formulation for the 119° glycol was the oxygen-bridged non-vicinal diol IV*a*, which would arise by intramolecular transannular attack of the tertiary hydroxyl group on the epoxide ring in the 1,2-diol precursor III. Structure IV*a* was confirmed by relating the 119° glycol to a known isocaryophyllene derivative in the following manner.

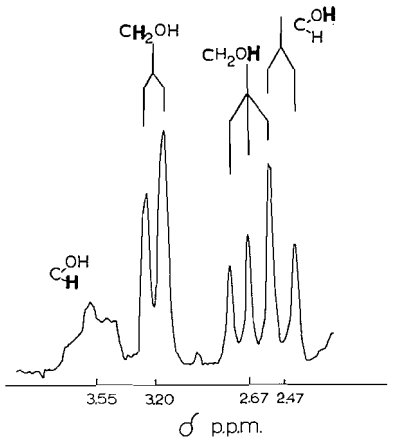


FIG. 1. The n.m.r. spectrum of Treibs' 119° glycol in the 2.4–4 p.p.m. region in deuteriochloroform solution.

Oxidation of the 119° glycol by the chromic acid – pyridine reagent produced a hydroxy ketone VI accompanied by a small amount of a keto aldehyde VII. Various attempts at reductive cleavage of the α-alkoxy group of ketone VI, including the use of zinc (or magnesium) – acetic acid or anhydride (8, 9), calcium – liquid ammonia (10), and potassium–*sec*-butylamine (11), gave starting material or acylated starting material, or else merely reduced the carbonyl group. Therefore, advantage was taken of the elimination that usually occurs in the Wolff–Kishner reduction of α-substituted ketones, including α-alkoxy ketones (9, 12), a particularly close analogy being the ketone VIII (13). Application of this reaction to the hydroxy ketone VI gave both the normal reduction product IX*a* (48%) and the reductive elimination product X (36%). The crystalline elimination product was a *vic*-diol, since it was oxidized by sodium metaperiodate to a liquid ketone XI. Proof of the structure of XI, as well as proof that the double bond had the *cis* configuration, was obtained by epoxidation of the double bond with monoperphthalic acid. From the reaction product was crystallized a keto epoxide XII*b*, m.p. 75–76°, $[\alpha]_D$ −13.8°, which was identical with a sample prepared from *cis*-caryophyllene via epoxidation to isocaryophyllene oxide-*b* (XIII*b*) and subsequent permanganate oxidation. The infrared and n.m.r. spectra (Table I) of the intermediates in the conversion of the 119° glycol into the *cis*-keto oxide XII*b* are all consistent with the structures proposed.

Provided that the oxirane ring is opened with inversion, the stereochemistry of the 119° glycol will be controlled by the hydroxyl configuration at C-1 in the 1,2-diol precursor. Of the two possibilities, Dreiding models show that stereoisomer IV*a* with the α-oriented oxygen bridge is free of angle strain,[4] whereas stereoisomer XV with the "β-oxygen bridge" has considerable angle strain[4] (four-carbon chain bridging the *trans*-2,6-positions

[4]*The discussion is restricted to angle strain over and above that present in the four-membered ring of all of these compounds.*

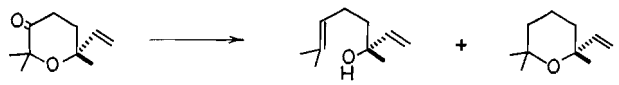
Can. J. Chem. Downloaded from www.nrcresearchpress.com by 210.87.254.6 on 09/05/12
For personal use only.

TABLE I

Nuclear magnetic resonance absorption of caryophyllene derivatives*

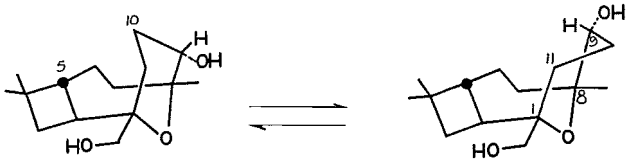
Compound	C-4 *gem*-dimethyl	C-8 methyl	C-9 H	C-12 H_2	Other peaks
Caryophyllene keto oxide II	1.03 s	1.29 s	?	—	—
142° glycol III	0.97 s	1.33 s	?	3.69 b s (2H)	2.38 b m (OH)
119° glycol IV*a*	1.02 s	1.20 s	3.55 m	3.20 s or d (2H)	2.89 b m (2H, OH)
119° glycol diacetate IV*b*	1.03 s	1.09 s	4.96 dd ($J \sim 3, 8$)	3.85 s (2H)	2.05 s (6H, $OOCCH_3$)
Hydroxy ketone VI	1.00 s	1.28 s	—	3.40 s (2H)	?
2,4-Dinitrophenylhydrazone of VI	0.96 s, 1.02 s	1.42 s	—	3.37 s (2H)	—
Keto aldehyde VII	1.01 s	1.32 s	—	9.52 s (1H)	—
Normal Wolff–Kishner product IX*a*	1.02 s	1.14 s	—	3.22 s (2H)	2.43 s (1H, OH)
Normal Wolff–Kishner acetate IX*b*	1.02 s	1.14 s	—	3.82 s (2H)	2.04 s (3H, $OOCCH_3$)
Unsaturated diol X	0.96 s	1.66 d ($J \sim 1$)	5.35 b m	3.60 d ($J \sim 1$)	2.58 b s (2H, OH)
Unsaturated ketone XI	1.00 s, 1.05 s	1.67 d ($J \sim 0.5$)	5.27 b m	—	—
Isocaryophyllene keto oxide XII*b*	1.01 s, 1.10 s	1.25 s	?	—	—

*Chemical shifts are given in parts per million from tetramethylsilane (= 0) for deuteriochloroform solutions. The symbol ? means that the peak position is not given because the assignment would be uncertain; s = singlet; d = doublet, b = broad, m = multiplet, and dd = doublet of doublets.



VIII

of a tetrahydropyran ring) and would not be expected to form readily. Furthermore, the failure of the keto alcohol VI to undergo reductive cleavage of the α-alkoxy group is in better agreement with an unstrained structure. Therefore, the 119° glycol is assigned the α-oxygen-bridged stereostructure IV*a* (IVA $\rightleftharpoons$ IVB).[5] This stereochemistry is consistent with, and supported by, some further experiments.



IVA IVB

[5]*The tetrahydropyran ring might prefer either a chair or a deformed boat conformation. In the more rigid chair form IVA, there is a very unfavorable interaction of the hydrogens on C-5 and C-10; in the distorted boat form IVB, this interaction is reduced, but the substituents on adjacent atoms C-8, C-9 and C-1, C-11 are more nearly eclipsed. Alleviation of these interactions in the ketone VI may account for the more rapid oxidation of the secondary relative to the primary hydroxyl group of IVa.*

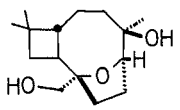
Can. J. Chem. Downloaded from www.nrcresearchpress.com by 210.87.254.6 on 09/05/12
For personal use only.

Can. J. Chem. Downloaded from www.nrcresearchpress.com by 210.87.254.6 on 09/05/12
For personal use only.

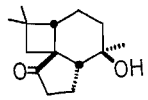
When the 142° diol from the permanganate oxidation was refluxed with methanolic sodium hydroxide, it was converted cleanly into the 119° glycol IV*a* with no detectable (n.m.r., thin-layer chromatography) amount of any other product. The stereostructure of the 142° glycol is therefore III, with the same configuration at C-1 as IV*a*. However, the formation of IV*a* from III in basic methanol solution is much slower than the formation of IV*a* in the basic permanganate oxidation of I, and it is presumably some manganese ester of III which is undergoing cyclization to IV*a* in this reaction. The conversion of III into IV*a* almost quantitatively was also catalyzed by dilute sulfuric acid in a rapid reaction, and, hence, the transannular cyclization of III is appreciably faster than pinacol rearrangement of the 1,2-diol or opening of the strained *trans*-epoxide to an allylic alcohol as in the isomerization of II to V (3).

Since the products from the oxidation of I could contain, at most, only traces of the other possible 1,2-diol or its derivatives, the attack of permanganate ion or osmium tetroxide apparently occurs only from the α-side of the exocyclic double bond. An inspection of a Stuart–Briegleb model of I shows that this is a reasonable restriction.

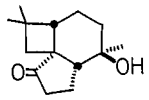
The intramolecular attack of the C-1 hydroxyl group of III exclusively at the *tertiary* carbon of the secondary–tertiary epoxide in basic solution is remarkable but can be rationalized. The product XVI of attack at the secondary carbon atom with inversion would be strained[4] (*trans* fusion of a ring across the 2,5-positions of a tetrahydrofuran ring), and the consequent increase in activation energy for its formation presumably overrides the usual preference for attack at the less-substituted oxide carbon atom in basic solution. The same explanation can be invoked to rationalize a long-known, closely related reaction in the chemistry of caryophyllene: the attack of the enolate anion of the keto oxide II at the *tertiary* carbon atom of the same oxide system to give XIV in over 90% yield (14, 15). Again, the compounds XVII (*trans* 6,5 fusion) and XVIII (*trans* 4,6 fusion) resulting from attack at the secondary carbon atom with inversion would be more strained[4] than the observed product XIV.



XVI



XVII



XVIII

The above rationalization does not take into account the following possible complication. The steric factors, which normally compel base-catalyzed *intermolecular* attack at the least substituted carbon atom of an oxirane ring (16), might be negligible in the case of the *intramolecular* reaction. If this is so, displacement at a tertiary carbon atom might become as facile as that at a secondary carbon atom. A test of this possibility can be provided by the 1,2-diols from the two isocaryophyllene oxides, provided that oxidation of XIII*a* and XIII*b* occurs from the α-side of the exocyclic double bond in these molecules too. The 1,2-glycol from isocaryophyllene oxide-*a* (XIII*a*) could give a strain-free[4] cyclic ether from attack of the C-1 hydroxyl group at either the secondary or tertiary oxirane carbon atom, and the proportion of products formed may be interpreted as a measure of the preference for secondary over tertiary displacement. On the other hand, the 1,2-glycol from isocaryophyllene oxide-*b* (XIII*b*) cannot give a strain-free[4] cyclic ether by attack of the C-1 hydroxyl group at either oxirane carbon atom, and therefore this reaction would not be expected to take place. These experiments are in progress.

Can. J. Chem. Downloaded from www.nrcresearchpress.com by 210.87.254.6 on 09/05/12
For personal use only.

EXPERIMENTAL

General

Melting points were taken on a Reichert microscope hot stage and are corrected. Optical rotations were measured with chloroform solutions, unless otherwise specified, in a 1 dm tube on a Rudolph model 80 polarimeter. Infrared spectra were recorded on a Beckman IR-5 or IR-5A spectrophotometer. The ultraviolet spectrum was taken on a Cary model 14 spectrophotometer. Nuclear magnetic resonance spectra were determined with deuteriochloroform solutions (20–30 mg/0.1 ml) on a Varian A-60 or DP-60 spectrometer. The spectra taken on the DP-60 instrument were calibrated by the audio side-band technique. Camag DF-5 silica gel with calcium sulfate binder was used for thin-layer chromatography (t.l.c.). Reported R_f values are taken from one plate on which all compounds were present, and which was developed in petroleum ether – ethyl acetate (40:60). The separations on this comparison plate are not necessarily the best obtained. Solutions in organic solvents were dried by washing them with saturated sodium chloride solution and then allowing them to stand with anhydrous magnesium sulfate. Petroleum ether refers to the fraction boiling at 60–80°. Microanalyses were carried out by Dr. A. Bernhardt, Mülheim, Germany.

Permanganate Oxidation of Caryophyllene Oxide (I)

The procedure of Treibs was followed (1). To a vigorously stirred solution of 12.3 g (56 mmoles) of caryophyllene oxide and 3.5 ml of water in 130 ml of acetone was added, in portions and with cooling, 26 g of powdered potassium permanganate over a period of 24 h. The reaction mixture was filtered through a sintered-glass funnel, and the colorless filtrate was evaporated to leave 8.5 g of oily product. Thin-layer chromatographic examination of the crude product revealed a spot corresponding to the keto epoxide II, a spot corresponding to both the 119° glycol IV*a* and the 142° glycol III, and a spot at the origin. The crude product was chromatographed on 240 g of Woelm neutral alumina (activity IV). Elution with petroleum ether gave 5.96 g (48%) of the keto epoxide II, m.p. 62–63°, $[\alpha]_D^{22}$ −148° (*c*, 1.95), R_f 0.85 (lit. (14) m.p. 62–63°, $[\alpha]_D$ −134° (chloroform)). Elution with benzene–chloroform (50:50) gave 0.64 g (4.5%) of the mixture of glycols. Recrystallization from benzene – petroleum ether gave a first crop of 220 mg of III which, after further recrystallization from the same solvent pair, had m.p. 138–139° and R_f 0.38 (lit. (1) m.p. 141°, $[\alpha]_D$ −72° (alcohol)). From the mother liquors of the first recrystallization above was obtained a second crop consisting of 118 mg of IV*a* which, after further recrystallization from benzene – petroleum ether, had m.p. 118–119°, $[\alpha]_D^{20}$ −7.2° (*c*, 1.91), $[\alpha]_D^{21}$ −5.3° (*c*, 2.21), $[\alpha]_D^{22}$ −10.4° (*c*, 2.12 in 95% ethanol), and R_f 0.40 (lit. (1) m.p. 119°, $[\alpha]_D$ −1.00° (alcohol)).

Continued elution of the chromatographic column with methanol – acetic acid gave 0.38 g of an oil. Trituration of this oil with chloroform gave 58 mg of white crystals, m.p. 181–182°, whose t.l.c. behavior corresponded to that of the spot remaining at the origin in the crude oxidation product.

A solution of 100 mg (0.39 mmole) of the 119° glycol IV*a* in 5 ml of methanol was treated with 160 mg (0.75 mmole) of sodium metaperiodate in 2 ml of water. After 8 h the clear solution was diluted with water and extracted with ether. Evaporation of the dried ether extract left 87 mg of recovered IV*a*, m.p. 117–118.5°, undepressed on admixture with starting material. The infrared spectrum of the product was identical with that of the 119° glycol and had no trace of carbonyl absorption.

Osmium Tetroxide Oxidation of Caryophyllene Oxide (I)

To a solution of 773 mg (3.04 mmoles) of osmium tetroxide in 1 ml of pyridine and 4 ml of ether was added 660 mg (3.00 mmoles) of pure caryophyllene oxide. The reaction mixture became warm and turned brown. Several days later, when brown crystals had appeared, the reaction mixture was diluted with ether and saturated with hydrogen sulfide. The black precipitate of osmium sulfide which precipitated was removed by filtration through Celite. The yellow filtrate was diluted further with ether, washed with dilute sulfuric acid and dilute potassium bicarbonate solutions, and dried. Evaporation of the solvent left 500 mg of white solid. Two recrystallizations from chloroform – petroleum ether gave 316 mg (41%) of colorless prisms of glycol IV*a*, m.p. 116–117.5°, undepressed on admixture with a sample, m.p. 117–118.5°, from the permanganate oxidation of I.

A second crop of 117 mg of crystals which was obtained from the mother liquors melted over a much wider range, <80–117°, although it gave a single spot corresponding to IV*a* on t.l.c. comparison. These facts together with the optical rotation, $[\alpha]_D^{21}$ −8.05° (*c*, 2.15), and the n.m.r. spectrum of this material show it to be almost pure 119° glycol IV*a* containing no noticeable amount of 142° glycol III. It is estimated that 3–5% of III could easily have been detected in the n.m.r. spectrum. The n.m.r. spectrum of the mother liquors from the second crop of crystals showed that they were also mainly 119° glycol IV*a* containing no detectable amount of 142° glycol III.

Oxidation of Caryophyllene Oxide with the Milas Reagent

The hydrogen peroxide – *t*-butyl alcohol reagent was prepared as described (5) and was assumed to contain 6.32% of peroxide. To 30 ml of the reagent was added a solution of 60 mg of osmium tetroxide in 2 ml of *t*-butyl alcohol, and the mixture was cooled to 0° in an ice–salt bath. Then 3.130 g (14.2 mmoles) of caryophyllene oxide was added in small portions during 5 min. The reaction mixture turned reddish brown and finally became a clear light-yellow after 30 min. It was then stored in a refrigerator at 4° for 96 h, whereupon it was diluted with ether. The organic solution was washed with 40 ml of 10% aqueous ferrous sulfate

Can. J. Chem. Downloaded from www.nrcresearchpress.com by 210.87.254.6 on 09/05/12
For personal use only.

solution to destroy excess peroxide, then with water, and finally dried. Removal of the solvent under reduced pressure left 3.13 g of crude product. Thin-layer chromatography in pure ethyl acetate gave two main spots, one corresponding to authentic keto oxide II and the other corresponding to the 119° and 142° glycol mixture. The crude product was chromatographed on 90 g of Woelm neutral alumina (activity IV) packed in petroleum ether (b.p. 60–80°). Petroleum ether eluted 1.87 g (59%) of keto epoxide II (single t.l.c. spot) which, on recrystallization from petroleum ether, gave long prisms, m.p. 62–63°, $\nu_{max}^{CS_2}$ 1 695 cm^{-1} (C=O). Further elution with benzene–chloroform (50:50) gave 990 mg of glycol fraction. Three recrystallizations from chloroform – petroleum ether gave 600 mg (16%) of glycol IV*a*, m.p. 117–117.5°, $[\alpha]_D^{20}$ −9.5° (*c*, 2.39), $[\alpha]_D^{22}$ −2.27° (*c*, 2.29 in 95% ethanol). The n.m.r. spectrum of the residue from the recrystallization mother liquors did not reveal any peaks from the 142° glycol III.

119° Glycol Diacetate IVb

A solution of 100 mg (0.39 mmole) of IV*a* in 2 ml of pyridine and 1 ml of acetic anhydride was allowed to stand at room temperature for 24 h. The reaction mixture was diluted with water and extracted with ether. The ethereal extracts were washed with dilute sulfuric acid and aqueous sodium bicarbonate, and dried. Evaporation of ether left 131 mg (98%) of colorless glass, $[\alpha]_D^{22}$ +8.8° (*c*, 2.09), $\nu_{max}^{CS_2}$ 1 740 cm^{-1} (ester C=O). A sample was evaporatively distilled at 75–80° and 0.01 mm for analysis.

Anal. Calcd. for $C_{19}H_{30}O_5$ (338.41): C, 67.43; H, 8.92. Found: C, 67.37; H, 8.96.

Chromic Acid – Pyridine Oxidation of 119° Glycol IVa

Chromium trioxide (3.2 g, 32 mmoles) was added to 35 ml of pyridine. To this slurry of the orange complex was added at room temperature a solution of 4.25 g (16.7 mmoles) of the 119° glycol IV*a* in 45 ml of pyridine. The color changed immediately to dark brown. After 24 h the reaction mixture was diluted with methylene chloride and filtered through a short column of Woelm neutral alumina (activity IV) to remove chromium salts. The eluate was evaporated under reduced pressure to leave 3.85 g of crude product. Thin-layer chromatography in ethyl acetate – petroleum ether (85:15) gave two intense spots and two very faint spots after charring. The crude product was chromatographed on a column of 160 g of silica gel (British Drug Houses) packed in chloroform. Elution with ether–chloroform (3:97) gave 175 mg (4%) of colorless crystalline keto aldehyde VII which was not quite free of VI. Four recrystallizations from petroleum ether gave colorless crystals, m.p. 84–86°, $[\alpha]_D$ +65° (*c*, 1.05), R_f 0.90, ν_{max} 2 700 cm^{-1} (CHO) and 1 724 cm^{-1} (broad, —CH=O, 6-ring C=O).

Anal. Calcd. for $C_{15}H_{22}O_3$ (250.32): C, 72.00; H, 8.85. Found: C, 72.30; H, 8.58.

Further elution of the column with the same solvent gave 2.70 g (67%) of colorless viscous liquid VI, $[\alpha]_D^{19}$ +76° (*c*, 2.96), R_f 0.80, $\nu_{max}^{CS_2}$ 3 484 cm^{-1} (OH) and 1 724 cm^{-1} (6-ring C=O). A sample was evaporatively distilled at 55–65° and 0.05 mm for analysis.

Anal. Calcd. for $C_{15}H_{24}O_3$ (252.34): C, 71.39; H, 9.59. Found: C, 71.11; H, 9.36.

The 2,4-dinitrophenyhydrazone was prepared and recrystallized from ethyl acetate – petroleum ether at −60° to give small yellow crystals, m.p. 80–82°.

Anal. Calcd. for $C_{21}H_{28}O_6N_4$ (432.47): C, 58.31; H, 6.52. Found: C, 57.73; H, 6.46.

Oxidation of IV*a* with chromium trioxide in acetic acid was more complex and gave acidic as well as neutral products; therefore it was not investigated further.

Attempted Reductive Cleavage of Hydroxy Ketone VI

The following reactions were carried out with the purpose of cleaving reductively the α-alkoxy group of the ketone VI: (*a*) 225 mg of VI, 5.5 ml acetic anhydride, and 5.25 g of zinc dust were refluxed for 6 h; (*b*) 160 mg of VI, 15 ml of acetic anhydride, and 4 g of zinc dust were refluxed for 48 h; (*c*) 180 mg of VI, 15 ml of propionic anhydride, and 4 g of zinc dust were refluxed for 36 h; (*d*) 185 mg of VI, 1.5 ml of glacial acetic acid, 25 ml of acetic anhydride, and 1 g of magnesium were refluxed for 18 h; (*e*) 210 mg of VI in 10 ml of toluene was added to 200 mg of calcium in 30 ml of liquid ammonia; and (*f*) 125 mg of VI in 25 ml of *sec*-butylamine was treated with 150 mg of potassium. Infrared spectra and t.l.c. examination indicated that, except for reaction *f*, the product of each reaction was starting material VI, or starting material with the primary alcohol acylated, or else the epimeric glycols of structure IV*a*.

Wolff–Kishner Reduction of Hydroxy Ketone VI

To a solution of 885 mg (3.50 mmoles) of hydroxy ketone VI in 30 ml of triethylene glycol were added 10 ml of hydrazine hydrate (85%) and 4.5 g of potassium hydroxide pellets. The mixture was refluxed in an oil bath at 130–135° for 3.7 h, after which the excess hydrazine hydrate was distilled out. The temperature of the oil bath was then raised to 230° and maintained at that temperature for 3 h. The cooled reaction mixture was diluted with water and extracted with ether. The combined ether extracts were washed with water and dried. Evaporation of the solvent left 818 mg of crude product. Thin-layer chromatography in ethyl acetate – petroleum ether (50:50) revealed two intense spots and one faint low-R_f spot. The crude product was chromatographed on 25 g of Woelm neutral alumina (activity IV) packed in petroleum ether. Elution with petroleum ether gave 400 mg (48%) of the normal reduction product IX*a* as a colorless liquid, $[\alpha]_D^{26}$ −19° (*c*, 2.00), R_f 0.85, $\nu_{max}^{CCl_4}$ 3 559 cm^{-1} (OH). A sample was evaporatively distilled at 50–60° and 0.01 mm for analysis.

Anal. Calcd. for $C_{15}H_{26}O_2$ (238.37): C, 75.58; H, 11.00. Found: C, 75.16; H, 10.96.

Further elution of the column with benzene – petroleum ether (75:25) gave 300 mg (36%) of solid reductive elimination product X. Five recrystallizations from petroleum ether gave small colorless needles, m.p. 91–92°, $[\alpha]_D^{24}$ −0.47° (*c*, 1.75), R_f 0.65, $\nu_{max}^{CCl_4}$ 3 390 cm^{-1} (OH) and 850 cm^{-1} (C=CH). Material of m.p. 92–93° could also be obtained by two sublimations of the crude product.

Anal. Calcd. for $C_{15}H_{26}O_2$ (238.37): C, 75.58; H, 11.00. Found: C, 76.02; H, 10.79.

Acetylation of Normal Reduction Product IXa

A solution of 250 mg (1.05 mmoles) of IX*a* in 2 ml of pyridine and 1.5 ml of acetic anhydride was refluxed for 1 h, cooled, and diluted with water. The product was removed by extraction with ether. The ether extracts were washed with dilute sulfuric acid and water. The dried ethereal solution was evaporated at reduced pressure to leave 280 mg (95%) of colorless liquid IX*b*, $[\alpha]_D^{20}$ −12.4° (*c*, 1.90), R_f 0.90, $\nu_{max}^{CCl_4}$ 1 751 cm^{-1} (ester C=O). A sample was evaporatively distilled at 60–65° and 0.05 mm for analysis.

Anal. Calcd. for $C_{17}H_{28}O_3$ (280.39): C, 72.82; H, 10.06. Found: C, 72.32; H, 9.84.

Periodate Cleavage of Reductive Elimination Product X

To a solution of 250 mg (1.05 mmoles) of the 1,2-diol X in 7 ml of methanol was added a solution of 500 mg (2.33 mmoles) of sodium metaperiodate in 5 ml of water. An exothermic reaction occurred, and a voluminous white suspension appeared almost immediately. The reaction mixture was left at room temperature for 9 h, after which it was diluted with water and extracted with ether. The water-washed and dried ethereal solution was evaporated at reduced pressure to yield 200 mg (92%) of a colorless liquid which was chromatographed on 6 g of Woelm neutral alumina (activity IV) packed in petroleum ether. Elution with the same solvent gave 151 mg of colorless liquid XI, $[\alpha]_D^{22}$ −77° (*c*, 2.26), λ_{max}^{EtOH} 235 mμ (ε 440),[6] $\nu_{max}^{CCl_4}$ 1 695 cm^{-1} (9-ring C=O) and 837 cm^{-1} (C=CH), R_f 0.90. During sulfuric acid charring of XI a characteristic mauve color appeared before carbonization. A sample was evaporatively distilled at 65–70° and 0.05 mm for analysis.

Anal. Calcd. for $C_{14}H_{22}O$ (206.32): C, 81.50; H, 10.75. Found: C, 81.37; H, 10.69.

Epoxidation of Unsaturated Ketone XI

To a solution of 103 mg (0.50 mmole) of XI in 5 ml of ether cooled to 0° was added 40 ml of a solution of monoperphthalic acid in ether (equivalent to 0.50 mmole of peracid). The reaction mixture was kept in the refrigerator for 60 h, after which it gave a negative starch–iodide test. Then the precipitated phthalic acid was removed by filtration. The filtrate was washed with sodium bicarbonate solution and with water. The dried ethereal solution was evaporated at reduced pressure to leave 95 mg of a mixture of the *cis* keto oxides XII*a* and XII*b*, which solidified when chilled. Two recrystallizations from petroleum ether gave 42 mg of colorless prisms of XII*b*, m.p. 75–76°, $[\alpha]_D^{15}$ −13.8° (*c*, 1.78 in methanol), R_f 0.80, $\nu_{max}^{CCl_4}$ 1 695 cm^{-1} (9-ring C=O). The mixed melting point with the authentic sample of isocaryophyllene keto epoxide-*b*, m.p. 77.5–78°, prepared as described below was undepressed. The infrared spectra of the two samples were identical.

Anal. Calcd. for $C_{14}H_{22}O_2$ (222.32): C, 75.63; H, 9.97. Found: C, 75.17; H, 10.01.

Isocaryophyllene (cis-Caryophyllene) (with V. Dave)

The procedure of Schreiner and Kremers (17) was followed in part. A solution of 22 g of combined caryophyllene fractions ($[\alpha]_D$ −9 to −9.5°) in 60 ml of petroleum ether (b.p. 35–60°) was stirred at room temperature with 25 ml of a saturated aqueous solution of sodium nitrite. To this suspension was added slowly 25 ml of glacial acetic acid. The reaction mixture became blue and then light green. After 25 min the solution was chilled and kept below 0° overnight. The reaction mixture was allowed to come to room temperature and was filtered to remove some crystalline material. The filtrate was diluted with water and extracted with ether. The dark-green ethereal solution was washed with several portions of 10% aqueous potassium hydroxide and with water. The ether was removed from the dried solution by distillation to leave 19 g of green oil. This residue was steam-distilled until the oily droplets in the distillate began to be denser than water. Extraction of the steam-distillate with ether yielded 9.89 g of yellow oil after removal of the ether. Fractional distillation through a 1 m Nester and Faust spinning spiral column gave four fractions totalling 4.8 g (22%) of colorless isocaryophyllene, b.p. 116° at 8.5 mm, $[\alpha]_D^{25.5}$ −22.2° (neat) (lit. (18) b.p. 125.5° at 14.5 mm, $[\alpha]_D^{19}$ −26.1° (neat)); ν_{max}^{neat} 3 060 cm^{-1} (vinyl H), 1 635 cm^{-1} (C=C), 885 cm^{-1} (C=CH$_2$), and 836 cm^{-1} (C=CH). Repetition of the isomerization process on this material did not change the optical rotation. The isocaryophyllene was 96.5% pure by vapor-phase chromatography, and the 3.5% of impurity was not caryophyllene or α- or β-humulene. On a 2 m × ¼ inch column of Chromosorb P (coated with silver nitrate – Carbowax 20M, 10% of each) at 162°, the compounds had the following retention times: isocaryophyllene, 8.0 min; impurity, 5.5 min; and caryophyllene, 8.8 min.

Authentic Isocaryophyllene Keto Epoxide-b (XIIb)

The procedure of Ramage and Whitehead (19) was followed. A solution of 4.03 g (19.7 mmoles) of isocaryophyllene in 25 ml of ether was cooled to 0° and treated with 65 ml (20 mmoles) of an ethereal solution of monoperphthalic acid. The reaction mixture was kept at 4° for 48 h, after which it was filtered to remove precipitated phthalic acid. The filtrate was washed successively with aqueous sodium bicarbonate and water

[6]*This chromophore is apparently an example of a σ-coupled p-electron system (20).*

Can. J. Chem. Downloaded from www.nrcresearchpress.com by 210.87.254.6 on 09/05/12
For personal use only.

before it was dried. Evaporation of the ether left 3.72 g of a residue which partially crystallized. Trituration of the crude product with cold petroleum ether and filtration left 1.10 g of crystalline material which was recrystallized once from petroleum ether to yield colorless crystals of isocaryophyllene oxide-*a* (XIII*a*), m.p. 73–75°, $[\alpha]_D^{20}$ −7.3° (*c*, 3.30 in methanol), R_f 0.90 (lit. (19) m.p. 77°, $[\alpha]_D$ −5° (methanol)).

The oily mother liquor, after separation of the crystalline isocaryophyllene oxide-*a*, contained mainly isocaryophyllene oxide-*b* (XIII*b*), and it was oxidized directly. To a solution of 1.31 g of the material and 1 ml of water in 25 ml of acetone was added 4.0 g of powdered potassium permanganate. The reaction was worked up as described for the oxidation of caryophyllene oxide above. The crude oily product (1.05 g) was chromatographed on 35 g of Woelm neutral alumina (activity IV) and yielded 80 mg[7] of isocaryophyllene keto epoxide-*b* (XII*b*), which had m.p. 77.5–78° and $[\alpha]_D^{20}$ −13.1° (*c*, 1.91 in methanol) (lit. (19) m.p. 78–79°, $[\alpha]_D$ −13° (methanol)) after two recrystallizations from petroleum ether.

Isomerization of 142° Glycol III

Basic Catalysis

A solution of 80 mg of III, m.p. 138–139°, and 250 mg of potassium hydroxide in 5 ml of methanol was refluxed for 168 h. Dilution with water and extraction with ether yielded 65 mg of a white solid, m.p. 114–117°, whose n.m.r. spectrum and t.l.c. behavior were identical with those of the 119° glycol IV*a*. Recrystallization from chloroform – petroleum ether raised the melting point to 116–117°, undepressed on admixture with authentic 119° glycol IV*a*.

When the isomerization was allowed to proceed for only 19 h, the reaction was incomplete and the product was a mixture of III and IV*a* (n.m.r. spectrum).

Acid Catalysis

A solution of 14 mg of III, m.p. 138–139°, and 2 ml of 5% aqueous sulfuric acid in 3 ml of acetone was refluxed for 2 h. Dilution with water and extraction with ether yielded 12 mg of colorless solid, m.p. 110–113°. Thin-layer chromatographic examination revealed only traces of two less-polar impurities besides the main III–IV*a* spot. Recrystallization from petroleum ether raised the melting point to 117–118°, undepressed on admixture with authentic 119° glycol IV*a*. Thin-layer chromatographic examination of the recrystallized product gave a single spot corresponding to III–IV*a*.

The melting point of a control mixture of III and IV*a* was depressed.

REFERENCES

1. W. Treibs. Ber. **80**, 56 (1947).
2. F. Šorm, L. Dolejš, and J. Plíva. Collection Czech. Chem. Commun. **15**, 186 (1950).
3. E. W. Warnhoff. Can. J. Chem. **42**, 1664 (1964).
4. R. Criegee, E. Höger, G. Huber, P. Kruck, F. Marktscheffel, and H. Schellenberger. Ann. **599**, 81 (1956).
5. N. A. Milas and S. Sussman. J. Am. Chem. Soc. **58**, 1302 (1936); **59**, 2345 (1937).
6. R. Criegee and W. Richter. Ann. **522**, 83 (1936).
7. L. M. Jackman. Applications of nuclear magnetic resonance spectroscopy in organic chemistry. Pergamon Press, Oxford, England. 1959. p. 55.
8. R. B. Woodward, F. Sondheimer, D. Taub, K. Heusler, and W. M. McLamore. J. Am. Chem. Soc. **74**, 4225 (1952).
9. E. W. Warnhoff and W. C. Wildman. J. Am. Chem. Soc. **82**, 1474 (1960).
10. J. H. Chapman, J. Elks, G. H. Phillipps, and L. J. Wyman. J. Chem. Soc. 4344 (1956).
11. R. A. Benkeser, C. Arnold, R. F. Lambert, and O. H. Thomas. J. Am. Chem. Soc. **77**, 6042 (1955).
12. N. J. Leonard and S. Gelfand. J. Am. Chem. Soc. **77**, 3269 (1955).
13. E. Klein, H. Farnow, and W. Rojahn. Ann. **675**, 75 (1964).
14. D. H. R. Barton and A. S. Lindsey. J. Chem. Soc. 2988 (1951).
15. D. H. R. Barton, T. Bruun, and A. S. Lindsey. J. Chem. Soc. 2210 (1952).
16. R. E. Parker and N. S. Isaacs. Chem. Rev. **59**, 737 (1959).
17. O. Schreiner and E. Kremers. Pharm. Arch. **2**, 282 (1899).
18. E. Deussen and A. Lewisohn. Ann. **359**, 245 (1908).
19. G. R. Ramage and R. Whitehead. J. Chem. Soc. 4336 (1954).
20. R. C. Cookson, J. Henstock, and J. Hudec. J. Am. Chem. Soc. **88**, 1060 (1966).

[7]*The low yield is due to loss during manipulation.*

Can. J. Chem. Downloaded from www.nrcresearchpress.com by 210.87.254.6 on 09/05/12
For personal use only.

Can. J. Chem. Downloaded from www.nrcresearchpress.com by 210.87.254.105 on 09/05/12
For personal use only.

STUDIES ON CHITAN (β-(1 → 4)-LINKED 2-ACETAMIDO-2-DEOXY-D-GLUCAN) FIBERS OF THE DIATOM THALASSIOSIRA FLUVIATILIS HUSTEDT.

II. PROTON MAGNETIC RESONANCE, INFRARED, AND X-RAY STUDIES[1]

MICHAEL FALK, D. G. SMITH, J. MCLACHLAN, AND A. G. MCINNES
Atlantic Regional Laboratory, National Research Council, Halifax, Nova Scotia

Received December 7, 1965

ABSTRACT

The extracellular fibers attached to the diatom *Thalassiosira fluviatilis* have been shown to be pure β-(1 → 4)-linked 2-acetamido-2-deoxy-D-glucan. This polysaccharide was given the systematic trivial name chitan to distinguish it from chitin, which is not a chemically distinct species and which has a radically different X-ray diffraction pattern and infrared spectrum. Proton magnetic resonance studies on the acid hydrolysis of chitan have established that the hydrolysis occurred in three distinct steps: (*a*) the degradation of the polysaccharide to smaller polymeric units, (*b*) the production of *N*-acetylglucosamine from the latter, and (*c*) the conversion of *N*-acetylglucosamine into glucosamine and acetic acid. X-ray and infrared studies have shown that chitan has a different macrostructure from that of arthropod chitin. Chitan is completely crystalline and can be converted irreversibly into a form indistinguishable from that of chitin by treatment with hot aqueous lithium thiocyanate. Boiling chitan in water converts it into a second crystalline modification, possibly a hydrate, which can be reconverted into the starting material by drying *in vacuo*. The exceptionally sharp infrared spectrum of chitan allows a more unequivocal assignment of a number of bands common to chitan and chitin, and provides information about the nature of the bands at 1 626 and 1 656 cm^{-1} in the spectrum of chitin. The correlation of the bands in the region of 840 to 890 cm^{-1} with the configuration at the anomeric center of glycopyranose derivatives is discussed.

INTRODUCTION

The biological importance of chitin, which is widely distributed among invertebrates and most fungi, is reflected in the large number of publications on this material since it was discovered by Braconnot in 1811 (1). Work on chitin falls into three broad categories. Firstly, there are investigations on the isolation, composition, and structure of chitin. Secondly, there are those dealing with its physical properties and macrostructure as determined largely by infrared and X-ray diffraction techniques. Finally, there are studies of the biochemical and biological role of chitin. Previous work has been reviewed (2–4).

We have previously described the isolation of fibers from *Thalassiosira fluviatilis* (5) and other diatoms (6) which we claimed were composed of *pure, homogeneously crystalline* β-(1 → 4)-linked 2-acetamido-2-deoxy-D-glucan. The polysaccharide was given the trivial name chitan to conform with modern nomenclature, and to distinguish it from chitin. Since most carbohydrate chemists seem to regard the above structure as being synonymous with chitin, an explanation for our choice of name is necessary. A critical survey of the literature offers no experimental justification for assuming, as some workers have (3, 4, 7), that chitin has the above composition. Indeed, all relevant studies on this material have actually established that it is a mixture of polysaccharides which contain variable amounts of *N*-acetylglucosamine and glucosamine (2, 8, 9). It is interesting to note that, although the presence of the latter is attributed to chemical degradation with a strong acid and (or) base, Giles (9) has found that even the use of enzymatic procedures to remove the protein associated with chitin gives a product which has been calculated to have 12.5% glucosamine. A striking feature of all preparations of chitin, moreover, is the

[1]*Issued as N.R.C. No. 9096.*

deviation of the elemental analyses from the theoretical values (2, 9). Some workers have drawn attention to these facts (2, 9), and have suggested that "native" chitin may always contain considerable amounts of glucosamine. In fact, Richards (10) goes so far as to question whether chitin can really be considered a "natural" chemical entity since it may be a degradation product of the various complexes in which it exists. Furthermore, any structure for chitin based on X-ray or infrared studies should be accepted with considerable reservation (see the section on macrostructure). Consequently, we feel that the name chitin should be reserved as a group name for those polysaccharides which contain glucosamine in addition to *N*-acetylglucosamine. The polysaccharide which we have isolated has a uniform composition, and its X-ray diffraction pattern and infrared spectrum are radically different from those of chitin. Consequently, we felt that this well-defined substance required a specific well-defined name, and for the sake of brevity the trivial name chitan was selected in addition to the somewhat lengthy systematic name.

In this communication we report the results of chemical, infrared, X-ray diffraction, and proton magnetic resonance (p.m.r.) studies which establish the composition and structure of chitan, and provide information on its macrostructure and the nature of the difference between this polysaccharide and arthropod chitin. Attempts to prepare oriented samples (fibers and films) suitable for future X-ray crystallographic and polarized infrared studies have been undertaken. Such studies should allow a more complete elucidation of the macrostructure of chitan.

EXPERIMENTAL

Materials

The methods used for the production and isolation of chitan fibres have been described in detail elsewhere (5). For elemental analysis the fibers were dried at 100° for 48 h under reduced pressure.

Anal. Calcd. for $(C_8H_{13}O_5N)_n$: C, 47.29; H, 6.45; N, 6.89. Found: C, 47.43; H, 6.40; N, 6.84.

Crustacean chitin was purchased from Brickman Co., Montreal. 2-Acetamido-2-deoxy-D-mannose (*N*-acetylmannosamine) had been synthesized previously in this laboratory (11). 2-Acetamido-2-deoxy-D-glucose (*N*-acetylglucosamine) was prepared from D-glucosamine hydrochloride (12).

Hydrolysis of Chitan at 40°

Chitan (50 mg) was weighed into a p.m.r. sample tube and triturated with 10.2 *N* HCl in D_2O (0.50 ml). A homogeneous solution was obtained when the mixture was warmed to 35°. The sample tube was capped with a "caplug", which supported a sealed capillary tube containing the external standard tetramethylsilane in $CDCl_3$, and was subsequently transferred to the probe of a Varian A60 nuclear magnetic resonance spectrometer equipped with a V-6057 variable-temperature accessory. Controlled hydrolysis of the chitan sample was carried out at 40°, and the progress of the reaction was followed by scanning the p.m.r. spectrum periodically. After an interval of 60 h glucosamine hydrochloride crystallized from the solution. This caused the p.m.r. spectrum to broaden, and prevented further quantitative measurements. After several days at 40° the mixture was taken to dryness under reduced pressure. The crystalline residue was dissolved in a minimum amount of distilled water, and ethanol and ether were added to induce crystallization. The p.m.r. and infrared spectra of the crystalline product (yield ≈70%) and an authentic sample of glucosamine hydrochloride were identical, and the former compound had $[\alpha]_D^{25}$ +72.0°, which is in excellent agreement with the reported values (13). Assignments of the signals for the products of hydrolysis of chitan were made by comparing the p.m.r. spectra with those obtained for authentic mixtures of *N*-acetylglucosamine, glucosamine, and acetic acid.

Hydrolysis of Chitan at 80°

The general procedure used in these experiments was the same as that described for the experiments at 40°. However, 8.2 *N* HCl in D_2O was used for the hydrolysis, and under these conditions no precipitation of glucosamine hydrochloride occurred as the reaction progressed. The hydrolysis of chitan was carried out in a sealed p.m.r. sample tube, and the reaction solution contained sodium 3-trimethylsilyl-1-propane sulfonate as an internal standard.

Hydrolysis of Chitin at 40° and 80°

The hydrolysis experiments described above for chitan were repeated for crustacean chitin under identical experimental conditions.

Can. J. Chem. Downloaded from www.nrcresearchpress.com by 210.87.254.105 on 09/05/12
For personal use only.

Specific Rotations of Chitan and Chitin

Chitan had $[\alpha]_D^{20}$ −19° (*c*, 1.07 in 10 *N* HCl) and crustacean chitin had $[\alpha]_D^{20}$ −21° (*c*, 1.03 in 10 *N* HCl). Both of these rotations were determined 30 min after the addition of the acid. Chitan immediately formed a gel in the presence of acid and had to be heated at 40° for a longer period (≈4 min) than chitin (≈0.5 min) before it dissolved. Considerable degradation of the polysaccharide had undoubtedly occurred during preparation of the solutions, and the rotations are only reported for the purpose of comparison. The change in $[\alpha]_D$ with time reached a plateau after approximately 100 h, at which time both solutions had $[\alpha]_D^{20}$ +56°. It was not possible to follow the hydrolysis to completion (glucosamine hydrochloride has $[\alpha]_D^{20}$ +72° in 10.2 *N* HCl) because the solution became highly colored and material precipitated.

Formation of Chitosan from Chitan

Chitan mats were treated with a boiling 50% potassium hydroxide solution for 1 h. The precipitated chitosan was removed from the solution, subsequently washed with dilute hydrochloric acid, distilled water, and acetone, and finally dried over phosphorus pentoxide under reduced pressure.

Infrared Technique

The chitan was studied in the form of unoriented fibrous mats prepared as described previously (5). The thickness of the mats was about 2.5 μ (calculated from their diameter (3.8 cm), their weight (4 mg), and the density of chitin (1.6 g/cm³)). The mats possessed sufficient mechanical strength to withstand boiling in water and various chemical treatments without disintegration. After the various chemical manipulations the mats were washed thoroughly with water and acetone and finally air-dried. More thorough drying in vacuum over phosphorus pentoxide had no further effect on the spectrum. The hydrogen–deuterium exchange was studied by immersing a mat in D_2O at various temperatures for various periods of time. The mats were then washed with acetone and air-dried.

Crustacean chitin, chitosan, *N*-acetylglucosamine, and *N*-acetylmannosamine were studied with potassium bromide pellets and Nujol mulls. The last two compounds were also studied as vitreous films prepared by the evaporation of drops of aqueous solution on silver chloride plates.

The infrared spectra were recorded from 4 000 to 250 cm^{-1} on a Perkin–Elmer model 521 spectrophotometer equipped with a frequency marker. The calibration of the instrument was accurate to 1 cm^{-1} below 2 000 cm^{-1} and to 2 cm^{-1} above 2 000 cm^{-1}. All frequencies reported are the average of at least three recordings.

X-ray Diffraction Technique

Measurements on chitan and lithium thiocyanate treated chitan were carried out on mats of fibers stacked to a thickness of 40 μ, whereas crustacean chitin was studied as a powder sprinkled to about the same thickness on a thin film of Mylar. Front-reflection patterns were obtained with CuK_α or CoK_α radiations, using a Laue camera with a rotating specimen holder (specimen to film distance, 3.75 cm). Thin aluminium foils were used for calibration.

RESULTS AND DISCUSSION

Structure of Chitan

In contrast to the chemical and (or) enzymatic procedures used in the preparation of chitin, the purification of chitan fibers was accomplished by a simple solvent wash followed by drying them *in vacuo*. The elemental analysis of these fibers then conformed to the molecular formula for poly-*N*-acetylglucosamine, namely $(C_8H_{13}O_5N)_n$.

Proton magnetic resonance studies on the acid hydrolysis of chitan, with an internal standard, enabled the number of hydrogen atoms directly attached to the carbon of each type in the repeating unit to be determined, and at the same time provided useful information on the mechanism of hydrolysis. It was necessary to carry out the hydrolysis in deuterium oxide, because the intense side bands of the signal from the hydroxyl protons of water obscured the p.m.r. spectrum of chitan.

The signals in the spectrum of chitan (Fig. 1A) could be assigned to the anomeric hydrogen on C-1 (τ 4.80) of each repeating unit, the four hydrogens in the pyranose ring together with those of the two methylene hydrogens at C-6 (τ 5.70), and the three methyl hydrogens of the *N*-acetyl group at C-2 (τ 7.10). Slight hydrolysis of chitan had also given rise to smaller signals for the methyl hydrogens of acetic acid (τ 7.47) and the α-anomeric hydrogens of *N*-acetylglucosamine (τ 4.25). The signal for the β-anomeric hydrogen of the latter was hidden under the envelope at τ 4.80, and that for the anomeric

Can. J. Chem. Downloaded from www.nrcresearchpress.com by 210.87.254.105 on 09/05/12
For personal use only.

hydrogens of glucosamine, which should have one-third the intensity of the signal at τ 7.47, was too weak to be observed. Figure 1B effectively illustrates the conversion of chitan into glucosamine and *N*-acetylglucosamine. The signals for the α-anomeric hydrogens of *N*-acetylglucosamine and glucosamine were doublets centered at τ 4.25 (spacing 2.4 c.p.s.) and τ 4.04 (spacing 3.6 c.p.s.), whereas the corresponding doublets for the β-anomers occurred at higher field and were centered at τ 4.65 (spacing 7.6 c.p.s.) and τ 4.49 (spacing 8.0 c.p.s.). These assignments were based on the spectra of the pure compounds and the hydrolysis products of an authentic sample of *N*-acetylglucosamine (see Fig. 1C). The pyranose ring and methylene hydrogens (on C-6) of glucosamine and its *N*-acetyl derivative appeared at higher field with an average τ value of 5.72, and the methyl hydrogens of the *N*-acetyl group and acetic acid could be assigned to the sharp singlets at τ 7.10 and τ 7.48. No signals were obtained for any hydroxyl protons because of exchange with deuterium oxide. It should be noted that the p.m.r. evidence established that *N*-acetylglucosamine, glucosamine, and acetic acid were the *only* products of hydrolysis, and the use of an internal standard established that 1 mole of acetic acid was produced per $C_8H_{13}O_5N$ repeating unit. Glucosamine hydrochloride could also be isolated in an excellent yield after the hydrolysis reaction was complete. Results obtained for the hydrolysis of crustacean chitin under the same experimental conditions were identical with those reported above, except that the yield of acetic acid was significantly lower than the theoretical amount.

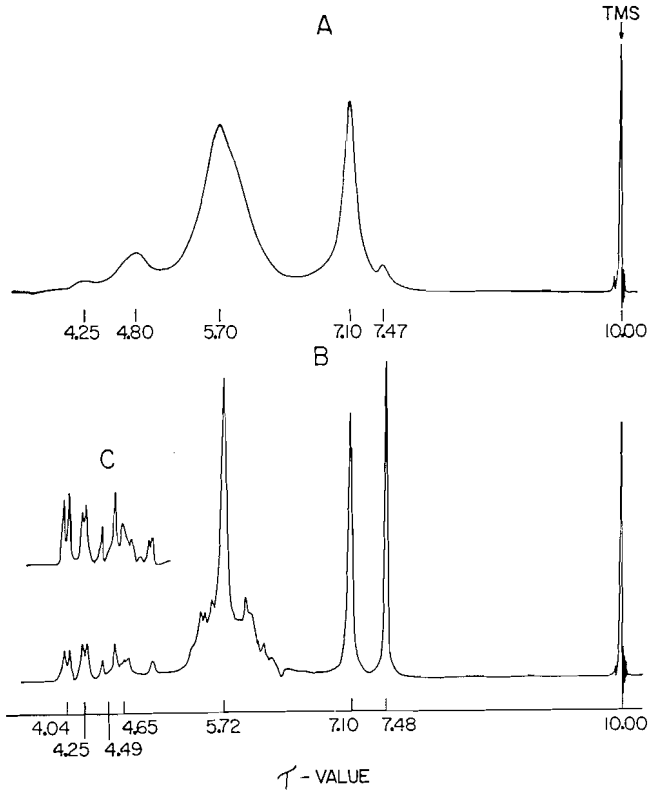


FIG. 1. The p.m.r. spectra of chitan after 1.7 h (A) and 32 h (B) in 10.2 *N* HCl at 40°. A section of the spectrum from the hydrolysis products (ca. 4 h at 50°) of an authentic sample of *N*-acetylglucosamine is shown in the insert (C). TMS = tetramethysilane.

Can. J. Chem. Downloaded from www.nrcresearchpress.com by 210.87.254.105 on 09/05/12
For personal use only.

Can. J. Chem. Downloaded from www.nrcresearchpress.com by 210.87.254.105 on 09/05/12
For personal use only.

The breadth of the signal for the anomeric hydrogen in chitan (τ 4.80; see Fig. 1A) obscured the spin–spin coupling with the neighboring hydrogen on C-2, and did not permit the configuration at the anomeric position to be derived from the magnitude of the coupling constant (14). Nevertheless, the data in the literature (15, 16) and experience in this laboratory suggest that under comparable experimental conditions the chemical shifts of anomeric hydrogens in oligosaccharides and polysaccharides containing a glycopyranose repeating unit occur within approximately ± 0.2 p.p.m. of the corresponding α- or β-anomeric hydrogens of the free glycopyranoses. In contrast, the chemical shifts of the α- and β-anomeric hydrogens differ by 0.4 to 1.0 p.p.m. Also, equatorial anomeric hydrogens usually occur at lower field than the corresponding axial hydrogens (17). The signals for the axial anomeric hydrogens of β-glucosamine and β-*N*-acetylglucosamine occur at higher field (τ 4.49 and τ 4.65) than those for the corresponding α-anomers. It can be concluded that the signal for the anomeric hydrogen of chitan at τ 4.80 indicates an axial orientation for this hydrogen, and therefore a β-configuration at the anomeric center of each repeating unit. Chitin is known to have a β-configuration at the anomeric center of each repeating unit. The identity of the chemical shifts for the anomeric hydrogens of crustacean chitin and chitan therefore provides supporting evidence for a β-configuration in the latter. The optical rotation data for chitan and crustacean chitin are also indicative of a β-D-configuration in these compounds (3, p. 379). These data establish that chitan is β-linked 2-acetamido-2-deoxy-D-glucan.

The only structural feature of chitan which has still to be considered is the type of linkage between the *N*-acetylglucosamine residues. It was found experimentally, however, that the p.m.r. spectra of chitan and crustacean chitin were superposable except for differences in the intensity of the signals for the methyl hydrogens of the *N*-acetyl groups. The identity of the chemical shifts for the hydrogens in the two polysaccharides provides strong evidence that they have the same type of linkage. It should be remembered that slight degradation and deacetylation of chitan had occurred before its p.m.r. spectrum was recorded (see Fig. 1A). In other words, chitan had been degraded by dissolving it in concentrated hydrochloric acid. Further evidence that the linkage in chitan is the same as in chitin was obtained by infrared studies. When chitan was treated with strong base it was converted into a material which gave a characteristic van Wisselingh iodine color test for chitosan (8), and an infrared spectrum identical with that reported (18) for the latter. Moreover, hot aqueous lithium thiocyanate converted chitan into a material giving an infrared spectrum indistinguishable from that of crustacean chitin (see the section on macrostructure). Chitosan and chitin are considered to be β-(1 $\rightarrow$ 4)-linked (3, p. 380; 19), although we believe that the type of linkage has not been elucidated unambiguously. Since the experimental conditions for the conversion of chitan into chitin and chitosan could not result in changes in the anomeric configuration or type of linkage, and keeping in mind our reservations on the validity of the proof for the type of linkage, we have assigned the structure β-(1 $\rightarrow$ 4)-linked 2-acetamido-2-deoxy-D-glucan to chitan.

Chitan remained unchanged when heated to a temperature of 300°. It has a molecular weight of approximately 3×10^7, as calculated from the average length of 80 μ for the microfibers (5) and an assumed value of 10 Å for the length of the repeating unit in the polysaccharide as compared with 10.4 Å for cellulose. Chitan will therefore contain approximately 8×10^4 repeating units if the polymer chain is fully extended. Chitan does not dissolve in any organic solvents.

Mechanism of Hydrolysis of Chitan

Some information on the mechanism of hydrolysis of chitan can be deduced from the data in Fig. 2. The rate of production of *N*-acetylglucosamine was the same as the rate of disappearance of polymer over the initial reaction period of 4.5 h. At this time, the *N*-acetylglucosamine concentration was at a maximum, and thereafter showed a gradual decrease with time because the rate of hydrolysis to glucosamine and acetic acid exceeded the rate of formation from chitan. A maximum concentration of *N*-acetylglucosamine was

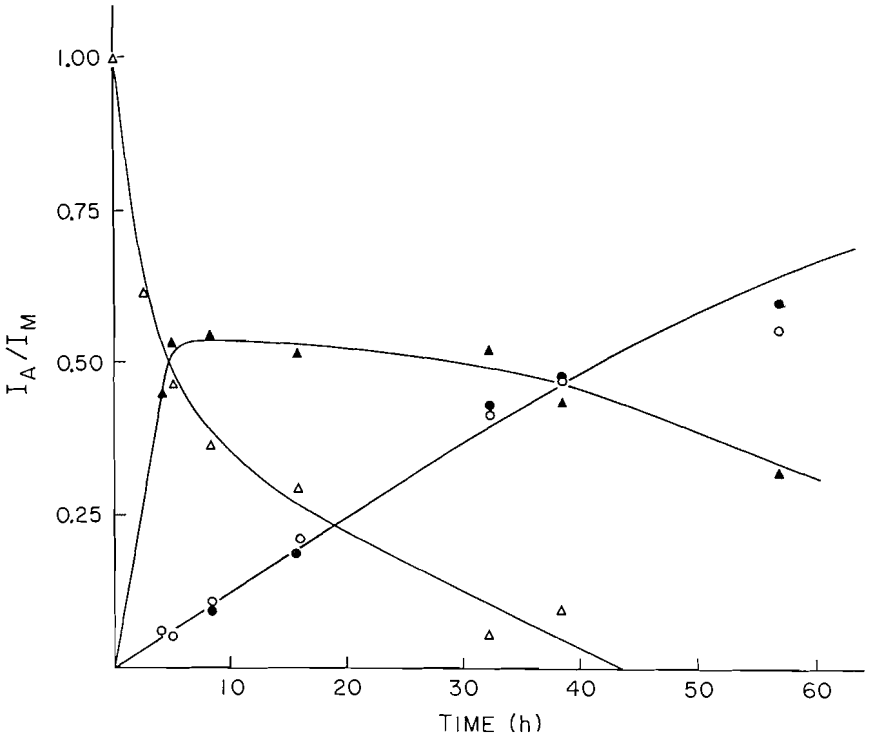


FIG. 2. Rate curves, calculated from the p.m.r. data, for the hydrolysis of chitan $((C_8H_{13}O_5N)_n)$ in 10.2 *N* HCl at 40°, showing the disappearance of chitan (△) and the formation of *N*-acetylglucosamine (▲), glucosamine (●), and acetic acid (○). The curves are a plot of I_A/I_M against time, where I_A represents the total anomeric hydrogen for each carbohydrate (or the methyl hydrogens of acetic acid), and I_M the total methyl hydrogens present in the acetic acid and *N*-acetyl groups.

obtained when 50% of the polymer was hydrolyzed. The rates of production of acetic acid and glucosamine, on the other hand, were the same within experimental error, and initially were considerably less than the rate of appearance of *N*-acetylglucosamine. It can be concluded, therefore, that most of the acetic acid was produced by the hydrolysis of *N*-acetylglucosamine, rather than by direct hydrolysis of the *N*-acetyl groups in the polymer. The data also established that good yields of *N*-acetylglucosamine cannot be obtained by controlled acid hydrolysis of chitan (or chitin).

It was observed experimentally that the p.m.r. signals for chitan sharpened appreciably after a short reaction time, and that this change in the spectrum was accompanied by a decrease in the viscosity of the reaction solution. The latter effect was undoubtedly due to the polymer chain being hydrolyzed indiscriminately along the chain length, with the

Can. J. Chem. Downloaded from www.nrcresearchpress.com by 210.87.254.105 on 09/05/12
For personal use only.

production of smaller polymeric units, and it is reasonable to conclude that the *N*-acetylglucosamine units which were being produced during hydrolysis were not being removed by preferential hydrolysis at the end of the polymer chain. These results are in agreement with those obtained by other workers, who followed the hydrolysis of chitin by a colorimetric procedure (20). The direct observation of the p.m.r. spectrum not only offers the advantage of following the reaction with more precision, but also enables all of the components in the system to be observed and analyzed simultaneously.

Macrostructure of Chitan

Comparison of Chitan and Crustacean Chitin

The infrared spectrum of chitan is shown in Fig. 3, and its X-ray diffraction pattern in Fig. 4. Chitan has extremely sharp infrared absorption bands and X-ray diffraction rings.

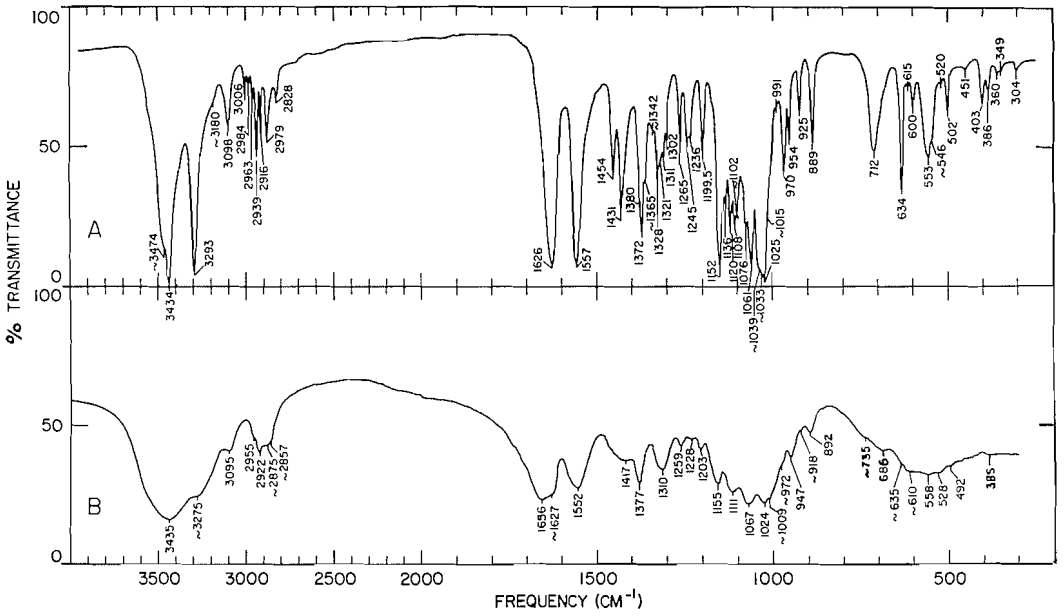


FIG. 3. The infrared absorption spectrum of chitan (A) and chitin (B).

Such sharpness is rare in polymers of biological origin and is characteristic of pure, crystalline compounds. In contrast, the far more diffuse infrared spectra and X-ray diffraction patterns of chitin point to a much less highly ordered macrostructure. The differences in the frequencies and intensities of the infrared bands (Fig. 3) and in the positions and intensities of the X-ray diffraction rings (Table I) show that chitan must have a macrostructure different from that of crustacean chitin.

It should be noted that the infrared spectrum of chitin reflects mainly the macrostructure of the fully *N*-acetylated regions, because the spectral contributions of a small number of glucosamine residues are lost in the presence of broad and intense bands caused by the bulk of the polysaccharide. The X-ray diffraction pattern of chitin, on the other hand, is obtained exclusively from the more highly ordered regions of the polysaccharide, which need not be representative of the bulk of the sample. Because of these limitations, previous conclusions about the macrostructure of chitin derived from X-ray diffraction and infrared studies (21–27) are suspect, and in any case are not relevant to chitan.

Can. J. Chem. Downloaded from www.nrcresearchpress.com by 210.87.254.105 on 09/05/12
For personal use only.



FIG. 4. The X-ray diffraction pattern of chitan obtained with CoK_{α} radiation.

It is possible to transform chitan into a form with an infrared spectrum and X-ray diffraction pattern indistinguishable from those of crustacean chitin. Such a transformation occurred when chitan mats were immersed in hot aqueous lithium thiocyanate (50%). The transformation was completed within a few seconds and was irreversible. Longer immersion of the mats in hot or cold aqueous lithium thiocyanate, immersion of the lithium thiocyanate treated mats in hot or cold water or organic solvents, and drying *in vacuo* at temperatures up to 200° caused no further spectral changes. A similar transformation also occurred when chitan was immersed in hot aqueous solutions of strong acids and alkalis, though more slowly than in lithium thiocyanate solutions. Immersion of chitan in hot concentrated aqueous solutions of lithium iodide, lithium perchlorate, urea, and other strong denaturing agents had no effect on chitan. It appears, therefore, that the transformation may involve some deacetylation in addition to a complete destruc-

Can. J. Chem. Downloaded from www.nrcresearchpress.com by 210.87.254.105 on 09/05/12
For personal use only.

TABLE I

X-ray reflections (Å) of chitan, lithium thiocyanate treated chitan, and crustacean chitin

Chitan	Lithium thiocyanate treated chitan	Crustacean chitin
9.01 vw*		
	8.89 m	9†
6.85 vw	6.84 m	6.8 w
5.16 m	5.12 w	5.1 vw
4.80 vs		
	4.58 vs	4.57 s
4.43 vs		
		4.24 vw
4.05 m		
3.74 vw	3.75 m	3.73 vw
3.53 m		
3.35 vw	3.35 vs	3.37 s
3.22 s		
	3.00 vw	3.01 vw
2.97 vw		
2.75 m	2.75 w	2.76 vw
2.59 vw		
	2.55 m	2.55 vw
2.48 vw		
2.39 w		
2.32 vw		
2.24 vw	2.25 w	
2.17 vw		

*Abbreviations: vw, very weak; w, weak; m, medium; s, strong; vs, very strong.
†Overlaid by a broad reflection from Mylar.

tion of the macrostructure of chitan. Acids and alkalis are known to cause deacetylation, and aqueous lithium thiocyanate, which has a pH of about 9, may have a similar effect.

The conclusion that chitan, but not chitin, is completely crystalline is supported by hydrogen–deuterium exchange experiments. When mats of chitan were immersed in deuterium oxide at 21°, only about 25% of the hydroxyl protons and 6% of those in the NH groups were exchanged after 1 month. The lithium thiocyanate treated mats exchanged many times faster. Analogous experiments with cellulose (28) have established that the rate of deuterium exchange is much faster for amorphous than for crystalline samples.

OH Stretching Bands

The infrared spectrum of chitan shows two absorption bands at 3 474 and 3 434 cm^{-1} caused by the OH stretching vibrations of the two hydroxyl groups in each *N*-acetylglucosamine residue. Deuterium exchange caused a slow diminution of both bands at about the same rate, with the concomitant appearance of the bands of the two corresponding OD vibrations at 2 565 and 2 545 cm^{-1}. The absence of absorption above 3 500 cm^{-1} in chitan shows that there are no "free" hydroxyl groups, i.e. that all of the hydroxyl groups in chitan are involved in hydrogen bonds.

The sharpness of the OH stretching bands is particularly remarkable. The half-widths of the OH bands (about 20 cm^{-1}) and of the corresponding OD bands (about 10 cm^{-1}) are smaller by an order of magnitude than those of OH bands in the spectra of most biopolymers. Indeed, *these may be the sharpest such bands ever observed for hydrogen-bonded OH groups at room temperature.* The sharpness of the OH absorption bands shows that each type of hydroxyl group in chitan, in contrast to chitin, has an identical environment.

Can. J. Chem. Downloaded from www.nrcresearchpress.com by 210.87.254.105 on 09/05/12
For personal use only.

Can. J. Chem. Downloaded from www.nrcresearchpress.com by 210.87.254.105 on 09/05/12
For personal use only.

Amide Group Bands

Amide groups in chitan give sharp infrared bands at 3 293, 1 557, and 712 cm^{-1} which are due to the NH stretching vibration, the amide II vibration (largely the in-plane NH bending), and the amide V vibration (largely the out-of-plane NH bending). The behavior of chitan is similar to that of other hydrogen-bonded secondary amides such as proteins and polypeptides (29), which exhibit slow rates of isotope exchange of the NH protons in the presence of deuterium oxide at room temperature. For example, only 6% of these protons in chitan are replaced by deuterium after 1 month at 21°, although there is a marked temperature dependence which results in the exchange of almost 40% of the NH protons in 2 h at 100°. The diminution of the NH bands is accompanied by the appearance of the corresponding ND vibrations at 2 462 – 2 428 (doublet), 1 479, and 522 cm^{-1}. Doublet formation in the ND stretching region is probably due to Fermi resonance. These frequencies are characteristic of hydrogen-bonded NH groups in polyamides and polypeptides (30, 31), and clearly establish the absence of free NH groups. Frequencies similar to those discussed above are observed in the spectrum of chitin, although the bands are much broader.

One of the most distinctive features of the infrared spectrum of chitan is the single, sharp, intense band at 1 626 cm^{-1}, which is due to the amide I vibration (largely C=O stretching). The sharpness of the band indicates immediately that the amide groups in this polysaccharide are in an equivalent environment. Crystalline *N*-acetylglucosamine also exhibits a single absorption band at 1 626 cm^{-1}, and so does its 2-epimer *N*-acetylmannosamine at 1 623 cm^{-1}. It seems probable, therefore, that this band position is characteristic of monomeric or polymeric 2-amino-2-deoxy-glycopyranoside units *in the crystalline state*. The position of the amide I band in this class of compounds appears to be insensitive to the configuration at C-2 of the hexosamine residue, and suggests that the factors influencing this mode of vibration are largely confined to the amide group itself. A recent X-ray study (32) indicates that the plane of the amide group in crystalline *N*-acetylglucosamine is perpendicular to the plane of the pyranose ring of the hexose residue, and that a network of hydrogen bonds exists between the NH and C=O groups in neighboring molecules. An analogous *interchain* system of hydrogen bonds is likely to be present in chitan. Certainly, the characteristic vibrations associated with the amide groups in the latter are consistent with the presence of a hydrogen-bonded secondary amide (30, 31, 33), and the presence of a system of C=O · · · HN hydrogen bonds in a plane perpendicular to the plane of the pyranose ring is supported by a consideration of the molecular models.

The Chitin Bands at 1 626 and 1 656 cm^{-1}

In contrast to the spectrum of chitan, which has only one band in the C=O stretching (amide I) region, that of chitin contains bands at 1 626 and 1 656 cm^{-1} which have been the source of some disagreement. The band at higher frequency has previously (22–24) been attributed to the amide I vibration. On the other hand, the band at 1 626 cm^{-1} has been assigned to a C=N stretching vibration (22), an overtone or combination mode (23), an amide C=O group hydrogen-bonded to an OH group (21), or the C=O group of a rotational isomer of the aminoacetyl group (22), or has been completely ignored (25). The present evidence strongly indicates that these two bands are in fact both due to amide I vibrations, but correspond to two different classes of amide groups. This conclusion is supported by the following observations. (*a*) Chitan has only one band, that at 1 626 cm^{-1}, and crystalline *N*-acetylglucosamine and *N*-acetylmannosamine also have a single amide I band at very nearly the same frequency. (*b*) Treatment of chitan with lithium thiocyanate

and with other reagents causes a simultaneous appearance of the new band at 1 656 cm^{-1}, and a decrease in the intensity at 1 626 cm^{-1}. (*c*) Reprecipitation of chitin from hydrochloric acid causes an intensification of the band at 1 656 cm^{-1}, with a corresponding decrease at 1 626 cm^{-1}. (*d*) The band at 1 626 cm^{-1} has been observed to disappear more rapidly than does the band at 1 656 cm^{-1} on progressive deacetylation and during nitration (21). (*e*) The two bands differ in their relative intensities and dichroism in different preparations of chitin (10, 21–24, 34).

It has been suggested that the band at 1 656 cm^{-1} in chitin may be due to water of hydration (34). However, we have found that prolonged drying at 110° under vacuum has no effect whatsoever on the intensity of this band in samples of crustacean chitin or of lithium thiocyanate treated chitan. The reported diminution of this band upon partial deuteration of chitin (34) was reproduced in our laboratory, but may correspond to the usual decrease in the frequency of an amide I band upon deuteration (31, 33). There was certainly no appearance of the corresponding bands of HDO near 1 450 cm^{-1} and of D_2O near 1 200 cm^{-1} as deuteration proceeded. Thus the band at 1 656 cm^{-1} cannot be due to water of hydration.

The amide I vibrations of neighboring amide groups within a unit cell are often strongly coupled, in which case the coupled vibrations may be removed as much as 20 cm^{-1} from the frequency of the uncoupled vibrations (35–37). It is thus possible that the band at 1 626 cm^{-1} in chitan (as well as the band at 1 626 cm^{-1} in chitin, at 1 626 cm^{-1} in crystalline *N*-acetylglucosamine, and at 1 623 cm^{-1} in crystalline *N*-acetylmannosamine) may represent one of two coupled vibrations of the unit cell, the other vibration being infrared inactive. The band at 1 656 cm^{-1} in chitin may represent the uncoupled vibration in the vicinity of "missing" *N*-acetyl groups or in the noncrystalline or less-regular regions of the sample. This would certainly explain the variation of the ratio of intensities of the 1 656 and 1 626 cm^{-1} bands in chitin and the absence of the 1 656 cm^{-1} band in chitan.

We have also observed that *N*-acetylglucosamine and *N*-acetylmannosamine in the vitreous form have a single broad amide I band at about 1 640 cm^{-1}, some 14 to 17 cm^{-1} higher than the corresponding sharp band in the spectra of the crystalline form of these compounds. The 1 640 cm^{-1} band is probably due to uncoupled amide I vibrations in these compounds. The magnitude of the coupling constants observed in our compounds (30 cm^{-1} for chitin, 14 cm^{-1} for *N*-acetylglucosamine, and 17 cm^{-1} for *N*-acetylmannosamine) agrees with the values calculated for the amide I vibrations in polyglycine (18 cm^{-1} (38)), nylon (11 cm^{-1} (37)), and horsehair keratin (13 cm^{-1} (37)).

Whether the above explanation of the nature of the two amide I bands in chitin is correct, the two bands do appear to correspond to two distinct classes of amide groups in chitin, originating in distinct structural regions which may differ in their degree of order and which need not both contribute to the X-ray diffraction pattern of chitin.

The 840–890 cm^{-1} Region

It has been claimed that the frequency of the deformation mode of an anomeric axial (891 ± 7 cm^{-1}) or equatorial (844 ± 8 cm^{-1}) CH can be used to characterize the configuration at the anomeric center of the glycopyranose residues (39–42). Since chitan absorbs at 889 cm^{-1}, this empirical correlation would indicate that the sugar residues in this polysaccharide have a β-configuration at the anomeric center. However, during deuterium exchange studies on chitan it was observed that progressive substitution of the hydrogen atoms of the hydroxyl groups by deuterium resulted in the gradual disappearance of the band at 889 cm^{-1}, with the simultaneous appearance of a band at 843 cm^{-1}. Similar results were also obtained on deuteration of chitin. Since the isotope exchange does not

Can. J. Chem. Downloaded from www.nrcresearchpress.com by 210.87.254.105 on 09/05/12
For personal use only.

involve a change in the macrostructure of chitan, it is clear that one or both of the modes of vibration associated with the two bands must contain a contribution from the motion of the hydroxyl groups at C-3 or C-6 in the repeating unit of the polysaccharide. It should be noted that the band at 893 cm^{-1}, on deuteration, actually moved to a position claimed to be characteristic of an α- rather than a β-configuration at the anomeric center. A vibrational mode which is sensitive to change at other sites in the molecule does not, in our opinion, constitute reliable evidence for assigning the configuration at C-1 in a glycopyranose unit. Consequently, the above empirical correlation should be used only if both anomers are analyzed, and even then the evidence for configuration should be accepted with reservation in the absence of other supporting evidence.

Effect of Boiling on Chitan

When chitan is immersed in water at 100° for several hours or at 90° for several days, it is transformed into a material having an infrared spectrum different from those of chitan and chitin. The sharp absorption bands in the spectrum are still characteristic of a crystalline rather than an amorphous material. The spectrum of the boiled material differs from that of chitan by having an additional band in the OH stretching region at 3 400 cm^{-1} (possibly the antisymmetric stretching vibration of water molecules), two bands in the carbonyl stretching region at 1 645 and 1 664 cm^{-1}, and two bands in the NH stretching region at 3 295 and 3 337 cm^{-1}, as well as by the doubling of some other bands present in the spectrum of chitan. On prolonged heating at 110° and 10^{-3} Torr, the material reverts to the original chitan structure. Consequently, the new material is probably a hydrate.

State of Chitin in Nature

The methods employed in the past for the isolation of arthropod chitin have generally included boiling with aqueous acids and alkalis (10, 21–25, 34, 43, 44). The present results indicate that even much less drastic treatment, such as boiling in pure water, may produce extensive changes. The macrostructure of chitin, as previously isolated (21–27), may therefore be an artifact formed in the process of isolation. In particular, the so-called α-, β-, and γ-types of chitin, isolated from some organisms and reported to have different X-ray diffraction patterns and infrared spectra (34, 43, 44), may be unrelated to the native state of chitin in these organisms. Certainly, until samples of chitin are isolated and purified by milder (e.g. enzymatic) procedures, the state of chitin in arthropods and elsewhere in nature must be considered to be uncertain. It is very likely that crystalline chitan may be present in many other organisms in addition to the two genera of diatoms (5, 6) in which it has so far been found.

ACKNOWLEDGMENTS

We thank Professor O. Knop and Mrs. J. M. Hartley, Chemistry Department, Dalhousie University, Halifax, for assistance in recording the X-ray diffraction patterns.

REFERENCES

1. H. Braconnot. Ann. Chim. Paris, **79**, 265 (1811).
2. K. M. Rudall. Advan. Insect Physiol. **1**, 257 (1963).
3. A. B. Foster and J. M. Webber. Advan. Carbohydrate Chem. **15**, 371 (1960).
4. C. Jeuniaux. Chitin et chitinolyse. Masson et Cie, Paris. 1963.
5. J. McLachlan, A. G. McInnes, and M. Falk. Can. J. Botany, **43**, 707 (1965).
6. J. McLachlan and J. S. Craigie. *In* Some contemporary studies in marine science. *Edited by* H. Barnes. George Allen & Unwin, Ltd., London. 1966. p. 511.
7. R. L. Whistler and C. L. Smart. Polysaccharide chemistry. Academic Press, Inc., New York. 1963. p. 367.
8. M. V. Tracey. Methods of plant analysis. Vol. 2. Springer-Verlag, Berlin. 1955. p. 266.

Can. J. Chem. Downloaded from www.nrcresearchpress.com by 210.87.254.105 on 09/05/12
For personal use only.

9. C. H. GILES, A. S. A. HASSAN, M. LAIDLAW, and R. V. R. SUBRAMANIAN. J. Soc. Dyers Colourists, **74**, 647 (1958).
10. A. G. RICHARDS. The integument of arthropods. University of Minnesota Press, Minneapolis. 1951. p. 127.
11. A. N. O'NEILL. Can. J. Chem. **37**, 1747 (1959).
12. Y. INOUYE, K. ONODERA, S. KITAOKA, and S. HIRANO. J. Am. Chem. Soc. **78**, 4722 (1956).
13. J. C. IRVINE and J. C. EARL. J. Chem. Soc. **121**, 2370 (1922).
14. R. U. LEMIEUX, R. K. KULLNIG, H. J. BERNSTEIN, and W. G. SCHNEIDER. J. Am. Chem. Soc. **80**, 6098 (1958).
15. J. M. VAN DER VEEN. J. Org. Chem. **28**, 564 (1963).
16. C. A. GLASS. Can. J. Chem. **43**, 2652 (1965).
17. L. D. HALL. Advan. Carbohydrate Chem. **19**, 63 (1964).
18. S. E. DARMON and K. M. RUDALL. Discussions Faraday Soc. **9**, 251 (1950).
19. M. L. WOLFROM, J. R. VERCELLOTTI, and D. HORTON. J. Org. Chem. **29**, 547 (1964).
20. J. A. RUPLEY. Biochim. Biophys. Acta, **83**, 245 (1965).
21. S. E. DARMON and K. M. RUDALL. Discussions Faraday Soc. **9**, 251 (1950).
22. R. H. MARCHESSAULT, F. G. PEARSON, and C. Y. LIANG. Biochim. Biophys. Acta, **45**, 499 (1960).
23. F. G. PEARSON, R. H. MARCHESSAULT, and C. Y. LIANG. J. Polymer Sci. **43**, 101 (1960).
24. D. CARLSTRÖM. J. Biophys. Biochem. Cytol. **3**, 669 (1957).
25. N. E. DWELTZ. Biochim. Biophys. Acta, **44**, 416 (1960).
26. D. CARLSTRÖM. Biochim. Biophys. Acta, **59**, 361 (1962).
27. G. N. RAMACHANDRAN and C. RAMAKRISHNAN. Biochim. Biophys. Acta, **63**, 307 (1962).
28. J. MANN and H. J. MARRINAN. Trans. Faraday Soc. **52**, 481 (1956); **52**, 487 (1956); **52**, 492 (1956).
29. A. BERGER and K. LINDERSTRØM-LANG. Arch. Biochem. Biophys. **69**, 106 (1957).
30. L. J. BELLAMY. The infra-red spectra of complex molecules. 2nd ed. Methuen & Co. Ltd., London. 1958.
31. C. H. BAMFORD, A. ELLIOTT, and W. E. HANBY. Synthetic polypeptides. Academic Press, Inc., New York. 1956. p. 208.
32. L. N. JOHNSON and D. C. PHILLIPS. Nature, **202**, 588 (1964).
33. M. BEER, H. B. KESSLER, and G. B. B. M. SUTHERLAND. J. Chem. Phys. **29**, 1097 (1958).
34. K. M. RUDALL. Advan. Insect Physiol. **1**, 257 (1963).
35. T. MIYAZAWA. J. Chem. Phys. **32**, 1647 (1960).
36. T. MIYAZAWA and E. R. BLOUT. J. Am. Chem. Soc. **83**, 712 (1961).
37. E. M. BRADBURY and A. ELLIOTT. Polymer, **4**, 47 (1963).
38. S. KRIMM. J. Mol. Biol. **4**, 528 (1962).
39. S. A. BARKER, A. B. FOSTER, M. STACEY, and J. M. WEBBER. J. Chem. Soc. 2218 (1958).
40. S. A. BARKER, E. J. BOURNE, M. STACEY, and D. H. WHIFFEN. J. Chem. Soc. 171 (1954).
41. A. B. FOSTER and J. M. WEBBER. Advan. Carbohydrate Chem. **15**, 371 (1960).
42. H. SPEDDING. Advan. Carbohydrate Chem. **19**, 23 (1964).
43. N. OKAFOR. Biochim. Biophys. Acta, **101**, 193 (1965).
44. N. E. DWELTZ. Biochim. Biophys. Acta, **51**, 283 (1961).

Can. J. Chem. Downloaded from www.nrcresearchpress.com by 210.87.254.105 on 09/05/12
For personal use only.

Can. J. Chem. Downloaded from www.nrcresearchpress.com by 210.87.254.105 on 09/05/12
For personal use only.

A STUDY OF THE SUBSTITUTION REACTIONS OF BENZO[*b*]THIOPHENE AND ITS DERIVATIVES

GERRIT VAN ZYL, C. J. BREDEWEG, R. H. RYNBRANDT, AND D. C. NECKERS
Department of Chemistry, Hope College, Holland, Michigan

Received April 13, 1966

ABSTRACT

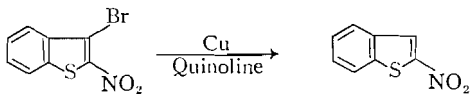
The nitration, halogenation, and amination reactions of benzo[*b*]thiophene and some of its derivatives are reported. Several new benzo[*b*]thiophenes have been prepared and directional influences of groups in the thiophene portion of the nucleus confirmed.

In a continuation of our interest in substitution reactions of benzo[*b*]thiophene and its derivatives, we have reinvestigated the isomer distribution in the nitration and halogenation of benzo[*b*]thiophene. It was of interest to study the orientation effects in reactions of electrophilic reagents with benzo[*b*]thiophene derivatives which were substituted on the thiophene portion of the benzo[*b*]thiophene ring system.

RESULTS AND DISCUSSION

Nitration of Benzo[b]thiophene

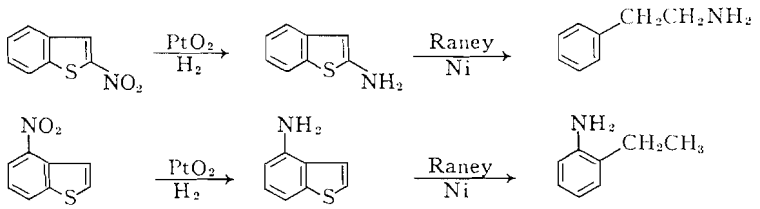
The nitration of benzo[*b*]thiophene (1–8) has been reported to give 3-nitrobenzo[*b*]-thiophene. No other mononitro derivatives have been isolated. Recently, an infrared study (8) suggested that the nitration reaction mixture contained about 61% 3-nitrobenzo[*b*]thiophene and 16% 5-nitrobenzo[*b*]thiophene. The 2-nitro derivative was also assumed to be present in the nitration mixture (9, 10). Since 2-nitrobenzo[*b*]thiophene has not been characterized previously, its synthesis was necessary to establish its presence in the nitration mixture. 2-Nitrobenzo[*b*]thiophene was prepared by an unambiguous synthesis involving a copper–quinoline dehalogenation (11) of 3-bromo-2-nitrobenzo[*b*]-thiophene (eq. [1]).

[1] 

The nitration of benzo[*b*]thiophene with fuming nitric acid – acetic acid mixtures at 60–70° results in the formation of mononitrated benzo[*b*]thiophene (85% yield). The mixture was shown to contain 2-, 3-, and 4-nitrobenzo[*b*]thiophene. Infrared analysis of the reaction mixture indicated that the products included 10–15% 2-nitrobenzo[*b*]thiophene, 60–65% 3-nitrobenzo[*b*]thiophene, and 20–30% of other components, mainly 4-nitrobenzo[*b*]thiophene.

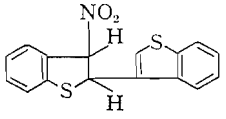
The presence of 4- and 2-nitrobenzo[*b*]thiophene in the nitration mixture was confirmed by chemical degradation. Thus, the nitration mixture was catalytically reduced over platinum oxide, followed by Raney nickel desulfurization, to give a mixture of aromatic amines including 2-phenylethylamine and *o*-aminoethylbenzene (eq. [2]).

Although 3-nitrobenzo[*b*]thiophene is also known to be in the nitration mixture, none of the corresponding degradation product, α-phenylethylamine, was observed. The reduction product of 3-nitrobenzo[*b*]thiophene, 3-aminobenzo[*b*]thiophene, reportedly

[2] 

cannot be distilled (2, 12), and is too unstable to be isolated in the pure form (3, 13, 14). No evidence was obtained for the presence of 5-nitrobenzo[*b*]thiophene or other isomers in the nitration mixture.

Optimum yields of the 3-nitrobenzo[*b*]thiophene were obtained when the nitration of benzo[*b*]thiophene was carried out above room temperature. At lower temperatures the formation of I, an unstable intermediate observed earlier by Komppa (3), was competitive with 3-nitrobenzo[*b*]thiophene formation.

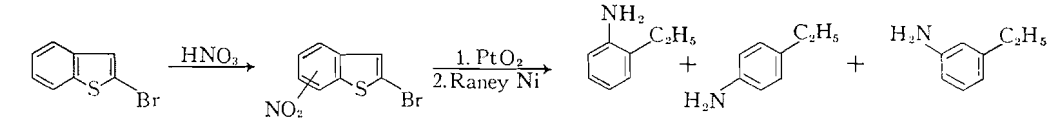


I

3-Nitrobenzo[*b*]thiophene undergoes no further nitration with fuming nitric acid and glacial acetic acid at 105°. Therefore, the possibility of the presence of dinitro products in the nitration mixture is doubtful. This is substantiated by the fact that no residue remained after the distillation of the mononitro products from the reaction mixture of nitric acid and benzo[*b*]thiophene at 60–70°.

Nitration of 2- and 3-Bromobenzo[b]thiophene

Although the nitration of 3-bromobenzo[*b*]thiophene occurs with preferential attack at the 2 position of the thiophene nucleus,[1] the nitration of 2-bromobenzo[*b*]thiophene yields several products. Vapor-phase chromatographic analysis, after dehalogenation, reduction, and desulfurization, confirmed the presence of *o*-aminoethylbenzene, *p*-aminoethylbenzene, and *m*-aminoethylbenzene. These products result from 4-nitro-2-bromobenzo[*b*]thiophene, 6-nitro-2-bromobenzo[*b*]thiophene, and 5(or 7)-nitro-2-bromobenzo[*b*]thiophene, respectively. Although no α-aminoethylbenzene was found, this does not prove that 3-nitro-2-bromobenzo[*b*]thiophene was not formed, because of the possible instability of the intermediate amino derivative mentioned previously (eq. [3]).

[3] 

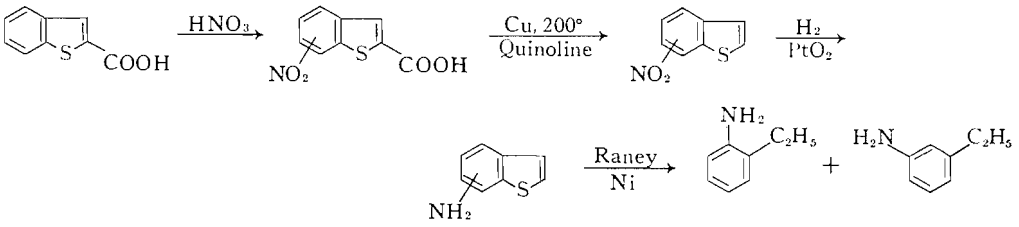
From the nitration mixture of 2-bromobenzo[*b*]thiophene, three distinct mononitro-2-bromobenzo[*b*]thiophenes were isolated. After debromination of the nitration mixture (11) one of the isolated compounds had a melting point corresponding to that of 4-nitrobenzo[*b*]thiophene. This fact further supports the postulate that 4-nitro-2-bromobenzo[*b*]thiophene was one of the original nitration products.

[1]*Reference 3 reports the 3-bromo-2-nitro derivative, but the 3-bromo derivative, which is a liquid, is incorrectly listed as a solid melting at 146–156°.*

Can. J. Chem. Downloaded from www.nrcresearchpress.com by 210.87.254.105 on 09/05/12
For personal use only.

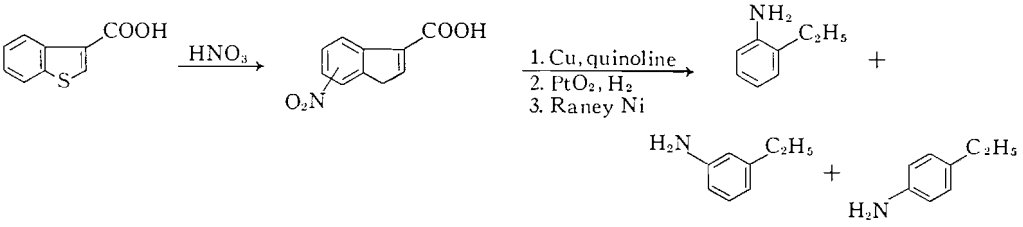
Nitration of 2- and 3-Benzo[b]thiophenecarboxylic Acids

Nitration of benzo[*b*]thiophene-2-carboxylic acid also produced a mixture of products. Structural elucidation was effected by decarboxylation to the corresponding nitrobenzo-[*b*]thiophenes followed by reduction and desulfurization as previously described (eq. [4]).

[4] 

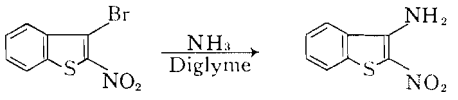
The *o*- and *m*-aminoethylbenzenes which were obtained correspond to 4-nitrobenzo[*b*]-thiophene-2-carboxylic acid and either 5- or 7- (or a mixture of both) nitrobenzo[*b*]thiophene-2-carboxylic acid. No *p*-aminoethylbenzene was found. Again, the 3-nitrobenzo-[*b*]thiophene-2-carboxylic acid cannot be eliminated, because of the unstable intermediate, 3-aminobenzo[*b*]thiophene.

Nitration of benzo[*b*]thiophene-3-carboxylic acid also led to a mixture of mononitro derivatives. By the decarboxylation, reduction, and desulfurization technique previously outlined, *o*-aminoethylbenzene was obtained as the major product. Minor quantities of *m*- and *p*-aminoethylbenzene, corresponding to 4-nitro-, 5- or 7-nitro-, and 6-nitrobenzo[*b*]thiophene-3-carboxylic acid, were also obtained (eq. [5]).

[5] 

Preparation of Amino Derivatives of 2-Nitrobenzo[b]thiophene

Heating 3-bromo-2-nitrobenzo[*b*]thiophene in diglyme with anhydrous ammonia gives 3-amino-2-nitrobenzo[*b*]thiophene by a simple aromatic nucleophilic substitution reaction (eq. [6]).

[6] 

3-Amino-2-nitrobenzo[*b*]thiophene was shown by its infrared spectrum to exist only in the tautomeric amino form. Recent reports indicate that 2-aminobenzo[*b*]thiophene also exists in the amino form (15). In addition to the known aminobenzo[*b*]thiophenes (16), 3-diethylamino and 3-phenylamino derivatives were also prepared by heating 3-bromo-2-nitrobenzo[*b*]thiophene with diethylamine and aniline, respectively.

Halogenation of Benzo[b]thiophene

Although the chlorination (3, 17, 18), bromination (3, 4, 19–22), and iodination (23–25) of benzo[*b*]thiophene have been reported, no isomer distributions are known. In

Can. J. Chem. Downloaded from www.nrcresearchpress.com by 210.87.254.105 on 09/05/12
For personal use only.

the chlorination and bromination of benzo[*b*]thiophene, we observed the formation of small quantities of 2-substituted and disubstituted products. Substitution in the 3 position is predominant. In the iodination of benzo[*b*]thiophene, no evidence for any 2-substitution or disubstitution products was obtained. Table I lists the isomer distributions obtained upon halogenation of benzo[*b*]thiophene.

TABLE I

Halogenation distribution products of benzo[*b*]thiophene

Halogen	2-Substitution (%)	3-Substitution (%)	2,3-Disubstitution (%)
Chlorine	3	69	28
Bromine	3	87	10
Iodine	0	100	0

EXPERIMENTAL[2]

Preparation of Mononitrobenzo[b]thiophenes

To a heated (60–70°) solution of 50 ml acetic acid and 12 ml fuming nitric acid was added dropwise, with stirring, 15 g (0.11 mole) benzo[*b*]thiophene which had been diluted with an equal volume of acetic acid. After the addition of the nitric acid solution was complete, the reaction mixture was stirred for an additional 2 h at 60–70° and then poured into ice water. The oily layer was extracted with chloroform, neutralized with an aqueous solution of sodium bicarbonate, and dried over anhydrous magnesium sulfate. An 85% yield of yellow mononitrobenzo[*b*]thiophenes was obtained upon distillation at 105–110° and 0.1 mm.

Preparation of Aminobenzo[b]thiophenes

A solution of 17 g (0.09 mole) of the mononitration mixture in 150 ml of acetone was reduced with 0.2 g of platinum oxide as catalyst in a Parr hydrogenation apparatus for 1 h at 50 p.s.i. hydrogen pressure. The reaction mixture was filtered and concentrated under vacuum. Vacuum distillation of the residue gave a mixture of aminobenzo[*b*]thiophenes; yield 11.9 g (81%), b.p. 110–115° at 0.2 mm.

Preparation of Aminoethylbenzenes

A mixture of 12 g (0.08 mole) of the aminobenzo[*b*]thiophenes, 800 ml of methanol, and 150 g of Raney nickel was refluxed for 0.5 h. After the Raney nickel was removed by filtration, the resulting filtrate was distilled *in vacuo* to give a mixture of aminoethylbenzenes; b.p. 49–53° at 0.1 mm. The aminoethylbenzenes were shown to consist of a mixture of 2-phenylethylamine and *o*-aminoethylbenzene in a ratio of about 2:1, as determined by vapor-phase chromatography with a 2 m Carbowax column.

Preparation of Mononitro-2-bromobenzo[b]thiophenes

A mixture of 5 ml of fuming nitric acid and 5 ml of acetic acid was added dropwise to a cooled (5–10°) solution of 5 g (0.02 mole) of 2-bromobenzo[*b*]thiophene in 20 ml of acetic anhydride. The reaction mixture was stirred for 2 h at room temperature and the resulting yellow solution poured into an ice–water mixture. After the yellow precipitate was washed with water and sodium carbonate solutions, 6 g of solid yellow product was obtained. From column chromatography with activated alumina, three mononitro-2-bromobenzo[*b*]thiophenes were obtained. They possessed the following melting points: 124.5–125°, 148°, and 164.0–164.5°.

Anal. Calcd. for $C_8H_4NO_2BrS$: C, 37.27; H, 1.56; S, 12.43; N, 5.43; Br, 30.97. Found:

Melting point	C	H	S	N	Br
124.5–125°	37.63	1.78	12.05	5.32	31.13
148°	37.17	1.71	12.05	5.17	30.69
164.0–164.5°	37.33	1.75	12.60	5.31	31.03

Debromination of the Nitration Products of 2-Bromo[b]thiophene

A mixture of 10 g of the nitration product of 2-bromo-[*b*]thiophene, 3.3 g of copper bronze powder, and 55 ml of quinoline was heated to 135° under a nitrogen atmosphere for 30 min. After the reaction mixture was cooled, dilute hydrochloric acid and benzene were added. The benzene layer was evaporated and the residue distilled at 0.1 mm. The resulting solid yellow material was chromatographed on activated alumina. A fraction melting at 85–86° was obtained (lit. (7, 26, 27) m.p. 84–85° and 88° for 4-nitrobenzo[*b*]thiophene).

[2]*All melting points are uncorrected. Analyses were performed by Schwarzkopf Microanalytical Laboratory. Infrared spectra were obtained with a Perkin–Elmer model 137 Infracord. Vapor-phase chromatographic analyses were performed with a Burrell model K-2 chromatograph equipped with thermal conductivity detectors.*

Can. J. Chem. Downloaded from www.nrcresearchpress.com by 210.87.254.105 on 09/05/12
For personal use only.

Preparation of Aminoethylbenzenes from Mononitro-2-bromobenzo[b]thiophenes

Reduction and desulfurization of the mononitration products of 2-bromobenzo[*b*]thiophene were carried out under conditions similar to those used for the mononitration products of benzo[*b*]thiophene. Vapor-phase chromatographic analysis of the products indicated the presence of *o*-aminoethylbenzene, *p*-aminoethylbenzene, and *m*-aminoethylbenzene by comparison of their retention times with those of known samples. No α-aminoethylbenzene was observed.

Nitration of 3-Bromobenzo[b]thiophene

A solution of 23 ml of fuming nitric acid and 23 ml of acetic acid was added dropwise, with stirring, to a cooled (5–10°) mixture of 20 g (0.095 mole) of 3-bromobenzo[*b*]thiophene and 80 ml of acetic anhydride. The reaction mixture was stirred for 1 h and poured onto ice. The yellow solid was recrystallized from ethanol and sublimed, m.p. 164–165° (4).

When a mixture of 3-bromo-2-nitrobenzo[*b*]thiophene and 20% sodium hydroxide was refluxed, 3-hydroxy-2-nitrobenzo[*b*]thiophene was obtained, m.p. 104–105° (decomp.) (lit. (28) m.p. 104–105° (decomp.)).

Preparation of 2-Nitrobenzo[b]thiophene

A mixture of 6 g (0.02 mole) of 3-bromo-2-nitrobenzo[*b*]thiophene, 1.8 g of copper bronze powder, and 30 ml of quinoline was vigorously stirred under a nitrogen atmosphere, gradually heated to 150°, and maintained at that temperature for 45 min. The reaction mixture was then cooled, made acidic with dilute hydrochloric acid, and extracted with benzene. After the benzene was removed, the residue was distilled at 105° and 0.1 mm. After recrystallization from methanol and sublimation, the yellow crystals melted at 117°; yield 25%.

Anal. Calcd. for $C_8H_5NO_2S$: C, 53.62; H, 2.81; S, 17.89; N, 7.82. Found: C, 53.83; H, 2.98; S, 17.93; N, 7.85.

Preparation of Mononitrobenzo[b]thiophene-2-carboxylic Acids

To a cold (0–5°) solution of 10 g (0.055 mole) of benzo[*b*]thiophene-2-carboxylic acid (19, 29) in 75 ml of acetic anhydride was added 10 ml of fuming nitric acid in 10 ml of acetic acid. After the solution was stirred for 30 min at 0°, it was allowed to warm to room temperature; the stirring was continued for an additional 2½ h. The mixture was poured into ice water, filtered, and washed. A 68% yield of a yellow mixture of mononitrocarboxylic acids, m.p. 230–240°, was obtained.

Anal. Calcd. for $C_9H_5NSO_4$: N, 6.28; S, 14.35. Found: N, 6.56; S, 14.35.

Decarboxylation of the Mixture of Mononitrobenzo[b]thiophene-2-carboxylic Acids

A mixture of 10 g (0.045 mole) of the mononitrobenzo[*b*]thiophene-2-carboxylic acids (30, 31) was decarboxylated with 2.5 g of copper bronze powder and 50 ml of quinoline by heating it at 190° for 30 min in a nitrogen atmosphere. At the end of this period, the reaction mixture was poured into a mixture of 250 g of ice and 50 ml of concentrated hydrochloric acid. The resulting yellow precipitate was filtered off, dried, and distilled *in vacuo* to give 4 g (50% yield) of mononitrobenzo[*b*]thiophenes, b.p. 105–110° at 0.1 mm, m.p. 50–70°.

Anal. Calcd. for $C_8H_5NSO_2$: N, 7.82; S, 17.90. Found: N, 7.89; S, 17.80.

Reduction and Desulfurization of the Mixture of the Decarboxylation Products from the Mononitrobenzo[b]thiophene-2-carboxylic Acids

The reduction and desulfurization procedure for the mononitrobenzo[*b*]thiophenes was the same as that described earlier.

Nitration of Benzo[b]thiophene-3-carboxylic Acid

The nitration procedure for benzo[*b*]thiophene-3-carboxylic acid was the same as that used for benzo[*b*]-thiophene-2-carboxylic acid (32). A 75% overall yield of a mixture of mononitrobenzo[*b*]thiophene-3-carboxylic acids, m.p. 192–225°, was obtained.

Anal. Calcd. for $C_9H_5NSO_4$: N, 6.28; S, 14.35. Found: N, 6.38; S, 13.93.

Decarboxylation of the Nitration Products of Benzo[b]thiophene-2-carboxylic Acid

A 62% yield of a mixture of mononitrobenzo[*b*]thiophenes was obtained by a decarboxylation procedure analogous to that used for the nitration mixture of benzo[*b*]thiophene-2-carboxylic acid.

Anal. Calcd. for $C_8H_5NSO_2$: N, 7.82; S, 17.90. Found: N, 7.91; S, 18.00.

Reduction and Desulfurization of the Decarboxylation Products from the Mononitrobenzo[b]thiophene-3-carboxylic Acids

Catalytic reduction and Raney nickel desulfurization were carried out by the previously described techniques. A 60% yield of aminobenzo[*b*]thiophenes was obtained, b.p. 120–123° at 0.5–0.3 mm. A 52% yield of aminoethylbenzene resulted after desulfurization, b.p. 48–52° at 0.1 mm. The aminoethylbenzenes consisted of mostly *o*- and minor amounts of *m*- and *p*-aminoethylbenzenes.

Can. J. Chem. Downloaded from www.nrcresearchpress.com by 210.87.254.105 on 09/05/12
For personal use only.

Gas Chromatographic Analysis

A 2½ m glass column packed with 20% Carbowax 4000 on Chromosorb W was used in all cases. Identifications were made by comparison of peaks with those of authentic compounds under the same experimental conditions (150° and a helium flow rate of 90 ml/min). The compounds used for comparison, α-phenylethylamine, 2-phenylethylamine, *o*-aminoethylbenzene, and *p*-aminoethylbenzene, were commercially available. *m*-Aminoethylbenzene was prepared from *m*-nitroacetophenone.

3-Amino-2-nitrobenzo[b]thiophene

A mixture of 10 g (0.039 mole) of 3-bromo-2-nitrobenzo[*b*]thiophene and 100–150 ml of diglyme was heated to 120°, and dry ammonia was passed into the solution for 3 h. After the solution was added to ice water, the crude solid was filtered off and dried. The crude material, which melted near 200°, was chromatographed on grade 3 activated alumina, yielding yellowish-orange crystals, m.p. 218.0–218.5°.

Anal. Calcd. for $C_8H_6N_2O_2S$: C, 49.47; H, 3.11; N, 14.43; S, 16.51. Found: C, 49.53; H, 3.17; N, 14.70; S, 16.24.

3-Phenylamino-2-nitrobenzo[b]thiophene

A mixture of 1 g (3.9 mmoles) of 2-nitro-3-bromobenzo[*b*]thiophene and 1.8 g (19.4 mmoles) of aniline was heated for 15 min at 100°. Dilute hydrochloric acid was added and the resulting mixture was extracted with benzene. After the benzene was evaporated, the residue was recrystallized from a mixture of chloroform and ethanol, to give a quantitative yield of bright-orange needles, m.p. 210–211°.

Anal. Calcd. for $C_{14}H_{10}N_2O_2S$: C, 62.21; H, 3.73; S, 11.86; N, 10.35. Found: C, 62.11; H, 3.56; S, 11.90; N, 10.50.

3-Diethylamino-2-nitrobenzo[b]thiophene

The procedure was the same as that used for the preparation of 3-phenylamino-2-nitrobenzo[*b*]thiophene, except that diethylamine was used instead of aniline; yield quantitative, m.p. 54°.

Halogenation of Benzo[b]thiophene

Benzo[*b*]thiophene was chlorinated, brominated, and iodinated according to the procedures of Schlesinger and Mowry (17), Szmuszkovicz and Modest (21), and Gaertner (24), respectively. Vapor-phase chromatographic analysis of the reaction products was accomplished on a 7 ft column packed with 20% Carbowax 4000 on Chromosorb W. The retention times of the various halobenzo[*b*]thiophenes were determined with authentic samples, and these times were compared with those of the various components found in the halogenation mixture.

Preparation of 2-Chlorobenzo[b]thiophene

An ethereal solution of *n*-butyllithium was prepared by the gradual addition, with stirring, of 20.0 g (0.2 mole) of *n*-butyl chloride in 40 ml of anhydrous ether to 3.7 g (0.5 mole) of lithium ribbon suspended in 100 ml of anhydrous ether. One milliliter of *n*-butyl bromide was added as catalyst and the mixture was allowed to reflux for 1 h. The solution was then cooled to 0–5°, and 13.5 g (0.10 mole) of benzo[*b*]thiophene in 30 ml of ether was added with stirring. The mixture was kept at 0° for 1 h. Into the above solution was bubbled 7.1 g (0.10 mole) of chlorine gas, during which time the temperature was maintained between −30° and −20°. The ether solution was washed with 200 ml of water and dried, and the solvent was removed *in vacuo*. Distillation gave 5 g (30% conversion, 48% yield) of 2-chlorobenzo[*b*]thiophene, b.p. 60–70° at 0.1 mm, m.p. 34°.

Anal. Calcd. for C_8H_5SCl: C, 57.0; H, 2.97; S, 19.0; Cl, 21.0. Found: C, 56.7; H, 3.16; S, 18.2; Cl, 20.8.

The picrate melted at 97°. The 1-dioxide was prepared by hydrogen peroxide oxidation, m.p. 141–142° (lit. (17) m.p. 142–143°).

ACKNOWLEDGMENT

This research was supported by a grant from the Petroleum Research Fund administered by the American Chemical Society.

REFERENCES

1. G. Komppa. Acta Soc. Sci. Fennicae, **23**, 1 (1897).
2. K. Fries and E. Hemmecke. Ann. **470**, 1 (1929).
3. G. Komppa. J. Prakt. Chem. **122**, 319 (1929).
4. E. B. Middleton and G. A. Dawson. U.S. Patent No. 2,424,483 (July 1947); Chem. Abstr. **42**, 1141 (1949).
5. W. Davies, N. W. Gamble, and W. E. Savige. J. Chem. Soc. 4678 (1952).
6. T. Sakan, H. Katake, A. Fujino, and T. Matsuura. J. Inst. Polytech. Osaka City Univ. **1**, 31 (1950); Chem. Abstr. **46**, 2047 (1952).
7. W. Davies and Q. N. Porter. J. Chem. Soc. 828 (1957).
8. R. Zahradnik, C. Parkanyi, V. Horak, and J. Koutecky. Collection Czech. Chem. Commun. **28**, 776 (1963).

Can. J. Chem. Downloaded from www.nrcresearchpress.com by 210.87.254.105 on 09/05/12
For personal use only.

9. H. D. HARTOUGH and S. L. MEISEL. Compounds with condensed thiophene rings. Interscience Publishers, Inc., New York. 1954. p. 48.
10. G. VAN ZYL, J. W. VAN DYKE, G. E. HEASLEY, D. DE JONGH, C. J. BREDEWEG, and D. C. NECKERS. 4th Report on Research under Sponsorship of Petroleum Research Funds. American Chemical Society, Washington, D.C. 1960. p. 39.
11. S. NISHIMURA, R. MOTOYAMA, and E. IMOTO. Bull. Univ. Osaka Prefect., Ser. A, **6**, 127 (1958).
12. W. KÖNIG and G. HAMPRECHT. Ber. **B63**, 1546 (1930).
13. P. FRIEDLÄNDER. Ann. Chem. **351**, 412 (1907).
14. R. ZAHRADNIK, C. PARKANYI, V. HORAK, and J. KOUTECKY. Collection Czech. Chem. Commun. **28**, 51 (1963).
15. G. W. STACY, F. W. VILLAESCUSA, and T. E. WOLLNER. J. Org. Chem. **30**, 4074 (1965).
16. B. B. LAMPERT. Ph.D. Thesis, Northwestern University, Evanston, Illinois. 1951.
17. A. H. SCHLESINGER and D. T. MOWRY. J. Am. Chem. Soc. **73**, 2615 (1951).
18. R. F. MCCLEARY and J. A. PATTERSON. U.S. Patent No. 2,571,742 (October 1951); Chem. Abstr. **46**, 8152 (1952).
19. E. M. CROOK and W. DAVIES. J. Chem. Soc. 1697 (1937).
20. BUU-HOI and J. LECOCQ. Compt. Rend. **222**, 1441 (1946).
21. J. SZMUSZKOVICZ and E. J. MODEST. J. Am. Chem. Soc. **72**, 571 (1950).
22. D. A. SHIRLEY and M. D. CAMERSON. J. Am. Chem. Soc. **74**, 664 (1952).
23. R. T. VAN VLECK. U.S. Patent No. 2,557,708 (June 1951); Chem. Abstr. **46**, 547 (1952).
24. R. GAERTNER. J. Am. Chem. Soc. **74**, 4950 (1952).
25. R. D. SCHUETZ and L. CIPORIN. J. Org. Chem. **23**, 206 (1958).
26. H. STANGE. Ph.D. Dissertation, Northwestern University, Evanston, Illinois. 1950.
27. K. FRIED, H. HEERING, E. HEMMECKE, and G. SIEBERT. Ann. **527**, 83 (1937).
28. J. L. D'SILVA and E. W. MCCLELLAND. J. Chem. Soc. 2883 (1932).
29. A. SCHÖNBERG, E. PETERSON, and H. KALTSCHMITT. Ber. **B66**, 233 (1933).
30. F. G. BORDWELL and C. J. ALBISETTI, JR. J. Am. Chem. Soc. **70**, 1955 (1948).
31. L. F. FIESER and R. G. KENNELLY. J. Am. Chem. Soc. **57**, 1611 (1935).
32. G. KOMPPA and S. WECKMAN. J. Prakt. Chem. **138**, 109 (1933).

Can. J. Chem. Downloaded from www.nrcresearchpress.com by 210.87.254.105 on 09/05/12
For personal use only.

Can. J. Chem. Downloaded from www.nrcresearchpress.com by 210.87.254.42 on 09/05/12
For personal use only.

THE WATER-SOLUBLE POLYSACCHARIDES OF DERMATOPHYTES

V. GALACTOMANNANS II FROM TRICHOPHYTON GRANULOSUM, TRICHOPHYTON INTERDIGITALE, MICROSPORUM QUINCKEANUM, TRICHOPHYTON RUBRUM, AND TRICHOPHYTON SCHÖNLEINII[1]

C. T. BISHOP AND M. B. PERRY

Division of Biosciences, National Research Council, Ottawa, Canada

AND

F. BLANK

The Skin and Cancer Hospital, Temple University School of Medicine, Philadelphia, Pennsylvania

Received June 2, 1966

ABSTRACT

Polysaccharides obtained from each of the organisms designated in the title have been resolved into three groups: galactomannans I, galactomannans II, and glucans. The five galactomannans II were homogeneous under conditions of electrophoresis, and had positive specific rotations. Methylation and hydrolysis of the five galactomannans II yielded varying amounts of the following: 2,3,5,6-tetra-*O*-methyl-D-galactose, 2,3,4,6-tetra-*O*-methyl-D-mannose, 2,3,4-tri-*O*-methyl-D-mannose, 3,4,6-tri-*O*-methyl-D-mannose, 3,5-di-*O*-methyl-D-mannose, and 3,4-di-*O*-methyl-D-mannose. The galactomannans II were therefore very similar to each other in their gross structural features. The unbranched portions of the polysaccharides were formed by $1 \rightarrow 2$ and $1 \rightarrow 6$ linked α-D-mannopyranose units, with the former predominating. Branch points were formed through substitutions at the C-2 and C-6 positions of D-mannofuranose and D-mannopyranose, and branches were terminated by D-galactofuranose and D-mannopyranose units. The presence of $1 \rightarrow 2$ linked α-D-mannopyranose units in the linear portions of the galactomannans II constitutes a major structural difference between this group of polysaccharides and the galactomannans I. The two groups of galactomannans differ serologically.

It was reported earlier that each of five dermatophytes had a similar pattern of water-soluble polysaccharides, specifically, two galactomannans and a glucan (1). The previous paper in this series described the properties and gross structural features of one group of the galactomannans (called galactomannan I) (2).

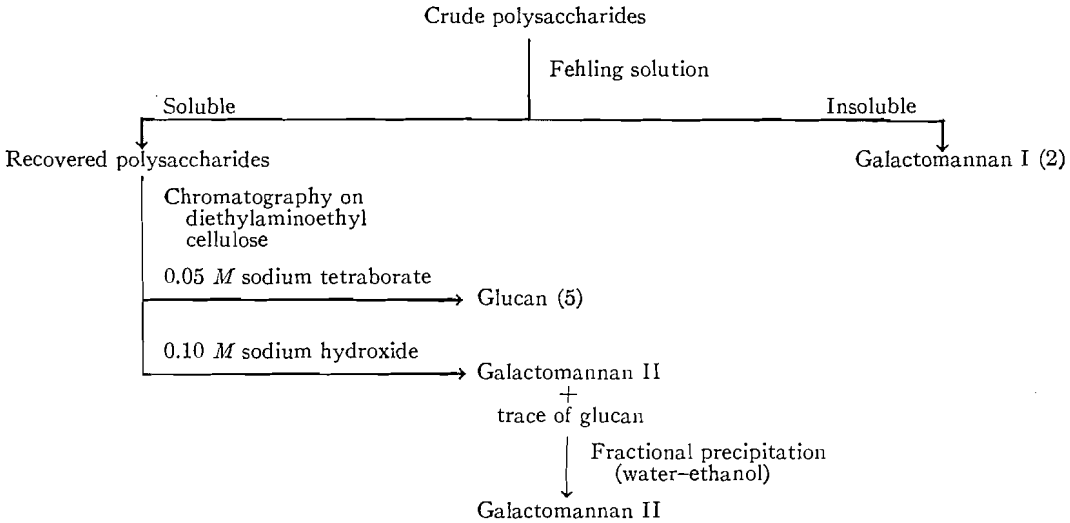
The present paper describes the separation of the three groups of polysaccharides and reports the properties and gross structural features of the second group of galactomannans (called galactomannan II) from *Trichophyton granulosum* Sabouraud, 1909, *Trichophyton interdigitale* Priestley, 1917, *Microsporum quinckeanum* (Zopf) Guiart and Grigorakis, 1928, *Trichophyton rubrum* (Castellani) Sabouraud, 1911, and *Trichophyton schönleinii* (Lebert) Langeron and Milochevitch, 1930.

Crude polysaccharides were extracted from powdered cells of the organisms in yields of 5–10% as described previously for *T. granulosum* (3). The procedure was designed to yield polysaccharide preparations which were free of lipid and protein. The aim of this continuing program is to relate structures to serological properties in the polysaccharides from dermatophytes. The presence of any contaminating lipid or protein, bound or free, could interfere in the serological tests and cause difficulties in interpreting the results of structural studies.

The crude polysaccharides were resolved into two galactomannans and a glucan by the procedure shown in Reaction Scheme 1. Addition of Fehling solution to aqueous solutions of the crude polysaccharides precipitated galactomannans I as insoluble copper complexes (2). The polysaccharides which were soluble in Fehling solution were recovered and

[1]*Issued as N.R.C. No. 9108.*

resolved, by chromatography on diethylaminoethyl cellulose (4), into glucans and the second group of galactomannans (galactomannans II). The latter still contained traces of glucan, but fractional precipitation from aqueous solutions by addition of ethanol yielded homogeneous samples of galactomannans II. The properties and structures of the five glucans are described in the next paper in this series (5).



REACTION SCHEME 1. Separation of the polysaccharides of dermatophytes.

Table I shows the yields and some of the properties of the galactomannans II. This group of polysaccharides formed roughly the same proportion of the crude polysaccharides in each organism. The specific rotations were positive and, except for the galactomannan II of *M. quinckeanum*, were lower than the specific rotations of the galactomannans I (2). The amounts of D-galactose in galactomannans II (23–33%) were higher than in the galactomannans I (0–13%). The results of periodate oxidation were not included because the galactomannans II showed extensive overoxidation, probably because of the malondialdehyde structure resulting from periodate oxidation of terminal D-galactofuranose units. Extrapolated values could not be used because it was impossible to decide which portion of the curve (oxidant consumption plotted against time) should be extrapolated. The galactomannans II were indistinguishable by electrophoresis, having the same mobility in borate buffer.

The galactomannans II were methylated fully and then hydrolyzed to yield mixtures of D-mannose and D-galactose methyl ethers. These mixtures were analyzed by a combination of paper electrophoresis and gas–liquid and thin-layer chromatography, and the

TABLE I

Yields and properties of galactomannans II from dermatophytes

Organism	Yield*	$[\alpha]_D$ (in water)	Hydrolysis products (%). D-Galactose	D-Mannose
T. granulosum	27.6	+16°	29.1	70.9
T. interdigitale	22.0	+6.5°	32.9	67.1
M. quinckeanum	32.6	+58°	31.2	68.8
T. rubrum	20.2	+26°	23.3	76.7
T. schönleinii	24.0	+23°	25.2	74.8

*Percentage of crude polysaccharide.

Can. J. Chem. Downloaded from www.nrcresearchpress.com by 210.87.254.42 on 09/05/12
For personal use only.

results are shown in Table II. The ratio of tetra- to tri- to di-*O*-methyl sugars was obtained by integration of the peaks on gas–liquid chromatograms and was checked by preparative thin-layer chromatography. The relative amounts of the two tetra-*O*-methyl sugars were determined by both gas–liquid and thin-layer chromatography. The amounts of 2,3,4- and 3,4,6-tri-*O*-methyl-D-mannoses in the tri-*O*-methyl fraction were determined by preparative paper electrophoresis. The di-*O*-methyl-D-mannoses were analyzed by gas–liquid chromatography. Except for the four minor di-*O*-methyl-D-mannoses, each compound was characterized by isolation of a crystalline derivative.

The results in Table II showed that the five galactomannans II were very similar in structure. Each one contained branch points formed primarily through substitutions at

TABLE II

Methylation studies on galactomannans II

	mole %				
O-Methyl sugar	*T. granulosum*	*T. interdigitale*	*T. rubrum*	*T. schönleinii*	*M. quinckeanum*
2,3,5,6-Tetra-*O*-methyl-D-galactose	27.3	27.9	23.0	24.0	29.0
2,3,4,6-Tetra-*O*-methyl-D-mannose	7.4	2.1	6.7	2.7	7.5
2,3,4-Tri-*O*-methyl-D-mannose	17.6	22.0	15.6	19.2	14.9
3,4,6-Tri-*O*-methyl-D-mannose	24.4	25.7	35.6	29.3	26.6
3,5-Di-*O*-methyl-D-mannose	10.4	11.0	9.2	6.0	10.4
3,4-Di-*O*-methyl-D-mannose	6.8	7.1	5.5	13.3	7.0
Four di-*O*-methyl-D-mannoses*	6.1	4.2	5.3	5.5	4.7

*Each of these four di-*O*-methyl-D-mannoses amounted to less than 2% of the total mixture of *O*-methyl sugars. The amount were too small to permit identification.

the C-2 and C-6 positions of D-mannofuranose and D-mannopyranose units, giving rise to the 3,5- and 3,4-di-*O*-methyl-D-mannoses, respectively. Most of these branch points occurred at the D-mannofuranose units in each galactomannan II, except in that from *T. schönleinii*. The presence of 3,4,6- and 2,3,4-tri-*O*-methyl-D-mannoses showed that the unbranched portions of the polysaccharides were formed by $1 \rightarrow 2$ and $1 \rightarrow 6$ linkages, with the former predominating. D-Mannopyranose and D-galactofuranose units formed the nonreducing terminal units of the galactomannans II, as shown by the presence of 2,3,4,6-tetra-*O*-methyl-D-mannose and 2,3,5,6-tetra-*O*-methyl-D-galactose. The latter compound was the only derivative of D-galactose found in the hydrolysis products from the methylated galactomannans II, and showed that this sugar was present in the polysaccharide exclusively as furanosidic nonreducing end groups.

The simplest general structure that can be proposed for the galactomannans II is shown in Fig. 1. The basic chain consists of $1 \rightarrow 6$ and $1 \rightarrow 2$ linked α-D-mannopyranose units. The sequence of these linkages cannot be determined from the present evidence, but $1 \rightarrow 2$ linkages predominate in the unbranched portions of the polysaccharides and some of them must therefore occur consecutively. Similarly, the length and distribution of the side chains must remain unknown at this stage of the work.

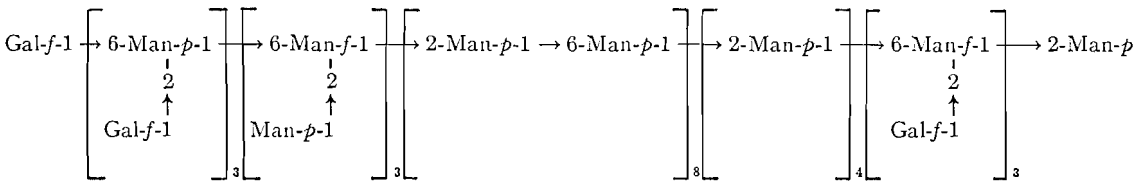


FIG. 1. General structure for galactomannans II.

Can. J. Chem. Downloaded from www.nrcresearchpress.com by 210.87.254.42 on 09/05/12
For personal use only.

Like the galactomannans I (2, 3), the galactomannans II appear to be unique among naturally occurring polysaccharides. The two groups of galactomannans resemble each other in having D-galactofuranoside nonreducing end groups, but the quantity of these units is higher in the galactomannans II. Both groups of galactomannans also contain $1 \rightarrow 6$ linked α-D-mannopyranose units but in different amounts. However, in the galactomannans II, $1 \rightarrow 2$ linked α-D-mannopyranose units predominate in the linear portions of the polysaccharide, and no such units occurred in galactomannans I. This constitutes a major structural difference between the two groups and demonstrates that two different galactomannans were present. Because of this basic structural difference it would be impossible for one galactomannan to be converted into the other by inadvertent chemical modification (e.g. removal of the acid-labile D-galactofuranoside units) during extraction or fractionation.

Preliminary tests have shown that the two groups of galactomannans have different serological properties, undoubtedly because of the major structural difference described above. There are only slight differences between the galactomannans within each group, as revealed by the studies of gross structure reported here and in the previous part (2) of this series. If the galactomannans within a group prove to have different serological properties, then further studies on the length of side chains and sequence of linkages may be required to explain the serological differences on a structural basis.

EXPERIMENTAL

Paper chromatograms were run by the descending method with the following solvent systems (v/v): (A) pyridine – ethyl acetate – water (1:2.5:2.5) (upper phase), and (B) butanone saturated with water. Whatman 3 MM paper was used for paper electrophoresis (6) in 0.1 *M* sodium tetraborate at a potential gradient of 25 V/cm for 1.5 h. A Tiselius-type, Spinco model H apparatus was used for moving-boundary electrophoresis in 0.05 *M* borate buffer (7). A Pye argon chromatograph and an F and M model 500 chromatograph were used for gas–liquid chromatography (8); the column packings were (*a*) 10% Carbowax 6000 on Chromosorb W, 100–120 mesh, and (*b*) 15% polyphenyl ether on Gas Chrom A, 100–120 mesh. Thin-layer chromatograms were on silica gel G with benzene–acetone (1:1) as developing solvent (9). Preparative thin-layer chromatography was carried out as previously described (2). Sugars on paper chromatograms, electrophoretograms, and thin-layer templates were detected by the *p*-anisidine hydrochloride spray reagent (10). Solvents were evaporated at 35–40 °C under reduced pressure; melting points are corrected; specific rotations are equilibrium values unless otherwise specified.

Isolation of Crude Polysaccharides

The growth and harvesting of the organisms and the extraction of mixtures of crude polysaccharides have been described in earlier papers in this series (1, 3).

Separation of Polysaccharides

The polysaccharides from each organism were resolved into two galactomannans and a glucan according to the scheme shown in Reaction Scheme 1. The first step, precipitation of galactomannans I as their insoluble copper complexes, was described in detail in part IV of this series (2). The water washings from the precipitates were combined with the individual supernatants, and the cooled solutions were acidified with concentrated hydrochloric acid at such a rate that the temperature never rose above 10 °C. The clear solutions were diluted with methanol until precipitation was complete. The precipitates were allowed to settle and the supernatants were decanted and discarded. The precipitates were then redissolved in the minimum amount of water and the solutions were deionized by passage through columns of Rexyn-101 (H^+) and Duolite-A4 (OH^-) ion-exchange resins. The deionized solutions were concentrated to thin syrups, to which ethanol was then added until precipitation was complete. The precipitates were centrifuged, washed successively with ethanol and ether, and air-dried to yield the polysaccharides soluble in Fehling solution (Reaction Scheme 1).

The recovered polysaccharides were chromatographed on diethylaminoethyl cellulose (4) (6 g per run on a 29 × 9 cm column containing 240 g of diethylaminoethyl cellulose). The sample was applied to the column as a 10% solution in 0.01 *M* sodium tetraborate, and the column was washed with a further 1 l of the same buffer; the eluate gave a negative anthrone test for carbohydrate. The buffer was then changed to 0.05 *M* sodium tetraborate, which displaced a polysaccharide (fraction 1). Elution with the same buffer was continued until the eluate gave a negative anthrone test (ca. 2.5 l), and the eluent was then changed to 0.1 *M* sodium hydroxide. Approximately 3.5 l of the latter was required to elute all of the second polysaccharide fraction (fraction 2).

Can. J. Chem. Downloaded from www.nrcresearchpress.com by 210.87.254.42 on 09/05/12
For personal use only.

Can. J. Chem. Downloaded from www.nrcresearchpress.com by 210.87.254.42 on 09/05/12
For personal use only.

The solution containing fraction 1 was passed over Rexyn-101 (H^+) ion-exchange resin and evaporated to dryness. Boric acid was removed from the residue by repeated addition and evaporation of methanol. The polysaccharide residue was then dissolved in the minimum volume of water and the solution was poured into a 10-fold volume of ethanol. The precipitated polysaccharide was then dried by solvent exchange with ethanol and ether. Samples (5 mg) of this fraction from each organism were hydrolyzed by *N* hydrochloric acid at 100 °C in sealed tubes for 10 h. D-Glucose was the only sugar detectable in the hydrolysates by paper chromatography (solvent A) or paper electrophoresis. The glucans behaved as homogeneous polysaccharides on moving-boundary electrophoresis, each with the same mobility ($\mu = 3.1 \times 10^{-5}$ cm^2 V^{-1} s^{-1}). Part VI of this series (5) describes other properties of the glucans and the investigation of their structures.

The solution containing fraction 2 from the diethylaminoethyl cellulose chromatography was neutralized by passage over Rexyn-101 (H^+) ion-exchange resin and evaporated to a thin syrup. Ethanol was added until precipitation was complete; the precipitated polysaccharides were centrifuged and dried by solvent exchange with ethanol and ether. Small samples of this fraction from each organism were hydrolyzed as described above for the glucans. Paper chromatography (solvent A) showed the presence of D-galactose, D-mannose, and small amounts of D-glucose.

The polysaccharides from fraction 2 were fractionally precipitated from aqueous solution by the stepwise addition of ethanol (11). A typical fractionation was as follows. The polysaccharide (6 g) was stirred in water (600 ml) and the solution was then centrifuged to remove a small, insoluble fraction (0.36 g). The addition of ethanol to the clarified aqueous solution yielded precipitates at the following ethanol concentrations: 50% (0.80 g), 60% (0.98 g), 65% (0.90 g), 70% (2.1 g), and 85% (0.31 g); recovery, 5.45 g (91%). The fraction that was insoluble in water and the one precipitated by 50% ethanol yielded D-glucose and smaller amounts of D-galactose and D-mannose on hydrolysis. The fractions precipitated by higher concentrations of ethanol (60–85%) yielded only D-galactose and D-mannose on hydrolysis, and were combined to give the galactomannans II.

Properties of Galactomannans II

The yields, based on the percentage of crude polysaccharides, and specific rotations of the galactomannans II are given in Table I. Samples (ca. 5 mg) of each galactomannan II were hydrolyzed by *N* hydrochloric acid (1 ml) in sealed tubes at 100 °C for 10 h. Sugars in the hydrolysates were separated by paper chromatography (solvent A) and their relative amounts, shown in Table I, were determined by the phenol – sulfuric acid method (12). The enantiomorphic forms of the sugars were established by isolation of crystalline derivatives of their *O*-methyl ethers as described below.

Galactomannans II were oxidized by periodate as described previously for the galactomannans I (2). Periodate was determined spectrophotometrically (13), and formic acid was determined by titration at the end of the oxidation. The following data indicated that extensive overoxidation occurred.

	Periodate consumed[2]					Formic acid produced[2]
Galactomannan II	2 h	10 h	18 h	24 h	48 h	
T. granulosum	0.72	1.33	1.42	1.51	—	0.41
T. interdigitale	1.34	1.52	1.68	1.80	1.92	1.04
M. quinckeanum	1.22	1.36	1.46	1.52	1.68	0.68
T. rubrum	1.15	1.34	1.45	1.52	1.76	0.68
T. schönleinii	1.19	1.37	1.54	1.66	1.91	0.63

Each galactomannan II gave a single, sharp symmetrical peak on moving-boundary electrophoresis in 0.05 *M* sodium tetraborate (electrophoretic mobility = 8.1×10^{-5} cm^2 V^{-1} s^{-1}). The galactomannans II also gave identical infrared spectra.

Methylation of Galactomannans II

Samples of the galactomannans II were methylated, first by the Haworth procedure (14) and then by the method of Falconer and Adams (15). Recoveries and methoxyl contents were as follows (calcd. methoxyl, 45.6%).

Galactomannan II	Original sample (g)	Recovered from methylation (g)	Methoxyl (%)
T. granulosum	0.50	0.28	45.2
T. interdigitale	2.60	1.48	42.8
M. quinckeanum	2.00	1.12	44.4
T. rubrum	2.00	1.30	45.5
T. schönleinii	1.97	1.30	43.3

These methylated galactomannans II showed no hydroxyl absorption in the infrared and had degrees of polymerization of 45–50, as determined by osmometry in chloroform solution with a Mechrolab vapor-pressure osmometer.

[2]*In moles per mole anhydrohexose.*

Hydrolysis Products from Methylated Galactomannans II

(i) Quantitative Estimation

The methylated galactomannans II were each hydrolyzed by sulfuric acid under conditions least likely to cause degradation or demethylation (16). A small portion (ca. 50 mg) of each mixture of hydrolysis products was boiled under reflux in 2% methanolic hydrogen chloride (2 ml) for 6 h. The methanolysates were neutralized by Duolite-A4 ion-exchange resin and then examined by gas–liquid chromatography (columns *a* and *b*). The following products were detected (with retention volumes relative to methyl 2,3,4,6-tetra-*O*-methyl-α-D-mannoside): column *a* (175 °C)—methyl tetra-*O*-methyl hexosides (1.00, 1.26); methyl tri-*O*-methyl mannosides (2.32, 2.82); methyl di-*O*-methyl mannosides (3.61, 5.33, 7.58, 9.32, 10.9, 13.7); column *b* (175 °C)—methyl 2,3,5,6-tetra-*O*-methyl-α,β-D-galactosides (0.94); methyl 2,3,4,6-tetra-*O*-methyl-α-D-mannoside (1.00); methyl tri-*O*-methyl mannosides (1.29, 1.50); methyl di-*O*-methyl mannosides (1.79, 2.11). Quantitative results were obtained by triangulation of the peaks on the gas–liquid chromatograms; the separation on column *a* provided the relative amounts of the methyl di-*O*-methyl mannosides, in which there were two major components: those with retention volumes of 7.58 and 13.7. Each of the other methyl di-*O*-methyl-D-mannosides amounted to less than 2% of the total mixture of methylated sugars. The separation on column *b* gave the ratio of di- to tri- to tetra-*O*-methyl-D-mannose methyl glycosides, and also permitted estimation of the methyl tetra-*O*-methyl-D-galactosides. Preparative thin-layer chromatography of the hydrolysates gave the same separation as column *b* and provided (by weight) the following check on the quantitative results for one of the mixtures; the others gave similar results.

	mole %	
Compound	Thin-layer chromatography	Gas–liquid chromatography
2,3,5,6-Tetra-*O*-methyl-D-galactose	29.7	28.3
2,3,4,6-Tetra-*O*-methyl-D-mannose	7.8	7.2
Tri-*O*-methyl-D-mannoses	40.5	42.5
Di-*O*-methyl-D-mannoses	22.2	22.0

The tri-*O*-methyl fraction contained two compounds which were not separable by paper or thin-layer chromatography or by gas–liquid chromatography of their methyl glycosides. However, the relative amounts of 2,3,4- and 3,4,6-tri-*O*-methyl-D-mannoses in the tri-*O*-methyl fractions were determined by the amounts recovered from preparative paper electrophoresis as described below. The quantitative results are summarized in Table II.

(ii) Isolation and Identification

The methylated sugars in each of the five mixtures were isolated and characterized by the same procedure. The mixtures of *O*-methyl sugars from hydrolysis of the methylated galactomannans II were resolved by preparative thin-layer chromatography to give the following fractions, in order of greatest mobility.

Fraction I.—The syrupy product gave a single spot on paper chromatography (solvent B) and a grey color with the spray reagent. Oxidation by bromine water yielded a syrupy lactone, which was converted into an amide in methanol saturated with ammonia. The amide crystallized spontaneously after evaporation of the solvent and was recrystallized from butanone to yield 2,3,5,6-tetra-*O*-methyl-D-galactonamide (17), m.p. 155–156 °C, $[\alpha]_D^{25}$ +6° (*c*, 3 in water).

Fraction II.—The syrupy product gave a single spot on paper chromatography (solvent B) and a red color with the spray reagent. A portion (ca. 5 mg) of the compound was boiled under reflux for 18 h in methanol containing Rexyn-101 (H^+) ion-exchange resin. The product had the same mobility on gas–liquid chromatography (column *b*) as methyl 2,3,4,6-tetra-*O*-methyl-α-D-mannoside. The rest of fraction II was converted into its anilide, which was recrystallized from ethyl acetate – light petroleum to yield *N*-phenyl-2,3,4,6-tetra-*O*-methyl-D-mannosylamine (18), m.p. 145–146 °C.

Fraction III.—The syrup gave one spot on paper chromatography (solvent B) and its methanolysate gave a single peak on gas–liquid chromatography (columns *a* and *b*). Paper electrophoresis showed the presence of two compounds, one migrating and one non-migrating, which were separated by preparative paper electrophoresis. The sections of the electrophoretograms containing the two compounds were eluted with water; the eluates were deionized (Rexyn-101 and Duolite-A4) and evaporated to dryness to yield the migrating (fraction III*a*) and non-migrating (fraction III*b*) components. The amounts recovered from each of the five mixtures provided the ratios of the two tri-*O*-methyl-D-mannoses.

Fraction III*a* crystallized spontaneously; recrystallization from ether–hexane (2:1) yielded 3,4,6-tri-*O*-methyl-D-mannose (19), m.p. 104–106 °C, $[\alpha]_D^{25}$ +35° (*c*, 2.17 in methanol).

Fraction III*b* was oxidized by bromine water and the product was esterified by 2% methanolic hydrogen chloride. The methyl ester was converted into the amide by methanol saturated with ammonia, and the amide was recrystallized from butanone to yield 2,3,4-tri-*O*-methyl-D-mannonamide (20), m.p. 142–144 °C.

Fraction IV.—Gas–liquid chromatography of the methyl glycosides of this fraction showed the presence of six components, two of which were present in larger amounts than the other four (see Table II). The

Can. J. Chem. Downloaded from www.nrcresearchpress.com by 210.87.254.42 on 09/05/12
For personal use only.

two major components were isolated by preparative paper chromatography in solvent A, which yielded fraction IV*a*, R_G 0.88, and fraction IV*b*, R_G 0.77. The latter fraction showed a streak on the chromatogram probably caused by the other minor components, which were not resolved; the streak was not collected.

Fraction IV*a* gave a brown color on the chromatograms with the *p*-anisidine hydrochloride spray. On paper electrophoresis it gave a single spot of the same mobility (M_G 0.42) as authentic 3,4-di-*O*-methyl-D-mannose. After methanolysis fraction IV*a* gave a single peak on gas–liquid chromatography, with the same retention volume as methyl 3,4-di-*O*-methyl-α-D-mannoside. Oxidation of fraction IV*a* with 4 moles of periodate at room temperature for 10 h gave a product which had the same mobility and color reactions on paper chromatograms as 2,3-di-*O*-methyl-L-arabinose. The syrupy product crystallized when seeded with an authentic sample of 3,4-di-*O*-methyl-D-mannose (21). Recrystallized from ethyl acetate, it had m.p. 71–73 °C, unchanged on admixture with an authentic sample.

Fraction IV*b* crystallized spontaneously; recrystallization from ethyl acetate yielded 3,5-di-*O*-methyl-D-mannose (22), m.p. 126–127 °C, unchanged on admixture with an authentic sample.

Serological Tests

Antisera produced in rabbits to autoclaved mycelial suspensions of each of these dermatophytes were used for analysis of these polysaccharides. By immunodiffusion and immunoelectrophoretic analyses, galactomannans I and galactomannans II were shown to be serologically distinct polysaccharides.

ACKNOWLEDGMENT

This work was, in part, supported by a grant from the John A. Hartford Foundation, Inc., New York.

REFERENCES

1. H. Alfes, C. T. Bishop, and F. Blank. Can. J. Chem. **41**, 2621 (1963).
2. C. T. Bishop, M. B. Perry, F. Blank, and F. P. Cooper. Can. J. Chem. **43**, 30 (1965).
3. C. T. Bishop, F. Blank, and M. Hranisavljevic-Jakovljevic. Can. J. Chem. **40**, 1816 (1962).
4. H. Neukom, H. Deuel, W. J. Heri, and W. Kündig. Helv. Chim. Acta, **43**, 64 (1960).
5. C. T. Bishop, M. B. Perry, R. K. Hulyalkar, and F. Blank. Can. J. Chem. This issue.
6. A. B. Foster. Advan. Carbohydrate Chem. **12**, 81 (1957).
7. D. H. Northcote. Biochem. J. **58**, 353 (1954).
8. C. T. Bishop. Advan. Carbohydrate Chem. **19**, 95 (1964).
9. R. Tschesche and G. Balle. Tetrahedron, **19**, 2323 (1963).
10. L. Hough, J. K. N. Jones, and W. H. Wadman. J. Chem. Soc. 1702 (1950).
11. R. L. Whistler and J. N. BeMiller. J. Am. Chem. Soc. **78**, 1163 (1956).
12. M. Dubois, K. A. Gilles, J. K. Hamilton, P. A. Rebers, and F. Smith. Anal. Chem. **28**, 350 (1956).
13. G. O. Aspinall and R. J. Ferrier. Chem. Ind. London, 1216 (1957).
14. W. N. Haworth. J. Chem. Soc. **107**, 8 (1915).
15. E. L. Falconer and G. A. Adams. Can. J. Chem. **34**, 338 (1956).
16. I. Croon, G. Herrström, G. Kull, and B. Lindberg. Acta Chem. Scand. **14**, 1338 (1960).
17. R. W. Humphreys, J. Pryde, and E. T. Waters. J. Chem. Soc. 1298 (1931).
18. J. C. Irvine and D. McNicoll. J. Chem. Soc. **97**, 1449 (1910).
19. H. G. Bott, W. N. Haworth, and E. L. Hirst. J. Chem. Soc. 1395 (1930).
20. W. N. Haworth, E. L. Hirst, F. A. Isherwood, and J. K. N. Jones. J. Chem. Soc. 1878 (1939).
21. P. A. J. Gorin and A. S. Perlin. Can. J. Chem. **34**, 1796 (1956).
22. B. Urbas, G. A. Adams, and C. T. Bishop. Can. J. Chem. **42**, 2093 (1964).

Can. J. Chem. Downloaded from www.nrcresearchpress.com by 210.87.254.42 on 09/05/12
For personal use only.

Can. J. Chem. Downloaded from www.nrcresearchpress.com by 210.87.254.6 on 09/05/12
For personal use only.

THE WATER-SOLUBLE POLYSACCHARIDES OF DERMATOPHYTES

VI. GLUCANS FROM TRICHOPHYTON GRANULOSUM, TRICHOPHYTON INTERDIGITALE, MICROSPORUM QUINCKEANUM, TRICHOPHYTON RUBRUM, AND TRICHOPHYTON SCHÖNLEINII[1]

C. T. BISHOP, M. B. PERRY, AND R. K. HULYALKAR[2]
Division of Biosciences, National Research Council, Ottawa, Canada

AND

F. BLANK
The Skin and Cancer Hospital, Temple University School of Medicine, Philadelphia, Pennsylvania

Received June 2, 1966

ABSTRACT

Polysaccharides obtained from each of the organisms designated in the title have been resolved into three groups: galactomannans I, galactomannans II, and glucans. The five glucans were homogeneous under conditions of electrophoresis, and had identical electrophoretic mobilities and infrared spectra. Methylation and hydrolysis of the glucans yielded varying amounts of the following: 2,3,4,6-tetra-*O*-methyl-D-glucose, 2,3,4-tri-*O*-methyl-D-glucose, 2,4,6-tri-*O*-methyl-D-glucose, and 2,4-di-*O*-methyl-D-glucose. The glucans were therefore branched polysaccharides, with branches formed by substitution at the C-3 and C-6 positions of D-glucopyranose units and terminated by D-glucopyranose units. The linear portions of the glucans contained $1 \rightarrow 6$ and $1 \rightarrow 3$ linkages but in varying amounts. These differences and some variation in the degrees of branching constituted the only dissimilarities detectable in the glucans by these structural studies.

Previous papers in this series have described the separation of three groups of polysaccharides from five dermatophytes: two galactomannans and a glucan (1,2). Structural studies on the galactomannans I have been reported (3,4), and the galactomannans II were described in part V of this series (2). The present paper describes the properties and gross structural features of the glucans from *Trichophyton granulosum* Sabouraud, 1909, *Trichophyton interdigitale* Priestley, 1917, *Microsporum quinckeanum* (Zopf) Guiart and Grigorakis, 1928, *Trichophyton rubrum* (Castellani) Sabouraud, 1911, and *Trichophyton schönleinii* (Lebert) Langeron and Milochevitch, 1930. A study of the glucan from *M. quinckeanum* was reported previously (1), and the results are included in the present paper to provide a full comparison of the glucans from the five organisms.

Mixtures of the three polysaccharides were extracted from powdered cells of the organisms as described previously (5), and separated into two galactomannans and glucans as reported in part V of this series (2).

Table I shows the yields and some of the properties of the glucans. The glucans were obtained in only 3–7% yields as compared with 30% for the galactomannans I (4) and 25% for the galactomannans II (2), and therefore constituted the smallest of the three groups of polysaccharides in the crude mixture. The specific rotations of the glucans showed considerable variation, the glucan from *T. granulosum* being singularly different in showing a positive value. The glucans showed no tendency to overoxidation by periodate; the values given for periodate consumption and formic acid production were constant over the period 24–42 h. The glucans were indistinguishable by electrophoresis; each one had the same mobility in borate buffer ($\mu = 3.1 \times 10^{-5}$ cm^2 V^{-1} s^{-1}).

[1]*Issued as N.R.C. No. 9109.*
[2]*National Research Council Postdoctorate Fellow, 1963–1965.*

TABLE I

Yields and properties of glucans from dermatophytes

Organism	Yield*	$[\alpha]_D$ (in water)	Periodate consumed†	Formic acid produced†
T. granulosum	6.5	+43°	1.54	0.72
T. interdigitale	5.0	−16°	1.46	0.76
M. quinckeanum	6.8	±0°	1.53	0.70
T. rubrum	2.8	−37°	1.12	0.52
T. schönleinii	4.0	−27°	1.50	0.67

*Percentage of crude polysaccharides.
†In moles per mole anhydroglucose unit.

The glucans were methylated fully and then hydrolyzed to yield mixtures of *O*-methyl-D-glucoses. These mixtures were analyzed by gas–liquid and paper chromatography to give the results shown in Table II. The ratio of tetra- to tri- to di-*O*-methyl-D-glucoses was determined by preparative paper chromatography; the relative amounts of the two isomers in the tri-*O*-methyl fraction were determined by gas–liquid chromatography of their methyl glucosides. Each of the *O*-methyl-D-glucoses was characterized by isolation of a crystalline derivative. The results showed that each glucan contained each of the structural features shown below and differed only in the relative amounts of them.



Thus, the glucans were branched polysaccharides, the branches occurring at the 3 and 6 positions of a D-glucopyranose unit (IV) and giving rise to the 2,4-di-*O*-methyl-D-glucose after methylation and hydrolysis. The branches were terminated by D-glucopyranose units (I), as shown by the presence of 2,3,4,6-tetra-*O*-methyl-D-glucose. The linear portions of the glucans contained $1 \rightarrow 6$ (II) and $1 \rightarrow 3$ (III) linkages, as represented by 2,3,4- and 2,4,6-tri-*O*-methyl-D-glucose, respectively. However, the relative amounts of $1 \rightarrow 6$ and $1 \rightarrow 3$ linkages in the linear portions varied from one glucan to another. The ratios of $1 \rightarrow 6$ to $1 \rightarrow 3$ linkages in the different glucans were as follows: *T. granulosum*, 1:0.72; *T. interdigitale*, 1:0.91; *M. quinckeanum*, 1:0.38; *T. rubrum*, 1:4.1; *T. schönleinii*, 1:1.32. These differences and some variation in the degree of branching, as represented by the amount of 2,4-di-*O*-methyl-D-glucose, constituted the only dissimilarities detectable in the glucans by the methods used.

TABLE II

Hydrolysis products of methylated glucans

	mole %				
	T. granulosum	*T. interdigitale*	*M. quinckeanum*	*T. rubrum*	*T. schönleinii*
2,3,4,6-Tetra-*O*-methyl-D-glucose	21.0	12.2	10.2	16.8	15.8
2,3,4-Tri-*O*-methyl-D-glucose	34.9	40.5	57.7	13.1	30.1
2,4,6-Tri-*O*-methyl-D-glucose	25.1	37.2	22.2	53.4	39.7
2,4-Di-*O*-methyl-D-glucose	19.0	10.2	8.1	16.7	14.4

Can. J. Chem. Downloaded from www.nrcresearchpress.com by 210.87.254.6 on 09/05/12
For personal use only.

Can. J. Chem. Downloaded from www.nrcresearchpress.com by 210.87.254.6 on 09/05/12
For personal use only.

The observed values for periodate oxidation of the original glucan (Table I) were all higher by about 0.5 mole than the values calculated from the methylation data. This is difficult to explain; any degradation that might have occurred under the alkaline conditions of methylation would be expected to cleave the periodate-resistant $1 \rightarrow 3$ linked units in preference to those joined by $1 \rightarrow 6$ glycosidic bonds (6). Such a degradation would therefore give a product for which the calculated periodate consumption was higher than the observed values.

The structural units I–IV could be joined together in a number of ways, and variations in the sequence of linkages could occur in the different glucans. There may also be some variation in the relative amounts of α- and β-glucosidic bonds, as shown by the specific rotations of the glucans (Table I). From those values it would appear that the glucans from *T. granulosum* and *M. quinckeanum* contained a higher proportion of α-linkages than the other three glucans. The five glucans gave identical infrared spectra, but the bands in the range 960–730 cm^{-1}, reported to be indicative of anomeric configuration (7), were not resolved.

The glucans from these five dermatophytes differ from most glucans that have been isolated from other microorganisms. They are distinguished by their specific rotations from the highly dextrorotary bacterial dextrans (8) and from *pullulan*, a glucan from the yeast-like fungus *Pullularia pullulans* (9, 10). However, a β-glucan has also been isolated from cultures of *Pullularia pullulans* and shown to contain $1 \rightarrow 6$ and $1 \rightarrow 3$ linkages in a highly branched structure (11) similar to those of the glucans from dermatophytes. Glucans from species of *Agrobacteria* contain a preponderance of β-$1 \rightarrow 2$ linkages (12), and an intracellular glucan from *Brucella suis* was shown to have β-$1 \rightarrow 4$ or β-$1 \rightarrow 2$ linkages but no $1 \rightarrow 6$ glycosidic bonds (13). A glucan from the fungus *Polyporus betulinus* contained mainly $1 \rightarrow 3$ linkages, but small amounts of other linkages could not be excluded (14).

The glucans from dermatophytes resemble the glucans isolated from the yeasts *Saccharomyces cerevisiae* (15, 16) and *Candida albicans* (17), a glucan produced by the fungus *Claviceps purpurea* (18), and a glucan from another unidentified fungus (19), in containing $1 \rightarrow 3$ and $1 \rightarrow 6$ linkages. Differences occur only in the relative amounts of these two linkages and in the degrees of branching in the polysaccharides. The glucans from *Claviceps purpurea* (18) and from the unidentified fungus (19) were shown to have a basic chain of $1 \rightarrow 3$ linked D-glucopyranose units, with single unit branches of D-glucopyranose attached by $1 \rightarrow 6$ linkages. Further work is required to determine whether a similar arrangement of $1 \rightarrow 3$ and $1 \rightarrow 6$ linkages occurs in the glucans from dermatophytes.

EXPERIMENTAL

Paper chromatograms were run by the descending method with the following solvent systems (v/v): (A) pyridine – ethyl acetate – water (1:2.5:2.5) (upper phase), and (B) butanone saturated with water. Sugars were detected on chromatograms by the *p*-anisidine hydrochloride spray reagent (20). Whatman 3 MM paper was used for paper electrophoreses, which were run in 0.1 *M* sodium tetraborate at 750 V (potential gradient, 25 V/cm) and 25–40 mA for 1.5 h (21). A Pye argon chromatograph was used for gas–liquid chromatography (22); the column packing was 10% of neopentyl glycol sebacate on Gas Chrom Z (100–120 mesh), the column temperature was 165 °C, and the flow rate was 100 ml argon/min. Solvents were evaporated at 35–40 °C under reduced pressure; melting points are corrected; specific rotations are equilibrium values unless otherwise specified. R_G values represent movement relative to 2,3,4,6-tetra-*O*-methyl-D-glucose on paper chromatograms.

Isolation and Properties of Glucans

The organisms were cultured and polysaccharides were extracted from the dried mycelia as reported previously (5). The separation of the glucans from the two galactomannans was described in the preceding paper (2). Yields, based on crude polysaccharides, and specific rotations of the glucans are shown in Table

I. A Tiselius-type, Spinco model H apparatus was used for moving-boundary electrophoresis of the glucans in 0.05 *M* sodium tetraborate (23); each glucan gave a single, sharp symmetrical peak of mobility = 3.1 $\times 10^{-5}$ cm^2 V^{-1} s^{-1}. Hydrolysis of these glucans yielded D-glucose exclusively, as shown by paper chromatography (solvent A) and paper electrophoresis.

Periodate Oxidations

Samples (11–12 mg) of each glucan were dissolved in 0.015 *M* sodium periodate (10 ml) and stored in the dark at room temperature. At intervals aliquots (0.1 ml) were removed and diluted to 25 ml with water, and periodate was determined spectrophotometrically (24). Periodate consumptions reached the values given in Table I after 24 h and were unchanged after 42 h. The amount of formic acid was determined by titration of the remaining oxidation solutions to a phenolphthalein end point after destruction of the excess periodate by the addition of 2 drops of butan-1,3-diol.

Methylation

Glucans from the five dermatophytes were dissolved in water and reduced by potassium borohydride (50 mg) to protect them from alkaline degradation (6). The reduced glucans were then methylated, first by dimethyl sulfate and 40% sodium hydroxide (25), then by dimethyl sulfate and solid sodium hydroxide in tetrahydrofuran (26). Recoveries and methoxyl contents were as follows (calcd. methoxyl, 45.6%).

Organism	Glucan	Methylated glucan	Methoxyl (%)
T. granulosum	100 mg	83.7 mg	43.3
T. interdigitale	1.1 g	0.48 mg	41.8
M. quinckeanum (1)	3.5 g	1.8 g	44.3
T. rubrum	400 mg	175.5 mg	44.8
T. schönleinii	801 mg	240 mg	42.9

The methylated glucans showed only traces of hydroxyl absorption in the infrared.

Hydrolysis Products from Methylated Glucans

The methylated glucans were hydrolyzed by sulfuric acid under the conditions reported as causing minimum degradation and demethylation (27). Paper chromatography (solvent B) of the hydrolysate showed the presence of the following products: 2,3,4,6-tetra-*O*-methyl-D-glucose (R_G 1.00), 2,3,4-tri-*O*-methyl-D-glucose (R_G 0.70), 2,4,6-tri-*O*-methyl-D-glucose (R_G 0.60), 2,4-di-*O*-methyl-D-glucose (R_G 0.23). Small portions (ca. 5 mg) of each hydrolysate were boiled under reflux for 6 h with 2% methanolic hydrogen chloride (1 ml). Acid was removed by silver carbonate and the methyl glucosides in the solution were examined by gas–liquid chromatography to give the relative amounts of the two tri-*O*-methyl isomers. Complete analysis of the mixture could not be obtained with the open injection system because some of the methyl di-*O*-methyl glucosides were either preferentially adsorbed or destroyed. The closed injection apparatus used in the earlier investigation of the glucan from *M. quinckeanum* (1) was not available at this time.

The rest of the hydrolysates were resolved by preparative paper chromatography in solvent B; the amounts recovered gave the mole percentage compositions shown in Table II. The compounds were identified as follows.

2,3,4,6-Tetra-O-methyl-D-glucose

The compound crystallized and was recrystallized from *n*-hexane to yield 2,3,4,6-tetra-*O*-methyl-D-glucose (28), m.p. 93–94 °C, $[\alpha]_D^{24}$ +83° (*c*, 1 in water).

2,3,4-Tri-O-methyl-D-glucose

The syrupy product yielded a crystalline anilide that was recrystallized from ether to give *N*-phenyl-2,3,4-tri-*O*-methyl-D-glucosylamine (29), m.p. 144–145 °C, $[\alpha]_D^{24}$ +70° (*c*, 1 in ethanol).

2,4,6-Tri-O-methyl-D-glucose

This product crystallized spontaneously and was recrystallized from ether to yield 2,4,6-tri-*O*-methyl-D-glucose (30), m.p. 121–122 °C, $[\alpha]_D^{25}$ +71° (*c*, 1 in water).

2,4-Di-O-methyl-D-glucose

The syrupy product was boiled under reflux for 6 h with 2% methanolic hydrogen chloride. The resulting mixture of methyl 2,4-di-*O*-methyl-α,β-glucosides crystallized when seeded with a crystal of methyl 2,4-di-*O*-methyl-α-D-glucoside obtained previously (1). Recrystallization from ether yielded methyl 2,4-di-*O*-methyl-α-D-glucoside (31), m.p. 79–80 °C, $[\alpha]_D^{24}$ +160° (*c*, 0.3 in acetone).

ACKNOWLEDGMENT

This work was, in part, supported by a grant from the John A. Hartford Foundation, Inc., New York.

Can. J. Chem. Downloaded from www.nrcresearchpress.com by 210.87.254.6 on 09/05/12
For personal use only.

REFERENCES

1. H. Alfes, C. T. Bishop, and F. Blank. Can. J. Chem. **41**, 2621 (1963).
2. C. T. Bishop, M. B. Perry, and F. Blank. Can. J. Chem. This issue.
3. F. Blank and M. B. Perry. Can. J. Chem. **42**, 2862 (1964).
4. C. T. Bishop, M. B. Perry, F. Blank, and F. P. Cooper. Can. J. Chem. **43**, 30 (1965).
5. C. T. Bishop, F. Blank, and M. Hranisavljevic-Jakovljevic. Can. J. Chem. **40**, 1816 (1962).
6. R. L. Whistler and J. N. BeMiller. Advan. Carbohydrate Chem. **13**, 289 (1958).
7. S. A. Barker, E. J. Bourne, M. Stacey, and D. H. Whiffen. J. Chem. Soc. 171 (1954).
8. M. Stacey and S. A. Barker. Polysaccharides of micro-organisms. Oxford University Press, London. 1960.
9. H. O. Bouveng, H. Kiessling, B. Lindberg, and J. McKay. Acta Chem. Scand. **16**, 615 (1962).
10. W. Sowa, A. C. Blackwood, and G. A. Adams. Can. J. Chem. **41**, 2314 (1963).
11. H. O. Bouveng, H. Kiessling, B. Lindberg, and J. McKay. Acta Chem. Scand. **17**, 1351 (1963).
12. P. A. J. Gorin, J. F. T. Spencer, and D. W. S. Westlake. Can. J. Chem. **39**, 1067 (1961).
13. N. D. Gory, L. L. Kupferberg, and L. H. Graf. J. Bacteriol. **76**, 359 (1958).
14. R. B. Duff. J. Chem. Soc. 2592 (1952).
15. D. J. Bell and D. H. Northcote. J. Chem. Soc. 1944 (1950).
16. S. Peat, J. R. Turvey, and J. M. Evans. J. Chem. Soc. 3868 (1958).
17. C. T. Bishop, F. Blank, and P. E. Gardner. Can. J. Chem. **38**, 869 (1960).
18. A. S. Perlin and W. A. Taber. Can. J. Chem. **41**, 2278 (1963).
19. J. Johnson, S. Kirkwood, A. Misaki, T. E. Nelson, J. V. Scaletti, and F. Smith. Chem. Ind. London, 820 (1963).
20. L. Hough, J. K. N. Jones, and W. H. Wadman. J. Chem. Soc. 1702 (1950).
21. A. B. Foster. Advan. Carbohydrate Chem. **12**, 81 (1957).
22. C. T. Bishop. Advan. Carbohydrate Chem. **19**, 95 (1964).
23. D. H. Northcote. Biochem. J. **58**, 353 (1954).
24. G. O. Aspinall and R. J. Ferrier. Chem. Ind. London, 1216 (1957).
25. W. N. Haworth. J. Chem. Soc. **107**, 8 (1915).
26. E. L. Falconer and G. A. Adams. Can. J. Chem. **34**, 338 (1956).
27. I. Croon, G. Herrström, G. Kull, and B. Lindberg. Acta Chem. Scand. **14**, 1338 (1960).
28. J. C. Irvine and J. W. H. Oldham. J. Chem. Soc. **119**, 1744 (1921)
29. S. Peat, E. Schluchterer, and M. Stacey. J. Chem. Soc. 581 (1939).
30. W. N. Haworth and W. G. Sedgwick. J. Chem. Soc. 2573 (1926).
31. M. H. Adams, R. E. Reeves, and W. F. Goebel. J. Biol. Chem. **140**, 653 (1941).

Can. J. Chem. Downloaded from www.nrcresearchpress.com by 210.87.254.6 on 09/05/12
For personal use only.

Can. J. Chem. Downloaded from www.nrcresearchpress.com by 210.87.254.42 on 09/05/12
For personal use only.

SUBSTITUTIONS ÉLECTROPHILES EN SÉRIE NAPHTALÈNIQUE

III. SUR LE DI-*t*-BUTYL-2,7 NAPHTALÈNE[1]

LUCIEN ERICHOMOVITCH, MARCEL MÉNARD[2] ET FRANCIS L. CHUBB
Frank W. Horner Ltée, Montréal, Québec

ET

YVON PÉPIN ET JEAN-CLAUDE RICHER
Département de Chimie, Université de Montréal, Montréal, Québec

Reçu le 16 mai 1966

RÉSUMÉ

Les produits de réaction entre le di-*t*-butyl-2,7 naphtalène d'une part et l'acide nitrique, le brome, le chlorure de sulfuryle ou le chlorure d'iode d'autre part ont été examinés. La structure des produits obtenus a été établie grâce à la résonance magnétique nucléaire.

INTRODUCTION

Dans des travaux précédents (1, 2), il a été démontré que les réactions de monosubstitution sur le diméthoxy-2,7 naphtalène (I) conduisent aux dérivés du type II, alors que la sulfonation du di-*t*-butyl-2,7 naphtalène (III), qui est stériquement plus empêché, conduit au produit IV*a*. Un autre effet stérique a été noté au cours de ces travaux; en effet, alors que la dinitration du diméthoxy-2,7 naphtalène (I) conduit au dinitro-1,8 diméthoxy-2,7 naphtalène (V), la réaction de dibromuration pour sa part conduit au dibromo-1,6 diméthoxy-2,7 naphtalène (VI). Il s'avérait donc intéressant d'examiner la nature des produits de monosubstitution sur le di-*t*-butyl-2,7 naphtalène (III) et l'effet des substituants déjà présents sur les réactions de di- et de tri-substitution dans la série du di-*t*-butyl-2,7 naphtalène. Les résultats rapportés dans le présent travail auront donc trait aux réactions de nitration, chloruration, bromuration et iodation du di-*t*-butyl-2,7 naphtalène. De plus, certains dérivés des produits originaux de substitution seront aussi décrits.

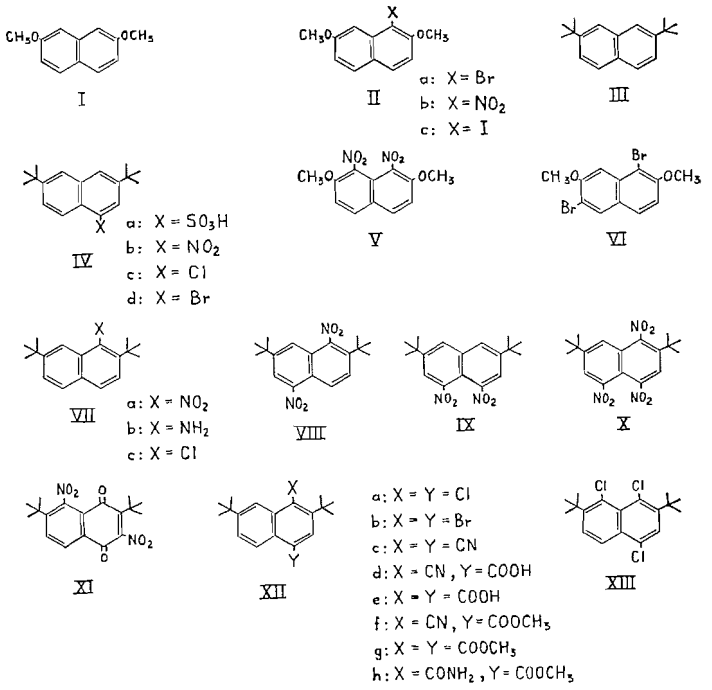
RÉSULTATS

La mononitration de l'hydrocarbure III conduit à deux isomères, l'un nitré en position 1 (VII*a*) et l'autre nitré en position 4 (IV*b*). Les proportions relatives de chacun, telles que déterminées par résonance magnétique nucléaire sur l'huile du mélange réactionnel, seraient de 56% de produit VII*a* et 44% du produit IV*b*; une détermination par infrarouge utilisant les bandes à 837 et 826 cm^{-1} pour les nitro-1 (VII*a*) et nitro-4 (IV*b*) di-*t*-butyl-2,7 naphtalène, respectivement, conduisent à des conclusions semblables. Une nitration plus poussée du di-*t*-butyl-2,7 naphtalène (III) conduit à un mélange contenant les dinitro-1,5 (VIII), dinitro-4,5 (IX) et trinitro-1,4,5 (X) di-*t*-butyl-2,7 naphtalènes aux côtés de la dinitro-3,8 di-*t*-butyl-2,7 naphtoquinone-1,4 (XI); en plus de ces produits, la chromatographie sur couche mince permet de détecter cinq autres produits qui sont présents en faible quantité et qui n'ont pas été isolés. Il est à noter que la nitration du nitro-4 di-*t*-butyl-2,7 naphtalène (IV*b*) conduit exclusivement aux dinitro-1,5 (VIII) et dinitro-4,5 (IX) di-*t*-butyl-2,7 naphtalènes, alors que la nitration du nitro-1 di-*t*-butyl-2,7

[1]*Les résultats rapportés dans cette communication sont extraits, en partie, du mémoire soumis par Yvon Pépin à la Faculté des Sciences de l'Université de Montréal, Montréal, en vue de l'obtention du grade de Maître ès Sciences (mars 1966).*

[2]*Adresse actuelle: Laboratoires Bristol du Canada, Candiac, Québec.*

naphtalène (VII*a*) conduit principalement au dinitro-1,5 di-*t*-butyl-2.7 naphtalène (VIII) et à la quinone dinitrée XI. La chromatographie sur couche mince permet dans chacun des cas de distinguer la présence des isomères à l'état de traces. Pour fins de comparaison, le nitro-1 di-*t*-butyl-2,7 naphtalène (VII*a*) a été réduit par l'étain et l'acide chlorhydrique en amino-1 di-*t*-butyl-2,7 naphtalène (VII*b*).



Lors de la chloruration du di-*t*-butyl-2,7 naphtalène (III) par 1 mole de chlorure de sulfuryle, un seul produit à savoir le chloro-1 di-*t*-butyl-2,7 naphtalène (VII*c*) a pu être isolé de l'huile provenant du mélange réactionnel. La dichloruration conduit aussi à un seul produit à savoir le dichloro-1,4 di-*t*-butyl-2,7 naphtalène (XII*a*); la réaction est toutefois assez délicate en ce sens que l'on est toujours en présence d'un mélange de monochloro-1 et de trichloro-1,4,8 di-*t*-butyl-2,7 naphtalène et qu'il est assez difficile d'arrêter la réaction au moment opportun. Quant à la trichloruration elle conduit au trichloro-1,4,8 di-*t*-butyl-2,7 naphtalène (XIII). D'autres produits seraient présents dans le mélange réactionnel mais n'ont pu être isolés.

Un essai d'iodation du di-*t*-butyl-2,7 naphtalène (III) par ICl ne conduit qu'au chloro-4 di-*t*-butyl-2,7 naphtalène (IV*c*). La chloruration de ce dérivé conduit au dichloro-1,4 di-*t*-butyl-2,7 naphtalène (XII*a*) obtenu précédemment.

La réaction du di-*t*-butyl-2,7 naphtalène (III) avec 1 mole de brome conduit exclusivement au bromo-4 di-*t*-butyl-2,7 naphtalène (IV*d*). Si des conditions réactionnelles plus énergiques sont utilisées, le dibromo-1,4 di-*t*-butyl-2,7 naphtalène (XII*b*) est isolé. La réaction de ce dérivé dibromé avec le cyanure cuivreux dans la diméthylformamide selon la méthode de Friedman et Schecter (3) conduit au dicyano-1,4 di-*t*-butyl-2,7 naphtalène (XII*c*), qui peut être hydrolysé par l'acide sulfurique pour conduire à un mélange d'acide cyano-1 di-*t*-butyl-2,7 naphtalène carboxylique-4 (XII*d*), d'acide di-*t*-butyl-2,7 naphtalène dicarboxylique-1,4 (XII*e*) et de leurs dérivés.

Can. J. Chem. Downloaded from www.nrcresearchpress.com by 210.87.254.42 on 09/05/12
For personal use only.

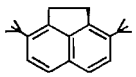
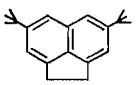
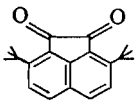
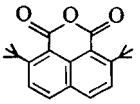
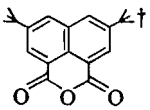
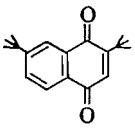
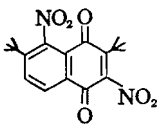
Can. J. Chem. Downloaded from www.nrcresearchpress.com by 210.87.254.42 on 09/05/12
For personal use only.

DISCUSSION

1. Sur la structure des composés obtenus

La structure de chacun des produits est attribuée d'une manière générale en se basant sur le patron de couplage des bandes des hydrogènes aromatiques dans la résonance magnétique nucléaire. Dans le cas des dérivés nitrés, la position des bandes dues à ces

TABLEAU I
Spectres r.m.n. des produits obtenus*

Di-*t*-butyl-2,7 naphtalène	H_1	H_3	H_4	H_5	H_6	H_8	*t*-Bu	
Hydrocarbure	7.82	7.50	7.76	7.76	7.50	7.82		
Nitro-1	—	7.68	7.95	7.98	7.68	7.37	1.32	1.43
Nitro-4	8.29	8.29	—	8.28	7.75	8.06	1.41	1.43
Dinitro-1,5	—	8.07	8.44	—	8.54	7.65	1.44	1.49
Dinitro-4,5	8.62	8.45	—	—	8.45	8.62	1.50	
Trinitro-1,4,5	—	8.77	—	—	8.78	7.71	1.45	1.54
Amino-1	—	7.00	7.29	7.60	7.38	8.04	1.38	1.47
Chloro-1	—	7.70	7.93	7.97	7.88	8.48	1.41	1.58
Chloro-4	8.12	7.82	—	8.20	7.82	8.02	1.39	
Dichloro-1,4	—	7.84	—	8.25	7.95	8.51	1.40	1.57
Trichloro-1,4,8	—	7.69	—	7.98	7.71	—	1.61	
Bromo-4	7.97	7.97	—	8.07	7.70	7.90	1.39	
Dibromo-1,4	—	7.92	—	8.10	7.79	8.51	1.42	1.61
Dicarboxylique-1,4	—	8.34	—	8.89	7.73	7.89	1.35	1.55
Cyano-1 carboxylique-4	—	8.25	—	8.87	7.88	8.25	1.44	1.66
Cyano-1 méthoxycarbonyle-4	—	8.25	—	8.74	7.90	8.25	1.45	1.65
Sulfonamide-4	8.26	8.08	—	8.65	7.62	7.98	1.41	
Sulfonate de cyclohexyle-4	8.30	8.23	—	8.44	7.70	8.07	1.40	1.43
	—	7.43	7.43	7.43	7.43	—	1.42	
	7.54	7.35	—	—	7.35	7.54	1.38	
	—	7.80	8.28	8.28	7.80	—	1.56	
	—	7.98	8.35	8.35	7.98	—	1.62	
	8.55	8.02	—	—	8.02	8.55	1.47	
	—	6.75	—	7.94	7.68	8.10	1.38	
	—	—	—	8.15	7.97	—	1.37–1.43	

*Des solutions dans la diméthylacétamide ont été utilisées.
†$CDCl_3$.

Can. J. Chem. Downloaded from www.nrcresearchpress.com by 210.87.254.42 on 09/05/12
For personal use only.

hydrogènes a aussi été utilisée; en effet, grâce à la méthode empirique de Wells et Alcorn (4), il est possible de prévoir quelles devraient être les positions d'absorption pour les différents hydrogènes aromatiques de ces molécules. Ces prédictions ainsi que les valeurs expérimentales observées sont résumées dans le Tableau II. La concordance entre les valeurs calculées et les valeurs expérimentales dans le cas des nitro-4 (IV*b*), dinitro-1,5 (IX) et trinitro-1,4,5 (X) di-*t*-butyl-2,7 naphtalènes est à la fois surprenante et convaincante. Cette méthode empirique échoue toutefois si elle est appliquée à l'isomère (VII*a*); l'explication plausible pour cette anomalie serait que, dans le nitro-1 di-*t*-butyl-2,7 naphtalène (VII*a*), le groupe nitro ne se trouve pas, comme dans les autres dérivés nitrés, dans le plan de la molécule à cause du groupe *t*-butyle en position 2. Il y aurait alors inhibition stérique de la résonance et l'effet du groupe nitro sur les hydrogènes aromatiques s'en trouverait pour autant diminué spécialement pour l'hydrogène en position 8, qui est maintenant retrouvé vers les champs élevés contrairement aux calculs qui le placent vers les champs les plus bas (Tableau II). Le déplacement de l'hydrogène en position 8 est aussi observé (2) dans le cas du nitro-1 diméthoxy-2,7 naphtalène (II*b*), et Wells et Alcorn (4) rapportent le même effet pour différents nitro-1 naphtalènes ayant un substituant alkyle en position 2. La réduction du groupe nitro en amine (composé VII*b*) ramène la bande due à l'hydrogène 8 vers les bas champs. Cependant, l'effet de déplacement de l'ensemble des pics disparaît aussi (Tableau II).

TABLEAU II
Comparaison des valeurs expérimentales avec les valeurs calculées

Di-*t*-butyl-2,7 naphtalène		H_1	H_3	H_4	H_5	H_6	H_8
Nitro-4 (IV*b*)	Calculé	8.24	8.24	—	8.23	7.76	8.07
	Trouvé	8.29	8.29	—	8.28	7.75	8.06
Dinitro-1,5 (VIII)	Calculé	—	7.94	8.42	—	8.42	7.79
	Trouvé	—	8.07	8.44	—	8.54	7.65
Dinitro-4,5 (IX)	Calculé	8.54	8.55	—	—	8.49	8.48
	Trouvé	8.62	8.45	—	—	8.45	8.62
Trinitro-1,4,5 (X)	Calculé	—	8.81	—	—	8.80	7.90
	Trouvé	—	8.77	—	—	8.78	7.71
Nitro-1 (VII*a*)	Calculé	—	7.70	8.18	8.01	7.78	8.29
	Trouvé	—	7.68	7.95	7.98	7.68	7.37
Amino-1 (VII*b*)	Trouvé	—	7.00	7.29	7.60	7.38	8.04

La structure du chloro-1 di-*t*-butyl-2,7 naphtalène (VII*c*) a été attribuée en se basant sur le fait que, dans le spectre de résonance magnétique nucléaire (r.m.n.) de ce composé, un système AB, avec constantes de couplage de 9 c.p.s., se retrouve superposé aux bandes attendues pour le système ABX des hydrogènes en position 5, 6 et 8. De même, dans le spectre r.m.n. du chloro-4 di-*t*-butyl-2,7 naphtalène (IV*c*), un système AB (J = 2 c.p.s.) est superposé aux bandes attendues pour le système ABX des hydrogènes en positions 5, 6 et 8. La structure du dichloro-1,4 di-*t*-butyl-2,7 naphtalène (XII*a*) est déduite du fait que les chloro-1 (VII*c*) et chloro-4 (IV*c*) di-*t*-butyl-2,7 naphtalènes conduisent au même dérivé dichloré; de plus, la présence dans le spectre r.m.n. de ce composé d'un pic sous forme de singulet suggère la présence de deux atomes de chlore attachés au même noyau. La présence dans le spectre r.m.n. du trichloro di-*t*-butyl-2,7 naphtalène (XIII) d'un singulet superposé aux bandes d'un système AB (J = 9 c.p.s.) n'est compatible qu'avec la présence des trois atomes de chlore dans les positions 1, 4 et 8. Les structures des bromo-4 (IV*d*) et dibromo-1,4 (XII*b*) di-*t*-butyl-2,7 naphtalènes ont été attribuées principalement à cause de la similitude très grande des spectres infrarouges de ces produits avec ceux des dérivés chlorés correspondants (IV*c* et XII*a*). Le

spectre r.m.n. du dibromo-1,4 di-*t*-butyl-2,7 naphtalène (XII*b*) est en accord avec la structure proposée. Les spectres r.m.n. du dicyano-1,4 di-*t*-butyl-2,7 naphtalène (XII*c*) et ses dérivés (XII*d* et XII*e*) obtenus à partir du dibromo-1,4 di-*t*-butyl-2,7 naphtalène (XII*b*) sont aussi en parfait accord avec les structures proposées.

2. Sur le mécanisme de formation des différents composés

Le premier fait important à noter est qu'alors que la chloruration de l'hydrocarbure III par SO_2Cl_2 ne conduit qu'au chloro-1 di-*t*-butyl-2,7 naphtalène (VII*c*) et que la nitration de III conduit aussi à des quantités importantes de nitro-1 di-*t*-butyl-2,7 naphtalène (VII*a*), les réactions de bromuration, sulfonation et chloruration par ICl ne conduisent qu'aux produits substitués en position 4 (IV*d*, IV*a* et IV*c*). Ces résultats indiqueraient que les intéractions stériques qui se développent entre certains réactifs et le groupe *t*-butyle peuvent déplacer le point d'attaque de la réaction de la position 1 vers la position 4 au fur et à mesure de l'augmentation de la grosseur du réactif.

Il est connu depuis longtemps (5) que la nitration du nitro-1 naphtalène conduit aux dinitro-1,8 et dinitro-1,5 naphtalènes. Par conséquent, la nitration du nitro-1 di-*t*-butyl-2,7 naphtalène (VII*a*) devrait conduire aux dinitro-1,5 (VIII) et dinitro-1,8 di-*t*-butyl-2,7 naphtalènes, alors que le nitro-4 di-*t*-butyl-2,7 naphtalène (IV*b*) devrait fournir les dinitro-1,5 (VIII) et dinitro-4,5 (IX) di-*t*-butyl-2,7 naphtalènes. Les résultats obtenus confirment ces prédictions en ce qui a trait à la formation des dinitro-1,5 (VIII) et dinitro-4,5 (IX) di-*t*-butyl-2,7 naphtalènes; toutefois, le dinitro-1,8 di-*t*-butyl-2,7 naphtalène ne semble pas se former, alors qu'une quantité appréciable de dinitro-3,8 di-*t*-butyl-2,7 naphtoquinone-1,4 (XI) est isolée du mélange réactionnel de la nitration du nitro-1 di-*t*-butyl-2,7 naphtalène (VII*a*). L'examen de ces résultats expérimentaux suggère que la quinone XI se forme à partir du nitro-1 di-*t*-butyl-2,7 naphtalène (VII*a*) et non pas à partir du nitro-4 di-*t*-butyl-2,7 naphtalène (IV*b*).

La formation de trinitro-1,4,5 di-*t*-butyl-2,7 naphtalène (X) indique que l'introduction d'un deuxième groupe nitro en position α d'un groupement *t*-butyle s'avère très difficile.

Le chlore offrant un encombrement stérique plus petit que celui d'un groupe nitro, l'approche de l'halogène vers la position 1 serait facilitée. Il n'est donc pas surprenant d'obtenir en prédominance la substitution en position 1 du chlore au cours de la monochloruration par le chlorure de sulfuryle.

Lors de la réaction de ICl avec l'hydrocarbure III les conditions sont telles que l'iodation du noyau aromatique s'effectuerait mais l'iode dans le complex intermédiaire serait aussitôt substitué par un atome de chlore pour donner le chloro-4 di-*t*-butyl-2,7 naphtalène. Ce genre de réaction a déjà été observé à plusieurs reprises par Andrews et Keefer (6). Ces résultats pourraient aussi être rapprochés à ceux rapportés par Lambourne et Robertson (7); ces auteurs ont notés que, lorsque le centre réactionnel est adjacent à une position portant un substituant volumineux, des réactions de chloruration plutôt que d'iodation sont observées. L'iode réagissant en premier, la réaction serait orientée de la même manière que la réaction de bromuration à savoir vers la position 4, qui est stériquement moins encombrée que la position 1, et le dérivé chloré provenant du remplacement de l'iode par un atome de chlore aurait donc la structure du chloro-4 di-*t*-butyl-2,7 naphtalène (IV*c*). Cette explication permettrait de justifier ce qui aurait pu apparaître comme une anomalie à savoir que la réaction de chloruration de III par le chlorure de sulfuryle conduit à un dérivé chloré en position 1 (VII*c*), alors que la réaction de chloruration par ICl conduit au chloro-4 di-*t*-butyl-2,7 naphtalène (IV*c*).

Il est toutefois surprenant que la dichloruration se produise sur le même noyau

Can. J. Chem. Downloaded from www.nrcresearchpress.com by 210.87.254.42 on 09/05/12
For personal use only.

Can. J. Chem. Downloaded from www.nrcresearchpress.com by 210.87.254.42 on 09/05/12
For personal use only.

aromatique. Il est bien connu en effet que les halogènes désactivent le noyau sur lequel ils sont substitués et devraient orienter un deuxième substituant sur le noyau adjacent. Les effets mésomériques des groupes *t*-butyles étant très faibles et leur encombrement stérique grand, les positions 3, 6 et 8 du chloro-1 di-*t*-butyl-2,7 naphtalène (VII*c*) peuvent être considérées comme défavorisées par opposition aux positions 4 et 5. Le fait que le deuxième atome de chlore s'introduise en position 4 pourrait être expliqué en admettant que l'effet inductif du chlore en position 1 est faible comparé à son effet mésomérique. La position 4 serait alors relativement peu désactivée mais serait quand même fortement polarisée par le chlore en position 1, qui favoriserait ainsi une disubstitution dans les positions 1 et 4. Il est intéressant de noter ici qu'une deuxième substitution sur un noyau portant déjà un atome de brome a été notée (8) dans la dibromuration du diméthoxy-1,7 naphtalène. De plus, dans des travaux antérieurs certains auteurs (9) ont supposé que les réactions de substitutions sur des halogéno-1 naphtalènes conduiraient aux naphtalènes substitués dans les positions 1 et 4. Il est probable que d'autres résultats seront nécessaires pour expliquer complètement cette réactivité.

La monobromuration donnant exclusivement l'isomère en position 4 peut être expliquée par le fait que le brome est beaucoup plus volumineux que le chlore et l'approche vers la position 1 est alors plus difficile et le brome est alors orienté vers la position 4. Si des conditions énergiques sont utilisées pour effectuer la réaction, il est alors possible d'introduire un deuxième atome de brome en position 1. La disubstitution sur le même noyau pourrait être expliquée par les mêmes raisons invoquées précédemment pour la dichloruration. Les expériences effectuées avec le diméthoxy-2,7 naphtalène ont montré que deux bromes ne peuvent s'accommoder en positions péri à savoir 1, 8 et 4, 5. Il ne reste donc alors que les positions 3 et 6 de disponibles pour une réaction de trisubstitution. Ces positions étant des positions β et encombrées, il n'est pas surprenant qu'aucun tribromo ne se soit formé même dans les conditions de réaction poussées.

Parmi les effets stériques dus aux groupes *t*-butyles qui ont été notés dans le présent travail, il convient de mentionner la stabilité relativement grande de groupes cyano vis-à-vis les réactions d'hydrolyse. En effet, dans les conditions où l'hydrolyse d'un des deux groupes cyano s'effectue complètement, des quantités considérables de produits qui n'ont pas été hydrolysés sont présentes; il est suggéré que le groupe cyano en position 1, qui est soumis à l'encombrement stérique du groupe *t*-butyle, est celui qui résiste le mieux à l'hydrolyse.

Il est donc évident que les groupes *t*-butyles dans les positions 2 et 7 influençent d'une façon prépondérante sur le cours des réactions de substitution sur ce noyau aromatique et provoquent aussi un ralentissement des vitesses de réaction des groupes attachés en position α.

PARTIE EXPÉRIMENTALE

Les spectres infra-rouges ont été mesurés à l'aide d'un spectrophotomètre Beckman, modèle IR-8, à double réseau. Les spectres ultra-violets ont été mesurés dans l'éthanol 95% à l'aide d'un appareil Bausch & Lomb Spectronic 505. Les spectres r.m.n. ont été déterminés à l'aide d'un spectromètre, modèle A-60, de la compagnie Varian. Les déplacements chimiques (δ) sont exprimés en parties par million et le tétraméthylsilane est utilisé comme référence interne. Les points de fusion ont été mesurés sur un "Hot Stage Apparatus" de la compagnie Reichert (Autriche). Les analyses élémentaires ont été effectuées par le Docteur Claude Daesslé, Montréal.

1. Nitrations

1.1. Mononitration du di-t-butyl-2,7 naphtalène

Un mélange de 3 g (12.5 mmoles) d'hydrocarbure III dans 200 ml d'acide acétique et 100 ml d'acide nitrique concentré est agité à la température de la pièce pendant 2 h. Après extraction à l'éther et cristallisation dans l'éthanol, 1.87 g (53% du rendement théorique) de produit mononitré sont obtenus. Par

cristallisation fractionnée dans l'éthanol, il est possible d'isoler le nitro-4 di-*t*-butyl-2,7 naphtalène (IV*b*), p.f. 68–69°C, et le nitro-1 di-*t*-butyl-2,7 naphtalène (VII*a*), p.f. 81–82 °C.

1.2. Dinitration du di-t-butyl-2,7 naphtalène

Un mélange de 1 g (4.2 mmoles) d'hydrocarbure III dans 30 ml d'acide acétique et 20 ml d'acide nitrique concentré est agité sur un bain-marie pendant 1 h. Le mélange est alors refroidi et extrait à l'éther. Par cristallisation de l'huile résiduelle dans l'éthanol, les dinitro-4,5 di-*t*-butyl-2,7 naphtalène (IX), p.f. 216–218 °C, dinitro-1,5 di-*t*-butyl-2,7 naphtalène (VIII), p.f. 76–78 °C, et dinitro-3,8 di-*t*-butyl-2,7 naphtoquinone-1,4 (XI), p.f. 225 °C, sont obtenus avec des rendements respectifs de 11%, 12% et 14% du rendement théorique.

1.3. Trinitration du di-t-butyl-2,7 naphtalène

Un mélange de 3 g (12.5 mmoles) d'hydrocarbure III dans 20 ml d'acide acétique et 30 ml d'acide nitrique fumant est chauffé sur un bain-marie pendant 30 min. Après refroidissement le mélange est extrait à l'éther; par recristallisation de l'huile résiduelle par de l'éthanol, 250 mg (6% du rendement théorique) de trinitro-1,4,5 di-*t*-butyl-2,7 naphtalène (X), p.f. 260 °C, et 500 mg (11% du rendement théorique) de dinitro-3,8 di-*t*-butyl-2,7 naphtoquinone-1,4 (XI), p.f. 225 °C, sont obtenus.

1.4. Nitration du nitro-1 di-t-butyl-2,7 naphtalène (VIIa)

Un mélange de 1 g (3.5 mmoles) de produit nitré VII*a* dans 50 ml d'acide acétique et 50 ml d'acide nitrique concentré est chauffé pendant 15 min sur un bain-marie. Le mélange est alors refroidi et extrait à l'éther; par cristallisation de l'huile obtenue à l'aide d'éthanol, 286 mg (22% du rendement théorique) de dinitro-3,8 di-*t*-butyl-2,7 naphtoquinone-1,4 (XI), p.f. 225 °C, et 106 mg (9% du rendement théorique) de dinitro-1,5 di-*t*-butyl-2,7 naphtalène (VIII), p.f. 76–78 °C, sont obtenus.

1.5. Nitration du nitro-4 di-t-butyl-2,7 naphtalène (IVb)

Un mélange de 500 mg (1.75 mmoles) de dérivé nitré IV*b* dans 10 ml d'acide acétique et 10 ml d'acide nitrique concentré est chauffé sur un bain-marie pendant 1 h. L'extraction à l'éther conduit à 450 mg (75% du rendement théorique) de produits dinitrés. Le spectre infra-rouge de ce produit brut ne révèle la présence d'aucune bande due à la dinitro-3,8 di-*t*-butyl-2,7 naphtoquinone-1,4; cependant, la présence des deux isomères dinitrés en proportion relative d'environ 50:50 est observée. La recristallisation de ce produit brut dans l'éthanol conduit à 153 mg (25% du rendement théorique) de dinitro-4,5 di-*t*-butyl-2,7 naphtalène (IX), p.f. 216–218 °C, et 110 mg (18% du rendement théorique) de dinitro-1,5 di-*t*-butyl-2,7 naphtalène (VIII), p.f. 76–78 °C.

1.6. Amino-1 di-t-butyl-2,7 naphtalène (VIIb)

A 1.0 g (3.5 mmoles) de nitro-1 di-*t*-butyl-2,7 naphtalène (VII*a*) dans 10 ml d'éthanol et 2 g d'étain en poudre, 20 ml d'acide chlorhydrique 20% sont ajoutés. Le mélange est alors chauffé pendant 10 min sur un bain-marie tout en maintenant une agitation. Après extraction des produits à l'éther et lavage avec de la soude 10%, 500 mg (50% du rendement théorique) d'amine VII*b*, p.f. 118–122 °C, sont isolés.

TABLEAU III

Analyse des produits nouveaux

	Point de fusion (°C)	C (%)		H (%)		Autre (%)	
		Calculé	Trouvé	Calculé	Trouvé	Calculé	Trouvé
Nitro-1	81–82	75.76	75.86	8.12	8.44	4.91 (N)	5.11
Nitro-4	68–69	75.76	75.36	8.12	7.98	4.91 (N)	5.09
Dinitro-1,5	76–78	65.44	65.98	6.71	7.13	8.48 (N)	8.40
Dinitro-4,5	216–218	65.44	65.40	6.71	7.00	8.48 (N)	8.81
Trinitro-1,4,5	260	57.59	57.97	5.64	5.70	11.19 (N)	11.34
Dinitro naphtoquinone	225	59.99	60.29	5.59	5.70	7.77 (N)	7.86
Chloro-1	80–81	78.66	78.61	8.44	8.10	12.90 (Cl)	13.03
Chloro-4	63–65	78.66	78.39	8.44	8.18	12.90 (Cl)	13.13
Dichloro-1,4	88–89	69.94	69.51	7.18	7.10	22.95 (Cl)	22.94
Trichloro-1,4,8	105–109	62.90	62.65	6.16	6.12	30.95 (Cl)	30.90
Bromo-4	69–70	67.71	67.66	7.27	7.02	25.03 (Br)	25.44
Dibromo-1,4	90–91	54.29	54.21	5.57	5.29	40.14 (Br)	39.92
			54.37		5.77		39.89
Dicyano-1,4	147–148	82.71	82.68	7.64	7.89	9.65 (N)	9.96
Cyano-1 carboxylique	234–236	77.56	77.55	7.47	7.28	4.52 (N)	5.01
Dicarboxylique-1,4	322–325	73.16	73.86	7.36	7.14		
Cyano-1 methoxycarbonyle-4	147–150	77.98	78.13	7.79	7.69	4.33 (N)	4.34
Carboxamide-1 methoxy-carbonyle-4	256–258	73.87	73.82	7.97	7.87	4.01 (N)	4.48
Dimethoxycarbonyle-1,4	Liquide	74.12	74.23	7.91	7.61		

Can. J. Chem. Downloaded from www.nrcresearchpress.com by 210.87.254.42 on 09/05/12
For personal use only.

2. Chlorurations

2.1. Chloro-1 di-t-butyl-2,7 naphtalène (VIIc)

Un mélange de 3 g (12.5 mmoles) d'hydrocarbure III dans 10 ml de chloroforme et 3.1 ml de chlorure de sulfuryle est laissé dans la glace pendant 2 h. Pour décomposer l'excès de chlorure de sulfuryl 25 ml d'éther et 10 ml d'eau sont alors ajoutés. L'extraction à l'éther et l'évaporation des solvants conduit à 3 g d'une huile qui, après recristallisation dans l'éthanol, donne 1.52 g (45% du rendement théorique) de chloro-1 di-*t*-butyl-2,7 naphtalène (VII*c*), p.f. 80–81 °C.

2.2. Chloro-4 di-t-butyl-2,7 naphtalène (IVc)

A 5 g (21 mmoles) d'hydrocarbure III dans 150 ml d'acide acétique, une solution contenant 3 équivalents de ICl (préparée à partir de 15 g de dichloroamine-*T* et 18.75 g d'iodure de sodium) dans 250 ml d'acide acétique est ajoutée. Le mélange est maintenu à la température de 55 °C pendant 2 h; après dilution avec 1 l d'eau le produit est extrait à l'éther. La recristallisation des produits dans l'éthanol conduit premièrement à la *p*-toluène sulfonamide, p.f. 137 °C, et puis à 2.41 g (42% du rendement théorique) de chloro-4 di-*t*-butyl-2,7 naphtalène (IV*c*), p.f. 63–65 °C.

2.3. Dichloro-1,4 di-t-butyl-2,7 naphtalène (XIIa)

Un mélange de 3 g (12.5 mmoles) d'hydrocarbure III dans 10 ml de chloroforme et 2.05 ml de chlorure de sulfuryle est laissé à la température de la pièce pendant 4 h. L'extraction des produits à l'éther conduit à une huile qui, après cristallisation dans l'éthanol, donne 750 mg (20% du rendement théorique) de dichloro-1,4 di-*t*-butyl-2,7 naphtalène (XII*a*), p.f. 88–89 °C. Du chloro-1 di-*t*-butyl-2,7 naphtalène (VII*c*, 900 mg) est aussi recueilli.

2.4. Trichloro-1,4,8 di-t-butyl-2,7 naphtalène (XIII)

A 3 g (12.5 mmoles) d'hydrocarbure III dans 10 ml de chloroforme, 9 ml de chlorure de sulfuryle sont ajoutés lentement. Après l'addition, le mélange est chauffé à reflux pendant 10 min, puis refroidi et extrait à l'éther. L'huile ainsi obtenue est cristallisée dans l'éthanol et conduit à 730 mg (19% du rendement théorique) de trichloro-1,4,8 di-*t*-butyl-2,7 naphtalène (XIII), p.f. 105–109 °C.

3. Bromurations

3.1. Bromo-4 di-t-butyl-2,7 naphtalène (IVd)

A 5 g (21 mmoles) d'hydrocarbure III dans 200 ml de chloroforme, 1.4 ml (21 mmoles) de brome dans 50 ml de chloroforme sont ajoutés. Le mélange est agité à reflux pendant 7 h et puis refroidi. L'extraction des produits et la cristallisation de l'huile résiduelle dans l'éthanol conduit à 3.07 g (45% du rendement théorique) de bromo-4 di-*t*-butyl-2,7 naphtalène (IV*c*), p.f. 69–70 °C. Le reste est du produit qui n'a pas réagi.

3.2. Dibromo-1,4 di-t-butyl-2,7 naphtalène (XIIb)

Bromuration dans l'acide acétique.—A une solution de 2 g (8.3 mmoles) d'hydrocarbure III dans 100 ml d'acide acétique, 3 ml (45 mmoles) de brome dissous dans 50 ml d'acide acétique sont ajoutés. Le mélange est agité sur un bain-marie pendant 2 h, puis refroidi et extrait à l'éther. L'excès de brome est détruit par du thiosulfate de sodium, et l'huile obtenue après extraction à la manière habituelle conduit à 1.62 g (50% du rendement théorique) de dibromo-1,4 di-*t*-butyl-2,7 naphtalène (XII*b*), p.f. 90–91 °C.

Bromuration dans le tétrachlorure de carbone.—Un mélange de 25 g d'hydrocarbure III dans 400 ml de tétrachlorure de carbone est traité par 15 ml de brome et chauffé à 80 °C pendant 4 h. Le mélange réactionnel est laissé à la température de la pièce pour la nuit et le produit alors extrait à la manière habituelle. La cristallisation à l'aide d'éthanol de l'huile obtenue conduit à 12 g (30% du rendement théorique) de dibromo-1,4 di-*t*-butyl-2,7-naphtalène, p.f. 90–92 °C; l'huile résiduelle distillée à 174 °C et 0.5 mm Hg montre un spectre infra-rouge identique à celui du solide précédent.

3.3 Essai de tribromuration du di-t-butyl-2,7 naphtalène

Un mélange de 3 g (12.5 mmoles) de di-*t*-butyl-2,7 naphtalène et de 6 ml (110 mmoles) de brome dans 50 ml d'acide acétique est chauffé sur un bain-marie pendant 5 h. Après extraction à la manière habituelle, un spectre infra-rouge du produit brut de la réaction a été déterminé et s'avérait en tous points semblable à celui du dibromo-1,4 di-*t*-butyl-2,7 naphtalène. La cristallisation du produit brut dans l'éthanol redonne du dibromo-1,4 di-*t*-butyl-2,7 naphtalène.

4. Dérivés du dibromo-1,4 di-t-butyl-2,7 naphtalène

4.1. Préparation du dicyano-1,4 di-t-butyl-2,7 naphtalène (XIIc)

Le dibromo-1,4 di-*t*-butyl-2,7 naphtalène (XII*b*, 200 g) est traité par du cyanure cuivreux dans la diméthylformamide selon la méthode de Friedman et Schecter (3) et fournit 93 g (76% du rendement théorique) de dicyano-1,4 di-*t*-butyl-2,7 naphtalène (XII*c*), p.f. 147–148 °C, après cristallisation dans l'éthanol.

4.2. Préparation de l'acide cyano-1 di-t-butyl-2,7 naphtalène carboxylique-4 (XIId)

Par l'action d'un mélange d'acide sulfurique 70% et d'acide acétique glacial sur le dicyano-1,4 di-*t*-butyl-2,7 naphtalène à l'ébullition pendant 6 h, un solide de point de fusion entre 220 et 290 °C est obtenu par cristallisation dans l'éthanol du produit brut de la réaction. La recristallisation de ce solide dans un excès

Can. J. Chem. Downloaded from www.nrcresearchpress.com by 210.87.254.42 on 09/05/12
For personal use only.

d'acide acétique glacial bouillant fournit l'acide cyano-1 di-*t*-butyl-2,7 naphtalène carboxylique-4 (XII*d*), p.f. 234–236 °C. Le solide qui ne s'est pas dissous dans l'acide acétique bouillant fond entre 305 et 320 °C. Après plusieurs recristallisations de ce solide dans l'éthanol, l'acide di-*t*-butyl-2,7 naphtalène dicarboxylique-1,4 (XII*e*), p.f. 322–325 °C, est obtenu.

4.3. Préparation du cyano-1 méthoxycarbonyle-4 di-t-butyl-2,7 naphtalène (XIIf)

A 3 g du nitrile acide XII*d* obtenu dans la section précédente, une solution éthérée de diazométhane en excès est ajoutée. Après évaporation de l'éther, 2.5 g de l'ester attendu XII*f* sont obtenus sous forme de solide blanc, p.f. 147–150 °C.

4.4. Préparation du diméthoxycarbonyle-1,4 di-t-butyl-2,7 naphtalène (XIIg)

Une solution éthérée contenant 3 g du produit fondant entre 305 et 320 °C obtenu dans la section 4.2 est traitée par une solution éthérée de diazométhane. L'évaporation de l'éther conduit à une huile qui laisse précipiter 0.4 g d'un solide, p.f. 256–258 °C, dont l'analyse correspondrait à celle du méthoxy-carbonyl-4 di-*t*-butyl-2,7 naphtalène carboxamide-1 (XII*h*). L'huile résiduelle, qui distille sans décomposition à 250 °C et 0.1 mm Hg, fournit 1.5 g de diméthoxycarbonyle-1,4 di-*t*-butyl-2,7 naphtalène (XII*g*), dont le spectre infra-rouge est exempt des pics dûs au groupe NH.

REMERCIEMENT

Les auteurs remercient sincèrement le Conseil National de Recherches pour l'aide financière apportée sous forme d'octroi (A-1295).

BIBLIOGRAPHIE

1. M. MÉNARD, L. MITCHELL, J. KOMLOSSY, A. WRIGLEY et F. L. CHUBB. Can. J. Chem. **39**, 729 (1961).
2. J.-C. RICHER et Y. PÉPIN. Can. J. Chem. **43**, 3443 (1965).
3. L. FRIEDMAN et H. SCHECTER. J. Org. Chem. **26**, 2522 (1961).
4. P. R. WELLS et P. G. E. ALCORN. Australian J. Chem. **19**, 1108 (1963).
5. H. H. HODGSON et J. WALKER. J. Chem. Soc. 1346 (1933).
6. L. J. ANDREWS et R. M. KEEFER. J. Am. Chem. Soc. **86**, 4158 (1964); **79**, 1412 (1957).
7. L. J. LAMBOURNE et P. W. ROBERTSON. J. Chem. Soc. 1167 (1947).
8. J.-C. RICHER et C. LAMARRE. Can. J. Chem. **43**, 715 (1965).
9. G. SCHIERMANN, W. GUEFFROY et W. WINKELMULLER. Liebigs Ann. Chem. **487**, 270 (1931).

Can. J. Chem. Downloaded from www.nrcresearchpress.com by 210.87.254.42 on 09/05/12
For personal use only.

THE THERMAL REVERSIBILITY OF THE MICHAEL REACTION

V. THE EFFECT OF THE STRUCTURE OF CERTAIN THIOL ADDUCTS ON CLEAVAGE

C. F. H. ALLEN

Department of Chemistry, Rochester Institute of Technology, Rochester, New York

AND

W. J. HUMPHLETT

Research Laboratories, Eastman Kodak Co., Rochester, New York

Received October 22, 1965

ABSTRACT

A large number of Michael adducts have been prepared from β-morpholinoethanethiol and α,β-unsaturated compounds bearing a variety of functional groups. The extent of cleavage of 23 of these under reversal conditions has been determined quantitatively. The relation between structure and amount of cleavage has been discussed. A few heterocyclic thiols were also employed, to extend the generality of the reactions. With the latter, the thiol-cleaved product was separated and identified, to show that the cleavage was normal.

Can. J. Chem. Downloaded from www.nrcresearchpress.com by 210.87.254.5 on 09/05/12
For personal use only.

It has been noted earlier that an arrangement of functional groups in the order of their activation of the Michael reaction would be useful (1). In our previous paper (2), morpholinoethanethiol adducts of α,β-unsaturated ketones (chalcones) having substituents in the ortho, meta, and para positions of both aromatic rings were described. Furthermore, the extent of their cleavage (reversibility of the Michael reaction) in hot water was determined. Adducts Nos. 1–4 (Table I) (2) illustrate similar reactivity in the present work. It was noted that related Michael adducts lacking an aryl group in the beta position were cleaved slightly or not at all under the same conditions, but were converted, in varying degrees, into their components in aqueous alkaline solution. To compare adducts with and without beta substituents, a study was made of a considerable number of such adducts lacking β-aryl groups. The addend, β-morpholinoethanethiol, was always the same so that the reversal would depend upon only the structure of the acceptor molecule (2); thus the functional groups in the latter were varied. The α,β-unsaturated compounds included those bearing open-chain (COAr, $COCH_3$) and cyclic ketonic, acidic ($CONH_2$, COOH), and neutral (CN, NO_2, $COOC_2H_5$) groups as well as two sulfones and three vinylpyridines. The degrees of cleavage of the substances investigated are shown in Table I. The adducts of heterocyclic mercaptans (Table II) underwent a similar reversal. In some of these instances, the reaction was not observed analytically, but instead, the resulting mercaptan was isolated and identified.

DISCUSSION OF RESULTS

Study suggests that the reversal reactions reached equilibrium rapidly at reflux, thus minimizing the dependency of the comparisons on rates. The data determined after 1 h of reflux (Table I) appear to represent equilibrium. The comparison of substituent effects was made under these conditions.[1] Previously, few quantitative data have been available on the position of the equilibrium (3).

[1]*A referee has suggested that: "It would be risky to equate relative yields after a fixed reaction period with relative reactivities. Discussion of substituent effects must relate to potential-energy variations, but it is entirely possible that two reactions could have the same energy of activation, thus leading to rate differences which have nothing to do with electronic effects of substituents. In the absence of a demonstration that all the reported reversals have similar entropies of activation, a correlation of relative yields with substituent effects may or may not be valid; some reservations should be expressed concerning the correlation."*

Can. J. Chem. Downloaded from www.nrcresearchpress.com by 210.87.254.5 on 09/05/12
For personal use only.

TABLE I

Determination of the extent of reversal of the conjugate addition of mercaptans (or thiols); % cleavage
(adduct = $R'CR''HCH_2R$, where R' = —$SCH_2CH_2NC_4H_8O \cdot HCl$)

No.	β-Substituent	R	Boiling H_2O for 2 min	20 ml of 0.1 *N* NaOH for 1 h		40 ml each of 1 *N* NaOH and C_2H_5OH		
						At 25 °C		
				At 25 °C	At reflux	For 0.5 h	For 1 h	At reflux for 1 h
		Ketones						
1	C_6H_5	COC_6H_5[d]	18, 18.5					
2	C_6H_5	COC_6H_5	58.2, 59.8					
3	C_6H_5	$COC_6H_4CH_3$-4	36.2					
4	C_6H_5	COC_6H_4OH-4	38.9					
5	C_6H_5	$COCH_3$				95.6[a]		95.8
6	None	$COCH_3$		48.5		65.9	65.7	78.2
7	None	COC_6H_5				65.3	65.3	88.5
8	None	$COC_6H_4OCH_3$-4				60.6	60.0	80.6
		Esters						
9	None	$(COOC_2H_5)_2$[c]				66.2[a]	65.3	65.0
10	C_6H_5	$(COOC_2H_5)_2$[c]				94.0[a]	95.0	94.5
11	4-$CH_3OC_6H_4$	$(COOCH_3)_2$[c]				93.5[a]	94.5	97.5
12	None	$COOCH_3$		2.3	16.0		0.7	7.0
		Nitrile						
13	None	CN		6.6	42.2		23.4	69.8
		Amide						
14	None	$CONH_2$		4.1	28.4		10.9	55.8
		Acids						
15	None	COOH		0	16.0		0	3.0
16	None	α-$C_6H_4NO_2$-4[b]COOH					49.8	70.6
		Nitro compound						
17	C_6H_5	NO_2				14.9[a]	23.9	60.2
		Sulfones						
18	None	$SO_2C_2H_5$					17.8	73.7
19	None	$SO_2C_6H_5$					20.5	78.0
		Heterocyclic rings						
20	None	Maleimide					5.0	66.3
21	None	2-Vinylpyridine·2HCl		0	20.5		0	4.5
22	None	4-Vinylpyridine·2HCl		0	89.0		0	48.4
23	None	4-Vinylpyridine·$2CH_3I$		79.5			19.9	

[a]For 10 min.
[b]α-Substituent.
[c]Malonate adducts; have the chain $R'CR''HCHR_2$.
[d]Free base.

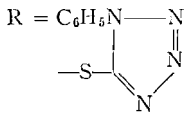
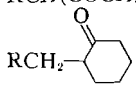
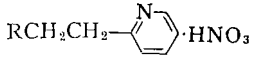
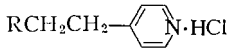
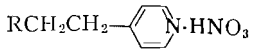
Can. J. Chem. Downloaded from www.nrcresearchpress.com by 210.87.254.5 on 09/05/12
For personal use only.

TABLE II

R = —SCH$_2$CH$_2$N⟨O⟩	Yield (%)	Melting point (°C)	Empirical formula	Analyses (%) Calculated C	Calculated H	Calculated N	Found C	Found H	Found N
A. Adducts of 2-morpholinoethanethiol									
RCH$_2$CH$_2$COCH$_3$	53								
RCH$_2$CH$_2$COCH$_3$·HCl	82	118–119[a]	$C_{10}H_{20}ClNO_2S$	47.3	7.9	5.5[p]	47.6	8.0	5.6
RCH(C$_6$H$_5$)CH$_2$COCH$_3$·HCl	59	124–125[a]	$C_{16}H_{24}ClNO_2S$	58.3	7.3	4.2	57.9	8.1	4.4
RCH$_2$CH$_2$COC$_6$H$_5$·HCl	83	186[b]	$C_{15}H_{22}ClNO_2S$	57.0	7.0	4.4	57.1	7.1	4.5
RCH$_2$CH$_2$COC$_6$H$_4$OCH$_3$-4·HCl	81	147[b]	$C_{16}H_{24}ClNO_3S$	55.6	7.0	4.1	55.5	7.3	3.8
RCH$_2$CH$_2$CN	86	123 at 0.05[a]	$C_9H_{15}N_2OS$	54.0	8.0	14.0[q]	54.4	8.3	14.1
RCH$_2$CH$_2$CN·HCl	78	134–135[a]	$C_9H_{17}ClNO_2S$	45.7	7.2	11.8	45.7	6.8	11.6
RCH$_2$CH$_2$CN·HClO$_4$	33	82–84[c]	$C_9H_{17}ClNO_2S$			9.3			9.1
RCH$_2$CH$_2$CONH$_2$	96	89–90[d]	$C_9H_{17}N_2O_2S$	49.5	8.3	12.8	49.0	8.5	12.7
RCH$_2$CH$_2$CONH$_2$·HCl	91	130[a]	$C_9H_{18}ClN_2O_2S$	42.4	7.5	13.9	42.5	7.6	13.9
RCH$_2$CH$_2$CONH$_2$·HClO$_4$	100	97–99[c]	$C_9H_{18}ClN_2O_6S$			8.8			9.1
RCH$_2$CH$_2$CO$_2$CH$_3$	76	114 at 0.05[o]	$C_{10}H_{19}NO_3S$	51.5	8.3	6.0[r]	51.8	8.4	5.6
RCH$_2$CH$_2$CO$_2$CH$_3$·HCl	61	144–145[b]	$C_{10}H_{20}ClNO_7S$		13.1	5.2		13.2	5.6
RCH$_2$CH$_2$CO$_2$CH$_3$·HClO$_4$	88	85–87[c]	$C_{10}H_{20}ClNO_7S$			4.2			3.8
RCH$_2$CH$_2$COOH	82	75[b]	$C_9H_{17}NO_3S$	49.3	7.8	6.4	49.0	7.8	6.7
RCH$_2$CH$_2$COOH·HCl	97	122–123[b]	$C_9H_{18}ClNO_3S$	42.3	7.1	5.5	42.3	7.0	5.4
RCH$_2$CH$_2$COOH·HClO$_4$	68	83–88[a]	$C_9H_{18}ClNO_7S$		10.8	4.2		11.2	3.8
RCH$_2$CH(C$_6$H$_4$NO$_2$-4)COOH·HCl	91	162[f]	$C_{15}H_{21}ClN_2O_5S$	47.8	5.6	7.4	48.1	5.9	7.6
RCH$_2$CH(COOC$_2$H$_5$)$_2$·HCl	61	122–123[a]	$C_{14}H_{26}ClNO_5S$	47.2	7.4	3.9	46.8	7.0	3.4
RCH(C$_6$H$_5$)CH(COOCH$_3$)$_2$·HCl	94	167	$C_{18}H_{26}ClNO_5S$	53.5	6.5	3.5	53.8	6.6	3.5
RCH(C$_6$H$_5$)CH(COOC$_2$H$_5$)$_2$·HCl	93	130[g]	$C_{20}H_{30}ClNO_5S$	55.7	6.8	3.2	55.9	7.1	3.1
RCH(C$_6$H$_4$OCH$_3$-4)CH(COOCH$_3$)$_2$·HCl	89	165[a]	$C_{19}H_{28}ClNO_6S$	52.6	6.5	3.1	52.5	6.4	3.2
RCH$_2$CH$_2$SO$_2$C$_2$H$_5$·HCl	85	134[b]	$C_{10}H_{22}ClNO_3S_2$	39.5	7.3	4.6	39.9	7.4	4.6
RCH$_2$CH$_2$SO$_2$C$_6$H$_5$·HCl	50	122[b]	$C_{14}H_{22}ClNO_3S_2$	47.8	6.3	4.0	48.0	6.4	3.8
RCH(C$_6$H$_5$)CH$_2$NO$_2$·HCl	86	182–183[b]	$C_{14}H_{21}ClN_2O_3S$	50.5	6.4	8.4	50.5	6.4	8.7
RCH$_2$CH$_2$⟨N⟩·2HCl	68	217[h]	$C_{13}H_{22}Cl_2N_2OS$	48.0	6.8	8.6	47.8	7.1	8.5
RCH$_2$CH$_2$⟨N⟩·2HCl	56	229[h]	$C_{13}H_{22}Cl_2N_2OS$	48.0	6.8	8.6	47.9	6.9	8.9
RCH$_2$CH$_2$⟨N⟩·2CH$_3$I	49	191[h]	$C_{15}H_{26}I_2N_2OS$	33.6	4.8	5.2	33.8	5.2	4.9
R⟨NH⟩	30	89–90[b]	$C_{10}H_{16}N_2O_3S$	49.2	6.6		49.0	6.5	
R⟨NH·HCl⟩	30	190–191	$C_{10}H_{17}ClN_2O_3S$	42.8	6.1		43.1	6.4	

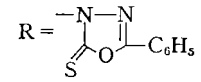
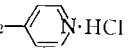
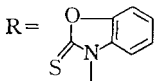
Can. J. Chem. Downloaded from www.nrcresearchpress.com by 210.87.254.5 on 09/05/12
For personal use only.

TABLE II (*Continued*)

	Yield (%)	Melting point (°C)	Empirical formula	Analyses (%) Calculated C	H	N	Found C	H	N
B. Adducts of heterocyclic thiols									
R = 									
$RCH_2CH_2COCH_3$	86	72[i]	$C_{11}H_{12}N_4OS$	53.2	4.9	22.6	53.1	5.3	22.5
$RCH_2CH_2COC_6H_5$	65	95[i]	$C_{16}H_{14}N_4OS$	61.9	4.5	18.0	61.8	4.9	18.3
$RCH_2CH_2COC_6H_4OCH_3$-4	62	114[b]	$C_{17}H_{16}N_4O_2S$	60.0	4.7	16.5	60.0	4.8	16.8
$RCH(COCH_3)CH_2COCH_3$	51	93[j]	$C_{16}H_{14}N_4OS$	53.8	4.9	19.3	53.6	5.1	19.6
	42	77[k]	$C_{14}H_6N_4OS$	58.3	5.6	19.4	58.5	5.6	19.8
	40	129[b]	$C_{13}H_{14}N_4OS$	56.9	5.1	20.4	57.2	5.3	21.0
	43	128[b]	$C_{14}H_{16}N_4OS$	48.5	4.1	24.3	48.9	4.3	24.5
	90	200[l]	$C_{14}H_{14}ClN_4S$	52.6	4.4	21.9	52.6	4.5	22.0
	56	122[b]	$C_{14}H_{16}N_4OS$	48.5	4.1	24.3	48.5	4.2	24.3

Can. J. Chem. Downloaded from www.nrcresearchpress.com by 210.87.254.5 on 09/05/12
For personal use only.

TABLE II (*Concluded*)

	Yield (%)	Melting point (°C)	Empirical formula	Analyses (%) Calculated C	H	N	Found C	H	N
R = 									
$RCH_2CH_2COCH_3$	52	55[l]	$C_{11}H_{12}N_2O_2S$	58.0	4.9	11.2	58.0	4.8	11.3
$RCH_2CH(COOCH_3)_2$	45	99[h]	$C_{14}H_{14}N_2O_5S$	52.2	4.4		52.5	4.7	
$RCH_2CH(COOC_2H_5)_2$	67	80[h]	$C_{16}H_{18}N_2O_5S$	54.8	5.2		55.2	5.1	
RCH_2CH_2—  ·HCl	45	200[b]	$C_{15}H_{24}ClN_2OS$	56.3	4.4	13.1	56.5	4.5	13.3
R = 									
$RCH_2CH(COOC_2H_5)_2$	17	67–68[h]	$C_{15}H_{17}NO_5S$	55.7	5.3		55.6	5.6	
$RCH_2CH_2SO_2CH_2CH_2R$	38	168[m]	$C_{18}H_{16}N_2O_4S_3$	51.4	3.8	6.7	51.6	3.8	7.0

[a]Recrystallized from methanol – ethyl acetate.
[b]Recrystallized from ethanol.
[c]Recrystallized from water.
[d]Recrystallized from benzene.
[e]Recrystallized from ethanol–benzene–ether.
[f]Recrystallized from ether–ethanol.
[g]Recrystallized from ethyl acetate.
[h]Recrystallized from methanol–ethanol.
[i]Recrystallized from ether.
[j]Recrystallized from ether–ligroin (b.p. 35–60°).
[k]Recrystallized from methanol.
[l]Recrystallized from ligroin (b.p. 35–60°).
[m]Recrystallized from xylene.
[n]n_D^{25} 1.5118.
[o]n_D^{25} 1.4968.
[p]Anal. Calcd.: S, 12.6. Found: S, 12.7.
[q]Anal. Calcd.: S, 16.0. Found: S, 16.4.
[r]Anal. Calcd.: S, 13.7. Found: S, 14.0.

In general, activation of the α-hydrogen atom appears to activate the adduct towards reversal, as expected by electronic theory. Thus, the cleavage may largely be predicted. The order of cleavage indicated is ketone > nitrile > amide > acid. Esters are not included within this order because of their probable hydrolysis to carboxylic acids (cf. Nos. 12 and 15). However, the adduct of methyl vinyl ketone was observed to reverse upon attempted distillation, whereas the adducts of acrylonitrile and methyl acrylate were unchanged upon distillation. These orders support that of Connor's generalization: ketones > esters > nitriles (1). The activating influence of a β-phenyl group is evident from a comparison of the ketones (Nos. 5 and 6). The adduct of a phenyl ketone (No. 7) appears to be more reactive than that of a methyl ketone (No. 6). An electron-repelling group in the para position (No. 8) measurably decreases the activity. On this basis, the relative reactivities of ketones is expected to be $-COC_6H_4NO_2$-4 > $-COC_6H_5$ > $-COCH_3$ = $-COC_6H_4OCH_3$-4. The adduct of acrylic acid (No. 15) is practically stable, whereas the derivative bearing a strong electron-attracting alpha substituent (No. 16) shows activation towards cleavage. Cleavage is particularly large because of activation by two carbonyl groups, as in the adducts of methylenemalonic esters (Nos. 9–11). A β-phenyl effect is also evident (No. 10). The cleavage reactivity of adducts of conjugated sulfones (Nos. 18 and 19) suggests significant α-hydrogen activity. The adducts of the heterocyclic unsaturated compounds (Nos. 21–23) indicate that the adduct from 4-vinylpyridine is more reactive than that from 2-vinylpyridine. The forming of a quaternary ammonium salt is expected to increase the reactivity.

EXPERIMENTAL

Adduct Formation

Mercaptans have been used to a limited extent in Michael additions (4–6); they add to α,β-unsaturated ketones without a catalyst more readily than to esters (7). In this work the procedure was varied depending upon the components. β-Morpholinoethanethiol was added to the second component, even to acrylic acid, simply by refluxing in alcohol; the amine moiety probably functioned as a catalyst (method A). Similarly, heterocyclic mercaptans were added to 2- and 4-vinylpyridine. The addition failed, however, with methyl cinnamate, methyl crotonate, and cinnamonitrile. A similar failure has been noted when nitromethane and an amine catalyst were used (8). 5-Mercapto-1-phenyltetrazole and 2-mercapto-5-phenyl-1,3,4-oxadiazole were added to conjugated ketones effectively in acetic acid (method B). In a few instances, when sodium acetate and refluxing in acetic acid were used (method C), appropriate Mannich bases served as the source of vinyl ketones. The addition of 2-mercaptobenzoxazole was catalyzed by sodium methoxide (method D).

Dimethyl malonate (9), dimethyl benzalmalonate (10), diethyl methylenemalonate (11), β-dimethylaminopropiophenone hydrochloride (12), maleimide (13), ethyl vinyl sulfone (14), and phenyl vinyl sulfone (15) were prepared as described in the literature. Diethyl benzalmalonate and dimethyl p-methoxybenzalmalonate were preferably prepared by the use of a continuous reactor (16). The latter ester solidified after distillation, b.p. 130–135° at 0.03 mm, m.p. 59–60° after crystallization from ethanol (66% yield).

Anal. Calcd. for $C_{13}H_{14}O_5$: C, 62.4; H, 5.6. Found: C, 62.4; H, 5.7.

Method A

Equimolar amounts of the acceptor component and β-morpholinoethanethiol in absolute ethyl alcohol were refluxed for 1 h and the solvent was removed under reduced pressure. Volatile products were fractionated through a 10 cm column filled with glass helices. Nonvolatile products, whether oils or solids, were dissolved in ether, and converted into salts with hydrogen chloride. Perchlorates were prepared by treating the hydrochlorides in methanol with sodium perchlorate.

Method B

Equimolar amounts of the acceptor molecule and β-morpholinoethanethiol in acetic acid were refluxed for 1 h, unless the acceptor had a low boiling point (methyl vinyl ketone, methyl acrylate); in these instances the reaction mixture was maintained at 70–80° for 30 min and then boiled for 10 min. Most of the solvent was removed under reduced pressure. When the residue was allowed to stand overnight, the crude product crystallized.

Method C

(*i*) A suspension of 0.2 mole of either component (42.6 g of β-dimethylaminopropiophenone hydrochloride or 54.8 g of the corresponding p-methoxypropiophenone hydrochloride), 29.5 g of β-morpholinoethanethiol, and 19.5 g of dry potassium acetate in 500 ml of xylene was refluxed for 1 h, during which time the solids

Can. J. Chem. Downloaded from www.nrcresearchpress.com by 210.87.254.5 on 09/05/12
For personal use only.

became a fine powder. The reflux condenser was removed and the mixture was boiled to remove the dimethylamine. After filtration of the precipitated potassium chloride, the solvent was removed under reduced pressure, leaving a brown oil. Addition of hydrogen chloride to a solution of this oil in ether gave the hydrochloride, which crystallized after being allowed to stand for 1 h. β-Dimethylamino-*p*-methoxypropiophenone hydrochloride was made by the usual procedure and used without purification.

(*ii*) A mixture of 0.04 mole of β-dimethylamino-α-(*p*-nitrophenyl)propionic acid (17), 6.9 g of β-morpholinoethanethiol, 4.1 g of potassium acetate, and 100 ml of acetic acid was maintained at 80° for 15 min, and then boiled for 10 min. Hydrogen chloride was passed through the cooled mixture, and sufficient ether was then added to precipitate the hydrochloride as an oil. After the oil had been decanted, addition of a small amount of ether–alcohol caused crystallization. The product was collected and recrystallized, after filtration of any salt present.

(*iii*) 5-Mercapto-1-phenyltetrazole formed adducts (Table IIB) on treatment of the hydrochlorides of β-dimethylaminopropiophenone, β-dimethylamino-*p*-methoxypropiophenone, and β-dimethylaminomethylcyclohexanone (18) in the following manner. Equimolar amounts of the Mannich base and potassium acetate in acetic acid were boiled for 15 min and then poured into 15 volumes of ice water. The product crystallized when allowed to stand overnight.

Method D

Sufficient sodium methoxide was added to a solution of 11.8 g (0.1 mole) of divinyl sulfone and 30.2 g (0.2 mole) of 2-mercaptobenzoxazole in 300 ml of hot ethanol to make the solution basic. The adduct began to separate as the mixture was refluxed for 1 h. The reaction mixture was then concentrated and the product was collected.

Cleavage of Adducts

Iodometric Estimation of Thiols

About 1 meq of adduct was placed in the alkaline solution, at the temperature and for the time indicated (Table I). An equivalent of hydrochloric acid was added, to render the solution approximately neutral, followed by 60 ml of acetic acid. Five milliliters of 0.25% starch indicator was then added, and the mixture was titrated with 0.1 *N* iodine solution to a blue end point. The results are shown in Table I.

Identification of Thiols

One gram (0.004 mole) of β-(1-phenyltetrazolyl-5-thio)propiophenone was dissolved in 10 ml of methanol, and a solution of 0.5 g of potassium hydroxide in 5 ml of water was added. The mixture was diluted with 15 ml of water and stirred for 10 min at room temperature. After removal of the methanol under reduced pressure, the mixture was acidified with hydrochloric acid. The precipitated 5-mercapto-1-phenyltetrazole (0.62 g, 87%) was collected; the melting point was 155°, and the mixture melting point was not depressed. Satisfactory elemental and infrared analyses of the compound, after it had been recrystallized from xylene, were obtained. Related adducts obtained from 3-hexene-2,5-dione, β-dimethylaminomethylcyclohexanone, and 2-cyclohexanone (Table IIB) gave a similar result. An analogous treatment of 1 g (0.0029 mole) of 2-(5-phenyl-1,3,4-oxadiazolyl-2-thio)-1,1-dicarbethoxyethane in 200 ml of methanol, with 1 g of potassium carbonate in 200 ml of water, yielded 0.4 g (79%) of 2-mercapto-5-phenyl-1,3,4-oxadiazole, m.p. 215–217°; the mixture melting point was not depressed.

REFERENCES

1. R. Connor and W. R. McLellan. J. Org. Chem. **3**, 570 (1939).
2. C. F. H. Allen, J. O. Fournier, and W. J. Humphlett. Can. J. Chem. **42**, 2616 (1964).
3. E. D. Bergmann, D. Ginsburg, and R. Pappo. Org. Reactions, **10**, 187 (1959).
4. E. J. Morgan and E. Friedmann. J. Biochem. **32**, 733 (1938).
5. C. D. Hurd and L. L. Gershbein J. Am. Chem. Soc. **69**, 2328 (1947).
6. L. L. Gershbein and C. D. Hurd. Org. Syn. Collective Vol. **3**, 458 (1955).
7. B. H. Nicolet. J. Am. Chem. Soc. **57**, 1098 (1935).
8. M. C. Kloetzel. J. Am. Chem. Soc. **70**, 3571 (1948).
9. W. J. Humphlett and C. V. Wilson. J. Org. Chem. **26**, 2507 (1961).
10. C. F. H. Allen and W. J. Humphlett. Bull. Soc. Chim. France, 961 (1961).
11. M. Masuno and T. Asahara. Bull. Chem. Soc. Japan, 2219 (1953); Chem. Abstr. **49**, 1780 (1955).
12. C. E. Maxwell. Org. Syn. Collective Vol. **3**, 305 (1955).
13. P. O. Tawney, R. H. Snyder, C. E. Bryan, R. P. Conger, F. S. Dovell, R. J. Kelly, and C. H. Stitler. J. Org. Chem. **25**, 56 (1960).
14. A. H. Ford-Moore. J. Chem. Soc. 2433 (1949).
15. A. H. Ford-Moore. J. Chem. Soc. 1754 (1949).
16. C. F. H. Allen and W. J. Humphlett. Org. Syn. Collective Vol. **4**, 80 (1962).
17. C. Mannich and L. Stein. Ber. **58**, 2659 (1925).
18. C. Mannich and R. Braun. Ber. **53**, 1874 (1920).

Can. J. Chem. Downloaded from www.nrcresearchpress.com by 210.87.254.5 on 09/05/12
For personal use only.

Can. J. Chem. Downloaded from www.nrcresearchpress.com by 210.87.254.5 on 09/05/12
For personal use only.

THE STRUCTURES OF TWO SELF-CONDENSATION PRODUCTS FROM *o*-AMINOBENZALDEHYDE

S. G. McGeachin
Department of Chemistry, University of Alberta, Edmonton, Alberta
Received July 13, 1965

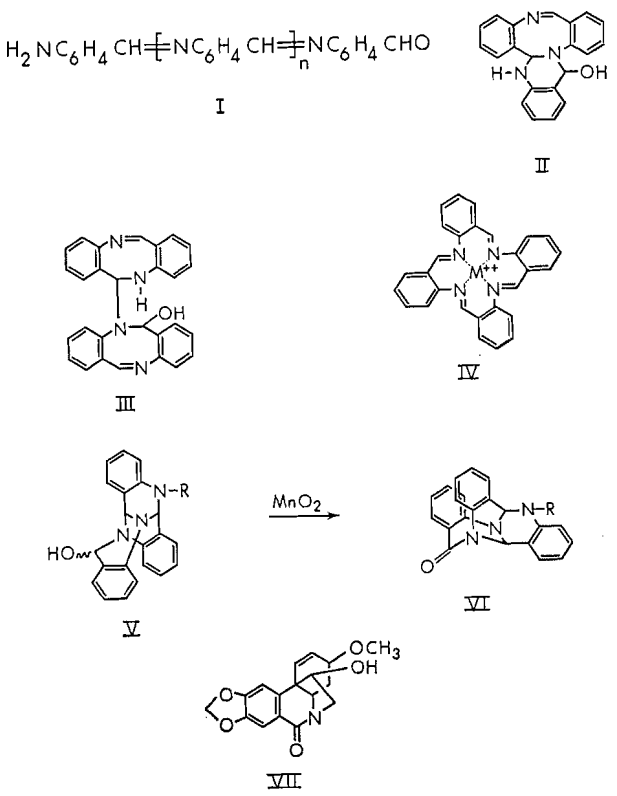
ABSTRACT

The nature of two self-condensation products of *o*-aminobenzaldehyde (one a bisanhydro trimer and the other a trisanhydro tetramer) formed under different conditions of acid catalysis has been reexamined Spectroscopic evidence is presented to support the assignment of structures V (R = H) and VIII (R = R′ = H) to these.

There exists considerable literature on self-condensation products formed from *o*-aminobenzaldehyde (1 and references therein). The number and nature of these were considerably clarified by the work of Seidel (1), who isolated and characterized a bisanhydro trimer and trisanhydro tetramer of the parent compound. Chemical evidence was interpreted in terms of simple linear Schiff base formation among three or four molecules of *o*-aminobenzaldehyde to give structures I ($n = 1$) and I ($n = 2$). These were later amended to the cyclic formulae II and III (2). Melson and Busch (3) have described self-condensation products formed in the presence of certain metal ions. These are the macrocyclic tetramer IV and an analogous trimer in which the nitrogen atoms are coordinated around the cation in a planar array. The two condensation products described by Seidel have now been reexamined and new structures assigned on the basis of evidence detailed below.

According to Seidel's method the first of these was most conveniently prepared by weakly acidifying an aqueous solution of *o*-aminobenzaldehyde, from which it precipitated in a crystalline form. Its formulation as a bisanhydro trimer followed from a correct elemental analysis for $C_{21}H_{17}N_3O$. The infrared spectrum, with bands at 3 560 and 3 390 cm^{-1}, indicated the presence of a hydroxyl and at least one NH group. That there was only one NH group was shown by the preparation of an *O,N*-diacetyl derivative which possessed no further NH band in the infrared spectrum. The nature of the remaining 15 hydrogens was apparent from the nuclear magnetic resonance (n.m.r.) spectrum of a deuterated sample, which exhibited complex 12-proton absorption between τ 2.58 and 3.50, assigned to the aromatic hydrogens, and three closely spaced one-proton singlets between τ 4.43 and 4.60, assigned to hydrogens of the type (Ar, Y_2)C*H* (Y = N or O). The ultraviolet spectrum, with maxima at 241 mμ (ϵ 14 600) and 285 mμ (ϵ 2 300), resembled that of *N*-ethyl-*o*-toluidine, which has maxima at 244 mμ (ϵ 7 200) and 291 mμ (ϵ 2 450) (4). These data indicated that the three units of *o*-aminobenzaldehyde must be joined by bonds formed between the aldehyde and amino functions only, and that no aldimine groups (—CH=N—) were present in the product. It follows that, of the three original aldehyde carbons, one must carry the hydroxyl function and be linked to nitrogen, and the other two must each be bonded to two nitrogens. If the reasonable assumption is made that no aldehyde carbon is linked to the nitrogen of the same unit, this allows only one structure for the trimer, namely V (R = H).

When stirred with methanol containing a catalytic amount of *p*-toluenesulfonic acid, the trimer gave an *O*-methyl ether consistent with its formulation as a carbinolamine.



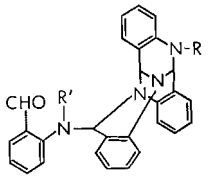
Reaction of the monoacetylbisanhydro trimer V (R = $COCH_3$) with manganese dioxide yielded a dehydro derivative (VI, R = $COCH_3$), $C_{23}H_{17}N_3O_2$, in which the hydroxyl had been oxidized to a carbonyl function, $\nu_{max}^{CCl_4}$ 1 714 cm^{-1}. Examination of a molecular model indicated that this compound belongs to the rare class of lactams in which steric requirements prevent overlap of the nitrogen lone-pair electrons with the carbonyl π bond. This results in their behaving more as aminoketones than as lactams. The position of the carbonyl band in the infrared spectrum is one consequence of this. The shift to higher frequencies than would be normal even for an aromatic ketone is probably caused by the inductive effect of the directly attached but unconjugated nitrogen atom. In the ultraviolet spectrum the band at longest wavelength, λ_{max} 333 mμ, lies between that of *o*-dimethylaminoacetophenone at 350 mμ and that of *o*-dimethylaminobenzamide at 315 mμ (5). In keeping with its behavior as a ketone, the lactam was reduced by sodium borohydride to the starting alcohol. Another example of such a "lactam" is oxohaemanthidine (VII), which has ν_{max}^{Nujol} 1 695 cm^{-1} (6).

The second self-condensation product was obtained, according to Seidel's method, through the action of 50% sulfuric or hydrochloric acids on *o*-aminobenzaldehyde or on the bisanhydro trimer. This led to the formation of red crystalline salts, from which the free base was liberated by treatment with water. Analysis of this substance and a molecular weight determination on its monoacetyl derivative confirmed its formulation as a trisanhydro tetramer, $C_{28}H_{22}N_4O$. The most important observations from the infrared spectrum were two NH bands at 3 380 and 3 310 cm^{-1}, and a carbonyl band at 1 665 cm^{-1}. The nature of the carbonyl function as a formyl group was apparent from the presence in the n.m.r. spectrum of a one-proton singlet at τ 0.10, and from the preparation of an oxime of the monoacetyl derivative which underwent ready dehydration to

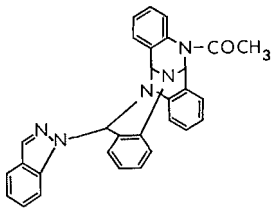
Can. J. Chem. Downloaded from www.nrcresearchpress.com by 210.87.254.5 on 09/05/12
For personal use only.

Can. J. Chem. Downloaded from www.nrcresearchpress.com by 210.87.254.5 on 09/05/12
For personal use only.

a nitrile. In the n.m.r. spectrum of the tetramer there also appeared resonances for the two hydrogens attached to nitrogen, one a broad band centered at τ 5.1, and the other a doublet (J = 5 c.p.s.) at τ 0.93 coupled to one of three one-proton resonances in the τ 4.3–4.7 region, all three ascribed, as in the trimer, to the system (Ar, Y_2)C*H*. A multiplet of weight 16 between τ 1.90 and 3.50 was also present for the aromatic hydrogens. It was apparent that the bonds joining the four units were once more between amino and formyl groups. By virtue of the presence of a formyl group one unit must be linked to the rest of the molecule by one or two bonds from its nitrogen atom. The former possibility requires that the molecule as a whole have two separate NH groups, whereas the latter requires either this or the presence of one NH_2 function. The very different positions of the NH resonances in the n.m.r. spectrum, the fact that the low-field NH exchanged much more slowly with deuterium, and its coupling to an aliphatic CH favored the presence of two separate NH groups. Under a variety of conditions, however, only a monoacetyl derivative of the tetramer could be obtained. A convincing answer came from nitrosation of this monoacetyl compound. This yielded an *N*-nitroso compound which had no NH absorption in its infrared spectrum. The absence in its ultraviolet spectrum of the long-wavelength band at 369 mμ characteristic of the *o*-aminobenzaldehyde chromophore suggested that the nitroso group was bonded to the nitrogen of this unit, which therefore was attached to the rest of the molecule by only one bond. The disappearance of this band or its appearance at shorter wavelengths on attachment of an electron-withdrawing substituent to the nitrogen is to be expected (7), and can be observed, for example, in *N*-acetyl-*o*-aminobenzaldehyde, which has its longest wavelength band at 330 mμ. The attachment of one of the four units by only a single bond from its nitrogen to the aldehyde carbon of a second, and the requirement that the aldehyde carbons of the remaining three units be linked each to two nitrogens permits, with the same assumption used in deriving the structure of the trimer, only one structure (VIII, R = R′ = H) for the tetramer. The *N*-acetyl compound and its nitroso derivative are therefore VIII (R = $COCH_3$, R′ = H) and VIII (R = $COCH_3$, R′ = NO), respectively. Since, in the latter, the relationship of nitroso to aldehyde functions is critical for the deduction of structure, it was desirable to confirm this chemically. Reduction



VIII



IX

of the nitroso group with zinc in acetic acid gave a substance, $C_{30}H_{23}ON_5$, which possessed no NH bands and no carbonyl band (other than that of the *N*-acetyl group) in the infrared spectrum. Its n.m.r. spectrum was similar to that of the parent nitroso compound, but in place of the signal assigned to the formyl proton at τ 0.10 there was a new one-proton doublet at τ 1.88 (J = 0.8 c.p.s.). The formula and spectra indicated that it was the desired indazole derivative IX. The lowest field signal at τ 1.88 in the n.m.r. spectrum is assigned to the C-3 hydrogen of the indazole ring and is in reasonable agreement with that reported for C-3 of indazole itself at τ 1.94 (doublet, J = 0.8 c.p.s.) (8).

Although the ring systems of both the trimer and tetramer remain unaltered during

the mild chemical transformations described above, the inherent lability in protonic solvents is seen on treatment with cupric nitrate in refluxing ethanol. Under these conditions they give the macrocyclic tetramer IV (M = Cu) that was obtained directly from *o*-aminobenzaldehyde by Melson and Busch (3).

EXPERIMENTAL

General

Melting points were taken on a Kofler melting point apparatus and are uncorrected. Infrared, ultraviolet, and n.m.r data were obtained on Perkin–Elmer model 337, Perkin–Elmer model 202, and Varian Associates model A-60 spectrometers, respectively.

Bisanhydro Trimer (V, R = H)

Freshly prepared *o*-aminobenzaldehyde (9) (4.5 g) was dissolved in water (700 ml) at 50°. The solution was placed under a nitrogen atmosphere, cooled to 25°, and acidified with a solution of concentrated hydrochloric acid (6 ml) in water (50 ml). The mixture was seeded with the bisanhydro trimer and allowed to stand for 1 h until precipitation was complete. The product was collected, washed with 2% aqueous sodium bicarbonate solution, and dried. Crystallization from acetone–methanol gave the bisanhydro trimer (3.1 g). The analytical sample formed prisms when recrystallized from the same solvents, and had m.p. 233–237°.

Anal. Calcd. for $C_{21}H_{17}N_3O$: C, 77.04; H, 5.23; N, 12.84. Found: C, 76.85; H, 5.51; N, 13.09.[1]

Ultraviolet spectrum: λ_{max}^{MeOH} 241 mμ (ε 14 600), 285 mμ (ε 2 300), with a shoulder at 304 mμ (ε 1 400). Infrared spectrum: $\nu_{max}^{CH_2Cl}$ 3 560 (OH), 3 390 (NH) cm^{-1}; ν_{max}^{Nujol} 3 300 (broad, NH and OH) cm^{-1}. Nuclear magnetic resonance spectrum of a deuterated sample in CD_3SOCD_3: τ 2.58–3.50 (12H, complex), τ 4.43 (1H, singlet), τ 4.45 (1H, singlet), τ 4.60 (1H, singlet).

N-Acetylbisanhydro Trimer (V, R = $COCH_3$)

The bisanhydro trimer (100 mg) was stirred with acetic anhydride (0.5 ml) at room temperature for 4 h. The monoacetyl derivative was collected by filtration and purified by crystallization from acetone. The analytical sample formed prisms when recrystallized from acetone, m.p. 227–229°.

Anal. Calcd. for $C_{23}H_{19}N_3O_2$: C, 74.78; H, 5.18; N, 11.38. Found: C, 75.05; H, 4.97; N, 11.36.

Infrared spectrum: $\nu_{max}^{CH_2Cl}$ 3 550 (OH), 1 660 ($NCOCH_3$) cm^{-1}; ν_{max}^{Nujol} 3 200 (broad), 1 660 cm^{-1}. Nuclear magnetic resonance spectrum on a deuterated sample in CD_3SOCD_3: τ 2.25–3.25 (12H, complex), τ 3.42 (1H, singlet), τ 4.40 (1H, singlet), τ 4.44 (1H, singlet), τ 7.40 (3H, singlet).

O,N-Diacetylbisanhydro Trimer

The bisanhydro trimer (100 mg) was acetylated in 1:1 pyridine – acetic anhydride (0.5 ml) for 12 h at room temperature. Addition of a few drops of water gave the diacetyl derivative in a crystalline form. The analytical sample formed needles when crystallized from dichloromethane–methanol, and had m.p. 222–225°.

Anal. Calcd. for $C_{25}H_{21}N_3O_3$: C, 72.98; H, 5.14; N, 10.21. Found: C, 72.86; H, 5.12; N, 10.03.

Infrared spectrum: $\nu_{max}^{CH_2Cl_2}$ 1 740 ($OCOCH_3$), 1 660 ($NCOCH_3$) cm^{-1}. Nuclear magnetic resonance spectrum ($CDCl_3$): τ 2.50–3.33 (14H, complex), τ 4.43 (1H, singlet), τ 7.48 (3H, singlet), τ 7.70 (3H, singlet).

O-Methylbisanhydro Trimer

The bisanhydro trimer (150 mg) was suspended in a solution of *p*-toluenesulfonic acid (10 mg) in methanol (5 ml), and the mixture stirred for 3 days at room temperature. After dilution with benzene it was washed with dilute aqueous sodium bicarbonate and water, and dried. Removal of the solvent and crystallization from dichloromethane–ether gave the product (105 mg). The analytical sample formed prisms when recrystallized from the same solvents, and had m.p. 228–230°.

Anal. Calcd. for $C_{22}H_{19}ON_3$: C, 77.39; H, 5.61. Found: C, 77.15; H, 5.77.

The Lactam (VI, R = $COCH_3$)

A solution of the monoacetylbisanhydro trimer (89 mg) in dichloromethane (50 ml) was stirred at room temperature with manganese dioxide (3 g) for 4 h. After filtration through Celite the solution was evaporated to dryness *in vacuo* and the residue crystallized from dichloromethane–ether to yield the lactam (40 mg). The analytical sample separated from the same solvent mixture as prisms, m.p. 229–231°.

Anal. Calcd. for $C_{23}H_{17}N_3O_2$: C, 75.19; H, 4.66; N, 11.44. Found: C, 74.93; H, 4.90; N, 11.65.

Ultraviolet spectrum: λ_{max}^{MeOH} 210 mμ (ε 34 900), 238 mμ (ε 25 900), 333 mμ (ε 2 800). Infrared spectrum: $\nu_{max}^{CCl_4}$ 1 714 (lactam C=O), 1 678 ($NCOCH_3$) cm^{-1}. Nuclear magnetic resonance spectrum ($CDCl_3$): τ 1.88 (1H, multiplet belonging to an aromatic hydrogen ortho to the lactam carbonyl), τ 2.25–3.00 (12H, complex), τ 4.11 (1H, singlet), τ 7.46 (3H, singlet).

A sample of the lactam (30 mg) was dissolved in dioxane (1 ml) and water (0.2 ml), and reduced with sodium borohydride (11.5 mg) for 15 min at room temperature. The solution was poured onto ice and

[1]*Analyses are by Galbraith Laboratories, Inc., P.O. Box 4187, Knoxville, Tennessee 37921, and by Miss D. Roberts, Chemistry Department, University of Alberta, Edmonton.*

Can. J. Chem. Downloaded from www.nrcresearchpress.com by 210.87.254.5 on 09/05/12
For personal use only.

the product (19 mg) collected and dried. On examination by thin-layer chromatography (alone and admixed with monoacetylbisanhydro trimer) it showed one spot. It was crystallized once from acetone, and was found to be identical with the monoacetyl compound by comparison of their infrared spectra and melting points.

Trisanhydro Tetramer (VIII, R = R′ = H)

A mixture of *o*-aminobenzaldehyde (2.5 g) and 1:1 sulfuric acid – water (10 ml) was stirred until solution was complete (ca. 0.5 h). Water (10 ml) was added and the solution was allowed to stand for 1 day until crystallization of the salt was complete. This was filtered off, washed with anhydrous ethanol, and dried, yield 2.05 g. It was converted quantitatively (as shown by thin-layer chromatography) into the trisanhydro tetramer by shaking it with water and chloroform. The free base was isolated from the chloroform solution and was crystallized once from chloroform–methanol. An analytical sample was obtained from the same solvent mixture, and had m.p. 235–236.5°.

Anal. Calcd. for $C_{28}H_{22}N_4O$: C, 78.12; H, 5.15; N, 13.02. Found: C, 77.92; H, 5.02; N, 12.83.

Ultraviolet spectrum: λ_{max}^{MeOH} 210 mμ (ε 44 000), 237 mμ (ε 32 700), 267 mμ (ε 11 000), 286 mμ (ε 2 700), 369 mμ (ε 6 900). Infrared spectrum: $\nu_{max}^{CH_2Cl_2}$ 3 380 (NH), 3 310 (NH), 2 740 (aldehyde CH stretch), 1 665 (CHO) cm^{-1}; ν_{max}^{Nujol} 3 370, 3 555, 3 315 (NH), 1 665 (CHO) cm^{-1}. Nuclear magnetic resonance spectrum ($CDCl_3$): τ 0.10 (1H, singlet), τ 0.93 (1H, doublet, J = 5 c.p.s.), τ 1.90–3.50 (16H, complex), τ 4.26 (1H, doublet, J = 5 c.p.s.), τ 4.33 (1H, singlet), τ 4.66 (1H, singlet), τ 5.1 (1H, broad band). Deuteration removed the doublet at τ 0.93 and the band at τ 5.1 from the spectrum, and collapsed the doublet at τ 4.26 to a singlet.

Similar results were obtained by using the bisanhydro trimer in place of *o*-aminobenzaldehyde.

Acetyltrisanhydro Tetramer (VIII, R = $COCH_3$, R′ = H)

The trisanhydro tetramer (730 mg) was acetylated overnight in 1:1 acetic anhydride – pyridine (2 ml) at room temperature. Addition of a little water precipitated a crystalline product which, after one recrystallization from dichloromethane–methanol, gave the pure acetyl derivative. The analytical sample formed plates, m.p. 255–259°, when crystallized from the above solvent mixture.

Anal. Calcd. for $C_{30}H_{24}N_4O_2$: C, 76.25; H, 5.12; N, 11.86; mol. wt. 472. Found: C, 75.93; H, 5.11; N, 11.57; mol. wt. 469 (osmometric).

Infrared spectrum: $\nu_{max}^{CCl_4}$ 3 300 (NH), 1 668 ($NCOCH_3$) cm^{-1}; ν_{max}^{Nujol} 3 325, 1 675 cm^{-1}. Nuclear magnetic resonance spectrum ($CDCl_3$): τ 0.05 (1H, singlet), τ 0.92 (1H, doublet, J = 5 c.p.s.), τ 2.0–3.25 (17H, complex), τ 4.20 (1H, doublet, J = 5 c.p.s.), τ 4.25 (1H, singlet), τ 7.5 (3H, singlet). Deuteration removed the doublet at τ 0.92, and collapsed that at τ 4.20 to a singlet.

An oxime was obtained by reaction of *N*-acetyltrisanhydro tetramer (150 mg) with hydroxylamine hydrochloride (145 mg) in pyridine (1 ml) for 12 h at room temperature. The analytical sample formed prisms, m.p. 248–250°, when crystallized from dichloromethane–ether.

Anal. Calcd. for $C_{30}H_{25}O_2N_5$: C, 73.90; H, 5.17; N, 14.37. Found: C, 73.76; H, 5.30; N, 14.20.

A sample of the oxime (115 mg) was dehydrated with toluenesulfonyl chloride (50 mg) in dry pyridine (1 ml) at 0° for 24 h. The solution was poured onto ice, and the product was collected by filtration and crystallized from dichloromethane–methanol to give the corresponding nitrile (107 mg). The analytical sample formed colorless prisms, m.p. 232–234°, when recrystallized from these solvents.

Anal. Calcd. for $C_{30}H_{23}ON_5$: C, 76.74; H, 4.94; N, 14.92. Found: C, 76.28; H, 5.08; N, 15.02.

Infrared spectrum: $\nu_{max}^{CH_2Cl_2}$ 3 420 (NH), 2 225 (CN), 1 675 ($NCOCH_3$) cm^{-1}.

N-Acetyl-N′-nitrosotrisanhydro Tetramer (VIII, R = $COCH_3$, R′ = NO)

Dry nitrosyl chloride was passed slowly during 4 min into a well-stirred ice-cold solution of acetyltrisanhydro tetramer (244 mg) in pyridine (6 ml). The solution was kept at 0–5° for a further 30 min, and then poured onto ice to give the product. This was purified by crystallization from dichloromethane–benzene, giving 205 mg of the *N*-nitroso derivative. The analytical sample formed prisms when recrystallized from benzene, m.p. 192–195°.

Anal. Calcd. for $C_{30}H_{23}N_5O_3$: C, 71.86; H, 4.62; N, 13.96 Found: C, 71.95; H, 4.86; N, 14.24.

Ultraviolet spectrum: λ_{max}^{EtOH} 209 mμ (ε 61 800), with shoulders at 240 mμ (ε 28 600), 275 mμ (ε 6 000), and 283 mμ (ε 5 300). Infrared spectrum: $\nu_{max}^{CCl_4}$ 1 704 (CHO), 1 675 ($NCOCH_3$). Nuclear magnetic resonance spectrum ($CDCl_3$): τ 0.10 (1H, singlet), τ 1.65–3.40 (18H, complex), τ 4.57 (1H, singlet), τ 7.50 (3H, singlet).

The Indazole (IX)

A mixture of zinc dust (460 mg) and *N*-acetyl-*N′*-nitrosotrisanhydro tetramer (210 mg) was added to a solution of anhydrous sodium acetate (750 mg) in glacial acetic acid (6 ml). The mixture was stirred for 0.5 h and poured onto ice; the crude product was filtered off and dried. It was purified by filtration through a column of grade III alumina (10 g) followed by crystallization from acetone to yield 155 mg of product. The analytical sample formed needles, m.p. 255–257°, when recrystallized from acetone.

Anal. Calcd. for $C_{30}H_{23}ON_5$: C, 76.74; H, 4.94; N, 14.92. Found: C, 76.22; H, 4.94; N, 14.97.

Can. J. Chem. Downloaded from www.nrcresearchpress.com by 210.87.254.5 on 09/05/12
For personal use only.

Ultraviolet spectrum: λ_{max}^{EtOH} 207 mμ (ε 61 500), 282 mμ (ε 5 800), 287 mμ (ε 5 750), and 300 mμ (ε 3 650), with shoulders centered at 245 mμ (ε 16 000) and 292 mμ (ε 5 000). Nuclear magnetic resonance spectrum (100 mCi in $CDCl_3$): τ 1.88 (1H, doublet, J = 0.8 c.p.s.), τ 2.1–3.4 (18H, complex), τ 3.27 (1H, singlet), τ 7.44 (3H, singlet).

Macrocyclic Tetramer (IV, M = Cu)

A solution of cupric nitrate trihydrate (53 mg) in ethanol (1 ml) was added to a refluxing suspension of trisanhydro tetramer (93 mg) in ethanol (2 ml). After 6 h at reflux temperature the solution was cooled and crystalline (IV, M = Cu) nitrate (121 mg, 93%) collected. The product was identical in its solid-state infrared spectrum with that obtained directly from *o*-aminobenzaldehyde by the method of Melson and Busch (3).

By using an equivalent amount of the bisanhydro trimer the same product was obtained in an 85% yield.

REFERENCES

1. F. Seidel. Chem. Ber. **59**, 1894 (1926).
2. F. Seidel and W. Dick. Chem. Ber. **60**, 2918 (1927).
3. G. H. Melson and D. H. Busch. Proc. Chem. Soc. 223 (1963); J. Am. Chem. Soc. **86**, 4830 (1964); **86**, 4834 (1964); **87**, 1706 (1965).
4. F. W. Holly and A. C. Cope. J. Am. Chem. Soc. **66**, 1875 (1944).
5. P. Grammaticakis. Bull. Soc. Chim. France, [5], **20**, 94 (1953); **20**, 207 (1953).
6. S. Uyeo, H. M. Fales, R. S. Highet, and W. C. Wildman. J. Am. Chem. Soc. **80**, 2590 (1958).
7. W. A. Schroeder, P. E. Wilcox, K. N. Trueblood, and A. O. Dekker. Anal. Chem. **23**, 1740 (1951).
8. P. J. Black and M. L. Heffernan. Australian J. Chem. **16**, 1052 (1963).
9. L. I. Smith and J. W. Opie. Org. Syn. **28**, 11 (1948).

Can. J. Chem. Downloaded from www.nrcresearchpress.com by 210.87.254.5 on 09/05/12
For personal use only.

THE INTERCONVERSION OF 5-CHLORO- AND 5-HYDROXY-DIPYRRYLMETHENES[1]

A. MARKOVAC,[2,3] B. D. KULKARNI,[2,4] K. B. SHAW,[2,5] AND S. F. MACDONALD
Division of Pure Chemistry, National Research Council, Ottawa, Canada

Received June 22, 1966

ABSTRACT

Like the known II, the 5-halo-dipyrrylmethenes IV, X, and XI were obtained conventionally by halogenating the pyrroles I and IX. The 5-free dipyrrylmethene VIII, a new type of intermediate in such halogenations, was obtained from the pyrrole ester VII. The four 5-halo-dipyrrylmethenes were hydrolyzed to the 5-hydroxy derivatives VI and XIII, and these were reconverted into 5-chloro-dipyrrylmethenes.

INTRODUCTION

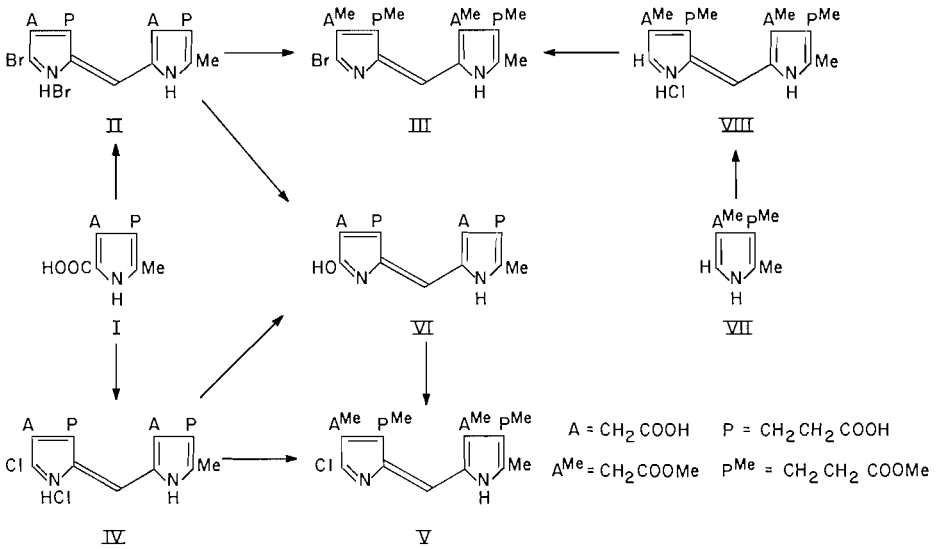
We have tried to obtain the dipyrrylmethene II (CH_2Br for CH_3) and its isomers as intermediates for the syntheses of polypyrranes related to porphobilinogen. They were attractive because, in their analogues, the bromomethyl group condensed with pyrroles (1, pp. 106 and 619; 2), and reduction converted the stable 5-bromo-dipyrrylmethenes into the labile 5-free dipyrrylmethanes (3, 4). Such bromomethyl-dipyrrylmethenes are often obtained by brominating either 5-methyl-dipyrrylmethenes or 2-methyl-pyrroles. However, these methods frequently fail, as in the case of XIV*b* (5), which has only recently been obtained as its ester by brominating 5-*t*-butoxycarbonyl-2,4-dimethyl-pyrrole-3-propionic acid methyl ester (6).

Having failed to halogenate the methyl groups in II or III, we prepared IV, X, and XI to study their halogenation. These were obtained, like II, from the pyrroles I and IX with bromine or sulfuryl chloride. For better characterization, they were esterified and then converted into the free bases III, V, and XII. The hydrochlorides IV and XI dissolved in water, but rapidly precipitated again as the rather unstable free bases, in which the halogen content tended to be low (lower still after recrystallization, the recovery being poor). The free base derived from XIV*a* is reportedly too unstable to be isolated (7).

The investigation of routes to the 5-halomethyl-dipyrrylmethenes was diverted when it was found that 2 moles of VII reacted with 1 mole of sulfuryl chloride to give the 5-free dipyrrylmethene VIII (43%). This was further identified as the free base and by conversion into the authentic 5-bromo-dipyrrylmethene III. It is thus clearly distinguished from another conceivable (cf. ref. 8) product, the ester of 5,5′-dimethyl-dipyrrylmethene-3,3′-diacetic acid 4,4′-dipropionic acid. The occurrence of this 5-free dipyrrylmethene cannot be reconciled with previous assumptions about the course of such halogenations: that the pyrrole is first halogenated in the 5-position and then in the 2-methyl group, and that the 2-halomethyl group (whether arising directly (1, p. 62) or indirectly (8)) then forms the bridge. However, the 5-free dipyrrylmethene would be a possible intermediate if anionotropy (cf. ref. 9, p. 588) made the 5-halo-2-methyl-pyrrole equivalent to the 5-free 2-halomethyl-pyrrole.

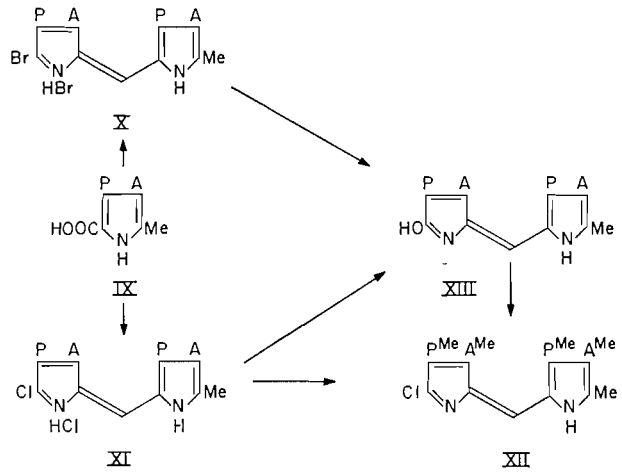
Another diversion occurred when the analysis of the hydrochloride XI showed that the ring halogen was unexpectedly labile, both chlorine atoms being determined as chloride

[1]*Issued as N.R.C. No. 9138.*
[2]*National Research Council Postdoctorate Fellow.*
[3]*Present address: Ash Stevens Inc., Detroit Research Park, 5861 John C. Lodge Freeway, Detroit, Michigan.*
[4]*Present address: National Chemical Laboratory, Poona 8, India.*
[5]*Present address: Defence Chemical, Biological and Radiation Laboratories, Shirley's Bay, Ontario.*



by adding mercuric nitrate and titrating the excess of mercury ion (10).[6] This observation was followed up, for we had had an interest in the likely product: the 5-hydroxy-dipyrrylmethene XIII. These 5-hydroxy-dipyrrylmethenes may have unexploited synthetic possibilities, because the nucleus is stable, the 5-position is blocked, and the reactivity at the 5′-position is similar to that of pyrroles (1, pp. 125, 136, 668, 670, 706, and 710). Other substituents may have the same effect as hydroxy (11). The 5-hydroxy-dipyrrylmethenes would then be attractive as intermediates if the hydroxy groups could be replaced by halogen and thus by hydrogen. However, there was no clear evidence that the replacement by halogen was possible (5, 12).

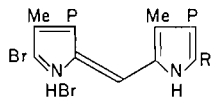
As well as being prepared directly from pyrroles, 5-methoxy- and 5-hydroxy-dipyrrylmethenes have been obtained from 5-bromo-dipyrrylmethenes by refluxing them with methanolic potash (5) or with potassium or silver acetate in acetic acid (13), or by heating them with alkali above 150° (1, p. 135). However, XV, the 5-hydroxy-dipyrrylmethene most closely related to VI, had been obtained from XIV*a* in only a 15% yield (5, 13).



[6]*We owe this observation to Mr. H. Séguin.*

By using mercuric nitrate at room temperature, the 5-chloro-dipyrrylmethene XI was rapidly converted into the 5-hydroxy-dipyrrylmethene XIII, but this method failed with the 5-bromo-dipyrrylmethene X. However, the 5-halo-dipyrrylmethenes II, IV, X, and XI were converted into the corresponding 5-hydroxy-dipyrrylmethenes VI and XIII by Dowex 3 (a weakly basic resin) in boiling 50% ethanol, the chloro derivatives giving more consistent yields (50–60%). This method too is not general, for we did not obtain XV (5, 13) from XIV*a* by using either mercuric nitrate or Dowex 3.

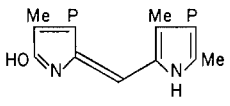
It is difficult to rationalize these and analogous preparations of 5-hydroxy-dipyrrylmethenes. The rates of reaction (2) and the yields have been influenced strongly by the other substituents (13) and by the purity of the materials (14), and 5-hydroxy-dipyrrylmethenes may be oxidized further to tetrapyrroles (13). The variable stability of the 5-halo-dipyrrylmethenes may be important, for X lost nearly all of its halogen when treated with mercuric nitrate but, unlike XI, did not yield XIII. Earlier methods suggest that base catalysis is involved, but sodium hydroxide removed the halogen from IV and XI slowly and incompletely, and the recovery was poor. It was also possible that acid catalysis might be effective, as with the 4-chloroquinazolines (15), because the halogen in the free base of the methyl ester derived from XIV*a* was easily replaced by aniline though not by methylamine or ammonia (5). Apparently, the halogen in 5-bromo-5′-carbethoxy-4,4′-dimethyl-dipyrrylmethene-3,3′-dipropionic acid is more readily hydrolyzed in acidic than in alkaline media, but the report (16) is confused, and this behavior might be conditioned by the 5′-carbethoxy group. The above hydrolysis with mercuric nitrate suggests electrophilic catalysis (cf. ref. 9, p. 357), but there was no evidence of such when XVI*a* was hydrolyzed to XVI*b* with silver acetate rather than with potassium acetate (17).



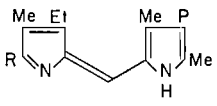
XIV

a, R = Me

b, R = CH_2Br



XV

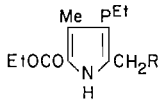


XVI

a, R = Br (Hydrobromide)

b, R = OH

c, R = OMe

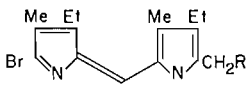


XVII

a, R = Br

b, R = N_3

P^{Et} = CH_2CH_2COOEt



XVIII

a, R = Br (Hydrobromide)

b, R = N_3 (Hydrozoate)

The hydroxyl groups in VI and XIII were replaced with chlorine by methanolic hydrogen chloride at room temperature, the products being isolated as the methyl esters V and XII (30%). This was surprising because the hydroxy groups in the dipyrrylmethenes studied earlier (13, 17) were unchanged under these conditions; there the initial products were the hydrochlorides of 5-hydroxy-dipyrrylmethenes, which readily lost hydrogen chloride to give the 5-hydroxy-dipyrrylmethenes. It is unlikely that these hydrochlorides were actually very easily hydrolyzed 5-chloro-dipyrrylmethenes, for 5-chloro-4,3′,5′-trimethyl-3,4′-diethyl-dipyrrylmethene is not that easily hydrolyzed (18). A reaction

related to the above is the conversion of XVI*c* into XVI*b* by methanolic hydrogen chloride (17).

Attempts were made to improve the synthesis of uroporphyrin 1, which had been obtained in a 5.9% yield from II at 118° (19). At 135° the yield from II was 3%, and at 118° the yields from X and from IV were, respectively, 5.3% and <0.1%. In a preliminary experiment modelled on a synthesis of coproporphyrin 1 (20), no porphyrin was obtained from VIII with 6% potassium methoxide in methanol at 180°.[7]

Few meaningful comparisons have been made between 5-chloro- and 5-bromo-dipyrrylmethenes, although the differences are significant. We obtained better yields of 5-hydroxydipyrrylmethenes from the former, whereas the latter have given better yields of porphyrins (cf. ref. 18). Apparently, the labilities of the halogens are not very different, but the 5-bromo-dipyrrylmethenes are more prone to other changes (but less so as esters).

As one projected use of compounds such as II (CH_2Br for CH_3) involved replacing the side-chain halogen with an amino group, we treated XVII*a* and XVIII*a* with sodium azide to obtain XVII*b* and XVIII*b*.

EXPERIMENTAL

5'-Methyl-dipyrrylmethene-4,3'-diacetic Acid-3,4'-dipropionic Acid Tetramethyl Ester Hydrochloride (VIII)

Methyl cryptopyrrole dicarboxylate (VII, 238 mg, 2 moles (21)) in 10 ml of chloroform was treated with 0.04 ml (1 mole) of sulfuryl chloride in 2 ml of chloroform. After 20 h at 20°, the solvent was evaporated *in vacuo* and the crystalline residue recrystallized from chloroform–ether. For analysis, the product (110 mg, 43%, m.p. 156–158°) was recrystallized as red prisms, m.p. 164–165°.

Anal. Calcd. for $C_{24}H_{31}O_8N_2Cl$: C, 56.41; H, 6.12; N, 5.48; Cl, 6.94. Found: C, 56.59; H, 6.00; N, 5.60; Cl (total or ionic (10)), 7.00.

To obtain the *free base*, 100 mg was dissolved in 3 ml of methanol and neutralized with ammonia, and the solution cooled. The product which separated was recrystallized from methanol as yellow needles (55 mg), m.p. 125–127°.

Anal. Found: Cl, 0.00.

5-Bromo-5'-methyl-dipyrrylmethene-4,3'-diacetic Acid-3,4'-dipropionic Acid Tetramethyl Ester (III)

(*a*) 5-Bromo-5'-methyl-dipyrrylmethene-4,3'-diacetic acid-3,4'-dipropionic acid hydrobromide (II, 350 mg (19)) was dissolved in methanol (5 ml) containing acetyl bromide (0.25 ml), and the solution was kept for 24 h at 20°. The solvent was removed *in vacuo* and the residue dissolved in chloroform. The solution was washed with aqueous sodium bicarbonate, and dried (sodium sulfate), and the solvent was evaporated. The residue was recrystallized from methanol as yellow needles (310 mg, 92%), m.p. 127–128°, with solid-phase changes at about 122°.

Anal. Calcd. for $C_{24}H_{29}O_8N_2Br$: C, 52.08; H, 5.28; Br, 14.44. Found: C, 52.35; H, 5.25; Br, 14.97.

A solution of this ester in methanol – acetyl bromide quickly set as a mass of brown prismatic needles of the *hydrobromide*, m.p. 158–163°.

Anal. Calcd. for $C_{24}H_{30}O_8N_2Br_2$: C, 45.44; H, 4.77; Br, 25.20. Found: C, 45.20; H, 4.72; Br, 24.95.

(*b*) 5'-Methyl-dipyrrylmethene-4,3'-diacetic acid-3,4'-dipropionic acid tetramethyl ester hydrochloride (VIII, 100 mg) was suspended in 2 ml of acetic acid, treated with 0.03 ml of bromine in 0.1 ml of acetic acid, and allowed to stand for 3 h at 20°. The solvent was removed *in vacuo*, the residue left overnight in 5 ml of methanol containing 0.25 ml of acetyl bromide, and the product (free base) isolated as in method *a* above to give orange-yellow needles (80 mg, 74%), m.p. 126–127°.

Anal. Found: Br, 14.47.

The products from methods *a* and *b* gave identical X-ray powder photographs and their mixed melting point was undepressed.

5-Bromo-5'-methyl-dipyrrylmethene-3,4'-diacetic Acid-4,3'-dipropionic Acid Hydrobromide (X)

5-Carboxy-hemopyrrole-dicarboxylic acid (IX, 500 mg (22)) was suspended in 3 ml of acetic acid at 50–60°, and 0.16 ml of bromine in 1 ml of acetic acid was added. After 20 min at this temperature, scratching induced crystallization, and the mixture was then left for 16 h in a partially evacuated vacuum desiccator over NaOH. The orange-brown rods (285 mg, 50%, m.p. 190–191° (decomp.)) were washed with acetic acid and then with ether. For analysis, it was recrystallized three times from acetic acid containing some formic acid, m.p. 197–198°.

Anal. Calcd. for $C_{20}H_{22}N_2O_8Br_2$: C, 41.54; H, 3.84; N, 4.85; Br, 27.64. Found: C, 41.26; H, 3.95; N, 4.91; Br, 27.65.

[7]*This was carried out by Dr. B. Gregorovich.*

5-Chloro-5'-methyl-dipyrrylmethene-3,4'-diacetic Acid-4,3'-dipropionic Acid Hydrochloride (XI)

Sulfuryl chloride (0.09 ml) was added to a suspension of 5-carboxy-hemopyrrole-dicarboxylic acid (IX, 245 mg) in 5 ml of acetic acid at 50–60°. After the evolution of gas ceased (about 10 min) the solution was left overnight in a partially evacuated vacuum desiccator over NaOH. The crystalline product (140 mg, 58%, m.p. 175° (decomp.)) was separated and washed with acetic acid and then with ether. For analysis, it was recrystallized from methanol–ether as red-brown prisms, m.p. 179–180° (decomp.), λ_{max} 481 mμ (in methanol).

Anal. Calcd. for $C_{20}H_{22}O_8N_2Cl_2$: C, 49.09; H, 4.53; N, 5.73; Cl, 14.49. Found: C, 49.17; H. 4.69; N, 5.63; Cl, 14.29.

To obtain the *free base*, 100 mg of the hydrochloride was dissolved in 2 ml of water to give a clear solution. After a few seconds the base separated as yellow-brown needles (60 mg), m.p. 191–193° (decomp.) (block preheated to 180°), λ_{max} 462 mμ (in methanol).

Anal. Calcd. for $C_{20}H_{21}O_8N_2Cl$: Cl, 7.83. Found: Cl, 7.31.

The Methyl Ester of the Free Base (XII)

(A) This was prepared from 100 mg of XI and 5 ml of 5% HCl in methanol by the same method as III, except that it was crystallized from ether–*n*-hexane instead of from methanol. It formed yellow prismatic rods (85 mg, 82%), m.p. 101°. For analysis it was recrystallized in the same way, m.p. 103–104°.

Anal. Calcd. for $C_{24}H_{29}N_2O_8Cl$: C, 56.63; H, 5.74; N, 5.50; Cl, 6.97. Found: C, 56.83; H, 5.59; N, 5.66; Cl, 6.80.

(B) 5-Hydroxy-5'-methyl-dipyrrylmethene-3,4'-diacetic acid-4,3'-dipropionic acid (XIII), prepared by methods *a*, *b*, and *c* below, was used. In each case 100 mg of the hydroxy-dipyrrylmethene was dissolved in 10 ml of 10% methanolic hydrogen chloride, and the solution was allowed to stand for 48 h at 20°. The solvent was removed *in vacuo* at 20°. The solution of the residue in chloroform was washed with aqueous sodium bicarbonate, dried, and evaporated. The resulting residue was extracted with 20 ml of ether. The ether was evaporated, leaving the product, which was crystallized from ether–*n*-hexane as yellow prisms (35 mg, 30%), m.p. 100–101°, mixed melting point with the product from method A above 100–101°. The X-ray powder photographs of the products from methods A and B (using XIII prepared by method *b* below from XI and Dowex 3) were identical.

The material insoluble in ether was recrystallized from chloroform–*n*-hexane to give a yellow product (15 mg) which was halogen free, m.p. 220° ("urobilirubin"? (cf. ref. 13)).

5-Chloro-5'-methyl-dipyrrylmethene-4,3'-diacetic Acid-3,4'-dipropionic Acid Hydrochloride (IV)

This was prepared in the same way as its isomer (above), except that 5-carboxy-cryptopyrrole-dicarboxylic acid (I (23)) was used. The crystalline product (200 mg, 81%), m.p. 179–180° (decomp.), was recrystallized for analysis from methanol–ether as orange-brown prisms, m.p. 180–181° (decomp.).

Anal. Calcd. for $C_{20}H_{22}O_8N_2Cl_2$: C, 49.09; H, 4.53; N, 5.73; Cl, 14.49. Found: C, 49.29; H, 4.52; N, 5.66; Cl, 14.45.

The *free base*, like its isomer above, was formed by dissolving the hydrochloride in water, from which the base separated as brown needles (68 mg), m.p. 195–200° (decomp.) (block preheated to 180°).

Anal. Calcd. for $C_{20}H_{21}O_8N_2Cl$: Cl, 7.83. Found: Cl, 7.29.

The Methyl Ester of the Free Base (V)

(A) This was prepared from 100 mg of IV and 5 ml of 5% HCl in methanol by the same method as III, except that it was crystallized from ether–*n*-hexane instead of from methanol. It formed orange-yellow prismatic needles (87 mg, 84%), m.p. 117–118°. Recrystallized for analysis, it formed yellow needles, m.p. 119–120°.

Anal. Calcd. for $C_{24}H_{29}O_8N_2Cl$: C, 56.63; H, 5.74; N, 5.50; Cl, 6.97. Found: C, 56.51; H, 5.69; N, 5.59; Cl, 6.82.

(B) 5-Hydroxy-5'-methyl-dipyrrylmethene-4,3'-diacetic acid-3,4'-dipropionic acid (VI), prepared by methods *a* and *b* below, was used. In each case 100 mg of the hydroxy-dipyrrylmethene was converted into the crude 5-chloro-dipyrrylmethene in the same manner as the isomeric XIII was converted into XII (see above). After the chloroform was evaporated the black crude product was extracted several times with ether. When the extract was evaporated a brown crystalline product remained which was recrystallized three times from ether–*n*-hexane as yellow needles (35 mg, 30%), m.p. 118–119°, undepressed on admixture with the product from method A above. Of the two products here, that of the sequence IV → VI → V was analyzed.

Anal. Found: C, 56.91; H, 6.17; N, 5.33; Cl, 6.82.

The nuclear magnetic resonance spectra of the product from method A and the two products from method B above showed the same chemical shifts.

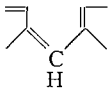
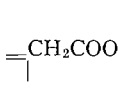
The Behavior of the 5-Chloro-dipyrrylmethenes IV and XI with Sodium Hydroxide

The dipyrrylmethene XI (100 mg) was allowed to stand at 20° for 1 h in 2 ml of 10% sodium hydroxide, and the product (60 mg containing 6.33% Cl) was then precipitated with acetic acid. This product (60 mg) was twice recycled in the same way, allowing the solution to stand for 3 h (45 mg recovered, 3.42% Cl) and then overnight (20 mg recovered, 0.1% Cl).

When IV was given the same three treatments, the final product contained 0.3% Cl.

TABLE I

Chemical shifts of dipyrrylmethenes (p.p.m., τ scale)

				OCH_3	CH_2CH_2COO		Solvent
V	3.12	—	6.38, 6.51	6.30, 6.33	7.25	7.67	$CDCl_3$ + tetramethysilane
XII	3.18	—	6.40, 6.52	6.31, 6.33	7.29	7.69	$CDCl_3$ + tetramethylsilane
VI	3.92	—	6.62, 6.78	—	7.52	7.85	D_2O/Na + CH_3CN
XIII	3.85	—	6.53, 6.72	—	7.55	7.80	D_2O/Na + CH_3CN
VIII (HCl)	2.55		6.28, 6.22, 6.18		7.30, 7.75		$CDCl_3$
VIII (base)	3.10	2.72	6.27, 6.35		7.33	7.63	$CDCl_3$

5-Hydroxy-5'-methyl-dipyrrylmethene-3,4'-diacetic Acid-4,3'-dipropionic Acid (XIII)

(a) With mercuric nitrate.—The corresponding 5-chloro-dipyrrylmethene hydrochloride (XI, 100 mg) was dissolved in 10 ml of 80% ethanol and the pH adjusted to 9–10 with 5% sodium hydroxide, giving a clear solution. The pH was then brought to 3.6 with 0.1% nitric acid, and 20 ml of mercuric nitrate solution (10) was added. The dark solution was concentrated and the crystalline product (40 mg, 45%) separated. It was extracted into methanol (thimble) and the solution was concentrated, filtered while hot, and cooled. The product (30 mg) formed yellow prisms, m.p. 230° (decomp.) (block preheated to 210°).

Anal. Calcd. for $C_{20}H_{22}O_9N_2$: C, 55.30; H, 5.11; N, 6.45; Cl, 0.00. Found: C, 55.18; H, 5.29; N, 6.60; Cl, 0.00.

(b) With Dowex 3 and aqueous ethanol.—The 5-chloro-dipyrrylmethene hydrochloride (XI, 500 mg) was dissolved in 50 ml of 50% ethanol, and 2.5 g (dry weight) of Dowex 3 was added. The mixture was refluxed on the steam bath for 30 min with occasional shaking. The resin was filtered off and washed well with water, and the combined filtrate and washings were evaporated in a rotary evaporator to give the yellow crystalline product (266 mg, 60%). It was recrystallized from methanol (thimble) or from hot water as yellow prisms, m.p. 231–232° (decomp.) (block preheated to 210°) alone or admixed with the product from method *a* above.

Anal. Found: C, 55.57; H, 5.28; N, 6.23; Cl, 0.00.

(*c*) The 5-bromo-dipyrrylmethene hydrobromide (X, 500 mg) was heated with Dowex 3 and 50% ethanol as under method *b* above. When the very-dark filtered solutions and washings were evaporated a brown residue (250 mg) remained. This was extracted with methanol (from a thimble, above a second thimble containing Darco), and the methanol concentrated. The product (100 mg, 27%) separated as yellow prisms, m.p. 230° (decomp.) (block preheated to 210°) alone or admixed with the product from method *a* above.

Anal. Found: Br, 0.00.

The Dowex 3 had been washed well with water. Some lots of the resin adsorb the products, and the apparent yields are low. In this case, the products were extracted from the resin by leaving it overnight in dilute ammonia. The resin was then washed with water as long as the washings were yellow. The extracts (500 ml) were evaporated in a rotary evaporator, the residue was dissolved in a little water, and the product was precipitated with acetic acid.

The products obtained by methods *a*, *b*, and *c* above, λ_{max} 421 mμ (in water), showed the same chemical shifts in their nuclear magnetic resonance spectra and were converted into the same 5-chloro-dipyrrylmethene methyl ester (XII, see above).

5-Hydroxy-5'-methyl-dipyrrylmethene-4,3'-diacetic Acid-3,4'-dipropionic Acid (VI)

(*a*) The 5-chloro-dipyrrylmethene hydrochloride (IV, 500 mg) was refluxed in 50% ethanol with Dowex 3 in the same manner as its isomer (above), and a crude brown product (270 mg) was isolated. It was recrystallized from methanol as yellow-brown prisms (250 mg, 56%), m.p. 238° (decomp.) (block preheated to 220°). For analysis it was again recrystallized as yellow prisms, m.p. 238–240° (decomp.).

Anal. Calcd. for $C_{20}H_{22}O_9N_2$: C, 55.30; H, 5.11; N, 6.45; Cl, 0.00. Found: C, 55.25; H, 5.38; N, 6.60; Cl, 0.00.

(*b*) The 5-bromo-dipyrrylmethene hydrobromide (II, 500 mg) was treated as in method *a*. The crude brown product (220 mg) was extracted with methanol (thimble, above a second thimble containing Darco), and the extract concentrated. The product (200 mg, 53%) separated as brownish-yellow prisms, m.p. 236–238° (decomp.) (block preheated to 220°) alone or admixed with the product from method *a* above.

Anal. Found: Br, 0.00.

The products obtained by methods *a* and *b* above, λ_{max} 419 mμ (in water), showed the same chemical shifts in their nuclear magnetic resonance spectra, and were converted into the same 5-chloro-dipyrrylmethene methyl ester (V, see above).

Uroporphyrin 1 Octamethyl Ester

(*a*) 5-Bromo-5'-methyl-dipyrrylmethene-3,4'-diacetic acid-4,3'-dipropionic acid hydrobromide (X) was heated with methylsuccinic acid at 118°, and the product was isolated in the same way as was that from the isomeric dipyrrylmethene II (19), 5.3%, m.p. 282–285°, raised to 284–285° (lit. (19) m.p. 285–286°) after several recrystallizations.

Anal. Calcd. for $C_{48}H_{54}O_{16}N_4$: C, 61.14; H, 5.77; N, 5.94; OMe, 26.33. Found: C, 61.06; H, 5.68; N, 5.90; OMe, 26.18.

This uroporphyrin methyl ester was degraded to coproporphyrin 1 methyl ester, m.p. 251–254° (lit. (19) m.p. 251–252°).

(*b*) 5-Chloro-5'-methyl-dipyrrylmethene-4,3'-diacetic acid-3,4'-dipropionic acid hydrochloride (IV, 250 mg) was heated with 1 g of methylsuccinic acid at 118° and the melt worked up as above. The product (0.13 mg, 0.06% (estimated spectroscopically)) did not crystallize.

2-Azidomethyl-4-methyl-5-carboxy-pyrrole-3-propionic Acid Diethyl Ester (XVIIb)

Powdered sodium azide (1 g) was warmed in 240 ml of dimethylformamide (distilled over P_2O_5) until it dissolved. A solution of 5 g of 2-bromomethyl-4-methyl-5-carboxy-pyrrole-3-propionic acid diethyl ester (XVII*a* (24)) in 10 ml of warm dimethylformamide was added. The solution was heated on the steam bath for 2 h and the solvent then removed at 50° in a rotary evaporator. The residue was washed with

water (2 × 10 ml), and then extracted with 60 ml of chloroform. The chloroform solution was washed with water (3 × 10 ml), and dried with sodium sulfate; then the solvent was evaporated. This residue was dissolved in 10 ml of warm chloroform, and 45 ml of pentane was added. The product (3.38 g) separated slowly as stable colorless needles, m.p. 110–110.5°.

Anal. Calcd. for $C_{14}H_{20}O_4N_4$: C, 54.53; H, 6.54; N, 18.17. Found: C, 54.64; H, 6.44; N, 18.20.

5-Bromo-5′-azidomethyl-4,3′-dimethyl-3,4′-diethyl-dipyrrylmethene Hydrazoate (XVIIIb)

The hydrobromide of 5-bromo-5′-bromomethyl-4,3′-dimethyl-3,4′-diethyl-dipyrrylmethene (XVIII*a*, 480 mg (4)) and 140 mg of sodium azide were refluxed in 20 ml of acetone and 5 ml of water for 1 h. The solvent was evaporated *in vacuo* and the residue, after being washed with water, crystallized from 85% acetone. This product (300 mg), m.p. 125–126°, was recrystallized three times to give brown rods, m.p. 129–130° (decomp.).

Anal. Calcd. for $C_{16}H_{21}N_8Br$: C, 47.41; H, 5.22; N, 27.65; Br, 19.72. Found: C, 47.52; H, 5.16; N, 27.42; Br, 19.60.

The *free base*, though crystalline, was quite unstable.

ACKNOWLEDGMENTS

We are indebted to Dr. Maria Przybylska for the X-ray powder photographs, and to Mr. H. Séguin for the microanalyses.

REFERENCES

1. H. Fischer and H. Orth. Chemie des Pyrrols. Vol. II. Akademische Verlagsgesellschaft, Leipzig. 1937. Part I.
2. H. Fischer and H. Reinecke. Z. Physiol. Chem. **258**, 243 (1939).
3. G. P. Arsenault, E. Bullock, and S. F. MacDonald. J. Am. Chem. Soc. **82**, 4384 (1960).
4. A. Markovac and S. F. MacDonald. Can. J. Chem. **43**, 3364 (1965).
5. H. Fischer and W. Fröwis. Z. Physiol. Chem. **195**, 49 (1931).
6. J. Ellis, A. H. Jackson, A. C. Jain, and G. W. Kenner. J. Chem. Soc. 1935 (1964).
7. H. Fischer, H. Friedrich, W. Lamatsch, and K. Morgenroth. Ann. **466**, 147 (1928).
8. A. H. Corwin and P. Viohl. J. Am. Chem. Soc. **66**, 1137 (1944).
9. C. K. Ingold. Structure and mechanism in organic chemistry. Cornell University Press, Ithaca, New York. 1953.
10. D. C. White. Mikrochim. Acta, 449 (1960).
11. F. Endermann and H. Fischer. Ann. **538**, 172 (1939).
12. W. Siedel and H. Möller. Z. Physiol. Chem. **259**, 121 (1939).
13. H. Fischer and E. Adler. Z. Physiol. Chem. **210**, 139 (1932).
14. H. Fischer and G. Fries. Z. Physiol. Chem. **231**, 231 (1935).
15. R. C. Elderfield and I. Serlin. J. Org. Chem. **16**, 1669 (1951).
16. H. Fischer and J. Aschenbrenner. Z. Physiol. Chem. **229**, 71 (1934); **245**, 107 (1937).
17. H. Fischer and E. Adler. Z. Physiol. Chem. **197**, 237 (1931).
18. H. Fischer, E. Baumann, and H. J. Riedl. Ann. **475**, 205 (1929).
19. S. F. MacDonald and R. J. Stedman. Can. J. Chem. **32**, 896 (1954).
20. H. Fischer and H. Berg. Ann. **482**, 213 (1930).
21. S. F. MacDonald and K. H. Michl. Can. J. Chem. **34**, 1671 (1956).
22. S. F. MacDonald and R. J. Stedman. Can. J. Chem. **33**, 458 (1955).
23. S. F. MacDonald. J. Chem. Soc. 4184 (1952).
24. F. Morsingh and S. F. MacDonald. J. Am. Chem. Soc. **82**, 4377 (1960).

Can. J. Chem. Downloaded from www.nrcresearchpress.com by 210.87.254.5 on 09/05/12
For personal use only.

A NOVEL SYNTHESIS OF SOME MIXED ARYLMETHYL–ALKYL ETHERS

K. G. RUTHERFORD, O. A. MAMER, J. M. PROKIPCAK, AND R. A. JOBIN

During an investigation into the synthesis of optically active trityl systems, it was found that triphenylcarbinol could be converted into its methyl ether in an excellent yield by treatment with iodine in methanol. Although the reaction appeared to be an obvious one, a survey showed that such a procedure had not as yet been recorded in the literature. It became of interest, then, to study this ether-forming reaction with other arylcarbinols which have become available in our laboratory.

Table I indicates the mixed ethers synthesized by this procedure. Although iodine was shown to be a catalyst by titration with standard sodium thiosulfate, the best results were obtained when it was used in approximately equimolar amounts. The arylcarbinol was dissolved in a mixture of acetone and aliphatic alcohol, iodine was added, and the reaction mixture was stirred at room temperature for periods of up to 2 h.

TABLE I

Properties of the mixed ethers

Ether	Melting point (°C)		Boiling point (°C)		Yield (%)
	Reported	Observed	Reported	Observed	
$(R)_3COCH_3$ (I)	80–82 (1)	81.5–82.5			90
$(R)_3COC_2H_5$ (II)	84.5 (2)	82.5–83.5			80
$(R)_3CO$—*n*-Pr (III)	56 (3)	54–55			78
$(R)_3CO$—*i*-Pr (IV)	111–113 (4)	112–113			45
$(R)_3COCH_2R$ (V)	106–107 (2)	105–106			50
$RR_1R_4COCH_3$* (VI)	120–121 (5)	50–52			Quantitative
RR_1CHOCH_3† (VII)			160–165 at 10 mm (6)	160–162 at 10 mm	96
$(R)_2CHOCH_3$‡ (VIII)			147–148 at 17 mm (7)	147–149 at 17 mm	70
$(R)_2CHOC_2H_5$ (IX)			160–161 at 19 mm (2)	157–159 at 19 mm	52
$(R)_2CHO$—*n*-Pr (X)			161 at 11 mm (8)	160–162 at 11 mm	42
RR_2CHOCH_3§ (XI)	Not reported	27–29			85
$R_2R_3CHOCH_3$‖ (XII)	Not reported	87–88			Quantitative
$R_7CH_2OCH_3$¶ (XIII)			225.5 at 758 mm (9)	220–225 at 745 mm	80

NOTE: R = C_6H_5—, R_1 = 4-CH_3—C_6H_4—, R_2 = 4-Cl—C_6H_4—, R_3 = 4-Br—C_6H_4—, R_4 = 1-naphthyl—, R_5 = 4-NO_2—C_6H_4—, R_6 = 4-*t*-Bu—C_6H_4—, R_7 = 4-$CH_3OC_6H_4$—.

The following alcohols could not be converted into the corresponding methyl ethers by this procedure: RCH_2OH, R_3R_5CHOH, RR_6CHOH, and R_5R_6CHOH.

*Anal. Calcd. for $RR_1R_4COCH_3$: C, 88.73; H, 6.54. Found: C, 88.70; H, 6.61.

†Anal. Calcd. for RR_1CHOCH_3: C, 84.87; H, 7.60. Found: C, 84.9; H, 7.49.

‡n_D^{25} 1.5648 (reported (7) n_D^{25} 1.5653).

§Anal. Calcd. for RR_2CHOCH_3: C, 72.32; H, 5.67. Found: C, 72.26; H, 5.52.

‖Anal. Calcd. for $R_2R_3CHOCH_3$: C, 54.00; H, 3.88. Found: C, 54.29; H, 3.68.

¶$n_D^{18.5}$ 1.5150.

It is apparent from the table that ether formation coincides quite favorably with what would be expected from the structure of the arylcarbinol and the ease of carbonium ion formation. Thus methyl ethers I, VI, VII, VIII, XI, XII, and XIII are obtained in good yields from the corresponding arylcarbinols. Again, those arylcarbinols which were nitro substituted did not undergo reactions under the conditions employed.

A definite trend towards a decrease in the yield of ether formation is observed from methyl, ethyl, *n*-propyl, and *i*-propyl alcohols. This effect could well be a manifestation of

the progressive decrease in the dielectric constant (32.63, 24.3, 20.1, and 18.3, respectively, (10)), although *i*-propyl alcohol presents a formidable steric effect as well. No *t*-butyl ether could be made from the reaction of *t*-butyl alcohol and the arylcarbinols employed. Undoubtedly, iodine-catalyzed dehydration of *t*-butyl alcohol was a competing reaction. A very unfavorable steric effect is also operative in this case.

The mechanism of the reaction is probably best represented by the sequence of reactions shown in eqs. [1]–[4].

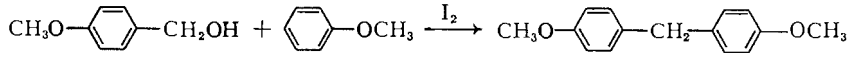
[1] $$R{-}OH + I_2 \rightleftharpoons R{-}\overset{\displaystyle I}{\underset{|}{O}}{-}H^+ + I^-$$

[2] $$R{-}\overset{\displaystyle I}{\underset{|}{O}}{-}H^+ \rightleftharpoons R^+ + HOI$$

[3] $$R^+ + R'OH \rightarrow R{-}O{-}R' + H^+$$

[4] $$HOI + HI \rightleftharpoons H_2O + I_2$$

This mechanism is essentially the same as that proposed by Dhar and his co-workers (11) for the iodine-catalyzed dehydration of alcohols, and accounts for the trends in the yields of methyl ether formation previously discussed as well as for the catalytic activity of iodine. Further support for the carbonium ion nature of the reaction (eq. [2]) was found when 4-methoxybenzyl alcohol was reacted with anisole in the presence of iodine. Bis-(4-methoxyphenyl)-methane was isolated in 82% yield (eq. [5]). To our knowledge, this is the first recorded example of an iodine-catalyzed Friedel–Crafts reaction.

[5] 

All of the ethers prepared by this method were well characterized by infrared spectrometry, elemental analysis, and (in all cases where possible) mixed melting point determinations with authentic samples which were prepared according to known procedures.

EXPERIMENTAL

All melting points were determined on the Fisher–Johns melting point apparatus and are uncorrected. Analyses were performed by Schwarzkopf Microanalytical Laboratory, Woodside 77, New York.

Triphenylcarbinol was obtained from commerical sources. Phenyl-*p*-tolyl-1-naphthylcarbinol was obtained by the reaction of 1-naphthylmagnesium bromide with 4-methylbenzophenone. The appropriate carbinols were obtained by the reduction of the appropriate ketones with sodium borohydride. This reagent does not reduce the nitro groups.

Authentic samples of the mixed ethers were prepared by the well-known reaction of arylmethyl chlorides with aliphatic alcohols in the presence of pyridine.

The general procedure for the synthesis of the mixed ethers by the iodine-catalyzed method involved dissolution of the arylcarbinol in an excess of the aliphatic alcohol. Iodine was added and the reaction mixture was stirred for approximately 2 h, whereupon it was poured onto a mixture of crushed ice and sodium thiosulfate solution. The product was isolated by crystallization or distillation. The preparation of the methyl ethers of triphenylcarbinol and 4-methoxybenzyl alcohol is given below.

Methyl Ether of Triphenylcarbinol

A solution of 10 g (0.0385 mole) of triphenylcarbinol, 10 g (0.039 mole) of iodine, and 50 ml of methanol was stirred at room temperature for 2 h. The reaction mixture was poured slowly, with stirring, into a cold solution of sodium thiosulfate (50 g $Na_2S_2O_3$ in 500 ml water). The methyl ether was recovered by filtration. Recrystallization from ethanol gave 9.5 g (90%) of the methyl ether, m.p. 81.5–82.5°.

Methyl Ether of 4-Methoxybenzyl Alcohol

A solution of 10 g (0.082 mole) of 4-methoxybenzyl alcohol, 15 g (0.059 mole) of iodine, 50 ml of methanol, and 50 ml of acetone was stirred at room temperature for 18 h, after which it was poured slowly into a solution of 50 g of sodium thiosulfate in 500 ml of water. The resultant mixture was extracted twice with 50 ml

Can. J. Chem. Downloaded from www.nrcresearchpress.com by 210.87.254.5 on 09/05/12
For personal use only.

portions of methylene chloride. These extracts were combined, dried over anhydrous sodium sulfate, and subjected to fractional distillation. The fraction boiling in the range of 223–225° at 745 mm was collected (reported (9) b.p. 225.5° at 758 mm). A yield of 8.1 g (80%), η_D^{20} 1.5150, was obtained.

Bis-(4-methoxyphenyl)-methane

A mixture of anisole (5.4 g, 0.05 mole), 4-methoxybenzyl alcohol (6.9 g, 0.05 mole), and iodine (12.7 g, 0.05 mole) was dissolved in 40 ml acetone, whereupon the temperature rose quickly to 45°. The mixture was allowed to stand, with stirring, for 30 min and then was poured into a solution of excess sodium thiosulfate and ice water. The mixture was extracted twice with 50 ml portions of ether. The ether extracts were dried over anhydrous potassium carbonate, treated with Norit, and evaporated *in vacuo* to an oil which crystallized when allowed to stand (9.4 g, 82%), m.p. 35–41°. The product was dissolved in hot ethanol and the solution was cooled to give white crystals of bis-(4-methoxyphenyl)-methane, m.p. 44–46° (recorded (12) m.p. 46–47°). The infrared spectrum showed the following bands: aromatic ring skeletal vibrations at 1 613, 1 585, 1 506, and 1 464 cm^{-1}, multiple CO stretching bands in the region of 1 300 to 1 030 cm^{-1}, methoxyl CH stretching at 2 830 cm^{-1}, and aromatic CH "out of plane" bending overtones at 1 875 and 1 775 cm^{-1}, which corresponds to 1,4-disubstitution on the benzene nucleus.

The structure of the product was confirmed by oxidation with chromic oxide in acetic acid to 4,4′-dimethoxybenzophenone, m.p. 144–145° (recorded (13) m.p. 143.5–145°).

ACKNOWLEDGMENTS

The financial support given by the National Research Council of Canada and by the Petroleum Research Fund (grant No. 1575-A4) administered by the American Chemical Society is gratefully acknowledged.

1. A. H. Hatt. J. Chem. Soc. 483 (1938).
2. G. L. Stadnikov. Ber. **57B**, 1 (1924).
3. B. Helferich, P. E. Speidel, and W. Toeldte. Ber. **56B**, 767 (1923).
4. J. F. Norris and R. C. Young. J. Am. Chem. Soc. **46**, 2582 (1924).
5. W. Dilthey, E. Haussler, E. Hausdorfer, and O. Reeh. J. Prakt. Chem. **109**, 273 (1925).
6. A. G. Davies, J. Kenyon, B. J. Lyons, and T. A. Rohan. J. Chem. Soc. 3474 (1954).
7. E. Bergmann and J. Hervey. Ber. **62B**, 893 (1929).
8. G. L. Stadnikov. J. Prakt. Chem. **88**, 2 (1913).
9. von S. Cannizzaro. Ann. **137**, 246 (1866).
10. N. A. Lange. Handbook of chemistry. 9th ed. Handbook Pubs., Inc., Sandusky, Ohio. 1956. p. 1222.
11. M. L. Dhar, E. D. Hughes, C. K. Ingold, A. M. Mandour, G. A. Maw, and L. I. Wolf. J. Chem. Soc. 2113 (1948).
12. P. D. Bartlett and J. D. McCollum. J. Am. Chem. Soc. **78**, 1448 (1956).
13. E. M. Arnett and G. B. Klingensmith. J. Am. Chem. Soc. **87**, 1028 (1965).

Received November 15, 1965.
Department of Chemistry,
University of Windsor,
Windsor, Ontario.

A ONE-STEP CONVERSION OF CYCLOHEXENE OXIDE INTO *cis*-1,2-DICHLOROCYCLOHEXANE

J. R. Campbell, J. K. N. Jones, and Saul Wolfe

cis-1,2-Dichlorocyclohexane (I) can be prepared by reacting *trans*-cyclohexene chlorohydrin with hydrochloric acid (1) or with thionyl chloride and pyridine (2), or by the photodegradation of 1-chlorocyclohexene (3). In each case, however, the yields are low and the *cis* dichloride is contaminated with substantial amounts of the *trans* isomer.

In connection with various problems under investigation in our laboratories, we required very pure samples of I and of other *cis* dichlorides, and have therefore tried to improve the stereospecificity of the preparation of I. The purpose of this note is to report that the

Can. J. Chem. Downloaded from www.nrcresearchpress.com by 210.87.254.5 on 09/05/12
For personal use only.

portions of methylene chloride. These extracts were combined, dried over anhydrous sodium sulfate, and subjected to fractional distillation. The fraction boiling in the range of 223–225° at 745 mm was collected (reported (9) b.p. 225.5° at 758 mm). A yield of 8.1 g (80%), η_D^{20} 1.5150, was obtained.

Bis-(4-methoxyphenyl)-methane

A mixture of anisole (5.4 g, 0.05 mole), 4-methoxybenzyl alcohol (6.9 g, 0.05 mole), and iodine (12.7 g, 0.05 mole) was dissolved in 40 ml acetone, whereupon the temperature rose quickly to 45°. The mixture was allowed to stand, with stirring, for 30 min and then was poured into a solution of excess sodium thiosulfate and ice water. The mixture was extracted twice with 50 ml portions of ether. The ether extracts were dried over anhydrous potassium carbonate, treated with Norit, and evaporated *in vacuo* to an oil which crystallized when allowed to stand (9.4 g, 82%), m.p. 35–41°. The product was dissolved in hot ethanol and the solution was cooled to give white crystals of bis-(4-methoxyphenyl)-methane, m.p. 44–46° (recorded (12) m.p. 46–47°). The infrared spectrum showed the following bands: aromatic ring skeletal vibrations at 1 613, 1 585, 1 506, and 1 464 cm^{-1}, multiple CO stretching bands in the region of 1 300 to 1 030 cm^{-1}, methoxyl CH stretching at 2 830 cm^{-1}, and aromatic CH "out of plane" bending overtones at 1 875 and 1 775 cm^{-1}, which corresponds to 1,4-disubstitution on the benzene nucleus.

The structure of the product was confirmed by oxidation with chromic oxide in acetic acid to 4,4′-dimethoxybenzophenone, m.p. 144–145° (recorded (13) m.p. 143.5–145°).

ACKNOWLEDGMENTS

The financial support given by the National Research Council of Canada and by the Petroleum Research Fund (grant No. 1575-A4) administered by the American Chemical Society is gratefully acknowledged.

1. A. H. Hatt. J. Chem. Soc. 483 (1938).
2. G. L. Stadnikov. Ber. **57B**, 1 (1924).
3. B. Helferich, P. E. Speidel, and W. Toeldte. Ber. **56B**, 767 (1923).
4. J. F. Norris and R. C. Young. J. Am. Chem. Soc. **46**, 2582 (1924).
5. W. Dilthey, E. Haussler, E. Hausdorfer, and O. Reeh. J. Prakt. Chem. **109**, 273 (1925).
6. A. G. Davies, J. Kenyon, B. J. Lyons, and T. A. Rohan. J. Chem. Soc. 3474 (1954).
7. E. Bergmann and J. Hervey. Ber. **62B**, 893 (1929).
8. G. L. Stadnikov. J. Prakt. Chem. **88**, 2 (1913).
9. von S. Cannizzaro. Ann. **137**, 246 (1866).
10. N. A. Lange. Handbook of chemistry. 9th ed. Handbook Pubs., Inc., Sandusky, Ohio. 1956. p. 1222.
11. M. L. Dhar, E. D. Hughes, C. K. Ingold, A. M. Mandour, G. A. Maw, and L. I. Wolf. J. Chem. Soc. 2113 (1948).
12. P. D. Bartlett and J. D. McCollum. J. Am. Chem. Soc. **78**, 1448 (1956).
13. E. M. Arnett and G. B. Klingensmith. J. Am. Chem. Soc. **87**, 1028 (1965).

Received November 15, 1965.
Department of Chemistry,
University of Windsor,
Windsor, Ontario.

A ONE-STEP CONVERSION OF CYCLOHEXENE OXIDE INTO *cis*-1,2-DICHLOROCYCLOHEXANE

J. R. Campbell, J. K. N. Jones, and Saul Wolfe

cis-1,2-Dichlorocyclohexane (I) can be prepared by reacting *trans*-cyclohexene chlorohydrin with hydrochloric acid (1) or with thionyl chloride and pyridine (2), or by the photodegradation of 1-chlorocyclohexene (3). In each case, however, the yields are low and the *cis* dichloride is contaminated with substantial amounts of the *trans* isomer.

In connection with various problems under investigation in our laboratories, we required very pure samples of I and of other *cis* dichlorides, and have therefore tried to improve the stereospecificity of the preparation of I. The purpose of this note is to report that the

Can. J. Chem. Downloaded from www.nrcresearchpress.com by 210.87.254.105 on 09/05/12
For personal use only.

reaction of cyclohexene oxide with sulfuryl chloride and pyridine or with thionyl chloride and pyridine produces the 1,2-dichlorocyclohexanes in satisfactory yield, with the *cis* isomer predominating. Depending on the conditions, the proportion of the *cis* isomer can be increased to greater than 99.5%. This is therefore a convenient route to a *cis* dichloride. The application of the conditions worked out in the present study to other epoxides[1] indicates that the reaction is a general one and proceeds with inversion of configuration at both termini of the epoxide.

Table I summarizes the results of a number of experiments performed in the absence of a solvent, using various quantities and modes of addition of the reagents at different temperatures. These results indicate that, with sulfuryl chloride, higher yields of dichloride are obtained with an excess of the halide, but the stereospecificity is greater when equivalent amounts of the three reactants are used. Equivalent amounts of oxide and sulfuryl chloride with an excess of pyridine (run 5) led to a poor yield of dichloride, which consisted mainly of the *trans* isomer. The proportions of the *cis* and *trans* isomers are not temperature dependent. However, the reaction is more difficult to control at the lower temperatures and the yields are not as good. Replacing sulfuryl chloride with thionyl chloride had no significant effect on the yield or the stereospecificity (runs 3 and 13) when equal amounts of the reactants were used. Excess thionyl chloride caused a reduction in the yield but not in the stereospecificity (runs 9 and 13).

TABLE I

The neat reaction of cyclohexene oxide with thionyl chloride and pyridine and with sulfuryl chloride and pyridine

Run	mmoles of reactant			Mode of addition	Temperature* (°C)	% yield of dichlorides	% *cis* in the dichlorides
	Oxide	Pyridine	Halide				
1	10.2	20.4	20.4†	A‡	73	89	82
2§	10.2	20.4	40.4†	A	75	71	83
3	10.2	10.2	10.8†	A	73	61	93
4	10.2	10.2	10.8†	A	25	55‖	—
5	10.2	40.8	10.8†	B¶	73	10	10
6	10.2	10.2	10.8†	B	25	34	93
7	10.2	20.4	16.2†	B	73	41	82
8	4.8	4.8	4.8†	A	−20	37**	95
9	10.2	10.2	20.4††	A	72	35	94
10	10.2	15.2	30.4††	A	90	39	86
11	10.2	10.2	10.2††	A	100	53	94
12	10.2	10.2	10.2††	A	100	57	91
13	10.2	10.2	10.2††	A	72	56	90
14	10.2	10.2	10.2††	B	72	52	91

*Refers to the external temperature.
†SO_2Cl_2.
‡Oxide and pyridine added to the halide.
§This run was performed in the presence of 10.2 mmoles of added pyridine hydrochloride.
‖The reaction mixture spontaneously warmed to 75°.
¶Halide added to the oxide and pyridine.
**A violent evolution of gas occurred as the reaction mixture was being brought to room temperature.
††$SOCl_2$.

The data summarized in Table II show that there is a dramatic improvement in the stereospecificity when the reaction is mediated by a solvent. Chloroform is more effective than carbon tetrachloride (runs 15 and 17) and, in chloroform, sulfuryl chloride is more effective than thionyl chloride (runs 18 and 19). The optimum conditions for the reaction appear to be those of run 18.

[1]*S. S. Ali and J. K. N. Jones, to be published.*

Can. J. Chem. Downloaded from www.nrcresearchpress.com by 210.87.254.105 on 09/05/12
For personal use only.

TABLE II

Effect of solvent on the conversion of cyclohexene oxide into the dichlorocyclohexanes

Run	mmoles of reactant: Oxide	Pyridine	Halide	Solvent (ml)	Temperature (°C)	% yield of dichlorides	% *cis* in the dichlorides
15	10.2	10.2	11.2*	$CHCl_3$ (5)	−20†	51	99.5
16	10.2	10.2	11.2*	$CHCl_3$ (5)	−20‡	66	99.3
17	10.2	10.2	11.2*	CCl_4 (5)	25‡	38	91
18	10.2	10.2	11.2*	$CHCl_3$ (10)	Reflux	70	99.0
19	10.2	10.2	11.2§	$CHCl_3$ (10)	Reflux	50	93.5

*SO_2Cl_2.
†The mixture was maintained at this temperature for 45 min and then refluxed for 2.5 h.
‡The mixture was maintained at this temperature for 15 min and then refluxed for 2.5 h.
§$SOCl_2$.

A comparison of the above results with those shown in Table III indicates that when cyclohexene chlorohydrin is used as the substrate both the yields and the stereospecificity are lower (2).

TABLE III

The conversion of cyclohexene chlorohydrin into the dichlorocyclohexanes

Run	mmoles of reactant: Chlorohydrin	Pyridine	Halide	Temperature (°C)	Solvent (ml)	% yield of dichlorides	% *cis* in the dichlorides
20	74.3	148.6	148.6*	73	None	38.0	84.2
21	111.8	223.6	223.6*	73	None	35.0	82.0
22	148.6	148.6	148.6*	75	None	†	80.8
23	10.2	10.2	11.2*	Reflux‡	$CHCl_3$ (10)	0	—
24	10.2	10.2	11.2*	Reflux§	$CHCl_3$ (10)	62	88
25	10.2	10.2	11.2‖	Reflux‡	$CHCl_3$ (10)	65	93

*$SOCl_2$.
†Not determined.
‡Reaction time of 2 h.
§Reaction time of 16 h.
‖SO_2Cl_2.

The reaction of iodobenzene dichloride with olefins may yield either a *cis* (4) or a *trans* (5) dichloride depending on the structure of the substrate. With cyclohexene this reagent produced the highest stereospecificity of any chlorinating agent which we have used, the product containing *no detectable amount of the cis isomer*. Table IV shows this result together with the results obtained from the action of other chlorinating agents on cyclohexene.

TABLE IV

The reaction of cyclohexene with various chlorinating agents

Source of chlorine	mmoles of reactant: Olefin	Chlorinating agent	Solvent (ml)	Temperature (°C)	% *trans* in the dichlorides
$C_6H_5ICl_2$	6.1	6.1	$CHCl_3$ (5)	Reflux	>99
	6.1	6.1	Tetrahydrofuran (5)	0	>99.5
SO_2Cl_2	36.6	36.6	CH_2Cl_2 (25)	Reflux	85.5
	12.2	12.2	CH_2Cl_2 (8)	5	85.5
Cl_2	29.2	29.2*	CS_2 (16)	Reflux†	97
	29.2	29.2*	CS_2 (16)	Reflux‡	98

*By titration.
†Reaction mixture was illuminated with a Photoflood light source.
‡Light was excluded.

Can. J. Chem. Downloaded from www.nrcresearchpress.com by 210.87.254.105 on 09/05/12
For personal use only.

Can. J. Chem. Downloaded from www.nrcresearchpress.com by 210.87.254.105 on 09/05/12
For personal use only.

EXPERIMENTAL

Preparation of Reagents

Commercial *pyridine* was purified by refluxing over sodium hydroxide (1 g/10 ml) and distillation, the fraction boiling at 115.0–115.5° being retained.

Commercial *sulfuryl chloride* was purified by distillation, the fraction boiling at 68.5–69.2° being retained.

Thionyl chloride was purified by distillation, the fraction boiling at 78.6–79.1° being retained.

Cyclohexene oxide was prepared by reacting cyclohexene bromohydrin with 20% sodium hydroxide (6), and was purified by distillation, the fraction boiling at 131.5–132.5° being retained.

Iodobenzene dichloride was prepared by the addition of chlorine to iodobenzene (7).

Cyclohexene chlorohydrin was prepared by reacting cyclohexene with aqueous *N*-chlorosuccinimide (8), and was purified by distillation, b.p. 67.0–68.0° at 5 mm.

Analytical Procedure

The dichlorides were analyzed by gas chromatography on a 6 ft column packed with 15% butanediol succinate on Embacel. The instrument used was a Beckman GC2 gas chromatograph operated at 130° and 30 p.s.i. of helium. The appearance times were: *trans*, 10.3 min; *cis*, 22.2 min. The ratios were determined by the triangulation method (9).

General Procedure

(a) Without Solvent

A solution of cyclohexene oxide (15.8 g, 0.161 mole) in pyridine (25.45 g, 0.322 mole) was added during a 40 min period to sulfuryl chloride (43.1 g, 0.322 mole) at 75° (gentle reflux). A gas was evolved and the mixture darkened. After a further 1.5 h at 75°, water was cautiously added and the organic layer was extracted with ether. The ether extract was washed with 10% sodium carbonate and water, and was then dried over anhydrous magnesium sulfate. Concentration gave 18.5 g of a brown oil which consisted of 88.4% of *cis*-1,2-dichlorocyclohexane and 11.6% of *trans*-1,2-dichlorocylohexane. The *cis* dichloride was freed from the *trans* isomer by preparative gas chromatography (Fisher preparative partitioner) and was then distilled at 75.0–75.3° and 3–4 mm.

Anal. Calcd. for $C_6H_{10}Cl_2$: C, 47.08; H, 6.59. Found: C, 46.92; H, 6.31.

The infrared spectrum of the *cis* isomer (10% in carbon disulfide) showed a single peak at 13.6 μ; the *trans* compound showed a doublet in this region, at 13.5 μ and 13.6 μ.

(b) In Chloroform

Sulfuryl chloride (1.51 g, 11.2 mmoles) was added during 5 min to a refluxing solution of cyclohexene oxide (1.0 g, 10.2 mmoles) and pyridine (0.81 g, 10.2 mmoles) in chloroform (10 ml). There was no darkening during the addition. The reaction mixture was refluxed for 16 h and was then diluted with water (15 ml) and ether (35 ml). The organic layer was dried over anhydrous magnesium sulfate and concentrated to give 1.08 g of material which was chromatographed on neutral alumina (activity III). Elution with petroleum ether gave 0.68 g (45%) of the dichlorocyclohexanes which contained 99.0% of the *cis* isomer.

ACKNOWLEDGMENT

We thank the National Research Council for support of this work and for the award of a studentship.

1. G. A. Russell, A. Ito, and R. Konaka. J. Am. Chem. Soc. **85**, 2988 (1963).
2. B. Carroll, D. G. Kubler, H. W. Davis, and A. M. Whaley. J. Am. Chem. Soc. **73**, 5382 (1951). H. C. Stevens and O. Grummitt. J. Am. Chem. Soc. **74**, 4876 (1952).
3. R. V. Lindsey, Jr. and J. N. Ingraham. J. Am. Chem. Soc. **75**, 5613 (1955).
4. D. H. R. Barton and E. Miller. J. Am. Chem. Soc. **72**, 370 (1950).
5. S. J. Cristol, F. R. Stermitz, and P. S. Ramey. J. Am. Chem. Soc. **78**, 4939 (1956).
6. C. O. Guss and R. Rosenthal. J. Am. Chem. Soc. **77**, 2549 (1955).
7. A. I. Vogel A textbook of practical organic chemistry. 3rd ed. Longmans, Green & Co., Inc., New York. 1957. p. 541.
8. E. J. Langstaff. M.Sc. Thesis, Queen's University, Kingston, Ontario. 1964.
9. L. Condal-Bosch. J. Chem. Educ. **41**, A235 (1964).

Received May 24, 1966.
Department of Chemistry,
Queen's University,
Kingston, Ontario.

REARRANGEMENT STUDIES WITH ^{14}C
XXVIII. SOLVOLYSES OF 1-^{14}C-1-PROPYL *p*-TOLUENESULFONATE

C. C. LEE AND JAMES E. KRUGER[1]

In the deamination of isotopically labeled 1-propylamine, published data (1, 2) have suggested the possible occurrence of 1,3-hydride shifts in accounting for the isotope position rearrangements observed in the resulting 1-propanol. More recent studies (3–5), however, have demonstrated that such rearrangements arose from some involvement of protonated cyclopropanes rather than 1,3-hydride shifts. It is of interest to investigate the possible isotopic rearrangements that may accompany solvolyses of 1-^{14}C-1-propyl *p*-toluenesulfonate (I) so as to assess the role, if any, of protonated cyclopropanes in such reactions.

1-^{14}C-1-Propanol was purchased commercially or prepared by the lithium aluminium hydride reduction of 1-^{14}C-propionic acid obtained from the reaction of ethylmagnesium bromide with ^{14}C-carbon dioxide. The alcohol was converted into the *p*-toluenesulfonate I, which was then subjected to solvolysis in acetic acid at 110 °C for 42 h or in refluxing formic acid for 18 h. The product, 1-propyl acetate or formate, was separated from minor amounts of 2-propyl acetate (less than 1%) or formate (1–2%) by preparative vapor-phase chromatography. After alkaline hydrolysis of these esters, the resulting 1-propanol was oxidized to propionic acid which was, in turn, degraded to acetic acid and methylamine as previously described (1, 3, 4). The propionic acid, acetic acid, and methylamine were converted into the appropriate solid derivatives, which were purified by repeated crystallizations until their specific activities were constant. The activity of the acetic acid served as a measure of the rearrangement of the ^{14}C-label from C-1 to C-2 and C-3, and the activity of the methylamine indicated the rearrangement to C-3. The results are summarized in Table I.

TABLE I

Rearrangements in the solvolyses of 1-^{14}C-1-propyl *p*-toluenesulfonate (I)

Expt.	Reaction	Specific activity (c.p.m./mmole)*			% ^{14}C on C-2 and C-3	% ^{14}C on C-3
		CH_3CH_2COOH†	CH_3COOH†	CH_3NH_2‡		
1	Acetolysis	60 300	170		0.3	
2	Acetolysis	523 000	200	170	0.04	0.03
3	Formolysis§	695 000	6 860		0.99	
4	Formolysis‖	4 095 000	33 800	27 300	0.83	0.68

*Measured by a liquid scintillation counter.
†Assayed as the *p*-bromophenacyl ester.
‡Assayed as the *N*-methyl *p*-toluenesulfonamide.
§The starting material I was prepared from commercially obtained 1-^{14}C-1-propanol, a control degradation of which gave CH_3COOH containing an appreciable amount of activity.
‖The starting material I was prepared from 1-^{14}C-1-propanol synthesized in this laboratory; a controlled degradation gave CHC_3COOH with negligible activity.

In the first acetolysis run (expt. 1, Table I), the specific activities of the compounds assayed were such that the degradation product, the solid *p*-bromophenacyl ester of acetic acid, showed an actually observed net activity, for samples weighing about 15 mg, of only about 10 c.p.m., whereas the background activity was of the order of 15–20 c.p.m.

[1]*Holder of a National Research Council of Canada studentship, 1965-1966.*

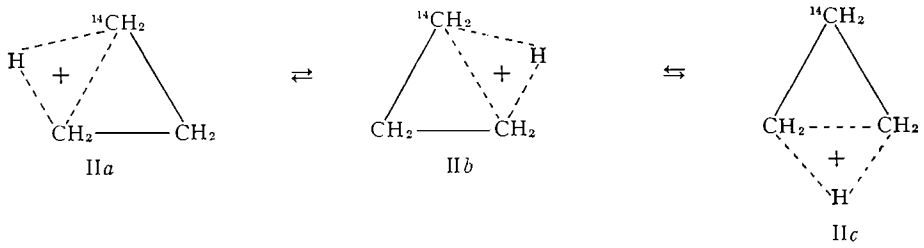
Can. J. Chem. Downloaded from www.nrcresearchpress.com by 210.87.254.6 on 09/05/12
For personal use only.

Can. J. Chem. Downloaded from www.nrcresearchpress.com by 210.87.254.6 on 09/05/12
For personal use only.

The reliability of the apparent rearrangement of 0.3% from this experiment was thus questionable. In expt. 2, starting material of much higher specific activity was employed, and the results indicated an essentially negligible isotopic rearrangement in the 1-propyl acetate from the acetolysis of I.

In the formolysis studies, a preliminary run with I of relatively lower specific activity suggested the possible presence of rearranged ^{14}C on both C-2 and C-3. Further experiments with starting materials of higher specific activities were carried out. In expt. 3, I was prepared from commercially obtained 1-^{14}C-1-propanol, the degradation of which, however, gave a sample of acetic acid containing an appreciable amount of radioactivity (about 0.2–0.3%). The formolysis product from expt. 3 was therefore degraded only to acetic acid, and not to methylamine. For expt. 4, 1-^{14}C-1-propanol of very high specific activity was synthesized in the laboratory. Its degradation to essentially inactive acetic acid showed that all of the ^{14}C-label was located on C-1. The alcohol was then converted into I and subjected to formolysis. The results from this experiment indicated a total of 0.83% ^{14}C-rearrangement from C-1 to C-2 and C-3 in the 1-propyl formate. From the activity on C-3, it was deduced that 0.15% and 0.68% of the rearranged ^{14}C were located on C-2 and on C-3, respectively. Although the magnitudes of these rearrangements were small, the reliability of these values was good (because of the high activities involved). The difference between the specific activities of the solid derivatives of acetic acid and methylamine was beyond experimental error. It can therefore be concluded that the formolysis of I gave 1-propyl formate showing a small amount of isotopic rearrangement, the rearranged ^{14}C being located on both C-2 and C-3, with the amount of ^{14}C on C-3 greater than that on C-2.

The absence of isotopic rearrangement in the acetolysis and the observation of only minor amounts of rearrangement in the formolysis showed the expected similarity with the solvolyses of 1-^{14}C-ethyl *p*-toluenesulfonate, which gave no detectable isotopic scrambling (6). These findings, coupled with the low yields of the 2-propyl products (which have also been reported by Huisgen and Ruchardt (7) for acetolysis), may be regarded as being consistent with a direct displacement as the major reaction pathway in the solvolyses of I. Alternatively, the results could also be interpreted in a manner similar to that discussed by Streitwieser (8) for the acetolysis and formolysis of optically active 1-*d*-1-butyl *p*-bromobenzenesulfonate. According to this view (8), solvolyses of even primary substrates in solvents of low nucleophilic character, such as acetic and formic acids, are not necessarily direct displacements of the S_N2 type. The structure usually regarded as the transition in an S_N2 displacement, a "covalently solvated carbonium ion", may be considered as the initial *intermediate*. For a primary central carbon with its low steric requirements and relative inability to delocalize a positive charge, the major reaction path would lead to an inverted product, the same as in a direct displacement. In the 1-propyl system, 1,2-hydride shifts in the solvated carbonium ion would account for the small amount of the 2-propyl product. The isotopic rearrangements observed in the formolysis could be interpreted as arising from some involvement of edge-protonated cyclopropanes. The initially formed protonated cyclopropane, II*a*, would give rise to the isotopically rearranged 3-^{14}C-1-propyl formate and the unrearranged 1-^{14}C-1-propyl formate. Subsequent equilibration of the three equivalent edge-protonated cyclopropanes (II*a* $\rightleftarrows$ II*b* $\rightleftarrows$ II*c*) would result in the distribution of the rearranged ^{14}C over all three carbon positions. In the formolysis of I, more formate was derivated from the initially formed edge-protonated cyclopropane, thus accounting for a greater amount of the rearranged ^{14}C on C-3 than on C-2.



In the deamination of 1-propylamine (3–5), the decomposition of the alkyldiazonium ion gave stable nitrogen and a highly energetic or vibrationally excited "hot" carbonium ion. In contrast to solvolyses, more 1,2-hydride shifts as well as a greater involvement of protonated cyclopropanes were noted. More 1,2-hydride shifts in the deamination of 1-^{14}C-ethylamine (9) than in the solvolyses of 1-^{14}C-ethyl *p*-toluenesulfonate (6) have also been observed. In the deamination of 1-propylamine, that portion of the reaction which proceeds via protonated cyclopropane apparently results from a more complete equilibration of II*a*–II*c*, giving rise to a rearranged 1-propanol with an isotopic distribution approaching that expected for a complete equivalence of all three carbon positions (3–5).

EXPERIMENTAL

1-^{14}C-1-Propyl p-Toluenesulfonate (I)

1-^{14}C-1-Propanol was prepared by the lithium aluminium hydride reduction of 1-^{14}C-propionic acid obtained from the reaction of ethylmagnesium bromide with carbon dioxide generated from sodium carbonate containing 10 mCi of ^{14}C. Treatment of the alcohol with *p*-toluenesulfonyl chloride in pyridine gave I, b.p. 136–140 °C at 2 mm (lit. (7) b.p. 102–109 °C at 0.01 mm).

Anal. Calcd. for $C_{10}H_{14}O_3S$: C, 56.05; H, 6.58; S, 14.96. Found: C, 56.05; H, 6.65; S, 14.93.

Acetolysis

A solution of 16.95 g (0.079 mole) of I in 75 ml of glacial acetic acid containing 8.75 g of potassium acetate was heated under reflux, with stirring, in a bath at 110 °C for 42 h. The material was poured into a 500 ml flask containing 150 ml of ice water; the resulting mixture was distilled, the fraction boiling between 80 and 99 °C being collected. The distillate was saturated with potassium carbonate and the upper organic layer was separated. After the organic material was dried over anhydrous magnesium sulfate, it was redistilled. Analytical vapor-phase chromatography showed that the major product was 1-propyl acetate, the amount of 2-propyl acetate being less than 1%. Final purification was effected by preparative vapor-phase chromatography with a column packed with 20% didecyl phthalate on Chromosorb P. The recovery of 1-propyl acetate was 5.12 g (63%).

Formolysis

A solution of 13.80 g (0.064 mole) of I in 55 ml of formic acid (reagent grade, 98–100% HCOOH, redistilled) was gently refluxed for 18 h. The material was poured into 150 ml of ice water and then extracted with four 30 ml portions of ether. The extract was carefully treated with solid potassium carbonate, washed with a small amount of water, and dried over anhydrous magnesium sulfate. After removal of the ether, the residue was fractionated, the fraction boiling between 65 and 83 °C being collected. Analytical vapor-phase chromatography showed that the major product was 1-propyl formate, the amount of 2-propyl formate being about 1–2%. Final purification was effected by preparative vapor-phase chromatography with a column packed with 20% Carbowax 20M on Chromosorb P. The recovery of 1-propyl formate was 1.30 g (23%).

Degradation

Samples of 1-propyl acetate or formate were hydrolyzed by refluxing them in 10% sodium hydroxide for 3 h. The resulting mixture was steam-distilled to give an aqueous solution of 1-propanol, which was used directly for oxidation to propionic acid (1, 3, 4). Where necessary, some inactive 1-propanol was added as carrier before the oxidation. The propionic acid was, in turn, degraded to acetic acid and methylamine by previously described methods (1, 3, 4).

ACKNOWLEDGMENT

The financial support given by the National Research Council of Canada is gratefully acknowledged.

Can. J. Chem. Downloaded from www.nrcresearchpress.com by 210.87.254.6 on 09/05/12
For personal use only.

1. O. A. REUTOV and T. N. SHATKINA. Tetrahedron, **18**, 237 (1962).
2. G. J. KARABATSOS and C. E. ORZECH, JR. J. Am. Chem. Soc. **84**, 2838 (1962).
3. C. C. LEE, J. E. KRUGER, and E. W. C. WONG. J. Am. Chem. Soc. **87**, 3985 (1965).
4. C. C. LEE and J. E. KRUGER. J. Am. Chem. Soc. **87**, 3986 (1965).
5. G. J. KARABATSOS, C. E. ORZECH, JR., and S. MEYERSON. J. Am. Chem. Soc. **87**, 4394 (1965).
6. C. C. LEE and M. K. FROST. Can. J. Chem. **43**, 526 (1965).
7. R. HUISGEN and C. RUCHARDT. Ann. **601**, 1 (1956).
8. A. STREITWISER, JR. J. Am. Chem. Soc. **77**, 1117 (1955).
9. J. D. ROBERTS and J. A. YANCEY. J. Am. Chem. Soc. **74**, 5943 (1952).

RECEIVED MAY 5, 1966.
DEPARTMENT OF CHEMISTRY AND CHEMICAL ENGINEERING,
UNIVERSITY OF SASKATCHEWAN,
SASKATOON, SASKATCHEWAN.

Can. J. Chem. Downloaded from www.nrcresearchpress.com by 210.87.254.6 on 09/05/12
For personal use only.

POLYFLUORINATED AROMATIC ESTERS
PREPARATION AND CARBONYL STRETCHING FREQUENCIES

ROBERT FILLER, JAMES F. WHITE, ANDREW J. KACMAREK, AND IRVINE J. SOLOMON

As part of studies currently in progress on the chemistry of highly fluorinated aromatic compounds, we have prepared a number of esters and have examined their infrared spectra with reference to the influence of pentafluorophenyl substitution on the carbonyl frequency. The role of perfluoroalkyl groups in shifting the ester carbonyl band to higher frequencies has been discussed previously (1–4).

In this note we report the preparation and infrared spectral data for phenyl benzoates in which a pentafluorophenyl group is located in the acid and (or) phenolic portions of the ester, as well as data for several other esters containing the C_6F_5 group. The results are summarized in Table I.

TABLE I
Carbonyl frequencies of pentafluorophenyl esters

Compound	$\nu_{C=O}$ (cm^{-1})
$C_6H_5CO_2C_6H_5$	1 740
$C_6F_5CO_2C_6H_5$	1 770
$C_6H_5CO_2C_6F_5$	1 765
$C_6F_5CO_2C_6F_5$	1 780
$C_6F_5CO_2CH_2CH_3$	1 741
$C_6F_5CO_2CH_2CF_3$	1 760, 1 765
$CF_3CO_2C_6F_5$	1 787

The data may be rationalized in terms of both the inductive and mesomeric effects. If we consider the canonical structures *a–d*, we see that, when R = alkyl, electron release causes the relative contribution of structure *d* to be much more significant than when R = C_6H_5, thereby enhancing the single-bond character of the $\rangle C{=}O$ group (lower frequency). Thus, methyl benzoate exhibits carbonyl absorption at 1 724 cm^{-1} (5), whereas in phenyl benzoate the band shifts to 1 740 cm^{-1}. Comparison of ethyl pentafluorobenzoate with phenyl pentafluorobenzoate provides a second example.

When the phenyl group is replaced by the C_6F_5 group in the acid portion of the ester,

1. O. A. REUTOV and T. N. SHATKINA. Tetrahedron, **18**, 237 (1962).
2. G. J. KARABATSOS and C. E. ORZECH, JR. J. Am. Chem. Soc. **84**, 2838 (1962).
3. C. C. LEE, J. E. KRUGER, and E. W. C. WONG. J. Am. Chem. Soc. **87**, 3985 (1965).
4. C. C. LEE and J. E. KRUGER. J. Am. Chem. Soc. **87**, 3986 (1965).
5. G. J. KARABATSOS, C. E. ORZECH, JR., and S. MEYERSON. J. Am. Chem. Soc. **87**, 4394 (1965).
6. C. C. LEE and M. K. FROST. Can. J. Chem. **43**, 526 (1965).
7. R. HUISGEN and C. RUCHARDT. Ann. **601**, 1 (1956).
8. A. STREITWISER, JR. J. Am. Chem. Soc. **77**, 1117 (1955).
9. J. D. ROBERTS and J. A. YANCEY. J. Am. Chem. Soc. **74**, 5943 (1952).

RECEIVED MAY 5, 1966.
DEPARTMENT OF CHEMISTRY AND CHEMICAL ENGINEERING,
UNIVERSITY OF SASKATCHEWAN,
SASKATOON, SASKATCHEWAN.

Can. J. Chem. Downloaded from www.nrcresearchpress.com by 210.87.254.6 on 09/05/12
For personal use only.

POLYFLUORINATED AROMATIC ESTERS
PREPARATION AND CARBONYL STRETCHING FREQUENCIES

ROBERT FILLER, JAMES F. WHITE, ANDREW J. KACMAREK, AND IRVINE J. SOLOMON

As part of studies currently in progress on the chemistry of highly fluorinated aromatic compounds, we have prepared a number of esters and have examined their infrared spectra with reference to the influence of pentafluorophenyl substitution on the carbonyl frequency. The role of perfluoroalkyl groups in shifting the ester carbonyl band to higher frequencies has been discussed previously (1–4).

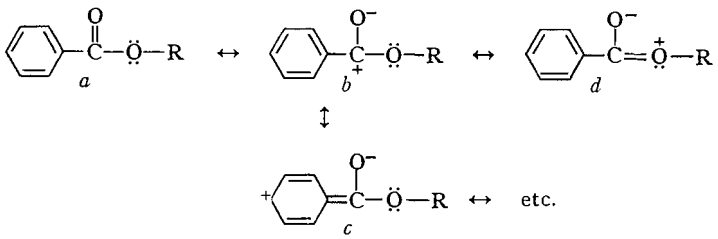
In this note we report the preparation and infrared spectral data for phenyl benzoates in which a pentafluorophenyl group is located in the acid and (or) phenolic portions of the ester, as well as data for several other esters containing the C_6F_5 group. The results are summarized in Table I.

TABLE I
Carbonyl frequencies of pentafluorophenyl esters

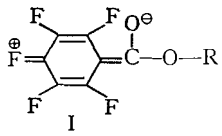
Compound	$\nu_{C=O}$ (cm^{-1})
$C_6H_5CO_2C_6H_5$	1 740
$C_6F_5CO_2C_6H_5$	1 770
$C_6H_5CO_2C_6F_5$	1 765
$C_6F_5CO_2C_6F_5$	1 780
$C_6F_5CO_2CH_2CH_3$	1 741
$C_6F_5CO_2CH_2CF_3$	1 760, 1 765
$CF_3CO_2C_6F_5$	1 787

The data may be rationalized in terms of both the inductive and mesomeric effects. If we consider the canonical structures *a–d*, we see that, when R = alkyl, electron release causes the relative contribution of structure *d* to be much more significant than when R = C_6H_5, thereby enhancing the single-bond character of the $\rangle C{=}O$ group (lower frequency). Thus, methyl benzoate exhibits carbonyl absorption at 1 724 cm^{-1} (5), whereas in phenyl benzoate the band shifts to 1 740 cm^{-1}. Comparison of ethyl pentafluorobenzoate with phenyl pentafluorobenzoate provides a second example.

When the phenyl group is replaced by the C_6F_5 group in the acid portion of the ester,



the strong electron-attracting inductive effect serves to diminish the contributions of structures *b*, *c*, and *d*, thus enhancing the double-bond character of the carbonyl group relative to that of the C_6H_5-substituted ester. However, the mesomeric effect operates in the opposite direction and increases contributions of type *c*, as indicated in structure I (and its ortho analogues).



I

In other recent experiments, we have demonstrated that the inductive effect is considerably stronger than the mesomeric effect in the C_6F_5 group. Therefore, the observed increase in the carbonyl stretching frequency is to be expected. When R = C_6F_5, structure *d* is strongly destabilized by the inductive effect. This is substantiated by the pronounced shift to higher frequency of pentafluorophenyl benzoate (1 765 cm^{-1}) compared with phenyl benzoate (1 740 cm^{-1}). Pentafluorophenyl pentafluorobenzoate, the first stable, completely fluorinated ester, reflects the influence of the C_6F_5 group at both ends of the molecule (1 780 cm^{-1}), but the effect is somewhat less than additive.

EXPERIMENTAL

Infrared Spectra

All compounds were measured as 5% solutions in carbon tetrachloride. The spectra were obtained on two instruments, a Beckman IR-8 grating spectrometer and a Perkin–Elmer 21 double-beam spectrometer equipped with sodium chloride optics.

Phenyl Pentafluorobenzoate

Pentafluorobenzoyl chloride (4.58 g) and phenol (1.88 g) were heated under reflux for 1.5 h in a 25 ml flask, with occasional shaking. After the flask was cooled, its contents were dissolved in ether, washed successively with water, 5% sodium carbonate solution, and again with water, and dried over anhydrous sodium sulfate; then the ether was removed. The residue was crystallized from hot methanol to give 1.4 g (24.6%) of ester, m.p. 66–67°.

Anal. Calcd. for $C_{13}H_5O_2F_5$: C, 54.13; H, 1.73. Found: C, 54.01; H, 1.95.

Pentafluorophenyl Benzoate[1]

Pentafluorophenol (3.68 g) and benzoyl chloride (2.8 g) were heated under reflux for 1.5 h. The contents of the flask were dissolved in ether and worked up as described above to give 1.0 g (17.5%) of ester, m.p. 73.0–73.5°.

Anal. Calcd. for $C_{13}H_5O_2F_5$: C, 54.13; H, 1.73. Found: C, 54.01; H, 1.87.

Pentafluorophenyl Pentafluorobenzoate

A mixture of 10.57 g of pentafluorobenzoyl chloride and 7.86 g of pentafluorophenol was heated under reflux for 3 days to give 16.0 g (99%) of pentafluorophenyl pentafluorobenzoate, b.p. 67–69° at 10^{-5} mm, m.p. 36.5–37.5°.

Anal. Calcd. for $C_{13}O_2F_{10}$: C, 41.30; F, 50.25; mol. wt. 378. Found: C, 41.34; F, 50.31; mol. wt. (osmometry in benzene) 371, 374.

[1]*Birchall and Haszeldine (6) reported m.p. 74–75° and* $\nu_{C=O}$ *(mull) 1 773* cm^{-1}.

Can. J. Chem. Downloaded from www.nrcresearchpress.com by 210.87.254.6 on 09/05/12
For personal use only.

Ethyl Pentafluorobenzoate

Pentafluorobenzoyl chloride (8.0 g, 0.035 mole) was added during 30 min to 1.7 g (0.037 mole) of absolute ethanol in a three-necked flask fitted with a dropping funnel, a reflux condenser, and a magnetic stirrer. The mixture was heated under reflux during the addition, and heating was continued for an additional 3 h at 70–80°. The solution was cooled, poured into 3 ml of water, and then washed with two 3 ml portions of a saturated sodium bicarbonate solution and two 3 ml portions of water. After the solution was dried over anhydrous sodium sulfate, distillation gave 4.5 g (54%) of ethyl pentafluorobenzoate, b.p. 93–94° at 10 mm.

Trifluoroethyl Pentafluorobenzoate

To a mixture of 5.0 g (0.022 mole) of pentafluorobenzoyl chloride and 2.2 g (0.022 mole) of trifluoroethanol was added, in small portions, 1.0 g of powdered anhydrous aluminium chloride. The mixture was heated under reflux overnight, cooled, poured into 6 *N* hydrochloric acid, and extracted with ether. The ether extracts were combined, washed with a 2% solution of sodium bicarbonate until neutral to litmus, and then washed with water. After the solution was dried over anhydrous sodium sulfate, the ether was removed and the product distilled to give 5.0 g (78%) of trifluoroethyl pentafluorobenzoate, b.p. 184–186° at 750 mm, 52–54° at 13 mm.

Anal. Calcd. for $C_9H_2O_2F_8$: C, 36.75; H, 0.69. Found: C, 37.45; H, 0.87.

Pentafluorophenyl Trifluoroacetate

Pentafluorophenol and trifluoroacetyl chloride reacted at −28° (carbon tetrachloride – dry ice) during 2.5 h. After the mixture was warmed to room temperature, it was dissolved in ether and washed thoroughly with water. The ether layer was dried over anhydrous sodium sulfate. Distillation gave two main fractions, b.p. 65–86° at 10 mm and 85–100° at 10 mm, both of which exhibited a single peak in the carbonyl region at 1 787 cm^{-1}.

ACKNOWLEDGMENTS

The authors thank the National Science Foundation for financial support to J. F. W. as an Undergraduate Research Participant during the summer of 1964. This work was supported in part by contract No. AF 49(638)-1175 and Public Health Service grant GM-12146.

1. G. Rappaport, M. Hauptschein, J. F. O'Brien, and R. Filler. J. Am. Chem. Soc. **75**, 2695 (1953).
2. R. Filler. J. Am. Chem. Soc. **76**, 1376 (1954).
3. E. T. McBee and D. L. Christman. J. Am. Chem. Soc. **77**, 755 (1955).
4. R. Filler and S. M. Naqvi. Tetrahedron, **19**, 879 (1963).
5. L. J. Bellamy. The infrared spectra of complex molecules. Methuen & Co. Ltd., London. 2nd ed. 1958. p. 182.
6. J. M. Birchall and R. N. Haszeldine. J. Chem. Soc. 13 (1959).

Received March 17, 1966.
Departments of Chemistry,
Illinois Institute of Technology and IIT Research Institute,
Chicago, Illinois.

SYNTHESIS AND CHROMATOGRAPHIC PROPERTIES OF *N*-ALKYL-L-ASPARAGINES[1]

Roderich Walter, Irving L. Schwartz, Louis J. Trauth,
Mervyn C. Berman, and David H. Schlesinger

Biochemical and physiological studies in this laboratory required a series of *N*-alkyl-L-asparagines. Unlike the *N*-alkyl-DL-asparagines, which are readily synthesized (1–4), the L-antipodes, in spite of recent interest in their potential role in biological systems (5–7), are scarcely documented. To our knowledge, only the syntheses of *N*-ethyl-L-asparagine (6) and *N*-phenyl-L-asparagine (8) have been reported. We therefore investigated a

[1]*The abbreviations are derived in accordance with the rules proposed by the commission on the nomenclature of biological chemistry, J. Am. Chem. Soc., 82, 5575 (1960).*

Can. J. Chem. Downloaded from www.nrcresearchpress.com by 210.87.254.6 on 09/05/12
For personal use only.

Ethyl Pentafluorobenzoate

Pentafluorobenzoyl chloride (8.0 g, 0.035 mole) was added during 30 min to 1.7 g (0.037 mole) of absolute ethanol in a three-necked flask fitted with a dropping funnel, a reflux condenser, and a magnetic stirrer. The mixture was heated under reflux during the addition, and heating was continued for an additional 3 h at 70–80°. The solution was cooled, poured into 3 ml of water, and then washed with two 3 ml portions of a saturated sodium bicarbonate solution and two 3 ml portions of water. After the solution was dried over anhydrous sodium sulfate, distillation gave 4.5 g (54%) of ethyl pentafluorobenzoate, b.p. 93–94° at 10 mm.

Trifluoroethyl Pentafluorobenzoate

To a mixture of 5.0 g (0.022 mole) of pentafluorobenzoyl chloride and 2.2 g (0.022 mole) of trifluoroethanol was added, in small portions, 1.0 g of powdered anhydrous aluminium chloride. The mixture was heated under reflux overnight, cooled, poured into 6 *N* hydrochloric acid, and extracted with ether. The ether extracts were combined, washed with a 2% solution of sodium bicarbonate until neutral to litmus, and then washed with water. After the solution was dried over anhydrous sodium sulfate, the ether was removed and the product distilled to give 5.0 g (78%) of trifluoroethyl pentafluorobenzoate, b.p. 184–186° at 750 mm, 52–54° at 13 mm.

Anal. Calcd. for $C_9H_2O_2F_8$: C, 36.75; H, 0.69. Found: C, 37.45; H, 0.87.

Pentafluorophenyl Trifluoroacetate

Pentafluorophenol and trifluoroacetyl chloride reacted at −28° (carbon tetrachloride – dry ice) during 2.5 h. After the mixture was warmed to room temperature, it was dissolved in ether and washed thoroughly with water. The ether layer was dried over anhydrous sodium sulfate. Distillation gave two main fractions, b.p. 65–86° at 10 mm and 85–100° at 10 mm, both of which exhibited a single peak in the carbonyl region at 1 787 cm^{-1}.

ACKNOWLEDGMENTS

The authors thank the National Science Foundation for financial support to J. F. W. as an Undergraduate Research Participant during the summer of 1964. This work was supported in part by contract No. AF 49(638)-1175 and Public Health Service grant GM-12146.

1. G. Rappaport, M. Hauptschein, J. F. O'Brien, and R. Filler. J. Am. Chem. Soc. **75**, 2695 (1953).
2. R. Filler. J. Am. Chem. Soc. **76**, 1376 (1954).
3. E. T. McBee and D. L. Christman. J. Am. Chem. Soc. **77**, 755 (1955).
4. R. Filler and S. M. Naqvi. Tetrahedron, **19**, 879 (1963).
5. L. J. Bellamy. The infrared spectra of complex molecules. Methuen & Co. Ltd., London. 2nd ed. 1958. p. 182.
6. J. M. Birchall and R. N. Haszeldine. J. Chem. Soc. 13 (1959).

Received March 17, 1966.
Departments of Chemistry,
Illinois Institute of Technology and IIT Research Institute,
Chicago, Illinois.

SYNTHESIS AND CHROMATOGRAPHIC PROPERTIES OF *N*-ALKYL-L-ASPARAGINES[1]

Roderich Walter, Irving L. Schwartz, Louis J. Trauth,
Mervyn C. Berman, and David H. Schlesinger

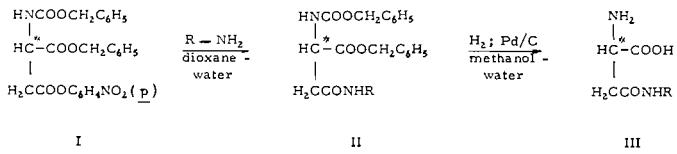
Biochemical and physiological studies in this laboratory required a series of *N*-alkyl-L-asparagines. Unlike the *N*-alkyl-DL-asparagines, which are readily synthesized (1–4), the L-antipodes, in spite of recent interest in their potential role in biological systems (5–7), are scarcely documented. To our knowledge, only the syntheses of *N*-ethyl-L-asparagine (6) and *N*-phenyl-L-asparagine (8) have been reported. We therefore investigated a

[1]*The abbreviations are derived in accordance with the rules proposed by the commission on the nomenclature of biological chemistry, J. Am. Chem. Soc., 82, 5575 (1960).*

Can. J. Chem. Downloaded from www.nrcresearchpress.com by 210.87.254.42 on 09/05/12
For personal use only.

method of converting a protected β-activated aspartate into the corresponding *N*-alkyl-L-asparagine derivative by treatment with the appropriate amine. The protecting groups of the activated ester were chosen in such a way that all of them could be eliminated in the final step.

For the synthesis of the protected amino acid intermediate N^2-carbobenzoxy-*N*-methyl-L-asparagine benzyl ester (II, R = CH_3), α-benzyl β-*p*-nitrophenyl *N*-carbobenzoxy-L-aspartate (I) (9) was treated with aqueous methylamine in dioxane (Reaction Scheme 1).



I II III

REACTION SCHEME 1.

Similarly, the *p*-nitrophenyl ester was allowed to react with higher alkyl amines (Table I). Some of the characteristic stretching bands in the infrared spectra of these protected *N*-alkyl-L-asparagines were located at 3 325 – 3 315 cm^{-1} (secondary NH), 1 755 – 1 744 cm^{-1} (ester carbonyl), 1 695 – 1 690 cm^{-1} (carbobenzoxy carbonyl), and 1 646 cm^{-1} (*N*-alkylamido carbonyl) (10).

In this study, the protecting groups were removed from the N^2-carbobenzoxy-*N*-alkyl-L-asparagine benzyl esters by catalytic hydrogenation in aqueous methanol to yield the *N*-alkyl-L-asparagines (Table II). The infrared spectra of these amino acids exhibited a pattern of strong absorption bands very similar to that already reported for *N*-ethyl-L-asparagine (3 330 – 3 280 cm^{-1}, 1 645 cm^{-1}, 1 610 – 1 585 cm^{-1}, and 1 570 – 1 550 cm^{-1}) (6). The *N*-alkyl-L-asparagines were subjected to paper chromatcgraphy in two solvent systems: phenol saturated with water, and *n*-butanol – acetic acid – water (4:1:5 v/v/v). The elution behavior of these amino acids during ion-exchange chromatography by the method of Spackman *et al.* (11) was also investigated. Increasing the hydrophobicity of the *N*-alkyl-L-asparagines by lengthening the alkyl chain resulted in an increase in the retention time. Pertinent details and physical properties of the individual *N*-alkyl-L-asparagines are listed in Table II.

EXPERIMENTAL[2]

Preparation of N^2-Carbobenzoxy-N-alkyl-L-asparagine Benzyl Ester (II)

Ester I (8.4 mmoles) was dissolved in 50 ml of dioxane at room temperature. The appropriate primary alkylamine (9.2 mmoles in 10 ml of water) was added over a period of 1 h. Stirring was continued for 24 h and the solvent was evaporated to dryness under reduced pressure. The residue was crystallized from a minimum amount of hot ethanol. After two or three recrystallizations the melting point remained unchanged. Pertinent data for the protected *N*-alkyl-L-asparagines are summarized in Table I.

Preparation of N-Alkyl-L-asparagine (III)

N^2-Carbobenzoxy-*N*-alkyl-L-asparagine benzyl ester (5.0 mmoles) was dissolved in 40 ml of methanol at 40°. To the clear solution, 10 ml of water and 0.2 g of 10% palladium on charcoal, suspended in 10 ml of methanol, were added. This mixture was hydrogenated for 3 h at 40°. The catalyst was removed by filtration, and the filtrate and aqueous washings were taken to dryness under reduced pressure. *N*-Butyl- and *N*-amyl-L-asparagines were extracted from the catalyst by additional washings with methanol. The *N*-alkyl-L-asparagine was dissolved in a small amount of water (or aqueous methanol), and alcohol or acetone was added until the solution turned turbid. After two recrystallizations the melting point remained constant. The yields were consistently high.

[2]*All melting points were determined with a Thomas–Hoover capillary melting point apparatus and are uncorrected. The infrared spectra were measured in pressed disks of potassium bromide at a concentration of 0.3% for the protected asparagines and 0.23% for the free asparagines. The optical rotations were determined with a Carl Zeiss photoelectric precision polarimeter (0.005°), code 550300. The elementary analyses were carried out by Galbraith Laboratories, Knoxville, Tennessee.*

Can. J. Chem. Downloaded from www.nrcresearchpress.com by 210.87.254.42 on 09/05/12
For personal use only.

Can. J. Chem. Downloaded from www.nrcresearchpress.com by 210.87.254.42 on 09/05/12
For personal use only.

TABLE I

N^2-Carbobenzoxy-*N*-alkyl-L-asparagine benzyl esters

R	Melting point (°C)	Formula	Calculated (%)			Found (%)			$[\alpha]_D^{24}$ (*c*, 1 in dimethylformamide)	Yield (%)
			C	H	N	C	N	N		
CH_3	145–146	$C_{20}H_{22}N_2O_5$	64.9	5.99	7.56	65.2	6.34	7.73	−11.5	77
CH_3CH_2	126–127	$C_{21}H_{24}N_2O_5$	65.6	6.29	7.29	65.4	6.44	7.54	−10.7	68
$CH_3CH_2CH_2$	119–120	$C_{22}H_{26}N_2O_5$	66.3	6.58	7.03	66.2	6.76	7.12	−7.20	81
$(CH_3)_2CH$	127–128	$C_{22}H_{26}N_2O_5$	66.3	6.58	7.03	66.4	6.63	7.04	−4.48	96
$CH_3(CH_2)_3$	115–116	$C_{23}H_{28}N_2O_5$	67.0	6.84	6.79	66.8	6.90	6.83	−6.68	84
$(CH_3)_2CHCH_2$	133–134	$C_{23}H_{28}N_2O_5$	67.0	6.84	6.79	67.1	7.01	6.88	−5.49	93
$CH_3(CH_2)_4$	115–116	$C_{24}H_{30}N_2O_5$	67.6	7.09	6.57	67.8	7.16	6.70	−6.62	81

TABLE II

N-Alkyl-L-asparagines

R	Melting point (decomp.) (°C)	Formula	Calculated (%)			Found (%)			$[\alpha]_D^{24}$	Descending chromatography[a]		Ion-exchange chromatography	
			C	H	N	C	H	N		R_f[b]	R_f[c]	Elution time (min)	*C* value
CH_3	252–253[d]	$C_5H_{10}N_2O_3$	41.1	6.90	19.2	41.0	6.92	18.9	−5.36°[e]	0.74	0.23	94	83.5 (6)
CH_3CH_2[f]	254–255[d,g]	$C_6H_{12}N_2O_3$	45.0	7.55	17.5	45.3	7.81	17.5	−3.95°[e]	0.80	0.36	101	82.5 (4)
$CH_3CH_2CH_2$	266–267[h,i]	$C_7H_{14}N_2O_3$	48.3	8.10	16.1	48.2	7.94	16.4	−2.24°[e]	0.83	0.50	126	85.2 (6)
$(CH_3)_2CH$	249–250[d]	$C_7H_{14}N_2O_3$	48.3	8.10	16.1	48.0	8.28	16.2	−2.36°[e]	0.82	0.50	102	75.4 (4)
$CH_3(CH_2)_3$	259–260[j,k]	$C_8H_{16}N_2O_3$	51.1	8.57	14.9	50.9	8.52	15.0	+39.2°[l]	0.84	0.62	186	91.1 (4)
$(CH_3)_2CHCH_2$	257–258[h,m]	$C_8H_{16}N_2O_3$	51.1	8.57	14.9	51.4	8.71	14.7	+41.1°[l]	0.85	0.61	147	73.9 (4)
$CH_3(CH_2)_4$	258–259[j]	$C_9H_{18}N_2O_3$	53.5	8.97	13.9	53.4	9.08	13.6	+38.6°[l]	0.87	0.72	241	80.6 (4)

[a]Descending chromatography on Whatman No. 1 paper. Developed with 0.2% ninhydrin in ethanol. All the above compounds gave a compact violet (contrasting with brown for asparagine) spot during development at room temperature.
[b]SOLVENT: phenol saturated with water.
[c]SOLVENT: *n*-butanol – acetic acid – water (4:1:5, upper phase).
[d]After recrystallization from water–ethanol.
[e]*c*, 2 in water.
[f]See ref. 6.
[g]Darkened at 244°.
[h]After recrystallization from water–acetone.
[i]Darkened at 258°.
[j]After recrystallization from water–methanol–acetone.
[k]Darkened at 250°.
[l]*c*, 2 in 6 *N* hydrochloric acid.
[m]Color change at 254°.

Elution of N-Alkyl-L-asparagines from Ion-Exchange Resin

The *N*-alkyl-L-asparagines were chromatographed on the Beckman–Spinco model 120C amino acid analyzer, using Beckman custom research resin PA-28 packed in a 56 × 0.9 cm column. Color values ($H \times W/\mu$mole = C value) are the constants per micromole of ninhydrin-positive compound. The time from the start of all chromatograms to the change to pH 4.25 buffer was 165.0 min, and to temperature change from 30° to 55° 100.0 min. The flow rate of buffer for the experiments was set at 50.0 ml/h, and of ninhydrin reagent 25.0 ml/h; the total flow rate was found to be 7.5 ± 0.8 ml/h. The calculated developing time of the ninhydrin color was 10.5 min. The elution times are reported in minutes. On our instrument, aspartic acid, glycine, and leucine were eluted at 81, 166, and 259 min, respectively, and the buffer (pH 4.25) front appeared at 229 min. The C values and elution times for each *N*-alkyl-L-asparagine are recorded in the last two columns of Table II. The numbers in parentheses indicate the number of determinations.

ACKNOWLEDGMENTS

This work was supported by the U.S. Public Health Service grant No. AM 10080-02 of the National Institute of Arthritis and Metabolic Diseases and by the U.S. Atomic Energy Commission. One of us (M. C. B.) acknowledges an Eli Lilly International Fellowship. The authors thank Miss P. Herling for determining the optical rotations.

1. Y. Liwschitz, A. Zilkha, and E. Nemes. Bull. Res. Council Israel, Sect. A, **10**, 107 (1961).
2. Y. Liwschitz, Y. Edlitz-Pfefferman, and Y. Lapidoth. J. Am. Chem. Soc. **78**, 3069 (1956).
3. P. Desnuelle and G. Bonjour. Biochim. Biophys. Acta, **9**, 356 (1952).
4. F. E. King and D. A. A. Kidd. J. Chem. Soc. 2976 (1951).
5. R. L. Wickremasinghe and T. Swain. J. Sci. Food Agr. **16**, 57 (1965).
6. D. O. Gray and L. Fowden. Nature, **189**, 401 (1961).
7. N. De Groot and N. Lichtenstein. Biochim. Biophys. Acta, **40**, 92 (1960); **40**, 99 (1960).
8. F. Weygand, P. Klinke, and I. Eigen. Chem. Ber. **90**, 1896 (1957).
9. G. Losse, H. Jeschkeit, and D. Knopf. Chem. Ber. **97**, 1789 (1964).
10. C. N. R. Rao. Chemical applications of infrared spectroscopy. Academic Press, Inc., New York. 1963. Chaps. III and IV.
11. D. H. Spackman, W. H. Stein, and S. Moore. Anal. Chem. **30**, 1190 (1958).

Received June 2, 1966.
Mount Sinai Medical and Graduate Schools,
New York, New York,
and
Brookhaven National Laboratory,
Upton, New York.

NOTE SUR LE CLIVAGE DE L'OZONIDE PRIMAIRE DU STYRÈNE

S. Fliszár

D'après les vues de Criegee (1), et si nous postulons les deux modes de réaction *a* et *b*, les produits engendrés par le clivage de l'ozonide primaire[1] du styrène[2] seraient ceux représentés par le schéma suivant.

Des ozonolyses du styrène effectuées dans du CCl_4 révèlent les quantités appréciables de Ph—CHO et de HCHO formés (Tableau I). On note également que la proportion des composés à O actif (ozonides et peroxydes) engendrés est, dans chaque cas, inférieure à celle de l'oléfine consommée; puisque, à la suite du clivage de l'ozonide primaire, il se

[1]*Nous adoptons cette représentation schématique uniquement dans le but de faciliter l'exposé de nos résultats expérimentaux et non pas avec l'intention d'aborder ainsi le fond des problèmes très complexes (dont la revue de Bailey (2) résume l'ampleur) se rattachant à la structure de l'ozonide primaire et au mécanisme de son clivage.*

[2]*Un travail étendu portant sur le clivage de nombreuses oléfines asymétriques (et, notamment, des styrènes substitués) sera présenté ultérieurement.*

Can. J. Chem. Downloaded from www.nrcresearchpress.com by 210.87.254.42 on 09/05/12
For personal use only.

Elution of N-Alkyl-L-asparagines from Ion-Exchange Resin

The *N*-alkyl-L-asparagines were chromatographed on the Beckman–Spinco model 120C amino acid analyzer, using Beckman custom research resin PA-28 packed in a 56 × 0.9 cm column. Color values ($H \times W/\mu$mole = C value) are the constants per micromole of ninhydrin-positive compound. The time from the start of all chromatograms to the change to pH 4.25 buffer was 165.0 min, and to temperature change from 30° to 55° 100.0 min. The flow rate of buffer for the experiments was set at 50.0 ml/h, and of ninhydrin reagent 25.0 ml/h; the total flow rate was found to be 7.5 ± 0.8 ml/h. The calculated developing time of the ninhydrin color was 10.5 min. The elution times are reported in minutes. On our instrument, aspartic acid, glycine, and leucine were eluted at 81, 166, and 259 min, respectively, and the buffer (pH 4.25) front appeared at 229 min. The C values and elution times for each *N*-alkyl-L-asparagine are recorded in the last two columns of Table II. The numbers in parentheses indicate the number of determinations.

ACKNOWLEDGMENTS

This work was supported by the U.S. Public Health Service grant No. AM 10080-02 of the National Institute of Arthritis and Metabolic Diseases and by the U.S. Atomic Energy Commission. One of us (M. C. B.) acknowledges an Eli Lilly International Fellowship. The authors thank Miss P. Herling for determining the optical rotations.

1. Y. Liwschitz, A. Zilkha, and E. Nemes. Bull. Res. Council Israel, Sect. A, **10**, 107 (1961).
2. Y. Liwschitz, Y. Edlitz-Pfefferman, and Y. Lapidoth. J. Am. Chem. Soc. **78**, 3069 (1956).
3. P. Desnuelle and G. Bonjour. Biochim. Biophys. Acta, **9**, 356 (1952).
4. F. E. King and D. A. A. Kidd. J. Chem. Soc. 2976 (1951).
5. R. L. Wickremasinghe and T. Swain. J. Sci. Food Agr. **16**, 57 (1965).
6. D. O. Gray and L. Fowden. Nature, **189**, 401 (1961).
7. N. De Groot and N. Lichtenstein. Biochim. Biophys. Acta, **40**, 92 (1960); **40**, 99 (1960).
8. F. Weygand, P. Klinke, and I. Eigen. Chem. Ber. **90**, 1896 (1957).
9. G. Losse, H. Jeschkeit, and D. Knopf. Chem. Ber. **97**, 1789 (1964).
10. C. N. R. Rao. Chemical applications of infrared spectroscopy. Academic Press, Inc., New York. 1963. Chaps. III and IV.
11. D. H. Spackman, W. H. Stein, and S. Moore. Anal. Chem. **30**, 1190 (1958).

Received June 2, 1966.
Mount Sinai Medical and Graduate Schools,
New York, New York,
and
Brookhaven National Laboratory,
Upton, New York.

NOTE SUR LE CLIVAGE DE L'OZONIDE PRIMAIRE DU STYRÈNE

S. Fliszár

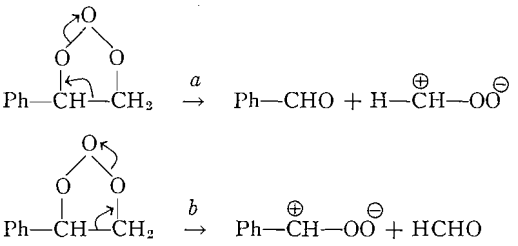
D'après les vues de Criegee (1), et si nous postulons les deux modes de réaction *a* et *b*, les produits engendrés par le clivage de l'ozonide primaire[1] du styrène[2] seraient ceux représentés par le schéma suivant.

Des ozonolyses du styrène effectuées dans du CCl_4 révèlent les quantités appréciables de Ph—CHO et de HCHO formés (Tableau I). On note également que la proportion des composés à O actif (ozonides et peroxydes) engendrés est, dans chaque cas, inférieure à celle de l'oléfine consommée; puisque, à la suite du clivage de l'ozonide primaire, il se

[1]*Nous adoptons cette représentation schématique uniquement dans le but de faciliter l'exposé de nos résultats expérimentaux et non pas avec l'intention d'aborder ainsi le fond des problèmes très complexes (dont la revue de Bailey (2) résume l'ampleur) se rattachant à la structure de l'ozonide primaire et au mécanisme de son clivage.*

[2]*Un travail étendu portant sur le clivage de nombreuses oléfines asymétriques (et, notamment, des styrènes substitués) sera présenté ultérieurement.*

Can. J. Chem. Downloaded from www.nrcresearchpress.com by 210.87.254.5 on 09/05/12
For personal use only.



forme 1 mole de composés à O actif par mole de styrène ozoné, on reconnait ainsi la réduction d'une partie de zwitterion, tout comme cela avait été montré dans le cas du stilbène (3) et du diphényl-1,4 butène-2 (4).

En vue de déterminer dans quelles proportions les voies de clivage *a* et *b* sont suivies, nous avons avantage à effectuer les ozonolyses en présence de CH_3OH (Tableau II). Dans des conditions expérimentales adéquates, les zwitterions sont alors quantitativement transformés en méthoxyhydroperoxydes stables, qui n'engendrent pas des molécules d'aldéhyde et ne consomment pas les molécules d'aldéhyde ayant pris naissance par le clivage de l'ozonide primaire. Nous nous sommes encore assuré que dans nos conditions

TABLEAU I

Ozonation de 20 ml de solution de styrène dans du CCl_4 à 25 (±0.1) °C

[Styrène] (*M*)	Débit O_3	Styrène consommé	Oxygène actif	Ph—CHO formé	HCHO formé
0.25	0.170	1.49	1.26	0.36	0.09
0.25	0.163	3.24	2.44	0.61	0.26
0.50	0.037	3.58	3.18	0.68	0.55
0.50	0.135	5.72	4.58	0.86	0.76
0.50	0.143	9.17	7.02	1.21	1.50

NOTONS: Débit O_3, millimoles/minute; les quantités de styrène consommé, d'oxygène actif, de Ph—CHO et de HCHO formés sont indiquées en millimoles.

expérimentales ([styrène] = 0.2 *M*, $[CH_3OH]$ = 1.0 *M*, température 15–35 °C, débit O_3 0.084–0.114 mmole/min) il n'y a pas de réduction appréciable de $Ph—\overset{\oplus}{C}H—OO^{\ominus}$ en Ph—CHO, en effectuant des ozonolyses de *trans*-stilbène dans les mêmes conditions; ces expériences ont montré qu'il se forme 1.0 mole d'hydroperoxyde et 1.0 mole de Ph—CHO par mole de stilbène consommé.[3] Finalement, les résultats du Tableau II indiquent bien que les quantités d'hydroperoxyde formé sont égales aux quantités d'oléfine consommée, aux erreurs expérimentales près.

Dès lors pouvons-nous considérer l'aldéhyde benzoïque[4] observé comme étant celui formé lors du clivage de l'ozonide primaire selon la voie *a* et n'ayant pas pu être utilisé par les zwitterions qui ont réagi avec le méthanol. Par conséquent, les rendements[5] en Ph—CHO (rapportés à l'oléfine consommée) expriment également le pourcentage de clivage de l'ozonide primaire selon la voie *a*.

[3]*Ces résultats étant en tous points comparables à ceux déjà publiés, nous renvoyons à cette étude (3) pour plus de détails.*

[4]*Nous n'avons malheureusement pas pu doser le formaldéhyde engendré lors des expériences faites en présence de méthanol. Toutefois, bien que n'étant pas entraîné par le courant gazeux (comme cela avait été le cas lors des expériences effectuées dans le* CCl_4*), et en raison de sa rapide conversion en hémiacétal, cet aldéhyde ne gêne pas les dosages spectrographiques de l'aldéhyde benzoïque; en effet, une solution 0.1 M de* HCHO *dans du* CCl_4*, en présence de* CH_3OH *1.0 M, ne présente pas de bande dans la région des fréquences du groupement carbonyle.*

[5]*Ces rendements ont été calculés en divisant "*PhCHO *formé" par la moyenne entre "styrène consommé" et "hydroperoxyde formé".*

Can. J. Chem. Downloaded from www.nrcresearchpress.com by 210.87.254.5 on 09/05/12
For personal use only.

TABLEAU II

Ozonation de 4.0 mmoles de styrène (solvant, solution 1.0 *M* de CH_3OH dans du CCl_4)

Température (°C)	Débit O_3	Styrène consommé	Hydroperoxyde formé	Benzaldéhyde formé	% voie *a*
15±0.1	0.087	1.40	1.39	0.59	42.1
	0.088	2.30	2.16	0.89	39.9
	0.093	3.34	3.29	1.30	39.3
25±0.1	0.095	0.96	0.96	0.39	40.4
	0.110	1.67	1.65	0.69	41.5
	0.112	2.47	2.45	0.99	40.4
	0.114	3.10	3.06	1.25	40.5
35±0.1	0.110	1.24	1.22	0.51	41.4
	0.084	2.36	2.25	0.96	41.7
	0.085	3.30	3.20	1.34	41.2

NOTONS: Débit O_3, millimoles/minute. Les quantités de styrène, d'hydroperoxyde et de benzaldéhyde s'entendent en millimoles.

L'analyse statistique des résultats du Tableau II ne permet pas de conclure à une variation significative de ce pourcentage avec la température entre 15 et 35 °C. Ainsi retiendrons-nous, avec une limite de confiance de 95%, que l'ozonation de 1 mole de styrène dans les conditions décrites conduit à la formation de 0.408 (±0.007) mole de Ph—CHO, ce calcul tenant compte de l'ensemble des résultats de ce tableau.

Cette production d'aldéhyde benzoïque, tout en confirmant les vues généralement admises (selon lesquelles le clivage du styrène par l'ozone se ferait préférentiellement selon le mécanisme engendrant l'aldéhyde formique (voie *b*)), fait cependant ressortir la contribution importante (40.8%) du clivage aboutissant à la formation de benzaldéhyde (voie *a*).

PARTIE EXPÉRIMENTALE

La technique d'ozonation et le dosage de l'ozone et des hydroperoxydes ont été décrits précédemment (5), ainsi que la méthode de dosage de l'oxygène actif (4).

L'aldéhyde benzoïque a été dosé par voie spectrographique infrarouge, d'après les mesures des densités optiques de la bande de vibration du groupement carbonyle vers 1 705 – 1 708 cm^{-1}; les courbes de calibration ont été établies au moyen de solutions de benzaldéhyde dans le CCl_4, ou dans du CCl_4 en présence de CH_3OH 1.0 *M*, ce dernier solvant étant utilisé lors des mesures faites sur des systèmes ozonés en présence de méthanol.

L'aldéhyde formique engendré lors des ozonations du styrène dans le CCl_4 est entraîné par le gaz d'ozonation et receuilli par de l'eau à 0 °C contenue dans un flacon laveur placé sur le circuit du gaz. Un balayage de la solution ozonée par un courant de N_2 sec (pendant 15 min) permet de receuillir pratiquement quantitativement le HCHO dans l'eau. Le dosage est ensuite effectué selon Signer (6) par iodométrie.

Le styrène a été dosé par chromatographie en phase gazeuse, au moyen d'un appareil F & M, modèle 810, avec détecteur à flamme ionisante, comprenant une colonne d'Hyprose 10% de 2.5 m, température du four 100 °C. Les solutions ozonées ont été diluées dans du CCl_4 dans la proportion de 1:25 (ou de 1:50 pour des solutions dont la concentration en styrène est supérieure à 0.2 *M*) et injectées en raison de 5.0 µl. Les intensités des pics chromatographiques du styrène, mesurées à l'aide d'un planimètre, ont été comparées à une courbe de calibration établie dans les mêmes conditions expérimentales avec des solutions de styrène de concentrations connues (0.05–0.2 *M*), ce qui permet de déterminer les concentrations en styrène des solutions ozonées. Chaque analyse a été faite 3–5 fois, avec une reproductibilité illustrée par l'exemple suivant, se rapportant à 5 mesures faites sur une solution 0.1 *M* de styrène dans les conditions décrites; surfaces mesurées: 12.35, 12.49, 12.80, 12.32 et 12.50 cm^2.

REMERCIEMENTS

Nous remercions Mlle S. Horoupian de son assistance technique précieuse, et le Conseil National de Recherches du Canada pour une subvention qui a permise ces recherches.

Can. J. Chem. Downloaded from www.nrcresearchpress.com by 210.87.254.5 on 09/05/12
For personal use only.

1. R. CRIEGEE. Record Chem. Progr. Kresge-Hooker Sci. Lib. **18**, 111 (1957).
2. P. S. BAILEY. Chem. Rev. **58**, 926 (1958).
3. S. FLISZÁR, D. GRAVEL et E. CAVALIERI. Can. J. Chem. **44**, 1013 (1966).
4. S. FLISZÁR et B. J. CHYLIŃSKA. A paraître.
5. S. FLISZÁR, D. GRAVEL et E. CAVALIERI. Can. J. Chem. **44**, 67 (1966).
6. R. SIGNER. Helv. Chim. Acta, **13**, 43 (1930).

REÇU LE 3 JUIN 1966.
DÉPARTEMENT DE CHIMIE,
UNIVERSITÉ DE MONTRÉAL,
MONTRÉAL, QUÉBEC.

Can. J. Chem. Downloaded from www.nrcresearchpress.com by 210.87.254.5 on 09/05/12
For personal use only.

ADDENDUM: IMPROVED SYNTHESIS OF *N*-ALKYL-ASPARTIC ACIDS

C. J. ABSHIRE AND L. BERLINGUET

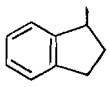
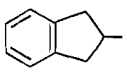
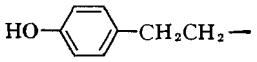
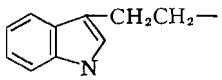
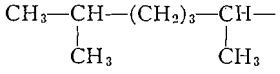
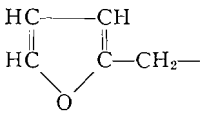
(Ref. Can. J. Chem. 40, 163 (1962))

The following, additional new compounds have been prepared by the methods previously described (1, 2).

TABLE I

N-Susbtituted aspartic acid β-methyl esters

$CH_3OOCCH_2CHCOOH$
|
NH
|
R

	R	Formula	Yield (%)	Melting point (°C)	% nitrogen Calculated	% nitrogen Found
I		$C_{14}H_{17}NO_4$	54	188–189	5.32	5.51
II		$C_{14}H_{17}NO_4$	71	224–225	5.32	5.52
III		$C_{13}H_{17}NO_5$	95	207–208	5.24	5.27
IV		$C_{15}H_{18}N_2O_4$	77	148–150	9.65	10.00
V		$C_{13}H_{25}NO_4$	45	152–154	5.40	5.70
VI		$C_{10}H_{13}NO_5$	45	186–187	6.17	6.36

1. R. CRIEGEE. Record Chem. Progr. Kresge-Hooker Sci. Lib. **18**, 111 (1957).
2. P. S. BAILEY. Chem. Rev. **58**, 926 (1958).
3. S. FLISZÁR, D. GRAVEL et E. CAVALIERI. Can. J. Chem. **44**, 1013 (1966).
4. S. FLISZÁR et B. J. CHYLIŃSKA. A paraître.
5. S. FLISZÁR, D. GRAVEL et E. CAVALIERI. Can. J. Chem. **44**, 67 (1966).
6. R. SIGNER. Helv. Chim. Acta, **13**, 43 (1930).

REÇU LE 3 JUIN 1966.
DÉPARTEMENT DE CHIMIE,
UNIVERSITÉ DE MONTRÉAL,
MONTRÉAL, QUÉBEC.

Can. J. Chem. Downloaded from www.nrcresearchpress.com by 210.87.254.6 on 09/05/12
For personal use only.

ADDENDUM: IMPROVED SYNTHESIS OF *N*-ALKYL-ASPARTIC ACIDS

C. J. ABSHIRE AND L. BERLINGUET

(Ref. Can. J. Chem. 40, 163 (1962))

The following, additional new compounds have been prepared by the methods previously described (1, 2).

TABLE I

N-Susbtituted aspartic acid β-methyl esters

$CH_3OOCCH_2CHCOOH$
|
NH
|
R

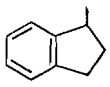
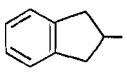
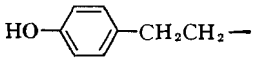
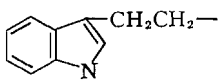
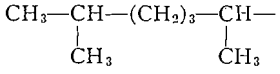
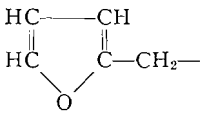
	R	Formula	Yield (%)	Melting point (°C)	% nitrogen Calculated	% nitrogen Found
I		$C_{14}H_{17}NO_4$	54	188–189	5.32	5.51
II		$C_{14}H_{17}NO_4$	71	224–225	5.32	5.52
III		$C_{13}H_{17}NO_5$	95	207–208	5.24	5.27
IV		$C_{15}H_{18}N_2O_4$	77	148–150	9.65	10.00
V		$C_{13}H_{25}NO_4$	45	152–154	5.40	5.70
VI		$C_{10}H_{13}NO_5$	45	186–187	6.17	6.36

TABLE I (*Concluded*)

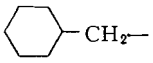
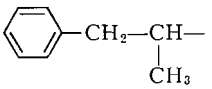
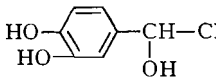
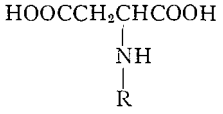
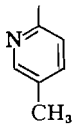
	R	Formula	Yield (%)	Melting point (°C)	% nitrogen Calculated	% nitrogen Found
VII		$C_{12}H_{21}NO_4$	45	184–185	5.76	5.93
VIII		$C_{14}H_{19}NO_4$	37	186–189	5.28	5.26
IX	$HO-(CH_2)_5-CH_2-$	$C_{11}H_{21}NO_5$	67	180–182	5.66	5.79
X		$C_{13}H_{17}NO_7$	34	139–140	4.68	4.98

TABLE II

N-Substituted aspartic acids



R*	Formula	Yield (%)	Melting point (°C)	% nitrogen Calculated	% nitrogen Found
I	$C_{13}H_{15}NO_4$	60	213–214	5.62	5.42
II	$C_{13}H_{15}NO_4$	53	200–206	5.62	5.67
III	$C_{12}H_{15}NO_5$	78	206–207	5.53	5.30
IV	$C_{14}H_{16}N_2O_4$	61	226–227	10.14	10.20
V	$C_{12}H_{23}NO_4$	72	168–170	5.71	5.57
VI	$C_9H_{11}NO_5$	58	155–157	6.57	6.50
VII	$C_{11}H_{19}NO_4$	53	194–195	6.11	6.10
VIII	$C_{13}H_{17}NO_4$	90	160–165	5.57	5.36
IX	$C_{10}H_{19}NO_5$	95	72–74	6.01	5.80
X	$C_{12}H_{15}NO_7$	77	>300	4.91	4.61
	$C_{10}H_{12}N_2O_4$	49	168–170	12.50	12.30

*For the structure, see Table I.

ACKNOWLEDGMENTS

The authors are indebted to the Medical Research Council of Canada and to The National Cancer Institute of Canada for financial assistance.

1. R. Laliberté and L. Berlinguet. Can. J. Chem. **40**, 163 (1962).
2. A. Zilkha and M. D. Bachi. J. Org. Chem. **24**, 1096 (1959).

Department of Biochemistry,
Faculty of Medicine,
Laval University,
Quebec, Quebec.

Can. J. Chem. Downloaded from www.nrcresearchpress.com by 210.87.254.6 on 09/05/12
For personal use only.

Can. J. Chem. Downloaded from www.nrcresearchpress.com by 210.87.254.105 on 09/05/12
For personal use only.

Canadian Journal of Chemistry

Issued by THE NATIONAL RESEARCH COUNCIL OF CANADA

VOLUME 44 OCTOBER 15, 1966 NUMBER 20

THE THERMAL DECOMPOSITION OF ETHANE

PART II. THE UNIMOLECULAR DECOMPOSITION OF THE ETHANE MOLECULE AND THE ETHYL RADICAL

M. C. LIN AND M. H. BACK

Department of Chemistry, University of Ottawa, Ottawa, Canada

Received May 5, 1966

ABSTRACT

The rate of the elementary dissociation of ethane into two methyl radicals has been measured in its pressure-dependent region at temperatures from 913–999 °K and at pressures from 1–200 mm. The high-pressure first-order rate constant obtained by extrapolation was in agreement with that obtained at lower temperatures,

$$k_1^{\infty} = 1.0 \times 10^{16}\, e^{-86000/RT}\, s^{-1}.$$

Comparison with calculated Kassel curves showed that the best fit of the data was obtained with the Kassel parameter $s = 12 \pm 1$. The high-pressure first-order rate constant for the decomposition of the ethyl radical was obtained by extrapolation of the data reported in Part I, assuming the rate constant for combination of ethyl radicals is independent of temperature.

$$k_3^{\infty} = 3.8 \times 10^{13}\, e^{-38000/RT}\, s^{-1}.$$

From the measured constant for the dissociation of ethane, the rate constant for the combination of methyl radicals was calculated and compared with the values measured in a lower temperature region. Differences in the values of the rate constants and in the shapes of the unimolecular falloff curves are discussed.

INTRODUCTION

In Part I of this study (1) the rates of initiation and termination in the decomposition of ethane were measured and the following mechanism, previously proposed (2, 3), was confirmed.

[1] $C_2H_6 \rightarrow 2CH_3$

[2] $CH_3 + C_2H_6 \rightarrow CH_4 + C_2H_5$

[3] $C_2H_5 \rightarrow C_2H_4 + H$

[4] $H + C_2H_6 \rightarrow H_2 + C_2H_5$

[5*a*] $C_2H_5 + C_2H_5 \rightarrow C_4H_{10}$

[5*b*] $\rightarrow C_2H_4 + C_2H_6$

There was some indication in the temperature range reported in Part I that pressure dependence of reaction [1] was observed at low pressures. We now report more extensive results on this pressure dependence over the temperature range 913–999 °K and at pressures from 1–200 mm.

Measurements of the rate of combination of methyl radicals at temperatures in the neighborhood of 500 °K (4, 5) have indicated that pressure dependence begins to occur at pressures below about 10 mm of acetone. Measurements at 1 273 °K have shown a

linear dependence on pressure in the range 3–15 mm of helium and a negative temperature coefficient of 1.5 kcal/mole (6). Between these temperature regions the results relating to the combination of methyl radicals are obtained by indirect kinetic evidence and are somewhat conflicting (7). The measurement of the rate of the reverse reaction, the dissociation of ethane, which is conveniently measured in the intermediate temperature region, should allow a more exact interpretation of the effect of temperature on the rate of stabilization of the energy-rich ethane molecule.

EXPERIMENTAL

The apparatus and procedure have been described in Part I. Initial pressures of ethane in the range 5–20 mm were determined by expansion of a small volume of ethane into the reaction vessel. The pressure readings were calibrated at each temperature with carbon dioxide. For initial pressures less than 5 mm a smaller calibrated volume was used and the resulting pressure in the reaction vessel was calculated from the ideal gas law. The measured pressure before expansion was always greater than 50 mm.

RESULTS

Ethane

Initial rates of methane formation in the temperature region 893–999 °K and at pressures from 1–200 mm are shown as a function of initial pressure of ethane in a double logarithmic plot in Fig. 1. Initial rates were obtained by extrapolation to zero time by methods described in Part III. The dotted lines were calculated using the equation for the first-order rate constants for methane production reported in Part I.

$$k_1^{\infty} = 1.00 \times 10^{16}\, e^{-86000/RT}\ s^{-1}$$

The effect of addition of carbon dioxide on the first-order rate coefficients at 958 °K is shown in Fig. 2. The results indicate that carbon dioxide is equally as effective as ethane in the intermolecular transfer of energy. The fact that the first-order coefficient is increased

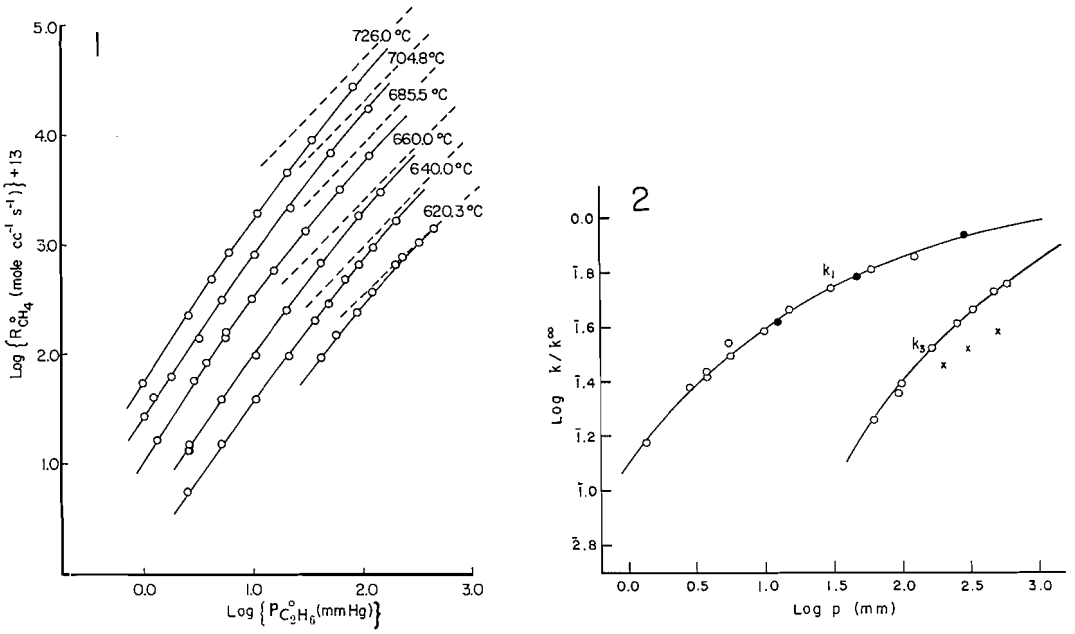
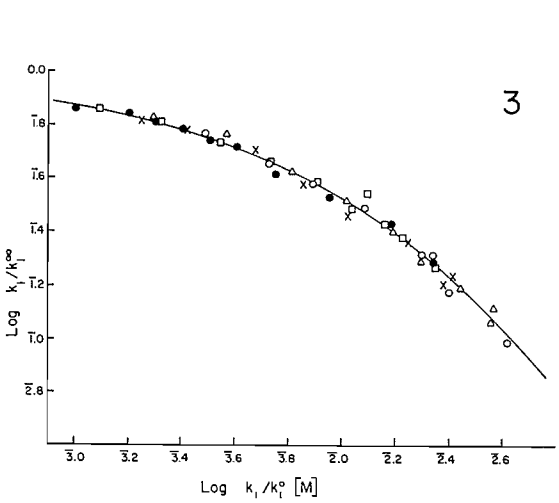


FIG. 1. Double logarithmic plot of the initial rate of methane formation against the ethane pressure.
FIG. 2. Effect of addition of carbon dioxide on the first-order rate coefficients k_1 and k_3 at 958 °K. Abscissa refers to total pressure. (○) Pure ethane; (●) 3.8 mm $C_2H_6 + CO_2$; (×) 100 mm $C_2H_6 + CO_2$.

Can. J. Chem. Downloaded from www.nrcresearchpress.com by 210.87.254.105 on 09/05/12
For personal use only.

by addition of inert gas is strong evidence that the dissociation reaction is pressure-dependent in this region of pressure. If the decrease in the rate of methane production were due to incomplete scavenging of methyl radicals by ethane, inert gas would not increase the rate of production of methane.



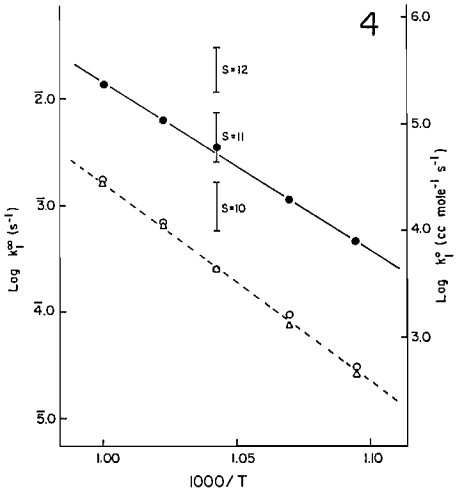


FIG. 3. Application of Powell's method of extrapolation to k_1. (○) 726.0 °C; (△) 704.8 °C; (□) 685.5 °C; (×) 660.0 °C; (●) 640.0 °C.

FIG. 4. Arrhenius plot of k_1^∞ and k_1^0. (-) Calculated from $k_1^\infty = 1.00 \times 10^{16}\ e^{-86000/RT}\ s^{-1}$; (○, ●) Powell extrapolation with $s' = 6$; (△) Lindemann–Hinshelwood extrapolation; (I) calculated from eq. [1].

The extrapolation of the first-order rate coefficient as expressed by Kassel's integral to obtain the first- and second-order rate constants was done using the approximation suggested by Powell (8). A discussion of the relation of the parameter s' used by Powell to the Kassel parameter s is given in the Appendix. Figure 3 shows the results at each temperature fitted to Powell's curve with parameter $s' = 6$. The first-order rate constants obtained in this way were in exact agreement with those obtained in the high-pressure region at lower temperatures. The first- and second-order rate constants are shown in an Arrhenius plot in Fig. 4. The Lindemann–Hinshelwood method of extrapolation gave very similar first-order rate constants and is a reasonably reliable method when the extrapolation is not long.

The second-order rate constants obtained by extrapolation could be represented by

$$k_1^0 = 1.82 \times 10^{21}\ e^{-(72500\pm1500)/RT}\ \text{cc mole}^{-1}\ s^{-1}.$$

The data are shown in Fig. 4 along with the range of values calculated for $\sigma = 4 \pm 1$ Å at 958 °K from the equation (9),

$$[1] \qquad k^0 = \lambda Z\left(\frac{E^\infty}{RT}\right)^{s-1}\frac{1}{(s-1)!}e^{-E^\infty/RT},$$

for various values of s, assuming the collision efficiency $\lambda = 1$. The best fit of the extrapolated and calculated values is obtained with $\sigma = 3.3$ Å and $s = 11$.

This value for the collision diameter was consequently used to evaluate Kassel curves for each temperature. The values of A and E were those obtained in the high-pressure region. Calculations were made using an IBM-650 computer.[1] The calculated curves are

[1]*The authors thank Dr. D. F. Swinehart, University of Oregon, for supplying the program for the Kassel integrals, and Mr. James Muirhead-Gould for suitable modifications.*

Can. J. Chem. Downloaded from www.nrcresearchpress.com by 210.87.254.105 on 09/05/12
For personal use only.

shown in Fig. 5 with the experimental points superimposed. The best fit of the experimental points was obtained with $s = 13$. The data of Dexter and Trenwith (10) are in reasonable agreement with this value of s, although these authors preferred a higher value of 15 or 16.

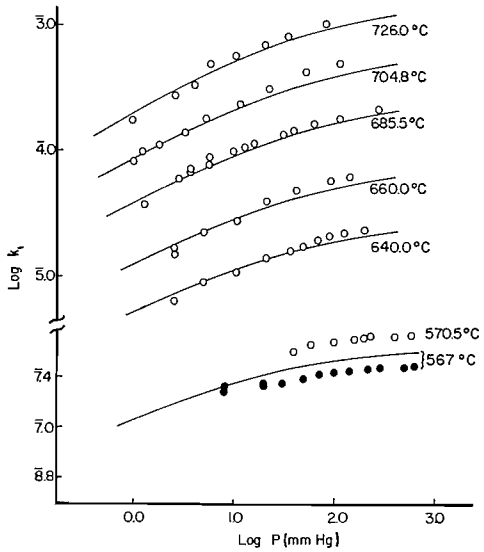


FIG. 5. Comparison of experimental results with calculated Kassel curves. Solid lines are curves calculated with $s = 13$. (○) Present results; (●) Dexter and Trenwith.

The values of the parameter s obtained from eq. [1] and from the direct comparison of the Kassel curves with k_1 are in satisfactory agreement in view of the uncertainties involved in the extrapolation to k_1^0 and in the application of the Kassel theory to reactions with high-frequency factors (11).

Recently Setser and Rabinovitch (12) evaluated theoretical curves for $\log k_1/k_1^\infty$ vs. $\log P$ at 873 and 1 273 °K based on the theory proposed by Marcus and Rice (13, 14). The expressions used for k_1^∞ were

$$k_1^\infty(873\ ^\circ\text{K}) = 1.0 \times 10^{17}\, e^{-85300/RT}\ s^{-1}$$

$$k_1^\infty(1\ 273\ ^\circ\text{K}) = 1.3 \times 10^{17}\, e^{-85300/RT}\ s^{-1}.$$

Their calculated curves are shown in Fig. 6 along with the present results at 958 °K. The difference between the calculated and the experimental results indicates that the model of the activated complex described by Setser and Rabinovitch is too "loose".

TABLE I

Activation energy as a function of pressure

	E_1 (kcal/mole)	
P (mm)	Obs.	Calcd. (Kassel curves)
0	72.5	—
2.0	82.4	79.9
6.3	83.5	81.0
20.0	84.3	83.2
63.0	84.6	83.9
100.0	84.9	84.4
200.0	85.4	84.4
∞	86.0	(86.0)

Can. J. Chem. Downloaded from www.nrcresearchpress.com by 210.87.254.105 on 09/05/12
For personal use only.

The activation energy was determined at several pressures and is compared in Table I with the activation energy evaluated from the series of Kassel curves with $s = 13$.

Ethyl Radical

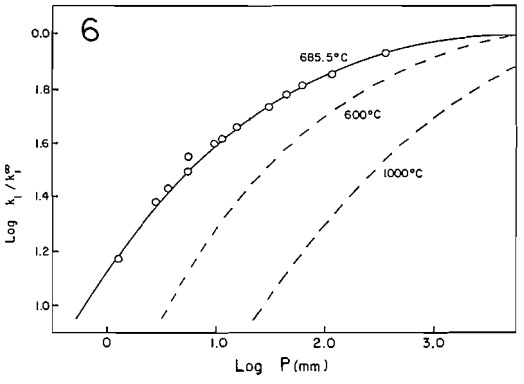
The rate constant for decomposition of the ethyl radical, k_3, was measured over the temperature range 823–913 °K and the pressure range 50–600 mm and was given in Part I. The rate constant was found to be pressure-dependent over the whole range and the order of the decomposition with respect to ethane varied from 0.38 to 0.59. The effect of addition of CO_2 on the first-order rate coefficient is shown in Fig. 2. In this case CO_2 appears to be less efficient than ethane in the deactivation of the energy-rich ethyl radical. It may be that ethane is unusually effective in the deactivation of a radical where chemical interaction may occur, whereas in the case of a molecule ethane and CO_2 are equally effective.

Powell's method of extrapolation was again applied and in Fig. 7 the experimental points are compared with the theoretical curve for parameter $s' = 3$. The values of k_3^∞ and k_3^0 thus obtained could be represented by the expressions

$$k_3^\infty = 3.8 \times 10^{13}\, e^{-38000/RT}\ s^{-1}$$

$$k_3^0 = 1.8 \times 10^{18}\, e^{-32400/RT}\ cc\ mole^{-1}\ s^{-1}$$

with an error of about ±2 kcal/mole in the activation energies, assuming the rate constant for the combination of ethyl radicals is 2.0×10^{13} cc mole^{-1} s^{-1} (15) for all temperatures studied.[2] The high-pressure rate constant is in reasonable agreement with that found by Bywater and Steacie (16), $k_3 = 1.4 \times 10^{14}\, e^{-39500/RT}\ s^{-1}$, and calculated by Benson (17), $k_3 = 2.4 \times 10^{13}\, e^{-40000/RT}\ s^{-1}$. Kerr and Trotman-Dickenson (18) recently obtained an



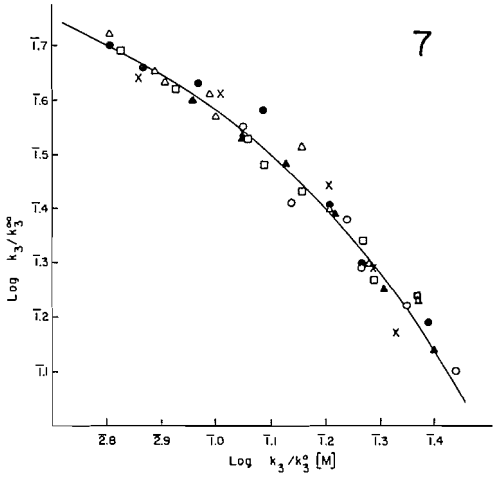


FIG. 6. Comparison of experimental results with curves calculated by Setser and Rabinovitch. (-) Calculated curves.

FIG. 7. Application of Powell's method of extrapolation to k_3. (○) 640.0 °C; (△) 620.3 °C; (●) 599.7 °C; (▲) 584.7 °C; (□) 570.5 °C; (×) 549.7 °C.

activation energy of 32.0 kcal/mole for the decomposition of the ethyl radical from a study of the photolysis of propionaldehyde. The pressure of reactant was low, about 45 mm, and comparison with the present values would suggest that in their experiments the decomposition was in the pressure-dependent region.

[2] *If* $k_{3a} = 1.5 \times 10^{14}\, e^{-2000/RT}$ *cc mole*$^{-1}$ *s*$^{-1}$ *(15), then* $k_3^\infty = 1.0 \times 10^{14}\, e^{-39000/RT}\ s^{-1}$.

Can. J. Chem. Downloaded from www.nrcresearchpress.com by 210.87.254.105 on 09/05/12
For personal use only.

The range of pressure over which k_3 was measured was not wide enough to allow a meaningful comparison with calculated Kassel curves. The parameter s of Kassel's theory may, however, be estimated from eq. [1] for the second-order rate constant. At 873 °K, using a value for $\sigma = 3.3$ Å, the closest approximation to the extrapolated values was obtained with $s = 6$ and was given by the following expression:

$$k_3^0 = 1.4 \times 10^{17}\, e^{-31800/RT} \text{ cc mole}^{-1}\text{ s}^{-1}.$$

The frequency factor would be increased by the use of a larger collision diameter. This result is consistent with that of Purnell and Quinn (19), who found, from a study of the thermal decomposition of butane, that a value of $s = 7$ gave the best fit to their data.

DISCUSSION

Comparison of Dissociation and Combination Rate Constants

For comparison with the rate constant for methyl radical combination, k_{-1} was calculated from the measured k_1 and the equilibrium constant.

$$C_2H_6 \underset{k_{-1}}{\overset{k_1}{\rightleftharpoons}} 2CH_3$$

$$K_1 = k_1/k_{-1} = (\exp(\Delta S_1^0/R))\,(\exp(-\Delta H_1^0/RT))$$

Recent calculations of S^0 for methyl radicals (20) were used to determine ΔS_1^0. There is some doubt about the exact relation between the measured activation energy, the dissociation energy of the bond broken, and the enthalpy change of the reaction at any temperature. In Part I we related the activation energy for the dissociation of ethane to the dissociation energy, D, as follows (21),

$$D + RT \geqslant E_1 \geqslant D,$$

and under our experimental conditions where $Nh\nu/RT \approx 1$, we took

$$D = E_1 - \tfrac{1}{2}RT = 85.0 \pm 0.5 \text{ kcal/mole}.$$

Since

$$\Delta H_1^0 = \Delta E_1^0 + RT,$$

$$\Delta H_1^0 = D + \tfrac{3}{2}RT = 85.0 + \tfrac{3}{2}RT.$$

Values of $(\Delta H_1^0)_T$ calculated in this way are given under column A in Table II. Use of the more exact relation

$$(\Delta H_1^0)_T = (\Delta H_1^0)_{T=0} + \int_0^T (\Delta C_p^0)\, dT$$

or

$$E_1 - E_{-1} + RT = D + \int_0^T (\Delta C_p^0)\, dT$$

leads to very similar values for $(\Delta H_1^0)_T$ which are shown in column B in Table II. Values for ΔC_p^0 were taken from JANAF (22). In column C ΔH_1^0 has been calculated from this equation using a value of $\Delta H_1^0(CH_3) = 34.0$ kcal/mole at 298 °K recently obtained (23, 24). It may be pointed out that the classical correction to the enthalpy based on the assumption that the vibrational degrees of freedom are not appreciably excited (25) is not valid at the temperatures considered here even for a molecule as small as ethane.

In Fig. 8 the values of k_{-1} thus obtained from the present measurements of k_1 are compared with k_{-1} measured at 520 °K (5) relative to abstraction from acetone. The latter

Can. J. Chem. Downloaded from www.nrcresearchpress.com by 210.87.254.105 on 09/05/12
For personal use only.

TABLE II

Thermodynamic quantities for the equilibrium $C_2H_6 \rightleftharpoons 2CH_3$

T (°K)	ΔS_1^0 (cal mole^{-1} deg^{-1})*	$(\overline{\Delta C_p^0})_T T$ (kcal mole^{-1})	ΔH_1^0 (kcal mole^{-1})		
			A	B	C
0	0	0	85.0	84.5	86.2
298.16	17.93	1.98	85.9	86.5	88.2
500	19.52	2.72	86.5	86.7	88.9
700	19.66	3.06	87.1	87.6	89.3
900	19.31	3.15	87.7	87.7	89.4
1 000	19.06	3.14	88.0	87.6	89.3

*Standard state: 1 mole cc^{-1} of ideal gas.

constant has been calculated relative to the value of 2.2×10^{13} cc mole^{-1} s^{-1} for the methyl combination constant in the pressure-independent region (26). The measurements of Dodd and Steacie give the most extensive data in the pressure-dependent region and hence were chosen for comparison.

(a) The Magnitude of k_1 and k_{-1}

From the quantities in Table II the present measurements of k_1 give a value of $k_{-1} = 1.1 \times 10^{12}$ cc mole^{-1} s^{-1} at 500 °K. The difference in the combination rate constants from the two types of measurements is much greater than can be accounted for by the estimated errors for each method and indicates a fundamental error in one of the four quantities, k_{-1}, k_1, ΔS_1^0, or ΔH_1^0. The most reliable of these four quantities is probably the entropy change of the reaction. The constants describing the structure of the methyl radical are well established and the estimated error in the calculation of S^0 for CH_3 was ± 0.5 e.u. (entropy unit) (20). Taking $A_{-1} = 2.2 \times 10^{13}$ cc mole^{-1} s^{-1} at 298 °K, the observed ratio of frequency factors corresponds to an entropy change of 12.2 e.u. (standard state: 1 mole cc^{-1}) or 5.7 e.u. less than the calculated value. It seems very unlikely that the calculated standard entropy of a methyl radical is too large by 2.9 e.u.

An error in k_1 might arise in several ways. First, k_1 might be low by a factor of 20

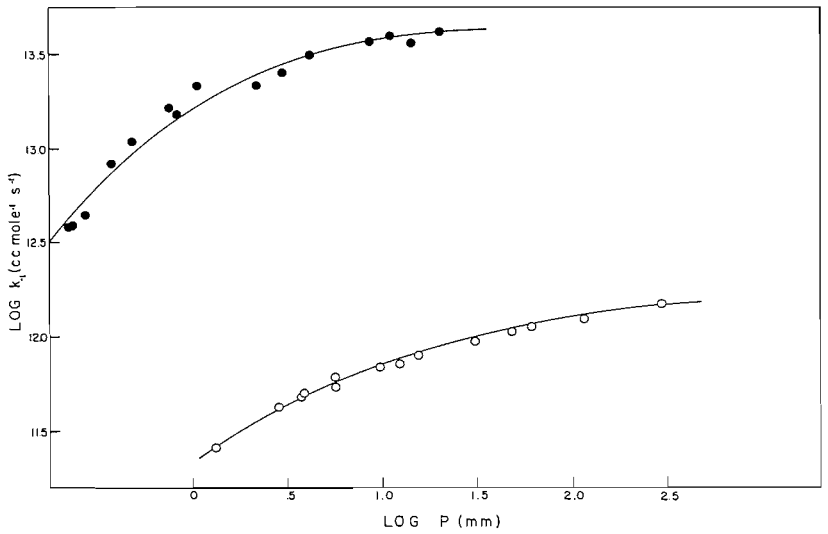


FIG. 8. Comparison of k_{-1} measured at different temperatures. (●) Dodd and Steacie; (○) present results.

Can. J. Chem. Downloaded from www.nrcresearchpress.com by 210.87.254.105 on 09/05/12
For personal use only.

throughout the whole temperature range. This would raise A_1 to satisfy the entropy requirements, $\log A_1/A_{-1} = \Delta S_1^0/2.3R$, and maintain E_1 at a value which agrees with the enthalpy change. The two most recent measurements of k_1 (3, 27) are in excellent agreement with the present values and at 828 °K are within 20%. These values of k_1 were all obtained by the measurement of the initial rate of production of methane from the pyrolysis of ethane, although the methods of analysis were different. This indicates that the measurement itself is reliable and an error of a factor of 20 in the rate constant would have to arise from a basic fault in the mechanism.

Secondly, a slight temperature-dependent error in the present results might give rise to a low activation energy and hence a low frequency factor. In fact the measurements of k_1 by Quinn (3) give a frequency factor of 2.8×10^{17} s^{-1}, which is in good agreement with the calculated entropy change. However, the activation energy of 91.7 kcal/mole thus obtained leads to a value of $\Delta H_f^0(CH_3) = 37.1$ kcal/mole at 0 °K and $D(CH_3—H) = 104.7$ kcal/mole at 0 °K or 105.6 kcal/mole at 298 °K. This is outside the error currently attributed to this quantity. The most recent measurement of $\Delta H_f^0(CH_3)$ of 34.1 kcal/mole at 298 °K (24), which is probably an upper limit, leads to $E_1 = 88.0$ kcal/mole at about 858 °K. With the values of k_1 from three independent measurements (3, 27) this activation energy gives a frequency factor of 3×10^{16} s^{-1}, which is still much below the predicted value.

To sum up, mutual consistency with the present measured k_1 and the currently accepted values of ΔS_1^0, ΔH_1^0, and k_{-1} is not attained within the estimated errors. It is not clear from the evidence where the error is most likely to occur.

(b) The Pressure Dependence of k_{-1}

The comparison of the pressure dependence of k_{-1} between the two systems involves two effects, both of which are imperfectly understood. Firstly, the efficiency of ethane and acetone in the deactivation of the excited ethane molecule is not the same. The results of Dodd and Steacie (5) suggest that ethane is much less efficient than acetone in this process. For two different third bodies of efficiencies λ and λ' it can be shown that

$$\lambda\omega = \lambda'\omega',$$

where ω is the collision frequency, defined as $z[X]$, and where [X] is the concentration of third body. This difference means that at the same temperature, pressure dependence of k_{-1} would be observed at a higher pressure in a system containing ethane than in one containing acetone. The effect in various systems has been discussed by Wieder and Marcus (28).

TABLE III

Values of s obtained from the equation $\log p_1/p_2 = (s - \frac{1}{2}) \log T_1/T_2$

	s	
k_1/k_1^∞	(*a*) $T_1 = 958.5$ °K and $T_2 = 520$ °K	(*b*) $T_1 = 999$ °K and $T_2 = 913$ °K
0.80	5.5	11.5
0.50	5.0	8.0
0.20	3.1	6.5

Secondly, the effect of increasing temperature on the lifetime of the activated molecule acts to shift the pressure-dependent region to higher pressures for any given system. The

Can. J. Chem. Downloaded from www.nrcresearchpress.com by 210.87.254.105 on 09/05/12
For personal use only.

pressure at which the first-order rate coefficient for a unimolecular reaction has declined to a certain fraction of its high pressure value is related to the temperature by the parameter s as follows (29)

$$\log p_1/p_2 = (s - \tfrac{1}{2}) \log T_1/T_2, \qquad [2]$$

where s refers to the parameter as defined by Kassel. Table III shows some values for s obtained for three ratios of k/k^∞ by two methods, (*a*) by comparison of the present results with those for the combination of methyl radicals and (*b*) using the largest temperature difference available in the present work. The value of s is very much smaller than that obtained by fitting the curves to the Kassel integral and the discrepancy is well outside the errors of the estimation. This emphasizes the weakness of the simple theories in dealing with changes in the lifetime of the activated molecule with changing temperature.

This result might be accounted for if the value of the parameter s increases with temperature. As s increases the pressure at which falloff is observed is decreased. This effect would tend to counteract the effect described by eq. [2] which shifts the falloff curve to higher pressures as the temperature is increased. The result would be a smaller pressure change and hence a smaller value of s than obtained by curve-fitting at a given temperature. In fact, different values of s were obtained at 520 and 958 °K, as is easily seen from the shape of the two curves in Fig. 8. At 520 °K the best value of s was about 9, whereas in the temperature region of the pyrolysis of ethane the value was 12 ± 1. The different shape of the curves also accounts for the trend to lower values of s at lower fractional declines.

Recent calculations of the decline in the first-order rate coefficient for methane and fluoroform (30) indicated that the parameter s increased with temperature and approached the total number of vibrational degrees of freedom in the molecules. This effect has been explained as the relaxation of quantum restrictions with rise of temperature (31). The trend has been demonstrated by the measurements of the rates of decomposition of molecules with large amounts of excess energy, which lead to the conclusion that under such conditions intramolecular energy transfer is very rapid and involves virtually all the normal modes of vibration in the molecule (32).

NOTE ADDED IN PROOF: A similar though larger discrepancy between dissociation and combination rate constants has been reported by Tsang (33). The rate constants measured were as follows:

$$\text{hexamethylethane} \rightarrow 2t\text{-}C_4H_9 \qquad k = 10^{16.3}\, e^{-68500/RT}\ s^{-1}$$

$$\text{2,2,3-trimethylbutane} \rightarrow t\text{-}C_4H_9 + i\text{-}C_3H_7 \qquad k = 10^{16.2}\, e^{-73000/RT}\ s^{-1}$$

$$\text{neopentane} \rightarrow t\text{-}C_4H_9 + CH_3 \qquad k = 10^{16.1}\, e^{-78200/RT}\ s^{-1}.$$

The frequency factors were a factor of 10^3 lower than calculated from the combination rate constants. The heat of formation of the methyl radical derived from these results was $\Delta H_f(CH_3)_{298} = 31.6$ kcal/mole.

ACKNOWLEDGMENTS

The authors thank Prof. K. J. Laidler for much helpful advice and Drs. R. A. Back and F. P. Lossing of the National Research Council for many valuable discussions. The work was supported by a grant from the National Research Council and one of us (M. C. L.) thanks the Ontario Research Foundation for the award of a fellowship.

Can. J. Chem. Downloaded from www.nrcresearchpress.com by 210.87.254.105 on 09/05/12
For personal use only.

Can. J. Chem. Downloaded from www.nrcresearchpress.com by 210.87.254.105 on 09/05/12
For personal use only.

APPENDIX

The fractional decline in the first-order rate coefficient was expressed by Kassel as

$$\frac{k}{k^\infty} = \frac{1}{(s-1)!}\int_0^\infty \frac{x^{s-1}\,e^{-x}\,dx}{1+\frac{k^\pm}{Z[M]}\left(\frac{x}{b+x}\right)^{s-1}},$$

where $x = (\epsilon - \epsilon^*)/kT$, $b = \epsilon^*/kT$, $k^\infty = k^\pm e^{-\epsilon^*/kT}$.

To obtain an expression convenient for extrapolation to k^∞ and k^0, Powell made the assumption that

$$\frac{x}{b+x} \approx \frac{x}{b} \quad \text{or} \quad \frac{\epsilon-\epsilon^*}{\epsilon} \approx \frac{\epsilon-\epsilon^*}{\epsilon^*}.$$

This implies that few molecules contain energy much in excess of the critical energy for dissociation. Replacing $(s-1)$ by s', he then obtained the expression (8)

$$\frac{k}{k^\infty} = \int_0^\infty \frac{e^{-x}\,dx}{\frac{(s')!}{x^{s'}}+\frac{1}{m}},$$

where $$m = \frac{k^0[M]}{k^\infty} \text{ and } k^0 = Z\left(\frac{\epsilon^*}{kT}\right)^{s'}\frac{1}{(s')!}e^{-\epsilon^*/kT}.$$

Powell's assumption is not strictly obeyed in any dissociation and it is not surprising that different values of $(s-1)$ and s' may be obtained by fitting experimental values of k/k^∞ to calculated Kassel curves and to calculated Powell curves. Only the parameter obtained by fitting to the Kassel curves has the physical significance intended in the development of the theory. The extrapolation to k^∞ and k^0 by the simplified expression is strictly reliable only insofar as the approximation is valid. The extrapolations to k_1^∞ and k_3^∞ are, however, in reasonable agreement with previous measurements. The extrapolated values of k_1^0 and k_3^0 are in accord with the predictions of the theory, but are not necessarily exact.

REFERENCES

1. M. C. Lin and M. H. Back. Can. J. Chem. **44**, 505 (1966).
2. H. G. Davis and K. D. Williamson. World Petrol. Congr. Proc. 5th, N.Y. 1959. 1960. Vol. IV. p. 37.
3. C. P. Quinn. Proc. Roy. Soc. London. Ser. A, **275**, 190 (1963).
4. G. B. Kistiakowsky and E. K. Roberts. J. Chem. Phys. **21**, 1637 (1953).
5. R. E. Dodd and E. W. R. Steacie. Proc. Roy. Soc. London, Ser. A, **223**, 283 (1954).
6. K. U. Ingold, I. H. S. Henderson, and F. P. Lossing. J. Chem. Phys. **21**, 2239 (1953).
7. M. H. Back, M. Eusuf, and K. J. Laidler. Symp. Kinetics Pyrolytic Reactions. University of Ottawa, Ottawa, Canada. 1964.
8. R. E. Powell. J. Chem. Phys. **30**, 724 (1959).
9. K. J. Laidler. Chemical kinetics. McGraw-Hill Book Co., Inc., New York and London. 1965.
10. R. W. Dexter and A. B. Trenwith. Proc. Chem. Soc. 392 (1964).
11. C. Steel and K. J. Laidler. J. Chem. Phys. **34**, 1827 (1961).
12. D. W. Setser and B. S. Rabinovitch. J. Chem. Phys. **40**, 2427 (1964).
13. R. A. Marcus and O. K. Rice. J. Phys. Colloid Chem. **55**, 894 (1951).
14. R. A. Marcus. J. Chem. Phys. **20**, 359 (1952).
15. A. Shepp and K. O. Kutschke. J. Chem. Phys. **26**, 1020 (1957).
16. S. Bywater and E. W. R. Steacie. J. Chem. Phys. **19**, 326 (1951).
17. S. W. Benson. The foundations of chemical kinetics. McGraw-Hill Book Co., Inc., New York and London. 1960.
18. J. A. Kerr and A. F. Trotman-Dickenson. J. Chem. Soc. 1611 (1960).
19. J. H. Purnell and C. P. Quinn. Proc. Roy. Soc. London, Ser. A, **270**, 267 (1962).
20. J. H. Purnell and C. P. Quinn. J. Chem. Soc. 4049 (1964).
21. M. Szwarc. Chem. Rev. **47**, 75 (1950).

22. D. R. STULL (*Editor*). JANAF Interim thermochemical tables. Dow Chemical Co., Midland, Mich. 1963.
23. G. C. FETTIS, J. H. KNOX, and A. F. TROTMAN-DICKENSON. J. Chem. Soc. 4177 (1960).
24. D. M. GOLDEN, R. WALSH, and S. W. BENSON. J. Am. Chem. Soc. **87**, 4053 (1965).
25. T. L. COTTRELL. The strengths of chemical bonds. Butterworths Scientific Publications, London. 1958.
26. A. SHEPP. J. Chem. Phys. **24**, 939 (1956).
27. A. S. GORDON. Symp. Kinetics Pyrolytic Reactions. University of Ottawa, Ottawa, Canada. 1964.
28. G. M. WIEDER and R. A. MARCUS. J. Chem. Phys. **37**, 1835 (1962).
29. N. B. SLATER. Theory of unimolecular reactions. Cornell Univ. Press, Ithaca, N.Y. 1959. p. 162.
30. D. W. PLACZEK, B. S. RABINOVITCH, G. Z. WHITTEN, and E. TSCHUIKOW-ROUX. J. Chem. Phys. **43**. 4071 (1965).
31. B. S. RABINOVITCH, D. W. SETSER, and F. W. SCHNEIDER. Can. J. Chem. **39**, 2609 (1961).
32. B. S. RABINOVITCH, R. F. KUBIN, and R. E. HARRINGTON. J. Chem. Phys. **38**, 405 (1963).
33. W. TSANG. J. Chem. Phys. **44**, 4283 (1966).

Can. J. Chem. Downloaded from www.nrcresearchpress.com by 210.87.254.105 on 09/05/12
For personal use only.

Can. J. Chem. Downloaded from www.nrcresearchpress.com by 210.87.254.6 on 09/05/12
For personal use only.

THE THERMAL DECOMPOSITION OF ETHANE

PART III. SECONDARY REACTIONS

M. C. LIN AND M. H. BACK
Chemistry Department, University of Ottawa, Ottawa, Canada

Received May 5, 1966

ABSTRACT

The kinetics of the secondary reactions producing methane, butane, and butene-1 in the pyrolysis of ethane have been investigated over the temperature range 550–726 °C and at pressures from 600–10 mm. The rate of secondary methane production was second order in ethylene at high pressures but was first order in ethylene at low pressures and high temperatures. In the latter region it is concluded that isomerization of the *n*-butyl radical to *sec*-butyl with subsequent decomposition to $CH_3 + C_3H_6$ was the main source of methane. The rate of butane formation increased with time at low temperatures and decreased with time at high temperatures. It is shown that the decrease in rate was mainly due to the thermal dissociation of butane. The main source of butene-1 was probably decomposition of the *n*-butyl radical.

INTRODUCTION

Because ethylene is much more reactive than ethane, secondary reactions occur at an early stage in the pyrolysis of ethane. These secondary reactions produce mainly methane, propylene (1), butane, butene, butadiene, and acetylene. Most of the secondary products probably arise from addition of radicals to ethylene with subsequent decomposition of or abstraction by the radicals so formed. The purpose of the present study was firstly to distinguish the primary products from the secondary products and to separate the primary and secondary rates of formation of those products, mainly methane and butane, which are produced by both mechanisms, and secondly, to evaluate the mechanisms for formation of the secondary products.

EXPERIMENTAL

The apparatus and procedure have been described in Part I (2). The additional products, butene-1, butadiene, and acetylene, were analyzed by vapor phase chromatography on the column described for the analysis of butane in Part I. The yields were measured over the temperature range 550–726 °C and at pressures from 600–10 mm. In the experiments in which acetylene was measured the distillation procedure described in Part I was not followed in order to avoid losses of acetylene. The present method of separation of the products was not sufficient to obtain a quantitative measure of the yield of propylene.

RESULTS AND DISCUSSION

The effect of added ethylene on the rates of formation of hydrogen, methane, butane, butene, and butadiene at 570 °C is shown in Fig. 1. The rates were obtained with a constant ethane pressure and a constant reaction time of 100 s. This shows that methane and butane are both primary and secondary products, whereas butene and butadiene are secondary products only. The mechanism for the formation of each product will be discussed separately.

(a) Inhibition of the Rate of Hydrogen Production

The decrease in the rate of production of hydrogen with reaction time may be satisfactorily explained by the addition of reactions [−3] and [−4] to the mechanism proposed in Part I.

[1] $$C_2H_6 \rightarrow 2CH_3$$

[2] $$CH_3 + C_2H_6 \rightarrow CH_4 + C_2H_5$$

[3] $$C_2H_5 \rightarrow C_2H_4 + H$$

[4] $H + C_2H_6 \rightarrow H_2 + C_2H_5$

[5a] $C_2H_5 + C_2H_5 \rightarrow C_4H_{10}$

[5b] $\rightarrow C_2H_4 + C_2H_6$

[−3] $H + C_2H_4 \rightarrow C_2H_5$

[−4] $C_2H_5 + H_2 \rightarrow C_2H_6 + H$

On the assumption that $[C_2H_4] = [H_2]$ and $[C_2H_5]$ and [H] are independent of reaction time, the yield of hydrogen is given as

$$[1] \qquad [H_2] = \frac{a}{b}(1 - e^{-bt})$$

where $a = k_3[C_2H_5]$ and $b = k_{-3}[H]$. If t^3 and higher terms are neglected, eq. [1] leads to

$$[2] \qquad [H_2]/t = R_{H_2} = a - \frac{ab}{2}t.$$

The rate of hydrogen production will thus be a linear function of time in the early stages of decomposition. Typical plots of R_{H_2} against t are shown in Fig. 2 and from the linear

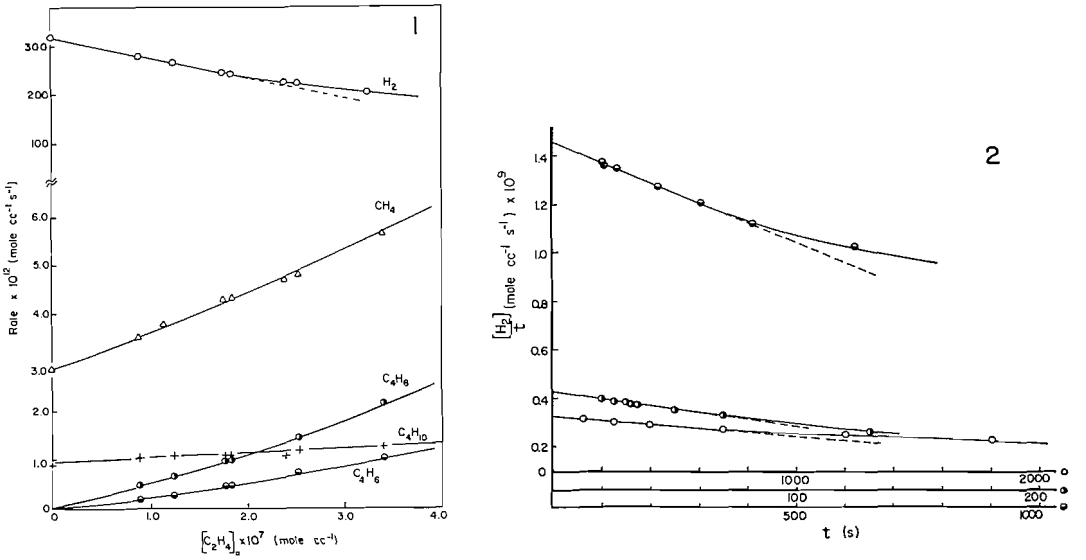


FIG. 1. Effect of added ethylene on the rates of formation of hydrogen, methane, butane, butene, and butadiene at 570 °C.
FIG. 2. Rate of hydrogen production against time.

portion values of a and b for each temperature and pressure were obtained. From eq. [1] the yield of hydrogen was then calculated beyond the short time interval over which a and b were obtained. These calculated yields agreed with the experimental yields up to 30% conversion. Since a and b were obtained assuming $[C_2H_5]$ and [H] were independent of time, it may be concluded that the decrease in the rate of hydrogen production is mainly the result of the back reactions [−3] and [−4] and not to a reduction in the steady-state radical concentration.

From eq. [2] the slope $ab/2 = \frac{1}{2}k_3k_{-3}[C_2H_5][H]$. Inserting the steady-state concentration of $[C_2H_5]$ and [H] yields

$$ab/2 = k_1(k_3)^3/2K_3k_4k_5.$$

Can. J. Chem. Downloaded from www.nrcresearchpress.com by 210.87.254.6 on 09/05/12
For personal use only.

Double-logarithmic plots of $ab/2$ against pressure of ethane, given in Fig. 3, showed a marked pressure dependence, as would be expected from the dependence on pressure of k_3 observed in Part I. At 570 °C and 400 mm the order of $ab/2$ was 1.32. Under the same conditions the order of k_3 was 0.45, whereas the other rate constants were pressure-independent. The temperature coefficient of $ab/2$ was found to be 139 kcal/mole at both 400 and 200 mm. Using the relevant values from Table I we calculated $E_{ab} = 138.7$ kcal/mole.

(b) Secondary Production of Methane

Two processes were found to be responsible for the secondary production of methane. At high pressures the secondary rate of production was proportional to the square of the ethylene concentration, whereas at low pressures this rate was linear with ethylene concentration. The first process was observed by Quinn (1) and he proposed a mechanism involving the isomerization of *n*-hexyl radicals.

[6] $C_2H_5 + C_2H_4 \rightleftharpoons n\text{-}C_4H_9$

[7] $n\text{-}C_4H_9 + C_2H_4 \rightleftharpoons n\text{-}C_6H_{13}$

[8] $n\text{-}C_6H_{13} \rightleftharpoons sec\text{-}C_6H_{13}$

[9] $sec\text{-}C_6H_{13} \rightarrow n\text{-}C_3H_7 + C_3H_6$

[10] $n\text{-}C_3H_7 \rightleftharpoons CH_3 + C_2H_4$

This mechanism accounted for the fact that no C_5 products were observed and that the yields of propylene and secondary methane were almost equal (1). It also explained the dependence of the secondary yield of methane on the square of the ethylene concentration.

TABLE I

Summary of values used and obtained in this work

Reaction	E (kcal/mole)	A (s^{-1} or cc $mole^{-1}$ s^{-1})	ΔH^0 (kcal/mole)	ΔS^{0*} (e.u.)	Reference
1	86.0	1.0×10^{16}			(2)
3	32.7 (p=200–400 mm)		38.6	1.7	(2)
4	6.8	3.4×10^{12}			(10)
5	0	2.3×10^{13}			(11)
5*a*	0	2.0×10^{13}			(11)
6			−22	−10.0	Assumed
7			−22	−10.6	Assumed
8			0	0	Assumed
9	26	3.2×10^{13}			This work
11	41	5.2×10^{14}			This work
13	15±4	5×10^{11}			This work
19	40±4	10^{14}			This work

*Note: standard state 1 mole/cc.

It can be shown that the equilibrium [6] is probably established under the present experimental conditions. In other words, the dissociation of the *n*-butyl radical into ethylene and ethyl radical is faster than the dissociation into butene and a hydrogen atom or the reaction with ethane or ethylene. Similar considerations show that reactions [7] and [−7] are also probably at equilibrium. To obtain a simple expression for the concentration of $sec\text{-}C_6H_{13}$ radicals, Quinn (1) assumed that $k_{-8} \gg k_9$. If the activation energy for reaction [−8] is comparable to that for hydrogen-atom abstraction from paraffins by large alkyl radicals, about 15 kcal/mole (3), while the activation energy for the decomposition of

Can. J. Chem. Downloaded from www.nrcresearchpress.com by 210.87.254.6 on 09/05/12
For personal use only.

sec-C_6H_{13} radical is in the range 25 kcal/mole (4), then this assumption is quite reasonable, provided only that A_9/A_{-8} is not greater than 10^3.

Thus $[sec\text{-}C_6H_{13}] = K_6K_7K_8\,[C_2H_5][C_2H_4]^2$. The rate of formation of methane is thus given by the expression:

$$d[CH_4]/dt = 2k_1[C_2H_6] + k_9\,K_6K_7K_8\,[C_2H_5]\,[C_2H_4]^2.$$

In the early stages of the decomposition while the concentration of the ethyl radical is constant

$$[CH_4] = ct + d\int_0^t [C_2H_4]^2\,dt = ct + d\overline{[C_2H_4]^2}t,$$

where $c = 2k_1[C_2H_6]$ and $d = k_9\,K_6K_7K_8\,[C_2H_5]$. From eq. [1] for the concentration of ethylene as a function of time,

$$[CH_4] = ct + d\int_0^t [\frac{a}{b}(1 - e^{-bt})]^2\,dt.$$

Integrating and dividing by t yields

$$[3] \qquad [CH_4]/t = c + \frac{a^2d}{b^3}\frac{1}{t}[bt - (1 - e^{-bt}) - \tfrac{1}{2}(1 - e^{-bt})^2]$$

$$= c + \frac{a^2d}{b^3}f(t).$$

When t is small eq. [3] becomes

$$[CH_4]/t = c + \frac{a^2d}{3}t^2.$$

The rate of methane production may thus be plotted against $\overline{[C_2H_4]^2}$ obtained graphically, against $f(t)$ using the values of b obtained from the hydrogen rates, and against t^2. Examples of these three methods are shown in Figs. 4, 5, and 6 respectively. The initial rates, c, obtained from the intercepts by these three methods agreed within 2%. In the temperature range 550–660 °C the initial rates of methane production were obtained by the t^2 plots. At temperatures higher than 685 °C, however, the rate of methane formation is approximately a linear function of time. This is the result of the rapid decomposition of ethane itself which compensates for the increase in rate due to the secondary reactions. Consequently, in this region initial rates were obtained by extrapolation of the rate against time.

The slopes of these plots together with values of a and b obtained from the hydrogen rates yield values for the quantity d.

$$d = k_9K_6K_7K_8(k_1/k_5)^{1/2}\,[C_2H_6]^{1/2}$$

A plot of logarithm of d against logarithm of the ethane pressure is shown in Fig. 7, which includes the results obtained by Quinn (1). At high pressures the order is fairly close to 1/2 as predicted, but at low pressures it becomes negative and a change in mechanism must therefore occur.

The two high-pressure values of d at 640 and 620 °C give a temperature coefficient of 27 kcal/mole. If the heat change in reactions [6] and [7] are taken equal to those of the following reactions (5),

Can. J. Chem. Downloaded from www.nrcresearchpress.com by 210.87.254.6 on 09/05/12
For personal use only.

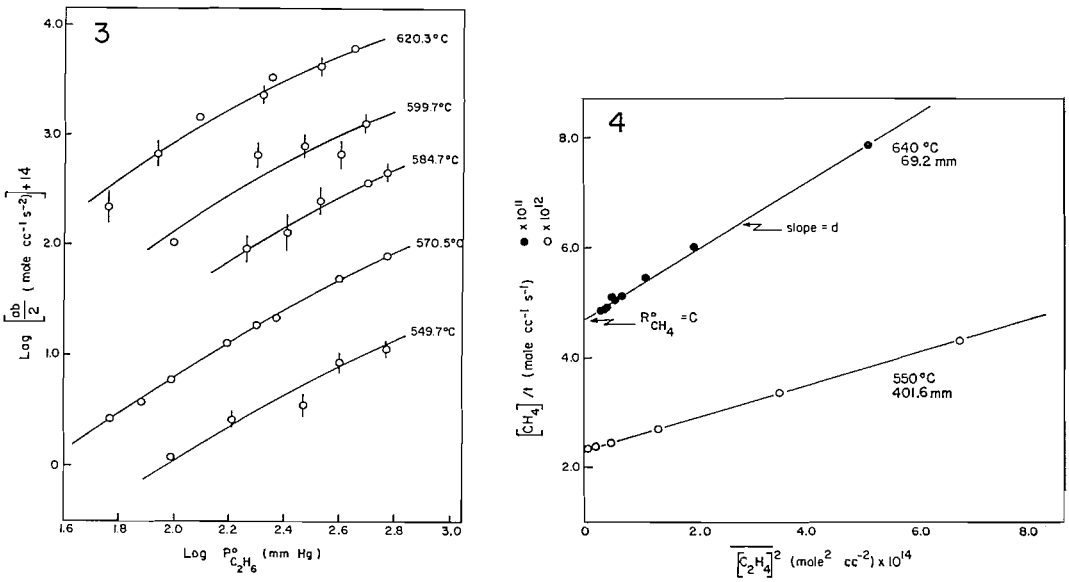


FIG. 3. Double-logarithmic plots of $ab/2$ against pressure.
FIG. 4. Rate of methane production as a function of $\overline{[C_2H_4]^2}$.

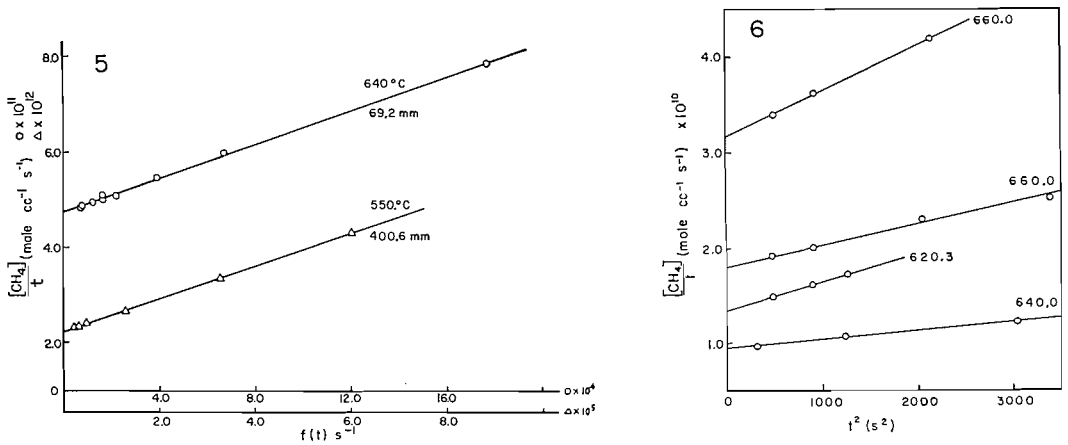


FIG. 5. Rate of methane production against $f(t)$.
FIG. 6. Rate of methane production as a function of t^2. From top to bottom, pressures and temperatures were: 145.2 mm, 660.0 °C; 91.1 mm, 660.0 °C; 448.3 mm, 620.3 °C; 123.3 mm, 640.0 °C.

[6′] $$C_2H_6 + C_2H_4 \rightleftharpoons n\text{-}C_4H_{10}$$

[7′] $$n\text{-}C_4H_{10} + C_2H_4 \rightleftharpoons n\text{-}C_6H_{14},$$

then $\Delta H_6^0 = \Delta H_7^0 = -22$ kcal/mole. If the entropy changes for reactions [6] and [7] are also equal to those for reactions [6′] and [7′] respectively, then at 640 °C $\Delta S_6^0 = -10.0$ e.u. (entropy units) and $\Delta S_7^0 = -10.6$ e.u. (5) (standard state 1 mole/cc). Using the relevant values from Table I and the data at 640 °C gives

$$E_9 = 26 \text{ kcal/mole and } A_9 = 3.2 \times 10^{13} \text{ s}^{-1}.$$

Can. J. Chem. Downloaded from www.nrcresearchpress.com by 210.87.254.6 on 09/05/12
For personal use only.

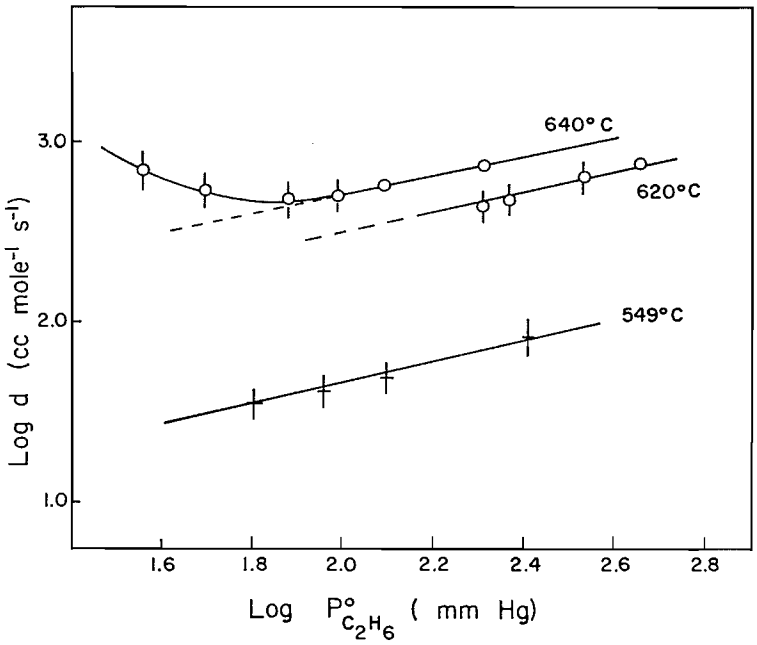


FIG. 7. Plot of log d against log of the ethane pressure. (O) This experiment; (+) Quinn.

At high temperatures and low pressures the rate of methane production increased linearly with $[C_2H_4]$ and may be expressed as

$$\mathrm{d}\,[CH_4]/\mathrm{d}t = c + d'\,[C_2H_4].$$

The same three methods of plotting the rates were again used and are shown in Figs. 8 and 9. The function $g(t) = [bt + e^{-bt} - 1]/t$ is that obtained by substitution of eq. [1] for the concentration of ethylene. The extrapolated rate was the same from all three plots and values of d' were in good agreement.

The change in the order of the rate of secondary methane formation indicates that the mechanism suggested by Quinn is no longer effective under these conditions of temperature and pressure. As the pressure is lowered the isomerization of the *n*-butyl radical to *sec*-butyl may compete with its addition to ethylene. Although *n*-butyl radicals do not decompose to yield methyl radicals (6), *sec*-butyl radicals may rapidly decompose to give propylene and a methyl radical (7, 8). The rate of production of methane thus formed would be proportional to the concentration of ethylene. The mechanism may then be represented by reactions [1]–[5] and the following.

[6] $\quad C_2H_5 + C_2H_4 \rightleftharpoons n\text{-}C_4H_9$

[11] $\quad n\text{-}C_4H_9 \rightarrow sec\text{-}C_4H_9$

[12] $\quad sec\text{-}C_4H_9 \rightarrow CH_3 + C_3H_6$

It may be argued that the decomposition may occur essentially in one step without the separate formation of a *sec*-butyl radical (4). However, the appearance of small amounts of *cis*- and *trans*-butene-2 at high conversions would suggest that *sec*-butyl radicals are formed in the system and hence would favor the mechanism as written.

Can. J. Chem. Downloaded from www.nrcresearchpress.com by 210.87.254.6 on 09/05/12
For personal use only.

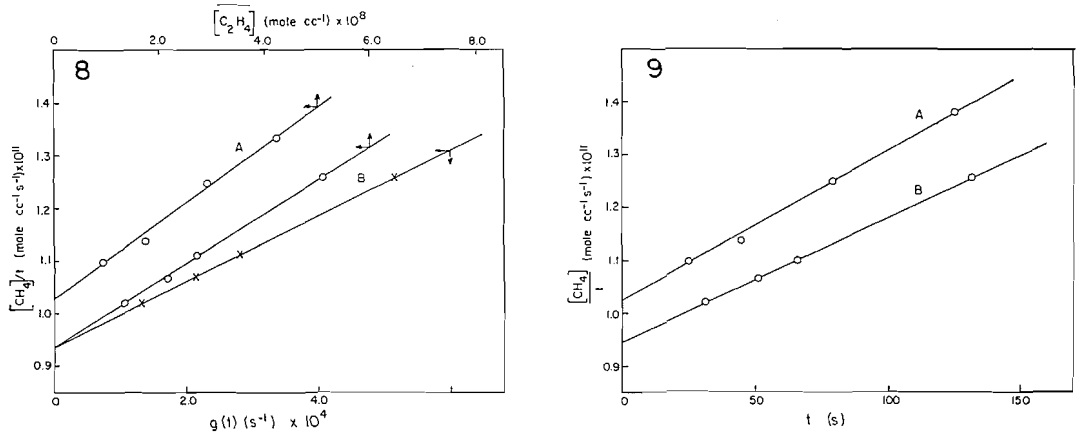


FIG. 8. Rate of methane formation as a function of $\overline{[C_2H_4]}$ and of $g(t)$. (A) 660 °C, 10.7 mm; (B) 640 °C, 20.7 mm.
FIG. 9. Rate of methane formation as a function of time. (A) 660 °C, 10.7 mm; (B) 640 °C, 20.7 mm.

The rate of formation of methane is now given as

$$d[CH_4]/dt = 2k_1 [C_2H_6] + k_{11}K_6 [C_2H_5] [C_2H_4].$$

Hence,
$$d' = k_{11}K_6 [C_2H_5] = k_{11}K_6(k_1/k_5)^{1/2} [C_2H_6]^{1/2}.$$

Since at these pressures and temperatures k_1 is no longer a first-order rate constant the ratio $d'/(k_1/k_5)^{1/2} [C_2H_6]^{1/2}$ was evaluated at 640 and 660 °C using the values of k_1 from Part II. The temperature coefficient of this ratio was 19 kcal/mole, from which values of E_{11} and A_{11} were calculated and are shown in Table I. The formation of propylene from *n*-butyl radicals was not observed, in a slightly different reaction system (6), at temperatures up to 450 °C, and it is not surprising that the activation energy for this process is rather large It may be pointed out that the present system is more favorable for the observation of isomerization since the equilibrium [6] is probably established and the decomposition into C_2H_5 and C_2H_4 is not a competing reaction.

(c) Secondary Reactions Producing Butane

At temperatures below 585 °C the rate of butane production increased with reaction time, whereas at higher temperatures the rate decreased as the reactions proceeded. Typical plots of the rate against time are shown in Fig. 10. The increase in production of butane may be ascribed to the abstraction reaction of a *n*-butyl radical

[13] $$n\text{-}C_4H_9 + C_2H_6 \rightarrow n\text{-}C_4H_{10} + C_2H_5,$$

whereas the decrease in yield may be caused by attack of radicals, mainly the ethyl radical, or thermal dissociation:

[14] $$R + C_4H_{10} \rightarrow RH + C_4H_9$$

[−5*a*] $$C_4H_{10} \rightarrow 2C_2H_5$$

The rate of butane production is thus given by

$$d[C_4H_{10}]/dt = k_{5a}[C_2H_5]^2 + k_{13}[n\text{-}C_4H_9][C_2H_6] - (k_{14}[R] + k_{-5a})[C_4H_{10}].$$

If one assumes equilibrium between *n*-butyl radicals, ethyl radicals, and ethylene as

Can. J. Chem. Downloaded from www.nrcresearchpress.com by 210.87.254.6 on 09/05/12
For personal use only.

discussed earlier, $k_{13}[n\text{-}C_4H_9] = k_{13}K_6[C_2H_5][C_2H_4]$. Substituting eq. [1] for the concentration of ethylene and integrating at short reaction times yields

$$[4] \qquad [C_4H_{10}]/t = R^0_{C_4H_{10}} + \frac{k_3k_{13}K_6[C_2H_5]^2[C_2H_6] - R^0_{C_4H_{10}}(k_{14}[R] + k_{-5a})}{2}\,t.$$

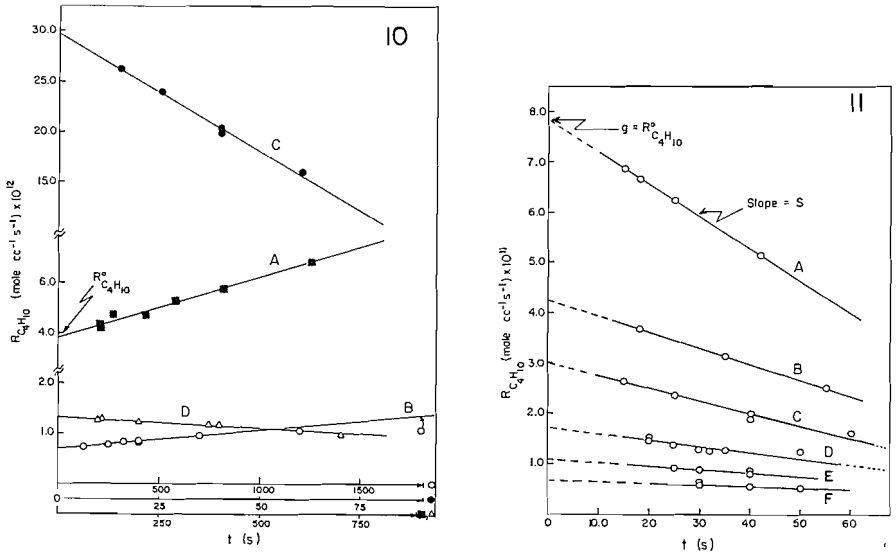


FIG. 10. Rate of butane production as a function of time. (A) 570.5 °C, 590.5 mm; (B) 549.7 °C, 401.5 mm; (C) 640.0 °C, 91.2 mm; (D) 584.7 °C, 100.0 mm.
FIG. 11. Rate of butane production as a function of time at 640 °C.

At 640 °C the rates of butane production decrease linearly with time at all pressures, as shown in Fig. 11. The ratios of slope to intercept for each pressure, given by the expression

$$[5] \qquad \frac{\text{slope}}{\text{intercept}} = \frac{k_3k_{13}K_6[C_2H_6]}{2k_{5a}} - \frac{(k_{14}[R] + k_{-5a})}{2},$$

are independent of pressure over the range 200–36 mm. The only term in [5] which is independent of pressure is k_{-5a} and it is concluded that at this temperature the unimolecular decomposition of butane is responsible for the decrease in the rate of butane formation. The ratio of slope to intercept therefore equals $\frac{1}{2}k_{-5a}$.

At 640 °C the value obtained is $(1.53 \pm 0.05) \times 10^{-2}$ s^{-1}. Assuming an activation energy for dissociation of butane of 80.0 kcal/mole (9) leads to

$$[6] \qquad k_{-5a} = (2.2 \pm 0.1) \times 10^{17}\, e^{-80000/RT}\ s^{-1}.$$

At 570 °C where the rate increased as the reaction proceeded, the first term in eq. [5] must be contributing to the butane yield and the ratio of slope to intercept should be dependent on the pressure. Since k_3 is roughly proportional to the square root of the ethane pressure in this region (2) the ratio should be approximately proportional to $[C_2H_6]^{3/2}$. This relation was obeyed at 570 °C and the value of the intercept, $(k_{14}[R] + k_{-5a})$, was 3.8×10^{-4} s^{-1}. This is close to the value of k_{-5a} at this temperature calculated from equation [6] and indicates that the dissociation of butane may still be an important factor in lowering the yield of butane even at 570 °C.

Can. J. Chem. Downloaded from www.nrcresearchpress.com by 210.87.254.6 on 09/05/12
For personal use only.

If therefore for the term $(k_{14}[R] + k_{-5a})$ the calculated value of k_{-5a} from equation [6] is used the ratio $k_{13}K_6/k_{5a}^{1/2}$ may be calculated from the ratio of slope to intercept of plots of $R_{C_4H_{10}}$ against t. Making the substitution $k_3[C_2H_5] = R^0_{H_2}$, we obtain

$$\frac{\text{slope}}{\text{intercept}} = \frac{k_{13}K_6[C_2H_6]R^0_{H_2}}{2k_{5a}^{1/2}(R^0_{C_4H_{10}})^{1/2}} - \frac{k_{-5a}}{2}.$$

An Arrhenius plot of the ratio $k_{13}K_6/k_{5a}^{1/2}$ gives a temperature coefficient of -7 ± 4 kcal/mole, which leads to $E_{13} = 15 \pm 4$ kcal/mole, and $A_{13} = 5 \times 10^{11}$ cc mole^{-1} s^{-1}. This is a reasonable value for a hydrogen abstraction reaction by larger alkyl radicals.

(d) Production of Butene-1, Butadiene, and Acetylene

These products were produced by secondary reactions only. Butene-1 was the first secondary product observed, and butadiene and acetylene became important at higher temperatures. Being very reactive, these unsaturated products themselves disappear rapidly and the kinetics becomes complex even in the early stages of decomposition. It is difficult therefore to draw definite conclusions regarding their origins.

Typical yields of secondary products as a function of time are shown in Figs. 12 and 13. The following reactions are proposed to account for the main features of the rates of formation.

[15] $H + C_2H_4 \rightarrow H_2 + C_2H_3$

[16] $C_2H_5 + C_2H_4 \rightarrow C_2H_6 + C_2H_3$

[17] $C_2H_3 + C_2H_4 \rightarrow C_4H_7$

[18] $C_2H_3 + C_2H_5 \rightarrow C_4H_8$

[19] $n\text{-}C_4H_9 \rightarrow C_4H_8 + H$

[20] $C_4H_7 \rightarrow C_4H_6 + H$

[21] $C_2H_3 + C_2H_3 \rightarrow C_4H_6$

[22] $C_2H_3 \rightarrow C_2H_2 + H$

Steady-state treatment yields

$$R_{C_4H_8} = k_{19}[n\text{-}C_4H_9] + k_{18}[C_2H_3][C_2H_5]$$

$$R_{C_4H_6} = k_{17}[C_2H_3][C_2H_4] + k_{21}[C_2H_3]^2$$

$$R_{C_2H_2} = k_{22}[C_2H_3].$$

Substituting the steady-state concentrations of n-C_4H_9 and C_2H_3 radicals yields

$$d[C_4H_8]/dt = k_{19}K_6[C_2H_5][C_2H_4] + \frac{k_{18}(k_{15}[H] + k_{16}[C_2H_5])[C_2H_4]}{k_{-16}[C_2H_6] + k_{17}[C_2H_4] + k_{18}[C_2H_5] + k_{22}},$$

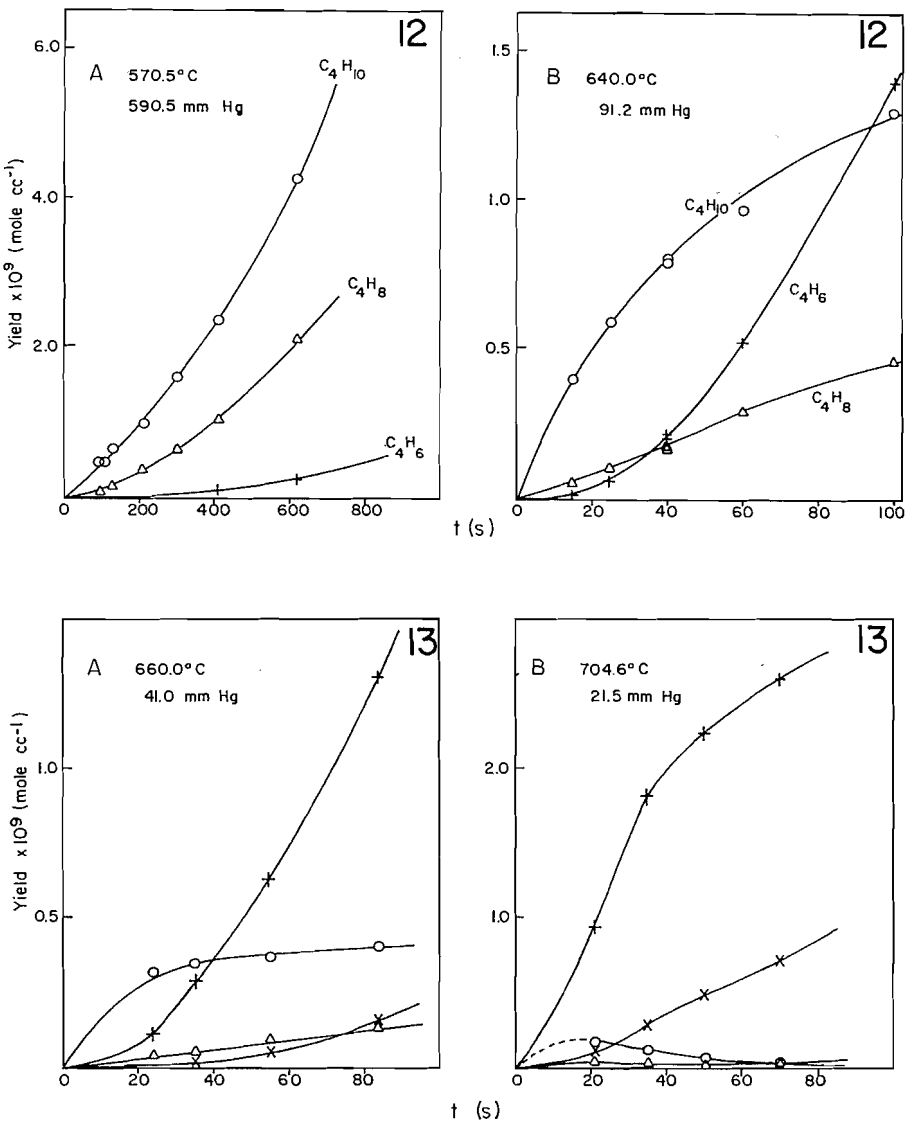
which may be written as

$$d[C_4H_8]/dt = (n + p)[C_2H_4].$$

The rate will be a linear function of $[C_2H_4]$ if $n \gg p$ or if the term $k_{17}[C_2H_4]$ is small compared with the other terms in the denominator of p. Plots of $R_{C_4H_8} = [C_4H_8]/t$ against $\overline{[C_2H_4]}$, the average ethylene concentration, at 550 °C are shown in Fig. 14 where linearity is observed only at short reaction times. Since the rate decreases at higher conversions, the reaction

$$C_4H_7 + C_2H_6 \rightarrow C_4H_8 + C_2H_5,$$

Can. J. Chem. Downloaded from www.nrcresearchpress.com by 210.87.254.6 on 09/05/12
For personal use only.



FIGS. 12 and 13. Yields of secondary products as a function of time. (○) Butane; (△) butene-1; (+) butadiene; (×) acetylene.

which gives an increasing rate of butene production with increasing ethylene concentration, is probably not important at these temperatures. At lower temperatures where the rate of butene does increase with time this reaction may occur.

In the linear portion of the plot of $R_{C_4H_8}$ against $\overline{[C_2H_4]}$ it may be assumed that the term $k_{17}[C_2H_4]$ is unimportant and the following expression may thus be obtained,

$$\left(\frac{R_{C_4H_8}}{[C_2H_4]}\right)_0 \Big/ (R^0_{C_4H_{10}})^{1/2} = \frac{k_{19}K_6}{k_{5a}^{1/2}} + \frac{k_{18}(k_{15}[H] + k_{16}[C_2H_5])}{k_{5a}^{1/2}(k_{-16}[C_2H_6] + k_{18}[C_2H_5] + k_{22}[C_2H_5])}.$$

Can. J. Chem. Downloaded from www.nrcresearchpress.com by 210.87.254.6 on 09/05/12
For personal use only.

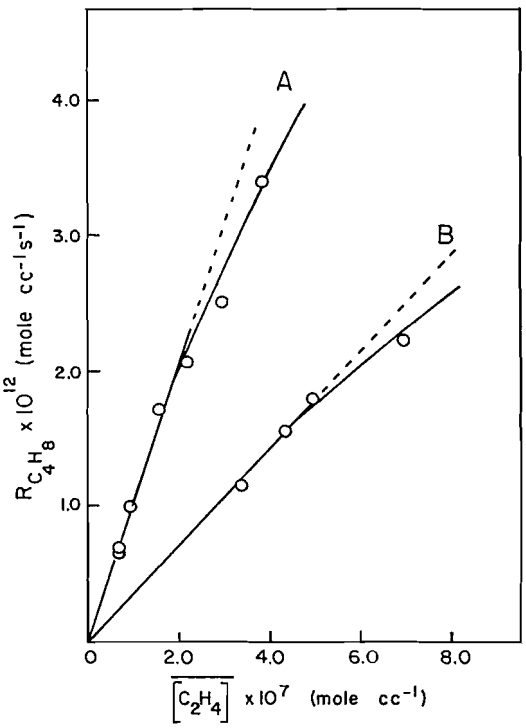


FIG. 14. Rate of butene formation against $\overline{[C_2H_4]}$ at 550 °C. Scale expanded 10 times for B. (A) 590 mm; (B) 96 mm.

TABLE II

$\left(\frac{R_{C_4H_8}}{\overline{[C_2H_4]}}\right)_0 \Big/ (R^0_{C_4H_{10}})^{1/2}$ as a function of temperature and pressure

T (°C)	P (mm)	$\left(\frac{R_{C_4H_8}}{\overline{[C_2H_4]}}\right)_0 \Big/ (R^0_{C_4H_{10}})^{1/2}$ (cc mole^{-1} s^{-1})$^{1/2}$
549.7	401.6	4.4±0.3
550.7	590.5	5.2±0.5
	400.0	5.1±0.3
	199.0	4.9±0.5
	96.3	5.2±0.3
584.7	341.8	6.9±0.3
	168.1	7.1±0.2
599.7	402.1	8.4±0.6
	298.9	8.3±0.3
	203.1	9.2±0.7
	99.9	5.3±1.5
620.3	335.1	10.4±0.3
	209.8	10.7±0.3

It may be shown that the predominant term in the denominator of the second ratio is $k_{-16}[C_2H_6]$ and hence this ratio should be dependent on pressure. The left-hand side was,

Can. J. Chem. Downloaded from www.nrcresearchpress.com by 210.87.254.6 on 09/05/12
For personal use only.

however, independent of pressure over the range 100–590 mm as given in Table II. Thus it may be concluded that

$$\left(\frac{R_{C_4H_8}}{[C_2H_4]}\right)_0 \Big/ (R^0_{C_4H_{10}})^{1/2} = \frac{k_{19}K_6}{k_{5a}^{1/2}}.$$

The temperature coefficient of this ratio was 18 ± 4 kcal/mole, from which values for E_{19} and A_{19} were calculated and are given in Table I. The main conclusion is that reaction [19] is more important than reaction [18] in the formation of butene-1. The decrease in butene production at higher conversions may be due to its unimolecular decomposition or to radical-addition reactions.

At 640 °C the rate of butadiene production was found to be proportional to $\overline{[C_2H_4]^2}$. The measurements of the rates of butadiene and acetylene, however, were not sufficiently extensive to suggest a mechanism for their formation.

The authors wish to thank the National Research Council and the American Petroleum Fund for grants in support of this work. One of us (M. C. L.) thanks the Ontario Research Foundation for a fellowship.

REFERENCES

1. C. P. Quinn. Trans. Faraday Soc. **59**, 2543 (1963).
2. M. C. Lin and M. H. Back. Can. J. Chem. **44**, 505 (1966).
3. V. N. Kondrat'ev. Chemical kinetics of gas reactions. Pergamon Press, Ltd., London. 1964.
4. J. A. Kerr and A. F. Trotman-Dickenson. Progr. Reaction Kinetics. Vol. 1. Pergamon Press, Ltd., London. 1961.
5. Selected Values of Physical and Thermodynamic Properties of Hydrocarbons and Related Compounds. American Petroleum Institute, Pittsburgh. 1953.
6. A. S. Gordon and J. R. McNesby. J. Chem. Phys. **33**, 1882 (1960).
7. J. R. McNesby, C. M. Drew, and A. S. Gordon. J. Chem. Phys. **24**, 1260 (1956).
8. J. T. Gruver and J. G. Calvert. J. Am. Chem. Soc. **78**, 5208 (1956).
9. A. F. Trotman-Dickenson. Gas kinetics. Butterworth Scientific Publications, London. 1955.
10. M. R. Berlie and D. J. LeRoy. J. Chem. Phys. **20**, 200 (1952).
11. A. Shepp and K. O. Kutschke. J. Chem. Phys. **26**, 1020 (1957).

Can. J. Chem. Downloaded from www.nrcresearchpress.com by 210.87.254.6 on 09/05/12
For personal use only.

Can. J. Chem. Downloaded from www.nrcresearchpress.com by 210.87.254.6 on 09/05/12
For personal use only.

REACTIONS OF ALKOXY RADICALS

I. HYDROGEN ATOM ABSTRACTION FROM SUBSTITUTED TOLUENES[1]

B. R. KENNEDY[2] AND K. U. INGOLD
Division of Applied Chemistry, National Research Council, Ottawa, Canada

Received June 2, 1966

ABSTRACT

The relative rates of hydrogen atom abstraction from ten substituted toluenes by *t*-butoxy radicals in carbon tetrachloride at 40 °C have been measured and the data fitted to the Hammett equation. A much better correlation is obtained with the σ^+ constants than with the σ constants of the substituents. In this respect, therefore, the reaction is similar to the majority of hydrogen atom abstraction reactions by radicals of moderate and high electron affinity. That is, the polar properties of the substituents are much more important than their stabilizing effect on the benzyl radical formed in the reaction.

The cumyloxy radical has a similar reactivity to the *t*-butoxy radical. The *p*-nitrocumyloxy radical appears to be slightly more reactive and also slightly more susceptible to the polar effects of substituents than are *t*-butoxy or cumyloxy radicals.

The relative rates of hydrogen atom abstraction from compounds of the type XC_6H_4YH by free radicals can frequently be correlated by means of the Hammett $\rho\sigma$ relationship. Data for a wide variety of such relations were summarized in a recent paper from this laboratory (1). It was shown that with few exceptions, notably hydrogen abstraction by *t*-butoxy radicals from substituted toluenes (2, 3), a better correlation was usually obtained with σ^+ constants rather than with σ constants.[3] Further support for this generalization has been provided by Russell and Williamson (5) who specifically pointed out that for the *t*-butoxy radical the proper substituents had not been examined to distinguish clearly between a σ- and a σ^+-correlation. With this point in mind we decided to reinvestigate this reaction with particular attention to those substituents having significantly different σ and σ^+ constants. While this work was in progress a similar study by Gilliom and Ward appeared (6). However, we feel that our results and conclusions differ sufficiently from theirs to warrant the present communication.

EXPERIMENTAL

Reagents

Toluene, *m*-xylene, *p*-xylene, ethylbenzene, and cumene were Phillips Research Grade materials. *m*-Chlorotoluene, *p*-chlorotoluene, *m*-nitrotoluene, *p*-nitrotoluene, and *p*-methoxytoluene were obtained from Eastman. These compounds were used as supplied, their purity being checked by gas–liquid chromatography (g.l.c.). Toluene-α-d_3 was obtained from Merck, Sharp & Dohme; it contained over 95% trideuterotoluene. We are grateful to the Benzol Products Company for a generous sample of *p*-methoxybenzyl chloride.

p-Phenoxytoluene was prepared by the method of Russell and Williamson (5). *p*-Cyanotoluene was prepared by the dehydration of *p*-tolualdehyde oxime with acetic anhydride (cf. ref. 7). *t*-Butyl hypochlorite was prepared as described by Teeter and Bell (8). Cumyl hypochlorite and *p*-nitrocumyl hypochlorite were prepared from the corresponding alcohols by the method of Zavitsas and Seltzer (9). The *p*-nitrocumyl alcohol was prepared from cumene by nitration (10) followed by oxidation of the purified *p*-nitrocumene by the method of Kwart and Francis (11). The complete esterification of the three alcohols to their hypochlorites was checked by infrared spectroscopy. Baker and Adamson Reagent Grade carbon tetrachloride was used as the solvent throughout this work.

[1]*Issued as N.R.C. No. 9120.*
[2]*National Research Council Postdoctorate Fellow 1965–1966.*
[3]*The suggestion that such free radical reactions might be correlated with σ^+ constants was first put forward by G. A. Russell (4).*

Chlorination Procedure

Relative reactivities were determined by competitive experiments in sealed, degassed ampoules. Solutions of the reactants were made by weight. The initial concentrations were 0.1 *M* in hypochlorite and 0.5 *M* in each of two toluenes. Excess hydrocarbon was used to prevent polychlorination (3) while the relatively dilute solutions ensured that any solvent effects caused by changing the reactants were held to a minimum. The ampoules were placed in a water bath at 40 °C and were irradiated with a 100 W tungsten filament lamp for not less than 4 h. All experiments were performed in duplicate.

Analytical Procedures

After irradiation the reaction solutions were generally analyzed for benzyl chlorides by g.l.c. on Chromosorb-supported columns containing di-isodecyl phthalate or diethyleneglycol succinate polyester. Relative reactivities were calculated from the relative yields of benzyl chlorides. The reactivities of *m*- and *p*-xylene, *m*- and *p*-chlorotoluene, and *p*-cyanotoluene were all measured directly against toluene. The reactivities of *m*- and *p*-nitrotoluene were measured against *p*-cyanotoluene. The reactivity of *p*-phenoxytoluene relative to diphenylmethane was determined by hydrocarbon consumption using benzonitrile as an internal standard. (Reactivity of diphenylmethane to toluene under these conditions = 3.46 per benzylic hydrogen (12), cf. a value of 4.70 given by Walling and Jacknow (3).) The reactivity of *p*-methoxytoluene was determined by nuclear magnetic resonance spectroscopy (13) since its chloride is too reactive for analysis by g.l.c. That is, the relative concentrations of benzyl chloride and *p*-methoxybenzyl chloride were determined by integrating the area of the peaks corresponding to their benzylic hydrogens on a Varian Associates model A-60 nuclear magnetic resonance spectrometer. Most of the CCl_4 was removed at low temperature under vacuum before analysis. This procedure gave satisfactory results with *t*-butyl hypochlorite but the spectra of the chlorides from the cumyl hypochlorite and the *p*-nitrocumyl hypochlorite reactions were not sufficiently well resolved for analysis.

The reactivities of the benzylic hydrogens of ethylbenzene and cumene were determined in competitive experiments with toluene by measuring the total concentration of benzylic chlorine by solvolysis and the concentration of benzyl chloride (compared to an internal standard) by g.l.c. The benzylic chlorine was determined by the following procedure. An aliquot of the irradiated solution (1.0 ml) was cooled to $-45° \pm 5$ °C and all the CCl_4 was removed under high vacuum (1 h). The residue was diluted with 25 ml ethanol and hydrolyzed with 0.5 *M* aqueous NaOH (10 ml) under reflux for 2 h. The solution was then acidified and the chloride ion concentration determined by potentiometric titration with *N*/100 silver nitrate.

All the relative reactivities given in this paper represent the average of not less than four analyses on duplicate experiments. All were reproducible to better than ±10%.

RESULTS

The relative reactivities obtained in this work for the reaction of substituted toluenes with *t*-butoxy radicals at 40 °C are compared in Table I with the data of Walling and Jacknow (3) and Gilliom and Ward (6). The agreement between the three sets of data is fairly good except for *p*-phenoxytoluene and *p*-chlorotoluene. In the latter case, no significant variation in the measured reactivity was found over a fourfold change in the ratio [*p*-chlorotoluene]/[toluene] and over a twofold change in the total extent of reaction. It is possible that the differences in reactivity are connected with a solvent effect. The much higher reactivity of *p*-phenoxytoluene found in the present work (compared with the value reported by Gilliom and Ward) has an important bearing on the choice between a correlation of the reaction with σ or σ^+ constants since there are relatively few substituents that can be employed in free radical reactions to draw this distinction.[4] The different reactivities are probably due to the different analytical methods employed. Thus, Gilliom and Ward compared *p*-phenoxytoluene with cyclohexane by selective solvolysis of the benzyl chloride and comparison of this with the total chloride. By this method, chlorination of the *p*-phenoxytoluene in either ring would give an apparently low reactivity.[5] In contrast, our analysis for hydrocarbon consumption will give somewhat

[4]*Substituents such as* OH *and* NH_2 *are unsuitable because they react rapidly with alkoxy radicals and the resultant phenoxy and anilino radicals do not continue the reaction chain. The p-dimethylamino group, which has a very large difference between its* σ *and* σ^+ *constants, was also unsuitable as the toluene was found to react directly with* CCl_4 *(cf. refs. 14 and 15).*

[5]*In this connection it is interesting to note that we have found diphenyl ether to be an unsatisfactory solvent for kinetic studies of chlorination with t-butylhypochlorite, since the ether appears to undergo a slow direct reaction with the hypochlorite. Anbar and Ginsberg (16) have reported that phenols and other reactive aromatics undergo electrophilic substitution with hypochlorites to give aryl chlorides.*

Can. J. Chem. Downloaded from www.nrcresearchpress.com by 210.87.254.6 on 09/05/12
For personal use only.

too high a reactivity if ring chlorination is significant. However, this difficulty does not arise in the method used in this work for measuring the reactivity of *p*-methoxytoluene (see Experimental). The high reactivity of this compound lends support to a high reactivity for *p*-phenoxytoluene.

TABLE I

Relative reactivities of substituted toluenes toward *t*-butyl hypochlorite at 40 °C

Substituent	This work	Ref. 3	Ref. 6
p-CH_3O	3.2	—	—
p-C_6H_5O	2.13	—	1.42
p-CH_3	1.47*	1.53*	1.52*
m-CH_3	1.07*	1.17*	1.14*
None	1.00†	1.00†	1.00†
p-Cl	0.89	0.71	0.67
m-Cl	0.59	0.52	0.52
p-CN	0.36	—	0.29
m-NO_2	0.29	—	—
p-NO_2	0.25	—	—
Solvent	CCl_4	Reactants	Benzene

*Experimental result divided by statistical factor of 2.
†Assumed.

The reactivity of some substituted toluenes towards *t*-butoxy radicals, cumyloxy radicals, and *p*-nitrocumyloxy radicals are compared in Table II. The deuterium isotope effects for hydrogen abstraction from toluene and toluene-α-d_3, which are also recorded in this table were calculated from competitive experiments with toluene-α-d_3 and *p*-xylene. Brook and Glazebrook (17) have reported a very rough value in the range 3.3–6.1 for this isotope effect with *t*-butoxy radicals at 135 °C (cf. also ref. 18).

TABLE II

Relative reactivities of substituted toluenes toward *t*-alkoxy radicals at 40 °C

Substituent	*t*-Butoxy	Cumyloxy	*p*-Nitrocumyloxy
p-CH_3	1.47*	1.50*	1.72*
None	1.00†	1.00†	1.00†
p-Cl	0.89	0.91	0.91
p-CN	0.36	0.39	0.35
k_H/k_D	2.4	2.6	1.7

*Experimental result divided by a statistical factor of 2.
†Assumed.

DISCUSSION

The present data on the relative reactivities of substituted toluenes towards *t*-butoxy radicals were fitted to the Hammett equation.[6] The following correlations were obtained:

[1] $$\log k/k_0 = -0.86\sigma + 0.08;\ s, 0.259;\ r, 0.972$$

[2] $$\log k/k_0 = -0.68\sigma^+ - 0.02;\ s, 0.012;\ r, 0.999.$$

The differences in the standard deviations (s) and correlation coefficients (r) for the σ and σ^+ equations leave little doubt that the substituent effect is best represented by σ^+ constants. The reaction of *t*-butoxy radicals with substituted toluenes in CCl_4 is therefore

[6]*The σ constants are from ref. 19, σ^+ constants from ref. 20 except for the p-phenoxy substituent for which the σ^+ constant was taken from ref. 5.*

Can. J. Chem. Downloaded from www.nrcresearchpress.com by 210.87.254.6 on 09/05/12
For personal use only.

similar to the majority of hydrogen atom abstraction reactions which involve radicals of moderate to high electron affinity (1, 5). If the transition state is represented by the following extreme resonance forms (4) then the correlation with σ^+ constants implies

$$\underset{\text{I}}{XC_6H_4CH_2{:}H\cdot OBu^t} \leftrightarrow \underset{\text{II}}{XC_6H_4\overset{+}{C}H_2\cdot H\,\dot{:}\,\bar{O}Bu^t} \leftrightarrow \underset{\text{III}}{XC_6H_4CH_2\cdot H{:}OBu^t}$$

that structure II makes a very important contribution to the transition state (1, 4, 5). This conclusion differs from that of Gilliom and Ward whose data give a slightly better fit with σ than with σ^+ constants.[7] It seems unlikely that this difference could be due to a solvent effect, although it would appear that carbon tetrachloride is a more satisfactory solvent than benzene for *t*-butyl hypochlorite chlorinations as CCl_4 does not enter into the chain reaction even with quite reactive alkyl radicals (21). The kinetics for the hypochlorite–toluene reaction are more complex in benzene than in CCl_4 which implies that benzene may enter into the reaction (22).

None of the values found for the toluenes studied in this work deviate substantially from the line defined by eq. [2]. This implies that in no case is the reactivity significantly affected by the stability of the resultant benzyl radical (cf. ref. 23) even though the two methylbenzyl radicals and the *p*-cyanobenzyl radical are stabilized by over 1 kcal/mole relative to the benzyl radical.[8] Gilliom and Ward (6) (cf. also ref. 25) reported that *p*-phenyltoluene showed a large positive deviation from both their σ and σ^+ Hammett equations. This is attributed to the radical-stabilizing ability of the *p*-phenyl group.[9] However, their relative reactivity for *p*-phenyl toluene of 1.64 deviates by only +0.12 log units from our Hammett relationship defined by eq. [2]. Although the *m*-chloro group does not stabilize the benzyl radical (24) our result with *m*-chlorotoluene deviates from eq. [2] by +0.06 log units. The deviation of the *p*-phenyltoluene is therefore hardly significant.[10] That is, in the transition state of this reaction radical stabilization by substituents (structure III) does not play a very important role compared with their polar effects (structure II).

The relative reactivities listed in Table II suggest that *t*-butoxy and cumyloxy radicals are equally sensitive to polar effects. The *p*-nitrocumyloxy radical may be slightly more sensitive but the difference is small since the inductive effect of the *p*-nitro group must be considerably attenuated at the radical center. Cumyloxy also has a similar reactivity to *t*-butoxy in its abstraction of other benzylic hydrogens. For example, the reactivities (per α-hydrogen relative to toluene) of ethylbenzene and cumene were 4.25 and 7.4 respectively, for cumyloxy and 3.7 and 6.4, respectively, for *t*-butoxy.[11] The significantly

[7] *That is, Gilliom and Ward report*

$$\log k/k_0 = -0.750\sigma - 0.007;\ s,\ 0.047;\ r,\ 0.984.$$
$$\log k/k_0 = -0.599\sigma^+ - 0.066;\ s,\ 0.092;\ r,\ 0.953.$$

[8] *Hodgkins and Megarity's (24) ultraviolet measurements on substituted benzyl radicals give the following stabilities (in kcal/mole relative to the unsubstituted radical): p-CN 1.55; p-CH_2 1.23; m-CH_3 1.17; p-Cl 0.28; and m-Cl 0.0.*

[9] *The p-C_6H_5 group stabilizes the benzyl radical by 2.15 kcal/mole (24).*

[10] *Deviations from the Hammett equation are generally attributed to any factor that will conveniently rationalize the results, for example, experimental error or special interactions between solvent and substituent. However, the electronic contribution of a substituent cannot really be represented by a single constant since the resonance contribution will vary from one reaction to another depending on the electron demand at the reaction center. This is particularly the case for the p-phenyl substituent since the magnitude of the angle between the two phenyl nuclei is strongly dependent on electron demand (26). In view of the potential variation in the electronic contribution of a substituent, the general success of the σ^+ treatment in correlating hydrogen atom abstractions by electrophilic radicals is really quite surprising.*

[11] *For t-butoxy, Walling and Jacknow (3) give 3.18 and 6.84, respectively, and Johnston and Williams (25) give 3.9 and 9.3, respectively (at 110 °C).*

Can. J. Chem. Downloaded from www.nrcresearchpress.com by 210.87.254.6 on 09/05/12
For personal use only.

smaller deuterium isotope effect obtained with the *p*-nitrocumyloxy radical suggests that it is probably rather more reactive than the *t*-butoxy and cumyloxy radicals. A similar increase in reactivity for radicals containing electron-attracting groups has been observed previously in the reaction of substituted polystyryl peroxy radicals with 2,6-di-*t*-butyl-4-methylphenol (27).

REFERENCES

1. J. A. HOWARD and K. U. INGOLD. Can. J. Chem. **41**, 1744 (1963).
2. K. M. JOHNSTON and G. H. WILLIAMS. J. Chem. Soc. 1446 (1960).
3. C. WALLING and B. B. JACKNOW. J. Am. Chem. Soc. **82**, 6113 (1960).
4. G. A. RUSSELL. J. Org. Chem. **23**, 1407 (1958).
5. G. A. RUSSELL and R. C. WILLIAMSON, JR. J. Am. Chem. Soc. **86**, 2357 (1964).
6. R. D. GILLIOM and B. F. WARD, JR. J. Am. Chem. Soc. **87**, 3944 (1965).
7. L. A. COHEN. J. Org. Chem. **22**, 1333 (1957).
8. H. M. TEETER and E. W. BELL. Org. Syn. **32**, 20 (1952).
9. A. A. ZAVITSAS and S. SELTZER. J. Am. Chem. Soc. **86**, 3836 (1964).
10. H. C. BROWN and W. H. BONNER. J. Am. Chem. Soc. **76**, 605 (1954).
11. H. KWART and P. S. FRANCIS. J. Am. Chem. Soc. **77**, 4907 (1955).
12. J. A. HOWARD. Unpublished results.
13. R. E. PEARSON and J. C. MARTIN. J. Am. Chem. Soc. **85**, 3142 (1963).
14. T. G. BONNER and R. A. HANCOCK. Chem. Ind. London, 267 (1965).
15. M. ASSCHER. Chem. Ind. London, 1430 (1965).
16. M. ANBAR and D. GINSBERG. Chem. Rev. **54**, 925 (1954).
17. J. H. T. BROOK and R. W. GLAZEBROOK. Trans. Faraday Soc. **56**, 1014 (1960).
18. S. H. WILEN and E. L. ELIEL. J. Am. Chem. Soc. **80**, 3309 (1958).
19. D. H. MCDANIEL and H. C. BROWN. J. Org. Chem. **23**, 420 (1958).
20. Y. OKAMOTO and H. C. BROWN. J. Am. Chem. Soc. **80**, 4979 (1958).
21. A. A. ZAVITSAS. J. Org. Chem. **29**, 3086 (1964).
22. D. J. CARLSSON, J. A. HOWARD, and K. U. INGOLD. Unpublished results.
23. C. WALLING. Free radicals in solution. John Wiley & Sons, Inc., New York. 1957. p. 139.
24. J. E. HODGKINS and E. D. MEGARITY. J. Am. Chem. Soc. **87**, 5322 (1965).
25. K. M. JOHNSTON and G. H. WILLIAMS. J. Chem. Soc. 1446 (1960).
26. L. M. STOCK and H. C. BROWN. J. Am. Chem. Soc. **84**, 1242, 3298 (1962).
27. J. A. HOWARD and K. U. INGOLD. Can. J. Chem. **43**, 2737 (1965).

Can. J. Chem. Downloaded from www.nrcresearchpress.com by 210.87.254.6 on 09/05/12
For personal use only.

SOME STUDIES OF SLOW ROTATIONS AROUND BONDS IN AMIDES

T. H. SIDDALL III

Savannah River Laboratory, E. I. du Pont de Nemours and Co., Aiken, South Carolina

AND

R. H. GARNER

Department of Chemistry, University of Alabama, University, Alabama

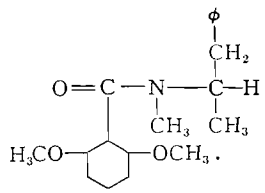
Received May 19, 1966

ABSTRACT

Studies were made of the relative rates of rotation around the benzene-to-carbonyl, carbonyl-to-nitrogen, and nitrogen-to-benzene bonds in some α-naphthamides, *o*-substituted benzamides, and related compounds. In general bulky substituents on the nitrogen atom tend to increase the rate of rotation around the carbonyl-to-nitrogen bond, but to decrease the rate around the benzene-to-carbonyl bond. Naphthanilides with *o*-substitution in the benzene ring have a rapid rate of rotation around the naphthalene-to-carbonyl bond compared with other naphthamides. Relative rates of rotation can be rationalized on the basis of combined steric and electronic effects.

INTRODUCTION

In preliminary work (T. H. Siddall III and R. H. Garner, submitted to Tetrahedron Letters) it was established that rotation is slow around the ring-carbonyl bond in the benzamide,



This paper reports the further exploration of the factors that affect the rotation around this bond and the carbonyl-to-nitrogen (amide) bond in various benzamides and related compounds, and compares qualitatively the rate of rotation around the ring-carbonyl bond with the rate around other bonds within the same molecule.

EXPERIMENTAL

The amides in this paper were prepared and purified by techniques described previously (1). All proton magnetic resonance spectra were taken on a Varian A-60 spectrometer equipped with a variable temperature insert.

RESULTS

Results are given in Table I (some additional information is included in the figures). The symbol $\langle \nu_a - \nu_b \rangle$ denotes the chemical shift in p.p.m. between non-equivalent methylene protons with AB patterns. The symbol $\langle \nu_1 - \nu_9 \rangle$ is the distance between the first and ninth signals (because of overlap this is actually the first and seventh) of the ABC_3 pattern for the non-equivalent methylene protons of ethyl groups. Where two amide isomers exist, the signals for the more abundant (major) isomer have been set in italics. Coupling constants are given in c.p.s. With only a few exceptions, $J_{AB} = 14$ c.p.s. for both the AB and ABC_3 patterns (ABX_3 approximation). Except where specifically noted, $CDCl_3$ was the solvent. The only other solvent employed was *sym*-tetrachloroethane. The concentration was 250 mg/ml for all solutions. Relative abundance

Can. J. Chem. Downloaded from www.nrcresearchpress.com by 210.87.254.5 on 09/05/12
For personal use only.

of isomers is expressed as a ratio (such as 1.3:1 for compound VI). Tetramethylsilane was used as a reference.

DISCUSSION

Rotation around Amide Bond

The effects of slow rotation around the carbonyl-to-nitrogen (amide) bond is observable in all compounds except VIII, for which rotation around this bond may be rapid, even at −40°. For the 2-substituted benzamides, coalescence of amide signals in general occurs at about the same or a slightly higher temperature than it does in acetamides (2; 3; also, unpublished work from this laboratory) and at a somewhat higher (as much as 50°) temperature than for benzamides not substituted in the ring. For the 2,6-dimethoxy benzamides (IX and X), coalescence occurs above 100 °C, in the same range as for formamides.

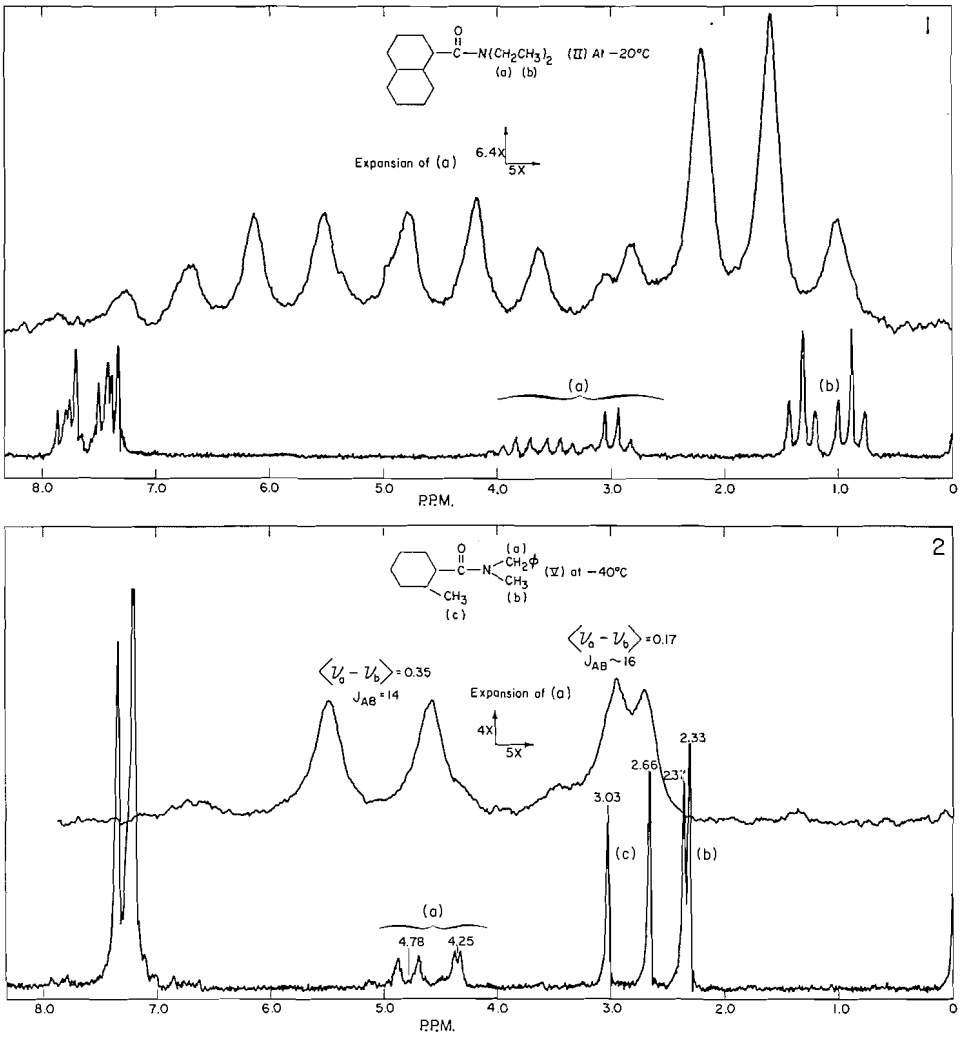
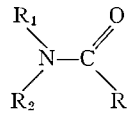


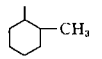
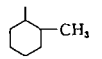
FIG. 1. Proton magnetic resonance spectrogram for compound II.
FIG. 2. Proton magnetic resonance spectrogram for compound V.

Can. J. Chem. Downloaded from www.nrcresearchpress.com by 210.87.254.5 on 09/05/12
For personal use only.

Can. J. Chem. Downloaded from www.nrcresearchpress.com by 210.87.254.5 on 09/05/12
For personal use only.

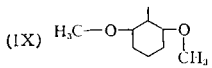
TABLE I

Proton magnetic resonance data for amides, 

No.	Amide R	Amide R_1	Amide R_2	Data and observations: R	Data and observations: R_1	Data and observations: R_2	Interpretation
(I)		Ethyl	Ethyl	—CH_3 at 2.31 at −40° 2.28 at −20° 2.27 at 0° 2.27 at 40° 2.26 at 60°	—CH_2— is two sets at −40°: 3.59, 3.13; 3.59 is non-equivalent, $\langle \nu_1 - \nu_9 \rangle = 0.64$, $J_{AB} = 14$ CH_3— is two sets: 1.27, 1.03 —CH_2— is two sets at −20°: 3.57, 3.10; 3.57 is non-equivalent, $\langle \nu_1 - \nu_9 \rangle = 0.60$ —CH_2— at 0° is broad hump + clear quartet: 3.11 —CH_2— at 40° is two quartets: 3.55, 3.08. CH_3— at 1.24, 1.00 —CH_2— at 60° is two broad humps. CH_3— one broad hump		—CH_2— non-equivalent in ethyl *cis* to R below about 0°, but coalescence is almost complete at 40°. Coalescence due to increasing rotation rate around amide bond begins at about 40°. but is not complete at 60°
(II)		Ethyl	Ethyl		—CH_2— is two sets at −20°: 3.60, 3.01; 3.60 is non-equivalent, $\langle \nu_1 - \nu_9 \rangle = 0.47$, $J_{AB} = 14$ CH_3 is two sets: 1.31, 0.90 (see Fig. 1) —CH_2— is two sets at 0°: much same as at −20°; CH_3— also —CH_2— 3.60 set very broad quartet at 40°; rest of signals slightly blurred At 60° all signals badly blurred		Rate of rotation around amide bond about same as I, but around ϕ-to-CO* bond is definitely slower than for I
(III)		2-Propyl	2-Propyl	—CH_3 at 2.32 at −40° 2.29 at 25° 2.30 at 40° 2.30 at 60°	At −40° two methine sets: 3.63, 3.51. Three CH_3— sets: 1.59, 1.11, 1.07; intensity 2:1:1 At 25° two methine: 3.63, 3.48. Three CH_3: 1.57, 1.09, 1.04; 1.09, 1.04 slightly broad At 40° methine partly coalesced. *Two* CH_3: 1.57, 1.08 (very broad) At 60° one methine set; 3.56. CH_3 broad hump		CH_3's non-equivalent in 2-propyl *cis* to R below about 40°. Rotation rate around amide bond faster than for I. Rotation rate around ϕ-to-CO bond much slower than for I
(IV)		2-Propyl	2-Propyl		At −20° two methine sets: 3.57, 3.55. Four equal CH_3— sets: 1.72, 1.65, 1.03, 0.97 At −20° two methine sets: 3.57, 3.54. Four equal CH_3— sets: 1.69, 1.62, 1.02, 0.97 sharp, but not ringing At 40° one broad methine set; four partly coalesced CH_3— sets At 60° one methine set: 3.57. Two humps for CH_3—		Rate of rotation around amide bond slightly faster than for III. Rate around ϕ-to-CO bond slower than for III

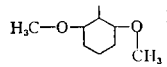
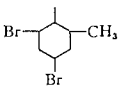
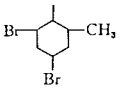
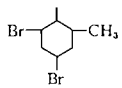
Can. J. Chem. Downloaded from www.nrcresearchpress.com by 210.87.254.5 on 09/05/12
For personal use only.

TABLE I (*Continued*)

	Amide				Data and observations		
No.	R	R_1	R_2	R	R_1	R_2	Interpretation
(V)		Benzyl	Methyl		See Fig. 2 for data at −40° —CH_2— non-equivalent in both isomers up to −10°. At 0° major has coalesced; minor still just resolved into two signals	(Signals for major isomer in italics here and for all entries that follow.)	Two amide isomers 1.4:1 at 25°, 1.3:1 at −20° (probably not at equilibrium). Amide coalescence well under way at 60°. Rotation around ϕ—CO much, much more rapid than around amide bond. Rotation around ϕ—CO more rapid in major amide isomer than it is in minor
(VI)		Benzyl	Methyl		—CH_2— is two sets at −30°: 4.85 (equivalent), *4.26* (AB pattern, blurred, $(\nu_a-\nu_b) \sim 0.1$); coalesces at 20° at 4.18 —CH_2— is two sets at 40°: 4.19, *4.80*	*3.10*, 2.60 at −30° 3.06, *2.68*	Two amide isomers 1.3:1 at 40°, but decreases below 1:1 at low temperatures (probably not at equilibrium at −30°). Rotation around ϕ—CO (4.26 at −30°) slower than in V (4.25 at −40°)
(VII)		Benzyl	2-Propyl	—CH_3 at *2.39*, 2.28 at −40° *2.37*, 2.27 at −30° 2.37, 2.26 at −20° 2.38, 2.23 at −20°	—CH_2— is *4.71*, 4.28 at −40°, −30°, −20°: *4.71* non-equivalent, $(\nu_a-\nu_b) = 0.2$, $J_{AB} = 16$; 4.28 equivalent. —CH_2— is *4.67* (singlet), 4.26 at 20°	CH_3— two broad doublets: 1.29, 1.09; one doublet: *0.098* at −20°, −30°, −40°. Coalesce to two doublets: 1.23, *0.99*, at 20°. Methine two sets: *3.80*, other mixed with —CH_2—	Two amide isomers 3:1 (signals for major isomer in italics). Major —CH_2—, minor βCH_3— non-equivalent at low temperature. Rotation around amide bond about same rate as in III; around ϕ-to-CO bond rotation is very much ($\geqslant$10?) faster
(VIII)		Benzyl	*t*-Butyl	—CH_3 at 2.35 at −40°	One signal: 4.48 at −40°, all blurred at 40 °C	One signal: 1.51 at −40°	No evident isomerism. Rotation rapid around all bonds
(IX)		Ethyl		At 40° —O—CH_3 at 3.79, *3.76*, *3.57*	At 40° two non-equivalent —CH_2—: *3.84*, $(\nu_1-\nu_9) = 1.21$; 3.7, $(\nu_1-\nu_9) = 0.41$. Two CH_3—: *1.17* 0.96	At 40° CH_3— at 2.36, *2.28*	Two amide isomers 2.4:1 in $CDCl_3$ at 40°. Two amide isomers 1.3:1 in *sym*-$C_2H_2Cl_4$, coalescence begins at about 90° and is complete at about 140 °C. Coalescence *not* in two separable stages

Can. J. Chem. Downloaded from www.nrcresearchpress.com by 210.87.254.5 on 09/05/12
For personal use only.

TABLE I (*Concluded*)

No.	Amide R	Amide R_1	Amide R_2	Data and observations R	Data and observations R_1	Data and observations R_2	Interpretation
(X)		Benzyl			See Fig. 4 for data in $CDCl_3$ at 60° —CH_2— two AB patterns: $(\nu_a-\nu_b)$ = 1.72 (−20°), *1.45 (60)*, 0.29 (−20°); partly coalesced (60°)		Amide isomers 2.9:1 in $CDCl_3$ at 60°; in *sym*-$C_2H_2Cl_4$ ratio is 1.8:1. Otherwise spectrum qualitatively same as in $CDCl_3$. Behavior with temperature is complex. Single sets of signals at 145°, but —CH_2— one broad hump. Rotation rates are: ϕ—N (minor) > amide bond > ϕ—CO (major)
(XI)		Ethyl		At 40° —CH_3 at 2.40 (note assignment with —CH_3 of R_2 may be interchanged)	At 40° two non-equivalent —CH_2—: *3.81*, $(\nu_1-\nu_9)$ = 0.95; ~3.4 (mixed with high field half of *3.81* set); $(\nu_1-\nu_9)$ much less than 0.95. CH_3—: *1.20*, 0.93	At 40° CH_3— at 2.33, *2.21* (see note under R)	Two amide isomers 3.2:1 at 40°; 2.3:1 at 0°. High field CH_3— (R_1) broad at −25°, −50° (third signal set?). In *sym*-$C_2H_2Cl_4$ isomer ratio is 1.2 at 40°. —CH_2— broad quartet at 145°; other signals are sharp, single sets. Rotation around amide bond more rapid than around ϕ—N.
(XII)		Methyl		At −20° —CH_3 at 2.57, *2.46*	At −20° —CH_3 at *3.53*, 3.17		Amide isomers 10:1 at −20°. Essentially same spectrum at −40°. No indication of additional isomerism
(XIII)				At 35° —CH_3 at *2.40*, 2.15	At 35° one non-equivalent set: ~3.7, overlaps a quartet *3.48* for —CH_2— CH_3— at 1.23, *0.97*	CH_3— at 35°: 2.46, *2.50*, ring-H two AB patterns with overlap, coupled to CH_3—, ~0.6 c.p.s.	Two amide isomers 2.0:1. No evidence for further isomerism even at −20°
(XIV)		Ethyl			See Fig. 3 for data in $CDCl_3$ at −40° and 25°	CH_3— at *2.47* broad at −10°, two definite signals but blurred at −20°. No additional signals even at ~−70°	Two amide isomers; equilibrium at 25° is 1.3:1 in $CDCl_3$, 1.3:1 at 60 °C in *sym*-$C_2H_2Cl_4$, 2:1 at 100°. Amide coalescence starts between 100–130°, but is not complete at 145°. ϕ—CO coalescence at −10 to 0°; rotation much, much faster than around amide bond
(XV)		Methyl			At 25° 3.39, *2.94* At −60° 3.47, *3.01* (broad)	At 25° CH_3— at *2.42*, 2.03 At −60° CH_3— at 2.54, 2.45, *2.07* (very broad) At −40° CH_3 at 2.47, just not quite two peaks At −45° CH_3 at 2.50, 2.44, *2.06*	Two amide isomers; equilibrium at 25° is 1.1:1 in $CDCl_3$, 1.7:1 at 100° in *sym*-$C_2H_2Cl_4$. Coalescence starts >100 °C, is not complete at 145°. ϕ—CO coalescence at −40 °C. Rotation many factors of 10 faster around ϕ—CO than around amide bond

*Aryl group to carbonyl bond.

It seems reasonable to conclude that the slower rotation around the amide bond (higher coalescence temperature) with increasing ortho substitution in the benzene ring attached to the carbonyl group reflects two effects. First, because of "steric inhibition of resonance", substitution decreases the effect of cross conjugation of the benzene ring with the carbonyl group (4) and thereby increases the double-bond character of the amide bond. Second, substitution on the benzene ring tends to lock the substituents on the nitrogen atom into a plane with the carbonyl group. This effect has already been noted for mesitamides (5).

This steric effect is evidently quite pronounced in favorable situations, even for cases with substitution on only one side of the ring. Essentially pure amide isomers were crystallized from ether for XV and from ethanol for XIV. On dissolution in $CDCl_3$ at 25° the equilibration of isomers was measured by observing the growth and decay of the separate signals. Both the N-methyl signals (3.39 grows in, while *2.94* decays) and the ring-methyl signals (2.03 grows in, while *2.42* decays) were utilized to monitor the equilibration for XV (see Fig. 3) while the ring-methyl signals only were used for XIV (1.98

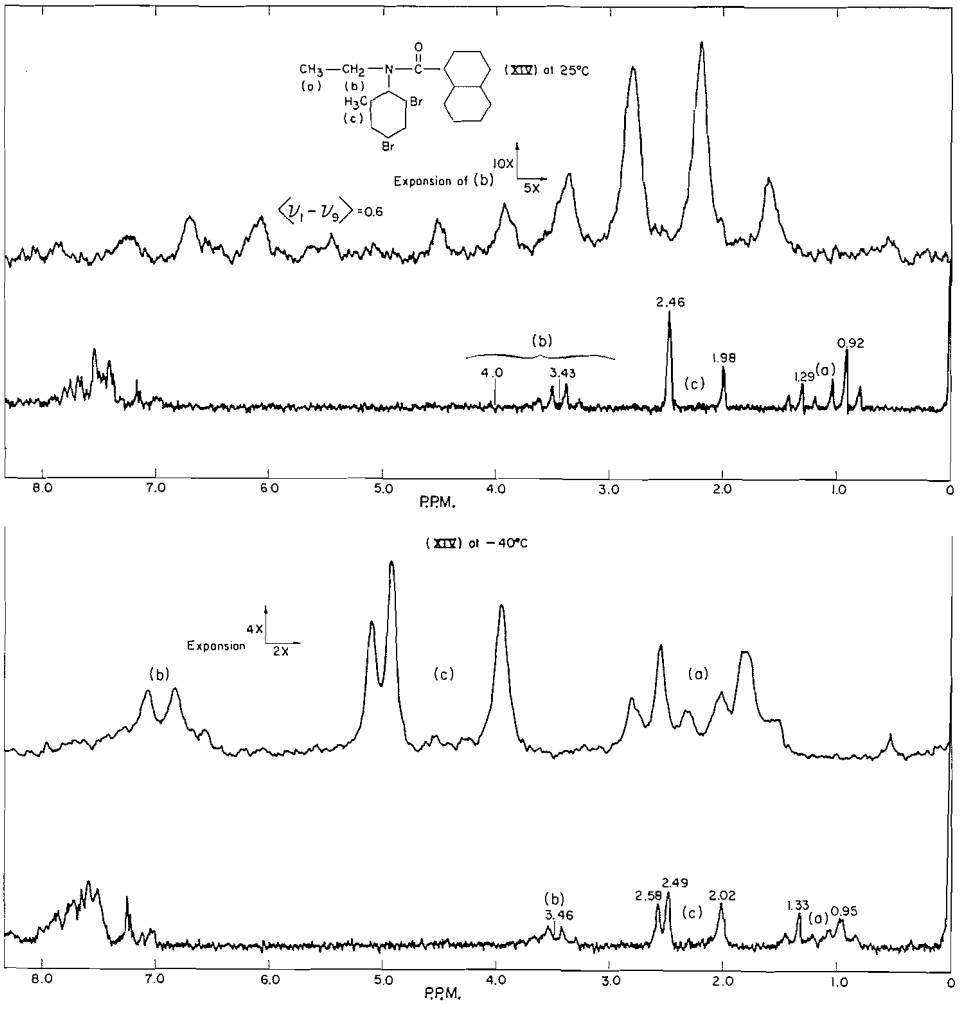


FIG. 3. Proton magnetic resonance spectrograms for compound XIV.

Can. J. Chem. Downloaded from www.nrcresearchpress.com by 210.87.254.5 on 09/05/12
For personal use only.

grows in, while *2.46* decays). The half-life of the forward reaction (major isomer to minor isomer) for XV is 70 min, whereas for the reverse reaction it is 60 min. For XIV the corresponding values are 22 min and 17 min. These half-lives lie in the same range as those obtained in this laboratory for N-ethyl-N-2,6-dimethylformanilide (6) and by Mannschreck (5) for N-methyl-N-benzyl mesitamide. The rotation around the amide bond in XIV is more rapid than in XV, as might be expected on the basis of steric factors.

Rotation around Benzene-to-Nitrogen Bond

Rotation around the benzene-to-nitrogen bond (IX through XV) occurs at about the same rate as rotation around the amide bond. However, since separate coalescence could not be clearly observed, it is not possible to make a more definite statement.

Rotation around the Ring-Carbonyl Bond

Appropriate comparisons between compounds I through VII show that increased size of substituents on nitrogen slows rotation around the ring-carbonyl bond. This effect could be predicted on the basis that the activated state for rotation around this bond would presumably place this benzene ring in the amide plane. As the amide plane becomes more crowded by larger substituents, the activated state for rotation at the benzene-to-carbonyl bond is pushed to a higher energy. However, with VIII, apparently the entire 360° of rotation has become crowded; there is no evidence for slow rotation around either the amide bond or the benzene-to-carbonyl bond.

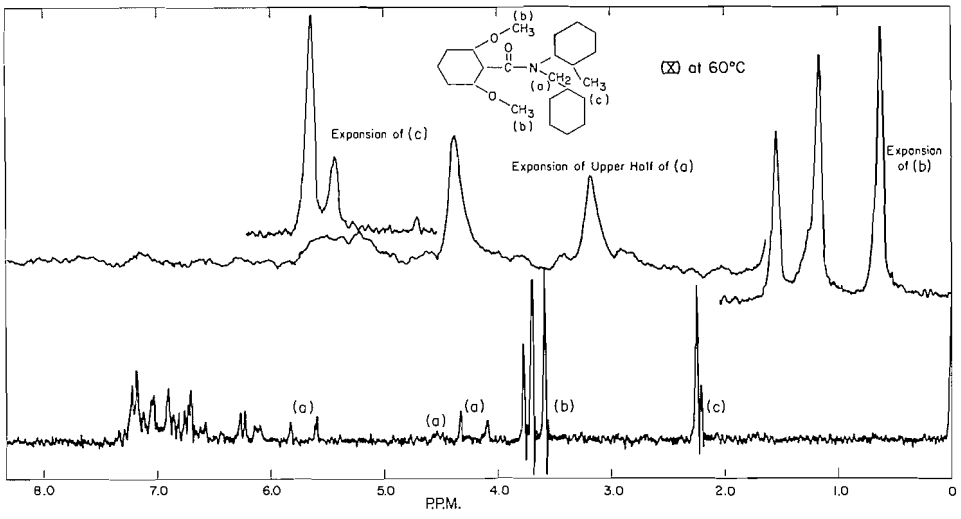


FIG. 4. Proton magnetic resonance spectrogram for compound X.

The spectra of XI, XIV, and XV show part of a third set of signals and, therefore, evidence for slow rotation around the ring-carbonyl bond.[1] However, this effect occurs only at much lower temperature than it does for I through VII.

[1]*Ortho substitution in both positions slows the half-life for rotation around the nitrogen-to-benzene bond to the order of 100 h even at 100 °C (7). However, for epimers to exist, as demonstrated by more than two sets of signals, rotation at the other asymmetry center (the ring-carbonyl bond) must also be slow.*

Can. J. Chem. Downloaded from www.nrcresearchpress.com by 210.87.254.5 on 09/05/12
For personal use only.

Interaction between Rotation Modes

There are several cases where it was possible to see clearly separate stages of coalescence for the two or three rotational modes and therefore to make qualitative assignments of relative rotation rates. For V, rotation around the ring-carbonyl bond was more rapid in the major than in the minor amide isomer. Even though the slow exchange chemical shift ($\langle \nu_a - \nu_b \rangle$) is greater for the geminal protons of the major isomer (see Fig. 2), the AB pattern for the major isomer coalesces at a lower temperature.

The spectrograms of compound X also permit considerable, detailed interpretation of relative rotation rates, as shown in Table I. Unfortunately the $\langle \nu_a - \nu_b \rangle$ for the major amide isomer for this compound is so much greater than other shifts associated with other rotational combinations that even qualitative comparison involving this particular rotation are difficult. However, after very close study of the spectrograms, assignment of the relative rotation rates is ring—N (minor) > ring—N (major) $\sim$ amide bond > ring—CO (major). Since only one signal is observable for the methoxy protons of the minor isomer, no assignment of relative rotation rate for the ring-carbonyl bond in the minor isomer can be made. More quantitative information can probably be obtained by changing substituents and (or) solvent.

ACKNOWLEDGMENT

The information contained in this article was obtained during the course of work under contract AT(07-2)-1 with the U.S. Atomic Energy Commission.

REFERENCES

1. T. H. SIDDALL III and C. A. PROHASKA. J. Am. Chem. Soc. **88**, 1172 (1966).
2. H. S. GUTOWSKY and C. H. HOLM. J. Chem. Phys. **25**, 1228 (1956).
3. A. G. WHITTAKER and S. SIEGEL. J. Chem. Phys. **43**, 1575 (1965).
4. M. T. ROGERS and J. C. WOODBREY. J. Phys. Chem. **66**, 540 (1962).
5. H. MANNSCHRECK. Tetrahedron Letters, 1341 (1965).
6 T. H. SIDDALL III. Inorg. Nucl. Chem. Letters, **1**, 155 (1965).
7. T. H. SIDDALL III. Tethrahedron Letters, 4515 (1965).

Can. J. Chem. Downloaded from www.nrcresearchpress.com by 210.87.254.5 on 09/05/12
For personal use only.

Can. J. Chem. Downloaded from www.nrcresearchpress.com by 210.87.254.105 on 09/05/12
For personal use only.

THE IONIZATION BEHAVIOR OF AMIDES IN CONCENTRATED SULFURIC ACIDS

III. INDICATOR ACTIVITY COEFFICIENT VARIATION

LINDA M. SWEETING[1] AND KEITH YATES
Department of Chemistry, University of Toronto, Toronto, Ontario

Received May 10, 1966

ABSTRACT

Activity coefficient data for ten substituted benzamides and two benzamide salts have been obtained from solubility measurements in 0–70% sulfuric acid. The ionic activity coefficients have been referred to a standard ion, the tetraethylammonium ion. The variations of activity coefficient with acid concentration are discussed and compared with available data for anilines and anilinium ions. Estimates have been made of the relative importance of the various terms contributing to the total acidity function for sulfuric acid. Up to 40% acid the order of importance of these terms is $f_{H^+} > f_{AH^+} > C_{H^+} > f_A$ and in more concentrated acids becomes $f_{H^+} \gg f_{AH^+} \gg f_A > C_{H^+}$.

Hammett-type acidity functions such as H_0 (1, 2), which is based on the ionization of a set of primary aniline indicators $B + H^+ \rightleftharpoons BH^+$ and is defined by

$$[1] \qquad H_0 = -\log a_{H^+} f_B / f_{BH^+} = pK_{BH^+} - \log C_{BH^+}/C_B,$$

have recently been shown to be more sensitive to variations in indicator structure than was at one time supposed. Although Hammett (3) originally pointed out that different acidity scales would be required for positive, neutral, and negatively charged indicator bases, it has recently been demonstrated that several different scales can be established even for neutral Brönsted bases which are structurally different (4–6). These have been shown to depend particularly on the nature of the site protonated in the equilibrium $In + H^+ \rightleftharpoons InH^+$. The acidity function determined using a set of primary amide indicators (6), and defined in an analogous way,

$$[2] \qquad H_A = -\log a_{H^+} f_A / f_{AH^+} = pK_{AH^+} - \log C_{AH^+}/C_A$$

is quite different from that based on primary amines. This is not unexpected, since amides have been shown to be protonated on the carbonyl oxygen (7) and are therefore oxonium type bases.

From eqs. [1] and [2], the dependence of the measured acidity of an aqueous mineral acid solution on indicator structure may be correlated with the variation in the activity coefficients of the species involved in the protonation equilibria. If it is assumed that a_{H^+} is a function only of the acid concentration, then

$$[3] \qquad H_0 - H_A = \log f_{BH^+} f_A / f_B f_{AH^+}.$$

Further, such differences in activity coefficient behavior may be related qualitatively to the hydration requirements of the base and conjugate acid forms (6, 8).

Boyd (9) has recently measured the activity coefficients of indicators of several types and has found that within a particular group of bases such as substituted anilines there are quite large variations in the individual values of $\log f$ for both neutral bases and conjugate acids, although the ratio $\log f_{BH^+}/f_B$ must have a similar medium dependence

[1]*Present address: Department of Chemistry, University of California, Los Angeles, California 90024.*

for each indicator. We have now investigated the activity coefficient behavior of several amides to determine the extent to which H_A is dependent on f_A and f_{AH^+} and to compare the relative importance of the amide and aniline activity coefficient terms in eq. [3]. Although it is generally assumed that differences such as that in eq. [3] in the measured acidity of a medium towards different types of base are essentially due to the conjugate acid terms, the relative importance of the log f_{InH^+} and log f_{In} terms has never been established, although Boyd's results show that variation in the log f_B terms is by no means negligible.

DETERMINATION OF ACTIVITY COEFFICIENTS

Activity coefficients were determined from the solubilities of the indicators in sulfuric acid – water solutions, essentially as described by Boyd (9). For any two saturated solutions the activities of a solute i in equilibrium with pure solid i are equal, hence

$$a_i(1) = f_i(1)C_i(1) = f_i(2)C_i(2) = a_i(2).$$

Therefore if the reference state ($f = 1$) is taken to be a dilute solution of the indicator in pure water (w), the activity coefficient in any sulfuric acid solution (a) is given by

$$f_i(a) = C_i(w)/C_i(a).$$

For a 1:1 electrolyte, the mean ionic activity coefficient is similarly

$$f_\pm(a) = C_\pm(w)/C_\pm(a),$$

where $f_\pm^2 = f_+f_-$. Since the cation and anion terms are inseparable, the single ion activity coefficients can only be estimated indirectly. If the electrolyte is highly dissociated in the medium used, it is possible to estimate the cation activity coefficient behavior by comparing two cations which have a common anion, since

$$f_\pm^2(BA)/f_\pm^2(CA) = f_{B^+}f_{A^-}/f_{C^+}f_{A^-} \cong f_{B^+}/f_{C^+}$$

if the ionic activity coefficients are reasonably independent of each other. In solvents of such high dielectric constant as sulfuric acid – water mixtures, the assumption of separability of the cation and anion activity coefficients is quite reasonable for comparisons of dilute solutions of cations of similar charge and size, since their interactions with the anion should be similar and tend to cancel (10). Following Boyd's example we have chosen the 1,1,2,3,3-pentacyanopropenide ion (PCP^-) as counter ion since this is a large charge-delocalized anion which is not protonated over the entire acid range used and would not be expected to interact specifically with other species in the medium. Similarly we have used the tetraethylammonium ion (TEA^+) as standard cation, so that all our cationic activity coefficients are referred back to this standard ion, i.e.

$$f_{AH^+}f_{PCP^-}/f_{TEA^+}f_{PCP^-} = f_{AH^+}/f_{TEA^+} = f^*_{AH^+}$$

Thus our results can be compared directly with Boyd's log $f^*_{BH^+}$ values for the anilinium ions.

The range of acid solutions over which log f_A and log f_{AH^+} values can be measured is limited experimentally by the protonation equilibria of these bases. The compounds studied must remain essentially unprotonated or protonated (depending on whether f_A or f_{AH^+} is being measured) over the particular range of acid investigated. Therefore only the weaker bases can be used to study f_A over a reasonable range, and only the stronger bases to study f_{AH^+}. A particular difficulty with the amides arises because these are considerably

Can. J. Chem. Downloaded from www.nrcresearchpress.com by 210.87.254.105 on 09/05/12
For personal use only.

weaker bases than the corresponding anilines, and no amide is available whose cation will remain unhydrolyzed in dilute aqueous acids. Therefore estimates of $\log f_{AH^+}$ are particularly difficult to obtain. The method by which this can be circumvented will be described in a later section.

EXPERIMENTAL

Preparation of Amides and Salts

The substituted benzamides were either obtained commercially, or prepared from the corresponding benzoic acids as described previously (6) and were recrystallized from aqueous ethanol to constant melting point.

Tetraethylammonium and pyridinium pentacyanopropenides were prepared by the method of Middleton *et al.* (11) and recrystallized from water. Melting points were 222–223.5 °C for TEA^+PCP^- and 165.5–167 °C for Py^+PCP^-.

The pentacyanopropenide salts of benzamide and *p*-methoxybenzamide were prepared by mixing equivalent amounts of the amide and pyridinium pentacyanopropenide dissolved in the minimum volumes of warm sulfuric acid and cooling to 0 °C. The amidonium pentacyanopropenides precipitated as yellow needles, which, however, could not be completely dried of the concentrated sulfuric acid required to ensure complete protonation of the amide before mixing. These needles were filtered off and washed with further sulfuric acid before being used to make up saturated solutions in the sulfuric acids of interest. Attempts to prepare pure pentacyanopropenide salts of the other more strongly basic amides were unsuccessful. Since preparation requires precipitation of the least soluble of four salts, the amide salts are subject to contamination by pyridinium and bisulfate salts. This could be detected by comparing the ratio of optical densities at the amide conjugate acid and PCP^- maxima (412 mμ). If the ratio D_{amide}/D_{412} was independent of the concentration of acid used to prepare the salt, it was assumed that only AH^+PCP^- had been precipitated, and in the cases of all the benzamide and some of the *p*-methoxybenzamide solutions the total ultraviolet absorption corresponded to that expected for AH^+ and PCP^- absorption. Contamination by bisulfate ion (which is transparent in the region of the spectrum investigated) resulted in too high a D_{amide}/D_{412} ratio, and contamination by pyridinium ion resulted in a low ratio and a peak at 250 mμ. If was not considered worthwhile to prepare salts of the weakly basic nitro- and dinitro-substituted amides since their range of usefulness would be too limited by hydrolysis even in moderately concentrated acids.

Preparation of Solutions

Sulfuric acid – water solutions were prepared by diluting CIL reagent grade acid ($\geqslant 98$ %) and concentrations determined by titrating weighed samples with standard sodium hydroxide.

Saturated solutions of both amides and salts were obtained by shaking mixtures of the solid with the appropriate acid solution for about 15–20 h in a water bath at 25 ± 0.5 °C. Samples were taken during this time and analyzed spectrophotometrically until the concentration of solute no longer increased. In a few cases the concentration began to decrease slowly after prolonged exposure to the sulfuric acid, presumably due to hydrolysis. In these cases log *D* was extrapolated to zero time to obtain corrected values for the solubility.

Samples of the saturated solutions were obtained by filtering carefully through fine glass wool into temperature-equilibrated flasks. A 1.0 ml aliquot was then withdrawn by means of a calibrated Hamilton syringe with Chaney adaptor and diluted to a known volume with water. Concentrations were then determined from the ultraviolet absorbance at the amide maximum for the neutral amides and at the pentacyanopropenide maximum for the salts.

Simple corrections were applied to take account of protonation in the case of the f_A determinations and hydrolysis in the case of the f_{AH^+} determinations, but in most solutions studied protonation or hydrolysis was less than 10%.

RESULTS AND DISCUSSION

Activity Coefficients of Neutral Amides

The bases investigated were all substituted benzamides, since these were predominantly used as indicators in establishing the H_A acidity scale (6). The solubility data and calculated activity coefficients ($\log f_A$ values) are listed in Table I. The results show generally that the neutral amide is "salted in" by the acid, except at the lower acid concentrations in a few cases. A plot of typical $\log f_A$ behavior with increasing acid concentration is shown in Fig. 1 for compounds containing different numbers of nitro substituents. This indicates that log *f* values for amides are generally more negative and decrease more rapidly with acid concentration than those for the corresponding aniline type bases. The $\log f_B$ values for 2,4-dichloro-6-nitroaniline and 2,4-dinitroaniline are shown for comparison (9). Like

Can. J. Chem. Downloaded from www.nrcresearchpress.com by 210.87.254.105 on 09/05/12
For personal use only.

Can. J. Chem. Downloaded from www.nrcresearchpress.com by 210.87.254.105 on 09/05/12
For personal use only.

TABLE I

Activity coefficient data for neutral amides

% acid	C_{obs}[a]	C_{corr}[b]	$\log f_A$	C_{obs}	C_{corr}	$\log f_A$
	o-Toluamide (λ_{max} = 253 mμ)			*p*-Chlorobenzamide (λ_{max} = 238 mμ)		
0.0	4.92	4.92	0.000	0.819	0.819	0.000
10.1	4.36	4.23	0.065	0.756	0.740	0.045
19.7	4.46	3.94	0.095	0.777	0.756	0.061
24.1	4.63	3.05	0.206			
29.1	6.70	2.41	0.248	1.05	0.664	0.004
40.1				2.87	1.45	−0.249
	m-Nitrobenzamide (λ_{max} = 263 mμ)			*p*-Nitrobenzamide (λ_{max} = 266 mμ)		
0.0	1.56	1.56	0.000	0.518	0.518	0.000
4.9	1.52	1.52	0.012	0.522	0.521	−0.004
10.1	1.58	1.57	−0.004	0.543	0.539	−0.018
19.7	1.80	1.74	−0.048	0.595	0.575	−0.047
29.1	2.44	2.22	−0.152	0.810	0.732	−0.151
40.1	5.69	4.15	−0.425	1.97[c]	1.45	−0.455
52.8				9.45[c]	3.55	−0.836
	Benzamide (λ_{max} = 227 mμ)			2,4-Dinitrobenzamide (λ_{max} = 240 mμ)		
0.0	10.16	10.16	0.000	0.411	0.411	0.000
4.9	10.08	10.08	0.019			
10.1	10.1	9.87	0.023	0.451	0.451	−0.040
16.1	10.1	9.27	0.041			
19.7				0.521	0.518	−0.108
20.4	14.6	12.75	−0.098			
28.6	17.8	12.73	−0.098			
34.4				0.959	0.934	−0.356
48.3				3.50	3.08	−0.876
	3,5-Dinitrobenzamide (λ_{max} = 217 mμ)			3,5-Dinitro-4-methylbenzamide (λ_{max} = 217 mμ)		
0.0	0.36	0.36	0.000	0.881	0.881	0.000
4.9	0.42	0.42	−0.067	0.729	0.728	0.083
10.1	0.43	0.43	−0.068	0.719	0.716	0.090
16.1	0.52	0.52	−0.165			
20.4	0.58	0.58	−0.205	0.907	0.889	−0.004
28.6	0.94	0.93	−0.410	1.33	1.26	−0.156
38.9	2.03	1.94	−0.731	3.13	2.65	−0.478
45.3	4.10	3.73	−1.02	6.21	4.61	−0.719
51.7	9.25	7.68	−1.33			
55.1	15.98	12.01	−1.52			
	3,5-Dinitro-2,4-dichlorobenzamide (λ_{max} = 216 mμ)			3,4,5-Trimethoxybenzamide (λ_{max} = 257 mμ)		
0.0	1.05	1.05	0.000	0.589	0.589	0.000
4.9				0.562	0.527	0.048
10.1	1.61	1.61	−0.186	0.563	0.545	0.034
16.1				0.542	0.497	0.074
20.4	1.84	1.84	−0.243	0.638	0.556	0.024
28.6	2.32	2.31	−0.342	1.03	0.731	−0.094
38.9	3.02	2.97	−0.452			
45.3	5.52	5.34	−0.706			
51.7	10.2	9.54	−0.959			
55.1	14.4	12.98	−1.09			
64.1	46.3	33.3	−1.50			

[a]All concentrations are in $10^2 \times M$ of the saturated solution based on D at wavelength given for each amide.
[b]Corrected for protonation using pK values in ref. 6.
[c]Concentrations obtained by extrapolation of log D to zero time.

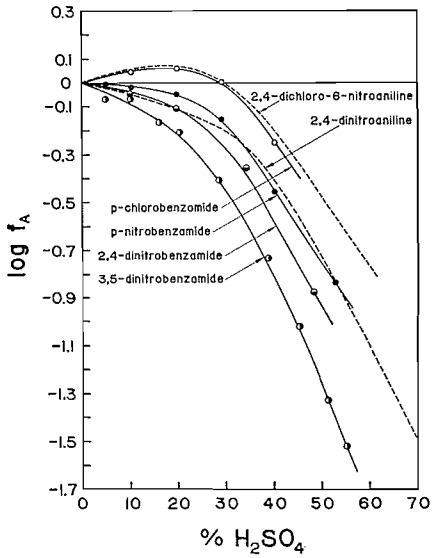
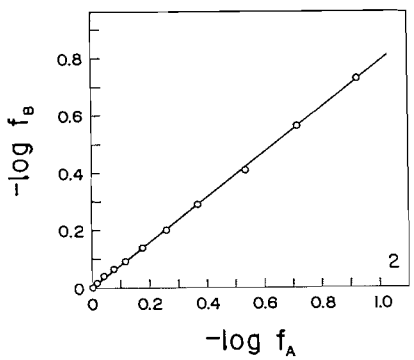


FIG. 1. Typical activity coefficient variation with acid concentration for substituted benzamides.

the aniline indicators, the amides give increasingly negative log f values as the number of nitro groups is increased. This is presumably due to strong hydrogen-bond interactions between these groups and the acidic solvent. The only direct comparison which can be made between log f_A and log f_B values for two bases with identical substituents is shown in Fig. 2, where log f_A for 2,4-dinitrobenzamide is plotted against log f_B for 2,4-dinitroaniline. Since the two compounds were studied in different acid solutions, interpolated values have been used. The remarkable straight line obtained shows that the two types of base respond qualitatively in the same way to changes in the medium, but the less than unit slope shows that the amino group is more sensitive than the amido group to decreases in the water content of the medium (i.e. anilines are "salted in" less rapidly with increasing acid than amides).

Activity Coefficients of Salts

Solubility and activity coefficient data for benzamidonium, *p*-methoxybenzamidonium, and tetraethylammonium pentacyanopropenides are listed in Table II. For the latter



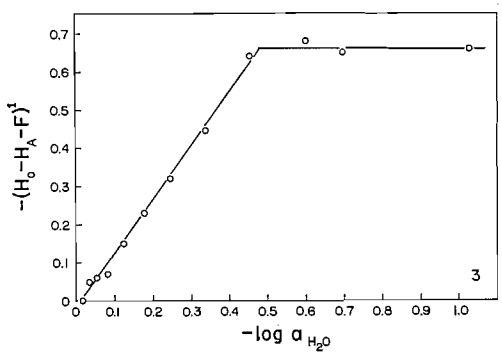


FIG. 2. Relationship between log f_A for 2,4-dinitrobenzamide and log f_B for 2,4-dinitroaniline.
FIG. 3. Water activity variation of the function $(H_0 - H_A - F)^1$ using first approximate log $f^1_{AH^+}/f_{TEA^+}$ values.

Can. J. Chem. Downloaded from www.nrcresearchpress.com by 210.87.254.105 on 09/05/12
For personal use only.

TABLE II*a*

Activity coefficient data for tetraethylammonium pentacyanopropenide

% acid	$10^2 \times D^a$	$\log f_{\pm}$
0.0	0.500	0.000
4.8	0.725	−0.161
9.6	0.810	−0.210
19.0	0.905	−0.258
29.1	1.11	−0.346
40.0	2.39	−0.680
43.7	2.90[b]	−0.763
50.5	5.87	−1.070
58.3	11.4[b]	−1.358
60.2	16.9[c]	−1.528
67.4	24.3[b]	−1.687
70.0	57.8[c]	−2.063

[a]All absorbance values based on PCP^- absorption at 412 mμ.
[b]Data obtained in the present work.
[c]Corrected values obtained from R. H. Boyd (14). Values for these acids in ref. 9 are incorrect.

TABLE II*b*

Activity coefficient data for benzamidonium and *p*-methoxybenzamidonium pentacyanopropenide

% acid	$10^2 \times D^a$	$10^2 \times D_{corr}{}^b$	$\log f_{\pm}$	$\log f^{\circ}_{AH^+}/f_{TEA^+}$
Benzamidonium pentacyanopropenide				
52.8	5.54	4.76	0.000	0.00
58.3	5.86	5.49	−0.062	0.38
62.7	6.65	6.42	−0.130	0.78
67.4	8.86	8.71	−0.263	1.06
72.5	14.11	14.01	−0.469	1.26
p-Methoxybenzamidonium pentacyanopropenide				
43.7	3.09	2.61	0.000	0.00
52.8	4.70	4.39	−0.225	0.16
62.7	2.70	2.66	−0.008	0.87

[a]Values obtained by extrapolation of log *D* to zero time for benzamide.
[b]Corrected for hydrolysis using p*K* values in ref. 6.

compound Boyd's original data have been supplemented and in some cases corrected. The data for the *p*-methoxybenzamidonium salt is limited because of the coprecipitation problem discussed earlier, and only the data for benzamidonium pentacyanopropenide is suitable for estimation of $\log f_{AH^+}$ values. Calculation of $\log f_{AH^+}/f_{TEA^+}$ for this compound is complicated by the fact that benzamides are much weaker bases than anilines. Therefore the benzamidonium ion is completely hydrolyzed in dilute aqueous solution and the usual standard state for the activity coefficients is experimentally inaccessible. A convenient first reference state can be defined as the lowest acid concentration in which the salt can be studied without serious interference from hydrolysis. These values are designated as $\log f^0_{AH^+}$. To obtain a set of values for $\log f_{AH^+}$ based on the same standard state as the $\log f_{BH^+}$ values for anilines, the following procedure was used. As a first approximation, all activity coefficients for the benzamidonium ion up to and including the above reference acid (52.8% sulfuric acid) were assumed to be the same as those for the anilinium ion itself. This first approximation is designated as $\log f^1_{AH^+}$ in Table III. Since according to

Can. J. Chem. Downloaded from www.nrcresearchpress.com by 210.87.254.105 on 09/05/12
For personal use only.

TABLE III

Calculation of the function $(H_0 - H_A - F)^1$

% acid	$-\log f_A$[a]	$-\log f_B$[b]	$\log f_{BH^+}/f_{TEA^+}$[c]	$\log f^1_{AH^+}/f_{TEA}$	$-(H_0-H_A-F)^1$[d]
10	0.03	0.03	0.23	0.23	0.00
15	0.06	0.06	0.32	0.32	0.05
20	0.11	0.09	0.42	0.42	0.06
25	0.18	0.13	0.68	0.68	0.07
30	0.27	0.20	0.97	0.97	0.15
35	0.39	0.29	1.32	1.32	0.23
40	0.55	0.41	1.71	1.71	0.32
45	0.73	0.56	1.98	1.98	0.44
50	0.94[e]	0.73	2.21	2.21	0.64
55	1.21[e]	0.92	2.41	2.54	0.68
60	1.45[e]	1.10	2.55	2.93	0.65
65	1.70[e]	1.30	2.65	3.26	0.66
70				3.52	

[a]From the data in Table I for 2,4-dinitrobenzamide.
[b]From the data in ref. 9 for 2,4-dinitroaniline.
[c]From the data in ref. 9 for anilinium ion.
[d]Values of H_0 and H_A taken from refs. 2 and 6.
[e]Obtained from a short extrapolation of the line in Fig. 2.

eq. [3] the experimentally observed difference between the H_0 and H_A functions must be accounted for entirely by the activity coefficient ratio

$$F = \log f_{BH^+} f_A / f_B f_{AH^+}$$

the function $(H_0 - H_A - F)$ was calculated for all concentrations up to 65% sulfuric acid, using the data for the 2,4-dinitro compounds for the neutral base activity coefficients and the unsubstituted compounds for the conjugate acids. (Since the first approximate values for the $\log f_{AH^+}$ were used, this function is designated in Table III as $(H_0 - H_A - F)^1$.) Ideally all the bases and conjugate acids for such a calculation should have the same substituents but it is experimentally impossible to study both the base and conjugate acid of any one compound in the same range of acid concentrations. However, it was hoped that by choosing each pair of bases or conjugate acids with the same substituents any large effect of substituents on the individual activity coefficients would cancel.

Since activity coefficients are usually a smooth function of the water activity, $(H_0 - H_A - F)^1$ was plotted against $\log a_{H_2O}$ as shown in Fig. 3. The figure consists of two linear portions: from dilute aqueous solution up to the first reference state (52.8% acid) the function has a slope of 1.44 (correlation coefficient 0.996) and for all acids above the first reference state it is essentially constant with a value of -0.66 ± 0.01. Since the function plotted should be constant over the whole range and hence independent of the water activity this value represents a constant difference in activity coefficient between that of the first reference state and that of dilute aqueous solution. The first part of the curve gives the correction for the error made in the 0–50% range by assuming $f_{AH^+} = f_{BH^+}$ below the reference state concentration. Smoothing all these values by least squares and adding them to $\log f_{AH^+}/f_{TEA}$ gives $\log f_{AH^+}/f_{TEA^+}$ values for the whole acid range, now based on dilute aqueous solution as standard state (Table IV). Using these values the function $H_0 - H_A - \log f_{BH^+} f_A / f_B f_{AH^+}$ now has the value 0.00 ± 0.01 over the range 0–65% acid and the estimated values of $\log f_{AH^+}/f_{TEA^+}$ are a smooth function of the acid concentration over the entire range as shown in Fig. 4. The corresponding curve for anilinium ion is included for comparison. This shows that the benzamidonium ion is "salted

Can. J. Chem. Downloaded from www.nrcresearchpress.com by 210.87.254.105 on 09/05/12
For personal use only.

TABLE IV

Final values of activity coefficients for benzamidonium ion

% acid	$-(H_0-H_A-F)$[1] [a]	$\log f_{AH^+}/f_{TEA^+}$	$H_0 - H_A - \log f_{BH^+}f_A/f_Bf_{AH^+}$
10	0.01	0.24	0.00
15	0.03	0.35	−0.03
20	0.06	0.48	0.00
25	0.10	0.78	+0.03
30	0.16	1.13	+0.01
35	0.23	1.55	0.00
40	0.33	2.04	+0.01
45	0.46	2.44	+0.01
50	0.63	2.84	−0.01
55	0.66	3.20	−0.02
60	0.66	3.59	+0.01
65	0.66	3.92	0.00
70	0.66	4.18	
			Mean 0.00±0.01

[a]Smoothed values obtained from least squares plot in Fig. 3 using water activity data in ref. 15.

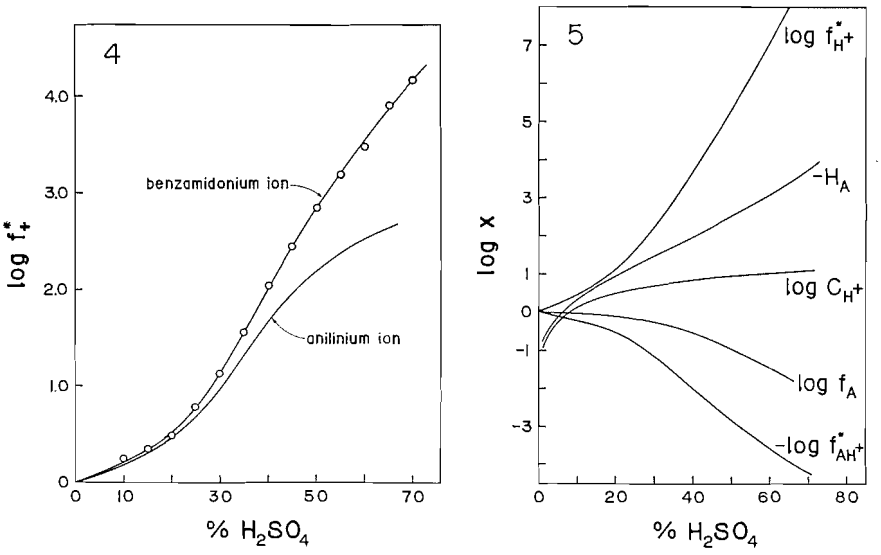


FIG. 4. Comparison of the concentration dependence of $\log f^*_{AH^+}$ for benzamide and $\log f^*_{BH^+}$ for aniline.

FIG. 5. Concentration dependence of individual terms contributing to the H_A acidity function $(-H = \log f^*_{H^+} + \log C_{H^+} + \log f_A - \log f^*_{AH^+})$.

out" more rapidly than anilinium ion, especially above 40% acid. Thus the amide ions are appreciably more sensitive to decreasing water content of the medium than the corresponding anilinium ions.

Analysis of Acidity Function Variation

We are now in a position to assess the relative importance of the various terms which contribute to the total acidity of aqueous sulfuric acids towards these organic bases. The H_A function can be expressed as

$$[4] \qquad -H_A = \log f_{H^+} + \log C_{H^+} + \log f_A - \log f_{AH^+}.$$

Can. J. Chem. Downloaded from www.nrcresearchpress.com by 210.87.254.105 on 09/05/12
For personal use only.

Values of log C_{H^+} can be calculated by assuming that the first dissociation of H_2SO_4 is essentially complete in the range 0–70% acid, and by using the known value of K_2. An estimate of log f_A can be made from the data in Table I either by averaging log f_A values for all the amides studied or by choosing one amide as representative. The latter seems preferable since a smoother function of concentration is obtained. Since the log f_A curve for 2,4-dinitrobenzamide occupies a central position when all the data in Table I is plotted against % H_2SO_4, its behavior was chosen as typical. No direct estimates can be made of the ionic terms in eq. [4] since the log $f^*_{AH^+}$ values are all related to the standard ion TEA^+. However, if the equation is rewritten as

$$-H_A = \log f_{H^+}/f_{TEA^+} + \log C_{H^+} + \log f_A - \log f_{AH^+}/f_{TEA^+},$$

values of log $f^*_{AH^+}$ for benzamidonium ion can be used to calculate values of log f_{H^+}/f_{TEA^+}. Since there is no possibility of obtaining single ion activity coefficients such as f_{TEA^+}, only the relative importance of the various contributions to H_A can be estimated. These are plotted in Fig. 5 as a function of acid concentration. Since there is reason to believe that the tetraethylammonium ion would not show large activity coefficient variation with medium (9, 12) it is unlikely that the positions of these curves would be changed greatly even if the correct values were accessible. It is reasonable to expect that TEA^+ would be "salted in" over most of the range studied, so that the curves for log f_{H^+}/f_{TEA^+} and log a_{AH^+}/f_{TEA^+} should probably be shifted upwards. It is also unlikely that substitution of log f_A or log $f^*_{AH^+}$ data for other compounds would change the relative positions of these two curves greatly.

It can be seen from Fig. 5 that except for the very dilute acid range where all values of f approach unity the most important single contribution to the acidity function is the f_{H^+} term. In the 5–40% range the order of importance is

$$f_{H^+} > f_{AH^+} \geqslant C_{H^+} > f_A$$

and in the more concentrated region it is

$$f_{H^+} \gg f_{AH^+} \gg f_A > C_{H^+}.$$

Although the f_{H^+} term is clearly the most important, it is clear that the variation of log f_{AH^+} has a powerful moderating effect on the magnitude of the acidity function. Although it is frequently assumed that activity coefficient variations of the neutral indicators are of little importance, it can be seen that log f_A contributes approximately half as much as log f_{AH^+} to the overall logarithmic acidity scale. The least important term (except for very dilute solutions) is that involving the stoichiometric hydronium ion concentration. The major influence of increasing the acid concentration results from the corresponding decrease in the water activity. As the available water is drastically reduced, the free energies of the ionic species are greatly increased, due to their inability to achieve sufficient solvation through hydrogen bonding. This is most pronounced for the hydronium ion which can form three very strong hydrogen bonds to other water molecules (13).

A similar treatment of the H_0 function can be made using Boyd's data for the anilines (9). The results are qualitatively similar to those in Fig. 5. The reason for the marked differences in acidity of aqueous mineral acids towards anilines (H_0) and amides (H_A) is twofold. Firstly, the AH^+ species is "salted out" to a greater extent than BH^+, especially in the more concentrated acids. This leads to the conclusion that amide conjugate acids are more strongly hydrated than the corresponding anilinium ions. Secondly, and equally important, is the fact that neutral amides are "salted in" to a greater extent than neutral

Can. J. Chem. Downloaded from www.nrcresearchpress.com by 210.87.254.105 on 09/05/12
For personal use only.

anilines. Thus the free amides are less strongly hydrated than the corresponding anilines. Therefore differences in hydration of both the neutral and cationic species contribute almost equally to the greater overall hydration changes (6, 8) produced when amides are protonated as compared with the protonation of anilines.

ACKNOWLEDGMENTS

We wish to thank the National Research Council for financial support. We are also grateful to the Province of Ontario for the award of a Graduate Fellowship to one of us (L.M.S.).

REFERENCES

1. L. P. HAMMETT and A. J. DEYRUP. J. Am. Chem. Soc. **54**, 2721 (1932).
2. M. J. JORGENSON and D. R. HARTTER. J. Am. Chem. Soc. **85**, 878 (1963).
3. L. P. HAMMETT. Physical organic chemistry. McGraw-Hill Book Co., Inc., New York and London. 1940. p. 269.
4. R. L. HINMAN and J. LANG. J. Am. Chem. Soc. **86**, 3796 (1964).
5. E. M. ARNETT and G. W. MACH. J. Am. Chem. Soc. **86**, 2671 (1964).
6. K. YATES, J. B. STEVENS, and A. R. KATRITZKY. Can. J. Chem. **42**, 1957 (1964). K. YATES and J. B. STEVENS. Can. J. Chem. **43**, 529 (1965).
7. T. BIRCHALL and R. J. GILLESPIE. Can. J. Chem. **41**, 2642 (1963).
8. E. M. ARNETT and G. W. MACH. J. Am. Chem. Soc. **88**, 1177 (1966).
9. R. H. BOYD. J. Am. Chem. Soc. **85**, 1555 (1963).
10. H. S. FRANK. J. Phys. Chem. **67**, 1554 (1963).
11. W. J. MIDDLETON, E. L. LITTLE, D. D. COFFMAN, and V. A. ENGELHARDT. J. Am. Chem. Soc. **80**, 2795 (1958).
12. N. C. DENO, H. E. BERKHEIMER, W. L. EVANS, and H. J. PETERSON. J. Am. Chem. Soc. **81**, 2344 (1958).
13. R. P. BELL. The proton in chemistry. Cornell Univ. Press, Ithaca, N.Y. 1959. pp. 83–84.
14. R. H. BOYD. Personal communication.
15. R. A. ROBINSON and R. H. STOKES. Electrolyte solutions. 2nd ed. Butterworths, London. 1959. p. 477.

Can. J. Chem. Downloaded from www.nrcresearchpress.com by 210.87.254.105 on 09/05/12
For personal use only.

Can. J. Chem. Downloaded from www.nrcresearchpress.com by 210.87.254.6 on 09/05/12
For personal use only.

SOLVENT SHIFTS IN CHARGE-TRANSFER SPECTRA. INFLUENCE OF DONOR STRENGTH

H. M. ROSENBERG, E. EIMUTIS, AND D. HALE
Air Force Materials Laboratory, Research and Technology Division, Wright-Patterson Air Force Base, Ohio
Received June 6, 1966

ABSTRACT

The charge-transfer transition energies for a series of methylbenzene–tetracyanoethylene complexes in four solvents are reported. The charge-transfer transition energies are found to decrease with increasing solvent refractive index. The magnitude of the decrease appears to be a function of donor strength. It is inferred that the excited state dipole moment decreases with increasing donor strength for these complexes.

A number of authors have attempted to account for the influence of solvent on electron donor-acceptor complex spectra (1). Thus, solvent shifts have been attributed to dielectric constant of solvent (1*a*, *b*, *f*), solvent interaction with donor and acceptor species (1*c*), *Z*-value of solvent (1*d*, *f*), and specific solvent interaction (1*e*). None of these hypotheses provide a satisfactory description of experimentally observed solvent shifts. In a previous study of aromatic hydrocarbon – tetracyanoethylene (TCNE) complexes (2), we found that the charge-transfer absorption bands vary monotonically with index of refraction of solvent, the transition energy decreasing with increasing index of refraction. Support for this relationship was found in published data for other π-complexes (3). Voigt has recently confirmed these observations (4). We interpreted these results by postulating an interaction between the induced solvent dipole and the excited state of the complex (2, 3).

The magnitude of the solvent shifts observed in our first study appeared to depend on the donor. This paper reports the results of a detailed investigation of this effect for methylbenzene-TCNE complexes.

RESULTS AND DISCUSSION

Consistent with our previous observations (2, 3), the transition energies of the complexes decrease with increasing solvent refractive index. The decrease in the transition energies in going from acetonitrile to chloroform is shown in the last column of Table I. The energy changes appear to be a function of donor ionization potential, being greatest for the benzene–TCNE complex and least for the hexamethylbenzene–TCNE complex. The same trend is exhibited for the solvent shifts between any pair of solvents in Table I. The gas-to-solution frequency shifts for methylbenzene–TCNE complexes are reported by Voigt (4). These shifts are consistent with our data.

A number of theoretical relationships have been derived for correlating electronic spectral shifts with solvent properties (5). Experimental support for the Bilot and Kawski equation (5*c*) was advanced in a recent study (6). For molecules of similar size this treatment yields the following approximation:

$$[1] \qquad \frac{\Delta E(\mathrm{I})}{\Delta E(\mathrm{II})} = \frac{\mu_e^2(\mathrm{I}) - \mu_g^2(\mathrm{I})}{\mu_e^2(\mathrm{II}) - \mu_g^2(\mathrm{II})}$$

where ΔE is the energy difference for an electronic transition in two nonpolar solvents; μ_e and μ_g are excited and ground state dipole moments respectively; I and II identify different complexes. The literature μ_g values for methylbenzene–TCNE complexes show

TABLE I

Charge-transfer transition energies* of TCNE complexes in various solvents

Donor	I_D†	CH_3CN	*n*-Hexane	CH_2Cl_2	$CHCl_3$	$E_\pi(CH_3CN) - E_\pi(CH_3Cl)$
Solvent n_D‡		1.346	1.375	1.424	1.446	
Benzene	9.25	3.51	3.28	3.22	3.16	0.35
Toluene	8.82	3.21	3.07	3.01	2.99	0.22
o-Xylene	8.56	2.98	2.92	2.82	2.81	0.17
m-Xylene	8.56	3.02	2.90	2.82	2.82	0.20
p-Xylene	8.45	2.84	2.68	2.62	2.65	0.19
1,2,3-Trimethylbenzene	8.48	2.79	2.72	2.64	2.63	0.16
Mesitylene	8.39	2.79	2.72	2.65	2.64	0.15
Pentamethylbenzene	7.92	2.51	2.46	2.38	2.39	0.12
Hexamethylbenzene	7.85	2.38	2.36	2.29	2.28	0.10

*Energy at absorption maxima, eV.
†Donor ionization potential, eV. Data from ref. 11.
‡Solvent index of refraction at 20°.

a maximum value of 1.35 D for the hexamethylbenzene–TCNE complex (7) compared with $\mu_e \approx 11$ D for the hexamethylbenzene - tetrachlorophthalic anhydride complex (8). Therefore:

$$[2] \qquad \frac{\Delta E(\mathrm{I})}{\Delta E(\mathrm{II})} \approx \frac{\mu_e^2(\mathrm{I})}{\mu_e^2(\mathrm{II})}$$

Application of eqs. [1] and [2] requires that the charge-transfer transition energy for a given complex show a linear dependence on $(n^2 - 1)/(2n^2 + 1)$ for the choice of solvents, where n is solvent refractive index.

Voigt has reported charge-transfer transition data for several methylbenzene–TCNE complexes in two sets of solvents which satisfy the above condition (4). From the ratio of the slopes obtained from the plot of charge-transfer energy vs. $(n^2 - 1)/(2n^2 + 1)$, (ref. 4) and assuming μ_e value of 12.0 D for the benzene–TCNE complex, we calculated from eq. [2] the μ_e values shown in Table II. These computed data have no absolute significance but show relative values based on an arbitrary choice of μ_e for the benzene–TCNE complex. The maximum value of μ_e is 15.3 D, based on an interplanar distance of 3.2 Å. The actual value is reduced by resonance and inductive effects. It is noteworthy that the calculated values for μ_e show a decreasing trend with decreasing ionization potential of donor.

According to Mulliken (9) the wave functions for the ground and excited states of a complex can be represented as follows:

$$[3] \qquad \psi_N \approx a\psi_0(\mathrm{D, A}) + b\psi_1(\mathrm{D^+ - A^-})$$

$$[4] \qquad \psi_E \approx a^*\psi_1(\mathrm{D^+ - A^-}) - b^*\psi_0(\mathrm{D, A})$$

where $a^2 \gg b^2$; $a^{*2} \gg b^{*2}$; neglecting overlap, $a^* \approx a$; $b^* \approx b$.

Briegleb has shown that the excited state dipole moment can be expressed as follows:

$$[5] \qquad \mu_e = \mu_1(a^{*2} + a^*b^*S) \approx a^{*2}\mu_1$$

where μ_1 is the dipole moment of the dative form of the complex (10).

Since the interplanar distances in π-complexes are generally similar, the dipole moments of the dative forms, which represent a complete electron transfer, can be considered constant. The excited state dipole moments are therefore proportional to a^*. It is reasonable to assume that the ground state resonance contribution of the dative canonical form

Can. J. Chem. Downloaded from www.nrcresearchpress.com by 210.87.254.6 on 09/05/12
For personal use only.

will vary directly with donor strength, i.e. b increases and a decreases with donor strength. This premise is supported by μ_g data for π-complexes with methyl benzene donors (10). Since $a^* \approx a$ and $b^* \approx b$, a^* and b^* should exhibit the same dependence on donor strength.[1] It is therefore predicted that as donor strength of a complex increases, μ_g should increase and μ_e decrease. The computed values presented in Table II are consistent with these deductions, and the ΔE_π data shown in Table I are also in good qualitative agreement. Quantitative μ_e comparisons, through use of eq. [2], cannot be made for these data since polar solvents were used in obtaining these measurements.

TABLE II

Excited state dipole moments of TCNE complexes

Donor	$\Delta E_\pi/\Delta f(n)$*	μ_e†
Benzene	1.11	12‡
p-Xylene	0.87	10
Mesitylene	0.80	10
Durene	0.74	10
Hexamethylbenzene	0.52	8.3

*Data from ref. 4; E_π in $cm^{-1} \times 10^{-3}$; $f(n) = (n^2 - 1)/(2n^2 + 1)$; n is solvent index of refraction; hydrocarbon solvents.
†Debye units.
‡Assumed value (arbitrary).

EXPERIMENTAL

All solvents were spectroquality grade reagents and all donors were the highest purity commerically available hydrocarbons and were used without further purification. The TCNE was sublimed twice *in vacuo*. Solutions were prepared to give charge-transfer bands having optical densities of 0.4 to 0.5, using excess donor. Spectra were measured on a Cary model 11 spectrophotometer in tared 1 cm quartz cells, with pure solvent as reference. Where there was evidence for overlapping double bands, spectra were resolved according to the method of Voigt and Reid (10). Data for charge-transfer transition energies at the absorption maxima are given in Table I together with donor photoionization potentials (taken from ref. 11).

REFERENCES

1. (*a*) J. N. MURRELL. Quart. Rev. London, **15**, 191 (1961).
(*b*) S. F. MASON. Quart. Rev. London, **15**, 287 (1961).
(*c*) K. M. C. DAVIS and M. C. R. SYMONS. J. Chem. Soc. 2079 (1965).
(*d*) P. H. EMSLIE and R. FOSTER. Rec. Trav. Chim. **85**, 255 (1965).
(*e*) C. C. THOMPSON, JR. and P. A. D. DE MAINE. J. Phys. Chem. **69**, 2766 (1965).
(*f*) E. M. KOSOWER. J. Am. Chem. Soc. **80**, 3253 (1958).
2. H. M. ROSENBERG and D. HALE. J. Phys. Chem. **69**, 2490 (1965).
3. H. M. ROSENBERG. Chem. Commun. **14**, 312 (1965).
4. E. M. VOIGT. J. Phys. Chem. **70**, 598 (1956).
5. (*a*) E. LIPPERT. Z. Naturforsch. **10a**, 541 (1957).
(*b*) E. G. MCRAE. J. Phys. Chem. **61**, 562 (1957).
(*c*) VON L. BILOT and A. KAWSKI. Z. Naturforsch. **17a**, 621 (1962).
(*d*) Y. OOSHIKA. J. Phys. Soc. Japan, **9**, 594 (1954).
(*e*) N. G. BAKHSCHIEV. Opt. i Spekroskopiya, **10**, 717 (1961).
6. H. M. ROSENBERG and E. EIMUTIS. Spectrochim. Acta. In press.
7. L. J. ANDREWS and R. M. KEEFER. Molecular complexes in organic chemistry. Holden-Day, Inc., San Francisco. 1964. p. 111.
8. G. BRIEGLEB. Elektronen-Donator-Acceptor Komplexe. Springer-Verlag, Berlin. 1961. p. 19.
9. R. S. MULLIKEN. J. Chim. Phys. **61**, 20 (1964).
10. E. M. VOIGT and C. REID. J. Am. Chem. Soc. **86**, 3930 (1964).
11. K. WANTANABE. J. Chem. Phys. **26**, 542 (1957).

[1]*For calculated values of a^* and b^* see ref. 8.*

Can. J. Chem. Downloaded from www.nrcresearchpress.com by 210.87.254.6 on 09/05/12
For personal use only.

Can. J. Chem. Downloaded from www.nrcresearchpress.com by 210.87.254.6 on 09/05/12
For personal use only.

HIGH RESISTANCE ANODIC OXIDE FILMS ON ALUMINIUM

A. C. HARKNESS
British Columbia Research Council, Vancouver, British Columbia

AND

L. YOUNG
Electrical Engineering Department, University of British Columbia, Vancouver, British Columbia

Received October 25, 1965

ABSTRACT

The thicknesses of oxide films formed in aqueous borate solutions were obtained by the spectrophotometric method after developing the interference colors by evaporating a very thin film of gold or bismuth onto the oxide. The refractive index of the stripped films was determined by the Becke immersion method as 1.57 to 1.58 at 5 900 Å wavelength. The dielectric constant was estimated as 9.8 ± 0.5. Experimental data on the steady state ionic current density, I, through the oxide as a function of the field strength, E, in the oxide could be represented by $I = I_0 \exp -(W - qaE)/kT$ where $I_0 = 2.24 \times 10^7$ A cm^{-2}, $W = 1.3 \pm 0.15$ eV, $q = 3e$, $a = 2.95 \pm 0.15$ Å.

INTRODUCTION

The aim of this work was to investigate, as a contribution to the comparative study of the various film-forming metals, the dielectric and ionic conduction properties of the films formed on aluminium in dilute aqueous borate solutions. The anodic behavior of aluminium is far more sensitive to the nature of the electrolyte than is that of tantalum, and it is probable that different results would have been obtained with other electrolytes which give high resistance films. The present films are, of course, quite different from the low resistance films which are produced in sulfuric acid and some other electrolytes.

The high resistance films have been reported by Franklin (1) to resemble the low resistance films in having a cell (or honeycomb) structure, though without pores. It is not clear how general this result is, and an earlier report (2) of cell structure in high resistance films shows that it is not invariably present. If it is present, the thickness determinations presumably refer to a mean value, and the associated differences in the solubility of the film material in Altenpohl's reagent (chromic plus phosphoric acid) at different places in the cells introduces a further complication. The present films were formed to comparatively small thicknesses at which they are reported to be amorphous; crystalline oxide is reported (3) to appear only at greater thicknesses (apart from any hydrated oxide present before anodization).

Several investigations have been made of the kinetics of formation, and several other investigations have been concerned with determining the "angstroms per volt" at a single current density. The first work was by Güntherschulze and Betz (4) who used the capacity to determine the thickness. The dielectric constant was taken as the mean of 7.04 and 7.85 obtained from thickness calibrations by weight gain determinations, and by measurement of electrical resistance changes, respectively. The current efficiencies reported were quite low as was to be expected from the purity of the available metal. These measurements were of interest in establishing that the dependence of I on E could be represented by

$$I = A \exp BE \qquad [1]$$

where I = ionic current density and E = field strength in the oxide. Charlesby (5) obtained data by several methods and based his field strengths on the value of Güntherschulze and Betz at $I = 10\ \mu A\ cm^{-2}$. Bernard and Cook (6) used substantially non-aqueous solutions and estimated thickness by weighing, capacity, and Faraday's Law methods. They found $(\partial E/\partial \log I)_T$ to be constant, in accordance with eq. [1]. Dignam, Goad, and Sole (7) have presented evidence to show that with Bernard and Cook's electrolyte the behavior of aluminium is better described by an equation of the form proposed by Young (8, p. 99) for tantalum.

Among the determinations of thickness and other properties, reference is made to the work of Hennig (9) using an interference method (Köster double prism) and to the work of Van Geel and Schelen (10) who found the dielectric constant to be 8.7 with various methods of determining the thickness.

EXPERIMENTAL PROCEDURES

The specimens were cut from 99.99% purity sheet by a die in the shape of a rectangle with a small tab at one end. A wire lead was spot welded to the tab. Several methods of surface preparation were tried. Finally, the specimens were etched in a 10% sodium hydroxide solution, chemically polished in a bath of concentrated orthophosphoric, sulfuric, and nitric acids in the volume ratio 70:25:5 at 85° for 5 min, and then formed to 200 V. The wire lead and the tab were covered with Picien wax. The exposed specimen of about 2 cm^2 in area was then etched in 1:1 hydrofluoric acid and reformed to 200 V. The etching and forming procedure was repeated several times with the final etching being done just before use. This method tended to give a more constant rate of voltage rise during formation at constant current density than did the other methods tried. The electrolyte was a 20 g/l recrystallized orthoboric acid solution which was adjusted to a pH of 7 with concentrated ammonium hydroxide. The measurement of pH was done on a small portion of the electrolyte to avoid contamination of the main body of the electrolyte by chloride ions.

The films were formed at constant current using an automatic electronic control which terminated the formation at the required potential with respect to a reference electrode and which indicated the time to traverse the successive 1 or 10 V intervals during formation. A specimen was inserted into the cell with care being taken to avoid touching the large concentric cylinder of platinized platinum which served as the cathode during formation and as the counter electrode for capacity measurements. The cell was immersed in a constant temperature bath. During formation the electrolyte was stirred to avoid heating effects. The specimen was formed to 10 V at 10 mA cm^{-2} and the capacity measured. The specimen was then formed to a higher voltage at the current density of the experiment and the capacity measured again. A different specimen was used for each formation voltage.

The films, as formed, showed only very faint interference colors. This is evidently due to the comparatively low refractive index of the oxide which causes the Fresnel coefficient for the oxide/air interface, r_1, to be small compared with that for the oxide/metal interface, r_2. The colors, as was shown by Güntherschulze and Betz, may be rendered quite intense by laying down by evaporation a very thin, invisible layer of metal. This process evidently increases the magnitude of r_1. A layer of bismuth was used in the first experiments, but in the later work gold was used instead since it was found to give sharper and more reproducible minima in the specular reflectivity. There was no significant difference between the wavelength of the minimum obtained with gold and that obtained with bismuth. Tests made with varying small amounts of the two metals showed no significant variation, so that the process was considered to be sufficiently controlled for the present purpose. The scatter is greater than for tantalum or niobium which do not require such treatment to enhance their colors and which are less sensitive to impurities in the solution. The peaks were moderately sharp from 2 700 Å to 4 000 Å. The measurements could be carried to 2 700 Å before interference from the intrinsic absorption of the oxide.

RESULTS AND DISCUSSION

The function $[Q\Delta(1/C)]^{1/2}$, where Q is the charge to form an increment of thickness starting with a film formed to 10 V at 10 mA cm^{-2} and $\Delta(1/C)$ is the change in the reciprocal of the capacity at 1 kc/s, gives a measure of the increments of thickness of the film (8, p. 78). This measure is in terms of ρ/ϵ, the ratio of the density of the film to its dielectric constant, and is independent of the knowledge of the surface area. This assumes 100% current efficiency, an assumption which we justify later.

Figure 1 shows a plot of grouped averages for many specimens of $[Q\Delta(1/C)]^{1/2}$ plotted against the wavelengths of minimum reflectivity. Each point covers a wavelength range of 400 to 900 Å and includes from 4 to 12 specimens. Specimens formed at 0 and 25 °C

Can. J. Chem. Downloaded from www.nrcresearchpress.com by 210.87.254.6 on 09/05/12
For personal use only.

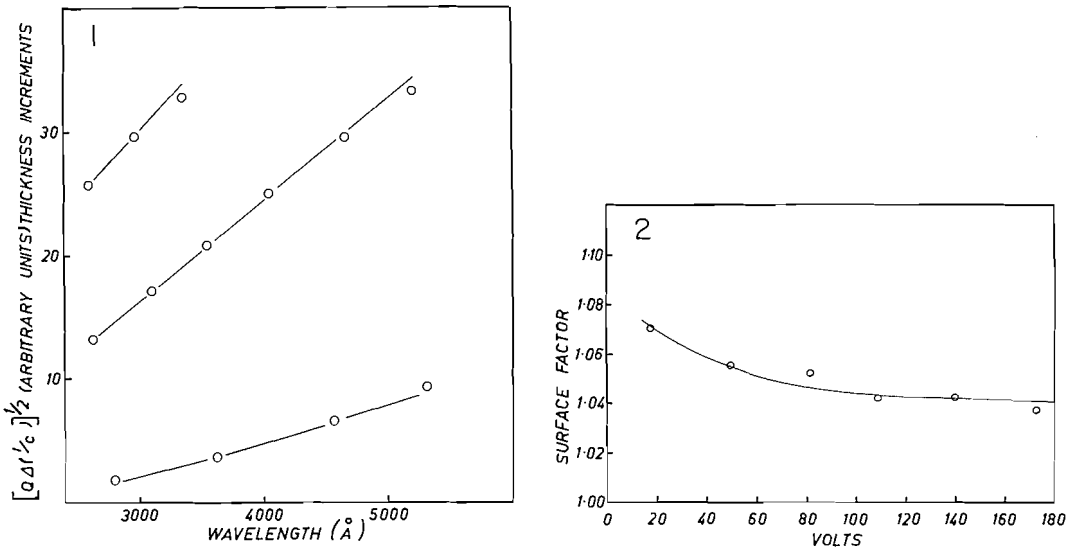


FIG. 1. Grouped averages of thickness increments from charge and capacity data vs. wavelength of minimum reflectivity of films.

FIG. 2. Grouped averages of the ratio of effective to apparent area calculated from charge and capacity data vs. formation voltage.

with current densities from 0.1 to 10 mA cm^{-2} were included. The units of $[Q\Delta(1/C)]^{1/2}$ are arbitrary in that time was measured in counts (120 s^{-1}) and capacities in microfarads.

The increment in thickness at a wavelength λ between consecutive orders of interference is $\lambda/2n \cos\theta$, if the refractive index, n, is constant, and where θ = angle of refraction. The refractive index of films isolated by using a bromine and methanol mixture to dissolve the metal was found by the Becke immersion method to be 1.57 to 1.58. The standard reference liquids were calibrated using an Abbé refractometer. Using a monochromator, the anomalous decrease in n at 4 360 Å reported by Hennig (9) was not detectable. The above value for n agrees with Hennig's value at the same wavelength but not with that of Van Geel and Schelen (10). The variation between the values reported by different authors is so large that it appears to be beyond experimental error; very probably the films formed under different conditions are different in structure.

Taking $n = 1.58$ at 3 600 Å, which is justified by the low dispersion of the oxide in this region shown by Hennig's results and confirmed by the present results, we obtain a value of $\rho/\epsilon = 0.306$. Taking a round number value of $\rho = 3.0$ g cm^{-3} (which is within about 5% of values reported by Van Geel and Schelen and by Bernard and Cook) we obtain $\epsilon = 9.8$ with about $\pm 5\%$ uncertainty. With these values the ordinate of Fig. 1 may be converted to cm by multiplying by 6.52×10^{-7}.

The function $[Q/\Delta(1/C)]^{1/2}$ measures the effective area (8, p. 78). Data averaged in groups of the ratio of effective to apparent area are shown in Fig. 3. These indicate that the effective area is only a few percent greater than the apparent area. The larger ratios found by Plumb (11) are for abraded surfaces. The fact that the plotted quantity is only slightly greater than unity shows that the current efficiency must have been close to 100%.

The field strengths estimated with the thickness obtained from the capacity and the charge passed, respectively, using the apparent area, showed a tendency to increase and to decrease respectively with increasing thickness. However, when the area-independent function, $[Q\Delta(1/C)]^{1/2}$, was used to obtain the thickness the field strengths were substantially independent of thickness. Some results for experiments at 0 °C are shown in Fig. 3.

Can. J. Chem. Downloaded from www.nrcresearchpress.com by 210.87.254.6 on 09/05/12
For personal use only.

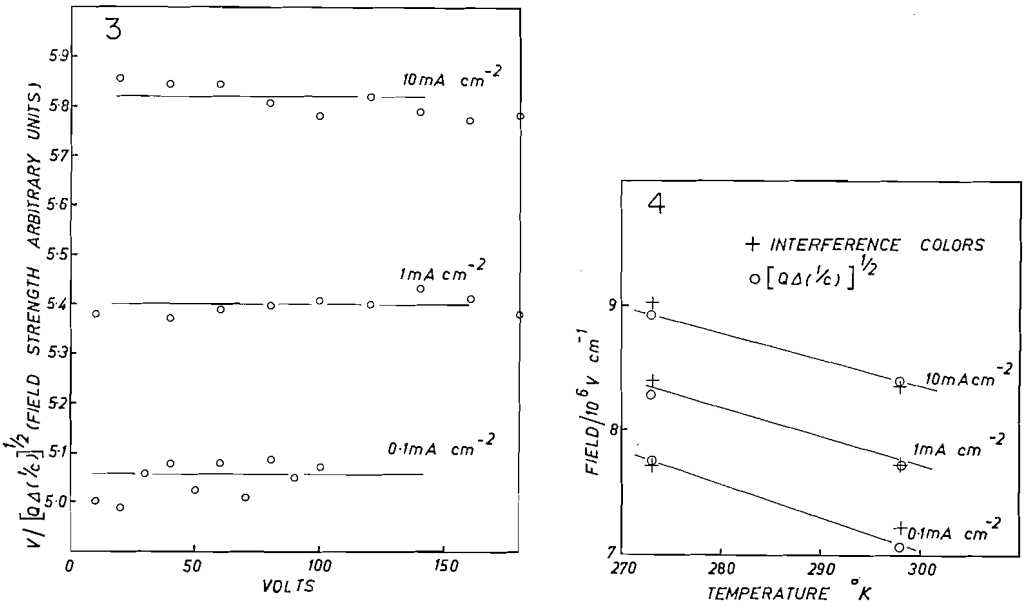


FIG. 3. Field strengths using $[Q\Delta(1/C)]^{1/2}$ for film thickness vs. formation voltage. Various current densities at 0 °C.

FIG. 4. Field strengths from $[Q\Delta(1/C)]^{1/2}$ and interference colors as a function of formation temperature. Colors made to agree with $[Q\Delta(1/C)]^{1/2}$ at 25 °C and 1 mA cm^{-2}.

(Field strengths in V cm^{-1} can be obtained by multiplying by 1.53×10^6.) The scatter was similar at 25 °C, but at 40 °C the results were more scattered and for films formed at temperatures above 40 °C the capacity changed markedly and continuously with the time—evidently due to hydrolysis.

Field strengths were also estimated by using estimates of the thickness obtained from the wavelengths of interference, taking a plot of wavelengths of interference vs. voltage for films formed at 1 mA cm^{-2} at 25 °C as a reference chart. The field was taken as the slope of plots of voltage vs. thickness.

Mean values of the field using $[Q\Delta(1/C)]^{1/2}$ excluding data from very small and from very large increments of thickness are shown in Fig. 4, together with fields estimated from the colors. Values at 40 °C were excluded since, as already stated, they were less reliable.

The straight lines shown in Fig. 4 correspond to

$$I = I_0 \exp - (W - qaE)/kT \qquad [2]$$

with $I_0 = 2.24 \times 10^7$ A cm^{-2}, $W = 1.3$ eV, and $a = 2.95$ Å, taking q as the valence charge $3e$. The uncertainties were estimated as ± 0.15 eV in W, ± 0.15 Å in a, and a corresponding error in I_0. These are the accuracies with which the constants are required to fit the results; the parameters are not independently determined to these accuracies.

The experimental data are consistent with the theoretical form, eq. [2], but the available temperature range was too small to detect whether the second order deviations which occur with tantalum and niobium also occur with aluminium. At 150 V and 25 °C in 30 wt. % ammonium pentaborate solution in ethylene glycol the data of Bernard and Cook derived from weight gain (with $\rho = 3.17 \pm 0.03$ g cm^{-3}), capacity (with $\epsilon = 8.4 \pm 0.2$), and Faraday's laws (with effective area taken as 1.03 times the apparent area from

Can. J. Chem. Downloaded from www.nrcresearchpress.com by 210.87.254.6 on 09/05/12
For personal use only.

comparison with chemically polished specimens) yield effective activation distances (defined by $a = BkT/q$ with $q = 3e$) of 4.1, 4.6, and 3.8 Å respectively. From weight gain and capacity, respectively, Bernard and Cook found $qa/kT = 4.8 \times 10^{-6}$ and 4.4×10^{-6} cm V^{-1} and the value of A in eq. [1] to be 10^{-22} and 10^{-20} A cm^{-2}.

In the present work from $A = I_0 \exp -(W/kT)$ we found the value of A at 25° to be $10^{-14.6}$ A cm^{-2}. It is easier to judge the significance of these results if the corresponding field strengths are calculated; the results are shown in Table I.

TABLE I

Field strength as a function of I

I (mA cm^{-2})	E (V $cm^{-1} \times 10^{-6}$)		
	Bernard and Cook (from weight gain)	Bernard and Cook (from capacity)	This work
10	9.60	9.64	8.44
1	9.11	9.10	7.77
0.1	8.64	8.57	7.10

The present data are about 15% lower which is evidently greater then experimental error. The fields are basically calibrated from the refractive index. Davies, Domeij, Pringle, and Brown (12) are therefore incorrect in suggesting the difference could be caused by the current efficiency being low. Their low current efficiencies were not obtained under comparable experimental conditions. It is noteworthy that, allowing for the different densities used, if we calculate the capacity to be expected for a film formed to a given voltage, the lower value of $\epsilon = 8.4 \pm 0.2$ found by Bernard and Cook as compared with the present value (9.8 ± 0.5) results in a compensation. These authors found that the capacity of films formed to a given voltage at a given current density in dilute aqueous solution of boric acid and in their non-aqueous solution were the same. This is found in analogous experiments with tantalum (13) though the films may differ markedly in optical thickness and in the charge required for their formation, so that it seems possible that there is a similar effect with aluminium. Randall, Bernard, and Wilkinson (14) have emphasized that the properties of anodic films depend on electrolyte composition even with dilute solutions and have found a similar inverse relation between dielectric constant and ionic resistivity for such dilute solutions.

Some of the results from the present work were quoted previously (8, p. 220).

ACKNOWLEDGMENT

We thank the Defence Research Board of Canada for supporting this work and for permission to publish it.

REFERENCES

1. R. W. Franklin. Nature, **180**, 1470 (1957).
2. F. Keller and A. H. Geisler. Trans. AIME, **156**, 82 (1944).
3. C. S. Taylor, C. M. Tucker, and J. D. Edwards. Trans. Electrochem. Soc. **88**, 325 (1945).
4. A. Güntherschulze and H. Betz. Z. Physik, **92**, 367 (1934).
5. A. Charlesby. Proc. Phys. Soc. London, B, **66**, 317, 533 (1953).
6. W. J. Bernard and J. W. Cook. J. Electrochem. Soc. **106**, 643 (1959).
7. M. J. Dignam, D. Goad, and M. Sole. Can. J. Chem. **43**, 800 (1965).
8. L. Young. Anodic oxide films. Academic Press, Inc., New York. 1961.
9. M. Hennig. Z. Physik, **144**, 296 (1956).
10. W. Ch. van Geel and B. J. J. Schelen. Philips Res. Rept. **12**, 240 (1957).
11. R. C. Plumb. J. Electrochem. Soc. **105**, 502 (1958).
12. J. A. Davies, B. Domeij, J. P. S. Pringle, and F. Brown. J. Electrochem. Soc. **112**, 675 (1965).
13. L. Young. Proc. Roy. Soc. London, Ser. A, **258**, 496 (1960).
14. J. J. Randall, Jr., W. J. Bernard, and R. R. Wilkinson. Electrochim. Acta, **10**, 183 (1965).

Can. J. Chem. Downloaded from www.nrcresearchpress.com by 210.87.254.6 on 09/05/12
For personal use only.

Can. J. Chem. Downloaded from www.nrcresearchpress.com by 210.87.254.5 on 09/05/12
For personal use only.

ELECTROPHILIC CATALYSIS IN SOLVOLYTIC REACTIONS

IX. INDUCTOMERIC EFFECT[1]

R. ANANTARAMAN AND M. R. NAIR[2]
Chemistry Department, University of Kerala, Trivandrum, India

Received March 16, 1966

ABSTRACT

The rates of solvolysis of 1-(*p*-alkylphenyl)ethyl chlorides (Alk = Me, Et, *i*-Pr, and *t*-Bu) in the presence and absence of mercuric chloride have been measured in aqueous acetone and ethanol solvents. In all cases, the Baker–Nathan order is followed. For all normal reactions and for the catalyzed reactions in 90% aqueous acetone and 90% aqueous ethanol there is an increase in the heats and entropies of activation as the series is ascended, while for the catalyzed reaction in 75% and 80% aqueous acetone, there is a decrease. It is suggested that in the more aqueous acetone solvents the catalyst calls into play an inductomeric effect. The effect of added chloride ions on the rate of hydrolysis has been studied and the results are discussed.

In a previous paper on the kinetics of mercuric chloride catalyzed hydrolysis of 1-phenylalkyl chlorides (Alk = Me, Et, *i*-Pr, and *t*-Bu), to understand the trend in the rates it was found necessary to postulate that the electrophilic catalyst brought into play an inductomeric mode of electron release from the alkyl groups (1). We have now studied the corresponding 1-(*p*-alkylphenyl)ethyl system from this standpoint.

RESULTS AND DISCUSSION

The first-order rate constants for the normal and catalyzed hydrolysis in aqueous acetone solvents and for the solvolysis in 90% aqueous ethanol, together with the values for the heats and entropies of activation, are given in Table I. Data for 1-phenylethyl chloride and *t*-butyl chloride are included for purposes of comparison. Considering first the data in 80% aqueous acetone, it can be seen that the rates for both reactions follow the Baker–Nathan order (2). The values for the ratios of rates of 1-*p*-tolylethyl chloride and *p*-*t*-butyl-α-chloro-α-methyltoluene at 25° for the normal and catalyzed hydrolysis are 2.75 and 2.43, respectively. Theoretically, however, the ratio for the catalyzed reaction should be larger than that for the normal reaction since the catalytic efficiency should increase with the ease of heterolysis of the C—Cl bond. This implies that in the catalyzed reaction, some factor has been introduced which favors the hydrolysis, the magnitude of which increases in the order Me < Et < *i*-Pr < *t*-Bu. An examination of the heats and entropies of activation also support this conclusion. The values for the normal reaction show the usual trend, which is similar to that found for the hydrolysis of *p*-alkylbenzhydryl chlorides (3). Provided both the normal and catalyzed reactions follow the S_N1 mechanism, as is the case here, the heat of activation for the catalyzed reaction for all four alkyl chlorides should be lower than that for the corresponding normal reaction while the trend in their values should be the same, i.e., the heats of activation should increase as the series is ascended; the entropy of activation values should be lower for the catalyzed reaction in all cases. 1-Phenylethyl chloride and *t*-butyl chloride are examples which obey this rule. The reason for expecting a decrease in the entropy of activation on passing from the normal to the catalyzed reaction is that the transition state for the latter will be more polar and so will be more highly solvated. With 1-*p*-tolylethyl chloride, while the heat of

[1]*Partial financial support from the U.G.C., India.*
[2]*Government of India Research Scholar.*

Can. J. Chem. Downloaded from www.nrcresearchpress.com by 210.87.254.5 on 09/05/12
For personal use only.

TABLE I

Kinetics of the solvolysis of alkyl chlorides, [RCl] = 0.025 M*, T = 25.0 °C, [$HgCl_2$] = 0.075 M

RCl	Normal			Catalyzed		
	10^6k_1 (s)	$\Delta H^{\ddagger}_{25°}$ (kcal/mole)	$\Delta S^{\ddagger}_{25°}$ (e.u.)	10^4k_1 (s)	$\Delta H^{\ddagger}_{25°}$ (kcal/mole)	$\Delta S^{\ddagger}_{25°}$ (e.u.)
(i) Solvent 75% v/v acetone–water						
CH(*p*-MePh)MeCl	107	—	—	106	17.8±0.2	−8±1
CH(*p*-*t*-BuPh)MeCl	37.6	—	—	40.4	16.3±0.2	−15±1
(ii) Solvent 80% v/v acetone–water						
CH(*p*-MePh)MeCl	36.3	20.3	−10.6	58.9	17.5±0.2	−10±1
CH(*p*-EtPh)MeCl	28.8	20.4	−10.7	43.4	16.9±0.3	−13±1
CH(*p*-*i*-PrPh)MeCl	22.4	20.6	−10.6	35.0	16.6±0.3	−14±1
CH(*p*-*t*-BuPh)MeCl	13.2	21.3	−9.5	24.6	16.4±0.2	−16±1
CHPhMeCl	0.846(ref. 1)	21.1(ref. 1)	−15.5(ref. 1)	0.724(ref. 1)	17.6(ref. 1)	−18.5(ref. 1)
t-BuCl	1.96	22.0(ref. 5)	−10.8(ref. 5)	0.975	17.9(ref. 5)	−17.1(ref. 5)
(iii) Solvent 90% v/v acetone–water						
CH(*p*-MePh)MeCl	2.35	19.9	−17.6	16.6	16.6±0.1	−15.6±0.5
CH(*p*-*t*-BuPh)MeCl	1.09	20.6	−16.6	9.00	16.9±0.1	−15.7±0.5
CHPhMeCl	—	—	—	0.271	16.8	−23.1
t-BuCl	—	21.9(ref. 15)	−16.8(ref. 15)	0.310	17.3	−21.2
(iv) Solvent 90% v/v ethanol–water						
CH(*p*-MePh)MeCl	110	20.0	−9.5	20.0	17.6±0.2	−12±1
CH(*p*-*t*-BuPh)MeCl	59.4	20.8	−7.9	12.9	19.0±0.2	−8±1

*For 80% v/v acetone–water, RCl = 0.050 M.

activation is lower than that for the normal reaction, the entropy factor remains practically constant. A likely explanation appears to be that the larger fractional charges in the transition state of the catalyzed reaction are effectively delocalized by C—H hyperconjugation. This would naturally reduce solvation and so will lead to a higher entropy value. As the series is ascended, in marked contrast to the trend noted for the normal hydrolysis, the heats of activation progressively decrease. It is suggested that this could be understood on the basis that the catalyst induces an inductomeric mode of electron release from the *p*-alkyl groups, the magnitude of which should obviously increase as the series is ascended. Consistent with this interpretation is the observed trend in the values of the entropy of activation. Again, in contrast to the normal reaction, where there is a slight increase in entropy as the series is ascended, the entropy values decrease markedly; the only exception is 1-*p*-tolylethyl chloride, as noted above. Now, the magnitude of C—H hyperconjugation should decrease, and that of the inductomeric effect increase along the series. The net result would be to accentuate the normal loss in entropy of activation which would be expected to occur on passing from the normal to the catalyzed reaction.

In 90% aqueous acetone also the Baker–Nathan order is observed for the normal and catalyzed reactions. The heats and entropies of activation have been determined only for 1-*p*-tolylethyl chloride and *p*-*t*-butyl-α-chloro-α-methyltoluene. Their trend for the normal reaction is quite similar to that in 80% aqueous acetone and so does not call for comment. However, the trend in the catalyzed reaction is similar to that in the normal reaction and opposite to that for the catalyzed reaction in 80% aqueous acetone. A simple explanation for the higher heat of activation noted for *p*-*t*-butyl-α-chloro-α-methyltoluene is that the solvent polarity is too low to call into play an appreciable inductomeric effect. However, this explanation alone is not adequate to account for the trend in the entropy values. For 1-*p*-tolylethyl chloride, the entropy of activation, as in 80% aqueous acetone, is essentially the same for both the normal and catalyzed reactions and C—H hyperconjugative effect can account for this observation. But in contrast to the position in 80% aqueous acetone, the entropy values for *p*-*t*-butyl-α-chloro-α-methyltoluene are also similar for both reactions. We suggest that this may be due to the operation of C—C hyperconjugation, the effect of which will increase the entropy of activation, and thus compensate the drop in entropy which should normally occur on passing from the normal to the catalyzed reaction. In the normal hydrolysis of *p*-alkylphenyldimethylcarbinyl chlorides, the heats and entropies of activation are practically the same for all four alkyl chlorides (Alk = Me, Et, *i*-Pr, and *t*-Bu). Brown has explained this by assuming an interplay of C—H and C—C hyperconjugation (4). In view of the different trends noted in the heats and entropies of activation in 80% and 90% aqueous acetone, data were also obtained in 75% aqueous acetone. The trends are quite similar to that in 80% aqueous acetone, thus supporting the above conclusion that the different behavior in 90% aqueous acetone is due to its low solvent polarity.

Since rates of mercuric chloride catalyzed solvolysis of alkyl chlorides are rather anomalous in aqueous ethanol (5), and aqueous alcohols generally (6), the kinetics of 1-*p*-tolylethyl chloride and *p*-*t*-butyl-α-chloro-α-methyltoluene were examined in 90% aqueous ethanol. In agreement with previous findings (5), the catalytic efficiency for both alkyl chlorides is much lower than in the aqueous acetone solvents. The rates follow the Baker–Nathan order for both the normal and catalyzed reactions. The trend in the heats and entropies of activation for the catalyzed reaction is quite similar to that for the normal reaction in this solvent, and the values are higher than for the catalyzed reaction in 90% aqueous acetone. This is to be expected because of the low catalytic efficiency, since not

Can. J. Chem. Downloaded from www.nrcresearchpress.com by 210.87.254.5 on 09/05/12
For personal use only.

only will there be no inductomeric effect, but even the reduction in the heats and entropies of activation normally associated with the catalyzed reaction will be largely absent.

The peculiar tendency of mercuric chloride to induce a mass-law effect in the hydrolytic reactions of alkyl chlorides (provided the structure of the alkyl chloride is sufficiently favorable) has been established (7) and given a probable theoretical basis (8). To determine whether the hyperconjugative effect can cause detectable difference in the stability of the carbonium ions derived from the four alkyl chlorides—such differences would obviously show themselves in the magnitude of the mass-law effect (9)—the effect of added chloride ions on their rates of catalyzed hydrolysis in 90% aqueous acetone was studied (Table II).

TABLE II

Effect of added chloride ions on the catalyzed hydrolysis, solvent 90% v/v acetone–water, $[HgCl_2] = 0.0750\ M$, $T = 20.00$ °C, $[RCl] = 0.0250\ M$

RCl	10^4k_1 (s)	% reduction in rate for varying [Cl]				
		0.0750 *M*	0.0625 *M*	0.0500 *M*	0.0375 *M*	0.0250 *M*
CH(*p*-MePh)MeCl	10.32	89.3	81.7	72.3	51.2	36.5
CH(*p*-EtPh)MeCl	8.86	90.1	83.2	72.0	—	—
CH(*p*-*i*-PrPh)MeCl	7.38	90.8	82.1	72.4	—	—
CH(*p*-*t*-BuPh)MeCl	5.40	91.3	80.7	71.1	51.5	36.7
CHPhMeCl	0.167	90.6	81.0	68.7	—	—
t-BuCl	0.187	84.7	70.7	52.1	32.6	28.9

A probable explanation for the results is as follows. Chloride ions reduce the rate of the catalyzed reaction in two ways, by inactivating the catalyst through complex formation, and by inducing a mass-law effect in suitable cases. The first effect is the sole cause with such substrates as benzyl (10) and *p*-chlorobenzyl chloride (11). *t*-Butyl chloride also does not show a mass-law effect presumably because of the low stability of the carbonium ion (12). So the smaller rate reductions for *t*-butyl chloride must mean that with the other alkyl chlorides part of the observed rate reductions must be due to a mass-law effect. At all chloride ion concentrations the rate reductions with the other five alkyl chlorides are closely similar, which must mean that the hyperconjugative effect, if present, is not great enough to affect the mass-law effect. This is understandable, since the hyperconjugative effect, like any other electronic effect, will have a polarizability component, and so its effect should be larger in the transition state of the hydrolytic reaction because of the presence of the powerful electrophilic catalyst. The mass-law effect, on the other hand, will depend on the stability of the carbonium ion and the differences on this account should be much smaller since only the polarization component of the hyperconjugative effect will be differentially involved.

EXPERIMENTAL

Materials

The nuclear-substituted alcohols were prepared by the Meerwein–Pondorff reduction of the corresponding ketones, and were purified through their acid phthalates. They were converted into the chlorides by reaction with thionyl chloride.

TABLE III

Physical constants of alkyl chlorides

Alkyl chloride	B.p. (°C)	n_D^{25}	d^{30}
CH(*p*-EtPh)MeCl	152 at 80 mm	1.5200	1.003
CH(*p*-*i*-PrPh)MeCl	180 at 176 mm	1.5155	0.9811
CH(*p*-*t*-BuPh)MeCl	179 at 130 mm	1.5140	0.9924

Can. J. Chem. Downloaded from www.nrcresearchpress.com by 210.87.254.5 on 09/05/12
For personal use only.

The physical constants of three alkyl chlorides are given in Table III. Data for the others have been given earlier (5).

Kinetic work

Details of purification of solvents, preparation of solvent mixtures, and technique of rate measurements have been given (5). It was noted that in the catalyzed hydrolysis of the nuclear-substituted alkyl chlorides, the rate coefficients steadily decreased during the course of the reaction. To obtain the initial rate, therefore, log k was plotted against log $(a - x)$ (13) and the best straight line was obtained by the method of least squares. As a check on the accuracy of the measurements, the initial rates were also evaluated graphically. The agreement between the two values was always good. An illustrative kinetic run is given in Table IV. All runs for the catalyzed reaction were conducted in triplicate and the others in duplicate. The average deviation of the rate in the replicate runs is: for about two-thirds <1%; for the rest between 1 and 2%. For the catalyzed reaction in 80% and 90% aqueous acetone, measurements at four temperatures were carried out, the range being 15°. The errors quoted for the heats and entropies of activation are probable errors obtained from least square calculations (14) rounded off to the values shown in Table I.

TABLE IV

Illustrative kinetic run for the mercuric chloride catalyzed hydrolysis of 1-*p*-tolylethyl chloride in 90% v/v acetone–water at 20.0° C (initial [alkyl chloride] = 0.0250 *M*, [$HgCl_2$] = 0.0750 *M*)

t (s)	NaOH titer (ml)*	10^4k_1
0	1.42	—
240	3.08	9.39
360	3.74	9.20
480	4.30	8.97
600	4.80	8.82
720	5.22	8.61
840	5.60	8.44
960	5.92	8.25
1 080	6.22	8.11
1 200	6.48	7.95
1 320	6.72	7.83
1 440	6.93	7.69
∞	9.65	
Initial rate (least squares)		10.3
Initial rate (graphical)		10.3

*Volume of 0.01295 *N* NaOH solution equivalent to 5.0 ml sample.

REFERENCES

1. R. ANANTARAMAN and K. SARAMMA. Tetrahedron, **21**, 535 (1965).
2. J. W. BAKER and W. S. NATHAN. J. Chem. Soc. 1844 (1935).
3. E. D. HUGHES, C. K. INGOLD, and A. D. SCOTT. J. Chem. Soc. 949 (1940).
4. H. C. BROWN and L. M. STOCK. J. Am. Chem. Soc. **79**, 1421 (1957).
5. R. ANANTARAMAN and K. SARAMMA. Can. J. Chem. **43**, 1770 (1965).
6. R. ANANTARAMAN and K. SARAMMA. Indian J. Chem. **3**, 567 (1965).
7. R. ANANTARAMAN. Ph.D. Thesis, University of London, London, Engl. 1950.
8. C. K. INGOLD. Structure and mechanism in organic chemistry. Cornell Univ. Press, Ithaca, N.Y. 1953. p. 359. C. A. BUNTON. Nucleophilic substitution at a saturated carbon atom. Eslevier Pub. Co., Inc., Amsterdam. 1963. p. 154.
9. L. C. BATEMAN, M. G. CHURCH, E. D. HUGHES, C. K. INGOLD, and N. A. TAHER. J. Chem. Soc. 979 (1940).
10. S. KOSHY and R. ANANTARAMAN. J. Am. Chem. Soc. **82**, 1574 (1960).
11. R. ANANTARAMAN and K. SARAMMA. Z. Physik. Chem. Leipzig, A, **216**, 21 (1961).
12. C. G. SWAIN and B. R. MOSELY. J. Am. Chem. Soc. **77**, 3727 (1955). C. A. BUNTON and B. NAYAK. J. Chem. Soc. 1915 (1959).
13. K. J. LAIDLER. Reaction kinetics. Vol. I. The Pergamon Press, Ltd., London. 1963. p. 18.
14. H. MARGENAU and G. M. MURPHY. The mathematics of physics and chemistry. 2nd ed. D. Van Nostrand Co., Inc., Princeton. 1956. p. 519.
15. S. WINSTEIN and A. H. FAINBERG. J. Am. Chem. Soc. **80**, 5937 (1957).

Can. J. Chem. Downloaded from www.nrcresearchpress.com by 210.87.254.5 on 09/05/12
For personal use only.

Can. J. Chem. Downloaded from www.nrcresearchpress.com by 210.87.254.5 on 09/05/12
For personal use only.

EFFECT OF THERMIONIC EMISSION ON ELECTROCHEMICAL MEASUREMENTS AT HIGH TEMPERATURES[1]

S. G. WHITEWAY AND C. R. MASSON
Atlantic Regional Laboratory, National Research Council, Halifax, Nova Scotia
Received May 9, 1966

ABSTRACT

In the measurement of electromotive forces at temperatures over 1 000° spurious contact potentials, which may be asymmetric, are sometimes encountered. As an example of these, contact potentials between solid oxides and electrically grounded portions of their environment were measured at temperatures between 1 000° and 1 450°. Their variation with temperature, gaseous environment, and impedance of the measuring circuit is presented and interpreted in terms of thermionic emission.

INTRODUCTION

Electrochemical measurements at high temperatures (> 1 000°) are subject to errors not encountered at lower temperatures. An example is the presence of "asymmetry potentials" (1, 2) in electrochemical cells. This effect is most troublesome when the internal resistance of the cell is high and it becomes necessary to use a potentiometer of high impedance for the measurements. If one side of the circuit is grounded, contact potentials (2) can develop between parts of the cell and grounded parts of the high temperature environment. These may not be the same for each side of the cell so that the difference can appear as an asymmetry contribution to the electromotive force even if a non-grounded instrument is used for the measurements.

An analogous effect influences measurements of electrical conductivity if the conductivity of the gaseous environment is high in comparison with that of the test specimen (3, 4). Loup and Anthony (5) have concluded that gaseous conduction may be initiated by thermal emission of electrons from heated surfaces, leading to ionization of the gas phase.

Although contact potentials exist even at low temperatures they are normally difficult to measure because of the extremely high source impedances involved (6). It seemed likely that their ready detection at high temperatures was due also to thermionic emission.

EXPERIMENTAL

Ceramic test pieces of size about 1.5 × 0.5 × 0.5 cm were suspended by two platinum leads inside an impervious alumina tube heated by a platinum–rhodium element. The leads were wound in grooves cut near the ends of the piece and were secured by twisting. Most of the experiments were performed with magnesia (Norton Co. optical grade), but ZrO_2 – 15 mole % CaO (made by pressing and sintering the powders) and FeO (made by melting a stoichiometric mixture of Fe and Fe_2O_3 under argon) were also used.

A grounded cylinder of Pt – 20% Rh, normally placed within the alumina tube, shielded the specimen from the electrical field of the furnace and also served as a reference point for potentials. Electrical leads outside of the furnace were also protected by grounded shields. Various arrangements involving test piece, shield, and auxiliary probe were employed, as shown schematically in Fig. 1 and described more fully below. Temperatures were recorded with a Pt – 13% Rh thermocouple placed outside the furnace tube.

Potentials were normally measured with a Leeds and Northrup recording potentiometer of sensitivity 5×10^9 Ω/V. Resistances for small applied voltages (up to 1.5 V) were determined by measuring the current with a galvanometer of sensitivity 1.75×10^{-11} A/mm deflection at 1 m. Resistances at a much higher voltage (135 V) were measured with an AVO meter.

[1]*Issued as N.R.C. No. 9135.*

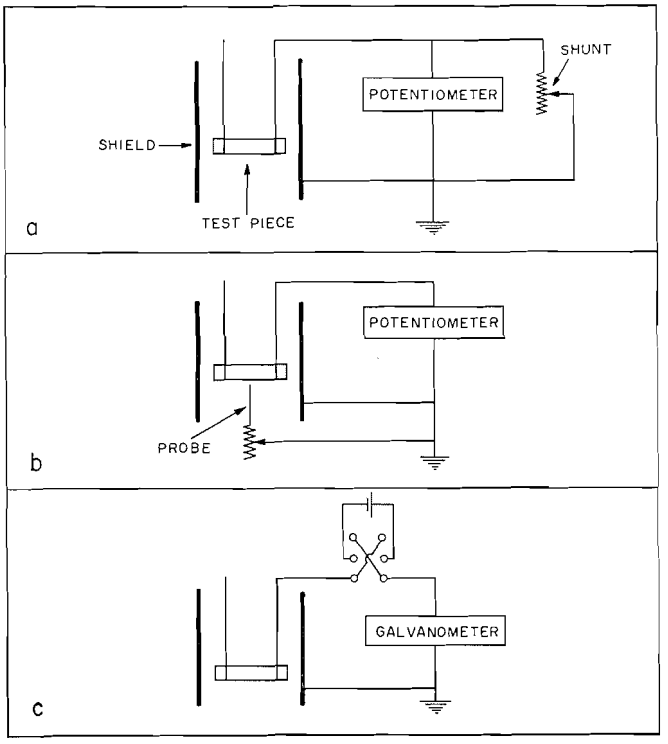


FIG. 1. Typical measuring circuits.

EXPERIMENTAL RESULTS AND DISCUSSION

Effect of Temperature and Impedance of Measuring Circuit

Typical data for the potential on MgO in air are shown in Fig. 2. The potential was measured between one end and the shield (Fig. 1*a*) while being shunted with resistances of 10, 20, 50, 90 and ∞ MΩ. In the last case the effective impedance of the measuring circuit would be that of the potentiometer itself, 1 000 MΩ.

The potential exhibited a maximum with temperature, V_{max}, which decreased as the input impedance of the measuring circuit was lowered. At the same time the position of V_{max} shifted to higher temperatures with decreasing impedance. It is apparent that the potential of the magnesia with respect to the shield increased with decreasing temperature but that below a certain temperature the potential decreased because of the current drawn by the measuring circuit. Potentials tended toward zero at temperatures of 1 400° rather than continued decreasing to negative values.

Negative potentials which became more positive with increasing temperature were encountered when a platinum wire probe, connected to ground, was placed a few millimeters from the MgO test piece (Fig. 1*b*). This arrangement was chosen to simulate the effect of a thermocouple in the vicinity of the test piece. The results are shown in Fig. 3. As the probe was isolated more and more from the shield by resistances of 10, 20, 90, and ∞ (open circuit between probe and ground) MΩ, the MgO tended to assume the potential it had in the absence of the probe.

Can. J. Chem. Downloaded from www.nrcresearchpress.com by 210.87.254.5 on 09/05/12
For personal use only.

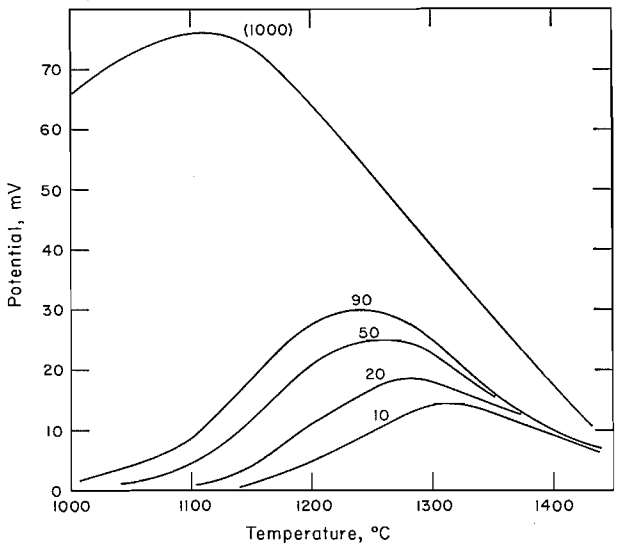


FIG. 2. Temperature variation of potential on MgO in air, with respect to shield, for various circuit impedances. Number beside each curve is impedance in megohms.

Relationship of Potential to Thermionic Emissivity

The above experiments indicated that the magnitude and sign of the potential, and its variation with temperature, depended on the material which constituted the nearest "ground", and it is likely that differences in the work functions of the two surfaces were responsible for the potential difference. Since the work function is related to the emission current by the Richardson–Dushman equation

$$[1] \qquad j = BT^2 \, e^{-\phi/kT}$$

(j = current density, B a constant, T the absolute temperature, ϕ the work function, and k the Boltzmann constant), measurements of the ratio of emission currents from test piece and shield should be related to the potential.

When direct current voltages between 0 and 1.5 V were applied first in one direction and then in the other between one end of the test piece and the shield, emission currents could be measured with the galvanometer (Fig. 1*c*). The potential for zero current agreed with potentials obtained with the recording potentiometer. The calculated resistances for electron flow from and to the test piece were equal near this equilibrium potential, but differed at higher applied potentials: the resistance to electron flow was greater in the direction: test piece to shield. Currents were non-ohmic but were not saturation currents within this voltage range.

Resistances at an applied voltage high enough to ensure that currents were saturation currents were measured with an AVO meter at 135 V. Resistances were measured, in both directions, between each end of the test piece and the shield, as well as across the test piece itself. In all experiments the shield was at ground potential. The results are given in Table I and are for an MgO test piece in air. Shown also are the equilibrium potentials between each end of the test piece and the shield, as measured with the recording potentiometer.

Can. J. Chem. Downloaded from www.nrcresearchpress.com by 210.87.254.5 on 09/05/12
For personal use only.

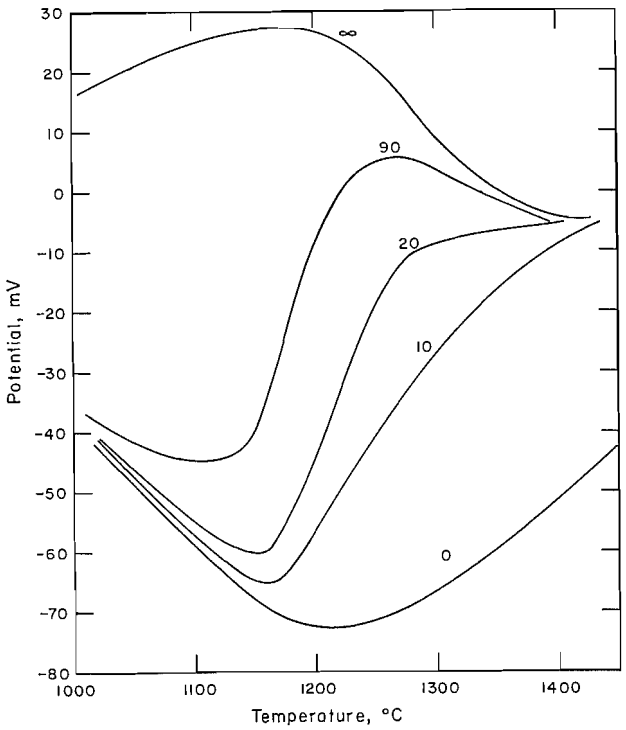


FIG. 3. Temperature variation of potential on MgO in air, with respect to shield–probe combination. Probe isolated from ground by resistances, in megohms, shown beside curves.

It may be noted that none of the resistances in Table I are simple. For example, the path for electron flow from end 1 to shield is shunted by the path consisting of the test piece in series with end 2 to shield. Ignoring these effects, the ratio "resistance test piece to shield / resistance shield to test piece", R_2/R_1, was calculated for each end. This ratio is a measure of the electron-emitting power of the shield compared with the test piece, and it is evident that as the ratio increases the equilibrium potential of the test piece becomes more negative.

From eq. [1] it may be shown that the ratio of resistances is related to the difference in emissivities of the two surfaces by

$$[2] \qquad \log_{10} R_2/R_1 = C + \frac{\phi_2 - \phi_1}{kT},$$

where the constant C involves the respective areas. If the contact potential between shield and test piece is proportional to $(\phi_2 - \phi_1)$, a plot of $\log_{10} R_2/R_1$ against potential / absolute temperature should be linear. As shown in Fig. 4 this is approximately true, although the relationship appears to break down at the lower temperatures where the potential is difficult to measure.

It is concluded that the sign of the potential assumed by the test piece is negative if it can emit fewer electrons/cm^2 than the reference surface, positive if it can emit more, and that the magnitude of the potential is a function of the ratio of the two emissivities. The equilibrium potential is established when the two surfaces are in thermionic equilibrium and no current flows between them. This equilibrium potential cannot be measured

Can. J. Chem. Downloaded from www.nrcresearchpress.com by 210.87.254.5 on 09/05/12
For personal use only.

Can. J. Chem. Downloaded from www.nrcresearchpress.com by 210.87.254.5 on 09/05/12
For personal use only.

TABLE I

Potentials on MgO in air, and resistance to electron emission

	Between end 1 and shield				Between end 2 and shield					
		Resistance*				Resistance			Resistance across test piece	
Temp. (°C)	Equilibrium potential on MgO for no applied voltage (mV)	R_2 (test piece to shield)	R_1 (shield to test piece)	Ratio R_2/R_1	Equilibrium potential on MgO for no applied voltage (mV)	R_2 (test piece to shield)	R_1 (shield to test piece)	Ratio R_2/R_1	End 1 to end 2	End 2 to end 1
1 100	+29.5	120	46	2.60	+30	190	80	2.4	46	48
1 150	+12.0	92.5	35.5	2.60	+13				26.0	27.7
1 172 (A)	−6.0	100	33.5	3.0	−7				16.9	17.2
1 172 (B)	−1.1	90	32	2.8	+1.0	100	40	2.5	17.5	18.1
1 200	−8.0	100	31	3.2	+2.5	100	37.8	2.65	13.6	13.8
1 300	−41.5	28	3.41	8.2	−39.0	29.5	3.85	7.66	3.30	3.34
1 400	−63.0	0.465	0.036	12.9	−54.0	0.557	0.046	12.1	0.445	0.505

*Resistances, in megohms, are quoted in the direction of electron flow, i.e. for R_2 the negative side of the applied voltage was connected to the test piece.

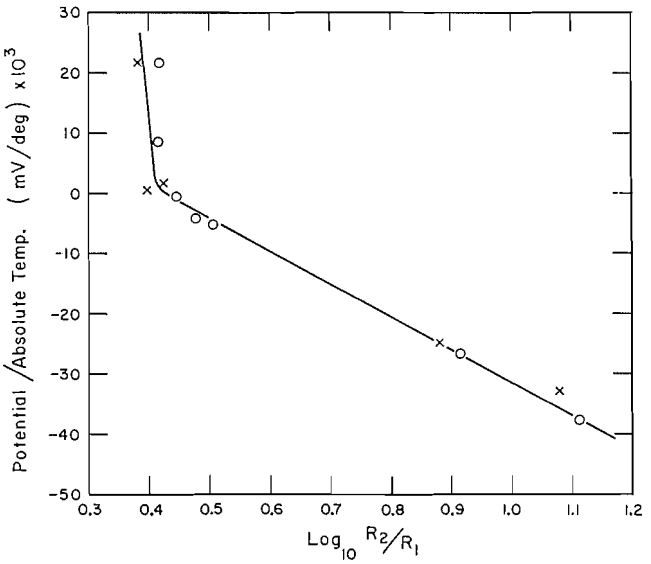


FIG. 4. Potential / absolute temperature vs. log resistance ratio. MgO in air. (○) End 1, (×) end 2.

exactly by a device which draws current, and at low temperatures may not be detected at all. At higher temperatures the potential tends to zero and it is likely that thermal ionization of the gaseous environment dissipates the electron double layers responsible for the equilibrium potential difference.

Asymmetry Potentials

From Table I it can be seen that an asymmetry potential existed across the piece itself, amounting to 9 mV at 1 400°. This behavior was characteristic of MgO and presumably was related to local differences in emissivities in the system. The asymmetry was neither predictable nor reproducible, although the end of the test piece which was more positive tended to remain that way during an experiment.

It might be expected that such a potential difference could only be maintained if the specimen itself had sufficient resistance compared to the resistance of the path: test piece to shield. In line with this, asymmetry potentials were smaller or absent when ZrO_2–CaO or FeO was used in place of MgO, although the contact potentials themselves were similar. The specific conductivities of these materials are much higher than for MgO.

Effect of Atmosphere

Potentials between magnesia and shield were similar in argon, helium, and air. When air was replaced by hydrogen the potential generally became negative, but was very erratic. It is possible that this was due partly to enhanced emissivity of the platinum, since hydrogen reduces the work function of platinum (6) by about 2 eV. Other possible effects of hydrogen in creating anion vacancies and excess electrons in the magnesia have been discussed elsewhere (2).

A further serious effect of atmosphere on the measurement of electromotive forces at high temperatures may be due to the short-circuiting effect of the ionized environment. This is the effect which also renders conductivity measurements difficult, and may be minimized by the use of a gas of high molecular weight, such as argon, which has a low mobility. Mitoff (4) has devised a guard circuit to prevent such short-circuiting.

Can. J. Chem. Downloaded from www.nrcresearchpress.com by 210.87.254.5 on 09/05/12
For personal use only.

REFERENCES

1. PHYSICAL CHEMISTRY OF METALLIC SOLUTIONS AND INTERMETALLIC COMPOUNDS. National Physical Laboratory Symposium, No. 9. H. M. Stationery Office, London. 1960. 6F. p. 12.
2. M. COLL-PALAGOS and C. R. MASSON. Trans. Faraday Soc. **57**, 1621 (1961).
3. D. W. PETERS, L. FEINSTEIN, and C. PELTZER. J. Chem. Phys. **42**, 2345 (1965).
4. S. P. MITOFF. J. Chem. Phys. **41**, 2561 (1964).
5. J. L. LOUP and A. M. ANTHONY. Rev. Hautes Temp. Refractaires, **1**, 15 (1964); **1**, 193 (1964).
6. N. K. ADAM. The physics and chemistry of surfaces. 3rd ed. Oxford University Press, London. 1941. pp. 308–314.

Can. J. Chem. Downloaded from www.nrcresearchpress.com by 210.87.254.5 on 09/05/12
For personal use only.

Can. J. Chem. Downloaded from www.nrcresearchpress.com by 210.87.254.6 on 09/05/12
For personal use only.

TETRASUBSTITUTED-CYCLOPENTADIENONE AND -*p*-BENZOQUINONE COMPLEXES OF RHODIUM(I)

S. McVey and P. M. Maitlis[1]
Chemistry Department, McMaster University, Hamilton, Ontario
Received June 20, 1966

ABSTRACT

The preparation of tetraphenylcyclopentadienone rhodium chloride, tetraphenylcyclopentadienone rhodium carbonyl chloride, duroquinone rhodium chloride, and 2,3,5,6-tetraethyl-*p*-benzoquinone rhodium chloride from rhodium dicarbonyl chloride dimer and the appropriate organic ligand are described. The properties of these complexes and some of their reactions are discussed.

During our investigation of the reactions of acetylenes with rhodium dicarbonyl chloride dimer (I), we obtained some new organo-rhodium(I) complexes (1). We here present details of the chemistry of some of these compounds.

As briefly reported (1), the main product obtained from the reaction of diphenylacetylene with I was 2,3,4,5-tetraphenylcyclopentadienone rhodium chloride dimer (III).[2] This we also synthesized directly from tetraphenylcyclopentadienone (tetracyclone) (II) and I. The yield of III was highest (65%) when the reaction was carried out in refluxing benzene; at 50° in benzene only 30% of III and at 25° in benzene 25% of III were obtained. The other product, obtained from the two latter reactions in 57% and 71% yield respectively, was identified as tetracyclone rhodium carbonyl chloride (IV).

The infrared spectrum of IV showed the presence of a terminal metal carbonyl at 2 062 cm^{-1}; this together with the reactions described below and the extreme insolubility of the compound lead us to formulate it as a chlorine-bridged polymer (IV).

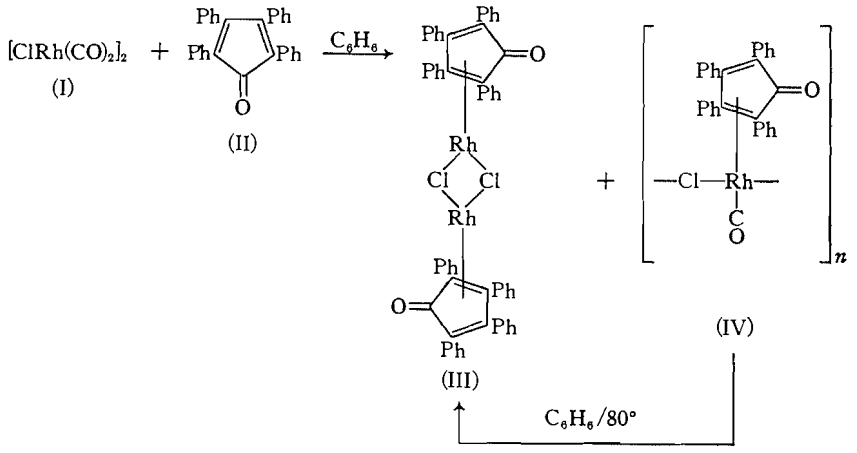
On heating, IV readily lost carbon monoxide and III was formed. The further reactions of III and IV with chlorine-bridge-splitting reagents are shown in the chart. Pyridine reacted with either III or IV to give bis-pyridine tetracyclone rhodium chloride (V), whereas thallous acetylacetonate (Tlacac) reacted with both to give the same rhodium acetylacetonate complex (VI). Triphenylphosphine, in contrast, gave the expected monomeric adduct (VII) from III, but this was not formed when IV was reacted with only 1 mole of triphenylphosphine. Instead disproportionation occurred and the products obtained were tetracyclone (II), the complex (III), and bis(triphenylphosphine)rhodium carbonyl chloride (VIII). This curious result must be due to the extremely strong tendency for the formation of VIII, which has already been commented on by Wilkinson *et al.* (3) and others (4) and has been used in the decarbonylation of aldehydes and similar molecules.

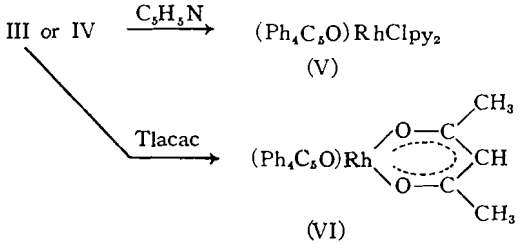
One other result of interest is that if tetracyclone is assumed to occupy two coordination positions, then the complexes (III), (VI), and (VII) are four-coordinate (and presumably square planar) while the bis-pyridine adduct (V) is five-coordinate. This may be due to the relative sizes of the various ligands.

2,3,5,6-Tetramethyl-*p*-benzoquinone (duroquinone) (IX, R=Me) reacted slowly in benzene with rhodium dicarbonyl chloride dimer (I) to give duroquinone rhodium chloride

[1]*Author to whom any correspondence should be addressed.*

[2]*The exact structure for a cyclopentadienone metal complex is still the subject of considerable dispute (2a; 2b and references therein). The most reasonable structure, based on X-ray structure determinations, appears to be one where the five-membered ring is linked to the metal by two partial σ-bonds and one π-bond. However, for simplicity of representation here, and since the detailed structure of III is not known, we have chosen to represent it as shown.*





$$III + Ph_3P \rightarrow (Ph_4C_5O)RhClPPh_3$$

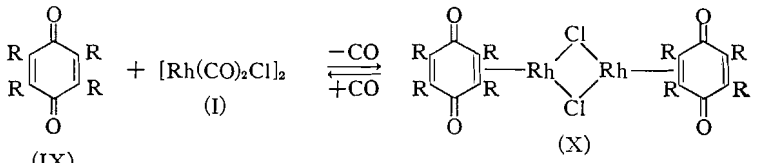
(VII)

$$\tfrac{1}{n}IV + PPh_3 \rightarrow III + II + (Ph_3P)_2RhCOCl$$

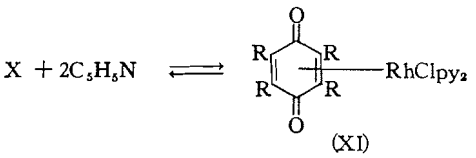
(VIII)

dimer (X, R=Me) in 83% yield. The compound (X, R=Me) was characterized by analysis, infrared, and ^1H nuclear magnetic resonance (n.m.r.) spectra and by the reversal of the reaction leading to its formation when it was treated with carbon monoxide. A rather unstable bis-pyridine adduct (XI, R=Me) was also obtained.

Duroquinone rhodium chloride has already been described by Schrauzer and Dewhirst (5), who prepared it from rhodium trichloride and duroquinone in ethanol. Their reaction, which we have verified, gave a product similar to the one described above. However, the compound from rhodium trichloride in ethanol is virtually insoluble in all but complexing solvents and must be formulated as a halogen-bridged linear polymer, as the authors



(IX) (I) (X)



(XI)

Can. J. Chem. Downloaded from www.nrcresearchpress.com by 210.87.254.6 on 09/05/12
For personal use only.

suggest. In contrast, X (R=Me) is quite readily soluble in organic solvents and molecular weight determinations show it to be dimeric in solution. This type of behavior, while unusual, is not without precedent, thus tetramethylcyclobutadiene nickel chloride has been shown to exist in the crystal (containing benzene of solvation) as a chlorine-bridged dimer (6). However, Criegee and Schroeder (7) report that in bromoform solution a molecular weight corresponding to $[(Me_4C_4)NiCl_2]_{10}$ is obtained. No doubt other examples of this type of behavior also exist.

2,3,5,6-Tetraethyl-*p*-benzoquinone (IX, R=Et) also reacted with I to give the complex (X, R=Et), which was again dimeric in solution. However, while the ^1H n.m.r. spectrum of IX (R=Et) showed the typical A_3B_2 spectrum expected for a molecule with equivalent ethyl groups, that of X (R=Et) was quite unusual. The methyl protons appeared as a triplet centered at 8.75 τ, but in the methylene region, instead of the expected quartet, a nonet centered at 7.90 τ with intensities 1:2.3:3.3:4.6:4.6:4.3:3.0:1.5:1 was observed. The total integrated intensities of the methyl and methylene protons remain as 3:2. This suggests that when IX (R=Et) is complexed to a metal, the methylene carbons are no longer free to rotate and hence the methylene protons become non-equivalent. Examination of a molecular model shows that this is indeed the case. This effect is increased if the carbonyl groups are also somewhat bent away from the metal, as was suggested by Schrauzer and Dewhirst (5) for the duroquinone complexes to account for the split carbonyl stretching frequency in the infrared. The n.m.r. spectrum of X (R=Me) was normal.

Tetraethyl-*p*-benzoquine and rhodium dicarbonyl chloride dimer were obtained when X (R=Et) was treated with carbon monoxide. The complex (X, R=Et) gave a bis-pyridine adduct (XI, R=Et) more unstable than XI (R=Me) and for which good analyses could not be obtained.

EXPERIMENTAL

Reaction of Rhodium Dicarbonyl Chloride with Diphenylacetylene

Rhodium dicarbonyl chloride dimer (I) (0.5 g, 1.25 mmole) and diphenylacetylene (1.35 g, 7.5 mmole) were refluxed in 20 ml of benzene for 24 h. A dark-brown solid (0.11 g, 12%), decomposing at 340°, was filtered off; this was insoluble in common organic solvents; it showed a strong infrared maximum at 2 015 cm^{-1} (terminal CO).[3]

Anal. Calcd. for $(C_{15}H_{10}ClORh)_n$: C, 52.2; H, 2.9; Rh, 29.9. Found: C, 51.8; H, 3.0; Rh, 31.4.

Chromatography of the filtrate on Florisil in benzene gave hexaphenyl benzene (0.12 g, 9%) and a red solid which eluted with methylene chloride – ethanol (9:1). Recrystallization from cyclohexane gave tetraphenylcyclopentadienone rhodium chloride (III) (0.63 g, 47%), m.p. 316–318°. The complex showed ν_{CO} at 1 621 cm^{-1} (KBr) and 1 647 cm^{-1}($CHCl_3$ solution).

Anal. Calcd. for $C_{58}H_{40}Cl_2O_2Rh_2$: C, 66.6; H, 3.8; Cl, 6.9; Rh, 19.7; mol. wt., 1 044. Found: C, 65.7; H, 4.8; Cl, 6.7; Rh 18.6; mol. wt., 1 085.

Reaction of Rhodium Dicarbonyl Chloride with Tetracyclone

Tetracyclone (II) (1.05 g, 3 mmole) and rhodium dicarbonyl chloride dimer (I) (0.5 g, 1.25 mmole) were heated at 50° in 30 ml of benzene for 42 h. A crystalline yellow solid (IV) (0.85 g, 57%), m.p. 328–330° (decomp.), was filtered off. This was purified by washing with benzene. The complex showed ν_{CO} at 2 062, 1 666 (sh), and 1 642 cm^{-1} (KBr).

Anal. Calcd. for $(C_{30}H_{20}ClO_2Rh)_n$: C, 65.0; H, 3.7; Cl, 6.4; Rh, 18.6. Found: C, 64.8; H, 3.8; Cl, 6.7; Rh, 19.2.

The filtrate was reduced to small bulk and chromatographed on Florisil to give, in addition to unchanged tetracyclone, a dark-red crystalline solid eluted with methylene chloride – ethanol (9:1). Recrystallization from cyclohexane gave tetracyclone rhodium chloride (III) (0.42 g, 30%), mixed melting point with the compound described above 316–318°.

Tetracyclone rhodium carbonyl chloride was smoothly converted to tetracyclone rhodium chloride in refluxing benzene or xylene.

[3]*Further details on this interesting compound will be published shortly.*

Can. J. Chem. Downloaded from www.nrcresearchpress.com by 210.87.254.6 on 09/05/12
For personal use only.

Bis-Pyridine Tetracyclone Rhodium Chloride (V)

A suspension of tetracyclone rhodium carbonyl chloride (IV) (0.15 g) in 25 ml of methylene chloride was treated with 2 ml of pyridine for 2 h at 25°. Filtration, removal of the solvent, and the addition of petrol gave bis-pyridine tetracyclone rhodium chloride (V) (0.175 g, 90%), m.p. 286–288°. Mixed melting point with the compound obtained under identical conditions from tetracyclone rhodium chloride 282–284°. The infrared spectrum showed ν_{CO} at 1 623, 1 603 cm^{-1} (KBr), and 1 621 cm^{-1} ($CHCl_3$ solution).

Anal. Calcd. for $C_{39}H_{30}ClN_2ORh$: C, 68.8; H, 4.4; N, 4.1; mol. wt., 680. Found: C, 68.6; H, 4.6; N, 4.1; mol. wt., 730.

Tetracyclone Rhodium Acetylacetonate (VI)

Tetracyclone rhodium carbonyl chloride (IV) (0.15 g) was suspended in 20 ml of benzene and a solution of thallous acetylacetonate (0.11 g) in 10 ml of hot benzene was added. The mixture was stirred overnight to give a red precipitate which was filtered off and extracted with methylene chloride. Removal of the methylene chloride followed by recrystallization of the residue from methylene chloride and petroleum ether gave tetracyclone rhodium acetylacetonate (VI) (0.14 g, 88%), m.p. 269–271° (softening at 257°). Mixed melting point with the product obtained under the same conditions from tetracyclone rhodium chloride 255–270° (decomp.). The n.m.r. spectrum ($CDCl_3$) showed, in addition to phenyl absorption, two singlets at 8.1 τ and 8.62 τ with relative intensities 1:5.5. The infrared spectrum shows ν_{CO} at 1 650 cm^{-1} (KBr) and 1 637 cm^{-1} ($CHCl_3$ solution).

Anal. Calcd. for $C_{34}H_{27}RhO_3$: C, 69.7; H, 4.6; mol. wt., 586. Found: C, 70.2; H, 5.4; mol. wt., 611.

Triphenylphosphine Tetracyclone Rhodium Chloride (VII)

Tetracyclone rhodium chloride (0.1 g) was dissolved in 20 ml of hot benzene, and triphenylphosphine (0.094 g) in 5 ml of benzene was added. The mixture was filtered after stirring for 30 min, and the solvent removed to give a dark red solid. Recrystallization from methylene chloride and petroleum ether gave triphenylphosphine tetracyclone rhodium chloride (VII) as red needles (0.125 g, 83%), m.p. 260–262° (effervescence). The infrared spectrum showed ν_{CO} at 1 645 cm^{-1} (KBr) and 1 642 cm^{-1} ($CHCl_3$ solution).

Anal. Calcd. for $C_{47}H_{35}ClOPRh$: C, 71.9; H, 4.5; mol. wt., 784. Found: C, 71.7; H, 4.3; mol. wt., 748.

Reaction of Tetracyclone Rhodium Carbonyl Chloride with Triphenylphosphine

Tetracyclone rhodium carbonyl chloride (IV) (0.1 g) suspended in 10 ml of benzene was treated with triphenylphosphine (47 mg, exactly 1 molar equivalent) in 2 ml of benzene and the mixture was stirred at 20° for 15 min. Filtration and removal of the solvent gave a red oil. Upon addition of methylene chloride yellow needles of bis(triphenylphosphine)rhodium carbonyl chloride (30 mg, 24%) were obtained, m.p. 282°; mixed melting point with an authentic sample 290–294°. The infrared spectrum was identical with that of the authentic sample.

The solvent was removed from the filtrate and the resultant brown residue was recrystallized from methylene chloride and petroleum ether to yield tetracyclone rhodium chloride (III) (24 mg, 25%), m.p. 291–295°, mixed m.p. 316–320°. Removal of the solvent from the mother liquor gave a small amount of impure purple solid whose infrared spectrum was identical with that of tetracyclone.

Duroquinone Rhodium Chloride (X, R=Me)

Rhodium dicarbonyl chloride (0.5 g, 1.25 mmole) and duroquinone (0.47 g, 2.5 mmole) were refluxed in 25 ml of benzene for 4 days. Removal of the solvent to small bulk gave a red crystalline solid (0.65 g, 83%). Recrystallization from benzene gave duroquinone rhodium chloride dimer (X, R=Me), m.p. > 300° (decomp. from 200°). The n.m.r. spectrum ($CDCl_3$) showed one methyl resonance at 8.36 τ. The infrared spectrum showed ν_{CO} at 1 608 cm^{-1} (KBr) and 1 658 cm^{-1} (CH_2Cl_2 solution).

Anal. Calcd. for $C_{20}H_{24}Cl_2O_4Rh_2$: C, 39.7; H, 4.0; mol. wt., 605. Found: C, 39.7; H, 3.9; mol. wt., 582.

2,3,5,6-Tetraethyl-p-Benzoquinone Rhodium Chloride (X, R=Et)

2,3,5,6-Tetraethyl-*p*-benzoquinone (0.55 g, 2.5 mmole) (1) and rhodium dicarbonyl chloride (0.5 g, 1.25 mmole) were refluxed in 20 ml of benzene for 4 days. The mixture was worked up as described above to yield the complex (X, R=Et) (0.6 g, 65%), m.p. 224–225° after recrystallization from benzene. The infrared spectrum showed ν_{CO} at 1 610 cm^{-1} (KBr) and 1 656 cm^{-1} (CH_2Cl_2 solution).

Anal. Calcd. for $C_{28}H_{40}Cl_2O_4Rh_2$: C, 46.9; H, 5.6; mol. wt., 717. Found: C, 46.8; H, 5.5; mol. wt., 678.

Treatment of methylene chloride solutions of either X (R=Me) or X (R=Et) with carbon monoxide for 30 min at 25° yielded quantitative amounts of the respective *p*-benzoquinone (IX, R=Me or Et) and rhodium dicarbonyl chloride dimer.

Bis-Pyridine Duroquinone Rhodium Chloride (XI, R=Me)

Duroquinone rhodium chloride dimer (X, R=Me) (0.1 g) was dissolved in methylene chloride (10 ml) and pyridine (2 ml) was added. After 5 min the solvent was removed to small bulk and petroleum ether added to give an orange crystalline solid. Recrystallization from methylene chloride and petroleum ether containing a few drops of pyridine gave XI (R=Me) as orange needles (0.11 g, 87%), m.p. > 300° (softens at 187°). The n.m.r. spectrum ($CDCl_3$) showed in addition to phenyl resonances a singlet at 8.62 τ. The infrared spectrum showed ν_{CO} at 1 939 and 1 600 cm^{-1} (KBr).

Anal. Calcd. for $C_{20}H_{22}ClN_2O_2Rh$: C, 52.1; H, 4.8; N, 6.0. Found: C, 51.1; H, 4.9; N, 6.5.

Can. J. Chem. Downloaded from www.nrcresearchpress.com by 210.87.254.6 on 09/05/12
For personal use only.

ACKNOWLEDGMENTS

We thank the National Research Council for the award of a Postdoctoral Fellowship (to S. M.) and Johnson, Matthey and Mallory for the loan of rhodium trichloride.

REFERENCES

1. P. M. MAITLIS and S. MCVEY. J. Organometal. Chem. **4**, 254 (1965).
2. (*a*) G. N. SCHRAUZER. Inorg. Chem. 4, 264 (1965). (*b*) S. F. A. KETTLE and R. MASON. J. Organometal. Chem. **5**, 97 (1966).
3. M. C. BAIRD, D. N. LAWSON, J. T. MAGUE, J. A. OSBORN, and G. WILKINSON. Chem. Commun. 129 (1966).
4. A. RUSINA and A. A. VLCEK. Nature, **206**, 295 (1965). J. TSUJI and K. OHNO. Tetrahedron Letters, 3969 (1965).
5. G. N. SCHRAUZER and K. C. DEWHIRST. J. Am. Chem. Soc. **86**, 3267 (1964).
6. J. C. DUNITZ, H. C. MEZ, O. S. MILLS, and H. M. M. SHEARER. Helv. Chim. Acta, **45**, 647 (1962).
7. R. CRIEGEE and G. SCHROEDER. Ann. **623**, 1 (1959).

Can. J. Chem. Downloaded from www.nrcresearchpress.com by 210.87.254.6 on 09/05/12
For personal use only.

Can. J. Chem. Downloaded from www.nrcresearchpress.com by 210.87.254.6 on 09/05/12
For personal use only.

THE INFRARED SPECTRUM AND THERMAL DECOMPOSITION OF HYDRAZINE PERCHLORATE HEMIHYDRATE[1]

P. W. M. JACOBS[2] AND A. RUSSELL-JONES[3]
Department of Chemistry, Imperial College, London, England

Received April 28, 1966

ABSTRACT

The infrared spectrum of hydrazine perchlorate hemihydrate (HPH) has been determined and an assignment of the absorption bands made. *In vacuo*, HPH will partially dehydrate even at room temperature; when heated the remainder of the half-mole of water is lost at 61 °C. The dehydrated salt melts at 138 °C and decomposition ensues. The kinetics of decomposition may be followed in the temperature range 180–280 °C. The activation energy is 36.3 kcal/mole. At low temperatures the decomposition is represented by the chemical equation

$$2N_2H_5ClO_4.\tfrac{1}{2}H_2O = 0.8NH_4ClO_4 + 0.7O_2 + 1.6N_2 + 0.6Cl_2 + 4.4H_2O,$$

but when the temperature is high enough the rate of decomposition of the ammonium perchlorate formed becomes appreciable also. Possible reaction mechanisms are discussed.

There have been no previous investigations of either the infrared spectrum or the decomposition kinetics of hydrazine perchlorate hemihydrate (HPH). This is remarkable because it is a substance of both chemical and technological interest. As the fourth member of the series nitronium perchlorate, hydroxylamine perchlorate, ammonium perchlorate, hydrazine perchlorate it contains the smallest excess of oxidant. Because of its greater hydrogen content it would be expected to be more unstable than ammonium perchlorate and thus to be a potentially useful, but possibly dangerous, additive to solid rocket propellants. The anhydrous salt (HP) is more sensitive to impact than pentaerythritol tetranitrate and is also highly friction-sensitive, being said to explode violently on gentle rubbing in a porcelain mortar (1). The burning of HP has been studied by Shidlovskii *et al.* (1), and by Levy *et al.* (2). The heat of formation of HP was found to be $\Delta H_{298} = -42.9 \pm 0.2$ kcal/mole (1), in good agreement with a previous value of -42 kcal/mole obtained by Medard (3). From measurements of the vaporization rate Levy *et al.* (2) deduced an enthalpy of vaporization for the equilibrium

$$N_2H_5ClO_4\ (l) = N_2H_4\ (g) + HClO_4\ (g)$$

of 59.2 kcal/mole.

HPH was found (2) to burn in a reasonably stable manner in the presence of small amounts of fuel (e.g. stabilized formaldehyde polymers) even at atmospheric pressure, the burning rate being some 15 times greater than the extrapolated rate at 1 atm for ammonium perchlorate (AP). The measured flame temperature (2) was $2\,275 \pm 50$ °K, indicative of thermodynamic equilibrium which corresponded closely to the stoichiometric equation

$$N_2H_5ClO_4 = N_2 + HCl + 2H_2O + O_2.$$

The burning rate of HP mixed with manganese dioxide or cuprous chloride is a factor of 2–3 times faster than similar mixtures with AP (1). Mixtures of AP and HP containing 30–60% of the latter will burn steadily, if ignited, at room temperature and pressure (1).

Ammonium perchlorate decomposes by first dissociating into ammonia and perchloric

[1]*British Crown Copyright, reproduced with the permission of the Controller Her Britannic Majesty's Stationery Office.*
[2]*Present address: Department of Chemistry, University of Western Ontario, London, Ontario.*
[3]*Present address: John and E. Sturge Ltd., Wheeleys Road, Edgbaston, Birmingham, England.*

acid (4). At low temperatures ($< \sim 300$ °C) decomposition is incomplete and, if sublimation is suppressed, a residue of AP, representing about 70% of the original material, remains. At higher temperatures this residue itself decomposes through the evaporation of ammonia and perchloric acid into the gas phase and the oxidation of the former by radicals from the pyrolysis of the latter. Catalysts, such as copper chromite, promote the reaction by substituting heterogeneous reactions for these gas-phase reactions (4). In view of the chemical similarity between ammonia and hydrazine it was interesting to see if a similar mode of reaction applied for hydrazine perchlorate.

EXPERIMENTAL

Because of its instability and shock sensitivity the main batches of HPH used were prepared at the Explosives Research and Development Establishment at Waltham Abbey. We had previously prepared small amounts of the material using essentially the same method, which was the neutralization of 60% aqueous perchloric acid with hydrazine. The recrystallized powder was pressed into pellets of mass 40 mg at Waltham Abbey. The normal precautions used in the storage and handling of unstable materials were observed. Storage in a desiccator is not recommended, since the dehydrated salt is considerably more sensitive than the hydrate.

Two methods were used to study the kinetics of the thermal decomposition of HPH. Pellets were dropped *in vacuo* into a reaction vessel (pyrex glass or silica) surrounded by an electronically controlled electric furnace and the ensuing pressure changes at constant volume were measured either with a glass spiral gauge or with a recording mercury manometer. In the latter, the surface of the mercury in the limb connected to the reaction vessel was protected from attack by chlorine by a layer of silicone oil. Alternatively the reaction was followed thermogravimetrically at 1 atm pressure with a Stanton automatic recording thermobalance.

At first an attempt was made to record the infrared spectrum of HPH by the KBr disc method but the measured spectrum corresponded to that of a mixture of potassium perchlorate and hydrazine bromide. Accordingly, mulls in Nujol, hexachlorobutadiene, and Fluorolube were employed. Among them these three provided sufficient peak-free zones for a complete spectrum to be determined. A Perkin–Elmer model 21 with a fluorite prism was used for the 4 000 – 2 000 cm^{-1} region and a Perkin–Elmer model 137 with a sodium chloride prism from 2 000 – 650 cm^{-1}.

RESULTS

Infrared Spectrum

The complete spectrum is shown in Fig. 1. The band due to N—H and O—H stretching frequencies is very broad and complex, the general shape being similar to that found by Decius and Pearson (5) for hydrazine hydrochloride. There is a well-defined pair of peaks between 6 and 7 μ and a second broad absorption band between 8 and 10 μ, with another sharp peak at 960 cm^{-1} and a broad band of low intensity at 765 cm^{-1}.

Kinetics

The kinetics of thermal decomposition was followed by pressure measurements in the temperature range 196 to 280 °C with an initial pressure of 10^{-6} Torr. The rate of decomposition in a silica vessel was significantly greater than that in one made of pyrex glass.

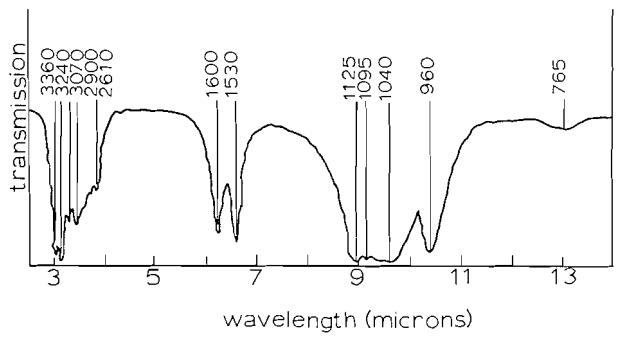


FIG. 1. Infrared spectrum of hydrazine perchlorate hemihydrate. The frequencies of the principal absorption peaks are given in cm^{-1}.

Can. J. Chem. Downloaded from www.nrcresearchpress.com by 210.87.254.6 on 09/05/12
For personal use only.

The evolution of the water of crystallization was clearly marked either on the recorder trace or by a sudden deflection of the light spot reflected from the mirror on the spiral gauge and this was taken as zero time for the decomposition. After this very rapid evolution of water the pressure–time curve followed a deceleratory course until the reaction was virtually complete. A typical plot of α (the fraction decomposed in time t) against t is shown in Fig. 2. As these $\alpha(t)$ curves did not appear to fit any of the usual kinetic equations, rate constants were determined as the initial slopes of the $\alpha(t)$ plots. These are plotted in the form log k vs. T^{-1}, with k in min^{-1}, in Fig. 3. This figure shows (*a*) the reproducibility achieved with two separate preparations of HPH and (*b*) the faster rate of reaction in silica vessels. The activation energies in silica and in pyrex vessels were found to be 36.4 and 36.6 kcal/mole respectively.

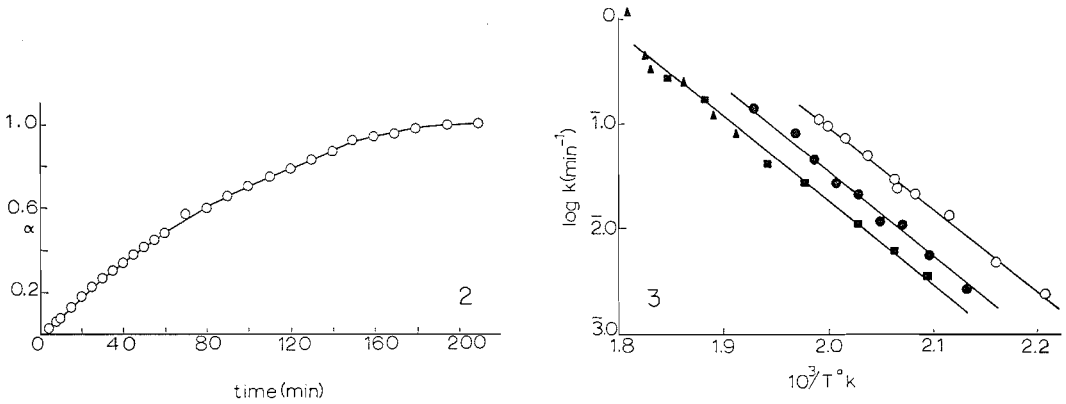


FIG. 2. Thermal decomposition of HPH in a silica vessel at 215 °C. The fractional decomposition α is plotted as a function of time.

FIG. 3. Logarithm of the initial rate of decomposition of HPH as a function of reciprocal temperature. Pressure measurements: pyrex vessel, batch I (▲); pyrex vessel, batch II (■); silica vessel (●); thermogravimetry (○).

Analysis of gaseous products was carried out by doing runs with a liquid nitrogen trap in the system. When reaction was complete, the permanent gas pressure was measured. The permanent gases were then pumped off and the system re-isolated. The liquid nitrogen was then replaced by a series of coolants, the equilibrium pressure being measured after each replacement. The quantity of gas released could then be calculated from the effective volume of the system at each trap temperature. The trap temperatures (78 °K, 90 °K, 147.5 °K, 156 °K, 175.4 °K, 195.2 °K, 250.8 °K, and 297 °K) were chosen so as to provide a separation of all likely products, but the only temperatures at which gases were evolved were 195.2 °K (chlorine) and 297 °K (water). At first both the chlorine and water balances were low: these were traced, respectively, to attack of Apiezon grease by chlorine and partial dehydration of the HPH during the pre-run room-temperature outgassing. As a check of this a pellet of HPH was outgassed for 60 h under hard vacuum. The pellet lost 6.05% of its weight, compared with 6.35% expected for complete dehydration.

The reaction was also studied in the temperature range 180 to 229 °C by thermogravimetry. The kinetics were again deceleratory throughout and did not conform to any of the usual rate equations. Rate constants were therefore again determined from initial slopes. A point of inflection was observed in the weight-loss curve at $\alpha = 0.33$. The infrared spectrum of the solid residue at this stage of the reaction contained none of the strong peaks characteristic of HPH: the spectrum did, however, conform to that of ammonium perchlorate. X-ray powder photographs of HPH, AP, and the residue were therefore

Can. J. Chem. Downloaded from www.nrcresearchpress.com by 210.87.254.6 on 09/05/12
For personal use only.

taken. That for pure HPH proved difficult to analyze since it was evident that the structure was one of low symmetry (6, 7). It was clear from a comparison of the powder photographs, however, that the residue at $\alpha = 0.33$ was not HPH but ammonium perchlorate, in confirmation of the infrared spectra.

The weight loss data and the gas analyses lead to the following chemical equation for the decomposition of HPH.

[1] $$2N_2H_5ClO_4.\tfrac{1}{2}H_2O = 0.8NH_4ClO_4 + 0.7O_2 + 1.6N_2 + 0.6Cl_2 + 4.4H_2O$$

The activation energy for the decomposition, as determined by thermogravimetry, is 35.8 kcal/mole, in good agreement with that found by pressure measurements.

DISCUSSION

Infrared Spectrum

Interpretation of this spectrum is facilitated by a comparison of the spectra of related compounds for which data are available. In Table I such a comparison is effected with spectra for $KClO_4$ (8–10), $NaClO_4.H_2O$ (8), NH_4ClO_4 (8), NH_4NO_3 (11), and N_2H_5Cl (5). The HPH spectrum can be divided conveniently into four regions.

(i) 4 000 to 2 000 cm^{-1}

Neglecting intermolecular coupling we should expect to find a maximum of six peaks in this region. The first band at 3 360 cm^{-1} is clearly due to the $(O—H)_s$ vibration though it may also include some contribution from the highest $(N—H)_s$ vibration which occurs at 3 261 cm^{-1} in hydrazine chloride. In AP and in ammonium nitrate the $(N—H)_s$ vibrations are all degenerate under T_d symmetry and give rise to bands at 3 330 and 3 260 cm^{-1} respectively. Because of the lack of symmetry in $(N_2H_5^+)$, a maximum of five peaks from the $(N—H)_s$ vibrations is expected. Four of these are clearly resolved. With better resolution one might see more than six peaks and thus would indicate intermolecular coupling, possibly through hydrogen bonding to the O atoms of the ClO_4^- ions.

(ii) 2 000 to 1 300 cm^{-1}

In this region we expect to find the $(O—H)_d$ frequency (1 630 cm^{-1} in $NaClO_4.\frac{1}{2}H_2O$) and $(H—N—H)_d$ frequencies. The degenerate asymmetric deformation of the NH_4^+ ion gives rise to absorption peaks at 1 420 and 1 435 cm^{-1} respectively in NH_4ClO_4 and NH_4NO_3. In N_2H_5Cl three $(H—N—H)_d$ peaks are observed at 1 500, 1 584, and 1 638 cm^{-1}. The 1 530 cm^{-1} peak in HPH is therefore due to this vibration also, whereas the 1 600 cm^{-1} peak is presumably due to both $(O—H)_d$ and $(H—N—H)_d$. In N_2H_5Cl two $(H—N—N)_b$ frequencies are detected at 1 246 and 1 417 cm^{-1} but these were not resolved in HPH.

(iii) 1 200 to 900 cm^{-1}

This is the most complicated region of the spectrum since the group-bending frequencies of the NH_3^+ group (1 101 and 1 124 cm^{-1} in N_2H_5Cl) are overlapped by the asymmetric stretching frequency of the ClO_4^- ion (1 135 cm^{-1} in NH_4ClO_4). We resolve three peaks at 1 125, 1 095, and 1 040 cm^{-1}. The first of these at 1 125 cm^{-1} is due to unresolved components from $(ClO_4^-)_s$ and $(NH_3^+)_b$, the second at 1 095 cm^{-1} arises from $(NH_3^+)_b$, and the third component at 1 040 cm^{-1} is due (9) to a combination of the asymmetric and symmetric deformations of the ClO_4^- ion. The frequency of the former is 624–628 cm^{-1} and thus beyond the range of our measurements, whereas the latter is of course observed only in Raman spectroscopy (461 cm^{-1} in $KClO_4$). Well resolved from this group of peaks is one at 960 cm^{-1} due to the $(N—N)_s$ vibration.

Can. J. Chem. Downloaded from www.nrcresearchpress.com by 210.87.254.6 on 09/05/12
For personal use only.

Can. J. Chem. Downloaded from www.nrcresearchpress.com by 210.87.254.6 on 09/05/12
For personal use only.

TABLE I

Observed frequencies (in cm^{-1}) in the infrared spectrum of HPH and in spectra used to effect assignments

$NaClO_4.\frac{1}{2}H_2O$ (8)*	$KClO_4$ (9)	$KClO_4$ (8)*	$KClO_4$ (10)†	NH_4ClO_4 (8)	NH_4NO_3 (11)‡	N_2H_5Cl (5)	$N_2H_5ClO_4.\frac{1}{2}H_2O$	Assignment
			461					$(ClO_4^-)_d$
628	624	637	628	624				$(ClO_4^-)_d$§
						763	765	$(N_2H_5^+)$ vib.
			938					$(ClO_4^-)_s$
						973	960	$(N—N)_s$
1 100‖	1 090	1 075	1 073	1 060			1 040	$(ClO_4^-)_d + (ClO_4^-)_d$
						1 101	1 095	$(NH_3^+)_b$
						1 124		$(NH_3^+)_b$
							1 125	
1 100‖	1 140	1 140	1 121	1 135				$(ClO_4^-)_s$
						1 246		$(H—N—N)_b$
						1 417		$(H—N—N)_b$
				1 420	1 435			$(NH_4^+)_d$
						1 500	1 530	$(H—N—H)_d$
						1 584		$(H—N—H)_d$
						1 638		$(H—N—H)_d$
							1 600	
1 630								$(O—H)_d$
						2 716	2 610	
						2 950	2 900	
				3 330	3 260	3 034	3 070	$(N—H)_s$
						3 150		
						3 261	3 240	
3 570							3 360	$(O—H)_s$

*Two very small bands reported by Miller and Wilkins at 2 030 cm^{-1} in $NaClO_4.\frac{1}{2}H_2O$ and at 1 990 cm^{-1} in $KClO_4$ have been omitted.
†Raman spectrum.
‡Phase IV; only NH_4^+ frequencies shown.
§Beyond the range of our determination.
‖Not resolved in $NaClO_4.\frac{1}{2}H_2O$.

(iv) Below 900 cm^{-1}

The only peak observed is one at 795 cm^{-1}, which is due to a vibrational mode of the $N_2H_5^+$ ion since it correlates well with the 763 cm^{-1} peak in N_2H_5Cl.

Mechanism of Decomposition

The first step in the decomposition of HPH is dehydration which occurs partially during outgassing at room temperature and is completed at a temperature of 61 °C. The anhydrous HP then melts at 138 °C. The vapor pressure of HP has been calculated by Levy *et al.* (2) from measurements of the rate of sublimation. They give values of 1.16 $\times$ 10^{-4} Torr at 180 °C and 33.4 $\times$ 10^{-4} Torr at 235 °C. The heat of vaporization for the dissociative equilibrium

$$N_2H_5^+ClO_4^- \text{ (l)} = N_2H_4 \text{ (g)} + HClO_4 \text{ (g)} \quad [2]$$

found from these vapor pressure measurements is $\Delta H_v = 59.2$ kcal/mole (2), in agreement with the value of 60.4 kcal/mole calculated from thermodynamic data. We first examine the available evidence to try and decide if reaction occurs in the melt or in the gas phase (including heterogeneous reactions on the walls of the reaction vessel).

If the mechanism of decomposition of HP involved the decomposition of hydrazine and perchloric acid in the gas phase with the vaporization step rate determining, then the experimental activation energy E would be 30 kcal/mole ($\frac{1}{2}\Delta H_v$). Similarly, if the gas-phase reaction were a bimolecular one between hydrazine and perchloric acid with vaporization rate determining, then E would be 60 kcal/mole. If the vapor is in equilibrium with the melt and the decomposition of one of the vapor species is rate determining (rate = $k'p_{N_2H_4}$ or rate = $k'p_{HClO_4}$), then the experimental activation energy E would be $E' + 30$ kcal/mole where E' is the activation energy corresponding to the rate constant k'. Since $E = 36.3$ kcal/mole, this is a theoretically possible situation, whereas a mechanism in which vaporization is rate determining is excluded ($E \neq \frac{1}{2}\Delta H_v$ or ΔH_v). Further evidence that vaporization is not rate determining comes from a comparison of the kinetics obtained from pressure measurements and from weight loss. The pressure measurements give the true reaction rate of the slowest step which leads to an increase in pressure and it is impossible to say from these alone whether the vaporization step or the subsequent gas-phase reactions are rate determining. Weight-loss measurements give the loss of material from the sample whether by reaction or vaporization. If the ambient pressure over the sample is increased by introducing an inert gas, then the rate of vaporization will be reduced. Thus, if vaporization were rate determining, the reaction rate determined from weight loss measurements under 1 atm pressure would be much lower than that found by pressure measurements at low pressures. In fact (Fig. 3) the rate is practically the same. (The rate determined by weight loss is actually higher than that found by pressure measurements, but the discrepancy is only of the same order as occurs on changing from a pyrex to a quartz reaction vessel and we do not therefore regard it as very significant.) For the above reasons we conclude that vaporization is not rate determining. One would like to support this conclusion quantitatively using the measured vaporization rates of Levy *et al.* (2), but unfortunately we do not know the surface area A of our molten HP. The order of magnitude of A may be 1 cm^2. If we assume a surface area of 1.5 cm^2 then the initial vaporization rate is faster than the initial reaction rate at all temperatures at which measurements were carried out. If we choose $A = 0.6$ cm^2 then the initial vaporization rate is faster than the initial reaction rate in a pyrex vessel at all temperatures, but marginally slower than the rate in quartz at the top two temperatures.

Another hypothesis which is consistent with the above facts is that the rate-determining

Can. J. Chem. Downloaded from www.nrcresearchpress.com by 210.87.254.6 on 09/05/12
For personal use only.

Can. J. Chem. Downloaded from www.nrcresearchpress.com by 210.87.254.6 on 09/05/12
For personal use only.

reaction occurs in the melt. The vaporization experiments of Levy *et al.* (2) were carried out in the temperature range 180–235 °C, which covers about the lower two thirds of our temperature range. Run durations varied from 315 to 37 min and it is clear from our kinetic experiments (e.g. Fig. 1) that substantial decomposition would have occurred during times of this order of magnitude. In fact, Levy *et al.* (2) analyzed both condensate and residue: they recovered 97–99% of their original charge and both condensate and residue contained 95–100% HP. This means that when the hydrazine and perchloric acid evaporate from the melt directly on to a cold finger, substantially no decomposition occurs. The above considerations thus show that reaction occurs not in the melt but in the gas phase (or on the reaction-vessel walls) after evaporation and that it is the rate of these chemical processes rather than the evaporation process which is rate determining in the temperature range of our experiments.

Although the chemical processes after evaporation cannot be established in complete detail certain general features of the reaction are clear. The homogeneous thermal decomposition of perchloric acid is not involved. Between 357 and 439 °C the reaction is first order (12) with a rate constant k given by

$$k = 5.8 \times 10^{13} \exp(-45100/RT)\ \mathrm{s}^{-1}. \qquad [3]$$

The extrapolated rate in our temperature range is two orders of magnitude lower than the rate of decomposition of HP. Below 350 °C, however, Levy's results (12) show a considerable scatter and a sensitiveness to the nature and pretreatment of the reaction vessel, both of which indicate the onset of a heterogeneous reaction. Superimposing a plot of our rate constants for the decomposition of HP on to Levy's data (12) shows that they lie between the rather wide limits indicated by his results. Of the nine points within our temperature range six lie below our lines, one is between the pyrex and quartz lines, and the other two lie above the quartz line. Thus we conclude that in the decomposition of HP, perchloric acid becomes adsorbed on the walls of the reaction vessel adjacent to the melt and that partial but not complete decomposition of $HClO_4$ ensues. The stoichiometric equation for this reaction is

$$HClO_4 = \tfrac{1}{2}Cl_2 + 1\tfrac{3}{4}O_2 + \tfrac{1}{2}H_2O. \qquad [4]$$

The mechanism of the heterogeneous reaction has not been established, but the primary step in the homogeneous reaction is the splitting of the HO—ClO_3 bond, which requires $\sim$ 45 kcal/mole, followed by decomposition of ClO_3. In this (or a likely alternative) route O atoms will be produced. Recombination of O atoms on the walls will occur and we may thus safely presume the presence of oxygen molecules, and possibly O atoms, from the decomposing perchloric acid.

The homogeneous decomposition of hydrazine may be safely excluded as a possible contributory feature. It has been studied (13) in the range 630–780 °C using toluene carrier gas to react with the NH_2 radicals produced by N—N bond fission, which requires 60 kcal/mole. The heterogeneous thermal decomposition occurs on silica between 270 and 310 °C (14). The stoichiometric equation for the reaction is

$$3N_2H_4 = 4NH_3 + N_2, \qquad [5]$$

but because it is first order (15) and does not involve free radicals[4] the mechanism probably involves the formation of an activated complex by one N_2H_4 molecule approaching two adsorbed N_2H_4 molecules (12). The activation energy of this reaction [5] is in doubt but is

[4]*Decomposition of hydrazine in the presence of para hydrogen (16) does not cause any para–ortho conversion; neither does randomization of nitrogen isotopes occur in the decomposition of* $H_2{}^{15}N{}^{14}NH_2$ *(17).*

variously estimated to be 18 kcal/mole (12) and 9.3 or 15.7 kcal/mole (15). Ammonia produced on the walls from this reaction will react with adsorbed but unreacted perchloric acid to produce the deposit of ammonium perchlorate observed at the bottom of the reaction tube.

The remaining reaction is the oxidation of hydrazine by oxygen from the perchloric acid. The chief uncertainty about the whole process is whether this involves O atoms or O_2 molecules. The vapor-phase reaction between hydrazine and molecular oxygen has been investigated by Bowen and Birley (18) who found the reaction approximately first order with respect to each component and with an activation energy of 38 kcal/mole falling to 20.5 kcal/mole at 'higher temperatures'. (The temperature range investigated was 100–160 °C.) Winning (19) investigated the same reaction between room temperature and 100 °C and found it to be second order and heterogeneous with an activation energy of 6.4 kcal/mole. The reaction of hydrazine with O atoms does not appear to have been studied, but there is substantial evidence that hydrogen abstraction from hydrazine is substantially easier (by several orders of magnitude) than from ammonia. Schiavello and Volpi (20) found that whereas the reaction of H atoms with ammonia proceeds only with difficulty at 150 °C, that with hydrazine goes at a measurable velocity in the range 25–150 °C. Estimated bimolecular rate constants at 150 °C are 3.5×10^{10} mole^{-1} cm^3 s^{-1} for $H + N_2H_4$ and 10^7 mole^{-1} cm^3 s^{-1} for $H + NH_3$. Similarly Gray and Thynne (21) found that at 150 °C CH_3 radicals will abstract H atoms from N_2H_4 450 times faster than from ammonia. Bimolecular rate constants for $O + NH_3$ are known from the work of Wong and Potter (22), but it is impossible to estimate the possible contribution of this reaction since the concentrations of O and NH_3 during the reaction are unknown. The main products, as would be expected, are water and nitric oxide (22) and because of the absence of NO in the products from the decomposition of HP, we conclude that this reaction does not occur either because it is much slower than the comparable reaction with hydrazine or because of the more rapid combination reaction

[6] $$O + O + M = O_2 + M.$$

Hydrazine is sufficiently reactive to be oxidized by molecular oxygen (18, 19) even if the O-atom concentration is negligible. The reaction probably occurs both heterogeneously on the walls and homogeneously in the gas phase.

The overall stoichiometry of the decomposition of HP in the temperature range 180–280 °C is thus satisfied by the following mechanism:

[2] $$N_2H_5^+ClO_4^- (l) = N_2H_4 (g) + HClO_4 (g)$$

[4] $$0.6HClO_4 = 0.3Cl_2 + 0.3H_2O + 1.05O_2$$

[7] $$0.7N_2H_4 + 0.7O_2 = 0.7N_2 + 1.4H_2O$$

[5] $$0.3N_2H_4 = 0.1N_2 + 0.4NH_3$$

[8] $$0.4NH_3 + 0.4HClO_4 = 0.4NH_4^+ClO_4^-.$$

Reactions [4], [5], [8], and probably [7] are heterogeneous. The oxygen produced in [4] will be initially present in part as O atoms. It is uncertain whether reaction [7] involves oxygen molecules or O atoms or both, since this depends on the relative speeds of the reactions $O + O + M = O_2 + M$ and $O + N_2H_4 =$ products.

ACKNOWLEDGMENTS

We are indebted to Dr. J. Powling for his support and encouragement of this research and to members of the staff of the Explosives Research and Development Establishment for undertaking the preparation and pelleting of the hydrazine perchlorate hemihydrate.

Can. J. Chem. Downloaded from www.nrcresearchpress.com by 210.87.254.6 on 09/05/12
For personal use only.

REFERENCES

1. A. A. SHIDLOVSKII, V. I. SEMISHIN, and L. F. SHMAGIN. Zh. Prikl. Khim. **35**, 756 (1962); J. Appl. Chem. USSR, English Transl. **35**, 734 (1962).
2. J. B. LEVY, G. VON ELBE, R. FRIEDMAN, T. WALLIN, and S. J. ADAMS. Advan. Chem. Ser. **54**, 55 (1966).
3. L. MEDARD. Mem. Artillerie Franc. 2me Fasc. 447 (1954).
4. P. W. M. JACOBS and A. RUSSELL-JONES. Symp. Combust. 11th.
5. J. C. DECIUS and D. P. PEARSON. J. Am. Chem. Soc. **75**, 2436 (1953).
6. U. PANICHI. Z. Kryst. Mineral. **50**, 495 (1912); Rivista Miner. Crist. Ital. **36**, 88 (1909).
7. J. CONANT and K. HOOGSTEEN. *Quoted by* M. Stammler and D. Orcutt. Advan. X-Ray Anal. **5**, 133 (1962).
8. F. A. MILLER and C. H. WILKINS. Anal. Chem. **24**, 1253 (1952).
9. H. COHN. J. Chem. Soc. 4282 (1952).
10. D. J. MILLEN. J. Chem. Soc. 2606 (1950).
11. A THEORET and C. SANDORFY. Can. J. Chem. **42**, 57 (1964).
12. J. B. LEVY. J. Phys. Chem. **66**, 1092 (1962).
13. M. SZWARC. Proc. Roy. Soc. London, Ser. A, **198**, 267 (1949).
14. P. J. ASKEY. J. Am. Chem. Soc. **52**, 970 (1930).
15. T. J. HANRATTY, J. N. PATTISON, J. W. CLEGG, and A. W. LEMMON. Ind. Eng. Chem. **43**, 1113 (1951).
16. E. A. B. BIRSE and H. W. MELVILLE. Proc. Roy. Soc. London, Ser. A, **175**, 164 (1940).
17. A. KANT and W. J. MCMAHON. J. Inorg. Nucl. Chem. **15**, 305 (1960).
18. E. J. BOWEN and A. W. BIRLEY. Trans. Faraday Soc. **47**, 580 (1951).
19. W. I. H. WINNING. J. Chem. Soc. 926 (1954).
20. M. SCHIAVELLO and G. G. VOLPI. J. Chem. Phys. **37**, 1510 (1962).
21. P. GRAY and J. C. J. THYNNE. Trans. Faraday Soc. **60**, 1047 (1964).
22. E. L. WONG and A. E. POTTER, JR. J. Chem. Phys. **39**, 2211 (1963).

Can. J. Chem. Downloaded from www.nrcresearchpress.com by 210.87.254.6 on 09/05/12
For personal use only.

Can. J. Chem. Downloaded from www.nrcresearchpress.com by 210.87.254.105 on 09/05/12
For personal use only.

ON THE POSSIBLE CONTRIBUTION OF A MOLECULAR MECHANISM TO THE PHOTODECOMPOSITION OF NITROGEN DIOXIDE[1]

K. F. PRESTON AND R. J. CVETANOVIĆ

INTRODUCTION

Experimental investigations (1) of the photolysis of NO_2 have been mainly confined to the wavelength (λ) region 3 000 Å – 4 500 Å. The importance of [1]

[1] $$NO_2 + h\nu \rightarrow NO + O(^3P)$$

as a primary process in this wavelength region, suggested by the appearance of diffuseness in the absorption spectrum of NO_2 at 3 980 Å, has been established by several workers (1). The results of a recent investigation by Pitts, Jr., Sharp, and Chan (2) imply that even at wavelengths longer than the threshold for $O(^3P)$ production, photodecomposition of NO_2 takes place entirely by way of an oxygen atom route, and that the contribution from reactions of excited molecules (NO_2^*) of the form

[1*a*] $$NO_2^* + NO_2 \rightarrow 2NO + O_2$$

is negligible. In a search for suitable sources of excited oxygen atoms, we have had occasion to study the photolysis of NO_2 at wavelengths in the region beyond the second onset of diffuseness in the absorption spectrum (2 490 Å), which we (3) believe corresponds to the predissociation

[1*b*] $$NO_2 + h\nu \rightarrow NO + O(^1D).$$

The photooxidation of butene-1 by nitrogen dioxide[2] exhibits distinct behavior not only at wavelengths at which reaction [1*b*] is energetically possible ($< 2\,490$ Å) but also at and in the neighborhood of 2 537 Å. In view of these observations we have thought it necessary to determine the extent of O-atom exchange during the photolysis of mixtures of NO_2 and O_2^{36} at 2 537 Å and at other wavelengths. This method, which is similar to that of Pitts, Jr. *et al.* (2), is based on the underlying assumption that only free oxygen atoms are capable of exchange with O_2^{36} while other potential intermediates (such as, for example, NO_2^*) are not. The exchange reaction is therefore used as a test for the involvement of free oxygen atoms in the photolysis of NO_2.

EXPERIMENTAL

The isotopic composition of the oxygen remaining after the photolysis at 27 ± 2 °C of mixtures of NO_2 and O_2^{36} at 2 288 Å, 2 537 Å, 3 660 Å, 4 047 Å, and at $\lambda > 4\,200$ Å was determined by mass spectrometry. Corrections ($< 10\%$) for the formation of small amounts of O_2^{34} in the mass spectrometer by exchange reactions between O_2^{32} and O_2^{36} were taken from a plot of ΔO_2^{34} against $[O_2^{32}] \times [O_2^{36}]$ obtained by analysis of synthetic mixtures of the 32 and 36 isotopes of oxygen.

A 325 cc cylindrical quartz vessel was used for photolyses at 2 288 Å and a 180 cc cylindrical quartz vessel for photolyses at all other wavelengths. Initial pressures of NO_2 were in the range 3–10 mm Hg; the total initial pressure was usually 11 mm Hg and never exceeded 30 mm Hg. Exposure times varied from a few minutes for runs at 3 660 Å to a maximum of 3 h for some runs at 2 537 Å, but photolysis of NO_2 was never allowed to proceed to more than 15% of complete decomposition. (Extents of decomposition were estimated from the atom % ^{18}O in initial and final oxygen.) The isotopic composition of the O_2^{36} at the

[1]*Issued as N.R.C. No. 9151.*
[2]*K. F. Preston and R. J. Cvetanović. To be published.*

end of a 4 h dark run with initial pressures, $NO_2 = O_2^{36} = 8$ mmHg, NO = 1 mm Hg, was identical within experimental error to the starting composition (the parenthetical values): O_2^{34} 1.31 (1.30), O_2^{35} 0.65 (0.65), O_2^{36} 98.04 (98.05). The dark exchange among the molecules NO, NO_2, and O_2^{36} was therefore negligible.

The following lamps and filter combinations were used: cadmium lamp and chlorine filter (3) for 2 288 Å; low-pressure Hg-resonance lamp with 4 cm Cl_2 (600 mm Hg), 3 cm $NiSO_4.6H_2O$ at 200 g/l H_2O and Corning C.S. 9-54 for 2 537 Å; Hanovia medium-pressure Hg lamp (673A-10) with Corning C.S. 0-52 and C.S. 7-39 for 3 660 Å; Hanovia medium-pressure Hg lamp with C.S. 7-51 and C.S. 3-74 for 4 047 Å; Hanovia medium-pressure Hg lamp with C.S. 3-73 for $\lambda > 4\,200$ Å. In all cases the transmission characteristics of the filter combinations were checked with an ultraviolet spectrophotometer to ensure that only light of the desired wavelength range was obtained from the lamps.

Full details of the apparatus and experimental procedure have been given elsewhere (3).

RESULTS AND DISCUSSION

The ratio of the yields of O_2^{32} and O_2^{34} (R_{32}/R_{34}) resulting from the photolysis of mixtures of NO_2 and O_2^{36} was determined as a function of the concentration ratio $[NO_2]/[O_2^{36}]$ for several wavelengths. The results are plotted in Fig. 1, where the abscissae refer to average ratios of $[NO_2]$ to $[O_2^{36}]$ during the course of a run. Apart from the results for $\lambda > 4\,200$ Å, the experimental data for all wavelengths are consistent with the following simple mechanism:

[1] $$NO_2 + h\nu \rightarrow NO + {}^{16}O$$

[2] $${}^{16}O + NO_2 \rightarrow NO + O_2^{32}$$

[3] $${}^{16}O + O_2^{36} \rightarrow O_2^{34} + {}^{18}O$$

[4] $${}^{18}O + NO_2 \xrightarrow{(a)} NO + O_2^{34}$$
$$\xrightarrow{(b)} N^{18}O + O_2^{32}$$
$$\xrightarrow{(c)} N^{16}O^{18}O + {}^{16}O$$

Formation and subsequent reactions of ozone have been ignored since stabilization of the intermediate O_3* for [3] is negligible compared with decomposition at the pressures used here (4). For similar reasons (5, 6) we have chosen to neglect reactions of NO_3* other than unimolecular decomposition.

For stationary concentrations of ^{16}O and ^{18}O the reaction scheme predicts:

$$R_{32}/R_{34} = \frac{k_{4b}}{(k_4 + k_{4a})} + \frac{k_2 k_4}{k_3(k_4 + k_{4a})} \times \frac{[NO_2]}{[O_2^{36}]},$$

and Fig. 1 shows that such a linear relation is obeyed at all wavelengths shorter than 4 200 Å. The fact that all the data for $\lambda < 4\,200$ Å fit the *same* relationship suggests very strongly that the oxygen atom mechanism is operative at all wavelengths and accounts for the entire extent of decomposition. (An alternative possibility that a molecular path may exist and account for precisely the same fraction of photodecomposition at all wavelengths is unlikely.) This confirms the earlier work of Pitts, Jr., Sharp, and Chan (2). On the other hand, for light of wavelength > 4 200 Å (principally 4 358 Å) there is evidently some production of oxygen molecules without the intermediate participation of oxygen atoms, suggesting the importance of reactions of type [1*a*]. No attempt was made to measure the quantum yield of O_2 production at 4 358 Å, although Pitts, Jr., *et al.* (2) found it to be very small. They believed that the small quantum yields which they observed for photolysis by "monochromatic" 4 358 Å light were actually due to traces of 4 047 Å light transmitted by their filter combination. Such an explanation cannot

Can. J. Chem. Downloaded from www.nrcresearchpress.com by 210.87.254.105 on 09/05/12
For personal use only.

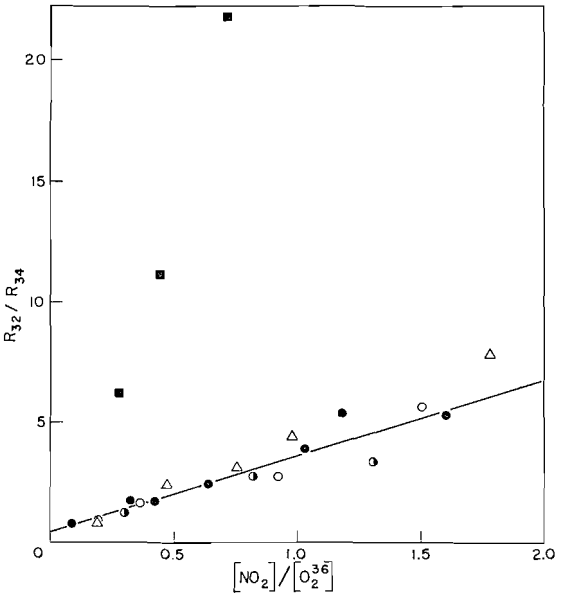


FIG. 1. Plot of R_{32}/R_{34} against $[NO_2]/[O_2^{36}]$ (27 ± 2 °C): (△) 2 288 Å, (●) 2 537 Å, (○) 3 660 Å, (◑) 4 047 Å, (■) > 4 200 Å.

account, however, for the large differences observed in this work between the extents of scrambling at 4 047 Å and 4 358 Å. It is possible, of course, that some photolysis and some or all of the scrambling for $\lambda > 4\,200$ Å was caused by extraneous 4 047 Å light, but we conclude that absorption at 4 358 Å does result in some (although admittedly (2) very small) decomposition and that it occurs at least in part by way of a molecular mechanism.

The results of Fig. 1 show that the overall mechanism for photolysis at 2 537 Å is essentially the same as at 4 047 Å and 3 660 Å, where an O-atom mechanism holds. Reactions of type [1*a*] do not then contribute to the photodecomposition at 2 537 Å. However, in principle, NO_2^* may still be an important intermediate, provided it participates in an indirect production of oxygen atoms, for example by

$$[1c] \qquad NO_2^* + NO_2 \rightarrow [N_2O_3 + O(^3P)] \rightarrow NO_2 + NO + O(^3P).$$

The implication of these results on the photooxidation of butene-1 by NO_2 at 2 537 Å will be discussed elsewhere.[2] A reaction analagous to [1*c*] has been proposed by Ford and Jaffe (5) to explain oxygen atom formation in the photolysis of NO_2 at 4 047 Å. (Reaction [1*a*] rather than [1*c*] is evidently necessary to explain the present results at $\lambda > 4\,200$ Å.)

A least-squares treatment of the data in Fig. 1 for 2 537 Å, 3 660 Å, and 4 047 Å gives a value for $k_2k_4/k_3(k_4 + k_{4a})$ of 3.1 ± 0.3. Klein and Herron (6) have measured k_3 at 37 °C and have determined k_2 as a function of temperature. From their value of k_2/k_3 and their estimate (6) of the contributions of *a*, *b*, and *c* to [4] we calculate $k_2k_4/k_3(k_4 + k_{4a}) = 4.5$ at 37 °C, in fair agreement with our value.

The fit of the 2 288 Å data to the straight line in Fig. 1 is somewhat surprising. We (3) have shown that $O(^1D)$ atoms participate in the photolysis of NO_2 at 2 288 Å, and have estimated that approximately 40% of the atoms generated in the primary step are in the excited state. One might expect the ratio of the rate constants k_2/k_3 for $O(^1D)$ (denoted in this case by k_2^*/k_3^*) to be closer to unity than the value of k_2/k_3 for $O(^3P)$

Can. J. Chem. Downloaded from www.nrcresearchpress.com by 210.87.254.105 on 09/05/12
For personal use only.

(4.0 derived from this work) and, in consequence, the values of R_{32}/R_{34} for 2 288 Å to be smaller than those observed at longer wavelengths. Consideration of a revised mechanism including reactions of $O(^1D)$ atoms shows, however, that the values of R_{32}/R_{34} for 2 288 Å will deviate by less than 10% from the values at longer wavelengths provided $6 > k_2^*/k_3^* > 3$. This inequality is very much dependent on the value assumed for the percentage of atoms generated in the ^1D state, which is not known precisely (3). Thus, for 10% $O(^1D)$, deviations from the straight line in Fig. 1 will be $< 10\%$ provided $k_2^*/k_3^* > 1.5$. It is possible that some deactivation of $O(^1D)$ by O_2[36] occurs without exchange and this will tend to reduce the predicted lower limit for k_2^*/k_3^*. For 40% $O(^1D)$ generation and equal rates of quenching of $O(^1D)$ by O_2[36] with and without exchange it can be shown that $3 > k_2^*/k_3^* > 1.4$.

ACKNOWLEDGMENT

We wish to express our thanks to Dr. R. Pottie and Mr. R. Sander for carrying out the mass spectrometric analyses.

1. J. G. CALVERT and J. N. PITTS, JR. Photochemistry. Wiley & Sons, Inc., New York. 1966.
2. J. N. PITTS, JR., J. H. SHARP, and S. I. CHAN. J. Chem. Phys. **42**, 3655 (1964).
3. K. F. PRESTON and R. J. CVETANOVIĆ. J. Chem. Phys. To be published.
4. M. C. SAUER, JR. and L. M. DORFMANN. J. Am. Chem. Soc. **87**, 3801 (1965).
5. H. W. FORD and S. JAFFE. J. Chem. Phys. **38**, 2935 (1963).
6. F. S. KLEIN and J. T. HERRON. J. Chem. Phys. **41**, 1285 (1964); **44**, 3645 (1966).

RECEIVED JUNE 29, 1966.
DIVISION OF APPLIED CHEMISTRY,
NATIONAL RESEARCH COUNCIL,
OTTAWA, CANADA.

Can. J. Chem. Downloaded from www.nrcresearchpress.com by 210.87.254.105 on 09/05/12
For personal use only.

Can. J. Chem. Downloaded from www.nrcresearchpress.com by 210.87.254.5 on 09/05/12
For personal use only.

Canadian Journal of Chemistry

Issued by THE NATIONAL RESEARCH COUNCIL OF CANADA

VOLUME 44 NOVEMBER 1, 1966 NUMBER 21

THE ELUCIDATION OF THE STRUCTURES OF OCHOTENSINE AND OCHOTENSIMINE

STEWART MCLEAN AND MEI-SIE LIN
Department of Chemistry, University of Toronto, Toronto, Ontario

AND

RICHARD H. F. MANSKE
Research Laboratories, Dominion Rubber Company Limited, Guelph, Ontario

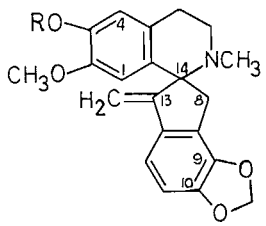
Received June 15, 1966

ABSTRACT

A combination of physical and chemical techniques has led unequivocally to the demonstration that ochotensimine and ochotensine have structures I and II, respectively.

Ochotensine and ochotensimine were isolated from *Corydalis ochotensis* Turcz. more than 25 years ago (1). Ochotensimine, $C_{22}H_{23}NO_4$, was shown to be the *O*-methyl ether of the phenolic ochotensine, and it was possible to convert ochotensimine methiodide into a crystalline degradation product under Emde conditions; however, other common degradative methods for determining structure gave no useful results when applied to these alkaloids.

When we examined these alkaloids again after a considerable lapse of time, we found that they were particularly susceptible to an attack by spectroscopic techniques. The nuclear magnetic resonance (n.m.r.) spectra were particularly useful, and it was mainly on the basis of an examination of these that we proposed structures I and II for ochotensimine and ochotensine, respectively (2). Our proposals have recently been completely confirmed by an X-ray crystallographic study of ochotensine methiodide (3). We now report in detail on the chemical and spectroscopic results we used to elucidate the structures of these alkaloids.



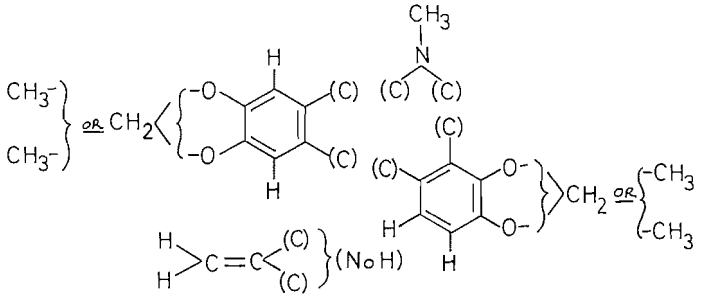
I R = Me (ochotensimine)
II R = H (ochotensine)

Ochotensimine is an optically active base which could not be induced to crystallize. The source of the alkaloid led us to anticipate that its structure would be based on a benzylisoquinoline skeleton, and the infrared and ultraviolet spectra did not contradict this, although in the latter case, because of the high intensity of the peaks, we suspected

that either the usual benzenoid chromophores had been modified or an additional chromophore was superimposed on the usual spectrum. However, the mass spectrum did not show a close correspondence with that of any class of benzylisoquinoline alkaloids studied previously (4); the spectrum was, in fact, almost devoid of positive information regarding structure since it showed the molecular ion to be the strongest peak by far, and showed few other peaks of significant intensity (see Experimental). The 60 MHz n.m.r. spectrum, on the other hand, gave a wealth of information; when this was amplified by results obtained at 100 MHz we were able to make a working hypothesis for the structure of the alkaloid. The two *O*-methyl groups and the *N*-methyl group were immediately recognized from the singlets with τ values of 6.17, 6.38, and 7.87, and the methylenedioxy protons appeared unsplit at τ 4.03. The general features of the substitution around the two aromatic rings followed from the observation that a two-proton AB quartet at τ 3.04 (J = 8.0 Hz, with an internal chemical shift of 19 Hz at 60 MHz) and two one-proton singlets at τ 3.47 and 3.70 required one ring to be tetra-substituted with two ortho-related hydrogens and the other to be tetra-substituted with two para-related hydrogens.

The appearance of two one-proton singlets at τ 4.37 and 5.10 was at first puzzling, since it suggested that there were two protons, uncoupled to any others, on two independent ethylenic systems. This appeared to be completely incompatible with the other evidence. However, the dilemma was resolved when it was found that these peaks did not appear in the spectrum of the product of the catalytic hydrogenation of ochotensimine (*vide infra*), which exhibited instead the methyl signal of a $CH_3CH\langle$ grouping at τ 9.05 (J = 7.2 Hz). The signals in ochotensimine must therefore arise from a $H_2C{=}C\langle$ grouping in which J_{gem} is zero (5), and furthermore, the two protons must be situated in rather different environments within the molecule and be too distant from other protons to couple with them.

The data reported so far showed that ochotensimine has the following partial structure.



From the molecular formula it was clear that four of the bracketed carbon atoms in the partial structure corresponded to sites that had been represented more than once and that two more rings had to be incorporated into the skeleton. If the presence of the structural feature $ArCH_2CH_2N\langle$ (common to most benzylisoquinoline alkaloids) could be assumed, then structure I possessed the only skeleton that satisfied all the data, although there were, however, still several ways in which the oxygen functions could be distributed.

We recognized that, if this were the correct structure, the C-8 methylene protons should appear as a clean AB quartet near τ 7. However, all six remaining protons gave rise to a complex pattern in this region, and it was only when the 100 MHz spectrum

Can. J. Chem. Downloaded from www.nrcresearchpress.com by 210.87.254.5 on 09/05/12
For personal use only.

was examined that the presence of the quartet could be established conclusively. It appeared at τ 6.80 (J = 18.0 Hz, with an internal chemical shift of 50 Hz); the A and B components could be decoupled by double irradiation, and it was clear that neither proton was coupled to any other outside the AB group. The proposal was thus placed on firm ground as far as ring C was concerned. The four protons still unaccounted for were presumably part of a complex multiplet arising from the postulated $ArCH_2CH_2N<$ grouping. It was necessary to carry out a rational degradation to prove that this structural feature was, in fact, present and so establish unequivocally that ochotensimine has the skeleton shown in structure I.

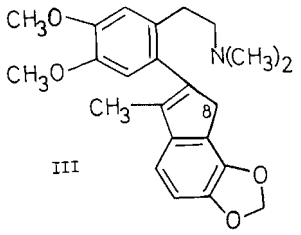
In the presence of palladium on charcoal catalyst, ochotensimine consumed 1 equivalent of hydrogen and formed the dihydro derivative referred to above. This was clearly the *C*-methyl compound produced by reduction of the $>C{=}CH_2$ grouping in I, and the difference in base strength between ochotensimine (pK_a 6.7) and dihydroochotensimine (pK_a 7.4) was of the magnitude anticipated for a molecule with the double bond and the basic center related as in I. Dihydroochotensimine had the predicted ultraviolet spectrum, with peaks of considerably lower intensity than ochotensimine. It was not possible to obtain crystalline dihydroochotensimine, and several hydrogenation experiments with different batches of catalyst gave products which were not completely identical with that already described. These bases formed methiodides that did not crystallize well, and led to poor and unreproducible microanalytical results. However, as far as we can ascertain, all samples were equally suitable for the degradation that is described next.

Hofmann degradation of dihydroochotensimine methiodide with potassium hydroxide in aqueous ethanol gave rise to an optically inactive base, $C_{23}H_{27}NO_4$, identical with the product previously obtained by reduction of ochotensimine methiodide with sodium amalgam (1). We now found that reduction of ochotensimine methiodide by hydrogenation in the presence of pre-reduced platinum oxide or by treatment with sodium borohydride also gave this product in an excellent yield.

Spectroscopic data clearly indicated that the Hofmann product had structure III (with the same reservations as before concerning the positions of the oxygen functions). The *C*-methyl signal in the n.m.r. spectrum had the appearance of a closely spaced triplet at τ 8.07, the cyclic CH_2 produced a multiplet (probably an incompletely resolved quartet) at τ 6.42, and there was no evidence for the presence of a vinyl proton. This compound is the expected Hofmann product of dihydroochotensimine methiodide; it should be recalled that, if any of the Δ^8 isomer of III were formed, it would be expected to rearrange to III under the conditions of the reaction (6). The formation of III by the reduction of ochotensimine methiodide can be accounted for by assuming that the C—N bond, which is both benzylic and allylic, is extremely susceptible to hydrogenolysis when the nitrogen is quaternized. The methyleneindane so formed would then rapidly isomerize to the methylindene III, which is resistant to further reduction; alternatively, 1,4 hydrogenation would lead directly to III.

The methiodide of III underwent a further Hofmann degradation and yielded the expected nitrogen-free styrene. Spectroscopic data for this compound supported the proposed structure, the most important evidence coming from the n.m.r. spectrum, which was almost superimposable on that of styrene in the vinyl region, but very slightly shifted to higher field. Catalytic hydrogenation readily converted the sytrene into a dihydro derivative in which the vinyl side chain had been transformed into an ethyl group attached directly to an aromatic ring (a triplet at τ 8.87 and a quartet at τ 7.48 with J = 7.8 Hz in the n.m.r. spectrum). This evidence establishes unequivocally that ochotensimine has the postulated $ArCH_2CH_2N<$ grouping; since the presence of this feature was the only

Can. J. Chem. Downloaded from www.nrcresearchpress.com by 210.87.254.5 on 09/05/12
For personal use only.

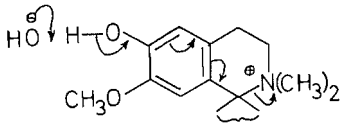


III

assumption made initially, it follows that the alkaloid has the skeleton depicted in structure I. However, as has been pointed out already, the oxygen functions can still be distributed in a number of ways. Presumptive evidence for this distribution has been obtained by a chemical degradation but, in agreement with previous experience (1), it was impossible to carry out a rational degradative sequence that would establish this point unambiguously. We have subjected ochotensimine and several of its transformation products to a variety of oxidative degradations; however, with one exception, either the conditions were too mild to affect the compounds or they were so severe that they apparently degraded the molecule indiscriminately at several sites and led to intractable mixtures or tars. The tetra-substituted double bond of III and its transformation products was particularly inert to chemical attack.

As has been described previously (1), the Hofmann degradation of ochotensimine methiodide led to an amorphous product. However, we now found that treatment of this product with permanganate gave a low yield of metahemipinic acid. This is good evidence that ochotensimine has ring A substituted as in I, but it is not conclusive since it is based on the assumption that ochotensimine, by analogy with other benzylisoquinoline alkaloids, is 2,3 disubstituted. Furthermore, even if this is so, ring D may be 9,10 or 11,12 disubstituted.

We did little work with ochotensine itself, but we succeeded in converting it into a crystalline methiodide which proved to be suitable for the X-ray crystallographic investigation (3) that led to the elucidation of the structures of both ochotensine and, as a corollary, ochotensimine. Information which we obtained from this methiodide led us to suspect at an early stage that ochotensine had structure II rather than the isomeric 2-hydroxy-3-methoxy structure; the ultraviolet spectrum of ochotensine methiodide showed λ_{max} 290 mμ which, on addition of aqueous alkali, shifted to a longer wavelength and underwent a complex sequence of changes with time; these changes were not reversed by neutralization of the sample. This suggested that the following type of cleavage was occurring.



Since the X-ray crystallographic investigation has confirmed completely the deductions based on other evidence, even those made very tentatively, the attempts to obtain unequivocal proof of structure for ochotensine and ochotensimine by degradative methods have been discontinued. However, it may be noted that, since these alkaloids have a unique skeleton (at least for the present), the biosynthetic pathways leading to them are obviously of great interest, and suitable rational degradations will have to be found before this feature can be studied adequately.

Can. J. Chem. Downloaded from www.nrcresearchpress.com by 210.87.254.5 on 09/05/12
For personal use only.

Can. J. Chem. Downloaded from www.nrcresearchpress.com by 210.87.254.5 on 09/05/12
For personal use only.

EXPERIMENTAL

Melting points were determined on a micro hot stage apparatus. Nuclear magnetic resonance spectra of samples in deuteriochloroform solution were obtained on a Varian A60 spectrometer, unless otherwise indicated.[1] A Beckman IR8 spectrometer was used to record infrared spectra, and samples were dissolved in chloroform unless otherwise indicated. A Bausch and Lomb Spectronic 505 spectrometer was used to record ultraviolet spectra, and a Hilger polarimeter was used to obtain optical rotations. In the mass spectra, the *m/e* value of a peak and its intensity (as a percentage of that of the base peak) are recorded if the intensity is 10% or greater and the *m/e* value is above 50.[2]

Ochotensine and Ochotensimine

The isolation of these alkaloids has been described previously (1). Ochotensimine, which formed a hydriodide, m.p. 190°, and a perchlorate, m.p. 172°, had pK_a 6.7 (by potentiometric titration with *p*-toluenesulfonic acid in 50% aqueous ethanol). Spectroscopic data: infrared 6.14 (sh), 6.20 (m) μ; ultraviolet λ_{max}^{MeOH} 226 (ϵ 25 700), 287 (ϵ 13 100) mμ; n.m.r. τ 3.04 (2 H; AB quartet, J = 8.0 Hz, with an internal chemical shift of 19 Hz), 3.47 (1 H), 3.70 (1 H), 4.03 (2 H), 4.37 (1 H), 5.10 (1 H), 6.17 (3 H), 6.38 (3 H), 6.65 to 7.3 (6 H; complex), 7.87 (3 H); at 100 MHz, the 4.03 peak is broadened and a peak at 6.80 (2 H; AB quartet, J = 18.0 Hz, with an internal chemical shift of 50 Hz; confirmed by decoupling) becomes apparent; mass spectrum 366 (24%), 365 (base), 364 (40%), 363 (14%), 350 (18%), 337 (10%), 336 (18%), 334 (10%), 205 (10%), 148 (16%), 85 (50%), 83 (24%).

Ochotensine, which is remarkably insoluble in most solvents, showed the following spectroscopic features: infrared (KBr pellet) 6.06 (sh), 6.23 (s) μ; mass spectrum 352 (24%), 351 (base), 350 (50%), 349 (48%), 348 (22%), 336 (24%), 334 (16%), 323 (10%), 322 (24%), 321 (12%), 320 (26%), 308 (10%), 306 (14%), 305 (14%), 191 (16%), 190 (18%), 189 (16%), 176 (16%), 148 (34%), 103 (16%), 102 (16%), 99 (16%), 94 (22%), 83 (14%), 78 (14%), 77 (16%), 76 (14%), 65 (12%), 63 (14%).

Ochotensine in dimethylformamide was allowed to react with excess methyl iodide at room temperature for 4 days. Evaporation of the solvent yielded a residue which, after repeated recrystallizations from methanol, formed crystals, m.p. 215° (the melting point was not well defined and depended on the rate at which the sample was heated).

Anal. Calcd. for $C_{22}H_{24}NO_4I$: C, 53.56; H, 4.87; N, 2.84; I, 25.74. Found: C, 53.69; H, 5.06; N, 2.94; I, 25.28.

The ultraviolet spectrum, λ_{max}^{MeOH} 290 mμ (ϵ 18 100) shifted to λ_{max} 360, 265, and 250 mμ on the addition of 2 drops of 5 *N* aqueous NaOH; the spectrum continued to change with time and the addition of hydrochloric acid did not regenerate the original chromophore.

Dihydroochotensimine

Ochotensimine (75 mg, 0.20 mmole) in 10 ml of 95% ethanol was hydrogenated at atmospheric pressure and room temperature in the presence of 30% palladium on charcoal (30 mg). After 20 h, 0.18 mmole hydrogen had been consumed, and dihydroochotensimine (74 mg) was isolated in the usual manner. This material, $[\alpha]_{Hg}^{22}$ +112° (*c*, 0.7 in $CHCl_3$), pK_a 7.4 (by potentiometric titration with *p*-toluenesulfonic acid in 50% aqueous ethanol), could not be induced to crystallize. With methyl iodide at room temperature it formed a methiodide (yield 70–80%) which, after several recrystallizations, formed white crystals, m.p. 169–175°.

Anal. Calcd. for $C_{23}H_{28}NO_4I$: C, 54.23; H, 5.50; N, 2.75. Found: C, 53.13, 53.61; H, 5.41, 5.02; N, 3.24, 2.71.

Spectroscopic data for dihydroochotensimine: infrared 6.20 (m) μ; ultraviolet λ_{max}^{MeOH} 223 (shoulder) (ϵ 12 400), 282 (ϵ 5 900) mμ; n.m.r. τ 3.45 (2 H; complex), 3.63 (1 H), 3.88 (1 H), 4.13 (2 H), 6.32 (3 H), 6.63 (3 H), 6.4 to 7.5 (7 H; complex), 7.65 (3 H), 9.05 (3 H; doublet, J = 7.2 Hz); mass spectrum 368 (25%), 367 (base), 366 (28%), 352 (28%), 339 (18%), 338 (76%), 337 (32%), 336 (50%), 322 (12%), 218 (18%), 206 (12%), 204 (16%), 163 (18%), 162 (54%), 149 (12%).

First Hofmann Degradation

A solution of dihydroochotensimine methiodide (133 mg) in 20 ml of 50% ethanol containing 0.6 g potassium hydroxide was refluxed for 21 h. The crude product (72 mg) was isolated in the usual way and recrystallized from a mixture of acetone and hexane. It formed crystals, m.p. 91–92°, $[\alpha]_D$ 0°, which were identical with the Emde product reported previously (1). Spectroscopic data: ultraviolet λ_{max}^{MeOH} 278 (ϵ 12 700), 316 (inflection) (ϵ 4 800) mμ; n.m.r. τ 3.17 (3 H), 3.34 (1 H), 4.02 (2 H), 6.10 (3 H), 6.18 (3 H), 6.42 (2 H; complex, width 8 Hz), 7.3 to 7.6 (4 H; complex), 7.84 (6 H), 8.07 (3 H; 1:2:1 triplet, J = 2.0 Hz).

The same product was conveniently prepared by hydrogenation of ochotensimine methiodide (400 mg) in 15 ml of 95% ethanol in the presence of pre-reduced platinum oxide (30 mg) for 44 h at room temperature and atmospheric pressure. The solid obtained after the solvent had been evaporated was treated with 4%

[1]*We are grateful to Professor R. U. Lemieux, University of Alberta, Edmonton, for the spectrum obtained at 100 MHz.*

[2]*We are grateful to Professor D. B. MacLean, McMaster University, Hamilton, for obtaining these spectra for us. A Hitachi Perkin–Elmer RMU-6A spectrometer was used.*

aqueous sodium carbonate and the resulting product was extracted with chloroform. The crude residue (258 mg), after evaporation of the chloroform, yielded, on recrystallization, a product identical with that described above. Alternatively, a suspension of ochotensimine methiodide in methanol was converted into the same product in a quantitative yield by treatment with excess sodium borohydride.

With methyl iodide at room temperature overnight, the base formed a methiodide which melted at 157–160°, resolidified at 175°, and remelted at 233–236°.

Anal. Calcd. for $C_{24}H_{30}NO_4I$: C, 55.07; H, 5.73; N, 2.67. Found: C, 54.88; H, 5.81; N, 2.70.

Second Hofmann Degradation

The methiodide (200 mg) just described was dissolved in 30 ml of 50% ethanol containing 1.0 g potassium hydroxide. The solution was refluxed for 2 h and the crude product (102 mg) was isolated in the usual way. Recrystallization of the product from a mixture of acetone and hexane yielded crystals, m.p. 142–144°.

Anal. Calcd. for $C_{21}H_{20}O_4$: C, 74.98; H, 5.99. Found: C, 75.17; H, 5.74.

Spectroscopic data: infrared 6.25 (m) μ; ultraviolet λ_{max}^{MeOH} 266 (ϵ 14 400), 274 (inflection) (ϵ 14 000), 300 (broad shoulder) (ϵ 10 000) mμ; n.m.r. τ 2.86 (1 H), 3.17 (2 H), 3.30 (1 H), 4.03 (2 H), 6.07 (3 H), 6.14 (3 H), 6.44 (2 H; 1:3:3:1 quartet, J = 2.0 Hz), 8.10 (3 H; 1:2:1 triplet, J = 2.0 Hz); in addition, the signals from the three vinylic protons (ABC) of a styrene can be recognized and analyzed approximately: τ 3.35 (A), 4.39 (B), 4.89 (C); $J_{AB(trans)}$ = 18.0 Hz, $J_{AC(cis)}$ = 11.0 Hz, $J_{BC(gem)}$ = 1.5 Hz.

Dihydro Derivative

The above material (145 mg, 0.43 mmole) in 10 ml of 95% ethanol containing 3 ml chloroform was hydrogenated at atmospheric pressure and room temperature in the presence of pre-reduced platinum oxide (30 mg). After 3 h, 0.44 mmole hydrogen had been consumed and the product was isolated as crystals, m.p. 110.5–112°.

Anal. Calcd. for $C_{21}H_{22}O_4$: C, 74.53; H, 6.55. Found: C, 74.67; H, 6.68.

Spectroscopic data: infrared 6.25 (m) μ; ultraviolet λ_{max}^{MeOH} 277 (ϵ 16 100), 289 (shoulder) (ϵ 13 700), 310 (inflection) (ϵ 5 800) mμ; n.m.r. τ 3.13 (3 H), 3.27 (1 H), 4.00 (2 H), 6.07 (3 H), 6.14 (3 H), 6.42 (2 H; 1:3:3:1 quartet, J = 2.0 Hz), 7.48 (2 H; 1:3:3:1 quartet, J = 7.8 Hz), 8.07 (3 H, 1:2:1 triplet, J = 2.0 Hz), 8.87 (3 H; 1:2:1 triplet, J = 7.8 Hz).

Metahemipinic Acid

Ochotensimine methiodide suspended in methanol was treated with slightly more than 1 equivalent of potassium hydroxide. Warming caused a brown resinous mass to separate, and precipitation was completed by the addition of water. A solution of this amorphous residue in acetone was treated with saturated aqueous potassium permanganate until the color of the solution was retained for 1 h. The mixture was filtered, the filtrate was diluted with water, and the acetone was removed by distillation. The cold aqueous solution was then oxidized with further potassium permanganate solution until a permanent color was produced. Excess calcium chloride was added (to remove any oxalic acid) and the mixture was filtered again. Acidification of the filtrate and extraction with ether yielded a partly crystalline acid which was treated with excess ethylamine and then sublimed *in vacuo*. The resulting colorless stout prisms (yield ca. 5%) melted sharply at 232° either alone or on admixture with *N*-ethylmetahemipinimide.

ACKNOWLEDGMENTS

Research support from the National Research Council and the Ontario Research Foundation is gratefully acknowledged.

REFERENCES

1. R. H. F. MANSKE. Can. J. Res., B, **18**, 75 (1940).
2. S. McLEAN and M.-S. LIN. Tetrahedron Letters, 3819 (1964).
3. S. McLEAN, M.-S. LIN, A. C. MACDONALD, and J. TROTTER. Tetrahedron Letters, 185 (1966).
4. M. OHASHI, J. M. WILSON, H. BUDZIKIEWICZ, M. SHAMMA, W. A. SLUSARCHYK, and C. DJERASSI. J. Am. Chem. Soc. **85**, 2807 (1963).
5. T. SCHAEFER. Can. J. Chem. **40**, 1 (1962).
6. G. BERGSON and A.-M. WEIDLER. Acta Chem. Scand. **17**, 862 (1963).

Can. J. Chem. Downloaded from www.nrcresearchpress.com by 210.87.254.5 on 09/05/12
For personal use only.

Can. J. Chem. Downloaded from www.nrcresearchpress.com by 188.143.235.115 on 09/06/12
For personal use only.

AZAINDOLES

I. PREPARATION OF 7-AZAINDOLES BY THERMAL INDOLIZATION OF 2-PYRIDYLHYDRAZONES

A. H. Kelly and J. Parrick[1]

Department of Chemistry and Metallurgy, Rutherford College of Technology, Newcastle-upon-Tyne, England

Received May 6, 1966

ABSTRACT

The preparation of 2-pyridylhydrazones and their thermal indolization to 2- and 3-monosubstituted and 2,3-disubstituted 7-azaindoles, and to 3,3-disubstituted and 2,3,3-trisubstituted 7-azaindolenines are described. Attempts to cause thermal indolization of two 2-(5-nitropyridyl)hydrazones were unsuccessful.

Azaindoles of the types I, II, III, and IV are of chemical interest because they contain the π-electron deficient pyridine nucleus fused to the π-electron excessive pyrrole nucleus (1), and their relationship to indole adds biochemical interest. In the cases of I and II additional similarities to purine are apparent. The biological activity of azaindoles might be expected to be similar to that of the corresponding indoles and purines but with potentially useful differences. The possible use of azaindoles as purine antimetabolites has stimulated other investigations (2), and some evidence of noteworthy biological activity of 7-azatryptophan (I*a*) is available (3). Neither the parent heterocycles nor simple derivatives of azaindoles seem to occur in nature, but the presence of the β-carboline nucleus V in certain alkaloids is well known (4).

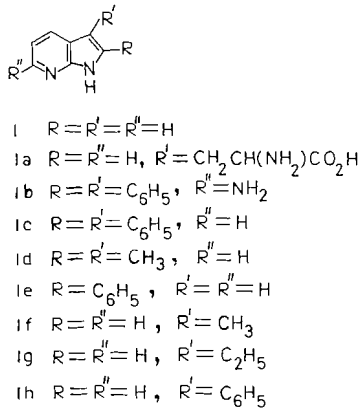
Several investigations of azaindoles (I, II, III, and IV) have been reported by Clemo (5), Herz (6), Möller (7), and Robison (8), and currently by Albert (9) and Badger (2). Numerous 2,3-dihydroazaindole derivatives have been reported by Yakhontov and Rubtsov (10), and Ficken and Kendall (11) have prepared some azaindolenines (e.g. VI*b*). The methods employed in the preparations of azaindoles have been predominantly adaptations of standard indole syntheses and involve the formation of the pyrrole ring on the pyridine ring. For example, preparations based on the Madelung (9, 12), Fischer (8*b*, 11, 13), and Reissert (14) indole syntheses have been reported (the recent successful application of the last method (14) is in contrast to the earlier reports of failures when this technique was applied to azaindole syntheses (2, 6)). An interesting method involving photochemical ring contraction to give azaindoles has been developed (7). Synthetic approaches involving the formation of a pyridine ring on an existing pyrrole nucleus have met with only modest success (15).

7-Azaindoles have received more attention than the other azaindoles, and the parent heterocycle I is available in a good yield by a modification of the Madelung synthesis (12) and by reaction of 3-pyridylacetylene with sodamide (16), or, less readily, through the photochemical route (7*b*). The base occurs in coal tar (17) and as a pyrolysis product of nicotine (18). The 2-, 3-, 4-, 5-, and 6-methyl-7-azaindoles have been prepared by the Madelung technique (5*a*, 9, 19), and 6-amino-2,3-diphenyl-7-azaindole (I*b*) was obtained in a high yield from 2,6-diaminopyridine and benzoin in the presence of the diaminopyridine hydrochloride (20).

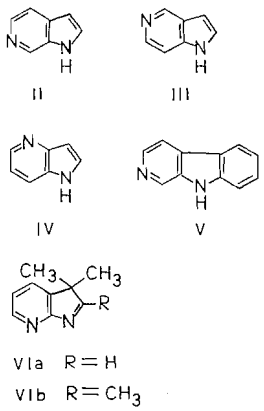
Probably the most useful method for the preparation of indoles is the Fischer synthesis

[1]*Present address: Department of Chemistry, Brunel College, Acton, London, W.3, England.*

(21). However, adaptations of this technique to the synthesis of azaindoles while using the usual acid catalysts have met with only limited success: 2,3-diphenyl-7-azaindole (I*c*) (8*a*) and 6,7,8,9-tetrahydro-α-carboline (VII*b*) (8*a*, 13) were obtained in a moderate yield, and the technique has been used for the preparation of azaindolenines (VI*b*) (11).

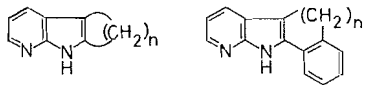


I $R=R'=R''=H$
Ia $R=R''=H$, $R'=CH_2CH(NH_2)CO_2H$
Ib $R=R'=C_6H_5$, $R''=NH_2$
Ic $R=R'=C_6H_5$, $R''=H$
Id $R=R'=CH_3$, $R''=H$
Ie $R=C_6H_5$, $R'=R''=H$
If $R=R''=H$, $R'=CH_3$
Ig $R=R''=H$, $R'=C_2H_5$
Ih $R=R''=H$, $R'=C_6H_5$



II III IV V

VIa $R=H$
VIb $R=CH_3$



VIIa $n=3$
VIIb $n=4$

VIIIa $n=1$
VIIIb $n=2$

The purely thermal indolization technique reported by Fitzpatrick and Hiser (22) appeared to offer advantages for the synthesis of azaindoles from pyridylhydrazones, since this method avoids the deactivation caused by quaternization of the pyridyl nitrogen atom. A brief study of the thermal indolization of pyridylhydrazones as part of a more general investigation of thermal indolization (23) gave encouraging results, and the application of this method to the synthesis of 7-azaindoles has been investigated in more detail.

2-Pyridylhydrazine was prepared from 2-chloropyridine (24) and then quickly converted into the 2-pyridylhydrazones of acetone, ethyl methyl ketone, isopropyl methyl ketone, acetophenone, cyclopentanone, α-indanone, α-tetralone, propionaldehyde, butyraldehyde, isobutyraldehyde, phenylacetaldehyde, pyruvic acid, and ethyl pyruvate by the usual techniques. Refluxing a solution of these 2-pyridylhydrazones in a high-boiling solvent gave the corresponding 7-azaindole in most cases (Table II). (Unless indicated in this table an inert atmosphere was not necessary to obtain the yields quoted.)

TABLE I

2-Pyridylhydrazone of:	Melting point	Formula	Calculated (%) C	H	N	Found (%) C	H	N
Cyclopentanone	91–92°	$C_{10}H_{13}N_3$	68.6	7.43		68.2	7.54	
α-Indanone	87–88°	$C_{14}H_{13}N_3$			18.8			18.5
α-Tetralone	112–114°	$C_{15}H_{15}N_3$			17.7			17.7
Propionaldehyde	54–55.5°	$C_8H_{11}N_3$	64.4	7.38		64.4	7.59	
Butyraldehyde	42–43°	$C_9H_{13}N_3$	66.3	7.97		66.5	7.99	
Phenylacetaldehyde	79–80°	$C_{12}H_{11}N_3$			19.9			19.6

NOTE: The 2-pyridylhydrazones of ethyl methyl ketone, isopropyl methyl ketone, and isobutyraldehyde were obtained only as oils and were not analyzed; those of acetone, acetophenone, pyruvic acid, and ethyl pyruvate had melting points in agreement with the literature values (25).

Can. J. Chem. Downloaded from www.nrcresearchpress.com by 188.143.235.115 on 09/06/12
For personal use only.

Can. J. Chem. Downloaded from www.nrcresearchpress.com by 188.143.235.115 on 09/06/12
For personal use only.

TABLE II

2-Pyridylhydrazone of:	Thermal indolization		Azaindole	Yield (%)	Melting point	Formula	Calculated (%)			Found (%)		
	Solvent*	Time (h)					C	H	N	C	H	N
Ethyl methyl ketone	DEG	7	I*d*	43†	137.5–138.5°	$C_9H_{10}N_2$	74.0	6.85		74.1	6.82	
Isopropyl methyl ketone	DEG (N_2)	2.5	VI*b*	5†	82–83° (77.5–78° (11*b*))	$C_{10}H_{12}N_2$			17.5			17.7
Acetophenone	TEG	4	I*e*	63†	201–202°	$C_{13}H_{10}N_2$			14.4			14.6
Cyclopentanone	DEG	9	VII*a*	67†	162.5–163.5°	$C_{10}H_{12}N_2$	75.9	6.33		75.8	6.55	
α-Indanone	DEG	7	VIII*a*	95§	266–268°	$C_{14}H_{10}N_2$			13.8			13.7
α-Tetralone	DEG (N_2)	2	VIII*b*	77‡	210–211°	$C_{15}H_{12}N_2$	81.8	5.45	12.7	81.3	5.47	12.4
Propionaldehyde	DEG (N_2)	14	I*f*	25†	126–128° (130.5–132° (19))	$C_8H_8N_2$			21.2			21.5
Butyraldehyde	DEG (N_2)	22	I*g*	37‖								
Isobutyraldehyde	DEG (N_2)	12.5	VI*a*	47‖	136–137°	$C_9H_{10}N_2$	74.0	6.85		73.6	6.92	
Phenylacetaldehyde	DEG	9	I*h*	88‡	192–5.193.5°	$C_{13}H_{10}N_2$	80.4	5.15		80.7	5.12	

*DEG = diethylene glycol; TEG = triethylene glycol.
†Crystallized from petroleum ether (b.p. 60–80°).
‡Crystallized from ethanol.
§Crystallized from acetone.
‖Obtained as an oil, b.p. 90–110° at 0.5 mm.
NOTE: Liquid 3-ethyl-7-azaindole (I*g*) yielded a picrate by reaction with ethanolic picric acid. Recrystallization from ethanol gave yellow needles, m.p. 221–222.5°.
Anal. Calcd. for $C_{15}H_{11}N_5O_7$: C, 48.0; H, 3.47. Found: C, 47.8; H, 3.57.

Several attempts were made to cause indolization of acetone 2-pyridylhydrazone under a variety of conditions; in no case was an azaindole isolated, but the pyridylhydrazone was recovered in some experiments. This result is in marked contrast to the fairly ready thermal indolization of acetone phenylhydrazone (22). All attempts to obtain an azaindole from the 2-pyridylhydrazones of pyruvic acid and ethyl pyruvate were unsuccessful.

2-(5-Nitropyridyl)hydrazine, prepared from 2-chloro-5-nitropyridine, gave the nitropyridylhydrazones on reaction with cyclohexanone and ethyl methyl ketone. Again, all attempts to cause indolization failed, though extensive decomposition did occur. In this connection it is interesting that cyclohexanone *p*-nitrophenylhydrazone gives only a poor yield of 6-nitro-1,2,3,4-tetrahydrocarbazole by a purely thermal technique (23) but gives a high yield when both an elevated temperature and an acidic medium are used (24).

These results are in agreement with the idea that protonation of the hydrazino nitrogen atom is not essential in the Fischer indole synthesis but may be necessary for success when indolization is difficult (21). However, when pyridylhydrazones are used, the acidic reaction medium deactivates the nucleus for the electrophilic cyclization stage of the reaction, thus making the purely thermal method particularly useful in this series, though not successful, in the examples examined, where the pyridyl nucleus contains an electron-withdrawing nitro substituent, nor when enehydrazine formation is difficult (as is presumably the case for acetone 2-pyridylhydrazone).

EXPERIMENTAL

2-Pyridylhydrazones

Equimolecular quantities of 2-pyridylhydrazine (25) and the aldehyde or ketone were warmed on a water bath for 30 min, and then benzene was added and the water removed by azeotropic distillation. The hydrazones (Table I) were obtained in a crystalline form (except those from ethyl methyl ketone, isopropyl methyl ketone, and isobutyraldehyde) either directly or after distillation under reduced pressure.

Indolization Procedure

In a typical experiment the hydrazone (3 g) was dissolved in a suitable solvent (30 ml) and the mixture boiled under reflux. After the mixture was cooled, it was poured into ice water and the oil crystallized. Recrystallization (charcoal) gave colorless crystals (Table II). (Analytical samples were sublimed under reduced pressure.)

2-(5-Nitropyridyl)hydrazine

Hydrazine hydrate (98%, 4 g) was added to 2-chloro-5-nitropyridine (3.2 g) (26) dissolved in ethanol (100 ml) and the mixture refluxed gently for 8 h. After the mixture was cooled, the solid was filtered off and crystallized from a large volume of ethanol as yellow prisms (2.1 g), m.p. 199–200° (27).

2-(5-Nitropyridyl)hydrazones

The aforementioned hydrazine and a small excess of the ketone were mixed in ethanol and then heated on a boiling water bath for 1 h.

Ethyl methyl ketone 2-(5-nitropyridyl)hydrazone was crystallized from a small volume of ethanol as yellow needles, m.p. 92–93°.

Anal. Calcd. for $C_9H_{12}N_4O_2$: C, 52.0; H, 5.78. Found: C, 52.3; H, 5.53.

Cyclohexanone 2-(5-nitropyridyl)hydrazone was crystallized from ethanol as yellow needles, m.p. 114–116°.

Anal. Calcd. for $C_{11}H_{14}N_4O_2$: C, 55.5; H, 5.99. Found: C, 55.2; H, 6.17.

ACKNOWLEDGMENT

We are grateful to the Newcastle-upon-Tyne Education Committee for the award of a research studentship to A. H. K.

REFERENCES

1. A. ALBERT. Heterocyclic chemistry. The Athlone Press, London. 1959.
2. G. M. BADGER and R. P. RAO. Australian J. Chem. **17**, 1399 (1964).
3. A. B. PARDEE, V. G. SHORE, and L. S. PRETIDGE. Biochim. Biophys. Acta, **21**, 406 (1956).
   A. BERECZ and C. GODIN. Can. J. Biochem. Physiol. **40**, 153 (1962).

Can. J. Chem. Downloaded from www.nrcresearchpress.com by 188.143.235.115 on 09/06/12
For personal use only.

4. R. A. ABRAMOVITCH and I. D. SPENSER. *In* Advances in heterocyclic chemistry. Vol. 3. *Edited by* A. R. Katritzky. Academic Press, Inc., London. 1964.
5. (*a*) G. R. CLEMO and G. A. SWAN. J. Chem. Soc. 603 (1945). (*b*) G. R. CLEMO and G. A. SWAN. J. Chem. Soc. 198 (1948).
6. W. HERZ and D. R. K. MURTY. J. Org. Chem. **26**, 122 (1961).
7. (*a*) O. SÜS and K. MÖLLER. Ann. **599**, 233 (1956). (*b*) K. MÖLLER and O. SÜS. Ann. **612**, 153 (1958).
8. (*a*) S. OKUDA and M. M. ROBISON. J. Am. Chem. Soc. **81**, 740 (1959). (*b*) S. OKUDA and M. M. ROBISON. J. Org. Chem. **24**, 1008 (1959).
9. A. ALBERT and R. E. WILLETTE. J. Chem. Soc. 4063 (1964).
10. L. N. YAKHONTOV and M. V. RUBTSOV. Zh. Obshch. Khim. **34**, 493 (1964).
11. (*a*) G. E. FICKEN and J. D. KENDALL. J. Chem. Soc. 584 (1961). (*b*) G. E. FICKEN and J. D. KENDALL. J. Chem. Soc. 3202 (1959).
12. R. R. LORENZ, B. F. TULLAR, C. F. KOELSCH, and S. ARCHER. J. Org. Chem. **30**, 2531 (1965).
13. F. G. MANN, A. F. PRIOR, and T. J. WILCOX. J. Chem. Soc. 3830 (1959).
14. B. FRYDMAN, M. E. DESPUY, and H. RAPOPORT. J. Am. Chem. Soc. **87**, 3530 (1965).
15. W. HERZ and S. TOCKER. J. Am. Chem. Soc. **77**, 6353 (1955).
16. J. REISCH. Ber. **97**, 2717 (1964).
17. O. KRUBER. Ber. **76B**, 128 (1943).
18. C. H. JARBOE and C. J. ROSENE. J. Chem. Soc. 2455 (1961).
19. M. M. ROBINSON and B. L. ROBISON. J. Am. Chem. Soc. **77**, 457 (1955).
20. J. BERNSTEIN, B. STEARNS, E. SHAW, and W. A. LOTT. J. Am. Chem. Soc. **69**, 1151 (1947).
21. B. ROBINSON. Chem. Rev. **63**, 373 (1963).
22. J. T. FITZPATRICK and R. D. HISER. J. Org. Chem. **22**, 1703 (1957).
23. A. H. KELLY, D. H. MCLEOD, and J. PARRICK. Can. J. Chem. **43**, 296 (1965).
24. D. S. DEOHRA and S. S. JOSHI. J. Org. Chem. **26**, 3527 (1961).
25. R. G. FARGHER and R. FURNESS. J. Chem. Soc. **107**, 688 (1915).
26. M. A. PHILLIPS. J. Chem. Soc. 9 (1941).
27. M. COLONNA and D. D. M. CASONI. Boll. Sci. Fac. Chim. Ind. Bologna, **5**, 35 (1944–1947).

Can. J. Chem. Downloaded from www.nrcresearchpress.com by 188.143.235.115 on 09/06/12
For personal use only.

Can. J. Chem. Downloaded from www.nrcresearchpress.com by 210.87.254.42 on 09/05/12
For personal use only.

THE ESSENTIAL OIL OF ILLICIUM ANISATUM LINN.

W. B. Cook and A. S. Howard
Department of Chemistry, Montana State University, Bozeman, Montana

Received June 13, 1966

ABSTRACT

The oil of the Japanese star anise tree, *Illicium anisatum* Linn., was analyzed by gas–liquid chromatography. The major constituents were found to be cineole (18.1%), linalool (10.1%), methyleugenol (9.8%), α-terpenyl acetate (6.8%), safrole (6.6%), and a sesquiterpene hydrocarbon of unknown constitution (7.2%). The composition of this oil differs widely from that of the commercially used star anise oil obtained from *Illicium verum* Hooker. The most striking difference between the two oils is found in the anethole content, which constitutes 88% of the commercial oil but only 1.2% of the oil here investigated.

INTRODUCTION

The Japanese star anise tree, *Illicium anisatum* Linn. (botanical synonym *Illicium religiosum* Sieb. and Zucc. (1)) is commercially cultivated for the fruit, which is used in the preparation of incense sticks and mixed with the fruit of the Chinese star anise tree as a spice in cooking (2, p. 378). It has long been known, however, that the fruit has poisonous properties, and the structure of the active principle, anisatin, has recently been elucidated by Yamada *et al.* (3). In connection with other investigations on this plant, we recently separated the steam-volatile oil and here report its composition.

The oil of *Illicium anisatum* has not been used much commercially (2, p. 378), but that of the botanically closely related Chinese star anise tree, *Illicium verum* Hooker, is widely used. It has been known for many years (2, p. 373) that the major constituent of the Chinese oil is *trans*-anethole (approximately 90%). Recently, Porsch *et al.* (4) analyzed the oil by gas chromatographic techniques and identified a further 17 compounds, most of which were monoterpene hydrocarbons. The general characteristics of the Japanese oil have been reported (5, 6) and a few compounds identified (7), but no detailed investigation appears to have been performed. It was with this object in mind that the present study was undertaken.

EXPERIMENTAL

Apparatus

Analytical gas chromatograms were carried out on an F & M Biomedical gas chromatograph, model 400, equipped with a flame ionization detector and a Disc integrator. Preparative gas chromatography was performed on an Aerograph model A-700 "Autoprep".

Infrared spectra were recorded with a Beckman IR-4 infrared spectrophotometer. The samples were mounted as liquid films between salt plates or in a 0.025 mm path length mercury amalgam cell. In the cases of some of the minor constituents, the samples were measured as carbon tetrachloride solutions in a 0.1 mm path length cavity cell. Nuclear magnetic resonance spectra were measured in carbon tetrachloride or deuteriochloroform solutions on a Varian model A-60 analytical nuclear magnetic resonance spectrometer.

Analytical gas chromatography was performed with 180 cm by 0.4 cm internal diameter glass columns. The solid support in each case was 100–120 mesh Gas Chrom Q, and the following liquid phases were used: Carbowax 20 M, SE 30, S.A.I.B., and F.F.A.P., each 16% (w/w); Hyprose SP 80, 4.5% (w/w); and β,β′-oxidipropionitrile, 20% (w/w). For the preparative work, a 10 ft × $\frac{3}{8}$ inch aluminium column packed with 20% (w/w) Carbowax 20 M on 60–80 mesh potassium hydroxide washed Chromosorb W and a 20 ft × $\frac{1}{4}$ inch copper column containing 20% (w/w) β,β′-oxidipropionitrile on 60–80 mesh acid-washed Chromosorb W were used. Samples were collected by passing the effluent gas through a U-tube suspended in a liquid air bath or by bubbling it through a solvent, usually pentane, cooled in an acetone – dry ice bath.

Isolation of the Oil

The dried seeds and husks (1 kg), obtained from the Applications Development Corporation, Washington, D.C., were ground to a powder and steam-distilled in the normal manner. The distillate, saturated with sodium chloride and extracted with ether, yielded, after it was dried over sodium sulfate and the solvent

removed, 4.5 g (0.45%) of a harsh-smelling yellow oil. This was separated into neutral (96%) and acidic (4%) fractions by extraction of an ethereal solution with 5% sodium carbonate.

Oils obtained separately from the seeds and husks showed only minor quantitative differences in some of the constituents.

Percentage Composition

This was calculated from the areas under the peaks, measured with a Disc integrator, in temperature-programmed runs using the Carbowax column and an Aerograph 200 equipped with a thermal conductivity detector. The results are the average of five runs. When compounds were not resolved under these conditions, the relative amounts of these particular compounds were obtained using different conditions or columns.

Preliminary Fractionation

The oil (1.00 g) was dissolved in pentane and adsorbed onto a column of silicic acid (15 g) deactivated with Carbowax 20 M (2% w/w), and the hydrocarbon fraction (230 mg) was eluted with pentane (120 ml). Further development with ethyl acetate (100 ml) and methanol (70 ml) eluted the oxygenated compounds (762 mg). Collection of the ethyl acetate eluent in smaller fractions allowed the partial separation of the esters and ethers from the alcohols.

Separation into Individual Compounds

This was performed by means of preparative gas–liquid chromatography under optimum conditions of temperature, gas flow rate, and amount of material injected.

Hydrocarbons

Initially, these were divided into monoterpene and sesquiterpene fractions on the Carbowax 20 M column. Separation into individual compounds was done on either of the preparative columns. The β,β'-oxidipropionitrile column was particularly useful in the separation of the monoterpenes.

Oxygenated Compounds

These were separated on the Carbowax column.

Identification of Compounds

In all cases, the purity of the isolated materials was checked on at least two of the analytical columns, and unless otherwise specified, all identifications are based on the comparison of the infrared spectrum of the isolated compound with that of an authentic specimen. In the cases where identifications are based on the retention times, at least three analytical columns were used.

The Acid Fraction

This was analyzed on the 16% F.F.A.P. column at 152 °C. The compounds were identified by comparison of their retention times with those of authentic acids.

RESULTS AND DISCUSSION

Originally, the separation of the oil into hydrocarbons and oxygenated compounds was performed according to the procedure of Kugler and Kovats (8). However, under these conditions, considerable losses of materials, in particular the monoterpene hydrocarbons, resulted, and it was necessary to increase the amount of impregnated Carbowax 20 M to 2% (w/w). Under these conditions, a clean separation was obtained and no significant loss of material or isomerization was observed.

Analysis of the acidic fraction of the oil indicated that only simple aliphatic acids were present. Straight-chain acids from C_2 to C_6 inclusive and isobutyric and isovaleric acids were identified.

The complex composition of the neutral fraction is illustrated in Fig. 1, and Table I provides a summary of the percentages of the individual components. A comparison between these results and those of Porsch *et al.* (4) for the oil of *Illicium verum* reveals that very considerable differences exist. The most striking of these is in the anethole content, which is 1.2% in the present case and 88% in the Chinese oil. This clearly indicates why the Japanese oil is not an acceptable substitute for the Chinese variety. Other aromatic ethers (peaks 23, 24, 27, and 29) constitute approximately 21% of the Japanese oil, and it is interesting to note that they all contain the allyl rather than the propenyl side chain found in anethole (1-methoxy-4-propenylbenzene). The major differences in composition between the two oils are summarized in Table II.

Can. J. Chem. Downloaded from www.nrcresearchpress.com by 210.87.254.42 on 09/05/12
For personal use only.

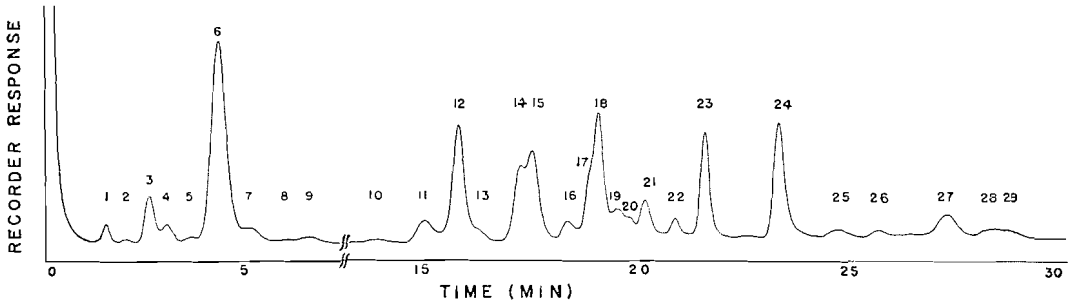


FIG. 1. Gas chromatograph of the neutral fraction of Japanese star anise oil on a 180 cm Carbowax 20 M column; temperature 90 °C for 10 min, then programmed to 200 °C at 5 °C per min; gas flow rate 65 ml per min.

TABLE I

Composition of the Japanese star anise oil

Peak No.*	Compound	%	Peak No.*	Compound	%
1	α-Pinene†	0.4	15	Sesquiterpene hydrocarbon	7.2
1*a*	α-Thujene†	0.4	16	Terpinen-4-ol acetate	1.5
2	Camphene†	Trace	17	α-Terpineol	3.3
3	β-Pinene	0.3	18	α-Terpinyl acetate	6.8
3*a*	Sabinene	1.4	18*a*	Sesquiterpene hydrocarbon	2.1
4	Myrcene	0.6	19	α,β-Unsaturated ketone	1.1
5	α-Terpinene	0.3	20	Sesquiterpene hydrocarbon	1.8
6	Cineole	18.1	21	Unidentified	2.7
6*a*	Limonene	1.5	22	*trans*-Anethole	1.2
6*b*	β-Phellandrene	1.4	23	Safrole	6.6
7	γ-Terpinene	1.3	24	Methyleugenol	9.8
8	*p*-Cymene	0.4	25	Unidentified mixture	1.5
9	Terpinolene	0.7	26	Sesquiterpene alcohol	1.3
10	Sesquiterpene hydrocarbon	0.4	26*a*	Unidentified	
11	Sesquiterpene hydrocarbon	2.2	27	Myristicin‡	3.5
12	Linalool	10.1	28	Sesquiterpene alcohol	2.8
13	Sesquiterpene hydrocarbon	1.0	29	5-Methoxy-methyleugenol‡	
14	Terpinen-4-ol	3.9	29*a*	Unidentified	
14*a*	Sesquiterpene hydrocarbon	1.3			

*Peak numbers are those shown in Fig. 1. Where the peaks contain more than one compound, this is indicated by the letters *a* and *b*.
†Identified by means of relative retention times and thin-layer chromatography according to Attaway *et al.* (9).
‡Identified by interpretation of their infrared and nuclear magnetic resonance spectra. No authentic specimens were available.

TABLE II

Main differences in the composition of Japanese and Chinese star anise oils

Compound	% content	
	Japanese oil	Chinese oil
Cineole	18.1	0.5
Linalool	10.1	1.0
α-Terpenyl acetate	6.8	Nil
trans-Anethole	1.2	88.0
Safrole	6.6	Nil
Methyleugenol	9.8	Nil

Can. J. Chem. Downloaded from www.nrcresearchpress.com by 210.87.254.42 on 09/05/12
For personal use only.

As can be seen from Table I, sesquiterpene hydrocarbons (peaks 10, 11, 13, 14*a*, 15, 18*a*, and 20) make up approximately 15% of the oil, and small samples of all of these compounds have been isolated in a pure state. On the basis of the information available at present, it appears that these compounds are not the bisabolenes and cadinenes reported to be present in the oil of *Illicium verum* (4), and it seems probable that at least some of them are new compounds. The constitutions of these compounds will be the subject of a later publication.

ACKNOWLEDGMENTS

Support of this work by a grant from the Geschickter Fund for Medical Research is gratefully acknowledged. In addition, the National Science Foundation is to be thanked for grant No. GP-3632 to cover the purchase of the Aerograph model A-700 "Auotprep". Finally, the authors are indebted to Messrs. Fritzsche Brothers, Inc., Hercules Powder Co., The Glidden Company, and Givaudan Corporation for the supply of numerous terpene samples.

REFERENCES

1. A. C. SMITH. Sargentia, **7**, 1 (1947).
2. E. GUENTHER. The essential oils. Vol. V. D. Van Nostrand Company, Inc., New York. 1952.
3. K. YAMADA, S. TAKADA, S. NAKAMURA, and Y. HIRATA. Tetrahedron Letters, **52**, 4785 (1965).
4. F. PORSCH, H. FARNOW, and H. WINKLER. Dragoco Rept. **12**, 123 (1965).
5. J. F. EYKMAN. Pharm. J. **11**, 1046 (1880).
6. K. K. CHEN. J. Am. Pharm. Assoc. **15**, 861 (1926).
7. J. A. CONCHA and L. WUNGWIRA. J. Philippine Pharm. Assoc. **50**, 361 (1964).
8. E. KUGLER and E. SZ. KOVATS. Helv. Chim. Acta, **46**, 1480 (1963).
9. J. A. ATTAWAY, L. J. BARABAS, and R. W. WOLFORD. Anal. Chem. **37**, 1289 (1965).

Can. J. Chem. Downloaded from www.nrcresearchpress.com by 210.87.254.42 on 09/05/12
For personal use only.

Can. J. Chem. Downloaded from www.nrcresearchpress.com by 210.87.254.40 on 09/05/12
For personal use only.

THIAZOLOISOQUINOLINES

I. THE SYNTHESIS OF THIAZOLO[4,5-*c*]ISOQUINOLINE[1]

CATHERINE E. HALL[2] AND ALFRED TAURINS
Department of Chemistry, McGill University, Montreal, Quebec

Received May 13, 1966

ABSTRACT

Thiazolo[4,5-*c*]isoquinoline (I), a new heterocyclic ring system, has been synthesized from 3-aminoisoquinoline (II) in four steps by reaction with potassium thiocyanate and bromine to give 3-amino-4-thiocyanoisoquinoline (VII), cyclization with hydrochloric acid to yield 2-aminothiazolo[4,5-*c*]isoquinoline (VIII), Sandmeyer reaction to give 2-chlorothiazolo-[4,5-*c*]isoquinoline (IX), and finally reduction with hydrogen iodide and red phosphorus to yield I. The attempted preparation of I via 3-amino-4-bromoisoquinoline was unsuccessful. Various 2-substituted derivatives of I were prepared by nucleophilic displacement of the chlorine atom in 2-chlorothiazolo[4,5-*c*]isoquinoline. The nuclear magnetic resonance and ultraviolet spectra of I and some of its derivatives were studied.

INTRODUCTION

Although all four isomers of thiazolopyridines (1–8) and many of the isomers of thiazoloquinolines (9–16) are known, thiazoloisoquinolines, of which eight isomers are possible, have remained an unknown class of heteroaromatic compounds, even in the form of derivatives. However, some thiazoloisoquinolinium compounds are known (17, 18). The synthesis of various isomers of thiazoloisoquinolines was undertaken to study the chemical, physical, and spectral properties of this new class of compounds. The first isomer chosen was thiazolo[4,5-*c*]isoquinoline (I).

RESULTS AND DISCUSSION

The preparation of thiazolopyridines and thiazoloquinolines is usually accomplished by reaction of the appropriate *o*-aminoarylthiol with carboxylic acids or their derivatives, such as the acid chlorides or the anhydrides (2, 5, 8, 10–12). The cyclization of *o*-thiocyanoarylamines to yield 2-aminothiazolo compounds has also been used (1, 13, 14). The former method was first chosen for the synthesis of thiazolo[4,5-*c*]isoquinoline (I), but difficulties were encountered in the attempted preparation of the intermediate 3-aminoisoquinoline-4-thiol (III).

The preparation of III was attempted with 3-amino-4-bromoisoquinoline as an intermediate. The method of Johnson and Nasutavicus (19) was used to prepare 3-aminoisoquinoline (II) from 2-cyanobenzyl cyanide. Bromination of II with bromine in carbon tetrachloride gave a 73% yield of 3-amino-4-bromoisoquinoline (IV). The bromine atom was proven to be in the 4-position in IV by infrared and nuclear magnetic resonance (n.m.r.) spectral evidence. In the infrared, a strong band at 750 cm^{-1}, indicative of an *o*-disubstituted benzene ring, showed that the bromine atom was in the heterocyclic ring. Since the resulting compound was different from the known 3-amino-1-bromoisoquinoline (19), it must be 3-amino-4-bromoisoquinoline. Comparison of the n.m.r. spectrum of IV

[1]*This work received financial assistance from the National Research Council of Canada, Ottawa. Presented before the meeting of the Royal Society of Canada, section III, held at Charlottetown, Prince Edward Island, June 9, 1964. Taken from a portion of the thesis submitted by C. E. Hall to the Faculty of Graduate Studies and Research, McGill University, Montreal, in partial fulfilment of the requirements for the Ph.D. degree.*
[2]*Holder of a National Research Council studentship, 1962–1963 and 1963–1964.*

with that of 3-aminoisoquinoline confirmed this assignment (Figs. 1A and 1B). 3-Aminoisoquinoline (II) shows a singlet at 1.15 τ for proton 1, a complex multiplet at 2.16 to 2.95 τ for the four protons on the carboxylic ring (H-5, H-6, H-7, and H-8), a singlet at 3.31 τ for the proton ortho to the amino group (H-4), and a broad singlet at 5.65 τ for the amino group protons. 3-Amino-4-bromoisoquinoline (IV) has a singlet at 1.38 τ for proton 1, a multiplet at 2.18 to 3.00 τ for the carboxylic ring protons, and a broad singlet at 5.00 τ for the amino group protons. Loss of the singlet at 3.31 τ, corresponding to proton 4 in II, proves that the bromine atom must be in the 4-position in IV.

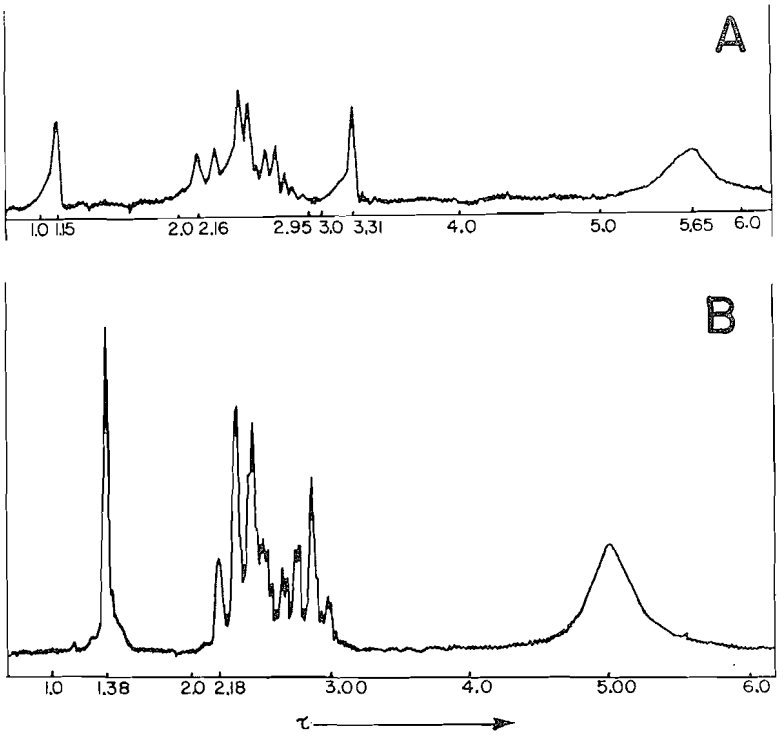


FIG. 1. The n.m.r. spectra (in $DCCl_3$) of (A) 3-aminoisoquinoline and (B) 3-amino-4-bromoisoquinoline.

Acetylation of 3-amino-4-bromoisoquinoline with acetic anhydride in the presence of pyridine gave a mixture of 3-monoacetamido-4-bromoisoquinoline (V) and 3-*N*,*N*-diacetylamino-4-bromoisoquinoline (VI). The infrared spectrum of V showed a strong band at 1 663 cm^{-1} (C=O stretching) and a medium-intensity band at 3 240 cm^{-1} (N—H stretching). Its n.m.r. spectrum (in a $CDCl_3$ and $(CD_3)_2SO$ mixture) exhibited a singlet at 1.04 τ for H-1, a multiplet at 1.88 to 2.61 τ for the four aromatic protons of the benzenoid ring plus the proton on the acetamido nitrogen, and a singlet at 7.60 τ for the methyl protons. After exchange with deuterium oxide, one proton was lost from the aromatic region (1.88 to 2.61 τ), thus confirming that the amide proton absorbed in this region.

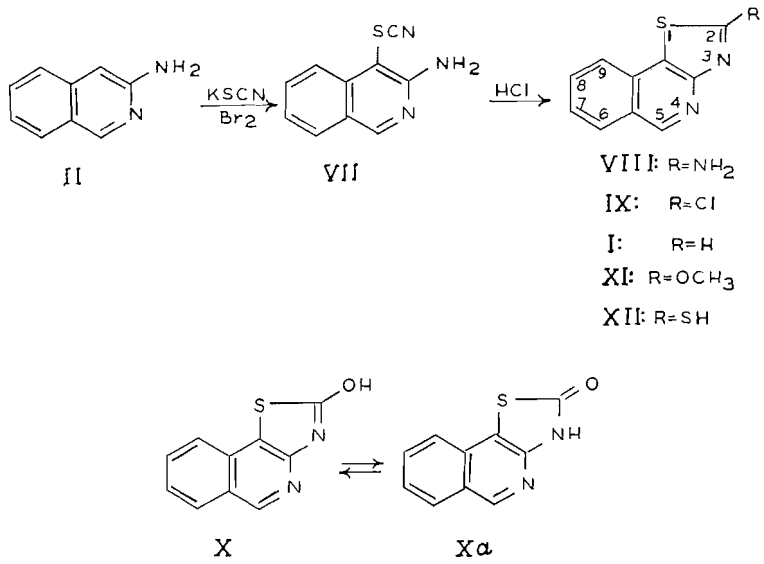
The attempted reaction of 3-acetamido-4-bromoisoquinoline (V) with thiourea to obtain 3-acetamidoisoquinoline-4-thiol was unsuccessful.

The infrared spectrum of 3-*N*,*N*-diacetylamino-4-bromoisoquinoline (VI) had a strong doublet at 1 705 and 1 725 cm^{-1} in the solid state (KBr pellet), but only a single strong

Can. J. Chem. Downloaded from www.nrcresearchpress.com by 210.87.254.40 on 09/05/12
For personal use only.

band at 1 725 cm^{-1} in either carbon tetrachloride or carbon disulfide solution. The n.m.r. spectrum of VI (in $CDCl_3$) exhibited a singlet at 0.94 τ for H-1, a complex multiplet at 1.80 to 2.43 τ for the four remaining aromatic protons, and a sharp singlet at 7.78 τ for the six methyl protons.

The synthesis of thiazolo[4,5-*c*]isoquinoline (I) was successfully accomplished via 3-amino-4-thiocyanoisoquinoline (VIII) (Reaction Scheme 1). The latter was obtained by the reaction of 3-aminoisoquinoline with potassium thiocyanate and bromine (20). The structure of VII was proven by infrared and n.m.r. spectroscopy. Thus, its infrared spectrum showed a strong band at 753 cm^{-1} characteristic of an *o*-disubstituted benzene ring, as well as a band at 2 143 cm^{-1} for the thiocyano group (21) and bands at 3 433 and 3 270 cm^{-1} for the amino group. In the n.m.r. spectrum of 3-amino-4-thiocyanoisoquinoline (VII) (in chloroform-*d* solution), a singlet at 1.29 τ was assigned to proton 1, a complex multiplet at 2.03 to 2.96 τ to the four benzenoid ring protons, and a broad singlet at 4.65 τ to the amino group protons.



REACTION SCHEME 1.

The cyclization of the thiocyano and amino groups in compound VII was achieved by refluxing VII in aqueous ethanolic hydrochloric acid. The resulting 2-aminothiazolo-[4,5-*c*]isoquinoline (VIII) was obtained in a 73% yield. Diazotization of VIII followed by reaction with cuprous chloride gave 2-chlorothiazolo[4,5-*c*]isoquinoline (IX). Reduction of IX with hydriodic acid and red phosphorus produced the parent compound of this series, thiazolo[4,5-*c*]isoquinoline (I). The n.m.r. spectrum of I (Fig. 2) exhibits a doublet at 0.87 and 0.92 τ with an area corresponding to two protons (assigned to H-2 and H-5), and a complex ABCD pattern of bands at 1.93 to 2.64 τ with an area corresponding to four protons of the benzenoid ring. It is not possible to state definitely whether H-2 absorbs at lower field than H-5, or vice versa. It was noted that, in the n.m.r. spectrum of I recorded in an acetone solution, the band for one of these protons moves downfield more than the other (two peaks at 0.44 and 0.60 τ).

The preparation of other 2-substituted derivatives of thiazolo[4,5-*c*]isoquinoline was accomplished by displacement of the chlorine atom of IX with various nucleophilic

Can. J. Chem. Downloaded from www.nrcresearchpress.com by 210.87.254.40 on 09/05/12
For personal use only.

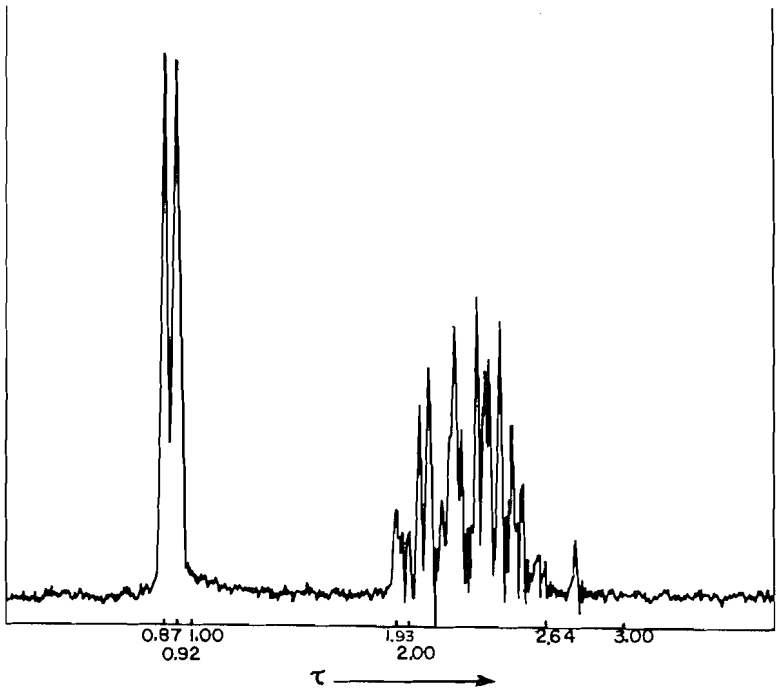


FIG. 2. The n.m.r. spectrum of thiazolo[4,5-*c*]isoquinoline (in $DCCl_3$).

reagents. For example, reaction of IX with sodium hydroxide gave the 2-hydroxy derivative X, and reaction of IX with sodium methoxide gave the 2-methoxy derivative XI. Reaction of IX with thiourea yielded the 2-mercapto derivative XII. The 2-hydroxythiazolo[4,5-*c*]isoquinoline (X) was shown, by infrared and other evidence (which will be the subject of a future publication in this series), to exist mainly in the lactam form X*a* rather than the hydroxy form. By analogy, 2-mercaptothiazolo[4,5-*c*]isoquinoline (XII) also probably exists as the thiolactam.

The chemical shifts of the protons of I and some of its derivatives are summarized in Table I. In all the compounds studied, the proton on the carbon atom adjacent to the heterocyclic nitrogen atom absorbs at lower field than the benzenoid protons. This is in agreement with the observations of other workers (22).

TABLE I

Proton chemical shifts of thiazolo[4,5-*c*]isoquinoline and some 2-substituted derivatives

Compound	Solvent	Chemical shift (τ)			
		H-2	H-5	H-6, H-7, H-8, H-9	Other
Thiazolo[4,5-*c*]-isoquinoline	$CDCl_3$	0.87 or 0.92	0.87 or 0.92	1.93 to 2.64	—
Thiazolo[4,5-*c*]-isoquinoline	Acetone	0.44 or 0.60	0.44 or 0.60	1.48 to 2.37	—
Derivatives					
2-Chloro	$CDCl_3$	—	0.73	1.81 to 2.38	—
2-Chloro	CH_3SOCH_3	—	0.50	1.46 to 2.22	—
2-Amino	CH_3SOCH_3	—	0.83	1.73 to 2.46	NH_2*
2-Hydroxy	CD_3SOCD_3	—	1.05	1.95 to 2.64	−2.58 (NH)
2-Methoxy	$CDCl_3$	—	0.78	1.80 to 2.59	5.62 (OCH_3)

*Superimposed upon the H-5, H-6, H-7, and H-8 bands.

Can. J. Chem. Downloaded from www.nrcresearchpress.com by 210.87.254.40 on 09/05/12
For personal use only.

The ultraviolet spectra of thiazolo[4,5-*c*]isoquinoline and its 2-substituted derivatives (Table II) generally show three groups of absorption bands, which are classified as the α-, *p*-, and β-bands (23). All the bands of I occur at longer wavelengths than do the corresponding bands of isoquinoline (α-band, 319 mμ and 308 mμ; *p*-band, 268 mμ; β-band, 220 mμ (24)). Annealing the thiazole ring to benzene, quinoline, and naphthalene similarly results in a bathochromic displacement of the bands from those of the parent compounds (25, 26). Electron-donating substituents, such as chlorine, give rise to bathochromic displacements of all the bands of the parent compound (I), as expected.

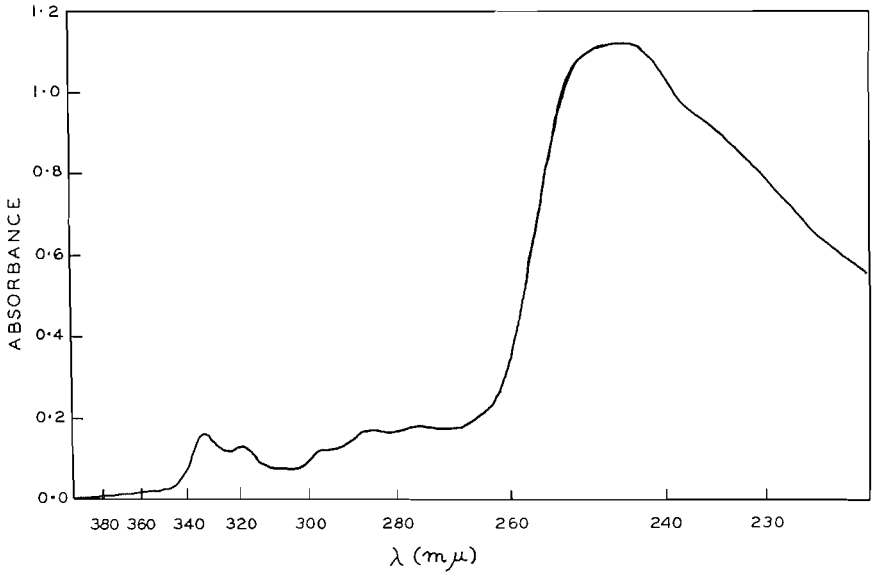


FIG. 3. The ultraviolet spectrum of thiazolo[4,5-*c*]isoquinoline (in ethanol).

EXPERIMENTAL

Melting points were determined on a Gallenkamp melting point apparatus and are corrected. Infrared spectra were recorded on a Perkin–Elmer model 421 grating spectrophotometer in KBr disks. Ultraviolet spectra were obtained on a Perkin–Elmer model 350 spectrophotometer with absolute ethanol as solvent. Nuclear magnetic resonance spectra were determined on Varian high-resolution n.m.r. spectrometers, model HR-60 or model A60. Solvents used for the n.m.r. work were chloroform-*d*, dimethyl sulfoxide, and dimethyl sulfoxide-d_6; tetramethylsilane was used as an internal reference. Elemental analyses were carried out by Dr. C. Daesslé, Montreal, and by A. Bernhardt, Mülheim, Germany.

Preparation of 3-Amino-4-bromoisoquinoline (IV)

3-Aminoisoquinoline (2.90 g, 0.02 mole) was dissolved in 100 ml of glacial acetic acid in a 500 ml three-necked flask equipped with an air condenser, a dropping funnel, and a mechanical stirrer. To this stirred solution was added dropwise, over 45 min, 210 ml of 0.1 *M* bromine solution in carbon tetrachloride.

The reaction mixture was stirred for an additional 5 min and then poured into 500 ml of a sodium acetate solution. The organic layer was separated and the aqueous layer extracted once with carbon tetrachloride. The organic extract was dried over sodium sulfate and filtered, and the solvent was evaporated, leaving 4.46 g of a black solid. Crystallization from hexane gave 3.25 g (73% yield) of 3-amino-4-bromoisoquinoline (IV) as yellow needles, m.p. 120.5–122°.

Anal. Calcd. for $C_9H_7BrN_2$: C, 48.46; H, 3.16; Br, 35.83; N, 12.55. Found: C, 48.24; H, 3.01; Br, 35.71; N, 12.61.

Acetylation of 3-Amino-4-bromoisoquinoline

3-Amino-4-bromoisoquinoline (2.32 g, 0.01 mole) was dissolved in a mixture of 32 ml of acetic anhydride and 16 ml of pyridine, and the resulting solution was heated at 90–95° for 4 h. It was cooled to room temperature and poured into an excess of dilute ammonium hydroxide solution, whereupon a crystalline substance

Can. J. Chem. Downloaded from www.nrcresearchpress.com by 210.87.254.40 on 09/05/12
For personal use only.

TABLE II

Positions of the ultraviolet absorption maxima and corresponding log ϵ values of thiazolo[4,5-*c*]isoquinoline and its derivatives (solvent, ethanol)

Compound	α-Band		p-Band		β-Band	
	mμ	log ϵ	mμ	log ϵ	mμ	log ϵ
Thiazolo[4,5-*c*]-isoquinoline	334 320	3.56 3.52	298 286 276	3.54 3.69 3.70	245 237 sh	4.45 4.37
Derivatives						
2-Amino	360	3.48	311 299 288 sh	3.98 3.90 3.66	259	4.57
2-Acetamido	343	3.81	311 302 290 sh	4.01 3.97 3.86	266 258	4.44 4.42
2-Chloro	337 324	3.70 3.63	304 292 282 sh	3.72 3.77 3.72	249 232 sh	4.51 4.39
2-Hydroxy	350	3.66	301 288 278	3.55 3.60 3.56	246.5 235 sh	4.45 4.36
2-Methoxy	345 335	3.61 3.61	301 289 278	3.73 3.79 3.71	247	4.63
2-Thiol*	344	—	290 283	— —	249	—

*Because of very low solubility, log ϵ could not be calculated.

precipitated. This was filtered off to yield 1.33 g (43% yield) of tan needles, m.p. 105–108°. Recrystallization from hexane gave colorless needles of the diacetyl derivative VI, m.p. 107–108.5°.

Anal. Calcd. for $C_{13}H_{11}BrN_2O_2$: C, 50.83; H, 3.61; N, 9.12. Found: C, 50.57, 50.73; H, 3.15, 3.33; N, 9.48, 9.41.

Evaporation of most of the filtrate from the crude reaction product above yielded 1.22 g (46% yield) of the monoacetyl derivative V as colorless needles, m.p. 166–168° (crystallized from ethanol).

Anal. Calcd. for $C_{11}H_9BrN_2O$: C, 49.83; H, 3.42; N, 10.57. Found: C, 49.83, 49.74; H, 3.11, 3.35; N, 10.80, 10.60.

Attempted Reaction of 3-Acetamido-4-bromoisoquinoline (V) with Thiourea

3-Acetamido-4-bromoisoquinoline (0.50 g, 0.0019 mole) was refluxed with 0.17 g (0.0022 mole) of thiourea in 15 ml of absolute ethanol for 7 h. Evaporation of the solvent and recrystallization of the residue from ethanol gave colorless needles, m.p. 165–168°, the infrared spectrum of which was identical with that of the starting 3-acetamido-4-bromoisoquinoline.

Preparation of 3-Amino-4-thiocyanoisoquinoline (VII)

3-Aminoisoquinoline (12.9 g, 0.09 mole) and potassium thiocyanate (34.8 g, 0.36 mole) were dissolved in 165 ml of 95% acetic acid in a 500 ml three-necked flask equipped with a mechanical stirrer, a reflux condenser, and a dropping funnel. The resulting solution was cooled to −5 to −10°, and bromine (5.10 ml, 0.09 mole) in 25 ml of 95% acetic acid was added dropwise to the stirred solution over a period of 35 min. After the reaction mixture was stirred for a further 15 min, it was poured into 1 500 ml of water. The resulting precipitate was filtered off and recrystallized from ethanol to give 11.74 g (65% yield) of 3-amino-4-thiocyanoisoquinoline as yellow needles, m.p. 158.5–160.5°. Two more recrystallizations from ethanol gave pale-yellow needles, m.p. 163–164°.

Anal. Calcd. for $C_{10}H_7N_3S$: C, 59.68; H, 3.51; N, 20.88. Found: C, 59.84; H, 3.67; N, 20.77.

When the original reaction mixture was allowed to stand overnight at room temperature, no cyclization of 3-amino-4-thiocyanoisoquinoline to 2-aminothiazolo[4,5-*c*]isoquinoline (VIII) was observed.

Can. J. Chem. Downloaded from www.nrcresearchpress.com by 210.87.254.40 on 09/05/12
For personal use only.

Preparation of 2-Aminothiazolo[4,5-c]isoquinoline (VIII)

3-Amino-4-thiocyanoisoquinoline (11.8 g, 0.06 mole) was dissolved in 900 ml of boiling ethanol, and 510 ml of 15% hydrochloric acid was added. The resulting solution was refluxed for 6 h. It was cooled to room temperature, diluted with 1 500 ml of water, and basified with solid sodium carbonate. The resulting precipitate was filtered off, dried, and washed with benzene to yield 8.57 g (73% yield) of yellow needles. Recrystallization from a large volume of benzene gave VIII as colorless needles, m.p. 240–242°.

Anal. Calcd. for $C_{10}H_7N_3S$: C, 59.68; H, 3.51; N, 20.88. Found: C, 59.87; H, 3.54; N, 20.76.

The acetyl derivative of VIII was prepared by refluxing VIII (1.00 g, 0.005 mole) in a mixture of 16 ml of acetic anhydride and 8 ml of pyridine for 5 h. The starting material did not appear to dissolve, but a new insoluble product was formed. Filtration of the cooled reaction mixture gave 0.85 g (75% yield) of tan needles, m.p. 326.7°. Recrystallization from absolute ethanol gave pale-tan needles of the monoacetyl derivative of VIII, m.p. 327–328°.

Anal. Calcd. for $C_{12}H_9N_3OS$: C, 59.24; H, 3.73; N, 17.27; S, 13.18. Found: C, 59.34; H, 3.51; N, 17.53; S, 13.03.

Preparation of 2-Chlorothiazolo[4,5-c]isoquinoline (IX)

Cuprous chloride was prepared in the usual manner from 1.32 g of sodium chloride, 6.00 g of hydrated cupric sulfate, 1.08 g of sodium bisulfite, and 0.72 g of sodium hydroxide, and was dissolved in 10 ml of concentrated hydrochloric acid.

2-Aminothiazolo[4,5-*c*]isoquinoline (2.40 g, 0.012 mole) was dissolved in a mixture of 80 ml of 85% phosphoric acid and 20 ml of 70% nitric acid, and then cooled to 0–5°. Sodium nitrite (0.88 g, 0.013 mole) in 8 ml of water was added over a 15 min period to the cooled stirred solution. The reaction mixture was stirred for another 20 min at 0–5°. The cold diazonium solution was then added over 20 min, with stirring, to the cuprous chloride solution at 0–5°. A vigorous reaction occurred during the addition. The reaction mixture was stirred for 1 h longer at room temperature. It was then basified with 10% sodium hydroxide solution, with cooling, and the basic mixture extracted with three 200 ml portions of ether. The organic extract was dried over sodium sulfate and the solvent evaporated, leaving 1.53 g of an oily brown solid. Extraction of this solid with boiling hexane gave 1.20 g (45% yield) of pale-yellow 2-chlorothiazolo[4,5-*c*]isoquinoline (IX), m.p. 114–117°. Recrystallization from hexane followed by vacuum sublimation gave colorless crystals of IX, m.p. 116.5–118°.

Anal. Calcd. for $C_{10}H_5ClN_2S$: C, 54.42; H, 2.28; Cl, 16.07; N, 12.70. Found: C, 54.36; H, 2.13; Cl, 15.97; N, 12.59.

Preparation of Thiazolo[4,5-c]isoquinoline (I)

2-Chlorothiazolo[4,5-*c*]isoquinoline (0.51 g, 2.3 mmoles) was dissolved in a mixture of 8 ml of 47% hydriodic acid, 4 ml of water, and 4 ml of acetic acid, and 0.28 g of red phosphorus was added. The resulting mixture was refluxed for 3½ h. It was cooled to room temperature, diluted with 250 ml of water, and filtered. The filtrate was basified with solid sodium carbonate and extracted with two 200 ml portions of ether. After the extract was dried over sodium sulfate, the ether was evaporated, leaving 0.39 g (91% yield) of a tan solid. Chromatography of 0.21 g of this material on 10 g of alumina (Woelm, activity 1) with benzene–ether (1:1) as eluent gave 0.18 g of a colorless solid. Recrystallization from hexane gave colorless needles of thiazolo-[4,5-*c*]isoquinoline (I), m.p. 117–118°.

Anal. Calcd. for $C_{10}H_6N_2S$: C, 64.49; H, 3.25; N, 15.05. Found: C, 64.68; H, 3.50; N, 15.08.

2-Hydroxy[4,5-c]isoquinoline (X)

2-Chlorothiazolo[4,5-*c*]isoquinoline (0.16 g, 0.7 mmole) was refluxed in 30 ml of 0.1 *N* sodium hydroxide solution for 5 h. The resulting solution was filtered while hot, cooled to room temperature, and acidified with dilute acetic acid. The flocculent precipitate was filtered off, washed with water, and dried to give 0.11 g (79% yield) of a tan solid, m.p. 285–285.5°. Recrystallization from ethanol–water gave pale-yellow needles of 2-hydroxythiazolo[4,5-*c*]isoquinoline (X), m.p. 286.7°.

Anal. Calcd. for $C_{10}H_6N_2OS$: C, 59.38; H, 2.99; N, 13.85; S, 15.86. Found: C, 59.34; H, 3.20; N, 13.87; S, 15.79.

2-Methoxy[4,5-c]isoquinoline (XI)

2-Chlorothiazolo[4,5-*c*]isoquinoline (0.20 g, 0.9 mmole) was dissolved in 15 ml of absolute methanol, and a solution of 0.05 g (1.2 mmoles) of sodium in 5 ml of absolute methanol was added. After the mixture was stirred at room temperature for 1 h, the clear-yellow solution was neutralized with dilute acetic acid, diluted with water, and dried to give 0.15 g (79% yield) of 2-methoxythiazolo[4,5-*c*]isoquinoline, m.p. 147–148.5°. Recrystallization from methanol gave pale-yellow needles, m.p. 149.5–150.5°.

Anal. Calcd. for $C_{11}H_8N_2OS$: C, 61.09; H, 3.73; N, 12.96; S, 14.83. Found: C, 61.04; H, 3.51; N, 13.11; S, 14.76.

Thiazolo[4,5-c]isoquinoline-2-thiol (XII)

A solution of 2-chlorothiazolo[4,5-*c*]isoquinoline (0.20 g, 0.9 mmole) and thiourea (0.10 g, 1.3 mmoles) in 10 ml of ethanol was refluxed for 1 h. The reaction mixture was cooled to room temperature and filtered.

Can. J. Chem. Downloaded from www.nrcresearchpress.com by 210.87.254.40 on 09/05/12
For personal use only.

The crystalline precipitate was dissolved in 40 ml of 1 *N* sodium hydroxide solution and filtered. Acidification of the filtrate with acetic acid gave a flocculent precipitate, which was filtered off, washed with water, and dried to give 0.14 g (70% yield) of pale-yellow thiazolo[4,5-*c*]isoquinoline-2-thiol, m.p. 323–326°. After this compound was dissolved in sodium hydroxide again and reprecipitated with acetic acid, the melting point was 324–326°.

Anal. Calcd. for $C_{10}H_6N_2S_2$: C, 55.03; H, 2.77; N, 12.84. Found: C, 55.05; H, 2.75; N, 12.80.

REFERENCES

1. J. A. BAKER and S. A. HILL. J. Chem. Soc. 3464 (1962).
2. T. TAKAHASHI and K. UEDA. J. Pharm. Soc. Japan, **73**, 442 (1953); Chem. Abstr. **48**, 5187*h* (1954).
3. T. TAKAHASHI, Y. YATSUKA, and Y. ONUMA. J. Pharm. Soc. Japan, **64**, 235 (1944); Chem. Abstr. **45**, 4717*e* (1951).
4. S. G. FRIDMAN. Zh. Obshch. Khim. **26**, 864 (1956); Chem. Abstr. **50**, 14753*a* (1956).
5. Y. YAMAMOTO. J. Pharm. Soc. Japan, **71**, 916 (1951); Chem. Abstr. **46**, 8109*g* (1952).
6. S. G. FRIDMAN. Zh. Obshch. Khim. **26**, 613 (1956); Chem. Abstr. **50**, 13906*g* (1956).
7. T. TAKAHASHI, K. UEDA, and T. ICHIMOTO. Pharm. Bull. Tokyo, **2**, 196 (1954); Chem. Abstr. **50**, 1000*i* (1956).
8. T. TAKAHASHI and K. UEDA. Pharm. Bull. Tokyo, **4**, 216 (1956); Chem. Abstr. **51**, 2732*i* (1957).
9. CH. GRÄNACHER, A. OFNER, and A. KLOPFENSTEIN. Helv. Chim. Acta, **8**, 883 (1925).
10. I. TĂNĂSESCU and I. DÉNES. Chem. Ber. **91**, 1601 (1958).
11. I. TĂNĂSESCU, I. DÉNES, and GH. RUSU. Chem. Ber. **90**, 1295 (1957).
12. G. B. BACHMAN, D. E. WELTON, G. L. JENKINS, and J. E. CHRISTIAN. J. Am. Chem. Soc. **69**, 365 (1947).
13. A. MAGGIOLO. J. Am. Chem. Soc. **73**, 5815 (1951).
14. Y. KASHIDA, K. YOKOTA, and H. S. HAI. J. Pharm. Soc. Japan, **71**, 553 (1951); Chem. Abstr. **46**, 4546*a* (1952).
15. K. FRIES and A. WOLTER. Ann. **527**, 60 (1936).
16. H. ERLENMEYER and H. UEBERWASSER. Helv. Chim. Acta, **23**, 328 (1940).
17. F. KRÖHNKE and H. STEUERNAGEL. Angew. Chem. **73**, 26 (1961).
18. R. HUISGEN, R. GRASHEY, and E. STEINGRUBER. Tetrahedron Letters, 1441 (1963).
19. F. JOHNSON and W. A. NASUTAVICUS. J. Org. Chem. **27**, 3953 (1962).
20. H. P. KAUFMANN. Arch. Pharm. **266**, 197 (1928).
21. C. N. R. RAO. Chemical applications of infrared spectroscopy. Academic Press, Inc., New York. 1963. p. 268.
22. G. G. HALL, A. HARDISSON, and L. M. JACKMAN. Tetrahedron Suppl. **2**, 101 (1963).
23. S. F. MASON. *In* Physical methods in heterocyclic chemistry. Vol. 2. A. R. Katritzky (*Editor*). Academic Press, Inc., New York. 1963. pp. 35–59.
24. J. P. PHILLIPS and F. C. NACHOD. Organic electronic spectral data. Vol. 4. Interscience Publishers, Inc., New York. 1958–1959. p. 204.
25. A. CERNIANI and R. PASSERINI. J. Chem. Soc. 2261 (1954).
26. W. A. BOGGUST, W. COCKER, J. C. P. SCHWARZ, and E. R. STUART. J. Chem. Soc. 680 (1950).

Can. J. Chem. Downloaded from www.nrcresearchpress.com by 210.87.254.40 on 09/05/12
For personal use only.

Can. J. Chem. Downloaded from www.nrcresearchpress.com by 210.87.254.40 on 09/05/12
For personal use only.

THIAZOLOISOQUINOLINES

II. THE SYNTHESIS OF THIAZOLO[5,4-*c*]ISOQUINOLINE[1,2]

CATHERINE E. HALL[3] AND ALFRED TAURINS
Department of Chemistry, McGill University, Montreal, Quebec

Received May 13, 1966

ABSTRACT

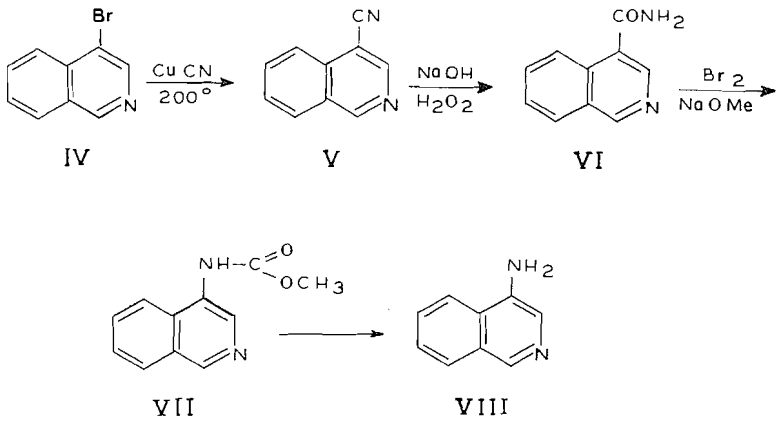
Thiazolo[5,4-*c*]isoquinoline (I) has been synthesized by cyclization of 4-amino-3-thiocyanoisoquinoline (IX) to 2-aminothiazolo[5,4-*c*]isoquinoline (X), which was converted into I via the 2-chloro derivative XI. Some 2-substituted derivatives of I were obtained by displacement of the chlorine atom in XI. The attempted preparation of 3-chloro-4-nitroisoquinoline as an intermediate in the synthesis of I was unsuccessful. Nuclear magnetic resonance and ultraviolet spectra of I and its derivatives were investigated.

In a continuation of our work on the synthesis of thiazoloisoquinolines, the preparation of thiazolo[5,4-*c*]isoquinoline (I) was undertaken. It was planned to arrive at I by cyclization (with formic acid) of 4-aminoisoquinoline-3-thiol, which could be prepared from 3-chloro-4-nitroisoquinoline (II) via 4-nitroisoquinoline-3-thiol. It was hoped that nitration of 3-chloroisoquinoline would yield the required 3-chloro-4-nitroisoquinoline. The starting material, 3-chloroisoquinoline, was prepared from homophthalimide (1) by way of 1,3-dichloroisoquinoline (2, 3). Nitration of 3-chloroisoquinoline with potassium nitrate in sulfuric acid gave a mononitro derivative which, from its nuclear magnetic resonance (n.m.r.) spectrum ($CDCl_3$), was established to be 3-chloro-5-nitroisoquinoline (III) rather than the desired 3-chloro-4-nitroisoquinoline (II). The singlet at 0.96 τ is attributed to proton 1, the multiplet at 1.43 to 1.54 τ to H-4 plus H-6, the doublet centered at 1.79 τ (J = 6.9 c.p.s.) to H-8, and the triplet centered at 2.37 τ (J = 6.9 c.p.s.) to H-7. The low-field absorption of H-4, caused by the diamagnetic anisotropy of the 5-nitro group, eliminates any position other than C-5 for the nitro group. In 5-nitroisoquinoline, H-4 was found to absorb in the region 1.1 to 1.4 τ, whereas in 3-chloroisoquinoline it appeared in the region 2.2 to 2.5 τ.

The infrared spectrum of III exhibited bands at 1 326 and 1 514 cm^{-1} (NO_2 group), 880 cm^{-1} (2,4,5-trisubstituted pyridine ring), and 686 and 760 cm^{-1} (1,2,3-trisubstituted benzene ring).

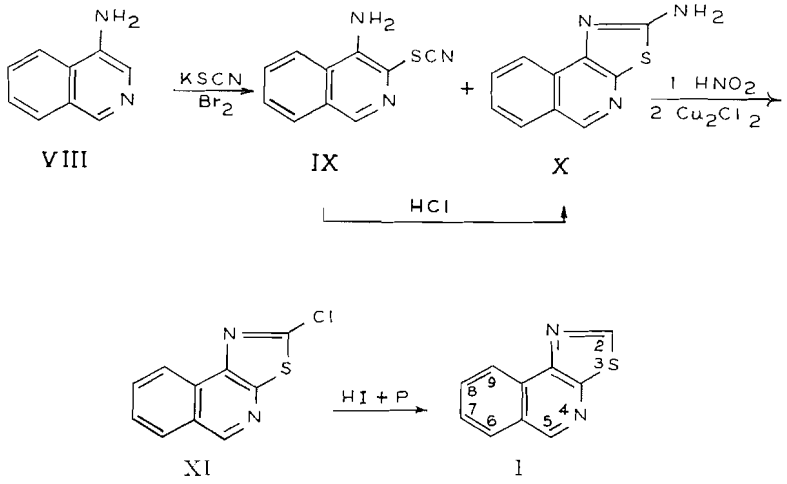
Since 3-chloro-4-nitroisoquinoline did not appear to be prepared as easily as originally envisaged, the synthesis of thiazolo[5,4-*c*]isoquinoline (I) via 4-aminoisoquinoline-3-thiol was abandoned in favor of the method involving 4-amino-3-thiocyanoisoquinoline (IX) as an intermediate (4). The synthesis of IX required 4-aminoisoquinoline (VIII) as a precursor; this compound was prepared as shown in Reaction Scheme 1. The conversion of isoquinoline into isoquinoline-4-carboxamide (VI) via the 4-bromo (IV) and 4-cyano (V) derivatives followed known procedures (5–7). The Hofmann rearrangement of VI with bromine and sodium hydroxide was unsuccessful and led to only resinous products. However, the use of bromine and sodium methoxide in methanol gave methyl isoquinoline-4-carbamate (VII), which was subsequently hydrolyzed to VIII with 93% sulfuric acid.

[1]*This work received financial assistance from the National Research Council of Canada, Ottawa. Taken from a portion of the Ph.D. Thesis of C. E. Hall.*
[2]*For part I, see ref. 9.*
[3]*Holder of a National Research Council studentship, 1962–1963 and 1963–1964.*



REACTION SCHEME 1.

The conversion of 4-aminoisoquinoline (VIII) into thiazolo[5,4-*c*]isoquinoline (I) is shown in Reaction Scheme 2. Thiocyanation of VIII produced a mixture of 4-amino-3-thiocyanoisoquinoline (IX) (33% yield) and 2-aminothiazolo[5,4-*c*]isoquinoline (X) (21% yield). 4-Amino-3-thiocyanoisoquinoline (IX) was characterized by its infrared spectrum, which showed thiocyano absorption at 2 143 cm^{-1} (8), as well as bands at 755 cm^{-1} for an *o*-disubstituted benzene ring and 3 460, 3 315, and 3 210 cm^{-1} for a primary amino group. The n.m.r. spectrum of IX (in a $CDCl_3$ and $(CH_3)_2SO$ mixture) had a singlet at 1.50 τ for H-1, a multiplet at 1.66 to 2.42 τ for the carbocyclic ring protons, and a broad singlet at 3.98 τ for the amino group protons. The presence of the singlet at 1.50 τ for H-1 excluded the possibility that the thiocyano group could be in the 1-position.



REACTION SCHEME 2.

The infrared spectrum of 2-aminothiazolo[5,4-*c*]isoquinoline (X) no longer showed thiocyano absorption at 2 143 cm^{-1}; however, a primary amino group was indicated by bands at 3 050, 3 215, and 1 662 cm^{-1}. A band at 747 cm^{-1} showed the presence of an *o*-disubstituted benzene ring.

Can. J. Chem. Downloaded from www.nrcresearchpress.com by 210.87.254.40 on 09/05/12
For personal use only.

Can. J. Chem. Downloaded from www.nrcresearchpress.com by 210.87.254.40 on 09/05/12
For personal use only.

4-Amino-3-thiocyanoisoquinoline (IX) could be converted into 2-aminothiazolo[5,4-*c*]-isoquinoline (X) by refluxing it in aqueous–ethanolic hydrogen chloride. It is significant that X was formed in the original thiocyanation reaction, whereas none of the cyclized 2-aminothiazolo[4,5-*c*]isoquinoline was formed in the thiocyanation of 3-aminoisoquinoline even after the reaction mixture was allowed to stand overnight at room temperature (9). This is attributed to a decreased electron density about the amino nitrogen in the intermediate 3-amino-4-thiocyanoisoquinoline in the latter case, which inhibits the nucleophilic attack of this nitrogen on the carbon of the thiocyano group.

Diazotization of 2-aminothiazolo[5,4-*c*]isoquinoline (X) followed by reaction with cuprous chloride gave 2-chlorothiazolo[5,4-*c*]isoquinoline (XI). Reduction of XI with hydriodic acid and red phosphorus gave the unsubstituted thiazolo[5,4-*c*]isoquinoline (I), a new heteroaromatic parent compound.

Several other 2-substituted derivatives of I were prepared by reaction of the 2-chloro derivative XI with various nucleophiles. For example, reaction with sodium hydroxide gave the 2-hydroxy derivative XII, and reaction with sodium methoxide gave the 2-methoxy compound XIII. Reaction with thiourea produced the 2-mercapto derivative XIV. The 2-hydroxy derivative XII was shown, by infrared and other evidence (which will be presented in a future paper), to exist predominantly in the lactam form. By analogy, the 2-mercapto derivative XIV probably exists mainly as the thiolactam.

The chemical shifts in the proton magnetic resonance spectra of thiazolo[5,4-*c*]isoquinoline (I) and some of its 2-substituted derivatives are presented in Table I. The n.m.r. spectrum of the parent compound I (in $CDCl_3$) (Fig. 1) shows two singlets at 0.80 and 0.83 τ integrating for two protons, an octet centered at 1.27 τ integrating for one proton, and a multiplet at 1.80 to 2.47 τ integrating for three protons. The singlets at 0.80 and 0.83 τ are assigned to the protons on the carbon atoms adjacent to the heterocyclic nitrogen atoms (H-2 and H-5), the octet to H-9 of the carbocyclic ring, and the multiplet to the three remaining aromatic protons (H-6, H-7, and H-8). The difference in chemical shift between protons H-2 and H-5 is very small in deuteriochloroform, although this difference is increased somewhat in acetone. However, it was not ascertained which proton absorbed at lower field. A similar result was observed for the corresponding protons of the isomeric thiazolo[4,5-*c*]isoquinoline (9).

The four benzenoid protons of thiazolo[5,4-*c*]isoquinoline (I) exhibit an ABCX pattern in contrast to the corresponding protons of thiazolo[4,5-*c*]isoquinoline, which show an ABCD pattern (9). The X part of the spectrum of I and its derivatives occurs at lower field than the ABC part and is assigned to H-9. The 9-position of I is comparable to the 10-position of benzo[*f*]quinoline, in which H-10 absorbs at much lower field than the other aromatic protons (10). This deshielding was attributed to the field effect of the "angularly opposite" hetero atom (10).

The ultraviolet spectra of thiazolo[5,4-*c*]isoquinoline (I) (Fig. 2) and its 2-substituted derivatives (Table II) generally show three groups of absorption bands, which are classified as the α-, p-, and β-bands (11). All three bands of I occur at shorter wavelengths than do the corresponding bands of thiazolo[4,5-*c*]isoquinoline (9). This is especially notable in the short-wavelength β-band, and it may be attributed to the overall greater length of conjugation in thiazolo[4,5-*c*]isoquinoline. Both electron-donating and electron-withdrawing substituents in the 2-position of thiazolo[5,4-*c*]isoquinoline give bathochromic displacements of the bands as expected.

The work on the synthesis and properties of other thiazoloisoquinolines is being continued.

Can. J. Chem. Downloaded from www.nrcresearchpress.com by 210.87.254.40 on 09/05/12
For personal use only.

TABLE I

Chemical shifts of the protons of thiazolo[5,4-*c*]isoquinoline and some 2-substituted derivatives

Compound	Chemical shift (τ)					Solvent†
	H-2	H-5	H-6, H-7, H-8	H-9	Other	
Thiazolo[5,4-*c*]isoquinoline	0.80 or 0.83	0.80 or 0.83	1.80 to 2.47	1.27	—	$DCCl_3$
Thiazolo[5,4-*c*]isoquinoline	0.50 or 0.66	0.50 or 0.66	1.50 to 2.33	1.17	—	Acetone
2-Chlorothiazolo[5,4-*c*]isoquinoline	—	1.15	2.05 to 2.66	1.68	—	$DCCl_3$
2-Aminothiazolo[5,4-*c*]isoquinoline	—	1.19	1.71 to 2.46	*	NH_2‡	DMSO
2-Hydroxythiazolo[5,4-*c*]isoquinoline	—	1.13	1.85 to 2.61	*	−2.60 (NH)	DMSO-d_6
2-Methoxythiazolo[5,4-*c*]isoquinoline	—	0.99	1.92 to 2.66	1.52	5.73 (OCH_3)	$DCCl_3$

*H-9 absorbs in the same region as H-6, H-7, and H-8.
†DMSO = dimethyl sulfoxide; DMSO-d_6 = dimethyl sulfoxide-d_6.
‡The amino group protons absorb in the same region as H-6, H-7, and H-8.

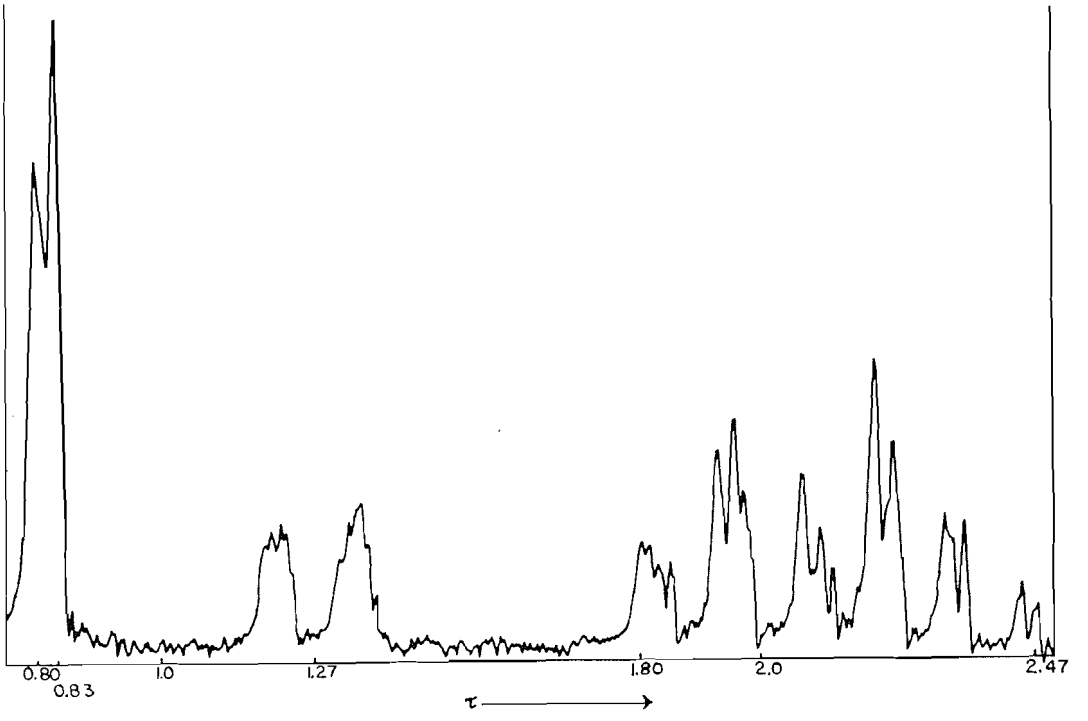


FIG. 1. The n.m.r. spectrum of thiazolo[5,4-*c*]isoquinoline (in $DCCl_3$).

TABLE II

Positions of the ultraviolet absorption maxima and corresponding log ε values of thiazolo[5,4-*c*]isoquinoline and its derivatives (solvent, ethanol)

	α-Band		p-Band		β-Band	
Compound	mμ	log ε	mμ	log ε	mμ	log ε
Thiazolo[5,4-*c*]isoquinoline	332.5	3.72	292.5	3.69	243 inf	4.42
	328 sh	3.64	281	3.75	233	4.66
	319	3.64	271	3.69		
Derivatives						
2-Amino	348	4.02	317 sh	3.66	251.5	4.46
			303 sh	3.60	238 sh	4.41
					230 sh	4.43
					222	4.47
2-Acetamido	345	4.14	305	3.87	249 sh	4.50
	333	4.07	293	3.94	241.5	4.54
			280	3.94	221	4.45
			272 sh	3.90		
2-Chloro	335.5	3.85	297	3.77	241 inf	4.52
	330 sh	3.77	285	3.79	234.5	4.69
	321	3.75	274	3.68	230 sh	4.64
2-Hydroxy	346	3.82	304	3.59	261 inf	3.82
			293	3.58	240	4.51
2-Methoxy	338	3.85	299	3.66	263 sh	3.52
	330 sh	3.80	287.5	3.69	237.5	4.73
			278 sh	3.59		
2-Thiolo	368	4.22	320 sh	3.97	249	4.29
			314	3.98		

Can. J. Chem. Downloaded from www.nrcresearchpress.com by 210.87.254.40 on 09/05/12
For personal use only.

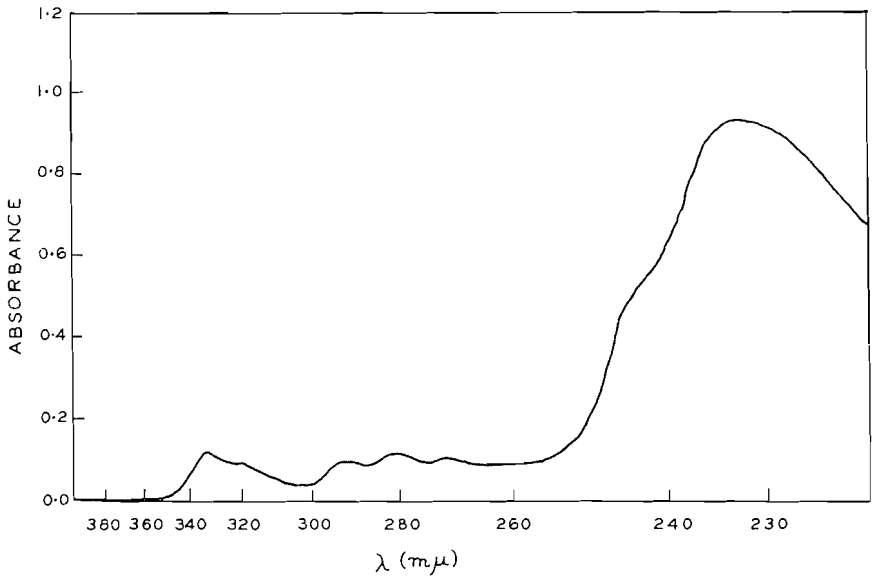


FIG. 2. The ultraviolet spectrum of thiazolo[5,4-*c*]isoquinoline (in ethanol).

EXPERIMENTAL

Melting points were determined on a Gallenkamp melting point apparatus and are corrected. Infrared spectra were recorded on a Perkin–Elmer model 421 grating spectrophotometer as KBr disks. Ultraviolet spectra were obtained on a Perkin–Elmer model 350 spectrophotometer with absolute ethanol as solvent. Nuclear magnetic resonance spectra were determined on Varian high-resolution n.m.r. spectrometers, model HR-60 or model A60. Solvents used were chloroform-*d*, dimethyl sulfoxide, and dimethyl sulfoxide-d_6. Tetramethylsilane was used as an internal standard. Elemental analyses were carried out by A. Bernhardt, Mülheim, Germany.

Nitration of 3-Chloroisoquinoline

3-Chloroisoquinoline (0.25 g, 1.5 mmoles) was dissolved in 4.0 ml of concentrated sulfuric acid, and potassium nitrate (0.19 g, 1.9 mmoles) in 3.0 ml of concentrated sulfuric acid was added dropwise to the stirred solution. The reaction mixture was stirred for 1 h at room temperature. It was then poured onto ice and basified with concentrated ammonium hydroxide solution, with cooling. Filtration yielded 0.30 g of a crude yellow product. Crystallization from hexane–benzene gave 0.23 g (74% yield) of 3-chloro-5-nitroisoquinoline (III) as pale-yellow needles, m.p. 162–164°. A second recrystallization raised the melting point to 163–165°.

Anal. Calcd. for $C_9H_5ClN_2O_2$: C, 51.81; H, 2.42; N, 13.43. Found: C, 51.75; H, 2.30; N, 13.22.

Hofmann Reaction of Isoquinoline-4-carboxamide (VI)

(a) In Sodium Hydroxide

Bromine (0.97 g, 0.006 mole) was added dropwise to 8 ml of a cooled (0–5°) stirred 10% sodium hydroxide solution. Isoquinoline-4-carboxamide (0.83 g, 0.005 mole) was added all at once to this cool, vigorously stirred solution. The reaction mixture was stirred for a further 15 min at this temperature, and was then heated to 55–70° and kept there for 25 min. During this time a black resinous material precipitated.

The reaction mixture was cooled to room temperature, and the resinous material was separated and dissolved in dilute sulfuric acid. The acid solution was filtered and the filtrate basified with solid sodium carbonate. The resulting flocculent precipitate was insoluble in boiling benzene, and thus was not the desired 4-aminoisoquinoline (10).

(b) In Methanol

Sodium methoxide was prepared by adding 19.5 g (0.85 mole) of sodium to 800 ml of absolute methanol in a 2 l three-necked flask equipped with a reflux condenser, a mechanical stirrer, and a dropping funnel. Isoquinoline-4-carboxamide (67.0 g, 0.39 mole) in 800 ml of absolute methanol was added all at once. Bromine (65.6 g, 0.41 mole) was then added dropwise to the stirred solution over a period of 13 min. The resulting solution was refluxed on the steam bath for 20 min.

The reaction mixture was cooled to room temperature and made just acidic with acetic acid, whereupon a small amount of a white solid precipitated. This was filtered off and dried *in vacuo* over calcium chloride to

Can. J. Chem. Downloaded from www.nrcresearchpress.com by 210.87.254.40 on 09/05/12
For personal use only.

give 25.6 g of methyl isoquinoline-4-carbamate (VII), m.p. 201–206°. Evaporation of the filtrate left a brown residue which was washed with water, filtered, and dried to give another 36.3 g of a tan-colored product. The total yield of crude methyl isoquinoline-4-carbamate was thus 61.9 g (79% yield). Recrystallization from ethanol gave colorless needles, m.p. 205–206°.

Anal. Calcd. for $C_{11}H_{10}N_2O_2$: C, 65.33; H, 4.98; N, 13.86. Found: C, 65.31; H, 5.11; N, 13.81.

Preparation of 4-Aminoisoquinoline (VIII)

Methyl isoquinoline-4-carbamate (VII) (66.3 g, 0.32 mole) and water (15 ml) were placed in a 1 l round-bottomed flask, and 365 ml of concentrated sulfuric acid was added. The resulting dark mixture was heated at 110° for 21 h. It was cooled to room temperature and poured into an equal volume of water, with cooling. The resulting mixture was carefully basified with concentrated ammonium hydroxide solution and extracted with three 800 ml portions of benzene. The benzene extract was dried over sodium sulfate and filtered, and the solvent was evaporated, leaving a viscous brown oil which later solidified. Crystallization from benzene gave 18.1 g (39% yield) of tan-colored crystals of 4-aminoisoquinoline, m.p. 101–106°. Sublimation gave colorless needles, m.p. 104.5–106.5° (lit. (10) m.p. 108°).

Thiocyanation of 4-Aminoisoquinoline

4-Aminoisoquinoline (VIII) (17 g, 0.12 mole) and potassium thiocyanate (45.9 g, 0.47 mole) were dissolved in 245 ml of 95% acetic acid in a 500 ml three-necked flask equipped with a reflux condenser, a mechanical stirrer, and a dropping funnel. Bromine (6.8 ml, 0.12 mole) in 35 ml of 95% acetic acid was added to this stirred solution at −5 to −10° over a period of 40 min. The reaction mixture was stirred for a further 20 min at this temperature and then poured into 2 100 ml of water.

The resulting precipitate was filtered off to give an orange solid. Extraction of this solid with boiling benzene gave 2.70 g of yellow needles, the infrared spectrum of which showed thiocyano absorption at 2 143 cm^{-1}. The benzene-insoluble material was crystallized from ethanol to give a mixture of yellow needles and brown amorphous material. The infrared spectrum of the yellow needles showed strong thiocyano absorption at 2 060 cm^{-1}, and that of the brown amorphous material was identical with the spectrum of 2-aminothiazolo-[5,4-*c*]isoquinoline (X) prepared as described below. The mixture was washed with sodium carbonate solution, then dissolved in 15% hydrochloric acid, and reprecipitated with solid sodium carbonate. The resulting yellow solid (5.15 g, 21% yield) showed an infrared spectrum identical with that of authentic 2-aminothiazolo-[5,4-*c*]isoquinoline.

The filtrate from the original acetic acid reaction mixture was basified with solid sodium carbonate, and the resulting precipitate was filtered off and dried *in vacuo*. Crystallization from benzene gave 5.13 g of pale-yellow needles, m.p. 148–149°. The infrared spectrum of this compound was identical with that of the benzene-soluble material obtained above. This was 4-amino-3-thiocyanoisoquinoline (IX), and the total yield was 7.83 g (33% yield).

Anal. Calcd. for $C_{10}H_7N_3S$: C, 59.68; H, 3.51; N, 20.88. Found: C, 59.68; H, 3.33; N, 20.75.

Preparation of 2-Aminothiazolo[5,4-c]isoquinoline (X)

4-Amino-3-thiocyanoisoquinoline (IX) (7.83 g, 0.039 mole) was refluxed for 2 h in a mixture of 315 ml of 15% hydrochloric acid and 315 ml of ethanol. The reaction mixture was cooled to room temperature and basified with solid sodium carbonate. The resulting yellow solid was filtered off, washed with water, and dried to give 6.48 g (83% yield) of 2-aminothiazolo[5,4-*c*]isoquinoline (X). Recrystallization from benzene gave yellow needles, m.p. 292–294°.

Anal. Calcd. for $C_{10}H_7N_3S$: C, 59.68; H, 3.51; N, 20.88. Found: C, 59.57; H, 3.43; N, 20.87.

The monoacetyl derivative of X was prepared by refluxing 0.25 g (1.2 mmoles) of X in a mixture of 5 ml of acetic anhydride and 2 ml of pyridine for 70 min. The reaction mixture was cooled and filtered to give 0.30 g (100% yield) of a tan solid, which was purified by dissolving it in hot glacial acetic acid, filtering, and diluting the filtrate with water, whereupon colorless needles precipitated, m.p. 361–362°.

Anal. Calcd. for $C_{12}H_9N_3OS$: C, 59.24; H, 3.73; N, 17.27; S, 13.18. Found: C, 59.60; H, 3.48; N, 17.23; S, 13.08.

Preparation of 2-Chlorothiazolo[5,4-c]isoquinoline (XI)

Cuprous chloride was prepared in the usual way from 2.64 g of sodium chloride, 10.00 g of hydrated cupric sulfate, 2.16 g of sodium bisulfite, and 1.44 g of sodium hydroxide, and was dissolved in 40 ml of concentrated hydrochloric acid.

2-Aminothiazolo[5,4-*c*]isoquinoline (X) (4.80 g, 0.024 mole) was dissolved in 160 ml of 85% phosphoric acid, and 40 ml of 70% nitric acid was added. The resulting solution was cooled to 0–5°, and sodium nitrite (1.76 g, 0.026 mole) in 16 ml of water was added, with stirring, over a period of 10 min. The reaction mixture was stirred for another 10 min at this temperature, and then it was added over 20 min to the stirred solution of cuprous chloride in hydrochloric acid at 0–5°.

The reaction mixture was stirred for 1 h at room temperature. It was then basified with 20% sodium hydroxide solution, with cooling. The basic mixture was extracted with three 500 ml portions of ether. The ether extract was washed once with water, dried over sodium sulfate, and filtered; then the ether was evaporated, leaving a tan-colored solid. This was extracted with 250 ml of boiling hexane and the hexane evaporated,

Can. J. Chem. Downloaded from www.nrcresearchpress.com by 210.87.254.40 on 09/05/12
For personal use only.

leaving 3.56 g (67% yield) of a crude yellow solid, m.p. 89–92°. Vacuum sublimation gave colorless 2-chlorothiazolo[5,4-*c*]isoquinoline, m.p. 91.5–93°.

Anal. Calcd. for $C_{10}H_5ClN_2S$: C, 54.42; H, 2.28; Cl, 16.07; N, 12.70. Found: C, 54.31; H, 2.19; Cl, 16.45; N, 12.57.

Preparation of Thiazolo[5,4-c]isoquinoline (I)

2-Chlorothiazolo[5,4-*c*]isoquinoline (1 g, 4.5 mmoles) was dissolved in a mixture of 16 ml of 47% hydriodic acid, 8 ml of glacial acetic acid, and 8 ml of water; then 0.56 g of red phosphorus was added. The resulting mixture was refluxed for 3½ h. It was filtered while hot, cooled to room temperature, diluted with 125 ml of water, and filtered again. The filtrate was basified with solid sodium carbonate, and the resulting flocculent precipitate (0.48 g, 57% yield) was filtered off, washed with water, and dried. The crude product was chromatographed on 20 g of alumina (Woelm, activity 2–3) and eluted with benzene to give 0.33 g of a colorless product, m.p. 96–98°. Recrystallization from hexane gave fine white needles of thiazolo[5,4-*c*]isoquinoline (I), m.p. 97–98°.

Anal. Calcd. for $C_{10}H_6N_2S$: C, 64.49; H, 3.25; N, 15.05. Found: C, 64.56; H, 3.13; N, 14.92.

2-Hydroxythiazolo[5,4-c]isoquinoline (XII)

2-Chlorothiazolo[5,4-*c*]isoquinoline (1 g, 4.5 mmoles) was refluxed in 75 ml of 0.5 *N* sodium hydroxide for 3 h. The reaction mixture was filtered while hot, cooled to room temperature, and acidified with dilute acetic acid. The resulting flocculent precipitate was filtered off, washed with water, and dried to give 0.61 g (67% yield) of 2-hydroxythiazolo[5,4-*c*]isoquinoline (XII), m.p. 309–311°. Recrystallization from ethanol–water gave fine yellow needles, m.p. 310–311°.

Anal. Calcd. for $C_{10}H_6N_2OS$: C, 59.38; H, 2.99; N, 13.85; S, 15.86. Found: C, 59.21; H, 3.05; N, 13.77; S, 15.89.

2-Methoxythiazolo[5,4-c]isoquinoline (XIII)

2-Chlorothiazolo[5,4-*c*]isoquinoline (1 g, 4.5 mmoles) was dissolved in 70 ml of absolute methanol, and 0.25 g (6.2 mmoles) of sodium in 25 ml of absolute methanol was added. After the reaction mixture was stirred magnetically at room temperature for 1½ h, it was neutralized with dilute acetic acid and cooled with several ice cubes. The resulting flocculent yellow precipitate was filtered off and dried to give 0.80 g (82% yield) of 2-methoxythiazolo[5,4-*c*]isoquinoline (XIII), m.p. 101–103°. Recrystallization from methanol followed by vacuum sublimation gave pale-yellow needles, m.p. 105.5–106.5°.

Anal. Calcd. for $C_{11}H_8N_2OS$: C, 61.09; H, 3.73; N, 12.96; S, 14.83. Found: C, 61.24; H, 3.73; N, 12.98; S, 14.74.

Thiazolo[5,4-c]isoquinoline-2-thiol (XIV)

2-Chlorothiazolo[5,4-*c*]isoquinoline (0.20 g, 0.9 mmole) and thiourea (0.10 g, 13 mmoles) were refluxed in 10 ml of ethanol for 3 h. The reaction mixture was cooled and filtered to give 0.10 g of an orange solid. This solid was dissolved in 1 *N* sodium hydroxide solution, the mixture was filtered, and the filtrate was acidified with acetic acid. The resulting precipitate was filtered off and dried to give 0.08 g (42% yield) of pale-yellow thiazolo[5,4-*c*]isoquinoline-2-thiol (XIV), m.p. 299–300.5°.

Anal. Calcd. for $C_{10}H_6N_2S_2$: C, 55.03; H, 2.77; N, 12.84. Found: C, 54.99; H, 2.95; N, 12.75.

REFERENCES

1. B. R. Harriman, R. S. Shelton, M. G. Van Campen, and M. R. Warren. J. Am. Chem. Soc. **67**, 1481 (1945).
2. S. Gabriel. Ber. **19**, 2355 (1886).
3. R. D. Haworth and S. Robinson. J. Chem. Soc. 777 (1948).
4. H. P. Kaufmann. Arch. Pharm. **266**, 197 (1928).
5. J. J. Craig and W. E. Cass. J. Am. Chem. Soc. **64**, 783 (1942).
6. F. T. Tyson. J. Am. Chem. Soc. **61**, 183 (1939).
7. F. W. Bergstrom and J. H. Rodda. J. Am. Chem. Soc. **62**, 3030 (1940).
8. C. N. R. Rao. Chemical applications of infrared spectroscopy. Academic Press, Inc., New York. 1963. p. 268.
9. C. E. Hall and A. Taurins. Can. J. Chem. This issue.
10. E. V. Donckt, R. H. Martin, and F. Geerts-Evrard. Tetrahedron, **20**, 1499 (1964).
11. S. F. Mason. *In* Physical methods in heterocyclic chemistry. Vol. 2. A. R. Katritzky (*Editor*). Academic Press, Inc., New York. 1963. pp. 35–59.

Can. J. Chem. Downloaded from www.nrcresearchpress.com by 210.87.254.40 on 09/05/12
For personal use only.

Can. J. Chem. Downloaded from www.nrcresearchpress.com by 210.87.254.6 on 09/05/12
For personal use only.

SOLVOLYSES OF 2-(2,4-DIMETHOXYPHENYL)-1,1-d_2-ETHYL AND 2-(3,5-DIMETHOXYPHENYL)-1,1-d_2-ETHYL *p*-BROMOBENZENESULFONATES; ION-PAIR RETURNS IN SOLVOLYSES OF 2-ARYLETHYL SYSTEMS

C. C. LEE AND L. NOSZKÓ[1]

Department of Chemistry and Chemical Engineering, University of Saskatchewan, Saskatoon, Saskatchewan

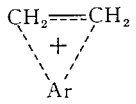
Received July 5, 1966

ABSTRACT

Acetolysis and formolysis of 2-(2,4-dimethoxyphenyl)-1,1-d_2-ethyl and 2-(3,5-dimethoxyphenyl)-1,1-d_2-ethyl *p*-bromobenzenesulfonates were allowed to proceed for about two half-lives, and the corresponding acetate and formate products as well as the unsolvolyzed sulfonate esters were recovered and analyzed by nuclear magnetic resonance. In the 2,4-dimethoxy substituted system, both acetolysis and formolysis gave products showing practically equal distributions of the deuterium in the C-1 and C-2 positions of the ethyl chain. For the 3,5-dimethoxy substituted system, deuterium isotope position rearrangements from C-1 to C-2 in the products were found to be 14 and 26%, respectively, for acetolysis and formolysis. These results provide more quantitative verifications of earlier conclusions, based on kinetic data, regarding the extents of involvement of bridged ions as reaction intermediates. The unsolvolyzed sulfonate ester recovered from the acetolysis of either the 2,4- or 3,5-dimethoxy substituted system showed a significant amount of deuterium rearrangement from C-1 to C-2, indicating the occurrence of ion-pair returns. On the other hand, such rearrangements were negligibly small in the sulfonates recovered after partial formolysis. By utilizing data on isotopic rearrangements in the recovered sulfonates obtained from the present work or from the literature, values of k_a/k_t, the ratio of the total reaction rate to the titrimetric rate, were calculated for a number of 2-arylethyl systems. Implications of the present results on a general mechanism for the solvolyses of 2-arylethyl arenesulfonates are also discussed.

INTRODUCTION

From considerations of relative rates and entropies of activation, Winstein and Heck (1) concluded that the chief contributor to the rate of both acetolysis and formolysis of 2-(2,4-dimethoxyphenyl)-ethyl *p*-bromobenzenesulfonate (I-OBs) is the anchimerically assisted rate constant (k_Δ), whereas for 2-(3,5-dimethoxyphenyl)-ethyl *p*-bromobenzenesulfonate (II-OBs), acetolysis is chiefly anchimerically unassisted (k_s) and both k_s and k_Δ contribute to the formolysis of II-OBs. The anchimerically assisted process involves a nonclassical, bridged ion, such as the ethylene-2,4-dimethoxyphenonium ion, as an intermediate (1). Such bridged ions may be generalized for 2-arylethyl systems, as shown by III, which may be termed an ethylenearonium ion. These qualitative conclusions



III

derived from kinetic data can be verified more quantitatively by isotope position rearrangement studies. In the present work, 2-(2,4-dimethoxyphenyl)-1,1-d_2-ethyl and 2-(3,5-dimethoxyphenyl)-1,1-d_2-ethyl *p*-bromobenzenesulfonates (I-OBs-1-d_2 and II-OBs-1-d_2, respectively) were subjected to acetolysis and formolysis, and the deuterium distributions in the ethyl chain of the resulting products were determined to ascertain the extents of involvement of III.

The solvolyses of I-OBs-1-d_2 and II-OBs-1-d_2 were interrupted before completion and

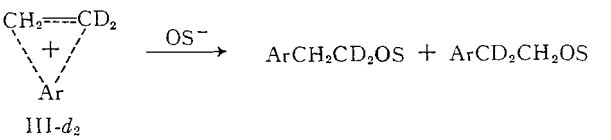
[1]*Visiting scientist, 1964–1965. Present address: Central Research Institute for Chemistry, Hungarian Academy of Sciences, Budapest, Hungary.*

the deuterium distributions in the recovered *p*-bromobenzenesulfonates gave indications of the extents of return from ion-pairs to covalent bonding. The return processes for optically active systems which proceed via symmetrical bridged ions, such as in the solvolyses of *threo*-3-phenyl-2-butyl and *threo*-3-anisyl-2-butyl arenesulfonates (2, 3), have been measured by a comparison of the polarimetric rate constant (k_α) and the titrimetric rate constant (k_t). Recently, Smith and Showalter (4) have utilized data on isotopic rearrangements to calculate an equivalent of k_α/k_t for the acetolysis of *erythro*-3-phenyl-2-butyl *p*-toluenesulfonate. In studies with 2-arylethyl systems, it is impossible to evaluate k_α because of the lack of optical activity. The method of Smith and Showalter (4), however, can be employed. This treatment is applied to the present results on returns as well as to other 2-arylethyl systems for which isotopic rearrangement data on returns are available from the literature.

RESULTS AND DISCUSSION

I-OBs-1-d_2 and II-OBs-1-d_2 were prepared from the corresponding deuterated alcohols, which were obtained, respectively, from the lithium aluminium deuteride reduction of 2,4-dimethoxyphenylacetic acid (IV) and 3,5-dimethoxyphenylacetic acid (V). As indicated by Winstein and Heck (1), IV was prepared from 2,4-dimethoxybenzaldehyde by the azlactone method (5) and V was obtained from 3,5-dimethoxybenzoic acid by way of the corresponding benzyl alcohol, benzyl chloride, and nitrile. Acetolysis and formolysis of I-OBs-1-d_2 and II-OBs-1-d_2 were interrupted after the reactions had proceeded for about two half-lives (see Experimental). The resulting acetates and formates (I-OAc-*x*-d_2, II-OAc-*x*-d_2, I-OCHO-*x*-d_2, and II-OCHO-*x*-d_2) as well as the recovered unsolvolyzed sulfonates (I-OBs-*x*-d_2 and II-OBs-*x*-d_2) were examined by nuclear magnetic resonance (n.m.r.). The pertinent parts of typical sets of spectra are shown in Figs. 1 and 2. Integration of a number of such sets of spectra gave the averaged deuterium distributions in the C-1 and C-2 positions of the ethyl chain of the various compounds analyzed. The results are given in Table I.

The reaction of III-d_2 from I-OBs-1-d_2 or II-OBs-1-d_2 could give rise to products with an equal amount of deuterium at the C-1 and C-2 positions (eq. [1]). This prediction is fully

[1] 

III-d_2

met in both the acetolysis and formolysis of I-OBs-1-d_2, confirming the earlier conclusion based on kinetic data (1). The small excess over 50% of deuterium at C-2 (Table I) for I-OAc-*x*-d_2 and I-OCHO-*x*-d_2 may be attributable to an isotope effect, the reaction with III-d_2 being slightly more favorable at the carbon position containing hydrogen than at the one containing deuterium.

The isotope position rearrangements of deuterium in the products from the acetolysis and formolysis of II-OBs-1-d_2 indicate the partial involvement of III, again confirming the conclusion (1) that k_s competes favorably with k_Δ in this system. Winstein and Heck (1) have pointed out that a *m*-methoxy group on a participating phenyl group may give rise to either a small retardation or a small acceleration of the rate, depending on the relative influence of the inductive and resonance effects. In the formolysis of II-OBs, it was noted that the two *m*-methoxy groups in the 2-phenylethyl system decreased the rate by a factor

Can. J. Chem. Downloaded from www.nrcresearchpress.com by 210.87.254.6 on 09/05/12
For personal use only.

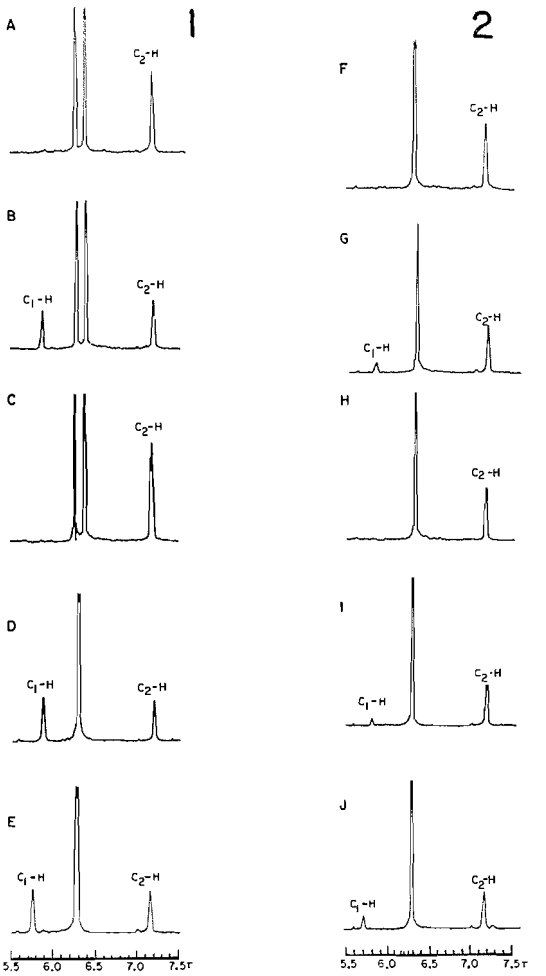


FIG. 1. Pertinent parts of the n.m.r. spectra obtained on the HA-100 spectrometer: A, 2-(2,4-dimethoxyphenyl)-1,1-d_2-ethyl *p*-bromobenzenesulfonate (I-OBs-1-d_2); B, I-OBs-x-d_2 recovered from acetolysis after 70.6% reaction; C, I-OBs-x-d_2 recovered from formolysis after 77.6% reaction; D, I-OAc-x-d_2 product from acetolysis; E, I-OCHO-x-d_2 product from formolysis. The undesignated peaks shown are caused by methoxyl hydrogens.

FIG. 2. Pertinent parts of the n.m.r. spectra obtained on the HA-100 spectrometer: F, 2-(3,5-dimethoxyphenyl)-1,1-d_2-ethyl *p*-bromobenzenesulfonate (II-OBs-1-d_2); G, II-OBs-x-d_2 recovered from acetolysis after 74.7% reaction; H, II-OBs-x-d_2 recovered from formolysis after 71.2% reaction; I, II-OAc-x-d_2 product from acetolysis; J, II-OCHO-x-d_2 product from formolysis. The undesignated peaks shown are caused by methoxyl hydrogens.

of 3 and that, when the $\Delta S^{\ddagger}$ values are considered, the formolysis rate for II-OBs "is not so predominantly composed of k_Δ as in the case of the parent $C_6H_5CH_2CH_2OBs$ system" (1). This statement is borne out more quantitatively by a comparison of the present results with known data from ^{14}C-labeled 2-phenylethyl *p*-toluenesulfonate (VI-OTs); the formolysis of II-OBs-1-d_2 gave 26% isotopically rearranged II-OCHO-2-d_2 (Table I) whereas the formolysis of VI-OTs-1-^{14}C resulted in 45% isotope position rearrangement to VI-OCHO-2-^{14}C (6).

Can. J. Chem. Downloaded from www.nrcresearchpress.com by 210.87.254.6 on 09/05/12
For personal use only.

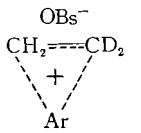
TABLE I

Rearrangements of deuterium from C-1 to C-2 in the products and recovered *p*-bromobenzenesulfonates from the solvolyses of 2-(2,4-dimethoxyphenyl)-1,1-d_2-ethyl and 2-(3,5-dimethoxyphenyl)-1,1-d_2-ethyl *p*-bromobenzenesulfonates (I-OBs-1-d_2 and II-OBs-1-d_2, respectively)

Reactant	Reaction	Compound analyzed	% deuterium at C-2*
I-OBs-1-d_2	Acetolysis	I-OAc-x-d_2	51
		I-OBs-x-d_2	40
I-OBs-1-d_2	Formolysis	I-OCHO-x-d_2	52
		I-OBs-x-d_2	<0.5
II-OBs-1-d_2	Acetolysis	II-OAc-x-d_2	14
		II-OBs-x-d_2	15
II-OBs-1-d_2	Formolysis	II-OCHO-x-d_2	26
		II-OBs-x-d_2	<0.5

*Corresponding to the proton content in the C-1 position, as measured by n.m.r.

Ion-pair returns involving III-d_2 and its counter ion will result in the location of some deuterium at the C-2 position of the recovered sulfonate (eq. [2]). The data in Table I

[2]  $\rightarrow$ $ArCH_2CD_2OBs + ArCD_2CH_2OBs$

show that such returns are significant in the acetolyses of both I-OBs-1-d_2 and II-OBs-1-d_2, but are negligible in the formolyses. Similar studies on the solvolyses of other 2-arylethyl systems labeled with ^{14}C, including 2-(*p*-anisyl)-1-^{14}C-ethyl, 2-(α-naphthyl)-1-^{14}C-ethyl, and 2-(β-napthyl)-1-^{14}C-ethyl *p*-toluenesulfonates (VII-OTs-1-^{14}C, VIII-OTs-1-^{14}C, and IX-OTs-1-^{14}C, respectively) (7–9), also resulted in significant returns for acetolysis and negligible returns for formolysis. The fact that acetic acid is an optimum medium for ion-pair returns has been discussed in the early formulation of the theory on such processes (10). Returns from ionic intermediates to covalent starting material have also been studied in the solvolyses of 2-phenyl-1-^{14}C-ethyl *p*-toluenesulfonate (VI-OTs-1-^{14}C) (11, 12). In this case, significant returns were observed for formolysis. By investigating the formolysis of VI-OTs-1-^{14}C in the presence of added sodium ^{35}S-*p*-toluenesulfonate, it was shown that the major contributor to the return processes may be intermolecular external return involving exchangeable *p*-toluenesulfonate anion, rather than intramolecular internal return from intimate ion-pairs (12).

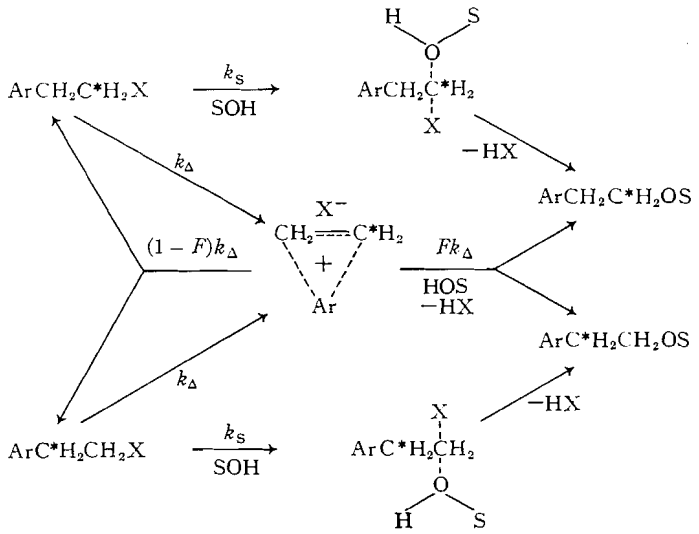
Following the mechanistic schemes given by Jenny and Winstein (7) and by Clayton and Lee (12), the processes occurring during the solvolyses of 2-arylethyl arenesulfonates are shown in Reaction Scheme 1, with the asterisk designating the isotopic label, either ^{14}C or D.

As pointed out earlier, the ionization rate constant (k_Δ) for optically active systems which proceed via symmetrical bridged ions can be followed polarimetrically as k_α. Because of the return processes, k_α is greater than the titrimetric rate constant (k_t) (2, 3). According to the scheme shown in Reaction Scheme 1, one can define k_α as the total reaction rate constant (eq. [3]) whereas the titrimetric rate constant is given by eq. [4]. Again, if returns occur ($F < 1$), k_α will be greater than k_t. Values for the k_α so defined can

[3] $$k_\alpha = k_\Delta + k_s$$

[4] $$k_t = Fk_\Delta + k_s$$

Can. J. Chem. Downloaded from www.nrcresearchpress.com by 210.87.254.6 on 09/05/12
For personal use only.



REACTION SCHEME 1.

be calculated according to the method of Smith and Showalter (4). For example, in the present studies, the acetolysis of I-OBs-1-d_2 was interrupted after 3 h at 60.6 °C when the reaction was 70.6% complete ($k_t = 1.13 \times 10^{-4}$ s^{-1}). The recovered sulfonate (I-OBs-x-d_2) showed 40% isotope position rearrangement of the deuterium label, which indicated that $2 \times 40 = 80\%$ of the recovered sulfonate has been involved in the return processes. Since the amount of sulfonate remaining was $100 - 70.6 = 29.4\%$, $(80/100) \times 29.4 = 23.5\%$ of the reactant would have been involved in returns. The total involved would be the sum of the percentage solvolyzed and the percentage return, namely, $70.6 + 23.4 = 94.0\%$. The total reaction rate constant would thus be $k_\alpha = (2.303/(3 \times 3\,600))(\log 100/(100 - 94.0)) = 2.5 \times 10^{-4}$ s^{-1}. These calculations can be summarized by eqs. [5]–[7].

[5] % return = 2(% rearrangement in recovered sulfonate/100) × (100 − % solvolyzed)

[6] % total involved = % solvolyzed + % return

[7] $k_\alpha = (2.303/\text{time})(\log 100/(100 - \%\text{ total involved}))$

In this way, k_α as well as k_α/k_t can be evaluated for the acetolysis of I-OBs-1-d_2, II-OBs-1-d_2, VII-OTs-1-^{14}C, VIII-OTs-1-^{14}C, and IX-OTs-1-^{14}C. These data are summarized in Table II.

It can be seen from Table II that, for the three acetolyses of VII-OTs-1-^{14}C which were interrupted at different stages of completion, the calculated values of k_α and k_α/k_t were quite constant. Also, as expected, k_α/k_t decreased markedly when the acetolyses of VII-OTs-1-^{14}C were carried out in the presence of lithium perchlorate. The latter salt is believed to prevent return from solvent-separated ion-pairs, but does not prevent returns from intimate ion-pairs (3, 7). According to eqs. [3] and [4], $k_\alpha/k_t = (k_\Delta + k_s)/(Fk_\Delta + k_s)$. In systems to which k_s does not contribute significantly, such as in the solvolyses of I-OBs-1-d_2 and VII-OTs-1-^{14}C, k_α/k_t would be equal to $1/F$. For the acetolysis of VII-OTs-1-^{14}C, the calculated k_α/k_t of about 3.9 is in reasonably good agreement with the value of 3.77 for $1/F$ reported by Jenny and Winstein (7).

Can. J. Chem. Downloaded from www.nrcresearchpress.com by 210.87.254.6 on 09/05/12
For personal use only.

Can. J. Chem. Downloaded from www.nrcresearchpress.com by 210.87.254.6 on 09/05/12
For personal use only.

TABLE II

Calculated k_α and k_α/k_t for the acetolyses of a number of labeled 2-arylethyl arenesulfonates

Reactant*	Reaction time (h)	Reaction temperature (°C)	% solvolyzed	$10^5 k_t$ (s^{-1})	% rearrangement†	% return	% total involved	$10^5 k_\alpha$ (s^{-1})	k_α/k_t
I-OBs-1-d_2	3	60.6	70.6	11.3	40	23.4	94.0	25	2.2
II-OBs-1-d_2	37	100.0	74.7	1.03	15	7.5	82.3	1.3	1.3
VII-OTs-1-^{14}C‡	3	75.00	7.3	0.70	10.0	18.5	25.8	2.8	4.0
VII-OTs-1-^{14}C‡	6.1	75.00	13.7	0.67	17.5	30.2	43.9	2.6	3.9
VII-OTs-1-^{14}C‡	19.3	75.00	38.0	0.69	38.0	47.1	85.1	2.7	3.9
VII-OTs-1-^{14}C‡,§	10	75.00	43	1.6	15.9	18.1	61.1	2.6	1.6
VII-OTs-1-^{14}C‡,‖	7.5	75.00	49	2.5	5.0	5.1	54.1	2.9	1.2
VII-OTs-1-^{14}C‡,¶	6	75.00	51	3.3	2.3	2.3	53.3	3.5	1.06
VII-OTs-1-^{14}C‡,**	6	75.00	58	4.0	2.0	1.7	59.7	4.2	1.05
VIII-OTs-1-^{14}C††	12.33‡‡	110.6	45.6	1.37	38	41.3	86.9	4.6	3.4
IX-OTs-1-^{14}C§§	18.5	110.6	50.0	1.04	31	31.0	81.0	2.5	2.4

*I-OBs-1-d_2 and II-OBs-1-d_2 are, respectively, 2-(2,4-dimethoxyphenyl)-1,1-d_2-ethyl and 2-(3,5-dimethoxyphenyl)-1,1-d_2-ethyl *p*-bromobenzenesulfonates; VII-OTs-1-^{14}C, VIII-OTs-1-^{14}C, and IX-OTs-1-^{14}C are, respectively, 2-(*p*-anisyl)-1-^{14}C-ethyl, 2-(α-naphthyl)-1-^{14}C-ethyl, and 2-(β-naphthyl)-1-^{14}C-ethyl *p*-toluenesulfonates.

†Isotope position rearrangement from C-1 to C-2 in the recovered arenesulfonate.

‡Data from ref. 7.

§In the presence of 0.002 *M* $LiClO_4$.

‖In the presence of 0.01 *M* $LiClO_4$.

¶In the presence of 0.03 *M* $LiClO_4$.

**In the presence of 0.06 *M* $LiClO_4$.

††Data from ref. 8.

‡‡In ref. 8, this reaction time was erroneously reported as one half-life based on the preliminary kinetic work carried out before the active runs. More accurate kinetic data show that the reaction was 45.6% complete.

§§Data from ref. 9.

Can. J. Chem. Downloaded from www.nrcresearchpress.com by 210.87.254.6 on 09/05/12
For personal use only.

For the 2-phenylethyl system, in the earlier work on ion-pair returns during the solvolyses of VI-OTs-1-^{14}C (11), kinetic measurements were not made in conjunction with isotopic rearrangement studies. From the later investigation on the formolysis of VI-OTs-1-^{14}C (12), both kinetic data and isotope position rearrangements in the recovered sulfonate are available. In this case, however, intermolecular external return involving exchangeable *p*-toluenesulfonate anion may be chiefly responsible for the rearrangements observed in the recovered sulfonate (12). In such an event, the rate for that portion of the reaction proceeding via the bridged ion should be dependent upon the *p*-toluenesulfonate anion concentration, as given in eq. [8] (13), where k_1, k_2, and k_3 are, respectively, the rate constants for ionization, for return from the carbonium ion to the starting material, and for product formation from the carbonium ion.

$$\text{Rate} = \frac{k_1[\text{ArOTs}]}{(k_2/k_3)[\text{OTs}^-] + 1} \qquad [8]$$

However, if $(k_2/k_3)[\text{OTs}^-]$ is small compared with 1, first-order kinetics would still be observed. Apparently, this condition may have been met in the formolysis of VI-OTs-1-^{14}C, because the extent of return was not large and no significant downward drift in the rate was detectable during a kinetic run (12). It is thus possible to apply the first-order kinetic treatments, as given by eqs. [5]–[7], to calculate k_α for the formolysis of VI-OTs-1-^{14}C.

Summarized in Table III are the results from the formolysis of 0.350 *M* VI-OTs-1-^{14}C at 74 °C carried out with no added salt (12). The k_α values calculated from the data obtained after the reaction was interrupted at various stages of completion may be regarded as satisfactorily constant, the average being 3.4×10^{-5} s^{-1}. Since k_t, under the same conditions, has been found to be 3.0×10^{-5} s^{-1} (12), k_α/k_t is about 1.1. This average value of k_α/k_t gave at least a correct indication of the order of magnitude for the return processes; the factor *F*, which is the fraction of the bridged ion proceeding to products, has been evaluated as 0.91 (12).

TABLE III

Calculated k_α for the formolysis of 0.350 *M* 2-phenyl-1-^{14}C-ethyl p-toluenesulfonate (VI-OTs-1-^{14}C) at 74 ± 0.2 °C with no added salt*

Reaction time (min)	% solvolyzed	% rearrangement†	% return	% total involved	$10^5 k_\alpha$ (s^{-1})
51	10.0	0.17	0.3	10.3	3.5
167	29.7	0.76	1.1	30.8	3.7
275	42.9	1.83	2.1	45.0	3.6
600	66.4	3.37	2.3	68.7	3.2
600	65.6	3.30	2.3	67.9	3.2
900	80.0	5.78	2.3	82.3	3.2
1 155	89.9	8.60	1.7	91.6	3.6
1 200	88.5	8.88	2.0	90.5	3.3
				Average	3.4

*Experimental data from ref. 12.
†Isotope position rearrangement from C-1 to C-2 in the recovered *p*-toluenesulfonate.

Recently, Brown and his co-workers (14) have emphatically questioned the existence of nonclassical, bridged phenonium ions as intermediates, and special attention was directed to the 3-phenyl-2-butyl and 2-phenylethyl systems. As an alternative to nonclassical ions, these workers have suggested rapidly equilibrating classical ions. On the other hand, Cram (15) has strongly stated the case for phenonium ions. The existence of bridged ions has not been questioned in systems in which anchimeric rate enhancements have definitely been

established, such as in the solvolyses of I-OBs and VII-OTs. Moreover, the recent direct observation of the n.m.r. spectrum of the carbonium ions derived from the 3-phenyl-2-butyl system under highly acidic conditions at low temperatures favored the bridged-ion formulation (16). The present results on deuterium scrambling in the products of the solvolyses of I-OBs-1-d_2 and II-OBs-1-d_2 also further strengthen the already known correlation that the extents of isotope position rearrangement generally are closely related to the extents of involvement of bridged ions predicted from structural, kinetic, or stereochemical considerations. The phenomena of returns from ionic intermediates to covalent starting materials are also adequately explained by bridged ions. Finally, for the 2-phenylethyl system, Jensen and Ouellette (17) have reported significant rate enhancements for the solvolyses of 2-phenylethylmercuric perchlorate in acetic acid and in formic acid. It is of interest to point out that preliminary work in this laboratory on the acetolysis and formolysis of 2-phenyl-1-^{14}C-ethylmercuric perchlorate gave products in which the ^{14}C-label was almost equally distributed in the C-1 and C-2 positions.[2] From all of these considerations, it appears quite reasonable to conclude that, for 2-arylethyl systems, the nonclassical ethylenearonium ion III may be utilized confidently to correlate the existing experimental data.

EXPERIMENTAL

2-(2,4-Dimethoxyphenyl)-1,1-d_2-ethyl and 2-(3,5-Dimethoxyphenyl)-1,1-d_2-ethyl p-Bromobenzenesulfonates (I-OBs-1-d_2 and II-OBs-1-d_2)

2,4-Dimethoxyphenylacetic acid or 3,5-dimethoxyphenylacetic acid was reduced to the corresponding alcohol as described by Winstein and Heck (1), except that lithium aluminium deuteride instead of lithium aluminium hydride was used as the reducing agent. These alcohols were treated with *p*-bromobenzenesulfonyl chloride in pyridine, again by the procedure of Winstein and Heck (1), to give the desired sulfonate esters. 2-(2,4-Dimethoxyphenyl)-1,1-d_2-ethyl *p*-bromobenzenesulfonate (I-OBs-1-d_2), m.p. 73° C (lit. (1) m.p. 72–73 °C), was obtained in a 48% yield, and the yield of 2-(3,5-dimethoxyphenyl)-1,1-d_2-ethyl *p*-bromobenzenesulfonate (II-OBs-1-d_2), m.p. 76 °C (lit. (1) m.p. 76.5–77.5 °C), was 43%. Deuterium analyses[3] showed the presence of 1.92 and 1.90 deuterium atoms per molecule in I-OBs-1-d_2 and II-OBs-1-d_2, respectively.

Acetolysis of I-OBs-1-d_2

A solution of 6.0 g (0.015 mole) of I-OBs-1-d_2 in 500 ml of reagent-grade glacial acetic acid was heated in a water bath at 60.6 °C for 3 h (70.6% solvolyzed). The mixture was poured into 2 l of ice water and then extracted with two 500 ml portions of ether. The extract was washed three times with cold water, twice with cold, diluted sodium carbonate solution, and finally once more with cold water. After the solution was dried over anhydrous magnesium sulfate, the ether was removed *in vacuo* at room temperature. The residue was triturated in 6 ml of a 1:2 solution of ether – petroleum ether (b.p. 40–60 °C) and then allowed to remain in the refrigerator for 2 days. The crystalline unsolvolyzed sulfonate ester was collected by filtration and recrystallized from ether – petroleum ether. The recovery was 1.4 g (79% based on 70.6% solvolyzed).

The filtrate obtained after the removal of the unsolvolyzed sulfonate was evaporated to an oil which, on vacuum distillation, gave 1.6 g (67% based on 70.6% solvolyzed) of 2-(2,4-dimethoxyphenyl)-*x*-d_2-ethyl acetate (I-OAc-*x*-d_2), b.p. 144° at 2 mm. The corresponding protio acetate isolated from a similar run boiled at 142 °C and 2 mm.

Anal. Calcd. for $C_{12}H_{16}O_4$: C, 64.27; H, 7.19. Found: C, 64.22; H, 7.21.

Acetolysis of II-OBs-1-d_2

A solution of 6.0 g (0.015 mole) of II-OBs-1-d_2 in 500 ml of reagent-grade glacial acetic acid was heated in a thermostated oil bath at 100.0 °C for 37 h (74.7% solvolyzed). The reaction mixture was worked up in the same manner as described for the acetolysis of I-OBs-1-d_2. The recovery of unsolvolyzed sulfonate ester was 1.2 g (79% based on 74.9% solvolyzed). The yield of acetate product (II-OAc-*x*-d_2), b.p. 148–150 °C at 2 mm, was 1.3 g (52% based on 74.7% solvolyzed). The corresponding protio acetate obtained from a similar run boiled at 146 °C and 1.5 mm.

Anal. Calcd. for $C_{12}H_{16}O_4$: C, 64.27; H, 7.19. Found: C, 64.20; H, 7.14.

[2]*Results of R. J. Tewari, to be published.*
[3]*By Josef Nemeth, Urbana, Illinois.*

Can. J. Chem. Downloaded from www.nrcresearchpress.com by 210.87.254.6 on 09/05/12
For personal use only.

Formolysis of I-OBs-1-d_2

A solution of 6.0 g (0.015 mole) of I-OBs-1-d_2 in 500 ml of reagent-grade 98–100% formic acid was kept at 25.0 °C in a water bath for 1 h (77.6% solvolyzed). The reaction mixture was worked up as described for the acetolyses. The recovery of unsolvolyzed sulfonate was nearly quantitative (1.3 g), and the yield of formate product (II-OCHO-x-d_2), b.p. 138 °C at 1.5 mm, was 1.5 g (60% based on 77.6% solvolyzed). The corresponding protio formate obtained in an analogous experiment boiled at 140° and 2 mm.

Anal. Calcd. for $C_{11}H_{14}O_4$: C, 62.84; H, 6.71. Found: C, 62.58; H, 6.78.

Formolysis of II-OBs-1-d_2

A solution of 6.0 g (0.015 mole) of II-OBs-1-d_2 in 500 ml of reagent-grade 98–100% formic acid was heated in a water bath at 60.0 °C for 50 h (71.2% solvolyzed). The reaction mixture was worked up in the same way as described above. The recovery of unsolvolyzed sulfonate was again essentially quantitative (1.7 g). Some technical difficulty was experienced in the isolation of the formate product, and the yield of purified formate (II-OCHO-x-d_2), b.p. 150–152° at 3.5 mm, was only 0.5 g (22% based on 71.2% solvolyzed). The corresponding protio formate boiled at 152 °C and 3.5 mm.

Anal. Calcd. for $C_{11}H_{14}O_4$: C, 62.84; H, 6.71. Found: C, 62.93; H, 6.85.

Nuclear Magnetic Resonance Analyses

The n.m.r. analyses of the various compounds were carried out in deuteriochloroform solution with Varian Associates HR-100 and HA-100 spectrometers by Mr. G. W. Bigam of the Department of Chemistry, University of Alberta, Edmonton, Alberta, and by Mr. M. Mazurek of the Prairie Regional Laboratory, National Research Council, Saskatoon, Saskatchewan.

ACKNOWLEDGMENT

The financial assistance given by the National Research Council of Canada is gratefully acknowledged.

REFERENCES

1. S. WINSTEIN and R. HECK. J. Am. Chem. Soc. **78**, 4801 (1956).
2. S. WINSTEIN and K. C. SCHREIBER. J. Am. Chem. Soc. **74**, 2165 (1952).
3. S. WINSTEIN and G. C. ROBINSON. J. Am. Chem. Soc. **80**, 169 (1958).
4. W. B. SMITH and M. SHOWALTER. J. Am. Chem. Soc. **86**, 4136 (1964).
5. R. PSCHORR and G. KNÖFFLER. Ann. **382**, 50 (1911).
6. C. C. LEE, G. P. SLATER, and J. W. T. SPINKS. Can. J. Chem. **35**, 1417 (1957).
7. E. F. JENNY and S. WINSTEIN. Helv. Chim. Acta, **41**, 807 (1958).
8. C. C. LEE and A. G. FORMAN. Can. J. Chem. **43**, 3387 (1965).
9. C. C. LEE and A. G. FORMAN. Can. J. Chem. **44**, 841 (1966).
10. W. G. YOUNG, S. WINSTEIN, and H. L. GOERING. J. Am. Chem. Soc. **73**, 1958 (1951).
11. C. C. LEE, R. TKACHUK, and G. P. SLATER. Tetrahedron, **7**, 206 (1959).
12. J. W. CLAYTON and C. C. LEE. Can. J. Chem. **39**, 1510 (1961).
13. J. HINE. Physical organic chemistry. 2nd ed. McGraw-Hill Book Co., Inc., New York. 1962. pp. 132–134.
14. H. C. BROWN, K. J. MORGAN, and F. CHLOUPEK. J. Am. Chem. Soc. **87**, 2137 (1965).
15. D. J. CRAM. J. Am. Chem. Soc. **86**, 3767 (1964).
16. G. A. OLAH and C. U. PITTMAN, JR. J. Am. Chem. Soc. **87**, 3509 (1965).
17. F. R. JENSEN and R. J. OUELLETTE. J. Am. Chem. Soc. **85**, 367 (1963).

Can. J. Chem. Downloaded from www.nrcresearchpress.com by 210.87.254.6 on 09/05/12
For personal use only.

Can. J. Chem. Downloaded from www.nrcresearchpress.com by 210.87.254.40 on 09/05/12
For personal use only.

SECONDARY KINETIC ISOTOPE EFFECTS IN THE SOLVOLYSES OF 2-(2,4-DIMETHOXYPHENYL)-1,1-d_2-ETHYL AND 2-(3,5-DIMETHOXYPHENYL)-1,1-d_2-ETHYL *p*-BROMOBENZENESULFONATES

C. C. LEE AND L. NOSZKÓ[1]

Department of Chemistry and Chemical Engineering, University of Saskatchewan, Saskatoon, Saskatchewan

Received July 5, 1966

ABSTRACT

The secondary α-deuterium kinetic isotope effects in the acetolyses and formolyses of 2-(2,4-dimethoxyphenyl)-ethyl and 2-(3,5-dimethoxyphenyl)-ethyl *p*-bromobenzenesulfonates (I-OBs and II-OBs, respectively) and their corresponding 1,1-dideuterio analogues (I-OBs-1-d_2 and II-OBs-1-d_2) were determined. The observed k_H/k_D values are compared with similar data from the literature for 2-phenylethyl and 2-*p*-anisylethyl *p*-toluenesulfonates (III-OTs and IV-OTs, respectively). In the formolyses of III-OTs, IV-OTs, and I-OBs, which proceed either chiefly or exclusively by way of bridged ions as intermediates, the isotope effects appear to increase slightly with increasing bridged-ion stability. For I-OBs and I-OBs-1-d_2, acetolyses gave smaller k_H/k_D values than formolyses because of deuterium scrambling caused by ion-pair returns during the acetolysis. Acetolyses and formolyses of II-OBs and II-OBs-1-d_2 gave lower isotope effects than the corresponding reactions with I-OBs and I-OBs-1-d_2. The magnitudes of the observed isotope effects in relation to transition-state structures are discussed.

INTRODUCTION

The possibility of utilizing kinetic isotope effects to probe the structures of the rate-determining transition states in the solvolyses of 2-arylethyl systems has been suggested (1–3). In conjunction with the studies on isotope position rearrangements in the acetolyses and formolyses of 2-(2,4-dimethoxyphenyl)-1,1-d_2-ethyl and 2-(3,5-dimethoxyphenyl)-1,1-d_2-ethyl *p*-bromobenzenesulfonates (I-OBs-1-d_2 and II-OBs-1-d_2, respectively) (4), it is of interest to determine also the secondary kinetic isotope effects of α-deuterium substitution in these solvolytic reactions.

RESULTS AND DISCUSSION

The kinetic isotope effects, as measured by k_H/k_D, the ratio of the rate constants for the protio and the corresponding 1,1-dideuterio analogues, for the acetolyses and formolyses of I-OBs, I-OBs-1-d_2, II-OBs, and II-OBs-1-d_2 are summarized in Table I. For comparison, similar data from the literature for the solvolyses of 2-phenyl-1,1-d_2-ethyl and 2-*p*-anisyl-1,1-d_2-ethyl *p*-toluenesulfonates (III-OTs-1-d_2 and IV-OTs-1-d_2, respectively) are also given in Table I.

The influence of aryl participation on the kinetic isotope effects in the solvolyses of III-OTs-1-d_2 and IV-OTs-1-d_2 has been discussed (1–3) in terms of Streitwieser's proposal that such isotope effects arise mainly out of the change in hydridization from sp^3 to sp^2 at the α-carbon during ionization (5). Although other factors, including inductive (6, 7) and steric (8) effects, may play some role in the interpretation of isotope effects, the present results can be explained adequately by the suggestions advanced by Streitwieser (3, 5). According to this theory (3, 5), the secondary α-deuterium kinetic isotope effect can be ascribed largely to the decrease in a bending force constant from a starting tetrahedral C—H bending vibration to the generally lower frequency out-of-plane bending

[1] *Visiting scientist, 1964–1965. Present address: Central Research Institute for Chemistry, Hungarian Academy of Sciences, Budapest, Hungary.*

Can. J. Chem. Downloaded from www.nrcresearchpress.com by 210.87.254.40 on 09/05/12
For personal use only.

TABLE I

Kinetic isotope effects in the solvolyses of protio and 1,1-dideuterio 2-arylethyl arenesulfonates

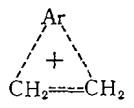
Compound solvolyzed	α-deuterium atoms/molecule	Acetolysis				Formolysis			
		Temperature (°C)	10^5k_H (s^{-1})	10^5k_D (s^{-1})	k_H/k_D	Temperature (°C)	10^5k_H (s^{-1})	10^5k_D (s^{-1})	k_H/k_D
$PhCH_2CH_2OTs$ (III-OTs)*	1.83	93.9			1.03‡	75.25			1.17‡
p-$CH_3OPhCH_2CH_2OTs$ (IV-OTs)†	2.00	75.0			1.18‡,§	50.0			1.20‡
2,4-$(CH_3O)_2PhCH_2CH_2OBs$ (I-OBs)	1.92	50.0	3.89±0.09	3.39±0.09	1.15	20.0	27.5±0.6	22.0±0.2	1.25
2,4-$(CH_3O)_2PhCH_2CH_2OBs$ (I-OBs)	1.92	50.0	3.91±0.09	3.43±0.04	1.14	20.0	27.4±0.1	22.1±0.6	1.24
2,4-$(CH_3O)_2PhCH_2CH_2OBs$ (I-OBs)	1.92	60.6	12.7±0.2	11.3±0.1	1.12	25.0	50.9±0.7	41.5±0.7	1.23
2,4-$(CH_3O)_2PhCH_2CH_2OBs$ (I-OBs)	1.92	60.6	12.9±0.2	11.4±0.1	1.13	25.0	51.4±0.1	41.7±0.1	1.23
3,5-$(CH_3O)_2PhCH_2CH_2OBs$ (II-OBs)	1.90	90.0	0.427±0.004	0.411±0.008	1.04	60.0	0.818±0.003	0.689±0.003	1.19
3,5-$(CH_3O)_2PhCH_2CH_2OBs$ (II-OBs)	1.90	90.0	0.420±0.002	0.411±0.007	1.02	60.0	0.825±0.003	0.696±0.003	1.18
3,5-$(CH_3O)_2PhCH_2CH_2OBs$ (II-OBs)	1.90	100.0	1.09±0.01	1.03±0.01	1.06	75.0	2.99±0.07	2.57±0.07	1.16
3,5-$(CH_3O)_2PhCH_2CH_2OBs$ (II-OBs)	1.90	100.0	1.09±0.01	1.03±0.01	1.06	75.0	3.04±0.02	2.67±0.07	1.14

*Data from ref. 1.
†Data from ref. 2.
‡Average of two or three runs.
§The reaction mixture, 0.05 M in p-toluenesulfonate ester, contained 0.06 M $LiClO_4$ to suppress ion-pair returns.

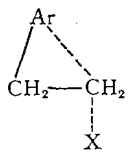
Can. J. Chem. Downloaded from www.nrcresearchpress.com by 210.87.254.40 on 09/05/12
For personal use only.

motion in the transition state leading to the carbonium ion. It is also postulated that the out-of-plane C—H vibration in the transition state can be impeded by the proximity of the leaving or the entering group; the closer these groups are to the developing carbonium ion, the stiffer the out-of-plane C—H bending motion and the lesser the isotope effect. For an isolated carbonium ion, k_H/k_D has been calculated to be about 1.4 per α-deuterium atom (5). In limiting S_N1 solvolyses, the observed k_H/k_D is about 1.15 per α-deuterium atom, and the decrease from 1.4 may be attributed largely to the influence of the nearby leaving group. For direct S_N2 displacements, the presence of both entering and leaving groups in the transition state causes the virtual disappearance of the isotope effect. It is also predicted that anchimerically assisted solvolyses should show values of k_H/k_D less than 1.15 per α-deuterium atom, since the participating neighboring group may be counted as an entering group (3).

The formolyses of I-OBs (4, 9) and IV-OTs (10) are exclusively anchimerically assisted (k_Δ), and the chief contributor to the formolysis of III-OTs is also k_Δ (9, 11). These three reactions all show k_H/k_D values of less than 1.15 per α-deuterium atom (Table I). There is also a trend towards a higher isotope effect as the 2-aryl group is changed in the order of phenyl, *p*-anisyl, and 2,4-dimethoxyphenyl (k_H/k_D per α-deuterium atom about 1.09, 1.10, and 1.12, respectively). The findings suggest that the proximity of the participating aryl group is progressively farther from C-1 in the transition states for the formolysis of III-OTs, IV-OTs, and I-OBs. According to Hammond's hypothesis (12), the transition state in a carbonium ion reaction should resemble the intermediate ion more than the tetrahedral reactant. As developed by Streitwieser (3, pp. 66–68), this hypothesis, when applied to solvolytic reactions, also suggests that the more stable the intermediate carbonium ion, the farther away is the transition state from the intermediate along the reaction coordinate. Thus, in reactions involving bridged ions as intermediates, if the bridged ion is more stable, the bridging would be less developed in the transition state. In a 2-arylethyl system with the symmetrical bridged ion V as intermediate, the transition state could be written as VI (2). As the aryl group is changed in the order of phenyl,



V



VI

p-anisyl, and 2,4-dimethoxyphenyl, the stability of the corresponding bridged ion will also increase in that order. Thus, in the transition state, the distance between Ar and C-1, and hence the isotope effect, will increase in the order of increasing bridged-ion stability. Such arguments have been presented by Streitwieser (3, pp. 171–175) to explain the slightly higher k_H/k_D values for the formolyses of IV-OTs and IV-OTs-1-d_2 as compared with those for the formolyses of III-OTs and III-OTs-1-d_2. The present data on isotope effects in the formolyses of I-OBs and I-OBs-1-d_2 fit into this pattern, and thus further strengthen the applicability of such interpretations of α-deuterium kinetic isotope effects.

As in the formolysis, the acetolysis of I-OBs is exclusively anchimerically assisted via a bridged ion as intermediate (4, 9). One might then expect that both the acetolyses and formolyses of I-OBs and I-OBs-1-d_2 would give similar isotope effects. However, from Table I, it can be seen that the observed k_H/k_D value for the acetolyses of this system (about 1.14) is much lower than that for the formolyses (about 1.24). This decrease most

Can. J. Chem. Downloaded from www.nrcresearchpress.com by 210.87.254.40 on 09/05/12
For personal use only.

likely arises from the occurrence of ion-pair returns. Such returns, highly significant in the acetolysis of I-OBs-1-d_2 but negligible in the formolysis, cause a "scrambling" of the deuterium from C-1 to C-2 in the reactant, the *p*-bromobenzenesulfonate ester (4). Since deuteration at C-2 gave no isotope effect in the solvolyses of analogous systems (III-OTs and IV-OTs) (1, 2), scrambling of deuterium to C-2 through ion-pair returns would cause a decrease in the k_H/k_D value, as is observed for the acetolyses of I-OBs and I-OBs-1-d_2. It is of interest to note that, when the acetolyses of IV-OTs and IV-OTs-1-d_2 were carried out in the presence of lithium perchlorate to suppress ion-pair returns, the difference in k_H/k_D for acetolysis and formolysis almost disappeared (2) (see Table I). Similarly, identical α-deuterium isotope effects for the 2,2-diphenylethyl system were observed for formolysis and for acetolysis in the presence of lithium perchlorate (2).

The solvolyses of II-OBs and II-OBs-1-d_2 show smaller isotope effects than the corresponding reactions with I-OBs and I-OBs-1-d_2 (Table I). This is to be expected, because k_s competes significantly with k_Δ in the solvolyses of II-OBs (4, 9). The acetolysis of III-OTs is largely due to k_s (9, 13), and the α-deuterium isotope effect is very small (1). Isotopic rearrangements of the C-1 label to C-2 in the solvolysis products have been found to be 14 and 5.5%, respectively, for the acetolyses of II-OBs-1-d_2 (4) and III-OTs-1-^{14}C (13), suggesting a greater extent of involvement of bridged ion V in the II-OBs system. Also, ion-pair returns are quite significant in the acetolysis of II-OBs-1-d_2 (4). When all this information is considered collectively, it is not surprising to note that the observed k_H/k_D value for the acetolyses of the II-OBs system appears to be slightly higher than that for the acetolyses of III-OTs and III-OTs-1-d_2, and is much lower than the α-deuterium isotope effects for the cases where involvement of the bridged ion V predominates.

The formolysis of II-OBs-1-d_2 gave 26% isotopic rearrangement in the product as compared with 14% of such rearrangement in its acetolysis, and there is no significant ion-pair returns in the formolysis (4). One would therefore expect a higher α-deuterium isotope effect for the formolyses than for the acetolyses; this is observed (Table I). The observed k_H/k_D value for the formolyses of II-OBs and II-OBs-1-d_2 ranged from 1.14 to 1.19. This range encompasses the k_H/k_D value for the formolyses of III-OTs and III-OTs-1-d_2 (1). From isotopic rearrangement data (4, 13), it can be estimated that the extents of involvement of bridged ion V in the formolyses of II-OBs and III-OTs are, respectively, 52 and 89%. Thus, the k_s contribution is greater in the formolysis of II-OBs than in that of III-OTs. If the k_s process involving the reaction with solvent were regarded as an S_N2 direct displacement with no isotope effect, one would expect that, in the formolyses, the k_H/k_D value would be smaller for the II-OBs system than for the III-OTs system; apparently this is not the case. A possible explanation of this observation may be as follows. Solvolyses of primary systems in nucleophilic solvents, such as alcohols, may be "pure" S_N2 or direct displacements with no α-deuterium kinetic isotope effects. However, solvolyses in highly ionizing solvents, such as formic acid, may proceed through a solvated carbonium ion as an *intermediate*, even for a primary system such as 1-butyl *p*-bromobenzenesulfonate (14). The k_s process in the formolysis of II-OBs or III-OTs could be regarded as proceeding via a solvated carbonium ion intermediate. In the transition state leading to such an intermediate, the separation between the entering solvent and C-1, and possibly also between the leaving group and C-1, would be greater than the corresponding separations in the transition states for solvolyses in more nucleophilic solvents, such as acetic acid or alcohols. Hence, in the formolyses of II-OBs and III-OTs, even the k_s process will give rise to some α-deuterium isotope effect, and the overall magnitude of k_H/k_D will not be very sensitive to variations in the relative contributions of k_s and k_Δ.

Finally, it may be pointed out that, in the present work, each system investigated was studied at two different temperatures (Table I). Because the temperature ranges employed were not large, extensive treatment of the limited data with regard to the effects of varying temperatures may not be justified. It is, however, of interest to note that, except for the acetolyses of II-OBs and II-OBs-1-d_2, which proceed largely by nucleophilic solvolysis with a relatively low isotope effect, the other reactions (acetolyses and formolyses of I-OBs and I-OBs-1-d_2 and formolyses of II-OBs and II-OBs-1-d_2) all appear to give a somewhat lower k_H/k_D value at a higher temperature. A similar trend of a slight decrease in the secondary α-deuterium kinetic isotope effect with increasing temperature has also been observed previously in this laboratory for the solvolyses of *exo*- and *endo*-norbornyl and 2-(Δ^3-cyclopentenyl)ethyl arenesulfonates (15–17).

EXPERIMENTAL

Preparations of the Sulfonate Esters

2-(2,4-Dimethoxyphenyl)-ethyl and 2-(3,5-dimethoxyphenyl)-ethyl *p*-bromobenzenesulfonates (I-OBs and II-OBs, respectively) were prepared by the methods outlined by Winstein and Heck (9). The syntheses of the corresponding 1,1-dideuterio analogues (I-OBs-1-d_2 and II-OBs-1-d_2) have been described in the preceding paper (4).

Kinetic Studies

The corresponding protio and dideuterio compounds (I-OBs and I-OBs-1-d_2 or II-OBs and II-OBs-1-d_2) were solvolyzed simultaneously at each temperature. About 0.03 *M* solutions of the appropriate compounds in either reagent-grade glacial acetic acid or reagent-grade 98–100% formic acid were heated in a water or an oil bath thermostated at the desired temperature, which remained constant within ±0.02 °C. The reaction rates were followed titrimetrically by known procedures (9, 16, 17). The specific rate constants were obtained from least-squares plots as described earlier (16).

ACKNOWLEDGMENT

The financial support given by the National Research Council of Canada is gratefully acknowledged.

REFERENCES

1. W. H. Saunders, Jr., S. Ašperger, and D. H. Edison. J. Am. Chem. Soc. **80**, 2421 (1958).
2. W. H. Saunders, Jr. and R. Glaser. J. Am. Chem. Soc. **82**, 3586 (1960).
3. A. Streitwieser, Jr. Solvolytic displacement reactions. McGraw-Hill Book Co., Inc., New York. 1962.
4. C. C. Lee and L. Noszkó. Can. J. Chem. This issue.
5. A. Streitwieser, Jr., R. H. Jagow, R. C. Fahey, and S. Suzuki. J. Am. Chem. Soc. **80**, 2326 (1958).
6. E. A. Halevi. Tetrahedron, **1**, 174 (1957).
7. E. A. Halevi. Progr. Phys. Org. Chem. **1**, 101 (1963).
8. L. S. Bartell. J. Am. Chem. Soc. **83**, 3567 (1961).
9. S. Winstein and R. Heck. J. Am. Chem. Soc. **78**, 4801 (1956).
10. E. F. Jenny and S. Winstein. Helv. Chim. Acta, **41**, 807 (1958).
11. J. W. Clayton and C. C. Lee. Can. J. Chem. **39**, 1510 (1961).
12. G. S. Hammond. J. Am. Chem. Soc. **77**, 334 (1955).
13. C. C. Lee, G. P. Slater, and J. W. T. Spinks. Can. J. Chem. **35**, 1417 (1957).
14. A. Streitwieser, Jr. J. Am. Chem. Soc. **77**, 1117 (1955).
15. C. C. Lee and E. W. C. Wong. J. Am. Chem. Soc. **86**, 2752 (1964).
16. C. C. Lee and E. W. C. Wong. Tetrahedron, **21**, 539 (1965).
17. C. C. Lee and E. W. C. Wong. Can. J. Chem. **43**, 2254 (1965).

Can. J. Chem. Downloaded from www.nrcresearchpress.com by 210.87.254.40 on 09/05/12
For personal use only.

Can. J. Chem. Downloaded from www.nrcresearchpress.com by 210.87.254.105 on 09/05/12
For personal use only.

THE REDUCTIVE DIMERIZATION OF *N*-BENZYLIDENE ANILINE[1]

JAMES G. SMITH AND C. DOREEN VEACH
Exploratory Research Laboratory, Dow Chemical of Canada, Limited, Sarnia, Ontario
Received May 3, 1966

ABSTRACT

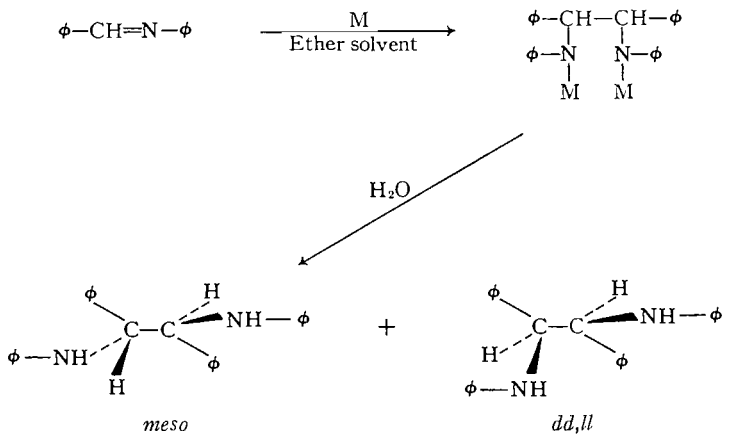
The formation of alkali metal adducts of *N*-benzylidene aniline in several inert solvents is studied by protonolysis of the adducts and analysis of the reaction products, the diastereomeric *N,N'*,1,2-tetraphenylethylenediamines. With sodium and potassium metal in polar solvents, the product is predominantly the *dd,ll* diamine. With lithium metal or with solvents of low polarity, the product contains approximately equal quantities of the two diastereomers.

It is demonstrated that the initially formed diastereomeric mixture generally contains appreciable amounts of the *meso* isomer. In polar solvents with sodium, isomerization to the stable *dd,ll* diastereomer occurs. However, with lithium or with sodium in nonpolar solvents, the isomerization does not occur. The reasons for the preponderance of the *dd,ll*-disodio compound in the equilibrating systems are discussed.

INTRODUCTION

Under certain conditions the reduction of *N*-benzylidene aniline proceeds with dimerization to give a diastereomeric mixture of *N,N'*,1,2-tetraphenylethylenediamines. This reaction occurs with alkali metals (1, 2), magnesium – magnesium iodide (3, 4), and aluminium amalgam (5, 6) as reducing agents. It has been reported (6) that the reduction product is approximately a 50:50 mixture of the two diastereomeric diamines.

A recent study in this laboratory (7) involved the preparation of the alkali metal adducts of *N*-benzylidene aniline (1, 2) (Reaction Scheme 1). Protonolysis of these adducts produced a diastereomeric mixture of diamines which was predominantly the *dd,ll*-*N,N'*,1,2-tetraphenylethylenediamine. This observation prompted a more detailed examination of the formation and protonolysis of these adducts by taking advantage of the facile analysis provided by the nuclear magnetic resonance spectra of the crude reaction product. A similar study has recently been described by Eisch (8). However, the conclusions reached here concerning the processes involved in the reductive dimerization differ somewhat from those of Eisch.



REACTION SCHEME 1.

[1]*Contribution No. 140 from the Exploratory Research Laboratory.*

Can. J. Chem. Downloaded from www.nrcresearchpress.com by 210.87.254.105 on 09/05/12
For personal use only.

RESULTS AND DISCUSSION

Initially, the influence of different alkali metals and solvents on the ratio of the diastereomeric diamines was investigated. Since the sodium adduct is appreciably more soluble than either the lithium or potassium adduct, the effect of concentration on the diastereomeric ratio was examined. The diastereomeric ratio remained constant within the concentration range studied (0.1–0.3 *m*) with the exception of one experiment, in which the adduct precipitated from solution. Wherever possible, solutions of the adducts have been selected for quenching and subsequent analysis; the notable exception is the potassium adduct, which appears to be quite insoluble.

Table I presents the results obtained with various metals and solvents. Broadly speaking, the product compositions fall into two groups, the one consisting of approximately equal parts of the two diastereomeric diamines, and the other consisting of mainly the *dd,ll* diastereomer. The agreement with Eisch's results is fair; the differences are possibly due to the somewhat different conditions of preparation.

TABLE I

Effect of alkali metal and solvent on the diastereomeric ratio*

		Composition		Previous data†	
Metal	Solvent	% *meso*	% *dd,ll*	% *meso*	% *dd,ll*
Li	Ether	59	41		
Na	Ether	46	54	42	53
K	Ether	No reaction			
Li	Tetrahydrofuran	53	47	41	46
Na	Tetrahydrofuran	7	93	6	90
K	Tetrahydrofuran‡	0	100		
Na	Benzene§	51	49	41	53
Na	Dioxane	12	88		
Na	1,2-Dimethoxyethane	4	96		

*Reaction time, 16 h; concentration, 0.1–0.15 *m* in *N*-benzylidene aniline; reaction temperature, 25–30 °C.
†Reference 8; reaction time, 22 h; concentration, 0.57 *m* in *N*-benzylidene aniline; reaction temperature, 45–50 °C.
‡Reaction precipitated.
§Reaction incomplete.

The reason for these two widely divergent groups of compositions becomes apparent when the composition is examined as a function of time (Table II). The adduct formation in an ether solvent (7, 9) is very rapid, and generally complete in 1 or 2 h. In the more polar solvents, a simultaneous isomerization of the originally formed diastereomeric mixture occurs to produce predominantly the *dd,ll* diastereomer. This does not occur in the less-polar solvent diethyl ether even after 5 days of reaction. In dioxane, the isomerization reaction is slow but readily observable, whereas in tetrahydrofuran the reaction is quite rapid.

The data of Table II also show that at lower temperatures in tetrahydrofuran the rate of isomerization is slowed appreciably. The initially formed composition is close to that formed in dioxane. The rate of isomerization at higher temperatures has been studied, but only a slight shift of the diastereomeric composition occurs. Some cleavage of the bond connecting the benzylic carbons is observed, with the formation of *N*-benzylaniline, if the reaction time is extended for unusually long periods of time (greater than 5 days).

When isomerization occurs, it proceeds only in the direction of an increased *dd,ll* content of the product (Table III). Thus, preparation of the sodium adduct at 0 °C produces a product containing 30% *meso*-*N,N'*-disodio-*N,N'*,1,2-tetraphenylethylenediamine. Permitting the solution to warm to 25 °C effects isomerization to an 8% *meso* content; cooling this solution to 0 °C has no effect on the composition.

TABLE II

Variation of the diastereomeric composition with time and temperature

Metal	Solvent	Temperature (°C)	% *meso* at time (h) 1	2	4	8	24
Na	Tetrahydrofuran	−15	30*	29	26	—	—
		0	—	31	25	25†	—
		25	23‡	18	7	—	7
		40	—	9	—	9	—
Na	Dioxane	25	32	—	28	25	19
Na	Ether	25	—	—	41	—	42§
		35	—	—	44		
Li	Tetrahydrofuran	25	—	56	53	—	54
		40	—	53	—	47	—
		60	—	50	47	—	—
Li	Ether	25	59	57†	59‖	60	57

*Reaction 85% completed.
†Precipitated.
‡28% *meso* in 0.25 h, reaction 65% completed.
§44% *meso* in 5 days.
‖Reaction 86% completed.

TABLE III

Reversibility of the isomerization

System	Treatment	Composition (% *meso*) Before	After	Final solvent
Na, tetrahydrofuran*	Warmed to 25° for 1 h	30	20	—
	Warmed to 25° for 16 h		8	—
Na, tetrahydrofuran†	Cooled to 0° for 21 h	11	11	—
Na, Et_2O	Tetrahydrofuran added	46	20	52% Et_2O
			29	69% Et_2O
Na, tetrahydrofuran†	Et_2O added	11	10	55% Et_2O
			11	69% Et_2O
			11	90% Et_2O

*Prepared at 0°.
†Prepared at 25°.

Addition of tetrahydrofuran to an ether solution of the sodium adduct causes the composition to be enriched in the *dd,ll* diastereomer. On the other hand, addition of ether to a tetrahydrofuran solution of the adduct does not change the composition.

Eisch has suggested (8) that the radical–ion, initially generated by an electron transfer from the alkali metal to *N*-benzylidene aniline, dimerizes either on the surface of the metal or, if it becomes solvated, in solution. In the former case, the protonolysis product consists of approximately equal amounts of the two diastereomeric *N,N'*,1,2-tetraphenylethylenediamines; in the latter case, the product is predominantly *dd,ll*.

The product composition is indeed affected by the solvent and metal used, as may be seen by comparing the initial compositions of the sodium–dioxane, sodium–ether, and lithium–tetrahydrofuran systems (Table II). However, the isomerization observed in polar solvents is at least an equally important factor. In these instances, the observed product composition is established largely after dimerization has occurred and not before. Dimerization of the radical–ion on the surface of the metal or in solution may affect the composition of the initially formed material, but the data on the initial compositions are insufficient to establish this.

The isomerization is probably effected[2] by the amide ion derived from the alkali metal

[2]*A referee has drawn our attention to the possibility that isomerization may occur through a reversion of the dimeric reduction product to its monomeric radical–ion followed by recoupling to the isomerized dimer. The present experimental data do not distinguish between this possibility and the one discussed above.*

Can. J. Chem. Downloaded from www.nrcresearchpress.com by 210.87.254.105 on 09/05/12
For personal use only.

adduct acting as its own isomerizing agent. Attempts have been made (Table IV) to prepare the *meso*-*N*,*N*′-disodio compound by treating the *meso*-*N*,*N*′,1,2-tetraphenylethylenediamine with sodium hydride. However, isomerization occurs too rapidly and is accompanied by some cleavage of the bond joining the benzylic carbon atoms, with the formation of *N*-benzylaniline.

TABLE IV

Isomerization of *meso*-*N*,*N*′,1,2-tetraphenylethylenediamine

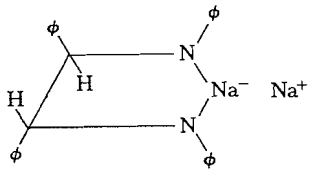
Agent	Mole ratio	Conditions	Final composition (% *meso*)
NaH	2.2	Refluxing tetrahydrofuran, 3 h	60
	4.0	Refluxing tetrahydrofuran, 3 h	9*
Sodium adduct	1.0	2 h in tetrahydrofuran, 25°	51†
		17 h in tetrahydrofuran, 25°	38
		42 h in tetrahydrofuran, 25°	31
Sodium adduct	1.0	2 h in tetrahydrofuran, 25°	48†
Sodium	2.0	17 h in tetrahydrofuran, 25°	17‡

*17% *N*-benzylaniline formed.
†In the absence of isomerization, the final composition should be 54% *meso*.
‡7% *N*-benzylaniline formed.

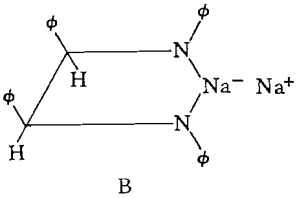
In a second attempt to prepare high concentrations of the *meso*-*N*,*N*′-disodio compound the *meso*-*N*,*N*′,1,2-tetraphenylethylenediamine was treated with an equivalent amount of preformed *N*,*N*′-disodio compound. An exchange would be expected to occur between the existing sodium compound and the amine to convert the added *meso* diamine into its corresponding *meso*-*N*,*N*′-disodio compound. As this occurs, the newly formed *N*,*N*′-disodio derivative is isomerized to the *dd*,*ll*-disodio derivative. As a consequence, the overall composition of the system becomes richer in the *dd*,*ll* diastereomer.

The final composition is not the 8% *meso* observed in the preparation of the adduct itself, but then the system contains only half the amount of sodium necessary for all the amine groups. An appreciably greater degree of isomerization occurs if the excess sodium metal from the adduct preparation is allowed to remain in the reaction mixture. In this case, the amine groups of the *meso* diamine probably react to some extent with the sodium, thereby bringing the system to a closer resemblance with the *N*,*N*′-disodio compound itself.

An explanation for the greater stability of the *dd*,*ll* diastereomer in polar solvents may lie in the ability of the compound to adopt conformation A or B, in which one sodium



A



B

atom is solvated by the ether solvent and the other is coordinated intramolecularly to the two nitrogen atoms. It will be noted that conformation A arises from the *dd*,*ll* isomer and conformation B from the *meso* isomer. The greater steric interaction of the phenyl groups in B as compared with A would be expected to shift any equilibrium between the two in the direction of A. In a somewhat similar suggestion, Eisch (8) proposes that the radical-ions cluster in a specific manner before the benzylic carbon bond is formed.

In contrast to the behavior of the *N*,*N*′-disodio compound, the addition of either *meso*- or *dd*,*ll*-*N*,*N*′,1,2-tetraphenylethylenediamine to a solution of the *N*,*N*′-dilithio compound

Can. J. Chem. Downloaded from www.nrcresearchpress.com by 210.87.254.105 on 09/05/12
For personal use only.

does not result in any significant isomerization of the added diamines (Table V). The small changes in composition observed in these systems are due to cleavage of the bond connecting the benzylic carbons of the diamines and (or) their *N,N'*-dilithio analogues, with the formation of *N*-benzylaniline. No indication of an equilibrium between the two diastereomeric *N,N'*-dilithio compounds was observed.

TABLE V

Experiments with *N,N'*-dilithio-*N,N'*,1,2-tetraphenylethylenediamine*

Treatment	Composition (% *meso*) Before	After
Added 1 equivalent of *meso* diamine	72.5	72 (6 h) 63 (18 h)†
Added 1 equivalent of *dd,ll* diamine	29	27 (6 h) 22 (18 h)†
Shaken with Na	52	51
Sodium adduct (1 equivalent) prepared in the same solution	30‡	29

*All experiments were conducted in tetrahydrofuran.
†9% *N*-benzylaniline present.
‡Calculated by averaging the composition of lithium adduct (53% *meso*) and the sodium adduct (7% *meso*).

Somewhat more surprising is the observation that the lithium adduct is unaffected by the presence of sodium metal or even by the preparation of the sodium adduct in a solution of the lithium adduct. There must be very little, if any, exchange of the lithium bonded to the nitrogen with either elemental sodium or sodium bonded to nitrogen. If such an exchange occurred, then the new *N,N'*-disodio compound thereby formed should isomerize to its equilibrium composition. It is possible to rationalize these observations by assuming that the N—Li bond has a high degree of covalent character so that the system contains a very low concentration of the corresponding amide ion. As a consequence, both isomerization and exchange of sodium for lithium would be very slow.

Eisch demonstrated (8) that, if the dimerization of *N*-benzylidene aniline is effected by the transfer of lithium from preformed lithium–biphenyl adduct (i.e. a homogeneous system), the protonolysis product contains appreciably more *dd,ll* diamine than if the lithium metal alone is used (i.e. a heterogeneous system). Although Eisch cites this as evidence for the dimerization of the radical-ion in solution to yield a *dd,ll*-rich product, it seems equally possible that the strong base lithium–biphenyl is isomerizing the *N,N'*-dilithio-*N,N'*,1,2-tetraphenylethylenediamine during the experiment.

In summary, the nitrogen–lithium bond of the *N,N'*-dilithio-*N,N'*1,2-tetraphenylethylenediamines behaves as a covalent bond, showing little tendency to form the amide ion and thus isomerize. The sodium–nitrogen bond of the corresponding *N,N'*-disodio compound possesses a much greater degree of ionic character as long as relatively polar solvents such as tetrahydrofuran are used. When less-polar solvents such as dioxane and diethyl ether are employed, the concentration of amide ion is reduced so that the isomerization of the initially formed *N,N'*-disodio compounds is slowed or halted.

The inability of diethyl ether to shift the equilibrium composition in tetrahydrofuran from its predominantly *dd,ll* composition indicates the exceptional stability of the *dd,ll*-amide ion once it is formed. The ether must not only displace the solvating tetrahydrofuran but also break the intramolecular coordination of the two nitrogen atoms to the sodium. This it does not appear to be able to do.

Can. J. Chem. Downloaded from www.nrcresearchpress.com by 210.87.254.105 on 09/05/12
For personal use only.

EXPERIMENTAL

The preparation of the alkali metal adducts has been described previously (7). Reference samples of *meso-* and *dd,ll-N,N'*,1,2-tetraphenylethylenediamine were prepared by reductive dimerization of *N*-benzylidene aniline with aluminium amalgam in wet ether (6) followed by separation of the individual components by means of their complexes with dimethylformamide (10). The reduction product, after isolation, was analyzed by means of its nuclear magnetic resonance spectrum taken on a Varian A-60 spectrometer in a manner similar to that described by Eisch (8).

Time Studies (Table II)

The time studies were carried out in a flask equipped with a mechanical stirrer and a stopcock at the bottom for withdrawing samples. Solutions were prepared in a dry box from freshly distilled solvents and *N*-benzylidene aniline. These were transferred from the dry box in a sealed separatory funnel and introduced into the reaction vessel under nitrogen. The metal was freshly cut in the dry box and transferred in a sealed test tube equipped with a standard taper joint. The metal was introduced into the reaction vessel by connecting the transfer tube to a side neck and gently tapping the tube to cause the metal to drop into the stirred solution. Color changes indicative of adduct formation were obvious within 2–3 min.

Weighed samples were withdrawn, quenched in 1:1 ethanol–water, and titrated with standard acid to determine the extent of reaction. The titrated samples were then extracted and analyzed as previously described (8).

In the case of the run at 0 °C, the entire reaction vessel was immersed in a Dewar flask filled with ice and water. Reactions at −15° and 40° were carried out in jacketed flasks through which methanol–water or water at the desired temperature was circulated.

In the experiments of Table IV, the adduct was first prepared in a modified Schlenk tube and then transferred to a second tube to which the second alkali metal was added. In the case of the experiments of Table V, the prepared adduct was transferred to a flask containing the second reagent, *dd,ll-* or *meso-N,N'*,1,2-tetraphenylethylenediamine.

ACKNOWLEDGMENTS

We are indebted to Dr. J. S. McIntyre of this laboratory for suggesting the analytical procedure, and to Dr. McIntyre and Mr. H. Mak for the determination of the nuclear magnetic resonance spectra.

REFERENCES

1. W. SCHLENK, J. APPRENRODT, A. MICHAEL, and A. THAL. Ber. **47**, 473 (1914).
2. W. SCHLENK and E. BERGMANN. Ann. **463**, 281 (1928).
3. W. E. BACHMANN. J. Am. Chem. Soc. **53**, 2672 (1931).
4. H. THIES, H. SCHOENENBERGER, and K. H. BAUER. Arch. Pharm. **291**, 620 (1958).
5. O. ANSELMINO. Ber. **41**, 623 (1908).
6. W. STUHMER and G. MESSWARB. Arch. Pharm. **286**, 221 (1953).
7. J. G. SMITH. Can. J. Chem. **44**, 59 (1966).
8. J. J. EISCH, D. D. KASKA, and C. J. PETERSON. J. Org. Chem. **31**, 453 (1966).
9. K. ZIEGLER and O. SCHAEFER. Ann. **479**, 175 (1930).
10. R. JAUNIN. Helv. Chim. Acta, **39**, 111 (1956).

Can. J. Chem. Downloaded from www.nrcresearchpress.com by 210.87.254.105 on 09/05/12
For personal use only.

Can. J. Chem. Downloaded from www.nrcresearchpress.com by 210.87.254.105 on 09/05/12
For personal use only.

A COMMENT ON THE INADEQUACY OF THE CORRELATION BETWEEN PHYLLO-TYPE SPECTRUM AND *meso*-SUBSTITUTION IN THE PORPHYRIN SERIES

R. Bonnett, I. A. D. Gale, and G. F. Stephenson
Chemistry Department, Queen Mary College, London, E.1, England

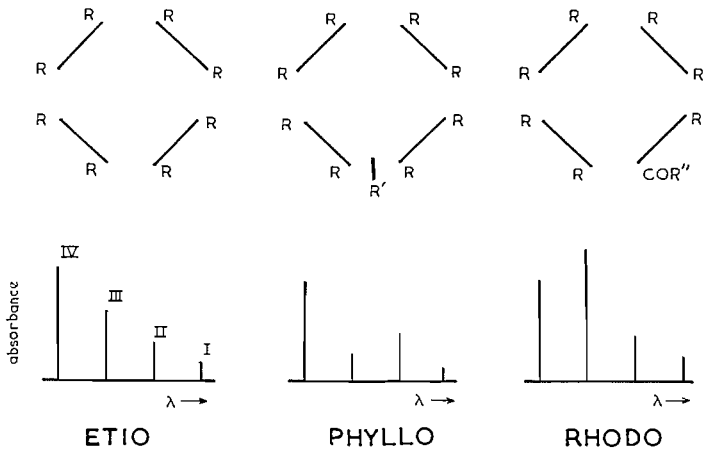
Received June 21, 1966

ABSTRACT

The empirical correlation between *meso*-substitution and the phyllo-type spectrum in the porphyrin series is shown to be much less general than had previously been supposed. The variation of the spectrum with the electronic nature of the substituent is discussed.

It became apparent at an early stage in our study of the nitration (1) of octa-substituted porphyrins that deductions from visible and nuclear magnetic resonance spectra were in conflict. Thus, although the nuclear magnetic resonance spectrum of nitrooctaethylporphyrin clearly corresponded to a *meso*-substituted structure, the visible spectrum was of an etio type, whereas, on the basis of the correlation proposed by Stern and Wenderlein (2), a phyllo-type spectrum (Fig. 1) would have been expected. Indeed, Stern and Molvig (3) had applied this correlation to reject, incorrectly as it now emerges (1, 4), the *meso*-nitro structure for nitroetioporphyrin I. It thus became desirable to reconsider the correlation between *meso*-substitution and the phyllo-type spectrum.

The general correlation, which was proposed in 1936, and which has in recent years (5, 6) received a certain amount of theoretical interpretation, is summarized in Fig. 1. It is well documented (2, 7, 8)[1] for both the etio- and rhodo-type assignments, where it operates effectively in the sense that all porphyrins of the stated substitution pattern are expected


R
R
R

to have the spectral type shown. When the phyllo-type correlation was suggested, however, Stern and his colleagues had catalogued only five examples (examples 1–5 in Table I) which demonstrated the effect of a *meso*-substituent in the absence of a "rhodofying" group, and, of these, two (examples 2 and 3, both possessing the isocyclic ring) did not possess typical phyllo-type spectra in that band I was more intense than band II. Thus, the correlation in the phyllo case appears to have been based rather inadequately. Later work has shown that phyllo-type spectra may be observed in the absence of *meso*-substitution (e.g. porphyrin (6), noted by Stern (2)) and, more significantly, has provided many examples of *meso*-substituted porphyrins which do not possess phyllo-type spectra.

Some relevant spectra are summarized in Tables I and II. The original measurements and correlations refer to dioxane solutions (Table I), but in recent years spectra have frequently been recorded in chloroform (Table II). As examples in the tables suggest, solvent dependence in this case is significant but not marked; in a borderline case, there may be a change in spectral type in going from one solvent to another. This happens with α-chlorooctaethylporphyrin, which has an intermediate etio–phyllo type spectrum ($\epsilon_{III} = \epsilon_{II}$) in dioxane but has a phyllo-type spectrum in chloroform. However, inspection of the extinction coefficients shows that the numerical change from one solvent to another is rather small.

The following points emerge from a consideration of Tables I and II.

(*i*) The phyllo-type spectrum is often associated with mono *meso*-alkylated porphyrins. Some authors (18, 19) have, indeed, restricted the correlation in this way, but as examples

TABLE I

Visible spectra of *meso*-substituted porphyrins in dioxane (wavelength in mμ ($\epsilon \times 10^{-2}$))

Example		IV	III	II	I	Type*	*R*†	Reference
1	γ-Phylloporphyrin methyl ester	502 (159.8)	533.5 (50.6)	573.5 (60.7)	627 (15.3)	P	1.66	9
2	Desoxophylloerythrin methyl ester	496 (166.7)	530 (35.6)	564 (62.9)	615 (65.4)	U		9
3	4-Desethyldesoxo-phylloerythrin methyl ester‡	496 (164)	529 (27)	564 (56.9)	613 (73.1)	U		10
4	2-Desethyldesoxo-phylloerythrin methyl ester	499 (158.2)	531.5 (36.2)	562.5 (64.8)	614.5 (57.8)	P		11
5	α,γ-Dimethyldeutero-etioporphyrin II	507 (144.8)	539 (30)	579 (53.5)	633 (6.4)	P		11
6	δ-Phylloporphyrin	502 (149.2)	534 (50)	573 (52.8)	624 (14)	P	1.47	12
7	6-Ethyl-γ-phyllo-porphyrin methyl ester	503 (135.6)	536 (54.8)	576 (50.6)	628 (16.6)	E		12
8	α-Chlorooctaethyl-porphyrin	505 (153)	536 (57)	576 (57)	628 (12)	EP	1.59	§
9	α-Bromooctaethyl-porphyrin	508 (134)	540 (55)	580 (50)	629 (17)	E	1.37	§
10	α-Nitroetioporphyrin I	500 (132.4)	532 (85.3)	570 (62.3)	623 (52.2)	E	1.16	3
11	α-Nitrooctaethyl-porphyrin	501 (140)	533 (91)	571 (64)	623 (57)	E	1.11	§
12	α-Benzoxycopro-porphyrin I tetramethyl ester	497 (180.7)	528 (58)	570 (62)	622 (20)	P	1.59	12

*SPECTRAL TYPES: P = phyllo; E = etio; EP = etio–phyllo intermediate type ($\epsilon_{II} = \epsilon_{III}$); U = unclassified.

†For definition see the text. Extinction values for the parent porphyrins in dioxane are taken from the Stern and Pruckner collection; Pruckner's data (22) (rather than Stern's) (23) for octaethylporphyrin are confirmed by our own measurements (λ 497 (ε 13 600), 529 (ε 10 000), 567 (ε 6 300), 593 (ε 1 300), and 619 mμ (ε 5 300)) and are therefore employed. The data in chloroform solutions were taken from ref. 1 (octaethylporphyrin) and ref. 16 (etioporphyrin I).

‡Also bands at 659 mμ (ε 410) and 590 mμ (ε 1 250).

§Present work; the spectra were recorded on a Unicam SP800B spectrophotometer and calibrated with a holmium filter.

Can. J. Chem. Downloaded from www.nrcresearchpress.com by 210.87.254.105 on 09/05/12
For personal use only.

TABLE II

Visible spectra of *meso*-substituted porphyrins in chloroform (wavelength in mμ ($\epsilon \times 10^{-2}$))

Example		IV	III	II	I	Type*	*R**	Reference
13	δ-Phylloporphyrin methyl ester	505 (1.0)†	539.5 (0.39)†	576 (0.42)†	628 (0.08)†	P		14
8*a*	α-Chlorooctaethyl-porphyrin	507 (148)	540 (53)	578 (56)	628 (16)	P	1.62	15
10*a*	α-Nitroetioporphyrin I	504 (119)	538 (79.5)	573 (59)	627 (49.1)	E	1.23	4
11*a*	α-Nitrooctaethyl-porphyrin	504 (125)	538 (84)	571 (63)	623 (53)	E	1.17	1
14	α-Formyletio-porphyrin I	509 (97)	538 (69)	577 (66)	633.5 (42)	E	1.49	16
15	α-Cyanoetioporphyrin I	515 (99.6)	553 (134)	587 (57.6)	640.5 (133)	U	0.72	16
16	α-Hydroxymethyl-etioporphyrin I	504 (133)	536.5 (88)	569.5 (67.9)	623 (41.2)	E	1.23	16
17	α-Aminooctaethyl-porphyrin	519 (113)	555 (52)	588 (36)	644 (58)	U	1.08	1
18	α-Hydroxyoctamethyl-porphyrin			583 (89)	630 (155)	U		17
19	α-Acetoxyoctamethyl-porphyrin	499 (102)	532 (43)	570 (42)	625 (11)	E		17

*See Table I.
†Extinction ratios.

7 and 16 show, even in this form there are exceptions, and many of the spectra are only marginally of the phyllo type (e.g. examples 6 and 13). Such exceptions have become significant in the structural work (13, 14) on porphyrins derived from the *Chlorobium* chlorophylls 660, in which the spectra (in ether) of various δ-phylloporphyrin homologues have been shown to have $\epsilon_{II} \simeq \epsilon_{III}$.

(*ii*) Many of the compounds, especially the *meso*-alkyl- and *meso*-halo-porphyrins, nevertheless show the development of phyllo character, although this does not necessarily extend as far as the phyllo-type spectrum. This can be demonstrated by observing in a given solvent the effect of introducing a *meso*-substituent into a porphyrin, e.g. by comparing in each case the extinction coefficient of band III with that of band II, the latter being rather insensitive to substituent changes (5, 8). Thus, the ratio (R) of ($\epsilon_{IIIp}/\epsilon_{IIp}$) to ($\epsilon_{IIIm}/\epsilon_{IIm}$), where p and m refer to the parent porphyrin and the *meso*-substituted porphyrin, respectively, is greater than unity in all but 1 (example 15) of the 14 instances where the comparison has been made (Tables I and II). The unusual nature of the spectrum of α-cyanoetioporphyrin I (example 15) has been remarked upon by Johnson and Oldfield (16); it is presumably associated with a combination of features (large negative spectroscopic moment (5) and low steric requirement) found with this substituent.

(*iii*) More bulky groups which are mesomerically electron withdrawing (e.g. NO_2 (examples 10, 11, 10*a*, and 11*a*)) appear to give spectra which are clearly of the etio type[2] (even though R is greater than unity, as indicated above). This may be rationalized in terms of the composition of the rhodo and phyllo effects *attributable to a single substituent*. The composition of such effects caused by two different substituents (as in chloroporphyrin e_6 trimethyl ester; etio-type spectrum in dioxane (9)) has numerous examples.

(*iv*) A *meso*-hydroxy substituent gives a spectrum of an unclassified type in which "band I" dominates the visible spectrum. Tautomeric forms (17) of such compounds may well be important, since in the acyl derivatives (e.g. example 18 → example 19) the spectrum returns to an etio type with pronounced phyllo character. In *meso*-aminoporphyrins this effect is much less marked (4).

[2]*Johnson and Oldfield discuss this point (4) and give several additional examples (in chloroform) (16).*

Can. J. Chem. Downloaded from www.nrcresearchpress.com by 210.87.254.105 on 09/05/12
For personal use only.

(*v*) The introduction of the maximum number of *meso*-substituents is not associated with the development of a phyllo-type spectrum. Thus, Eisner (20) has noted that the spectrum of $\alpha,\beta,\gamma,\delta$-tetramethylporphyrin (in chlorobenzene) is of an unclassified type. This point is further illustrated (Table III) by the chloro derivatives. The phyllo character of the spectrum increases somewhat on proceeding from α-chlorooctaethylporphyrin to the α,γ-dichloro derivative; however, the $\alpha,\beta,\gamma,\delta$-tetrachloro compound has a spectrum of an unclassified type in which the bands have suffered a considerable bathochromic shift. The extent of the shift suggests that it is not merely due to the electronic effect of the substituents; possibly, this is a further example (21) where departure from coplanarity (caused by peripheral overcrowding (15)) results in a bathochromic shift because the diminution of the ground-state stabilization reduces the energy gap between the ground and excited states.

TABLE III

Visible spectra of *meso*-substituted octaethylporphyrins in dioxane (wavelength in mμ ($\epsilon \times 10^{-2}$))

Example		IV	III	II	I	Type*	Reference*
8	α-Chloro	505 (153)	536 (57)	576 (57)	628 (12)	EP	Present work
20	α,γ-Dichloro	513 (123)	544 (36)	585 (41)	635 (7)	P	Present work
21	$\alpha,\beta,\gamma,\delta$-Tetrachloro†	548 (115)	597 (112)	640 (43)	712 (41)	U	Present work

*See Table I.
†Also band at ~520 mμ (ϵ 7 000).

REFERENCES

1. R. BONNETT and G. F. STEPHENSON. J. Org. Chem. **30**, 2791 (1965).
2. A. STERN and H. WENDERLEIN. Z. Physik. Chem. Leipsig, **A176**, 81 (1936).
3. A. STERN and H. MOLVIG. Z. Physik. Chem. Leipsig, **A177**, 365 (1936).
4. A. W. JOHNSON and D. OLDFIELD. J. Chem. Soc. 4303 (1965).
5. J. R. PLATT. *In* Radiation biology. Vol. 3. *Edited by* A. Hollaender. McGraw-Hill Book Co., Inc., New York. 1956. p. 102. M. GOUTERMAN. J. Chem. Phys. **30**, 1139 (1959).
6. C. RIMINGTON, S. F. MASON, and O. KENNARD. Spectrochim. Acta, **12**, 65 (1958).
7. R. LEMBERG and J. E. FALK. Biochem. J. **49**, 674 (1951). R. LEMBERG, P. CLEZY, and J. BARRETT. *In* Haematin enzymes. *Edited by* J. E. Falk, R. Lemberg, and R. K. Morton. The Pergamon Press, Ltd., London. 1961. p. 344.
8. J. E. FALK. Porphyrins and metalloporphyrins. Elsevier Pub. Co., Ltd. London. 1964. p. 91.
9. A. STERN and H. WENDERLEIN. Z. Physik. Chem. Leipsig, **A174**, 81 (1935).
10. A. STERN and H. WENDERLEIN. Z. Physik. Chem. Leipsig, **A174**, 321 (1935).
11. A. STERN and H. WENDERLEIN. Z. Physik. Chem. Leipsig, **A175**, 405 (1936).
12. F. PRUCKNER. Z. Physik. Chem. Leipsig, **A190**, 101 (1942).
13. A. S. HOLT, J. W. PURDIE, and J. W. F. WASLEY. Can. J. Chem. **44**, 88 (1966).
14. J. L. ARCHIBALD, D. M. WALKER, K. B. SHAW, A. MARKOVAC, and S. F. MACDONALD. Can. J. Chem. **44**, 345 (1966).
15. R. BONNETT, I. A. D. GALE, and G. F. STEPHENSON. J. Chem. Soc., Sect. C. In press.
16. A. W. JOHNSON and D. OLDFIELD. J. Chem. Soc., Sect. C, 794 (1966).
17. P. S. CLEZY and A. W. NICHOL. Australian J. Chem. **18**, 1835 (1965).
18. H. FISCHER and H. ORTH. Die Chemie des Pyrrols. Vol. II. Akademische Verlagsgesellschaft, Leipzig. 1937. p. 582.
19. A. S. HOLT. *In* Chemistry and biochemistry of plant pigments. *Edited by* T. W. Goodwin. Academic Press, Inc., London. 1965. p. 13.
20. U. EISNER. J. Chem. Soc. 854 (1957).
21. A. I. SCOTT. Interpretation of the ultraviolet spectra of natural products. The Pergamon Press, Ltd., London. 1964. p. 170.
22. F. PRUCKNER. Z. Physik. Chem. Leipsig, **A187**, 257 (1940).
23. A. STERN and H. WENDERLEIN. Z. Physik. Chem. Leipsig, **A170**, 337 (1934).

Can. J. Chem. Downloaded from www.nrcresearchpress.com by 210.87.254.105 on 09/05/12
For personal use only.

Can. J. Chem. Downloaded from www.nrcresearchpress.com by 210.87.254.42 on 09/05/12
For personal use only.

QUINODIMETHANE CHEMISTRY

THE GENERATION AND TRAPPING OF QUINODIMETHANES FROM SUBSTITUTED AROMATIC HYDROCARBONS WITH HIGH-POTENTIAL QUINONES

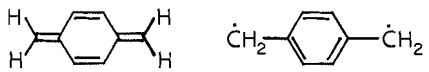
J. W. Lown and A. S. K. Aidoo
Department of Chemistry, University of Alberta, Edmonton, Alberta

Received June 17, 1966

ABSTRACT

9,10-Dimethylanthracene and 9,10-dimethyl-9,10-dihydroanthracene react with 2 and 3 moles, respectively, of tetrachloro-1,2-benzoquinone to give the same 1:1 adduct of 9,10-anthraquinodimethane with the quinone, the structure of which was proved by ozonolysis. A lower limit for the rate of adduct formation in 1,2-dichlorobenzene at 80° is 4.22×10^{-2} l mole^{-1} s^{-1}. 7,12-Dimethylbenzanthraquinodimethane was generated in a similar way and the structure of the 1:1 adduct proved by ozonolysis and by mass spectrometry. The reaction of 9,10-anthraquinodimethane with a *p*-quinone gave a 1:2 adduct. 9-Methylanthracene reacts with high-potential quinones by hydride abstraction at the methyl group with the formation of an ether.

Quinodimethanes or *p*-xylylenes are of considerable interest both from the theoretical and experimental standpoints. The first evidence of their existence was obtained from the pyrolysis of *p*-xylene (1, 2), and subsequent investigations of the pyrolysis of related compounds proved that analogues of *p*-xylylene can be produced by similar techniques (2–5). More recently, *p*-xylylenes have been produced as reactive intermediates by the reaction of magnesium with 4-methoxymethylbenzyl chloride (6) and the decomposition of trimethyl-4-methylbenzyl ammonium hydroxide (7–10). Errede and Landrum (11) discovered that solutions of *p*-xylylene are relatively stable at low temperatures. That *p*-xylylene exists in the quinodimethane form I rather than as a diradical II is shown by its spectra and its diamagnetism. It is extremely reactive and polymerizes readily, but controlled polymerization leads to compounds of low molecular weight, including [2,2]-paracyclophane.

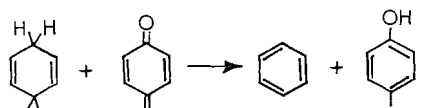


I II

Recently, a novel method has been introduced by Millar and Wilson (12, 13) and Stille and Foster (14), namely, the dehydration of the appropriate tertiary diols in high-boiling solvents such as diethyl phthalate. In this way, quinodimethanes derived from the anthracene and phenanthrene series have been generated and trapped by dienophiles, such as maleic anhydride, benzoquinone, and dimethyl acetylene dicarboxylate.

An interest in the homogeneous dehydrogenation of hydroaromatic compounds with high-potential quinones (15) led us to investigate the dehydrogenation of aromatic hydrocarbons as a method of generating quinodimethanes.

The driving force for the hydrogen transfer reaction, represented schematically below,



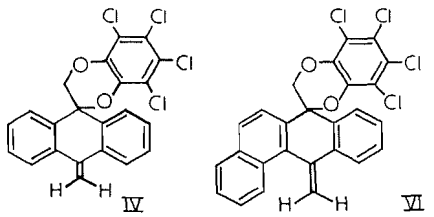
III

is provided by the gain in resonance energy of both reactants (15). Molecular orbital calculations predict that the resonance energy of *p*-xylylenes is comparable with that of the benzenoid precursor (16) (e.g. *p*-xylylene itself has a resonance energy of 38 kcal/mole compared with ca. 36 kcal/mole for *p*-xylene). Therefore, the dehydrogenation of a dimethyl aromatic hydrocarbon to a quinodimethane is energetically feasible. The generating reactant also acts as a dienophile, and therefore will trap the quinodimethane. Since the reaction is homogeneous, unlike the various methods described above, order-of-magnitude estimates may be made of the rate of the reaction between the quinodimethane and the dienophile, as shown below. By using different quinones, information is obtained on the steric requirements of the subsequent reactions.

9,10-Anthraquinodimethane

Previous attempts to prepare anthraquinodimethane by the pyrolysis of 9,10-dimethylanthracene were unsuccessful (2). Dehydration of 9,10-dimethyl-9,10-dihydroxy-9,10-dihydroanthracene in boiling diethyl phthalate in the presence of a dienophile gave 1:1 or 1:2 adducts (13, 17). We have observed that *cis*-9,10-dimethyl-9,10-dihydroanthracene (18) reacts readily with 3 moles of tetrachloro-1,2-benzoquinone and that the reaction is not confined to a simple dehydrogenation to 9,10-dimethylanthracene. The product mixture was complex, but by repeated chromatography in benzene on alumina a colorless crystalline compound, $C_{22}H_{12}Cl_4O_2$, could be isolated in a pure form in a 16.2% yield. The low yield reflects the difficulty of separation from other components of high molecular weight (estimated ca. 880), presumably arising from rapid polymerization of the anthraquinodimethane, as has often been observed in other methods of generating this type of intermediate (1, 2, 13, 14).

The nuclear magnetic resonance (n.m.r.) spectrum of the compound exhibited singlets which were each equivalent to two protons in the regions characteristic (19) of olefinic protons and protons of the type —CH_2—O—, respectively. There was also a complex band arising from eight aromatic protons. The infrared spectrum contained no bands attributable to carbonyl stretching, but exhibited a very strong band at 1 422 cm^{-1} characteristic of a tetrachlorobenzodioxin (20). The ultraviolet spectrum was compatible with the presence of a 1,1-diphenylethylene chromophor. This evidence leads to the formulation IV as the structure of this compound, and its formation is attributed to the addition of 1 mole of tetrachloro-1,2-benzoquinone to the carbon–carbon double bond at the 9 position of the anthraquinodimethane intermediate.



IV VI

The structure was confirmed by ozonolysis, which gave formaldehyde (isolated as the dimedone derivative) and a yellow solid V, $C_{21}H_{10}Cl_4O_3$, the n.m.r. spectrum of which resembles that of IV except for the absence of the olefinic band. The infrared spectrum of V shows a strong carbonyl absorption, as expected.

9,10-Dimethylanthracene similarly reacts with 2 moles of tetrachloro-1,2-benzoquinone to give IV as the main isolable product. The deep-red color of the quinone allows measurement of the reaction rates by a simple spectrokinetic procedure, the details of which have

Can. J. Chem. Downloaded from www.nrcresearchpress.com by 210.87.254.42 on 09/05/12
For personal use only.

been presented elsewhere (21). It was thus shown that *cis*- and *trans*-9,10-dimethyl-9,10-dihydroanthracene undergo rapid, triply consecutive, second-order reactions with 3 moles of the quinone, with a relatively slow initial step. The reaction of 9,10-dimethylanthracene and tetrachloro-1,2-benzoquinone, which was bimolecular, consecutive second order with a fast second step (i.e. Diels–Alder reaction of the quinodimethane with the quinone), was 30–60 times faster than the reaction of the dihydrodimethylanthracenes.

On the basis of the evidence of the isolated product and the rate data, the following two series of reactions can be postulated.

Scheme 1

$$RH_4 + Q \xrightarrow{k_1} RH_2 + QH_2$$

$$RH_2 + Q \xrightarrow{k_2} RH_2Q$$

$$RH_2Q + Q \xrightarrow{k_3} QH_2 + RQ$$

k_2 and $k_3 \gg k_1$

Scheme 2

$$RH_4 + Q \xrightarrow{k_1} RH_2 + QH_2$$

$$RH_2 + Q \xrightarrow{k_2} R + QH_2$$

$$R + Q \xrightarrow{k_3} RQ$$

k_2 and $k_3 \gg k_1$

RH_4 represents 9,10-dihydro-9,10-dimethylanthracene, RH_2 represents 9,10-dimethylanthracene, R represents 9,10-anthraquinodimethane, and RQ represents the isolated product IV. Scheme 1 implies the formation of an intermediate Diels–Alder addition compound (RH_2Q) of 9,10-dimethylanthracene and tetrachloro-1,2-benzoquinone, which is then attacked at the CH_3 groups by a further molecule of quinone with the formation of IV. Scheme 2 represents the simpler mechanism, in which 9,10-dimethylanthracene is dehydrogenated directly to the 9,10-anthraquinodimethane (R), which undergoes Diels–Alder addition with the quinone to yield IV. Scheme 1 is rendered unlikely by the following observation. 9,10-Dimethyl-9,10-dihydro-9,10-ethanoanthracene-11,12-dicarboxylic anhydride (i.e. the Diels–Alder addition compound of 9,10-dimethylanthracene and maleic anhydride), in which the CH_3 groups are in an environment similar to that in the hypothetical intermediate RH_2Q, is completely inert to the action of tetrachloro-1,2-benzoquinone in 1,2-dichlorobenzene at 101° for 44 h. Since the rate data obtained are consistent only when k_3 is much greater than k_1, scheme 1 is rejected; the results are therefore interpreted in terms of scheme 2 involving the intermediacy of 9,10-anthraquinodimethane (see Experimental). Therefore, a lower limit for the reaction rate of 9,10-anthraquinodimethane with tetrachloro-1,2-benzoquinone in 1,2-dichlorobenzene at 80° is 4.22×10^{-2} l mole^{-1} s^{-1}.

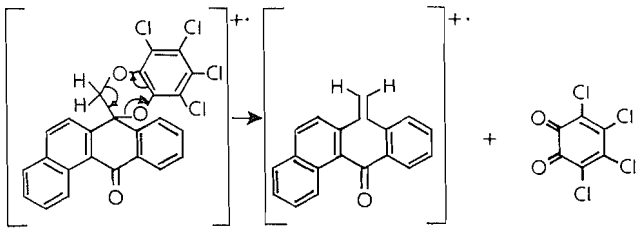
The reaction of anthraquinodimethane, generated *in situ* by refluxing 9,10-dimethyl-9,10-dihydroxy-9,10-dihydroanthracene in ethyl phthalate, with tetrachloro-1,2-benzoquinone led only to tars. This result is not unexpected since the chloroquinone is sensitive to water and can undergo a variety of side reactions.

7,12-Benzanthraquinodimethane

7,12-Dimethylbenzanthracene reacted readily with tetrachloro-1,2-benzoquinone in benzene, and the main product was a colorless crystalline solid, $C_{26}H_{14}O_2Cl_4$, the spectral properties of which confirmed a 1:1 adduct of benzanthracenequinodimethane and tetrachloro-1,2-benzoquinone. Considerations of steric hindrance predict an orientation for the quinone at the double bond remote from the fused benzo ring corresponding to VI. This assignment is supported by the n.m.r. spectrum, which shows the olefinic protons to be non-equivalent owing to the different effects of the ring current from the angular benzene ring, in contrast to the equivalent protons shown by IV. Treatment with ozone

Can. J. Chem. Downloaded from www.nrcresearchpress.com by 210.87.254.42 on 09/05/12
For personal use only.

followed by decomposition of the ozonide with steam gave a yellow solid, the n.m.r. spectrum of which showed the absence of vinyl protons; the infrared spectrum showed a new carbonyl. Mass spectrometry showed a molecular ion peak measuring 499.9543, compared with 499.9540 calculated for $C_{25}H_{12}O_3Cl_4$. A strong peak in the spectrum at *m/e* 256 was expected and is due to the following fragmentation.



This interpretation is based on the very recent analogy provided by the mass spectrum of an adduct of tetrachloro-1,2-benzoquinone and abietic acid (22).

Reactions with Other Quinones

It was anticipated that the reaction of anthraquinodimethane with a *p*-quinone would give rise to different adducts owing to the different geometrical requirements of the dienophile. 9,10-Dimethylanthracene reacts very readily with 2,3-dichloro-5,6-dicyanobenzoquinone, and a bright-yellow solid, $C_{32}H_{12}N_4Cl_4O_4$, was isolated from the reaction mixture. The infrared spectrum exhibited bands characteristic of C≡N and enedione groupings. The n.m.r. spectrum (Fig. 1) was compatible with structure VIII, i.e. a

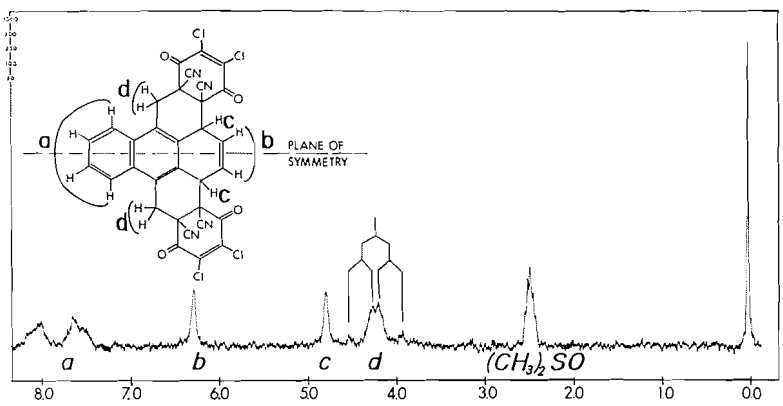
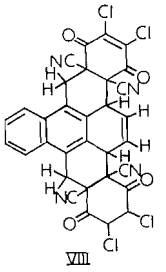


FIG. 1.

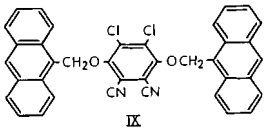
4,5-benzpyrene skeleton. The structure is analogous to similar 1:2 adducts obtained by Millar and Wilson by the reaction of anthraquinodimethane, generated by the dehydration of 9,10-dimethyl-9,10-dihydroxy-9,10-dihydroanthracene, with various dienophiles (12, 13). The simplicity of the n.m.r. spectrum supports the proposed 4,5-benzpyrene structure, which has a plane of symmetry, if the quinone rings are *cis* to one another and if both are *cis*-fused at the carbons bearing the nitrile groups (as expected) or, less likely, symmetrically *trans*-fused. The orientation of the 2,3-dichloro-5,6-dicyanobenzoquinone moieties

Can. J. Chem. Downloaded from www.nrcresearchpress.com by 210.87.254.42 on 09/05/12
For personal use only.

is based, by analogy, on the studies of Ansell (23), in which the powerfully electron-attracting nitrile groups so enhance the dienophilic character of the double bond to which they are attached that addition takes place exclusively at this bond. Attempts to prove this point by the base-catalyzed elimination of hydrocyanic acid were unsuccessful owing to the general lability of the substance towards the action of strong bases.



VIII



IX

The reactivity of the 9-methyl group in anthracene derivatives towards hydride abstraction is not confined to 9,10-disubstituted compounds. 9-Methylanthracene reacted readily with 2,3-dichloro-5,6-dicyanobenzoquinone and gave a yellow solid, $C_{38}H_{22}Cl_2N_2O_2$, the infrared spectrum of which showed bands characteristic of ether and nitrile linkages. The material is assigned structure IX by analogy with a similar ether obtained by the reaction of 2,2-dimethylindane with the same quinone (20), and the structure was proved by cleavage of the ether linkage with hydriodic acid and reduction of the resulting 9-iodomethyleneanthracene with lithium aluminium hydride to 9-methylanthracene.

The scope of the above method of generating *p*- and *o*-quinodimethanes in other systems, particularly the phenanthrene and acepleiadylene series, is being investigated.

EXPERIMENTAL

Melting points were taken on a Fisher–Johns apparatus and are uncorrected. Infrared spectra were recorded on a Perkin–Elmer model 421 spectrophotometer. Only the principal, sharply defined peaks are reported. Nuclear magnetic resonance spectra were recorded on a Varian A-60 analytical spectrometer operating at a fixed radiofrequency of 60 Mc.p.s. The spectra were measured on an approximately 15% (w/v) solution in an appropriate solvent, with tetramethylsilane as a standard. Line positions are reported in parts per million from the reference. Absorption spectra were recorded in 'spectro'-grade solvents on a Beckman DB recording spectrophotometer. Mass spectra were obtained on an AEI-MS-9 high-resolution mass spectrometer. Microanalyses were carried out by Dr. C. Daesslé, Organic Microanalyses Ltd., Montreal, Quebec, and by Miss D. Roberts, Microanalytical Laboratory, Chemistry Department, University of Alberta, Edmonton, Alberta.

Reaction of 9,10-Dimethylanthracene with Tetrachloro-1,2-benzoquinone

A mixture of 4.506 g (0.022 mole) of 9,10-dimethylanthracene and 10.822 g (0.044 mole) of tetrachloro-1,2-benzoquinone in 100 ml of sodium-dried benzene was refluxed under nitrogen for 2 days, cooled, diluted with 150 ml of *n*-hexane, and filtered to remove hydroquinone. The filtrate was concentrated *in vacuo* to ca. 40 ml and passed down a column of grade I alumina to remove hydroquinone and unreacted quinone. Elution with 1:1 benzene–*n*-hexane and evaporation of the solvents gave a pale-yellow crystalline solid (2.3 g) as the first fraction. Careful chromatography of this fraction on alumina in 1:2 benzene–*n*-hexane gave, as the main component, a colorless crystalline solid (1.75 g, 18% yield), which was purified by recrystallization from ethyl acetate, m.p. 240° (decomp.).

Anal. Calcd. for $C_{22}H_{13}Cl_4O_2$ (450.12): C, 58.6; H, 2.9; Cl, 31.50. Found: C, 58.4; H, 3.2; Cl, 31.9; mol. wt. (ebullioscopic in benzene) 444.4.

Infrared spectrum: ν_{max} ($CHCl_3$) 1 422 cm^{-1} (s) (characteristic (20) of a six-membered tetrachlorobenzodioxan structure); no absorption in the region expected for OH or C=O. Nuclear magnetic resonance spectrum ($CDCl_3$): 5.80 (2H, singlet, vinyl protons), 3.94 (2H, singlet, $—CH_2—O$), 7.44 (8H, complex aromatic absorption). Absorption spectrum (cyclohexane): λ_{max} 302 mμ (log ε 3.48), 253 mμ (sh) (log ε 4.20), 230 mμ (sh) (log ε 4.59).

Subsequent fractions of the chromatogram consisted of mixtures of minor, higher molecular weight, colored products which could not be separated.

Can. J. Chem. Downloaded from www.nrcresearchpress.com by 210.87.254.42 on 09/05/12
For personal use only.

Reaction between cis-9,10-Dimethyl-9,10-dihydroanthracene and Tetrachloro-1,2-benzoquinone

A mixture of 1.032 g (0.0048 mole) of *cis*-9,10-dimethyl-9,10-dihydroanthracene (obtained by the reduction of 9,10-dimethylanthracene with sodium and ethanol (18) and 3.786 g (0.0154 mole) of tetrachloro-1,2-benzoquinone in 30 ml of dry benzene was refluxed for 12 h, then cooled, diluted with 100 ml *n*-hexane, and filtered. The filtrate was concentrated to ca. 40 ml and passed down a column of grade I alumina. Elution with 1:1 benzene–*n*-hexane and evaporation of the eluate gave a yellow solid (0.52 g), shown by thin-layer chromatography to be a mixture. Careful re-chromatography of this fraction on alumina in 1:2 benzene–*n*-hexane gave, as the main component, a colorless crystalline solid, which was purified by recrystallization from ethyl acetate (0.35 g, 16.2% yield), m.p. 240°, mixed m.p. with the pure product isolated from the previous reaction 240°. The spectral properties of the two samples were identical.

Again, subsequent fractions of both chromatograms proved to be complex mixtures of high molecular weight components, and no attempt was made to separate them.

Ozonolysis of the Adduct of Anthraquinodimethane and Tetrachloro-1,2-benzoquinone

A slow stream of dry ozone (from a Welsbach T-23 ozonator) was passed successively through a solution of 223 mg (0.0005 mole) of the adduct dissolved in 80 ml ethyl acetate in a 250 ml Dreschel bottle and a second bottle containing 50 ml of water, until ozone was detected in the effluent with moist starch – potassium iodide paper. The two liquids were combined and subjected to steam-distillation; a yellow solid separated in the flask. The steam-distillate was made neutral to phenolphthalein, and a solution of 3 g of 5,5-dimethyl-1,3-cyclohexanedione in 50 ml of 50% ethanol added. After 60 min the precipitate of formaldehyde dimedone was collected, washed with 5 ml of 20% aqueous ethanol, and dried (0.102 g, 0.7 mole).

The yellow solid was collected, dried, and purified by recrystallization from acetonitrile (0.180 g, 80% yield), m.p. 270°.

Anal. Calcd. for $C_{21}H_{10}O_3Cl_4$: C, 55.79; H, 2.23; Cl, 31.36. Found: C, 55.81; H, 2.48; Cl, 31.05.

Infrared spectrum: ν_{max} (KBr disk) 1 422 cm^{-1} (s) (characteristic of a six-membered tetrachlorobenzodioxin structure (20)), 1 672 cm^{-1} (C=O stretching). Nuclear magnetic resonance spectrum ($CDCl_3$): 4.06 (2H, singlet, $—CH_2O—$), 7.45 (8H, complex aromatic absorption); no vinyl absorption was present. Absorption spectrum (CH_3CN): λ_{max} 3.05 mμ (sh) (log ε 3.42), 264 mμ (log ε 4.68), 230 mμ (sh) (log ε 4.38).

Reaction of 7,12-Dimethylbenzanthracene and Tetrachloro-1,2-benzoquinone

A solution of 1 g (0.0032 mole) of 7,12-dimethylbenzanthracene and 2.06 g (0.0084 mole) of tetrachloro-1,2-benzoquinone in 20 ml of dry benzene was refluxed for 3 days, then cooled, and chromatographed on grade I alumina. The column was developed and eluted with 1:1 benzene–*n*-hexane. Evaporation of the first fraction gave a pale-yellow crystalline solid, which gave a single spot on thin-layer chromatography in a variety of solvents and was recrystallized from 1:1 benzene–*n*-hexane, m.p. 247° (decomp.) (0.375 g, 19% yield). Subsequent chromatographic fractions gave a yellow material, which was shown by thin-layer chromatography to be a complex mixture of minor products which were not investigated further.

Anal. Calcd. for $C_{26}H_{14}O_2Cl_4$: C, 62.43; H, 2.82; Cl, 28.77. Found: C, 62.57; H, 2.70; Cl, 28.90.

Infrared spectrum: ν_{max} ($CHCl_3$) 1 422 cm^{-1} (s) (characteristic of a six-membered tetrachlorobenzodioxan structure (20)). Nuclear magnetic resonance spectrum ($CDCl_3$): 4.10 (2H, singlet, $—CH_2—O$), 5.93 and 6.12 (1H, each narrow doublets, $J_{ab} < 1$ c.p.s., vinyl protons), 7.30–8.00 (10H, complex aromatic absorption). Absorption spectrum (cyclohexane): λ_{max} 302 mμ (log ε 4.07), 290 mμ (sh) (log ε 3.98), 232 mμ (log ε 4.86).

Ozonolysis of the Adduct of Benzanthraquinodimethane and Tetrachloro-1,2-benzoquinone

A solution of 47 mg (0.000095 mole) of the adduct in 70 ml of ethyl acetate was subjected to ozonolysis under conditions similar to those described for the anthraquinodimethane adduct. Decomposition of the ozonide with steam gave a yellow crystalline solid (27 mg, 51% yield), m.p. 253°. The mass spectrum showed a parent peak with an isotopic pattern typical of four chlorine atoms, measured as 499.9543 (calcd. for $C_{25}H_{12}O_3Cl_4$: 499.9540). A strong peak at *m/e* 256 was caused by the retro-Diels–Alder fragmentation typical of this type of adduct, as described in the Discussion.

Infrared spectrum: ν_{max} (KBr disk) 1 422 cm^{-1} (s) (characteristic of a six-membered tetrachlorobenzodioxin structure (20), 1 670 cm^{-1} (C=O). Nuclear magnetic resonance spectrum ($CDCl_3$): 4.16 (2H, singlet, $—CH_2—O—$), 7.3–8.1 (10H, complex aromatic absorption); no vinyl absorption was present. Absorption spectrum (CH_3CN): λ_{max} 292 mμ (log ε 3.55), 258 mμ (sh) (log ε 3.59), 232 mμ (sh) (log ε 3.99).

Reaction of 9,10-Dimethylanthracene with 2,3-Dichloro-5,6-dicyanobenzoquinone

A solution of 2.027 g (0.0099 mole) of 9,10-dimethylanthracene in 75 ml of warm benzene was added to a solution of 6.79 g (0.03 mole) of 2,3-dichloro-5,6-dicyanobenzoquinone in 225 ml of warm benzene, with shaking. There was an immediate darkening of the solution caused by charge transfer complexing; then a copious yellow precipitate separated. The mixture was refluxed for 7 h and cooled, and the solid was collected. Extraction of the solid with hot acetone left the insoluble brown hydroquinone, and evaporation of the extract gave adduct VIII as a bright-yellow crystalline solid (1.86 g, 28.2% yield), m.p. 217° (decomp.).

Anal. Calcd. for $C_{32}H_{12}O_4N_4Cl_4$ (658.38): C, 58.38; H, 1.85; N, 8.51; Cl, 21.54. Found: C, 58.44; H, 2.30; N, 8.36; Cl, 21.74; mol. wt. (by mass spectrometry) 656 (^{35}Cl).

Can. J. Chem. Downloaded from www.nrcresearchpress.com by 210.87.254.42 on 09/05/12
For personal use only.

Can. J. Chem. Downloaded from www.nrcresearchpress.com by 210.87.254.42 on 09/05/12
For personal use only.

Infrared spectrum: ν_{max} (Nujol mull) 1 726 cm^{-1} (br) (enedione C=O), 2 245 cm^{-1} (m) (C≡N). Nuclear magnetic resonance spectrum ($(CD_3)_2SO$): 4.82 (2H, singlet, 'angular' protons), 6.32 (2H, singlet, vinyl protons), 7.50–8.30 (4H, A_2B_2 aromatic protons), AB quartet, J = 16 c.p.s., centers of gravity at 4.17 and 4.37 (CH_2 protons). (See Fig. 1.) Absorption spectrum (CH_3CN): λ_{max} 375 mμ (log ε 3.19), 278 mμ (log ε 4.31), 260 mμ (sh) (log ε 4.25), 234 mμ (log ε 4.75).

Reaction of 9-Methylanthracene with 2,3-Dichloro-5,6-dicyanobenzoquinone

A solution of 2.4 g (0.0106 mole) of 2,3-dichloro-5,6-dicyanobenzoquinone in 45 ml of dry benzene was added to a solution of 1 g (0.0052 mole) of 9-methylanthracene in 5 ml of dry benzene. The solution darkened, and after it was refluxed for 10 min a light-yellow precipitate separated. The mixture was refluxed for 2 h and cooled, and the solid was collected by filtration. The major product was insoluble in chloroform, methanol, acetonitrile, dimethyl sulfoxide, and benzene, and was purified by Sohxlet extraction from it of impurities with methanol, leaving a bright-yellow solid (1.1 g, 34.6% yield), m.p. 215° (decomp.).

Anal. Calcd. for $C_{38}H_{22}Cl_2N_2O_2$ (609.482): C, 74.87; H, 3.61; Cl, 11.66; N, 4.61. Found: C, 74.74; H, 3.88; Cl, 11.98; N, 4.42; mol. wt. (by mass spectrometry) 608 (^{35}Cl).

Infrared spectrum: ν_{max} (KBr disk) 1 425 cm^{-1} (s) (C—O—C linkage (20)), 2 216 cm^{-1} (C≡N).

Adduct IX (0.227 g, 0.00036 mole) was refluxed with a mixture of 5 ml of 57% hydriodic acid and 3 ml of water for 8 h. White crystals of 9-iodomethyleneanthracene (45 mg), m.p. 65–66°, which had sublimed into the condenser were removed and dried *in vacuo*. The substance, without further purification, was dissolved in 10 ml of dry ether, treated with a solution of 85 mg of lithium aluminium hydride, and stirred for 4 h. The mixture was cooled, unreacted hydride decomposed with water, and the organic layer removed. Evaporation of the ether gave yellow crystals of 9-methylanthracene, m.p. 74–75°, mixed m.p. with authentic 9-methylanthracene 74–75°. The n.m.r. spectrum in $CDCl_3$ was identical with that of an authentic sample of the hydrocarbon.

Control Reaction of 9,10-Dimethyl-9,10-dihydro-9,10-ethanoanthracene-11,12-dicarboxylic Anhydride with Tetrachloro-1,2-benzoquinone

A mixture of 1.18 g (0.0039 mole) of 9,10-dimethyl-9,10-dihydro-9,10-ethanoanthracene-11,12-dicarboxylic anhydride and 1.65 g (0.0068 mole) of the quinone in 45 ml of dry 1,2-dichlorobenzene was heated in a constant-temperature bath at 101° for 44 h. The mixture was concentrated to a small volume and cooled, and the white crystalline solid was collected and washed with benzene, yielding the unchanged adduct (1.09 g, 92% recovery), m.p. 330°, mixed m.p. with an authentic sample 330° (lit. (25) m.p. 333–335°).

Kinetic Experiments

Materials

Pure 1,2-dichlorobenzene was distilled from sodium and had b.p. 177–178° at 750 mm, n_D^{22} 1.5518 (24). Commercial samples of tetrachloro-1,2-benzoquinone and 2,3-dichloro-5,6-dicyanobenzoquinone were purified by sublimation and by recrystallization from benzene–*n*-hexane, respectively, the benzene of crystallization being removed in a vacuum desiccator.

Reaction Rates

The rates were determined by following spectrophotometrically the disappearance of the colored quinone. The E_0 values were determined by graphical extrapolation. The experimental method used and detailed treatment of the rate data have been described previously (21).

Kinetic Equations Employed

Let a mole l^{-1} = the initial concentration of quinone; let b mole l^{-1} = the initial concentration of hydrocarbon; let x mole l^{-1} = the amount of quinone consumed at time t; let the initial extinction of the quinone at 5 600 Å be E_0; let the extinction of the quinone at 5 600 Å at time t be E. The meaning of the symbols RH_2, RH_2, and R used below is explained in the Discussion.

Bimolecular, Consecutive, Second-Order Reaction with Fast Second Step

$$\underset{(b-x)}{RH_2} + \underset{(a-x)}{Q} \xrightarrow{k} \underset{x}{R} + \underset{x}{QH_2}; \quad \underset{x}{R} + \underset{x}{Q} \xrightarrow{k_2} \underset{(a-x)}{RQ}$$

The overall rate expression when $k_2 \gg k$ is

$$dx/dt = k(b - x)(a - 2x).$$

Integration leads to

$$k = \frac{1}{(2b - a)t} \ln \left(\frac{a}{b} \cdot \frac{b - x}{a - 2x} \right).$$

$E_0 = \lambda a$; $E = \lambda(a - 2x)$; therefore, $E + E_0 = 2\lambda(a - x)$, where λ is a proportionality constant.

When $(b - x) = a\left(\frac{b}{a} - 1\right) + (a - x)$ is substituted,

$$k = \frac{1}{(2b - a)t} \ln \left[\frac{a}{b} \cdot \frac{E_0\left(\frac{b}{a} - 1\right) + \frac{E_0 + E}{2}}{E}\right]$$

$$k = \frac{1}{(2b - a)t} \ln\left[\frac{a}{b} \cdot \frac{E_0\left(\frac{2b}{a} - 1\right) + E}{2E}\right].$$

If $a = b$, then

$$k = \frac{1}{at} \ln\left[\frac{E_0 + E}{2E}\right].$$

Triply Consecutive, Second Order Reaction with Slow Initial Step

$$RH_4 + Q \xrightarrow{k_1} RH_2 + QH_2$$
$$RH_2 + Q \xrightarrow{k_2} R + QH_2$$
$$R + Q \xrightarrow{k_3} RQ$$

The overall rate expression when k_2 and $k_3 \gg k_1$ is $dx/dt = k_1(b - x)(a - 3x)$.
Integration leads to $(b > a)$

$$k = \frac{1}{(3b - a)t} \ln\left[\frac{a}{b} \cdot \frac{b - x}{a - 3x}\right].$$

$E_0 = \lambda a$; $E = \lambda(a - 3x)$; $(b - x) = a\left(\frac{b}{a} - 1\right) + (a - x)$; $(a - x) = 2E_0 + E/3\lambda$. Therefore,

$$k = \frac{1}{(3b - a)t} \ln\left[\frac{a}{b} \cdot \frac{E_0\left(\frac{b}{a} - 1\right) + \frac{2E_0 + E}{3}}{E}\right]$$

$$k = \frac{1}{(3b - a)t} \ln\left[\frac{a}{b} \cdot \frac{E + E_0\left(\frac{3b}{a} - 1\right)}{3E}\right].$$

Summary of Rate Constants

The units for the following rates are liters per mole per second. The initial concentration of hydrocarbon and quinone in 1,2-dichlorobenzene was 0.0100 *M*.

cis-9,10-Dihydro-9,10-dimethylanthracene

$T°$	76.4	77.0	79.4	82.0	88.1	90.6
10^3k	7.76	8.13	9.33	11.00	15.10	17.40

trans-9,10-Dihydro-9,10-dimethylanthracene

$T°$	75.2	77.5	82.8	87.1	89.9	93.9
10^3k	3.80	4.47	6.02	7.94	9.33	11.75

9,10-Dimethylanthracene

$T°$	49.4	55.1	60.5	75.6	8.16	85.0
10^2k	0.74	1.00	1.48	3.35	4.62	5.45

Arrhenius Rate Parameters

The Arrhenius parameters were computed by the method of least squares and their precision (standard

Can. J. Chem. Downloaded from www.nrcresearchpress.com by 210.87.254.42 on 09/05/12
For personal use only.

deviation) by the equations set out in in a previous paper (21). The values of $k_{obs.}$ at 80° were obtained by least-squares interpolation.

Hydrocarbon	$k_{80°}$ (l mole^{-1} s^{-1})	E (kcal/mole)	$\log_{10} B$
cis-9,10-Dihydro-9,10-dimethylanthracene	$9.98\pm0.18\times10^{-3}$	14.65 ± 0.53	7.03
trans-9,10-Dihydro-9,10-dimethylanthracene	$5.27\pm0.16\times10^{-3}$	15.00 ± 0.40	6.97
9,10-Dimethylanthracene	$4.22\pm0.10\times10^{-2}$	12.96 ± 0.16	6.65

ACKNOWLEDGMENTS

This research was supported by a National Research Council of Canada grant to J. W. L. Preliminary work in this study was carried out while one of us (J. W. L.) was in the Chemistry Department of Imperial College, London. The n.m.r. and mass spectra were measured by R. N. Swindlehurst and Dr. A. Hogg of this laboratory, respectively.

REFERENCES

1. M. Szwarc. Discussions Faraday Soc. **2**, 46 (1947).
2. M. Szwarc. J. Polymer Sci. **6**, 319 (1951).
3. M. Szwarc. J. Chem. Phys. **16**, 128 (1948).
4. L. Errede and B. F. Landrum. J. Am. Chem. Soc. **79**, 4952 (1957).
5. Roper. U.S. Patent No. 2,798,052 (1957).
6. F. G. Mann and F. H. C. Stewart. J. Chem. Soc. 2826 (1954).
7. H. E. Winberg, F. S. Fawcett, W. E. Mochel, and C. W. Theobald. J. Am. Chem. Soc. **82**, 1428 (1960).
8. P. D. Gardner and H. Sarrafizadeh. J. Am. Chem. Soc. **82**, 4287 (1960).
9. D. J. Cram and G. R. Knox. J. Am. Chem. Soc. **83**, 2204 (1961).
10. L. A. Errede. J. Am. Chem. Soc. **83**, 949 (1961).
11. L. A. Errede and B. F. Landrum. J. Am. Chem. Soc. **79**, 4952 (1957).
12. I. T. Millar and K. V. Wilson. Proc. Chem. Soc. 217 (1963).
13. I. T. Millar and K. V. Wilson. J. Chem. Soc. 2121 (1964).
14. T. K. Stille and R. T. Foster. J. Org. Chem. **28**, 2708 (1963).
15. L. M. Jackman. *In* Advances in organic chemistry. Vol. II. Interscience Publishers, Inc., New York. 1960. p. 329, and references therein.
16. C. A. Coulson, D. P. Craig, A. Maccoll, and A. Pullman. Discussions Faraday Soc. **2**, 36 (1947).
17. I. T. Millar and K. E. Richards. Chem. Commun. **15**, 369 (1965).
18. L. M. Jackman and J. W. Lown. J. Chem. Soc. 3776 (1962).
19. L. M. Jackman. Applications of nuclear magnetic resonance spectroscopy in organic chemistry. Pergamon Press, New York. 1959.
20. E. A. Braude, L. M. Jackman, R. P. Linstead, and G. Lowe. J. Chem. Soc. 3123 (1960).
21. E. A. Braude, L. M. Jackman, R. P. Linstead, and J. S. Shannon. J. Chem. Soc. 3116 (1960).
22. T. R. Kasturi, E. Raghavan, S. Dev, and D. K. Banerjee. Tetrahedron, **22**, 745 (1966).
23. M. F. Ansell, G. C. Culling, B. W. Nash, and J. W. Lown. Proc. Chem. Soc. 405 (1960).
24. T. Carswell. Ind. Eng. Chem. **20**, 728 (1928).
25. W. E. Bachmann and M. C. Kloetzel. J. Am. Chem. Soc. **60**, 481 (1938).

Can. J. Chem. Downloaded from www.nrcresearchpress.com by 210.87.254.42 on 09/05/12
For personal use only.

Can. J. Chem. Downloaded from www.nrcresearchpress.com by 210.87.254.5 on 09/05/12
For personal use only.

STEROIDS AND STEROIDASES

III. DICYCLOHEXYLCARBODIIMIDE – DIMETHYL SULFOXIDE OXIDATIONS OF ALCOHOLS AND THIOLS[1]

J. BRYAN JONES AND DONALD C. WIGFIELD

Lash Miller Laboratories, Department of Chemistry, University of Toronto, Toronto, Ontario

Received July 4, 1966

ABSTRACT

A survey of methods for the preparation of acid- and base-labile steroid Δ^5-3-ketones showed that oxidation of the appropriate Δ^5-3β-alcohols with dicyclohexylcarbodiimide – dimethyl sulfoxide (Moffatt reagent) was the most satisfactory, giving yields of 60–70% of the required ketones with little or no isomerization to the corresponding Δ^4-3-ketones. From the oxidation of 3β-hydroxyandrost-5-en-17-one, the product of a Pummerer rearrangement, 3β-(methylthiomethoxy)-androst-5-en-17-one, was isolated. The Moffatt reagent also was convenient for the oxidation of thiols to the corresponding disulfides.

In connection with studies related to the mechanism of action and specificity of the Δ^5-3-ketosteroid isomerase of *Pseudomonas testosteroni*, it became necessary to prepare several Δ^5-3-ketosteroids in a high state of purity. In the past, this has presented some difficulty because of the ease with which these compounds isomerize to the corresponding Δ^4-3-ketosteroids in the presence of traces of acid or base or when heat was applied. The problem is particularly acute for androst-5-ene-3,17-dione (II*a*), which is the substrate normally used in assaying the isomerases derived from both bacterial and mammalian sources (1).

Before 1963, the routes followed in the preparation of II*a* were those of Djerassi and his co-workers (2), using chromium trioxide oxidation of the 3β-alcohol I*a*, and of Butenandt and Schmidt-Thomé (3), in which the double bond of I*a* was protected by reaction with bromine before oxidation of the 3β-hydroxyl group. The physical properties reported in the literature for II*a* prepared by these methods were not consistent, and it was decided to investigate both routes to establish the optimum conditions for the preparation of the pure Δ^5-3-keto substrates.

Application of the chromic acid method (2) to 3β-hydroxyandrost-5-en-17-one (I*a*) gave a product whose melting point and specific rotation were identical with those reported previously (2, 4). However, thin-layer chromatographic analysis showed it to be a mixture of the starting alcohol, the required Δ^5-3-ketone II*a*, and some of the product of the subsequent acid-catalyzed isomerization, androst-4-ene-3,17-dione (III). Isolation of a pure sample of II*a* from the mixture could not be achieved.

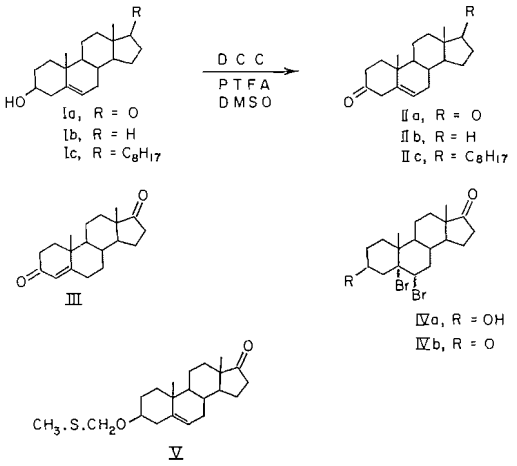
The alternative method, involving addition of bromine to I*a*, followed by chromic acid oxidation of the dibromide IV*a* and subsequent debromination of IV*b* with zinc, proved to be rather tedious, but by using a modification (5) of the original (3) method, low yields of thin-layer chromatographically pure II*a* were obtained. The difficulties encountered in this method were due mainly to the instability of the intermediate dibromoketone IV*b*, which rapidly underwent considerable photolytic decomposition (cf. ref. 6).

Fortunately, the elegant procedure reported in 1963 by Pfitzner and Moffatt (7) with DCC,[2] PTFA, and DMSO enabled the oxidation of the 3β-alcohols I to be carried out

[1]*For part II, see J. B. Jones, V. Vlasinich, and J. D. Leman, Can. J. Biochem., 44, 1183 (1966).*

[2]*The following abbreviations have been used: DCC, N,N'-dicyclohexylcarbodiimide; DMSO, dimethyl sulfoxide; PTFA, pyridinium trifluoroacetate; t.l.c., thin-layer chromatography.*

under mild neutral conditions, thereby obviating most of the problems associated with the preparation of Δ^5-3-ketosteroids. By the application of slightly modified conditions for the Moffat oxidation, good yields (~70%) of androst-5-ene-3,17-dione (II*a*), androst-5-en-3-one (II*b*), and cholest-5-en-3-one (II*c*) have been obtained from the 3β-alcohols I*a*, I*b*, and I*c*, respectively.



During a survey carried out to determine the molar proportion of DCC required for optimum yields of the Δ^5-3-ketones, an oxidation was attempted with equimolar proportions of the alcohol I*a*, DCC, and PTFA. Under these conditions, only a 5% yield of the β,γ-unsaturated ketone II*a* was produced together with 5% of 3β-(methylthiomethoxy)-androst-5-en-17-one. Structure V was assigned to the latter compound on the basis of its acid hydrolysis to I*a* and its spectral data.[3] The formation of methylthiomethoxy compounds as by-products of the Moffatt oxidation of several other alcohols has now been reported (7–11).

The data currently available (7–12) indicate that the methylthiomethoxy compounds are formed by Pummerer rearrangement (13) of intermediates such as VI. Formation of a methylthiomethoxy derivative from this type of intermediate can occur either by rearrangement through an ion pair such as VII (path A, Diagram 1) or intramolecularly as shown in path B, Diagram 1.[4] From the data of Johnson (14) and Parham (15) and their collaborators and by analogy with the cleavage–recombination mechanisms proposed for the Stevens and Wittig reactions (16), to which the Pummerer rearrangement seems closely related, it would appear that path A is the more probable. *N*-Trifluoroacetyl-*N*,*N*′-dicyclohexylurea (IX), which arises by rearrangement of the first-formed isourea VIII (7, 17), could be isolated from all oxidations in which DCC and PTFA were used. Its structure was confirmed by comparison with an authentic sample obtained by reaction of DCC with trifluoroacetic acid.

DCC–PTFA–DMSO mixtures were also effective in oxidizing thiols to disulfides. Treatment of benzylthiol (α-toluenethiol, XI*a*) with the reagent gave dibenzyl disulfide (XII*a*) in a quantitative yield. Since the coupling of thiol residues to form disulfide bridges plays such an important role in determining the tertiary structure of proteins, the possible application of this mild reagent for the oxidation of the thiol side chains of

[3]*Details of the proof of structure have been given in a preliminary communication (8).*

[4]*The two pathways may be differentiated formally by considering whether rearrangement occurs by migration of the* OR *group with (path A) or without (path B) the electrons of the* S—OR *bond.*

Can. J. Chem. Downloaded from www.nrcresearchpress.com by 210.87.254.5 on 09/05/12
For personal use only.

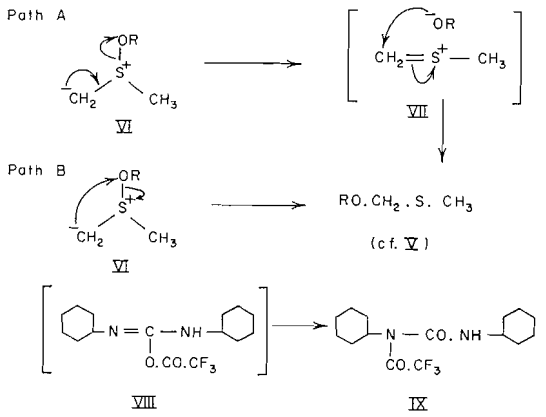


DIAGRAM 1.

cysteine derivatives was considered. The model compound selected, methyl *N*-acetyl-L-cysteinate (XI*b*), was prepared from *N*-acetyl-L-cysteine with anhydrous methanolic hydrogen chloride. On treatment with the Moffatt reagent it gave dimethyl *N*,*N*′-diacetyl-L-cystinate (XII*b*) in a high yield with little or no racemization.

The oxidation of the biologically important dithiol 6,8-dimercaptooctanoamide (XIII) to 6,8-dithiooctanoamide (XIV, lipoamide) was also investigated. Even though the reaction proceeded smoothly, the Moffatt reagent cannot be recommended for this particular oxidation, because isolation of the required lipoamide XIV from the dicyclohexylurea by-products proved to be extremely tedious and the final yields of pure material were very low.

While this communication was in preparation, Pfitzner and Moffatt (7) reported that thiols were not oxidized by the DCC–DMSO reagent. One of the mercaptans studied, *p*-chlorobenzylthiol, closely resembled the compound, benzylthiol, for which facile oxidation occurred in our hands. In view of these conflicting data, oxidation of the other mercaptan, octan-1-thiol (XI*c*), investigated by Moffatt and his co-workers was repeated. The reaction was found to proceed normally, and a 66% yield of dioctyl disulfide (XII*c*) was obtained.

The analytical method normally used for monitoring oxidations with the DCC–DMSO reagent, viz. t.l.c., was not wholly satisfactory for the above sulfur compounds since, surprisingly, some of the thiols and their corresponding disulfides, of which octan-1-thiol and dioctyl disulfide are examples, were found to have coincidental R_F values on chromatograms developed with the commonly used solvent systems.[5] Acidic spray reagents were not suitable for the t.l.c. detection of thiol–disulfide mixtures, but exposure of the plates to iodine vapor proved to be a convenient nonselective method for the detection of all the sulfur compounds studied. The disulfides could be distinguished from their thiol precursors by selective visualization of the latter with a sodium nitroprusside spray reagent. In all the reactions carried out, analysis by a combination of infrared and proton magnetic resonance spectroscopy enabled the mercaptans and their oxidation products to be identified unambiguously.

Since treatment of thiols with DMSO alone, usually for an extended period or at an elevated temperature, is known (18) to give the corresponding disulfides in a good yield,

[5]*The use of the usually reliable t.l.c. analytical methods alone for following their reactions undoubtedly misled Pfitzner and Moffatt (7) into concluding that thiols were not oxidized by the DCC–DMSO reagent.*

Can. J. Chem. Downloaded from www.nrcresearchpress.com by 210.87.254.5 on 09/05/12
For personal use only.

control experiments in which DCC and PTFA were omitted were carried out for each of the above thiols. In no case was a disulfide product detected, and the starting mercaptans were recovered unchanged.

These results, together with those of Wallace and his co-workers (18, 19), who showed that oxidation of thiols by DMSO alone proceeded via ionic intermediates with the formation of dimethyl sulfide,[6] suggest that the initial stages of thiol oxidation by DCC–DMSO are similar to those established for alcohols (12), as indicated in Diagram 2.

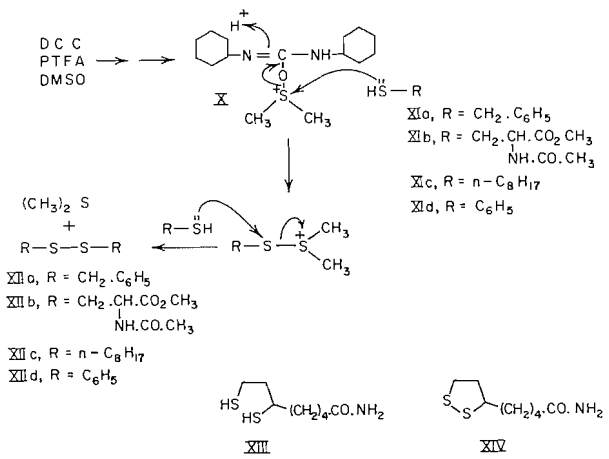


DIAGRAM 2.

The results of the studies carried out on the mechanism by which the Moffatt reagent effects oxidation (7, 9, 12) are in accord with the formation of the intermediate X. In an attempt to obtain further evidence for its existence, various mixtures of DCC, PTFA, and DMSO were examined by infrared and proton magnetic resonance spectroscopy. Solutions of DCC in DMSO possessed the spectra to be expected from a physical mixture of the unreacted components, but on addition of PTFA protonation of the DCC occurred immediately, as evidenced by the disappearance of the diimide infrared absorption at 2 114 cm^{-1}. However, no infrared or proton magnetic resonance peaks which could be ascribed to X were observed.

For the oxidation of thiophenol (XI*d*) to phenyl disulfide (XII*d*), it was not necessary to use the Moffatt reagent, since treatment with DMSO alone at room temperature (18) gave the disulfide in a quantitative yield.

EXPERIMENTAL

Melting points were determined on a Fisher–Johns block and are corrected. Infrared spectra were obtained on a Beckman IR.8 or a Perkin–Elmer 237-B spectrophotometer, and proton magnetic resonance spectra in deuteriochloroform, with tetramethylsilane as the internal standard, on a Varian A-60 instrument. Thin-layer and preparative layer chromatography were performed on silica gel G to which 3% of General Electric phosphor No. 118-2-7 had been added to facilitate the detection of ultraviolet-absorbing compounds. When the latter technique was not suitable, the compounds were visualized with the appropriate spray reagent (100% (w/v) aqueous toluene-*p*-sulfonic acid or concentrated sulfuric acid) or with iodine vapor. Selective detection of compounds containing a free thiol group was achieved with a sodium nitroprusside spray (20). Solvents for chromatography were redistilled, and the DMSO used (Fisher reagent grade) was stored over molecular sieves. All compounds were purified until t.l.c. and, where appropriate, gas–liquid chromatography showed no impurities. Gas–liquid chromatograms were obtained on an F and M 400 biomedical unit equipped with 3% SE-30 and 1% QF-1, on silanized Chromosorb G, columns.

[6]*During the oxidations, with DCC–PTFA–DMSO, of all the thiols surveyed a strong odor of dimethyl sulfide became apparent as each reaction proceeded.*

Can. J. Chem. Downloaded from www.nrcresearchpress.com by 210.87.254.5 on 09/05/12
For personal use only.

Can. J. Chem. Downloaded from www.nrcresearchpress.com by 210.87.254.5 on 09/05/12
For personal use only.

Pyridinium Trifluoroacetate

Pyridinium trifluoroacetate, m.p. 78°, was obtained in a quantitative yield by the reaction of pyridine with trifluoroacetic acid in dry ether (21).

Androst-5-en-3β-ol (Ib)

A solution of 3β-hydroxyandrost-5-en-17-one (9 g), potassium hydroxide (13 g), and 85% hydrazine hydrate (22 ml) in diethylene glycol (130 ml) was refluxed for 3 h. The bath temperature was then raised gradually to 200° and maintained at this level until nitrogen evolution ceased (4.5 h). The mixture was cooled and poured into water (600 ml), and the precipitate was filtered off and washed with water until the washings were neutral. The residue (7.1 g) was recrystallized from aqueous methanol to give androst-5-en-3β-ol as prisms (5.3 g), m.p. 133.5–134.5°, $[\alpha]_D^{22}$ −74° (*c*, 1 in dioxane), $\nu_{max}^{CHCl_3}$ 3 597 cm^{-1} (lit. (22) m.p. 136.5–137°, $[\alpha]_D$ −75° (dioxane)).

Androst-5-en-3-one (IIb)[7]

Androst-5-en-3β-ol (1.1 g, 4 mmoles), DCC (2.47 g, 12 mmoles), and PTFA (0.39 g, 2 mmoles) were dissolved in DMSO (10 ml) and benzene (10 ml), and the mixture was heated at 50° for 2 h. Ethyl acetate (40 ml) was added and the precipitated dicyclohexylurea, m.p. 236–237° after recrystallization from ethanol, ν_{max}^{DMSO} 1 660 cm^{-1}, was removed by filtration. The solution was extracted with 0.1 *M* phosphate buffer (2 × 10 ml, pH 7.2) and then with water (2 × 10 ml). The dried ($MgSO_4$) solution was rotary evaporated and the residue was recrystallized[8] from methanol (10 ml) to give androst-5-en-3-one as plates (0.74 g), m.p. 129–131°,[8] $[\alpha]_D^{20}$ −32° (*c*, 0.7 in methanol), $\nu_{max}^{CHCl_3}$ 1 712 cm^{-1}.

Anal. Calcd. for $C_{19}H_{28}O$ (272.4): C, 83.77; H, 10.36. Found: C, 83.97; H, 10.54.

Androst-5-ene-3,17-dione (IIa) and Cholest-5-en-3-one (IIc)

Androst-5-ene-3,17-dione (plates from methanol, m.p. 150–155°,[8] $[\alpha]_D^{21}$ 50° (*c*, 1.2 in chloroform), $\nu_{max}^{CHCl_3}$ 1 736 and 1 715 cm^{-1}) and cholest-5-en-3-one (prisms from methanol, m.p. 120–122°, $[\alpha]_D^{21}$ −3.5° (*c*, 0.8 in chloroform), $\nu_{max}^{CHCl_3}$ 1 712 cm^{-1}) were prepared by the method described above (60–70% yields) from the 3β-alcohols I*a* and I*c*, respectively.

Attempted Oxidation of 3β-Hydroxyandrost-5-en-17-one (Ia) with 1 Mole of DCC; Isolation of 3β-(Methylthiomethoxy)-androst-5-en-17-one (V) and N-Trifluoroacetyl-N,N′-dicyclohexylurea (IX)

A solution of 3β-hydroxyandrost-5-en-17-one (5 g, 17.4 mmoles), DCC (3.6 g, 17.4 mmoles), and PTFA (3.36 g, 17.4 mmoles) in DMSO (100 ml) was heated at 50° for 2 h. The mixture was then poured into water (1 l) and extracted with *n*-pentane (5 × 100 ml), and the combined pentane solutions were washed with water (3 × 100 ml) and dried ($MgSO_4$). Rotary evaporation yielded a solid (1.6 g), which was shown by t.l.c. to contain several compounds, including some unchanged starting material I*a*. (A further 4.5 g of the starting alcohol was recovered from the original aqueous mixture by ether extraction.) After repeated chromatography of the pentane-derived mixture on Florisil, using benzene with increasing proportions of ether as the elution solvents, *N*-trifluoroacetyl-*N*,*N*′-dicyclohexylurea (230 mg) and 3β-(methylthiomethoxy)-androst-5-en-17-one (192 mg) were isolated. The latter was recrystallized from hexane as needles, m.p. 171.5–172°, $\nu_{max}^{CHCl_3}$ 1 733 and 1 047 cm^{-1}; proton magnetic resonance δ 0.88 and 1.04 (3 H, singlets, C_{18}—CH_3 and C_{19}—CH_3), 2.17 (3 H, singlet, CH_3—S), 3.5 (1 H, multiplet, C_3—α-H), 4.67 (2 H, singlet, S—CH_2—O), and 5.4 p.p.m. (1 H, multiplet, C_5—H).

Anal. Calcd. for $C_{21}H_{32}O_2S$ (348.6): C, 72.34; H, 9.26; S, 9.20. Found: C, 72.03; H, 9.31; S, 9.39; mol. wt. (mass spectrum) 348.

The trifluoroacetylurea IX gave needles, m.p. 139°, when crystallized from hexane; $\nu_{max}^{CHCl_3}$ 3 425, 1 724, and 1 695 cm^{-1}; proton magnetic resonance δ 3.8 (22 H, multiplet, cyclohexyl protons) and 6.5 p.p.m. (1 H, multiplet, N—H). The material was identical in all respects with an authentic sample prepared from DCC (1 mole) and trifluoroacetic acid (1 mole) in refluxing pyridine.

Anal. Calcd. for $C_{15}H_{23}F_3N_2O_2$ (320.4): C, 56.26; H, 7.23; F, 17.79; N, 8.74. Found: C, 56.31; H, 7.44; F, 17.93; N, 8.77.

Acid Hydrolysis of 3β-(Methylthiomethoxy)-androst-5-en-17-one (V)

3-β-(Methylthiomethoxy)-androst-5-en-17-one (25 mg) dissolved in methanol (8 ml) and concentrated hydrochloric acid (2 ml) was kept overnight at 20°. The mixture was then poured into water (200 ml) and extracted with ether (2 × 50 ml), and the ethereal extracts were washed, first with saturated aqueous sodium bicarbonate (2 × 20 ml) and then with water (20 ml), and dried ($MgSO_4$). Rotary evaporation yielded

[7]*All glassware used in the preparation and purification of the Δ⁵-3-ketosteroids was washed with dilute aqueous potassium hydroxide during the final stages of the normal cleaning cycle. This was necessary because the traces of acid absorbed on the surfaces of glassware not treated in this way were sufficient to effect partial isomerizations of the desired β,γ-unsaturated ketones.*

[8]*Isomerization also occurred when heat was applied, and during all operations, especially recrystallization, the temperature was not allowed to exceed 50° for any extended period. Accordingly, melting point determinations of Δ⁵-3-ketones were carried out with the temperature increasing at 6°/min. Isomerization of Δ⁵-3-ketones during melting point determinations has been reported previously (7).*

3β-hydroxyandrost-5-en-17-one (17 mg) which, on recrystallization from hexane, gave prisms, m.p. 150–151°, identical in all respects with an authentic sample.

Oxidation of Benzyl Mercaptan (XIa) to Dibenzyl Disulfide (XIIa)

Benzyl mercaptan (1 g, 8.1 mmoles), DCC (5 g, 24.3 mmoles), and PTFA (1.6 g, 8.1 mmoles) were dissolved in DMSO (40 ml), and the mixture was heated at 50° for 6 h. Water (400 ml) was then added and the precipitate extracted with ether (3 × 50 ml). The ether solution was filtered to remove undissolved dicyclohexylurea, then washed with water (3 × 25 ml), and dried ($MgSO_4$). Evaporation yielded a white solid, from which the desired product was extracted with petroleum ether (b.p. 40–60°). Final purification was achieved by preparative layer chromatography, with benzene – petroleum ether (b.p. 40–60°) (1:3) as the developing solvent, followed by recrystallization from petroleum ether (b.p. 40–60°) to give dibenzyl disulfide as rhombs (0.95 g), m.p. 68–70° (lit. (18) m.p. 69–70°), proton magnetic resonance δ 3.57 (4 H, singlet, $(—CH_2—S—)_2$) and 7.23 p.p.m. (10 H, singlet, C_6H_5). Benzyl mercaptan was recovered unchanged when a control experiment without DCC was carried out under identical conditions.

Oxidation of Octan-1-thiol (XIc) to Dioctyl Disulfide (XIIc)

A solution of octan-1-thiol (2 g, 13.6 mmoles), DCC (9.6 g, 41.2 mmoles), and PTFA (1.4 g, 7.2 mmoles) in DMSO (50 ml) was kept at 25° for 24 h. Anhydrous ether (250 ml) was then added followed by oxalic acid (3.7 g, 42 mmoles) in methanol (25 ml). After the gas evolution had ceased the mixture was diluted with water (250 ml) and the precipitated *N,N'*-dicyclohexylurea filtered off. The ether layer was separated, washed with water (3 × 30 ml), dried ($MgSO_4$), and rotary evaporated. *n*-Hexane (20 ml) was added to the residue and the mixture was filtered to remove *N*-trifluoroacetyl-*N,N'*-dicyclohexylurea. Evaporation of the hexane solution followed by distillation gave dioctyl disulfide (1.3 g), b.p. 140° at 0.5 mm (lit. (23) b.p. 160–163° at 1.5 mm), proton magnetic resonance δ 2.63 p.p.m. (4 H, triplet, J = 7 c.p.s., $(—CH_2—S—)_2$). No oxidation occurred when a solution of octan-1-thiol alone in DMSO was kept for 24 h at room temperature.

Methyl N-Acetyl-L-cysteinate (XIb)

N-Acetyl-L-cysteine (15.1 g) in methanol (150 ml) was saturated with hydrogen chloride at 0°. The solution was refluxed for 20 min and was then concentrated to 75 ml under reduced pressure (nitrogen bleed). Solid sodium bicarbonate was added to neutralize the remaining acid and the mixture was again evaporated to dryness under reduced pressure (nitrogen bleed). The residue was extracted with methylene chloride (6 × 30 ml), and the combined extracts were dried ($MgSO_4$) and evaporated to a crystallizing oil (15.2 g). Recrystallization from isopropyl ether, followed by washing of the crystals with cold *n*-hexane to facilitate solvent evaporation, gave methyl *N*-acetyl-L-cysteinate as feathery needles (8.7 g), m.p. 79–80°, $[\alpha]_D^{22}$ −24° (*c*, 1 in methanol); $\nu_{max}^{CHCl_3}$ 3 436, 2 398, 1 745, and 1 678 cm^{-1}; proton magnetic resonance δ 1.62 (1 H, triplet, J = 9 c.p.s., S—H), 2.05 (3 H, singlet, —CO—CH_3), 2.95 (2 H, multiplet, —CH_2—S), 3.77 (3 H, singlet, O—CH_3), 4.90 (1 H, multiplet, α-CH), and 7.35 p.p.m. (1 H, multiplet, —CO—NH—).

Anal. Calcd. for $C_8H_{11}NO_3S$ (177.2): C, 40.68; H, 6.26; N, 7.91; S, 18.08. Found: C, 40.61; H, 6.18; N, 7.84; S, 18.23.

Oxidation of Methyl N-Acetyl-L-cysteinate to Methyl N-Acetyl-L-cystinate (XIIb)

A solution of methyl *N*-acetyl-L-cysteinate (1 g, 5.7 mmoles), DCC (3.5 g, 17.1 mmoles), and PTFA (1.1 g, 5.7 mmoles) in DMSO (20 ml) was heated at 50° for 2 h, after which time the precipitated dicyclohexylurea was filtered off. Methylene chloride (75 ml) was added to the filtrate, and the mixture was washed with water (4 × 20 ml), dried ($MgSO_4$), and rotary evaporated. The resulting syrup was washed with boiling *n*-hexane to remove unchanged DCC and *N*-trifluoroacetyl-*N,N'*-dicyclohexylurea, and the residue (0.9 g) was recrystallized from isopropyl ether – acetone to remove most of the dicyclohexylurea impurity. Subsequent recrystallization from ethyl acetate gave methyl *N*-acetyl-L-cystinate as needles (508 mg), m.p. 129–130° (lit. (24) m.p. 128–129°), $[\alpha]_D^{20}$ −121° (*c*, 1 in methanol); $\nu_{max}^{CHCl_3}$ 3 448, 1 730, and 1 678 cm^{-1}; proton magnetic resonance δ 2.07 (3 H, singlet, —CO—CH_3), 3.22 (2 H, doublet, J = 6 c.p.s., —CH_2—S), 3.78 (3 H, singlet, O—CH_3), 4.90 (1 H, multiplet, α-CH), and 7.05 p.p.m. (1 H, multiplet, CO—NH—).

Anal. Calcd. for $C_{12}H_{20}N_2O_6S_2$ (352.4) (sample dried at 100° *in vacuo* to remove ethyl acetate of crystallization): C, 40.90; H, 5.72; N, 7.95; S, 18.20. Found: C, 41.14; H, 5.91; N, 7.81; S, 18.36.

Methyl *N*-acetyl-L-cysteinate was recovered unchanged from a control experiment in which DCC was omitted.

Oxidation of Thiophenol (XId) to Diphenyl Disulfide (XIId)

Thiophenol (560 mg) in DMSO (20 ml) was heated at 50° for 17 h. The mixture was poured into water (250 ml) and extracted with ether (3 × 50 ml), and the ether extracts were washed with water (2 × 25 ml) and dried ($MgSO_4$). Rotary evaporation gave a solid (500 mg) which, on recrystallization from petroleum ether (b.p. 40–60°), yielded diphenyl disulfide as rhombs (420 mg), m.p. 58–59° (lit. (18) m.p. 60°), proton magnetic resonance δ 7.1–7.6 p.p.m. (multiplets, C_6H_5). In a control experiment carried out under identical conditions, but with benzene replacing DMSO as solvent, the thiophenol was recovered unchanged.

Can. J. Chem. Downloaded from www.nrcresearchpress.com by 210.87.254.5 on 09/05/12
For personal use only.

ACKNOWLEDGMENTS

We thank the National Research Council, the Ontario Research Foundation, and the Upjohn Company for their generous support, and Dr. F. Colton for a gift of 3β-hydroxyandrost-5-en-17-one. The award (to D. C. W.) of a Commonwealth Scholarship by the Canadian Universities Foundation is also gratefully acknowledged.

REFERENCES

1. P. TALALAY. Ann. Rev. Biochem. **34**, 348 (1965).
2. C. DJERASSI, R. R. ENGLE, and A. BOWERS. J. Org. Chem. **21**, 1547 (1956).
3. A. BUTENANDT and J. SCHMIDT-THOMÉ. Chem. Ber. **69**, 882 (1936).
4. W. R. NES, E. LOESER, R. KIRDANI, and J. MARSH. Tetrahedron, **19**, 299 (1963).
5. F. S. KAWAHARA. *In* Methods in enzymology. Vol. 5. Academic Press, Inc., New York. 1962. p. 527.
6. L. F. FIESER. Org. Syn. **35**, 43 (1955).
7. K. E. PFITZNER and J. G. MOFFATT. J. Am. Chem. Soc. **85**, 3027 (1963); **87**, 5661 (1965); **87**, 5670 (1965).
8. J. B. JONES and D. C. WIGFIELD. Tetrahedron Letters, 4103 (1965).
9. J. D. ALBRIGHT and L. GOLDMAN. J. Am. Chem. Soc. **87**, 4214 (1965).
10. M. G. BURDON and J. G. MOFFATT. J. Am. Chem. Soc. **87**, 4656 (1965).
11. K. E. PFITZNER, J. P. MARINO, and R. A. OLOFSON. J. Am. Chem. Soc. **87**, 4658 (1965).
12. A. H. FENSELAU and J. G. MOFFATT. J. Am. Chem. Soc. **88**, 1762 (1966).
13. R. PUMMERER. Ber. **43**, 1401 (1910).
14. C. R. JOHNSON and W. G. PHILLIPS. Tetrahedron Letters, 2101 (1965).
15. W. E. PARHAM and S. H. GROEN. J. Org. Chem. **30**, 728 (1965).
16. D. J. CRAM. Fundamentals of carbanion chemistry. Academic Press, Inc., New York. 1965. pp. 223–233.
17. D. F. DETAR and R. SILVERSTEIN. J. Am. Chem. Soc. **88**, 1013 (1966).
18. T. J. WALLACE. J. Am. Chem. Soc. **86**, 2018 (1964).
19. T. J. WALLACE and J. J. MAHON. J. Am. Chem. Soc. **86**, 4099 (1964); J. Org. Chem. **30**, 1502 (1965).
20. I. W. GROTE. J. Biol. Chem. **93**, 25 (1931).
21. E. J. BOURNE, M. STACEY, J. C. TATLOW, and R. WORRALL. J. Chem. Soc. 2008 (1954).
22. M. FÉTIZON and M. GOLFIER. Bull. Soc. Chim. France, 167 (1963).
23. F. H. MCMILLAN and J. A. KING. J. Am. Chem. Soc. **70**, 4143 (1948).
24. N. W. PIRIE. Biochem. J. **25**, 618 (1931).

Can. J. Chem. Downloaded from www.nrcresearchpress.com by 210.87.254.5 on 09/05/12
For personal use only.

Can. J. Chem. Downloaded from www.nrcresearchpress.com by 210.87.254.40 on 09/05/12
For personal use only.

ORMOSIA ALKALOIDS

III. CHEMISTRY OF ORMOSANINE AND ORMOJANINE; DEHYDROGENATION TO 3,6,8-TRIALKYLATED QUINOLINES[1]

Z. VALENTA, P. DESLONGCHAMPS, M. H. RASHID, R. H. WIGHTMAN, AND J. S. WILSON
Department of Chemistry, University of New Brunswick, Fredericton, New Brunswick

Received July 8, 1966

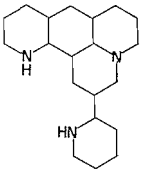
ABSTRACT

Degradations of ormosanine, $C_{20}H_{35}N_3$, are described which are in agreement with structure II (8) for this alkaloid. Nuclear magnetic resonance study of *N*-acetyl and *N*-nitroso derivatives has been used to clarify the environment of the secondary nitrogen atoms. Chemical and spectroscopic evidence leads to the formulation XV*b* for the related alkaloid ormojanine, $C_{20}H_{31}N_3$.

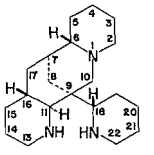
Both alkaloids were found to give 3-*n*-pentyl-6,8-dipropylquinoline together with the corresponding 3-*n*-butyl derivative in a catalytic dehydrogenation. The possible mechanism of formation of these dehydrogenation products is discussed and their synthesis is described.

The presence of a large number of alkaloids in *Ormosia jamaicensis* (1, 2), *O. panamensis* (3), and *O. dasycarpa* (4) has recently been reported. Three of the alkaloids were identified with lupin alkaloids of known structure: augustifoline (1, 2, 5, 6), epihydroxylupanine (2, 5), and (−)-sparteine (4). It thus became of great interest to investigate the C_{20}-alkaloids of unknown structure which are also present in the *Ormosia* plants (2, 3) and which could be expected to be formed by an interesting variation of the lupin alkaloid biogenesis.

In a preliminary communication (7), we proposed formula I as a representation of our physical and chemical data obtained for ormosanine, $C_{20}H_{35}N_3$, m.p. 179–181°, an alkaloid of *Ormosia jamaicensis*, and an unsaturated version of I for ormojanine, $C_{20}H_{31}N_3$, m.p. 124–126°, another alkaloid from the same plant. Recently, Karle and Karle reported an X-ray crystallographic investigation of jamine, the homo-derivative of ormosanine, on the basis of which ormosanine was assigned structure II (8). Using structure II, Wildman and his co-workers then explained their degradative and correlative work with alkaloids from *O. panamensis* (9, 10).



I



II

We now wish to describe our own degradative results (which are in agreement with the formulation II for ormosanine), to develop the structure of ormojanine, and to report an unusual dehydrogenative rearrangement which had been the cause of the incorrect placement of two C—C bonds in our previous structural proposal.[2]

[1]*For part II in this series, see P. Deslongchamps, J. S. Wilson, and Z. Valenta, Tetrahedron Letters, 3893 (1964).*

[2]*The stereochemistry of Ormosia alkaloids is discussed in the following communication (11).*

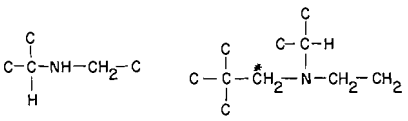
Can. J. Chem. Downloaded from www.nrcresearchpress.com by 210.87.254.40 on 09/05/12
For personal use only.

Ormosanine

The alkaloid $C_{20}H_{35}N_3$, which was isolated from the plant in its racemic form (9), was found to have three features common to lupin alkaloids: it contains no *C*-methyl groups and no *N*-alkyl groups, and its molecular composition fits the general formulation $(C_5N)_x + C_5$. No double bonds are present in the alkaloid, which must therefore be pentacyclic.

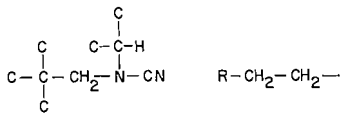
Treatment with acetic anhydride in pyridine converted the alkaloid into *N*-acetyl-ormosanine, $C_{22}H_{37}N_3O$, m.p. 202–204°, and *N*,*N*′-diacetylormosanine, $C_{24}H_{39}N_3O_2$, m.p. 164–166°; *N*,*N*′-dinitroso-ormosanine, $C_{20}H_{35}N_5O_2$, m.p. 171–173°, was formed in a reaction with sodium nitrite and hydrochloric acid. Since the diacetyl and dinitroso derivatives are basic and their infrared spectra contain no NH signals, the alkaloid contains one tertiary and two secondary basic nitrogens. This is confirmed by two reactions in which a bridging of the two secondary nitrogen atoms is achieved. Treatment of ormosanine with formic acid and formaldehyde yielded homo-ormosanine, $C_{21}H_{35}N_3$, m.p. 148–149°,[3] in which the grouping N—CH_2—N had been created, whereas a treatment with phosgene and triethylamine in benzene gave the corresponding urea, homoxy-ormosanine, $C_{21}H_{33}N_3O$, m.p. 178–180°. These two derivatives could not be acetylated or nitrosated. The infrared spectrum of homoxy-ormosanine contained an amide maximum at 1 640 cm^{-1}, showing that the two secondary nitrogens in ormosanine must be separated by at least three carbon atoms.

The nuclear magnetic resonance study of the above derivatives provided an interesting method for the elucidation of the structural environment of the nitrogen atoms. Although the spectrum of ormosanine contains no absorption below 6.8 τ, both dinitroso- and diacetyl-ormosanine contain six deshielded hydrogen atoms with signals below 6.8 τ. These signals, furthermore, can be divided into two groups: a multiplet corresponding to two hydrogens appearing below 5.5 τ, and a multiplet corresponding to four hydrogens appearing between 5.9 and and 6.65 τ in both spectra.[4,5] It is reasonable to assume that these signals correspond to methine and methylene groups, respectively. Since the spectrum of monoacetylormosanine shows one methine hydrogen (5.66 τ) and two methylene hydrogens (6.50–6.80 τ), it can be concluded that two groupings III are contained in the structure of ormosanine.



III

IV



V: R = Br
VI: R = OAc
VII: R = OH

[3]*Wildman and his co-workers found homo-ormosanine to be identical with the alkaloid jamine (9).*

[4]*The nitroso derivative is particularly well resolved; the method should be of general use for the nuclear magnetic resonance study of secondary bases.*

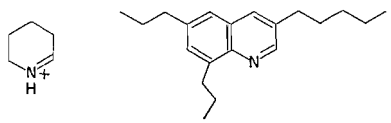
[5]*It should be noted that, in contrast, only two hydrogen atoms are deshielded (5.65 τ) in the spectrum of the cyclic urea, homoxy-ormosanine. Clearly, some neighboring hydrogen atoms must lie in the shielding region of the carbonyl group within the rigid cyclic framework of this derivative.*

The spectra of ormosanine and all the above derivatives contain a two-hydrogen singlet in the 7.5 τ region. This is best explained by the presence, in ormosanine, of a methylene group connected to the tertiary nitrogen atom and to a quaternary carbon (C_{10} in structure II).[6] The remaining features of the tertiary nitrogen environment were revealed by the von Braun degradation of homoxy-ormosanine. The crystalline cyanobromo adduct, $C_{22}H_{33}N_4BrO$, m.p. 184–186°, showed a cyanamide (2 200 cm^{-1}) and a urea peak (1 648 cm^{-1}) in its infrared spectrum. The nuclear magnetic resonance spectrum contained, in addition to the two hydrogens deshielded by the urea function (5.6 τ), a total of five deshielded hydrogen atoms in a partially resolved multiplet (6.1–6.9 τ). This assignment could be confirmed by further transformations of the cyanobromo adduct. Treatment with potassium acetate gave the oily cyanoacetate, $C_{24}H_{36}N_4O_3$, showing infrared peaks at 2 225 (cyanamide), 1 740 (acetate), and 1 647 cm^{-1} (urea), which was converted on mild hydrolysis into the crystalline cyanoalcohol, $C_{22}H_{34}N_4O_2$, m.p. 225–227°. The nuclear magnetic resonance spectra of both these compounds again showed a total of seven hydrogen atoms absorbing below 7.0 τ. Thus, the tertiary nitrogen in ormosanine must be joined to two methylene groups and one methine group.

A more detailed study of the unshielded region showed a two-hydrogen signal, with the appearance of a narrow triplet at 6.62 τ for the bromide, at 6.39 τ for the alcohol, and at 5.97 τ for the acetate. Furthermore, oxidation of the cyanobromo compound with pyridine-*N*-oxide gave an aldehyde which again contained the aldehydic hydrogen atom as a triplet (0.21 τ). The above evidence can thus be summarized by partial formulae IV, V, VI, and VII representing the transformations of the tertiary nitrogen.

The sharp singlet in the spectra of ormosanine and its acetyl and nitroso derivatives corresponding to the methylene at C* in formula IV (C_{10} in formula II) is not present in the spectra of the cyanamides. This can most likely be attributed to the change from an A_2 to an AB pattern. The A part of this pattern can, in fact, be discerned clearly in the deshielded region of the cyanobromo adduct (6.22 τ; doublet, J_{AB} = 12 c.p.s.).

It now remained to perform degradations which would reveal the skeleton of ormosanine. Several interesting products were obtained in the dehydrogenation of ormosanine with palladium on charcoal at 275° in a sealed tube. The presence of pyridine and β-picoline in the volatile basic fraction could be established by vapor-phase chromatography. Mass spectroscopy provided additional information about this fragmentation. The most prominent peak in the mass spectrum of ormosanine at *m/e* 84 is best explained by the ion VIII, and the presence of an α-monosubstituted piperidine in ormosanine is thus strongly indicated.



VIII IX

An even more diagnostic product was obtained from the nonvolatile fraction of the above dehydrogenation. A high-boiling quinoline could be obtained in a relatively pure form as a result of its unusual solubility properties. It is so weakly basic that only sulfuric acid stronger than 40% (by weight) would extract it efficiently from ether. After chromatography, the weakly basic fraction was converted into the picrate, and recrystallized from ether to a constant melting point (108–110°). Surprisingly, the liberated free base

[6] *Unfortunately, we had originally not considered this feature as sufficiently diagnostic, and it was therefore not incorporated into our first ormosanine formulation (structure I).*

Can. J. Chem. Downloaded from www.nrcresearchpress.com by 210.87.254.40 on 09/05/12
For personal use only.

Can. J. Chem. Downloaded from www.nrcresearchpress.com by 210.87.254.40 on 09/05/12
For personal use only.

was found by vapor-phase chromatography to be a mixture of two compounds in which the higher boiling one predominated. Their separation was finally achieved by a nine-funnel countercurrent distribution between ether and sulfuric acid.

The structural elucidation of these two compounds proved relatively simple. The ultraviolet spectrum, with maxima at 237 (ϵ 31 600), 298 (ϵ 3 900), 310 (ϵ 3 700), and 322 mμ (ϵ 3 400) (λ_{max} in HCl at 248 and 322.5 mμ), indicated a substituted quinoline. The nuclear magnetic resonance spectra of both compounds contained the following diagnostic peaks: a doublet at 1.48 τ (1 H, J = 2 c.p.s.), a doublet at 2.42 τ (1 H, J = 2 c.p.s.), a sharp singlet at 2.85 τ (2 H's), a triplet at 6.88 τ (2 H's, J = 6 c.p.s.), a triplet at 7.32 τ (4 H's, J = 6 c.p.s.), and a triplet at 9.0 τ (9 H's, J = 6 c.p.s.). A multiplet centered at 8.6 τ was different in the two compounds.

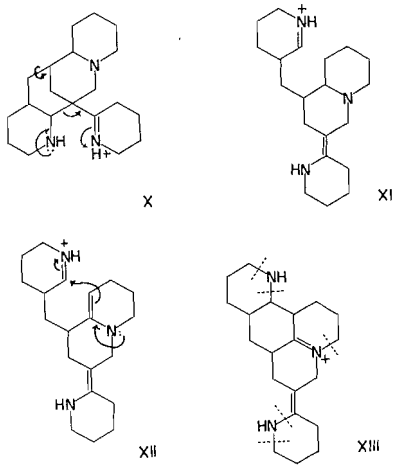
Integration of the nuclear magnetic resonance spectra, together with mass spectroscopy, showed the two quinolines to have the composition $C_{20}H_{29}N$ and $C_{19}H_{27}N$, respectively. A comparison of the aromatic region with that of model methylquinolines showed that the two quinolines must be 3,6,8-trisubstituted. Differently substituted quinolines gave distinctly different absorption patterns. In particular, only hydrogen atoms at C_5 and C_7 of the quinoline nucleus have a precisely identical τ value. Since the compounds only contain three methyl groups, the chains must be unbranched, and since no methyl group resonates below 9 τ, all chains must be longer than ethyl.

Because of the presence, in ormosanine, of an α-monosubstituted piperidine ring (*vide supra*), the higher boiling component should be an *n*-pentyl-dipropylquinoline. The three possible compounds were therefore synthesized in an unambiguous way from *p*-propyl- and *p*-*n*-pentyl-aniline,[7] and the degradation product was found to be identical in all respects with 3-*n*-pentyl-6,8-dipropylquinoline (IX). Furthermore, the lower boiling product was identified with authentic 3-*n*-butyl-6,8-dipropylquinoline, which was synthesized in a similar way. To our knowledge, 3,6,8-trialkylated quinolines have not been described previously.

Quinoline IX contains all 20 carbons of ormosanine. Although its formation can be explained easily on the basis of structure I for ormosanine and was, in fact, our key evidence for the formulation I, the crystallographically determined structure II does not contain the skeleton of IX. The question now arises whether formula II can be correct and, if so, how quinoline IX is formed from ormosanine. Two facts strongly favor formula II. Firstly, the above-mentioned nuclear magnetic resonance singlet corresponding to a methylene group joined to the tertiary nitrogen is only in accord with formula II. Secondly, and more significantly, several stereoisomers of ormosanine can be prepared, all of which are capable of forming the corresponding homoxy derivatives.[8] Whereas formula II allows this variety, it is clear from model inspection that, at best, two stereoisomers of formula I would be capable of forming a bridged compound of a sufficiently high stability.

It therefore follows that our faith in the stability of the ormosanine skeleton under the dehydrogenation conditions (7) was not justified, and that the molecule undergoes a deep-seated rearrangement in a relatively high yield (5–10% of quinoline). This can be illustrated by the scheme II → X → XI → XII → XIII, in which the exact sequence of steps and the precise oxidation level of all intermediates is, of course, not implied. The hypothetical intermediate XIII can be transformed into IX by the breakage of five C—N bonds (dotted lines in formula XIII) and a further dehydrogenation. Although the individual steps in this sequence are unexceptional, the total yield of the transformation is remarkable.

[7]*Synthetic details and physical properties of the synthetic compounds are given in the Experimental.*
[8]*These isomers are described in the following communication (11).*



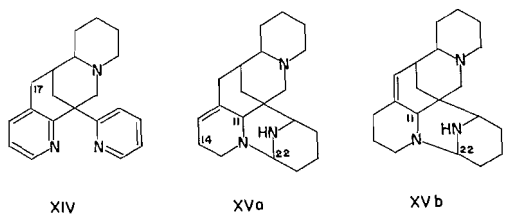
Ormojanine

The alkaloid $C_{20}H_{31}N_3$ contains two more unsaturated centers than ormosanine and is optically active (2). It can be reduced to dihydro-ormojanine, $C_{20}H_{33}N_3$, m.p. 127–129°, on careful hydrogenation of its hydrochloride with platinum, and to tetrahydro-ormojanine, $C_{20}H_{35}N_3$, m.p. 107–109°, on prolonged hydrogenation.

The following dehydrogenation results leave no doubt that tetrahydro-ormojanine and ormosanine have the same skeletal structure. Dehydrogenation of tetrahydro-ormojanine at 275° also yielded the quinoline IX, again accompanied by the corresponding *n*-butyl derivative. Even more significantly, a dehydrogenation of dihydro-ormojanine at 200° with palladium on charcoal gave a high yield of a crystalline pyridine, $C_{20}H_{23}N_3$, m.p. 130–132°. Its ultraviolet spectrum (inflection 256 mμ, λ_{max} 262 mμ (ϵ 5 600) and 268 mμ (ϵ 5 300), inflection 278 mμ) shows the presence of two pyridine rings in the molecule, and the position of the absorption maxima together with the number of aromatic hydrogen atoms in the nuclear magnetic resonance spectrum clearly indicates one α-monosubstituted and one α,β-disubstituted pyridine ring.

This dehydrogenation product must possess structure XIV for the following reasons. Wildman reported that the dehydrogenation of ormosanine at 250° (10) gave a dehydro-ormosanine, for which he proposed structure XIV. We now find that this dehydrogenation product of racemic ormosanine is identical in ultraviolet, infrared, and nuclear magnetic resonance spectra with our product from optically active ormojanine. With the structure of ormosanine known (II), the dipyridine must undoubtedly be XIV, provided no rearrangement occurs during the dehydrogenation. This possibility is eliminated by our finding that the dipyridine can be reduced back to tetrahydro-ormojanine.[9] It is thus established that tetrahydro-ormojanine is a stereoisomer of ormosanine (II).

Nuclear magnetic resonance spectroscopy provides important information about the nature of the two unsaturated centers in ormojanine. The spectrum of the alkaloid



[9]*The reduction and stereochemistry of XIV are discussed in the following communication (11).*

Can. J. Chem. Downloaded from www.nrcresearchpress.com by 210.87.254.40 on 09/05/12
For personal use only.

Can. J. Chem. Downloaded from www.nrcresearchpress.com by 210.87.254.40 on 09/05/12
For personal use only.

contains, in the region below 7.0 τ, a doublet at 4.65 τ (1 H, J = 6 c.p.s.), a broad singlet at 6.46 τ (1 H), and a sharp singlet at 6.84 τ (1 H). Of these three peaks, only the doublet remains in the spectrum of dihydro-ormojanine (4.68 τ), and the spectrum of tetrahydro-ormojanine contains no signals below 7.0 τ.

Ormojanine forms an oily *N*-monoacetyl derivative, $C_{22}H_{34}N_3O$, and an *N*-mononitroso derivative, $C_{20}H_{30}N_4O$, m.p. 178–181°. Thus, in contrast to ormosanine, only one secondary nitrogen atom is present in the molecule. Both these derivatives show the doublet at approximately 4.6 τ and a sharp singlet in the 6.6–6.8 τ region in their nuclear magnetic resonance spectra. However, the broad singlet found at 6.46 τ in the spectrum of ormojanine appears at 4.71 τ in the spectrum of the mononitroso derivative, which also shows an additional broad singlet at 5.27 τ (1 H).[10]

These findings only agree with formula XV*a* or XV*b* for ormojanine.[11] The shape and position of the sharp singlet at 6.84 τ indicate its correspondence to the hydrogen atom at C_{11}, placed between a double bond, a nitrogen atom, and a quaternary carbon atom. C_{11} cannot be alpha to the secondary nitrogen atom, since the signal does not shift significantly on nitrosation or acetylation. The hydrogen atom corresponding to the broad singlet at 6.46 τ in ormojanine can be assigned with confidence to C_{22} because of its low-field position and the fact that its signal shifts downfield on nitrosation and acetylation. The nuclear magnetic resonance study does not allow an unambiguous decision between XV*a* and XV*b*. The fact that the vinylic hydrogen appears as a doublet in the spectrum of ormojanine (4.65 τ) and all its derivatives favors formula XV*b*, but model inspection shows clearly that one of the hydrogen atoms at C_{14} in structure XV*a* forms a dihedral angle close to 90° with the vinylic hydrogen and need therefore not give any observable splitting.

On the basis of the above formulation, dihydro-ormojanine has structure XVI*a* or XVI*b* and tetrahydro-ormojanine, as stated above, a structure stereoisomeric with II. In agreement with this assignment, the corresponding bridged compounds, homodihydro-ormojanine, $C_{21}H_{33}N_3$, homoxydihydro-ormojanine, $C_{21}H_{31}N_3O$, m.p. 173–174° (infrared maximum at 1 645 cm^{-1}), homotetrahydro-ormojanine, $C_{21}H_{35}N_3$, m.p. 100–101°, and homoxytetrahydro-ormojanine, $C_{21}H_{33}N_3O$, m.p. 203–205° (infrared maximum at 1 640 cm^{-1}), could be prepared from the two reduction products under appropriate conditions.

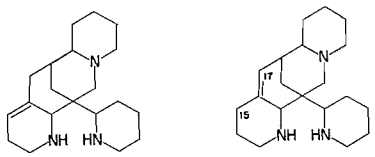
The following degradation gives support for the formulation of ormojanine as XV*b* and of dihydro-ormojanine as XVI*b*. The urea derivative of XVI, homoxydihydro-ormojanine, was subjected to a Hofmann degradation, achieved by a dry distillation of the corresponding metho-hydroxide. The resulting product, m.p. 135–138°, obtained in a good yield, was found to be a conjugated diene. Its ultraviolet spectrum, with maxima at 225 mμ (ϵ 11 600) and 253 mμ (ϵ 11 700) in a neutral solution and at 243 mμ (ϵ 16 600) in acid, indicates a transoid arrangement of the two double bonds and a probable interaction of the electron pair on the basic nitrogen atom with the conjugated π-electron system. This and the nuclear magnetic resonance spectrum, showing one vinylic hydrogen at 3.85 τ (singlet) and one at 4.79 τ (triplet), are best explained by formula XVII for the Hofmann diene.[12]

It is clear that formula XVI*b* for dihydro-ormojanine provides a more satisfactory explanation for the formation of diene XVII in a good yield. Although XVII could, in

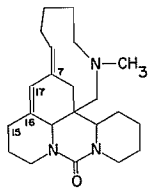
[10] *A similar situation is found in the spectrum of the acetyl derivative; the signals, however, are not as well resolved.*

[11] *The presence of an* N—C—N *linkage in unsaturated Ormosia alkaloids was postulated for the first time in our first publication of this series (7); Wilson (12) later correctly concluded that this linkage is also present in the alkaloid panamine.*

[12] *An alternative formulation, with double bonds at* C_{15}—C_{16} *and* C_{17}—C_7, *appears less likely on the basis of our evidence.*



XVIa XVIb



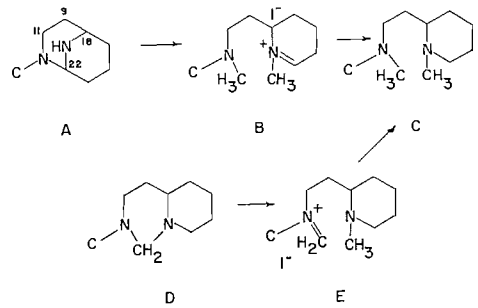
XVII

principle, be formed from XVIa via a non-conjugated diene, the necessary base-catalyzed double-bond migration does not appear to be probable under the experimental conditions used.

Our preference for formulae XV*b* and XVI*b* is somewhat tempered by the finding that the reduction of XVI with platinum and deuterium gas in acetic acid-OD, followed by a dehydrogenation of the product with palladium, gave deuterated compound XIV containing no deuterium at C_{17} or at any of the aromatic carbon atoms (nuclear magnetic resonance spectroscopy; see Experimental). This negative result, however, is not convincing, since a palladium-catalyzed hydrogen exchange at C_{17}, taking place during or after the formation of the pyridine ring, can readily be visualized.[13]

Further chemical evidence relevant to the environment of the secondary nitrogen atom in ormojanine is depicted in Scheme I, in which only partial formulae are used for the sake of brevity. Treatment of ormojanine (A) with methyl iodide in benzene gave the salt B, which could be reduced with sodium borohydride to *N*,*N*-dimethyldihydro-ormojanine (C), m.p. 120–122°. In another series, homodihydro-ormojanine (D), prepared by treatment of dihydro-ormojanine with formaldehyde and formic acid (see above), was converted, on treatment with methyl iodide in benzene, into the salt E, which could be reduced with sodium borohydride to a compound identical in all respects with *N*,*N*-dimethyldihydro-ormojanine (C).

In summary, dehydrogenation experiments have shown that tetrahydro-ormojanine is



SCHEME 1.

[13]*The two structural possibilities for ormojanine, XVa and XVb, are discussed by P. Deslongchamps in his Ph.D. thesis, University of New Brunswick, 1964; Wilson (13) recently concluded that our evidence leads to XVb as the most probable structure for ormojanine, but unfortunately did not support this conclusion with additional experimental evidence. It is hoped that a rigorous proof for the position of the double bond in ormojanine will be obtained by synthesis.*

Can. J. Chem. Downloaded from www.nrcresearchpress.com by 210.87.254.40 on 09/05/12
For personal use only.

a stereoisomer of ormosanine (II). Our chemical and spectroscopic evidence has revealed the nature of the two additional unsaturations in ormojanine, which can be represented by formula XV. Of the two possible positions of the double bond (XV*a* and XV*b*), that in XV*b* is favored by our evidence. The configuration of all the asymmetric centers in ormojanine and related alkaloids is reported in the following communication (11).

EXPERIMENTAL

Nuclear magnetic resonance spectra were recorded in $CDCl_3$ on a Varian HR-60 spectrometer, and chemical shifts are reported in parts per million relative to an internal tetramethylsilane reference. Infrared spectra were obtained with Perkin–Elmer model 21 and 137B Infracord instruments, and ultraviolet spectra were recorded on a Beckman DK-2 instrument and mass spectra on a Hitachi Perkin–Elmer RMU-6D instrument. All melting points are uncorrected.

Extraction of Ormosanine and Ormojanine

Ground beans of *Ormosia jamaicensis* Urb. (5 kg) were extracted for 24 h with petroleum ether (b.p. 65–110°) in a Soxhlet apparatus and the extract was discarded. The ground material was then subjected for 60 h to a Soxhlet extraction with methanol; the solvent was then evaporated, the residue dissolved in water (3 l), and the solution acidified to pH 2 with hydrochloric acid. Exhaustive extraction with chloroform removed acidic and neutral material. The aqueous solution was then neutralized with potassium carbonate and made alkaline (pH 10) with concentrated ammonium hydroxide. A continuous ether extraction (70 h) of the aqueous solution yielded, after drying and removal of the ether, fraction A, 117.0 g of a viscous oil. Extraction of the aqueous solution with five portions of chloroform, drying, and evaporation of the solvent yielded fraction B, 26.8 g of an amorphous residue. Examination by paper chromatography and thin-layer chromatography (t.l.c.) revealed at least seven different compounds (three major constituents) in fraction A and five compounds (two comparable to components of fraction A) in fraction B.

The ether-soluble bases (fraction A) were crystallized from acetone to yield crude ormosanine, m.p. 165–178° (5.8 g, 0.12% of the original ground material). An extensive study of various purification methods showed that the mother liquors of fraction A could best be purified by a countercurrent separation. Distribution of 70 g of evaporated mother liquors between McIlvain's buffer (pH 7.8) and ether (2 l of each phase in each funnel) in 15 funnels yielded crude crystalline ormojanine, m.p. 115–125° (9 g, 0.18% of the original ground material) from funnels 12–15 (crystallized from acetone) and a small amount of crystalline ormosanine from funnels 8–10. A redistribution of the mother liquors from the crystallization of ormojanine with buffer (pH 8) yielded additional crystalline ormojanine.

Ormosanine (2, 3) was recrystallized from acetone and melted at 179–181°.

Anal. Calcd. for $C_{20}H_{35}N_3$: C, 75.65; H, 11.11; N, 13.24; 2 active H's, 0.628. Found: C, 75.35; H, 11.00; N, 13.29; active H, 0.475; no oxygen, O—CH_3, N—CH_3, C—CH_3.

Mass spectrum: 317 (molecular ion), 84 (largest peak).

Ormojanine (2) was recrystallized from acetone (or ethyl acetate) and melted at 124–126°.

Anal. Calcd. for $C_{20}H_{31}N_3$: C, 76.62; H, 9.97; N, 13.40; 1 active H, 0.319. Found: C, 75.65; H, 10.00; N, 13.40; active H, 0.444; no oxygen, O—CH_3, N—CH_3, C—CH_3.

Mass spectrum: 313 (molecular ion).

Acetylation of Ormosanine

(*a*) Ormosanine (105 mg) was acetylated for 8 h in 2 ml of dry pyridine with 2 ml of acetic anhydride at room temperature. Evaporation *in vacuo* followed by a separation into basic and nonbasic material by a distribution between aqueous hydrochloric acid and ether yielded 128 mg of a basic residue. Paper chromatography, with *n*-butanol – concentrated hydrochloric acid – water (100:20:36 by volume) (3) on Whatman No. 1 filter paper, showed two compounds with R_f 0.65 and 0.90. Crystallization from ethyl acetate gave pure acetylormosanine, m.p. 202–204°, R_f 0.65.

Anal. Calcd. for $C_{22}H_{37}N_3O$: C, 73.49; H, 10.38; N, 11.69; O, 4.45. Found: C, 73.55; H, 10.32; N, 12.66; O, 3.72.

(*b*) Acetylation of ormosanine (400 mg) for 16 h in 8 ml of dry pyridine and 8 ml of acetic anhydride, followed by a work-up as under method *a*, gave pure *N,N'*-diacetylormosanine, m.p. 164–166°, R_f 0.90 (420 mg).

Anal. Calcd. for $C_{24}H_{39}N_3O_2$: C, 71.79; H, 9.79; N, 10.47; O, 7.97. Found: C, 72.00; H, 9.91; N, 10.33; O, 7.71.

N,N'-Dinitroso-ormosanine

An aqueous solution of sodium nitrite (145 mg in 2 ml) was added during a period of 30 min to a solution of ormosanine (226 mg) in 3 ml of 1 *N* hydrochloric acid at 0°. After standing for 1 h at room temperature and 5 min at 60°, the solution was diluted with water (30 ml), extracted with ether to remove impurities, basified with sodium hydroxide, and extracted with ether. The basic ether extract (265 mg) was shown by

Can. J. Chem. Downloaded from www.nrcresearchpress.com by 210.87.254.40 on 09/05/12
For personal use only.

paper chromatography to consist of one major and four minor products. Elution with benzene from basic alumina gave *N,N'*-dinitroso-ormosanine (170 mg), which, after crystallization from ether or methanol, melted at 171–173°.

Anal. Calcd. for $C_{20}H_{35}N_5O_2$: C, 63.96; H, 8.86; N, 18.65; O, 8.52. Found: C, 64.01; H, 8.85; N, 18.17; O, 8.30.

Homo-ormosanine

A solution of ormosanine (120 mg) in formic acid (5 ml, 90%) and formaldehyde (3 ml, 40% in water) was boiled for 3 h; additional formic acid (2.5 ml) and formaldehyde (1.5 ml) were added and reflux was continued for 12 h. The reaction mixture was then diluted with water (50 ml), non-basic impurities were removed by extraction with ether, and the aqueous solution was basified with sodium hydroxide and extracted with ether. The basic ether extract (130 mg) was crystallized from acetone to give pure homo-ormosanine, m.p. 148–149° (R_f comparable to that of ormosanine).

Anal. Calcd. for $C_{21}H_{35}N_3$: C, 76.55; H, 10.71; N, 12.75. Found: C, 76.84; H, 10.61; N, 12.66; no oxygen.

Homoxy-ormosanine

Phosgene was bubbled for 1 h into a stirred solution of ormosanine (500 mg) and triethylamine (10 ml) in dry benzene (65 ml) at 0°. The viscous orange-colored solution was then allowed to stand at room temperature for 3 h, and then washed with dilute aqueous hydrochloric acid and with water. The combined aqueous layers were washed with benzene, then basified with sodium hydroxide, and extracted with ether. The basic extract (524 mg) was homoxy-ormosanine, recrystallized from petroleum ether (b.p. 50–70°) to m.p. 178–180°.

Anal. Calcd. for $C_{21}H_{33}N_3O$: C, 73.43; H, 9.69; N, 12.23; O, 4.66. Found: C, 73.98; H, 10.18; N, 11.60; O, 5.06.

von Braun Degradation of Homoxy-ormosanine

A solution of homoxy-ormosanine (450 mg) in dry benzene (25 ml) was added over a period of 4 h to a refluxing solution of cyanogen bromide (1.5 g) in dry benzene (75 ml). The solution was refluxed for an additional 16 h, and then washed with dilute aqueous hydrochloric acid and water. The benzene layer, on evaporation, gave 517 mg of a neutral residue which crystallized from ethyl acetate to give the pure cyanobromo adduct, m.p. 184–186°.

Anal. Calcd. for $C_{22}H_{33}N_4BrO$: C, 58.79; H, 7.40; N, 12.47; O, 3.56; Br, 17.78. Found: C, 58.74; H, 7.47; N, 12.55; O, 3.78; Br, 17.58.

Treatment of the cyanobromo compound (60 mg) with pyridine-*N*-oxide (1.0 g) in boiling acetonitrile (25 ml) for 24 h, followed by addition of triethylamine (15 ml) and a 5 h reflux, yielded 60 mg of a neutral material which was chromatographed twice on acid-washed alumina (Shawinigan). Chloroform–ether (4:1) eluted the crude oily cyanoaldehyde (15 mg), infrared maxima (carbon tetrachloride) at 2 730 (aldehyde), 2 210 (cyanamide), 1 742 (aldehyde), and 1 650 cm^{-1} (urea); nuclear magnetic resonance maximum at 0.21 (aldehyde, triplet).

Cyanoacetate

A solution of the cyanobromo compound (100 mg) and potassium acetate (400 mg) in 95% ethanol (60 ml) was refluxed for 24 h, then evaporated to a small volume, and diluted with water (75 ml). After acidification with hydrochloric acid, the aqueous solution was extracted with ether. The oily ether extract (80 mg) was chromatographed on basic alumina (Merck). Chloroform eluted the homogeneous oily cyanoacetate.

Cyanoalcohol

A solution of the cyanoacetate (80 mg) and potassium carbonate (200 mg) in methanol (10 ml) and water (5 ml) was allowed to stand at room temperature for 45 min. The methanol was then removed *in vacuo* and the resulting solution was diluted to 75 ml with water. After acidification with hydrochloric acid, the aqueous phase was extracted with chloroform to give 72 mg of the crude cyanoalcohol, which crystallized from ethyl acetate and melted at 225–227°.

Dehydrogenation of Ormosanine

Ormosanine (4 × 0.5 g) was intimately mixed with a palladium catalyst (4 × 0.7 g; 10% palladium on charcoal, L. Light and Co.) and heated in four sealed Carius tubes at 275° for 9 h. After these were opened (strong smell of ammonia), the contents were washed out with ether, and the tubes were crushed and extracted in a Soxhlet apparatus with ether for 24 h. Most of the ether was then carefully evaporated from the combined ether extracts through a Vigreux column, and the residue was distilled at 85° under reduced pressure. Volatile amines were condensed in a dry ice – acetone trap; treatment of the volatile fraction with ethanolic picric acid gave a picrate, m.p. 155–165° (230 mg). Decomposition of the picrate gave a basic fraction containing at least five compounds (shown by vapor-phase chromatography (v.p.c.)). The major component showed a retention time identical with that of pyridine, and one of the minor components was comparable with β-picoline.

Can. J. Chem. Downloaded from www.nrcresearchpress.com by 210.87.254.40 on 09/05/12
For personal use only.

Can. J. Chem. Downloaded from www.nrcresearchpress.com by 210.87.254.40 on 09/05/12
For personal use only.

The nonvolatile residue (725 mg of brown oil) was shown to contain two major components and at least 23 additional compounds by v.p.c. The residue was dissolved in ether (30 ml) and shaken in a five-funnel countercurrent system between five portions of ether, three portions of sulfuric acid (20% by weight), and two portions of water. All layers had a volume of 30 ml and all ether layers were shaken with five aqueous layers. The combined ether layers contained 211 mg of material. The combined aqueous layers were neutralized with potassium carbonate, basified with sodium hydroxide, and extracted with ether to give 420 mg of a brown oil, which, according to ultraviolet analysis, contained mainly pyridines.

The weakly basic, ether-soluble fraction (211 mg) was chromatographed on basic alumina (18 g, Merck); petroleum ether (b.p. 40–60°) – benzene (9:1) eluted a colorless oil (106 mg) which readily formed a crystalline picrate. The salt (82 mg) was recrystallized 15 times from ether, the last five melting points remaining constant at 108–110°. The liberated free base (basic alumina, Woelm) was subjected to a v.p.c. analysis (25% silicone SE-30 on Chromosorb W; 12 ft × $\frac{1}{8}$ in. outside diameter column; 280°; N_2, 40 ml/min), which showed the presence of two compounds with the peak area ratio of 1.65:1 and retention times of 14 min 37 s and 11 min 57 s, respectively.

The quinoline mixture (30 mg) was subjected to a nine-funnel countercurrent distribution with ether (50 ml) and sulfuric acid (50 ml, 23.5% by volume) in each funnel, sulfuric acid being the moving phase. The first four funnels contained 5 mg of pure (v.p.c.) 3-*n*-pentyl-6,8-dipropylquinoline, picrate m.p. 115–116°, and the last funnel contained pure (v.p.c.) 3-*n*-butyl-6,8-dipropylquinoline, picrate m.p. 110–112°. The structure of these two compounds was established by comparing their identity with synthetic specimens (see below).

Synthesis of 3-n-Pentyl-6,8-dipropylquinoline (IX)

4-n-Propylaniline

Aniline (9.3 g, distilled from zinc dust) and fused zinc chloride (9.54 g) (14) in *n*-propanol (7.21 g) were placed into a Carius tube, which was sealed under nitrogen, and then heated to 240° for 9 h. After the tube was cooled and opened (caution, high pressure), the contents (a reddish paste) were washed with water to remove unreacted zinc chloride and with ether to remove non-primary amines. The resulting crystalline zinc salt was dissolved in concentrated sodium hydroxide and the solution was extracted with ether. Evaporation of the ether gave a residue (4 g) which, on distillation at atmospheric pressure, gave pure 4-*n*-propylaniline, b.p. 224–230°; nuclear magnetic resonance maxima at 3.20 (2 meta H's, doublet, J = 7 c.p.s.), 3.67 (2 ortho H's, doublet, J = 7 c.p.s.), 6.70 (NH_2, singlet), 7.58 (2 benzylic H's, triplet, J = 7 c.p.s.), 8.55 (—CH_2—, multiplet), and 9.10 τ (—CH_3, triplet, J = 6 c.p.s.).

No alkylation of aniline was observed when the reaction was carried out at 200°, whereas heating to 270° produced equal amounts of *n*-propyl- and isopropyl-aniline.

N-Allyl-4-propylaniline

4-Propylaniline (7.36 g) and allyl chloride (20.9 g) (15) were heated under reflux for 13 h in a nitrogen atmosphere, then basified with aqueous sodium hydroxide (5 *N*, 100 ml), and extracted with ether. The separation of starting material and its *N*-allyl and *N*,*N*-diallyl derivatives was effected by distillation at atmospheric pressure. *N*-Allyl-4-propylaniline was obtained in a 45% yield, b.p. 248–254°; infrared maximum (chloroform) at 3 400 cm^{-1} (NH); ultraviolet maxima (ethanol) at 253 (ϵ 10 500) and 303 mμ (ϵ 1 600); nuclear magnetic resonance absorption for 3 olefinic protons.

2-Allyl-4-propylaniline

N-Allyl-4-propylaniline (3.58 g) was heated under reflux with anhydrous zinc chloride (2.78 g) in xylene (10 ml) for 15 h (15). The reaction mixture was treated with a 5 *N* sodium hydroxide solution and extracted with ether; then the ether extract was distilled to give the desired product (1.6 g), b.p. 125–130° at 14 mm.

2,4-Dipropylaniline

2-Allyl-4-propylaniline (1.6 g) was hydrogenated in glacial acetic acid (25 ml) and concentrated hydrochloric acid (1 ml) in the presence of platinum oxide (200 mg) at atmospheric pressure and room temperature for 4 h. The mixture was filtered and evaporated to dryness; then the residue was dissolved in 5 *N* sodium hydroxide solution and extracted with ether. Evaporation of the ether gave a quantitative yield of 2,4-dipropylaniline; nuclear magnetic resonance maxima at 3.34 (H's at C_3 and C_5, multiplet), 3.63 (1 H at C_6, doublet, J = 8 c.p.s.), 6.78 (NH_2, singlet), 7.62 (4 benzylic H's, triplet, J = 7 c.p.s.), 8.52 (4 methylene H's, multiplet), and 9.05 τ (6 methyl H's, triplet, J = 6 c.p.s.).

n-Pentylmalonic Acid Diethyl Ester

Sodium (14 g), cut in thin slices, was gradually added to 350 ml of absolute ethanol in a flame-dried flask protected from moisture (16). Diethyl malonate (100 g) was then added slowly through a dropping funnel. Under vigorous stirring, *n*-pentyl bromide (90 g) was then added during a 30 min period. The mixture was then refluxed until the solution was neutral to litmus (about 2 h). Ethanol was then evaporated, water added, and the separated organic layer distilled under reduced pressure. The desired product was obtained in a 90% yield, b.p. 130–133° at 14 mm.

2,4-Dihydroxy-3-n-pentyl-6,8-dipropylquinoline

To a refluxing solution (255°) of diethyl *n*-pentylmalonate (12 g) in diphenyl ether (150 ml) (17) was added dropwise, over a period of 4 h, a solution of 2,4-dipropylaniline (1.88 g) in diphenyl ether (100 ml) under

nitrogen. The solution was refluxed for an additional hour, cooled, and extracted with four 100 ml portions of dilute sodium hydroxide. The combined aqueous layers were acidified with hydrochloric acid and extracted with ether. Evaporation of the ether gave the desired dihydroxyquinoline (1.6 g), which crystallized after sublimation, m.p. 160–162°; ultraviolet maxima (ethanol) at 234 (ε 53 700), 278 (ε 10 000), 290 (sh), 322 (ε 7 200), and 330 mμ (sh).

A faster addition of the dipropylaniline in the above condensation resulted in an extensive formation of the corresponding diamide (two molecules of aniline reacting with one molecule of malonate).

2,4-Dichloro-3-n-pentyl-6,8-dipropylquinoline

A mixture of 2,4-dihydroxy-3-*n*-pentyl-6,8-dipropylquinoline (150 mg), phosphorus pentachloride (680 mg), and phosphorus oxychloride (0.5 ml) was heated to 100° for 4 h in a flask protected from moisture. The cooled reaction mixture was decomposed with water, and the solution was basified with sodium carbonate and extracted with ether. Evaporation of the ether yielded 142 mg of product, which, on the basis of t.l.c. on alumina with petroleum ether as eluent, consisted of two compounds, showing R_f values of 0.9 and 0.2, respectively. A clean separation was achieved on a column of basic alumina (Woelm); the desired oily dichloroquinoline (R_f 0.9) was obtained in a 20% yield; ultraviolet maxima (ethanol) at 245 (ε 44 600), 280–305 (broad, ε 3 200), 315 (ε 2 800), and 330 mμ (ε 2 200); nuclear magnetic resonance maxima in the aromatic region at 2.30 (1 H, singlet) and 2.70 τ (1 H, singlet); no infrared absorption in the 3 400 – 3 600 cm^{-1} region.

The second compound (R_f 0.2) proved to be the corresponding chloro-hydroxyquinoline and could be recycled to give an additional amount of the dichloroquinoline.

The dichlorination could not be achieved in the absence of phosphorus pentachloride.

3-n-Pentyl-6,8-dipropylquinoline (IX)

The dichloroquinoline (98 mg) was hydrogenated in the presence of 15% palladium on charcoal (100 mg) and potassium hydroxide (200 mg) in ethanol (15 ml) for 15 h at room temperature and normal pressure. After filtration, the ethanol was evaporated and the residue distributed between ether and 5 *N* sodium hydroxide solution. Evaporation of the ether gave 80 mg of the desired quinoline, which formed a picrate, m.p. 115–116°, in methanol. Mass spectrum: 283 (molecular ion), 268, 255 (largest peaks).

The higher boiling quinoline obtained in the dehydrogenation of ormosanine proved to be identical with this compound in picrate melting point, mixed melting point, mass spectrum, infrared spectrum, ultraviolet spectrum, and v.p.c. retention time.

Synthesis of 3-n-Butyl-6,8-dipropylquinoline

This compound was prepared by a method identical with that used for the synthesis of IX, only using diethyl *n*-butylmalonate (16) for the condensation with 2,4-dipropylaniline.

The oily quinoline gave a picrate, m.p. 110–112°. The lower boiling quinoline obtained in the dehydrogenation of ormosanine proved to be identical with this compound in picrate melting point, mixed melting point, infrared spectrum, ultraviolet spectrum, and v.p.c. retention time.

Synthesis of 6-n-Pentyl-3,8-dipropylquinoline

Only minor variations from the synthesis of IX were necessary. The required starting material, 4-*n*-pentylaniline, was prepared by a reaction of aniline (7.0 g) with amyl alcohol (8.0 g) and zinc chloride (7.2 g) in a sealed Carius tube at 240° for 9 h. Distillation at atmospheric pressure gave the desired aniline in a 20% yield, b.p. 255–265°. This was then refluxed with 5 moles of allyl chloride for 15 h, and the resulting *N*-allyl-4-*n*-pentylaniline, after purification by fractional distillation (5.92 g), was heated under reflux with zinc chloride (4.0 g) in xylene (25 ml) for 10 h. Vacuum distillation of the product gave 2.7 g of 2-allyl-4-*n*-pentylaniline, which was hydrogenated to 4-*n*-pentyl-2-propylaniline with platinum oxide (300 mg) in glacial acetic acid (25 ml) and hydrochloric acid (2 ml).

Diethyl propylmalonate, b.p. 100–105° at 14 mm, needed for the condensation reaction, was prepared in an 85% yield by a reflux of propyl bromide with an equivalent amount of the sodium salt of diethyl malonate in dry ethanol (see above).

Condensation of 4-*n*-pentyl-2-propylaniline (700 mg) with diethyl propylmalonate (3.45 g) in 170 ml of diphenyl ether gave the dihydroxyquinoline (600 mg), which, on treatment with phosphorus pentachloride (1.1 g) and phosphorus oxychloride (2 ml), followed by chromatography on basic alumina, yielded the pure 2,4-dichloro-6-*n*-pentyl-3,8-dipropylquinoline (178 mg). Its hydrogenolysis with 15% palladium on charcoal (200 mg) and potassium hydroxide (400 mg) in ethanol (20 ml) then gave the required 6-*n*-pentyl-3,8-dipropylquinoline (163 mg), picrate m.p. 103–104°. Mass spectrum: 283 (molecular ion), 268, 255 (largest peaks).

The compound was found to be distinctly different from IX in picrate melting point, nuclear magnetic resonance spectrum (8–9 τ), and infrared and mass spectra. Ultraviolet spectra and v.p.c. retention times were identical.

Synthesis of 6-n-Butyl-3,8-dipropylquinoline

The required starting material, 4-*n*-butylaniline, was prepared by a reaction of aniline with butyl alcohol and zinc chloride as described above. The previously described steps, including condensation with diethyl propylmalonate, then gave the quinoline, picrate m.p. 130–131°.

Can. J. Chem. Downloaded from www.nrcresearchpress.com by 210.87.254.40 on 09/05/12
For personal use only.

Can. J. Chem. Downloaded from www.nrcresearchpress.com by 210.87.254.40 on 09/05/12
For personal use only.

The lower boiling quinoline from ormosanine was distinctly different from this compound in picrate melting point and infrared spectrum. Ultraviolet spectra and v.p.c. retention times were identical.

Synthesis of 8-n-Pentyl-3,6-dipropylquinoline

The required starting material, 2-*n*-pentyl-4-propylaniline, was not attainable by the above *N*-allylation–rearrangement sequence. 4-Propylaniline (5.08 g; preparation, see above) was therefore heated directly with amyl alcohol (3.98 g) and fused zinc chloride (5.12 g) in a sealed Carius tube to 240° for 11 h. The resulting solid was dissolved in 10 *N* sodium hydroxide solution, which was extracted with ether. Vapor-phase chromatographic analysis (10% D.C. on Chromosorb W; 210°; N_2, 60 ml/min) of the ether extract showed the presence of over 20 compounds, with the two major components being starting material and what was later found to be the required product. A series of three fractional distillations produced v.p.c. pure 2-*n*-pentyl-4-propylaniline (610 mg), which, after condensation with diethyl propylmalonate, chlorination, and reduction as described above, gave the desired 8-*n*-pentyl-3,6-dipropylquinoline, picrate m.p. 130–132°. Mass spectrum: 283 (molecular ion), 254, 240, 227 (largest peaks).

The compound was found to be distinctly different from IX in picrate melting point, nuclear magnetic resonance, infrared, and mass spectra, and v.p.c. (IX is 13 s slower in a 4 min run).

Dihydro-ormojanine

Ormojanine (2.362 g) was dissolved in ethanol (50 ml) and treated with an excess of gaseous hydrochloric acid. The solution was then evaporated to dryness, and the hydrochloride was dissolved in 50 ml of ethanol and hydrogenated in the presence of platinum oxide (400 mg) at room temperature and normal pressure. The hydrogenation was stopped when 1 mole of hydrogen was absorbed, and the solution was filtered and evaporated. The residue was distributed between ether and a 2 *N* sodium hydroxide solution, the ether evaporated, and the solid residue crystallized from acetone to give pure dihydro-ormojanine, m.p. 127–129° (1.856 g).

Anal. Calcd. for $C_{20}H_{33}N_3$: C, 76.13; H, 10.55; N, 13.32. Found: C, 75.89; H, 10.71; N, 13.72.

Tetrahydro-ormojanine

Hydrogenation of ormojanine in ethanol in the presence of platinum oxide at room temperature and normal pressure for 2 days gave an almost quantitative yield of tetrahydro-ormojanine, m.p. 107–109° (crystallized from acetone).

Anal. Calcd. for $C_{20}H_{35}N_3$: C, 75.65; H, 11.11; N, 13.24. Found: C, 76.03; H, 11.07; N, 13.02.

Dehydrogenation of Ormojanine Derivatives

(*a*) Treatment of tetrahydro-ormojanine (2.0 g) with palladium on charcoal (15%, 3.0 g) at 275° for 18 h (sealed Carius tubes), followed by isolation and purification procedures similar to those described for the dehydrogenation of ormosanine (see above), resulted in the isolation of 3-pentyl- and 3-butyl-6,8-dipropyl-quinolines.

(*b*) Dihydro-ormojanine (4 × 1.025 g) was mixed with palladium on charcoal (15%, 4 × 1.15 g) and benzene (4 × 4.5 ml) and sealed under nitrogen in four Carius tubes. The tubes were heated to 200° for 12 h, cooled, opened, and washed with ether. After filtration, the ether solution was evaporated to give 1.53 g of a residue. Elution with 1% to 25% ether in benzene from basic alumina (Woelm, activity 1, 150 g) gave pure dipyridine XIV, m.p. 130–132° (700 mg).

Anal. Calcd. for $C_{20}H_{23}N_3$: C, 78.69; H, 7.61; N, 13.70. Found: C, 78.87; H, 7.93; N, 13.24.

Infrared maxima (chloroform) at 2 800 (s), 2 750 (s), 1 590 (s), 1 580 (s); nuclear magnetic resonance maxima (carbon tetrachloride) in the aromatic region at 1.53 and 1.89 τ (2 alpha H's, multiplets) and 2.50–3.20 τ (3 beta H's and 2 gamma H's, multiplet).

Dipyridine XIV was found to be identical in ultraviolet, infrared, and nuclear magnetic resonance spectra with (racemic) dipyridine, m.p. 146–147° and 154°, prepared from ormosanine according to Wildman *et al.* (10).

A further purification (countercurrent distribution) of later fractions of the above chromatogram gave a small amount (8 mg) of a t.l.c. pure material which, on the basis of its ultraviolet spectrum (inflection 262, maximum at 268 (ϵ 3 400), inflection 275 mμ) and the absence of NH absorption in the infrared spectrum, is very likely a C_{15} compound corresponding to XIV, but with the monosubstituted pyridine ring removed. Molecular weight (found by Mechrolab 301 osmometer): 235. Calcd. for $C_{15}H_{20}N_2$: 228.

N-Acetylormojanine

Ormojanine (165 mg) was acetylated with acetic anhydride (1.5 ml) in pyridine (1.5 ml). Evaporation of the solvents was followed by a distribution of the residue between ether and aqueous hydrochloric acid. Basification of the aqueous layer and extraction with ether gave 173 mg of the oily *N*-acetyl derivative, which appeared homogeneous by t.l.c. and paper chromatography.

Anal. Calcd. for $C_{22}H_{33}N_3O$: C, 73.90; H, 9.86; N, 11.75. Found: C, 73.51; H, 9.76; N, 11.82.

Infrared maximum (chloroform) at 1 630 cm^{-1} (s).

N-Nitroso-ormojanine

A solution of sodium nitrite (150 mg) in 1 ml of water was added during 30 min to a solution of ormojanine (200 mg) in 1 *N* hydrochloric acid (3 ml) at 0°. After standing for 1 h, the solution was heated to 100° for

5 min, cooled, diluted with water (75 ml), and extracted with ether. The ether extract (180 mg) crystallized from ether. Recrystallization gave the pure nitroso compound, m.p. 178–181°.

Anal. Calcd. for $C_{20}H_{30}N_4O$: C, 70.13; H, 8.83; N, 16.36. Found: C, 70.05; H, 8.92; N, 15.42.

Homoxydihydro-ormojanine

A solution of ethyl chloroformate (1 ml) in dry benzene (5 ml) was added dropwise to a well-stirred solution of dihydro-ormojanine (166 mg) in dry benzene (5 ml) containing triethylamine (1 ml). The mixture was stirred for 5 h at room temperature. Additional amounts of triethylamine (1 ml) and ethyl chloroformate (0.5 ml) in benzene were added after 2 h. The precipitated triethylamine hydrochloride was then filtered off, the filtrate evaporated to dryness, and the residue distributed between ether and 2 *N* hydrochloric acid. The aqueous layer was basified with sodium carbonate and extracted with ether. Evaporation of the ether gave 182 mg of a residue which, after recrystallization from petroleum ether, melted at 173–174°.

Anal. Calcd. for $C_{21}H_{31}N_3O$: C, 73.96; H, 9.16; N, 12.32; O, 4.69. Found: C, 73.30; H, 9.20; N, 13.09; O, 4.59.

Infrared maximum (KBr) at 1 645 cm^{-1}; nuclear magnetic resonance maxima below 7 τ at 4.49 (1 H, doublet, J = 5 c.p.s.), 5.20–5.81 (2 H's, multiplet), and 6.51 τ (1 H, singlet).

Homotetrahydro-ormojanine

Tetrahydro-ormojanine (143 mg) was boiled under reflux with formic acid (90%, 10 ml) and formaldehyde (40%, 6 ml) for 3 h. Additional formic acid (5 ml) and formaldehyde (3 ml) were then added and the solution was boiled for a further 7 h. Dilution with water (75 ml) and work-up in the usual manner gave 196 mg of a basic material, which, after recrystallization from acetone, melted at 100–101°.

Anal. Calcd. for $C_{21}H_{35}N_3$: C, 76.55; H, 10.71; N, 12.75. Found: C, 76.55; H, 10.54; N, 12.54.

The nuclear magnetic resonance spectrum contains an AB quadruplet for 2 protons centered at 6.69 τ (δ_{AB} = 17 c.p.s.; J_{AB} = 9 c.p.s.).

Homoxytetrahydro-ormojanine

The compound was prepared by the same method as that used for homoxydihydro-ormojanine (see above), using 334 mg of tetrahydro-ormojanine, 3 ml of ethyl chloroformate, 4 ml of triethylamine, and 30 ml of dry benzene. The basic extract (377 mg) crystallized from ether; recrystallization from ether gave pure homoxytetrahydro-ormojanine, m.p. 203–205°.

Anal. Calcd. for $C_{21}H_{33}N_3O$: C, 73.43; H, 9.69; N, 12.23; O, 4.66. Found: C, 73.64; H, 9.73; N, 11.87; O, 4.96.

Mass spectrum: 343 (molecular ion); infrared maximum (chloroform) at 1 640 cm^{-1}.

Hofmann Degradation of Homoxydihydro-ormojanine

Homoxydihydro-ormojanine (2.10 g) was converted into the methiodide by a reflux in benzene solution (10 ml) with methyl iodide (10 ml) for 3 days. The supernatant liquid was then decanted from the semi-crystalline precipitate, which was washed repeatedly with dry ether. The precipitated methiodide, which could be crystallized from water, was converted into the corresponding quaternary hydroxide on a column of basic Amberlite IRA-300 in methanol. After evaporation of the methanol, the residue was sublimed at 180–185° and 0.1 mm Hg.

The sublimate (1.56 g, amorphous solid) was subjected to an 11-funnel countercurrent distribution, using ether and McIlvain's buffer (pH 6.1) with the aqueous solution as a moving phase. The material in funnels 2–5 was recrystallized from ether – petroleum ether to give pure diene XVII, m.p. 135–138° (0.74 g).

Anal. Calcd. for $C_{22}H_{33}N_3O$: C, 74.43; H, 9.37; N, 11.84; O, 4.51; one N—CH_3, 4.22. Found: C, 74.43; H, 9.42; N, 11.85; O, 4.54; N—CH_3, 4.50.

Diagnostic nuclear magnetic resonance maxima at 3.85 (1 H, singlet), 4.79 (1 H, triplet, J = 7 c.p.s.), and 7.74 τ (N—CH_3, singlet).

Dehydrogenation of Deuterated Dihydro-ormojanine

Dihydro-ormojanine (620 mg) was reduced with deuterium gas in the presence of platinum oxide (1 g) in CH_3COOD (25 g) for 2 weeks at room temperature and normal pressure. The mixture was filtered, the filtrate evaporated to dryness, and the residue distributed between ether and a 5 *N* sodium hydroxide solution. The ether residue was crystallized from acetone to give deuterated dihydro-ormojanine, m.p. 107–109°. The infrared spectrum (carbon tetrachloride) shows strong deuterium absorption bands at 2 170 (sharp) and 2 000 cm^{-1} (broad).

The deuterated compound (245 mg) was mixed with palladium on charcoal (10%, 270 mg) and heated in a 10 ml test tube in a Wood's metal bath to 250° for 20 min. After cooling, the tube contents were washed exhaustively with benzene, and the solution was filtered and evaporated to dryness. Distribution between ether and aqueous acid and base in the usual manner gave 174 mg of a basic material which was chromatographed on neutral alumina (Woelm, activity 3, 10 g). Elution with benzene – petroleum ether (3:1) gave fractions containing pure deuterated dipyridine XIV, m.p. 130–132°. Deuterium analysis showed the presence of 2.3 deuterium atoms per molecule. The presence of deuterium is confirmed by weak infrared bands (chloroform) at 2 170 and 2 000 cm^{-1}. However, a quantitative comparison of the nuclear magnetic resonance spectra of deuterated XIV and of XIV prepared by dehydrogenation of dihydro-ormojanine (see above)

Can. J. Chem. Downloaded from www.nrcresearchpress.com by 210.87.254.40 on 09/05/12
For personal use only.

showed that the deuterium atoms are definitely not located on the pyridine rings (identical 1.45–3.20 τ region) or on C_{17} (identical 6.80–7.30 τ region). All these hydrogens are clearly visible in both spectra. It can reasonably be concluded that the deuterium atoms were incorporated in a position alpha to the tertiary nitrogen atom (C_2, C_6, and (or) C_{10}).[14]

Formation of N,N-Dimethyldihydro-ormojanine

(*a*) Ormojanine (370 mg) was methylated with methyl iodide (2 ml) in dry benzene for 20 h at room temperature. The supernatant liquid was then decanted from the precipitated salt, which was washed repeatedly with fresh dry benzene. The dried salt was dissolved in methanol (50 ml) and reduced with sodium borohydride (470 mg) at reflux temperature for 1 h. Most of the solvent was then evaporated and the residue was distributed between ether and a 2 *N* sodium hydroxide solution. The ether extract (350 mg) crystallized from acetone to give pure *N,N*-dimethyldihydro-ormojanine, m.p. 120–122°.

Anal. Calcd. for $C_{22}H_{37}N_3$: C, 77.03; H, 10.75; N, 12.25; two N—CH_3 groups, 8.80. Found: C, 76.88; H, 10.62; N, 12.09; N—CH_3, 7.50.

Diagnostic nuclear magnetic resonance maxima at 4.40 (1 H, doublet, J = 6 c.p.s.), 6.66 (1 H, singlet), 7.38 (N—CH_3, singlet), and 7.79 τ (N—CH_3, singlet).

The above quaternary iodide could be converted into an unstable enamine by percolation through basic Amberlite IRA-300 in methanol. The enamine could be crystallized from acetone and showed a moderately strong absorption at 1 645 cm^{-1} in the infrared spectrum (KBr).

(*b*) Dihydro-ormojanine (77 mg) was boiled under reflux in formic acid (88%, 1 ml) and formaldehyde (37%, 2 ml); additional amounts of formic acid (2 ml) and formaldehyde (4 ml) were added in two portions at 3 h intervals, with the total reflux time being 9 h. The mixture was then diluted with water (25 ml) and extracted with ether. The aqueous layer was basified with sodium hydroxide and extracted with ether. The oily ether extract (74 mg) proved homogeneous on t.l.c. and was identified as homodihydro-ormojanine (D) by spectroscopy. The infrared spectrum (carbon tetrachloride) showed the absence of an NH group, and the nuclear magnetic resonance spectrum showed absorption typical for the N—CH_2—N grouping (AB quadruplet centered at 6.62 τ, δ_{AB} = 20 c.p.s., J_{AB} = 7 c.p.s.).

The homo derivative was boiled under reflux with methyl iodide (1 ml) in dry benzene (3 ml) for 3 h. After evaporation of the benzene, the resulting salt was dissolved in methanol (10 ml) and reduced with sodium borohydride (50 mg) at reflux for 1 h. Purification in the usual manner, followed by crystallization from acetone, gave 30 mg of a product identical in all respects with *N,N*-dimethyldihydro-ormojanine (see above).

ACKNOWLEDGMENTS

The authors are grateful to the National Research Council, Ottawa, and to Smith, Kline and French Laboratories, Philadelphia, for the financial support of this work. Support to one of us (P. D.) in the form of a Shell Oil Graduate Fellowship is also gratefully acknowledged.

REFERENCES

1. H. A. Lloyd and E. C. Horning. J. Org. Chem. **25**, 1959 (1960).
2. C. H. Hassall and E. M. Wilson. Chem. Ind. London, 1358 (1961).
3. H. A. Lloyd and E. C. Horning. J. Am. Chem. Soc. **80**, 1506 (1958).
4. R. T. Clarke and M. F. Grundon. J. Chem. Soc. 41 (1960).
5. L. Marion, M. Wiewiorowski, and M. D. Bratek. Tetrahedron Letters, **19**, 1 (1960).
6. F. Bohlmann and E. Winterfeldt. Chem. Ber. **93**, 1956 (1960).
7. Z. Valenta, P. Deslongchamps, M. H. Rashid, R. H. Wightman, and J. S. Wilson. Tetrahedron Letters, 1559 (1963).
8. T. L. Karle and J. Karle. Tetrahedron Letters, 2065 (1963).
9. P. Naegeli, W. C. Wildman, and H. A. Lloyd. Tetrahedron Letters, 2069 (1963).
10. P. Naegeli, R. Naegeli, W. C. Wildman, and R. J. Highet. Tetrahedron Letters, 2075 (1963).
11. P. Deslongchamps, Z. Valenta, and J. S. Wilson. Can. J. Chem. This issue.
12. E. M. Wilson. Chem. Ind. London, 472 (1965).
13. E. M. Wilson. Tetrahedron, **21**, 2561 (1965).
14. J. Reilly and W. Hickinbottom. J. Chem. Soc. **117**, 103 (1920).
15. C. Hurd and W. Jenkins. J. Org. Chem. **22**, 1418 (1957).
16. R. Adams and C. Marvel. J. Am. Chem. Soc. **42**, 310 (1920).
17. R. Baker, G. Lappin, and B. Riegel. J. Am. Chem. Soc. **68**, 1284 (1946).

[14] *For additional evidence of the lability of* C_6—H, *see the following communication (11) and part II in this series.*

Can. J. Chem. Downloaded from www.nrcresearchpress.com by 210.87.254.40 on 09/05/12
For personal use only.

Can. J. Chem. Downloaded from www.nrcresearchpress.com by 210.87.254.105 on 09/05/12
For personal use only.

ORMOSIA ALKALOIDS

IV. STEREOCHEMISTRY OF ORMOJANINE; STRUCTURE AND STEREOCHEMISTRY OF PIPTANTHINE, DASYCARPINE, AND ORMOSININE[1]

P. DESLONGCHAMPS, Z. VALENTA, AND J. S. WILSON
Department of Chemistry, University of New Brunswick, Fredericton, New Brunswick

Received July 8, 1966

ABSTRACT

By using the known structure and stereochemistry of the alkaloid ormosanine, $C_{20}H_{35}N_3$ (I), as reference, the structure and stereochemistry of the isomeric compounds piptanthine (II), tetrahydro-ormojanine (XIV), isotetrahydro-ormojanine (XIII), and dasycarpine (XX) have been elucidated by isomerization and reduction experiments. Three additional $C_{20}H_{35}N_3$ bases possessing the ormosanine skeleton have been prepared by the reduction of pyridine VII. Thus, of the 15 possible stereoisomers of ormosanine, 7 are now known.

The study leads to the stereo-formula XIX for the alkaloid ormojanine, $C_{20}H_{31}N_3$. The alkaloid ormosinine has been found to be a dimer of panamine.

Stereochemical aspects of the catalytic and chemical reductions of the double bonds and pyridine rings contained in the described compounds are discussed. A possible biogenetic intermediate is proposed which explains the presence of both antipodal series of *Ormosia* alkaloids in nature.

The isolation of a number of alkaloids with the empirical formula $C_{20}H_{35}N_3$ has been reported; these are ormosanine from *Ormosia jamaicensis* (1), piptanthine from *Piptanthus nanus* (2), and dasycarpine from *Ormosia dasycarpa* (3). Recently, the structure and stereochemistry of ormosanine were found by X-ray crystallography to be as represented in I (4).[2] It appeared to be an interesting challenge to use the known structure and configuration of ormosanine as a point of departure and to establish the structure and stereochemistry of all the isomeric bases by correlative experiments and configurational arguments. Our interest in this problem was enhanced by the fact that we obtained two additional $C_{20}H_{35}N_3$ bases, tetrahydro-ormojanine and isotetrahydro-ormojanine, in reduction experiments on ormojanine, $C_{20}H_{31}N_3$, another constituent of *O. jamaicensis*.

Disregarding absolute configuration[2] and taking account of the fact that the two asymmetric centers C_7 and C_9 are configurationally interdependent, one arrives at 16 possible compounds containing the ormosanine skeleton. It now remains to establish whether tetrahydro-ormojanine, isotetrahydro-ormojanine, piptanthine, and dasycarpine all possess the same skeleton as ormosanine and, if so, to select for each of these compounds the correct configuration out of the 15 remaining stereochemical possibilities.

Piptanthine

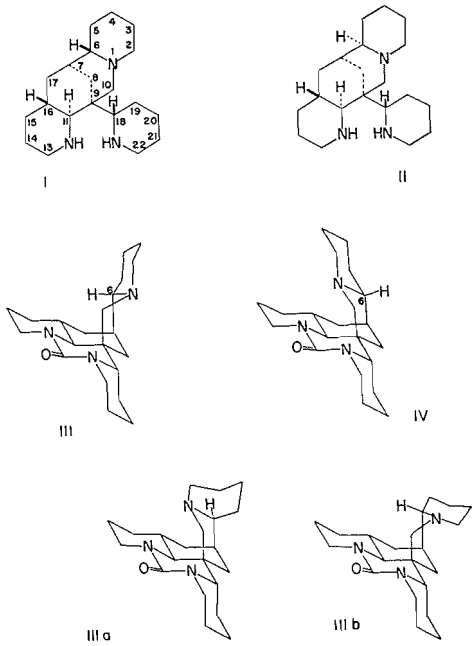
The solution in the case of the alkaloid piptanthine proved to be remarkably easy. We have been able to show (5) that a prolonged treatment of ormosanine with platinum in acetic acid in a hydrogen atmosphere at room temperature converted it into piptanthine.[3] On the basis of this isomerization, the structure and stereochemistry of piptanthine must be II for the following reasons.

Homoxy-ormosanine (III), the urea derivative of ormosanine (8), was found to undergo the same catalytic isomerization to homoxypiptanthine (IV). Consequently, C_6 must be

[1]*For part III in this series, see ref. 8.*

[2]*The absolute configuration of ormosanine and related compounds is unknown, and none is implied in any of the formulae in this communication.*

[3]*Since natural ormosanine is racemic (6), the catalytically produced piptanthine is also racemic. Piptanthine from P. nanus is levorotatory ($[\alpha]_D$ −24.3°) (7).*



considered the most likely reaction center, since this process, which probably proceeds via dehydrogenation–hydrogenation, can be expected to be sufficiently rapid only in the vicinity of the basic nitrogen atom. The configurational assignments at C_6 are confirmed by infrared spectroscopy. A potassium bromide pellet spectrum of homoxy-ormosanine shows bands in the 2 800 cm^{-1} region characteristic of the *trans*-diaxial arrangement of the tertiary nitrogen electron pair and at least two α-hydrogen atoms (9), in agreement with conformation III (4). A spectrum of homoxy-ormosanine in chloroform, on the other hand, shows no bands in this region and indicates that the compound assumes conformation III*a* or III*b* in solution. In contrast, the infrared spectrum of homoxypiptanthine shows the diagnostic bands both in solid state and in solution, in agreement with the stable all-chair all-*trans* conformation IV (5).

This difference in spectroscopic behavior and the selectivity and efficiency of this essentially irreversible isomerization process can only be explained by the configuration II for piptanthine. It should be added parenthetically that a direct proof for the platinum-catalyzed exchange of hydrogen atoms situated alpha to the tertiary nitrogen atom in *Ormosia* alkaloids is also available. During our investigation of the alkaloid ormojanine, dihydro-ormojanine (VI) was reduced with deuterium gas and platinum in CH_3COOD and the product was dehydrogenated with palladium on charcoal to the pyridine VII (8). A nuclear magnetic resonance study of the resulting pyridine showed a complete absence of deuterium in the aromatic rings and at C_{17}, whereas analysis indicated the presence of 2.3 deuterium atoms in the molecule (8). Since the deuteration was done under very mild conditions (normal pressure and room temperature), it appears reasonable to assume that the incorporated deuterium atoms must be situated alpha to the tertiary nitrogen atom (C_2, C_6, and (or) C_{10}).

It is also interesting to note that the deep-seated rearrangement taking place during the catalytic dehydrogenation of ormosanine and tetrahydro-ormojanine to 3-pentyl-6,8-dipropylquinoline requires the removal of the C_6-hydrogen atom as one of the initial steps (8).

Can. J. Chem. Downloaded from www.nrcresearchpress.com by 210.87.254.105 on 09/05/12
For personal use only.

Can. J. Chem. Downloaded from www.nrcresearchpress.com by 210.87.254.105 on 09/05/12
For personal use only.

Tetrahydro-ormojanine and Isotetrahydro-ormojanine

As reported in the accompanying communication (8), the gross structure of the alkaloid ormojanine, $C_{20}H_{31}N_3$, a constituent of *O. jamaicensis*, can be represented by formula V.[4] The following three compounds were obtained by the reduction of ormojanine. A short catalytic reduction yielded dihydro-ormojanine (VI), whereas a longer hydrogenation saturated the double bond and gave pure tetrahydro-ormojanine (8, 10). A reduction of dihydro-ormojanine (VI) with lithium in boiling ethylene diamine (17) also saturated the double bond and gave an isomeric $C_{20}H_{35}N_3$ compound, isotetrahydro-ormojanine, in a good yield. The two isomeric reduction products were found to be distinctly different from ormosanine (I) and piptanthine (II) in their physical and chemical properties.

Dehydrogenation experiments showed clearly that ormosanine and ormojanine possess the same skeleton (8). Dehydrogenation of ormosanine and of tetrahydro-ormojanine at 280° with palladium on charcoal yielded 3-*n*-pentyl-6,8-dipropylquinoline (8, 10), whereas both ormosanine and dihydro-ormojanine gave the pyridine VII on dehydrogenation with the same catalyst at a lower temperature (8, 11). It should be noted that the hydrogen atom at C_6 in pyridine VII is assigned a configuration *cis* to the C_7—C_9 bridge, requiring an isomerization at C_6 during the dehydrogenation of ormosanine (5). This configuration follows from the presence of strong bands in the 2 800 cm^{-1} region of the infrared spectrum of pyridine VII both in solid state and in solution, in complete analogy to the spectral properties of piptanthine (see above), and is proved by the reduction study described below.

The question now arises whether ormojanine and its reduction products have the ormosanine or the piptanthine configuration at C_6. Several lines of evidence clearly show that the C_6-hydrogen atom is *cis* to the C_7—C_9 bridge (analogous to II and VII) in ormojanine and all its derivatives.

(*a*) Ormojanine and all its reduction products show infrared bands in the 2 800 cm^{-1} region analogous to those of piptanthine (II) and pyridine VII.

(*b*) Neither tetrahydro-ormojanine nor isotetrahydro-ormojanine change under conditions used for the ormosanine–piptanthine isomerization.

(*c*) Isomerization of dasycarpine to isotetrahydro-ormojanine (see below) proves that the C_6-hydrogen atom in the latter is *cis* to the C_7—C_9 bridge.

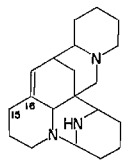
(*d*) Catalytic reduction of dihydro-ormojanine gives only one compound, tetrahydro-ormojanine.

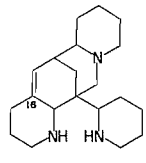
(*e*) The absence of an isomerization at C_6 during the catalytic reduction of ormojanine to dihydro-ormojanine is proved by the following evidence. *N*,*N*-Dimethyldihydro-ormojanine has been prepared from dihydro-ormojanine in three steps (8, 10). The identical dimethyl compound has also been prepared from ormojanine itself in a sequence in which no catalytic reduction was involved (8, 10).

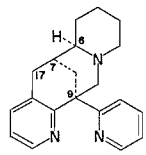
If tetrahydro-ormojanine, isotetrahydro-ormojanine, and piptanthine (II) have the same relative configuration at C_6, C_7, and C_9, they must obviously differ at some or all of the asymmetric centers C_{11}, C_{16}, and C_{18}. In other words, with the structure of piptanthine determined as II, tetrahydro-ormojanine and isotetrahydro-ormojanine must be two of the seven remaining possible compounds represented by formula VIII. Since the pyridine VII possesses the same configuration at C_6, C_7, and C_9 as the three compounds in question, it is clear that a detailed study of its reduction could provide a complete solution to the problem.

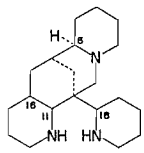
This opportunity was exploited in the following way. Pyridine VII was first reduced under mild catalytic conditions, which saturated only the monosubstituted pyridine ring.

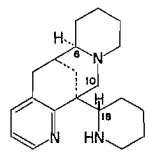
[4] *An alternative position of the double bond at* C_{15}—C_{16} *in ormojanine is not rigorously excluded by our evidence.*

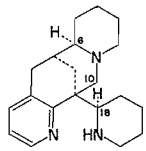

V


VI


VII


VIII


IX


X

Clearly, this reduction could be expected to give two compounds, IX and X, differing only in the configuration at C_{18}. In fact, the reduction product gave only one spot in thin-layer chromatography and was also reported (11) to appear homogeneous in vapor-phase chromatography. We have found, however, that acetylation of the reduction product gave two acetyl derivatives which could be separated chromatographically. To facilitate a reconversion into the secondary amines, the procedure was repeated with the corresponding carbobenzyloxy derivatives, which were separated by column chromatography and individually hydrogenolyzed to pure IX and pure X. The two secondary amines have the same R_f value in thin-layer chromatography, but show distinct differences in their infrared and nuclear magnetic resonance spectra. Most significantly, the two hydrogen atoms at C_{10} appear as a singlet (A_2) at 8.2 τ in the spectrum of one of the isomers and as a quadruplet (AB) centered at 8.11 τ (δ_{AB} = 19 c.p.s., J_{AB} = 10 c.p.s.) in the spectrum of the other isomer.

It must now be established which of these isomers is IX and which is X. To simplify the discussion, the results of the subsequent reduction experiments are anticipated; these demonstrate unambiguously that the isomer showing a singlet corresponding to the C_{10}-methylene group is X, and that the other isomer (quadruplet corresponding to C_{10}-methylene) is IX.

Pyridine IX was reduced catalytically with platinum in acetic acid at high pressure. Since the resulting mixture of completely saturated bases did not appear to be sufficiently stable for an extended experimentation, it was immediately treated with phosgene and thus converted into the corresponding cyclic urea derivatives. Purification by chromatography yielded two crystalline ureas, A_1 and A_2. Reduction of pyridine IX with sodium and isoamyl alcohol, followed by a treatment with phosgene and chromatography, also yielded A_1 and A_2.

Similarly, a high-pressure hydrogenation of pyridine X, followed by a treatment with

Can. J. Chem. Downloaded from www.nrcresearchpress.com by 210.87.254.105 on 09/05/12
For personal use only.

phosgene and chromatography, yielded two crystalline ureas, B_1 and B_2, whereas the chemical reduction of X with sodium and isoamyl alcohol resulted, after treatment with phosgene, in two ureas, B_1 and B_3.

These transformations can be summarized by the following scheme.

$$A_1, A_2 \xleftarrow[2.\ COCl_2]{1.\ H_2/Pt} IX \xrightarrow[2.\ COCl_2]{1.\ Na/alcohol} A_1, A_2$$

$$B_1, B_2 \xleftarrow[2.\ COCl_2]{1.\ H_2/Pt} X \xrightarrow[2.\ COCl_2]{1.\ Na/alcohol} B_1, B_3$$

The five homoxy derivatives (ureas) obtained in this way are all pure, stable compounds with the expected molecular ion in their mass spectra (*m/e* 343) and showing distinct differences in thin-layer chromatography and infrared and nuclear magnetic resonance spectroscopy. Furthermore, their spectra show the complete absence of olefinic or aromatic hydrogen atoms. They must therefore be the homoxy derivatives of five of the eight possible $C_{20}H_{35}N_3$ isomers depicted by the general formula VIII.

Comparison with known compounds has shown that A_1 is identical with homoxy-piptanthine (IV) and that B_3 is identical with homoxytetrahydro-ormojanine. Since the complete stereochemistry of piptanthine is known, it is clear that these findings rigorously differentiate between the two monopyridines IX and X. Furthermore, ormojanine and its reduction products must clearly have a configuration at C_{18} opposite to that of piptanthine.

Just as significantly, however, the homoxy derivatives of ormosanine, dasycarpine, and isotetrahydro-ormojanine were found not to be identical with any one of the remaining reduction products, A_2, B_1, and B_2. The absence of homoxy-ormosanine (III) was to be expected and confirms our assignment of a configuration at C_6 in pyridine VII opposite to that of ormosanine (I) (5). Homoxy-dasycarpine cannot be expected to be present among the hydrogenation products on the basis of experiments described below.

The absence of the urea of isotetrahydro-ormojanine among the reduction products of X was, however, unexpected. It must be remembered that isotetrahydro-ormojanine is produced by the chemical reduction of dihydro-ormojanine (VI), whereas tetrahydro-ormojanine results from a catalytic reduction of VI. Since we now know that ormojanine possesses the more stable configuration at C_6 and since, furthermore, there is no evidence in our work of any isomerizations under the conditions of a chemical reduction, it must be assumed that the two tetrahydro isomers differ only in the configuration at the reduced center C_{16}.[5] It follows, therefore, that isotetrahydro-ormojanine must correspond to the missing fourth possible reduction product of X (B_4).

This postulate gives rise to a paradoxical situation. Since isotetrahydro-ormojanine is formed in a high yield in the chemical reduction of VI, it should be more stable than tetrahydro-ormojanine. How is it possible, then, that the less-stable compound, tetrahydro-ormojanine, is formed in the chemical reduction of pyridine X and that the more stable compound, isotetrahydro-ormojanine, is not obtained from X at all?

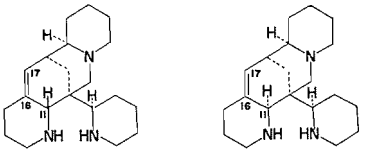
Actually, there is one, and only one, satisfactory solution to this dilemma. First of all, as stated above, the results of the hydrogenation of pyridines IX and X clearly show that the ormojanine series has a configuration at C_{18} opposite to that of ormosanine (I) and piptanthine (II). Dihydro-ormojanine (VI) can therefore definitely be represented by one of two complete stereo-formulae, XI and XII, differing in the configuration at C_{11}.

[5]*That isotetrahydro-ormojanine has a configuration at* C_6 *identical with that of X also follows clearly from our work on dasycarpine (see below).*

Can. J. Chem. Downloaded from www.nrcresearchpress.com by 210.87.254.105 on 09/05/12
For personal use only.

Scheme 1 now shows the tetrahydro compounds to be expected from the two possibilities. Clearly, XI would, on reduction, give rise to XIII and XIV, whereas XII would be reduced to XV and XVI.

Should XI be the correct representation of dihydro-ormojanine, then XIII must be the formula for isotetrahydro-ormojanine and XIV for tetrahydro-ormojanine for the following reasons. Clearly, a catalytic reduction of the C_{16}—C_{17} double bond in XI should proceed from the less-hindered side. In this case, the two rings containing the tertiary nitrogen

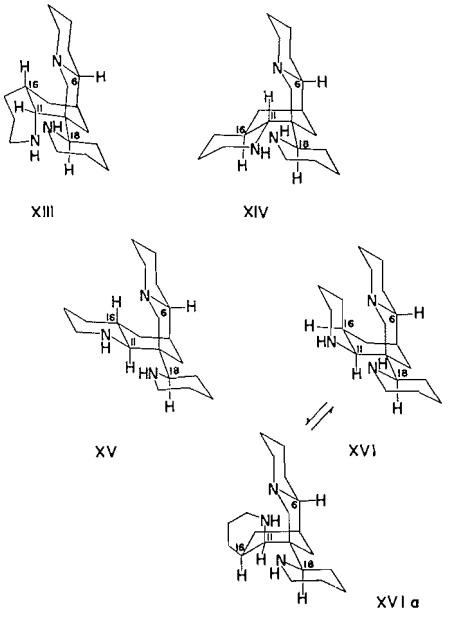


XI XII

atom completely screen the upper side of the molecule, and the catalytic addition of hydrogen, which is found to be completely stereospecific, must therefore take place from the bottom. Thus, tetrahydro-ormojanine would be XIV. On the other hand, the chemical reduction of the C_{16}—C_{17} double bond in XI would be expected to give the more stable compound, and an inspection of models shows that XIII could well be more stable than XIV. This leads to formula XIII for isotetrahydro-ormojanine.

Similar considerations apply if XII were the structure of dihydro-ormojanine. Again, the catalytic reduction would be expected to proceed from the side opposite to the two rings containing the tertiary nitrogen; tetrahydro-ormojanine would therefore be XVI. Furthermore, XV is clearly more stable than XVI; isotetrahydro-ormojanine would thus have structure XV.

The decision between these two possibilities is now quite simple. It can be seen that the



XIII XIV XV XVI XVIa

SCHEME 1.

Can. J. Chem. Downloaded from www.nrcresearchpress.com by 210.87.254.105 on 09/05/12
For personal use only.

Can. J. Chem. Downloaded from www.nrcresearchpress.com by 210.87.254.105 on 09/05/12
For personal use only.

configuration at the important centers C_6, C_{11}, and C_{16} in formula XV is identical with that of piptanthine (II).[6] Since piptanthine is produced both by a catalytic and a chemical reduction of pyridine IX (see above), it can be expected that compound XV would be formed by both reductions, or at the very least one of the reductions, of pyridine X. Since B_3 is identical with homoxytetrahydro-ormojanine, structure XV must therefore definitely correspond to one of the two remaining reduction products of pyridine X, B_1 or B_2. However, neither B_1 nor B_2 are identical with homoxyisotetrahydro-ormojanine (see above); *isotetrahydro-ormojanine must therefore have structure XIII, tetrahydro-ormojanine structure XIV, and dihydro-ormojanine structure XI.*[7] Mechanistic considerations (see below), furthermore, clearly indicate that formula XV must correspond to reduction product B_1 and formula XVI to reduction product B_2.

It still remains to be explained, however, why the chemical reduction of pyridine X gives no isotetrahydro-ormojanine (XIII). It can be seen immediately that this and all other reported facts find a ready explanation when the reasonable assumption is made that the reduction of the pyridine ring with sodium and alcohol is a multistage process in which the tetrahydro-pyridines XVII and XVIII (or the corresponding dihydro-pyridines with an additional double bond at C_{13}—C_{14}) are intermediates.[8] The reduction of XVII can give XIII and XV, but if XV is the more stable compound of the two, only XV and no isotetrahydro-ormojanine (XIII) will be produced. Similarly, the reduction of XVIII can give XIV and XVI; only tetrahydro-ormojanine (XIV) will be produced if it is more stable than compound XVI.

The apparent paradox is thus seen to arise because, in the chemical reduction of dihydro-ormojanine, the stability of isotetrahydro-ormojanine is compared with that of tetrahydro-ormojanine, whereas in the chemical reduction of pyridine X, it is compared with that of isomer XV. In the first case, isotetrahydro-ormojanine is the more stable compound; in the second case, it is the less-stable one.

The above analysis thus explains all the known experimental facts satisfactorily and provides a unique solution of the stereochemistry of the ormojanine reduction products. *Based on the previously deduced gross structure V, ormojanine itself can then be represented by the complete formula XIX.* The opposite configuration at C_{22} in this structure is sterically impossible.

It is interesting to note that, on the basis of the hydrogenation study described above, the synthesis of pyridine VII will represent the total synthesis of one natural product, piptanthine, and four alkaloid reduction products, including tetrahydro-ormojanine. Stereochemically, the synthesis thus simplifies to the preparation of two possible diastereoisomers (VII and its epimer at C_6), which are furthermore connected by the described isomerization at C_6.

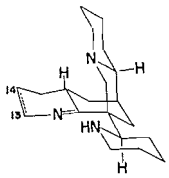
Dasycarpine

After the stereochemical relationships in the ormojanine series had been clarified, the structure and stereochemistry of dasycarpine, $C_{20}H_{35}N_3$, an alkaloid of *Ormosia dasycarpa* (3), were solved in the following simple way. A sample of dasycarpine was subjected to a

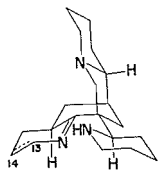
[6]*The two compounds only differ in their configuration at* C_{18}, *and this difference would not be expected to affect significantly the following arguments.*

[7]*Another argument, independent of the piptanthine series, leads to the same conclusion. The assignment of formula XV to isotetrahydro-ormojanine and of XVI to tetrahydro-ormojanine cannot be correct, since it requires that compound XVI not be formed in the catalytic reduction of pyridine X, although an addition of two* α*-hydrogen atoms during this hydrogenation would be expected to be particularly favorable.*

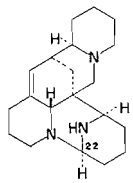
[8]*It is known that the reduction of pyridines with sodium and alcohol proceeds via 1,4-dihydropyridines (12), and it can be expected that an enamine–imine isomerization will precede further reduction.*



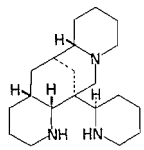
XVII



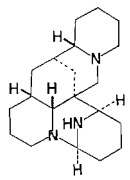
XVIII



XIX



XX



XXI

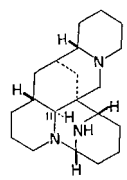
prolonged treatment with platinum in acetic acid in a hydrogen atmosphere at room temperature under conditions identical with those necessary for the ormosanine–piptanthine isomerization. The resulting product was found to be isotetrahydro-ormojanine. *Dasycarpine is therefore epimeric with isotetrahydro-ormojanine at* C_6 *and can be represented by the stereo-formula XX.*

An oily alkaloid isolated from *O. jamaicensis* has been found to give dasycarpine in a mild hydrogenation. This compound is probably identical with ormosajine, $C_{20}H_{33}N_3$, which has been isolated and hydrogenated to dasycarpine by Hassall and Wilson (13, 14). Since the presence of an N—C—N linkage in this alkaloid is indicated by spectroscopy, it can be assigned the structure and stereochemistry XXI.

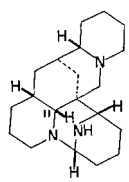
Panamine and Ormosinine

These two alkaloids of *Ormosia panamensis* have been studied under the assumption that they both have the composition $C_{20}H_{33}N_3$ (6, 15).

On the basis of the fact that panamine is converted into ormosanine by a reduction with sodium borohydride (6), and to ormosanine (6) and piptanthine (5) by catalytic hydrogenation, structure XXII was proposed for panamine (15). A recent X-ray analysis (16) confirmed the correctness of this proposal. Thus, panamine is a simple oxidative derivative of ormosanine.



XXII



XXIII

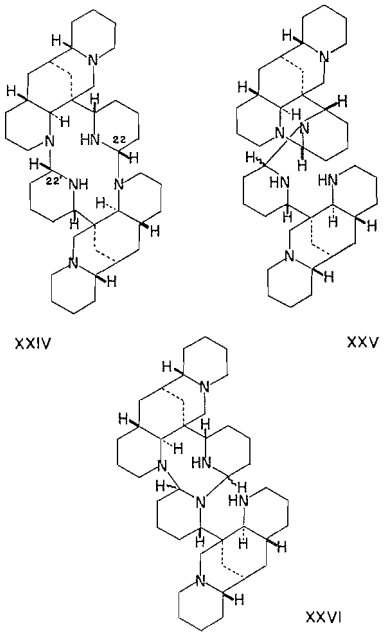
It was furthermore proposed that the alkaloid ormosinine can be represented by formula XXIII (15). The conversion of ormosinine into some derivatives of panamine (6), which requires an epimerization at C_{11} on the basis of this structural assignment, was explained by rather involved isomerization mechanisms (15).

Can. J. Chem. Downloaded from www.nrcresearchpress.com by 210.87.254.105 on 09/05/12
For personal use only.

Our own interest in ormosinine was based on the following considerations. Should XXIII be the correct representation of this alkaloid, then one of its hydrogenation products would clearly be a C_{18}-epimer of dasycarpine and should, after isomerization at C_6, fit into our pyridine reduction series A. We have, however, found that vigorous hydrogenation of ormosinine produces, in addition to ormosanine and piptanthine, two reduction products, neither of which gives A_2 on conversion into the corresponding urea derivatives.

All published data and the above hydrogenation can readily be explained by the fact that *ormosinine is not an isomer but a dimer of panamine.* This follows from the following new findings. (*a*) Sublimation of ormosinine in a high vacuum gave pure panamine. (*b*) A molecular weight determination with a Mechrolab osmometer gave a value of 640 for ormosinine.

The identity of the mass spectra of panamine and ormosinine (6) and the conversion of ormosinine into panamine derivatives (6) can thus be explained in a very simple way.



SCHEME 2.

The only remaining question is the exact nature of the dimer. There are several ways in which two molecules of panamine (in the open imine form) can dimerize, and the available evidence does not lead to a unique solution. The structural possibilities are given in Scheme 2.[9] On the basis of steric considerations and a study of urea formation (see Experimental), we consider formula XXIV as the most probable structure of ormosinine.

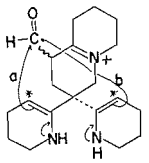
Biogenesis

One of the unusual aspects of *Ormosia* alkaloid stereochemistry is the fact that the natural alkaloid ormosanine is racemic (6). Furthermore, our work has shown (5) that piptanthine from *Piptanthus nanus* and panamine from *Ormosia panamensis* belong to antipodal series.[10]

[9] *Additional structures with an opposite configuration at* C_{22} *and (or)* $C_{22'}$ *in XXIV are also sterically possible.*

[10] *Piptanthine form P. nanus is levorotatory (7), whereas piptanthine formed by the reduction and isomerization of panamine is dextrorotatory (5, 6).*

Can. J. Chem. Downloaded from www.nrcresearchpress.com by 210.87.254.105 on 09/05/12
For personal use only.



XXVII

It is interesting to note that the existence of both antipodal series in this class of alkaloids can be explained in a particularly simple manner by the postulate of a biogenetic intermediate of the type XXVII, formed by the condensation of four lysine units (10, 15). The enol of aldehyde XXVII has a plane of symmetry, and the two corresponding enantiomeric aldehydes can condense with the appropriate C*-atom (arrows *a* or *b* in formula XXVII) to give the two antipodal pentacyclic derivatives.

EXPERIMENTAL

Nuclear magnetic resonance spectra were recorded in $CDCl_3$ on a Varian HR-60 spectrometer, and chemical shifts are reported in parts per million relative to an internal tetramethylsilane reference. Infrared spectra were obtained with Perkin–Elmer model 21 and 137B Infracord instruments, and ultraviolet spectra were recorded on a Beckman DK-2 instrument and mass spectra on a Hitachi Perkin–Elmer RMU-6D instrument. All melting points are uncorrected.

Isomerization of Ormosanine

Ormosanine (35 mg) was stirred in a hydrogen atmosphere in acetic acid (10 ml) in the presence of platinum oxide (100 mg) at room temperature and normal pressure for 1 day. The catalyst was removed by filtration and the solution evaporated. Distribution between ether and 1 *N* hydrochloric acid, followed by basification of the aqueous layer with ammonia and its extraction with ether gave 29 mg of a basic material. To convert it into the corresponding urea, the residue was dissolved in dry benzene, one drop of triethylamine was added, and phosgene gas was bubbled through the solution for 1 min. The solution was then extracted with 1 *N* hydrochloric acid, and the aqueous layer was basified with ammonia and extracted with ether. The resulting mixture of two homoxy-derivatives (thin-layer chromatography (t.l.c.)) was purified by preparative t.l.c., using alumina and ether–benzene (1:4).

The faster moving fraction (11 mg) crystallized from petroleum ether and was found to be identical with homoxypiptanthine (IV) (2)[11] in t.l.c. and infrared and nuclear magnetic resonance spectra.

The slower moving fraction (8 mg) was homoxy-ormosanine (III) (8) on the basis of melting point, t.l.c., and infrared spectrum.

The same catalytic isomerization was performed, starting with homoxy-ormosanine (52 mg). Preparative t.l.c. again gave pure homoxypiptanthine (7 mg) and homoxy-ormosanine (27 mg).

Chemical Reduction of Dihydro-ormojanine

Dihydro-ormojanine (200 mg) (8) and ethylene diamine (40 ml) were heated to 90 °C in a purified nitrogen atmosphere in a dried apparatus protected with a mercury seal. Lithium wire (2.5 g) was then added in small portions to the stirred solution over a period of 45 min, the temperature being maintained at 90–100° (17). The mixture was then refluxed for 1 h and allowed to stand at room temperature for 15 h. After a careful addition of water under ice cooling, the mixture was acidified with concentrated hydrochloric acid and extracted with ether. The aqueous layer was basified with sodium hydroxide and extracted with ether to give 110 mg of a basic material. Crystallization from acetone gave pure isotetrahydro-ormojanine, m.p. 135–136°. The mass spectrum shows the expected molecular ion peak at *m/e* 317. Infrared maximum (CCl_4) at 3 300 cm^{-1} (NH, sharp).

Treatment of isotetrahydro-ormojanine with phosgene in the usual manner gave the homoxy derivative, showing a molecular ion peak at *m/e* 343 in its mass spectrum and an amide maximum at 1 610 cm^{-1} in its infrared spectrum ($CHCl_3$).

Isotetrahydro-ormojanine was found to be distinctly different from tetrahydro-ormojanine (8), ormosanine (1), and piptanthine (2) in melting point and infrared and nuclear magnetic resonance spectra.

Catalytic Reduction of Pyridine VII

Pyridine VII (1.08 g), prepared by the dehydrogenation of dihydro-ormojanine (8), was hydrogenated in the presence of platinum oxide (100 g) in acetic acid (70 ml) for 20 h at room temperature and normal pressure. The solution was filtered and evaporated, and the residue was distributed between aqueous ammonia and ether. The dried ether extract (1.10 g) showed only one spot in t.l.c. Maxima in the nuclear magnetic

[11] *We thank the Czech workers for a sample of piptanthine from P. nanus.*

Can. J. Chem. Downloaded from www.nrcresearchpress.com by 210.87.254.105 on 09/05/12
For personal use only.

resonance spectrum (CCl_4) at 1.83 (1 H, multiplet) and 2.80–3.40 τ (2 H's, multiplet) together with the ultraviolet spectrum (inflection 263, λ_{max} 268 (ϵ 3 400), inflection 275 mμ) clearly show that only one (α,β-substituted) pyridine ring is present in the product. Purification and characterization of this product as a mixture of pyridines IX and X is described below.

N-Acetyl Derivatives of Pyridines IX and X

The above mixture (68 mg) was acetylated with acetic anhydride (5 ml) in pyridine (5 ml) for 15 h at room temperature. The usual work-up gave 65 mg of a basic material which showed two spots in t.l.c. on alumina with benzene–ether (1:1) as eluent. Preparative t.l.c. gave one compound (R_f 0.6) as an oil (26 mg).

Anal. Calcd. for $C_{22}H_{31}N_3O$: C, 74.74; H, 8.88; O, 4.53; N, 11.88. Found: C, 74.12; H, 8.73; O, 4.42; N, 10.89.

Nuclear magnetic resonance maxima at 1.73 (1 H, multiplet), 2.70–3.20 (2 H's, multiplet), and 7.80 τ (*N*-acetyl, singlet).

The second acetyl derivative (R_f 0.4) weighed 31 mg and, after crystallization from ether, melted at 195–197°.

Anal. Found: C, 74.26; H, 8.60; O, 4.39; N, 10.99.

Nuclear magnetic resonance maxima at 1.70 (1 H, multiplet), 2.70–3.20 (2 H's, multiplet), and 7.65 and 7.70 τ (*N*-acetyl, two singlets).

N-Carbobenzyloxy Derivatives of Pyridines IX and X

The above mixture of pyridines IX and X (1.10 g) was dissolved in methylene chloride (175 ml), and the solution was mixed with water (50 ml) and magnesium oxide (280 mg). Benzyl chloroformate (3.6 g) in methylene chloride (75 ml) was added to the stirred mixture over a period of 90 min at ice-bath temperature. The stirring was continued for an additional hour, the mixture was acidified with dilute hydrochloric acid, and the organic layer was extracted exhaustively with 2 *N* hydrochloric acid. The combined aqueous layers were basified with ammonia and extracted with ether to give 1.54 g of a basic material. Thin-layer chromatography on alumina with ether indicated two compounds different from the starting material.

These were separated by column chromatography on neutral alumina (Woelm, activity 2, 80 g), taking 100 ml fractions and analyzing them by t.l.c. Elution with benzene – petroleum ether (1:2 (2.5 l) and 1:1 (500 ml)) gave pure *N*-carbobenzyloxy IX (630 mg), elution with benzene – petroleum ether (3:1, 800 ml) gave a mixture of the two isomers (120 mg), and elution with ether (500 ml) gave pure *N*-carbobenzyloxy X (790 mg). The two compounds, which could not be induced to crystallize, were found to be homogeneous by t.l.c. and showed the expected ultraviolet (λ_{max} 268 mμ), infrared (maxima at 1 680 and 1 580 cm^{-1}), and nuclear magnetic resonance spectra (a multiplet at 1.7 τ for 1 H, a multiplet at 2.8–3.3 τ for 7 H's, and a broad singlet at 5.0 τ for the benzylic CH_2).

Pyridines IX and X

N-Carbobenzyloxy IX (200 mg) was hydrogenolyzed in acetic acid (95%, 10 ml) with palladium on charcoal (10%, 40 mg) in a hydrogen atmosphere for 12 h. The usual work-up gave 140 mg of pure oily pyridine IX, homogeneous in t.l.c. Infrared maxima (CCl_4) at 3 300 (NH) and 1 560 cm^{-1} (broad); nuclear magnetic resonance maxima (CCl_4) at 1.81 (1 H, multiplet), 2.8–3.3 (2 H's, multiplet), and 8.11 τ (C_{10}-methylene, quadruplet).

N-Carbobenzyloxy X (156 mg) was hydrogenolyzed in the same manner to give 108 mg of pure oily pyridine X. Infrared maxima (CCl_4) at 3 300 (NH) and 1 560 cm^{-1} (broad); nuclear magnetic resonance maxima at 1.83 (1 H, multiplet), 2.8–3.3 (2 H's, multiplet), and 8.20 τ (C_{10}-methylene, singlet).

The pyridines IX and X show identical R_f values in all t.l.c. systems tried; their separation was therefore found to be possible only through the above derivatives.

Catalytic Reduction of IX

Pyridine IX (75 mg) was hydrogenated in acetic acid (10 ml) with platinum oxide (110 mg) at 100° and 2 200 p.s.i. for 12 h. The usual work-up gave 58 mg of a basic material. Since a preliminary study indicated that the product slowly decomposed on chromatography, it was immediately treated with phosgene and triethylamine in benzene (see above). The product (50 mg) was shown to be a mixture of two homoxy derivatives by t.l.c.

Separation was achieved by preparative t.l.c., using alumina and benzene–ether (1:1). The faster moving fraction was further purified by a second preparative t.l.c. under the same conditions, and the resulting crystalline product, A_1 (12 mg), m.p. 153–155°, was found to be identical in infrared spectrum and t.l.c. with homoxypiptanthine (2).

The second compound, A_2 (8 mg), crystallized from petroleum ether and melted at 164–165°. Its mass spectrum (molecular ion peak at *m/e* 343) confirms its composition. Its infrared spectrum contains the urea maximum at 1 620 cm^{-1} ($CHCl_3$); the fingerprint region, furthermore, shows that A_2 is not identical with the homoxy derivative of any of the known $C_{20}H_{35}N_3$ *Ormosia* isomers.

Chemical Reduction of IX

To a solution of pyridine IX (200 mg) in boiling isoamyl alcohol (30 ml) was added sodium (2.0 g) in small pieces during 90 min. The cooled solution was extracted with 1 *N* hydrochloric acid, and the aqueous

Can. J. Chem. Downloaded from www.nrcresearchpress.com by 210.87.254.105 on 09/05/12
For personal use only.

layer was washed with ether, basified, and extracted with ether. The residue was treated with phosgene in the usual way to give 156 mg of two homoxy derivatives (t.l.c.).

The faster moving fraction was obtained in a pure state (39 mg) by column chromatography with benzene on neutral alumina (Woelm, grade 2, 7.5 g) and identified as homoxypiptanthine, A_1.

The second compound could not be obtained in a pure state by column chromatography. The preparative t.l.c. method gave the pure product (10 mg), identical in all respects with A_2 (see above).

Catalytic Reduction of X

Pyridine X (76 mg) was hydrogenated in acetic acid (10 ml) with platinum oxide (20 mg) at 115° and 2 500 p.s.i. for 3 days. The usual work-up gave 40 mg of a basic material, which was immediately treated with phosgene as above. The product (40 mg), containing two compounds (t.l.c.), was subjected to preparative t.l.c. on alumina, with benzene–ether (1:1) as eluent.

The faster moving fraction, B_2 (15 mg), crystallized from petroleum ether and melted at 224–225°. Its mass spectrum shows the expected molecular ion peak at *m/e* 343; the infrared spectrum ($CHCl_3$) shows the urea peak at 1 610 cm^{-1}.

The second fraction, B_1 (11 mg), crystallized from petroleum ether and melted at 158–159°. Its mass spectrum shows the expected molecular ion peak at *m/e* 343, and its infrared spectrum ($CHCl_3$) contains the urea peak at 1 610 cm^{-1}.

The physical properties of B_1 and B_2 (melting point and infrared, nuclear magnetic resonance, and mass spectra) clearly show the non-identity of these compounds with the homoxy derivatives of ormosanine, piptanthine, tetrahydro-ormojanine, and isotetrahydro-ormojanine.

Chemical Reduction of X

Sodium (1.2 g) was added in small pieces during 90 min to a boiling solution of pyridine X (108 mg) in isoamyl alcohol (15 ml). The usual work-up (see above) gave 100 mg of a basic material, which was subjected to an additional reduction with sodium (1.2 g) in isoamyl alcohol (15 ml). The resulting basic material (70 mg) was subjected to preparative t.l.c. on silica, using 4% dimethylamine in petroleum ether as eluent.

The faster moving fraction (10 mg) was treated with phosgene as described above, and the resulting homoxy derivative was purified by preparative t.l.c. on alumina with benzene–ether (1:1). The pure product (7 mg) melted at 158–159° and was found to be identical with B_1, produced by the catalytic reduction of pyridine X.

The second fraction (7 mg) was also treated with phosgene and the product purified by preparative t.l.c. on alumina with benzene–ether (1:1). The resulting pure compound (4 mg) crystallized from petroleum ether and melted at 203–205°. This compound, B_3, was found to be identical in all respects (melting point, t.l.c., and infrared and mass spectra) with homoxytetrahydro-ormojanine (8).

Isomerization of Dasycarpine

(*a*) Dasycarpine (34 mg) (3)[12] was stirred in a hydrogen atmosphere in acetic acid (10 ml) in the presence of platinum oxide (100 mg) at room temperature and normal pressure for 3 weeks. The usual work-up gave 34 mg of a basic material, which was treated with phosgene as described above. Thin-layer chromatographic analysis of the product on alumina with ether – petroleum ether (1:1) as eluent showed the presence of two compounds with R_f values of 0.4 and 0.5, respectively.

Preparative t.l.c. on alumina with ether – petroleum ether (7:3) as eluent achieved a complete separation. The faster moving compound was found to be identical in all respects with homoxyisotetrahydro-ormojanine (see above). The slower moving compound was homoxydasycarpine (3). The two compounds were isolated in approximately equal quantities.

Although homoxyisotetrahydro-ormojanine shows a strong band at 2 750 cm^{-1} in the infrared spectrum ($CHCl_3$), this band is completely absent from the spectrum of homoxydasycarpine. This is analogous to the piptanthine–ormosanine pair.

(*b*) Mother liquors from the crystallization of ormosanine and ormojanine from *O. jamaicensis* (8) were subjected to a nine-funnel countercurrent distribution, using ether and McIlvaine's buffer (pH 7.3), with the buffer as a moving phase. Fraction 7 (1.95 g from 13.5 g of the original mixture) contained a foam which was homogeneous in t.l.c. and showed an R_f value of 0.4 on alumina with 4% methanol in benzene. Sublimation in a high vacuum gave a colorless oil; nuclear magnetic resonance maximum at 6.50 τ (1 H, broad singlet). This compound is probably identical with the alkaloid ormosajine (13, 14).

The oily sublimed alkaloid (215 mg) was hydrogenated for 16 h in 2% aqueous hydrochloric acid (40 ml) in the presence of platinum oxide (400 mg) at room temperature and normal pressure. The usual work-up gave 200 mg of a basic material which, on the basis of t.l.c. analysis (3% diethylamine in petroleum ether on silica), consisted of approximately equal amounts of two products with R_f values of 0.4 and 0.3, respectively.

Preparative t.l.c. with the above system achieved a complete separation. The component, R_f 0.3, was found to be identical with dasycarpine (3), and the second component, R_f 0.4, was isotetrahydro-ormojanine.

[12]*We thank Drs. Clarke and Grundon for this sample.*

Can. J. Chem. Downloaded from www.nrcresearchpress.com by 210.87.254.105 on 09/05/12
For personal use only.

Ormosinine

The alkaloids ormosinine, m.p. 219–220°, and panamine were isolated from *O. panamensis* by the procedure reported by Lloyd and Horning (18). Ormosinine shows a strong sharp NH maximum at 3 300 cm^{-1} in the infrared spectrum (CCl_4) and a broad singlet at 6.56 τ characteristic of the N—CH—N grouping in the nuclear magnetic resonance spectrum.

A molecular weight determination with Mechrolab osmometer model 301 in carbon tetrachloride (four independent measurements) gave a value of 640 ∓ 30 for ormosinine.

Sublimation of ormosinine at 250° and 0.4 mm gave a quantitative yield of panamine (sublimate), identified by infrared and nuclear magnetic resonance spectra.

Thin-layer chromatographic analysis of crystalline ormosinine on silica with 7% diethylamine in petroleum ether (double elution) revealed the presence of two components, R_f 0.5 and 0.45, respectively. It is not yet certain whether crystalline ormosinine consists of two different dimers or whether a partial conversion takes place during chromatography.

Vigorous hydrogenation of ormosinine in acetic acid with platinum oxide at 40° and 1 850 p.s.i. for 20 h gave, in addition to starting material, four reduction products. After the conversion of the mixture into the corresponding homoxy derivatives, homoxy-ormosanine and homoxypiptanthine were isolated from the mixture by column chromatography on alumina. The two remaining compounds were separated by preparative t.l.c. on alumina, with ether as eluent. One of them crystallized from petroleum ether and melted at 245°, and the second one remained oily. Both compounds are almost certainly dimeric, since their mass spectra show fragments with *m/e* above 400.

Homoxy-ormosinine

Ormosinine (130 mg) was treated in the usual way with phosgene in dry benzene (15 ml) and triethylamine (0.5 ml). The usual extraction gave a quantitative yield of a basic material. The infrared spectrum of the product in chloroform showed a carbonyl absorption at 1 720 and a double maximum at 1 630 cm^{-1}. Although it has so far not been possible to achieve a separation, it appears possible that the maxima at 1 630 cm^{-1} indicate the presence of ureas formed after a partial opening of the dimer, and the maximum at 1 720 cm^{-1} corresponds to the homoxy derivative of XXIV, in which the geometry of the relevant orbitals would not allow the usual amide resonance.

Hydrogenation of Panamine

Panamine (18) (1.4 g) was hydrogenated in 4% hydrochloric acid (50 ml) in the presence of platinum oxide (550 mg) at room temperature and normal pressure for 16 h. The resulting basic material, obtained in a quantitative yield, was converted into the homoxy derivative on treatment with phosgene and triethylamine in benzene (see above). Separation of a portion of this product by t.l.c. on alumina with ether – petroleum ether (1:1) gave pure homoxy-ormosanine and pure homoxypiptanthine.

The original hydrogenation mixture could, without conversion into ureas, be separated by preparative t.l.c. on silica with 5% diethylamine in petroleum ether. The two components were identified as ormosanine and piptanthine.

ACKNOWLEDGMENT

The authors are grateful to the National Research Council, Ottawa, for the financial support of this work.

REFERENCES

1. H. A. Lloyd and E. C. Horning. J. Org. Chem. **25**, 1959 (1960).
2. U. Eisner and F. Sorm. Collection Czech. Chem. Commun. **24**, 2348 (1959).
3. R. T. Clarke and M. F. Grundon. J. Chem. Soc. 41 (1960); 535 (1963).
4. I. L. Karle and J. Karle. Tetrahedron Letters, 2065 (1963).
5. P. Deslongchamps, J. S. Wilson, and Z. Valenta. Tetrahedron Letters, 3893 (1964).
6. P. Naegeli, W. C. Wildman, and H. A. Lloyd. Tetrahedron Letters, 2069 (1963).
7. R. A. Konovalova, B. S. Diskina, and M. S. Rabinovich. Zh. Obshch. Khim. **21**, 773 (1951).
8. Z. Valenta, P. Deslongchamps, M. H. Rashid, R. H. Wightman, and J. S. Wilson. Can. J. Chem. This issue.
9. F. Bohlmann. Chem. Ber. **91**, 2157 (1958).
10. Z. Valenta, P. Deslongchamps, M. H. Rashid, R. H. Wightman, and J. S. Wilson. Tetrahedron Letters, 1559 (1963).
11. P. Naegeli, R. Naegeli, W. C. Wildman, and R. J. Highet. Tetrahedron Letters, 2075 (1963).
12. B. D. Shaw. J. Chem. Soc. **127**, 215 (1925).
13. C. H. Hassall and E. M. Wilson. Chem. Ind. London, 1358 (1961).
14. C. H. Hassall and E. M. Wilson. J. Chem. Soc. 2657 (1964).
15. E. M. Wilson. Tetrahedron, **21**, 2561 (1965).
16. I. L. Karle and J. Karle. Tetrahedron Letters, 1659 (1966).
17. L. Reggel, R. A. Friedel, and I. Wender. J. Org. Chem. **22**, 891 (1957).
18. H. A. Lloyd and E. C. Horning. J. Am. Chem. Soc. **80**, 1506 (1958).

Can. J. Chem. Downloaded from www.nrcresearchpress.com by 210.87.254.105 on 09/05/12
For personal use only.

Can. J. Chem. Downloaded from www.nrcresearchpress.com by 210.87.254.105 on 09/05/12
For personal use only.

ISOTOPE EFFECT STUDIES ON ELIMINATION REACTIONS

V. THE MECHANISM OF THE CARBONYL ELIMINATION REACTION OF 9-FLUORENYL NITRATE WITH ACETATE ION[1]

P. J. SMITH[2] AND A. N. BOURNS

Department of Chemistry, Hamilton College, McMaster University, Hamilton, Ontario

Received June 30, 1966

ABSTRACT

The carbonyl elimination reaction ($E_{CO}2$) of 9-fluorenyl nitrate with acetate ion in anhydrous ethanol was found to be second order and to give at 30° primary nitrogen-15 and deuterium isotope effects of 1.0091 ± 0.0007 and 4.3 ± 0.2, respectively. The ester showed no deuterium exchange with solvent under the reaction conditions. A change in solvent to 85 volume % ethanol–water increased the nitrogen isotope effect to 1.0131 ± 0.0007 without changing the deuterium effect. These results exclude any form of two-stage carbanion intermediate mechanism, but are in accord with a concerted process.

INTRODUCTION

Nitrate esters of benzyl alcohol and its ring-substituted derivatives show competing reactions of substitution and elimination when treated with a strong base (1, 2).

Substitution (S_N2):

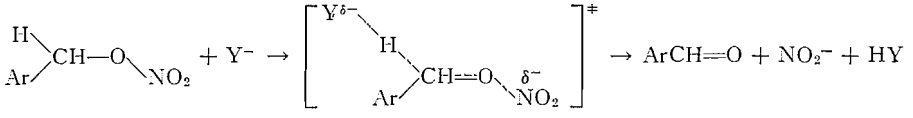
[1] $$ArCH_2ONO_2 + Y^- \rightarrow ArCH_2Y + NO_3^-$$

Carbonyl elimination ($E_{CO}2$):

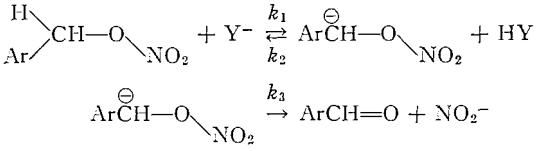
[2] $$ArCH_2ONO_2 + Y^- \rightarrow ArCH{=}O + NO_2^- + HY$$

By analogy with other second-order elimination processes, two mechanisms have been considered for the latter.

Concerted mechanism:

[3] 

Two-step mechanism:

[4] 

In a previous investigation (3) in our laboratory, the combination of a test for deuterium exchange and the determination of the nitrogen isotope effect successfully distinguished between the two mechanisms for the reaction of benzyl nitrate with ethoxide ion in anhydrous ethanol. It was found that ester recovered from a reaction carried part way to completion in ethanol-O-*d* contained a barely detectable amount of the tracer. This virtual absence of exchange can be accommodated by the two-step mechanism only if the formation of the intermediate were to be rate determining ($k_3 \gg k_2[HY]$), a condition which is excluded by the observation of a primary nitrogen isotope effect of

[1] *For Part IV in this series, see A. N. Bourns and P. J. Smith, Proc. Chem. Soc., 366 (1964).*

[2] *Holder of a National Research Council studentship, 1963–1964.*

2% ($k^{14}/k^{15} = 1.020$). These results, however, as well as a deuterium isotope effect, k^H/k^D, of 5.0, are in accord with the concerted mechanism.

For base-promoted β-elimination reactions forming a carbon–carbon double bond, the concerted mechanism (E2) has been found to have broad generality and to be supplanted by a two-step process (E1*cb*) only in very infrequently encountered cases where the reactant has structural features which give exceptional stability to an intermediate carbanion (4, 5). In the carbonyl elimination of nitrate esters, however, reaction by the latter pathway might be expected to be more favorable because of the strong acidifying effect of the electron-withdrawing nitrate group. It was with the objective of exploring this possibility that the study has now been extended to 9-fluorenyl nitrate, which has previously been shown to undergo carbonyl elimination to give fluorenone in a high yield on treatment with methanolic potassium hydroxide (6) or with benzylamine, morpholine, or pyridine in acetonitrile (7, 8). A rough indication of the relative acidity of fluorenyl and benzyl nitrates is found from a comparison of the acid dissociation constants of the corresponding parent hydrocarbons. The pK_a of fluorene has been estimated variously as 25 (9) and 31 (10), whereas that of toluene is at least 37 (11) and is probably very much higher (10). It seems inherently reasonable, therefore, that the two esters might react by different mechanisms.

Unfortunately, the reaction of fluorenyl nitrate with alkoxide ion was found to be too rapid for a deuterium exchange test and nitrogen isotope effect measurements at ester concentrations suitable for such experiments. Also, the use of an amine as base seemed to be unsuitable because of possible contamination of the nitrogen from the nitrite ion by nitrogen from the amine in the isotope effect studies. A satisfactory base, however, was found in acetate ion in anhydrous and aqueous ethanol. In the anhydrous solvent, the carbonyl elimination reaction gives nitrite ion in about a 90% yield and is in competition with an S_N2 reaction giving nitrate ion. In aqueous ethanol, the carbonyl elimination accounts for less than 70% of the total reaction, and nitrate ion is formed by solvolysis as well as by a displacement with acetate ion. Despite these complications, it is possible, by using the methods described in the previous paper (3), to determine both the nitrogen and deuterium isotope effects associated with the elimination process. Measurements were made in both aqueous and anhydrous ethanol, since it was hoped that the influence of the medium on the magnitude of the isotope effects might provide further insight into the mechanism of the process.

RESULTS

Kinetics of the Reaction of Fluorenyl Nitrate with Acetate Ion in Anhydrous and Aqueous Ethanol

The kinetics of the reaction were studied under pseudo first order conditions with a large excess of acetate ion. The total reaction rate (carbonyl elimination and substitution) was followed spectrophotometrically and the fraction of each was determined by measuring the yields of nitrite and nitrate ions. In anhydrous ethanol, nitrate ion was formed only by S_N2 displacement with acetate ion. In 85% ethanol, however, solvolysis was significant and accounted for approximately one-third of the nitrate ion produced (10% of the total reaction rate).

The results of these kinetic experiments are shown in Table I. It is seen that in anhydrous ethanol the second-order rate constant ($k_2 = k_1/[\mathrm{MOAc}]$, where k_1 is the pseudo first order constant and [MOAc] is the concentration of acetate salt) decreases significantly with increasing concentration of the acetate salt. Furthermore, a comparison of the results of expts. 5 and 6 shows that this effect is found even when the ionic strength

Can. J. Chem. Downloaded from www.nrcresearchpress.com by 210.87.254.105 on 09/05/12
For personal use only.

of the medium is kept constant by addition of lithium perchlorate. A similar situation has been observed by Berliner (12) in the bromination of naphthalene and fluorene in aqueous acetic acid, and it has been attributed to a primary salt effect, which is different for acetate and perchlorate salts. Although this may be the origin of the trend in rate constants found in the present study, an alternative explanation is an increased dissociation at higher dilutions of ion pairs (and triplets and higher aggregates) to the more reactive dissociated acetate ion. It is also noteworthy that the second-order rate constants for reaction in both anhydrous and aqueous ethanol are higher the lower the concentration of fluorenyl nitrate (compare expts. 7 and 8, and 9 and 10). The reason for this is not clear, although it may only be a medium effect.

TABLE I

Kinetic results for the reaction of 9-fluorenyl nitrate with acetate ion

Expt. No.	Temperature (°C)	[Ester] (M)	[KOAc] (M)	[$LiClO_4$] (M)	% E_{CO2} reaction	$k_2 \times 10^4$ (l mole^{-1} s^{-1}) Total	$k_2 \times 10^4$ (l mole^{-1} s^{-1}) E_{CO2}
			Solvent: anhydrous EtOH				
1	40.5	0.011	0.12	—	93	11.4	10.6
2	40.5	0.011	0.17	—	93	10.9	10.1
3	40.5	0.012	0.24	—	93	10.3	9.6
4	40.5	0.014	0.29	—	93	9.8	9.1
5	40.5	0.005	0.090*	0.045	88	10.3	9.0
6	40.5	0.009	0.135*	—	88	9.1	8.0
7	30.0	0.017	0.31	—	94	3.4	3.2
8	30.0	0.005	0.31	—	94	3.9	3.7
			Solvent: 85 volume % EtOH–N_2O				
9	30.0	0.024	0.37	—	67	1.38	0.92
10	30.0	0.005	0.37	—	70	1.57	1.10

*LiOAc was used in place of KOAc.

Finally, the rates in both solvents were found to be reduced only very slightly by addition of acetic acid. This establishes that it is acetate ion and not ethoxide or hydroxide ion which is acting as the base in the elimination reaction.

Deuterium Isotope Effects

The deuterium isotope effects for reaction with potassium acetate in anhydrous ethanol and 85 volume % ethanol–water at 30° were determined by separately measuring the rate constants for the reaction of 9-fluorenyl nitrate and 9-fluorenyl-9-*d* nitrate by the method described in the previous section. In every case, the reactions with labelled and unlabelled compounds were run in parallel. The results are shown in Table II.

TABLE II

Hydrogen–deuterium isotope effects in the carbonyl elimination reaction of 9-fluorenyl nitrate with acetate ion at 30°

	Anhydrous ethanol*		85 volume % ethanol–water†	
	$C_{12}H_8CHONO_2$	$C_{12}H_8CDONO_2$	$C_{12}H_8CHONO_2$	$C_{12}H_8CDONO_2$
% E_{CO2}	95.2	87.4	67.7	42.7
$10^5 k_{total}$‡	33.1	8.47	15.5	5.78
$10^5 k_{E_{CO2}}$‡	31.5	7.40	10.5	2.47
$(k_H/k_D)_{E_{CO2}}$	4.26±0.20§		4.25±0.20§	

*[Ester] = 0.013 M; [KOAc] = 0.29 M.
†[Ester] = 0.006 M; [KOAc] = 0.42 M.
‡Rate constants are in liters mole^{-1} second^{-1}.
§Estimated maximum uncertainty based on the reproducibility of nitrite ion yields and rate constant values.

Can. J. Chem. Downloaded from www.nrcresearchpress.com by 210.87.254.105 on 09/05/12
For personal use only.

Deuterium Exchange Tests

Deuterium exchange tests were carried out in anhydrous C_2H_5OD at 40° and in 85% C_2H_5OD – 15% D_2O at 30°. Reactant recovered after approximately one half-life was found to have no isotopic enrichment within the limits of detection, which were less than 0.04 atom %.

Kinetic Nitrogen Isotope Effects

The nitrogen isotope effect for the carbonyl elimination reaction in each of three solvents (anhydrous ethanol, 92 volume % ethanol–water, and 85 volume % ethanol–water) was obtained by comparing the $^{14}N/^{15}N$ ratio of fluorenyl nitrate of natural isotopic abundance with that of nitrite ion formed in the reaction of the ester carried to some known extent of completion. Selective reduction of the nitrite ion to ammonia accomplished the separation of the nitrogen of this ion from that of the nitrate ion formed in the simultaneous S_N1 and S_N2 displacement reactions (3). The ammonia was then converted into nitrogen gas, which was analyzed by mass spectrometry. The isotopic abundance for the reactant was obtained by analysis of the nitrogen gas similarly formed from nitrite plus nitrate ion produced in a reaction which had been allowed to proceed to completion. Different preparations of ester were used for measurements in anhydrous and aqueous ethanol, and isotopic analyses were performed on each. The results given in Table III show an isotope effect, k^{14}/k^{15}, of 1.009 in anhydrous ethanol, increasing to 1.013 in 85% aqueous ethanol. These values may be compared with 1.020 found previously (3) for the reaction of benzyl nitrate with ethoxide ion.

TABLE III

$^{14}N/^{15}N$ ratios and the kinetic isotope effects in the carbonyl elimination reaction of 9-fluorenyl nitrate with potassium acetate at 30°

Expt. No.	volume % EtOH	Total reaction (%)	$^{14}N/^{15}N$* $NO_2^- + NO_3^-$	$^{14}N/^{15}N$* NO_2^-	k^{14}/k^{15}
Ester preparation A					
1	100	100	266.04		
2	100	100	266.22		
3	100	100	266.22		
4	100	100	266.22		
5	100	100	266.48		
			Mean 266.24±0.16†		
6	100	13		268.72	1.0098
7	100	13		268.50	1.0086
8	100	13		268.66	1.0095
9	100	13		268.34	1.0084
10	100	13		268.72	1.0098
					Mean 1.0091±0.0007†
Ester preparation B					
11	100	100	268.40		
12	100	100	268.52		
13	100	100	268.60		
14	100	100	268.42		
			Mean 268.49±0.10†		
15	92	16		271.12	1.0106
16	92	20		271.08	1.0104
					Mean 1.0105
17	85	20		271.54	1.0123
18	85	18		271.96	1.0139
19	85	26		271.68	1.0133
20	85	22		271.70	1.0129
					Mean 1.0131±0.0007†

*The isotopic ratios are relative to a standard nitrogen source whose $^{14}N/^{15}N$ ratio was arbitrarily chosen as 136.500.
†The limits shown are standard deviations of the mean.

Can. J. Chem. Downloaded from www.nrcresearchpress.com by 210.87.254.105 on 09/05/12
For personal use only.

Test for Nitrogen Isotopic Exchange Between NO_2^- and NO_3^-

Since fluorenol–fluorenone is a good oxidation system, it was necessary to establish that there is no isotopic exchange between nitrite and nitrate ions under the reaction conditions and in the subsequent work-up. A solution containing ^{15}N-enriched sodium nitrate, isotopically normal sodium nitrite, potassium acetate, acetic acid, fluorenone, and fluorenol in absolute ethanol was maintained at 30° for 1 h. Nitrite and nitrate ions were separated by the method used in the isotope effect studies, and the nitrogen isotopic abundance of the recovered nitrate was compared with that of the original material. From the results shown in Table IV, it is concluded that there is no significant isotopic exchange between the two ions.

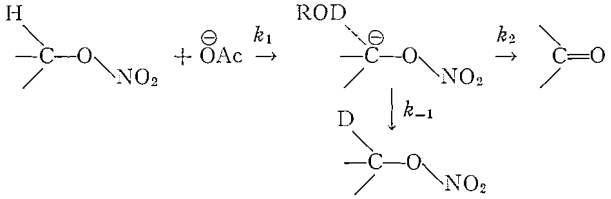
TABLE IV

Test for isotopic exchange between NO_3^- and NO_2^-

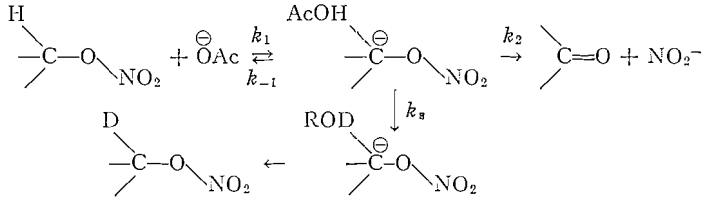
Nitrate samples	atom % ^{15}N
Original	2.28
	2.31
Recovered	2.35
	2.34

DISCUSSION

The absence of detectable deuterium exchange with the solvent, ROD, coupled with a primary nitrogen isotope effect of 0.9% or more, excludes reaction by way of a carbanion intermediate which is hydrogen bonded at the 9-position by a molecule of solvent (eq. [5]). If $k_2 \gg k_{-1}$, there would be no isotope effect, whereas any other relationship of these rate constants would result in some incorporation of deuterium in the unreacted ester. One is not jusified, however, on the basis of these observations alone, in concluding

[5] 

that the fluorenyl nitrate reaction is a concerted process, since there is a modification of the two-step mechanism which could give rise to a primary nitrogen isotope effect without requiring hydrogen exchange with the solvent. This is a reaction via a carbanion which is specifically hydrogen bonded to the acetic acid molecule formed by abstraction of a proton by acetate ion (eq. [6]). If this intermediate were to lose nitrite ion very much

[6] 

faster than it exchanges the hydrogen-bonded acetic acid molecule for a molecule of solvent ($k_2 \gg k_s$), there would be no observable deuterium exchange. Furthermore, if the rate of decomposition of the intermediate to product were not much greater than

Can. J. Chem. Downloaded from www.nrcresearchpress.com by 210.87.254.105 on 09/05/12
For personal use only.

its rate of return to reactants, so as to make the O—N bond rupture step at least partially rate determining, there would be an isotope effect associated with the leaving group.

Such a specifically hydrogen-bonded species has been invoked by Cram (13) to account for the very low or reverse hydrogen isotope effects which have been observed in certain hydrogen exchange reactions. It can be seen that, if this species were formed in a pre-equilibrium step ($k_2 \gg k_{-1}$), the hydrogen isotope effect would be given by $K^H/K^D \cdot k_2^H/k_2^D$, where the K's are equilibrium constants for the first step of eq. [6]. Both of these isotopic ratios would be small; indeed, that for the equilibrium step might even be less than unity, since the vibrational stretching frequency of the O—H bond is greater than that of the original C—H bond (13).

Such a pre-equilibrium formation of the specifically hydrogen-bonded carbanion is precluded in the fluorenyl nitrate reaction by the observation of a deuterium isotope effect, k^H/k^D, of 4.25 at 30°. On the other hand, a rate-determining formation of this intermediate ($k_{-1} \ll k_2$) is also precluded by the observation of the primary nitrogen isotope effect. It should be noted, however, that both isotope effects are small in comparison with those found in the reaction of benzyl nitrate with ethoxide ion (3); in absolute ethanol, the nitrogen effect is 0.9% compared with 2.0% for the latter reaction, and k^H/k^D is 4.25 compared with 5.94.[3] It is possible, therefore, that these smaller effects might arise in a reaction proceeding by the mechanism of eq. [6] in the particular circumstance that the rate constants k_{-1} and k_2 are approximately equal, that is, that the C—H and O—N bond rupture processes are both partially rate determining. However, in this region of approximate equality of the rates for return of the intermediate to reactant and decomposition to product, the isotope effects would be very dependent upon the actual value of the k_{-1}/k_2 ratio, which in turn would be expected to depend upon the medium in which the reaction is carried out. Consequently, the proposed mechanism predicts that *both* the nitrogen and the hydrogen isotope effects should be very sensitive to changes in the solvent.

It can be seen from Table II that the nitrogen isotope effect increases by almost 50% in going from absolute ethanol to 85% aqueous ethanol as solvent. In terms of the mechanism of eq. [6], this would mean an increase in the k_{-1}/k_2 ratio, and therefore a much closer approach to a pre-equilibrium formation of the carbanion intermediate. This, however, would be expected to cause a large decrease in the hydrogen isotope effect (*vide supra*), which is not observed. As shown in Table III, the k^H/k^D ratio is the same within experimental error in the two solvents. Therefore, it is concluded that the reaction of fluorenyl nitrate with acetate ion does not proceed by way of any type of carbanion intermediate and, like the reaction of benzyl nitrate with ethoxide ion, is a concerted process.

That the leaving group isotope effect should be so sensitive to the change in solvent whereas the hydrogen isotope effect remains constant is surprising and requires comment. The nitrogen isotope effect is a measure of the extent to which the composite force constant of the O—N bond is decreased in going from the initial to the transition state (14), and the larger value of the effect in the more ionizing solvent is possibly a consequence of a greater solvation of the incipient nitrite ion tending to weaken this bond. Compensating factors must be responsible for the insensitivity of the hydrogen isotope effect to a change in the medium. There will be a smaller electron density associated with the

[3]*The previously reported effect of 5.04 for benzyl nitrate was for a reaction at 60° (3). A value of 5.94 has been found by the present authors at 30°.*

Can. J. Chem. Downloaded from www.nrcresearchpress.com by 210.87.254.105 on 09/05/12
For personal use only.

three-center system, C---H---O, of the transition state in aqueous ethanol, because of both the smaller base strength of the acetate ion (15) and the greater transfer of charge to nitrogen. This will result in lower bending frequencies associated with the proton being transferred and an increased hydrogen isotope effect (16). The symmetrical stretching frequency of the three-center system also will be solvent dependent, probably in the direction of a higher value in the more aqueous solvent, since the relatively large decrease in the base strength of the acetate ion might be expected to result in a more unsymmetrical transition state, C---H--O (17). This would tend to decrease the hydrogen isotope effect (18–20,). It should be pointed out, however, that our understanding of the relative importance of the different factors which determine the magnitude of hydrogen isotope effects, particularly in multicenter systems such as β-eliminations, is very incomplete (21), and the situation is undoubtedly much more complicated than has been indicated.

EXPERIMENTAL

Materials

9-Fluorenyl Nitrate

This compound was prepared by the action of silver nitrate on 9-bromofluorene in acetonitrile (6) and was recrystallized from petroleum ether (b.p. 30–60°), m.p. 89–90° (lit. m.p. 88–89° (8)).

9-Fluorenyl-9-^{2}H Nitrate

The deuterated compound was prepared by the following reaction sequence: (*a*) reduction of 9-fluorenone to 9-fluorenol-9-^{2}H with lithium aluminium deuteride; (*b*) conversion of the alcohol into 9-bromofluorene-9-^{2}H by means of acetyl bromide; and (*c*) reaction of the bromo compound with silver nitrate. The overall yield of 9-fluorenyl-9-^{2}H nitrate was 60%. The product, recrystallized from petroleum ether, had a melting point of 88.5–89.5° and was at least 99% deuterated in the 9-position, as shown by nuclear magnetic resonance analysis.

9-Fluorenol-9-^{2}H

9-Fluorenone (7.9 g, 0.044 mole) was treated for 8 h with lithium aluminium deuteride (0.92 g, 0.022 mole) in 300 ml of diethyl ether which had been dried by distillation from lithium aluminium hydride. The complex was decomposed by addition of water, the precipitated salts were removed by filtration, and the product was isolated from the ether solution. Recrystallization from benzene gave 7.5 g of 9-fluorenol-9-^{2}H (94% yield), m.p. 157–157.5° (lit. m.p. 156° (22)).

9-Bromofluorene-9-^{2}H

Acetyl bromide (8.3 g, 0.067 mole) was added all at once to 9-fluorenol-9-^{2}H (7.5 g, 0.041 mole) and the flask stoppered. A vigorous reaction set in, and in a short time the mixture solidified. The reaction was completed by warming the mixture on a steam bath, and acetic acid and excess reagents were removed under reduced pressure. The residue was recrystallized from petroleum ether (b.p. 30–60°), giving 8.3 g (83% yield) of 9-bromofluorene, m.p. 102–102.8° (lit. m.p. 102–103° (23)).

Kinetic Measurements

The total reaction rate was followed spectrophotometrically by measuring the optical density of the reaction solutions at 380 mμ, the λ_{max} of the elimination product fluorenone. Since a large excess of acetate ion was used, the concurrent reactions of carbonyl elimination, S_N2 displacement, and solvolysis all follow first-order kinetics, and the rate constant for the nitrite ion forming elimination is given by the product of the rate constant for the disappearance of fluorenyl nitrate and the mole fraction of nitrite ion.

A solution of 9-fluorenyl nitrate (0.005–0.024 *M*) and potassium or lithium acetate (0.09–0.42 *M*) in anhydrous or aqueous ethanol, prepared by mixing temperature-equilibrated solutions of each reactant, was maintained in a constant-temperature bath at $\pm$0.02°. At suitable time intervals 5 ml samples were removed and immediately diluted to 50 ml with ethanol. The optical density of these solutions was measured on either a Beckman model D.U. or a Perkin–Elmer Hitachi spectrophotometer. Also, several times during the reaction 10 ml samples of the reaction solution were withdrawn and added to 15 ml of ether and 15 ml of water. The aqueous layer was separated and washed twice with 5 ml portions of ether. The combined ether layers were extracted 3 times with 5 ml portions of water, and the combined aqueous solutions were analyzed for nitrite and nitrate ions by the method of differential reduction to ammonia described previously (3). As expected, the ratio of nitrite and nitrate ion concentrations remained constant throughout the reaction.

The pseudo first order rate constants for the disappearance of fluorenyl nitrate were determined by plotting log ($OD_\infty - OD_t$) against time for the equation $kt = 2.303 \log ((OD_\infty - OD_0)/(OD_\infty - OD_t))$, where OD_0, OD_∞, and OD_t are the optical densities at time zero, infinity, and t, respectively. The best

Can. J. Chem. Downloaded from www.nrcresearchpress.com by 210.87.254.105 on 09/05/12
For personal use only.

fit of the data was obtained by the method of least squares. These constants were converted into second-order constants by dividing by the concentration of the acetate salt, and the second-order constants were multiplied by $[NO_2^-]/([NO_2^-] + [NO_3^-])$ to give the second-order constants for the carbonyl elimination reaction.

Somewhat less precise rate constants were evaluated from the actual amounts of nitrite and nitrate ions formed at different reaction times. The agreement between these and the constants obtained by the method described in the preceding paragraph was within 3%.

Deuterium Exchange Tests

A solution of potassium acetate in anhydrous C_2H_5OD, prepared by the action of deuterium oxide on sodium ethoxide (3), or 85% C_2H_5OD – 15% D_2O was added to a solution of 9-fluorenyl nitrate in the corresponding solvent, and the reaction[4] was allowed to proceed for approximately one half-life. The reaction was quenched by cooling to 0°, and the solution was then added to an ice-cold mixture of 100 ml of ether and 100 ml of water. The ether layer was separated and the water layer washed thoroughly with fresh ether. The combined ether extracts were washed 5 times with 50 ml portions of water, and the ether solution was dried and concentrated to yield a crude solid nitrate ester. This solid was dissolved in 15 ml of ethanol and extracted 4 times with 25 ml portions of petroleum ether (b.p. 30–60°), with a little water present to cause separation of the layers. The petroleum ether was concentrated to 10 ml and fluorenyl nitrate allowed to crystallize. The ester was recrystallized 5 times from petroleum ether. This elaborate procedure was required to remove fluorenone and to ensure no contamination by the deuterated solvent.

Deuterium analyses were carried out by combustion of the recovered fluorenyl nitrate diluted with some unlabelled ester and measuring the deuterium content of the resulting water by either infrared spectroscopy (24) or by the falling-drop method.[5]

Nitrogen Isotope Effects

The procedure was essentially that previously described (3) for the reaction of benzyl nitrate, with the exception that acetate ion replaced ethoxide, sodium bicarbonate was not used to neutralize base, and separation of the organic compounds from inorganic ions was achieved by partition between diethyl ether – water rather than petroleum ether – water.

The kinetic isotope effect was calculated by using the expression

$$\frac{k^{14}}{k^{15}} = \frac{\ln\left(1 - \frac{f(1-p)}{1-fp}\right)}{\ln\left(1 - \frac{rf(1-p)}{1-fp}\right)},$$

where f is the mole fraction of the ester which has undergone reaction, p is the fraction of the total reaction which is substitution, and r is $(^{14}N/^{15}N)_{reactant}/(^{14}N/^{15}N)_{NO_2^-}$ (25). This is a modification of an expression derived by Stevens and Attree (26), and takes into account the fact that the reactant is being consumed by reactions other than that whose isotope effect is being measured.

ACKNOWLEDGMENT

This work was supported by the National Research Council of Canada.

REFERENCES

1. J. W. Baker and D. M. Easty. J. Chem. Soc. 1193 (1952); 1208 (1952).
2. J. W. Baker and T. G. Heggs. J. Chem. Soc. 616 (1955).
3. E. Buncel and A. N. Bourns. Can. J. Chem. **38**, 2457 (1960).
4. D. V. Banthorpe. Elimination reactions. Elsevier Press, Inc., New York. 1963. p. 78.
5. F. G. Bordwell, R. L. Arnold, and J. B. Biranowski. J. Org. Chem. **28**, 2496 (1963).
6. J. P. Freeman. J. Org. Chem. **21**, 471 (1956).
7. G. W. H. Cheeseman. Chem. Ind. London, 1390 (1956).
8. G. W. H. Cheeseman. J. Chem. Soc. 448 (1959).
9. W. K. McEwen. J. Am. Chem. Soc. **58**, 1124 (1936).
10. A. Streitwieser, Jr., W. C. Langworthy, and J. I. Brauman. J. Am. Chem. Soc. **85**, 1761 (1963).
11. A. Streitwieser, Jr. Tetrahedron Letters, **6**, 23 (1960).
12. E. Berliner and M. C. Beckett. J. Am. Chem. Soc. **79**, 1425 (1957). U.-J. Zimmerman and E. Berliner. J. Am. Chem. Soc. **84**, 3953 (1962).
13. D. J. Cram, D. A. Scott, and W. D. Nielsen. J. Am. Chem. Soc. **83**, 3696 (1961).
14. J. Bigeleisen and M. Wolfsberg. Advan. Chem. Phys. **1**, 15 (1958).
15. M. Kilpatrick. Chem. Rev. **30**, 159 (1942).

[4]*In anhydrous solvent: [ester] = 0.02 M, [KOAc] = 0.4 M, temperature = 40.5°; in 85% ethanol: [ester] = 0.06 M, [KOAc] = 0.3 M, temperature = 30°.*

[5]*The latter was performed by J. Nemeth, Urbana, Illinois.*

Can. J. Chem. Downloaded from www.nrcresearchpress.com by 210.87.254.105 on 09/05/12
For personal use only.

16. R. F. W. BADER. Can. J. Chem. **42**, 1822 (1964).
17. C. G. SWAIN and E. R. THORNTON. J. Am. Chem. Soc. **84**, 817 (1962).
18. F. H. WESTHEIMER. Chem. Rev. **61**, 265 (1961).
19. L. MELANDER. Isotope effects on reaction rates. The Ronald Press Co., New York. 1960. p. 24.
20. K. B. WIBERG and E. L. MOTELL. Tetrahedron, **19**, 2009 (1963).
21. R. P. BELL. Discussions Faraday Soc. **39**, 16 (1965).
22. C. L. ARCUS and J. V. EVANS. J. Chem. Soc. 789 (1958).
23. W. E. BACHMANN and J. C. SHEEHAN. J. Am. Chem. Soc. **62**, 2687 (1940).
24. R. N. JONES and M. A. MACKENZIE. Talanta, **3**, 356 (1960).
25. B. T. BALIGA. Ph.D. Thesis, McMaster University, Hamilton, Ontario. 1961.
26. W. H. STEVENS and R. W. ATTREE. Can. J. Res., Sect. B, **27**, 807 (1949).

Can. J. Chem. Downloaded from www.nrcresearchpress.com by 210.87.254.105 on 09/05/12
For personal use only.

Can. J. Chem. Downloaded from www.nrcresearchpress.com by 210.87.254.40 on 09/05/12
For personal use only.

ARYLATION DES QUINONES PAR LES SELS DE DIAZONIUM

VIII. SUR LES 3-ARYL-1,2-NAPHTOQUINONES

JACQUES ASSELIN, PAUL BRASSARD ET PHILIBERT L'ECUYER
Département de Chimie, Université Laval, Québec, Québec

Reçu le 12 mai 1966

RÉSUMÉ

Les 3-aryl-1,2-naphtoquinones se sont avérées les seuls produits de la réaction des sels de benzènediazonium avec la 1,2-naphtoquinone. Ces résultats sont différents des données antérieures. Nous avons recherché le meilleur milieu réactionnel pour effectuer la substitution et nous avons discuté la portée des résultats sur le mécanisme de la réaction.

ABSTRACT

The arylation of 1,2-naphthoquinone by benzenediazonium salts, in contrast to previously published results, gave only 3-aryl-1,2-naphthoquinones with poor to fair yields. The best reaction medium has been sought and the implications of the results with regard to the reaction mechanism are discussed.

La réaction des quinones avec les sels de diazonium aromatiques présente encore certains problèmes. En particulier, les mécanismes radicalaires proposés (1, 2) pour la réaction de Meerwein ne lui semblent pas appropriés. En effet, au cours de travaux sur les quinones (3 et la présente communication), nous avons observé que, contrairement à ce qui se produit dans la réaction de Meerwein avec d'autres composés carbonylés α,β-insaturés, l'addition de sels cuivriques au milieu réactionnel n'améliore pas le rendement de la réaction. Nous avons constaté également que les réactions des sels de benzènediazonium avec la chloroquinone, la toluquinone ou la 1,2-naphtoquinone, de même que les réactions des sels de benzènediazonium substitués en position ortho, ainsi que d'autres peu réactifs, avec la benzoquinone même donnent lieu à la formation d'un intermédiaire dans le mélange réactionnel. Cet intermédiaire, qui apparaît d'abord sous la forme d'un solide ou d'un liquide visqueux, dégage lentement de l'azote pour devenir éventuellement cristallin.

Nous avons déjà souligné (3) que la nature de l'anion du sel de diazonium n'influe pas sur le cours de la réaction avec les quinones, alors qu'un chlorure ou un bromure est nécessaire à la réaction de Meerwein. De plus, Bergmann et Weizman (4) ont démontré que la stabilité des sels de diazonium constitue le plus important des facteurs qui influencent le cours de la réaction. Nous avons au contraire observé que la nature de la quinone joue aussi un rôle considérable. Ainsi, dans des conditions identiques, la réaction du chlorure de benzènediazonium avec la benzoquinone est complète en 30 min; avec la chloroquinone le dégagement gazeux ne cesse qu'au bout de 24 h, tandis qu'avec la toluquinone la réaction dure plusieurs jours.

Toutes ces données expérimentales semblent favoriser un mécanisme différent de celui de la réaction de Meerwein. Elles permettent en outre d'en formuler un (7, 8) qui rend compte de toutes ces divergences (Schéma 1).

Nous avons pensé que la présence d'un substituant sur le noyau de la quinone pourrait influencer la direction de la substitution, mais nos expériences sur l'arylation de quelques quinones substituées (5 et résultats inédits) n'ont pas donné les résultats significatifs escomptés. Celles-ci ont montré que la substitution est peu sensible aux effets directeurs d'un substituant et qu'elle donne naissance à tous les isomères bisubstitués possibles.

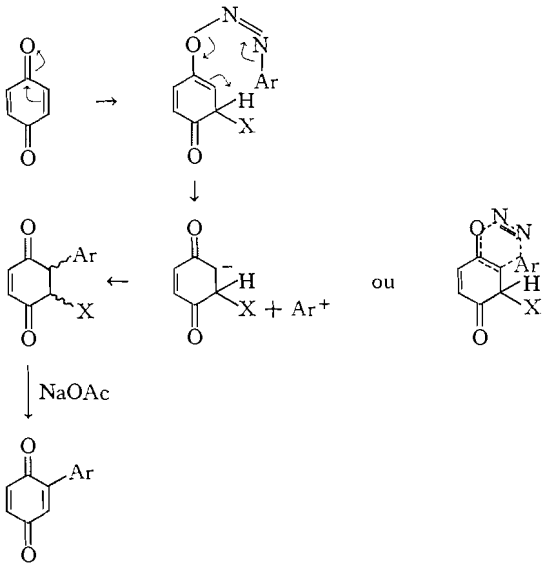


SCHÉMA 1.

Il est par contre bien établi que la 1,2-naphtoquinone subit la substitution électrophile (nitration) en position 3 et la substitution nucléophile (réaction de Thiele) en position 4. Un mécanisme radicalaire devrait conduire à la substitution en position 3.

Kvalnes (6) avait déjà trouvé que la substitution de la 1,2-naphtoquinone à l'aide du sel de *p*-carboxybenzènediazonium dans l'acide acétique en solution aqueuse n'aboutissait qu'à un dérivé bisubstitué. Toutefois, une étude de cette réaction avec d'autres sels de diazonium dans divers milieux réactionnels et à différentes températures nous a donné les produits monosubstitués en position 3. Nous n'avons pu déceler que des traces de produits bisubstitués. Ici encore, la présence de sels cuivriques dans le milieu réactionnel n'affecte pas le rendement mais elle permet, cependant, d'obtenir un produit plus facile à purifier. Les solutions d'acétone à 65% en volume, à 0°, et d'acide formique à 55% en volume, à 20°, dans l'eau se sont avérées les meilleurs solvants.

Les réactions représentées au Schéma 2 nous ont permis d'établir les structures des naphtoquinones ainsi obtenues.

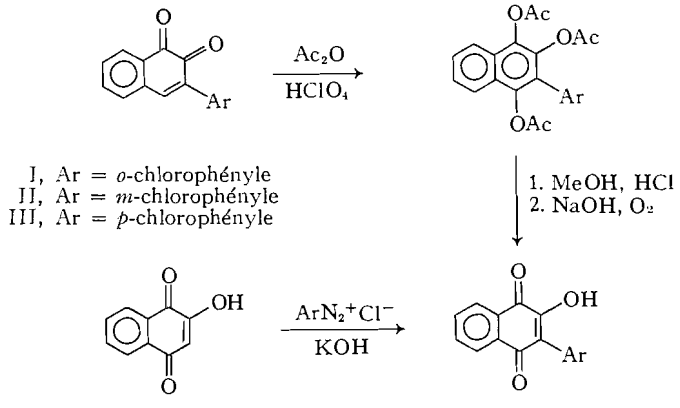


SCHÉMA 2.

Can. J. Chem. Downloaded from www.nrcresearchpress.com by 210.87.254.40 on 09/05/12
For personal use only.

Can. J. Chem. Downloaded from www.nrcresearchpress.com by 210.87.254.40 on 09/05/12
For personal use only.

PARTIE EXPÉRIMENTALE

Arylation de la 1,2-naphtoquinone

Le sel de diazonium se prépare de la façon habituelle par addition lente d'une solution de nitrite de sodium (1.6 g) dans de l'eau (10 ml) à un mélange de l'amine (0.02 mole), de 5.0 ml d'acide chlorhydrique concentré et de 25 ml d'eau. On ajoute goutte à goutte la solution ainsi obtenue à un mélange, maintenu entre 20 et 25°, de 3.2 g (0.02 mole) de 1,2-naphtoquinone, de 4.9 g (0.06 mole) d'acétate de sodium, de 0.5 g de chlorure cuivrique, de 80 ml d'acide formique et de 25 ml d'eau. On agite ensuite à la température ambiante jusqu'à ce que l'évolution d'azote soit complète (environ 12 h); puis on refroidit, on filtre et on triture le résidu avec un peu de méthanol glacé. La purification par chromatographie (gel de silice–benzène) n'améliore pas sensiblement le rendement.

3-o-Chlorophényl-1,2-naphtoquinone (I)

La substance cristallise en feuillets jaune-orangé (5%) dans l'éthanol à 70%, p.f. 171–172°; $\lambda_{max}^{CHCl_3}$ 5.87, 5.96, 6.02, 6.26 μ.

Anal. Calc. pour $C_{16}H_9O_2Cl$: C, 71.52; H, 3.38; Cl, 13.20. Trouvé: C, 71.63; H, 3.51; Cl, 13.11.

3-m-Chlorophényl-1,2-naphtoquinone (II)

Cristallisée dans l'acide acétique à 75% puis dans le benzène, la substance est obtenu en aiguilles rouges (17%), p.f. 197–198°; $\lambda_{max}^{CHCl_3}$ 5.88, 5.96, 6.02, 6.27 μ.

Anal. Calc. pour $C_{16}H_9O_2Cl$: C, 71.52; H, 3.38. Trouvé: C, 71.76; H, 3.46.

3-p-Chlorophényl-1,2-naphtoquinone (III)

La substance cristallise dans l'acide acétique à 75% en fines aiguilles rouges (37%), p.f. 214.5–215.0°; $\lambda_{max}^{CHCl_3}$ 5.88, 5.96, 6.27 μ.

Anal. Calc. pour $C_{16}H_9O_2Cl$: C, 71.52; H, 3.38; Cl, 13.20. Trouvé: C, 71.30; H, 3.40; Cl, 13.34.

TABLEAU I

2-Hydroxy-3-aryl-1,4-naphtoquinones

Groupe substituant	$\lambda_{max}^{CHCl_3}$ (μ)	Point de fusion et point de fusion mélangé	Point de fusion (littérature)
3-*o*-Chlorophényle	3.94, 5.99, 6.24	195–196°	194–195.5° (9)
3-*m*-Chlorophényle*	3.94, 5.99, 6.23	151.5–152.5°	203–204° (9)
3-*p*-Chlorophényle	3.93, 6.00, 6.24	190.5–191.5°	187.4–188° (9)

*Anal. Calc. pour $C_{16}H_9O_3Cl$: C, 67.50; H, 3.19; Cl, 12.45. Trouvé: C, 67.59; H, 3.16; Cl, 12.65.

Les 2-Hydroxy-3-aryl-1,4-naphtoquinones

On ajoute 0.5 g de 3-aryl-1,2-naphtoquinone à un mélange d'anhydride acétique (10 ml) et de 5 gouttes d'acide perchlorique à 70%, et la température est élevée lentement jusqu'à dissolution complète; puis on refroidit et verse dans de l'eau. Le triacétate brut est ensuite décomposé par chauffage à reflux dans un mélange de méthanol (10 ml) et d'acide chlorhydrique concentré (0.3 ml) pendant 1 h. On évapore à sec sous vide, on ajoute 30 ml d'eau, on porte le pH à 8 par addition d'une solution d'hydroxyde de sodium à 5% et l'on fait passer un courant d'air dans la solution pendant 1 h. Les 2-hydroxy-3-aryl-1,4-naphtoquinones (60–70%) obtenues après acidification sont identiques aux substances (point de fusion mélangé et spectres infrarouges) préparées d'après Fieser et Leffler et leurs collaborateurs (9) (Tableau I). La 2-hydroxy-3-(*m*-chlorophényl)-1,4-naphtoquinone obtenue par cette méthode diffère toutefois sensiblement par son point de fusion de la substance déjà décrite.

REMERCIEMENTS

Nous remercions le Ministère de l'Education de la Province de Québec pour une bourse de perfectionnement accordée à l'un de nous (J. A.), ainsi que le Conseil National de Recherches du Canada pour l'octroi de subventions qui ont permis la réalisation de ce travail.

BIBLIOGRAPHIE

1. J. K. Kochi. J. Am. Chem. Soc. **79**, 2942 (1957).
2. S. C. Dickerman, K. Weiss et A. K. Ingberman. J. Am. Chem. Soc. **80**, 1904 (1958).
3. P. Brassard et Ph. L'Ecuyer. Can. J. Chem. **36**, 700 (1958).
4. F. Bergmann et J. Weizman. J. Org. Chem. **9**, 415 (1944).
5. P. Brassard et Ph. L'Ecuyer. Can. J. Chem. **36**, 814 (1958).
6. D. E. Kvalnes. J. Am. Chem. Soc. **56**, 2478 (1934).
7. P. Brassard. Thèse de doctorat, Université Laval, Québec. 1957.
8. J. F. Bagli et Ph. L'Ecuyer. Can. J. Chem. **39**, 1037 (1961).
9. L. F. Fieser et M. T. Leffler *et al.* J. Am. Chem. Soc. **70**, 3203 (1948).

Can. J. Chem. Downloaded from www.nrcresearchpress.com by 210.87.254.105 on 09/05/12
For personal use only.

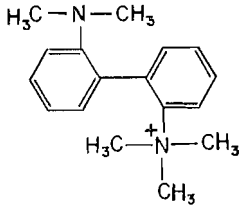
DEUTERIUM ISOTOPE EFFECT ON THE RACEMIZATION OF A HIGHLY HINDERED BIPHENYL DERIVATIVE[1]

C. HEITNER AND K. T. LEFFEK

Suggestions that certain kinetic secondary deuterium isotope effects were manifestations of the steric differences between the normal and deuterated molecules (1, 2) have led to a search for such isotope effects which are unambiguously steric in origin. Recently, Mislow *et al.* (3, 4) found rate ratios (k_H/k_D) between 0.86 and 0.88 for 9,10-dihydro-4,5-dimethyl-d_6-phenanthrene under various conditions of solvent and temperature; almost simultaneously, the results of Melander and Carter (5, 6) on 2,2′-dibromo-4,4′-dicarboxybiphenyl-6,6′-d_2 appeared, for which they observed an 18% inverse isotope effect ($k_H/k_D = 0.82$) in several solvents. These rate changes are in the direction predicted by the greater steric requirements of carbon–hydrogen relative to carbon–deuterium bonds.

Mislow *et al.* concluded (4) that steric isotope effects would appear only in severely crowded situations, in contrast to Bartell's hypothesis (2) that steric factors contribute to many, if not all, isotopic rate changes.

In the present work, the rate of racemization of optically active *o*-(2-dimethyl-d_6-aminophenyl)-phenyltrimethyl-d_9-ammonium *d*-camphor-10-sulfonate (I) has been measured and compared with that of the normal compound. The cation is an ortho-substituted biphenyl more highly hindered than those previously studied.



I

RESULTS AND DISCUSSION

The rate constants and rate ratios for compound I are presented in Table I. The rate constants for the normal compound, together with those of Leffler and Graham (7), give a good straight-line plot for $\log_{10} k/T$ versus $1/T$, which yields $\Delta H^{\ddagger} = 27.46$ kcal (standard error = 0.06) and $\Delta S^{\ddagger} = -5.04$ cal mole^{-1} degree^{-1} (standard error = 0.05).

The rate constants for the normal and deuterated molecules are not significantly different in the two solvents, water and dimethyl sulfoxide, or at temperatures of 100 and 120 °C in water. Although there may be a small normal isotope effect in water at 120 °C, the rate difference is no bigger than twice the standard deviation.

In view of the isotope effects already observed in biphenyl systems, it is unlikely that

[1]*Presented at the 49th annual conference of the Chemical Institute of Canada, Saskatoon, Saskatchewan, June 1966.*

TABLE I

Kinetic isotope effects in the racemization of *d*-*o*-(2-dimethyl-d_6-aminophenyl)-phenyltrimethyl-d_9-ammonium *d*-camphor-10-sulfonate

Solvent	No. of runs	10^5k_H (s^{-1})	$10^5\sigma_H$* (s^{-1})	10^5k_D (s^{-1})	$10^5\sigma_D$* (s^{-1})	k_H/k_D	σ*
H_2O at 100.0 °C	6	5.19	0.02				
	2			5.21	0.03	0.99_6	0.007
H_2O at 119.9 °C	3	34.0	0.3				
	4			33.2	0.2	1.02	0.01
Dimethyl sulfoxide at 100.1 °C	2	14.7	0.1_5				
	2			14.6	0.1_5	1.01	0.01_5

*Standard error.

the rate ratio of unity found for compound I means that the normal and deuterated molecules are identical. Melander and Carter (6), following Bartell (2), successfully accounted for their results in terms of the isotopic difference in the mean-square amplitude of the vibration between carbon–hydrogen and carbon–deuterium. If this is present in 2,2′-dibromo-4,4′-dicarboxybiphenyl-6,6′-d_2, it must also exist in compound I, although the isotopic difference may be slightly smaller in this case, since the inductive effect of the positive charge on the nitrogen should tend to weaken both the carbon–hydrogen and the carbon–deuterium bonds relative to an uncharged molecule. However, bond weakening is not extensive under the reaction conditions, because no isotope exchange was observed (see Experimental).

Qualitatively, the results may be rationalized in two ways: either the non-bonded interactions during racemization are so great that they are not significantly changed by deuteration, or a second effect occurs in the molecule with deuteration which compensates for the change in the mean-square amplitude. Although a discussion of such a second effect can only be speculatory, it is of interest to note the data of Mislow *et al.* (3, 4), which show opposing changes in the activation parameters ($(\Delta H_H^{\ddagger} - \Delta H_D^{\ddagger}) = 0.24$ kcal mole^{-1} and $(\Delta S_H^{\ddagger} - \Delta S_D^{\ddagger}) = 0.53$ cal mole^{-1} degree^{-1}) for 9,10-dihydro-4,5-dimethyl-d_6-phenanthrene in benzene. The results in Table I cannot be used to derive analogous figures for compound I, but if reasonable values are chosen (e.g. $(\Delta H_H^{\ddagger} - \Delta H_D^{\ddagger}) = 0.17$ kcal mole^{-1} and $(\Delta S_H^{\ddagger} - \Delta S_D^{\ddagger}) = 0.46$ cal mole^{-1} degree^{-1}) the rate ratios (k_H/k_D) at 100 °C and 120 °C would be 1.00 and 1.01, respectively. Hence, our results are not as inconsistent with those of Mislow *et al.* as they appear to be at first sight. The latter workers, understandably, did not attempt to explain the isotope effect on the entropy of activation. Further, it should be noted that Melander and Carter *assumed* their isotope effect to be on the enthalpy of activation, the proof being beyond the limits of their experiments.

It appears probable that secondary deuterium isotope effects in biphenyl systems may be more complicated than simply steric effects. The present results are useful in that they help to demonstrate this point, and also the limitations of Mislow's conclusion (4) "that steric hydrogen isotope effects are plainly operative only under special conditions of severe overcrowding", since Melander and Carter's system (6), which is not severely crowded, shows a large rate change per deuterium, whereas compound I, which is more severely crowded, shows none.

EXPERIMENTAL

Materials

2,2′-Diaminobiphenyl

2,2′-Dinitrobiphenyl (m.p. 125–126.5 °C), prepared in an 89% yield from *o*-chloronitrobenzene by the method of Kornblum and Kendall (8), was reduced with hydrogen catalytically (9) to yield 2,2′-diaminobiphenyl (m.p. 78–80 °C) in an 86% yield after recrystallization from ethanol.

Can. J. Chem. Downloaded from www.nrcresearchpress.com by 210.87.254.105 on 09/05/12
For personal use only.

Methyl-d_6 Sulfate

Methyl-d_3 iodide was prepared by the method of Cotton *et al.* (10). The deuterium content was monitored by mass spectrometric analysis and was always 98% or greater.

Methyl-d_6 sulfate was prepared by mixing methyl-d_3 iodide with dry silver sulfate, whereupon the methyl-d_3 iodide refluxed spontaneously for 1½ h. Extraction with ether and distillation gave methyl-d_6 sulfate in a 74% yield.

dl-o-(2-Dimethyl-d_6-aminophenyl)phenyltrimethyl-d_9-ammonium Iodide

Methylation of the 2,2′-diaminobiphenyl with methyl-d_6 sulfate according to the procedure of Shaw and Turner (11) gave 2,2′-bisdimethyl-d_6-aminobiphenyl (m.p. 71–72 °C) in a 93% yield. This was then quaternized with methyl-d_3 iodide by the method of Leffler and Graham (7). The product melted at 185–186 °C and the yield was 93% with respect to the biphenyl when carried out on a scale of 0.005 mole.

d-o-(2-Dimethyl-d_6-aminophenyl)phenyltrimethyl-d_9-ammonium d-Camphor-10-sulfonate

This compound was prepared by the method of Shaw and Turner (11), m.p. 190–191 °C (uncorrected), $[\alpha]^{25}_{5461}$ +59.2° (in water).

The protium compound was prepared in the same manner, m.p. 189–190 °C (uncorrected), $[\alpha]^{25}_{5461}$ +59.5° (in water).

Kinetic Method

The kinetic runs were carried out at a concentration of 0.02 *M*, since at higher concentrations than this the first-order rate constant is not independent of the initial concentration (7).

Solution samples were sealed under nitrogen in tubes and, after they were preheated, were placed in a constant-temperature bath. After temperature equilibrium had been reached, 3 tubes were withdrawn to mark the kinetic zero, and thereafter 10 or 11 tubes were withdrawn at regular intervals. Three samples were left in the bath for 10 half-lives to give the optical rotation for the complete reaction.

The optical activity of each sample was measured with a Bendix–Ericsson ETL-NPL automatic polarimeter, type 143A, which gives an electric current directly proportional to the optical rotation. This current was passed through a resistance and the potential across it measured with a Croydon potentiometer, type P3. The system was calibrated with sucrose of a known specific rotation. The average of 20 readings was taken as the rotation for each sample. The rate constant was calculated by the method of least squares from the equation

$$2kt = 2.303 \log_{10}\left(\frac{\alpha_0 - \alpha_\infty}{\alpha_t - \alpha_\infty}\right),$$

where k is the first-order rate constant, t is the time, and α_0, α_t, and α_∞ are the optical rotations at the kinetic zero, time t, and after 10 half-lives, respectively. An illustrative run is shown in Table II.

TABLE II

Racemization of *d-o-*(2-dimethyl-d_6-aminophenyl)-trimethyl-d_9-ammonium *d*-camphor-10-sulfonate in water at 100.0 °C*

Time (s) × 10^{-2}	Optical rotation × 10^2	Time (s) × 10^{-2}	Optical rotation × 10^2
0	5.018°†	72.21	3.110°
12.00	4.592°	84.00	2.894°
24.00	4.230°	96.00	2.696°
36.00	3.890°	108.00	2.562°
48.00	3.615°	120.00	2.416°
60.01	3.342°	∞	1.402°†

*Run 28, concentration ca. 0.02 *M*, cell length 1 cm.
†Mean of three separate samples.
NOTE: From a least-squares calculation, $k_1 = 5.26 \times 10^{-5}$ s (standard error = 0.04×10^{-5} s).

Usually two runs, identical except for the isotopic composition of the substrate molecule, were carried out simultaneously. After one such pair of runs, the solvent was removed and a nuclear magnetic resonance spectrum, in deuterium oxide solution, was obtained for both the normal and deuterated compound. The normal compound showed two peaks at 6.38 τ and 7.42 τ for the $\overset{+}{N}(CH_3)_3$ and the $N(CH_3)_2$ hydrogens, respectively (12). The spectrum for the deuterated compound was identical except for the absence of the above peaks. Thus, the deuterated compound was at least 98% isotopically pure, and also no exchange took place with the solvent water under the reaction conditions.

Can. J. Chem. Downloaded from www.nrcresearchpress.com by 210.87.254.105 on 09/05/12
For personal use only.

ACKNOWLEDGMENTS

The authors are grateful for financial support of this work by the National Research Council, and thank Dr. W. D. Jamieson for the determination of the mass spectra and Mr. D. G. Smith for running the nuclear magnetic resonance spectra.

1. K. T. LEFFEK, J. A. LLEWELLYN, and R. E. ROBERTSON. J. Am. Chem. Soc. **82**, 6315 (1960).
2. L. S. BARTELL. Iowa State J. Sci. **36**, 137 (1961).
3. K. MISLOW, R. GRAEVE, A. J. GORDON, and G. H. WAHL, JR. J. Am. Chem. Soc. **85**, 1190 (1963).
4. K. MISLOW, R. GRAEVE, A. J. GORDON, and G. H. WAHL, JR. J. Am. Chem. Soc. **86**, 1733 (1964).
5. L. MELANDER and R. E. CARTER. J. Am. Chem. Soc. **86**, 295 (1964).
6. L. MELANDER and R. E. CARTER. Acta Chem. Scand. **18**, 1138 (1964).
7. J. E. LEFFLER and W. H. GRAHAM. J. Phys. Chem. **63**, 687 (1959).
8. N. KORNBLUM and D. L. KENDALL. J. Am. Chem. Soc. **74**, 5782 (1952).
9. A. E. BLOOD and C. R. NOLLER. J. Org. Chem. **22**, 711 (1957).
10. F. A. COTTON, J. H. FORSNACHT, W. D. HORCOCKS, JR., and N. A. NELSON. J. Chem. Soc. 4138 (1959).
11. F. R. SHAW and E. E. TURNER. J. Chem. Soc. 135 (1933).
12. L. M. JACKMAN. Applications of nuclear magnetic resonance spectroscopy in organic chemistry. Pergamon Press, New York. 1959. p. 56.

RECEIVED JUNE 30, 1966.
DEPARTMENT OF CHEMISTRY,
DALHOUSIE UNIVERSITY,
HALIFAX, NOVA SCOTIA.

Can. J. Chem. Downloaded from www.nrcresearchpress.com by 210.87.254.105 on 09/05/12
For personal use only.

A STUDY OF THE MANNICH REACTION WITH PROPARGYL ALCOHOL

R. L. SALVADOR AND D. SIMON

Although 1-alkynes are known to partake in the Mannich reaction, the seeming inertness of propargyl alcohol in undergoing this condensation prompted us to investigate the mechanism of this reaction. During this investigation we applied these theoretical aspects to the synthesis of a group of aminobutynols of the type $R_2N—CH_2—C\equiv C—CH_2OH$. The sequence of events in the Mannich reaction has been subject to many debates, two explanations being offered. One possible course is an aldol condensation of the active hydrogen component I with formaldehyde, followed by reaction of the acetylenic alcohol II with a secondary amine to produce the Mannich base III.

$$\underset{\text{I}}{R'—C\equiv C—H} + HCOH \rightarrow \underset{\text{II}}{R'—C\equiv C—CH_2OH} + R_2NH \rightarrow \underset{\text{III}}{R'—C\equiv C—CH_2—NR_2}$$

The alternative is the formation of the methylol derivative of the amine IV, followed by its reaction with the active hydrogen compound (1).

$$HCHO + HNO_2 \rightarrow \underset{\text{IV}}{HO—CH_2—NR_2} + \underset{\text{I}}{R'—C\equiv C—H} \rightarrow \underset{\text{III}}{R'—C\equiv C—CH_2—NR_2}$$

Since the acetylenic compound, in our case, was propargyl alcohol, it seemed probable that the second type of reaction was followed. Formation of the hydroxymethyl derivative of the acetylenic compound would lead to the production of 2-butyne-1,4-diol, with the probability of amination of both ends of the chain. The high yields of the expected products, however, precluded this line of reasoning. Also, attempts to isolate 2-butyne-1,4-diol were unsuccessful. Although the Mannich reaction proceeds well for 3-alkyl- and

ACKNOWLEDGMENTS

The authors are grateful for financial support of this work by the National Research Council, and thank Dr. W. D. Jamieson for the determination of the mass spectra and Mr. D. G. Smith for running the nuclear magnetic resonance spectra.

1. K. T. LEFFEK, J. A. LLEWELLYN, and R. E. ROBERTSON. J. Am. Chem. Soc. **82**, 6315 (1960).
2. L. S. BARTELL. Iowa State J. Sci. **36**, 137 (1961).
3. K. MISLOW, R. GRAEVE, A. J. GORDON, and G. H. WAHL, JR. J. Am. Chem. Soc. **85**, 1190 (1963).
4. K. MISLOW, R. GRAEVE, A. J. GORDON, and G. H. WAHL, JR. J. Am. Chem. Soc. **86**, 1733 (1964).
5. L. MELANDER and R. E. CARTER. J. Am. Chem. Soc. **86**, 295 (1964).
6. L. MELANDER and R. E. CARTER. Acta Chem. Scand. **18**, 1138 (1964).
7. J. E. LEFFLER and W. H. GRAHAM. J. Phys. Chem. **63**, 687 (1959).
8. N. KORNBLUM and D. L. KENDALL. J. Am. Chem. Soc. **74**, 5782 (1952).
9. A. E. BLOOD and C. R. NOLLER. J. Org. Chem. **22**, 711 (1957).
10. F. A. COTTON, J. H. FORSNACHT, W. D. HORCOCKS, JR., and N. A. NELSON. J. Chem. Soc. 4138 (1959).
11. F. R. SHAW and E. E. TURNER. J. Chem. Soc. 135 (1933).
12. L. M. JACKMAN. Applications of nuclear magnetic resonance spectroscopy in organic chemistry. Pergamon Press, New York. 1959. p. 56.

RECEIVED JUNE 30, 1966.
DEPARTMENT OF CHEMISTRY,
DALHOUSIE UNIVERSITY,
HALIFAX, NOVA SCOTIA.

Can. J. Chem. Downloaded from www.nrcresearchpress.com by 210.87.254.42 on 09/05/12
For personal use only.

A STUDY OF THE MANNICH REACTION WITH PROPARGYL ALCOHOL

R. L. SALVADOR AND D. SIMON

Although 1-alkynes are known to partake in the Mannich reaction, the seeming inertness of propargyl alcohol in undergoing this condensation prompted us to investigate the mechanism of this reaction. During this investigation we applied these theoretical aspects to the synthesis of a group of aminobutynols of the type $R_2N—CH_2—C\equiv C—CH_2OH$. The sequence of events in the Mannich reaction has been subject to many debates, two explanations being offered. One possible course is an aldol condensation of the active hydrogen component I with formaldehyde, followed by reaction of the acetylenic alcohol II with a secondary amine to produce the Mannich base III.

$$\underset{\text{I}}{R'—C\equiv C—H} + HCOH \rightarrow \underset{\text{II}}{R'—C\equiv C—CH_2OH} + R_2NH \rightarrow \underset{\text{III}}{R'—C\equiv C—CH_2—NR_2}$$

The alternative is the formation of the methylol derivative of the amine IV, followed by its reaction with the active hydrogen compound (1).

$$HCHO + HNO_2 \rightarrow \underset{\text{IV}}{HO—CH_2—NR_2} + \underset{\text{I}}{R'—C\equiv C—H} \rightarrow \underset{\text{III}}{R'—C\equiv C—CH_2—NR_2}$$

Since the acetylenic compound, in our case, was propargyl alcohol, it seemed probable that the second type of reaction was followed. Formation of the hydroxymethyl derivative of the acetylenic compound would lead to the production of 2-butyne-1,4-diol, with the probability of amination of both ends of the chain. The high yields of the expected products, however, precluded this line of reasoning. Also, attempts to isolate 2-butyne-1,4-diol were unsuccessful. Although the Mannich reaction proceeds well for 3-alkyl- and

3-aryl-1-alkynes (2) and for some hydroxy-1-alkynes (3), the method is not available if the hydroxy group of the latter is propargylic.

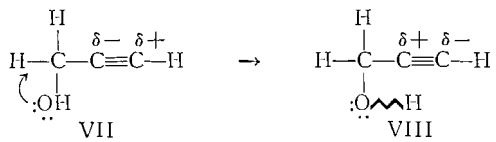
Although McLeod and Robinson (4) and Fernandez *et al.* (5) have shown that ethers of the type $R_2N—CH_2—O—R$ are formed under conditions similar to those of the Mannich reaction, and although it has been shown that propargyl alcohol reacts with amine and formaldehyde preferentially at the hydroxylic group rather than the acetylenic C—H, under the conditions described in this paper we were unable to isolate these ethers from the reaction mixture even without the copper catalyst, the bis-aminomethane $R_2N—CH_2—NR_2$ being the main product isolated. We must therefore conclude that the preferential reaction cited above does not obtain under these conditions. The limitation imposed upon the reaction with propargylic alcohols was overcome by esterifying (3) or etherifying (6) the hydroxyl function.

We have circumvented these steps by the use of cupric sulfate as a catalyst, following, to a limited extent, a German patent (7). The process was greatly modified. The elucidation of this process threw light upon the mechanism of the Mannich reaction. It is well understood that 1-alkynes may be envisioned as possessing two polarization forms V and VI, in which form VI accounts for the "acidity" of the acetylenic hydrogen. A hydroxy group propargylic to the acetylenic function prevents formation of the "acidic" polariza-



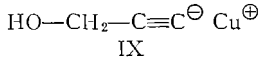
V VI

tion form VI by virtue of an electron shift involving an unbound electron pair on the oxygen atom. This phenomenon probably accounts for the well-known acidity of the hydrogen on a propargylic hydroxyl function. The electron shift would, incidentally, reverse the polarization pattern of the molecule and preclude the existence of an active acetylenic hydrogen (VII to VIII). However, since the Mannich reaction depends



VII VIII

precisely upon the presence of such a labile hydrogen, the condensation does not take place. The sharp and strong band at 2 118 cm^{-1} in the infrared absorption spectrum of propargyl alcohol shows that the acetylenic bond is strongly polarized, but the absence of condensation implies that it exists mainly as form VIII, which can account for both the acidity of the hydroxyl hydrogen and the lack of acidity of the acetylenic hydrogen. The formation of the copper salt IX (8) would produce, however, a labile center, or in essence a carbanion, which would react with the aminomethylol formed between the secondary amine and formaldehyde. The identical copper salt was produced by the reaction of cupric sulfate

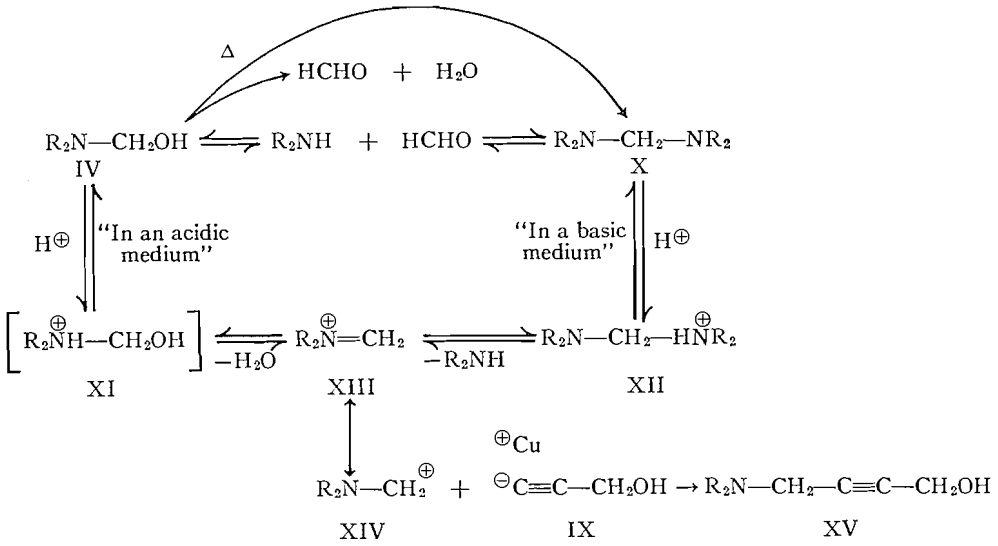


IX

and propargyl alcohol alone in a basic medium, even at room temperature. In this case, reduction of the cupric ion is probably effected by the acetylene itself. Since the reaction was carried out in an aqueous medium, insoluble reaction products could be isolated and identified. An oily layer was immediately produced during the preparation of 4-piperidino-2-butyne-1-ol. Upon distillation of this layer, a vigorous evolution of formaldehyde was noted, and the distillate was identified as bis-piperidinomethane (1). The amine and

Can. J. Chem. Downloaded from www.nrcresearchpress.com by 210.87.254.42 on 09/05/12
For personal use only.

formaldehyde were not introduced in a 2:1 ratio, however, and the initial product was identified as piperidinomethanol. This product was identified by its infrared spectrum, which was identical with that of the piperidinomethanol produced by the method of Henry (9). Attempts to prepare 4-piperidino-2-butyne-1-ol from piperidinomethanol and propargyl alcohol in the presence of cupric ion in a basic medium resulted in inferior yields, whereas the preparation from the bis-piperidinomethane gave yields similar to those of the whole reaction itself (some yield was obtained even in the cold). It was therefore concluded that the principal species involved in this reaction, when run in a slightly basic medium, is the bis-piperidinomethane formed from the aminomethylol under the influence of heat, and the following mechanism is proposed for the reaction. Although the existence of these intermediates has been postulated by Wagner (10) and reviewed by Helman and Opitz (1), and although the properties of the stable species have been studied in some detail, we have isolated and identified the above-mentioned intermediates from the reaction itself.



It must be understood that the different species IV and X have different stabilities. Whereas IV is unstable in an acidic medium, rapidly reverting to the amine salt and formaldehyde, X will actually form a stable salt. Thus, the pathways of the reaction in acidic and basic media are somewhat different. The reaction in a slightly acid medium contributes to two species at differing rates. The reversible reaction involving IV to regenerate the amine and formaldehyde predominates. However, the formation of the carbenium species XIII by way of the unstable methylol salt XI is also accomplished, but at a much slower rate, as evidenced by the long reaction time in this medium. In a slightly basic medium, X is formed in the reaction, and also by the thermal decomposition of IV. This bis-aminomethane rapidly forms the carbenium species XIII through the intermediate salt XII. It is postulated that the carbenium ion XIV, stabilized by resonance with XIII, is the reactive species in both reactions (1). The carbanion IX formed from cupric sulfate and the 1-alkyne would then enter into reaction with XIV to produce the desired Mannich base XV. A similar series of events was noted during the synthesis of the diisopropyl analogue. By following the changes in the pH values during the preparation of the reaction, it was noted that the introduction of formalin, even when carefully

Can. J. Chem. Downloaded from www.nrcresearchpress.com by 210.87.254.42 on 09/05/12
For personal use only.

neutralized, brought about an abrupt drop in pH. The resultant solutions were strongly resistant to subsequent change in pH by the addition of excess amine until the amount of amine calculated to produce the bis-aminomethane was introduced. This strongly indicates a parallel course for all the reactions in the series, even those whose bis-aminomethanes are soluble in water.

The effect of pH on the yield in the reaction was studied. The diethyl analogue was prepared several times at varying initial pH values. It was established that at a pH greater than 8, the reaction, as evidenced by the precipitation of metallic copper, was complete after 55 min. At a pH less than 7 the reaction required at least 5½ h, and at pH 3 no reaction occurred. At a pH greater than 9 the yield decreased. It was decided to run all future reactions at pH 8.4.

TABLE I

Effect of pH on the yield of 4-diethylamino-2-butyne-1-ol

Initial pH	Yield (%)	Time of run	Remarks
9.0	62	55 min	Metallic copper precipitates
8.4	80	"	Some precipitation of metallic copper
7.9	80	5½ h	Some copper propargylate remains
6.0	80	"	Some copper propargylate remains
5.0	77	"	Copper propargylate slow to form
4.5	75	"	Copper propargylate slow to form
3.8	65	"	Copper propargylate slow to form
3.0	0	"	Copper propargylate does not form
7.0	0	"	No copper ion present

It should be noted, therefore, that the reaction should be run in a medium which is acidic enough to form and stabilize the postulated carbenium ion but not acidic enough to prevent the formation of the acetylide.

EXPERIMENTAL

The melting points were measured by the capillary method in an electrothermal apparatus and are uncorrected. Carbon–hydrogen analyses were determined by Dr. C. Daesslé, 5757 Decelles Avenue, Montreal. Amine nitrogen was determined by direct titration in acetic acid, using a Radiometer pH meter with a standard glass electrode and a sleeve-type calomel electrode filled with saturated potassium chloride in anhydrous acetic acid. The hydrochloride salt (compound 6, Table II) was determined by the mercuric acetate – acetic acid method of Pifer and Wollish (11) with the same titrating apparatus.

4-Dimethylamino-2-butyne-1-ol

Dimethylamine (1.2 moles) was dissolved in 80 ml of water and the solution was brought to pH 9 by the addition of a solution of 50% sulfuric acid. One and six-tenth moles of 40% formalin solution was added to the mixture followed by 1 mole of propargyl alcohol. A solution of 5 g of anhydrous cupric sulfate in 50 ml of water was admixed with the contents of the reaction vessel, and the pH adjusted to 8.4 by the addition of excess dimethylamine solution.

The reaction mixture was heated at 80° under reflux (dry ice condenser), with stirring, until the greenish precipitate, which gradually turned yellow, showing the formation of copper propargylate, was succeeded by the deposition of metallic copper (55 min). The mixture was cooled and poured into 300 ml of cold concentrated aqueous ammonia. The combined aqueous solutions were then extracted for 9 h with ether in a liquid–liquid extractor. The ether extract was separated and dried over anhydrous magnesium sulfate, and the solvent was evaporated. The residue was distilled *in vacuo* to yield 91.5 g (81%) of the aminobutynol, b.p. 76–78° at 1.5 mm, n_D^{23} 1.4765, $d_4^{22.5}$ 0.941 (reported (12) b.p. 101° at 1.5 mm, $n_D^{27.5}$ 1.4732).

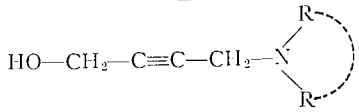
4-Diethylamino-2-butyne-1-ol

This substance was prepared by the general procedure described above, except that the reflux condenser was replaced by a regular Allihn water condenser. A 1 mole run, based on propargyl alcohol, gave 112.8 g (80%) of the desired aminoalcohol, b.p. 92–93° at 2 mm, $n_D^{21.7}$ 1.4784, $d_4^{21.7}$ 0.975 (reported (7) b.p. 105° at 2 mm).

Can. J. Chem. Downloaded from www.nrcresearchpress.com by 210.87.254.42 on 09/05/12
For personal use only.

Can. J. Chem. Downloaded from www.nrcresearchpress.com by 210.87.254.42 on 09/05/12
For personal use only.

TABLE II



R	Boiling point (°C)	Yield (%)	Melting point (°C)		Formula (benzilate)	Analysis (%)					
						Calculated			Found		
			Naphthylurethane*	Benzilate ester		C	H	N	C	H	N
1. Methyl	76–78 at 1.5 mm	81	101.5–102†	103.5–104	$C_{20}H_{21}O_3N$	74.27	6.54	4.34	74.05	6.65	4.33
2. Ethyl	92–93 at 2 mm	80	76–76.5†	79.5–80	$C_{22}H_{25}O_3N$	75.18	7.17	3.98	75.09	6.99	4.07
3. Pyrrolidino	106–107 at 1.5 mm	84	126–126.5†	124.5–125	$C_{22}H_{23}O_3N$	75.61	6.63	4.01	75.38	6.31	4.17
4. Piperidino	112–113 at 1.5 mm	80	103.5–104†	116–116.5	$C_{23}H_{25}O_3N$	76.01	6.93	3.85	76.37	6.99	3.70
5. Morpholino	104–106 at 0.1 mm§	80	102–103‡	119.5–120	$C_{22}H_{23}O_4N$	72.31	6.34	3.83	72.17	6.53	3.78

R	Boiling point (°C)	Yield (%)	Melting point (°C)		Formula	Analysis (%)			
						Calculated		Found	
			Naphthylurethane	Hydrochloride*		N	Cl	N	Cl
6. Isopropyl	96–98 at 2 mm	87.5	77.5–78	144–144.5	$C_{10}H_{20}ONCl$	6.81	17.23	6.78	17.15

*Recrystallized from 2-propanol.
†Recrystallized from petroleum ether (b.p. 30–60°).
‡Recrystallized from benzene.
§Recrystallized from toluene–heptane, m.p. 51.5–52.5°.

4-Diisopropylamino-2-butyne-1-ol

This aminoalcohol was prepared by the general method described above. Sufficient triethylamine was added to bring the pH to 8 and to aid in the solubilization of the insoluble bis-aminomethane. The reaction was heated at 80° for 72 h. A 1 mole run based on propargyl alcohol gave 147.5 g (87.5%) of the product, $n_D^{21.7}$ 1.4811, $d_4^{21.5}$ 0.931.

4-Pyrrolidino-2-butyne-1-ol

This compound was prepared by the general method described for the dimethyl analogue. A 1 mole run, based on propargyl alcohol, gave 117 g (84%) of the desired aminobutynol, b.p. 106–107° at 1.5 mm, $n_D^{21.7}$ 1.5039, $d_4^{26.5}$ 1.013 (reported (13) b.p. 101–102° at 0.4 mm, n_D^{22} 1.5092).

4-Piperidino-2-butyne-1-ol

This substance was prepared in 50% dioxane–water by the general method described above. A 1 mole run, based on propargyl alcohol, gave 122.4 g (80%) of the product, b.p. 112–113° at 1.5 mm, $n_D^{24.7}$ 1.5095, $d_4^{26.5}$ 1.030 (reported (13) b.p. 112–113° at 0.9 mm).

4-Morpholino-2-butyne-1-ol

This aminoalcohol was prepared by the general method. A 1 mole run, based on propargyl alcohol, gave 124 g (80%) of the desired product, b.p. 104–106° at 0.1 mm, $n_D^{21.7}$ 1.5095 (supercooled liquid), m.p. 51.5–52.5° (reported (14) b.p. 104–106° at 0.1 mm, n_D^{25} 1.5087).

ACKNOWLEDGMENT

The authors are grateful to the National Research Council for their financial assistance in this part of a research project.

1. H. Helman and G. Opitz. Angew. Chem. **68**, 265 (1956).
2. C. Mannich and F. T. Chang. Ber. Deut. Chem. Ges. **66**, 418 (1933).
3. E. R. H. Jones, I. Marszak, and H. Bader. J. Chem. Soc. 1578 (1947).
4. C. M. McLeod and G. M. Robinson. J. Chem. Soc. 1470 (1921).
5. J. E. Fernandez, C. Powell, and J. S. Fowler. J. Chem. Eng. Data, **7**, 600 (1963).
6. J. P. Guermont. Bull. Soc. Chim. France, **20**, 386 (1953).
7. P. Dimrath, P. Duffner, R. Oster, and H. Pasedach. Ger. Patent No. 1,100,617 (March 2, 1961); Chem. Abstr. **55**, 19960*f* (1961).
8. L. Henry. Ber. Deut. Chem. Ges. **5**, 571 (1872).
9. L. Henry. Bull. Soc. Chim. France, [3], **13**, 158 (1895).
10. E. G. Wagner. J. Org. Chem. **19**, 1862 (1954).
11. C. W. Pifer and E. G. Wollish. Anal. Chem. **24**, 300 (1952).
12. I. Marszak, A. Marszak-Fleury, R. Epstein, J. P. Guermont, J. Jacob, and G. Montezin. Mem. Serv. Chim. Etat Paris, **36**, 411 (1951).
13. R. Dahlblom and R. Mollberg. Acta Chem. Scand. **17**, 916 (1963).
14. J. H. Biel, E. P. Sprengler, and H. L. Friedman. J. Am. Chem. Soc. **79**, 6184 (1957).

Received March 30, 1966.
Medicinal Chemistry Laboratory,
Faculty of Pharmacy,
University of Montreal,
Montreal, Quebec.

CONVERSION OF NEOABIETIC ACID INTO MANOOL

Ernest Wenkert, J. R. Mahajan, M. Nussim, and F. Schenker

As a consequence of our recent total synthesis of abietoid resin acids (1), various intermediates became available for possible conversion into other diterpenic natural products. Thus, for example, the synthetic ketoester I*a* (2, 3), also a product of the ozonolysis of methyl neoabietate (2–4), appeared to be a likely candidate for transformation into manool (II) and sclareol (III), especially since the more readily accessible sclareol degradation product IV had already been converted into sclareol (5) and the latter had previously

Can. J. Chem. Downloaded from www.nrcresearchpress.com by 210.87.254.42 on 09/05/12
For personal use only.

4-Diisopropylamino-2-butyne-1-ol

This aminoalcohol was prepared by the general method described above. Sufficient triethylamine was added to bring the pH to 8 and to aid in the solubilization of the insoluble bis-aminomethane. The reaction was heated at 80° for 72 h. A 1 mole run based on propargyl alcohol gave 147.5 g (87.5%) of the product, $n_D^{21.7}$ 1.4811, $d_4^{21.5}$ 0.931.

4-Pyrrolidino-2-butyne-1-ol

This compound was prepared by the general method described for the dimethyl analogue. A 1 mole run, based on propargyl alcohol, gave 117 g (84%) of the desired aminobutynol, b.p. 106–107° at 1.5 mm, $n_D^{21.7}$ 1.5039, $d_4^{26.5}$ 1.013 (reported (13) b.p. 101–102° at 0.4 mm, n_D^{22} 1.5092).

4-Piperidino-2-butyne-1-ol

This substance was prepared in 50% dioxane–water by the general method described above. A 1 mole run, based on propargyl alcohol, gave 122.4 g (80%) of the product, b.p. 112–113° at 1.5 mm, $n_D^{24.7}$ 1.5095, $d_4^{26.5}$ 1.030 (reported (13) b.p. 112–113° at 0.9 mm).

4-Morpholino-2-butyne-1-ol

This aminoalcohol was prepared by the general method. A 1 mole run, based on propargyl alcohol, gave 124 g (80%) of the desired product, b.p. 104–106° at 0.1 mm, $n_D^{21.7}$ 1.5095 (supercooled liquid), m.p. 51.5–52.5° (reported (14) b.p. 104–106° at 0.1 mm, n_D^{25} 1.5087).

ACKNOWLEDGMENT

The authors are grateful to the National Research Council for their financial assistance in this part of a research project.

1. H. Helman and G. Opitz. Angew. Chem. **68**, 265 (1956).
2. C. Mannich and F. T. Chang. Ber. Deut. Chem. Ges. **66**, 418 (1933).
3. E. R. H. Jones, I. Marszak, and H. Bader. J. Chem. Soc. 1578 (1947).
4. C. M. McLeod and G. M. Robinson. J. Chem. Soc. 1470 (1921).
5. J. E. Fernandez, C. Powell, and J. S. Fowler. J. Chem. Eng. Data, **7**, 600 (1963).
6. J. P. Guermont. Bull. Soc. Chim. France, **20**, 386 (1953).
7. P. Dimrath, P. Duffner, R. Oster, and H. Pasedach. Ger. Patent No. 1,100,617 (March 2, 1961); Chem. Abstr. **55**, 19960*f* (1961).
8. L. Henry. Ber. Deut. Chem. Ges. **5**, 571 (1872).
9. L. Henry. Bull. Soc. Chim. France, [3], **13**, 158 (1895).
10. E. G. Wagner. J. Org. Chem. **19**, 1862 (1954).
11. C. W. Pifer and E. G. Wollish. Anal. Chem. **24**, 300 (1952).
12. I. Marszak, A. Marszak-Fleury, R. Epstein, J. P. Guermont, J. Jacob, and G. Montezin. Mem. Serv. Chim. Etat Paris, **36**, 411 (1951).
13. R. Dahlblom and R. Mollberg. Acta Chem. Scand. **17**, 916 (1963).
14. J. H. Biel, E. P. Sprengler, and H. L. Friedman. J. Am. Chem. Soc. **79**, 6184 (1957).

Received March 30, 1966.
Medicinal Chemistry Laboratory,
Faculty of Pharmacy,
University of Montreal,
Montreal, Quebec.

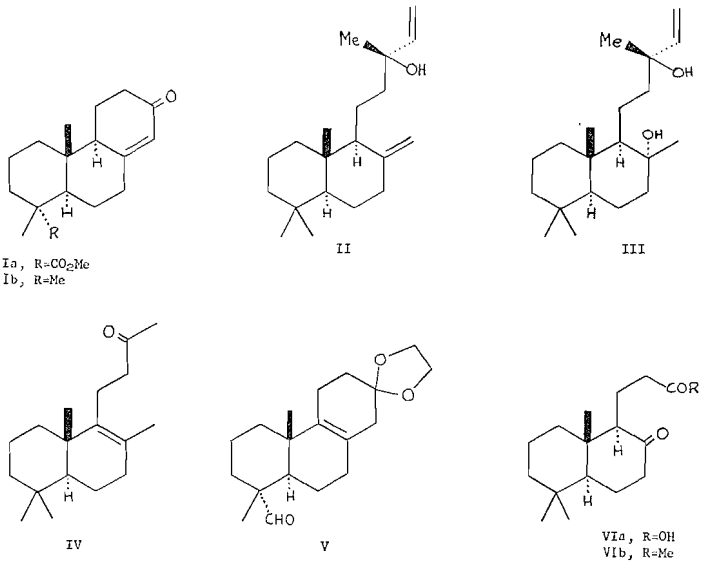
CONVERSION OF NEOABIETIC ACID INTO MANOOL

Ernest Wenkert, J. R. Mahajan, M. Nussim, and F. Schenker

As a consequence of our recent total synthesis of abietoid resin acids (1), various intermediates became available for possible conversion into other diterpenic natural products. Thus, for example, the synthetic ketoester I*a* (2, 3), also a product of the ozonolysis of methyl neoabietate (2–4), appeared to be a likely candidate for transformation into manool (II) and sclareol (III), especially since the more readily accessible sclareol degradation product IV had already been converted into sclareol (5) and the latter had previously

Can. J. Chem. Downloaded from www.nrcresearchpress.com by 210.87.254.105 on 09/05/12
For personal use only.

been transformed into manool (6). The present communication describes the transformation of I*a* into IV.



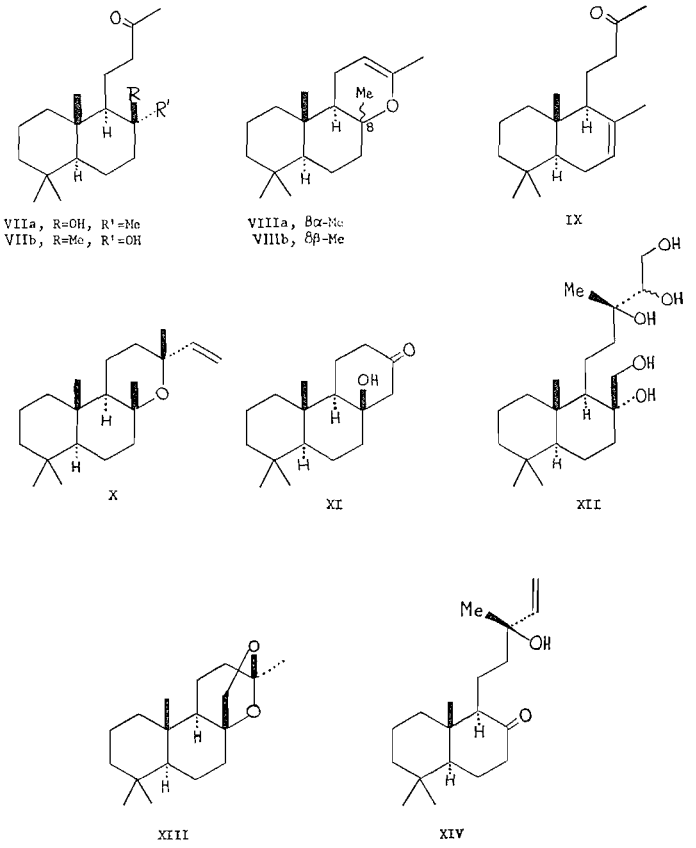
Ethylene glycol ketalation of I*a*, lithium aluminium hydride reduction of the ketal ester, and Sarett oxidation of the resultant ketal alcohol yielded the crystalline aldehyde V. The absence of any olefinic hydrogen signal in the proton magnetic resonance spectrum of the aldehyde indicated the tetra-substituted nature of its double bond. Wolff–Kishner reduction of the aldehyde, followed by acid-catalyzed deketalation, yielded the unsaturated ketone I*b*, a known product of the oxidative degradation of manool (II) (7–9). Although racemic I*b* has been converted into *d,l*-IV, only optically active ketone IV has been transformed into natural sclareol (III) (5), thus leaving the total synthesis of the natural product unfinished. As a consequence, the I*b*–IV transformation was repeated in the optically active series.

Ozonolysis of the ketone I*b* produced the ketoacid VI*a*, whose exposure to methyllithium yielded ketol VII*a* and enol ether VIII*a*. The latter was an 8-epimer of VIII*b* obtained by oxidation of sclareol (III) (*vide infra*) and dehydration of the intermediate ketol VII*b*. Acid-induced isomerization of either epimer VIII yielded a mixture of olefinic ketones IV and IX, only the former of which had been noted previously (5). This completed a formal total synthesis of sclareol (III), manool (II), and manoyl oxide (X) (10).

Both the present and related projects have depended on the availability of large quantities of tricyclic ketone I*b*. Although it has been prepared previously by oxidation of manool (II) (7, 8, 10–12), base treatment of the resultant diketone VI*b*, and acid-catalyzed dehydration of the intermediate ketol XI, the first step of the three-reaction sequence has been inefficient. As a consequence of a search for an improved procedure the oxidation of manool by osmium tetroxide – periodate (13) was investigated. Since initial experiments indicated the formation of mixtures of products, some of which could have arisen only from acid-induced chemical changes, a qualitative study of the pH dependence of the oxidation was undertaken.

t-Butanolic solutions of manool were adjusted to various pH values while being exposed to periodic acid in the presence of a trace quantity of osmium tetroxide. At high alkalinity the product was exclusively the pentol XII. This may have been the consequence of low

Can. J. Chem. Downloaded from www.nrcresearchpress.com by 210.87.254.105 on 09/05/12
For personal use only.



solubility of the product in the reaction medium. At pH 1 the oxidation yielded the diketone VI*b* along with the ketal XIII and a $C_{18}H_{30}O_4$ product whose structure was not investigated. In the pH range 6–8 the desired diketone VI*b* was the exclusive product. In a few experiments in which early nonhomogeneity of the reaction medium developed, hydroxyketone XIV appeared as a by-product. This product has not previously been obtained from oxidations of manool.

EXPERIMENTAL

All melting points are uncorrected. Unless otherwise stated, the optical rotations were carried out on chloroform solutions. A Beckman pH meter was used for the pH determinations.

Aldehyde V

A mixture of 1.26 g of the ketoester I*a*, 60 mg of *p*-toluenesulfonic acid, 5 ml of ethylene glycol, and 50 ml of benzene was refluxed for 18 h in the presence of a water separator. The mixture was cooled, washed with 10% sodium carbonate solution and with water, and evaporated. A solution of the residual (1.45 g), oily ketal ester in 30 ml of ether was added dropwise, with stirring, to a suspension of 0.5 g of lithium aluminium hydride in 20 ml of ether, and the mixture was refluxed for 3 h. After the usual work-up the mixture yielded 1.23 g of crude, gummy ketal alcohol. A solution of the latter in 13 ml of pyridine was added to a slurry of 1.2 g of chromic acid in 12 ml of pyridine, and the mixture was stirred at room temperature for 45 min. It then was extracted with ether and the extract washed successively with 10% sodium carbonate solution, water, 5% hydrochloric acid solution, and water once more. The extract was dried over sodium sulfate and evaporated to give 1.1 g of a pale-yellow, thick oil which became partly crystalline when allowed to stand. Several crystallizations from methanol yielded colorless needles of the ketal aldehyde V, m.p. 110–110.5°; $[\alpha]_D$ +90.0° (*c*, 1.5); μ (KBr) CH 3.67 (w), C=O 5.82 (s); δ C—CH_3 singlets at 1.02 and 1.04 p.p.m., ketal methylene broad singlet at 3.94 p.p.m., aldehyde CH singlet at 9.12 p.p.m.

Anal. Calcd. for $C_{19}H_{28}O_3$: C, 74.96; H, 9.27. Found: C, 75.10; H, 9.38.

Can. J. Chem. Downloaded from www.nrcresearchpress.com by 210.87.254.105 on 09/05/12
For personal use only.

Ketone Ib

A mixture of 0.74 g of crude ketal aldehyde, 8 ml of 95% hydrazine, and 32 ml of diethylene glycol was heated for 2 h at a bath temperature of 125–135°. After the addition of 4.0 g of potassium hydroxide pellets, heating (170–180°) was continued for 8 h. The usual work-up gave 0.64 g of a pale-yellow oil; chromatography of this oil on 10 g of alumina and elution with hexane yielded 0.38 g of an oil showing one spot on thin-layer chromatography. A solution of the product and 1.6 ml of sulfuric acid in 30 ml of methanol was refluxed for 30 min and then worked up in the usual manner. Chromatography of the resultant oil (0.29 g) on 8 g of alumina and elution with 20:1 hexane–ether yielded 205 mg of a solid. Several crystallizations from hexane yielded the enone *Ib*, m.p. and mixed m.p. 61.5–62.5°; its infrared spectrum was identical with that of an authentic sample.

Ketoacid VIa

An excess of ozone was bubbled for 20 min through a solution of 0.56 g of ketone *Ib* in 10 ml of glacial acetic acid and 15 ml of ethyl acetate cooled in an ice–salt bath. After the addition of 0.6 ml of 30% hydrogen peroxide and 5 ml of water, the mixture was left to stand at room temperature for 2 h and then heated at 60–70° for 5 min. Work-up gave 0.60 g of an acidic fraction and negligible amounts of neutral material. Chromatography of the former on silica gel and elution with 3:2 benzene–ether gave 0.48 g of a solid, m.p. 83–88°. Crystallization from hexane yielded ketoacid VI*a*, m.p. 90–92°; μ (KBr) OH 3.0–3.3 (m), 3.6–3.8 (m), C=O 5.85 (s, broad).

Anal. Calcd. for $C_{16}H_{26}O_3$: C, 72.14; H, 9.84. Found: C, 72.10; H, 9.79.

Ketones IV and IX

An ethereal solution of methyllithium (from 0.5 g of lithium) was poured through a glass-wool plug into a solution of 0.25 g of crude acid VI*a* in 15 ml of ether, and the mixture was refluxed for 3.5 h. The cooled mixture was poured onto ice and worked up in the usual manner. A hexane solution of the neutral product (0.23 g of a pale-yellow, viscous liquid) was treated with charcoal and filtered through 1.5 g of alumina. The hexane filtrate contained 106 mg of a semisolid mixture, and a subsequent ether eluate was composed of 102 mg of VII*a* (μ (KBr) OH 2.84 (m), C=O 5.87 (s)), m.p. 102–106° (softening at 95°). Despite crystallization from hexane and chromatographies over alumina the solid ketol could not be purified further. Chromatography of VII*a* and the earlier semisolid fraction (154 mg) on 5 g of alumina and elution with hexane yielded 86 mg of a colorless liquid which could be induced to crystallize. Unfortunately this substance, VIII*a*, m.p. 63–65° (μ (neat liquid) no OH, C=C 5.91 (m)), was as sensitive as its ketol precursor and could not be purified further. A solution of 85 mg of the enol ether and 1 ml of 5 *N* hydrochloric acid in 5 ml of 95% alcohol was kept at 70° under nitrogen for 2 h. The usual work-up gave 75 mg of a ketone mixture. Its gas-phase chromatography (20% polyester LAC 446 on WAW column, 225–300°, F. and M. model 500 apparatus) yielded IV as the major component (retention time 18 min; μ (neat) C=O 5.82 (s); δ C—CH_3 singlets at 0.83, 0.88, and 0.94 p.p.m., olefinic C—CH_3 singlet at 1.55 p.p.m., $COCH_3$ singlet at 2.13 p.p.m.) and IX as the minor component (retention time 22.8 min; μ (neat) C=O 5.80 (s); δ C—CH_3 singlets at 0.78, 0.86, and 0.87 p.p.m., olefinic C—CH_3 broad singlet at 1.67 p.p.m., $COCH_3$ singlet at 2.13 p.p.m., olefinic CH multiplet at 5.43 p.p.m.).

A 1% solution (2 ml) of osmium tetroxide in *t*-butanol was added to a solution of 200 mg of sclareol (III) in 50 ml of *t*-butanol. After the addition of a 0.5 *M* aqueous solution of periodic acid (8 ml) and enough 0.5 *M* sodium hydroxide solution to bring the mixture to pH 8, it was stirred at room temperature for 10 h. Some sodium sulfite and water were added and the mixture was extracted with ether. The extract was washed with water, dried over sodium sulfate, and evaporated to give 161 mg of a grey liquid. Gas-phase chromatographic analysis (see above) indicated a single peak, retention time 10.7 min, μ (neat) no OH, C=C 5.92 (m); hence it was VIII*b*. Acid-catalyzed isomerization of the latter in a manner identical with the isomerization of VIII*a* (see above) yielded also a mixture of IV and IX, identified and separated by gas-phase chromatography. As in the above case, IV was the major product, but much less so.

Osmium Tetroxide – Periodate Oxidations of Manool

A solution of osmium tetroxide (20 mg) in *t*-butanol (2 ml) was added to a solution of manool (200 mg) in *t*-butanol (50 ml). After the addition of a 0.5 *M* aqueous solution of periodic acid (15 ml) and a 0.5 *N* sodium hydroxide solution (100 ml) the mixture was stirred for 45 min. Within 5–10 min a fine precipitate appeared. The mixture was extracted with chloroform, and the extract was washed with saturated brine solution and dried over sodium sulfate. Evaporation of the solvent, chromatography of the residue (235 mg) on silica gel (8 g), and elution with chloroform–methanol (20:1) yielded a solid (196 mg) which, on crystallization from chloroform – ethyl acetate, gave pentol XII, m.p. 186–187° (lit. (10) m.p. 184–185°); $[\alpha]_D$ −9° (*c*, 0.80 in pyridine).

A solution of osmium tetroxide (50 mg) in *t*-butanol (5 ml) was added to a solution of manool (500 mg) in *t*-butanol (250 ml). After the addition of a 0.5 *M* aqueous solution of periodic acid (30 ml) and a 0.1 *N*

Can. J. Chem. Downloaded from www.nrcresearchpress.com by 210.87.254.105 on 09/05/12
For personal use only.

solution (225 ml) of sulfuric acid the clear mixture was left to stand for 22 h. It then was extracted with ether and worked up as above. Chromatography of the residue (505 mg) on silica gel (15 g) and elution with pentane–ether (50:1) gave a solid (177 mg) which, on crystallization from hexane, gave ketal XIII, m.p. 119–121° (lit. (12) m.p. 115–116°); $[\alpha]_D$ +26° (*c*, 0.52) (lit. (12) $[\alpha]_D$ +31° (*c*, 1.08)); its infrared and proton magnetic resonance spectra were identical with those reported (12).

Anal. Calcd. for $C_{18}H_{30}O_2$: C, 77.65; H, 10.86. Found: C, 77.92; H, 10.80.

Elution with pentane–ether (9:1) gave the diketone VI*b* (195 mg) as an oil, $[\alpha]_D$ −10.3° (*c*, 2.08) (lit. (10) $[\alpha]_D$ +36° (*c*, 1.0)); μ (neat) C=O 5.85 (s); δ C—CH_3 singlets at 0.71, 0.84, and 0.97 p.p.m., $COCH_3$ singlet at 2.08 p.p.m.

Anal. Calcd. for $C_{17}H_{28}O_2$: C, 77.22; H, 10.67. Found: C, 77.37; H, 10.44.

Elution with pentane–ether (4:1) gave a solid (52 mg) whose crystallization from acetone–hexane yielded crystals, m.p. 173–175°; $[\alpha]_D$ +40.5° (*c*, 0.83); μ (KBr) OH 2.76 (w), 2.91 (m); δ C—CH_3 singlets at 0.77, 0.81, 1.02, and 1.24 p.p.m., hydroxymethine broad singlet at 5.01 p.p.m., molecular ion *m/e* 310.

Anal. Calcd. for $C_{18}H_{30}O_4$: C, 69.64; H, 9.74. Found: C, 69.61, 69.55; H, 9.65, 9.53.

A solution of osmium tetroxide (40 mg) in *t*-butanol (4 ml) was added to a solution of manool (400 mg) in *t*-butanol (320 ml). After the addition of a 0.5 *M* aqueous solution of periodic acid (40 ml), the mixture was brought to pH 6.0 by the addition of 0.5 *N* sodium hydroxide solution and kept at this pH by the addition of a phosphate buffer solution (500 ml composed of 357.5 ml of a 0.1 *M* potassium dihydrogen phosphate solution, 10 ml of a 0.5 *N* sodium hydroxide solution, and 132.5 ml of water). The clear mixture was left to stand for 8 h and then treated with a solution of sodium sulfite (2 g) in water (50 ml), stirred for 2 min, and extracted with ether. Isolation as above led to the diketone VI*b* (332 mg).[1]

Execution of the pH 6 experiment as above, except for the use of only 200 ml of *t*-butanol and 20 ml of periodic acid (the reaction mixture remaining a suspension throughout the experiment), yielded diketone VI*b* (272 mg) and an oil (XIV), eluted with pentane–ether (5:1), $[\alpha]_D$ +36.9° (*c*, 2.05); μ (neat) OH 2.85 (m), C=O 5.84 (s), CH=CH_2 10.08 (m), 10.90 (m); δ C—CH_3 singlets at 0.71, 0.84, 0.97, and 1.25 p.p.m., vinyl 12-line signal at 4.93, 4.97, 5.05, 5.08, 5.12, 5.15, 5.35, 5.38, 5.77, 5.93, 6.05, and 6.23 p.p.m.

Anal. Calcd. for $C_{19}H_{32}O_3$: C, 78.03; H, 11.03. Found: C, 77.74; H, 11.29.

ACKNOWLEDGMENT

The authors are indebted to the U.S. National Science Foundation for support of the work at Indiana University.

1. E. Wenkert, A. Afonso, J. B. Bredenberg, C. Kaneko, and A. Tahara. J. Am. Chem. Soc. **86**, 2038 (1964).
2. E. Wenkert, R. W. J. Carney, and C. Kaneko. J. Am. Chem. Soc. **83**, 4440 (1961).
3. A. W. Burgstahler and L. R. Worden. J. Am. Chem. Soc. **86**, 96 (1964).
4. G. C. Harris and T. F. Sanderson. J. Am. Chem. Soc. **70**, 339 (1948). W. M. Hoehn. U.S. Patent No. 2,682,555 (June 29, 1954).
5. D. B. Bigley, N. A. J. Rogers, and J. A. Barltrop. J. Chem. Soc. 4613 (1960).
6. G. Büchi and K. Biemann. Croat. Chem. Acta, **29**, 163 (1957). G. Ohloff. Ann. **617**, 134 (1958); Helv. Chim. Acta, **41**, 845 (1958).
7. J. R. Hosking. Ber. **69**, 780 (1936).
8. P. K. Grant and R. Hodges. J. Chem. Soc. 5274 (1960).
9. J. A. Barltrop, D. Giles, J. R. Hanson, and N. A. J. Rogers. J. Chem. Soc. 2534 (1962).
10. O. Jeger, O. Dürst, and G. Büchi. Helv. Chim. Acta, **30**, 1853 (1947).
11. H. R. Schenk, H. Gutmann, O. Jeger, and L. Ruzicka. Helv. Chim. Acta, **35**, 817 (1952); **37**, 543 (1954).
12. V. Scheidegger, K. Schaffner, and O. Jeger. Helv. Chim. Acta, **45**, 400 (1962).
13. R. Pappo, D. S. Allen, R. Lemieux, and W. S. Johnson. J. Org. Chem. **21**, 478 (1956).

Received April 4, 1966.
Department of Chemistry,
Indiana University,
Bloomington, Indiana, U.S.A.,
and
Department of Organic Chemistry,
The Weizmann Institute of Science,
Rehovoth, Israel.

[1]*Experiments at pH 7.4 and 8.0 yielded similar results.*

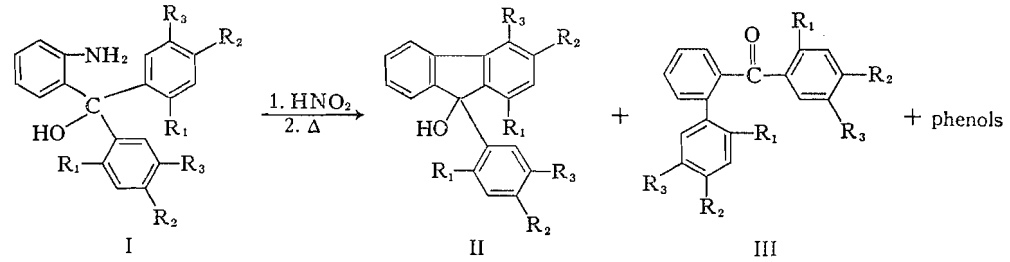
Can. J. Chem. Downloaded from www.nrcresearchpress.com by 210.87.254.105 on 09/05/12
For personal use only.

MOLECULAR REARRANGEMENT OF DIAZOTIZED *o*-AMINOPHENYLCARBINOLS

A. J. SISTI AND R. L. COHEN

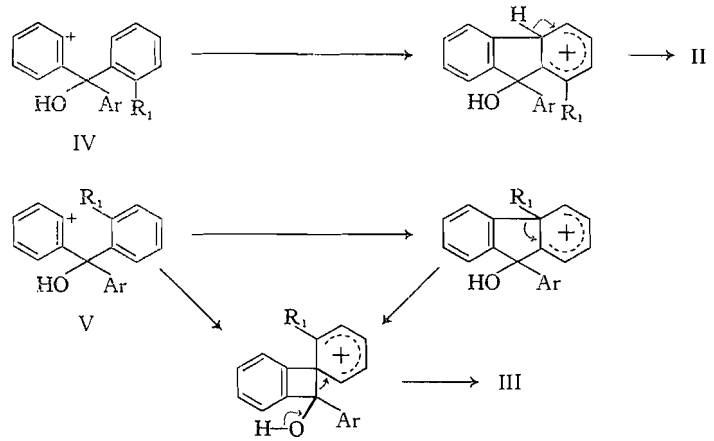
Two new reaction paths[1] have recently been observed in the decomposition of diazonium salts: in certain instances, molecular rearrangement (2, 3), and a fragmentation reaction yielding a benzyne intermediate (2, 4).

The first example of the rearrangement involved the conversion of 9-*o*-aminophenylfluorenol into tribenzotropone (5). More recently (2), the scope of the rearrangement was extended to a group of *o*-aminophenylcarbinols (I), yielding substituted 9-fluorenols II, ketones III (resulting from molecular rearrangement), and phenols (eq. [1]).

[1] 

I II III

The previous study demonstrated the necessity of an *o*-substituent (only the *o*-methyl substituent was studied (I, $R_1 = CH_3$)) for the production of ketone III. These results (Table I (*a*–*e*)) suggested that the lifetime of the aryl cation formed by the loss of nitrogen is very short compared with the time required for rotational equilibrium within the molecule (2). The following rationale was postulated.



Structures IV and V represent conformations in which the unsubstituted *o*-position is within and without incipient bonding distance to the aryl cation.[2]

Two new *o*-substituents, chloro and ethyl, were introduced to increase further the scope of the rearrangement and to offer more evidence to substantiate the previously postulated rationale.

[1] *For the more established reactions of the highly reactive aryl cation, see ref. 1.*
[2] *Structures IV and V are not intended to imply that the two rings are coplanar.*

Can. J. Chem. Downloaded from www.nrcresearchpress.com by 210.87.254.40 on 09/05/12
For personal use only.

The aminocarbinols listed in Table II were prepared from the corresponding Grignard reagents and acetyl anthranil, yielding the amido alcohols (6). The amido alcohols were subsequently hydrolyzed with alcoholic potassium hydroxide to the aminocarbinols.

The amino alcohols were diazotized in aqueous sulfuric acid and the diazonium salts were allowed to decompose at room temperature. Column chromatography on alumina was employed to separate the neutral materials.

Since all the diazonium salt decompositions were carried out in strong acid conditions, the heterolytic mechanism is most probably operating (1*c*).[3] The results are presented in Table I.

TABLE I

Yields of ketones and fluorenols from diazonium salts

	Amine I				
	R_1	R_2	R_3	% ketone III*	% fluorenol II†
a‡	H	H	H	0	46
b‡	H	OCH_3	H	0	48
c‡	CH_3	H	H	16.5 (15)	19
d‡	CH_3	CH_3	H	21.0 (16.6)	19
e‡	CH_3	OCH_3	H	28.6 (22.6)	21
f§	CH_3	OCH_3	CH_3	38 (27)	16
g	Cl	H	H	2.9	9.5
h	Cl	CH_3	H	8.8	9.9
i	Cl	OCH_3	H	11.0	8.7
j	CH_2CH_3	H	H	16.9 (13.0)	31.3
k	CH_2CH_3	OCH_3	H	33 (28)	28.4

*Yields in parentheses refer to recrystallized ketone; those without parentheses refer to chromatographed but not recrystallized material.
†In all cases, yields are based on recrystallized material.
‡Previously reported (2).
§This reaction, which was described previously (3), also gave a 7% yield of 2-(2,5-dimethyl-4-methoxybenzoyl)-2′,5′-dimethyl-4′-methoxyazobenzene.

The most significant feature of the results presented in Table I is that ketone is only obtained from the triphenylcarbinol derivatives possessing an *o*-substituent. The effect of the three *o*-substituents (chloro, methyl, and ethyl) cannot be solely electrical, since compound I*b*, containing the powerful electron-donating *p*-methoxyl group, yields no ketone. It may be noted that electron-donating substituents in the *p*-position of the migrating aryl group increase the yields of ketone significantly provided an *o*-substituent is present (I*d*, I*e*, I*h*, I*i*, and I*k*). In addition, one observes that ketone formation also appears to be dependent upon the electrical properties of the *o*-substituent (compare I*c* and I*j* with I*g*). These electrical effects are not unexpected since the rearrangement involves the migration of an aryl group to an electron-deficient site.

Another striking feature of Table I is that for a *given* *o*-substituent the yield of fluorenol remains unaltered when electron-donating *p*-substituents are introduced (I*g*–I*i*, I*c*–I*f*, and I*j*–I*k*). These data are consistent with the rationale previously postulated, based upon a very short lifetime for the aryl cation, the total number of free *o*-positions, and the relative populations of conformations IV and V. One additional observation, however, can be made. If the same relative population of conformations IV and V is assumed for R_1 = Cl, CH_3, and CH_2CH_3, the lower yield of fluorenol for *o*-chloro versus *o*-methyl and *o*-ethyl (I*g* versus I*c* and I*j*) may be ascribed to an adverse electrical effect.

The evidence presently available indicates that ketone formation resulting from the aryl cation is directly related to the total number of substituted *o*-positions and the electrical property of the *o*-substituent.

[3]*Recently an ion–diradical has been postulated as the intermediate (7).*

Can. J. Chem. Downloaded from www.nrcresearchpress.com by 210.87.254.40 on 09/05/12
For personal use only.

Can. J. Chem. Downloaded from www.nrcresearchpress.com by 210.87.254.40 on 09/05/12
For personal use only.

EXPERIMENTAL[4]

Aryl halides were prepared as follows: *o*-chlorobromobenzene (8), b.p. 197–200° (reported (8) b.p. 199–200°); 4-bromo-3-chlorotoluene (9), b.p. 75° at 2 mm (reported (9) b.p. 115–116° at 25 mm); 3-chloro-4-iodoanisole (10), b.p. 93–97° at 0.7 mm (reported (11) b.p. 127–130° at 6 mm); *o*-iodoethylbenzene (12), b.p. 56° at 0.7 mm (reported (12) b.p. 92–95° at 13 mm); 3-ethyl-4-iodoanisole, b.p. 125–126° at 5.5 mm (reported (10) b.p. 120–125° at 5 mm).

Synthesis of Acetamido Alcohols

All of the acetamido alcohols were prepared by the reaction of the appropriate arylmagnesium halide with acetyl anthranil (13). In each case a threefold excess of Grignard reagent was used. The ethereal solution of the Grignard reagent was cooled in an ice bath during the addition of a benzene solution of acetyl anthranil. The reactions were then completed by refluxing the solutions for 3 h followed by stirring at room temperature overnight. The reaction mixture was then hydrolyzed with an ammonium chloride solution, and the organic layer was separated and washed with 6 *M* sodium hydroxide followed by water. After the ether layer was dried over calcium sulfate and the solvent removed, the residue was crystallized, and recrystallized from benzene. The yields ranged from 18 to 32%. Three acetamido alcohols were characterized; the others were directly hydrolyzed to the amino alcohols listed in Table II.

The following acetamido alcohols were characterized.

2-Acetaminophenyldi-(2-chlorophenyl)carbinol had m.p. 188–189°.

Anal. Calcd. for $C_{21}H_{17}Cl_2NO_2$: C, 65.29; H, 4.44; N, 3.63. Found: C, 65.14; H, 4.55; N, 3.69.

2-Acetaminophenyldi-(2-chloro-4-methylphenyl)carbinol had m.p. 171–172°.

Anal. Calcd. for $C_{23}H_{21}Cl_2NO_2$: C, 66.68; H, 5.10; N, 3.38. Found: C, 66.57; H, 5.20; N, 3.40.

2-Acetaminophenyldi-(2-ethylphenyl)carbinol had m.p. 184–186°.

Anal. Calcd. for $C_{25}H_{27}NO_2$: C, 80.39; H, 7.29; N, 3.75. Found: C, 80.33; H, 7.28; N, 3.66.

Synthesis of Amino Alcohols

The amino alcohols listed in Table II were prepared by the hydrolysis of the corresponding acetamido alcohols. The hydrolysis was accomplished by refluxing the acetamido alcohols with a 20% alcoholic potassium hydroxide solution for 24–30 h. The mixture was then poured into water and extracted with ether, and the ether layer was dried over calcium sulfate. After removal of the ether the residue was crystallized from benzene – petroleum ether (b.p. 30–60°).

Diazotizations

The amino alcohols were diazotized in 100–150 ml of 5–10% sulfuric acid and 50 ml of dioxane at 0–5° with slightly more than an equivalent quantity of sodium nitrate. The aqueous acid (100–150 ml) was cooled to 0–5°, and the amino alcohol (8–17 mmoles) dissolved in 50 ml of dioxane was added. To the cooled solution was added the sodium nitrate in 10 ml of water. The solution was then allowed to stand at 0–10° for 1–2 h, after which time the solution was permitted to warm to room temperature and remain overnight. The mixture was then warmed to 40–50° to complete the decomposition (0.5–1 h). The mixture was extracted three times with ether and the ether extracts were washed with 5% sodium hydroxide to remove phenolic material, which was not characterized further. The dried ether solution was then evaporated and the residue examined as described below.

Products from Ig

The neutral residue was dissolved in 75% petroleum ether – benzene and adsorbed on alumina.[5] Elution with more of the same solvent mixture yielded 0.165 g (2.9%) of an oil, ν 1 685 cm^{-1} (chloroform). The oil resisted all attempts at crystallization. The ketone, however, was assigned the structure of *2-chloro-2′-(2-chlorophenyl) benzophenone* (III*g*).

Elution of the column with 70% benzene–chloroform gave an oil which was crystallized from benzene – petroleum ether, yielding 0.538 g (9.5%) of *1-chloro-9-(2-chlorophenyl)-9-fluorenol* (II*g*), m.p. 131–132°.

Anal. Calcd. for $C_{19}H_{12}Cl_2O$: C, 69.74; H, 3.70. Found: C, 69.44; H, 3.58.

A duplicate diazotization with Ig yielded essentially the same results: 3.2% ketone (III*g*) and 8.9% fluorenol (II*g*).

Products from Ih

The neutral residue was dissolved in equal volumes of benzene – petroleum ether and adsorbed on alumina. Elution with the same solvent mixture yielded 0.418 g (8.8%) of a yellow oil, ν 1 677 cm^{-1} (chloroform). The oil could not be crystallized; however, it was assigned the structure of *2-chloro-4-methyl-2′-(2-chloro-4-methylphenyl) benzophenone* (III*h*).

Elution of the column with benzene gave an oil which was crystallized from benzene – petroleum ether, yielding 0.470 g (9.9%) of *2-chloro-4-methyl-9-(2-chloro-4-methylphenyl)-9-fluorenol* (II*h*), m.p. 163–164°.

Anal. Calcd. for $C_{21}H_{16}Cl_2O$: C, 71.00; H, 4.54. Found: C, 70.88; H, 4.74.

[4]*Microanalyses were carried out by Spang Microanalytical Laboratory, Ann Arbor, Michigan. Melting points and boiling points are not corrected.*

[5]*All chromatograms described herein were conducted with ordinary Merck alumina (20 g/g of compound).*

Can. J. Chem. Downloaded from www.nrcresearchpress.com by 210.87.254.40 on 09/05/12
For personal use only.

TABLE II

Amino alcohols

	Melting point (°C)	% yield	Calculated (%)			Found (%)		
			C	H	N	C	H	N
2-Aminophenyldi-(2-chlorophenyl)carbinol (I*g*)	141.5–143	82	66.29	4.39	4.07	66.35	4.46	3.97
2-Aminophenyldi-(2-chloro-4-methylphenyl)carbinol (I*h*)	162–164	78	67.75	5.14	3.76	67.87	5.19	3.82
2-Aminophenyldi-(2-chloro-4-methoxyphenyl)carbinol (I*i*)	119–121	7	62.39	4.73	3.47	62.29	4.84	3.68
2-Aminophenyldi-(2-ethylphenyl)carbinol (I*j*)	100–102	54	83.34	7.60	4.23	83.33	7.65	4.36
2-Aminophenyldi-(2-ethyl-4-methoxyphenyl)carbinol (I*k*)	96–98	3	76.69	7.47	3.58	76.76	7.48	3.64

Products from Ii

The neutral residue was dissolved in equal volumes of benzene – petroleum ether and adsorbed on alumina. Elution with benzene yielded 0.301 g (11%) of a light-yellow oil, ν 1 672 cm^{-1} (chloroform). The oil resisted crystallization; however, it was assigned the structure of *2-chloro-4-methoxy-2'-(2-chloro-4-methoxyphenyl) benzophenone* (III*i*).

Elution of the column with equal volumes of benzene–chloroform gave, after recrystallization from benzene – petroleum ether, 0.249 g (8.7%) of *2-chloro-4-methoxy-9-(2-chloro-4-methoxyphenyl)-9-fluorenol* (II*i*), m.p. 191–193°.

Anal. Calcd. for $C_{21}H_{16}Cl_2O_3$: C, 65.13; H, 4.17. Found: C, 65.20; H, 4.28.

Products from Ij

The neutral residue was dissolved in 35% benzene – petroleum ether and adsorbed on alumina. Elution with petroleum ether yielded 0.803 g (16.9%) of a light-yellow oil, ν 1 685 cm^{-1} (chloroform). Recrystallization from petroleum ether yielded 0.616 g (13%) of *2-ethyl-2'-(2-ethylphenyl) benzophenone* (III*j*), m.p. 45–47°.

Anal. Calcd. for $C_{23}H_{22}O$: C, 87.86; H, 7.05. Found: C, 87.76; H, 7.04.

Further elution of the column with benzene yielded, after recrystallization from benzene – petroleum ether, 1.487 g (31.3%) of *2-ethyl-9-(2-ethylphenyl)-9-fluorenol* (II*j*), m.p. 91–93°.

Anal. Calcd. for $C_{23}H_{22}O$: C, 87.86; H, 7.05. Found: C, 87.67; H, 7.11.

Products from Ik

The neutral material was dissolved in equal volumes of benzene – petroleum ether and adsorbed on alumina. Elution with the same solvent mixture gave 0.928 g (33%) of a light-yellow oil, ν 1 665 cm^{-1} (chloroform). The oil was crystallized from ethanol, yielding 0.780 g (28%) of *2-ethyl-4-methoxy-2'-(2-ethyl-4-methoxyphenyl) benzophenone* (III*k*), m.p. 65–67°.

Anal. Calcd. for $C_{25}H_{26}O_3$: C, 80.18; H, 7.00. Found: C, 80.23; H, 7.09.

Elution of the column with equal volumes of benzene–chloroform yielded, after recrystallization from benzene – petroleum ether, 0.804 g (28.4%) of *2-ethyl-4-methoxy-9-(2-ethyl-4-methoxyphenyl)-9-fluorenol* (II*k*), m.p. 153–155°.

Anal. Calcd. for $C_{25}H_{26}O_3$: C, 80.18; H, 7.00. Found: C, 80.23; H, 7.09.

1. (*a*) J. F. Bunnett and R. E. Zahler. Chem. Rev. **49**, 273 (1951). (*b*) E. S. Lewis. J. Am. Chem. Soc. **80**, 1371 (1958). (*c*) D. F. Detar and D. I. Relyea. J. Am. Chem. Soc. **76**, 1680 (1954). (*d*) K. R. Brower. J. Am. Chem. Soc. **82**, 4535 (1960).
2. M. Stiles and A. J. Sisti. J. Org. Chem. **26**, 3639 (1961).
3. R. L. Cohen and A. J. Sisti. Can. J. Chem. **42**, 1388 (1964).
4. M. Stiles, R. G. Miller, and W. Burckhardt. J. Am. Chem. Soc. **85**, 1792 (1963).
5. M. Stiles and A. J. Libbey, Jr. J. Org. Chem. **22**, 1243 (1957).
6. W. Lothrup and P. Goodwin. J. Am. Chem. Soc. **65**, 363 (1943).
7. R. A. Abramovitch. Tetrahedron Letters, **23**, 1507 (1963); **23**, 1511 (1963).
8. J. L. Hartwell. *In* Organic syntheses. Collective Vol. III. John Wiley & Sons, Inc., New York. 1955. p. 185.
9. L. F. Fieser and D. M. Bowen. J. Am. Chem. Soc. **62**, 2103 (1940).
10. M. Oko and T. Sato. Bull. Chem. Soc. Japan, **30**, 508 (1957).
11. H. Faith, M. Bahler, and H. Florestano. J. Am. Chem. Soc. **77**, 543 (1955).
12. F. Weygand, H. Weber, E. Mackawa, and G. Eberhardt. Ber. **89**, 1994 (1956).
13. G. Walker. J. Am. Chem. Soc. **77**, 6698 (1955).

Received March 28, 1966.
Department of Chemistry,
Adelphi University,
Garden City, New York.

THE STRUCTURE OF THE MALEIC ANHYDRIDE – ACETYLACETONE ADDUCT

R. D. Bailey and G. M. Strunz

The reaction of maleic anhydride with acetylacetone was reported by Berner (1) in 1946 to give rise to a 2:1 adduct, m.p. 180° (decomp.), $C_{13}H_{12}O_8$. Similarly, ethyl acetoacetate was shown to give rise to an analogous adduct, $C_{14}H_{14}O_9$. The structures I*a* and I*b*, respectively, were assigned to these adducts, largely on the basis of their degradation

Can. J. Chem. Downloaded from www.nrcresearchpress.com by 210.87.254.40 on 09/05/12
For personal use only.

Products from Ii

The neutral residue was dissolved in equal volumes of benzene – petroleum ether and adsorbed on alumina. Elution with benzene yielded 0.301 g (11%) of a light-yellow oil, ν 1 672 cm^{-1} (chloroform). The oil resisted crystallization; however, it was assigned the structure of *2-chloro-4-methoxy-2'-(2-chloro-4-methoxyphenyl) benzophenone* (III*i*).

Elution of the column with equal volumes of benzene–chloroform gave, after recrystallization from benzene – petroleum ether, 0.249 g (8.7%) of *2-chloro-4-methoxy-9-(2-chloro-4-methoxyphenyl)-9-fluorenol* (II*i*), m.p. 191–193°.

Anal. Calcd. for $C_{21}H_{16}Cl_2O_3$: C, 65.13; H, 4.17. Found: C, 65.20; H, 4.28.

Products from Ij

The neutral residue was dissolved in 35% benzene – petroleum ether and adsorbed on alumina. Elution with petroleum ether yielded 0.803 g (16.9%) of a light-yellow oil, ν 1 685 cm^{-1} (chloroform). Recrystallization from petroleum ether yielded 0.616 g (13%) of *2-ethyl-2'-(2-ethylphenyl) benzophenone* (III*j*), m.p. 45–47°.

Anal. Calcd. for $C_{23}H_{22}O$: C, 87.86; H, 7.05. Found: C, 87.76; H, 7.04.

Further elution of the column with benzene yielded, after recrystallization from benzene – petroleum ether, 1.487 g (31.3%) of *2-ethyl-9-(2-ethylphenyl)-9-fluorenol* (II*j*), m.p. 91–93°.

Anal. Calcd. for $C_{23}H_{22}O$: C, 87.86; H, 7.05. Found: C, 87.67; H, 7.11.

Products from Ik

The neutral material was dissolved in equal volumes of benzene – petroleum ether and adsorbed on alumina. Elution with the same solvent mixture gave 0.928 g (33%) of a light-yellow oil, ν 1 665 cm^{-1} (chloroform). The oil was crystallized from ethanol, yielding 0.780 g (28%) of *2-ethyl-4-methoxy-2'-(2-ethyl-4-methoxyphenyl) benzophenone* (III*k*), m.p. 65–67°.

Anal. Calcd. for $C_{25}H_{26}O_3$: C, 80.18; H, 7.00. Found: C, 80.23; H, 7.09.

Elution of the column with equal volumes of benzene–chloroform yielded, after recrystallization from benzene – petroleum ether, 0.804 g (28.4%) of *2-ethyl-4-methoxy-9-(2-ethyl-4-methoxyphenyl)-9-fluorenol* (II*k*), m.p. 153–155°.

Anal. Calcd. for $C_{25}H_{26}O_3$: C, 80.18; H, 7.00. Found: C, 80.23; H, 7.09.

1. (*a*) J. F. Bunnett and R. E. Zahler. Chem. Rev. **49**, 273 (1951). (*b*) E. S. Lewis. J. Am. Chem. Soc. **80**, 1371 (1958). (*c*) D. F. Detar and D. I. Relyea. J. Am. Chem. Soc. **76**, 1680 (1954). (*d*) K. R. Brower. J. Am. Chem. Soc. **82**, 4535 (1960).
2. M. Stiles and A. J. Sisti. J. Org. Chem. **26**, 3639 (1961).
3. R. L. Cohen and A. J. Sisti. Can. J. Chem. **42**, 1388 (1964).
4. M. Stiles, R. G. Miller, and W. Burckhardt. J. Am. Chem. Soc. **85**, 1792 (1963).
5. M. Stiles and A. J. Libbey, Jr. J. Org. Chem. **22**, 1243 (1957).
6. W. Lothrup and P. Goodwin. J. Am. Chem. Soc. **65**, 363 (1943).
7. R. A. Abramovitch. Tetrahedron Letters, **23**, 1507 (1963); **23**, 1511 (1963).
8. J. L. Hartwell. *In* Organic syntheses. Collective Vol. III. John Wiley & Sons, Inc., New York. 1955. p. 185.
9. L. F. Fieser and D. M. Bowen. J. Am. Chem. Soc. **62**, 2103 (1940).
10. M. Oko and T. Sato. Bull. Chem. Soc. Japan, **30**, 508 (1957).
11. H. Faith, M. Bahler, and H. Florestano. J. Am. Chem. Soc. **77**, 543 (1955).
12. F. Weygand, H. Weber, E. Mackawa, and G. Eberhardt. Ber. **89**, 1994 (1956).
13. G. Walker. J. Am. Chem. Soc. **77**, 6698 (1955).

Received March 28, 1966.
Department of Chemistry,
Adelphi University,
Garden City, New York.

THE STRUCTURE OF THE MALEIC ANHYDRIDE – ACETYLACETONE ADDUCT

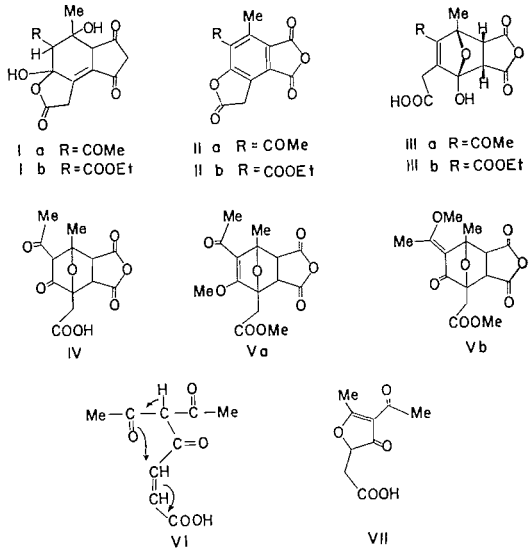
R. D. Bailey and G. M. Strunz

The reaction of maleic anhydride with acetylacetone was reported by Berner (1) in 1946 to give rise to a 2:1 adduct, m.p. 180° (decomp.), $C_{13}H_{12}O_8$. Similarly, ethyl acetoacetate was shown to give rise to an analogous adduct, $C_{14}H_{14}O_9$. The structures I*a* and I*b*, respectively, were assigned to these adducts, largely on the basis of their degradation

Can. J. Chem. Downloaded from www.nrcresearchpress.com by 210.87.254.105 on 09/05/12
For personal use only.

to the aromatic compounds II*a* and II*b* through the action of concentrated sulfuric acid. Recently, Bird and Molton (2) have proposed the bicyclic hemiketal structure III*b* for the ethyl acetoacetate adduct, the acetylacetone product being considered, by analogy, to be III*a*.

Both adducts have been found to yield a dimethyl derivative readily on treatment with ethereal diazomethane (1, 2). The product obtained by the British authors contains no hydroxyl group, and its structure has been proposed on the basis of its nuclear magnetic resonance spectrum in conjunction with mechanistic considerations. A rather unusual rearrangement is postulated to account for the formation of the aromatic substance II*b*. The formulation IV for the acetylacetone adduct appeared to us to be in closer accord with the results of Berner and Bird, and with the additional evidence described below. A close structural relationship between IV and I*a* is evident.



We have prepared the acetylacetone adduct, its dimethyl derivative, and the aromatic compound II*a* as described by Berner, and have established conclusively that the adduct is a β-dicarbonyl compound and that the diazomethane product is the enolether of a β-diketone, best formulated as IV and V (*a* and *b*), respectively.

The infrared spectrum of IV (KBr) shows broad absorption between 2 400 and 3 500 cm^{-1} and bands at 1 870, 1 835 (low intensity), 1 780, and 1 700 cm^{-1} (strong). A strong band at 1 230 cm^{-1} is in agreement with a cyclic five-membered ether and (or) anhydride (3). The ultraviolet chromophore (dioxane) clearly excludes the possibility that the compound is an α,β-unsaturated ketone. Absorption at 275 mμ (ε 2 100) is consistent with a slightly enolized β-dicarbonyl system.[1] Addition of a trace of aqueous base caused a change in the chromophore to λ_{max} 295 mμ (ε 11 400). Neutralization regenerated a chromophore closely similar to that of the starting material.

The dimethyl derivative V ($C_{15}H_{16}O_8$) shows infrared absorption (KBr) at 1 865, 1 830 (low intensity), 1 780, and 1 740 cm^{-1} (strong). Strong bands at 1 710 and 1 610 cm^{-1} are consistent with the carbonyl and C=C absorption, respectively, of the enolether formed by exocyclic enolization of an α-acetyl five-membered ketone (4).

[1]*The formulation IV allows for the existence of a lactol tautomer which might be involved in the enolization equilibrium.*

Can. J. Chem. Downloaded from www.nrcresearchpress.com by 210.87.254.105 on 09/05/12
For personal use only.

The ultraviolet absorption (dioxane) at 276 mμ (ϵ 10 000) is in excellent agreement with the predicted chromophore.

Two possible structures (V*a* and V*b*) can clearly arise from the reaction of IV with diazomethane. That the crystalline product of this reaction was a mixture of both isomers became evident from a study of its nuclear magnetic resonance spectrum. The methyl and —CH_2— protons attached to the bridgehead positions show three- and two-proton singlets at 8.11 and 6.96 τ, respectively. The ester methyl appears as a singlet at 6.25 τ. A pair of singlets at 7.84 and 7.56 τ in the ratio 1:4, together integrating for three protons, accounts respectively for the methyl hydrogens of the acetyl side chain of V*a* and the corresponding methyl protons of V*b*. The enolether methoxyls of these isomers appear as singlets in the same ratio, at 6.03 and 6.12 τ. An AB pattern (partially hidden) centered at 6.47 τ (J = 7.9 c.p.s.) accounts for the remaining two protons. It is not possible, on the basis of this coupling constant, to determine whether the configuration of the adduct is *exo* or *endo* (5).

By varying the conditions of reaction it was possible to increase the ratio of V*a* to V*b* to approximately 2:1, as determined by nuclear magnetic resonance spectroscopy. So far, only the isomer V*b* has been obtained in a pure state.

Finally, the mass spectrum of the crystalline isomer mixture V appears to be in agreement with the assigned structures. A weak molecular ion peak with *m/e* 324 can be observed. The major peaks in the higher mass region correspond to ions with *m/e* 226, 167, and 154.

We consider that one possible mode of formation of IV might involve an initial attack by the enol of acetylacetone on a maleic anhydride carbonyl, giving VI. The latter could conceivably cyclize as shown, yielding VII, which, as its 3-hydroxyfuran tautomer, could undergo Diels–Alder addition of a second molecule of maleic anhydride, giving rise to IV.

EXPERIMENTAL

Melting points were determined on a hot stage apparatus and are uncorrected. Infrared spectra were determined on a Perkin–Elmer Infracord model 137B spectrophotometer. Ultraviolet spectra were obtained on a Beckman DK-2 spectrophotometer. Nuclear magnetic resonance spectra were measured with a Varian Associates 56.4 Mc.p.s. spectrometer. The mass spectrum was obtained on a Hitachi Perkin–Elmer RMU-6D mass spectrometer. Microanalyses were performed by Spang Microanalytical Laboratory, Ann Arbor, Michigan.

The procedures of Berner (1) were followed for the preparation of IV, V, and II, and his experimental results were essentially duplicated.

Adduct IV had m.p. 176–181° (decomp.).

The dimethyl derivative V was prepared by addition of the powdered adduct IV (1.5 g) to approximately 5 equivalents of diazomethane in ether (200 ml). The crystalline product which separated had m.p. 142–150° and was used directly in the spectroscopic studies. An analytical sample (pure V*b*) was prepared by recrystallization from benzene, m.p. 148–154°.

Anal. Calcd. for $C_{15}H_{16}O_8$: C, 55.55; H, 4.97. Found: C, 55.47; H, 4.92.

By varying the concentration and excess of diazomethane, it was possible to vary the relative proportions of V*a* and V*b* formed. The presence of the isomer V*a* was manifested in both the infrared and nuclear magnetic resonance spectra.

ACKNOWLEDGMENTS

Grateful acknowledgment is made to the National Research Council of Canada for financial support. The authors thank Professors Z. Valenta and K. Wiesner for helpful discussions.

1. E. Berner. J. Chem. Soc. 1052 (1946).
2. C. W. Bird and P. Molton. Tetrahedron Letters, **17**, 1891 (1966).
3. M. St. C. Flett. Characteristic frequencies of chemical groups in the infrared. Elsevier Pub. Co., Inc., Amsterdam. 1963.

Can. J. Chem. Downloaded from www.nrcresearchpress.com by 210.87.254.105 on 09/05/12
For personal use only.

4. G. E. ARTH, G. I. POOS, and L. H. SARETT. J. Am. Chem. Soc. **77**, 3834 (1955).
5. P. LASZLO and P. VON R. SCHLEYER. J. Am. Chem. Soc. **86**, 1171 (1964).

RECEIVED JULY 8, 1966.
DEPARTMENT OF CHEMISTRY,
UNIVERSITY OF NEW BRUNSWICK,
FREDERICTON, NEW BRUNSWICK.

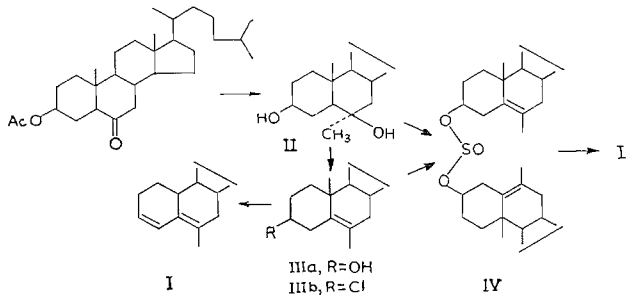
Can. J. Chem. Downloaded from www.nrcresearchpress.com by 210.87.254.105 on 09/05/12
For personal use only.

SYNTHESIS OF 6-METHYLCHOLESTA-3,5-DIENE; SOLVOLYSIS OF 6-METHYLCHOLESTERYL IODIDE[1]

GEORGE JUST AND EDWARD LEE-RUFF[2]

In connection with a study of the photolysis of substituted cholesta-3,5-dienes, we required a sample of 6-methylcholesteryl ethyl ether and adequate amounts of 6-methylcholesta-3,5-diene (I). The latter compound had been obtained by Bauslaugh (1) in an unsatisfactory yield.

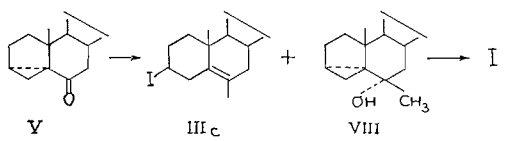
We therefore investigated an alternate pathway. 6α-Methylcholestan-3β,6β-diol (II) (2), obtained as outlined in Reaction Scheme 1, was submitted to various dehydrating agents. Treatment of II with 10% ethanolic hydrochloric acid gave 6-methylcholesterol (III*a*) (2) and 6-methylcholesteryl chloride (III*b*) (3) in 67 and 20% yields, respectively.



REACTION SCHEME 1.

Reaction of 6-methylcholesterol with thionyl chloride gave di(6-methylcholesteryl) sulfite (IV). The same product was obtained by reacting diol II with thionyl chloride. Its structure was proven by hydrolysis to III*a*. Pyrolysis of sulfite IV gave 6-methylcholesterol (III*a*) and diene I. Pyrolysis of 6-methylcholesterol with anhydrous copper sulfate gave a 1:1 mixture of the desired diene I and di(6-methylcholesteryl) ether.

The most convenient sequence proved to be that depicted in Reaction Scheme 2.



REACTION SCHEME 2.

[1]*We thank the National Research Council of Canada for financial support.*
[2]*Holder of a National Research Council of Canada bursary, 1964–1965, and studentship, 1965–1966.*

4. G. E. ARTH, G. I. POOS, and L. H. SARETT. J. Am. Chem. Soc. **77**, 3834 (1955).
5. P. LASZLO and P. VON R. SCHLEYER. J. Am. Chem. Soc. **86**, 1171 (1964).

RECEIVED JULY 8, 1966.
DEPARTMENT OF CHEMISTRY,
UNIVERSITY OF NEW BRUNSWICK,
FREDERICTON, NEW BRUNSWICK.

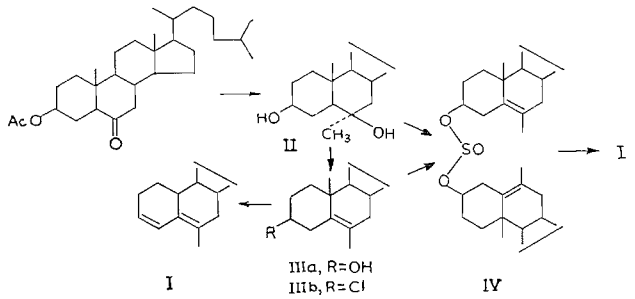
Can. J. Chem. Downloaded from www.nrcresearchpress.com by 210.87.254.5 on 09/05/12
For personal use only.

SYNTHESIS OF 6-METHYLCHOLESTA-3,5-DIENE; SOLVOLYSIS OF 6-METHYLCHOLESTERYL IODIDE[1]

GEORGE JUST AND EDWARD LEE-RUFF[2]

In connection with a study of the photolysis of substituted cholesta-3,5-dienes, we required a sample of 6-methylcholesteryl ethyl ether and adequate amounts of 6-methylcholesta-3,5-diene (I). The latter compound had been obtained by Bauslaugh (1) in an unsatisfactory yield.

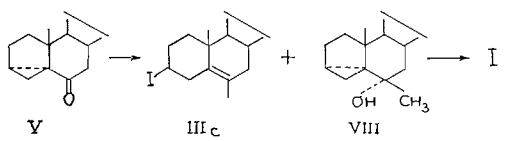
We therefore investigated an alternate pathway. 6α-Methylcholestan-3β,6β-diol (II) (2), obtained as outlined in Reaction Scheme 1, was submitted to various dehydrating agents. Treatment of II with 10% ethanolic hydrochloric acid gave 6-methylcholesterol (III*a*) (2) and 6-methylcholesteryl chloride (III*b*) (3) in 67 and 20% yields, respectively.



REACTION SCHEME 1.

Reaction of 6-methylcholesterol with thionyl chloride gave di(6-methylcholesteryl) sulfite (IV). The same product was obtained by reacting diol II with thionyl chloride. Its structure was proven by hydrolysis to III*a*. Pyrolysis of sulfite IV gave 6-methylcholesterol (III*a*) and diene I. Pyrolysis of 6-methylcholesterol with anhydrous copper sulfate gave a 1:1 mixture of the desired diene I and di(6-methylcholesteryl) ether.

The most convenient sequence proved to be that depicted in Reaction Scheme 2.



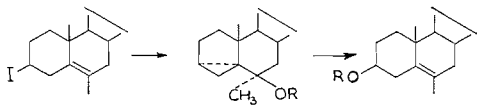
REACTION SCHEME 2.

[1]*We thank the National Research Council of Canada for financial support.*
[2]*Holder of a National Research Council of Canada bursary, 1964–1965, and studentship, 1965–1966.*

Reaction of 3α,5-cyclo-5α-cholestan-6-one (V) with methylmagnesium iodide gave 6β-methyl-3α,5-cyclo-5α-cholestan-6α-ol (VIII) (4) in a 75% yield. The minor product of this reaction was 6-methylcholesteryl iodide (III*c*). The assignment of the stereochemistry of alcohol VIII at C-6 was based on arguments similar to those used to explain the stereochemistry of the lithium aluminium hydride reduction of V (5). The formation of 6-methylcholesteryl iodide is easily rationalized, since the reaction medium contained iodide ions and a Lewis acid. Dehydration and rearrangement of the cyclopropyl carbinol was achieved by stirring alcohol VIII in dry benzene with phosphorus pentoxide. The desired 6-methylcholesta-3,5-diene (I) was obtained in over 90% yield.

*6-Methylcholesteryl Ethyl Ether; a Study of the Solvolysis of 6-Methylcholesteryl Iodide (III*c*)*

One of the by-products obtained above was 6-methylcholesteryl iodide (III*c*). Since a sample of 6-methylcholesteryl ethyl ether (VII*a*) was required for comparison purposes, we solvolyzed iodide IIIc in ethanol. The major product obtained was cycloether VI*a*, accompanied by small amounts of VII*a*. Cycloether VI*a* was not stable under the solvolysis conditions and was slowly transformed to VII*a*. When cycloether VI*a* was treated with acidified ethanol at room temperature, it was quantitatively converted into ether VII*a*. The methanolysis and hydrolysis of iodide III*c* proceeded in a similar fashion.



IIIc VIa, R=Et VIb, R=Me VIc, R=H VIIa, R=Et VIIb, R=Me

REACTION SCHEME 3.

The structure of 6-methylcholesteryl ether was proven by comparison with the product obtained from the reaction of the potassium salt of III*a* with ethyl iodide. The assignments of the structures of the cyclo compounds VI*a*–VI*c* were based on the infrared and nuclear magnetic resonance spectra (which all showed cyclopropyl absorptions at 3 080 and 3 020 cm^{-1} (infrared) and 0.4–0.6 p.p.m. (nuclear magnetic resonance)) and the fact that acid treatment resulted in the formation of cholesteryl derivatives (VII*a*, VII*b*, and III*a*).

When 6-methylcholesteryl *p*-toluenesulfonate was solvolyzed under conditions identical with those used for the hydrolysis of 6-methylcholesteryl iodide, the same relative yield of 6α-methyl-3α,5-cyclo-5α-cholestan-6β-ol (VI*c*) was obtained. It is therefore apparent that the same homoallylic carbonium ion is involved in both the iodide and tosylate solvolyses, and the low yields of VI*c* reported by Davis *et al.* can be rationalized by the decomposition of VI*c* to 6-methylcholesterol (III*a*) under the reported reaction and work-up conditions (4). These results are therefore quite similar to those reported by Summers in the spirostane series (6).

EXPERIMENTAL

The general experimental details have been given in ref. 7. All preparative thin-layer chromatography (t.l.c.) separations were performed with glass plates (20 × 20 cm) covered with silica gel (½ mm, E. Merck A.G.).

Acid Dehydration of Diol II

A solution of 1.5 g of diol II in 50 ml of ethanol containing 5 ml of concentrated hydrochloric acid was refluxed for 3 h. The reaction mixture was diluted with 200 ml of ether, washed with 5% aqueous sodium bicarbonate and water, and dried with anhydrous magnesium sulfate. The residue, after evaporation,

Can. J. Chem. Downloaded from www.nrcresearchpress.com by 210.87.254.5 on 09/05/12
For personal use only.

crystallized from ether–hexane, giving 1.05 g of 6-methylcholesterol (III*a*), m.p. 131–135°. Recrystallization from hexane gave an analytic sample, m.p. 139–141°; the mixed melting point with an authentic sample showed no depression; ν 3 550 and 1 050 – 1 060 cm^{-1} (OH); δ 3.55 p.p.m. (1 H, multiplet, C_3—H), 2.90 p.p.m. (1 H, half of an AB quartet, C_4—H), 1.85 p.p.m. (1 H, singlet, exchangeable with D_2O, —OH), and 1.65 p.p.m. (3 H, singlet, C=C—CH_3). Crystallization of the mother liquor from ethanol–ether gave 300 mg of 6-methylcholesteryl chloride, m.p. 101–104°. Recrystallization from ethanol raised the m.p. to 105–106°; ν 847 cm^{-1} (C—Cl); δ 3.65 p.p.m. (1 H, multiplet, C_3—H), 3.0 p.p.m. (1 H, half of an AB quartet, C_4—H), and 1.62 p.p.m. (3 H, singlet, C=C—CH_3).

Anal. Calcd. for $C_{28}H_{47}Cl$: C, 80.24; H, 11.21; Cl, 8.46. Found: C, 80.21; H, 11.21; Cl, 8.32.

Dehydration of Diol II with Thionyl Chloride – Pyridine

A solution of 200 mg of diol II in 15 ml of anhydrous pyridine was cooled to 0°, and 0.1 ml of thionyl chloride was added dropwise, with stirring. The reaction mixture was allowed to reach room temperature and the stirring was continued for an additional hour. The mixture was quenched with 20 ml of cold water, and the resulting white precipitate was filtered off, washed with water until neutral, and crystallized from ethanol–ether, giving 190 mg of di(6-methylcholesteryl) sulfite (IV), m.p. 191–192°; ν 1 200, 950, and 925 cm^{-1} (strong, sulfite); δ 4.25 p.p.m. (1 H, multiplet, C_3—H), 2.9 p.p.m. (1 H, half of an AB quartet, C_4—H), and 1.65 p.p.m. (3 H, singlet, C=C—CH_3).

Anal. Calcd. for $C_{56}H_{94}SO_3$: C, 79.40; H, 11.17; S, 3.80. Found: C, 79.29; H, 10.95; S, 4.10.

Dehydration of 6-Methylcholesterol (IIIa) with Thionyl Chloride – Pyridine

The same procedures as for the thionyl chloride dehydration of diol II were used for the dehydration of 100 mg of 6-methylcholesterol (III*a*). This yielded 90 mg of the diester sulfite IV, identical in all respects with the sample obtained above.

Acid Hydrolysis of Diester Sulfite IV

A solution containing 100 mg of IV in 20 ml of ethanol and 2 ml of concentrated hydrochloric acid was refluxed for 1 h. The reaction mixture was worked up in the usual manner, yielding 70 mg of 6-methylcholesterol (III*a*), identical in all respects with an authentic sample.

Pyrolysis of Diester Sulfite IV

A melting point tube containing 2 mg of IV was heated to 205°. The pyrolysate was dissolved in ether. Quantitative t.l.c. showed two stains, one having an R_f value identical with that of 6-methylcholesterol. The ultraviolet spectrum showed diene absorptions at 236, 242, and 249 mμ.

Pyrolysis of 6-Methylcholesterol (IIIa)

An intimate mixture of 500 mg of 6-methylcholesterol (III*a*) and 500 mg of anhydrous cupric sulfate was heated to 200° for 20 min. The residue was extracted with benzene and the extract chromatographed on silica gel. Hexane eluted 260 mg of 6-methylcholesta-3,5-diene, which was crystallized from an ethanol–ether mixture, m.p. 86–88°; ν 3 040 and 1 650 cm^{-1} (C=C—H); λ_{max}^{EtOH} 236 mμ (ϵ 18 220), 242 mμ (ϵ 19 800), and 249 mμ (ϵ 13 900); δ 6.42 p.p.m. (1 H, doublet, J = 10 c.p.s., C=C_4—H), 5.80 p.p.m. (1 H, broad signal, C=C_3—H), and 1.72 p.p.m. (3 H, singlet, C=C—CH_3).

Anal. Calcd. for $C_{28}H_{46}$: C, 87.88; H, 12.12. Found: C, 87.91; H, 12.28.

Hexane–benzene eluted 140 mg of di(6-methylcholesteryl) ether, which was crystallized from ether, m.p. 215–216°; ν 1 100 and 1 080 cm^{-1} (ether); δ 3.35 p.p.m. (1 H, multiplet, C_3—H), 2.87 p.p.m. (1 H, half of an AB quartet, C_4—H), and 1.65 p.p.m. (3 H, singlet, C=C—CH_3).

Anal. Calcd. for $C_{56}H_{94}O$: C, 85.86; H, 12.10. Found: C, 85.86; H, 11.88.

6β-Methyl-3α,5-cyclo-5α-cholestan-6α-ol (VIII)

A solution of 5 g of 3α,5-cyclo-5α-cholestan-6-one (V) in 100 ml of ether was added dropwise to 120 ml of an ethereal solution of methylmagnesium iodide (3.2 g magnesium turnings, 8.8 ml methyl iodide). The solution was heated under reflux for 2 h. The excess reagent was destroyed by slowing adding 50 ml of 10% aqueous ammonium chloride. The ether layer was washed with water until neutral, dried over anhydrous magnesium sulfate, and evaporated under reduced pressure. The oily residue was chromatographed on alumina (activity II–III, 140 g). Elution with hexane gave 6-methylcholesteryl iodide (III*c*) (1.1 g, 20%), m.p. 103–105°. Two crystallizations from ethanol–ether raised the melting point to 110–111°; δ 4.00 p.p.m. (1 H, broad signal, C_3—H), 2.95 p.p.m. (2 H, quartet, C_4—H), and 1.65 p.p.m. (3 H, singlet, C=C—CH_3).

Anal. Calcd. for $C_{28}H_{47}I$: C, 65.88; H, 9.21; I, 24.81. Found: C, 65.93; H, 9.33; I, 24.94.

Elution with benzene–ether gave 3.7 g of 6β-methyl-3α,5-cyclo-5α-cholestan-6α-ol (VIII), identical in all respects with an authentic sample (4), m.p. 91–91.5°, $[\alpha]_D^{19}$ +38.2° (*c*, 0.87).

6-Methylcholesta-3,5-diene (I)

A solution of 3.5 g of 6β-methyl-3α,5-cyclo-5α-cholestan-6α-ol (VIII) in 100 ml of anhydrous benzene containing 3 g of phosphorus pentoxide was stirred for 3 h at room temperature. Ether extraction and crystallization from ethanol gave 3.2 g of 6-methylcholesta-3,5-diene (I), identical in all respects with the sample prepared above.

Can. J. Chem. Downloaded from www.nrcresearchpress.com by 210.87.254.5 on 09/05/12
For personal use only.

Ethanolysis of 6-Methylcholesteryl Iodide (IIIc)

A solution of 300 mg of iodide III*c* in 50 ml of absolute ethanol containing 200 mg of potassium acetate was refluxed for 1 h. The mixture was diluted with 150 ml of ether, washed with water until neutral, dried over anhydrous magnesium sulfate, and evaporated under reduced pressure. The residue was chromatographed on two t.l.c. plates (hexane–benzene (1:1)), giving 188 mg of oily 6β-ethoxy-6α-methyl-3α,5-cyclo-5α-cholestane (VI*a*), ν 3 080 and 3 020 cm^{-1} (cyclopropane), 1 115 and 1 085 cm^{-1} (ether); δ 3.39 p.p.m. (2 H, two overlapping quartets, O—CHH′—CH_3) and 0.4–0.6 p.p.m. (multiplet, cyclopropyl protons).

Anal. Calcd. for $C_{30}H_{52}O$: C, 84.04; H, 12.23. Found: C, 84.03; H, 12.12.

6-Methylcholesteryl Ethyl Ether (VIIa)

From 6-Methylcholesterol (IIIa)

To a solution of 180 mg of 6-methylcholesterol (III*a*) in 50 ml of anhydrous benzene was added 200 mg of potassium chips. The mixture was refluxed for 3 h and cooled to room temperature, after which 1 ml of ethyl iodide was added. The mixture was refluxed for a further 24 h. After the solution was cooled, absolute ethanol was slowly added to destroy the excess potassium. The mixture was diluted with 100 ml ether, washed with water until neutral, dried over anhydrous magnesium sulfate, and evaporated. The residue (131 mg) was chromatographed on one t.l.c. plate (benzene), giving 52 mg of 6-methylcholesteryl ethyl ether (VII*a*), m.p. 95–96°; ν 1 105 cm^{-1} (ether); δ 3.42 p.p.m. (2 H, quartet, O—CH_2—CH_3), 2.80 p.p.m. (1 H, multiplet, C_3—H), and 1.55 p.p.m. (3 H, singlet, C=C—CH_3).

Anal. Calcd. for $C_{30}H_{52}O$: C, 84.04; H, 12.23. Found: C, 83.95; H, 12.10.

From Cycloether VIa

A solution of 100 mg of cycloether VI*a* in 25 ml of absolute ethanol containing 0.5 ml of 72% perchloric acid was stirred overnight. The resulting precipitate was filtered off, washed with water, and crystallized from ethanol–ether, giving 75 mg of 6-methylcholesteryl ethyl ether (VII*a*), identical in all respects with the sample prepared above.

Methanolysis of 6-Methylcholesteryl Iodide (IIIc)

A solution of 300 mg of iodide III*c* in 50 ml of absolute methanol containing 200 mg of potassium acetate was stirred at room temperature for 24 h. The reaction mixture was worked up in the usual manner, giving 290 mg of an oil, which was chromatographed on two t.l.c. plates (hexane–benzene (1:1)), yielding 135 mg of oily 6β-methoxy-6α-methyl-3α,5-cyclo-5α-cholestane (VI*b*), ν 3 080 and 3 020 cm^{-1} (cyclopropane), 1 089 cm^{-1} (ether); δ 3.11 p.p.m. (3 H, singlet, O—CH_3) and 0.3–0.6 p.p.m. (multiplet, cyclopropyl protons).

Anal. Calcd. for $C_{29}H_{50}O$: C, 83.99; H, 12.15. Found: C, 83.96; H, 12.06.

Acid Reaction of Cycloether VIb

The same procedures were followed as for the acid rearrangement of cycloether VI*a* (100 mg of VI*b* being used). This gave, after crystallization from methanol–ether, 65 mg of 6-methylcholesteryl methyl ether, m.p. 101–102°; ν 1 105 cm^{-1} (ether); δ 3.20 p.p.m. (3 H, singlet, O—CH_3), 2.75 p.p.m. (1 H, multiplet, C_3—H), and 1.57 p.p.m. (3 H, singlet, C=C—CH_3).

Anal. Calcd. for $C_{29}H_{50}O$: C, 83.99; H, 12.15. Found: C, 84.00; H, 12.05.

Hydrolysis of 6-Methylcholesteryl Iodide (IIIc)

A solution of 200 mg of iodide III*c* in 25 ml of acetone containing 5 ml of water and 50 mg of potassium bicarbonate was stirred for 72 h. This was worked up in the usual manner to give 184 mg of an oily residue. Chromatography of this residue on two t.l.c. plates (benzene) yielded 147 mg of oily cycloalcohol VI*c*, ν 3 620, 1 105, and 1 020 cm^{-1} (alcohol), 3 080 and 3 020 cm^{-1} (cyclopropane); δ 0.2–0.5 p.p.m. (multiplet, cyclopropyl protons).

Anal. Calcd. for $C_{28}H_{48}O$: C, 83.93; H, 12.08. Found: C, 84.06; H, 11.91.

Acid Rearrangement of Cycloalcohol VIc

A solution of 100 mg of cycloalcohol VI*c* in 50 ml of ether containing 1 ml of 72% perchloric acid was stirred overnight. The solution was diluted to 100 ml with ether, washed with 5% aqueous sodium bicarbonate, dried over anhydrous magnesium sulfate, and evaporated under reduced pressure, giving 95 mg of 6-methylcholesterol (III*a*), identical in all respects with the sample prepared above.

Solvolysis of 6-Methylcholesteryl p-Toluenesulfonate

The tosylate of 6-methylcholesterol was prepared according to the procedures of Davis *et al.* (4). A solution of 200 mg of the tosylate (m.p. 128–133°) in 25 ml of acetone containing 5 ml of water and 50 mg of potassium bicarbonate was stirred for 72 h. The usual work-up gave 194 mg of an oily residue, which was chromatographed on two t.l.c. plates, yielding 63 mg of unreacted 6-methylcholesteryl *p*-toluenesulfonate and 90 mg of cycloalcohol VI*c*, identical in all respects with the sample prepared above.

1. G. Bauslaugh. Ph.D. Thesis, McGill University, Montreal, Quebec. 1965.
2. L. F. Fieser and J. Rigaudy. J. Am. Chem. Soc. **73**, 4660 (1951).
3. M. Shiota. Nippon Kagaku Zasshi, **77**, 778 (1956); Chem. Abstr. **52**, 417 (1958).
4. M. Davis, S. Julia, and G. H. R. Summers. Bull. Soc. Chim. France, 742 (1960).

Can. J. Chem. Downloaded from www.nrcresearchpress.com by 210.87.254.5 on 09/05/12
For personal use only.

5. G. JUST and K. ST. C. RICHARDSON. Can. J. Chem. **42**, 456 (1964).
6. G. H. R. SUMMERS. J. Chem. Soc. 1821 (1961).
7. N. D. HALL and G. JUST. Steroids, **6**, 111 (1965).

RECEIVED JUNE 24, 1966.
DEPARTMENT OF CHEMISTRY,
MCGILL UNIVERSITY,
MONTREAL, QUEBEC.

Can. J. Chem. Downloaded from www.nrcresearchpress.com by 210.87.254.5 on 09/05/12
For personal use only.

A CONVENIENT METHOD FOR THE PREPARATION OF OPTICALLY ACTIVE BENZYL-α-*d* ALCOHOL

SAUL WOLFE AND ARVI RAUK

Optically active benzyl-α-*d* alcohol was synthesized some years ago and the levo enantiomer shown to have the *R* absolute configuration (I) by Streitwieser and his co-workers (1). Their method involved the preparation of benzaldehyde-*d* from benzonitrile (2), the reduction of (+)-camphor to (−)-isoborneol with lithium aluminium hydride (3), and then asymmetric reduction of the benzaldehyde-*d* with isobornyloxymagnesium bromide (4). (−)-Benzyl-α-*d* alcohol, $[\alpha]_D$ −0.715° (neat), was obtained after a lengthy isolation procedure. The optical purity of this material cannot be better than 45%, since Mosher and his co-workers have now found (5) that the optically active benzyl-α-*d* alcohol produced in the reduction of benzaldehyde-*d* with actively fermenting yeast has $[\alpha]_D^{24}$ 1.58° (neat). The same workers also obtained (+)-benzyl-α-*d* alcohol, $[\alpha]_D^{26}$ 0.32° (neat), in a 16% yield (average of two runs) from the reaction of benzaldehyde-α-*d* with the optically active Grignard reagent from (+)-1-chloro-2-methylbutane.

During another investigation, we recently had to prepare optically active benzyl-α-*d* alcohol. Since high optical purity was not essential for this study, an alternative to the Streitwieser procedure was worked out and forms the subject of this note. The new synthesis, which proceeds with 30% stereospecificity, has the advantage of providing the dextro alcohol in 1 day's working time, with all the reactions being performed in a single vessel. The deuterium source is sodium borodeuteride; from 0.5 g of this compound is obtained 1.1 g of (+)-benzyl-α-*d* alcohol. The actual reducing agent is (−)-diisopinocampheyldeuterioborane (II), prepared from (+)-α-pinene and deuterated diborane, the latter in turn prepared in tetrahydrofuran by the reduction of boron trifluoride with sodium borodeuteride.

Brown and his co-workers have shown (6, 7) that hydroboration of olefins with undeuterated II followed by the usual oxidative work-up (8) leads to optically active alcohols and (−)-isopinocampheol. The reduction of methyl ketones III to optically active secondary alcohols (11–30% excess of the *R* enantiomer, i.e. IV) was reported in a brief communication (9).[1] By analogy with this work, the reduction of benzaldehyde (VI) by II is expected to produce VII, i.e. *S*-(+)-benzyl-α-*d* alcohol.

No volatile compounds were obtained directly from the reaction of II with benzaldehyde, even after prolonged treatment with sodium hydroxide. Benzyl alcohol and isopinocampheol were readily obtained, however, when this alkaline mixture was treated with

[1]*Although it is not specifically stated in this communication that the reducing agent was (−)-diisopinocampheylborane and not the (+)-isomer V, we infer that the former was, in fact, used, since the preparation of V was not described until somewhat later (7).*

5. G. JUST and K. ST. C. RICHARDSON. Can. J. Chem. **42**, 456 (1964).
6. G. H. R. SUMMERS. J. Chem. Soc. 1821 (1961).
7. N. D. HALL and G. JUST. Steroids, **6**, 111 (1965).

RECEIVED JUNE 24, 1966.
DEPARTMENT OF CHEMISTRY,
MCGILL UNIVERSITY,
MONTREAL, QUEBEC.

Can. J. Chem. Downloaded from www.nrcresearchpress.com by 210.87.254.42 on 09/05/12
For personal use only.

A CONVENIENT METHOD FOR THE PREPARATION OF OPTICALLY ACTIVE BENZYL-α-*d* ALCOHOL

SAUL WOLFE AND ARVI RAUK

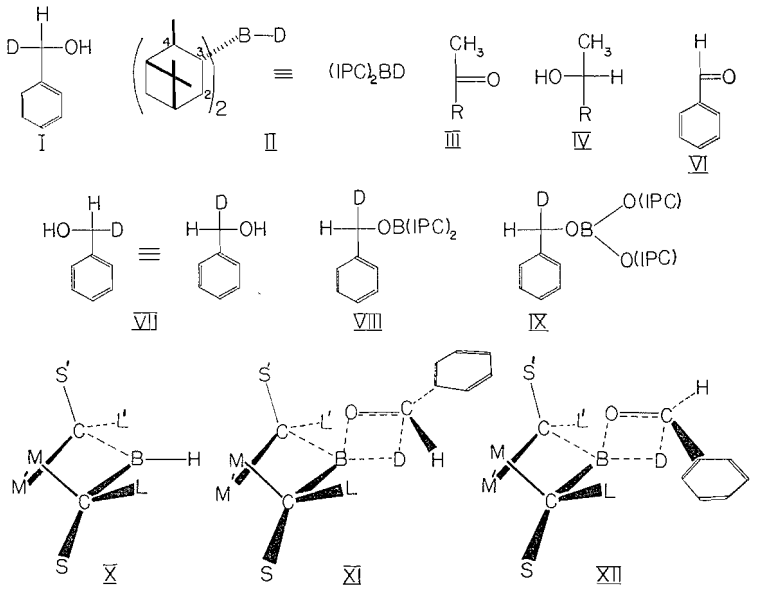
Optically active benzyl-α-*d* alcohol was synthesized some years ago and the levo enantiomer shown to have the *R* absolute configuration (I) by Streitwieser and his co-workers (1). Their method involved the preparation of benzaldehyde-*d* from benzonitrile (2), the reduction of (+)-camphor to (−)-isoborneol with lithium aluminium hydride (3), and then asymmetric reduction of the benzaldehyde-*d* with isobornyloxymagnesium bromide (4). (−)-Benzyl-α-*d* alcohol, $[\alpha]_D$ −0.715° (neat), was obtained after a lengthy isolation procedure. The optical purity of this material cannot be better than 45%, since Mosher and his co-workers have now found (5) that the optically active benzyl-α-*d* alcohol produced in the reduction of benzaldehyde-*d* with actively fermenting yeast has $[\alpha]_D^{24}$ 1.58° (neat). The same workers also obtained (+)-benzyl-α-*d* alcohol, $[\alpha]_D^{26}$ 0.32° (neat), in a 16% yield (average of two runs) from the reaction of benzaldehyde-α-*d* with the optically active Grignard reagent from (+)-1-chloro-2-methylbutane.

During another investigation, we recently had to prepare optically active benzyl-α-*d* alcohol. Since high optical purity was not essential for this study, an alternative to the Streitwieser procedure was worked out and forms the subject of this note. The new synthesis, which proceeds with 30% stereospecificity, has the advantage of providing the dextro alcohol in 1 day's working time, with all the reactions being performed in a single vessel. The deuterium source is sodium borodeuteride; from 0.5 g of this compound is obtained 1.1 g of (+)-benzyl-α-*d* alcohol. The actual reducing agent is (−)-diisopinocampheyldeuterioborane (II), prepared from (+)-α-pinene and deuterated diborane, the latter in turn prepared in tetrahydrofuran by the reduction of boron trifluoride with sodium borodeuteride.

Brown and his co-workers have shown (6, 7) that hydroboration of olefins with undeuterated II followed by the usual oxidative work-up (8) leads to optically active alcohols and (−)-isopinocampheol. The reduction of methyl ketones III to optically active secondary alcohols (11–30% excess of the *R* enantiomer, i.e. IV) was reported in a brief communication (9).[1] By analogy with this work, the reduction of benzaldehyde (VI) by II is expected to produce VII, i.e. *S*-(+)-benzyl-α-*d* alcohol.

No volatile compounds were obtained directly from the reaction of II with benzaldehyde, even after prolonged treatment with sodium hydroxide. Benzyl alcohol and isopinocampheol were readily obtained, however, when this alkaline mixture was treated with

[1]*Although it is not specifically stated in this communication that the reducing agent was (−)-diisopinocampheylborane and not the (+)-isomer V, we infer that the former was, in fact, used, since the preparation of V was not described until somewhat later (7).*



hydrogen peroxide. Apparently, the borate ester IX is considerably more susceptible to hydrolysis than is VIII, the presumed initial product of the reduction. (+)-Benzyl-α-*d* alcohol, $[\alpha]_D^{22}$ 0.33° (*c*, 10 in chloroform) was isolated by a countercurrent procedure, using petroleum ether and water, followed by chloroform extraction of the aqueous phase. Since (−)-isopinocampheol is the second product of the sequence of reactions, the observed dextro rotation of the benzyl alcohol is real and indicates a minimum stereospecificity for the reduction of 30%, assuming that rotations in chloroform and neat are comparable and correcting for the use of pinene which was 70% optically pure.

The direction of specificity in the reduction of benzaldehyde is thus the same as that observed earlier with the methyl ketones (9). It is noteworthy that both of these results are consistent with the model used by Brown and his co-workers to explain the stereospecific conversion of olefins into alcohols (7).

According to this model, (−)-diisopinocampheylborane can be represented as shown in X, where S and S′ are the hydrogens at C_3 and $C_{3'}$, M and M′ are the methylene groups at C_2 and $C_{2'}$, and L and L′ are the methyl groups at C_4 and $C_{4'}$. If it is assumed that the reduction of benzaldehyde by II proceeds via a four-centered transition state, then the two possibilities are XI and XII. In each of these, one of the substituents attached to the carbonyl group points towards L and the other substituent points towards L′. However, it is evident upon examination of molecular models that phenyl and L in XII are in closer proximity than are phenyl and L′ in XI. Therefore, it is concluded that XI, which leads to the observed *S*-benzyl-α-*d* alcohol, is more favorable sterically.

EXPERIMENTAL

To a suspension of finely powdered sodium borodeuteride (0.5329 g, 4.25 mmoles) in 25 ml of tetrahydrofuran (freshly distilled from lithium aluminium hydride) in a three-necked flask fitted with a pressure-equalizing dropping funnel, magnetic stirrer, thermometer, and condenser fitted with a calcium chloride drying tube was added dropwise, during a 20 min period at room temperature, a solution of freshly distilled boron trifluoride etherate (2.14 ml, 2.41 g, 5.67 mmoles) in 25 ml of dry tetrahydrofuran. Apart from a slight rise in temperature, there was no apparent reaction. The white suspension was stirred for 1 h and then a solution of 4.63 g (5.39 ml, 11.33 mmoles) of (+)-α-pinene, $[\alpha]_D^{25}$ 36° (71.3% optically pure (10)), in 25 ml of dry tetrahydrofuran was added dropwise, over a 20 min period. Again there was no apparent reaction apart

Can. J. Chem. Downloaded from www.nrcresearchpress.com by 210.87.254.42 on 09/05/12
For personal use only.

from a slight rise in temperature. The white suspension was stirred for 4 h at room temperature and cooled to 0°; a solution of freshly distilled benzaldehyde (1.72 ml, 1.80 g, 5.67 mmoles) in 25 ml of dry tetrahydrofuran was then added dropwise, during a 20 min period. A transient pale-green color appeared upon the addition of each drop of the benzaldehyde solution. The cooling bath was then removed and the reaction mixture was stirred overnight. Then, 5 ml of 3 *N* NaOH was added, the mixture was warmed to 50°, and 5 ml of 30% H_2O_2 was added dropwise.[2] After 1 h the clear colorless tetrahydrofuran layer was decanted from the viscous aqueous phase. The aqueous phase was extracted several times with ether and the combined organic extracts were concentrated to yield a viscous oil. This was shaken with a mixture of 100 ml of water and 50 ml of petroleum ether (b.p. 40–60°), and subjected to countercurrent extraction, using five separatory funnels. The aqueous phase was then extracted with chloroform, and the chloroform extract was dried over anhydrous magnesium sulfate and evaporated to give 1.63 g (88%) of a clear colorless oil which had a slightly negative rotation. The countercurrent procedure (three separatory funnels) and the chloroform extraction were therefore repeated, and the product then showed $[\alpha]_D^{23}$ 0.12° (*c*, 10 in chloroform). Distillation gave 1.10 g (59%) of benzyl-α-*d* alcohol, $[\alpha]_D^{22}$ 0.33° (*c*, 10 in chloroform), identified by gas chromatography and by its infrared and nuclear magnetic resonance spectra. When the optical purity of the α-pinene is taken into account, the stereospecificity of the present reduction is 30%, i.e. $\frac{100}{71} \times \frac{0.33}{1.58} \times 100$.

ACKNOWLEDGMENTS

We thank the National Research Council of Canada for the support of this work and the award of a studentship, G. E. Palmer for the (+)-α-pinene, and Professor H. S. Mosher for sending us a preprint of his paper.

1. A. Streitwieser, Jr., J. R. Wolfe, Jr., and W. D. Schaeffer. Tetrahedron, **6**, 338 (1959).
2. J. W. Williams. J. Am. Chem. Soc. **61**, 2248 (1939).
3. D. S. Noyce and D. B. Denney. J. Am. Chem. Soc. **72**, 5743 (1950).
4. A. Streitwieser, Jr. and J. R. Wolfe, Jr. J. Am. Chem. Soc. **79**, 903 (1957).
5. V. E. Althouse, D. M. Feigl, W. A. Sanderson, and H. S. Mosher. J. Am. Chem. Soc. **88**, 3595 (1966).
6. H. C. Brown and G. Zweifel. J. Am. Chem. Soc. **83**, 486 (1961).
7. H. C. Brown, N. R. Ayyangar, and G. Zweifel. J. Am. Chem. Soc. **86**, 397 (1964).
8. H. C. Brown. Hydroboration. W. A. Benjamin, Inc., New York. 1962.
9. H. C. Brown and D. B. Bigley. J. Am. Chem. Soc. **83**, 3166 (1961).
10. F. H. Turber and R. C. Thielke. J. Am. Chem. Soc. **53**, 1030 (1931).

Received May 24, 1966.
Department of Chemistry,
Queen's University,
Kingston, Ontario.

[2]*If the hydrogen peroxide was not added at this point, the subsequent work-up gave only traces of α-pinene and no other volatile product.*

CHLOROMETHYL–PHOSPHORUS COMPOUNDS SYNTHESIS AND INFRARED SPECTRA

Arlen W. Frank[1] and Irving Gordon

Chloromethyl–phosphorus compounds are of interest because of their accessibility from hydroxymethyl–phosphorus compounds and their unique chemical properties. The synthesis and infrared spectra of these compounds are discussed in this note.

Thionyl chloride is widely used for the replacement of hydroxyl by chlorine in organic compounds, but its use with organophosphorus compounds containing hydroxymethyl substituents sometimes gives surprisingly poor results. Hydroxymethylphosphonic acid, for example, gives a 56.6% yield of chloromethylphosphonic dichloride (I) when treated with thionyl chloride in the presence of pyridine (1), but no reaction takes place when the

[1]*Present address: Ohio Wesleyan University, Delaware, Ohio.*

Can. J. Chem. Downloaded from www.nrcresearchpress.com by 210.87.254.42 on 09/05/12
For personal use only.

from a slight rise in temperature. The white suspension was stirred for 4 h at room temperature and cooled to 0°; a solution of freshly distilled benzaldehyde (1.72 ml, 1.80 g, 5.67 mmoles) in 25 ml of dry tetrahydrofuran was then added dropwise, during a 20 min period. A transient pale-green color appeared upon the addition of each drop of the benzaldehyde solution. The cooling bath was then removed and the reaction mixture was stirred overnight. Then, 5 ml of 3 *N* NaOH was added, the mixture was warmed to 50°, and 5 ml of 30% H_2O_2 was added dropwise.[2] After 1 h the clear colorless tetrahydrofuran layer was decanted from the viscous aqueous phase. The aqueous phase was extracted several times with ether and the combined organic extracts were concentrated to yield a viscous oil. This was shaken with a mixture of 100 ml of water and 50 ml of petroleum ether (b.p. 40–60°), and subjected to countercurrent extraction, using five separatory funnels. The aqueous phase was then extracted with chloroform, and the chloroform extract was dried over anhydrous magnesium sulfate and evaporated to give 1.63 g (88%) of a clear colorless oil which had a slightly negative rotation. The countercurrent procedure (three separatory funnels) and the chloroform extraction were therefore repeated, and the product then showed $[\alpha]_D^{23}$ 0.12° (*c*, 10 in chloroform). Distillation gave 1.10 g (59%) of benzyl-α-*d* alcohol, $[\alpha]_D^{22}$ 0.33° (*c*, 10 in chloroform), identified by gas chromatography and by its infrared and nuclear magnetic resonance spectra. When the optical purity of the α-pinene is taken into account, the stereospecificity of the present reduction is 30%, i.e. $\frac{100}{71} \times \frac{0.33}{1.58} \times 100$.

ACKNOWLEDGMENTS

We thank the National Research Council of Canada for the support of this work and the award of a studentship, G. E. Palmer for the (+)-α-pinene, and Professor H. S. Mosher for sending us a preprint of his paper.

1. A. Streitwieser, Jr., J. R. Wolfe, Jr., and W. D. Schaeffer. Tetrahedron, **6**, 338 (1959).
2. J. W. Williams. J. Am. Chem. Soc. **61**, 2248 (1939).
3. D. S. Noyce and D. B. Denney. J. Am. Chem. Soc. **72**, 5743 (1950).
4. A. Streitwieser, Jr. and J. R. Wolfe, Jr. J. Am. Chem. Soc. **79**, 903 (1957).
5. V. E. Althouse, D. M. Feigl, W. A. Sanderson, and H. S. Mosher. J. Am. Chem. Soc. **88**, 3595 (1966).
6. H. C. Brown and G. Zweifel. J. Am. Chem. Soc. **83**, 486 (1961).
7. H. C. Brown, N. R. Ayyangar, and G. Zweifel. J. Am. Chem. Soc. **86**, 397 (1964).
8. H. C. Brown. Hydroboration. W. A. Benjamin, Inc., New York. 1962.
9. H. C. Brown and D. B. Bigley. J. Am. Chem. Soc. **83**, 3166 (1961).
10. F. H. Turber and R. C. Thielke. J. Am. Chem. Soc. **53**, 1030 (1931).

Received May 24, 1966.
Department of Chemistry,
Queen's University,
Kingston, Ontario.

[2]*If the hydrogen peroxide was not added at this point, the subsequent work-up gave only traces of α-pinene and no other volatile product.*

CHLOROMETHYL–PHOSPHORUS COMPOUNDS SYNTHESIS AND INFRARED SPECTRA

Arlen W. Frank[1] and Irving Gordon

Chloromethyl–phosphorus compounds are of interest because of their accessibility from hydroxymethyl–phosphorus compounds and their unique chemical properties. The synthesis and infrared spectra of these compounds are discussed in this note.

Thionyl chloride is widely used for the replacement of hydroxyl by chlorine in organic compounds, but its use with organophosphorus compounds containing hydroxymethyl substituents sometimes gives surprisingly poor results. Hydroxymethylphosphonic acid, for example, gives a 56.6% yield of chloromethylphosphonic dichloride (I) when treated with thionyl chloride in the presence of pyridine (1), but no reaction takes place when the

[1]*Present address: Ohio Wesleyan University, Delaware, Ohio.*

Can. J. Chem. Downloaded from www.nrcresearchpress.com by 210.87.254.105 on 09/05/12
For personal use only.

pyridine is absent (2). Tris(hydroxymethyl)phosphine oxide gives tris(chloromethyl)phosphine oxide (II) in only a 32–33% yield (3). Thionyl chloride is unsuitable for converting tetrakis(hydroxymethyl)phosphonium chloride into tetrakis(chloromethyl)phosphonium chloride (III), although it works well with other phosphonium salts containing hydroxymethyl groups (4).

We have now examined the missing member of this series, bis(hydroxymethyl)phosphinic acid. Treatment of this compound in a benzene suspension with thionyl chloride at reflux (procedure A) gave a good yield (75%) of bis(chloromethyl)phosphinic chloride (IV), provided, however, that sufficient time was allowed for the very viscous phase which formed to redissolve completely. The viscous intermediate tended to ball on the stirrer and climb the walls of the reaction vessel. Little difficulty was experienced as long as sufficient space was left above the surface of the liquid to allow for this.

These observations prompted a reexamination of the other members of the series to see whether they too formed a viscous, gummy phase, which might account for the low yields reported in the literature.

Contrary to Prat *et al.* (2), hydroxymethylphosphonic acid did react with thionyl chloride, giving a viscous, gummy substance similar in appearance to the one described above. It did not break, however, even after 25 h of refluxing. Tris(hydroxymethyl)phosphine oxide and tetrakis(hydroxymethyl)phosphonium chloride did not form viscous, gummy phases, but the products were partly liquid and yielded only 30.5% of II and 12% of III, respectively. The liquid portions contained sulfur as well as chlorine. It seems likely that the gummy or liquid products of these reactions represent sulfite cross-links between hydroxymethyl groups, as reported by Kuznetsov and Faizullin (5).

The formation of the gummy, viscous intermediate in the bis(hydroxymethyl)phosphinic acid reaction could be avoided by reversing the order of addition (procedure B). When the acid was added in portions to the thionyl chloride at reflux in the absence of a solvent, IV was obtained in a 93% yield. With III, however, no improvement in the yield was noted.

The detection of product formation in this work was facilitated by the discovery that the CH_2 deformation band in the infrared spectra of the chloromethyl–phosphorus compounds was shifted from its usual position at 1 465 cm^{-1} (6) to 1 400 cm^{-1}. The $ClCH_2$—P band occurred at 1 400 $\pm$ 3 cm^{-1} in most of the 20 compounds examined (Table I). In general, it was insensitive to the state of oxidation of the phosphorus and to the nature of the other substituents, with the exception of chlorine, which caused a shift to an even lower frequency (1 385 – 1 395 cm^{-1}). The band was absent in dichloromethylphosphonic dichloride.

The presence of a band in the neighborhood of 1 400 cm^{-1} should not, of course, be construed as proof of the presence of a $ClCH_2$—P group, in the absence of other supporting evidence, for conflicts in this region of the spectrum are inevitable.

EXPERIMENTAL

Melting points were taken on a Fisher–Johns apparatus, and are corrected. The thionyl chloride, unless otherwise stated, was purified by distillation from boiled linseed oil. The hydroxymethyl–phosphorus compounds were stripped of excess water on a steam bath under vacuum, and dried to constant weight.

Bis(chloromethyl)phosphinic Chloride (IV)

Procedure A

Bis(hydroxymethyl)phosphinic acid (252 g, 2 moles) was mixed with 2 l of benzene and distilled until about 500 ml of distillate was collected, to remove any water present as the azeotrope. Thionyl chloride (834 g, 7 moles) was then added dropwise over a 5 h period at reflux. The reaction mixture was kept at reflux until the gas evolution subsided (10 h) and the viscous contents, which had collected on the stirrer and climbed the walls of the reaction vessel, had completely redissolved. At the end, the solution was clear. The solvent was

Can. J. Chem. Downloaded from www.nrcresearchpress.com by 210.87.254.105 on 09/05/12
For personal use only.

TABLE I

Infrared absorption by the $ClCH_2$—P group

Compound	Frequency, cm^{-1}
$ClCH_2P(O)Cl_2$ (I)	1 389
$ClCH_2P(O)(OH)_2$	1 402
$ClCH_2P(O)(OCH_2Cl)Cl$	1 395
$ClCH_2P(O)(OCH_2Cl)_2$	1 398
$ClCH_2P(O)(OCH_2CH_2Cl)_2$	1 398
$ClCH_2P(O)(OC_3H_7\text{-}n)_2$	1 399
$ClCH_2P(O)(OC_4H_9\text{-}n)_2$	1 397
$ClCH_2P(O)(OCH_2CH(C_2H_5)C_4H_9)_2$	1 400
$ClCH_2P(O)(OCH_2CH{=}CH_2)_2$	~1 400*
$ClCH_2P(O)(OC_6H_5)_2$	1 398
$ClCH_2P(O)F_2$	1 400
$ClCH_2P(S)Cl_2$	1 385
$ClCH_2PCl_2$	1 393
$ClCH_2P(O)(C_6H_5)CH_2CH_2Cl$	1 400†
$(ClCH_2)_2P(O)Cl$ (IV)	1 389
$(ClCH_2)_2P(O)OH$	1 400
$(ClCH_2)_2P(O)OC_2H_5$	1 400
$(ClCH_2)_3P$	1 398
$(ClCH_2)_3PO$ (II)	1 391, 1 410
$(ClCH_2)_4PCl$ (III)	1 400

*Sadtler standard spectra, No. 14549, Sadtler Research Laboratories, Philadelphia, Pennsylvania.
†From ref. 7.

stripped off and the product distilled, giving 274 g (75%) of IV, b.p. 104–106° at 2 mm, n_D^{25} 1.5196. A portion of this product was redistilled for analysis.

Anal. Calcd. for $C_2H_4Cl_3OP$: C, 13.24; H, 2.22; Cl, 58.64; P, 17.08. Found: C, 13.32; H, 2.15; Cl, 58.9; P, 16.6.

Its infrared spectrum (neat) contained bands at 522 (vs) (P—Cl), 1 260 (vs) (P=O), and 1 389 (s) ($ClCH_2$—P) cm^{-1}. Moedritzer (8) prepared IV, b.p. 98–101° at 1 mm, from chloromethylphosphonous dichloride and paraformaldehyde in a 53.5% yield, and from bis(chloromethyl)phosphinic anhydride and phosphorus pentachloride in a 84.5% yield.

Procedure B

Bis(hydroxymethyl)phosphinic acid (126 g, 1 mole) was added in small portions to 595 g (5 moles) of technical-grade thionyl chloride over a 4 h period at reflux. Gas evolution was heavy, but no viscous phase separated. The reaction mixture was held at reflux until the gas evolution subsided (6 h), and was then distilled, giving 175 g (1.47 moles) of recovered thionyl chloride, b.p. 76–79°, n_D^{25} 1.5169, followed by 169 g (93%) of IV, b.p. 131–133° at 11 mm, n_D^{25} 1.5198.

Anal. Calcd. for $C_2H_4Cl_3OP$: Cl, 58.6 (total), 19.6 (hydrolyzable); P, 17.1. Found: Cl, 59.0 (total), 19.6 (hydrolyzable); P, 16.5.

The identity of the product was confirmed by hydrolysis to the known acid, bis(chloromethyl)phosphinic acid, m.p. 79–80° (lit. (8) m.p. 78°), and by esterification to the known ester, ethyl bis(chloromethyl)phosphinate, b.p. 104–106° at 1.5 mm, n_D^{25} 1.4780 (lit. (8) b.p. 115–116° at 1.5 mm).

Infrared Spectra

The infrared spectra were obtained on a Beckman IR-4 instrument (liquids neat and solids in Nujol). The $ClCH_2$—P band was readily distinguishable from the 1 378 cm^{-1} Nujol band, provided the latter was not too strong. The compounds in Table I not mentioned in the text were obtained from commercial sources or prepared by standard literature methods.

ACKNOWLEDGMENTS

We are grateful to Mr. Leon A. Zengierski and to Mr. Rudolph Mundhenke for technical assistance, and to Dr. Charles F. Baranauckas for his interest and encouragement.

1. R. A. B. Bannard, J. R. Gilpin, G. R. Vavasour, and A. F. McKay. Can. J. Chem. **31**, 976 (1953).
2. J. Prat, L. Bourgeois, and P. Ragon. Mem. Serv. Chim. Etat Paris, **34**, 393 (1948).
3. M. Reuter and F. Jakob. Ger. Patent No. 1,064, 511 (September 3, 1959).
4. H. Hellmann, J. Bader, H. Birkner, and O. Schumacher. Ann. **659**, 49 (1962).
5. E. V. Kuznetsov and I. N. Faizullin. USSR Patent No. 161,917 (April 1, 1964); Chem. Abstr. **61**, 8436 (1964).

Can. J. Chem. Downloaded from www.nrcresearchpress.com by 210.87.254.105 on 09/05/12
For personal use only.

6. L. J. BELLAMY. The infra-red spectra of complex molecules. 2nd ed. John Wiley & Sons, Inc., New York. 1958. p. 13.
7. H. HELLMANN and J. BADER. Tetrahedron Letters, 724 (1961).
8. K. MOEDRITZER. J. Am. Chem. Soc. **83**, 4381 (1961).

RECEIVED APRIL 22, 1966.
RESEARCH CENTER,
HOOKER CHEMICAL CORPORATION,
NIAGARA FALLS, NEW YORK.

Can. J. Chem. Downloaded from www.nrcresearchpress.com by 210.87.254.105 on 09/05/12
For personal use only.

Can. J. Chem. Downloaded from www.nrcresearchpress.com by 210.87.254.40 on 09/05/12
For personal use only.

Canadian Journal of Chemistry

Issued by THE NATIONAL RESEARCH COUNCIL OF CANADA

VOLUME 44 NOVEMBER 15, 1966 NUMBER 22

KINETICS AND MECHANISMS OF REACTIONS CATALYZED BY PANCREATIC RIBONUCLEASE

EILEEN N. RAMSDEN AND KEITH J. LAIDLER
Department of Chemistry, University of Ottawa, Ottawa, Canada

Received January 19, 1966

ABSTRACT

A kinetic study has been made of the ribonuclease-catalyzed hydrolyses of three cyclic nucleotides, cytidine-2′,3′-phosphate, uridine-2′,3′-phosphate, and N^6,$O^{5'}$-diacetyl cytidine-2′,3′-phosphate. Rates were measured at pH values ranging from 6 to 8.5. The variation of the kinetic parameters with pH showed that the free enzyme possesses two active groups, having pK values of 5.4 and 7.25. When the enzyme–substrate complex is formed, the pK values of the groups are increased to 6.6 and 8.4. The pK values identify these groups as imidazole groups and show that two histidine residues are present at the active site. Since both increase in pK on complex formation, it is concluded that the acid imidazole group binds the substrate, but that the basic imidazole group cannot be concerned in substrate binding and must function only in the hydrolytic step. The results indicate that the pyrimidine base is concerned in the hydrolytic step and not solely in binding, as had been postulated. It is concluded from all of the evidence that four specific sites are present at the active center of the enzyme; three are involved in binding and one in catalysis. It is proposed that the active site of ribonuclease is composed of: the histidine residue in position 12, which catalyzes the hydrolytic step; the histidine residue in position 119, which binds the 2′-ribose oxygen atom in the substrate; the lysine residue in position 41, which binds the phosphate group or anion; and the aspartic acid residue in position 121, which binds the nitrogen atom at N^1 in the pyrimidine base. A mechanism for enzyme–substrate complex formation and subsequent hydrolysis is proposed.

INTRODUCTION

The degradation of ribonucleic acid by pancreatic ribonuclease was shown by Vandendriessche (1) to be a multistage reaction with complex kinetics. In the course of the degradation, the 3′-pyrimidine nucleoside phosphodiesters are converted to the 3′-phosphomonoesters in two steps. Markham and Smith (2) and Brown and Todd (3) have shown that in the first step the diesters are converted to the cyclic 2′,3′-diesters; in the second step the cyclic diesters are hydrolyzed to the 3′-monoesters. The action of ribonuclease on ribonucleic acid is illustrated in Fig. 1. It is to be noted that if in the second stage H_2O is replaced by R′OH, the process is of the same character as the reverse of the first stage. It is therefore likely that the activated complex for the first stage is analogous to that for the second.

For reaction to occur, a pyrimidine base must be part of the nucleotide, and the phosphate ester linkage must be in the 3′ position. The essential structure for the substrate for the first stage of the reaction is represented in Fig. 2. Findlay *et al.* (4) explain this specificity in terms of a specific binding to the enzyme, and consider that the pyrimidine is not involved in the subsequent reaction. Witzel (5) on the other hand concludes that the pyrimidine base is concerned in the catalytic step.

The object of the present work was to throw further light on the reaction mechanism, in

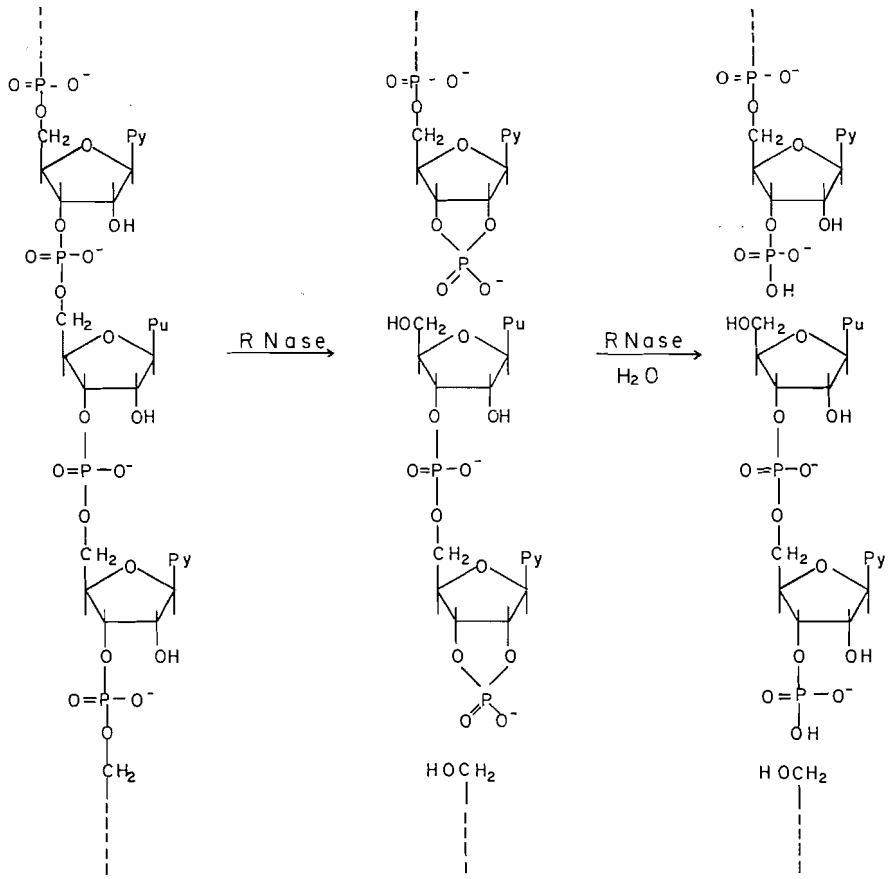


FIG. 1. Action of ribonuclease on ribonucleic acid. The pyrimidine bases (cytosine and uridine) and the purine bases (adenine and guanidine) are represented by Py and Pu respectively.

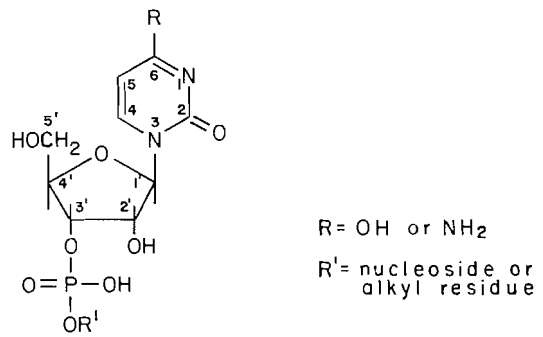


FIG. 2. Specific structure for a substrate of ribonuclease.

particular on the participation of the various groups in the binding and catalytic processes. It has been done with the three nucleotides represented in Fig. 3: (I) cytidine-2′,3′-phosphate (R = NH_2), (II) uridine-2′,3′-phosphate (R = OH), and (III) N^6,$O^{5'}$-diacetyl cytidine-2′,3′-phosphate (R = $NHCOCH_3$). A comparison of the inductive, mesomeric, and electromeric effects of the three R substituents leads to the conclusion that the polarity of the carbonyl group in the pyrimidine base will be greatest in I and least in III. If the reaction of the enzyme with the substrate depends on the presence of the carbonyl group, as

Can. J. Chem. Downloaded from www.nrcresearchpress.com by 210.87.254.40 on 09/05/12
For personal use only.

seems to be indicated by the specificity of ribonuclease for pyrimidine nucleotides, one would expect a slower reaction for the acetylated substrate. If, as postulated by Findlay *et al.* (4), the only function of the carbonyl group is to bind the substrate to the enzyme, the three substrates will differ in the value of the Michaelis constant, K_m, but not very much in the value of the rate constant k_2 for the subsequent catalytic step. If Witzel (5) is correct in concluding that the carbonyl group is involved in the hydrolytic step, the values of the rate

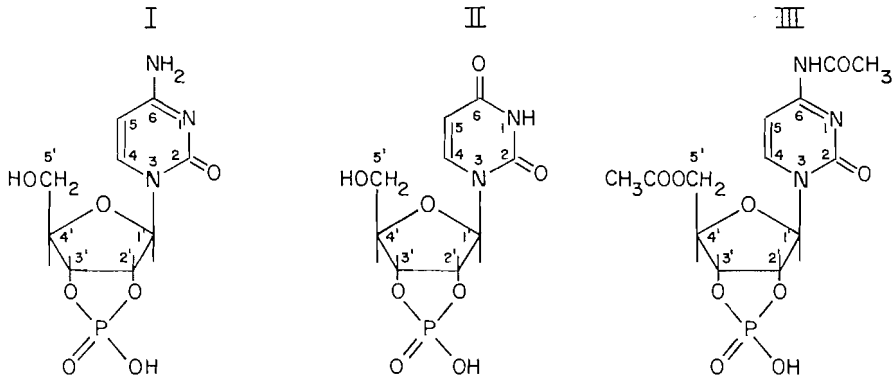


FIG. 3. Substrates employed in this work: (I) Cytidine-2′,3′-phosphate, (II) uridine-2′,3′-phosphate, (III) N^6,$O^{5'}$-diacetyl cytidine-2′,3′-phosphate.

constant k_2 for II and III will be lower than the value for I. That the changes in R have relatively little effect on the phosphate group is shown by the similarity of the acid dissociation constants of the phosphate group reported by Jordan (6). The substrates differ, however, in that I and II can exist in the form of zwitterions, whereas III cannot.

EXPERIMENTAL

Materials

Water was double distilled from glass, boiled out, and kept under nitrogen. AnalaR grades of anhydrous sodium sulfate, standard hydrochloric acid, and standard sodium hydroxide solution were used. The sodium hydroxide solution was opened each time under nitrogen, and the concentration was checked at intervals.

Ribonuclease A was supplied by Nutritional Biochemicals. Cytidine-2′,3′-phosphate and uridine-2′,3′-phosphate were supplied by Schwarz Bioresearch as the barium salts and converted to the sodium salts by precipitation with sodium sulfate solution. N^6,$O^{5'}$-Diacetyl cytidine-2′,3′-phosphate was prepared according to the method of Michelson (7).

Measurement of Reaction Rates

The pH-stat method was used. A Radiometer titrator TTT1a and titrigraph SBR 2c were used to control and record the addition of sodium hydroxide as reaction progressed. The cell was surrounded by a jacket through which circulated water at 20° from a thermostatted bath. Inserted into the cell were a glass electrode (Radiometer 202 C), a calomel electrode, a stirrer, a lead for sodium hydroxide solution, and a lead for nitrogen. The nitrogen was washed with alkali and then with water before it was passed in a slow stream over the surface of the reaction mixture. Sodium hydroxide (0.02 *N*) was delivered from a Radiometer syringe burette (SBU 1a) which gave a 100% scale reading for 0.50 ml. Manual addition, from a syringe, of a small volume of *N* acid or *N* alkali brought the pH to 0.1 below the desired value, and this was followed by adjustment to the exact value by the machine. The pH was read on a scale expander (Radiometer PHA 630 Ta) calibrated to 0.01 pH unit. The electrodes were standardized against potassium dihydrogen phosphate – sodium hydroxide buffer at pH 7.00. The ionic strength was adjusted to 0.20 with sodium sulfate solution.

After precipitation of the barium in the cytidine-2′,3′-phosphate barium salt by sodium sulfate, the substrate was made up to a standard volume in 1/3 *M* sodium sulfate solution. Ribonuclease was employed in a 1/3 *M* sodium sulfate solution, since the presence of an electrolyte helps to prevent the adsorption of ribonuclease on glass (8). Volumes of 1 ml of substrate solution and 1 ml of enzyme solution were used to make up a 10 ml reaction mixture in the cell.

The measured rate of addition of sodium hydroxide is not equal to the true rate of hydrolysis on account of titration of cytidine-3′-phosphate at pH values in the vicinity of the pK of this product of hydrolysis. A correction factor was used at each pH, using pK values of 6.00 and 5.88 for the secondary phosphate dissociations of cytidine-3′-phosphate and uridine-3′-phosphate respectively (6).

Can. J. Chem. Downloaded from www.nrcresearchpress.com by 210.87.254.40 on 09/05/12
For personal use only.

RESULTS

The results were interpreted in terms of a scheme for combination of an enzyme molecule and a substrate molecule to form a complex which reacts to give the product. The scheme can be expressed as

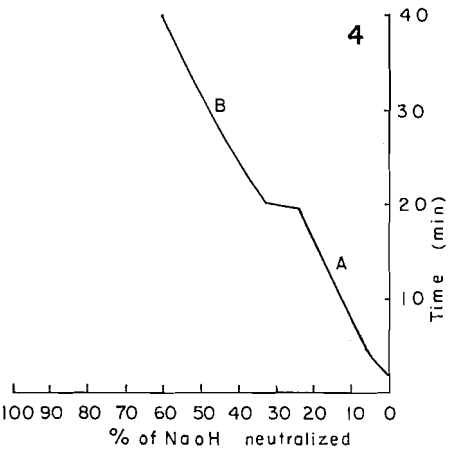
$$E + S \underset{k_{-1}}{\overset{k_1}{\rightleftharpoons}} ES \xrightarrow{k_2} E + P \quad .$$

The rate equation for this sequence of reactions is

$$v = \frac{\tilde{k}_2[E]_0[S]}{\tilde{K}_m + [S]},$$

where $\tilde{k}_2$ is the rate constant for the reaction of ES, $[E]_0$ the initial enzyme concentration, [S] the substrate concentration, and $\tilde{K}_m$ the Michaelis constant, equal to $(k_{-1} + k_2)/k_1$.

The parameters $\tilde{k}_2$ and $\tilde{K}_m$ were determined from a plot of $[S]/v$ against [S] according to one of the methods of Lineweaver and Burk (9). A typical recording for the hydrolysis of cytidine-2′-3′-phosphate is shown in Fig. 4. The gradual decrease in rate is caused by product inhibition, but the recording is sufficiently linear to allow the initial rate to be obtained. The plot of $[S]/v$ against [S] for this substrate is shown in Fig. 5. The intercept on the $[S]/v$ axis is $\tilde{K}_m/\tilde{k}_2[E]_0$, and the gradient is $1/\tilde{k}_2[E]_0$.



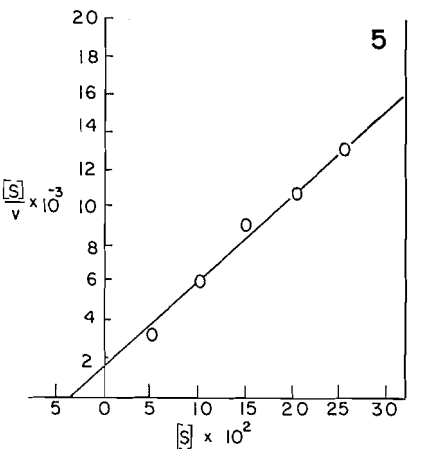


FIG. 4. Chart recording for the hydrolysis of cytidine-2′,3′-phosphate (2×10^{-2} *M*) in the presence of ribonuclease (0.5×10^{-7} *M*): (A) at pH 6.50, (B) at pH 6.75.

FIG. 5. Plot of $[S]/v$ against [S] for the hydrolysis of cytidine-2′,3′-phosphate at pH 6.50.

Information about the reactive groups in the enzyme can be obtained by studying the effect of changes in pH upon the rate of reaction. If the enzyme can exist in three states of ionization, E, EH, and EH_2, and the enzyme–substrate complex ES also has three states of ionization, then for a scheme which can be represented as

$$\begin{array}{ccc} & \overset{K_b}{\rightleftharpoons} & \overset{K_a}{\rightleftharpoons} \\ EH_2 & EH & E \\ & k_1[S] \uparrow\downarrow k_{-1} & \\ & \overset{K_b'}{\rightleftharpoons} & \overset{K_a'}{\rightleftharpoons} \\ EH_2S & EHS & ES \\ & & \downarrow k_2 \\ & & EH + P \end{array}$$

Can. J. Chem. Downloaded from www.nrcresearchpress.com by 210.87.254.40 on 09/05/12
For personal use only.

the steady state analysis (10) gives the rate expression:

$$v = \frac{k_2[E]_0[S]}{K_m\left(1 + \frac{[H^+]}{K_b} + \frac{K_a}{[H^+]}\right) + [S]\left(1 + \frac{[H^+]}{K_b'} + \frac{K_a'}{[H^+]}\right)}.$$

From this it follows that the experimentally determined parameters $\tilde{k}_2$ and $\tilde{K}_m$ are related to the pH-independent constants k_2 and K_m by the equations:

$$\tilde{k}_2 = \frac{k_2}{1 + \frac{[H^+]}{K_b'} + \frac{K_a'}{[H^+]}}$$

$$\tilde{K}_m = \frac{K_m\left(1 + \frac{[H^+]}{K_b} + \frac{K_a}{[H^+]}\right)}{1 + \frac{[H^+]}{K_b'} + \frac{K_a'}{[H^+]}}$$

$$\frac{\tilde{k}_2}{\tilde{K}_m} = \frac{k_2}{K_m\left(1 + \frac{[H^+]}{K_b} + \frac{K_a}{[H^+]}\right)}.$$

The variation with pH of log $\tilde{k}_2$, p$\tilde{K}_m$, and log $(\tilde{k}_2/\tilde{K}_m)$ allows the values of K_a', K_b', K_a, and K_b to be determined. The curves have an axis of symmetry, and the slopes approach $+1$ at low pH values and -1 at high ones.

TABLE I

Values of $\tilde{k}_2$ and $\tilde{K}_m$ for cytidine-2′,3′-phosphate at 25° and $I = 0.20$

pH	$\tilde{k}_2$ (s^{-1})	$\tilde{K}_m \times 10^2$ (M)	$\tilde{k}_2/\tilde{K}_m$
6.00	1.1±0.1	0.18±0.02	620±60
6.25	1.4±0.1	0.23±0.02	590±60
6.50	2.2±0.2	0.38±0.04	575±60
6.75	2.6±0.2	0.53±0.05	500±50
7.00	3.3±0.3	0.72±0.07	460±50
7.25	4.5±0.5	1.16±0.1	390±40
7.50	5.1±0.5	2.6 ±0.2	200±20
7.75	5.6±0.5	4.7 ±0.5	120±10
8.00	4.0±0.4	3.1 ±0.3	130±10
8.25	1.7±0.2	1.3 ±0.1	135±10

The values of the pH-dependent kinetic parameters for cytidine-2′,3′-phosphate are given in Table I, and are plotted against pH in Fig. 6. In drawing these curves use has been made of the fact that they must be symmetrical and that the limiting slopes are $+1$ and -1.

The results for uridine-2′,3′-phosphate are shown in Table II and Fig. 7. The results are uncertain at pH 7.0 and 7.25. The values of $\tilde{K}_m$ are of the order of 10^{-1} M, and the limiting velocity could not be attained since there is a concentration of substrate beyond which the precipitation of barium as barium sulfate is incomplete. The $\tilde{k}_2/\tilde{K}_m$ values could be obtained accurately from plots of rate against [S], but the individual values could be obtained less accurately. The procedure used at these pH values was to plot either $1/v$

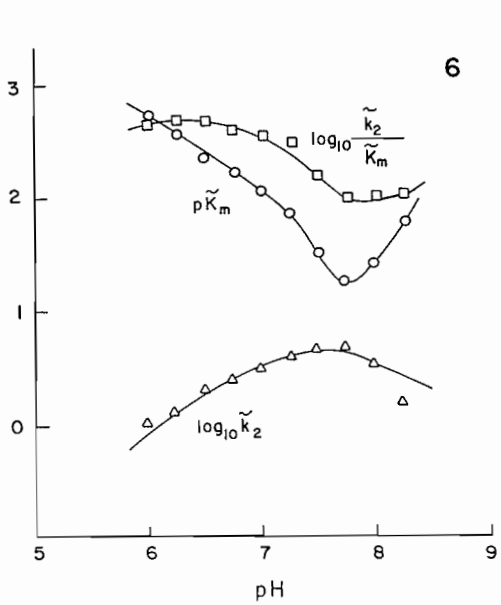
Can. J. Chem. Downloaded from www.nrcresearchpress.com by 210.87.254.40 on 09/05/12
For personal use only.

TABLE II

Values of $\tilde{k}_2$ and $\tilde{K}_m$ for uridine-2′,3′-phosphate at 25° and $I = 0.20$

pH	$\tilde{k}_2$ (s^{-1})	$\tilde{K}_m \times 10^2$ (M)	$\tilde{k}_2/\tilde{K}_m$
5.50	0.095±0.01	0.8 ± 0.08	12 ±1.0
5.75	0.18 ±0.02	1.0 ± 0.1	18 ±1.5
6.00	0.32 ±0.03	0.95± 0.1	34 ±2
6.25	0.54 ±0.05	1.6 ± 0.1	33 ±2
6.50	1 ±0.2	5 ± 1	23 ±2
6.75	2 ±1	10 ± 5	22 ±2
7.00	3 ±1	14 ± 7	24 ±2
7.25	4 ±2	17 ± 8	17 ±2
7.50	4 ±2	20 ±10	7.5±0.7
7.75	0.8 ±0.4	7 ± 3	10 ±1.0
8.00	0.8 ±0.4	11 ± 5	7.5±0.8
8.25	0.3 ±0.1	15 ± 3	4.6±0.5

against 1/[S] or [S]/v against [S] and to force the line to pass through the value of [S]/v at [S] = 0, obtained from the plots of rate against [S].



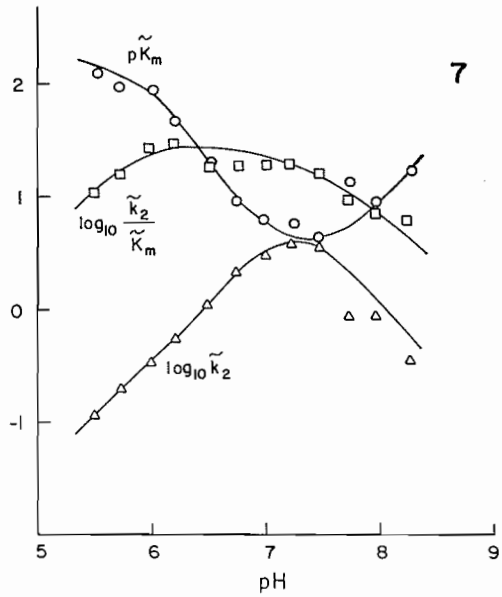


FIG. 6. Variation with pH of the logarithms of the kinetic parameters for the hydrolysis of cytidine-2′,3′-phosphate at 25° and $I = 0.20$.

FIG. 7. Variation with pH of the logarithms of the kinetic parameters for the hydrolysis of uridine-2′,3′-phosphate at 25° and $I = 0.20$.

The substrate N^6,$O^{5'}$-diacetyl cytidine-2′,3′-phosphate acts as a buffer from pH 6 to 7, and the method could not be used over this range. Results obtained at pH 8.0 are shown in Table III.

The pK values derived from the curves in Figs. 6 and 7 are given in Table IV. The pH independent parameters, k_2, K_m, and k_2/K_m are given in Table V. In calculating the values for N^6,$O^{5'}$-diacetyl cytidine-2′,3′-phosphate from the $\tilde{k}_2$ and $\tilde{K}_m$ values at a single pH, the assumption was made that this substrate involves the same groups in the enzyme, with the same values of pK_a, pK_b, pK_a', and pK_b' as for the other two substrates. This

Can. J. Chem. Downloaded from www.nrcresearchpress.com by 210.87.254.40 on 09/05/12
For personal use only.

seems a reasonable assumption, since the results for the other two substrates are very similar and $N^6,O^{5'}$-diacetyl cytidine-2′,3′-phosphate resembles cytidine-2′,3′-phosphate more than does uridine-2′,3′-phosphate.

DISCUSSION

The pK values of the groups in the enzyme that participate in the reaction are characteristic of imidazole groups, of which one must be active in the basic form and one in the acidic form. This conclusion was reached by Findlay *et al.* (11) on the basis of their work on the effect of solvent on the pK values of the enzyme. They showed that the protonated forms of both groups are cationic, which can only mean that one imidazole is acting in its non-protonated, and the other in its protonated, form.

TABLE III

Values of $\bar{k}_2$ and $\bar{K}_m$ for $N^6,O^{5'}$-diacetyl cytidine-2′,3′-phosphate at 25° and $I = 0.20$

pH	$\bar{k}_2$ (s^{-1})	$\bar{K}_m \times 10^2$ (M)	$\bar{k}_2/\bar{K}_m$
8.05	0.069±0.007	2.1±0.2	3.3±0.3

TABLE IV

pK values of ionizing groups at the active site of the enzyme

Cytidine-2′,3′-phosphate		
Free enzyme	$pK_b = 5.40$:	$pK_a = 7.25$
Enzyme–substrate complex	$pK_b' = 6.75$:	$pK_a' = 8.40$
Uridine-2′,3′-phosphate		
Free enzyme	$pK_b = 5.62$:	$pK_a = 7.50$
Enzyme–substrate complex	$pK_b' = 6.80$:	$pK_a' = 7.85$

TABLE V

Comparison of kinetic parameters for three substrates

	k_2 (s^{-1})	$K_m \times 10^2$ (M)	k_2/K_m
Cytidine-2′,3′-phosphate	7.2 ±0.7	0.87±0.09	810±80
Uridine-2′,3′-phosphate	2.1 ±0.6	4.6 ±1.5	44 ±4
$N^6,O^{5'}$-Diacetyl cytidine-2′,3′-phosphate	0.10±0.01	0.46±0.05	22 ±2

The fact that the pK of the acidic imidazole group increases on complex formation (i.e. $pK_a' > pK_a$) for both cytidine-2′,3′-phosphate and uridine-2′,3′-phosphate suggests that the proton on the imidazole forms a hydrogen bond with a group on the substrate: as a result, it is more difficult for the proton to leave.

The increase in pK of the basic group for both substrates, on the other hand, indicates that this group cannot become bound to a group on the substrate, since it would then be more difficult for the nitrogen atom to become protonated, and pK_b' would be less, and not greater, then pK_b. In the mechanism proposed later, this increase in the basicity of the basic imidazole group, on complex formation, is attributed to the fact that the nitrogen atom is brought into close proximity to two oxygen atoms on the substrate, and to an oxygen atom belonging to a water (or alcohol) molecule.

It is to be noted from Table V that the structure of the pyrimidine base has more effect on the catalytic constant k_2 than on the Michaelis constant K_m. The sequence of k_2 values

Can. J. Chem. Downloaded from www.nrcresearchpress.com by 210.87.254.40 on 09/05/12
For personal use only.

is cytidine > uridine ≫ N^6,$O^{5'}$-diacetyl cytidine, which is the order of polarity of the carbonyl groups. The sequence of K_m values is uridine ≫ cytidine > N^6,$O^{5'}$-diacetyl cytidine, which means that the uridine compound is much less strongly bound than the other two substrates. In the cytidine and N^6,$O^{5'}$-diacetyl cytidine compounds there can be zwitterion formation, with consequent enhancement of the binding power of the phosphate group; this is not possible with the uridine compound.

Mechanistic Information

Before considering the modes of interaction between the enzyme and substrate molecules during the reactions, it is convenient to summarize the main mechanistic information that must be taken into account:

(1) The specificity of the enzyme is for nucleotides of pyrimidine bases.

(2) The bond broken when the cyclic phosphate is hydrolyzed is the $C^{2'}$—OP bond (2, 3).

(3) A molecule of water or alcohol must participate in the reaction; in the latter case, the alcoholysis of a cyclic phosphate, the process is the reverse of the cyclic phosphate formation from the diester.

(4) Two histidine residues are involved in the reaction, one with the imidazole group in its acid form and the other with it in the basic form.

(5) Both the basic and acidic groups experience an increase in pK when the complex is formed.

(6) The rates for the three substrates studied in the present work and for others studied by Witzel and Barnard (12), show some variation in K_m and a much greater variation in k_2.

(7) Ukita *et al.* (13) have found significant variations in the efficiencies of inhibitors, as summarized in Table VI (cf. Fig. 8).

(8) The reaction is inhibited by zinc and copper ions (14).

(9) The cyclization of cytidine-3′-cytidine-5′-phosphate is much faster than the subsequent hydrolysis of the cytidine-2′,3′-phosphate formed (15).

(10) Chemical modification of known amino acid residues in the enzyme leads to loss of activity: further details are considered later.

The Binding Sites

To explain the inhibitor results of Ukita *et al.* (13), it is necessary to postulate three binding groups. Since all bases similar to uracil, possessing a —CO—NH—CO— group, inhibit reaction, there must be a site which binds to —CO—NH—CO—. The N^1—H bond is weakened by the polarity of the adjacent carbonyl groups, and it is very likely that this forms a hydrogen bond to a basic site on the enzyme. As cytidine is an inhibitor, whereas cytosine is not, there must be a sugar-binding site in the enzyme, and as 2′-deoxycytidine has half the inhibitory property of cytidine, this site probably binds the 2′-oxygen atom. The fact that 2′-deoxycytidine still has the ability to inhibit suggests that in this compound, where there is no hydrogen bond formation between the carbonyl group in the base and the 2′-hydroxyl group in the ribofuranose ring, there is free rotation about the N—$C^{1'}$ bond so that the 3′-OH group can occupy a position close to that occupied by the 2′-OH group in cytidine. Inhibition by inorganic phosphates shows that there must be a phosphate-binding site in the enzyme. Nucleotides are better inhibitors than nucleosides and purine and pyrimidine bases. A comparison of cytidine-2′-phosphate and uridine-2′-phosphate shows that, although cytidine-2′-phosphate can be bound to two of the proposed sites and uridine-2′-phosphate to three sites, the attachment at two sites must be sufficient to hold the molecule of cytidine-2′-phosphate in the position occupied by the substrate on the

Can. J. Chem. Downloaded from www.nrcresearchpress.com by 210.87.254.40 on 09/05/12
For personal use only.

enzyme. Also, zwitterion formation is possible in the cytidine phosphates (cf. Jordan (16)), and this will increase the binding by the phosphate anion in regions close to the isoelectric point.

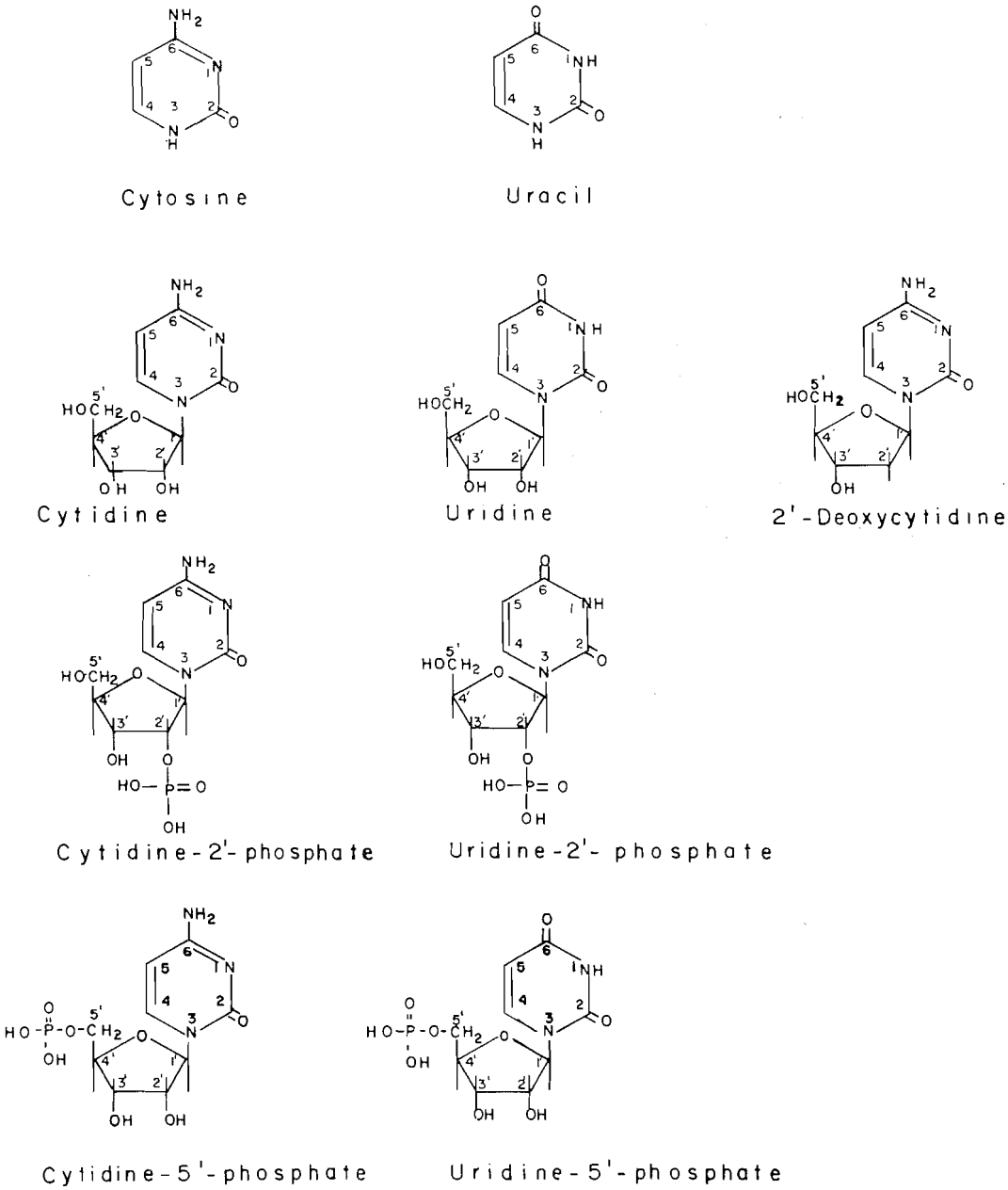


FIG. 8. The structures of some inhibitors of the enzymatic hydrolysis of cytidine-2′,3′-phosphate.

Inhibition studies thus establish a need for three binding groups, and kinetic studies demonstrate the participation of two groups, of which one, the basic imidazole, cannot fulfil any of these substrate-binding functions. It is, therefore, necessary to postulate a

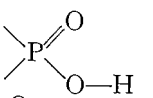
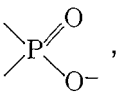
Can. J. Chem. Downloaded from www.nrcresearchpress.com by 210.87.254.40 on 09/05/12
For personal use only.

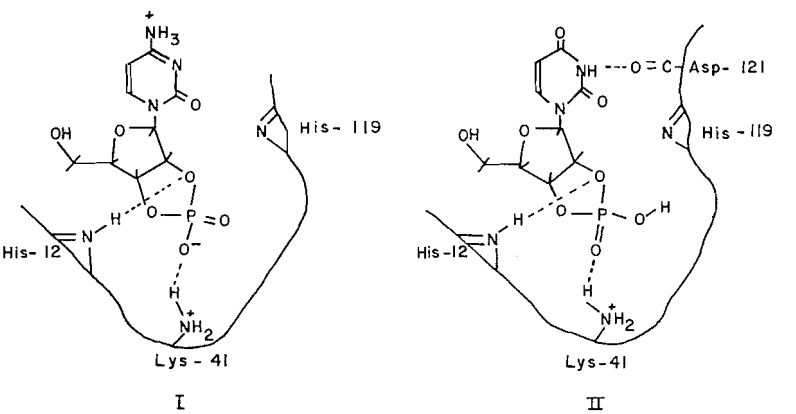
total of at least four groups, three involved in binding and one, the basic imidazole, in basic catalysis.

TABLE VI

Inhibition indices obtained by Ukita *et al.* (13) in the hydrolysis of cytidine-2′,3′-phosphate

Inhibitor	Inhibition index
Cytosine	0
Cytidine	37
2′-Deoxycytidine	19
Cytidine-2′-phosphate	82
Cytidine-5′-phosphate	68
Uracil	24
Uridine	29
Uridine-2′-phosphate	80
Uridine-5′-phosphate	57

Schemes for the structure of the ES complex for cytidine-2′,3′-phosphate and for uridine-2′,3′-phosphate are proposed below and illustrated in Fig. 9. The two substrates are different in that there is no binding by the pyrimidine base in cytidine-2′,3′-phosphate. The ring nitrogen, N^1, requires a basic site for binding. The ribose oxygen, $O^{2'}$, requires an acid site when it occurs in a $C^{2'}$—O—P grouping; it also requires an acid site when it occurs in a $C^{2'}$—O—H grouping, since the H atom is hydrogen bonded to the C^2=O group. The acid imidazole group, which is in evidence from the kinetics, can perform this function. The phosphate group can occur as  , which could form a hydrogen bond with an acid or a basic site, or as  , which could form a hydrogen bond with an acid site or with a basic group containing a hydrogen atom, such as $-NH_2$. There is so much



I II

FIG. 9. The suggested modes of enzyme–substrate complex formation for (I) cytidine-2′,3′-phosphate and (II) uridine-2′,3′-phosphate.

evidence for the participation of a lysine residue that it is reasonable to assign to it the function of binding the phosphate group or anion. Anfinsen (17) reported that dinitrobenzylation of the lysine residue in position 41 in the amino acid sequence determined by

Can. J. Chem. Downloaded from www.nrcresearchpress.com by 210.87.254.40 on 09/05/12
For personal use only.

Can. J. Chem. Downloaded from www.nrcresearchpress.com by 210.87.254.40 on 09/05/12
For personal use only.

Redfield and Anfinsen (18) and by Hirs *et al.* (19) destroyed the enzymatic activity, and that the lysine in position 41 does not react in the presence of phosphate ion. Hirs (20) showed that the ϵ-amino group of the lysine in position 41 is extremely reactive to alkylating reagents, and he deduced that it is part of or close to the anion-binding site in the active center. Reaction of this ϵ-amino group deactivates ribonuclease, and cytidylic acid protects ribonuclease from this deactivation. Hirs deduced that the lysine residues in positions 7 and 41 are close together in the enzyme from the fact that, although the lysine in position 7 does not react with alkylating reagents, it will react after the lysine in position 41 has been alkylated; this he attributed to a local unfolding of the enzyme molecule. The binding of the phosphate group by the basic group, a role which the lysine residue in position 41 seems able to play, must be a step in complex formation which is too fast to be rate determining. The binding of the pyrimidine N^1H by a basic site must also be a fast step. It is possible that the aspartic acid residue at position 121 performs this function since both Stein (21) and Anfinsen (22) have presented evidence that this residue is necessary for enzyme activity and since the carbonyl group would be able to form a strong hydrogen bond with a >NH group.

There is a great body of evidence to support the participation of the histidine residues at positions 12 and 119 at the active site. Richards and Vithayathil's (23) work on photooxidation of individual groups places the histidine in position 12 at the active site. Barnard and Stein (24) made a study of the deactivation following reaction of histidine with bromoacetate and placed the histidine in position 119 at the active site. Crestfield *et al.* (25) showed that alternative products in the reaction with bromoacetate are N^1-carboxymethyl histidine-119 and N^3-carboxymethyl histidine-12, and he deduced that the two histidine residues are 5 Å apart in the enzyme. The kinetics indicate the participation of two histidine residues. The fact that, on alkylation of the histidine in position 119, enzyme activity is destroyed, but the enzyme retains the ability to combine with substrate and inhibitors, as shown by shifts in the ultraviolet spectra studied by Ross *et al.* (26), indicates that it is the histidine in position 12 which binds the substrate, while the histidine in position 119 has a catalytic function.

The Catalytic Step

Complex formation is followed by hydrolysis. In the proposed mechanism, shown in Fig. 10, the carbonyl group of the pyrimidine ring holds a molecule of water or alcohol, by hydrogen bonding, in a favorable position close to the $O^{2'}$—P bond which is to be broken. The function of the basic imidazole group is to weaken further the H—OH or H—OR bond and assist in the transfer of the hydrogen atom from the molecule of water or alcohol to the 2′-oxygen atom of the sugar ring. The weakening of the H—OH or H—OR bond renders the hydroxyl or alkoxyl group sufficiently nucleophilic to attack the electrophilic phosphorus atom. In consequence, the $O^{2'}$—P bond, already weakened through binding of the acid imidazole group to $O^{2'}$, breaks and the 2′-oxygen atom forms a bond with the H atom.

The basic catalytic function of the imidazole group is exercised without the addition of a proton and consequent reionization of the group. It is envisaged as a lowering of the energy barrier to the transfer of a proton from the alkoxyl or hydroxyl oxygen to the sugar oxygen by first attracting the proton away from the alkoxyl oxygen and then releasing it to the sugar oxygen. When the imidazole nitrogen atom enters into an enzyme–substrate complex in which the nitrogen is in close proximity to three oxygen atoms, these negative atoms facilitate the approach of a proton and increase the basicity of the imidazole nitrogen.

This type of interaction can thus explain the increase in pK of the basic imidazole group on complex formation.

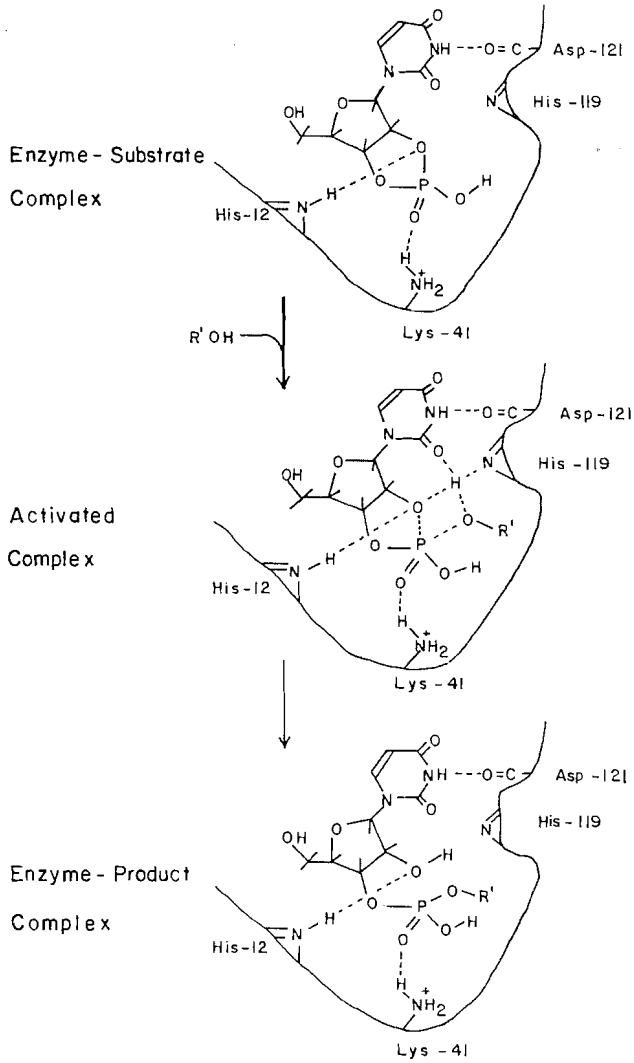


FIG. 10. The suggested mechanism of the catalytic step. In the activated complex the histidine-119 N atom, the oxygen atom of the water or alcohol molecule, the O atom attached to $C^{2'}$, and the O atom attached to C^{2} are envisaged as being roughly at the corners of a regular tetrahedron. In this way the histidine N atom aids the proton transfer.

Inhibition by zinc and copper ions (14) fits into this scheme, in that Tanford (27) has shown that zinc ions can be bound by an imidazole ring, and Ross *et al.* (26) have shown by a spectrophotometric study that zinc ions form a complex with the enzyme and with the enzyme–product complex.

Comparison with Other Mechanisms

In the mechanism proposed by Witzel (5) and by Witzel and Barnard (12), the substrate is bound to the enzyme only at the phosphate group. The carbonyl group of the pyrimidine ring functions by holding a molecule of water in the correct position for an attack on the

Can. J. Chem. Downloaded from www.nrcresearchpress.com by 210.87.254.40 on 09/05/12
For personal use only.

P—$O^{2'}$ bond, as in the mechanism proposed here. The imidazole groups are concerned only in the binding and not in the subsequent catalytic step.

There are two important features of the reaction that do not support this point of view. One is that binding only at the phosphate group does not account for the properties of known inhibitors, as discussed earlier. Secondly, if the C^2=O group is the only one involved in the catalytic step, the variations of the catalytic constants $\tilde{k}_2$ with pH would not reflect the changes in state of ionization of the enzyme: they would only relate to changes in the state of ionization of the substrate. There would be no reason why the $\tilde{k}_2$ values would vary with pH in much the same way for the different substrates. In fact, the groups in cytidine and uridine phosphates do not change their states of ionization over the pH range of 6 to 8 (6).

Shugar and Fox (28) suggested that the polarity of the carbonyl group is enhanced by coordination from a basic group in the enzyme to N^1H in uridine-2′,3′-phosphate or to —NH_2 in cytidine-2′,3′-phosphate. A combination of this type is not in accordance with the fact that cytidine is not an inhibitor.

Findlay *et al.* (4) proposed a specific binding to the enzyme at the pyrimidine nitrogen: the acid imidazole binds the 2′ oxygen atom, as in the present mechanism, while the basic imidazole holds a molecule of water. It was proposed that during the catalytic step the basic imidazole supplies electrons to break the H—OH bond, thus facilitating attack by the nucleophilic oxygen on the electrophilic phosphorus atom; electrons from the bond that is broken are attracted by the acidic imidazole.

The proposed specificity site, at N^1, is not, however, in accordance with the inhibition work (13), which shows that cytosine is not an inhibitor. In addition, since the carbonyl group is not envisaged as playing any role in reaction, substrates differing in the pyrimidine group R would be expected to differ in K_m rather than in k_2; this is contrary to the results of Barnard and Witzel (15) and to the present results.

The type of mechanism proposed by Findlay *et al.* is not one that would be expected to be of very high efficiency. During the catalytic step, the protonated imidazole group is considered to transfer its proton completely to the substrate, which in turn transfers a proton to the basic imidazole group. The enzyme thus ends up in an unnatural state of ionization, and will at once reionize. Since the pK values of the two groups differ by about 2 units the production of the enzyme in this unnatural state of ionization is done at the expense of about $2RT = 2.8$ kcal per mole of free energy, and this would have an adverse effect on the rate of a factor of about $10^{-2800/RT} = 10^{-2}$. This argument does not, of course, exclude mechanisms such as that of Findlay *et al.*: it merely shows that, other things being equal, a mechanism will be more efficient if the acidic and basic groups simply facilitate proton transfers without themselves undergoing a change in state of ionization. The mechanism proposed in the present paper is a scheme of this kind.

ACKNOWLEDGMENT

This work was supported by a grant from the National Cancer Institute of Canada.

REFERENCES

1. L. VANDENDRIESSCHE. Acta Chem. Scand. **7**, 699 (1963).
2. R. MARKHAM and J. D. SMITH. Biochem. J. **52**, 552 (1952).
3. D. M. BROWN and A. R. TODD. J. Chem. Soc. 2040 (1953).
4. D. FINDLAY, D. G. HERRIES, A. P. MATHIAS, B. R. RABIN, and C. A. ROSS. Biochem. J. **85**, 152 (1962).
5. H. WITZEL. Ann. Chem. **635**, 191 (1960); Intern. Congr. Biochem. 4th, Vienna, 1958. Abstr. Communs. **33** (1958); Progr. Nucleic Acid Res. **2**, 221 (1963).
6. D. O. JORDAN. The chemistry of the nucleic acids. Butterworths, London. 1960. pp. 135, 137.
7. A. M. MICHELSON. J. Chem. Soc. 3655 (1959).

Can. J. Chem. Downloaded from www.nrcresearchpress.com by 210.87.254.40 on 09/05/12
For personal use only.

8. R. SHAPIRA. Biochem. Biophys. Res. Commun. **1**, 236 (1959).
9. H. LINEWEAVER and D. BURK. J. Am. Chem. Soc. **56**, 658 (1934).
10. K. J. LAIDLER. The chemical kinetics of enzyme action. Clarendon Press, Oxford. 1958. p. 126.
11. D. FINDLAY, A. P. MATHIAS, and B. R. RABIN. Biochem. J. **85**, 139 (1962).
12. H. WITZEL and E. A. BARNARD. Biochem. Biophys. Res. Commun. **7**, 289 (1962).
13. T. UKITA, K. WAKU, M. IRIE, and O. HOSHINO. J. Biochem. Tokyo, **50**, 405 (1961).
14. F. F. DAVIES and F. W. ALLEN. J. Biol. Chem. **217**, 13 (1955).
15. E. A. BARNARD and H. WITZEL. Biochem. Biophys. Res. Commun. **7**, 295, (1962).
16. D. O. JORDAN. Progr. Biophys. **2**, 51 (1951).
17. C. B. ANFINSEN. Brookhaven Symp. Biol. **15**, 184 (1962).
18. R. R. REDFIELD and C. B. ANFINSEN. J. Biol. Chem. **221**, 385 (1956).
19. C. H. W. HIRS, S. MOORE, and W. H. STEIN. J. Biol. Chem. **235**, 633 (1960). D. H. SPACKMAN, W. H. STEIN, and S. MOORE. J. Biol. Chem. **235**, 648 (1960). D. G. SMYTH, W. H. STEIN, and S. MOORE. J. Biol. Chem. **237**, 1845 (1962); **238**, 227 (1963).
20. C. H. W. HIRS. Brookhaven Symp. Biol. **15**, 154 (1962).
21. W. H. STEIN. Brookhaven Symp. Biol. **13**, 104 (1960).
22. C. B. ANFINSEN. J. Biol. Chem. **221**, 405 (1956).
23. F. M. RICHARDS and P. J. VITHAYATHIL. Brookhaven Symp. Biol. **13**, 115 (1960).
24. E. A. BARNARD and W. D. STEIN. J. Mol. Biol. **1**, 339, 350 (1959).
25. A. M. CRESTFIELD, W. H. STEIN, and S. MOORE. J. Biol. Chem. **238**, 2413 (1963).
26. C. A. ROSS, A. P. MATHIAS, and B. R. RABIN. Biochem. J. **85**, 145 (1962).
27. C. TANFORD. J. Am. Chem. Soc. **74**, 211 (1952).
28. D. SHUGAR and J. J. FOX. Biochim. Biophys. Acta, **9**, 199, 369 (1962).

Can. J. Chem. Downloaded from www.nrcresearchpress.com by 210.87.254.40 on 09/05/12
For personal use only.

DEUTERIUM ISOTOPE EFFECTS ON HYDROGEN BONDING[1]

SURJIT SINGH[2] AND C. N. R. RAO[3]
Department of Chemistry, Indian Institute of Technology, Kanpur, India
Received March 7, 1966

ABSTRACT

The interaction of phenol and phenol-*d* with a number of donors of varying basicity has been studied in terms of the equilibrium constants, ΔS^0, ΔH^0, $\Delta\nu_{OH}$, and $\Delta\nu_{OD}$ and various aspects of deuterium isotope effects on hydrogen bonding have been discussed. The deuterium isotope effects are found to vary markedly with the basicity of the donor and the results are discussed in terms of the zero point contributions to the K_H/K_D.

INTRODUCTION

While isotope effects on chemical equilibria and kinetics have been reported in a variety of systems in the literature, information on deuterium isotope effects on hydrogen bonding, XH...Y, is limited. Bellamy and Rogasch (1) and Dahlgram and Long (2) have reported that deuterium bonds are comparatively weaker than the hydrogen bonds. Josien and co-workers (3) as well as Creswell and Allred (4) have found higher values of the equilibrium constants and the enthalpy and entropy changes for deuterium bonds in alcohols–hexamethylbenzene and fluoroform–tetrahydrofuran systems. Literature data (5) on self-association, however, show lower values of equilibrium constants and enthalpies for deuterium bonds.

In the models for proton transfer reactions, Westheimer (6) and Bigeleisen (7) have considered the importance of the symmetric stretching frequencies of X...Y in describing deuterium isotope effects. Recent work of Bader (8) has shown the possible importance of bending modes as well. We have now examined deuterium isotope effects on the thermodynamics (K, ΔH^0, ΔS^0) of hydrogen bonding equilibria as well as the frequency shifts of the stretching vibrations for the interaction of phenol with a number of donors, Y, of varying basicity. The dependence of isotope effects on the basicity of the donors was expected to throw some light on the importance of various zero point contributions to K_H/K_D.

EXPERIMENTAL

All the chemicals, with the exception of tetra-*n*-heptylammonium iodide and tetramethylthiourea, were commercially available and were purified before use. Tetraheptylammonium iodide was kindly provided by Professor P. V. R. Schleyer and tetramethylthiourea by Dr. M. J. Janssen. Deuterated phenol, C_6H_5OD, was prepared by repeated exchange of phenol with D_2O (supplied by Atomic Energy Establishment, Bombay). The exchange was found to be 80% by measurement of the intensity of the free OH stretching band at different concentrations as well as by quantitative estimation of the D_2O content of the water obtained by the combustion of the sample.

Infrared measurements in the OH and OD stretching regions were obtained with a Carl–Zeiss UR-10 spectrophotometer with LiF optics. The equilibrium constants of hydrogen bond formation were calculated using the expression similar to that of Becker (9) and the uncertainties in K are within ±10%. The optical densities of the monomer OH and OD bands in phenol and phenol-*d* solutions (solvent, CCl_4; concentration ~0.007 *M*) and in their solution with different donors of known concentration were measured in the overtone region using a Cary-14R spectrophotometer fitted with variable temperature cells (path length 10 cm). From the data on equilibrium constants at three temperatures (in the range 5–45 °C with an uncertainty in temperature of ±1 °C) the enthalpy of hydrogen bond formation was calculated. The uncertainty in enthalpy values was ±0.5 kcal mole^{-1}. The uncertainty in frequency shifts ($\Delta\nu_{OH}$ and $\Delta\nu_{OD}$) was ±5 cm^{-1}.

[1]*Taken in part from the Ph.D. thesis of S. Singh to be submitted to the Indian Institute of Technology.*
[2]*C.S.I.R. Senior Research Fellow.*
[3]*To whom all correspondence should be addressed.*

The experimental procedure and details of the method of evaluation of the equilibrium constants have been discussed in other publications from this laboratory (10).

RESULTS AND DISCUSSION

Thermodynamic data on the interaction of phenol and phenol-*d* with donors have been summarized in Table I along with the frequency shifts of the OH and OD stretching vibration bands, $\Delta\nu_{OH}$ and $\Delta\nu_{OD}$. It can be seen that the enthalpy of formation of 1:1 complexes is always greater in the case of hydrogen bonding than in deuterium bonding. This may be due to the longer O...Y distance in the deuterated species. The overlap in the hydrogen bond is expected to be greater than in the deuterium bond (11) and crystals containing deuterium bonds often show expansion of the unit cell (12, 13). Rightly enough, it has been pointed out that the barrier height in the double minimum potential (14) for the transfer of deuterium would be higher than for proton transfer due to the lower zero point energy of the O—D bond (15, 16).

The ratio of the equilibrium constants, K_H/K_D, is found to vary from donor to donor (Table I) and there appears to be no rule that the ratio be greater than unity. The results of this study show that the varied values of K_H/K_D in the literature probably are all valid and that K_H/K_D is a function of the basicity of the donor. The entropy change ΔS^0 is, however, always greater for the deuterium bonds than for the hydrogen bonds. The variation in equilibrium constants has to be interpreted in terms of the contributions from both the ΔH^0 and ΔS^0 since $\Delta F^0 = -RT \ln K = \Delta H^0 - T\Delta S^0$.

The frequency shift, $\Delta\nu_{OH}$, is always greater than $\Delta\nu_{OD}$. While this is in line with the earlier observation that $\Delta H^0_{OH...Y}$ is greater than $\Delta H^0_{OD...Y}$, the $\Delta\nu_{OH}$ and $\Delta\nu_{OD}$ do not show any simple linear relation with the ΔH^0 values. This is not unexpected since the linearity between $\Delta\nu_{OH}$ and ΔH^0 holds good only in a limited range of ΔH^0 (or $R_{O...Y}$) for the interaction of the same acceptor (proton donor) with donors of comparable basicity (ionization potential) (10). It should also be pointed out that $\Delta\nu_{OH}$ or $\Delta\nu_{OD}$ is determined by the barrier height in the double minimum potential and is not strictly related to the ΔH^0. It is quite conceivable to have a situation where the barrier height (or $\Delta\nu$) varies with little or no variation in $R_{X...Y}$ (or ΔH^0) (10).

Since the theories of Westheimer, Bigeleisen, and Bader on isotope effects refer to rate processes, they cannot be applied to the equilibrium data reported in this study. The isotope exchange equilibrium constant can, however, be estimated fairly accurately by employing the expression from statistical thermodynamics in terms of partition functions.

By neglecting all the factors in the partition functions other than the zero point energy contributions, one can write the expression for K_H/K_D for the equilibrium exchange reaction,

[1] $$C_6H_5OH + C_6H_5OD...Y \rightleftharpoons C_6H_5OD + C_6H_5OH...Y$$

[2] $$K_H/K_D = \exp -(\sum\Delta\nu_{XHY} + \sum\Delta\nu_{XH})/2kT,$$

where $\Delta\nu = \nu_H - \nu_D$ and the subscript XHY and XH refer to the hydrogen-bonded species and the free X—H monomer respectively. The sum in each case is over all the vibrations affected by isotopic substitution. In the case of the free monomer, these vibrations are the ν_{OH}, δ_{OH}, and γ_{OH}, and in the bonded species, the ν_{OH} is reduced appreciably from the monomer value. On hydrogen bonding δ_{OH} increases a little while γ_{OH} increases markedly. By using Δ' to denote the difference $\nu_H - \nu_D$ and Δ to denote the frequency change on hydrogen bonding, eq. [2] can be rewritten as

[3] $$2kT \ln (K_H/K_D) = -\Delta\Delta'\nu_{OH} - \Delta\Delta'\delta_{OH} - \Delta\Delta'\gamma_{OH}$$

TABLE I

Thermodynamic data* on the hydrogen and deuterium bond formation with different donors

Donors	I, eV†	Phenol-d K_D 25 °C	Phenol-d K_D 40 °C	Phenol-d $-\Delta H^0$	Phenol-d ΔS^0	Phenol-d $\Delta\nu_{OD}$	Phenol K_H 25 °C	Phenol K_H 40 °C	Phenol $-\Delta H^0$	Phenol $-\Delta S^0$	Phenol $\Delta\nu_{OH}$	K_H/K_D
1. $(n\text{-}C_7H_{15})_4N^+I^-$	6.0±1‡	89	78.4	1.5	4.0	225	382	239	5.9	8.0	380	4.3
2. $(C_2H_5)_3N$	7.5	32	25.7	2.7	−2.0	180	58	27.6	9.2	22.0	450	1.8
3. $(C_6H_5)_3P$	8.02	5.6	5	1.1	0.0	230	6	5.4	1.3	0.8	360	1.1
4. $[(CH_3)_2N]_2C{=}S$	8.12	16.5	15	1.1	2.0	220	14	10.5	3.1	5.0	310	0.8
5. $C_6H_5OH(D)$§	8.5	3.2	2.8	1.6	−3.0	80	0.74	0.5	5.1	18	120	0.2
6. $(CH_3)_2C{=}O$	9.69	27	25	0.8	3.7	150	14	8.7	4.5	10	210	0.5
7. C_5H_5N	9.85	33	30	1.1	3.3	310	41	20	9.0	23	475	1.2
8. CH_3CN	12.39	7.2	6.8	0.6	2.0	100	5	38	2.3	8	160	0.7

*Solvent is CCl_4; K in l mole^{-1}; ΔH^0 in kcal mole^{-1}; ΔS^0 in e.u. at 25 °C; $\Delta\nu_{OD}$ and $\Delta\nu_{OH}$ in cm^{-1}.
†Values of ionization potentials were taken from refs. 17–20.
‡The value of ionization potential of tetraheptylammonium iodide was estimated to be 6 ± 1 eV from the electronic spectrum of alkali iodide (21). The ionization potential of free I^- is, however, equal to minus the electron affinity of free iodine atom (3.2 eV).
§Data for dimerization.

In eq. [3]

$$\Delta\Delta'\nu_{OH} = [\nu_{OH(XHY)} - \nu_{OD(XDY)}] - [\nu_{OH(XH)} - \nu_{OD(XD)}]$$

and $\Delta\Delta'\nu_{OH}$ is negative since ν_{OH} decreases on hydrogen bonding. The terms $\Delta\Delta'\delta_{OH}$ and $\Delta\Delta'\gamma_{OH}$ are both positive since δ_{OH} and γ_{OH} increase on hydrogen bonding. Further, when $K_H/K_D > 1$ the proton is more tightly bound in the monomer, and when $K_H/K_D < 1$ it is more tightly bound in the complex. The deuterium is always concentrated in the species which has the largest zero point energy difference. Since only data on ν_{OH} have been obtained in the present study, it is not possible to discuss all the major zero point contributions; but the observed isotope effects can be understood in terms of the known isotope effects on the three vibrations discussed earlier.

If the isotope effects in terms of K_H/K_D, $\Delta H^0_{OH...Y}/\Delta H^0_{OD...Y}$ or $\Delta\nu_{OH}/\Delta\nu_{OD}$, are plotted against the ionization potentials of the donors (as measures of basicities), the plots show minima around 8.5 eV. It is difficult to rationalize the observation of these minima. The minima are likely to be fallacious since ionization potentials are probably not good measures of base strengths. On the other hand one may be justified in using $\Delta\nu_{OH}$ or $\Delta H^0_{OH...Y}$ as the measure of base strengths of the donors (10*a*).

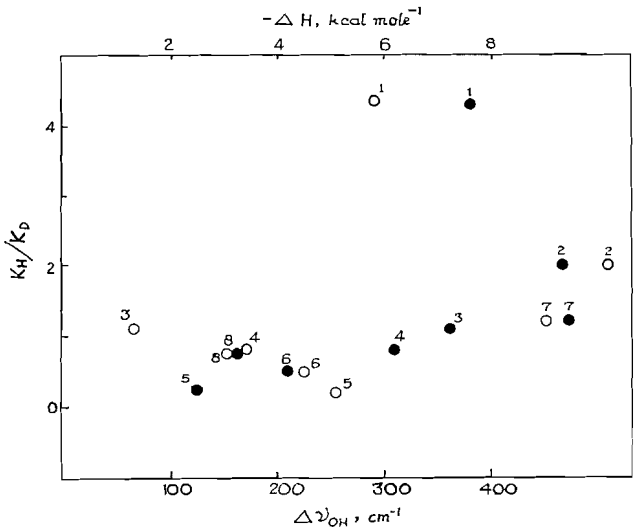


FIG. 1. Correlation of equilibrium isotope effect in hydrogen bonding with base strengths (in terms of $\Delta\nu_{OH}$ and enthalpies of formation of hydrogen bonds). ○, K_H/K_D vs. ΔH^0; ●, K_H/K_D vs. $\Delta\nu_{OH}$.

A plot of K_H/K_D against $\Delta\nu_{OH}$ or $\Delta H^0_{OH...Y}$, Fig. 1, shows that some proportionality exists (with the exception of the charged donor $(C_7H_{15})_4N^+I^-$ which falls out of line) between these quantities. This appears to be reasonable; as the hydrogen bond becomes stronger, the ν_{OH} is decreased and the γ_{OH} is increased. Apparently, for weak bases, the increase in γ_{OH} is greater than the decrease in ν_{OH} and the converse is true for the stronger bases. The positive slopes of the plots in Fig. 1 indicate that the proton is more tightly bonded in the free acid than in the hydrogen-bonded complex. This is indeed a new and interesting result, which needs to be examined more carefully by theory and further experimentation.

ACKNOWLEDGMENTS

The authors are thankful to the Council of Scientific and Industrial Research, India, for the award of a research grant. The authors' thanks are due to Dr. M. J. Janssen of Netherlands and Prof. P. V. R. Schleyer of Princeton University for gift samples of

tetramethylthiourea and tetraheptylammonium iodide respectively. Thanks are also due to Dr. A. B. King and Dr. J. G. Larson of the Gulf Research Laboratory, Pittsburgh, for determining the ionization potentials of tetramethylthiourea and triphenyl phosphine by the electron impact method.

The authors are particularly thankful to one of the referees for his suggestions regarding the interpretation of K_H/K_D.

REFERENCES

1. L. J. BELLAMY and P. F. ROGASCH. Proc. Roy. Soc. London, Ser. A, **257**, 98 (1960).
2. G. DAHLGRAM and F. A. LONG. J. Am. Chem. Soc. **82**, 1303 (1960).
3. J. P. LERCKMAN, J. LASCOMBE, and M. L. JOSIEN. Proc. Intern. Conf. Mol. Spectry. 4th Bologna, 1959, **2**, 858 (1962).
4. C. J. CRESWELL and A. L. ALLRED. J. Am. Chem. Soc. **84**, 3966 (1962).
5. G. C. PIMENTEL and A. L. MCCLELLAN. The hydrogen bond. W. H. Freeman & Co., San Francisco. 1960.
6. F. H. WESTHEIMER. Chem. Rev. **61**, 265 (1961).
7. J. BIGELEISEN. Paper presented at the I.A.E.A. Symposium, Vienna, Austria. 1963. S.M. 50/24.
8. R. F. W. BADER. Can. J. Chem. **42**, 1822 (1964).
9. E. D. BECKER. Spectrochim. Acta, **17**, 436 (1961).
10. (*a*) S. SINGH, A. S. N. MURTHY, and C. N. R. RAO. Trans. Faraday Soc. **62**, 1056 (1966).
    (*b*) S. SINGH and C. N. R. RAO. J. Am. Chem. Soc. **88**, 2142 (1966).
11. A. R. UBBELONDE and K. J. GALLAGHER. Acta Cryst. **8**, 11 (1955).
12. R. E. RUNDLE. J. Chem. Phys. **21**, 937 (1953).
13. C. E. NORDMAN and W. N. LIPSCOMB. J. Chem. Phys. **19**, 1422 (1951).
14. E. R. LIPPINCOTT and R. SCHROEDER. J. Phys. Chem. **61**, 921 (1957).
15. C. G. CANNON. Spectrochim. Acta, **10**, 341 (1958).
16. N. D. SOKOLOV. Opt. Spectry. USSR English Transl. **11**, 8 (1961).
17. A. STREITWEISER, JR. *In* Progress in physical organic chemistry. Vol. I. John Wiley & Sons, Inc., New York. 1964.
18. K. R. BHASKAR, S. N. BHAT, S. SINGH, and C. N. R. RAO. J. Inorg. Nucl. Chem. **28** (1966). In press.
19. K. R. BHASKAR, R. K. GOSAVI, and C. N. R. RAO. Trans. Faraday Soc. **62**, 29 (1966).
20. J. D. MORRISON and J. C. NICHOLSON. J. Chem. Phys. **20**, 1021 (1952).
21. J. FRANK, H. KUHEN, and G. ROLLEFSON. Z. Physik, **43**, 155 (1927).

Can. J. Chem. Downloaded from www.nrcresearchpress.com by 210.87.254.105 on 09/05/12
For personal use only.

PHASE TRANSITIONS OF ADSORBATES

I. SPECIFIC HEAT AND DIMENSIONAL CHANGES OF THE POROUS GLASS – WATER SYSTEM[1]

G. G. LITVAN

Division of Building Research, National Research Council, Ottawa, Canada

Received March 24, 1966

ABSTRACT

The specific heat and dimensional changes of the porous 96% silica glass – water system were measured simultaneously between −35 °C and +2 °C with coverages of 1.6, 4.0, 5.3, and 7.7 molecular layers. The specific heat of the adsorbate below the transition range was found to be higher than that of ice. No phase change was detected with the lowest concentration. At the higher coverages, transition always occurred near −9.5° and was of the anomalous first order type. The values of the specific latent heat of fusion, calculated by assuming that two monolayers do not freeze, are 49.4, 54.4, and 55.5 cal g^{-1}, depending on the concentration. The correlation between the results of calorimetric and dimensional change measurements was considered satisfactory.

INTRODUCTION

Phase transitions of water adsorbed on porous glass differ from those of other adsorbates in at least two aspects: (*a*) water has several freezing ranges (1, 2) while benzene (3) and xenon (1) have one, and (*b*) its melting point is not concentration dependent as is that of helium on jeweller's rouge (4), argon (5), nitrogen (6), and methane (7) on rutile. This anomalous behavior and the importance of the freezing phenomenon from a practical point of view seemed to warrant further studies.

The thermal properties and the dimensional changes of the partially and fully saturated systems were simultaneously measured to facilitate the correlation of the results.

EXPERIMENTAL

Apparatus

The adiabatic calorimeter incorporating a Tuckerman-type optical extensometer (8), manufactured by American Instrument Co., Silver Spring, Maryland, was similar to that described in ref. 2 but with several modifications. Instead of using the phototube controllers, the temperature of the envelope and the tube was regulated by a microswitch in the heating circuit actuated by a disc mounted on the slidewire shaft of a 0.1 mV Speedomax recorder and governed by the amplified e.m.f. of a seven-junction thermopile. The apparent temperature difference between the calorimeter and envelope was ±0.001 °C. In addition, the temperature of the reference block and the bath was made to follow automatically that of the calorimeter without the need of manual adjustments. Adiabatic conditions were thus better maintained during temperature changes.

The reported (2) 0.1° temperature lowering of the calorimeter that occurred overnight was eliminated. The temperature remained either constant or increased by 0.01° overnight so that the state of the adsorbate was not altered from one of desorption to one of adsorption.

Precision and Accuracy

The degree of precision increased as the tests progressed; the final precision varied between ±2% and ±0.02% depending on the working temperature range. The accuracy was determined by measuring the heat capacity of sodium chloride and it was found to be ±0.2%.

Materials

The porous 96% silica glass had a nitrogen surface area of 112.5 $m^2 g^{-1}$. The pore-size distribution, calculated from the nitrogen isotherm (9) showed that 66% of the total pore volume consisted of pores with radii between 28 and 20 Å. The distribution curve had a maximum at 21 Å. Prior to each series of measurements the glass was heated to 400 °C in air to burn off organic impurities and subsequently evacuated at 10^{-5} mm pressure for at least a day.

The water used was purified by several vacuum distillations. The amount adsorbed was determined with the aid of a burette (3), instead of gravimetrically (2).

[1]*Issued as N.R.C. No. 9150.*

Can. J. Chem. Downloaded from www.nrcresearchpress.com by 210.87.254.105 on 09/05/12
For personal use only.

CALCULATIONS

The heat capacity of the adsorbate was calculated by taking the difference between the heat capacity of the calorimeter system with and without the adsorbate. The total heat capacity of the system is given by the formula due to Morrison *et al.* (10).

$$[1] \qquad \frac{dQ}{dT} = c_{p_{cal}} + c_{p_g} + c_{N_s} - q_{st}\frac{dN_s}{dT} - V_g\frac{dp}{dT}$$

where

Q = heat supplied

$c_{p_{cal}}$ = heat capacity at constant pressure of the calorimeter and adsorbent

c_{p_g} = heat capacity at constant pressure of the gaseous phase

N_s = number of moles sorbed

c_{N_s} = heat capacity of the adsorbed phase at constant amount sorbed

q_{st} = isosteric heat of sorption

p = vapor pressure

T = temperature

V_g = volume of gaseous phase in the calorimeter.

Because of the experimental difficulties due to the small water vapor pressures at low temperatures, no data are available for q_{st}, N_s, and p. The maximum value, however, of dN_s/dT was $<1 \times 10^{-5}$ mole deg^{-1} and that of dp/dT was 0.14 mm deg^{-1} calculated with the saturation vapor pressure data (V_g = 310 ml). Consequently, the second, fourth, and fifth terms on the right-hand side of eq. [1] were considered negligible. The validity of the assumption that the adsorbent is inert, i.e. its heat capacity is not altered by the presence or the state of the adsorbate, was accepted due to necessity.

RESULTS

The heat capacity of the adsorbed water in fixed concentrations of 0.0511, 0.1266, 0.1676, and 0.2431 g/g were determined between −35 and +2 °C while heating the system. The system with the highest concentration was saturated. These concentrations are equivalent to 1.6, 4.0, 5.3, and 7.7 layers, respectively. Measurements of the fifth series with 0.1810 g/g (5.7 layers) were interrupted due to malfunctioning of the compressor. The specific heat vs. temperature plot is shown in Fig. 1.

The specific heat at temperatures below the heat anomaly is, in all cases, higher than that of bulk ice (0.45 cal deg^{-1}) but at temperatures above the anomaly it closely approaches the value of bulk water. For reasons yet unexplained the curve for 0.1676 g/g concentration lies above the others.

With the lowest amount of water present, equivalent to 1.6 layers, no anomaly takes place. At higher concentrations anomalously large heat absorption occurs, beginning a few degrees below −20 °C and extending over a temperature range of ~12 deg. The curve ascends gradually but descends sharply after the maximum which is near −9.5°. Normal behavior, except for a small minimum, is resumed at about −7°.

The entropy changes,

$$\int_{243}^{T} \frac{c_p}{T} dT,$$

are shown in Fig. 2 and the entropy of fusion values are given in column 5 of Table I.

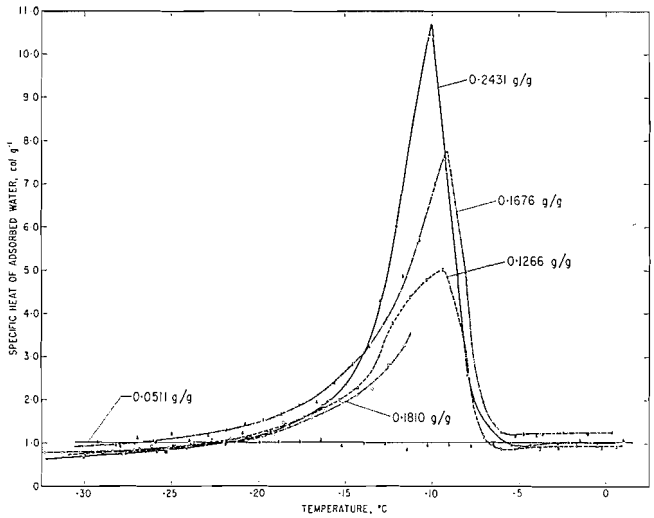


FIG. 1. Specific heat of adsorbed water vs. temperature. The numerical values indicate the water content of the adsorbent.

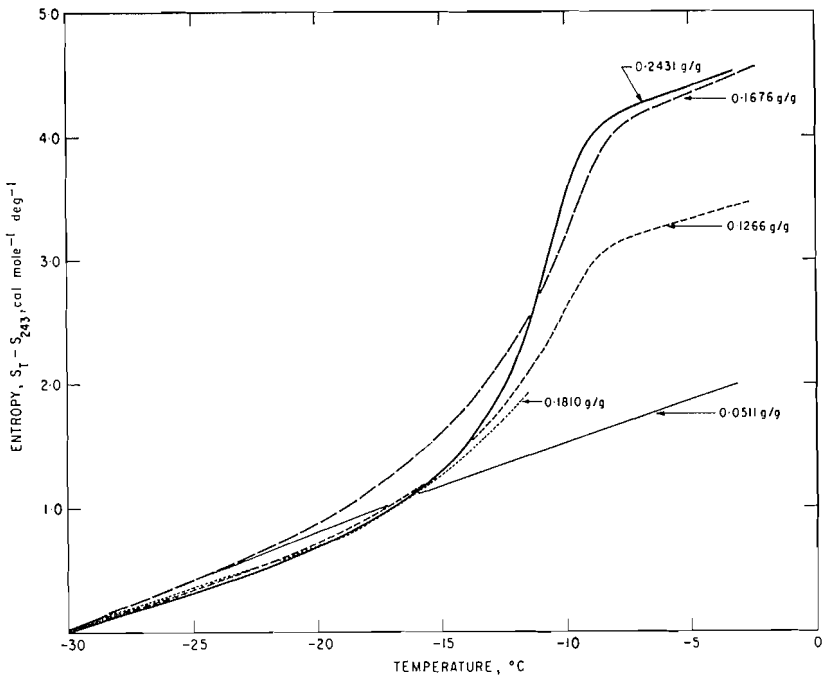


FIG. 2. Entropy change, $S_T - S_{243}$, of adsorbed water vs. temperature.

The latent heats of fusion (column 3, Table I) were determined by graphical integration of the area between the c_p vs. T curve and a straight line connecting the points at $-30°$ and -7 °C.

Figure 3 shows the expansion isosteres (fractional length changes plotted against temperature). At the lowest concentration no anomaly can be detected. In the case of higher concentrations, two anomalies occurred on cooling, one around $-20°$ and the other around $-7°$.

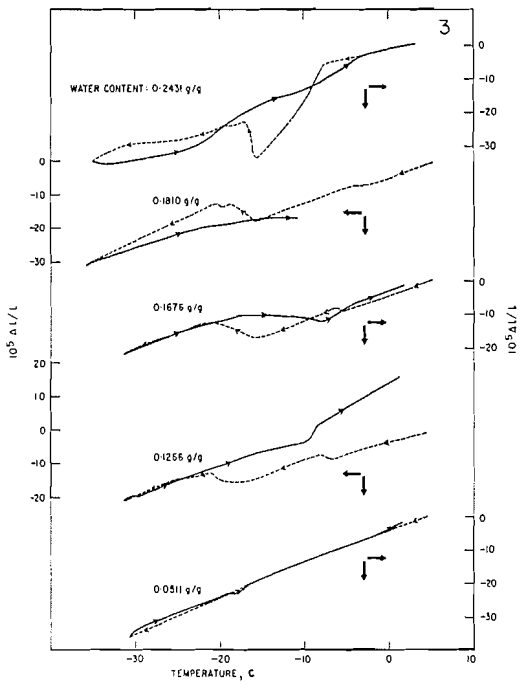
Can. J. Chem. Downloaded from www.nrcresearchpress.com by 210.87.254.105 on 09/05/12
For personal use only.

TABLE I

Specific latent heat and entropy of fusion of adsorbed water

Water adsorbed (g/g)	No. of layers	Heat of fusion (cal g^{-1})		Entropy of fusion (cal $mole^{-1}$ deg^{-1})
0.0511	1.6	0.0*	0.0†	
0.1266	4.0	26.32*	49.40†	1.74
0.1676	5.3	33.75*	54.42†	2.32
0.2431	7.7	41.82*	55.55†	2.76
Bulk		79.67		5.26

*Values calculated by assuming that all the water present has transformed.
†Values calculated by assuming that an amount of water equivalent to two monolayers has not transformed.



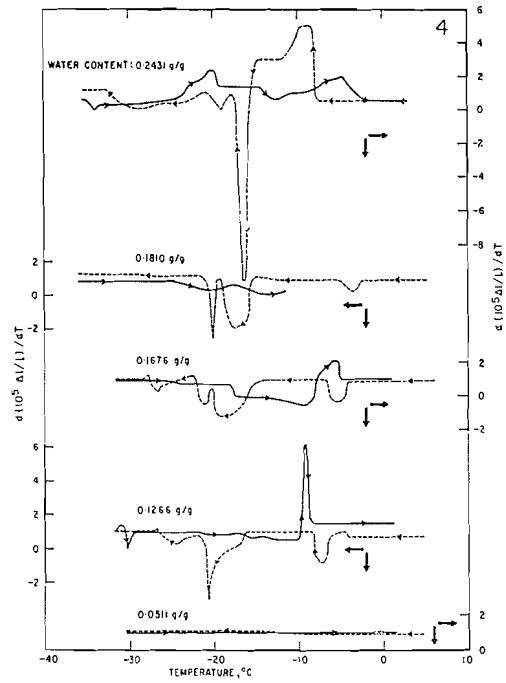


FIG. 3. Expansion isosteres. Individual points omitted.
FIG. 4. Derivative of the expansion isosteres.

From the temperature derivative of the fractional length changes (Fig. 4) it is apparent that the expansion occurring at high temperature is concentration dependent: it shifted to higher temperature and decreased in magnitude with increasing water concentration, and it vanished at saturation. This finding is in line with one previous study (1) but is only in partial agreement with another (2) where on the saturated system anomaly was found at −7°. The other anomaly, which always occurs around −20°, seems to have not one but two maxima at approximately −19° and −21° as indicated by Figs. 3 and 4.

On warming, only one expansion was observed around −8° and it became broader with increasing concentration. Pronounced hysteresis is exhibited with all except the lowest concentrations.

DISCUSSION

Absence of Transition

The finding that no transition occurs at a coverage of 1.6 layers is in accordance with findings of previous calorimetric (4–7) and dimensional change (1) measurements.

Can. J. Chem. Downloaded from www.nrcresearchpress.com by 210.87.254.105 on 09/05/12
For personal use only.

Presumably, the strong adsorbent–adsorbate interaction prevents the water from rearrangement necessary for transition. It is remarkable that the water–glass system behaves similarly in this respect to the rutile–nitrogen (5) and rutile–argon (6) systems where the onset of freezing occurs after the coverage exceeds two layers.

Heat of Fusion

When calculating ΔH the question arises whether the first two layers still do not suffer phase change with coverages exceeding this value. It is conceivable that the attractive forces between the solid and the first layers, at higher concentrations, are weakened by the water–water interaction and consequently the adsorbate achieves the mobility required for ice formation. The latent heat of fusion was, therefore, calculated in two ways: by assuming that (*a*) all the water froze and (*b*) only the water in the third and subsequent layers froze.[2] The results are given in columns 3 and 4 of Table I and the mean latent heat of fusion is plotted as the function of the water concentration in Fig. 5. For the present, assumption (*b*) is accepted without direct evidence. There are indications, however, that support this view.

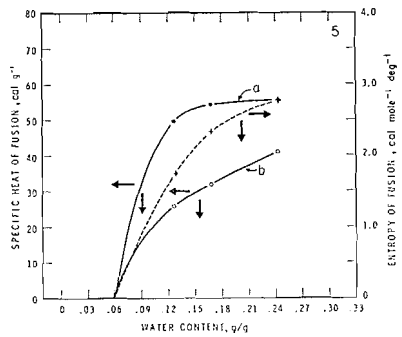


FIG. 5. Specific heat of fusion and entropy of fusion vs. water content (see test for explanation).

If the attractive force holding the adsorbate in the surface is higher than a first order function of the distance, the heat of fusion vs. concentration curve is expected to be of the saturation type as is the case with assumption (*b*) but not with (*a*) (Fig. 5). In addition, considering that in the bulk state the specific heat of water is approximately twice that of ice the high specific heat of the adsorbate at temperatures below the melting point may be viewed as an indication of the presence of unfrozen water.

Antoniou (2), when calculating the results for the saturated system, assumed the heat of fusion of the adsorbed water to be the same as that of the bulk and that the observed net heat change was therefore low because not two but three water layers remained unfrozen. Earlier extensometric measurements (1) showed, however, that the onset of freezing occurs at a coverage between 1.3 and 2.3 layers. Furthermore, application of this concept to the present case results in the improbable finding that 2.7, 3.1, and 3.7 layers, respectively, remained unfrozen, i.e. the amount of unfrozen water increased with increasing concentration.

The values for the heat of fusion are less than that for bulk ice; even at saturation they reach only ~70%. In other systems, such as argon–rutile (5), methane–rutile (7), and nitrogen trifluoride – anatase (11), ΔH is equal to the value for the bulk substance, presumably because of weaker adsorbent–adsorbate interaction.

[2]*For the specific heat of the unfrozen water in the first two layers the experimental values determined in the series with the lowest concentration were used.*

Can. J. Chem. Downloaded from www.nrcresearchpress.com by 210.87.254.105 on 09/05/12
For personal use only.

The small entropy of fusion values show that less disordering occurs in the adsorbed than in the bulk state. Since the absolute values are not known it cannot be decided whether the state of the solid or liquid or both phases are responsible for the smaller difference.

The transition is of the anomalous first order type (12) as indicated by the shape of the c_p vs. T curve. At least two conditions can account for such phase changes: (*a*) gradual disordering of a homogeneous phase and (*b*) the existence of domains with different properties.

Expansion Isosteres

The results of the length change measurements are in general accord with those obtained when cooling to −180 °C (1). Because in the present study the system was cooled only to −35 °C, the agreement implies that the portion of the water that froze below −35° also melted in the same region and had no detectable effect on the melting process at high temperatures.

The shape of the expansion isosteres (Figs. 3 and 4) changes gradually with concentration. The curve for the saturated system shows one special feature, namely, a contraction occurring on cooling near −16°. It is noteworthy that the disappearance of the menisci at saturation does not cause more significant changes.

In contrast to Antoniou's finding (2) the correlation between the expansion isosteres and heat capacity curves can be considered as satisfactory. At low temperatures the slope of the expansion isostere changes gradually corresponding to the slow increase of c_p. The expansion due to melting begins at the temperature of the maximum heat capacity (−9.5°) and takes place in the region where the c_p curve shows a minimum which is characteristic of anomalous transitions.

ACKNOWLEDGMENTS

The author is indebted to Mr. P. J. Sereda for helpful discussions, to Mr. B. Hurley for carrying out most of the measurements, and to Mr. H. F. Slade for technical assistance. This contribution is published with the approval of the Director, Division of Building Research, National Research Council of Canada.

REFERENCES

1. G. G. Litvan and R. McIntosh. Can. J. Chem. **41**, 3095 (1963).
2. A. A. Antoniou. J. Phys. Chem. **68**, 2754 (1964).
3. C. Hodgson and R. McIntosh. Can. J. Chem. **38**, 958 (1960).
4. H. P. R. Frederikse. Physica, **15**, 860 (1949).
5. J. A. Morrison and L. E. Drain. J. Chem. Phys. **19**, 1063 (1951).
6. J. A. Morrison, L. E. Drain, and J. S. Dugdale. Can. J. Chem. **30**, 890 (1952).
7. K. S. Dennis, E. L. Pace, and Ch. S. Baughman. J. Am. Chem. Soc. **75**, 3267 (1953).
8. L. B. Tuckerman. Proc. ASTM, **23**, II, 602 (1923).
9. C. Pierce. J. Phys. Chem. **57**, 149 (1953).
10. J. A. Morrison, J. M. Los, and L. E. Drain. Trans. Faraday Soc. **47**, 1023 (1951).
11. A. R. Siebert and E. L. Pace. J. Phys. Chem. **60**, 828 (1956).
12. J. E. Mayer and S. F. Streeter. J. Chem. Phys. **7**, 1019 (1939).

Can. J. Chem. Downloaded from www.nrcresearchpress.com by 210.87.254.105 on 09/05/12
For personal use only.

Can. J. Chem. Downloaded from www.nrcresearchpress.com by 210.87.254.42 on 09/05/12
For personal use only.

CATALYTIC HYDRODESULFURIZATION OF THIOPHENE

VI. COMPARISONS OVER MOLYBDENUM DISULFIDE, COBALT MOLYBDATE, AND CHROMIA CATALYSTS[1]

S. KOLBOE[2] AND C. H. AMBERG[3]

Division of Applied Chemistry, National Research Council, Ottawa, Canada

Received June 25, 1965

ABSTRACT

The hydrodesulfurization of thiophene over five molybdenum disulfide catalysts, an alumina-supported cobalt molybdate, and a chromia catalyst has been investigated. Comparisons on the basis of equal surface areas showed that desulfurization activity did not vary a great deal. It was established mainly by working at very low conversion levels that 1,3-butadiene was a product over all these catalysts, and that a mixture of butadiene, the three *n*-butenes, and *n*-butane constituted the actual *primary* reaction product. The reaction rate is strongly dependent on conversion, probably as the result of small quantities of product H_2S, the rate decreasing by a factor of 100 in going from 0.01% to 5% conversion in a typical flow experiment. A strong enhancement of the rate over MoS_2 was noted in the presence of oxygen.

INTRODUCTION

Following a series of studies of the hydrodesulfurization of thiophene over cobalt molybdate catalysts previously carried out in this laboratory (1–3) it was found to be of interest to investigate the catalytic properties of molybdenum disulfide itself, as this may well be the most important constituent in the sulfided cobalt molybdate.

Most of the experiments to be described below were carried out in the steady state and using much lower reaction rates than before; for this reason some comparative measurements using alumina-supported cobalt molybdate and pure chromia were included, these being the catalysts employed in the previous studies (1–5).

EXPERIMENTAL

(i) Apparatus

Modifications of the flow system which has been previously described (1) made it possible to pass a complete range of H_2/He mixtures through a thiophene saturator at flow rates varying from 1 to 200 ml/min at or near atmospheric pressure, flows and pressures being measurable with 1% precision or better. As before, pulse injection into a system in the steady state could take place from a syringe through a serum cap at the top of the microreactor. In addition, a simple syringe holder has been constructed, which permits additions to be sufficiently slow so that new steady states can again be attained over periods of several minutes. This is done by moving forward the plunger of the syringe with a screw (1 mm per turn) continuously or intermittently, depending on the requirements of a particular system. For the analysis of tail gases, when they are not passed directly to the gas chromatographic column, a commercial sampling valve (Perkin–Elmer) has now been incorporated in the apparatus.

The range of the apparatus was considerably extended by adding a flame ionization detector as an alternative to the Gow-Mac thermal conductivity detector. The flame ionization detector was a copy of one previously used by one of us (S. Kolboe. Unpublished). Using this combination of detectors, product concentrations from 3×10^{-12} up to 5×10^{-6} mole/ml (5×10^{-5} to 80 torr) were measurable; combined with the full range of flows available, reaction rates (product concentration $\times$ flow rate) from 5×10^{-14} to 1×10^{-3} mole/s were attainable, and these then represented the extreme limits of the apparatus.

An 8 ft propylene carbonate column (25% w/w) for C_4 analysis was used at 0 °C, the temperature being somewhat lower than that used earlier to minimize "bleeding" from the stationary phase, and a 6 ft squalane column (25% w/w) at 80–100 °C was again used for the analysis of sulfur compounds.

[1]*Issued as N.R.C. No. 9181.*

[2]*National Research Council Postdoctorate Fellow 1963–1964. Present address: Central Institute for Industrial Research, Oslo-Blindern, Norway.*

[3]*Present address: Department of Chemistry, Carleton University, Ottawa 1, Ontario.*

(ii) Catalysts

I. MoS_2 - "Molykote", a finely divided solid lubricant, used as received.

II. MoS_2 (Anachemia), as received.

III. Catalyst II doped with 1 mole % cobalt. Prepared by making a slurry with an aqueous solution of cobalt nitrate, drying, outgassing at 400–500 °C and then heating in a sealed quartz ampoule to 650 °C for 4 h.

IV. MoS_2 made by heating MoS_3 to 400 °C in a H_2/He mixture (6).

V. Prepared by heating catalyst IV to 650 °C for 1 h in a H_2/He mixture.

VI. Prepared by heating catalyst V to 800 °C for 12 h in a sealed quartz ampoule.

Although no changes in activity were observable in catalysts I–VI after the first 1 to 2 h of desulfurization at 300 °C, measurements were not made until after the first 5–10 h to ensure constant activity.

VII. Cobalt molybdate on alumina, Girdler No. G35A (1) crushed from pellets and using −65 mesh portion. Contains 1.3% Co + 6.1% Mo. Activated by heating in hydrogen to 400 °C and then stabilized (i.e. sulfided) with thiophene and H_2 for 16 h at a flow rate of 5 ml/min.

VIII. Chromia gel. Prepared by slowly adding a 10% ammonia solution to a 20% $Cr(NO_3)_3$ solution until pH = 9.0, filtering, washing, and drying.[4] Activated by slowly heating to 400 °C in hydrogen, and stabilized like catalyst VII.

The B.E.T. surface areas as well as spectrographic analyses of the catalysts are shown in Table I. The percentages given are an indication of order of magnitude only.

TABLE I

B.E.T. surface areas and semiquantitative spectrographic analysis of catalysts

Catalyst	I	II	III*	IV	V	VI	VII	VIII
Area ($m^2\ g^{-1}$)	2.2	3.3	3.3	157	67	12	241	150
% Mg	0.005–0.05			0.0005–0.005			—	0.001–0.01
% Mn	0.005–0.05			None			—	None
% Pb	0.01–0.1			0.001–0.01			—	0.005–0.05
% Si	0.1–1			None			—	0.05–0.5
% Fe	0.1–1			None			—	0.05–0.5
% Ge	0.01–0.1			None			—	None
% Bi	0.05–0.5			None			—	0.005–0.05
% Al	0.05–0.5			None			—	0.001–0.01
% Cu	0.05–0.5			0.001–0.01			—	0.0001–0.001
% Ag	0.001–0.01			0.005–0.05			—	None
% Ca	0.01–0.1			None			—	0.005–0.05
% Ni	None			None			—	0.001–0.01

*1% Co not shown in table.

All catalysts gave reproducible results and nos. I, II, III, V, VI, and VII showed no decrease in activity after being in use for 2 to 3 weeks.

(iii) Reagents

Thiophene, Eastman; this contained some C_4 impurities which were largely removed by bubbling dry air through the liquid until about one-third of it had evaporated. Any C_4 compounds remaining were negligible even for measurements at very low conversion. The other impurities have been reported in (2).

C_4 hydrocarbons, Phillips research grade; used as received. Hydrogen, Matheson Ultrapure; used as received. Helium, Matheson; dried over Anhydrone.

RESULTS AND DISCUSSION

In contrast to the work reported previously in this series, conditions were now chosen so as to achieve much lower reaction rates and conversions in order to avoid the complications arising from secondary reactions. This was made possible by the increase in analytical sensitivity and it was also, in part, facilitated by using low-area catalysts.

No appreciable cracking was noted for any of the catalysts, and quantities of isobutylene and isobutane formed were negligible. There was no indication of any polymerization of unsaturated hydrocarbons. The product distribution of the *n*-C_4 hydrocarbons depended greatly on the catalyst and the conditions of a given experiment.

[4]*A sample of this catalyst was kindly provided by Dr. Y. Amenomiya.*

Can. J. Chem. Downloaded from www.nrcresearchpress.com by 210.87.254.42 on 09/05/12
For personal use only.

Attempts to run the reactor under differential conditions failed because of the extremely strong dependence of reaction rate on conversion even down to very low conversions, as shown in Fig. 1 for all catalysts. This strong dependence on conversion is believed to be caused by the H_2S formed in the reaction. Hydrogen sulfide addition experiments have shown that this gas strongly depresses the reaction rate. The effect appears to be of the right magnitude for explaining the conversion behavior; unfortunately it has not been possible to reproduce the curves shown in Fig. 1 by independent H_2S additions, because

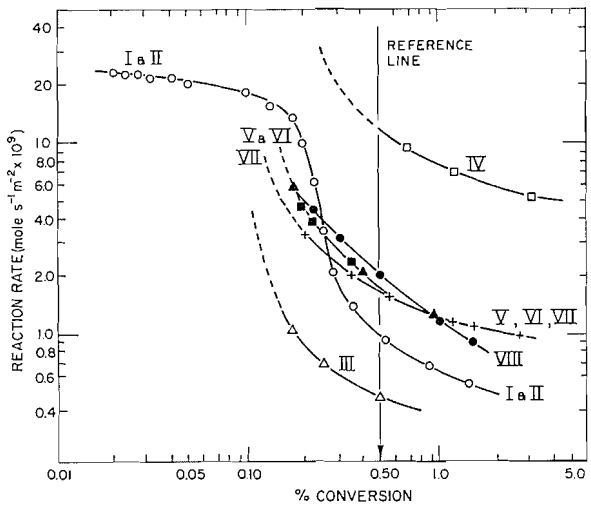


FIG. 1. Thiophene desulfurization as a function of conversion over various catalysts at 288 °C. Partial pressures: thiophene 20 torr; hydrogen 740–770 torr. Flows ranged from 2 to 200 ml/min, catalyst weights from 6 mg to 1.5 g. Roman numerals correspond to catalyst numbers. Extrapolations shown are based on measurements at 10–20 °C lower temperatures (identical curve shapes).

the required concentrations would have to be too small (the partial pressures of H_2S would have to lie in the region 0.02 to 0.2 torr). It has been possible to eliminate from consideration the effects of diffusion in the gas phase or in catalyst pores, temperature gradients within porous catalyst particles or from catalyst surface to ambient, as well as C_4-hydrocarbons generated by complete desulfurization of the 0.02% butanethiol impurity present in the thiophene. This was done by calculations and some ancillary experiments, such as employment of constant weight-to-flow ratios for different weights of catalyst.

It can be seen from Fig. 1 that unambiguous comparisons of catalyst activity cannot be made. However, for approximate comparisons under the same experimental conditions a region in which the curve shapes are similar has been arbitrarily selected (see "Reference Line" at 0.5% conversion); these comparative rates have been assembled in Table II. The most striking fact emerging from that table is the relatively slight variation of activities based on unit surface area of catalyst (column 5), particularly when compared with the rates based on unit weight of catalyst which vary by three orders of magnitude (column 4). This can be considered significant despite the uncertainties in the comparison of different catalysts discussed in connection with Fig. 1. Unless one makes the usual assumption that for the supported cobalt molybdate, VII, substantial coverage of the alumina surface has resulted from the impregnation processes employed, the good agreement in that case must be regarded as fortuitous. We are confident, however, that the assumption is correct and the comparison justified. The similarity in rates of desulfurization over all the catalysts

Can. J. Chem. Downloaded from www.nrcresearchpress.com by 210.87.254.42 on 09/05/12
For personal use only.

TABLE II

Reaction rates at 0.50% conversion and 288 °C. Hydrogen and thiophene pressures: 740 and 20 torr respectively; hydrogen flow rate: ~20 ml/min. Catalyst amounts varied from 10 mg to 1.5 g to give a total surface of 2–5 m^2

No.	Type	B.E.T. area ($m^2\ g^{-1}$)	Reaction rate (10^9 molc $s^{-1}\ g^{-1}$)	Reaction rate (10^9 mole $s^{-1}\ m^{-2}$)
I	MoS_2(Molykote)	2.2	2.2	1.0
II	MoS_2(Anach.)	3.3	3.0	0.90
III	MoS_2 + 1% Co	3.3	1.65	0.5
IV	MoS_2 from MoS_3(400°)	154	1 600	11
V	IV (650°)	67	107	1.6
VI	IV (800°)	12	18	1.5
VII	Cobalt molybdate on alumina (Girdler G35A)	241	400	1.65
VIII	Cr_2O_3	150	300	2.0

is strongly suggestive of the same basic mechanism being operative in all cases. In this connection it may be noted that an apparent activation energy of 24 kcal/mole was determined over catalyst V (MoS_2) in agreement with previously published values of 25 kcal/mole over VII (1) and 24 kcal/mole over a Cr_2O_3 catalyst (4) similar to VIII.

It is interesting to note, in passing, the decrease in activity per unit area when catalyst IV was pretreated by reduction in a H_2/He mixture at a higher temperature (catalyst V, 650°). In view of the common origin of the catalysts this decrease can be considered significant. It could be due to improved reduction, or to thermal destruction of unstable surface states in the MoS_2 crystallite, of surface impurities, or of micro-cracks accessible only to N_2; or combinations of these factors. Further sintering (catalyst VI, 800°), although decreasing the surface area by a factor of more than 5, had virtually no effect on activity per unit area or in other words on the catalytic nature of the surface.

The present set of experiments has thrown new light on the distribution of C_4 hydrocarbons over the various catalysts. Previously, both the *n*-butenes and *n*-butane had been identified as reaction products over a cobalt molybdate identical with catalyst No. VII (1), as well as over a chromia similar to No. VIII (4); moreover, butadiene had been found over chromia, and identified on catalyst VII during infrared studies carried out while the reaction was in progress (R. A. Siddiqui and C. H. Amberg. Unpublished). It had been assumed at the time that butadiene would occur in the gas phase also over the cobalt molybdate catalyst in significant amounts, but that it was being hydrogenated too fast for detection. Butadiene has now been definitely identified as a gas phase product over all the catalysts used.

Even though the C_4 distribution depends strongly on conditions, a single set is given in Table III for the same conditions as those specified in Table II for purposes of comparison.

In the earlier experiments in this series, the distribution of the *n*-butenes had always been close to equilibrium (1), although a tendency for 1-butene and *cis*-2-butene to occur slightly in excess had been observed (3). Present conditions of steady-state operation at very short contact times strongly accentuate this tendency, so that the distributions are far from equilibrium. Thus it can be calculated from Table III that the observed quantity of 1-ene exceeded the equilibrium value by factors of 3–6 (equilibrium distribution: 13.2% 1-ene, 32.2% *cis*-2-ene, 54.6% *trans*-2-ene).

The dependence of C_4 distribution on conversion can be appreciable even at conversions as low as 0.5%; this is borne out by Fig. 2, which is shown as an example. Care should be

Can. J. Chem. Downloaded from www.nrcresearchpress.com by 210.87.254.42 on 09/05/12
For personal use only.

TABLE III

Distribution of C_4 hydrocarbons from thiophene at 0.50% conversion and 288 °C. Hydrogen and thiophene pressures: 740 and 20 torr, respectively; hydrogen flow rate: ~20 ml/min

Catalyst	Butadiene (%)	1-Butene (%)	*cis*-2-Butene (%)	*trans*-2-Butene (%)	Butane (%)
I	6.2	42.6	21.7	22.0	9.1
II	6.9	42.5	22.3	19.2	8.8
III	8.4	55.6	14.0	17.4	4.7
IV	7.2	39.9	16.7	23.5	12.7
V	4.0	28.5	22.0	36.5	9.5
VI*	—	—	—	—	—
VII	2.2	47.5	19.8	24.3	6.2
VIII	7.7	31.3	11.8	11.8	37.4

*Product distributions for catalyst VI were only roughly surveyed, but did not appear to show significantly different trends.

taken not to extrapolate the curves in Fig. 2 to zero conversion, because in the interval not shown here, abnormal and yet completely reproducible inflections of the curves have been observed for some catalysts, for which we have at present no reasonable explanation. Catalysts IV, V, VI, and VII exhibited essentially the same dependence upon conversion as is demonstrated in Fig. 2, while catalysts I, II, III, and VIII varied to a lesser extent with conversion.

Consecutive reactions—if by this we mean further reaction with a product molecule which has been present in the gas phase—were found not to be the prime reason for the changing product distribution with conversion. Thus the isomerization and hydrogenation rates of 1-butene over catalyst V were examined by slowly admitting the gas to the reactor, simultaneously with the thiophene, and under the same conditions as were indicated for Fig. 2 except for a conversion level of 0.4%. It had been shown previously that olefins do

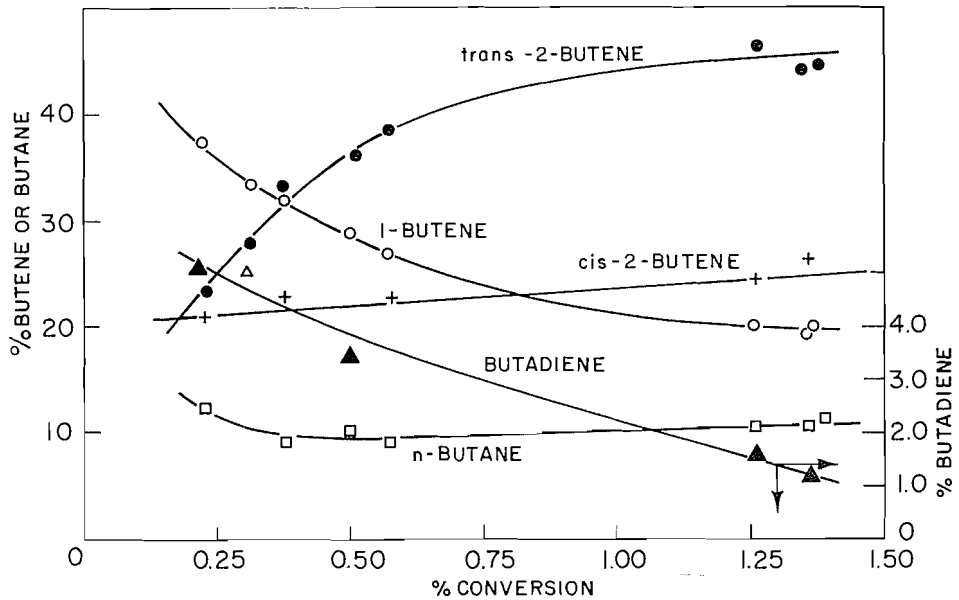


FIG. 2. Product distribution as a function of thiophene conversion over MoS_2 catalyst V at 288 °C. Partial pressures: thiophene 20 torr; hydrogen 740 torr. Flows 5–200 ml/min. Catalyst weights 20 and 75 mg.

Can. J. Chem. Downloaded from www.nrcresearchpress.com by 210.87.254.42 on 09/05/12
For personal use only.

not much affect the rate of hydrodesulfurization (1) and, in any case, the concentration of the added 1-butene was only about 1% of that of the thiophene. In this way no more than 1–2% of the added 1-butene was isomerized to *cis*- or *trans*-2-butene, the isomerization following first-order kinetics. No hydrogenation of the added butene could be detected. From somewhat different experiments performed with butadiene on the other hand one may deduce that a fair amount of gas-phase butadiene, say between 25 and 50%, would be hydrogenated under the above conditions. It must then be concluded that distributions of the type shown in Fig. 2 are essentially primary product distributions of the C_4 hydrocarbons as desorbed from the catalyst, the only exception being the fast reacting butadiene which shows too low a value. Considering that no hydrogenation of butene could be detected, it is remarkable that the fully hydrogenated butane forms a significant fraction of the reaction products. Since the other catalysts exhibited the same reaction pattern it can be stated that all of them yield a *primary* product consisting of a mixture of 1,3-butadiene, the three *n*-butenes, and *n*-butane. This result had been anticipated by an indirect calculation using data from experiments over chromia (4).

The fact that 1,3-butadiene was identified over all our catalysts (in amounts of up to 60%, depending on conditions) might indicate, as has been argued previously, that it is the first C_4-hydrocarbon formed from thiophene. If this is so, however, it can now be seen that only a part of the butadiene molecules can have desorbed from the surface prior to further hydrogenation. This is borne out by the following experiments over catalyst No. I: Butadiene was admitted to the system which was in the steady state with respect to thiophene desulfurization. The distribution of the butenes coming from the added butadiene was evaluated and found to be similar to that arising from thiophene desulfurization, but significantly lower in 1-butene (Table IV).

TABLE IV

Product distributions from thiophene and from added 1,3-butadiene over catalyst No. I at 320 °C and 1.5% conversion. Partial pressures: thiophene 20 torr, H_2 200 torr, He 540 torr; flow rate of hydrogen/helium carrier gas: 20 ml/min; catalyst weight: 1.5 g

Reactant	1-Butene (%)	*cis*-2-Butene (%)	*trans*-2-Butene (%)	Butane (%)
Thiophene	50.0	19.0	25.5	5.8
Thiophene (butenes only)	(53)	(20)	(27)	
1,3-Butadiene*	40	22	37	<0.5

*Mean of two experiments in which amount of butadiene added was, respectively, equal to and three times the total C_4 yield from thiophene.

The table shows that the behavior of butadiene is analogous to that of 1-butene, in that complete hydrogenation of the free gas can be almost totally suppressed under conditions in which thiophene desulfurization can still give rise to significant amounts of butane, provided these conditions are appropriately selected. Similar results were observed over catalyst V, which leads us to believe that the phenomenon is a general one for all our catalysts.

If we accept that the first C_4-hydrocarbon product from thiophene is adsorbed 1,3-butadiene, then the different product distributions from thiophene and from added butadiene shown in Table IV can only arise from two different surface configurations of the adsorbed butadiene molecule. Similar reasoning would apply to butenes from thiophene on the one hand, and butenes added or derived from hydrogenated butadiene on the other, if

Can. J. Chem. Downloaded from www.nrcresearchpress.com by 210.87.254.42 on 09/05/12
For personal use only.

and only if the hydrogenation route of thiophene proceeds through adsorbed butene. This is so, because thiophene can be made to yield butane under conditions where gas phase butene will not hydrogenate further. The above arguments are not invalidated by the possibility of a sulfur-containing adsorbate, say of the type

$$-S-CH=CH-CH=CH_2,$$

preceding the butadiene, if the latter is to be regarded as an intermediate member of the hydrogenation sequence (3). However, if butane were to be formed directly from the adsorbed diene-thiol a much more complex desulfurization mechanism than had been envisaged so far would have to be proposed. This will be discussed in a later publication (S. Kolboe. To be published).

It was noted previously that olefin hydrogenation was strongly suppressed in the presence of H_2S over supported cobalt molybdate (catalyst VII), and to a much lesser extent over chromia (4). The selective effect of H_2S has now been observed over pure MoS_2 (catalyst VI) and so may be assumed to be general for MoS_2 catalysts. The fact that butadiene was always fully hydrogenated to butenes and butane in the earlier studies was due to the very different reaction conditions employed then.

In an effort to reexamine the poisoning effect of ammonia on the desulfurization reaction (3) a 10 μl pulse of conc. aqueous NH_3 was injected into a steady-state system operating over catalyst IV (100 mg catalyst; 250 °C; hydrogen flow: 25 ml/min; partial pressure of thiophene: 20 torr). No effect whatever could be found after 2 min. On examining the hydrogenation and isomerization of 1-butene (pulse addition) in the absence of thiophene but otherwise under similar conditions over catalyst VI, an effect was observed with ammonia solution, but this lasted only about 10 min; moreover, water addition produced a similar effect. As before, H_2S acted as a much stronger and long-lasting poison.

The above observations indicate that the activity of pure MoS_2 does not reside in acid sites of the Brønsted type: one would not expect fast desorption of NH_3 from such sites at the relatively low temperatures employed. This is in contrast to the strong and persistent effect of pyridine found earlier with the cobalt molybdate on alumina catalyst (3). If the earlier results are to be interpreted on the basis of acid-site poisoning in the Brønsted sense—as was implied at the time—then it becomes necessary to invoke cooperative effects arising from the acidic sites of the alumina. This would be compatible with the fact that only a partial poisoning of the supported catalyst was observed. Obviously, however, a

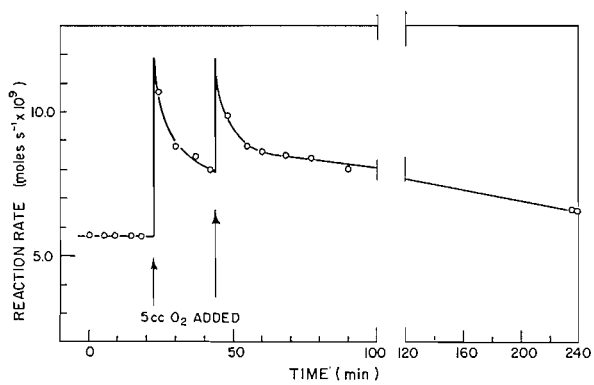


FIG. 3. Effect of oxygen pulses on the rate of desulfurization of thiophene over MoS_2 catalyst V at 289 °C and 1.2% conversion. Partial pressures: thiophene 20 torr; hydrogen 740 torr. Flow 21 ml/min. Catalyst weight 75 mg.

Can. J. Chem. Downloaded from www.nrcresearchpress.com by 210.87.254.42 on 09/05/12
For personal use only.

more detailed study is required before specific sites can be identified with any degree of confidence.

Finally it is worthy of note that oxygen addition, as demonstrated in Fig. 3, led to an immediate doubling of the desulfurization rate over catalyst V, followed by gradual return to the initial rate over a period of hours. At the same time the product composition was completely unchanged, indicating that desulfurization and hydrogenation sites, if distinct from each other, were affected to the same extent. Isomerization was too close to equilibrium for significant conclusions to be drawn regarding the sites pertinent to that reaction. Similar experiments performed during butene hydrogenation resulted in the same qualitative behavior, but the effect was much more marked in that the hydrogenation rate was increased by a factor of 50–100. We have at present no explanation of these results. However, since oxygen is a strong electron acceptor, it is tempting to find an answer in terms of the electronic properties of MoS_2 which is to be regarded as a semiconductor. An indirect promotion through water formation can probably be ruled out, because under all conditions which were tried water was found to act as a poison.

ACKNOWLEDGMENTS

We thank D. Kulawic for the measurement of surface areas and P. Tymchuk for spectrographic analyses.

REFERENCES

1. P. J. Owens and C. H. Amberg. Advan. Chem. Ser. **33**, 182 (1961).
2. P. Desikan and C. H. Amberg. Can. J. Chem. **41**, 1966 (1963).
3. P. Desikan and C. H. Amberg. Can. J. Chem. **42**, 843 (1964).
4. P. J. Owens and C. H. Amberg. Can. J. Chem. **40**, 941 (1962).
5. P. J. Owens and C. H. Amberg. Can. J. Chem. **40**, 947 (1962).
6. F. T. Eggertsen and R. M. Roberts. J. Phys. Chem. **63**, 1981 (1959).

Can. J. Chem. Downloaded from www.nrcresearchpress.com by 210.87.254.42 on 09/05/12
For personal use only.

Can. J. Chem. Downloaded from www.nrcresearchpress.com by 210.87.254.40 on 09/05/12
For personal use only.

ÉTUDE DES SPECTRES DE RÉSONANCE PARAMAGNÉTIQUE ÉLECTRONIQUE DE RADICAUX ALLYLIQUES POLYORIENTÉS

CLAUDE CHACHATY
Service de Chimie physique, Centre d'Études Nucléaires de Saclay,[1] *France*

ET

JEAN MARUANI
Centre de Mécanique Ondulatoire Appliquée,[2] *Paris, France*

Reçu le 20 avril 1966

RÉSUMÉ

On a étudié, à l'aide de calculs électroniques de formes de raies, les effets d'anisotropies hyperfines sur les spectres de résonance paramagnétique électronique de radicaux allyliques polyorientés. Les formes de raie calculées s'avèrent fortement dépendantes de l'orientation relative des tenseurs, donc susceptibles de caractériser les structures isomériques possibles. La comparaison entre les spectres calculés après introduction de l'anisotropie de **g** et ceux mesurés pour différents composés monoéthyléniques irradiés aux γ a permis d'identifier les radicaux allyliques produits et de montrer que, dans la plupart des cas, ces radicaux gardent la configuration géométrique de la molécule initiale.

ABSTRACT

The effect of the hyperfine coupling anisotropy on the shape of the electron spin resonance spectra of randomly oriented allyl radicals has been studied by means of electronic computer calculation. The line shape has been shown to be strongly dependent on the relative orientation of the tensor axes, and it can be used, therefore, to characterize the structural isomerism of the radical. The comparison of the computed spectra, taking account of the **g** tensor anisotropy, with the spectra recorded after γ irradiation of several monoethylenic compounds, allowed the identification of the produced allyl radicals and showed that, in most cases, these radicals keep the geometrical configuration of the corresponding undamaged molecules.

I. INTRODUCTION

Bien que les spectres de résonance paramagnétique electronique (r.p.e.) des radicaux produits dans des échantillons liquides (p.ex., 1) ou monocristallins (p.ex., 2, 3) fournissent des informations des plus précises sur la structure électronique et géométrique des espèces, ainsi que sur leurs interactions avec l'environnement, les physico-chimistes sont souvent amenés à faire des expériences sur des solides polycristallins ou amorphes. L'interprétation des spectres obtenus dans ces conditions peut présenter cependant de grandes difficultés, en raison d'effets d'anisotropie qui peuvent soit élargir plus ou moins asymétriquement les composantes, soit donner naissance à des singularités susceptibles d'être attribuées par erreur à une structure hyperfine mal résolue. Depuis une quinzaine d'années, un certain nombre d'études, aussi bien expérimentales que théoriques, ont été faites sur ce problème (p.ex., 4, 5). Les choses se simplifient considérablement lorsqu'on n'a qu'un petit nombre de tenseurs, de préférence axiaux, à axes principaux confondus, et que les raies "satellites" (p.ex., 5*d*) sont négligeables et l'élargissement des composantes (p.ex., 4*d*, 5*a*, 5*c*, 5*d*), peu important. Dans le cas, général, de plusieurs tenseurs hyperfins orientés dans tous les sens, avec possibilité de raies "satellites" et élargissement élémentaire important, le problème devient analytiquement inextricable, et sa seule méthode d'approche est le calcul électronique. Dans un article antérieur (6), on a étudié les diverses possibilités offertes par le calcul électronique des formes de raie associées à des

[1]*B.P n° 2, 91 Gif-sur Yvette.*
[2]*23 rue du Maroc, Paris 19e.*

hamiltoniens de spin supposés. Nous nous proposons ici de fournir une nouvelle application de cette méthode, à l'étude systématique des spectres de radicaux allyliques polyorientés.

Ce travail comporte deux parties: dans la première, on analyse les spectres calculés, pour l'ensemble des radicaux allyliques possibles à protons σ (p.ex., 8) seulement, en négligeant l'anisotropie de $\mathbf{g}$; dans la seconde, on se sert des spectres calculés pour identifier, après introduction de l'anisotropie de $\mathbf{g}$, les radicaux allyliques produits par irradiation γ de composés monoéthyléniques.

II. ANALYSE DES SPECTRES CALCULÉS

Nous allons étudier maintenant la structure des spectres calculés pour des radicaux produits par substitution aux protons du radical allyle de groupes ne contribuant pas à la structure hyperfine et ne perturbant pas les densités de spin π (p.ex., 8) sur les carbones centraux. Ces radicaux peuvent être définis par la donnée des positions des protons restants, repérés par leurs numéros dans la Fig. 1.

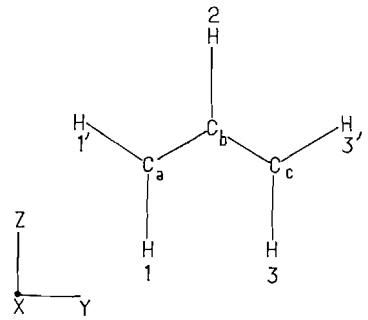


FIG. 1. Formule développée plane du radical allyle, avec représentation des axes principaux des tenseurs de H_1, H_2 et H_3.

Des radicaux de ce type ont été mis en évidence dans différentes matrices rigides (5*c*, 7). Un certain nombre d'études, tant expérimentales (1, 3) que théoriques (p.ex., 8), ont montré que la densité de spin π sur le carbone médian est négative et de l'ordre du tiers de celles, positives, sur les carbones extrêmes. Ces densités ne varient guère par substitution de groupes carboxyliques à des hydrogènes de l'allyle ($\rho_a = \rho_c = 0.58$, $\rho_b = -0.16$ pour l'allyl (1); $\rho_a = \rho_c = 0.57$, $\rho_b = -0.19$ pour le dérivé dicarboxylé en 1′,3′ (3)). Le paramètre Q_σ de l'interaction σ–π (p.ex., 8) n'étant pas non plus très modifié par de telles substitutions (1, 3), les couplages ne varieront guère quand on décrira la série ainsi constituée. Nous avons alors adopté, pour valeurs principales moyennes des tenseurs hyperfins:

pour les positions 1, 2 et 3, les valeurs mesurées sur le composé obtenu par substitution de groupes carboxyliques en 1′, 3′ (3):

$$c^x_{1,3} = -12.5\ \text{G},\ c^y_{1,3} = -18.9\ \text{G},\ c^z_{1,3} = -6.4\ \text{G},$$

$$c^x_2 = +2.5\ \text{G},\ c^y_2 = +6.1\ \text{G},\quad c^z_2 = \pm 4.3\ \text{G};$$

pour les positions 1′ et 3′, celles mesurées en 1 et 3 (3) modifiées pour tenir compte de la différence des interactions dipôlaires de 1 et 1′ avec ρ_c et, symétriquement, de 3 et 3′ avec ρ_a, soit:

$$c^x_{1',3'} = -13.0\ \text{G},\ c^{y',y''}_{1',3'} = -17.8\ \text{G},\ c^{z',z''}_{1',3'} = -5.8\ \text{G},$$

Can. J. Chem. Downloaded from www.nrcresearchpress.com by 210.87.254.40 on 09/05/12
For personal use only.

y' et y'' et z' et z'' désignant, respectivement, les directions perpendiculaires et parallèles aux liaisons $C_aH_{1'}$ et $C_cH_{3'}$. De cet ensemble de valeurs principales, on déduit les couplages isotropes:

$$a_{1,1',3,3'} = -12.45 \text{ G}, \quad a_2 = +4.3 \text{ G}.$$

Négligeant, ainsi, les effets spécifiques des substituants sur la distribution des densités de spin dans la molécule, nous avons, en particulier, considéré comme équivalents des protons symétriques par rapport au plan passant par l'axe médian et perpendiculaire au plan moléculaire, ce qui réduit le nombre des cas possibles. En outre, dans ce paragraphe, nous n'avons pas du tout tenu compte de l'anisotropie de $\mathbf{g}$, et, quant au reste, nous avons, pour les différents cas étudiés (Fig. 2), considéré les modifications subies par le spectre "isotrope" (ligne 1) à mesure que l'on introduit les différents effets liés à l'anisotropie des $\mathbf{c}_i$: l'élargissement *moyen* des composantes (ligne 2), leur élargissement *spécifique* (ligne 3), et les transitions du type $\Delta M_s = 1$, $\Delta M'_I = 1$ (ligne 4) (M'_I désignant la projection du spin nucléaire sur la résultante du champ externe et du champ interne créé par le spin électronique orienté). Nous définissons l'élargissement *moyen* comme un élargissement supplémentaire donné par:

$$[1] \qquad \sigma = 2\left(\frac{1}{3} M_2^d\right)^{1/2} = \left(\frac{1}{3}\sum_i \frac{1}{3}\sum_u (b_i^u)^2\right)^{1/2},$$

où les b_i^u sont les valeurs principales des parties dipôlaires des $\mathbf{c}_i$, M_2^d est le deuxième moment lié aux parties dipôlaires des tenseurs hyperfins, et le coefficient $\frac{1}{3}$ provient d'une optimisation de sa contribution à l'élargissement des différentes raies pour les différentes structures. Cette largeur s'ajoute à la largeur *élémentaire*, λ, pour donner la largeur *globale*, Λ, suivant la relation:

$$[2] \qquad \Lambda = (\sigma^2 + \lambda^2)^{1/2}$$

où λ a partout été pris égal à 3 G. Les spectres de la ligne 4 sont calculés pour la bande X ($H_c = 3\,300$ G, $H_p = 5.02$ G).

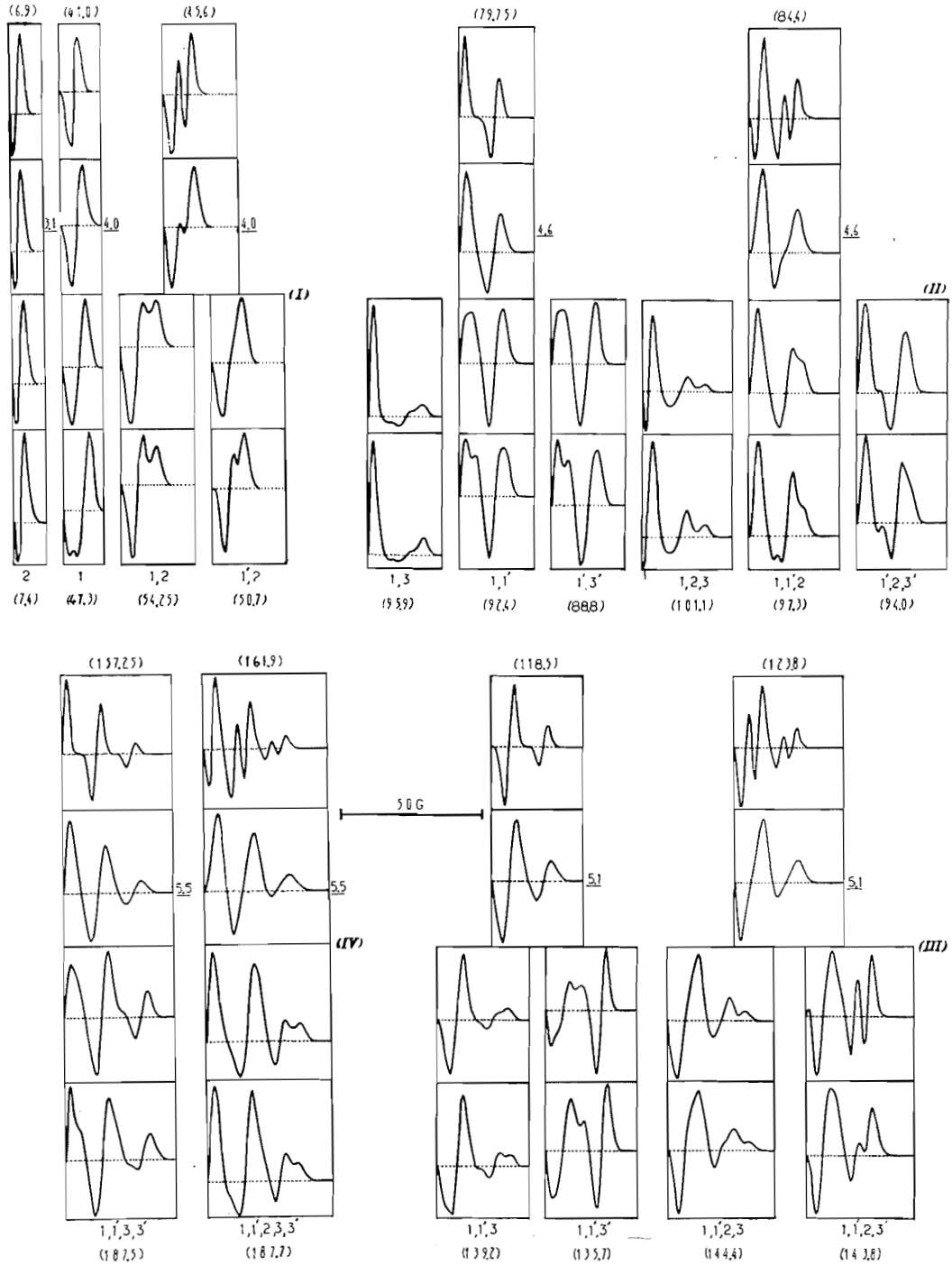
Avant de passer à l'analyse des spectres calculés, nous allons rappeler brièvement les notions de champs stationnaires et de deuxièmes moments, qui seront utilisées dans l'interprétation de certains d'entre eux. On démontre que, si un radical a un seul système d'axes privilégié pour ses tenseurs, les positions des singularités de son spectre polycristallin seront liées de manière simple aux valeurs principales de ceux-ci (p.ex., 4, 5), en raison du fait que les positions des raies "monocristallines" sont stationnaires par rapport à tout changement d'orientation quand le champ externe est aligné suivant l'un des axes (orientations canoniques) (p.ex., 2, 3). Les diagrammes de champs stationnaires consistent alors en la superposition des raies correspondant à ces orientations canoniques, à l'exclusion de toutes les autres (p.ex., 6, 9). On ne pourra constituer de diagrammes de champs stationnaires lorsque les tenseurs auront des axes principaux très différents, ou que les transitions "interdites" ($\Delta M_S = 1$, $\Delta M'_I = 1$), d'intensités toujours nulles aux orientations canoniques (p.ex., 2), contribueront de façon notable au spectre polycristallin. Nous utiliserons aussi la notion de deuxième moment: si $F(H)$ est une courbe d'absorption "polycristalline", son deuxième moment est défini par la relation:

$$[3] \qquad M_2 = \int_{-\infty}^{+\infty} F(H)(\Delta H)^2 \, dH,$$

et il est donné, en l'absence d'anisotropie de $\mathbf{g}$, et pour des noyaux de spin $\frac{1}{2}$, par l'expression (5*d*, 6):

$$[4] \qquad M_2 = \frac{1}{12}\sum_i \sum_u (c_i^u)^2 + \frac{\lambda^2}{4}.$$

Can. J. Chem. Downloaded from www.nrcresearchpress.com by 210.87.254.40 on 09/05/12
For personal use only.



Can. J. Chem. Downloaded from www.nrcresearchpress.com by 210.87.254.40 on 09/05/12
For personal use only.

FIG. 2. Formes de raie calculées, à l'aide de tenseurs hyperfins normalisés pour l'ensemble des radicaux allyliques possibles possédant des protons σ seulement. La position de ceux-ci est indiquée au bas de chaque colonne, à l'aide de la numérotation apparaissant Fig. 1. Seules les dérivées premières des courbes d'absorption ont été représentées. Les tenseurs hyperfins de H_1, H_2 et H_3 (Fig. 1) utilisés dans le calcul sont ceux mesurés sur un monocristal d'acide glutaconique irradié (3) omission étant ici faite de léger défaut de parallélisme entre leurs axes; ceux de H_1' et H_3' sont ceux de H_1 et H_3 modifiés pour tenir compte de l'interaction dipôlaire plus faible avec la densité de spin π sur le carbone opposé (la disposition relative de leurs axes étant déduite de la symétrie du système). Le tenseur **g** a été partout négligé, seule une moitié de chaque spectre étant alors calculée. Les spectres où l'on a tenu compte des transitions du type $\Delta M_I' = 1$ sont calculés pour la bande *X* seulement. La largeur monocristalline a été prise égale à celle qui fournira (courbe φ de la Fig. 4) la reconstitution la plus fidèle du spectre polycristallin expérimental (courbe *f* de la Fig. 4) de l'acide glutaconique irradié. Ligne 1: l'anisotropie des couplages hyperfins est omise; ligne 2: il en est tenu compte seulement par un élargissement supplémentaire moyen des composantes (souligné); ligne 3: l'anisotropie des couplages hyperfins est explicitement introduite, mais les transitions du type $\Delta M_I' = 1$, quoique non toujours "satellites" sont ici aussi négligées; ligne 4: on tient compte de toutes les transitions possibles. Les deuxièmes moments totaux des première et dernière lignes, exprimés en G^2, sont indiqués entre parenthèses.

Nous avons déjà employé cette expression pour définir la largeur globale des composantes isotropes d'un spectre.

Les différentes formes de raie calculées pour le cas d'un proton unique localisé en la position 2 sont constituées (Fig. 2,I) par une bande simple, de largeur sensiblement constante (comparer les seconds moments calculés pour les lignes supérieure et inférieure). Ceci n'est pas étonnant, si l'on considère que:

(*a*) la contribution au second moment de $\mathbf{c}_2$ est faible comparée à celle (2.25 G^2) de la largeur adoptée pour les composantes (ligne 2);

(*b*) la distance (0.9 G) entre les champs stationnaires correspondant aux trois valeurs principales de $\mathbf{c}_2$ est très inférieure à cette même largeur (ligne 3);

(*c*) la transition du type $\Delta M'_I = 1$ (qui se situe vers 5 G) est à une distance de la singularité la plus extrême (vers 3 G) elle aussi sensiblement inférieure à λ, et ne peut donc en être distinguée (ligne 4).

Le cas d'un proton unique en position 1 ou 1′ est un peu plus compliqué. Si, en effet, pour ce cas il n'y a guère de différence entre les spectres calculés aux lignes 1, 2 et 3—les distances entre champs stationnaires étant encore de l'ordre (3.1 G) de l'élargissement élémentaire—l'introduction de la transition supplémentaire produit (ligne 4) une complication du spectre, cette transition se produisant au voisinage (5.0 G) du champ stationnaire intermédiaire (6.4 G) de la bande principale.

Dans les colonnes suivantes, nous avons ajouté au proton 1, puis 1′, le proton 2 (les figures des deux premières lignes sont communes aux deux colonnes). La différence, sensible, entre les spectres relatifs aux différentes structures provient moins des écarts, petits, entre les valeurs de $\mathbf{c}_1$ et celles de $\mathbf{c}_{1'}$ que de l'écart, considérable, entre les orientations de leurs axes par rapport à ceux de $\mathbf{c}_2$. Le spectre correspondant à la structure 1,2 calculé sans raies "satellites" s'explique aisément par la méthode des champs stationnaires (Fig. 3*a*). Les spectres des deux autres structures pourraient eux aussi donner lieu à un diagramme approché de champs stationnaires, considérant que la plus petite valeur principale de chaque tenseur est, à 30° près, orientée comme la plus grande valeur principale de l'autre, les axes intermédiaires étant toujours confondus (ce qui explique que l'on n'observe que trois bandes binômiales sans structure). L'introduction des transitions supplémentaires modifie les spectres dans le même sens dans les deux cas. Comme on pourra le vérifier aussi dans les colonnes qui suivent, le remplacement de la partie anisotrope des tenseurs par un élargissement moyen supplémentaire (ligne 2) peut, dans certains des cas, permettre de reproduire, à peu de chose près, la moyenne des spectres calculés sans les transitions supplémentaires (ligne 3) (mais, naturellement, elle ne permet pas de distinguer entre les différentes structures).

Can. J. Chem. Downloaded from www.nrcresearchpress.com by 210.87.254.40 on 09/05/12
For personal use only.

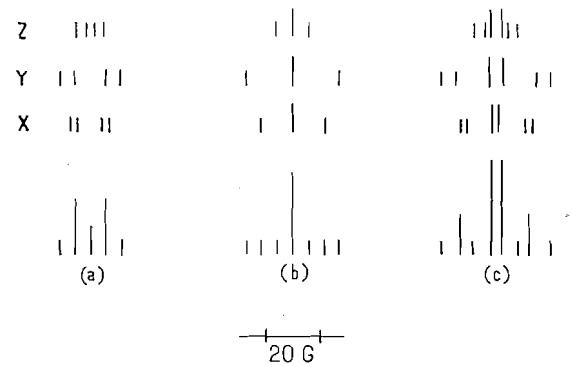


FIG. 3. Champs stationnaires des spectres des différentes structures radicalaires allyliques à liaisons C—H parallèles: (*a*) 1,2; (*b*) 1,3; (*c*) 1,2,3. De haut en bas sont indiqués les champs de résonance correspondant aux différentes orientations canoniques, indiquées à gauche en marge; les hauteurs des raies sont évaluées compte-tenu des dégénérescences. On a fondu, dans les derniers diagrammes (où les différents schémas sont superposés), les raies dont les distances sont inférieures à la largeur utilisée dans les calculs de formes de raie présentés dans Fig. 2. Les raies "satellites" ont été partout négligées.

Les trois colonnes qui suivent (Fig. 2,II) présentent les spectres calculés pour les trois structures comportant deux protons sur les carbones extrêmes 1,3; 1,1′ et 1′,3′. Remarquons que la légère différence entre les spectres calculés pour ces deux dernières est uniquement due aux petites différences entre les valeurs principales des tenseurs primés et non primés, les axes principaux ayant les mêmes orientations relatives dans les deux cas. Le spectre de 1,3 est, par contre, très différent, la bande centrale du triplet étant, cette fois, très mince—du même ordre de largeur que les composantes—et les deux bandes extrêmes, larges et bien structurées. Ces particularités peuvent aisément s'expliquer par des champs stationnaires très prononcés dans ce cas, les tenseurs étant strictement équivalents et ayant leurs axes parallèles (Fig. 3*b*). Les trois inflexions de chaque bande latérale correspondent, au recouvrement près, aux positions différentes de chaque raie extrême aux trois orientations canoniques, tandis que la raie centrale, la plus intense, garde la même position à toutes les orientations. Pour les structures 1,1′ et 1′,3′, on ne peut appliquer qu'un diagramme approché de champs stationnaires, considérant que les deux protons sont, à 30° près, à angle droit: on arrive à expliquer ainsi la quasi-isotropie de la bande latérale et l'élargissement de la bande centrale. On peut encore noter que, comme on pouvait s'y attendre, d'après une remarque antérieure, l'introduction des raies "satellites" a, sur les spectres, un effet d'autant plus marqué que, toutes choses égales d'ailleurs, les champs stationnaires sont moins prononcés.

Si l'on ajoute un proton 2 aux structures qui viennent d'être décrites, on obtient les spectres présentés dans les colonnes qui suivent (Fig. 2,II). Le premier de ces spectres, calculé pour la structure 1,2,3 sans raies "satellites", peut encore s'expliquer par des champs stationnaires prononcés (Fig. 3*c*). On constate que, par l'introduction du proton 2, le pic central de chaque bande extrême se relève et s'élargit au détriment de sa singularité externe, tandis que la bande centrale se dédouble et s'élargit en recouvrant partiellement les singularités internes. Comme prévu, les raies "satellites" ne modifient pas fondamentalement ce schéma. Nous verrons plus loin (Fig. 4) l'effet produit par l'anisotropie de **g**. Les spectres des deux autres structures peuvent, eux aussi, être utilement comparés aux spectres des structures correspondantes sans proton 2. Le changement produit par l'introduction du proton 2 est plus considérable pour la structure 1,1′,2, où

Can. J. Chem. Downloaded from www.nrcresearchpress.com by 210.87.254.40 on 09/05/12
For personal use only.

$\mathbf{c}_2$ a les mêmes axes que $\mathbf{c}_1$, que la structure 1′,2,3′, où $\mathbf{c}_2$ a des axes intermédiaires entre ceux de $\mathbf{c}_{1'}$ et ceux de $\mathbf{c}_{3'}$ (et contribue donc surtout à élargir les bandes) et ce, aussi bien avec que sans raies "satellites". Bien entendu, la méthode des champs stationnaires n'est alors pas applicable.

Les deux premières colonnes de la Fig. 2,III se rapportent aux structures comportant trois protons sur les carbones extrêmes. La structure "en étoile," 1,1′,3′, devrait fournir des spectres très semblables à ceux calculés avec les seuls couplages isotropes (lignes 1 et 2), puisque, pour cette structure, les anisotropies hyperfines se compensent pour donner à toute orientation les mêmes décalages. Mais, curieusement, ce n'est pas ce qui se produit; les spectres 1,1′,3 ressemblent le plus aux spectres isotropes; la bande centrale est à peine élargie, seule la bande extrême acquérant une structure. Pour 1,1′,3′, la bande latérale reste bien isotrope, mais la bande centrale s'élargit en se structurant, faisant perdre au spectre son allure de quartet binômial. La méthode des champs stationnaires n'étant guère ici utilisable, on ne peut comprendre ces singularités qu'en se référant aux spectres, plus simples, des structures 1,3 et 1′,3′. Nous aurons à utiliser plus loin la différence, considérable, des spectres correspondant à ces deux structures, dans l'identification des radicaux produits par irradiation de poudres polycristallines.

L'adjonction d'un proton en 2 dans les structures qui précèdent produit une modification des spectres très sensible pour le composé "en étoile", mais plus légère—sensible surtout aux extrêmités—pour l'autre. Ici encore, c'est le spectre du dernier qui paraît le mieux reproduit dans l'approximation des composantes isotropes élargies (ligne 2), à l'épaulement latéral près. Les spectres de 1,1′,2,3 et de 1,1′,2,3′ peuvent encore être utilement comparés à ceux, précédemment étudiés, des structures 1,2,3; 1,1′,2 et 1′,2,3′. Pour 1,1′,2,3′, l'introduction des raies "satellites" paraît agir surtout en élargissant simplement les composantes. Ces spectres nous serviront eux-aussi ultérieurement.

Si l'on a deux protons sur chaque carbone extrême (Fig. 2,IV), une seule structure est possible, et l'on obtient par le calcul complet un spectre d'allure quasi-binômiale (dernière ligne de la première colonne). L'interprétation détaillée de ce spectre n'étant guère possible, nous ne nous y attarderons pas, retenant seulement que plus le nombre de protons d'un radical sera grand, mieux le spectre pourra être reproduit, à un élargissement moyen supplémentaire près, à l'aide de simples couplages isotropes. L'adjonction à ce composé d'un proton en 2, pour aboutir au radical allyle lui-même, n'apportera (deuxième colonne) que des différences de détail à la structure des spectres, en particulier un dédoublement de la bande extrême.

III. IDENTIFICATION DES RADICAUX PRODUITS

1. *Conditions expérimentales*

Nous avons irradié par les rayons γ du ^{60}Co une série de composés monoéthyléniques, afin de comparer les spectres théoriques décrits dans le paragraphe précédent à des spectres expérimentaux.

Les produits utilisés étaient l'alcool allylique, les acides crotonique, citraconique, mésaconique, glutaconique, itaconique et *trans*-aconitique, et l'anhydride *cis*-aconitique. A part le premier et le dernier composés, tous ont été purifiés par recristallisation dans l'eau ou l'acétone puis dessication sous vide pendant 24 heures. Les échantillons étaient dégazés et scellés sous vide avant irradiation dans des tubes en silice "Spectrosil".

Les irradiations ont été effectuées à 77 °K avec des doses allant de 2 à 3 Mrads et jusqu'à 10 Mrads pour les composés donnant des radicaux peu stables à température ordinaire.

Can. J. Chem. Downloaded from www.nrcresearchpress.com by 210.87.254.40 on 09/05/12
For personal use only.

Can. J. Chem. Downloaded from www.nrcresearchpress.com by 210.87.254.40 on 09/05/12
For personal use only.

Les mesures étaient effectuées à l'aide d'un spectromètre fonctionnant à 9 250 MHz, le champ magnétique étant mesuré par un magnétomètre à résonance nucléaire (Varian F 8) relié à un fréquencemètre. Les échantillons, pendant les mesures, étaient refroidis par l'azote liquide à 77 °K, et, entre 95 °K et 300 °K, en les plaçant dans un cryostat à azote refroidi situé dans la cavité du spectromètre.

2. Résultats obtenus

Nous avons rassemblé dans le Tableau I les différents types de composés étudiés et de radicaux allyliques pouvant en dériver par ruptures de liaisons simples, si l'on fait abstraction d'isomérisations éventuelles. Ces composés sont classés selon les nombres et positions des substituants. Les autres radicaux pouvant se former par arrachement d'hydrogène ou de groupement oxygéné sont de type σ. Il peut aussi se former des radicaux π, saturés, par addition sur la double laison éthylénique.*

Nous avons comparé les spectres obtenus par irradiation aux spectres étudiés dans le paragraphe précédent. Pour réaliser un meilleur accord entre spectres expérimentaux et théoriques, nous avons dû modifier la largeur monocristalline des composantes et introduire l'anisotropie de **g**. Les valeurs principales de ce tenseur étant sensiblement les mêmes, à l'approximation de Stone (10) près, pour tous les radicaux de cette série, nous avons adopté, simplement, pour ces valeurs celles mesurées sur un monocristal du composé dicarboxylé en 1′,3′ (3), soit:

$$g_x = 2.0021, \qquad g_y = g_z = 2.0036,$$

les axes principaux étant sensiblement ceux de $\mathbf{c}_1$, $\mathbf{c}_2$ et $\mathbf{c}_3$, définis prédédemment.

Les résultats obtenus sont les suivants (Fig. 4).

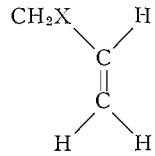
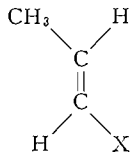
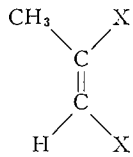
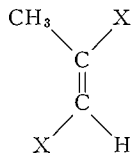
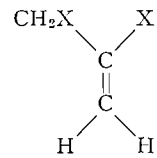
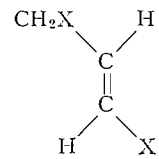
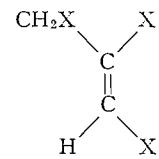
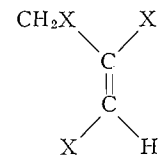
I,1, X = OH, alcool allylique (CH_2=CH—CH_2OH). Le spectre de l'alcool allylique irradié à 77 °K a été interprété (11) comme la superposition des spectres de l'allyle (CH_2=CH=CH_2) et de l'hydroxyallyle (CH_2=CH=$CHOH$). Par réchauffement progressif à 150 °K, ce spectre se transforme en un quartet dont les raies sont approximativement écartées de 12 à 13 G, correspondant au radical hydroxyallyle (11). Celui-ci pourrait présenter les deux formes: 1,1′,2,3 et 1,1′,2,3′; le spectre enregistré à 150 °K (courbe *b*), dont la résolution est optimum, fait nettement ressortir, à cette température, la prédominance de la deuxième forme (courbe β_1) sur la première (courbe β_2). La photolyse à 2 537 Å des radicaux produits par l'irradiation de l'alcool allylique conduit, au contraire, à une transformation du spectre observé à 77 °K en celui du radical allyle (11) (courbe *a*), en bon accord avec le spectre calculé pour cette structure (courbe α). Le nombre des radicaux étant inchangé, ceci est l'indice d'une transformation des radicaux hydroxyallyle, absorbant dans l'ultraviolet, en radicaux allyle.

I,2, X = COOH; acide trans-crotonique (CH_3—CH=CH—$COOH$). L'irradiation de l'acide *trans*-crotonique à 77 °K fournit un spectre complexe et mal résolu, que nous n'avons pu interpréter. La résolution de ce spectre augmente avec la température, et l'on obtient vers 0 °C un quartet binômial d'écart hyperfin 12–13 G (courbe *c*). Aucun des spectres calculés pour les deux formes isomères 1,1′,2,3 (courbe β_2) et 1,1′,2,3′ (courbe β_1), ne concordant de manière satisfaisante avec l'expérience, on a cherché à réaliser un meilleur accord en superposant, en proportions variables, les spectres correspondant à ces deux structures. Le meilleur accord est obtenu avec des proportions respectives de 60 et 40% (courbe γ). Ainsi, il semble qu'il y ait isomérisation partielle du squelette

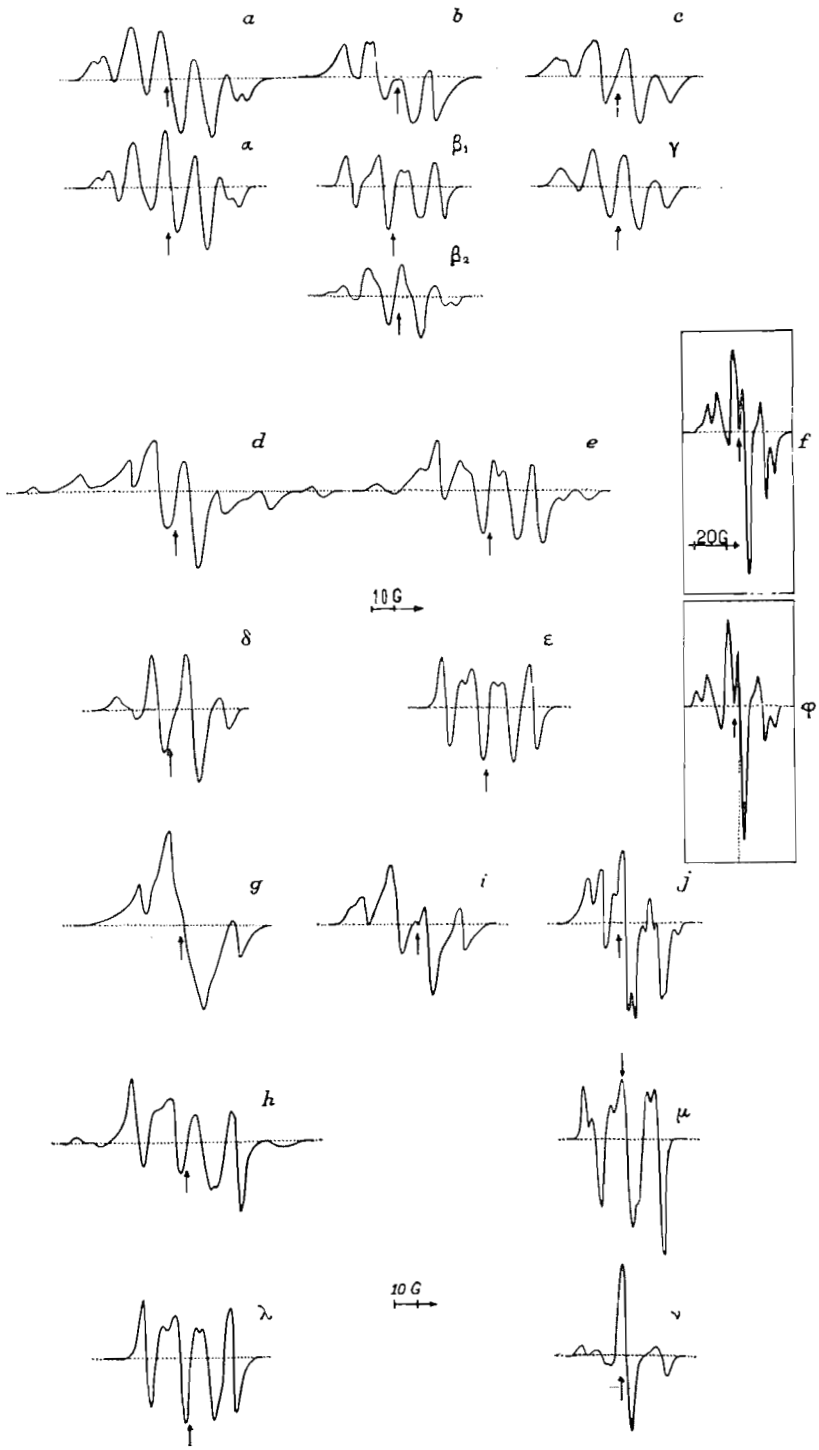
**On trouvera une définition des notions de radicaux π, radicaux σ, protons π, protons σ, densités de spin π, etc., dans, par exemple, les réfs. 8 et 13.*

TABLEAU I

Différents types de radicaux allyliques pouvant dériver de composés monoéthyléniques

	Composé monoéthylénique initial		Radicaux allyliques possibles (Fig. 1)
I	1		1,1′,2,3 1,1′,2,3′ 1,1′,2,3,3′
	2		1,1′,2,3
II	1		1,1′,3
	2		1,1′,3′
	3		1,1′,3′ 1,1′,3 1,1′,3,3′
	4		1,2,3 1′2,3 1,1′,2,3
III	1		1,3 1′3 1,1′,3
	2		1′,3′ 1′,3 1,1′,3′

Can. J. Chem. Downloaded from www.nrcresearchpress.com by 210.87.254.40 on 09/05/12
For personal use only.



Can. J. Chem. Downloaded from www.nrcresearchpress.com by 210.87.254.40 on 09/05/12
For personal use only.

FIG. 4. Identification des radicaux allyliques produits par irradiation de composé monoéthyléniques. Les lettres latines indiquent les spectres mesurés, les lettres grecques, les spectres calculés. Les traits marqués sous les spectres—expérimentaux et théoriques—indiquent le champ de résonance du DPPH (g = 2.0036). Les spectres théoriques sont calculés avec les mêmes couplages hyperfins et les mêmes champs de résonance qu'en Fig. 2 mais en tenant compte, cette fois, de l'anisotropie de **g** (supposée la même que celle mesurée sur un monocristal d'acide glutaconique irradié (3)). La largeur monocristalline, variable, est indiquée séparément pour chaque espèce. (*a*): alcool allylique irradié aux γ à 77 °K puis photolysé à 2 537 Å; (α) radical allyle (λ = 3.5 G, raies "satellites" négligées). (*b*): le même que précédemment mais réchauffé à 150 °K après irradiation; (β_1) et (β_2): radicaux 1,1′,2,3′ et 1,1′,2,3 (λ = 3.5 G et raies "satellites" introduites seulement dans le premier cas, où l'on néglige le proton 2). (*c*): acide *trans*-crotonique irradié à 77 °K puis réchauffé à 300 °K; (γ): mélange de 0.6(1,1′,2,3′) + 0.4(1,1′,2,3) (λ = 4.5 G et pas de raies "satellites"). (*d*), (*e*) et (*f*): acides citraconique, mésaconique et *trans*-glutaconique irradiés à température ordinaire; (δ), (ϵ) et (φ): radicaux 1,1′,3; 1,1′,3′ et 1,2,3 (λ = 4 G, 3.5 G et 3 G respectivement; raies "satellites" incluses dans le dernier cas seulement). (*g*), (*h*), (*i*) et (*j*): spectres mesurés après irradiation de l'acide *trans*-aconitique à 77 °K (*g*) et à 300 °K (*h*) et de l'anhydride *cis*-aconitique à 77 °K (*i*) et à 300 °K (*j*); (λ), (μ) et (ν): spectres calculés pour les structures 1,1′,3′ (λ = 3.5 G), 1,3′ (λ = 2.5 G) et 1,3 (même largeur), raies "satellites" incluses.

de l'acide crotonique lorsqu'on irradie à basse température puis qu'on réchauffe. Cette transformation n'apparaît qu'au voisinage de la température ordinaire, en même temps que les radicaux se recombinent.

II,1, X_2 et $X_{3'}$ = COOH, acide citraconique. Le spectre obtenu à 77 °K consiste principalement en un triplet binômial aux bandes écartées de 14 G, mais lorsqu'on élève progressivement la température, on observe un dédoublement des raies et, à partir de 150 °K, on obtient un quartet binômial aux raies écartées de 10 à 11 G (Fig. 5). Cette

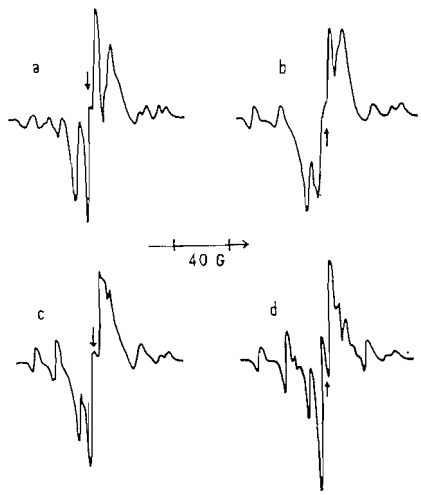


FIG. 5. Evolution réversible avec la température des spectres de l'acide citraconique irradié à 77 °K aux γ: (*a*) 77 °K; (*b*) 130 °K; (*c*) 140 °K; (*d*) 180 °K.

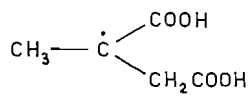
transformation, réversible entre 77 et 200 °K, peut s'expliquer par un non-planéité du radical initialement produit et une évolution progressive par réchauffement vers une forme plane, plus stable (l'interaction de l'électron célibataire s'effectuant principalement avec deux protons σ d'un CH_2 dans le premier cas et les trois protons σ du radical plan dans le second). A température ordinaire, le spectre (courbe *d*) comprend principalement un quartet binômial, qui peut être raisonnablement comparé à celui calculé pour la structure 1,1′,3 (courbe δ). Les bandes parasites observées à toutes température à 30–60 G de la partie centrale des spectres pourraient être dues à la présence, en

Can. J. Chem. Downloaded from www.nrcresearchpress.com by 210.87.254.40 on 09/05/12
For personal use only.

abondance moindre, d'un autre radical, formé par addition sur la double liaison éthylénique. Aux basses températures, la faible interaction de l'électron célibataire avec le proton 2 est prouvée par l'écart réduit des bandes, qui indique une densité de spin π notablement inférieure à 1 sur le carbone a (donc partiellement délocalisée sur C_c), et par le dédoublement partiel de la bande centrale (Fig. 5). La déviation de la planéité est donc faible. La continuité entre les parties principales des spectres mesurés entre 77 et 150 °K (Fig. 5) n'indique pas nécessairement que la transformation entre radical plan et radical distordu se fasse de manière continue; elle peut en effet se faire entre positions privilégiées, seules les proportions respectives des différentes formes variant continûment. Les spectres mesurés étant brouillés par des espèces parasites, et les spectres théoriques correspondant aux deux hypothèses dépendant de nombreux paramètres, il semble difficile de déterminer de manière simple laquelle est vérifiée. Lorsque l'acide citraconique est irradié à 77 °K et réchauffé à température ordinaire ($T \approx 280$ °K), ou irradié à cette température, le spectre obtenu est un quartet, qui ne redonne pas de triplet par refroidissement.

II,2, Acide mésaconique. Contrairement aux spectres obtenus avec l'acide citraconique, les spectres mesurés avec l'acide mésaconique varient assez peu avec la température. A température ordinaire, ils peuvent raisonnablement se comparer (courbe *e*) au spectre calculé pour la structure 1,1′,3′ (courbe ϵ). Ici encore se superpose au spectre allylique celui d'un autre radical, vraisemblablement aussi, saturé.

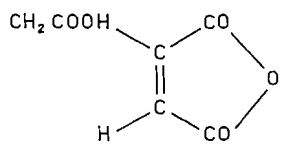
II,3, Acide itaconique. A température ordinaire, l'irradiation de ce composé donne un radical non allylique, de structure



(12). L'examen du spectre obtenu après irradiation à 77 °K suggère la formation simultanée d'un radical allylique, que nous n'avons pu identifier. De ceux que nous avons étudiés, ce composé est le seul avec l'alcool allylique qui contienne un groupe $=CH_2$, qu'on sait être particulièrement propice aux additions sur la liaison double.

II,4, Acide trans-glutaconique. La conformation *cis* ou *trans* du composé commercial n'est pas spécifiée, mais on sait qu'après recristallisation dans l'eau on obtient toujours le deuxième isomère. Le spectre obtenu après irradiation est indépendant de la température d'irradiation, de la température de mesure et du fait que l'acide utilisé a été recristallisé ou non (courbe *f*). Ce spectre, qui consiste principalement en un triplet de doublets, correspond visiblement à une seule espèce. Comme prévisible, il est très proche de celui calculé pour la structure 1,2,3 (courbe φ), toutes les données utilisées dans les calculs étant précisément celles mesurées sur un monocristal de ce composé (3). Ce résultat, conforme à celui démontré par Heller et Cole (3), indique que l'acide glutaconique est bien de la forme *trans*, la formation du radical 1,2,3 n'étant raisonnablement compatible qu'avec cette hypothèse.

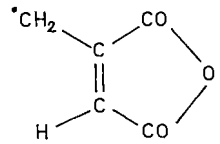
III,1, Anhydride cis-aconitique.



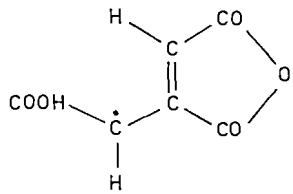
Le spectre enregistré après irradiation à 77 °K est un quartet mal résolu, d'écartement moyen 13 G, dont la résolution augmente avec la température. Sa forme (courbe *i*) est

Can. J. Chem. Downloaded from www.nrcresearchpress.com by 210.87.254.40 on 09/05/12
For personal use only.

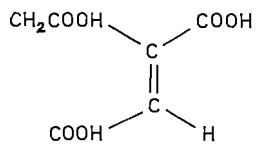
plus proche de celle de la courbe correspondant à la structure 1,1′,3 (courbe δ) que de celle correspondant à la structure 1,1′,3′ (courbe λ). Le radical principal formé dans ces conditions serait donc:



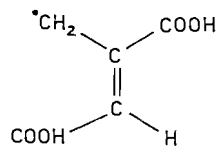
Par irradiation à température ordinaire avec des doses quatre fois plus élevées, on obtient un spectre beaucoup moins intense, comportant trois bandes principales (courbe j). Nous avons comparé ce spectre à ceux calculés pour les structures 1,3′ (courbe μ) et 1,3 (courbe ν). Le spectre expérimental paraît en meilleur accord avec la première forme qu'avec la seconde. Le radical formé serait donc:



III,2, Acide trans-aconitique.



L'irradiation à basse température donne un spectre mal résolu (courbe g), comprenant une bande centrale de 15 G de large et un spectre dont on ne distingue que les bandes extrêmes. Lorsqu'on élève la température, on observe une disparition progressive de la bande centrale, les deux bandes extrêmes étant conservées. Celles-ci s'avèrent faire partie d'un quartet de bandes d'écartement moyen 14 G, le spectre alors obtenu étant semblable à celui qu'on peut obtenir directement par irradiation à température ordinaire (courbe h). Ce dernier est très voisin de celui calculé pour la forme 1,1′,3′ (courbe λ), et correspond donc au radical:



Encore stable à température ordinaire, ce radical pourrait masquer celui qui résulterait, comme pour l'isomère *cis*, de l'arrachement d'un hydrogène. La large raie centrale observée à basse température pourrait être due au radical ·COOH.

IV. CONCLUSIONS

La reproduction exacte des formes de raie expérimentales des radicaux obtenus était rendue difficile par les approximations faites sur les paramètres de l'hamiltonien de spin et la présence, inévitable, d'autres radicaux, souvent non allyliques.

Le meilleur accord était obtenu pour le radical dérivé de l'acide glutaconique, pour lequel les valeurs exactes des tenseurs étaient connues et dont on savait qu'il était le

Can. J. Chem. Downloaded from www.nrcresearchpress.com by 210.87.254.40 on 09/05/12
For personal use only.

seul formé par l'irradiation. On peut cependant remarquer que, pour tous les composés que nous avons étudiés, la comparaison entre les spectres expérimentaux et théoriques nous a permis d'établir de manière à peu près sûre la nature des radicaux allyliques produits, et de déterminer leur configuration—*cis* ou *trans*—généralement la même que celle de la molécule initiale. La seule exception observée était celle du radical dérivé de l'acide *trans*-crotonique, dont le spectre a été interprété comme résultant de proportions comparables de radicaux de deux types. Remarquons d'ailleurs que ce spectra était pris au voisinage de la température de disparition des radicaux, zône dans laquelle les mouvements moléculaires, qui tendent à se libérer, peuvent faciliter l'isomérisation.

BIBLIOGRAPHIE

1. R. W. Fessenden et R. H. Schuler. J. Chem. Phys. **39**, 2147 (1963).
2. H. M. McConnell, C. Heller, T. Cole et R. W. Fessenden. J. Am. Chem. Soc. **82**, 766 (1960).
3. C. Heller et T. Cole. J. Chem. Phys. **37**, 243 (1962).
4. (*a*) B. Bleaney. Proc. Phys. Soc. London, A, **63**, 407 (1950). (*b*) R. H. Sands. Phys. Rev. **99**, 1222 (1955). (*c*) F. K. Kneubühl. J. Chem. Phys. **33**, 1074 (1960). (*d*) Ya. S. Lebedev. J. Strukt. Khim. **4**, 22 (1963).
5. (*a*) S. M. Blinder. J. Chem. Phys. **33**, 748 (1960). (*b*) H. Sternlicht. J. Chem. Phys. **33**, 1128 (1960). (*c*) E. L. Cochran, F. J. Adrian et V. A. Bowers. J. Chem. Phys. **34**, 1161 (1961). (*d*) R. Lefebvre. J. Chem. Phys. **33**, 1826 (1960).
6. R. Lefebvre et J. Maruani. J. Chem. Phys. **42**, 1480 (1965).
7. B. Smaller et M. S. Matheson. J. Chem. Phys. **28**, 1169 (1958). M. Fujimoto et D. J. E Ingram. Trans. Faraday Soc. **54**, 1034 (1958). K. A. Maas et D. H. Volman. Trans. Faraday Soc. **60**, 1 (1964). A. T. Bullock and L. H. Sutcliffe. Trans. Faraday Soc. **60**, 625 (1964). P. B. Ayscough et H. E. Evans. Trans. Faraday Soc. **60**, 801 (1964).
8. H. M. McConnell. J. Chem. Phys. **28**, 1188 (1958); Erratum: J. Chem. Phys. **30**, 328 (1960).
9. C. Chachaty. J. Chim. Phys. **62**, 728 (1965).
10. A. J. Stone. Mol. Phys. **7**, 311 (1964).
11. C. Chachaty. Compt. Rend. **259**, 2219, 2423 (1964).
12. M. Fujimoto. J. Chem. Phys. **39**, 826 (1963).
13. C. Heller et H. M. McConnell. J. Chem. Phys. **32**, 1535 (1960).

Can. J. Chem. Downloaded from www.nrcresearchpress.com by 210.87.254.40 on 09/05/12
For personal use only.

Can. J. Chem. Downloaded from www.nrcresearchpress.com by 210.87.254.5 on 09/05/12
For personal use only.

γ-RADIATION-INDUCED HYDROGEN EXCHANGE REACTION IN LIQUID CYCLOHEXANE – HYDROGEN CHLORIDE SOLUTIONS

J. W. FLETCHER AND G. R. FREEMAN
Department of Chemistry, University of Alberta, Edmonton, Alberta
Received June 15, 1966

ABSTRACT

The overall exchange reactions

$$HCl + c\text{-}C_6D_{12} \rightarrow DCl + c\text{-}C_6D_{11}H$$

and

$$DCl + c\text{-}C_6H_{12} \rightarrow HCl + c\text{-}C_6H_{11}D$$

have been initiated by radiolysis and measured by a nuclear magnetic resonance spectroscopic method. The reactions occur by a chain mechanism, with a chain length of $\sim 10^4$ in a 1 *M* solution of hydrogen chloride in cyclohexane. The mechanism is complex.

The exchange reaction can also be initiated by the photolysis of chlorine or of hydrogen chloride.

A chain exchange reaction does not occur between c-C_6H_{12} and DI, D_2S, or ND_3. These results are consistent with the suggestion that the exchange reaction in the cyclohexane – hydrogen chloride system occurs by a free radical chain mechanism.

This type of exchange reaction can cause difficulties in isotopic tracer studies.

INTRODUCTION

In recent studies of the effects of mineral acids on the radiolysis of organic compounds (J. W. Fletcher, unpublished results) it was noted that a radiation-induced hydrogen exchange reaction occurred between hydrogen chloride and cyclohexane. The reaction has a long chain-length in the liquid phase. Since this type of exchange reaction may give erroneous results in isotopic tracer studies, it was of interest to conduct a more detailed kinetic investigation.

The platinum-catalyzed exchange of H and D between c-C_6H_{12} and DCl is a relatively slow reaction (1).

EXPERIMENTAL

Materials

Eastman Spectrograde cyclohexane and Phillips Research grade cyclohexane treated with sulfuric acid to remove olefins were used in these experiments. They both gave the same results. The cyclohexane was saturated with D_2O then dried in vacuum with P_2O_5 which had been transferred in a dry atmosphere.

The perdeutero-cyclohexane, deuterium chloride, perdeutero-ammonia and deuterium sulfide were used as received from Merck, Sharpe and Dohme. Matheson hydrogen chloride and chlorine were fractionated in vacuum before use.

Deuterium iodide was prepared by heating deuterium and iodine with a platinum oxide powder catalyst.

Technique

The exchange reaction was followed by nuclear magnetic resonance (n.m.r.) spectroscopic observation of the buildup or loss of HCl.

The n.m.r. tubes were cleaned with a 3:1 solution of sulfuric and nitric acids and rinsed several times with doubly distilled water. They were then evacuated and heated to about 450 °C, then cooled. Approximately 0.1 ml of D_2O was distilled into each tube and left for 24 h to exchange with the H_2O on the walls. The D_2O was then pumped out and the tubes were heated to about 450 °C.

In the filled cells, the vapor space was kept to less than 10% of the total cell volume, to reduce the amount of hydrogen chloride in the vapor. The high acid concentration samples were contained in heavy wall n.m.r. tubes, to prevent breaking by the HCl pressure.

The acid concentrations are reported in units of molarity (*M*).

Can. J. Chem. Downloaded from www.nrcresearchpress.com by 210.87.254.5 on 09/05/12
For personal use only.

RESULTS

The results of each experiment were plotted in such a way that the pseudo-first order exchange rate constants were obtained.

In the c-C_6H_{12}–DCl system, the formation of HCl was observed. Representative samples, with different DCl concentrations, are shown in Fig. 1.

In the c-C_6D_{12}–HCl system, the destruction of HCl was observed. Representative samples, with different HCl concentrations, are shown in Fig. 2.

To verify that the reaction was indeed an exchange reaction, both the formation of c-$C_6D_{11}H$ and the disappearance of HCl were measured in one c-C_6D_{12}–HCl sample.

[1] $$c\text{-}C_6D_{12} + HCl \rightarrow c\text{-}C_6D_{11}H + DCl$$

The amount of c-$C_6D_{11}H$ formed was found to be equal to the amount of HCl destroyed. In Fig. 3, one set of points represents log ($[HCl]_0/[HCl]$), the other represents log ($[HCl]_0/[HCl]_0 - [c\text{-}C_6D_{11}H]$), and the two sets of points are equivalent to each other.

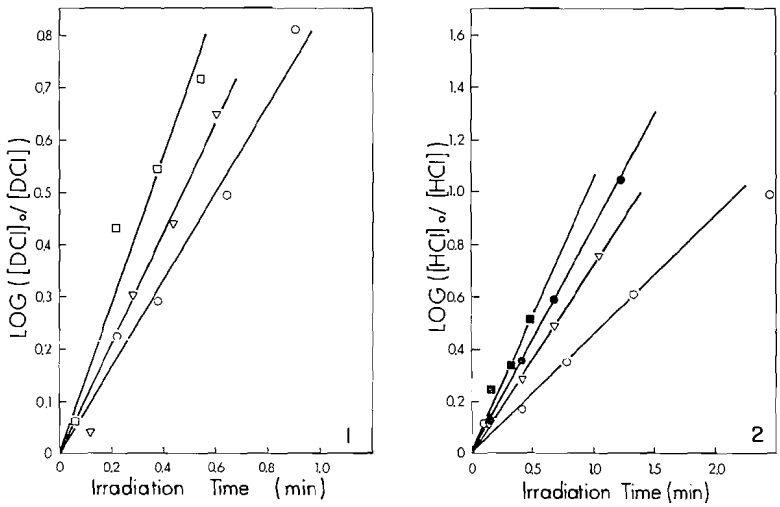


FIG. 1. Exchange of DCl with c-C_6H_{12}. $[DCl]_0$ represents initial DCl concentration. [DCl] = $[DCl]_0$ − [HCl]. Dose rate = 6.08×10^{17} eV/ml min. (□) $[DCl]_0 = 0.177$ M; (△) $[DCl]_0 = 0.200$ M; (○) $[DCl]_0 = 0.310$ M.

FIG. 2. Exchange of HCl with c-C_6D_{12}. $[HCl]_0$ represents initial HCl concentration. Dose rate = 6.08×10^{17} eV/ml min. (■) $[HCl]_0 = 0.075$ M; (●) $[HCl]_0 = 0.139$ M; (△) $[HCl]_0 = 0.351$ M; (○) $[HCl]_0 = 1.780$ M.

The initial rates of the exchange reactions were determined by multiplying the initial acid concentrations by the pseudo-first order rate constants obtained from the slopes of plots such as those in Figs. 1–3 ($k = 2.3 \times$ slope). The initial rates of exchange are plotted against initial acid concentration, at different dose rates, in Figs. 4 and 5. At all dose rates, and in both the c-C_6H_{12}–DCl and the c-C_6D_{12}–HCl systems, the rate–concentration plots have maxima.

The dose rate dependence of the c-C_6H_{12}–DCl exchange reaction is shown in Fig. 6. The rate of the reaction is proportional to approximately the first power of the dose rate.

The length of the chain is indicated by G(exchange) $= 1 \times 10^5$ at $[DCl]_0 = 0.5$ M, and a dose rate $= 6.08 \times 10^{17}$ eV/ml min. The addition of carbon tetrachloride to the system greatly decreased the rate of the exchange reaction (Table I). Carbon tetrachloride was more than 50-fold better as an inhibitor than was $CDCl_3$ (Table I).

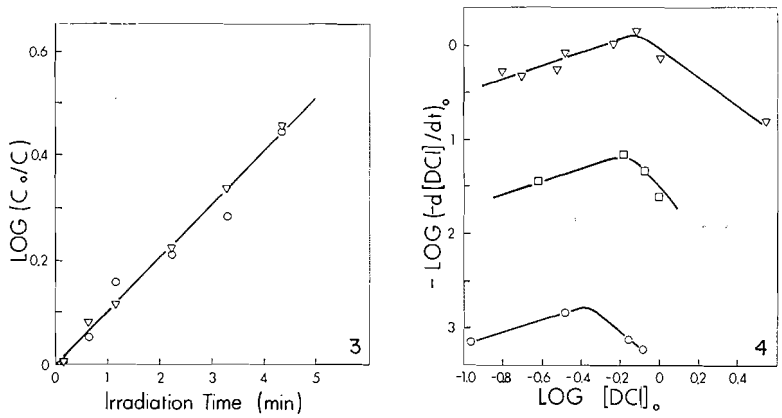


FIG. 3. Formation of c-$C_6D_{11}H$ and destruction of HCl in c-C_6D_{12}–HCl. Dose rate = 6.08×10^{17} eV/ml min. C_0 = initial concentration of HCl = 4.25 M. (△) C = [HCl]; (○) $C = C_0 - [c\text{-}C_6D_{11}H]$.

FIG. 4. The rate of exchange of DCl with c-C_6H_{12} as a function of DCl concentration at different dose rates. (△) 6.08×10^{17} eV/ml min; (□) 5.35×10^{16} eV/ml min; (○) 6.25×10^{14} eV/ml min.

TABLE I

Rate of exchange of c-C_6H_{12} with DCl in the presence of CCl_4 and of $CDCl_3$ ([DCl] = 0.5 M; dose rate = 6.08×10^{17} eV/ml min)

Concentration of additive (M)	$(dc/dt) \times 10^3$
0	1 000
$[CCl_4] = 0.080$	31
$[CCl_4] = 0.62$	6.7
$[CDCl_3] = 1.00$	355

The rate of formation of c-$C_6D_{11}H$ in n-C_6H_{14} containing 25 mole % c-C_6D_{12} and 0.30 M HCl was 1000-fold smaller than it was in a solution of 0.30 M HCl in c-C_6D_{12} (Table II). The corresponding reduction in neo-C_6H_{14} solvent was 200-fold (Table II).

Photolysis of a DCl–c-C_6H_{12} solution in a quartz tube with a 600 W mercury resonance lamp gave complete hydrogen exchange in 5 min. Under these conditions in an initially 1 M DCl solution, the final concentration of the major chain-termination product $C_6H_{11}Cl$ was 1×10^{-3} M. This indicates that the chain length was $\geqslant 10^3$.

TABLE II

Rate of exchange of c-C_6D_{12} with HCl in solution in n-hexane and in neo-hexane ([c-C_6D_{12}] = 25 mole %; [HCl] = 0.3 M; dose rate = 7.8×10^{17} eV/g min)

Solvent	$(d[c\text{-}C_6D_{11}H]/dt) \times 10^3$	G(exchange)
n-C_6H_{14}	0.44	50
Neo-C_6H_{14}	2.38	260
Pure c-C_6D_{12}	520	5.2×10^4

The exchange between DCl and c-C_6H_{12} was also induced by the photolysis of Cl_2, using a high-pressure mercury lamp and a Pyrex reaction cell. Complete exchange was observed in a solution 1 M in DCl and 10^{-2} M in Cl_2. This result indicated a chain length of greater than 10^2. More dilute solutions of Cl_2 were not used because of the difficulty of measuring small quantities of Cl_2.

Can. J. Chem. Downloaded from www.nrcresearchpress.com by 210.87.254.5 on 09/05/12
For personal use only.

A 1 *M* solution of DI in *c*-C_6H_{12} was irradiated for 40 min at a dose rate of 6.08×10^{17} eV/ml min. Within experimental error no exchange was observed, so $G(\text{exchange}) < 30$ in this system.

Similarly, no exchange was observed in a 0.3 *M* solution of D_2S in *c*-C_6H_{12}, after 11 h irradiation at 6.08×10^{17} eV/ml min. Thus, $G(\text{exchange}) < 1.5$ in this system.

In a 0.3 *M* solution of ND_3 in *c*-C_6H_{12}, $G(ND_2H) = 0.8$, within a factor of two.

DISCUSSION

The chain length of the hydrogen exchange reaction between hydrogen chloride and cyclohexane is of the order of 10^4 when the hydrogen chloride concentration is about 1 *M*. No reasonable ionic chain mechanism could be devised to explain the results. The most reasonable free radical chain-propagation steps are

$$[2] \qquad c\text{-}C_6H_{11} + DCl \rightarrow c\text{-}C_6H_{11}D + Cl$$

$$[3] \qquad Cl + c\text{-}C_6H_{12} \rightarrow HCl + c\text{-}C_6H_{11} \quad .$$

High concentrations of HCl (or DCl) inhibit the exchange (Figs. 4 and 5). This might be due to the formation of HCl_2,

$$[4] \qquad Cl + HCl \rightleftarrows HCl_2,$$

which would be less efficient in propagating the chain than is Cl, but which could enter into a chain-termination reaction.[1]

If chain termination occurred by the reactions [5]–[7],

$$[5] \qquad 2c\text{-}C_6H_{11} \rightarrow \text{products}$$

$$[6] \qquad Cl + c\text{-}C_6H_{11} \rightarrow \text{products}$$

$$[7] \qquad 2Cl + M \rightarrow Cl_2 + M,$$

the rate of exchange should have varied as (dose rate)$^{0.5}$. However, the rate of reaction varied approximately as (dose rate)$^{1.0}$ (Fig. 6). This is probably due to inhibition of the reaction by a trace of impurity, which is often observed in long chain processes (2, p. 356).

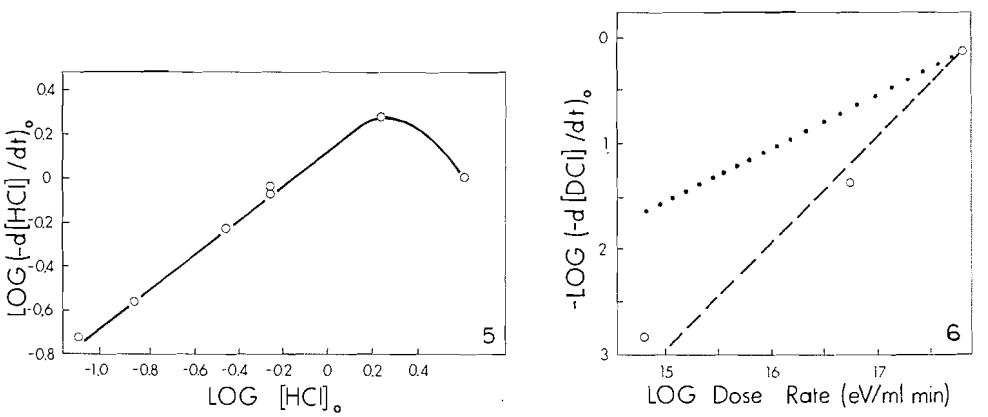


FIG. 5. The rate of exchange of HCl with *c*-C_6D_{12} as a function of HCl concentration at a dose rate of 6.08×10^{17} eV/ml min.

FIG. 6. The rate of exchange of DCl with *c*-C_6H_{12} as a function of dose rate. $[DCl]_0 = 0.3$ *M*. The slope of the broken line is 1.0; that of the dotted line is 0.5.

[1]*It was pointed out by a referee that inhibition could also be caused by association of the* HCl *molecules in the more concentrated* HCl *solutions. The rate of reaction of* *c*-C_6H_{11} *radicals with free* HCl *would probably be faster than with hydrogen-bonded* HCl. *The n.m.r. absorption frequency of the* HCl *proton was observed to shift to lower* τ*-values as the* HCl *concentration was increased. This confirms that the amount of association increased with increasing* HCl *concentration.*

Can. J. Chem. Downloaded from www.nrcresearchpress.com by 210.87.254.5 on 09/05/12
For personal use only.

The inhibition caused by carbon tetrachloride (Table I) can be explained by reactions [8]–[9].

[8] $$c\text{-}C_6H_{11} + CCl_4 \rightarrow c\text{-}C_6H_{11}Cl + CCl_3$$

[9] $$CCl_3 + c\text{-}C_6H_{12} \rightarrow CCl_3H + c\text{-}C_6H_{11}$$

CCl_3 is evidently a less efficient chain carrier than is c-C_6H_{11} and the chain length is shortened.

$CDCl_3$ is a less efficient inhibitor than is CCl_4 because the former is a less efficient chain-transfer agent than is the latter (2, p. 152).

The exchange of hydrogen between c-C_6D_{12} and HCl occurs five times more efficiently in neo-hexane solvent than it does in n-hexane solvent (Table II). This is consistent with the proposed free radical mechanism if the Cl atoms react predominantly with secondary hydrogens on the hydrocarbons.

[10] $$Cl + CH_3CH_2CH_2CH_2CH_2CH_3 \rightarrow HCl + sec\text{-}C_6H_{11}$$

[11] $$Cl + CH_3C(CH_3)_2CH_2CH_3 \rightarrow HCl + CH_3C(CH_3)_2\dot{C}HCH_3$$

The number of secondary hydrogens on a n-hexane molecule is four times as great as the number on a neo-hexane molecule.

Photolysis of DCl by the 1 847 Å mercury line or of Cl_2 by visible light produces atoms which initiate the chain exchange reaction. The Cl atoms undergo reaction [3] and the D atoms also react to produce cyclohexyl radicals.

One would not expect a free radical chain exchange reaction to occur between c-C_6H_{12} and DI, D_2S, or ND_3 because of the inefficiencies of the endothermic propagation steps [12]–[14].

[12] $$I + c\text{-}C_6H_{12} \rightarrow HI + c\text{-}C_6H_{11}$$

[13] $$DS + c\text{-}C_6H_{12} \rightarrow HDS + c\text{-}C_6H_{11}$$

[14] $$c\text{-}C_6H_{11} + ND_3 \rightarrow c\text{-}C_6H_{11}D + ND_2$$

No chain exchange reaction was observed in these systems.

All the experimental results are thus consistent with the suggestion that the hydrogen exchange between cyclohexane and hydrogen chloride occurs by a free radical chain mechanism.

Deuterated polar compounds have been (3, 4) and are currently being used as ion scavengers in radiolysis systems. The amount of ion scavenging that occurs is estimated from the yield of HD or of D_2 produced during radiolysis. This study illustrates the necessity to be aware of the possibility of exchange reactions in these systems. We conclude, however, that exchange reactions did not vitiate the results obtained by using ND_3 (3) or D_2S (4).

ACKNOWLEDGMENT

We are grateful to the National Research Council for giving financial assistance to this work.

REFERENCES

1. C. HORREX, R. K. GREENHALGH, and M. POLANYI. Trans. Faraday Soc. **35**, 511 (1939).
2. C. WALLING. Free radicals in solutions. John Wiley & Sons, Inc., New York. 1957.
3. F. WILLIAMS. J. Am. Chem. Soc. **86**, 3954 (1964).
4. A. MEISSNER and A. HENGLEIN. Ber. Bunsenges. Physik. Chem. **69**, 264 (1965).

Can. J. Chem. Downloaded from www.nrcresearchpress.com by 210.87.254.5 on 09/05/12
For personal use only.

Can. J. Chem. Downloaded from www.nrcresearchpress.com by 210.87.254.5 on 09/05/12
For personal use only.

KIHARA POTENTIAL AND LENNARD-JONES AND DEVONSHIRE EQUATION OF STATE OF LIQUIDS AND DENSE GASES

ISAMU NAGATA[1]
William Marsh Rice University, Department of Chemical Engineering, Houston, Texas
Received April 28, 1966

ABSTRACT

The Kihara potential has been applied to the Lennard-Jones and Devonshire cell theory in place of the Lennard-Jones potential. The expressions for the internal energy, heat capacity, and entropy, as well as the compressibility, are given in excess over those of a perfect gas. A comparison between experimental data and the present theory is made.

INTRODUCTION

It has been shown that the Kihara potential is in general better than the Lennard-Jones potential in the calculation of crystal properties (1), virial coefficients (2), and gas hydrate dissociation pressures (3). An extensive study on the Lennard-Jones and Devonshire cell theory has been carried out by Wentorf *et al.* (4); therefore the detailed discussion of this theory seems to be unwarranted. The present investigation shows how the formulae in the theory are altered by substituting the Kihara potential for the Lennard-Jones potential and compares the theoretical results with some of the experimental properties of argon.

CELL THEORY FOR THE KIHARA POTENTIAL

For simplicity only a spherical model for the Kihara potential is considered and it is further assumed that a molecule with spherical core of radius c roams in the cell and that the Z nearest neighbors distributed on the surface of the cell are point molecules. The interaction energy between the molecule in the cell and a molecule on the surface is assumed to be expressed by the Lennard-Jones 12–6 form as a function of the shortest distance between the molecules.

$$\Phi(R,c) = 4\epsilon\left[\frac{\sigma^{12}}{(R-c)^{12}} - \frac{\sigma^{6}}{(R-c)^{6}}\right] \qquad [1]$$

R is the distance between the center of the molecule in the cell and that of a surface molecule. ϵ is the potential minimum and σ is the position where $\Phi(R,c) = 0$. We obtain the spherically symmetrical potential for a molecule located a distance r from the center of the cell from eq. [2].

$$\psi(r) = \frac{Z}{4\pi}\int_0^{2\pi}\int_0^{\pi}\Phi(R,c)\sin\theta\,\mathrm{d}\theta\,\mathrm{d}\phi \qquad [2]$$

The origin of the coordinate system used in eq. [2] is the center of the cell. The detailed explanation on how to carry out the integral is given elsewhere (5). θ and ϕ are the orientation angles. If we consider a face-centered cubic lattice for the cell and take the contribution of the second- and third-shell molecules to the potential function into consideration, $\psi(r)$ is expressed as (4)

$$\psi(r) - \psi(0) = \sqrt{2}\epsilon\left[\left(\frac{N\sigma^3}{v}\right)^4 L(y) - 2\left(\frac{N\sigma^3}{v}\right)^2 M(y)\right], \qquad [3]$$

[1]*Present address: Department of Chemical Engineering, Kanazawa University, Kanazawa, Japan.*

where $\sqrt{2}v = Na^3$, $y = (r/a)^2$, $c^* = c/a$, and a is the cell radius.

[4] $$L(y) = l(y) + (1/128)l(y/2) + (2/729)l(y/3)$$

[5] $$M(y) = m(y) + (1/16)m(y/2) + (2/27)m(y/3),$$

where $l(y)$ and $m(y)$ are given by McKoy and Sinanoğlu (6)

[6] $$l(y) = \frac{c^*}{20y^{1/2}}\left[\frac{1}{(1-y^{1/2}-c^*)^{10}} - \frac{1}{(1+y^{1/2}-c^*)^{10}}\right] - \frac{1}{(1-c^*)^{11}} + \frac{1}{22y^{1/2}}\left[\frac{1}{(1-y^{1/2}-c^*)^{11}} - \frac{1}{(1+y^{1/2}-c^*)^{11}}\right] - \frac{c^*}{(1-c^*)^{12}}$$

[7] $$m(y) = \frac{1}{8y^{1/2}}\left[\frac{1}{(1-y^{1/2}-c^*)^{4}} - \frac{1}{(1+y^{1/2}-c^*)^{4}}\right] - \frac{1}{(1-c^*)^{5}} + \frac{c^*}{10y^{1/2}}\left[\frac{1}{(1-y^{1/2}-c^*)^{5}} - \frac{1}{(1+y^{1/2}-c^*)^{5}}\right] - \frac{c^*}{(1-c^*)^{6}}.$$

Then we can obtain the expression for Pv/NkT by eq. [8].

[8] $$\frac{Pv}{NkT} = 1 - \left(12\frac{\epsilon}{kT}\right)\left\{2.4090\left(\frac{N\sigma^3}{v}\right)^2\left[\frac{1}{(1-c^*)^5} + c^*\left(\frac{2}{(1-c^*)^6} + \frac{c^*}{(1-c^*)^7}\right)\right] - 2.0219\left(\frac{N\sigma^3}{v}\right)^4\left[\frac{1}{(1-c^*)^{11}} + c^*\left(\frac{2}{(1-c^*)^{12}} + \frac{c^*}{(1-c^*)^{13}}\right)\right]\right\} - \left(48\frac{\epsilon}{kT}\right)\left[\left(\frac{N\sigma^3}{v}\right)^2\left(\frac{g_M}{g}\right) - \left(\frac{N\sigma^3}{v}\right)^4\left(\frac{g_L}{g}\right)\right] - \left(12v\frac{\epsilon}{kT}\right)\left[\left(\frac{N\sigma^3}{v}\right)^4\left(\frac{g_{L'}}{g}\right) - 2\left(\frac{N\sigma^3}{v}\right)^2\left(\frac{g_{M'}}{g}\right)\right]$$

For the one-shell calculation the factors of 2.4090 and 2.0219 of eq. [8] must be replaced by a factor of 2 (4). The functions g, g_L, g_M, $g_{L'}$, and $g_{M'}$ were calculated from the following formulas:

[9] $$g = \int_0^{0.30544} y^{1/2}\exp\{-[\psi(r) - \psi(0)]/kT\}\,dy$$

[10] $$g_L = \int_0^{0.30544} y^{1/2}L(y)\exp\{-[\psi(r) - \psi(0)]/kT\}\,dy$$

[11] $$g_M = \int_0^{0.30544} y^{1/2}M(y)\exp\{-[\psi(r) - \psi(0)]/kT\}\,dy$$

[12] $$g_{L'} = \int_0^{0.30544} y^{1/2}\frac{\partial L(y)}{\partial v}\exp\{-[\psi(r) - \psi(0)]/kT\}\,dy$$

[13] $$g_{M'} = \int_0^{0.30544} y^{1/2}\frac{\partial M(y)}{\partial v}\exp\{-[\psi(r) - \psi(0)]/kT\}\,dy.$$

If $c = 0$, then $g_{L'} = 0$ and $g_{M'} = 0$ ($\partial L(y)/\partial v = 0$ and $\partial M(y)/\partial v = 0$ at $c = 0$), and eq. [8] reduces to that for the point molecule model described by Wentorf *et al.* (eq. [2] of ref. 4).

Can. J. Chem. Downloaded from www.nrcresearchpress.com by 210.87.254.5 on 09/05/12
For personal use only.

It is convenient to define pressure, temperature, and volume in reduced forms.

[14] $$P^* = (Pv/NkT)T^*/v^*$$

[15] $$T^* = kT/\epsilon$$

[16] $$v^* = v/N\sigma^3$$

The expressions for the thermodynamic functions in excess over those of a perfect gas such as internal energy E', internal heat capacity c_v', and internal entropy S' are given easily (4, 7).

[17] $$E' = \tfrac{1}{2}N\psi^*(0) + N\chi(v,T)$$

Here $\frac{1}{2}\psi'(0)$ is the potential energy per molecule when all the molecules are at the centers of their cells.

[18] $$\psi^*(0) = \sqrt{2}\epsilon\left\{\frac{1.0109}{v^{*4}}\left(\frac{1}{(1-c^*)^{11}} + \frac{c^*}{(1-c^*)^{12}}\right) - \frac{2.4090}{v^{*2}}\left(\frac{1}{(1-c^*)^5} + \frac{c^*}{(1-c^*)^6}\right)\right\}$$

$\chi(v,T)$ is the average potential energy in a cell referred to the potential at the center as zero. The factors 1.0109 and 2.4090, which are obtained for the Lennard-Jones potential and are assumed to be valid for the Kihara potential in the present investigation, must be replaced by 1 and 2, respectively, for the one-shell calculation (4).

[19] $$\chi(v,T) = \sqrt{2}\epsilon\left[\frac{1}{v^{*4}}\left(\frac{g_L}{g}\right) - \frac{2}{v^{*2}}\left(\frac{g_M}{g}\right)\right]$$

[20] $$c_v' = \frac{\partial E'}{\partial T} = Nk\left(\frac{12}{T^*}\right)^2\left[\frac{1}{v^{*8}}\left(\frac{g_L{}^2g - g_L{}^2}{g^3}\right) - \frac{4}{v^{*6}}\left(\frac{g_{LM}g - g_Lg_M}{g^2}\right) + \frac{4}{v^{*4}}\left(\frac{g_M{}^2g - g_M{}^2}{g^2}\right)\right]$$

[21] $$g_{LM} = \int_0^{0.30544} y^{1/2}L(y)M(y)\exp\{-[\psi(r) - \psi(0)]/kT\}\,dy$$

[22] $$g_M{}^2 = \int_0^{0.30544} y^{1/2}M(y)M(y)\exp\{-[\psi(r) - \psi(0)]/kT\}\,dy$$

[23] $$g_L{}^2 = \int_0^{0.30544} y^{1/2}L(y)L(y)\exp\{-[\psi(r) - \psi(0)]/kT\}\,dy$$

[24] $$S'(v,T) = [N\chi(v,T)/T] + Nk\log(2\pi\sqrt{2}g)$$

These relations may be used as a basis for the calculation of the respective thermodynamic functions.

NUMERICAL CALCULATIONS

Simpson's rule was used in the numerical integration involved in the present investigation. All numerical calculations were programmed for the Rice University Research Computation Laboratory IBM 7040. The energy parameters and core size of the Kihara potential determined from second virial coefficient data for argon (2) are $\epsilon/k = 147.2$ °K, $\sigma = 2.946$ Å, $c = 0.184$ Å. The nearest distance between argon molecules in the critical region is 4.5 Å (8). The calculated critical values are compared with experimental results in Table I. This table shows that the present investigation results in unsuccessful prediction of critical constants.

Can. J. Chem. Downloaded from www.nrcresearchpress.com by 210.87.254.5 on 09/05/12
For personal use only.

TABLE I

Critical constants for argon

	T_c^*	V_c^*	P_c^*	$P_c^* V_c^*/T_c^*$
Experimental	1.025	4.844	0.062	0.291
Present calculation				
One shell	0.814	2.05	0.184	0.463
Three shells	1.294	1.95	0.402	0.605

TABLE II

Compressibility for argon

	Density (g/cc)			
	0.5642	0.7483	0.8975	1.1161
0 °C				
Experimental (4)	0.97	1.13	1.38	2.07
Present calculation				
One shell	1.40	1.61	1.87	2.18
Three shells	1.22	1.31	1.40	1.50
Wentorf *et al.* (4)	1.45	1.61	1.77	2.10
75 °C				
Experimental (4)	1.14	1.36	1.64	2.34
Present calculation				
One shell	1.50	1.78	2.07	2.41
Three shells	1.36	1.53	1.69	1.87
Wentorf *et al.* (4)	1.64	1.87	2.09	2.51
150 °C				
Experimental (4)	1.25	1.50	1.80	2.32
Present calculation				
One shell	1.54	1.88	2.18	2.54
Three shells	1.43	1.68	1.87	2.10
Wentorf *et al.* (4)	1.76	2.02	2.28	2.74

TABLE III

Excess internal energy for argon (cal/mole)

	Density (g/cc)			
	0.4995	0.7136	0.9277	1.1418
0 °C				
Experimental (4)	−429	−601	−769	−924
Present calculation				
One shell	−387	−495	−576	−690
Three shells	−453	−599	−715	−888
Wentorf *et al.* (4)	−445	−634	−826	−1 035
75 °C				
Experimental (4)	−402	−564	−718	−851
Present calculation				
One shell	−360	−462	−538	−641
Three shells	−427	−567	−678	−841
Wentorf *et al.* (4)	−415	−592	−769	−956
150 °C				
Experimental (4)	−386	−539	−680	−791
Present calculation				
One shell	−335	−429	−499	−592
Three shells	−401	−534	−640	−793
Wentorf *et al.* (4)	−386	−550	−712	−879

Can. J. Chem. Downloaded from www.nrcresearchpress.com by 210.87.254.5 on 09/05/12
For personal use only.

TABLE IV

Excess heat capacity for argon (cal/mole deg)

	Density (g/cc)			
	0.4995	0.7136	0.9277	1.1418
0 °C				
Experimental (4)	0.42	0.55	0.74	1.02
Present calculation				
One shell	0.36	0.44	0.51	0.65
Three shells	0.36	0.44	0.50	0.63
Wentorf *et al.* (4)	0.41	0.56	0.77	1.07
75 °C				
Experimental (4)	0.30	0.42	0.62	0.91
Present calculation				
One shell	0.35	0.44	0.51	0.65
Three shells	0.35	0.43	0.50	0.63
Wentorf *et al.* (4)	0.40	0.56	0.76	1.04
150 °C				
Experimental (4)	0.16	0.26	0.43	0.69
Present calculation				
One shell	0.33	0.44	0.52	0.65
Three shells	0.33	0.43	0.51	0.63
Wentorf *et al.* (4)	0.38	0.56	0.76	1.02

TABLE V

Excess entropy for argon (cal/mole deg)

	Density (g/cc)			
	0.4995	0.7136	0.9277	1.1418
0 °C				
Experimental (4)	−1.23	−1.86	−2.60	−3.48
Present calculation				
One shell	−0.51	−1.19	−1.72	−2.53
Three shells	−0.50	−1.17	−1.71	−2.50
Wentorf *et al.* (4)	−0.66	−1.70	−2.75	−3.92
75 °C				
Experimental (4)	−1.15	−1.74	−2.43	−3.24
Present calculation				
One shell	−0.42	−1.08	−1.60	−2.37
Three shells	−0.42	−1.07	−1.58	−2.35
Wentorf *et al.* (4)	−0.54	−1.56	−2.57	−3.67
150 °C				
Experimental (4)	−1.10	−1.67	−2.33	−3.08
Present calculation				
One shell	−0.36	−0.99	−1.50	−2.25
Three shells	−0.35	−0.98	−1.49	−2.23
Wentorf *et al.* (4)	−0.48	−1.45	−2.42	−3.46

The saturation pressures were obtained by using the rule of equal areas on the figure plotting P^* against v^* in the two-phase region for each subcritical isotherm. The relationship between the logarithm of vapor pressure P^* and $1/T^*$ may be represented by

[25] $$\log_{10} P^* = 1.09 - 2.37/T^* \quad \text{(experimental)}$$

[26] one shell $$\log_{10} P^* = 3.61 - 3.54/T^* \quad \text{(present calculations)}$$

[27] three shells $$\log_{10} P^* = 2.55 - 3.82/T^* \quad \text{(present calculations)}$$

The experimental vapor pressure data for argon were obtained from Cook (9).

Can. J. Chem. Downloaded from www.nrcresearchpress.com by 210.87.254.5 on 09/05/12
For personal use only.

Tables II to V show the results for Pv/NkT, E', c_v', and S' at 0 °C, 75 °C, and 150 °C together with experimental values and the results by Wentorf *et al.* (4). It is apparent that the assumption underlying the Lennard-Jones and Devonshire theory is applicable at high temperatures and high densities. These tables demonstrate that the results of the three-shell calculation are often not so good as the results of the one-shell calculation and that the present more complicated approach often does not give appreciably better agreement with the experimental values than the original simple Lennard-Jones and Devonshire theory.

ACKNOWLEDGMENT

Financial support was made through the National Aeronautics and Space Administration Research Grant NSG 6–59.

REFERENCES

1. T. KIHARA. Adv. Chem. Phys. **5**, 147 (1963).
2. A. E. SHERWOOD and J. M. PRAUSNITZ. J. Chem. Phys. **41**, 429 (1964).
3. I. NAGATA and R. KOBAYASHI. Ind. Eng. Chem. Fundamentals, **5**, 344 (1966).
4. R. H. WENTORF, JR., R. J. BUEHLER, J. O. HIRSCHFELDER, and C. F. CURTISS. J. Chem. Phys. **18**, 1484 (1950).
5. H. EYRING, D. HENDERSON, B. J. STOVER, and E. M. EYRING. Statistical mechanics and dynamics. John Wiley, New York. 1964. p. 371.
6. V. MCKOY and O. SINANOĞLU. J. Chem. Phys. **38**, 2946 (1963).
7. J. E. LENNARD-JONES and A. F. DEVONSHIRE. Proc. Roy. Soc. London, Ser. A, **163**, 53 (1937).
8. A. EISENSTEIN and N. S. GINGRICH. Phys. Rev. **62**, 261 (1942).
9. G. A. COOK. Argon, helium and the rare gases. Vol. 1. Interscience, New York. 1961.

Can. J. Chem. Downloaded from www.nrcresearchpress.com by 210.87.254.5 on 09/05/12
For personal use only.

Can. J. Chem. Downloaded from www.nrcresearchpress.com by 210.87.254.105 on 09/05/12
For personal use only.

KINETICS OF HYDROGEN ABSTRACTION FROM PROTON DONORS BY DPPH[1]

SURJIT SINGH, K. R. BHASKAR, AND C. N. R. RAO[2]
Department of Chemistry, Indian Institute of Technology, Kanpur, India

Received April 28, 1966

ABSTRACT

The kinetics and energetics of the interaction of DPPH with a variety of hydroxylic compounds have been investigated by electronic and e.s.r. spectroscopy. Deuterium isotope effects on the kinetics have been examined. A model involving hydrogen bonded complexes has been suggested for the hydrogen abstraction reaction.

INTRODUCTION

The interaction of DPPH with proton donors has been investigated by several workers (1–6) in recent years, although there is limited information on the energetics of the reaction. While it was believed earlier (2) that the interaction of proton donors with DPPH involved hydride ion transfer and formation of carbonium ions, recent work of Russell and co-workers (3, 4, 6) has shown that this reaction involves the formation of radicals by hydrogen abstraction from a hydrogen bonded complex initially formed between the proton donors and DPPH. Thus, Russell and coworkers (6) have identified the formation of the stable 2,4,6-tri-*t*-butylphenoxy radical in the interaction of 2,4,6-tri-*t*-butylphenol with DPPH by electron spin resonance (e.s.r.) spectroscopy.

We have now investigated the kinetics and energetics of the interaction of DPPH with a variety of proton donors: (i) substituted phenols with varying basicity, (ii) sterically hindered phenols, (iii) 4-substituted-2,6-di-*t*-butylphenols, (iv) sterically hindered alcohols, (v) ortho-substituted (intramolecularly hydrogen bonded) phenols, and (vi) aniline and aniline-d_2, phenol and phenol-*d*, and oxalic acid and oxalic acid-d_2.

In addition to providing useful kinetic information, these studies were expected to throw some light on the nature of the hydrogen bonded complexes which act as intermediates or activated complexes in the hydrogen abstraction reaction.

EXPERIMENTAL

DPPH was prepared by the lead oxide oxidation of diphenyl picryl hydrazine. 2,2,4,4-Tetramethyl-3-isopropyl-3-pentanol was prepared by the method described in the literature (7). Deuterated compounds were obtained from the Atomic Energy Establishment, Bombay. All the other chemicals used were obtained commercially and were purified before use.

DPPH gives violet colored solutions in organic solvents and is stable up to about 80 °C. The solutions show an absorption maximum around 520 mμ with an extinction coefficient of $\sim$12 000 l mole^{-1} cm^{-1}. Another high intensity absorption maximum appears at $\sim$330 mμ. The 520 mμ band was used to determine the concentration of DPPH in the kinetic studies of the interaction of DPPH with proton donors.

The measurements of electronic spectra were made with a Beckman DU spectrophotometer, fitted with a variable temperature cell compartment. The pseudo-first order kinetics of interaction of DPPH with proton donors were followed (for less than the first 30–40% of the reaction) in carbon tetrachloride solutions in the presence of excess of proton donors. The concentration of DPPH was generally $\sim 10^{-5} M$ while that of proton donors varied between $\sim 10^{-4}$ and $\sim 0.1 M$. The rate constants for the second order reactions were then calculated employing an expression similar to that of McGowan, Powell, and Raw (2).

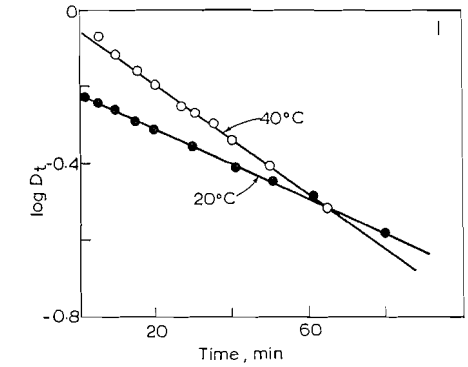
$$k_{II} = \frac{2.303}{t} \log \frac{a}{a - x} \times \frac{1}{D}$$

$$= \frac{2.303}{t} \log \frac{D_0}{D_t} \times \frac{1}{D}$$

[1]*Taken in part from the Ph.D. Thesis of S. Singh submitted to the Indian Institute of Technology, Kanpur.*
[2]*To whom all correspondence should be addressed.*

where a and $(a - x)$ are the initial and final molar concentrations of DPPH after t minutes when D moles of proton donor has been allowed to react with it. Typical plots of log D_t against time are shown in Fig. 1.

The rate constants were also calculated by noting the rate of disappearance (decrease in the peak height of the first derivative curve) of the electron spin resonance signal of DPPH with time. Generally, there was no interference in the e.s.r. spectrum due to the phenoxy or other radicals, except in the case of 2,4,6-tri-*t*-butylphenoxy radical (6). Since the kinetics in such cases were also examined by electronic spectroscopy, there was no difficulty in obtaining good rate constants. Typical e.s.r. signals of DPPH as a function of time in presence of phenol are shown in Fig. 2. A Varian H-4500 spectrometer operating at 100 kc/s was employed for this purpose.



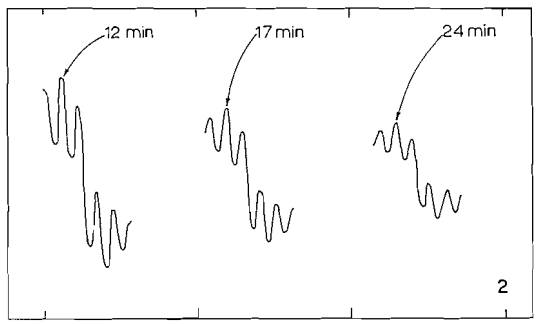


FIG. 1. Typical first order plots for the reaction of DPPH with 2,6-di-*t*-butylphenol at two temperatures.
FIG. 2. Time dependence of the e.s.r. signal of DPPH ($\sim 10^{-4}$ M) in the presence of phenol (~ 0.05 M, solvent CCl_4).

The rate constants have an uncertainty less than $\pm 10\%$. Reverse reactions of phenoxy and other radicals do not affect the k values appreciably since the proton donors were present in excess and since the rate data were taken only for the initial few percent of the reaction. Rate constants were determined at three temperatures in the 20–40 °C range and the energy of activation was calculated using the Arrhenius equation. Rate constants at only one temperature have been shown in the tables for purpose of brevity. The uncertainty in the energy of activation is ± 1 kcal mole^{-1}.

The hydrogen bonding data given in Tables I–VI are from the studies in this laboratory (7, 8).

RESULTS AND DISCUSSION

The interaction of a proton donor, RXH, with DPPH may be visualized to proceed as follows. (i) The RXH first forms a hydrogen bonded complex, X—H...N, with DPPH. (ii) the hydrogen of this complex is then transferred completely to the nitrogen atom forming the hydrazine and a radical, through a transition state where the X—H bond is more polarized than in the initial hydrogen bonded complex. Such an activated complex may be considered to be similar to the symmetrical hydrogen bond X...H...N. (iii) The facility with which the hydrogen abstraction takes place is determined by several factors. A low free energy of formation (ΔF^0) of the initial hydrogen bonded complex should

Can. J. Chem. Downloaded from www.nrcresearchpress.com by 210.87.254.105 on 09/05/12
For personal use only.

increase the rate constant since the rate will be proportional to the concentration of the hydrogen bonded species. Strong hydrogen bonds (high enthalpy of formation of the complex, $-\Delta H^0$) should lower the energy of activation, E_a, for the hydrogen abstraction reaction since a stronger hydrogen bond will approximate a symmetrical hydrogen bond more closely. The stability of the radical produced by hydrogen abstraction should also favor the hydrogen abstraction due to obvious thermodynamic reasons. All these ideas regarding the hydrogen abstraction reaction between DPPH and proton donors have been summarized in the form of a potential energy diagram in Fig. 3. In the present discussion the reverse reaction of the phenoxy or other radicals with the hydrazine (6) will not be considered, and the rate data presented are only for the forward reaction of DPPH with the proton donors.

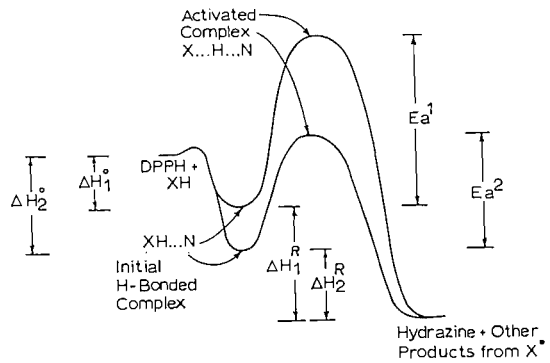


FIG. 3. Potential energy diagram for the interaction of DPPH with proton donors. DPPH and a proton donor XH initially form a hydrogen bonded complex XH...N which then forms an activated complex, X...H...N ($R_{X...H}$) R_{X-H}) resembling a symmetric hydrogen bond. Two cases have been considered, one with a high and another with a medium value for the enthalpy of formation ($-\Delta H^\circ$)of the initial hydrogen bonded complex. The energy levels of the hydrazine and other products formed by the new radicals are shown to be the same for both cases for the purpose of simplicity. ΔH^R is the enthalpy change for the reaction giving rise to the hydrazine and the products from X•.

From these arguments it is clear that one should not expect a simple relationship between the data on hydrogen bonding and the kinetics of hydrogen abstraction. However, in certain systems, one may see some relation between the ΔH^0 (also $\Delta\nu_{OH}$) and ΔF^0 of hydrogen bonding and the energy of activation. In systems where the radicals produced have nearly the same stabilities, it is possible that ΔH^0 of hydrogen bonding as well as $\Delta\nu_{OH}$ may be inversely proportional to the energy of activation for hydrogen abstraction.

Interaction of DPPH with p-Substituted Phenols

The kinetic data for the interaction of DPPH with *p*-substituted phenols are given in Table I. It can be seen that there is no simple relationship between the rate constant or the energy of activation and the electrical properties of the *p*-substituents. This is probably due to the operation of several of the factors discussed earlier. Comparison of these kinetic data with the hydrogen bonding data of these proton donors with benzophenone, however, shows that *p*-chlorophenol which forms the strongest hydrogen bond (being the most acidic of the four phenols studied) does not show the lowest value of the energy of activation.

Interaction of DPPH with Sterically Hindered Phenols and Alcohols

The data for the interaction of DPPH with sterically hindered phenols are given in Table II. Although there is no simple relationship between the rate constants or the energies of activation with the bulk of the ortho substituents, it can be seen that the

Can. J. Chem. Downloaded from www.nrcresearchpress.com by 210.87.254.105 on 09/05/12
For personal use only.

TABLE I

Interaction of substituted phenols (RC_6H_4OH) with DPPH

R	σ (9)	$k_{20°C}$,* min^{-1}	E_a, kcal $mole^{-1}$	$-\Delta S^{\neq}$, e.u.	Benzophenone hydrogen bonding (8) $K_{25°C}$, l $mole^{-1}$	$\Delta\nu_{OH}$, cm^{-1}	$-\Delta H^0$, kcal $mole^{-1}$
4-Cl†	0.23	5.5 (5.6)	6.5	43	14	190	4.9
H‡	0.00	2.9 (2.7)	6.9	45	7.7	175	4.4
4-CH_3 (2)	−0.17	55.0	9.8	27	6.3	160	—
4-OCH_3§	−0.27	3 350 (3 860)	6.5	31	7.3	170	4.4

*Values of k in parentheses are from e.s.r. measurements.
†k from ref. 2 is 1.1 at 20 °C.
‡k from ref. 2 is 4.0 at 20 °C.
§The reaction was not pseudo-first order in this case since the concentration of the phenol and DPPH were nearly the same. The value found by other workers (2) is 14 000 which is very high because they calculated k treating the reaction as pseudo-first order.

TABLE II

Interaction of sterically hindered phenols ($R_1R_2C_6H_3OH$) with DPPH*

R_1	R_2	$k_{20°C}$, min^{-1}	E_a, kcal $mole^{-1}$	$-\Delta S^{\neq}$, e.u.	THF hydrogen bonding (7) $K_{25°C}$, l $mole^{-1}$	$-\Delta H^0$, kcal $mole^{-1}$
H	2-*t*-Bu	36	6.4	39	7	5
2-Me	6-Me†	82 (83)	7.0	36	2.5	—
2-*i*-Pr	6-*i*-Pr	79 (81)	11	22	1.8	5
2-*t*-Bu	6-*t*-Bu‡	15 (19)	3.7	50	0.5	8

*Values of k in parentheses are from e.s.r. measurements.
†The k at 20 °C from ref. 2 is 117.
‡The k at 30 °C from ref. 4 is 1.2 and from ref. 2 is 12.0.

2,6-di-*t*-butylphenol which forms the strongest hydrogen bond (high $-\Delta H^0$) shows the lowest energy of activation for hydrogen abstraction. The rate constant, however, is low in this case probably due to the very low equilibrium constant of formation of the hydrogen bonded complex.

The kinetics of hydrogen abstraction of a sterically hindered alcohol with DPPH are compared in Table III with the data on ethanol.

Although the reaction of ethanol gives complex products, one can treat the reaction as of pseudo-first order. The value of k has been given here only to show the large difference

TABLE III

Interaction of aliphatic alcohols with DPPH

	$k_{25°C}$, min^{-1}	E_a, kcal $mole^{-1}$	$-\Delta S^{\neq}$, e.u.	Benzophenone hydrogen bonding $K_{25°C}$, l $mole^{-1}$	$10^{-3}\Delta\nu/\nu$
2,2,4,4-Tetramethyl-3-isopropyl-3-pentanol	3×10^{-3}	20	13	0.6	17.1
Ethanol (5)	4×10^{-10}	9.6	79	1.9	23.6

Can. J. Chem. Downloaded from www.nrcresearchpress.com by 210.87.254.105 on 09/05/12
For personal use only.

in rates between the two alcohols. The sterically hindered alcohol shows a much faster rate. The energy of activation is high possibly because of a lower enthalpy of formation of the hydrogen bonded complex.

It has been found earlier that there was no systematic variation of the equilibrium constant or the $\Delta\nu_{OH}$ in the hydrogen bonding equilibrium of *p*-substituted 2,6-di-*t*-butylphenols with donors (7). It is interesting to see, however, that the energy of activation of hydrogen abstraction varies roughly in the same fashion as the $\Delta\nu_{OH}$ (Table IV). 2,4,6-Tri-*t*-butylphenol is slightly out of line and the value of the energy of activation is not as low as one would have expected.

TABLE IV

Interaction of *p*-substituted (R) 2,6-di-*t*-butylphenols with DPPH

					THF hydrogen bonding (7)	
4-R	σ (10)	$k_{20°C}$, min^{-1}	E_a, kcal $mole^{-1}$	$-\Delta S^{\neq}$, e.u.	$K_{25°C}$ l $mole^{-1}$	$10^3\Delta\nu/\nu$
NO_2	1.24	1.3	8.6	39	1.3	27.6
CN	0.88	9.6	11	27	1.3	28.9
COOEt*	0.64	15	6.9	39	1.1	26.1
H	0.00	15	3.7	50	0.5	23.0
t-Bu (6)	−0.14	7.2	6.5	42	0.5	22.0

*The rate constant determined by e.s.r. was 16 min^{-1}.

TABLE V

Interaction of intramolecularly hydrogen bonded phenols $R_1R_2C_6H_3OH$ with DPPH

R_1	R_2	$k_{20°C}$, min^{-1}	E_a kcal $mole^{-1}$	$-\Delta S^{\neq}$, e.u.
H	2-Cl	0.21	11	32
2-Cl	6-Cl	2.2	7	44
2-Br	6-Br	1.5	4	54
H	2-$COCH_3$	0.02	8	49
H	2-NO_2*	0.002	3	69

*The rate constant determined by e.s.r. was found to be 0.003 min^{-1}.

Interaction of DPPH with Intramolecularly Hydrogen Bonded ortho-Substituted Phenols

Studies on the intramolecularly hydrogen bonded ortho-substituted phenols show that hydrogen can be abstracted from even the stronger intramolecular hydrogen bonds (Table V). 2,6-Dichlorophenol which can exist only in the bonded *cis* form, shows a much lower rate constant as well as energy of activation for hydrogen abstraction compared with ortho-chlorophenol which can exist either in the *cis* (hydrogen bonded) or the *trans* form. It appears as though the E_a decreases with an increase in the energy of the intramolecular hydrogen bond. 2-Nitrophenol which probably has the strongest intramolecular hydrogen bond also shows the lowest value of E_a. It is possible that in the case of 2-nitrophenol, it forms the strongest intermolecular hydrogen bond with DPPH as well. The low rate constant, however, is likely to be due to the low concentration of the hydrogen bonded species with DPPH since it will be more difficult to break a strong intramolecular hydrogen bond.

Deuterium Isotope Effects on the Hydrogen Abstraction Reaction

The results in Table VI clearly show that deuterium substitution lowers the rate constant for hydrogen abstraction and increases the E_a considerably. The k_H/k_D ratio varies

Can. J. Chem. Downloaded from www.nrcresearchpress.com by 210.87.254.105 on 09/05/12
For personal use only.

anywhere between 1 and 12. The lowering of the rate constant by deuterium substitution can be understood in terms of the kinetic isotope effects discussed in the literature (11). It is interesting to note that the equilibrium constants and enthalpies of formation of intermolecular hydrogen bonds are also considerably decreased by deuterium substitution (12).

TABLE VI

Deuterium isotope effects*

	X—H			X—D		
	$k_{20°C}$, min^{-1}	E_a, kcal $mole^{-1}$	$-\Delta S^{\neq}$, e.u.	$k_{20°C}$, min^{-1}	E_a, kcal $mole^{-1}$	$-\Delta S^{\neq}$, e.u.
Phenol	2.9	6.1	45	2.1	8.9	40
2,4,6-Tri-*t*-butylphenol (6)	7.2	6.5	42	0.60	7.7	43
Aniline†	0.06	6.6	51	0.04	13	29
Oxalic acid‡	0.19	9.4	40	0.10	2.5	64

*CCl_4 was used throughout as the solvent except in the case of oxalic acid where CH_3CN was used.
†McGowan, Powell, and Raw (2) have treated the reaction of primary amines with DPPH as a third order reaction. In the present study it has been found that better fits of the rate data are obtained if the reaction is treated as second order.
‡In oxalic acid there is the possibility of formation of a diradical which would mean a third order reaction. Here, values have been calculated assuming a second order reaction only.

Entropy of Activation of the Hydrogen Abstraction Reaction

In all the systems examined in the present study, the entropies of activation for hydrogen abstraction calculated from the Eyring equation (11) are large negative numbers. This appears reasonable since the activated complex (symmetric hydrogen bond) is more polar than the initial hydrogen bond complex between the proton donor and DPPH (Fig. 3).

CONCLUDING REMARKS

Although the hydrogen abstraction reaction of DPPH with proton donors seems to be fairly well understood (3–6), the detailed mechanism of the interaction is difficult to establish from kinetic studies alone. While it is possible to visualize a plausible mechanism (Fig. 3), the kinetics in most instances seem to be affected by more than one factor. In some instances, however, it is possible to show some relation between the kinetic data and the hydrogen bonding data.

ACKNOWLEDGMENTS

The authors' thanks are due to the C.S.I.R. (India) for the award of a research grant, and to Dr. L. A. Cohen of the National Institutes of Health, Bethesda, for the samples of 4-substituted 2,6-di-*t*-butylphenols.

REFERENCES

1. K. E. Russell. J. Phys. Chem. **58**, 437 (1954).
2. J. C. McGowan, T. Powell, and R. Raw. J. Chem. Soc. 3103 (1959).
3. J. C. Hogg, D. H. Lohmann, and K. E. Russell. Can. J. Chem. **39**, 1588 (1961).
4. R. A. Bird, G. A. Harpell, and K. E. Russell. Can. J. Chem. **40**, 701 (1962).
5. P. J. Proll and L. H. Sutcliff. Trans. Faraday Soc. **59**, 2090 (1962).
6. P. B. Ayscough and K. E. Russell. Can. J. Chem. **43**, 3039 (1965).
7. S. Singh and C. N. R. Rao. J. Am. Chem. Soc. **88**, 2142 (1966).
8. S. Singh, A. S. N. Murthy, and C. N. R. Rao. Trans. Faraday Soc. **62**, 1056 (1966).
9. D. H. McDaniel and H. C. Brown. J. Org. Chem. **23**, 420 (1958).
10. L. A. Cohen and W. M. Jones. J. Am. Chem. Soc. **85**, 3397 (1963).
11. S. Glasstone, K. J. Laidler, and H. Eyring. The theory of rate processes. McGraw-Hill Book Co., Inc., New York and London. 1941.
12. S. Singh and C. N. R. Rao. Can. J. Chem. This issue.

Can. J. Chem. Downloaded from www.nrcresearchpress.com by 210.87.254.105 on 09/05/12
For personal use only.

Can. J. Chem. Downloaded from www.nrcresearchpress.com by 210.87.254.40 on 09/05/12
For personal use only.

COORDINATION COMPOUNDS OF OLEFINS WITH ANHYDROUS SILVER SALTS

III. KINETICS OF THE GAS–SOLID REACTION PRODUCING $AgBF_4.2C_3H_6$[1]

C. A. JULL, R. J. KOMINAR,[2] N. K. MAINLAND,[3] AND H. W. QUINN[4]
Exploratory Research Laboratory, Dow Chemical of Canada, Limited, Sarnia, Ontario
Received May 31, 1966

ABSTRACT

A study has been made of the pressure and temperature dependence of the rate of combination of propylene with silver tetrafluoroborate to produce $AgBF_4.2C_3H_6$. Dependent upon the prior history of the salt, the reaction may proceed via predominantly diffusion control, predominantly kinetic control, or a combination of the two mechanisms. With both mechanisms, the adsorption of the olefin on the salt surface appears to exert a rate-controlling influence.

INTRODUCTION

For many years there has been much interest in the kinetics of gas–solid reactions. The resulting investigations have covered both reversible and irreversible combination and dissociation reactions. Those effected prior to 1955 have been well reviewed by Garner (1).

While many investigators (2–6) have concerned themselves with the kinetics of dissociation, study of the combination reactions has received more attention in recent years. The reactions investigated have included the rehydration of $CuSO_4$ (7), $NiSO_4$ (8), alum (9), and K_2CO_3 (10), the formation of $CaCO_3$ and $CdCO_3$ (11) and of the ammoniates of $CdCl_2$ (11) and $AgNO_3$ (12) and the reaction of UF_6 with NaF (14).

Although most of these studies have resulted in determination of the temperature dependence of the reaction rates as expressed by the activation energy, relatively few have included an adequate assessment of the pressure dependence. With combination reactions in particular such information might be expected to provide a better basis for discussion of the reaction mechanism.

Our interest in the coordination compounds formed by interaction of olefins with silver tetrafluoroborate (15, 16) and the observation that these could be formed reversibly by exposure of the solid salt to olefin vapor suggested the applicability of this system to a study of the kinetics of the gas–solid reaction. This paper reports on the temperature and pressure dependence of the rate of the propylene combination reaction,

$$\tfrac{1}{2}AgBF_4 + C_3H_6 \rightarrow \tfrac{1}{2}AgBF_4.2C_3H_6 \ (\Delta H^\circ = -10.08 \text{ kcal/mole } C_3H_6).$$

The product of this reaction, having a 1:2 silver ion to olefin ratio, has earlier (15) been established to be the most stable propylene complex of $AgBF_4$.

EXPERIMENTAL

Anhydrous silver tetrafluoroborate was prepared from silver fluoride and boron trifluoride according to the method of Olah and Quinn (17) with the exception that it was recovered by fractional crystallization from the nitromethane solvent rather than by complete removal of the solvent under vacuum.

Propylene and cyclohexene were Phillips pure grade materials of 99% minimum purity. Prior to use they were dried by passage in the vapor phase through a column packed with phosphorus pentoxide and freeze-degassed at liquid nitrogen temperature.

[1]*Contribution No. 143 from Dow Chemical of Canada, Limited.*
[2]*Present address: Department of Chemistry, University of Windsor, Windsor, Ontario.*
[3]*Present address: Engineering Division, Imperial Oil Enterprises Ltd., Sarnia, Ontario.*
[4]*Author to whom communications regarding this paper should be directed.*

Procedure

The 200–600 mg sample of silver salt, wet with petroleum ether, was placed in a quartz pan suspended from a quartz spiral of sensitivity 5.571 mg/mm and evacuated. The spiral was enclosed in a jacketed chamber thermostatted to ±0.1 °C by liquid pumped from a constant temperature bath capable of control over the range from −5° to 60 °C. After suitable treatment of the sample in order to achieve reproducible kinetics (*vide infra* under Preparation of Sample), propylene was admitted at constant pressure through two solenoid valves in series actuated by platinum contacts in mercury manometers. By maintaining the pressure in the first manometer at not more than 10 mm above the system pressure, surging upon opening of the second valve was prevented and the system pressure could be controlled to ±0.5 mm.

The spiral extension was measured to ±0.02 mm with a cathetometer.

Preparation of Sample

Experimentation established that, in order to obtain kinetic reproducibility, it was necessary to expose the sample of $AgBF_4$ to several complex formation–dissociation cycles. As illustrated in Fig. 1, the rate of the combination reaction is much more rapid in the second cycle than in the first. An explanation of this will be offered in the Discussion section. Microscopic examination of the $AgBF_4$ crystals has revealed that the complex formation–dissociation cycle results in a net volume expansion (the linear dimensions increase by a factor of about 1.3) and the particles appear to develop a very rough surface. The B.E.T. plots of krypton adsorption isotherms at liquid nitrogen temperature (18) revealed, as the result of a single formation–dissociation cycle, an increase of almost 40-fold (from 0.1 to 3.9 m^2/g) in the surface area of the salt. While the X-ray diffraction powder patterns of the salt are identical in samples taken before and after this cyclic operation, that obtained with the before sample is spottier in character indicating larger particle size than in the after sample.

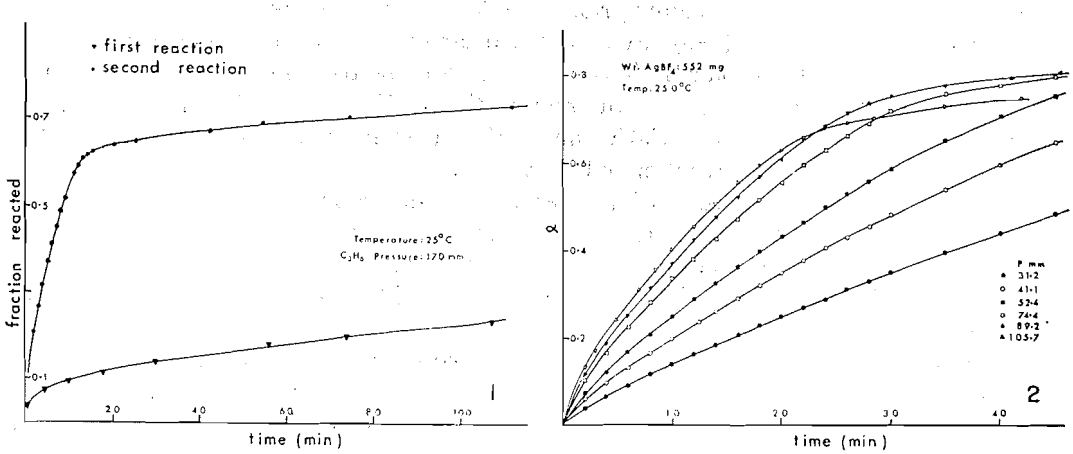


FIG. 1. Plot of fraction reacted versus time for consecutive reactions illustrating the effect of activation.
FIG. 2. Plot of fraction reacted versus time for propylene-activated $AgBF_4$ (sample 2).

The lattice expansion attending complex formation followed by contraction upon dissociation apparently results in breakdown of the crystal or particle size of the $AgBF_4$ thus creating more surface area and probably a rather porous structure. After four or five such cycles, the reaction rates are quite reproducible indicating no further change in the surface structure of the salt.

For the benefit of further discussion, the process of development of the solid surface will be termed activation. With each sample employed, the activation process was effected at 25 °C and, regardless of the temperature at which the rate data for the combination reactions were obtained, the subsequent dissociation step was carried out at 25 °C.

To evaluate the dependence of the kinetics of the propylene complex upon the activation history of the salt, some samples were activated with cyclohexene, an olefin molecule larger than propylene, by formation and dissociation of the complex $AgBF_4.2C_6H_{10}$. As might be expected, there is a greater volume expansion of the salt when this complex forms than is observed with propylene.

RESULTS

Rate determinations on propylene-activated samples of $AgBF_4$ were made at temperatures over the range from 2.3 to 55.0 °C and at pressures of C_3H_6 from about 13 to 200 mm Hg.

Can. J. Chem. Downloaded from www.nrcresearchpress.com by 210.87.254.40 on 09/05/12
For personal use only.

Figure 2 shows the plot of the fraction (α) of $AgBF_4$ reacted versus time in minutes for a typical sample at 25 °C and at a number of pressures. It is evident that there is no induction period required for the reaction and that the rate decreases continuously from the beginning. Some of the higher pressure lines are observed to intersect lower pressure ones at α values of 0.6 to 0.7.

Of the various expressions which have been employed for treatment of rate data for gas–solid reactions (1, 5, 6, 14, 19), the linear rate law,

$$1 - (1 - \alpha)^{1/3} = k_1 t,$$

has been found to apply for this reaction for values of α up to at least 0.4 and ranging upward to greater than 0.9, dependent upon the prior history of the sample. For spherical particles, k_1 is inversely proportional to the particle radius. The data of Fig. 2 deviate from the linear plot of $1 - (1 - \alpha)^{1/3}$ versus time (Fig. 3) only above $\alpha = 0.7$ with the exception of those obtained at the highest pressure when deviation occurs at about $\alpha = 0.55$. It has been found in general that this deviation occurs at lower values of α for the higher pressure determinations.

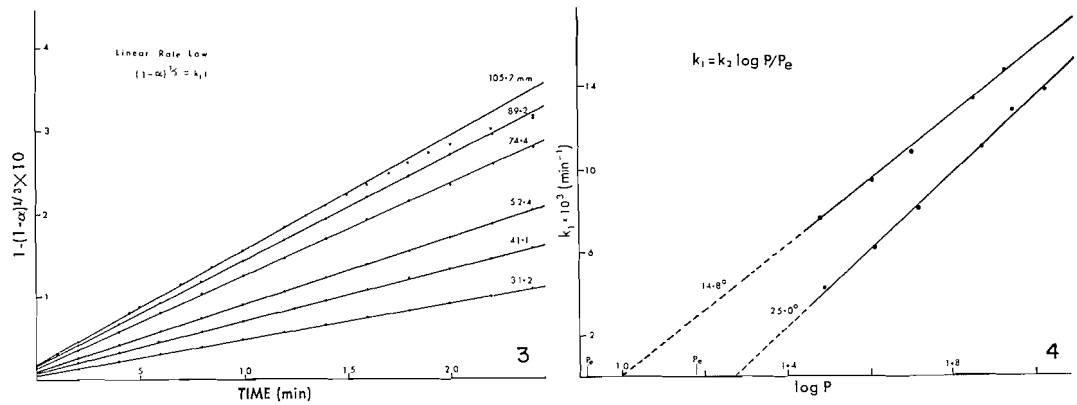


FIG. 3. Linear rate law plots of the data of Fig. 2.
FIG. 4. Pressure dependence of the slope of the linear rate law plots.

The value of the slope, k_1, has been found to be directly proportional to the logarithm of the applied pressure, P (Fig. 4). The linear plot of k_1 versus log P intersects the log P axis at a point just slightly above that corresponding to log P_e, the equilibrium dissociation pressure of the complex. (The equilibrium pressure–temperature relationship for $AgBF_4 \cdot 2C_3H_6$ is

$$\log P_e \text{ (mm)} = 8.5661 - 2202.8/T,$$

yielding P_e values of 8.27 mm at 14.8 °C and 15.1 mm at 25.0 °C.)[5] The slopes and intercepts of these plots were obtained by a least squares treatment of the k_1 vs. log P data. While one would expect k_1 to be positive at any pressure greater than P_e, one might try to rationalize the intercept on the log P axis at a point above P_e in terms of the sample temperature being somewhat above that of its surroundings because of the exothermic nature of the reaction. This discrepancy would diminish, however, as the reaction proceeded and also would be more marked at higher than at lower pressures. The fact that with the most reactive samples, the linear law plots have been found to be linear up to

[5]*Data obtained in this laboratory.*

Can. J. Chem. Downloaded from www.nrcresearchpress.com by 210.87.254.40 on 09/05/12
For personal use only.

$\alpha = 0.9$ suggests that the sample temperature must remain essentially constant throughout the reaction. Also, the good fit of the k_1 vs. log P data to a straight line suggests that the temperature is essentially constant over the range of pressures employed. Despite the small discrepancy, one can consider that the expression

$$[1] \qquad k_1 = k_2 \log P/P_e$$

very nearly expresses the pressure dependence of the reaction rate at constant temperature, with k_2 as the temperature-dependent rate constant. As Fig. 4 illustrates, k_2 increases slightly with increasing temperature, from 15.8×10^{-3} min^{-1} at 14.8 °C to 18.6×10^{-3} min^{-1} at 25.0 °C. Similar behavior is demonstrated in Fig. 5 by data obtained with a different sample over a wider temperature range.

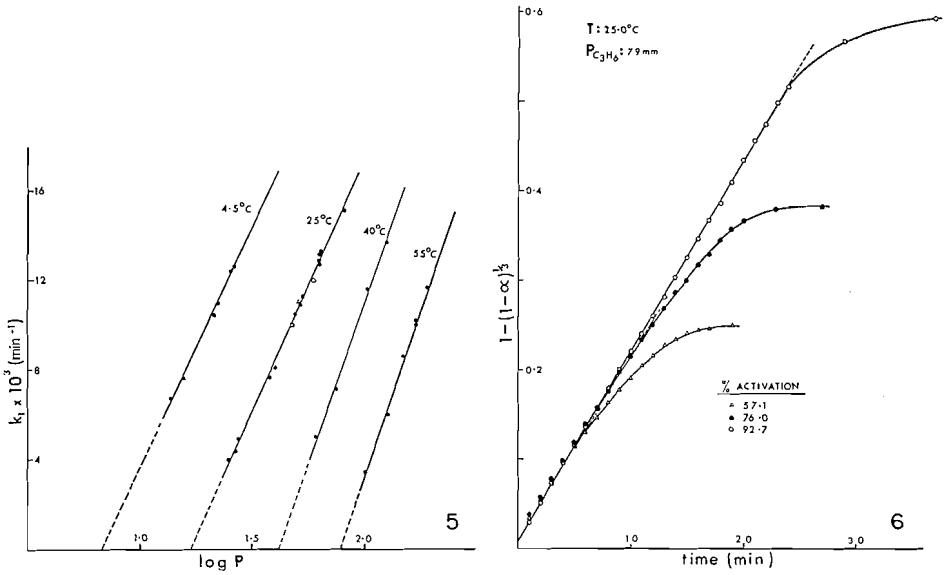


FIG. 5. Temperature dependence of the k_1 versus log P plot (sample 10). (25 °C points, ○, □, △, obtained after determinations at 4.5, 40, and 55 °C respectively).
FIG. 6. Effect of varying cyclohexene activation on range of applicability of linear rate law.

TABLE I

Dependence of rate constant k_2 on sample weight and history (25 °C)

Sample No.	Activating olefin	Sample weight (mg)	$10^3 k_2$ (min^{-1})
3	Propylene	228	31.9
1	Propylene	513	21.4
2	Propylene	552	18.6
4	Cyclohexene	232	40.5
8	Cyclohexene	340	31.4

It has been observed (Table I) that the value of k_2 at a given temperature generally increases with decreasing sample weight and that for samples of comparable weight it is somewhat greater for cyclohexene activation.

In an attempt to determine the dependence of the reaction kinetics upon the activation history of the $AgBF_4$, the kinetics of the propylene reaction were determined on a sample

Can. J. Chem. Downloaded from www.nrcresearchpress.com by 210.87.254.40 on 09/05/12
For personal use only.

after varying amounts of cyclohexene activation. The results are shown in Fig. 6. While the rate, k_1, increases somewhat from 19.2×10^{-3} min^{-1} to 20.9×10^{-3} min^{-1} upon increasing the extent of activation from 57.1% to 92.7%, there is a more marked effect on the value of α at which deviation from the linear rate law occurs. This increases from 0.34 at 57.1% activation to 0.88 at 92.7% activation.

It was found that with complete cyclohexene activation, deviation did not occur below $\alpha = 0.9$.

Deviation of the data from the linear rate law indicates the onset of a second rate-controlling process. It has been observed by others (10, 14, 19) that gas–solid reactions can be in part or largely subject to diffusion control. The rate of the reaction is thus assumed to be a function of the thickness of the product layer through which diffusion must occur and the rate data are often found to obey the parabolic rate law

$$[1 - (1 - \alpha)^{1/3}]^2 = k_d t.$$

For spherical particles, k_d is inversely proportional to the square of the particle radius.

Treatment of the data for the propylene–$AgBF_4$ combination reaction according to the parabolic rate law has established that for non-activated samples, a plot of $[1 - (1 - \alpha)^{1/3}]^2$ versus time is linear over most of the reaction. The data obtained for the first reaction depicted in Fig. 1 obey the parabolic law after only 7.5% reaction. It was found impossible, however, to determine the pressure and temperature dependence of k_d for non-activated $AgBF_4$ since each determination required a new sample, slightly different from the others in physical characteristics.

While in general it was found that the activated samples of $AgBF_4$ gave rate data which deviated from the linear rate law at the higher values of α, most of these did not obey the parabolic rate law alone over a significant range of α. With one sample, however, a plot of the rate data according to the parabolic law demonstrated linear regions from which values of the rate constant, k_d, for the diffusion-controlled reaction could be obtained. The data for determinations at several pressures at 25.0 °C are shown in Fig. 7. The upward deviation from the parabolic law at high values of α may indicate some opening up of the sample due to expansion.

In Table II are reported data at 25.0 °C for the slopes, k_1, of the linear law plots, the value of α, α_1, at which deviation from the linear law begins, the slope, k_d, of the parabolic

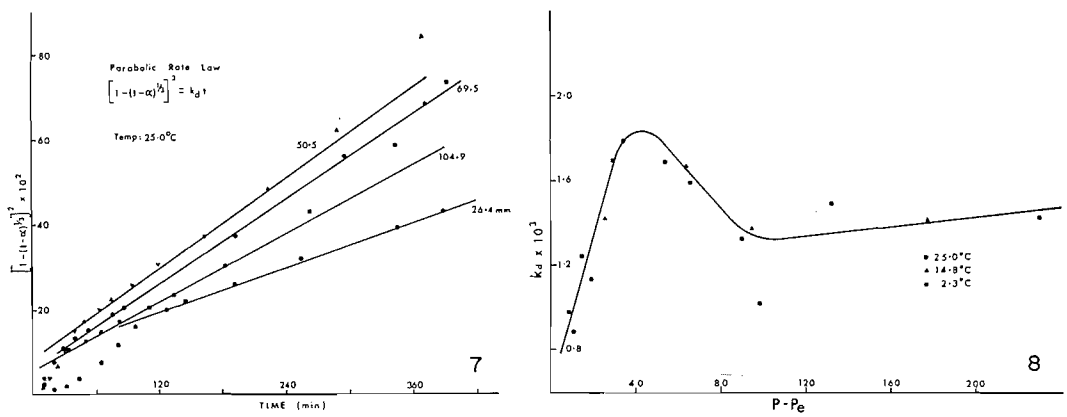


FIG. 7. Parabolic rate law plots (sample 1).
FIG. 8. Pressure dependence of rate constant for diffusion-controlled reaction.

Can. J. Chem. Downloaded from www.nrcresearchpress.com by 210.87.254.40 on 09/05/12
For personal use only.

rate law plots and the range of values of α, α_2 to α_3, over which that law applies (for sample 1 of Table I). It is apparent that while α_1 decreases somewhat with increasing propylene pressure, there is a much more marked decrease in α_2, the value of α at which the diffusion-controlled reaction alone obtains; this changes from 0.85 at 26.4 mm Hg to 0.50 at 245.2 mm Hg. The earlier observation that the α versus time plots for higher pressure determinations intersected those at lower pressures might be explained by the earlier onset of diffusion control at higher pressures.

TABLE II

Kinetic data for propylene combination reaction at 25.0 °C (sample 1)

Pressure (mm Hg)	Linear rate law		Parabolic rate law		
	10^3k_1 (min^{-1})	α_1*	10^3k_d (min^{-1})	α_2†	α_3†
26.4	4.12	0.523	0.90	0.847	0.959
34.1	6.30	0.518	1.14	0.780	0.947
50.5	10.2	0.587	1.79	0.810	0.972
69.5	13.3	0.462	1.69	0.689	0.995
104.9	17.1	0.474	1.32	0.687	0.910
147.0	20.2	0.458	1.48	0.580	0.912
245.2	23.1	0.423	1.41	0.497	0.907

*The quantity α_1 is value of α at which deviation from linear law observed.
†The quantities α_2 and α_3 are respectively the lowest and highest values of α for which the parabolic law applies.

With this sample, as with all others, k_1 varies logarithmically with P ($k_2 = 21.4 \times 10^{-3}$ min^{-1} and, by extrapolation, $k_1 = 0$ when $P = 16.7$ mm Hg). The value of k_1 at the highest value of P fell below the linear k_1 vs. log P plot.

Over a short range of pressure, k_d was found to vary essentially linearly with P, subsequently passing through a maximum and decreasing to a point beyond which there was little dependence on pressure. The variation of k_d with $P - P_e$ at various temperatures is illustrated in Fig. 8. The temperature dependence of k_d is not very marked.

DISCUSSION

While the parabolic rate law describes the reaction kinetics for most of the reaction of propylene with non-activated samples of $AgBF_4$, the linear rate law applies for most of the reaction with activated samples. The linear rate law indicates a kinetically controlled reaction since the rate is proportional to the area, and thus to the concentration of unreacted salt, at the reaction interface. The parabolic rate law, on the other hand, indicates a diffusion-controlled reaction. The effect of varying degrees of activation (Fig. 6) upon the value of α at which deviation from kinetic control is observed establishes a progressive change from diffusion to kinetic control as activation proceeds.

There is marked similarity between the variation with pressure of the rate constant, k_d, for the diffusion-controlled reaction (Fig. 8) and the well-known variation of the diffusion coefficient with amount of adsorption for transport of a gas through a porous plug on which it is adsorbed. This phenomenon has been reviewed by Field, Watts, and Weller (20). It has been observed that the diffusion coefficient increases with surface coverage, reaches a maximum at the monolayer coverage and shows relatively little variation with further adsorption. This behavior has been interpreted in terms of transport via a surface diffusion process, the rate of which increases with increasing adsorption until the monolayer is formed with very little further change as a result of multilayer adsorption.

As a result of this similarity, it is suggested that, for those samples of $AgBF_4$ which demonstrate diffusion control, the rate-controlling mechanism is the surface diffusion of

Can. J. Chem. Downloaded from www.nrcresearchpress.com by 210.87.254.40 on 09/05/12
For personal use only.

adsorbed gas molecules through the pore structure rather than diffusion through the reaction product. It would be expected that the activation process which involves an expansion followed by a contraction of the salt lattice would markedly change the pore structure of the salt particles. The observed net volume expansion and increased surface area as well as the decreased particle size of the sample resulting from activation indicate that the original salt particles have been converted to expanded porous bodies composed of smaller particles.

When the activated salt is reacted with propylene, the C_3H_6 molecules must be able initially to reach the reaction interface without being subject to the control of surface diffusion. As the reaction proceeds, however, the concommitant lattice expansion reduces the average pore size and, at some point in the reaction, surface diffusion begins to play a rate-controlling role. The observation that diffusion control occurs at lower values of α at the higher pressures can be explained by the greater adsorption at those pressures which brings surface diffusion into play at an earlier stage. Similarly in nonactivated or semi-activated samples, earlier onset of diffusion control can be explained by a greater proportion of small pores in the system. The fact that most activated samples have not demonstrated significant regions of pure diffusion control indicates that they contain some pores of diameter sufficiently large that, even toward the end of the reaction, the propylene molecules can pass through without being subject to the control of surface diffusion. The observation that deviation from the linear rate law occurred at higher values of α for cyclohexene-activated than for propylene-activated samples can equally well be attributed to a larger average pore diameter in the former.

The observation by Pavlyuchenko and Torgonskaya (13) that the reaction

$$AgNO_3 + 3NH_3 \rightarrow AgNO_3.3NH_3$$

is entirely diffusion-controlled at -20 °C and 0 °C but initially, kinetically controlled at 25 °C and 56 °C suggests that the diffusion control in this system may be also the result of adsorption; with increasing temperature, the decreasing adsorption will reduce the controlling effect of surface diffusion.

The adherence of the rate data to the linear rate law for much of the reaction of activated salt indicates that the contracting sphere model (21) may be satisfactorily employed to visualize the reaction mechanism. It has been reported by several investigators (6, 11) that, for kinetically controlled reactions, the rate is often directly proportional to the difference between the imposed pressure and the equilibrium dissociation pressure of the compound, i.e. for combination reactions to $P - P_e$. Our observation that the rate at constant temperature, k_1, is proportional to log P suggests that the driving force is something other than the simple pressure differential between the outside of the reacting particle and the reaction interface. The log P relationship suggests, in fact, that the propylene molecules are supplied to the reaction interface from an adsorbed film on the particle surface. The earlier indication that surface diffusion may be the rate-controlling process when diffusion control is operative further substantiates the view that the gas is adsorbed on the solid surface. It has been recognized (1) that adsorption of the gaseous component on the surface of a solid will affect the rate of a dissociation reaction. While it is not surprising, then, that for this combination reaction the propylene is adsorbed, it is nonetheless interesting that the reaction rate demonstrates a pressure dependence that may be that shown by the adsorption process.

Of the adsorption isotherms which might apply for this system, the two most probable are the Freundlich isotherm

Can. J. Chem. Downloaded from www.nrcresearchpress.com by 210.87.254.40 on 09/05/12
For personal use only.

$$\log \theta = AT \log P + BT \quad [2]$$

and the Temkin isotherm

$$\theta = A'T \log P + B'T \quad [3]$$

where θ represents the surface coverage. The Freundlich isotherm is based on the assumption that the heat of adsorption, q, decreases logarithmically with increasing θ, while the Temkin isotherm assumes a linearly decreasing q (22) and is valid only when θ is approximately 0.5. Because of the reaction of C_3H_6 with $AgBF_4$, it has not been possible to determine directly the form which the adsorption isotherm takes in this system.

For the sake of simplicity one might tend to assume that the rate of reaction is proportional to the difference between the amounts of adsorption at P and P_e, i.e.,

$$k_1 = k'(\theta_P - \theta_{P_e}). \quad [4]$$

Equation [4] in combination with equation [1] suggests Temkin adsorption. Because, however, the Temkin isotherm is valid only in the vicinity of 50% surface coverage, it is unlikely that it can adequately represent the rate-determining adsorption process. This is particularly so if the maximum in the k_d versus $P - P_e$ plot (Fig. 8) can be considered to represent the point at which monolayer formation is complete.

The suggestion then that the Freundlich isotherm may apply infers that k_1 is proportional to the difference between the heats of adsorption at P and P_e rather than to the difference between the surface coverages, i.e.,

$$k_1 = K(q_P - q_{P_e}). \quad [5]$$

From eqs. [1], [2], and [5], one deduces the expression

$$k_2 = KAT. \quad [6]$$

The observed dependence of the magnitude of k_2 on sample size may be due to a decrease in the surface area to weight ratio as the sample size increases.

It has been observed by a number of investigators (1) that, for a truly reversible dissociation reaction at a solid–solid interface, the activation energy is equivalent to the heat of reaction. Consequently, it has been suggested (1) that there should be zero activation energy for the reverse combination reaction. Since the $AgBF_4.2C_3H_6$ complex formation is reversible, one would then expect this combination reaction to show zero activation energy also.

An Arrhenius plot of the values of k_2 from Fig. 5 shows considerable scatter about a straight line with a slope such that the activation energy calculated therefrom is <2 kcals/mole. It is probable then that the temperature dependence of k_2 is simply that of the adsorption of propylene as suggested by eq. [6].

It is apparent that, for Freundlich adsorption as defined by eq. [2], T/k_2 should be constant. It was found, however, that for the propylene reaction, T/k_2 decreases with increasing temperature (Table III). Halsey (23) has stated that if the partition function for the adsorbed molecules is not constant but is a function of θ, the Freundlich isotherm can be of the form

$$\log \theta = A \frac{T}{(1 - rT)} \log P + B \frac{T}{(1 - rT)}$$

where r is a constant. Should this expression apply for adsorption in the propylene–$AgBF_4$ system, one would predict a linear decrease of T/k_2 with increasing T. With the exception of the point at 40 °C the data of Table III obey this relationship.

Can. J. Chem. Downloaded from www.nrcresearchpress.com by 210.87.254.40 on 09/05/12
For personal use only.

TABLE III

Variation of rate constant k_2 with temperature (data of Fig. 5 after correction for adsorption)

T (°K)	$10^3 k_2$ (min^{-1})	$10^{-4} T/k_2$
277.7	17.9	1.55
298.2	21.4	1.39
313.2	26.8	1.17
328.2	29.2	1.12

The temperature and pressure dependence of the rate data certainly indicate that the propylene is being supplied to the reaction interface from an adsorbed film rather than from the gas phase. The earlier suggestion that, if Freundlich adsorption applies, the rate of reaction is proportional to the difference between the heats of adsorption at P and P_e may be suggestive of the mechanism of transport of the olefin molecules from the particle surface to the reaction interface. If the transfer involves successive combination and dissociation reactions between the olefin molecules and silver ions in the salt lattice, it is possible that the activation energy for the initial dissociation step is provided by the heat of adsorption. Because of the electronic interaction involved, the olefin molecules can be considered, at least to the point of monolayer formation, to be chemisorbed rather than just physically adsorbed on the salt surface, and the heat of adsorption would probably exceed the value of $\Delta H°$ for complex formation ($\simeq$10 kcal/mole) since lattice energy changes would be less for surface reaction than for bulk complex formation.

Although the suggested mechanism is very speculative, this study has established that the rate of reaction of propylene with silver tetrafluoroborate is markedly dependent upon the adsorption state of the system whether the reaction is kinetically controlled or diffusion controlled. This same behavior might be expected for many other gas–solid combination reactions since a marked adsorption of the gas on the solid surface would be anticipated.

ACKNOWLEDGMENT

The authors are very grateful to Dr. H. Watts for helpful discussion relating to the diffusion control observed in this study.

REFERENCES

1. W. E. Garner. Chemistry of the solid state. Butterworths, London. 1955, pp. 213–231.
2. J. A. Allen. Australian J. Chem. **14**, 20 (1961).
3. P. Barret and L. Bonnetain. Bull. Soc. Chim. France, 576 (1961).
4. P. J. Anderson and R. F. Horlock. Trans. Faraday Soc. **58**, 1993 (1962).
5. N. A. Warner and T. R. Ingraham. Can. J. Chem. Eng. **40**, 263 (1962).
6. T. R. Ingraham and P. Marier. Can. J. Chem. Eng. **41**, 170 (1963).
7. W. A. Davis and J. V. Eyre. Proc. Roy. Soc. London, Ser. A, **104**, 512 (1923).
8. B. N. Ghosh. J. Indian Chem. Soc. **18**, 472 (1941).
9. A. Bielanski and F. C. Thompkins. Trans. Faraday Soc. **46**, 1072 (1950).
10. M. M. Pavlyuchenko and E. M. Borisenko. Geterogennye Khim. Reaktsii, 203 (1961).
11. J. Zawadski and S. Bretsynajder. Trans. Faraday Soc. **34**, 951 (1938).
12. M. M. Pavlyuchenko and T. I. Torgonskaya. Geterogennye Khim. Reaktsii, 184 (1961).
13. M. M. Pavlyuchenko and T. I. Torgonskaya. Geterogennye Khim. Reaktsii, 190 (1961).
14. F. E. Massoth and W. E. Hensel. J. Phys. Chem. **63**, 697 (1959).
15. H. W. Quinn and D. N. Glew. Can. J. Chem. **40**, 1103 (1962).
16. H. W. Quinn, J. S. McIntyre, and D. J. Peterson. Can. J. Chem. **43**, 2896 (1965).
17. G. A. Olah and H. W. Quinn. J. Inorg. Nucl. Chem. **14**, 295 (1960).
18. F. W. Bloecher. Mining Eng. **3**, 255 (1951).
19. R. L. Farrar and H. A. Smith. J. Phys. Chem. **59**, 763 (1955).
20. G. J. Field, H. Watts, and K. R. Weller. Rev. Pure Appl. Chem. **13**, 1 (1963).
21. W. D. Spencer and B. Topley. J. Chem. Soc. 2633 (1929).
22. D. O. Hayward and B. M. W. Trapnell. Chemisorption. Butterworths, London. 1964. p. 159.
23. G. Halsey. Advan. Catalysis, **4**, 259 (1952).

Can. J. Chem. Downloaded from www.nrcresearchpress.com by 210.87.254.40 on 09/05/12
For personal use only.

Can. J. Chem. Downloaded from www.nrcresearchpress.com by 210.87.254.42 on 09/05/12
For personal use only.

CYCLOBUTADIENE–METAL COMPLEXES

PART VIII.[1] SYNTHESIS OF TETRAPHENYLCYCLOBUTADIENE NICKEL HALIDES BY LIGAND-EXCHANGE REACTIONS

D. F. POLLOCK AND P. M. MAITLIS[2]

Chemistry Department, McMaster University, Hamilton, Ontario

Received July 5, 1966

ABSTRACT

The preparation of cyclobutadiene nickel halide complexes $(R_4C_4NiX_2)_2$, where R is phenyl or substituted phenyl, by reaction of the palladium complexes, $[R_4C_4PdX_2]_2$, with a *tert*-phosphine metal complex, e.g. $(n\text{-}Bu_3P)_2NiX_2$, is described. The reaction proceeds according to the equation

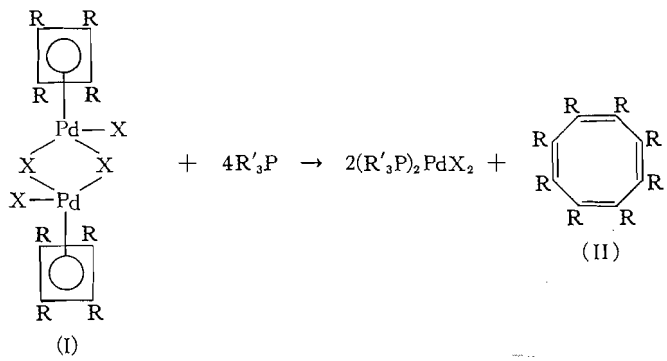
$$[R_4C_4PdX_2]_2 + 2(Bu_3P)_2NiX_2 \rightarrow [R_4C_4NiX_2]_2 + 2(Bu_3P)_2PdX_2.$$

Possible mechanisms are suggested.

INTRODUCTION

When this work was started (1962), little was known about the chemistry of cyclobutadiene–metal complexes, mainly because of the difficulty in preparing representative complexes with (*a*) different substituents on the four-membered ring and (*b*) different metals complexed to the cyclobutadiene. The problems associated with the synthesis of various substituted cyclobutadiene complexes of a given metal have now been largely overcome though serious practical difficulties often remain (1). The syntheses used were for the most part specific for one metal, and in order to obtain a series of complexes with the same ligand attached to different metals it was necessary to devise a means of transferring the cyclobutadiene ring from one metal to another. This problem has been solved to a great extent by the ligand-transfer reactions which have been described previously (2). Before the discovery of these reactions, however, we developed the novel ligand-exchange reactions which form the subject of this paper.

The preparation and properties of the tetraphenylcyclobutadiene palladium halides (I, R = Ph) have been adequately described by ourselves (3) and others (4). One of the most interesting reactions which these compounds undergo is with a *tert*-phosphine (5). In refluxing benzene the cyclobutadiene–palladium bond is broken and the products isolated are the bis(*tert*-phosphine)palladium halides and a dimer of tetraphenylcyclobutadiene, later identified as octaphenylcyclooctatetraene (II, R = Ph) (6).

[1] 

(I) (II)

[1]*Part VII. A. Efraty and P. M. Maitlis. Tetrahedron Letters, 4025 (1966).*
[2]*Author to whom correspondence should be addressed.*

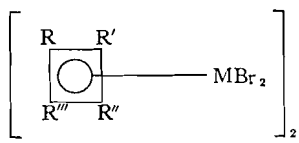
This reaction, which proceeded in high yield, suggested that if the phosphine complex of a metal in which the phosphine was labile were used in place of the free phosphine it might be possible to get complete exchange of ligands between the two metals, thus

[2] $$(R_4C_4PdX_2)_2 + 2(R'_3P)_2NiX_2 \rightarrow (R_4C_4NiX_2)_2 + 2(R'_3P)_2PdX_2 \ .$$

(I) (III) (IV) (V)

RESULTS

Preliminary experiments with $(R'_3P)_2NiX_2$, where X = halogen and R′ = Ph or $(R'_3P)_2$ = $Ph_2PCH_2CH_2PPh_2$, indicated that this exchange was feasible. The products from these reactions, though, were nearly impossible to separate. However, use of $(n\text{-}Bu_3P)_2NiBr_2$ as the source of the phosphine also led to the desired reaction and gave products which were easy to separate. The reaction was most conveniently carried out in refluxing chlorobenzene; a color change from red [the color of the mixture of the cyclobutadiene complex (I, R = Ph) and the nickel complex (III)] to green [mainly the color of IV since V is yellow] occurred very rapidly. Heating was continued for 2 h to ensure completion of the reaction. After removal of the chlorobenzene the products were separated either by chromatography or by solvent extraction, the complex (V, R′ = *n*-Bu) being exceedingly soluble whereas IV (R = Ph) was only slightly soluble in most solvents. The nickel complex (IV, R = Ph) was identified by analysis and by comparison with an authentic sample. This reaction was extended to the synthesis of other complexes (IV, R = *p*-ClC_6H_4, *p*-$MeOC_6H_4$, and *p*-$CH_3C_6H_4$, and VI, M = Ni)[3] since the required palladium complexes were readily accessible by modification of the routes used to prepare I (R = Ph).



(VI)

The bromide complexes (I, X = Br) were usually used and the yields ranged from 72–90%. In one case (I, R = Ph, X = Cl), the chloride complex was used; here the yield was slightly lower than for the bromide. These reactions are, however, probably quantitative, since in no case was any by-product detected, and the lower yields obtained are due to some difficulty in isolating and purifying the products.

The results are presented in Table I.

DISCUSSION

The first step in both the ligand-displacement reaction (eq. [1]) and in the ligand-exchange reaction (eq. [2]) is probably the attack of a phosphine at the palladium. In the latter case this must be formed by dissociation of the nickel complex.

$$(R'_3P)_2NiX_2 \rightleftharpoons R'_3P + R'_3PNiX_2$$

Once the phosphine is complexed to the palladium the metal–cyclobutadiene bond is weakened since, despite a number of attempts, no stable tetraphenylcyclobutadiene palladium halide – phosphine complexes, $R_4C_4PdX_2PR'_3$, could be obtained. The next

[3] *VI (M = Ni) was prepared from VI (M = Pd) which was obtained from palladium chloride and o-methoxydiphenylacetylene. VI is therefore probably a mixture of the 1,2-bis(o-anisyl)-3,4-diphenylcyclobutadiene (R = R′ = o-anisyl, R″ = R‴ = phenyl) and the 1,3-bis(o-anisyl)-2,4-diphenylcyclobutadiene (R = R″ = o-anisyl, R′ = R‴ = phenyl).*

Can. J. Chem. Downloaded from www.nrcresearchpress.com by 210.87.254.42 on 09/05/12
For personal use only.

TABLE I

Ligand-exchange reactions

Reactants			Analysis of product, $[R_4C_4NiX_2]_2$					
			Found			Calculated		
$[R_4C_4PdX_2]_2$	$(n\text{-}Bu_3P)_2NiX_2$	Yield (%)	C	H	Mol. wt.	C	H	Mol. wt.
R = Ph, X = Br	X = Br	90	58.27	3.40	—	58.49	3.51	—
R = Ph, X = Cl	X = Cl	82	69.02	4.32	—	69.18	4.16	—
R = *p*-ClC_6H_4, X = Br	X = Br	72	47.03	2.34	1 390	47.24	2.26	1 425
R = *p*-$MeOC_6H_4$, X = Br	X = Br	77	54.87	4.50	1 340	54.97	4.26	1 390
R = *p*-MeC_6H_4, X = Br	X = Br	73	56.74	3.98	1 210	56.61	4.16	1 262
VI, M = Pd	X = Br	75	56.56	3.62	1 220	56.72	3.81	1 270

step, however, is less obvious since there are two main mechanisms by which the reaction can proceed. The first assumes that free tetraphenylcyclobutadiene is transiently formed and that this then adds to a coordinatively unsaturated nickel complex.

$$4R'_3P + [R_4C_4PdX_2]_2 \rightarrow 2(R'_3P)_2PdX_2 + 2R_4C_4$$

Either

$$R_4C_4 + R'_3PNiX_2 \rightarrow \tfrac{1}{2}[R_4C_4NiX_2]_2 + R'_3P.$$

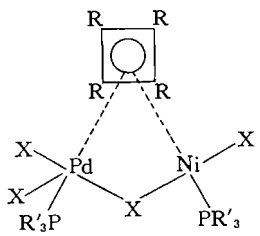
Or

$$2R_4C_4 \rightarrow R \text{ (VII)} R \rightarrow \text{II.}$$

(VII)

The formation of the cyclooctatetraene (II) can be visualized as arising by a similar route.

The second reaction path does not assume that the cyclobutadiene becomes completely detached from the metal at any time but rather that it proceeds via an intermediate such as VIII in which both metals are attached to the ring (either from the same side, as shown, or from opposite sides).



(VIII)

Pettit and his co-workers (7) have recently obtained evidence to show that free cyclobutadiene, obtained by oxidation of its iron tricarbonyl complex, is capable of existence, though only for a short time. This might suggest that a free tetraphenylcyclobutadiene, which would be expected to be more stable than cyclobutadiene itself, would be capable of existing for a short time and might well be an intermediate in the above reaction. However, attempts to trap any tetraphenylcyclobutadiene produced from I, according to eq. [1], with a dienophile have been surprisingly unsuccessful (8). Adducts have been obtained but in low yield and usually together with II despite the large preponderance of the dienophile. In some cases, however, even the expected adducts are not found; thus reaction of tetraphenylcyclobutadiene palladium bromide (I, R = Ph, X = Br) with tributylphosphine in

Can. J. Chem. Downloaded from www.nrcresearchpress.com by 210.87.254.42 on 09/05/12
For personal use only.

refluxing benzene gave no trace of hexaphenylbenzene when conducted in the presence of a 10 *M* excess of diphenylacetylene. A 92% yield of the cyclooctatetraene (II, R = Ph) was obtained. One of us has recently suggested (9) that the diradical (VII) supposed to be the precursor to II may well be formed inside a metal complex and that the successful reactions with dienophiles may also start when both dienophile and the cyclobutadiene are complexed to the metal.

This argument, accompanied by the absence of any by-products in the ligand-exchange reactions, notably II, makes us favor the second mechanism for the ligand-transfer reaction. Further studies are in progress which it is hoped will shed some light on this problem.

Attempts to extend these reactions to form the cyclobutadiene complexes of cobalt(II) and iron(II) have not, as yet, proved successful.

EXPERIMENTAL

The palladium complexes (I, R = Ph) and (I, R = *p*-ClC_6H_4) were prepared by published methods (3). The remaining complexes were prepared from the acetylenes in similar ways, full details of which will be published shortly. Since the method of carrying out the ligand-exchange reactions did not vary greatly, a representative procedure is given. The results of the other reactions are presented in Table I.

Tetraphenylcyclobutadiene Nickel Bromide (IV, R = Pd, X = Br)

A suspension of 1.0 g (0.8 mmole) of tetraphenylcyclobutadiene palladium bromide dimer in 200 ml of chlorobenzene was refluxed for 5 min under nitrogen to remove air dissolved in the solvent. 1.0 g (1.6 mmoles) of bis(tri-*n*-butylphosphine)nickel bromide (10) was added; the solution changed color from red to dark green almost immediately. Refluxing was continued for 2 h to complete the reaction.

The hot solution was then filtered (negligible residue) and the volume of the filtrate reduced to 50 ml on a rotary evaporator. This solution was then chromatographed on a silica column. Methylene chloride eluted the yellow and extremely soluble bis(tri-*n*-butylphosphine)palladium bromide, whereas the less soluble tetraphenylcyclobutadiene nickel bromide (IV, R = Ph, X = Br) was eluted by 1:1 methylene chloride – tetrahydrofuran. The yield of the cyclobutadiene nickel halide dimeric complex was 0.83 g (0.72 mmole, 90%). The identity of the complex was shown by analysis (a molecular weight determination was not possible because of its insolubility), decomposition point 317°, and comparison of the infrared spectrum with that of an authentic sample (11). Crystalline bis(tri-*n*-butylphosphine)palladium bromide was isolated in 46% yield, but the mother liquors still contained a large amount of this very soluble compound. The identity of the phosphine complex was established by comparison of its infrared spectrum with that of an authentic sample; it had m.p. 71–73°, mixed melting point with an authentic sample 72–74°.

Formation of Octaphenylcyclooctatetraene (II, R = Ph) in the Presence of Diphenylacetylene

Tetraphenylcyclobutadiene palladium bromide dimer (I, R = Ph, X = Br) (0.30 g, 0.24 mmole) and diphenylacetylene (0.86 g, 4.8 mmoles) were refluxed in 100 ml of benzene under nitrogen. Tri-*n*-butylphosphine (0.20 g, 0.98 mmole) was added; the suspension rapidly turned yellow and the solid dissolved. The solution was refluxed for 30 min and then filtered hot to leave 0.11 g of a white crystalline solid shown to be octaphenylcyclooctatetraene (II, R = Ph) by its infrared spectrum. The solvent was removed on a rotary evaporator and the residue extracted with a few milliliters of ethanol in which both the cyclooctatetraene (II, R = Ph) and hexaphenylbenzene are totally insoluble. The insoluble residue (0.05 g) was shown to be exclusively octaphenylcyclooctatetraene by its characteristic infrared spectrum. Total yield of II (R = Ph) obtained was 0.16 g, 92% theoretical. Thin layer chromatography of the ethanol-soluble material showed the presence only of bis(tributylphosphine)palladium bromide and diphenylacetylene.

ACKNOWLEDGMENT

We thank the National Research Council for their support of this work, Johnson, Matthey and Mallory for the loan of palladium chloride, and M and T Chemicals for a gift of tributylphosphine.

REFERENCES

1. P. M. MAITLIS. Advan. Organometal. Chem. **4**, 103 (1966).
2. P. M. MAITLIS and M. L. GAMES. J. Am. Chem. Soc. **85**, 1887 (1963); Chem. Ind. London, 1624 (1963). P. M. MAITLIS and A. EFRATY. J. Organometal. Chem. **4**, 172, 175 (1965).
3. A. T. BLOMQUIST and P. M. MAITLIS. J. Am. Chem. Soc. **84**, 2329 (1962). P. M. MAITLIS and M. L. GAMES. Can. J. Chem. **42**, 183 (1964). P. M. MAITLIS, D. POLLOCK, M. L. GAMES, and W. J. PRYDE. Can. J. Chem. **43**, 470 (1965).

Can. J. Chem. Downloaded from www.nrcresearchpress.com by 210.87.254.42 on 09/05/12
For personal use only.

4. L. MALATESTA, G. SANTARELLA, L. M. VALLARINO, and F. ZINGALES. Atti Accad. Nazl. Lincei, Rend. Classe Sci. Fis. Mat. Nat. **27**, 230 (1959); Angew. Chem. **72**, 34 (1960). L. M. VALLARINO and G. SANTARELLA. Gazz. Chim. Ital. **94**, 252 (1964). R. C. COOKSON and D. W. JONES. Proc. Chem. Soc. 115 (1963); J. Chem. Soc. 1881 (1965). R. HÜTTEL and H. J. NEUGEBAUER. Tetrahedron Letters, 3541 (1964).
5. P. M. MAITLIS and F. G. A. STONE. Proc. Chem. Soc. 330 (1962).
6. G. A. PAWLEY, W. N. LIPSCOMB, and H. H. FREEDMAN. J. Am. Chem. Soc. **86**, 4725 (1964). P. J. WHEATLEY. J. Chem. Soc. 3136 (1965).
7. L. WATTS, T. D. FITZPATRICK, and R. PETTIT. J. Am. Chem. Soc. **87**, 3254 (1965).
8. R. C. COOKSON and D. W. JONES. J. Chem. Soc. 1881 (1965).
9. P. M. MAITLIS. Advan. Organometal. Chem. **4**, 128 (1966).
10. K. A. JENSEN, P. H. NIELSEN, and C. T. PEDERSEN. Acta Chem. Scand. **17**, 1115 (1963).
11. H. H. FREEDMAN. J. Am. Chem. Soc. **83**, 2194 (1961).

Can. J. Chem. Downloaded from www.nrcresearchpress.com by 210.87.254.42 on 09/05/12
For personal use only.

Can. J. Chem. Downloaded from www.nrcresearchpress.com by 210.87.254.6 on 09/05/12
For personal use only.

KINETIC ASPECTS OF THE COPOLYMERIZATION OF TETRAHYDROFURAN WITH PROPYLENE OXIDE. I

L. P. BLANCHARD, J. SINGH,[1] AND M. D. BAIJAL[2]
Département de Génie Chimique, Université Laval, Québec, P.Q.
Received December 14, 1964, and, as revised, July 11, 1966

ABSTRACT

Tetrahydrofuran and propylene oxide were copolymerized in the presence of the catalyst boron fluoride ethyl ether, and various co-catalysts, such as 1,2-propanediol, 1,3-propanediol, and 1,4-butanediol. Ethylene chloride was used as a solvent and as an internal reference for analytical purposes. Reactions were carried out at 0 °C and at atmospheric pressure. Monomer concentrations were determined by vapor phase chromatography, and copolymer molecular structure analyses were carried out by physical and chemical methods including infrared spectroscopy, vapor pressure osmometry, hydroxyl end-group analysis, and chemical reduction of unsaturated linkages.

The homopolymerization of tetrahydrofuran did not take place, whereas that of propylene oxide proceeded at a rapid rate. In the copolymerization of tetrahydrofuran with propylene oxide, the rate of disappearance of tetrahydrofuran was found to be independent of its concentration, but varied directly with the concentration of propylene oxide. Under similar conditions, the rate of disappearance of propylene oxide was found to be (*a*) proportional to the square of its concentration, and (*b*) inversely proportional to the concentration of tetrahydrofuran.

Reactivity ratios varied between 1.3 and 1.8 for propylene oxide and between 0.1 and 0.6 for tetrahydrofuran. Molecular weights obtained by vapor pressure osmometry ranged between 460 and 740, and those obtained by hydroxyl end-group analysis ranged between 520 and 1 660. Infrared spectra confirmed the presence of hydroxyl groups and ether linkages in the copolymers prepared. Results on terminal unsaturation were negative.

RÉSUMÉ

La copolymérisation du tétrahydrofuran et de l'oxyde de propylène fut effectuée en présence du catalyseur l'éthérate du fluorure de bore, et de cocatalyseurs tels le 1,2-propanediol, le 1,3-propanediol et le 1,4-butanediol. Le chlorure d'éthylène servait de solvant et d'étalon interne pour fins d'analyse. Les concentrations de monomères furent suivies, en fonction du temps, par la chromatographie en phase vapeur. L'analyse des copolymères a porté surtout sur l'étude de la structure au moyen de techniques physiques et chimiques telles que la spectroscopie infrarouge, l'osmométrie à tension de vapeur, l'analyse chimique des groupements hydroxyles terminaux et la réduction chimique des liaisons doubles.

L'homopolymérisation du tétrahydrofuran n'a pu être effectuée, tandis qu'avec l'oxyde de propylène seul, dans les conditions de réaction adoptées, la réaction s'est poursuivie à grande vitesse. Dans la copolymérisation du tétrahydrofuran avec l'oxyde de propylène, la vitesse de disparition du tétrahydrofuran était indépendante de sa concentration et variait directement avec la concentration d'oxyde de propylène. Dans les mêmes conditions, la vitesse de disparition de l'oxyde de propylène était (*a*) proportionnelle au carré de sa concentration et (*b*) inversement proportionnelle à la concentration du tétrahydrofuran.

Les rapports de réactivité de l'oxyde de propylène ont varié de 1.3 à 1.8 et ceux du tétrahydrofuran de 0.1 à 0.6. Les poids moléculaires obtenus par osmométrie à tension de vapeur étaient compris entre 460 et 740 et ceux obtenus par analyse chimique des groupements hydroxyles terminaux entre 520 et 1 660. Les spectres infrarouges ont confirmé la présence des groupements hydroxyles et des liaisons éther internes.

Les résultats des tests d'insaturation terminale ont été négatifs.

INTRODUCTION

Copolymerization reactions of alkylene oxides and tetrahydrofuran with boron fluoride ethyl ether as catalyst have been investigated by a number of groups (1–4); no work, however, has been reported on the kinetics of the copolymerization reaction of tetrahydrofuran with propylene oxide. Copolyetherdiols obtained from the copolymerization

[1]*Present address: Department of Agriculture, Government of Canada, Ottawa, Canada.*
[2]*National Research Council Postdoctorate Fellow.*

of alkylene oxides and tetrahydrofuran have been used in the preparation of polyurethanes (1, 3). It has been reported (1) that diols prepared from tetrahydrofuran and propylene oxide present two advantages when used as intermediates in the preparation of polyurethanes. They reduce cold hardening or crystallinity in the solid, and facilitate efficient mixing and good molding of the uncured ingredients.

Since the mechanism of preparation of these low molecular weight copolyetherdiols has not been established yet, the copolymerization reaction of tetrahydrofuran with propylene oxide was studied. The results obtained throw light (*a*) on the chemistry of preparation, and (*b*) on the composition and structure of these polyols.

EXPERIMENTAL

Materials

The following substances were used for this study:

(*a*) comonomers: propylene oxide (Anachemia, polymerization grade), tetrahydrofuran (Anachemia, b.p. 64–66°);

(*b*) catalyst: boron fluoride ethyl ether (Eastman, purified);

(*c*) co-catalysts: 1,2-ethanediol (Fisher, U.S.P.), 1,2-propanediol (Fisher, U.S.P.), 1,3-propanediol (Eastman, practical), 1,4-butanediol (Eastman, practical);

(*d*) solvent: ethylene dichloride (Fisher certified reagent).

Methods

Solvent and comonomers were always blended in equal molar ratios (0.4 mole of ethylene chloride (EC) with 0.4 mole of tetrahydrofuran – propylene oxide mixtures). These mixtures were prepared in the following

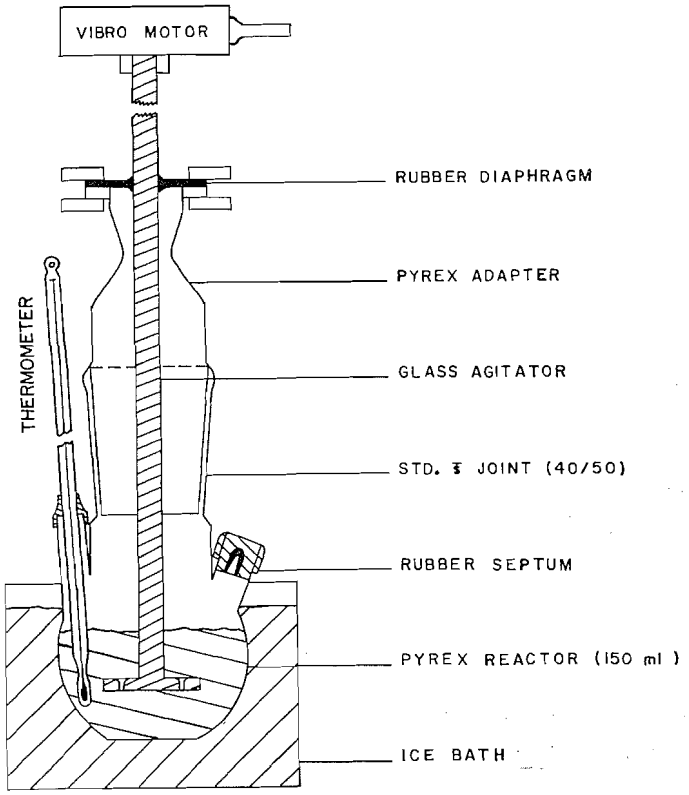


FIG. 1. Schematic diagram of reactor used for polymerization reactions.

Can. J. Chem. Downloaded from www.nrcresearchpress.com by 210.87.254.6 on 09/05/12
For personal use only.

molar ratios: 1:0, 1:1, 1:2, 1:4, 2:1, 4:1, and 0:1. The amount of catalyst added was usually 7×10^{-4} mole, and that of co-catalyst was always 2.4×10^{-2} mole (6 mole % of the comonomers charged).

The reactions were carried out at 0 °C and at atmospheric pressure in a 150 ml round bottom pyrex flask with three openings (Fig. 1). One of the lateral openings was covered with a self-sealing rubber septum through which reactants were admitted and samples were withdrawn by Luer-Lok syringes for analysis, the other opening was used to insert a thermometer. The large mouth of the flask served to introduce an all-glass stirrer activated by an appropriate vibro motor.

The disappearance of reactants was followed with a Perkin–Elmer vapor fractometer (model 154-C) equipped with thermistor detectors, a Westronics two-pen recorder (type DU/11A) and a Self-Organizing-Systems electronic integrator (type RI 220). Five microliter samples of the reactants, withdrawn with a Hamilton syringe (type 705N), were separated on a column (P.E. type R), 2 m long ($\frac{1}{4}$ in. outside diameter), containing polypropylene glycol (UCON LB-550-X), and maintained at 125 °C. Helium was used as the carrier gas at a flow rate of 100 cc/min. Calibration curves for quantitative estimations were prepared by a simple method involving pure substances alone (5). The concentrations at zero time were obtained from reference mixtures having no catalyst. When concentration changes became insignificantly small, the reaction was presumed to be terminated, and this was taken as the completion time of the reaction. Residual reactants and solvent were removed from the copolymer by evaporation under reduced pressure and at room temperature, first using a water aspirator and later a high-vacuum mechanical pump.

The rates of disappearance, D_1 and D_2, for tetrahydrofuran and propylene oxide during the copolymerization reactions were obtained from the initial slopes of monomer concentration versus time curves.

Reactivity ratios of propylene oxide (r_1) and tetrahydrofuran (r_2) were obtained by using experimental data at 5% conversion of propylene oxide. The composition of the copolymer formed at this point was calculated from the amount of each comonomer consumed. The ratio of the comonomers in the mixture, on the other hand, was assumed to be that existing when $2\frac{1}{2}$% of the propylene oxide was consumed. The Mayo and Lewis copolymerization equation (6) was transformed[3] to isolate one of the reactivity ratios, then used to trace a line of r_2 versus r_1. This procedure was followed for the various comonomer mixtures studied, and the points of intersection of these lines yielded average values for the monomer reactivity ratios.

Number-average molecular weights of the copolymers were determined by a Mechrolab vapor pressure osmometer (Model 301A) and by hydroxyl end-group analysis using the phthalation procedure (7).

The vapor pressure osmometer was operated at 37 °C with methyl ethyl ketone. The calibration constant of the instrument 440 ohms/mole l was obtained by using substances of known molecular weights: polypropylene glycols (PPG 425 and 2 025), polyethylene glycols (PEG 200, 600, and 1 000), and benzil (210). The molecular weights of copolymers were obtained using the standard method described in the vapor pressure osmometer manual.

Molecular weights by hydroxyl end-group analysis were determined assuming 100% bifunctionality. This assumption was supported in part by negative unsaturation tests.

Qualitative tests for unsaturation in the copolymer were made by two methods, one using bromine in carbon tetrachloride, and the other using aqueous solutions of potassium permanganate. Quantitative estimations using mercuric acetate in methanol were made at the Canadian Armament Research and Development Establishment (C.A.R.D.E.).

Infrared spectra of the liquid copolymers were obtained at C.A.R.D.E., in Valcartier, Quebec, with a Perkin–Elmer double-beam recording spectrophotometer (Model 21) equipped with sodium chloride optics.

RESULTS AND DISCUSSION

The effect of the concentration of catalyst on the rate of copolymerization was investigated to determine the concentration range in which isothermal conditions could be maintained. This range and the completion time for each reaction, with rates of disappearance of each monomer, is given in Table I. The initial rates of disappearance of tetrahydrofuran (D_1) and propylene oxide (D_2) have been plotted as a function of the concentration of catalyst in Fig. 2. To a first approximation, these rates follow a first order law.

The homopolymerization of tetrahydrofuran could not be brought about under the reaction conditions adopted[4] (Fig. 3). Other reports (8, 9), however, show that it can be polymerized in a highly acidic medium. Homopolymerization of propylene oxide under the

[3]*Modified Mayo and Lewis equation:* $r_2 = [M_1]/[M_2][d[M_2]/d[M_1](1 + [M_1]r_1/[M_2]) - 1]$ *where* $[M_1]$ = *propylene oxide (PO), and* M_2 = *tetrahydrofuran (THF).*

[4]*The reaction conditions adopted were: 2:1:1 (EC:THF:PO)* $+ 7 \times 10^{-4}$ *mole (catalyst)* $+ 2.4 \times 10^{-2}$ *mole (co-catalyst), 0 °C and atmospheric pressure.*

Can. J. Chem. Downloaded from www.nrcresearchpress.com by 210.87.254.6 on 09/05/12
For personal use only.

TABLE I

The influence of the concentration of boron fluoride ethyl ether on the completion time of the copolymerization reaction at 0 °C in 2:1:1 mixtures of ethylene chloride, tetrahydrofuran, and propylene oxide, along with 1,2-propanediol

Concentration of catalyst (mole/l) × 10^2	Completion time of the reaction (min)	D_1(THF) × 10^3 (moles/l min)	D_2(PO) × 10^3 (moles/l min)
0.24	2 686	2.4	4.4
0.50	507	7.6	11.6
1.00	487	13.8	21.6
1.50	148	21.8	32.0

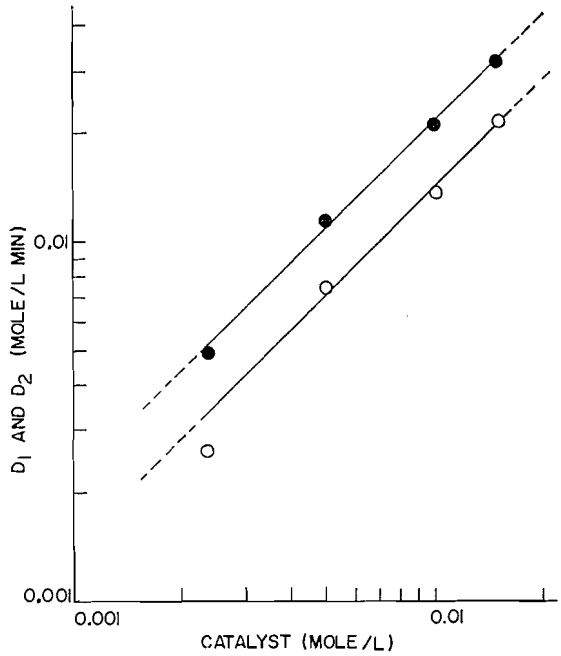


FIG. 2. Influence of the concentration of catalyst on the initial rates of disappearance of comonomers. The reactions were carried out at 0 °C, in 2:1:1 mixtures of EC:THF:PO, in the presence of 1,2-propanediol. (●) D_2(PO), (○) D_1(THF).

reaction conditions adopted[4] proved to be a very fast reaction (Fig. 3). These observations are understandable in the light of thermodynamic calculations of Small *et al.* (10) who pointed out that the opening of five-membered rings as found in tetrahydrofuran calls for more drastic reaction conditions than those required for the opening of three-membered rings as in propylene oxide.

After attempts to homopolymerize each monomer were completed, monomer mixtures were copolymerized in the presence of different diols. Monomer concentrations, as determined by gas chromatography, are given as a function of time in Figs. 4, 5, and 6. These figures show that the consumption of tetrahydrofuran ceases when propylene oxide has

Can. J. Chem. Downloaded from www.nrcresearchpress.com by 210.87.254.6 on 09/05/12
For personal use only.

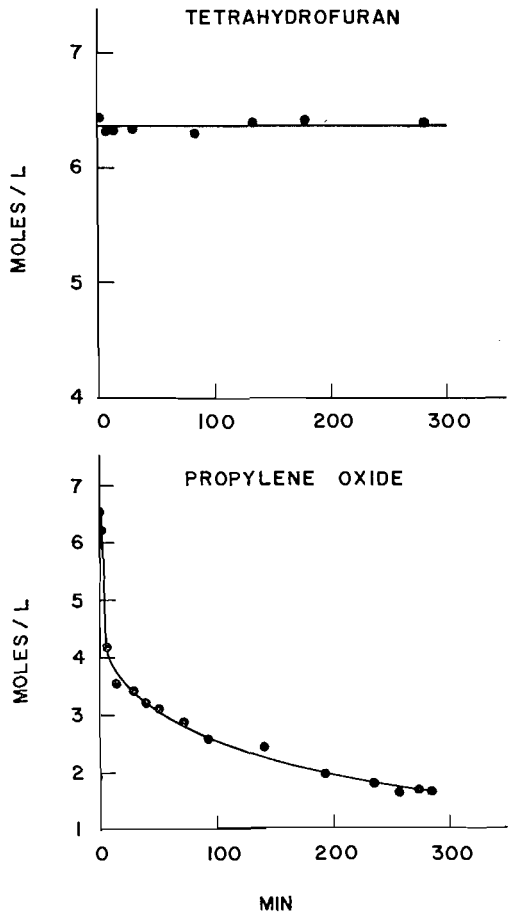


FIG. 3. Concentration versus time plots for the homopolymerization of tetrahydrofuran and propylene oxide. The reactions were carried out at 0 °C, in the presence of 1,3-propanediol.

been totally consumed. This observation emphasized the fact that the presence of propylene oxide is essential for the consumption of tetrahydrofuran under the reaction conditions adopted.[4]

The rates of disappearance of comonomers (D_1 and D_2) have been plotted as a function of their initial concentrations in Figs. 7 and 8. For the three co-catalysts used, the rate of disappearance of propylene oxide was found to be (*a*) proportional to the square of its initial concentration, and (*b*) inversely proportional to the initial concentration of tetrahydrofuran when the concentration of the latter does not exceed 3 moles/l. Above this value, this rate rapidly goes to zero. The rate of disappearance of tetrahydrofuran, on the other hand, varies directly with the initial concentration of propylene oxide but is independent of its initial concentration.

Various plots obtained using the modified Mayo and Lewis equation are given in Fig. 9 for the three diols. The average reactivity ratios obtained from these plots are given in Table II. The variation observed in the reactivity ratios may be explained in terms of the

Can. J. Chem. Downloaded from www.nrcresearchpress.com by 210.87.254.6 on 09/05/12
For personal use only.

Can. J. Chem. Downloaded from www.nrcresearchpress.com by 210.87.254.6 on 09/05/12
For personal use only.

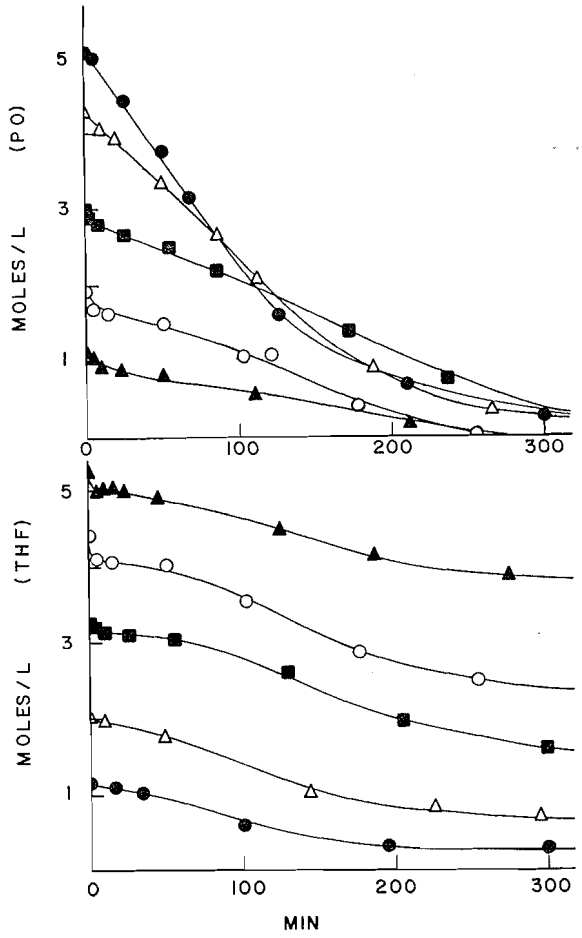


FIG. 4. Concentration versus time plots for the copolymerization of tetrahydrofuran with propylene oxide. The reactions were carried out at 0 °C, in the presence of 1,2-propanediol. Ratios THF:PO are: (▲) 4:1, (○) 2:1, (■) 1:1, (△) 1:2, (●) 1:4.

TABLE II

Average reactivity ratios of propylene oxide (r_1) and tetrahydrofuran (r_2)

Reactivity ratios	Co-catalysts		
	1,2-Propanediol	1,3-Propanediol	1,4-Butanediol
r_1(PO)	1.8	1.4	1.3
r_2(THF)	0.6	0.1	0.5

Can. J. Chem. Downloaded from www.nrcresearchpress.com by 210.87.254.6 on 09/05/12
For personal use only.

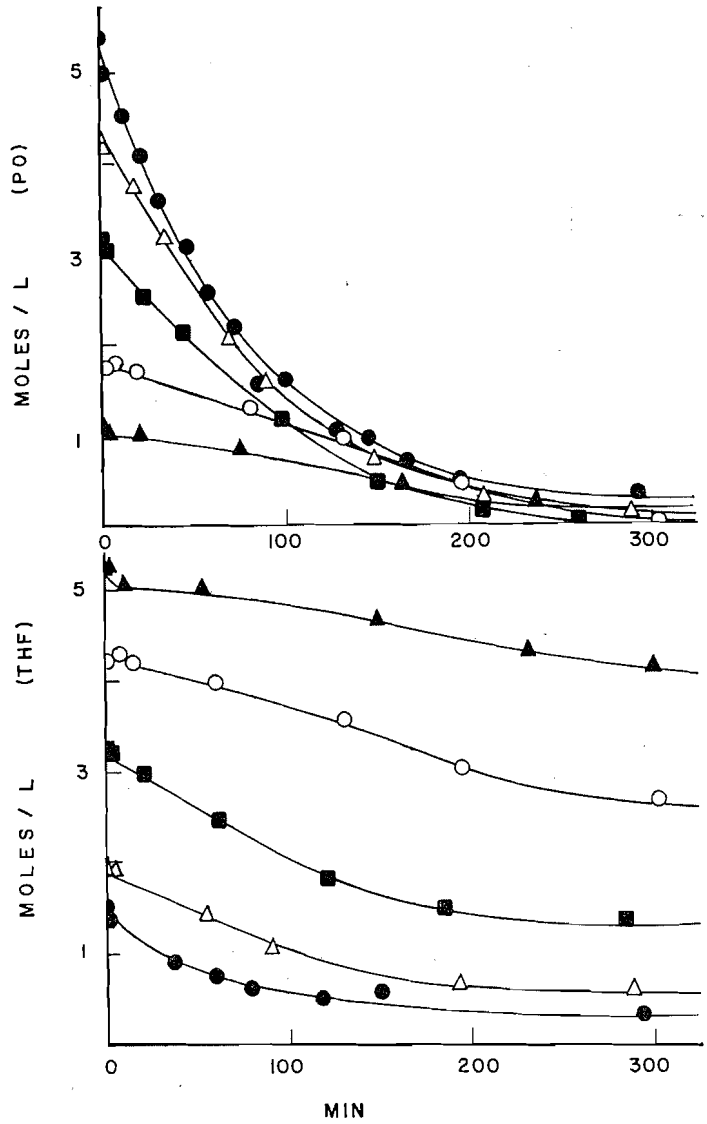


FIG. 5. Concentration versus time plots for the copolymerization of tetrahydrofuran with propylene oxide. The reactions were carried out at 0 °C, in the presence of 1,3-propanediol. Ratios THF:PO are: (▲) 4:1, (○) 2:1, (■) 1:1, (△) 1:2, (●) 1:4.

end effects resulting from the production of low molecular weight species. It is probable that r_2 is equal to the reciprocal value of r_1, and that the most probable value of r_2 is 1/1.5 or about 0.67.

The molecular weights determined by means of the vapor pressure osmometer and hydroxyl end-group analysis are given in Table III.

Variation of the comonomer ratio influences the molecular weights somewhat. From 1:1 to 1:4, the molecular weight remains essentially constant, and from 1:4 to 4:1 it decreases.

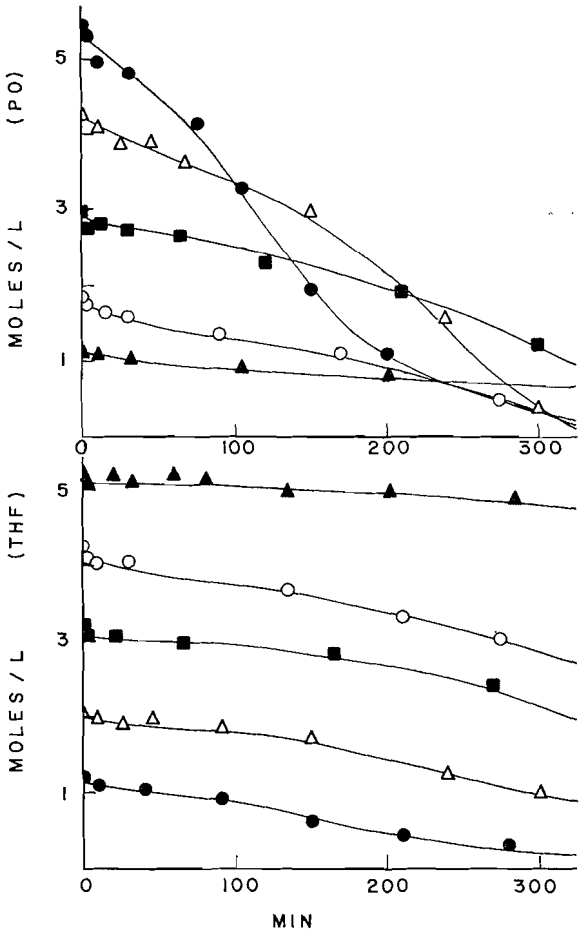


FIG. 6. Concentration versus time plots for the copolymerization of tetrahydrofuran with propylene oxide. The reactions were carried out at 0 °C, in the presence of 1,4-butanediol. Ratios THF:PO are: (▲) 4:1, (○) 2:1, (■) 1:1, (△) 1:2, (●) 1:4.

The use of different co-catalysts does not substantially alter the molecular weights of the copolyetherdiols obtained, except in the case of ethanediol. Increasing the concentration of catalyst does not affect the molecular weights. This agrees with the work of Murbach and Adicoff (3) who obtained similar results with copolymers of tetrahydrofuran and ethylene oxide. As a whole, the experimental molecular weights are low but this is due to the large amount of co-catalyst used.

There is considerable discrepancy between the molecular weights obtained by vapor pressure osmometry and hydroxyl end-group analysis. A preliminary gel permeation chromatographic analysis of the copolyetherdiols prepared in this laboratory has indicated that there is a secondary product (of low molecular weight) formed during these copolymerization reactions. The discrepancy between the molecular weight values is due to the dilution effects introduced by the low molecular weight product (11).

Infrared spectra of tetrahydrofuran – propylene oxide copolymers were recorded.

Can. J. Chem. Downloaded from www.nrcresearchpress.com by 210.87.254.6 on 09/05/12
For personal use only.

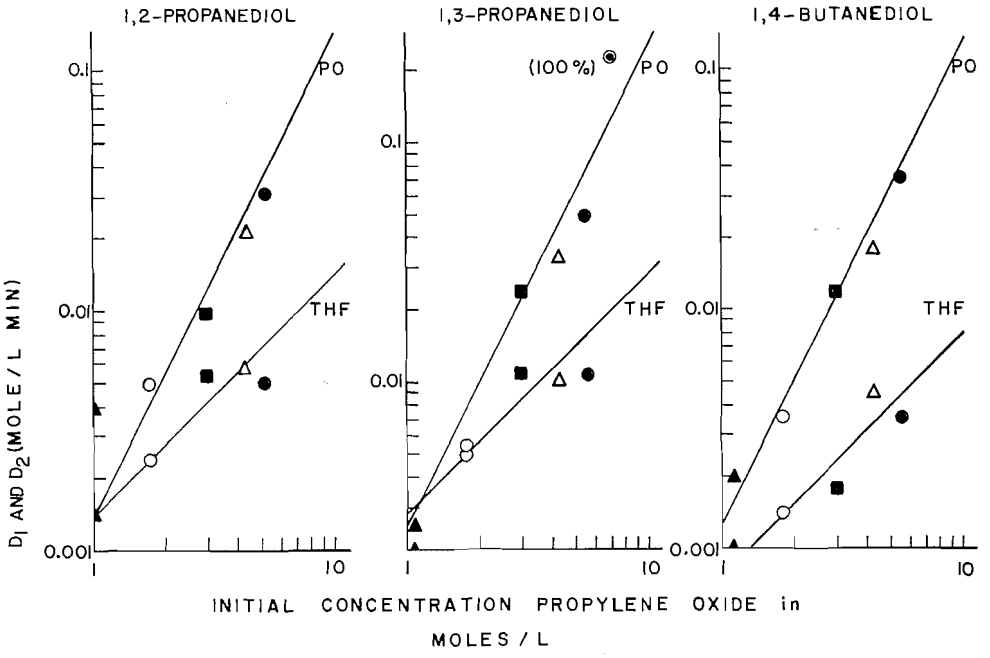


FIG. 7. Rates of disappearance of tetrahydrofuran and propylene oxide (D_1 and D_2) as a function of the initial concentration of propylene oxide. The reactions were carried out at 0 °C, in the presence of 1,2-propanediol, 1,3-propanediol, and 1,4-butanediol. Ratios THF:PO are: (▲) 4:1, (○) 2:1, (■) 1:1, (△) 1:2, (●) 1:4.

Bands were observed at the following wave numbers:

(*a*) 1 110 cm^{-1}: strong and broad, carbon oxygen – carbon ether linkages;

(*b*) 1 380 and 1 450 cm^{-1}: weak, symmetrical, and unsymmetrical deformation of CH_2 and CH_3 groups;

(*c*) 2 850 cm^{-1}: strong, carbon hydrogen stretching;

(*d*) 3 440 cm^{-1}: weak, hydroxyl stretching.

No bands were observed to indicate the presence of unsaturation.

The mechanism of this acid-catalyzed copolymerization of tetrahydrofuran with propylene oxide has been described elsewhere (12). The main features of this mechanism are: (i) 'Initiation' leading to the formation of oxonium ion intermediates; (ii) 'Propagation' involving ring-opening reactions and copolymer formation; (iii) 'Termination' involving the formation of a loose complex of the anion (nucleophile) with the oxonium-terminated copolymer, and subsequent reorganization to yield hydroxyl-terminated copolymer.

ACKNOWLEDGMENTS

The authors gratefully acknowledge the financial assistance received from the Defence Research Board of Canada under Grant No. 9530-32, and from the National Research Council of Canada under Grant No. A 1260. They are also indebted to Mrs. Jacqueline Dumas for the splendid work carried out both in the laboratory and in the preparation of this paper. The authors thank Dr. F. Maine (who is now with Glidden Co. Ltd.) and Dr. J. Levesque of the Propulsion Wing at C.A.R.D.E., for their assistance with physical and chemical analyses, and for many stimulating discussions.

Can. J. Chem. Downloaded from www.nrcresearchpress.com by 210.87.254.6 on 09/05/12
For personal use only.

TABLE III

Effects of operating reaction parameters on the molecular weights of copolymers*

Operating reaction parameters	Reaction time (min)	% reactants† consumed THF – PO	Number-average molecular weights	
			Vapor pressure osmometry	Hydroxyl end-group analysis
A. Comonomer ratios‡,§				
THF:PO				
1:0	∞	0–0	—	—
1:1	345	59–100	720	940
1:2	377	72–100	730	960
1:4	1 388	81–92	740	960
2:1	415	39–100	590	820
4:1	368	24–100	460	610
0:1	442	0–42	440	520
B. Co-catalysts‡,‖				
1,2-Ethanediol	1 390	40–96	460	470
1,2-Propanediol	560	45–100	600	710
1,3-Propanediol	415	39–100	590	820
1,4-Butanediol	425	43–100	550	610
C. Catalyst‖,¶				
Boron fluoride ethyl ether (mole/l × 10^2)				
0.24	2 686	54–100	630	770
0.50	507	54–97	640	730
1.00	487	62–100	650	770
1.50	148	53–99	600	740

*Reactions done at 0 °C.
†Calculated on a mole basis.
‡Catalyst, boron fluoride ethyl ether, 7×10^{-4} mole.
§Co-catalyst, 1,3-propanediol, 2.4×10^{-2} mole.
‖Proportion, EC:THF:PO, 2:1:1.
¶Co-catalyst, 1,2-propanediol, 2.4×10^{-2} mole.

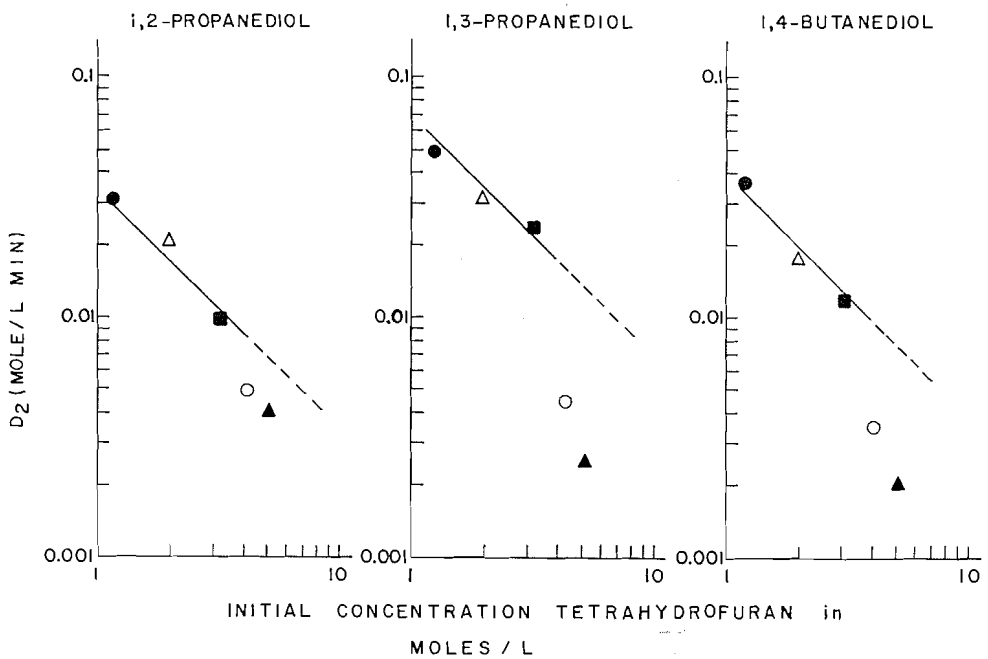


FIG. 8. Rate of disappearance of propylene oxide (D_2) as a function of the initial concentration of tetrahydrofuran. The reactions were carried out at 0 °C, in the presence of 1,2-propanediol, 1,3-propanediol, and 1,4-butanediol. Ratios THF:PO are: (▲) 4:1, (○) 2:1, (■) 1:1, (△) 1:2, (●) 1:4.

Can. J. Chem. Downloaded from www.nrcresearchpress.com by 210.87.254.6 on 09/05/12
For personal use only.

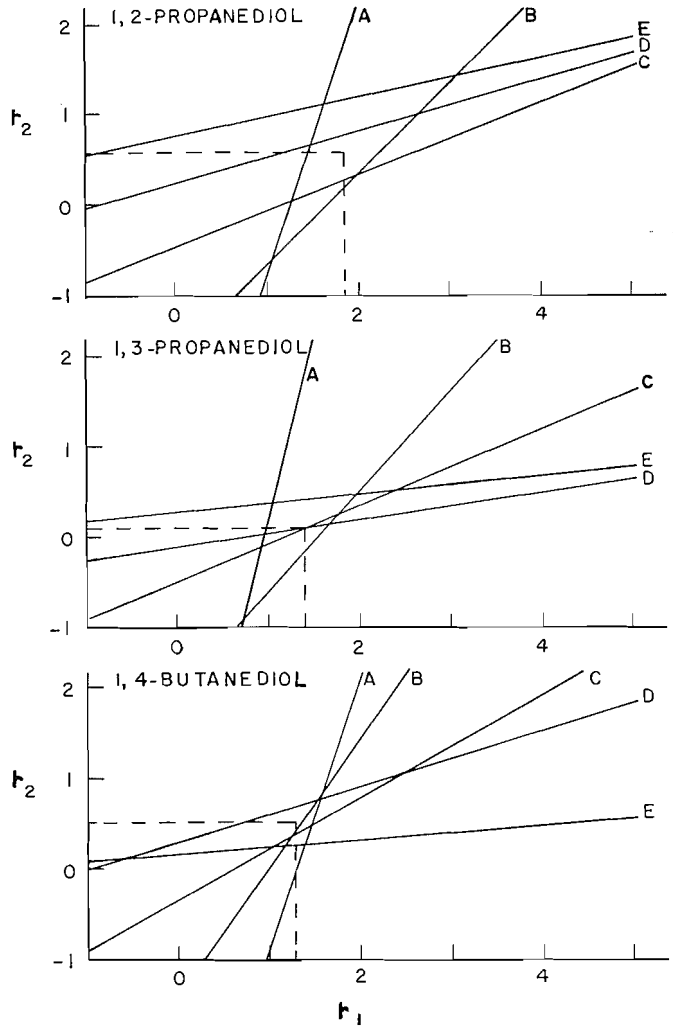


FIG. 9. Plots of the reactivities ratios: r_2(PO) versus r_1(THF). Proportions of THF:PO are as follows: (A) 1:4, (B) 1:2, (C) 1:1, (D) 2:1, and (E) 4:1.

REFERENCES

1. L. A. DICKINSON. J. Polymer Sci. **58**, 857 (1962).
2. H. MORSCHEL, H. MEERWEIN, and D. DELFS. Ger. Patent No. 914,438 (July 1, 1954).
3. W. J. MURBACH and A. ADICOFF. Ind. Eng. Chem. **52**, 772 (1960).
4. T. SEAGUSA, H. IMAI, and J. FURUKAWA. Makromol. Chem. **56**, 55 (1962); Kogyo Kagaku Zasshi, **65**, 699 (1962).
5. L. P. BLANCHARD. Nat. Res. Council Can. Ann. Rept. A-1260 (January, 1964).
6. F. R. MAYO and F. M. LEWIS. J. Am. Chem. Soc. **66**, 1594 (1944).
7. L. P. BLANCHARD and M. D. BAIJAL. J. Polymer Sci. Pt. B. In press.
8. H. HAMANN. Angew. Chem. **63**, 231 (1951).
9. H. MEERWEIN. Angew Chem. **59**, 168 (1947).
10. P. A. SMALL, T. R. E. DEVLIN, and F. S. DAINTON. Trans. Faraday Soc. **51**, 1710 (1955).
11. L. P. BLANCHARD and M. D. BAIJAL. N.Y. A.C.S. Polymer preprints. 7(2), 944 (1966).
12. M. D. BAIJAL and L. P. BLANCHARD. IUPAC Intern. Macromol. Symp. Tokyo, 1966.

Can. J. Chem. Downloaded from www.nrcresearchpress.com by 210.87.254.6 on 09/05/12
For personal use only.

Can. J. Chem. Downloaded from www.nrcresearchpress.com by 210.87.254.6 on 09/05/12
For personal use only.

THE REACTIONS OF ACTIVE NITROGEN WITH ETHYLENE AND DEUTERATED ETHYLENES[1]

KENNETH D. FOSTER, P. KEBARLE, AND H. B. DUNFORD
Department of Chemistry, University of Alberta, Edmonton, Alberta

Received June 30, 1966

ABSTRACT

The reaction of active nitrogen with ethylene and deuterated ethylenes has been investigated by use of a mass spectrometer. The rate of disappearance of atomic nitrogen in the presence of ethylene appears to obey the equation

$$-\mathrm{d[N]}/\mathrm{d}t = k_{app}[\mathrm{N}]\,[\text{ethylene}]_0,$$

where k_{app} is an apparent second order rate constant and $[\text{ethylene}]_0$ is the initial concentration of added ethylene. However, exceptions to this equation are found at 0.6 Torr either for short reaction times or for small concentrations of added ethylene, and apparently for short reaction times at 2.6 Torr when a large excess of ethylene is added. Where the above equation is obeyed, $k_{app} = (3 \pm 1) \times 10^{-13}$ cc molecule^{-1} s^{-1}. The formation of C_2D_4 in the reaction of active nitrogen with C_2D_3H is interpreted as further evidence for the importance of hydrogen atom reactions in intermediate steps of the reaction of active nitrogen with ethylene.

INTRODUCTION

The reaction of active nitrogen with ethylene has been studied by several workers (1–3). The initial steps in the reaction were believed to be

[1] $$\mathrm{N} + \mathrm{C_2H_4} \rightarrow \mathrm{HCN} + \mathrm{CH_3}$$

[2] $$\mathrm{N} + \mathrm{CH_3} \rightarrow \mathrm{HCN} + 2\mathrm{H} \quad .$$

The yield of hydrogen cyanide from the reaction of active nitrogen with excess ethylene has been taken as a measure of the nitrogen atom content in active nitrogen. However, the nitric oxide titration consistently indicates higher values for the nitrogen atom concentration (3). The possibility that the discrepancy is caused by catalyzed recombination of nitrogen atoms in the presence of ethylene has been ruled out on the ground that the $\Delta[\mathrm{N}]/[\mathrm{HCN}]$ ratio is independent of the initial nitrogen atom concentration (1, 3). Herron (1) detected H atoms with a mass spectrometer in the reaction of active nitrogen with ethylene. He proposed the following reactions in addition to [1] and [2].

[3] $$\mathrm{H} + \mathrm{C_2H_4} \rightarrow \mathrm{C_2H_5}$$

[4] $$\mathrm{H} + \mathrm{C_2H_5} \rightarrow 2\mathrm{CH_3}$$

[5] $$\mathrm{N} + \mathrm{C_2H_5} \rightarrow \mathrm{C_2H_4} + \mathrm{NH}$$

[6] $$\mathrm{N} + \mathrm{NH} \rightarrow \mathrm{N_2} + \mathrm{H}$$

followed by atom and radical termination reactions.

There remain, however, certain puzzling features of the discrepancy between the NO and HCN methods of measurement of nitrogen atom concentrations (4) and in particular of the mechanism of the reaction of active nitrogen with ethylene. In an attempt to resolve some of these problems, we report here on the use of a mass spectrometer to examine the reaction of active nitrogen with C_2D_4, C_2D_3H, and C_2H_4, as well as the results of product analyses obtained by using the combined techniques of gas–liquid chromatography and mass spectrometry.

[1]*Presented at the 49th Canadian Chemical Conference, Saskatoon, Saskatchewan, June, 1966. Financial support from the National Research Council is acknowledged.*

EXPERIMENTAL

Linde prepurified nitrogen was passed through a U trap filled with glass helices. In most experiments the trap was maintained at −195°. Nitric oxide was purified by repeated distillation through U traps at −160°. Reagent grade C_2D_4 and C_2D_3H (Merck, Sharpe and Dohme of Canada) were degassed prior to use. C_2H_4 was purified by repeated distillation through U traps at −130°.

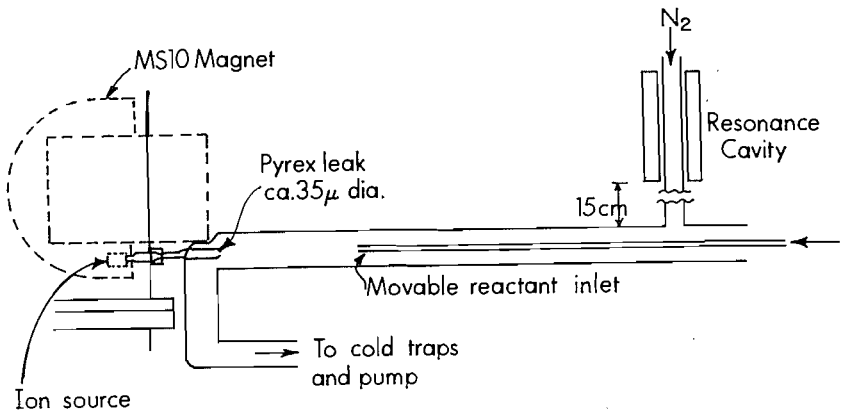


FIG. 1. Diagram of reaction system.

Nitrogen was partially dissociated in a fast-flow system by passage through a microwave resonance cavity (Ophthos Instrument Co.) coupled with a microwave exciter (Baird Atomic) of 2 450 Mc/s output. It then passed into a cylindrical reaction vessel of 18 mm inside diameter where a movable reactant inlet was located. Downstream from the inlet, a leak into the mass spectrometer was located. A diagram of the reaction chamber coupled to the mass spectrometer is shown in Fig. 1. The MS 10 instrument was modified so as to locate the leak as close as possible to the ion source. A 5 cm long pyrex lead was used between the leak and ion source. This lead could not be made shorter because of the design of the spectrometer. The ion source of the MS 10 instrument, which is normally of quite open construction, was closed off by the insertion of metal strips which formed the walls of an ion box. This was done since the pumping speed near the ion source is only moderate (approximately 15 l/s). The closed construction increased the probability that only freshly arriving sample entered the ion source. All mass spectrometric determinations on this instrument were conducted with an electron beam energy of 20 eV, except for ionization efficiency studies. The sensitivity of the mass spectrometer to various gases was determined from parent peak heights observed after mixing known amounts of the gases with the correct amount of nitrogen. Experiments were performed at 0.6 and 2.6 Torr of nitrogen. Flow rates of nitrogen in the reaction tube were 34.5 and 225 μmoles/s, respectively, which gave average linear velocities of 422 and 666 cm/s at the two different pressures. Flow rates of reactants were calculated from their partial pressures and the flow rate of molecular nitrogen, based on the assumption that the latter remained unchanged upon the addition of reactant. The sensitivity of the mass spectrometer to nitrogen atoms was determined by use of the nitric oxide titration.

For a typical experiment, the nitrogen flow and discharge were started. When a constant ion current at $m/e = 14$ was obtained, reactant was added through a fine control needle valve (Edwards High Vacuum Corp.) behind the movable inlet tube. A constant reactant flow rate was maintained by keeping the liquefied reactant at some low temperature such that it had a constant vapor pressure of ca. 100–200 Torr behind the Edwards valve.

The correlation between peak height at $m/e = 14$ from active nitrogen and afterglow intensity was tested. A portable photosensitive search head (Photovolt Corporation), strapped to the reaction tube near the mass spectrometer leak, was used to make the relative intensity measurements. The photo search head, placed upstream from the ethylene inlet, was also used to obtain relative initial nitrogen atom concentrations in some experiments where the ratio of N atoms destroyed to ethylene destroyed was studied as a function of initial nitrogen atom concentration.

In some experiments, products of the reaction were collected in a trap cooled in liquid nitrogen, then fractionated by distillation through a U trap at −130°. Products volatile at −130° were separated by gas–liquid chromatography on a medium activity silica gel column. Products not volatile at −130° were separated on a dibutyl maleate column. Fractions obtained from the gas–liquid chromatographic apparatus were then analyzed on a mass spectrometer. A few of these experiments were conducted specifically to test for C_2D_4 formation in the reaction of active nitrogen with C_2D_3H. For these experiments a medium activity silica gel column 10 ft in length was used. Mass spectra of the ethylene fractions were taken, both

Can. J. Chem. Downloaded from www.nrcresearchpress.com by 210.87.254.6 on 09/05/12
For personal use only.

from the reaction and from blank experiments in which the discharge was off. Parent peak heights at $m/e = 32$ and 31, corrected for the blank were used as measures of C_2D_4 and C_2D_3H concentrations, respectively.

RESULTS AND DISCUSSION

The ionization efficiency curves for $m/e = 14$, obtained with the discharge on and off, showed clearly the presence of ^4S nitrogen atoms in active nitrogen. The voltage separation of the curves below 0.1% intensity was about 9.7 eV, which is very close to $D(N_2) = 9.75$ eV. We did not observe a discontinuity corresponding to that found by Jackson and Schiff (5). However, this may be due to the difference in excitation sources, since these authors used the more energetic condensed discharge.

A good linear plot was obtained when afterglow intensity was plotted against the square of the $m/e = 14$ ion current (6). In experiments conducted at 0.6 Torr, with the incoming nitrogen passed through the glass helices at −196°, it was found that the NO titration indicated no decay of atomic nitrogen along the reaction tube in the absence of reactant.

Traces of acetylene and ethane were observed as products volatile at −130° (7). Traces of ammonia were detected in the less volatile fraction. The predominant reaction product was always hydrogen (or deuterium) cyanide. Some ion current at $m/e = 41$, believed to be CH_3CN (1), was observed.

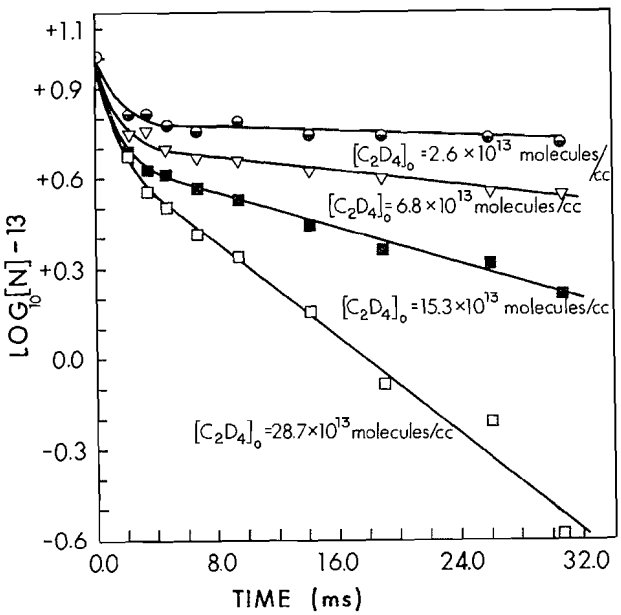


FIG. 2. Pseudo first order decay of N atoms at $P_{N_2} = 0.63$ Torr.

The deuterated ethylenes make no contribution to the $m/e = 14$ ion current and so their use facilitated precise measurement of the decay of atomic nitrogen in the reaction zone. The rates of decay of N atoms at 0.63 Torr total pressure for different rates of input of C_2D_4 are summarized in Fig. 2.[2] A feature of these logarithmic plots of nitrogen atom concentration vs. time is the transition, at a reaction time of about 4 ms, from a process

[2]*Photocopies of all of the original data discussed in this paper may be obtained in tabular form upon request to: Depository of Unpublished Data, National Science Library, National Research Council, Ottawa, Canada.*

Can. J. Chem. Downloaded from www.nrcresearchpress.com by 210.87.254.6 on 09/05/12
For personal use only.

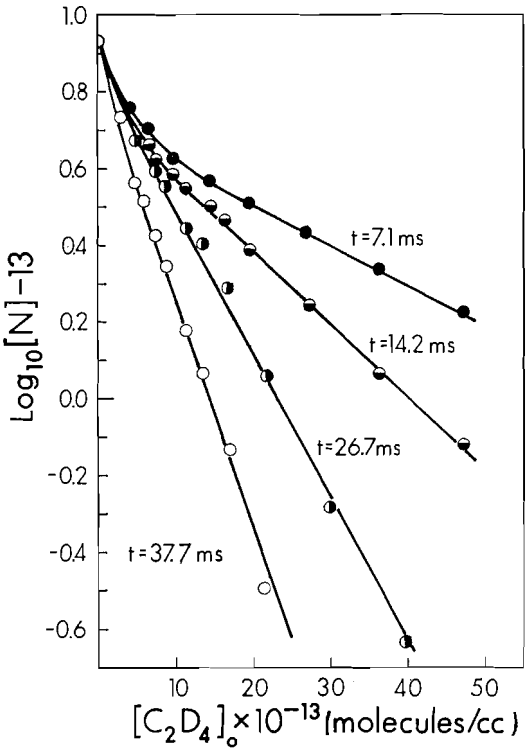


FIG. 3. Logarithmic dependence of N on $[C_2D_4]_0$ at P_{N_2} = 0.63 Torr.

(or processes) of apparent order greater than one to apparent first order decay of nitrogen atoms. One might suspect, however, at this low pressure, that this phenomenon may not be chemical in nature but possibly due to anomalous flow behavior at low ethylene input rates. The concentration of nitrogen atoms for zero reaction time is obtained from a measurement of the nitrogen atom concentration in the absence of C_2D_4. Since the C_2D_4 decomposition is always less than 13% of the initial concentrations of ethylene, $[C_2D_4]_0$, we can divide the slopes of the linear portions of the four plots in Fig. 2 by the appropriate values of $[C_2D_4]_0$, multiply by 2.303, and obtain four values of an apparent second order rate constant. These are given in Table IA. In Fig. 3, each of the curves was obtained at a fixed position of the reactant inlet by varying the partial pressure of ethylene. A slight but discernible trend to apparent order higher than first for N-atom decay is present for small values of $[C_2D_4]_0$ in Fig. 3. For higher values of $[C_2D_4]_0$, linear logarithmic plots are observed. By use of the appropriate reaction times four values for the apparent second order specific rate constant for the rate of decay of N atoms in the presence of C_2D_4 at 0.6 Torr total pressure are obtained from the linear plots in Fig. 3. These values are also given in Table IB.

The rate of decay of N atoms for two different $[C_2D_4]_0$ values at a total pressure of 2.6 Torr is shown in Fig. 4 and is plotted in logarithmic form in Fig. 5. The linear portions of the latter curves lead to apparent second order rate constants, shown in Table IC, in good agreement with those observed at low pressure. As shown in Fig. 4, the initial rate of disappearance of N atoms appears to be zero order at 2.6 Torr for the higher value of $[C_2D_4]_0$. Thus, the higher than first order disappearance of N atoms in the presence of ethylene was only observed for short reaction times at 0.6 Torr.

Can. J. Chem. Downloaded from www.nrcresearchpress.com by 210.87.254.6 on 09/05/12
For personal use only.

TABLE I

Apparent second order specific rate constants, k_{app}, for the disappearance of nitrogen atoms in the presence of ethylene, in cc molecule^{-1} s^{-1}

(A) $[N]_0 = 10.2 \times 10^{13}$ atoms/cc, $P_{N_2} = 0.63$ Torr

$[C_2D_4]_0$ (molecules/cc)	k_{app}
2.6×10^{13}	2.1×10^{-13}
6.8×10^{13}	2.0×10^{-13}
15.3×10^{13}	2.2×10^{-13}
28.7×10^{13}	3.0×10^{-13}

(B) $[N]_0 = 8.6 \times 10^{13}$ atoms/cc with C_2D_4, $P_{N_2} = 0.63$ Torr

t (ms)	k_{app}
7.1	3.5×10^{-13}
14.2	3.2×10^{-13}
26.7	3.2×10^{-13}
37.7	3.2×10^{-13}

(C) $[N]_0 = 10.8 \times 10^{13}$ atoms/cc, $P_{N_2} = 2.6$ Torr

$[C_2D_4]_0$ (molecules/cc)	k_{app}
13.6×10^{13}	3.5×10^{-13}
31.4×10^{13}	5.1×10^{-13}

(D) $[N]_0 = 72 \times 10^{13}$ atoms/cc, $P_{N_2} = 2.6$ Torr, $t = 21.2$ ms

	k_{app}
"Poisoned" system	4.4×10^{-13}
"Unpoisoned" system	4.4×10^{-13}

(E) Herron's result (8) multiplied by two

$k_{app}(2k_1)$
1.9×10^{-13}

All of the above results were obtained using nitrogen which was passed through glass helices at −196°. Some of the results obtained using C_2D_3H as reactant were obtained with the glass helices maintained at room temperature, so that traces of water vapor were admitted into the vacuum system. These experiments can be described as occurring in a "poisoned" system, whereas when the liquid nitrogen was placed on the nitrogen line, the experiments can be described as occurring in an "unpoisoned" system. For experiments in the "poisoned" system, the nitrogen atom concentration was approximately 60% higher than it was when the system was "unpoisoned", for the same power output on the microwave exciter.

The decay of N atoms in the presence of varying amounts of C_2D_3H, summarized in Fig. 6, is shown in the form of a logarithmic plot in Fig. 7. The same apparent second order specific rate constant for the rate of disappearance of N atoms is obtained from the plots in Fig. 7 for the poisoned and unpoisoned systems and is shown in Table ID. The effect of poisoning appears to be negligible on the reaction of active nitrogen with ethylene. It might be noted that the concentration of N atoms used in studying the reaction with

Can. J. Chem. Downloaded from www.nrcresearchpress.com by 210.87.254.6 on 09/05/12
For personal use only.

Can. J. Chem. Downloaded from www.nrcresearchpress.com by 210.87.254.6 on 09/05/12
For personal use only.

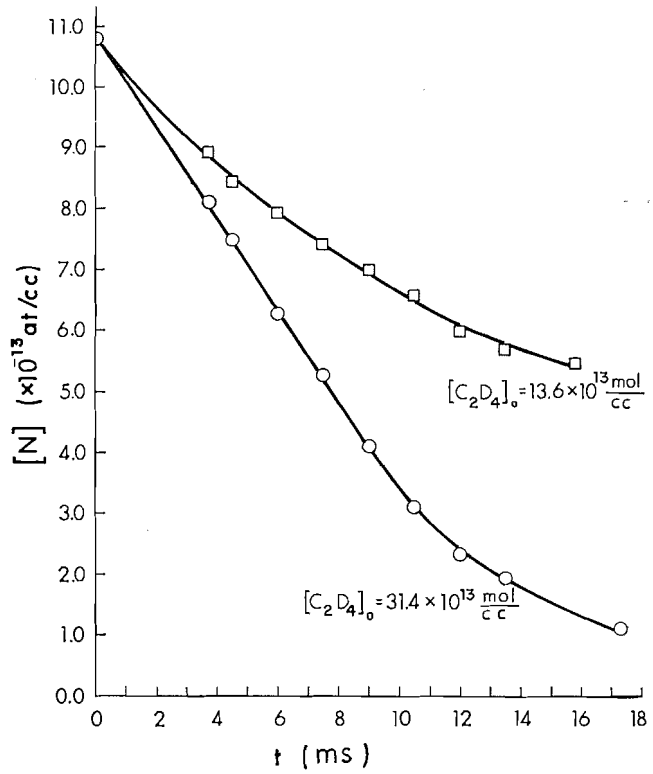


FIG. 4. Decay of N atoms in the presence of C_2D_4 at P_{N_2} = 2.6 Torr.

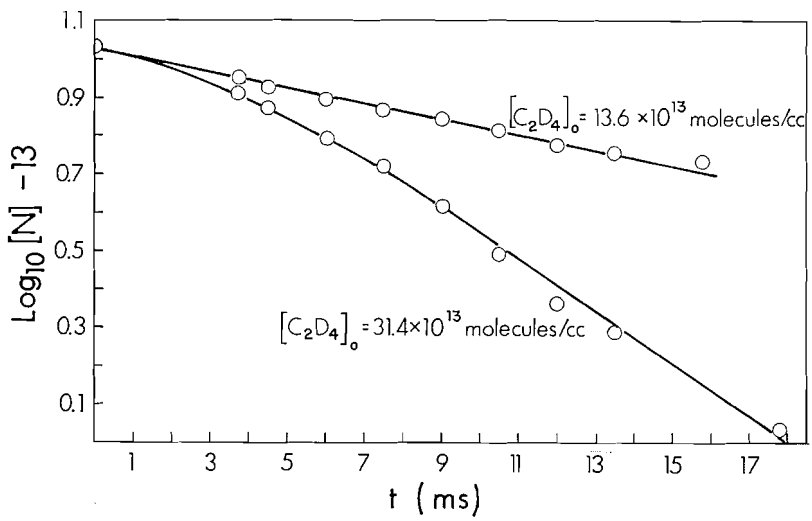


FIG. 5. Logarithmic decay of N atoms in the presence of C_2D_4 at P_{N_2} = 2.6 Torr.

C_2D_3H was roughly eight times that used when C_2D_4 was the reactant. Within experimental error, the same *apparent* second order specific rate constant for the rate of disappearance of N atoms in the presence of ethylene is obtained under a wide variety of experimental conditions, as is apparent from the data of Table I. The constants reported in Table I were obtained where our data appeared to fit the rate expression

$$-\mathrm{d[N]}/\mathrm{d}t = k_{app}[\mathrm{N}]\,[\mathrm{ethylene}]_0.$$

However, no assumptions about the actual reaction mechanism have been made.

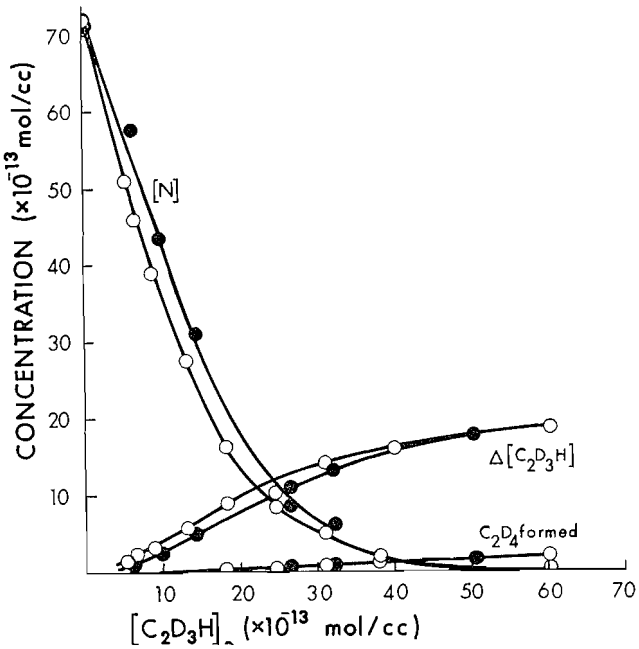


FIG. 6. Dependence of reagent concentrations on $[C_2D_3H]_0$ for poisoned (○) and unpoisoned (●) systems at P_{N_2} = 2.6 Torr. Reaction time 21.2 ms.

The rate constant for N-atom disappearance in the reaction of active nitrogen with ethylene, measured by Herron (8), is directly comparable to our apparent rate constants when multiplied by two, since he assumed in this earlier work that two N atoms disappear for every ethylene molecule destroyed. This apparent specific rate constant is also reported in Table IE. The interpretation of apparent specific rate constants in terms of reaction mechanisms is discussed below.

The Accuracy of the NO Titration and HCN Yields as Measures of N-Atom Concentration

The NO titration has been shown by the electron spin resonance work of Westenburg and deHaas (9) and by the work of Elias (10) to give an accurate measure of N-atom concentrations in active nitrogen produced in a microwave discharge. There appeared to be evidence, however, that $A^3\Sigma_u^+$ nitrogen molecules with a half-life of about 0.1 s are formed in a condensed discharge in appreciable amounts (11). The reaction of these triplet state molecules with nitric oxide was postulated by Fersht and Back (4) to account for their experimental results. It has been pointed out by Brennan and Kistiakowsky (12) that the data on triplet state nitrogen molecules (11) is also consistent with a mechanism in which

Can. J. Chem. Downloaded from www.nrcresearchpress.com by 210.87.254.6 on 09/05/12
For personal use only.

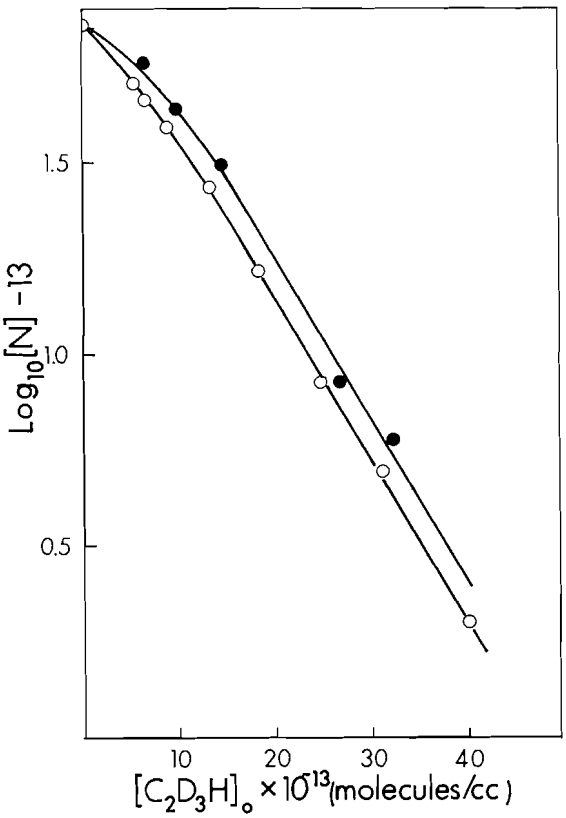


FIG. 7. Logarithmic dependence of [N] on $[C_2D_3H]_0$ for poisoned (○) and unpoisoned (●) systems at P_{N_2} = 2.6 Torr. $[N]_0 = 72 \times 10^{13}$ atoms/cc; reaction time 21.2 ms.

they are formed almost exclusively by nitrogen atom recombination, and have a collisional half-life of the order of a millisecond, a conclusion which they reach from their own studies. With such a short half-life, the concentration of $A^3\Sigma_u^+$ molecules would not be large enough to compete with atomic nitrogen in its extremely rapid reaction with NO (13), as postulated by Fersht and Back.[3]

In the case of C_2D_3H, the amount of C_2D_4 formed does not alter the conclusions we draw from Fig. 8, which shows a plot of $\Delta[N]/\Delta(C_2D_3H]$ vs. $[C_2D_3H]_0^{-1}$. Herron's results show a similar dependence of $\Delta[N]/[HCN]$ on $[C_2H_4]_0$. If nitrogen atoms only disappeared with the resultant formation of hydrogen (or deuterium) cyanide, then the plot in Fig. 8 would have zero slope and an intercept of two. It can be seen that the plot has a finite slope, and that for the highest rates of input of ethylene the ratio $\Delta[N]/\Delta[C_2D_3H]$ is about four. We also conclude that the NO titration always indicates the correct N-atom concentration in active nitrogen which exhibits the normal Lewis–Rayleigh afterglow.

On the Mechanism of the Reaction of Active Nitrogen with Ethylene

We have reexamined the apparent independence of $\Delta[N]/[HCN]$, or of approximate equivalence, $\Delta[N]/\Delta[C_2D_4]$, on the initial concentration of atomic nitrogen. The results

[3]*It has recently been postulated that triplet state nitrogen molecules are destroyed rapidly in the reaction (14)*

$$N + N_2^* \rightarrow N_2 + N.$$

Can. J. Chem. Downloaded from www.nrcresearchpress.com by 210.87.254.6 on 09/05/12
For personal use only.

are shown in Fig. 9. It can be seen that $\Delta[N]/\Delta[C_2D_4]$ varies with $[N]_0$, particularly at low flow rates of ethylene. These results indicate that catalyzed recombination of atomic nitrogen can occur in its reaction with ethylene, but that catalysis tends not to occur in the presence of a large excess of ethylene, in agreement with the data of Verbeke and Winkler (3). That the intercept in Fig. 9 is >3 provides strong evidence in support of Herron's conclusion that the extent of HCN production is not a valid measure of the nitrogen atom concentration in active nitrogen.

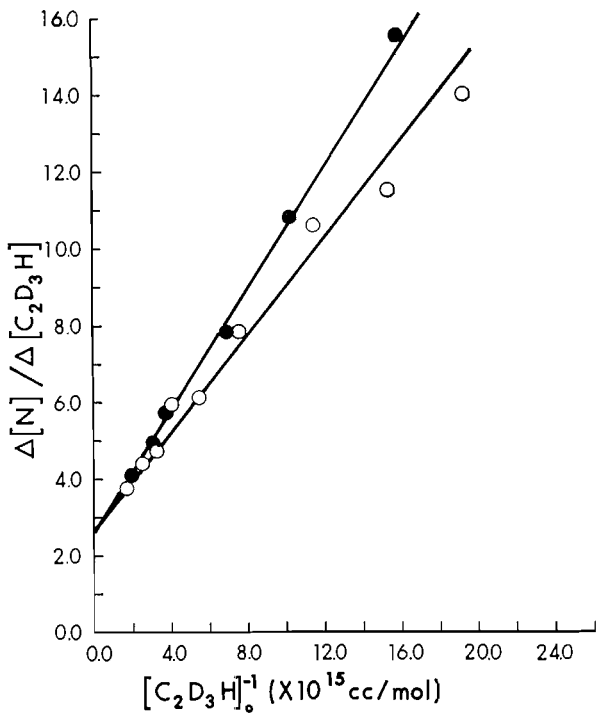


FIG. 8. Dependence of $\Delta[N]/\Delta[C_2D_3H]$ ratio on the reciprocal of the initial ethylene input. $P_{N_2} = 2.6$ Torr; $[N]_0 = 72 \times 10^{13}$ atoms/cc. (○) Poisoned system; (●) unpoisoned system.

In no experiments, either in a poisoned or in an unpoisoned system, was it possible to detect deuterium atoms in the reaction system. The MS 10 instrument is not suited for detection of hydrogen atoms ($m/e = 1$) unless it is modified so that a higher accelerator voltage is attainable. Such a modification was not made. A concentrated effort was not made to detect other radicals such as CH_3 ($m/e = 15$) or C_2H_5 ($m/e = 29$) in our system. Since our molecular leak is a substantial distance from the ion source (5 cm), radicals recombining bimolecularly would probably evade detection. There are various possible explanations for the generation of C_2D_4 in the reaction of active nitrogen with C_2D_3H. A plausible intermediate for C_2D_4 formation would appear to be the ethyl radical, C_2D_4H, which requires deuterium atom addition to C_2D_3H for its formation. Abstraction of its hydrogen atom by a nitrogen atom (analogous to reaction [5] proposed by Herron) or by a deuterium atom could occur. Alternatively, the exchange reaction $D + C_2D_3H \rightarrow C_2D_4 + H$ might take place. In any case, the presence of deuterium atoms is required. Although we have been unable to observe directly the presence of H or D atoms in our studies, the production of C_2D_4 in the reaction of active nitrogen with C_2D_3H provides further evidence

Can. J. Chem. Downloaded from www.nrcresearchpress.com by 210.87.254.6 on 09/05/12
For personal use only.

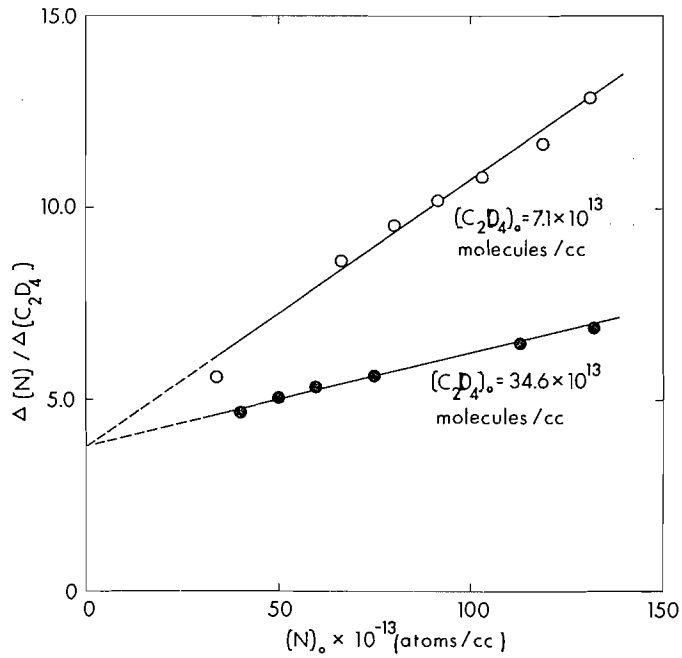


FIG. 9. Dependence of $\Delta[N]/\Delta[C_2D_4]$ on $[N]_0$. P_{N_2} = 2.6 Torr; reaction time = 42 ms.

in support of Herron's conclusion that hydrogen atoms play a role in the reaction of active nitrogen with ethylene (1).

The precise role of hydrogen atoms remains in doubt, however. The addition of hydrogen atoms to active nitrogen is known to destroy atomic nitrogen and yield ammonia (15). Yet Herron's Figs. 1 and 4, shown in ref. 1, show the same concentration of atomic nitrogen reaching the ion source of the mass spectrometer whether or not hydrogen is mixed with the nitrogen passing through the discharge. There must be an enhanced concentration of atomic nitrogen at the discharge when hydrogen is present to account for this result. Preliminary experiments in this laboratory with a separate discharge for hydrogen have shown that the initiation of the hydrogen discharge depletes the [N] by ca. 40%. Therefore, the enhanced yield of HCN when hydrogen is added is perhaps not entirely attributable to the effect of atomic hydrogen.

Our data can be compared with that obtained in the recent contribution by Herron (1) if we assume that his mechanism is correct. For example, if we evaluate our data obtained from the reaction of active nitrogen with C_2D_3H in a similar manner to Herron's use of his integrated rate expression, we obtain a value of $k_1 = 1.7 \times 10^{-14}$ cc molecule^{-1} s^{-1}, compared with his value of $k_1 = 1.2 \times 10^{-14}$ cc molecule^{-1} s^{-1} for reaction [1]. However, since there remain many unexplained features of the reaction of active nitrogen with ethylene (16), such an evaluation should be treated with caution.

REFERENCES

1. J. T. HERRON. J. Phys. Chem. **69**, 2736 (1965).
2. E. M. LEVY and C. A. WINKLER. Can. J. Chem. **40**, 686 (1962).
3. G. J. VERBEKE and C. A. WINKLER. J. Phys. Chem. **64**, 319 (1960).
4. E. FERSHT and R. A. BACK. Can. J. Chem. **43**, 1899 (1965).
5. D. S. JACKSON and H. I. SCHIFF. J. Chem. Phys. **23**, 2333 (1955).
6. J. BERKOWITZ, W. A. CHUPKA, and G. B. KISTIAKOWSKY. J. Chem. Phys. **25**, 457 (1956).

Can. J. Chem. Downloaded from www.nrcresearchpress.com by 210.87.254.6 on 09/05/12
For personal use only.

7. J. VERSTEEG and C. A. WINKLER. Can. J. Chem. **31**, 1 (1953).
8. J. T. HERRON. J. Chem. Phys. **33**, 1273 (1960).
9. A. A. WESTENBERG and N. DEHAAS. J. Chem. Phys. **40**, 3087 (1964).
10. L. ELIAS. J. Chem. Phys. **44**, 3810 (1966).
11. H. B. DUNFORD. J. Phys. Chem. **67**, 258 (1963).
12. W. R. BRENNAN and G. B. KISTIAKOWSKY. J. Chem. Phys. **44**, 2695 (1966).
13. M. A. A. CLYNE and B. A. THRUSH. Proc. Roy. Soc. London, Ser. A, **261**, 259 (1961).
14. R. A. YOUNG. Can. J. Chem. **44**, 1171 (1966).
15. W. STEINER. Z. Elektrochem. **36**, 807 (1930).
16. J. DUBRIN, C. MACKAY, and R. WOLFGANG. J. Chem. Phys. **44**, 2208 (1966).

Can. J. Chem. Downloaded from www.nrcresearchpress.com by 210.87.254.6 on 09/05/12
For personal use only.

PLATINUM(II) COMPLEXES CONTAINING α-HYDROXYACETYLENES

A. D. ALLEN AND T. THEOPHANIDES[1]
Lash Miller Chemical Laboratories, University of Toronto, Toronto, Ontario
Received April 14, 1966

ABSTRACT

The structures of complexes of the types M[$PtCl_3$ac] and *trans*-[$PtCl_2$ac(amine)], where ac = a tertiary α-hydroxyalkyl- or α-methoxyalkyl-acetylene, are described. The coordination of the ligands to the metal is through both the triple bond and the hydroxyl groups. The infrared spectra of the complexes in the O—H stretching region (3 000 – 3 800 cm^{-1}) and the effect on the spectra of the addition of bases to solutions of the free ligand and complexes strongly indicate that the hydroxyl groups are coordinated through the oxygen atom to the metal.

Structures of complexes of the types M[$PtCl_3$ac] and *trans*-[$PtCl_2$ac(amine)], where ac = a tertiary α-hydroxyalkyl- or α-methoxyalkyl-acetone, have recently been discussed in some detail (1). Such compounds have been known for many years (2, 3) and the unexpected stability of the complex formed by the dihydroxyacetylene HO.Me_2C—C≡C—CMe_2.OH has been attributed to a direct interaction between the hydroxyl groups and the rest of the complex, in addition to coordination by the triple bond to the metal. To account for the lowering of the O—H stretching frequency on coordination (by about 125 cm^{-1}) Chatt and his co-workers (4) originally suggested either (*a*) coordination by the oxygen of the hydroxyl groups to the metal atom, or (*b*) hydrogen bonding between the hydroxyl groups and the metal atom. In their recent paper (1) these authors propose that the interaction is (*c*) a hydrogen bond between the hydroxyl groups and the *cis*-chlorines of the complex, and they give diagrams showing the three possible interactions. Possibility *a* is rejected on the basis of infrared evidence that the hydrogen of the hydroxyl group is not free to form a hydrogen bond with a base such as dioxane (0.1 *M*) in carbon tetrachloride. We shall show that this is not the case if higher concentrations of base, or stronger bases, are used. It was also found that the hydroxyl proton resonance in the complex *trans*-[$PtCl_2$ac.py] (py = pyridine) is at lower field than in the free ligand, consistent with structures *a* or *c* but not with *b*, and that it did not change with concentration. The free ligand shows a decrease in τ value for the hydroxyl hydrogen as the concentration is increased, and since this ligand obviously contains free hydroxyl groups this contrast in behavior was taken as evidence that the proton was intramolecularly bonded in the complex. It appeared that this evidence could only be explained on the basis of structure *c*, involving hydrogen bonds to the *cis*-chlorines. Our infrared spectra (Table I) show that, whereas intermolecular hydrogen bonding between the hydroxyl groups of the free glycol is essentially absent at low concentrations in chloroform, a strong band due to this interaction appears when higher concentrations are used (up to 1 *M*). This accounts for the change in the nuclear magnetic resonance spectrum. By contrast the above complex shows only one band at 3 479 cm^{-1} (Table I) even in a saturated solution in $CHCl_3$ or $CDCl_3$, indicating that intermolecular hydrogen bonds do not form between the molecules of the complex. This is consistent with both of the structures *a* and *c*, since in structure *a* the oxygen atoms of the hydroxyl groups are already coordinated to the metal atom. There is, therefore, little possibility of hydrogen

[1]*Present address: Département de Chimie, Université de Montréal, Montréal, Québec.*

TABLE I

Stretching frequencies O—H (cm^{-1})

Solvent	Ligand (ac)	*trans*-[$PtCl_2$ac.py]	*trans*-[$PtCl_2$ac.2,6-lut]
C_6H_6	3 578 s	3 482 s	3 480 s
C_6H_6 + 20% pyridine	3 575 m, 3 255 s,b	3 481 s, 3 210 b,	3 480 s, 3 210 b
C_6H_6 + 20% pyridine*	3 575 m, 3 255 s,b	3 574 m, 3 255 s,b	3 575 m, 3 260 s,b
C_6H_6 + 20% 2,6-lutidine	3 576 m, 3 250 s,b	3 480 s, 3 210 vs	3 480 s, 3 210 b
C_6H_6 + 33% ether	3 576 m, 3 447 s,b	3 481 s, 3 410 sh	3 481 s, 3 410 sh
CCl_4	3 612 s	3 502 m	3 490 m
CCl_4 + 20% ether	3 612 m, 3 440 s,b	3 500 m, 3 415 b	
CCl_4 + 20% dioxane	3 604 m, 3 445 s	3 475 b, 3 420 vb	
$CHCl_3$	3 596 s (0.01 *M*)	3 479 s (0.2 *M*)	3 480 s (0.1 *M*)
$CHCl_3$	3 594 m, 3 390 s,b (1 *M*)	—	—
Ether	3 447 s	3 486 m, 3 410 sh	3 486 m, 3 410 sh
Pyridine	3 266 vs,b	3 210 vs,b	3 210 vs,b
2,6-Lutidine	3 250 vs,b	—	3 200 vs,vb

NOTE: Abbreviations used in Tables I–IV: s, strong; m, medium; b, broad; sh, shoulder; v, very; w, weak.
*Spectrum taken after several hours.

bonding between one molecule and another, at room temperature, and a constant spectrum and proton resonance signal would be expected. This evidence does not, therefore, distinguish between structures *a* and *c*.

The proposed structure *c* was supported (1) by a study of the platinum(0) compound [$Pt(PPh_3)_2$ac], where ac = MeEtC(OH)C≡CC(OH)MeEt. The O—H stretching frequency in this compound is identical with that of the free glycol, showing that the hydroxyl groups are not directly involved in bonding, and, incidentally, showing that coordination by the triple bond alone does not affect the O—H stretching frequency. Thus it is clear that the platinum atom in this compound does not interact with the hydroxyl groups. This cannot be taken as evidence that coordination of oxygen to the metal does not occur in the bivalent platinum chloro complexes, since it is well known that the nature of the metal atom in the two types of complexes is very different. For example, the acetylene–platinum(0) compounds are strongly stabilized by electron-withdrawing groups attached to the triple bond (5), but acetylene–platinum(II) compounds are stabilized by electron-releasing groups in the coordinated acetylene. This implies, as one might expect, a much greater electron-accepting power of the metal in the platinum(II) complexes, and hence the tendency to coordinate the oxygen atom of the hydroxyl group will be similarly greater than in the platinum(0) compound. Chatt *et al.* (1) found that stepwise substitution of phenyl for the α-methyl groups in the hydroxyacetylene gives rise to complexes of the same form in which the O—H stretching frequency is progressively lowered. They concluded that the phenyl groups reduce the donor capacity of the triple bond, and that this is partly offset by a strengthening of the hydroxyl-group interaction. A reduction in the donor capacity of the triple bond would result in the platinum atom bearing an increased positive charge: this would tend to strengthen a coordinate bond from oxygen to the metal, which would lead to a greater lowering of the O—H stretching frequency, as observed. The presence of an increased positive charge on the metal would also increase the covalency of the bond between the metal and the *cis*-chlorines, which would reduce the tendency of the chlorines to form a hydrogen bond wih the hydroxyl groups. We would, therefore, expect the presence of phenyl groups to weaken the hydroxyl-group interaction if it occurred through an intramolecular hydrogen bond with the *cis*-chlorines, and the O—H stretching frequency would not be lowered to the same extent. This is contrary to the experimental results.

It was felt that the published data ruled out structure *b*, but that it did not distinguish clearly between structures *a* and *c*. We have, therefore, examined the infrared spectra of a series of compounds of this general type and have studied the effect of addition of bases to solutions containing them. Our results indicate very strongly that structure *a*, involving coordination by oxygen to the metal atom, is correct.

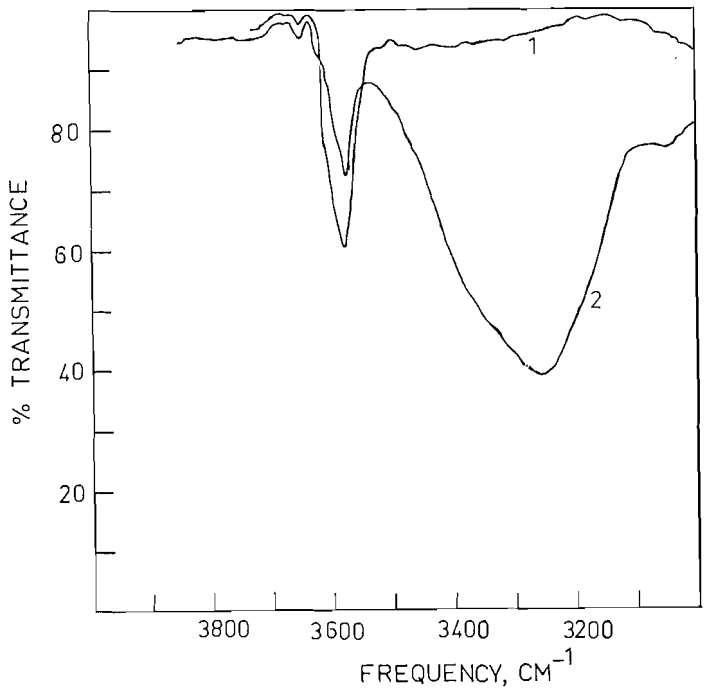


FIG. 1. Spectra of $Me_2C(OH)C{\equiv}CC(OH)Me_2$: (1) in benzene, (2) in benzene + 20% pyridine.

To simplify the discussion we shall deal first with one case, the compound *trans*-[$PtCl_2$ac.py] (where ac = the glycol $Me_2C(OH)C{\equiv}CC(OH)Me_2$), and its spectra in benzene with and without the addition of bases. Figure 1 shows the spectra of a dilute solution of the glycol in benzene and in benzene containing 20% (by volume) pyridine. In benzene the glycol has a single sharp peak at 3 578 cm^{-1}, the O—H stretching frequency of the free hydroxyl group: in the presence of pyridine this peak is reduced in intensity but remains at essentially the same frequency (3 575 cm^{-1}). The appearance of an additional strong broad band at about 3 255 cm^{-1} shows that considerable, but not complete, hydrogen bonding occurs between the hydroxyl groups and the base. The fact that some free hydroxyl groups persist, even in the presence of a high concentration of a strong base, is no doubt due to the fact that these are essentially tertiary alcohols so that steric hindrance tends to decrease the degree of association. Spectra of the complex formed by this glycol in the same solutions are shown in Fig. 2*a*. In benzene there is a single sharp band at 3 482 cm^{-1}, about 100 cm^{-1} lower than for the free ligand. The shape of this band is much more typical of a free hydroxyl group than of a hydrogen-bonded hydroxyl group, which are commonly strong but broad bands. The occurrence of this single sharp band shows clearly that the interaction of the hydroxyl group with the rest of the complex is essentially complete, i.e. any equilibrium between free and bound hydroxyl groups is very strongly displaced towards the bound hydroxyl groups. This implies that the interaction is energetically important in the total binding of the ligand. When pyridine is added this band is

immediately reduced in intensity, but remains at the same frequency (3 481 cm^{-1}) and a new strong broad band appears at about 3 210 cm^{-1}, 45 cm^{-1} lower than in the free ligand with pyridine. On standing at room temperature in the presence of this base (Fig. 2*a*), both bands slowly increase in frequency until the spectrum is the same as that of the free ligand in this medium, indicating that the glycol has been displaced from the complex. It is clear from the shape and position of the bands that, on the addition of pyridine, the glycol forms a hydrogen bond to the base while it is still an integral part of the complex.

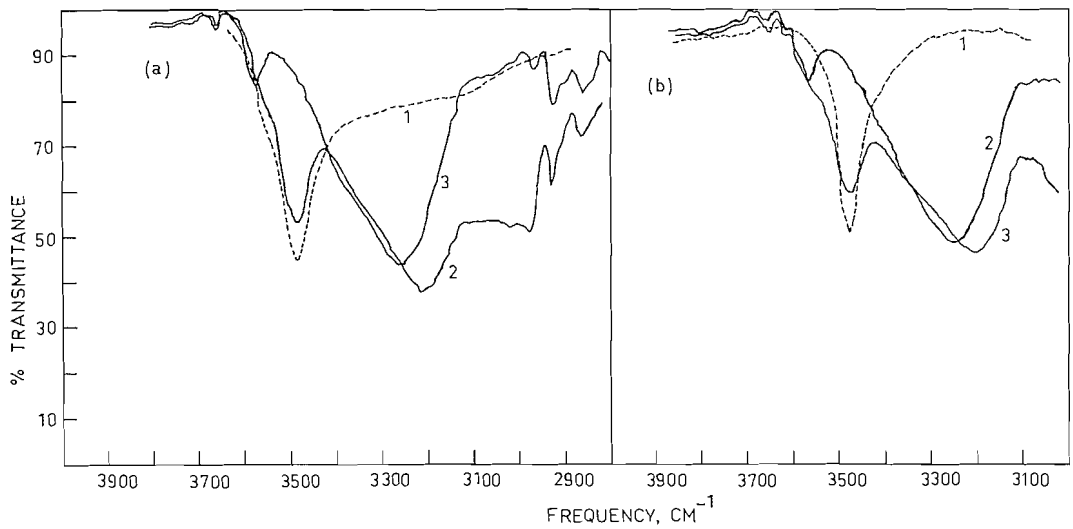


FIG. 2. (*a*) Spectra of *trans*-[$(Me_2C(OH)C{\equiv}CC(OH)Me_2)PtCl_2py$]: (1) in benzene, (2) in benzene + 20% pyridine (immediately), (3) in benzene + 20% pyridine (after 8 h). (*b*) Spectra of *trans*-[$(Me_2C(OH)C{\equiv}CC(OH)Me_2)PtCl_2$(2,6-lut)]: (1) in benzene, (2) in benzene + 20% pyridine (after 12 h), (3) in benzene + 20% pyridine (immediately).

We can discount the possibility that the pyridine causes rupture of an intramolecular hydrogen bond (e.g. to chlorine) and then forms a new hydrogen bond to the "freed" hydroxyl group. The only link between the glycol and the complex would be through the triple bond, and it is extremely unlikely that this could cause the hydrogen bond to pyridine to be 45 cm^{-1} lower than that for the free ligand with pyridine. The O—H stretching frequency observed by Chatt *et al.* (1) in their platinum(0) compound, in which only the triple bond is involved in the metal–ligand bond, is in exactly the same position as the free ligand, and it is well established that drastic changes in the nature of the organic group to which a hydroxyl group is attached produce very small changes in the O—H stretching frequency (6). The clear difference in the position of this hydrogen-bonded band in the free and bound glycol can only be accounted for if the hydroxyl groups are simultaneously linked to both the complex and the added base, and this is only possible if the oxygen of the hydroxyl groups is coordinated to the metal, leaving the hydrogen free to form a hydrogen bond to the base. It is also significant that the hydrogen bond to the base is formed immediately (in the time necessary to record the spectrum) and that the spectrum then changes slowly with time. If a hydrogen bond to the *cis*-chlorines were the important stabilizing factor in the link between the glycol and the metal, it is unlikely that the compound could exist for so long after this bond had been broken and in the presence of so large an excess of a powerful reagent. The relative intensities of the bands

shown in Fig. 2*a* provide an indication that, as expected from steric reasons, the extent of hydrogen bonding to the added base is greater with the free ligand than its complex.

Table I summarizes the above data, and shows the results obtained with other solvents and bases. Steric effects are shown clearly when 2,6-lutidine (2,6-lut) is used instead of pyridine either as part of the complex or as the reagent, or both. The spectra of the complex [PtacCl$_2$2,6-lut] in benzene and with added pyridine closely resembles that of the pyridine complex (see Fig. 2*b* and Table I). When this complex is treated with 2,6-lutidine (Fig. 3) the spectrum remains essentially the same for several days and the complex can be recovered from the solution.

The spectra of the free glycol and the complexes in mixtures of benzene–ether or carbon tetrachloride with ether and dioxane give similar results (Table I). It is clear from these spectra that the oxygen bases do form hydrogen bonds to the coordinated glycol, but that they do so to a lesser extent than the stronger nitrogen bases.

TABLE II

Infrared spectra taken in CCl_4 (cm^{-1})

Compound	ν_{O-H}	$\Delta\nu_{O-H}$	$\nu_{C\equiv C}$	$\Delta\nu_{C\equiv C}$	$\nu_{C=C}$	$\Delta\nu_{C=C}$
$Me_2C(OH)C{\equiv}CC(OH)Me_2$(ac)	3 612 s		2 248†			
trans-[acPtCl$_2$py]	3 502 m	110	2 040 w	208		
trans-[acPtCl$_2$(2,6-lut)]	3 490 m	122	2 045 w	203		
trans-[acPtBr$_2$(2,6-lut)]	3 497 s	115	2 035 w	213		
trans-[acPtBr$_2$py]*	3 497	115	2 032	216		
MeEtC(OH)C≡CC(OH)EtMe(ac′)	3 620 s		2 235 w			
trans-[ac′PtCl$_2$py]	3 492 s	128	2 035 m, 1 996 w	200, 239		
trans-[ac′PtCl$_2$(2,6-lut)]	3 489 s	131	2 037 w, 1 978 w	198, 257		
$Et_2C(OH)C{\equiv}CC(OH)Et_2$(ac″)	3 619 s		‡			
trans-[ac″PtCl$_2$py]	3 490 vs	129	‡			
trans-[ac″PtCl$_2$(2,6-lut)]	3 480 vs	139	‡			
$CH_2{=}CHCH_2OH$ (ol)	3 620 s				1 648 w	
trans-[olPtCl$_2$py]§	3 470 vs	150			1 482 w	166
trans-[olPtCl$_2$(2,6-lut)]	3 462 s	158			1 490 w	158

*Taken from ref. 8.
†Taken in CCl_4 (7).
‡Not visible.
§Taken in $CDCl_3$.

Table II records data on the stretching frequencies ν_{O-H}, $\nu_{C\equiv C}$, and $\nu_{C=C}$ to several α-hydroxy compounds (free ligands and their complexes) in carbon tetrachloride, and shows the changes in frequency ($\Delta\nu$) that occur on coordination.

A number of other observations have been made on these systems, some of which help in the interpretation of their structure.

(i) Spectra of the analogous bromo complexes *trans*-[PtacBr$_2$(amine)] (Table II) show O—H stretching frequencies which are almost identical with those of the chloro complexes. If there were a hydrogen bond to the halogen we would expect a greater difference in the two complexes (9).

(ii) A structure in which there are hydrogen bonds to the *cis*-chlorines involves some twisting $(CH_3)_2C(OH)$— group about the axis of the triple bond, and might be expected to give rise to different resonance signals for the two sets of methyl hydrogens. We find only one resonance signal for these protons at room temperature and at $-50°$ (10) which indicates a symmetrical environment.

(iii) Complexes containing the methoxy ether of the glycol K[PtCl$_3$($Me_2C(OMe)$-$C{\equiv}CC(OMe)Me_2$)] and *trans*-[PtCl$_2$(amine)($MeOME_2CC{\equiv}CCMe_2OMe$)] are at least as stable as the complexes of the glycol (11), which is surprising if hydrogen bonding is

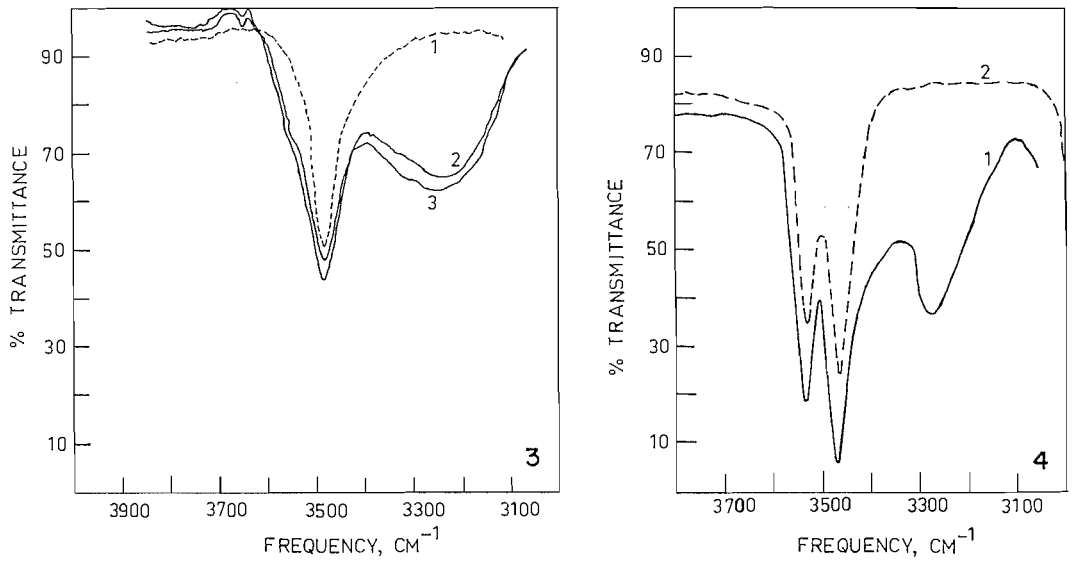


FIG. 3. Spectra of *trans*-[$(Me_2C(OH)C{\equiv}CC(OH)Me_2)PtCl_2$(2,6-lut)]: (1) in benzene, (2) in benzene + 20% 2,6-lutidine (immediately), (3) in benzene + 20% 2,6-lutidine (after 28 h).
FIG. 4. Spectra of $K^+[(Me_2C(OH)C{\equiv}CC(OH)Me_2)PtCl_3]^-$ in Nujol and KBr: (1) at 90 °K, (2) at 300 °K.

important. In their latest paper Chatt *et al.* (1) propose, from dipole moment evidence, that the methoxyl groups are directed away from the rest of the complex, and do not take part in the bonding. Our experiments do not shed further light on the structure of this compound, but circumstantial evidence indicates a great similarity between the nature of the bonding in the hydroxy and methoxy compounds. It is difficult to predict the effect the methyl group would have on the ability of oxygen to coordinate the metal, because of conflicting steric and electronic effects. If, in contrast to the glycol, only the triple bond is involved in the bonding and this is strong enough to compensate for the absence of hydrogen bonding, we would expect the frequency of the triple bond to be very strongly affected on coordination. In fact the reduction in the triple bond stretching frequency is greater for the glycol (about 200 cm^{-1}) than it is for the dimethyl ethyl of the glycol (100–150 cm^{-1}). Data for the stretching frequencies ν_{C-H} (of the methoxyl group) and $\nu_{C{\equiv}C}$ for the methoxy ether and its compounds are given in Table III.

TABLE III

Stretching frequencies (spectra taken in C_4Cl_6 mulls), cm^{-1}

Compound	ν_{C-H} for OCH_3	$\Delta\nu_{C-H}$	$\nu_{C{\equiv}C}$	$\Delta\nu_{C{\equiv}C}$
$Me_2C(OMe)C{\equiv}CC(OMe)Me_2$*	2 828 vs		2 144 m	
$K[Me_2C(OMe)C{\equiv}CC(OMe)Me_2PtCl_3]$	2 832 vs	4	1 996 m	148
trans-$[Me_2C(OMe)C{\equiv}CC(OMe)Me_2PtCl_2py]$	2 840 s*	12	2 043 m	101
	2 841 m	13	†	
trans-$[Me_2C(OMe)C{\equiv}CC(OMe)Me_2PtCl_2$(2,6-lut)]	2 839 s*	11	2 021 m	123
	2 840 m	12	†	

*Spectra taken in CCl_4.
†Not visible.

(iv) Infrared spectra in the OH stretching region of the salt $K[PtacCl_3]$ in the solid state at 300 °K and 90 °K are shown in Fig. 4. At room temperature the OH stretching frequency is split into two sharp bands at 3 523 and 3 453 cm^{-1} possibly because of a coupling of the vibrations of the two hydroxyl groups. At 90 °K the above two bands become sharper and more intense and also a third new broad band appears at 3 270 cm^{-1}. It is difficult to explain the presence of the new medium strength band at 3 270 cm^{-1} which is observed on cooling the sample at 90 °K. A possible explanation is that it could be the result of intermolecular hydrogen bonding, which may be possible at this low temperature because of a contraction in the interionic distances of the crystal.

TABLE IV

Stretching frequencies O—H cm^{-1} for allyl alcohol (ol) and *trans*-$[PtCl_2(ol)2,6\text{-lut}]$

Solvent	CH_2=CH—CH_2OH	*trans*-$[PtCl_2(ol)2,6\text{-lut}]$
C_6H_6	3 594 s	3 456 s
C_6H_6 + pyridine	3 595 s, 3 300 vs,b*	3 456 s, 3 255 vb†
		3 597 m, 3 300 b‡
C_6H_6 + 20% 2,6-lutidine	3 596 s, 3 270 vs,b	3 456 s, 3 235 b‖
C_6H_6 + 33% ether	3 596 s, 3 470 vs,b	3 460 s
CCl_4	3 620 s	3 462 m
Ether	3 472 s,b	3 460 s, 3 350 w,vb
Pyridine	3 300 vs,b	3 300 vs,b§
2,6-Lutidine	3 270 vs,b	3 230 vs,b

*20% pyridine.
†2% pyridine.
‡After 10 min.
‖Stable for 12 h.
§After reaction with solvent.

(v) Complexes with allyl alcohol, an α-hydroxyolefin, are very similar to those of the α-hydroxyacetylenes (Table IV). The spectra in the OH stretching frequency region show the same behavior.

We conclude from these studies that the interaction of the α-hydroxyl groups, in the complexes, is through coordination of the oxygen atom to the metal. We consider that no other structure can account for the spectral observations we have made, and that this structure is consistent with all previously published data.

EXPERIMENTAL

Materials

Most of the compounds used have been reported previously (11, 12). The following compounds were prepared by similar methods.

trans-Dibromo-(2,5-dimethyl-3-hexyne-2,5-diol)2,6-lutidine platinum(II): yellow-orange prisms, recrystallized from ether, m.p. 140–142°.

Anal. Calcd. for $C_{15}H_{23}O_2Br_2NPt$: C, 29.8; H, 3.8; Br, 26.4. Found: C, 30.8; H, 3.3; Br, 25.2.

trans-Dichloro-(3,6-dimethyl-4-octyne-3,6-diol)2,6-lutidine platinum(II): bright yellow, recrystallized from ether, m.p. 115–118°.

Anal. Calcd. for $C_{17}H_{27}O_2Cl_2NPt$: C, 37.6; H, 5.0. Found: C, 37.5; H, 5.2.

trans-Dichloro-(3,6-diethyl-4-octyne-3,6-diol)pyridine platinum(II); yellow, recrystallized from ether, m.p. 53–56°.

Anal. Calcd. for $C_{17}H_{27}O_2Cl_2NPt$: C, 37.5; H, 5.0. Found: C, 36.6; H, 4.9.

trans-Dichloro-(3,6-diethyl-4-octyne-3,6-diol)2,6-lutidine platinum(II): yellow, recrystallized from ether, m.p. 126°.

Anal. Calcd. for $C_{19}H_{31}O_2Cl_2NPt$: C, 39.9; H, 5.5. Found: C, 39.6; H, 5.4.

trans-Dichloro-(2,5-dimethyl-2,5-dimethoxy-3-hexyne)2,6-lutidine platinum(II): yellow, m.p. 140–145° (decomp.).

Anal. Calcd. for $C_{17}H_{27}Cl_2O_2NPt$: C, 37.6; H, 5.0. Found: C, 37.5; H, 4.9.

trans-Dichloro-(2,5-dimethyl-2,5-dimethoxy-3-hexyne)pyridine platinum(II): yellow, m.p. 95–97° (lit. m.p. 101–103° (decomp.) (1)).

Anal. Calcd. for $C_{15}H_{23}Cl_2O_2NPt$: C, 34.9; H, 4.5. Found: C, 34.5; H, 4.25.

Spectra

Infrared spectra were recorded with a Perkin–Elmer 221 prism-grating spectrometer using standard settings, calibrated against polystyrene film. For the solid state spectrum at 90 °K a Perkin–Elmer 21 spectrometer was used. A conventional low temperature cell (13) was used for the spectrum at liquid nitrogen temperature.

REFERENCES

1. J. CHATT, R. G. GUY, L. A. DUNCANSON, and D. T. THOMSON. J. Chem. Soc. 5170 (1963).
2. A. D. HEL'MAN, S. V. BUKHOVETS, and E. MEILAKH. Compt. Rend. Acad. Sci. U.R.S.S. **46**, 105 (1945).
3. S. V. BUKHOVETS. Izvest. Sektora Platiny i Drug. Blagorod. Metal. Inst. Obshcheĭ Neorg. Khim. Akad. Nauk S.S.S.R. **29**, 55 (1955).
4. J. CHATT, L. A. DUNCANSON, and R. G. GUY. Nature, **184**, 526 (1959).
5. J. CHATT, G. A. ROWE, and A. A. WILLIAMS. Proc. Chem. Soc. 208 (1957).
6. L. J. BELLAMY. The infra-red spectra of complex molecules. 2nd ed. Methuen & Co. Ltd., London; John Wiley & Sons, Inc., New York. 1958. p. 97.
7. F. F. CLEVELAND and M. J. MURRAY. J. Am. Chem. Soc. **62**, 3186 (1940).
8. J. CHATT, L. A. DUNCANSON, and R. G. GUY. Proc. Symp. Chem. Co-ord. Compounds, Agra, India. Part I, 118 (1959).
9. G. ROSSMY, W. LUTTKE, and R. MECHE. J. Chem. Phys. **21**, 1606 (1953). A. NICKON. J. Am. Chem. Soc. **79**, 243 (1957).
10. J. A. POPLE, W. G. SCHNEIDER, and H. J. BERNSTEIN. High-resolution nuclear magnetic resonance. McGraw-Hill Book Co., New York. 1959. p. 101.
11. A. D. ALLEN and T. THEOPHANIDES. Can. J. Chem. **43**, 290 (1965).
12. A. D. ALLEN and T. THEOPHANIDES. Can. J. Chem. **42**, 1551 (1964).
13. E. L. WAGNER and D. F. HORNING. J. Chem. Phys. **18**, 296 (1950).

Can. J. Chem. Downloaded from www.nrcresearchpress.com by 210.87.254.105 on 09/05/12
For personal use only.

DEPENDENCE OF BOND ANGLES ON OVERLAP INTEGRALS FOR SOME COVALENT HYDRIDES

D. A. HUTCHINSON
Department of Chemistry, University of Victoria, Victoria, British Columbia
Received June 27, 1966

ABSTRACT

An explicit relationship, between bond angles and overlap integrals, is developed for covalent hydrides of C_{3v} and C_{2v} symmetries. From this relationship it is argued that the bond angle depends on the overlap integrals of s and p functions with hydrogen 1s functions. The results of calculations of these overlap integrals are given; the calculations were first performed with Slater functions and repeated with approximate self-consistent-field functions. Arguments, based on the results of these calculations, are advanced as an additional explanation of why ammonia and water have larger bond angles than phosphine and hydrogen sulfide.

1. INTRODUCTION

The simplest description of bonding in the NH_3, H_2O, PH_3, and H_2S molecules is provided by the overlap of p orbitals of the central atom with H-atom 1s orbitals. This description predicts bond angles of 90° in all cases. Heath and Linnett (1) showed that repulsive interactions between the H atoms make a significant contribution to the opening of the bond angle from 90° in the case of H_2O. The bond lengths of NH_3 and H_2O are shorter than the bond lengths of PH_3 and H_2S, thus the HH repulsive interactions in NH_3 and H_2O should be larger than those for PH_3 and H_2S. An additional contribution to larger HH repulsions for NH_3 and H_2O is that the NH and OH bonds have more ionic character than the PH and SH bonds. The greater ionic character of the NH and OH bonds is due to the higher electronegativity of the N and O atoms. The larger HH repulsive interactions for NH_3 and H_2O provide one explanation why the HNH bond angle, 107°, exceeds the HPH bond angle, 93.5°, and why the HOH bond angle, 104.5°, exceeds the HSH bond angle, 92°. The values for the bond angles are quoted from Sutton's (2) tables.

A more accurate view of bonding in the above covalent hydrides is provided by viewing the bond as the overlap of an H atom 1s orbital with a hybrid orbital of the central atom. The angle between a pair of hybrid orbitals is related to the amounts of s and p orbitals in each hybrid. Also, the overlap integral between a hybrid orbital and an H atom 1s orbital depends on the amounts of s and p orbitals in each hybrid. Thus if the strength of a bond is related to the overlap integral, then the bond strength depends on the bond angle through the hybridization. Moreover, the relative values of the overlap integrals of a p orbital and an s orbital with an H-atom 1s orbital will affect the bond angle. The details of these arguments are presented in the next section.

2. HYBRIDIZATION AND BOND ANGLES

The general expression

$$[1] \qquad |t_r\rangle = U_{1r}|\mathrm{s}\rangle + U_{2r}|\mathrm{p}_x\rangle + U_{3r}|\mathrm{p}_y\rangle + U_{4r}|\mathrm{p}_z\rangle$$

for a hybrid orbital $|t_r\rangle$, consisting of s and p orbitals, suggests that 16 arbitrary coefficients are involved in the description of four hybrid orbitals. However, as a matter of convenience one usually imposes four normalization conditions and six orthogonality constraints

$$\langle t_r|t_s\rangle = \delta_{rs}.$$

Now the hybridization of an s and three p orbitals involves only six independent variables.

The 16 transformation coefficients U_{jr} form an orthogonal 4×4 matrix if the orthonormality constraints are imposed. An $n \times n$ orthogonal matrix M and an $n \times n$ antisymmetric matrix A both have $n(n+1)/2$ independent elements. Ferrar (3) shows that if $(1 + A)$ is non-singular, then an $n \times n$ orthogonal matrix M can be constructed from an $n \times n$ antisymmetric matrix A by the prescription

$$M = (1 - A)(1 + A)^{-1}.$$

This procedure allows one to express each transformation coefficient U_{jr} as a function of six independent variables. It is possible to simplify the situation even further (4). Three conditions are required to orient the hybrids $|t_1\rangle$, $|t_2\rangle$, $|t_3\rangle$, and $|t_4\rangle$ with respect to the basis vectors $\boldsymbol{i}, \boldsymbol{j}$, and $\boldsymbol{k}$ defining the x, y, and z directions. These three conditions are not relevant because the physically significant features of the hybrid orbitals are the amounts of s and p character in each hybrid orbital and the orientations of the hybrid orbitals with respect to each other. Rotation of the basis vectors $\boldsymbol{i}, \boldsymbol{j}, \boldsymbol{k}$ will alter neither the s and p characters of the hybrid orbitals nor the relative orientations of the hybrid orbitals. Of the six independent hybridization parameters, only three are of physical interest. The other three can be fixed by choosing a particular set of basis vectors $\boldsymbol{i}, \boldsymbol{j}, \boldsymbol{k}$; the choice is motivated by the consideration of convenience. The result of a particularly convenient choice of basis vectors $\boldsymbol{i}, \boldsymbol{j}, \boldsymbol{k}$ are the hybrid orbitals

$$\begin{aligned} |t_1\rangle &= N(|\mathrm{s}\rangle - \lambda_1|\mathrm{p}_x\rangle - \lambda_2|\mathrm{p}_y\rangle - \lambda_3|\mathrm{p}_z\rangle), \\ |t_2\rangle &= N(\lambda_1|\mathrm{s}\rangle + |\mathrm{p}_x\rangle - \lambda_3|\mathrm{p}_y\rangle + \lambda_2|\mathrm{p}_z\rangle), \\ |t_3\rangle &= N(\lambda_2|\mathrm{s}\rangle + \lambda_3|\mathrm{p}_x\rangle + |\mathrm{p}_y\rangle - \lambda_1|\mathrm{p}_z\rangle), \\ |t_4\rangle &= N(\lambda_3|\mathrm{s}\rangle - \lambda_2|\mathrm{p}_x\rangle + \lambda_1|\mathrm{p}_y\rangle + |\mathrm{p}_z\rangle), \\ N &= (1 + \lambda_1^2 + \lambda_2^2 + \lambda_3^2)^{-1/2}. \end{aligned} \qquad [2]$$

The directional p orbitals behave as vectors whereas the s orbital is spherically symmetric. Consequently the directional properties of a hybrid orbital arise from the contributions of the p orbitals. The direction, with respect to the basis vectors $\boldsymbol{i}, \boldsymbol{j}, \boldsymbol{k}$ of the general hybrid orbital $|t_r\rangle$ of eq. [1], is given by the unit vector

$$\boldsymbol{e}_r = (U_{2r}^2 + U_{3r}^2 + U_{4r}^2)^{-1/2}(U_{2r}, U_{3r}, U_{4r}).$$

The angle θ_{rs} between two hybrid orbitals $|t_r\rangle$ and $|t_s\rangle$ is given by

$$\begin{aligned} \cos\theta_{rs} &= \boldsymbol{e}_r \cdot \boldsymbol{e}_s \\ &= \left(\sum_{i=2}^{4} U_{ir}^2\right)^{-1/2}\left(\sum_{j=2}^{4} U_{js}^2\right)^{-1/2}\sum_{k=2}^{4} U_{kr}U_{ks}. \end{aligned} \qquad [3]$$

A more extensive discussion on angles between hybrid orbitals can be found in a paper by Coulson (5).

For the remainder of this discussion the hybrid orbitals $|t_3\rangle$ and $|t_4\rangle$ are chosen as the hybrids involved in bonds between a central atom A and an H atom. It is convenient to use the difference ϕ_{34} between the angle θ_{34} and 90°,

$$\phi_{34} = \theta_{34} - 90°, \qquad [4]$$

instead of θ_{34} itself. The relationship between ϕ_{34} and the hybridization parameters is

$$\sin\phi_{34} = \lambda_2\lambda_3(1 + \lambda_1^2 + \lambda_2^2)^{-1/2}(1 + \lambda_1^2 + \lambda_3^2)^{-1/2}, \qquad [5]$$

Can. J. Chem. Downloaded from www.nrcresearchpress.com by 210.87.254.105 on 09/05/12
For personal use only.

this follows immediately from eqs. [2], [3], and [4]. The overlap integral $\langle t_4|h\rangle$ between the hybrid orbital $|t_4\rangle$ and the hydrogen 1s orbital $|h\rangle$ is

$$\langle t_4|h\rangle = N(\lambda_3\langle s|h\rangle + (1 + \lambda_1^2 + \lambda_2^2)^{1/2}\langle p_\sigma|h\rangle). \quad [6]$$

$|p_\sigma\rangle$ is a p orbital in the direction of the hybrid orbital $|t_4\rangle$. From eqs. [5] and [6] it is seen that the bond angle and overlap integrals are related through the hybridization parameters λ_j.

The four molecules of interest have either C_{3v} symmetry or C_{2v} symmetry. A consequence of either symmetry is that the hybridization can be described by a single parameter μ. In the case of C_{3v} symmetry, the three hybrids which bond to the H atoms, say $|t_2\rangle$, $|t_3\rangle$, $|t_4\rangle$, are equivalent; that is each one has the same amount of s character. Consequently

$$\lambda_1 = \lambda_2 = \lambda_3 = \mu. \quad [7]$$

The angle ϕ and the overlap integral $\langle t_4|h\rangle$ are obtained by substituting eq. [7] into eqs. [5] and [6] respectively,

$$\sin\phi = \mu^2(1 + \mu^2)^{-1}, \quad [8]$$

$$\langle t_4|h\rangle = (1 + 3\mu^2)^{-1/2}(\langle s|h\rangle + (1 + 2\mu^2)^{1/2}\langle p_\sigma|h\rangle). \quad [9]$$

From eqs. [8] and [9], the overlap integral can be written directly in terms of the deviation ϕ of the bond angle from 90°

$$\langle t_4|h\rangle = (1 + \sin\phi)^{-1/2}(\langle s|h\rangle\sin^{1/2}\phi + \langle p_\sigma|h\rangle). \quad [10]$$

If the same arguments are used for the case of C_{2v} symmetry, an identical result is obtained for the overlap integral in terms of ϕ. Whereas for a C_{3v} hydride $0 \leqq \phi \leqq 30°$, for a C_{2v} hydride $0 \leqq \phi \leqq 90°$.

Although hybridizing the s and p orbitals increases the energy of the central atom, a greater amount of energy is recovered from the formation of a more stable bond; a large overlap integral is associated with a strong chemical bond. If the ratio $\langle s|h\rangle/\langle p_\sigma|h\rangle$ is large, energy considerations will favor a larger deviation ϕ from 90° for the bond angle than if the ratio $\langle s|h\rangle/\langle p_\sigma|h\rangle$ is small.

The ratio $\langle 2s|h\rangle/\langle 2p_\sigma|h\rangle$ for NH_3 and H_2O is larger than the ratio $\langle 3s|h\rangle/\langle 3p_\sigma|h\rangle$ for PH_3 and H_2S. These results are valid for both Slater functions and Clementi's (6) approximate self-consistent-field (s.c.f.) functions. Thus, the preceding arguments offer an additional explanation why the bond angles of NH_3 and H_2O exceed those of PH_3 and H_2S. The results of calculations of the relevant overlap integrals are presented in the following section.

3. OVERLAP INTEGRALS

The overlap integrals were first calculated with orthogonalized Slater functions; the simple Slater functions were orthogonalized by the Schmidt procedure. The orbital exponents were determined by applying Slater's (7) rules. The bond lengths, used in the overlap integral calculations, were obtained from Sutton's (2) tables; these bond lengths are given in Table I. The results of the calculations for orthogonalized Slater functions are also given in Table I.

The argument, for relative bond angles based on the ratio $\langle s|h\rangle/\langle p_\sigma|h\rangle$ of overlap integrals, would be more convincing if the results are also valid for atomic functions other than orthogonalized Slater functions. Clementi (6) has published results for approximate s.c.f. functions which employ a basis set consisting of several Slater-type orbitals (s.t.o.'s). Clementi's 2s function consists of two 1s and four 2s s.t.o.'s and his 2p function consists of

Can. J. Chem. Downloaded from www.nrcresearchpress.com by 210.87.254.105 on 09/05/12
For personal use only.

TABLE I
Results of overlap integral calculations

	Function			Function	
	Slater	Clementi		Slater	Clementi
NH in NH_3 (R = 1.905 atomic units)			OH in H_2O (R = 1.811 atomic units)		
$\langle 2s\|h\rangle$	0.546	0.555	$\langle 2s\|h\rangle$	0.508	0.521
$\langle 2p_\sigma\|h\rangle$	0.406	0.456	$\langle 2p_\sigma\|h\rangle$	0.348	0.413
PH in PH_3 (R = 2.685 atomic units)			SH in H_2S (R = 2.521 atomic units)		
$\langle 3s\|h\rangle$	0.504	0.459	$\langle 3s\|h\rangle$	0.507	0.460
$\langle 3p_\sigma\|h\rangle$	0.523	0.550	$\langle 3p_\sigma\|h\rangle$	0.496	0.511

four 2p s.t.o.'s. The 3s function consists of one 1s and seven 3s s.t.o.'s and the 3p function consists of one 2p and seven 4p s.t.o.'s. For the calculations in this paper the values chosen for the various orbital exponents and expansion coefficients were Clementi's results for the ground states of the N, O, P, and S atoms. The results of the calculations of the respective overlap integrals with Clementi's functions are also given in Table I.

After the preceding calculations were completed, the referee pointed out to the author that the qualitative nature of the results in Table I are still valid if a different value for the orbital exponent of the hydrogen 1s function is chosen. In numerous molecular calculations an orbital exponent of 1.2 is preferable to one of unity; it would be useful to know what effect this has on the results. If an orbital exponent of 1.2 is chosen for the hydrogen 1s orbital, the overlap integrals with the Clementi functions are somewhat less, but the relative magnitudes in the 2s/2p series and the 3s/3p series remain the same. In addition, the referee's results indicate that only minor variations occur if one chooses the Clementi functions for states, other than the ground state, of the lowest electronic configurations of the nitrogen, oxygen, phosphorous, and sulfur atoms.

Since both the orthogonalized Slater functions and the fairly sophisticated Clementi functions lead to the same conclusion, namely

$$[11] \qquad (\langle 2s|h\rangle/\langle 2p_\sigma|h\rangle > (\langle 3s|h\rangle/\langle 3p_\sigma|h\rangle)$$

for NH_3 versus PH_3 and H_2O versus H_2S, it seems probable the result would be valid for any reasonable choice of atomic functions. Thus, arguments based on the result of eq. [11] contribute toward an explanation of the observation that the bond angles in NH_3 and H_2O are respectively larger than those of PH_3 and H_2S. In Table I it is interesting to note that for N and O, the $\langle 2s|h\rangle$ overlap integral is considerably larger than the $\langle 2p_\sigma|h\rangle$ overlap integral. Conceivably, this could provide an appreciable contribution towards the large deviations of the HNH and HOH bond angles from 90°. For PH_3 and H_2S, the small deviations from 90° most likely arise mainly from HH repulsions since the $\langle 3s|h\rangle$ overlap integral is smaller than the $\langle 3p_\sigma|h\rangle$ overlap integral. As a last word, it should be kept in mind that the arguments presented in this paper, while perhaps interesting, are subsidiary to those based on repulsions between the H atoms and other causes such as the variation of the kinetic energy term.

ACKNOWLEDGMENTS

The author is grateful to Professor C. A. Coulson for some valuable discussions and in addition for many helpful suggestions which led to an improvement on the original manuscript. Also the author thanks the referee for performing a number of additional calculations, the results of which add support to the conclusions of this paper.

Can. J. Chem. Downloaded from www.nrcresearchpress.com by 210.87.254.105 on 09/05/12
For personal use only.

REFERENCES

1. D. F. HEATH and J. W. LINNETT. Trans. Faraday Soc. **44**, 556 (1948).
2. L. E. SUTTON. Tables of interatomic distances. Chemical Society, London. 1958. Special Publication No. 11.
3. W. L. FERRAR. Algebra. Oxford University Press, London. 1946 pp. 164–166.
4. D. A. HUTCHINSON. Ph.D. Thesis, University of Oxford, Oxford, England. 1963. pp. 16–22.
5. C. A. COULSON. Victor Henri commemorative volume "Contributions to the study of molecular structure". Desoer, Liège, Belgium. 1952.
6. E. CLEMENTI. Tables of atomic functions. IBM, San Jose, California. 1965.
7. J. C. SLATER. Phys. Rev. **36**, 57 (1930).

Can. J. Chem. Downloaded from www.nrcresearchpress.com by 210.87.254.105 on 09/05/12
For personal use only.

Can. J. Chem. Downloaded from www.nrcresearchpress.com by 210.87.254.6 on 09/05/12
For personal use only.

INFRARED ABSORPTION OF SINGLE CRYSTALS OF ANHYDROUS SODIUM FORMATE

T. L. CHARLTON[1] AND K. B. HARVEY
Department of Chemistry, University of British Columbia, Vancouver, British Columbia

Received June 6, 1966

ABSTRACT

The infrared absorption of single crystals of sodium formate has been measured in the region of 250 cm^{-1} to 4 000 cm^{-1}. Thin sections cut perpendicular to the unique axis were employed and spectra were recorded with light polarized at various angles in this plane. It has been possible to assign unambiguously all of the infrared active internal fundamentals of the formate ion including the overlapping ν_2 and ν_5 modes. In addition, three lattice modes at 57, 107, and 138 cm^{-1} have been identified.

RÉSUMÉ

On a étudié par spectroscopie infrarouge des cristaux uniques de formiate de sodium dans la région de 250 à 4 000 cm^{-1}. L'absorption par des lames minces taillées perpendiculairement à l'axe unique a été mesurée en lumière polarisée à divers angles dans ce plan. On a réussi à identifier sans ambiguité toutes les fréquences fondamentales de l'ion formiate actives en infrarouge, y compris les modes ν_2 et ν_5 qui se recouvrent. De plus on a enregistré trois vibrations du réseau cristallin à 57, 107 et 138 cm^{-1}.

INTRODUCTION

The vibrational spectrum of sodium formate has been the subject of investigation of a number of workers (1–9) but only in Newman's studies were single crystals and polarized radiation used. Some of the results are summarized in Table I. It should be noted that we have assigned the symbol ν_1 to the C—H stretching frequency in conformity with the usual convention. Some confusion has arisen in the past due to the assignment of ν_1 to the lower C—O stretching frequency which in Table I is given the symbol ν_2.

TABLE I

Previous data on the infrared and Raman spectra of sodium formate (wave numbers in cm^{-1})

	Ito and Bernstein		Newman*	Fonteyne		Harvey	
Mode	I.R. cryst.	R. H_2O†	I.R. single crystal	$NaHCO_2$ R. H_2O	$NaDCO_2$ R. H_2O	$NaHCO_2$ I.R. cryst.	$NaDCO_2$ I.R. cryst.
$\nu_3(\delta COO)a_1$	772	762 p	784 b	773	757	769	762
$\nu_6(\rho CH)b_2$	1 073	1 066 d	1 070⊥	1 069	918	1 062	912
$\nu_2(\nu CO)a_1$	1 366	1 349 p	1 377 b	1 352	1 329	1 355	1 327
$\nu_5(\omega CH)b_1$	1 377	1 380 d	1 365 ‖	1 386	1 028	1 385	1 010
$\nu_4(\nu CO)b_1$	1 567	—	1 620 ‖	1 584	1 580	1 590	1 580
$2\nu_6$	2 134	—	—	2 126	1 831	—	—
$\nu_2+\nu_6$	2 435	—	—	—	—	—	—
$2\nu_5$	2 720	—	2 750 ‖	2 732	2 032	2 715	2 017
$\nu_1(\nu CH)a_1$	2 841	2 803 p	2 870 b	2 825	2 122	2 828	2 130
$\nu_4+\nu_5$	2 953	—	—	—	—	2 950	—
$\nu_1+\nu_3$	3 611	—	—	—	—	—	—
$3\nu_5$	4 085	—	—	—	—	—	—
$\nu_1+\nu_5$	4 200	—	—	—	—	—	—
$\nu_2+\nu_4+\nu_5$	4 313	—	—	—	—	—	—

*The symbols are those used by Newman to refer to activity: b means parallel to the b axis (twofold axis) of the crystal; ‖ and ⊥ refer to directions in the (010) plane parallel and perpendicular to the plane of the molecule.
†In this column p = polarized and d = depolarized.

[1]*Present address: Chemistry Department, University of Alberta, Edmonton, Alberta.*

Can. J. Chem. Downloaded from www.nrcresearchpress.com by 210.87.254.6 on 09/05/12
For personal use only.

The overall agreement in the frequency and the assignment of the fundamentals is quite good. The major exception is the assignment by Newman (8) of the higher frequency member of the pair of bands in the 1 350 – 1 400 cm^{-1} region to ν_2. This assignment based on the apparent activity of this mode in the crystal is in conflict with the assignments of Fonteyne (2) and Bernstein (4) who attributed the 1 380 cm^{-1} absorption to ν_5. The latter authors based their assignments on a vibrational analysis (2) and Raman depolarization ratios (4). Bernstein quotes measured depolarization ratios of 0.29 and 0.80 for the 1 349 cm^{-1} and 1 380 cm^{-1} scattering respectively. This is clear-cut evidence for the assignment of the 1 349 cm^{-1} scattering to the symmetric C—O stretching mode ν_2.

Ito and Bernstein also observed many overtones and combinations in the infrared absorption spectrum of crystalline sodium formate and a number of these are also listed in Table I. We have altered the assignments in some cases to give better agreement with the spectrum of the deutero-formate ion. In addition Bernstein observed several combination and difference bands involving low frequency lattice modes at 60 cm^{-1} and 140 cm^{-1}.

Crystal Structure of Sodium Formate

The crystal structure of sodium formate is described by Zachariasen (10) as being monoclinic and belonging to the space group $C\,2/c$ (C_{2h}^6). The cell parameters and the coordinates of the generating atomic positions of sodium formate are listed below. The hydrogen atom positions were calculated by us on the assumption of a value of 1.09 Å for the C—H bond length.

Space group: $C\,2/c$ (C_{2h}^6)
$a = 6.19$ Å; $b = 6.72$ Å; $c = 6.49$ Å; $\beta = 121°42'$
Generating positions:
Origin at $\bar{1}$ on glide plane n.
8 O atoms at: (0.043, 0.194, 0.185)
4 Na^+ ions at: (1/4, −0.139, 1/4)
4 C atoms at: (1/4, 0.283, 1/4)
4 H atoms at: (1/4, 0.445, 1/4)

As shown in Fig. 1, the symmetry axis of the formate ions is co-linear with the twofold axis of the crystal while the plane of the molecule is approximately perpendicular (103°) to the c axis. The formate ion parameters were calculated by us to be r(C—O) = 1.27 Å and $\angle$OCO = 124°.

Since the unit cell of Fig. 1 is compound, an alternative unit cell based on a lattice with shorter translation vectors may be chosen. The single unit of pattern of such a cell forms

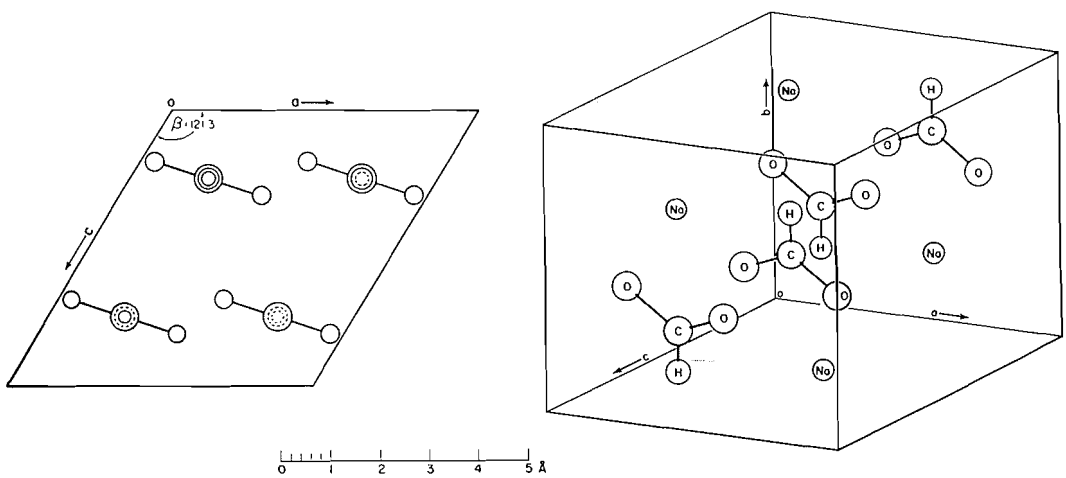


FIG. 1. Crystal structure of sodium formate.

the basis for the vibrational analysis. As shown in Fig. 2, each unit of pattern contains two formate ions and two sodium ions symmetrically related by a center of symmetry. The space group is $P\,\bar{1}$ (C_i^1) and the cell parameters are $a = 4.57$ Å, $b = 6.72$ Å, $c = 6.49$ Å, $\alpha = 90°$, $\beta = 110°52'$, and $\gamma = 42°40'$. The higher overall symmetry of the structure is reflected in the nonaccidental value of 90° for the angle α. In the unit of pattern each sodium ion is separated by a distance of 2.80 Å from the hydrogen atom of the formate ion on the same twofold axis. The distances between the atoms related by the center of symmetry are: r(Na—Na) = 3.57 Å; r(H—H) = 5.22 Å; r(C—C) = 7.07 Å; r_1(O—O) = 8.25 Å; r_2(O—O) = 7.68 Å. A distance of 2.50 Å separates the sodium ion from the oxygen atoms of the formate ion in the adjacent unit of pattern lying on the same twofold axis. The nearest oxygen atoms of formate ions lying on adjacent twofold axes are somewhat closer than this at 2.35 Å and 2.45 Å.

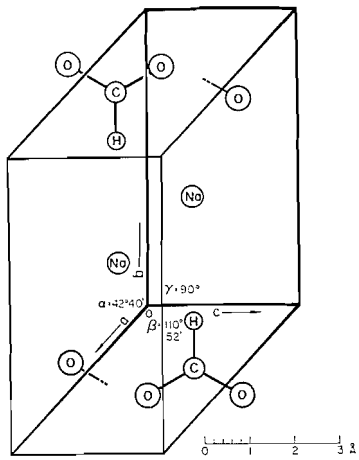


FIG. 2. Primitive unit cell of sodium formate. The b and c axes are the same as those of the centered unit cell of Fig. 1.

EXPERIMENTAL

Preparation of Crystals

Reagent grade (Baker and Adamson) sodium formate was used without further purification except the removal of insoluble impurities by filtration. The crystals studied were obtained by crystallization from aqueous solution at 40° C to avoid forming the dihydrate which has been reported obtained at temperatures below 28 °C (11). Using specially selected untwinned seed crystals and slow evaporation (several weeks) of the aqueous solution large crystals of tabular habit 2 to 10 mm wide, 20 to 30 mm long, and 2 or 3 mm thick were obtained. X-Ray diffraction photographs showed that the principal face of these crystals was the (010) face elongated in the c direction.

Crystals with as few internal flaws as possible were selected and reduced to the proper thickness by grinding. To accomplish this the flat crystal was glued to a rock-salt window with C.I.L. Household Cement and a planar surface obtained by grinding on successively finer grades of emery paper (150 C, 360 A and 4/0). The surface was then polished on a ground glass lap and finally on a velvet lap using fine abrasives. The kerosene used as a lubricant in these operations also served to protect the slightly hygroscopic sodium formate.

The crystal was next removed from the rock-salt window, using acetone as a solvent for the cement, and the polished surface glued to the window. This required considerable care since shrinkage of the cement on drying often led to glue-free pockets between the crystal and the window. The crystals usually cracked through lack of support at these points during the final grinding and polishing. We are still looking for a more satisfactory glue for this application. The second face of the crystal was prepared in the same manner as the first except that considerably more care was required in the final stages. In regions where the glue did not absorb, it was possible to examine the spectrum of the crystal and the polishing process was continued until the desired intensity of absorption was observed.

The thin crystal was now floated free of the rock-salt window in an acetone bath, placed over a slit 10 mm × 2 mm in a brass disc and glued sparingly at the edges. The disc was designed to fit the keys on the spectrometer mounting so that it could be placed as close to the entrance slit as possible.

Can. J. Chem. Downloaded from www.nrcresearchpress.com by 210.87.254.6 on 09/05/12
For personal use only.

A polarizing microscope was used to determine the relative orientation of the crystal axes and to confirm the quality of the crystal. In all cases the crystals were clear, except for surface scratches, and exhibited sharp extinction. Observation of interference figures also allowed us to confirm that crystals were ground to within 1° or 2° of the perpendicular of the axis of observation. The thickness of the crystals was measured on a Zeiss Light-section microscope and found to be approximately 40 μ.

Infrared Spectrometer

Spectra were recorded in the region of 4 000 to 250 cm^{-1} using a Perkin–Elmer 421 spectrometer with two dual-grating interchanges. The polarizer, constructed in our shop, consisted of two three-sheet stacks of 0.5 mm silver chloride plates mounted in the form of a V (12) to prevent displacement of the spectrometer beam. Measurements in the visible region against a Wollaston prism indicate that <5% of the component perpendicular to the desired component and the beam is passed. Measurements of the convergence of the sample beam showed that <1% of the component parallel to the beam direction would be introduced by the convergence.

The spectrometer was calibrated against known spectra (13) at the scanning speeds and response times used in obtaining the crystal spectra to minimize errors due to response time effects. Spectral slit widths are indicated for the individual spectra. The error of measurement is estimated to be ± 2 cm^{-1}; much smaller, in most cases, than the uncertainty introduced due to the overlapping of adjacent bands.

RESULTS AND DISCUSSION

Vibrational Analysis

The primitive unit cell of sodium formate contains 10 atoms so that there will be a total of 30 vibrations. Under the factor group or finite space group (C_{2h}) the structure of the representation formed by the cartesian coordinates is $\Gamma = 6a_g + 9b_g + 6a_u + 9b_u$ (Table II). If the unique axis of the crystal (b) is chosen to coincide with the y axis of the

TABLE II

Character table and factor-group analysis for sodium formate

C_{2h}	E	C_2	i	σ_h	n_i*	$n_i(T)$	$n_i(T')$	$n_i(R')$	n_i'	
a_g	1	1	1	1	6	0	2	1	3	$\alpha_{xx}\alpha_{yy}\alpha_{zz}\alpha_{xz}$
b_g	1	−1	1	−1	9	0	4	2	3	$\alpha_{yz}\alpha_{yx}$
a_u	1	1	−1	−1	6	1	1	1	3	T_y
b_u	1	−1	−1	1	9	2	2	2	3	T_x, T_z

*where n_i = total number of vibrations of symmetry species i under the factor group analysis,
$n_i(T)$ = number of purely translational modes of symmetry species i,
$n_i(T')$ = number of lattice modes of translational origin of symmetry species i,
$n_i(R')$ = number of lattice modes of rotational origin of symmetry species i, and
n_i' = number of internal formate vibrations of symmetry species i.

Cartesian system then the translation in the y direction (T_y) will be of species a_u while T_x and T_z are of species b_u. The remaining translational motions yield nine normal vibrations: $2a_g + 4b_g + a_u + 2b_u$. Rotational motions of the ions give six normal vibrations: $a_g + 2b_g + a_u + 2b_u$. This leaves 12 normal vibrations associated with internal motions of the formate ions $3a_g + 3b_g + 3a_u + 3b_u$. There are in other words 12 internal formate ion vibrations and 15 lattice vibrations. These are illustrated schematically in Fig. 3 for the unit of pattern shown in Fig. 2. Since most of these vibrations should be observable in the Raman or infrared spectra of the crystal they have been numbered consecutively from ν_1 to ν_{27}. Where possible the usual numbering convention has been followed but until more quantitative data is available the numbering of the lattice modes must be regarded as only tentative.

The 12 internal normal vibrations may be considered to arise from 6 normal vibrations of the "free" formate ion through a dynamic crystal effect resulting from the presence of two formate ions in the unit of pattern. The two ions may execute the same internal vibration in phase or out of phase to give crystal modes of g or u symmetry respectively. Since the g modes are Raman active and the u modes infrared active the Raman and infrared spectra will in principle be different in frequency. In practice, the observed frequencies

Can. J. Chem. Downloaded from www.nrcresearchpress.com by 210.87.254.6 on 09/05/12
For personal use only.

Can. J. Chem. Downloaded from www.nrcresearchpress.com by 210.87.254.6 on 09/05/12
For personal use only.

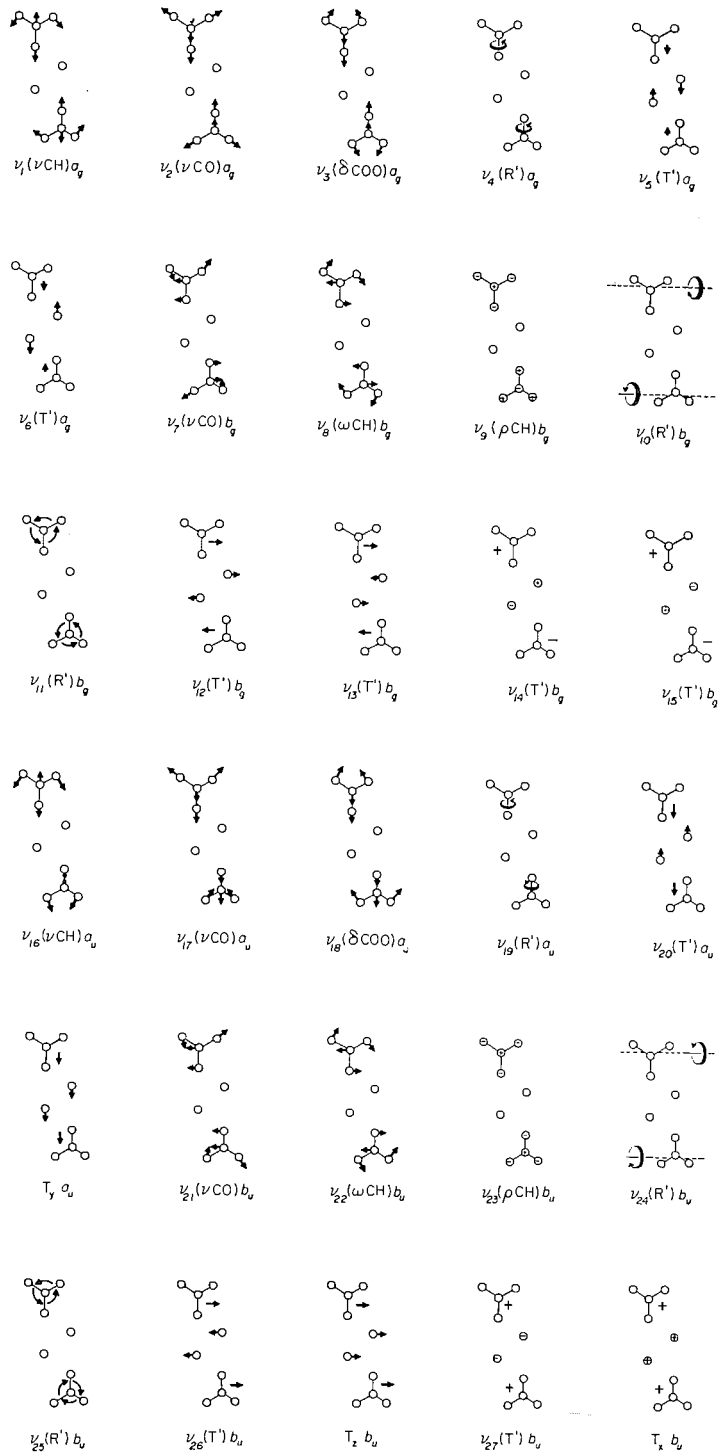


FIG. 3. Normal vibrations of the sodium formate crystal. See text regarding the numbering of the lattice vibrations and the form of ν_{10} to ν_{15} and ν_{24} to ν_{27}.

are not expected to differ by more than a small amount, but this difference will be a direct measure of the dynamic crystal effect or correlation field splitting.

In the same way the three possible rotations of the "free" formate ion are doubled to give three g and three u lattice modes of rotational origin. Because of its symmetry, the sodium ion may execute translational but not rotational motion hence there are 12 lattice modes of translational origin. Three of the u modes are pure translations, however, so that there will be only 3 infrared active lattice modes of translational origin but 6 Raman active modes of this type.

Single Crystal Spectra

In considering the spectra of single crystals it is necessary to take account of the orientation of the ions with respect to the crystal axes. The formate ions lie on sites of C_2 symmetry with the symmetry axis of the ion collinear with the unique axis of the crystal (Table III). As a result the totally symmetric modes of the "free" ion of species a_1 become a_g (ν_1,ν_2,ν_3) and a_u ($\nu_{16},\nu_{17},\nu_{18}$) in the crystal and are most strongly infrared active for light polarized with the electric vector parallel to the $y(b)$ direction. There should be no absorption for light polarized in the $xz(ac)$ plane.

Since the crystal is monoclinic there is no unique axis in the ac plane and the b_1 and b_2 modes of the free ion are not distinguished by group theoretical analysis of the vibrations of the crystal. Thus, each of the asymmetric modes gives rise to a b_g and a b_u mode in the crystal. The intensity behavior with polarized light will be quite different, however, for the in-plane and out-of-plane "free" ion modes. The in-plane internal modes (ν_{21},ν_{22}) will show maximum infrared absorption for light polarized with the electric vector parallel to the plane of the molecule and perpendicular to the twofold axis. On the other hand, absorption due to the out-of-plane vibration (ν_{23}) will be a maximum with the electric vector perpendicular to the plane of the molecule.

The intensity behavior of the lattice modes is not as easily predicted as that of the internal modes. The two a_u modes arising from translation parallel to the twofold axis (ν_{20}) and rotation about the twofold axis (ν_{19}) will show maximum absorption for light polarized parallel to this axis. In the case of the four b_u modes (ν_{24} to ν_{27}), however, the directions of translation and the axes of rotation of the vibrations are constrained only to the $ac(xz)$ plane. The pairs of transition moments will be perpendicular to one another but their orientation relative to the crystal axes will be a function of the physical parameters of the system. (This behavior may be compared with that of the refractive index ellipsoid of a monoclinic crystal. The two are obviously related.) The actual vibrations will, therefore, be linear combinations of those illustrated. Similar considerations apply, of course, to the corresponding Raman active vibrations.

While the crystal field effects are relatively minor, the intensity variations arising from the orientation of the ions in single crystals will be quite large and readily observable experimentally. Even relative intensity measurements will permit unambiguous assignment of the frequencies of the fundamental vibrations. More important perhaps is the fact that such data will also fix uniquely the orientation of the formate ion in the crystal.

Combinations and Overtones of Internal Fundamentals

All of the first overtones will be of a_g symmetry and inactive in the infrared spectrum (Table IV). Combinations of the corresponding in-phase (g) and out-of-phase (u) pairs such as $\nu_1 + \nu_{16},\nu_2 + \nu_{17}$ etc. will be infrared active and their frequency should be approximately the same as the corresponding overtones; $2\nu_{16} \simeq \nu_1 + \nu_{16}$ etc. These will be of a_u symmetry, however, and it is unlikely they will be observed for the ac cut crystals used in this investigation.

Can. J. Chem. Downloaded from www.nrcresearchpress.com by 210.87.254.6 on 09/05/12
For personal use only.

Can. J. Chem. Downloaded from www.nrcresearchpress.com by 210.87.254.6 on 09/05/12
For personal use only.

In the same way it can be deduced that any combination of the infrared active (u) modes or any combination of the Raman active (g) modes will have a_g or b_g symmetry and be infrared inactive. The remaining combinations will all be infrared active but the combinations $a_g + a_u$ or $b_g + b_u$ will have a_u symmetry and are unlikely to be observed. This leaves 18 combinations of b_u symmetry ($b_g + a_u$ or $a_g + b_u$) which will be infrared active. These occur in pairs with approximately the same frequency ($\nu_7 + \nu_{16} \approx \nu_1 + \nu_{21}$ for example) so that only nine absorption peaks (possibly doubled) arising from combinations of internal fundamentals are to be expected.

In principle the frequencies of the infrared inactive a_g and b_g modes could be inferred from the infrared active combinations. Any such estimate must be very rough, however, because the anharmonicity and crystal field splitting will be of the same order of magnitude.

Combinations of Internal Fundamentals and Lattice Modes

Sum and difference modes of the low-frequency lattice vibrations and the internal fundamentals will give rise to a series of weaker peaks on the high- and low-frequency sides of the absorption peak assigned to the internal fundamental. The transition probabilities for the difference modes are the same as those of the corresponding sum modes but the intensities are expected to be less because of the smaller populations of the excited lattice-mode energy levels at which the transitions originate.

The satellite structure of an internal a_u mode will, in principle, exhibit 15 peaks in the infrared spectrum arising from combinations: 3 of species a_u, $(a_u + a_g)$; $6b_u$, $(a_u + b_g)$; $2a_u$, $(a_g + a_u)$; and $4b_u$, $(a_g + b_u)$. Only the 10 b_u modes should be observable with the electric vector of the polarized light perpendicular to the b axis. There will in addition be 10 corresponding difference modes.

The situation is similar for an internal b_u mode. The 15 possible active combinations with lattice modes are: $3b_u$, $(b_u + a_g)$; $6a_u$, $(b_u + b_g)$; $2b_u$, $(b_g + a_u)$; and $4a_u$ $(b_g + b_u)$. Only the five b_u modes should be observable with the ac cut crystals, along with the five corresponding difference modes.

It should be noted that extending the arguments of the factor group analysis to the combinations and overtones is open to criticism since the implicit assumption that the wave-vector k is zero may not be valid in these cases.

Assignment of Internal Fundamentals

The symmetric modes ν_{16}, ν_{17}, and ν_{18} of a_u symmetry should be inactive for light polarized in the ac plane but because of the slight convergence of the spectrometer beam they are observed as weak but very sharp peaks at 2 831 cm^{-1}, 1 376 cm^{-1}, and 782 cm^{-1}

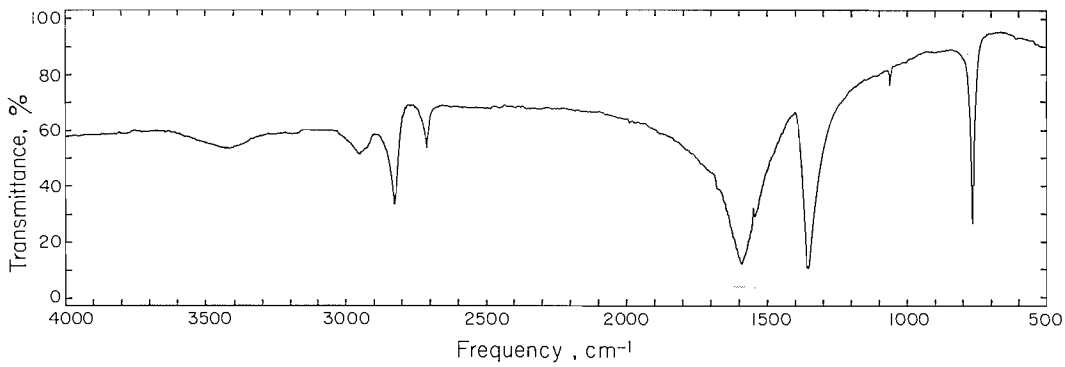


FIG. 4. Infrared absorption of powdered sodium formate. The spectral slit width varies from approximately 2.3 cm^{-1} in the high-frequency region to a minimum of 1.0 cm^{-1} in the low-frequency region.

TABLE III

Correlation table for sodium formate

Molecular group C_{2v}	Site group C_2	Factor group C_{2h}
$(\nu_1,\nu_2,\nu_3)a_1$	a	a_g
a_2		b_g
$(\nu_4,\nu_5)b_1$	b	a_u
$(\nu_6)b_2$		b_u

TABLE IV

Symmetry species of combinations and overtones

	a_g	b_g	a_u	b_u
a_g	a_g	b_g	a_u	b_u
b_g	b_g	a_g	b_u	a_u
a_u	a_u	b_u	a_g	b_g
b_u	b_u	a_u	b_g	a_g

respectively. All three of these peaks change very little in intensity as the angle of polarization relative to the c axis is changed (Fig. 5). The peaks adjacent to ν_{16} at 2 950 cm^{-1} and 2 720 cm^{-1}, for example, vary markedly in intensity as the polarizer angle is changed in the manner expected of b_u modes. Confirmation of these assignments is provided by noting that the three a_u fundamentals are much more prominent in the powder spectrum than in the single crystal spectra.

The wagging mode, ν_{22}, overlaps the symmetric C—O stretching mode ν_{17} and in the powder spectrum the two are very difficult to resolve. Figure 5*a* shows clearly, however, that ν_{17} is at 1 376 cm^{-1} and that the lower frequency component of the overlapping bands is of b_u symmetry. Since the intensity of absorption is a maximum when the polarized light vector is parallel to the plane of the molecule it must be an in-plane mode and we have assigned it to ν_{22}. The frequency of maximum absorption is estimated to be at 1 356 cm^{-1}. The order of these assignments is in agreement with the results of Newman but is the reverse of all other assignments. The assignments of Bernstein's Raman spectrum are supported by the measured depolarization ratios suggesting that solvent effects produce a downward shift of about 27 cm^{-1} in $\nu_{17}(\nu_2)$ while $\nu_{22}(\nu_5)$ undergoes an upward shift of 24 cm^{-1}.

The remaining in-plane mode, $\nu_{21}(\nu\mathrm{CO})b_u$, is overlapped by absorption arising from combination modes. The absorption peak is strong and relatively broad for light polarized in the plane of the molecule making difficult an accurate estimate of the frequency of maximum absorption. The value of 1 595 cm^{-1} quoted in Table V is the frequency of a weak shoulder observed in spectra taken with the electric vector of the polarized light nearly perpendicular to the plane of the molecule.

The only out-of-plane mode, $\nu_{23}(\rho\mathrm{CH})b_u$, is readily identifiable as absorbing at 1 066 cm^{-1} since this peak exhibits maximum intensity when the polarized light vector is perpendicular to the plane of the molecule. This is the least strongly absorbing of all of the internal fundamentals and is observed in powder spectra only with difficulty.

Can. J. Chem. Downloaded from www.nrcresearchpress.com by 210.87.254.6 on 09/05/12
For personal use only.

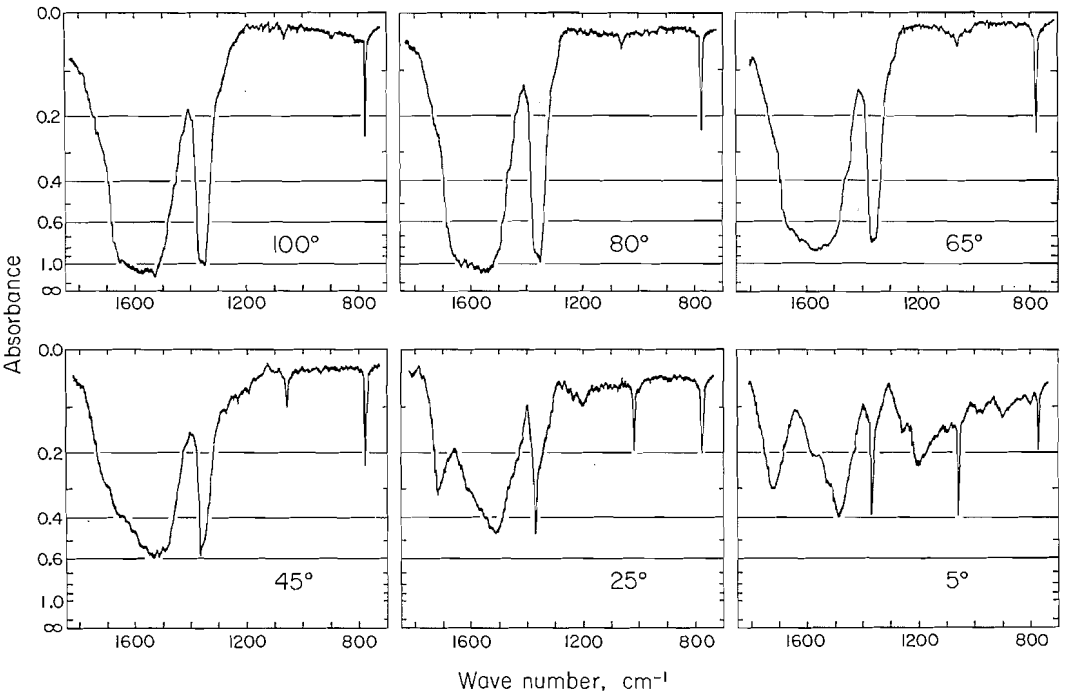


FIG. 5*a*. Infrared absorption of a thin section of sodium formate cut perpendicular to the *b* axis. The electric vector of the polarized light is perpendicular to the *b* axis and at the angles indicated to the *c* axis: 700 – 1 900 cm^{-1} region, spectral slit width approximately 1.1 ± 0.2 cm^{-1}.

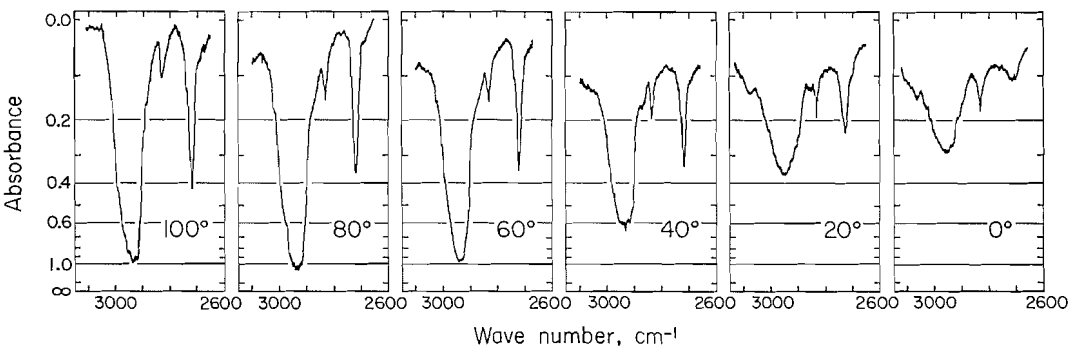


FIG. 5*b*. As for Fig. 5*a*, for the 2 600 – 3 200 cm^{-1} region, spectral slit width approximately 1.8 ± 0.2 cm^{-1}.

Assignment of Combinations

Spectra obtained under optimum conditions (small spectral slit width, slow scanning speed etc.) exhibit a larger number of absorption peaks, in addition to the fundamentals, which range in intensity from medium to very weak. Only those reproducible in several traces taken from the same sample and in samples of different thickness are reported here. Most of these absorption peaks must arise from b_u modes but very little information is available regarding the direction of the transition moment because of the overlapping which occurs. The majority of the weaker peaks were observed in spectra taken with the light polarized parallel to the *c* axis of the crystal but this is undoubtedly due to the

Can. J. Chem. Downloaded from www.nrcresearchpress.com by 210.87.254.6 on 09/05/12
For personal use only.

TABLE V

Frequencies of formate ion internal fundamentals in sodium formate

Mode		Wave number (cm^{-1})
C_{2v}	C_{2h}	
$\nu_1(\nu CH)a_1$	$\nu_{16}(\nu CH)a_u$	2 831
$\nu_2(\nu CO)a_1$	$\nu_{17}(\nu CO)a_u$	1 376
$\nu_3(\delta COO)a_1$	$\nu_{18}(\delta COO)a_u$	782
$\nu_4(\nu CO)b_1$	$\nu_{21}(\nu CO)b_u$	1 595
$\nu_5(\omega CH)b_1$	$\nu_{22}(\omega CH)b_u$	1 356
$\nu_6(\rho CH)b_2$	$\nu_{23}(\rho CH)b_u$	1 066

relative weakness of the absorption of the in-plane b_u modes, ν_{21} and ν_{22}, under these conditions.

Since all of the first order combinations involve Raman active modes, it is difficult to make definitive assignments. The assignments of Table VI were made on the assumption that the frequencies of the corresponding Raman and infrared active internal modes were approximately the same. Results obtained in this laboratory on calcium formate (T. L. Charleton and B. K. Harvey, to be published) indicate that the correlation field splitting is small so that this assumption is probably reasonable.

TABLE VI

Infrared absorption of single crystals of sodium formate

Assignment	Wave number (cm^{-1})	Assignment	Wave number (cm^{-1})	Assignment	Wave number (cm^{-1})
	531	ν_{17}	1 374		2 470
	586		1 389		2 630
ν_{18}	781	$\nu_{22}+57$	1 415	$\nu_{16}-138$, $\nu_8+\nu_{22}$	2 701
$\nu_{18}+57$	838	$\nu_{21}-138$	1 452	$\nu_{16}-107$	2 723
$\nu_{18}+107$	880	$\nu_{22}+107$	1 465	$\nu_2+\nu_{17}$	2 741
$\nu_{18}+138$	913	$\nu_{22}+138$, $\nu_{21}-107$	1 490	$\nu_{16}-57$	2 776
$\nu_{23}-107$	960	$\nu_{21}-57$	1 540	ν_{16}	2 834
$\nu_{23}-57$	1 009	ν_{21}	1 597	$\nu_{16}+57$	2 893
ν_{23}	1 066	$\nu_{21}+57$	1 645		2 923
$\nu_{23}+57$	1 125		1 670	$\nu_{16}+107$	2 944
$\nu_{23}+107$	1 169	$\nu_{21}+107$	1 718	$\nu_2+\nu_{21}$, $\nu_{16}+138$	2 959
$\nu_{22}-138$	1 225	$\nu_{21}+138$	1 734		2 985
	1 241		1 740		3 012
$\nu_{22}-107$	1 250		1 780		3 061
	1 278	$\nu_3+\nu_{23}$	1 850	$\nu_7+\nu_{21}$	3 190
	1 284	$\nu_3+\nu_{22}$	2 146		3 687
$\nu_{22}-57$	1 303	$\nu_3+\nu_{21}$	2 354	$\nu_1+\nu_{23}$	3 882
ν_{22}	1 357	$\nu_2+\nu_{23}$	2 428		
			2 445		

The majority of the absorption peaks observed arise from combinations of internal formate modes with pure lattice vibrations. We have been able to identify three of these at 57 cm^{-1}, 107 cm^{-1}, and 138 cm^{-1}. These are to be compared with the two observed by Bernstein at 60 cm^{-1} and 140 cm^{-1}.

Clearly, a complete explanation of the crystal vibrational spectrum of sodium formate will require considerably more data. To this end we are currently investigating: (i) the Raman spectrum, (ii) the long-wavelength infrared spectrum, and (iii) the effect of temperature on the infrared spectrum of sodium formate.

Can. J. Chem. Downloaded from www.nrcresearchpress.com by 210.87.254.6 on 09/05/12
For personal use only.

The authors wish to acknowledge with thanks the financial support of the National Research Council of Canada and of the University of British Columbia. We are also grateful to Mr. R. Muelchen for his able assistance in the design and construction of the polarizer.

REFERENCES

1. J. LECOMTE. Cahiers Phys. **17**, 1 (1943).
2. R. FONTEYNE. Natuurw. Tijdschr. Ghent, **25**, 173 (1943).
3. R. FONTEYNE. Naturwiss. **31**, 441 (1943).
4. K. ITO and H. J. BERNSTEIN. Can. J. Chem. **34**, 170 (1956).
5. C. S. VENKATESWAREN. Proc. Ind. Acad. Sci. **2**, 173 (1935).
6. R. M. HAMMAKER and J. P. WALTERS. Spectrochim. Acta, **20**, 1311 (1964).
7. J. GUPTA. Indian J. Phys. **10**, 117 (1936).
8. R. NEWMAN. J. Chem. Phys. **20**, 1663 (1952).
9. K. B. HARVEY, B. A. MORROW, and H. F. SHURVELL. Can. J. Chem. **41**, 1181 (1963).
10. W. H. ZACHARIASEN. J. Am. Chem. Soc. **62**, 1011 (1940).
11. A. SEIDELL. Solubilities of inorganic and metal-organic compounds. Vol. I. D. Van Nostraud Co., Inc., New York. 1940.
12. E. CHARNEY. J. Opt. Soc. Am. **45**, 980 (1955).
13. E. K. PLYLER, A. DANTI, L. R. BLAINE, and E. D. TIDWELL. J. Res. Natl. Bur. Std. A, **64**, 27 (1960).

Can. J. Chem. Downloaded from www.nrcresearchpress.com by 210.87.254.6 on 09/05/12
For personal use only.

Can. J. Chem. Downloaded from www.nrcresearchpress.com by 210.87.254.40 on 09/05/12
For personal use only.

THE CORRELATION OF ABSORPTION SPECTRA AND STRUCTURE OF COPPER(II AND I)-2,2′-BIQUINOLINE COMPLEXES IN ACETONE MEDIA

G. H. FAYE

Analytical Chemistry Subdivision, Mineral Sciences Division, Mines Branch, Department of Mines and Technical Surveys, Ottawa, Canada

Received April 15, 1966

ABSTRACT

A study of the absorption spectra of copper(II and I)–2,2′-biquinoline complexes in acetonic media has revealed that in the presence of excess ligand the predominant structure for both oxidation states of copper is probably that of a trigonal bipyramid. A crystalline mono-biquinoline complex containing pseudo-octahedrally coordinated copper(II) has been isolated from solutions containing chloride ion. Evidence has been obtained that suggests the existence of a tris-biquinoline–copper(I) complex in which one biquinoline acts as a monodentate ligand.

INTRODUCTION

Although 2,2′-biquinoline (Biq) is used widely as a reagent for the spectrophotometric determination of copper(I), the complexes formed in the copper–Biq system do not seem to have been well characterized. For example, the author has found only a single reference (1) to a copper(II)–Biq complex. This is surprising because a comparison of the structure of bulky Biq complexes with those formed with unsubstituted bipyridine and phenanthroline and with their 2,9-substituted derivatives should be of interest to coordination chemists.

The author has recently used elementary ligand field theory in the interpretation of the spectra of copper(II)–halogeno (2) and phenanthroline (Phen) (3) complexes and it seemed worthwhile to use the same approach in an attempt to elucidate the nature of the species formed in the copper–Biq system.

The results of the present work indicate that in an acetone medium, copper(II) forms a pseudo-octahedral mono-Biq complex and a trigonal bipyramidal bis-Biq complex. It is considered that in the presence of chloride ion the binuclear species $[(Biq)_2Cu—Cl—Cu(Biq)_2]^{3+}$ containing five-coordinate copper(II) forms, and this rearranges in the presence of excess chloride to give crystalline $CuBiqCl_2$ and $[Cu(Biq)_2Cl]^+$. A study of charge transfer bands (including that used for analytical purposes) suggests that copper(II) forms a bis- and tris-Biq complex, each being trigonal bipyramidal but with one monodentate Biq in the tris species.

EXPERIMENTAL

With the exception of solutions of Biq in acetone and freshly prepared aqueous solutions of ascorbic acid, the materials, apparatus, and experimental procedure were similar to those described previously in spectrophotometric studies of copper(II)–halogeno (2) and Phen (3) complexes in acetone media.

As in previous work, extinction coefficients were calculated using total copper concentrations.

Preparation and Properties of $CuBiqCl_2$

As indicated later in the paper, solid $CuBiqCl_2$ is formed under certain conditions in copper–Biq–chloride systems in acetone solutions. For analytical and X-ray diffraction studies, samples of this material were prepared at room temperature by mixing 50 ml of a 2×10^{-4} *M* solution of $CuCl_2.2H_2O$ in acetone with a similar volume of a 2×10^{-4} *M* acetonic solution of Biq. The orange acicular crystals that formed immediately were allowed to settle for several minutes and were then recovered in a filter crucible, washed with acetone, and dried at approximately 100 °C. Approximately 80% of the copper was recovered in the product.

The orange material formed as above was found on analysis to contain 16.3% Cu and 18.0% Cl and to contain one molecule of Biq per copper. Therefore, the crystalline material may be formulated as $CuBiqCl_2$, a compound that requires 16.4% Cu and 18.2% Cl.

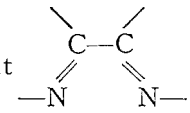
X-ray diffraction studies indicate that $CuBiqCl_2$ is monoclinic, and the tentative unit-cell dimensions are: $a = 13.7$ Å, $b = 15.2$ Å, $c = 7.90$ Å, and $\beta \simeq 90°$. The extinctions are consistent with the space group $P2_1/n$.

RESULTS AND DISCUSSION

Copper(II)–Biq Complexes

In Acetone Solutions

Octahedral Mono- and Trigonal Bipyramidal Bis-Complexes

Because the functional or "bonding" unit  is common to Biq and variously substituted bipyridines (Bips) and phenanthrolines (Phens), it is to be expected that the structure and "d–d" absorption spectra of corresponding copper(II) complexes formed with such ligands should be qualitatively similar. Indeed, spectra A and B in Fig. 1 are directly analagous to copper(II)–Phen complexes formed under similar conditions (3).

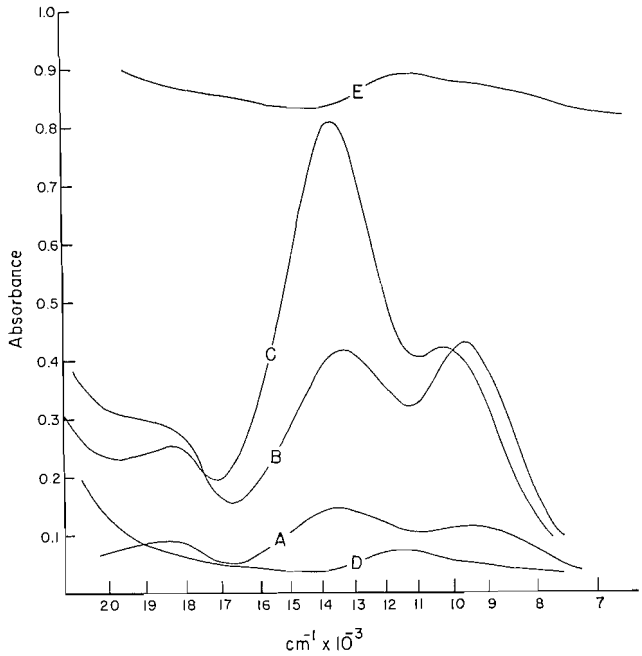


FIG. 1. d-d spectra of copper(II)–biquinoline complexes.

		$[Cu^{2+}]_{total}$	[Biq]/[Cu^{2+}]	[Cl^-]/[Cu^{2+}]	Band max. (cm^{-1})	$\sim \epsilon_{max}$ (l/mole cm)
A	$[CuBiq(OH_2)_3solv]^{2+}_{oc}$	4×10^{-3} *M*	0.8	—	13 700	40
B	$[Cu(Biq)_2solv]^{2+}_{trig\ bipy}$	4×10^{-3} *M*	2.5	—	13 300 and 9 650	110
C	$[Cu(Biq)_2Cl]^{2+}_{trig\ bipy}$	4×10^{-3} *M*	4.0	1.0	13 600 and 10 250	200
D	$CuCl_2.2H_2O$ + Biq in acetone $[CuBiqCl_2(solv)_2]_{\sim oct}$	4×10^{-4} *M*	—	—	11 500	150
E	$CuBiqCl_2$ (Nujol mull)	—	—	—	11 500	—

Spectrum A is considered to be due largely to the pseudo-octahedral complex $[Cu(Biq)(OH_2)_3ac]^{2+}$. Evidence for a 1:1 combination of Cu(II) and Biq is given in Fig.

Can. J. Chem. Downloaded from www.nrcresearchpress.com by 210.87.254.40 on 09/05/12
For personal use only.

2*a*. As in previous studies (2, 3), undried reagent grade acetone was used as the solvent and this was the source of the waters in the mono-Biq species.

Spectrum B is that of an approximately trigonal bipyramidal entity, $[Cu(Biq)_2solv]^{2+}$. Figure 2*a* confirms the conclusion, based on the comparison of spectrum B with that of the bis-Phen complex (3), that the absorbing species is a 2:1 entity.

That a pseudo-octahedral bis-Biq complex is not detected when $[Biq]/[Cu^{2+}] > 1$ is considered to be due partly (as previously for the copper(II)–Phen system (3)) to the greater ligand field stabilization energy inherent in a trigonal bipyramidal structure.

From Fig. 2*a* it is evident that there is no tendency for a pseudo-octahedral tris-species to form and this is probably a consequence of steric hindrance introduced by the projecting carbocyclic parts of Biq. This finding is similar to that of James and Williams (1), who found no evidence for a 3:1 complex with Phen substituted in the 2,9-positions.

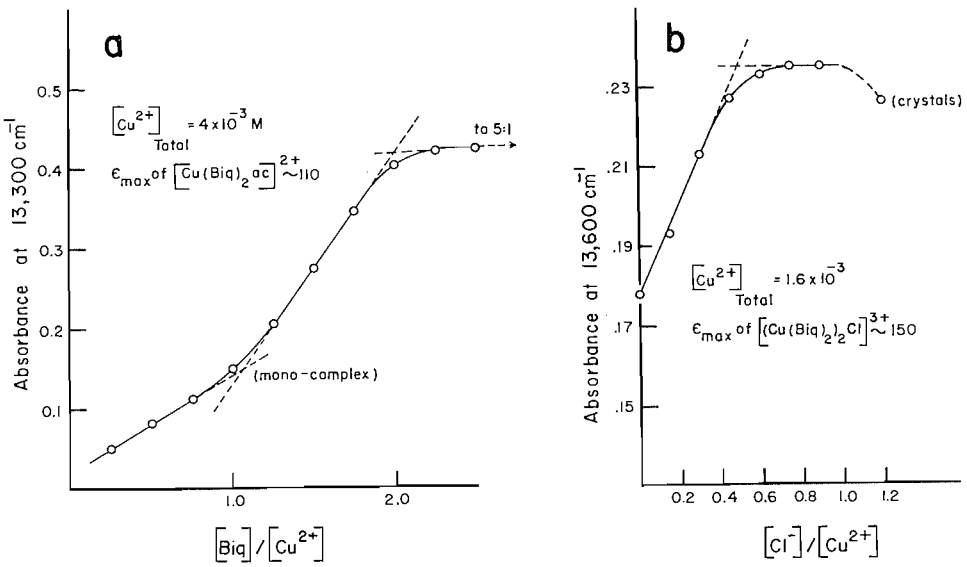


FIG. 2. Mole ratio plots.

It will be seen later that the shoulder at 18 300 cm^{-1} in spectrum B is an electron-transfer band due to the bis(Biq)–copper(I) complex. It is estimated that approximately 1% of the total copper existed as the cuprous complex at the time of the scan of spectrum B.

In the $Cu(ClO_4)_2$–Phen system in acetone solutions (3) a turquoise crystalline compound, $[Cu(Phen)_2ClO_4]ClO_4$, forms when $[Phen]/[Cu^{2+}]$ is in the range 1 to 3. A corresponding solid is not formed under comparable conditions in the $Cu(ClO_4)_2$–Biq system, and this is probably a consequence of the larger size of the bis-Biq complex.

In Acetone – Hydrochloric Acid Solutions

Trigonal Bipyramidal Bis-Biq–Monochlorocopper(II) Complex

On the addition of an acetone solution of hydrochloric acid (10^{-3} *M*) to a solution in which $[Biq]/[Cu^{2+}] \geqslant 2$ the spectrum of the absorbing species gradually changes from B to C in Fig. 1 as $[Cl^-]/[Cu^{2+}]$ is increased to ~ 1. As $[Cl^-]/[Cu^{2+}]$ is increased from 1 to 2.5, an increasing fraction of the total copper (original concentration 10^{-3} *M* or higher) forms the orange crystalline compound $CuBiqCl_2$. The spectrum of the copper complex remaining in solution is qualitatively the same as C.

Can. J. Chem. Downloaded from www.nrcresearchpress.com by 210.87.254.40 on 09/05/12
For personal use only.

From the two bands and their energies, it is evident that spectrum C is also due to an essentially trigonal bipyramidal entity, one in which Cl^- has replaced a solvent molecule in the trigonal plane to give $[Cu(Biq)_2Cl]^+$ (or possibly a dimer as we will see below).

Solid $CuBiqCl_2$

The single maximum (and its energy) in the mull spectrum (E) of $CuBiqCl_2$ in Fig. 1 suggests that Cu(II) is in an approximately octahedral environment, i.e. probably in a unit such as that depicted in Fig. 3.

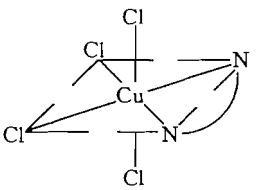


FIG. 3. Immediate environment of copper(II) in $CuBiqCl_2$.

Evidence for Dimer

The effect of adding Cl^- to an acetone solution containing $[Cu(Biq)_2solv]^{2+}$ is shown in Fig. 2*b*. The plot indicates that the combining ratio of chloride to copper is 0.5 and this strongly suggests the formation of a chloride-bridged dimer containing two trigonal bipyramidal units, i.e. $[(Biq)_2Cu—Cl—Cu(Biq)_2]^{3+}$.

From the experimental evidence cited above, it is proposed that the following reactions occur as $[Cl^-]/[Cu^{2+}]$ is increased from 0 to 1.5 in an acetone solution containing the trigonal bipyramidal species, $[Cu(Biq)_2solv)^{2+}$:

$$2[Cu(Biq)_2solv]^{2+} + Cl^- \rightleftarrows [(Biq)_2Cu—Cl—Cu(Biq)_2]^{3+}$$

$$+ Cl^-$$

$$\Updownarrow$$

$$2[Cu(Biq)_2Cl]^+ + Cl^- \leftrightarrows CuBiqCl_2 + [Cu(Biq)_2Cl]^+ + Biq.$$

The Study of Charge-Transfer Bands of Copper(II)–Biquinoline Complexes

Figure 4 shows some charge-transfer bands arising from the copper(II)–Biq complexes discussed above. Mole ratio vs. absorbance plots confirmed that spectra A and B are those bis-Biq complexes and spectrum C is that of a mono-complex.

Because the frequency of the band maxima (28 000 cm^{-1}) remains constant and the ϵ_{max} values are approximately proportional to the number of Biqs per copper (i.e. 2.2–2.5 $\times$ 10^4 l/mole cm per Biq) it is concluded that the bands represent charge-transfer processes within the coordinated Biq molecules. From A it is apparent that there are three closely spaced components within the band and these have their maxima at approximately 28 600, 28 000, and 27 200 cm^{-1} respectively. It is of interest to note that the intensity of the three transitions are such as to give a band of high symmetry in spectrum C. As we will see later three similar transitions occur in copper(I)–Biq complexes and this is further evidence that the charge-transfer processes are not of the ligand $\rightarrow$ metal type (because the d orbitals of Cu(I) are filled).

Spectra C and C-1 are those of solutions in which the absorbing species was considered to contain hexa-coordinated copper(II) in $[CuBiqCl_2(solv)_2]$. It is to be noted that a few minutes after scanning C-1, orange crystals formed which proved to be $CuBiqCl_2$ (D and E in Fig. 1). The shoulder at approximately 25 000 cm^{-1} is probably due to a $Cl^- \rightarrow Cu(II)$ charge-transfer process as its ϵ value is of the same order of magnitude as those of other copper(II) halogeno complexes (2).

Can. J. Chem. Downloaded from www.nrcresearchpress.com by 210.87.254.40 on 09/05/12
For personal use only.

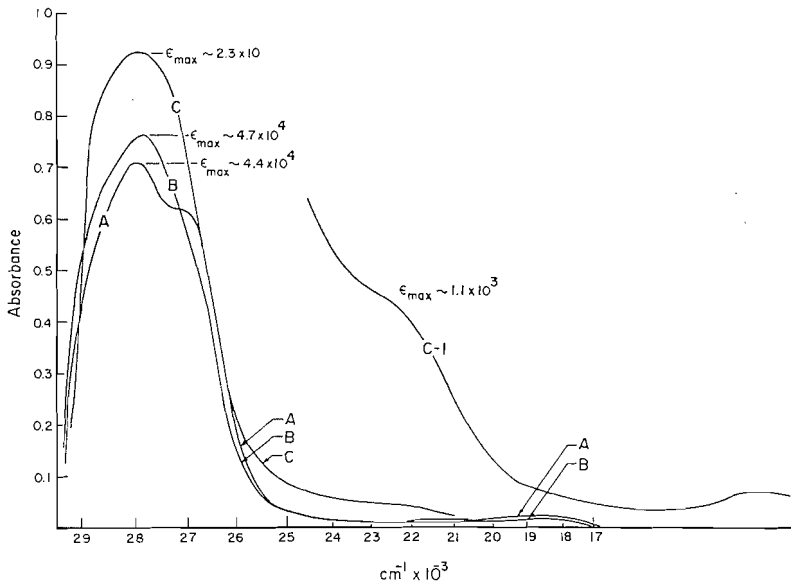


FIG. 4. Charge-transfer spectra of copper(II)–Biq complexes.

		$[Cu^{2+}]_{total}$	[Biq]/$[Cu^{2+}]$	$[Cl^-]/[Cu^{2+}]$	Band max. (cm^{-1})	$\sim \epsilon_{max}$ (l/mole cm)
A	$[Cu(Biq)_2ac]^{2+}_{trig\ bipy}$	1.6×10^{-5} *M*	2.5	—	28 000	4.4×10^4
B	$[Cu(Biq)_2Cl]^{2+}_{trig\ bipy}$	1.6×10^{-5} *M*	4	1	27 900	4.7×10^4
C	$CuCl_2.2H_2O$ + Biq in acetone $[CuBiqCl_2(solv)_2]_{\sim oct}$	4×10^{-5} *M*	20	2	28 000	2.3×10^4
C-1	$CuCl_2.2H_2O$ + Biq in acetone $[CuBiqCl_2(solv)_2]_{\sim oct}$	4×10^{-4} *M*	2	2	23 000 (s)	1.1×10^3

COPPER(I)–BIQ COMPLEXES

A number of spectrophotometric methods for the determination of copper are based on the formation of the purple bis-Biq–copper(I) complex (4–6), a species whose structure has been assumed to be that of a regular tetrahedron (7).

The resolvable charge-transfer bands arising from the copper(I)–Biq species formed in water–acetone (A and A-1) and in acetone (B) solutions are given in Fig. 5; these will be discussed in some detail later. The band at approximately 18 500 cm^{-1} is responsible for the purple color and is the one used for analytical purposes.

While the present study is concerned mainly with the constitution and geometry of the species formed in the copper–Biq system, certain aspects of the work in the water–acetone medium, to be described below, were undertaken with the hope that the results might have some analytical value.

Reduction of Copper with Ascorbic Acid

In many analytical methods involving Biq, hydroxylamine hydrochloride or hydrazine hydrochloride is used to reduce copper(II) to copper(I) in an aqueous solution having a pH $> \sim 4$. The copper(I) solution is then shaken with a solution of Biq in a solvent such as amyl alcohol, whereupon the purple complex forms in the organic phase.

Biq is essentially insoluble in water but has a relatively high solubility in acetone, therefore it was decided to attempt the formation of the purple species in a mixture of the two solvents and thereby avoid the necessity of the extraction step.

Preliminary experiments indicated that ascorbic acid added to an aqueous solution of

Can. J. Chem. Downloaded from www.nrcresearchpress.com by 210.87.254.40 on 09/05/12
For personal use only.

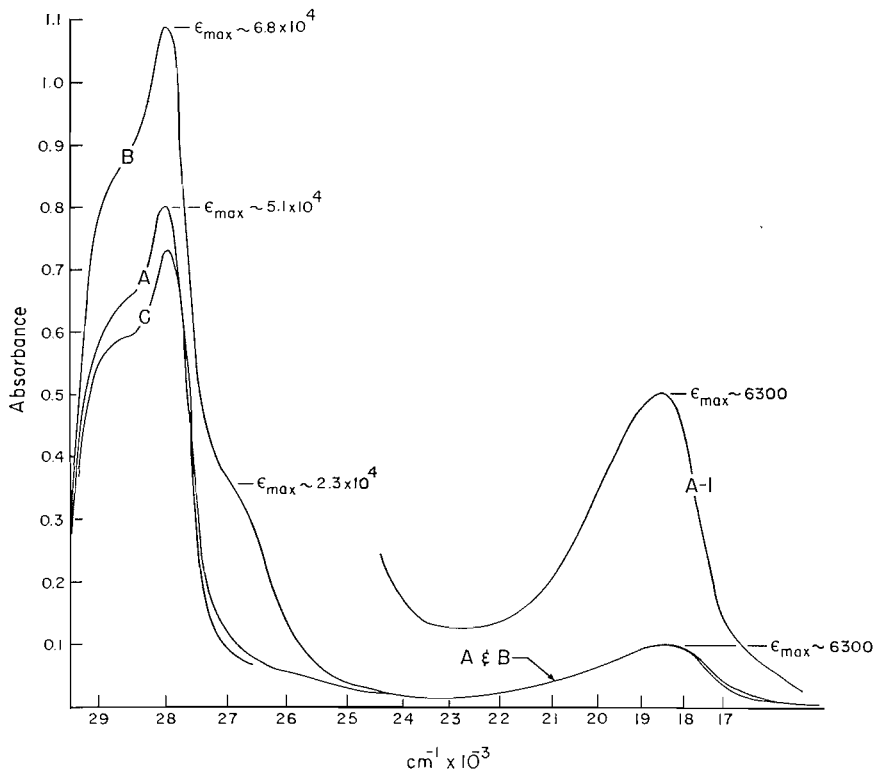


FIG. 5. Charge-transfer spectra of Cu(I)–Biq complexes.

		$[Cu]_{total}$	[Biq]/[Cu]	Band max. (cm^{-1})	$\sim \epsilon_{max}$ (l/mole cm)
A	$[Cu(Biq)_2solv]^+$	1.6×10^{-5} *M*	5	28 000	5.1×10^4
A-1	$[Cu(Biq)_2solv]^+$	8×10^{-5} *M*	5	18 500	6.25×10^3
B	$[(Biq)_2CuBiq]^+$	1.6×10^{-5} *M*	5	28 000	6.8×10^4
				~27 000 (s)	2.3×10^7
C	$[Cu(Biq)_2solv]^+$	1.6×10^{-5} *M*	2	~27 000 (s)	2.3×10^7

$CuCl_2.2H_2O$ is effective as a reducing agent for copper over a considerably greater pH range (1.4 to 9+) than is hydroxylamine, therefore ascorbic acid was used in subsequent experiments.

Frequently in analytical practice the aqueous copper-bearing sample solution contains an appreciable concentration of chloride ion, therefore an aqueous stock solution of $CuCl_2.2H_2O$ was used in the mixed-solvent experiments rather than one of copper perchlorate. It can be assumed that the initial complex was mainly $[Cu(OH_2)_6]^{2+}$ (8).

By measuring the absorbance of test solutions at 18 500 cm^{-1} ($\epsilon_{max} \sim 6\,300$ l/mole cm), it was established that excess ascorbic acid added as a freshly prepared aqueous solution or as crystals effects essentially complete formation of the purple bis-Biq–copper(I) complex when added to a water–acetone solution containing copper(II) and excess Biq, and when the mole fraction of water is 0.5–0.85. At mole fraction < 0.5 it is considered that conditions are suitable for the coordination of chlorines in the copper complex and this inhibits the reducing power of the ascorbic acid. At mole fraction > 0.85, Biq crystallizes from solution.

A plot of the mole ratio of ascorbic acid:total copper vs. absorbance measured under conditions such as those described above clearly indicated that 1 mole of ascorbic acid

Can. J. Chem. Downloaded from www.nrcresearchpress.com by 210.87.254.40 on 09/05/12
For personal use only.

reduces 2 moles of copper(II). This suggests the possibility of ascorbic acid (asc) acting as a bridge between two trigonal bipyramidal bis-Biq–copper(I) groups at the time of reduction, i.e. $[(Biq)_2Cu—asc—Cu(Biq)_2]^{2+}$.

In experiments similar to those above but using a stock solution of $Cu(ClO_4)_2$ in acetone, it has been found that crystalline ascorbic acid is an effective reducing agent in acetone solution (no water added) containing $[Cu(Biq)_2solv]^{2+}$. In this medium too, 0.5 mole of ascorbic acid reduces 2 moles of copper(II).

Speculations on the Existence of a tris-Biq–Copper(I) Complex Containing One Monodentate Biq

Spectra A and B in Fig. 5 are those of the complexes formed in water–acetone ($CuCl_2.2H_2O$) and in acetone ($Cu(ClO_4)_2$) media respectively. The mole ratio plots for the 28 000 cm^{-1} bands are given in Fig. 6 and from these it is evident that combining ratios of [Biq]:[Cu^+] are 2 and 3 for the species giving rise to spectra A and B respectively. However, similar plots for the 18 500 cm^{-1} band indicate a 2:1 combination of Biq and Cu(I) for both complexes in the presence of excess Biq.

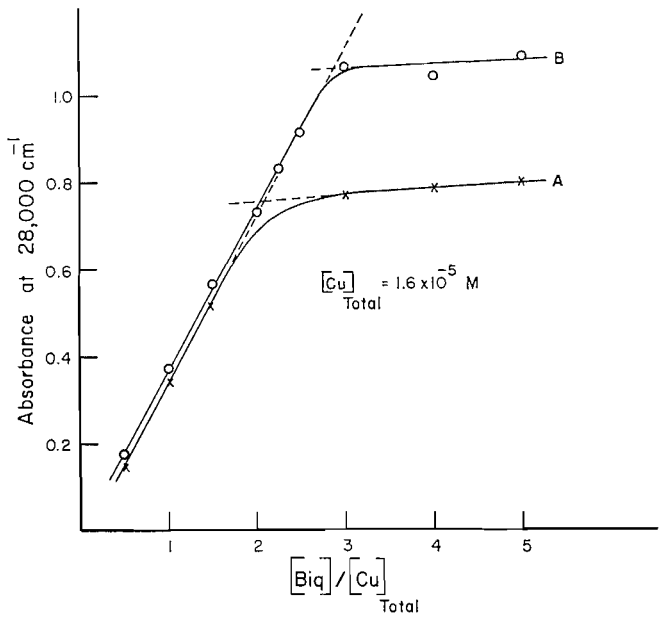


FIG. 6. Mole ratio plots. (A) Complex formed in H_2O–acetone medium in which mole fraction of H_2O = 0.5 and $[Cl^-]/[Cu^{2+}]$ = 2. (B) Complex formed in acetone solution initially containing $[Cu(Biq)_2solv]^{2+}$.

The apparent anomaly can be resolved by a study of the three-transition band between 25 000 – 29 000 cm^{-1}. As in the case of the copper(II) complexes, the electronic transitions are considered to occur within the bound Biq molecules because their frequency changes little with radical changes in the nature of the complex.

It was pointed out previously that the ϵ value of the 28 000 cm^{-1} maximum increased by $\sim 2.3 \times 10^4$ l/mole cm for each bound Biq in the copper(II) species. The same relationship holds for the copper(I) complexes as values of 5×10^4 and 6.8×10^4 l/mole cm are consistent with Biq:Cu(I) ratios of 2 and 3 respectively for complexes giving spectra A and B in Fig. 5.

Can. J. Chem. Downloaded from www.nrcresearchpress.com by 210.87.254.40 on 09/05/12
For personal use only.

It is of interest to note that the 27 200 cm^{-1} transition in the spectra of copper(II) complexes in Fig. 4 (see A especially) is absent in spectra A and C of the bis-Biq–copper(I) species shown in Fig. 5. However, in spectrum B, a shoulder at 27 200 cm^{-1} with $\epsilon \sim 2.3 \times 10^4$ l/mole cm appears and this is evidently the result of the bonding of a third molecule of Biq.

To account for the formation of a tris-Biq–copper(I) complex, it seems necessary to assume that the structure remain essentially that of a trigonal bipyramid because an approximately octahedral one is sterically unlikely. However, the five-coordinate structure requires that two Biq molecules be bound in a bidentate fashion and a third "dangling" Biq be bound by a single Cu—N bond in the trigonal plane. This proposal is supported by the fact that the band with maximum at 18 500 cm^{-1} seems to be associated with the two bidentately bound Biq molecules.

Spontaneous Reduction of Copper(II) by Biq

During the work on the copper(II)–Biq complexes, it was observed that the purple color (18 500 cm^{-1}) of the bis-Biq–copper(I) species formed gradually in the test solutions and it appeared that Biq acted as the reducing agent.

Experiments with 1.6×10^{-5} M solutions of $Cu(ClO_4)_2$ in acetone showed that after 20 h approximately 80% of the copper was present as the purple complex when $[Biq]/[Cu]_{total} = 3$. However, under similar conditions, but with sufficient Cl^- added to make $[Cl^-]/[Cu_{total}] = 1$, only about 50% of the copper existed as the cuprous species.

That the rate of reduction is decreased in the presence of Cl^- suggests that the partial transfer of charge from bound chlorines to copper(II) renders a similar process from Biq to copper(II) less efficient.

Although the experimental evidence presented above does not conclusively establish the existence of trigonal bipyramidal copper(I)–Biq complexes, such a structure seems to be more likely than the tetrahedral one proposed, without evidence, for the bis-species (7).

ACKNOWLEDGMENTS

The author thanks Mr. J. F. Rowland, Physical Chemistry Section, Mineral Sciences Division, for the X-ray work performed on crystalline $CuBiqCl_2$ and George F. Morris, Analytical Chemistry Research Branch, Department of Agriculture, for the determination of chlorine on samples of the same material.

REFERENCES

1. B. R. James and R. J. P. Williams. J. Chem. Soc. 2007 (1961).
2. G. H. Faye. Can. J. Chem. **44**, 1643 (1966).
3. G. H. Faye. Can. J. Chem. **44**, 2165 (1966).
4. J. G. Breckenridge, R. W. J. Lewis, and L. A. Quick. Can. J. Res. B, **17**, 258 (1939).
5. R. J. Guest. Anal. Chem. **25**, 1484 (1953).
6. R. T. Pflaum, A. I. Popov, and N. C. Goodspeed. Anal. Chem. **27**, 253 (1955).
7. H. Diehl and G. F. Smith. *In* The copper reagents: cuproine, neucuproine, bathocuproine. G. Frederick Smith Chemical Co., Columbus, Ohio. 1958. p. 6.
8. J. Bjerrum, C. J. Ballhausen, and C. K. Jorgensen. Acta Chem. Scand. **8**, 1275 (1954).

Can. J. Chem. Downloaded from www.nrcresearchpress.com by 210.87.254.40 on 09/05/12
For personal use only.

Can. J. Chem. Downloaded from www.nrcresearchpress.com by 210.87.254.42 on 09/05/12
For personal use only.

THE SUBSTITUENT EFFECT ON VICINAL PROTON COUPLING CONSTANTS IN MONOSUBSTITUTED BENZENES

ROBERT R. FRASER
Department of Chemistry, University of Ottawa, Ottawa, Canada
Received July 4, 1966

ABSTRACT

The magnitude of the coupling constants between adjacent ring protons in several monosubstituted benzenes has been determined. The values for the interaction between protons ortho and meta to the substituents were in the range of 8.1–8.4 c.p.s. The interaction between protons in the meta and para positions varied from 7.27–7.8 c.p.s. Although the relative insensitivity of these coupling constants to the character of the substituent precludes any accurate assessment of the cause of this variation, the changes in coupling constants are thought to be mainly a reflection of changes in π-electron distribution.

The nuclear spin–spin interaction between adjacent protons in an aromatic ring (vicinal coupling constant, J) has been examined from both the theoretical and experimental point of view. McConnell (1) has proposed that the interaction occurs primarily through the sigma bonds. He estimated the contribution to vicinal coupling by the pi electrons to be of the order of 0.5 c.p.s. in benzene, using valence-bond calculations. A large number of spectra of aromatic compounds have been analyzed, and the vicinal coupling constants were found to fall in the range of 7 to 10 c.p.s. (2). Two systematic studies of the variations in J with a change in substituents have been reported (3, 4). Martin and Dailey (3) examined the spectra of over 40 disubstituted benzenes. From a detailed analysis of these spectra they found the variation in J with structure to be rather small, less than 2 c.p.s. They concluded this to be an indication of the invariant geometry of the ring. Cox (4) found that, in a number of para disubstituted benzenes, the coupling constants increased with increasing substituent electronegativity. Similar electronegativity effects have been noted in furans (5), thiophenes (2), and pyridines (6). It is noteworthy that the vicinal coupling constants are known for only 2 monosubstituted benzenes, biphenyl (7) and phenylacetylene (8). We wish to report the determination of J_{vicinal} for several additional compounds.

The exact analysis of a five-spin system is rather tedious and, in instances where chemical shifts are small, may be of limited accuracy. We have used the technique of "massive deuteration" (9) to produce benzene derivatives from whose spectra the coupling constants are readily obtained. Previously, massive deuteration was employed to enable the accurate determination of chemical shifts by observing the single peaks due to the ortho, meta, and para isomers of monoprotiotetradeuterioaniline and phenol (10). To obtain the vicinal coupling constants, one requires vicinal diprotiotrideuterio compounds. These are obtained in the following manner as, for example, in the case of fluorobenzene. Aniline-d_7 was prepared by reaction with heavy water in the presence of platinum. Four such exchanges gave 99% deuterated aniline. This material was converted to fluorobenzene-d_5 via the diazonium fluoborate. The fluorobenzene-d_5 was then reacted with ordinary water and platinum for 3.5 h at 85 °C and the product was found to consist of 56% fluorobenzene-d_5, 33% d_4, 10% d_3, and 1% d_2 by mass spectral analysis. The nuclear magnetic resonance spectrum of this material was measured during simultaneous irradiation of the deuterium nuclei to remove all coupling between hydrogen and deuterium

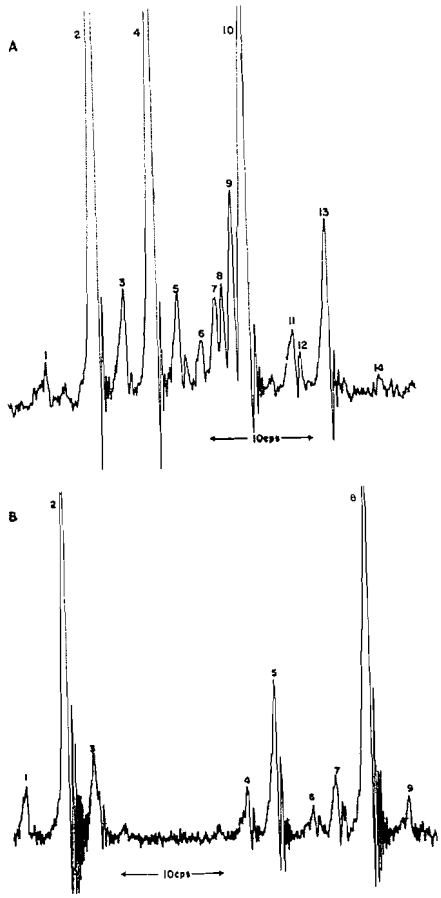


FIG. 1. (A) Spectrum of "massively deuterated" fluorobenzene; (B) spectrum of "massively deuterated" aniline.

nuclei. This spectrum is shown in Fig. 1A. Peaks 2 and 4 comprise the doublet ($J_{\text{H-F}_{\text{meta}}} = 5.7 \pm 0.09$ c.p.s.) for the protons meta to fluorine in fluorobenzene-d_4. Peaks 9 and 13 are the doublet ($J_{\text{H-F}_{\text{ortho}}} = 9.05 \pm 0.07$ c.p.s.) representing the lesser concentration of protons ortho to fluorine in fluorobenzene-d_4. The single peak 10 shows no resolvable splitting ($J_{\text{H-F}_{\text{para}}} = 0$ c.p.s.) and is due to para monoprotonated product. It is from the 10% of d_3 material that the vicinal coupling constants are determined. The peaks 1, 3, 5, 7, 8, 11, 12 represent the absorption of 2,5,6-trideuteriofluorobenzene. These appear as the AB part of an ABX spectrum and as such are readily analyzed as two pairs of AB patterns, one resulting from fluorine nuclei with spin 1/2, the other resulting from fluorine nuclei with spin $-1/2$. One of the eight lines is obscured by peak 2. The coupling constant, $J_{3,4}$[1] is equal to the separation between peaks 1 and 3, 7 and 11, 8 and 12 and has the value 7.48 ± 0.07 c.p.s. Unfortunately, the proportion of 3,4,5-trideuteriofluorobenzene is too small to allow an accurate determination of $J_{2,3}$ which is estimated to be 8.4 ± 0.25 c.p.s. (peak 11 obscures two of the four peaks due to the ortho protons). The others are peaks 6 and 14. It is interesting to note that one can obtain all

[1]*We wish to use subscripts to denote the position of the two interacting protons in relation to the substituent in position 1. Thus, $J_{3,4}$ represents the coupling between protons meta and para to the substituent.*

Can. J. Chem. Downloaded from www.nrcresearchpress.com by 210.87.254.42 on 09/05/12
For personal use only.

H—F coupling constants, two H—H coupling constants, and three chemical shifts from this one spectrum. By calculating ν_{para} from the AB patterns of trideuterio compound and comparing it with ν_{para} for tetradeuterio material, it is found that the effect of replacing a vicinal proton by deuterium is to increase the chemical shift by 0.08 c.p.s. In aniline the same effect is 0.10 c.p.s. (This isotope effect is small compared with the geminal isotope effect of 0.75 c.p.s. (11).)[2]

The spectrum of deuterated aniline is shown in Fig. 1B. Here peaks 2, 5, and 8 represent meta, para, and ortho isomers of monoprotiotetradeuterioaniline. Peaks 1, 3, 4, and 6 represent the AB pattern for 4,5,6-trideuterioaniline and peaks 1, 3, 7, and 9 the AB pattern for 4,5,6-trideuterioaniline. The coupling constants $J_{2,3}$ and $J_{3,4}$ are given by the separation of peaks 7 and 9, and 4 and 6 respectively. The other substituted benzenes were analyzed in the same way and all the results are shown in Table I. Only the deuterated anilines and nitrobenzenes contained a sufficient concentration of ortho protons to allow determination of $J_{2,3}$. Table I also contains for comparison the coupling constants reported for biphenyl (7), phenylacetylene (8), and benzene (12).

TABLE I

Vicinal coupling constants in C_6H_5X

Substituent (X)	$J_{3,4}$*	$J_{2,3}$*	E_X†	σ_R
$N(CH_3)_2$	7.27 (0.09)		3.0‡	−0.93
NH_2	7.38 (0.05)	8.09 (0.05)	2.95	−0.76
OCH_3	7.38 (0.05)		3.31	−0.51
C_6H_5	7.45 (0.17)	7.84 (0.17)	2.75	−0.11
F	7.48 (0.07)	8.4 (0.25)	4‡	−0.41
Cl	7.52 (0.18)		3.25	−0.24
NO_2	7.55 (0.07)	8.41 (0.08)	3.7	+0.16
$COOCH_3$	7.57 (0.20)		2.6	+0.11
H	7.7 (0.10)	7.7 (0.10)	2.1	0
CN	7.78 (0.09)		2.5	+0.10
C≡CH	7.59 (0.04)	7.76 (0.05)	2.5§	‖

*Figures in parenthesis represent the standard deviation.
†Except where noted, taken from the work of Cavanaugh and Dailey (24).
‡Pauling's values.
§Calculated from data of Narasimhan and Rogers (25).
‖Not available.

TABLE II

Coupling constants for aniline in various solvents

Solvent	$J_{2,3}$	$J_{3,4}$
Neat	8.09±0.05	7.38±0.04
Carbon tetrachloride	8.08±0.04	7.39±0.05
Deuterochloroform	8.06±0.05	7.45±0.08
Methanol	8.17±0.05	7.38±0.07
Dimethyl formamide	8.09±0.11	7.29±0.07

The possibility that $J_{vicinal}$ might be solvent dependent was investigated in view of the recent report by Hutton and Schaefer (13) on such an effect for para-nitroanisole. The results which are given in Table II show that for aniline there is no detectable variation in $J_{2,3}$ or $J_{3,4}$ with a change in solvent.

[2]*One must also consider the possibility of an isotope effect on the vicinal coupling constant. This has always been assumed to be unobservable, an assumption which is supported by the observation that the effect of deuterium substitution on* J^{13}_{C-H} *in toluene is less than 0.4 c.p.s. or 0.3% of its value, 126 c.p.s. (11). A vicinal isotope effect would be expected to be an order of magnitude smaller.*

Can. J. Chem. Downloaded from www.nrcresearchpress.com by 210.87.254.42 on 09/05/12
For personal use only.

Can. J. Chem. Downloaded from www.nrcresearchpress.com by 210.87.254.42 on 09/05/12
For personal use only.

According to Karplus (14), the size of a vicinal coupling constant depends on many structural features including carbon–carbon bond lengths, bond angles, hybridization, electronegativity of substituents, average excitation energy, π-electron distribution, and molecular vibrations. Within the range of compounds we have studied, the variation in the first three factors is minimal. This is illustrated by the data of Bak and co-workers (15, 16) who analyzed and interpreted the microwave spectrum of fluorobenzene and benzonitrile. In all portions of the molecule the bond angles deviate less than 2 degrees and the bond lengths deviate less than 0.01 Å from those of benzene. If we assume then that geometrical effects are relatively constant, we can consider our results in relation to the remaining variables.

The data in Table I reveals two effects which the substituents exert on vicinal coupling. Replacement of a hydrogen by each substituent causes an increase in $J_{2,3}$ and a decrease in $J_{3,4}$ except for cyano and ethynyl which do not affect $J_{3,4}$ and $J_{2,3}$ respectively. It is unlikely that the electronegativity of a substituent would be of major importance in influencing $J_{3,4}$ via the σ electrons, since the effect would have to be transferred through two intervening carbon–carbon bonds. Indeed the $J_{3,4}$ values do not appear to correlate well with the substituent electronegativities, particularly for the nitro group. This can be seen from a consideration of dimethylamino, nitro, and cyano substituents which cause $J_{3,4}$ to increase in that order, even though nitro is far more electronegative than either of the other two groups. Of the remaining factors affecting vicinal coupling constants, a change in π-electron distribution would best explain the observed variations. The larger value of $J_{2,3}$ over $J_{3,4}$ could be a reflection of a larger bond order in this position. Calculations for nitrobenzene (17) and aniline (18) predict slightly larger bond orders between ortho and meta carbon atoms, than between meta and para carbon atoms. There does appear to be some relation between the size of $J_{3,4}$ and the Taft σ_R values (19) with the nitro group again providing the exception. These parameters are a measure of the electron-donating (negative) or electron-withdrawing (positive) ability of the substituent, through resonance interaction with the aromatic π-electrons. The observed correlation between $J_{3,4}$ and σ_R would therefore be a reflection of a relation between $J_{3,4}$ and π-electron density as influenced by the substituent. It must be emphasized that the above discussion pertains to coupling constants which vary over a narrow range only slightly greater than the limits of accuracy of the measurements. For this reason, reliable conclusions cannot be made with certainty. With this in mind we can only say that the observed variation in coupling constants is consistent with a variation in π-electron density. McConnell's estimate of the π-electron contribution to J is likely conservative.

Recently Cohen and Schaefer (20) published an interesting review in which they examined the effect of electronegativity (E) on vicinal coupling constants. They were able to show that in aliphatic and olefinic compounds an increase in E caused an increase in $J_{2,3}$ and a slight decrease in $J_{3,4}$. From the works of Cox and of Martin and Dailey they pointed out that in aromatic compounds, too, an increase in E caused an increase in $J_{2,3}$. They further proposed that the results for ortho dihalobenzenes suggested that again $J_{3,4}$ will decrease with an increase in E. Our data provides evidence that such is *not* the case. Rather, the effect of π-electron distribution appears to be of equal if not greater importance than electronegativity.

Finally, we would like to compare our results for fluorobenzene with those already in the literature. Bak, Shoolery, and Williams (21) found $J_{H-F_{ortho}} = 9.4$, $J_{H-F_{meta}} = 5.8$, and $J_{H-F_{para}} = 0$. They also reported $J_{2,3} = 8.9$ but were not able to determine $J_{3,4}$. Since their accuracy was quoted as ± 0.2 c.p.s., our results are in ageement with theirs.

EXPERIMENTAL

All spectra were measured on a Varian DA-60 nuclear magnetic resonance spectrometer equipped with an external locking system for field stabilization. Double irradiation experiments were carried out using an NMR Specialties SD-60 spin decoupler operating at 9.2 Mc.p.s. Each coupling constant is reported as the average of at least six and usually eight traces. The samples were measured as neat liquid whenever the amount available permitted, otherwise they were measured as solutions of maximum possible concentration in cyclohexane. The experimental details of the deuteration methods are reported in a separate paper (22). Deuterated nitrobenzene was obtained by oxidation of deuterated aniline by the peracetic method of Emmons (23).

ACKNOWLEDGMENTS

The preparative work was done by Mr. R. N. Renaud. The financial assistance of the National Research Council of Canada is gratefully acknowledged.

REFERENCES

1. H. M. McConnell. J. Chem. Phys. **30**, 126 (1959).
2. R. A. Hoffman and S. Gronowitz. Arkiv Kemi, **16**, 562 (1961).
3. J. Martin and B. P. Dailey. J. Chem. Phys. **37**, 2594 (1962).
4. P. J. Cox. J. Am. Chem. Soc. **85**, 380 (1963).
5. A. J. Abraham and H. J. Bernstein. Can. J. Chem. **39**, 905 (1961).
6. W. Brügel. Z. Elektrochem. **66**, 159 (1962).
7. R. E. Mayer and J. H. Goldstein. Mol. Phys. **10**, 301 (1966).
8. S. Castellano and J. Lorenc. J. Phys. Chem. **69**, 3552 (1965).
9. G. V. D. Tiers. J. Chem. Phys. **29**, 963 (1958).
10. J. L. Garnett, D. J. Henderson, W. A. Sollich, and G. V. D. Tiers. Tetrahedron Letters, **15**, 516 (1961).
11. G. Fraenkel and W. Burlant. J. Chem. Phys. **42**, 3724 (1965); **43**, 4541 (1965).
12. H. J. Bernstein and R. Reavill. Private communication.
13. H. M. Hutton and T. Schaefer. Can. J. Chem. **43**, 3116 (1965).
14. M. Karplus. J. Am. Chem. Soc. **85**, 2870 (1963).
15. B. Bak, D. Christensen, L. Hansen-Nygaard, and E. Tannenbaum. J. Chem. Phys. **26**, 134 (1957).
16. B. Bak, D. Christensen, W. B. Dixon, L. Hansen-Nygaard, and J. Rastrup-Andersen. J. Chem. Phys. **37**, 2027 (1962).
17. T. E. Peacock. Proc. Phys. Soc. London, **78**, 460 (1961).
18. H. C. Longuet-Higgins and C. A. Coulson. Trans. Faraday Soc. **43**, 87 (1947).
19. R. W. Taft, Jr., N. C. Deno, and P. S. Skell. Ann. Rev. Phys. Chem. **9**, 292 (1958).
20. A. D. Cohen and T. Schaefer. Mol. Phys. **10**, 209 (1966).
21. B. Bak, J. N. Shoolery, and G. A. Williams. J. Mol. Spectry. **2**, 525 (1958).
22. R. R. Fraser and R. N. Renaud. J. Am. Chem. Soc. In press.
23. W. D. Emmons. J. Am. Chem. Soc. **79**, 5528 (1957).
24. J. R. Cavanaugh and B. P. Dailey. J. Chem. Phys. **34**, 1099 (1961).
25. P. T. Narasimhan and M. T. Rogers. J. Chem. Phys. **33**, 727 (1960).

Can. J. Chem. Downloaded from www.nrcresearchpress.com by 210.87.254.42 on 09/05/12
For personal use only.

Can. J. Chem. Downloaded from www.nrcresearchpress.com by 210.87.254.5 on 09/05/12
For personal use only.

DOUBLE AND TRIPLE RESONANCE EXPERIMENTS ON 2-BROMO-5-CHLOROTOLUENE

SIGNS OF THE RING AND RING-METHYL PROTON COUPLING CONSTANTS

G. KOTOWYCZ[1] AND T. SCHAEFER

Department of Chemistry, University of Manitoba, Winnipeg, Manitoba

Received July 15, 1966

ABSTRACT

Tickling and decoupling (triple resonance) techniques show that the ortho, meta, and para proton coupling constants have the same sign in 2-bromo-5-chlorotoluene. If the ortho coupling in the ring is positive, then decoupling experiments show that the methyl proton couplings to the ring protons in the ortho and para position to the methyl group are negative, while that to the meta position is positive. These signs are in agreement with the σ–π exchange polarization mechanism.

INTRODUCTION

Long range coupling between the methyl and ring protons in substituted benzenes is known (1–3). Hoffman (1) attributed such coupling in mesitylene to hyperconjugation. Calculations by McConnell (4, 5) invoked a σ–π exchange polarization mechanism for long range couplings like the para coupling of ring protons. Acrivos (6) found that the magnitudes of the ring-methyl proton couplings in mesitylene were predicted satisfactorily by the same mechanism, as did Cohen and McLauchlan (3) for 2-carbomethoxy-5,6-dimethylbenzofuran. Theory (5, 6) also predicts the signs of the couplings. While the relative signs of methyl proton couplings with protons on the furan (7) and thiophene rings are known (8, 9), such is not the case for the benzene ring, although there have been a few careful determinations of the magnitudes of these couplings (3, 10).

The ortho coupling between the protons on the benzene ring is positive (11–13) as are the meta and para couplings in all known cases (14–17). We describe experiments here which determine the sign of the ring-methyl proton couplings and of the meta and para couplings relative to the ortho coupling in 2-bromo-5-chlorotoluene.

EXPERIMENTAL

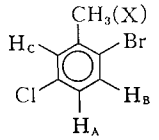
Measurements were made on a degassed, 10 mole % solution of 2-bromo-5-chlorotoluene in carbon disulfide, with tetramethylsilane (TMS) as internal reference. Decoupling and tickling experiments, some of them involving triple resonance, were performed with a DA-60-I Varian spectrometer according to standard procedures (18–22). The temperature of the sample was 28.5 °C as determined using an ethylene glycol sample.[2]

RESULTS

The parameters obtained are (shifts relative to internal TMS):

$\nu_A = -6.919 \pm 0.005$ p.p.m.
$\nu_B = -7.317 \pm 0.005$ p.p.m.
$\nu_C = -7.097 \pm 0.005$ p.p.m.
$\nu_X = -2.313 \pm 0.005$ p.p.m.

J_{AB}[3] $= +8.48 \pm 0.03$ c.p.s. $= J_{H,H}^{o}$
$J_{AC} = +2.55 \pm 0.03$ c.p.s. $= J_{H,H}^{m}$
$J_{BC} = +0.33 \pm 0.03$ c.p.s. $= J_{H,H}^{p}$



$J_{CX} = -0.63 \pm 0.03$ c.p.s. $= J_{H,CH_3}^{o}$
$J_{BX} = +0.40 \pm 0.03$ c.p.s. $= J_{H,CH_3}^{m}$
$J_{AX} = -0.58 \pm 0.03$ c.p.s. $= J_{H,CH_3}^{p}$

[1]*Holder of an N.R.C. Studentship, 1965–1966.*
[2]*A calibration graph of shift versus temperature was used as given by Varian Associates, Palo Alto, California.*
[3]*Assumed positive.*

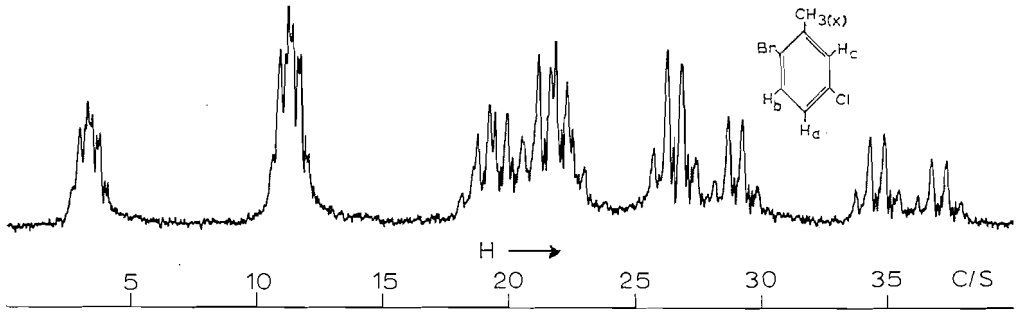


FIG. 1. Ring proton spectrum of a 10 mole % solution of 2-bromo-5-chlorotoluene in CS_2 recorded by sweeping the frequency ω_1.

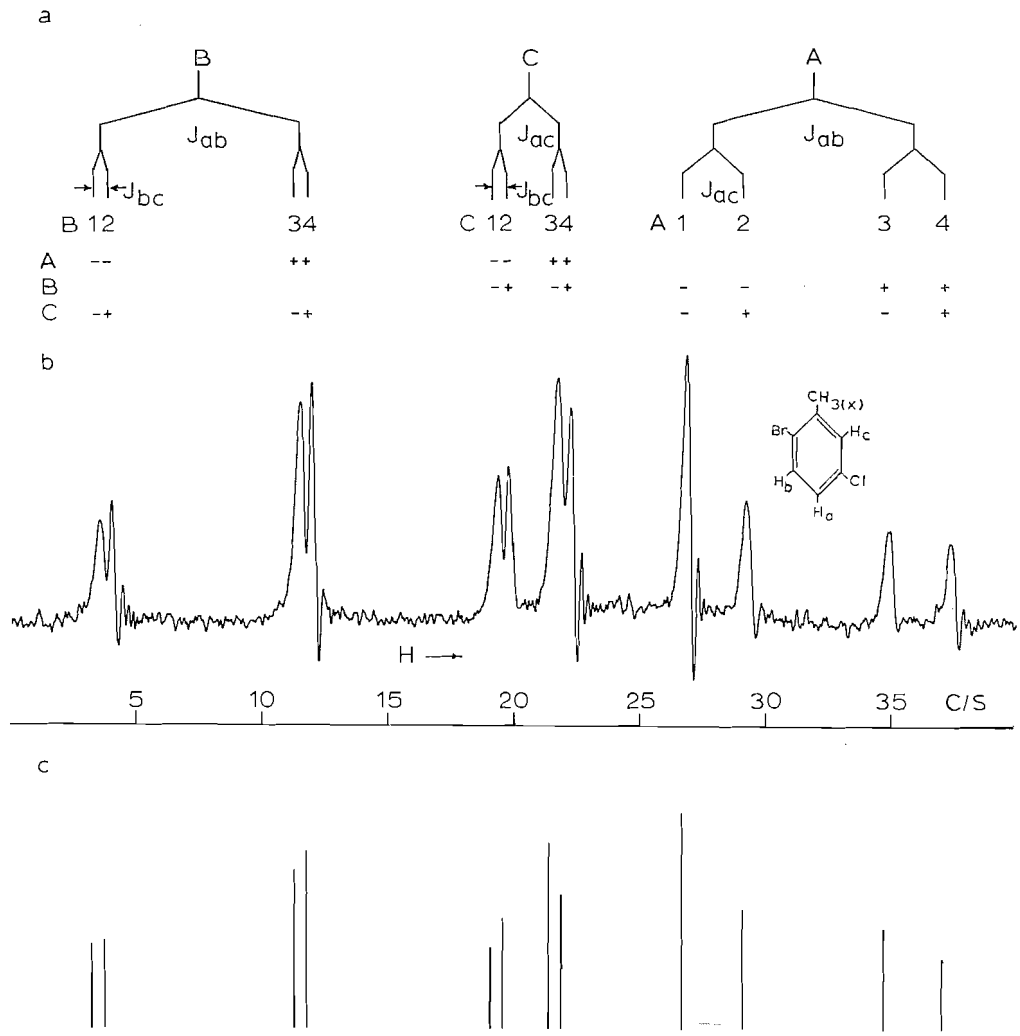


FIG. 2. The ABC (ring proton) part of the spectrum of 2-bromo-5-chlorotoluene in CS_2 with the methyl group decoupled (*b*). In *a*, the A, B, and C quartets and their respective transitions are labelled and the spin states of the two neighboring protons during each transition are indicated. The three ring proton couplings are all positive. The calculated spectrum is shown in *c*.

Can. J. Chem. Downloaded from www.nrcresearchpress.com by 210.87.254.5 on 09/05/12
For personal use only.

Can. J. Chem. Downloaded from www.nrcresearchpress.com by 210.87.254.5 on 09/05/12
For personal use only.

Figure 1 gives the ring proton spectrum using the frequency sweep mode. It is a loosely coupled ABC part of an $ABCX_3$ spectrum. The ring-methyl proton couplings were therefore found from this spectrum by simple spacing rules and were found to reproduce the methyl proton spectrum satisfactorily (Fig. 4A). The errors given above are standard deviations obtained from a large number of runs.

In Fig. 2*b*, the methyl protons have been decoupled and the resulting ABC ring proton spectrum, analyzed exactly by the method of Castellano and Waugh (23), gave the parameters above. The calculated spectrum is shown in Fig. 2*c*. In Fig. 2*a*, the A, B, and C quartets are labelled and the spin states of the two neighboring protons during each transition are indicated, assuming all ring couplings positive.

Figure 3 gives the spectrum obtained by tickling transition B1 of the ring proton spectrum while the methyl group is decoupled. The observed spectrum shows that the ring proton couplings are all of the same sign. Similar tickling experiments on other transitions served to confirm this result.[4]

Fig. 4A shows the single resonance spectrum of the methyl group. The lines are numbered from low to high field. Because of the magnitudes of the ring–methyl couplings there is overlapping of two transitions in two cases, resulting in six instead of eight observed transitions. In Fig. 4B, the quartet centered on B1 (Figs. 1 and 2*a*), arising from the long range coupling between the methyl protons and proton B, is irradiated by a decoupling field. Transitions 5 and 6 of the methyl resonance collapse into a single line, showing that $J_{H,CH_3}{}^o$ and $J_{H,CH_3}{}^p$ are of opposite sign to the ring proton couplings. In Fig. 4C, a similar decoupling field is applied to the quartet centered on transition A1. Transitions 3 and 5 collapse and overlap transition 4 in the methyl resonance, showing that $J_{H,CH_3}{}^m$ is of the same sign, while $J_{H,CH_3}{}^o$ is of opposite sign, to the ring proton couplings. (A confirming experiment was performed by irradiating the quartet centered on transition C1.)

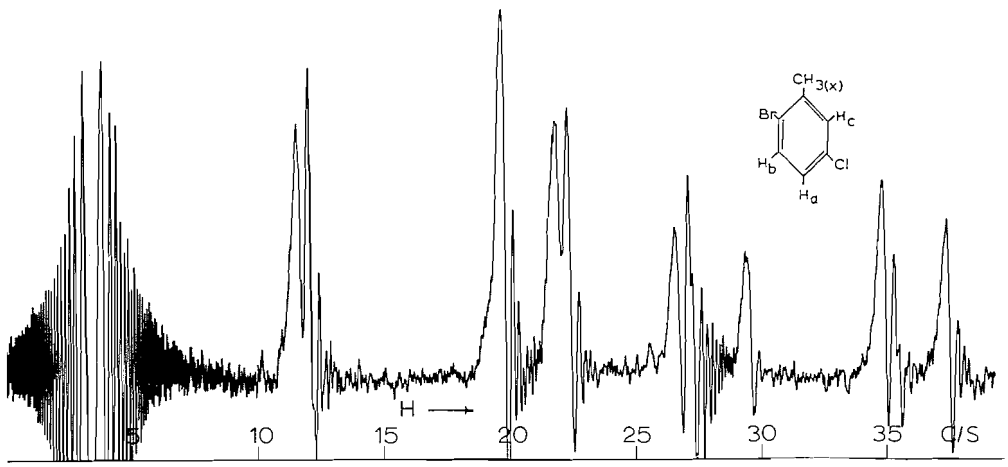


FIG. 3. Spectrum obtained by tickling transition B1 of the ring proton spectrum while the methyl group is decoupled, a triple resonance. The spectrum is observed by sweeping the frequency ω_1, the methyl group is decoupled with a second oscillator at its resonant frequency ω_2, while the spin tickling is carried out by a third frequency irradiating transition B1 at its resonant frequency ω_3.

In summary, if $J_{H,H}{}^o$ is positive, the other two ring couplings are positive. The couplings between the methyl and the ortho and para ring protons are negative, while the coupling with the meta proton is positive.

[4]*Freeman and Anderson (20) describe the arguments needed to find the relative signs. B2 is obscured by tickling B1, but there is no doubt that B1 is the tickled transition in Fig. 3.*

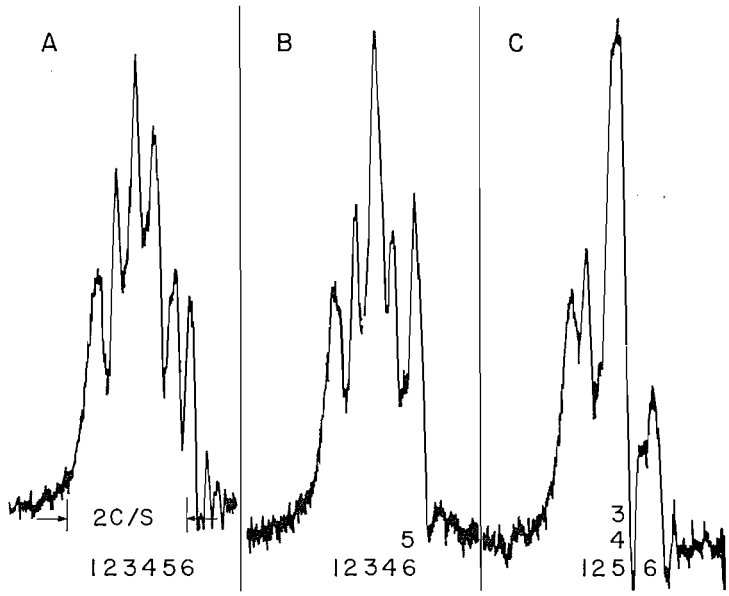


FIG. 4. The methyl group proton spectrum observed by sweeping the frequency ω_1. The lines are numbered from low to high field. (A) Unperturbed spectrum. (B) The methyl group proton spectrum observed when the decoupling frequency ω_2 irradiates the quartet centered on transition B1 which arises from the long range coupling between the methyl protons and proton B. Transitions 5 and 6 collapse into a singlet. (C) Spectrum observed with the quartet centered on transition A1 decoupled. Transitions 3 and 5 collapse and overlap transition 4.

DISCUSSION

Our conclusion from spin tickling and detailed spectral analysis of the same sign, presumably positive, of couplings within the ring agrees with earlier work on substituted benzenes using spectral analysis (14–16) and decoupling techniques (17). The suggestion is that $J_{H,H}^{p}$ arises from a σ–π mechanism (5, 6) since coupling through the σ electrons alone is expected to be negligible (4, 24).

The signs found for the ring-methyl proton couplings are in agreement with the Dirac vector model (25), more likely to be relevant to long range "through-bond" couplings (26). The simple molecular orbital calculation (4, 27) of the σ–π interaction predicts negative values for J_{H,CH_3}^{o} and J_{H,CH_3}^{p} as we find, but $J_{H,CH_3}^{m} = 0$. The latter is supported by data on acenaphthene (27). However, the more refined calculations (5, 6) predict J_{H,CH_3}^{m} to be positive and this is supported by our results.

Cohen and McLauchlan came to a similar conclusion from the proton spectrum of 2-carbomethoxy-5,6-dimethylbenzofuran but their argument was based on the magnitude of J_{H,CH_3}^{m} only (3). The signs obtained here agree with those found in methylfurans and methylthiophenes (7, 9). The sign reversal of the coupling to the para proton when the methyl group replaces a hydrogen is also in agreement with a valence-bond calculation by Karplus (24).

ACKNOWLEDGMENTS

We thank Drs. H. M. Hutton and F. H. Hruska for help with the interpretation of the double and triple resonance results and are grateful to the National Research Council for financial aid.

Can. J. Chem. Downloaded from www.nrcresearchpress.com by 210.87.254.5 on 09/05/12
For personal use only.

Can. J. Chem. Downloaded from www.nrcresearchpress.com by 210.87.254.5 on 09/05/12
For personal use only.

REFERENCES

1. R. A. HOFFMAN. Mol. Phys. **1**, 326 (1958).
2. T. SCHAEFER and W. G. SCHNEIDER. Can. J. Chem. **37**, 2078 (1959).
3. A. D. COHEN and K. A. MCLAUCHLAN. Mol. Phys. **9**, 49 (1965).
4. H. M. MCCONNELL. J. Mol. Spectry. **1**, 11 (1957).
5. H. M. MCCONNELL. J. Chem. Phys. **30**, 26 (1959).
6. J. V. ACRIVOS. Mol. Phys. **5**, 1 (1962).
7. S. RODMAR, S. FORSÉN, B. GESTBLOM, S. GRONOWITZ, and R. A. HOFFMAN. Acta Chem. Scand. **19**, 485 (1965).
8. B. GESTBLOM and B. MATHIASSON. Acta Chem. Scand. **18**, 1905 (1965).
9. B. GESTBLOM, S. GRONOWITZ, R. A. HOFFMAN, and B. MATHIASSON. Arkiv Kemi, **23**, 517 (1965).
10. H. ROTTENDORF and S. STERNHELL. Australian J. Chem. **17**, 1315 (1964).
11. A. D. BUCKINGHAM and K. A. MCLAUCHLAN. Proc. Chem. Soc. 144 (1963).
12. A. SAUPE and G. ENGLERT. Z. Naturforsch. Pt. a, **19**, 172 (1964).
13. L. C. SNYDER and E. W. ANDERSON. J. Am. Chem. Soc. **86**, 5023 (1964).
14. C. N. BANWELL, A. D. COHEN, N. SHEPPARD, and J. J. TURNER. Proc. Chem. Soc. 266 (1959).
15. J. S. MARTIN and B. P. DAILEY. J. Chem. Phys. **37**, 2594 (1962). D. M. GRANT, R. C. HIRST, and H. S. GUTOWSKY. J. Chem. Phys. **38**, 470 (1963).
16. P. F. COX. J. Am. Chem. Soc. **85**, 380 (1963).
17. R. FREEMAN, N. S. BHACCA, and C. A. REILLY. J. Chem. Phys. **38**, 293 (1963).
18. J. P. MAHER and D. F. EVANS. Proc. Chem. Soc. 208 (1961).
19. R. FREEMAN and D. H. WHIFFEN. Mol. Phys. 4, 321 (1961).
20. R. FREEMAN and W. A. ANDERSON. J. Chem. Phys. **37**, 2053 (1962).
21. J. D. BALDESCHWIELER and E. W. RANDALL. Chem. Rev. **63**, 81 (1963).
22. R. A. HOFFMAN, B. GESTBLOM, S. G. GRONOWITZ, and S. FORSÉN. J. Mol. Spectry. **11**, 454 (1963).
23. S. CASTELLANO and J. S. WAUGH. J. Chem. Phys. **34**, 295 (1961).
24. M. KARPLUS. J. Chem. Phys. **33**, 1842 (1960).
25. H. M. MCCONNELL. J. Chem. Phys. **23**, 2454 (1955).
26. C. N. BANWELL and N. SHEPPARD. Discussions Faraday Soc. **34**, 115 (1962).
27. M. J. S. DEWAR and R. C. FAHEY. J. Am. Chem. Soc. **85**, 2704 (1963).

Can. J. Chem. Downloaded from www.nrcresearchpress.com by 210.87.254.42 on 09/05/12
For personal use only.

FORMATION OF ^{7}Be IN NUCLEAR REACTIONS INDUCED BY 85-MeV PROTONS[1]

M. S. LAFLEUR, N. T. PORILE,[2] AND L. YAFFE
Radiochemistry Laboratory, Department of Chemistry, McGill University, Montreal, Quebec

Received July 6, 1966

ABSTRACT

Cross sections were measured for the formation of ^{7}Be in targets bombarded with 85-MeV protons. The variation of these cross sections with the mass and neutron-to-proton ratio of the target was investigated.

Cross-section calculations were performed on the assumption that ^{7}Be is emitted from the irradiated target as an evaporated particle. Calculated and measured cross sections were in good agreement for medium and heavy targets ($A > 55$). The calculation underestimated the production of ^{7}Be in light targets ($27 < A < 55$).

I. INTRODUCTION

The emission of multiply charged fragments ($Z > 3$) has been observed in many nuclear reactions induced by projectiles with a wide range of energies. There is no consensus on the mechanism of fragment emission; its characteristics have been explained both in terms of slow and fast reactions.

Cross sections for fragment formation have been calculated on the assumption that fragments are evaporated from the excited products of the knock-on cascade. Monte Carlo calculations of nuclear evaporation (1) have been modified to include the emission of complex particles (2–4) and the calculated relative cross sections were in good agreement with the dependence on target mass displayed by the experimental values in most cases. Recently Katcoff *et al.* (5) performed a detailed cascade–evaporation calculation to predict angular and energy distributions of ^{8}Li fragments emitted from targets irradiated with GeV protons. The calculated and experimental energy distributions agreed at the peak energies but the shape of the distributions differed at the low- and high-energy ends of the spectra. Because of the failure of the calculation to account for the emission of high-energy fragments and its inability to match the strong forward peaking of the angular distribution, the authors concluded that either a substantial fraction of the fragments is emitted by a process other than evaporation, or the emission is by a mechanism intermediate between evaporation and fast fragmentation.

The asymmetry of fragment angular distributions has been interpreted as due to the quasi-elastic ejection of fragments on the assumption of the existence of instantaneous substructures in the nucleus; fragments are produced by the nuclear cascade process. Makarov (6) performed a calculation based on the cascade model with allowance for various groupings inside the nucleus, assuming some probability for their production and a momentum distribution for each grouping within the nucleus. The calculation could not be carried out completely because of the lack of data for the differential scattering cross sections for all the particles participating in the cascade. However, the calculation was able to predict kinematic relations such as the energy spectra of particles emitted at a certain angle and the relation between the energy and emission angle of the scattered particles. A comparison of the calculated and experimental results indicated that, for incident protons of less than 100 MeV, the fragments are produced by collisions with

[1]*Financial assistance received from the National Research Council of Canada.*
[2]*Present address: Department of Chemistry, Purdue University, Lafayette, Indiana.*

secondary nucleons. The decrease in asymmetry with energy was also attributed to this process.

There has been little radiochemical investigation of fragment emission induced by low-energy protons. We have chosen to study the variation of the ^{7}Be formation cross section with target mass for 85-MeV incident protons. The process of fragment emission is simplified at this energy, since the nuclear cascade is not yet well developed and since the energy is well below the threshold for meson production. At the present time, the lack of knowledge of the relevant differential scattering cross sections prohibits the calculation of cross sections for fragment formation according to a cascade process and it is not possible to determine fully the applicability of this mechanism. As a detailed test for the mechanism of evaporation, the dependence of cross section on the neutron-to-proton ratio of the target was investigated in a restricted mass region, and comparisons made with evaporation calculations.

II. EXPERIMENTAL

(A) Targets and Irradiations

Nuclei were chosen to span the nuclear mass range from oxygen ($A = 16$) to uranium ($A = 238$) with special interest in nuclei with masses from 48 to 65. For this mass region and incident particle energy, fragment emission is not obscured by the formation of fragments as residues while the expected cross sections indicate reasonable counting rates. Target nuclei are listed in Table I.

TABLE I

Target characteristics

Target	Isotopes present: A	Abundance (%)	Thickness (mg/cm^2)	Impurity (%)
O (CuO)	16	99.76	58*	Ni 0.0002; Fe 0.0001
Al	27	100	22.01	Ag 0.001; Cu 0.001; Fe 0.001; Mg 0.001
Ti	46	7.93	8.06	Cu 0.001; Fe 0.001; Mn 0.001
	47	7.28		
	48	73.94		
	49	5.51		
	50	5.34		
V	51	99.76	30.16	Cu 0.01; Fe 0.001
Fe	54	5.82	39.93	Cu 0.001; Ni 0.001; In 0.001; Mn 0.01
	56	91.66		
	57	2.19		
	58	0.33		
Co	59	100	58.09	
Ni	58	67.88	41.77	Co 0.1; Cu 0.01; Fe 0.01; Mg 0.1; Mn 0.1
	60	26.23		
Cu	63	69.09	45.37	Ag 0.001; Fe 0.001; Ni 0.0001
	65	30.91		
Cu	63	99.9	67.17	Al 0.02; Fe 0.03; Ni 0.01; Sr 0.02
	65	0.1		
Ag	107	51.35	55.20	Cu 0.1; Fe 0.001; Mg 0.001; Pb 0.01
	109	48.65		
Au	197	100	106.80	Ag 0.1; Cu 0.1; Fe 0.001; Ni 0.001; Pb 0.01; Pt 0.001
U	238	99.27	51.19	—

*Approximate thickness estimated for CuO powder.

Contamination of the target material by medium and heavy elements, determined by spectroscopic analysis,[3] is negligible as is shown in Table I. However, a spectroscopic analysis does not detect the presence of many light elements which have a relatively high ^{7}Be formation cross section. Such contamination may lead to false cross-section values, especially for the heavier targets. The oxygen layer on metal foils is a particular problem. All foils were cleaned to remove this layer and the targets were stored in an oxygen-free environ-

[3]*The authors are indebted to Brookhaven National Laboratory for these analyses.*

Can. J. Chem. Downloaded from www.nrcresearchpress.com by 210.87.254.42 on 09/05/12
For personal use only.

ment until irradiation. To detect the presence of gross light-element contamination, the difference in the shape of the excitation functions of light and heavier nuclei was exploited. Oxygen, a representative light element, was irradiated at proton energies from 30 to 85 MeV. The resultant excitation function is shown in Fig. 1. For our purposes the significant portion of the function is its negative slope from 65 to 85 MeV. The excitation function of ^{7}Be from a heavier element, aluminium, shown in Fig. 2, was constructed using our two cross-section values and the values of other workers. In this case the slope of the function is positive from 65 to 85 MeV. Previous high-energy results show that the cross section for formation of ^{7}Be from targets

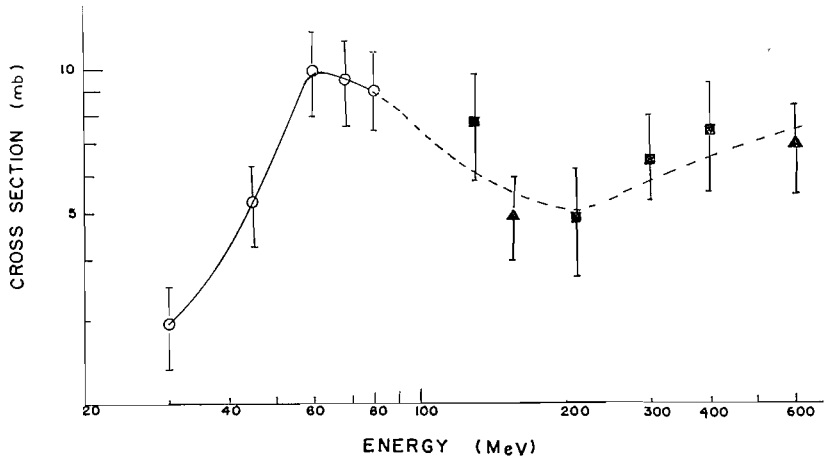


FIG. 1. Excitation function for the production of ^{7}Be in the proton bombardment of oxygen. (○) Present data, (■) Rayudu (7), (▲) Ligonniere *et al.* (8).

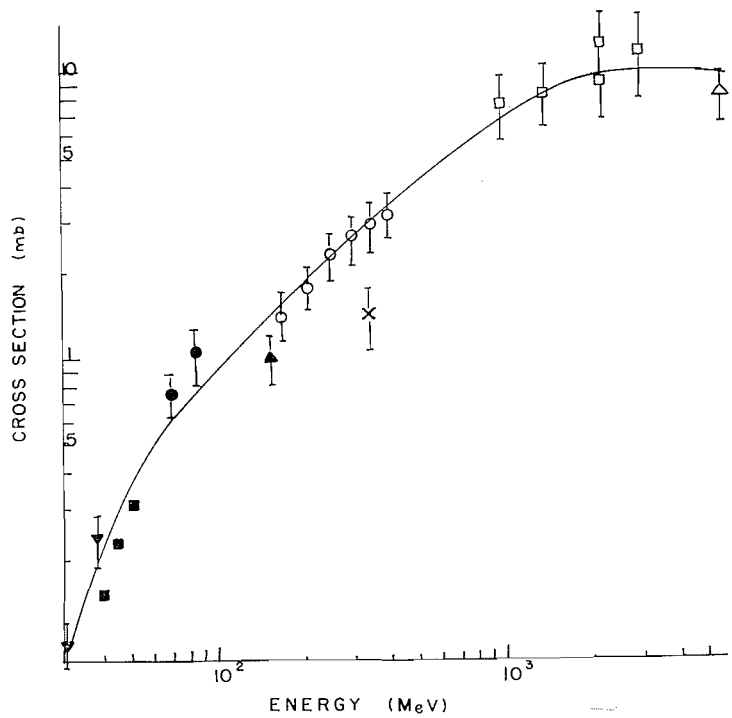


FIG. 2. Excitation function for the production of ^{7}Be in the proton bombardment of aluminium. (●) Present data, (▲) Benioff (9), (□) Friedlander, Hudis, and Wolfgang (10), (○) Gray (11), (×) Baker, Friedlander, and Hudis (12), (△) Ligonniere, Vassent, and Bernas (8), (▼) Lindsay and Neuzil (13), (■) Furukawa, Kume, and Ogawa (14).

Can. J. Chem. Downloaded from www.nrcresearchpress.com by 210.87.254.42 on 09/05/12
For personal use only.

heavier than aluminium always increases with energy up to the BeV region while the slope of the curve increases with increasing target mass. As a test for oxygen (and other light-element contamination), all targets were irradiated at 65 as well as at 85 MeV. If the resultant excitation functions in this energy region are plotted for all the targets, the slopes of the functions are expected to increase with increasing target mass. It was anticipated that any deviations from this trend would indicate gross oxygen contamination. The presence of oxygen in the target would increase the cross-section value at 65 MeV relative to the value at 85 MeV.

All target nuclei with the exception of oxygen were irradiated as foils. The reaction $^{27}Al(p,3pn)^{24}Na$ was used to monitor the proton beam, and the cross-section values given by Cumming (15) were used.

The enriched copper (99.9% ^{63}Cu) was obtained from Oak Ridge National Laboratory.

The target assembly consisted of three foils of aluminium (5.44 mg/cm^2 each) and three foils of the target element (x mg/cm^2 each). Thus the target foil and the monitor foil were both sandwiched between guard foils which served to minimize ^7Be loss by recoil from the target and to eliminate ^7Be gain by recoil from the aluminium foil. The monitor guard foils were used to avoid ^{24}Na recoil loss.

Generally the target was irradiated downstream from the monitor foil. For several irradiations an additional monitor (with guard foils) was placed downstream from the target foil but no difference was observed in the activity of the 'forward' and 'backward' monitor foils.

The foils were stacked, clamped, and carefully cut to ensure alignment, especially at the leading edge. The distribution of activity from the leading edge was determined, and accordingly after irradiation the first 1/8 in. of the leading edge was cut off and used. This portion, which was retained for use, contained 96% of the foil activity. The variation in foil area presented to the beam was found to be of the order of 1%.

On the basis of the activity distribution, ^7Be recoil loss from the leading edge was calculated to be less than 0.5%.

The thickness, x, of the target was chosen by imposing two limiting conditions, one tending to minimize x, the other to maximize it.

(i) Beam degradation.—x was chosen so that the energy degradation of the beam was less than the energy spread of the McGill synchrocyclotron (±2 MeV). The degradation of 85-MeV protons in various materials was estimated from the data of Aron *et al.* (16).

(ii) Recoil loss of ^7Be.—x was also chosen so that the target was thick enough to minimize loss of ^7Be from the foil surface. To estimate the recoil loss from the total target assembly (target plus guard foils), an approximation of the Sugarman, Campos, and Wielgoz (17) expression was used.

$$2W(F + B) = R, \qquad [1]$$

where $W = 3x$ = thickness of target foil stack, F = recoil loss in the forward direction (with respect to the beam), B = recoil loss in the backward direction, and R = range of recoil fragment.

To calculate the range of ^7Be in various target materials, it was assumed that the ^7Be fragments were emitted with energy equal to the coulomb barrier. The range–energy curves of Hower (18) for ^9Be in Al and Au were used to get approximate values for ^7Be. It was always possible to choose W so that the recoil loss from the target stack was less than 5% while satisfying the first condition. Hence the recoil loss from the target foil itself was negligible. Foil thicknesses used are given in Table I.

Oxygen was irradiated as CuO powder wrapped in gold foil. The 'specpure' CuO was obtained from Johnson, Mathey and Co., Ltd. Impurities are listed in Table I as detected by spectrographic analysis. To correct for ^7Be produced from copper and gold, blank irradiations of Cu powder in gold foil were made at 70 and 85 MeV. The reaction $^{65}Cu(p,pn)^{64}Cu$ was employed to monitor the beam and Meadows' cross-section values, as corrected by Meghir and Yaffe (19), were used as standards.

Irradiations were performed using the internal beam of the McGill synchrocyclotron. To produce observable amounts of ^7Be the irradiation time for each target was estimated on the basis of the expected cross section and the beam intensity of approximately 5×10^{12} protons/s. The duration of bombardments was ½ to 2 h. The energy of the incident protons was obtained from a known radius–energy relation (20).

(B) Chemical Separations

(1) Beryllium

The target was dissolved in a suitable acid and a known amount of beryllium carrier (about 15 mg) was added.

Separation methods given by Baker, Friedlander, and Hudis (12) were used to purify ^7Be from other radioactive nuclides.

The major contaminating activity in aluminium targets is ^{22}Na. Its 511-keV annihilation γ-ray interferes with the measurement of the 477-keV γ-ray of ^7Be. Beryllium and aluminium were separated from sodium by precipitation of beryllium and aluminium hydroxides with ammonia. Aluminium was precipitated as $AlCl_3.6H_2O$ by addition of ether and HCl (gas). Beryllium was then purified by extracting basic beryllium acetate with chloroform. The chloroform was evaporated, the residue dissolved in acid, and $Be(OH)_2$ was precipitated with a slight excess of ammonia.

The separation from all other targets (CuO, Ti, V, Fe, Ni, Co, Cu, Ag, Au, and U) was essentially the same. $Be(OH)_2$ was precipitated a number of times with ammonia. The final precipitate was dissolved in

Can. J. Chem. Downloaded from www.nrcresearchpress.com by 210.87.254.42 on 09/05/12
For personal use only.

concentrated hydrochloric acid and the solution was passed through a Dowex-1X-10 ion–exchange column. $Be(OH)_2$ was again precipitated and dissolved, then a ferric hydroxide scavenging precipitation with NaOH performed. Beryllium acetylacetonate was extracted in the presence of excess ethylenediaminetetraacetic acid at pH 4–5 into benzene. Beryllium was back-extracted with 6 *N* HCl and $Be(OH)_2$ was precipitated after evaporation steps with nitric acid and the separation steps were repeated if the ^{7}Be sample was not radiochemically pure.

The chemical yields of beryllium were determined by the spectrophotometric method described by Sandell (21) using the complexing agent *p*-nitrobenzeneazoorcinol.

(2) Sodium

Chemical separation of sodium from the aluminium monitor foils was not necessary. Because of the short half-lives of other radioactive nuclides likely to be produced in the bombardment, no interfering activity is present if ^{24}Na ($t_{1/2}$ = 15 h) is measured 24 h after bombardment.

(3) Copper

It was necessary to separate the copper monitor from the CuO targets. After $Be(OH)_2$ precipitation, $Cu(OH)_2$ was precipitated from the solution, dissolved in concentrated HCl, and evaporated to a small volume. The copper was then purified by absorption on a Dowex-1X-10 column with 4.5 *M* HCl and elution from the column with 1.5 *M* HCl.

The chemical yields of the copper were determined by titration with the disodium salt of ethylenediaminetetraacetic acid using a murexide indicator (22).

(C) Activity Measurements

The activity of all samples was obtained by γ-ray scintillation spectrometry.

^{7}Be decays by K-capture to ^{7}Li with 10.32% of the decays going to the 477-keV state and the remainder to the ground state (23). The decay is characterized by a 53.6-day half-life. The internal conversion coefficient is negligibly small ($\alpha_K = 5.8 \times 10^{-7}$).

Since a high detection efficiency was required, the activity of ^{7}Be samples was measured using a $1\frac{3}{4}$ in. × 2 in. NaI(Tl) crystal with a center well 5/8 in. in diameter and $1\frac{1}{2}$ in. deep in conjunction with a single channel pulse-height analyzer set to accept pulses about the 477-keV photopeak.

A standard ^{7}Be source was used to calibrate the well counter and to check its day-to-day stability. The absolute gamma activity of the standard source was obtained in two ways: (i) The activity of the source was measured by a 3 in. × 3 in. NaI crystal coupled to a 100-channel pulse-height analyzer. The assembly had been calibrated to yield the detection efficiencies for gamma rays of various energies by Grant (24), who had calibrated the counter for standard gamma sources against a $4\pi\beta$ proportional counter. (ii) The absolute gamma activity of a standard ^{7}Be source was determined by Dr. D. Santry[4] of the Chalk River Nuclear Laboratory of Atomic Energy of Canada Limited. The two independent measurements agreed within 5%.

The background counting rate of the counter was about 14.5 c.p.m. Samples with net count rates as low as 2 c.p.m. could be measured with reasonable accuracy.

The purity of ^{7}Be samples was indicated by the 53.6-day half-life found. The decay was followed for at least seven half-lives. The gamma activity of sufficiently active samples was checked on the 100-channel analyzer and the resultant spectra compared with that of the standard ^{7}Be source.

The 1.368-MeV γ-ray of ^{24}Na was detected and measured by the 100-channel analyzer assembly.

A γ–γ coincidence counter was used to measure the 511-keV annihilation γ-radiation of ^{64}Cu. The γ-γ coincidence unit was calibrated against a $4\pi\beta$ counter using ^{22}Na.

III. RESULTS

The gamma activities at the end of bombardment were converted to disintegration rates and cross sections were determined in the usual manner.

Errors involved in the cross-section determinations may be classified as systematic and random.

(1) Systematic Errors

Systematic errors are associated with monitor cross sections, detection efficiencies, branching ratios, internal conversion coefficients, and half-life values.

The limit quoted by Cumming (15) for the reaction ^{27}Al(p,3pn)^{24}Na cross section is ±6.5%, whereas the limit quoted by Meghir (25) for the reaction ^{65}Cu(p,pn)^{64}Cu is ±14%. An error of ±5% was quoted by Grant (24) for the determination of the detection efficiency of the 3 in. × 3 in. crystal. An error of ±5% was also assessed for the detection

[4]*The authors are indebted to Dr. Santry for performing the measurement.*

Can. J. Chem. Downloaded from www.nrcresearchpress.com by 210.87.254.42 on 09/05/12
For personal use only.

efficiency of the well crystal. Taylor and Merritt (23) cite an error of ±1% for their value of the branching ratio of ^{7}Be. The errors in the branching ratio values for ^{24}Na and ^{64}Cu have been given as ±1% and ±2% (25) respectively. The magnitude of other systematic errors was negligible.

(2) Random Errors

Random errors are connected with light-element contamination, gamma activity determinations, chemical yields, foil thickness measurements, alignment accuracy, and dilution factors.

The error associated with light-element contamination of the target is difficult to assess in most cases. In the following section it is seen that there is evidence of light-element contamination of certain targets. The corresponding cross-section values for ^{7}Be production from these targets were corrected for ^{7}Be production from the light-element contamination. In each case an estimate was made of the uncertainty associated with the measured cross-section value. At least 10 000 counts were accumulated in each gamma measurement so that statistical fluctuations in the count rate were reduced to ±1%. The error in the determination of the area of the 1.368-MeV photopeak was estimated to be ±6%. An error of ±3% was assigned to count rates determined by coincidence technique (26). Chemical yields were determined in duplicate and sometimes in triplicate. They agreed within 3–5%. The uncertainty in the determination of superficial density was ±1%. The variation in foil area presented to the beam was 1%. The error associated with pipetting and diluting was ±1%.

The total error was calculated by taking the square root of the sum of the squares of the individual errors cited above for both ^{7}Be and the monitor. The uncertainty in the measured cross sections for ^{7}Be from oxygen was estimated to be ±17% (the monitor was copper). The lower limit of the uncertainty in the measured cross sections for ^{7}Be from the other targets was estimated to be ±13% (the monitor was aluminium). The uncertainty associated with the cross-section values corrected for light-element contamination is given in the following section. Table II contains the results of the cross-section measurements. The ^{7}Be cross section, $\sigma_{^{7}\mathrm{Be}}$, is listed for each target and relevant proton bombarding energy, E_{p}. The mean value of the cross section, $\bar{\sigma}_{^{7}\mathrm{Be}}$, is given if more than one cross section was obtained at a given energy; the deviation of cross-section values from the mean is also given. Duplicate measurements agreed within the limits estimated above.

The presence of oxygen and (or) light-element contamination in the target was indicated by the comparison of the cross-section measurements at 65 and 85 MeV. The cross-section values are plotted as a function of energy in Fig. 3. For each target a straight line drawn through the points approximates the excitation function in the energy region. As previously discussed in Section II, A, the slope of the excitation function for ^{7}Be formation is expected to be a function of target mass. In Fig. 3, the slope of the O(p,^{7}Be) excitation function is negative; the slope of the Al(p,^{7}Be) excitation function is positive, whereas the slope of the excitation functions of ^{7}Be from V, Ni, Co, and Cu increase in steepness with increasing target mass. However, the slope of the Ti(p,^{7}Be) excitation function is steeper than expected from the general trend, whereas the Ag(p,^{7}Be) excitation function is much flatter than expected.

Titanium is known to have a tenacious surface layer of oxygen. The observed ^{7}Be cross section for the two irradiations at 85 MeV was higher than expected. Therefore for the irradiation at 65 MeV the surface of the target was cleaned after as well as before irradiation. To obtain a corrected cross-section value at 85 MeV, denoted $(\bar{\sigma}_{^{7}\mathrm{Be}})_{\mathrm{c}}$, the cross-section value at 65 MeV was then extrapolated to 85 MeV using a straight line of the same

Can. J. Chem. Downloaded from www.nrcresearchpress.com by 210.87.254.42 on 09/05/12
For personal use only.

slope as the V(p,^{7}Be) excitation function. The error associated with the corrected cross-section value was large, estimated to be ±40%.

TABLE II

Cross sections for the production of ^{7}Be in targets bombarded with low-energy protons

Target	E_P (MeV)	$\sigma_{^{7}Be}$ (mb)	$\bar{\sigma}_{^{7}Be}$ (mb)	$(\bar{\sigma}_{^{7}Be})_c$ (mb)
O (CuO)	30	2.9		
	45	5.3		
	60	9.9		
	70	9.5		
	85	9.0		
Al	70	0.76		
	85	1.08	1.06±0.01	
	85	1.05		
Ti	65	0.074		
	85	0.245	0.25±0.01	0.18
	85	0.260		
V	65	0.061		
	85	0.155	0.147±0.007	
	85	0.140		
Fe	85	0.108		
Co	65	0.036		
	85	0.081	0.089±0.008	
	85	0.098		
Ni	65	0.039		
	85	0.089	0.095±0.01	
	85	0.101		
^{63}Cu	65	0.019		
	85	0.064	0.065±0.01	
	85	0.066		
Cu	65	0.023		
	85	0.054		
	85	0.069	0.068±0.014	
	85	0.081		
^{65}Cu*	85	0.074		
Ag	65	0.024		
	85	0.032		
	85	0.025	0.028±0.004	0.0067
	85	0.027		
Au	65	0.0031		
	85	0.0045	0.0035±0.001	0.0008
	85	0.0026		
U	65	0.021		
	85	0.013	0.02±0.007	
	85	0.027		

*Obtained by calculation from experimental values for ^{63}Cu and Cu.

For the Ag(p,^{7}Be) reaction, the measurements at 65 and 85 MeV were made under the same conditions. The similarity of the two results definitely indicates light-element contamination in the silver target. It was assumed that at 65 MeV the measured ^{7}Be was produced mainly from the light elements. The amount of ^{7}Be produced from light elements at 85 MeV was calculated by extrapolating the measured cross-section value at 65 MeV to 85 MeV using a straight line with the same slope as the O(p,^{7}Be) excitation function; this cross-section value was then subtracted from the observed cross section to yield an estimate of the ^{7}Be cross section from silver. The error associated with the corrected cross-section value is also very large, estimated to be ±100%.

Can. J. Chem. Downloaded from www.nrcresearchpress.com by 210.87.254.42 on 09/05/12
For personal use only.

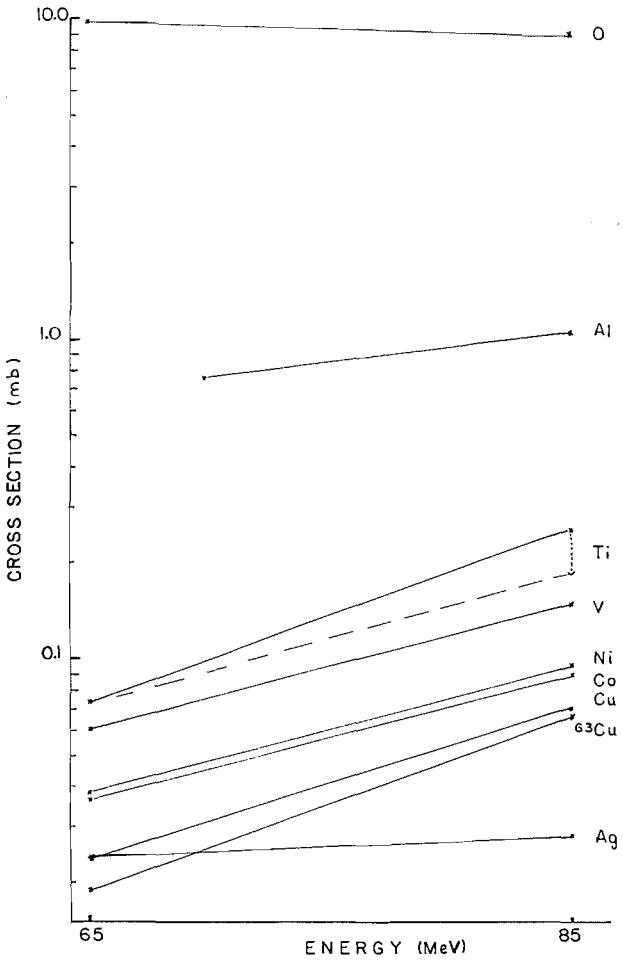


FIG. 3. ^{7}Be cross sections plotted against energy of the incident proton.

The same procedure was used to obtain a very rough estimate of the ^{7}Be cross section from gold. The error associated with the corrected cross-section value was estimated to be $\pm 300\%$.

It was not possible to obtain even an estimate of the cross-section value for uranium because of the low ^{7}Be production and the high contamination of the target.

The variation of the ^{7}Be formation cross section with target mass number A is shown in Fig. 4 for bombarding protons of 65 and 85 MeV energy. The uncertainty in the cross-section value is shown by the vertical bar.

III. DISCUSSION

(A) Evaporation Calculations

According to evaporation theory (27), the cross section for the emission of ^{7}Be from an excited nucleus is given by

$$[4] \qquad \sigma_{^{7}\mathrm{Be}} = \sigma_{F} \times \frac{\Gamma_{^{7}\mathrm{Be}} + \Gamma_{^{7}\mathrm{Be}^{*}}}{\sum_{j} \Gamma_{j}},$$

where σ_{F} = formation cross-section of the excited nucleus.

Can. J. Chem. Downloaded from www.nrcresearchpress.com by 210.87.254.42 on 09/05/12
For personal use only.

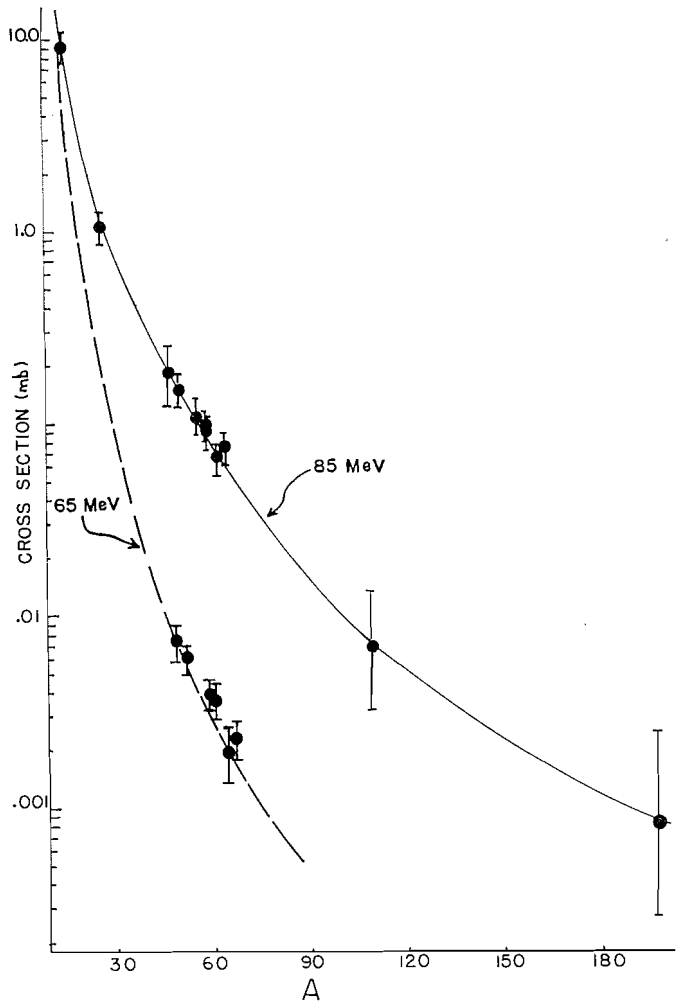


FIG. 4. Cross section plotted against mass number, A, for the production of ^{7}Be in targets irradiated with 65- and 85-MeV protons.

Γ_j = emission width for particle j

$$= \frac{g_j m_j}{\pi^2 \hbar^3} \int \sigma^*(E_j) \times \frac{\omega(E_f)}{\omega(E_i)} \times E_j \times \mathrm{d}E_j \qquad [5]$$

where g_j = number of spin states of particle j, m_j = mass of particle j, $\sigma^*(E_j)$ = cross section for the inverse reaction, E_j = kinetic energy of particle j, $\omega(E_f)$,$\omega(E_i)$ = level densities of the final and initial nuclei at their respective excitation energies.

$\Gamma_{^{7}\mathrm{Be}^*}$ refers to the excited state of ^{7}Be, 0.43 MeV above the ground level. (The production of excited states of heavy particles as well as the ground state must be considered.)

The starting point for evaporation calculations is the spectrum of excited nuclides left after the completion of the knock-on cascade.

The *maximum* energy available for the evaporation of ^{7}Be from a residual nucleus (i.e. the maximum kinetic energy of the outgoing ^{7}Be) may be approximated as (28):

$$R_{^{7}\mathrm{Be}} \sim E^* - Q_{^{7}\mathrm{Be}} - \delta_{^{7}\mathrm{Be}}, \qquad [6]$$

Can. J. Chem. Downloaded from www.nrcresearchpress.com by 210.87.254.42 on 09/05/12
For personal use only.

where E^* = excitation energy of residual nucleus, $Q_{^7Be}$ = separation energy of ^7Be from residual nucleus, $\delta_{^7Be}$ = nucleon-pairing correction.

According to the sharp cutoff approximation, the *minimum* kinetic energy of a ^7Be particle is given by the effective coulomb barrier, $k_{^7Be}V_{^7Be}$.

The difference between the maximum and minimum energy may be regarded as the energy available for a residual nucleus to evaporate a particle. The factor $(R_{^7Be} - k_{^7Be}V_{^7Be})$ was estimated for residual nuclei which were formed by specific types of cascades. Average excitation energies of residual nuclei, calculated by Metropolis *et al.* (29), were used to give an average value of $R_{^7Be}$. The factor $k_{^7Be}V_{^7Be}$ was calculated in the manner described in the following section. The estimation was performed for 82-MeV protons incident on the targets Al, Cu, and U, and the results are shown in Table III.

TABLE III

Average energy available for the evaporation of ^7Be from residual nuclei formed by specific-type cascades (82-MeV incident protons)

	$\bar{R}_{^7Be} - k_{^7Be}V_{^7Be}$ (MeV)		
Type of cascade	Al	Cu	U
Compound nucleus formation	49.8	49.4	40.5
p,n	0.7	10.2	7.2
p,p′	−0.5	3.4	−4.6
p,2n	−2.7	−1.2	−10.6
p,pn	−12.0	−11.6	−22.8
p,2p	−14.6	−14.4	

As seen in Table III, it is unlikely that ^7Be will be evaporated from nuclei which have been formed with the ejection of cascade particles. To simplify the present calculation, it is assumed that ^7Be is evaporated solely after compound nucleus formation.

Energy considerations also suggest that ^7Be is most probably evaporated from the compound nucleus itself but may also be evaporated from the product nuclei formed by particle evaporation.

(1) Cross Section for the Formation of ^7Be from the Compound Nucleus

The cross section for the emission of ^7Be from the compound nucleus was calculated according to eq. [4]: The important factors to be evaluated in this equation are the inverse cross section and the level density.

(i) $\sigma^*(E)$ – inverse cross section.—The inverse cross section was assumed equal to the total reaction cross section for particles incident upon a nucleus in its ground state.

The variation of charged-particle capture cross sections with energy and atomic number was approximated according to the well-known sharp cutoff expression

$$[7] \qquad \sigma^*(E_j) = \begin{cases} 0 & \text{for } E_j < k_jV_j \\ \pi R^2(1 + c_j)(1 - k_jV_j/E_j) & \text{for } E_j > k_jV_j \end{cases}$$

where c_j and k_j are parameters that are functions of atomic number, z, and V_j is the coulomb barrier. Dostrovsky, Fraenkel, and Friedlander (28) determined the values of the parameters c_j and k_j for protons, alphas, ^3H, and ^3He particles by the best fit of eq. [7] to tabulated continuum theory cross sections of Shapiro (30) and Blatt and Weisskopf (31). The classical barrier, V, was calculated by the formula

$$[8] \qquad V = zZe^2/R,$$

Can. J. Chem. Downloaded from www.nrcresearchpress.com by 210.87.254.42 on 09/05/12
For personal use only.

Can. J. Chem. Downloaded from www.nrcresearchpress.com by 210.87.254.42 on 09/05/12
For personal use only.

where z, Z = atomic number of outgoing particle and residual nucleus respectively, e = electron charge, and $R = r_0A^{1/3} + \rho$ = interaction radius between nucleus and charged particle. r_0 was set equal to 1.5×10^{-13} cm, ρ was taken equal to zero for protons and equal to 1.2×10^{-13} cm for all other emitted particles, and A = mass number of residual nucleus.

No calculations have been performed to evaluate the dependence of the reaction cross-section of ^{7}Be on energy and atomic number. Therefore the parameters $c_{^{7}\mathrm{Be}}$ and $k_{^{7}\mathrm{Be}}$ were determined in the following way:

Experimentally the reaction of 85-MeV protons incident on various targets was studied. The reaction is represented as p(A,^{7}Be)B. ^{7}Be was emitted with kinetic energies ranging from $k_{^{7}\mathrm{Be}}V_{^{7}\mathrm{Be}}$ (the energy required to overcome the coulomb barrier) to $R_{^{7}\mathrm{Be}}$ (the maximum kinetic energy of emission given in eq. [10]). The computer program of D. R. Sachdev[5] was used to evaluate the reaction cross-section of ^{7}Be incident on various targets, B, with energy ranging from $k_{^{7}\mathrm{Be}}V_{^{7}\mathrm{Be}}$ to $R_{^{7}\mathrm{Be}}$. The calculation followed the outline described by Thomas (32) for the square-well potential model. Thomas found reasonable agreement with experiment for the radius parameter $r_0 = 1.5 \times 10^{-13}$ cm, hence this value was used. The computation was performed by an IBM 7040. For each target the reaction cross section of ^{7}Be was evaluated at 1-MeV intervals between the energy limits. In Fig. 5 the calculated cross section of ^{7}Be is plotted as a function of energy for ^{7}Be particles incident on $^{42}_{19}$K. As is shown in the figure a good fit to the curve was obtained using eq. [7] with $(1 + c_{^{7}\mathrm{Be}}) = 0.974$ and $k_{^{7}\mathrm{Be}} = 0.983$. The classical barrier was calculated using eq. [8] with $\rho = 2.43 \times 10^{-13}$ cm (33). The calculated cross-section curve was fitted with eq. [7] for each case of interest and the resultant values of $1 + c_{^{7}\mathrm{Be}}$ and $k_{^{7}\mathrm{Be}}$ are listed in Table IV.

TABLE IV

Parameters in eq. [11] for ^{7}Be cross sections

A	Z	$1 + c_{^{7}\mathrm{Be}}$	$k_{^{7}\mathrm{Be}}$
21	10	1.013	0.949
42	19	0.974	0.983
45	20	0.988	1.018
53	24	0.977	1.015
52	25	0.975	1.018
54	25	0.977	1.030
57	26	0.975	1.024
59	26	0.973	1.023
101	44	0.940	1.046
103	44	0.940	1.046
191	76	0.898	1.046
232	89	0.875	1.043

In every instance a good fit to the calculated curve was obtained and the fit was always remarkably good in the low-energy region where the sharp cutoff approximation is the weakest.

The energy and mass number dependence of neutron capture cross sections as given by continuum theory (31) was approximated according to Dostrovsky *et al.* (28).

$$\sigma^*(E_n) = \alpha(1 + \beta/E_n)\pi R^2, \qquad [9]$$

where $\alpha = 0.76 + 2.2A^{-1/3}$, and $\beta = (2.12A^{-2/3} - 0.050)/(0.76 + 2.2A^{-1/3})$ MeV.

[5]*The authors are indebted to Mr. D. R. Sachdev for the use of his computer program.*

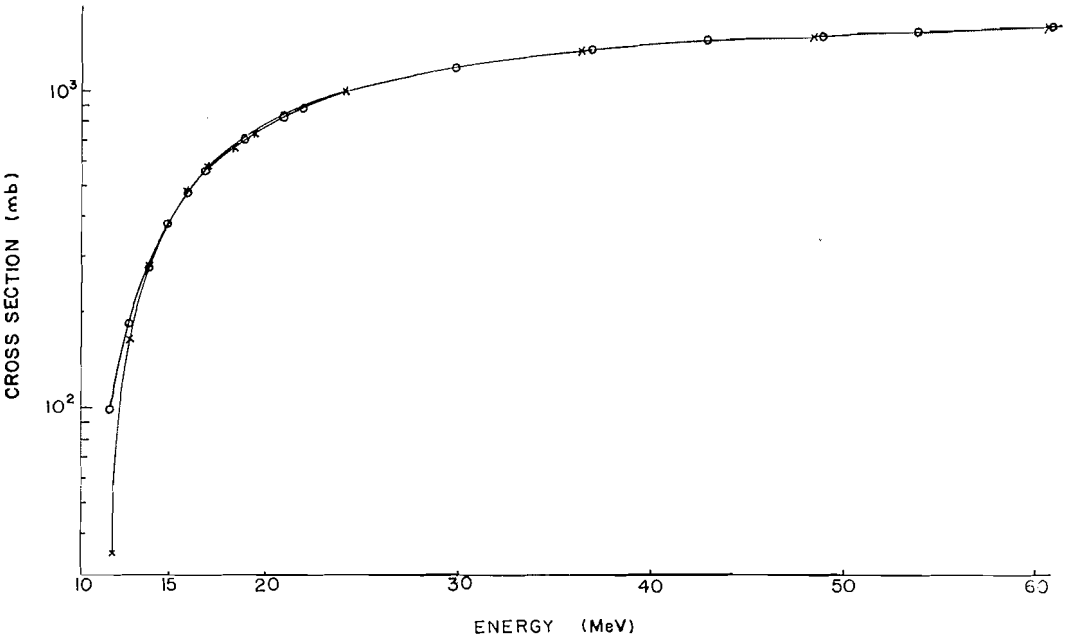


FIG. 5. Reaction cross section for ^{7}Be particles incident on $^{42}_{19}$K as a function of energy. (○) Cross section computed according to outline described by Thomas (32) for the square-well potential model, (×) $\sigma = \pi R^2(1 + c_{^7\mathrm{Be}})(1 - k_{^7\mathrm{Be}}V_{^7\mathrm{Be}}/E_{^7\mathrm{Be}})$.

(ii) $\omega(E)$ – level density.—We have chosen to use a level density formulation based on the Fermi-gas model (34–36).

$$\omega(E) = C(E - \delta)^{-2} \exp\left[2\{a(E - \delta)\}^{1/2}\right], \qquad [10]$$

where C = constant, E = excitation energy, a = level density parameter, and $\delta = 0$ for odd–odd nuclei and $\delta > 0$ for all other types. The value of δ is usually taken to be the pairing energies for neutrons and protons. Cameron's (37) tabulation of pairing energies for even values of Z and N has been used in the present calculations.

In order to explain the effect of shell structure on level densities observed at the neutron binding energy, the level density parameter has been formulated by Newton (38) and Lang (35) as

$$a = 0.0748(\bar{j}_n + \bar{j}_p + 1)A^{2/3}, \qquad [11]$$

where $\bar{j}_n$ and $\bar{j}_p$ are mean values of the spins of the neutron and proton shell-model states which correspond to a particular $A = N + Z$. The values of $\bar{j}_n$ and $\bar{j}_p$ are obtained from Klinkenberg's (39) shell-model scheme based on a study of nuclei in or near their ground states. The influence of shell effects is expected to disappear with increasing excitation energy, but it is not known up to what energies shell effects are important.

Two values of the level density parameter have been used in the present calculation: $a = A/10$ and $a = 0.0748\,(\bar{j}_n + \bar{j}_p + 1)A^{2/3}$.

The emission width was computed by substituting the inverse cross section as given by eqs. [7] and [9] and the level density as given by eq. [10] into eq. [5].

$$\Gamma_j = \frac{g_j m_j}{\pi\hbar^2} r_o^2 A_j^{2/3} \times (E - \delta_o)^2 \exp\left[-2\{a_o(E - \delta_o)\}^{1/2}\right] C_j \qquad [12]$$

$$\times \int_{k_jV_j}^{E_j} (E_j + \beta - k_jV_j) \exp\left[2\{a_j(E - Q_j - \delta_j - E_j)\}^{1/2}\right](E - Q_j - \delta_j - E_j)^{-2} \times dE_j,$$

Can. J. Chem. Downloaded from www.nrcresearchpress.com by 210.87.254.42 on 09/05/12
For personal use only.

where subscripts o and j refer to the original and residual nucleus respectively. For neutrons, C_j denotes α and $k_j = 0$; for protons, C_j denotes $(1 + c_j)$ and $\beta = 0$.

Because the integration of eq. [12] in closed form is not possible, its integral was approximated by the summation:

$$[13] \quad \sum_{k_j V_j}^{R_j} (E_j + \beta - k_j V_j) \exp\{2(a_j(E - Q_j - \delta_j - E_j)]^{1/2}\} (E - Q_j - \delta_j - E_j)^{-2} \Delta E_j.$$

The summation was performed by an IBM type 7040 computer for $E_j = 0.1$ MeV. Sample emission widths were calculated for values of ΔE_j ranging from 0.01 to 1.0 MeV. Emission width was plotted as a function of ΔE_j and the value of the emission width for $\Delta E_j = 0$ was determined by extrapolation. It was found that the emission width calculated for $\Delta E_j = 0.1$ MeV differed from the estimated emission width for $\Delta E_j = 0$ MeV by 0.001%. Smaller values of ΔE_j greatly increased the computer time required to perform the summation.

Separation energies, Q, were computed on the basis of experimental atomic mass data compiled by Konig *et al.* (40). For nuclei for which experimental mass values were not available, masses computed from Levy's (41) empirical mass formula were used.

The emission width was determined for two values of the level density parameter. For $a = 0.0748\ (\bar{j}_n + \bar{j}_p + 1)A^{2/3}$, emission width was determined for neutrons, protons, deutrons, tritons, alphas, ^{3}He, ^{7}Be, and ^{7}Be* particles. The probability of ^{7}Be emission,

$$P_{^7\mathrm{Be}} = \frac{\Gamma_{^7\mathrm{Be}} + \Gamma_{^7\mathrm{Be}^*}}{\sum_j \Gamma_j},$$

was then calculated. The inclusion of the emission width of tritons and ^{3}He particles to the sum $\sum_j \Gamma_j$ made little difference to the value obtained for $P_{^7\mathrm{Be}}$. Hence for the level density parameter $a = A/10$, emission width determination was confined to neutrons, protons, deuterons, alphas, ^{7}Be, and ^{7}Be* particles.

The formation cross section of the compound nucleus was determined according to

$$[14] \quad \sigma_F = \sigma_R F_{CN},$$

where σ_R = proton-reaction cross section, and F_{CN} = fraction of reaction which yields compound nucleus formation.

The proton-reaction cross section was calculated using eq. [7] with $r_o = 1.5 \times 10^{-13}$ cm.

The fraction yielding compound nucleus formation was obtained from the results of the Monte Carlo calculations on intranuclear cascades of Metropolis *et al.* (29) and Turkevich (42).

The calculated quantities for the proton-reaction cross section, σ_R, the fraction of compound nucleus formation, F_{CN}, the probability of ^{7}Be emission from the compound nucleus, $(P_{^7\mathrm{Be}})^{CN}$, and the cross section for ^{7}Be emission from the compound nucleus, $(\sigma_{^7\mathrm{Be}})^{CN}$, are presented in Table V.

For the level density parameter $a = 0.0748(\bar{j}_n + \bar{j}_p + 1)A^{2/3}$, calculated and experimental ^{7}Be cross sections are plotted as a function of target mass number, A, in Fig. 6. This value of the level density parameter fails to predict the observed variation of cross section for ^{7}Be formation with target element. There is no relation between calculation and experiment. The shell effects observed at low energies and represented by the Newton–Lang formulation do not persist then to the excitation energies encountered here. This was predicted by Ericson (43), who cautioned about the use of the Newton formula for excitation energies much above neutron-binding energies.

Can. J. Chem. Downloaded from www.nrcresearchpress.com by 210.87.254.42 on 09/05/12
For personal use only.

Can. J. Chem. Downloaded from www.nrcresearchpress.com by 210.87.254.42 on 09/05/12
For personal use only.

TABLE V

Comparison between experimental cross sections and those obtained with various values of a

Target	σ_R (mb)	F_{CN}	$a = 0.0748\,(\bar{j}_n + \bar{j}_p + 1)A^{2/3}$		$a = A/10$			Expt.
			$(P_{^7Be})^{CN}$	$(\sigma_{^7Be})^{CN}$ (mb)	$(P_{^7Be})^{CN}$	$(\sigma_{^7Be})^{CN}$ (mb)	$\sigma_{^7Be}$ (mb)	$\sigma_{^7Be}$ (mb)
^{27}Al	862.8	0.05	3.96×10^{-3}	0.17	3.32×10^{-3}	0.143	0.248	1.064
^{48}Ti	1 069.0	0.107	5.52×10^{-7}	0.63×10^{-4}	4.86×10^{-4}	0.056	0.073	
Natural Ti								0.182
^{51}V	1 097.3	0.115	2.6×10^{-6}	0.33×10^{-4}	3.62×10^{-4}	0.044	0.052	0.147
^{59}Co	1 139.7	0.133	1.25×10^{-3}	0.189	3.21×10^{-4}	0.044	0.056	0.089
^{58}Ni	1 134.2	0.131	8.16×10^{-3}	1.22	5.8×10^{-4}	0.087	0.104	
^{60}Ni	1 139.8	0.136	8.17×10^{-3}	1.26	6.1×10^{-4}	0.094	0.108	
Natural Ni				1.23		0.089	0.105	0.095
^{63}Cu	1 166.3	0.143	2.23×10^{-3}	0.37	4.41×10^{-4}	0.073	0.099	0.065
^{65}Cu	1 169.2	0.147	3.03×10^{-3}	0.52	2.05×10^{-4}	0.035	0.045	0.074
Natural Cu				0.42		0.062	0.082	0.068
^{107}Ag	1 420.1	0.23	1.22×10^{-7}	4.0×10^{-5}	2.13×10^{-5}	0.0070	0.0084	
^{109}Ag	1 439.3	0.233	2.67×10^{-7}	8.95×10^{-5}	0.69×10^{-5}	0.0023	0.0026	
Natural Ag				6.38×10^{-5}		0.0047	0.0066	0.0067
^{197}Au	1 696.0	0.375	9.36×10^{-6}	5.95×10^{-3}	2.06×10^{-9}	1.3×10^{-6}		$\sim$0.0008
^{238}U	1 792.7	0.45	1.085×10^{-11}	7.85×10^{-9}	3.77×10^{-10}	3.04×10^{-7}		—

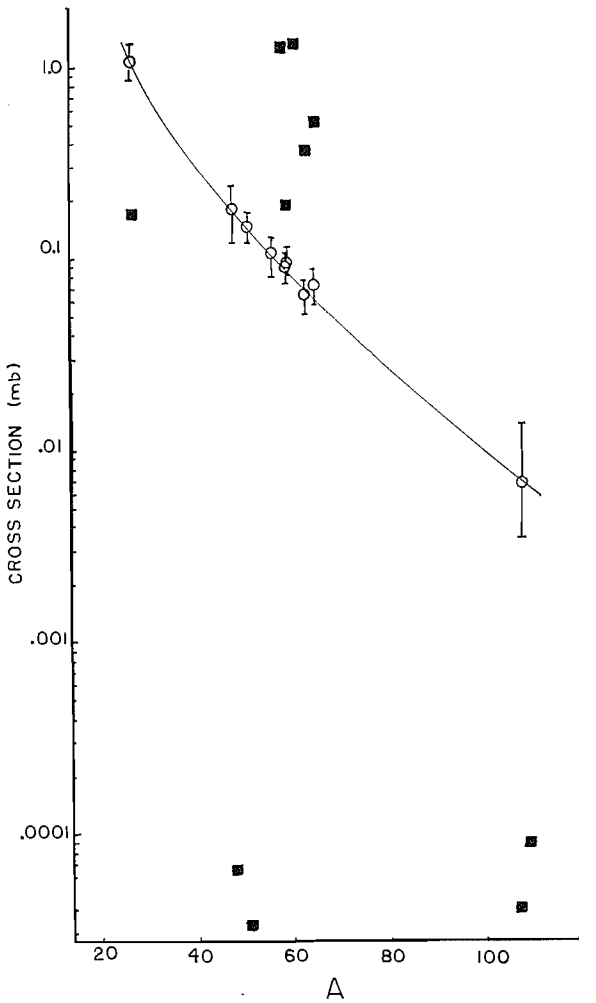


FIG. 6. Cross sections plotted against mass number, A. (○) Experimental cross-section values, (■) calculated cross sections for ^{7}Be formation from the compound nucleus, $(\sigma_{^7\mathrm{Be}})^{\mathrm{CN}}$, for $a = 0.0748(\bar{j}_n + \bar{j}_p + 1)A^{2/3}$.

(2) Estimate of the Total Cross Section for Formation of ^{7}Be

The contribution to the ^{7}Be cross section for ^{7}Be evaporated after particle emission was estimated in the following approximate manner:

In the first step of the evaporation chain, the compound nucleus de-excites by evaporating a particle of varying kinetic energy. The excitation energy of the product nucleus so formed is a function of this kinetic energy. The most probable kinetic energy, E_{mp}, of the evaporated particle has been given by Dostrovsky, Fraenkel, and Friedlander (28) as

$$[15] \qquad E_{mp} = V + a_j^{-1}[(a_j R_j + 1/4)^{1/2} - \tfrac{1}{2}],$$

where $V = k_j V_j$ for charged particles, and $V = -\beta$ for neutrons. For each compound nucleus of interest, the most probable excitation energy of the product nuclei formed by neutron, proton, deuteron, and alpha emission was thus determined. The probability of ^{7}Be emission from each product, $(P_{^7\mathrm{Be}})j$, at its most probable excitation energy, was calculated as in the preceding section.

Can. J. Chem. Downloaded from www.nrcresearchpress.com by 210.87.254.42 on 09/05/12
For personal use only.

Can. J. Chem. Downloaded from www.nrcresearchpress.com by 210.87.254.42 on 09/05/12
For personal use only.

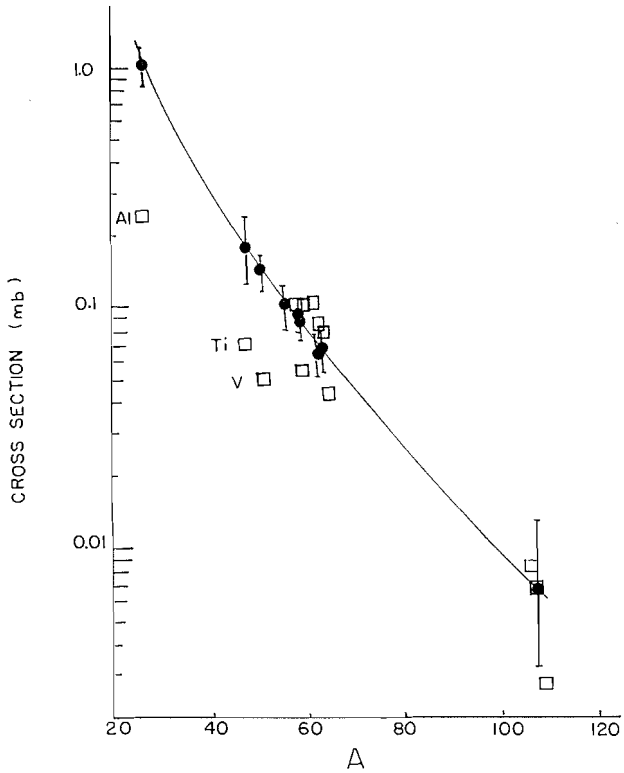


FIG. 7. Cross section plotted against mass number, A. (●) Experimental cross-section values, (□) calculated cross sections for $a = A/10$.

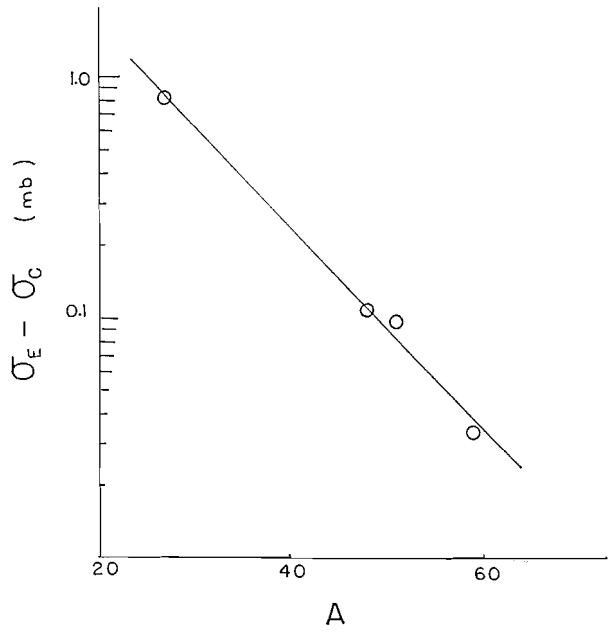


FIG. 8. ($\sigma_E - \sigma_C$) plotted against mass number, A.

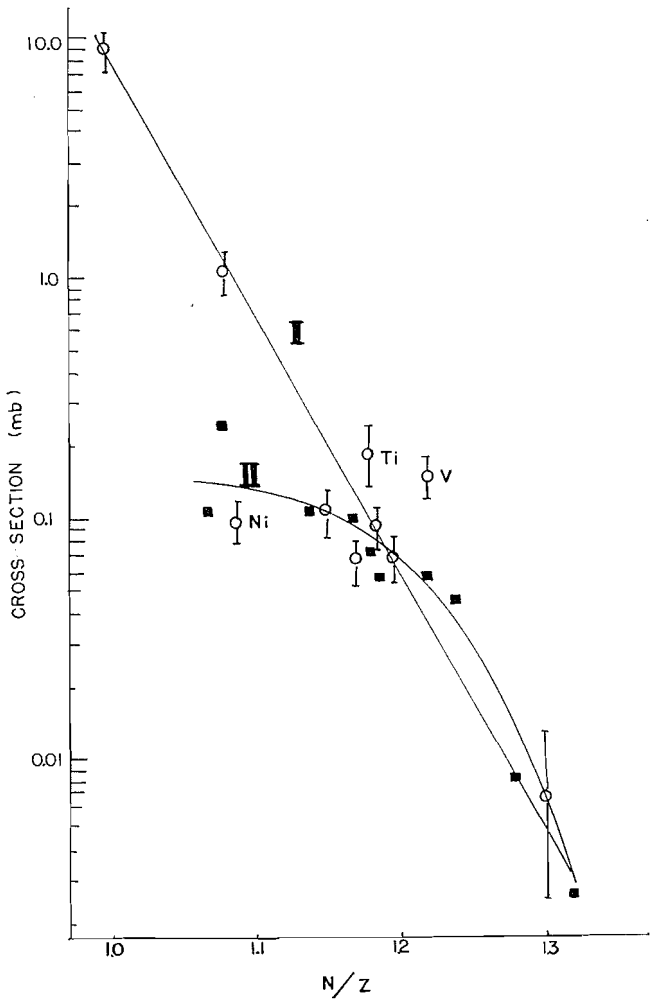


FIG. 9. Cross sections plotted against target neutron-to-proton ratio, N/Z. (○) Experimental cross-section values, (■) calculated cross sections for $a = A/10$.

The contribution from ^{7}Be emission further along the evaporation chain was assumed to be negligible on the basis of energy considerations.

The total ^{7}Be cross section was then estimated to be:

$$[16] \quad \sigma_{^{7}\mathrm{Be}} = \{(P_{^{7}\mathrm{Be}})^{\mathrm{CN}} + (P_{\mathrm{n}})^{\mathrm{CN}}(P_{^{7}\mathrm{Be}})^{\mathrm{n}} + (P_{\mathrm{p}})^{\mathrm{CN}}(P_{^{7}\mathrm{Be}})^{\mathrm{p}} + (P_{\mathrm{d}})^{\mathrm{CN}}(P_{^{7}\mathrm{Be}})^{\mathrm{d}} + (P_{\alpha})^{\mathrm{CN}}(P_{^{7}\mathrm{Be}})^{\alpha}\}\sigma_{\mathrm{F}}.$$

The cross section for ^{7}Be formation, $\sigma_{^{7}\mathrm{Be}}$, was estimated according to eq. [16] for the level density parameter $a = A/10$ and is given in Table V.

In Fig. 7, calculated and experimental ^{7}Be cross sections are plotted as a function of target mass number, A. With the exception of the light elements there is reasonable agreement between calculated and experimental values. However, the experimental points vary smoothly with A, whereas the calculated points are scattered. Scatter of the experimental points may be masked by the experimental error. Dostrovsky *et al.*[4](4)

Can. J. Chem. Downloaded from www.nrcresearchpress.com by 210.87.254.42 on 09/05/12
For personal use only.

found that cross sections for fragment production in irradiations with high-energy protons were a smoother function of the target neutron-to-proton ratio, N/Z, than the target mass, A. In the following section, experimental and calculated ^{7}Be cross sections are plotted as a function of N/Z.

The calculation underestimates the production of ^{7}Be from the light targets Al, Ti, and V. The underestimation does not seem to be due to the fact that the contribution of ^{7}Be evaporation following knock-on cascade was neglected. Examination of Table V indicated that after the knock-on cascade more energy is available for ^{7}Be evaporation from irradiated Cu than Al. In Fig. 8, the difference between the calculated and experimental ^{7}Be cross sections, $(\sigma_E - \sigma_C)$, is plotted against target mass number, A. Although the points are limited and the errors are large, the trend seems to indicate a straight line, suggesting that a mechanism other than evaporation contributes to the formation of ^{7}Be in these targets.

(B) Variation of the Cross Section for ^{7}Be Emission With The Neutron-to-Proton Ratio of the Target

Dostrovsky *et al.* (4) observed a dependence of the cross section for the formation of the neutron-excess fragments ^{9}Li, ^{16}C, and ^{17}N on the neutron-to-proton ratio of the target in irradiations with GeV protons. Hence calculated ($a = A/10$) and experimental values of the ^{7}Be cross section are plotted as a function of target neutron-to-proton ratio, N/Z, in Fig. 9. A straight line, I, may be drawn through the experimental points for the targets O, Al, Co, Cu, and Ag. There is considerable scatter of the rest of the points about this line. Points for the neutron-rich targets Ti and V are above the line. The point for the neutron-poor Ni is substantially below the line.

However, as was shown in Fig. 8, it seems highly possible that a mechanism other than evaporation contributes significantly to the production of ^{7}Be in the irradiated targets Al, Ti, and V, while spallation accounts for a large fraction of the production of ^{7}Be from O. A curve, II, may be drawn through the experimental points for the remaining targets as well as the calculated points.

The variation of ^{7}Be cross section with target neutron-to-proton ratio seems to suggest that more than one mechanism is responsible for ^{7}Be formation. However, the data are too limited to be conclusive.

As shown in Fig. 7, evaporation theory does predict the N/Z dependence of ^{7}Be cross sections for medium mass targets ($A > 55$). According to evaporation theory, the dependence of cross section on target neutron-to-proton ratio arises primarily from differences in the binding energies of ^{7}Be in the evaporating nuclei. The decrease in cross section with target mass for the neutron-deficient fragment ^{7}Be may be partly attributed to the fact that, as the target mass increases, the neutron-to-proton ratio of the fragment becomes further removed from the neutron-to-proton ratio of the stability valley of the target region (the decrease in cross section is also attributable to the increase in the factor $k_{^7\mathrm{Be}}V_{^7\mathrm{Be}}$).

(C) Concluding Remarks

The present work adds to the evidence that more than one mechanism contributes to fragment formation. Evaporation as a mechanism for ^{7}Be emission from medium and heavy targets ($A > 55$) has successfully predicted cross-section magnitudes and the variation of cross section with the neutron-to-proton ratio of the target. However, the latter does not uniquely indicate an evaporation mechanism. Indeed the asymmetry of fragment angular distribution (44) contradicts such a process.

This asymmetry has suggested that fragments are produced by the direct process of

Can. J. Chem. Downloaded from www.nrcresearchpress.com by 210.87.254.42 on 09/05/12
For personal use only.

the scattering of nucleons on nucleon clusters. The effect of collisions with clusters is expected to be more important in interactions with light nuclei where the cascade is likely to consist of one, two, or three collisions. In heavy nuclei, collisions with single nucleons are expected to increase with target mass. This explains the decrease in fragment asymmetry with increase in target mass, and, for the non-evaporation mechanism, the decrease in fragment production with target mass shown in Fig. 8.

ACKNOWLEDGMENTS

The authors wish to thank Professor R. E. Bell, Director, Foster Radiation Laboratory, for permission to use the McGill synchrocyclotron, and Mr. R. H. Mills, who cheerfully performed the irradiations. One of us (M. S. L.) wishes to thank the National Research Council of Canada for studentships held during 1959–1963.

REFERENCES

1. I. Dostrovsky, P. Rabinowitz, and R. Bivins. Phys. Rev. **111**, 1659 (1958).
2. I. Dostrovsky, Z. Fraenkel, and P. Rabinowitz. Phys. Rev. **118**, 791 (1960).
3. I. Dostrovsky, Z. Fraenkel, and J. Hudis. Phys. Rev. **123**, 1452 (1961).
4. I. Dostrovsky, R. Davis, Jr., A. M. Poskanzer, and P. L. Reeder. Phys. Rev. **139**, B1513 (1965).
5. S. Katcoff, E. W. Baker, and N. T. Porile. Phys. Rev. **140**, B1549 (1965).
6. M. M. Makarov. Zh. Eksperim. i Teor. Fiz. **44**, 962 (1962); Soviet Phys. JETP English Transl. **17**, 653 (1963).
7. G. V. S. Rayudu. Can. J. Chem. **42**, 1149 (1964).
8. M. Ligonniere, B. Vassent, and R. Bernas. Compt. Rend. **259**, 1406 (1964).
9. P. A. Benioff. Phys. Rev. **119**, 316 (1960).
10. G. Friedlander, J. Hudis, and R. Wolfgang. Phys. Rev. **99**, 263 (1955).
11. J. Gray. Progress Report. Carnegie Institute of Technology. 1962.
12. E. Baker, G. Friedlander, and J. Hudis. Phys. Rev. **112**, 1319 (1958).
13. R. H. Lindsay and E. F. Neuzil. Phys. Rev. **127**, 1269 (1962).
14. M. Furukawa, S. Kume, M. Ogawa. Nucl. Phys. **69**, 362 (1965).
15. J. B. Cumming. Ann. Rev. Nucl. Sci. **13**, 261 (1963).
16. W. A. Aron, B. G. Hoffman, and F. C. Williams. U.S. At. Energy Comm. Rept. AECU-663 (1951).
17. N. Sugarman, M. Campos, and K. Wielgoz. Phys. Rev. **101**, 388 (1956).
18. C. Hower. Ph.D. Thesis, University of Washington, Seattle, Washington. 1962.
19. S. Meghir and L. Yaffe. To be published.
20. R. E. Bell. Private communication.
21. E. B. Sandell. Colorimetric determination of traces of metals. 3rd ed. (revised). Interscience Publishers, Inc., New York. 1959.
22. F. J. Welcher. The analytical uses of ethylenediaminetetraacetic acid. D. Van Nostrand Co., Inc., Princeton, New Jersey. 1958.
23. J. G. V. Taylor and J. S. Merritt. Can. J. Phys. **40**, 926 (1962).
24. G. R. Grant. Ph.D. Thesis, McGill University, Montreal, Quebec. 1961.
25. S. Meghir. Ph.D. Thesis, McGill University, Montreal, Quebec. 1962.
26. G. B. Saha. Ph.D. Thesis, McGill University, Montreal, Quebec. 1965.
27. V. Weisskopf. Phys. Rev. **52**, 295 (1937).
28. I. Dostrovsky, Z. Fraenkel, and G. Friedlander. Phys. Rev. **116**, 683 (1959).
29. N. Metropolis, R. Bivins, M. Storm, A. Turkevich, J. M. Miller, and G. Friedlander. Phys. Rev. **110**, 185 (1958).
30. M. M. Shapiro. Phys. Rev. **90**, 171 (1953).
31. J. Blatt and V. F. Weisskopf. Theoretical nuclear physics. John Wiley and Sons, Inc., New York. 1952.
32. T. D. Thomas. Phys. Rev. **116**, 703 (1959).
33. L. Dresner. Oak Ridge Natl. Lab. Rept. ORNL-TM-196 (1961).
34. H. A. Bethe. Rev. Mod. Phys. **9**, 69 (1937).
35. D. W. Lang. Nucl. Phys. **26**, 434 (1961).
36. H. Hurwitz and H. A. Bethe. Phys. Rev. **81**, 898 (1951).
37. A. G. W. Cameron. Can. J. Phys. **36**, 1040 (1958).
38. T. D. Newton. Can. J. Phys. **34**, 804 (1956).
39. P. F. A. Klinkenberg. Rev. Mod. Phys. **24**, 63 (1952).
40. L. A. Konig, J. H. E. Mattauch, and A. H. Wapstra. Nucl. Phys. **31**, 18 (1962).
41. H. B. Levy. Phys. Rev. **106**, 1265 (1957). J. Riddell. Numerical tables. At. Energy Can. Ltd. AECL 339 (1956).
42. A. Turkevich. Private communication.
43. T. Ericson. Phil. Mag. Suppl. **9**, 425 (1960).
44. M. M. Makarov. Zh. Eksperim. i Teor. Fiz. **45**, 56 (1963); Sov. Phys. JETP English Transl. **18**, 41 (1964).

Can. J. Chem. Downloaded from www.nrcresearchpress.com by 210.87.254.42 on 09/05/12
For personal use only.

Can. J. Chem. Downloaded from www.nrcresearchpress.com by 210.87.254.105 on 09/05/12
For personal use only.

ERRATUM: STUDIES OF THE DISSOCIATION OF OXIDE SURFACES AT THE LIQUID–SOLID INTERFACE

SYED M. AHMED

(Ref. Can. J. Chem. 44, 1663 (1966))

On page 1664, the first part of eq. [2]

$$d\gamma = -(q^{\pm} . /dE^{\pm})_{\mu_{K^+,NO_3^-}}$$

should read as

$$d\gamma = -(q^{\pm}\, dE^{\pm})_{\mu_{K^+,NO_3^-}}$$

and eq. [4]

$$\gamma - \gamma_0 = \left(\int_{E_0}^{E} q^{\pm}\, dE^{\pm} \right)_{\mu_{K^+,NO_3^-}} = -\infty - \left(\int_{-\infty}^{\mu} \Gamma_{K^+,NO_3^-} \cdot d\mu_{K^+,NO_3^-} \right)_E .$$

should read as

$$\gamma - \gamma_0 = \left(\int_{E_0}^{E} q^{\pm}\, dE^{\pm} \right)_{\mu_{K^+,NO_3^-}=-\infty} - \left(\int_{-\infty}^{\mu} \Gamma_{K^+,NO_3^-} \cdot d\mu_{K^+,NO_3^-} \right)_E .$$

MINES BRANCH,
DEPARTMENT OF MINES AND TECHNICAL SURVEYS,
OTTAWA, CANADA.

CHEMICAL SHIFT CHANGES IN FLUOROANIONS OF SOME DIAMAGNETIC SALTS[1]

RIZWANUL HAQUE AND L. W. REEVES

INTRODUCTION

In most processes occurring in electrolyte solutions the nuclear magnetic resonance signal observed for a solvent or solute nucleus is a time average of all environments rather than a series of separate peaks. Gutowsky and Saika (1) used this fact to measure dissociation constants of acids and Shoolery and Alder (2) interpreted the changes in chemical shift of the proton resonance in water as a function of the concentration of diamagnetic electrolyte added as a sum of several time-averaged processes. In this note we shall present results pertaining to the solute resonance peaks in simple and complex fluoroanions.

For the solvent proton resonance (3–6) changes in chemical shift are due to breaking of hydrogen bonds and a polarization effect due to the distortion of water molecules near a positive ion. Axtmann (7) has correlated the proton chemical shift changes in water with the pK of the salt. Taube and co-workers (8–10) and Connick and co-workers (11–14) have

[1]*Research supported by the National Research Council of Canada and the Petroleum Research Fund of the American Chemical Society.*

measured both the relaxation characteristics and the resonance positions for enriched ^{17}O water in aqueous solutions of electrolytes. They have been able to determine hydration numbers of diamagnetic cations and rates of exchange of water molecules between the bulk solution and the first coordination sphere.

In this work we shall present some chemical shift measurements as a function of concentration for the fluorine magnetic resonance in the ions F^-, BF_4^-, and SiF_6^{2-} with a variety of cations. Shoolery and Alder (2) made similar measurements on potassium fluoride solutions. Later studies of Carrington and co-workers (15, 16) and Connick and Poulson (17) indicated that the direction of the ^{19}F chemical shift change for KF and NaF in water were in opposite sense. The chemical shift change to low field for KF in water was reversed at high concentrations ($>5\ m$), however, and Craig and Richards (18) note a change in chemical shift with time when glass sample tubes are used. No satisfactory explanation of the unique ^{19}F chemical shift behavior of KF in water has been advanced.

Solvent resonances from ^{17}O or ^{1}H isotopes in water have been correlated to a certain extent with ionic size or polarizability (3–5, 19) of dissolved electrolytes. Since ions can approach to close distances in concentrated electrolyte solutions, it would seem appropriate to attempt some correlation of 1 m ^{19}F shifts with the factor (charge/radius^3) for the cation.

EXPERIMENTAL

Materials

Solutions were prepared by dissolving a known weighed quantity in double-distilled water. NaF, NH_4F, and KF were analytical grade B.D.H. reagents. Most of the fluoroborates were supplied by Allied Chemical Company, N.Y. Fluoroborate solutions were standardized by precipitation as nitron fluoroborate. Most of the hexafluorosilicates were prepared by dissolving carbonates or hydroxides of metal in hexafluorosilicic acid and further crystallization (20).

Apparatus and Technique

^{19}F spectra were recorded on a Varian HR-60 spectrometer at 56.4 and 40 Mc. Chemical shifts were measured by side-band technique and details are given earlier (21). Samples were kept in a 3 mm internal diameter pyrex nuclear magnetic resonance tube. All the chemical shifts were measured using a fine capillary of 10 m KF (for F^- ion), saturated $NaBF_4$ (for BF_4^- ion), or 3.3 m $ZnSiF_6$ (for SiF_6^{2-} ion) as an external standard. For each sample an average of five or six spectra were recorded and the mean of chemical shift was taken. The experiments were performed at room temperature ($\approx$ 25 °C).

RESULTS AND DISCUSSION

The ^{19}F chemical shift for the anions F^-, BF_4^-, and SiF_6^{2-} have been measured as a function of concentration in water for several cations. The results for the fluoroborates and hexafluorosilicates are shown in Fig. 1. The results for the fluorides are not plotted but will be quoted in terms of their shifts at 1 m concentration. The dilution shift curves are not linear in general over the range 0 to 1 m. Any interionic effects will, if present, dominate the chemical shift change although rearrangements of solvent may also occur around the ion. The trend of shifts is to low field with fluoroborates and hexafluorosilicates but two salts of small univalent cations Li^+ and Na^+ give high field shifts. With the fluoroborates there is an obvious trend of increasing low field shift with the size of the cation. To introduce some order into these shifts we have taken the shift change from 0 to 1 m concentration for each salt and plotted this against the charge/(radius)^3 of the cation in Fig. 2. In this way any connection between the chemical shift changes and ability of the cation to polarize the anion will be evident. At present the results are scattered and limited by the solubility and availability of the necessary salts. Definite trends can be observed. This is most clearly seen for the fluoroborates of cadmium, tin, and lead. As the cation of the same charge increases in size the 1 m shift to low field is more pronounced. Formation of inner sphere complexes where the anion replaces water of hydration at the

Can. J. Chem. Downloaded from www.nrcresearchpress.com by 210.87.254.105 on 09/05/12
For personal use only.

cation is suggested. The larger the cation of the same charge the more the equilibrium for this process will favor ion pairs.

$$[M[H_2O)_x]^{n+} + A^{m-} \rightleftharpoons [M(H_2O)_{x-y}A]^{(n-m)+} + yH_2O$$

Further evidence for ion pair formation with the heavy metal ions can be inferred from the fact that the ^{19}F resonance of the BF_4^- ion shows a partially collapsed scalar coupling to the ^{11}B nucleus. The electric field gradient of T_d symmetry is perturbed by the adjacent positive ion and the increased rate of quadrupolar relaxation of the ^{11}B nucleus results in a collapse of ^{11}B—^{19}F coupling. This effect has been previously observed by Muetterties and Packer (22) for the salts of AsF_6^- ion.

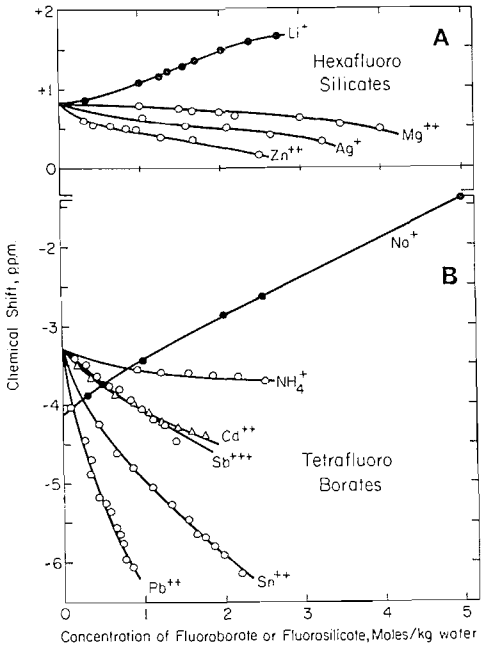


FIG. 1. (A) Concentration dependence of ^{19}F chemical shift of diamagnetic hexafluorosilicates. (B) Concentration dependence of ^{19}F chemical shift of diamagnetic fluoroborates.

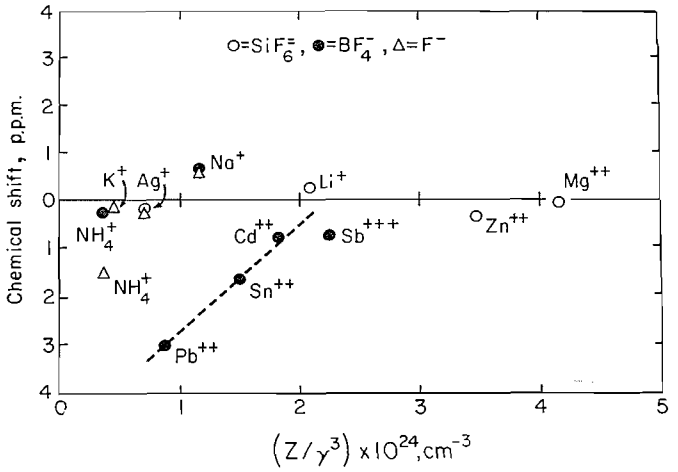


FIG. 2. Graph showing relation between molal chemical shift of a salt and charge/(ionic radius)^3 of cation. (Ionic radii are Goldschmidt radii.)

Can. J. Chem. Downloaded from www.nrcresearchpress.com by 210.87.254.105 on 09/05/12
For personal use only.

In salts of the same anion, the cation of smallest size produces an overall change in chemical shift which is small. It is likely that these ions do not form inner sphere complexes and thus the large chemical shift changes in the anion due to a cation in close proximity are absent. The preservation of the T_d symmetry in $NaBF_4$ at all concentrations is indicated by a long transverse relaxation time T_2 with resolution of a sharp quartette, the components of which have a line width ~ 0.5 c.p.s. Close contact between cation and anion is ruled out (21).

Changes in chemical shift with concentration in the salts of SiF_6^{2-} are always small even with the large and polarizable Ag^+ ion. This is particularly pronounced in the Zn^{2+} and Mg^{2+} salts, where we expect outer sphere complexes since these ions are strongly hydrated.

An unusual feature of the results presented in Fig. 1(B) is the fact that at infinite dilution the chemical shift is unique in $NaBF_4$ solutions. This effect has been noted before (21, 23). The exceptional variation of the coupling constant and chemical shift changes with concentration in this salt have been presented separately (21, 23).

1. H. S. Gutowsky and A. Saika. J. Chem. Phys. **21**, 1688 (1953).
2. J. N. Shoolery and B. J. Alder. J. Chem. Phys. **23**, 805 (1955).
3. B. P. Fabricand and S. Goldberg. J. Chem. Phys. **34**, 1624 (1961).
4. J. C. Hindman. J. Chem. Phys. **36**, 1000 (1962).
5. M. S. Bergqvist and E. Forslind. Acta Chem. Scand. **16**, 2069 (1962).
6. H. G. Hertz. Ber. Bunsenges Physik Chem. **67**, 311 (1963).
7. R. C. Axtmann. J. Chem. Phys. **30**, 340 (1959).
8. W. B. Lewis, J. A. Jackson, and H. Taube. J. Chem. Phys. **32**, 553 (1960).
9. W. B. Lewis, J. A. Jackson, F. Lemons, and H. Taube. J. Chem. Phys. **36**, 694 (1962).
10. J. H. Swinheart and H. Taube. J. Chem. Phys. **37**, 1579 (1962).
11. R. E. Connick and R. E. Poulson. J. Chem. Phys. **30**, 759 (1959).
12. R. E. Connick and D. E. Stover. J. Phys. Chem. **65**, 2075 (1961).
13. T. J. Swift and R. E. Connick. J. Chem. Phys. **37**, 307 (1962).
14. R. E. Connick and D. N. Fiat. J. Chem. Phys. **39**, 1349 (1963).
15. A. Carrington and T. Hines. J. Chem. Phys. **28**, 727 (1958).
16. A. Carrington, F. Dravnicks, and M. C. R. Symons. Mol. Phys. **3**, 174 (1960).
17. R. E. Connick and R. E. Poulson. J. Phys. Chem. **62**, 1002 (1958).
18. R. A. Craig and R. E. Richards. Trans. Faraday Soc. **59**, 1075 (1959).
19. Z. Luz and G. Yagil. J. Phys. Chem. **70**, 554 (1966).
20. N. T. L. Ten Broeck, Jr. and P. A. van der Muelen. J. Am. Chem. Soc. **53**, 3596 (1931).
21. R. Haque and L. W. Reeves. J. Phys. Chem. **70** (1966). In press.
22. K. J. Packer and E. L. Muetterties. Proc. Chem. Soc. 147 (1964).
23. K. Kuhlmann and D. M. Grant. J. Phys. Chem. **68**, 3208 (1964).

Received June 15, 1966.
Department of Chemistry,
University of British Columbia,
Vancouver, British Columbia.

SOLVENT DEPENDENCE OF ^{29}Si—^{19}F COUPLING CONSTANT IN SILICON TETRAFLUORIDE. THE IMPORTANCE OF INTERMOLECULAR DISPERSION INTERACTIONS

H. M. Hutton,[1] E. Bock, and T. Schaefer

Solvent dependent nuclear spin–spin coupling constants are observable in a variety of neutral molecules (1–16). For the most part, the interpretation of these observations are qualitative or even speculative in nature, but Watts and Goldstein (10) attempt to show that the geminal proton–proton coupling in α-chloroacrylonitrile depends on the reaction

[1]*Research Associate, Summer 1966. Permanent address: Brandon College, Brandon, Manitoba.*

Can. J. Chem. Downloaded from www.nrcresearchpress.com by 210.87.254.105 on 09/05/12
For personal use only.

In salts of the same anion, the cation of smallest size produces an overall change in chemical shift which is small. It is likely that these ions do not form inner sphere complexes and thus the large chemical shift changes in the anion due to a cation in close proximity are absent. The preservation of the T_d symmetry in $NaBF_4$ at all concentrations is indicated by a long transverse relaxation time T_2 with resolution of a sharp quartette, the components of which have a line width ~ 0.5 c.p.s. Close contact between cation and anion is ruled out (21).

Changes in chemical shift with concentration in the salts of SiF_6^{2-} are always small even with the large and polarizable Ag^+ ion. This is particularly pronounced in the Zn^{2+} and Mg^{2+} salts, where we expect outer sphere complexes since these ions are strongly hydrated.

An unusual feature of the results presented in Fig. 1(B) is the fact that at infinite dilution the chemical shift is unique in $NaBF_4$ solutions. This effect has been noted before (21, 23). The exceptional variation of the coupling constant and chemical shift changes with concentration in this salt have been presented separately (21, 23).

1. H. S. Gutowsky and A. Saika. J. Chem. Phys. **21**, 1688 (1953).
2. J. N. Shoolery and B. J. Alder. J. Chem. Phys. **23**, 805 (1955).
3. B. P. Fabricand and S. Goldberg. J. Chem. Phys. **34**, 1624 (1961).
4. J. C. Hindman. J. Chem. Phys. **36**, 1000 (1962).
5. M. S. Bergqvist and E. Forslind. Acta Chem. Scand. **16**, 2069 (1962).
6. H. G. Hertz. Ber. Bunsenges Physik Chem. **67**, 311 (1963).
7. R. C. Axtmann. J. Chem. Phys. **30**, 340 (1959).
8. W. B. Lewis, J. A. Jackson, and H. Taube. J. Chem. Phys. **32**, 553 (1960).
9. W. B. Lewis, J. A. Jackson, F. Lemons, and H. Taube. J. Chem. Phys. **36**, 694 (1962).
10. J. H. Swinheart and H. Taube. J. Chem. Phys. **37**, 1579 (1962).
11. R. E. Connick and R. E. Poulson. J. Chem. Phys. **30**, 759 (1959).
12. R. E. Connick and D. E. Stover. J. Phys. Chem. **65**, 2075 (1961).
13. T. J. Swift and R. E. Connick. J. Chem. Phys. **37**, 307 (1962).
14. R. E. Connick and D. N. Fiat. J. Chem. Phys. **39**, 1349 (1963).
15. A. Carrington and T. Hines. J. Chem. Phys. **28**, 727 (1958).
16. A. Carrington, F. Dravnicks, and M. C. R. Symons. Mol. Phys. **3**, 174 (1960).
17. R. E. Connick and R. E. Poulson. J. Phys. Chem. **62**, 1002 (1958).
18. R. A. Craig and R. E. Richards. Trans. Faraday Soc. **59**, 1075 (1959).
19. Z. Luz and G. Yagil. J. Phys. Chem. **70**, 554 (1966).
20. N. T. L. Ten Broeck, Jr. and P. A. van der Muelen. J. Am. Chem. Soc. **53**, 3596 (1931).
21. R. Haque and L. W. Reeves. J. Phys. Chem. **70** (1966). In press.
22. K. J. Packer and E. L. Muetterties. Proc. Chem. Soc. 147 (1964).
23. K. Kuhlmann and D. M. Grant. J. Phys. Chem. **68**, 3208 (1964).

Received June 15, 1966.
Department of Chemistry,
University of British Columbia,
Vancouver, British Columbia.

SOLVENT DEPENDENCE OF ^{29}Si—^{19}F COUPLING CONSTANT IN SILICON TETRAFLUORIDE. THE IMPORTANCE OF INTERMOLECULAR DISPERSION INTERACTIONS

H. M. Hutton,[1] E. Bock, and T. Schaefer

Solvent dependent nuclear spin–spin coupling constants are observable in a variety of neutral molecules (1–16). For the most part, the interpretation of these observations are qualitative or even speculative in nature, but Watts and Goldstein (10) attempt to show that the geminal proton–proton coupling in α-chloroacrylonitrile depends on the reaction

[1]*Research Associate, Summer 1966. Permanent address: Brandon College, Brandon, Manitoba.*

Can. J. Chem. Downloaded from www.nrcresearchpress.com by 210.87.254.5 on 09/05/12
For personal use only.

field of the medium. Temperature studies on this molecule throw some doubt on this explanation (15). In the case of directly bonded nuclei, Evans (2) presents evidence that hydrogen bonding is a factor in the solvent dependence of $^{13}C—^{1}H$ coupling in chloroform, whereas Bell and Danyluk (14) argue for the dependence of $^{13}C—^{1}H$ and $^{13}C—^{19}F$ couplings in *cis*- and *trans*-dichlorofluoroethylene on the reaction field of the solvent.

Coyle, Johannesen, Brinckman, and Farrar (16) demonstrate a substantial change in the $^{29}Si—^{19}F$ coupling in SiF_4 as a function of solvent and suggest that specific interactions between solute and solvent molecules may be responsible. Since SiF_4 is nonpolar, the data afford an opportunity to see whether intermolecular dispersion interactions affect the coupling, perhaps by a mechanism similar to that affecting the chemical shift (17–21). The calculation of these interactions involves a knowledge, among other things, of the polarizability, the ionization potential, certain absorption frequencies, and intermolecular distances of approach for the solute–solvent system. For most of the solvents employed by Coyle *et al.* (16) this information is not available.

However, Buckingham, Schaefer, and Schneider (17) find a rough proportionality between the gas-to-solvent shift of methane in a number of halogenated solvents and the heat of vaporization, H_b, of the solvent at its boiling point chosen to approximate "corresponding" states. H_b is a measure of the interaction between like solvent molecules but, if the interactions are simple dispersion forces, a proportionality of the corresponding interaction of the solvent molecules with the common solute molecule may be expected. H_b can be calculated from the formula

$$[1] \qquad H_b \text{ (cal)} = 17.0T_b + 0.009T_b^2,$$

as shown by Hildebrand and Scott (22). Linder (23) shows that there is a rough correlation between the dispersion free energy and the energy of vaporization of the solvent. By this means it can be tested whether the change in the $^{29}Si—^{19}F$ coupling is dependent on dispersion forces in solution.

In Fig. 1 the values of the $^{29}Si—^{19}F$ coupling in SiF_4 from Coyle *et al.* (16) are plotted versus H_b as obtained from the boiling points of the solvent. The mean deviation from the illustrative straight line is about 10% of the total variation of the coupling. The measurements were made at 28 °C and those solvents with calculated H_b values of less than 6 kcal/mole all boil below this temperature at 1 atm. The largest scatter occurs in this region of the plot.[2] Note also that a considerable variation of the coupling with temperature is found in $CClF_3$ (see Fig. 1). As the density of the solvent changes the dispersion interactions will also change, as is found in chemical shift measurements (24).[3] Further, the concentration of SiF_4 may deviate considerably from the estimated 15% (16) in this region. Finally, the calculated H_b is not a completely faithful measure of dispersion interactions between the nonpolar SiF_4 molecule and the, for the most part, polar solvent molecules.[4]

In view of the above remarks we consider the plot to indicate that the variation in the $^{29}Si—^{19}F$ coupling can be attributed mainly to time varying electric fields, i.e. dispersion interactions, which alter the net electronic state of the SiF_4 molecule. Because of the scatter in Fig. 1, however, specific interactions with donor solvent molecules cannot be ruled out in all cases.

From Fig. 1 it is evident that the magnitude of the $^{29}Si—^{19}F$ coupling in c.p.s. increases as the intermolecular dispersion interactions increase. For first row nuclei, Pople and

[2] C_6F_6 *deviates particularly strongly, as do those molecules containing* only *fluorine as halogen.*
[3] *A better temperature of measurement would be at the boiling point of each solvent.*
[4] *Thus, chloroform, with a dipole moment of 1.02 D, has an electrostatic energy of 0.24 kcal/mole at its normal boiling point (23).*

Can. J. Chem. Downloaded from www.nrcresearchpress.com by 210.87.254.5 on 09/05/12
For personal use only.

Santry (25) calculate a negative reduced coupling to fluorine, which is the coupling in c.p.s. divided by the product of the magnetogyric ratios of the coupled nuclei. Since this product is negative for Si—F, the measured coupling in c.p.s. will be positive[5] *if* the Pople and Santry theory holds. In terms of their theory, an increased dispersion interaction with solvent molecules leads to a lower excitation energy between the highest bonding and lowest anti-bonding molecular orbitals in the Si—F bond (this may be a result of the expansion of the electron clouds in the molecule by the dispersion interactions). Such a possibility should stimulate someone with ^{19}F resonance equipment to make similar measurements on CF_4.

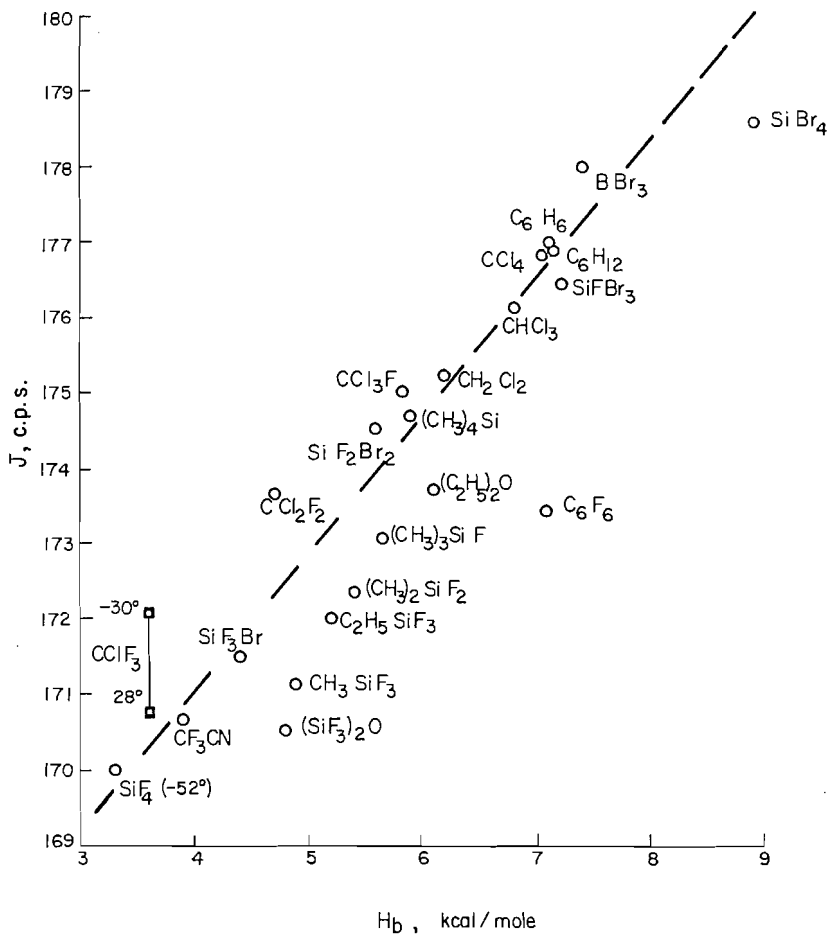


FIG. 1. The ^{29}Si—^{19}F coupling constant in c.p.s. in SiF_4 is plotted versus the heat of vaporization, H_b, in kcal/mole of the solvent as calculated from eq. [1] in the text. The concentrations are roughly 15% and the temperature of measurement, unless otherwise indicated, is 28 °C. The precision of the coupling constant values is at least ±0.1 c.p.s.

ACKNOWLEDGMENTS

We thank a referee for helpful comments. We are grateful to the National Research Council for financial aid.

[5]*Danyluk (26) shows that this is very likely true by double resonance experiments.*

Can. J. Chem. Downloaded from www.nrcresearchpress.com by 210.87.254.5 on 09/05/12
For personal use only.

1. H. M. HUTTON and T. SCHAEFER. Can. J. Chem. **41**, 684 (1963).
2. D. F. EVANS. J. Chem. Soc. 5575 (1963).
3. V. S WATTS, G. S. REDDY, and J. H. GOLDSTEIN. J. Mol. Spectry. **11**, 325 (1963).
4. B. L. SHAPIRO, S. J. EBERSOLE, and R. M. KOPCHIK. J. Mol. Spectry. **11**, 326 (1963); J. Chem. Phys. **39**, 3154 (1963).
5. S. G. FRANKISS. J. Phys. Chem. **67**, 752 (1963).
6. P. BATES, S. CAWLEY, and S. S. DANYLUK. J. Chem. Phys. **40**, 2415 (1964).
7. G. J. MARTIN and M. L. MARTIN. J. Chim. Phys. **61**, 1222 (1964).
8. S. NG, J. TANG, and C. H. SEDERHOLM. J. Chem. Phys. **42**, 79 (1965).
9. V. S. WATTS, J. LOEMKER, and J. H. GOLDSTEIN. J. Mol. Spectry. **17**, 348 (1965).
10. V. S. WATTS and J. H. GOLDSTEIN. J. Chem. Phys. **42**, 228 (1965).
11. S. L. SMITH and R. H. COX. J. Mol. Spectry. **16**, 216 (1965).
12. P. LASZLO and H. J. T. BOS. Tetrahedron Letters, 1325 (1965).
13. H. M. HUTTON and T. SCHAEFER. Can. J. Chem. **43**, 3116 (1965).
14. C. L. BELL and S. S. DANYLUK. J. Am. Chem. Soc. **88**, 2344 (1966).
15. K. A. MCLAUCHLAN, L. W. REEVES, and T. SCHAEFER. Can. J. Chem. **44**, 1473 (1966).
16. T. D. COYLE, R. B. JOHANNESEN, F. E. BRINCKMAN, and T. C. FARRAR. J. Phys. Chem. **70**, 1682 (1966).
17. A. D. BUCKINGHAM, T. SCHAEFER, and W. G. SCHNEIDER. J. Chem. Phys. **32**, 1227 (1960).
18. B. B. HOWARD, B. LINDER, and M. T. EMERSON. J. Chem. Phys. **36**, 485 (1962).
19. W. T. RAYNES, A. D. BUCKINGHAM, and H. J. BERNSTEIN. J. Chem. Phys. **36**, 3481 (1962).
20. L. PETRAKIS and H. J. BERNSTEIN. J. Chem. Phys. **37**, 2731 (1962); **38**, 1562 (1963).
21. F. H. A. RUMMENS and H. J. BERNSTEIN. J. Chem. Phys. **43**, 2971 (1965).
22. J. H. HILDEBRAND and R. L. SCOTT. The solubility of nonelectrolytes. 3rd. ed. Dover Publications, Inc., New York. 1964. p. 427.
23. B. LINDER. J. Chem. Phys. **33**, 668 (1960).
24. S. GORDON and B. P. DAILEY. J. Chem. Phys. **34**, 1084 (1961).
25. J. A. POPLE and D. P. SANTRY. Mol. Phys. **8**, 1 (1964).
26. S. S. DANYLUK. J. Am. Chem. Soc. **86**, 4504 (1964).

RECEIVED JUNE 21, 1966.
CHEMISTRY DEPARTMENT,
UNIVERSITY OF MANITOBA,
WINNIPEG, MANITOBA.

PREPARATION AND CHARACTERIZATION OF SOME BINARY AND TERNARY COMPLEXES OF BENZOYLTRIFLUOROACETONE AND PHOSPHORUS ESTERS[1]

G. N. RAO AND N. C. LI

As part of our program (1–3) on the investigation of metal complexes involved in solvent extraction, we report here the preparation and characterization of several binary and ternary metal complexes of benzoyltrifluoroacetone and phosphorus compounds. The isolation and investigation of solid complexes are important because any information about their stoichiometry, stability, solubility, and spectral characteristics is a contribution to the problems of synergism in solvent extraction.

EXPERIMENTAL

Materials

Benzoyltrifluoroacetone (HBTA), tri-*n*-octyl phosphine oxide (TOPO), and triphenyl phosphine oxide (TPPO) were obtained from Peninsular ChemResearch, Inc. Their infrared spectra agree with those reported in the literature. Carbon tetrachloride, benzene, and acetone were Spectranalyzed Fisher Certified.

Instrumental

Infrared spectra were obtained with a Perkin–Elmer Model 137 spectrophotometer using Nujol mull. Absorption spectra were taken on a Cary Model 14 spectrophotometer with 5 cm cells at room temperature (25°). Proton magnetic resonance measurements were obtained with an A-60 NMR spectrometer. Chemical shifts of the signals were measured with respect to tetramethylsilane as an internal standard.

[1]*This investigation was supported by the U.S. Atomic Energy Commission Contract No. AT(30-1)-1922. Paper No. NYO-1922-36.*

Can. J. Chem. Downloaded from www.nrcresearchpress.com by 210.87.254.5 on 09/05/12
For personal use only.

1. H. M. HUTTON and T. SCHAEFER. Can. J. Chem. **41**, 684 (1963).
2. D. F. EVANS. J. Chem. Soc. 5575 (1963).
3. V. S WATTS, G. S. REDDY, and J. H. GOLDSTEIN. J. Mol. Spectry. **11**, 325 (1963).
4. B. L. SHAPIRO, S. J. EBERSOLE, and R. M. KOPCHIK. J. Mol. Spectry. **11**, 326 (1963); J. Chem. Phys. **39**, 3154 (1963).
5. S. G. FRANKISS. J. Phys. Chem. **67**, 752 (1963).
6. P. BATES, S. CAWLEY, and S. S. DANYLUK. J. Chem. Phys. **40**, 2415 (1964).
7. G. J. MARTIN and M. L. MARTIN. J. Chim. Phys. **61**, 1222 (1964).
8. S. NG, J. TANG, and C. H. SEDERHOLM. J. Chem. Phys. **42**, 79 (1965).
9. V. S. WATTS, J. LOEMKER, and J. H. GOLDSTEIN. J. Mol. Spectry. **17**, 348 (1965).
10. V. S. WATTS and J. H. GOLDSTEIN. J. Chem. Phys. **42**, 228 (1965).
11. S. L. SMITH and R. H. COX. J. Mol. Spectry. **16**, 216 (1965).
12. P. LASZLO and H. J. T. BOS. Tetrahedron Letters, 1325 (1965).
13. H. M. HUTTON and T. SCHAEFER. Can. J. Chem. **43**, 3116 (1965).
14. C. L. BELL and S. S. DANYLUK. J. Am. Chem. Soc. **88**, 2344 (1966).
15. K. A. MCLAUCHLAN, L. W. REEVES, and T. SCHAEFER. Can. J. Chem. **44**, 1473 (1966).
16. T. D. COYLE, R. B. JOHANNESEN, F. E. BRINCKMAN, and T. C. FARRAR. J. Phys. Chem. **70**, 1682 (1966).
17. A. D. BUCKINGHAM, T. SCHAEFER, and W. G. SCHNEIDER. J. Chem. Phys. **32**, 1227 (1960).
18. B. B. HOWARD, B. LINDER, and M. T. EMERSON. J. Chem. Phys. **36**, 485 (1962).
19. W. T. RAYNES, A. D. BUCKINGHAM, and H. J. BERNSTEIN. J. Chem. Phys. **36**, 3481 (1962).
20. L. PETRAKIS and H. J. BERNSTEIN. J. Chem. Phys. **37**, 2731 (1962); **38**, 1562 (1963).
21. F. H. A. RUMMENS and H. J. BERNSTEIN. J. Chem. Phys. **43**, 2971 (1965).
22. J. H. HILDEBRAND and R. L. SCOTT. The solubility of nonelectrolytes. 3rd. ed. Dover Publications, Inc., New York. 1964. p. 427.
23. B. LINDER. J. Chem. Phys. **33**, 668 (1960).
24. S. GORDON and B. P. DAILEY. J. Chem. Phys. **34**, 1084 (1961).
25. J. A. POPLE and D. P. SANTRY. Mol. Phys. **8**, 1 (1964).
26. S. S. DANYLUK. J. Am. Chem. Soc. **86**, 4504 (1964).

RECEIVED JUNE 21, 1966.
CHEMISTRY DEPARTMENT,
UNIVERSITY OF MANITOBA,
WINNIPEG, MANITOBA.

PREPARATION AND CHARACTERIZATION OF SOME BINARY AND TERNARY COMPLEXES OF BENZOYLTRIFLUOROACETONE AND PHOSPHORUS ESTERS[1]

G. N. RAO AND N. C. LI

As part of our program (1–3) on the investigation of metal complexes involved in solvent extraction, we report here the preparation and characterization of several binary and ternary metal complexes of benzoyltrifluoroacetone and phosphorus compounds. The isolation and investigation of solid complexes are important because any information about their stoichiometry, stability, solubility, and spectral characteristics is a contribution to the problems of synergism in solvent extraction.

EXPERIMENTAL

Materials

Benzoyltrifluoroacetone (HBTA), tri-*n*-octyl phosphine oxide (TOPO), and triphenyl phosphine oxide (TPPO) were obtained from Peninsular ChemResearch, Inc. Their infrared spectra agree with those reported in the literature. Carbon tetrachloride, benzene, and acetone were Spectranalyzed Fisher Certified.

Instrumental

Infrared spectra were obtained with a Perkin–Elmer Model 137 spectrophotometer using Nujol mull. Absorption spectra were taken on a Cary Model 14 spectrophotometer with 5 cm cells at room temperature (25°). Proton magnetic resonance measurements were obtained with an A-60 NMR spectrometer. Chemical shifts of the signals were measured with respect to tetramethylsilane as an internal standard.

[1]*This investigation was supported by the U.S. Atomic Energy Commission Contract No. AT(30-1)-1922. Paper No. NYO-1922-36.*

Can. J. Chem. Downloaded from www.nrcresearchpress.com by 210.87.254.6 on 09/05/12
For personal use only.

Preparation of Solid Complexes

The following compounds have *not* been reported previously.

Binary Complexes

$UO_2(BTA)_2$.—To a solution of uranyl acetate (4.24 g) in 100 ml water, HBTA (4.32 g) in 50 ml ethanol was added slowly with stirring. The yellow precipitate which was formed immediately was filtered off, washed with water and ethanol, and dried over P_2O_5 in a vacuum desiccator. When this compound was heated at 115° for 2 h, the anhydrous compound $UO_2(BTA)_2$ was obtained; m.p. 156°. The infrared spectrum of this compound shows no peaks in the OH-stretching region.

Anal. Calcd. for $UC_{20}H_{12}O_6F_6$: C, 34.28; H, 1.73. Found: C, 34.32; H, 2.12.

The following binary complexes were prepared in a similar manner.

$Cd(BTA)_2.2H_2O$.—Anal. Calcd. for $CdC_{20}H_{16}O_6F_6$: C, 41.50; H, 2.65; Cd, 19.44. Found: C, 41.45; H, 2.80; Cd, 19.50. Melting point 99°.

$Zn(BTA)_2.2H_2O$.—Anal. Calcd. for $ZnC_{20}H_{16}O_6F_6$: C, 45.18; H, 3.43; Zn, 12.31. Found: C, 45.01; H, 3.36; Zn, 12.45. Melting point 118°.

$Pb(BTA)_2$.—Anal. Calcd. for $PbC_{20}H_{12}O_4F_6$: C, 37.70; H, 1.90. Found: C, 37.83; H, 2.00. Melting point 194°.

Ternary Complexes

$UO_2(BTA)_2.TOPO$.—Uranyl acetate (4.24 g) dissolved in 100 ml water was shaken with 100 ml of a hexane solution containing HBTA (4.32 g) and TOPO (3.87 g). The intense yellow-colored hexane layer was separated and evaporated to about 1/10 of its volume. The ternary complex separated out after keeping the hexane solution for 1 day in a refrigerator. The solid was filtered off, washed with hexane, and dried over P_2O_5 in a vacuum desiccator; m.p. 59°.

Anal. Calcd. for $UC_{44}H_{63}O_7F_6P$: C, 48.60; H, 5.84. Found: C, 48.73; H, 5.78.

The following compounds were prepared in the manner described for $UO_2(BTA)_2.TOPO$.

$UO_2(BTA)_2.TBP$.—Anal. Calcd. for $UC_{32}H_{39}O_{10}F_6P$: C, 39.74; H, 4.06. Found: C, 39.80; H, 3.96. Melting point 89°.

$Zn(BTA)_2.TPPO$.—Anal. Calcd. for $ZnC_{38}H_{27}O_5F_6P$: C, 58.95; H, 3.51; Zn, 8.45. Found: C, 59.15; H, 3.71; Zn, 8.33. Melting point 168°.

$Cd(BTA)_2(TPPO)_2$.—Anal. Calcd. for $CdC_{56}H_{42}O_6F_6P_2$: C, 61.20; H, 3.82; Cd, 10.23. Found: C, 61.30; H, 3.89; Cd, 10.30. Melting point 185°.

In the above preparations with TPPO as adduct, benzene was used instead of hexane. The metal content was analyzed by complexometric titration with ethylenediaminetetraacetic acid. Analysis for carbon and hydrogen was done by A. Bernhardt, Germany.

$Cd(BTA)_2.TOPO$ and $Zn(BTA)_2.TOPO$ were obtained as oils. The proton magnetic resonance spectrum of $Zn(BTA)_2.TOPO$ in CCl_4 was integrated and the ratio of the vinyl proton signal in BTA to those of the tri-*n*-octyl protons in TOPO was 2:50 (calcd. 2:51). The agreement between the experimental and calculated ratios establishes the ratio of BTA:TOPO in $Zn(BTA)_2.TOPO$.

RESULTS AND DISCUSSION

Infrared Spectra

The infrared spectra of most of the complexes reported in this paper were measured as Nujol mulls. The spectra of $Cd(BTA)_2.2H_2O$, $Zn(BTA)_2.2H_2O$, and $Mn(BTA)_2.2H_2O$ show broad peaks in the 3 350 – 3 500 cm^{-1} region, which are assigned to the OH-stretching frequency of coordinated water. For the ternary complexes $UO_2(BTA)_2.TBP$, $UO_2(BTA)_2.TOPO$, $Cd(BTA)_2(TPPO)_2$, $Cd(BTA)_2.TOPO$, $Zn(BTA)_2.TPPO$, and $Zn(BTA)_2.TOPO$, the 3 500 cm^{-1} region is free of absorption, indicating the absence of coordinated water in these adducts.

The displacement of the phosphoryl (P → O) stretching frequencies in TBP, TPPO, and TOPO to lower frequencies, on formation of the above ternary complexes, had been observed. This could indicate that oxygen is bonded directly to the metal, and has been pointed out by Ferraro and Healy (4) for the ternary complexes of metal thenoyltrifluoroacetone–phosphorus ester.

Since previous investigators (5–7) have discussed the relation between the order of carbonyl stretching frequency to the stability order of metal acetylacetonates, it is interesting to examine such a relation for the metal benzoyltrifluoroacetonates, $M(BTA)_2.2H_2O$. The order of C=O stretching frequency is: Cd = Zn = Pb, 1 613; Mn, 1 610; Cu, 1 597 cm^{-1}. On the other hand, the order (8) of stability constants (as log of

Can. J. Chem. Downloaded from www.nrcresearchpress.com by 210.87.254.6 on 09/05/12
For personal use only.

formation constants) is: Zn, 7.30; Cd, 7.60; Mn, 8.20; Cu, 13.2. Thus it is seen that a qualitative relation exists between the strength of metal–oxygen bond, as obtained from stability constants, and the frequency of the perturbed carbonyl absorptions. On the other hand the magnitudes of the frequency shifts do not match the differences in stability constants, so that there is no apparent quantitative agreement. Nakamoto, McCarthy, and Martell (7) have assumed that for the metal acetylacetonates, correlation of stability with frequency would occur only for metals of similar covalent radii and similar mass.

Visible Spectral Studies

The visible spectra of $Cu(BTA)_2$ in benzene, in the presence of varying amounts of TBP, reveal the presence of a single well-defined isosbestic point at 611 mμ. A plot of ϵ at 675 mμ vs. 1/[TBP] gave a limiting value of $\epsilon_\infty = 61.7$. By the method of Graddon and Watton (9), we have calculated the equilibrium constant K of the reaction

$$Cu(BTA)_2 + TBP = Cu(BTA)_2.TBP$$

to be 80.7 ± 2.2 l mole^{-1}.

The visible spectra of $Cu(BTA)_2$ (2×10^{-3} M in benzene) in the presence of increasing amounts of TOPO ($2\text{–}100 \times 10^{-3}$ M) were also obtained. In contrast to the $Cu(BTA)_2$.TBP system, however, no single isosbestic point was observed. With increasing amount of TOPO, the spectra shifted to longer wavelengths. The intensity of absorption maxima increased and then decreased as the concentration of TOPO was increased. The possibility of formation of adducts containing more than 1 mole of TOPO is indicated. In the region of [TOPO] = $4\text{–}15 \times 10^{-3}$ M, the equilibrium constant of the reaction

$$Cu(BTA)_2 + TOPO = Cu(BTA)_2.TOPO$$

was determined to be 770 ± 45. When the adduct is TPPO instead of TOPO, the visible spectra gave results similar to the TOPO system, and the value of K was determined to be 505 ± 65 l mole^{-1} at 25°.

The values of K for $Cu(BTA)_2$.TBP, $Cu(BTA)_2$.TPPO, and $Cu(BTA)_2$.TOPO indicate therefore that the electron-donor ability of the phosphorus compounds increases in the order TBP < TPPO < TOPO, and is in agreement with the order of stability constants found for $Cu(TTA)_2$.TBP, $Cu(TTA)_2$.TPPO, and $Cu(TTA)_2$.TOPO (10), where TTA is thenoyltrifluoroacetone anion. This order also agrees with the finding of Li, Wang, and Walker (3) that in the Zn–TTA system, the efficiency in synergistic solvent extraction on adding a phosphorus compound falls in the order: TBP < TPPO < TOPO.

Solubility Studies

The binary $M(BTA)_2$ and $M(BTA)_2.2H_2O$ complexes are slightly soluble in carbon tetrachloride, benzene, chloroform, hexane, alcohol, and water, but dissolve in acetone and dimethyl sulfoxide. The metal–BTA adducts with TOPO, however, are highly soluble in hexane and CCl_4. This enhanced solubility in the nonpolar organic phase of neutral metal–BTA chelates caused by adduct formation with a phosphorus compound is considered to play an important part in the synergistic extraction of metals, and has been pointed out for metal–TTA systems by Walker and Li (2).

ACKNOWLEDGMENTS

The authors thank the U.S. Atomic Energy Commission for support of this research, and acknowledge the assistance of a U.S. National Science Foundation equipment grant for the purchase of a Cary Model 14 spectrophotometer. We also wish to thank Dr.

Can. J. Chem. Downloaded from www.nrcresearchpress.com by 210.87.254.6 on 09/05/12
For personal use only.

S. M. Wang for a helpful discussion and for a proton magnetic resonance analysis of the ternary complex $Zn(BTA)_2.TOPO$.

1. R. L. Scruggs, T. Kim, and N. C. Li. J. Phys. Chem. **67**, 2194 (1963).
2. W. R. Walker and N. C. Li. J. Inorg. Nucl. Chem. **27**, 411 (1965).
3. N. C. Li, S. M. Wang, and W. R. Walker. J. Inorg. Nucl. Chem. **27**, 2263 (1965).
4. J. R. Ferraro and T. V. Healy. J. Inorg. Nucl. Chem. **24**, 1463 (1962).
5. H. F. Holtzclaw and J. P. Collman. J. Am. Chem. Soc. **79**, 3318 (1957).
6. R. West and R. Riley. J. Inorg. Nucl. Chem. **5**, 295 (1958).
7. K. Nakamoto, P. J. McCarthy, and A. E. Martell. J. Am. Chem. Soc. **83**, 1272 (1961).
8. A. E. Martell and M. Calvin. Chemistry of the metal chelate compounds. Prentice-Hall Inc., New York. 1952.
9. D. P. Graddon and E. C. Watton. J. Inorg. Nucl. Chem. **21**, 49 (1961).
10. C. H. Ke and N. C. Li. J. Inorg. Nucl. Chem. In press.

Received May 10, 1966.
Department of Chemistry,
Duquesne University,
Pittsburgh, Pennsylvania.

THE INITIATION OF PROPYLENE PYROLYSIS

R. M. Marshall, J. H. Purnell, and B. C. Shurlock

Possible homogeneous initiation steps in the pyrolysis of propylene are:

[1] $$C_3H_6 \rightarrow CH_2{=}CH{-}\dot{C}H_2 + H\cdot$$

[2] $$C_3H_6 \rightarrow CH_3\cdot + C_2H_3\cdot$$

[3] $$C_3H_6 \rightarrow CH_2{=}\dot{C}{-}CH_3 + H\cdot$$

[4] $$2C_3H_6 \rightarrow CH_2{=}CH{-}CH_2\cdot + n\text{-}C_3H_7\cdot \quad .$$

Reaction [3] may be discounted immediately since, although its A factor is likely to compare with that of [1], its activation energy must be substantially higher because there is no possibility of resonance stabilization of the resulting radicals.

Until recently, reaction [1] has been favored over all others (1) because of the belief that the allyl resonance energy (Q) was about 22 kcal mole^{-1} (2). Recent kinetic studies (3), however, yield results which are more consistent with a value of about 12 kcal mole^{-1}. This finding leads us to reassess the relative importance of reactions [1] and [2] and it is appropriate also to consider reaction [4], since the reaction comparable with [−4], involving ethyl and allyl radicals, has recently been studied (4).

The thermochemical data employed in the calculations are listed in Table I.

TABLE I

Thermodynamic data used in calculations*

	H·	CH_3·	C_2H_3·	C_2H_4†	C_3H_5·	C_3H_6†	n-C_3H_7·
S_{873}^0	32.7	58.6	73.2	69.1	89.6	88.8	97.3
$H_{873}^0 - H_{298}^0$	2.8	6.8‡	9.5	9.5	14.2	14.2	15.9‡
ΔH_{298f}^0	52.1	32.0§	65‖	12.5	50.2−Q¶	4.9	20.5¶

*All enthalpies in kcal mole^{-1}; entropies quoted are for the ideal gas at 1 atm pressure.
†Reference 7.
‡Calculated from the structural assignments in ref. 5.
§Reference 9.
‖Reference 8.
¶From data of ref. 6.

Can. J. Chem. Downloaded from www.nrcresearchpress.com by 210.87.254.6 on 09/05/12
For personal use only.

S. M. Wang for a helpful discussion and for a proton magnetic resonance analysis of the ternary complex $Zn(BTA)_2$.TOPO.

1. R. L. Scruggs, T. Kim, and N. C. Li. J. Phys. Chem. **67**, 2194 (1963).
2. W. R. Walker and N. C. Li. J. Inorg. Nucl. Chem. **27**, 411 (1965).
3. N. C. Li, S. M. Wang, and W. R. Walker. J. Inorg. Nucl. Chem. **27**, 2263 (1965).
4. J. R. Ferraro and T. V. Healy. J. Inorg. Nucl. Chem. **24**, 1463 (1962).
5. H. F. Holtzclaw and J. P. Collman. J. Am. Chem. Soc. **79**, 3318 (1957).
6. R. West and R. Riley. J. Inorg. Nucl. Chem. **5**, 295 (1958).
7. K. Nakamoto, P. J. McCarthy, and A. E. Martell. J. Am. Chem. Soc. **83**, 1272 (1961).
8. A. E. Martell and M. Calvin. Chemistry of the metal chelate compounds. Prentice-Hall Inc., New York. 1952.
9. D. P. Graddon and E. C. Watton. J. Inorg. Nucl. Chem. **21**, 49 (1961).
10. C. H. Ke and N. C. Li. J. Inorg. Nucl. Chem. In press.

Received May 10, 1966.
Department of Chemistry,
Duquesne University,
Pittsburgh, Pennsylvania.

THE INITIATION OF PROPYLENE PYROLYSIS

R. M. Marshall, J. H. Purnell, and B. C. Shurlock

Possible homogeneous initiation steps in the pyrolysis of propylene are:

[1] $$C_3H_6 \rightarrow CH_2{=}CH{-}\dot{C}H_2 + H\cdot$$

[2] $$C_3H_6 \rightarrow CH_3\cdot + C_2H_3\cdot$$

[3] $$C_3H_6 \rightarrow CH_2{=}\dot{C}{-}CH_3 + H\cdot$$

[4] $$2C_3H_6 \rightarrow CH_2{=}CH{-}CH_2\cdot + n\text{-}C_3H_7\cdot \quad .$$

Reaction [3] may be discounted immediately since, although its A factor is likely to compare with that of [1], its activation energy must be substantially higher because there is no possibility of resonance stabilization of the resulting radicals.

Until recently, reaction [1] has been favored over all others (1) because of the belief that the allyl resonance energy (Q) was about 22 kcal mole^{-1} (2). Recent kinetic studies (3), however, yield results which are more consistent with a value of about 12 kcal mole^{-1}. This finding leads us to reassess the relative importance of reactions [1] and [2] and it is appropriate also to consider reaction [4], since the reaction comparable with [−4], involving ethyl and allyl radicals, has recently been studied (4).

The thermochemical data employed in the calculations are listed in Table I.

TABLE I

Thermodynamic data used in calculations*

	H·	CH_3·	C_2H_3·	C_2H_4†	C_3H_5·	C_3H_6†	n-C_3H_7·
S_{873}^0	32.7	58.6	73.2	69.1	89.6	88.8	97.3
$H_{873}^0 - H_{298}^0$	2.8	6.8‡	9.5	9.5	14.2	14.2	15.9‡
ΔH_{298f}^0	52.1	32.0§	65‖	12.5	50.2−Q¶	4.9	20.5¶

*All enthalpies in kcal mole^{-1}; entropies quoted are for the ideal gas at 1 atm pressure.
†Reference 7.
‡Calculated from the structural assignments in ref. 5.
§Reference 9.
‖Reference 8.
¶From data of ref. 6.

Can. J. Chem. Downloaded from www.nrcresearchpress.com by 210.87.254.5 on 09/05/12
For personal use only.

In the absence of reliable values for the entropy and enthalpy of vinyl and of allyl radicals we assume that these are the same as those of the parent olefin except where symmetry and electron degeneracy corrections are needed. As is usual in considering radical–radical reactions, reactions [−1] and [−2] are regarded, at this stage, as proceeding with no energy of activation and with unit collision efficiency. For the disproportionation reaction [−4] calculations, we have employed the measured ratio of disproportionation to combination for the similar reaction of ethyl with allyl at 150 °C (4), whereas for the combination reaction we have again made the assumption stated above. On this basis we obtain the rate parameters listed in Table II.

TABLE II

Calculated rate parameters

	Reaction		
	[1]	[2]	[4]
$\text{Log}_{10}A$*	15.7	17.8	14.4
E†	$100-Q$	94	$63-Q$

*Units of cc mole s.
†Units of kcal mole^{-1} rounded to nearest whole number.

At 873 °K, roughly the midpoint of the temperature range used in static experiments, the tabulated data yield $k_2 = 10^{-5.7}$ s^{-1}. In order that $k_1 > k_2$ it follows that $E_1 < 85$ kcal mole^{-1}. Thus $Q > 15$ kcal mole^{-1}. It follows that reaction [2] is, if anything, to be considered more important than [1] if recent estimates of Q are to be accepted. However, even allowing for the possible uncertainties in the calculations, it is quite certain that reaction [2] can never be neglected in comparison with [1] on the basis of present evidence.

Assuming that $Q = 12$ kcal mole^{-1}, the calculated rate of reaction [4] at about 100 mm Hg initial pressure at 873 °K is $10^{-9.8}$ mole cc^{-1} s^{-1} which may be compared with the calculated rate of reaction [2], $10^{-11.4}$ mole cc^{-1} s^{-1} for the same conditions. Obviously, therefore, reaction [4] would appear to be highly favored over [1] and [2]. However, this conclusion does not accord with the kinetic evidence.

The overall order of propylene pyrolysis in the region of 873 °K is 1.4 (1*c*, 10) and is pressure independent over the range 7–300 mm Hg. Goldfinger *et al.* (11) have shown that such a result is consistent with any of the possibilities shown in Table III.

TABLE III

Possibilities for propylene pyrolysis in the region of 873 °K

	Initiation order	Radicals involved in termination	Overall order
(*a*)	1	$\beta\beta$	3/2
(*b*)	2	$\beta\mu$	3/2
(*c*)	2	$\beta\beta$M	3/2

A detailed analytical investigation (10) of propylene pyrolysis has shown that the major termination reaction is the combination of methyl with allyl radicals, i.e. $\beta\beta$ in the above terminology. Hence, only case *a* is acceptable.

It thus follows that our calculated rate of reaction [4] must be much too high and hence also that of [−4]. This implies, in contrast to the assumptions made earlier, that radical combination reactions involving allyl proceed with either or both entropy and energy of activation. This conclusion is also drawn from different evidence elsewhere (10).

Can. J. Chem. Downloaded from www.nrcresearchpress.com by 210.87.254.5 on 09/05/12
For personal use only.

A consequence of the above considerations is that the rate of reaction [1] is also overestimated in the calculation. Thus reaction [2] should be considered the predominant initiation step on the basis of present evidence. The measured rate (10) of methyl–allyl combination, $10^{-10.4}$ mole cc^{-1} s^{-1}, at 100 mm Hg and 873 °K is found to be of the same order of magnitude as the presently calculated rate of reaction [2] in the same conditions, which must be regarded as reasonable agreement in view of the uncertainties in the thermochemical data available. Finally, since the overall rate of pyrolysis of 100 mm Hg propylene at 873 °K is $10^{-8.7}$ mole cc^{-1} s^{-1} (10), it is apparent that the pyrolysis of propylene must be regarded as a long-chain process.

The authors gratefully acknowledge the provision of maintenance grants from the Science Research Council (R. M. M.) and Central Electricity Generating Board (B. C. S.).

1. (*a*) M. Szwarc. J. Chem. Phys. **17**, 284 (1949). (*b*) K. J. Laidler and B. Wojciechowski. Proc. Roy. Soc. London, Ser. A, **259**, 257 (1961). (*c*) A. Amano and M. Uchiyama. J. Phys. Chem. **67**, 1242 (1963).
2. M. Szwarc and A. H. Sehon. J. Chem. Phys. **18**, 237 (1950). A. S. Gordon, S. R. Smith, and J. R. McNesby. J. Am. Chem. Soc. **81**, 5059 (1959).
3. R. J. Ellis and H. M. Frey. J. Chem. Soc. 5579 (1964). K. W. Egger, D. M. Golden, and S. W. Benson. J. Am. Chem. Soc. **86**, 5420 (1964). F. H. Dorer and B. S. Rabinovitch. J. Phys. Chem. **69**, 1952 (1965).
4. D. G. L. James and G. E. Troughton. Trans. Faraday Soc. **62**, 145 (1966).
5. J. H. Purnell and C. P. Quinn. J. Chem. Soc. 4049 (1964).
6. S. W. Benson and A. Amano. J. Chem. Phys. **36**, 3464 (1962).
7. F. D. Rossini *et al.* Selected values of physical and thermodynamic properties of hydrocarbons and related compounds. American Petroleum Institute, Pittsburgh. 1953.
8. A. G. Harrison and F. P. Lossing. J. Am. Chem. Soc. **82**, 519 (1960). F. W. Lampe and F. H. Field. J. Am. Chem. Soc. **81**, 3238 (1959).
9. A. F. Trotman-Dickinson. Gas kinetics. Butterworths Scientific Publications, London. 1955.
10. A. S. Kallend, J. H. Purnell, and B. C. Shurlock. To be published.
11. P. Goldfinger, M. Letort, and M. Niclause. Volume commémoratif Victor Henri, contribution a l'étude de la structure moléculaire. 1948. p. 283.

Received May 30, 1966.
Department of Chemistry,
University College of Swansea,
Singleton Park,
Swansea, Glam, U.K.

ERRATUM: ^{35}Cl AND ^{37}Cl MAGNETIC RESONANCE OF SIMPLE CHLORINE COMPOUNDS

Yasukazu Saito

(Ref. Can. J. Chem. 43, 2530 (1965))

A standard value of the chemical shift of chlorine magnetic resonance obtained by extrapolating the quadrupole coupling constants of a series of chloromethanes to zero in the equation

[i] $$\delta = \delta_d + K(\Delta E^{-1})(e^2qQ)$$

was reported previously (1).

Since the author considered that the standard value of δ_d derived above corresponded to a hypothetical state with spherical distribution of electrons of chlorine atom (not anion), a correction term was added in order to obtain the chemical shift of spherical

Can. J. Chem. Downloaded from www.nrcresearchpress.com by 210.87.254.5 on 09/05/12
For personal use only.

A consequence of the above considerations is that the rate of reaction [1] is also overestimated in the calculation. Thus reaction [2] should be considered the predominant initiation step on the basis of present evidence. The measured rate (10) of methyl–allyl combination, $10^{-10.4}$ mole cc^{-1} s^{-1}, at 100 mm Hg and 873 °K is found to be of the same order of magnitude as the presently calculated rate of reaction [2] in the same conditions, which must be regarded as reasonable agreement in view of the uncertainties in the thermochemical data available. Finally, since the overall rate of pyrolysis of 100 mm Hg propylene at 873 °K is $10^{-8.7}$ mole cc^{-1} s^{-1} (10), it is apparent that the pyrolysis of propylene must be regarded as a long-chain process.

The authors gratefully acknowledge the provision of maintenance grants from the Science Research Council (R. M. M.) and Central Electricity Generating Board (B. C. S.).

1. (*a*) M. Szwarc. J. Chem. Phys. **17**, 284 (1949). (*b*) K. J. Laidler and B. Wojciechowski. Proc. Roy. Soc. London, Ser. A, **259**, 257 (1961). (*c*) A. Amano and M. Uchiyama. J. Phys. Chem. **67**, 1242 (1963).
2. M. Szwarc and A. H. Sehon. J. Chem. Phys. **18**, 237 (1950). A. S. Gordon, S. R. Smith, and J. R. McNesby. J. Am. Chem. Soc. **81**, 5059 (1959).
3. R. J. Ellis and H. M. Frey. J. Chem. Soc. 5579 (1964). K. W. Egger, D. M. Golden, and S. W. Benson. J. Am. Chem. Soc. **86**, 5420 (1964). F. H. Dorer and B. S. Rabinovitch. J. Phys. Chem. **69**, 1952 (1965).
4. D. G. L. James and G. E. Troughton. Trans. Faraday Soc. **62**, 145 (1966).
5. J. H. Purnell and C. P. Quinn. J. Chem. Soc. 4049 (1964).
6. S. W. Benson and A. Amano. J. Chem. Phys. **36**, 3464 (1962).
7. F. D. Rossini *et al.* Selected values of physical and thermodynamic properties of hydrocarbons and related compounds. American Petroleum Institute, Pittsburgh. 1953.
8. A. G. Harrison and F. P. Lossing. J. Am. Chem. Soc. **82**, 519 (1960). F. W. Lampe and F. H. Field. J. Am. Chem. Soc. **81**, 3238 (1959).
9. A. F. Trotman-Dickinson. Gas kinetics. Butterworths Scientific Publications, London. 1955.
10. A. S. Kallend, J. H. Purnell, and B. C. Shurlock. To be published.
11. P. Goldfinger, M. Letort, and M. Niclause. Volume commémoratif Victor Henri, contribution a l'étude de la structure moléculaire. 1948. p. 283.

Received May 30, 1966.
Department of Chemistry,
University College of Swansea,
Singleton Park,
Swansea, Glam, U.K.

ERRATUM: ^{35}Cl AND ^{37}Cl MAGNETIC RESONANCE OF SIMPLE CHLORINE COMPOUNDS

Yasukazu Saito

(Ref. Can. J. Chem. 43, 2530 (1965))

A standard value of the chemical shift of chlorine magnetic resonance obtained by extrapolating the quadrupole coupling constants of a series of chloromethanes to zero in the equation

$$\delta = \delta_d + K(\Delta E^{-1})(e^2qQ) \quad [i]$$

was reported previously (1).

Since the author considered that the standard value of δ_d derived above corresponded to a hypothetical state with spherical distribution of electrons of chlorine atom (not anion), a correction term was added in order to obtain the chemical shift of spherical

Can. J. Chem. Downloaded from www.nrcresearchpress.com by 210.87.254.105 on 09/05/12
For personal use only.

chlorine anion by use of Dickinson's (2) calculation. Indeed, the paramagnetic term of the Ramsey (3) equation becomes zero if the distribution of electrons of the atom has spherical symmetry. However, the above hypothetical state is not appropriate to be taken as the standard state, since the free atom has one electron missing from the closed shell, and all chlorine compounds, including chloromethanes and chlorine aqueous ion, ought to have a common reference from the viewpoint of chemical bonds. Either the free chlorine ion or the chlorine nucleus should be regarded as the standard state of chlorine chemical shifts (4–6). The purpose of this note is to correct the results reported in ref. 1, and for this purpose the free chloride ion is adopted as the standard reference state. This state is derived, in accordance with eq. [1], by extrapolating the experimental chlorine resonance measurements for various compounds to zero quadrupole coupling constant. Since the experimental chemical shift data, δ, were measured relative to aqueous chloride ion, extrapolation according to eq. [1] yields δ_d, the diamagnetic shift of the free chloride ion relative to aqueous chloride ion. The value of δ_d, the diamagnetic screening of the free chloride ion relative to the bare nucleus, has been calculated by Dickinson (2) to be +1.15 p.p.t. (parts per thousand).

The extrapolated value for δ_d obtained from Fig. 1 of the previous paper (1) is 2.60 p.p.t. This is a more accurate value than the former value, 2.90 p.p.t., which was erroneously given as −2.90 p.p.t. in the earlier paper (1).

When Saika and Slichter's (4) equation

[ii] $$\delta_p = -(2/3)(e^2\hbar^2/m^2c^2)(1 - i)\langle r^{-3}\rangle_{av}\Delta E^{-1},$$

where i is the ionic character of the atom, is applied to some chlorine compounds, calculated values of chlorine chemical shifts can be derived from the extrapolated value. The results are shown in Table I.

TABLE I

Paramagnetic shifts in some chlorine compounds

Compound	Ionic character* (%)	ΔE† (eV)	Shift (p.p.t.) Calcd.	Obs.
Cl_2	0.0	3.67	−2.17	−2.91
CCl_4	7.0	5.25	−1.41	−3.16
$CHCl_3$	8.8	5.42	−1.34	−3.01
CH_2Cl_2	11.7	5.77	−1.22	−2.82
CH_3Cl	17.1	6.0	−1.1	−2.64

*Data were taken from ref. 10.
†Data of electronic absorption were used, including an assumed value for CH_3Cl from extrapolation. References were cited in the previous paper (1).

The paramagnetic contribution to the chemical shift of the chlorine aqueous ion due to hydration is −2.60 p.p.t. and this value can be compared with the analogous parameter for the fluorine ion shown by Saika and Slichter (4) to be −1.45 p.p.t. Paramagnetic shifts of simple chlorine compounds on the present revised basis are compared with the corresponding fluorine compounds in Fig. 1. Experimental data of fluorine chemical shifts (7–9) were rearranged, with Saika and Slichter's F^- ion as standard.

The author is very much indebted to Dr. R. G. Kidd for pointing out the error and ambiguity in the previous paper and is also thankful to Dr. W. G. Schneider and Dr. A. Saika for their comments.

Can. J. Chem. Downloaded from www.nrcresearchpress.com by 210.87.254.105 on 09/05/12
For personal use only.

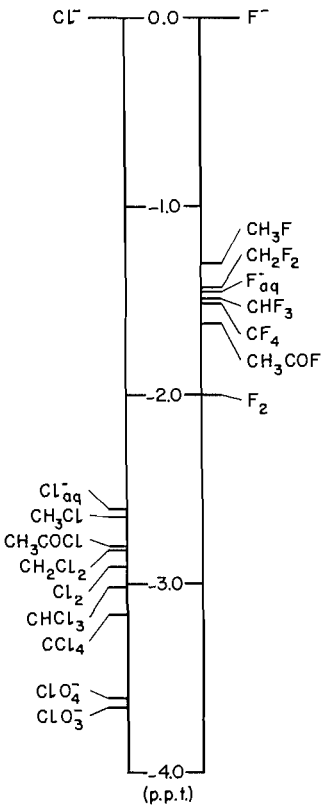


FIG. 1. Paramagnetic shifts of some chlorine and fluorine compounds.

1. Y. SAITO. Can. J. Chem. **43**, 2530 (1965).
2. W. C. DICKINSON. Phys. Rev. **80**, 563 (1950).
3. N. F. RAMSEY. Phys. Rev. **78**, 699 (1950).
4. A. SAIKA and C. P. SLICHTER. J. Chem. Phys. **22**, 26 (1954).
5. M. R. BAKER, C. H. ANDERSON, and N. F. RAMSEY. Phys. Rev. **133**, A1533 (1964).
6. C. D. CORNWALL. J. Chem. Phys. **44**, 874 (1966).
7. H. S. GUTOWSKY and C. J. HOFFMAN. J. Chem. Phys. **19**, 1259 (1951).
8. L. H. MEYER and H. S. GUTOWSKY. J. Phys. Chem. **57**, 481 (1953).
9. G. A. OLAH, S. J. KUHN, W. S. TOLGYESI, and E. B. BAKER. J. Am. Chem. Soc. **84**, 2736 (1962).
10. EIICHI HAMANO. Nippon Kagaku Zasshi, **77**, 746 (1956).

DEPARTMENT OF SYNTHETIC CHEMISTRY,
FACULTY OF ENGINEERING,
UNIVERSITY OF TOKYO,
HONGO, BUNKYO-KU,
TOKYO, JAPAN.

Can. J. Chem. Downloaded from www.nrcresearchpress.com by 210.87.254.105 on 09/05/12
For personal use only.

Can. J. Chem. Downloaded from www.nrcresearchpress.com by 210.87.254.6 on 09/05/12
For personal use only.

Canadian Journal of Chemistry

Issued by THE NATIONAL RESEARCH COUNCIL OF CANADA

VOLUME 44 DECEMBER 1, 1966 NUMBER 23

THE ELECTROLYSIS OF *o*-HALOGENOPHENYL-SUBSTITUTED ACIDS

R. G. WOOLFORD AND W. S. LIN

Department of Chemistry, University of Waterloo, Waterloo, Ontario

Received June 15, 1966

ABSTRACT

The synthesis and electrolysis of a series of *o*-chloro- and *o*-bromo-phenyl-substituted acids with two to five carbon chain lengths have been studied. The main products, under the experimental conditions used, were the Kolbe dimers. A complete isolation and identification of all of the important by-products is recorded. Methanol and methanol–pyridine were the solvents for electrolysis.

This work represents the first study of the behavior of aromatic halogen substituents during the Kolbe electrolysis. In contrast to many reactions involving aliphatic halogen substituents, no free halogen was produced and no products were obtained, even in trace amounts, where halogen had been lost from the aromatic nucleus. During this investigation, 18 previously unreported compounds were synthesized and their properties were determined.

Recently, there has been an increase in interest in the electrolysis reactions of aryl-substituted aliphatic acids (refs. 1–4 and articles cited therein). In part, this interest has involved efforts to observe other than normal Kolbe coupling reactions, and in particular to study phenyl migration in free radicals and homolytic cyclization of the radicals involved. No studies were undertaken with halogenated aromatic rings.

Past work (5, 6) has shown that halogen is readily lost during electrolysis of some ω-halogenated aliphatic acids. It was expected that halogen would be more stable and thus less easily lost from an aromatic ring than from an aliphatic chain. However, because of the complete lack of work in this area, it was felt worthy of investigation. As a start, efforts were concentrated on *o*-chloro- and *o*-bromo-phenyl-substituted acids of two to five carbon chain lengths. It was hoped to learn something of the radicals produced, their reactions, and to what extent this class of organic acids might be used in the synthesis of Kolbe-type halogenated hydrocarbons.

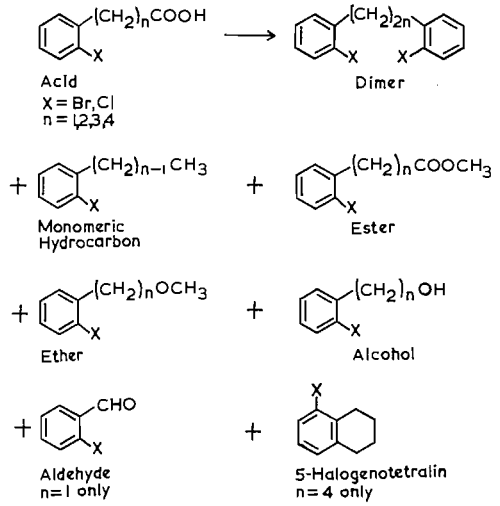
It is difficult to produce and separate large quantities of pure ortho isomers from the ortho–para mixture obtained on direct halogenation of an aromatic ring. Thus, the acids used were all synthesized from starting materials with the halogen substituent already on the ring.

Two new acids were prepared: 4-*o*-bromophenylbutanoic acid and 5-*o*-bromophenylpentanoic acid. All other acids had been synthesized previously. Misra and Shukla (7) prepared *o*-halogenated phenylacetic acids by reacting *o*-halogenated benzyl bromide and chloride with sodium cyanide; hydrolysis gave the desired acids. This method was used to prepare the necessary substituted acetic acids and extended to produce the halogenophenylbutanoic acids.

Can. J. Chem. Downloaded from www.nrcresearchpress.com by 210.87.254.6 on 09/05/12
For personal use only.

Various workers (8–11) have synthesized *o*-halogenophenylpropanoic acids from the corresponding *o*-halobenzyl halides and diethyl malonate, although not on the scale of reaction used in the present work. Granger (12) extended the method to prepare 5-*o*-chlorophenylpentanoic acid, but gave no experimental details. The necessary propanoic and pentanoic acids were prepared by this route.

The *o*-halogenophenyl-substituted acids were electrolyzed in methanol and methanol–pyridine solution. The products are illustrated in Reaction Scheme 1, and the yields are described in Table I.



REACTION SCHEME 1.

Previous electrolyses of *o*-substituted phenylacetic acids have indicated that the size of the ortho substituent is a very important factor in dimer formation. If the group is small, considerable dimer is formed; if the group is large, little or no dimer is formed. The best yield of dimer from the electrolysis of phenylacetic acid itself (i.e. when the ortho substituent is hydrogen) was 55% in methanol solvent (13) and 59% in dimethylformamide (4). Mesitylacetic acid (i.e. two *o*-methyl groups) gives (4) 44% dimer, and 2,4,6-triisopropylphenylacetic acid (i.e. two *o*-isopropyl groups) gives only 31% dimer (4). Wladislaw (2) found that the bulky nitro substituent in 2-nitrophenylacetic acid suppressed dimer formation completely; this was also true with nitro groups in the 2,4-positions, but with a 4-nitro substituent alone, 33% dimer was produced. However, this effect may not be entirely a steric one, since a 3-nitro substituent also suppresses dimer formation completely (Wladislaw concluded that more information was needed to justify any general discussion of how substituents influence the electrolysis products from substituted phenylacetic acids). In our work, an *o*-bromo substituent, which is relatively large, but still smaller than nitro, suppresses dimer formation but does not completely eliminate it. An *o*-chloro substituent, which is considerably smaller, allows more dimer formation, but still less than that with unsubstituted phenylacetic acid. Any steric hindrance vanishes once the chain length of the acid is increased by one carbon or more; this is borne out in most cases by the increased yields of dimer for the other *o*-halogenophenyl-substituted acids studied.

In the past, the Kolbe reaction of an acid RCOOH has been regarded usually as a relatively simple free-radical process involving the production, at the anode, of radicals

Can. J. Chem. Downloaded from www.nrcresearchpress.com by 210.87.254.6 on 09/05/12
For personal use only.

TABLE I

Electrolysis products from *o*-halogenophenyl-substituted acids

Acid used	Solvent†	Product yields (%)*							
		Dimer	Monomeric hydrocarbon	Ester	Ether	Alcohol	Aldehyde	5-Halogeno-tetralin	Unidentified polymer‡
o-Bromophenylacetic acid	M	3.4	—	6.1	10.0	—	7.8	—	40
o-Chlorophenylacetic acid	M	15.1	—	11.8	13.8	—	Trace	—	29
3-*o*-Bromophenylpropanoic acid	M	23.6	8.0	6.8	12.9	Trace	—	—	32
3-*o*-Chlorophenylpropanoic acid	M	25.2	10.3	7.4	17.0	—	—	—	21
4-*o*-Bromophenylbutanoic acid	M	14.0	10.5	15.0	9.4	1.3	—	—	27
4-*o*-Chlorophenylbutanoic acid	M	24.0	13.0	10.0	6.2	3.0	—	—	30
5-*o*-Bromophenylpentanoic acid	M	9.2	10.7	13.0	1.9	1.4	—	4.0§	45
5-*o*-Bromophenylpentanoic acid	M–P	22.6	10.9	8.3	6.2	1.8	—	6.2§	22
5-*o*-Chlorophenylpentanoic acid	M	10.2	9.8	9.0	4.6	4.7	—	7.0§	31
5-*o*-Chlorophenylpentanoic acid	M–P	28.8	12.8	6.7	2.1	0.9	—	3.5§	20

*Calculated in the usual manner based on the amount of acid reacting. The yields of unidentified polymeric fractions are based on a weight ratio exclusively (i.e. weight polymer/weight acid reacting) and hence cannot be regarded as accurate; they do give a good indication of the extent of polymer formation.

†M = methanol; M–P = methanol–pyridine.

‡The term polymer is used for convenience. The fraction consists of ether-insoluble material that settles on the electrodes during electrolysis plus the high-boiling, tarry residue left when the total neutral product is first distilled. Sodium fusion tests and infrared spectra showed the presence of halogen and ortho aromatic substitution in both components, but no further identification was made.

§No trace of unsubstituted tetralin was found.

Can. J. Chem. Downloaded from www.nrcresearchpress.com by 210.87.254.6 on 09/05/12
For personal use only.

RCOO· and R· and their subsequent reaction. In methanol solvent, oxidation of CH_3O^- or CH_3OH to CH_3O· has been an additional factor assumed to be important in product formation and subsequently confirmed (e.g. ref. 14 and articles contained therein). However, recent studies indicate that the Kolbe reaction is often a much more complicated process, or at least it has the potential to be so under the experimental conditions used. Where R· is a normal primary alkyl radical, the formation of products can be reconciled with radical intermediates; except under strong alkaline conditions (the Hofer–Moest reaction, where alcohol production is the major process), there is little experimental evidence to suggest appreciable further oxidation of such a primary radical to R^+. Where R· is secondary, tertiary, allylic, or benzylic, there is considerable evidence to suggest that further oxidation to R^+ is an important factor in at least some of the product formations (for an excellent summary of possible reaction paths, see ref. 4). Eberson (15, 16) and others (17, 18) have also shown that, under the usual Kolbe conditions, not only $RCOO^-$ and solvent but also un-ionized RCOOH and added substrate such as aromatic rings, as well as primary R·, can be oxidized easily to R^+. These latter processes do not always occur to a marked extent even though the experimentally applied voltage is sufficient. However, sometimes they can be important. For example, in the acetoxylation of aromatic substrates under Kolbe conditions (15, 17, 18), instead of a simple radical attack of CH_3COO· on ArH, the reaction involves a two-electron transfer from ArH to the anode, giving ArH^{2+}, which reacts with acetate ion to give $ArOCOCH_3$ and H^+.

In the present work involving electrolysis of *o*-halogenophenyl-substituted acids, the products are those that have been explained traditionally by free-radical intermediates, e.g. $Ar(CH_2)_nCOO$· attack on methanol to give methyl esters, and, by decarboxylation, production of $Ar(CH_2)_{n-1}CH_2$·, which reacts with an identical species to give dimer, with methanol to give monomeric hydrocarbon[1] by hydrogen abstraction, and with CH_3O·, from the oxidation of methanol, to give methyl ether. For the acids other than the substituted phenylacetic acids, there is no evidence to suspect any major involvement of carbonium ions, although they cannot be ruled out completely. We could postulate ether formation by $Ar(CH_2)_{n-1}CH_2^+$ attack on methanol, or tetralin formation by cyclization of $Ar(CH_2)_{n-1}CH_2^+$, but this would involve oxidation of primary radicals to carbonium ions. The reactions are more probably radical combination of $Ar(CH_2)_{n-1}CH_2$· and CH_3O·, and radical cyclization of $Ar(CH_2)_{n-1}CH_2$· to give the substituted tetralin. Bunyan and Hey (1) found that unsubstituted 5-phenylpentanoic acid, on electrolysis, gave small amounts (3.8–4.5%) of tetralin, and postulated radical cyclization in its production. We isolated similar low yields (3.5–7.0%) of the corresponding 5-halogenotetralins.

The formation of alcohols was small, which is in accord with past work. In an acid medium, alcohol formation is rarely pronounced and appears to come from reaction with the small amounts of water, either present in the methanol solvent or else often added to decrease cell resistance and improve current flow. Aldehyde products have only been important when aryl-substituted acetic acids were used; this was explained (19) on the basis of peroxide formation from the more stable benzyl-type radicals produced. *o*-Bromo- and *o*-chloro-phenylacetic acids both gave aldehyde products in a low yield (only a trace from *o*-chlorophenylacetic acid), and no aldehydes were detected in any of the other reactions.

The electrolysis products from the *o*-halogenophenylacetic acids were similar to those

[1]*Commonly used to describe this by-product and used here to indicate the character of the side chain even though a halogen substituent is present on the ring.*

from the longer chain acids and can be explained by purely radical processes. However, electrolytically generated benzyl radicals appear to be oxidized to carbonium ions with great ease; hence, carbonium ion intermediates should not be ruled out, especially in ether formation. It should be noted that we did not isolate, as have other workers with substituted phenylacetic acids, products which clearly are not derived from radical processes.

In all of our electrolyses, ester formation was small; although control reactions indicate ester formation to be minor in the absence of the passage of current, it could possibly take place by attraction of the un-ionized acid to the anode and reaction there with methanol. Other workers (1, 2) have encountered polymer formation during electrolysis, although our yields of polymer were never as high as have been reported (up to 90%). Polymer formation seems to occur readily when phenyl substitution is present. Our results and those of other workers could possibly involve oxidation of the aromatic ring, leading to high-boiling, polymeric products. This is only speculation, however, and further comment must await a more detailed analysis of the polymeric fractions obtained. No other products were isolated where oxidation of the aromatic ring was involved.

Two conclusions regarding the effect of the *o*-halogen substituent on electrolysis reactions of phenyl-substituted acids can be made. First, the halogen substituent is perfectly stable during electrolysis; no products, even in trace amounts, were found in which either chlorine or bromine was displaced from the aromatic ring. Even in the case of the substituted pentanoic acids, where internal cyclization of the alkyl radical occurs to give small yields of tetralins, it was always hydrogen which was displaced, never halogen. This stability is not surprising, but it is the first time it has been demonstrated by experimental work. Secondly, there is a more-uniform spread of yields among all of the normal by-products than other workers have usually found during Kolbe-type electrolyses, where often only one by-product (usually the ester) predominates. This spread of products is possibly due to the increase in the molecular weight of the acids used when a halogen substituent is present. The acid therefore moves through the solution to the electrodes more slowly and the electrolysis is less efficient. The solvent carries more than its normal share of the current. Methoxy radical concentration, and hence ether formation, increases. Also, a decrease in the alkyl radical concentration at the electrode occurs and attack on the solvent takes place more readily, with a resultant decrease in dimer formation. However, with the *o*-halogenophenylacetic acids, the stability of the benzyl-type radical or carbonium ion may be a more important factor in determining the products.

The work described herein represents the first detailed study of the electrolyses of a series of *o*-halogenophenyl-substituted acids. The low yields and spread of products probably mean that the reactions should not be regarded as good synthetic ones for the production of the appropriate Kolbe dimers. In some individual cases, however, since other synthetic methods for these compounds do not exist presently, the reactions might be used conveniently for small-scale preparations.

EXPERIMENTAL

Physical constants and analytical data for new compounds are given in Table II. Melting points were determined on a Leitz hot stage and are corrected; boiling points are uncorrected. Analyses were performed by Schwarzkopf Mircoanalytical Laboratory, Woodside, New York. Infrared spectra were taken with Beckman IR-5 and IR-9 infrared spectrophotometers. An Aerograph Autoprep model 700 gas chromatograph was used with either a 10 or 20 ft × ⅜ inch column of 30% SE-30 silicone gum rubber on 60–80 mesh Chromosorb W; separated components were collected by means of the fraction collector, with external cooling.

Can. J. Chem. Downloaded from www.nrcresearchpress.com by 210.87.254.6 on 09/05/12
For personal use only.

Can. J. Chem. Downloaded from www.nrcresearchpress.com by 210.87.254.6 on 09/05/12
For personal use only.

TABLE II

Physical constants and analytical results of new compounds

Compound	Boiling point (°C)	n_D^{25} or melting point (°C)	Analytical results (%) C Calculated	C Found	H Calculated	H Found	Cl or Br Calculated	Cl or Br Found
Starting acids								
4-*o*-Bromophenylbutanoic acid		85–86	49.40	49.59	4.56	4.82	32.88	33.01
5-*o*-Bromophenylpentanoic acid		43–44	51.38	51.60	5.10	5.26	31.09	30.99
Reference compounds								
Methyl 5-*o*-chlorophenylpentanoate	104–108 at 0.2 mm	1.5249	63.57	63.81	6.67	6.87	15.64	15.12
4-*o*-Bromophenylbutan-1-ol	102–103 at 0.2 mm	1.5577	52.42	52.68	5.72	5.77	32.88	32.72
4-*o*-Bromophenylbutyl methyl ether	98–100 at 0.5 mm	1.5300	54.33	54.62	6.22	6.24	32.87	32.70
4-*o*-Chlorophenylbutyl methyl ether	85–86 at 0.5 mm	1.5112	66.49	66.21	7.61	7.34	17.85	17.58
Electrolysis products								
Methyl *o*-bromophenylacetate	73–75 at 0.2 mm	1.5465	47.18	47.03	3.96	3.69	34.89	34.31
Methyl 3-*o*-bromophenylpropanoate	90–95 at 0.3 mm	1.5408	49.40	49.74	4.56	4.45	32.88	32.38
Methyl 4-*o*-bromophenylbutanoate	92–94 at 0.2 mm	1.5345	51.38	51.93	5.09	5.15	31.08	30.90
Methyl 4-*o*-chlorophenylbutanoate	105–110 at 0.2 mm	1.5245	62.11	62.08	6.16	6.26	16.67	16.92
Methyl 5-*o*-bromophenylpentanoate		44–45	53.15	53.40	5.58	5.56	29.47	29.18
1,4-Di-(*o*-bromophenyl)-butane		68–69.5	52.20	52.54	4.38	4.52	43.42	43.21
1,6-Di-(*o*-bromophenyl)-hexane		31.5–32	54.56	54.53	5.08	5.11	40.36	40.16
1,6-Di-(*o*-chlorophenyl)-hexane	162–165 at 0.2 mm	1.5582	70.35	70.25	6.56	6.58	23.09	22.91
1,8-Di-(*o*-bromophenyl)-octane	190–192 at 0.3 mm	1.5690	56.62	56.60	5.70	5.76	37.68	37.57
1,8-Di-(*o*-chlorophenyl)-octane	170–175 at 0.15 mm	1.5512	71.64	71.77	7.21	7.22	21.15	20.98
2-*o*-Chlorophenylethyl methyl ether	47–49 at 0.3 mm	1.5185	63.64	63.42	6.49	6.58	20.78	20.90
3-*o*-Chlorophenylpropyl methyl ether	60–62 at 0.4 mm	1.5155	65.04	64.94	7.09	7.01	19.24	19.30

Syntheses of o-Halogenophenyl-Substituted Acids

o-Halogenophenyl-Substituted Acetic and Propanoic Acids

o-Bromo- and *o*-chloro-phenylacetic acids, prepared according to the procedure of Misra (7), had melting points of 104–105.5° and 94–95°, respectively. Misra found melting points of 104–105.5° and 93–94°. The malonate procedure (9, 10) gave 3-*o*-bromophenylpropanoic acid, m.p. 96–98° (lit. m.p. 97–98° (9)), and 3-*o*-chlorophenylpropanoic acid, m.p. 95–96.5° (lit. m.p. 95–96° (10)).

4-o-Bromophenylbutanoic Acid

3-*o*-Bromophenylpropyl bromide (94.0 g, 0.34 mole), prepared by the procedure of Beeby and Mann (20), was added to sodium cyanide (20.0 g, 0.40 mole) in 40 ml of hot water and 100 ml of ethanol over 30 min. The mixture was heated under reflux for 5 h, cooled, and filtered. Ethanol was distilled under vacuum, giving crude 4-*o*-bromophenylbutanonitrile, which was heated under reflux with a solution of equal volumes (80 ml each) of concentrated sulfuric acid, acetic acid, and water for 12 h, and set aside overnight. An oily layer separated after addition of 1 000 ml of water. This layer and two ethereal extracts of the aqueous layer were dried over magnesium sulfate. Distillation gave a colorless liquid, b.p. 124–130° at 1.5 mm, which solidified when allowed to stand. Purified 4-*o*-bromophenylbutanoic acid (67.2 g, 81%) was obtained by recrystallization from carbon tetrachloride (Table II).

4-o-Chlorophenylbutanoic Acid

By a reaction similar to that described above, 4-*o*-chlorophenylbutanoic acid, m.p. 92–93.5°, was obtained (lit. m.p. 94–95° (21)).

5-o-Bromophenylpentanoic Acid

The malonate procedure described in refs. 9 and 10 was used, although on a larger scale, and gave 146 g (72%) of diethyl 3-*o*-bromophenylpropylmalonate (b.p. 186–201° at 1.5 mm) from 190 g (0.68 mole) of 3-*o*-bromophenylpropyl bromide. Hydrolysis and decarboxylation of the crude malonic acid gave 5-*o*-bromophenylpentanoic acid, b.p. 146–162° at 1.0 mm, m.p. 40–42°. Recrystallization from carbon tetrachloride gave 74.6 g (61%) of pure acid (Table II).

5-o-Chlorophenylpentanoic Acid

In a similar manner, 3-*o*-chlorophenylpropyl bromide (200 g, 0.86 mole) gave diethyl 3-*o*-chlorophenylpropylmalonate (154 g, 58%), b.p. 185–190° at 1.5 mm. Hydrolysis and decarboxylation yielded 5-*o*-chlorophenylpentanoic acid, b.p. 155–160° at 0.6 mm, m.p. 43–46°. Recrystallization from carbon tetrachloride gave m.p. 45.5–46.5° (lit. m.p. 46°, b.p. 166–167° at 1.0 mm (12)) and a yield of 73.4 g (61%).

Syntheses of Authentic Reference Compounds

Esters of o-Halogenophenyl-Substituted Acids

Concentrated sulfuric acid (2 ml) was added cautiously to 1.5–2.0 g of the appropriate acid in 15 ml of methanol. Heating under reflux for 1 h and work-up in the usual manner gave the pure ester, on distillation, in yields of 85–90%. Esters of all the acids previously described were prepared. New compounds are listed in Table II.

4-o-Bromophenylbutan-1-ol

4-*o*-Bromophenylbutanoic acid (10 g, 0.041 mole) in 100 ml of anhydrous ether was added to a stirred suspension of lithium aluminium hydride (2.5 g) in 100 ml of anhydrous ether, maintaining gentle reflux. The reaction mixture was heated under reflux for 1 h. After removal of 100 ml of ether, the cooled reaction mixture was hydrolyzed with 20 ml of water, followed by 50 ml of 10% sulfuric acid. After filtration, the ethereal layer was separated, washed with 10% sodium carbonate solution and then water, and dried over magnesium sulfate. Distillation gave 7.79 g (83%) of pure 4-*o*-bromophenylbutan-1-ol (Table II).

4-o-Chlorophenylbutan-1-ol

Preparation from 4-*o*-chlorophenylbutanoic acid, as described above, gave a colorless liquid, b.p. 113–115° at 0.9 mm, n_D^{25} 1.5351 (lit. b.p. 150–151° at 12 mm (22) and b.p. 97–98° at 0.7 mm (23)).

3-o-Bromophenylpropyl Methyl Ether and 3-o-Chlorophenylpropyl Methyl Ether

The 3-*o*-halophenylpropyl bromides were methylated with sodium methoxide (20). The resulting bromoether had b.p. 68–71° at 0.5 mm, n_D^{25} 1.5334 (lit. b.p. 127–129° at 15 mm (20)), and the chloroether is described in Table II.

4-o-Bromophenylbutyl Methyl Ether

4-*o*-Bromophenylbutan-1-ol (3.0 g, 0.0014 mole) was dissolved in methyl iodide (20 ml) and stirred with silver oxide (6.0 g) and anhydrous calcium sulfate (10 g) for 24 h. The crude product was chromatographed on silicic acid (2.5 × 20 cm), with benzene as eluent. Evaporation of the first 50 ml of eluent left a colorless liquid, which was distilled to give 1.23 g (36%) of the pure ether (Table II).

4-o-Chlorophenylbutyl Methyl Ether

4-*o*-Chlorophenylbutan-1-ol was methylated as described immediately above. Similar purification gave the ether (Table II).

Electrolysis of o-Halogenophenyl-Substituted Acids

General Method of Electrolysis

The cell used was fully described previously (6). The acid was dissolved in methanol, along with enough sodium to produce 5% neutralization. By using a D.C. supply of 50–80 V, 0.5–1.0 A was passed for about

Can. J. Chem. Downloaded from www.nrcresearchpress.com by 210.87.254.6 on 09/05/12
For personal use only.

3 times the theoretical. The temperature was kept below 40°. During the electrolysis, insoluble, apparently polymeric material deposited on the anode, causing the current to fall below the stated minimum periodically. The current was stopped, the anode deposit removed, and the reaction started again.

Isolation of products into acidic and neutral fractions was carried out as described before (6), except that continuous ether extraction for 24 h gave the neutral component. Negligible starting material was usually returned. The neutral fraction was distilled under vacuum, giving four to five major fractions plus a non-distillable, tarry residue.

Isolation and Identification of Products

Two general procedures were used to purify the crude distillation fractions from above. Gas–liquid chromatography (g.l.c.) indicated that the substituted acetic and propanoic acid products were fairly well separated by the first distillation. The first three fractions were redistilled and the fourth recrystallized or treated to column chromatography. The *o*-bromophenylacetic acid reaction is described in detail as representative, and others similar to it in only enough detail to show some physical constants and important variations. The substituted butanoic and pentanoic acid products were not well separated by the first distillation, and chromatography was necessary, both column and g.l.c. with fraction collection. The 4-*o*-bromophenylbutanoic acid reaction is representative, and other similar ones are only briefly described. Percentage yields are found in Table I. In some cases, the yields were estimated from the relative peak areas of the g.l.c. chromatograms, but wherever possible, the actual weights of pure collected fractions were used.

The products were identified by matching g.l.c. behavior, physical constants, and infrared spectra with those of authentic samples as well as literature values. The infrared spectra were as expected and are not described. New compounds were submitted for elemental analysis (see Table II for analysis figures and physical constants). As an additional confirmation of the identity of the esters, small-scale hydrolysis to the free acids and mixed melting points were used.

Electrolysis of o-Halogenophenyl-Substituted Acetic and Propanoic Acids

Electrolysis of *o*-bromophenylacetic acid (20.0 g, 0.093 mole) in 150 ml methanol yielded four initial distillation fractions: 1, 1.46 g, b.p. 40–59° at 0.35 mm; 2, 1.34 g, b.p. 60–85° at 0.35 mm; 3, 1.05 g, b.p. 95–115° at 0.35 mm; 4, 0.55 g, b.p. 125–135° at 0.35 mm. The tarry residue weighed 3.95 g, and 4.13 g (22%) of starting acid was returned. Polymeric material (2.35 g) deposited on the anode during the reaction. Fraction 1 was a mixture of *o*-bromobenzaldehyde (1.06 g) and methyl *o*-bromobenzyl ether (0.40 g), as estimated by g.l.c. Redistillation of *o*-bromobenzaldehyde gave b.p. 49–50° at 0.2 mm, n_D^{25} 1.5931 (lit. b.p. 118–119° at 12 mm, m.p. 22° (24)). Gas–liquid chromatography indicated that fraction 2 was methyl *o*-bromobenzyl ether containing some ester. After the ester was removed by basic hydrolysis, the ether was redistilled, b.p. 65–66° at 0.2 mm, n_D^{25} 1.5505, 1.08 g (lit. b.p. 106–107° at 16 mm (25)). Fraction 3 was mainly methyl *o*-bromophenylacetate, and redistillation gave 0.98 g. Fraction 4 was passed through a silicic acid chromatography column (20 × 2.5 cm). Elution with 1:1 *n*-hexane–benzene gave 2,2′-dibromodibenzyl (0.42 g), which, on recrystallization from methanol, had m.p. 84–84.5° (lit. m.p. 84.5° (20)).

The electrolyses of *o*-chlorophenylacetic, 3-*o*-bromophenylpropanoic, and 3-*o*-chlorophenylpropanoic acids were similar. The following variations in procedure or in physical constants are noteworthy: 2-*o*-bromophenylethyl methyl ether had n_D^{25} 1.5429 (no literature value) and 1,4-di-*o*-(bromophenyl)-butane was chromatographed on neutral alumina with elution by hexane; methyl 3-*o*-chlorophenylpropanoate had b.p. 65–66° at 0.3 mm, n_D^{25} 1.5170 (lit. b.p. 255° (26)), and no column chromatography was necessary, only recrystallization, to give 1,4-di-(*o*-chlorophenyl)-butane, m.p. 53.5–54° (lit. m.p. 51–52° (27)).

Electrolysis of o-Halogenophenyl-Substituted Butanoic and Pentanoic Acids

Electrolysis of 4-*o*-bromophenylbutanoic acid (15.0 g, 0.062 mole) in 130 ml methanol yielded four initial distillation fractions: 1, 2.43 g, b.p. 40–80° at 0.4 mm; 2, 1.83 g, b.p. 70–98° at 0.3 mm; 3, 1.84 g, b.p. 106–135° at 0.3 mm; 4, 1.92 g, b.p. 186–200° at 0.3 mm. The tarry residue weighed 1.71 g to go with 2.35 g deposited during electrolysis. Fraction 1 was chromatographed on the alumina column previously described, and eluted with hexane to give *o*-bromo-*n*-propylbenzene, 0.95 g, b.p. 51–52° at 0.7 mm, n_D^{25} 1.5405 (lit. b.p. 217–220°, n_D^{25} 1.5395 (28)), as well as 1.38 g of a yellow liquid, which appeared to be identical (by g.l.c.) with fraction 2 and was added to it. Fraction 2, now 3.22 g, was separated by g.l.c. with temperature programming from 200 to 300° on the 10 ft column; the yields were estimated from the chromatogram. *o*-Bromo-*n*-propylbenzene (0.35 g), 3-*o*-bromophenylpropyl methyl ether (1.33 g), 3-bromophenylpropan-1-ol (0.17 g), and methyl 4-*o*-bromophenylbutanoate (0.74 g) plus an unidentified component (0.71 g) were obtained. Fraction 3 was redistilled, giving 1.56 g of methyl 4-*o*-bromophenylbutanoate. Fraction 4, on recrystallization from methanol, gave 1.72 g of 1,6-di-(*o*-bromophenyl)-hexane.

The electrolyses of 4-*o*-chlorophenylbutanoic, 5-*o*-bromophenylpentanoic, and 5-*o*-chlorophenylpentanoic acids were similar, but, for the latter two acids, the g.l.c. separations were carried out on the 20 ft column at 250–320° and 200–300°, respectively. Significant variations in physical constants were: *o*-chloro-*n*-propylbenzene, b.p. 33–35° at 0.5 mm, n_D^{25} 1.5130 (lit. b.p. 79° at 10 mm, n_D^{16} 1.5213 (29)), and *o*-chloro-*n*-butylbenzene, b.p. 38–40° at 0.3 mm, n_D^{25} 1.5117 (lit. b.p. 53–54° at 2 mm, n_D^{25} 1.5087 (30)).

Can. J. Chem. Downloaded from www.nrcresearchpress.com by 210.87.254.6 on 09/05/12
For personal use only.

ACKNOWLEDGMENTS

The authors are indebted to the National Research Council of Canada for financial support.

REFERENCES

1. P. J. BUNYAN and D. H. HEY. J. Chem. Soc. 1360 (1962).
2. B. WLADISLAW and A. GIORA. J. Chem. Soc. 1037 (1964).
3. W. A. BONNER and F. D. MANGO. J. Org. Chem. **29**, 430 (1964).
4. L. RAND and A. F. MOHAR. J. Org. Chem. **30**, 3885 (1965).
5. F. L. M. PATTISON, J. B. STOTHERS, and R. G. WOOLFORD. J. Am. Chem. Soc. **78**, 2255 (1956).
6. R. G. WOOLFORD. Can. J. Chem. **40**, 1846 (1962).
7. G. S. MISRA and J. S. SHUKLA. J. Indian Chem. Soc. **28**, 480 (1951).
8. L. F. FIESER and A. M. SELIGMAN. J. Am. Chem. Soc. **57**, 2174 (1935).
9. F. G. HOLLIMAN, F. G. MANN, and D. A. THORNTON. J. Chem. Soc. 9 (1960).
10. R. HUISGEN and H. KONIG. Chem. Ber. **92**, 203 (1959).
11. M. NAKAZAKI, K. YAMAGAMI, and S. ISOE. Bull. Chem. Soc. Japan, **34**, 1189 (1961).
12. R. GRANGER, H. ORZALESI, and A. MURATELLE. Compt. Rend. **252**, 1478 (1961).
13. R. P. LINSTEAD, B. R. SHEPHARD, and B. C. L. WEEDON. J. Chem. Soc. 3624 (1952).
14. S. TSUTSUMI and T. INOUE. Bull. Chem. Soc. Japan, **38**, 661 (1965).
15. L. EBERSON and K. NYBERG. J. Am. Chem. Soc. **88**, 1686 (1966).
16. L. EBERSON. Acta Chem. Scand. **17**, 2004 (1963).
17. S. D. ROSS, M. FINKELSTEIN, and R. C. PETERSEN. J. Am. Chem. Soc. **86**, 4139 (1964).
18. H. W. SALZBERG and M. LEUNG. J. Org. Chem. **30**, 2873 (1965).
19. A. J. VAN DER HOEK and W. T. NAUTA. Rec. Trav. Chim. **61**, 845 (1942).
20. M. H. BEEBY and F. G. MANN. J. Chem. Soc. 411 (1951).
21. F. G. BADDAR, L. S. EL-ASSAL, and N. A. DOSS. J. Chem. Soc. 1027 (1959).
22. J. F. BUNNETT and J. A. SKORCZ. J. Org. Chem. **27**, 3836 (1962).
23. H. KONIG and R. HUISGEN. Chem. Ber. **92**, 429 (1959).
24. O. L. BRADY, A. N. COSSON, and A. J. ROPER. J. Chem. Soc. 2427 (1925).
25. F. G. HOLLIMAN and F. G. MANN. J. Chem. Soc. 1634 (1947).
26. F. MAYER, H. PHILIPPS, F. W. RUPPERT, and A. T. SCHMITT. Ber. **61**, 1966 (1928).
27. R. A. BARNES and M. D. KONORT. J. Am. Chem. Soc. **75**, 303 (1953).
28. J. H. LAMNECK. J. Am. Chem. Soc. **76**, 1106 (1954).
29. C. D. NENITZESCU and D. A. ISACESCU. Ber. **66**, 1102 (1933).
30. D. F. DETAR and C. WEIS. J. Am. Chem. Soc. **78**, 4296 (1956).

Can. J. Chem. Downloaded from www.nrcresearchpress.com by 210.87.254.6 on 09/05/12
For personal use only.

Can. J. Chem. Downloaded from www.nrcresearchpress.com by 210.87.254.6 on 09/05/12
For personal use only.

THE CHEMISTRY OF YLIDS

XV. MECHANISM OF THE REACTION OF IMINOPHOSPHORANES WITH CARBONYL COMPOUNDS[1-3]

A. WILLIAM JOHNSON[4] AND SIMON C. K. WONG

Division of Natural Sciences, University of Saskatchewan, Regina Campus, Regina, Saskatchewan, and Chemistry Department, University of North Dakota, Grand Forks, North Dakota

Received July 19, 1966

ABSTRACT

The pK_a values of two series of iminophosphoranes, *N*-(substituted phenyl)-iminotriphenylphosphoranes (VI) and *N*-phenyliminotri-(substituted phenyl)-phosphoranes (VII), have been correlated with σ^0 and σ, respectively, giving ρ values of +3.5 and +9.3. A kinetic study of the reaction of VI and VII with benzaldehydes indicates that a betaine intermediate (V) is involved. The rate-limiting step of the reaction changes, the result of a delicate balance between the nucleophilicity of the nitrogen atom and the electrophilicity of the phosphorus atom. The involvement of $d\pi$–$p\pi$ bonding is indicated.

INTRODUCTION

In earlier papers in this series (1), we have been concerned with the chemistry of methylenephosphoranes (phosphonium ylids) (I), especially those characteristics that reflect the nature of the "ylid bond". Our attention has focused on the basicity and nucleophilicity of the ylid carbanion as influenced by its substituents. We report herein the initial results of our parallel investigations of the chemistry of iminophosphoranes (phosphinimines) (II). The latter are isoelectronic with phosphonium ylids.



I II

Iminophosphoranes were first prepared by Staudinger and Meyer (2) in 1919. As indicated in a recent review (3), several groups have examined the chemistry of iminophosphoranes qualitatively. These results have indicated the substances to be typical nucleophiles, undergoing reactions such as alkylation, acylation, halogenation, and protonation all on the nitrogen atom. However, there has been no correlation of structure with nucleophilicity in the imines. We report such a correlation in this work.

Staudinger and Meyer (2) had reported that *N*-phenyliminotriphenylphosphorane reacted with diphenylketene to yield triphenylketenimine and triphenylphosphine oxide (eq. [1]). Since that early work, only a few others have studied the reaction between imino-

$$\begin{array}{ccc} C_6H_5N{=}P(C_6H_5)_3 & & C_6H_5N{=}C{=}C(C_6H_5)_2 \\ + & \rightarrow & + \\ (C_6H_5)_2C{=}C{=}O & & (C_6H_5)_3PO \end{array} \qquad [1]$$

phosphoranes and carbonyl compounds to form Schiff bases and phosphine oxides (4–9). Nonetheless, it has become a useful and well-accepted reaction. Its scope has been expanded to include reaction with ketones, aldehydes, isocyanates, carbon dioxide, and carbon

[1] *For part XIV in this series, see A. Wm. Johnson and R. T. Amel, Tetrahedron Letters, 819 (1966).*

[2] *Presented in part at the 151st meeting of the American Chemical Society, Pittsburgh, Pennsylvania, March 1966, and at the 49th conference of the Chemical Institute of Canada, Saskatoon, Saskatchewan, June 1966.*

[3] *From the dissertation of S. C. K. Wong submitted to the Graduate School of the University of North Dakota in partial fulfillment of the requirements for the degree of Doctor of Philosophy, January 1966.*

[4] *To whom inquiries should be addressed at the first location.*

disulfide. In all cases, a C=N bond is formed to replace a C=O or C=S bond, the driving force appearing to be the formation of phosphine oxide or sulfide.

It has been assumed (8, 9), without valid proof, that the mechanism of these reactions parallels that of the Wittig Reaction between methylenephosphoranes and carbonyl compounds to yield olefins and phosphine oxide (3, 10). Specifically, it has been assumed that the carbonyl carbon undergoes attack by the nitrogen of the imine to yield a betaine intermediate (V). The latter was thought to be converted into products by oxygen transfer to phosphorus (see eq. [3] in Discussion).

We have undertaken a detailed study of the mechanism of the reaction of iminophosphoranes with carbonyl compounds. We report herein the preparation of the necessary imines and our initial kinetic studies on the reaction.

RESULTS

A series of *N*-(substituted phenyl)-iminotriphenylphosphoranes (VI) were prepared in 55–90% yields by reaction of triphenylphosphine with the appropriate substituted phenyl azide, a procedure originally used by Staudinger and Meyer (2) (eq. [2]). A series of *N*-phenyliminotri-(substituted phenyl)-phosphoranes (VII) also were prepared in 60–87% yields, but by reaction of phenyl azide with the appropriate substituted triphenylphosphine. The properties of these imines are listed in Table I and the Experimental.

$$(C_6H_5)_3P + XC_6H_4N_3 \rightarrow (C_6H_5)_3P{=}NC_6H_4X + N_2 \qquad [2]$$

$X{-}C_6H_4{-}N{=}P(C_6H_5)_3$

VI*a* X = *p*-NO_2
VI*b* X = *m*-NO_2
VI*c* X = *m*-Cl
VI*d* X = *p*-Br
VI*e* X = H
VI*f* X = *p*-CH_3
VI*g* X = *p*-CH_3O

$C_6H_5N{=}PR_3$

VII*a* R = *m*-$CH_3C_6H_4$
VII*b* R = C_6H_5
VII*c* R = *p*-BrC_6H_4
VII*d* R = *p*-ClC_6H_4

The pK_a values of the hydrochlorides of the two series of imines were determined by potentiometric titration in 95% ethanol solution. The pK_a values ranged from 4.55 to 8.36 and are reported in Table I. These determinations were confirmed by using a spectrophotometric method (11). A plot of pK_a versus σ^0 gave a ρ value of +3.5 for the imines of type VI, and a plot of σ versus pK_a gave a ρ value of 9.3 for those of type VII (Figs. 1 and 2).

The imines (VI and VII) all reacted with *p*-nitrobenzaldehyde to yield the expected and known substituted *N*-(*p*-nitrobenzylidene) anilines in 60–95% yields (see Experimental). The rate of disappearance of VI*e* in its reaction with *p*-nitrobenzaldehyde was determined in absolute ethanol at 40.5° by potentiometric titration of the imine. The reaction was second order, first order each in imine (VI*e*) and in aldehyde. The reaction was subject to a solvent effect, the k_{rel} values in ethanol, chloroform, and benzene being 29:15:1, respectively.

Activation parameters for the reaction of VI*e* with benzaldehyde were obtained from the rate data taken at three temperatures (30, 40.5, and 50 °C). The E_a was 8.46 kcal/mole and the $\Delta S^{\ddagger}$ was −42.0 e.u. at 40.5°. Rate data were accumulated for the reaction of VI*e* with a series of substituted benzaldehydes (Table II). A plot of log k/k_0 versus σ gave a Hammett plot with a ρ value of +2.1.

The effect of the imine structure on the rate of reaction with *p*-nitrobenzaldehyde was examined. The rate constants are summarized in Table I. A Hammett plot for the *P*-phenyl substituents (i.e. VII) versus σ gave a ρ value of −0.70 (Fig. 3). A similar plot for the *N*-phenyl substituents did not give a straight line, the curve being concave down (Fig. 4).

Can. J. Chem. Downloaded from www.nrcresearchpress.com by 210.87.254.6 on 09/05/12
For personal use only.

Can. J. Chem. Downloaded from www.nrcresearchpress.com by 210.87.254.6 on 09/05/12
For personal use only.

TABLE I

Properties of iminophosphoranes (VI and VII)

	$R_3P{=}NC_6H_4X$					Reaction with *p*-nitrobenzaldehyde		
Compound	R	X	Melting point	Reference	pK_a	$k_{obs} \times 10^2$ (l/mole s)	Solvent	Temperature
VI*a*	C_6H_5	*p*-NO_2	158–159°	12	4.55±0.05	Too slow	EtOH	40.5°
VI*b*	C_6H_5	*m*-NO_2	136–137°	12	5.32±0.05	2.03±0.08	EtOH	40.5°
VI*c*	C_6H_5	*m*-Cl	119–120°	12	6.36±0.01	16.7±0.3	EtOH	40.5°
VI*d*	C_6H_5	*p*-Br	126–127°	13	6.68±0.01	24.0±0.5	EtOH	40.5°
VI*e*	C_6H_5	H	133–134°	12	7.61±0.01	34.6±0.6	EtOH	40.5°
						18.1±0.7	$CHCl_3$	40.5°
						1.20±0.05	C_6H_6	40.5°
						0.87*±0.01	EtOH	30°
						1.37*±0.01	EtOH	40.5°
						2.09*±0.02	EtOH	50°
VI*f*	C_6H_5	*p*-CH_3	136–137°	12	7.92±0.01	23.3±0.6	EtOH	40.5°
VI*g*	C_6H_5	*p*-CH_3O	119–120°	12	8.20±0.05	19.3±0.3	EtOH	40.5°
VII*a*	*m*-$CH_3C_6H_4$	H	135–136°	†	8.36±0.05	41.6±0.3	EtOH	40.5°
VII*b*	C_6H_5	H	133–134°	12	7.61±0.01	34.6±0.6	EtOH	40.5°
VII*c*	*p*-BrC_6H_4	H	166–167°	†	5.55±0.05	25.8±0.6	EtOH	40.5°
VII*d*	*p*-ClC_6H_4	H	160–161°	†	5.58±0.05	25.8±0.6	EtOH	40.5°

*Rate for the reaction with benzaldehyde.
†Previously unknown compound.

Can. J. Chem. Downloaded from www.nrcresearchpress.com by 210.87.254.6 on 09/05/12
For personal use only.

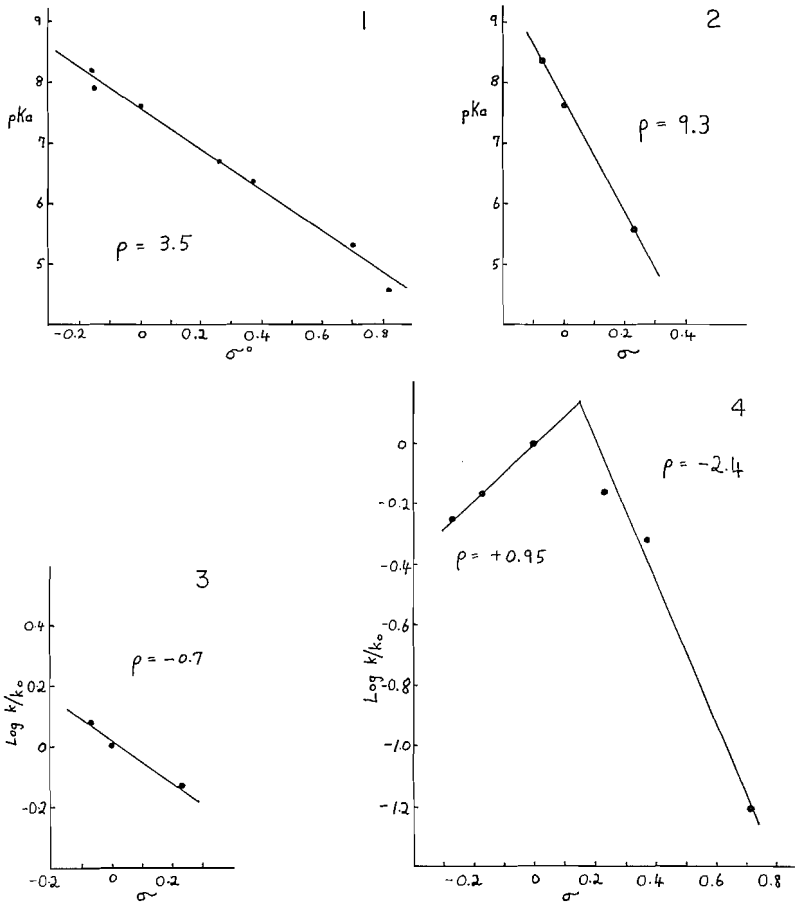


FIG. 1. pK_a of *N*-(substituted phenyl)-iminotriphenylphosphoranes versus σ^0.
FIG. 2. pK_a of *N*-phenyliminotri-(substituted phenyl)-phosphoranes versus σ.
FIG. 3. Rate of reaction of VII*a*–VII*d* with *p*-nitrobenzaldehyde versus σ.
FIG. 4. Rate of reaction of VI*b*–VI*g* with *p*-nitrobenzaldehyde versus σ.

TABLE II

Reaction of *N*-phenyliminotriphenyl-phosphorane with substituted benzaldehydes ($(C_6H_5)_3P{=}NC_6H_5 + RC_6H_4CHO$)

R	$k_{obs} \times 10^2$ (l/mole s)
p-NO_2	34.6±0.6
p-CN	27.9±0.7
m-Cl	8.82±0.04
H	1.37±0.01
p-CH_3	0.66±0.01
p-CH_3O	0.17±0.01

DISCUSSION

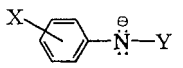
Basicity of Iminophosphoranes

As indicated in Fig. 1, the pK_a values of the *N*-(substituted phenyl)-iminotriphenyl-phosphoranes (VI) correlated well with σ^0, the "normal substituent constant" (14), giving a ρ value of +3.5. This is equivalent to saying the imine basicities also correlated and

implies, as expected, that the more delocalization given the anionic center, the less basic is that imine (and the more acidic is its conjugate acid).

The observation that the use of σ values or σ^- values gave rise to less-satisfactory correlations with the pK_a values of VI is significant. The point for the *p*-nitro imine (VI*a*) lay below the line when the σ value of +0.78 was used, above the line when the σ^- value of +1.27 was used, and nearly on the line when a σ^0 value of +0.82 was used. A value of +0.92 would have fallen on the best line. This observation is consistent with that of van Bekkum *et al.* (15), who observed that in a series of reactions the substituent constant for the *p*-nitro group varied from 0.766 to 1.378 depending on the degree of resonance interaction of the substituent with the reaction site. Clearly, there is more than a simple inductive interaction between the imine group and the nitro group in VI*a*. There would appear to be a demand for some, but not an excessive amount of, resonance interaction (the amount being considerably less than that required for a phenoxide ion).

The successful use of σ^0 values in the correlation of pK_a values of VI attests to the modest demand for delocalization exerted by the nitrogen anion on the *N*-phenyl substituents. The modest level of this demand probably is due in part to the fact that nitrogen is able to sustain a charge. The major factor, however, probably is a result of the phosphonium group providing considerable stabilization for the anionic center by virtue of $p\pi$–$d\pi$ overlap between phosphorus and nitrogen. Stewart and O'Donnell (16) have reported similar behavior for the *N*-(substituted phenyl)-2,4,6-trinitroanilines (VIII), the acidities of which correlated with σ^0. In this instance, the modest demand for delocalization by the substituent was attributed to the presence of the highly stabilizing 2,4,6-trinitrophenyl



VI, Y = $(C_6H_5)_3P$

VIII, Y = $C_6H_2(NO_2)_3$ (2,4,6)

group. We previously observed that σ^0 would correlate with the pK_a values for substituted fluorenyltriphenylphosphonium bromides, the phosphonium group providing a major source of stabilization for the carbanion (1).

The ρ value of +3.5 from the plot of the pK_a values of VI versus σ^0 is smaller than the +5.0 value obtained by us (1) for the triphenylphosphoniumfluorenylide system. This is to be expected when the anionic center is changed from carbon to nitrogen. However, the value is larger than the +1.7 value reported by Stewart and O'Donnell (16) for the acidity of the *N*-(substituted phenyl)-2,4,6-trinitroanilines (VIII). The difference may imply that the triphenylphosphonium group provides somewhat less delocalization than does the 2,4,6-trinitrophenyl group for the anionic center. Concomitantly, the substituents (X in VI and VIII) would be called on for more interaction in VI than in VIII, leading to a larger ρ value.

As indicated in Fig. 2, the pK_a values of the *N*-phenyliminotri-(substituted phenyl)-phosphoranes (VII) were linearly correlated with a ρ value of +9.3. The effect per substituent is one-third as large, the ρ value being +3.1. This observation indicates that electron-withdrawing substituents on the *P*-phenyl groups decrease the basicity of the nitrogen anion. We attribute this stabilization of the phosphinimine to $p\pi$–$d\pi$ overlap between the filled 2p-orbitals of nitrogen and the vacant 3d-orbitals of phosphorus. Furthermore, the sign of the ρ value is consistent with the proposal by Craig and Magnusson (17) that the attachment of more electronegative groups to a phosphonium atom would permit better $d\pi$-bonding. Such a correlation was observed in our earlier work with phosphoniumfluorenylides (1), and the generalizations indicated therein probably apply to this work. We conclude that a measure of imine basicity is a convenient and reliable indication of the degree of $p\pi$–$d\pi$ overlap in the imine P—N bond.

Can. J. Chem. Downloaded from www.nrcresearchpress.com by 210.87.254.6 on 09/05/12
For personal use only.

Can. J. Chem. Downloaded from www.nrcresearchpress.com by 210.87.254.6 on 09/05/12
For personal use only.

The ρ value per substituent of +3.1 is larger than that of +1.7 found for the correlation of the pK_a values of the 9-fluorenyltri-(substituted phenyl)-phosphonium salts. This is to be expected, however, since fluorene is more acidic than aniline.

The mode of interaction of the *P*-phenyl groups and their substituents with the phosphorus atom in VII is made apparent by these results. Normally, when a substituent interacts through a benzenoid ring with an electron-deficient center, linear free energy correlations are best obtained by using σ^+ values (18, p. 203). In spite of the direct attachment of an electron-deficient phosphorus atom to the benzenoid ring in VII, the pK_a values did not correlate with σ^+. Furthermore, a better correlation was obtained with σ than with σ^0 values. Together these observations indicate that there is little direct resonance interaction between the *P*-phenyl substituents and the phosphorus atom. The conclusion is similar to that drawn in the fluorenylide case (1); the phosphorus substituents were exerting mainly an inductive effect on the phosphorus atom, although it undoubtedly contained both a σ and a π component.

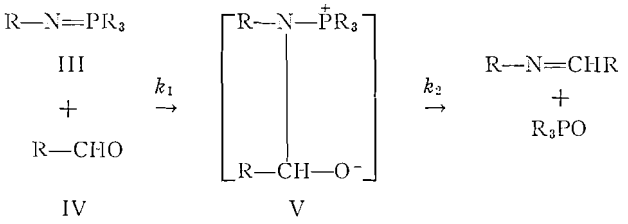
It may be concluded that the basicity of iminophosphoranes is dependent on the nature of both the nitrogen and phosphorus substituents. There can be stabilization of such structures by delocalization of the charge from nitrogen by inductive effects, by $p\pi$–$p\pi$ overlap with nitrogen substituents, and by $p\pi$–$d\pi$ overlap with phosphonium groups.

The results from this work and our earlier work on fluorenylides (1) are pertinent to the question of electronic interactions of organic substituents with quaternary phosphorus. We conclude, on the basis of earlier arguments (3, 19), that there is $p\pi$–$d\pi$ resonance interaction between quaternary phosphorus and a carbanion (in ylids) or a nitrogen anion (in iminophosphoranes). However, at the same time we conclude from our own work that interaction of the same quaternary phosphorus atom with phenyl substituents is of a different nature, devoid of strong resonance interactions. This interaction can be rationalized by the proposal that there is little $p\pi$–$d\pi$ overlap between the phenyl group and phosphorus, perhaps caused by steric interference in the ring orientation required for maximum overlap. (This would leave inductive effects as the major observed mode of interaction.) Alternatively, there may be $p\pi$–$d\pi$ interaction between phenyl and phosphorus, but the effects created thereby are inefficiently reflected at the carbanion (the carbanion is our probe to the phosphorus atom by a measure of its basicity). This latter view is consistent with earlier work (20) in phosphoryl systems, in which it was concluded that substituents could conjugate weakly with phosphorus but that there was no direct conjugation with the phosphorus–oxygen bond. There is insufficient evidence available at present to permit a choice between these (and perhaps other) rationalizations.

Reaction with Carbonyl Compounds

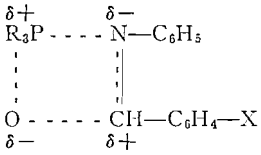
The substituted iminophosphoranes (VI and VII) all reacted with a series of benzaldehydes. A typical reaction, that between *N*-phenyliminotriphenylphosphorane (VI*e*) and *p*-nitrobenzaldehyde in ethanolic solution, was first order in each component. The reaction rates were subject to a solvent effect, in that the reaction was twice as fast in ethanol as in chloroform, and 30 times as fast in ethanol as in benzene. These observations are analogous to those made by Speziale and Bissing (10) for the reaction of carbethoxymethylenetriphenylphosphorane with benzaldehyde. They are consistent with a proposal of increased charge localization in the transition state. In other words, these data are in agreement with the proposed intermediacy of a betaine (V). It is also consistent with the latter's formation in the slow step of the reaction (i.e. $k_2 > k_1$).

The reaction of *N*-phenyliminotriphenylphosphorane (VI*e*) with benzaldehyde showed

[3] 

a small activation energy (8.46 kcal/mole) and a large negative entropy of activation (−42.0 e.u. at 40.5°). This trend also was found by Speziale and Bissing for the Wittig reaction (10). It indicates that the transition state probably is highly structured (i.e. the phosphorus and oxygen probably are eclipsed as a result of electrostatic attraction). Rate-limiting betaine formation implies considerable concentration of charge, which would require significantly increased solvation. Both of these factors would lead to a negative entropy of activation. Furthermore, they also imply that $k_2 > k_1$.

The substituent effect observed by reacting various benzaldehydes with *N*-phenyliminotriphenylphosphorane also indicated that $k_2 > k_1$. A ρ value of +2.1 was obtained (Table II) from a plot of log k/k_0 versus σ for substituted benzaldehydes. The sign of the ρ value indicates that the aldehyde was subjected to nucleophilic attack on the carbonyl carbon in the slow step. The magnitude of the ρ value compares favorably with that (+2.7) reported by Speziale and Bissing (10) for the Wittig reaction, a reaction involving slow, reversible betaine formation and rapid betaine decomposition. The ρ value is larger than, and of the opposite sign to, that expected for a reaction in which the second step, betaine decomposition, was the slow step ($k_1 > k_2$). In such an instance, a transition state such as IX would be involved. The effect of electron-donating groups (X) would be to lower the energy of the



IX

species and speed the reaction. Our observations are just the opposite.

A plot of $-pk_{BH^+}$ for the substituted benzaldehydes (21) versus log k/k_0 for the reaction between VI*e* and the appropriate benzaldehydes gave a straight line with a slope of +0.85. This observation clearly ruled out an alternate mechanism involving nucleophilic attack by carbonyl oxygen on phosphorus. It is consistent with the proposed nucleophilic attack by imine on the carbonyl carbon in the rate-limiting step.

Additional evidence for betaine formation being the slow step was provided by a Hammett plot of log k/k_0 versus σ for the reaction of a series of *N*-phenyliminotri-(substituted phenyl)-phosphoranes (VII*a*–VII*d*) with *p*-nitrobenzaldehyde (Table I). A ρ value of −0.70 was obtained, the effect per substituent being one-third as large. The sign of the ρ value indicates that electron-withdrawing groups slowed the reaction. On the basis of our pK_a studies, it would be expected that such substituents would decrease the nucleophilicity of the imine. Reduced nucleophilicity would be expected to decrease k_1, but the same substitution would be expected to increase the rate of betaine decomposition (k_2) (22). That the former expectation was reflected in the observed data argues for betaine formation (k_1) being the slow step of the reaction.

Can. J. Chem. Downloaded from www.nrcresearchpress.com by 210.87.254.6 on 09/05/12
For personal use only.

Can. J. Chem. Downloaded from www.nrcresearchpress.com by 210.87.254.6 on 09/05/12
For personal use only.

The small magnitude of the reaction constant, especially when contrasted with the large ρ value for the pK_a values of the same imines (VII), may be indicative that, although betaine formation may be the slow step ($k_2 > k_1$), there is not much difference between k_1 and k_2. The smaller magnitude of the ρ value for the effect of benzaldehyde substituents compared with that reported by Speziale and Bissing (10) supports this hypothesis. The smaller solvent effect (a factor of 29 from benzene to ethanol in this work compared with a factor of 927 from benzene to ethanol reported by Speziale and Bissing (10)) also is consistent with the difference in k_1 and k_2 being less than that for ylids. It would appear that the *P*-phenyl substituents in VII are exerting opposing effects on the two steps of the reaction, betaine formation and betaine decomposition, thereby causing little change in k_{obs}.

The effect of the *N*-phenyl substituents in VI on the rate of reaction of imines with *p*-nitrobenzaldehyde clearly indicated a change in mechanism and supports the hypothesis that k_1 and k_2 are very similar. A plot of log k/k_0 versus σ for the substituents *p*-nitro, *m*-nitro, *m*-chloro, *p*-bromo, and hydrogen in VI gave a straight line with a ρ value of -2.4. This indicated that the more nucleophilic imine (VI*e*) reacted fastest, as would be expected for $k_2 > k_1$, i.e. imine nucleophilicity was reflected mainly in the first (and slow) step. However, a plot of log k/k_0 versus σ for the substituents *p*-methoxy, *p*-methyl, and hydrogen gave a straight line with a ρ value of $+0.95$. This observation, the more nucleophilic imine (VI*g*) giving a slower rate, is inconsistent with betaine formation being the slow step. The complete plot is concave down, a pattern previously observed for a change in the rate-limiting step but not for a complete change in the mechanism of a reaction (18, pp. 189–190; 23).

The pattern of substituent effects elaborated above may be rationalized as follows. With unsubstituted imine (VI*e* and VII*b*) betaine formation may be the rate-limiting step (i.e. $k_2 > k_1$). Accordingly, changes in the solvent polarity and changes in the electrophilicity of the carbonyl group would be reflected in k_{obs}. Under a fixed set of conditions (i.e. a common solvent and common aldehyde), changes in the imine structure theoretically could be reflected to the greatest degree in k_1 or k_2. Imine structure affects k_1 through alterations in the nucleophilicity such that electron-withdrawing substituents on the *P*-phenyl or *N*-phenyl groups decrease the electron density both on phosphorus and on nitrogen. This leads to a less nucleophilic nitrogen (i.e. smaller k_1) but to a phosphorus more susceptible to oxyanion attack (i.e. larger k_2). Thus, k_1 remains the rate-limiting step, and alterations in k_1 are reflected directly in k_{obs}. However, electron-donating substituents on the *P*-phenyl or *N*-phenyl groups increase the electron density about both phosphorus and nitrogen. This leads to a more nucleophilic nitrogen (i.e. larger k_1) but to a phosphorus less susceptible to oxyanion attack (i.e. smaller k_2). Therefore, k_2 becomes the rate-limiting step, and alterations in k_2 are reflected directly in k_{obs}.

On the basis of this rationale, the change of the rate-limiting step can be explained. At some point, as the electron density on nitrogen becomes sufficiently large, the rate-limiting step changes from betaine formation to betaine decomposition. Examination of our data indicates that $k_2 > k_1$ when the *P*-phenyl group carries any kind of substituent and when the *N*-phenyl group carries no substituent or an electron-withdrawing substituent. When the *N*-phenyl group carries electron-donating substituents it appears that $k_1 > k_2$.

The situation just described is not novel. Similar changes in the rate-limiting step appear to prevail in methylenephosphoranes (3). Whereas "stabilized" phosphonium ylids such as carbomethoxymethylenetriphenylphosphorane (10) and fluorenylidenetriphenylphosphorane (24) react with carbonyl compounds by a mechanism involving

rate-limiting betaine formation, non-stabilized ylids such as methylenetriphenylphosphorane undergo the same reaction but with rapid betaine formation and rate-limiting decomposition (25). However, the work reported herein on the reaction of iminophosphoranes with carbonyl compounds is the first describing a change in the rate-limiting step through a continuous series of "ylidic" substances.

We are continuing our study of this reaction with a view to investigating its reversibility, elaborating further on the relative values of the rate constants, and providing more convincing evidence for the intermediacy of a betaine.

EXPERIMENTAL

General

Melting points are uncorrected. Analyses were performed by Alfred Bernhardt Microanalytical Laboratory, Mülheim (Ruhr). All pH determinations were carried out with a Beckman model 76 expanded-scale pH meter equipped with glass and saturated calomel electrodes and standardized with a standard buffer of pH 7.02 at 25° in an aqueous medium.

Preparation of Iminophosphoranes

The *N*-phenyliminotri-(substituted phenyl)-phosphoranes (VII) were prepared by adding an ethereal solution of the phosphine to an equimolar ethereal solution of phenyl azide (26). After the solution was heated under reflux for 2 h to ensure complete evolution of the nitrogen, the solvent was evaporated and the residue was crystallized from absolute ethanol.

The phosphines required for these syntheses have been described in our earlier work (1).

N-Phenyliminotri-(*m*-tolyl)-phosphorane, pale-yellow microcrystals, m.p. 135–136°.

Anal. Calcd. for $C_{27}H_{26}PN$: C, 82.00; H, 6.59; P, 7.85; N, 3.54. Found: C, 81.13; H, 6.53; P, 8.26; N, 3.70.

N-Phenyliminotri-(*p*-bromophenyl)-phosphorane, yellow microcrystals, m.p. 166–167°.

Anal. Calcd. for $C_{24}H_{17}PNBr_3$: C, 48.90; H, 2.88; P, 5.25; N, 2.38; Br, 40.60. Found: C, 48.62; H, 2.98; P, 5.05; N, 3.14; Br, 40.98.

N-Phenyliminotri-(*p*-chlorophenyl)-phosphorane, pale-yellow microcrystals, m.p. 160–161°.

Anal. Calcd. for $C_{24}H_{17}PNCl_3$: C, 63.00; H, 3.72; P, 6.56; N, 3.10; Cl, 23.30. Found: C, 62.97; H, 3.73; P, 6.57; N, 3.27; Cl, 23.46.

The *N*-(substituted phenyl)-iminotriphenylphosphoranes (VI) were prepared by adding an ethereal solution of triphenylphosphine to an equimolar ethereal solution of the substituted phenyl azide. After the solution was heated under reflux for 2 h and the nitrogen evolution had ceased, the solvent was removed *in vacuo* and the residue was crystallized from absolute ethanol. By this means the seven imines (VI*a*–VI*g*) listed in Table I were prepared. In all cases the physical constants agreed with those in the literature.

The substituted phenyl azides were prepared from the appropriate substituted aniline by treatment with nitrous acid and then sodium azide as previously described (27). The crude azides were isolated, but not purified, and then treated directly with triphenylphosphine.

pK_a Determinations

Three different methods were employed. The most reproducible method was back titration, whereby 0.1 mmole of imine was dissolved in 40 ml of absolute ethanol. After the addition of 6.5 ml of 0.0205 *N* hydrochloric acid, the solution was titrated with 0.0173 *N* potassium hydroxide. A plot of the volume of titrant versus pH was prepared. From this titration curve the point of half-neutralization could be determined. At that point the concentration of imine and its conjugate acid would be equal. Therefore, the pK_a of the imine would equal the pH of the solution (28). The pK_a values so obtained are reported in Table I.

The imines also were titrated directly with 0.0205 *N* hydrochloric acid. The pK_a values thereby determined were consistently lower than those obtained by back titration, although a plot of pK_a versus σ gave nearly the same ρ value (+3.3).

Spectrophotometric determination of the pK_a values of the imines was carried out as reported in our earlier work (1). The pK_a values thereby obtained were within 0.3 pK_a unit of those reported in Table I. A plot of pK_a versus σ gave nearly the same ρ value (+3.3).

Reaction of Imines with Aldehydes

A general procedure was used for all such reactions. A solution of 2.5 mmoles of imine and 2.5 mmoles of aldehyde in 50 ml of ethanol was heated under reflux for 3 h. Evaporation of half of the solvent and then cooling the rest led to the precipitation of the Schiff base. Reaction of *p*-nitrobenzaldehyde with the imines VI*a*–VI*g* gave the following products, respectively: 80% of *p*-nitro-*N*-(*p*-nitrobenzylidene)-aniline, m.p. 200–201° (lit. (29) m.p. 199–200°); 77% of *m*-nitro-*N*-(*p*-nitrobenzylidene)-aniline, m.p. 154–155° (lit. (29) m.p. 152–153°); 60% of *m*-chloro-*N*-(*p*-nitrobenzylidene)-aniline, m.p. 110–111° (Anal. Calcd. for $C_{13}H_9N_2O_2Cl$: C, 59.80; H, 3.45; N, 10.70; Cl, 13.20. Found: C, 59.48; H, 3.44; N, 10.51; Cl, 12.77); 84% of *p*-bromo-*N*-(*p*-nitrobenzylidene)-aniline, m.p. 159–160° (lit. (30) m.p. 160–161°); 68% of

Can. J. Chem. Downloaded from www.nrcresearchpress.com by 210.87.254.6 on 09/05/12
For personal use only.

N-(*p*-nitrobenzylidene)-aniline, m.p. 91–91.5° (lit. (31) m.p. 93°); 78% of *N*-(*p*-nitrobenzylidene)-*p*-toluidine, m.p. 123–124° (lit. (30) m.p. 122.5°); and 95% of *N*-(*p*-nitrobenzylidene)-*p*-anisidine, m.p. 134–135° (lit. (32) m.p. 139°). Reaction of benzaldehyde with VIe gave *N*-benzylideneaniline in an 82% yield, m.p. 49–50° (lit. (33) m.p. 48°).

Kinetic Measurements

Reagent-grade materials were used and purified where necessary. Ethanol was distilled from magnesium filings.

The rates of reaction of the imines (VI and VII) with the benzaldehydes were determined by following the rates of disappearance of the imine. The imine concentration was determined by quenching the reaction solution with hydrochloric acid and then back titrating as described for the pK_a determinations. In control experiments it was shown that the ethanol–water ratio did not influence this titration between 5% and 50% water. Furthermore, the presence of the other reactant, the benzaldehyde, or the presence of the products, *N*-benzylidene aniline and the phosphine oxide, did not alter the reliability of this titration.

The order of the reaction was determined by the differential method (34, p. 14). The integrated form of the rate equation for a second-order reaction was used to calculate the reaction rates (34, p. 12). Standard means were used to obtain the energy (E_a) and entropy ($\Delta S^{\pm}$) of activation (35), the reaction temperatures being 30.0 ± 0.2°, 40.5 ± 0.2°, and 50.0 ± 0.2°.

In a typical experiment 0.5 mmole of the imine and 0.5 mmole of the aldehyde were separately dissolved in exactly 100 ml of absolute ethanol and brought to 40.5 ± 0.2° in a water bath shaker. For the $t = 0$ determination 20 ml of each solution was withdrawn with a syringe and added to a beaker containing 6.5 ml of 0.0205 *N* hydrochloric acid. The acid converted the imine into its conjugate base, thereby preventing any reaction with the aldehyde. The quenched solution was then titrated potentiometrically with 0.0173 *N* potassium hydroxide. The remaining ethanolic solutions of imine and aldehyde were mixed in the water bath. Aliquots were withdrawn periodically, quenched with 6.5 ml of standard hydrochloric acid, and then titrated potentiometrically.

The reaction rates are recorded in Table I.

ACKNOWLEDGMENTS

We are grateful for the financial support provided by the Petroleum Research Fund, administered by the American Chemical Society, and by the National Science Foundation (grant No. GP-1321). We acknowledge helpful discussions with Dr. J. A. Stewart.

REFERENCES

1. A. Wm. Johnson, S. Y. Lee, R. A. Swor, and L. D. Royer. J. Am. Chem. Soc. **88**, 1953 (1966).
2. H. Staudinger and J. Meyer. Helv. Chim. Acta, **2**, 635 (1919).
3. A. Wm. Johnson. Ylid chemistry. Academic Press, Inc., New York. 1966.
4. E. Bergmann and H. A. Wolff. Chem. Ber. **63**, 1176 (1930).
5. L. Horner and A. Gross. Ann. **591**, 117 (1955).
6. R. Appel and A. Hauss. Chem. Ber. **93**, 405 (1960).
7. R. Appel and R. Schollhorn. Angew. Chem. **76**, 991 (1964).
8. T. W. Campbell, J. J. Monagle, and V. S. Foldi. J. Am. Chem. Soc. **84**, 3673 (1962).
9. J. J. Monagle, T. W. Campbell, and H. F. McShane, Jr. J. Am. Chem. Soc. **84**, 4288 (1962).
10. A. J. Speziale and D. E. Bissing. J. Am. Chem. Soc. **85**, 3878 (1963).
11. L. A. Flexser, L. P. Hammett, and A. Dingwall. J. Am. Chem. Soc. **57**, 2103 (1935).
12. L. Horner and H. Oediger. Ann. **627**, 142 (1959).
13. G. W. Brown, R. C. Cookson, I. D. R. Stevens, T. C. W. Mak, and J. Trotter. Proc. Chem. Soc. 87 (1964).
14. R. W. Taft, Jr. J. Phys. Chem. **64**, 1805 (1960).
15. H. van Bekkum, P. E. Verkade, and B. M. Wepster. Rec. Trav. Chim. **78**, 815 (1959).
16. R. Stewart and J. P. O'Donnell. Can. J. Chem. **42**, 1694 (1964).
17. D. P. Craig and E. A. Magnusson. J. Chem. Soc. 4895 (1956).
18. J. E. Leffler and E. Grunwald. Rates and equilibria of organic reactions. John Wiley & Sons, Inc., New York. 1963.
19. R. F. Hudson. Structure and mechanism in organophosphorus chemistry. Academic Press, Inc., New York. 1965. p. 83.
20. E. A. C. Lucken and M. A. Whitehead. J. Chem. Soc. 2459 (1961).
21. K. Yates and R. Stewart. Can. J. Chem. **37**, 664 (1959).
22. A. Wm. Johnson and V. L. Kyllingstad. J. Org. Chem. **31**, 334 (1966).
23. B. M. Anderson and W. P. Jencks. J. Am. Chem. Soc. **82**, 1773 (1960).
24. A. Wm. Johnson and R. B. LaCount. Tetrahedron, **9**, 130 (1960).
25. S. Fliszar, R. F. Hudson, and G. Salvadori. Helv. Chim. Acta, **46**, 1580 (1963).
26. R. O. Lindsay and C. F. H. Allen. Org. Syn. Collective Vol. **III**, 710 (1955).
27. P. A. S. Smith and J. H. Boyer. Org. Syn. Collective Vol. **IV**, 75 (1963).

Can. J. Chem. Downloaded from www.nrcresearchpress.com by 210.87.254.6 on 09/05/12
For personal use only.

28. H. H. WILLARD, L. L. MERRITT, JR., and J. A. DEAN. Instrumental methods of analysis. D. Van Nostrand Company, Inc., New York. 1960. p. 416.
29. C. K. INGOLD and H. A. PIGGOTT. J. Chem. Soc. **121**, 2793 (1922).
30. A. LOWY and C. G. KING. J. Am. Chem. Soc. **43**, 627 (1921).
31. O. FISCHER. Chem. Ber. **14**, 2526 (1881).
32. F. G. POPE and R. FLEMING. J. Chem. Soc. **93**, 1917 (1908).
33. F. TIEMANN and K. PIEST. Chem. Ber. **15**, 2029 (1882).
34. K. J. LAIDLER. Chemical kinetics. McGraw-Hill Book Co., Inc., New York. 1950.
35. S. GLASSTONE, K. J. LAIDLER, and H. EYRING. The theory of rate processes. McGraw-Hill Book Co., Inc., New York. 1941. p. 195.

Can. J. Chem. Downloaded from www.nrcresearchpress.com by 210.87.254.6 on 09/05/12
For personal use only.

Can. J. Chem. Downloaded from www.nrcresearchpress.com by 210.87.254.6 on 09/05/12
For personal use only.

THE CHEMISTRY OF THE INDOLE GRIGNARD REAGENT

I. THE REACTION OF INDOLE MAGNESIUM IODIDE WITH ETHYL CHLOROFORMATE[1]

S. KAŠPÁREK[2] AND R. A. HEACOCK

Atlantic Regional Laboratory, National Research Council, Halifax, Nova Scotia

Received July 22, 1966

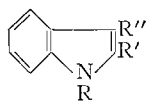
ABSTRACT

In contrast to previous reports in the literature, it has been shown that both 1- and 3-carbethoxyindole are obtained from the reaction of indole magnesium iodide with 1 or 2 moles of ethyl chloroformate. The formation of 1-carbethoxyindole was favored at low temperatures (i.e. −10°), whereas maximum yields of 3-carbethoxyindole were obtained at 10°. Significant quantities of 1,3-dicarbethoxyindole are only formed in the presence of 2 equivalents of ethyl chloroformate and when the reaction is carried out at higher temperatures (i.e. 35°).

Paper and gas–liquid chromatographic systems have been developed for the qualitative and quantitative analysis of mixtures containing indole, 1-, 2-, and 3-carbethoxyindole, and 1,3-dicarbethoxyindole.

The main product of the reaction between indole magnesium iodide and ethyl chloroformate was originally reported to be 2-carbethoxyindole (I) by Oddo and Sessa more than 50 years ago (1). However, Majima and Kotake subsequently claimed that the major product was not I but 3-carbethoxyindole (II) (2, 3), and that under ideal conditions yields of up to 78% of this ester could be obtained (3). The Japanese authors further reported that 1,3-dicarbethoxyindole (III) was invariably formed together with the monoester II, and that when the reaction was carried out in the presence of 2 moles of ethyl chloroformate the diester III was formed in sufficient quantity to allow its isolation from the final reaction mixture by fractional crystallization (3).

In the 36 years that have elapsed since Majima and Kotake's second paper appeared, several authors have employed essentially the same method for the preparation of II, without reporting precise reaction conditions or yields obtained (cf. refs. 4–6). However, Brown and Garrison claimed that the procedure described by Majima and Kotake was



I R = R'' = H; R' = $COOC_2H_5$
II R = R' = H; R'' = $COOC_2H_5$
III R' = H; R = R'' = $COOC_2H_5$
IV R = R' = R'' = H
V R = $COOC_2H_5$; R' = R'' = H
VI R = $CONH_2$; R' = R'' = H
VII R = $C_6H_5CONHCO$; R' = R'' = H

unsatisfactory and that better results were obtained by carrying out the reaction between −15 and −5° (5) instead of at the higher temperature (up to 35°) employed previously by the Japanese workers. Noland and Rieke prepared II by Majima and Kotake's method in an unspecified yield, but reported that the melting point of II could be raised from 118–119° to 126–127° by chromatographic purification on alumina (6).

In our hands, the yields of II obtained by the interaction of ethyl chloroformate and indole magnesium iodide, under the conditions previously described, were lower than anticipated. This fact, together with the general confusion in the literature on this subject, indicated that a comprehensive investigation of the effect of the systematic variation of several of the more important reaction parameters on the nature and composition of the

[1]*Issued as N.R.C. No. 9219.*
[2]*National Research Council Postdoctorate Fellow, 1965–1967.*

products would be of value. A series of experiments was therefore performed in which the reaction between equivalent quantities of indole magnesium iodide and ethyl chloroformate was carried out at a number of different temperatures (between −10 and 20°) for a series of reaction times (between 5 and 140 min). The reaction mixtures were worked up in the usual way, and in each case the products were analyzed by means of paper and gas–liquid chromatographic procedures.

Satisfactory separations of authentic samples of all possible expected components of the reaction mixtures (i.e. indole (IV), 3-carbethoxyindole (II), 1,3-dicarbethoxyindole (III), and 2-carbethoxyindole (I)) could readily be obtained by radial paper chromatography with a formamide/(benzene – light petroleum (1:1)) system (cf. ref. 7). The chromogenic reagents commonly employed for the detection of indoles on developed chromatograms, such as Ehrlich's reagent, cinnamaldehyde, and *p*-dimethylaminocinnamaldehyde, were unsatisfactory in this case, since I, II, and III gave either no color or weak ill-defined colors with these reagents. However, these esters and unchanged indole gave characteristic colors with Gibb's reagent (*N*,2,6-trichloro-*p*-quinoneimine) and could easily be located on developed chromatograms by spraying with this reagent.

Gas–liquid chromatography has not so far been employed extensively for the analysis of indole derivatives, but simple indoles have been separated satisfactorily with silicone oil (8, 9) or "Versamid 900" (10, 11) as stationary phases. In the current investigation it was observed that IV and the esters I, II, and III could be separated on a 6 ft × $\frac{1}{8}$ in. column with the silicone gum rubber (SE-30) (5% on Chromosorb W) as the stationary phase. This stationary phase has previously been employed for the gas chromatography of tryptamine derivatives (12).

Paper chromatographic analysis of the products obtained from the interaction of indole magnesium iodide and 1 or 2 moles of ethyl chloroformate invariably indicated the presence of at least three main components (II, IV, and a substance or substances which travelled with the solvent front, gave a yellow color with Gibb's reagent, and was assumed to be the diester III). It appeared, at first, that gas chromatographic analysis of the reaction mixtures confirmed these results, but a careful study of the temperature dependence of the retention times of indole (IV), authentic samples of the expected reaction products I, II, and III (see Fig. 3), and the components of the reaction mixtures (see Fig. 1) indicated that, although II and IV were always present among the reaction products, the third main product was not the diester III. The gas chromatographic investigation further showed that, unless the reaction was carried out with 2 moles of ethyl chloroformate, only traces of III were formed (see Table II), and that only when the reaction was carried out at 35° were significant quantities of III formed (see Fig. 1B).

A careful reexamination of the paper chromatographic behavior of all the substances under investigation indicated that the component of the reaction mixture previously assumed to be III gave a somewhat different shade of yellow color with Gibb's reagent, and that the colored derivative was more stable than that obtained from an authentic sample of III. It was not possible to differentiate between these two compounds on formamide- or dimethylformamide-treated paper with a variety of nonpolar running solvents (see Table I).

The preparation of suitable calibration curves enabled a quantitative analysis of the reaction mixtures to be made by gas–liquid chromatography. In this manner it was ascertained that, in the reaction between indole magnesium iodide and 1 mole of ethyl chloroformate, between 20 and 30% of the original indole (IV) was invariably recovered unchanged, and that the yields of 3-carbethoxyindole (II) varied between 27 and 45%, the

Can. J. Chem. Downloaded from www.nrcresearchpress.com by 210.87.254.6 on 09/05/12
For personal use only.

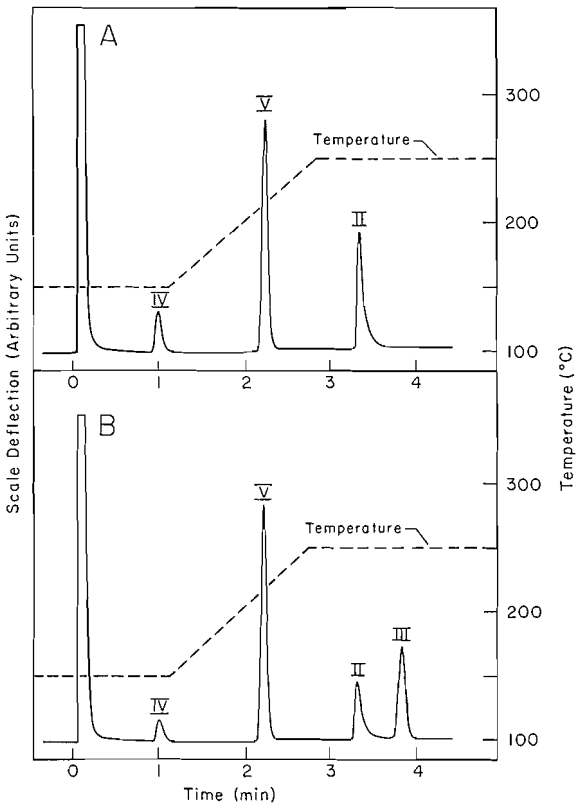


FIG. 1. Gas–liquid chromatograms of the ether-soluble products from the reaction of indole magnesium iodide with (A) 1 or 2 moles of ethyl chloroformate at temperatures below 0°, and (B) 2 moles of ethyl chloroformate at 35°. II = 3-carbethoxyindole; III = 1,3-dicarbethoxyindole; IV = indole; V = 1-carbethoxyindole.

maximum yield of II being obtained when the reaction was carried out at 10° for 100 min. This finding is in contrast to one of the more recent previous reports, which suggests that low temperatures favor the formation of II (5). However, under all the reaction conditions studied, significant quantities of the third component were always formed, and it appeared to be the main product when the reaction was carried out below −5°. It was possible to separate this substance from the other components by column chromatography on alumina or "Polyclar AT". The infrared spectrum of this product, which was obtained as a colorless oil, exhibited a strong ester carbonyl peak at 1 735 cm^{-1}, but showed no peaks in the NH stretching region. The proton magnetic resonance (p.m.r.) spectrum of the oil indicated the presence of four aromatic protons and the indole α and β protons (see Fig. 2) (cf. refs. 13–17). The spectroscopic results, together with the microanalytical data, suggest that the new product is the hitherto undescribed 1-carbethoxyindole (V),[3] which was obtained in a 30–40% yield and which gave indole (IV) on hydrolysis with aqueous alkali and a white crystalline solid, probably indole-1-carboxamide (VI), on treatment with aqueous ammonia. A substance reported to be the amide VI had previously been obtained by Dutcher and Kjaer by the hydrolysis of *N*-benzoylindole-1-carboxamide (VII) (18). However,

[3]*At the conclusion of our investigation we became aware of the fact that, although 1-carbethoxyindole had not previously been described in the literature, it was available commercially from the Regis Chemical Co., Chicago, Illinois, U.S.A.*

Can. J. Chem. Downloaded from www.nrcresearchpress.com by 210.87.254.6 on 09/05/12
For personal use only.

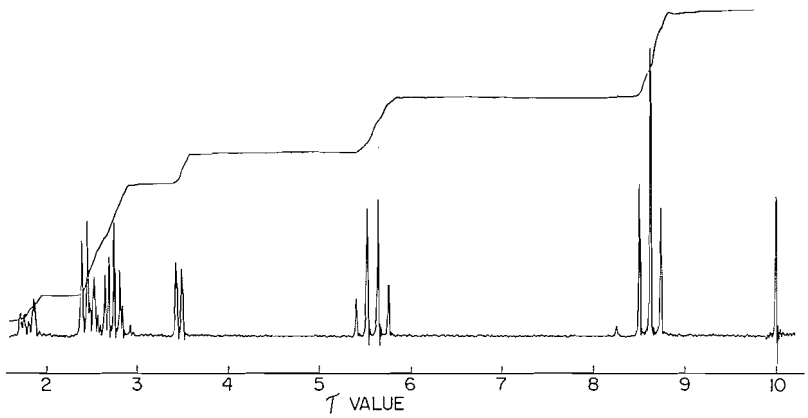


FIG. 2. The p.m.r. spectrum of 1-carbethoxyindole (V) in $CDCl_3$ (recorded on a Varian A-60-A instrument with tetramethylsilane as an internal standard).

these authors reported a slightly different melting point and different ultraviolet spectroscopic data for their product (18).

In conclusion, it may be stated, with regard to the reaction between indole magnesium iodide and either 1 or 2 moles of ethyl chloroformate, that (*i*) at low temperatures (i.e. $< -5°$) and for reaction times between 5 and 60 min the main product is 1-carbethoxyindole (V); (*ii*) 3-carbethoxyindole (II) is always formed, but in yields not exceeding 46%, the formation of II being favored by higher reaction temperatures (ca. 10°); (*iii*) some unreacted indole was always recovered unchanged; and (*iv*) significant quantities of 1,3-dicarbethoxyindole (III) are only formed when the reaction is carried out at temperatures of not less than 35° with 2 moles of ethyl chloroformate.

EXPERIMENTAL

The infrared spectra were recorded on a Perkin–Elmer model 237 recording spectrophotometer; the ultraviolet spectra were recorded on either a Bausch and Lomb "Spectronic 505" or a Beckman DU spectrophotometer, and the p.m.r. spectrum on a Varian A-60-A instrument.

Carbethoxyindoles

3-Carbethoxyindole (II)

A solution of indole-3-carboxylic acid (3 g) in dry ethanol (125 ml), saturated with hydrogen chloride, was boiled under reflux, in the dark, under anhydrous conditions for 2 h. The deep-red solution was then evaporated to dryness *in vacuo*, the residues were dissolved, as far as possible, in ether (200 ml), and the ether solution was washed with aqueous sodium bicarbonate solution and water. Recrystallization of the solid obtained on concentration of the dried (Na_2SO_4) ether solution from 50% ethanol gave 3-carbethoxyindole (1.57 g, 45%), m.p. 123–124°, ν_{max}^{Nujol} 3 250 cm^{-1} (NH) and 1 670 cm^{-1} (C=O), $\lambda_{max}^{C_2H_5OH}$ 282 and 288 mμ. As far as the authors are aware, there are no previous reports in the literature of the preparation of 3-carbethoxyindole by the direct esterification of indole-3-carboxylic acid, the compound having previously been obtained by the Grignard reaction described in this paper. The literature melting points for 3-carbethoxyindole are 118–119° (2), 124° (19), and 126–127° (6).

2-Carbethoxyindole (I)

2-Carbethoxyindole (m.p. 121–123°, ν_{max}^{Nujol} 3 300 cm^{-1} (NH) and 1 690 cm^{-1} (C=O), $\lambda_{max}^{C_2H_5OH}$ 293 mμ) was prepared by the method of Fischer and Pistor (20).

1,3-Dicarbethoxyindole (III)

1,3-Dicarbethoxyindole (m.p. 103–104°, ν_{max}^{Nujol} 1 750 and 1 715 cm^{-1} (C=O); $\lambda_{max}^{C_2H_5OH}$ 274, 285, and 292 (sh) mμ) was prepared by the method of Majima and Kotake (3).

1-Carbethoxyindole (V)

Freshly distilled ethyl chloroformate (1.1 ml) in dry ether (5 ml) was added, with stirring, at −10° during 15 min to indole magnesium iodide (prepared from indole (1.18 g) by the method of Doyle *et al.* (21)) in dry ether (10 ml). After 90 min at a temperature between −9 and −5°, crushed ice was added; the reaction mixture was acidified with dilute acetic acid and extracted with ether (3 × 30 ml). The combined ether extracts were washed with aqueous sodium bicarbonate and water, dried (Na_2SO_4), and concentrated *in*

Can. J. Chem. Downloaded from www.nrcresearchpress.com by 210.87.254.6 on 09/05/12
For personal use only.

vacuo. The residue was dissolved in benzene (5 ml) and adsorbed on "Polyclar AT"[4] (24 × 3 cm). Elution of the column with benzene – light petroleum[5] (1:3) (100 ml) gave 1-carbethoxyindole (0.75 g, 40%), which was obtained as a colorless oil (b.p. 150–151° at 13–14 mm)[6] on vacuum distillation of the crude product, ν_{max}^{Nujol} 1 735 cm^{-1} (C=O); $\lambda_{max}^{C_2H_5OH}$ 254, 260, 284, and 291 mμ ($\epsilon_{max}^{C_2H_5OH}$ 10 898, 10 599, 3 693, and 5 365). The p.m.r. spectrum in $CDCl_3$ indicated the presence of six protons in the region between τ 1.78 and 3.45; the doublet of doublets observed at τ 3.45 with splittings of 3.7 ($J_{2,3}$) and 0.7 ($J_{3,7}$) c.p.s. can be assigned to the β indole proton, and the complex multiplet with an average τ value of 1.78 is probably caused by the 7-proton (cf. ref. 22). The signals caused by the α indole proton and the remaining aromatic protons are observed as a complex series of peaks between τ 2.83 and 2.34 (see Fig. 2).

Anal. Calcd. for $C_{11}H_{11}NO_2$: C, 69.82; H, 5.85; N, 7.40. Found: C, 69.62; H, 5.65; N, 7.64.

Indole (0.3 g) and 3-carbethoxyindole (0.6 g) could also be obtained by further elution of the column with benzene – light petroleum (1:1) mixtures and benzene, respectively.

Ammonolysis of 1-Carbethoxyindole

A suspension of 1-carbethoxyindole (0.7 g) in concentrated aqueous ammonia solution (20 ml) was stirred at room temperature for 8 h. A white solid was obtained which gave indole-1-carboxamide (VI) (0.2 g) as colorless plates, m.p. 174–175° (hot stage microscope), after repeated recrystallizations from ether – light petroleum (b.p. 60–80°); ν_{max}^{Nujol} 3 340, 3 175 (amide NH_2), 1 728, 1 625, 1 605, 1 588, and 1 530 cm^{-1}; $\lambda_{max}^{C_2H_5OH}$ 256, 262, 284, and 292 mμ.

Anal. Calcd. for $C_9H_8N_2O$: C, 67.49; H, 5.03; N, 17.49. Found: C, 67.85; H, 4.72; N, 17.65.

Dutcher and Kjaer obtained a product described as indole-1-carboxamide by the alkaline hydrolysis of *N*-benzoyl-(1-carbamylindole) (VII), but reported a melting point (198–199°) and ultraviolet spectroscopic absorption maxima (18) which differed from those obtained in the current investigation.

Alkaline Hydrolysis of 1-Carbethoxyindole

A suspension of 1-carbethoxyindole (0.1 g) in 10% aqueous sodium hydroxide (10 ml) was heated on a boiling water bath for 1 h. The reaction mixture was cooled, neutralized with dilute sulfuric acid, and extracted with ether. Paper and gas–liquid chromatographic examination of the dried (Na_2SO_4) ether extracts indicated the presence of indole and unchanged 1-carbethoxyindole.

Paper Chromatography

The R_f values of 1-, 2-, and 3-carbethoxyindole and of 1,3-dicarbethoxyindole are given in Table I. The following notes apply.

Radial development with a suitable nonpolar solvent on paper pretreated with either formamide or dimethylformamide was used, the general procedure being the same as that described for the indole derivatives by Heacock and Mahon (7) (development time ~30 min). The esters (and indole) could be located on the developed chromatograms by spraying with Gibb's reagent (a 2% solution of *N*,2,6-trichloro-*p*-quinoneimine in ethanol).

TABLE I

R_f values* of indole and some carbethoxyindoles

	I	II	III	IV	V
System A†	0.96	0.50	1.00	0.75	1.00
System B‡	0.48	0.13	1.00	0.27	1.00

*Radial development.
†System A = formamide/(benzene – light petroleum (b.p. 60–80°) (1:1)).
‡System B = dimethylformamide–*n*-hexane.
NOTE: Colors given with Gibb's reagent: (I) brown, turning grey after 24 h; (II) brown; (III) yellow-green; (IV) violet; (V) yellow.

Gas–Liquid Chromatography

Determination of Retention Times

A Varian Aerograph model 204 dual-column instrument fitted with two hydrogen-flame ionization detectors was used. The 6 ft × ⅛ in. stainless-steel columns (5% SE-30 on 60–80 Chromosorb W) were used independently. The injector and detector temperatures were maintained at 270 and 250°, respectively. The nitrogen carrier gas flow rate was 14 ml/min and the hydrogen flow rate was 25 ml/min. The column was maintained at the appropriate temperatures during the determination of the relative retention times of I, II, III, IV, and V as a function of the column temperature. The dependence of the retention times of these compounds on column temperature is shown in Fig. 3.

[4]*"Polyclar AT" is a cross-linked polyvinylpyrrolidone, obtained from Chemical Developments of Canada Ltd. (Montreal). Similar separations could be obtained on activated alumina (Peter Spence, type "H", 100–200 mesh).*

[5]*British Drug Houses Analar grade (b.p. 60–80°).*

[6]*The commercial product (Regis Chemical Co.) has a boiling point of 155° at 14 mm. The melting point of 153–155° quoted in the 1965 Regis Chemical Co. catalogue was due to a misprint (personal communication from Dr. W. F. Gannon).*

Can. J. Chem. Downloaded from www.nrcresearchpress.com by 210.87.254.6 on 09/05/12
For personal use only.

Can. J. Chem. Downloaded from www.nrcresearchpress.com by 210.87.254.6 on 09/05/12
For personal use only.

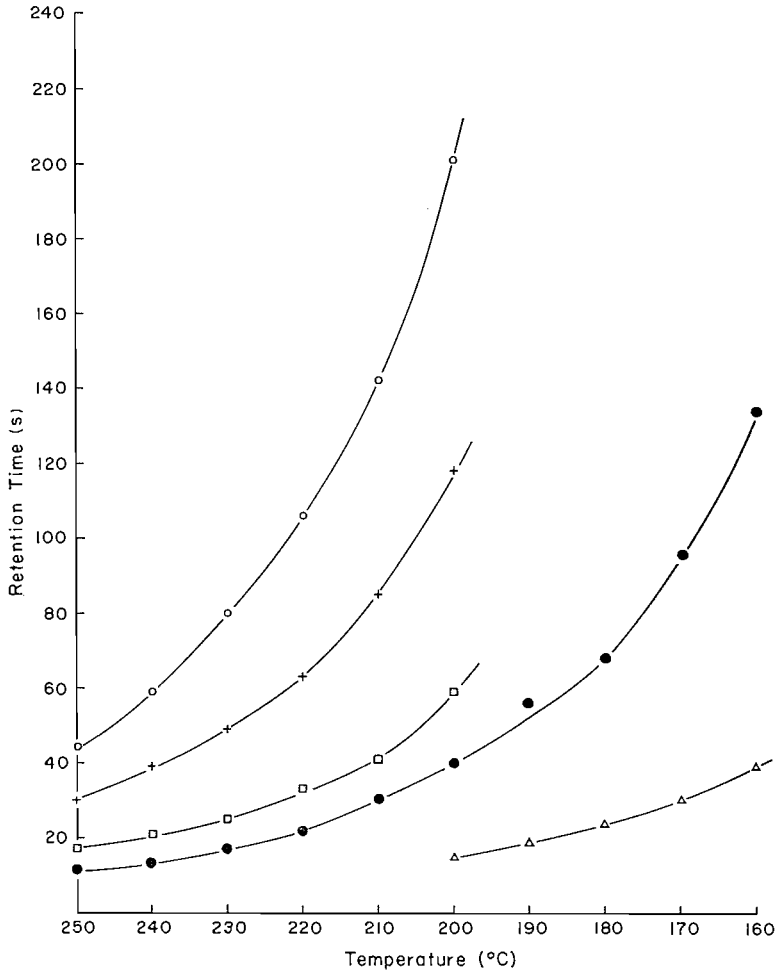


FIG. 3. Temperature dependence of the retention times (measured from the leading edge of the solvent peak) of: △, indole; ●, 1-carbethoxyindole; □, 2-carbethoxyindole; +, 3-carbethoxyindole; ○, 1,3-dicarbethoxyindole.

Analysis of Reaction Products

The reaction between indole magnesium iodide (prepared from 1.18 g indole) and ethyl chloroformate (1.1 ml) was carried out for the times and at the temperatures specified in Table II, in the manner described above for the preparation of 1-carbethoxyindole. The resulting mixture of products was dissolved in absolute ethanol (200 ml), and 1 μl samples of this solution were used for both qualitative and quantitative analysis. The gas flow rates and the temperatures of the injection compartment and the detector were as previously specified.

For *qualitative* analysis, the temperature of the column was maintained at 150° after injection of the sample until the peak caused by indole was observed; the column temperature was then raised during 105 s to 250° and finally maintained at this temperature for several minutes. The second peak observed (when the column temperature reached ca. 220°) was caused by 1-carbethoxyindole, and finally peaks caused by 3-carbethoxyindole and 1,3-dicarbethoxyindole, respectively, were observed with the column temperature at 250°.

For *quantitative* analysis of all four possible components of the reaction mixture, suitable calibration curves were prepared by the peak height method. A slight modification of the procedure used for the qualitative analysis was employed for the quantitative work. One sample was used for the determination of indole and 1-carbethoxyindole, and a second sample for the determination of the other two components. In the first case, the sample was injected with the column temperature at 150°; after the indole peak was observed the temperature was rapidly raised to 220° to obtain the peak caused by 1-carbethoxyindole. In the second case, the peaks caused by 3-carbethoxyindole and 1,3-dicarbethoxyindole were obtained with isothermal runs at

250°, the early peaks caused by the other two components being disregarded. The two-stage procedure was used to ensure maximum peak sharpness; some tailing of the peaks caused by 3-carbethoxyindole and 1,3-dicarbethoxyindole was observed when the initial column temperature was 150°. Each value was based on an average of not less than six determinations. In each case the yields of all the products could be estimated by reference to the calibration curves, and the results are shown in Table II.

TABLE II

Reaction temperature (°C)	Time required for the addition of ethyl chloroformate (min)	Reaction time (min)	% yield*	
			II	V
−10	5	0	27.0	32.8
−10	5	60	30.0	39.6
−10	5	90	30.0	36.0
0	10	30	29.6	32.8
0	10	60	28.6	32.8
0	10	90	29.6	34.4
0	10	120	33.9	31.8
10	10	30	30.7	31.8
10	10	60	35.0	31.8
10	10	90	46.6	32.8
10	10	120	43.4	35.4
20	20	30	37.0	31.8†
20	20	60	39.0	31.8†
20	20	90	37.0	31.8†
20	20	120	37.0	34.4†

*In all cases 20–30% of the original indole was recovered unchanged. II = 3-carbethoxyindole; V = 1-carbethoxyindole. These yields are considerably higher if one allows for the recovered starting material.
†Traces of 1,3-dicarbethoxyindole formed.

ACKNOWLEDGMENTS

The authors express their thanks to Dr. A. McCulloch and Mr. D. G. Smith for assistance in the recording and interpretation of the p.m.r. spectrum.

REFERENCES

1. B. Oddo and L. Sessa. Gazz. Chim. Ital. **41**, 234 (1911).
2. R. Majima and M. Kotake. Ber. **55B**, 3865 (1922).
3. R. Majima and M. Kotake. Ber. **63B**, 2237 (1930).
4. E. Leete and L. Marion. Can. J. Chem. **31**, 775 (1953).
5. R. K. Brown and R. A. Garrison. J. Am. Chem. Soc. **77**, 3839 (1955).
6. W. E. Noland and R. D. Rieke. J. Org. Chem. **27**, 2250 (1962).
7. R. A. Heacock and M. E. Mahon. Can. J. Biochem. Physiol. **38**, 1500 (1960).
8. F. Mossini and T. Vitali. Ric. Sci. Rend. **1**, 244 (1961).
9. R. D. De Moss and V. Gage. Anal. Biochem. **13**, 116 (1965).
10. L. E. Powell. Plant Physiol. **39**, 836 (1964).
11. B. B. Stowe and J. F. Schilke. *In* Regulateurs naturels de la croissance végétale. Colloques internationaux du centre national de la recherche scientifique. Centre National de la Recherche Scientifique, Paris. 1964. No. 123. p. 409.
12. H. M. Fales and J. J. Pisano. Anal. Biochem. **3**, 337 (1962).
13. L. A. Cohen, J. W. Daly, H. Kny, and B. Witkop. J. Am. Chem. Soc. **82**, 2184 (1960).
14. R. V. Jardine and R. K. Brown. Can. J. Chem. **41**, 2067 (1963).
15. J. A. Elvidge and R. G. Foster. J. Chem. Soc. 981 (1964).
16. J. Hutton and W. A. Waters. J. Chem. Soc. 4253 (1965).
17. R. A. Heacock and O. Hutzinger. Can. J. Chem. **43**, 2535 (1965).
18. J. D. Dutcher and A. Kjaer. J. Am. Chem. Soc. **73**, 4139 (1951).
19. F. Millich and E. I. Becker. J. Org. Chem. **23**, 1096 (1958).
20. H. Fischer and K. Pistor. Ber. **56B**, 2317 (1923).
21. F. P. Doyle, W. Ferrier, D. O. Holland, M. D. Mehta, and J. H. C. Nayler. J. Chem. Soc. 2853 (1956).
22. S. McLean. Can. J. Chem. **38**, 2278 (1960).

Can. J. Chem. Downloaded from www.nrcresearchpress.com by 210.87.254.6 on 09/05/12
For personal use only.

THE REACTION OF SULFUR DICHLORIDE WITH *cis,cis*-1,5-CYCLOOCTADIENE

F. LAUTENSCHLAEGER
Dunlop Research Centre, Sheridan Park, Ontario
Received March 28, 1966

ABSTRACT

Transannular additions of sulfur dichloride to various cyclic and bicyclic di- and poly-olefins have been disclosed recently. Our observations on the reaction product from *cis,cis*-cyclooctadiene are reported inasmuch as they supplement the previous findings.

INTRODUCTION

Attempts to synthesize novel sulfur-containing heterocyclic compounds have led us to the observation of the transannular addition of sulfur dichloride to bicycloheptadiene (2). This addition reaction of sulfur dichloride provides a convenient synthesis for a large number of novel cyclic β,β'-dichlorosulfides (1–4). The versatility of that reaction and unusual features of the reaction products were reported recently (4).

RESULTS AND DISCUSSION

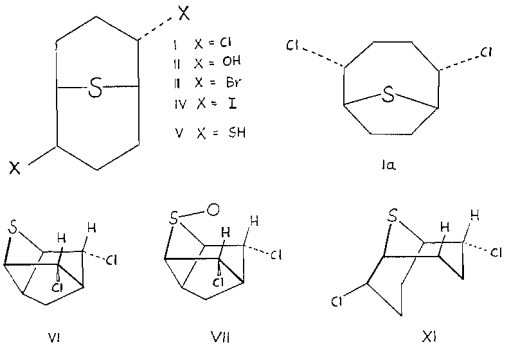
One of the first questions in the structural evaluation of the products from the intramolecular addition reaction of a diolefin with sulfur dichloride is to ascertain which of the possible ring systems is formed. For this, a simple approach was considered, which is of general validity for the resulting ring systems and is of particular value if the reaction products cannot be converted into a known sulfide.

Addition to a cyclic diolefin can lead to a dichlorosulfide with both chlorine atoms either on one side (I*a*) or on both sides (I) of the sulfur atom. Two sulfoxides should be obtained in the first case, but only one in the latter, provided a symmetric diolefin such as *cis,cis*-cyclooctadiene-1,5 is considered. The sulfoxides are interconvertible with triethyloxonium fluoroborate in the first case, but no isomer is obtained in the second case. In the nuclear magnetic resonance spectrum, shielding by the sulfoxide oxygen affects either both CHCl groups or none in the first type, but only one CHCl group should be affected in the second. An example of the first type is the reaction product from bicycloheptadiene (2). The product obtained from cyclooctadiene-1,5, the structure of which was demonstrated by a sequence of unambiguous reactions (1, 3), provides an example of the second type.

The nuclear magnetic resonance spectrum of I at 70 °C on a Varian A-60 spectrophotometer shows a multiplet for the —CHCl— proton at 4.62 p.p.m., whereas its sulfone IX (1) exhibits that proton at 4.43 p.p.m. In contrast, the nuclear magnetic resonance spectrum of its sulfoxide VIII (1) at 70 °C in hexachlorobutadiene shows two resonances for the —CHCl— groups, of equal intensity, at 4.63 p.p.m. and 4.06 p.p.m., respectively. The chemical shifts are independent of temperature (20 and 150 °C) and remain unchanged on dilution (5 and 10 mole %). The magnitude of the observed shielding effect of the sulfoxide oxygen on the —CHCl— group (Δ = 0.57 p.p.m.) is in very good agreement with that effect observed on *exo,exo*-4,8-dichloro-2-thiatricyclo[3.2.1.$0^{3,7}$]octane 2-oxide (VII) (Δ = 0.53 p.p.m.) (2), suggesting the similar proximity of the sulfoxide oxygen

Can. J. Chem. Downloaded from www.nrcresearchpress.com by 210.87.254.105 on 09/05/12
For personal use only.

to the hydrogen of the —CHCl— group in both ring systems, and therefore identical configuration of the chlorine atoms with respect to the sulfur atom and identical conformation. In contrast, in the hypothetical sulfoxides of I*a*, the proton of both —CHCl— groups is symmetrically oriented with respect to the sulfoxide oxygen in all conformations, provided the chlorine groups are *cis* to each other. The significant shielding of only one —CHCl— group cannot therefore be explained on the basis of the [4.2.1] ring system.



As expected, attempted inversion of the sulfoxide to an isomer by its reaction with triethyloxonium fluoroborate failed (5). The successful inversion of a tricyclic β,β-dichlorosulfoxide under identical conditions was reported previously (2).

Although a dipole moment determination is not expected to distinguish between the [4.2.1] and [3.3.1] ring systems, conclusions about the conformation and configuration of the dichlorosulfide can be drawn from the observed moment if the [3.3.1] system is accepted. The twin-chair conformation for I has been suggested on the basis of the coupling constants between the proton of the —CHCl— group and the adjacent methylenic protons (3), and on the basis of the 'abnormal' infrared band at 1 485 $\pm$ 5 cm^{-1} (1) which results from non-bonding interaction between the two methylenic groups in that conformation. This conclusion is supported by the observed dipole moment.

A moment of 0.85 D for I in benzene at 20 °C is very close to the value of 0.8 D for VI (1). The thiane ring in the latter compound has a rigid chair conformation, with both chlorine atoms equatorial (2). Inspection of molecular models of I and VI shows that the resultant moment of both chlorine groups forms an angle of 180° with the moment angle of C—S—C in the twin-chair conformation XI and in the rigid system VI. The observed moment is therefore best explained by the assumption of a twin-chair conformation for I. The moment is lower than calculated (1.4 D), assuming group moments of 1.8 D for C—Cl (6) and 1.6 D for C—S—C (7). Moments of 1.6 D and 1.9 D are calculated for the chair–boat and boat–boat conformations of I, respectively. For a configuration with the chlorine groups *trans* to each other, a moment of 2.6 D is calculated for the chair–boat conformation, 2.1 D for the chair–chair conformation, and 1.3 D for the boat–boat conformation. The isomer with both chlorine atoms *cis* to each other and *cis* with respect to the sulfur atom would show moments of 3.7 D for the chair–chair, 3.8 D for the chair–boat, and 1.6 D for the boat–boat conformations.

The dichlorosulfide I was shown to exhibit the characteristic reactivity of β,β'-dichlorosulfides towards nucleophilic substitution (1). The diol II can be obtained in polymorphic forms with melting points from 188 to 256 °C. The low-melting polymorph melts with decomposition by elimination of water. A sample melting close to that reported by Weil (1) was obtained by hydrolysis with aqueous sodium carbonate. Recrystallization of the low- and high-melting species from toluene did not affect their melting points. Whereas

Can. J. Chem. Downloaded from www.nrcresearchpress.com by 210.87.254.105 on 09/05/12
For personal use only.

the high-melting polymorph is unaffected by crystallization from methanol or water, the melting point of the low-melting polymorph is increased to 248–250 °C on a single crystallization from methanol and to 215–220 °C on crystallization from water. Both diols show identical infrared absorption in potassium bromide, although in Nujol small differences in the relative intensities of several peaks appear, particularly those of the three unidentified peaks at 865, 880, and 895 cm^{-1}. Both the higher and lower melting polymorphs show a single peak for the OH stretching frequency at 3 443 $\pm$ 2 cm^{-1} in dioxane and at 3 620 $\pm$ 2 cm^{-1} in carbon tetrachloride. The diol was oxidized to its sulfone X with hydrogen peroxide in glacial acetic acid. The nuclear magnetic resonance spectrum of the sulfone X shows a single resonance at 4.45 p.p.m. in pyridine for the proton alpha to the hydroxy group, which is 0.13 p.p.m. downfield from the resonance of that proton in the diol II.

The dimercaptan V was obtained from the dichlorosulfide I via its thiouronium salt in a yield of 41%.

Attempts to isolate the isomeric [4.2.1] ring system were unsuccessful. The absence of the isomeric dichlorosulfide I*a* in the reaction product of sulfur dichloride and cyclooctadiene was indicated by gas chromatographic analysis, which shows a single peak for I. Also, no evidence for the [4.2.1] ring system was found in products resulting from heterolytic substitution reactions in which isomerization via an intermediate episulfonium ion was expected (8). The diol II was recovered from its solution in 97% sulfuric acid in a yield of 68% by neutralization with aqueous sodium bicarbonate. Treatment of II with concentrated hydrochloric acid leads to I in a yield of 97%. The crude product shows a melting point of 99–101 °C, compared with 101–102 °C for I. Similarly, the bromide III and the iodide IV (1) were obtained from II in yields of 80 and 64%, respectively, by use of the corresponding acids. The iodide IV is identical with the product obtained from the chloride I with sodium iodide in acetone. Hydrolysis of the iodide IV with aqueous sodium bicarbonate leads to II in a yield of 60%.

The participation of the free electrons on sulfur in the stabilization of the carbonium ion is demonstrated by comparison of the reactivity in nucleophilic reactions of sulfide versus sulfoxide and sulfone. In contrast to the dihydroxysulfide II, the dihydroxysulfone X can be recovered unchanged from its solution in concentrated hydrochloric acid. Also, the dichlorosulfoxide VIII is not hydrolyzed in hot aqueous sodium carbonate, although rapid hydrolysis of I to II proceeds under these conditions.

The absence of the [4.2.1] ring system is surprising if an episulfonium ion is involved in the addition of sulfur dichloride to the diene and in substitution reactions. Both the [4.2.1] and [3.3.1] ring systems of bicyclononane were isolated in the acetolysis of 4-cyclooctene-1-methylbrosylate (9), and a bridged intermediate was suggested on the basis of the observed products. Analogous to the reaction of sulfur dichloride with bicycloheptadiene, an *endo* approach of the chlorosulfenium ion (10) is suggested in the addition step. The flexibility of the bicyclic ring system obtained from cyclooctadiene allows the formation of a configuration and conformation of the most favorable staggering of the carbon–hydrogen bonds, which could be the deciding factor in the observed formation of the [3.3.1] ring system in preference to the [4.2.1] ring system, and which distinguishes between the reaction of sulfur dichloride with cyclooctadiene and that with bicycloheptadiene.

EXPERIMENTAL

The dielectric constants were determined with the instruments described earlier (11). The melting points were determined in a Hallenkamp block and are uncorrected. Gas chromatographic analysis was carried out on a Perkin–Elmer 800 chromatograph at 175 °C, with Apiezon as the stationary phase and helium as the carrier gas.

Can. J. Chem. Downloaded from www.nrcresearchpress.com by 210.87.254.105 on 09/05/12
For personal use only.

Can. J. Chem. Downloaded from www.nrcresearchpress.com by 210.87.254.105 on 09/05/12
For personal use only.

2,6-Dichloro-9-thiabicyclo[3.3.1]nonane (I)

A suspension of 1.75 g (0.01 mole) of the diol II (m.p. 188 °C) in 50 ml of concentrated hydrochloric acid was stirred for 8 h at room temperature, and the product was filtered off and air-dried to give 2.05 g (97%) of I, m.p. 99–101 °C. The product was identified as I by mixed melting point with a sample obtained from the reaction of cyclooctadiene-1,5 and sulfur dichloride, and by its infrared absorption in potassium bromide. Gas chromatographic analysis of that product and a crude reaction product of sulfur dichloride and cyclooctadiene showed a single peak for I.

This agrees with the result of the thin-layer chromatography reported by Corey and Block (3).

9-Thiabicyclo[3.3.1]nonane-2,6-diol (II)

(*a*) To a refluxing solution of 6.2 g (0.05 mole) of sodium carbonate in 100 ml of water was added 10.5 g (0.05 mole) of I, with high-speed stirring, over a period of 10 min. A clear solution formed, from which colorless crystals separated when it was cooled, yield 7 g (80%), m.p. 189 °C (decomp.). The aqueous solution was continuously extracted with diethyl ether to give another 1.1 g (13%) of the dihydroxy compound, m.p. 205 °C (decomp.).

Anal. Calcd. for $C_8H_{14}O_2S$: C, 55.13; H, 8.10; S, 18.40. Found (for the fraction with m.p. 189 °C): C, 55.36; H, 8.02; S, 18.52.

(*b*) Hydrolysis under the same conditions in a repeat experiment led, with a yield of 87%, to a diol having m.p. 252–253 °C.

Anal. Found: C, 55.20; H, 8.15; S, 18.3.

(*c*) To a solution of 5.3 g (0.025 mole) of I in 100 ml of tetrahydrofuran were added 10 ml of water and 2 g of sodium bicarbonate. The suspension was refluxed, with stirring, for 64 h, and evaporated to dryness on a rotary evaporator; the residue was ground and exhaustively extracted with 400 ml of benzene. After evaporation of the benzene solutions, 1.6 g of II was obtained, m.p. 188 °C (decomp.). The benzene-insoluble residue was extracted three times with 50 ml of acetone. On evaporation, another 2.35 g of II was obtained, m.p. 254–256 °C. When a solution of the high-melting product in boiling methanol or water was allowed to evaporate, the melting point of the recovered material was unchanged. Similar solutions of the low-melting material led to a product with a melting point of 248–250 °C after recovery from methanol, and 215–220 °C after recovery from water.

(*d*) A suspension of 12 g (0.03 mole) of IV in 100 ml of water containing 16.8 g (0.2 mole) of sodium bicarbonate was stirred under reflux for 10 min. The solution was filtered to remove traces of undissolved material, and continuously extracted with diethyl ether. The ether solution was dried with magnesium sulfate and evaporated to give 3.4 g (65%) of II, m.p. 255–257 °C, shown by its infrared absorption in potassium bromide and by mixed melting point to be identical with the product described under method *c*.

II (2 g) was dissolved in 10 g of 97% sulfuric acid at room temperature. The clear, colorless solution was allowed to drop into 50 ml of a saturated sodium bicarbonate solution with rapid stirring, the internal temperature being kept at 5–10 °C. The resulting suspension was continuously extracted with diethyl ether, and the extract was dried and evaporated to give 1.6 g (80%) of a product which, on exhaustive sublimation, yielded 1.28 g (64%) of diol, m.p. 196–203 °C (decomp.). The diol was identified as II by its infrared spectrum in potassium bromide and Nujol.

2,6-Dibromo-9-thiabicyclo[3.3.1]nonane (III) from II with Hydrobromic Acid

In 50 ml of fuming hydrobromic acid was dissolved 3.5 g (0.02 mole) of II (m.p. 255–257 °C). The suspension was stirred for 2 h and filtered, and the residue was washed with water and dried over calcium chloride to yield 5.8 g (97%) of product, m.p. 124 °C (decomp.). By sublimation, 1.2 g of polymeric material was separated. An analytical sample was obtained by recrystallization of 2.5 g from 25 ml of hexane, m.p. 136–137.5 °C.

Anal. Calcd. for $C_8H_{12}SBr_2$: C, 32.02; H, 4.03; Br, 53.27; S, 10.68. Found: C, 32.21; H, 3.89; Br, 53.05; S, 10.60.

2,6-Diiodo-9-thiabicyclo[3.3.1]nonane (IV) from II with Hydriodic Acid

Into 50 ml of 47% hydriodic acid was stirred 3.5 g (0.02 mole) of II (m.p. 255–257 °C). After the solution was stirred for 2 h at room temperature, the colorless product was filtered off, washed with water, and dried over calcium chloride to yield 7.8 g (99%), m.p. 128 °C (decomp.). Sublimation (an initial colored fraction was discarded) produced a colorless sample, yield 5 g (64%), m.p. 143–145 °C.

The product was shown to be identical by mixed melting point and infrared absorption with the product obtained from I with potassium iodide (1).

9-Thiabicyclo[3.3.1]nonane-2,6-thiouronium Chloride

To a solution of 4.22 g (0.02 mole) of I in 100 ml of ethanol was added 6.1 g (0.08 mole) of thiourea; the suspension was refluxed for 14 h, allowed to cool to room temperature, and filtered; the residue was washed with ethanol and air-dried to give 4.8 g (61%), m.p. 232 °C (decomp.) (A). The solvent was evaporated from the combined ethanol solutions, and the crystalline residue was extracted with 50 ml of tetrahydrofuran and 50 ml of hot ethyl acetate to leave another 2.4 g (30%) of product, m.p. 200–212 °C (decomp.) (B).

Anal. Calcd. for $C_{10}H_{20}S_2N_4Cl_2$: H, 5.51; S, 26.48. Found: H, 5.30; S, 26.83.

2,6-Dimercapto-9-thiabicyclo[3.3.1]nonane (V)

To a solution of 5.4 g (0.015 mole) of the thiouronium salt A in 25 ml of water was added 25 ml of concentrated ammonium hydroxide. Traces of insoluble material were filtered off and the filtrate was acidified with dilute hydrochloric acid, with cooling, the internal temperature being kept between +5 and +10 °C. The crystalline product was separated with 20 ml of methylene chloride, and the extract was washed with water, dried with magnesium sulfate, and evaporated to give 2.5 g of a crystalline product, m.p. 25–43 °C. Sublimation gave 1.5 g (41%) of V, m.p. 44–46 °C. An analytical sample was obtained by drying over paraffin chips and repeated sublimation.

Anal. Calcd. for $C_8H_{14}S_3$: C, 46.55; H, 6.84; S, 46.61. Found: C, 46.84; H, 6.88; S, 46.86.

Attempted Hydrolysis of VIII

A suspension of 2.27 g (0.01 mole) of VIII in a solution of 10 g of sodium carbonate in 50 ml of water was refluxed, with high-speed stirring, for 30 min. After the solution was cooled, 2.05 g of VIII was recovered, m.p. 121.5–122.5 °C, identified as VIII by mixed melting point and by its infrared absorption.

Attempted Conversion of VIII

To a solution of 3 g (0.013 mole) of VIII in 50 ml of methylene chloride was added 2.85 g (1.5 moles) of triethyloxonium fluoroborate (12). After the solution had stood for 8 h, 1.5 g (26%) of a crystalline adduct was filtered off, m.p. 163 °C (decomp.). On complete evaporation, another 3.2 g of product was obtained.

Anal. Calcd. for $C_{10}H_{17}Cl_2F_4OS$: C, 35.0; H, 5.00. Found: C, 34.8; H, 5.07.

To a solution of 0.2 g of sodium hydroxide (0.05 mole) in 20 ml of water was added 1.1 g (0.0032 mole) of the adduct. After the solution was stirred at 30 °C for 15 min, the crystalline product was filtered off, washed with water, and air-dried to give 0.7 g (96%) of VIII, m.p. 122.5–123.5 °C. The product was identified by mixed melting point and by its infrared and nuclear magnetic resonance spectra in carbon tetrachloride.

2,6-Dihydroxy-9-thiabicyclo[3.3.1]nonane 9,9-Dioxide (X)

To a solution of 17.5 g (0.1 mole) of II (m.p. 255–257 °C) in 500 ml of glacial acetic acid was added 17 g of 50% aqueous hydrogen peroxide. The solution was stirred at room temperature for 48 h and then allowed to evaporate to dryness to give 20 g (100%) of crude X, m.p. 160–190 °C (decomp.); 15 g was recrystallized from 80 ml of dioxane to give a first fraction of 4 g. A second fraction of 4 g was obtained by reducing the volume of the dioxane solution to 40 ml. An analytical sample was obtained by a second recrystallization from dioxane and drying at 60 °C and 0.1 mm for 54 h. The compound is discolored when heated above 250 °C.

Anal. Calcd. for $C_8H_{14}SO_2$: C, 46.57; H, 6.83; S, 15.54. Found: C, 46.87; H, 6.79; S, 15.53.

The dihydroxysulfone X is recovered unchanged from its solution in concentrated hydrochloric acid (0.5 g in 5 ml) after evaporation of the solution.

ACKNOWLEDGMENTS

The author is greatly indebted to Prof. J. K. Stille and Prof. N. Kharasch for the discussions of various aspects of this work, to Prof. G. F Wright for measuring the dielectric constants of I, to Dr. R. T. Woodhams for guidance and encouragement, to members of the analytical departments of the Dunlop Research Centre and the Ontario Research Foundation for supplying spectroscopic data, and to Dr. E. Weil of Hooker Chemical Corporation for a copy of his manuscript on 2,6-dichloro-9-thiabicyclo[3.3.1]-nonane in advance of publication.

REFERENCES

1. E. D. Weil, K. J. Smith, and R. J. Gruber. J. Org. Chem. **31**, 1669 (1966).
2. F. Lautenschlaeger. J. Org. Chem. **31**, 1679 (1966).
3. E. J. Corey and E. Block. J. Org. Chem. **31**, 1663 (1966).
4. F. Lautenschlaeger. The Princeton University Conference on The Chemistry of Sulfides, June 29, 1966.
5. C. R. Johnson and D. McCants, Jr. J. Am. Chem. Soc. **87**, 1109 (1965).
6. C. P. Smyth. Dielectric behaviour and structure. McGraw-Hill Book Co., Inc., New York. 1955.
7. C. W. N. Cumper and A. I. Vogel. J. Chem. Soc. 3521 (1959).
8. A. G. Osten, E. R. Holiday, J. St. L. Philot, and L. A. Stocken. Trans. Faraday Soc. **44**, 45 (1948).
9. A. C. Cope, D. L. Nealy, P. Scheiner, and G. Wood. J. Am. Chem. Soc. **87**, 3130 (1965).
10. S. N. Nabi and M. A. Khaleque. J. Chem. Soc. 3626 (1965).
11. C. C. Meredith, L. Westland, and G. F Wright. J. Am. Chem. Soc. **79**, 2385 (1957). C. C. Meredith and G. F Wright. Can. J. Technol. **33**, 182 (1955).
12. H. Meerwein, E. Battenberg, H. Gold, E. Pfeil, and G. Williams. J. Prakt. Chem. **154**, 83 (1939).

Can. J. Chem. Downloaded from www.nrcresearchpress.com by 210.87.254.105 on 09/05/12
For personal use only.

Can. J. Chem. Downloaded from www.nrcresearchpress.com by 210.87.254.105 on 09/05/12
For personal use only.

REACTIONS OF OZONIDES

IV. OZONIZATION OF ALKYLCYCLOALKENES[1,2]

D. G. M. DIAPER
Department of Chemistry, Royal Military College of Canada, Kingston, Ontario

Received July 20, 1966

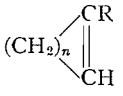
ABSTRACT

Oxidative ozonolysis of some 1-alkylcyclopentenes, 1-alkylcyclohexenes, and 1-methylcycloheptene gives keto acids ($RCO(CH_2)_nCOOH$) and by-product derived esters now identified as $RCO(CH_2)_nCOO(CH_2)_nCOR$. The mechanisms of formation of esters from zwitterion and carbonyl intermediates are discussed in terms of dimeric zwitterions. Cycloalkanones also present in the neutral by-product are attributed to alkylidenecycloalkanes.

INTRODUCTION

A flexible unambiguous general method for the synthesis of keto acids uses oxidation of the ozonolysis products from 1-alkylcycloalkenes in participating solvents (1). Attempts to extend this method to the preparation of diketoalkanedioic acids and alkylalkanedioic acids (2) met with little success, chiefly because of a side reaction giving a nonacidic by-product other than the anticipated keto aldehyde (3). By-product formation was more serious for reactions involving two rings than for those involving one, not only because of greater by-product yields but also because of complication of the problem of isolating the desired dioic acid.

These side products have now been studied in the oxidation of the olefins I*a*–I*e* and of 1,2-dimethylcyclohexene, and four hypotheses of their origin were considered. The first concerns the possible participation of the equilibrium endocyclic isomer of the starting material (for example, ethylidenecyclohexane in 1-ethylcyclohexene). The second postulates cyclodehydration or dimerization of keto aldehyde intermediates II*a*–II*e*. The third and fourth hypotheses both suggest ester formation, either through "abnormal molozonide stabilization", as put forward by Fields for unsubstituted cycloalkene ozonization (4), or through peracid and peranhydride intermediates, as suggested by Pasero (5–8), giving III*a*–III*e*.



I

$RCO(CH_2)_nCHO$

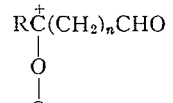
II

$RCO(CH_2)_nCOO(CH_2)_nCOR$

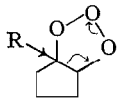
III

$RCO(CH_2)_n\overset{+}{C}H—O—O^-$

IV



V



VI

a R = CH_3, *n* = 3
b R = CH_3, *n* = 4
c R = CH_3, *n* = 5
d R = CH_3CH_2, *n* = 3
e R = CH_3CH_2, *n* = 4

[1]*Presented at the Saskatoon meeting of the Chemical Institute of Canada, June 1966.*
[2]*The financial support of Defence Research Board grant 9530-17 is gratefully acknowledged.*

Can. J. Chem. Downloaded from www.nrcresearchpress.com by 210.87.254.105 on 09/05/12
For personal use only.

EXPERIMENTAL

Preparation of 1-Alkylcycloalkenes

The required alkylmagnesium bromide (0.5 mole) was treated during 4–5 h with the cycloalkanone (0.45 mole) in ether containing 30–40% benzene at −20 to −10°. These conditions help to minimize reduction of the ketone to the secondary alcohol (9) and minimize clogging of the flask with precipitate. After the mixture was mechanically stirred for 1 h at room temperature, it was added to ice, water, and ammonium chloride (1.5 moles) and quickly separated. Work-up of the Grignard reaction with acid causes premature dehydration. The ether and benzene were removed from the washed and dried solution, and the residual liquid was fractionally distilled through a 12 in. Widmer column to separate the 1-alkylcycloalkanol from the secondary alcohol and unchanged ketone. 1-Ethylcyclohexanol was obtained as a solid, m.p. 34.5–35° (lit. (10) m.p. 33°), and purified by low-temperature crystallization from petroleum ether. The others were liquid. All were dehydrated by heating under reflux without solvent in the presence of a few milligrams of iodine under a water separator. When reaction was complete, the liquid was again fractionated. The physical constants were as follows: I*a*, b.p. 74–77°; I*b*, b.p. 110–111°, n_D^{21} 1.4490; I*c*, b.p. 137°, n_D^{20} 1.4599; I*d*, b.p. 105.5° at 751 mm, n_D^{24} 1.4410; I*e*, b.p. 136–139°, n_D^{20} 1.4578; 1,2-dimethylcyclohexene, b.p. 136°, n_D^{20} 1.4578. Each was examined by vapor-phase chromatography (v.p.c.) and infrared spectroscopy to detect alcohol and ketone impurities. Fractionation was repeated, if necessary, until these were absent. The olefins were stored at 0° in the dark under nitrogen.

Oxidative Ozonolysis

The olefin (10–20 g) dissolved in dry methylene chloride (50–100 cc) was ozonized to completion, as shown by the rapid evolution of iodine in a potassium iodide trap and by the failure of an aliquot to decolorize a bromine solution. The solvent and ozone were removed by entrainment in a dry nitrogen stream at room temperature and finally by evaporation under reduced pressure. The residual viscous water-white liquid was divided by weight into two approximately equal portions. One was oxidized by slowly raising the temperature to 95° while a very slow stream of oxygen was passed through (5) (autoxidized sample). The other (performic acid oxidation sample) was diluted with ether (5–10 g in 50 cc) and treated with formic acid (10 cc) and 70% hydrogen peroxide in excess (10 cc). Heat was evolved. It was allowed to stand at room temperature for 3 days, after which aldehyde could no longer be detected. The autoxidized samples were generally found to be free of aldehyde after 24 h at 95° with a slow stream of oxygen passing through, but were treated for a further 24 h if necessary. Each sample was divided into acidic and nonacidic fractions for titration.

The v.p.c. traces of the neutral products from I*a*, I*b*, and I*c* showed two minor volatile substances in each case (identified as the starting material and corresponding ketone). The infrared spectra had broad or double peaks in the carbonyl region. Negative aldehyde tests were obtained from the autoxidized products and from those oxidized with performic acid, but a trace of aldehyde was detected in each of the products from the emulsion ozonization. The neutral fractions were tested with silver nitrate and found to be free of halogen. Saponification titrations in ethanol with approximately 0.1 g aliquots were performed with 0.2 *N* ethanolic potassium hydroxide, and the results, expressed as percentage yields of esters III, are presented in the first two columns of Table I.

TABLE I

Ester by-products in ozonization

	Ester yields (% of starting material)		
	Autoxidation in O_2	Performic acid oxidation	Emulsion
1-Methylcyclopentene (I*a*)	8.13	4.42	0.34
1-Methylcyclohexene (I*b*)	16.7	6.05	0.21
1-Methylcycloheptene (I*c*)	17.4	5.32	0.55
1-Ethylcyclopentene (I*d*)	22.0	7.18	0.37
1-Ethylcyclohexene (I*e*)	11.6	7.02	0.81
1,2-Dimethylcyclohexene	0.58	0.31	0.44

There was a polymeric peroxide fraction in the performic acid oxidation experiments (for example, 4.38 g of acid, 0.76 g of peroxy polymer, and 0.25 g of neutral product were obtained from 7.5 g of 1-methylcycloheptene). The peroxide was insoluble in ether and in aqueous potassium carbonate, but dissolved in acetone.

Emulsion Ozonization

The third column of Table I contains the ester values of samples of alkylcycloalkenes ozonized in an aqueous alkaline emulsion. For example, 10 g of 1-methylcycloheptene was suspended in 60 cc of water containing 5.6 g of sodium hydroxide, 10 cc of hydrogen peroxide (70%), and 0.1 g of non-ionic detergent.

Ozone was passed through at 0° until the upper layer was reduced in bulk to about 1 cc of a viscous scum. The nonacidic hexane-soluble fraction was separated for the saponification titration. In each case, there was a considerable amount of fluffy white insoluble polymeric peroxide.

Isolation and Saponification of $CH_3CO(CH_2)_5COO(CH_2)_5COCH_3$

The neutral fraction (4.74 g) from autoxidation at 95° of the ozonization product from 1-methylcycloheptene (18.97 g) was distilled without fractionation at 150–170° and 0.4 mm. The saponification titration value of this distillate was 3.03 meq/g (theory 3.71). It was redistilled in a micro-apparatus with the thermometer as the fractionating element,[3] and the middle fraction, b.p. 159–167° at 0.6 mm, had a saponification titration value of 3.40 meq/g. Its nuclear magnetic resonance (n.m.r.) spectrum had a sharp singlet, attributable to CH_3CO, at 2.08 p.p.m. (cf. 2.12 for methyl isobutyl ketone) and broad signals (attributed to CH_2O and CH_2CO) superimposed downfield and the other methylenes upfield. There were no signals attributable to aldehyde or vinylic protons. A bromine test was negative and permanganate decolorization was slow.

A sample (1.3 g) was saponified and the acid product converted into the semicarbazone, m.p. 124–125° (decomp.) when recrystallized from ethanol.

Anal. Found: N, 19.17; acid equiv. 218. $C_9H_{17}O_3N_3$ requires N, 19.52; acid equiv. 215.

The oily residue from the neutral saponification layer had a peak attributable to ketone carbonyl in its infrared spectrum. It was treated in ether with a large excess (0.5 g) of lithium aluminium hydride and the product, after solvent removal (0.11 g), was treated with phenyl isocyanate. The phenylurethane melted at 93–95°, undepressed on admixture with authentic heptane-1,6-diol phenylurethane obtained from methyl 6-ketoheptanoate (m.p. 95–96°).

The presence of 7-ketooctanal was demonstrated through a solid derivative as follows. The unoxidized ozonization product of another sample of 1-methylcycloheptene was treated with 2,4-dinitrophenylhydrazine, giving the bis-2,4-dinitrophenylhydrazone of 7-ketooctanal, m.p. 152–153° when recrystallized from pyridine – carbon tetrachloride.

Anal. Found: N, 21.33. $C_{20}H_{22}O_8N_8$ requires N, 21.59.

In a similar way, the neutral product from the oxidative ozonolysis (autoxidation method) of 1-methylcyclohexene was distilled (b.p. 135–145° at 0.4 mm) (2.92 meq ester/g before distillation and 3.61 after; theory 4.13). Its n.m.r. spectrum similarly showed a singlet at 1.90 p.p.m. and broad CH_2 signals on each side. Aldehyde and vinylic proton signals were not observed. The ester was hydrolyzed and the acid product was found to give a methyl ester whose v.p.c. retention time was identical with that of authentic methyl 6-ketoheptanoate. Hexane-1,5-diol was identified with an authentic sample by v.p.c. of their trifluoroacetyl derivatives. The authentic sample was obtained by reduction of methyl 5-ketohexanoate; the reduction mixture was saponified and the neutral material distilled. The phenylurethane could not be crystallized.

1-Methylcyclopentene gave a neutral by-product, b.p. 130–145° at 12 mm (4.01 meq ester/g; theory 4.68), whose n.m.r. spectrum was similar. Resolution was poorer because of its low solubility in carbon tetrachloride containing 1% tetramethylsilane, the solvent used for all spectra. Its acidic hydrolysis product was 5-ketohexanoic acid, and the reduced neutral hydrolysis product gave a phenylurethane melting at 126–128° (lit. (21) m.p. 124.5–126°).

Ozonolysis of 1,2-Dimethylcyclohexene

When treated as above, the oxidative ozonolysis product was almost entirely free from acid. The emulsion ozonization mixture contained a white fluffy peroxide which decomposed when heated. The ester values were negligible and the product was not examined further.

DISCUSSION OF RESULTS

The equilibrium concentration of methylene cyclopentane in 1-methylcyclopentene is 0 (11), 0.6 or 0.7 (12), and 0.8% (13). For methylenecyclohexane in 1-methylcyclohexene it is 3 or 5 (11), 0 (14), and 1.8% (13), and the heat of conversion is 3.6 kcal. For 1-methylcycloheptene the isomer was found in 1.27 or 1.33% concentration (15). The exocyclic olefin concentration in 1-ethylcyclopentene and 1-ethylcyclohexene is, respectively, 10.9% (13) and 6 (11) or 8.5% (13) or 0.5% (14). Even so, they are not large enough to account for all the neutral by-product observed. 1,2-Dimethylcyclohexene has no detectable exocyclic olefin impurity. In all cases, the gas chromatogram of the neutral product of oxidative ozonolysis showed some of the corresponding ketone (for example, cyclohexanone from 1-methylcyclohexene and 1-ethylcyclohexene), and the reaction route is doubtless through the carbonyl and zwitterion fragments of scission of the exocyclic olefin. Present

[3]*Kontes Bantam Ware.*

Can. J. Chem. Downloaded from www.nrcresearchpress.com by 210.87.254.105 on 09/05/12
For personal use only.

Can. J. Chem. Downloaded from www.nrcresearchpress.com by 210.87.254.105 on 09/05/12
For personal use only.

evidence indicates that inductive effects would favor cycloalkanone production, and possible fates of zwitterion fragments will be discussed later. Cycloalkanone was not the major constituent.

Self-condensation of keto aldehyde II*a* would give 2-cyclohexenone, II*b* 1-acetylcyclopentene, and II*c* 1-acetylcyclohexene. These compounds have the common feature of a conjugated unsaturated carbonyl system, and would be expected to have an appropriate strong absorption peak in the ultraviolet. No such peak was detected in the ultraviolet spectra of the neutral products from oxidative ozonolysis of the corresponding olefins. Furthermore, the n.m.r. spectra did not show the expected characteristic vinylic proton triplet. These n.m.r. data also rule out bimolecular keto aldehyde condensation products.

Acyl chlorides are among the products of the reaction of ozone with aldehydes in halogenated solvents (16), but were not present in the neutral fraction of the present study, which was free of halogen.

Saponification titration (Table I) showed that a major neutral by-product contained ester groups. Fields (4) found an 8% yield of valerolactone from oxidative ozonization of cyclohexene, and 15% of 7-hydroxyheptanoic acid from cyclooctene (under hydrolyzing conditions). Interestingly, no ester side products were detected in emulsion oxidative ozonolysis of cyclohexene-4,5-dicarboxylic acid, and another ozonization study of acidic cyclohexene derivatives (17) shows peracids to be the main product. For production of esters from unsubstituted cycloalkenes, a mechanism of ring enlargement and "abnormal molozonide stabilization" has been put forward (4). Such a mechanism would predict that product yields would depend markedly on the size of the original ring. No such correlation was found in the cases studied. Analogous "abnormal molozonides" from the substrates I*a*, I*b*, and I*c* would be acetates of ω-hydroxyaldehydes or formates of ω-hydroxyketones. The anticipated n.m.r. signals of the HCO protons were not found.

Identification of the major neutral by-product as the diketo ester III rests on four pieces of evidence. The saponification equivalents are in reasonable agreement with the theoretical, and the n.m.r. signals agree with this structure. Isolation of the keto acid after saponification and identification of the neutral saponification product through the derived diol confirm the structure. Such ester products are analogous to those reported by Pasero from oleic acid derivatives and are thought to be formed by the following process (5–8):

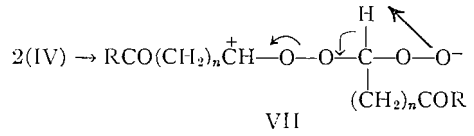
$$RCHO \rightarrow RCO_3H \rightarrow (RCO)_2O_2 \rightarrow RCOOR + CO_2.$$

There is an important difference between the compounds of the present study and those hitherto studied. The carbonyl and zwitterion fragments of the latter were separate, and it was only aldehydes that were invoked as the ester precursors. Here the carbonyl and zwitterion residues are joined in the same molecule, and the possibilities of derivation of ester from both functions will now be discussed.

The Criegee ozonization mechanism would predict the two carbonyl zwitterions IV and V to be the key intermediates in conversion of the immediate ozonization product (here represented as a 1,2,3-trioxolane) such as VI into both the keto acid and diketo ester end products observed. Present evidence about inductive effects on the direction of cleavage would predict that V would be formed in a greater concentration than IV, but, irrespective of relative proportions, possible mechanisms must be considered for the reduction of the zwitterion function of V to ketone and conversion of the zwitterion function of IV into aldehyde, acid, or peracid, the latter being the precursor of the ester function observed (5).

The oxidation level of the zwitterion function is two electrons higher than that of an aldehyde or ketone, and equal to that of an acid or its anion. It is two electrons below the peracid level. The environment in the present study was in all cases an oxidizing one.

In non-participating solvents, two processes for the interaction of two zwitterion fragments have been proposed. Dimeric ring peroxide (18) is the product of one process, and mutual reduction to two carbonyl products with oxygen evolution is the other (19). Monoalkylated zwitterions, of which IV is an example, undergo mutual reduction more easily than dialkylated zwitterions, to which class V belongs (20). Both processes call for an initial dimeric zwitterion to be formed (for example, VII) by condensation of two

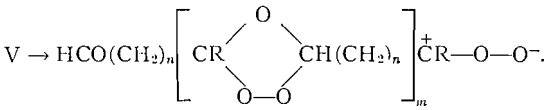


VII

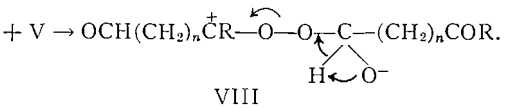
zwitterions IV. Break-up of VII as shown can give an aldehyde function and a peracid function. A route for conversion of zwitterion IV into both keto acid and diketo ester end products is thus possible, for aldehyde is autoxidized to peracid and the latter is the common precursor of acid and ester. VII can also break up to give 1 mole of oxygen and 2 moles of keto aldehyde II, as previously suggested (19, 20).

A product resembling VII can be obtained by condensation of the negative oxygen of zwitterion V with the positive carbon atom of zwitterion IV. Its decomposition will give keto aldehyde and keto peracid fragments identical with those derived from VII.

Carbonyl–zwitterion reversible condensation processes offer several plausible routes for the conversion of the zwitterion function of V into ketonic carbonyl. Self-condensation to give a monomeric ozonide having a 1,2,4-trioxolane system as part of a bridged ring is unlikely on steric grounds for the larger rings. If it occurred, however, dissociation to give IV is one possible route for conversion of zwitterion into ketone. A sterically more likely reaction of V with itself is polymerization as follows:



The rings of the polymer can similarly dissociate to give ketone functions. Condensation of V with II will proceed as follows:



VIII

VIII may close the trioxolane ring and reopen to give a ketonic carbonyl as discussed above. It may also decompose as shown by the arrows, giving keto aldehyde as before, but keto acid this time rather than peracid. In effect, the zwitterion function has thus been reduced to ketone with simultaneous oxidation of the aldehyde to acid. VIII will be formed in preference to the isomeric condensation product of II and V because the aldehyde function is more susceptible to nucleophilic attack than the ketone function.

The observed products of alkylcycloalkene oxidative ozonolysis are thus explicable in terms of the Criegee intermediates if zwitterion–carbonyl and zwitterion–peracid conversion through dimeric zwitterions occurs as indicated.

REFERENCES

1. D. G. M. Diaper. Can. J. Chem. **33**, 1720 (1955).
2. D. G. M. Diaper and A. Kuksis. Chem. Rev. **59**, 89 (1959).
3. A. S. Bailey, D. G. M. Diaper, and M. V. H. Schwemin. Can. J. Chem. **39**, 1147 (1961).

Can. J. Chem. Downloaded from www.nrcresearchpress.com by 210.87.254.105 on 09/05/12
For personal use only.

4. M. I. FREMERY and E. K. FIELDS. J. Org. Chem. **28**, 2537 (1963).
5. J. PASERO. Thesis, University of Marseilles, Marseilles, France. 1963.
6. J. PASERO and M. NAUDET. Rev. Franc. Corps Gras, **7**, 189 (1960).
7. J. PASERO and M. NAUDET. Rev. Franc. Corps Gras, **10**, 453 (1963).
8. J. PASERO, L. COMEAU, and M. NAUDET. Bull. Soc. Chim. France, 493 (1965).
9. M. S. KHARASCH and O. REINMUTH. Grignard reactions of non-metallic substances. Prentice-Hall, Inc., New York. 1954. p. 143.
10. P. SABATIER and A. MAILHE. Ann. Chim. Phys., [8], **10**, 527 (1907).
11. V. J. TRAYNELIS, W. L. HERGENROTHER, H. T. HANSON, and J. A. VALICENTI. J. Org. Chem. **29**, 123 (1964).
12. J. SHABTAI and E. GIL-AV. Tetrahedron Letters, 467 (1964).
13. E. GIL-AV and J. SHABTAI. Chem. Ind. London, 1630 (1959).
14. W. A. MOSHER. J. Am. Chem. Soc. **62**, 552 (1940).
15. A. C. COPE, D. AMBROS, E. CIGANEK, C. F. HOWELL, and Z. JACURA. J. Am. Chem. Soc. **82**, 1750 (1960).
16. H. M. WHITE and P. S. BAILEY. J. Org. Chem. **30**, 3037 (1965).
17. E. BERNATEK, T. LEDAAL, and T. SOLBJØR. Acta Chem. Scand. **19**, 1998 (1965).
18. P. S. BAILEY. Chem. Rev. **58**, 925 (1958).
19. S. FLISZAR, D. GRAVEL, and E. CAVALIERI. Can. J. Chem. **44**, 1013 (1966).
20. S. FLISZAR, D. GRAVEL, and E. CAVALIERI. Can. J. Chem. 44, 67 (1966).
21. A. LEMKE and D. V. TISCHTSCHENKO. J. Gen. Chem. USSR Engl. Transl. **7**, 1998 (1937).

Can. J. Chem. Downloaded from www.nrcresearchpress.com by 210.87.254.105 on 09/05/12
For personal use only.

THE PREPARATION OF 4,6-*O*-BENZYLIDENE-D-GLUCAL AND THE REACTION OF METHYLLITHIUM WITH METHYL 2,3-ANHYDRO-4,6-*O*-BENZYLIDENE-α-D-ALLOPYRANOSIDE

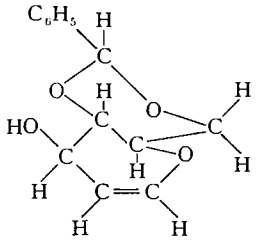
M. SHARMA[1] AND R. K. BROWN
Department of Chemistry, University of Alberta, Edmonton, Alberta
Received July 6, 1966

ABSTRACT

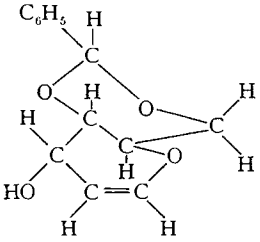
4,6-*O*-Benzylidene-D-glucal has been prepared by the reaction of benzaldehyde with D-glucal. The reaction of commercial methyllithium with methyl 2,3-anhydro-4,6-*O*-benzylidene-α-D-allopyranoside produces the C_2-methylated 1,2-unsaturated compound 4,6-*O*-benzylidene-1,2-didehydro-1,2-dideoxy-2-methyl-D-*ribo*-hexopyranose. Their structures have been proven by first-order analyses of their nuclear magnetic resonance spectra.

INTRODUCTION

4,6-*O*-Benzylidene-1,2-didehydro-1,2-dideoxy-D-*arabino*-hexopyranose (4,6-*O*-benzylidene-D-glucal, I) and 4,6-*O*-benzylidene-1,2-didehydro-1,2-dideoxy-D-*ribo*-hexopyranose (4,6-*O*-benzylidene-D-allal, II) were required as reference compounds for some work in progress in our laboratories.



I



II

Compound II has been prepared recently by the reaction of methyllithium with methyl 2,3-anhydro-4,6-*O*-benzylidene-α-D-allopyranoside (1). However, to our knowledge, no report exists describing the formation of compound I. This paper shows a successful preparation of I and, as well, our results of a reexamination of the reaction of methyllithium with methyl 2,3-anhydro-4,6-*O*-benzylidene-α-D-allopyranoside.

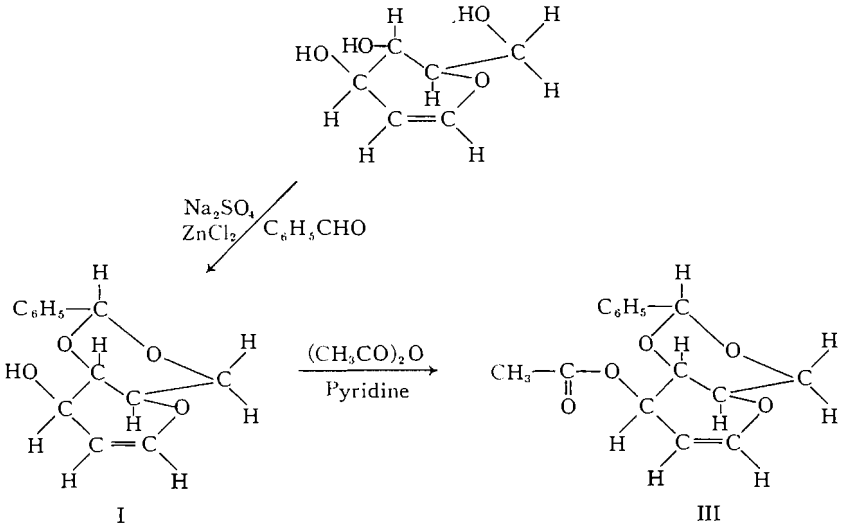
RESULTS AND DISCUSSION

4,6-O-Benzylidene-D-glucal (I)

The reaction of freshly distilled benzaldehyde with D-glucal in the presence of anhydrous zinc chloride and anhydrous sodium sulfate gave I in a 30% yield (Reaction Scheme 1). The following evidence supported the structure assigned.

The infrared spectrum in $CHCl_3$ showed a rather narrow band at 3 590 cm^{-1} (OH), and a sharp, intense band at 1 645 cm^{-1}. The latter agrees with the position (~1 650 cm^{-1}) and intensity (strong) of the absorption band that is found generally for glycals and which is caused by their vinyl ether structural feature, $-\overset{|}{C}-\underset{|}{C}=\underset{|}{C}-O-$ (2). The infrared spectrum in Nujol showed two broad overlapping bands with maxima at 3 190 cm^{-1} and

[1]*Postdoctorate Fellow.*



REACTION SCHEME 1.

3 290 cm^{-1} (OH), a sharp, intense band at 1 650 cm^{-1} (—C—C=C—O—), and two sharp bands at 697 cm^{-1} and 747 cm^{-1} characteristic of the 4,6-*O*-benzylidene aromatic group (3).

Integration of the 60 Mc.p.s. nuclear magnetic resonance (n.m.r.) spectrum in $CDCl_3$ gave a ratio of aromatic protons to total protons of 5 to 14. The H_1 and H_2 signals appeared as an AB spectrum consisting of a pair of doublets centered at τ 3.67 and τ 5.27 ($J_{1,2}$ = 6 c.p.s.) and both split by the allylic H_3 ($J_{1,3}$ = 1.8 c.p.s. and $J_{2,3}$ = 2.0 c.p.s.). The aromatic protons appeared as a multiplet between τ 2.35 and τ 2.83. The benzylidene proton signal was a sharp singlet at τ 4.43, and the OH proton gave a broad "singlet" at τ 7.32 (half width, 6 c.p.s.). The remaining proton signals appeared as a complicated multiplet between τ 5.4 and τ 6.3. In pyridine, the n.m.r. spectrum at 60 Mc.p.s. (Fig. 1) gave a clearly separated signal for the H_3 proton centered at τ 5.23 (multiplet), and signals for the H_1 and H_2 quartets at τ 3.58 and τ 4.98 (Table I). At 100 Mc.p.s., the H_3 signal was clearly resolved into a pair of triplets each showing additional small splitting caused by long-range coupling.[2] Double irradiation definitely showed that this proton was coupled to both H_1 and H_2, and thus identified it as H_3. The spectrum (Fig. 1) was amenable to first-order analysis[3] and gave the observed chemical shifts and coupling constants shown in Table I. The large values of $J_{3,4}$ (7.5 c.p.s.) and $J_{4,5}$ (~9.0 c.p.s.) support the *trans* diaxial arrangement of the protons on C_3 and C_4 as well as the half-chair H1 structure (4) shown in I.

[2]*"Virtual coupling" (J. I. Musher and E. J. Corey, Tetrahedron, 18, 791 (1962)) with* C_5H *may be responsible for the multiplicity of the signal for* H_3 *beyond that of a pair of triplets.*

[3]*Although first-order analysis is generally not recommended unless the ratio of the chemical shift difference (δ) to the coupling constant (J) is >6 (E. D. Beker, J. Chem. Educ., 42, 591 (1965)), a number of papers have appeared in which reasonable values of couplings and chemical shifts have been extracted by using first-order analysis even though in some cases* $\delta/J < 6$ *(D. Horton and W. N. Turner, J. Org. Chem., 30, 3387 (1965); R. J. Abraham, K. A. McLauchlan, L. D. Hall, and L. Hough, Chem. Ind. London, 213 (1962); R. J. Ferrier, W. G. Overend, and G. H. Sankey, J. Chem. Soc., 2830 (1965); L. D. Hall, Advan. Carbohydrate Chem., 19, 58 (1964)). In the present work, the configuration of the molecules is known. The similarities in the structures of all six molecules, and recognition of repetitive patterns of signals for such key positions as* H_3, H_{6c}, *and* H_{6a}, *along with a comparison of the multiplets with those expected, enabled us to pick out a unique arrangement in each case which agreed with the structure. The general agreement in the first-order analysis among the six spectra led us to believe that this approach was reasonably sound.*

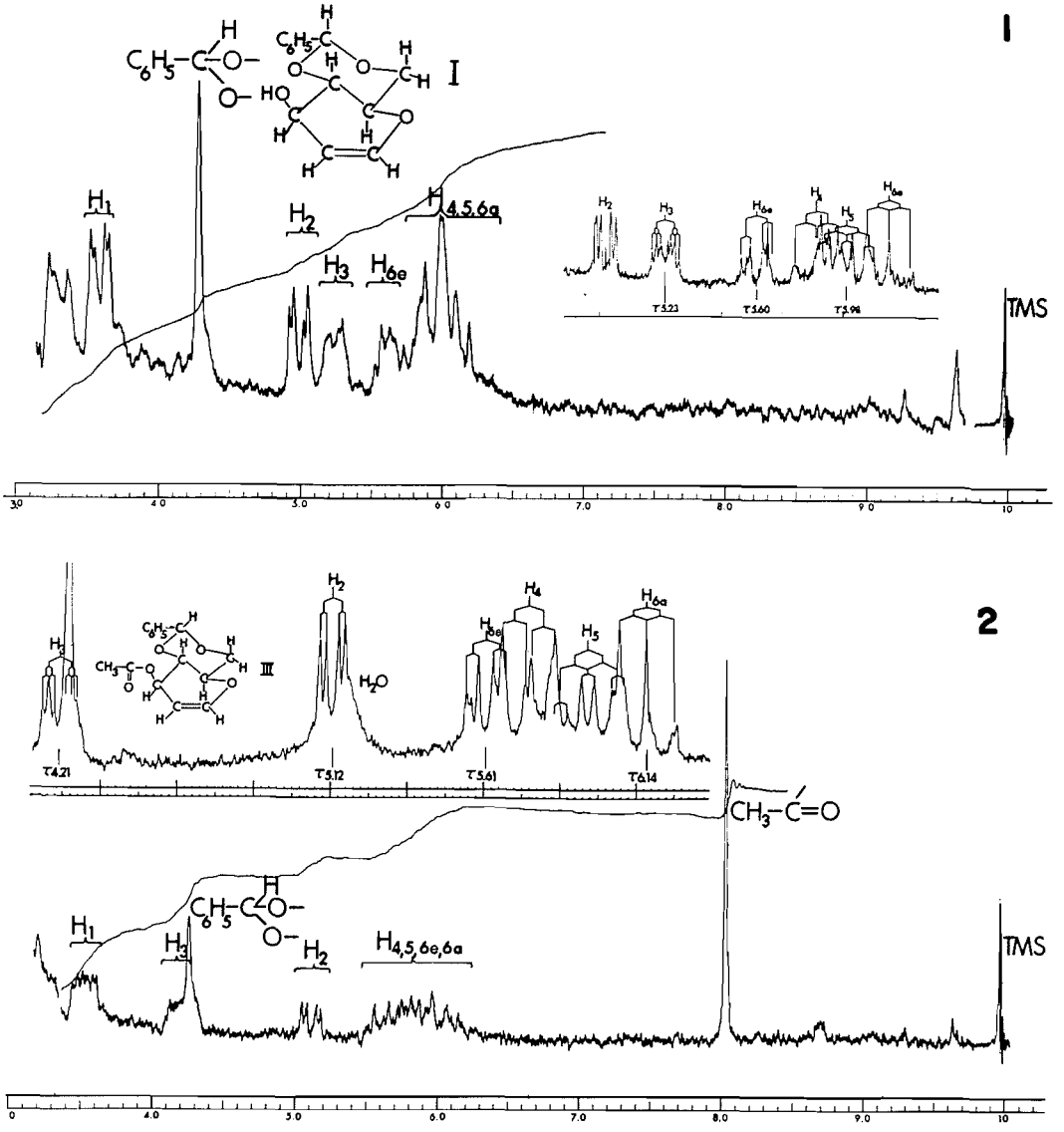


FIG. 1. Nuclear magnetic resonance spectrum at 60 Mc.p.s. of 4,6-*O*-benzylidene-1,2-didehydro-1,2-dideoxy-D-*arabino*-hexopyranose (I) in pyridine. Inset, 100 Mc.p.s. spectrum in pyridine.

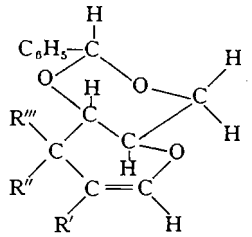
FIG. 2. Nuclear magnetic resonance spectrum at 60 Mc.p.s. of 3-*O*-acetyl-4,6-*O*-benzylidene-1,2-didehydro-1,2-dideoxy-D-*arabino*-hexopyranose (III) in pyridine. Inset, 100 Mc.p.s. spectrum in pyridine.

Acetylation of I gave III, whose infrared spectrum in Nujol showed no absorption for OH. Strong bands appeared at 1 652 cm^{-1} (—C—C=C—O—) and 1 742 cm^{-1} (C=O). The presence of the 4,6-*O*-benzylidene group was indicated by bands at 698 cm^{-1} and 753 cm^{-1}. Double irradiation was used to locate the signals for specific protons in the 100 Mc.p.s. spectrum of III in pyridine (Fig. 2). A first-order analysis was possible and gave the observed coupling constants and chemical shifts shown in Table I. The large values of

TABLE I

Nuclear magnetic resonance and infrared data for several 1,2-unsaturated hexopyranoses

X =



X	Solvent	Chemical shift* referred to tetramethylsilane (τ)										
		H_1	H_2	H_3	H_4	H_5	H_{6e}	H_{6a}	Benzylidene	Acetyl CH_3	C_2—CH_3	OH
I R′=R″=H R‴=OH	Pyridine	3.58 q	4.98 q	5.23 s	5.85 q	5.98 sx	5.60 q	6.15 t	4.27 s	—	—	?
III R′=R″=H R‴=CH_3—C(=O)—O—	Pyridine	3.56 q	5.12 q	4.21 s	5.75 q	5.94 sx	5.61 q	6.14 t	4.25 s	8.03 s	—	—
II R′=R‴=H R″=OH	$CDCl_3$	3.62 d	5.05 t	5.81 q	6.23 q	5.83 sx	5.57 q	6.20 t	4.41 s	—	—	7.47 s
IX R′=R‴=H R″=CH_3—C(=O)—O—	$CDCl_3$	3.54 q	5.01 t	4.57 q	6.05 q	5.80 sx	5.53 q	6.18 t	4.42 s	7.95 s	—	—
V R′=CH_3 R″=OH R‴=H	$CDCl_3$	3.82 d	—	5.99 d	6.28 q	5.94 sx	5.59 q	6.26 t	4.44 s	—	8.30 q J_{1,CH_3} = 1.5 c.p.s. J_{3,CH_3} = 0.3 c.p.s.	7.48 s
VI R′=CH_3 R″=CH_3—C(=O)—O— R‴=H	$CDCl_3$	3.75 d J_{1,CH_3} = 1.5 c.p.s.	—	4.48 d	6.12 q	5.98 sx	5.58 q	6.24 t	4.48 s	7.92	8.38 d J_{1,CH_3} = 1.5 c.p.s.	—

TABLE I (*Concluded*)

			Coupling constants (c.p.s.)							Infrared absorption† (cm^{-1})		
X	Solvent	$J_{1,2}$	$J_{1,3}$	$J_{2,3}$	$J_{3,4}$	$J_{4,5}$	$J_{5,6c}$	$J_{5,6a}$	$J_{6c,6a}$	C=C	$C_6H_5C(O-)(H)(O-)$	OH
I R′=R″=H R‴=OH	Pyridine	6.0	1.8	2.0	7.5	9.0	4.0	9.0	9.0	1650 S	697, 747	3190, 3290
III R′=R″=H R‴=CH_3—C(=O)—O—	Pyridine	6.0	1.8	2.0	7.5	9.0	4.0	9.0	9.0	1652 S	698, 753	—
II R′=R‴=H R″=OH	$CDCl_3$	6.0	~0	6.0	3.5	9.5	4.5	9.5	10.0	1640 S	705, 753	3170
IX R′=R‴=H R″=CH_3—C(=O)—O—	$CDCl_3$	6.0	0.5	5.7	3.5	9.5	4.4	9.5	9.5	1638 S	697, 763	—
V R′=CH_3 R″=OH R‴=H	$CDCl_3$	—	1.5	—	3.5	9.5	4.5	9.5	9.5	1670 S	698, 753	3550
VI R′=CH_3 R″=CH_3—C(=O)—O— R‴=H	$CDCl_3$	—	?	—	3.0	9.5	3.0	9.5	9.5	1668 S	755, 697	—

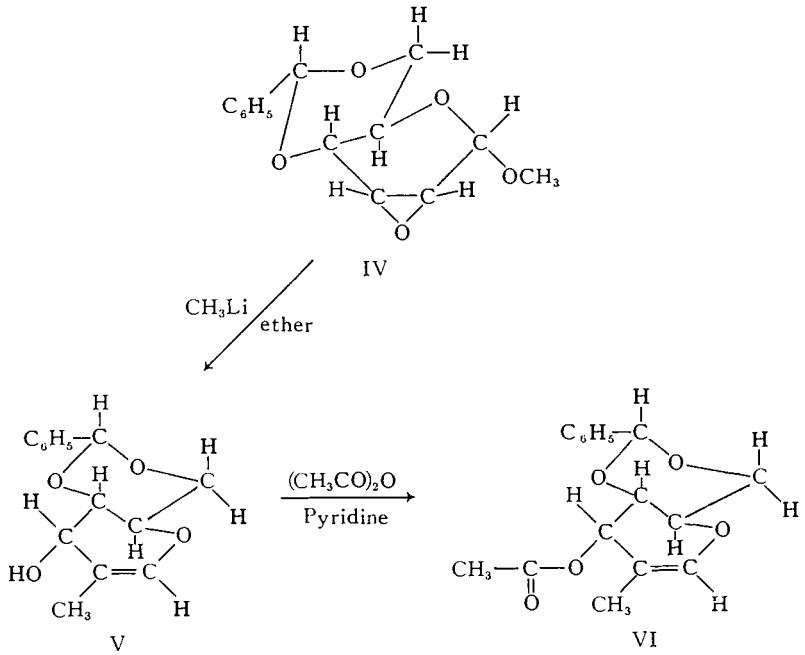
*s = singlet; d = doublet; t = triplet; q = quartet; sx = sextet.
†In Nujol; calibrated against polystyrene, 1601 cm^{-1}; S = strong.

$J_{3,4}$ (7.5 c.p.s.) and $J_{4,5}$ (9.0 c.p.s.) are in agreement with the *trans* diaxial arrangement of the protons attached to C_3, C_4, and C_5. The signal for the proton on C_3, upon acetylation of the C_3—OH group, was shifted markedly downfield (from τ 5.3 (Fig. 1) to τ 4.21 (Fig. 2)), providing proof that the OH group at C_3 was unsubstituted in II and hence that the benzylidene group involved the hydroxyl functions on C_4 and C_6.

The above information leaves no doubt that 4,6-*O*-benzylidene-D-glucal has been formed by the reaction of D-glucal with benzaldehyde under our conditions.

The Reaction of Methyllithium with 2,3-Anhydro-4,6-O-benzylidene-α-D-allopyranoside

The reaction of commercial methyllithium[4] with methyl 2,3-anhydro-4,6-*O*-benzylidene-α-D-allopyranoside (IV) according to the directions described in the literature (1), or by adding the methyllithium to an ether solution of IV directly, gave a compound whose analytical data showed it to be 4,6-*O*-benzylidene-1,2-didehydro-1,2-dideoxy-2-methyl-D-*ribo*-hexopyranose (V) rather than II (Reaction Scheme 2).



REACTION SCHEME 2.

The infrared spectrum in Nujol showed a broad band at 3 550 cm^{-1} (OH), a sharp, intense band at 1 670 cm^{-1} (vinyl ether), and bands at 698 cm^{-1} and 753 cm^{-1} (benzylidene). The n.m.r. spectrum in $CDCl_3$, with the aid of spin decoupling and resolution of the signals at 100 Mc.p.s., was amenable to complete first-order analysis (Fig. 3). The observed chemical shifts and coupling constants are listed in Table I. The coupling constants $J_{3,4}$ (3.5 c.p.s.) and $J_{4,5}$ (9.5 c.p.s.) are in agreement with the half-chair H1 structure V.

Acetylation of V gave VI, whose infrared spectrum showed no absorption in the OH region; strong absorption occurred at 1 742 cm^{-1} (C=O) and 1 668 cm^{-1} (vinyl ether) as

[4]*Obtained from the Lithium Corporation of America via Alfa Inorganics Inc., 8 Congress Street, Beverly, Massachusetts, U.S.A.*

well as at 755 cm^{-1} and 697 cm^{-1} (benzylidene). First-order analysis of the n.m.r. spectrum (Fig. 4) in $CDCl_3$ gave coupling constants and chemical shifts (Table I) in complete agreement with the half-chair H1 structure VI. Acetylation of C_3OH shifted the C_3H signal markedly from τ 5.99 to τ 4.48.

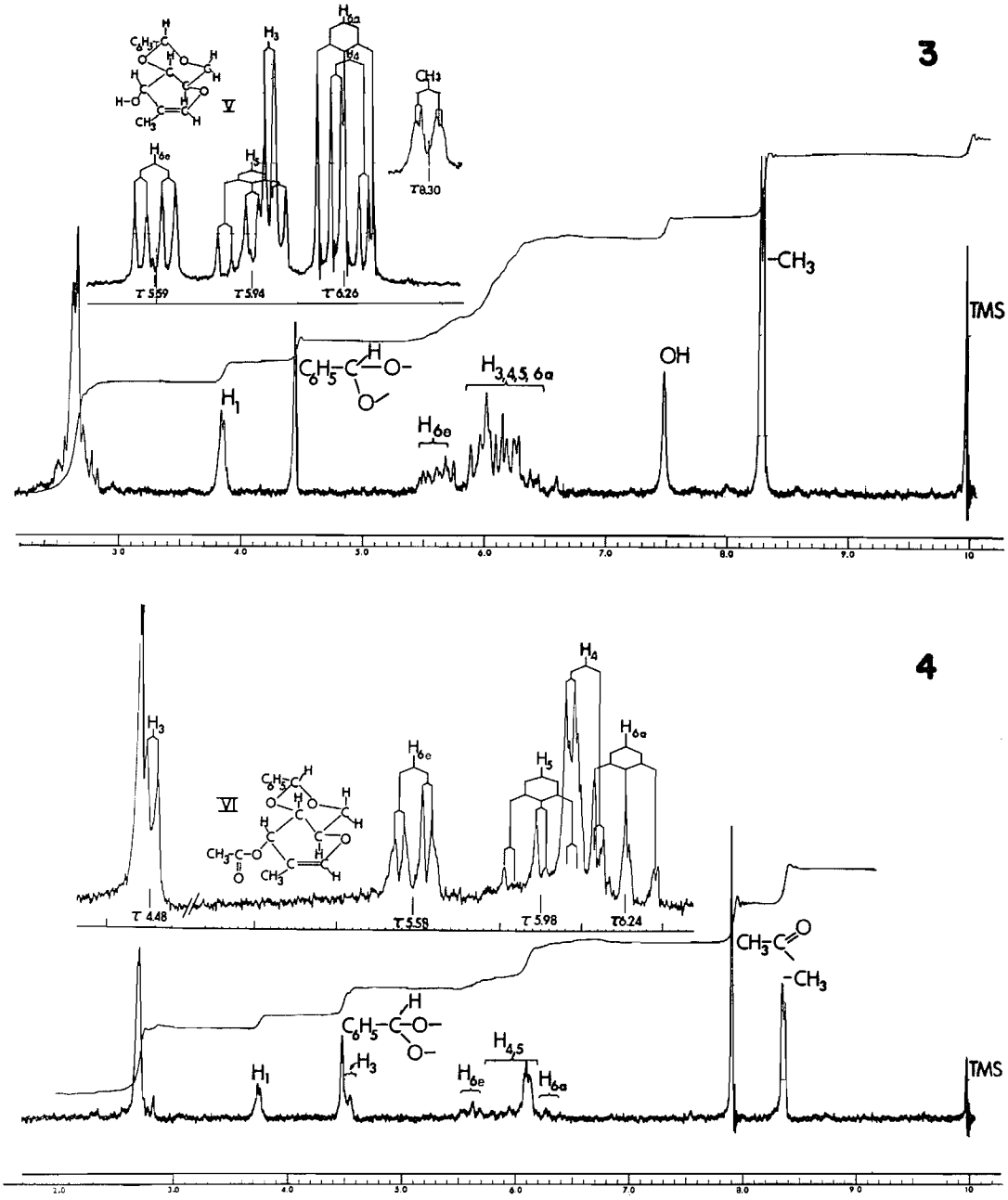
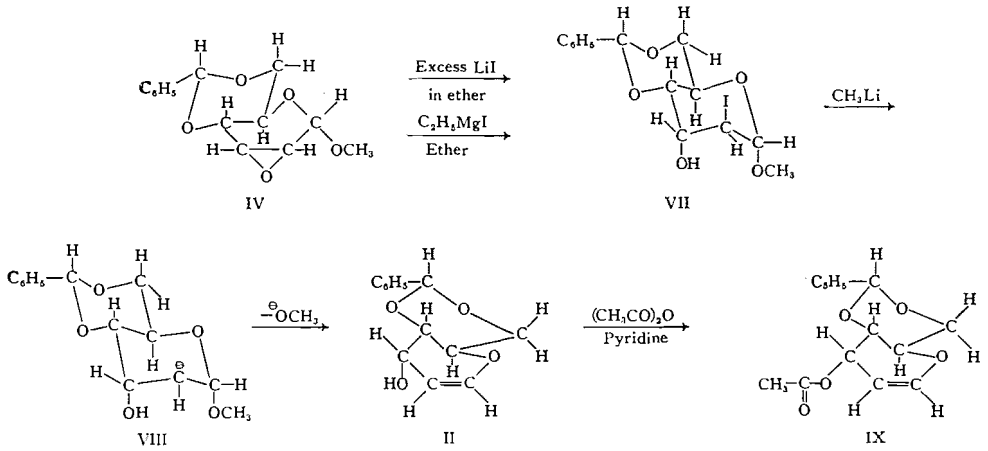


FIG. 3. Nuclear magnetic resonance spectrum at 60 Mc.p.s. of 4,6-*O*-benzylidene-1,2-didehydro-1,2-dideoxy-2-methyl-D-*ribo*-hexopyranose (V) in $CDCl_3$. Inset, 100 Mc.p.s. spectrum in $CDCl_3$.

FIG. 4. Nuclear magnetic resonance spectrum at 60 Mc.p.s. of 3-*O*-acetyl-4,6-*O*-benzylidene-1,2-didehydro-1,2-dideoxy-2-methyl-D-*ribo*-hexopyranose (VI) in $CDCl_3$. Inset, 100 Mc.p.s. spectrum in $CDCl_3$.

The formation of V rather than II and the fate of the rest of IV are under investigation and will be reported upon later.

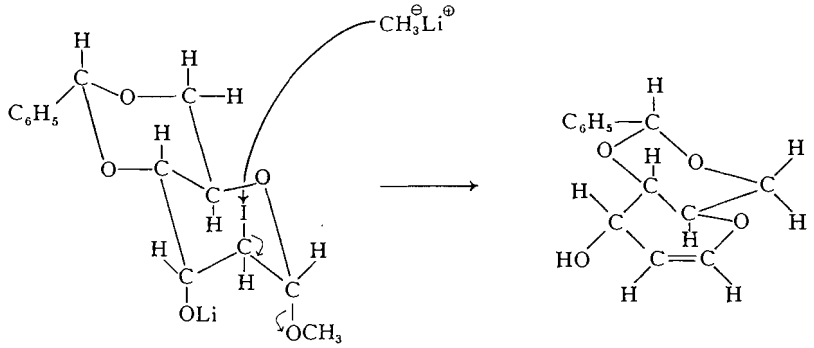
Compound II could be obtained by the reaction of methyl 2,3-anhydro-4,6-*O*-benzylidene-α-D-allopyranoside (IV) with methyllithium prepared according to the directions of Feast *et al.* (1), or by the reaction of commercial methyllithium with the iodohydrin VII. The iodohydrin could be prepared according to published directions (5) by the reaction of ethylmagnesium iodide with methyl 2,3-anhydro-4,6-*O*-benzylidene-α-D-allopyranoside (IV), or more conveniently by treatment of an ether solution of IV with lithium iodide in fourfold excess to force the equilibrium towards VII. No doubt, the conversion of VII into II involved lithium–iodine exchange to produce the carbanion VIII, which would eliminate the methoxide anion to form the α,β-unsaturated ether II (Reaction Scheme 3).[5] The formation of II by the reaction of the 2,3-anhydroallopyranoside IV with methyllithium, as found by Feast *et al.* (1), will be discussed in an early communication by R. U. Lemieux of our department.



REACTION SCHEME 3.

First-order analysis of the n.m.r. spectra of II (Fig. 5) and its acetylated derivative IX (Fig. 6) gave the coupling constants and chemical shifts listed in Table I. These, along with the infrared spectra, corroborated the structures II and IX. In both cases, the coupling constants $J_{3,4}$ (3.5 c.p.s. and 3.0 c.p.s.) and $J_{4,5}$ (9.5 c.p.s.) support the "gauche" arrangement of H_3 and H_4 and the *trans* diaxial configuration of H_4 and H_5.

[5]*The referee pointed out that IX might be obtained via a concerted reaction such as*



rather than by stepwise formation of the carbanion intermediate.

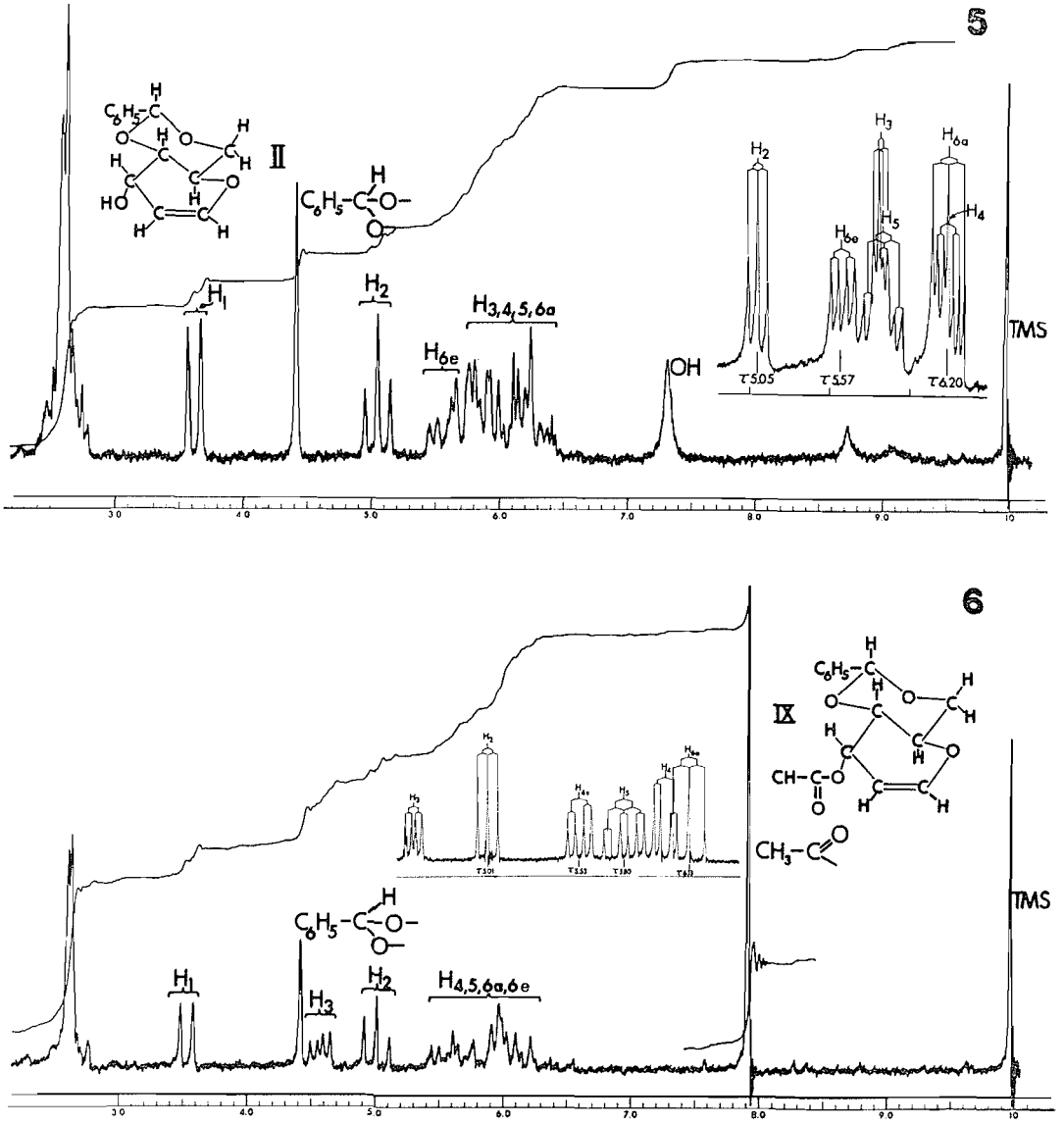


FIG. 5. Nuclear magnetic resonance spectrum at 60 Mc.p.s. of 4,6-*O*-benzylidene-1,2-didehydro-1,2-dideoxy-D-*ribo*-hexopyranose (II) in $CDCl_3$. Inset, 100 Mc.p.s. spectrum in $CDCl_3$.

FIG. 6. Nuclear magnetic resonance spectrum at 60 Mc.p.s. of 3-*O*-acetyl-4,6-*O*-benzylidene-1,2-didehydro-1,2-dideoxy-D-*ribo*-hexopyranose (IX) in $CDCl_3$. Inset, 100 Mc.p.s. spectrum in $CDCl_3$.

It is interesting that in compounds I and III, where H_3 and H_4 are *trans* diaxial, the signal for H_4 is downfield from that for H_5, whereas in compounds II and IX as well as V and VI, where H_3 is "gauche" to H_4, the H_4 signal lies upfield from that for H_5. This observation has been of some utility in locating both the H_4 and H_5 signals in several compounds to be reported upon later.

EXPERIMENTAL

Melting points are uncorrected. Infrared spectra were obtained with a model 421 Perkin–Elmer spectrometer. Nuclear magnetic resonance spectra were obtained with Varian Associates A60 and HR100 spectrometers. Elemental analyses were performed by Miss Darlene Roberts, Department of Chemistry, University of Alberta, Edmonton. Rotations were found with a Perkin–Elmer model 141 polarimeter.

D-*Glucal*

The following modification of the published procedure (6) gave better results.

Pure tri-*O*-acetyl-D-glucal (5 g) (7) was stirred at room temperature for 18 h with anhydrous sodium carbonate (5 g) in dry methanol (75 ml). The mixture was filtered and the solid residue washed with dry methanol. The combined washings and filtrate were freed from methanol and the residue was extracted with hot ethyl acetate. When this extract was concentrated under reduced pressure and allowed to stand in the refrigerator, 2.0 g (70%) of D-glucal slowly separated as crystals. These were pure enough for the next reaction, m.p. 57–59° (lit. m.p. 57–59° (6)). A mixed melting point gave no depression.

4,6-O-Benzylidene-D-glucal (I)

A mixture of pure D-glucal (1 g), benzaldehyde freshly distilled under nitrogen (2 ml), freshly fused zinc chloride (600 mg), and anhydrous sodium sulfate (heated to drive off residual moisture) (500 mg) was stirred for 12 h at room temperature under nitrogen. (The presence of the dry sodium sulfate was thought to be necessary to remove water which might otherwise react with the glucal double bond. Later experiments showed that its absence made little difference in the yield of product.) The solid materials, except sodium sulfate, slowly dissolved, giving a pale-green solution. An aqueous solution of sodium carbonate (10%, 10 ml) was stirred into the mixture, which then stood for 10 min. The white precipitate of zinc hydroxide was removed by filtration, and washed with water and then with ether. The organic layer was separated from the combined washings and filtrate and the aqueous portion (~50 ml) extracted with ether (5 × 50 ml). The combined ether solutions were washed twice with water and then dried (Na_2SO_4). The ether was removed and the residue was freed from benzaldehyde by passage of the material through a column of neutral alumina (grade II, 15 g) and elution of the column with *n*-hexane until the eluent was free from benzaldehyde. The 4,6-*O*-benzylidene-D-glucal was removed from the column with diethyl ether. Evaporation of the ether gave a colorless solid, m.p. 136–138°, yield 31%. Crystallization from ether–hexane raised the melting point to 142–143°; $[\alpha]_D^{27}$ −20° (*c*, 1 in $CHCl_3$).

Anal. Calcd. for $C_{13}H_{14}O_4$: C, 66.70; H, 6.02. Found: C, 66.72; H, 5.77.

3-O-Acetyl-4,6-O-benzylidene-D-glucal (III)

To 4,6-*O*-benzylidene-D-glucal (120 mg) in dry pyridine (2 ml) was added acetic anhydride (0.5 ml), and the mixture was allowed to stand at room temperature for 12 h. It was then poured into ice water, from which, after 1 h, was obtained a solid (100 mg, 70%). The solid was separated, washed with water, and crystallized from acetone–hexane, m.p. 136–137°, $[\alpha]_D^{27}$ −85° (*c*, 1 in $CHCl_3$).

Anal. Calcd. for $C_{15}H_{16}O_5$: C, 65.21; H, 5.84. Found: C, 65.19; H, 5.50.

4,6-O-Benzylidene-1,2-didehydro-1,2-dideoxy-2-methyl-D-ribo-hexopyranose (V)

To a suspension of 2 g of methyl 2,3-anhydro-4,6-*O*-benzylidene-α-D-allopyranoside (IV) (8) in anhydrous ether (50 ml) was added an ether solution of methyllithium (100 ml of a 4.5% solution, Lithium Corporation of America) at 0 to 5° under a nitrogen atmosphere. Ten minutes later the mixture was refluxed for a period of 8 h, during which time the alloside slowly dissolved. The yellow mixture was poured slowly, with stirring, into ice water (50 ml). The ether layer was separated and the aqueous portion extracted four times with ether. The combined ether layers were washed with water, dried (Na_2SO_4), and freed from solvent. The residual syrup, upon trituration with hexane, gave a crystalline solid, m.p. 120–122° (400 mg, 22%). Crystallization from ether–hexane gave 370 mg (20%) of material melting at 126–127°; $[\alpha]_D^{27}$ +175° (*c*, 1 in $CHCl_3$).

Anal. Calcd. for $C_{14}H_{16}O_4$: C, 67.73; H, 6.50. Found: C, 67.52; H, 6.25.

3-O-Acetyl-4,6-O-benzylidene-1,2-didehydro-1,2-dideoxy-2-methyl-D-ribo-hexopyranose (VI)

Acetic anhydride (0.5 ml) was added to a solution of V (120 mg) in dry pyridine (2 ml). The mixture was left overnight at room temperature, and then poured into ice water. After 1 h, the crystalline product was separated by filtration, washed with water, and air-dried (120 mg, 85%), m.p. 70–72°. When crystallized from hexane it melted at 74–75° (100 mg, 76%); $[\alpha]_D^{27}$ +185° (*c*, 1 in $CHCl_3$).

Anal. Calcd. for $C_{16}H_{18}O_5$: C, 66.20; H, 6.25. Found: C, 66.42; H, 6.16.

Methyl 4,6-O-Benzylidene-2-deoxy-2-iodo-α-D-altropyranoside (VII)

A mixture of methyl 2,3-anhydro-4,6-*O*-benzylidene-α-D-allopyranoside (IV) (1.32 g) and dry lithium iodide (2.6 g) in anhydrous ether (80 ml) was refluxed for 1 h. The clear solution was cooled, washed with water until neutral to litmus, and then dried (Na_2SO_4). Removal of the ether gave a syrup which crystallized on trituration with hexane (1.5 g, 76%), m.p. 102–104°. Recrystallization from ether–hexane gave a melting point of 104–105° (lit. m.p. 105–106° (5)). A mixed melting point was undepressed.

Attempted Methylation of the 2-Iodoaltroside VII

To a solution of VII (1.96 g) in 1,2-dimethoxyethane (40 ml, distilled from potassium metal) and methyl iodide (5 g) was added sodium hydride (0.5 g, obtained as a 55% dispersion in mineral oil, from which the mineral oil was first removed with dry hexane). A white solid appeared immediately after the addition of the first portion of the sodium hydride. After the addition of the hydride, the mixture was stirred for 2 h at room temperature and filtered; then the residue (1 g) was washed with water. Crystallization from chloroform–ether gave methyl 2,3-anhydro-4,6-*O*-benzylidene-α-D-allopyranoside, m.p. 199–200°. A further quantity was

recovered from the filtrate, total yield 89%. A mixed melting point with an authentic sample (8) was undepressed. No methylated material was obtained.

*4,6-O-Benzylidene-1,2-didehydro-1,2-dideoxy-*D*-ribo-hexopyranose (4,6-O-Benzylidene-*D*-allal, II)*

Method A

To a stirred solution of the 2-iodoaltroside VII (1.95 g) in dry ether (50 ml), cooled in an ice bath, was added moderately slowly and under nitrogen a solution of *n*-butyllithium (10 ml of a 15% solution). The solution slowly became cloudy. It was refluxed for 2 h, cooled, and poured into ice water. The ether layer was separated and the aqueous portion extracted with ether. The combined ether solutions were washed with water, dried (Na_2SO_4), and freed from ether. The light-yellow syrupy residue crystallized slowly as fine long needles. Recrystallization from ether–hexane gave a melting point of 84–85°; yield 1.1 g (93%). A mixed melting point with an authentic sample (1) was undepressed.

When methyllithium replaced *n*-butyllithium, similar results were obtained.

Method B

A mixture of methyl 2,3-anhydro-4,6-*O*-benzylidene-α-D-allopyranoside (IV) (3.5 g) and dry lithium iodide (6 g) in anhydrous ether (250 ml) was stirred and refluxed under nitrogen for 1 h. The clear, light-yellow solution was cooled in an ice bath; to this was added an ether solution of *n*-butyllithium (40 ml of a 15% solution) at a moderate rate. After the addition, the cloudy solution was refluxed for 2 h, cooled, and poured into ice water. The ether layer was separated and the aqueous portion extracted with ether. The combined organic layers were washed with water, dried (Na_2SO_4), and freed from solvent. The semisolid residue (3.0 g, 94%) was crystallized from ether–hexane, m.p. 84–85°, yield 2.85 g (89%).

Similar results were obtained when methyllithium was added in place of *n*-butyllithium.

Example of the Method for the First-Order Analysis (with Compound IX)

The signal at low field (τ 3.54) is no doubt caused by H_1. The signal for H_3 was located by its change of position from τ 5.81 (for compound II) to τ 4.57 on acelylation of II to produce IX. The signal for H_2 must then be that at τ 5.01.

Irradiation at τ 3.54 (H_1) converted the triplet at τ 5.01 (H_2) into a doublet ($J_{2,3}$ = 5.7 c.p.s.). Irradiation at τ 4.57 (H_3) changed the triplet at τ 5.01 (H_2) to a doublet ($J_{1,2}$ = 6.0 c.p.s.). Irradiation at τ 4.57 converted the quartet at τ 6.05 into a doublet with a coupling of 9.5 c.p.s. ($J_{4,5}$), eliminating the two small couplings of 3.5 c.p.s. ($J_{3,4}$) and thus indicating that the signal for H_4 was at τ 6.05 and that H_3 and H_4 have an equatorial–axial (gauche) steric relationship. The large coupling of 9.5 c.p.s. is no doubt caused by coupling of H_4 with H_5, thus indicating that these protons are *trans* diaxial.

The quartet at τ 5.53 is most likely that for H_{6e} since it agrees with the expected quartet for H_{6e}, and the triplet at τ 6.18 would be that expected for H_{6a} if this proton were coupled equally to H_{6e} and H_5. On this assumption, H_5 must be centered at τ 5.80 with $J_{4,5}$ = 9.5 c.p.s. (as indicated above) and $J_{5,6a}$ = 9.5 c.p.s., giving a triplet which, in turn, is split by coupling of H_5 with H_{6e} by 4.5 c.p.s. caused by their gauche arrangement.

Irradiation at τ 5.53 (H_{6e}) caused a strong collapse at both the τ 5.80 and τ 6.18 regions.

With the aid of this information, and the use of similar reasoning along with a careful comparison of all of the spectra, the HR100 spectra of the remaining compounds were analyzed to give multiplets which agreed reasonably well with those expected.

ACKNOWLEDGMENTS

The authors appreciate the financial assistance given by the National Research Council of Canada and the Defence Research Board of Canada. Thanks are due to R. N. Swindlehurst and his assistants for the A60 n.m.r. as well as the infrared spectra, and to G. Bigam for the HR100 n.m.r. spectra. We also appreciate the assistance given by G. Bigam in the interpretation of the HR100 n.m.r. spectra.

REFERENCES

1. A. A. J. Feast, W. G. Overend, and N. R. Williams. J. Chem. Soc. 7378 (1965).
2. R. J. Ferrier. J. Chem. Soc. 5443 (1964).
3. U. G. Nayak and R. K. Brown. Can. J. Chem. **44**, 591 (1966).
4. R. J. Ferrier and W. G. Overend. Quart. Rev. London, **13**, 265 (1959).
5. G. N. Richards and L. F. Wiggins. J. Chem. Soc. 2442 (1953).
6. F. Shafizadeh and M. Stacey. J. Chem. Soc. 3608 (1952).
7. B. Helferich, E. N. Mulcahy, and H. Ziegler. Ber. **87**, 233 (1954).
8. N. K. Richtmeyer and C. S. Hudson. J. Am. Chem. Soc. **63**, 1727 (1941).

Can. J. Chem. Downloaded from www.nrcresearchpress.com by 210.87.254.6 on 09/05/12
For personal use only.

PHOTOCHEMICAL TRANSFORMATIONS OF DIENES

VII. STEREOCHEMISTRY OF ADDITION OF ALCOHOL, AND EFFECT OF SUBSTITUENTS AND ACIDS ON THE PHOTOCHEMISTRY OF CHOLESTA-3,5-DIENES[1,2]

G. BAUSLAUGH,[3] G. JUST, AND E. LEE-RUFF[4]
Department of Chemistry, McGill University, Montreal, Quebec

Received July 19, 1966

ABSTRACT

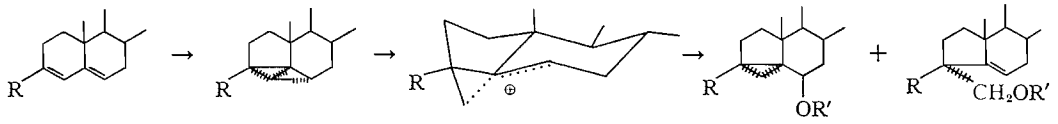
Results for the photolysis of 6-methylcholesta-3,5-diene are described. The photolysis of these and other dienes proceeds by a unimolecular process, giving bicyclobutanes, or a bimolecular process, giving carbonium ions. Reaction of the bicyclobutane with a protic solvent results in stereospecific incorporation of a proton (4β), whereas direct abstraction of a proton by a photo-excited species results in non-stereospecific abstraction. In the presence of small amounts of acid, more or in part new products, derived from the bimolecular pathway, are obtained.

It was noted that the normal chromatographic elution sequence (alumina) of epimeric alcohols was reversed when thin-layer chromatography (silica gel) was used.

The photolysis of cholesta-3,5-dienes (I) proceeds through at least two different pathways: a unimolecular process (A) and a bimolecular process (B), in which a photo-excited species abstracts a proton from solvents such as alcohols.

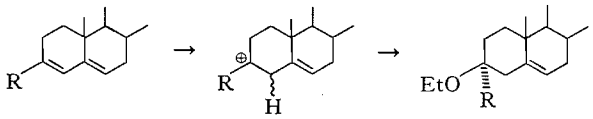
Process A is characteristic of the photolysis of cholesta-3,5-diene (I*a*), which gives bicyclobutane (II*a*) in at least a 75% yield (1). Treatment of II*a* with water or alcohol gives homoallylic carbonium ion III*a*, in which the protonation has occurred stereospecifically (2). Coordination with solvent then gives ethers or alcohols IV*a* and V*a* (R′ = H or C_2H_5).

Mechanism A



I*a*, I*b* II*a*, II*b* III*a*, III*b* IV*a*, IV*b* V*a*, V*b*

Mechanism B



I*b*, I*c* VI*b*, VI*c* VII*b*, VII*c*

a, R = H; *b*, R = CH_3; *c*, R = OCH_3 or OC_2H_5

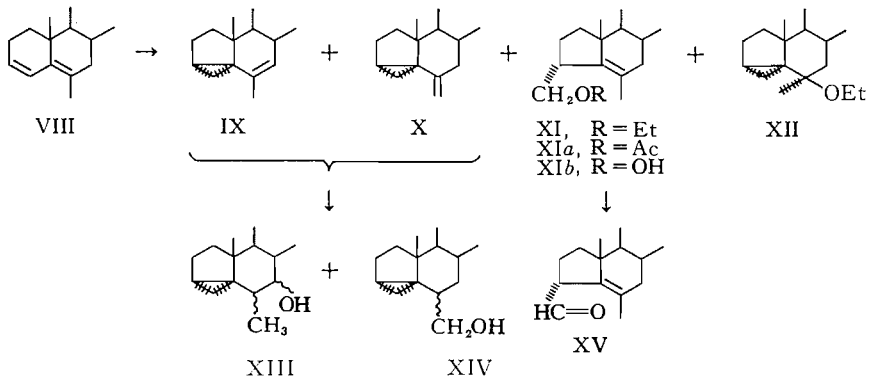
Process B is typical of the photolysis of 3-alkoxycholesta-3,5-dienes (I*c*) (3). No bicyclobutane can be detected in that reaction. An excited polar species abstracts a proton from solvent non-stereospecifically, giving a carbonium ion (VI), which then coordinates with solvent.

[1]*This work was supported by the National Research Council of Canada.*
[2]*For part VI in this series, see G. Just and C. Pace-Asciak, Tetrahedron, 22, 1069 (1966).*
[3]*Holder of a Shell Oil of Canada fellowship, 1963–1964. Present address: Bishop's University, Lennoxville, Quebec.*
[4]*Holder of a National Research Council of Canada bursary, 1964–1965, and studentship, 1965–1966.*

In this paper, we shall examine the influence of a 6-methyl substituent on the photoreaction. The stereochemistry of the protonation and of the coordination of solvent will be discussed, as well as the effect of acid on the photolysis.

Photolysis of 6-Methylcholesta-3,5-diene (VIII)

The photolysis of diene VIII (4) in a pentane–ethanol mixture gave two ethers XI and XII in 17 and 5% yields, and two hydrocarbons IX and X in 40 and 20% yields, respectively. The ether with the lower yield was identified as 6β-ethoxy-6α-methyl-3β,5-cyclo-5β-cholestane (XII) by spectroscopic means,[5] and by analogy with similar reactions of cholesta-3,5-diene (20). This is the expected product from the ethanolysis of the bicyclobutane intermediate formed from VIII.



The second major photoether was identified as 3α-ethoxymethyl-6-methyl-A-norcholest-5-ene (XI), also an expected photo product, based on the following evidence. Treatment with boron trifluoride etherate in acetic anhydride (5) converted XI into 3α-acetoxymethyl-6-methyl-A-norcholest-5-ene (XI*a*) in a quantitative yield.

The magnetic non-equivalence of protons B and C, including the large difference in the values of J_{AB} and J_{AC} in the nuclear magnetic resonance (n.m.r.) spectrum of acetate XI*a* (Fig. 1), indicated that the rotation of the acetoxymethyl group was hindered.

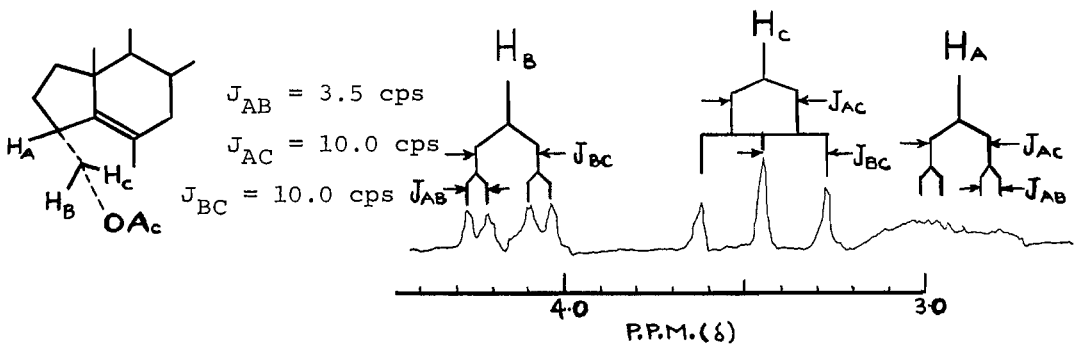


FIG. 1. Nuclear magnetic resonance spectrum of acetate XI*a*.

Acetate XI*a* could be hydrolyzed to alcohol XI*b*. Alcohol XI*b*, upon re-acetylation, gave acetate XI*a*, and was converted into photoether XI by treating its potassium salt

[5]*Relevant spectroscopic data for all the compounds described are given in the Experimental.*

Can. J. Chem. Downloaded from www.nrcresearchpress.com by 210.87.254.6 on 09/05/12
For personal use only.

Can. J. Chem. Downloaded from www.nrcresearchpress.com by 210.87.254.6 on 09/05/12
For personal use only.

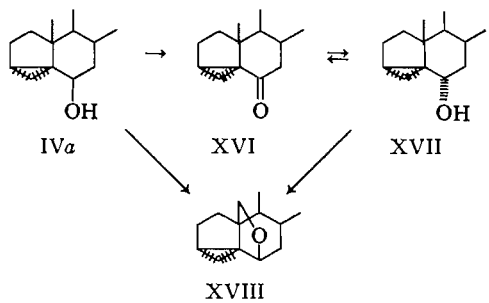
with ethyl iodide. A mild Jones oxidation of alcohol XI*b* gave aldehyde XV. The alcohol XI*b* was stable to manganese dioxide and to 10% ethanolic hydrochloric acid, indicating that it was not allylic (6, 7). Dehydration with phosphorus pentoxide in pyridine converted XI*b* into the cycloolefin IX, whereas treatment with phosphorus pentoxide in benzene gave 6-methylcholesta-3,5-diene (VIII). This latter reaction was also observed with the corresponding 3α-hydroxymethyl-A-norcholest-5-ene (1*a*). These dehydrations most likely proceed through the intermediacy of a homoallylic carbonium ion similar to III, which, under acidic conditions (phosphorus pentoxide – benzene), would rearrange to diene VIII.

The hydrocarbon fraction from the photolysis could not be resolved into its two components on a preparative scale. However, thin-layer chromatography (t.l.c.) did reveal two overlapping stains of slightly different colors. Vapor-phase chromatography (v.p.c.) showed two sharp peaks with an intensity ratio of 2:1. The major and less-polar olefin was assigned the structure of 6-methyl-3β,5-cyclo-5β-cholest-6-ene (IX), and the more polar olefin the structure of 6-methylene-3β,5-cyclo-5β-cholestane (X), based on n.m.r. and infrared spectral data. Hydroboration of the olefin mixture gave, in low yields, two alcohols, XIII and XIV, which were separated on a silica gel column and identified by n.m.r. and infrared spectra.

Stereochemistry

Mechanism A

The highly strained bicyclobutane derivatives II*a* and II*b* are rapidly solvolyzed in protic solvents. The stereochemistry of solvolysis products of the type IV and V has been well established (8). Using alcohol IV*a* (R′ = H), Dauben and Wipke (2) showed that the n.m.r. coupling constants between the proton at C_6 and those at C_7 were typical of a 6β alcohol ($J_{AX} = J_{BX} = 3$ c.p.s.). We oxidized alcohol IV*a* (R′ = H) to ketone XVI, which was then reduced with lithium aluminium hydride to the previously unreported alcohol XVII. Alcohol XVII could be reoxidized to ketone XVI, and hence was epimeric with alcohol IV*a*. The n.m.r. spectrum of alcohol XVII showed typical coupling constants



(9) (10.8 and 4.2 c.p.s.) for an axial 6β proton, and therefore confirmed the 6β configuration for the hydroxyl group in IV*a*. Supporting evidence was obtained by observing the position of the peak of the C_{19} methyl group in the n.m.r. spectrum of epimers IV*a* (R′ = H) and XVII. In IV*a* (R′ = H) the peak was located at 1.2 p.p.m., whereas in XVII it was found at 1.0 p.p.m. The lower field position is indicative of a 6β substituent (e.g. see ref. 10).

Lead tetraacetate oxidations of steroidal 6β alcohols are known to give 6β,19 ethers (11). When 3β,5-cyclo-5β-cholestan-6β-ol (IV*a*) was treated with lead tetraacetate, a 66%

yield of the cyclic ether XVIII was obtained. However, the 6α alcohol XVII gave the same ether in a comparable yield, indicating the unreliability of this method for stereochemistry assignments. Also, t.l.c. (on Merck silica gel G) showed that the 6α alcohol XVII (equatorial) moved faster than its 6β epimer IV*a*. This result is somewhat unexpected since the axial epimer usually has a higher chromatographic mobility on aluminium oxide. Kosower and Winstein (12), for example, showed that 3α,5-cyclo-5α-cholestan-6β-ol has a higher mobility on aluminium oxide than its 6α epimer. However, these 3α,5-cyclo compounds also showed the reverse order of mobility when chromatographed on thin-layer silica gel.

Dauben and Wipke (2) studied the stereochemistry of the addition of hydrogen to C_4 by carrying out the solvolysis in heavy water, giving IV*a*-4-d_1 (R′ = H). They tentatively assigned the 4β configuration to the deuterium on the basis of the coupling constant between the remaining C_4 proton and the C_3 proton, assuming that the *trans* coupling in cyclopropanes is always smaller than the *cis* coupling. However, typical chemical shift values for bicyclo[3.1.0]hexanes (20) suggested the opposite assignment. We have obtained more conclusive evidence by examining the n.m.r. spectra of XVII and XVII-4-d_1. Whereas in the spectrum of alcohol IV*a* peaks for both C_4 cyclopropyl protons appeared (+0.31 and −0.22 p.p.m.) and no higher field signal was present in the monodeuterated product, both XVII and XVII-4-d_1 showed absorption for only one C_4 proton. Hence the proton in XVII which becomes deuterated in XVII-4-d_1 is shifted to an abnormally low field by the presence of a 6α-hydroxyl group. Models show that a 6α-hydroxyl group is in close proximity to the 4β proton, and therefore the deuterium is in the 4β position. To show that the disappearance of one of the two C_4 protons was caused by a 6α substituent, we examined the spectra of the 6β-acetoxy-, 6β-benzoyloxy-, 6β-ethoxy-, and unsubstituted 3β,5-cyclo-5β-cholestanes. All showed both C_4 proton signals.

When 6β-ethoxy-3β,5-cyclo-5β-cholestane-4β-d_1 (IV*a*-4β-d_1, R′ = Et) was hydrolyzed with acid and the resulting ring-contracted alcohol V*a*-4β-d_1 (R′ = H) converted into its *p*-toluenesulfonate and solvolyzed in aqueous acetone, the n.m.r. spectrum of the resultant cycloalcohol IV*a*-4β-d_1 (R′ = H) showed one doublet at 0.32 p.p.m., indicating that the deuterium was still attached to the 4β position. This proves that at no stage in the solvolysis is there a classical carbonium ion which would have altered the stereochemistry at C_4.

We therefore believe that the most likely mechanism for the solvolysis of the bicyclobutanes II involves initial protonation at the 4β position to give homoallylic carbonium ion III, followed by attack of solvent at C_4 or C_6, as demonstrated by Whitham (8).

Mechanism B

The photolyses of 3-alkoxycholesta-3,5-dienes (I*c*) in alcohol give 3,3-dialkoxycholest-5-enes (VII*c*). Deuterium labelling experiments showed non-stereospecific addition of deuterium at C_4 (3*b*). The photolysis of 3-methylcholesta-3,5-diene (I*b*) is reported (13) to give 20% of products derived from bicyclobutane II*b* (mechanism A) in which deuterium has been introduced stereospecifically at C_4, and 20% of 3β-ethoxy-3α-methylcholest-5-ene (VII*b*) (mechanism B). We now have obtained evidence that deuterium addition in VII*b* is nonspecific by carrying out the photolysis in deuterated ethanol. The n.m.r. spectrum of VII*b* (Fig. 2) shows half of the expected AB quartet, with peaks at 2.68 and 2.45 p.p.m. The spectrum of VII*b*-4-d_1 shows a peak of one-half the relative area of the previous two at their approximate center of gravity.

Therefore, dienes I*b* and I*c* both apparently react in part by a similar mechanism (mechanism B), which likely involves bimolecular reactions between an excited state and ethanol.

Can. J. Chem. Downloaded from www.nrcresearchpress.com by 210.87.254.6 on 09/05/12
For personal use only.

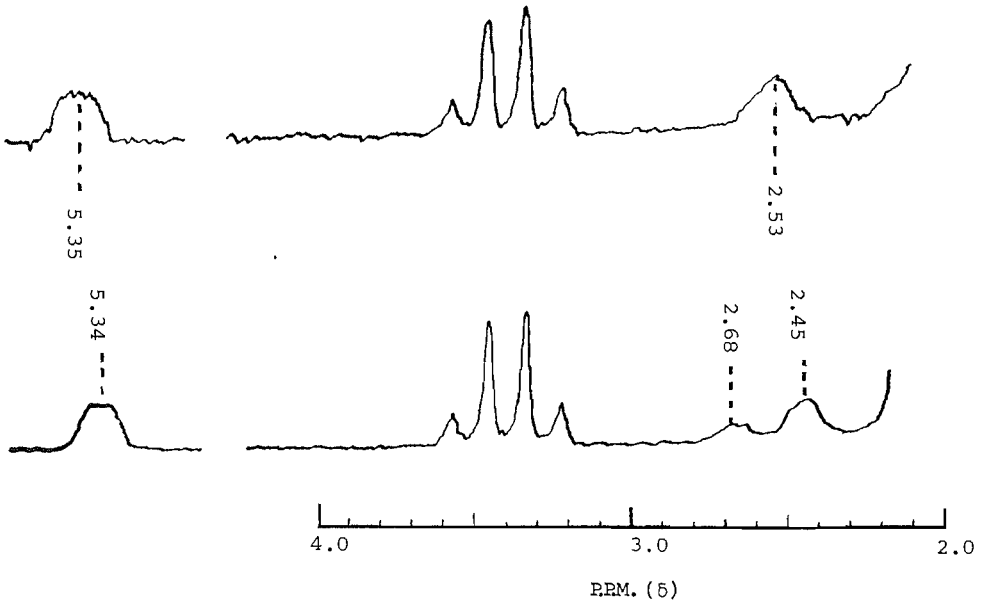


FIG. 2. Nuclear magnetic resonance of ethers VII*b* and VII*b*-4-d_1.

Effect of Acid on the Photolyses of Cholesta-3,5-dienes

To test the hypothesis that a polar excited state abstracts a proton from solvent in a bimolecular reaction, we carried out the photolysis of 3-methylcholesta-3,5-diene (I*b*) in acidic ethanol. The yield of ether VII*b* increased from about 20% (in pure ethanol) to 37%.

Photolysis of cholesta-3,5-diene in ethanol gives only bicyclobutane cleavage products IV and V. However, photolysis in acidic ethanol gave 29% of ether IV*a* (R′ = Et), traces of ether V*a* (R′ = Et), and 31% of a new ether, 3β-ethoxycholest-4-ene. The structure was confirmed by hydrogenation of this ether in the presence of sodium nitrite to suppress hydrogenolysis (14). Cholestane and 3β-ethoxycholestane were obtained and identified by comparison with authentic samples, the latter being obtained by reduction of cholesteryl ethyl ether. More cholestane was obtained when no sodium nitrite was added to the hydrogenation mixture.

The photolysis of 6-methylcholesta-3,5-diene (VIII) is similar to that of cholesta-3,5-diene in that it gave only products IX, X, XI, and XII derived from a bicyclobutane of type II. When the photolysis of this diene was carried out in acidic ethanol, 6-methylcholesteryl ethyl ether was formed in a 20% yield in addition to 30% of the ring-contracted ether XI.[6] The structure of the former ether was proven by comparison with a synthetic sample (4).

The starting material and all products from the photolyses of dienes I*a*, I*b*, and VIII were subjected to the acidic reaction conditions. None of the polar reaction products VII*b*, 3β-ethoxycholest-4-ene, and 6-methyl-cholesteryl ethyl ether were obtained.

It seems, therefore, that the formation of 3β-ethoxycholest-4-ene, 3β-ethoxy-3α-methylcholest-5-ene (VII*b*), ketal VII*c*, and 6-methylcholesteryl ethyl ether from dienes I*a*, I*b*, I*c*, and VIII, respectively, proceeds by a bimolecular reaction mechanism.

From the photolyses of 3-substituted cholestadienes, it appears that strong electron-donating substituents favor the bimolecular mechanism (OEt > CH_3 > H). Since

[6]*Ether XII is not stable to acidic ethanol and is transformed into XI.*

Can. J. Chem. Downloaded from www.nrcresearchpress.com by 210.87.254.6 on 09/05/12
For personal use only.

6-methylcholestadiene resembles cholestadiene (Table I), it must be concluded that the effect of substituents in the polar excited state is localized.

TABLE I

Comparison of product yields from mechanisms A and B in the photolyses of cholesta-3,5-dienes

Diene	In neutral media		In acidic media	
	Total yield of products from mechanism A (%)	Total yield of products from mechanism B (%)	Total yield of products from mechanism A (%)	Total yield of products from mechanism B (%)
Cholesta-3,5-diene (I*a*)	75	0	29	31
3-Methylcholesta-3,5-diene (I*b*)	20	20	9	37
3-Alkoxycholesta-3,5-diene (I*c*)	0	65–90	—	—
6-Methylcholesta-3,5-diene (VIII)	87	0	30	20

EXPERIMENTAL

For general experimental details, see ref. 15. All v.p.c. experiments were performed on a F and M laboratory chromatograph model 700 under the following conditions: glass column (6 ft × ¼ in.) packed with silicon gum SE-30 on Chromosorb W; column temperature 280°; injection port temperature 300°; detector temperature 300°; helium flow 50 ml/min. All preparative t.l.c. separations were performed with glass plates (20 × 20 cm) covered with silica gel (½ mm, E. Merck AG).

Photolysis of 6-Methylcholesta-3,5-diene (VIII) in Ethanol–n-Pentane

Diene VIII (3 g) in 100 ml of spectrograde *n*-pentane and 400 ml of absolute ethanol was irradiated with a 450 W high-pressure mercury arc lamp[7] until there was no appreciable absorption in the ultraviolet between 200 and 400 mμ (96 h). Evaporation gave an oily residue (3.05 g), which was chromatographed on alumina (activity II–III, 100 g). Elution with hexane gave 1.9 g of a hydrocarbon mixture containing 6-methyl-3β,5-cyclo-5β-cholest-6-ene (IX) and 6-methylene-3β,5-cyclo-5β-cholestane (X). Vapor-phase chromatography resolved two sharp peaks with retention times of 57 and 77 s and relative areas of 2:1; ν 3 030 (C=C_7—H), 3 070, 1 645, and 885 cm^{-1} (C=CH_2); δ 1.67 p.p.m. (singlet, C=C—CH_3), 0.25 p.p.m. (doublet, J = 5 c.p.s., C_4 cyclopropyl H in IX), and 0.6 p.p.m. (doublet, J = 5 c.p.s., C_4 cyclopropyl H in X). In addition, signals for vinyl protons at 5.36 p.p.m. (doublet, J = 11 c.p.s., C_7—H) and 5.06 and 4.45 p.p.m. (finely split singlet, J = 2 c.p.s., C_6=CH_2) appeared with relative areas of 1:1, respectively.

Benzene eluted 0.663 g of an oil which contained a mixture of ethers. This mixture was separated by preparative t.l.c. (benzene). The faster moving band (130 mg) was identified as 6β-ethoxy-6α-methyl-3β,5-cyclo-5β-cholestane (XII); ν 3 010, 3 075 (cyclopropane), and 1 080 cm^{-1} (C—O—C); δ 0.0 p.p.m. (2H, overlapping doublets, cyclopropyl protons) and 3.32 p.p.m. (2H, poorly resolved quartet, C_6—O—CH_2). Ether XII was quite labile towards traces of moisture so that no satisfactory analysis could be obtained.

The slower moving band (505 mg, XI) could not be crystallized; ν 1 108 cm^{-1} (C—O—C); δ 1.60 p.p.m. (3H, singlet, C=C—CH_3), 2.85 p.p.m. (2H, doublet, ethoxymethyl protons), and 3.40 p.p.m. (2H, quartet, O—*CH_2*—CH_3); v.p.c. showed one peak with a retention time of 118 s.

Anal. Calcd. for $C_{30}H_{52}O$: C, 84.04; H, 12.23. Found: C, 83.82; H, 12.06.

3α-Acetoxymethyl-6-methyl-A-norcholest-5-ene (XIa)

To 8 ml of acetic anhydride and 1.5 ml of boron trifluoride etherate cooled to −18° was added a solution of 200 mg of ether XI in 2 ml of anhydrous ether. The reaction mixture was stirred for 3 min at −18°. An ice chip was carefully added and the mixture was stirred at room temperature for a further 2 h. The reaction mixture was diluted with 50 ml of ether and the ethereal solution washed with water, 5% aqueous sodium carbonate, and water. The ethereal solution was then dried over anhydrous magnesium sulfate and evaporated under reduced pressure, giving 190 mg of amorphous 3α-acetoxymethyl-6-methyl-A-norcholest-5-ene (XI*a*); ν 1 230, 1 030, and 1 735 cm^{-1} (acetate).

Anal. Calcd. for $C_{30}H_{50}O_2$: C, 81.39; H, 11.38. Found: C, 81.32; H, 11.23.

3α-Hydroxymethyl-6-methyl-A-norcholest-5-ene (XIb)

A solution of 100 mg of acetate XI*a* in 30 ml of 5% methanolic potassium hydroxide was heated under reflux for 3 h. Extraction and evaporation gave 97 mg of an oil which crystallized from methanol–ether,

[7]*The lamp was cooled by running water in a quartz jacket, supplied by Hanovia Lamp Division, 100 Chestnut St., Newark, New Jersey. The container was further cooled by immersion in a cold-water bath.*

Can. J. Chem. Downloaded from www.nrcresearchpress.com by 210.87.254.6 on 09/05/12
For personal use only.

m.p. 109–110°; ν 3 640, 1 165, and 1 015 cm^{-1} (primary OH); δ 1.59 p.p.m. (3H, singlet, C=C—CH_3), 2.93 p.p.m. (1H, multiplet, C_3—H), and 3.45 p.p.m. (2H, multiplet, CH_2—OH).

Anal. Calcd. for $C_{28}H_{48}O$: C, 83.93; H, 12.08. Found: C, 84.02; H, 12.08.

Acetylation of alcohol XI*b* (5 mg) with pyridine and acetic anhydride overnight gave acetate VII*a*, identical in all respects with a sample obtained above from photoether XI.

Attempted Dehydration of Alcohol XIb with Acid

A solution of 5 mg of alcohol XI*b* in 10 ml of absolute ethanol containing 1 ml of concentrated hydrochloric acid was heated under reflux for 4 h. Starting material was recovered.

Attempted Oxidation of Alcohol XIb with Manganese Dioxide

A solution of 10 mg of alcohol XI*b* in 5 ml of tetrahydrofuran containing 50 mg of manganese dioxide (21) was heated under reflux overnight. Filtration of the manganese and evaporation of the ether gave starting material.

Etherification of Alcohol XIb

To a solution of 10 mg of alcohol XI*b* in 5 ml of anhydrous benzene were added potassium chips (100 mg). The mixture was stirred and heated under reflux for 2 h. Ethyl iodide (1 ml) was added and the reaction mixture was refluxed for an additional hour. The mixture was cooled and ethanol was slowly added to decompose the excess potassium. Ether extraction gave an oily residue, which was purified by t.l.c. (benzene). The fast-moving band (2 mg) was identified as 3α-ethoxymethyl-6-methyl-A-norcholest-5-ene (XI). Its infrared spectrum was identical with that of photoether XI, and v.p.c. gave identical retention times.

Oxidation of Alcohol XIb

To a solution of 80 mg of alcohol XI*b* in 5 ml of acetone (freshly distilled over potassium permanganate) cooled to −10° was added dropwise 0.5 ml of Jones reagent (22) diluted with 2.5 ml of acetone. The solution was stirred for 10 min at −10°, after which 1.3 ml of 2-propanol was added followed by 7.5 ml of water. Ether extraction and purification by t.l.c. (benzene) gave 35 mg of 3α-formyl-6-methyl-A-norcholest-5-ene (XV), m.p. 82–84°; ν 2 830, 2 700, and 1 720 cm^{-1} (saturated aldehyde); λ_{max}^{EtOH} 214 mμ (ϵ 2 500); δ 9.24 p.p.m. (3H, singlet, C=C—CH_3).

Anal. Calcd. for $C_{28}H_{46}O$: C, 84.35; H, 11.63. Found: C, 84.22; H, 11.50.

Dehydration of Alcohol XIb

(a) With Phosphorus Pentoxide and Benzene

To a solution of 10 mg of alcohol XI*b* in 5 ml of anhydrous benzene was added 100 mg of phosphorus pentoxide. The mixture was stirred at room temperature for ½ h. This was worked up in the normal manner, giving 8 mg of 6-methylcholesta-3,5-diene (VIII), identified by comparison with an authentic sample.

(b) With Phosphorus Pentoxide and Pyridine

A solution of 7 mg of alcohol XI*b* in 5 ml of anhydrous pyridine containing 100 mg of phosphorus pentoxide was heated under reflux for 4 h. After addition of 5 ml of water to the cooled solution, it was extracted with ether. Evaporation gave 7 mg of an oil showing an infrared spectrum identical with that of the hydrocarbon fraction obtained from the photolysis, except that peaks for the exomethylene group at 3 070 and 885 cm^{-1} were missing. Vapor-phase chromatography showed that the retention time was identical with that of hydrocarbon IX.

Dehydration of 3α-Hydroxymethylcholest-5-ene with Phosphorus Pentoxide in Benzene

The same procedures used for the dehydration of alcohol XI*b* with phosphorus pentoxide in benzene were followed to give cholesta-3,5-diene (19) in a quantitative yield.

Hydroboration of the Photo-olefin Mixture (IX and X)

Diborane, generated by the addition of 1.52 g of sodium borohydride in 30 ml of diglyme to 7.2 g of boron trifluoride etherate in 40 ml of diglyme, was passed through a solution of 50 ml of ether containing 1 g of the photo-olefin mixture (IX and X) over a period of 30 min. The reaction mixture was stirred at room temperature for a further 30 min. To this solution, 4 ml of 3 *M* aqueous sodium hydroxide was added followed by the slow addition of 4 ml of 30% aqueous hydrogen peroxide. The mixture was extracted with ether, and the ethereal extract was washed with water until neutral, dried over anhydrous magnesium sulfate, and evaporated under reduced pressure, giving a colorless oil which was chromatographed on silica gel. Hexane eluted 0.900 g of starting material. Benzene–ether eluted 80 mg of an oil identified as alcohol XIII; ν 3 600, 1 000 (hydroxyl), and 3 050 cm^{-1} (cyclopropyl); δ 3.45 p.p.m. (1H, broad multiplet, $C_7(OH)H$), 0.00 p.p.m. (multiplet, C_4 cyclopropyl protons), and 0.50 p.p.m. (multiplet, C_3 cyclopropyl proton).

Ether eluted 50 mg of an oil identified as alcohol XIV; ν 3 630, 1 010 (hydroxyl), and 3 060 cm^{-1} (cyclopropyl); δ 3.60 p.p.m. (2H, doublet, C_6—CH_2—O) and 0.40 p.p.m. (multiplet, C_4 cyclopropyl protons).

3β,5-Cyclo-5β-cholestan-6β-ol (IVa)

A solution of 5.7 g of cholesta-3,5-diene (I*a*) in wet pentane was irradiated under a helium atmosphere until no diene could be detected by ultraviolet (14 h). Chromatography on alumina (activity II–III) gave

Can. J. Chem. Downloaded from www.nrcresearchpress.com by 210.87.254.6 on 09/05/12
For personal use only.

two crystalline samples: 3β,5-cyclo-5β-cholestan-6β-ol (IV*a*) in a 30–40% yield from the early hexane–benzene (1:1) fractions, and 3α-hydroxymethyl-A-norcholest-5-ene (V*a*) in a 10–20% yield from the later hexane–benzene (1:1) fractions.

The photoalcohol IV*a* was purified by forming the benzoate (benzoyl chloride and pyridine). The benzoate was purified by crystallization several times from ether, and was then reconverted into the alcohol IV*a* by refluxing for 1 h in 25 ml of 5% methanolic potassium hydroxide under nitrogen. Addition of water and extraction with ether yielded a residue, which was purified by t.l.c. (hexane–ether, 9:1). Slow crystallization from ether gave crystals, m.p. 98–100°; $[\alpha]_D$ +21.1° (*c*, 1.61 in $CHCl_3$) (lit. (16) m.p. 98–100.5° and $[\alpha]_D$ 23°); ν_{CCl_4} 3 622 (OH stretching) and 1 032 cm^{-1} (C—O stretching). The n.m.r. spectrum showed C_4 cyclopropyl quartets at +0.35 (*J* 3.0 and 4.6 c.p.s.) and −0.14 p.p.m. (*J* 4.6 and 7.4 c.p.s.). The equatorial C_6 proton appeared at 3.39 p.p.m. as a poorly resolved quartet.

Anal. Calcd. for $C_{27}H_{46}O$: C, 83.87; H, 11.99. Found: C, 84.28; H, 12.09.

The photoalcohol was identical in all respects (melting point, t.l.c., infrared, n.m.r.) with the solvolysis product prepared by Whitham (16).

For purposes of examining their n.m.r. spectra, the following derivatives of IV*a* were prepared.

3β,5-Cyclo-5β-cholestan-6β-acetate

3β,5-Cyclo-5β-cholestan-6β-ol (290 mg) was left overnight in 4 ml of pyridine and 2 ml of acetic anhydride. The solution was then poured into 100 ml of ice water, left for 1 h, and extracted twice with 100 ml portions of ether. The ether phases were washed five times with 5% hydrochloric acid, twice with 5% sodium hydroxide, and twice with water (100 ml each). Drying with sodium sulfate and removal of the solvent left an oily residue of 315 mg. Crystallization from hexane gave 86 mg of the acetate, m.p. 91.5–92.0°; ν_{CCl_4} 1 735, 1 225, and 1 020 cm^{-1} (acetate); δ_{CCl_4} 1.98 p.p.m. (acetate methyl group), and 0.40 and 0.05 p.p.m. (poorly resolved quartets, C_4 cyclopropyl protons).

Anal. Calcd. for $C_{29}H_{48}O_2$: C, 81.24; H, 11.29. Found: C, 81.33; H, 11.27.

3β,5-Cyclo-5β-cholestan-6β-benzoate

3β,5-Cyclo-5β-cholestan-6β-ol (600 mg) was left for 3 h in 5 ml of pyridine and 2.5 ml of bonzoyl chloride. After the solution was poured into ice water and allowed to stand for an additional hour, the benzoate was extracted twice with 100 ml portions of ether. The ether phases were washed twice with 5% sodium hydroxide (100 ml each) and once with water. Drying and removal of the solvent gave a crude, oily product which was crystallized from ether–methanol, giving 318 mg, m.p. 125–125.5°; $[\alpha]_D$ +9.9° (*c*, 0.87 in $CHCl_3$); ν_{CCl_4} 1 710, 1 260, and 1 110 cm^{-1} (benzoate); δ_{CCl_4} 8.17 and 7.56 p.p.m. (benzoate), unresolved peaks at 4.89 p.p.m. (C_6 proton), poorly resolved quartets at 0.49 and 0.19 p.p.m. (C_4 cyclopropyl protons).

Anal. Calcd. for $C_{34}H_{50}O_2$: C, 83.21; H, 10.27. Found: C, 83.01; H, 10.36.

3β,5-Cyclo-5β-cholestan-6-one (XVI)

To a solution of chromium trioxide (100 mg) in 1 ml of chilled pyridine was added, with stirring, a solution of 120 mg of 3β,5-cyclo-5β-cholestan-6β-ol (IV*a*) in 4 ml of pyridine. Stirring was continued for 30 min, and then the mixture was allowed to stand for 16 h. Water and ether were added (100 mg of each) and the ether layer was washed five times with 10% hydrochloric acid (50 ml each) and twice with water. Drying and removal of the solvent left an oily residue, which was crystallized several times from hexane to give XII, m.p. 107–108°; $[\alpha]_D$ +111° (*c*, 0.63 in $CHCl_3$) (lit. (16) m.p. 109–110°, $[\alpha]_D$ +80°); ν_{CCl_4} 1 705 cm^{-1} (ketone); $\delta_{benzene}$ several weak peaks at 0.51 and 0.22 p.p.m. (C_4 cyclopropyl protons).

Anal. Calcd. for $C_{27}H_{44}O$: C, 84.31; H, 11.53. Found: C, 83.93; H, 11.53.

3β,5-Cyclo-5β-cholestan-6α-ol (XVII)

3β,5-Cyclo-5β-cholestan-6-one (45 mg) was dissolved in 7 ml of dry ether, and 10 mg of lithium aluminium hydride was added. After the solution was stirred for 2 h, the excess hydride was destroyed with a little ethyl acetate. Water and ether (100 ml of each) were added, and the ether phase was washed with 5% sodium hydroxide (100 ml), 2% hydrochloric acid (100 ml), and water, and then dried with sodium sulfate. An oily residue of 45 mg was obtained. Crystallization from hexane gave about 20 mg of XVII, m.p. 130–132°; $[\alpha]_D$ +34° (*c*, 0.93 in $CHCl_3$); ν_{CCl_4} 3 622 (OH stretching) and 1 110 cm^{-1} (C—O stretching); δ 3.95 p.p.m. (quartet, 6β proton, $J_{6\beta,7\alpha}$ 10.2 c.p.s., $J_{6\beta,7\beta}$ 4.8 c.p.s.) and 0.11 p.p.m. (quartet, 4α cyclopropyl proton).

Anal. Calcd. for $C_{27}H_{46}O$: C, 83.87; H, 11.99. Found: C, 83.27; H, 11.89.

The 6α alcohol (XVII) was oxidized as described for the 6β alcohol (IV*a*). The ketone was identical with XVI (mixed melting point, t.l.c., infrared).

3β,5-Cyclo-5β-cholestan-6β,19-oxide (XVIII)

A sample of lead tetraacetate was dried for several hours under vacuum, and then 50 mg was added to a solution of 120 mg of 3β,5-cyclo-5β-cholestan-6β-ol (IV*a*) in dry benzene. The mixture was refluxed for 20 h, after which the excess lead tetraacetate was destroyed with 2 ml of ethylene glycol. The insoluble residue was filtered off and washed with benzene. Ether (100 ml) was added to the filtrate and it was washed once with 5% sodium bicarbonate and twice with water (100 ml each). The ether phase was dried with sodium sulfate and, after removal of the solvent, yielded 125 mg of an oily residue. Separation on one thin-layer plate (hexane–

Can. J. Chem. Downloaded from www.nrcresearchpress.com by 210.87.254.6 on 09/05/12
For personal use only.

ether, 9:1) gave 80 mg of XVIII, which was crystallized from ethyl acetate – methanol to give 40–50 mg, m.p. 78–81°; $[\alpha]_D$ +37° (*c*, 1.06 in $CHCl_3$); infrared showed cyclopropyl absorption at 3 020 and 3 050 cm^{-1}, and no peaks could be definitely assigned to the ether group. The n.m.r. spectrum in benzene showed two groups of ether absorption, a complex absorption at 3.98 p.p.m., and a doublet at 3.40 p.p.m. However, when taken in pyridine, as suggested by Slomp and Mackellar (17), the C_6 proton showed up as an unevenly split band around 4.00 p.p.m., and the AB quartet for the two nonequivalent C_{19} protons was clearly seen at 3.15 and 3.49 p.p.m. (J_{AD} 6.9 c.p.s.). Similar observations were made by Tadanier (11) for the n.m.r. spectra of 6β,19-oxido-3α,5-cyclo-5α-steroids. Complex cyclopropyl absorption from about 0.2 to 0.7 p.p.m. was also noted in the n.m.r. spectrum of XVII.

Anal. Calcd. for $C_{27}H_{44}O$: C, 84.31; H, 11.53. Found: C, 84.11; H, 11.64.

The 6α alcohol XVII, when treated with lead tetraacetate, also gave XVIII in a similar yield. The product was identified by mixed melting point and comparison of its thin-layer chromatograph and infrared spectrum with an authentic sample of XVIII (from the 6β alcohol).

6β-Ethoxy-3β,5-cyclo-5β-cholestane-4β-d_1 (IVa-4β-d_1, R′ = Et)

Cholesta-3,5-diene (I*a*) (6 g) was irradiated in *n*-pentane–deuterioethanol (9:1) until the reaction was 90% complete (21 h). Chromatography on 300 g of silica gel gave 2.5 g of crude IV*a*-4β-d_1 (R′ = Et); this was further purified by t.l.c., with hexane as eluent. Crystallization from hexane gave 420 mg of pure IV*a*-4β-d_1 (R′ = Et), m.p. 102–104°. The identity was verified by mixed melting point with an authentic sample of IV*a* (R′ = Et) (from previous photolyses), and by t.l.c. and infrared spectra. The n.m.r. spectrum showed only a doublet at 0.37 p.p.m. (*J* 3.1 c.p.s.) in the cyclopropyl region, and was otherwise identical with that of IV*a* (R′ = Et).

3α-Hydroxymethyl-A-norcholest-5-ene-4-d_1 (Va-d_1, R′ = H)

6β-Ethoxy-3β,5-cyclo-5β-cholestane-4β-d_1 (120 mg) was dissolved in a solution of 50 ml of acetone and 5 ml of water, and 12 mg of *p*-toluenesulfonic acid was added. After the solution was refluxed overnight, water and ether were added (100 ml of each). The ether phase was washed twice with 5% sodium hydroxide (100 ml each) and once with water, and then dried with magnesium sulfate. Separation on one thin-layer plate (hexane–ether, 3:2) gave 100 mg of 3α-hydroxymethyl-A-norcholest-5-ene-4-d_1 (V*a*-d_1, R′ = H), m.p. 102–103°. This had an identical thin-layer chromatograph and infrared spectrum with a sample of V*a* (R′ = H) obtained by solvolysis (16), and the mixed melting point showed no depression.

3β,5-Cyclo-5β-cholestan-6β-ol-4β-d_1 (IVa-4β-d_1, R′ = H)

The tosylate of the ring-contracted alcohol V*a*-d_1 (R′ = H) was prepared by allowing the alcohol to stand for 24 h in 5 ml of pyridine containing 100 mg of *p*-toluenesulfonyl chloride. Water (100 ml) was added, the tosylate was extracted with ether (100 ml), and the ether phase was washed five times with 5% hydrochloric acid (50 ml each) and twice with water. After the ether phase was dried with magnesium sulfate, it yielded a residue of 100 mg which was dissolved in a solution of 15 ml of acetone, 5 ml of water, and 500 mg of potassium acetate. The solution was refluxed overnight, and then 100 ml of water was added. Extraction by ether (100 ml) gave a solution which, after it was washed with 100 ml of 10% sodium bicarbonate and dried, yielded a residue, which was immediately separated on one thin-layer plate (hexane–ether, 3:2), giving 46 mg of IV*a*-4β-d_1 (R′ = H), m.p. 96–98°. This product was identified by comparison (mixed melting point, t.l.c., and infrared) with a sample of IV*a* (R′ = H) (from solvolysis (16)). The n.m.r. spectrum showed, in the cyclopropyl region, one doublet at 0.00 p.p.m. Otherwise, the spectrum was the same as that for IV*a* (R′ = H).

3β,5-Cyclo-5α-cholestan-6α-ol-4β-d_1 (XVII-4β-d_1)

Oxidation of the deuterated 6β alcohol IV*a*-4β-d_1 and reduction of the resulting ketone XVI-4β-d_1 to the 6α alcohol XVII-4β-d_1 were carried out as for the non-deuterated compounds. The identity of XVII-4β-d_1 was established by comparing its melting point, infrared spectrum, and thin-layer chromatograph with those of XVII. The n.m.r. spectrum of XVII-4β-d_1 was indistinguishable from that of XVII.

3β,5-Cyclo-5β-cholest-6-ene

6β-Ethoxy-3α,5-cyclo-5β-cholestane (IV*a*, R′ = Et) (840 mg) was dissolved in hexane and passed through a column of 50 g of alumina (activity I). Elution with a total of 300 ml of hexane gave 274 mg, m.p. 105–107°, of the crystalline hydrocarbon 3β,5-cyclo-5β-cholest-6-ene (lit. (1*a*) m.p. 109.5–110.2°).

3β,5-Cyclo-5β-cholestane

Platinum oxide (150 mg) was added to a solution of 254 mg of 3β,5-cyclo-5β-cholest-6-ene in 20 ml of acetic acid, and the mixture was shaken under 55 p.s.i. of hydrogen at 30° for 10 h. The platinum oxide was filtered off, ether (100 ml) was added, and the solution was washed three times with 5% sodium hydroxide (50 ml each) and twice with water. After the solution was dried, an oily residue of 245 mg was obtained; this was crystallized from acetic acid to give 185 mg of 3β,5-cyclo-5β-cholestane, m.p. 77–78°. Infrared showed only a saturated hydrocarbon. The n.m.r. spectrum showed the two C_4 cyclopropyl proton quartets at 0.00 and 0.42 p.p.m.

Can. J. Chem. Downloaded from www.nrcresearchpress.com by 210.87.254.6 on 09/05/12
For personal use only.

6β-Ethoxy-3α-methyl-3β,5-cyclo-5β-cholestane-4β-d_1 (IVb-4β-d_1, R′ = Et) and 3β-Ethoxy-3α-methylcholest-5-ene-4-d_1 (VIIb-4-d_1, R′ = Et)

A solution of 10 g of 3-methylcholesta-3,5-diene (I*b*) in 550 ml of *n*-pentane–deuterioethanol (9:1) was irradiated in a helium atmosphere for 48 h, at which time no diene chromophore could be detected in the ultraviolet. Removal of the solvent gave an oil which was chromatographed on 500 g of silica gel. Benzene eluted first 850 mg of crystalline IV*b*-4β-d_1 (R′ = Et), and then about 200 mg of crystalline[8] VII*b*-4-d_1 (R′ = Et).

Recrystallization of the first fraction from hexane gave 322 mg of IV*b*-4β-d_1 (R′ = Et), m.p. 123–126°. The sample was identified by comparison of its melting point, thin-layer chromatograph, and infrared spectrum with those of an authentic sample of IV*b* (R′ = Et) (10). The n.m.r. spectrum showed one cyclopropyl proton as a singlet, around 0.50 p.p.m. The rest of the spectrum was identical with that of IV*b*. Recrystallization of the second chromatographic fraction from hexane gave 120 mg of VII*b*-4-d_1 (R′ = Et), m.p. 120–122°. This was also identified by comparing its melting point, thin-layer chromatograph, and infrared spectrum with those of an authentic sample of VII*b* (R′ = Et) (13); ν 2 170 cm^{-1} (C_4—D). The n.m.r. spectrum of VII*b*-4-d_1 (R′ = Et) is reproduced in Fig. 2.

Photolysis of 3-Methylcholesta-3,5-diene (Ib) in Acid

3-Methylcholesta-3,5-diene (I*b*) (500 mg) dissolved in 500 ml of ethanol and 1 ml of 72% perchloric acid was photolyzed under helium until 10% of the original diene remained (7 h). Ether (500 ml) was added, and the solution was washed twice with 500 ml portions of 5% sodium hydroxide and twice with water. After the solution was dried with magnesium sulfate, the solvent was removed and the resulting oil separated on three thin-layer plates (hexane–ether, 39:1). Crystalline products of 6β-ethoxy-3α-methyl-3β,5-cyclo-5β-cholestane (IV*b*, R′ = Et) and 3β-ethoxy-3α-methylcholest-5-ene (VII*b*, R′ = Et) were obtained in yields of 9% (50 mg) and 37% (190 mg), respectively. These products were identified by mixed melting points and comparison of their thin-layer chromatographs and infrared spectra with those of authentic samples of IV*b* (R′ = Et) and VII*b* (R′ = Et).

A 500 mg sample of I*b* was photolyzed in an identical manner, except that no acid was added until the photolysis was completed (7 h). The same work-up procedure was then followed, and the yields were 7% (40 mg) of IV*b* (R′ = Et) and 13% (70 mg) of VII*b* (R′ = Et).

Samples of the diene I*b*, ether IV*b* (R′ = Et), and ether VII*b* (R′ = Et) (50 mg each) were allowed to stand for 2 days in 50 ml of ethanol containing 0.1 ml of 72% perchloric acid. No change in the samples could be detected by t.l.c.

Photolysis of Cholesta-3,5-diene (Ia) in Acid

Cholesta-3,5-diene (I*a*) (2.9 g) was photolyzed in 500 ml of ethanol and 1 ml of 72% perchloric acid under helium until 3% of the original diene remained (5 h). Ether (1 l) was added and the solution was washed with water, twice with 5% bicarbonate, and again with water (500 ml each). The ether phase was dried with sodium sulfate and the solvent removed, giving 3.1 g of an oil. Chromatography on 100 g of alumina (activity II–III) gave, in the hexane eluate, 2.3 g of a crude mixture of 6β-ethoxy-3β,5-cyclo-5β-cholestane (IV*a*, R′ = Et) and 3β-ethoxycholest-4-ene. Separation by t.l.c. (hexane–ether, 39:1) yielded 29% of IV*a* (R′ = Et) (identical with an authentic sample (1*a*) according to mixed melting point, infrared spectrum, and t.l.c.) and 31% of 3β-ethoxycholest-4-ene (pure by t.l.c.). Two crystallizations of this ether from ethyl acetate gave a product, m.p. 63°; $[\alpha]_D$ +27° (*c*, 0.78 in $CHCl_3$); ν_{CCl_4} equally intense peaks at 1 092 and 1 110 cm^{-1} (ether); $\delta_{pyridine}$ a singlet for one proton at 5.64 p.p.m. (C_4 vinyl proton), a weak, highly split band at 4.03 p.p.m. (C_3 proton), and a quartet centered at 3.68 p.p.m. (ethoxy quartet).

Anal. Calcd. for $C_{29}H_{50}O$: C, 83.96; H, 12.17. Found: C, 83.02; H, 11.73.

Hydrogenation of 3β-Ethoxycholest-4-ene

Hydrogenation was carried out on 200 mg of 3β-ethoxycholest-4-ene in 50 ml of acetic acid under 60 p.s.i. of hydrogen, with 150 mg of platinum oxide as catalyst. Sodium nitrite (15 mg) was added to suppress hydrogenolysis and the mixture was shaken for 27 h at room temperature. The platinum oxide was filtered off and ether (100 ml) was added. Washing three times with 5% bicarbonate (50 ml each) and twice with water, drying with sodium sulfate, and removal of the solvent gave a residue which was separated on one plate (hexane). Cholestane (38 mg, R_f 1) and 3β-ethoxycholestane (130 mg, R_f 0.25) were obtained.

The cholestane sample was crystallized twice from methanol, m.p. 78–79° (lit. (7) m.p. 80°). The melting point was undepressed when mixed with an authentic sample of cholestane. The 3β-ethoxycholestane fraction was crystallized twice from ethyl acetate – methanol, m.p. 80–81°; $[\alpha]_D$ +16.7° (*c*, 0.56 in $CHCl_3$) (lit. (18) m.p. 81–83°, $[\alpha]_D$ +23.8°); ν_{CCl_4} 1 097 and 1 115 cm^{-1} (ether); δ_{CCl_4} a two-proton quartet at 3.33 p.p.m. (ethoxy) and a highly split, weak absorption at about 3.00 p.p.m. (C_3 proton). The sample was identical (melting point, mixed melting point, t.l.c., and infrared) with a sample prepared by hydrogenating cholesteryl ethyl ether.

Anal. Calcd. for $C_{29}H_{52}O$: C, 83.56; H, 12.59. Found: C, 83.94; H, 12.54.

A hydrogenation was also carried out on 33 mg of 3β-ethoxycholest-4-ene in 10 ml of acetic acid with 25 mg

[8]*The low yield of the reaction is probably due to the fact that the deuterioethanol, prepared from diethyl sulfate and deuterated water, still contained some sulfuric acid or sulfur dioxide.*

Can. J. Chem. Downloaded from www.nrcresearchpress.com by 210.87.254.6 on 09/05/12
For personal use only.

of platinum oxide under 55 p.s.i. of hydrogen. No sodium nitrite was added, resulting in considerably more hydrogenolysis. The product consisted of 15 mg of cholestane and 18 mg of 3β-ethoxycholestane.

Photolysis of 6-Methylcholesta-3,5-diene (VIII) in Acidic Ethanol

Diene VIII (1.1 g) in 500 ml of ethanol–pentane (10:1) containing 1 ml of 72% perchloric acid was photolyzed for 72 h, when only 16% of the original diene absorption at 242 mμ remained. The solution was evaporated to 50 ml, diluted with 200 ml ether, and washed with 5% aqueous sodium bicarbonate and water. The etheral solution was dried over anhydrous magnesium sulfate and evaporated under reduced pressure, giving 1.05 g of an oily residue, which was chromatographed on alumina (activity II–III, 30 g). Elution with hexane gave a hydrocarbon fraction (200 mg) which contained 80% of unreacted diene (ultraviolet and infrared spectra). Benzene eluted 0.520 g of an oil which contained a mixture of ethers. This mixture was separated by preparative t.l.c. (benzene). The faster moving band (310 mg) was identified as ring-contracted ether XI, by comparison with a sample obtained previously. The slower moving band (200 mg) crystallized from ethanol–ether, m.p. 95–96°, and was identical with 6-methylcholesteryl ethyl ether (mixed melting point and infrared and n.m.r. spectra) prepared from 6-methylcholesterol (4).

REFERENCES

1. (*a*) W. G. Dauben and J. A. Ross. J. Am. Chem. Soc. **81**, 6521 (1959).
   (*b*) W. G. Dauben and F. G. Wiley. Tetrahedron Letters, **20**, 893 (1962).
2. W. G. Dauben and W. T. Wipke. Organic photochemistry. Butterworths, London. 1965.
3. (*a*) G. Just and C. C. Leznoff. Can. J. Chem. **42**, 79 (1964).
   (*b*) C. C. Leznoff and G. Just. Can. J. Chem. **42**, 2801 (1964).
4. G. Just and E. Lee-Ruff. Can. J. Chem. **44**, 2587 (1966).
5. C. R. Narayanan and K. N. Iyer. Tetrahedron Letters, **14**, 759 (1964).
6. L. F. Fieser and M. Fieser. Advanced organic chemistry. Reinhold Publishing Corp., New York. 1962. p. 302.
7. L. F. Fieser and M. Fieser. Steroids. Reinhold Publishing Corp., New York. 1959. pp. 28 and 263.
8. G. H. Whitham and J. A. F. Wickramasinghe. J. Chem. Soc. 1655 (1964).
9. J. Tadanier and W. Cole. J. Org. Chem. **27**, 4610 (1962).
10. D. J. Collins, J. J. Hobbs, and S. Sternhell. Tetrahedron Letters, **4**, 197 (1963).
11. J. Tadanier. J. Org. Chem. **28**, 1744 (1963).
12. E. M. Kosower and S. Winstein. J. Am. Chem. Soc. **78**, 4347 (1956).
13. G. Just and V. DiTullio. Can. J. Chem. **42**, 2153 (1964).
14. G. Just and V. DiTullio. Can. J. Chem. **42**, 2695 (1964).
15. N. D. Hall and G. Just. Steroids, **6**, 111 (1965).
16. G. H. Whitham. Proc. Chem. Soc. 330 (1962).
17. G. Slomp and F. Mackellar. J. Am. Chem. Soc. **82**, 999 (1960).
18. G. R. Pettit and T. R. Kasturi. J. Org. Chem. **26**, 4553 (1961).
19. F. S. Spring and G. Swan. J. Chem. Soc. 83 (1941).
20. W. G. Dauben and W. T. Wipke. Pure Appl. Chem. **9**, 539 (1964).
21. F. Sondheimer *et al.* J. Chem. Soc. 2189 (1953).
22. W. G. Jones *et al.* J. Am. Chem. Soc. **81**, 2151 (1959).

Can. J. Chem. Downloaded from www.nrcresearchpress.com by 210.87.254.6 on 09/05/12
For personal use only.

Can. J. Chem. Downloaded from www.nrcresearchpress.com by 210.87.254.6 on 09/05/12
For personal use only.

ACTION DES ORGANOMAGNÉSIENS SUR LES COMPOSÉS β-DICARBONYLÉS

I. OBTENTION DES β-DIOLS BITERTIAIRES PAR ACTION DES ARYLMAGNÉSIENS ET DES ALKYLMAGNÉSIENS SUR LES β-DICÉTONES SYMETRIQUES

P. Canonne et H. Bilodeau
Département de Chimie, Université Laval, Québec, Québec

Reçu le 25 janvier 1966

RÉSUMÉ

La réaction d'addition des organomagnésiens au dibenzoylméthane et à l'acétylacétone a été réétudiée. Outre les produits de scission, nous avons constaté, dans le cas de l'acétylacétone, la présence de β-diols. Le dibenzoylméthane n'a conduit qu'à l'obtention de l'hydroxycétone.

ABSTRACT

The addition of Grignard reagents to dibenzoylmethane and acetylacetone has been reinvestigated. Apart from cleavage products, it has been found that, in the case of acetylacetone, the reaction leads to the corresponding β-ditertiary diols. On the other hand, dibenzoylmethane yields only the β-hydroxyketone.

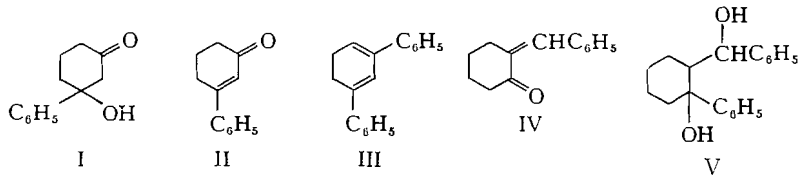
INTRODUCTION

L'action des organomagnésiens sur les cétones est considérée, depuis de nombreuses années, comme la meilleure méthode de préparation des alcools tertiaires. A l'opposé, les études consacrées à l'action des organomagnésiens sur les β-dicétones ont été très peu poussées. Pourtant, les β-hydroxycétones et les β-diols, ainsi que les composés qui en dérivent, présentent à cause de leurs propriétés un intérêt non négligeable pour la synthèse organique.

Aussi avons-nous jugé utile, dans le cadre d'une reprise de l'étude de l'action des organomagnésiens sur les composés β-dicarbonylés, de compléter les travaux précédents par des expériences originales.

Après avoir rappelé les recherches de Zelinski (1), Smedley (2) et Vorländer *et al.* (3), en 1931 Kohler et Erickson (4) publièrent que des dicétones non substituées, tel le dibenzoylméthane, réagissaient avec deux molécules du réactif de Grignard pour fournir des β-hydroxycétones, alors que les dicétones substituées formaient des produits de scission. L'action de l'iodure de méthylmagnésium sur l'acétylacétone donnait naissance à l'hydroxycétone correspondante (hydroxy-4 méthyl-4 pentanone-2) avec un rendement de 92%.

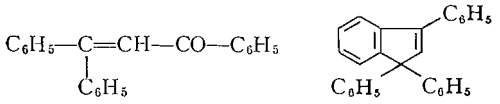
En 1948, Woods et Tucker (5), en faisant agir le bromure de phénylmagnésium sur la cyclohexanedione-1,3, isolèrent trois produits (I, II et III).



Chaney et Astle (6) traitèrent (1951) le bromure d'éthylmagnésium avec quatre dicétones asymétriques du type R—CO—CH_2—CO—CH_3 (R = C_2H_5, *n*-C_5H_9, *t*-C_4H_9 et C_6H_5). Ils obtinrent des mélanges d'hydroxycétones, sauf dans le cas où R = C_6H_5.

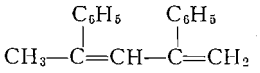
Aucun de ces produits ne fut isolé; les auteurs tentèrent, cependant, de les identifier par les produits de scission, qui sont des cétones connues.

Dreiding et Nickel (7) obtinrent en 1954, en faisant réagir le bromure de phénylmagnésium sur l'hydroxyméthylène-2 cyclohexanone et son éther isopropylique, deux composés (IV et V). Une année auparavant (1953), Dreiding et Hartman (8) avaient annoncé la présence de glycols lors de la réduction de composés β-dicarboxylés par l'hydrure de lithium et d'aluminium.



VI

VII



VIII

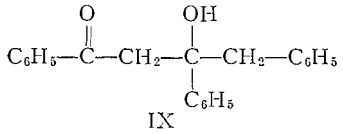
Au cours d'un examen de l'action du bromure de phénylmagnésium en grand excès et dans le benzène sur les β-cétoesters d'une part et sur les β-dicétones d'autre part, Freeman (9) rapporta la préparation de la β-phénylchalcone (VI) et du triphényl-1,1,3 indène (VII) à partir du dibenzoylméthane. Avec l'acétylacétone et dans les mêmes conditions, il obtint une huile jaune qui ne fut pas purifiée mais qui, déshydratée avec de l'anhydride acétique, donna la diphényl-2,4 pentadiène-1,3 (VIII). Dans les conditions habituelles et dans l'éther, la même réaction conduisit à la formation de la phényl-4 hydroxy-4 pentanone-2, qui fut déshydratée en la cétone insaturée et fut ainsi caractérisée (1958).

Au cours du présent travail, nous avons réétudié la réaction de Grignard sur les β-dicétones afin de (*i*) isoler et caractériser les β-hydroxycétones autrement que par la scission ou la déshydratation; (*ii*) déterminer un procédé d'obtention des diols; et (*iii*) formuler, si possible, une hypothèse originale sur la formation de ces diols.

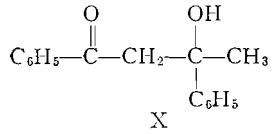
RÉSULTATS

Nous avons fait agir le bromure de phénylmagnésium, le bromure de benzylmagnésium et l'iodure de méthylmagnésium sur l'acétylacétone et sur le dibenzoylméthane choisis, à dessein, pour leur structure différente.

Les deux β-hydroxycétones IX et X ont été aisément obtenues à partir du dibenzoyl-



IX



X

méthane sous l'action des trois magnésiens. Leur pureté a été contrôlée par chromatographie sur couches minces. Leur structure a été démontrée à l'aide des spectres infrarouge et de résonance magnétique nucléaire.

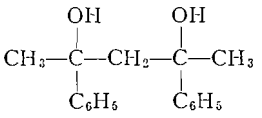
Les produits huileux obtenus à partir de l'acétylacétone furent distillés sous pression réduite. Dans la première fraction, on trouva des cétones de scission sans aucune trace de l'acétylacétone de départ. La deuxième fraction se composait, en majeure partie, de β-hydroxycétones encore impures. Etant donné la relative fragilité de ces composés, leur purification par distillation et par chromatographie en phase gazeuse à l'échelle préparatoire ne s'est pas avérée concluante. (Nous poursuivons actuellement d'autres travaux de purification.)

Dans la troisième fraction, des cristaux se déposèrent par refroidissement; ils correspondent à deux des β-diols bitertiaires (XI et XII); le troisième β-diol (XIII), impur,

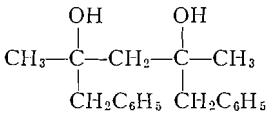
Can. J. Chem. Downloaded from www.nrcresearchpress.com by 210.87.254.6 on 09/05/12
For personal use only.

était un liquide. Les structures des β-diols XI et XII ont été établies à l'aide de leurs spectres infrarouges et de résonance magnétique nucléaire, et leur pureté fut contrôlée par chromatographie sur couches minces. Une preuve supplémentaire de structure a été apportée en faisant agir l'iodure de méthylmagnésium sur le dibenzoylméthane. Après purification et caractérisation de l'hydroxy-3 phényl-3 butyrophénone (X), l'addition de ce produit à une autre solution d'iodure de méthylmagnésium conduisit à un β-diol bitertiaire identique au XI, dont les spectres infrarouge et de résonance magnétique nucléaire sont rigoureusement superposables.

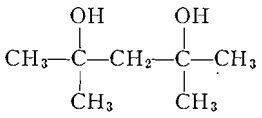
Avec le dibenzoylméthane, aucun des trois diols XI, XIV et XV ne put être isolé des milieux réactionnels des trois organomagnésiens. Pour identifier les produits recherchés



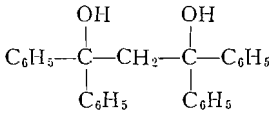
XI



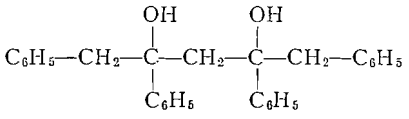
XII



XIII



XIV



XV

(XIV et XV), nous avons entrepris leur synthèse par voie indirecte, de la même manière que nous avions procédé pour le produit XI.

Remarquons que chacune de nos expériences fut refaite trois fois et que, aux erreurs expérimentales près, les résultats concordent.

DISCUSSION

Des résultats mentionnés ci-dessus, il apparaît qu'il existe une différence marquée entre les comportements respectifs du dibenzoylméthane et de l'acétylacétone à l'égard des réactifs de Grignard. L'acétylacétone produit des hydroxycétones et des β-diols bitertiaires, alors que le dibenzoylméthane donne seulement des hydroxycétones et aucun diol isolable.

Ces résultats nous permettent de confirmer certains travaux rapportés dans la littérature (1, 2, 7, 8) et de faire disparaître une contradiction apparente avec certains autres résultats (4–6, 9).

En effet, si l'idée qu'un diol peut être formé à partir d'un composé β-dicarbonylé provient de Zelinsky (1), il n'utilisa pas les organomagnésiens pouvant conduire à des β-diols solides et assez facilement isolables.

Nous sommes, en outre, tentés de faire une corrélation entre ces résultats et le pourcentage de la forme dicétonique de l'équilibre cétoénolique de l'acétylacétone. Nous savons, d'une part, que l'acétylacétone se trouve sous deux formes tautomères possibles (la forme dicétonique et la forme cétoénolique, cette dernière en majeure partie sous forme chélatée (10–14)). D'autre part, le pourcentage de chaque forme éthérée en solution est de 85:15 (10, 12), tandis que le dibenzoylméthane existe seulement sous sa forme énolique entièrement chélatée; ce qui conduit à formuler l'hypothèse selon laquelle les diols correspondent à la forme dicétonique de l'équilibre tautomère tandis que les hydroxycétones correspondent à la forme cétoénolique. Cette hypothèse, si elle est vérifiée, nous conduira à une seconde: les réactifs de Grignard réagissent si rapidement que l'équilibre

Can. J. Chem. Downloaded from www.nrcresearchpress.com by 210.87.254.6 on 09/05/12
For personal use only.

reste inchangé, ou encore, les vitesses de réaction des deux groupements (dicétonique et cétoénolique) sont égales.

Nous espérons que nos travaux postérieurs permettront d'apporter quelques nouvelles contributions à l'étude des réactions des organomagnésiens sur les β-dicétones, de vérifier éventuellement nos hypothèses, et dans l'affirmative de les préciser.

PARTIE EXPERIMÉNTALE

Les points de fusion ont été déterminés dans des tubes capillaires au moyen d'un appareil Thomas Hoover; ils ne sont pas corrigés. Les spectres infrarouges ont été pris à l'aide d'un appareil Beckman à double faisceau, modèle IR-4. Les spectres de résonance magnétique nucléaire ont été pris avec un appareil Varian, modèle A-60, en solution dans le deutériochloroforme. Les déplacements chimiques sont exprimés en parties par million, le tétraméthylsilane servant de référence. La position des signaux correspondant au proton "hydroxyle" a été mise en évidence par addition d'eau lourde. La chromatographie sur couches minces a été réalisée sur des plaques de gel de silice G de Merck, les révélateurs étant la lumière ultraviolette et l'acide sulfurique concentré, ainsi que leur combinaison.

Diphényl-2,4 pentanediol-2,4 (XI)

Une solution de Grignard est préparée sous atmosphère d'azote à partir de 18 g (0.75 g-atome) de tournures de magnésium et 118 g (0.75 mole) de bromobenzène dans 400 ml (3.75 moles) d'éther anhydre.

Après filtrage de l'excès de magnésium, on ajoute lentement 25 g (0.25 mole) d'acétylacétone diluée dans 100 ml d'éther anhydre pour éviter des projections sur les parois du ballon. Une agitation vigoureuse est maintenue tout en surveillant la température afin qu'elle ne dépasse pas 5 °C et en ayant soin de placer le dispositif réactionnel sous atmosphère d'azote. On chauffe ensuite à reflux pendant 1 h et l'on agite à la température ambiante pendant 12 h. Si les précautions ont été respectées lors de l'addition, le milieu réactionnel reste en solution.

L'hydrolyse se fait avec une solution saturée de chlorure d'ammonium à une température ne dépassant pas 5 °C. On extrait trois fois la couche aqueuse avec 100 ml d'éther; puis on lave deux fois avec 100 ml d'eau saturée de chlorure de sodium. On sèche sur sulfate de magnésium anhydre et l'on évapore l'éther et le benzène sous vide. Une huile jaune (60 g) est recueillie. Après distillation sous vide poussé (0.05 mm Hg) à une température ne dépassant pas 100 °C, des fractions liquides sont obtenues (40 g) qui contiennent des composés cétoniques (acétophénone et β-hydroxycétone). Le résidu, dont le point d'ébullition est supérieur à 100 °C, est traité sous vide (0.05 mm Hg) par 100 ml d'éther de pétrole (p.é. 37–55 °C). Des cristaux jaune-brun se forment immédiatement; on refroidit et l'on filtre. On obtient ainsi un composé (9 g) dont le spectre montre seulement une bande OH. Après purification, on isole 8 g d'un solide blanc qui cristallise en paillettes, p.f. 106 °C.

La pureté de ce composé (diphényl-2,4 pentanediol-2,4) a été contrôlée par chromatographie sur couches minces avec le *n*-hexane et l'acétate d'éthyle (90:10) comme solvants, en prenant comme témoins le biphényle, l'acétophénone et la benzophénone. Aucun de ces produits n'a souillé le composé pur. La pureté de ce β-diol bitertiaire a été contrôlée par résonance magnétique nucléaire. Il présente, outre les signaux dûs aux protons aromatiques, trois singulets à 1.22, 2.37 et 4.05 p.p.m. correspondant, respectivement, aux groupements méthyles, méthylène et hydroxyle, dont le pourcentage se trouve dans un rapport de 40:8.5:8.5:28. Le spectre infrarouge présente une bande à 3 475 cm^{-1} (OH) et une à 1 170 cm^{-1} (COH).

Anal. Calc. pour $C_{17}H_{20}O_2$: C, 79.90; H, 7.80. Trouvé: C, 79.52; H, 7.61.

Diphényl-1,5 diméthyl-2,4 pentanediol-2,4 (XII)

La solution de Grignard est préparée en prenant soin de maintenir le dispositif toujours sous courant d'azote, et en maintenant l'éther en faible ébullition et en grande quantité pour éviter la formation du dibenzyle. On utilise 124.7 g (0.75 mole) de bromure de benzyle, 18 g (0.75 g-atome) de tournures de magnésium et 690 ml (6.5 moles) d'éther. Après filtrage de l'excès de magnésium, on ajoute 25 g (0.25 mole) d'acétylacétone dissous dans 100 ml d'éther anhydre en prenant les mêmes précautions que précédemment et en travaillant lentement.

Après hydrolyse et évaporation du solvant, on obtient une huile jaune (65 g) que l'on distille à pression réduite (0.05 mm Hg). On recueille ainsi des fractions volatiles, constituées en majeure partie de la β-hydroxycétone et de la phénylacétone. On arrête la distillation lorsque la température augmente, c'est-à-dire avant qu'elle atteigne 100 °C. On obtient 9.6 g d'un résidu qui se solidifie en refroidissant et donne des cristaux incolores après traitement à la Norit A et recristallisation dans un mélange d'éthanol et d'eau (80:20). La pureté de ce composé (diphényl-1,5 diméthyl-2,4 pentanediol-2,4) a été contrôlée par son point de fusion (94 °C) et par son spectre infrarouge, qui ne présente aucune bande cétonique mais, par contre, les bandes à 3 475 cm^{-1} (OH) et à 1 175 cm^{-1} (COH). La chromatographie sur couches minces ne révèle aucune contamination par des composés voisins. Le spectre de résonance magnétique nucléaire présente, outre les protons aromatiques, trois singulets à 1.30 p.p.m. (CH_3), 2.78 p.p.m. (CH_2) et 3.08 p.p.m. (OH), ainsi qu'un multiplet de 1.50 à 2.00 p.p.m. (H_2), dans un rapport de protons de 65:10:10:40:22:106.

Anal. Calc. pour $C_{19}H_{24}O_2$: C, 80.29; H, 8.44. Trouvé: C, 80.11; H, 8.38.

Can. J. Chem. Downloaded from www.nrcresearchpress.com by 210.87.254.6 on 09/05/12
For personal use only.

Hydroxy-3 phényl-3 butyrophénone (X)

Selon la méthode habituelle, la solution de Grignard a été préparée à partir de 4.3 g (0.177 g-atome) de magnésium et 25.1 g (0.177 mole) d'iodure de méthyle dans 147 ml (1.416 moles) d'éther anhydre. Après filtrage des traces de magnésium, on ajoute lentement et à la température ambiante 10 g (0.0442 mole) de dibenzoylméthane dissous dans 100 ml d'éther. Après addition, on chauffe à reflux pendant 3 h; puis on refroidit dans la glace et hydrolyse avec une solution saturée de NH_4Cl à une température ne dépassant pas 5 °C. Après extraction et évaporation du solvant, on obtient une masse cristalline (10 g). Une recristallisation dans l'éther de pétrole (p.é. 37–55 °C) donne des paillettes incolores d'hydroxy-3 phényl-3 butyrophénone, p.f. 59–60 °C.

Cette masse cristalline a été chromatographiée sur plaques de gel de silice G avec un mélange de *n*-hexane et d'acétate d'éthyle, et ne révélait aucune trace du β-diol bitertiaire (diphényl-2,4 pentanediol-2,4).

Le spectre infrarouge présente une bande à 1 663 cm^{-1} (C=O) et une à 3 450 cm^{-1} (OH). Le spectre de résonance magnétique nucléaire montre les signaux dûs aux protons aromatiques et deux singulets à 1.60 p.p.m. (CH_3) et 4.8 p.p.m. (OH) ainsi qu'un multiplet de 3.1 à 3.92 p.p.m. (CH_2), dont les intensités sont dans un rapport de 34:11:3:111.

Anal. Calc. pour $C_{16}H_{16}O_2$: C, 80.01; H, 6.66. Trouvé: C, 79.54; H, 6.32.

Diphényl-2,4 pentanediol-2,4 (XI)

A la solution de Grignard préparée à partir de 1 g de magnésium et 6 g d'iodure de méthyle, selon la méthode habituelle, on ajoute 2.4 g d'hydroxy-3 phényl-3 butyrophénone (X) en solution dans l'éther puis on chauffe à reflux pendant 3 h. Après hydrolyse et évaporation de l'éther, on obtient une huile qui cristallise par addition d'éther de pétrole (1.5 g). Après recristallisation dans un mélange d'éthanol et d'eau, on obtient des cristaux blancs dont le point de fusion est de 106 °C.

Hydroxy-3 diphényl-3,3 propiophénone (XVI)

Dans les conditions habituelles, une solution de Grignard est préparée à partir de 6.5 g (0.266 g-atome) de magnésium, 40 g (0.25 mole) de bromobenzène et 165 ml (1.6 mole) d'éther anhydre. A la température ambiante, on ajoute lentement 15.7 g (0.07 mole) de dibenzoylméthane dissous dans 100 ml d'éther; puis on chauffe à l'ébullition pendant 1 h. La solution est maintenue sous agitation pendant 1 nuit. Après hydrolyse de la manière habituelle et évaporation de l'éther et du benzène, on recueille 19.5 g d'une huile jaune contenant des cristaux. On refroidit le tout, puis ajoute de l'éther de pétrole pour aider à la cristallisation. Après filtrage et recristallisation dans un mélange de méthanol et d'eau, on obtient un solide blanc (12.4 g), l'hydroxy-3 diphényl-3,3 propiophénone, p.f. 119–119.5 °C (3, 4).

Une chromatographie sur couches minces de ces cristaux et du mélange réactionnel ne donne qu'une tache jaune-foncé par pulvérisation d'acide sulfurique, tandis que le diol correspondant à un R_f inférieur se colore en bleu-vert en utilisant le gel de silice comme support et un mélange de *n*-hexane et d'acétate d'éthyle (90:10) comme éluant. Le spectre infrarouge présente une bande d'absorption à 1 670 cm^{-1} (C=O) et une à 3 475 cm^{-1} (OH). En résonance magnétique nucléaire, on retrouve, outre les signaux dûs aux protons aromatiques, deux singulets à 3.92 p.p.m. (CH_2) et à 5.43 p.p.m. (OH) dans un rapport de 7:3.5.

Anal. Calc. pour $C_{21}H_{18}O_2$: C, 83.45; H, 5.95. Trouvé: C, 83.31; H, 5.86.

Déshydratation de l'hydroxy-3 diphényl-3,3 propiophénone et préparation de la diphényl-3,3 acrylophénone (VI)

On dissout 1 g d'hydroxy-3 diphényl-3,3 propiophénone (XVI) dans 25 ml de benzène anhydre; puis on ajoute 5 ml d'anhydride acétique et 2 gouttes d'acide sulfurique concentré. La déshydratation est instantanée à la température ambiante. L'excès d'anhydride acétique est détruit par 50 ml d'eau. On extrait à l'éther (50 ml); puis on lave avec du bicarbonate de sodium à 10% et avec de l'eau saturée de sel et l'on cristallise dans l'éthanol. On obtient ainsi la β-phénylchalcone (VI), p.f. 86–87 °C (9), dont le spectre ultraviolet révèle le système des chalcones et le spectre infrarouge présente à 1 655 cm^{-1} une bande de groupement cétonique conjugué. En résonance magnétique nucléaire, on retrouve trois singulets dans la région de 7 p.p.m. qui correspondent bien aux protons aromatiques.

Anal. Calc. pour $C_{21}H_{16}O$: C, 88.73; H, 5.63. Trouvé: C, 88.32; H, 5.49.

Tétraphényl-1,1,3,3 propanediol-1,3 (XIV)

La solution de Grignard est préparée dans les conditions habituelles à partir de 6.5 g (0.266 g-atome) de magnésium, 40 g (0.25 mole) de bromobenzène et 200 ml (1.9 moles) d'éther anhydre. On ajoute lentement 15.8 g (0.050 mole) de l'hydroxycétone XVI dissoute dans 150 ml d'éther et l'on chauffe à reflux pendant 45 min; puis on laisse sous agitation pendant 1 nuit à la température ambiante. Après hydrolyse et évaporation, on obtient une huile (18.4 g) qui cristallise par addition de *n*-hexane. Après cristallisation dans l'éthanol et l'eau, on obtient un solide blanc, le tétraphényl-1,1,3,3 propanediol-1,3 (XIV), p.f. 124 °C (4, 15). La pureté de ce diol a été établie par chromatographie sur couches minces dans un système de *n*-hexane et d'acétate d'éthyle comme solvants. Seule la présence du diol est révélée par la tache bleu-vert caractéristique de ce composé sous pulvérisation d'acide sulfurique. Le R_f est beaucoup plus petit que celui de l'hydroxycétone de départ et que celui du diphényle.

Le spectre infrarouge présente une bande d'absorption à 3 450 cm^{-1} (OH) et le spectre de résonance magnétique nucléaire montre, à part les protons aromatiques à 7–15 p.p.m., deux singulets à 3.36 p.p.m. (CH_2) et à 4.10 p.p.m. (OH) d'intensité de 17 mm chacun.

Anal. Calc. pour $C_{27}H_{24}O_2$: C, 85.27; H, 6.31. Trouvé: C, 85.01; H, 5.49.

Can. J. Chem. Downloaded from www.nrcresearchpress.com by 210.87.254.6 on 09/05/12
For personal use only.

Hydroxy-3 diphényl-3,4 butyrophénone (IX)

Une solution de Grignard est préparée dans les mêmes conditions qu'habituellement à partir de 6.5 g (0.266 g-atome) de magnésium, 31.55 g (0.25 mole) de chlorure de benzyle et 200 ml (1.9 moles) d'éther anhydre. On ajoute lentement 7 g (0.0312 mole) de dibenzoylméthane dissous dans 50 ml d'éther anhydre. Par le procédé décrit précédemment, on obtient 5.1 g de cristaux blancs d'hydroxy-3 diphényl-3,4 butyrophénone, p.f. 122 °C.

Le spectre infrarouge présente une bande à 1 660 cm^{-1} (CO) et une à 3 450 cm^{-1} (OH). En résonance magnétique nucléaire, on a deux singulets à 3.12 p.p.m. (CH_2) et à 4.9 p.p.m. (OH), non couplés, et un multiplet de 3.05 à 4.08 p.p.m. (CH_3) qui est couplé avec les protons précédents. L'intensité de ces protons est proportionnelle pour chaque type de proton et prouve donc la pureté du composé. Cette pureté a été contrôlée par chromatographie sur couches minces en utilisant un système de *n*-hexane et d'acétate d'éthyle (90:10) comme solvant.

Anal. Calc. pour $C_{22}H_{20}O_2$: C, 83.55; H, 6.32. Trouvé: C, 83.33; H, 6.21.

Tétraphényl-1,2,4,5 pentanediol-2,4 (XV)

A la solution de Grignard préparée de la façon habituelle à partir de 6.5 g (0.266 g-atome) de magnésium, 31.54 g (0.25 mole) de chlorure de benzyle et 165 ml (1.6 moles) d'éther anhydre, on ajoute 15.8 g (0.05 mole) de l'hydroxycétone IX dissous dans 150 ml d'éther. On chauffe pendant 45 min et laisse sous agitation pendant 1 nuit. Après hydrolyse, on obtient une huile (18.1 g) qui cristallise par addition de *n*-hexane, le tétraphényl-1,2,4,5 pentanediol-2,4, p.f. 141 °C. La structure de ce diol a été prouvée par le spectre infrarouge (bande à 3 475 cm^{-1} (OH)) et par le spectre de résonance magnétique nucléaire, qui présente un singulet à 3.55 p.p.m. (OH) et deux multiplets légèrement superposés, entre 2.45 et 3.45 p.p.m., dûs aux groupements CH_2. L'intensité de ces signaux est proportionnelle au nombre de protons. La pureté de ce diol a été également contrôlée par chromatographie sur couches minces (*n*-hexane – acétate d'éthyle (90:10)).

Anal. Calc. pour $C_{29}H_{28}O_2$: C, 85.29; H, 6.85. Trouvé: C, 85.03; H, 6.75.

REMERCIEMENTS

Nous remercions le Conseil National de Recherches pour l'aide financière apportée sous forme de subventions. Nous exprimons notre gratitude au Dr L. C. Leitch et à son collaborateur M. R. N. Renaud pour la mesure des spectres de résonance magnétique nucléaire, ainsi qu'à M. H. Seguin pour les analyses élémentaires.

BIBLIOGRAPHIE

1. N. Zelinsky. Ber. **35**, 2138 (1902).
2. I. Smedly. J. Chem. Soc. **97**, 1493 (1910).
3. D. Vorländer, J. Osterburg et O. Meye. Ber. **56**, 1136 (1923).
4. E. P. Kohler et I. L. E. Erickson. J. Am. Chem. Soc. **53**, 2301 (1931).
5. G. P. Woods et I. W. Tucker. J. Am. Chem. Soc. **70**, 2174 (1948).
6. A. Chaney et M. J. Astle. J. Org. Chem. **16**, 57 (1951).
7. A. Dreiding et S. N. Nickel. J. Am. Chem. Soc. **76**, 3965 (1954).
8. A. Dreiding et J. A. Hartman. J. Am. Chem. Soc. **75**, 939 (1953).
9. J. P. Freeman. J. Am. Chem. Soc. **80**, 1926 (1958).
10. T. H. Zerewitinoff. Ber. **41**, 2243 (1908).
11. L. N. Ferguson. The modern structural theory of organic chemistry. 2nd ed. Prentice-Hall, Inc., New York. 1964. pp. 153 et 370.
12. A. S. N. Murthy, A. Balasubramanian, C. N. R. Rao et T. R. Kasturi. Can. J. Chem. **40**, 2267 (1962).
13. E. S. Gould. Mechanism and structure in organic chemistry. Holt, Rinehart & Winston Inc., New York. 1964. p. 376.
14. W. Gordy. J. Chem. Phys. **8**, 518 (1940).
15. J. English, Jr. et F. V. Brutcher, Jr. J. Am. Chem. Soc. **74**, 4279 (1952).

Can. J. Chem. Downloaded from www.nrcresearchpress.com by 210.87.254.6 on 09/05/12
For personal use only.

Can. J. Chem. Downloaded from www.nrcresearchpress.com by 210.87.254.105 on 09/05/12
For personal use only.

^{13}C N.M.R. STUDIES

VIII. ^{13}C SPECTRA OF SOME SUBSTITUTED ANISOLES[1,2]

K. S. DHAMI[3] AND J. B. STOTHERS
Department of Chemistry, University of Western Ontario, London, Ontario

Received July 29, 1966

ABSTRACT

The ^{13}C nuclear magnetic resonance spectra of a series of 40 substituted anisoles have been obtained to investigate the effects of substitution on the aromatic and methoxyl carbon shieldings. This work extends our studies on the variations of chemical shifts of carbon nuclei in side chains of aryl derivatives. The question of steric hindrance to conjugative interaction of a methoxyl group with an aromatic ring is considered on the basis of the present results. Evidence of a steric effect in compounds in which *both* ortho positions are substituted is presented.

INTRODUCTION

As an extension of a general survey of the ^{13}C chemical shifts for a variety of aromatic systems, it was of interest to examine the effects of substitution on the shieldings of the methoxyl and aryl carbon nuclei in a series of anisoles. There are two major features to be investigated. Lauterbur has demonstrated the existence of an additive relationship for the effects of substituents on aryl carbon shieldings in a number of benzene derivatives (1, 2), which holds very well provided the substituent groups are not ortho to each other (1–5). Since the chemical shifts for the aromatic carbons in several monosubstituted benzenes have been reported by Spiesecke and Schneider (6), it is possible to predict the shieldings in other derivatives by using these data and assuming additivity. It seemed worthwhile to test these predictions for a number of anisoles, since only a few have been reported (1, 7). For the same series we have determined the variation of the methoxyl carbon shieldings with substitution to find if these are sensitive to substituent polarity. Proton nuclear magnetic resonance studies have shown that methoxyl proton shifts are linearly related to the Hammett σ parameter (8).

The second feature concerns the effects of substituents on carbon shieldings in ortho-substituted systems. In general, it is found that the shielding effects of substituents on the aryl carbons are no longer additive, but it appears that the magnitude of the deviation from additivity is a crude measure of the steric hindrance to electronic interactions (2–5, 9). An examination of the ^{13}C spectra of a series of ortho-substituted anisoles could therefore provide information on the steric inhibition of resonance of the methoxyl function. In addition, changes in the shielding of the methoxyl carbon nucleus itself should provide information about this point.

For these reasons the ^{13}C spectra of 11 meta- and para-substituted anisoles, 14 ortho-substituted examples, and 15 diortho-substituted anisoles have been obtained. The chemical shifts for the methoxyl and aryl carbon nuclei have been measured. These results are the subject of this paper.

EXPERIMENTAL

Nuclear Magnetic Resonance Spectra

The ^{13}C spectra were determined at a spectrometer frequency of 15.085 Mc/s with samples containing ^{13}C in natural abundance. The detailed procedure has been described (3). For the most part, the spectra were obtained with the neat liquids. In the case of solids, saturated solutions in either CS_2 or $CHCl_3$ were examined.

[1] *For part VII in this series, see G. W. Buchanan, D. A. Ross, and J. B. Stothers, J. Am. Chem. Soc., in press.*
[2] *Some of these results were reported at the 47th annual conference of the Chemical Institute of Canada, Kingston, Ontario, 1964.*
[3] *Petroleum Research Fund Predoctorate Fellow, 1962–1964.*

Two solutes were studied in each of these to test for the presence of a significant solvent effect. The shielding data are given on the CS_2 scale (δ_{CS_2} = 0 p.p.m.) and are judged to be accurate to ±0.5 p.p.m.

Materials

Anisole and its 3-methyl, 4-methyl, and 4-bromo derivatives are commercially available and were used directly. Most of the others were prepared from the corresponding phenol by methylation with dimethyl sulfate by the method outlined below. A few of the hindered phenols were methylated by reaction of the phenoxide with methyl iodide as described by Kornblum and Seltzer (10). 2,6-Dimethyl-4-nitro- and 2,6-di-*t*-butyl-4-nitro-anisole were prepared according to the sequence reported by Bruice *et al.* (11), in which the 2,6-dialkyl phenol is converted into its 4-bromo derivative, methylated, and then treated with nitric acid in acetic anhydride to give the desired compound. For five of the compounds which have not been reported previously, the method of preparation, their physical properties, and analytical data are collected in Table I. For the others, their properties agreed well with those reported in the literature.

Methylation Procedure

To the phenol (0.11 mole) dissolved in 20 ml of Claisen's alkali (12) was added dimethyl sulfate (0.12 mole). The mixture was refluxed for 3 h, cooled, and poured over chipped ice. After ether extraction, the combined ethereal extracts were washed with 20% NaOH and water, and dried over $CaCl_2$. After removal of the solvent, the product was distilled *in vacuo* on a 16 in. spinning-band column.

RESULTS

The observed chemical shifts for the aromatic and methoxyl carbon nuclei for the meta- and para-substituted anisoles are given in Table II. The data for a number of ortho-substituted examples appear in Table III, and the results for 15 diortho-substituted anisoles are collected in Table IV. These three types will be considered separately in the Discussion; for clarity, the aromatic and methoxyl carbon nuclei are discussed under separate sub-headings. Since some of the compounds are solids and were examined as saturated solutions in either $CHCl_3$ or CS_2, two solutes, anisole and *p*-nitroanisole, were run in both solvents; the results are given in Table V.

DISCUSSION

The effects of structure on ^{13}C shieldings in general have been reviewed recently (13), and the present results are considered on the basis of these general trends. Following the discussion of the chemical shift results, the question of steric hindrance to resonance interaction of a methoxyl group with an aromatic ring is considered in the light of these and other recent findings for related compounds (2–5, 9).

Meta- and Para-Substituted Anisoles

Aromatic Carbon Nuclei

For the ^{13}C spectrum of anisole itself, the unequivocal assignment of the appropriate absorption peaks to specific nuclei has been established by Spiesecke and Schneider (6), and the present data are in excellent agreement with these, except for the shielding of C-1, the carbon bearing the methoxyl group. Our value is intermediate between the two which have been reported (1*b*, 6) and, after a number of measurements, we feel that it is reliable within our limits of experimental uncertainty. The observed chemical shift changes caused by the methoxyl group at the various positions on the aromatic ring relative to the shift of benzene carbons have been discussed (1*b*, 6) and require no further comment. It is important, however, to draw attention to the pronounced shielding at the para position, indicative of electron release to the ring by methoxyl.

The data for the mono-substituted anisoles included in Table II provide more examples to confirm the existence of the additive nature of substituent effects on aryl carbon shieldings. Most of these are para-substituted examples, for which the assignments are straightforward and unequivocal because the effects of substituents at the meta positions are known to be small (1–6). Thus the absorption for C-2 and C-6 is expected to be centered

Can. J. Chem. Downloaded from www.nrcresearchpress.com by 210.87.254.105 on 09/05/12
For personal use only.

Can. J. Chem. Downloaded from www.nrcresearchpress.com by 210.87.254.105 on 09/05/12
For personal use only.

TABLE I

Preparative method, physical properties, and analytical data of some substituted anisoles prepared for this study

Substituents	Preparative method*	Yield (%)	Physical constants: Boiling point (m.p.)	Physical constants: n_D^{25}	Analyses† (%): Carbon: Found	Carbon: Calculated	Hydrogen: Found	Hydrogen: Calculated	Other: Element	Other: Found	Other: Calculated
2,3-$(CH_3)_2$-4-Cl	A	70	130–131° at 30 mm	1.5417	63.19	63.35	6.54	6.45	Cl	20.99	20.82
2,6-$(CH_3)_2$-4-Cl	A	83	117° at 29 mm	1.5220	63.28	63.35	6.43	6.45	Cl	20.77	20.82
2,6-$(t$-$C_4H_9)_2$-4-Cl	B	73	135° at 8 mm	1.5178	70.71	70.72	9.05	9.10	Cl	14.10	13.92
2,6-$(t$-$C_4H_9)_2$-4-Br	B	60	149–150° at 9 mm	1.5329	60.61	60.20	7.16	7.68	Br	27.02	26.77
2,6-$(t$-$C_4H_9)_2$-4-NO_2	C	30	(67–69°)	—	67.82	67.89	8.95	8.74	N	5.28	5.28

*Methods used: A, ArOH in Claisen's alkali + $(CH_3)_2SO_4$ (see Experimental); B, ArOH in *t*-BuO–*t*-BuOH + CH_3I (10); C, ArOH → *p*-BrArOH → *p*-BrArOCH$_3$ → *p*-NO_2ArOCH$_3$ (11).
†Performed by Alfred Bernhardt and Associates, Mülheim, Germany.

TABLE II

^{13}C shieldings of methoxyl and aryl carbon nuclei in some meta- and para-substituted anisoles (in p.p.m. from CS_2)

Substituent	Methoxyl carbon	Aromatic carbons			
		C-1	C-2, C-6	C-3, C-5	C-4
H	138.8	33.9	79.6	64.1	73.0
4-CH_3	138.5	35.3	79.5	63.3	64.1
4-Cl	138.1	34.9	77.9	63.8	68.3
4-Br	138.0	34.5	77.2	60.7	80.3
4-NO_2*	136.2	27.9	78.3	67.1	53.7
4-$COCH_3$†	137.9	29.7	79.5	62.7	62.9
4-CHO	137.6	29.0	79.2	63.2	63.5
4-$COOCH_3$†	137.9	30.0	79.4	61.9	70.5
4-$CH{=}CH_2$	138.7	33.8	79.2	66.0	62.4
4-CH_2Cl	138.5	33.9	79.3	63.3	63.6
3-CH_3	139.2	34.1	79.1 (C-2) 82.9 (C-6)	55.0 (C-3) 64.8 (C-5)	72.6
3-$COCH_3$	138.5	34.0	81.1 (C-2) 74.0 (C-6)	55.1 (C-3) 64.1 (C-5)	74.0

*Saturated solution in CS_2.
†Saturated solution in $CHCl_3$.

TABLE III

Methoxyl and aryl carbon shieldings for ortho-substituted anisoles (in p.p.m. from CS_2)

Substituent(s)	Methoxyl carbon	Aromatic nuclei					
		C-1	C-2	C-3	C-4	C-5	C-6
2-CH_3	139.1	36.1	67.7	63.3	72.9	66.5	83.6
2-CH_3-4-Cl	138.8	37.4	68.5	63.8	65.1	67.0	82.9
2-CH_3-4-Br*	137.8	35.7	63.6	59.6	79.6	63.1	81.3
2,3-$(CH_3)_2$	138.4	36.0	68.4	56.0	71.1	67.5	85.5
2,3-$(CH_3)_2$-4-Cl*	138.5	37.6	67.0	58.7	67.0	67.0	85.2
2,4-$(CH_3)_2$	138.9	37.5	67.2	62.0	64.5	66.1	83.5
2,5-$(CH_3)_2$	139.3	35.8	70.2	62.9	73.0	57.6	83.3
2-(C_2H_5)	139.1	36.2	61.0	64.2	72.0	66.3	83.2
2-(i-C_3H_7)	138.8	36.7	57.0	67.1	72.9	67.1	83.3
2-(t-C_4H_9)	138.9	35.3	55.6	67.0	72.9	67.0	82.2
2-(t-C_4H_9)-4-Cl	138.3	36.2	53.3	66.3	67.6	66.3	80.6
2-(t-C_4H_9)-4-Br	138.0	35.4	52.6	63.3	79.6	63.6	79.6
2-CHO	138.8	32.9	70.3	66.7	73.9	58.2	82.5
2-$COCH_3$	138.2	34.3	65.1	63.2	73.1	59.7	81.4

*Saturated solution in $CHCl_3$.

close to the value found for anisole, 79.6 p.p.m., and the remaining doublet in the aromatic region of these spectra must arise from C-3 and C-5. The assignment of the two singlets for each of C-1 and C-4 follows readily because of the marked deshielding effect of the methoxyl group on C-1. In each case, this peak is the lowest field signal in the aromatic region. The assigned shifts may be compared with those predicted by the assumption of additivity of substituent effects at the various aromatic positions. The latter values are calculated from the changes observed for the monosubstituted cases by using the data in the literature (3, 5, 6). For example, the aryl carbons in chlorobenzene exhibit absorption at -6.4, -0.2, -1.0, and $+2.0$ p.p.m., relative to benzene, for C-1 (C—Cl), the ortho carbons, the meta carbons, and the para carbon, respectively (6). For p-chloroanisole, the calculated values for the aryl shieldings (the results for anisole itself being used as the base case) become 66.6 (C-4), 63.9 (C-3, C-5), 78.6 (C-2, C-6), and 35.9 (C-1) p.p.m. from CS_2. These values agree closely with those observed for p-chloroanisole (see Table II), with the largest

Can. J. Chem. Downloaded from www.nrcresearchpress.com by 210.87.254.105 on 09/05/12
For personal use only.

TABLE IV

Methoxyl and aryl carbon shieldings for some 2,6-disubstituted anisoles (in p.p.m. from CS_2)

Substituents	Methoxyl carbon	Aromatic carbons			
		C-1	C-2, C-6	C-3, C-5	C-4
2,6-$(CH_3)_2$	134.9	36.6	63.5	65.2	70.2
2,4,6-$(CH_3)_3$	134.7	38.5	63.5	64.3	61.2
2,3,5,6-$(CH_3)_4$*	133.0	36.6	66.5	65.8	66.4
2,3,4,5,6-$(CH_3)_5$†	133.0	37.4	66.6	60.2	60.2
2,6-$(CH_3)_2$-4-Cl	134.3	37.1	60.1	64.5	64.5
2,6-$(CH_3)_2$-4-Br	134.3	37.0	60.3	61.9	77.2
2,6-$(CH_3)_2$-4-NO_2*	132.6	30.9	60.5	68.5	49.5
2,6-$(i\text{-}C_3H_7)_2$	131.6	38.3	51.9	69.1	69.1
2,6-$(i\text{-}C_3H_7)_2$-4-Cl	132.1	40.4	50.2	69.4	64.1
2,6-$(i\text{-}C_3H_7)_2$-4-Br	131.7	39.7	49.8	66.3	75.5
2,6-$(t\text{-}C_4H_9)_2$	129.1	33.9	50.2	66.9	70.1
2,4,6-$(t\text{-}C_4H_9)_3$†	128.5	35.7	49.6	68.8	49.6
2,6-$(t\text{-}C_4H_9)_2$-4-Cl	128.9	35.0	48.0	66.6	64.2
2,6-$(t\text{-}C_4H_9)_2$-4-Br	128.8	34.0	47.1	63.4	75.8
2,6-$(t\text{-}C_4H_9)_2$-4-NO_2†	128.1	28.2	47.4	70.8	—

*Saturated solution in $CHCl_3$.
†Saturated solution in CS_2.

TABLE V

^{13}C shieldings of anisole and *p*-nitroanisole in different media (in p.p.m. from CS_2)

Compound	Carbon nuclei	Solvent				
		Nil	$CHCl_3$		CS_2	
			75%*	50%*	75%*	50%*
Anisole	C-1	33.9	33.8	33.9	32.8	32.7
	C-2, C-6	79.5	79.4	79.2	78.6	78.8
	C-3, C-5	64.1	63.8	63.9	63.1	63.1
	C-4	72.9	72.4	72.3	72.2	72.0
	OCH_3	138.8	138.6	138.2	138.3	138.0
p-Nitroanisole†	C-1		28.1		27.9	
	C-2, C-6		78.3		78.3	
	C-3, C-5		67.0		67.1	
	C-4		51.4		53.7	
	OCH_3		136.9		136.2	

*Percentage anisole by volume.
†Saturated solutions in both $CHCl_3$ and CS_2.

discrepancy being 1.7 p.p.m. for the C-4 nucleus. A similar comparison of the results in Table II with calculated shieldings shows that, with two exceptions, the deviations are <2 p.p.m. Somewhat larger deviations of 2.6 and 2.3 p.p.m. are found for C-1 in *p*-vinylanisole and C-3 and C-5 in *p*-nitroanisole, respectively. This difference for the vinyl derivative may be an indication that the electronic effect of the vinyl group is reversed in this system relative to that for styrene itself. This possibility was discussed in our earlier paper on the ^{13}C spectra of substituted styrenes (5). An additional feature of the *p*-vinylanisole results is that the difference between the calculated and observed shifts for C-4 is 2.0 p.p.m. Both of these differences are negative in the sense that the calculated shielding is greater than the experimental figure, indicative of a lower electron density at these positions than that predicted, in agreement with the above hypothesis.

In summary, it is found that, of the 32 comparisons between the calculated and experimental results for the para-substituted examples, 30 are within 2 p.p.m. Thus one can

Can. J. Chem. Downloaded from www.nrcresearchpress.com by 210.87.254.105 on 09/05/12
For personal use only.

conclude that Lauterbur's original suggestion (1*b*) that this additive relation can be used to predict aromatic carbon nuclear shieldings receives further confirmation.

For the two meta derivatives, the deviations between the experimental shifts and those calculated are less than 1.7 p.p.m. Since the additive relation is utilized for the assignments in these cases, the agreement cannot be taken as evidence in support of the additivity of substituent effects. For these cases, specifically labelled materials would be required to make unequivocal assignments. In view of the apparent generality of the additive relation, however, it appears that the present assignments are the most probable.

Methoxyl Carbons

The assignments for the methoxyl carbon absorptions present no difficulty. Because of the effective deshielding by oxygen, these appear in a region of the spectrum which, for this series, is devoid of other absorption patterns. From the data in Table II it is apparent that the methoxyl carbon chemical shifts are not highly sensitive to meta and para substitution on the ring. The methoxyl absorption is found over the rather narrow range of 136.2–139.2 p.p.m., which is about half the shielding change observed for the β-carbon in similarly substituted styrenes (5). There is little doubt that the electron density about the methoxyl oxygen nucleus depends on the ring substituent, and it would be surprising indeed if this were not reflected, however slightly, at the methoxyl carbon. It is expected that electron-withdrawing groups on the ring decrease the shielding at the oxygen nucleus, since the conjugative electron release by oxygen will be enhanced, and therefore the methoxyl carbon would also be deshielded. Although this general trend is observed, the changes are small. A plot of the methoxyl carbon shifts versus the Hammett σ values for the various substituents reveals an approximate relation between the two parameters, but a good linear correlation is not obtained. The situation is not improved if σ^+ values are employed. This finding is interesting in the light of the report that methoxyl proton shifts show a fair correlation with σ values for a series of substituted anisoles (8). For the carbon shieldings, however, we can only conclude that these exhibit a weak dependence on substituent polarity, and that other factors may exert some influence.

Ortho-Substituted Anisoles

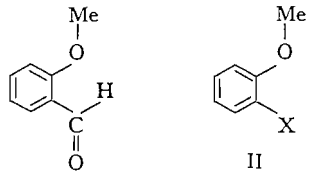
Aromatic Carbons

For the ortho-substituted anisoles having only one substituent ortho to the methoxyl group, the observed aryl carbon shieldings differ somewhat from those predicted by assuming additivity of the substituent effects. The deviations between the calculated and observed values, however, appear to follow a definite pattern.

At the C-4 and C-5 positions the observed shieldings are, for the most part, within 1.5 p.p.m. of the calculated values and, for more than half of these, the deviations are <0.5 p.p.m. This is true even for those cases in which substituents are bonded to these nuclei. But for two exceptions, a similar situation obtains for the C-3 shieldings. The exceptions are 2,3-dimethyl-4-chloroanisole and 2-formylanisole, for which the differences between the calculated and observed shifts are $+4.2$ and $+3.8$ p.p.m., respectively (i.e. the absorption is found at significantly higher field than that calculated). This change for 2,3-dimethyl-4-chloroanisole is analogous to the behavior found for other aromatic systems (1, 3–5) in which a substituted aryl carbon is flanked by two substituted aromatic nuclei, and apparently may be attributed to the crowding of the substituent methyl groups. For 2-formylanisole, it seems probable that the preferred planar conformation will be that in which the carbonyl oxygen and methoxyl methyl group are as far apart as possible. In this conformation (I), the carbonyl oxygen will be relatively close to C-3 and could affect its

Can. J. Chem. Downloaded from www.nrcresearchpress.com by 210.87.254.105 on 09/05/12
For personal use only.

shielding. Since the data for suitable model compounds are lacking, it is not possible to confirm this proposal at the present time, but it would appear to be a reasonable suggestion.



I II

The shieldings found for C-6 are interesting because, in all examples, the observed values lie at higher field than those calculated. The differences range from +1.7 to +4.6 p.p.m. The average deviation is +3.4 p.p.m., more than twice that normally found for meta- and para-substituted molecules. In these ortho-substituted cases, however, the C-2 substituent could interfere with the methoxyl group such that the preferred conformation would be that in which the methoxyl carbon is "turned away" from the ortho group, as in II. It appears reasonable to suggest, therefore, that the consistent shift of the C-6 nuclei to higher field is caused by the location of the methoxyl carbon. If a planar conformation is assumed, the distance separating the methoxyl and C-6 carbon nuclei is approximately the same as that between two ortho-oriented methyl groups on an aromatic ring. For the latter case, it is well established that these nuclei are abnormally shielded (1, 3–5, 14). The remarkable consistency of the data for the C-6 nuclei suggests a common origin for this shielding effect in all cases.

The remaining aromatic carbons, C-1 and C-2, exhibit moderate departures from the behavior predicted by the additive relation. For C-1, the deviations are not much larger than the worst cases in the meta- and para-substituted series, ranging up to a maximum of ±3 p.p.m. There is no obvious trend with substituent and, in a few cases, the differences are less than 1 p.p.m. At C-2, however, all of the experimental values are lower than those calculated, and the differences range from −0.3 to −5.2 p.p.m., with an average deviation of −2.6 p.p.m. It is interesting that this change is directionally opposite to that found for the C-6 nuclei, and it is conceivable that at least part of the difference is caused by the conformation of the methoxyl group. For anisole and its meta- and para-substituted derivatives, the methoxyl group can exist in two possible planar conformations, the relative populations of which will be comparable. Thus, if the methoxyl carbon exerts a shielding effect through space at the ortho carbons, the effect will be comparable at both positions. In an ortho-substituted compound, however, one of the planar conformations (II) may be much more stable than the other, and it follows that C-6 will become more shielded relative to C-2 owing to the suggested effect operative through space. As found for C-6, the deviations for the C-2 shieldings are consistently in one direction, a fact that is required by our proposal but, of course, does not confirm it.

Methoxyl Carbons

As the results in Table III show, the presence of an ortho substituent produces virtually no change in the methoxyl carbon chemical shift relative to the value for anisole itself. With one possible exception, all of these values are indistinguishable within the limits of our experimental error. The exception is 2,3-dimethylanisole, whose methoxyl absorption is found at 137.8 p.p.m. in comparison with that of anisole at 138.8 p.p.m. Since, in general, closely crowded carbons tend to absorb at higher field than chemically similar but less-crowded carbons, it appears, therefore, that the preferred conformation for these examples

Can. J. Chem. Downloaded from www.nrcresearchpress.com by 210.87.254.105 on 09/05/12
For personal use only.

is that in which the distance between the methoxyl carbon and the ortho substituent is a maximum (as in II).

Diortho-Substituted Anisoles

Aromatic Carbons

This particular series of compounds was chosen for study because there is no ambiguity in the assignments of the absorption patterns to specific carbon nuclei. For most cases, the strongest doublet in the aromatic region arises from the meta carbons (C-3, C-5), and the strongest singlet is the absorption of the ortho carbons (C-2, C-6). As before, the lowest field singlet is the C-1 signal, and the remaining pattern arises from C-4. Only in the case of the tetramethyl and pentamethyl derivatives is there a chance of incorrect assignments, for which the ortho and meta carbons could perhaps be reversed. We have assigned these signals on the basis of previous results for polymethylated benzene derivatives (3–5). No major conclusions drawn from these results, however, depend on these particular assignments.

In contrast to the results for each of the two preceding series, most of the aryl carbon shieldings for the 2,6-disubstituted examples differ markedly from the values calculated by assuming additivity of the substituent effects. Uniformly large differences, in the range of -5.8 to -9.5 p.p.m., are found for the C-2 and C-6 nuclei. It is interesting that all are negative in the sense that the signals appear at lower field than predicted. A similar uniformity is found for the differences between the calculated and observed shieldings of the para carbons (C-4), for which the deviations are in the range of -0.6 to -5.4 p.p.m. At the other sites, the deviations are not directionally uniform, but rather range from -8.1 to $+8.6$ p.p.m. and there are few cases in which the differences are less than ± 1.5 p.p.m. Clearly, the additive relationship breaks down completely. It follows, therefore, that the electronic effect of one or more substituents has been altered substantially. Since the differences between the calculated and observed shieldings are negative at the 2, 4, and 6 positions in every case, it is reasonable to conclude that the major factor causing these deviations is a perturbation of the interaction of the methoxyl group with the aromatic ring. This conclusion is based on the fact that alkyl groups do not affect the shielding of aryl carbons ortho to the substituted center nearly as much as the methoxyl group, which shields the ortho carbons by 14.7 p.p.m. in anisole. The deviations of up to -9.5 p.p.m. for the C-2 and C-6 nuclei clearly indicate that the methoxyl – aryl ring interaction is altered for the 2,6-disubstituted series.

Methoxyl Carbons

There are marked changes in the methoxyl carbon shieldings for this series, in distinct contrast to the behavior observed for each of the preceding groups of substituted anisoles. A strong dependence of these shieldings on the size of the ortho substituent is apparent from the data in Table IV. The absorption pattern for the methoxyl carbon nucleus is shifted to progressively lower field as the bulk of the ortho substituents increases from methyl to isopropyl to *t*-butyl. The observed range of 6.8 p.p.m. (128.1–134.9 p.p.m.) is much larger than that found for either of the other series, and the lowest field signals (i.e. the 2,6-di-*t*-butyl derivatives) are 10 p.p.m. downfield from that of the anisole methoxyl carbon.

It is interesting that the data fall into a number of separate groupings depending on the ortho substituents. With the *p*-NO_2 derivatives as exceptions, the 2,6-di-*t*-butyl compounds exhibit methoxyl absorption at 128.8 ± 0.3 p.p.m., the 2,6-di-isopropyl examples at 131.8 ± 0.3 p.p.m., and the 2,6-dimethyl cases at 134.6 ± 0.3 p.p.m., excluding the two

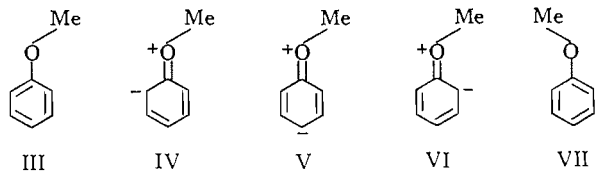
Can. J. Chem. Downloaded from www.nrcresearchpress.com by 210.87.254.105 on 09/05/12
For personal use only.

durene derivatives. The latter, 2,3,5,6-tetramethyl- and 2,3,4,5,6-pentamethyl-anisole, absorb at 133.0 p.p.m. It would appear that the additional methyl groups at the 3 and 5 positions tend to accentuate the deshielding trend, although both were examined in solution, which may account for part of the difference between these and the other 2,6-dimethylated examples. For the two *p*-NO_2 examples, the low-field shift of 1.0–1.7 p.p.m. relative to the corresponding 2,6-dialkyl compounds is slightly less than the difference between *p*-nitroanisole and anisole when the latter are examined in the same medium (see Table V), and can be attributed to the electron-withdrawing inductive effect of the NO_2 grouping. In any event, there is a clear dependence of the methoxyl carbon shieldings on the size of the ortho substituents for those cases in which both ortho positions are substituted.

It is more difficult, however, to account for the trend to lower field relative to the less highly substituted examples. The origin of this deshielding effect is not evident to us, although its significance with respect to the question of the most probable conformations of these structures may be intimated. This aspect is considered in the concluding section of this paper. To judge from the aryl carbon shieldings it appears that conjugative electron release by oxygen to the aromatic ring is strongly affected by the presence of two ortho substituents, and it follows that the hybridization of the oxygen may be altered in the more hindered systems. If the electron-releasing tendency is reduced, one would expect the methoxyl carbon to be more shielded; if the hybridization of the oxygen is changed from something close to sp^2 to sp^3, one would expect the shielding of the methoxyl carbon to increase. Both expectations are contrary to the experimental results. This raises the question of whether the shift to lower field could arise from a "through space" effect of the ortho alkyl carbon nuclei. If so, it would be a remarkably large factor if the above suppositions are reasonable. Because of a lack of suitable model compounds, it is difficult to estimate the importance of a field effect, but it is known that closely crowded methyl carbons tend to absorb at *higher* field than in chemically equivalent but less-crowded systems (3, 5, 14). Thus, the qualitative rationalizations normally used to interpret ^{13}C nuclear shieldings predict variations opposite to those found for the methoxyl carbon shifts in the 2,6-disubstituted examples. Perhaps the appearance of more data for related systems will provide an answer for these apparently anomalous observations.

Steric Inhibition of Resonance

In the preceding discussion, a number of observations were noted which indicate that the interaction of the methoxyl oxygen with the benzene ring is altered in the highly substituted examples relative to that in the meta-, para-, and mono-ortho-substituted cases. For a compound in which there is no interference by substituents, several canonical forms can be written. The more important of these are shown as structures III–VII.



III IV V VI VII

Besides these, there are three, corresponding to IV–VI, having the methyl group as in VII, and two other Kekulé forms corresponding to III and VII. The aromatic shieldings for anisole are readily explicable in terms of the contributing forms IV–VI, since an increase in the electron density is expected at the ortho and para positions, and since these positions

Can. J. Chem. Downloaded from www.nrcresearchpress.com by 210.87.254.105 on 09/05/12
For personal use only.

are considerably shielded in the anisole molecule relative to the value for benzene carbons. In addition, the methoxyl carbon absorbs at lower field than that found for methoxyl groups in many saturated systems.[4] Any factor which could interfere with the conjugative electron release from oxygen to the ring may be expected to decrease these relatively high shieldings at the ortho- and para-carbon nuclei. Changes in the shift of the methoxyl carbon would also be expected. The results of the present series can be considered on this basis.

It would seem reasonable to assume that the interactions of the substituents are normal for all cases in which the additive relationship holds for the aryl carbon chemical shifts. In particular, one could expect the shielding of the carbon para to the methoxyl group to reflect a significant perturbation of the methoxyl – aryl ring interaction. If electron release from the methoxyl oxygen were reduced, the para-carbon shielding would be expected to decrease. Although a similar change should be observed for the ortho carbons, predictions are more difficult because of the very real possibility that a part of the observed shielding arises through a field effect of the methoxyl function. Support for this argument is given by the data for the 2-substituted series, for which it is found that the para-carbon results are in good agreement with those calculated by assuming additivity of the substituent effects, whereas the ortho-carbon values are not. The consistency of the deviations for C-2 and C-6, as discussed earlier, point to the existence of an appreciable influence of the methoxyl group through space. We conclude, therefore, that the conjugative interaction of the methoxyl group with the aromatic ring is operative in the mono-ortho-substituted examples, although there may be only one planar conformation (II) in which this interaction can be appreciable. The fact that the methoxyl carbon shieldings are very similar for all of these mono-substituted examples (meta, para, and ortho) is completely consistent with this conclusion.

For the 2,6-disubstituted derivatives, the observed shielding changes strongly suggest an important difference in the electronic interactions. For each case, the para carbon absorbs at lower field than that expected, and the deviations from the calculated values are large (up to -5.4 p.p.m.). Similar trends for the para-carbon shieldings in other hindered aromatic derivatives have been noted previously (2–4) and have been attributed to steric inhibition of resonance. For the present series, the changes are precisely those expected for cases in which the contribution of resonance form V is small. The relatively large differences in the methoxyl carbon shieldings are also indicative of a major change in the electronic nature of the methoxyl oxygen. To illustrate the magnitude of these differences, a summary of the methoxyl carbon shieldings for a number of the examples relative to the methoxyl shift for anisole are given in Table VI. From these data it is clear that appreciable changes occur upon the introduction of substituents at both ortho positions. Furthermore, the magnitude of the change for a particular case is strongly dependent on the size of the ortho groups. The maximum difference is found for the 2,6-di-*t*-butyl derivatives. We conclude, therefore, that there is steric interference of the ortho groups with the methoxyl function in the 2,6-disubstituted anisoles such that electron release by the methoxyl oxygen is significantly reduced.

One of the more usual approaches to an investigation of steric hindrance to conjugative interactions is an examination of the electronic spectra of a series of model compounds. The question of steric inhibition of resonance in substituted anisoles has been studied by a number of workers by using ultraviolet spectroscopy, and a marked decrease in the molar extinction coefficient (ϵ_{max}) of the absorption near 260–270 mμ has been attributed to a steric effect (15–17). A comparison of these data with the ^{13}C shielding results reveals a

[4]*G. W. Buchanan, D. A. Ross, and J. B. Stothers, unpublished observations.*

Can. J. Chem. Downloaded from www.nrcresearchpress.com by 210.87.254.105 on 09/05/12
For personal use only.

TABLE VI

^{13}C shieldings of the methoxyl carbons in some substituted anisoles (in p.p.m. relative to anisole)

Substitution		Para substituents			
C-2	C-6	H	Cl	Br	NO_2
H	H	0.0	−0.7	−0.8	−2.6*
Me	H	+0.3	0.0	−1.0†	—
Et	H	+0.3	—	—	—
i-Pr	H	0.0	—	—	—
t-Bu	H	+0.1	−0.5	−0.8	—
Me	Me	−3.9	−4.5	−4.5	−6.2†
i-Pr	*i*-Pr	−7.2	−6.7	−7.1	—
t-Bu	*t*-Bu	−9.7	−9.9	−10.0	−10.7*

*Saturated solution in CS_2.
†Saturated solution in $CHCl_3$.

very good linear correlation between the ϵ_{max} values and the methoxyl carbon shieldings, as illustrated in Fig. 1. The existence of this relation offers further support for our conclusion regarding steric hindrance to resonance in the 2,6-disubstituted systems.

Another report bearing on this question has appeared (18) and warrants comment in the light of our present results. Baliah and Uma claim, on the basis of dipole moment data for some anisoles, that a single ortho substituent causes an exaltation of methoxyl conjugation with the aryl ring. These authors, however, have chosen to ignore the small, but nevertheless real, contribution of an ortho substituent to the total dipole moment of the molecule,

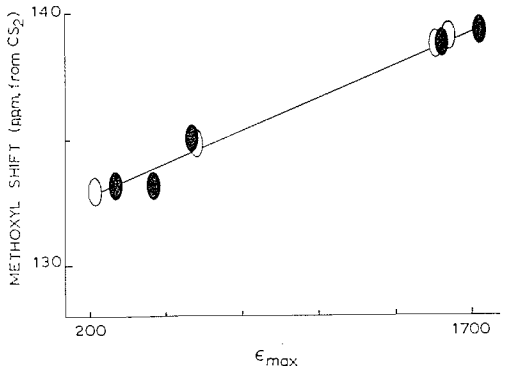


FIG. 1. Plot of methoxyl carbon shieldings versus ϵ_{max} of the ultraviolet absorption near 260 mμ. LEGEND: ●, ultraviolet data from ref. 16; ○, data from ref. 18.

and we suggest that this neglected factor may be sufficient to account for the observations. We find it difficult to accept the concept of an exaltation of conjugation by ortho-alkyl substitution. On the basis of our ^{13}C results and the available ultraviolet spectral data, it appears that significant differences in the conjugative interaction of the methoxyl group with the aromatic ring occur only if both ortho positions are occupied by substituents.

ACKNOWLEDGMENTS

We thank the donors of the Petroleum Research Fund, administered by the American Chemical Society, and the Ontario Research Foundation for operating funds and a major equipment grant, respectively.

Can. J. Chem. Downloaded from www.nrcresearchpress.com by 210.87.254.105 on 09/05/12
For personal use only.

REFERENCES

1. (*a*) P. C. LAUTERBUR. J. Am. Chem. Soc. **83**, 1838 (1961). (*b*) P. C. LAUTERBUR. J. Am. Chem. Soc. **83**, 1846 (1961).
2. P. C. LAUTERBUR. J. Chem. Phys. **38**, 1406 (1963); **38**, 1415 (1963); **38**, 1432 (1963).
3. K. S. DHAMI and J. B. STOTHERS. Can. J. Chem. **43**, 479 (1965).
4. K. S. DHAMI and J. B. STOTHERS. Can. J. Chem. **43**, 498 (1965).
5. K. S. DHAMI and J. B. STOTHERS. Can. J. Chem. **43**, 510 (1965).
6. H. SPIESECKE and W. G. SCHNEIDER. J. Chem. Phys. **35**, 731 (1961).
7. G. B. SAVITSKY. J. Phys. Chem. **67**, 2723 (1963).
8. C. HEATHCOCK. Can. J. Chem. **40**, 1865 (1962).
9. K. S. DHAMI and J. B. STOTHERS. Tetrahedron Letters, No. 12, 631 (1964).
10. N. KORNBLUM and R. SELTZER. J. Am. Chem. Soc. **83**, 3668 (1961).
11. T. C. BRUICE, N. KHARASCH, and R. J. WINZLER. J. Org. Chem. **18**, 83 (1953).
12. L. F. FIESER. Experiments in organic chemistry. 3rd ed. D. C. Heath & Co., Boston, Massachusetts. 1957. p. 310.
13. J. B. STOTHERS. Quart. Rev. London, **19**, 144 (1965).
14. W. R. WOOLFENDEN and D. M. GRANT. J. Am. Chem. Soc. **88**, 1496 (1966).
15. A. BURAWOY and J. T. CHAMBERLAIN. J. Chem. Soc. 2310 (1952).
16. J. C. DEARDEN and W. F. FORBES. Can. J. Chem. **37**, 1305 (1959).
17. L. J. FROLEN and L. GOODMAN. J. Am. Chem. Soc. **83**, 3405 (1961).
18. V. BALIAH and M. UMA. Tetrahedron Letters, No. 25, 21 (1960).

Can. J. Chem. Downloaded from www.nrcresearchpress.com by 210.87.254.105 on 09/05/12
For personal use only.

Can. J. Chem. Downloaded from www.nrcresearchpress.com by 210.87.254.42 on 09/05/12
For personal use only.

SUR LES PRÉSUMÉS *cis*-DIHALOGÉNURES DE QUINONES

J. Y. Savoie et P. Brassard
Département de Chimie, Université Laval, Québec, Québec

Reçu le 18 mai 1966

RÉSUMÉ

En se basant sur des données de nature surtout spectrale, on a déjà conclu à une addition *cis* du chlore à la benzoquinone. Le *cis*-dichlorure, en solution alcoolique, se transformerait en son isomère *trans*, qui par la suite s'énoliserait en l'hydroquinone correspondante. Après avoir répété les travaux antérieurs et isolé les intermédiaires et les produits de la réaction en solution alcoolique, nous pouvons réaffirmer que, dans diverses conditions, le *trans*-dichlorure est le seul isomère décelable formé lors de la chloration. Les changements observés en solution alcoolique sont dûs à une élimination suivie d'une réduction photochimique. L'étude des dibromures correspondants à conduit à des conclusions semblables.

ABSTRACT

It has been proposed, mainly on the basis of spectral evidence, that the addition of chlorine to *p*-benzoquinone gives the *cis*-dichloride, and that in an alcoholic solution this substance isomerizes to the *trans*-dichloride, which then enolizes to the corresponding hydroquinone. Upon reexamination of the evidence and isolation of the intermediates and end products of the reaction in an alcoholic solution, it can now be reasserted that the *trans*-dichloride is the only detectable isomer resulting from chlorination under various conditions. The observed changes in an alcoholic solution have been proven to be the result of elimination followed by photochemical reduction. Similar conclusions have been reached in the case of quinone dibromides.

Il est bien connu, depuis la fin du siècle dernier, que l'action du chlore et du brome sur les quinones conduit à des produits d'addition 1,2 (1–3). Plus tard, l'oxydation permanganique des dichlorures de *p*-benzoquinones en acide *dl*-dichlorosuccinique permettait à Dimroth *et al.* (4) de leur assigner la configuration *trans*. En 1954, ter Borg (5) aurait isolé les deux isomères du dichlorure de la benzoquinone; il leur assigna les configurations *cis* et *trans* et élabora une interprétation des transformations observées en solution alcoolique.

Selon ter Borg, l'isomère *cis* s'obtiendrait par la méthode de Clark (3) et se décomposerait à 120° (λ_{max} 250 mμ (ϵ 4 300)); l'action du chlorure de sulfuryle sur l'hydroquinone donnerait l'isomère *trans* (λ_{max} 252 mμ (ϵ 14 750)), qui se décomposerait à 130°. De plus, il nie catégoriquement l'existence d'un dichlorure qui, pourtant, avait été décrit à plusieurs reprises, p.f. 143° (2) et 146° (3, 4). L'hypothèse de la transformation du *cis*-dichlorure en l'isomère *trans* et finalement en 2,3-dichlorohydroquinone est basée sur l'examen périodique du spectre d'absorption dans l'ultraviolet de cette substance en solution alcoolique.

Dans le cadre d'un projet sur les 2,3-dihydroquinones, nous avons répété le travail de ter Borg, mais nous n'avons pu reproduire ses résultats en dépit de nombreuses tentatives. Nous pouvons, en conséquence, proposer les mises au point suivantes.

Préparation des dihalogénures de quinones

Nous avons refait la préparation du dichlorure de la *p*-benzoquinone d'après la méthode de Clark (3), une méthode préconisée également par ter Borg. Nous y avons apporté en outre un grand nombre de modifications (variations de température et de vitesse d'addition, emploi de divers solvants, etc.) sans réussir à isoler autre chose que le dichlorure décrit par Clark. De plus, lors d'une réaction faite à $-20°$, nous avons obtenu ce dichlorure pur directement du milieu réactionnel (λ_{max} 230 mμ (ϵ 9 800)). Cette seule et même substance s'obtient également par l'action du chlorure de sulfuryle sur l'hydroquinone et par celle du dichlorure d'iodobenzène, qui donne généralement un produit d'addition *cis* (6), sur la

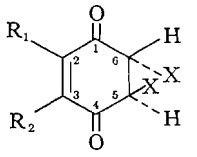
p-benzoquinone. Des résultats semblables ont été obtenus pour les dichlorures de la toluquinone, de l'*o*-xyloquinone et de la α-naphtoquinone, de même que pour les dibromures de ces quinones. En outre, des préparations présentant les caractéristiques décrites par ter Borg ont été obtenues à l'occasion, mais leur spectre infrarouge a démontré qu'elles étaient impures et contenaient des quantités certaines d'hydroquinones.

Spectroscopie

Ter Borg avait signalé et étudié la variation du spectre d'absorption dans l'ultraviolet du dichlorure de la benzoquinone en solution alcoolique. Toutefois, le spectre que nous avons observé diffère sensiblement de celui déjà publié. Les bandes d'absorption notées par ter Borg (5) pour le dichlorure de la benzoquinone (λ_{max} 250 mμ (ϵ 4 300)), par Vischer (7) pour le dibromure de la benzoquinone (λ_{max} 256 mμ) et par Andrews *et al.* (8) pour le dibromure de l'*o*-xyloquinone (λ_{max} 275 mμ (ϵ 8 300)) sont identiques à celles que nous avons observées environ 1 h après la préparation de la solution et correspondent aux monohalogénoquinones correspondantes. Des solutions fraîches de ces trois substances révèlent des bandes d'absorption à 230 mμ, à 220 mμ et à 225 et 271 mμ. Ces bandes persistent, par ailleurs, lorsque l'on emploie des solvants non polaires comme le *n*-hexane.

La différence marquée entre les dibromures et les dichlorures de quinones lorsque l'on tente de les énoliser nous a incité à en rechercher la cause par la détermination des caractéristiques spectrales de ces substances (Tableau I) et des dicétotétrahydronaphtalènes (Tableau II). Mais, en l'absence de toute indication dans la littérature sur la conformation des ènediones homocisoïdes, nous nous contenterons de signaler quelques effets.

TABLEAU I

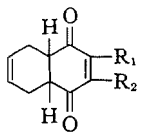
	λ_{max}^{EtOH} (mμ)	$\lambda_{max}^{n\text{-hexane}}$ (mμ)	ϵ (*n*-hexane)	ν_{max}^{KBr} (cm^{-1})	$\nu_{max}^{CHCl_3}$ (cm^{-1})
$R_1 = R_2 = H$, X = Cl	230	230	9 800	1 719	1 717
$R_1 = CH_3$, $R_2 = H$, X = Cl	247	246–247	12 000	1 699, 1 718 (doublet)	1 705
$R_1 = R_2 = CH_3$, X = Cl	259	205 259	11 500	(1 680), 1 695	1 694
R_1, R_2 = benzo, X = Cl	232 264 310			1 715	
$R_1 = R_2 = H$, X = Br	220	220	10 400	1 695, 1 705 (doublet)	1 707
$R_1 = CH_3$, $R_2 = H$, X = Br	230 255	227 252	7 100 6 400	1 680, 1 700 (doublet)	(1 690), 1 704
$R_1 = R_2 = CH_3$, X = Br	225 271	222 267	5 900 8 400	1 697	1 699
R_1, R_2 = benzo, X = Br	235–236 268–270 310	234–235 263 308	16 000 6 300 210	1 710	1 701

Spectres ultraviolets

La cyclohex-2-ène-1,4-dione, λ_{max}^{EtOH} 233 mμ, $\lambda_{max}^{iso\text{-octane}}$ 219 mμ (9), donne lieu à un effet de solvant considérable; par contre, nous avons noté une absence de cet effet dans le cas des dihalogénures de quinones. On pourrait peut-être attribuer ceci à une faible polarité de ces molécules, qui serait compatible avec une conformation dans laquelle les atomes d'halogène seraient axiaux.

Can. J. Chem. Downloaded from www.nrcresearchpress.com by 210.87.254.42 on 09/05/12
For personal use only.

TABLEAU II



	$\lambda_{max}^{EtOH\ 95\%}$ (mμ)	$\lambda_{max}^{n\text{-hexane}}$ (mμ)	ν_{max}^{KBr} (cm^{-1})	$\nu_{max}^{CHCl_3}$ (cm^{-1})
$R_1 = R_2 = H$	222–223	221	1 685	1 695
$R_1 = CH_3$, $R_2 = H$	238–239	235	1 678	1 678
$R_1 = R_2 = CH_3$	250–251	246	1 668, 1 677 (doublet)	1 678
R_1, R_2 = benzo	224	221	1 695	1 700

La règle modifiée de Fieser (10) s'applique bien aux dicétotétrahydronaphtalènes et assez bien aux dichlorures de quinones mais à condition de donner aux atomes de chlore un effet constant; ceci impliquerait que tous les dichlorures ont la même conformation. Elle ne s'applique pas aux dibromures car, à l'exception de celui de la *p*-benzoquinone, ils montrent deux bandes assez mal définies.

Spectres infrarouges

La cyclohex-2-ène-1,4-dione montre une bande, ν^{CCl_4} 1 690 cm^{-1}, qui concorde bien avec celle du dicétotétrahydronaphtalène, $\nu_{max}^{CHCl_3}$ 1 695 cm^{-1}; mais, toute corrélation entre l'orientation de l'atome d'halogène et la fréquence d'absorption du groupe carbonyle devient hasardeuse à défaut de substance isomère ou de structure établie auxquelles on peut se référer (cf. réf. 11, par exemple).

La régularité de la diminution de la fréquence $\nu_{C=O}$ (Tableau I) (11–12 cm^{-1} pour les dichlorures et 3–5 cm^{-1} pour les dibromures de quinones) suggère que dans chacun de ces groupes les substances ont la même conformation et que les différences de réactivité ne sont pas d'ordre conformationnel.

La 2,3,5,6-tetrabromocyclohexane-1,4-dione (1) et le composé chloré correspondant (3) ($\nu_{C=O}^{KBr}$ 1 750 cm^{-1} et $\nu_{C=O}^{KBr}$ 1 754 cm^{-1}, respectivement) montrent, par ailleurs, des bandes d'absorption caractéristiques de cétones α,α'-dihalogénées dans lesquelles les atomes d'halogène sont nettement équatoriaux (12).

Elimination

Par l'emploi de solutions alcooliques plus concentrées de dichlorures et de dibromures de quinones, nous avons pu, après la disparition de la bande d'absorption originale, isoler, pour quelques substrats, la monohalogénoquinone correspondante. La vitesse d'élimination augmente avec la proportion d'eau dans le solvant et aussi par addition d'halogénures alcalins. L'effet du fluorure de sodium est particulièrement frappant (Tableau III). Lorsque les solutions sont placées dans l'obscurité, la bande d'absorption, due à la quinone, ne varie plus pour toute fin pratique. Mais à la lumière, elle fait lentement place à une troisième bande dans la région caractéristique des hydroquinones. Dans quelques cas, cette hydroquinone a été isolée et était identique à la monohalogénohydroquinone correspondante.

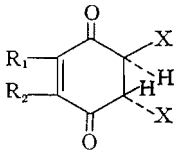
La réduction photochimique des quinones est bien connue (réf. 13, par exemple) et ne surprend pas si ce n'est par sa facilité, car elle ne nécessite ni source lumineuse, ni lumière directe du soleil.

Enolisation

On a déjà souligné que le dibromure de la benzoquinone ne s'énolise pas en 2,3-bromohydroquinone (4, 5) et, en dépit de nombreuses tentatives, nous n'avons pu modifier ce résultat. Toutefois l'oxydation permanganique de ce dibromure de benzoquinone en acide

Can. J. Chem. Downloaded from www.nrcresearchpress.com by 210.87.254.42 on 09/05/12
For personal use only.

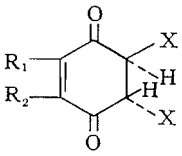
TABLEAU III



Solvant	Première bande, λ_{max} (t = 2 min)	Deuxième bande, λ_{max}, t à ϵ_{max}	Troisième bande, λ_{max}, t à ϵ_{max}
$R_1 = R_2 = H$, X = Cl	EtOH 80%	230	251, 30 min	296, ~48 h
$R_1 = R_2 = H$, X = Cl	EtOH 99%	230	251, 72 h	296, >7 jours
$R_1 = R_2 = H$, X = Cl	EtOH 99% à l'obscurité	230	251, 72 h	—
$R_1 = R_2 = H$, X = Br	EtOH 80%	220	256, 40 min	296, ~48 h
$R_1 = R_2 = H$, X = Br	EtOH 95%	220	256, 25 h	296, >3 jours
$R_1 = R_2 = H$, X = Cl	EtOH 80% à l'obscurité	220	256, 40 min	—
$R_1 = R_2 = H$, X = Cl	EtOH 80% + NaF 0.01 M	—	251, 2 min	296, 15 h

dl-dibromosuccinique lui assigne pourtant la même configuration qu'au dichlorure. Nous avons, par ailleurs, observé que les énolisations peuvent se faire rapidement au moyen de l'acide sulfurique concentré ou de l'acide bromhydrique sec dans l'éther. Dans ces conditions le dibromure de l'*o*-xyloquinone se transforme en 5,6-dibromo-*o*-xylohydroquinone, à l'instar des dichlorures. Par contre, avec le dibromure de la benzoquinone on peut isoler un intermédiaire passablement stable (il n'a pu être analysé), dont les caractéristiques spectrales seraient celles de la 2,3,5-tribromocyclohexane-1,4-dione. Dans les mêmes conditions expérimentales, cet intermédiaire se transforme éventuellement en 2,5-dibromohydroquinone; dans l'alcool, il se convertit en 2,5-dibromobenzoquinone. Il semble donc que le cours de la transposition puisse être plus complexe qu'on ne l'avait supposé (4) et que l'élimination d'un molécule de HBr soit suivie de l'addition 1,2 de cette substance à une autre molécule de dibromure plutôt qu'à la bromobenzoquinone. D'ailleurs, l'addition de HBr à la bromobenzoquinone donnerait surtout la 2,6-dibromohydroquinone (14) (Tableau IV).

TABLEAU IV



Méthode	Produits (hydroquinones)	Quinones correspondantes
$R_1 = CH_3$, $R_2 = H$, X = Cl	A,B	2-Méthyl-5,6-dichloro- 112.0–112.5° (110.7–111.5°) (18)	78.0–78.2° (77.7–78.5°) (18)
$R_1 = R_2 = CH_3$, X = Cl	A,B	2,3-Diméthyl-5,6-dichloro- 168.5–169.0° (163–164°) (19)	167–168° (159°) (19)
$R_1 = R_2 = H$, X = Br	A,B	2,5-Dibromo- 187–188° (186–187°) (20)	188–190° (188°) (20)
$R_1 = CH_3$, $R_2 = H$, X = Br	A	2-Méthyl-5-bromo- 179° (179°) (3)	104° (105–106°) (3)
$R_1 = CH_3$, $R_2 = H$, X = Br	B	Methyltribromo- 203° (203°) (3)	234–235° (234°) (21)
$R_1 = R_2 = CH_3$ X = Br	A,B	2,3-Diméthyl-5,6-dibromo- 164–165° (163–164°) (17)	151–152° (152.5–153.0°) (22)

Can. J. Chem. Downloaded from www.nrcresearchpress.com by 210.87.254.42 on 09/05/12
For personal use only.

Can. J. Chem. Downloaded from www.nrcresearchpress.com by 210.87.254.42 on 09/05/12
For personal use only.

PARTIE EXPÉRIMENTALE

Les points de fusion corrigés ont été déterminés en tube capillaire (appareil Thomas Hoover). Les spectres infrarouges ont été réalisés avec un appareil Beckman, modèle IR-4, et ont été calibrés à l'aide d'un film de polystyrène. Les spectres ultraviolets ont été déterminés avec un appareil Beckman, modèle DK-1A.

1. Addition du chlore aux quinones

Dichlorure de la p-benzoquinone (5,6-dichlorocyclohex-2-ène-1,4-dione)

Méthode A.—On fait barboter rapidement du chlore dans une solution de 10.8 g (0.1 mole) de *p*-benzoquinone dans 60 ml de chloroforme anhydre pendant 1 h à −20°. Après avoir entraîné l'excès de chlore dans un courant d'azote, filtré et lavé les cristaux avec un peu de chloroforme glacé, on obtient le dichlorure pur (10.8 g, 60%), p.f. 146.0–146.5° (litt. p.f. 143° (2), 146° (3)).

Méthode B.—On dissout la *p*-benzoquinone (10.8 g) dans un minimum de chloroforme sec (20 ml) à 25° et on sature de chlore un volume égal du même solvant. Après avoir réuni les deux solutions, on fait barboter du chlore dans le mélange pendant 10 min; puis on y ajoute 10 ml d'éther de pétrole (p.é. 30–60°). On isole le dichlorure (80%) comme ci-dessus, p.f. 145–146°.

Méthode C (5).—On ajoute goutte à goutte 24.0 g de chlorure de sulfuryle à une solution de 10.0 g de *p*-benzoquinone dans 100 ml d'éther anhydre. Après avoir agité pendant 1 h, on constate que la quinhydrone formée au début de la réaction s'est transformée en un précipité blanc du dichlorure. On refroidit, filtre et lave avec un peu d'éther glacé. Le dichlorure ainsi obtenu (40%) est pur, p.f. 146–146.5°.

Méthode D.—On ajoute par petites portions 5.5 g (0.02 mole) de dichlorure d'iodobenzène à une solution de 2.2 g (0.02 mole) de *p*-benzoquinone dans 20 ml d'acide acétique à 50°. Au moment de l'apparition d'une teinte rouge, on refroidit rapidement, on dilue avec de l'eau et l'on extrait avec du chloroforme (100 ml). Le dichlorure (1.5 g, 40%) cristallise dans un mélange de chloroforme et d'éther de pétrole (p.é. 66–70°), p.f. 145–146°.

Pour les autres dichlorures, l'emploi de la méthode B donne les meilleurs résultats. Toutefois dans chaque cas, les trois premières méthodes conduisent au même produit. Les rendements varient de 70 à 80%.

5,6-Dichloro-2-méthylcyclohex-2-ène-1,4-dione (dichlorure de la toluquinone), p.f. 134.5° (litt. p.f. 135–136° (3)). *5,6-Dichloro-2,3-diméthylcyclohex-2-ène-1,4-dione (dichlorure de l'o-xyloquinone)*, p.f. 194.5°. *2,3-Dichloro-1,2,3,4-tétrahydronaphtalène-1,4-dione*, p.f. 178–180° (décomp.) (litt. p.f. 176° (15)).

2. Addition du brome aux quinones

5,6-Dibromocyclohex-2-ène-1,4-dione (dibromure de la p-benzoquinone)

A une solution de 10.8 g (0.1 mole) de *p*-benzoquinone dans 200 ml de CCl_4 anhydre, on ajoute un mélange de 16.0 g de brome, de 150 ml de CCl_4 et de 15 ml d'éther anhydre. On évapore aussitôt sous vide la moitié du solvant et l'on précipite le dibromure par addition d'éther de pétrole (p.é. 30–60°), p.f. 84.5–85.0° (26.8 g, 100%). Après avoir cristallisé deux fois dans l'éther de pétrole (p.é. 66–70°), la substance fond à 85.5–86.0° (litt. p.f. 86° (1)). L'oxydation permanganique de cette substance d'après la méthode de Dimroth *et al.* (4) conduit à l'acide *dl*-dibromosuccinique, p.f. et p.f. mixte 165–167° (litt. p.f. 166–167° (16)).

Les autres dibromures se préparent de façon analogue; les rendements sont supérieurs à 90%.

5,6-Dibromo-2-méthylcyclohex-2-ène-1,4-dione (dibromure de la toluquinone), p.f. 62.5° (litt. p.f. 61–62° (3)). *5,6-Dibromo-2,3-diméthylcyclohex-2-ène-1,4-dione (dibromure de l'o-xyloquinone)*, p.f. 103–103.5° (litt. p.f. 104–105° (8)). *2,3-Dibromo-1,2,3,4-tétrahydronaphtalène-1,4-dione*, p.f. 100–101° (litt. p.f. 92° (15)).

3. Réactions des dihalogénures de quinones dans l'éthanol

Les transformations des dihalogénures de quinones en solution alcoolique contenant de 1 à 20% d'eau ont été étudiées par la détermination périodique des spectres d'absorption dans l'ultraviolet. Une solution strictement fraîche (t = 2 min) de chaque dihalogénure révèle une ou deux bandes d'absorption à des longueurs d'onde plus faibles que celles déjà mentionnées (5, 7, 8). Après un temps qui varie en fonction de la concentration en eau du solvant et sous l'effet des halogénures alcalins, ces bandes font place à l'absorption caractéristique des quinones monohalogénées correspondantes. Ces effets ainsi que celui de la lumière sur la persistance de ces dernières bandes sont résumés au Tableau III.

4. Identification des produits d'élimination et de réduction photochimique

Monohalogénoquinones

On dissout 3.0 g de dichlorure de la *p*-benzoquinone dans 100 ml d'éthanol à 80%. Après avoir agité pendant 1 h, on évapore l'alcool sous vide et l'on extrait le résidu avec du chloroforme. L'analyse chromatographique de cette solution (gel de silice, éther de pétrole (p.é. 30–60°)) ne révèle qu'un seul produit, la chloro-*p*-benzoquinone, p.f. et p.f. mixte 56–57° (litt. p.f. 57°), λ_{max}^{EtOH} 250 mμ (ϵ 12 500).

Dans les mêmes conditions, le dibromure de la *p*-benzoquinone se transforme en bromo-*p*-benzoquinone, p.f. et p.f. mixte 56.0–56.5° (litt. p.f. 55–56°), λ_{max}^{EtOH} 256 mμ (ϵ 11 600).

D'une solution de dichlorure de l'*o*-xyloquinone (0.8 g) dans 100 ml d'éthanol à 80%, on isole après 2 semaines la chloro-*o*-xyloquinone, p.f. et p.f. mixte 50.0–50.5°, λ_{max}^{EtOH} 267 mμ (ϵ 13 300).

D'une façon analogue, on obtient la bromo-*o*-xyloquinone, p.f. et p.f. mixte 41–42° (litt. p.f. 42–43° (8)), λ_{max}^{EtOH} 275 mμ (ϵ 13 400).

Monohalogénohydroquinones

On dissout 3.0 g de dichlorure de la *p*-benzoquinone dans 1 l d'éthanol à 80%. Après avoir laissé séjourner la solution à la lumière pendant 1 mois, on évapore l'alcool sous vide et l'on extrait le résidu avec du benzène. Après plusieurs cristallisations dans le chloroforme, la chlorohydroquinone est obtenue à l'état pur, p.f. et p.f. mixte 105° (litt. p.f. 106°), λ_{max}^{EtOH} 296 mμ. Di-acétate, p.f. et p.f. mixte 71.0–71.5° (litt. p.f. 72°).

De la même façon, le dibromure de la *p*-benzoquinone se transforme en bromohydroquinone, p.f. et p.f. mixte 112.5–113.5° (litt. p.f. 111°), λ_{max}^{EtOH} 296 mμ. Di-acétate, p.f. et p.f. mixte 75.0–75.5° (litt. p.f. 71–73°).

5. Enolisation des dihalogénures de quinones

Méthode A

On fait barboter de l'acide bromhydrique gazeux et sec dans une suspension de 5.4 g (0.05 mole) de dichlorure de la *p*-benzoquinone dans 100 ml d'éther anhydre jusqu'à ce que la substance se dissolve. On entraîne l'excès d'acide bromhydrique dans un courant d'azote, on évapore la solution à sec et l'on cristallise la 2,3-dichlorohydroquinone (5.2 g) dans le benzène, p.f. 147–148° (litt. p.f. 147–148° (17)).

On dissout la 2,3-dichlorohydroquinone dans un mélange d'eau et d'acide acétique et l'on y ajoute un excès d'une solution 1.3 *M* de $FeCl_3$ pour obtenir la 2,3-dichloro-*p*-benzoquinone (5.0 g), p.f. 101–102° (litt. p.f. 99–100° (14)).

Méthode B

On dissout par petites portions 2.2 g (0.02 mole) de dichlorure de la *p*-benzoquinone dans 25 ml d'acide sulfurique concentré à 0°. Après avoir agité pendant 20 min, on y ajoute 25 g de glace, on filtre et on lave le résidu avec très peu d'eau glacée. On obtient ainsi 2.1 g de 2,3-dichlorohydroquinone, p.f. 146–147°.

Méthode C

On dissout 10.0 g de dibromure de la *p*-benzoquinone dans 350 ml d'éther anhydre, on y fait barboter un courant rapide de HBr sec pendant 10 s et l'on agite à température ambiante pendant 30 min. On filtre et triture le résidu (7.5 g) dans de l'éther, p.f. 158–159° (décomp.), $\lambda_{max}^{EtOH\,95\%}$ 283 mμ; ν_{max}^{KBr} 1 750, 1 730 et 1 692 cm^{-1}. La substance n'est pas très stable; il n'a donc pas été possible de la soumettre à l'analyse élémentaire. Il s'agit sans doute de la 2,3,5-tribromocyclohexane-1,4-dione puisque le spectre infrarouge n'indique pas d'insaturation et qu'elle se transforme rapidement en 2,5-dibromohydroquinone par l'emploi de la méthode A décrite ci-dessus.

REMERCIEMENT

Nous remercions le Conseil National des Recherches pour l'octroi d'une bourse de recherche à l'un de nous (J. Y. S.) et de subventions.

BIBLIOGRAPHIE

1. J. U. Nef. Am. Chem. J. **12**, 463 (1890).
2. J. U. Nef. Am. Chem. J. **13**, 422 (1891).
3. T. H. Clark. Am. Chem. J. **14**, 553 (1892).
4. O. Dimroth, H. Eber et K. Wehr. Ann. **446**, 132 (1926).
5. A. P. ter Borg. Rec. Trav. Chim. **73**, 5 (1954).
6. C. J. Berg et E. S. Wallis. J. Biol. Chem. **162**, 638 (1946).
7. E. B. Vischer. J. Chem. Soc. 815 (1953).
8. K. J. M. Andrews, D. H. Mariam et D. R. Maxwell. J. Chem. Soc. 1844 (1956).
9. E. W. Garbisch, Jr. J. Am. Chem. Soc. **87**, 4971 (1965).
10. A. I. Scott. Interpretation of the ultraviolet spectra of natural products. The Macmillan Co., New York. 1964. p. 61.
11. D. N. Kirk et V. Petrow. J. Chem. Soc. 1334 (1958).
12. R. N. Jones, D. A. Ramsay, F. Herling et K. Dobriner. J. Am. Chem. Soc. **74**, 2828 (1952).
13. L. Paoloni et G. B. Marini-Bettolo. Gazz. Chim. Ital. **87**, 395 (1957).
14. A. N. Grinev et A. B. Terent'ev. Vestn. Mosk. Univ. Ser. Mat. Mekhan. Astron. Fiz. i Khim. **12**, 147 (1957); Chem. Abstr. **53**, 3187 (1959).
15. T. Zincke et M. Schmidt. Ber. **27**, 2753 (1894).
16. A. McKenzie. J. Chem. Soc. **101**, 1196 (1912).
17. A. Eckert et R. Endler. J. Prakt. Chem., [2], **104**, 81 (1922).
18. J. Cason, R. E. Harman, P. T. Adams et S. Goodwin. J. Org. Chem. **16**, 328 (1951).
19. A. Claus. J. Prakt. Chem., [2], **43**, 563 (1891).
20. E. Sarauw. Ann. **209**, 93 (1881).
21. F. Fichter et M. Rinderspracher. Helv. Chim. Acta, **10**, 41 (1927).
22. L. I. Smith et F. L. Austin. J. Am. Chem. Soc. **64**, 528 (1942).

Can. J. Chem. Downloaded from www.nrcresearchpress.com by 210.87.254.42 on 09/05/12
For personal use only.

Can. J. Chem. Downloaded from www.nrcresearchpress.com by 210.87.254.40 on 09/05/12
For personal use only.

METABOLITES OF PATHOGENIC FUNGI

V. ISOLATION AND TENTATIVE STRUCTURES OF VIOXANTHIN AND VIOPURPURIN, TWO COLORED METABOLITES OF TRICHOPHYTON VIOLACEUM[1,2]

F. BLANK, A. S. NG, AND G. JUST

Skin and Cancer Hospital, Temple University Health Sciences Center, Philadelphia, Pennsylvania, and Department of Chemistry, McGill University, Montreal, Quebec

Received August 3, 1966

ABSTRACT

Two new pigments, vioxanthin and viopurpurin, were isolated from *Trichophyton violaceum*, and tentative structures are proposed. Xanthomegnin was found to be the major component of the pigment mixture.

As part of our continuing program of investigating the constituents of dermatophytes, the pigments of *Trichophyton violaceum* Sabouraud, apud Bodin, 1902, have been studied.

Mycelium of *Trichophyton violaceum* was grown on a modified Sabouraud glucose medium, autoclaved, washed, freeze-dried, and milled. Extraction followed by chromatographic procedures yielded, in addition to large amounts of xanthomegnin (previously isolated from *T. megnini* in our laboratory (1)), two new pigments. A brownish-yellow pigment, vioxanthin, was obtained from the acetone extract, and the acetic acid extract yielded a dark-red pigment, viopurpurin. In addition, several other pigments were obtained and are being purified.

Vioxanthin

The molecular formula of vioxanthin is $(C_{15}H_{13}O_5)_2$. The molecular weight, which was determined by osmometry, and the nuclear magnetic resonance (n.m.r.) spectrum of vioxanthin, which indicated the presence of 13 protons, showed that the molecule consisted of two identical moieties linked by an odd number of bonds.

The n.m.r. spectrum of vioxanthin showed the presence of a $CH_3—\underset{\displaystyle O}{\underset{|}{CH}}—CH_2—Ph$ group (δ 1.50 p.p.m. (CH_3, doublet) and 2.96 p.p.m. and 4.70 p.p.m. (—CH_2— and —CH, multiplets)), two aromatic protons at 6.70 and 6.96 p.p.m., a methoxy group at 3.80 p.p.m., and two exchangeable protons at 9.70 and 13.84 p.p.m. The infrared spectrum showed a strong peak in the carbonyl region at 1 640 cm^{-1}, which shifted to 1 725 cm^{-1} upon acetylation. The carbonyl function is assigned to a hydrogen-bonded six-membered lactone[3] (2–4). Absorption at 3 415 cm^{-1} (CCl_4) caused by the phenol groups was not shifted upon dilution, indicating that all the hydroxy groups were hydrogen bonded.

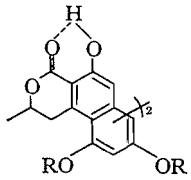
Vioxanthin formed a tetraacetate, ν 1 780 cm^{-1}, δ 2.00 and 2.46 p.p.m. The ultraviolet spectra of vioxanthin (λ_{max}^{EtOH} 268 mμ (ϵ 50 000) and 380 mμ (ϵ 14 000)) and its tetraacetate (λ_{max}^{EtOH} 262.5 mμ (ϵ 112 000) and 320 mμ (ϵ 27 000)) were uninformative, but compatible with a naphthalene derivative (6).

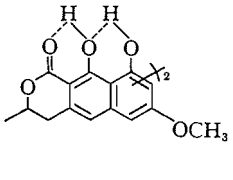
[1]*This work was supported by U.S. Public Health Service research grants 5 R01 AI 05378 and AI 04050, and a grant from the John A. Hartford Foundation, Inc., New York.*

[2]*For part IV in this series, see G. Bauslaugh, G. Just, and F. Blank, Nature, 202, 1218 (1964).*

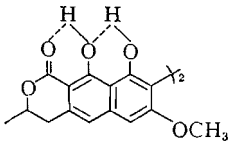
[3]*The low-field exchangeable proton at 13.84 p.p.m. is in good agreement with a phenolic proton hydrogen bonded to a carbonyl function.*

If it is assumed that vioxanthin results from dimerization of two moieties formed from seven acetate units and that the oxygenation pattern is not altered during its biosynthesis, the following partial structures can be proposed.





It is known that the δ value of hydrogens ortho, meta, and para to phenolic hydroxyl groups is shifted upon acetylation towards lower field by 0–0.2, 0, and 0.4–0.5 p.p.m., respectively (5). The two aromatic protons in vioxanthin were shifted downfield upon acetylation by 0.4 and 0.54 p.p.m., respectively. We therefore conclude that the protons must have been para to the phenolic groups. These considerations suggest the following structure for vioxanthin (I).



I

Viopurpurin

Viopurpurin is a very insoluble, dark-red pigment. Its insolubility precluded further purification; a n.m.r. spectrum could not be obtained for the same reason. Its infrared spectrum showed a peak at 1 725 cm^{-1} for a lactone and peaks at 1 675 and 1 635 cm^{-1} for a quinone function.

Upon acetylation, an orange triacetate was obtained. Elemental analysis and molecular weight determination by osmometry indicated the molecular formula $C_{35}H_{26}O_{14}$. The infrared spectrum of the triacetate showed the presence of phenolic acetates at 1 775 cm^{-1}, a lactone group at 1 725 cm^{-1}, and an α,β-unsaturated carbonyl or quinone function at 1 675 cm^{-1}. The n.m.r. spectrum indicated the presence of two lactone rings identical with those of vioxanthin, two acetate groups at 2.5 p.p.m. and one at 2.65 p.p.m., one methoxy group at 4.05 p.p.m., and two aromatic protons at 7.60 p.p.m. and 8.04 p.p.m.

Reductive acetylation with zinc in acetic anhydride gave dihydro-viopurpurin penta-acetate, which differed in its n.m.r. spectrum from the triacetate in that the two aromatic protons had almost merged (δ 7.63 p.p.m. (broad, 2H)). Its infrared spectrum showed strong peaks in the carbonyl region at 1 785 cm^{-1} and 1 730 cm^{-1} only.

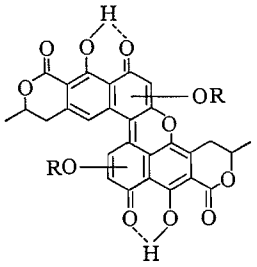
One can conclude, therefore, that viopurpurin must be composed of two similar moieties, each consisting of a six-membered lactone ring fused to an aromatic or quinoid system, but differing in that one half has one methoxy and one phenolic hydroxy group, whereas the other half has two phenolic hydroxy groups. Since reductive acetylation resulted in the formation of two more acetate groups, the quinoid system must have extended over two rings. This extended chromophore is also reflected by the intense absorption in the visible region.

Analysis of the molecular formula ($C_{35}H_{26}O_{14} - 3C_2H_2O$ (acetate) $- CH_2$ (methoxy) $= C_{28}H_{18}O_{11}$) shows that the "stripped skeleton" of viopurpurin contains two halves linked by a double bond and a single bond. Since 10 oxygen atoms are accounted for by two lactones, four hydroxy groups (OCH_3 + 3OAc of the viopurpurin triacetate), and the

Can. J. Chem. Downloaded from www.nrcresearchpress.com by 210.87.254.40 on 09/05/12
For personal use only.

extended quinone, the 11th oxygen must be an ether function, most likely linking the two ring systems.

At the present time, the scarcity of this pigment precludes further degradative work, but the available data suggest viopurpurin can be represented by the following structure (II).



II, R = H or CH_3

EXPERIMENTAL

Amberlite 120 ion-exchange resin was used for the ion-exchange column, and ion-exchange cellulose (No. 78 cm type 40, Carl Schleicher and Schuell Co.) for the washing columns. Infrared spectra were determined with a Perkin–Elmer model 337 grating spectrophotometer. All the spectra were taken in potassium bromide pellets. Nuclear magnetic resonance spectra were taken with a Varian A-60 n.m.r. spectrometer. Deuterated chloroform was used as the solvent. Ultraviolet spectra were measured with a Beckman recording spectrophotometer, model DK. Melting points were taken on a Kofler hot stage. Microanalyses were carried out by Beller Mikroanalytisches Laboratorium, Theaterstrasse 23, 34 Gottingen, Germany.

Trichophyton violaceum was grown in 500 ml Erlenmeyer flasks containing 250–300 ml of medium at room temperature for 5–6 weeks. The medium consisted of 4% crude glucose (cerelose), 2% neopeptone (Difco), 0.05% yeast extract (Difco), 0.005% inositol, 0.001% thiamine, and 2% agar. The cultures were autoclaved, and the harvested mycelium was washed free of adhering medium by boiling three times in water. After the mycelium was pressed, it was freeze-dried and milled in a ball mill.

The extraction was carried out by stirring dry powdered mycelium (first batch, 875 g; second batch, 286 g) at room temperature successively with hexane, diethyl ether, acetone, methanol, and glacial acetic acid. The yields are summarized in Table I.

TABLE I

Solvent	Time (days)	Yield (g)		Yield (% of dry mycelium)		Pigments isolated
		First batch	Second batch	First batch	Second batch	
Hexane	7	12.98	6.93	1.49	2.42	
Ether	7	13.41	4.5	1.53	1.57	
Acetone	2×7	15.9	5.4	1.82	1.89	Xanthomegnin, vioxanthin
Methanol	7	9.5	1.93	1.08	0.68	Xanthomegnin
Glacial acetic acid	2	45	3.7	5.14	1.29	Xanthomegnin, viopurpurin

Acetone Extract

The dried, brownish extract (5.4 g) was washed with hexane and diethyl ether to remove fatty materials. The residue was then dissolved in chloroform and the organic layer washed three times with each of the following: 3% aqueous HCl, distilled water, 5% aqueous Na_2CO_3 solution, distilled water, and 3% aqueous NaOH solution.

Evaporation of the washed chloroform extract gave 1.4 g of crude xanthomegnin, which, upon purification, was identified by comparison of its infrared spectrum with that of an authentic sample.

The 5% aqueous Na_2CO_3 solution wash and following water wash were acidified with concentrated HCl (pH 2) and extracted with diethyl ether. The ether solution was washed with water until it was neutral, and evaporated to dryness. The resulting solid (1.36 g) was washed with hexane to remove residual fatty materials. It was then extracted with carbon tetrachloride and the solution evaporated. The residual solid (1 g)

Can. J. Chem. Downloaded from www.nrcresearchpress.com by 210.87.254.40 on 09/05/12
For personal use only.

from the carbon tetrachloride solution was dissolved in a minimum amount of chloroform. Judicious addition of diethyl ether and hexane resulted in the formation of a crystalline brownish material. Recrystallization from the same solvent system gave pure vioxanthin, m.p. 190–195° (decomp.), λ_{max}^{EtOH} 268 mμ (ε 50 000) and 380 mμ (ε 14 000).

Anal. Calcd. for $C_{30}H_{26}O_{10}$: C, 65.93; H, 4.80; O, 29.28; mol. wt. 546.51. Found: C, 66.04; H, 4.83; O, 29.10; mol. wt. (osmometric) 554.

Vioxanthin Tetraacetate

A solution of vioxanthin (50 mg) in 2 ml of pyridine and 6 ml of acetic anhydride was warmed to 60 °C for 15 min and stirred at room temperature overnight. Excess acetic anhydride was hydrolyzed by pouring the solution onto ice chips, with stirring. Filtration gave 45 mg of vioxanthin tetraacetate, m.p. 210 °C (decomp.), λ 262.5 mμ (ε 112 000) and 320 mμ (ε 27 000). No suitable solvent was found for recrystallization. An analytical sample was dried at 68 °C in a high vacuum overnight.

Anal. Calcd. for $C_{38}H_{34}O_{14}$: C, 64.00; H, 4.70; O, 31.30; mol. wt. 714.27. Found: C, 64.26; H, 4.66; O, 30.98; mol. wt. (osmometric) 752.

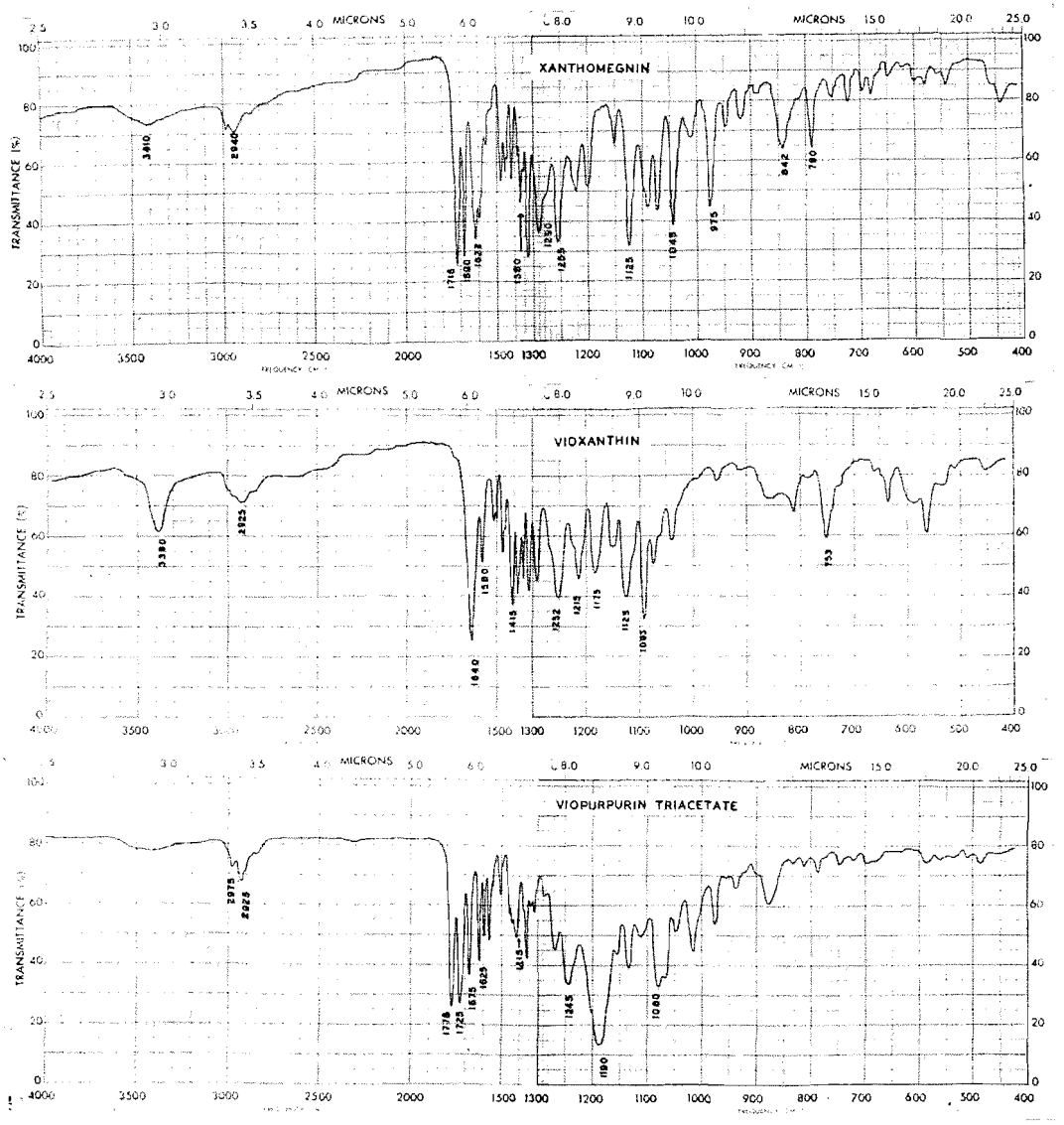


FIG. 1. Top, infrared spectrum of xanthomegnin; center, infrared spectrum of vioxanthin; bottom, infrared spectrum of viopurpurin triacetate.

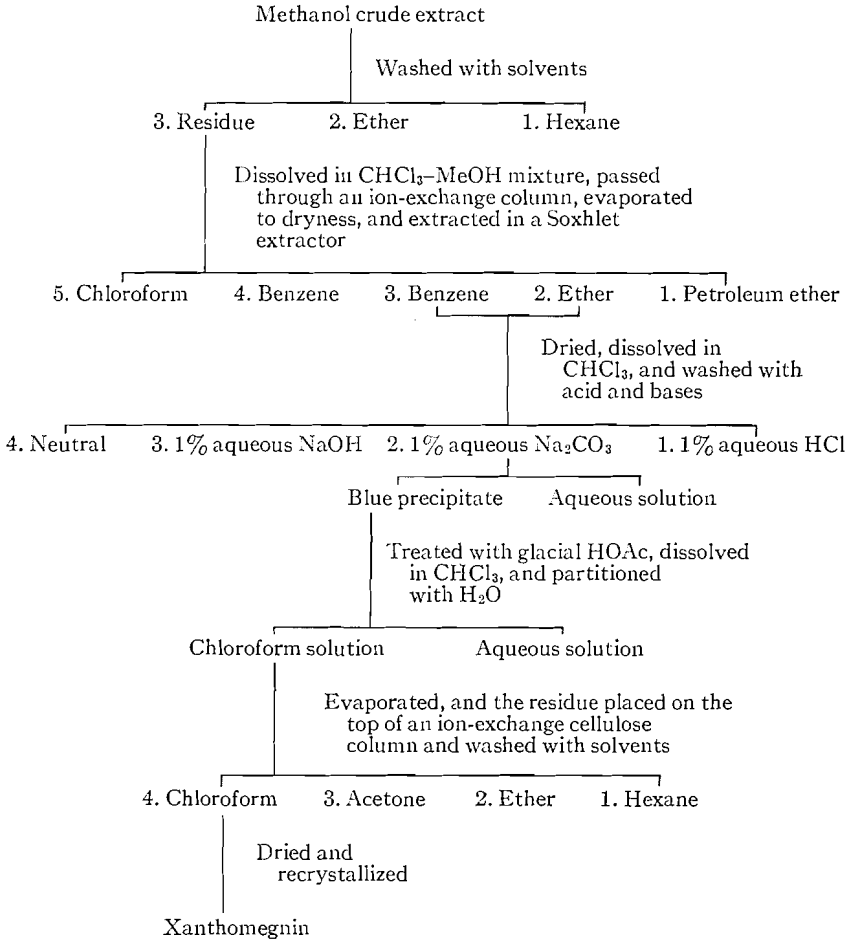
Can. J. Chem. Downloaded from www.nrcresearchpress.com by 210.87.254.40 on 09/05/12
For personal use only.

Methanol Extract

The crude methanol extract was washed successively with petroleum ether and diethyl ether to remove fatty materials. The solid residue (9.5 g) was dissolved in 1 l of chloroform, and 1 l of methanol was then added to the chloroform solution. The chloroform–methanol solution was passed through a 4 × 60 cm Amberlite 120 column. The organic solution was then partitioned with distilled water. From the organic layer, 6.0 g of solid was obtained. The residue was extracted successively in a Soxhlet extractor with petroleum ether, benzene, and chloroform. Each extraction was performed for a 2 day period. The benzene extraction was interrupted halfway, and the first fraction was combined with the ether extract.

The residual solid (2.89 g) from the ether extract and the first half of the benzene extract was dissolved in 1 500 ml of chloroform. The chloroform solution was then washed successively with 1% aqueous HCl, water–methanol (3:1 v/v), 1% aqueous Na_2CO_3 solution, 1% aqueous NaOH solution, and distilled water.

During the washing with the 1% aqueous Na_2CO_3 solution, a bluish insoluble solid precipitated. It was filtered off and, after being dried, weighed 1.1 g.



SCHEME 1. Isolation of xanthomegnin from the methanol extract.

Insoluble Bluish Precipitate from 1% Aqueous Na_2CO_3 Wash

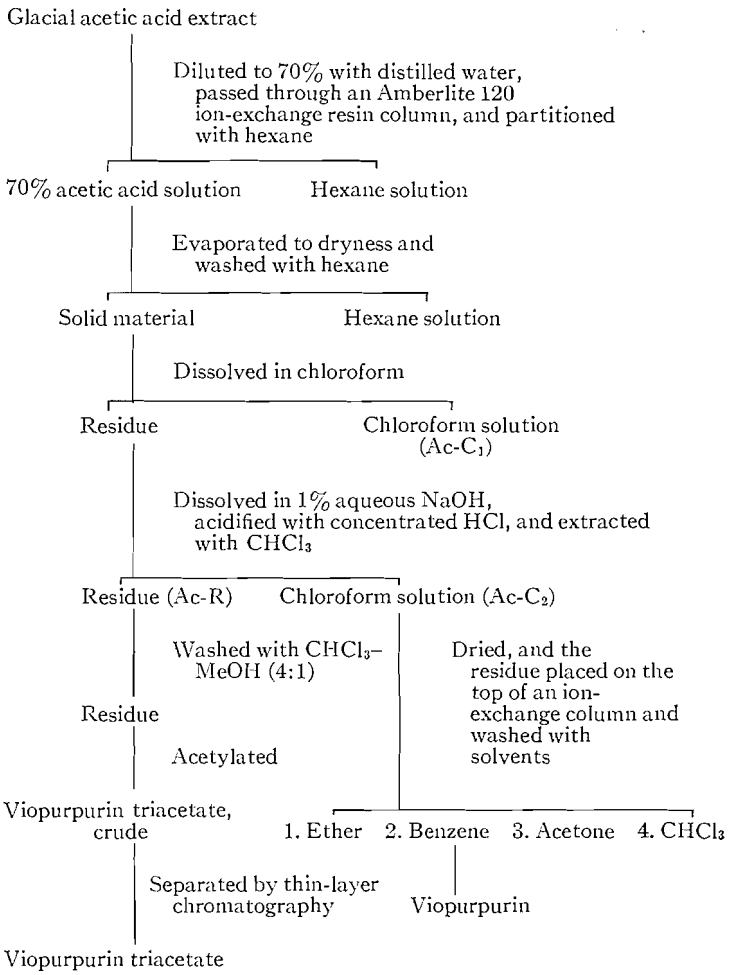
The bluish residue (1.1 g) was dissolved in 5 ml of glacial acetic acid, the acetic acid was evaporated, and chloroform (700 ml) was then added to the resulting yellowish residue. The chloroform solution was washed with water, and methanol was added to destroy the emulsion formed. Evaporation gave 0.82 g of a residue. It was placed on the top of an ion-exchange cellulose column and washed successively with hexane, ether, acetone, and chloroform. The chloroform wash gave 304 mg of a solid. Crystallization from methanol gave 200 mg of xanthomegnin.

Glacial Acetic Acid Extract

The crude glacial acetic acid solution (2 800 ml) was diluted with 1 200 ml of water, and passed in two batches through a 4 × 60 cm Amberlite 120 ion-exchange resin column. The deionized aqueous acetic acid

Can. J. Chem. Downloaded from www.nrcresearchpress.com by 210.87.254.40 on 09/05/12
For personal use only.

solution was partitioned with hexane to remove fatty materials. Evaporation of the acetic acid solution gave 45 g of a wet solid. This was reextracted with hexane to remove residual fatty materials, and then dissolved in chloroform (Ac-C_1).[4] The chloroform-insoluble residue was filtered off and dissolved in 1% aqueous NaOH. Careful acidification of the basic solution with concentrated HCl gave a dark-colored precipitate. The aqueous suspension was extracted with chloroform, and the insoluble residue (Ac-R,[4] 3.5 g) was filtered off. The chloroform solution was separated from the aqueous phase, giving, upon evaporation, 1 g of a residue (Ac-C_2).[4]



SCHEME 2.

Ac-R Fraction

The residue (3.5 g) was washed with chloroform–methanol (4:1) to remove soluble materials. A highly insoluble dark residue of impure viopurpurin (1 g) was obtained. It could not be purified further because of its insolubility, and was therefore acetylated by stirring overnight in 15 ml of acetic anhydride and 4 ml of pyridine. The excess anhydride was decomposed by pouring the solution onto ice chips, with stirring. The product was filtered off and washed with distilled water to give 500 mg of crude viopurpurin triacetate.

Ac-C_2 Fraction

Fraction Ac-C_2[4] (1 g) obtained above was put on a 3 × 30 cm ion-exchange cellulose column, and washed successively with ether, benzene, acetone, chloroform, and pyridine. The benzene fraction contained crude viopurpurin. A triacetate derivative (300 mg) was prepared by the method mentioned above.

[4]*Code numbers refer to Scheme 2.*

Can. J. Chem. Downloaded from www.nrcresearchpress.com by 210.87.254.40 on 09/05/12
For personal use only.

Purification of Viopurpurin Triacetate

A chloroform solution of crude viopurpurin triacetate was applied to silica gel plates which had been sprayed with 1% hydrochloric acid before brief activation. Benzene–acetone (7:3) was used for developing. A yellow-orange band was collected and the pigment dissolved out with chloroform. No suitable solvent was found for crystallization of viopurpurin triacetate, m.p. 280–285 °C; λ_{max}^{EtOH} 217 mμ (ε 5 600), 270 mμ (ε 9 300), and 277 mμ (ε 9 300).

Anal. Calcd. for $C_{35}H_{26}O_{14}$: C, 62.69; H, 3. 91; O, 33.40; mol. wt. 670.56. Found: C, 62.80; H, 3.78; O, 33.55; mol. wt. (osmometric) 698.

Reductive Acetylation of Viopurpurin Triacetate

To a solution of 70 mg of viopurpurin triacetate in 5 drops of pyridine and 15 ml of acetic anhydride, 200 mg of zinc dust was added in portions, with stirring. The mixture was allowed to stand for 30 h, filtered, and poured onto ice chips, with stirring, to hydrolyze the excess acid anhydride. After the ice had melted (1 h), the product was filtered off and washed with distilled water. After being dried, 61 mg of dihydroviopurpurin pentaacetate was obtained. It could not be recrystallized, m.p. 200–203 °C (decomp.); λ_{max}^{EtOH} 286 mμ (ε 30 200), 296 mμ (ε 39 400), and 365 mμ (ε 5 020).

Anal. Calcd. for $C_{39}H_{32}O_{16}$: C, 61.90; H, 4.26; O, 33.83; mol. wt. 756.65. Found: C, 61.00; H, 4.38; O, 33.70; mol. wt. (osmometric) 776.

ACKNOWLEDGMENT

We thank Mr. K. Valentin for taking the n.m.r. spectra.

REFERENCES

1. F. BLANK, W. C. DAY, and G. JUST. J. Invest. Dermatol. **40**, 133 (1963). G. JUST, W. C. DAY, and F. BLANK. Can. J. Chem. **41**, 74 (1963).
2. A. L. PORTE, H. S. GUTOWSKY, and I. M. HUNSBERGER. J. Am. Chem. Soc. **82**, 5057 (1960).
3. I. M. HUNSBERGER. J. Am. Chem. Soc. **72**, 5626 (1950).
4. J. R. MERRILL. J. Phys. Chem. **65**, 2023 (1961).
5. A. GAUDEMER and J. POLONSKY. Bull. Soc. Chim. France, 1918 (1963).
6. E. A. BRAUDE. J. Chem. Soc. 379 (1950).

Can. J. Chem. Downloaded from www.nrcresearchpress.com by 210.87.254.40 on 09/05/12
For personal use only.

Can. J. Chem. Downloaded from www.nrcresearchpress.com by 210.87.254.5 on 09/05/12
For personal use only.

RADICALS DERIVED FROM HETEROAROMATIC SYSTEMS

I. THIENYL RADICALS

DONALD MACKAY
Department of Chemistry, University of Waterloo, Waterloo, Ontario

Received July 27, 1966

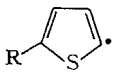
ABSTRACT

The decomposition of 3-thenoyl and 5-nitro-2-thenoyl peroxides in aromatic solvents leads to 3-thenoyloxy and 5-nitro-2-thenoyloxy radicals, which decarboxylate to some extent to 3-thienyl (I) and 5-nitro-2-thienyl (II*a*) radicals, respectively. Attack of these radicals on the solvent leads to the corresponding aryl thenoates and arylthiophenes. The Gomberg reaction of 5-carbomethoxy-2-thienylamine or the silver oxide oxidation of the related thienylhydrazine leads to 5-carbomethoxy-2-thienyl radicals (II*b*). A mechanism for the formation of biphenyl, formed in small quantities in the decomposition of 5-nitro-2-thenoyl peroxide in benzene, is proposed.

Little attention has been paid to homolytic reactions giving rise to free radicals with the unpaired electron on a heteroaromatic ring. The thermal decomposition of a few heterocyclic dicarbonyl peroxides in a variety of solvents has been studied as a possible route to such radicals (cf. the reactions of benzoyl peroxide). Thus, nicotinoyl peroxide leads to 3-pyridyl radicals in a good yield (1). 2-Furoyl peroxide, however, gave only intractable products in benzene (2). 2-Coumariloyl (3) and 5-methyl-1-phenyl-1,2,3-triazole-4-carbonyl (4) peroxides in aromatic solvents gave products derived from the related acyloxy radicals, but there was no conclusive evidence for decarboxylation of the latter. Likewise, 2-thenoyl peroxide reacts with solvents mainly through 2-thenoyloxy radicals, although there was also some indication of the involvement of 2-thienyl radicals (5). Other methods for generating heteroaryl radicals have apparently not been investigated. Evidence is now given for the production of the 3-thienyl (I), the 5-nitro-2-thienyl (II*a*), and the 5-carbomethoxy-2-thienyl (II*b*) radicals.



I



II*a*, R = NO_2
II*b*, R = CO_2CH_3

Schuetz and Teller (6) prepared a number of thenoyl peroxides, including 3-thenoyl and 5-nitro-2-thenoyl peroxides, and examined the kinetics of their decomposition in carbon tetrachloride; however, product analyses were not undertaken. The decomposition products of both these peroxides in representative aromatic solvents have now been investigated (Table I). 3-Thenoyl peroxide was decomposed in benzene, chlorobenzene, toluene, and thiophene, and its behavior was strikingly similar to that found for 2-thenoyl peroxide (5). Thus, carbon dioxide evolution was rather low (33 mole %[1] in benzene), and much amorphous high molecular weight material was formed in benzene and chlorobenzene, whereas in toluene and thiophene the reaction was cleaner and the yields of carboxylic acid were correspondingly higher. Aryl 3-thenoates were produced in all cases, in a very low yield (<2%) except in thiophene (13%), indicating nuclear attack of 3-thenoyloxy

[1] *Yields are based for convenience on the reaction*

$$(RCO_2)_2 \rightarrow RCO_2^{\cdot} + R^{\cdot} + CO_2.$$

radicals on the solvent. From toluene, only the *o*-tolyl ester was isolated, but from chlorobenzene all three chlorophenyl 3-thenoates were shown to be formed, the *m*- and *p*-isomers predominating; from thiophene, the 2-thienyl ester seemed to be formed exclusively. In the chlorobenzene reaction a small amount of *phenyl* 3-thenoate was also produced, showing that the 3-thenoyloxy radical, like the 2-thenoyloxy radical (5), can displace halogen from halogenobenzene.

In contrast to the rather scanty evidence for the formation of 2-thienyl radicals by decarboxylation of 2-thenoyloxy radicals, clearcut evidence for the analogous formation of 3-thienyl radicals was provided by the production, albeit in a low yield, of 3-phenylthiophene in benzene, all three chlorophenylthiophenes in chlorobenzene, and 2,3′- and 3,3′-bithienyl in thiophene; in chlorobenzene, moreover, the *o*-isomer predominated, as is normally found (7) in a free-radical arylation process.

In the decomposition products from toluene the presence of traces of tolylthiophenes was inferred by gas–liquid chromatography (g.l.c.), but was not conclusively proven. The main product was bibenzyl (22%), formed from benzyl radicals derived by hydrogen abstraction from toluene, mainly by 3-thenoyloxy radicals; this accounted for the rather high yield of 3-thenoic acid. In addition, the carboxylic acid fraction contained a small amount of another acid, identified as 2- or 5-benzyl-3-thenoic acid (by decarboxylation to 2-benzylthiophene), which could arise by attack of benzyl radicals either on 3-thenoic acid or on undecomposed peroxide; the affinity of the thiophene nucleus for benzyl radicals has already been noted (5). Another minor reaction of the benzyl radicals in this decomposition was their coupling with 3-thenoyloxy radicals to give benzyl 3-thenoate.

The formation of thiophene in benzene and, more efficiently, in toluene represents further evidence for the involvement of 3-thienyl radicals in the peroxide decompositions (a control experiment showed that *no* decarboxylation of 3-thenoic acid to thiophene occurred under the conditions of these experiments). The source of hydrogen is undoubtedly the side chain in the toluene reaction; in benzene it is probably complex material obtained by radical (e.g. 3-thenoyloxy) *addition* to the substrate, a process which would lead to the accumulation of di- and tetra-hydrothiophene containing nuclei, providing a source of abstractable "aliphatic" hydrogen; such hydrogen would also account for the high yields of 3-thenoic acid, relative to those of diaryls and esters, in both the benzene and chlorobenzene reactions. Complex sulfur-containing material of this kind was found in earlier work (5) to cause reduction of 2-thenoyl peroxide to the anhydride, but no 3-thenoic anhydride could be detected in any of the present experiments.

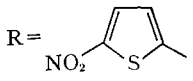
The 2,3′- and 3,3′-bithienyls (7% and <1%, respectively) found in the decomposition in thiophene undoubtedly arise through attack of 3-thienyl radicals on the solvent, the relative degree of attack at the 3-position being much less than at the 2-position, as has been noted by other workers (8, 9). The isolation of 2,2′-bithienyl (9%), however, was rather unexpected as it implies the involvement of 2-thienyl radicals. This product is in accordance with a recent report by Griffin and Martin (9), who found that 2,2′- and lesser amounts of 2,3′-bithienyl were formed in the benzoyl peroxide phenylation of thiophene, and attributed their formation to a process of oxidation by the benzoyloxy radical of thiophene to the radical cation $C_4H_4S^{+\cdot}$, with ready conversion of this into the 2-thienyl radical $C_4H_3S^{\cdot}$ by benzoate anion. A similar process with 3-thenoate anion as the proton-removing species could occur here, leading to the 2,2′-bithienyl and to a *small part* of the 2,3′-bithienyl found; the yield of the latter (relative to that of the 2-isomer) is too great to be accounted for by this process alone. An alternative mechanism for the formation of the bithienyls from thiophene is proposed below.

Can. J. Chem. Downloaded from www.nrcresearchpress.com by 210.87.254.5 on 09/05/12
For personal use only.

Can. J. Chem. Downloaded from www.nrcresearchpress.com by 210.87.254.5 on 09/05/12
For personal use only.

TABLE I

Decomposition products of heterocyclic diacyl peroxides in aromatic solvents (mole %)

Peroxide ($(RCO_2^-)_2$)	Solvent (ArH)	CO_2	Acid (RCO_2H)	RH	Diaryl (RAr) (isomer distribution)	Ester (RCO_2Ar) (isomer distribution)	Other
R = 	PhH	33	91	1	2.3	1.8	
	PhCl		63		7.5 (63% 2-, 37% 3- + 4-)	1.6 (22% 2-, 78% 3- + 4-)	1.7 phenyl ester
	$PhCH_3$		150*	6	Trace	2 (2- only)	22 bibenzyl
	C_4H_4S		134		7 (90% 2-, 10% 3-)	13 (2- only)	9 2,2′-bithienyl
R = 	PhH	19	104	0	5	11	9 biphenyl†
	$PhCH_3$	19	122	Trace			14 benzyl ester

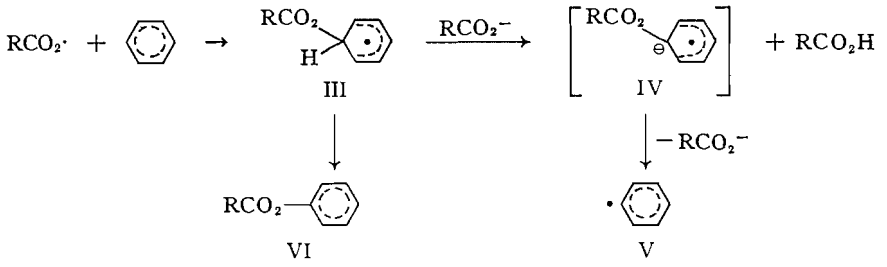
*Contains a small amount of 2- or 5-benzyl-3-thenoic acid.
†Scheme 1 requires the stoichiometry $2RCO_2^{\cdot} + 2PhH \rightarrow 2RCO_2H + Ph_2$, on which this yield is based.

Can. J. Chem. Downloaded from www.nrcresearchpress.com by 210.87.254.5 on 09/05/12
For personal use only.

The decomposition reactions of 5-nitro-2-thenoyl peroxide in benzene and in toluene (Table I) followed the general pattern described for 3-thenoyl peroxide. Carbon dioxide evolution was scanty (19%), and yields of the carboxylic acid, especially in toluene, were high, indicating that 5-nitro-2-thenoyloxy was the main radical species involved. Benzene was attacked to give the phenyl ester in a moderate yield (11%). In toluene, however, nuclear attack was not observed, the ester fraction consisting entirely of benzyl 5-nitro-2-thenoate (14%), and the yield of bibenzyl was correspondingly low (3%), suggesting that the 5-nitro-2-thenoyloxy radical has a very high affinity for the benzyl radical.

Like the 3-thenoyloxy radicals, the 5-nitro-2-thenoyloxy radicals decarboxylate to some extent; evidence for the resulting 5-nitro-2-thienyl radicals (II*a*) rests in the formation of 2-phenyl-5-nitrothiophene (5%) in benzene, and of 2-nitrothiophene (a trace) in toluene. The phenylnitrothiophene was not isolated, but its presence was confirmed by comparative g.l.c. with the mixture of the three isomeric phenyl-2-nitrothiophenes obtained in the decomposition of benzoyl peroxide in 2-nitrothiophene, the least volatile of these isomers being identical under all conditions with the product from the nitrothenoyl peroxide decomposition in benzene.

The isolation of biphenyl from the nitrothenoyl peroxide decomposition in benzene represents the first case in which a diaryl, Ar_2, of which both Ar groups are derived from a monocyclic[2] benzenoid solvent, ArH, has been detected in the products from the reaction of an aroyl peroxide. This implies the abstraction of phenyl hydrogen to give a phenyl radical, which then forms biphenyl with the solvent in the usual way. The direct abstraction of a hydrogen atom is a process requiring much energy, and seems unlikely. An alternative in which this is accomplished indirectly can be envisaged. If the product of the initial attack of the acyloxy radical on benzene (Scheme 1) is the σ-complex (III, R = 5-nitro-2-thienyl), as seems reasonable by analogy with the attack of the aryl radical in arylation (12), then deprotonation by carboxylate anion could occur to give the radical anion (IV), with concerted or subsequent loss of carboxylate anion from IV to give the phenyl radical (V). The loss of a stabilized leaving group (the anion) would constitute a driving force for III → V, which would be absent for the analogous σ-complex in an arylation reaction. The route III → V would compete with the "normal" process of the oxidation of III to product ester VI, which occurs either directly by abstraction of a hydrogen atom or, as now seems more likely (11, 12, 13), by disproportionation. In the decomposition of aroyl peroxides in benzene, esters (VI) are only trace products; this means that the amount of III formed is correspondingly very small, and hence biphenyl is unlikely to be detectable. This mecha-



SCHEME 1.

[2]*All three binaphthyls were isolated by Hey et al. from the decomposition products of benzoyl peroxide in naphthalene, their formation being attributed to hydrogen abstraction by benzoyloxy radicals to give the naphthyl radicals, which then attacked naphthalene (10); an alternative mechanism for this has been suggested by de Tar (11).*

nism could explain analogously the bithienyls obtained from thiophene in this work with 3-thenoyl peroxide[3] and in Griffin and Martin's (9) experiments with benzoyl peroxide, already described, as well as the binaphthyls found by Hey *et al.* (10) in the benzoyl peroxide decomposition in naphthalene. The dihydro derivative corresponding to III would be expected to form even more readily from thiophene and naphthalene than from benzene, and esters are in fact major products in all three decompositions (5, 10).

Most of the recognized routes to aryl radicals start ultimately either from the carboxylic acid by way of the aroyloxy radical which then loses CO_2, or from the amine by converting it into some arylazo derivative capable of losing nitrogen. Of the latter type, the alkaline decomposition of diazonium solutions (the Gomberg reaction) and the thermal decomposition of *N*-nitrosoacylarylamines have been the most widely used. An excellent alternative to these, giving good yields of diaryls in aromatic solvents, uses the oxidation of arylhydrazines with heavy metal oxides, particularly silver oxide, the azo intermediate involved being the diimide derivative ArN=NH (14).

Thienylamines are quite unstable unless the ring is also substituted with electron-withdrawing groups (15, p. 229); contrary to an earlier report (16), the diazotization of 2-thienylamine (as its stannichloride complex) does *not* proceed normally (17). This precludes the use of thienyldiazonium solutions as a route to unsubstituted thienyl radicals, either by the Gomberg reaction or by reduction to the thienylhydrazines. The only thienylhydrazines so far described have been prepared by displacement with hydrazine of suitably activated halogen, e.g. 3-nitro- and 3,5-dinitro-2-thienylhydrazines (18).

Reduction of methyl 5-nitro-2-thenoate gave the amine, which, as expected, was stable and could be diazotized. The diazonium solution, on treatment with benzene and alkali, gave methyl 5-phenyl-2-thenoate (8%) (the Gomberg product diagnostic of the radical 5-carbomethoxy-2-thienyl (II*b*)), and, on reduction with tin(II) chloride in concentrated hydrochloric acid, gave methyl 5-hydrazino-2-thenoate, which decomposed in air, but was stable as its hydrochloride. Oxidation of the hydrochloride, as a suspension in benzene, with silver oxide also gave the methyl phenylthenoate, in an excellent yield (85%). That the homolytic nature of this type of oxidation is unchanged when the hydrochloride is used in place of the free hydrazine (a modification which involves the immediate *in situ* liberation of the latter) was shown by oxidizing phenylhydrazine hydrochloride in nitrobenzene with silver oxide; the mixture of nitrobiphenyls was found to contain 54% of the *o*-isomer, in agreement with other phenylation procedures (7).

With 5-nitro-2-thenoic acid as a starting point, efforts were directed to making 5-nitro-2-thienylamine, and from it 5-nitro-2-thienylhydrazine, both of which would be expected to be stable and to provide potential sources of 5-nitro-2-thienyl radicals. The Schmidt reaction with hydrazoic acid, however, failed to give the amine, the carboxylic acid being recovered. 5-Nitro-2-thenoyl azide was readily prepared from the acid chloride and sodium azide, and in solution in inert solvents at temperatures above 70° it lost nitrogen. The Curtius rearrangement to 5-nitro-2-thienyl isocyanate had in fact evidently occurred, for the resulting solution gave the expected urethane and urea derivatives with methanol and aniline, respectively; however, efforts to isolate the isocyanate failed, only colored high molecular weight material being obtained when the solvent was evaporated. Similarly,

[3]*After the manuscript of this paper had been prepared, the decomposition products from 3-thenoyl peroxide in benzene were reexamined by g.l.c.; a small amount of biphenyl is in fact formed, in line with the result found for the nitrothenoyl peroxide in benzene. Furthermore, if the thenoyl peroxide decomposition is carried out in the presence of a large excess of added 3-thenoic acid, there is a substantial increase in the yield of biphenyl, relative to that of phenyl 3-thenoate, as would be predicted by Scheme 1.*

Can. J. Chem. Downloaded from www.nrcresearchpress.com by 210.87.254.5 on 09/05/12
For personal use only.

direct hydrolysis of the azide with aqueous hydrochloric or sulfuric acids led to intractable products and not the amine.

Most of the thiophene derivatives involved in this work have not been described previously. Detailed infrared studies on some of them in the region of 1 000 to 400 cm^{-1} have been reported elsewhere (19). The aryl esters of 3-thenoic and 5-nitro-2-thenoic acids listed in Table II, all of which are new, had carbonyl stretching frequencies (singlet or doublet) between 1 743 and 1 752 cm^{-1}, rather higher than the values typical for the aryl esters of aromatic carboxylic acids (20).

EXPERIMENTAL

General

Solvents were purified by conventional methods and fractionated. Melting points were taken on a Kofler block and are corrected. Gas–liquid chromatography was carried out on a Beckman GC-2A or an F & M 810 chromatograph. For high-resolution infrared spectra, either a Beckman IR-9 or a Perkin–Elmer 237 spectrometer was used.

3-Phenylthiophene was prepared by ring closure of sodium phenylsuccinate with phosphorus pentasulfide (21), and had m.p. 91° (lit. (21) m.p. 91–92°) after two crystallizations from petroleum ether;[4] *3-o-chlorophenylthiophene* was similarly prepared from the salt of *o*-chlorophenylsuccinic acid (22) of m.p. 171–173° (lit. (22) m.p. 173–174°) and had b.p. 103° at 1.0 mm, n_D^{20} 1.6394.

Anal. Calcd. for $C_{10}H_7ClS$: C, 61.7; H, 3.6; Cl, 18.2; S, 16.5. Found: C, 61.7; H, 3.7; Cl, 18.2; S, 16.7.

2,3′-Bithienyl was made as described by Teste and Lozac'h (23) and had m.p. 63–63.5° (lit. (23) m.p. 65°, (24) 61.5–63°) after crystallization from petroleum ether and then from aqueous ethanol. 3,3′-Bithienyl was kindly supplied by Professor S. Gronowitz, University of Lund, Sweden.

3-Thenoyl Chloride

Treatment of 3-thenoic acid (25), m.p. 138–139.5°, with thionyl chloride gave the acid chloride in an almost quantitative yield; purification by distillation and crystallization from petroleum ether gave large prisms, m.p. 52–52.5° (lit. (26) m.p. 51–52°).

Details of the method of preparation and physical constants of esters derived from the acid chloride are listed in Table II.

3-Thenoyl Peroxide

A mixture of the acid chloride (6.0 g), dissolved in ether (150 ml), and aqueous hydrogen peroxide (100 volumes, 5 ml) was cooled with crushed ice (50 g), and 1 *N* sodium hydroxide (45 ml, 1.1 equiv.) was added dropwise, with vigorous stirring and external cooling, over 15 min. After a further 30 min stirring, more ether (50 ml) was added, and the ethereal solution of the peroxide was separated, washed well with water, dried ($MgSO_4$),[5] and evaporated under reduced pressure. The crystalline residue (4.1 g) was dissolved in chloroform (20 ml) and precipitated by the addition, with stirring, of petroleum ether (40 ml) as colorless prisms (3.2 g, 62%), m.p. 121–122° (with decomposition) (detonation if determined in a capillary tube) (lit. (6) m.p. 120°); ν (CCl_4) 1 792 and 1 772 cm^{-1} (carbonyl doublet).

Anal. Calcd. for $C_{10}H_6O_4S_2$: equiv. wt. (iodometric) 127. Found: equiv. wt. 127.

3-Thenoic Anhydride

Treatment of 3-thenoic acid with a large excess of refluxing acetic anhydride gave 3-thenoic anhydride; it formed prisms, m.p. 55.5–56.5° (lit. (27) m.p. 54.5–56°), when recrystallized from petroleum ether.

5-Nitro-2-thenoic Acid

2-Diacetoxymethyl-5-nitrothiophene was prepared as described by Tirouflet and Fournari (28) from 2-thenaldehyde (15, p. 509), and was recrystallized to a constant melting point of 73.5–74° (lit. (28) m.p. 73°) from ethanol or ether – petroleum ether as yellow prisms.

Anal. Calcd. for $C_9H_9O_6NS$: C, 41.7; H, 3.6. Found: C, 42.15; H, 3.7.

Hydrolysis with 4 *N* sulfuric acid gave 5-nitro-2-thenaldehyde, purified by steam distillation, as faintly yellow needles, m.p. 74–75.5° directly (lit. (28) m.p. 74°), unchanged on recrystallization from aqueous ethanol; ν (CCl_4) 2 840, 2 805 (aldehyde CH), and 1 695 cm^{-1} (carbonyl).

The diacetate (20 g) was vigorously stirred with 4 *N* sulfuric acid (200 ml) at 100°, and aqueous hydrogen peroxide (30 volumes, 100 ml) was run in over 30 min; a clear deep-yellow solution was obtained which was refluxed for a further 30 min with charcoal. The filtered solution, cooled to 0°, gave 5-nitro-2-thenoic acid (9.4 g, 70%, average over many runs) as light-yellow needles, m.p. 160–161°, raised to 160.5–161.5° (lit. (29) m.p. 157–158°) by further recrystallization from water and then from toluene. The use of hydrochloric instead of sulfuric acid gave a much less pure product.

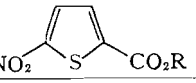
[4] *Unless otherwise stated, b.p. 35–60°.*

[5] *Used as the drying agent throughout.*

Can. J. Chem. Downloaded from www.nrcresearchpress.com by 210.87.254.5 on 09/05/12
For personal use only.

TABLE II

Esters of thiophene carboxylic acids

R in 	Melting point (°C)	Method of preparation*	Crystallization solvent†	C=O stretching (cm^{-1})‡	Formula	% analysis									
						Calculated					Found				
						C	H	N	S	Cl	C	H	N	S	Cl
C_6H_5	57	A	PE	1 747	$C_{11}H_8O_2S$	64.7	3.95	—	15.7	—	64.7	4.3	—	15.4	—
2-Thienyl	47–47.5	B	PE	1 746	$C_9H_6O_2S_2$	51.4	2.9	—	30.5	—	51.6	3.0	—	30.7	—
m-C_6H_4Cl	70–71	A	PE	1 752	$C_{11}H_7O_2ClS$	55.35	3.0	—	—	14.85	55.2	3.0	—	—	14.7
p-C_6H_4Cl	77.5–78	B	PE	1 751	$C_{11}H_7O_2ClS$	55.35	3.0	—	—	14.85	55.6	3.1	—	—	14.8
o-$C_6H_4CH_3$	52.5–53	A	PE	1 743	$C_{12}H_{10}O_2S$	66.05	4.6	—	14.7	—	66.15	4.8			14.6
m-$C_6H_4CH_3$	60–61.5	A	PE	1 748	$C_{12}H_{10}O_2S$	66.05	4.6	—	14.7	—	65.9	4.5	—	—	14.8
p-$C_6H_4CH_3$	90–91	A	PE	1 748	$C_{12}H_{10}O_2S$	66.05	4.6	—	14.7	—	65.6	4.6	—	—	14.8
$C_6H_5CH_2$	b.p. 140–142° at 1 mm	C	PE	1 728	$C_{12}H_{10}O_2S$	66.05	4.6	—	—	—	65.9	4.1	—	—	—
R in 															
C_6H_5	93–94	B	E–PE	1 752, 1742	$C_{11}H_7O_4NS$	53.0	2.8	—	—	—	52.9	2.85	—	—	—
m-C_6H_4Cl	92–93	B	PE	1 750	$C_{11}H_6O_4NClS$	46.6	2.1	—	—	12.5	46.7	2.25	—	—	12.4
p-C_6H_4Cl	99.5–100.5	B	PE	1 752	$C_{11}H_6O_4NClS$	46.6	2.1	—	—	12.5	46.5	2.21	—	—	12.7
o-$C_6H_4CH_3$	57–58	B	PE	1 750, 1 742	$C_{12}H_9O_4NS$	54.8	3.45	5.3	—	—	54.3	3.4	5.4	—	—
m-$C_6H_4CH_3$	62.5–63.5	B	EtOH	1 750, 1 742	$C_{12}H_9O_4NS$	54.8	3.45	5.3	—	—	54.8	3.7	5.5	—	—
p-$C_6H_4CH_3$	93–94	B	EtOH	1 752, 1 745	$C_{12}H_9O_4NS$	54.8	3.45	5.3	—	—	54.7	3.55	5.44	—	—
$C_6H_5CH_2$	90–91	C	EtOH	1 730	$C_{12}H_9O_4NS$	54.8	3.45	5.3	—	—	54.8	3.7	5.15	—	—

*From the acid chloride and the phenol in A, cold aqueous sodium hydroxide; B, refluxing pyridine. C, refluxing the acid chloride in excess of benzyl alcohol.
†PE, petroleum ether; E, diethyl ether; EtOH, aqueous ethanol.
‡CCl_4 or CS_2 used as solvents.

Can. J. Chem. Downloaded from www.nrcresearchpress.com by 210.87.254.5 on 09/05/12
For personal use only.

5-Nitro-2-thenoyl Chloride

Refluxing the acid with an excess of thionyl chloride for 3 h gave the acid chloride (90%), which was distilled, b.p. 90–91° at 0.4 mm, and crystallized, m.p. 51–52° directly (lit. (29*b*) m.p. 52–53°), unchanged on recrystallization from ether – petroleum ether.

The esters prepared from the acid chloride are described in Table II.

5-Nitro-2-thenoyl Peroxide

To a solution of sodium carbonate (2.2 g, 0.02 mole) and aqueous hydrogen peroxide (100 volumes, 4 ml) in water (30 ml) was added crushed ice (30 g), followed by a solution of the acid chloride (3.8 g, 0.02 mole) in ether (10 ml); the whole was shaken vigorously for 20 min. Petroleum ether (10 ml) was added and the product was collected, washed with water, dried, and precipitated from solution in chloroform (15 ml) by the addition, with stirring, of petroleum ether (15 ml) as faintly lemon-yellow prisms (2.8 g, 80%), m.p. 121–121.5° (with decomposition) (violent detonation if determined in a capillary tube) (lit. (6) m.p. 120–122°).

Anal. Calcd. for $C_{10}H_4O_8N_2S_2$: equiv. wt. (iodometric) 172. Found: equiv. wt. 170.5.

5-Nitro-2-thenoic Anhydride

The acid chloride and an equivalent weight of the sodium salt of the acid were refluxed together in toluene for 1 h. The toluene-soluble material was crystallized 3 times from benzene, giving the *anhydride* as a buff crystalline powder, m.p. 134–135.5°; ν ($CHCl_3$) 1 800 and 1 720 cm^{-1} (carbonyl doublet).

Anal. Calcd. for $C_{10}H_4O_7N_2S_2$: C, 36.6; H, 1.2; N, 8.5. Found: C, 36.7; H, 1.25; N, 8.5.

5-Nitro-2-thenoyl Azide

A solution of the acid chloride (1.92 g) in acetone (10 ml) was run into a stirred solution of sodium azide (1.0 g, 1.5 equiv.) in water (5 ml). An oil separated and, after the mixture was stirred for 15 min, ice was added and the *azide* crystallized (1.83 g, 93%), m.p. 61–63°. It formed yellow prisms, m.p. 62–63°, on recrystallization from ether – petroleum ether; ν (CCl_4) 2 160 (azide) and 1 701 cm^{-1} (carbonyl).

Anal. Calcd. for $C_5H_2O_3N_4S$: C, 30.3; H, 1.0; N, 28.3. Found: C, 30.4; H, 1.2; N, 27.9.

The azide rapidly gave off 1 equivalent of nitrogen in refluxing benzene or toluene; the residue, on evaporation of the solvent, could not be crystallized, and developed an intense orange-yellow color in air. When a solution of the azide in toluene was refluxed briefly and then treated with dry methanol, the resulting solution gave *methyl 5-nitro-2-thienylcarbamate* as a deep-yellow solid, which, after crystallization from aqueous methanol and then benzene–chloroform, had m.p. 184–188° (with decomposition); ν ($CHCl_3$) 3 415 (NH) and 1 740 cm^{-1} (carbonyl).

Anal. Calcd. for $C_6H_6O_4N_2S$: C, 35.65; H, 3.0; N, 13.9. Found: C, 35.8; H, 3.1; N, 14.1.

When aniline was used in place of methanol, *N-phenyl-N'-(5-nitro-2-thienyl)-urea* was obtained, which gave small orange prisms when recrystallized from chloroform–methanol; this compound had no melting point, decomposing slowly at >230°; ν (Nujol) 3 225, 3 300 (NH), and 1 714 cm^{-1} (carbonyl).

Anal. Calcd. for $C_{11}H_9O_3N_3S$: C, 50.2; H, 3.45; N, 16.0; mol. wt. 263. Found: C, 50.4; H, 3.4; N, 15.3; mol. wt. 269.

Methyl 5-Amino-2-thenoate

A methanolic solution of 5-nitro-2-thenoic acid containing concentrated sulfuric acid was refluxed for 6 h and poured into water to give the methyl ester (directly pure), m.p. 74.5–75° (lit. (29*a*) m.p. 76°). A solution of the ester (5 g) in methanol (50 ml) was saturated with hydrogen chloride, and the gas stream was maintained while zinc (12 g, in coarse lumps) was added in portions over 30 min, with external cooling. The solution was allowed to stand for a further 30 min, and was then concentrated and treated with 2 *N* hydrochloric acid (100 ml). The slightly cloudy solution was clarified by shaking it with methylene chloride, from which unreacted ester (0.9 g) was recovered, and crushed ice and an excess of concentrated ammonia were added to the aqueous layer. The base was extracted with benzene and precipitated from the dried solution as the granular *hydrochloride* (2.6 g, 60%), m.p. 181–184° (with decomposition), unaltered by recrystallization from methanol, from which it formed colorless plates.

Anal. Calcd. for $C_6H_5O_2ClNS$: Cl, 18.3; N, 7.2. Found: Cl, 18.5; N, 7.1.

The hydrochloride, suspended in ether, was shaken with an excess of 3 *N* ammonia, and the ether layer was separated, washed well with water, dried, and evaporated, giving *methyl 5-amino-2-thenoate* (90%, based on hydrochloride), which crystallized as faintly buff needles, m.p. 85.5–86°, from ether – petroleum ether; ν (CCl_4) 3 480, 3 393 (NH), and 1 710 cm^{-1} (carbonyl).

Anal. Calcd. for $C_6H_7O_2NS$: C, 45.9; H, 4.5; N, 8.9. Found: C, 45.7; H, 4.4; N, 8.8.

Treatment of the amine with benzaldehyde in boiling aqueous methanol gave the *azine*, which formed deep-yellow prisms, m.p. 107.5–108.5°, when recrystallized from methanol.

Anal. Calcd. for $C_{13}H_{11}O_2NS$: N, 5.7. Found: N, 5.7.

Acetylation of the amine with acetic anhydride – acetic acid (1:1) gave the *N-acetyl derivative*, which, after two crystallizations from aqueous methanol, had m.p. 172–173°.

Anal. Calcd. for $C_8H_9O_3NS$: C, 48.2; H, 4.55; N, 7.0. Found: C, 48.3; H, 4.8; N, 7.1.

Can. J. Chem. Downloaded from www.nrcresearchpress.com by 210.87.254.5 on 09/05/12
For personal use only.

Methyl 5-Hydrazino-2-thenoate Hydrochloride

The amine hydrochloride (1.9 g), dissolved in 12 *N* hydrochloric acid (20 ml), was diazotized by the addition of a solution of sodium nitrite (0.75 g, 1.1 equiv.) in water (10 ml), the internal temperature being kept between 0 and 5°. The hydrochloride dissolved to give an orange-red solution, which was filtered and then immediately added, with stirring, to a solution of tin(II) chloride (10 g) in 12 *N* hydrochloric acid (20 ml). A finely divided suspension formed rapidly, which was filtered off and washed with a small amount of cold 12 *N* hydrochloric acid. Crystallization from methanol containing a small amount of hydrochloric acid gave the *hydrazine hydrochloride* as colorless plates, decomposing above 183° without a definite melting point. Efforts to liberate the free hydrazine with base gave a solid which rapidly darkened and decomposed.

Anal. Calcd. for $C_6H_9O_2ClN_2S$: Cl, 17.0; N, 13.4. Found: Cl, 16.9; N, 13.2.

Equimolar amounts of the hydrochloride and benzophenone were refluxed in aqueous acetic acid to give the *hydrazone*, which crystallized as yellow prisms, m.p. 169.5–170°, from aqueous methanol.

Anal. Calcd. for $C_{19}H_{16}O_2N_2S$: C, 67.85; H, 4.8; N, 8.3. Found: C, 67.3; H, 5.0; N, 8.5.

Gomberg Reaction of Amino-ester in Benzene

The amine hydrochloride (0.79 g) was diazotized as above, and the diazonium solution was filtered and stirred into a mixture of benzene (50 ml) and a solution of an excess of sodium acetate (15 g) in water (30 ml); stirring was continued for over 18 h. The dark-colored benzene layer was washed with dilute sodium hydroxide, dried, and evaporated, and the residue was then refluxed in methanol with charcoal. The methanol solution yielded a light-orange solid (0.14 g), which, on crystallization from petroleum ether (b.p. 60–80°), gave *methyl 5-phenyl-2-thenoate* (0.070 g, 8%) as colorless prisms, m.p. 95–97°.

Anal. Calcd. for $C_{12}H_{10}O_2S$: C, 66.0; H, 4.6; S, 14.7. Found: C, 65.85; H, 4.6; S, 14.95.

Alkaline hydrolysis of a portion of the methyl phenylthenoate gave 5-phenyl-2-thenoic acid, which crystallized from toluene as small plates, m.p. 189–190° (lit. (30) m.p. 187–188°), and which, on decarboxylation with soda lime, gave 2-phenylthiophene, m.p. 34° on admixture with an authentic specimen.

Silver Oxide Oxidation of Hydrazino-ester Hydrochloride in Benzene

The hydrazine hydrochloride (1.05 g) was suspended in dry benzene (25 ml) in a vessel connected to a gas burette, and silver oxide (4.6 g, 4 equiv.) was added. The mixture was stirred for 3 h while the temperature was raised from 20 to 55°, by which time the evolution of nitrogen (91%) was complete, and was then refluxed for 30 min. The faintly yellow solution obtained on filtration was washed with dilute hydrochloric acid (the washings were found to contain no amine) and then with water. After the solution was dried and the solvent evaporated, a crystalline residue of almost pure methyl 5-phenyl-2-thenoate (0.83 g, 85%) was left, m.p. 94–96°, raised to 97–98° by recrystallization from petroleum ether (b.p. 80–100°); it was identical in all respects with the product from the Gomberg reaction.

Silver Oxide Oxidation of Phenylhydrazine Hydrochloride in Nitrobenzene

When the hydrochloride was stirred with silver oxide (2 equiv.) in nitrobenzene at 50°, an exothermic reaction occurred. The whole was then heated at 100° for 2 h and filtered. Gas–liquid chromatographic analysis (silicone gum rubber on Chromosorb W) showed all three nitrobiphenyls in the percentage ratios 54 ortho : 14 meta : 32 para.

Decomposition Reactions of 3-Thenoyl and 5-Nitro-2-thenoyl Peroxides

Dilute solutions of the peroxides in representative solvents were heated at temperatures up to 100° in the dark until decomposition was at least 97% complete (iodometric test). The residues, after removal of the solvent, were extracted with ether; the carboxylic acid was removed from the ethereal solution by repeated shaking with saturated aqueous potassium hydrogen carbonate, and was purified by crystallization from water (3-thenoic acid) or from aqueous ethanol (5-nitro-2-thenoic acid). The neutral ether-soluble fractions were worked up in each case as described below, and the products are summarized in Table I. All yields are in mole percentage of peroxide.

3-Thenoyl Peroxide

Benzene

A solution of the peroxide (15 g) in benzene (1 500 ml) was refluxed for 10 h. The carbon dioxide evolved (33%) was adsorbed on Carbosorb, dry nitrogen being used as the carrier gas. The solution was concentrated at atmospheric pressure and the distillate was analyzed colorimetrically for thiophene (<1%) with isatin – concentrated sulfuric acid (15, p. 16). The residue, on complete removal of the solvent, was extracted with ether (3.3 g insoluble polymer), the ethereal solution giving 3-thenoic acid (91%) and a neutral fraction (3.0 g), which was chromatographed on Norit – Hyflo Super Cel (1:1) with elution by petroleum ether (b.p. 60–80°) followed by chloroform. Only a crude separation was achieved, but re-chromatography on Norit alone gave 3-phenylthiophene as waxy plates, m.p. and mixed m.p. 90°, and phenyl 3-thenoate as prisims, m.p. and mixed m.p. 57°, both being crystallized from petroleum ether. Quantitative g.l.c. (Silicone 550 on C_{22} Firebrick) of the original neutral fraction gave the phenylthiophene (2.3%) and the ester (1.8%).

Can. J. Chem. Downloaded from www.nrcresearchpress.com by 210.87.254.5 on 09/05/12
For personal use only.

Toluene

The peroxide (2.55 g) was heated in toluene (255 ml) for 48 h. The first few milliliters of distillate collected at atmospheric pressure was shown by g.l.c. (silicone gum rubber on Chromosorb W) to contain 6% of thiophene. A control experiment, in which 3-thenoic acid was refluxed in toluene for 48 h, showed that no thiophene was produced by decarboxylation. The carboxylic acid fraction (1.95 g), m.p. 125–132°, could not be purified by crystallization, but the main component, 3-thenoic acid (ca. 150%), was isolated in a pure state by sublimation. A portion of the crude acid mixture was refluxed with copper powder in quinoline for 30 min, and the filtered solution was diluted with an excess of dilute hydrochloric acid and extracted with ether, the ethereal solution yielding, on evaporation at 100°, a discolored oil, identified as 2-benzylthiophene by comparison of its infrared spectrum with that of an authentic sample (31); it gave a chloromercuric deviative having m.p. and mixed m.p. 182–183° (32). This established that the acidic contaminant was 2- or 5-benzyl-3-thenoic acid. The neutral fraction (1.63 g) was chromatographed on alumina and eluted with petroleum ether, giving bibenzyl as the only crystalline substance, identified by its mixed melting point. Gas–liquid chromatographic analysis (diethylene glycol succinate on Chromosorb W) showed that this was the main volatile component (0.40 g, 22%), only minor peaks being observed which might be caused by benzyl- or tolyl-thiophenes; at longer retention times two further peaks appeared which comparative g.l.c. with reference samples showed to be caused by *o*-tolyl 3-thenoate (ca. 2%) and benzyl 3-thenoate (a trace). The *m*- and *p*-esters could not be detected.

Chlorobenzene

The peroxide (15 g) was heated in chlorobenzene (1 500 ml) for 30 h. Much tar was formed which was not ether soluble, and the carboxylic acid fraction, on precipitation from the bicarbonate extracts, also formed tar which could not be redissolved in ether; the soluble acid (63%) consisted of 3-thenoic acid only. The neutral ether-soluble material was an orange oil (1.6 g). A portion was chromatographed on Norit – Hyflo Super Cel (1:1) with elution by petroleum ether (b.p. 60–80°) and then chloroform. The first fractions were oily and consisted mainly of 3-chlorophenylthiophenes; the next fractions crystallized and were identified as phenyl 3-thenoate, which crystallized from petroleum ether as prisms, m.p. 55.5–57° and mixed m.p. 56–57° with authentic ester. The final fractions, presumably the chlorophenyl 3-thenoates, were noncrystalline and not amenable to further purification.

A further portion of the neutral oil (0.79 g) was refluxed for 16 h with methanolic sodium hydroxide. After removal of the methanol, the residue was separated into a neutral, a phenolic, and a carboxylic acid fraction. The neutral fraction consisted of a mixture of pure 3-chlorophenylthiophenes (0.44 g, 7.5%).

Anal. Calcd. for $C_{10}H_7ClS$: C, 61.7; H, 3.6; Cl, 18.2; S, 16.5. Found: C, 61.5; H, 3.7; Cl, 18.35; S, 16.6.

Gas–liquid chromatography (diethylene glycol succinate on Chromosorb W) showed 63% of the *o*-isomer, its identity being established by comparison with the synthetic isomer, and 37% of the *m*- plus *p*-isomers, the peaks for these being incompletely resolved. The phenolic fraction, on g.l.c. analysis, gave, in order, *o*-chlorophenol (corresponding to an overall yield of 0.4% *o*-chlorophenyl 3-thenoate), phenol (1.6%), and a mixture of *m*- and *p*-chlorophenyl esters (1.4%, incompletely resolved). The amount of the carboxylic acid fraction (0.29 g) corresponded with the amount of phenols.

Thiophene

Decomposition of the peroxide (4.0 g) in thiophene (100 ml) for 20 h gave 3-thenoic acid (134%) and neutral material, which was thoroughly extracted with hot petroleum ether. A portion of the extracts was chromatographed on Norit – Hyflo Super Cel (1:1) with petroleum ether and chloroform as eluents, giving initially liquid fractions and then crystalline 2-thienyl 3-thenoate, m.p. and mixed m.p. 48–48.5°, after recrystallization (twice) from petroleum ether. Re-chromatography of the liquid under the same conditions gave first a waxy solid melting from 30 to 50°, which was shown (infrared) to be a mixture of 2,2′- and 2,3′-bithienyls, and then pure 2,2′-isomer, mixed m.p. 32° with reference material. Quantitative g.l.c. (diethylene glycol succinate on Chromosorb W) of the original neutral fraction gave, in order, three initial unidentifiable peaks (all in the order of 2 to 7%) (possibly partially reduced bithienyls), 2,2′-bithienyl (8.9%), 2,3′-bithienyl (6.7%), a trace of 3,3′-bithienyl (<1%), and 2-thienyl 3-thenoate (13.4%).

5-Nitro-2-thenoyl Peroxide

Benzene

The peroxide (6.9 g) was refluxed in benzene (400 ml) for 48 h (19% carbon dioxide evolved). After removal of the 5-nitro-2-thenoic acid (104%), the neutral products were extracted with benzene and the benzene-soluble material was chromatographed on Norit – Hyflo Super Cel (1:1). Elution with petroleum ether (b.p. 60–80°) gave crystalline material consisting essentially of biphenyl (0.27 g), m.p. and mixed m.p. 68°, after crystallization from petroleum ether; further elution with petroleum ether – benzene (3:1) gave crystalline phenyl 5-nitro-2-thenoate (0.51 g, 11%), recrystallized from petroleum ether as prisms, m.p. 92–92.5°, undepressed on admixture with authentic ester.

Gas–liquid chromatographic analysis (silicone gum rubber on Chromosorb W) of the benzene solution of neutral products showed the biphenyl, a compound identified as 2-phenyl-5-nitrothiophene (see below), and the phenyl ester, but no 2-nitrothiophene.

Benzoyl peroxide (2 g) was heated in 2-nitrothiophene (10 g) for 48 h. The whole was then dissolved in

Can. J. Chem. Downloaded from www.nrcresearchpress.com by 210.87.254.5 on 09/05/12
For personal use only.

benzene, and benzoic acid was removed in the usual way. Distillation of the neutral solution to remove most of the 2-nitrothiophene gave a residue, which was chromatographed on alumina with ether – petroleum ether to give residual 2-nitrothiophene and then a mixture of isomeric phenylnitrothiophenes (directly pure) melting between 113 and 130°.

Anal. Calcd. for $C_{10}H_7O_2NS$: C, 58.5; H, 3.4; N, 6.8; S, 15.6. Found: C, 58.4; H, 3.7; N, 6.7; S, 15.3.

Gas–liquid chromatographic analysis showed three components; the least volatile was identical under all conditions of chromatography with the above compound found in the chromatogram of the nitrothenoyl peroxide decomposition products. This compound, 2-phenyl-5-nitrothiophene, was the least abundant of the three phenylation products, the ratios of which were, in order, 5:16:1.

Toluene

The peroxide (6.1 g) was heated in toluene (610 ml) for 48 h (19% carbon dioxide evolved). The carboxylic acid (122%) was removed, and the neutral residue from the toluene solution was dissolved in benzene and analyzed by g.l.c. (silicone gum rubber on Chromosorb W). The chromatogram showed 2-nitrothiophene (<1%, but a control experiment proved that it did *not* arise by decarboxylation of the acid), bibenzyl (3.4%), and the much less volatile benzyl ester, in larger amounts. Column chromatography on Norit – Hyflo Super Cel (1:1) with petroleum ether as eluent gave oily fractions containing 2-nitrothiophene and bibenzyl, and with petroleum ether – benzene as eluent gave crystalline benzyl 5-nitro-2-thenoate (14%), m.p. 90–90.5°, after recrystallization from petroleum ether, undepressed on admixture with reference ester, with which it had an identical infrared spectrum.

ACKNOWLEDGMENT

The author thanks the National Research Council of Canada for financial support.

REFERENCES

1. M. C. FORD and D. MACKAY. J. Chem. Soc. 1294 (1958).
2. D. H. HEY. Private communication.
3. M. C. FORD and W. A. WATERS. J. Chem. Soc. 824 (1951).
4. M. C. FORD and D. MACKAY. J. Chem. Soc. 1290 (1958).
5. M. C. FORD and D. MACKAY. J. Chem. Soc. 4620 (1957).
6. R. D. SCHUETZ and D. M. TELLER. J. Org. Chem. **27**, 410 (1962).
7. G. H. WILLIAMS. Homolytic aromatic substitution. The Pergamon Press, Ltd., London. 1960. p. 46.
8. J. DEGANI, M. PALLOTTI, and A. TUNDO. Ann. Chim. Rome, **51**, 434 (1961).
9. C. E. GRIFFIN and K. R. MARTIN. Chem. Commun. 154 (1965).
10. D. I. DAVIES, D. H. HEY, and G. H. WILLIAMS. J. Chem. Soc. 1878 (1958).
11. D. F. DE TAR and R. A. J. LONG. J. Am. Chem. Soc. **80**, 4742 (1958).
12. E. L. ELIEL, M. EBERHARDT, O. SIMAMURA, and S. MEYERSON. Tetrahedron Letters, **17**, 749 (1962).
13. E. L. ELIEL, S. MEYERSON, Z. WELVART, and S. H. WILEN. J. Am. Chem. Soc. **82**, 2936 (1960).
14. R. L. HARDIE and R. H. THOMSON. J. Chem. Soc. 2512 (1957).
15. H. D. HARTOUGH. The chemistry of heterocyclic compounds. Thiophene and its derivatives. Interscience Publishers, Inc., New York. 1952.
16. N. I. PUTOKHIN and V. I. YAKOVLEV. Dokl. Akad. Nauk SSSR, **98**(1), 89 (1954); Chem. Abstr. **49**, 12431*c* (1955).
17. G. V. SHISHKIN and V. P. MAMAEV. Izv. Sibirsk. Otd. Akad. Nauk SSSR, **2**, 112 (1962); Chem. Abstr. **58**, 2421*f* (1963).
18. H. BEYER, S. MELDE, and K. DITTRICH. Z. Chem. **1**, 191 (1961).
19. H. ROSATZIN. Spectrochim. Acta, **19**, 1107 (1963).
20. L. J. BELLAMY. The infra-red spectra of complex molecules. 2nd ed. Methuen & Co. Ltd., London. 1958. p. 179.
21. A. CHRZASZCZEWSKA. Roczniki Chem. **5**, 33 (1925); Chem. Abstr. **20**, 1078 (1926).
22. M. NAPS and I. B. JOHNS. J. Am. Chem. Soc. **62**, 2450 (1940).
23. J. TESTE and N. LOZAC'H. Bull. Soc. Chim. France, 492 (1954).
24. H. WYNBERG and A. BANTJES. J. Org. Chem. **24**, 1421 (1959).
25. E. CAMPAIGNE and W. M. LESUER. Org. Syn. **33**, 95 (1953).
26. E. CAMPAIGNE and W. M. LESUER. J. Am. Chem. Soc. **70**, 1555 (1948).
27. W. STEINKOPF and H. F. SCHMITT. Ann. **533**, 264 (1938).
28. J. TIROUFLET and P. FOURNARI. Compt. Rend. **243**, 61 (1956).
29. (*a*) I. J. RINKES. Rec. Trav. Chim. **51**, 1134 (1932). (*b*) I. J. RINKES. Rec. Trav. Chim. **52**, 538 (1933).
30. E. E. CAMPAIGNE and R. E. CLINE. J. Org. Chem. **21**, 39 (1956).
31. W. STEINKOPF and W. HANSKE. Ann. **541**, 238 (1939).
32. W. STEINKOPF. Ann. **424**, 23 (1921).

Can. J. Chem. Downloaded from www.nrcresearchpress.com by 210.87.254.5 on 09/05/12
For personal use only.

Can. J. Chem. Downloaded from www.nrcresearchpress.com by 210.87.254.5 on 09/05/12
For personal use only.

CYCLIZATIONS OF DIALDEHYDES WITH NITROMETHANE

XIII. SYNTHESIS OF TREHALOSE-TYPE DISACCHARIDES CONTAINING NITROGENOUS HEPTULOSES[1,2]

HANS H. BAER AND ALAUDDIN AHAMMAD[3]
Department of Chemistry, University of Ottawa, Ottawa, Canada

Received July 25, 1966

ABSTRACT

The dialdehyde II that arises from a partial lead tetraacetate cleavage of sucrose has been cyclized with nitromethane to give a stereoisomeric mixture of nitro disaccharides IV via their sodium nitronates III. Upon catalytic hydrogenation a single amino disaccharide, α-D-glucopyranosyl 4-amino-4-deoxy-β-D-*gluco*-heptulopyranoside hydrochloride (V), was isolated. Various derivatives of the nitrogenous heptulose components of IV and V were prepared by methanolysis and hydrolysis. The configuration of V was established by a degradation of its *N*-acetylated hydrolysis product, 4-acetamido-4-deoxy-α-D-*gluco*-heptulose (VII), which gave 2-amino-2-deoxy-D-arabinose hydrochloride, and by reduction of VII, which gave the two epimeric acetamido heptitols XIII and XIV.

INTRODUCTION

In a continuation of studies concerned with the cyclization of dialdehydes with nitromethane (1), a method which has proved to be particularly useful for the synthesis of nitrogenous sugars and cyclitols (2, 3), it was decided to approach the synthesis of disaccharides that belong to the nonreducing trehalose type. This project appeared of interest not only from the viewpoint of broadening the scope of the nitromethane synthesis by application to the disaccharide field but also because of the discovery (4) of an antibiotic, α,α-trehalosamine (I), which stimulated research on nonreducing amino disaccharides, a class that has received scant attention to date.

It was considered that the dialdehyde II, which, according to Mitra and Perlin (5), is readily obtainable from sucrose by partial lead tetraacetate oxidation, should give rise to disaccharides of the general structure IV. This structure is related to I, although the nitrogen function is in a different position and the nitrogenous moiety is a heptulose rather than a hexose. Apart from any potential biological activity, the synthesis of such a structure would, in itself, be of interest. It would be the first example of an oligosaccharide containing a nitrogenous seven-carbon sugar. Moreover, the nitro and amino heptuloses that could conceivably be obtained from it should add to a relatively sparse knowledge about this type of sugar, of which the first few derivatives[4] have only recently become available (6).

RESULTS

Synthesis

Dialdehyde II was cyclized with nitromethane in methanolic solution in the presence of sodium methoxide, and a mixture of *aci*-nitro disaccharide sodium salts III was obtained in a yield of 58%. Since the glucose moiety of the original sucrose is not involved in the reactions leading to II and III, and since the configurations at C-2 and C-5 of the fructose

[1]*For part XII in this series, see ref. 1.*
[2]*A brief account of this work has been given by H. H. Baer before the International Symposium on Nitro Compounds, Warsaw, Poland, September 1963 (2). This work forms part of a Ph.D. thesis submitted by A. Ahammad to the University of Ottawa, Ottawa, 1964.*
[3]*Recipient of a Canadian Commonwealth Scholarship, 1961–1964.*
[4]*These are the 2,7-anhydro-4-nitro(and amino)-4-deoxy-β-D-heptulopyranoses with allo, altro, and gulo configurations.*

moiety can also be presumed to remain unaffected, the salts III may be designated as α-D-glucopyranosyl 4-*aci*-nitro-4-deoxy-β-D-heptulopyranoside sodium salts. Deionization of this mixture of nitronates gave an amorphous mixture of the corresponding free-nitro disaccharides IV; paper chromatography revealed the presence of two components in similar quantities.

Catalytic hydrogenation of IV to the corresponding amines proceeded readily, and from the hydrogenated mixture a pure disaccharide crystallized as the hydrochloride (yield, 23% based on starting sucrose). The compound proved to be α-D-glucopyranosyl 4-amino-4-deoxy-β-D-*gluco*-heptulopyranoside hydrochloride (V), as will be demonstrated in a subsequent section. *N*-Acetylation produced a crystalline *N*-acetate VI. One has to assume that at least a second, stereoisomeric amino disaccharide arose from the mixture IV, but no attempt has been made to isolate or characterize it.

Hydrochloric acid hydrolysis of V produced D-glucose and (amorphous) 4-amino-4-deoxy-D-*gluco*-heptulose hydrochloride. The former was detected by paper chromatography and the latter was characterized as the crystalline *N*-acetate, 4-acetamido-4-deoxy-α-D-*gluco*-heptulose (VII), after isolation by means of a cation-exchange resin. The anomeric configuration of VII was assigned on the basis of a downward mutarotation, $[\alpha]_D$ +66 → +55°.

Methanolysis of V catalyzed by 5% hydrogen chloride gave crystalline methyl α-D-glucopyranoside and methyl 4-amino-4-deoxy-α-D-*gluco*-heptulopyranoside hydrochloride (VIII). The glycoside VIII gave a pentaacetate IX and was converted, by successive hydrolysis and *N*-acetylation, into the reducing acetamido sugar VII.

The same amino glycoside hydrochloride VIII was also obtained in another way. Methanolysis of the mixture of nitro disaccharides IV gave, besides methyl α-D-glucopyranoside, a nitro heptuloside X which crystallized upon purification via its 1,3;5,7-di-*O*-benzylidene derivative XI. Catalytic reduction of X in the presence of 1 equivalent of hydrochloric acid then produced VIII, thus proving X to be methyl 4-deoxy-4-nitro-α-D-*gluco*-heptulopyranoside.

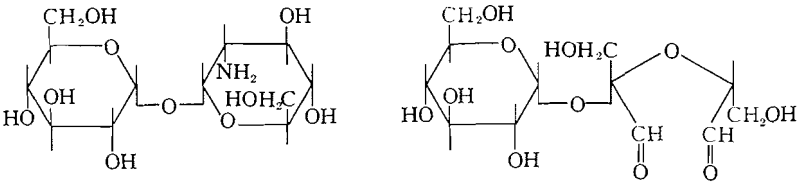
The α-anomeric configuration of VIII (and therefore also of X) follows from a consideration of the molecular rotations. The disaccharide V (M_D +42 054) may be regarded as a methyl α-D-glucopyranoside (M_D +30 691) in which a 4-amino-4-deoxy-β-D-*gluco*-heptulopyranosyl residue (as its hydrochloride) has been substituted for the optically inactive methyl group. The difference in the M_D values (+11 363) may serve as an approximate value for the contribution made by the β-heptuloside moiety in the disaccharide. Since the M_D value of VIII (+25 613) is considerably more positive, it is concluded that VIII is the α-anomer.

Establishment of the gluco Configuration

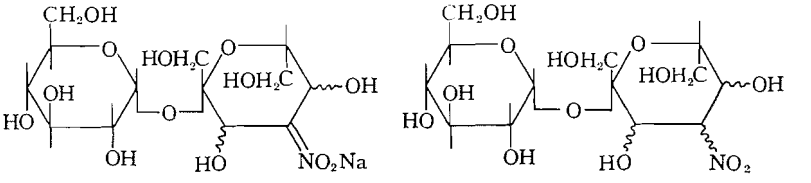
The key compound used for the establishment of the configuration of V–XI was the reducing acetamido heptulose VII. It was necessary to determine only the stereochemistry at its carbon atoms 3, 4, and 5, the configuration at C-6 being known from the origin of the molecule, namely, the D-fructofuranosyl moiety of sucrose.

The configurations at C-4 and C-5 were elucidated, and that of C-6 was confirmed, by a partial lead tetraacetate (LTA) oxidation. Perlin and Brice (7) have demonstrated that ketoses are cleaved, by a limited amount of oxidant, preferentially between the reducing center and the adjacent ring carbon (and not the adjacent hydroxymethyl group). The degradation thus results in removal of the top two carbons of the ketose chain, producing a lower aldose. In the present case, VII gave rise to known 2-acetamido-2-deoxy-D-arabinose and, upon acid hydrolysis, to known 2-amino-2-deoxy-D-arabinose hydrochloride (XII).

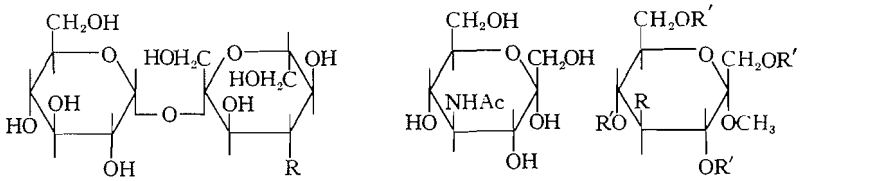
Can. J. Chem. Downloaded from www.nrcresearchpress.com by 210.87.254.5 on 09/05/12
For personal use only.



I II



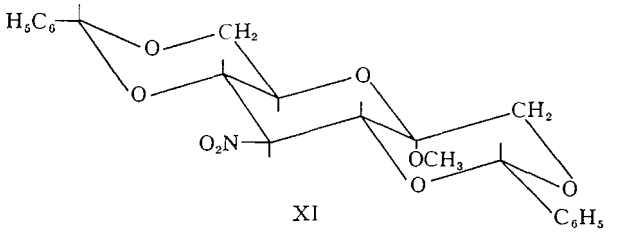
III IV



V R = NH_3Cl
VI R = NHAc

VII

VIII R = NH_3Cl, R′ = H
IX R = NHAc, R′ = Ac
X R = NO_2, R′ = H



XI

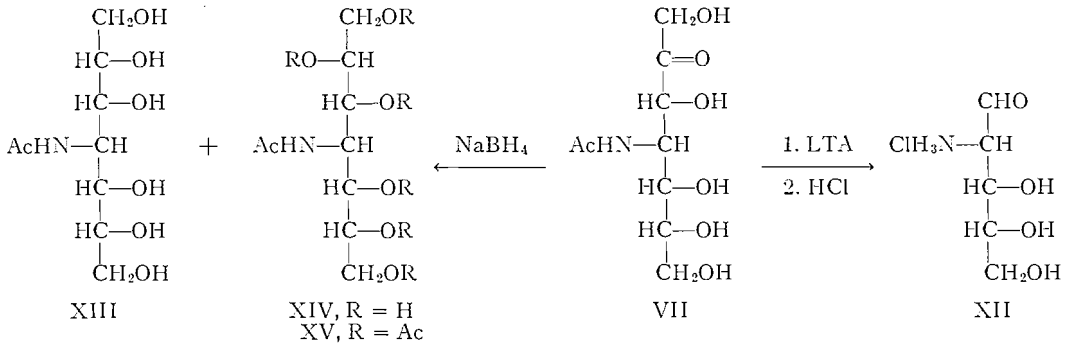
Since C-2, C-3, and C-4 in D-arabinosamine correspond to C-4, C-5, and C-6, respectively, in the heptulose, the only remaining configuration yet to be determined was at C-3. It was possible to make this assignment upon reduction of VII with sodium borohydride, whereby two epimeric 4-acetamido-4-deoxy heptitols (XIII and XIV) were formed.[5] One of these crystallized directly and was found to be *optically inactive*; the other was obtained from the mother liquor as an optically active ($[\alpha]_D$ +30°) crystalline heptaacetate. This result requires VII to possess the D-*gluco* configuration (i.e. the hydroxyl on C-3 to the right in the Fischer projection), for only then can an inactive (*meso*) heptitol arise. The inactive product must be 4-acetamido-4-deoxy-D-*glycero*-D-*gulo*-heptitol (XIII), and its active epimer must be 4-acetamido-4-deoxy-D-*glycero*-D-*ido*-heptitol (XIV). If VII had possessed the D-*manno* configuration (i.e. with the hydroxyl on C-3 to the left), then two optically active reduction products would have been expected.

EXPERIMENTAL

Melting points were determined in an electrically heated aluminium block apparatus. All evaporations were done *in vacuo* at 35–40° (bath temperature) unless otherwise indicated. Paper chromatography was performed by the descending technique on Whatman No. 1 paper. The nitro compounds were irrigated with 1-butanol – acetic acid – water (4:1:5 v/v/v, upper layer) and made visible by spraying with alkali (*N* sodium hydroxide – methanol – 1-butanol (1:4:5 v/v/v) and inspection under an ultraviolet lamp. The

[5] *We are obliged to Mr. F. Kienzle for carrying out these experiments.*

Can. J. Chem. Downloaded from www.nrcresearchpress.com by 210.87.254.5 on 09/05/12
For personal use only.



amino compounds were irrigated with the Fischer–Dörfel system (8) and detected with ninhydrin (R_{gm} is the speed relative to glucosamine hydrochloride). The acetamido compounds were chromatographed with 1-butanol–pyridine–water (6:4:3 v/v/v) and indicated according to Pan and Dutcher (9).

Lead Tetraacetate Oxidation of Sucrose to Dialdehyde II (5)

To a solution of sucrose (10 g, 29.2 mmoles) in 500 ml of water was added 500 ml of glacial acetic acid and then, with vigorous stirring, 12.4 g (28 mmoles) of lead tetraacetate. The oxidation was allowed to proceed for 30 min at room temperature. Divalent lead was removed by stirring the solution with about 130 ml of Rexyn RG 50 (H^+ form). The filtrate was concentrated, and most of the remaining solvent was removed by several co-distillations with ethanol and toluene. A white solid was obtained that was suitable for the next step without purification, as a possible presence of some unreacted sucrose was considered unobjectionable.

α-D-Glucopyranosyl 4-aci-Nitro-4-deoxy-β-D-heptulopyranoside Sodium Salts (III)

The crude dialdehyde II (from 10 g of sucrose) was dissolved in 85 ml of absolute methanol. The solution was chilled in an ice bath, and 1.6 ml of nitromethane and 23 ml of sodium methoxide solution (3 g of sodium per 100 ml of methanol) were added, with stirring. The amounts of reagents added corresponded to 1 equivalent each, based on the amount of starting sucrose. A yellowish-white precipitate began to appear within about 15 min. Cooling and stirring were continued for 1 h, after which the stoppered flask was kept in a refrigerator for another 4 h. The precipitate was collected on a Büchner funnel, washed quickly with ice-cold methanol, and immediately placed in a vacuum desiccator. The dried product (III) weighed 7.2 g (yield, 58.5% based on sucrose), showed $[\alpha]_D^{23}$ +46.9° (*c*, 1 in water), and decomposed on heating, with darkening around 100° and foaming at 119–120°. Unless proper care is taken during isolation, the material tends to absorb moisture and become syrupy; when carefully washed and dried, however, the solid is fairly stable and can be stored in a desiccator in the cold. In an aqueous solution, the salt exhibits strong ultraviolet absorption which undergoes a peculiar bathochromic shift on heating (λ_{max} 250 → 299 mμ). This phenomenon has been investigated recently (10).

Anal. Calcd. for $C_{13}H_{22}O_{13}NNa$ (423.3): N, 3.31; Na, 5.43. Found: N, 3.26; Na, 5.39.

α-D-Glucopyranosyl 4-Nitro-4-deoxy-β-D-heptulopyranosides (IV)

Sodium salt III (5 g) was suspended in about 100 ml of methanol, and the suspension was treated at ice-bath temperature with an excess (50 ml) of Rexyn RG 50 (H^+ form) that had been washed well with methanol. The salt dissolved, and the deionized, faintly yellowish filtrate from the resin was evaporated to give a syrup that was further evaporated with two successive additions of ethanol. There resulted a near-colorless, hygroscopic froth which sintered at about 60° and foamed at 85°, $[\alpha]_D^{23}$ +73.4° (*c*, 1 in water). Paper chromatography showed two spots, R_f 0.23 and 0.30, presumed to represent stereoisomeric disaccharides IV.

α-D-Glucopyranosyl 4-Amino-4-deoxy-β-D-gluco-heptulopyranoside Hydrochloride (V)

A sample of the disaccharide mixture IV (1.26 g) in 5 ml of water was added to 31 ml of 0.1 *N* hydrochloric acid (1 equivalent) containing prehydrogenated catalyst from 1 g of platinum dioxide. Hydrogenation was performed, with efficient shaking, at normal temperature and pressure over a period of 3.5 h, during which 186 ml of hydrogen was consumed. The catalyst was filtered off and the solution was evaporated to give a colorless syrup. Excess acid was removed by several co-evaporations with water. Finally, the syrup was evaporated twice with ethanol to give a white solid that crystallized from methanol – ethyl acetate containing a few drops of water. The yield was 500 mg. The product was recrystallized by dissolution in the minimum amount of water and dropwise addition of glacial acetic acid to incipient turbidity, m.p. 197° (decomp.), R_{gm} 0.88, $[\alpha]_D^{23}$ +103.2° (*c*, 0.5 in water).

Anal. Calcd. for $C_{13}H_{26}O_{11}NCl$ (407.5): C, 38.31; H, 6.45; N, 3.43; Cl, 8.71. Found: C, 38.36; H, 6.58; N, 3.63; Cl, 8.62.

Can. J. Chem. Downloaded from www.nrcresearchpress.com by 210.87.254.5 on 09/05/12
For personal use only.

α-D-Glucopyranosyl 4-Acetamido-4-deoxy-β-D-gluco-heptulopyranoside (VI)

Amino dissacharide hydrochloride V (314 mg) was dissolved in 4.5 ml of water and 0.6 ml of methanol. *N*-Acetylation (11) was carried out by treatment with 5 ml of Dowex-1 (CO_3^{2-} form) and 0.1 ml of acetic anhydride for 90 min, at 3°, with magnetic stirring. The resin was filtered off and washed exhaustively with water, and the combined filtrate and washings were stirred briefly with 2 ml of Dowex-50 (H^+ form). The filtrate was evaporated to a colorless syrup that was dehydrated with ethanol, giving an amorphous solid. Crystallization occurred from ethanol (2 ml) upon addition of a few drops of ethyl acetate, m.p. 151–152°, $[\alpha]_D^{23}$ +84° (*c*, 0.5 in water). The product VI was chromatographically uniform, R_f 0.32.

Anal. Calcd. for $C_{15}H_{27}O_{12}N$ (413.4): C, 43.57; H, 6.58; N, 3.39. Found: C, 43.52; H, 6.71; N, 3.23.

Hydrolysis of Disaccharide V

In a preliminary experiment, a 1% solution of V in 2 *N* hydrochloric acid was heated on a steam bath, and samples for chromatography were withdrawn from time to time. The absence of V was noted after 20 min of hydrolysis.

Disaccharide V (535 mg) in 50 ml of 2 *N* hydrochloric acid was heated on a steam bath for 50 min. The slightly yellow hydrolysate, which reduced Fehling solution strongly, was evaporated, the excess acid being removed by several subsequent evaporations with water. The resulting syrup was dissolved in 4 ml of water and poured onto a narrow column containing 22 ml of Rexyn RG 50 (H^+ form). The column was eluted with 250 ml of water at a rate of 30 drops per min. Evaporation of this eluate gave a syrupy residue that weighed 210 mg upon dehydration with absolute ethanol and drying in a high vacuum. The material gave a negative ninhydrin test and was indistinguishable from glucose on paper chromatograms sprayed with aniline hydrogen phthalate.

Elution of the column was then continued with 250 ml of *N* hydrochloric acid. The colorless, ninhydrin-positive eluate was brought to a syrup, and residual acid was removed by several evaporations with water. Finally, the syrup was evaporated with ethanol to give an amorphous powder (310 mg) of 4-amino-4-deoxy-D-*gluco*-heptulose hydrochloride, which failed to crystallize from common solvents.

4-Acetamido-4-deoxy-α-D-gluco-heptulose (VII)

The amorphous amino sugar hydrochloride just described was *N*-acetylated (11) by treating its solution in 8 ml of water and 1 ml of methanol with 9 ml of Dowex-1 (CO_3^{2-} form) and 0.18 ml of acetic anhydride. The procedure was the same as that given above for the preparation of VI. The *N*-acetate VII crystallized from ethanol (2 ml) containing a few drops of ethyl acetate, in a yield of 150 mg. Upon one recrystallization from ethanol it had m.p. 171–172° (decomp.), $[\alpha]_D^{23}$ +66.0 (3 min) → +55.0° (45 min, final; *c*, 0.5 in water), and R_f 0.48.

Anal. Calcd. for $C_9H_{17}O_7N$ (251.2): C, 43.02; H, 6.77; N, 5.58. Found: C, 43.10; H, 6.91; N, 5.70.

The compound reduced Fehling and Benedict solutions, but did not respond to an *o*-naphthoresorcinol test in which (nitrogen-free) ketoses usually produce a red color.

Methanolysis of Disaccharide V

A sample of disaccharide V (240 mg) was refluxed for 7.75 h with 20 ml of methanol containing 1 g of hydrogen chloride. The brown solution was brought to dryness, and the residue was evaporated with water several times, decolorized with activated charcoal, and brought to dryness again. From ethanol – ethyl acetate crystallized[6] 25 mg of needles having m.p. 173–174° (decomp.), R_{gm} 1.15, and $[\alpha]_D^{23}$ +98.0° (*c*, 0.5 in water). The identity of the product with methyl 4-amino-4-deoxy-α-D-*gluco*-heptulopyranoside hydrochloride (VIII) obtained from X (below) was confirmed by comparison of the infrared spectra and by an undepressed mixture melting point.

A second crop of crystals (30 mg) was deposited when the mother liquor was allowed to stand in a refrigerator, m.p. 158–160°, $[\alpha]_D^{23}$ +126.5° (*c*, 0.5 in water). Chromatographically, this crop showed only one ninhydrin-positive spot (R_{gm} 1.18). The infrared spectrum was slightly different from that of VIII. Possibly, the material was VIII accompanied by some methyl glucopyranoside; it was not investigated further.

Addition of some more ethyl acetate to the mother liquor and continued storage at 4° gave a third crop of crystals (20 mg), which melted at 161–162°. Recrystallization from ethanol gave needles of pure methyl α-D-glucopyranoside, m.p. 166°, $[\alpha]_D^{23}$ +158.0° (*c*, 0.5 in water), in agreement with the literature (12).

Methanolysis of the Disaccharide Mixture IV

Nitro disaccharide mixture IV (4.3 g) was refluxed for 3.5 h in 400 ml of methanol containing 8 g of hydrogen chloride. The dark-brown solution was treated with activated charcoal, whereby it became pale yellow; it was then evaporated, with several additions of water towards the end. The resulting syrup still was acidic; it was therefore dissolved in 100 ml of water, and the pH was adjusted to about 5 by stirring the solution with Amberlite IR-45 (OH^- form). The resin was washed well with water, the filtrate evaporated, and the syrupy residue freed from remnant water by means of ethanol. The material was then dissolved in a small amount of hot ethanol; addition of a little ethyl acetate and cooling (4°) gave 0.9 g of crystals that were identified, after one recrystallization from ethanol, as methyl α-D-glucopyranoside, having m.p. 166° and $[\alpha]_D^{23}$ +158.8° (*c*, 1 in water) (12).

[6] *Upon seeding with VIII that had been obtained from X (see a subsequent section).*

Can. J. Chem. Downloaded from www.nrcresearchpress.com by 210.87.254.5 on 09/05/12
For personal use only.

Methyl 1,3;5,7-Di-O-benzylidene-4-nitro-4-deoxy-α-D-gluco-heptulopyranoside (XI)

The ethanol – ethyl acetate mother liquor of the preceding experiment was presumed to contain X and probably one or more isomers. Evaporation gave a noncrystallizable syrup (3 g). Zinc chloride (3.6 g) and benzaldehyde (15 ml) were added to the syrup, and the mixture was stirred at room temperature for 24 h. Water (40 ml) and petroleum ether (20 ml, b.p. 30–60°) were then added, and the heterogeneous system was stirred for 15 min. This resulted in the separation of a semicrystalline mass, which was collected and washed twice with water and twice with petroleum ether. The crude product, when air-dried and recrystallized from chloroform, gave pure dibenzylidene derivative XI as fine needles (1.0 g), m.p. 285–286°. Compound XI was soluble in hot chloroform, hot dimethylformamide, and hot dioxane, but only sparingly so in hot ethanol. Solubility in cold solvents was very slight.

Anal. Calcd. for $C_{22}H_{23}NO_8$ (429.4): C, 61.53; H, 5.36; N, 3.26. Found: C, 61.45; H, 5.52; N, 3.18.

Methyl 4-Nitro-4-deoxy-α-D-gluco-heptulopyranoside (X)

A suspension of dibenzylidene derivative XI (3.05 g) in 450 ml of methanol–water (4:1 v/v) was magnetically stirred and heated under reflux with 18 g of Dowex 50W-X8 (H^+ form) for 44 h. Evaporation of the reaction solution gave a crystalline residue, which was freed from the last traces of water by two evaporations with ethanol. Recrystallization from ethyl acetate gave 1.39 g of debenzylidenated nitro glycoside X, m.p. 157–158°, $[\alpha]_D^{23}$ +102° (*c*, 0.5 in water). (For the ultraviolet absorption spectrum of X in alkaline solution and its change upon heating, see ref. 10.)

Anal. Calcd. for $C_8H_{15}O_8N$ (253.2): C, 37.95; H, 5.93; N, 5.53. Found: C, 38.19; H, 6.00; N, 5.60.

Methyl 4-Amino-4-deoxy-α-D-gluco-heptulopyranoside Hydrochloride (VIII)

Nitro glycoside X (1.13 g) in 5 ml of water and 45 ml of 0.1 *N* hydrochloric acid was hydrogenated with 0.60 g of prehydrogenated platinum dioxide catalyst. The hydrogen consumption at room temperature and atmospheric pressure was 300 ml. The filtrate was treated with a small amount of Amberlite IR-45 (OH^- form) to adjust the pH to about 5. Evaporation, ultimately with added ethanol, gave a crystalline residue, that was recrystallized from ethanol – ethyl acetate with a few drops of water to give 700 mg of fine needles of VIII, m.p. 170–172° (decomp.), R_{gm} 1.15, $[\alpha]_D^{23}$ +98.7° (*c*, 0.5 in water).

Anal. Calcd. for $C_8H_{18}NO_6Cl$ (259.5): C, 36.99; H, 6.93; N, 5.39. Found: C, 37.20; H, 6.93; N, 5.19.

Conversion of VIII into VII

Amino glycoside hydrochloride VIII (842 mg) was hydrolyzed with 85 ml of 2 *N* hydrochloric acid on a steam bath for 1 h. Removal of the acid by evaporation gave an amorphous, reducing amino sugar (R_{gm} 0.95), which was *N*-acetylated under the conditions described above for the preparations of VII and VI. In the present case, 19 ml of water, 2.25 ml of methanol, 0.42 ml of acetic anhydride, and 21 ml of Dowex-1 (CO_3^{2-} form) were employed. Acetamido sugar VII (550 mg) crystallized from 5 ml of ethanol upon addition of a small amount of ethyl acetate, m.p. 173–175° (decomp.), R_f 0.48, $[\alpha]_D^{23}$ +66.6 (3 min) → +53° (45 min, final; *c*, 0.5 in water). An undepressed mixture melting point and a comparison of infrared spectra confirmed its identity with VII obtained from V.

Methyl 4-Acetamido-4-deoxy-1,3,5,7-tetra-O-acetyl-α-D-gluco-heptulopyranoside (IX)

Amino glycoside hydrochloride VIII (250 mg) was acetylated in 5 ml of pyridine and 2 ml of acetic anhydride for 24 h at room temperature. The reaction mixture was poured onto 40 g of crushed ice and, after decomposition of the excess anhydride, it was extracted with four 15 ml portions of chloroform. The extract was dried over sodium sulfate and evaporated, the last traces of pyridine being removed by co-distillation with toluene. The pentaacetate IX was obtained as a gel from ethanol; drying in a high vacuum gave 140 mg of a microcrystalline white powder having m.p. 191–192°, R_f 0.86, and $[\alpha]_D^{23}$ +75° (*c*, 0.5 in chloroform).

Anal. Calcd. for $C_{18}H_{27}NO_{11}$ (433.4): C, 49.88; H, 6.28; N, 3.24. Found: C, 49.85; H, 6.37; N, 3.19.

Degradation of 4-Acetamido-4-deoxy-D-gluco-heptulose (VII) to 2-Amino-2-deoxy-D-arabinose Hydrochloride (XII)

Acetamido heptulose VII (249 mg) was dissolved in 2.1 ml of water, and 120 ml of glacial acetic acid was added. Into the stirred solution was introduced 444 mg (1 equivalent) of finely powdered lead tetraacetate. After 10 min a 10% solution of oxalic acid in glacial acetic acid was added dropwise until no more lead oxalate precipitated; stirring was continued for another 30 min. The lead oxalate was filtered off and washed with glacial acetic acid, and the filtrate was evaporated with several additions of water. The material so obtained was treated briefly with 12 ml of Dowex-1 (HCO_3^- form) in about 20 ml of water. The colorless filtrate and washings from the resin were combined, concentrated to a volume of 15 ml, and then warmed with 120 mg of sodium bicarbonate for 30 min at 50°. Upon deionization with Dowex 50W-X8 (H^+ form) and evaporation, a colorless syrup was obtained that gave a positive Morgan–Elson color test for 2-acetamido sugars and had the same mobility on paper as a co-chromatographed authentic sample[7] of 2-acetamido-2-deoxy-D-arabinose. The syrup was then hydrolyzed for 2 h on a steam bath with 21 ml of 0.3 *N* hydrochloric acid. The hydrolysate was brought to dryness and dissolved in a small amount of methanol. A few drops of

[7]*Kindly provided by Prof. Richard Kuhn and Dr. G. Baschang, Heidelberg.*

Can. J. Chem. Downloaded from www.nrcresearchpress.com by 210.87.254.5 on 09/05/12
For personal use only.

ethanol were added, and crystallization was allowed to take place slowly in an open dish. Crystalline 2-amino-2-deoxy-D-arabinose hydrochloride (XII) was collected in a yield of 68 mg (washed with ethanol and dried). The melting point, 155–156° (decomp.), and rotation, $[\alpha]_D^{23}$ −123° (*c*, 0.5 in water), were in agreement with the literature data (13), m.p. 154–157° and $[\alpha]_D$ −124°. A mixed melting point with an authentic sample[7] was 155–156° (decomp.), and identical infrared spectra and R_{gm} values (1.08) were obtained.

*Sodium Borohydride Reduction of 4-Acetamido-4-deoxy-*D*-gluco-heptulose*

*4-Acetamido-4-deoxy-*D*-glycero-*D*-gulo-heptitol (XIII)*

Acetamido heptulose VII (100 mg) and sodium borohydride (100 mg) were dissolved in 7 ml of water at room temperature. After 18 h the solution was deionized with 5 ml of Rexyn RG 50 (H^+ form) and evaporated. The residue was evaporated six times with 10 ml portions of methanol to remove the boric acid. Slow crystallization of XIII occurred during several days when a concentrated aqueous solution was left in a small dish in the air. The crystals were isolated by trituration with water-containing ethanol and melted at 149–151°; yield, 47 mg. For analysis the product was recrystallized from 95% ethanol, giving long prisms that melted at 154°. Thin-layer chromatography on silica gel G with 1-butanol–pyridine–water (2:1.2:0.7 v/v/v) gave only one spot. The optical rotation was found to be zero in water (*c*, 1.3) as well as in half-saturated sodium tetraborate solution (*c*, 0.65).

Anal. Calcd. for $C_9H_{19}NO_7$ (253.3): C, 42.69; H, 7.56. Found: C, 42.62; H, 7.80.

*4-Acetamido-4-deoxy-1,2,3,5,6,7-hexa-O-acetyl-*D*-glycero-*D*-ido-heptitol (XV)*

The aqueous ethanol with which the crystals of XIII had been triturated for isolation gave, on thin-layer chromatography, a weak spot of XIII and a strong spot that moved more slowly and was presumed to represent the isomer XIV. Evaporation yielded 51 mg of an amorphous material having $[\alpha]_D^{23}$ +9.8° (*c*, 1.25 in water). The material was acetylated with 0.5 ml of acetic anhydride in 1 ml of pyridine (18 h, room temperature). Work-up by the common chloroform extraction procedure resulted in a syrupy acetate (XV), which crystallized as fine, colorless needles (30 mg, m.p. 139–140°) from ethyl acetate – petroleum ether (b.p. 30–60°). Recrystallization from the same solvents yielded 22 mg of XV melting at 140° and having $[\alpha]_D^{23}$ +30° (*c*, 0.8 in chloroform).

Anal. Calcd. for $C_{21}H_{31}NO_{13}$ (505.5): C, 49.90; H, 6.14. Found: C, 49.88; H, 6.31.

ACKNOWLEDGMENTS

Support of this work by the National Institutes of Health, United States Public Health Service (grant AI-4697), is gratefully acknowledged. A. A. thanks the Canadian Commonwealth Scholarship Council for the award of a scholarship.

REFERENCES

1. H. H. Baer and B. Achmatowicz. J. Org. Chem. **29**, 3180 (1964). H. H. Baer and A. Ahammad. Can. J. Chem. **41**, 2931 (1963).
2. H. H. Baer. *In* Nitro compounds. T. Urbański (*Editor*). Pergamon Press, New York. 1964. p. 263.
3. F. W. Lichtenthaler. Angew. Chem. Intern. Ed. **3**, 211 (1964).
4. F. Arcamone and F. Bizioli. Gazz. Chim. Ital. **87**, 896 (1957).
5. A. K. Mitra and A. S. Perlin. Can. J. Chem. **37**, 2047 (1959).
6. H. H. Baer. J. Org. Chem. **28**, 1287 (1963). H. H. Baer, L. D. Hall, and F. Kienzle. J. Org. Chem. **29**, 2014 (1964).
7. A. S. Perlin and C. Brice. Can. J. Chem. **34**, 541 (1956).
8. F. G. Fischer and H. Dörfel. Z. Physiol. Chem. **301**, 224 (1955).
9. S. C. Pan and J. D. Dutcher. Anal. Chem. **28**, 836 (1956).
10. H. H. Baer and F. Kienzle. Ann. **695**, 192 (1966).
11. S. Roseman and J. Ludowieg. J. Am. Chem. Soc. **76**, 301 (1954).
12. E. Fischer. Ber. **26**, 2406 (1893).
13. R. Kuhn and G. Baschang. Ann. **628**, 193 (1959).

Can. J. Chem. Downloaded from www.nrcresearchpress.com by 210.87.254.5 on 09/05/12
For personal use only.

Can. J. Chem. Downloaded from www.nrcresearchpress.com by 210.87.254.40 on 09/05/12
For personal use only.

THE ORTON REARRANGEMENT IN APROTIC SOLVENTS

III. THE ACID-CATALYZED CHLORINATION OF ANISOLE BY A SERIES OF 4-SUBSTITUTED *N*-CHLOROACYLANILIDES

JOHN M. W. SCOTT AND JUNE G. MARTIN
Memorial University of Newfoundland, St. John's, Newfoundland

Received January 5, 1966

ABSTRACT

Anisole has been chlorinated with a sequence of chlorinating agents generated by the reaction of a series of 4-substituted *N*-chloroacylanilides (4-X-C_6H_4NClAc (X = Me, H, and CN)) with a series of carboxylic acids (R—COOH (R = CF_3, CCl_3, CH_2Cl, and CH_3)). The isomer ratios of the 2- and 4-chloroanisoles produced in these reactions have been measured for each *N*-chloroacylanilide – carboxylic acid pair, and are found to be dependent on the strength of the catalyzing acid but independent of the structure of the *N*-chloroacylanilide within the precision of the reported data. These observations are consistent with both the termolecular scheme proposed in part II of this series and the Soper mechanism. However, evidence derived from these and other observations suggests that the termolecular scheme is still the most probable mechanism for the chlorine transfer reaction.

INTRODUCTION

In a previous communication (1) the acid-catalyzed bromination of anisole by a sequence of reagents generated by the reaction of a series of 4-substituted *N*-bromoacylanilides (NBAA's) with a series of carboxylic acids was investigated. These experiments demonstrated that the product ratio of 2-bromoanisole to 4-bromoanisole depended on the structure of both the NBAA and the carboxylic acid, which suggested that the mechanism originally proposed by Soper and his co-workers (2) was inadequate. The new results were interpreted in terms of a product-determining termolecular transition state, and the mechanism involving the intermediate production of acylhypobromites was rejected. A similar study has now been carried out with a series of *N*-chloroacylanilides (NCAA's), and the results of this investigation are reported below.

EXPERIMENTAL

General

Melting points were determined on a Fisher–Johns apparatus and are uncorrected. Nuclear magnetic resonance spectra were measured on a Varian A.60 instrument, and peaks are reported on the τ scale.

Product analyses were determined by vapor-phase chromatography as described in part II (1) of the present series. The measurement of the product ratio (*R*) of 2- to 4-chloroanisole required the following instrument conditions: column oven 95 °C, detector oven 158 °C, and injector oven 184 °C. The inlet pressure was 20 p.s.i. and the flow rate was 25 ml He min^{-1}. The retention times for the three monosubstituted chloroanisoles and 2,4-dichloroanisole under these conditions are given in Table I. Biphenyl was used as an internal standard in the determination of the yield of the chloroanisoles with the following instrument conditions: column oven 139 °C, injector oven 196 °C, and detector oven 167 °C. The helium flow rate was the same as that given above. Under the latter conditions 4-chloroanisole had a retention time of 5.66 min, and biphenyl 8.30 min.

Materials

Acetanilides

The acetanilides used in the present study either were commercial samples or were obtained by acylation of the appropriate amine with acetic anhydride. The melting points of these materials were in satisfactory agreement with those previously reported.

N-Chloroacetanilides

The 4-substituted *N*-chloroacetanilides were prepared by dissolving the anilide in the minimum amount of 1,2-dimethoxyethane and adding this solution dropwise, with vigorous stirring, to a twofold excess of aqueous NaClO–$NaHCO_3$ cooled to 0 °C. The precipitated *N*-chloro compound was collected, thoroughly washed

with cold water, and then dried in a vacuum over anhydrous calcium chloride. Samples were then purified by crystallization from chloroform and light petroleum (b.p. 40–60°), and the active chlorine was determined iodometrically.

Chloroanisoles

2-Chloroanisole was obtained commercially. 3-Chloroanisole was prepared by the Sandmeyer reaction from 3-anisidine, and 4-chloroanisole was obtained by methylating 4-chlorophenol with dimethyl sulfate. 2,4-Dichloroanisole was prepared by chlorinating 4-chloroanisole in carbon tetrachloride. All these materials gave a single peak when examined by vapor-phase chromatography. The physical properties of these materials are reported in Table I.

Acid Solutions

These were identical with those used in part II of the present series.

Method

The reactions were carried out as described for the NBAA experiments (1). The thermostat temperature was raised to 50.00 ± 0.02 °C so that the reactions were complete in a convenient period of time. The chloroanisole isomer ratios for each NCAA–acid pair are reported in Tables II–IV together with the ratios for the photochemical chlorinations, which were considerably less than those observed for the acid-catalyzed substitutions. The photochemical R values for *N*-chloroacetanilide and *N*-chloro-4-methylacetanilide were identical, but the R value for *N*-chloro-4-cyanoacetanilide for the light-catalyzed reaction was smaller than that observed for the 4-methyl and the unsubstituted NCAA. In view of the fact that R (photochemical) $< R$ (acid-catalyzed) in all cases, this anomaly was not investigated further. The recovery of the nitrogen-bound chlorine as chloroanisoles averaged 80–90%. The fate of the remaining chlorine was not established, but the possibility of some rearrangement accompanying the chlorine transfer reaction cannot be ruled out (cf. part II and ref. 2).

TABLE I

The physical properties of some chloroanisoles

Substance	Boiling point (°C)	Retention time* (min)	Nuclear magnetic resonance data†	
			MeO	Aromatic protons
2-Chloroanisole	101 at 25 mm	12.90	6.39	2.6–3.5
3-Chloroanisole	84 at 13 mm	9.53	6.50	2.8–3.5
4-Chloroanisole	45 at 1 mm	10.32	6.47	3.66 (2H) 2.88 (3H)
2,4-Chloroanisole	—	29.57	—	—

*For instrument conditions see the Experimental.
†Neat samples containing tetramethylsilane.

Kinetic Experiments

Some kinetic experiments were carried out with *N*-chloroacetanilide and *N*-chloro-4-cyanoacetanilide by the method described in part II of this series. In neither case did the rate of disappearance of the NCAA obey first-order kinetics. Both compounds displayed the type of behavior described by Bell and Dankwerts (3), who used chlorobenzene as the solvent.

DISCUSSION

An examination of the results in Tables II–IV reveals that the R values for each individual NCAA are dependent on the structure of the catalyzing acid, and that the R values decrease as the pK_a of the catalyzing acid increases. In this respect the NCAA series is analogous to the NBAA series (1). For each NCAA the acid-catalyzed R values approximately obey a type of Brönsted equation of the form

$$\log R = \alpha \log K_a + C'', \quad [1]$$

where K_a is the dissociation constant of the acid and C'' is a constant. These correlations are illustrated graphically in Fig. 1, and the least-squares values of α and C'' for each NCAA are reported in Tables II–IV. In the NBAA series the Brönsted exponent α proved to be sensitive to the substituent at the 4-position of the NBAA, but, in contrast, the α

Can. J. Chem. Downloaded from www.nrcresearchpress.com by 210.87.254.40 on 09/05/12
For personal use only.

Can. J. Chem. Downloaded from www.nrcresearchpress.com by 210.87.254.40 on 09/05/12
For personal use only.

TABLE II

Isomer distributions and product analyses for the acid-catalyzed chlorinations of anisole with *N*-chloroacetanilide (purity of *N*-chloroacetanilide, 100%)

Acid*	[Ca] (*M*)	Weight of NCAA (g)	Recovery of anilide: Weight of anilide (g)	Recovery of anilide: % yield	Recovery of anilide: Melting point† (°C)	Analysis of 2- and 4-chloroanisoles‡: Weight (g)	Analysis of 2- and 4-chloroanisoles‡: % yield	Analysis of 2- and 4-chloroanisoles‡: *R*
CF_3COOH (*a*)	0.443	0.853	—	—	—	0.594	83±4	0.163±0.002
CCl_3COOH (*b*)	0.535	0.812	—	—	—	0.592	87±3	0.172±0.001
$CH_2ClCOOH$ (*c*)	0.509	0.822	—	—	—	0.578	84±3	0.141±0.009
CH_3COOH (*d*)	0.377	0.827	0.081	12	113–114	0.620	89±4	0.078±0.002
Light-catalyzed reaction		0.807	0.330	51	112.5–114	0.659	93±5	0.061±0.005

*pK_a of *a* = 0.23, pK_a of *b* = 0.65, pK_a of *c* = 2.86, pK_a of *d* = 4.76 (4).
†Literature m.p. 114 °C.
‡No 3-chloroanisole or 2,4-dichloroanisole was detected in these experiments. Least-squares line for the Brönsted correlation: log R = 0.070 ± 0.01, log K_a = −0.73 ± 0.04. The probable errors in the parameters for the Brönsted equation were calculated as described in part II.

TABLE III

Isomer distributions and product analyses for the acid-catalyzed chlorinations of anisole with *N*-chloro-4-methylacetanilide (purity of *N*-chloro-4-methylacetanilide, 98%)

Acid	[Ca] (*M*)	Weight of NCAA (g)	Recovery of anilide: Weight of anilide (g)	Recovery of anilide: % yield	Recovery of anilide: Melting point* (°C)	Analysis of 2- and 4-chloroanisoles†: Weight (g)	Analysis of 2- and 4-chloroanisoles†: % yield	Analysis of 2- and 4-chloroanisoles†: *R*
CF_3COOH	0.443	0.929	—	—	—	0.616±0.02	90±4	0.157±0.003
CCl_3COOH	0.535	0.928	—	—	—	0.596±0.02	87±4	0.168±0.006
$CH_2ClCOOH$	0.509	0.930	0.268	36	148–150	0.611±0.02	89±3	0.135±0.006
CH_3COOH	0.377	0.932	0.510	69	147–151	0.598±0.03	87±5	0.087±0.003
Light-catalyzed reaction		0.928	0.593	80	149–153	0.607±0.02	88±3	0.061±0.003

*Literature m.p. 154 °C.
†No 3-chloroanisole or 2,4-dichloroanisole was detected in these experiments. Least-squares line for the Brönsted correlation: log R = 0.058 ± 0.01, log K_a = −0.75 ± 0.03. The probable errors in the parameters for the Brönsted equation were calculated as described in part II.

Can. J. Chem. Downloaded from www.nrcresearchpress.com by 210.87.254.40 on 09/05/12
For personal use only.

TABLE IV

Isomer distributions and product analyses for acid-catalyzed chlorinations of anisole with *N*-chloro-4-cyanoacetanilide (purity of *N*-chloro-4-cyanoacetanilide, 98%)

Acid	[Ca] (*M*)	Weight of NCAA (g)	Recovery of anilide: Weight of anilide (g)	Recovery of anilide: % yield	Recovery of anilide: Melting point* (°C)	Analysis of 2- and 4-chloroanisoles†: Weight (g)	Analysis of 2- and 4-chloroanisoles†: % yield	Analysis of 2- and 4-chloroanisoles†: *R*
CF_3COOH	0.443	0.972	0.695	89	210–215	0.689	99±0	0.185±0.007
CCl_3COOH	0.535	0.973	0.720	92	204–205	0.646	93±3	0.160±0.008
$CH_2ClCOOH$	0.509	0.980	0.726	92	207–208	0.654	93±3	0.139±0.009
CH_3COOH	0.377	0.981	0.740	93	206–207	0.677	96±2	0.076±0.000
No acid	—	0.978	0.745	95	204–206	0.684	98±4	0.047±0.001

*Literature m.p. 205 °C.

†No 3-chloroanisole or 2,4-dichloroanisole was detected in these experiments. Least-squares line for the Brönsted correlation: $\log R = 0.077 \pm 0.01$, $\log K_a = -0.71 \pm 0.03$. The probable errors in the parameters for the Brönsted equation were calculated as described in part II.

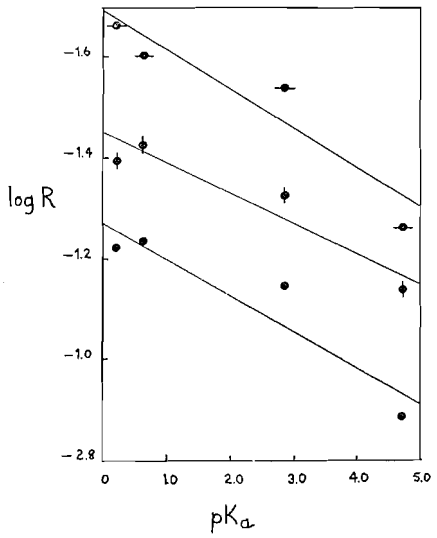


FIG. 1. The correlation between the isomer ratio parameter R and the pK_a of the catalyzing acid. LEGEND: ●, *N*-chloroacetanilide; ●, *N*-chloro-4-methylacetainilide; –●–, *N*-chloro-4-cyanoacetanilide. The curves for *N*-chloro-4-methylacetanilide and *N*-chloro-4-cyanoacetanilide have been displaced upwards by 0.2 and 0.4 log unit on the R axis, respectively.

values for the NCAA's are identical within the precision of the present results. The operation of the Soper mechanism (eq. [2]) offers a tempting explanation of the insensitivity

[2] $$\mathrm{ArNClCOCH_3 + RCOOH \rightleftarrows ArNHAc + RCOOCl}$$
$$\mathrm{RCOOCl + C_6H_5OMe \rightarrow 2\text{-}ClC_6H_4OMe + 4\text{-}ClC_6H_4OMe + RCOOH}$$

of R to the structure of the NCAA. However, a more detailed examination of the problem suggests other possibilities. In part II of the present series, the Brönsted α appropriate to each 4-substituted NBAA was shown to correlate with the Brown and Okamoto σ^+ parameter, giving an equation of the form

[3] $$\alpha = \rho^+\sigma^+ + C',$$

where the symbols ρ^+ and σ^+ have their usual significance and C' is a constant. Combining eqs. [1] and [3] gives eq. [4], which provides a means of expressing the dependence of R on

[4] $$\log R = (\rho^+\sigma^+ + C') \log K_a + C''$$

both the structure of *N*-halogenoacylanilide and the carboxylic acid within the framework of a single equation. From the relationship

[5] $$\log R = \log \frac{2k_o}{k_p},$$

where k_o and k_p are, respectively, the specific rate constants for the product-determining step in the anisole chlorination at the 2 and 4 positions, it is possible to split eq. [4] into two separate equations of the form

[6] $$\log k_o = (\rho_o{}^+\sigma^+ + C_o') \log K_a + C_o''$$

and

[7] $$\log k_p = (\rho_p{}^+\sigma^+ + C_p') \log K_a + C_p'',$$

Can. J. Chem. Downloaded from www.nrcresearchpress.com by 210.87.254.40 on 09/05/12
For personal use only.

where

[8] $$\rho^+ = \rho_o^+ - \rho_p^+,$$

[9] $$C' = C_o' - C_p',$$

and

[10] $$C'' = C_o'' + \log 2 - C_p''.$$

Equation [8] provides the basis for a systematic discussion of the dependence of the R parameter on the structure of the N-halogenoacylanilide in terms of the parameters ρ_o^+ and ρ_p^+. There are three distinct possibilities with regard to these parameters, which are conveniently summarized by eqs. [11]–[13]. The first condition (eq. [11]) is one in which the

[11] $$\rho_o^+ = \rho_p^+ = 0; \text{ therefore, } \rho^+ = 0$$

[12] $$\rho_o^+ = \rho_p^+; \text{ therefore, } \rho^+ = 0$$

[13] $$\rho_o^+ \neq \rho_p^+; \text{ therefore, } |\rho^+| > 0$$

rate constants k_o and k_p are completely independent of structural variations of the N-halogenoacylanilide; this is clearly a necessary condition for the operation of the Soper mechanism. The second possibility (eq. [12]) requires that k_o and k_p both have identical sensitivities to structural variations at the 4 position of N-halogenoacylanilide. This condition leads to the same situation with regard to the parameter ρ^+, i.e. $\rho^+ = 0$; this is now seen to be a necessary, but not a sufficient, condition for the operation of the Soper mechanism. The third possibility (eq. [13]) is that observed in the case of the NBAA series (1), and this situation is incompatible with a mechanism involving the intermediate production of acylhypohalites. In cases where both ρ_o^+ and ρ_p^+ are small, but where $\rho_o^+ \neq \rho_p^+$, the situation represented by eq. [13] will be difficult to distinguish from those represented by eqs. [11] and [12]; in these circumstances no clear-cut distinction between the Soper and the termolecular scheme (see part II) will be possible.

On the basis of other evidence, Dewar and Couzens (5, 6) have rejected acylhypobromites as intermediates in both the bromination and rearrangement reactions of NBAA's. Although the evidence for the rejection of hypochlorites in the case of NCAA's is less compelling, the reduction of the Brönsted exponent by the N—Cl link relative to the N—Br link (see Tables II–IV and ref. 1) is similar to the effect of electron-withdrawing substituents attached to the aromatic ring in the case of the NBAA's (1). We interpret this observation by postulating that the N—Cl linkage saturates this effect to the extent that various substituents attached to the para position of the aromatic ring of the NCAA's produce no *observable* change in the magnitude of the Brönsted exponents. This explanation of the small and constant Brönsted exponents in the NCAA series, combined with the close chemical analogy generally displayed by bromine and chlorine, suggests that a rejection of the termolecular scheme in favor of a rationalization of the experimental data based on the Soper mechanism would be premature. Any revival of the Soper mechanism must await the accumulation of less-ambiguous experimental evidence in its favor.

ACKNOWLEDGMENTS

The authors thank the National Research Council for financial support, and Mr. T. Buckley for measuring the nuclear magnetic resonance spectra. We also thank our colleagues for their continued interest.

Can. J. Chem. Downloaded from www.nrcresearchpress.com by 210.87.254.40 on 09/05/12
For personal use only.

REFERENCES

1. J. M. W. Scott and J. G. Martin. Can. J. Chem. **48**, 732 (1965).
2. G. C. Israel, A. W. N. Tuck, and F. G. Soper. J. Chem. Soc. 547 (1945).
3. R. P. Bell and P. V. Dankwerts. J. Chem. Soc. 1774 (1939).
4. H. C. Brown, D. H. MacDaniel, and O. Hafliger. Determination of organic structures by physical methods. *Edited by* E. A. Braude and F. C. Nachod. Academic Press, Inc., New York. 1955. Chap. 14. p. 579.
5. M. J. S. Dewar. Kekule Symposium; International Union of Pure and Applied Chemistry. Butterworth Scientific Publications, London. 1959. p. 179.
6. P. J. Couzens. Ph.D. Thesis, University of London, London, England. 1959.

Can. J. Chem. Downloaded from www.nrcresearchpress.com by 210.87.254.40 on 09/05/12
For personal use only.

Can. J. Chem. Downloaded from www.nrcresearchpress.com by 210.87.254.40 on 09/05/12
For personal use only.

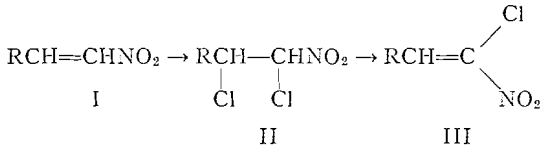
THE SYNTHESES OF 1-CHLORO-1-NITROALKENES

F. I. Carroll and J. A. Kepler
Natural Products Laboratory, Research Triangle Park, North Carolina
Received August 26, 1966

ABSTRACT

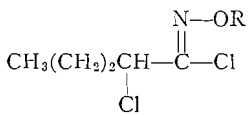
Chlorination of 1-nitroalkenes in acetic acid at 0° in the presence of hydrogen chloride gives the corresponding 1,2-dichloro-1-nitroalkanes in good yields. If the reaction is carried out at higher temperatures, an α-chlorohydroxamoyl chloride, resulting from the reaction of the nitroalkene with hydrogen chloride, is obtained as a side product. Base-catalyzed elimination of hydrogen chloride from the 1,2-dichloro-1-nitroalkenes gave the corresponding 1-chloro-1-nitroalkenes in high yields.

In a recent paper (1) we described an improved synthesis of 1,4-dinitro-1,4-dichlorobutadiene, a biologically active material.[1] As an extension of this work we have now prepared some simple 1-nitro-1-chloroalkenes (III) by the sequence shown in Reaction Scheme 1.

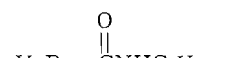


Reaction Scheme 1.

Chlorination of the nitroolefins (I) in carbon tetrachloride or acetic acid at r oom tem perature was very slow. Increasing the temperature to 40° did not accelerate the reaction to any appreciable extent. However, when hydrogen chloride and chlorine were simultaneously passed through an acetic acid solution of I (R = $CH_3(CH_2)_2$–), an exothermic reaction occurred. Distillation of the reaction mixture gave a 41% yield of the desired 1,2-dichloro-1-nitropentane and 20% of a higher boiling component C_5H_9ClNO. We have shown this product to be 2-chloropentanehydroxamoyl chloride (IV), based largely on the infrared spectrum, which showed absorption at 3 550 (OH) and 1 630 cm^{-1} (C=N), and the nuclear magnetic resonance (n.m.r.) spectrum, which showed a triplet at δ 4.70 (1H, J = 7 c.p.s., $-CH_2\underset{|}{CH}-Cl$) and a broad singlet at 8.73 p.p.m. (1H, OH) in addition to the methyl and methylene resonances. 2-Chloropentanehydroxamoyl chloride gradually decomposed, even at −10°, and a satisfactory analysis could not be obtained. Treatment of



IV, R = H



V, R =

[1]*The nature of this activity will be described in a future publication by H. W. Spurr and J. A. Durden, Olefins Division, Union Carbide Corporation.*

Can. J. Chem. Downloaded from www.nrcresearchpress.com by 210.87.254.40 on 09/05/12
For personal use only.

IV with phenylisocyanate gave the urethane V, which was quite stable. The analysis and infrared and n.m.r. spectra of this compound are in agreement with the assigned structure. Heath and Rose (2) have reported that nitroolefins containing an α-hydrogen are converted into the corresponding α-chlorohydroxamoyl chloride when treated with dry hydrogen chloride in anhydrous ether. The 2-chloropentanehydroxamoyl chloride (IV) we obtained undoubtedly arose from the reaction of hydrogen chloride with the 1-nitropentene, since a 54% yield of IV could be obtained by treating an acetic acid solution of I (R = $CH_3(CH_2)_2$–) with dry hydrogen chloride in the absence of chlorine. We found that this side reaction could be prevented and the yield of the 1,2-dichloropentane increased to 51% if the reaction was performed at ice-bath temperature with a solvent ratio of 375 ml of acetic acid for each 0.1 mole of nitroolefin. By using this procedure, the 1,2-dichloro-1-nitroalkanes listed in Table I were prepared. The n.m.r. spectra of these dichloro derivatives showed a doublet at δ 5.75–5.85 (1H, J = 8.5 c.p.s., —$CH(Cl)NO_2$) and a multiplet at 4.32–4.46 p.p.m. (1H, –CH_2–CH—CH—). Other physical constants are tabulated in Table I.

Treatment of the 1,2-dichloronitroalkanes with triethylamine or pyridine in ether gave the corresponding 1-chloro-1-nitroalkenes (III) in 70–88% yields. The n.m.r. spectrum of the olefins (III) showed a multiplet at δ 2.39–2.44 for the allylic methylene proton and a triplet at 7.39–7.49 p.p.m. (J = 7.5 c.p.s.) for the olefinic proton. The 1-chloro-1-nitroalkenes (III) prepared, along with their analyses and physical constants, are given in Table II.

EXPERIMENTAL

The melting points were obtained on a Kofler hot stage and are corrected. The boiling points are uncorrected. The infrared spectra were obtained with a Perkin–Elmer model 221 spectrophotometer. The n.m.r. spectra were obtained on a Varian A-60 spectrometer with samples dissolved in deuteriochloroform (internal standard, tetramethylsilane). The ultraviolet spectra were obtained with a Bausch and Lomb model 505 spectrophotometer. The gas chromatograms were run on a F & M model 700 chromatograph, and thin-layer chromatograms were obtained with silica gel HF. The microanalyses were carried out by Micro-Tech Laboratories, Inc., Skokie, Illinois.

Preparation of Nitroolefins

The nitroolefins used in the preparation of the 1,2-dichloro-1-nitroalkanes were prepared according to the procedure of Carroll *et al.* (3). The olefins were obtained in a reasonable yield and purity by one distillation.

Chlorination of 1-Nitropentene at Room Temperature

Chlorine and hydrogen chloride were passed simultaneously through a solution of 10.0 g (0.087 mole) of 1-nitropentene in 48 ml of acetic acid. The solution turned blue and the temperature rose to 85° and then dropped as the blue color disappeared. After ½ h, a vapor-phase chromatograph (6 ft column of 5% SE-30 on 60–80 Chromosorb P) indicated that all of the nitroolefin had reacted and showed two new peaks. Nitrogen was passed through the solution to displace the excess chlorine and hydrogen chloride. The acetic acid was separated from the products by distillation at 16 mm. The remaining liquid was distilled under a high vacuum to give 6.64 g (41%) of 1,2-dichloro-1-nitropentane (see Table I for analysis and physical constants), b.p. 61–62° at 3 mm, and 2.29 g (20%) of 2-chloropentanehydroxamoyl chloride, b.p. 50–51° at 0.05 mm. This compound gradually decomposed with the evolution of hydrogen chloride and precipitation of hydroxylamine hydrochloride.

A phenylurethan was obtained by heating a sample of 2-chloropentanehydroxamoyl chloride with phenylisocyanate, and was recrystallized from hexane, m.p. 96–98°. The infrared spectrum (CH_2Cl_2) showed absorption at 3 400 (NH) and 1 775 cm^{-1} (C=O). The n.m.r. ($CDCl_3$) showed a triplet at δ 0.92 (3H, J = 7.5 c.p.s., CH_3—CH_2), a multiplet at 1.41 (1.9H, CH_3CH_2), a multiplet at 2.0 (2.1H, CH_2CH—Cl), a triplet at 4.75 (1H, J = 7.5 c.p.s., CH_2CH—Cl), a multiplet at 7.31 (5.4H, Ar—H), and a singlet at 7.88 p.p.m. (1H, NH).

Anal. Calcd. for $C_{12}H_{14}Cl_2N_2O_2$: C, 49.84; H, 4.88; N, 9.69. Found: C, 49.69; H, 4.63; N, 9.84.

Preparation of 2-Chloropentanehydroxamoyl Chloride from the Reaction of 1-Nitropentene with Hydrogen Chloride

Hydrogen chloride was passed into a solution of 10 g (0.087 mole) of 1-nitropentene in 50 ml of acetic acid. The solution turned blue and the temperature rose to 85° and then dropped as the blue color disappeared.

Can. J. Chem. Downloaded from www.nrcresearchpress.com by 210.87.254.40 on 09/05/12
For personal use only.

TABLE I

$CH_3(CH_2)_nCH(Cl)—CHNO_2(Cl)$

n	% yield	Boiling point (°C)	n_D^{25}	Molecular formula	Carbon (%)		Hydrogen (%)		Nitrogen (%)		Chlorine (%)	
					Calculated	Found	Calculated	Found	Calculated	Found	Calculated	Found
2	51	35–37 at 0.03 mm	1.4600	$C_5H_9Cl_2NO_2$	32.29	32.52	4.88	4.94	7.53	7.46	38.12	38.01
3	58	46–47 at 0.06 mm	1.4612	$C_6H_{11}Cl_2NO_2$	36.01	35.99	5.54	5.51	7.00	7.06	35.44	35.61
4	74	56–57 at 0.05 mm	1.4607	$C_7H_{13}Cl_2NO_2$	39.27	39.35	6.12	6.18	6.54	6.85	33.12	33.12
5	85	67–68 at 0.05 mm	1.4610	$C_8H_{15}Cl_2NO_2$	42.12	42.38	6.63	6.70	6.14	6.14	31.09	31.06
6	92	91–93 at 0.04 mm	1.4618	$C_9H_{17}Cl_2NO_2$	44.64	44.86	7.07	6.95	5.79	5.56	29.28	29.19

TABLE II

$CH_3(CH_2)_nCH{=}C(Cl)(NO_2)$

n	% yield	Boiling point (°C)	n_D^{25}	$\lambda_{max}^{n\text{-hexane}}$ (mμ)	ϵ_{max}	Molecular formula	Carbon (%)		Hydrogen (%)		Nitrogen (%)		Chlorine (%)	
							Calculated	Found	Calculated	Found	Calculated	Found	Calculated	Found
2	74	40–41 at 1.0 mm	1.4735	256	4 425	$C_5H_5ClNO_2$	40.14	40.19	5.39	5.35	9.36	9.07	23.70	23.96
3	70	56–56.5 at 0.7 mm	1.4725	256	4 032	$C_6H_{10}ClNO_2$	44.05	44.31	6.16	6.22	8.56	8.67	21.67	21.48
4	75	55–56 at 0.2 mm	1.4719	258	4 822	$C_7H_{12}ClNO_2$	47.33	47.01	6.81	6.81	7.89	7.53	19.96	19.71
5	83	69 at 0.2 mm	1.4724	258	5 104	$C_8H_{14}ClNO_2$	50.12	50.05	7.35	7.32	7.30	7.19	18.50	18.67
6	88	82–84 at 0.08 mm	1.4716	258	5 013	$C_9H_{16}ClNO_2$	52.51	52.17	7.91	7.78	6.81	6.81	17.22	16.96

The acetic acid and excess hydrogen chloride were removed under vacuum. The remaining liquid was distilled under a high vacuum to give 7.98 g (54%) of 2-chloropentanehydroxamoyl chloride (IV), b.p. 55–58° at 0.15 mm. The infrared and n.m.r. spectra were identical with those of IV prepared in the experiment above.

General Procedure for the Preparation of 1,2-Dichloro-1-nitroalkanes from 1-Nitroalkenes

The 1-nitroalkene (0.2 mole) was dissolved in 750 ml of acetic acid (distilled from potassium permanganate). The solution was cooled in an ice bath, and hydrogen chloride and chlorine were bubbled through the solution simultaneously. The reaction mixture was then subjected to thin-layer chromatography (petroleum ether – benzene (2:1)). When the reaction was complete (1–3 h), the ice bath was removed and the excess chlorine and hydrogen chloride were expelled from solution by passing nitrogen through the reaction mixture. The acetic acid was then removed on the freeze-dryer and the residual colorless oil distilled. The 1,2-dichloro-1-nitroalkanes were obtained as colorless liquids in reasonable yields (Table I).

A modified work-up procedure was used in the preparation of 1,2-dichloro-1-nitropentane. The reaction mixture was diluted with 3 l of water after the excess chlorine and hydrogen chloride had been expelled from the solution. The oily layer was separated, dissolved in ether, and dried over magnesium sulfate. The aqueous layer was washed with 3 × 500 ml of ether. The ether was removed on the flash evaporator, leaving an acetic acid solution of the desired product. This solution was concentrated to approximately one-half of its original volume by distillation at the water pump. The concentrate was further purified by distilling the acetic acid from it on a spinning-band column at 15 mm pressure. The pot residue from the spinning-band distillation was combined with the oil that separated upon dilution of the original acetic acid solution. Distillation of this mixture gave the desired product in a 51% yield. The infrared spectra of the 1,2-dichloro-1-nitroalkanes were all very similar and showed absorption at 1 570 and 1 360 cm^{-1} (saturated NO_2).

General Procedure for the Preparation of 1-Chloro-1-nitroalkenes from 1,2-Dichloro-1-nitroalkanes

The 1,2-dichloro-1-nitroalkane (0.05 mole) was dissolved in 500 ml of dry ether, and the solution was cooled in an ice bath. Triethylamine (0.05 mole) in 250 ml of dry ether was added dropwise to the well-stirred solution over a 1–3 h period. Filtration of the reaction mixture gave a quantitative yield of triethylamine hydrochloride. The filtrate was washed with dilute hydrochloric acid and 3 × 100 ml of water. The ether solution was dried and the solvent removed to give the desired products. The olefins were purified by vacuum distillation (Table II). The 1-chloro-1-nitroalkenes gradually decompose at room temperature, but seem to be relatively stable when kept at −10°.

Pyridine rather than triethylamine was used as the base for the preparation of 1-chloro-1-nitrohexene. Consequently, the reaction was allowed to proceed for a longer time and at room temperature.

The infrared spectra of the 1-chloro-1-nitroalkenes were all very similar and were characterized by the following bands: 1 630 (double bond) and 1 540 and 1 340 cm^{-1} (conjugated nitro).

ACKNOWLEDGMENTS

We thank Dr. Monroe E. Wall, Director of this laboratory, for his kind encouragement and support of this work. Part of the work was supported by the Union Carbide Chemicals Corporation, South Charleston, West Virginia. Expert technical assistance was provided by Mrs. Rebecca Stephenson.

REFERENCES

1. F. I. Carroll, S. C. Kerbow, and M. E. Wall. Can. J. Chem. **44**, 2115 (1966).
2. R. L. Heath and J. D. Rose. J. Chem. Soc. 1485 (1947).
3. F. I. Carroll, J. D. White, and M. E. Wall. J. Org. Chem. **28**, 1236 (1963).

Can. J. Chem. Downloaded from www.nrcresearchpress.com by 210.87.254.40 on 09/05/12
For personal use only.

Can. J. Chem. Downloaded from www.nrcresearchpress.com by 210.87.254.40 on 09/05/12
For personal use only.

SOME STEAM-VOLATILE COMPONENTS OF THE EXTRACTIVES FROM POPULUS TREMULOÏDES HEARTWOOD

R. A. Abramovitch and O. A. Koleoso

The extractives from the heartwood of *Populus tremuloïdes* (aspen poplar) have been the subject of a systematic investigation (1–3). It was shown that saponification of the acetone extractives gave a steam-volatile portion which could be resolved into four major components by gas-phase chromatography (1). It has since been established that one of the major components of this mixture was isophorone, which was an artifact formed during the extraction procedure. We now report a study of the composition of the steam-volatile fraction of the benzene extractives of the heartwood, from which fatty acids had been removed with sodium bicarbonate.

The mixture was subjected to a preliminary preparative gas chromatographic separation to give nine components, the first four of which were collected together as fraction I and later rechromatographed. The other peaks were collected individually as fractions II, III, IV, V, and VI, respectively (increasing retention times). Fractions IV and VI appeared to be mixtures which could not be resolved further and were not examined at this time. Fractions II, III, and V were rechromatographed on Apiezon L columns; II and V were single compounds, and III was resolved into four fractions: III^A, III^B, III^C, and III^D.

Compound II had bands in the infrared characteristic of a primary alcoholic group and a monosubstituted phenyl ring. Its nuclear magnetic resonance (n.m.r.) spectrum exhibited a 5H singlet at τ 2.9 and a 2H singlet at τ 5.7, suggesting that it was benzyl alcohol, which was confirmed by comparison of the spectra with those of an authentic sample. Similarly, compound III^A was shown to be phenol, and compound III^B β-phenylethanol. Compound III^C exhibited a weak band at 3 500 cm^{-1} (OH), a band of medium intensity at 2 720 cm^{-1} (C(=O)—H), and a strong band at 1 680 cm^{-1}, suggesting the presence of an α,β-unsaturated aldehyde function. It had an ultraviolet absorption maximum at 274 mμ, suggestive of an α- or β-hydroxy-α,β-unsaturated aldehyde (4). It formed a 2,4-dinitrophenylhydrazone and a semicarbazone, the melting points of which were very close to those of the corresponding derivatives of isophorone. The infrared and ultraviolet spectra of III^C, however, were quite different from those of isophorone. Unfortunately, there were insufficient amounts of III^C to carry out any further structural studies. Compound V had bands in the infrared characteristic of a phenolic hydroxyl group and a para-disubstituted benzene ring. Its n.m.r. spectrum showed a 4H quartet at τ 3.2, a 2H quartet at τ 7.5 (Ar—$C\underline{H}_2$—), and a 3H triplet at τ 8.9 (—CH_2—CH_3). These data were compatible with the compound being *p*-ethylphenol; this was confirmed by direct comparison with an authentic sample.

Fraction I was rechromatographed at a lower temperature and resolved into nine components (fractions I^A–I^I). Fractions I^B, I^D, I^F, and I^I were collected, since they were the most abundant (the first fraction was present in appreciable quantities but was clearly a mixture), and purified by further preparative gas chromatography. Fractions I^B and I^D were identified as *n*-hexyl and *n*-heptyl alcohols, respectively. Fraction I^F was not obtained

in sufficient quantities to permit its characterization, but its infrared absorption spectrum suggested the presence of a hydroxyl group and an α,β-unsaturated aldehyde function. The ultraviolet absorption maximum at 220 mμ indicated that the hydroxyl group was not on the α- or β-carbon of the α,β-unsaturated aldehyde. On the basis of its infrared and n.m.r. spectra, fraction I^I could be characterized as methyl benzoate; this was confirmed by comparison with an authentic sample.

None of the compounds isolated in this study were observed in the other fractions already investigated (1–3). The presence of phenol, *p*-ethylphenol, benzyl alcohol, and β-phenylethanol in the heartwood may be of taxonomic significance.

EXPERIMENTAL

Extraction and Isolation

The dried sawdust (8 kg) from *Populus tremuloïdes* heartwood was extracted continuously with benzene for 8 days. Evaporation of the solvent gave a brown semisolid residue (120 g, 1.5% by weight of the sawdust). This was steam-distilled for 5 h, the distillate being collected in an ice–salt mixture. The steam-distillate was extracted with ether, and the ether solution was shaken with a saturated aqueous sodium bicarbonate solution, washed with water, and dried ($MgSO_4$). Evaporation of the ether gave a yellow oil (4 g, 0.05% by weight of the sawdust).

Gas Chromatographic Separation of the Steam-Volatile Oil

A preliminary resolution was achieved on a 6 ft × $\frac{1}{4}$ in. column packed with 15% ethylene glycol adipate on Chromosorb W and operated at 150° and a helium flow rate of 46 ml/min. The first four components were collected together as fraction I. The last five (retention times 6, 7.2, 10.5, 13.7, and 14.5 min, respectively) were collected individually as fractions II, III, IV, V, and VI. Fractions II and III were rechromatographed on a 6 ft × $\frac{1}{4}$ in. column packed with 25% Apiezon L on Chromosorb W and operated at 145° and a helium flow rate of 20 ml/min. Fraction II gave a single component (retention time 11 min), collected as a colorless liquid (24 mg), b.p. 106° at 20 mm. Fraction III was resolved into four components: III^A, III^B, III^C, and III^D (retention times 7, 10.5, 16, and 41.5 min, respectively), III^A and III^C being the major ones. Fraction V was rechromatographed on a 6 ft × $\frac{3}{16}$ in. column packed with 20% Apiezon L on Chromosorb W and operated at 135° and a helium flow rate of 81 ml/min. Only a single peak, retention time 4.3 min, was observed. Fractions IV and VI could not be resolved cleanly into their components by using different columns.

Fraction I was rechromatographed on a 6 ft × $\frac{1}{4}$ in. column packed with 15% ethylene glycol adipate on Chromosorb W and operated at 125° and a helium flow rate of 60 ml/min. Nine peaks (corresponding to fractions I^A–I^I) were observed, the first of which was a broad band consisting of a mixture of compounds. The other peaks had retention times of 3.2, 4.2, 5.0, 6.0, 6.8, 8.0, 10.6, and 14 min, respectively. The fractions giving rise to peaks 2, 4, 5, 6, and 9 were collected and rechromatographed, and pure fractions I^B, I^D, I^F, and I^I were thus obtained.

Fraction II (Benzyl Alcohol)

The infrared and n.m.r. spectra were identical with those of authentic benzyl alcohol.

Fraction III^A (Phenol)

This fraction (22 mg), b.p. 75° at 14 mm, m.p. 39–40°, had bands in the infrared (liquid film) at 3 420 (s) (OH), 3 050 (w), 1 595 (s), 1 220 (s), 750 (s), and 690 cm^{-1} (s). In the ultraviolet it had a band at λ_{max} 272 mμ (95% ethanol), and the n.m.r. spectrum (measured on a CCl_4 solution) had a 5H doublet at τ 3.15 and a 1H singlet at τ 4.7. A direct comparison with phenol showed the two compounds to be identical in all respects.

Fraction III^B (β-Phenylethanol)

This fraction (20 mg) exhibited bands in the infrared (liquid film) at 3 350 (s), 3 070 (s), 3 030 (s), 2 940 (s), 2 880 (s), 1 600 (s), 1 490 (s), 1 450 (s), 1 370 (w), 1 170 (m), 1 040 (s), 740 (s), and 690 cm^{-1} (s), which corresponded to those of an authentic sample. The retention times of both compounds were also identical.

Fraction III^C

This was a colorless liquid (5 mg) whose infrared spectrum (liquid film) exhibited bands at 3 500 (br) (w), 3 020 (w), 2 960 (s), 2 920 (s), 2 860 (s), 2 720 (m), 1 680 (s), 1 635 (s), 1 450 (m), 1 375 (w), 1 155 (s), 1 140 (s), 1 005 (s), and 980 cm^{-1} (s). It absorbed at λ_{max} 274 mμ in the ultraviolet. The 2,4-dinitrophenylhydrazone, recrystallized from an ethyl acetate – ethanol mixture, had m.p. 138–139°. The semicarbazone (crystallized from aqueous ethanol) had m.p. 188–189°.

Fraction V (p-Ethylphenol)

This fraction (21 mg) had b.p. 104° at 13 mm and m.p. 44–45°. It exhibited the following bands in the infrared (KBr disk): 3 320 (s), 3 020 (w), 2 960 (s), 2 930 (s), 2 870 (s), 1 610 (s), 1 230 (s), 1 108 (s), and 820 cm^{-1} (s). It absorbed at 280 mμ in the ultraviolet (95% ethanol solution). The following CH lines were present in the n.m.r. spectrum: 4H quartet at τ 3.2, 2H quartet at τ 7.5, and a 3H triplet at τ 8.9. These data were identical with those for authentic *p*-ethylphenol.

Can. J. Chem. Downloaded from www.nrcresearchpress.com by 210.87.254.40 on 09/05/12
For personal use only.

Fractions I^B and I^D

Fraction I^B (18 mg), b.p. 58–60° at 11 mm, was shown by infrared and n.m.r. spectroscopy as well as by gas chromatography to be identical with *n*-hexyl alcohol. Similarly, fraction I^D (58 mg), b.p. 68–70° at 11 mm, was shown to be *n*-heptyl alcohol.

Fraction I^F

This was a colorless liquid (23 mg), b.p. 70° at 11 mm. It had infrared absorption bands (liquid film) at 3 500 (s), 2 960 (sh), 2 920 (s), 2 860 (s), 2 720 (m), 1 680 (s), 1 630 (s), 1 450 (s), 1 375 (m), 1 140 (s), 1 090 (m), 980 (s), and 720 cm^{-1} (m), and an ultraviolet absorption band at 220 mμ with shoulders at 274 and 320 mμ.

Fraction I^I (Methyl Benzoate)

The infrared and n.m.r. spectra and retention times of this fraction (17 mg, b.p. 76° at 13 mm) were identical with those of an authentic sample of methyl benzoate.

ACKNOWLEDGMENT

This work was supported financially by a grant from the Saskatchewan Research Council.

1. R. A. Abramovitch, R. G. Micetich, and S. J. Smith. Tappi, **46**, 37 (1963).
2. R. A. Abramovitch and R. G. Micetich. Can. J. Chem. **40**, 2017 (1962).
3. R. A. Abramovitch and R. G. Micetich. Can. J. Chem. **41**, 2362 (1963).
4. C. N. Rao. Ultraviolet and visible spectroscopy. Butterworths, London. 1961.

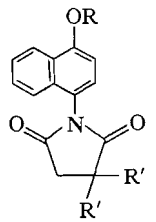
Received August 9, 1966.
Department of Chemistry,
University of Saskatchewan,
Saskatoon, Saskatchewan.

Can. J. Chem. Downloaded from www.nrcresearchpress.com by 210.87.254.40 on 09/05/12
For personal use only.

DERIVATIVES OF 4-AMINO-1-NAPHTHOL

M. A. Abdelkader, M. Khalifa, and Y. M. Abou-Zeid

Although 4-acetamido-1-ethoxynaphthalene, commonly known as naphthacetin, as well as the methoxy analogue has been found to possess analgesic properties, they are too toxic to be used as medicines (1), and the need arose for less-toxic derivatives. In the hope of realizing such an objective and because of the importance which has been attached to the use of succinimides as anticonvulsants (2, 3), the acetamido group was replaced by succinimido while the classical ether groupings were retained.



R = H, CH_3, C_2H_5, CH_2—CH=CH_2, or $COCH_3$
R′ = H or CH_3

Derivatives having the above general formula were synthesized by condensing succinic anhydride or the α,α-dimethyl derivative with the hydrochloride of 4-amino-1-naphthol.

Fractions I^B and I^D

Fraction I^B (18 mg), b.p. 58–60° at 11 mm, was shown by infrared and n.m.r. spectroscopy as well as by gas chromatography to be identical with *n*-hexyl alcohol. Similarly, fraction I^D (58 mg), b.p. 68–70° at 11 mm, was shown to be *n*-heptyl alcohol.

Fraction I^F

This was a colorless liquid (23 mg), b.p. 70° at 11 mm. It had infrared absorption bands (liquid film) at 3 500 (s), 2 960 (sh), 2 920 (s), 2 860 (s), 2 720 (m), 1 680 (s), 1 630 (s), 1 450 (s), 1 375 (m), 1 140 (s), 1 090 (m), 980 (s), and 720 cm^{-1} (m), and an ultraviolet absorption band at 220 mμ with shoulders at 274 and 320 mμ.

Fraction I^I (Methyl Benzoate)

The infrared and n.m.r. spectra and retention times of this fraction (17 mg, b.p. 76° at 13 mm) were identical with those of an authentic sample of methyl benzoate.

ACKNOWLEDGMENT

This work was supported financially by a grant from the Saskatchewan Research Council.

1. R. A. Abramovitch, R. G. Micetich, and S. J. Smith. Tappi, **46**, 37 (1963).
2. R. A. Abramovitch and R. G. Micetich. Can. J. Chem. **40**, 2017 (1962).
3. R. A. Abramovitch and R. G. Micetich. Can. J. Chem. **41**, 2362 (1963).
4. C. N. Rao. Ultraviolet and visible spectroscopy. Butterworths, London. 1961.

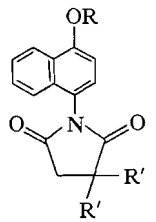
Received August 9, 1966.
Department of Chemistry,
University of Saskatchewan,
Saskatoon, Saskatchewan.

Can. J. Chem. Downloaded from www.nrcresearchpress.com by 210.87.254.6 on 09/05/12
For personal use only.

DERIVATIVES OF 4-AMINO-1-NAPHTHOL

M. A. Abdelkader, M. Khalifa, and Y. M. Abou-Zeid

Although 4-acetamido-1-ethoxynaphthalene, commonly known as naphthacetin, as well as the methoxy analogue has been found to possess analgesic properties, they are too toxic to be used as medicines (1), and the need arose for less-toxic derivatives. In the hope of realizing such an objective and because of the importance which has been attached to the use of succinimides as anticonvulsants (2, 3), the acetamido group was replaced by succinimido while the classical ether groupings were retained.



R = H, CH_3, C_2H_5, CH_2—CH=CH_2, or $COCH_3$
R′ = H or CH_3

Derivatives having the above general formula were synthesized by condensing succinic anhydride or the α,α-dimethyl derivative with the hydrochloride of 4-amino-1-naphthol.

Can. J. Chem. Downloaded from www.nrcresearchpress.com by 210.87.254.6 on 09/05/12
For personal use only.

TABLE I
Yields, melting points,* and analyses† for 4-amino-1-naphthol and derivatives

Chemical name	R	R′	Yield (%)	Melting point (°C)	Formula	Analysis (%) Calculated C	H	N	Found C	H	N
4-(3,3-Dimethylsuccinimido)-1-acetoxynaphthalene	$COCH_3$	CH_3	96	149–150	$C_{18}H_{17}NO_4$	69.45	5.46	4.50	69.10	5.59	4.46
4-(3,3-Dimethylsuccinimido)-1-allyloxynaphthalene	CH_2—CH=CH_2	CH_3	85	130–132	$C_{19}H_{19}NO_3$	73.78	6.15	4.53	73.88	6.25	4.76
4-(3,3-Dimethylsuccinimido)-1-ethoxynaphthalene	C_2H_5	CH_3	88	144–146	$C_{18}H_{19}NO_3$	72.69	6.39	4.71	72.77	6.47	4.71
4-(3,3-Dimethylsuccinimido)-1-methoxynaphthalene	CH_3	CH_3	90	183–185	$C_{17}H_{17}NO_3$	72.08	6.00	4.94	71.87	6.05	5.00
4-(3,3-Dimethylsuccinimido)-1-naphthol	H	CH_3	76	205–207	$C_{16}H_{15}NO_3$	71.37	5.57	5.20	71.28	5.69	5.24
4-Succinimido-1-acetoxynaphthalene	$COCH_3$	H	90	174–176	$C_{16}H_{13}NO_4$	67.84	4.99	4.94	67.76	4.75	4.91
4-Succinimido-1-allyloxynaphthalene	CH_2—CH=CH_2	H	90	155–157	$C_{17}H_{15}NO_3$	72.59	5.34	4.98	72.09	5.34	5.03
4-Succinimido-1-ethoxynaphthalene	C_2H_5	H	96	210–212	$C_{16}H_{15}NO_3$			5.20			4.78
4-Succinimido-1-methoxynaphthalene	CH_3	H	95	212–214	$C_{15}H_{13}NO_3$	70.50	5.09	5.49	70.60	5.01	5.47
4-Succinimido-1-naphthol	H	H	80	260–262	$C_{14}H_{11}NO_3$	69.70	4.56	5.80	69.59	4.48	5.88

*All melting points are uncorrected.
†The microanalyses were performed by Dr. C. Janssen, Beerse, Belgium.

The resulting product was either acetylated by heating it with acetic anhydride or converted into the ether by treating the naphthoxide with the alkyl iodide or, alternatively, the free naphthol in acetone with the alkyl iodide in the presence of potassium carbonate. α,α-Dimethylsuccinic acid was prepared in 70% yield according to two reported procedures (4, 5). The dicarboxylic acid was converted into the anhydride in 80% yield by the acetyl chloride method (6*a*). α-Phenylsuccinic acid was prepared by Higson and Thorpe's procedure (6*b*) in an overall yield of 78%, calculated on the basis of the mandilonitrile. An attempt to convert it into the anhydride by the method of Dehn and Thorpe (7) did not give satisfactory results. However, the anhydride was obtained in 80% yield by heating the acid with excess acetic anhydride at 100° for 8 h instead of heating it at 140° for 6 h as reported (7). Among the methods reported for the acylation of amines with inner anhydrides is the direct fusion method (8). However, the aminonaphthol is oxidized by atmospheric oxygen, especially at the fusion temperature. To overcome this difficulty, the aminonaphthol was replaced by its hydrochloride and the succinoylation was successfully achieved by refluxing the hydrochloride with succinic anhydride or the α,α-dimethyl derivative in dry pyridine. On the other hand, when α-phenylsuccinic anhydride was used, no condensation took place with the hydrochloride or the aminonaphthol.

EXPERIMENTAL

4-Succinimido-1-naphthol and Derivatives

General Procedure

A mixture of equimolecular amounts of succinic anhydride (or the α,α-dimethyl derivative) and the hydrochloride of 4-amino-1-naphthol was suspended in dry pyridine (about 7 ml pyridine per 1 g mixture) and heated at 100° for 2–3 h. The pyridine was distilled off *in vacuo*, and the residue was crystallized from aqueous ethanol and then finally either acetylated or etherified as described above. The products were also crystallized from aqueous ethanol (see Table I).

1. F. RADT. Elsevier's encyclopedia of organic chemistry. Vol. 12B. Elsevier Press, Inc., New York. 1950. Ser. III. p. 1647.
2. K. W. HEATHFIELD and E. C. JEWESBURY. Brit. Med. J. **2**, 565 (1961)
3. C. A. MILLER and M. L. LORN. J. Am. Chem. Soc. **73**, 4895 (1951).
4. I. VOGEL. J. Chem. Soc. 2019 (1928).
5. P. A. SMITH and J. P. HORWITZ. J. Am. Chem. Soc. **71**, 3418 (1949).
6. (*a*) A. HIGSON and J. F. THORPE. J. Chem. Soc. **89**, 1468 (1906). (*b*) A. HIGSON and J. F. THORPE. J. Chem. Soc. **89**, 1471 (1906).
7. F. B. DEHN and J. E. THORPE. J. Chem. Soc. **89**, 1882 (1906).
8. J. H. BILLMAN and W. F. HARTING. J. Am. Chem. Soc. **70**, 1473 (1948).

RECEIVED FEBRUARY 25, 1966.
PHARMACY DEPARTMENT, FACULTY OF MEDICINE,
ASSIUT UNIVERSITY,
CAIRO, UNITED ARAB REPUBLIC.

THE STRUCTURE OF SUCCINYL DICHLORIDE

GEORGE H. SCHMID

The existence of two forms of succinyl dichloride was originally proposed (1) to account for the cyclic products obtained in the reactions of succinyl dichloride with Lewis acids. The cyclic product could result from the small amount of the more reactive cyclic form of succinyl dichloride, which was in a facile equilibrium with the acyclic form.

Can. J. Chem. Downloaded from www.nrcresearchpress.com by 210.87.254.6 on 09/05/12
For personal use only.

The resulting product was either acetylated by heating it with acetic anhydride or converted into the ether by treating the naphthoxide with the alkyl iodide or, alternatively, the free naphthol in acetone with the alkyl iodide in the presence of potassium carbonate. α,α-Dimethylsuccinic acid was prepared in 70% yield according to two reported procedures (4, 5). The dicarboxylic acid was converted into the anhydride in 80% yield by the acetyl chloride method (6*a*). α-Phenylsuccinic acid was prepared by Higson and Thorpe's procedure (6*b*) in an overall yield of 78%, calculated on the basis of the mandilonitrile. An attempt to convert it into the anhydride by the method of Dehn and Thorpe (7) did not give satisfactory results. However, the anhydride was obtained in 80% yield by heating the acid with excess acetic anhydride at 100° for 8 h instead of heating it at 140° for 6 h as reported (7). Among the methods reported for the acylation of amines with inner anhydrides is the direct fusion method (8). However, the aminonaphthol is oxidized by atmospheric oxygen, especially at the fusion temperature. To overcome this difficulty, the aminonaphthol was replaced by its hydrochloride and the succinoylation was successfully achieved by refluxing the hydrochloride with succinic anhydride or the α,α-dimethyl derivative in dry pyridine. On the other hand, when α-phenylsuccinic anhydride was used, no condensation took place with the hydrochloride or the aminonaphthol.

EXPERIMENTAL

4-Succinimido-1-naphthol and Derivatives

General Procedure

A mixture of equimolecular amounts of succinic anhydride (or the α,α-dimethyl derivative) and the hydrochloride of 4-amino-1-naphthol was suspended in dry pyridine (about 7 ml pyridine per 1 g mixture) and heated at 100° for 2–3 h. The pyridine was distilled off *in vacuo*, and the residue was crystallized from aqueous ethanol and then finally either acetylated or etherified as described above. The products were also crystallized from aqueous ethanol (see Table I).

1. F. Radt. Elsevier's encyclopedia of organic chemistry. Vol. 12B. Elsevier Press, Inc., New York. 1950. Ser. III. p. 1647.
2. K. W. Heathfield and E. C. Jewesbury. Brit. Med. J. **2**, 565 (1961)
3. C. A. Miller and M. L. Lorn. J. Am. Chem. Soc. **73**, 4895 (1951).
4. I. Vogel. J. Chem. Soc. 2019 (1928).
5. P. A. Smith and J. P. Horwitz. J. Am. Chem. Soc. **71**, 3418 (1949).
6. (*a*) A. Higson and J. F. Thorpe. J. Chem. Soc. **89**, 1468 (1906). (*b*) A. Higson and J. F. Thorpe. J. Chem. Soc. **89**, 1471 (1906).
7. F. B. Dehn and J. E. Thorpe. J. Chem. Soc. **89**, 1882 (1906).
8. J. H. Billman and W. F. Harting. J. Am. Chem. Soc. **70**, 1473 (1948).

Received February 25, 1966.
Pharmacy Department, Faculty of Medicine,
Assiut University,
Cairo, United Arab Republic.

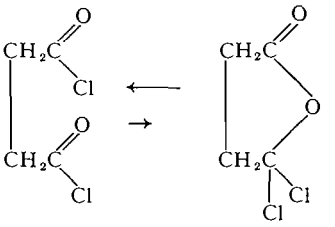
THE STRUCTURE OF SUCCINYL DICHLORIDE

George H. Schmid

The existence of two forms of succinyl dichloride was originally proposed (1) to account for the cyclic products obtained in the reactions of succinyl dichloride with Lewis acids. The cyclic product could result from the small amount of the more reactive cyclic form of succinyl dichloride, which was in a facile equilibrium with the acyclic form.

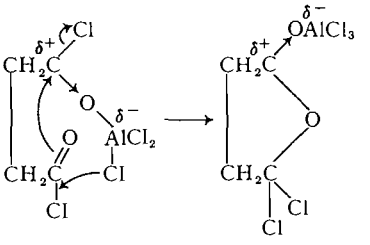
Can. J. Chem. Downloaded from www.nrcresearchpress.com by 210.87.254.105 on 09/05/12
For personal use only.

Nuclear magnetic resonance has shown (2) that neat succinyl dichloride exists predominantly in the acyclic form (I). The possibility of an equilibrium between the proposed cyclic (II) and acyclic (I) forms of succinyl dichloride could not be ruled out, since it was



I II

not possible to detect nuclear magnetic resonance signals from both forms simultaneously. To obtain more information about this proposed equilibrium, it was desirable to obtain the cyclic form II. The reaction of succinyl dichloride with aluminium chloride seemed an attractive method to effect the isomerization of I to II by the [3.2.1] bicyclic path recently established by Newman (3) for similar isomerizations.



The infrared spectrum of a solution of aluminium chloride in succinyl dichloride is shown in Fig. 1. The principal bands in the carbonyl region are listed in Table I.

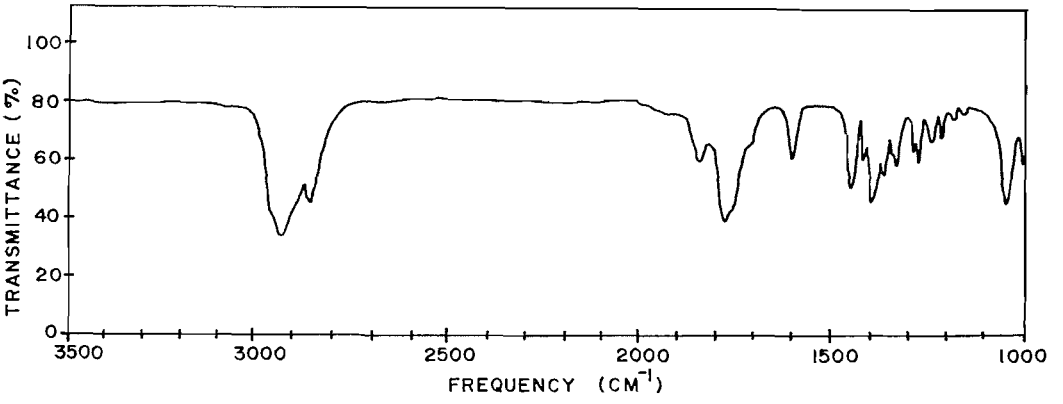


FIG. 1.

The addition of aluminium chloride to succinyl dichloride causes the appearance of a new absorption band in the infrared region at 1 601 cm^{-1}. This band can be attributed to a polarized complex between the acyclic succinyl dichloride and aluminium chloride. Such a

Can. J. Chem. Downloaded from www.nrcresearchpress.com by 210.87.254.105 on 09/05/12
For personal use only.

TABLE I

	$\nu_{C=O}$ (cm^{-1})	Reference
$[CH_2COCl]_2$	1 790 vs* 1 861 m, sh	This work
$[CH_2COCl]_2AlCl_3$	1 601 s 1 710 s, sh 1 783 vs 1 861 s	This work
CH_3COCl	1 808 vs	4
$CH_3COCl{\cdot}AlCl_3$	1 779 m 1 637 vs	4

*m = medium, s = strong, vs = very strong, sh = shoulder.

band has been found by Cook (4) and Olah (5) in the infrared spectra of numerous acyl halides in the presence of Lewis acids. The lowering of the frequency of the carbonyl band when the complex is formed is 183 cm^{-1}. Shifts of $\nu_{C=O}$ of a similar magnitude in carbonyl – Lewis acid complexes have been reported by Susz and Cooke (6).

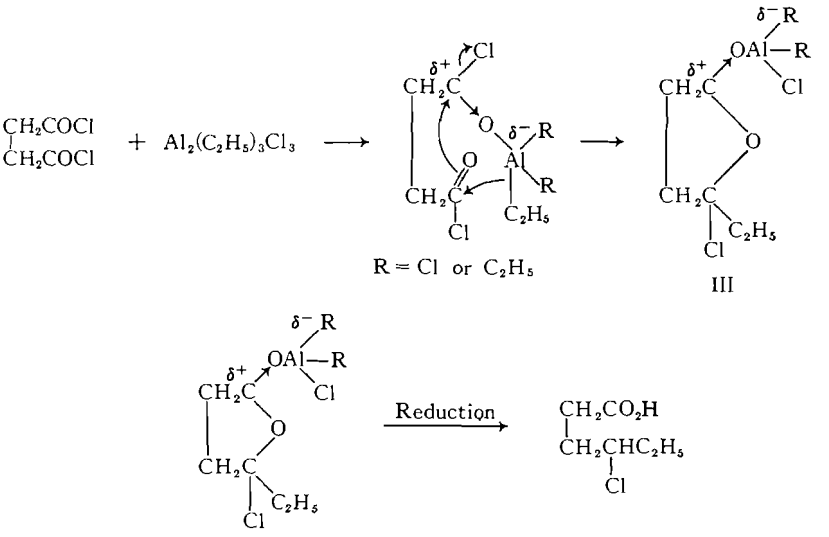
The cyclic form of succinyl dichloride, if formed, would be expected to show a strong γ-lactone carbonyl absorption band in the region of 1 800 cm^{-1} (7–9). No such band for the cyclic form is found in the infrared spectrum. There is a possibility that the strong carbonyl band at 1 783 cm^{-1} might hide the carbonyl band of the cyclic form. This possibility is ruled out by the nuclear magnetic resonance spectrum of a solution of succinyl dichloride and aluminium chloride in nitromethane. In addition to the nitromethane proton peak, there are two peaks. One, a singlet at 3.36 p.p.m., is caused by the excess succinyl dichloride. The other, a broad unresolved peak centered at 3.58 p.p.m., is consistent (5) with the formation of a polarized donor–acceptor complex with the acyclic form of succinyl dichloride. The protons of the cyclic form, if present, would be expected to be more shielded and should be found upfield from the acyclic form. The methylene, methoxyl, and methyl protons of cyclic pseudo methyl levulinate have been shown (2) to be upfield by approximately 0.30 p.p.m. from the acyclic methyl levulinate. The absence of peaks upfield from the proton peak of succinyl dichloride, in addition to the infrared data, rules out the presence of the cyclic isomer of succinyl dichloride.

There is really no reason to postulate the existence of a cyclic form of succinyl dichloride. Cyclic products can be accounted for by means of the [3.2.1] bicyclic reaction path starting with the acyclic form. For example, the mechanism of the reaction of succinyl dichloride with ethyl aluminium sesquichloride to form γ-chlorocaproic acid as the major product rather than the expected octane-3,6-dione has been postulated as starting from the cyclic form (10). An alternate mechanism is the reaction of succinyl dichloride with the

$$\begin{matrix}CH_2COCl\\ |\\ CH_2COCl\end{matrix} + Al_2(C_2H_5)_3Cl_3 \rightarrow \begin{matrix}Cl\\ |\\ CH_2CHC_2H_5\\ |\\ CH_2CO_2H\end{matrix} + \begin{matrix}CH_2CO_2CH_5\\ |\\ CH_2COC_2H_5\end{matrix}$$

aluminium compound to form a 1:1 polarized complex. This complex could react by a [3.2.1] bicyclic reaction path to form the cyclic complex (III), which could be reduced to the observed product. Further support for this mechanism is the fact that compounds of type III have been shown to exist predominantly in the cyclic form (2, 3). An analogous

Can. J. Chem. Downloaded from www.nrcresearchpress.com by 210.87.254.105 on 09/05/12
For personal use only.



[3.2.1] bicyclic mechanism starting with the acyclic form can be postulated for other reactions of succinyl dichloride with Lewis acids that result in cyclic products.

It is therefore unnecessary to postulate the existence of a cyclic form of succinyl dichloride, since (*i*) there is no physical evidence to support its existence, and (*ii*) the reaction products can be explained satisfactorily without its intervention.

EXPERIMENTAL

Boiling points are uncorrected. Nuclear magnetic resonance spectra were taken on a Varian A-60 spectrometer, with tetramethylsilane as an internal standard. Infrared spectra were taken on a Perkin–Elmer model 521 spectrophotometer.

Succinyl dichloride was prepared by the method of Cason and Reist (11) in an 80% yield, b.p. 65–67° at 2 mm (lit. (11) b.p. 65° at 5 mm).

Preparation of the Succinyl Dichloride – Aluminium Chloride Complex

All operations were carried out in a dry box. To 0.55 g (0.004 mole) of aluminium chloride was added 2.05 g (0.013 mole) of succinyl dichloride. The mixture was allowed to stand at room temperature, with occasional shaking, until all the aluminium chloride had dissolved. The infrared spectrum of the resulting oil was examined as the neat liquid between NaCl plates. The nuclear magnetic resonance sample was prepared by adding the liquid complex to nitromethane, which was purified by the method of Olah (5).

ACKNOWLEDGMENT

This research was supported by the National Research Council of Canada.

1. B. H. Chase and D. H. Hey. J. Chem. Soc. 553 (1952), and references therein.
2. G. H. Schmid and L. S. J. Weiler. Can. J. Chem. **43**, 1242 (1965).
3. M. S. Newman and C. Courduvelis. J. Am. Chem. Soc. **88**, 781 (1966).
4. D. Cook. Can. J. Chem. **37**, 48 (1959).
5. G. A. Olah, S. J. Kuhn, W. S. Tolgyesi, and E. B. Baker. J. Am. Chem. Soc. **84**, 2733 (1962).
6. B. P. Susz and I. Cooke. Helv. Chim. Acta, **37**, 1273 (1954).
7. M. Hauptschein, C. S. Stokes, and A. V. Grosse. J. Am. Chem. Soc. **74**, 1974 (1952).
8. A. Winston *et al.* J. Org. Chem. **30**, 2784 (1965).
9. S. J. Cristol and R. F. Helmreich. J. Am. Chem. Soc. **74**, 4084 (1952).
10. H. Reinheckel. Angew. Chem. **76**, 646 (1964).
11. J. Cason and E. J. Reist. J. Org. Chem. **23**, 1492 (1958).

Received August 5, 1966.
Department of Chemistry,
University of Toronto,
Toronto, Ontario.

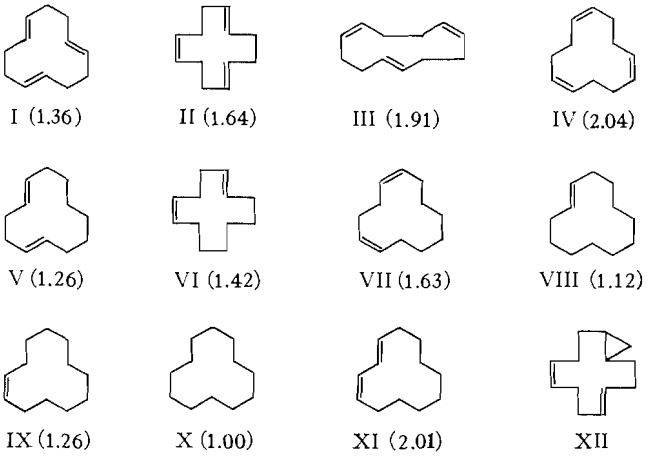
Can. J. Chem. Downloaded from www.nrcresearchpress.com by 210.87.254.105 on 09/05/12
For personal use only.

DIIMIDE REDUCTION OF 12-MEMBERED CYCLIC OLEFINS

H. NOZAKI, Y. SIMOKAWA, T. MORI, AND R. NOYORI

Diimide reduction (1) of *cis,trans,trans*-1,5,9-cyclododecatriene (II) gives *cis*-cyclododecene (IX) in preparative yields (2), whereas *cis,trans*-bicyclo[10.1.0]trideca-4,8-diene (XII) is completely inert to this treatment (3).[1] To gain further information regarding the selectivity in addition reactions of 12-membered cyclic olefins (3, 4), we have now investigated the diimide reduction of 1,5,9-cyclododecatriene isomers (I–IV) and *trans*- and *cis*-cyclododecenes (VIII and IX).

Reinvestigation of the reduction of *cis,trans,trans*-1,5,9-cyclododecatriene (II) was carried out under four different modes of generating diimide. These methods were (A) air oxidation of hydrazine hydrate in the presence of cupric salts (2*a*), (B) oxidation of hydrazine hydrate with 30% hydrogen peroxide (5), (C) thermal or basic decomposition of iodohydrazine in various solvents (6), and (D) decomposition of tosylhydrazine in the presence of bases (1). All products were analyzed by gas–liquid chromatography (g.l.c.) ($AgNO_3$-treated polyethylene glycol 6000), and the results are summarized in Table I. The relative retention times with reference to that of X are shown in parentheses under each structural formula.



The selective formation of *cis*-cyclododecene was consistently observed in every method of generating diimide irrespective of reaction temperatures and solvents. No detectable amount of the *trans* isomer VIII was formed. The first attack of diimide occurs at one of the *trans* bonds to produce *cis,trans* diene VI, which is further hydrogenated at another *trans* bond. Thermal decomposition of tosylhydrazine (method D) gives *p*-toluenesulfinic acid as a counterpart of the diimide species. This acid has been found to be an active reagent of *cis–trans* isomerization of olefins (7). Therefore, the presence of bases such as potassium carbonate is essential in method D; otherwise the selectivity is completely lost because of the isomerization of compounds at each reduction stage to thermally more stable isomers.

Of the four different methods, method D gave the highest yields of reduction products

[1]*This bicyclic diene has now been found to be inert under the conditions of methods B and D as well as those of method A previously reported.*

Can. J. Chem. Downloaded from www.nrcresearchpress.com by 210.87.254.40 on 09/05/12
For personal use only.

Can. J. Chem. Downloaded from www.nrcresearchpress.com by 210.87.254.40 on 09/05/12
For personal use only.

TABLE I

Diimide reduction of *cis,trans,trans*-1,5,9-cyclododecatriene (II)*

Method†	Solvent	Base	Reaction temperature (°C)	Reaction time (h)	Mole ratio diimide/II	Recovery of C_{12}-fraction (%)‡	Abundance ratio (%)§			
							II	VI‖	IX‖	X‖
A	EtOH	—	30 to 50	50	30	85	0	0	93	7
B	EtOH	—	0	0.5	1	88	90	10¶	0	0
B	EtOH	—	0	1	10	75	6	33	59	2
C	EtOH	NaOH	20 to 25	7	12	62	35	47	18	0
C	Et_2O	NaOH	35	8	12	70	8	34	55	3
C	AcOH	—	40 to 45	27	12	25	47	43	10	0
D	$EtO(CH_2)_2OH$	K_2CO_3	95 to 100	4	1	77	35	48	17	0
D	$EtO(CH_2)_2OH$	K_2CO_3	95 to 100	7	3	62	0	0	69	31

*Contaminated with 2% all-*trans* triene I.
†For methods A–D, see the text.
‡This is the ratio of the weight of the recovered C_{12}-fraction, b.p. 100–110° at 13 mm, to the weight of the triene II subjected to the reduction.
§Calculated on the basis of the peak areas of g.l.c. of the C_{12}-fraction.
‖Identified by comparison of the g.l.c. retention times and infrared spectra with those of an authentic specimen.
¶This was the sole product at early stages of the reduction, and the *trans,trans* isomer V was not produced.

Can. J. Chem. Downloaded from www.nrcresearchpress.com by 210.87.254.40 on 09/05/12
For personal use only.

TABLE II

Diimide reduction of other 1,5,9-cyclododecatriene isomers (I,* III,† and IV‡)

Triene	Method§	Mole ratio diimide/triene	Recovery of C_{12}-fraction (%)‖	Abundance ratio (%)¶								
				I	III	IV	V**	VI**	VII††	VIII**	IX**	X**
I	B	10	75	24	—	—	32	—	—	26	—	18
I	D	1	76	50	—	—	33	—	—	14	—	3
I	D	3	70	4	—	—	16	—	—	24	—	56
III	B	7	78	—	40	—	—	10	43	—	7	0
III	B	12	69	—	7	—	—	7	59	—	27	0
III	D	1	73	—	39	—	—	11	43	—	7	0
III	D	3	62	—	0	—	—	0	16	—	60	24
IV	D	1	70	—	—	42	—	Trace‡‡	52	—	6	0
IV	D	3	60	—	—	12	—	—	69	—	19	0

*Contaminated with 1% *cis,trans,trans* isomer II.
†Contaminated with 4% *cis,trans,trans* isomer II.
‡Contaminated with 10% *cis,cis,trans* isomer III.
§For methods B and D, see the text and Table I.
‖The ratio of the weight of recovered C_{12}-fraction, b.p. 100–110° at 13 mm, to the weight of the respective olefin subjected to the reduction.
¶Calculated on the basis of the peak areas of g.l.c. of the C_{12}-fraction.
**Identified by comparison of the g.l.c. retention time with that of an authentic sample.
††The structure was tentatively assigned (see Experimental).
‡‡This originates from the isomer III.

TABLE III

Diimide reduction of cyclododecenes VIII and IX and 1,3-cyclododecadiene (XI)

Olefin	Method*	Mole ratio diimide/olefin	Recovery of C_{12}-fraction (%)†	Abundance ratio (%)‡			
				VIII	IX	X	XI
VIII + IX (50:50)	B	3	79	41	49	10	—
VIII + IX (50:50)	D	0.3	77	43	49	8	—
VIII + IX (50:50)	D	1	73	23	46	31	—
XI	D	0.5	70	4	5	Trace	91
XI	D	2	65	16	51	26	7

*For methods B and D, see the text and Table I.
†The ratio of the weight of the recovered C_{12}-fraction, b.p. 100–110° at 13 mm, to the weight of the respective olefins subjected to the reduction.
‡Calculated on the basis of the peak areas of g.l.c. analyses of the recovered C_{12}-fraction.

based on the diimide-generating reagents. In view of the ease in operation and of reproducible results, methods B and D were preferred in the following experiments.

Partial hydrogenation of *cis,cis,trans*-1,5,9-cyclododecatriene (III) (8) was expected to provide a means of preparing *cis,cis*-1,5-diene VII under such strictly preferential attack of the *trans* bond as observed with II. As shown in Table II, however, a fair amount of *cis,trans*-1,5-diene VI was produced by the attack of the *cis* bond. All-*trans* triene I (8) and all-*cis* triene IV (9) were also susceptible to diimide reduction. Facile formation of the totally saturated product X characterized the reduction of the all-*trans* isomer.

Table III involves the diimide reduction of a mixture of equal amounts of *trans*- and *cis*-cyclododecene (VIII and IX). The data clearly show that the *trans* olefin VIII is much more susceptible to the reduction than the *cis* isomer IX. The reduction similarly proceeded with *cis,trans*-1,3-cyclododecadiene (XI),[2] which yielded a considerable amount of completely saturated cyclododecane X. Presumably, the *cis* bond is nearly as reactive as the *trans* bond in the first attack of diimide on the 1,3-diene XI,[3] and *trans* monoene VIII produced by the attack of the *cis* bond is then converted into cyclododecane X.

In summary, we may conclude that the *trans* double bond is ordinarily much easier to reduce than the *cis* one in the diimide reduction of 12-membered cyclic olefins. The approach of the diimide molecule is very sensitive to the steric environment of the double bond to be attacked, as has been pointed out previously (12). Clearly, the ring structures outside of the reacting site are also controlling the susceptibility. This has been most dramatically exemplified by the behavior of XII, which is inactive toward the diimide reduction but smoothly reacts with carbenes and Simmons–Smith reagent at the *cis* bond (3, 4). Such an effect apparently distinguishes these large ring olefins from the ones of common rings or of open chains (13).

EXPERIMENTAL

Both all-*trans* triene I and *cis,cis,trans* triene III were prepared by isomerizing *cis,trans,trans* triene II photochemically (7, 8), and triene IV was prepared by the method of Untch and Martin (9). *trans*-Cyclododecene (VIII) was obtained by isomerization of the *cis* olefin IX (7). *cis,trans*-1,3-Cyclododecadiene (XI) (14) and authentic samples of 1,5-diene V (15) and VI (16) were prepared by known methods, respectively.

Though *cis,cis*-1,5-diene VII could not be isolated in an analytically pure state, the structure tentatively assigned was supported by the infrared spectrum of the mixture of IV, VII, and IX obtained by the reduction of all-*cis* triene IV, which indicated the absence of the *trans* double bond. Furthermore, ozonolysis of the same mixture yielded practically no products other than succinic acid, suberic acid, and dodecanedioic acid, which were identified as their respective methyl esters. Cyclododecane, m.p. 60–61°, was the sole isolable product obtained by exhaustive catalytic hydrogenation of this partial reduction mixture (IV, VII, and IX).

Gas–liquid chromatographic analyses of the recovered C_{12}-fractions were performed on a 2 m column of polyethylene glycol 6000 treated with silver nitrate, helium being used as the carrier gas at 130°. The results are summarized in Tables I–III.

Diimide reduction by means of air oxidation of hydrazine hydrate (method A) was carried out as previously described (2*a*). General procedures of the diimide reduction of cyclododecatrienes by means of methods B–D are illustrated below.

Oxidation of Hydrazine Hydrate by 30% Hydrogen Peroxide (Method B)

To a solution of each cyclododecatriene (0.8 g, 5 mmoles), 80% hydrazine hydrate (0.32 g, 5 mmoles), and 1% aqueous cupric sulfate (1 ml) in 99% ethanol (30 ml) kept at 0° was added 30% hydrogen peroxide at a rate of 0.1 ml per min, with stirring. For completion of the reaction, 0.6–0.8 ml hydrogen peroxide was required. After nitrogen evolution had ceased, the mixture was treated with water, and extracted with *n*-hexane. The hexane extracts were dried (Na_2SO_4), passed through a short alumina column, and distilled *in vacuo* to give 0.5–0.6 g of the C_{12}-fraction as a colorless oil, b.p. 100–110° at 13 mm, which was subjected to g.l.c. analysis.

Decomposition of Iodohydrazine (Method C)

To a mixture of each cyclododecatriene (1.6 g, 10 mmoles), 80% hydrazine hydrate (6 g, 96 mmoles), and

[2]*To the authors' best knowledge the only known example of diimide reduction of a conjugated diene is that of cyclopentadiene (see ref. 10).*

[3]*No example of 1,4-addition of diimide is known. For example, the reduction of sorbic acid gives mainly 4-hexenoic acid and Δ^2-isomer, 3-hexenoic acid not being detected (see ref. 11).*

Can. J. Chem. Downloaded from www.nrcresearchpress.com by 210.87.254.40 on 09/05/12
For personal use only.

sodium hydroxide (2.0 g, 50 mmoles) in ethanol (100 ml), a 20% ethanol solution of I_2 was added dropwise at 20–25°, with stirring. The color of I_2 immediately disappeared. At the point when this color discharge was no longer perceptible, the mixture was treated with water and extracted with *n*-hexane. The combined extracts were washed with water and aqueous $Na_2S_2O_3$, dried (Na_2SO_4), and passed through a short alumina column. After concentration, the residual oil was distilled *in vacuo* to yield ordinarily 0.8–1.0 g of the C_{12}-fraction, b.p. 100–110° at 13 mm, which was analyzed by g.l.c.

Basic Decomposition of Tosylhydrazine (Method D)

To a mixture of each cyclododecatriene (0.8 g, 5 mmoles) and tosylhydrazine (0.8 g, 5 mmoles) in ethyl cellosolve (25 ml) was added saturated aqueous K_2CO_3 (0.8 g, 5 mmoles); then the mixture was heated at 95–100°, with stirring, until the gas evolution had ceased. The reaction mixture was treated with water and extracted with ether, and the ether extracts were washed with water, dried, and concentrated *in vacuo*. The residue was dissolved in *n*-hexane, and the hexane solution was passed through an alumina column and distilled to give 0.5–0.6 g of the C_{12}-fraction as a colorless oil, which was subjected to g.l.c. analysis.

Diimide Reduction of Cyclododecenes

An equimolar mixture of *trans*- and *cis*-cyclododecenes (VIII and IX) was prepared from each pure isomer and subjected to diimide reduction as shown below.

Method B

To a solution of cyclododecenes (50:50 mixture, 0.8 g, 5 mmoles), 80% hydrazine hydrate (1.0 g, 15 mmoles), and 1% aqueous cupric sulfate (1 ml) in ethanol (30 ml), 30% hydrogen peroxide was added at a rate of 0.1 ml per min, with stirring, at 0°. After 0.8 ml of hydrogen peroxide was added, the reaction mixture was diluted with water and extracted with *n*-hexane. The extracts were dried (Na_2SO_4) and distilled *in vacuo* to give a colorless oil (0.63 g, 79% recovery), b.p. 103–110° at 13 mm, which was subjected to g.l.c. analysis.

Method D

A solution of cyclododecenes (50:50 mixture, 0.8 g, 5 mmoles) and tosylhydrazine (0.8 g, 5 mmoles) in ethyl cellosolve (25 ml) containing K_2CO_3 (0.8 g, 5 mmoles) was heated at 95°, with stirring, for 5 h. The reaction mixture was treated with water and extracted with ether. The ethereal solution was washed, dried (Na_2SO_4), and concentrated. The residue was dissolved in a small amount of *n*-hexane, passed through a short alumina column, and distilled *in vacuo* to yield a colorless oil (0.58 g, 73% recovery), b.p. 101–106° at 13 mm, which was analyzed by g.l.c.

Diimide Reduction of cis,trans-1,3-Cyclododecadiene

A solution of the cyclododecadiene (0.8 g, 5 mmoles), tosylhydrazine (1.6 g, 10 mmoles), and aqueous K_2CO_3 (1.6 g, 10 mmoles) in ethyl cellosolve (25 ml) was heated at 95°, with stirring, during 7 h. The mixture was treated with water and extracted with ether. The combined extracts were washed, dried (Na_2SO_4), and concentrated *in vacuo*. The residual oil was dissolved in *n*-hexane and passed through an alumina column. The hydrocarbon fractions were collected and distilled to yield a colorless oil (0.52 g, 65% recovery), b.p. 100–105° at 13 mm, which was analyzed by g.l.c.

ACKNOWLEDGMENT

The authors are grateful to Prof. K. Sisido for help and encouragement.

1. S. HÜNIG, H. R. MÜLLER, and W. THIER. Angew. Chem. **77**, 368 (1965). C. E. MILLER. J. Chem. Educ. **42**, 254 (1965).
2. (*a*) H. NOZAKI and R. NOYORI. J. Org. Chem. **30**, 1652 (1965). (*b*) M. OHNO, M. OKAMOTO, and S. TORIMITSU. Bull. Chem. Soc. Japan, **39**, 316 (1966).
3. H. NOZAKI, M. KAWANISI, and R. NOYORI. J. Org. Chem. **30**, 2216 (1965).
4. H. NOZAKI, S. KATÔ, and R. NOYORI. Can. J. Chem. **44**, 1021 (1966).
5. L. F. FIESER. *In* Organic experiments. Maruzen Asian ed. Maruzen, Tokyo. 1965. p. 192.
6. H. ROTTENDORF and S. STERNHELL. Australian J. Chem. **16**, 647 (1963).
7. H. NOZAKI, Y. NISIKAWA, M. KAWANISI, and R. NOYORI. To be published.
8. H. NOZAKI, Y. NISIKAWA, Y. KAMATANI, and R. NOYORI. Tetrahedron Letters, 2161 (1965).
9. K. G. UNTCH and D. J. MARTIN. J. Am. Chem. Soc. **87**, 3518 (1965).
10. E. J. COREY, W. L. MOCK, and D. J. PASTO. Tetrahedron Letters, 347 (1961).
11. T. TAKAGI. 19th Annual Meeting of the Chemical Society of Japan, Yokohama, Japan, March 31 to April 3, 1966. Abstr. Papers. Part III. p. 298.
12. E. E. VAN TAMELEN and R. J. TIMMONS. J. Am. Chem. Soc. **84**, 1067 (1962).
13. E. W. GARBISCH, JR., S. M. SCHILDCROUT, D. B. PATTERSON, and C. M. SPRECHER. J. Am. Chem. Soc. **87**, 2932 (1965).
14. W. R. FAWCETT and J. O. HARRIS. J. Chem. Soc. 2673 (1954).
15. W. F. ERMAN and H. C. KRETSCHMAR. Tetrahedron Letters, 1717 (1965).
16. W. STUMPF and K. ROMBUSCH. Liebigs Ann. Chem. **687**, 136 (1965).

RECEIVED MAY 16, 1966.
DEPARTMENT OF INDUSTRIAL CHEMISTRY,
KYÔTO UNIVERSITY,
KYÔTO, JAPAN.

Can. J. Chem. Downloaded from www.nrcresearchpress.com by 210.87.254.40 on 09/05/12
For personal use only.

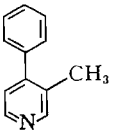
ERRATUM: AROMATIC SUBSTITUTION

XIV. THE HOMOLYTIC PHENYLATION OF 3- AND 4-PICOLINE. A QUANTITATIVE STUDY OF ISOMER AND TOTAL RATE RATIOS

R. A. ABRAMOVITCH AND MAITREYI SAHA

(Ref. Can. J. Chem. 44, 1765 (1966))

On page 1766, the methyl group is missing in the structural formula of compound V. Compound V should read as follows:



DEPARTMENT OF CHEMISTRY,
UNIVERSITY OF SASKATCHEWAN,
SASKATOON, SASKATCHEWAN.

Canadian Journal of Chemistry. Volume 44 (1966)

Can. J. Chem. Downloaded from www.nrcresearchpress.com by 210.87.254.105 on 09/05/12
For personal use only.

Can. J. Chem. Downloaded from www.nrcresearchpress.com by 210.87.254.105 on 09/05/12
For personal use only.

Canadian Journal of Chemistry

Issued by THE NATIONAL RESEARCH COUNCIL OF CANADA

VOLUME 44 DECEMBER 15, 1966 NUMBER 24

KINETICS OF THE DECOMPOSITIONS OF ETHANE AND PROPANE SENSITIZED BY AZOMETHANE

THE DECOMPOSITION OF THE NORMAL PROPYL RADICAL

M. C. LIN AND K. J. LAIDLER

Department of Chemistry, University of Ottawa, Ottawa, Canada

Received June 14, 1966

ABSTRACT

The azomethane-sensitized pyrolysis of ethane was studied at low temperatures from 280 to 350 °C. Measurements were made of initial rates of formation of methane, nitrogen, and butane. From the rate of nitrogen production the rate constant for the azomethane decomposition into $2CH_3 + N_2$ was

$$k = 2.4 \times 10^{14} e^{-47600/RT} s^{-1}.$$

A similar study of the propane decomposition, at temperatures from 260 to 300 °C, led to the value

$$k = 6.0 \times 10^{14} e^{-48300/RT} s^{-1},$$

in satisfactory agreement. The rate of decomposition of the *n*-propyl radical into CH_3 and C_2H_4 was obtained by comparing the rates of formation of C_2H_4 and *n*-C_6H_{14}; the rate constant was

$$k = 3.47 \times 10^{13} e^{-31400/RT} s^{-1}.$$

The activation energy of 31.4 kcal/mole, together with that of 8.9 kcal/mole for the reverse reaction obtained by Brinton, leads to a value of 20.3 kcal/mole for the dissociation energy of *n*-CH_3—CH_2 at 0 °K, and to a value of 22.8 at 25 °C. The corresponding values for the heats of formation of the *n*-propyl radical are 28.4 kcal/mole at 0 °K, and 23.1 kcal/mole at 25 °C. The dissociation energy of *n*-$CH_3CH_2CH_2$—H is deduced to be 99.4 kcal/mole at 0 °K and 99.9 kcal/mole at 25 °C. An energy diagram is constructed for the various reactions of *n*-C_3H_7 and *i*-C_3H_7.

INTRODUCTION

Azomethane decomposes at a convenient rate between 250° and 350°, and is therefore a suitable sensitizer for the decomposition of substances giving rise to a chain carrier that decomposes readily in this temperature range (1). The decomposition of acetaldehyde, for example, occurs at a convenient rate at these temperatures in the presence of small amounts of azomethane (2, 3). The present paper describes studies of the azomethane-sensitized decompositions of ethane and propane. In the ethane decomposition, the ethyl radical decomposition, which has an activation energy of about 40 kcal/mole, does not occur sufficiently rapidly, but the investigation is of interest in providing information about the kinetics of decomposition of the azomethane molecule into a nitrogen molecule and two methyl radicals.

Propyl radicals, on the other hand, decompose more rapidly, and the study of the propane decomposition in the presence of azomethane therefore provides information about the kinetic parameters for the decomposition of this radical.

The activation energy for the decomposition of the *n*-propyl radical has been measured in a variety of ways, and values ranging from 20 to 35 kcal/mole have been obtained (4–8).

From this activation energy the carbon–carbon bond dissociation energy in the radical, $D^0(CH_3—CH_2CH_2)$, and the primary carbon–hydrogen bond energy in propane, $D^0(CH_3CH_2CH_2—H)$, can be deduced; values for the latter range from 110 to 95 kcal/mole. The present work leads to what is considered to be reliable values for these quantities.

EXPERIMENTAL

Apparatus

The reactions were studied in a conventional static system. The reaction vessel was a quartz bulb 511.5 ml in volume, enclosed in an electrically heated steel cylinder 2 cm in thickness. The temperature of the vessel was controlled within 0.2 °C with a Thermoelectric regulator. The pressure of the system after evacuation was measured by a Pirani gauge. Before each run, the system was evacuated to a pressure of less than 10^{-4} mm Hg.

Materials

Phillips research grade ethane and propane were subjected to several trap-to-trap distillations and were finally degassed thoroughly at −160 °C. Azomethane was obtained from Merck, Sharp and Dohme of Canada Limited. It was prepared in a similar manner to ethane and propane, but was degassed at a higher temperature (−130 °C) to remove all traces of ethane. The purified azomethane, which showed no impurity in vapor-phase chromatographic tests, was stored at −78 °C. The mixtures of azomethane and alkanes were stored in black-painted bulbs and were degassed from time to time.

Procedure and Analysis

The reaction was quenched by passing the reaction mixture through a spiral trap maintained at −196 °C. It was connected in series with a LeRoy still, a pump-down trap (−210 °C), a mercury-diffusion pump, and a Toepler pump with a gas burette. The noncondensable products, methane and nitrogen, were first measured with the gas burette and then analyzed by vapor-phase chromatography using a 1 ft 60–80 mesh silica gel column.

The condensable products resulting from the ethane decomposition were distilled in the LeRoy still at −160 °C. The residues from the distillation, mainly butane and the remaining fraction of ethane, were then transferred to the vapor-phase chromatograph. A 12 ft column of 30% (by weight) 2,5-hexane-dione was used at 0 °C.

The condensable products obtained from the propane decomposition were subjected to distillation at −135 °C. The C_2 fractions, ethane and ethylene, and parts of the C_3 fraction trapped in the −210 °C trap, were analyzed by vapor-phase chromatography with the same silica gel column as used in the methane determination. The residues of the distillation, containing mainly hexanes, azomethane, and other nitrogen compounds, were analyzed by vapor-phase chromatography using a 2 ft di-2-ethylhexylsebacate column maintained at 34 °C.

n-Hexane could be separated satisfactorily from two other possible isomers, diisopropyl and 2-methylpentane, whose peaks, however, overlapped each other. Appreciable amounts of $CH_3N_2C_4H_9$ were identified and measured by mass spectrometry. An attempt, which turned out to be unsuccessful, was made to separate diisopropyl from 2-methylpentane by using two of the 2 ft di-2-ethylhexylsebacate columns connected in series.

RESULTS AND DISCUSSION

The Ethane Decomposition

Ethane containing 0.507% azomethane was pyrolyzed at low temperatures from 280 to 350 °C. The products measured were nitrogen, methane, and butane. Initial rates were obtained by extrapolating the plots of rate against time to zero time, and the results are summarized in Table I.

The results are explained by the mechanism

[1] $$CH_3N_2CH_3 \rightarrow N_2 + 2CH_3$$

[2] $$CH_3 + C_2H_6 \rightarrow CH_4 + C_2H_5$$

[3] $$CH_3 + CH_3 \rightarrow C_2H_6$$

[4] $$CH_3 + C_2H_5 \rightarrow C_3H_8 \text{ or } CH_4 + C_3H_6$$

[5] $$C_2H_5 + C_2H_5 \rightarrow C_4H_{10} \text{ or } C_2H_6 + C_2H_4 \quad .$$

Reactions between radicals and azomethane can be neglected in view of the low concentration of azomethane.

Can. J. Chem. Downloaded from www.nrcresearchpress.com by 210.87.254.105 on 09/05/12
For personal use only.

That the rate of nitrogen formation is exactly first order with respect to azomethane was shown by plots of $\log_{10}([A]_0—[N_2])/[A]_0$ against time; $[A]_0$ is the initial concentration of azomethane and $[N_2]$ the concentration of nitrogen at time t. The value of the rate constant obtained from such plots agreed within 1% with the rate constant calculated from the initial rates of nitrogen production.

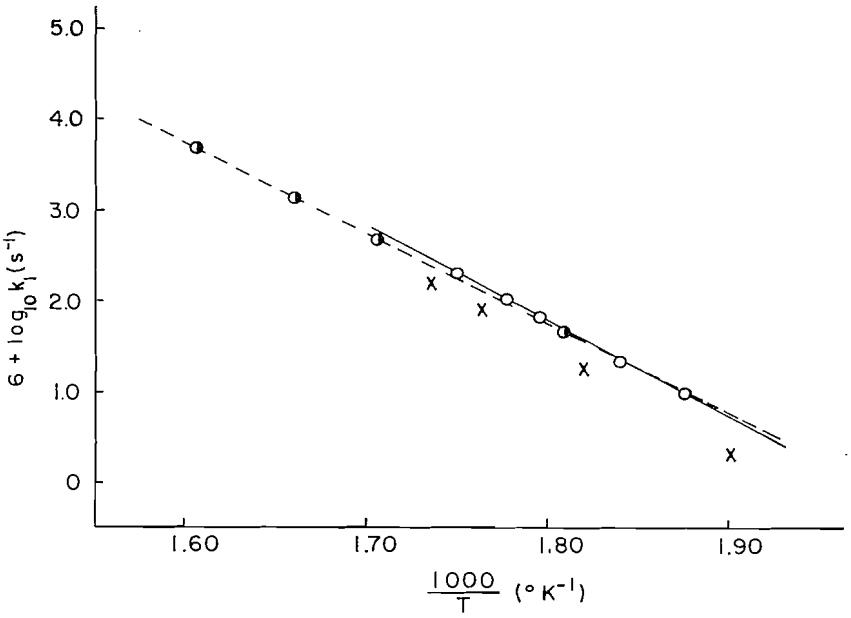


FIG. 1. Arrhenius plots of k_1 values obtained in different investigations: ◑, results obtained for ethane + 0.507% azomethane; ○, those for propane + 2.31 and 3.39% azomethane; ×, results of Forst and Rice (9) for the azomethane decomposition inhibited by nitric oxide.

An Arrhenius plot for these rate constants is shown in Fig. 1. The rate constant is given by

$$k_1 = 2.4 \times 10^{14}\, e^{-47600/RT}\ s^{-1}.$$

This differs significantly from the expression

$$k_1 = 1.9 \times 10^{17}\, e^{-55400/RT}\ s^{-1}$$

obtained by Forst and Rice (9) from a study of the azomethane decomposition inhibited by nitric oxide. The results of Forst and Rice are included in Fig. 1.

Owing to the difficulty of determining propane in the presence of a large excess of ethane, the rates of propane production were estimated from the rates of methane and butane formation using the relationship

[*i*] $$v^*_{C_3H_8} = \frac{k_4}{k_2[C_2H_6]k_5^{1/2}}\, v_{CH_4} v^{1/2}_{C_4H_{10}}.$$

Similarly the rate of combination of methyl radicals was calculated from

[*ii*] $$v^*_{C_2H_6} = \frac{k_3}{k_2^2}\,\frac{v^2_{CH_4}}{[C_2H_6]^2}.$$

The methane produced from reaction [4] amounts to less than 2% of the total, and was neglected.

Can. J. Chem. Downloaded from www.nrcresearchpress.com by 210.87.254.105 on 09/05/12
For personal use only.

The rate constants used were

$$k_2 = 4.25 \times 10^{10}\, T^{1/2}\, e^{-11300/RT} \text{ cc mole}^{-1}\text{ s}^{-1} \quad (10)$$

$$k_3 = 2.2 \times 10^{13} \text{ cc mole}^{-1}\text{ s}^{-1} \quad (11)$$

$$k_4 = 4.2 \times 10^{13} \text{ cc mole}^{-1}\text{ s}^{-1} \quad (12)$$

$$k_5 = 2.0 \times 10^{13} \text{ cc mole}^{-1}\text{ s}^{-1} \quad (13).$$

Equations [*i*] and [*ii*] also allow one to calculate $2v_1$, the rate of methyl production, which is equal to the sum of the rates of the processes by which methyl radicals disappear:

[*iii*] $$2v_1 = v_{CH_4} + 2v^*_{C_2H_6} + v^*_{C_3H_8}.$$

The results are given in Table I, and it is to be seen that the ratio v_1/v_{N_2} is approximately unity as expected from the mechanism.

The Propane Decomposition

The work with propane was done with two azomethane–propane mixtures, one containing 2.31% of azomethane and the other 3.39%. The following products were observed and the rates of their formation were measured: nitrogen, methane, ethane, ethylene, *n*-hexane, diisopropyl [$(CH_3)_2CHCH(CH_3)_2$], and 2-methylpentane. Some initial rates of reaction are given in Table II.

The overall kinetics of the pyrolysis of propane has been studied by Laidler, Sagert, and Wojciechowski (14) and in the light of their reaction scheme the following mechanism can be proposed for the azomethane-sensitized reaction.

[1] $$CH_3N_2CH_3 \rightarrow N_2 + 2CH_3$$

[6*a*] $$CH_3 + C_3H_8 \rightarrow CH_4 + CH_3CH_2CH_2$$

[6*b*] $$CH_3 + C_3H_8 \rightarrow CH_4 + CH_3CHCH_3$$

[7] $$CH_3CH_2CH_2 \rightarrow CH_3 + C_2H_4$$

[8] $$2CH_3CH_2CH_2 \rightarrow CH_3CH_2CH_2CH_2CH_2CH_3$$

[9] $$CH_3CH_2CH_2 + CH_3CHCH_3 \rightarrow CH_3CH_2CH_2CH(CH_3)_2$$

[10] $$2CH_3CHCH_3 \rightarrow (CH_3)_2CHCH(CH_3)_2$$

[3] $$CH_3 + CH_3 \rightarrow C_2H_6$$

[11] $$CH_3 + CH_3CH_2CH_2 \rightarrow CH_3CH_2CH_2CH_3$$

[12] $$CH_3 + CH_3CHCH_3 \rightarrow CH_3CH(CH_3)_2$$

This mechanism is seen to account for the products obtained in the present investigation. Significant amounts of $C_4H_9N_2CH_3$ were formed, so that reactions such as

[13] $$CH_3 + CH_3N_2CH_3 \rightarrow CH_4 + CH_2N_2CH_3$$

[14] $$C_3H_7 + CH_2N_2CH_3 \rightarrow C_4H_9N_2CH_3$$

probably also occur. The radical $CH_3N_2CH_2$ will be stabilized by resonance, and will disappear largely by combination with radicals.

The double-logarithmic plot in Fig. 2 shows that the order of nitrogen production is again unity. The Arrhenius plot for the rate constants for the azomethane decomposition, obtained in the work with propane, was included in Fig. 1, and is shown to be consistent with the results found in the ethane experiments. The rate constant derived from the propane results can be expressed as

$$k_1 = 6.0 \times 10^{14}\, e^{-48300/RT}\, s^{-1}.$$

This is in satisfactory agreement with the result obtained with ethane.

Can. J. Chem. Downloaded from www.nrcresearchpress.com by 210.87.254.105 on 09/05/12
For personal use only.

Can. J. Chem. Downloaded from www.nrcresearchpress.com by 210.87.254.105 on 09/05/12
For personal use only.

TABLE I

Initial rates of product formation in the decomposition of ethane sensitized by 0.507% azomethane (all rates in 10^{-11} mole cc^{-1} s^{-1})

T (°C)	Pressure (mm Hg)	$[A]_0 \times 10^8$ (mole/cc)	$[C_2H_6] \times 10^6$ (mole/cc)	v_{N_2}	v_{CH_4}	$v_{C_4H_{10}}$	$v^*_{C_2H_6}$‡	$v^*_{C_3H_8}$‡	$2v_1$‡	v_1/v_{N_2}
280.5	302.5	4.42	8.72	0.165	0.308	0.078	0.000	0.008	0.316	0.96
313.5	203.3	2.80	5.53	1.32	2.09	0.750	0.008	0.150	2.25	0.85
330.0	187.5	2.52	4.95	3.47	6.30	2.18	0.063	0.739	7.16	1.03
349.8	214.7	2.80	5.50	12.9	22.2	9.05	0.272	3.14	25.8	1.00
349.8	154.4	2.02	3.95	9.28	15.7	5.80	0.259	2.45	18.7	1.00
349.8	104.6	1.37	2.68	6.29	9.25	2.84	0.198	1.50	11.3	0.91
349.8	72.2	0.94	1.85	4.24	5.60	1.71	0.156	1.04	6.95	0.80

‡$v^*_{C_2H_6}$, $v^*_{C_3H_8}$, and $2v_1$ are calculated as explained in the text (eqs. [*i*], [*ii*], and [*iii*]).

TABLE II

Initial rates of product formation in the decomposition of propane at 300 °C sensitized by azomethane (all rates in mole cc^{-1} s^{-1})

Initial total pressure (mm Hg)	$[A]_0 \times 10^7$ (mole cc^{-1})	$v_{CH_4} \times 10^{11}$	$v_{N_2} \times 10^{11}$	$v_{C_2H_4} \times 10^{12}$	$v_{C_2H_6} \times 10^{12}$	$v_{n\text{-}C_6H_{14}} \times 10^{13}$	$(v_9 + v_{10}) \times 10^{12}$	$v_{C_4H_9N_2CH_3} \times 10^{12}$
195.5	12.7	5.30	2.67	6.75	12.2	7.42	4.70	3.5
155.6	10.1	4.10	2.25	5.60	9.82	5.20	3.87	2.7
123.1	7.96	3.45	1.60	4.74	6.35	3.66	3.75	1.9
89.3	8.48	3.38	1.60	4.97	7.45	3.97	2.62	1.5
55.5	5.25	1.85	1.00	3.54	3.50	2.10	1.56	0.67

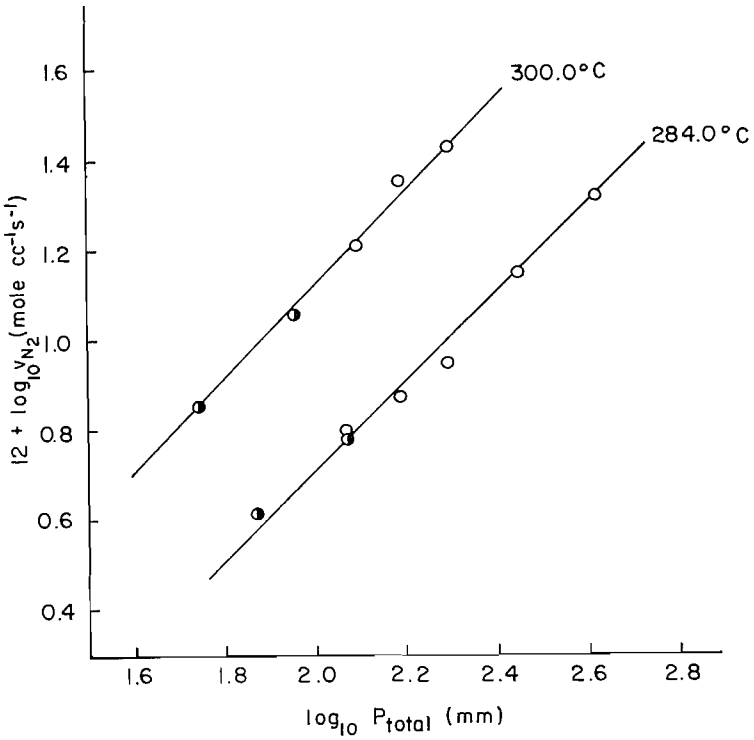


FIG. 2. Order plots for nitrogen production at 300.0 and 284.0 °C: ○, results from 2.31% azomethane + propane; ◑, those from 3.39% azomethane + propane normalized to 2.31% of azomethane.

Decomposition of the n-C_3H_7 Radical

The isopropyl radical is known to be much more stable than the *n*-propyl radical (15, 16); in the temperature range of the present experiments the process

[15] $$CH_3CHCH_3 \rightarrow CH_3 + C_2H_4$$

is 10^2 to 10^3 times slower than reaction [7]. The initial rate of formation of ethylene is therefore equal to the initial rate v_7 of reaction [7].

The rate of reaction [7] can be measured by using the relationship

[*iv*] $$v_{C_2H_4}/v_{n\text{-}C_6H_{14}}^{1/2} = k_7/k_8^{1/2}.$$

Typical yield–time plots for ethylene and *n*-hexane are given in Figs. 3 and 4. The rates of both processes decline rapidly as reaction proceeds, especially at higher temperatures; this is attributed to the decomposition of azomethane. Initial rates were obtained by the extrapolation of plots of rate against time, as shown in Fig. 5, and the results for all temperatures and pressures are given in Table III. As expected, the ratio $v_{C_2H_4}/v_{n\text{-}C_6H_{14}}^{1/2}$ is independent of the amount of azomethane in the system. It is also independent of pressure under the present conditions, although pressure dependence of k_7 has been observed by Kerr and Calvert (7) at below 15 mm pressure of $(n\text{-}C_3H_7)_2N_2$. The data in Table III, with k_8 taken as 2.2×10^{13} cc mole^{-1} s^{-1}, lead to

$$k_7 = 3.47 \times 10^{13}\, e^{-31400/RT}\ s^{-1}.$$

The Arrhenius plot is shown in Fig. 6.

Can. J. Chem. Downloaded from www.nrcresearchpress.com by 210.87.254.105 on 09/05/12
For personal use only.

TABLE III

Initial rates of formation of ethylene and *n*-hexane from various azomethane-propane mixtures (all rates in moles $cc^{-1}\,s^{-1}$)

T (°C)	Initial pressure (mm Hg)	% azomethane	$v_{C_2H_4} \times 10^{12}$	$v_{n\text{-}C_6H_{14}} \times 10^{13}$	$(v_{C_2H_4}/v^{1/2}_{n\text{-}C_6H_{14}}) \times 10^6$
300.0	195.5	2.31	6.75	7.42	7.83
	155.6	2.31	5.60	5.20	7.77
	123.1	2.31	4.74	3.66	7.83
	89.1	3.39	4.97	3.97	7.88
	55.5	3.39	3.54	2.10	7.73
290.0	195.5	2.31	3.02	4.00	4.80
284.0	194.8	2.31	1.44	1.58	3.62
	154.4	2.31	1.30	1.29	3.62
	114.2	2.31	1.04	0.893	3.66
270.5	154.7	2.31	0.485	0.695	1.84
260.0	154.1	3.39	0.193	0.360	1.02

TABLE IV

Kinetics parameters for the decomposition of n-C_3H_7 into $CH_3 + C_2H_4$

Methods of investigation	A^* (s^{-1})	E (kcal/mole)	$(k_7)_{300°C}$	References
Hg-photosensitized decomposition of C_3H_8	3×10^9	20	70.3	Bywater and Steacie (4)
Photolysis of $CH_3N_2CH_3$ in the presence of n-C_3H_7CHO	5.4×10^{15}	34.9	268	Calvert and Sleppy (5)
Photolysis of n-C_3H_7CHO	5.0×10^{11}	25.3	124	Kerr and Trotman-Dickenson (6)
Photolysis of n-$C_3H_7N_2C_3H_7$	1.6×10^{15}	34.5	113	Kerr and Calvert (7)
Hg-photosensitized decomposition of C_3H_8	4×10^9	22	16.3	Back and Takamuku (8)
Thermochemical estimation based on the results of ref. 6	8.0×10^{13}	31	124	Jackson and McNesby (17)
$CH_3N_2CH_3$-sensitized decomposition of C_3H_8	3.47×10^{13}	31.4 ± 0.30	37.2	This work

*The values given are recalculated from the original results, using the value of 2.2×10^{13} cc $mole^{-1}$ s^{-1} for the rate constant of the n-C_3H_7 radical combination.

Table IV lists the very divergent kinetic parameters for the $CH_3CH_2CH_2$ decomposition, obtained by a variety of methods. Our activation energy agrees well with that estimated by Jackson and McNesby (17) from thermochemical data. It is much higher than the values of 20–22 kcal/mole obtained from the results of the mercury-photosensitized decomposition of propane (4, 8). The latter values are unreliable since they involve the assumption that the radical concentration is independent of temperature. In the present study, however, the concentration of the radical of interest was monitored by direct measurements of the rate of recombination.

Our activation energy is somewhat lower than the values obtained by Calvert and coworkers from studies with *n*-propionaldehyde (5) and azo-*n*-propane (7), and it is to be noted from Table IV that significantly higher rate constants were obtained in their work. It is possible that error arises in the aldehyde work from the presence of the radicals $CH_2CH_2CH_2CHO$ and CH_3CH_2CHCHO, which may decompose into $C_2H_4 + CH_2CHO$ and $CH_3 + CH_2CHCHO$ respectively; there would therefore be higher rates of formation of methane and ethylene. Similar side reactions may also occur in the azo-*n*-propane system. The work with propane is free from complications of this kind, especially since, as discussed above, the isopropyl radical breaks down very slowly.

Can. J. Chem. Downloaded from www.nrcresearchpress.com by 210.87.254.105 on 09/05/12
For personal use only.

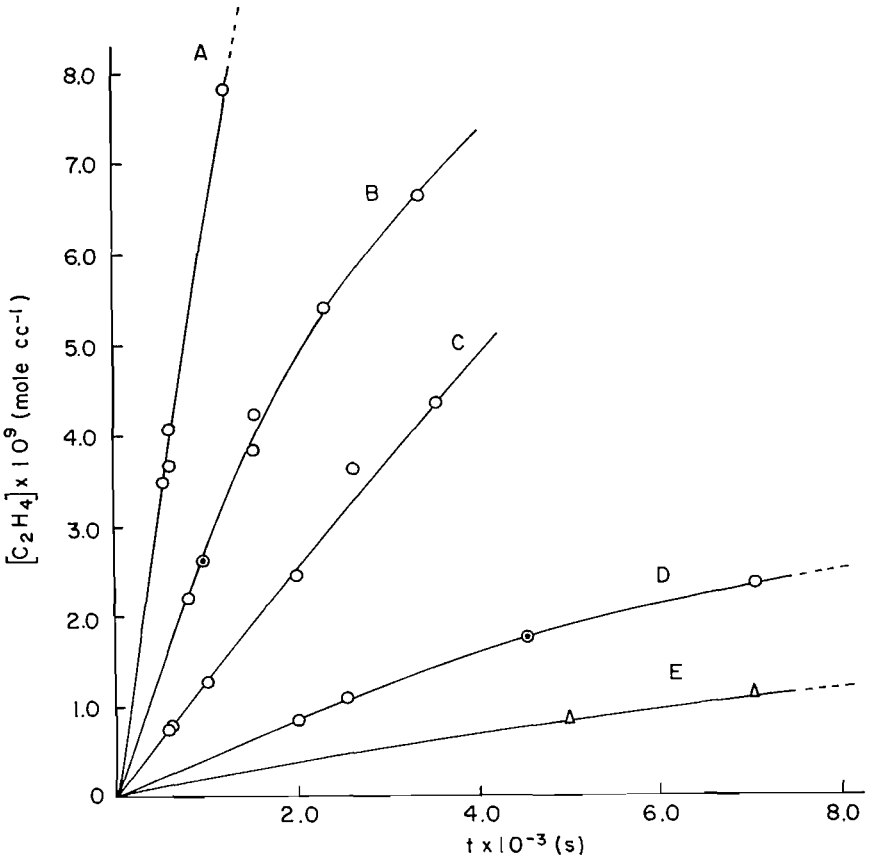


FIG. 3. Typical plots of yield against time for C_2H_4 formation at different temperatures and pressures. The results obtained from the 2.31% mixtures are shown as ○, and those from 3.39% as △. (A) 300.0 °C, 195.3 mm; (B) 290.0 °C, 195.5 mm; (C) 284.4 °C, 154.4 mm; (D) 270.5 °C, 154.7 mm; (E) 260.0 °C, 154.1 mm.

The Relative Concentrations of n-C_3H_7 and i-C_3H_7

The relative rates of production of i-C_3H_7 and n-C_3H_7 are given by (18)

[v] $$v_{6b}/v_{6a} = k_{6b}/k_{6a} = 0.43\, e^{1750/RT}.$$

This ratio is higher than unity in the temperature range of the present experiments. Estimates indicate, however, that the concentrations of i-C_3H_7 are lower than those of n-C_3H_7 at temperatures below about 550 °K. The ratio $[i\text{-}C_3H_7]/[n\text{-}C_3H_7]$ can be estimated from the relationship

[vi] $$[i\text{-}C_3H_7]/[n\text{-}C_3H_7] = (v_{10}/v_8)^{1/2} = (v_{\text{diisopropyl}}/v_{n\text{-}C_6H_{14}})^{1/2},$$

the rate constants k_8 and k_{10} being assumed equal. In the present study diisopropyl could not be determined by vapor-phase chromatography, because its peak was overlapped completely by that of 2-methylpentane; it was possible, however, to measure $v_9 + v_{10}$, the sum of the rates of formation of these substances. The rates of formation of diisopropyl were estimated using the relationship (19)

[vii] $$v_9/(v_8 v_{10})^{1/2} = 2.0$$

Can. J. Chem. Downloaded from www.nrcresearchpress.com by 210.87.254.105 on 09/05/12
For personal use only.

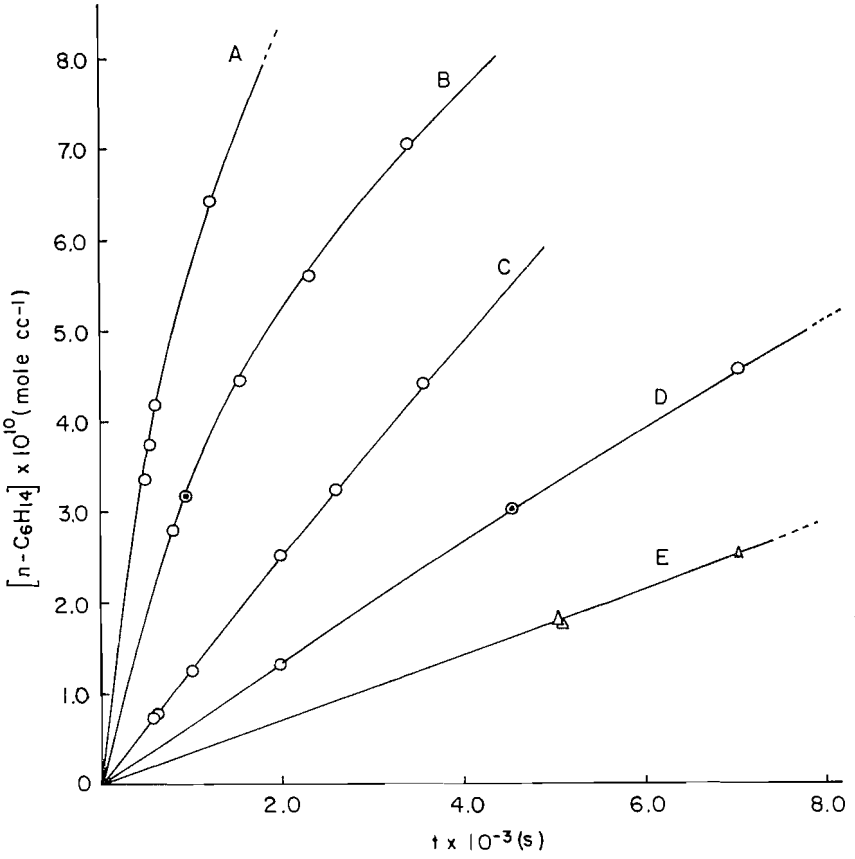


FIG. 4. Typical plots of yield against time for n-C_6H_{14} formation at different temperatures and pressures. The results obtained from the 2.31% mixture are shown as ○, and those from 3.39% as △. (A) 300.0 °C, 195.3 mm; (B) 290.0 °C, 195.5 mm; (C) 284.0 °C, 154.4 mm; (D) 270.5 °C, 154.7 mm; (E) 260.0 °C, 154.1 mm.

and from the known values of $v_9 + v_{10}$. The results obtained in this way are shown in Fig. 7, which leads to the relationship

[*viii*] $$[i\text{-}C_3H_7]/[n\text{-}C_3H_7] \approx 5 \times 10^6\, e^{-17000/RT}.$$

Frey, Danby, and Hinshelwood (20) found in work at higher temperatures that the reactions

[16] $$n\text{-}C_3H_7 + C_3H_8 \underset{[-16]}{\overset{[16]}{\rightleftharpoons}} C_3H_8 + i\text{-}C_3H_7$$

are sufficiently rapid that the radicals n-C_3H_7 and i-C_3H_7 are at equilibrium with one another. The present results, however, show that in the temperature range of our experiments the concentrations of these radicals differ from the equilibrium concentrations. If these reactions were so fast that equilibrium was established, the n-C_3H_7 radical concentration would be reduced to a few percent of that of i-C_3H_7, which is more stable by 3.5 kcal/mole (21). It therefore appears that under the present conditions reactions [16] and [−16] are not sufficiently rapid to establish equilibrium. The temperature coefficient of the ratio $[i\text{-}C_3H_7]/[n\text{-}C_3H_7]$, corresponding to 17 kcal/mole, is related to the increasing rate of

Can. J. Chem. Downloaded from www.nrcresearchpress.com by 210.87.254.105 on 09/05/12
For personal use only.

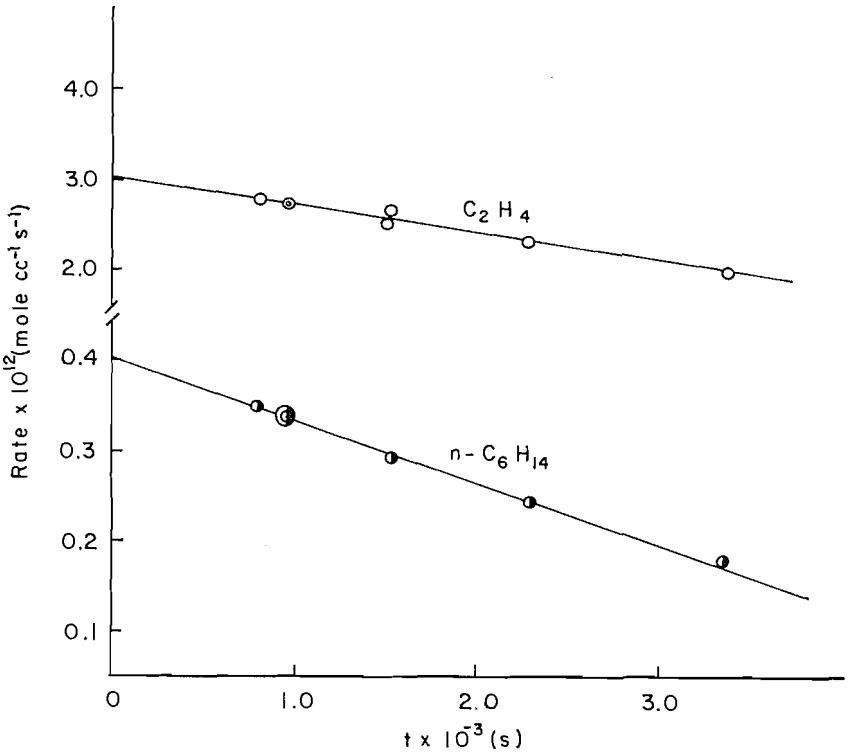


FIG. 5. Typical plots of rate against time for C_2H_4 and n-C_6H_{14} formation at 290.0 °C; 195.5 mm of 2.31% azomethane–propane mixture.

breakdown of the n-C_3H_7 radical as the temperature increases. This throws further light on why the procedure of Bywater and Steacie (4, 8) led to too low a value for E_7.

Energy Levels for the Reactions of Propyl Radicals

The activation energy $E_7 = 31.4$ kcal/mole is related to the standard enthalpy change ΔH_7^0 for reaction [7] by

$$[ix] \qquad \Delta H_7^0 = E_7 - E_{-7} + RT$$

$$[x] \qquad = \Delta H_{7,0}^0 + \int_0^T \Delta C_p^0 \, dT$$

where $\Delta H_{7,0}^0$ is the standard enthalpy change at 0 °K. By definition

$$[xi] \qquad \Delta H_{7,0}^0 = D_0^0(n\text{-}CH_3\text{—}CH_2CH_2)$$

where D_0^0 denotes the dissociation energy at 0 °K. Therefore,

$$[xii] \qquad D_0^0(n\text{-}CH_3\text{—}CH_2CH_2) = E_7 - E_{-7} + RT - \int_0^T \Delta C_p^0 \, dT.$$

At 550 °K (the middle of the present temperature range), substitution of $E_7 = 31.4$ and $\int_0^T \Delta C_p^0 \, dT = 3.3$ (on the assumption that C_p^0 is the same for n-C_3H_7 as for C_3H_8), and use of the heat capacities of C_2H_4 and C_3H_8 (22) and of CH_3 (23) gives

$$D_0^0(n\text{-}CH_3\text{—}CH_2CH_2) = 29.2 - E_{-7} \text{ kcal/mole.}$$

Can. J. Chem. Downloaded from www.nrcresearchpress.com by 210.87.254.105 on 09/05/12
For personal use only.

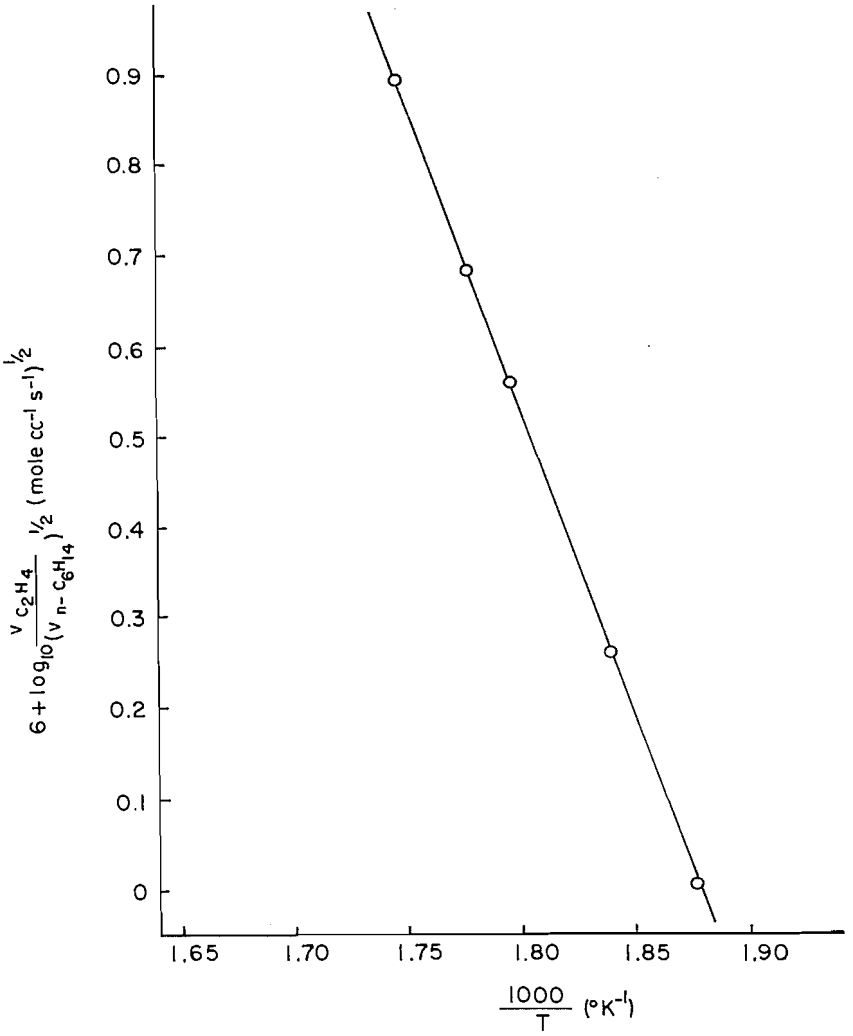


FIG. 6. Plot of $\log_{10} \frac{v_{C_2H_4}}{v_{n\text{-}C_6H_{14}}^{1/2}}$ against $1/T$.

Mandelcorn and Steacie (24) obtained a value of 7.0 ± 1.5 kcal/mole for E_{-7}, while Brinton (25), from a more extensive study, obtained a value of 8.9 kcal/mole, which is about the upper limit of the former.

Use of $E_{-7} = 8.9$ kcal/mole leads to

$$D_0^0(n\text{-}CH_3\text{—}CH_2CH_2) = 20.3 \text{ kcal/mole.}$$

This value together with $\Delta H_{f,0}^0(CH_3) = 34.2$ kcal/mole (26) and the heats of formation of ethylene and propane at 0 °K gives

$$\Delta H_{f,0}^0(n\text{-}C_3H_7) = 28.4 \text{ kcal/mole}$$

and

$$D_0^0(n\text{-}C_3H_7\text{—}H) = 99.4 \text{ kcal/mole,}$$

which is in excellent agreement with the value of 99.5 kcal/mole obtained by Stevenson

Can. J. Chem. Downloaded from www.nrcresearchpress.com by 210.87.254.105 on 09/05/12
For personal use only.

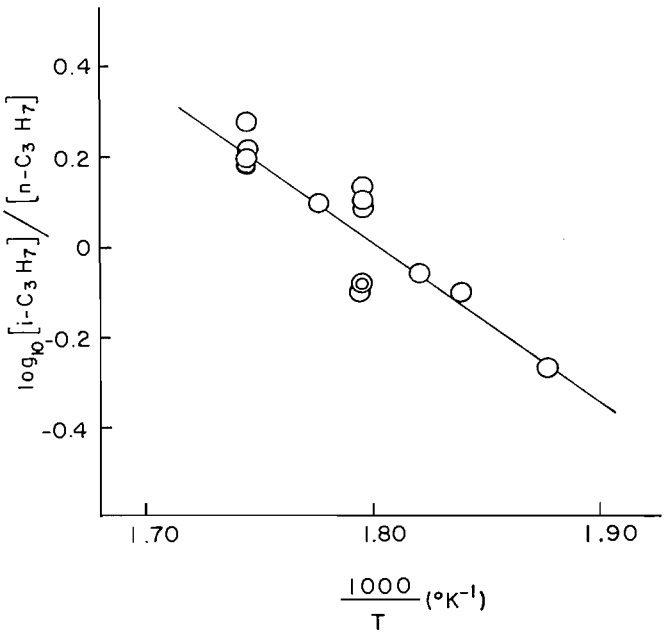


FIG. 7. Plot of $\log_{10}([i\text{-}C_3H_7]/[n\text{-}C_3H_7])$ against $1/T$.

(27). The values of $\Delta H_f^0(n\text{-}C_3H_7)$, ΔH_7^0, and ΔS_7^0 (28) are tabulated for various temperatures in Table V, together with ΔH_{17}^0 for the heat of dissociation of the primary C—H bond in propane.

[17] $$CH_3CH_2CH_2—H \rightarrow n\text{-}C_3H_7 + H$$

TABLE V

Thermodynamic quantities at various temperatures (reactions [7] and [17])

T (°K)	ΔS_7^{0*} (e.u.)	$(\Delta C_p^0)_T T$† (kcal/mole)	ΔH_7^0 (kcal/mole)	$\Delta H_f^0(n\text{-}C_3H_7)$ (kcal/mole)	ΔH_{17}^0 (kcal/mole)
0	0	0	20.3	28.4	99.4
298.16	9.48	2.45	22.8	23.1	99.9
400	9.56	2.89	23.2	21.5	100.0
500	9.37	3.16	23.5	20.3	100.3
600	9.06	3.34	23.6	19.2	100.4
700	8.78	3.43	23.7	18.4	100.5

*Standard state: 1 mole cc^{-1} of ideal gas.

†$(\Delta C_p^0)_T T = \int_0^T \Delta C_p^0 \, dT$.

An energy diagram for the system of reactions involving the $n\text{-}C_3H_7$ and $i\text{-}C_3H_7$ radicals is shown in Fig. 8. It is based on the values derived above, on the fact that the difference between the primary and secondary C—H bond dissociation energies is 3.5 kcal/mole (21), and on the result that the activation energy for the addition of a hydrogen atom to propylene

[18] $$H + C_3H_6 \rightarrow CH_3CHCH_3$$

is 1.5 kcal/mole (29). The diagram relates to 298 °K.

The activated complexes for reactions [18] and

[19] $$H + CH_3CHCH_2 \rightarrow CH_3CH_2CH_2$$

Can. J. Chem. Downloaded from www.nrcresearchpress.com by 210.87.254.105 on 09/05/12
For personal use only.

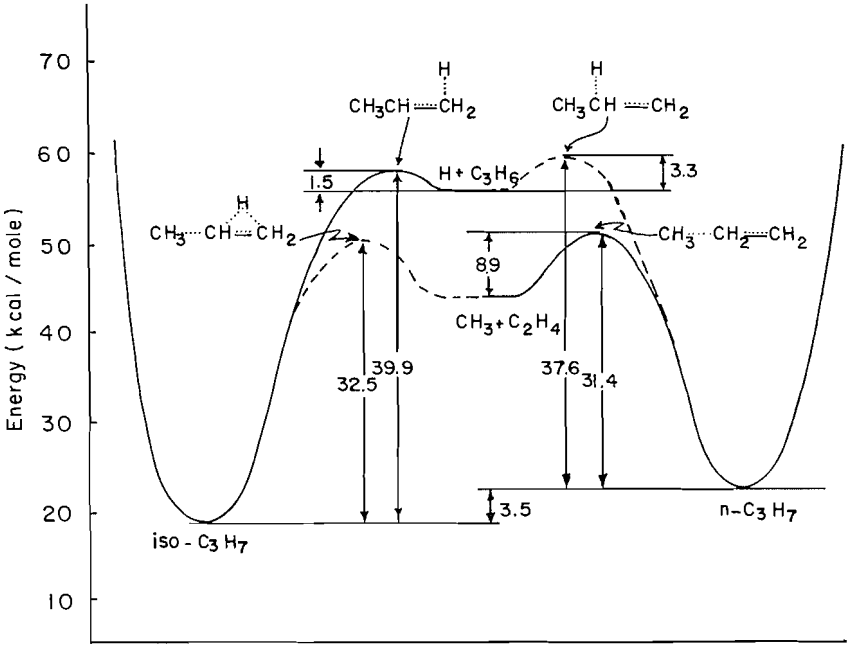


FIG. 8. Schematic energy diagram for the reactions of n-C_3H_7 and i-C_3H_7 radicals at 298.16 °K.

have structures that may be represented as

$$CH_3\overset{\overset{H}{|}}{C}H{=}CH_2 \quad \text{and} \quad CH_3\overset{\overset{H}{|}}{C}H{=}CH_2$$

Since the entropy of n-C_3H_7 at 298 °K is only 1.8 e.u. (entropy unit) greater than that of i-C_3H_7 (28), it is reasonable to assume equal entropies for these two activated complexes. From the relative rates of [18] and [19] it can then be estimated that the activation energy of [19] is about 3.3 kcal/mole, as compared with 1.5 for [18]. When a hydrogen atom reacts with propylene at room temperature there will therefore be formed 5% n-C_3H_7 and 95% i-C_3H_7 (30). These values lead to a value of 37.6 kcal/mole for the activation energy of the reverse of reaction [19] and of 39.9 kcal/mole for the reverse of that of reaction [18]. These values are about 3 kcal/mole higher from previously reported values (4, 6, 8, 15).

There is still controversy about the Arrhenius parameters for reaction [15].

[15] $$CH_3CHCH_3 \rightarrow CH_3 + C_2H_4$$

Kerr and Trotman-Dickenson (15) obtained

$$k_{15} = 2.0 \times 10^{10}\, e^{-29500/RT}\ s^{-1},$$

whereas Heller and Gordon (16) obtained

$$k_{15} = 1.0 \times 10^{12}\, e^{-32500/RT}\ s^{-1}.$$

In both investigations the frequency factor is low, probably because of the tightness of the structure produced during the simultaneous breaking of two bonds.

[15] $$CH_3CHCH_3 \rightarrow CH_3\text{---}\overset{\overset{H}{|}}{C}H\text{---}CH_2 \rightarrow CH_3 + C_2H_4$$

Can. J. Chem. Downloaded from www.nrcresearchpress.com by 210.87.254.105 on 09/05/12
For personal use only.

Because of this low entropy of the activated state the reverse reaction is of negligible importance compared with

[−7] $$CH_3 + C_2H_4 \rightarrow CH_3CH_2CH_2$$

even though the reverse of [15] may be slightly favored energetically. No i-C_4H_{10} or diisopropyl was obtained in the reaction of CH_3 with ethylene (25).

ACKNOWLEDGMENTS

The authors thank Drs. M. H. Back and J. L. Holmes for valuable help with the vapor-phase chromatography and mass spectrometry respectively. The work was supported by grants from the American Petroleum Fund and from the National Research Council of Canada.

REFERENCES

1. E. W. R. Steacie. Atomic and free radical reactions. Vol. 1. Reinhold Publishing Corp., New York. 1954.
2. A. O. Allen and D. V. Sickman. J. Am. Chem. Soc. **56**, 2031 (1934).
3. D. G. Milne and O. K. Rice. C.I.C. Symposium on the Kinetics of Pyrolytic Reactions. Ottawa. September, 1964.
4. S. Bywater and E. W. R. Steacie. J. Chem. Phys. **19**, 319 (1951).
5. J. G. Calvert and W. C. Sleppy. J. Am. Chem. Soc. **81**, 1544 (1959).
6. J. A. Kerr and A. F. Trotman-Dickenson. Trans. Faraday Soc. **55**, 592 (1959).
7. J. A. Kerr and J. G. Calvert. J. Am. Chem. Soc. **83**, 3391 (1961).
8. R. A. Back and S. Takamuku. J. Am. Chem. Soc. **86**, 2558 (1964).
9. W. Forst and O. K. Rice. Can. J. Chem. **41**, 562 (1963).
10. J. R. McNesby and A. S. Gordon. J. Am. Chem. Soc. **77**, 4719 (1955).
11. A. Shepp. J. Chem. Phys. **24**, 939 (1956).
12. J. A. Kerr and A. F. Trotman-Dickenson. Progr. Reaction Kinetics, **1**, 119 (1961).
13. A. Shepp and K. O. Kutschke. J. Chem. Phys. **26**, 1020 (1957).
14. K. J. Laidler, N. H. Sagert, and B. W. Wojciechowski. Proc. Roy. Soc. London, Ser. A, **270**, 242 (1962).
15. J. A. Kerr and A. F. Trotman-Dickenson. Trans. Faraday Soc. **55**, 921 (1959).
16. C. A. Heller and A. S. Gordon. J. Phys. Chem. **62**, 709 (1958).
17. W. M. Jackson and J. R. McNesby. J. Am. Chem. Soc. **83**, 4891 (1961).
18. W. M. Jackson, J. R. McNesby, and B. de B. Darwent. J. Chem. Phys. **37**, 1610 (1962).
19. S. W. Benson and W. B. DeMore. Ann. Rev. Phys. Chem. **16**, 397 (1965).
20. H. M. Frey, C. J. Danby, and C. N. Hinshelwood. Proc. Roy. Soc. London, Ser. A, **234**, 301 (1956).
21. S. W. Benson. J. Chem. Educ. **42**, 505 (1965).
22. F. D. Rossini *et al.* Selected values of physical and thermodynamic properties of hydrocarbons and related compounds. American Petroleum Institute, Pittsburgh. 1953.
23. Janaf Interim Table. Thermal Laboratory of Dow Chemical Co., Midland, Michigan. 1961.
24. L. Mandelcorn and E. W. R. Steacie. Can. J. Chem. **32**, 474 (1954).
25. R. K. Brinton. J. Chem. Phys. **29**, 781 (1958).
26. M. C. Lin and M. H. Back. Can. J. Chem. **44**, 505 (1966).
27. D. P. Stevenson. Trans. Faraday Soc. **10**, 35 (1951).
28. J. H. Purnell and C. P. Quinn. J. Chem. Soc. 4049 (1964).
29. K. Yang. J. Am. Chem. Soc. **87**, 719 (1962).
30. R. E. Harrington, B. S. Babinovitch, and H. M. Frey. J. Chem. Phys. **33**, 1271 (1960).

Can. J. Chem. Downloaded from www.nrcresearchpress.com by 210.87.254.105 on 09/05/12
For personal use only.

THE KINETICS OF SORPTION AND DESORPTION OF WATER VAPOR BY LEAD STYPHNATE

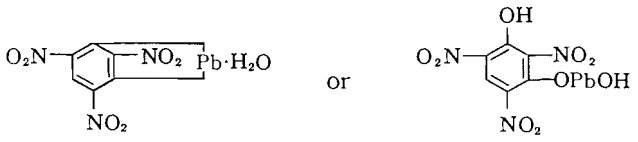
TED B. FLANAGAN
Chemistry Department, University of Vermont, Burlington, Vermont
Received June 6, 1966

ABSTRACT

The kinetics of dehydration and rehydration of lead styphnate monohydrate have been studied as a function of the number of cycles of dehydration and rehydration. The activation energy for dehydration of a repeatedly dehydrated sample is 14.6 kcal/mole compared with 21.7 kcal/mole for the virgin hydrate. Mechanisms for these sorption and desorption phenomena are discussed.

INTRODUCTION

In a previous study (1) of the dehydration of the primary explosive lead styphnate monohydrate, it was observed that the virgin monohydrate, as crystallized from solution,



(I) (II)

lost water at an approximately linear rate (100–130 °C). (I is the usually accepted structure of lead styphnate monohydrate; however, recent work indicates that II may be a more likely structure (1, 2).) The activation energy for the dehydration of virgin monohydrate is 21.7 kcal/mole (1). It was also noted that the subsequent dehydration of rehydrated samples occurred more readily and with different kinetics than the original dehydration (1). Because of the general paucity of information about such systems (3), i.e. systems capable of dehydration and rehydration (exclusive of true zeolites), the behavior of lead styphnate upon repeated cycles of dehydration–rehydration was investigated in some detail.

EXPERIMENTAL

The experimental apparatus was similar to the one previously described (1). The quartz helix balance (Microchemical Specialties, Berkeley, California) had a sensitivity of 1.0 cm/mg. After evacuation to 10^{-6} mm of mercury at room temperature, the samples (approximately 6 mg of powder, average particle size 7 microns) were dehydrated *in vacuo* at the temperature of the run. The preparation of the lead styphnate used for those studies has previously been described (1).

RESULTS

Dehydration

Figure 1 shows a series of dehydration runs with the same sample of lead styphnate monohydrate (119.3 °C). The rate of dehydration is greatly enhanced upon repeated dehydration–rehydration cycles until after approximately 6 or 7 cycles the rate appears to have become reproducible. In reality, however, the rate continues to increase slowly, e.g. after approximately 30 cycles the rate of dehydration increased to a value twice that of the apparent maximum rate shown in Fig. 1. It was noted earlier that the kinetics of dehydration are zero and first order, with respect to time, for the first (the original) and

Can. J. Chem. Downloaded from www.nrcresearchpress.com by 210.87.254.5 on 09/05/12
For personal use only.

the second dehydration respectively (1). This finding was confirmed here and the rate of the dehydration is approximately the same as in the original study after storage for 3 years. The extent of the agreement of the dehydration data with a first order rate law increases with the number of cycles, e.g. in Fig. 1 curve *b* is described by a first order rate equation from approximately 10 to 75% dehydration whereas curve *c* is well described by a first order equation from 10 to 90%. The behavior shown in Fig. 1 is reproducible, i.e. another sample exhibited the same sequence of behavior with rates closely identical with those of Fig. 1 for each run of the sequence.

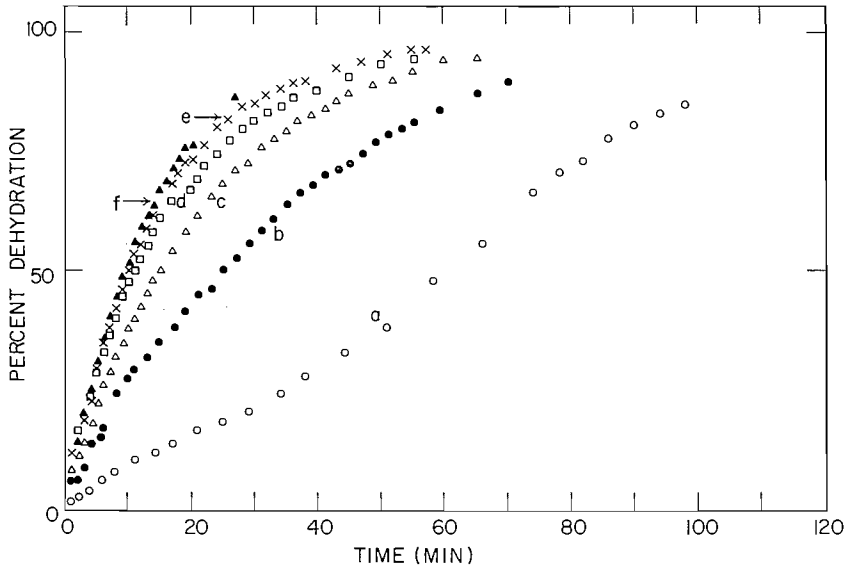


FIG. 1. Repeated dehydration runs of lead styphnate monohydrate (119.3 °C); *a* represents the dehydration of the virgin monohydrates and *b* represents the second dehydration run with the same sample, etc. The samples were rehydrated between runs at 22.5 °C and $P_r = 0.66$. Before dehydration the samples were evacuated at room temperature.

The change in the rate of dehydration after run *f* (curve *f*, Fig. 1) was small enough to allow the determination of a meaningful activation energy (Fig. 2). The determinations were made at random temperatures to minimize the effect due to the slow increase in rate. The first order rate constants are shown as an Arrhenius plot (Fig. 2); the energy of activation is 14.6 kcal/mole. The linearity of the plot suggests that self-cooling is not significant. Since the presence of small pressures of water vapor accelerates the virgin dehydration, impedance effects are believed to be negligible in this system. Evidence for this is that the addition of a series of pressures (20 mm to 150 mm) of methyl chloride accelerated the rate slightly, but the effect was not as marked as would be expected if impedance was a dominant feature of the reaction. Interruption and resumption of a run did not introduce any new features.

Rehydration

It was of interest to determine the kinetics of rehydration during the approach to "constant activity". Percent rehydration – time curves ($P_r = P/P_0 = 0.66$, where P is the actual vapor pressure employed and P_0 is the saturation water vapor pressure at 22.5 °C) are shown in Fig. 3. It is seen that, as for dehydration, the kinetics change

Can. J. Chem. Downloaded from www.nrcresearchpress.com by 210.87.254.5 on 09/05/12
For personal use only.

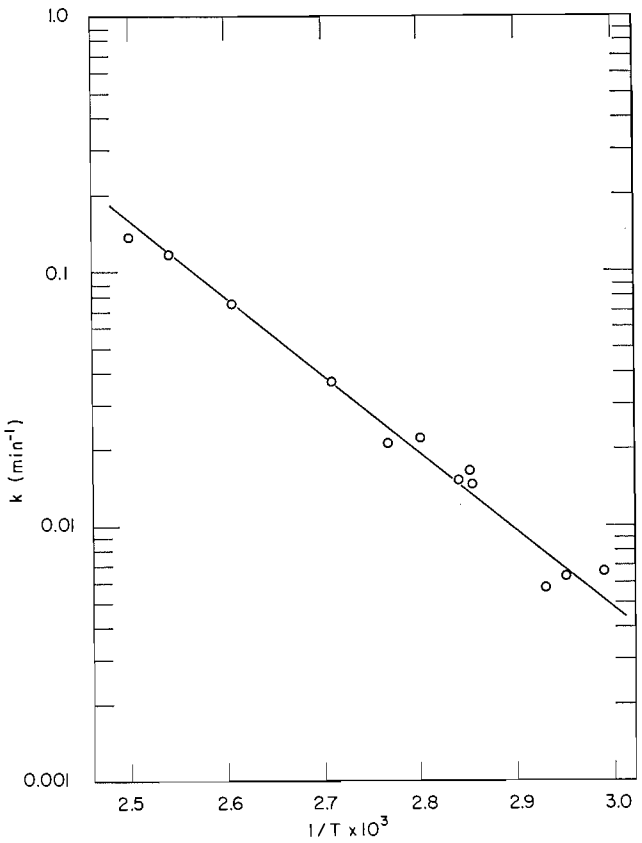


FIG. 2. The Arrhenius plot for the dehydration of a sample of lead styphnate monohydrate of "constant activity".

markedly with the number of cycles of dehydration–rehydration. After the initial rehydration, the data, e.g. curves *b* and *c*, may be described by a linear dependence of percent rehydration upon time as was reported earlier (1). (Since the kinetics were not systematically investigated as a function of the number of cycles of dehydration–rehydration in the earlier study, the linear rehydration rate was the only behavior noted in several runs with different samples.) The initial rehydration curve differs markedly from the subsequent curves. The amount of rehydration of this run in its initial stages is greater than for subsequent runs, whereas during the final stages of this rehydration the rate is slower than the subsequent runs.

After a sample of "constant activity" is attained, the dependence of percent rehydration upon time is best described by a diffusion-controlled slow step. The kinetics shown in curves *d* and *e* (Fig. 3) are well described by a $t^{\frac{1}{2}}$ rate law (4).

Equilibration with Water Vapor

During rehydration studies of the anhydride it was noted that rehydration did not go to completion under some conditions. This incomplete rehydration was investigated by allowing an anhydride of "constant activity" to equilibrate with a constant water vapor pressure (13.6 mm) at various temperatures for at least 24 h. Results are shown in Fig. 4 as a plot of log K versus $1/T$. K is taken as the percentage of water in the styphnate

Can. J. Chem. Downloaded from www.nrcresearchpress.com by 210.87.254.5 on 09/05/12
For personal use only.

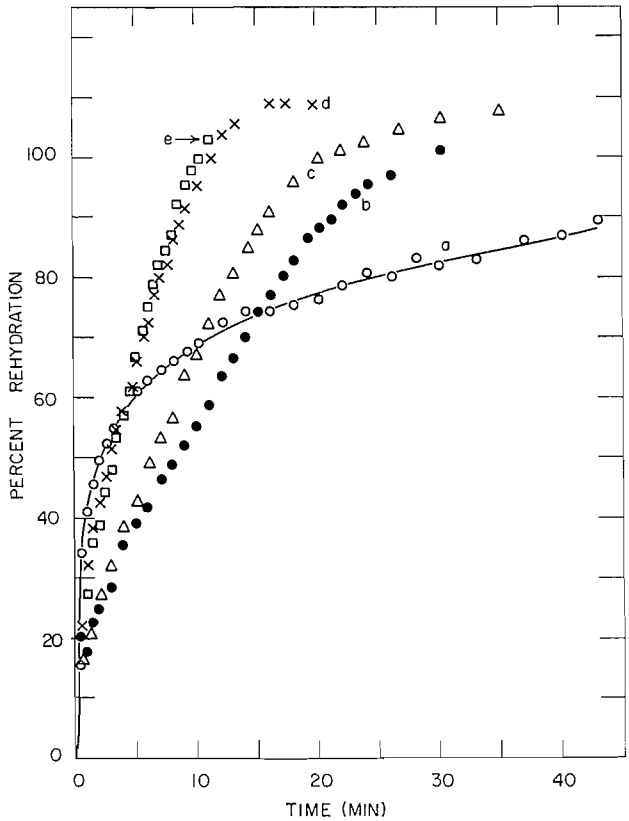


FIG. 3. Repeated rehydration runs of lead styphnate anhydride (22.5 °C, $P_r = 0.66$). The solid curve *a* shows the first rehydration run and *b* represents the second rehydration, etc. Before rehydration the samples were dehydrated *in vacuo* at 119.3 °C.

matrix; the water vapor pressure (constant) and factors for the conversion of percentage of water into concentration units are incorporated into the value of K. It should be noted that this approach is somewhat unorthodox for such a system, and if the anhydride and the monohydrate always existed as distinct crystalline phases one would not be able to vary the temperature at an arbitrary water vapor pressure (Fig. 4) because it would constitute a violation of the phase rule. Apparently below approximately 15% rehydration, the rehydrated species does not have the characteristics of a distinct crystalline phase. It can be argued that not enough time has been allowed for complete reaction; however, at lower temperatures where the rate processes are slower, complete rehydration occurs rapidly (Fig. 3).

The sharp increase of K below 70 °C (Fig. 4) should be noted. Several other determinations in the 60 to 65° temperature ranged showed that the rehydration went to completion and therefore supported the behavior exhibited in Fig. 4. Figure 5 shows the approach to equilibrium of a sample at a temperature in the nonlinear region of Fig. 4, 61.7°, compared with a run which did not go to completion, 73.2°. The acceleratory nature of the former curve indicates that a cooperative effect is operating. It is suggested that in the nonlinear region enough of the hydrate is found in localized regions of the lattice for it to attain the characteristics of a distinct phase, and therefore a violation of the phase rule occurs; further rehydration then readily occurs at the hydrate nuclei formed at localized regions

Can. J. Chem. Downloaded from www.nrcresearchpress.com by 210.87.254.5 on 09/05/12
For personal use only.

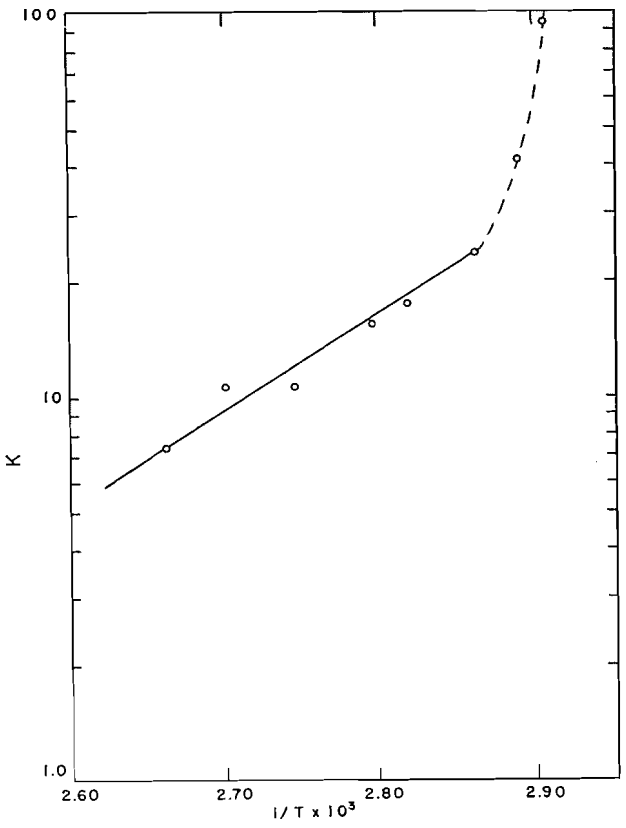


FIG. 4. A plot of the equilibration of water vapor (13.6 mm) with the anhydride as a function of temperature.

of the lattice. The acceleratory portion of Fig. 5 represents the rapid growth of the second phase. The subsequent kinetics and absolute rate of dehydration of the sample rehydrated at 61.7° were comparable with samples rehydrated at 22.5°, although the latter samples did not exhibit acceleratory behavior in their rehydration–time curves (Fig. 3).

The slope of the linear portion of the plot (75 to 100 °C, Fig. 4) yields a heat of ~ 12 kcal/mole. It seems reasonable that ~ -12 kcal/mole should represent ΔH for the recombination of water vapor with a styphnate matrix having the crystal structure of the anhydride, provided that this heat of recombination is independent of the percentage reaction over the range from 0 to 15% of sorbed water. Ideally, "sorption" isotherms should be determined at a series of temperatures to obtain the isosteric heats of "sorption"; in their absence, the limited equilibrium data of the present study should mainly be regarded as showing that an equilibrium is established between sorbed water and gaseous water under the conditions obtaining in Fig. 4 and that this equilibrium breaks down at a critical composition of sorbed water when the second solid phase appears.

Previous deductions based on examination of X-ray powder patterns of the anhydride and rehydrated species indicated that these species were closely similar (1). The evidence presented above shows, however, that these species can exist as distinct crystalline phases (Fig. 4). It must be concluded therefore that the hydrate and anhydride have very

Can. J. Chem. Downloaded from www.nrcresearchpress.com by 210.87.254.5 on 09/05/12
For personal use only.

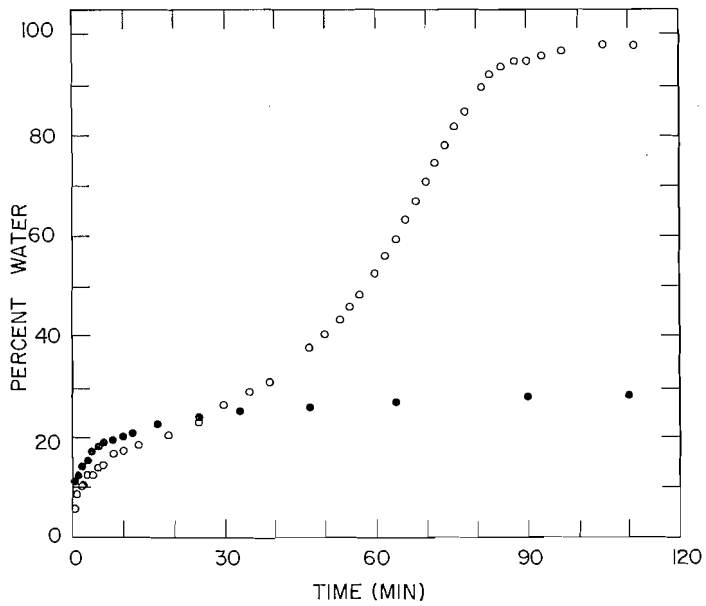


FIG. 5. Rehydration of lead styphnate (13.6 mm water vapor): (●) 73.2 °C, (○) 61.7 °C.

closely related structures as indicated by the ease of their interconversion and similarities of X-ray powder patterns.

Sorption of Other Vapors

The quasi-zeolitic behavior of lead styphnate indicates that lead styphnate may be capable of sorbing other vapors. Barrer and co-workers (5) have found that potassium benzene sulfonate monohydrate can sorb many vapors after dehydration. After dehydration *in vacuo*, the same sample used for the above studies was exposed to ethanol (22.5°) at $P_r = 0.66$. After approximately 60 h of equilibration, the extension of the helix indicated that $\alpha' = 10\%$ (where α' is the percentage reaction assuming a 1:1 addition compound); half of this ethanol was desorbed by evacuation at room temperature.

Methanol was sorbed to a much greater extent than ethanol and after equilibration for 20 h ($P_r = 0.66$, 22.5 °C), $\alpha' = 90\%$. The rates of both the sorption and the subsequent desorption were much slower than the corresponding reactions of water; the desorption of methanol is shown in Fig. 6 (114.0 °C). The run shown in Fig. 6 is the last of a series of methanol sorption and desorption runs. The dehydration run (114.0°) shown on Fig. 6 was made immediately after the methanol run and the rate was considerably faster than that of the dehydration runs prior to the methanol sorption studies, although these, too, were faster than the methanol desorption. A first rate equation describes the removal of methanol from near the commencement of the desorption to approximately 60% reaction.

DISCUSSION

It is of interest to consider the mechanism of dehydration of repeatedly dehydrated–rehydrated samples. A valid mechanism must account for the result that compared with the virgin dehydration process, which proceeds by an interfacial mechanism (1), the activation energy for dehydration of dehydrated–rehydrated samples is decreased by 7.3 kcal/mole while the absolute rate of dehydration is increased only by a factor of

Can. J. Chem. Downloaded from www.nrcresearchpress.com by 210.87.254.5 on 09/05/12
For personal use only.

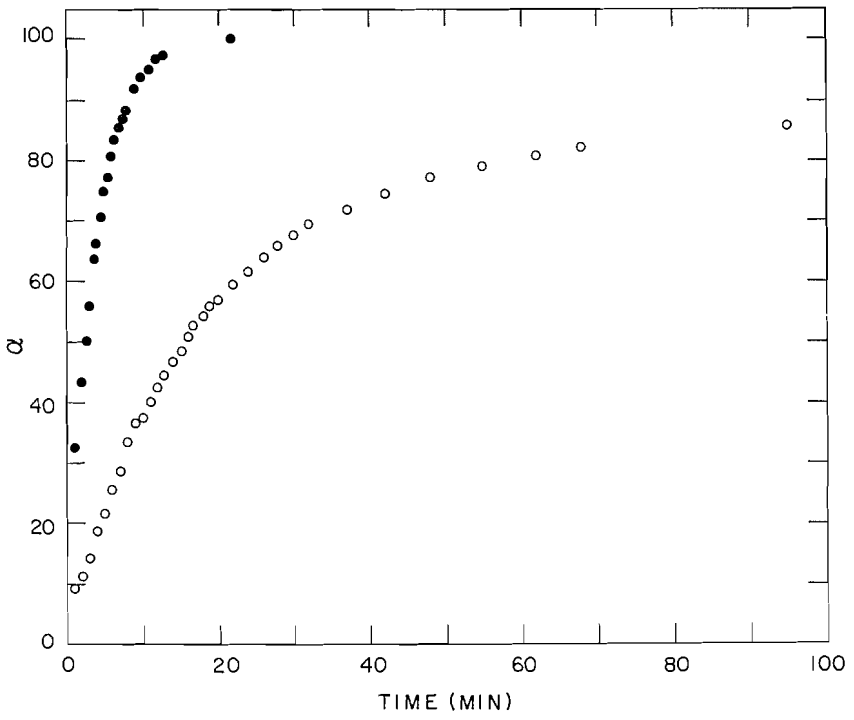


FIG. 6. Comparison of the desorption kinetics of methanol and water (114.0 °C): (○) methanol, (●) water.

approximately 7. This implies that an entirely new mechanism must be operative, since it is difficult to explain such changes by a normal interfacial mechanism. It should be mentioned that a true first order reaction, such as observed here for the entire dehydration process, is quite rare in solid state decomposition reactions, and since there appear to be only two mechanisms to account for these kinetics in this system they will be discussed in some detail below.

One possible mechanism which must be considered is random nucleation of the well-separated blocks of rehydrated material. In view of the tendency found in the styphnates for one-dimensional growth (1, 6), it is not unreasonable to suppose that after random nucleation, one-dimensional growth will occur. At small times such a mechanism leads to (7)

$$[1] \qquad \alpha = (2k_2/k_1c)[(\exp -k_1t) + k_1t - 1],$$

where k_1 and k_2 are the rate constants for growth and nucleation respectively and c is the dimension of the block in the growth direction. For $t > c/2k_2$ eq. [1] becomes (7)

$$[2] \qquad \alpha = 1 + (2k_2/k_1c)[1 - (\exp (k_1c/2k_2))](\exp -k_1t).$$

A plot of $\log (1 - \alpha)$ versus t gives first order kinetics with slope k_1 and intercept $\log \{(2k_2/k_1c)[(\exp (k_1c/2k_2)) - 1]\}$ from which $2k_2/c$ can be obtained. For eq. [2] to describe the data of the present investigation below 110 °C, $2k_2/c$ must be negative, which is untenable. In addition since eq. [1] itself does not fit the data at small times this implies that for eq. [2] to be applicable the blocks which were nucleated at $t = 0$ have decomposed immediately, again an unreasonable conclusion.

Can. J. Chem. Downloaded from www.nrcresearchpress.com by 210.87.254.5 on 09/05/12
For personal use only.

Can. J. Chem. Downloaded from www.nrcresearchpress.com by 210.87.254.5 on 09/05/12
For personal use only.

An alternative mechanism which leads to first order kinetics is that the entire reaction takes place by desorption of water molecules from the surface of the blocks. The surface, or some active fraction of the surface, is supplied by diffusion of highly mobile water molecules from within the rehydrated lattice. At any time the concentration of water molecules on the surface of the blocks is proportional to the fraction of hydrate within the blocks or, more accurately, the chemical potential of water on the surface is the same as the chemical potential within the solid blocks. The rate is proportional to the chemical potential. An activation energy for surface desorption of 14.6 kcal/mole is not unreasonable, i.e. it is comparable to the heat of the recombination of water with the anhydride lattice, $\sim$ 12 kcal/mole (Fig. 4). Furthermore, since only a small fraction of the surface need be active for this process, the absolute rate could be much smaller than would correspond to desorption from the entire surface. The important and unusual requisite for this mechanism is the high degree of mobility of water molecules within the rehydrated matrix. Water vacancies will be generated during dehydration and their mobility may be high, judging from the rapidity of the rehydration reaction at, for example, 22.5 °C (Fig. 3).

The remarkable ease of rehydration of this system is of considerable interest. In contrast to zeolitic systems, evidence has been presented here to indicate that two distinct solid phases can be formed. What is the nature of the transport processes which occur during rehydration? Are water molecules transported through the hydrate phase to the growing internal interface? These questions, which have relevance to non-zeolitic solid state rehydration processes in general, can be considered here only in a speculative fashion.

The results shown in Fig. 5 are of interest with regards to the mechanism of rehydration. The fact that a cooperative process occurs (61.7 °C) suggests that nucleation and growth are the slow steps and diffusion to the nuclei must be rapid. The rehydration behavior up to the onset of the autocatalytic portion is describable by a diffusion-controlled slow step. If the nuclei are situated within the anhydride matrix, growth of the nuclei could occur through the maintenance of an "equilibrium" concentration of water molecules within the anhydride matrix. That such an "equilibrium" concentration exists is shown by the "equilibrium" constant studies (Fig. 4). Because the nuclei are located within the anhydride matrix their formation and growth may be slow compared with diffusion resulting from internal strain. In contrast to 61.7 °C the rehydration behavior shown at lower temperatures, e.g. curves *d* and *e* of Fig. 3, is describable solely in terms of diffusion as the slow step, whereas it would be expected that here the nucleation and growth processes would be even slower relative to diffusion than at 61.7 °C. A possible explanation is that a different sequence of events occurs at the lower temperatures; because of the greater degree of supersaturation immediate nucleation occurs adjacent to the surface at low temperatures and diffusion now takes place through the hydrate lattice rather than through the anhydride lattice as at higher temperatures. Diffusion through the hydrate lattice proceeds via water vacancies. These vacancies are continually generated at the internal interface as rehydration proceeds. The assumption of a relatively constant supply of vacancies and the thickening hydrate layer which is formed as rehydration proceeds leads to the $t^{\frac{1}{2}}$ rate law.

ACKNOWLEDGMENTS

Since this is the last of several papers dealing with the kinetics of dehydration and decomposition of lead styphnate, this is an appropriate opportunity to acknowledge a

debt of gratitude to Dr. D. A. Young of Imperial College, London, for his stimulating and helpful comments concerning these papers.

REFERENCES

1. T. B. FLANAGAN. Trans. Faraday Soc. **55**, 114 (1959).
2. R. ZINGARO. J. Am. Chem. Soc. **76**, 816 (1954).
3. W. E. GARNER. *In* Chemistry of the solid state. *Edited by* W. E. Garner. Butterworths, London. 1955.
4. R. M. BARRER and B. E. F. FENDER. J. Phys. Chem. Solids, **21**, 1 (1961).
5. R. BARRER, J. DRAKE, and T. WHITTAM. Proc. Roy. Soc. London, Ser. A, **219**, 32 (1953).
6. F. C. TOMPKINS and D. A. YOUNG. Trans. Faraday Soc. **52**, 1245 (1956).
7. P. W. M. JACOBS and F. C. TOMPKINS. *In* Chemistry of the solid state. *Edited by* W. E. Garner. Butterworths, London. 1955.

Can. J. Chem. Downloaded from www.nrcresearchpress.com by 210.87.254.5 on 09/05/12
For personal use only.

Can. J. Chem. Downloaded from www.nrcresearchpress.com by 210.87.254.5 on 09/05/12
For personal use only.

XENON YIELDS IN THE FISSION OF HEAVY ELEMENTS BY MEDIUM-ENERGY PROTONS[1]

J. H. FORSTER,[2] N. T. PORILE,[3] AND L. YAFFE
Radiochemistry Laboratory, Department of Chemistry, McGill University, Montreal, Quebec

Received July 7, 1966

ABSTRACT

Independent yields for ^{133}Xe and ^{135}Xe and cumulative yields for ^{133}I and ^{135}I in fission of ^{233}U, ^{235}U, ^{238}U, and ^{232}Th with protons of energies 20–85 MeV were measured. Values of Z_p, the most probable charge, were obtained by two different methods. The behavior of Z_p for ^{235}U and ^{233}U differed considerably from that of ^{238}U and ^{232}Th. Total chain yields were obtained for $A = 133$ and $A = 135$.

INTRODUCTION

A large contribution has been made to the study of fission by the measurement of the yields of fission products. Many more data are still required to improve the understanding of the distributions of fission products with their mass and charge and their dependence on excitation energy.

An important part of the existing data has been collected for the rare gases, krypton and xenon. They are both formed in good yield in fission and are particularly suitable for quick, efficient extraction after, or even during, an irradiation. In 1960, Momyer (1) reviewed the extensive radiochemistry of the rare gases and, more recently, many additional techniques have been reported (2–5). Very important data for the fractional cumulative yields of short-lived isotopes of krypton and xenon have been obtained by the emanation technique of Wahl *et al.* (6).

For thermal neutron fission, several measurements (7–11) have been made of the independent yield of ^{135}Xe and the cumulative yield (9, 12) of ^{133}Xe. For a few medium-energy systems, independent yields have been measured (10, 13) for ^{135}Xe and ^{133}Xe (10). Cumulative yields have been obtained for the iodine parents of these two xenon isotopes (10, 13–15). Cumulative yields of ^{133}Xe and ^{135}Xe have been measured (16) for the fission of ^{238}U by 14.7-MeV neutrons.

The present research was a radiochemical study of xenon yields in proton-induced fission of ^{323}Th, ^{238}U, ^{235}U, and ^{233}U, for which no values have been reported previously.

Nuclear charge distribution in the proton-induced fission of ^{235}U and ^{233}U at medium energies had not been studied heretofore. However, considerable data have been obtained in this laboratory for the charge distribution of fission products with $A = 130$–143, formed in proton-induced fission of ^{232}Th (15, 17) and ^{238}U (18, 19). The conclusions from these previous studies could usefully be compared with those, for the same fission systems, from the present work which involved different fission products and different correlation methods. The method used here to determine Z_p, the most probable charge, was similar to that of Storms (10) and of Nethaway and Levy (20). In all three of these studies insufficient yield data were available to construct charge distribution curves and they were assumed to be given by the Gaussian function

$$[1] \qquad f[Z] = \frac{1}{\sqrt{(\pi C)}} \exp\left[-(Z - Z_p)^2 C\right],$$

[1]*Financial assistance was received from the U.S. Air Force, Grant No. AF–AFOSR 62–24.*
[2]*Present address: Central Instrument Research Lab., Imperial Chemical Industries, Bozedown House, Whitchurch Hill, Reading, Berks, England.*
[3]*Present address: Department of Chemistry, Purdue University, Lafayette, Indiana.*

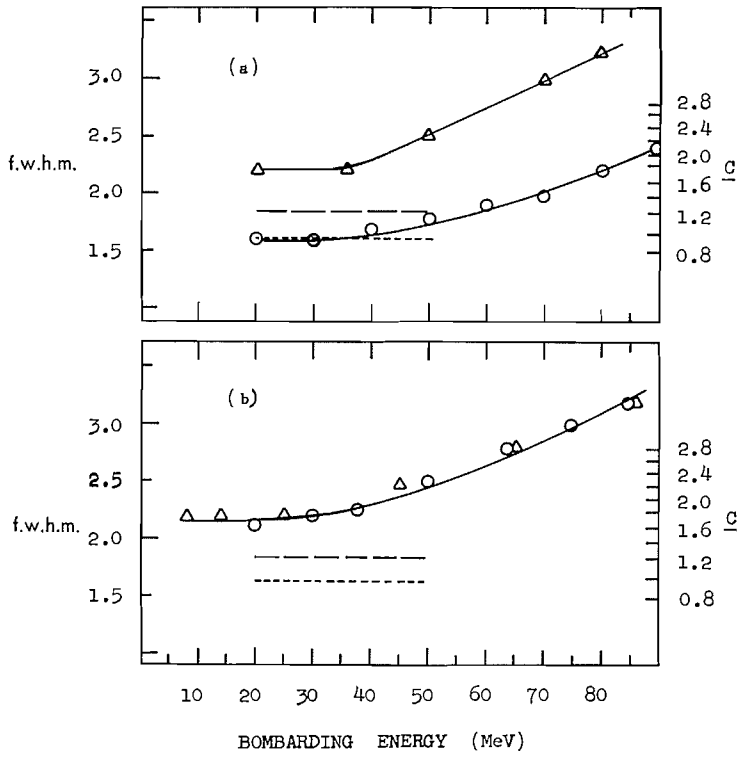


FIG. 1. (*a*) f.w.h.m. of function [1] from previous studies of charge distribution in the fission of ^{238}U with protons: (△) Davies and Yaffe (18); (○) Parikh (19). (*b*) f.w.h.m. of function [1] from previous studies of the fission of ^{232}Th with protons: (△) Pate, Foster, and Yaffe (15); (○) Benjamin (17). Shown for comparison in (*a*) and (*b*) are the f.w.h.m. used in other medium-energy fission systems: (— —) Storms (10); (--) McHugh (13). In (*a*) and (*b*), the alternative ordinates, f.w.h.m. and *C*, were related by eq. [1].

where $f[Z]$ represents the fractional chain yield of an isobar of charge Z. For the present systems, the value of C was estimated from empirical curves in the studies briefly reviewed below.

The first empirical charge distribution curves for individual mass chains were constructed by Wahl and co-workers (6, 21). They obtained the yields of two or three isobaric fission products and fitted the data to the function in eq. [1]. For 10 mass chains the average value of C was 0.86 ± 0.04. Wolfsberg (22) obtained similar empirical curves for fission induced by 14-MeV neutrons. McHugh (13) has made a precise mass spectrometric study of charge distribution in medium-energy fission for the initial 'compound nucleus' ^{236}U. He obtained for chain 135 the yields of iodine, xenon, and cesium and fitted the data to the same Gaussian function with C values from 0.9–1.0 for a range of excitation energy 18–40 MeV. Previous studies in our laboratory have shown a similar constancy in the width of charge distribution curves up to excitation energies of about 40 MeV, for proton-induced fission of ^{232}Th and ^{238}U. However, most of these curves now appear to be too wide, from the evidence of McHugh (13) and of Wolfsberg (22) and also from the latest of the studies in this laboratory (19), in which narrower curves were obtained. There is an interesting parallel here with the history of charge distribution at low energy, in which the earlier curves were shown to be too wide as more precise data were obtained.

Can. J. Chem. Downloaded from www.nrcresearchpress.com by 210.87.254.5 on 09/05/12
For personal use only.

The Gaussian curves used in several studies are characterized in Fig. 1 (*a* and *b*) by their full width at half maximum (f.w.h.m.) and the corresponding C value in eq. [1].

EXPERIMENTAL

1. Targets and Irradiation

The targets were irradiated in the internal circulating beam of protons in the McGill 82-in. synchrocyclotron. For ^{233}U, the target material was finely powdered uranium oxide (5–12 mg) wrapped in aluminium foil of surface density 5.5 mg/cm^2. These irradiations were not monitored, but in the other irradiations the beam intensity (0.5–1.0 μA) was monitored by the reaction $^{65}Cu(p,pn)^{64}Cu$ for the entire proton energy range of 20–85 MeV. The target foils of ^{232}Th, ^{238}U, and ^{235}U and the copper monitor foil had surface densities of 80.8, 46.4, 104.0, and 45.9 mg/cm^2 respectively. A target was assembled by clamping in an aluminium holder a copper monitor foil and a heavy metal foil held in an envelope of aluminium foil (5.5 mg/cm^2). The foils were pressed between aluminium plates in a vise and then carefully sheared to ensure edge alignment. The holder was screwed on to a water-cooled probe and positioned in the cyclotron tank at a radius corresponding to the required proton energy (23). The time of irradiation was from 5–25 min.

2. Chemical Processing

The irradiated target was rapidly removed from the cyclotron to the chemistry laboratory where it was sheared from the holder. The heavy metal and catcher foils were immediately introduced into the gas-sweeping apparatus. The copper foil was processed the following day.

Xenon

Two timed separations of xenon were made, sweeps (*a*) and (*b*), by techniques similar to those used by Dostrovsky and Stoenner (24). The procedure falls into three parts, shown schematically in Fig. 2.

Part 1. Extraction of Xenon and Krypton

To minimize the amount of xenon grown from iodine precursors, the rare gases were separated from the target and other fission products as quickly as possible after the bombardment, while still permitting a complete extraction from the target and catcher foils. Figure 3 gives more details of this part of the experiment. Helium was passed through the following components (from right to left in the figures).

(i) A mercury manostat which maintained the helium pressure at 2–3 cm above atmospheric.

(ii) A steel-float flowmeter capable of measuring rates of up to 100 cc/min.

(iii) A carrier gas injection system. This consisted of a standard column connected to a mercury manometer and a reservoir which contained the carrier gas of spec-pure xenon and krypton in known ratio. A known amount of carrier gas could be injected into the helium stream by diverting it through this system.

(iv) Dissolver and halogen trap. The helium flowed through tap T_1 into these units, each consisting of a simple bubbler attached to a removable flask and to a funnel for introducing liquids. The irradiated materials were put in the dissolver which was evacuated before the rapid introduction of an acid mixture of concentrated HCl, concentrated HNO_3, and 6 M HBr (15:5:1). During the addition of the acid the loss of rare gas was negligible because the initial attack of the foils was slow and was further inhibited by the aluminium wrapping. Helium containing a known amount of carrier gas had a flow rate of 80 cc/min. The metals could be dissolved in less than 5 min by heating the dissolver with an air-blower. Halogens which were swept out of the dissolver were held in the halogen trap containing a concentrated alkaline reducing solution (KOH and $KHSO_3$).

(v) Drier and purifier. The gas stream was purified and dried by solid KOH, CaO, and $Mg(ClO_4)_2$ and by an oil-free titanium sponge at 800 °C and copper oxide at 500 °C. The gases left the unit through tap T_2.

(vi) Adsorption column and thermal conductivity cell. The loading of xenon and krypton on to the adsorption column was indicated on a recorder in a simple bridge circuit by a Gow-Mac AEL 9677 thermal conductivity cell (T.C.C. in Figs. 2–4). The column was a glass U tube containing activated charcoal (Columbia, grade L, 40–60 mesh). This was cooled in liquid air and a similar cold trap used to purify the helium at the beginning of the flow system, while another was used as a safety trap at the end of the system.

At the end of sweep (*a*), taps T_1 and T_2 were closed and the helium stream diverted through taps T_3 and T_4 during part 2 of the experiment. The time, t_1, from the end of bombardment to the end of this sweep (*a*) was usually less than $\frac{1}{2}$ h. There was no further need for fast procedures; parts 2 and 3 each took about 1 h.

Part 2. Separation of Xenon from Krypton

This part of the experiment is outlined in Fig. 2, part 2, and described in more detail in Fig. 4, which also includes a table giving the temperatures, helium flow rates, and times used for the desorption of first the krypton and then the xenon. The separate fractions were collected on activated charcoal in cold traps 1 and 2, and the unloading was indicated on the recorder. Then, trap 2 was kept at liquid air temperature and evacuated for 10 min, which removed helium but caused no measurable loss of xenon.

Can. J. Chem. Downloaded from www.nrcresearchpress.com by 210.87.254.5 on 09/05/12
For personal use only.

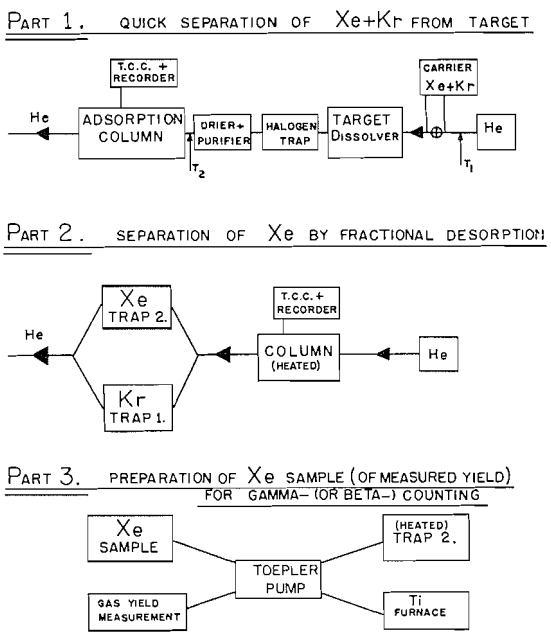


FIG. 2. Part 1: Quick separation of Xe + Kr from target. Part 2: Separation of Xe by fractional desorption. Part 3: Preparation of Xe sample (of measured yield) for gamma (or beta) counting.

Part 3. Preparation of Xenon Sample

Figure 2, part 3, gives a simple description of this part of the experiment. Trap 2 was heated to 120–150 °C for 45 min and the desorbed xenon transferred with an automatic Toepler pump to a quartz furnace for purification over oil-free titanium at 800–900 °C. The chemical yield of the cooled, purified xenon was measured in a gas burette and a sample for gamma spectrometry was prepared by condensing and sealing the xenon into a pyrex glass vial cooled in liquid air. These vials were of standard dimensions and had a volume of approximately 2 cc. Appendix B describes the preparation of xenon samples for beta activity measurements in a gas phase proportional counter.

After about 30 h a similar procedure was followed in which a sweep (*b*) was taken to prepare a sample of xenon formed purely from decay of iodine precursors. Taps T_1 and T_2 were reopened and for about 45 min helium was bubbled at a rate of 80 cc/min through the dissolver and halogen trap, both warmed with the air-blower. The procedure for the sweep (*b*) and the subsequent parts 2 and 3 was the same as described above. The time, t_2, was taken from the end of sweep (*a*) to the end of sweep (*b*).

Some further experimental details are now described. After a complete experiment the dissolver, halogen trap, purifier, and drier units were dismantled for cleaning, decontamination, re-greasing, and replacement of chemicals. When the apparatus was not in use, the adsorption of impurities on the charcoal was avoided by keeping the traps under vacuum and heated to about 120 °C. In an experiment the helium was passed through the tested flow system for about 1 h before the processing of a target.

The extraction of xenon in sweeps (*a*) and (*b*) was assumed to be quantitative. These techniques had been tested previously by Dostrovsky and Stoenner (24). In the present work the high efficiency of the xenon separation was confirmed by two methods. (i) Two xenon fractions were found by mass spectrometric analysis to contain only 1–2% of krypton. (ii) No xenon activity was detected in a krypton fraction from sweep (*a*). This sample was prepared in a sealed vial and the γ-activity measured only a few hours after bombardment. The 249-keV gamma ray of $^{135}Xe^{g}$ was not detected, though this had a very intense activity in the xenon fractions from sweep (*a*). It is unlikely that there was a significant loss of xenon from the target before processing. Recoiling fission products were held in the relatively thick aluminium catcher foils. Diffusion losses of xenon have been shown (25, 10, 13) to be very small for foil targets, though more significant for powdered targets of uranium oxide. No correction was made for these small losses; however, for ^{233}U they may have a small effect on the relative yields of iodine and xenon.

Copper

The copper foil was weighed and then dissolved and separated from other spallation products on an anion-exchange resin (26). The chemical yield was determined by ethylenediametetraacetic acid titrations with murexide indicator.

Can. J. Chem. Downloaded from www.nrcresearchpress.com by 210.87.254.5 on 09/05/12
For personal use only.

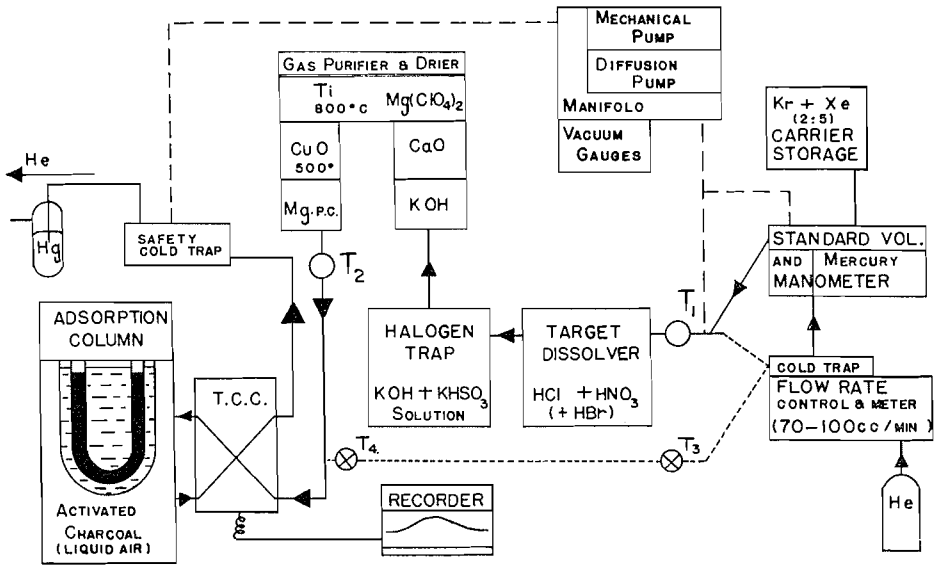


FIG. 3. Extraction of Kr and Xe from the target.

TABLE I

Xenon isotopes (27) contributing to the gamma spectra in the present study

Isotope	Half-life	Gamma energy (MeV)	% abundance	α_K	α_K/α_{LM}
$^{133}Xe^m$	2.3 d	0.233	100	4.4±1.4*	2.2
$^{133}Xe^g$	5.3 d	0.080	100	1.5±0.2	5
$^{135}Xe^g$	9.2 h	0.250	97	0.054	6.5
		(0.610)	3	—	—
$^{131}Xe^m$	12.0 d	0.164	100	29	2
$^{129}Xe^m$	8.0 d	0.196	100	10	2
$^{127}Xe^g$	36.0 d	0.173	25	0.13	—
		0.205	73	0.09	—
		(0.378)	21	0.01	—

*Experimental value which may be too low.

3. Radiation Measurements

The gamma activity of xenon and copper was measured by a 3 in. × 3 in. NaI crystal linked to a multichannel analyzer. Table I gives the xenon species that contributed to the gamma spectra in this work. The efficiency, for measurement of their gamma activities, was determined with a calibrated gas phase β-proportional counter. Appendix B describes these determinations and explains why the gamma and not the beta activity of fission product xenon was measured. The counting efficiency for the 511-keV annihilation radiation of ^{64}Cu (12.8 h) was known (23).

RESULTS AND DISCUSSION

For a xenon sample from sweep (*a*), a composite photopeak, due to the 249-keV gamma ray of $^{135}Xe^g$ and the highly converted 233-keV gamma ray of $^{133}Xe^m$, gave a decay curve with two components of half-lives 9.2 h and 2.3 d. The resolution of this curve became increasingly difficult for proton energies lower than 35 MeV, where the yield of ^{133}Xe decreased rapidly. Longer bombardments could not be used to increase the activity of $^{133}Xe^m$ because this would also increase the difficulties due to the growth of $^{133}Xe^g$ from ^{133}I. When most of the $^{133}Xe^m$ had decayed to the ground state, the 80-keV photopeak due to $^{133}Xe^g$ gave a simple decay curve with a half-life of 5.3 d. The gamma rays of $^{131}Xe^m$ and $^{129}Xe^m$ are highly converted and ^{127}Xe

Can. J. Chem. Downloaded from www.nrcresearchpress.com by 210.87.254.5 on 09/05/12
For personal use only.

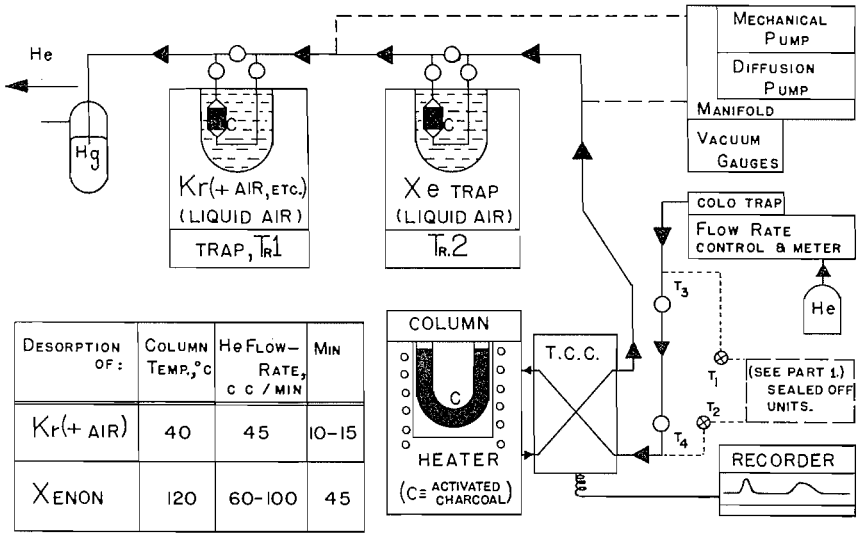


FIG. 4. Separation of Xe from Kr.

is formed in relatively low yield. The yield of more neutron-deficient isotopes increases with increasing proton energy and with decreasing (N/Z) of the target. However, these activities interfered significantly only above about 70 MeV for ^{235}U and above about 30 MeV for ^{233}U. A satisfactory correction could be made even in the worst case, ^{233}U with 70-MeV protons, in which the correction to the $^{133}Xe^{m}$ peak was about 25%. No such interference occurred in the samples of decay-product xenon from sweep (*b*).

For a xenon sample from sweep (*b*), a negligible amount of $^{133}Xe^{m}$ was detected. The 249-keV peak of $^{135}Xe^{g}$ and the 80-keV peak of $^{133}Xe^{g}$ decayed with half-lives of 9.2 h and 5.3 d respectively.

Appendix A describes the calculations of relative and absolute cross sections from the activity data.

Information was obtained on fission yields and their variations in chains 133 and 135, for the fission of ^{232}Th, ^{238}U, ^{235}U, and ^{233}U with protons of energy 20–85 MeV. A study of the relative independent yields of the isomers of ^{133}Xe will be published shortly.

The growth from ^{135}I was always relatively small during the short time $(t_0 + t_1)$. Figure 5 shows the excitation functions for ^{135}Xe (independent) and ^{135}I (cumulative). Table II and Fig. 6 give values of the ratio, $R_{c/I}{}^{135}$, of the cumulative yield of ^{135}I to the corrected independent yield of ^{135}Xe. This ratio was used in a new method to obtain values of Z_p, to be discussed later.

Table III gives the cross sections for the more complex chain 133, and Table II the cross sections for the 135 chain. For unmonitored irradiations, yields are shown relative to the cumulative cross section of ^{135}I, Y (experimental number). The simplified correction for growth from ^{133}I is given in Appendix A. This overcorrects slightly the yield of $^{133}Xe^{g}$, but the correction was of the same order as the experimental error.

The values of the cross section of $^{133}Xe^{m}$, and therefore of $^{133}Xe^{g}$ and of total ^{133}Xe, were dependent upon the value of α_K for the 233-keV γ-radiation from $^{133}Xe^{m}$. Rose's (30) theoretical value of 6.7 is much higher than the only reported (31) experimental value of 4.4 $\pm$ 1.4. Figure 7 shows the cross sections of ^{133}Xe with $\alpha_K = 4.4$ and 6.4 for the fission of

Can. J. Chem. Downloaded from www.nrcresearchpress.com by 210.87.254.5 on 09/05/12
For personal use only.

Can. J. Chem. Downloaded from www.nrcresearchpress.com by 210.87.254.5 on 09/05/12
For personal use only.

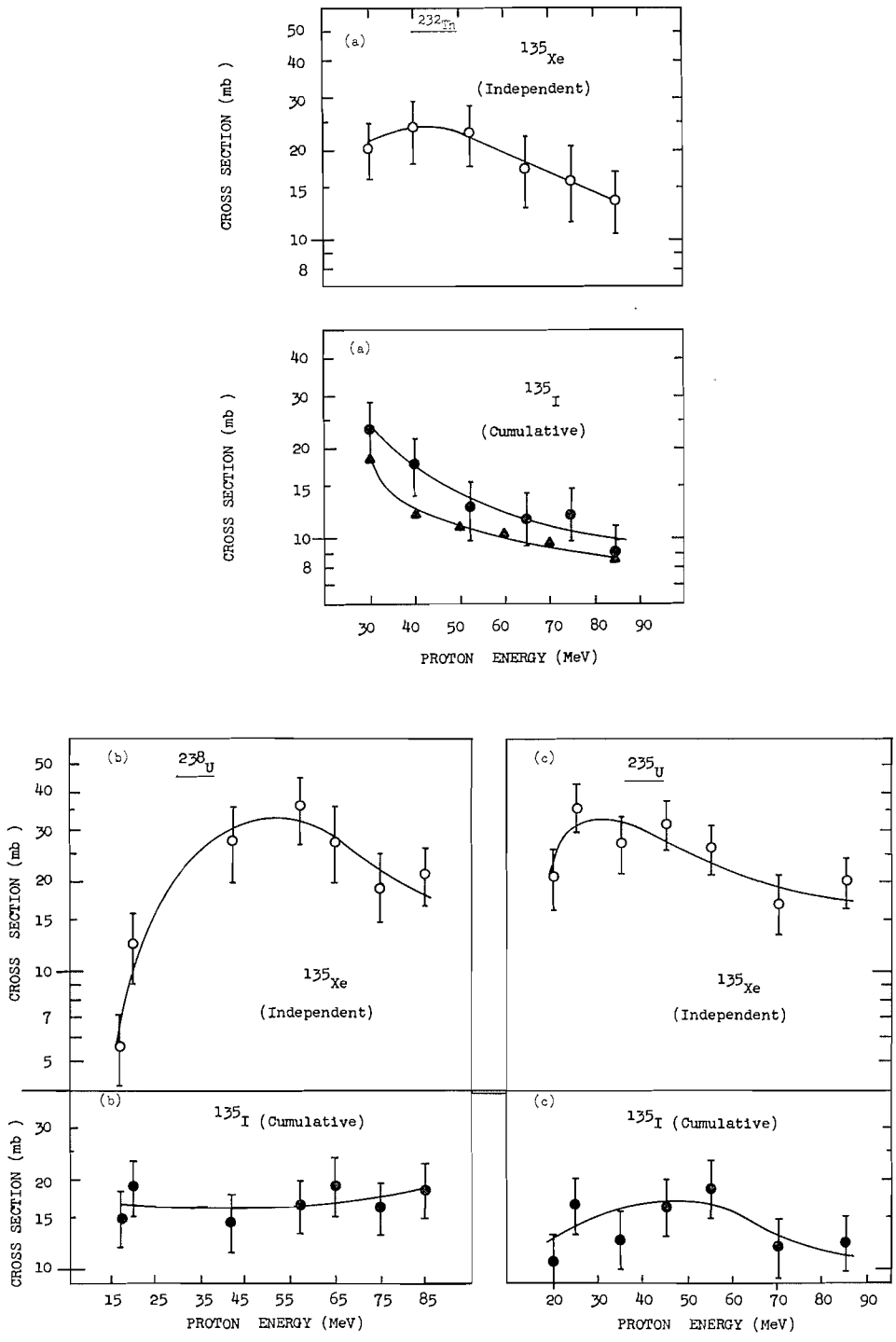


FIG. 5. Excitation functions for the cumulative formation of ^{135}I, and the independent formation of ^{135}Xe (corrected for growth from the decay of ^{135}I). (*a*) ^{232}Th: (●) present work; (▲) reference 15. (*b*) ^{238}U. (*c*) ^{235}U.

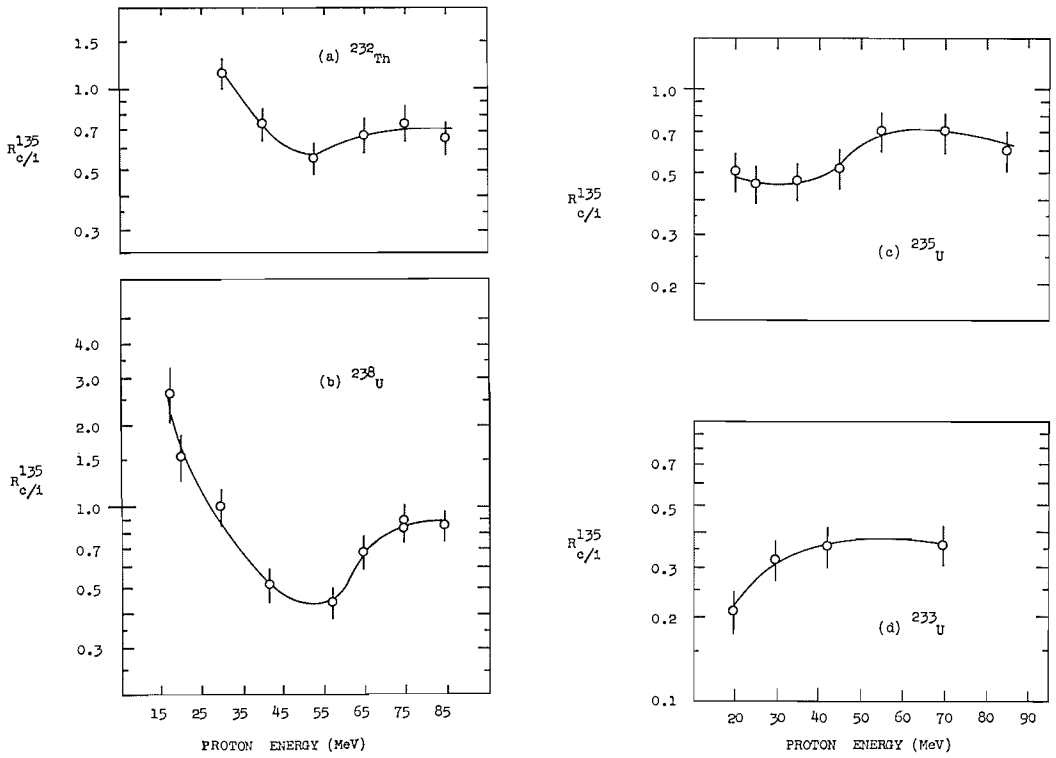


FIG. 6. Dependence of the relative formation of ^{135}I and ^{135}Xe upon proton energy, expressed in the form

$$R_{c/i}^{135} = \frac{\text{cumulative yield of } ^{135}\text{I}}{\text{independent yield of } ^{135}\text{Xe, corrected}}:$$

(*a*) ^{232}Th; (*b*) ^{238}U; (*c*) ^{235}U; (*d*) ^{233}U.

^{232}Th. It also shows that the uncertainty in α_K introduces only a relatively small error within the experimental error. Figure 8 gives the formation cross sections for ^{133}Xe in the fission of ^{238}U and ^{235}U. The uncertainty in α_K introduced only small errors in the ratio, $R_{c/i}^{133}$, of the cumulative yield of ^{133}I to the independent yield of ^{133}Xe. Figure 9 illustrates these ratios. The solid lines are for $\alpha_K = 4.4$ and, for ^{232}Th, the broken line is for $\alpha_K = 6.4$.

Only two of the excitation functions presented here have been reported previously. By a totally different method, using solid iodide sources, Pate, Foster, and Yaffe (15) determined the cumulative yields of ^{133}I and ^{135}I for the fission of ^{232}Th with 10–85 MeV protons. Their excitation functions are plotted in Figs. 5(*a*) and 7 and can be directly compared with the present data, since Meghir (29) has shown that little systematic error exists between the monitor cross sections used in the two studies. The previous results were slightly lower for ^{135}I and considerably lower for ^{133}I than the present values which were obtained from much simpler decay curves and are therefore probably more reliable.

The cross sections had an uncertainty of $\pm 25\%$, which was compounded from estimated errors in the beam monitoring, in the measurement of activities and chemical yields, and in analyses of γ-ray spectra and decay curves. The estimated uncertainty does not include the important systematic error due to uncertainty in the value of α_T for ^{133}Xe^m. A larger uncertainty existed for the lowest energy experiments in which activities were lower and decay

Can. J. Chem. Downloaded from www.nrcresearchpress.com by 210.87.254.5 on 09/05/12
For personal use only.

TABLE II

Cross sections for the independent formation of ^{135}Xe and the cumulative formation of ^{135}I

Expt. No.	E_p (MeV)	σ (mb) ^{64}Cu	Independent σ (mb), ^{135}Xe Uncorrected	Independent σ (mb), ^{135}Xe Corrected	Cumulative σ (mb), ^{135}I	$R_{c/i}^{135}$
^{232}Th						
T6	30	390	21.1	20.3	23.3	1.15
T3	40	270	24.9	24.0	17.9	0.75
T4	52	205	23.6	23.0	12.9	0.56
T1	65	173	17.9	17.3	11.7	0.68
T5	75	150	16.5	15.9	12.0	0.75
T2	85	140	14.2	13.7	9.1	0.66
^{238}U						
R10	15	—	0.32 Y^{R10}	0.25 Y^{R10}	1.0 Y^{R10}	3.94
R15	17	(100)	6.5	(5.6)*	(14.8)*	2.64
R14	20	(240)	13.3	(12.3)*	(19.1)*	1.55
R18	30	—	1.03 Y^{R18}	0.99 Y^{R18}	1.0 Y^{R18}	1.01
R8	42	250	28.9	27.8	14.4	0.52
R17	57	190	37.0	36.2	16.4	0.45
R9	65	170	28.6	27.5	19.0	0.69
R11	75	150	20.2	19.2	16.1	0.84
R16	75	—	1.16 Y^{R16}	1.12 Y^{R16}	1.0 Y^{R16}	0.89
R12	85	140	22.8	21.6	18.6	0.86
^{235}U						
E10	20	(240)	21.5	(21.1)*	(10.7)*	0.51
E9	25	488	36.6	36.0	16.7	0.46
E7	35	310	28.2	27.5	12.8	0.47
E5	45	235	32.7	31.9	16.6	0.52
E3	55	195	28.0	26.8	19.0	0.71
E8	70	160	17.8	17.2	12.2	0.71
E4	85	140	21.6	20.8	12.6	0.61
^{233}U						
U5	20	—	4.77 Y^{U5}	4.74 Y^{U5}	1.0 Y^{U5}	0.21
U4	30	—	3.16 Y^{U4}	3.13 Y^{U4}	1.0 Y^{U4}	0.32
U3	42	—	2.83 Y^{U3}	2.79 Y^{U3}	1.0 Y^{U3}	0.36
U1	55	—	5.01 Y^{U1}	No sweep (*b*)	(1.0 Y^{U1})	—
U2	70	—	2.86 Y^{U2}	2.81 Y^{U2}	1.0 Y^{U2}	0.36

*Very large uncertainty in σ(^{64}Cu) at this energy.

errors larger. The main conclusions in this paper depend not on absolute yields but on the yield ratios $R_{c/i}^{133}$ and $R_{c/i}^{135}$, which could be obtained with an uncertainty of $\pm 15\%$.

Determination of Empirical Values of Z_p

An empirical charge distribution curve could not be constructed with the present data which consisted, for each fission system, of an independent yield of xenon and a cumulative yield of iodine for the chains 133 and 135. However, values of Z_p and fractional chain yields were obtained empirically by two methods which assumed that, for the present systems with proton energies below 55 MeV, the charge distribution curves were given by eq. [1] with $C = 1.20 \pm 0.25$. These curves on a $(Z - Z_p)$ plot allowed a more systematic analysis of the data for all four targets than would have been possible with the known empirical curves on an N/Z plot, which are available only for ^{232}Th and ^{238}U. Above 55 MeV, no attempt was made to extract Z_p values, because at these energies the broader and possibly asymmetric charge distribution curves are not very well defined.

The basis of method 1 to determine Z_p empirically was the relationship between Z_p and the yield ratio $R_{c/i}^{A}$ which is defined by the expression:

$$R_{c/i}^{A} = \frac{\text{cumulative yield of beta parent}}{\text{independent yield of daughter}}.$$

Can. J. Chem. Downloaded from www.nrcresearchpress.com by 210.87.254.5 on 09/05/12
For personal use only.

TABLE III

Cross sections for the cumulative formation of ^{133}I and independent formation of $^{133}Xe^{m}$ and $^{133}Xe^{g}$

Expt. No.	E_p (MeV)	Cumulative σ (mb), ^{133}I	Independent σ (mb), $^{133}Xe^{m}$	Independent σ (mb)			
				Uncorrected $^{133}Xe^{g}$	Overcorrected $^{133}Xe^{g}$	Uncorrected $^{133}Xe^{m+g}$	Overcorrected $^{133}Xe^{m+g}$
^{232}Th							
T6	30	38.9	2.7	3.1	2.7	5.8	5.4
T3	40	41.6	6.1	6.9	6.2	13.0	12.3
T4	52	33.4	9.7	10.1	9.6	19.7	19.2
T1	65	28.3	9.4	9.6	9.1	19.0	18.5
T5	75	27.2	9.6	9.1	8.6	18.7	18.2
T2	85	19.9	8.4	7.8	7.5	16.2	15.9
^{238}U							
R10	15	1.38 Y^{R10}	0.020 Y^{R10}	0.031 Y^{R10}	(0.003 Y^{R10})†	0.051 Y^{R10}	(0.023 Y^{R10})
R15	17	(21.1)*	0.5	0.7	0.3	1.2	(0.8)*
R14	20	(31.4)*	1.2	1.9	1.4	3.1	(2.6)*
R18	30	2.07 Y^{R18}	0.182 Y^{R18}	0.191 Y^{R18}	0.166 Y^{R18}	0.373 Y^{R18}	0.348 Y^{R18}
R8	42	36.6	8.1	9.8	8.9	17.9	17.1
R17	57	35.8	17.8	16.4	15.8	34.2	33.6
R9	65	40.9	13.8	15.0	14.3	28.8	28.1
R11	75	33.6	10.6	9.4	8.7	19.9	19.2
R16	75	2.13 Y^{R16}	0.613 Y^{R16}	0.540 Y^{R16}	0.513 Y^{R16}	1.15 Y^{R16}	1.12 Y^{R16}
R12	85	39.1	12.0	12.7	11.9	24.7	23.9
^{235}U							
E10	20	32.8	5.4	6.6	6.3	12.0	11.7
E9	25	49.5	12.8	14.5	14.0	27.2	26.7
E7	35	37.5	15.2	14.5	13.8	29.7	29.0
E5	45	44.2	20.2	21.2	20.5	41.4	40.7
E3	55	45.7	18.9	17.1	16.2	36.0	35.1
E8	70	29.2	12.0	10.9	10.4	22.9	22.4
E4	85	30.4	13.6	13.4	12.8	27.0	26.5
^{233}U							
U5	20	5.00 Y^{U5}	2.55 Y^{U5}	2.74 Y^{U5}	2.68 Y^{U5}	5.29 Y^{U5}	5.23 Y^{U5}
U4	30	4.30 Y^{U4}	2.14 Y^{U4}	2.42 Y^{U4}	2.36 Y^{U4}	4.56 Y^{U4}	4.50 Y^{U4}
U3	42	3.42 Y^{U3}	2.31 Y^{U3}	2.22 Y^{U3}	2.17 Y^{U3}	4.52 Y^{U3}	4.47 Y^{U3}
U1	55	6.57 Y^{U1}	3.68 Y^{U1}	3.80 Y^{U1}	No sweep (*b*)	7.48 Y^{U1}	—
U2	70	3.15 Y^{U2}	1.98 Y^{U2}	2.11 Y^{U2}	2.06 Y^{U2}	4.09 Y^{U2}	4.04 Y^{U2}

*Very large uncertainty in $\sigma(^{61}Cu)$ at this energy.
†The simple growth correction is not satisfactory at this energy.

If one assumes that the charge distribution is given by eq. [1],

$$[2] \qquad R_{c/I}{}^{A} = \frac{\sum_{Z_i=(Z'-1)}^{Z_i=(Z'-6)} \exp\left[-(Z_i - Z_p)^2/C\right]}{\exp\left[-(Z' - Z_p)^2/C\right]},$$

where Z' is the nuclear charge of a daughter isobar, and therefore $(Z' - 1)$ is the charge of the negative-beta parent. Figure 10 shows functions of $R_{c/I}{}^{A}$ versus $(Z' - Z_p)$ computed with five C values from 0.7–1.9. Now, if $R_{c/I}{}^{A}$ is known experimentally for a pair of adjacent isobars (e.g. $^{133}I/^{133}Xe$) the corresponding value of $(Z' - Z_p)$ for the daughter isobar may be read from one of the functions for a particular C value. Figure 10 also demonstrates the dependence of the empirical value of Z_p on the width of the assumed charge distribution curve. When the daughter nuclide has $(Z' - Z_p) \approx +0.7$, the empirical value of Z_p is shown to be almost independent of C.

Method 2 to determine Z_p empirically was similar to that described by Storms (10) who determined Z_p in chains 133 and 135, from data similar to those in this work. Simple Bateman equations (32) were used to construct two lengthy expressions for the measured activities of $^{133}Xe^{g}$ from sweeps (*a*) and (*b*). The two simultaneous equations could be solved for Z_p by

Can. J. Chem. Downloaded from www.nrcresearchpress.com by 210.87.254.5 on 09/05/12
For personal use only.

Can. J. Chem. Downloaded from www.nrcresearchpress.com by 210.87.254.5 on 09/05/12
For personal use only.

TABLE IV

Empirical values of $(Z - Z_p)$ for chains 133 and 135, from methods 2 and 1

Expt. No.	E_p (MeV)	$(Z - Z_p)$ from method 2								$(Z - Z_p)$ from method 1	
		^{135}Xe			^{133}Xe*						
		$C = 0.95$	$C = 1.20$	$C = 1.45$	$C = 0.95$	$C = 1.20$	$C = 1.45$	$R_{c/i}^{133}$	$R_{c/i}^{135}$	^{133}Xe $C = 1.20$	^{135}Xe $C = 1.20$
^{232}Th											
T6	30	0.51	0.48	0.44	1.22	1.32	1.40	7.21	1.15	1.32	0.48
T3	40	0.32	0.25	0.18	0.95	1.00	1.04	3.37	0.75	1.00	0.25
(T4)	(52)	0.20	0.10	−0.01	0.69	0.69	0.69	1.74	0.56	0.69	0.10
^{238}U											
R10	15	1.07	1.15	1.21	1.75	1.92	2.07	(61)	3.94	2.03	1.08
R15	17	0.91	0.96	0.99	1.60	1.75	1.88	(28)	2.64	1.80	0.90
R14	20	0.68	0.68	0.68	1.39	1.51	1.61	12.2	1.55	1.51	0.65
R18	30	0.46	0.41	0.36	1.15	1.24	1.31	5.93	1.01	1.24	0.41
R8	42	0.19	0.10	−0.01	0.77	0.79	0.80	2.15	0.52	0.79	0.05
(R17)	(57)	0.10	−0.02	−0.15	0.48	0.44	0.40	1.06	0.45	0.44	−0.02
^{235}U											
E10	20	0.15	0.04	−0.07	0.88	0.92	0.95	2.81	0.51	0.92	0.03
E9	25	0.10	−0.02	−0.14	0.71	0.72	0.72	1.85	0.46	0.72	−0.02
E7	35	0.11	−0.01	−0.13	0.56	0.54	0.52	1.27	0.47	0.54	0.00
E5	45	0.16	0.05	−0.06	0.49	0.45	0.41	1.09	0.52	0.45	0.05
(E3)	(55)	0.30	0.23	0.15	0.57	0.55	0.52	1.30	0.71	0.55	0.22
^{233}U											
U5	20	−0.26	−0.46	−0.57	0.43	0.39	0.33	0.96	0.21	0.39	−0.46
U4	30	−0.06	−0.22	−0.39	0.43	0.39	0.33	0.95	0.32	0.38	−0.22
U3	43	−0.01	−0.16	−0.31	0.34	0.27	0.19	0.76	0.36	0.27	−0.15

*Using $\alpha_K = 4.4$ ($\alpha_T = 6.3$).

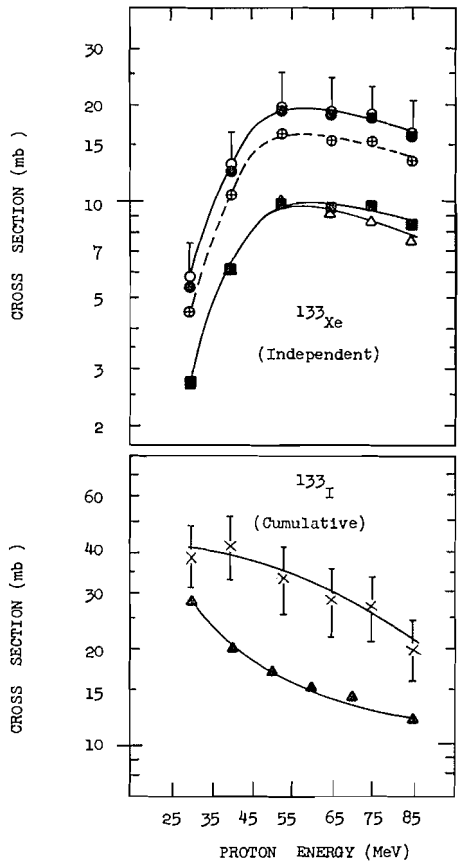


FIG. 7. Excitation functions for the cumulative formation of ^{133}I and the independent formation of ^{133}Xe^{m}, ^{133}Xe^{g}, and total ^{133}Xe from the proton-induced fission of ^{232}Th. $\alpha_K = 4.4$ ($\alpha_T = 6.3$): (△) overcorrected independent, ^{133}Xe^{g}; (■) independent, ^{133}Xe^{m}; (○) uncorrected independent total ^{133}Xe; (●) overcorrected independent total ^{133}Xe. $\alpha_K = 6.4$ ($\alpha_T = 9.3$): (⊕) overcorrected independent total ^{133}Xe; (×) cumulative cross sections of ^{133}I; (▲) reference 15.

assuming a Gaussian charge distribution for chain 133. The equations were similar to those used by Storms, except for a few minor revisions in parameters, but they were solved differently by a stepwise reiteration method. Initially, the value of $(Z - Z_p)$ for ^{133}Xe was set equal to +2.0 and was decreased in steps of 0.1, and finally in steps of 0.01, until the value of Z_p was consistent with the gamma activity data substituted in the two simultaneous equations. The above procedure and the method of programming it for the McGill I.B.M. 7044 computer were first tested with the simpler chain 135 and then applied to chain 133. The derived Z_p values for both chains were in excellent agreement with those from method 1.

Empirical Z_p Values for Chains 133 and 135

Table IV gives the value of $(Z - Z_p)$ for ^{133}Xe and ^{135}Xe, obtained empirically by method 2 with values of $C = 0.95$, 1.20, and 1.45. The table also gives the values obtained by method 1 with $C = 1.20$. The very good agreement between the two methods proved the reliability of method 1, which should be useful in future work, since accurate values of $R_{c/l}^{A}$ could be obtained for many pairs of adjacent isobars formed in fission. For the four targets studied, Fig. 11 shows the variation of Z_p with proton energy; the solid lines were obtained with

Can. J. Chem. Downloaded from www.nrcresearchpress.com by 210.87.254.5 on 09/05/12
For personal use only.

Can. J. Chem. Downloaded from www.nrcresearchpress.com by 210.87.254.5 on 09/05/12
For personal use only.

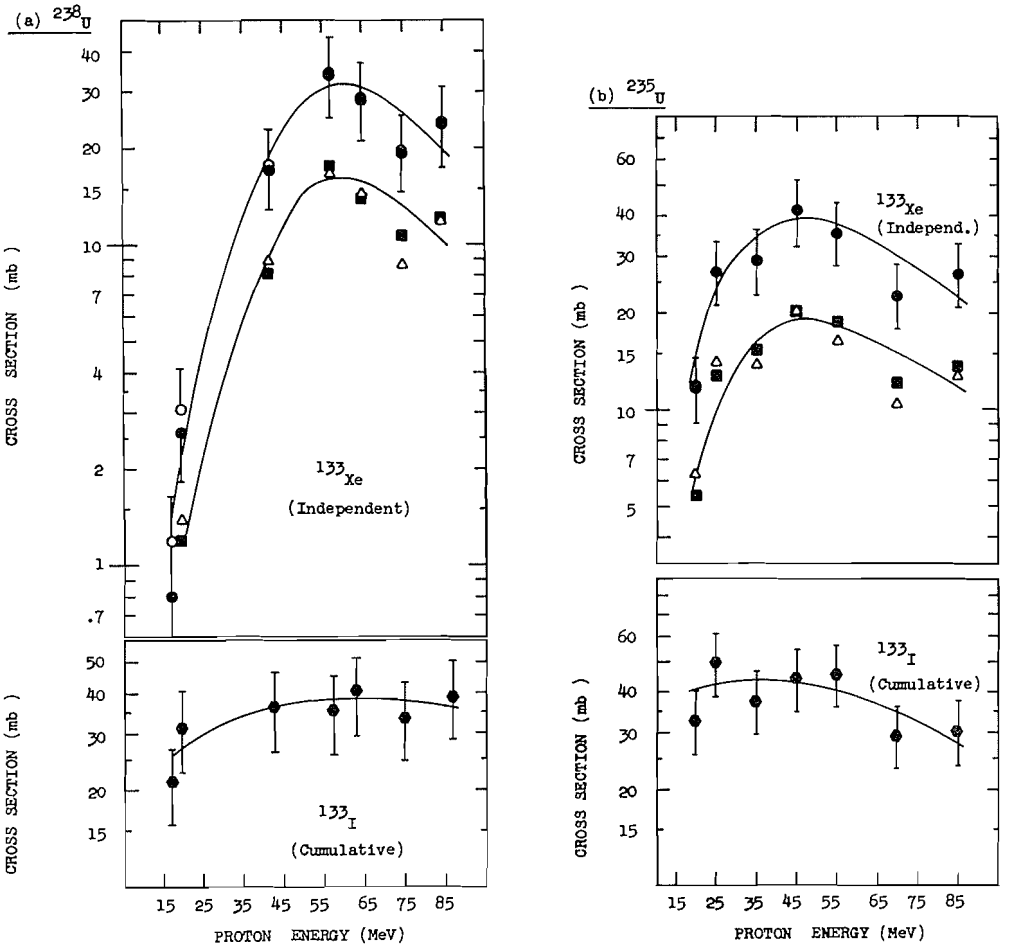


FIG. 8. Excitation functions for the cumulative formation of ^{133}I and the independent formation of ^{133}Xe^{m}, ^{133}Xe^{g}, and total ^{133}Xe: (*a*) ^{238}U; (*b*) ^{235}U. $\alpha_K = 4.4$ ($\alpha_T = 6.3$): (△) overcorrected independent, ^{133}Xe^{g}; (■) independent, ^{133}Xe^{m}; (○) uncorrected independent total ^{133}Xe; (●) overcorrected independent total ^{133}Xe.

$C = 1.20$ and the long and short broken lines with $C = 0.95$ and 1.45 respectively. The uncertainty in Z_p was estimated to be 0.1–0.2 charge units, depending on the value of $(Z - Z_p)$. As expected from Fig. 10, the variation of C had least effect on the empirical value of Z_p when $(Z - Z_p) \approx +0.7$, which for xenon isotopes reduces to $Z_p \approx 53.3$. For fission of ^{232}Th and ^{238}U, the displacement of the empirical value of Z_p from beta stability, Z_A, and the effect of proton energy are shown in Fig. 12 for the above results obtained with $C = 1.20$ and for results previously reported from this laboratory. Values of Z_A were taken from the same Z_A function (33, 34) which for Z_{133} and Z_{135} gave values 54.95 and 55.65. For ^{232}Th and ^{238}U, with protons of a particular energy the value of $(Z_A - Z_p)$ for chain 133 was approximately equal to that for chain 135. Thus, the change in Z_p for the mass chains 133 to 135 was about 0.7, since this was the corresponding change in Z_A. There is good agreement between the present and previous data for the same mass region. The rate of change of Z_p with energy, in this figure, was consistent with that obtained by McHugh (13) and by Nethaway and Levy (20) for some medium-energy fission systems.

Can. J. Chem. Downloaded from www.nrcresearchpress.com by 210.87.254.5 on 09/05/12
For personal use only.

TABLE V

Total chain yields for $A = 133$ and 135

Expt. No.	E_p (MeV)	Independent yields of ^{135}Xe			Cumulative yields of ^{133}I			$\left(\frac{\sigma}{f}\right)$ = total chain yields (mb)			
		σ (mb)	f (from method 2)		σ (mb)	f (from method 2)		$A = 135$		$A = 133$	
			$C = 1.20$	$C = 1.45$		$C = 1.20$	$C = 1.45$	$C = 1.20$	$C = 1.45$	$C = 1.20$	$C = 1.45$
^{238}U											
R15	17	6.5*	0.24	0.24	21.1*	0.96	0.96	27.1	27.1	22.0	22.0
R14	20	13.3*	0.35	0.34	31.4*	0.92	0.92	38.0	39.1	34.1	34.1
R8	42	28.9	0.51	0.47	36.6	0.66	0.65	56.6	61.4	55.4	56.3
(R17)†	57	37.0	0.52	0.46	35.8	0.47	0.45	71.1	80.4	76.2	79.5
^{232}Th											
T6	30	21.1	0.42	0.41	38.9	0.87	0.87	50.2	51.4	44.7	44.7
T3	40	24.9	0.49	0.46	41.6	0.76	0.75	50.8	54.2	54.7	55.4
(T4)†	52	23.6	0.51	0.47	33.4	0.60	0.59	46.3	50.3	55.6	56.7
^{235}U											
E10	20	21.5	0.51	0.47	32.8	0.72	0.71	42.2	45.7	45.6	46.2
E9	25	36.6	0.51	0.46	49.5	0.62	0.61	71.7	79.5	79.8	81.1
E7	35	28.2	0.51	0.46	37.5	0.52	0.51	55.3	61.3	72.1	73.5
E5	45	32.7	0.51	0.47	44.2	0.47	0.46	64.1	69.5	94.0	96.0
(E3)†	55	28.0	0.49	0.46	45.7	0.53	0.51	57.2	60.9	84.3	87.6

*Large uncertainty in monitor cross section at this energy.
†At this energy, charge distribution curves probably have $C \geqslant 1.45$.

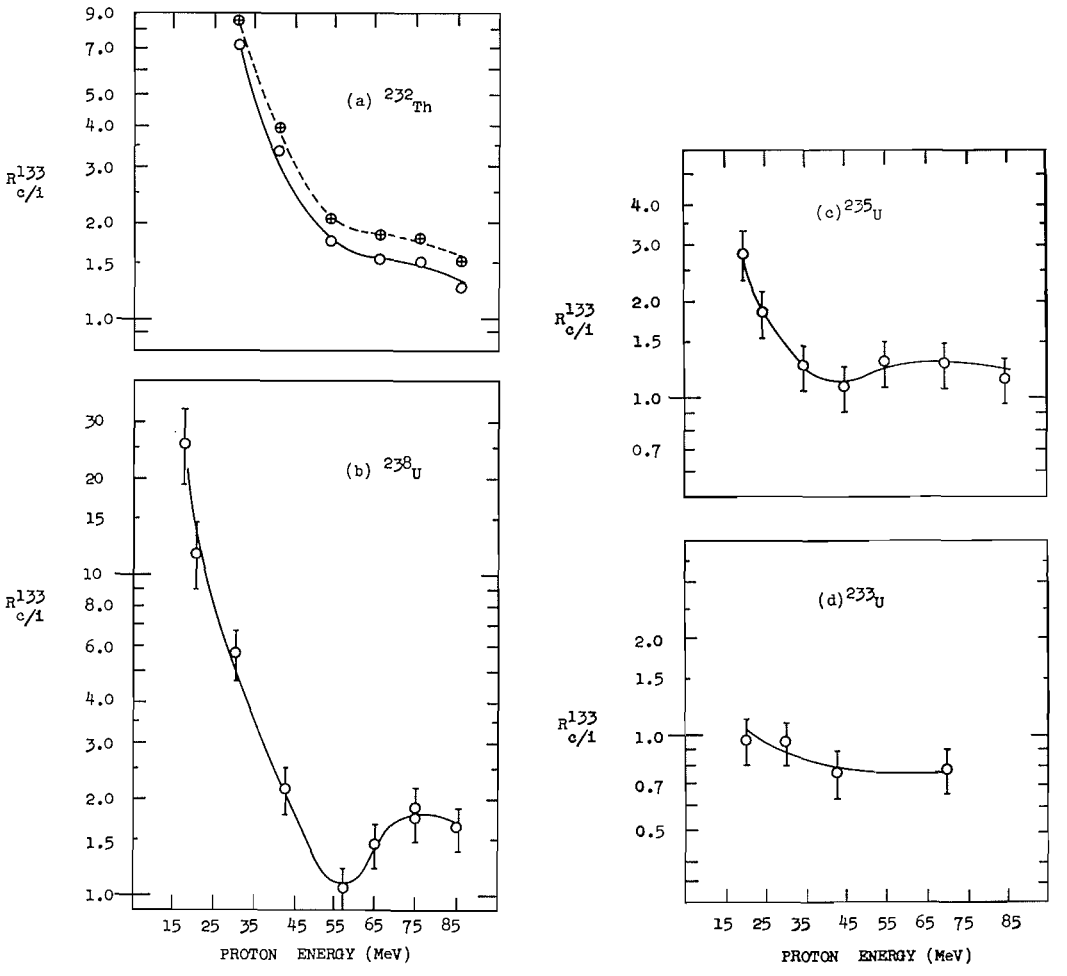


FIG. 9. The dependence of the relative formation of ^{133}I and ^{133}Xe upon proton energy

$$R_{c/I^{133}} = \frac{\text{cumulative yield of } ^{133}I}{\text{independent yield of } ^{133}Xe, \text{ overcorrected}};$$

(*a*) ^{232}Th; (*b*) ^{238}U; (*c*) ^{235}U; (*d*) ^{233}U. The data for ^{133}Xe were obtained with $\alpha_K = 4.4$ ($\alpha_T = 6.3$). In (*a*) the data were plotted also for $\alpha_K = 6.4$ ($\alpha_T = 9.3$): (○) $\alpha_K = 4.4$; (⊕) $\alpha_K = 6.4$.

For proton-induced fission of ^{235}U and ^{233}U, no Z_p values have been reported previously. However, the limited data collected here for these systems appear to be reliable because of the good agreement between previous and present data for ^{232}Th and ^{238}U. For the proton-induced fission of ^{235}U and ^{233}U, the variations of Z_p with energy are significantly different from the changes, which are now fairly well established, for the proton-induced fission of ^{238}U and ^{232}Th. Figure 12 shows that, at lower energies, the targets of lower (N/Z) had Z_p values closest to beta stability, but at 40–50 MeV the values of $(Z_A - Z_p)$ were almost equal for all four targets.

Observed charge distributions of fission products cannot yet be explained satisfactorily in terms of the distribution of charge at scission and the emission of pre- and post-fission neutrons. Little is known about neutron emission in the present fission systems, but rough

Can. J. Chem. Downloaded from www.nrcresearchpress.com by 210.87.254.5 on 09/05/12
For personal use only.

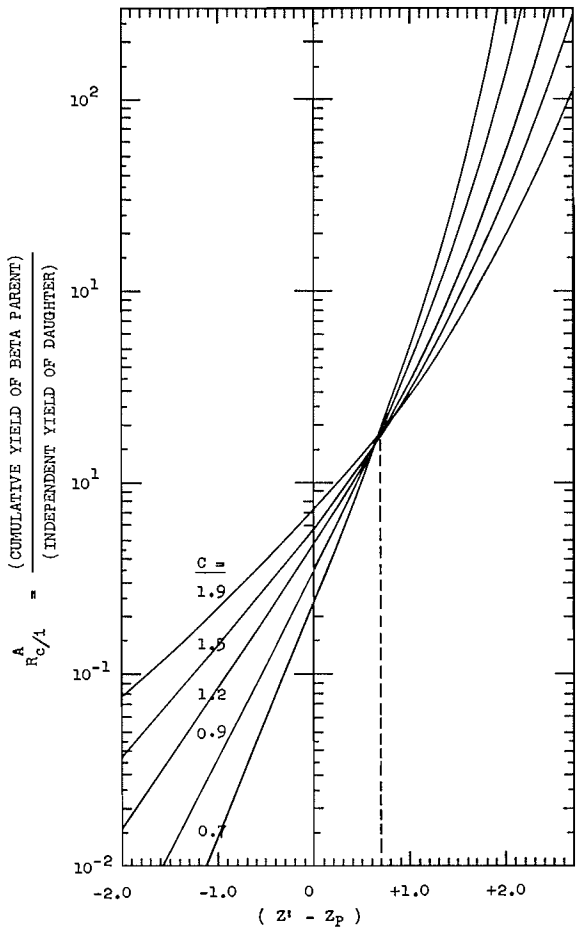


FIG. 10. Theoretical $R_{c/i}{}^A$ versus $(Z' - Z_p)$ from eq. [2] with values of $C = 0.7, 0.9, 1.2, 1.5$, and 1.9.

estimates could be made from the empirical Z_p values, if the latter were assumed to be given by the simple u.c.d. (unchanged charge division) postulate. This postulate (35) gives a very simple mechanism for fission in which the most probable initial fragments have the same value of (N/Z) as the fissioning nucleus. Although an exact formulation of this rule would involve a knowledge of the yields of pre- and post-fission neutrons, the rule may be closely approximated by the simplified expression

$$[3] \qquad (Z_p)_{f.p.} = (A_{f.p.}) \frac{(Z_{target} + Z_{projectile})}{(A_{target} + A_{projectile} - \bar{\nu}_T)} .$$

Here, $\bar{\nu}_T$ is the average total number of neutrons in a fission event leading to the fission product, f.p. The vertical lines on the right in Fig. 11 have divisions corresponding to values of Z_p for chains 133 and 135, which were postulated from eq. [3] with the values of $\bar{\nu}_T$ given by the numbers besides the lines. For a particular energy, the empirical Z_p was equated with a postulated Z_p in order to estimate directly from Fig. 11 the corresponding value of $\bar{\nu}_T$. Fig. 13 (*a* and *b*) shows the estimated average total neutron yields as a function of energy, obtained from two sets of data, one for chain 135 and the other for chain 133. There is evidence (21, 13) that for low- and medium-energy fission the u.c.d. postulate predicts values of

Can. J. Chem. Downloaded from www.nrcresearchpress.com by 210.87.254.5 on 09/05/12
For personal use only.

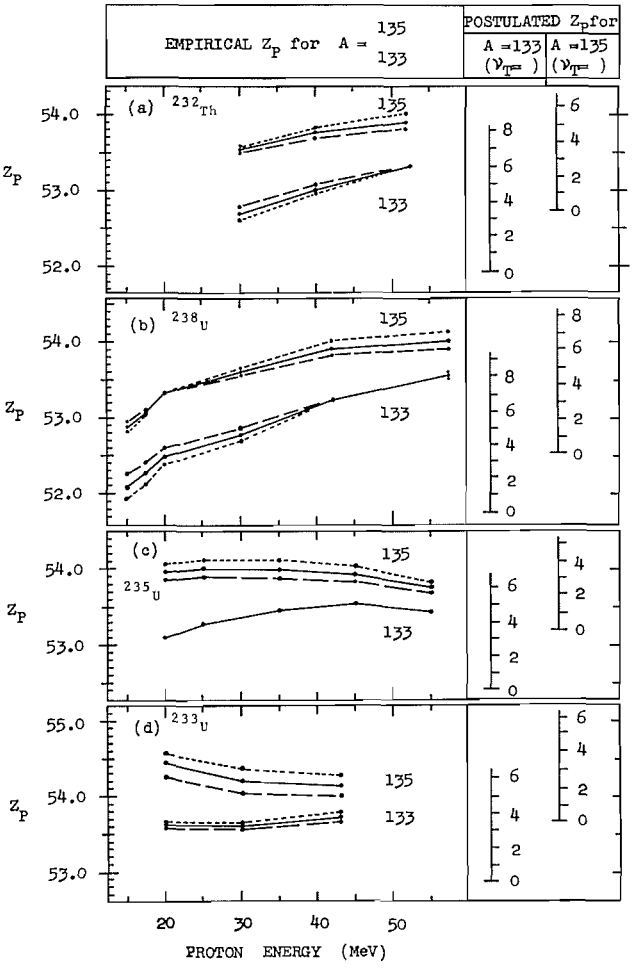


FIG. 11. The variation of the empirical value of Z_p with the proton energy: (*a*) ^{232}Th; (*b*) ^{238}U; (*c*) ^{235}U; (*d*) ^{233}U. The Z_p values were obtained by method 2: (——) $C = 0.95$; (—) $C = 1.20$; (--) $C = 1.45$. The divisions on the vertical lines, to the right of the figure, show Z_p values for chains 133 and 135 from the u.c.d. postulate. The numbers given beside these lines are the total number of fission neutrons, ν_T, used in postulating the corresponding Z_p values.

Z_p which are too high for heavy mass chains. Consequently the present rough estimates of $\bar{\nu}_T$ may be expected to be lower limits and serve primarily to compare the fission of the four targets. For ^{232}Th and ^{238}U, the rate of change with energy of $\bar{\nu}_T$ was consistent with the values, 0.13–0.16 neutrons per MeV, which have been reported previously for similar medium-energy fission systems (36–38). However, Fig. 13 shows that, as the energy increases, the rate ($d\bar{\nu}_T/dE$) is less for the targets of lower (N/Z). No attempt will be made to explain the rather surprising differences, for different targets, in the energy dependence of Z_p and $\bar{\nu}_T$ until the present preliminary conclusions have been confirmed by further work on ^{235}U and ^{233}U.

Fractional and Total Chain Yields for A = 133 and 135

For the monitored irradiations with proton energies below 55 MeV, total chain yields were determined by dividing the absolute cross sections by the fractional chain yields obtained

Can. J. Chem. Downloaded from www.nrcresearchpress.com by 210.87.254.5 on 09/05/12
For personal use only.

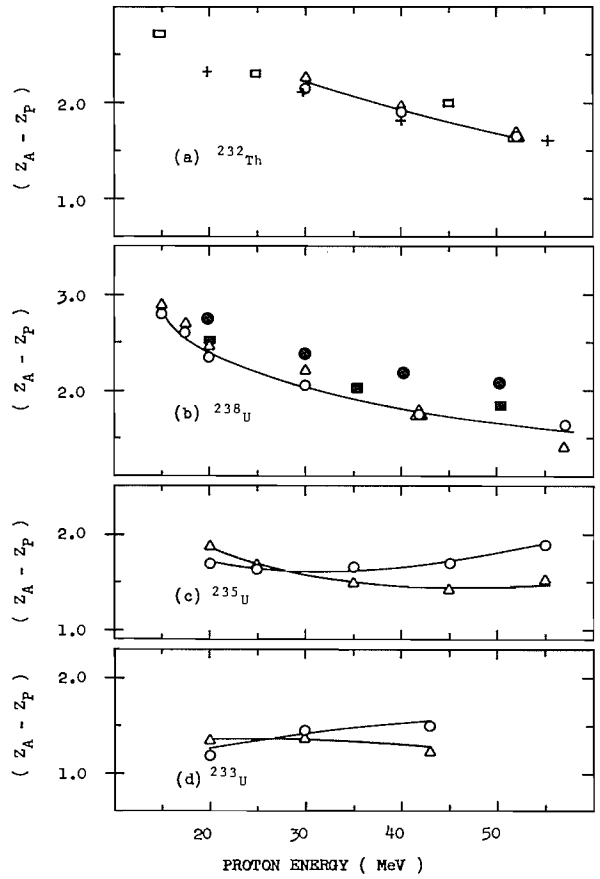


FIG. 12. The displacement of the empirical value of Z_p from beta stability, Z_A, and the effect of variations in the proton energy: (*a*) ^{232}Th; (*b*) ^{238}U; (*c*) ^{235}U; (*d*) ^{233}U. For the chains: (△) $A = 133$; (○) $A = 135$. (+) Reference 17; (□) ref. 15; (■) ref. 18; (●) ref. 19.

from the determined charge distribution curves. Table V gives these yields which were estimated to have an uncertainty of about 30%. Within this uncertainty, these data were consistent with a flat mass distribution in this mass region for fission of ^{232}Th and ^{238}U. James *et al.* (16) found that the chain yield for $A = 133$ was much higher than for $A = 135$, in the fission of ^{238}U with 14.7 MeV neutrons. However, their measurements for chain 133 may contain an error which is discussed in Appendix B.

For proton-induced fission, few chain yields have been reported previously. For ^{238}U, the present yields were in agreement with those, for the same mass region, determined previously in this laboratory (18, 19) and by Stevenson *et al.* (39). This agreement suggested there were no serious systematic errors in the present results.

ACKNOWLEDGMENTS

We are grateful to Prof. R. E. Bell, Director, Foster Radiation Laboratory, for permission to use the McGill synchrocyclotron and to Mr. R. H. Mills who cheerfully performed the irradiations. Our thanks go to Drs. I. Dostrovsky and R. Stoenner, Brookhaven National Laboratory, who gave much of their time advising us on experimental techniques. One of us

Can. J. Chem. Downloaded from www.nrcresearchpress.com by 210.87.254.5 on 09/05/12
For personal use only.

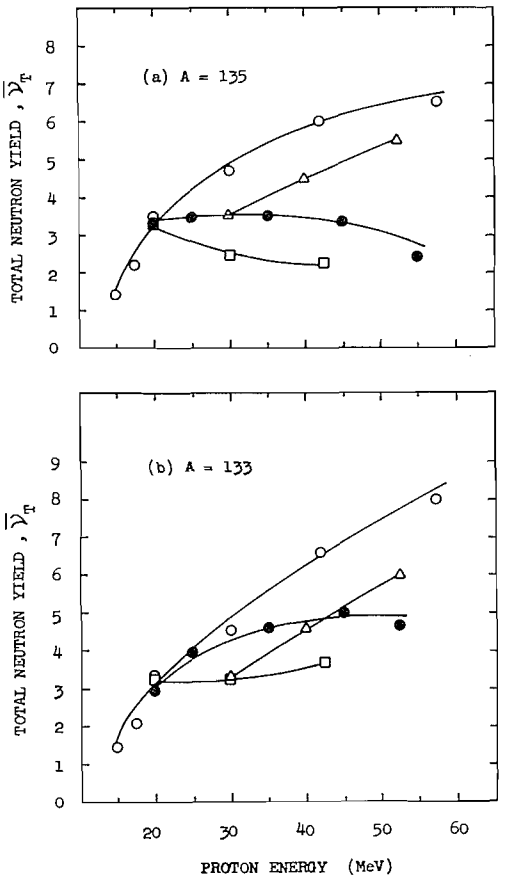


FIG. 13. Total neutron yields, $\bar{\nu}_T$, in the proton-induced fission of (△) ^{232}Th; (○) ^{238}U; (●) ^{235}U; (□) ^{233}U.

(J. H. F.) wishes to express his gratitude to the National Research Council of Canada for Studentships from 1963–66.

APPENDIX A

Equations to Calculate Relative and Absolute Cross Sections

A disintegration rate, D_N, of a product, N, was determined from the corresponding gamma activity, C_N, by the expression

$$[4] \qquad D_N = C_N \times \frac{1}{(\text{eff})} \times \frac{1}{Y_N} \times \frac{(1+\alpha_T)}{(\text{b.r.})}.$$

Here Y_N = the chemical yield of N, eff = photopeak efficiency for the particular source geometry, α_T = total internal conversion coefficient, b.r. = branching ratio. The values of eff for ^{64}Cu were known (28), but values for the xenon isotopes were determined as described in Appendix B.

The disintegration rate at the end of bombardment, $D_N{}^0$, was related to the formation cross section, σ_N, to the proton flux, F, and to the number, n_T, of target nuclei in the beam, by the expression

$$[5] \qquad D_N{}^0 = F n_T \sigma_N (1 - \exp - \lambda_N t_0)$$

Can. J. Chem. Downloaded from www.nrcresearchpress.com by 210.87.254.5 on 09/05/12
For personal use only.

Here λ_N is the decay constant of N, and the term $(1 - \exp -\lambda_N t_0)$ accounts for the decay of N during the bombardment of duration t_0. To obtain independent cross sections for the unshielded fission products, ^{135}Xe and $^{133}Xe^g$, the measured $D_{Xe}{}^0$ had to be corrected by subtracting the rates $((D_{Xe}{}^0)'$ and $(D_{Xe}{}^0)''$, due respectively to xenon which had grown from decay of the iodine parent during the times t_0 and t_1. Here t_1 is the time from the end of bombardment to the end of the first separation of xenon from iodine [i.e. to the end of sweep (*a*)]. These corrections are given by the equations

$$[6] \qquad (D_{Xe}{}^0)' = \frac{(D_I{}^0)_{cum}}{(1 - \exp -\lambda_I t_0)}\left[1 - \frac{\lambda_{Xe}\,(\exp -\lambda_I t_0) - \lambda_I\,(\exp -\lambda_{Xe} t_0)}{(\lambda_{Xe} - \lambda_I)}\right]$$

$$[7] \qquad (D_{Xe}{}^0)'' = (D_I{}^0)_{cum}\frac{\lambda_I}{(\lambda_{Xe} - \lambda_I)}\frac{(\exp -\lambda_I t_1)(\exp -\lambda_{Xe} t_2)}{\exp -\lambda_{Xe} t_1},$$

where $(D_I{}^0)_{cum}$ is the disintegration rate of the parent iodine nuclide at the end of bombardment. This value was obtained from the disintegration rate, $D_{Xe}{}^b$, at the end of sweep (*b*) for ^{135}Xe and $^{133}Xe^g$, by using the formula

$$[8] \qquad D_{Xe}{}^b = (D_I{}^0)_{cum}\frac{\lambda_{Xe}}{\lambda_{Xe} - \lambda_I}(\exp -\lambda_I t_1)[(\exp -\lambda_I t_2) - (\exp -\lambda_{Xe} t_2)].$$

The cumulative cross sections for ^{135}I and ^{133}I were obtained by substituting the corresponding values of $(D_I{}^0)_{cum}$ in eq. [5]. To use $(D_I{}^0)_{cum}$ from eq. [8] in eqs. [6] and [7], the assumption must be made that the decay precursors of iodine are very short-lived. This assumption is reasonable for the simple chain 135, but is not true for the more complex chain 133. In the latter chain, during the period $(t_0 + t_1)$ a fraction of the cumulative yield of ^{133}I is held back by the relatively long-lived isomers of ^{133}Te. Therefore the above correction procedure uses a value of $(D_{^{133}I}{}^0)_{cum}$ in eqs. [3] and [7] which is too high. Consequently the independent yield of $^{133}Xe^g$ is overcorrected and will be too low. This overcorrection introduces significant errors only when there is a large growth of $^{133}Xe^g$. Therefore the time t_1 was minimized in the present experiments. The above equations proved satisfactory for the present data.

A further correction for the growth resulting from decay of $^{133}Xe^m$ was made to the disintegration rate of $^{133}Xe^g$. This was given by

$$[9] \qquad (D_{^{133}Xe^g}{}^0)''' = [\lambda_{^{133}Xe^g}/(\lambda_{^{133}Xe^m} - \lambda_{^{133}Xe^g})][D_{^{133}Xe^m}{}^0].$$

Without a known value of F in eq. [5], only relative cross sections could be obtained.

Absolute Cross Sections

Absolute cross sections were measured for most irradiations by monitoring the proton beam with the reaction $^{65}Cu(p,pn)^{64}Cu$ with the revised cross sections of Meghir (29). Then F may be eliminated from eq. [5], if it is assumed that the same flux passed through the foil of copper and of the heavy metal target (h.m.t.). Then

$$[10] \qquad \sigma_N = \sigma_{^{64}Cu}\frac{D_N{}^0}{D_{^{64}Cu}{}^0}\frac{n_{^{65}Cu}}{n_{h.m.t.}}\frac{(1 - \exp -\lambda_{^{64}Cu} t_0)}{(1 - \exp -\lambda_N t_0)}.$$

The relative number of monitor and heavy target nuclei were given by

$$\frac{n_{^{65}Cu}}{n_{h.m.t.}} = \frac{(s.d.)_{Cu}}{(s.d.)_{h.m.t.}} \times \frac{(ab)_{^{65}Cu}}{(ab)_{h.m.t.}} \times \frac{A_{h.m.t.}}{A_{^{65}Cu}},$$

where s.d. is the surface density, A is the mass number, and ab is the abundance of the target isotope. For ^{65}Cu, ab equals 31.9% and, for the four heavy metals, ab was taken to be 100%.

Can. J. Chem. Downloaded from www.nrcresearchpress.com by 210.87.254.5 on 09/05/12
For personal use only.

The error caused in the present results for ^{235}U by the presence of about 5% of ^{238}U was estimated to be negligible.

APPENDIX B

Measurement of Beta Activity and Photopeak Efficiencies for Xenon

Efficiencies were determined for the photopeaks of energy 80 keV and 249 keV, due respectively to $^{133}Xe^g$ and $^{135}Xe^g$. Samples from sweep (*b*) were used for the measurements since they contained only $^{133}Xe^g$ and $^{135}Xe^g$. Their disintegration rates were measured with a gas phase beta proportional counter whose absolute efficiency was determined with a standard beta source of ^{85}Kr.

Equipment for Measurement of Beta Activity

The cylindrical glass counter was similar to one used previously (24, 29, 40, 41).

Beta samples were prepared in the same apparatus used for preparation of the gamma samples. The rare gas sample was measured in the gas burette and transferred with the Toepler pump to the counter. The pressure in the beta counter was then brought up to 1 atm with P-10 counting gas (argon/methane = 9/1). To obtain good plateau characteristics, the sample gases were first purified over titanium sponge at 850 °C. The plateau lengths were always about 200 V. The dead time of the counter was found by a paired-source method to be only about 20 μs.

The efficiency of the beta counter was found to be 97 $\pm$ 3% with samples of a standard beta source of ^{85}Kr. Previous studies (24, 40) used efficiencies of 98–100%. The active volume of the counter was found by weighing with toluene.

Efficiency of Xenon Photopeaks

A sample of xenon from sweep (*b*) was divided in the gas burette into a beta and a gamma sample. The absolute beta counting gave the disintegration rates for $^{135}Xe^g$ and $^{133}Xe^g$. The efficiency of the corresponding photopeaks was determined with an uncertainty of 10%. The efficiency for $^{133}Xe^g$ was confirmed in one experiment in which the gamma activity of a xenon sample was first measured for 12 d and then the vial broken *in vacuo* and quantitatively transferred to the beta counter. The efficiencies for the gas sample proved to be only slightly higher than for liquid samples of comparable geometry and gamma ray energy (28). The efficiency of the 233-keV photopeak was taken to be a few per cent higher than the measured value for the 249-keV gamma ray.

Measurement of Beta Activity of Xenon Produced in Fission

Although previous studies (10, 16) have measured fission product xenon with a beta counter, this technique was not used here, except for the above calibrations, because of the complexity of the decay curves for a sample from sweep (*a*). These contained the following components: (i) $^{135}Xe^g$ (9.2 h); (ii) $^{133}Xe^g$ (5.3 d), present at the end of separation (*a*), and grown from decay of $^{133}Xe^m$; (iii) $^{133}Xe^m$ (2.3 d); (iv) small but significant activities of longer-lived, more neutron-deficient xenon isotopes (Table I); these become more important at higher fission energies.

Storms (10) measured the beta activity of a xenon sample from 'sweep (*a*)' for only the first 2 d because his sample from 'sweep (*b*)' was then measured in the same counter. This was an unsatisfactory method because of the complexity of the beta decay curve in this early period, particularly as his samples often contained relatively short-lived krypton contamination. It was not surprising that his beta activity data did not indicate the presence of the 2.3-d $^{133}Xe^m$, but it was surprising that it was not detected in his gamma spectra. From his evidence he concluded that there was a negligible yield of $^{133}Xe^m$ in medium-energy fission.

Can. J. Chem. Downloaded from www.nrcresearchpress.com by 210.87.254.5 on 09/05/12
For personal use only.

This assumption now appears to be wrong as indicated by the present work on ^{133}Xe and from general considerations of isomeric yield ratios in fission.

Similarly the beta activity data for ^{133}Xe measured by James *et al.* (16) should be reviewed. However, their samples were measured for a much longer time than those of Storms and the error introduced by neglecting $^{133}Xe^{m}$ may be fortuitously small.

A disadvantage of gamma counting in this work was that the measured independent cross sections for $^{133}Xe^{m}$, and therefore for $^{133}Xe^{g}$, were very dependent on the poorly defined α_K for the highly converted gamma radiation of $^{133}Xe^{m}$. Integral beta counting has been shown to be an unsuitable alternative method of measurement. However, measurement by a beta spectrometer of the conversion electrons would eliminate some difficulties due to other xenon isotopes and to low gamma activities of $^{133}Xe^{m}$. Furthermore, the isomer ratios obtained would be far less sensitive to the value of α_K.

REFERENCES

1. F. F. Momyer, Jr. The radiochemistry of the rare gases. Nuclear Science Series NAS-NS 3025, National Research Council, Washington, D.C. 1960.
2. R. C. Koch and G. L. Grandy. Anal. Chem. **33**, 43 (1961).
3. R. Aubeau, L. Champeix, and J. Reiss. J. Chromatog. **6**, 209 (1961).
4. F. Felix and P. Schmeling. Joint Euratom/United States Program, EUR 111.e, Brussels. 1962.
5. I. Dostrovsky, S. Katcoff, and R. W. Stoenner. Phys. Rev. **136**, B44 (1964).
6. A. C. Wahl, R. L. Ferguson, D. R. Nethaway, D. E. Troutner, and K. Wolfsberg. Phys. Rev. **126**, 1112 (1962).
7. E. J. Hoagland and N. Sugarman. Radiochemical Studies. Vol. 9. National Nuclear Energy Series Div. IV. McGraw-Hill Book Co., Inc., New York. 1951. Paper 147.
8. F. Brown and L. Yaffe. Can. J. Chem. **31**, 242 (1953).
9. S. Katcoff and W. Rubinson. Phys. Rev. **91**, 1458 (1953).
10. H. A. Storms. Ph.D. Thesis, Massachusetts Institute of Technology, Cambridge, Mass. Unpublished. September, 1962.
11. J. G. Bayly, M. F. Duret, N. G. Poulsen, and R. H. Tomlinson. Can. J. Phys. **39**, 1391 (1961).
12. J. Macnamara, C. B. Collins, and H. G. Thode. Phys. Rev. **78**, 129 (1950).
13. J. A. McHugh, Jr. Ph.D. Thesis, University of California Radiation Laboratory Report. UCRL-10673. 1963.
14. L. J. Colby, Jr. and J. W. Cobble. Phys. Rev. **121**, 1410 (1961).
15. B. D. Pate, J. S. Foster, and L. Yaffe. Can. J. Chem. **36**, 1691 (1958).
16. R. H. James, G. R. Martin, and D. J. Silvester. Radiochim. Acta, **3**, 76 (1964).
17. P. P. Benjamin. Ph.D. Thesis, Department of Chemistry, McGill University, Montreal, Que. 1965.
18. J. H. Davies and L. Yaffe. Can. J. Phys. **41**, 762 (1963); Can. J. Chem. **41**, 1836 (1963).
19. S. Parikh. Ph.D. Thesis, Department of Chemistry, McGill University, Montreal, Que. 1966.
20. D. R. Nethaway and H. B. Levy. Phys. Rev. **139**, B1505 (1965).
21. A. C. Wahl. Symposium on the physics and chemistry of fission, I.A.E.A. Salzburg. Paper SM-60/22 (1965).
22. K. Wolfsberg. Phys. Rev. **137**, B929 (1965).
23. J. S. Kirkaldy. Ph.D. Thesis, Foster Radiation Laboratory, McGill University, Montreal, Que. 1954; and more recent private communications.
24. I. Dostrovsky. Private communications. 1962, 1963.
25. D. L. Gray. U.S.A.E.C. Report HW-62639 (1960).
26. K. A. Kraus and G. E. Moore. J. Am. Chem. Soc. **75**, 1460 (1953).
27. K. Way *(Editor)*. Nuclear Data Sheets. National Academy of Sciences, National Research Council, Washington, D.C., (1962), with later supplements.
28. G. Grant. Ph.D. Thesis, Department of Chemistry, McGill University, Montreal, Que. 1961.
29. S. Meghir. Ph.D. Thesis, Department of Chemistry, McGill University, Montreal, Que. 1962; and more recent communications.
30. M. E. Rose. International conversion coefficients. North-Holland Pub. Co., Amsterdam. 1958.
31. I. Bergstrom, S. Thulin, A. H. Wapstra, and B. Astrom. Arkiv Fysik, **7**, 255 (1954).
32. H. Bateman. Proc. Cambridge Phil. Soc. **15**, 423 (1910).
33. C. D. Coryell. Ann. Rev. Nucl. Sci. **2**, 305 (1953).
34. Y. Y. Chu. University of California Radiation Laboratory Report, UCRL-8926, (1959).
35. R. H. Goeckermann and I. Perlman. Phys. Rev. **73**, 1127 (1948); **76**, 628 (1949).
36. J. A. Powers. Ph.D. Thesis, Purdue University, Lafayette, Ind. 1962.
37. D. S. Mather, P. Fieldhouse, and A. Moat. Nucl. Phys. **66**, 149 (1965).
38. R. Batchelor, W. B. Gilboy, and J. H. Towle. Nucl. Phys. **65**, 236 (1965).
39. P. C. Stevenson, H. G. Hicks, W. E. Nervik, and D. R. Nethaway. Phys. Rev. **111**, 886 (1958).
40. W. Bernstein and R. Ballentine. Rev. Sci. Instr. **21**, 158 (1950).
41. S. Katcoff and W. Rubinson. J. Inorg. Nucl. Chem. **27**, 1447 (1965).

Can. J. Chem. Downloaded from www.nrcresearchpress.com by 210.87.254.5 on 09/05/12
For personal use only.

Can. J. Chem. Downloaded from www.nrcresearchpress.com by 210.87.254.5 on 09/05/12
For personal use only.

PHOTOOXIDATION OF PROPIONALDEHYDE AT LOW PARTIAL PRESSURES OF ALDEHYDE

A. P. ALTSHULLER, I. R. COHEN, AND T. C. PURCELL

Laboratory of Engineering and Physical Sciences, Robert A. Taft Sanitary Engineering Center, U.S. Department of Health, Education, and Welfare, Cincinnati, Ohio

Received May 24, 1966

ABSTRACT

Propionaldehyde at partial pressures of from 0.0006 to 0.04 mm was photooxidized at 3 100 Å in the presence of 150 mm of oxygen. The major products were ethyl hydroperoxide and carbon monoxide. Acetaldehyde was formed at intermediate concentrations and formaldehyde, ethanol, methanol, hydrogen peroxide, and ethane were minor products. No ozone, peroxy acids, or diacyl peroxides could be detected.

The results can be explained on the basis of a free-radical mechanism. Certain radical disproportionation reactions which are often postulated are unimportant because of the low partial pressures of propionaldehyde. An alternative mechanism involving direct chemical reaction of an oxygen molecule with the triplet state of the propionaldehyde may be of some significance, but cannot account for all of the products obtained. The present results indicate the importance of alkyl hydroperoxides as products in photooxidations at low partial pressures of aldehyde in the presence of large excesses of oxygen.

The photooxidation of aldehydes has been the subject of several investigations in recent years (1). Little work has been done at very low concentrations of the aldehyde. It was of interest to ascertain whether the mechanism for aldehyde photooxidation would be the same or somewhat different at low concentrations of an aldehyde, but at high partial pressures of oxygen. These conditions are of especial significance in atmospheric chemistry.

A problem in work at very low concentration (0.75 to 50 p.p.m., or 0.0006 to 0.04 mm) is the need for extended periods of irradiation to allow conversions sufficient for measurement of products. Irradiation periods as short as 10 min were occasionally used, but more typically periods of 30 to 180 min were required. It is reasonable to expect that secondary reactions occurred, particularly during the longest irradiation periods with large percentages of conversion.

EXPERIMENTAL

The irradiations were carried out at 23 ± 1° in the same thermostatted system used previously (2). In most of the experiments reported in this work, each of the two parallel light banks consisted of sunlight fluorescent lamps with an intensity maximum at 3 100 Å. The K_d value ($K_d = \phi K_a$, ϕ is the primary quantum yield and K_a the rate of light absorption) based on the initial rate of photolysis of nitrogen dioxide in nitrogen, was 0.08 ± 0.02 min^{-1} when 28 sunlight fluorescent lamps were used.

The plastic container for the reaction mixture was fabricated from FEP (fluorinated ethylene–propylene copolymer) film (2). The volume of the initial mixture usually was 50 l; 100 l volumes were occasionally used in calibrations and special experiments. The redistilled propionaldehyde was injected into an air stream by means of microsyringes, and the cylinder air was metered into the plastic bag. In some preliminary experiments, irradiations were carried out on mixtures in pyrex flasks or in FEP containers covered by Mylar film. The propionaldehyde partial pressures used were 0.0006, 0.003, 0.02, and 0.04 mm. The propionaldehyde was diluted to 750 (± 10) mm total pressure and 150 mm partial pressure of oxygen.

Analyses for acetaldehyde, propionaldehyde, and ethanol were made with a flame-ionization detector after separation of the components at 25 °C on a column packed with bis-2(2-methoxyethyl)adipate on C-22 firebrick. Carbon monoxide was separated on a molecular sieve column, hydrogenated to methane, and analyzed with a flame-ionization detector (2). Peroxy-type compounds were analyzed by several variations of the potassium iodide and ferrous thiocyanate methods. Formaldehyde was determined by the chromotropic acid method (2). Hydrogen peroxide was analyzed by a modification of the titanous sulfate method (3). After each irradiation period, the container was removed from the irradiation chamber and samples were removed for subsequent gas chromatographic or colorimetric analysis. Replicate gas chromatographic analyses were made on each sample, and were used to determine whether any loss of products occurred in the

dark period. The losses during the periods of time needed for the analyses were small and were well within the usual variations in replicate measurements in the p.p.m. range.

The ethyl hydroperoxide and *n*-butyl hydroperoxide were synthesized by the literature procedures (4, 5). Refractive indices and active oxygen contents were determined. The purity of the ethyl hydroperoxide was 54%; that of the *n*-butyl hydroperoxide was 93%.

RESULTS

Gas chromatographic analyses indicated the presence of acetaldehyde and ethanol along with traces of methanol and ethane. Carbon monoxide was a major product, and formaldehyde a minor product. A peroxy-type substance was shown to be a major product, determined by several colorimetric methods.

The moles of propionaldehyde consumed per mole of propionaldehyde initially present are summarized in Table I. A small but consistent increase in rate (moles consumed averaged over the various irradiation periods) occurred with increase in propionaldehyde concentrations from 0.75 p.p.m. (0.0006 mm) to 50 p.p.m. (0.04 mm). The general shapes of the curves for rate versus irradiation time appear to be very similar over the concentration range investigated.

TABLE I

Consumption of propionaldehyde during photooxidation*

Average concentration level (p.p.m.)	Moles of propionaldehyde consumed per mole initially present for various irradiation periods				
	30 min	60 min	90 min	120 min	180 min
0.75	—	0.30	—	0.55	0.70
4.3†	0.17	0.33	0.45	0.56	0.73
20	0.21	0.36	0.51	0.56	0.78
50	—	0.36	0.51	0.58	—

*750 mm total pressure, 150 mm partial pressure of oxygen.
†10 min irradiation, 0.06; 20 min irradiation, 0.12.

Much of the acetaldehyde and most or all of the ethanol analyzed by chromatography are produced by thermal decomposition of the ethyl hydroperoxide in the chromatographic system rather than by photochemically induced reactions. This conclusion is based in part on the results obtained with vapor mixtures of ethyl hydroperoxide in the p.p.m. range in air. This type of decomposition is also suggested by measurements indicating that the uncorrected product yields greatly exceed the amount of propionaldehyde consumed.

The peroxy-type product formed from the photooxidation of low concentrations of propionaldehyde in 150 mm oxygen reacted slowly with both neutral potassium iodide reagent and molybdate-catalyzed potassium iodide reagent, but reacted rapidly with a modified ferrous ammonium sulfate reagent. Ozone, peroxy acid, and hydrogen peroxide all reacted very rapidly (complete reaction in 3 min or less) in the catalyzed iodide reaction, whereas the peroxy-type product continued to react slowly for many hours. Ozone and peroxy acid also reacted almost immediately with neutral potassium iodide; hydrogen peroxide reacted more slowly, but still much more rapidly than the peroxy-type product. The latter reacted rapidly with ferrous ammonium sulfate reagent, as did ozone, peroxy acid, and hydrogen peroxide. However, diacetyl peroxide reacted slowly with the ferrous ammonium sulfate reagent. The alkyl hydroperoxides, ethyl and *n*-butyl, reacted at essentially the same rate as this peroxy-type product with catalyzed potassium iodide and the neutral iodide reagent. These hydroperoxides reacted rapidly with ferrous ammonium sulfate reagent. Ethyl hydroperoxide and *n*-butyl hydroperoxide cannot be differentiated by means of these chemical reactions; however, in the chromatographic procedure used,

Can. J. Chem. Downloaded from www.nrcresearchpress.com by 210.87.254.5 on 09/05/12
For personal use only.

n-alkyl hydroperoxides decomposed to form the aldehyde and alcohol having the same number of carbon atoms as the original hydroperoxide. The only aldehyde and alcohol detected in appreciable quantities from the reaction mixture were acetaldehyde and ethanol, which are products of the decomposition of ethyl hydroperoxide.

On the basis of these experimental results, ozone, peroxy acids, and diacyl peroxides can be excluded as significant products of the photooxidation of propionaldehyde at low partial pressures (0.0006 to 0.04 mm) in the presence of a large excess of oxygen. All of these measurements indicate that ethyl hydroperoxide is the major product containing the peroxy group.

The photooxidation of acetaldehyde also was investigated briefly in the same range of partial pressures as that used for propionaldehyde. Acetaldehyde photooxidized at about two thirds the rate of propionaldehyde to form a peroxy-type substance and formaldehyde as two of its major products. These two products were produced in almost equal amounts, and they accounted for somewhat over half of the acetaldehyde consumed. The photooxidation of formaldehyde also has been investigated and hydrogen peroxide identified as a significant reaction product (6). Traces of hydrogen peroxide were measured after large percentage conversions of propionaldehyde. Since formaldehyde was present as a minor product, it seems likely that the hydrogen peroxide was formed from the concurrent photooxidation of formaldehyde. These results indicate that small amounts of other peroxy-type substances were present in addition to the major oxidant, ethyl hydroperoxide, particularly after the larger conversions during the longer irradiation periods.

Most of the ethanol yields (0.05 to 0.2 mole of ethanol found per mole of propionaldehyde reacted) are believed to result from decomposition of the ethyl hydroperoxide. This conclusion is based on a comparison of the amounts of ethanol formed by passing either ethyl hydroperoxide or the reaction products directly into a chromatograph with the amounts formed by passing them first through a substrate of ferrous ammonium sulfate and then into the chromatograph. With the substrate, the amounts of ethanol obtained from either the ethyl hydroperoxide in air or the reaction products were reduced by two thirds to three quarters. Insignificant amounts of ethanol or acetaldehyde were lost when they were passed directly through the ferrous ammonium sulfate. This shift in composition probably results from a change in the relative amounts of homogeneous and heterogeneous decomposition occurring. The close similarity of results for ethyl hydroperoxide and reaction products indicates that most or all of the ethanol was not originally present as a photooxidation product. The ethyl hydroperoxide decomposed too slowly in the reaction container to account for these results. Therefore, it is believed that most of the decomposition occurred in the chromatographic system.

Formaldehyde was a minor product. Its yield increased from about 0.02 for 30 min irradiations to 0.06–0.07 for 180 min irradiations. Owing to the small concentrations produced, measurements could be made only at the higher reactant levels.

Carbon monoxide was a major product of the photooxidation of propionaldehyde in this study. Even at the shorter irradiation times, 1 mole of carbon monoxide was formed per mole of propionaldehyde consumed. At longer irradiation times the carbon monoxide yield exceeded 1.

At the lower propionaldehyde concentrations, 90 to 100% of the moles of propionaldehyde consumed could be accounted for as ethyl hydroperoxide (Fig. 1). High yields of ethyl hydroperoxide were obtained in both continuous and intermittent irradiations ranging from 10 to 180 min. However, the yield of ethyl hydroperoxide relative to propionaldehyde did decrease slowly with increasing irradiation time.

Can. J. Chem. Downloaded from www.nrcresearchpress.com by 210.87.254.5 on 09/05/12
For personal use only.

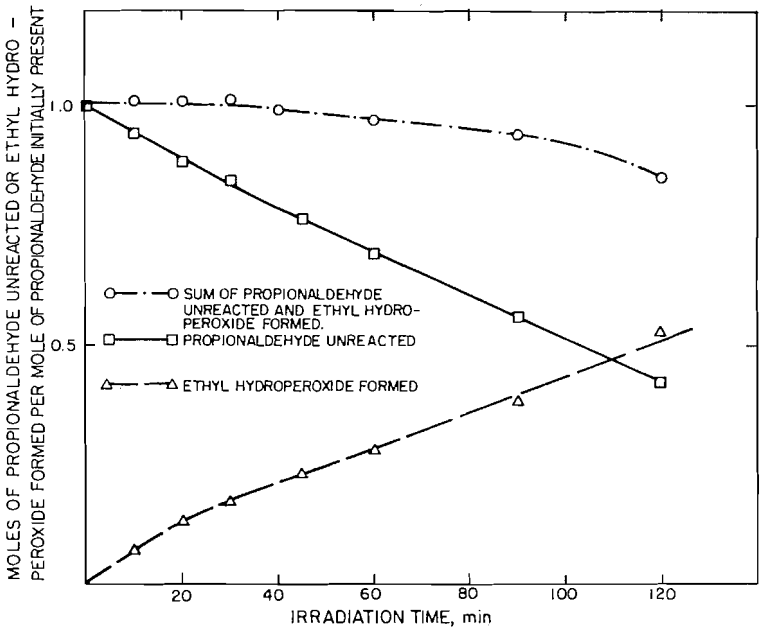


FIG. 1. Relative molar yields of unreacted propionaldehyde and of ethyl hydroperoxide formed after various reaction times. Initial conditions: propionaldehyde 0.003 mm; oxygen, 150 mm; total pressure, 150 mm.

At the higher propionaldehyde concentrations, the yield of ethyl hydroperoxide relative to propionaldehyde consumed varied from slightly below 0.5 to 0.8. Acetaldehyde was the only other two-carbon product detected, and it probably contributed the remainder of the two-carbon yield. Although no available procedure could accurately separate the photochemically produced acetaldehyde from that resulting from the decomposition of the ethyl hydroperoxide, significant amounts of acetaldehyde definitely were produced directly from the photooxidation.

DISCUSSION

The four primary processes usually considered in the photolysis of aldehydes (7) also should be considered in discussing the mechanism for the photooxidation of propionaldehyde.

$$C_2H_5CHO + h\nu \rightarrow C_2H_5CHO^*$$

[I] $$C_2H_5CHO^* \rightarrow CH_3CH_2 + HCO$$

[II] $$C_2H_5CHO^* \rightarrow C_2H_6 + CO$$

[III] $$C_2H_5CHO^* \rightarrow C_2H_4 + CH_2O$$

[IV] $$C_2H_5CHO^* \rightarrow CH_3 + CH_2CHO$$

Process [II] can occur to only a small extent, since less than 0.01 mole of ethane is produced per mole of propionaldehyde consumed. Therefore, very little of the large yield of carbon monoxide can be attributed to this reaction. Similarly, process [III] is excluded by the absence of ethylene as a detectable product. The formaldehyde produced must be formed by other processes. Process [IV] produces methyl radicals, which should react to form peroxymethyl radicals; these in turn could in part disproportionate and in part associate or decompose to produce substantial concentrations of formaldehyde or methanol. Since formaldehyde is a minor product, since only a trace of methanol is detectable, and

Can. J. Chem. Downloaded from www.nrcresearchpress.com by 210.87.254.5 on 09/05/12
For personal use only.

since no association product is detectable, process [IV] is at most of minor significance. Process [IV] has a primary quantum yield of 0.00 at 3 130 Å in the photolysis of propionaldehyde (7). Since the formaldehyde yield increases with increasing irradiation time, the formaldehyde and methanol are more likely formed by the photooxidation of acetaldehyde than by process [IV]. Thus, it appears that process [I] is by far the most important of these four processes, since the products observed can best be accounted for in terms of a mechanism involving this process.

One type of mechanism which is often used to explain photooxidation reactions involves a free-radical oxidation scheme. An alternative mechanism can involve direct chemical reaction of the oxygen molecule with the triplet state of the propionaldehyde. It can be postulated that an intermediate can be formed which will decompose into the two major products, ethyl hydroperoxide and carbon monoxide. While such a possibility is interesting, there is a lack of direct experimental evidence on the nature of chemical reactions of oxygen with the triplet state of aldehydes (1, 7, 8). This type of mechanism would not explain the presence of acetaldehyde and the small yields of other oxidation products. Nevertheless, chemical reaction of the oxygen with the triplet state must be considered as of some possible significance.

In considering a free-radical-type oxidation mechanism, the very low aldehyde pressures, high oxygen pressures, and inadequate light intensities in the present study tend to reduce the significance of certain reactions involving radical species. Because of the very low levels of radical concentrations, some of the reactions between radicals are not likely to be as important as they may be under other experimental conditions.

Since process [I] appears to be the only important primary process leading to products, the following steps can be suggested.

[1] $$C_2H_5CHO + h\nu \rightarrow C_2H_5CHO^*$$

[2] $$C_2H_5CHO^* \rightarrow C_2H_5 + HCO$$

The peroxyethyl radical should be formed (1, 8), particularly in the presence of high partial pressures of oxygen as in the present work.

[3] $$C_2H_5 + O_2 \rightarrow C_2H_5O_2^* \rightarrow C_2H_5O_2$$

Several possible reactions of formyl radical have been suggested (1), but only its reaction with oxygen to form carbon monoxide will be considered.

[4] $$HCO + O_2 \rightarrow CO + HO_2$$

Since 1 mole of carbon monoxide is produced per mole of formyl radical formed at smaller percentage conversions, reactions leading to carbon dioxide or to CHO_3 and then formic acid could not be significant.

Ethyl hydroperoxide can be formed by several steps which have been proposed. However, a reaction which is compatible with the experimental results is as follows.

[5] $$C_2H_5O_2 + HO_2 \rightarrow C_2H_5OOH + O_2$$

This reaction has been suggested by Watson and Darwent (9), Turner *et al.* (10), and Gray (11) to explain ethyl hydroperoxide formation in the mercury-photosensitized oxidation of ethane and ethylene. In reviewing the reactions of alkyl peroxy radicals, McMillan and Calvert (8) conclude that it is unlikely that alkyl peroxy radicals abstract hydrogen from molecules in low temperature reactions. The substances normally produced from reactions of the acyl radical formed by the hydrogen abstraction from propionaldehyde were not identified in this study.

Can. J. Chem. Downloaded from www.nrcresearchpress.com by 210.87.254.5 on 09/05/12
For personal use only.

At higher aldehyde concentrations (0.02 and 0.04 mm) or at higher percent conversions (greater than 50%), acetaldehyde becomes a significant product although ethyl hydroperoxide yields always exceed acetaldehyde yields. Acetaldehyde yields were higher than ethanol yields.

The often proposed disproportionation of RO_2 radicals

[6] $$2RO_2 \rightarrow 2RO + O_2$$

is needed to provide RO radicals which in turn react to form acetaldehyde. However, the disproportionation of RO_2 radicals must be significantly less important than their reaction to form ethyl hydroperoxide. The alkoxy radical levels should be lower than the RO_2 and HO_2 radical concentration levels. Consequently, disproportionations of RO with itself or with RO_2 should not be important. Such reactions lead to equal yields of ethanol and acetaldehyde or of ethyl hydroperoxide and acetaldehyde. Such yields are not in accord with the present experimental results. Reaction of the ethoxy radical with oxygen to form acetaldehyde appears more likely.

[8] $$C_2H_5O + O_2 \rightarrow CH_3CHO + HO_2$$

Acetaldehyde also could be formed by the reaction

[9] $$C_2H_5 + O_2 \rightarrow C_2H_5O_2^* \rightarrow CH_3CHO + OH,$$

but this reaction is unlikely to be important in room temperature reactions.

The small amount of ethanol which may be attributed to direct reaction could come from ethoxy radical disproportionation, but the reaction

[10] $$C_2H_5O + HO_2 \rightarrow C_2H_5OH + O_2$$

may be more important.

The formation of HO_2 radicals by reactions [4] and [8] exceeds its consumption by reaction [5] in experiments at higher aldehyde levels (0.02 and 0.04 mm) or larger percentage conversions (greater than 50%) at the lower levels (0.0006 and 0.003 mm). Although traces of hydrogen peroxide were detected after larger conversions (probably from formaldehyde photooxidation), no hydrogen peroxide could be detected earlier in the reaction. Therefore, gas-phase reaction of HO_2 radicals with themselves to produce hydrogen peroxide (and oxygen) is of no importance. Wall reactions of HO_2 radicals must be suggested to account for their consumption.

Acetaldehyde photooxidation would be a likely source of the additional carbon monoxide when its yield exceeds 1 as it does at large percentage conversions. The small yield of formaldehyde also can be attributed to its formation as a product of the photooxidation of acetaldehyde.

There is little point in discussing the various reactions leading to peroxyacetic acid or diacyl peroxides (12–15). These products could not be detected in the present investigation. Since ozone also was not detected, the reaction of RO_2 with oxygen to produce ozone could not have been significant (1, 8).

The present results differ from those of McDowell and co-workers (12–14) and of Calvert and Hanst (15). These investigators reported peroxy acids and diacetyl peroxide as products, but no hydroperoxides as products from the photooxidation of acetaldehyde (12, 13, 15) and propionaldehyde (14). Johnston and Heicklen (16) in a study of the photooxidation of acetaldehyde at lower partial pressures detected methyl hydroperoxide. Their measurements show a marked increase in methyl hydroperoxide relative to methanol, formic acid, and acetic acid as the partial pressure of the aldehyde decreases from 18 to

Can. J. Chem. Downloaded from www.nrcresearchpress.com by 210.87.254.5 on 09/05/12
For personal use only.

0.4 mm and as the partial pressure of oxygen increases. These latter measurements suggest that results similar to those found in the present study should be obtained in the photooxidation of acetaldehyde at very low partial pressures.

The present results provide evidence for the importance of alkyl hydroperoxides as major products in photooxidations at very low partial pressures of aldehyde. The results also indicate that reactions [4] and [5] may be very important steps in the photooxidation of aldehydes.

ACKNOWLEDGMENT

We wish to thank Dr. J. J. Bufalini for the preparation of *n*-butyl hydroperoxide and for a number of helpful suggestions.

REFERENCES

1. D. E. HOARE and G. S. PEARSON. Gaseous photochemical reactions. *In* Advances in photochemistry. Vol. 3. *Edited by* W. A. Noyes, Jr., G. S. Hammond, and J. N. Pitts, Jr. Interscience Publishers, New York. 1964. p. 83.
2. A. P. ALTSHULLER and I. R. COHEN. Intern. J. Air Water Pollution, **8**, 611 (1964).
3. I. R. COHEN and T. C. PURCELL. The analysis of the oxidant in photochemical reactions. Presented at 152nd Meeting, American Chemical Society, New York. Sept. 11–16, 1966.
4. G. J. MINKOFF. Proc. Roy. Soc. London, Ser. A, **224**, 176 (1954).
5. H. R. WILLIAMS and H. S. MOSHER. J. Am. Chem. Soc. **76**, 2984 (1954).
6. UNPUBLISHED RESULTS. Photochemistry and Kinetics Unit, Laboratory of Engineering and Physical Sciences, Div. of Air Pollution, Public Health Service.
7. J. G. CALVERT and J. N. PITTS, JR. Photochemistry. John Wiley & Sons, Inc., New York. 1966. p. 372.
8. G. R. MCMILLAN and J. G. CALVERT. Gas phase photo-oxidation. *In* oxidation and combustion reviews. Vol. I. *Edited by* C. F. H. Tipper. Elsevier Publishing Co., Amsterdam. 1965. p. 83.
9. J. S. WATSON and B. DEB. DARWENT. J. Phys. Chem. **61**, 577 (1957).
10. A. H. TURNER, A. B. CALLAR, and R. J. CVETANOVIC. *Cited by* H. Cerfontain and K. O. Kutschke. J. Am. Chem. Soc. **84**, 4017 (1962).
11. J. A. GRAY. J. Chem. Soc. 3150 (1952).
12. C. A. MCDOWELL and L. K. SHARPLES. Can. J. Chem. **36**, 251 (1958).
13. C. A. MCDOWELL and S. SIFNIADES. Can. J. Chem. **41**, 300 (1963).
14. C. A. MCDOWELL and L. K. SHARPLES. Can. J. Chem. **36**, 258 (1958).
15. J. G. CALVERT and P. L. HANST. Can. J. Chem. **37**, 1671 (1959).
16. H. S. JOHNSTON and J. HEICKLEN. J. Am. Chem. Soc. **86**, 4254 (1964).

Can. J. Chem. Downloaded from www.nrcresearchpress.com by 210.87.254.5 on 09/05/12
For personal use only.

CHEMICAL REACTIONS IN ELECTRICAL DISCHARGES[1]

II. THE STRUCTURE OF THE POSITIVE COLUMN IN D-C. GLOW DISCHARGES THROUGH FAST-FLOWING GASES

JOZEF L. PEETERS,[2] HOWARD W. RUNDLE,[3] AND JACQUES M. DECKERS
Lash Miller Chemical Laboratories, University of Toronto, Toronto, Ontario

Received September 30, 1965

ABSTRACT

After a brief summary of recent advances in the structure of the positive column of a d-c. glow discharge, general expressions are derived for rates of reaction and excitation produced by electron impact. These rate equations are expressed in terms of the easily measured electrical parameters of the discharge. Such expressions will be used in future studies of chemical reactions occurring in the positive column; a qualitative comparison to experiment is given, where possible.

A general expression for the axial electric field in the positive column is obtained by equating the energy gained by the electrons in this field to that lost by collisions. The main assumption made is that axial electron concentration be constant along the column.

In the second part of the paper, calculations are done which indicate that ion and electron concentration gradients exist in the positive column adjacent to the anode. It is pointed out that such a phenomenon will be pronounced only under special conditions of low transverse and high axial field, and will be enhanced with fast-flowing gases.

A sample calculation is presented using the expression for the rate of electronic excitation of a species by electron impact, assuming a Maxwell–Boltzmann energy distribution for the electrons and constant elastic and inelastic collision cross sections.

1. INTRODUCTION

In this paper we concern ourselves with the structure of the positive column of a d-c. glow discharge through fast-moving gases. Under such fast-flow conditions appreciable axial pressure and velocity gradients are found. If a gas or gas mixture, in which composition changes could take place, is passed through the discharge, a concentration gradient is established because of the finite rate of chemical reactions. Ionization processes also occur with finite rates and thus result in a gradient of the number density of charged species. Because of the occurrence of these gradients we shall observe changes in the physical and electrical properties of the discharge, or in the composition of the gases which pass through the discharge, as a function of the distance from the entrance point of the gas. From the measurement of these changes we can then derive the rates of the processes from which the observed phenomena are only the consequence. By making successive measurements at increasing distances from the entrance point of the gases in the discharge the actual rate of these processes can then be calculated. In other instances the observed quantity is solely determined by the local value of the parameters in the discharge. This is the case in particular for the emission of optically allowed transitions. These observations then provide us with the actual rate directly, without having to resort to differential measurements.

In a first paper in this series Bois D'Enghien and Deckers (1) have shown that when a methane–oxygen mixture was passed through the positive cloumn of a d-c. glow discharge the intensity of emission of the carbon monoxide spectrum increased while the gases proceeded downstream from the entrance point in the discharge. It was further established

[1]*Supported by grants from the U.S. Air Force Office of Scientific Research (AF–AFOSR 63-375, 64-375, and 65-375), the National Research Council of Canada, and the University of Toronto.*
[2]*Present Address: Department of Chemistry, Institut d'Aremberg, Université de Louvain, Louvain, Belgium.*
[3]*Holder of a N.R.C. Bursary, 1964–1965.*

Can. J. Chem. Downloaded from www.nrcresearchpress.com by 210.87.254.5 on 09/05/12
For personal use only.

that the emission intensity was proportional to the carbon monoxide mole fraction in the mixture; it is thus feasible to measure rates of chemical reactions occurring in the discharge. In this laboratory Ailliet and Deckers (2) have shown that changes in the intensity of emission of CO bands in fast-flowing $CO–O_2$ mixtures result from changes in the electron energy distribution. Methods for studying the field in the positive column, the electron energy distribution, and reactions under fast flow conditions have (1) or will (3) be reported. In this paper, after attempting to modify existing theories so as to take into account these fast-flow conditions, we derive suitable kinetic expressions which will allow us to obtain quantitative data for the rate of processes occurring in the discharge.

2. THEORY

(A) General

Before breakdown, the electric field in a gas is equal to the potential applied to the electrodes divided by the electrode separation. If the applied field is strong enough, an electron, generated in the gas by an external agent such as a cosmic ray or an energetic photon, will be accelerated and produce an increasing number of positive ions and electrons or negative ions, in equal number. The resulting plasma will partially screen the field, increasing its value near the electrodes and decreasing it in what is known as the positive column. In the positive column the electrons will initially diffuse laterally and reach the walls much faster than the heavy positive ions, setting up a transverse field. The ambipolar diffusion process, first proposed by Schottky (4, 5) in 1924, provides a mechanism by means of which ions and electrons will recombine at the walls. Besides the recombination at the wall, recombination in the gas phase will also occur in three-body collisions or in dissociative two-body collisions (6). The longitudinal field supplies energy to the electrons and in ionizing collisions with neutral molecules more electron–ion pairs will be produced. If the screening action of the plasma is too large not enough ions will be produced to maintain a steady-state concentration; thus the longitudinal field will be the one in which the electrons draw just enough energy from the field so that the rate of ionization equals the rate of loss of ions through recombination.

Spenke (7) has taken into account stepwise ionization processes and Seeliger (8) the presence of negative ions in electronegative gases. Further refinements and generalizations were proposed by Ecker (9), Ludwig (10), and Allbrecht, Ecker, and Müller (11).

Druyvesteyn and Penning (12, 13) attempted calculations of the longitudinal field by equating the energy loss through elastic and inelastic collisions to the energy gained by electrons from the field. Mohler (14) ascribed the difference between the power supplied to the discharge and that carried to the walls to losses by radiation. In a particular case, Schottky (5) himself showed that about 20% of the energy drawn from the field by the electrons was used in producing ions.

Seeliger and Wichmann (15) investigated the existence of two types of discharges in oxygen and Seeliger (8) points out the existence of negative ions in oxygen. Now, the rate of diffusion of the negative charges to the walls will be reduced when negative ions are formed; hence the ambipolar diffusion will also be reduced and the average lifetime of the positive ions increased; the longitudinal field, necessary to maintain a steady-state positive ion concentration is thus decreased. Rundle *et al.* (3) in this laboratory have obtained evidence for the existence of even more than two types of discharges in oxygen.

In a static gas, conditions are uniform along the positive column (16). Wilhelm (17) showed that the constancy of the longitudinal field was a consequence of the quasi-neutrality of the plasma; he also had to assume that the motion of charged particles was

Can. J. Chem. Downloaded from www.nrcresearchpress.com by 210.87.254.5 on 09/05/12
For personal use only.

only conditioned by diffusion in the field. To our knowledge the only paper in the literature dealing with measurements of the electrical properties in the positive column through fast-flowing gases is one by Maier (18) in which evidence is presented that the electrical conditions are not uniform in the positive column. In particular, he found a variation of the axial electric field along the positive column.

After having obtained an expression for the rates of reactions[4] induced by electron impact, we shall derive an expression for the influence of pressure and gas velocity upon the electric parameters, such as field and density of charged particles in the positive column.

(B) Energy-Transfer Processes

In this section we consider transfer of energy under various forms from the electrons to the gas molecules in the discharge, which is a system not in equilibrium (11, 19). Electrons having energy E will collide inelastically with molecules AB_i and result in molecules AB_j (i and j specifying all quantum numbers of the initial and final states respectively). In such a collision the electron loses energy E_{ij}. If $E_{ij} > 0$ (the electron energy is smaller after collision) the collision is referred to as an inelastic collision of the first kind. The inverse process is then a collision of the second kind, also called a superelastic collision. In a system in equilibrium a consequence of the principle of microreversibility is that both processes should occur with equal frequency. Because the positive column is not in equilibrium, there will be an excess of collisions of the first kind as was pointed out by Rompe and Schon (19). The overall energy balance will thus only be affected by the effective number of collisions, which is the excess of the number of collisions of the first kind over those of the second kind (Ludwig (10, 20)).

If, in an inelastic collision, the vibrational energy imparted to AB is larger than the bond energy or if AB_j is an antibonding electronic state, AB will dissociate into A + B (where A and B are atoms, molecules, radicals, and (or) ions). A very large number of different collisions ij are possible in a gas. The amount of energy lost by an electron in exciting the rotational or vibrational states of a molecule is always small compared with the electron's energy (21). Sampson (22) calculated the rotational energy loss to be anywhere between 100% and a negligible percentage of that due to elastic collision. In a particular case Anderson and Goldstein (23) using microwave techniques estimated the fractional energy loss to be about 5.5 times as large as the loss via elastic collisions for slow electrons ($E < 0.4$ eV). Losses via vibrational energy transfer are also small unless there exists a short-lived compound negative ion state, as found by Schultz (24, 25) for nitrogen and carbon monoxide. Even then, only vibrational levels below the energy of the compound state will be excited. Lifetimes of vibrationally excited ground state molecules are large and it is thus not excluded that cumulative excitation will take place. It is, however, not clear a priori if dissociation into atoms could take place via such a "ladder climbing" process. Since collision cross sections for electronic excitation are often rather large (of order 10^{-16} cm^2) (21), it is more probable that dissociation will occur more readily via excitation into an antibonding state.

The cross section for elastic collisions is of the order of 10^{-16} to 10^{-15} cm^2 (26). Because of the large mass ratio between the colliding partners the energy lost in such collisions will always be small (26, p. 44). For excitation of electronic states, however, the cross sections

[4]*In this paper the term reaction should be taken very broadly, including such processes as dissociation of molecules, excitation (electronic, vibrational, rotational), and ion production after electron impact. The electrons will be considered as a reacting species and treated as such in the rate laws.*

Can. J. Chem. Downloaded from www.nrcresearchpress.com by 210.87.254.5 on 09/05/12
For personal use only.

for electrons having energies above the threshold may become comparable to (if not larger than) the elastic collision cross section. In this case, once an electron acquires an energy E_{ij} from the field, the average number of elastic collisions it will suffer before undergoing the inelastic collision ij will be much smaller than the number of elastic collisions suffered during the time that it took the electron to acquire the energy E_{ij}.

The number of inelastic collisions per unit time and unit volume for electrons having an energy E is equal to the number density of electrons n_e times the ratio of the electron speed $(2E/m)^{1/2}$ to their free path $l_e \equiv (n_i Q_{ij})^{-1}$ where Q_{ij} is the inelastic collision cross section for process ij and n_i the number density of species i. If $f(E)\,dE$ is the fraction of electrons having energy between E and $E + dE$ (27) and dn_{ij}/dt is the rate of change of n_i due to process ij then

$$\frac{dn_{ij}}{dt} = n_i n_e \int_0^\infty f(E) Q_{ij} \left(\frac{2E}{m}\right)^{1/2} dE = k_{ij} n_i n_e. \qquad [2.1]$$

k_{ij} can be considered a rate constant averaged over the electron energy distribution. Thus

$$k_{ij} = \int_0^\infty f(E) Q_{ij} (2E/m)^{1/2}\, dE. \qquad [2.2]$$

If an electron takes a time t_{ij} to gain the energy E_{ij} from the field in the positive column we can define

$$f_{ij} = k_{ij} t_{ij}. \qquad [2.3]$$

Since k_{ij} is a bimolecular rate constant having dimensions of unit volume per number of molecules (inverse of a number density) per unit of time, f_{ij} will have the dimensions of the inverse of a number density. The discussion of the true significance of f_{ij} will be postponed till the end of Section 2D. Substituting [2.3] into [2.1] we obtain

$$dn_{ij}/dt = (f_{ij}/t_{ij}) n_i n_e. \qquad [2.4]$$

This explicitly shows that the number of inelastic collisions per unit volume will be inversely proportional to the time it takes the electron to acquire the energy involved in the inelastic collision.

The electron concentration is related to the current density J by

$$J = n_e \bar{v}_e e, \qquad [2.5]$$

where $\bar{v}_e$ and e are the drift velocity and the charge of an electron respectively. We consider the contribution of positive and negative ions to the overall current density to be negligibly small because of their much smaller drift velocities $\bar{v}_+$ and $\bar{v}_-$. We obtain from [2.4] and [2.5]

$$dn_{ij}/dt = f_{ij} J n_i / \bar{v}_e e t_{ij}. \qquad [2.6]$$

We proceed to calculate the rate of energy loss in the gas.

(i) Energy Loss in Elastic Collisions

$\bar{K}$ is the fraction of energy lost by an electron of energy E per elastic collision averaged over the impact parameter. The number of collisions suffered by an electron of energy E per unit time is given by $(\sum n_i Q_{0i})(2E/m)^{1/2}$, where Q_{0i} is the elastic collision cross section for molecules i. Thus, the energy lost per unit time and volume in elastic collisions is equal to

$$-\left(\frac{dE}{dt}\right)_{el} = n_e \left(\frac{2}{m}\right)^{1/2} \int_0^\infty f(E) \bar{K} E^{3/2} (\sum n_i Q_{0i})\, dE. \qquad [2.7]$$

Can. J. Chem. Downloaded from www.nrcresearchpress.com by 210.87.254.5 on 09/05/12
For personal use only.

(ii) Energy Loss in Inelastic Collisions

$$[2.8]\qquad -\left(\frac{dE}{dt}\right)_{inel} = n_e \sum_i \sum_j \frac{dn_i}{dt} E_{ij} = n_e \sum_i \left(n_i \sum_j k_{ij} E_{ij}\right)$$
$$= n_e \left(\frac{2}{m}\right)^{1/2} \sum_i n_i \left(\sum_j E_{ij} \int_0^\infty f(E) E^{1/2} Q_{ij}\, dE\right).$$

The energy loss in elastic collisions is proportional to the mass ratio $2m/M$ of the electron and its collision partner. This factor is never larger than 10^{-3} and is more often of order 10^{-5}. Since this corresponding ratio is of order one for collisions involving an ion, they will lose energy almost as fast as they gain it and very few energetic ions will be found in the gas.

(C) The Axial Field

In the absence of a field the scattering of electrons by a gas will be isotropic because each direction of impact is equally probable. Only if concentration gradients arise will an average electron drift result from diffusion processes. If an axial field is applied, the electrons will be accelerated between collisions and their flight path will be bent in the direction of the field. The projection of the free path on the field axis is thus the sum of two terms: the projection of the free path in the absence of a field and a net displacement along the field due to the acceleration suffered by the electron in the direction of the field. This displacement or drift in the field for an electron of energy E between two collisions averaged over all directions of motion (but not over the energy distribution) will be referred to hereafter as the drift distance λ. If the field is not too strong we can express the overall drift of the electrons as the sum of an isotropic term resulting in a zero drift and the average axial drift $\lambda(E)$ times the number of collisions per unit time. In writing this we neglect the possible anisotropy in the scattering which is introduced because the impact velocity vectors will no longer be completely random but somewhat peaked in the field direction. The error thus introduced, due to the "persistence of velocity", could become important at very low pressures or in very large fields.

The acceleration in a field X suffered by an electron is equal to Xe/m. If $t_E(E)$ is the time between collisions for an electron of energy E, the drift distance λ between two collisions is equal to $Xet_E^2/2m$. The time between two collisions t_E is equal to the ratio of the free path to the average speed. Thus $t_E = m^{1/2}(\sum n_i Q_{0i})^{-1}(2E)^{-1/2}$. The drift distance is then equal to

$$[2.9]\qquad \lambda = \frac{Xe}{4} \frac{1}{E(\sum n_i Q_{0i})^2}.$$

The energy gain per electron between two collisions dE/dN is equal to the force Xe times the displacement λ. The number of collisions is given by $1/t_E$. Per unit time and volume the energy gain becomes

$$[2.10]\qquad \frac{dE}{dt} = \frac{dE}{dN} n_e \frac{dN}{dt} = \frac{(Xe)^2 n_e}{(8m)^{1/2}} \int_0^\infty \frac{f(E)\, dE}{E^{1/2}(\sum n_i Q_{0i})}.$$

Equating the energy gained from the field [2.10] to that lost by collisions [2.7] + [2.8] and solving for X we obtain

$$[2.11]\quad X = \frac{2}{e}\left\{\frac{\sum_i \left[n_i \sum_j E_{ij} \int_0^\infty f(E) E^{1/2} Q_{ij}\, dE\right] + \sum_i \left[n_i \int_0^\infty f(E) \bar{K} E^{3/2} Q_{0i}\, dE\right]}{\int_0^\infty f(E) E^{-1/2} \left(\sum_i n_i Q_{0i}\right)^{-1} dE}\right\}^{1/2}.$$

Can. J. Chem. Downloaded from www.nrcresearchpress.com by 210.87.254.5 on 09/05/12
For personal use only.

The derivation of this equation implicitly assumes n_e to remain constant over the distance in which the electron acquires the energy E_{ij}. This calculation was first suggested by Mierdel (28) and was further extended by Wasserrab (29). It neglects the kinetic energy lost by the electrons hitting the wall. As long as the average electron temperature is not too large ($kT <$ ionization energy) the number of ionizing collisions will be much smaller than the total number of other inelastic collisions. The average energy per electron will also be smaller than the energy lost in an ionizing collision. In the absence of volume recombination, for each ionizing collision one electron hits the wall and thus the kinetic energy lost by the electrons to the wall will only be a very small fraction of the total energy lost in the gas and can then be neglected in the above calculation. All other energy losses, particularly the energy lost at the wall by ion recombination, are included in the energy balance. In fact Schottky (5) estimated the longitudinal field by equating the energy lost by the electrons in ionizing collisions to the energy liberated at the wall by the recombination of ions and electrons.

At low pressures the losses through elastic collisions are small compared with the losses through inelastic collisions (16, p. 133) and the second term on the right-hand side of [2.11] can be neglected. At higher pressures the number of elastic collisions will increase and both terms have to be considered. Also noteworthy is the fact that X is independent of the electron concentration.

(D) Rate of Excitation

In the absence of energy losses during elastic collisions an electron having an energy E will gain an energy E_{ij} from the field during the time t_{ij}. This time can be calculated using [2.10]:

$$[2.12] \qquad t_{ij} = \int_0^{t_{ij}} \mathrm{d}t = \frac{(8m)^{1/2}}{(Xe)^2} \int_{E_i}^{E_i+E_{ij}} \frac{\mathrm{d}E}{\int_0^\infty \frac{f(E)\,\mathrm{d}E}{E^{1/2}\sum_i n_i Q_{0i}}} = \frac{8m^{1/2}\,E_{ij}}{(Xe)^2 \int_0^\infty \frac{f(E)\,\mathrm{d}E}{E^{1/2}\sum_i n_i Q_{0i}}}.$$

If energy losses in elastic and (or) inelastic collisions are taken into account, one obtains an expression similar to [2.12] with two additional terms subtracted from the denominator; these terms contain the integrals appearing in [2.7] and [2.8]. Unless one or more of the n_i's are very large (high pressures) these terms are small: the term representing the loss through elastic collision contains $\bar{K}$ which is of order 10^{-5} and cross sections figuring in the third term are small (21).

[2.12] shows that t_{ij} is independent of the initial energy E of the electron. If we assume Q_{0i} independent of the impact energy of the electron, the value of the integral in the denominator becomes

$$\left(\sum n_i Q_{0i}\right)^{-1} \int_0^\infty f(E)\,E^{-1/2}\,\mathrm{d}E = \left(\sum n_i Q_{0i}\right)^{-1} \overline{1/E^{1/2}}.$$

Thus

$$[2.13] \qquad t_{ij} = \frac{(8m)^{1/2}\sum n_i Q_{0i}}{(Xe)^2\,\overline{1/E^{1/2}}} E_{ij}.$$

The drift velocity of an electron is equal to the drift distance between two collisions as given by [2.9] divided by the time between two collisions. The averaging over the electron energy distribution gives

$$[2.14] \qquad \bar{v}_e = \frac{Xe}{(8m)^{1/2}} \int_0^\infty \frac{f(E)\,\mathrm{d}E}{E^{1/2}\sum_i n_i Q_{0i}}.$$

Can. J. Chem. Downloaded from www.nrcresearchpress.com by 210.87.254.5 on 09/05/12
For personal use only.

This expression can also be obtained from [2.10] if we recall that $dE/dt = JX = n_e e \bar{v}_e X$. If we substitute [2.12] and [2.14] into [2.6] we obtain the rate expression for a process ij

$$[2.15] \qquad \frac{dn_{ij}}{dt} = \frac{f_{ij}\, Jn_i X}{E_{ij}} = \alpha_{ij} \frac{JX}{E_{ij}},$$

where $\alpha_{ij} = n_i f_{ij}$. If j is any state in the ionizing continuum this equation becomes identical to that used by Schottky (5) when he states that the rate of formation of ion pairs is proportional to a fraction of the current density and the potential gradient and inversely proportional to the ionization energy (his eq. [7]). We have shown here that this equation is quite general and applicable to any inelastic collision process.

An alternate expression for the rate of production of excited species is obtained by combining expression [2.1] with [2.14] and [2.5]:

$$[2.16] \qquad \frac{dn_{ij}}{dt} = \frac{4Jn_i \int_0^\infty f(E)\, Q_{ij} E^{1/2}\, dE}{Xe^2 \int_0^\infty f(E)\, E^{-1/2} \left(\sum n_i Q_{0i}\right)^{-1} dE}.$$

If observations are made in flowing gases through the discharge, the substitution $dt = dx/v_s$ (where v_s = stream velocity) can be made in all above expressions giving then the steady-state expressions.

Further insight into the meaning of f_{ij} and α_{ij} can be obtained by equating [2.15] to [2.16] and solving for f_{ij}

$$[2.17] \qquad f_{ij} = \frac{4E_{ij} \int_0^\infty f(E) Q_{ij} E^{1/2} dE}{X^2 e^2 \int_0^\infty f(E) E^{-1/2} \left(\sum n_i Q_{0i}\right)^{-1} dE}.$$

The value of the field was obtained in [2.11]. We obtain after multiplying by n_i

$$[2.18] \qquad \alpha_{ij} = n_i f_{ij} = \frac{\int_0^\infty f(E) E^{1/2} n_i Q_{ij} E_{ij}\, dE}{\int_0^\infty f(E) E^{1/2} \sum_i \left(n_i \sum_j Q_{ij} E_{ij}\right) dE}.$$

If we multiply both the denominator and the numerator of the right-hand side of [2.18] by $n_e(2/m)^{1/2}$ the denominator is equal to [2.8] and represents the energy spent in inelastic collisions per unit time and volume. The numerator is then the energy spent in the particular process ij and the dimensionless quantity α_{ij} represents the fraction of the total energy spent by electrons per unit volume and time on process ij. [2.15] then means that at constant field and current a constant fraction of the energy will be dissipated in process ij. f_{ij} and α_{ij} are functions of the electron energy distribution.

(E) The Pressure Gradient Due to the Flow

It is nearly impossible to determine a priori the conditions of the gas, or the pressure gradient downstream of the discharge. Indeed, a certain amount of cooling of the gas will occur for that part of the expansion which takes place adiabatically. On the other hand gas heating will occur as a result of electrons losing energy in elastic collisions or in inelastic collisions followed by energy-transfer processes. In addition to this a certain degree of turbulence will exist which will reduce the importance of transverse gradients in the concentration and the velocity of the gases in the tube.

Can. J. Chem. Downloaded from www.nrcresearchpress.com by 210.87.254.5 on 09/05/12
For personal use only.

Can. J. Chem. Downloaded from www.nrcresearchpress.com by 210.87.254.5 on 09/05/12
For personal use only.

As we are mainly interested experimentally in the stream velocity, and the way it varies while the gases proceed downstream, we prefer to measure the pressure gradient at a number of takeoff points along the discharge tube. Any decrease in pressure will be the result of a density decrease corrected for any change in temperature. The increase in stream velocity is then given empirically by the decrease in pressure. For analytical purposes it is convenient to have a mathematical expression to fit the measurements; this is easily done by expressing the pressure as a power series

$$p = \sum_n p_n x^n. \qquad [2.19]$$

If v_s is the stream velocity, D (in volume units per unit time at 760 Torr) the measured total flow of the gas admitted to the discharge, and A the cross section of the tube, then

$$v_s(x) = \frac{D}{A} \frac{760}{\sum_n p_n x^n}. \qquad [2.20]$$

(F) Ion and Electron Concentration in the Positive Column and Influence of the Flow

We assume the discharge tube to be cylindrical and of radius R. An ion formed at a distance r from the axis will drift in the transverse field during its lifetime τ a distance

$$R - r = \int_0^\tau (\bar{v}_+)_{Tr}(x,r)\, dt. \qquad [2.21]$$

x is the distance along the axis from the boundary separating the anode layer from the positive column. $(\bar{v}_+)_{Tr}$ and $(\bar{v}_+)_A$ are the drift velocities of the ions in the transverse and axial fields respectively. During this time τ an ion will drift a distance Λ in the axial direction where Λ is given by

$$\Lambda = \int_0^\tau (\bar{v}_+)_A(x,r)\, dt. \qquad [2.22]$$

In order to express $R - r$ as a function of x we calculate τ. Since $(\bar{v}_+)_A = dx/dt$, we have

$$\tau = \int_0^\tau dt = \int_0^x \frac{dx}{(\bar{v}_+)_A}. \qquad [2.23a]$$

By introducing this value of τ in the expression of $R - r$ (eq. [2.21]) we obtain the value of r as a function of x.

We can similarly write

$$\tau = \int_0^\tau dt = \int_r^R \frac{dx}{(\bar{v}_+)_{Tr}}. \qquad [2.23b]$$

When $r = 0$, that is when the ion is formed on the axis, $\tau \equiv \tau_0$. If this value τ_0 is introduced into [2.22] we obtain the maximum value of $\Lambda \equiv \Lambda_0$.

Although we have assumed a turbulent flow field, the molecular velocities are normally very much smaller than the ion drift velocities and we thus neglect the perturbation of the ion concentration profile due to turbulence of the gas stream. This approximation begins to break down in very small fields ($\lesssim 1$ V cm^{-1}). Under very fast flow conditions v_s, the stream velocity, cannot be neglected in the previous equations; $(\bar{v}_+)_A$ will then have to be replaced by the sum of the drift velocity and the stream velocity, viz. $(\bar{v}_+)_A + v_s$. Unless $\Lambda \ll (R - r)$, the ion concentration will increase in that part of the positive column in the vicinity of the anode. The above condition is realized when the transverse field is much larger than the axial field. This is usually the case in wide tubes in discharges through monatomic gases. However, in discharges through molecular gases or in dis-

charges in tubes of medium or small diameter (say less than 3 cm) and in electronegative gases, the transverse field is rather small and the last condition is nearly always realized. The ion concentration will then increase over a distance Λ_0 from the anode. We now calculate approximately the magnitude of this increase in concentration. In the absence of negative ions Schottky (5) has shown that, in a static gas, the ion number density $(n_+)(x, r)$ at a distance r from the axis of the discharge tube is equal to the ion density on the axis $n_+(x, 0)$ times a Bessel function of zero order in $r(a/D_a)^{1/2}$ (16, p. 122).

$$[2.24] \qquad (n_+)_{r=r} = (n_+)_{r=0} J_0[r(a/D_a)^{1/2}],$$

where D_a is the ambipolar diffusion coefficient and a the number of ions produced per unit time per electron. When $r(a/D_a)^{1/2} = 2.405$ the value of the Bessel function is zero and for larger values of $r(a/D_a)^{1/2}$, the function becomes negative. Since ion concentrations that are negative have no physical meaning we impose the further boundary condition that at $r = R$, the radius of the discharge tube, $R(a/D_a)^{1/2} = 2.405$. Thus

$$[2.25] \qquad (n_+)_{r=r} = (n_+)_{r=0} J_0\left(2.405 \frac{r}{R}\right).$$

Inherent in Schottky's theory is the assumption of uniform production of ions in a section of the discharge perpendicular to the axis.

We now calculate the increase in ion concentration when $0 < x < \Lambda_0$. The number of positive ions in a slice across the discharge of width dx at the point of entry of the gases in the positive column will be given by the integral from 0 to R, of the ion concentration in a ring $2\pi r\, dr$, viz.

$$\int_0^R 2\pi r n_+(0,0)\, J_0\left(2.405 \frac{r}{R}\right) dr\, dx.$$

At a point $x = x$ we obtain a similar expression with the term $n_+(x,0)$ replacing $n_+(0,0)$. The difference between these two terms is equal to the excess of ions formed over those lost by recombination at the walls. The number of ions formed while the gas proceeds from $x = 0$ to $x = x$ is given by [2.15] in which we make the substitution $dt = dx/(v_s + (\bar{v}_+)_A)$. v_s is given by [2.20]. The number of ions lost in this slice is equal to the number of ions which have reached the wall. Thus

$$[2.26] \quad \int_0^R 2\pi r n_+(0,0)\, J_0(2.405)\, dr\, dx = \int_0^R 2\pi r n_+(0,0)\, J_0\left(2.405 \frac{r}{R}\right) dr\, dx + \int_0^x \sum_i \frac{f_i}{v_s + (\bar{v}_+)_A} n_i \frac{JX}{E_1} \left\{ \int_0^R 2\pi r\, dr\, dx \right\} dx - \frac{1}{x} \int_0^x \int_r^R 2\pi r n_+(x,0)\, J_0\left(2.405 \frac{r}{R}\right) dr\, (dx)^2.$$

The second term on the right-hand side of this equation expresses the production of ions in the discharge, E_1 being the ionization energy; the last term is the loss term. Since $n_+(x,0)$ is independent of r we can integrate all terms with respect to r. If we remember that $xJ_0(x)\, dx = d(xJ_1(x))$ (30) and that $J_1(2.405) = 0.519$, eq. [2.26] becomes

$$[2.27] \quad n_+(x,0) = n_+(0,0) + 2.316 \int_0^x \frac{\sum_i f_i}{v_s + (\bar{v}_+)_A} \frac{n_i JX}{E_1} dx - \frac{1}{x} \int_0^x n_+(x,0) \left\{ 1 - \frac{1}{0.519} \frac{r}{R} J_1\left(2.405 \frac{r}{R}\right) \right\} dx.$$

Can. J. Chem. Downloaded from www.nrcresearchpress.com by 210.87.254.5 on 09/05/12
For personal use only.

In the above two equations the value of r in terms of x is given by [2.21] and [2.23a]. When $x = \Lambda_0$ this becomes

$$[2.28] \quad n_+(\Lambda_0,0) = n_+(0,0) + 2.316 \int_0^{\Lambda_0} \sum_i \frac{f_i}{v_s + (\bar{v}_+)_A} \frac{n_i JX}{E_i} \, dx - \frac{1}{\Lambda_0} \int_0^{\Lambda_0} n_+(x,0) \, dx.$$

For values of $x > \Lambda_0$ no further increase in ion concentration will occur if f_i is independent of x; that is the electron energy distribution remains constant.

If negative ions are present or volume recombination occurs Seeliger (8) has shown that the Bessel concentration profile will change to that given by an elliptic function. Qualitatively, however, this will not affect the above conclusions and we have not attempted to solve the equations under these conditions.

(G) Radical Concentration in the Positive Column

In addition to ions, a large number of molecules in excited states, atoms, and radicals will be formed in the discharge. The radicals formed in an impact may either further dissociate during subsequent electron impacts or they may react chemically with other molecules either in the gas phase or at the walls. Excited species will lose energy through the emission of photons. Steady-state conditions will be established as soon as the rate of production becomes equal to the rate of loss. The production term will be of the form [2.15] if the collision cross section for the reactive collision with an electron having the necessary energy is of the same order of magnitude as the elastic cross section for less energetic electrons; E is then the dissociation energy of the bond being broken. If dissociation occurs via an antibonding state this energy will be somewhat larger. The loss term will be the sum of all the rate expressions describing the disappearance of radicals or excited species. Some of these terms will be first-order in the radical concentration (reaction of radicals with other (stable) molecules or emission of a photon); second-order terms describe radical recombination in tri-body collisions or in radiative processes.

We assume that whenever a first-order process leading to the disappearance of radicals produced in the discharge can occur, the magnitude of the rate term will be such that it dominates the loss term; other terms, second order in radical concentration, will be, at most, small correction terms. Under these conditions concentration gradients and diffusion processes will be negligibly small. Only if no first-order process can occur (such as in the dissociation of a diatomic gas in the discharge), will recombination reactions become important. Recently Young and Sharpless (31) have obtained evidence that, even at low pressures, tri-body recombination processes have to be taken into account. Whenever the lifetime of an excited molecule or radical is small, deactivation will occur mostly via emission of a photon. Under these conditions the emission intensity will be proportional to the total concentration of the radical in the gas phase, unless a simultaneous production of the radical or molecule in the excited state takes place via a reactive collision or an energy-transfer process (chemiluminescent emission[5]).

Whenever processes first order in the radical concentration dominate the loss term, the change in number density with distance of an excited species or a radical n_i will be given by

$$[2.29] \quad \frac{dn_i}{dx} = \frac{f_i}{v_s + (\bar{v}_+)_A} \frac{n_i JX}{E_i} - k_{im}' n_i n_m.$$

[5] *Under fast-flow conditions the number of collisions between an impurity and excited molecules during the time the gas moves a small distance is small and hence excitation of these impurities via energy-transfer and chemiluminescent processes will be characterized by an emission intensity which increases over a greater distance than processes in which the excited state is produced by electron impact directly.*

Can. J. Chem. Downloaded from www.nrcresearchpress.com by 210.87.254.5 on 09/05/12
For personal use only.

k_{im}' is the bimolecular rate constant for the reaction of radical i (number density n_i) with molecules of type m (number density n_m). If one of the k_{im}' values in the loss term is very large and leads to a stable product, monitoring the increase in the number density of the product will permit a measure of the magnitude of the production term.

3. DISCUSSION AND COMPARISON WITH EXPERIMENT

In Section 2 we have derived a set of equations which will be helpful in evaluating and interpreting experimental results obtained in this laboratory. Although a detailed analysis at this time is not yet possible, it was felt necessary to present in an accompanying paper (3) the results of a general survey of the oxygen discharge, in which evidence is presented for some of the models which were analyzed in this paper. The extent of the inhomogeneous zone in the positive column due to the increase in the ion concentration in the vicinity of the anode, as analyzed in Section 2F, is controlled primarily by the size of the ratio of the longitudinal electric field to the transverse field. We have found that many discharge modes are possible in an oxygen discharge, and in one of them the above ratio is much larger than 1. In this discharge we have also obtained evidence of an increasing ion concentration at the head of the positive column, which is as expected. In most gases (especially the inert gases), however, the field ratio is much smaller and hence the inhomogeneous region will be much shorter; its observation will then become much more difficult, if at all possible. It should be pointed out that the stream velocity of the gas will cause an extension of this region, but this effect will be much smaller than the effect of the ratio of the electric fields. Quantitative calculations cannot be performed for oxygen as yet because of the presence of negative ions (32, 33). The eqs. [2.24] to [2.28] will have to be rederived for a non-Bessel ion-density profile (34).

We will also be interested in analyzing the results of spectroscopic and other measurements performed in this laboratory on flowing gases in the discharge. From [2.15] it is seen that a change in the emission intensity of a spectral feature in the positive column can be due to a change in any of the parameters appearing in that equation. By choosing a system which experimentally gives X and J constant, it is possible to study chemical reactions and excitation processes in the discharge. A chemical reaction causes a change in n_i, and the rate of these processes can thus be determined by monitoring this change. Two interfering effects are possible: (i) significant pressure gradients can be produced along the column if the tube diameter is relatively small and the pumping capacity large (they introduce a nonchemical change in the value of n_i); and (ii) any change in the electron energy distribution function would cause a change in the $\alpha_{ij} = n_i f_{ij}$ factor. In ref. 1 an example is given where it was shown that changes in the intensity of emission of atomic oxygen lines were proportional to the concentration of atomic oxygen while in ref. 2 it was shown that the change in intensity of emission of CO in a carbon monoxide – oxygen mixture was due to changes in the f_{ij} factor.

If the electron energy distribution is Maxwellian it can be written in terms of an electron temperature T, viz.

$$[3.1] \qquad f(E) = 2E^{1/2}(\pi k^3 T^3)^{-1/2} \exp(-E/kT).$$

We further assume that in a first approximation the elastic collision cross section Q_0 is constant. Experimentally it is found that $Q_0(E)$ varies by a factor of 2 or 3 over the energy range over which there is an appreciable population of electrons (26). The inelastic collision cross section can also be approximated by a constant in the interval $E_{ij} < E < \infty$ because at very high energy the electron population becomes vanishingly small; for values

Can. J. Chem. Downloaded from www.nrcresearchpress.com by 210.87.254.5 on 09/05/12
For personal use only.

of $E < E_{ij}$ the inelastic collision cross section is zero. Under these assumptions eq. [2.16] can be written

$$[3.2] \qquad \frac{dn_{ij}}{dx} = AkT\left(\frac{E_{ij}}{kT} + 1\right)\exp\left(-E_{ij}/kT\right),$$

where k is the Boltzmann constant and

$$[3.3] \qquad A = 4Jn_i \sum n_i Q_{ij} Q_{0i}/(v_s Xe^2).$$

The drift velocity [2.14] becomes

$$[3.4] \qquad \bar{v}_e = Xe/[(2\pi mkT)^{1/2} \sum n_i Q_{0i}].$$

If changes in the emission intensity of a species present in the discharge is due to a change in the electron temperature along the positive column, we can write the ratio of [3.2] for two values of x as

$$[3.5] \quad \ln \frac{(dn_{ij}/dx)_{x=0}}{(dn_{ij}/dx)_{x=x}} = \ln \frac{T_0}{T} + \left(\ln \frac{E_{ij}}{kT_0} + 1\right) - \left(\ln \frac{E_{ij}}{kT} + 1\right) - \frac{E_{ij}}{k}\left(\frac{1}{T_0} - \frac{1}{T}\right).$$

If the lifetime of the excited state j is short enough, we can put $\sum_i dn_{ij}/dx$ for all excitation processes leading into the state j proportional to the emission intensity from this state at any point in the discharge. Thus

$$[3.6] \qquad \ln \frac{I}{I_0} = \ln \frac{E_{ij} + kT}{E_{ij} + kT_0} - \frac{E_{ij}}{kT_0}\left(\frac{T_0 - T}{T}\right).$$

E_{ij} is the energy of excitation of level j, and i is the ground state of the emitting species. If T_0 is known we can thus calculate the drop in temperature associated with a given change in the intensity of emission along the positive column. If we assume E_{ij} to be about 12 eV and T to be 10 000 °K the decrease in temperature which accounts for a drop in intensity of about 40% is of the order of 200 °K while if $T_0 = 50\,000$ °K, the required decrease in electron temperature is about 4 000 °K.

ACKNOWLEDGMENTS

The authors wish to thank Professor J. P. Valleau for many stimulating discussions. He also read the manuscript and made many suggestions for its improvement.

It is a real pleasure to acknowledge support in the form of grants from the United States Air Force through the Office of Scientific Research (Propulsion Research Division), from the National Research Council of Canada, and from the University of Toronto.

One of us (J. L. P.) is indebted to Professor A. Van Tiggelen of the University of Louvain (Belgium) for allowing a year's leave of absence to study at the University of Toronto.

H. W. R. is indebted to the N.R.C. for the award of a bursary.

REFERENCES

1. P. A. Bois d'Enghien and J. M. Deckers. Can. J. Chem. **42**, 1792 (1964).
2. M. Ailliet and J. M. Deckers. To be published.
3. H. W. Rundle, K. A. Gillespie, R. M. Yealland, R. Sova, and J. M. Deckers. Can. J. Chem. This issue.
4. W. Schottky. Physik. Z. **25**, 342 (1924).
5. W. Schottky. Physik. Z. **25**, 635 (1924).
6. T. R. Conner and M. A. Biondi. Phys. Rev. **140**, A778 (1965).
7. E. Spenke. Z. Physik, **127**, 221 (1950).
8. R. Seeliger. Ann. Physik, **6**, 93 (1949).

Can. J. Chem. Downloaded from www.nrcresearchpress.com by 210.87.254.5 on 09/05/12
For personal use only.

9. G. ECKER. Proc. Phys. Soc. London, **67**, 485 (1954).
10. E. H. LUDWIG. Z. Angew. Phys. **5**, 377 (1953).
11. G. ALBRECHT, G. ECKER, and K. G. MÜLLER. Z. Naturforsch. Pt. a, **17**, 854 (1962).
12. M. J. DRUYVESTEYN. Physica, **3**, 65 (1936).
13. M. J. DRUYVESTEYN and F. M. PENNING. Rev. Mod. Phys. **12**, 87 (1940).
14. F. MOHLER. Bur. Standards, J. Research, **9**, 493 (1932).
15. R. SEELIGER and A. WICHMANN. Ann. Physik, **9**, 235 (1951).
16. G. FRANCIS. *In* Handbuch der physik. Vol. XXII. *Edited by* S. Flügge. Springer-Verlag, Berlin. 1956. p. 53.
17. J. WILHELM. Ann. Physik, **15**, 148 (1955).
18. E. MAIER. Z. Physik, **93**, 65 (1934).
19. R. ROMPE and M. SCHON. Z. Physik, **108**, 265 (1938).
20. E. H. LUDWIG. Z. Angew. Phys. **5**, 421 (1953).
21. W. P. ALLIS. *In* Handbuch der physik. Vol. XXI. *Edited by* S. Flügge. Springer-Verlag, Berlin. 1956. p. 401.
22. D. H. SAMPSON. Phys. Rev. **137**, A4 (1965).
23. J. M. ANDERSON and L. GOLDSTEIN. Phys. Rev. **102**, 388 (1956).
24. G. J. SCHULTZ. Phys. Rev. **116**, 1141 (1959).
25. G. J. SCHULTZ. Phys. Rev. **125**, 229 (1962).
26. J. B. HASTED. Physics of atomic collisions. Butterworths, London. 1964. p. 179.
27. H. S. W. MASSEY. *In* Handbuch der physik. Vol. XXXVI. Sect. 11. *Edited by* S. Flügge. Springer-Verlag, Berlin. 1956. p. 329.
28. G. MIERDEL. Wiss. Veröffentl. Siemens-Werken, **17**, 71 (1938).
29. T. WASSERRAB. Z. Physik, **127**, 324 (1950).
30. H. WAYLAND. Differential equations in science and engineering. D. Van Nostrand Co., Inc., New York. 1957. p. 170 (problem 5.21).
31. R. A. YOUNG and R. L. SHARPLESS. J. Chem. Phys. **39**, 1071 (1963).
32. J. B. THOMPSON. Proc. Roy. Soc. London, Ser. A, **262**, 503 (1961).
33. J. B. THOMPSON. Proc. Phys. Soc. London, **73**, 818 (1959).
34. G. ALBRECHT and G. ECKER. Z. Naturforsch. Pt. a, **17**, 848 (1962).

Can. J. Chem. Downloaded from www.nrcresearchpress.com by 210.87.254.5 on 09/05/12
For personal use only.

CHEMICAL REACTIONS IN ELECTRICAL DISCHARGES

III. THE POSITIVE COLUMN IN D-C. GLOW DISCHARGES THROUGH OXYGEN[1]

H. W. RUNDLE, K. A. GILLESPIE, R. M. YEALLAND, R. SOVA, AND J. M. DECKERS
Lash Miller Chemical Laboratories, University of Toronto, Toronto, Ontario

Received June 6, 1966

ABSTRACT

Discharges through fast-flowing oxygen have been investigated. It has been shown that the electrical field remains constant in the positive column of a particular mode, even in the presence of a large pressure gradient. It was found that five types of discharges could be distinguished and they can be characterized by fluctuations of the voltage at the electrodes. These oscillations are linked with the absence or presence of travelling waves in the column. The conditions of existence of the various discharges are outlined. It has also been shown that the structure of the positive column is not as homogeneous as previously thought. In particular, even at constant field, changes in the electron temperature and the number density of charged species are shown to occur. The change in electron temperature and the presence or absence of oscillations have been shown to affect the rate of production of atomic oxygen and the emission intensity of the spectrum of these discharges.

1. INTRODUCTION

In this paper we report our observations on the positive column of a glow discharge through fast-flowing oxygen. In 1927 Güntherschulze (1) reported the existence of two types of d-c. glow discharges in oxygen. In fairly narrow tubes he observed a grey-green discharge, whereas in wide tubes the discharge appeared violet. In that paper he also pointed out that the longitudinal field in the positive column was much larger in the grey-green discharge than in the violet one. Seeliger (2) and Seeliger and Wichmann (3) further investigated these two discharges and found that with increasing pressure and (or) with decreasing current, the discharge characterized by a high value of the field in the positive column (hereafter referred to as the high field discharge) would switch to the low field discharge. They described the high field discharge as blue and having a core lightly violet, whereas the low field discharge was described as grey blue. In the high field discharge the local value of the field, constant in time, was equal to the value of the field averaged over the whole length of the positive column; whereas in the low field discharge the local field value could deviate by as much as 20% from the average value. The high field discharges displayed predominantly the atomic oxygen spectrum and no ozone formation was observed. The low field discharge displayed the "negative band spectrum" and formed ozone in substantial amounts. Although they (2, 3) mentioned that oxygen could form negative ions, they did not suggest a mechanism by which these negative ions could be responsible for the occurrence of the two types of discharges.

Thompson (4, 5) has estimated the influence of the presence of negative ions on the positive column and he has shown both experimentally and theoretically that the transverse field in the presence of negative ions is much smaller than it is in non-electronegative gases. The ratio of the number density of negative ions to electrons under his operating conditions was estimated to be about 20 to 1. The influence of negative ions on the conditions in the positive column was further discussed theoretically by Albrecht and Ecker (6).

[1]*Supported by grants from the U.S. Air Force Office of Scientific Research (AF–AFOSR 63-375, 64-375, and 65-375), the National Research Council of Canada, and the University of Toronto.*

Can. J. Chem. Downloaded from www.nrcresearchpress.com by 210.87.254.5 on 09/05/12
For personal use only.

Can. J. Chem. Downloaded from www.nrcresearchpress.com by 210.87.254.5 on 09/05/12
For personal use only.

Oscillatory phenomena, occurring in the d-c. glow discharge, were observed by Dieke, Loh, and Crosswhite (7) and by Loh and Dieke (8); the correlation between the oscillations of the current density or the applied voltage and the emitted light intensity was established by Donahue and Dieke (9) and shown to be due to fast-moving striations ($\sim 10^5$ cm s^{-1}), even when the column appeared uniform and unstriated to the naked eye. Pekarek and Šicha (10) established the presence of fast-moving striations in the low field discharge described by Seeliger and Wichmann. No oscillations were found to occur in the high field discharge. Recently Miller (11) presented some data on the value of the electrical field in the positive column as a function of current and pressure.

We have extended these observations and found the oxygen discharge to be even more complicated. More specifically, there are two different low field discharges; the mixed discharges described by Seeliger and Wichmann (3) have some features which would indicate that they should be considered as a distinct type of discharge.

These various discharges can best be distinguished by the oscillations of the potential at the anode. They are characteristic of the type of discharge. In some instances, this oscillation was periodic with a frequency between 5 and 100 kcycles, whereas in other cases it could be completely aperiodic or totally absent. Under otherwise identical conditions the different types of discharges were shown to have different concentrations of oxygen atoms. This clearly established the importance of a better understanding and characterization of the positive column of the glow discharge itself, before attempting to investigate chemical effects produced by the discharge. Indeed, it has been shown by Peeters *et al.* (12) that in order to account quantitatively for the rate of excitation of molecules and for the rate of chemical reactions induced by electron impact in the discharge, the electron number density, the field, and the electron energy distribution must be determined.

2. EXPERIMENTAL

(A) Gas Supply and Handling

Oxygen, tapped from a cylinder (British Oxygen of Canada Ltd.), was passed through a trap, cooled by an acetone – dry ice bath, and used without further purification. In some instances Matheson ultra high purity oxygen was used. It was stated to be at least 99.95% pure, the impurities being N_2 (7.9 p.p.m.), CH_4 (15.8 p.p.m.), CO_2 (3.8 p.p.m.), Kr (13 p.p.m.), and other impurities combined (less than 0.9 p.p.m). After being metered by a capillary flowmeter, the gas expanded to the working pressure through a needle valve and entered the discharge tube through a side arm upstream of the electrode. After passing through the discharge tube, the gases were pumped out via another side arm by a mechanical pump. A throttling valve in the line to the pump allowed us to change the gas velocity and the pressure in the discharge tube. The pressure could be measured at either end of the discharge tube by means of a tilting-type McLeod gauge.

(B) The Discharge Tube

The discharge tubes were made from Pyrex tubing of various diameters. At both ends of the tube (Fig.1) the electrodes entered via rubber stoppers. These electrodes consisted of copper wire 2 mm in diameter and slightly tapered at the end. A small amount of vacuum grease coated part of the electrodes to facilitate sliding through the rubber stopper. In a few experiments the vacuum pump was connected to the downstream end of the discharge tube by moving the electrode into a side arm. This arrangement did not affect the conditions upstream of the location of the side arm, and permitted the use of electrodes with larger surfaces without interference with the gas stream. Use of these large surface electrodes would often stabilize the discharge. This arrangement was always used when we measured the number of oxygen atoms produced in the discharge.

In several discharge tubes, probes were sealed in every 5 to 10 cm. They consisted of small pieces of platinum wire of 0.1 to 0.25 mm diameter coated with Pyrex glass; the outside diameter of the coated probe was between 1 and 1.5 mm. The tip of the probe was left exposed over a length of 2 to 3 mm and was located as closely as possible to the axis of the discharge tube. To ensure a good vacuum seal at the Pyrex–platinum interface, the outside of the seal was further coated with glyptal paint.

The discharges were sustained by means of NJE regulated variable power supplies (model S326, 327 or 328). A chain of resistors in series with the discharge permitted us to adjust the resistance of the overall circuit. This was of great use when trying to obtain a particular type of discharge when more than one type could be sustained under the operating conditions. The current through the discharge could be adjusted most easily by varying the setting at the power supply.

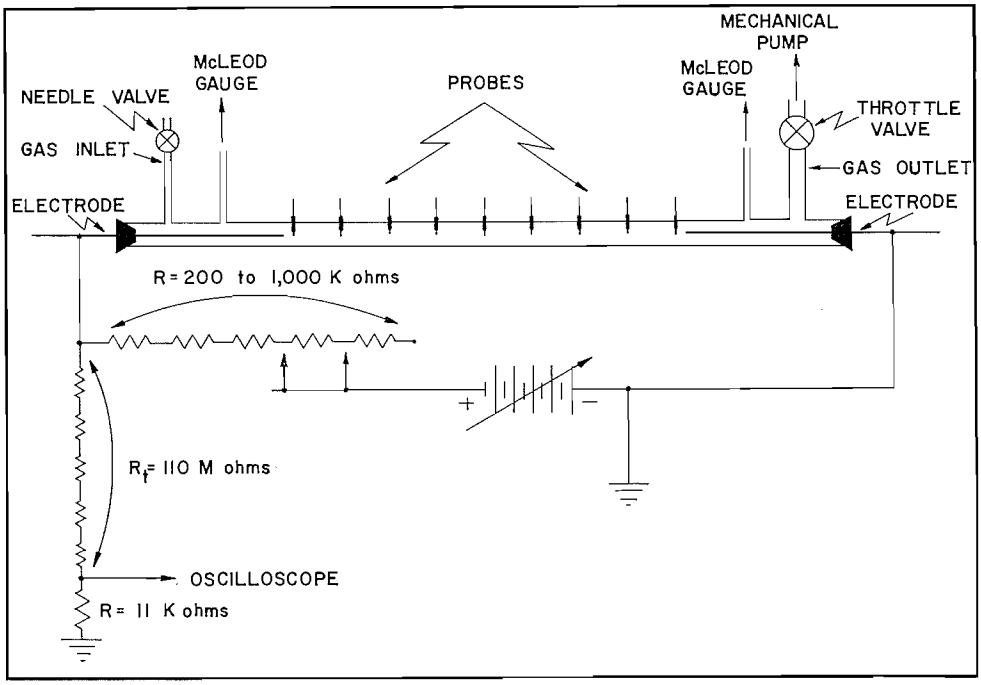


FIG. 1. Schematic of the apparatus.

For spectral measurements, a monochromator (Jarrell-Ash model 82000 with grating blazed at 5 000 Å) was mounted underneath the discharge tube. The spectrum was then recorded by either an 1P21 or an 1P28 photomultiplier tube.

(C) Field Measurements

The fields in the positive column were measured by two methods: the moving electrode and the floating potential techniques. The moving electrode technique consisted of increasing the distance between the two electrodes and measuring the increase in voltage necessary to maintain the discharge at constant current.

The electrode separation was increased a few centimeters at a time and the field determined either by measuring the slope of a plot of voltage versus electrode separation or by fitting a first-order equation to the experimental data by least squares using the IBM 7094 computer of the University of Toronto. The derivative of this equation was then equal to the field.

When using the floating potential technique, we measured the floating potential at a number of probes sealed every few centimeters in the discharge. The fields were then determined either from a plot of the measured potential versus probe location or, as above, by fitting the best first-order equation using the method of least squares. Voltage measurements were made with a Keithley model 610R electrometer, using when necessary, a 1000–1 divider probe having an input impedance of 10^{12} Ω.

(D) Langmuir Probe Measurements

By superimposing small voltages on one of the probes sealed in the discharge tube and by measuring the current drawn from the probe, we obtained the "Langmuir characteristics", from which electron temperatures could be calculated, assuming an equilibrium energy distribution. To superimpose a small voltage on the probe, a large resistance board was mounted in parallel with the discharge tube. It consisted of an arrangement of various size precision resistors. The power supply was left floating for these measurements and one of the takeoffs of this bleeder network, close to the floating potential of the probe, was grounded. The probe was then successively connected to various points of the bleeder and the current drawn from the discharge was measured by means of a Lange multiflex galvanometer (type MG1; sensitivity 2×10^{-8} A per scale division). The potential at the probe was simultaneously measured by means of a Cimron model 6200 A digital voltmeter. With this instrument measurements were always taken on the 0 to 10 V scale to insure an input resistance of 10^{12} Ω (at balance).

(E) Oscillations

To observe and measure the oscillations of the current and voltage, an oscilloscope (Tektronix RM 561 or Philips PM 3230) was connected by means of a voltage divider network (of input impedance not less than

Can. J. Chem. Downloaded from www.nrcresearchpress.com by 210.87.254.5 on 09/05/12
For personal use only.

10^8 Ω) to the off-ground electrode. Enough energy could also be picked up by the probe of the oscilloscope when it was located unconnected (as an antenna) close to the discharge tube itself, although background noise and other spurious signals were also picked up this way.

(F) Measurement of the Oxygen Atom Concentration

When the atomic oxygen produced in the discharge was measured, the downstream electrode was always mounted in a side arm of the discharge tube; the atom concentration was then measured a short distance downstream of the discharge region itself. Two different methods were used: the isothermal calorimeter probe technique (developed by Tollefson and Le Roy (13) and adapted to oxygen by Elias, Ogryzlo, and Schiff (14)) and the gas titration technique (developed by Kaufman (15, 16)).

The catalytic probe used in the isothermal calorimeter was tungsten wire coated with freshly prepared silver. Under these conditions Elias *et al.* (14) indicated that atoms and molecules in excited states would not be deactivated in measurable amounts at the probe. To establish the efficiency of the probe, a small amount of NO was added to the oxygen flow and the green glow due to the recombination reaction $NO + O \rightarrow NO_2^* \rightarrow NO_2 + h\nu$ fell off quite sharply at the probe, when viewed in total darkness. NO_2^* denotes an electronically excited NO_2 molecule.

The power supply for the bridge was an NJE QR-36-10, the potentiometer a Leeds and Northrup K33, and the bridge null detector a Lange multiflex type MG1 galvanometer (1 μV off-balance sensitivity). The probe itself could be moved closer to, or farther from, the discharge in order to determine the amount of recombination taking place between the discharge and the probe.

Gas titrations, using NO_2, were done through a small gas inlet located about 10 cm downstream of the side arm in which the downstream electrode was located. The extinction point of the NO_2 glow was determined by eye or by using a photomultiplier tube.

3. RESULTS

(A) General Survey of Types of Oxygen Discharges

In this section we will qualitatively categorize the various types of oxygen discharges that we observed between 0.5 and 5 Torr, listing their properties and the conditions under which they are obtained. A comparison of these results with those obtained by Seeliger and Wichmann (3) appears in Section 4.

These results are primarily those of observations taken in discharge tubes of 10 to 15 mm diameter and at a current density of about 5×10^{-3} A cm^{-2}. The pressure region investigated was 0.5 to 5 Torr, measured near the anode at the entrance point of the gas into the discharge. A pressure gradient of not more than 0.4 Torr (depending on the electrode separation, the stream velocity of the oxygen, and the tube diameter) was always present; the values quoted for the pressure were those taken at the anode unless otherwise stated. To observe the various types of discharges the mass flow of oxygen and the discharge current density were kept constant while the pressure was varied using the throttling valve in the pumping line. This was done for several mass flows of between 0.5 and 2.0 cm^3 s^{-1} at standard temperature and pressure, which represent upstream velocities in the range of 0 to 10 m s^{-1}. The observations are summarized in Table I and the different types of discharges have been assigned Roman numerals.

Below 1.5 Torr the type I discharge occurs exclusively. The positive column is a fairly intense pink color and appears uniform and unstriated at higher stream velocities. At lower stream velocities several stationary striations would appear on the anode side of the platinum probes and would become more prominent at lower pressures. The electric field in the column is quite constant and has values between 20 and 60 V cm^{-1} depending on the pressure (fields of this magnitude are referred to as high fields in Table I). No oscillations occur in the range 10 to 10^7 c.p.s. (other than some residual 60 c.p.s. noise of amplitude less than 0.01% of the anode potential). Under favorable conditions of electrode separation and current, it is often possible to obtain the type I discharge up to pressures of about 4 Torr. Above 1.5 Torr the high field discharge becomes unstable in that it might spontaneously shift to a type II or type III discharge. This phenomenon of switching to other types of discharges is less likely to occur at higher flow velocities and is also

Can. J. Chem. Downloaded from www.nrcresearchpress.com by 210.87.254.5 on 09/05/12
For personal use only.

TABLE I
Type of discharge and characteristics

Type	Pressure range (Torr)	Color of the positive column	Electric field in the positive column	Anode oscillations	
				Frequency (kcycles)	Amplitude (% of anode voltage)
I	0.5–4.0	Pink	High	Absent	
II	1.5–5.0	Grey-violet	Low	10–100	5–10% (20–100 *V*)
III	2.5–5.0	Grey-violet	Lower than II	Aperiodic	
IV*a*	1.6–1.8	Predominantly pink	High at anode lower at cathode		(200–400 *V*)
IV*b*	2.0	Pink near cathode grey-violet near anode	Low at anode higher at cathode	5–10	15–25%

sensitive to the presence of foreign material (e.g. sputtered copper or copper oxide from the electrodes) on the tube wall. To observe the high field discharge, the discharge tube had to be cleaned periodically with dilute nitric acid (followed by copious rinsing with distilled water).

Type II discharges are characterized by periodic oscillations of the anode potential in a frequency range of 10^4 to 10^5 c.p.s. The amplitude is small (5–10% of the anode voltage) and the wave form is rather complex. Although the oscillation frequency and the amplitude of the oscillations would remain fairly constant under given conditions, exact reproduction of the pattern is difficult, owing to a marked dependence upon discharge conditions. The electric field in the positive column is constant and in the range of 10 to 15 V cm^{-1} (referred to as low field discharge in Table I). The color of the column is quite different from that of type I discharges, but at the currents used its intensity is so low that the best description we could give it is a grey-violet color. It appears completely uniform and exhibits neither stationary nor visible moving striations under any conditions of pressure and gas stream velocity. The low field discharge, which is usually obtained, is the type III discharge. It is in many respects similar to a type II discharge, the main distinguishing feature being that the anode oscillations are completely aperiodic. The pressure ranges in which these two types of discharges are observed are almost the same, and spontaneous switching back and forth between the two discharges can occur. Again, switching to another type of discharge could be induced by the presence of a Tesla coil, keeping the potential across the discharge electrodes low compared with what is required for a type I discharge. The positive column is visually indistinguishable from a type II discharge and the electric field is in the same range.

In addition to the above types of oxygen discharges, two distinct transition regions could be observed. These have been labelled type IV*a* and IV*b* discharges in Table I.

Type IV*a* occurs over a wide pressure range (2–5 Torr) and has a characteristic anode oscillation which is nearly sinusoidal (although at times more or less distorted depending on the other discharge parameters). The frequency is lower than that of type II discharges ($\sim 10^4$ c.p.s.) but the amplitude of the oscillations is considerably larger (15 to 30% of the anode voltage). The electric field in the positive column is not constant axially. The positive column has two distinct regions, each of which has a different constant field. It is

Can. J. Chem. Downloaded from www.nrcresearchpress.com by 210.87.254.5 on 09/05/12
For personal use only.

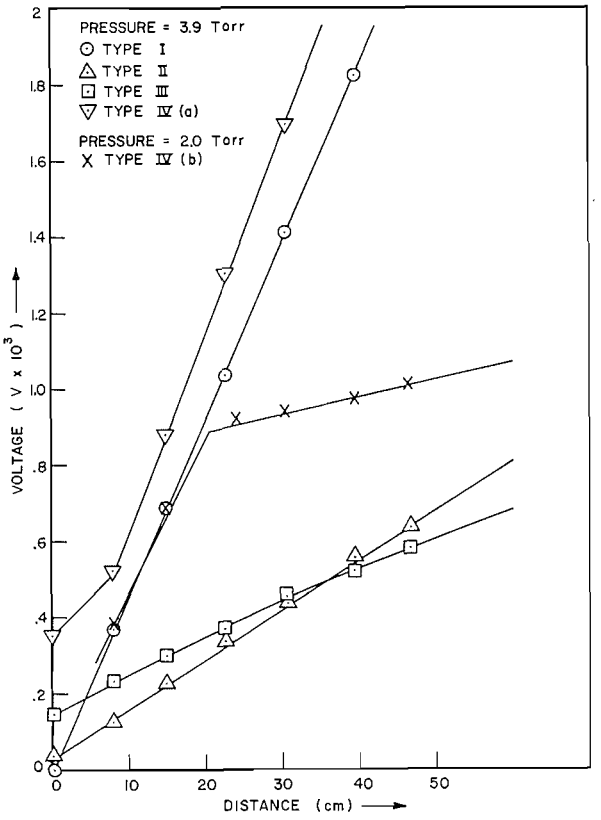


FIG. 2. Probe voltage versus distance along the positive column (from cathode to anode) for the various types of discharge. Tube diameter 12.6 mm; current density 7.4×10^{-3} A cm^{-2}; flow velocity 224 cm s^{-1}.

higher near the anode, and the value of the higher field is generally greater than the field of a type I discharge under similar conditions. The color of the column is predominantly pink and appears uniform, but because of the low intensity it is possible that it does contain some grey violet. A curious point of interest is that the platinum probes about halfway along the discharge tube (near the center of the column) would invariably be surrounded by a glow in this type of discharge. Unless the discharge parameters were changed very slowly the discharge would merely pass from a type II or type III directly into a type I discharge or vice versa, without establishing the characteristic pattern of a type IV discharge on the oscilloscope.

In addition to the above discharge, another more obvious transition type of discharge (IV*b*) could be obtained over a very narrow pressure range (1.5–2 Torr). The positive column is a visible mixture of pink near the cathode and grey violet near the anode. The electric field is high in the pink region and low in the grey violet. The low field part is similar to that of the type II or type III discharge but the value of the high field seems less than that of a type I discharge. Indeed, the anode oscillation was visibly flickering back and forth between the aperiodic pattern of the type III discharge and the kcycle pattern of the above-mentioned type IV*a* discharge. In many cases this made it impossible to obtain reliable field values. The probes near the center of the tube that would be glowing for the type IV*a* discharge would have a flickering glow in step with the anode flickering.

Can. J. Chem. Downloaded from www.nrcresearchpress.com by 210.87.254.5 on 09/05/12
For personal use only.

The region of stability of the type IV discharges often depends on other discharge parameters such as electrode separation and current. If the electrode separation is too small, only the low field discharge will appear. When the electrode separation is increased it is always the higher field portion of the positive column which extends.

Some rough measurements were taken at other tube diameters (up to 2.5 cm), and the observations are comparable. Values of the high and low field discharges will both increase or decrease when the radius of the discharge tube is decreased or increased respectively.

When very small amounts (0.1%) of gases more electronegative than O_2 such as NO_2 or Br_2 were added to the oxygen passing through a type I discharge at pressures at which other types of discharges could be obtained, the transition would immediately occur. At pressures below those at which type II or III discharges could be sustained, oscillation resembling those of type IV discharges would sometimes appear and the current density would increase. However, the operating conditions could not be made stable enough to actually measure the field.

(B) Field Measurements

Fields were measured by two methods: the moving electrode and the floating probe. Fields measured by both methods in identical discharges compare rather favorably, and the disagreement between the two methods could usually be traced to the accuracy to which the pressure, the flow, and the current density in the discharge could be reproduced or measured. Table II gives some values of fields measured by the floating probe technique at various discharge pressures and two values of the current. These measurements were taken at a stream velocity of 336 cm s^{-1}. It was observed that changing the stream velocity within the range investigated (1 to 10 m s^{-1}) had little effect on the field of a type I discharge. Several values of the fields in the different types of discharges are given for

TABLE II

The field X in the positive column of a d-c. glow discharge through oxygen as measured by the floating probe techniques for the various types of discharges (tube diameter 1.26 cm; flow velocity at anode 336 cm s^{-1}; pressure difference between anode and cathode 0.2 to 0.3 Torr)

	Electrical field (V cm^{-1}) for type of discharge				
			III*		
Pressure (Torr)	I	II	Anode	Cathode	IV*a* Anode
Current density 3.7 × 10^{-3} A cm^{-2}					
0.73	16.3				
1.27	26.0				
1.82	31.7				
2.37	38.7		12	—	
2.92	46.7		10.7	8	
3.65			9.5	9.5	
4.4			9.3	12.4	
4.9			9.0	12.8	
Current density 7.4 × 10^{-3} A cm^{-2}					
0.73	15.3				
1.27	23.5				
1.82	28.1				
2.37	33.8				
2.92	41.6				40.0
					43.3
3.65		9.5			
4.4			8.7	11.1	
4.9			11.6	11.6	

*Field changes slightly; the values given are at anode and cathode respectively.

Can. J. Chem. Downloaded from www.nrcresearchpress.com by 210.87.254.5 on 09/05/12
For personal use only.

comparison. Figure 2 illustrates the various types of discharge, giving some of the voltage versus distance curves from which the field values were calculated. The curves are labelled as to the type of discharge they represent and many of the features of the electrical field, which were mentioned in Section 3A, can be seen in them. Particularly noteworthy are the linearity of the type I, the change of the field in the type IV*a*, and the slight curvature of the type III curve.

As can be seen from Table II, there is a marked influence of the pressure on the value of the field in a type I discharge. The field is observed to increase with pressure approximately as $P^{2/3}$. To a slightly smaller degree there is also an influence of the pressure on the high field part of the type IV*a* discharge. Further studies on the pressure dependence of the field are now being carried out and will be reported when completed. The one curious feature to note is that despite the strong dependence of the field on the pressure and its slight dependence on the stream velocity, it remains constant along the positive column even in the presence of large pressure gradients.

This was particularly apparent in those measurements which were made at high flow velocities in a fairly narrow tube (inside diameter 7 mm) using the moving electrode technique. Under these conditions the pressure gradient is large (up to 1.5 Torr), and we expected the value of the field to be determined by the local pressure. However, this is not so, since a plot of applied potential versus electrode separation is linear within experimental error.

(C) Langmuir Probe Measurements

Figure 3 shows typical Langmuir characteristics taken in the positive column of a type I discharge in the immediate vicinity of the anode. The linearity of these curves establishes that the electron energy distribution is Maxwellian and hence an electron temperature has significance. Pressure limitations on the interpretation of the Langmuir characteristics restricted all probe measurements to type I discharges in the pressure range of 0.5 to 1.5 Torr.

Our results indicate that the electron temperature increases immediately adjacent to the anode (<1.0 cm) and then begins to decrease in the next few centimeters. Langmuir characteristics were also taken at various intervals further along the column (up to 30 cm from the anode). However, these curves became increasingly nonlinear beyond about 3 to 5 cm; a temperature could thus not be measured nor its variation established over the entire length of the positive column. The nonlinearity of the characteristics shows that the energy distribution becomes non-Maxwellian. It is probable that negative ions being formed by electron attachment are responsible for this behavior. An actual measurement of the distribution by the method of Boyd and Twiddy (17) should clarify the situation. The Langmuir characteristics have established that the electron temperature increases before decreasing along the positive column away from the anode. This variation will be interpreted in Section 4 in the light of other experimental observations made in this laboratory.

(D) Atom Concentration Measurements

Atom concentrations were measured by two methods: the calorimetric probe and the NO_2 gas titration technique. With the probe technique a 15 mm inside diameter discharge tube was connected at the downstream end to a tube 30 mm inside diameter in which the probe itself was mounted. The atom concentration was found to be independent of the probe location in the measuring section over a distance of 40 cm. It was thus concluded that no measurable amount of recombination occurred in the measuring section.

The isothermal probe was found to be more accurate than the NO_2 titration method.

Can. J. Chem. Downloaded from www.nrcresearchpress.com by 210.87.254.5 on 09/05/12
For personal use only.

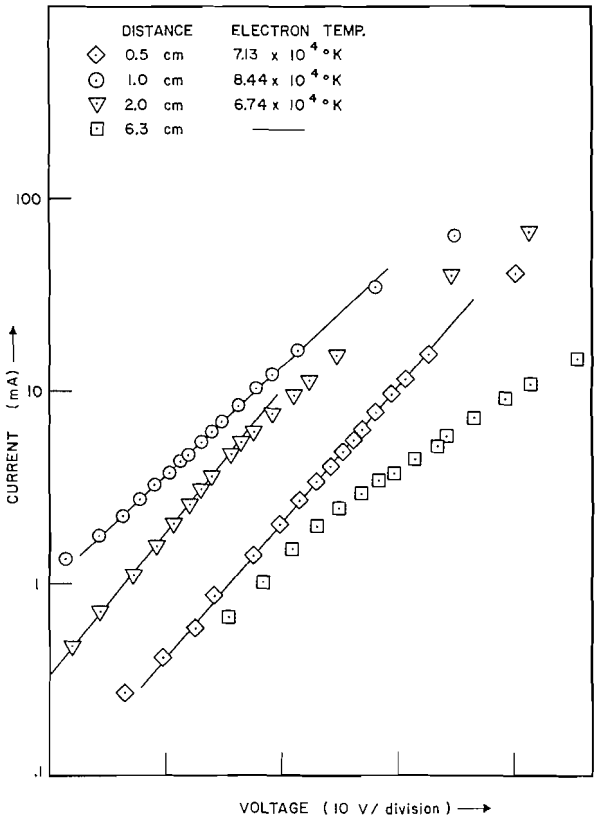


FIG. 3. Langmuir characteristics taken at various distances from the anode. Tube diameter 12.6 cm; current density 3.2 A cm^{-2}; pressure 1.0 Torr at anode.

However, for the particular probes used, only relatively small oxygen atom flows could be measured. Hence, both techniques were employed. The titration method was found to be relatively insensitive particularly in the presence of the yellow-green afterglow sometimes observed in the oxygen discharge (see Section 3E) and then its accuracy is questionable since both the NO_2 glow and the afterglow appear rather similar to the eye. The type of discharge had a significant influence upon the dissociation of oxygen. In Fig. 4 the percent dissociation is plotted against discharge current for a type I and a type IV discharge at various linear flow velocities. These results were obtained by means of NO_2 titration techniques. Hardly any dissociation could be detected in type II or III discharges.

By the probe technique the influence of the length of the positive column on the oxygen atom concentration was determined for various values of the current density (Fig. 5). As can be seen the percent dissociation increases linearly except during the first 15 cm. This decrease in slope in the first 15 cm is to be noted and is to be correlated with the decrease in electron temperature (see Section 4). For all discharges reported in this section the yellow-green afterglow was observed.

(E) Spectral Observations

General speaking only atomic oxygen lines were observed in any type of discharge although their emission intensity was very different. In type I and IV discharges a fair number of atomic oxygen lines were observed. In type II or III discharges the emission intensity was only 2 to 10% of that in type I or IV discharges and hence only the most

Can. J. Chem. Downloaded from www.nrcresearchpress.com by 210.87.254.5 on 09/05/12
For personal use only.

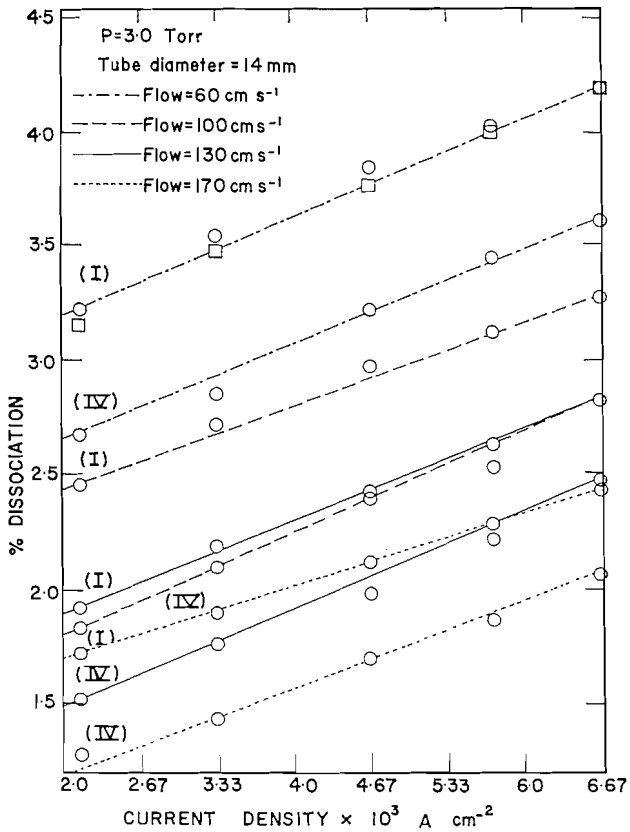


FIG. 4. Percent dissociation of oxygen versus discharge current in mA for a type I and a type IV discharge.

intense lines could then be observed. Even when using ultra pure oxygen containing less than 7.9 p.p.m. N_2, the second positive band system of N_2 could be observed at the downstream end of the discharge. Within the sensitivity of our apparatus no emission of the oxygen negative band spectrum has been observed.

Noteworthy is the fact that at times a yellow-green afterglow was observed. Under these conditions part of the positive column of the type I discharge was also yellowish green. This was particularly apparent at the downstream end, as if the emission was increasing with distance from the anode. The column was uniformly pink near the anode and towards the cathode the yellow-green glow would appear at the walls. Proceeding along the column, this glow spread to fill the tube. In larger tubes, the pink core would hardly be visible although in small tubes it could always be seen, no matter how strong the yellow glow. The presence or absence of the yellow glow under identical conditions does not seem to affect any of the parameters which we have measured, including the spectrum. The spectral features of the glow could not be measured with our equipment because their intensity was less than the noise level of our amplifier and recorder.

4. DISCUSSION OF THE RESULTS

In this section we discuss and interpret the observations reported in Section 3. In a previous paper in this series, Peeters *et al.* (12) have analyzed a model of the positive column. We shall make use of the equations derived in that paper and refer to them by

Can. J. Chem. Downloaded from www.nrcresearchpress.com by 210.87.254.5 on 09/05/12
For personal use only.

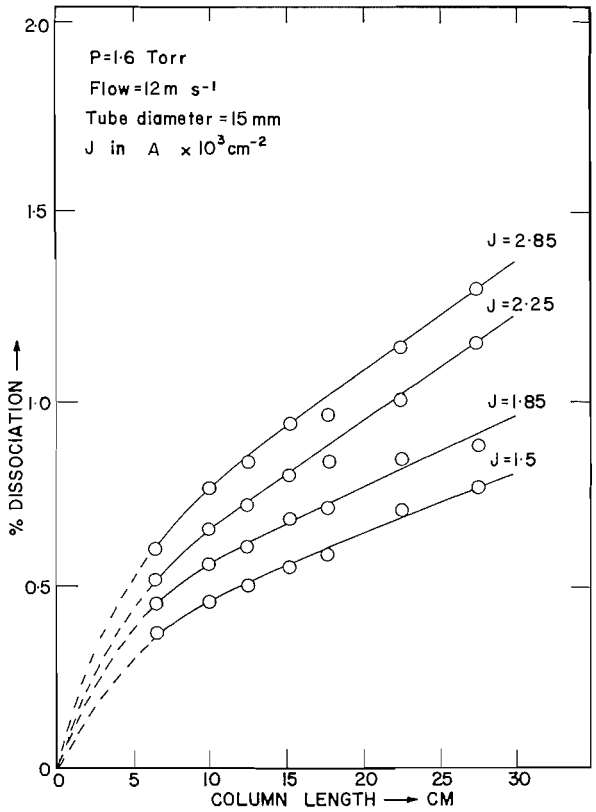


FIG. 5. Percent dissociation of oxygen versus positive column length.

preceding the numbering of the relevant equation by II. The meaning of the symbols is also the same as in II.

(A) General

Our observations of the various types of discharges in oxygen and the conditions under which they occur agree quite well with the observations of Seeliger and Wichmann (3). Discharge type I is their "H" form and types II and III are both the "T" form. The transition-type discharges containing H and T forms we have labelled type IV. In all cases, values of the field and conditions for occurrence of the various discharges agree. The most striking observation is the correlation existing between the different types of oscillations and the values of the field. These oscillations indicated two "T" types of discharges as the current density in the discharge varied with the type of oscillation. The discrepancies in the color of the discharge might be due to the lower currents used in our experiments.

A correspondence between voltage oscillations and moving striations has been established (18) and the oscillations observed here agree well with the findings of Pekarek and Šicha (10) in the different forms of the discharge in oxygen.

(B) The Electron Temperature

Since the radial field in oxygen has been shown to be very small (Thompson (4, 5), and also verified in this laboratory), Poisson's equation can be written in its one dimensional form

$$\nabla^2 V = \frac{\partial X}{\partial x} = \frac{e}{\epsilon_0}(n_+ - n_- - n_e),$$

Can. J. Chem. Downloaded from www.nrcresearchpress.com by 210.87.254.5 on 09/05/12
For personal use only.

where X is the axial field; n_+, n_-, and n_e the number densities of positive ions, negative ions, and electrons respectively; ϵ_0 the permittivity of free space; and e the electron charge. Hence, for a constant field X, any change in the concentration of positive ions will be balanced by an equal change in the concentration of negative species.

As the current density J is conserved and neglecting the part of the current carried by ions, it follows from [II 2.5] that an increase in n_e implies a decrease in the electron drift velocity $\bar{v}_e$ which, at constant gas density, then further implies an increase in the electron temperature [II 3.4]. Over relatively short distances ($\sim$5 cm) the pressure drop is negligible and the field remains constant, and so an increase in the positive ion concentration should be accompanied by an electron temperature rise in the vicinity of the anode. In II an analysis of the structure of the positive column in the area adjacent to the anode indicated an increase in the positive ion concentration. The observed increase in electron temperature is thus in agreement with this model.

Further downstream, the increasing nonlinearity of the Langmuir characteristics indicates a distribution of the electron energy which becomes progressively non-equilibrium. We think that this is due to the formation of negative ions. Thompson (4) has indicated that in an oxygen discharge the ratio n_-/n_e can be as high as 20/1. At constant field and positive ion density, this corresponds to an effective decrease of the electron temperature. Measuring the actual energy distribution will permit the verification of this hypothesis. But although we cannot conclude anything about the behavior of the electron energy distribution function further down the positive column, we expect it to shift to lower average energies in view of the following experimental observations previously mentioned: the rate of production of atomic oxygen remains constant except for a decrease over the first 15 cm and the change in the rate of production of oxygen atoms is the same as the change in the rate of growth of the emission intensity of atomic oxygen lines.

(C) The Field in the Positive Column

In the high field type I discharge the field is seen to increase monotonically with pressure (see Table II) and to be relatively independent of the flow velocity in the region studied. The surprising feature, however, is that the field remains constant along the whole positive column even in the presence of a pressure gradient. The measurements made in tubes of narrow diameter having large pressure gradients established this with certainty, since no variation in the field could be detected.

If [II 3.1] is introduced into [II 2.11] it is seen that the field should be a monotonically increasing function of the electron temperature. However, in the derivation of [II 2.11] it is implicitly assumed that the electron number density remains constant over the distance in which the electron gains an energy E_{ij} from the field (E_{ij} is the energy lost by an electron in an inelastic collision). The constancy of the current density J [II 2.5] implies that for any change in the drift velocity due to a change in the field, an opposite change in the electron number density will take place. As long as no space charge can develop, type I discharges are observed. The other types of discharges are oscillatory in character and striations travel along the column. Pekarek (19) has developed a theory which links the striations with oscillations travelling along the column. It is thus somewhat surprising that the time-average value of the field remains constant. The relation which is deduced in II between the electrical field and the electron temperature is to be used with caution, as the results of this work indicate that it cannot be applied under all conditions.

(D) The Production of Oxygen Atoms and the Emission Spectrum

The importance of properly characterizing the type of discharge when using it as a

Can. J. Chem. Downloaded from www.nrcresearchpress.com by 210.87.254.5 on 09/05/12
For personal use only.

tool to produce atoms, radicals, or other metastable or excited species is apparent from Figs. 4 and 5. Indeed, when the discharge is switched from a type I to a type IV discharge, the amount of atoms produced is significantly reduced and no dissociation is observed in type II or III discharges.

Bois D'Enghien and Deckers (20) previously reported that the emission intensity of certain bands or lines (e.g. atomic oxygen) increased linearly with the length of the positive column. The assumption was made that for oxygen the emission intensity of these lines was proportional to the atomic oxygen concentration. This assumption has now been confirmed as it can be seen from Fig. 5 that the atomic oxygen concentration varies linearly with distance.

The rate of production of oxygen atoms has been shown to decrease over the first 10 to 15 cm from the anode (as mentioned in Section 4C). The decrease in the rate of production of oxygen atoms is paralleled by a decrease of the emission intensity of the atomic oxygen lines, adding further support to the proportionality existing between the concentration of atomic oxygen and the emission intensity. We ascribe this decrease to the suspected change in electron temperature.

SUMMARY

We have shown that there exist more than two types of d-c. glow discharges through oxygen. The type of voltage oscillation at the anode is characteristic of the type of discharge. The electric field is different under a given set of conditions for the different types of discharges. The amount of oxygen atoms produced also depends on the characteristics of the discharge. The electron temperature varies at constant field near the anode.

ACKNOWLEDGMENTS

We acknowledge support in the form of grants from the United States Air Force through the Office of Scientific Research (Propulsion Research Division) and from the National Research Council of Canada. Help from B. H. Miller, K. L. Rabone, L. B. Stansfield, L. S. Moseley, L. Higgins, and Nguyen Thi Sen and technical assistance of A. Boorman and J. Gielisse are acknowledged. H. W. R. is indebted to the National Research Council of Canada for the award of a bursary. K. A. G. and R. M. Y. are holders of a Province of Ontario Graduate Fellowship.

REFERENCES

1. A. Günthersschulze. Z. Physik, **42**, 763 (1927).
2. R. Seeliger. Z. Naturforsch. Pt. a, **8**, 74 (1953).
3. R. Seeliger and A. Wichmann. Ann. Physik, **9**, 235 (1951).
4. J. B. Thompson. Proc. Phys. Soc. London, **73**, 818 (1959).
5. J. B. Thompson. Proc. Roy. Soc. London, Ser. A, **262**, 503 (1961).
6. G. Albrecht and G. Ecker. Z. Naturforsch. Pt. a, **17**, 848 (1962).
7. G. H. Dieke, H. Y. Loh, and H. M. Crosswhite. J. Opt. Soc. Am. **36**, 185 (1946).
8. H. Y. Loh and G. H. Dieke. J. Opt. Soc. Am. **37**, 837 (1947).
9. T. Donahue and G. H. Dieke. Phys. Rev. **81**, 248 (1951).
10. L. Pekarek and M. Sicha. Czech. J. Phys. Sect. B, **10**, 749 (1960).
11. H. G. Miller. Phys. Letters, **5**, 120 (1963).
12. J. L. Peeters, H. W. Rundle, and J. M. Deckers. This issue.
13. E. L. Tollefson and D. J. Le Roy. J. Chem. Phys. **16**, 1057 (1948).
14. L. Elias, E. A. Ogryzlo, and H. I. Schiff. Can. J. Chem. **37**, 1690 (1959).
15. F. Kaufman. Proc. Roy. Soc. London, Ser. A, **247**, 123 (1958).
16. F. Kaufman. J. Chem. Phys. **28**, 352 (1958).
17. R. L. F. Boyd and N. D. Twiddy. Proc. Roy. Soc. London, Ser. A, **250**, 53 (1959).
18. D. A. Lee, P. Bletzinger, and A. Garscadden. J. Appl. Phys. **37**, 377 (1966).
19. L. Pekarek. Czech J. Phys. Sect. B, **12**, 439 (1962).
20. P. A. Bois d'Enghien and J. M. Deckers. Can. J. Chem. **42**, 1792 (1964).

Can. J. Chem. Downloaded from www.nrcresearchpress.com by 210.87.254.5 on 09/05/12
For personal use only.

Can. J. Chem. Downloaded from www.nrcresearchpress.com by 210.87.254.6 on 09/05/12
For personal use only.

THE DEUTERIUM ISOTOPE EFFECT AND THE MOLECULAR DYNAMICS OF WATER IN BENZENE

D. C. MOULE[1]

Research Chemistry Branch, Atomic Energy of Canada, Limited, Chalk River, Ontario

Received August 24, 1966

ABSTRACT

Infrared spectra of H_2O and D_2O in benzene have been recorded and the solubilities of light and heavy water in benzene from 10 to 50 °C measured. Isotope fractionation factors for the distribution of HDO and H_2O between the vapor and liquid benzene phases were calculated from the relative solubilities and the vapor pressure ratios of pure H_2O and D_2O. The isotope equilibrium data was fitted to the expression $\ln \alpha = -A/T^2 + B/T$ and interpreted by the Bigeleisen formulism. The intramolecular B term was determined from the solvent shifts of the near infrared frequencies and the intermolecular A term calculated by a least squares fit to the isotope equilibrium data. Spectral and equilibrium data were combined to give 220 $cm^{-1} \simeq \nu_{Ry} > \nu_{Rx} > \nu_{Rz} \geq 120$ cm^{-1}.

INTRODUCTION

Kirschenbaum (1) has reported the solubilities of H_2O and D_2O in a series of organic solvents at room temperature. For some of the solvent systems it was found that HDO distributes preferentially from the liquid organic phase into the vapor phase by as much as 5%, whereas for other superficially similar systems it was found that HDO fractionates preferentially into the liquid phase. A theory of the phase equilibrium isotope effect for polyatomic molecules which could be applied to such two-component two-phase systems has recently been developed by Bigeleisen (2). In the simplest form of this theory isotope separation factors are expressed in terms of the $3N - 6$ normal vibrational modes in the liquid and vapor phases and the 3 external translational and the 3 librational condensed phase modes. Equilibrium isotope effect data can be compared and combined with the spectroscopic observations on the two phases and can provide information about the molecular dynamics of the condensed phase.

The benzene–water system was chosen as a representative example in which to confirm and extend the existing solubility results, and obtain information about the dynamics of water in liquid benzene. From an understanding of this system one might be able to predict whether large enough separation factors could occur in other solvent systems to make two-component two-phase equilibria a potentially useful method for separating heavy water from natural water.

EXPERIMENTAL

In a previous paper (3) the solubility of H_2O in C_6H_6 in the temperature range 10 to 50 °C was measured. The method used was an isotope dilution technique in which a quantity of benzene saturated with light water was equilibrated with a known amount of heavy water and the concentration change in the D_2O measured by infrared difference spectroscopy. Water solubility was calculated from the concentration change in the heavy water, and the quantities of heavy water and benzene. The solubility of D_2O in benzene has been measured in a similar fashion with light water replacing heavy water as the isotope exchange medium. It was estimated that the solubility of H_2O in C_6H_6 could be determined to ±0.8%, and D_2O in C_6H_6 to ±0.6%.

Far infrared spectra of H_2O and D_2O in C_6H_6 were recorded from 340 cm^{-1} to 95 cm^{-1} with a Perkin–Elmer 301 spectrophotometer. The path length of the infrared cells was approximately 3 mm and the benzene solutions were saturated with water at 20 °C. Near infrared spectra of H_2O and D_2O in C_6H_6 were obtained on a Perkin–Elmer 521 spectrophotometer. Path length of the water-saturated benzene solution was approximately 1 mm. The D_2O deformation mode ν_2 could not be observed because the 1 200 cm^{-1} region was opaque to infrared radiation.

[1]*Now at Brock University, St. Catharine's, Ontario.*

Can. J. Chem. Downloaded from www.nrcresearchpress.com by 210.87.254.6 on 09/05/12
For personal use only.

RESULTS

The solubilities of light and heavy water in benzene in parts per million (p.p.m.) by weight over the range 10 to 50° are given in Table I.

TABLE I

The solubilities of light and heavy water in benzene as a function of temperature

	Solubilities (p.p.m. by weight)	
T (°C)	H_2O	D_2O
9.44	442.5	388.4
14.98	530.2	475.3
20.10	639.2	581.5
24.54	726.0	665.2
29.52	848.0	790.3
34.88	1 017.1	941.7
40.06	1 177.8	1 134.6
43.78	1 333.7	1 268.3
49.45	1 570.6	1 495.8

Frequencies of the band centers of the modes υ_1, υ_2, and υ_3 of H_2O and υ_1 and υ_3 of D_2O in C_6H_6 are listed in column 3 of Table II along with the band origins of corresponding vapor phase modes (4) in column 2. Columns 4 and 5 show the solvent shift υ(vapor) − υ(benzene) and reduced solvent shifts [υ(vapor) − υ(benzene)]/υ(benzene). A value for $\upsilon_2(D_2O)$ in benzene was estimated from the assumption (5) that $\Delta\upsilon_2/\upsilon_2(H_2O) = \Delta\upsilon_2/\upsilon_2(D_2O)$.

TABLE II

Infrared frequencies of H_2O and D_2O in the vapor phase and in liquid benzene. Solvent shifts and reduced solvent shifts

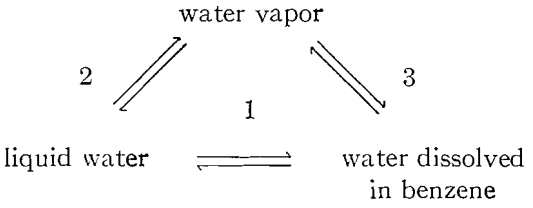
	Mode	υ(vapor) (cm^{-1})	υ(benzene) (cm^{-1})	$\Delta\upsilon$ (cm^{-1})	$\Delta\upsilon/\upsilon \times 10^2$
H_2O	υ_1	3 656.7	3 594.8±1	61.9	1.722
	υ_2	1 594.6	1 602.8±0.5	−8.2	−0.512
	υ_3	3 755.8	3 681.5±1	74.3	2.018
D_2O	υ_1	2 671.5	2 630.1±0.5	41.4	1.574
	υ_2	1 178.3	1 184.3±1*	−6.0	−0.512
	υ_3	2 788.1	2 734.3±0.5	53.8	1.968

*Estimated from reduced solvent shift.

Far infrared spectra of H_2O and D_2O in C_6H_6 from 320 cm^{-1} to 100 cm^{-1} are shown in Fig. 1. Broad peaks, centered at 220 cm^{-1} and 170 cm^{-1} respectively, appear in the spectra which are devoid of structure.

DISCUSSION

The isotope separation factors for the fractionation of H_2O and HDO in the equilibria



are related through

$$\alpha_1 = \alpha_2\alpha_3, \quad [1]$$

where

$$\alpha_1 = [(H_2O)/(HDO)]_{C_6H_6}/[(H_2O)/(HDO)]_{liq} \quad [2]$$

$$\alpha_2 = [(H_2O)/(HDO)]_{vap}/[(H_2O)/(HDO)]_{liq} \quad [3]$$

$$\alpha_3 = [(H_2O)/(HDO)]_{C_6H_6}/[(H_2O)/(HDO)]_{vap} \quad [4]$$

and the symbolism $(H_2O)_{C_6H_6}$ denotes the mole fraction of light water in benzene.

For equilibrium 2, the law of the isotope mean is assumed (6) and

$$\alpha_2 = \left[\left(\frac{P_{H_2O}}{P_{D_2O}}\right)\left(1 + \frac{P(B - V)}{RT}\right)\left(\frac{1 - (C_6H_6)_{H_2O}}{1 - (C_6H_6)_{D_2O}}\right)\right]^{1/2}, \quad [5]$$

where P_{H_2O} and P_{D_2O} are the vapor pressures of H_2O and D_2O, B the second virial coefficient for water vapor, which is assumed to be isotopically invarient, and V the molar volume of water in the condensed phase. The terms $(C_6H_6)_{H_2O}$ and $(C_6H_6)_{D_2O}$ are the solubilities of benzene in light and heavy water introduced through Raoult's law to correct for the vapor pressure lowering of water by dissolved benzene.

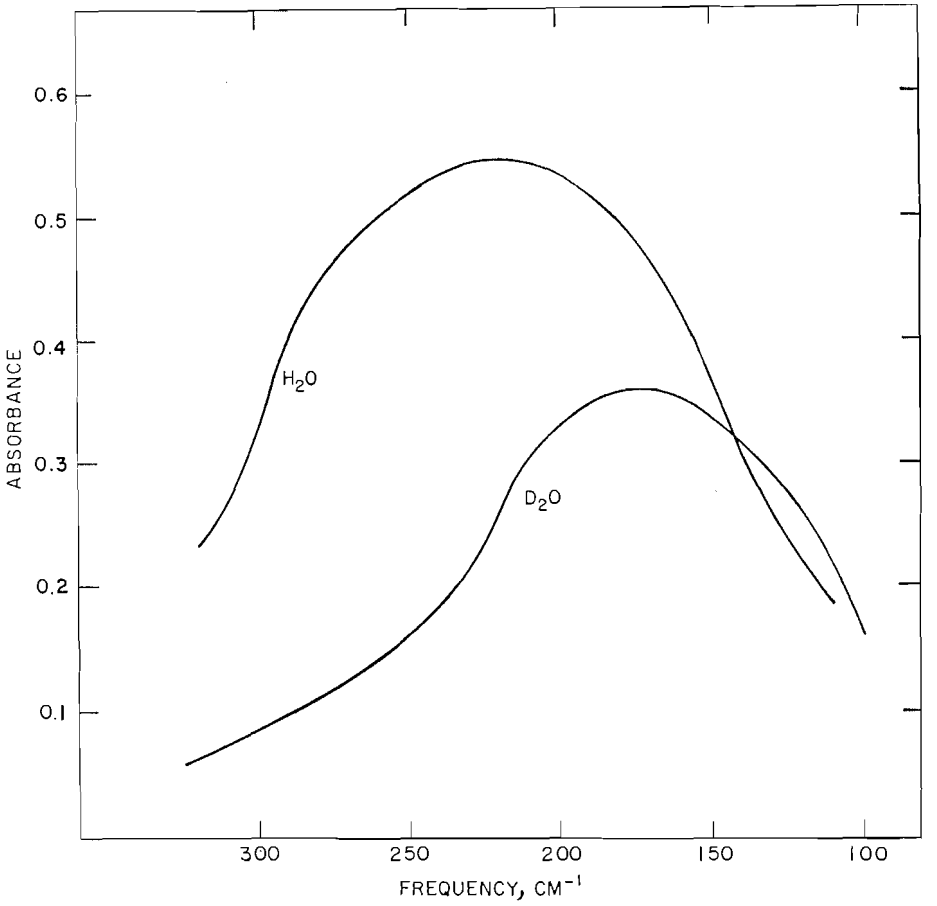


FIG. 1. Far infrared spectra of H_2O and D_2O in C_6H_6.

Can. J. Chem. Downloaded from www.nrcresearchpress.com by 210.87.254.6 on 09/05/12
For personal use only.

A theoretical treatment of the isotope fractionation of H_2O and HDO between the liquid phases of nonideal systems such as triethylamine–water has been given by Linderstrom-Lang (7). Applied to the benzene–water equilibrium his treatment yields

$$[6] \qquad \alpha_1 = \left[\left(\frac{(H_2O)_{C_6H_6}}{(D_2O)_{C_6H_6}}\right)\left(1 + (H_2O)_{C_6H_6}\frac{\partial \ln \gamma[(H_2O)_{C_6H_6}]}{\partial (H_2O)_{C_6H_6}}\right)\right]^{1/2}.$$

The first factor is the ratio of the molar solubilities of light and heavy water in benzene, while the second expresses the degree of ideality of water in benzene, $\gamma[(H_2O)_{C_6H_6}]$ being the activity coefficient of water in benzene.

There does exist some controversy over the state of water in benzene. On the basis of viscosity and specific volume measurements (8) and infrared data (9) it has been proposed that water is predominantly polymerized in benzene solution at concentrations near the solubility limit. On the other hand, evidence from infrared spectra (10) and freezing point (11) and vapor pressure measurements (12) indicate that water is monomeric in benzene. This difficulty appears to have been settled recently by Christian, Affsprung, and Johnson (13), who used an isopiestic method to measure the solubility of water in benzene over a range of partial pressures. These authors found $\ln \gamma[(H_2O)_{C_6H_6}]/(H_2O)_{C_6H_6} = 0$, which indicates that polymer formation is very improbable.

TABLE III
Fractionation factors

T (°C)	α_1	α_2	α_3	α_4
9.44	1.125	0.9159	1.030	1.061
14.98	1.114	0.9227	1.028	1.057
20.10	1.105	0.9292	1.027	1.055
24.54	1.101	0.9327	1.027	1.055
29.52	1.092	0.9374	1.024	1.049
34.88	1.096	0.9420	1.032	1.065
40.06	1.075	0.9462	1.017	1.034
43.78	1.082	0.9488	1.027	1.055
49.45	1.080	0.9525	1.029	1.059

Values of α_2 calculated from the vapor pressure ratio data for H_2O and D_2O (14), molar volume of liquid H_2O (14), the second virial coefficient of water vapor (15), and the solubility data for benzene in H_2O and D_2O (W. J. Wallace, unpublished data) are shown in the third column of Table III. Separation factors α_1 obtained from eq. [6] and the solubility data of Table I are listed in column 2 while α_3 calculated from eq. [1] is given in the fourth column of Table III. To compare the observed fractionation effect with that calculated from spectroscopic data we use the fraction factor

$$[7] \qquad \alpha_4 = [(H_2O)/(D_2O)]_{C_6H_6}/[(H_2O)/(D_2O)]_{vap}.$$

This represents the isotope fractionation when water is present in the system only as H_2O and D_2O, and is given with sufficient accuracy as

$$[8] \qquad \alpha_4 = \alpha_3^2.$$

Values of α_4 are listed in the last column of Table III.

Fractionation Factors from Spectroscopic Data

To relate α_4 to the hindered translational, librational, and vibrational frequencies of water in the condensed phase, we employ the equilibrium isotope effect theory for polyatomic molecules, which has been developed by Bigeleisen (2). The reduced partition

Can. J. Chem. Downloaded from www.nrcresearchpress.com by 210.87.254.6 on 09/05/12
For personal use only.

function ratio in this theory is expressed as a product over the $3N - 6$ internal and the 6 external reduced partition function ratios for each phase. In the liquid phase the molecules are assumed to be a collection of harmonic oscillators, each molecule possessing 3 hindered translational and 3 librational frequencies. In the gas phase all these frequencies are zero. The $3N - 6$ internal or normal vibrations of a polyatomic molecule retain their gas phase identity in the liquid phase although slightly shifted in frequency. When the external vibrations are small with respect to the experimental temperature ($h\upsilon/kT \lesssim 1$) and the internal vibrations large ($h\upsilon/kT > 1$), the phase equilibrium isotope effect equation reduces to the simple form

$$\ln \alpha_4 = -A/T^2 + B/T, \qquad [9]$$

provided that molar volume effects and vibrational anharmonicities are neglected. The intermolecular term, A, is given by

$$A = \frac{1}{24}\left(\frac{hc}{k}\right)^2 \sum^{3} \{[\upsilon(H_2O)^2 - \upsilon(D_2O)^2]_{trans} + [\upsilon(H_2O)^2 - \upsilon(D_2O)^2]_{rot}\}, \qquad [10]$$

where the summation extends over the 3 hindered translational and the 3 librational frequencies in the condensed phase. The intramolecular term B is given as

$$B = \frac{hc}{2k} \sum^{3N-6} \{[\upsilon(H_2O) - \upsilon(D_2O)]_{vap} - [\upsilon(H_2O) - \upsilon(D_2O)]_{C_6H_6}\}, \qquad [11]$$

the summation being taken over all of the internal frequencies in the separate phases.

Because of the scatter in the experimental data, it was not feasible to fit α_4 to the two-parameter eq. [9]. Instead B was determined from the solvent shifts of the normal frequencies and inserted into eq. [9], then A was obtained by a least squares fit of α_4 to the expression in only one parameter. The external frequencies derived from A were then compared with the transitions observed in the far infrared spectra.

From the solvent shifts for H_2O and D_2O in benzene listed in Table II and eq. [11], a value of $B = 27.91 \pm 1.97$ °K² was obtained. The least squares fit gave $A = 3\,600 \pm 580$ °K². The resulting fractionation factor curve and the experimental fractionation data are illustrated in Fig. 2.

To factor out the translational contribution from eq. [10] an estimate of 90 cm^{-1} was made for the hindered translational frequencies of water in benzene. On the supposition that the mass dependence of the translational frequencies is a function only of the molecular weight (2) and that the translational modes are degenerate, the translational contribution to A is 214 ± 30 °K². The equilibrium isotope effect for librational motion is $3\,600 - 214 = 3\,386 \pm 581$ °K².

In the simple case where the hydrogen-bonded proton lies in a field which is cylindrically symmetrical about the O—H · · · C group, it can be shown that to a good approximation the three frequencies will be equal (16). It follows from eq. [9] and from the approximation that the librational frequencies are inversely proportional to the square root of the average moments of inertia that $\upsilon_{Rx} = \upsilon_{Ry} = \upsilon_{Rz} = 166 \pm 14$ cm^{-1}.

From the isotope shift of the far infrared bands, illustrated in Fig. 1, $\upsilon(H_2O)/\upsilon(D_2O) = 1.29$; thus the rotational-like nature of the motion is established and the bands are assigned to a superposition of modes Ry and Rx. The Rz liberation does not involve a change in dipole moment and is not therefore infrared active. The lack of agreement between the observed centers of the far infrared bands and the calculated librational frequencies demonstrates that the average librational frequencies are widely different and that one librational frequency, presumably υ_{Rz}, must be about 120 cm^{-1}.

Can. J. Chem. Downloaded from www.nrcresearchpress.com by 210.87.254.6 on 09/05/12
For personal use only.

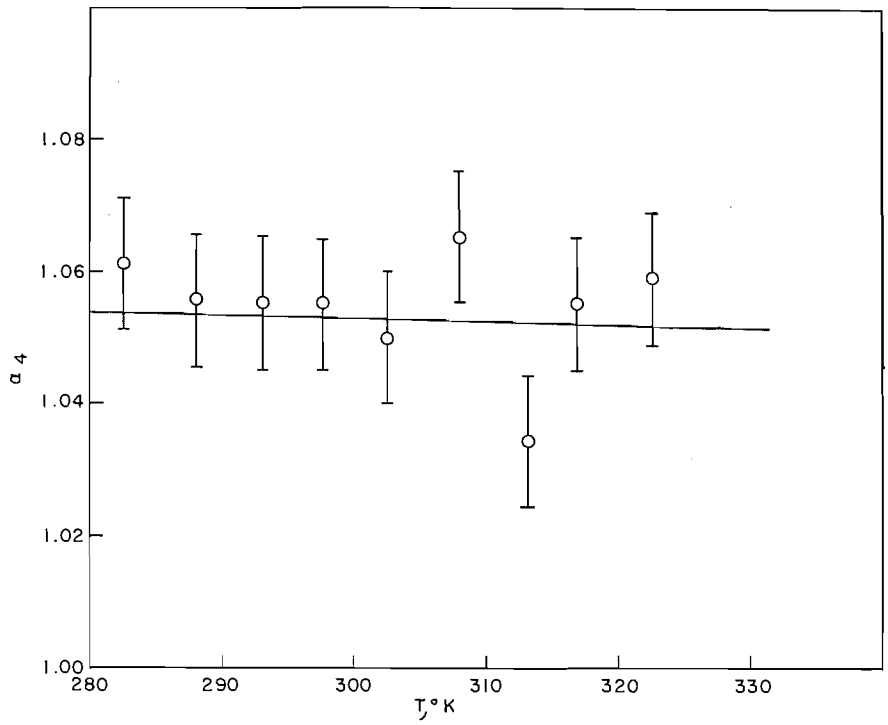


FIG. 2. The observed and calculated fractionation factors.

Van Hook and Phillips (17) have recently obtained separation factors for the distribution of C_2H_6 and C_2D_6 between the vapor phase and a variety of liquids by gas–liquid partition chromatography. They found that the isotope separation was strongly solvent dependent and that C_2H_6 was preferentially fractionated into the vapor phase with increasing solvent polarity. A similar correlation is evident in Table II. In the benzene–water system $\alpha_4(25\ °C) = 1.055$, whereas in a highly polar solvent such as liquid water, the fractionation changes direction and $\alpha_2^2(25\ °C) = 0.8699$. This is reflected in the inter- and intra-molecular terms for water in liquid water (18) and water in benzene, $A_{C_6H_6}/A_{H_2O} = 3600/33630$ and $B_{C_6H_6}/B_{H_2O} = 27.91/70.87$, which shows that the solvent shift contribution to the isotope effect is less sensitive to changes in solvent polarity than the corresponding contribution from librational motion. From eq. [9] and this correlation it follows that the most favorable solvent for separating HDO from natural water would be a nonpolar aliphatic hydrocarbon.

ACKNOWLEDGMENTS

The author wishes to thank Drs. J. E. Bertie and E. Whalley of the National Research Council, Ottawa, for recording the far infrared spectra, and Dr. R. N. Jones, also of N.R.C., for measuring the centers of the near infrared bands. The help of Mr. W. M. Thurston in constructing the absorption cell is acknowledged.

REFERENCES

1. I. KIRSHENBAUM. Physical properties and analysis of heavy water. McGraw-Hill Book Co., Inc., New York and London. 1951.
2. J. BIGELEISEN. J. Chem. Phys. **34**, 1485 (1961); J. Chim. Phys. **60**, 35 (1963).
3. D. C. MOULE and W. M. THURSTON. Can. J. Chem. **44**, 1361 (1966).
4. W. S. BENEDICT, N. GAILAR, and E. K. PLYLER. J. Chem. Phys. **24**, 1139 (1956).
5. A. D. BUCKINGHAM. Proc. Roy. Soc. London, Ser. A, **248**, 169 (1958).

Can. J. Chem. Downloaded from www.nrcresearchpress.com by 210.87.254.6 on 09/05/12
For personal use only.

6. L. MERLIVAT, R. BOTTER, and G. NIEF. J. Chim. Phys. **60**, 56 (1963).
7. C. U. LINDERSTROM-LANG. Acta Chem. Scand. **16**, 1730 (1962); Isotope and mass effects in chemistry and biology. IAEA, Vienna. 1963. p. 259.
8. M. GORDON, C. S. HOPE, L. D. LOAN, and R. J. ROE. Proc. Roy. Soc. London, Ser. A, **258**, 215 (1960).
9. T. ACKERMANN. Z. Physik. Chem. Frankfurt, **42**, 119 (1964).
10. E. GREINACHER, W. LUTTKE, and R. MECKE. Z. Elektrochem. **59**, 23 (1955).
11. J. M. PETERSON and W. H. RODEBUSH. J. Phys. Chem. **32**, 709 (1928).
12. B. D. CADDOCK and P. L. DAVIES. Nature, **184**, 2011 (1959).
13. S. D. CHRISTIAN, H. E. AFFSPRUNG, and J. R. JOHNSON. J. Chem. Soc. 1896 (1963).
14. E. WHALLEY. Proc. Conf. Thermodyn. Transport Properties Fluids, London, 1957. 1958. p. 15.
15. J. P. MCCULLOUGH, R. E. PENNINGTON, and G. WADDINGTON. J. Am. Chem. Soc. **74**, 4439 (1952).
16. R. W. BLUE. J. Chem. Phys. **22**, 280 (1954).
17. W. A. VAN HOOK and J. T. PHILLIPS. J. Phys. Chem. **70**, 1515 (1966).
18. W. M. JONES. Los Alamos Rept. (W-7405-eng-36) (1963).

Can. J. Chem. Downloaded from www.nrcresearchpress.com by 210.87.254.6 on 09/05/12
For personal use only.

Can. J. Chem. Downloaded from www.nrcresearchpress.com by 210.87.254.5 on 09/05/12
For personal use only.

ARSENIDES OF THE TRANSITION METALS

VIII. SOME BINARY AND TERNARY GROUP VIII DIARSENIDES AND THEIR MAGNETIC AND ELECTRICAL PROPERTIES

S. L. BENNETT[1] AND R. D. HEYDING

Department of Chemistry, Queen's University, Kingston, Ontario

Received May 13, 1966

ABSTRACT

The diarsenides of the cobalt and nickel families have been synthesized for magnetic susceptibility studies. The diffraction pattern of the low-temperature modification of nickel diarsenide differs from that of the mineral pararammelsbergite, although the space group is apparently identical and the unit cell dimensions comparable (orthorhombic D_{2h}^{15}-*Pbca*; $a = 5.770 \pm 0.007$, $b = 5.838 \pm 0.006$, $c = 11.419 \pm 0.008$ Å). These binary diarsenides exhibit temperature dependent diamagnetic or weakly paramagnetic behavior. Temperature dependence of electrical resistivity indicates that $PdAs_2$ is metallic while $PtAs_2$ is a semiconductor with an energy gap of ~0.17 eV.

Substitutional solid solution limits have been determined for various Group VIII transition metal atoms in the pyrite phases $PdAs_2$ and $PtAs_2$, and in the skutterudites $RhAs_3$ and $IrAs_3$. There is no substitution by Ru or Os in $PdAs_2$, by Ni or Pt in $PdAs_2$, by Ru or Ag in $RhAs_3$, or by Os in $IrAs_3$. Very limited substitutions were observed for Rh and Ag in $PdAs_2$, Pd in $PtAs_2$, Pd in $RhAs_3$, and Pt in $IrAs_3$. The limit of Co substitution in $PdAs_2$ is 8.2 ± 0.3 atom %, and of Ni in $PdAs_2$, 56.7 ± 0.3 atom %.

In the $Co_xPd_{1-x}As_2$ system, a temperature-dependent paramagnetic contribution corresponding to approximately one uncompensated spin per cobalt ion has been attributed to the t_{2g}^5 low-spin configuration of the Co ion in the pyrite structure. In the $Ni_xPd_{1-x}As_2$ system, the temperature-independent paramagnetic contribution by the nickel ions is not completely understood.

INTRODUCTION

The diarsenides of palladium and platinum crystallize in the C2 pyrite structure (1–3), while the monoclinic diarsenides of the cobalt family (4) are believed to be isomorphous with the EO_7 arsenopyrite-type diantimonides of Co, Rh, and Ir (5) and diphosphides of Rh and Ir (6).[2] Nickel diarsenide is polymorphic. The high-temperature modification, β-$NiAs_2$ (rammelsbergite), has the orthorhombic C18 marcasite structure with an abnormally large c/b ratio in comparison with the iron family marcasites. The low-temperature modification, α-$NiAs_2$, also orthorhombic, has been shown (7, 8) to have the same unit cell dimensions as the mineral pararammelsbergite (9, 10). A complete structure analysis of this modification has not yet been reported.

With the exception of the nickel compounds, the dipnictides of the nickel family form pyrite structures with octahedral configuration of pnigogen atoms about the metal atoms. These compounds and the cobalt family MZ_3 skutterudites are the only transition metal pnictides in which the metal atoms are completely surrounded by non-metal atoms, precluding metal–metal interaction.[3] In the arsenopyrite structure exhibited by the cobalt family dipnictides, pairs of metal atoms can be recognized, while in the marcasite structure exhibited by the iron family dipnictides, one-dimensional chains of metal atoms exist parallel to the c axis of the crystal. Recently, Hulliger and Mooser (11, 13) and

[1]*Present address: Department of Chemistry, University of Kansas, Lawrence, Kansas.*

[2]*The unit cell dimensions for* $CoAs_2$ *reported earlier (4) are in error. The correct values are:* $a = 5.918 \pm 0.005$; $b = 5.876 \pm 0.002$; $c = 5.964 \pm 0.005$ Å; $\beta = 116°27' \pm 5'$. *Complete structural analyses of the cobalt family diarsenides have not been reported.*

[3]*In their recent review article, Hulliger and Mooser list* $NiAs_3$ *as a skutterudite with metallic properties (11). However, in studies on the binary* Ni–As *system, Holmes (7), Heyding and Calvert (8), and Yund (12) did not observe any compound with this composition or structure.*

Pearson (14) have used the concepts of ligand field theory to explain virtually all of the structural, magnetic, and electrical properties of these compounds, including the diarsenides, which are diamagnetic or weakly paramagnetic (15, 16).

In an earlier paper, the homogeneity limits and the magnetic and electrical properties of the substituted cobalt skutterudites $(Ni,Co)As_3$, $(Fe,Co)As_3$, and $(Fe,Ni)As_3$ were reported (17). The substitution of iron or nickel for cobalt made it possible to examine the properties of these elements in an octahedral field, that is, in the absence of metal–metal interactions. Obviously, other transition metals might be examined in a similar manner by substitution in $RhAs_3$ or $IrAs_3$, or in the pyrite diarsenides $PdAs_2$ and $PtAs_2$, provided the range of solid solution were relatively large. In this paper we report the results of attempts to substitute several transition metal atoms for Rh and Ir in the triarsenides, and for Pd and Pt in the diarsenides, and record the magnetic properties in those two systems in which appreciable substitution was obtained. The magnetic susceptibilities of the diarsenides of Pd, Pt, Co, Rh, and Ir, and the electrical properties of Pt and Pd diarsenide have been redetermined.

EXPERIMENTAL

Sample Preparation

All elements were high purity (99.99+%). The arsenic was obtained from Cominco; Rh, Pd, Pt, Ag from A. D. Mackay Inc.; Co, Ni from Johnson, Matthey and Co.; Ru, Os, Ir from Engelhard Ind. Spectrographic analyses for arsenic revealed, in p.p.m., Si, 20; Fe, 5; Ni, 5; Ag, 5; and for the transition metals, the maximum impurities were Si, 20; Fe, 50; and Cu, 10.

The arsenic was sublimed and condensed under high vacuum to effect purification and to obtain a predominance of the amorphous forms which are easy to grind and handle. The charge was initially heated at 250 °C to remove traces of As_2O_3 that formed during manipulations, and then heated at ~400 °C. The arsenic was stored *in vacuo*.

Specimens were prepared in 2 g quantities by weighing calculated amounts of arsenic and metal powders and sealing in Vycor or quartz tubes under high vacuum. After an initial treatment at ~400 °C, the temperature was raised to 750°. After a week the samples were quenched, ground thoroughly, sampled for Debye–Scherrer patterns, resealed under vacuum, and annealed for periods of 1 week. This procedure was repeated until all diffraction lines due to extraneous phases had been eliminated and consecutive photographs showed no change in lattice parameter(s). Three annealing periods were generally sufficient for complete reaction. Most systems were investigated up to $x = 0.40$, except the Ni–Pd, Rh–Pd, and Pd–Pt diarsenide systems, for which the complete composition ranges were prepared.

Debye–Scherrer patterns were obtained in 11.46 cm Norelco cameras using Cu Kα ($\lambda(K\alpha_1) = 1.5405$ Å) radiation.

Magnetic Susceptibilities

Magnetic susceptibilities were determined by the Faraday (Curie) method using Henry pole caps described earlier (18). Apparent changes in weight were determined in a closed system under dry nitrogen at 380 torr using an Ainsworth vacuum semimicro balance, equipped with a transducer, acting as a null-point instrument. Temperatures were controlled to ±2° in the temperature range 84 to ~550 °K. Measurements were taken at high fields ($B_{min} > 8\,000$ G) in five field gradients, dB^2/dx, ranging from 30.3 to 48.8 $kG^2\,cm^{-1}$. The apparent susceptibilities were plotted against $1/(B_{max} + B_{min})$ and extrapolated to infinite field, allowing χ_g^∞ to be determined. The variation in the susceptibilities of all samples with field was $\sim 0.003 \times 10^{-6}$ cgs e.m.u./g; the loss in sample weight at the higher temperatures was <0.1%; the error in χ_g^∞ was $\pm 0.003 \times 10^{-6}$ cgs e.m.u./g.

The field was calibrated with a high-purity copper cylinder (impurities in p.p.m., Fe, 1; O, 1, H; 0.4; Ni, 1; and the balance <10) of the same dimensions and in the same position in the field as subsequent samples. The absolute mass susceptibility of Cu has been determined by Henry *et al.* (19, 20).

The powdered samples (~1 g) were contained in a light quartz bucket, which was calibrated as a function of magnet excitation current and temperature. Quartz as a container material has the advantage of an almost temperature-independent susceptibility.

RESULTS AND DISCUSSION

1. Solid Solution Studies

Results of the search for substitutional solid solutions in the cubic di- and tri-arsenides are summarized in Table I. Appreciable and unambiguous regions were observed in only

Can. J. Chem. Downloaded from www.nrcresearchpress.com by 210.87.254.5 on 09/05/12
For personal use only.

TABLE I

Substitution limits in $M_xM'_{1-x}As_2$ pyrite and $M_xM'_{1-x}As_3$ skutterudite phases

System	x at limit of solid solution		Phases present beyond solid solution region
$Ni_xPd_{1-x}As_2$	0.567±0.003	(750 °C)	Pd(Ni)As_2 (a = 5.863 Å), Pd-subst. α,β-$NiAs_2$ (see text)
$Co_xPd_{1-x}As_2$	0.082±0.003	(750°)	Pd(Co)As_2 (a = 5.965 Å), Co(Pd)As_{3-y} (a = 8.207 Å)
$Ru_xPd_{1-x}As_2$	~0	(750°)	$PdAs_2$,* $RuAs_2$
$Rh_xPd_{1-x}As_2$	<0.05	(750°)	See text
$Ag_xPd_{1-x}As_2$	<0.05	(750°)	Pd(Ag)As_2,* Ag_8As, As
$Os_xPd_{1-x}As_2$	~0	(750°)	$PdAs_2$,* $OsAs_2$
$Ni_xPt_{1-x}As_2$	~0	(750°)	$PtAs_2$,* β-$NiAs_2$
		(1 100°)	$PtAs_2$, NiAs, As
$Pd_xPt_{1-x}As_2$	~0	(750°)	
	~0.2	(1 100°)	Pt(Pd)As_2,* $PdAs_2$
	~0.5	(1 200°)	
$Pt_xPd_{1-x}As_2$	~0	(750°)	$PdAs_2$,* $PtAs_2$
	~0	(1 100°)	
$Ru_xRh_{1-x}As_3$	~0	(750°)	$RhAs_3$ (a = 8.452 Å),* $RuAs_2$, As
	~0	(1 050°)	
$Pd_xRh_{1-x}As_3$	~0.07	(750°)	Rh(Pd)As_3 (a = 8.455 Å), $PdAs_2$, As
	~0.07	(1 100°)	
$Ag_xRh_{1-x}As_3$	~0	(750°)	$RhAs_3$,* Ag_8As, As
$Pt_xIr_{1-x}As_3$	<0.1	(750°)	Ir(Pt)As_3 (a = 8.470 Å), $PtAs_2$, As
$Os_xIr_{1-x}As_3$	~0	(750°)	$IrAs_3$ (a = 8.468 Å),* $OsAs_2$, As

*No change in parameter.

2 of 14 systems studied. It is clear that $4d^6$ and $5d^6$ ions in the pyrite structure are not readily replaced by $4d^4$, $4d^5$, $5d^4$, and $5d^5$ ions.[4] It is remarkable that the $4d^6$ and $5d^6$ ions (Pd^{4+} and Pt^{4+}) are not mutually interchangeable even though both binary diarsenides have the same structure and almost the same unit cell volume, while there is appreciable mutual substitution of $3d^6$ and $4d^6$ ions (Ni^{4+} and Pd^{4+}) although the end members are not isostructural.

The phases observed above the solid solution regions (if formed) are those to be expected, except in the $Rh_xPd_{1-x}As_2$ system. In this system, the composition $x = 0.05$ yielded two pyrite phases: $PdAs_2$, with no change in parameter (5.985 Å), and a rhodium-substituted phase with a smaller parameter (5.976 Å). The compositions $0.10 \leqslant x \leqslant 0.50$ consisted of the latter pyrite phase and a skutterudite phase having the same parameter as pure $RhAs_3$ (8.452 Å). The composition $x \sim 0.55$ was single phase skutterudite, and with increasing Rh concentration, the phases present were skutterudite and $RhAs_2$. The diffraction patterns imply that in the three phase system skutterudites of the form $Rh_{0.55}Pd_{0.45}As_{3-y}$ exist with $y \sim 1$. The type of defect structure is not as yet known.

For the systems in which appreciable substitutions were obtained, (Co,Pd)As_2 and (Ni,Pd)As_2, precise lattice parameters were obtained by Nelson–Riley extrapolations. The results are summarized in Table II. Plots of these room temperature parameters as a function of composition (Figs. 1 and 2) show the limits of solid solution at 750 °C to be $x = 0.082 \pm 0.003$ in the system $Co_xPd_{1-x}As_2$, and $x = 0.567 \pm 0.003$ in the system $Ni_xPd_{1-x}As_2$. Extrapolation of these data to $x = 1.00$ gives a unit cell parameter of the hypothetical C2 pyrite $CoAs_2$ of $5.74_5 \pm 0.01$ Å, and a cell volume (189.6 ± 1.0 Å^3) slightly larger than that of the stable monoclinic diarsenide (185.7 ± 0.5 Å^3). Similarly, the unit cell dimension of the hypothetical C2 $NiAs_2$ is 5.796 ± 0.002 Å, and a cell volume (192.0 ± 0.2 Å^3) comparable to those of β-$NiAs_2$ (195.3 ± 0.3 Å^3) and α-$NiAs_2$ (192.3 ± 0.5 Å^3 for $Z = 4$; *vide infra*).

[4]*The formal cation oxidation number in the ionic model of the pyrite dipnictides is +4.*

Can. J. Chem. Downloaded from www.nrcresearchpress.com by 210.87.254.5 on 09/05/12
For personal use only.

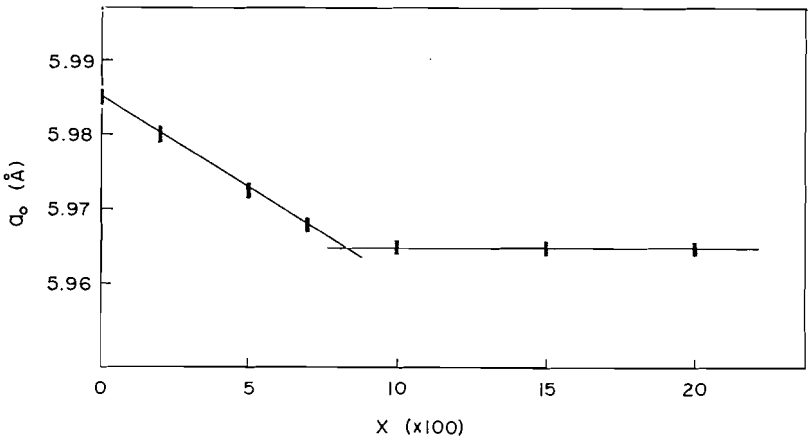


FIG. 1. Unit cell dimension as a function of composition in the cubic C2 phase $Co_xPd_{1-x}As_2$.

TABLE II

Compositions and cell parameters of the Co- and Ni-substituted $PdAs_2$ pyrite phases

$Co_xPd_{1-x}As_2$		$Ni_xPd_{1-x}As_2$	
x	a (Å)	x	a (Å)
0.00	$5.984_5 \pm 0.001$	0.00	$5.984_5 \pm 0.001$
0.02	5.980	0.05	5.975
0.05	5.972_5	0.10	5.964
0.07	5.968	0.20	5.943
0.10*	5.965	0.30	5.921
0.15*	5.965	0.40	5.900
0.20*	5.965	0.50	5.877
		0.60*	5.863
		0.70*	5.863

*From pyrite pattern in the two-phase region.

In the $Pd_xNi_{1-x}As_2$ system beyond the homogeneous pyrite phase, both α-Pd- and β-Pd-substituted nickel diarsenides were observed. The α,β transformation temperature is raised by the substitution of Ni by Pd (see Table III). The transformations in $Ni_{0.8}Pd_{0.2}As_2$ and $Ni_{0.9}Pd_{0.1}As_2$ were found to be relatively rapid (<8 d at 785°; <21 d at 750°; <50 d at 650 °C). As Yund observed (12), the transformation of β-$NiAs_2$ to α-$NiAs_2$ is extremely sluggish; no trace of the low-temperature modification could be detected after annealing at 500 °C for 150 d.

TABLE III

The system $Ni_xPd_{1-x}As_2$: effect of substitution of Pd for Ni on the α,β transformation in $NiAs_2$

T (°C)	$x = 0.80$	$x = 0.90$	$x = 1.00$
775	β	β	β
750	α	β	β
650	α	α	β
600	α	α	β
500	α	α	α*

*Synthesis from elements.

Can. J. Chem. Downloaded from www.nrcresearchpress.com by 210.87.254.5 on 09/05/12
For personal use only.

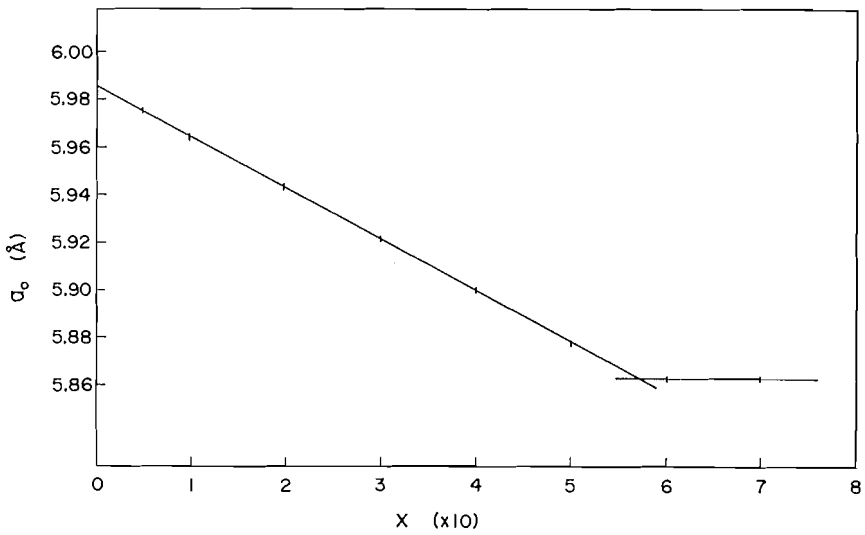


FIG. 2. Unit cell dimension as a function of composition in the cubic C2 phase $Ni_xPd_{1-x}As_2$.

2. The Binary Diarsenides. Pararammelsbergite and α-$NiAs_2$

The end members in the above systems, $PdAs_2$, $CoAs_2$, α-$NiAs_2$, and β-$NiAs_2$, and the compounds $PtAs_2$, $RhAs_2$, and $IrAs_2$ were synthesized with great care to ensure that the preparations were single phase.[5] Unit cell dimensions for these compounds are given in Table IV.

TABLE IV

Unit cell dimensions of the nickel and cobalt family diarsenides

Compound	Structure	a (Å)	b (Å)	c (Å)	β
β-$NiAs_2$	Orthorhombic C18	4.758±0.007	5.794±0.008	3.543±0.005	
α-$NiAs_2$	Orthorhombic	5.770±0.007	5.838±0.006	11.419±0.008	
$PdAs_2$	Cubic C2	5.984_5±0.001			
$PtAs_2$	Cubic C2	5.967±0.001			
$CoAs_2$	Monoclinic EO_7(?)	5.91_4±0.03_5	5.87_1±0.01	5.96_4±0.03_5	116.5°±0.5
$RhAs_2$	Monoclinic EO_7(?)	6.06_4±0.03_9	6.08_7±0.02_4	6.15_3±0.03_4	114.8°±0.5
$IrAs_2$	Monoclinic EO_7(?)	6.06_0±0.04	6.06_8±0.02_4	6.16_7±0.04_2	113.2°±0.6

Because the β ⟶ α-$NiAs_2$ transformation is slow, α-$NiAs_2$ was prepared by prolonged reaction of the elements below the transformation temperature with frequent grinding. The heating sequence: 2 d at 300 °C, 10 d at 400°, and a total of 61 d at 500 °C with periodic regrinding of the sample, produced the low-temperature modification free of NiAs and As. However, the diffraction pattern of this synthetic α-$NiAs_2$ did not agree well with the diffraction pattern of pararammelsbergite (10). Some additional reflections were present, and some of the intensities of reflections common to both patterns were at variance. It was shown that oxide, arsenate (24), and arsenite (25) impurities were absent, and that annealing the synthetic specimen at 600 °C produced pure β-$NiAs_2$. In studies on additional preparations, the parameters were found to be unchanged whether this phase was in equilibrium with NiAs or As, indicating a narrow homogeneity range.

[5]*The neighboring metal-rich phases, where known, are paramagnetic (21); the* MAs_3 *phases are diamagnetic (17). Polycrystalline arsenic is weakly paramagnetic at low temperatures and weakly diamagnetic at high temperatures (22, 23).*

Can. J. Chem. Downloaded from www.nrcresearchpress.com by 210.87.254.5 on 09/05/12
For personal use only.

Can. J. Chem. Downloaded from www.nrcresearchpress.com by 210.87.254.5 on 09/05/12
For personal use only.

TABLE V

Diffraction pattern of α-$NiAs_2$ (synthetic pararammelsbergite) orthorhombic; D_{2h}^{15}-$Pbca$; $a = 5.770 \pm 0.007$ Å; $b = 5.838 \pm 0.006$ Å; $c = 11.419 \pm 0.008$ Å; monochromatic Cu Kα radiation $\lambda(K\alpha_1) = 1.5405$ Å; Guinier–de Wolff focusing camera, diameter 11.46 cm; temperature 24 °C; internal standard As_2O_3 ($a = 11.075_5$ Å); low angle cutoff 40 Å; high angle cutoff 1.19 Å

I/I_1*	d_{obs} (Å)	d_{calc} (Å)	hkl
15	3.861	3.862	111
20(*a*)	2.900	2.898	020
22(*a*)	2.886	2.885	200
50	2.855	2.855	004
48	2.827	2.828	021
33(*a*)	2.793	2.791	113
45	2.602	2.600	022
41(*a*)	2.587	2.586	210
100(*a*)	2.559	2.559	104
45	2.541†	2.539	121
96	2.521	2.522	211
67	2.371	2.370	122
67	2.357	2.356	212
28(*a*)	2.345	2.344	114
16	2.317	2.316	023
15	2.151	2.149	123
11	2.054	2.052	220
11	2.042	2.041	024
20	2.031	2.029	204
20	2.020	2.020	221
36(*a*)	1.996	1.996	115
5(*a*)	1.918	1.917	214
52	1.821	1.820	131
15	1.807	1.807 1.806	106 223
36(*a*)	1.798	1.799	025
16(*a*)	1.755	1.755	132
66	1.741	1.740	312
39(*a*)	1.727	1.727	116
11(*a*)	1.714	1.712	215
15(*a*)	1.667	1.666	224
35(*a*)	1.660	1.659	133
35	1.648	1.647	313
35	1.613	1.613	230
43	1.596†	1.594	026
44(*a*)	1.549†	1.549	134
20(*v*)	1.539	1.539	314
45(*a*)	1.533	1.533	216
15(*v*)	1.526	1.526	225
43	1.485	1.485	233
15(*v*)	1.480†	1.480	323
24	1.448	1.448	041
25	1.442†	1.442	400
18(*a*)	1.434	1.435	135
32	1.427	1.427	008
20(*a*)	1.404	1.404	141
45(*a*)	1.380	1.380	217
30(*a*)	1.326	1.326	143
35(*a*)	1.318	1.318 1.318	235 316
16(*a*)	1.294	1.294	241
17(*a*)	1.279†	1.279	208
28	1.261	1.261	422
37	1.233	1.234	334
35	1.225	1.225	423
20	1.203	1.203	145

*Intensities determined by recording microphotometer; accuracy 5–10%. The reflections denoted by (*a*) are not present in the standard ASTM pattern for pararammelsbergite. The intensities of the reflections denoted by (*v*) were estimated visually because of poor photometric resolution.

†As_2O_3 overlap.

The focusing camera diffraction pattern is given in Table V. The pattern can be indexed on the orthorhombic pararammelsbergite cell, with all reflections, including the 'additional' reflections, conforming to the space group D_{2h}^{15}-*Pbca*. The unit cell volume is 384.6 ± 1.1 Å^3. With a cell content of eight formula units, the crystallographic density is 7.20 ± 0.02 g cm^{-3}. The observed density, measured by a helium displacement method (26), was 7.25 ± 0.07 g cm^{-3}.

Using these unit cell dimensions for α-$NiAs_2$, the enthalpy of the α,β transformation can be recalculated, using Yund's values for the parameters of β-$NiAs_2$, the transformation temperature (863 °K at 1 atm), and dP/dT for the univariant pararammelsbergite–rammelsbergite–niccolite curve of 45.5 bar deg^{-1} (12). Assuming the thermal expansion coefficients of the two forms are approximately equal, $\Delta V = 0.45 \pm 0.11$ cm^3 mole^{-1} and $\Delta H = 0.42 \pm 0.1$ kcal mole^{-1}. The $\alpha \rightarrow \beta$ transformation is too slow to be observed by differential thermal analysis.

3. *Magnetic Susceptibilities*

The System $Co_xPd_{1-x}As_2$

The magnetic properties of several compositions within the solid solution region of the $Co_xPd_{1-x}As_2$ system are shown in Fig. 3. $PdAs_2$ exhibits slightly temperature dependent diamagnetism. As Co is substituted for Pd, a paramagnetic contribution to the susceptibility is evident, especially at low temperatures. This behavior is indicative of the presence of localized moments on the solute ions.

To facilitate the interpretation of the magnetic data, the following terms are introduced (27): χ_M = molar susceptibility; $\chi_{xCo^{4+}}$ = paramagnetic susceptibility of cobalt in solid solution at a concentration of x cobalt ions; $\chi^D_{Co^{4+}}$ and $\chi^D_{Pd^{4+}}$ = diamagnetic core susceptibility per gram ion of cobalt and palladium; $\chi^D_{PdAs_2}$ = diamagnetic contribution

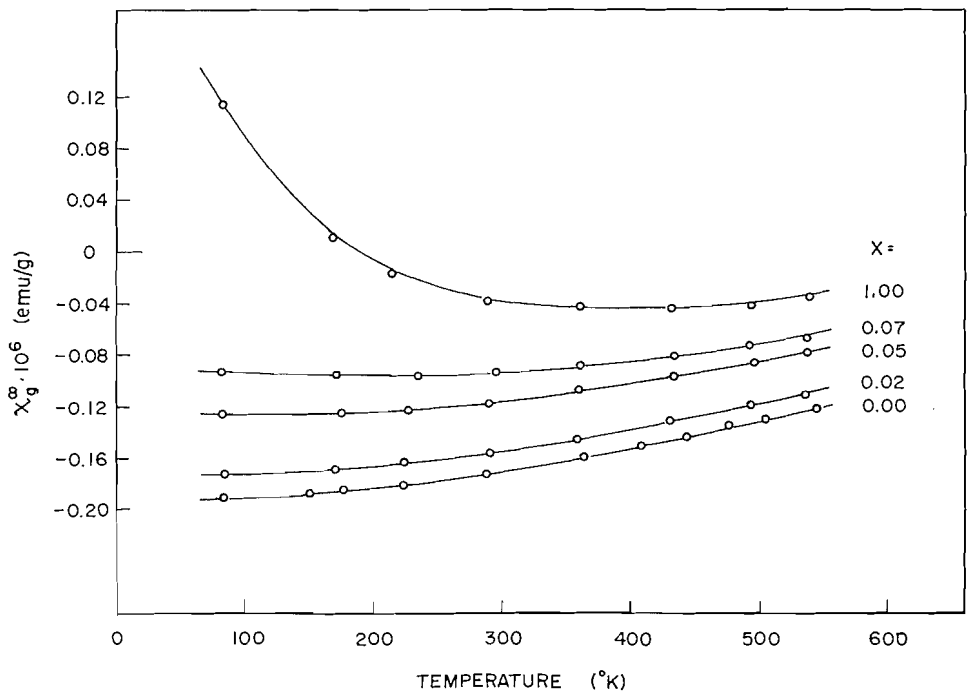


FIG. 3. Mass susceptibilities of $Co_xPd_{1-x}As_2$ solid solutions and of $CoAs_2$ as a function of temperature.

Can. J. Chem. Downloaded from www.nrcresearchpress.com by 210.87.254.5 on 09/05/12
For personal use only.

per gram molecule of $PdAs_2$; χ^D_x = diamagnetic contribution per gram molecule of solid solution defined by x cobalt ions. One can write

$$\chi_{xCo^{4+}} = \chi_M - \chi^D_x. \quad [1]$$

Now, χ^D_x can be written, using the additivity of diamagnetism, as

$$\chi^D_x = \sum_i n_i \chi^D_i + \varphi, \quad [2]$$

where n_i is the number of ions, χ^D_i is the diamagnetism of the ions, and φ is the structure term. Applying eq. [2] to the pyrite solid solution $Co_xPd_{1-x}As_2$,

$$\chi^D_x = [\chi^D_{Pd^{4+}} + \chi^D_{As_2^{4-}} + \varphi] + x\chi^D_{Co^{4+}} - x\chi^D_{Pd^{4+}},$$
$$= \chi^D_{PdAs_2} + x[\chi^D_{Co^{4+}} - \chi^D_{Pd^{4+}}].$$

The first term on the right-hand side represents the experimental molar susceptibility of $PdAs_2$[6] in which the term φ has necessarily been included. The diamagnetic contribution of the polyanion As_2^{4-} need not be known. Substituting into eq. [1],

$$\chi_{Co^{4+}} (\equiv \chi_{Co}) = (1/x)[\chi_M - \chi^D_{PdAs_2}] - \chi^D_{Co^{4+}} - \chi^D_{Pd^{4+}}. \quad [3]$$

Thus the molar susceptibility of $PdAs_2$ ($\chi^D_{PdAs_2}$) is subtracted from the molar susceptibility of $Co_xPd_{1-x}As_2$ (χ_M) at the temperature corresponding to the measured values of the latter. From these values are subtracted the difference in diamagnetic core susceptibilities of the cobalt and palladium ions. The latter have been calculated by the Slater–Angus method (28):

$$\chi^D_{Co^{4+}} \times 10^6 = -12.0 \quad \text{and} \quad \chi^D_{Pd^{4+}} \times 10^6 = -26.0 \text{ cgs e.m.u./gram-ion.}$$

For paramagnetic susceptibilities obeying the Curie–Weiss law $1/\chi = (T - \theta_w)/C$, a plot of $1/\chi_{Co}$ versus T gives a straight line of slope $1/C$. The graphs of $1/\chi_{Co}$ versus T are shown in Figs. 4 and 5 for the compositions $x = 0.05$ and 0.07.[7] The data have been fitted to a straight line by the method of least squares. For the composition $x = 0.05$, $1/\chi_{Co} = (T + 832)/0.307$. Since $p_{eff} = 2.83\sqrt{C}$ (where p_{eff} is the effective magnetic moment

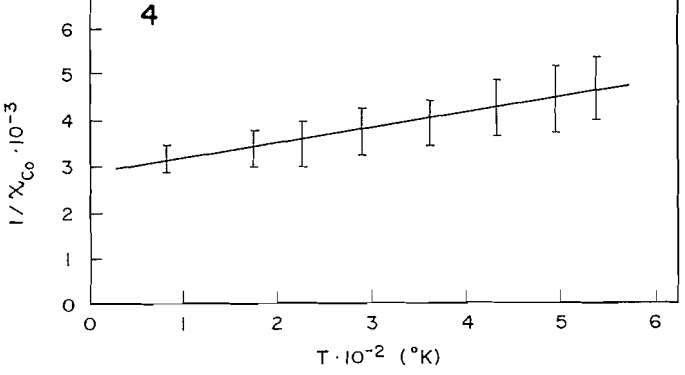


FIG. 4. Reciprocal paramagnetic susceptibility versus temperature for the composition $Co_{0.05}Pd_{0.95}As_2$.

[6]*Neither the magnitude of* χ^D *for* $PdAs_2$ *nor the temperature dependence of the susceptibility of* $PdAs_2$ *can, of course, be calculated with any certainty. That there is an electronic contribution to the susceptibility is also borne out by the resistivity data of* $PdAs_2$ *(vide infra).*

[7]*The magnetic data for the composition* $x = 0.02$ *has not been used to obtain an estimate of* p_{eff} *since the increase in susceptibility at low temperatures is almost within experimental error.*

Can. J. Chem. Downloaded from www.nrcresearchpress.com by 210.87.254.5 on 09/05/12
For personal use only.

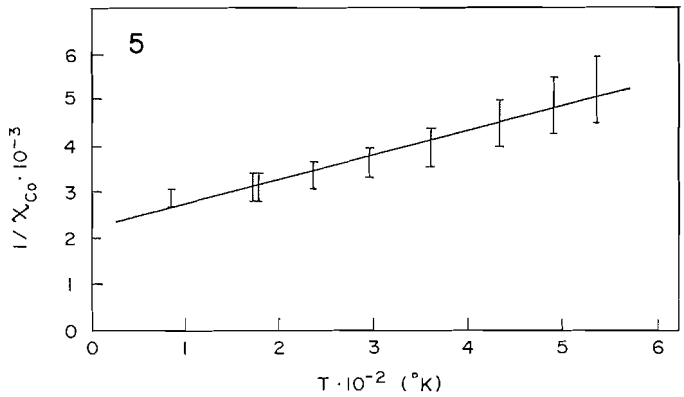


FIG. 5. Reciprocal paramagnetic susceptibility versus temperature for the composition $Co_{0.07}Pd_{0.93}As_2$.

per gram atom of Co), $p_{eff} = 1.5_7 \pm 0.4\ \mu_B$. For the composition $x = 0.07$, $1/\chi_{Co} = (T + 429)/0.196$, and $p_{eff} = 1.2_5 \pm 0.4\ \mu_B$.

The average value of p_{eff} is $1.4 \pm 0.4\ \mu_B$, and is, within experimental error, the moment arising from one free electron ($1.73\ \mu_B$), using the spin-only formula. Thus, as Co is substituted for Pd in $PdAs_2$, there is a temperature-dependent paramagnetic contribution to the susceptibility, which is attributed to the d^5 low-spin configuration of the cobalt atom in the pyrite structure. It is to be emphasized that the distance between metal atoms is large, and metal–metal interactions are precluded.

The System $Ni_xPd_{1-x}As_2$

The magnetic properties of several compositions within the solid solution region of the system $Ni_xPd_{1-x}As_2$ are shown in Fig. 6. In this system, a d^6 cation is being substituted by another d^6 cation, and one does not expect a paramagnetic contribution as in the foregoing system. With increased substitution of Ni for Pd, there is a progressive paramagnetic contribution to the susceptibility, but not of the Curie–Weiss type.

From the graph of gram susceptibilities versus temperature, values of χ^{∞}_M have been plotted against composition in Fig. 7, for the (randomly selected) temperatures $T = 84$, 290, 400, and 530 °K. Applying eq. [2] to this system,

$$\chi^D_x = \chi^D_{PdAs_2} + 14.2 \times 10^{-6}x,$$

where $\chi^D_{Ni^{4+}} \times 10^6 = -11.8$ cgs e.m.u./gram-ion, also calculated by the Slater–Angus method. This line is also shown in Fig. 7 for $T = 290$ °K. Now the increase in paramagnetism is much greater than that allowed for by the difference in diamagnetic core susceptibilities alone. However, only a rough estimate of this temperature-independent paramagnetic contribution can be made. If one assumes that the departure from linearity above $x \sim 0.3$ is anomalous, then extrapolation (for $T = 290°$) from $x = 0$ to $x = 1.0$ gives $\chi_M \times 10^6 = +35 \pm 5$ e.m.u./mole, and from eq. [3], $\chi_{Ni} \times 10^6 = +65 \pm 6$ e.m.u./gram-atom. The molar susceptibility is of the same order as that obtained for β-$NiAs_2$ (*vide infra*). The departure from linearity may be a result of the contraction of the crystal lattice on substitution of Ni for Pd. In $PdAs_2$ the As–As distance is 2.43 Å, i.e., twice the arsenic single bond radius. Provided the parameter of the As positions in the lattice is not altered on the formation of the solid solution, this interatomic distance is reduced to 2.38 Å at the homogeneity limit. If any compression of the arsenic pairs does occur, then neither φ nor $\chi^D_{As_2^{4-}}$ will be independent of concentration of Ni in the lattice, and eq. [2] will not be valid.

Can. J. Chem. Downloaded from www.nrcresearchpress.com by 210.87.254.5 on 09/05/12
For personal use only.

Can. J. Chem. Downloaded from www.nrcresearchpress.com by 210.87.254.5 on 09/05/12
For personal use only.

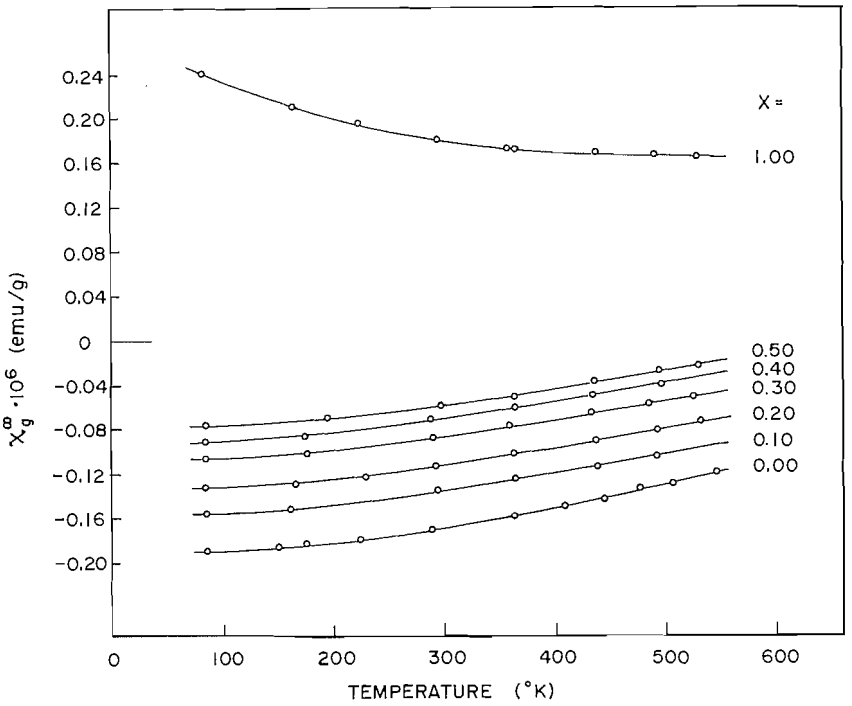


FIG. 6. Mass susceptibilities of $Ni_xPd_{1-x}As_2$ solid solutions and of β-$NiAs_2$ as a function of temperature.

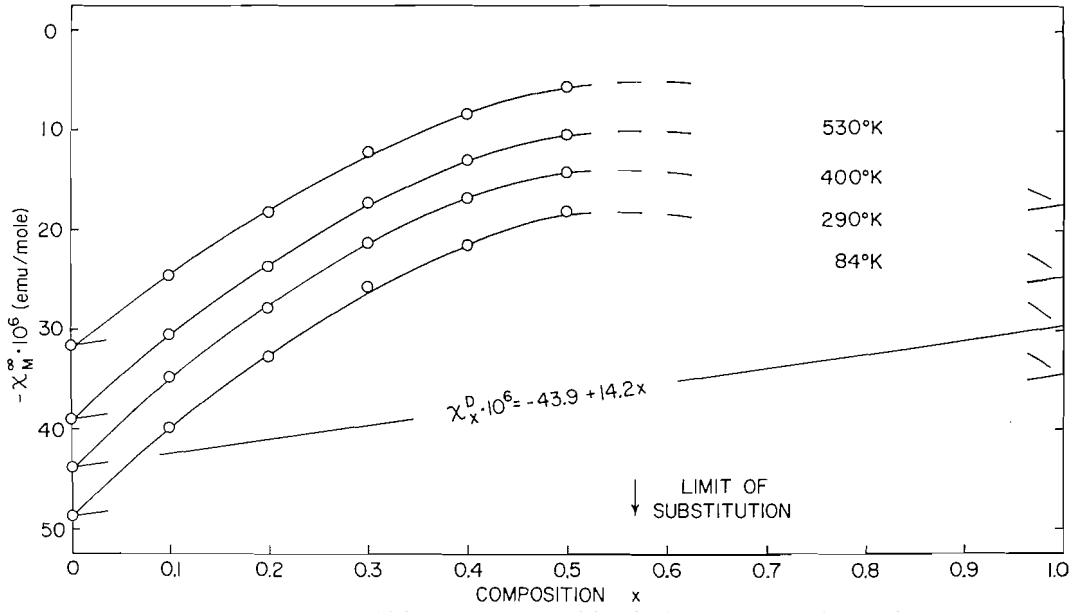


FIG. 7. Molar susceptibilities versus composition for $Ni_xPd_{1-x}As_2$ solid solutions.

Binary Transition Metal Diarsenides

The molar susceptibilities of the cobalt group and nickel group diarsenides as a function of temperature are shown in Figs. 8 and 9. All of the compounds are either diamagnetic or weakly paramagnetic. In the cases of β-$NiAs_2$ and $CoAs_2$, the hyperbolic form of the curves suggest that the Curie–Weiss law is approximately satisfied over certain temperature

Can. J. Chem. Downloaded from www.nrcresearchpress.com by 210.87.254.5 on 09/05/12
For personal use only.

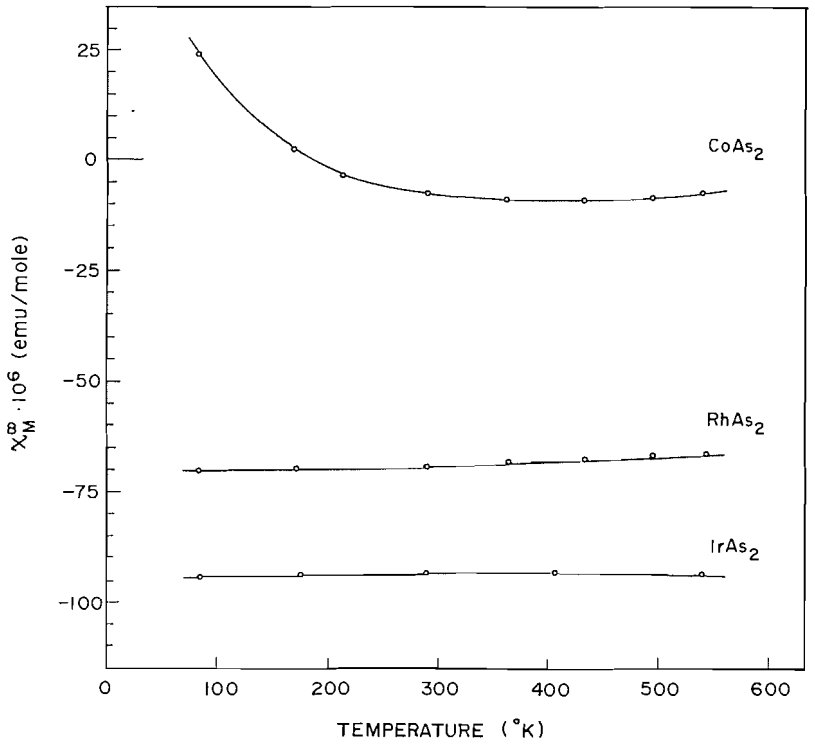


FIG. 8. Molar susceptibilities of the cobalt family diarsenides as a function of temperature.

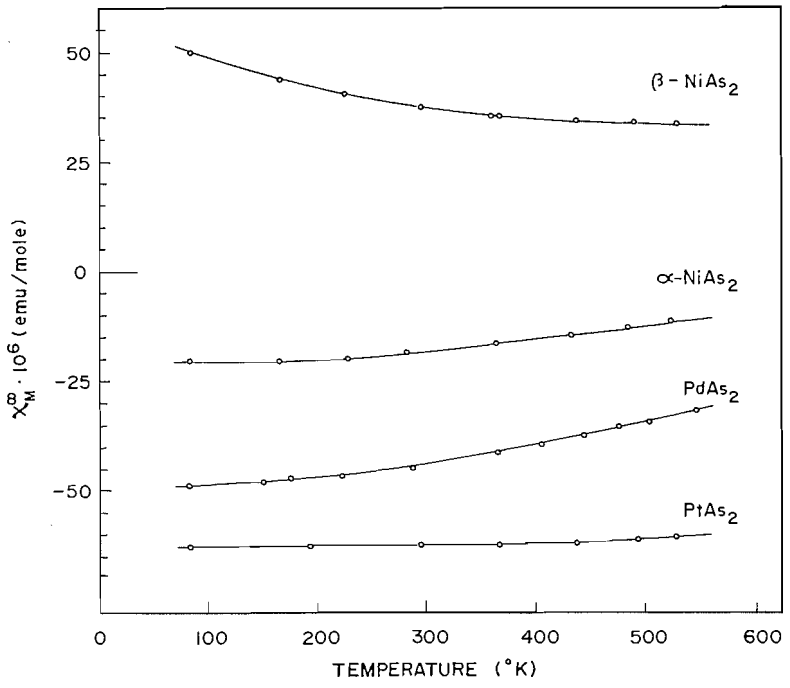


FIG. 9. Molar susceptibilities of the nickel family diarsenides as a function of temperature.

regions, but this is dependent upon the core diamagnetic susceptibility correction employed. To obtain an estimate of the magnetic moment in such cases, it is customary to replace the Curie–Weiss law by the expression $p_{eff}^2 = 8.01\chi_M T$, and p_{eff} approaches, with increasing temperature, the magnetic moment of the ion.[8] Even using the limiting diamagnetic corrections $\chi^D_{Ni^0} = -43.2$; $\chi^D_{Pd^0} = -52.7$; $\chi^D_{As^{3-}} = -63.3$ e.m.u./g ($\times 10^6$), p_{eff} approaches $\sim 0.8\ \mu_B$ at 550 °K for both β-$NiAs_2$ and $CoAs_2$. These values are maxima and are very approximate; nevertheless it is clear that these compounds have a magnetic moment of only a fraction of a Bohr magneton.

4. The Resistivity of $PdAs_2$ and $PtAs_2$

The resistivities of $PdAs_2$ and $PtAs_2$ shown in Fig. 10 were determined by a four probe method described by Pleass and Heyding (17). $PdAs_2$ is metallic in behavior, while $PtAs_2$ is semiconducting. Assuming $\rho \propto \exp(E_g/2kT)$ in the high-temperature region, an energy gap, E_g, of 0.17 eV is obtained for the latter. Hulliger (13, 15) reported that $PtAs_2$ was a semiconductor with an energy gap of 0.5 eV, and that $PdAs_2$ was "possibly metallic". More recently, Johnston *et al.* (29) measured the resistivity of $PtAs_2$ up to 1 200 °K, and found that the conductivity changed from *p*- to *n*-type at about 800 °K.

5. The Hulliger–Mooser–Pearson Model

Hulliger and Mooser (11, 13) and Pearson (14) have proposed that the metal ions in d^6 pyrites are in the low spin t_{2g} state, and that such compounds should be diamagnetic or weakly paramagnetic. The data for $PdAs_2$ and $PtAs_2$ are consistent with the model. Moreover, the substitution of a d^5 ion (Co^{4+}) for a d^6 ion (Pd^{4+}) in the pyrite structure introduces a moment indicating that the five non-bonding electrons in the d^5 ion are also in the t_{2g} energy levels. In the arsenopyrite-type diarsenides of the cobalt family, these authors suggest that the two singly occupied d levels of the neighboring cations in a hypothetical low-spin d^5 marcasite split up into a filled bonding and an empty antibonding level, giving rise to the cation pairs in the arsenopyrite structure. The pairing of the odd d electron gives each metal a filled t_{2g}^6 configuration, and consequently diamagnetic properties. Again the model is consistent with the observed susceptibilities of $CoAs_2$, $RhAs_2$, and $IrAs_2$.

Definitive comments on the magnetic behavior of α-$NiAs_2$ require a knowledge of its crystal structure. In all probability the lattice will be found to contain the arsenic pairs characteristic of all Group VIII diarsenides. The observation can be made that for the orthorhombic cell $a \sim b \sim c/2$, and a is approximately the dimension one would expect for a pyrite-type $NiAs_2$. The structure may be more closely related to the C2 structure than to the C18 structure.

According to the rule evolved by Pearson and Mooser for the semiconducting bond, all of the C2 and EO_7 diarsenides are potential semiconductors. The compounds $PdAs_2$ (metallic) and $PtAs_2$ (semiconducting) constitute an excellent example of the 'necessary-but-not-sufficient' nature of the rule. While the form of the Brillouin zones will be identical in both crystals, the rule does not predict the magnitude of the energy gap between the first zone (i.e., the valence band) and the second (the conduction band). If the periodic lattice potential is so small that energy states exist in the second zone below the maximum energy states in the first, the conduction and valence bands will be contiguous and metallic behavior will be observed. In isomorphous non-transition metal semiconductors and compound semiconductors the energy gap decreases with increasing atomic number in any

[8]*While this treatment of weak paramagnetic data is conventional, it has little merit other than to indicate the magnitude of the paramagnetic contribution expressed in terms of a spin-only model, regardless of the actual source of the moment.*

Can. J. Chem. Downloaded from www.nrcresearchpress.com by 210.87.254.5 on 09/05/12
For personal use only.

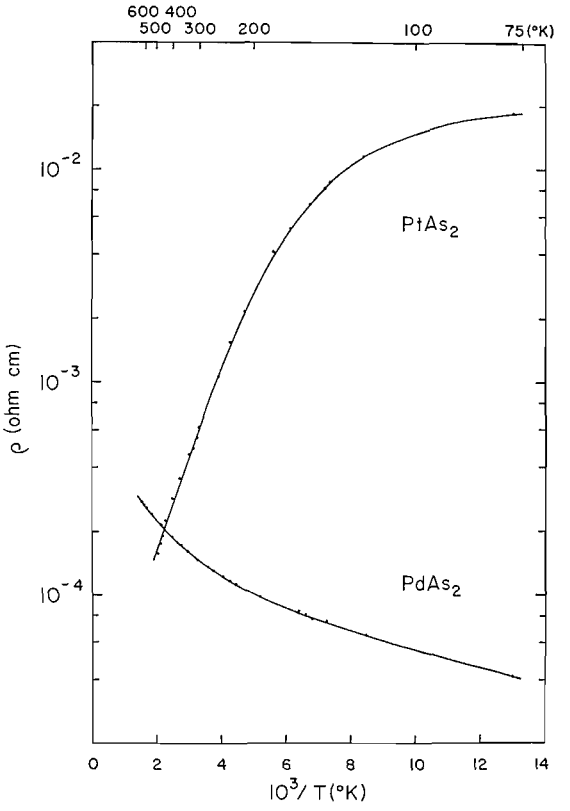


FIG. 10. Temperature dependence of resistivity of $PdAs_2$ and $PtAs_2$.

family, because the lattice potential energy decreases with increasing ionic radius. In these transition metal compounds, however, increasing atomic number of the metal ion from $PdAs_2$ to $PtAs_2$ is accompanied by an increase in lattice potential, because of the higher charge density associated with the $4f^{14}5d^6$ configuration of the Pt^{4+} ion. An increase in the magnitude of the energy gap in any family of transition metal semiconductors is to be expected when the transition metal ion in the second long period is replaced by the corresponding metal ion in the third long period.[9]

NOTE ADDED IN PROOF: Least squares lattice parameters and probable errors of α-$NiAs_2$, determined with an IBM 7040 computer (Univ. of Kansas), are $a = 5.770 \pm 0.001$, $b = 5.838 \pm 0.001$, and $c = 11.419 \pm 0.002$ Å.

ACKNOWLEDGMENTS

We wish to thank Dr. L. D. Calvert, National Research Council, Ottawa, for the Guinier – de Wolff diffraction patterns of α-$NiAs_2$. Operating grants from the National Research Council are gratefully acknowledged.

[9]*The experimental susceptibility data for these various systems have been placed in The Depository of Unpublished Data, National Science Library, National Research Council, Ottawa, Canada, and photocopies may be obtained upon request to the Depository.*

Can. J. Chem. Downloaded from www.nrcresearchpress.com by 210.87.254.5 on 09/05/12
For personal use only.

REFERENCES

1. CH. J. RAUB AND G. W. WEBB. J. Less-Common Metals, **5**, 271 (1963).
2. G. S. SAINI, L. D. CALVERT, R. D. HEYDING, and J. B. TAYLOR. Can. J. Chem. **42**, 620 (1964).
3. S. FURUSETH, K. SELTE, and A. KJEKSHUS. Acta Chem. Scand. **19**, 735 (1965).
4. J. C. QUESNEL and R. D. HEYDING. Can. J. Chem. **40**, 814 (1962).
5. N. N. ZHURAVLEV, G. S. ZHADANOV, and R. N. KUZ'MIN. Soviet Phys. Cryst. **5**, 532 (1960).
6. S. RUNDQVIST. Acta Chem. Scand. **15**, 451 (1961).
7. P. J. HOLMES. Bull. Geol. Soc. Am. **58**, 299 (1947).
8. R. D. HEYDING and L. D. CALVERT. Can. J. Chem. **38**, 313 (1960).
9. M. A. PEACOCK and C. E. MICHENER. Univ. Toronto Geol. Ser. No. 42, 95 (1939).
10. L. G. BERRY and R. M. THOMPSON. X-Ray powder data file. 8th set (1958). Card 9-8. Special Technical Publication 480G. A.S.T.M., Philadelphia, Pa.
11. F. HULLIGER and E. MOOSER. *In* Progress in solid state chemistry. Vol. 2. *Edited by* H. Reiss. Pergamon Press, New York. 1965. p. 330.
12. R. A. YUND. Econ. Geol. **56**, 1273 (1961).
13. F. HULLIGER and E. MOOSER. J. Phys. Chem. Solids, **26**, 429 (1965).
14. W. B. PEARSON. Z. Krist. **121**, 449 (1965).
15. F. HULLIGER. Nature, **200**, 1064 (1963).
16. F. HULLIGER. Phys. Letters, **4**, 282 (1963).
17. C. M. PLEASS and R. D. HEYDING. Can. J. Chem. **40**, 590 (1962).
18. R. D. HEYDING, J. B. TAYLOR, and M. L. HAIR. Rev. Sci. Instr. **32**, 161 (1961).
19. W. G. HENRY and J. L. ROGERS. Phil. Mag. **1**, 223 (1956).
20. M. GARBER, W. G. HENRY, and H. G. HOEVE. Can. J. Phys. **38**, 1595 (1960).
21. A. KJEKSHUS and W. B. PEARSON. *In* Progress in solid state chemistry. Vol. 1. *Edited by* H. Reiss. Pergamon Press, New York. 1964. p. 83.
22. J. B. TAYLOR, S. L. BENNETT, and R. D. HEYDING. J. Phys. Chem. Solids, **26**, 69 (1965).
23. S. L. BENNETT and R. D. HEYDING. J. Phys. Chem. Solids, **27**, 471 (1966).
24. J. B. TAYLOR and R. D. HEYDING. Can. J. Chem. **36**, 597 (1958).
25. S. STAHL. Arkiv Kemi Mineral. Geol. **17B**, No. 2, 1 (1943).
26. W. C. SCHUMB and E. S. RITTNER. J. Am. Chem. Soc. **65**, 1692 (1943).
27. P. POIX. Ann. Chim. Paris, **10**, 49 (1965).
28. W. R. ANGUS. Proc. Roy. Soc. London, Ser. A, **316**, 569 (1932).
29. W. D. JOHNSTON, R. C. MILLER, and D. H. DAMON. J. Less-Common Metals, **8**, 272 (1965).

Can. J. Chem. Downloaded from www.nrcresearchpress.com by 210.87.254.5 on 09/05/12
For personal use only.

Can. J. Chem. Downloaded from www.nrcresearchpress.com by 210.87.254.105 on 09/05/12
For personal use only.

A COMPARISON OF OPTIMIZATION METHODS FOR FITTING CURVES TO INFRARED BAND ENVELOPES[1]

J. PITHA[2] AND R. NORMAN JONES
Division of Pure Chemistry, National Research Council, Ottawa, Canada

Received August 8, 1966

ABSTRACT

A comparison has been made of seven numerical methods of fitting infrared absorption band envelopes with analytical functions using nonlinear least squares approximations. Gauss and Cauchy (Lorentz) band shape functions are used, and also sum and product combinations of the two. The methods have been compared with respect to both the degree of convergence and to the computation time needed to achieve an acceptable fit.

The most effective method has matched the overlap envelope of a steroid spectrum containing 16 bands; this necessitated the optimization of 65 variables. More complex spectra can be dealt with by a "moving subspace" modification in which only the parameters of a group of adjacent bands are adjusted at one time. Automatic computer programs have been written for five of the methods, and for the moving subspace modification. These will be published elsewhere.

If the computed curve is convoluted with the spectral slit function before making the least squares calculations, the distortion of the observed spectrum caused by the finite spectral slit width can be corrected. In some cases this method of diminishing the slit distortion is better than direct methods, particularly when dealing with strongly overlapped bands.

INTRODUCTION

In many applications of absorption spectrophotometry it is desirable to separate overlapping bands, and to approximate the band envelope by an analytical function. The simplest way to do this is by trial and error. Suitable mathematical functions are chosen for the component bands, the positional and shape parameters are adjusted empirically, and the contour of the composite band envelope is compared graphically with the measured spectrum. Moderately complex band systems have been analyzed in this fashion, both in vibrational spectra (1) and in electronic spectra (2). A more sophisticated adaptation of this method uses an analog computer to generate the component curves and match the band envelopes (3–5), but greater precision and flexibility can be introduced with digital techniques, and it is these that will concern us here.

In 1962 a general method for computing spectroscopic band envelopes was described by Stone (6) and further developed by Papoušek and Plíva (7).[3] Some aspects of this technique have been discussed by us previously (8) and also by Biggers and co-workers (9, 10). The basic mathematical problem is not specific to optical spectrophotometry, and similar methods have been applied to the approximation of electron paramagnetic resonance (11–13), nuclear magnetic resonance (14), and mass spectra (15), as well as to optical rotatory dispersion curves (16) and the envelopes of chromatographic recordings (17, and other references therein). Mathematically the problem calls for the application of least squares analysis to nonlinear functions, using iteration to achieve an acceptable fit. There is an extensive literature on this subject (18, 19), but no criteria exist for selecting the most efficient method for our particular purpose. Some comparisons of the effectiveness of different methods can be gleaned from the recent general literature on numerical analysis (20, 21) and from other specific applications, notably to automated lens design (22, 23).

[1]*Issued as N.R.C. No. 9204.*
[2]*National Research Council of Canada Postdoctorate Fellow.*
[3]*We wish to thank Drs. Papoušek, Plíva, and Toman for providing us with a preprint of this paper.*

In this article we compare seven techniques of nonlinear least squares analysis for fitting the envelopes of singlet and multiplet infrared absorption band systems.

METHODS AND RESULTS

Choice of the Band Shape Function

The theoretical treatment of infrared band shapes for condensed phase systems has been reviewed recently (24), and experimental measurements (25–27) support theory in indicating that isolated absorption bands are of Cauchy (Lorentz) form, on which secondary factors of both physical and instrumental origin impose a Gaussian perturbation. These basic shape functions are commonly expressed in the form

$$A(\nu)_c = a(b_c^2 + (\nu - \nu_0)^2)^{-1} \quad [1]$$

and

$$A(\nu)_g = a \cdot b_g^{-2} \cdot \exp\,[-(\nu - \nu_0)^2 \cdot \ln 2 \cdot b_g^{-2}], \quad [2]$$

in which ν_0 is the position of the band center, $2b$ the width of the band at half-maximal intensity, and a/b^2 the peak height.

For the least squares analysis it is preferable to generalize the variables as $x_1, x_2, \ldots x_n$. If we identify x_1 with the peak height, x_2 with the position of band center, x_3 and x_4 with band width parameters, eqs. [1] and [2] transform to

$$A(\nu)_c = x_1 \cdot (1 + x_3^2(\nu - x_2)^2)^{-1} \quad [3]$$

$$A(\nu)_g = x_1 \cdot \exp\,[-x_4^2(\nu - x_2)^2], \quad [4]$$

where $x_3 = b_c^{-1}$ and $x_4^2 = \ln 2 \cdot b_g^{-2}$.

The Gaussian perturbation of the Cauchy profile is most elegantly controlled by the Voigt convolution function (24, 28), or it can be developed theoretically in terms of correlation functions (29), but these are awkward to handle numerically. The product function $A(\nu)_p$ (eq. [5]), introduced by Abramowitz and Baumann (25), is more easily dealt with. This function was also employed by Papoušek and Plíva (7).

$$A(\nu)_p = x_1(1 + x_3^2(\nu - x_2)^2)^{-1} \cdot \exp\,[-x_4^2(\nu - x_2)^2] \quad [5]$$

In this equation the shape is defined by $x_3/(x_3 + x_4)$ which has a value of unity for a Cauchy curve and zero for a Gauss curve. There is no simple expression for the half-width, but it can be easily evaluated by an iterative process. We have used this product function in most of our calculations, but we have also investigated the sum function $A(\nu)_s$ (eq. [6]), which has five variables.

$$A(\nu)_s = x_1(1 + x_3^2(\nu - x_2)^2)^{-1} + x_5 \cdot \exp\,[-x_4^2(\nu - x_2)^2] \quad [6]$$

The contours of single Cauchy bands convoluted with a triangular slit function have been matched in good approximation by $A(\nu)_s$, with the restraining condition that x_4/x_3 is constant.[4] This reduces the number of adjustable parameters to four, as for $A(\nu)_p$.

Several methods are available for the treatment of asymmetric bands. Certain types of asymmetry can be conveniently controlled by introducing additional sets of parameters $(x_1 \ldots x_n)_i$, corresponding to additional bands; this is obviously the most physically meaningful way to take care of asymmetry resulting from weak unresolved bands. Cabana

[4]*Graphs of the error function ϕ plotted against x_4/x_3 in typical cases exhibit a broad flat minimum with x_4/x_3 in the range 0.7 to 0.8.*

Can. J. Chem. Downloaded from www.nrcresearchpress.com by 210.87.254.105 on 09/05/12
For personal use only.

and Sandorfy (30) dealt with the problem in a purely numerical way by using the Cauchy function [3] with different values of x_3 for $\nu > x_2$ and $\nu < x_2$. Stone (6) relaxed the requirement that the baseline must be horizontal and linear and used a function of the form

$$[7] \qquad E(\nu, \boldsymbol{x}) = \alpha + \beta\nu + \gamma\nu^2 + \sum_{j=1}^{N} A(\nu)_j,$$

where $E(\nu,\boldsymbol{x})$ defines the complete band envelope composed of N component bands each characterized by $A(\nu)_j$. This is an empirical, but effective, way to take account of slight asymmetries, particularly in systems where N is small.

The shape functions discussed above are all expressed in terms of absorbance, $\log_{10}(T_0/T)_\nu$, where T_0 is the intensity of the radiation entering and that leaving the sample and passing through the monochromator. Although it is desirable to store the finally computed intensity indices as absorbance ordinates, there are at least two reasons which make it preferable to perform the optimization computations in units of transmittance $(T/T_0)_\nu$.

$$(TT_0^{-1})_\nu = \exp[-2.303E(\nu,\boldsymbol{x})]$$

In these calculations the ordinates of the synthesized band envelope are summed from the individual component bands in absorbance units, and then converted to transmittance before evaluating the differences.

The first and main reason for computing in transmittance is because experiments with rotating sector photometers (31) have shown that for both single and double beam spectrometers the signal to noise ratio is approximately constant in transmittance, whereas on an absorbance scale it increases at high absorbance values and introduces maximal errors at the peaks. The second advantage of calculating in transmittance units is that it makes it practical to correct for the finite spectral slit distortion by convoluting the computed band envelope with the spectral slit function after each iteration, and performing the least squares analysis with respect to this convoluted band envelope. The synthesized band envelope then conforms to the "true" spectrum. For certain types of overlapping band systems this may be a more effective way of correcting for the finite slit distortion than methods based on the direct recovery from the experimentally measured spectrum (32–34). An illustration is given later in this paper.

EXPERIMENTAL

Our digitized spectra are obtained with a Perkin–Elmer model 521 spectrophotometer and digital data recorder. This permits the encoding of the spectra on eight-hole paper tape at constant wavenumber intervals in the range 10–0.1 cm^{-1}. In practice, logistical considerations of scanning rates and computation time limit this to minimal intervals of 0.5 cm^{-1} for extensive spectral ranges, though intervals of 0.2 or 0.1 cm^{-1} have occasionally been used over short wavenumber ranges. The intensity is encoded linearly in transmittance to three decimal places. The simulated curves considered in this paper were computed at 0.5 cm^{-1} intervals and the intensities rounded to 0.001 to conform with these conditions. The encoding of the transmission data to this order of precision is justified by the analysis of measurements obtained with a sector photometer (31), which has shown that the standard deviation in the reproducibility of the transmittance can be reduced below 0.002, if the random noise is averaged by repeated scanning.

The several techniques of least squares analysis discussed below were tested on a variety of simulated band systems and are illustrated for the set of singlet, quadruplet, and septuplet bands shown in Fig. 1. The characteristics of these curves are summarized in Table I.

Can. J. Chem. Downloaded from www.nrcresearchpress.com by 210.87.254.105 on 09/05/12
For personal use only.

Can. J. Chem. Downloaded from www.nrcresearchpress.com by 210.87.254.105 on 09/05/12
For personal use only.

TABLE I
Indices of test band systems*

	x_1	x_2	x_3	x_4	α	Half-width (cm^{-1})	Cauchy–Gauss ratio
Singlet	0.600 (0.720)	950.0 (952.0)	0.1 (0.15)	0.1 (0.15)	0.05 (0.06)	12.24 (8.16)	0.50 (0.50)
Quadruplet	0.300 (0.360)	970.0 (972.0)	0.2 (0.1)	0.1 (0.15)	0.05 (0.06)	8.28 (9.38)	0.67 (0.40)
	0.600 (0.720)	955.0 (957.0)	0.2 (0.1)	0.2 (0.30)		6.12 (5.27)	0.50 (0.25)
	0.300 (0.360)	940.0 (938.0)	0.1 (0.15)	0.1 (0.15)		12.24 (8.16)	0.50 (0.50)
	0.400 (0.480)	920.0 (918.0)	0.2 (0.1)	0.1 (0.05)		8.28 (16.55)	0.67 (0.67)
Septuplet	0.150 (0.180)	985.0 (987.0)	0.1 (0.15)	0.1 (0.05)	0.05 (0.06)	12.24 (12.11)	0.50 (0.75)
	0.400 (0.480)	970.0 (972.0)	0.2 (0.1)	0.2 (0.1)		6.12 (12.24)	0.50 (0.50)
	0.400 (0.320)	960.0 (958.0)	0.2 (0.1)	0.2 (0.1)		6.12 (12.24)	0.50 (0.50)
	0.200 (0.240)	950.0 (952.0)	0.2 (0.1)	0.1 (0.15)		8.28 (9.38)	0.67 (0.40)
	0.250 (0.300)	940.0 (942.0)	0.1 (0.15)	0.1 (0.15)		12.24 (8.16)	0.50 (0.50)
	0.400 (0.320)	930.0 (928.0)	0.2 (0.1)	0.2 (0.1)		6.12 (12.24)	0.50 (0.50)
	0.300 (0.360)	920.0 (918.0)	0.1 (0.15)	0.1 (0.15)		12.24 (8.16)	0.50 (0.50)

*The true values are listed first followed by the starting values in parentheses. x_1 = peak height in units of $\ln (T_0/T)_\nu$; x_2 = position of band center in cm^{-1}; x_3 and x_4 = band shape parameters (see eq. [5]); α = baseline displacement (see eq. [7] ($\beta = \gamma = 0$)).

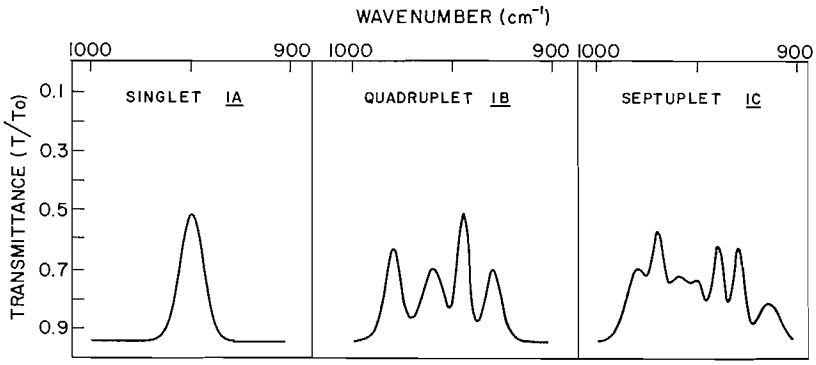


FIG. 1. Synthesized test curves.

The most effective method was tested on a 16-band section of the spectrum of 5β-androstan-17-one measured in carbon disulfide solution (Fig. 2). It becomes uneconomic in time, and possibly ineffective, to attempt to deal directly with spectra much more complex than this, but a system involving a "moving subspace", capable of computing longer sections of spectra, was later developed. The computer programs, which will be published separately (35), were written in Fortran IV and the computations were performed on an IBM 360–/50 computer.

Description of the Numerical Methods

Infrared band envelopes involve a large number of variables, but the accuracy of each ordinate measurement is relatively low, and these factors determine the most efficient method of computation. If $A(\nu)_p$ is used, or $A(\nu)_s$ with the restraining condition that x_3/x_4 is constant, a minimum of $4P$ variables are required to describe the envelope generated from P bands. This may be increased to $4P + 1$, $4P + 2$, or $4P + 3$ if, by the method of Stone (6), the baseline is freed from zero and, by addition of the α, $\alpha + \beta$, or $\alpha + \beta + \gamma$ terms, it is allowed to shift horizontally or with linear or quadratic slope.[5]

The agreement between the observed and calculated band envelope is given by

$$\phi = \sum_{i=1}^{M} f_i^2, \qquad [9]$$

where $f_i = I_i(\text{obs.}) - I_i(\text{calcd.})$, and M is the number of ordinate measurements. These ordinates will normally be in transmittance units, and we may consider that a maximal significant fit is achieved when $\phi \leqslant S^2 \cdot M$ (in which S is the standard deviation of the transmittance measurements). If this is taken as 0.002, the fit is optimized when $\phi \leqslant 4.10^{-6} M$. This is a conservative estimate, based on repetitive scan measurements with rotating sectors and, under normal conditions of recording it will be raised by the higher noise levels on the measured spectra (cf. Fig. 7).

The seven methods we have examined differ in the numerical procedure for optimization. In general they converge more rapidly with the ordinate data in absorbance than in transmittance units. This is to be expected since the absorbance functions are less seriously nonlinear, and the degree of nonlinearity has crucial importance for the efficiency

[5]*The use of the non-zero baseline is permissible if the sole purpose of the numerical analysis is to record the spectrum in a condensed form from which it can be regenerated. It is less acceptable if the analysis is intended to yield information of physical significance in the vibrational analysis of the absorbing molecule. One must also caution that these techniques of numerical analysis may lead to more than one acceptable solution, depending on the choice of the starting values. Again this is immaterial for documentational purposes, but the uniqueness of the solution would need to be checked carefully before any detailed physical interpretation is attempted.*

Can. J. Chem. Downloaded from www.nrcresearchpress.com by 210.87.254.105 on 09/05/12
For personal use only.

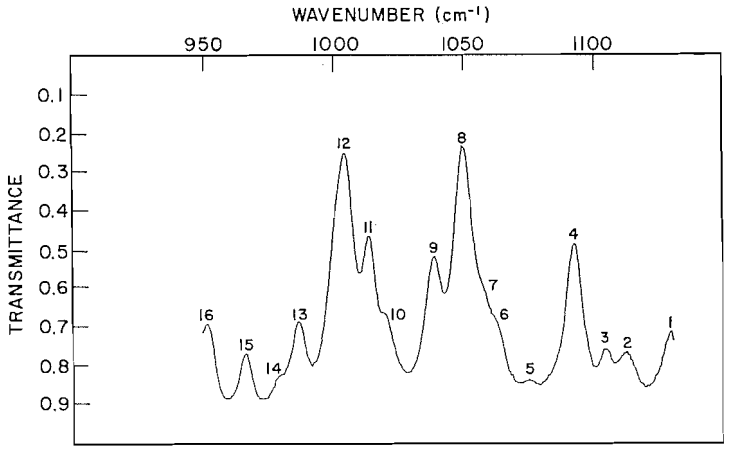


FIG. 2. Sixteen-band test spectrum of 5β-androsten-17-one in carbon disulfide solution. The curve was plotted from the digital tape by an S.D.S. 920 computer and Moseley plotter. The lettering and scales were added.

of the numerical procedures (21). In dealing with very complex band envelopes it may be necessary to take account of this, but we have preferred to work in transmittance units for the reasons discussed in the section on Methods and Results. In some cases the sum function (holding x_3/x_4 constant) converged more rapidly than the product functions, but there is an open question of choosing the x_3/x_4 value. The product function does not require this and was used in most of the calculations.

The mathematical discussion will be restricted to brief summaries of the methods, and the original papers should be consulted for details. Our nomenclature and symbolism are based on those used by Feder (22).

If ϕ is the function to be minimized, $\boldsymbol{x} = x_1, x_2 \ldots x_N$ is the vector of variables, $\boldsymbol{f}$ the vector of differences, where $f_i = I_{i(\text{obs})} - I_{i(\text{calcd})}$, we may write $\boldsymbol{f}^T \cdot \boldsymbol{f}$ for ϕ in eq. [9].

The central factor in the calculations is the $M \times N$ matrix $\boldsymbol{A}$ of partial derivative elements, where

$$A_{jk} = \partial f_j / \partial x_k, \qquad [10]$$

in which M is the total number of ordinate data points and N the total number of variables. Normally $M \gg N$. In the example of the septuplet band of Fig. 1C, $M = 200$ and $N = 28$ for a zero baseline, or $N = 31$ for non-zero values of α, β, and γ of eq. [7]. It is also necessary to define a matrix $\boldsymbol{B}$ where

$$\boldsymbol{B} = \boldsymbol{A}^T \cdot \boldsymbol{A}, \qquad [11]$$

and the vector $\boldsymbol{G}$ in which

$$\boldsymbol{G} = \boldsymbol{A}^T \cdot \boldsymbol{f} = 0.5 \text{ grad } \phi. \qquad [12]$$

Further discussion of these basic quantities and their interrelationships will be found in Feder's review article (22). The numerical calculations involve $\boldsymbol{B}$ and $\boldsymbol{G}$ only. To obtain these it is not necessary to store the complete $\boldsymbol{A}$ matrix in the computer. Memory places for one row only of the $\boldsymbol{A}$ matrix are needed; and $\boldsymbol{B}$ and $\boldsymbol{G}$ can be built up by gradual summation (36).

Can. J. Chem. Downloaded from www.nrcresearchpress.com by 210.87.254.105 on 09/05/12
For personal use only.

Method I

This was the first method we tested [8], and the calculations were performed in absorbance units.[6] It is a slight modification of the method described by Stone (6), in that we used the product function $A(\nu)_p$, whereas he used either pure Cauchy or pure Gauss functions.

The iteration step in the $(m + 1)^{th}$ convergence cycle is

$$\boldsymbol{x}_{m+1} = \boldsymbol{x}_m - p\boldsymbol{C}^{-1} \cdot \boldsymbol{G}_m, \quad [13]$$

where $\boldsymbol{C}$ is the diagonal matrix formed from $\boldsymbol{B}$ by setting the off-diagonal terms to zero. The scalar p determines the length of the step along the scaled gradient. If it is too large ϕ will not converge, but if it is too small the convergence will be slow. Stone commenced each iteration with a trial value of p (usually $p = 1$) and if the step was divergent he halved p progressively until convergence was obtained. In our experience this proved impractical in some cases, since it was necessary to reduce p to a value where the convergence became vanishingly small. Under these circumstances the overall minimization was improved when some of the parameters were held constant for a few cycles. Studies of several examples by this method revealed that the curve fit could be improved in all cases, but only exceptionally to a degree comparable with the experimental error of measurement. With highly inaccurate starting values, one or more bands might be eliminated by an extreme change in one of the variables (as for example displacement of a band position by 1 000 cm^{-1}). The calculated spectrum in the experimental range is then no longer sensitive to changes of the parameters of this band, and the band ceases to contribute to subsequent cycles of iteration. This difficulty can be overcome by setting quiescent boundary conditions (22).

Method II

This is an adaptation of the conjugated gradient method of Hestenes and Stiefel (37), which has been extensively employed in other applications of numerical analysis (22, 38). The iterative process is shown in eqs. [14]–[16].

$$\boldsymbol{D}_0 = -\boldsymbol{G}_0 \quad [14]$$

$$\boldsymbol{D}_m = -\boldsymbol{G}_m + (\boldsymbol{G}_m^2/\boldsymbol{G}_{m-1}^2) \cdot \boldsymbol{D}_{m-1} \quad [15]$$

$$\boldsymbol{x}_{m+1} = \boldsymbol{x}_m + h \cdot \boldsymbol{D}_m, \quad [16]$$

where h is chosen so that

$$\boldsymbol{D}_m^T \cdot \boldsymbol{G}_{m+1} = 0. \quad [17]$$

The technical difficulty in this method is the problem of choosing the scalar h. Feder (22) recommended that h be initially evaluated for a linear approximation of the system and then improved by interpolation. However, we found that for our functions such precalculated values of h could be in error by several orders of magnitude. In test cases, plots of $\boldsymbol{D}_m^T \cdot \boldsymbol{G}_{m-1}$ against h exhibited maxima, so that an interpolation starting from such a precalculated value of h may lead in the wrong direction. We overcame this difficulty by checking the degree of nonlinearity by eq. [18], by which $\boldsymbol{f}$ can be evaluated for linear conditions.

$$\boldsymbol{f}_{m+1} = \boldsymbol{A}(\boldsymbol{x}_{m+1} - \boldsymbol{x}_m) \times \boldsymbol{f}_m \quad [18]$$

If the value of ϕ computed from eq. [18] differed widely from the value of ϕ obtained by the calculation, the precalculated value of h was diminished by several orders of magnitude ($\sim 10^{-3}$) and this value used to improve h by interpolation.

[6] *All other calculations discussed in this paper were performed in transmittance units.*

Can. J. Chem. Downloaded from www.nrcresearchpress.com by 210.87.254.105 on 09/05/12
For personal use only.

We found this method gave better results than method I, but it was slower than methods III–VII examined later. A second disadvantage is that, in some cases, numerical errors accumulated to the point where a meaningful solution was lost. This is apt to happen when the components of $\boldsymbol{D}$ are widely different. Methods III–VII are less sensitive in this respect. Method II makes modest demands on the computer memory capacity, but because of the accumulation of errors it is not recommended for large systems, even when they are linear (38).

Method III

This method uses the procedure of Levenberg (39), which requires that the changes of the variables $\Delta\boldsymbol{x}^T \cdot \Delta\boldsymbol{x}$ be minimized as well as ϕ. Papoušek and Plíva (7) have devised a semiautomatic program based on this method. It calculates in absorbance units and has been applied to the five-component envelope of the C—H stretching bands in the infrared spectrum of *n*-decane.

The iteration step is

$$[19] \qquad \boldsymbol{x}_{m+1} = \boldsymbol{x}_m - (\boldsymbol{B}_m + p\boldsymbol{I})^{-1} \cdot \boldsymbol{G}_m,$$

with the scalar p chosen to minimize ϕ at each step. To make this method operate efficiently, a rapid procedure is needed to determine the optimal value of p. Papoušek and Plíva evaluated ϕ for a range of values of p and selected the best one. In our initial experiments we used a one-dimensional search, as described by Spang (19), but later we developed an interpolation procedure which is described in the Appendix. Method III proved to be superior to both I and II, but it failed to converge satisfactorily in some cases. Out of a series of 40 tests on systems containing 20–400 data points and 3–7 unknowns, three cases were encountered in which the convergence was extremely slow. It was also impracticably slow when used in the moving subspace technique developed for dealing with long band envelopes.

Method IV

This method was developed by Marquardt (40). The iteration step is

$$[20] \qquad \boldsymbol{x}_{m+1} \cdot \boldsymbol{C}_m^{1/2} = \boldsymbol{x}_m \cdot \boldsymbol{C}_m^{1/2} - (\boldsymbol{C}_m^{-1/2} \cdot \boldsymbol{B}_m \cdot \boldsymbol{C}_m^{-1/2} + p\boldsymbol{I})^{-1} \cdot \boldsymbol{G}_m \cdot \boldsymbol{C}_m^{-1/2}.$$

It differs from method III in that the matrix $\boldsymbol{C}$ is introduced as a scaling factor; $\boldsymbol{C}$ is the diagonal matrix formed from $\boldsymbol{B}$ by setting the off-diagonal terms to zero (cf. eq. [13]). The lowest value of p still giving a convergent ϕ is used. This method is available as I.B.M. SHARE program No. 3094, but as so written it could not be used with the large number of unknowns required in our application, and we reprogrammed it *ab initio*. This proved to be one of the more effective methods, as is seen from Figs. 3–5.

Method V

This is also a modification of method III. It was developed by Meiron (23) and employs different damping factors on different variables. The iteration step is

$$[21] \qquad \boldsymbol{x}_{m+1} = \boldsymbol{x}_m - (\boldsymbol{B}_m + p\boldsymbol{C}_m)^{-1} \cdot \boldsymbol{G}_m.$$

Here the unity matrix of method III is replaced by the matrix $\boldsymbol{C}$. This change takes account of the hyper-ellipsoidal form of the function ϕ which slows the convergence of method III. Equation [21] can be derived from eq. [20] by a simple algebraical transformation, and methods IV and V are mathematically equivalent. In V the *value of p producing the lowest value of* ϕ is determined at each step, whereas IV utilizes *the lowest value of p*. It is this operational difference that leads to more rapid convergence with method V.

Can. J. Chem. Downloaded from www.nrcresearchpress.com by 210.87.254.105 on 09/05/12
For personal use only.

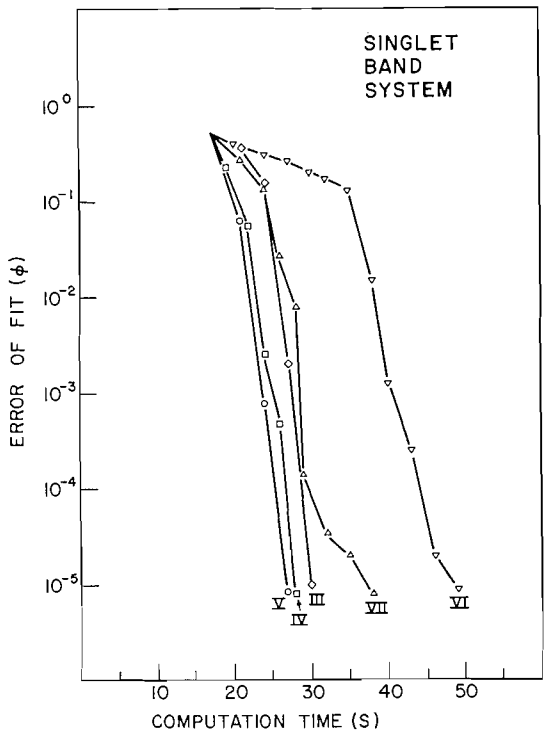


FIG. 3. Convergence of methods III–VII for the singlet band system. Consecutive iterations are indicated.

Our program normalizes the matrix (see eq. [20]), and automatically determines the optimal value of p as described in the Appendix. This method gives significantly faster convergence than any of the others we have investigated, as is seen from Figs. 3–5. Occasionally, where there were large differences in the magnitude of the diagonal elements of the $\boldsymbol{B}$ matrix, numerical difficulties developed during the computation, and it was then necessary to revert to method III.

Method VI

This is a metric variation method developed by Fletcher and Powell (41), and is based on the earlier work of Davidson (42). This method has been used extensively and has been claimed to be highly efficient (21).

The iteration step is

$$[22] \qquad \boldsymbol{x}_{m+1} = \boldsymbol{x}_m - h \cdot \boldsymbol{H}_m \cdot \boldsymbol{G}_m.$$

Here $\boldsymbol{H}_m$ modifies the metric of the parameter space. Initially $\boldsymbol{H}_0$ is a unity matrix and is iterated (41) to approximate the behavior of ϕ near the minimum point $\boldsymbol{x}_{\min}$.

$$[23] \qquad \boldsymbol{x}_{\min} - \boldsymbol{x} = -\boldsymbol{H} \cdot \boldsymbol{G}$$

The scalar h is adjusted to minimize ϕ in each iteration step.

Fletcher and Powell have used this method to obtain rapid convergence of systems of 100 variables. We have written it as an automatic program, but found it less efficient than method V in dealing with our $A(\nu)_D$ function, as is seen from Figs. 3–5.

Can. J. Chem. Downloaded from www.nrcresearchpress.com by 210.87.254.105 on 09/05/12
For personal use only.

Can. J. Chem. Downloaded from www.nrcresearchpress.com by 210.87.254.105 on 09/05/12
For personal use only.

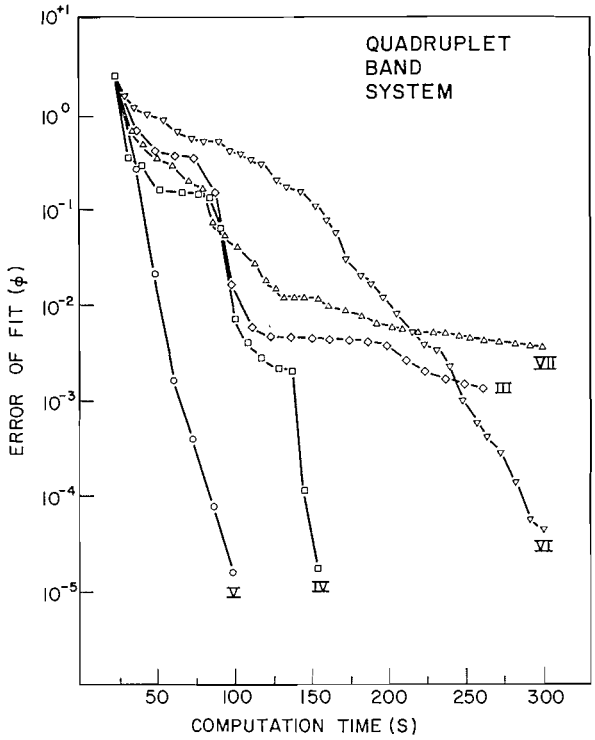


FIG. 4. Convergence of methods III–VII for the quadruplet band system. Consecutive iterations are indicated.

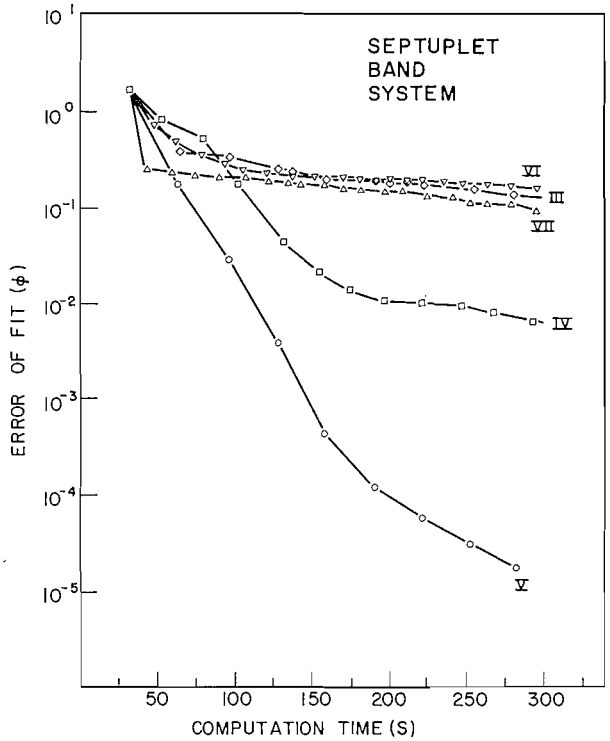


FIG. 5. Convergence of methods III–VII for the septuplet band system. Consecutive iterations are indicated.

Method VII

An analysis of the performance of method VI on the examples shown in Figs. 3–5 demonstrates the known fact (41) that the method is inefficient in the initial stages during which profound changes occur in the $\boldsymbol{H}$ matrix. In comparison with method III the iteration step takes less time and this only increases slowly with an increasing number of variables. It seemed reasonable to anticipate that the convergence in the initial stages might be accelerated by replacing $\boldsymbol{H}_0$ by $(\boldsymbol{B}_m + p\boldsymbol{I})^{-1}$ from method III (cf. eq. [19]). A duplex method was therefore developed using method III for the initial stages and later converting to method VI. It is seen from Figs. 3–5 that this does improve the slow initial stages of convergence of method VI, but not sufficiently to make it comparable with method V.

Comparison of the Methods

Reference has been made to the test cases of the singlet, quadruplet, and septuplet band systems of Fig. 1, and these may now be examined more closely. These curves were each synthesized from 200 data points and they were smooth to the limit of the rounding error (0.0005 transmittance units). The five most effective methods (III–VII) have been written as fully automatic programs in Fortran IV (35), using a standard form of input and output. The programs terminate the calculations when $f_{i(\max)} < 0.001$, or if a preselected time interval is exceeded. In Figs. 3–5 ϕ is plotted against the recorded computation time with the successive iterations indicated.

Figure 3 shows that for the single band all five methods converge rapidly. For 4 bands (Fig. 4) and 7 bands (Fig. 5) method V converges much faster than any of the others, and achieves an optimal significant fit in 3 iterations. Though methods IV and VI ultimately converge sufficiently in the 4-band case, 11 and 29 iterations are required respectively and neither of these methods can deal effectively with the 7-band system. Since this work was completed, Box (21) has compared the efficiency of eight optimization methods on highly nonlinear functions. Only one of his methods was identical with those we examined: this was the Davidson–Fletcher–Powell method (our method VI), which he found consistently better than his other seven. Since, in our hands, methods IV and V were superior to method VI, one is led to conclude that they would also be more efficient for our purpose than any of the other methods Box investigated.

Altogether about 100 sets of calculations have been made with a wide range of starting parameters. If these were too far removed from the true values, some of the bands were lost, as was noted in the discussion of method I. In general methods III–V were more stable in this respect than methods II, VI, and VII. Occasionally, when using the product function $A(\nu)_p$, negative values of x_3 and x_4 resulted (cf. eq. [5]), but this was not mathematically significant, since these variables enter the computations only as squared terms. The use of the sum function $A(\nu)_s$ occasionally resulted in negative Gauss components, but this could be avoided by diminishing the starting values of x_1 and x_5. The high stability of methods III–V may be associated with the fact that method III tends to follow closely the "natural valley path" of the parameter space (43), and the other methods presumably behave likewise.

In method VI, the final form of $\boldsymbol{H}$ describes the dependence of $\boldsymbol{G}$ on $\boldsymbol{x}$ near the minimum, and so provides an estimate of the precision of the final values of $\boldsymbol{x}$ (42). For methods III–V the procedure of Quenouille can be used to calculate the standard errors in the $\boldsymbol{x}$ vector terms (44). We have not pursued this because we were concerned only with the overall agreement, and this can be estimated sufficiently from ϕ, and $f_{i(\max)}$, the magnitude and wavenumber position of which was recorded by our programs.

Can. J. Chem. Downloaded from www.nrcresearchpress.com by 210.87.254.105 on 09/05/12
For personal use only.

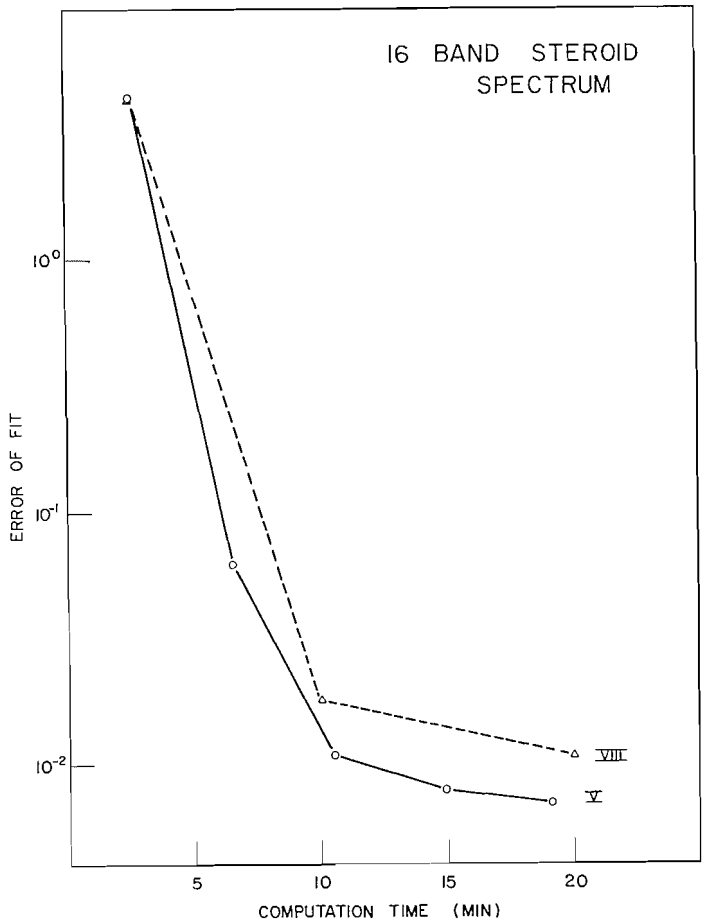


FIG. 6. Convergence of methods V and VIII for the 16-band steroid spectrum. (—) Method V. Consecutive iterations are indicated. (Two minutes must be added to the indicated times for the terminal output of the program.) (--) Method VIII. Terminal values after two consecutive 10 min computation periods are indicated.

Extension to the Analysis of Complex Real Spectra

Method V was found to deal effectively with the spectrum of 5β-androstan-17-one shown in Fig. 2. Sixteen bands can be discerned in the wavenumber range 1 132 – 950 cm^{-1}, and the matching of this band envelope calls for the optimization of 65 variables. Each iteration cycle was completed in approximately 4 min and the convergence is shown by the solid line of Fig. 6. Starting with guessed values of peak absorbance and band position taken from the normalized digital output from the spectrophotometer (34), and a guessed product band shape of 90% Cauchy/10% Gauss, 17 min computation reduced ϕ from 4.401 to 0.00788 and the maximal transmittance discrepancy ($f_{t(max)}$) from 0.287 to 0.016. A further 27 min computation only reduced these values slightly to 0.00723 and 0.0156. The error spectrum after 17 min is shown in Fig. 7A. In considering this it must be remembered that significant noise is present in the real band envelope as is seen from Fig. 2. The synthesized curve is smooth to the level of the round-off error, and it is difficult to separate the discrepancy due to the difference in the noise levels on the two curves from that associated with the misfit of the synthetic band envelope. A better indication of this misfit is provided by Fig. 7B

Can. J. Chem. Downloaded from www.nrcresearchpress.com by 210.87.254.105 on 09/05/12
For personal use only.

which shows the residual error after both the real spectrum and the synthesized band envelopes have been separately smoothed with a 5-point quadratic smoothing function. Earlier work (34) has shown that this type of smoothing induces only minor distortion in the shape of the band envelope, but diminishes the random noise, as is seen from Fig. 7C. The starting and ending values of the 65 variables are listed in Table II.

The Multiplet Method (Method VIII)

Comparison of the iteration time for method V in Figs. 2–6 suggests that the direct use of method V on still more complex band systems would become excessively slow. We have not investigated these yet but the difficulty in dealing with more complex spectra can be largely overcome by using a "moving subspace" method. In this (method VIII) the guessed variables for all the bands are initially introduced into the computation and the spectrum is treated as a whole. The variables of only a limited number of adjacent bands (usually four) are adjusted at one time; the α baseline term is included, but not β or γ. After a predetermined number of iterations with one of the standard methods the active subspace is moved to a neighboring set of bands, usually with one band overlap, and the minimized variables from the first section are incorporated into the $\boldsymbol{x}$ vector. This process is progressed cyclically through the spectrum and ϕ is computed throughout for the complete band system. As found previously, only method V was generally effective for optimizing the subspace variables. Method VIII was programmed to print out the variables after computing for a preselected time (usually 10 min) and the progress of the intermediate iterations was not monitored.

Method VIII was tested on the 16-band steroid system using the same starting values as for method V, and the convergence is shown by the broken line in Fig. 6. After 20 min, using 4-band subspace, ϕ was reduced to 0.011 and $f_{i(\max)}$ to 0.017, which compares satisfactorily with method V. Changing from a 4-band to a 3-band or 5-band subspace in the second 10 min cycle had negligible effect, and a third 10 min cycle produced no additional improvement. In a second series of calculations the guessed starting values for the peak heights were arbitrarily diminished by 10% to make a gross initial adjustment for the band overlap, but this also had no significant influence on the outcome after 10 min of computation.

It is seen from Table III that many of the parameters obtained by this calculation differ from those obtained by the direct application of method V to the complete spectrum. This suggests that these calculations may have led into a different minimization valley, or that the same minimum has been approached from a different direction. It demonstrates that the parameters obtained from nonlinear least squares analysis are not unique.

The major difference between the two sets of data summarized in Table III is the baseline parameter α. The systematic differences in the peak intensities (Δx_1) are clearly correlated with this, as also are the greater half-widths in the method VIII series. If the α variable had been omitted, and the computed curve constrained to lie on the zero baseline, the numerical agreement between the two sets of data would have been improved. This indicates the importance of the baseline in analyzing band shapes and intensities; it also suggests that uncertainty about the baseline position is the cause of much of the variation noted in experimental measurements of infrared band intensities (27). The error spectrum using method VIII is almost identical with that recorded for method V in Fig. 7 (A and B), except for a small region between 1 090 and 1 120 cm^{-1}.

Still other solutions are to be expected, and we have experimental evidence for this. In one series of calculations on the Fig. 2 curve we reduced ϕ to 0.0048 and $f_{i(\max)}$ to 0.0123,

Can. J. Chem. Downloaded from www.nrcresearchpress.com by 210.87.254.105 on 09/05/12
For personal use only.

Can. J. Chem. Downloaded from www.nrcresearchpress.com by 210.87.254.105 on 09/05/12
For personal use only.

TABLE II

Band indices for 5β-androstan-17-one spectrum (1 132 – 950 cm^{-1})

Band No.	Transmittance maximum	x_1	x_2	x_3	x_4	α	Half-width (cm^{-1})	Cauchy–Gauss ratio
Input values*								
1	0.713	0.14688	1130.0	0.22980	0.02550	0.00	8.5986	0.9001
2	0.766	0.11578	1113.0	"	"		"	"
3	0.759	0.11982	1104.5	"	"		"	"
4	0.488	0.31160	1092.5	"	"		"	"
5	0.837	0.07730	1075.5	"	"		"	"
6	0.668	0.17519	1061.5	"	"		"	"
7	0.593	0.22692	1057.5	"	"		"	"
8	0.239	0.62160	1050.0	"	"		"	"
9	0.520	0.28398	1039.0	"	"		"	"
10	0.668	0.17519	1020.5	"	"		"	"
11	0.468	0.32980	1014.0	"	"		"	"
12	0.253	0.59689	1004.0	"	"		"	"
13	0.686	0.16242	986.5	"	"		"	"
14	0.855	0.06801	977.5	"	"		"	"
15	0.770	0.11348	967.0	"	"		"	"
16	0.690	0.16212	952.0	"	"		"	"
Output values†								
1		0.13322	1129.9	0.18675	0.01603	−0.007	10.63	0.9210
2		0.09077	1112.9	0.17833	0.01023		11.18	0.9457
3		0.06639	1104.6	0.33432	0.02200		5.96	0.9382
4		0.28462	1092.5	0.25832	0.03763		7.58	0.8728
5		0.05006	1076.5	0.09004	0.02975		20.20	0.7516
6		0.08757	1062.9	0.23612	0.00862		8.46	0.9648
7		0.08746	1057.3	0.23689	0.08886		7.50	0.7272
8		0.57362	1049.9	0.29437	0.04113		6.67	0.8774
9		0.22896	1038.5	0.24916	0.01898		7.98	0.9292
10		0.11121	1020.8	0.18793	0.00634		10.63	0.9673
11		0.21688	1013.9	0.40105	0.01315		4.98	0.9682
12		0.56839	1003.7	0.23259	0.03989		8.36	0.8536
13		0.12959	986.8	0.28406	0.04277		6.89	0.8691
14		0.04676	978.9	0.18385	0.07908		9.38	0.6992
15		0.10133	966.4	0.25418	0.04723		7.61	0.8433
16		0.16161	951.5	0.23883	0.05127		8.02	0.8233

*The peak heights and transmittance measurements were taken directly from the normalized digital output from the spectrometer (34). x_1 = peak height in absorbance units ($\log_{10}(T_0/T)_{max}$; x_2 = position of band center; x_3 and x_4 = band shape parameters (see eq. [5]); α = baseline displacement (see eq. [7] ($\beta = \gamma = 0$)).

†These values for the indices were obtained by method V after four cycles of calculation (17 min of computation).

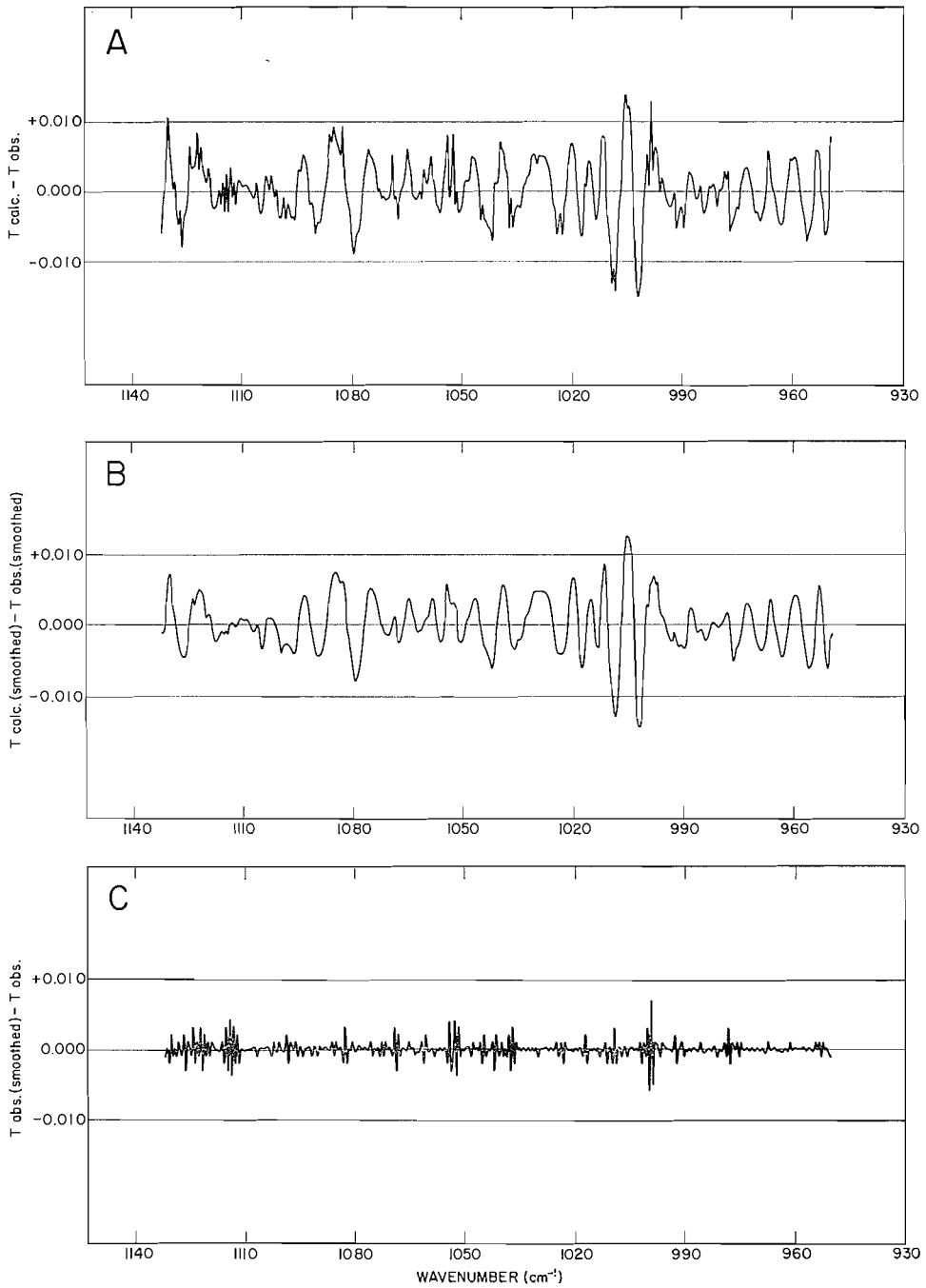


FIG. 7. Error spectrum for the data from Fig. 6 after 17 min computation by method V. Curve A: $I_{\text{calcd}} - I_{\text{obs}}$ as measured and computed. Curve B: $I_{\text{calcd}} - I_{\text{obs}}$ after each has been separately smoothed by a 5-point quadratic convoluting function to diminish the random noise on the real spectrum. Curve C: $I_{\text{obs(smoothed)}} - I_{\text{obs}}$.

Can. J. Chem. Downloaded from www.nrcresearchpress.com by 210.87.254.105 on 09/05/12
For personal use only.

Can. J. Chem. Downloaded from www.nrcresearchpress.com by 210.87.254.105 on 09/05/12
For personal use only.

TABLE III

Comparison of output indices for 5β-androstan-17-one spectrum computed by methods V and VIII*

Band No.	Δx_1	Δx_2	Δx_3	Δx_4	$\Delta\alpha$	Half-width difference (cm^{-1})	Cauchy–Gauss ratio difference
1	−0.031	−0.1	0.023	0.007	0.094	−1.54	−0.027
2	−0.029	0.0	0.040	0.000		−3.22	0.014
3	−0.005	0.5	0.048	−0.058		−0.56	0.016
4	−0.025	−0.1	0.014	0.019		−0.56	−0.056
5	−0.037	0.7	0.050	−0.030		−2.51	0.384
6	−0.022	0.1	0.024	−0.097		0.64	0.297
7	−0.008	0.1	0.182	−0.172		1.12	0.707
8	−0.048	0.0	0.013	0.006		−0.32	−0.012
9	−0.020	0.0	0.022	−0.008		−0.70	0.034
10	−0.023	0.3	0.044	−0.021		−2.96	0.127
11	0.010	0.0	−0.032	0.002		0.38	−0.006
12	−0.022	0.0	0.008	0.026		−0.53	−0.087
13	−0.010	0.0	0.020	0.030		−0.66	−0.086
14	−0.014	0.2	0.004	0.070		−1.69	−0.252
15	−0.015	0.0	0.028	0.037		−1.19	−0.113
16	−0.029	0.1	0.028	0.044		−1.14	−0.144

*The differences are given for the method V − method VIII indices.

TABLE IV

Comparison of input and output indices for synthesized overlapping doublet with slit function deconvolution*

	Starting values					Ending values				
	x_1	x_2	x_3	x_4	α	x_1	x_2	x_3	x_4	α
True values	—	—	—	—	—	1.1513 1.1513	997.5 1002.5	0.200 0.200	0.000 0.000	0.000
First experiment†	1.200 1.100	997.0 1002.0	0.18 0.18	0.02 0.02	0.01	1.154 1.148	997.5 1002.5	0.200 0.200	0.005 0.003	0.001
Second experiment‡	1.100 1.200	997.0 1002.0	0.18 0.18	0.02 0.02	0.01	1.153 1.149	997.5 1002.5	0.200 0.200	0.004 0.004	0.001
Third experiment‖	1.050 1.050	997.5 1002.5	0.15 0.15	0.15 0.15	0.01	1.150 1.149	997.5 1002.5	0.200 0.200	0.007 0.005	0.001

*See Fig. 9. Method V was used.
†The guessed values placed the inflection correctly on the right side of the band center.
‡The guessed values placed the inflection on the left side of the band center but this was corrected in the computations.
‖The guessed band shape was 50% Cauchy/50% Gauss but the Gaussian component was rejected in the computation.

but this necessitated starting values that had been refined by extensive preliminary calculations on separate sections of the spectrum. Where possible we have preferred to use starting values for x_1 and x_2 taken directly from the digitized output data from the spectrometer together with reasonable rounded values for x_3 and x_4; this gives an objectively defined starting point for the iterations. A search for better starting values is only attempted if the values of ϕ and $f_{i(\max)}$ obtained in this way are unacceptable in relation to the noise levels and other experimental errors in the measured spectrum.

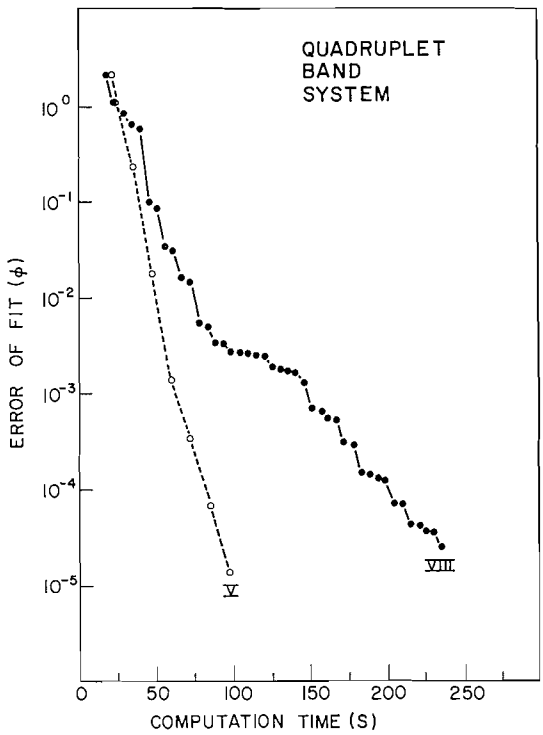


FIG. 8. Convergence of methods V and VIII for the quadruplet band system, using 2-band subspace for method VIII.

At present we cannot indicate at what degree of complexity method VIII surpasses method V. On the 16-band steroid spectrum they are almost equally efficient, with method V having a slight advantage. We have also compared methods V and VIII on the 4-band system of Fig. 1B using a 2-band subspace for method VIII. The convergence rates are compared in Fig. 8, and here method V is clearly the better, though method VIII does achieve an acceptable solution. The general superiority of method VIII probably becomes decisive around 17–20 bands, but this boundary may not be sharply defined and may depend on the type of computer used, particularly on its ability to deal with the $N \times N$ matrix $\boldsymbol{B}$. Beyond a certain degree of complexity the computation time for method VIII should increase approximately linearly with the number of bands, or with the total wavenumber scan, since the wing contributions of the more remote bands will become negligible.

Corrections for Slit Function Distortion

The measured spectrum is subject to systematic errors, the most important of which is the distortion resulting from the use of a finite spectral slit width. This may be expressed

$$T(\nu)_{\text{obs}} = \int p(\nu,\nu') \cdot T(\nu')_{\text{true}} \cdot d\nu', \qquad [25]$$

Can. J. Chem. Downloaded from www.nrcresearchpress.com by 210.87.254.105 on 09/05/12
For personal use only.

where $p(\nu,\nu')$ is the normalized spectral slit function. There is an extensive literature dealing with numerical methods of solving this equation for $T(\nu)_{true}$ (24, 32–34).

Instead of trying to obtain $T(\nu)_{true}$ directly, it is possible to use the least squares approximation method to obtain an analytical expression for $T(\nu)_{true}$ instead of $T(\nu)_{obs}$. To do this, the synthesized band envelope, derived from the initial guessed variables, is convoluted with the slit function before minimization of the variables, and this procedure is repeated at each iteration step. We thus obtain a band envelope which, after convolution with the slit function, conforms with the observed spectrum and is therefore equivalent to $T(\nu)_{true}$ within the limits of the approximation. The additional calculation slows the computation to an extent dependent on the type of numerical integration used.

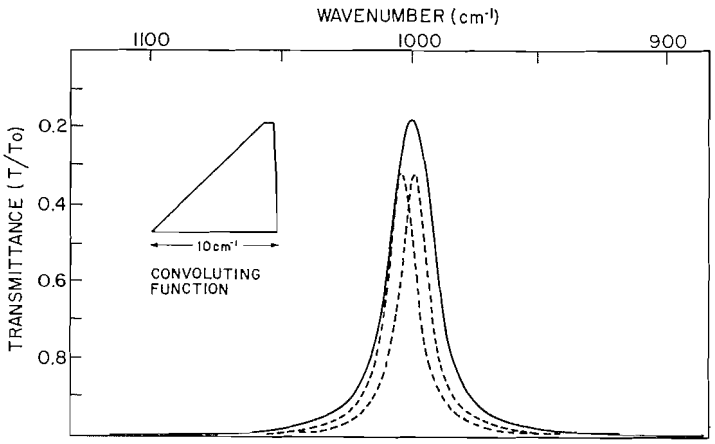


FIG. 9. Curves illustrating the analytical separation of closely overlapping bands generated from a doublet convoluted with a trapezoidal function.

We have tested this method on a few simple cases, but have concluded that for the more complex types of band envelope it is preferable to correct the measured spectrum directly by the pseudo-deconvolution method of numerical analysis discussed previously (34). On the other hand this method has proved to be very effective in dealing with band envelopes composed of a small number of strongly overlapped components.

This is illustrated by the example shown in Fig. 9 and Table IV. Here the slightly asymmetric single-peaked band envelope was constructed from a symmetrical pair of component bands by addition, with subsequent convolution using the highly asymmetric trapezoidal "convoluting function" shown in Fig. 9. In the computations, the presence of the two component bands was assumed, initial guessed variables were chosen, and the resultant curve adjusted by method V, convoluting with the trapezoidal function before evaluating ϕ, B, and G at each step. Highly satisfactory recoveries of the equivalent pair of component bands were obtained using widely different starting values, as is seen from the indices listed in Table IV. The "true" summation band was approximated from these by addition, with a maximal transmittance error less than 0.001.

CONCLUSIONS

With digital computers, it is possible to generate analytical expressions that will fit the contours of infrared band envelopes with a precision approaching that of the statistical uncertainty of the data measurements. The number of component bands that can be handled with reasonable speed will depend on the computing facilities available. The

Can. J. Chem. Downloaded from www.nrcresearchpress.com by 210.87.254.105 on 09/05/12
For personal use only.

computation time increases rapidly with the number of bands when the spectrum is analyzed as a single unit, and if the number of bands exceeds 17–20 it probably becomes more efficient to use a cyclical method, varying the parameters of a limited number of bands at a time. The choice of the initial guessed variables does not appear to effect the rate of convergence critically, though our experimental evidence for this is limited, particularly for the more complex band systems. More than one statistically acceptable solution is possible, and it would seem prudent to choose the starting values with care, since this should help to achieve a solution having the maximum physical meaning. Economic factors would appear to set the upper limit to the size of spectrum that can be handled by method VIII. The accuracy of the fit could almost certainly be improved by the use of closer wavenumber intervals. In all our work we have held this interval constant at 0.5 cm^{-1}. This was done mainly for technical reasons associated with the digital encoding of the spectrum. The use of smaller intervals (0.2–0.1 cm^{-1}) would considerably increase the computing time.

In this paper we have emphasized the digital approach to fitting band envelopes, though analog methods are also being used to deal with systems of moderate complexity (5). Analog methods could certainly help in recognizing weak component bands and in rapidly establishing input values for calculations of the kind discussed here.

The complete description of an infrared absorption spectrum containing P component bands by $4P$ or $4P + 1$ band "indices" would appear to be technically feasible and from these indices the spectrum can be regenerated on any chosen ordinate and abscissal scale using simple computing facilities: the limitations would seem to be economic rather than scientific. The spectroscopic value of this type of band classification will be determined by the extent to which each component band can be shown to have physical significance in relation to the vibrational behavior of the molecule, and this aspect of the problem needs careful and cautious investigation.

ACKNOWLEDGMENTS

We wish to thank Dr. S. D. Baxter and his colleagues at the N.R.C. Computation Center for their assistance with the computation measurements and also Mr. E. R. R. Funke of the Analysis Laboratory and the Control Systems Laboratory of the N.R.C. Division of Mechanical Engineering. Helpful discussions with Dr. J. W. Hopkins, Dr. J. Meiron, Dr. R. L. Somorjai, Dr. H. Stone, and Dr. C. M. Woodside are also gratefully acknowledged.

APPENDIX

Methods III and V. Selection of the Optimal Value of p

At the beginning of the computation ϕ_{initial} is calculated from the starting values of the variables. In the first cycle we arbitrarily set $p_0 = 10^{-1}$ and use it to compute $\phi_0(1)$ from eqs. [19] or [21]. If $\phi_0(1) < \phi_{\text{initial}}$ we take as second choice for p_0 the value $p_0(2) = p_0(1) \times 10^{-2}$, but if $\phi_0(1) \geqslant \phi_{\text{initial}}$ we take instead $p_0(2) = p_0(1) \times 10^{3}$. For the third trial value of p_0 we take $p_0(3) = p_0(1) \times 0.5$ or $p_0(3) = p_0(2) \times 0.5$ whichever gives the smaller value of ϕ_0. Having in this way obtained three values for p_0, the two which give the lower values for ϕ_0 are selected and interpolated with a cubic polynomial in the following manner. The coordinates ϕ and p^{-1} are used and the two best values of (ϕ, p^{-1}) provide two points defining the interpolation curve. The remaining condition is the relation that as $p^{-1} \rightarrow 0$, $\phi_m \rightarrow \phi_{m-1}$ and $d\phi_m/dp^{-1} = -2\boldsymbol{G}^T \cdot \boldsymbol{G}$, from which the slope of the cubic interpolation curve and its intercept with the y axis are known (39).

An additional value of p is obtained from the minimum of this interpolation curve, and

Can. J. Chem. Downloaded from www.nrcresearchpress.com by 210.87.254.105 on 09/05/12
For personal use only.

the corresponding ϕ computed. Normally the ϕ_0 calculated from this p_0 will be the lowest, but not necessarily so. Of the several values of p obtained by the above process, *that giving the lowest* ϕ is accepted, and the variables adjusted on this basis for the next cycle. The same procedure for obtaining the optimal value of p is followed in subsequent cycles, except that the p used in the preceding cycle is taken as starting point, instead of the arbitrarily chosen value of 10^{-1}.

REFERENCES

1. R. N. JONES. Spectrochim. Acta, **9**, 235 (1957).
2. C. SANDORFY and R. N. JONES. Can. J. Chem. **34**, 88 (1956).
3. F. W. NOBLE, J. E. HAYES, JR., and M. EDEN. Proc. Inst. Radio Engrs. **47**, 1952 (1959).
4. E. D. BECKER. Spectrochim. Acta, **17**, 436 (1961).
5. I. M. SARASOHN and S. DAY NOGARE. Pittsburgh Conference on Analytical Chemistry and Applied Spectroscopy Abstracts. 1966. p. 143.
6. H. STONE. J. Opt. Soc. Amer. **52**, 998 (1962).
7. D. PAPOUŠEK and J. PLÍVA. Collection Czech. Chem. Commun. **30**, 3007 (1965).
8. J. PITHA and R. N. JONES. Can. Spectry. **11**, 14 (1966).
9. J. T. BELL and R. E. BIGGERS. J. Mol. Spectry. **18**, 247 (1965).
10. R. E. BIGGERS, J. T. BELL, E. C. LONG, and O. W. RUSS. Mathematical resolution of complex overlapping spectra and spectral fine structure with non-linear least squares computer techniques. ORNL-3834. In preparation.
11. J. A. IBERS and J. D. SWALEN. Phys. Rev. **127**, 1914 (1962).
12. D. W. MARQUARDT, R. G. BENNETT, and E. J. BURRELL. J. Mol. Spectry. **7**, 269 (1961).
13. T. S. JOHNSTON and H. G. HECHT. J. Mol. Spectry. **17**, 98 (1965).
14. W. D. KELLER, T. R. LUSEBRINK, and C. H. SEDERHOLM. J. Chem. Phys. **44**, 782 (1966).
15. D. G. LUENBERGER and U. E. DENNIS. Anal. Chem. **38**, 715 (1966).
16. J. P. CARVER, E. SCHECHTER, and E. R. BLOUT. J. Am. Chem. Soc. **88**, 2550 (1966).
17. P. D. KLEIN and B. A. KUNZE-FALKNER. Anal. Chem. **37**, 1245 (1965).
18. J. F. TRAUB. Iterative methods for the solution of equations. Prentice-Hall, Inc., Englewood Cliffs, N.J. 1964.
19. H. A. SPANG III. SIAM Rev. **4**, 343 (1962).
20. R. N. MADISON. J. Assoc. Computing Machinery, **13**, 124 (1966).
21. M. J. BOX. Computer J. **9**, 67 (1966).
22. D. P. FEDER. Appl. Opt. **2**, 1209 (1963).
23. J. MEIRON. J. Opt. Soc. Am. **55**, 1105 (1965).
24. K. S. SESHADRI and R. N. JONES. Spectrochim. Acta, **19**, 1013 (1963).
25. S. ABRAMOWITZ and R. P. BAUMANN. J. Chem. Phys. **39**, 2757 (1963).
26. R. N. JONES, K. S. SESHADRI, N. B. W. JONATHAN, and J. W. HOPKINS. Can. J. Chem. **41**, 750 (1963).
27. J. T. SHIMOZAWA and M. KENT WILSON. Spectrochim. Acta. **22**, 1591 (1966).
28. W. VOIGT. Münch. Ber. 603 (1912).
29. H. SHIMIZU. J. Chem. Phys. **43**, 2453 (1965).
30. C. CABANA and C. SANDORFY. Spectrochim. Acta, **16**, 335 (1960).
31. Unpublished observations from this laboratory.
32. H. C. BURGER and P. H. VAN CITTERT. Z. Physik, **79**, 722 (1932); **80**, 428 (1933).
33. A. L. KHIDIR and J. C. DECIUS. Spectrochim. Acta, **18**, 1629 (1962).
34. R. N. JONES, R. VENKATARAGHAVAN, and J. W. HOPKINS. Spectrochim. Acta. In press.
35. R. N. JONES and J. PITHA. National Research Council of Canada Bulletin No. 12 (1967).
36. KADAKIA. Super least-squares program. I.B.M. SHARE Program No. 1435.
37. M. R. HESTENES and E. STIEFEL. J. Research Natl. Bur. Stds. **49**, 409 (1952).
38. F. S. BECKMAN. *In* Mathematical methods for digital computers. *Edited by* A. Ralston and H. S. Wilf. John Wiley & Sons, Inc., New York. 1960. p. 62.
39. K. LEVENBERG. Quart. Appl. Math. **2**, 164 (1944).
40. D. W. MARQUARDT. J. Soc. Ind. Appl. Math. **11**, 431 (1963).
41. R. FLETCHER and M. J. D. POWELL. Computer J. **6**, 163 (1963).
42. W. C. DAVIDON. Variable metric method for minimization. A.E.C. Research and Development Report. ANL-5990 (1959).
43. H. B. CURRY. Quart. Appl. Math. **2**, 258 (1944).
44. R. A. DAMKOEHLER. J. Biol. Chem. **241**, 1955 (1966).

Can. J. Chem. Downloaded from www.nrcresearchpress.com by 210.87.254.105 on 09/05/12
For personal use only.

SOME ADSORPTION PHENOMENA OF NITROANILINES ON ALKALINE EARTH COMPOUNDS

R. W. FREI
Department of Chemistry, Dalhousie University, Halifax, Nova Scotia

AND

H. ZEITLIN AND G. FUJIE
Department of Chemistry, University of Hawaii, Honolulu, Hawaii

Received July 8, 1966

Can. J. Chem. Downloaded from www.nrcresearchpress.com by 210.87.254.40 on 09/05/12
For personal use only.

ABSTRACT

The spectral behavior of *o*- and *p*-nitroanaline adsorbed on various alkaline earth compounds has been studied by reflectance spectroscopy. Regular bathochromic shifts in the diffuse reflectance spectra have been observed for the absorption maxima in the visible region in order of increasing size of the adsorbent cation. Progressive removal of coadsorbed moisture which competes for active adsorbent sites resulted in an enhancement of the bathochromic shifts. The intensity of the absorption maxima as measured by peak heights was found to be dependent upon the size of both cations and anions of the adsorbents. Interpretation of observed phenomena was advanced in terms of electronic polarization theory and varying surface area of the adsorbents.

INTRODUCTION

In recent studies Zeitlin and co-workers (1–3) have measured the reflectance spectra of various nitrophenols and their salts on a series of alkaline earth oxides and alkaline metal carbonates. In this work bathochromic shifts were reported for the absorption maxima of nitrophenols on both series with increasing size and decreasing effective nuclear change of the cation. These shifts proved to be more pronounced for mononitrophenols than for di- or tri-nitrophenols. The relative magnitude of the shifts was interpreted in terms of electronic polarization theory. Similar phenomena, however, were not observed for the sodium salts of the nitrophenols upon adsorption on alkaline metal carbonates. Zeitlin and Lieu (3) postulated that the spectra of the salts are those of the phenoxide anions in the adsorbed state, with little or no differentiating effect evident on the part of the cations.

To obtain a broader base for the support of the interpretation of Zeitlin and co-workers, it was decided to investigate nitro compounds containing a functional group other than OH. Nitroanilines were chosen as models for the study with the hope that data obtained with these compounds which contain a hydrogen bonded to nitrogen would reveal, on comparison with phenols, a common pattern of behavior upon adsorption on solid surfaces. It was also hoped to be able to correlate the height of absorption peaks with the cationic and anionic sizes of various adsorbents, an aspect not considered in the work with nitrophenols.

EXPERIMENTAL

The *p*-nitroaniline and *o*-nitroaniline used in this study were Eastman Organic Chemicals, recrystallized until the melting points indicated satisfactory purity. The adsorbents used and their sources were: beryllium oxide, anhydrous purified grade, Fisher Scientific Co.; magnesium oxide and calcium oxide, reagent grade, Baker Chemical Co.; strontium and barium oxide, anhydrous, purified grade, Fisher Scientific Co.; magnesium carbonate and magnesium sulfate, Baker analyzed reagent grade. The adsorbents were ground for approximately 15 min in an agate mortar to achieve a fine state of subdivision and then sieved through fine mesh screens; 200-mesh powders were used throughout this investigation. Samples of the pure adsorbent were dried at 300 and 600 °C to evaluate the effect of moisture on the systems to be examined. Additional samples were obtained in an air-dry state by exposure to ambient temperatures and humidity.

Samples of the preheated adsorbent were transferred to a desiccator containing P_2O_5. The nitroaniline, the pre-dried equipment, and the desiccator were placed in a dry box dried by dynamic adsorption through

activated silica gel for 12 h. In the dry box 0.04 g of the nitroaniline, which was weighed quickly on a Mettler balance to 1 mg to minimize moisture uptake before transfer to the dry box, was mixed thoroughly with 0.05 mole of each adsorbent in a mortar for about 1 min to attain a uniform distribution. The primary visual change that occurred was a rapid intensification of the color of the amine upon adsorption. Preliminary examination of the system showed that a period of about 1 h was sufficient to achieve a satisfactory state of equilibrium. The cell employed to pack the samples was similar to that described by Barnes *et al.* (4). The edges of the aluminium planchet were coated with silicon grease.

The diffuse reflectance spectra were measured with an automatic recording DK-2 spectrophotometer equipped with the standard reflectance attachment.

Magnesium oxide served as the reference standard throughout the investigation. The reproducibility was studied by measuring four replicates under similar conditions. The wavelength readings obtained for the adsorption maxima were reproducible to ± 3 mμ. The samples were measured again after 24 h exposure to the atmosphere and the spectra compared with that obtained from air-dry samples to establish whether a reversible adsorption process was taking place.

RESULTS AND DISCUSSION

Figures 1–4 contain the reflectance spectra of *o*- and *p*-nitroaniline adsorbed on the various adsorbents. Table I shows the absorption maxima of *o*-nitroaniline adsorbed on a series of alkaline earth oxides measured 1 h after mixing and preparation of the samples under various conditions.

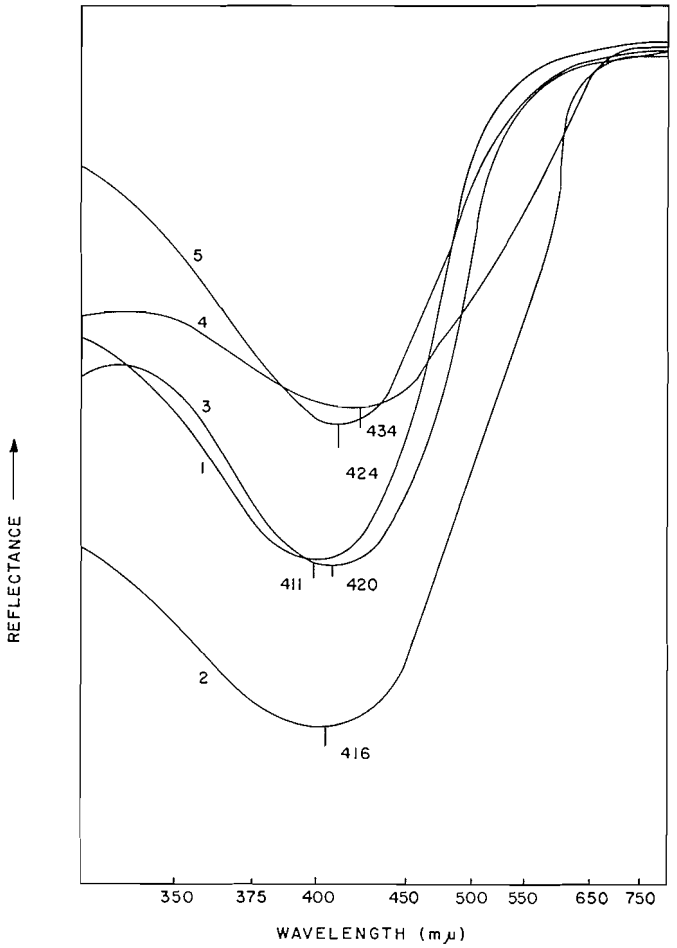


FIG. 1. Reflectance spectra of 0.04 g *o*-nitroaniline adsorbed on 0.05 mole of (1) BeO, (2) MgO, (3) CaO, (4) BaO, (5) SrO of 200-mesh particle size and regenerated at 300 °C.

Can. J. Chem. Downloaded from www.nrcresearchpress.com by 210.87.254.40 on 09/05/12
For personal use only.

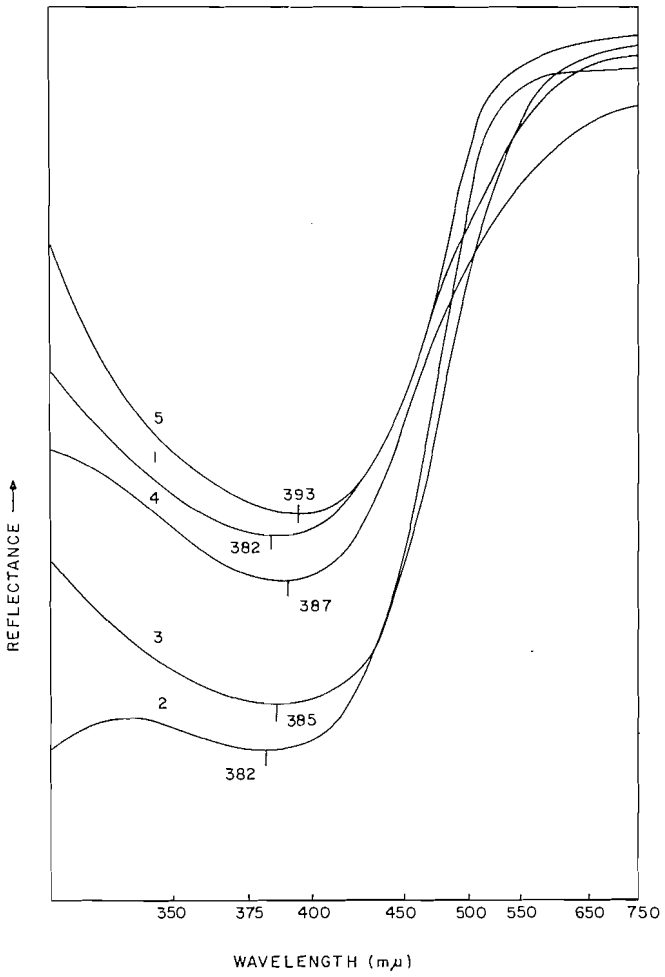


FIG. 2. Reflectance spectra of 0.04 g *p*-nitroaniline adsorbed on 0.05 mole of (1) BeO, (2) MgO, (3) CaO, (4) SrO, (5) BaO of 200-mesh particle size and regenerated at 300 °C.

An examination of the data in Table I shows a relatively small but evident bathochromic shift in going from smaller to larger cations. The actual order is BaO > SrO > CaO > MgO > BeO and agrees with the data found for *o*-nitrophenol on the same adsorbents (2). The same tendency is observed for a series of alkaline metal carbonates in connection with free nitrophenols (1, 3). The arguments which were put forward in these papers to account for the effect of the cations on the adsorbed species could therefore apply for both *o*- and *p*-aniline, which behaved similarly (Fig. 2). The acidity of the hydrogens on the amino nitrogen being weak, any stretching of the hydrogen–nitrogen bond as a result of the polarizing effect from the cations would be expected to be relatively light. Ionization and actual salt formation should be ruled out. It appears likely that the degree of perturbation of the nitrogen to hydrogen bond, which presumably involves stretching in varying degrees, is governed by the effective nuclear charge of the alkaline earth cation. The spectral data (Table I) show also the effect of the pretreatment of the adsorbent, which includes heating of the alkaline earth oxides at 300 °C and 600 °C prior to mixing with the

Can. J. Chem. Downloaded from www.nrcresearchpress.com by 210.87.254.40 on 09/05/12
For personal use only.

adsorbate, and the preparation of an air-dry system in which equilibration at room temperature and atmospheric moisture was achieved. A shift to larger wavelengths was observed in going from metaloxide (MO) air dry → MO 300 °C → MO 600 °C (see Table I). The results agree with the findings of Zeitlin *et al.* (2) for *o*-nitrophenol adsorbed on alkaline earth oxides.

TABLE I

Absorption maxima (mμ ± 3 mμ) of the reflectance spectra of *o*-nitroaniline adsorbed on alkaline earth oxides

	Air dry	300 °C*	600 °C*
BeO	409	412	415
MgO	412	416	421
CaO	416	420	424
SrO	419	424	430
BaO	425	434	—

*Temperature at which adsorbent is preheated and allowed to cool before mixing with nitroaniline.

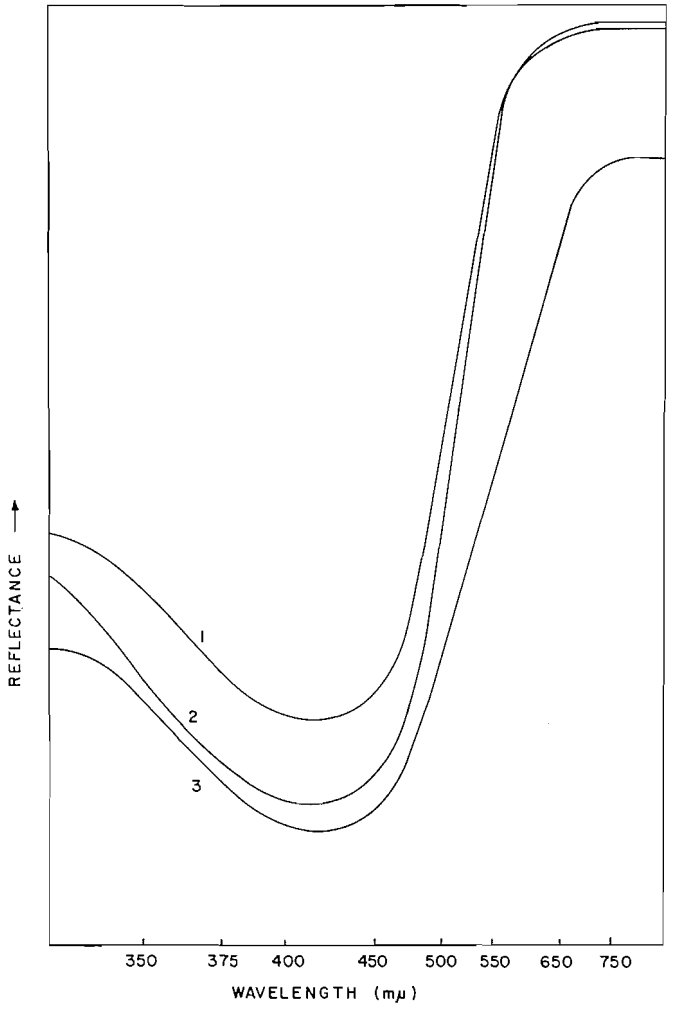


FIG. 3. Reflectance spectra of 0.04 g *o*-nitroaniline adsorbed on 0.05 mole of (1) $MgSO_4$, (2) $MgCO_3$, (3) MgO of 200-mesh particle size and regenerated at 200 °C.

Can. J. Chem. Downloaded from www.nrcresearchpress.com by 210.87.254.40 on 09/05/12
For personal use only.

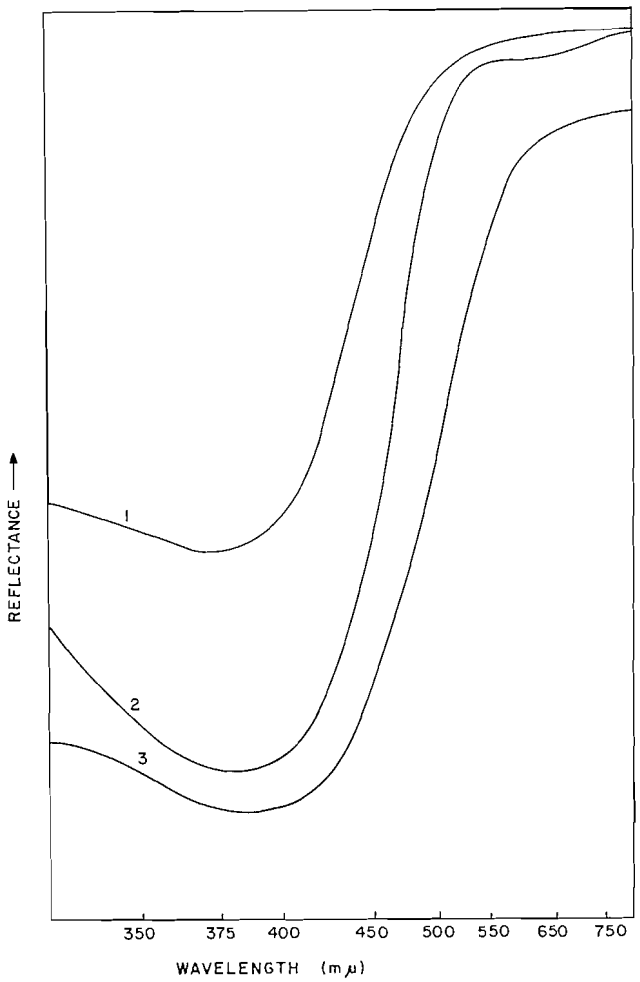


FIG. 4. Reflectance spectra of 0.04 g *p*-nitroaniline adsorbed on 0.05 mole of (1) $MgSO_4$, (2) $MgCO_3$, (3) MgO of 200-mesh particle size and regenerated at 200 °C.

The extent of this shift is believed to be governed by the amount of water coadsorbed with the adsorbate. According to Kortüm and co-workers (5–7), who observed similar phenomena on different systems, an equilibrium condition which is moisture dependent exists between unadsorbed and adsorbed species relative to the active adsorbent. The heat treatment results in partial or complete removal of the coadsorbed water which competes for the active surface sites and hence the nitroaniline is more effectively and directly exposed to the polarizing action of the adsorbent. It is believed that a transition from physical adsorption resulting from van der Waals forces to chemisorption, which takes place in the first monomolecular layer, is occurring. This phenomenon was tested for reversibility by exposing the dry sample to atmospheric humidity. After a period of 24 h the spectra were again identical to those obtained from air-dry systems. Similar observations were reported in 1932 by de Boer (8), who observed a reversible adsorption process for *p*-nitrophenol on $BaCl_2$ and suggested a non-destructive mode of adsorption.

In contrast to the previous studies of adsorption phenomena of nitrophenols (1–3), which were carried out on a qualitative base, it was attempted in this paper to ascertain

Can. J. Chem. Downloaded from www.nrcresearchpress.com by 210.87.254.40 on 09/05/12
For personal use only.

whether a correlation existed between intensity of the absorption maxima of the mononitroanilines and the adsorbent used. Figures 1 and 2 show the relative peak heights for equal mole ratios of *p*- and *o*-nitroaniline with alkaline earth oxides of 200-mesh particle size and measured under the same conditions (i.e. 300 °C regeneration) versus MgO as a reference standard. The observed trend shows a decrease in color intensity in the order MgO > CaO > SrO > BaO for both *p*- and *o*-nitroanilines with BeO being the only exception to the rule. Observation of such a trend is not new. Kortüm and Vogel (6) reported an increase in intensity of the absorption maxima of malachite green – *o*-carbonic acid lactone adsorbed on alkaline metal chlorides and sulfates of the same grain size in the order LiCl > NaCl > KCl > RbCl > CsCl and $MgSO_4$ > $CaSO_4$ > $BaSO_4$.

An explanation for the trends exhibited would be provided by the polarization theory whereby the intensity of the color formation is a function of the differentiating nuclear charge exerted by the various cations of the adsorbents. If the adsorption model which was used to explain the influence of moisture on changes in reflectance spectra is valid, it is reasonable to assume that the specific active surface of the adsorbent should exert an influence. The fact that BeO does not fit into the scheme supports such an assumption, since it is known that the alkaline earth oxides with the exception of BeO crystallize with the rock salt structure. In contrast BeO has the 4.4 coordinated zinc blend structure (9).

Further support is lent to this view by the spectra shown in Figs. 3 and 4, which exhibit a decrease in peak height with increasing size of the *anion* in the order MgO > $MgCO_3$ > $MgSO_4$ for both *p*- and *o*-nitroaniline.

ACKNOWLEDGMENTS

We are grateful to the Petroleum Research Fund administered by the American Chemical Society and to the National Research Council of Canada for financial support of this research.

REFERENCES

1. H. Zeitlin, N. Kondo, and W. Jordan. J. Phys. Chem. Solids, **25**, 641 (1964).
2. H. Zeitlin, R. Frei, and M. McCarter. J. Catalysis, **4**, 77 (1965).
3. H. Zeitlin and V. Lieu. J. Catalysis, **4**, 546 (1965).
4. I. L. Barnes, H. Goya, and H. Zeitlin. Rev. Sci. Instr. **34**, 292 (1963).
5. G. Kortüm, J. Vogel, and W. Braun. Angew. Chem. **70**, 651 (1958).
6. G. Kortüm and J. Vogel. Chem. Ber. **93**, 706 (1960).
7. G. Kortüm, W. Braun, and G. Herzog. Angew. Chem. **2**, 333 (1963).
8. J. H. de Boer. Z. Physik. Chem. Leipzig, **B16**, 397 (1932).
9. W. H. Zachariasen. Z. Physik. Chem. Leipzig, **A119**, 201 (1926).

Can. J. Chem. Downloaded from www.nrcresearchpress.com by 210.87.254.40 on 09/05/12
For personal use only.

Can. J. Chem. Downloaded from www.nrcresearchpress.com by 210.87.254.6 on 09/05/12
For personal use only.

EUROPIUM OXALATE ION ASSOCIATION IN WATER

P. G. MANNING
Mines Branch, Department of Mines and Technical Surveys, Ottawa, Canada
Received March 4, 1966

ABSTRACT

The partitioning of radiotracer $^{152/154}$Eu between aqueous sodium oxalate (Na_2L) solutions and toluene solutions of thenoyltrifluoroacetone (HTTA) has been studied as a function of the oxalate concentration. The pH of the aqueous phase was controlled by means of sodium acetate – acetic acid mixtures and the ionic strength (I) by NaCl or $NaClO_4$.

At low ionic strengths (~ 0.05) and $[L] \sim 10^{-4}$ M EuL^+ formed, but at $I = 0.95$ and $[L] \sim 10^{-3}$ M EuL_2^- also formed. Stability constants for the 1:1 and 1:2 (metal:ligand) complexes are reported.

The magnitudes of the stepwise stability constant ratios are discussed.

INTRODUCTION

Rare earth – oxalate complexing in solution has been studied extensively by Crouthamel and Martin (1) and by Sekine (2). The absolute magnitudes of the stability constants of the complexes cannot be compared directly because of the vastly different ionic strengths used in these works. However, the ratios of the stepwise stability constants are clearly at variance (Table I). The stepwise stability constant is defined as

$$K_n = [EuL_n]/[EuL_{n-1}][L], \quad [1]$$

where L is the ligand.

TABLE I
Stability constant ratios for oxalate complexes

Crouthamel and Martin		Sekine	
Ce	360	La	4.7
Nd	800	Eu	6.6
Yb	500	Lu	11

Bjerrum (3) has shown that for simple complexes

$$P = K_1{:}K_2 = S \times T \times R, \quad [2]$$

where S is a statistical factor and T is a measure of the work done in bringing a charged ligand from infinity to its equilibrium position in the 1:2 complex against the repulsive force exerted by already bound ligands. For singly charged ligands that bind to rare earth or transition metal ions it has been shown that $T = 1.6$ (4, 5). If the cation has N available sites and if, for example, the ligand is monodentate, $S = 2 \times N/(N - 1)$, i.e. $S > 2$. The factor of 2 arises because the probability of a ligand's leaving the 1:2 complex is twice that of a ligand's leaving the 1:1. The R factor, termed the rest effect, covers those contributions to P that are neither statistical nor electrostatic. R will be an important entity in stepwise reactions where, for example, the cation coordination number changed. Steric hindrance and metal–ligand covalency are other obvious contributors to R. The magnitudes of the ratios of the stepwise stability constants are discussed later in this paper.

The solvent extraction – radiotracer technique has proved useful in the study of rare earth ion association reactions in solution (6). The method is particularly applicable in the

present work because of the low solubility of europium oxalate. In this work [Eu] $\sim 10^{-7}$ M and [oxalate] $\sim 10^{-4}$ M.

EXPERIMENTAL

The experimental techniques have been described in detail in earlier publications (7). The organic phase was 0.035 M thenoytrifluoroacetone in toluene. Sodium perchlorate prepared from $HClO_4$ and NaOH was used to maintain a constant ionic strength, although in some "runs" at low I NaCl was used. The pH was kept constant by means of a 0.0040 M sodium acetate – acetic acid mixture. At low I values the pH was 4.69 and at high I the pH was 5.42. Sodium oxalate and sodium chloride were dried at 110 °C prior to use. All reagents were of analytical reagent grade, except for HTTA which was recrystallized from hexane. $^{152/154}$Eu of high specific activity was purchased from the Radiochemical Centre, Amersham, England.

The aqueous and pre-equilibrated organic phases were shaken for 3 h in erlenmeyer flasks fitted with polytetrafluoroethylene sleeves. The phases were separated and assayed for $^{152/154}$Eu with an annular-type scintillation assembly coupled to an automatic sample changer. At least 20 000 counts were recorded, giving a standard deviation of $\pm 0.7\%$. The temperature was 25 ± 0.5 °C.

THEORY

The distribution coefficient is defined as

$$D = [\mathrm{Eu}]_o/[\mathrm{Eu}]_w, \qquad [3]$$

where "o" and "w" designate organic and aqueous species respectively. Distribution coefficients were generally reproducible to $\pm 2\%$, although when [L] = 0 errors were greater, possibly because of tracer adsorption on the walls of the glass vessels. For this reason, at least two determinations were made of the distribution coefficient at [L] = 0.

When [L] = 0 and omitting ionic charges,

$$D^0 = \frac{[\mathrm{Eu(TTA)_3}]_o}{([\mathrm{Eu}] + [\mathrm{EuA}])_w}, \qquad [4]$$

where A = acetate ion. Only the 1:1 EuA species forms under these experimental conditions (7).

In the presence of oxalate,

$$D = \frac{[\mathrm{Eu(TTA)_3}]_o}{([\mathrm{Eu}] + [\mathrm{EuA}] + [\mathrm{EuL}] + [\mathrm{EuL_2}] + \ldots)_w}. \qquad [5]$$

From eqs. [1], [3], [4], and [5] it can be readily shown that (7)

$$F((D^0/D) - 1)/[\mathrm{L}] = K_1 + K_1K_2[\mathrm{L}] + \ldots, \qquad [6]$$

where F is a correction factor for lanthanide–acetate complexing; F is given by the equation

$$F = 1 + K_1'[\mathrm{A}], \qquad [7]$$

where K_1' is a stability constant for EuA.

Equation [6] shows that a plot of $F((D^0/D) - 1)/[\mathrm{L}]$ against [L] is horizontal if only EuL forms, linear with positive slope if EuL_2 forms, and curved, of ever-increasing curvature, if EuL_3 also forms.

RESULTS AND DISCUSSION

In Table II are listed D and [L] values for europium oxalate systems at different ionic strengths. Free oxalate concentrations were calculated from the expression

$$C_L/[\mathrm{L}] = 1 + ([\mathrm{H^+}]f_H f_L/K_{a2}f_{HL}), \qquad [8]$$

where C_L is the total ligand concentration, K_a is the dissociation constant of oxalic acid (8),

Can. J. Chem. Downloaded from www.nrcresearchpress.com by 210.87.254.6 on 09/05/12
For personal use only.

Can. J. Chem. Downloaded from www.nrcresearchpress.com by 210.87.254.6 on 09/05/12
For personal use only.

TABLE II

L, F, and $100/D$ values for europium oxalate

$I = 0.027$, $C_L/[L] = 1.176$, $F = 1.696$		$I = 0.036$, $C_L/[L] = 1.167$, $F = 1.63$		$I = 0.052$, $C_L/[L] = 1.155$, $F = 1.54$		$I = 0.054$, $C_L/[L] = 1.153$, $F = 1.53$		$I = 0.061$, $C_L/[L] = 1.149$, $F = 1.50$		$I = 0.95$, $C_L/[L] = 1.031$, $F = 1.34$	
10^5L	$100/D$	10^5L	$100/D$	10^5L	$100/D$	10^5L	$100/D$	10^5L	$100/D$	10^4L	$100/D$
0	1.73	0	2.63	0	2.81	0	2.89	0	8.92	0	0.147
0.680	5.47	0.917	6.10	1.385	8.99	1.39	10.86	1.39	34.0	3.88	4.04
0.850	7.20	1.145	8.02	1.73	10.61	1.735	12.88	1.74	37.55	7.77	9.80
1.70	11.50	2.29	14.31	3.46	17.42	3.47	19.71	3.48	66.35	9.70	13.13
2.55	15.88	3.43	17.60	5.19	22.96	5.20	39.04	5.22	87.3	19.4	31.94; 35.12
3.40	23.39	4.57	26.72	6.93	37.41	6.94	47.9	6.96	113.1	29.1	66.80; 61.86
4.25	26.98	5.72	31.91	8.66	43.10	8.67	49.0	8.70	136.8	38.8	106.8; 104.4

and f_H and f_L are activity coefficients. A second term involving $K_{a1} \times K_{a2}$ gives an insignificant contribution to $C_L/[L]$. The Davies' form of the Debye–Huckel expression (9) was used to calculate f values, namely

$$[9] \qquad -\log f = 0.509z^2\left(\frac{I^{1/2}}{1 + I^{1/2}} - 0.3I\right),$$

where z is the ionic charge. The $C_L/[L]$ values at different ionic strengths are listed in Table II. Free acetate ion concentrations were estimated from the relationship

$$[10] \qquad C_A/[A] = 1 + [H^+]f_H f_A/K_a',$$

where K_a' is the dissociation constant of acetic acid ($= \sim 1.74 \times 10^{-5}$ (10)).

To calculate F at low ionic strengths, K_1' values were evaluated by adjusting the K_1' value of Kolat and Powell (11) at $I = 0.1$ to the relevant I using eq. [9]. The applicability of eqs. [8] and [9] to the present work has been discussed in an earlier publication (6).

Plots of $F((D^0/D) - 1)/[L]$ against [L] were horizontal at the lower ionic strengths, indicating that EuL only formed. It follows from eq. [6] that when $K_2 = 0$, $1/D \propto [L]$. The best straight line of a $1/D$ against [L] plot was determined by the method of least squares. This method gave D^0 and also D at a given [L], and K_1 values were calculated by direct substitution of the parameters in eq. [6]. The K_1 values determined at different ionic strengths are listed in Table III, together with the thermodynamic K_1 value estimated using Davies' activity expression (9).

TABLE III
Stability constant for europium–oxalate complexes

	I					
	0.027	0.036	0.052	0.054	0.061	0.95
$10^{-5}K_1$	5.95	4.50	2.70	3.10	2.05	0.75
$10^{-2}K_2$						5.8
$K_1:K_2$						130
$10^{-6}K_1$ (thermodynamic)	3.85	3.60	2.95	3.55	2.55	
Average K_1 (thermodynamic) $= 3.3\ (\pm 0.5) \times 10^6$						

The thermodynamic K_1 value of 3.3×10^6 for europium oxalate (this work) may be compared with the K_1 values for Ce, Nd, and Yb oxalates of 3.3×10^6, 16×10^6, and 20×10^6 respectively, these values being those determined by Crouthamel and Martin (1). Europium lies between Nd and Yb in the rare earth series, so that agreement between our work and the solubility work of Crouthamel and Martin is poor. Thermodynamic K_1 values have also been reported (12, 13) for Erbium oxalate (6.6×10^4) and Yttrium oxalate (3.3×10^6), and this lack of agreement is characteristic of published K_1 values for these oxalate systems. Thus for Cerium oxalate, solubility measurements at $I = 2$ (14) give $K_1 = 1.1 \times 10^6$, whereas ion exchange measurements at $I = 1$ (15) give $K_1 = 1.1 \times 10^4$. A stability difference of two orders of magnitude seems impossibly large to be attributed to activity coefficients. However, our K_1 value for europium oxalate is in good agreement with that estimated for Y (3.3×10^6) by Feibush and co-workers (13) from solubility measurements.

Our solvent extraction results at $I = 0.95$ show that $EuC_2O_4^+$ and $Eu(C_2O_4)_2^-$ are formed, and K_1 and K_1K_2 values were estimated from the intercept and slope of a plot of

Can. J. Chem. Downloaded from www.nrcresearchpress.com by 210.87.254.6 on 09/05/12
For personal use only.

the left hand side of eq. [6] against [L]. The K_1 and K_2 values are listed in Table III. The K_1' value for EuA^{2+} has not been reported at $I = 1$ or $I = 2$, and Sonesson's K_1' value (16) for SmA^{2+} at $I = 2$ has been used. The F values were calculated, therefore, on the basis that $K_1' = 100$. The $C_L/[L]$ correction is small (3%), so that the calculation of activity coefficients at $I = 0.95$ using the Davies' equation (9) should not introduce too great an error. The estimated error in the quoted stability constants is probably less than 20%. Our K_1 value ($= 7.5 \times 10^4$) is in accord with the results of Sekine ($K_1 = 6 \times 10^4$ (2)).

The K_1:K_2 ratios are of interest, however. Our K_1:K_2 value at $I = 0.95$ is 4 times smaller than the values of Crouthamel and Martin and 20 times larger than the K_1K_2 value of Sekine (Tables I and II). A sampling of the P values for transition metal oxalates, listed in the Chemical Society tabulations of stability constants (17), shows that $P \sim 200$. Consequently, it would seem that P values in the range 100–500 are correct for rare earth and transition metal oxalates.

In an earlier publication it was shown that a T value = 1.6 explained the magnitudes of P values for rare-earth and transition metal complexes with some α-hydroxymonocarboxylates (4). This T value was also valid for some transition metal amino acid complexes (5). The T factor was independent of the nature of the (singly charged) ligand, and this was part of the evidence put forward to show that the factor of 1.6 was of mainly electrostatic character. Bjerrum (18) has shown that

$$\log T \propto \frac{e^2}{D_c r} \times \frac{1}{kK_T},$$

where e is the ligand charge, r the equilibrium separation of the ligands D_c the dielectric constant, k the Boltzmann constant, and K_T the absolute temperature. Assuming that r(oxalate) $\sim r$(α-hydroxymonocarboxylate), log T(oxalate) = 4 log T(α-hydroxymonocarboxylate), or T(oxalate) $= 1.6^4 \sim 6.5$. Hence, for six-coordinated metal ions, P(calcd.) $= 4.8 \times 6.5 \sim 30$, whereas for eight-coordinated ions, P(calcd.) $= 3.5 \times 6.5 \sim 25$. These P(calcd.) values are considerably smaller than the P(obs.) values ($= 130$) determined in this investigation. The P(calcd.) values are an order of magnitude smaller than the P(obs.) values of Crouthamel and Martin (1) and also the P(obs.) values for transition metal oxalates (17). Sekine's (2) results are indicative of a large stabilizing effect in the second association stage, but our P(obs.) values are in better agreement with those of Crouthamel and Martin (1) and those for transition metal oxalates (17). If $T = 1.0$, as has been suggested by Powell and Rowlands (19) from an analysis of P values for rare earth 1-hydroxycyclopentane carboxylic acid complexes, Sekine's results would be in fair agreement with theory. However, 1-hydroxycyclopentane carboxylic acid does not associate with rare earths in the same way as do the simpler hydroxymonocarboxylates, and it would be dangerous to put great faith in this T value ($= 1.0$). It is significant that the P(obs.) values for four transition metal 1-hydroxycyclopentane carboxylic acid complexes[1] average at 3.5 ± 0.2, suggesting a T value ~ 1.5. Sekine's (2) results would indicate that $R \sim 0.25$, and it is difficult to postulate a mechanism that preferentially aids the second associate stage. Such reactions as the disruption of the cation hydration sheath or changes in metal–oxalate bond length would be expected to confer increased stability on the 1:1 complex. It would seem, therefore, that rest effects are present in these rare earth and transition metal oxalate systems. Bjerrum (3) defined the rest effect as the influence of bound ligands on the binding power of the metal ion. Steric effects are negligible in these systems. It is possible that the strength of the metal–ligand bond is different in the first

[1] *J. E. Powell and D. L. G. Rowlands. Private communication.*

Can. J. Chem. Downloaded from www.nrcresearchpress.com by 210.87.254.6 on 09/05/12
For personal use only.

and second states of ion association. This effect would be due to a lengthening of the M—L bond length in the 1:2 complex, and, in the extreme case, one can imagine the M—L bonding changing from low covalent character in the 1:1 complex to more electrostatic character in the 1:2 complex.

CONCLUSION

Stepwise stability constants have been determined for europium–oxalate complexes in water. The solvent extraction – radiotracer technique was employed. The magnitudes of the ratios of stepwise stability constants suggest that the 1:2 complexes are weaker than expected from statistical and electrostatic considerations. The suggestion is made that the M—L bond length is greater in the 1:2 complex than the 1:1.

ACKNOWLEDGMENTS

The author is grateful to Mr. David Hanes, a summer student at the Mines Branch, for his mature assistance in the experimental aspects of this work.

REFERENCES

1. C. E. CROUTHAMEL and D. S. MARTIN. J. Am. Chem. Soc. **73**, 569 (1951).
2. T. SEKINE. J. Inorg. Nucl. Chem. **26**, 1463 (1964).
3. J. BJERRUM. Metal ammine formation in aqueous solution. P. Haase and Son, Copenhagen. 1941.
4. P. G. MANNING. Can. J. Chem. **43**, 3258 (1965).
5. P. G. MANNING. Can. J. Chem. **44**, 1975 (1966).
6. P. G. MANNING. Can. J. Chem. **41**, 2557 (1963).
7. P. G. MANNING and C. B. MONK. Trans. Faraday Soc. **58**, 938 (1962).
8. W. J. CLAYTON and W. S. VOSBURGH. J. Am. Chem. Soc. **59**, 2414 (1937).
9. C. W. DAVIES. J. Chem. Soc. 2093 (1938); Ion association. Butterworths, London. 1962.
10. M. LLOYD, V. WYCHERLEY, and C. B. MONK. J. Chem. Soc. 1786 (1951).
11. R. S. KOLAT and J. E. POWELL. Inorg. Chem. **1**, 293 (1962).
12. Z. F. ANDREEVA and I. V. KOLOSOR. Izv. Timiryazev. Sel'skokhoz. Akad. No. 1, 212 (1962).
13. A. M. FEIBUSH, K. ROWLEY, and L. GORDON. Anal. Chem. **30**, 1610 (1958).
14. A. K. BABKO and L. I. DUBOVENKO. Zh. Neorgan. Khim. **2**, 808 (1957).
15. K. B. ZABORENKO, A. V. Zaval'skaya, and V. V. Formin. Radiokhimiya, **1**, 387 (1959).
16. A. SONESSON. Acta Chem. Scand. **12**, 165 (1958).
17. J. BJERRUM, G. SCHWARZENBACH, and L. G. SILLEN (*Editors*). Stability constants. Vol. I. The Chemical Society, London. 1958.
18. N. BJERRUM. Z. Physik. Chem. Leipzig, **106**, 238 (1923).
19. J. E. POWELL and D. L. G. ROWLANDS. Inorg. Chem. **5**, 819 (1966).

Can. J. Chem. Downloaded from www.nrcresearchpress.com by 210.87.254.6 on 09/05/12
For personal use only.

MASS SPECTROMETRIC STUDY OF SUBLIMING SELENIUM[1]

H. FUJISAKI,[2] J. B. WESTMORE,[3] AND A. W. TICKNER
Division of Applied Chemistry, National Research Council, Ottawa, Canada
Received May 31, 1966

ABSTRACT

In the mass spectrum of the vapor from grey selenium subliming in the temperature range 102 to 187 °C all possible Se_n^+ ions between $n = 1$ and $n = 8$ were detected in measurable quantities. The ions Se_5^+, Se_6^+, Se_7^+, and Se_8^+ arise mainly from ionization of the corresponding parent molecules, which are believed to be cyclic. At 175 °C the composition of the vapor is $Se_5 \leqslant 29.0\%$, $Se_6 \geqslant 57.5\%$, $Se_7 \geqslant 11.4\%$, and $Se_8 \geqslant 2.0\%$. Thermodynamic data are reported for the sublimation of these molecules. Small amounts of Se_9^+ and Se_{10}^+ were also detected.

INTRODUCTION

In the condensed state, selenium can exist in a wide variety of different forms. The thermodynamically stable form at temperatures up to the melting point is grey, metallic, or hexagonal selenium (1, 2). In this variety the selenium atoms form spiral chains (3, 4) in which adjoining atoms form normal single bonds.

Red crystalline selenium is monoclinic and two forms have been found (5, 6). The α form is composed of Se_8 rings (7). According to Burbank (7) the β form consists of open Se_8 chains but Marsh, Pauling, and McCullough have found closed Se_8 rings. There appears to be little difference between the α and β forms (8). Monoclinic selenium transforms to grey selenium, taking 15 days at 80 °C and 12 h at 120 °C (9, 10). At 150 °C the transformation is rapid (11).

Vitreous selenium is formed by rapid cooling of molten selenium. Although various views on its structure have been proposed (12–18) it seems certain that the chain structure found in grey selenium exists in this variety but the chains have become enmeshed and intertwined. When it is dissolved in iodine the average length of the selenium chain is about 100 atoms (19). Vitreous selenium transforms to grey selenium, taking 20 days at 43°, 72 h at 55°, 12 h at 70° (10), and 1 h at 100 °C (20).

Red amorphous selenium also contains chains of selenium atoms (21), the spirals being slightly deformed and randomly placed along the axis of the chain (22). Berthelot (23) distinguishes two varieties of amorphous selenium.

Contradicting values have been given for the density of selenium vapor (24–29). However, all results indicate progressive dissociation into smaller molecules as the temperature rises.

Vapor pressures have been measured by several methods (29–38). Determinations involving the Knudsen technique involve a knowledge of the vapor composition and will be in error if the incorrect assumption is made. It has been proposed (30) that below 550 °C the vapor consists of Se_8 and between 550 and 800 °C the vapor consists of Se_6 and Se_2 in equilibrium. Metzger (39) has found that the average molecular weight of freely evaporating selenium is consistent with the formula $Se_{5\text{ to }6}$. On the basis of electron diffraction studies on selenium vapor at low pressures, Howe and Lark-Horovitz (40) propose Se_6

[1]*Issued as N.R.C. No. 9215.*
[2]*N.R.C. Postdoctorate Fellow 1963–64. Present address: Research Institute for Scientific Measurements, Tohoku University, Sendai, Japan.*
[3]*N.R.C. Postdoctorate Fellow 1961–63. Present address: Department of Chemistry, University of Manitoba, Winnipeg, Manitoba.*

Can. J. Chem. Downloaded from www.nrcresearchpress.com by 210.87.254.5 on 09/05/12
For personal use only.

rings to be present in the vapor. In a high frequency electrodeless discharge through selenium vapor at 10^{-4} to 10^{-5} Torr a band system which has been attributed to the molecule Se_4 has been found (41). An incomplete study of the mass spectrum of the vapor over grey selenium at 200 °C has been published (42) in which the ions Se_n^+ (n = 1 to 10) were found. No attempt was made to interpret the results. Thus, the composition of selenium vapor has not yet been established.

EXPERIMENTAL

The apparatus and method described previously by Mann and Tickner (43) were used with a few minor modifications (44). Experiments on powdered samples were performed in the seven-holed molybdenum crucible described in ref. 44. The ionizing electron beam passes through the vapor inside the effusion cell. This arrangement has the advantage of higher sensitivity over conventional arrangements in which the electron beam intersects the vapor beam outside the effusion cell. It is thus possible to work at lower temperatures and pressures. The apparatus is more suited to measuring the composition of the vapor leaving the surface than to measuring equilibrium compositions. Experiments on tablet samples were performed in a special sample holder designed so that the surface was parallel to, and about 2 mm from, the electron beam and so that very few collisions of vapor with the crucible wall would occur before ionization.

The selenium, in the form of small pellets, was obtained from the American Smelting and Refining Company and was 99.999% pure. X-ray diffraction showed the material to be amorphous, but a few faint lines were present because of some surface devitrification. Some initial sublimation experiments in the temperature range 120 to 185 °C were performed with the crushed sample. On removal from the mass spectrometer X-ray diffraction showed that extensive crystallization to the hexagonal form had occurred. In view of the preceding discussion this is not surprising. Since the sample must be maintained at these temperatures for a number of hours while the experiment is performed, it was not possible to study the sublimation of vitreous selenium. Consequently, this work is a study of the sublimation of grey selenium, 99.999% pure, annealed for 4 weeks at 150 °C in an evacuated quartz tube. The sample was kindly prepared by Dr. J. B. Taylor of this division. The samples were crushed to give particles passing through 100 mesh and retained on 200 mesh screens. Examination under a microscope showed the particles to be reasonably homogeneous in size and regular in shape. A specific area of the sample could be estimated though, because of irregularities in the surface, considerable uncertainty exists as to the true surface area. By placing the sample in just the center hole, or all seven holes, of the crucible, the effective area of the vaporizing surface could easily be varied.

Some experiments were also performed on red monoclinic selenium and tablets of monoclinic selenium, which were prepared by melting and casting in thin cylindrical forms 8 mm in diameter and 2 mm in thickness, in an evacuated quartz tube. These samples were also prepared by Dr. Taylor. In the mass spectrometer, these samples gave results not significantly different from the hexagonal form and it was found, not surprisingly, that they had indeed reverted to the hexagonal form.

RESULTS AND DISCUSSION

I. Mass Spectrum of the Vapor from Hexagonal Selenium

The mass spectrum was scanned up to $m/e \simeq 1\,000$ for electrons of 40 V energy. Ion currents due to the species Se_n^+, where n = 1 to 10, were found. Those for n = 9 and n = 10 were very small. The ratio of the ion currents for the different species was difficult to estimate accurately since selenium has six isotopes of masses 74, 76, 77, 78, 80, and 82. Moreover, since under the conditions of operation the resolving power of the instrument was less than 150, the mass spectra of the heavier ions species were largely unresolved. An estimate of the ion current ratios was obtained by assuming that the measured maximum ion current for the group of masses at each ion species was proportional to the relative abundance of the commonest mass of the group. It was also assumed that mass discrimination effects in the mass spectrometer were small. For 40 V electrons at 175 °C the results obtained are shown in Table I and compared with those of Goldfinger and Jeunehomme (42).

II. Appearance Potentials of the Ions

The ionization efficiency curves for Se_n^+ (n = 1 to 8) together with those of Xe^+ and Hg^+ are shown in Fig. 1 for electron energies up to 20 V. Appearance potentials were determined by the method of Lossing, Tickner, and Bryce (45) and corrected so that xenon

Can. J. Chem. Downloaded from www.nrcresearchpress.com by 210.87.254.5 on 09/05/12
For personal use only.

Can. J. Chem. Downloaded from www.nrcresearchpress.com by 210.87.254.5 on 09/05/12
For personal use only.

TABLE I

Relative ion currents for 40 V electrons at 175 °C, and appearance potentials of the ions from the vapor over hexagonal selenium

Species	Commonest mass	Relative abundance (%)	Ion current (arbitrary units)	Total ion current (arbitrary units)	Relative ion current ($Se_6^+ = 100$)	Appearance potential (V)	Goldfinger and Jeunehomme*
Se^+	80	49.8	354.0	710.8	7.02	—	4.1
Se_2^+	160	29.1	961.6	3 304.5	32.6	—	25.2
Se_3^+	238	21.3	358.9	1 685.0	16.6	11.6 ±0.3	11.5
Se_4^+	318	17.4	395.4	2 272.4	22.4	10.9 ±0.2	21.7
Se_5^+	396	14.5	619.4	4 271.8	42.2	9.2 ±0.2	39.0
Se_6^+	476	12.6	1 276	10 127.	100.0	9.08±0.05	100.0
Se_7^+	554	11.3	263.0	2 327.4	23.0	8.87±0.05	13.1
Se_8^+	634	10.4	48.9	470.2	4.7	8.97±0.05	2.36
Se_9^+		≃9.8	0.3	3.06	0.03	—	—
Se_{10}^+				Too small to be recorded			

*Relative ion currents ($Se_6^+ = 100$) for 70 V electrons at 200 °C.

had the literature value of 12.13 V (46). In this way the appearance potential of mercury (simultaneously introduced as a check in some final experiments) was found to be 10.45 V, in agreement with the spectroscopic ionization potential of 10.43 V (46). The appearance potentials of the ions Se_5^+, Se_6^+, Se_7^+, and Se_8^+ lie close together and much lower than the other ions and lower than the spectroscopic ionization potential of 9.81 V (46) for atomic selenium. The positions of the Se^+, Se_2^+, Se_3^+, and Se_4^+ curves indicate that these ions are electron impact fragments of a heavier species, although the shapes of the Se^+ and Se_2^+ curves at low electron energies may indicate the presence of small concentrations of Se and Se_2 in the vapor. Support for this view is given by an appearance potential of 10.21 V for Se_2^+ from the vapor over CdSe, which is shown to contain Se_2 molecules (47). As in the case of As_4 these small molecules probably arise by decomposition of a heavier molecule on the mass spectrometer filament (48, 44).

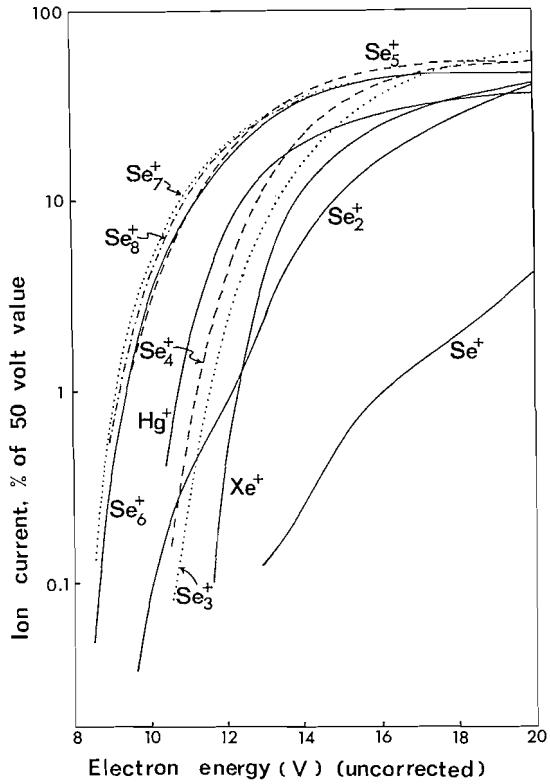


FIG. 1. Ionization efficiency curves for ions from vapor over selenium at 165 °C.

III. Variation of Partial Pressures with Temperature

The ion current due to a substance can be used as a quantity proportional to its concentration over a considerable temperature range as long as conditions in the ion source do not change. In practice, the efficiency of the ion source was found to vary with temperature and a reference concentration of xenon was maintained by allowing the gas to leak in from a reservoir in the sample line. The ion currents used in determining variations in partial pressure were obtained from the equation

$$I = I_m \times \frac{I_{Xe}^0}{I_{Xe}} \left(\frac{T^0}{T}\right)^{1/2} \frac{P_{Xe}}{P_{Xe}^0},$$

Can. J. Chem. Downloaded from www.nrcresearchpress.com by 210.87.254.5 on 09/05/12
For personal use only.

Can. J. Chem. Downloaded from www.nrcresearchpress.com by 210.87.254.5 on 09/05/12
For personal use only.

where I_m is the measured ion current at temperature T, I_{Xe} is the $^{132}Xe^+$ ion current at temperature T and reservoir pressure P_{Xe}, and the superscript zero indicates the corresponding quantities under the reference conditions. The temperature correction arises from the dependence of the steady state xenon concentration inside the effusion cell on temperature. Since the sample pressure is proportional to concentration multiplied by temperature then the sample pressure is proportional to IT. Hence, temperature coefficients can be obtained by plotting log IT against $1/T$. For each ion, log IT was plotted against $1/T$; the results for one experiment are shown in Fig. 2. For several experiments the results are summarized in Table II. The following conclusions may be drawn. The most abundant ion, Se_6^+, has one of the smallest temperature coefficients. The ions Se^+, Se_2^+, Se_3^+, and Se_4^+, which are known from their appearance potentials to be formed by fragmentation, have temperature coefficients of comparable magnitude and are presumably formed mainly from Se_6^+. The ion Se_5^+ has a significantly higher temperature coefficient than Se_6^+. In view of its low appearance potential, it is formed mainly by ionization of Se_5 molecules. It is not possible to estimate the contribution to Se_5^+ of fragmentation of heavier molecules but it is probably small, otherwise marked curvature of the log IT vs. $1/T$ plot for Se_5^+ would have been noticed. Support for this conclusion is given by the fragmentation of sulfur molecules under electron impact (49) where $S_5^+ < 0.25\%$ of S_6^+ when formed from S_6. Larger amounts of S_5^+ are formed from S_7 and S_8 but for selenium the corresponding parent molecules are present in low amounts. However, it is only possible to calculate an upper limit for the relative concentration of Se_5 in the vapor. Se_6^+ arises mainly from Se_6 molecules, contributions from fragmentation of heavier molecule ions being negligible. Similarly, Se_7^+ and Se_8^+ arise mainly from Se_7 and Se_8 molecules. (It is shown later that they are not formed in ion–molecule reactions.)

TABLE II

Slopes of log IT vs. $1/T$ plots for selenium ions from vapor over grey selenium (mean of 20 experiments covering the temperature limits 102 to 187 °C)

Ion	Slope (deg)
Se^+	7 530±150
Se_2^+	7 550±110
Se_3^+	7 705±100
Se_4^+	7 400±100
Se_5^+	7 920± 85
Se_6^+	7 410± 90
Se_7^+	8 390±100
Se_8^+	8 720±145

It has been shown previously (44) that the steady state pressure, p, in the effusion cell is given by

$$p = \frac{P}{1 + f/\alpha},$$

where P is the equilibrium vapor pressure, f is the ratio of effective effusion area to effective sample area, and α is the accommodation coefficient. The variation of p with temperature is then given by

$$\frac{\mathrm{d} \log p}{\mathrm{d}\,(1/T)} = -\frac{1}{2.303R}\left[\Delta H + \Delta H'\left(1 - \frac{1}{1 + f/\alpha}\right)\right],$$

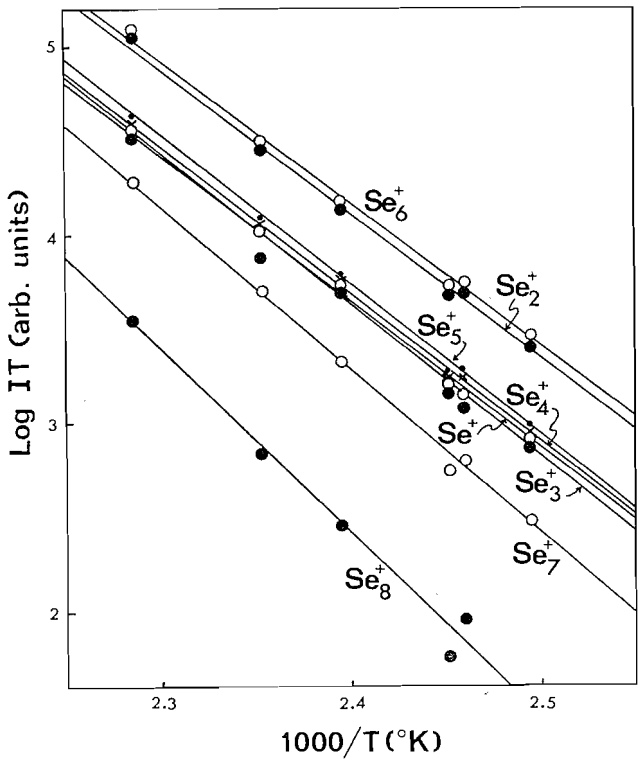


FIG. 2. Temperature coefficients for selenium ions (electron energy 40 V).

where ΔH is the heat of sublimation and $\Delta H'$ is the heat of a surface reaction which occurs before sublimation. The activation energy of sublimation is $\Delta H + \Delta H'$. The effect of varying f has been discussed before (44). It was found that neither the temperature coefficients nor the ion current ratios Se_5^+/Se_6^+, Se_7^+/Se_6^+, and Se_8^+/Se_6^+ varied as f was changed. Since the temperature coefficient for the sublimation of Se_6 in these experiments is close to the equilibrium value determined by other workers, it is concluded that the selenium species Se_5, Se_6, Se_7, and Se_8 have accommodation coefficients close to unity, $\Delta H'$ is very small, and the experimentally determined temperature coefficient does not depend on the value of f.

IV. Test for Ion–Molecule Reactions

It was verified that the ions Se_7^+ and Se_8^+ were not formed in ion–molecule reactions by measuring relative ion currents as a function of the voltage on a repeller electrode mounted inside the effusion chamber, 2 to 3 mm from the electron beam and opposite the ion-withdrawal slit. Little dependence on repeller voltage was found, whereas the current due to an ion formed in an ion–molecule reaction is proportional to the inverse square root of the repeller voltage (50, 51). Thus, at 165 °C, the temperature of the measurements, ion–molecule reactions are of little importance.

V. Calculation of Thermodynamic Quantities

Because of the complexity of the mass spectrum any numbers assigned to the composition of the vapor and heats of sublimation of each species may not be very precise. If we assume that Se_5, Se_6, Se_7, and Se_8 molecules have similar fragmentation patterns when

Can. J. Chem. Downloaded from www.nrcresearchpress.com by 210.87.254.5 on 09/05/12
For personal use only.

ionized, an assumption justified by the similarity of the ionization efficiency curves for Se_5^+, Se_6^+, Se_7^+, and Se_8^+, the ion currents due to Se_5^+, Se_6^+, Se_7^+, and Se_8^+ can be used as a measure of the relative concentrations of the respective molecules in the vapor. Such an approximation is probably good for Se_6, Se_7, and Se_8 but likely to be high for Se_5. Consequently, the value for Se_5 will be an upper limit and the values for the other molecules will be lower limits. In the absence of other data, it was assumed that the relative ionization cross sections of the other molecules were proportional to the number of atoms contained in them. The results are summarized in Table III. According to this approximation the molecules leaving the surface would have an average of 5.90 atoms of selenium at 175 °C, in good agreement with the value found by Metzger (39) for freely subliming selenium.

TABLE III

Heats of sublimation and relative abundances of subliming selenium molecules

Species	ΔH_{418} (kcal/mole)	Relative abundance at 175 °C	% in vapor at 175 °C
Se_5	36.2±0.5	50.6	29.1
Se_6	33.8±0.5	100.0	57.5
Se_7	38.4±0.5	19.7	11.4
Se_8	39.9±0.7	3.5	2.01
Se_9	—	0.02	0.012

For correcting the thermodynamic data to 298 °K the heat capacities of the gaseous molecules are required. For Se_6 an average value for the temperature range 298 to 418 °K was estimated from data given by Stull and Sinke (52). The vibrational contribution to C_p is about 90% of its maximum value and a similar contribution was assigned to the vibrational parts of C_p for Se_5, Se_7, and Se_8. These values, and heats of sublimation corrected to 298 °K, are given in Table IV. Stull and Sinke select heats of sublimation of 35.38 and 34.12 kcal/mole for Se_6 and Se_2, respectively, to give the best fit with entropy and vapor pressure data of other workers, with Se_6 being the most abundant species at the temperatures considered here. These results are consistent with those given here but the current results suggest that the equilibrium vapor composition is more complex than this, and an attempt will be made to present some more satisfying thermodynamic data. Furthermore, the conclusions of Illarionov and Lapina (29), who report equilibrium constants involving Se_2, Se_4, Se_6, and Se_8 vapor molecules, should be treated with suspicion.

The variation of vapor pressure with temperature is given by

$$\log \frac{P_T}{P_{298}} = -\left(\frac{\Delta H_{298}^0 - 298\Delta C_p}{2.303R}\right)\left(\frac{1}{T} - \frac{1}{298}\right) + \frac{\Delta C_p}{R} \log \frac{T}{298},$$

where the symbols have their conventional meanings. Unfortunately the present apparatus does not allow measurement of absolute vapor pressures. Consequently the relative partial pressures at 298 °K were calculated from those at 448 °K given in Table III, and their sum was equated to the value for Se_6 at 298 °K given by Stull and Sinke. The rest of the thermodynamic data in Table IV were then evaluated.

VI. Mechanism of the Sublimation

A mechanism of the sublimation is proposed which is consistent with the observed results. It is significant that the molecules Se, Se_2, Se_3, and Se_4 are not found in the subliming vapor, yet Se_5 is the second most abundant species. It is recalled that the solid

Can. J. Chem. Downloaded from www.nrcresearchpress.com by 210.87.254.5 on 09/05/12
For personal use only.

phase used in these studies consists of spirally wound chains of selenium atoms. A selenium atom at the end of a chain has an unpaired electron. A cyclic molecule could therefore be formed by the end selenium atom forming a bond with a selenium atom further along the chain at the same time that the bond between the latter atom and its neighbor is broken.

TABLE IV

Thermodynamic data for the sublimation of grey selenium

Species	Average C_p from 298 to 418 °K (cal deg^{-1})	Average ΔC_p (cal deg^{-1})	ΔH_{298}^0 (kcal/mole)	ΔF_{298}^0 (kcal/mole)	ΔS_{298}^0 (cal mole^{-1} deg^{-1})
Se_5	23.9	−8.2	37.2	21.8	51.7
Se_6	29.5	−9.0	34.9	20.6	48.0
Se_7	35.1	−9.9	39.6	23.2	55.1
Se_8	40.7	−10.6	41.2	24.8	55.1

Such a molecule would be held to the surface by van der Waals forces and could readily leave the surface. Such a process would be expected to be more energetically favorable than the formation of diradical chain molecules. Ignoring d orbital contributions the hybridization of a selenium atom in a chain or a ring will be mainly sp^3, and with two lone pairs the Se—Se—Se angle should be somewhat smaller than 109° 28′. In grey selenium this angle is 105°. A planar Se_5 ring requires bond angles of 108° and since any strains could be removed by puckering of the ring the molecule will be relatively unstrained. Similarly, Se_6 and larger cyclic molecules will be unstrained. Large strains would be present in a planar Se_4 ring, which could only be partially relieved by folding of the ring since then large repulsions between lone electron pairs would occur.[4] Thus molecules containing 5 or more atoms should be formed more readily than small molecules if the molecules are assumed to be cyclic. This is consistent with the results which show that 98% of the vapor subliming at 175 °C is composed of Se_5, Se_6, and Se_7 molecules. Dissociation of these molecules by collision with the walls of the effusion cell will be negligible at this temperature.

VII. Comparison with Sulfur Vapor

The mass spectrum of the vapor over sulfur shows that the vapor is as complex as that over selenium. Berkowitz and Marquart (53) have studied the equilibrium composition of sulfur vapor and summarized the results of earlier workers. They find the molecules S_2, S_3, S_4, S_5, S_6, S_7, and S_8, plus insignificant but detectable amounts of S_9 and S_{10}. The major species were S_8, S_6, and S_7 respectively. Free evaporation of sulfur has also been studied (49). Rhombic sulfur, which contains S_8 units, gives rise solely to S_8 vapor molecules. Engel's sulfur, which contains S_6 units, produces only S_6 vapor molecules. The evaporation coefficients of S_6 and S_7 from rhombic sulfur are very small, presumably because of a surface reaction in which they are formed from S_8. In the case of selenium the rate of transition of the unstable allotropes to the stable hexagonal form is too rapid to permit measurement of the composition of the subliming vapor from these unstable forms.

ACKNOWLEDGMENT

The authors wish to express their gratitude to Dr. J. B. Taylor for supplying the selenium samples and to Dr. L. D. Calvert for X-ray diffraction studies and helpful discussion of the crystalline states of these materials.

[4]*In a non-planar molecule with* Se—Se—Se *angles of 105° and* Se—Se *bond distances of 2.35 Å as found in grey selenium, the distance between the non-bonded selenium atoms in cyclic* Se_4 *would be 3.74 Å, which is less than twice the van der Waals radius of 2.00 Å. Since the lone pair orbitals of these atoms are directed toward each other considerable repulsion would exist.*

Can. J. Chem. Downloaded from www.nrcresearchpress.com by 210.87.254.5 on 09/05/12
For personal use only.

Can. J. Chem. Downloaded from www.nrcresearchpress.com by 210.87.254.5 on 09/05/12
For personal use only.

REFERENCES

1. A. P. SAUNDERS. J. Phys. Chem. **4**, 423 (1900).
2. J. D. MCCULLOUGH. Ph.D. Thesis, California Institute of Technology, Pasadena, Calif. 1936.
3. K. TANAKA. Mem. Coll. Sci, Univ. Kyoto, Ser. A, **17**, 59 (1934).
4. M. STRAUMANIS. Z. Krist. **102**, 432 (1940).
5. W. MUTHMANN. Ber. **20**, 990 (1887).
6. H. P. KLUG. Z. Krist. **88**, 128 (1934).
7. R. D. BURBANK. Acta Cryst. **4**, 140 (1951); **5**, 236 (1952).
8. R. E. MARSH, L. PAULING, and J. D. MCCULLOUGH. Acta Cryst. **6**, 71 (1953).
9. S. R. DAS and K. DAS GUPTA. Nature, **143**, 165 (1939).
10. K. DAS GUPTA, S. R. DAS, and B. B. RAY. Indian J. Phys. **15**, 389 (1941).
11. E. MITSCHERLICH. Ann. Chim. Phys. [3], **46**, 301, (1856).
12. G. BRIEGLEB. Naturwissenschaften, **17**, 51 (1929).
13. H. RICHTER. Physik. Z. **44**, 406 (1943).
14. K. LARK-HOROWITZ and E. P. MILLER. Phys. Rev. **51**, 380 (1936).
15. R. GLOCKER and H. HENDUS. Z. Elektrochem. **48**, 327 (1942).
16. H. HENDUS. Z. Physik, **119**, 265 (1942).
17. H. KREBS and F. SCHULTZE-GEBHARDT. Naturwissenschaften, **41**, 474 (1945); Acta Cryst. **8**, 412 (1955).
18. H. RICHER and F. HERRE. Naturwissenschaften, **44**, 31 (1957).
19. H. KREBS and W. MORSCH. Z. Anorg. Chem. **263**, 305 (1950).
20. M. COSTE. Compt. Rend. **149**, 674 (1909).
21. E. BILLIG. Proc. Phys. Soc. London, Sect. B, **65**, 216 (1952).
22. H. RICHTER, W. KULCKE, and H. SPECHT. Z. Naturforsch. Pt. a, **7**, 511 (1952).
23. D. BERTHELOT. Compt. Rend. **134**, 705 (1902).
24. H. ST. CLAIRE DEVILLE and L. TROOST. Compt. Rend. **91**, 83 (1880).
25. H. VON WARTENBERG. Z. Anorg. Chem. **56**, 320 (1907).
26. H. BILTZ. Z. Physik. Chem. Leipzig, **19**, 385 (1896).
27. E. SZAVARZY. Ber. **30**, 1244 (1897).
28. W. T. COOKE. Z. Phys. Chem. Leipzig, **55**, 537 (1906).
29. V. V. ILLARIONOV and L. M. LAPINA. Dokl. Akad. Nauk S.S.S.R. **114**, 1021 (1957).
30. G. PREUNER and I. BROCKMÜLLER. Z. Phys. Chem. Leipzig, **81**, 129 (1912).
31. J. JANNEK and J. MEYER. Z. Anorg. Chem. **83**, 51 (1913).
32. L. E. DODD. J. Am. Chem. Soc. **42**, 1579 (1920).
33. K. NEUMANN and E. LICHTENBERG. Z. Phys. Chem. Leipzig, **184**, 89 (1939).
34. M. DE SELINCOURT. Proc. Phys. Soc. London, **52**, 348 (1940).
35. K. NIWA and Z. SIBATA. J. Fac. Sci. Hokkaido Univ. Ser. III, **3**, 53 (1940).
36. T. SATO and H. KANEKO. Technol. Repts. Tôhoku Univ. **14**, 45 (1950).
37. L. S. BROOKES. J. Am. Chem. Soc. **74**, 227 (1952).
38. YU. A. PRISELKOV, V. V. KARELIN, A. V. TSEPLYAEVA, and YU. A. SAPOZHNIKOV. Izv. Vysshykh Uchebn. Zavedenii Khim. i Khim. Tekhnol. **3**, 447 (1960).
39. F. METZGER. Helv. Phys. Acta, **16**, 323 (1943).
40. J. D. HOWE and K. LARK-HOROVITZ. Phys. Rev. **51**, 380 (1937).
41. B. ROSEN and M. DÉSIRANT. Bull. Sci. Acad. Roy. Belgium, **21**, 436 (1935).
42. P. GOLDFINGER and M. JEUNEHOMME. *In* Advances in mass spectrometry. *Edited by* J. D. Waldron. The Pergamon Press, Ltd., London. 1959.
43. K. H. MANN and A. W. TICKNER. J. Phys. Chem. **64**, 251 (1960).
44. J. B. WESTMORE, K. H. MANN, and A. W. TICKNER. J. Phys. Chem. **68**, 606 (1964).
45. F. P. LOSSING, A. W. TICKNER, and W. A. BRYCE. J. Chem. Phys. **19**, 1254 (1951).
46. C. E. MOORE. Natl. Bur. Std. U.S., Circ. No. 467.
47. H. FUJISAKI and A. W. TICKNER. Unpublished results.
48. J. S. KANE and J. H. REYNOLDS. J. Chem. Phys. **25**, 342 (1956).
49. J. BERKOWITZ and W. A. CHUPKA. J. Chem. Phys. **40**, 287 (1964).
50. H. GUTBIER. Z. Naturforsch. Pt. a, **12**, 499 (1957).
51. D. P. STEVENSON and D. O. SCHISSLER. J. Chem. Phys. **23**, 1353 (1955); **29**, 282 (1958).
52. D. R. STULL and G. C. SINKE. Advances in Chem. Ser. No. 18, (1956). pp. 179–182.
53. J. BERKOWITZ and J. R. MARQUART. J. Chem. Phys. **39**, 275 (1963).

CONTRIBUTION À L'ÉTUDE DES SPECTRES DE VIBRATION DU DIBENZOFURANNE

GISÈLE DAVIDOVICS, JACQUES CHOUTEAU ET HENRI REYMOND

Laboratoire de Chimie Physiologique B.M.P.V. et Centre Technique de Spectrographie Infrarouge; Département de Chimie Organique, Faculté des Sciences de Marseille, France

Reçu le 20 juillet 1966

RÉSUMÉ

La plupart des fréquences de vibration fondamentales du dibenzofuranne ainsi que leur type de symétrie ont été déterminés par l'analyse des spectres infrarouges entre 4 000 et 200 cm^{-1} sous différents états, vapeur, liquide, solution et cristal, et par l'étude de la polarisation des raies Raman à l'état dissous.

ABSTRACT

The majority of fundamental vibration frequencies of dibenzofuran and their symmetry types were determined by the analysis of infrared spectra in vapor, liquid, solution, and solid states, and from the study of polarization ratios of Raman lines in the dissolved phase.

Les spectres infrarouges du dibenzofuranne ont été enregistrés de 4 000 à 400 cm^{-1} sous les états solution et vapeur, et jusqu'à 200 cm^{-1} en phases liquide et solide. Le spectre Raman du dibenzofuranne dissous a également été réalisé.

L'analyse de la structure rotationnelle des bandes d'absorption, de la polarisation des raies de diffusion et du dichroïsme en lumière polarisée d'un film cristallin orienté, nous ont permis de déterminer, pour la plupart des vibrations fondamentales de la molécule de dibenzofuranne, la classe de symétrie à laquelle elles appartiennent.

Les études par spectroscopie infrarouge de cette molécule sont peu nombreuses et ne concernent que quelques fréquences (1–4). Briggs et Colebrook (1) en relèvent quatre entre 1 300 et 840 cm^{-1}, Barnes *et al.* (2) et Groenewege (3) une entre 800 et 700 cm^{-1}, et Tschamler et Leutner (4), une également vers 1 200 cm^{-1}.

Les spectres de diffusion Raman du dibenzofuranne à l'état liquide (5), dissous (6) ou cristallisé (7), ont été publiés mais n'ont pas été analysés.

Teplyakov et Trisov (8) ont essayé de déterminer certaines des vibrations fondamentales et harmoniques du dibenzofuranne en comparant les spectres de phosphorescence obtenus par eux avec le spectre Raman publié par Donzelot et Chaix (5).

I. THÉORIE

D'après Cullinane et Plummer (9) et Merkel et Wiegan (10) la molécule de dibenzofuranne est vraisemblablement plane; elle aurait donc la symétrie C_{2v}. Le Tableau I résume pour cette classe de symétrie le nombre de vibrations appartenant à chaque type de symétrie et leur activité en spectroscopies Raman et infrarouge.

Le calcul des moments principaux d'inertie réalisé avec des paramètres choisis par comparaison avec le furanne (11) et le diphénylène (12) a permis de fixer l'orientation des axes principaux d'inertie (petit, moyen et grand) du dibenzofuranne, qui sont respectivement parallèles aux directions oy, ox, oz (cette dernière perpendiculaire au plan de l'hétérocycle) portées sur la Fig. 1.

On sait que dans le spectre infrarouge à l'état gazeux, la structure de vibration rotation des bandes d'absorption dépend de l'orientation du moment de transition M_x, M_y, M_z par rapport aux axes principaux d'inertie de la molécule (13). C'est ainsi que pour le dibenzofuranne, aux vibrations de symétrie A_1 doivent correspondre des bandes de type B, aux

Can. J. Chem. Downloaded from www.nrcresearchpress.com by 210.87.254.105 on 09/05/12
For personal use only.

TABLEAU I
Dénombrement des vibrations et activité pour la classe de symétrie C_{2v}

Mode de symétrie	Éléments de symétrie		Degrés de liberté		Mouvements d'ensemble de la molécule	Nombre de vibrations C—C	Nombre de vibrations C—H	Nombre de vibrations O—C	Activité des vibrations	
	C_2^z	σ_z	ω_z 6 fam. C 4 fam. H	α_z 1 fam. O					Raman	Infrarouge
A_1	s	s	2	1	T_z	11	8	1	P	M_z
A_2	s	a	1	0	R_z	5	4	0	D	i
B_1	a	s	2	1	R_zT_y	10	8	1	D	M_y
B_2	a	a	1	1	R_yT_z	4	4	1	D	M_z

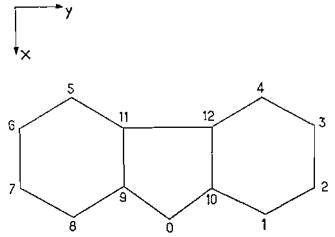


FIG. 1.

vibrations de mode B_1 des bandes de type A et aux oscillations de symétrie B_2 des enveloppes de type C.

II. RÉSULTATS EXPÉRIMENTAUX

Les spectres infrarouges de 1 700 à 200 cm^{-1} du dibenzofuranne sont représentés à l'état gazeux et liquide sur la Fig. 2, à l'état dissous sur la Fig. 3, à l'état solide et de cristal orienté sur la Fig. 4.

La Fig. 3 comporte également le spectre Raman du dibenzofuranne dissous dans le benzène.

La Fig. 5 représente les spectres infrarouges du dibenzofuranne sous différents états (liquide, solution, solide) dans la région de 3 150 à 3 000 cm^{-1}.

Les fréquences infrarouges (sous différents états) et Raman sont groupées dans les Tableaux II à IV. La structure des bandes à l'état gazeux, les coefficients d'extinction molaires et la polarisation des raies Raman sont indiqués dans le Tableau II.

Nos attributions sont résumées dans le Tableau V.

III. ATTRIBUTION DES VIBRATIONS

La distinction entre vibrations de symétrie A_1, B_1, B_2, A_2 a pu être faite à l'aide des critères suivants:

(1) Dans le spectre infrarouge à l'état vapeur, les enveloppes des bandes de vibration rotation correspondant aux mouvements de symétrie A_1, B_1, B_2 doivent être respectivement de types B, A et C, ainsi que nous l'avons dit ci-dessus.

(2) Les raies Raman polarisées doivent résulter de vibrations de mode A_1.

(3) Les vibrations de type A_2 sont actives dans le spectre de diffusion seulement; on peut les attendre en général au dessous de 1 100 cm^{-1}.

(4) Les vibrations de symétrie A_1, B_1, B_2 que leur structure rotationnelle ou la polarisation des raies Raman n'a pas permis de caractériser, ont pu être différenciées par l'étude en lumière polarisée du spectre infrarouge d'un film cristallin orienté.

Can. J. Chem. Downloaded from www.nrcresearchpress.com by 210.87.254.105 on 09/05/12
For personal use only.

(5) Les vibrations de valence ν(CH) doivent se manifester dans la région de 3 100 à 3 000 cm^{-1} (14). Dans le cas d'un couplage entre tous les vibrateurs CH, on peut attendre quatre mouvements de mode A_1 et quatre mouvements de mode B_1 (Tableau I). Par suite, au dessous de 1 700 cm^{-1}, 40 fréquences fondamentales infrarouges (16 A_1, 15 B_1, 9 B_2) et 49 fréquences fondamentales Raman, dont 9 de type A_2 sont attendues respectivement.

(A) Région de 1 700 à 200 cm^{-1}

(1) Spectres infrarouges sous les états vapeur, liquide et solution, et spectre Raman à l'état dissous (Fig. 2 et 3) (Tableau II)

Vibrations de symétrie A_1

La structure de type B des bandes de vibration rotation à 1 241 et 1 146 cm^{-1} ainsi que la polarisation des raies Raman correspondantes permettent d'attribuer ces fréquences à des mouvements de mode A_1. Les raies de diffusion polarisées à 1 485, 1 442, 1 307, 1 183, 1 098, 1 012, 847 et 746 cm^{-1} sont également attribuables à des vibrations de symétrie A_1; notons que par suite de leur faible intensité dans le spectre infrarouge, ou de recouvrements, les structures rotationnelles sont peu visibles pour ces fréquences.

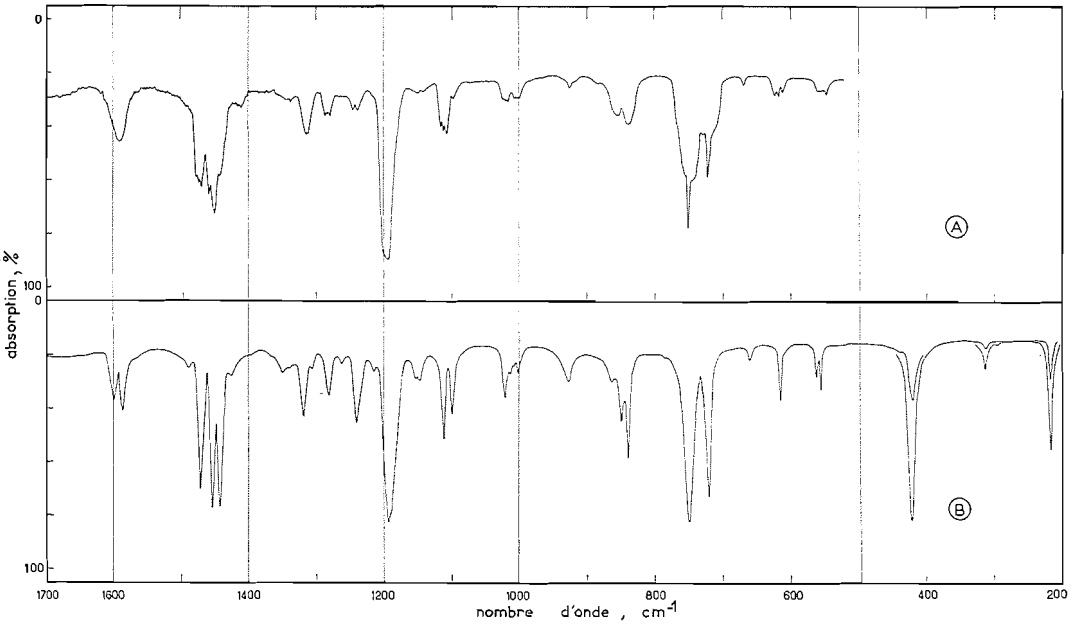


FIG. 2. Spectres infrarouges du dibenzofuranne de 1 700 à 200 cm^{-1}: (A) à l'état gazeux, (B) à l'état liquide, sous des épaisseurs de $\sim$ 10, 25 et 125 μ.

Vibrations de symétrie B_1

Nous attribuons à des oscillations de la classe B_1 les sept bandes d'absorption à 1 470, 1 318,[1] 1 282, 1 110, 1 022, 1 002 et 614 cm^{-1} en raison de leur structure rotationnelle de type A et les trois raies de diffusion à 1 635, 1 589 et 1 352 cm^{-1} en raison de leur dépolarisation. On remarque que la fréquence infrarouge correspondant à la forte raie de diffusion à 1 635 cm^{-1} est absente (Fig. 2, Tableau II).

[1]*Le spectre infrarouge du dibenzofuranne en solution montre deux bandes d'absorption à 1 318 cm^{-1} (ϵ = 100) et 1 306 cm^{-1} (ϵ = 18); une seule bande est observée à l'état vapeur à 1 312 cm^{-1}. Cette dernière, en raison de l'intensité faible du maximum à 1 306 cm^{-1}, ne peut correspondre qu'à la fréquence 1 318 cm^{-1} du spectre à l'état dissous.*

Can. J. Chem. Downloaded from www.nrcresearchpress.com by 210.87.254.105 on 09/05/12
For personal use only.

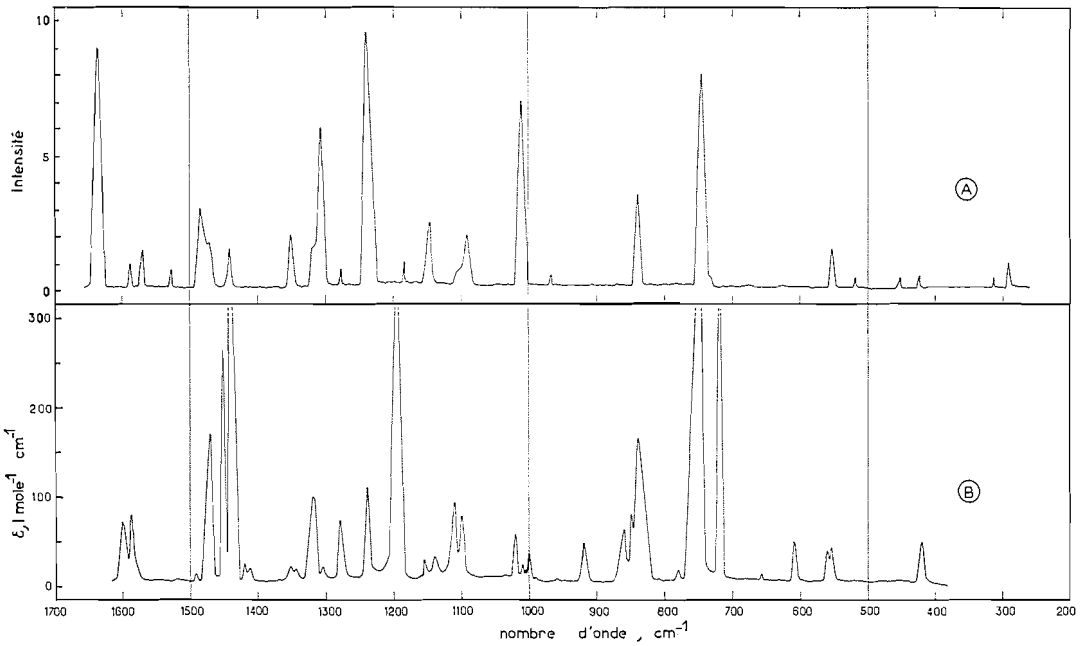


FIG. 3. Spectres Raman (A) et infrarouge (B) du dibenzofuranne en solution.

TABLEAU II
Spectres infrarouges et Raman du dibenzofuranne

Infrarouge			Raman		
Vapeur	Type de bande	Solution (1 *M*)	Solution (1 *M*)		Type de symétrie
			1 635 (9)	0.78	B_1
~1 592	?	1 599 (62)			
		1 586 (79)	1 589 (1)	0.78	B_1
			1 570 (3/2)	0.45	
			1 523 (3/4)	0.53	B_1
		1 491 (13)			
			1 485 (3)	0.36	A_1
1 478 1 475 1 471	A	1 470 (169)	1 472 (e)		B_1
~1 451	?	1 452 (263)			
1 444	?				
1 441	?	1 443 (433)	1 442 (3/2)	0.36	A_1
		1 422 (23)			
		1 415 (20)			
		1 370 (4)			
		1 353 (20)	1 352 (2)	0.57	B_1
		1 345 (18)			
~1 316 1 314 ~1 312	A ?	1 318 (100)	1 321 (e)		B_1 ?
		1 306 (18)	1 307 (6)	0.27	A_1
1 288 1 284 1 280	A	1 282 (72)	1 278 (3/4)	0.44	B_1
1 247 1 239	B	1 241 (110)	1 239 (10)	0.34	A_1
1 202 e 1 199 e 1 195	A ?	1 196 (310)			B_1 ?

Can. J. Chem. Downloaded from www.nrcresearchpress.com by 210.87.254.105 on 09/05/12
For personal use only.

TABLEAU II (*Conclu*)

Spectres infrarouges et Raman du dibenzofuranne

Infrarouge			Raman		
Vapeur	Type de bande	Solution (1 *M*)	Solution (1 *M*)		Type de symétrie
		1 188 e	1 183 (1)	0.29	A_1
		1 160 (15)			
		1 151 (29)			
1 152	B	1 146 (32)	1 146 (5/2)	0.17	A_1
1 143					
1 117					
1 113	A	1 110 (108)	†1 109 fff		B_1
1 108					
1 098	?	1 100 (77)	1 098 (2)	0.24	A_1
1 026					
1 022	A	1 022 (57)			B_1
1 018		1 012 (26)	1 012 (7)	0.08	A_1
		1 006 ff			
1 008					
1 004	A	1 002 (37)			B_1
1 000					
		990 (9)			
		964 (6)	969 (1/2)		
927	C ?	926 (48)			B_2 ?
		863 (34)			
854	?	850 (80)	847 (3,5)	0.19	A_1
840	?	840 (165)			
		785 (18)			
755					
750	C	750 (1 190)			B_2
743					
		740 e	746 (8)	0.08	A_1
			†734 fff		
		728 e			
728					
722	C	721 (450)			B_2
714					
		659 (11)			
620					
616	A	614 (50)			B_1
612					
561		561 (40)			
558					
555	?	555 (42)	552 (3/2)	0.63	
550					
		517* ff	517 (1/3)		
			451 (1/3)		
		421 (48)	423 (1/2)		
		314*	314 (1/3)		
		293*	295 (1)	0.7	
		218*			

NOTE: Les fréquences infrarouges à l'état dissous sont suivies du coefficient d'extinction molaire apparent. Les fréquences Raman sont suivies de l'intensité relative et du facteur de dépolarisation. ff = très faible, e = épaulement.

*Fréquences observées dans le spectre à l'état liquide.

†Ces fréquences sont tirées de ref. 5.

Vibrations de symétrie B_2

On peut attribuer à des oscillations de la classe B_2 les maximums infrarouges à 750 et 721 cm^{-1} qui donnent lieu dans le spectre à l'état gazeux à des enveloppes de type C. La bande de vibration rotation à 926 cm^{-1} semble également avoir une enveloppe de type C, elle pourrait donc appartenir à une vibration de type B_2.

Notons que Barnes *et al.* (2) et Groenewege (3) situent une vibration de déformation hors du plan γ(CH) du dibenzofuranne à 750 cm^{-1}.

Can. J. Chem. Downloaded from www.nrcresearchpress.com by 210.87.254.105 on 09/05/12
For personal use only.

Vibrations de symétrie A_2

Aucun maximum d'absorption infrarouge n'ayant été observé à 451 et 734 cm^{-1}, les raies Raman observées à ces fréquences sont attribuables à des vibrations de mode A_2.

TABLEAU III

Spectres infrarouges de 1 700 à 200 cm^{-1} du dibenzofuranne sous les états liquide et solide

Liquide (~ 82°)	Solide	Cristal orienté	Polarisation	Type de symétrie
1 599 m	1 594 m	1 593 m	∥	A_1
1 586 m	1 586 m			B_1
1 488 ff	1 484 f	1 485 f	∥	A_1
1 472 F	1 469 m			B_1
1 453 F	1 450 F			B_1
1 443 F	1 443 FF	1 442 F	∥	A_1
1 424 ff				
1 370 ef		1 372 ef	∥	A_1
1 350 f	1 351 e	1 350 e		
1 340 e	1 341 m	1 342 m	∥	A_1
1 319 m	1 321 F			B_1
1 307 f	1 306 m	1 307 m	∥	A_1
1 282 m	1 282 m			B_1
1 263 f	1 263 ff			
1 241 m	1 238 F	1 239 F	∥	A_1
1 226 e	1 225 e	1 226 e	∥	A_1
1 215 f	1 214 f			B_1
1 194 FF large	1 196 FF	1 196 f		B_1
1 188 e	~1 190 e	1 190 e	∥	A_1
1 152 m	1 152 F	1 152 ff		B_1
1 147 m	1 147 e 1 136 m	1 135 m	∥	A_1
1 111 m	1 112 f			B_1
1 101 m	1 098 m	1 097 m	∥	A_1
1 022 m	1 018 m			B_1
1 013 f				
1 008 ff	1 006 m	1 008 m	∥	A_1
1 002 m	997 m			B_1
992 e				
969 f	970 f	970 f	∥	A_1
929 m	926 F	929 F	⊥	B_2
864 m	862 f	863 f	∥	A_1
850 m	847 F	848 F	∥	A_1
840 F	838 F			B_1
787 e		783 f	⊥	B_2
768 e				
749 FF	753 F 746 FF	753 F 744 FF	⊥	B_2
722 F	721 FF	722 FF	⊥	B_2
660 f	658 f	658 f	∥	A_1
616 m	616 m			B_1
562 F	568 F 564 e	568 F 564 m	⊥	B_2
517 ff				
556 F	556 F			B_1
425 e	425 e			
421 m	423 m	421 F	⊥	B_2
314 ff	~318 ff			
293 ff				
218 f	220 m			
	217 e			

NOTE: Les intensités relatives des bandes d'absorption sont désignées par: FF = très forte, F = forte, m = moyenne, f = faible, ff = très faible, e = épaulement.

(2) Spectres infrarouges du dibenzofuranne à l'état solide (Fig. 4) (Tableau III)

Les spectres infrarouges du dibenzofuranne solide (dispersé dans du bromure de potassium) et liquide sont très peu différents. La plupart des bandes d'absorption du spectre du liquide se retrouvent dans celui du solide: trois doublets, cependant, vers

Can. J. Chem. Downloaded from www.nrcresearchpress.com by 210.87.254.105 on 09/05/12
For personal use only.

753–746 cm^{-1}, 568–564 cm^{-1} et 424–420 cm^{-1} se fondent en trois bandes d'absorption simples dans le spectre à l'état liquide. La présence des deux composantes dans le spectre du solide est sans doute due à un effet de cristal.

Un film cristallin orienté de dibenzofuranne a été réalisé; son spectre infrarouge présente par rapport au spectre du liquide des différences notables: en particulier, le spectre du cristal orienté ne comporte pas de bandes d'absorption de fréquences voisines de 1 586, 1 470, 1 353, 1 318, 1 282, 1 110, 1 022, 1 002 et 614 cm^{-1} qui ont été attribuées au cours de cette étude à des vibrations de symétrie B_1.

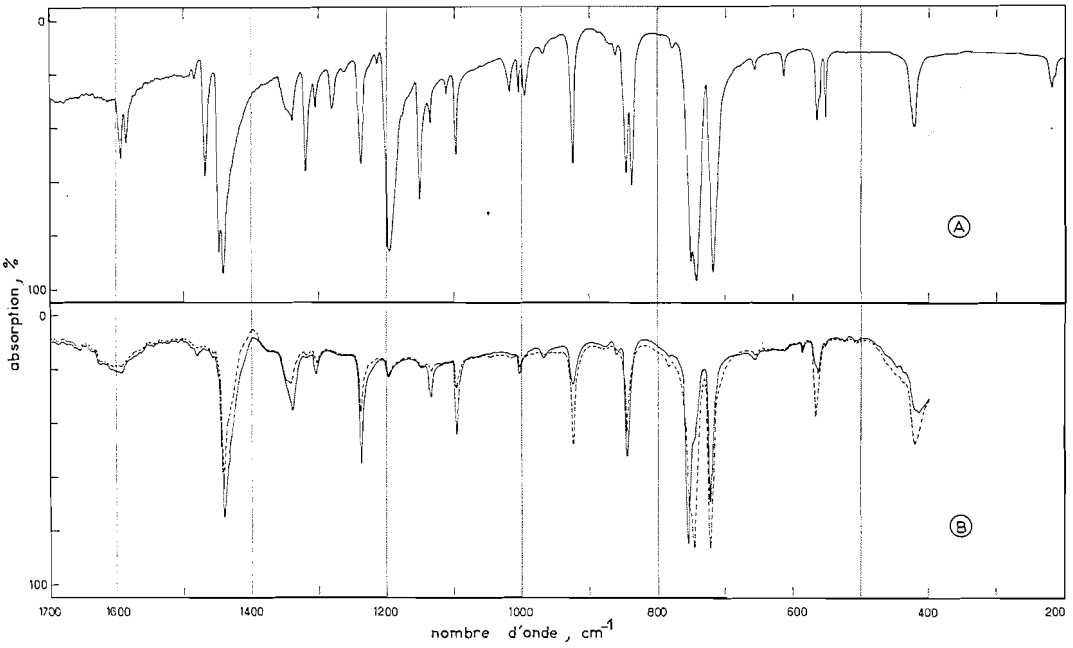


FIG. 4. Spectres infrarouges du dibenzofuranne (région 1 700 à 200 cm^{-1}) à l'état solide: (A) non orienté, (B) orienté: (- -) vecteur électrique ($\perp$), (—) vecteur électrique (||).

Le spectre du cristal orienté a été étudié en lumière polarisée pour deux orientations orthogonales du vecteur électrique. On voit sur les spectres de la Fig. 4 que pour la direction dite parallèle (||), du vecteur électrique, les bandes d'absorption de fréquences 1 485, 1 443, 1 306, 1 241, 1 146, 1 100, 1 012 et 850 cm^{-1}, relatives à des mouvements de symétrie A_1, sont plus intenses que lorsque le vecteur électrique est perpendiculaire ($\perp$) à cette première direction. Inversement, les bandes d'absorption correspondant aux vibrations de mode B_2 à 750 et 721 cm^{-1} ont une intensité maximum pour cette même orientation perpendiculaire ($\perp$) du vecteur électrique.

La structure cristalline du dibenzofuranne n'ayant pas été déterminée à notre connaissance, une interprétation rigoureuse du spectre du film cristallin orienté que nous avons réalisé est impossible, puisque le groupe spatial, le nombre et l'orientation des molécules dans la maille ne sont pas connus. Cependant, en raison du peu de différence constaté entre les spectres du dibenzofuranne sous les états solide et liquide, le couplage entre les vibrations des molécules dans la maille paraît négligeable, pour le plus grand nombre de mouvements, et le modèle de gaz "orienté", dans lequel la molécule est considérée comme isolée dans le cristal, semble applicable: donc, on peut admettre, que les vibrations de

Can. J. Chem. Downloaded from www.nrcresearchpress.com by 210.87.254.105 on 09/05/12
For personal use only.

même symétrie, doivent donner lieu à des maximums d'absorption, présentant un dichroïsme analogue, dans chaque classe de symétrie.

Vibrations de symétrie A_1

D'après ce qui précède, nous pensons que l'on peut attribuer à des mouvements de mode A_1 les maximums de fréquences 1 599, 1 345, 964, 863 et 659 cm^{-1} présentant un dichroïsme (||).

Vibrations de symétrie B_1

Nous attribuons à des oscillations de mode B_1 les bandes d'absorption vers 1 452, 1 196, 1 151, 840 et 555 cm^{-1} observées dans le spectre du dibenzofuranne liquide et qui manquent ou sont faibles dans le spectre du cristal orienté.

La fréquence 1 196 cm^{-1} a été attribuée par Tschamler et Leutner (4) à la vibration antisymétrique ν_a(C—O—C), ce qui est en accord avec notre interprétation.

Vibrations de symétrie B_2

En raison de leur dichroïsme, semblable à celui des bandes provenant des vibrations de mode B_2 à 750 et 722 cm^{-1}, les maximums à 926, 561 et 421 cm^{-1} doivent pouvoir être attribués à des mouvements de symétrie B_2. La bande faible à 782 cm^{-1} pourrait également, étant donné son dichroïsme, appartenir à une vibration de la classe B_2. Nous avions vu précédemment que la bande à 926 cm^{-1} avait une structure rotationnelle de type C probable.

(3) Discussion

L'analyse des spectres infrarouges (vapeur et solide) et du spectre Raman du dibenzofuranne a permis de dénombrer entre 1 700 et 200 cm^{-1} 15 vibrations de type A_1, 15 de type B_1, et, respectivement, 6 et 2 vibrations de modes B_2 et A_2. Mis à part les mouvements de mode A_2, 3 vibrations de mode B_2 et une de mode A_1 n'ont donc pas été identifiées.

Aux trois vibrations de mode B_2 on peut probablement faire correspondre les fréquences basses à 314, 295 et 218 cm^{-1}. Les deux premières sont communes aux spectres infrarouge et Raman, et la raie de diffusion à 295 cm^{-1} est nettement dépolarisée; la troisième fréquence n'est observée que dans le spectre infrarouge.

Les maximums de modes A_1 et B_1 sont attribuables à des oscillations de noyau et de déformation des hydrogènes dans le plan. Par analogie avec les composés aromatiques, on peut, en première approximation, situer les huit vibrations de déformation δ(CH) dans l'intervalle 1 300 – 1 000 cm^{-1}; cependant, la fréquence 1 196 cm^{-1} doit appartenir à une vibration de noyau mettant plus particulièrement en jeu la liaison (C—O—C), ainsi que nous l'avons indiqué (4).

Les vibrations de noyau et des hydrogènes hors du plan sont de symétries B_2 et A_2; les attributions faites pour les dérivés du benzène permettent de penser qu'aux vibrations γ(CH) devraient correspondre des fréquences comprises entre 926 et 726 cm^{-1}; au nombre de huit, si les vibrateurs CH sont couplés, et de quatre, s'ils sont indépendants.

(B) Region de 3 200 à 3 000 cm^{-1}

On peut envisager trois hypothèses pour interpréter les spectres de vibration du dibenzofuranne dans la région des oscillations de valence ν(CH).

(*a*) Tous les vibrateurs CH de la molécule sont couplés et donnent naissance à huit vibrations dont quatre de mode A_1 et quatre de mode B_1.

(*b*) Les vibrateurs CH d'un seul noyau sont couplés et donnent lieu à quatre vibrations de fréquences distinctes: deux de symétrie A_1 et deux de symétrie B_1.

Can. J. Chem. Downloaded from www.nrcresearchpress.com by 210.87.254.105 on 09/05/12
For personal use only.

(*c*) Les vibrateurs CH sont indépendants ce qui entraîne encore quatre vibrations de fréquences différentes : deux de symétrie A_1 tandis que les deux autres ont chacune deux composantes dirigées suivant les axes o*x* et o*y* de la molécule.

(1) Spectres infrarouges à l'état liquide et solution

Les spectres à l'état liquide et dissous (1 *M*) montrent cinq bandes d'absorption dont une bande faible à 3 064 cm^{-1}, dont l'intensité et la fréquence varient peu avec la dilution (Tableau IV).

TABLEAU IV

Fréquences de vibration du dibenzofuranne de 3 150 à 3 000 cm^{-1} sous différents états

Raman	Infrarouge						
		Solution			Cristal		
Solution (1 *M*)	liquide	1 *M*	0.01 *M*	Solide	orienté	Polarisation	Attributions
				3 117 ff	3 117 f	⊥	Combinaison
			3 108 ef				
			3 100 ef				
	3 086 f	3 091 (23)	3 091 (26)	3 087 m	3 086 m		
	3 071 f	3 075 (32)	3 075 (33)	3 071 e	3 069 e	∥	A_1 ν(CH)
3 068 (3/2) 0.14	3 064 e	3 066 e	3 066 e	3 065 F	3 064 F		A_1 ν(CH)
	3 050 F	3 054 (50)	3 054 (52)	3 050 F	3 049 F	∥	A_1 ν(CH)
				3 038 e	3 036 ff	⊥	Combinaison
	3 028 m	3 031 (23)	3 031 (27)	3 029 m	3 028 m	∥	A_1 ν(CH)
				3 018 m	3 017 m	⊥	Combinaison

NOTE : Les fréquences infrarouges à l'état dissous sont suivies du coefficient d'extinction molaire apparent. La fréquence Raman est suivie de l'intensité de la raie et du facteur de dépolarisation. F = forte, m = moyenne, f = faible, ff = très faible, e = épaulement.

(2) Spectre infrarouge à l'état vapeur

Le spectre de vibration rotation montre un massif d'absorption dont la structure rotationnelle est difficile à définir.

(3) Spectres Raman

Une raie de diffusion polarisée est présente dans les spectres Raman de la solution, à 3 068 cm^{-1} ; Behringer et Brandmuller (7) en observent une également à cette fréquence dans le spectre du solide.

(4) Spectres infrarouges à l'état solide

Les spectres sous les états solide et liquide diffèrent sensiblement dans la région de 3 150 à 3 000 cm^{-1} ; ceux du solide montrent en effet trois bandes d'absorption qui n'apparaissent pas dans le spectre du liquide à 3 117, 3 036 et 3 018 cm^{-1}, dues soit à un effet de cristal, soit à des modes de combinaison. On observe également une inversion d'intensité des deux maximums à 3 069 et 3 064 cm^{-1} ; ce dernier, intense dans le spectre du solide devient très faible dans les spectres sous les états liquide et dissous.

Les spectres entre 3 150 et 3 000 cm^{-1} du dibenzofuranne solide et à l'état de cristal orienté sont identiques. Or, nous avons vu précédemment (région de 1 700 à 400 cm^{-1}) que les bandes d'absorption qui apparaissaient simultanément dans le spectre du solide et dans celui du cristal orienté résultaient de vibrations de symétrie soit A_1, soit B_2. Il semblerait donc que le spectre infrarouge du dibenzofuranne ne présente pas d'absorptions de mode B_1 dans la région des vibrations de valence ν(CH), ce qui serait compatible avec l'hypothèse des vibrateurs (CH) indépendants seulement. Cependant, l'étude en lumière polarisée, des bandes d'absorption observées dans cette région, n'apporte aucune certitude. Le dichroïsme des maximums à 3 028, 3 049 et 3 069 cm^{-1} est assez net et

Can. J. Chem. Downloaded from www.nrcresearchpress.com by 210.87.254.105 on 09/05/12
For personal use only.

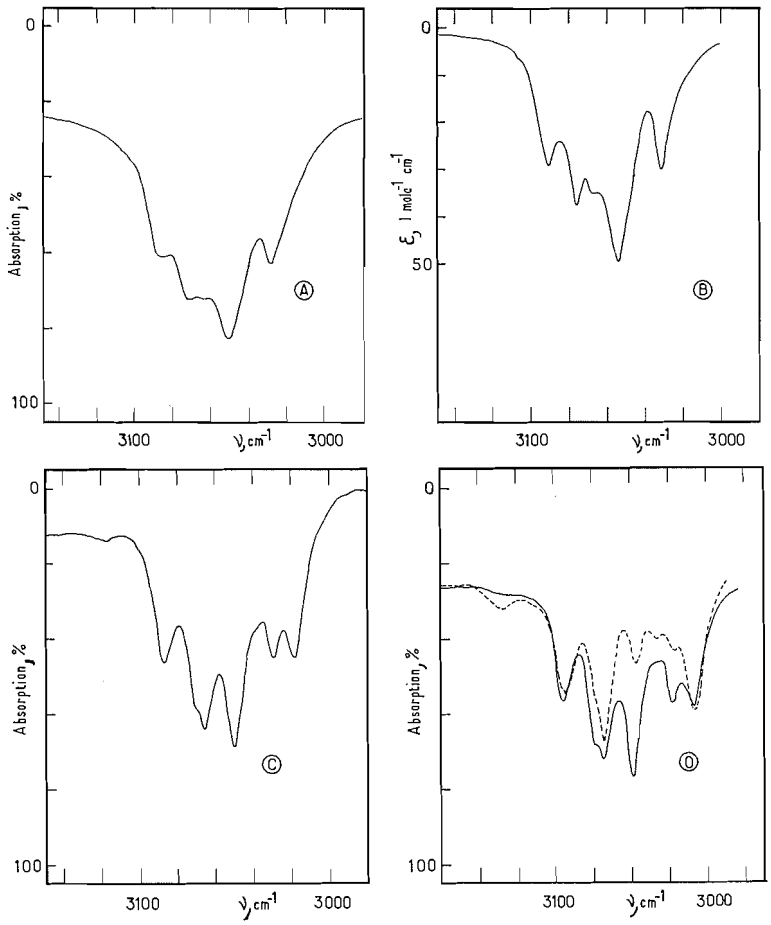


FIG. 5. Spectres infrarouges du dibenzofuranne dans la région de 3 150 à 3 000 cm^{-1}, sous les états: (A) liquide, (B) solution à 1 *M*, (C) solide (dans l'hexachlorobutadiène), (D) cristal orienté: (—) vecteur électrique (∥), (- -) vecteur électrique (⊥).

semblable à celui des vibrations de type A_1 (Fig. 5 et Tableau IV). La forte bande d'absorption de fréquence 3 064 cm^{-1} qui correspond vraisemblablement à la raie Raman polarisée à 3 068 cm^{-1}, du spectre à l'état dissous, devrait aussi appartenir à une vibration de mode A_1, bien que son dichroïsme ne permette pas de l'affirmer (Fig. 5).

(4) Discussion

Dans l'hypothèse des vibrateurs CH indépendants, il faudrait admettre que les autres maximums observés entre 3 150 et 3 000 cm^{-1} sont dus à des vibrations de combinaison ou à des effets de cristal, ce qui est certainement le cas pour les bandes à 3 017, 3 036 et 3 117 cm^{-1} qui n'apparaissent que dans le spectre du solide, mais rien ne permet de rattacher à des modes de combinaison l'absorption à 3 086 cm^{-1}, ni les épaulements à 3 108 et 3 100 cm^{-1} du spectre à l'état dilué.

CONCLUSION

Cette étude nous a permis de situer la plupart des vibrations de modes A_1, B_1, B_2 du dibenzofuranne (Tableau V).

Can. J. Chem. Downloaded from www.nrcresearchpress.com by 210.87.254.105 on 09/05/12
For personal use only.

TABLEAU V

Fréquences de vibration fondamentales du dibenzofuranne entre 1 700 et 200 cm^{-1}

Mode de symétrie			
A_1	B_1	B_2	A_2
1 599 (*b*)	1 635 (*a*)	926	734
1 485 (*b*)	1 586	785 probable	451
1 443 (*b*)	1 470	750	
1 345	1 452	721	
1 306 (*a*)	1 353 (*a*)	561	
1 241 (*a*)	1 318	421 (*a*)	
1 183	1 282	314 probable	
1 146 (*a*)	1 196	293 (*a*)	
1 100 (*a*)	1 151	218 (*a*) probable	
1 012 (*a*)	1 110		
964 (*a*)	1 022		
863	1 002		
850 (*a*)	840		
746 (*a*)	616		
659	555 (*a*)		

NOTE: les fréquences marquées (*a*) et (*b*) sont attribuées par Teplyakov (8): (*a*) à des vibrations fondamentales, (*b*) à des vibrations fondamentales ou de combinaison.

Notre interprétation des spectres de vibration du dibenzofuranne, vérifiant l'hypothèse de la symétrie C_{2v} de cette molécule, confirme sa structure très probablement plane.

Bien qu'en première approximation les vibrateurs CH paraissent indépendants dans les vibrations de valence ν(CH), les spectres ne permettent pas de conclure définitivement à l'absence de couplage.

Nous n'avons observé que deux vibrations de mode A_2. Rappelons que dans le cas où les vibrateurs CH ne seraient pas couplés dans les mouvements hors du plan γ(CH), cinq vibrations de mode A_2 seulement de fréquences distinctes seraient attendues (Tableau I).

CONDITIONS EXPÉRIMENTALES

Le dibenzofuranne utilisé dans ce travail est un produit Fluka; recristallisé d'après la technique de Cass *et al.* (15), il a un point de fusion de 81.5 à 82°.

Les spectres infrarouges ont été enregistrés sur spectrophotomètres Perkin–Elmer, double faisceau, à deux réseaux, modèle 125 de 4 000 à 400 cm^{-1} et modèle 225 de 400 à 200 cm^{-1}.

Ils ont été réalisés:

(*a*) À l'état gazeux à l'aide d'une cellule chauffante Perkin–Elmer, de 5 cm d'épaisseur à fenêtres de KBr à une température d'environ 190 °C.

(*b*) À l'état dissous dans le tétrachlorure de carbone pour les régions de 3 100 cm^{-1} et 1 500–1 250 cm^{-1}, le tétrachlorure d'éthylène entre 1 800 et 1 500 cm^{-1}; le sulfure de carbone entre 1 250 et 400 cm^{-1}.

(*c*) À l'état liquide, avec une cuve chauffante Perkin–Elmer à une température voisine de 82°.

(*d*) À l'état solide, sous forme de pastille de bromure de potassium et, entre 450 et 200 cm^{-1}, de dispersion dans l'hexachlorobutadiène.

(*e*) À l'état de cristal orienté, par fusion et refroidissement du produit entre deux fenêtres de KBr. Un domaine bien orienté a été délimité en examinant les lames entre deux polaroïds croisés. Les spectres de ce cristal ont été réalisés en lumière polarisée au moyen de polariseurs de transmission Perkin–Elmer en AgCl. Pour le premier enregistrement ($\parallel$), le cristal a été orienté de telle sorte que l'intensité de la bande d'absorption à 1 440 cm^{-1} soit maximum; le cristal a été tourné de 90° dans la deuxième expérience ($\perp$) (cf. Fig. 4).

Les spectres Raman ont été réalisés à l'état dissous (1 *M*) dans le benzène et le tétrachlorure de carbone avec un spectrographe Hilger et Watts, Type E–612, le tube Raman mesurait 22 cm de long et 9 mm de diamètre intérieur. Un filtre de nitrite de sodium permettant de sélectionner la raie excitatrice à 4 358 Å du mercure a été utilisé.

Les spectres ont été photographiés sur plaques à partir desquelles un enregistrement a été effectué à l'aide d'un microphotomètre Hilger L 470.

Les facteurs de dépolarisation ont été mesurés par la technique d'Edsall et Wilson (16) et corrigés d'après la méthode de Rank et Kagarise (17).

Can. J. Chem. Downloaded from www.nrcresearchpress.com by 210.87.254.105 on 09/05/12
For personal use only.

REMERCIEMENTS

Nous remercions Monsieur le Professeur Pesteil des échanges d'idées et discussions que nous avons eus avec lui au cours de ce travail et de sa rédaction.

BIBLIOGRAPHIE

1. L. H. Briggs et L. D. Colebrook. J. Chem. Soc. 2458 (1960).
2. R. B. Barnes, U. Liddel et V. Z. Williams. Ind. Eng. Chem. **15**, 659 (1943).
3. M. P. Groenewege. Spectrochim. Acta, **11**, 579 (1957).
4. H. Tschamler et R. Leutner. Monatsh. Chem. **83**, 1502 (1952).
5. P. Donzelot et M. Chaix. Compt. Rend. **202**, 851 (1936).
6. J. Behringer. Z. Elektrochem. **62**, 544 (1958).
7. J. Behringer et J. Brandmuller. Z. Angew. Phys. **14**, 674 (1962).
8. P. A. Teplyakov et V. V. Trisov. Opt. Spectry. **18**, 32 (1965).
9. N. M. Cullinane et C. A. J. Plummer. J. Chem. Soc. 63 (1938).
10. E. Merkel et C. Wiegan. Naturforscher, **3b**, 93 (1948).
11. V. Schomaker et L. Pauling. J. Am. Chem. Soc. **61**, 1769 (1939).
12. J. Waser et V. Schomaker. J. Am. Chem. Soc. **65**, 1451 (1943).
13. R. M. Badger et L. R. Zumwalt. J. Chem. Phys. **6**, 711 (1938).
14. R. N. Jones et C. Sandorfy. *Dans* Technique of organic chemistry. IX. *Édité par* A. Weissberger. Interscience, New York. 1958. p. 247.
15. R. C. Cass, S. E. Fletcher, C. T. Mortimer, H. D. Springall et T. R. White. J. Chem. Soc. 1406 (1958).
16. J. T. Edsall et E. B. Wilson. J. Chem. Phys. **6**, 124 (1938).
17. D. H. Rank et R. E. Kagarise. J. Opt. Soc. Am. **40**, 89 (1950).

Can. J. Chem. Downloaded from www.nrcresearchpress.com by 210.87.254.105 on 09/05/12
For personal use only.

Can. J. Chem. Downloaded from www.nrcresearchpress.com by 210.87.254.5 on 09/05/12
For personal use only.

NOTES

A STUDY BY ELECTRON PARAMAGNETIC RESONANCE SPECTROSCOPY OF RADICALS FORMED FROM ACETAMIDE AND FORMAMIDE[1]

P. SMITH AND P. B. WOOD

Previous electron paramagnetic resonance spectral studies in this laboratory have involved simple free radicals, with π-type delocalization, formed by hydroxyl-radical attack on aliphatic carboxylic esters (1) within an aqueous flow system, e.g. the radicals $\dot{C}H_2COOCH_3$ and $HCOO\dot{C}H_2$. For such radicals small long-range hyperfine couplings across the oxycarbonyl group were resolved. In an extension of the above work, this report presents the results for hydroxyl-radical attack on two simple aliphatic amides acetamide and formamide. Well-resolved spectra showing long-range couplings across the carbonyl group were obtained for both compounds. Acetamide gave a spectrum consistent with the radical $\dot{C}H_2CONH_2$; formamide, an absorption assigned to the radical $HC\dot{O}NH$. The latter appears to be the first case in which a radical resulting from abstraction of a hydrogen atom bonded to a nitrogen atom has been observed with aqueous flow techniques.

EXPERIMENTAL

The basic experimental arrangement has been described before (1). Hyperfine coupling constants were measured by means of the Varian Fieldial accessory. *g*-Factors were taken using a frequency meter (Hewlett Packard model X532B) by comparison with peroxylamine disulfonate on the assumption that its *g*-factor is 2.00550 (2), the procedure followed being similar to that of Sicilio *et al.* (3). The flow system was modified to include the mix-and-flow cell of Borg (4). Eastman white label acetamide was used as substrate before and after recrystallization from benzene – ethyl ether, the results obtained with both materials being indistinguishable. The formamide used as substrate was Fisher reagent grade. Unpurified formamide gave spectra suggesting the presence of a significant proportion of methanol impurity. This was effectively removed by fractional distillation under reduced pressure. The following reaction conditions were employed: total flow rate, 2–8 ml s^{-1}, this being kept equally divided between the two streams; reaction temperature, $25 \pm 2 - \sim 45$ °C; titanous chloride concentration in the reducing stream, 0.01–0.003 M; hydrogen peroxide concentration in the oxidizing stream, 0.04–0.3 M; added sulfuric acid concentration in both streams, 0.2–0.0 M. Apart from signal intensity changes, the only significant result produced by these variations was an improvement in the resolution of the small doublet splitting in the spectrum obtained from formamide, a consequence of lowering the titanous chloride concentration while raising that of the hydrogen peroxide to maintain a high enough signal level. Unless otherwise specified the results reported refer to the first listed value for each parameter. The substrates were included in both streams, the minimum concentrations necessary to quench the hydroxyl-radical signal being 1.0 and 0.4 M for acetamide and formamide, respectively.

[1]*This investigation was supported by United States Public Health Service Grant GM 07653, Division of General Medical Sciences.*

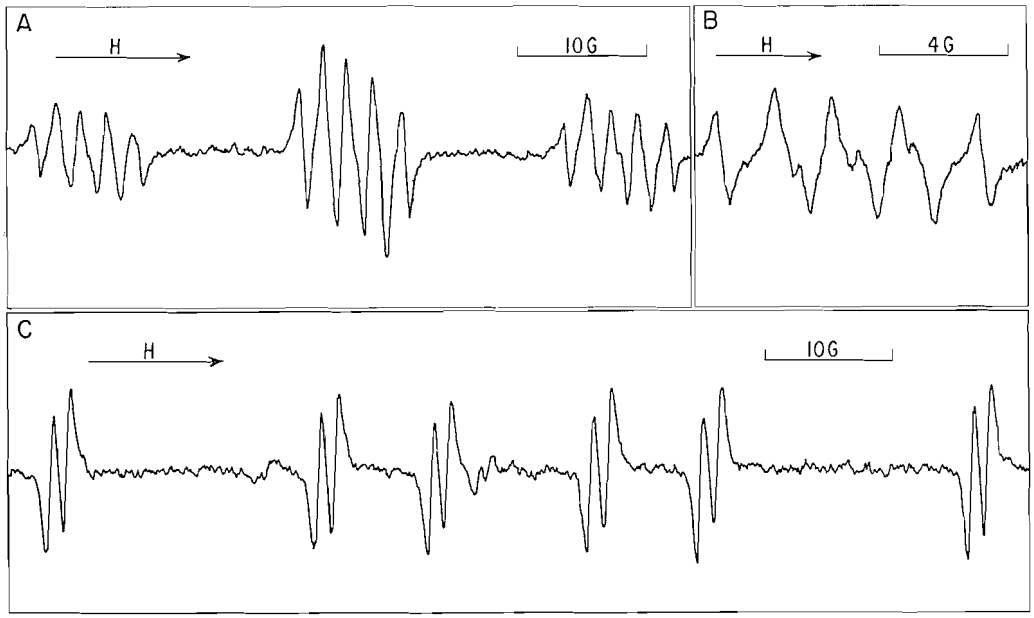


FIG. 1. First-derivative electron paramagnetic resonance spectra for the reaction of hydroxyl radicals with acetamide and formamide at 27 °C. (A) and (B). Acetamide. Concentrations in the reacting streams: CH_3CONH_2, 1.2 *M*; $TiCl_3$, 0.008 *M*; H_2O_2, 0.01 *M*; H_2SO_4, 0.1 *M*; (A) a complete spectrum; (B), a slower scan of the central quintet shown in (A) with reduced modulation. (C). Formamide. Concentrations in the reacting streams: $HCONH_2$, 0.4 *M*; $TiCl_3$, 0.006 *M*; H_2O_2, 0.2 *M*; H_2SO_4, 0.1 *M*.

RESULTS AND DISCUSSION

With acetamide as the substrate the spectrum observed under comparatively fast sweep conditions was a wide (21.3 G) triplet (1:2:1) of narrow ($\sim$ 2 G) apparent quintets (2:3:4:3:2), as shown in Fig. 1(A). Slower scans revealed that the central three lines of each quintet showed signs of extra, incompletely resolved splittings indicating a total of eight lines. For the central apparent quintet this feature is illustrated in Fig. 1(B). The size of the major triplet coupling and its intensity distribution are consistent with the radical $\cdot CH_2CONH_2$. For this radical trapped in irradiated amorphous acetamide Gordy and co-workers (5, 6) have found $a_H^{CH_2}$ to be $\sim$ 23 G (7). Moreover, in radicals of functional structure —ĊH—CO— values of 20–23 G for $a_H^{CH_2}$ are normal (1, 8), e.g. for the $\cdot CH_2COOH$ radical in aqueous solution $a_H^{CH_2}$ has been reported to be 21.3 G (1) and 21.7–21.8 G (8). The subsidiary eight-line patterns are attributed to the expected (1) π-type delocalization[2] which leads to hyperfine splitting due to the ^{14}N nucleus together with the possibility of extra splitting arising from coupling with the two amide protons. In this connection it would not be expected that more than two protons should be observed to couple under the employed reaction conditions since amides are very weak bases (10). The details of the eight-line patterns appear inconsistent with couplings of different size from ^{14}N and two equivalent protons, which would yield a triplet (1:1:1) of triplets (1:2:1). A more plausible interpretation is that they arise from a quartet (1:2:2:1) of doublets (1:1)

[2]*That* $a_H^{CH_2}(\cdot CH_2COOH)$ *is close to the size of* $a_H^{CH_2}(\cdot CH_2CONH_2)$ *suggests that about 10% of the unpaired electron density in* $\cdot CH_2CONH_2$ *is delocalized through the amide group, for a similar extent of delocalization into the carboxyl group occurs in the case of* $\cdot CH_2COOH$ *(1). The size of* $a_N(\cdot CH_2CONH_2)$ *is consistent with this extent of delocalization, for unit unpaired electron density on nitrogen in a planar radical gives* a_N *equal to 23.0 G (2). Furthermore, a recent single-crystal study (9) of the radical* $CH_2(CONH_2)\dot{C}HCONH_2$ *reports isotropic coupling constants,* $a_H^{CH_2}$ *and* a_N, *and a spin density on the α-amide-group nitrogen atom in general agreement with this present work.*

Can. J. Chem. Downloaded from www.nrcresearchpress.com by 210.87.254.5 on 09/05/12
For personal use only.

with coupling constants 2.0 and 2.5 G, respectively. The resultant overall theoretical intensity distribution (1:2:1:2:2:1:2:1) is in accord with that observed experimentally, considering the incomplete resolution achieved. A similar absorption would result if the ^{14}N nucleus and one amide-group proton had essentially equal coupling constants (2.0 G) and the remaining amide-group proton had a different coupling constant (2.5 G). Roughly equal splittings for ^{14}N and for protons bonded to ^{14}N are well known in the case of related radicals, e.g. $\cdot N_2H_4^+$ (2), $\cdot NH_3^+$ (11), and $\cdot ONH_2$ (12). The spectroscopic results obtained with acetamide are given in Table I.

TABLE I

Hyperfine coupling constants and g factors at 25 ± 2 °C for radicals formed by hydroxyl-radical attack on acetamide and formamide*

		Hyperfine coupling constants, G			
Radical	g-Factor†	$a_H^{CH_2}$	$a_N^{NH_2}$	$a_{H(1)}^{NH_2}$	$a_{H(2)}^{NH_2}$
$\cdot CH_2CONH_2$	2.0034	21.28	1.96‡	1.96‡	2.53‡

		Hyperfine coupling constants, G		
Radical	g-Factor	a_N^{NH}	a_H^{NH}	a_H^{CH}
$HC\dot{O}NH$	2.0016	21.65	30.55	1.22

*Each coupling constant given is the arithmetical mean of all measurements of that coupling constant taken from several field scans. Unless otherwise specified, the maximum uncertainty in each constant is ± ~0.05 G.
†The estimated maximum uncertainty is ±0.0002.
‡These values are not very precise because the absorption arising from the NH_2 group was only incompletely resolved; the maximum uncertainty in each of these values is estimated to be ±0.2 G.

The non-equivalence of the two amide-group protons is noteworthy and implies a considerable degree of hindered rotation about the C—N bond in the radical. Rotational isomerism arising from hindered rotation about the C—N bond is well established for many amides (12, 13). The π-type delocalization of the unpaired electron on to the nitrogen atom present in the radical $\cdot CH_2CONH_2$ should enhance this kind of rotational hindrance. Given this restriction to free rotation and the low molecular symmetry for this radical, assuming the normal planar-type structure of the parent molecule (10) to apply, the splittings from the two amide-group protons would not, a priori, be expected to be equal. The size of the ratio ($a_N/a_H^{NH_2}$) does not deviate far from the value of 1.06 expected for a planar radical with a sp^2-hybridized nitrogen atom (2). The fact that a_N and $a_H^{NH_2}$ for one amide-group proton are apparently equal, bearing in mind that the peak-to-peak line widths are ~ 0.5 G, must be coincidental.

The spectrum obtained from formamide was a wide (21.7 G) triplet of wide (30.6 G) doublets (1:1), each line of which displayed a narrow (1.2 G) doublet (1:1) splitting. A typical spectrum is shown in Fig. 1(C). Of the various conceivable, direct or indirect, products of hydroxyl-radical attack on formamide, the observed absorption seems most consistent with the radical $HC\dot{O}NH$. In view of the low reactivity toward hydroxyl radicals of acetamide relative to formamide, it is interesting that the site of hydrogen-atom abstraction is so clearly different for these two substrates. Perhaps the $HC\dot{O}NH$ radical is formed via some undetected species, e.g. by the rearrangement of the radical $\cdot CONH_2$. However, there is no evidence for any other radical species in spectra taken over the fullest possible range of conditions for both substrates. Other formyl substrates have been found to show particularly high reactivity in this reaction system. For example, formic acid is more reactive than acetic acid, their respective minimum molarities for quenching the hydroxyl-radical signal under conditions similar to those employed in this

Can. J. Chem. Downloaded from www.nrcresearchpress.com by 210.87.254.5 on 09/05/12
For personal use only.

work being 0.3 and 1.0 (P. Smith and P. B. Wood, unpublished results), in qualitative agreement with the relative reactivities of these acids toward hydroxyl-radical attack found by pulse radiolytic studies (14). However, the selectivity of hydroxyl-radical attack on these two acids has not yet been conclusively elucidated (1). The spectroscopic results obtained for formamide are given in Table I.

The value of a_N for HCONH is larger than those for the related radicals $\cdot NH_2$, $\cdot ND_2$, and $\cdot NF_2$ which have been studied in inert gas matrices at about 4 °K (15, 16). This is not considered to be inconsistent with the proposed assignment of the spectrum to HCONH, for it is clear that the size of a_N in radicals of this type is markedly dependent on radical structure (considerably larger ^{14}N couplings have been reported for iminoxy radicals in which a considerable proportion of the unpaired electron density is expected to reside on oxygen rather than nitrogen (17)). Further support for the proposed assignment is provided by the *g*-value for this radical, 2.0015, which is somewhat lower than those for species such as $\cdot NH_2$, 2.0048 (15), in harmony with the expected greater delocalization (18) of the unpaired electron in HCONH compared with $\cdot NH_2$. Extensive delocalization would result in a radical formally analogous to allyl, $\dot{C}H_2—CH=CH_2 \leftrightarrow CH_2=CH—\dot{C}H_2$, i.e. $O=CH—\dot{N}H \leftrightarrow \dot{O}—CH=NH$ in which the splitting from the central proton arises from exchange interaction with negative spin density on the central carbon nucleus (19). The formyl proton coupling constant in HCONH is approximately one quarter of that of the central proton in the allyl radical, suggesting that delocalization is appreciable but somewhat less than in allyl itself. π-Type delocalization should keep HCONH planar and thus constrict the formyl hydrogen atom to the modal plane of the π-system, thereby preventing any hyperconjugative interaction between the formyl hydrogen atom and the unpaired spin density on the nitrogen atom. It is hoped to present the results of molecular orbital treatments of the delocalization in radicals such as HCONH and $\dot{C}H_2CONH_2$ in a later publication dealing also with the extension of this investigation to a number of other simple aliphatic amides.

1. P. Smith, J. T. Pearson, P. B. Wood, and T. C. Smith. J. Chem. Phys. **43**, 1535 (1965).
2. J. Q. Adams and J. R. Thomas. J. Chem. Phys. **39**, 1904 (1963).
3. F. Sicilio, R. E. Florin, and L. A. Wall. J. Phys. Chem. **70**, 47 (1966).
4. D. C. Borg. Nature, **201**, 1087 (1964).
5. C. F. Luck and W. Gordy. J. Am. Chem. Soc. **78**, 3240 (1956).
6. I. Miyagawa and W. Gordy. J. Am. Chem. Soc. **83**, 1036 (1961).
7. M. T. Rogers, S.-J. Bolte, and P. S. Rao. J. Am. Chem. Soc. **87**, 1875 (1965).
8. W. T. Dixon, R. O. C. Norman, and A. L. Buley. J. Chem. Soc. 3625 (1964).
9. M. Kashiwagi. J. Chem. Phys. **44**, 2823 (1966).
10. L. Pauling. Nature of the chemical bond. 3rd ed. Cornell University Press, Ithaca, New York. 1960. p. 281.
11. T. Cole. J. Chem. Phys. **35**, 1169 (1961).
12. C. J. W. Gutch and W. A. Waters. J. Chem. Soc. 751 (1965).
13. J. A. Pople, W. G. Schneider, and H. J. Bernstein. High-resolution nuclear magnetic resonance. McGraw-Hill Book Company, Inc., New York. 1959. p. 366. R. J. Gillespie and T. Birchall. Can. J. Chem. **41**, 148 (1963).
14. G. E. Adams, J. W. Boag, J. Currant, and B. D. Michael. *In* Pulse radiolysis. *Edited by* M. Ebert. Academic Press, New York. 1965. p. 117.
15. S. N. Foner, E. L. Cochran, V. A. Bowers, and C. K. Jen. Phys. Rev. Letters, **1**, 91 (1958).
16. P. H. Kasai and E. B. Whipple. Mol. Phys. **9**, 497 (1965).
17. J. R. Thomas. J. Am. Chem. Soc. **86**, 1446 (1964).
18. T. Kawamura, S. Matsunami, T. Yon-Ezawa, and K. Fukui. Bull. Chem. Soc. Japan, **38**, 1935 (1965).
19. R. W. Fessenden and R. H. Schuler. J. Chem. Phys. **39**, 2147 (1963).

Received August 17, 1966.
Department of Chemistry,
Duke University,
Durham, North Carolina.

Can. J. Chem. Downloaded from www.nrcresearchpress.com by 210.87.254.5 on 09/05/12
For personal use only.